



13th World Congress on Computational Mechanics
2nd Pan American Congress on Computational Mechanics



New York City, NY • July 22 – 27, 2018

ABSTRACTS

13th World Congress on Computational Mechanics

July 22-27, 2018

New York City, NY

USA

The following abstracts were presented at the 13th World Congress on Computational Mechanics (WCCM2018), held in New York City, July 22-27, 2018. The document contains extended abstracts of approximately 12 pages each, in addition to one-page abstracts. All abstracts were reviewed by a congress organizer before acceptance.

The abstracts are in order of the presenting author.

Congress Organizers
WCCM2018

Integrated Nonlinear Multi-scale Material Modelling of Composite Materials Using Digimat

Laurent ADAM*

*MSC Software Belgium S.A. (e-Xstream engineering)

ABSTRACT

The simulation of composites has to master several characteristics of these materials (anisotropic behavior following the local microstructure, nonlinear behaviors and various failure mechanisms, effects of residual stresses, strain rate and temperature dependences, etc) in order to deliver predictive results. Multi-scale methods relying on continuum models which enable to account for the material microstructure and constituents properties are becoming standards across the industry. Amongst these methods, mean-field and full-field homogenization methods are used for years in order to predict the nonlinear stiffness and strength of heterogeneous materials like composites. Such methods are commonly used to perform material engineering, virtual testing and also ICME. In order to be used in the industry, such methods have not only to reach a sufficient level of TRL but also be efficient, available in smooth and easy to use workflows, and cover various application cases, from simple stress analysis over the investigation of crash performance of composite part. The current presentation will show latest advances in combining mean and full-field homogenization methods in order to predict composite stiffness and strength. Different linking and coupling methods will also be shown in order to propagate material behaviors in between the different scales as well as from the process to the structural simulation. These different coupling methods allows to balance CPU time with the richness of the generated results. Material variabilities can also be studied numerically by using such simulation chain so that, for example, allowable (A/B basis) can be computed. The supporting technologies are developed in Digimat and will be exposed during the presentation. Representative applications will also be illustrated.

Robust Water Flooding Reservoir Management Based on Surrogate Models

SILVANA AFONSO*, Jefferson Wellano**, Ramiro Willmersdorf***

*Federal University of Pernambuco, **Federal University of Pernambuco, ***Federal University of Pernambuco

ABSTRACT

A big challenge in water flooding reservoir optimization is the reservoir spatial variability and the uncertainties at geological parameters. An approach to reduce the uncertainties impact on the solutions is named robust optimization. In this work it will be built an automatic tool for optimal robust management based on a different optimization formulation. This is in contrast with most of works reported in literature in which robust optimization is based on uniobjective problem formulation, combining in a unique weight function the expected function and standard deviation of the net present value (NPV). Here, robust optimization will be conducted from a given set of realizations. The NPV is calculated for each realization considering pre-defined rate controls. A small subset of realizations is selected aiming time processing reduction for the statistics calculations. Two approaches of selecting a representative subset of realizations are done, one ranks the realizations according to the performance of each realization in terms of NPV (Net Present Value), the other is based on clustering the uncertain field, e.g. in terms of permeability field, using a K-means procedure. In order to reduce simulation costs due to several function calls required in the optimization process, data fitting based surrogate models are applied in the Sequential Approximated Optimization strategy. The optimization results based on the realizations subset is then applied to all existing realizations. It was found that the net present value evaluated at the robust optimization solution is almost independent of economical parameters such as produced oil costs, injected and produced water costs. This means that uncertainties found on NPV calculations are due to geological parameters. Finally, the technical applicability of the proposed tool will be checked against a benchmark example reported in literature.

Reliability-based Maintenance Optimization Planning of Logistic Corridor Bridges by Using Time-variant Reliability Analysis and Kriging Metamodeling

Younes AOUES*, Arnaud KNIPPEL **, Eduardo SOUZA DE CURSI***

*Normandie Univ, INSA Rouen Normandie, LMN, 76000 Rouen, France, **Normandie Univ, INSA Rouen Normandie, LMI, 76000 Rouen, France, ***Normandie Univ, INSA Rouen Normandie, LMN, 76000 Rouen, France

ABSTRACT

Logistic corridors fluidity depends on the reliability of infrastructure transportations. Highway bridges are considered the most critical and vital links in any transportation network, where a full or partial failure of these infrastructures leads to decrease the operational efficiency of the network and can provoke serious economic impacts. These infrastructures undergo various degradation (decay, aging, corrosion, fatigue) due to the weather conditions, natural disaster, the increase in traffic of the last decades. In the current economic context, the prolongation of infrastructure lifetime is based on the maintenance and rehabilitation operations. However, the scheduling management of several infrastructures throughout the life cycle involves the search of the best compromise between conflicting objectives and requirements. This study presents an efficient approach integrating uncertainty in the decision making of the maintenance planning optimization. The optimal planning of the maintenance and inspection actions is the best solution that minimizes the total expected total cost of an infrastructure network while fulfilling reliability and functionality requirements over the lifetime. The total expected cost is composed from the maintenance costs and the failure cost due to failure consequences. This approach is based on quantitative evaluation of the structural performance in term of reliability and risk, where the reliability-based maintenance optimization approach aims to provide the optimal and robust solution of the maintenance plan, that are less sensitive for the various uncertainties affecting the system. Predictive degradation models have already been used to predict maintenance operations. However, a purely deterministic approach limits the quality of the provided solution. Thus, the rational approach is to use the probability theory to predict the future condition. Time-variant reliability analysis can be used for predicting the performance of infrastructure components, systems and networks. The time variant reliability analysis allows to capture the time-dependence of the probability of failure and the uncertainty of the deterioration process. However, for realistic situation, the time-variant reliability analysis is very time consuming because it requires several evaluations of the mechanical model describing the structural behavior. Thus, Kriging metamodeling aims to overcome this issue, where the mechanical model is replaced by a simple analytical function that is easy to evaluate. This paper presents an original approach of the reliability-based maintenance optimization in conjunction with time-variant reliability analysis and kriging metamodels for programming maintenance actions. The proposed approach is used to find the optimal maintenance planning of bridges in order to increase the fluidity of the logistic corridors of the Normandy region.

Establishment of Bounds for the Statistical Moments of the Crack Size Using the Fast Bounds Crack Method According to the Collipriest Model

CLAUDIO ROBERTO AVILA DA SILVA JÚNIOR*, LUCAS GIMENIS DE MOURA**

*PPGEM/UTFPR-CURITIBA, **PPGEM/UTFPR-CURITIBA

ABSTRACT

The existence of cracks in a realistic approach of structures and mechanical components is admitted. Their presence is generally associated with the phenomenon of fatigue. There are several mathematical models that describe the propagation of cracks. In general, crack propagation models are classified by the type of loading, which can be a loading with constant amplitude of stress (CAS) or variable amplitude of stress (VAS). For many engineering applications, up to a certain point, it is not necessary to have great accuracy in predictions about the behavior of the evolution of a crack, but a reliable prediction, within certain limits, of such behavior. This work presents theoretical results consisting in obtaining lower and upper bounds that “envelop” the first and second order statistical moment estimators of the crack size function based on the Fast Bounds Crack method. These bounds are polynomials defined in the variable “number of cycles” that consider the uncertainties of the parameters that describe the crack propagation models. The performance of the bounds for the statistical moments of the crack size is evaluated through the relative deviation between the bounds and the approximate numerical solutions of the initial value problems (IVP) that describe the crack evolution laws. For this work, the Collipriest model will be used. Quantification of these uncertainties will be done with aid of the Monte Carlo method. In general, the definition of the function “factor of correction of the stress intensity factor” makes it impossible to obtain the explicit determination of the function “crack size”. Thus, the IVP solution describing the Collipriest model can be obtained through the use of numerical methods, such as the explicit fourth-order Runge-Kutta method (RK4). The use of a computational environment makes it possible to evaluate the computational time of the proposed methodology and the deviations of the bounds from the approximate solutions, confirming the efficiency of the method.

Density-based Topology Optimization of Coated Structures Subject to Dynamic Loading

Niels Aage^{*}, Malte Wollert Torp^{**}, Frank Edberg Olsen^{***}

^{*}Technical University of Denmark, ^{**}Technical University of Denmark, ^{***}Technical University of Denmark

ABSTRACT

Topology optimization and additive manufacturing forms a near perfect match, in which the design freedom from the material distribution methods complement the geometric freedom provided by 3D printing and vice versa. Therefore, many obvious directions for further extensions and research exist, with one of them being the design of optimized coating and infill patterns for light weight constructions as shown in e.g. [1,2]. The basic idea of the coating approach is to use the projected gradient of the density field to identify the coating region and to overlay this with the background density field to obtain a single-design field representation of interior, void and coating domains. The infill approach, on the other hand, consists of adding a local volume constraint to the interior domain through a second design variable field. The second design is filtered to ensure a prescribed level of design freedom and the locality is circumvented by a p-norm statement. Thus, one extra design field and one extra constraint is all that is needed compared to the standard minimum compliance problem. The novelty of the presented work consists of extending the above methodologies to cover dynamic loading and adding the possibility to have two distinct materials in the coating region; for example one with highly damping material properties (and a high cost) and one with standard material properties (and a low cost). Firstly, the dynamics are introduced as harmonic loading in the low frequency range. This, amongst others, means that full material utilization is no longer optimal for all problems. To alleviate this we introduce modifications to the interpolation functions and derive bounds on material property-ratios that ensure crisp material interfaces. Secondly, introducing the extra material in the coated region requires the addition of yet a design field as well as the development of new material interpolation functions. We show that this can be obtained by a total of ten filters/projections operations on a total of three globally defined design fields. The application of the proposed design methodology is demonstrated on a number of numerical examples in which different forms of dynamic compliance measures are minimized. [1] Clausen, A., Aage, N., & Sigmund, O. (2015). Topology optimization of coated structures and material interface problems. *CMAME*, 290, 524–541. [2] Wu, J., Aage, N., Westermann, U., & Sigmund, O. (2017). Infill Optimization for Additive Manufacturing –Approaching Bone-like Porous Structures. *IEEE Trans. Vis. Comput. Graph* 24(2), 1127–1140.

Planar 3D: A Scalable, Hybrid Parallel Simulator for Multiple Hydraulic Fractures

Safdar Abbas^{*}, Aman Verma^{**}, Anthony Peirce^{***}

^{*}Schlumberger, ^{**}Schlumberger, ^{***}University of British Columbia

ABSTRACT

Planar 3D models have been developed as an alternative to both simplistic pseudo 3D models and full 3D models to better predict fracture propagation in a vertical plane with different vertical layer properties. One of these planar 3D models has been enhanced recently with the possibility to simulate the propagation of multiple simultaneous fractures. The referenced model is distinguished from other planar 3D approaches by the more accurate treatment of the fracture front crossing the layered interfaces by incorporating a multilayer elasticity equation (spectral-based displacement discontinuity), fluid flow (2D finite difference method with zero flux boundary conditions), leakoff, and fracture propagation (a consistent volume of fluid formulation accounting for rock toughness and different fracture propagation regimes) in one fully coupled robust and efficient scheme. The proppant transport model also accounts for proppant packing and bridging. In this enhancement of the planar 3D approach, the fracture communication and impact of the fractures on each other's growth are modeled through a wellbore communication algorithm and the stress shadow effect. The enhanced fidelity and capabilities of the simulator would normally incur a significant computational expense. However parallel programming paradigms are leveraged to drastically reduce the simulation runtime. This enables engineers to explore the vast decision space in reasonable time for optimal completion design. Note that domain decomposition in the context of DDM is very challenging without Fast Multipole Methods. Hence a multi-level, hybrid parallel framework is designed to provide greater throughput from an efficient single fracture simulator. Each fracture can be simulated using multiple CPU cores and GPU on a single node. This is implemented using vectorization (AVX), shared memory parallelization (TBB, OpenMP) and offloading to GPU (CUDA). This single fracture simulator is encapsulated in an MPI based wrapper which enables the entire simulation to run on multiple, distributed nodes. This hybrid parallel simulator is shown to exhibit good performance scaling with the number of fractures. It has been commercially deployed in the public cloud (Microsoft, Google) for several years now. The robustness and scalability of the model are demonstrated by application to field cases.

Moment-Guided Isogeometric Analysis for the Boltzmann Equation

Michael Abdelmalik*, Thomas Hughes**

*ICES University of Texas at Austin; Eindhoven University of Technology, **ICES University of Texas at Austin

ABSTRACT

Kinetic theory of fluids is concerned with a generalized phase-space description of molecular flow. In kinetic theory, the description of fluid dynamics is based on the Boltzmann equation that governs a one-molecule phase-space distribution which depends on velocity, space and time variables. Of particular significance is the account provided by the Boltzmann equation for fluid dynamics that do not conform to continuum models. The equation is of fundamental importance in a range of high-tech applications, such as semiconductor photolithography devices. However, the velocity-space-time phase-space description of the flow renders a high dimensional problem setting. Moreover, the domain of the velocity variable is unbounded. The computational cost of resolving such high dimensional problems with unbounded domains using traditional numerical methods is prohibitive. In this presentation we consider a novel numerical approximation technique for the Boltzmann equation, in which the velocity discretization is based on a global moment-system approximation [1] and a local isogeometric-based refinement. The moment method infers an approximate distribution function that is consistent with macroscopic observables. Generally, moment-based approximations provide a sharper estimate of the tails than of the main-mass of the distribution; see [2] for more details. We use the statistical information provided by the moment-based approximation to guide a localized refinement strategy based on isogeometric analysis. The b-spline bases associated with isogeometric analysis provides an ideal candidate to enrich the moment-system approximation locally for the generally noteworthy accuracy per-degree-of-freedom of isogeometric discretizations. Further efficiency opportunities are provided by efficient integration rules that can be devised for integrating such b-spline bases [3]. We establish that the proposed velocity discretization preserves the fundamental properties of the Boltzmann equation, namely entropy dissipation and conservation of mass, momentum and energy. Furthermore, we show that the proposed velocity discretization facilitates the use of traditional numerical methods, such as finite-elements, to discretize the space and time variables. Finally, we will conclude this presentation with some numerical results to illustrate the approximation properties of the proposed method. [1] Abdelmalik, M.R.A. and van Brummelen, E.H. Moment closure approximations of the Boltzmann equation based on δ -divergences. *J. Stat. Phys.*, Vol. 164, pp. 77–104, (2016). [2] Brinks, R. On the convergence of derivatives of B-splines to derivatives of the Gaussian function *Comput & Appl Math* 27 (2008), pp. 79–92. [3] Calabro F., Sangalli G. and Tani, M. Fast formation of isogeometric Galerkin matrices by weighted quadrature. *Comput. Methods in Appl. Mech. Eng.*, Vol. 316, pp. 606-622, (2017).

Origin-Destination Matrix Estimation with Incomplete Signal Dataset for Microscopic Traffic Simulation

Kazuki Abe^{*}, Hideki Fujii^{**}, Shinobu Yoshimura^{***}

^{*}The University of Tokyo, ^{**}The University of Tokyo, ^{***}The University of Tokyo

ABSTRACT

Nowadays, multi-agent-based microscopic traffic simulators are useful for making decisions for solving traffic-related problems, e.g. traffic jams, evacuation planning, etc. Traffic demand is a sort of essential input data to use such simulators, which is described in the form of Origin-Destination (OD) matrix. Since the matrix cannot be observed directly, indirect estimation methods are indispensable. One of them is using link traffic volume, which is obtained by fixed-point observation. We have been proposing this type of OD estimation method using the traffic simulator, which estimates the input data for that simulator itself [1]. The proposed OD estimation method mainly consists of the following two processes: (1) a process of calculating estimated link traffic volume from the assumed OD matrix, and (2) a process of updating OD matrix with some constraints. In the process (1), a microscopic traffic simulator ADVENTURE_Mates [2] developed by the authors is used. In the process (2), a new OD matrix is obtained by solving a quadratic programming problem. In this process, the norm of residual between the simulated link traffic volume and observed one is minimized with the constraints of non-negative traffic volume in OD matrix satisfied. Until that norm satisfies a convergence criterion, the OD matrix is updated repeatedly. When microscopic traffic simulators are employed in the process (1), due to their precise resolution and route search algorithm, estimated results are easily affected from the congestion around intersections in the simulation. It sometimes causes unrealistic results. For instance, long waiting queues can be formed in a few links even if most of other links are vacant. To avoid this problem, we add a new feasible constraint to each link by comparing its traffic demand and the traffic capacity calculated from the light durations. Additionally, even if all of the signal datasets in the real world are not accessible, our proposed method provides the complemented ones simultaneously. Since the results of this completion and the OD estimation depend on each other, these methods are used alternately to solve the whole OD estimation problem. References: [1] K. Abe, H. Fujii and S. Yoshimura. Inverse Analysis of Origin-Destination Matrix for Microscopic Traffic Simulator. *Computer Modeling in Engineering and Science*. Vol. 113, No. 1, pp. 68-85, 2017. [2] H. Fujii, H. Uchida and S. Yoshimura. Agent-based Simulation Framework for Mixed Traffic of Cars, Pedestrians and Trams. *Transportation Research Part C: Emerging Technologies*, Vol. 85, pp. 234-248, 2017.

Adaptive Space-Time Discontinuous Galerkin Method for Unsteady Elliptic and Parabolic PDEs with First-Order Hyperbolic System Approach

Reza Abedi*, Alireza Mazaheri**, Robert Haber***

*University of Tennessee Space Institute, **NASA Langley Research Center, ***University of Illinois at Urbana-Champaign

ABSTRACT

We present a pseudo-time approach to relax elliptic and parabolic PDEs to hyperbolic equations. When an elliptic PDE is solved, the pseudo-time plays the role of physical time for a hyperbolic equation. However, for parabolic equation pseudo-time is added to the physical time and for each physical time advance the problem is solved in pseudo-time until it reaches steady state in pseudo-time. The relaxation times, target solutions for the hyperbolized discontinuous Galerkin method, and other aspects of the pseudo-time formulation are carefully chosen to optimize the convergence of the hyperbolized system to its steady state limit at each pseudo-time step [1]. In [1], this hyperbolic system is solved in pseudo-time using an implicit time marching scheme. Our main contribution will be to demonstrate, for the first time, an adaptive space-time discontinuous Galerkin for first-order system of hyperbolic equations. For this purpose, the spatial discretization is extruded in physical time to form implicit spacetime finite elements. We will also verify the order of accuracy of the solution and solution gradients for time-dependent problems. More specifically, we will demonstrate that the spatial order of accuracy of both solution and solution gradients is $(k+1)$ for P_k polynomial. When an elliptic problem is hyperbolized by the pseudo-time approach, the resulting system can also be solved with other spacetime discontinuous Galerkin formulations such as [2]. Therein, adaptivity in spacetime [3] can expedite the convergence of solution in pseudo-time. Thus, quality, order of accuracy, and efficiency of the proposed approach will be compared with those presented in [2] and [3].

References: [1] Alireza Mazaheri and Hiroaki Nishikawa. Efficient high-order discontinuous Galerkin schemes with first-order hyperbolic advection-diffusion system approach. *Journal of Computational Physics*, 321:729-54, 2016. [2] R. Abedi, B. Petracovici, and R.B. Haber, "A spacetime discontinuous Galerkin method for linearized elastodynamics with element-wise momentum balance", *Computer Methods in Applied Mechanics and Engineering*, 195:3247 – 3273, 2006. [3] R. Abedi, R. B. Haber, S. Thite, and J. Erickson. An h-adaptive spacetime discontinuous Galerkin method for linearized elastodynamics. *European Journal of Computational Mechanics*, 15(6):619-42, 2006.

Towards an Optimal Parameter Free Stabilisation for Systems of Nonlinear Conservation Laws: An Application of Neural Networks

Remi Abgrall^{*}, Maria Han Veiga^{**}, Karim Obrial^{***}

^{*}University of Zurich, ^{**}University of Zurich, ^{***}University of Zurich

ABSTRACT

We are interested in a parameter free limiter for hyperbolic conservation laws. We want to identify cells which are in need of limiting by just using the local structure of the solution as the eye of a good engineer would optimally do. If successful, we would put nonlinear stabilization only where really needed. Neural networks gained new popularity recently due to the computational tractability of back-propagation algorithm, used for the learning of weights and biases in a deep neural network, see [1] for example. Furthermore, it has been empirically shown to generate robust models for classification in many areas of application and theoretically, to generate universal classifiers and function approximators. Preliminary applications in the hyperbolic setting can also be found in [2]. In this work, we train a neural network using labelled data run on several CFD simulations, and use this to flag the trouble cells. In detail, we show how to construct a training dataset, perform feature selection and how to integrate this model with different CFD codes. We show the performance of this trouble cell indicator for three numerical methods, the Residual Distribution and Discontinuous Galerkin methods (denoting the necessary changes to the inference model), for scalar and systems in one and two dimensions. We also apply the same philosophy on a standard second order scheme where the dissipation ranges from the Lax-Wendroff ones to the pure upwind one, extending the work of Kurganov et al. [3]. It is our belief that these ideas can be applied to other problems which depend on certain local properties of the numerical solution, such as scheme stabilisation through addition of artificial viscosity or scheme blending, ultimately contributing towards CFD codes which are robust to different initial conditions and that require less parameter tuning to produce readily usable results. References: [1] Alex Krizhevsky, Ilya Sutskever, and Geoffrey E. Hinton. Imagenet classification with deep convolutional neural networks. In Proceedings of the 25th International Conference on Neural Information Processing Systems - Volume 1, NIPS'12, pages 1097–1105, USA, 2012. Curran Associates Inc. [2] D. Ray and J. Hesthaven. An artificial neural network as trouble-cell indicator. Journal of Computational Physics, 2017. submitted. [3] Alexander Kurganov and Yu Liu. New adaptive artificial viscosity method for hyperbolic systems of conservation laws. J. Comput. Phys., 231(24):8114–8132, 2012.

Structural Behavior of Composite Thin Walled Structures-An Experimental and Numerical Overview

Haim Abramovich*

*Aerospace Engineering, Technion, I.I.T., Israel

ABSTRACT

Laminated composite thin walled structures or sandwich based structures are today one of the most effective ways of reducing weight and increasing performance of aircraft and space launchers. To be able to realize this target, it is necessary to develop the appropriate reliable tools, which are complemented and validated by a sound experimental data base to correctly and safely predict the behavior of a laminated composite stringer-stiffened shells in the "deep" postbuckling region and its collapse load, which is characterized by the probable following failure modes : separation between the skin and the stringers, delaminations, crack propagations and matrix failure, as well as to get better insight and understanding of the phenomena associated with its behavior under repeated buckling, particularly in the range of "deep" postbuckling loading. During its normal service life, a fuselage, which is composed of many curved laminated composite stringer-stiffened panels, may experience no more than a few hundreds of buckling postbuckling cycles. In parallel, to safely enable an economical use of sandwich type shells ?? a reliable launcher structure, the knock-down factor associated with the behavior of thin walled shells has to be investigated and understood. Since 2000, the author had been part of 4 extensive campaigns sponsored by the EU to investigate the above topics. It started with the POSICOSS (Improved POSTbuckling Simulation for Design of Fibre Composite Stiffened Fuselage Structures) program, followed by the COCOMAT (Improved MATERIAL Exploitation at Safe Design of COMposite Airframe Structures by Accurate Simulation of COLLapse) and DAEDALOS (Dynamics in Aircraft Engineering Design and Analysis for Light Optimized Structures, and finalized with the DESICOS (New Robust DESign Guideline for Imperfection Sensitive COMposite Launcher Structures). Typical results from those programs will be highlighted, presenting effective ways of experimental and numerical investigations of stringer stiffened curved panels and sandwich shells and cones under compressive loading, with a focus on their buckling and postbuckling behavior. Emphasize will be made on various inherent characteristics of those structures, at buckling and beyond, like: skin-stringer separation, repeated buckling in the presence of prescribed delaminations, and deep postbuckling behavior. The effective width method adopted for laminated composite stringer stiffened panels, to calculate the collapse loads of the plates, will also be outlined and typical results will be presented.

Benchmark Numerical Solutions for Flows of Complex Fluids Governed by the Rolie-Poly Constitutive Model

Jade Abuga^{*}, Dr. Tirivanhu Chinyoka^{**}

^{*}University of Cape Town, ^{**}University of Cape Town

ABSTRACT

Polymer melts are a group of fluids that are classified as complex fluids. The understanding of the flow and properties of such fluids is essential due to their great importance in industrial sectors such as those involving plastic and food processing. It is thus of fundamental importance to understand the flow and physical properties of these fluids via appropriate scientific modelling techniques. It is only recently that the different forms of constitutive equations have been developed to describe molten polymers with the most adept mathematical models being the tube-based models which are derived from the Doi-Edwards tube-based model [2]. Examples of such models include the pom-pom [3] and the Rolie-Poly [1] constitutive equations. This work presents a validation for the developed solver for viscoelastic fluid flow computations, with particular focus on the flow of fluids governed by the Rolie-Poly constitutive equation. The solver is based on the finite volume method and is built on the open source software, OpenFoam platform. The two well-known benchmark problems used for this validation for the new numerical method are the lid-driven cavity flow and the 4:1 planar contraction flow. Additionally, we implement and investigate the efficiency of numerical stabilization techniques, with particular reference to the Discrete Elastic Viscous Stress Splitting (DEVSS) and the log-Conformation stabilization techniques. Comparison is done between our numerical results, obtained using each of the two stabilization techniques, against data from existing literature. The numerical results obtained for the contraction flow using the log-conformation reformulation approach are in good agreement with the existing literature for a wider range of Deborah numbers. For the lid-driven cavity flow, good agreement is observed for low Deborah numbers using either of the two stabilization techniques. References
1. Alexei E. Likhtman and Richard S. Graham. Simple constitutive equation for linear polymer melts derived from molecular theory: Rolie-poly equation. *Journal of Non-Newtonian Fluid Mechanics*, 114:1–12, 2003. 2. M. Doi and S. F. Edwards. *The theory of Polymer dynamics*. Oxford University Press, New York, 1986. 3. T. C. B. McLeish and R. G. Larson. Molecular constitutive equations for a class of branched polymers: The pom-pom polymer. *Journal of Rheology*, 42(1):81, 1998.

3D Method and Codes for Fluid Structure Interaction Problems in Euler Variables

Mustafa Abuziarov*

*research institute of mechanics Nizhny Novgorod State University

ABSTRACT

3D method and codes for fluid structure interaction problems in Euler variables M.H. Abuziarov Research institute for mechanics of Nizhny Novgorod State University, Russia. abouziar@mech.unn.ru The 3D codes based on the explicit numerical method for modeling shock wave and fluid structure interaction problems in Euler variables are presented. The method is based on the modified Godunov scheme of increased accuracy, uniform for solving equations of fluid dynamics and elastic-plastic flows [1]. The increase of the scheme accuracy is achieved by using 3D spatial time dependent solution of the discontinuity problem (3D space time dependent Riemann's solver). The same solution is used to calculate the interaction at the fluid-solid surface (Fluid Structure Interaction problem). These codes do not require complex 3D mesh generators, only the surfaces of the calculating objects as the STL files created by CAD systems, which greatly simplifies the preparing the task and makes it convenient to use directly by the designer at the design stage. To set the initial geometry and follow the deformation of the calculating domains in the process of interaction it is enough to take into account the interacting surfaces constituted by a set of triangles. Fixed Cartesian grid and local mobile grids associated with each triangle of the surface are used. The flow parameters are interpolated from the Cartesian grid to the local grids and vice versa. The results of the test solutions and applications related to the generation and extension of the detonation and shock waves, loading the constructions are presented. This work was supported by the RFBR grants (15-48-02333 R_povolzhe_a, 16-08-00458 a, 14-08-00197 a). References [1] Abouziarov M., Aiso H., Takahashi T. An application of conservative scheme to structure problems. Series from research institute of mathematics of Kyoto university. Mathematical analysis in fluid and gas dynamics. 2004, N2 1353, pp. 192-201

Efficient Computation of N-component Cahn-Hilliard Systems

Ruyam Acar*

*Okan University

ABSTRACT

We propose an algorithmic approach for efficient computation of N-component Cahn-Hilliard systems with constant surface tension. When pairwise surface tensions are homogeneous, diffusion term in the Cahn-Hilliard equation becomes isotropic and the energy term involves the summation of free energy contributions from each phase. Since diffusion is isotropic we suggest that instead of tracking the evolution of N phase variables it is sufficient to use a single parameter. Accordingly, we divide the value range of the phase parameter into N parts to represent N different components. In this way, for example values between 0 and 0.1 will correspond to phase one, values in range [0.1,0.2] will correspond to phase two and so on. Furthermore, in the energy term, we need to calculate the energy contribution only from the components in the diffusion range since components outside this range do not affect the current phase evolution. (Free energy values of these components also vanish in the N-component formulation. [1]) We can find the components that will contribute to the current energy with a simple neighborhood search in the local diffusion area based on the interface thickness. Once we find the relevant components, we can calculate the energy contribution from each component using the corresponding energy function defined in the given phase value range. In this way, we compute an N-component Cahn-Hilliard system by the evolution of a single parameter and using adaptive free energy calculations. Using one phase parameter also ensures mass conservation. We use a fast, stable, spectral method [2] based on a semi-implicit discretization for the numerical solution. Using a one-component solution provides a more efficient computation compared to the multigrid solution proposed for N-component systems in [1]. Furthermore, it allows flexibility in designing different physical properties for different components. [1] Lee, H.G., Choi, J-W and Kim, J., A practically unconditionally gradient stable scheme for the N-component Cahn-Hilliard system, Physica A 391, 2012, 1009–1019. [2] Badalassi , V., Cenicerros , H., and Banerjee , S. 2003. Computation of multiphase systems with phase field models. Phys. D. 190, 371–397.

Computer Simulation Model of Bone Osteoporosis and Drug Treatment for In-silico Experiment and Observation

Taiji Adachi^{*}, Yuki Miya^{**}, Yoshitaka Kameo^{***}, Tomoki Nakashima^{****}

^{*}Kyoto University, ^{**}Kyoto University, ^{***}Kyoto University, ^{****}Tokyo Medical and Dental University

ABSTRACT

Osteoporosis, loss of bone mass and functional structure, increases a risk of bone fractures caused by unbalance between osteoclastic resorption and osteoblastic formation. At the cellular level, complex couplings between mechanical and biochemical factors locally regulate cellular remodeling activities. To understand the mechanism of bone metabolism and remodeling in osteoporosis, in this study, we develop mathematical models incorporating biochemical regulatory factors combined with a mechano-adaptation model. In addition to this, drugs for osteoporosis treatment are modeled based on the diffusion-reaction type equations, some of which are mechanically regulated. Based on the model, we will discuss the applicability to predict effects of the drugs treatment for osteoporosis through in-silico experiment and observation. By introducing signaling molecules identified in bone metabolism, cellular activities in bone were modeled. Osteoclastogenesis, for example, is promoted by the binding of RANKL to its receptor RANK, whereas OPG acts as a decoy receptor. Semaphorin 3A (Sema 3A) exerts a protective effect on bone by suppressing osteoclastic bone resorption and increases osteoblastic bone formation. For these biochemical signaling molecules, production, degradation, diffusion, and binding terms are modeled to predict spatiotemporal evolution of their molecular concentrations. Addition to this, the expression of these biochemical factors was coupled with mechanical factors on the trabecular surface and numerically solved in cancellous bone discretized into voxel finite elements. In silico experiments and observations were conducted for a mouse distal femur model that was built based on the X-ray micro-CT image data. Cancellous bone region was uniaxially compressed and the trabecular remodeling and cellular activities were observed. By comparing with in vivo experimental data, we validated the proposed model as an in-silico tool for perturbation experiments as well as for time-course observations in 3D. In addition, we discuss the effect of drugs for osteoporosis on the cellular activities and the resulting bone microstructure. This work was supported in part by the AMED-CREST (Mechanobiology), Japan.

A Multiscale Shell Finite Element for Modeling the Out-of-plane Response of Masonry Walls

Daniela Addessi*, Paolo Di Re**, Elio Sacco***

*Sapienza University of Rome, Rome, Italy, **Sapienza University of Rome, Rome, Italy, ***University of Naples Federico II, Naples, Italy

ABSTRACT

The numerical simulation of nonlinear response of masonry structures is still an important and challenging task, as the stress/strain evolution in the material strongly depends on the progression of damage and micro-cracks in bricks and mortar as well as on the debonding phenomena at the brick/mortar interfaces, that influence the structural collapse. Masonry walls and vaults can experience different failure mechanisms, among which those out-of-plane are the most frequent. Multiscale finite element (FE) modeling [1,2] is a widely adopted and efficient procedure for the analysis of masonry structures, as it permits a detailed description of the nonlinear phenomena with a reasonable computational demand. This approach evaluates the response of a Unit Cell (UC), assumed as reference volume at the microscopic scale, and derives the response of the equivalent homogeneous medium at the macroscopic scale. Among the several proposals, shell-like models [3] have been widely developed based on proper homogenization procedures to link the responses at the micro and macro levels. This work proposes a thick shell FE based on a two-scale homogenization procedure to reproduce the out-of-plane response of masonry walls characterized by periodic textures. The constitutive relationship of the masonry assemblage is obtained through the homogenization process of three-dimensional UCs at the microscale, whose microscopic displacements are assumed as the sum of an assigned part, depending on the shell strains, and an unknown perturbation, due to the masonry heterogeneous nature. The bricks are considered as elastic, while a damage-friction model is used to reproduce the mortar response. The proposed FE model is implemented in a standard FE code and is used to perform numerical applications on masonry walls subjected to out-of-plane loading conditions. [1] Massart T.J., Peerlings R.H.J., and Geers M.G.D., "An enhanced multi-scale approach for masonry wall computations with localization of damage", Int J Numer Meth Eng, 69, 1022-1059 (2007). [2] Addessi D. and Sacco E., "A multi-scale enriched model for the analysis of masonry panel ", Int J of Solids Struct, 49, 865-880 (2012). [3] Petracca M., Pel L., Oller S., Camata G., and Spacone E., "Multiscale computational first order homogenization of thick shells for the analysis of out-of-plane loaded masonry walls ", Comput Method Appl M, 315, 273-301 (2017).

Data-driven Modeling & Uncertainty Quantification for Molecular Dynamics Simulations Using a Hierarchical Bayesian Framework

Yaser Afshar^{*}, Shaowu Pan^{**}, Karthik Duraisamy^{***}

^{*}University of Michigan, ^{**}University of Michigan, ^{***}University of Michigan

ABSTRACT

The goal of the present work is to obtain a better understanding of Li⁺ -ion transport and solvation in various electrolytes via molecular dynamics (MD) computations. The reliability of the simulations, however, critically depends on the accuracy of the interaction potential models. The functional form of the interaction potential is inferred from heterogeneous data, and the uncertainty in predictions is propagated to the outputs of the MD simulation. The derivation of potentials can be considered as a single or multi-objective optimization problem, where the calibration data is obtained from different types of experiments and quantum mechanical calculations. Hierarchical Bayesian uncertainty quantification is utilized for this purpose with a highly scalable framework based on the Transitional Markov chain Monte Carlo sampling for populating the posterior probability distribution of the MD force-field. A machine-learned surrogate model is proposed to reduce the computational cost associated with a large number of MD model runs.

Efficient Crack Propagation Simulations Using Well Conditioned Extended/Generalized Finite Elements and a Deflated Conjugate Gradient Solver

Konstantinos Agathos^{*}, Eleni Chatzi^{**}, Stéphane P. A. Bordas^{***}

^{*}ETH Zurich, ^{**}ETH Zurich, ^{***}University of Luxembourg

ABSTRACT

The incorporation of solution specific features in finite element approximations through partition of unity enrichment is known to significantly improve the approximation properties of the method, however it also introduces some numerical and implementation problems. Two important such problems are conditioning issues arising from linear dependencies between the enrichment functions and the finite element basis as well as blending problems between the standard and enriched part of the approximation. Since the early development of the extended/generalized finite element method (XFEM/GFEM) [1,2] several techniques have been proposed to handle the above issues, most of which require significant modifications to the original method thus increasing complexity and rendering application to existing codes problematic. In the present work two XFEM/GFEM variants are employed which significantly improve the conditioning of the resulting system matrices, while requiring only slight modifications to the original method. The discretization schemes are then combined to a deflated conjugate gradient (DCG) solver [3] and applied to 3D crack propagation problems where it is shown that a significant reduction in the computational time associated with solution of the linear systems can be achieved. Furthermore, since the schemes employed allow the application of geometrical enrichment, i.e. the use of singular enrichment functions in a fixed area around the crack front, a smoother variation of the stress intensity factors (SIFs) along the crack front is achieved, resulting in smoother crack paths. [1] Moës N, Dolbow J, Belytschko T. A finite element method for crack growth without remeshing. International Journal for Numerical Methods in Engineering 1999; 46(1): 131–150. [2] Strouboulis, T, Babuška, I, Copps, K. The design and analysis of the generalized finite element method. Computer methods in applied mechanics and engineering 2000; 181(1): 43-69. [3] Saad Y, Yeung M, Erhel J, Guyomarc 'h F. A deflated version of the conjugate gradient algorithm. SIAM Journal on Scientific Computing 2000; 21(5): 1909-1926.

Materials Informatics and Big Data: Realization of 4th Paradigm of Science in Materials Science

Ankit Agrawal^{*}, Alok Choudhary^{**}

^{*}Northwestern University, ^{**}Northwestern University

ABSTRACT

Abstract In this age of “big data”, large-scale experimental and simulation data is increasingly becoming available in all fields of science, and materials science is no exception to it. Our ability to collect and store this data has greatly surpassed our capability to analyze it, underscoring the emergence of the fourth paradigm of science, which is data-driven discovery. The need to use of advanced data science approaches in materials science is also recognized by the Materials Genome Initiative (MGI), further promoting the emerging field of materials informatics. In this talk, I would present some of our recent works employing state-of-the-art data analytics approaches such as deep learning for exploring processing-structure-property-performance (PSPP) linkages in materials, both in terms of forward models (e.g. predicting property for a given material) and inverse models (e.g. discovering materials that possess a desired property). In particular, I will focus on some examples of microstructure informatics such as learning data-driven multi scale localization/homogenization linkages, identifying prior deformation from discrete dislocation dynamics images, and microstructure optimization of a magnetostrictive Fe-Ga alloy. I will also demonstrate some materials informatics tools we have developed that deploy machine learning models to predict materials properties. Such data-driven analytics can significantly accelerate prediction of material properties, which in turn can accelerate the optimization process and thus help realize the dream of rational materials design. The increasingly availability of materials databases along with groundbreaking advances in data science approaches offers lot of promise to successfully realize the goals of MGI, and aid in the discovery, design, and deployment of next-generation materials. **Keywords** Materials informatics, big data, deep learning, PSPP relationships, prediction, optimization **Acknowledgment** We gratefully acknowledge support from NIST Award 70NANB14H012, AFOSR Award FA9550-12-1-0458, DARPA Award N66001-15-C-4036, NSF BigData Spoke Award IIS-1636909, and Northwestern Data Science Initiative. **References** A. Agrawal and A. Choudhary, “Perspective: Materials informatics and big data: Realization of the ‘fourth paradigm’ of science in materials science,” APL Materials, vol. 4, no. 053208, pp. 1–10, 2016.

Lipids Catalyze Mitochondrial Fission via Geometric Instability

Ashutosh Agrawal*, Ehsan Irajizad**, Rajesh Ramachandran***

*University of Houston, **University of Houston, ***Case Western Reserve University School of Medicine

ABSTRACT

Balanced mitochondrial fission is essential for apoptosis and its disruption is linked to lung cancer, cardiac dysfunction and neurogenerative disorders. Pioneering experimental studies have provided molecular insights into mitochondrial fission. The fission pathway is characterized by three key steps: i) the initial constriction carried out by actin polymerization and actomyosin contraction, ii) the intermediate constriction executed by Drp1 (dynamin-related protein 1), and iii) the final fission carried out by dynamin. While the fission proteins play an inarguably critical role, a growing body of evidence reveals that conical lipids, regulate mitochondrial morphology and fission. But how conical lipids contribute to fission remains an open question. Here, we computationally model tubular mitochondria to reveal a new buckling instability-based mechanism for achieving a stable geometry conducive for fission. Employing membrane physics and differential geometry, the study reveals that buckling instabilities, triggered synergistically by cylindrical curvatures from proteins and spherical curvatures from conical lipids, help achieve superconstrictions for fission. We validate the role of conical lipids by an in vitro study in which membrane tubules with reduced concentration of conical lipids (PE) fail to undergo necking despite the presence of Drp1 proteins.

A Comparative Study of Contact Problem Solution Based on Different Isogeometric Contact Formulations

Vishal Agrawal*, Sachin Singh Gautam**

*IIT Guwahati, India, **IIT Guwahati, India

ABSTRACT

Since the introduction of isogeometric analysis technique, it has been applied to a wide-range of contact problems due to its ability to exactly represent the complex shape of geometries and inherited tailorable continuity. It is observed that for the application of NURBS-based isogeometric analysis of different contact problems either the Gauss-Point-to-Surface (GPTS) [1] or the mortar based contact formulations [2] are most popularly employed for the treatment of contact constraints. However, it is known that the GPTS-based isogeometric analysis leads to excessive stiff and non-physical oscillations of the contact forces [2]. Hence, a post-processing scheme, which is developed within the spirit of mortar method in [3] and computes the regularized contact forces at the control points, is utilized with GPTS formulation and is denoted by GPTS(E). To the best of our knowledge, a comparative study between these formulations is not available and is the scope of present work. In this contribution, numerical behaviour, robustness, and accuracy of these two approaches are compared using the standard Hertz contact problem. For the enforcement of contact constraints penalty method is employed. It is found that mortar based contact formulation delivers slightly accurate results at a coarse mesh resolution in comparison to GPTS(E)-based formulation. As the mesh resolution is increased the former formulation approaches faster towards the exact solution than the latter one. Moreover, the distribution of contact pressure improves considerably in case of the mortar formulation with the order-elevation, whereas it remains unchanged for the GPTS(E)-based approach. It is shown that to achieve the numerical results similar to the former algorithm the contact boundary has to be discretized with a finer mesh resolution and a lower value of penalty parameter in the latter approach. But, as a result, the computational cost increases substantially. It is concluded that mortar based contact formulation delivers robust and superior quality result when compared with the GPTS(E)-based formulation. References [1] Fischer K. A., Wriggers P. Frictionless 2D contact formulations for finite deformations based on the mortar method. *Comput. Mech.*, 36:226–244, 2005. [2] De Lorenzis L., Temizer I., Wriggers P., Zavarise G. A large deformation frictional contact formulation using NURBS-based isogeometric analysis. *Int. J. Numer. Methods. Eng.*, 87:1278-1300, 2011. [3] Sauer R. A. Local finite element enrichment strategies for 2D contact computations and a corresponding post-processing scheme. *Comput. Mech.*, 52:301-319, 2013.

Wave Propagation in Geological Reservoirs with the Generalized Finite Difference Method

Adriano José Aguiar Marçal*, Deane Roehl**

*Institute Tecgraf at PUC-Rio, **Civil and Environmental Engineering Department at PUC-Rio

ABSTRACT

The Generalized Finite Difference (GFD) is a kind of mesh free method. Therefore, like the classical Finite Difference Method (FD), it is not restricted to a regular grid. In the GFD, we numerically solve the partial differential equations by a second-order approximation of the derivatives using a Taylor's series expansion for two or more variables. Hence, with the GFD, as with the Finite Element Method, we are capable of representing complex geological scenarios with more flexibility, keeping the computational efficiency of the classical Finite Difference Method. In most meshfree methods the assembly of the global system is very computationally intensive. In the classic FD method, since the mesh is structured, the approximation of the derivatives is calculated directly. On the other hand, the GFD requires the inversion of a local matrix at each point. Such matrix is small, symmetric and easy to solve numerically. However, to carry out an accurate discretization of complex geometries, we need thousands and even millions of points. Sometimes it is necessary to build a new point cloud. To mitigate the computational issues discussed above, we propose an analytical calculation of each local matrix. Following this procedure, we replace the numerical computation of inverse matrices by operations of product and sum of vectors, which are more efficient operations. We apply this methodology to model the propagation of seismic and electromagnetic waves in two-dimensional models using GFD. Such problems are common in geophysical simulations and of great interest to the oil and mining industry. Currently, these problems demand large investments in computer systems due to the complexity of geological scenarios.

GPU-accelerated Structural Topology Optimization for Frequency Response Problems with Parameter Uncertainty

Miguel Aguilo^{*}, Joshua Robbins^{**}, James Warner^{***}, Thomas Voth^{****}, Brett Clark^{*****}

^{*}Sandia National Laboratories, ^{**}Sandia National Laboratories, ^{***}NASA Langley Research Center, ^{****}Sandia National Laboratories, ^{*****}Sandia National Laboratories

ABSTRACT

The intersection of additive processes and design optimization has introduced revolutionary capabilities for design, product development, and manufacturing. ``Complexity is free '' has been a common mantra with additive manufacturing processes. However, anyone involved in the qualification or certification of additive processes or materials will acknowledge that complexity is currently not free due to the prevailing lack of understanding of advanced manufacturing processes. One approach to address the highly variable nature of additive processes is to improve process determinism. An alternate, complementary approach is to account for these inherent uncertainties early in the design process by providing designers with uncertainty aware computational design tools that generate solutions that insure performance requirements are met and margins are quantified. This work presents a graphics processing unit (GPU) accelerated structural topology optimization solver for frequency response problems under uncertainty. Uncertainty aware optimization problems are computationally complex due to the substantial number of model evaluations that are necessary to accurately quantify and propagate uncertainties due to design imperfections. This computational complexity is magnified if a high-fidelity, physics-based numerical model is used during synthesis optimization. This work combines a GPU-accelerated structural dynamic finite element solver and the stochastic reduced order model (SROM) method to design a structural component that matches a prescribed frequency response. Results will highlight how the GPU-accelerated structural dynamic finite element solver and SROM method effectively 1) alleviate the prohibitive computational cost associated with uncertainty aware structural topology optimization for frequency response problems; and 2) quantify and propagate the inherent uncertainties due to design imperfections.

Computation of the Energy Release Rate Using a Complex Stiffness Derivative Approach

Andres Aguirre Mesa*, Daniel Ramirez Tamayo**, Manuel J. Garcia Ruiz***, Harry Millwater****

*Universidad EAFIT, **University of Texas at San Antonio, ***University of Texas at San Antonio, ****University of Texas at San Antonio

ABSTRACT

A variation of the virtual crack extension method, based on the stiffness derivative approach, is proposed using Complex Taylor Series Expansion (CTSE). The stiffness derivative approach for computing the Energy Release Rate of a cracked system is derived from the total potential energy of a finite element solution, and requires the computation a stiffness derivate, i.e, a first order sensitivity of the stiffness matrix with respect to the crack tip area perturbation. Several variations of this classical approach have been proposed for the computation of the stiffness derivative, including finite difference approximations and analytical solutions. The alternative presented here uses CTSE to compute the stiffness derivative. This is obtained as the imaginary part of a complex version of the stiffness matrix, which is created by adding a small imaginary perturbation to a set of nodal coordinates in the crack tip area. The method was implemented in a user-defined element subroutine of the commercial finite element software Abaqus, and it is particularly useful for the computation of the ERR of multiple cracked specimens. Preliminary results show that the ERR obtained by the Complex Stiffness Derivative approach has the same accuracy and superior efficiency with respect to J-integral results. Parks, D. M. (1974). A stiffness derivative finite element technique for determination of crack tip stress intensity factors. *International Journal of Fracture*, 10(4), 487-502. Hellen, T. K. (1975). On the method of virtual crack extensions. *International Journal for numerical methods in engineering*, 9(1), 187-207. Lin, S. C., & Abel, J. F. (1988). Variational approach for a new direct-integration form of the virtual crack extension method. *International Journal of Fracture*, 38(3), 217-235.

Glycosaminoglycans in Aortic Dissection: A Model-Based Study Using Damage-based Smoothed Particle Hydrodynamics

Hossein Ahmadzadeh*, Manuel Rausch**, Jay Humphrey***

*Yale University, **University of Texas at Austin, ***Yale University

ABSTRACT

Aggregates of glycosaminoglycans (GAGs) localized within the medial layer of large arteries can sequester interstitial water and induce swelling of the intra-lamellar space. It is increasingly believed that this accumulation of GAGs, and the associated increase in the intramural mechanical stress field, can potentially trigger the damage and dissection that is often seen in thoracic aortic aneurysms. In this study, we present computational simulations using our previous smoothed particle hydrodynamics (SPH) model of soft tissues(1) that examine potential roles of pooled GAGs within the medial layer in initiating and propagating an intra-lamellar delamination. Mimicking the histological observations of the descending thoracic aorta of mouse models, the model aortic wall consists of an inner medial layer (composed of ~6-7 elastic laminae with associated smooth muscle cells and collagen fibers) and an outer collagen-rich adventitial layer. In order to elucidate the homeostatic in vivo state, the model aorta is initially axially stretched (60%) and subsequently pressurized intra-luminally (~12 kPa). The pooled GAGs are modeled by introducing a Gibbs-Donnan swelling pressure, which contributes to the stress field especially near the predefined GAG "particles". Our SPH model allows us to determine the evolution of the damage in discrete particles surrounding the GAGs. Specifically, in response to the swelling stress field induced by the GAGs, the maximum principal stretch of the neighboring particles is calculated and compared to a threshold value associated with the onset of the failure. The model shows that the swelling of intra-lamellar particles causes delamination between the elastic laminae, consistent with experimental observations. In addition, the damage experienced by the particles in the vicinity of the GAGs facilitates the propagation of the delamination in the circumferential direction. These results, combined with our sensitivity study on the input parameters of the model such as the luminal pressure and the size of the GAG pool, suggest that localized swelling can alter the mechanics in ways that eventually can cause catastrophic damage within the aortic wall. 1. Rausch, M.K., Karniadakis, G.E. & Humphrey, J.D. Biomech Model Mechanobiol (2017) 16: 249.

Three-dimensional Simulation of Spreading Dynamics of a Droplet on Substrate Using Multi-phase-field Model

Shintaro Aihara^{*}, Tomohiro Takaki^{**}, Naoki Takada^{***}

^{*}Kyoto Institute of Technology, ^{**}Kyoto Institute of Technology, ^{***}National Institute of Advanced Industrial Science and Technology

ABSTRACT

Phase-field method has attracted much attention as a model for simulating not only material microstructures but also multiphase flow, because it can easily express a complicated morphological change by introducing a diffuse interface. In the multiphase flow area, the phase-field method has been extensively used in a two-phase flow problem. Recently, we have developed a multi-phase-field model which can express a dynamics of multiphase flow with three or more phases by introducing multiple phase-field variables [S. Aihara, T. Takaki, N. Takada, submitting]. In the study, we performed two-dimensional simulations to obtain an equilibrium droplet shape on solid substrate and to see droplet floating dynamics through a liquid-liquid interface. As a result of those simulations, we have confirmed that the simulation results agree well with theoretical ones. In this study, we extend the two-dimensional multi-phase-field model to the three-dimensional model. In addition, we enable a GPU (graphics processing unit) computation of the model to accelerate the three-dimensional simulation. Using the developed method, we simulate a wetting spread phenomenon of a three-dimensional droplet on a flat solid surface. We validate the developed three-dimensional multi-phase-field model by comparing the simulation results to the experimental ones [T.D. Blake, J. Colloid interface Sci., 299 (2006), 1].

ICME for Automotive Composites – A Perspective

Venkat Aitharaju^{*}, Satvir Aashat^{**}, William Rodgers^{***}

^{*}General Motors, ^{**}ETA, Inc., ^{***}General Motors

ABSTRACT

Predictability of composite materials has been one of the bottlenecks hindering their large scale implementation in the industry. Several challenges exist in simulating the manufacturing and structural performance of these materials. The material properties of composites are a function of the manufacturing process used, and the performance predictability must include this aspect in great detail. Integrated Computational Materials Engineering (ICME) is an approach used to design the products, the materials that comprise them, and the associated material processing methods by linking material models at various length scales. ICME embraces a combined strategy of bottom-up and top-down modeling and simulation. Recently, there has been significant research in the area of ICME of automotive composite materials both in academia and at the national research labs. Some progress and success stories have been reported, but several unresolved issues, continue to prohibit the usage of these modeling developments in commercial industrial simulations. In the past, General Motors (GM) has successfully used composite materials for light-weighting of closures and non-critical structural composites in low volume applications. Additionally, GM is interested in evaluating carbon fiber composites in structural applications for potentially high volume vehicles. During service, these structural components are subject to complex long term loading conditions as well as potential crash events. Since the technology to validate the composite material designs in a virtual environment is not satisfactorily developed, GM has partnered with leading composite material simulation software companies, academia, and composite material molding companies (ESI, USC, Altair, CSP) through a Department of Energy funded project to develop state of the art probabilistic ICME tools to develop the required knowledge base and eliminate the current gaps. In this paper, a high level overview of the challenges and the progress realized in this project will be presented.

A Study on Finite Element Model Selection in Sequential State Estimation Based on the Ensemble Kalman Filter

Takeshi Akita*

*Chiba Institute of Technology

ABSTRACT

Numerical simulations based on the finite element (FE) models play an important role in various engineering fields. The key to building effective FE models is to identify various uncertainties in the systems, such as uncertain structural parameters. These uncertainties are often time-variant, in such cases, a sequential parameter estimation technique, where structural uncertainties are simultaneously identified at each measurement time step, is effective. The Kalman filter is widely used for sequential parameter estimation, however, the conventional Kalman filter is mainly applied for low-order and linear systems. Recently, the ensemble Kalman filter (EnKF) have been proposed for high-order and nonlinear systems [1]. The EnKF is based on a Monte-Carlo calculation and can be easily incorporated into nonlinear finite element analysis codes. The author has applied the EnKF to sequential parameter estimations of FE models, and has presented a self-tuning scheme for noise settings in the EnKF [2]. The self-tuning is performed by maximizing the likelihood function of the innovation sequence in the EnKF. In the previous research, the self-tuning is limited to the same FE models. In this research, we extend the scheme for FE model selection problems. We quantify the effectiveness of a FE model by evaluating its likelihood function of the innovation sequence in the EnKF, which gives us a basic criteria for the FE model selection. A simple example is given to validate the presented scheme. [1] G. Evensen, Sequential Data Assimilation with a Nonlinear Quasi-Geostrophic Model Using Monte Carlo Methods to Forecast Error Statistics, Journal of Geophysical Research, 1994, pp. 10143-10162. [2] T. Akita, R. Takaki, N. Kogiso, An Adaptive Estimation of Nonlinear Structural Deformations by Using the Ensemble Kalman Filter, Aerospace Technology Japan, Vol. 14 (2016), No. ists30.

A Computational Strategy for Solving Large Generalized Eigenvalue Problems in Fluid-structure Interactions

Quentin Akkaoui*, Evangéline Capiez-Lernout**, Christian Soize***, Roger Ohayon****

*Laboratoire Modélisation et Simulation Multi Echelle (MSME), **Laboratoire Modélisation et Simulation Multi Echelle (MSME), ***Laboratoire Modélisation et Simulation Multi Echelle (MSME), ****Conservatoire National des Arts et Métiers (CNAM)

ABSTRACT

For constructing reduced-order models of large-scale fluid-structure systems, computations of generalized eigenvalue problems are required [1]. For linear, and a fortiori for nonlinear dynamical systems, reduced-order models are essential for reducing the computational costs of the simulation in terms of CPU time and memory use. The algorithms and mathematical libraries involved for solving such generalized eigenvalue problems have demonstrated their efficiency and are suitable for analyzing large-scale models using parallel computers and massively parallel computers such as LAPACK. However, when dealing with a large-scale fluid-structure system, a stop of the calculation due to an out of memory can be encountered on mid-power and moderate-memory computers. For instance, this case occurred when trying to compute the generalized eigenvalue problems for a fluid-structure computational model with 2 million degrees of freedom on a workstation with 264GB of RAM and 12 processors. For circumventing this problem, the present work is devoted to revisiting the algorithms in order to be able to compute these generalized eigenvalue problems on a mid-power computer. The methods proposed [2] are algorithms based on double projection and subspace iteration methods [3], which efficiently allow for reducing the computational cost of these calculations and above all for avoiding the stop of the calculation due to an out of memory. In such context, after briefly recalling the existing algorithms used for solving the three generalized eigenvalue problems related to the displacement of the elastic structure, the pressure in the acoustic fluid, and the free-surface elevation of the fluid, a new adapted computational strategy [2] is described for reducing the numerical cost of each generalized eigenvalue problem. Finally, a detailed quantification of the computer resources required for computing the reduced-order projection basis with both classical and new method is presented, validating the efficiency of the proposed strategy. [1] R. Ohayon, C. Soize, Nonlinear model reduction for computational vibration analysis of structures with weak geometrical nonlinearity coupled with linear acoustic liquids in the presence of linear sloshing and capillarity, *Computers & Fluids* 141 (2016) 82-89 [2] Q. Akkaoui, E. Capiez-Lernout, C. Soize, R. Ohayon, Solving generalized eigenvalue problems for large scale fluid-structure computational models with mid-power computers, Submitted to publication, October 2017. [3] K.-J. Bathe, The subspace iteration method—Revisited, *Computers & Structures* 126 (2013) 177–183.

Monolithic Time-Integration of Two-Fluid Flow with Correct Energy Behavior

Ido Akkerman*, Marco ten Eikelder**

*Delft University of Technology, **Delft University of Technology

ABSTRACT

Stable energy behavior for two-fluid simulation is not trivial, intact most practical time stepping approaches have a hidden instability, see [1] for a clear demonstration of the issue. A monolithic two-fluid formulation is presented that exhibits correct kinetic and potential energy evolution. This is achieved by solving the interface evolution with special care. Additional to the standard convection of the interface essential constraints on the interface evolution are enforced using global Lagrange multipliers. In order to allow the method to be monolithic a special level-set formulation is used [2]. In this level-set formulation the difficult non-linear Eikonal problem is translated to a simple linear projection problem. The formulation with Lagrange multipliers is solved with a Quasi-newton method. This method partially decouples the constraints from the rest of the problem. This results in a favorable matrix structure and the ability to solve the constraint to a strict tolerance without increasing the global iteration count. Divergence conforming NURBS spatial discretization is adopted. This avoids ambiguities with regard to mass conservation and volume conservation, which should be equivalent in the incompressible case. The energy properties of the proposed method are verified with the tried and tested dambreak problem. Examining the convergence of the energy evolution demonstrates the potential of the proposed formulation. The testcase involves low Reynolds-number flow. High Reynolds number flow would require the use of a stabilized formulation. A stabilized formulation with correct energy behaviour for a single fluid has been developed in parallel [3]. A stabilized formulation for two-fluids is work in progress. [1] I. Akkerman, Y. Bazilevs, D.J. Benson, and M.W. Farthing C.E.Kees. Free-Surface flow and fluid object interaction modeling with emphasis on ship hydrodynamics. *Journal of Applied Mechanics*, 79, 2012. [2] I. Akkerman. Monotone level-sets on arbitrary meshes without redistancing. *Computers & Fluids*, 146:74 – 85, 2017. [3] M.F.P. ten Eikelder and I. Akkerman. Correct energy evolution of stabilized formulations: The relation between VMS, SUPG and GLS via dynamic orthogonal small-scales and isogeometric analysis. I: The convective-diffusive context. *Computer Methods in Applied Mechanics and Engineering*, 331(Supplement C):259 – 280, 2018.

Local Boundary Conditions in Nonlocal Problems

Burak Aksoylu^{*}, George Gazonas^{**}

^{*}U.S. Army Research Laboratory, ^{**}U.S. Army Research Laboratory

ABSTRACT

We present novel governing operators inspired by the theory of peridynamics (PD). They agree with the original PD operator in the bulk of the domain and simultaneously enforce local boundary conditions (BC). We present pure and mixed combinations of Neumann, Dirichlet, periodic, and antiperiodic BC. Our construction is systematic and easy to follow. We provide numerical experiments that validate our theoretical findings. The operators had been introduced in [1,2,3]. We extend the construction to more general inhomogeneous BC. We had proved that the nonlocal diffusion operator is a function of the classical operator. This observation opened a gateway to incorporate local BC to nonlocal problems on bounded domains. The main tool we use to define the novel governing operators is functional calculus, in which we replace the classical governing operator by a suitable function of it. We present how to apply functional calculus to general nonlocal problems in a methodical way. [1] B. Aksoylu and F. Celiker, Nonlocal problems with local Dirichlet and Neumann boundary conditions, *Journal of Mechanics of Materials and Structures*, 12(4) (2017), pp. 425-437. [2] B. Aksoylu, H.R. Beyer, and F. Celiker, Application and implementation of incorporating local boundary conditions into nonlocal problems, *Numerical Functional Analysis and Optimization*, 38(9) (2017), pp. 1077-1114. [3] B. Aksoylu, H.R. Beyer, and F. Celiker, Theoretical foundations of incorporating local boundary conditions into nonlocal problems, *Reports on Mathematical Physics*, 80(1) (2017), pp. 39-71.

Mechanics of Fluid Flow and Tissue Deformation inside a Solid Tumor

Meraj Alam^{*}, Bibaswan Dey^{**}, Raja Sekhar G. P.^{***}

^{*}Indian Institute of Technology, Kharagpur, India, 721302, ^{**}Indian Institute of Technology, Kharagpur, India, 721302, ^{***}Indian Institute of Technology, Kharagpur, India, 721302

ABSTRACT

Introduction: Present work reports a mathematical modeling for the interstitial hydrodynamics and mechanical behavior of the solid phase inside a solid tumor. Mainly, there are two types of continuum models to describe the mechanics of soft biological tissue (i) theory of poroelasticity and theory of mixture. We use the concept of mixture theory to model the problem. In case of mixture theory, soft biological tissues are assumed to be a continuum binary mixture of solid and fluid phases. One can study the density variations within the components to evaluate the evolution of the stresses and mechanical interactions among the constituents. We assume tumor tissue as a visco-poroelastic deformable living biomaterial with cellular phase and extracellular matrix (ECM) constitutes the solid phase (also small volume of blood vessels) and physiological extracellular fluid is the fluid phase. The intravascular fluid or blood and the interstitial fluid form a single fluid phase. We write down the mass and momentum balance equations for both the phases. The momentum equations are coupled due to the relative interaction (or drag) force between the phases. **Method:** In this study we establish well-posedness (existence, uniqueness, and stability of solution) of the govern mathematical models (which is a system of partial differential equations) in the weak sense under following assumptions (i) motion of interstitial fluid flow and solid phase deformation are slow and (ii) nutrient proliferation rate is much faster than the tumor cell growth. To show the well-posedness we use semi-discrete Galerkin method. Further, we simulate some analytical results corresponding to the one-dimensional spherical symmetry model. We have adopted standard eigenfunction expansion method to solve the one-dimensional spherical symmetry model. **Results:** We have discussed the temporal variation of interstitial fluid pressure (IFP) and composite velocity and justified that corresponding to a long duration of perfusion; convection does not play a significant role because IFP and composite velocity become constant beyond a certain time level. Our results on unsteady hydrodynamics model would give an idea about the time required for the necrosis formation from the initial stage of perfusion. **References:** 1. Helen Byrne and Luigi Preziosi. Modelling solid tumour growth using the theory of mixtures. *Mathematical Medicine and Biology*, 20(4):341–366, 2003. 2. Bibaswan Dey and GP Raja Sekhar. Hydrodynamics and convection enhanced macromolecular fluid transport in soft biological tissues: Application to solid tumor. *Journal of Theoretical Biology*, 395:62–86, 2016.

Modeling, Simulations and Experiments of Cell Bulk and Cortex Mechanics

Sebastian Aland*, Elisabeth Fischer-Friedrich**

*HTW Dresden, **TU Dresden

ABSTRACT

Cell shape changes are vital for many physiological processes such as cell proliferation, cell migration and morphogenesis. They emerge from an orchestrated interplay of cellular force generation and cellular force response, both mainly dictated by the actin cytoskeleton. To understand cellular force response from a mechanistic point of view, we describe cells as incompressible viscoelastic bulk domains surrounded by an impermeable elastic surface (the cortex) under active tension. A comparison of simulated and experimental shapes of cells in a flow channel, permits extraction of cell mechanical parameters. As the cell cortex is found to be the dominant mechanical element, we investigate the cortical force response of cells which are clamped between two plates. We compare simulation results to cell-mechanical measurements to extract the Young's surface modulus and the surface Poisson ratio of the cortex. Our results corroborate the idea of the cortex as a thin, isotropic, incompressible material and provide a route to new medical diagnostics by cell mechanics.

Exploring Mechanical Properties of Amorphous Materials through Molecular Dynamics and Eshelby Inclusions Analysis

Tristan Albaret^{*}, Francesca Boioli^{**}, Anne Tanguy^{***}, David Rodney^{****}

^{*}ILM-Physics Dept., Université Lyon 1, Villeurbanne, Auvergne-Rhône-Alpes , France., ^{**}ILM-Physics Dept., Université Lyon 1, Villeurbanne, Auvergne-Rhône-Alpes , France., ^{***}LAMCOS, INSA de Lyon, Villeurbanne, Auvergne-Rhône-Alpes , France., ^{****}ILM-Physics Dept., Université Lyon 1, Villeurbanne, Auvergne-Rhône-Alpes , France.

ABSTRACT

Understanding the mechanical properties of amorphous systems is tightly related with the identification and characterization of the elementary events that are at the origin of plasticity. Though these localized events involve rearrangements at the atomic scale, they can also be associated to mechanical heterogeneities in a continuous medium, also known as Eshelby inclusions. From molecular dynamics results we rebuild a representation in terms of Eshelby inclusions that is able to reproduce the stress-strain relations and give access, to some extent, to fine details such as the amplitude of the events, their size and their orientations. We used this mapping scheme to study the pressure dependence of plasticity in a model amorphous silicon bulk, or to inform mesoscopic models, for instance by determining activation volume through NEB calculations. I will also discuss more recent results on the Eshelby inclusion distributions as a function of the shear rate, in the first stages of plasticity. This should give an insight on the typical behaviour of the stress-strain relation in these regimes.

Cell-Based Topology Optimization Under the cgFEM Framework

José Albelda*, Mikel Barral**, Enrique Nadal***, Juan José Ródenas****

*Universitat Politècnica de València, **Universitat Politècnica de València, ***Universitat Politècnica de València,
****Universitat Politècnica de València

ABSTRACT

Today industries need to develop components meeting the needs of users each time faster. Therefore, companies need to generate optimal models for their components quickly. In this sense, various optimization processes are used in industry. The most usual of them is based on defining certain parameters characterizing the component and through a classical optimization process the combination of them that minimizes a certain objective function (weight, deflection, ...) is obtained. Another optimization technique, so called Topological Optimization (TO), has been used to optimize the geometry of various components. Unlike the previous one, the TO seeks the optimal distribution of a certain quantity of material maximizing the stiffness of the component. The results are much richer allowing important topological changes (appearance or collapse of holes) in a simple way. However, the optimization process entails a greater difficulty than other types of optimization, forcing the development of specific TO methods [1]. A problem of large structures so designed is that they need to be manufactured by additive manufacturing due to its complexity, which can be expensive. To alleviate this difficulty, this contribution proposes a method that, instead of obtaining the optimized structure of the whole component, subdivides the component into cells of manageable size and those cells are optimized by TO. All the software developed is integrated into the cgFEM environment [2], taking advantage of its computational performance. The process takes the following steps: i) a TO is carried out for the whole component with a certain parameter configuration so that it distributes the amount of material needed in each cell. ii) Using this information and the loads to which each cell is subjected to, a second TO process is launched at each cell defining the geometry of the same. iii) Finally, the global component is built by joining all cells together. In this way, additive manufacturing is only necessary for the construction of the cells and not for the entire component, thus being able to manufacture larger components. [1] O. Sigmund. A 99 line topology optimization code written in Matlab. *Structural and Multidisciplinary Optimization*. 21:120-127, 2001. [2] E. Nadal. Cartesian grid FEM (cgFEM): High performance h-adaptive FE analysis with efficient error control: application to structural shape optimization. Ph.D. Thesis, Universitat Politècnica de València, 2014. AK The financial support to this work of Generalitat Valenciana (PROMETEO/2016/007) and the Spanish Ministerio de Economía, Industria y Competitividad (DPI2017-89816-R) is greatly acknowledged.

Combined Modeling and Experimental Study of the Structural Mechanobiology of Blood Clot Contraction and Deformation

Mark Alber^{*}, Oleg Kim^{**}, Samuel Britton^{***}, Rustem Litvinov^{****}, John Weisel^{*****}

^{*}University of California Riverside, ^{**}University of California Riverside, ^{***}University of California Riverside,
^{****}University of Pennsylvania, ^{*****}litvinov@mail.med.upenn.edu

ABSTRACT

Blood clot contraction plays an important role in prevention of bleeding and in thrombotic disorders. In this talk, we will unveil and quantify the structural mechanisms of clot contraction at the level of single platelets. A key elementary step of contraction is sequential extension–retraction of platelet filopodia attached to fibrin fibers. In contrast to other cell–matrix systems in which cells migrate along fibers, we will demonstrate that the “hand-over-hand” longitudinal pulling causes shortening and bending of platelet-attached fibers, resulting in formation of fiber kinks. When attached to multiple fibers, platelets were shown in [1] to densify the fibrin network by pulling on fibers transversely to their longitudinal axes. Single platelets and aggregates will be shown to use actomyosin contractile machinery and integrin-mediated adhesion to remodel the extracellular matrix, inducing compaction of fibrin into bundled agglomerates tightly associated with activated platelets. The revealed platelet-driven mechanisms of blood clot contraction demonstrate an important new biological application of cell motility principles. Recently developed multi-scale discrete worm-like chain model will be used to demonstrate that non-linear mechanical properties of compressed fibrin network can originate from structural re-arrangements of the entire fibrin network, as well as from alterations of individual fibers including fiber buckling, bending and reorientation. Model simulation results support novel hypothesized mechanism of stress propagation through the network and quantify how rearrangement and linkage of fibrin fibers effects network stiffening. The new model was also used to determine how contractile function of platelets, their distribution within the fibrin network and fibrin properties affect mechanical response of a blood clot to applied stresses in blood flow. Lastly, a novel multi-phase computational model will be described that simulates active interactions between platelets and fibrin, to study the impact of various physiologically relevant blood shear flow conditions on deformation and embolization of a partially obstructive clot with variable permeability [2]. Simulations provide new insights into mechanisms underlying clot stability and embolization that cannot be studied experimentally at this time. References 1. Oleg V. Kim, Rustem I. Litvinov, Mark S. Alber and John W. Weisel [2017], Quantitative Structural Mechanobiology of Platelet-Driven Blood Clot Contraction, *Nature Communications* 8: 1274. <https://www.nature.com/articles/s41467-017-00885-x.pdf>. 2. Shixin Xu, Zhiliang Xu, Oleg Kim, Rustem I. Litvinov, John W. Weisel and Mark Alber [2017], Model Predictions of Deformation, Embolization, and Permeability of Partially Obstructive Blood Clots under Variable Shear Flow, *Journal of the Royal Society Interface* 14: 20170441. <http://rsif.royalsocietypublishing.org/content/14/136/20170441>.

Topology Optimization of Periodic Elastoplastic Energy Dissipating Microstructures

Ryan Alberdi^{*}, Kapil Khandelwal^{**}

^{*}University of Notre Dame, ^{**}University of Notre Dame

ABSTRACT

A framework for the design of periodic elastoplastic energy dissipating microstructures is developed using topology optimization. While the topology optimization of elastic microstructures has been carried out in numerous studies, microstructural design considering inelastic behavior is relatively untouched due to a number of reasons which are addressed in this study. An RVE-based homogenization approach is employed along with periodic boundary conditions, satisfying the Hill-Mandel principle. The plastic anisotropy which may be prevalent in materials fabricated through additive manufacturing processes is considered by modeling the constitutive behavior at the microscale with Hoffman plasticity. Discretization is done using enhanced assumed strain (EAS) elements to avoid locking from incompressible plastic flow under plane strain conditions and a Lagrange multiplier approach is used to enforce periodic boundary conditions in the discrete system. The design problem is formulated using a density-based design parameterization in conjunction with a SIMP-like material interpolation scheme. The total plastic work in the RVE is maximized and the path-dependent sensitivity analysis is carried out using an adjoint method. Attention is devoted to issues such as dependence on initial design, material and geometric symmetry and the enforcement of microstructural connectivity. A number of microstructural designs are obtained under different prescribed macroscopic strains.

A Flat-top Partition of Unity Method for Unit Cell Problems

Clelia Albrecht^{*}, Marc Alexander Schweitzer^{**}

^{*}Fraunhofer SCAI, ^{**}University of Bonn / Fraunhofer SCAI

ABSTRACT

In this presentation we are concerned with the application of the flat-top partition of unity method to unit cell problems which are solved in a representative volume element and subject to periodic boundary conditions. To use the full approximation power of the PUM, we use problem-dependent enrichment functions. We present techniques, implemented within the PUMA software framework, to construct these enrichment functions as well as to handle occurring stability problems of the resulting system matrices. To demonstrate the effectiveness of this approach, we discuss examples for unit cell problems like the solution of the Schrödinger equation for quantum mechanical calculations (collaboration with J. Pask and N. Sukumar) or the simulation of heterogeneous materials. For these examples, we examine their approximation properties as well as parallel performance.

A Discrete Element Approach for Modeling the 3D Thermal-induced Damage

Ghassan Alhaji Hassan*, Solange Humblet**, Grégory Martic***, Emmanuel Bellenger****, Willy Leclerc*****, Meric Tandja*****, Mohammed Guessasma*****, Christine Pelegris*****, Marc Duquennoy*****, Maurice Gonon*****

*LTI, UPJV, University of Picardie Jules Verne, France, **SIRRIS, Gosselies, Belgium, ***BCRC (Belgian Ceramic Research Centre), Belgium, ****LTI, UPJV, University of Picardie Jules Verne, France, *****LTI, UPJV, University of Picardie Jules Verne, France, *****LTI, UPJV, University of Picardie Jules Verne, France, *****LTI, UPJV, University of Picardie Jules Verne, France, *****LTI, UPJV, University of Picardie Jules Verne, France, *****IEMN/DOAE, UVHC, University of Valenciennes, France, *****Faculty of Engineering, University of Mons, Belgium

ABSTRACT

This work is treated in the framework of CUBISM project funded by INTERREG V program. The purpose of the project is to develop a pressure and humidity SAW sensor, in order to follow the drying of refractory materials under high temperature and pressure conditions. More precisely, we aim to describe and predict the thermo-mechanical behavior of the piezoelectric SAW substrate under such conditions for a full set of geometrical configurations and materials. Besides, we expect to take into account the micro-cracks resulting from thermal expansion mismatch between the substrate and its environment. However, at the microscopic scale, the finite element method is less suitable to describe discontinuities induced by micro-cracks. For that reason, we propose to study the thermo-mechanical behavior using the discrete elements method (DEM). This choice is also motivated by the advantage of DEM to describe the crack propagation. This contribution presents significant improvement for DEM to model the 3D thermal-induced damage due to thermal expansion. Furthermore, this study allows to follow the damage level of the material during its lifetime. Thanks to the MULTICOR3D++ code developed in our laboratory, a hybrid particulate-lattice model [1], based on the equivalence between a granular system and a network of cohesive beam elements, is generated. Our contribution is to introduce the linear thermal expansion at the scale of the contact by modifying the initial free length of each link, using the model introduced in 2D by [2]. Heat transfer by conduction is taken into account, what requires contact areas which can be computed using two approaches. The first one consists in calibrating a coefficient describing the mean ratio between particle and contact areas. The second one is to associate a polyhedral element to each particle, using the concept of representative elements. Besides, we study the characteristics of materials in terms of the number of discrete elements, also the equivalent stress and strain of each particle are determined using a representative area. In addition, a model of damage resulting from thermal expansion was introduced. We consider that the fracture occurs when the hydrostatic stress for local tensile solicitations is greater than a given tensile strength limit. [1] H. Haddad. Modélisation du comportement thermomécanique de l'interface de contact par une approche couplée MED-MEF. PhD thesis, France, 2013. [2] W. Leclerc, H. Haddad, M. Guessasma. On a Discrete Element Method to simulate thermal-induced damage in 2D composite materials, In Computers & Structures, 2017, ISSN 0045-7949.

Nonlinear Oscillations of a Biomimetic Scale Elastica

Hessein Ali^{*}, Hossein Ebrahimi^{**}, Ranajay Ghosh^{***}

^{*}University of Central Florida, ^{**}University of Central Florida, ^{***}University of Central Florida

ABSTRACT

Biomimetic scales are ubiquitous in nature and known to provide the organism several mechanical and multifunctional advantages. Such scales significantly change the curvature dependent properties of mechanical materials giving rise to complex nonlinearities that can be apparent even in small deformations due to scales engagement. Accordingly, mimicking such structures in materials has been of great interest to acquire high performance including stiffness gains and tunable elasticity. The essential source of these behaviors are difficult to model further than simple geometries due to the complexity arises from scales interaction. This work focuses on the dynamic behavior of such biomimetic systems. Furthering a deeper understanding of the origins of these nonlinearities for a scale-covered elastic can provide useful information towards controlling their deformation behavior in various twisting and bending modes. Such nonlinearities involve various aspect of scales interaction, geometrical sliding, interfacial friction and their combinations. In this study, we explore a special class of these materials, one which behave like nonlinear elastica. The vibrational characteristic and different nonlinearities will be discussed and suitable means of controlling them introduced.

Simulation of Blood Flow in Circle of Willis in Case of an Artery Stenosis

Aria Alimi^{*}, Olaf Wunsch^{**}

^{*}University of Kassel, ^{**}University of Kassel

ABSTRACT

Numerical simulation of blood flow in deformable arteries in human body can be used to study the effect of phenomena that change normal blood flow behavior in the body. One of these phenomena is the arterial stenosis that can occur in brain arteries. The main reason of brain stenosis is not known, but certain habits and conditions like smoking or unhealthy diet can increase the risk of this disease. In this work, numerical calculations are performed to study the blood flow in the main arteries of Circle of Willis in case of an artery stenosis. Intracranial arterial stenosis is the narrowing of the arteries inside the brain. It could be caused by buildup of a plaque inside of the artery on the inner wall. Stenosis may occur in any artery in the circle of Willis but the arteries that most likely are affected by stenosis are internal carotid artery (ICA), the middle cerebral artery (MCA), the vertebral arteries and the basilar artery [2][3]. Over time, the plaque would harden and get larger. Hence, it reduces or completely blocks the blood flow and could lead to a stroke. Different size of plaques and multiple locations are studied, and the results are discussed. Finite-Volume method is used for the calculations of the 3D model of arteries by means of foam-extend-3.1. Different arteries are assigned with in-vivo blood pressure read from the medical experiments on patients. Fluid-structure interaction simulation is used to study a more realistic behavior of the arteries. Brain is assumed to have a homogeneous, linear elastic incompressible material [1]. Blood is modeled to be an incompressible Newtonian fluid. As the plaques are hardened tissues stuck to the wall of the arteries, the stenosis cases are modeled by narrowing the arteries on the location that plaque exists.

Analysis of Functionally Graded Mindlin Sector Microplates under Transverse Loading

F. Alinaghizadeh^{*}, M. Shariati^{**}, Jacob Fish^{***}

^{*}Columbia University/Ferdowsi University of Mashhad, ^{**}Ferdowsi University of Mashhad, ^{***}Columbia University

ABSTRACT

In this work bending analysis of functionally graded sector microplates is studied. The modified couple stress theory with a single material length scale parameters is used to capture the size effect. The equilibrium equations are obtained based on the first-order shear deformation plate theory using principle of minimum total potential energy. Two types of Hooke 's law are considered in calculations. The material properties of the plates are considered to be graded through thickness direction according to a power-law distribution of the volume fraction of the constituents. The equilibrium equations of the microplates are a system of five forth-order partial differential equations. A polynomial based generalized differential quadrature method is employed to solve the equilibrium equations of the plates for different boundary conditions. The effects of power-law index, material length scale parameters and geometrical parameters on deflections of plates are investigated. It is observed that the effect of length scale parameter is to make the plate behavior stiffer. Furthermore, deflection values predicted by using the 3-D Hooke's law are less than those that are obtained by the Hooke's law.

A Coupled Chemo-Mechanical Cell-Matrix Model to Predict Mechanical Feedback Between Cells and Extracellular Matrices

Farid Alisafaei^{*}, Matthew Hall^{**}, Mingming Wu^{***}, vivek Shenoy^{****}

^{*}University of Pennsylvania, ^{**}University of Michigan, ^{***}Cornell University, ^{****}University of Pennsylvania

ABSTRACT

Introduction: Reciprocal mechanical interactions between cells and their surrounding extracellular matrices (ECMs) regulate various physiological and pathological processes such as cell motility, and tumor growth. Our recent study [1] reveals a mechanical cross-talk (feedback loop) between breast tumor cells and fibrous ECMs. Contractile cells pulling on their surrounding ECMs reorganize, align, and subsequently stiffen the fibrous collagen matrices in their immediate vicinity. In return, the matrix stiffening leads to greater cell force generation and cell stiffening. Here, we propose a novel nonlinear chemo-mechanical cell model, coupled with a fiber network-inspired continuum matrix model, to link the mechanics of the cell (stiffness and architecture) to its surrounding extracellular matrix. **Materials and Methods:** We engineer an array of type 1 collagen matrices with different microstructures modulated by altering; (i) collagen concentration, (ii) polymerization temperature, and (iii) cross-linking via preglycation with ribose. Using a parallel-plate oscillatory shear rheometer, we also measure the shear modulus of all nine collagen matrices. To study the interaction between cells and matrices, MDA-MB-231 breast cancer cells are embedded within the collagen matrices covalently bonded to fluorescent marker beads. Using a 3D particle tracking microscopy from the laboratory of M.W. and coworkers [1], the 3D displacements of ~10,000 beads are measured in the vicinity of each cell. **Results and Discussion:** As reported in [1], collagen matrices with larger pore sizes exhibit greater fiber alignment accompanied by an increased range of displacement propagation. Our experimental results also show that actin filaments are more aligned (along the cell's major axis) in stiffer matrices than in softer matrices indicating that cell body stiffness increases with matrix stiffness; cells actively respond to their stiffened surrounding by alignment of f-actin filament along the long axis of the cell. We propose a coupled cell-matrix model to qualitatively predict (i) displacement fields induced by pulling cells within their surrounding matrices, (ii) cell-generated forces, actin fiber alignment, and cell stiffening as functions of matrix stiffness, and (iii) strain-induced fiber alignment of fibrous matrices and its associated long-range displacement propagation. **References:** [1] M.S. Hall, F. Alisafaei, E. Ban, X. Feng, C-Y Hui, V.B. Shenoy, M. Wu, Proc Natl Acad Sci USA, 113:14043-14048, 2016.

A Study of Shear Band Broadening in Simulated Glasses

Darius Alix-Williams^{*}, Michael Falk^{**}

^{*}Johns Hopkins University, ^{**}Johns Hopkins University

ABSTRACT

We investigate the broadening of shear bands in three distinct glassy materials systems – a two-dimensional binary Lennard-Jones system, a Cu₆₄Zr₃₆ EAM system and a Stillinger-Weber silicon system. For each material system, three glassy configurations are prepared via quenches from well-equilibrated liquids to low temperature at various rates. These configurations are subsequently deformed in simple shear to 1000% strain and, in all cases, shear bands form and broaden. The rate of shear band broadening is inconsistent with an assumption that the band grows at a rate proportional to the strain rate within the band. This implies that additional time scales are important in determining the rate of band broadening. We explore potential causes for the discrepancy between the assumed model and our simulation results with the objective of constraining the underlying constitutive response theory appropriate for amorphous solids subject to large deformations.

Numerical Implementation of Thermomechanical Problem Considering Heterogeneous Media Using Multiscale Procedures Combined with eXtended Finite Element Method

Nasser Alkmim^{*}, Francisco Evangelista Junior^{**}

^{*}University of Brasilia, ^{**}University of Brasilia

ABSTRACT

In this work we present the description and a in-house implementation of a multi-scale procedure for modeling heterogeneous media considering linear and nonlinear material behavior. The model considers a weak coupling between temperature effects on the mechanical problem. All material nonlinearity that may result during analysis is solved only in the microscale problem, no constitutive equations are needed for the macroscale. The implemented approach relies on the XFEM (eXtended finite element method) with level-set functions to model material interfaces in the microscale of the material. The homogenized material properties at a quadrature points are obtained from the microscale analysis and used during construction of macroscale element stiffness matrices. The implemented solution -- \texttt{scikit-mechanics} -- was done using Python programming language which offers a highly legible syntax and benefits of object-oriented programming paradigm.

Modeling the Effects of Microstructure on Localization in Polycrystalline Stainless Steel

Coleman Alleman^{*}, James W. Foulk III^{**}, Alejandro Mota^{***}, Hojun Lim^{****}, David Littlewood^{*****}

^{*}Sandia National Laboratories, ^{**}Sandia National Laboratories, ^{***}Sandia National Laboratories, ^{****}Sandia National Laboratories, ^{*****}Sandia National Laboratories

ABSTRACT

In a polycrystalline aggregate, the heterogeneous plastic deformation introduced by the local anisotropy of the microstructure plays a critical role in the localization of the deformation. To accurately resolve this incipient stage of failure, it is therefore necessary to incorporate microstructure with sufficient resolution, including accurate representations of interfaces such as grain boundaries. However, modeling the entire body at the required level of resolution is computationally prohibitive. In this study, the authors demonstrate the use of concurrent multiscale modeling to incorporate explicit, finely resolved microstructure in a critical region while resolving the smoother mechanical fields outside this region with a coarser discretization to limit computational cost. The Schwarz alternating method is a well-established technique for the solution of elliptic PDEs by means of domain decomposition. This concurrent multiscale method enables the flow of information between fine and coarse scales to achieve strong two-way coupling, which is critical in the accurate simulation of localization of plastic deformation leading to void or crack initiation in the incipient failure regime. The Schwarz method avoids the use of Lagrange multipliers or gradients that afflict other coupling methods, instead directly imposing the solution of each domain on the others in a way that guarantees convergence of the combined problem. This presentation will discuss the formulation of the Schwarz method and its implementation in the open-source Albany finite element platform developed at Sandia National Laboratories and demonstrate the use of the method as an effective approach for concurrent coupling in finite deformation solid mechanics. In particular, the Schwarz method is applied in this study to analyze the behavior of stainless steel tension specimens undergoing the localization of plastic deformation during the necking process. The gauge section of the specimen where localization occurs is resolved at a scale where the polycrystalline microstructure is discretized explicitly, and an anisotropic crystal elasto-viscoplasticity constitutive model is employed. The far field domain is coarsely discretized, and a simplified, isotropic elastoplastic constitutive relation is employed to capture the aggregate response of a polycrystalline region in a phenomenological manner. A suite of microstructural realizations are simulated to investigate the effects of microstructural variability on the necking process.

Multiscale and Non-conforming Interface Coupling for the Non Invasive Global-local Analysis of Heterogeneous Structures

Olivier Allix^{*}, Maxence Wangermez^{**}, Pierre-Alain Guidault^{***}, Oana Ciobanu^{****}, Christian Rey^{*****}

^{*}LMT Cachan, ^{**}LMT Cachan / Safran Tech, ^{***}LMT Cachan, ^{****}Safran Tech, ^{*****}Safran Tech

ABSTRACT

This contribution presents an interface coupling technique between a heterogeneous microscopic (local) model and a first order homogenised (global) model, representative of the macroscopic behaviour of a structure. It addresses the problematic of replacing a local part of the homogenised macroscopic model where the RVE (Representative Volume Element) is not fully representative of the microstructure or where the first order homogenization hypothesis are no longer respected. The key point of this multiscale based coupling technique is that we operate a scale separation on the interfaces between models. An interface fields scale separation is performed into macroscopic and microscopic contributions and ensure perfect interface equilibrium between models in a macroscopic sense: continuity of macro-displacements and equilibrium of macro-forces. Then, we add a priori conditions on the microscopic interface quantities that depends on the locations and external loading of the microscopic details. The first situation corresponds to the one where the microscopic detail is far from the edges and submitted to large wavelength loading. The coupling technique is performed such that the local solution corresponds to the one of the standard first order periodic homogenization. For this the global and local models are tied through interface mean displacements. The complementary microscopic part which are incompatible are used to impose a priori periodic condition between opposite faces on the local model. As such the technique leads to a complex and non-standard formulation which, in turn, can be easily recovered in a non-intrusive way and therefore applied in legacy codes. The validation of the method is done on a 2D and 3D steady mechanical academic problem under linear elasticity assumption with matching geometries on the interface between local and global meshes. The non conforming interface coupling techniques along with its non-intrusive are currently extended to high gradient area implying macroscopic stress concentration as cracks, edges and so on.

A Coupled Multi-Scale Study of Lithium Ion Batteries to Evaluate Performance of Deformed Electrodes

Srikanth Allu^{*}, Hsin Wang^{**}, Srdjan Simunovic^{***}, John Turner^{****}

^{*}Oak Ridge National Laboratory, ^{**}Oak Ridge National Laboratory, ^{***}Oak Ridge National Laboratory, ^{****}Oak Ridge National Laboratory

ABSTRACT

Mechanical abuse of Lithium Ion Batteries (LIB) has become an important research topic mainly because of the commercialization of electric vehicles and increasing possibility of accidents involving large number of Li-ion cells. Since internal short can lead to the thermal runaway, extreme importance is given safety design aspect of LIB packs. It is important to fully understand the value of mechanical abuse simulation. In general, a Li-ion cell can be put under one of the three conditions after mechanical abuse: 1) short circuit is induced and followed by thermal runaway, 2) short circuit is induced without thermal runaway and cell slowly discharges, and 3) no short circuit is induced and the cell can still function. Most studies have been focused on the simulation of mechanical damages in the first two cases in which failure of the battery components led to discharge, thermal runaway, fire and explosion. But there has been no report on how the cells will function under the last case. In many cases, the multiple layer structure of the LIBs made them very tolerant to mechanical abuse. In fact, studies showed a typical battery take more than 80% compression without short circuit. In this talk we will present a coupled multi-physics model of species transport, charge conservation and chemical kinetics developed for lithium-ion batteries. The developed model is used to simulate the indentation damage and the consequences it has on electrochemical transport corresponding to capacity loss.

The Strong Form Collocation Method for the Prediction of Polycrystalline Solidification with the Diffuse-interface Approach

Ashkan Almasi^{*}, Jeong-Hoon Song^{**}

^{*}University of Colorado Boulder, ^{**}University of Colorado Boulder

ABSTRACT

Application of a diffuse-interface, or phase field, approach to modelling polycrystalline solidification has become a significant topic of interest in science and engineering research. Such modelling requires suitable computational methods to solve the relevant differential equations. In this study, we use the particle difference method (PDM) [1-2], a strong-form point collocation method, to model solidification of polycrystalline materials and perform a subsequent stress analysis. The PDM is a meshfree method based on Taylor polynomial expansion and the moving least square approach. One of its distinct features is that the PDM can directly discretize the strong form of governing partial differential equations. Consequently, the PDM neither performs domain integration nor constructs a mesh, thus saving computational time. After describing the formulation of the PDM and some techniques used in the subsequent analysis, this study takes advantage of these benefits of the PDM to predict the solidification process in two cases, one with 5 grains and the other with 36 grains, using grain growth kinetics [3]. Afterward, stress analysis is performed with the predicted polycrystalline morphology, yielding results for displacement, strain, stress, and Von Mises stress in the polycrystalline solid for various levels of discretization. Finally, these results are compared to results from the finite element method for verification, demonstrating that the PDM successfully predicts polycrystalline solidification and computes stress in the predicted morphology. References [1] Young-Cheol Yoon and Jeong-Hoon Song. Extended particle difference method for weak and strong discontinuity problems: part i. derivation of the extended particle derivative approximation for the representation of weak and strong discontinuities. *Computational Mechanics*, 53(6):1087–1103, 2014. [2] Young-Cheol Yoon and Jeong-Hoon Song. Extended particle difference method for moving boundary problems. *Computational Mechanics*, 54(3):723–743, 2014. [3] Danan Fan and L-Q Chen. Computer simulation of grain growth using a continuum field model. *Acta Materialia*, 45(2):611–622, 1997.

TOPOLOGY OPTIMIZATION OF PERIODIC PIEZOELECTRIC MATERIALS FOR ENERGY HARVESTING DEVICES

BRENO V. DE ALMEIDA^{*}, RENATO PAVANELLO[†]

^{*}School of Mechanical Engineering, University of Campinas
Cidade Universitaria Zeferino Vaz - Barao Geraldo, 13083-970
Campinas, Sao Paulo, Brazil
brenodealmeida4@gmail.com

[†]School of Mechanical Engineering, University of Campinas
Cidade Universitaria Zeferino Vaz - Barao Geraldo, 13083-970
Campinas, Sao Paulo, Brazil
pava@fem.unicamp.br

Key words: Piezoelectric, periodic, energy harvester

1 INTRODUCTION

There has been effort in the past decades to improve the performance of energy harvesting devices, in order to efficiently recharge or even independently power small electronic devices, thus decreasing the amount of batteries needed to power them, which can yield financial as well as environmental benefits. These devices work by converting ambient waste energy to useful electrical energy and there are three main phenomena which favor this process: electromagnetic, electrostatic and piezoelectric; of which the most advantageous, considering power density and ease of application, is piezoelectric^[1].

In the context of topology optimization of piezoelectric energy harvesting devices, Zheng et. al.^[2] optimized a beam-like piezoelectric harvester using a finite element (FE) mesh in three dimensions considering a static load and Noh and Yoon^[3] extended this analysis using the SIMP model and studying the effect of using different penalization factors for the interpolation of the piezoelectric properties, for both static and dynamic excitations. Lin et. al.^[4] optimized the harvester considering a range of base vibration frequencies, also in three dimensions but with only one element thickness per piezoelectric layer. Kiyono et. al.^[5] considered a multilayered shell element.

Most of these piezoelectric topology optimization articles used the SIMP method for the optimization problem and, to the best of the authors' knowledge, only perform topology optimization of the piezoelectric layers modelled as plate^[4], shell^[5] or using a three-dimensional model with only one or two elements per layer in the thickness direction^[2,3] and a FE analysis of the optimal topology for the thickness direction is seldom done. This

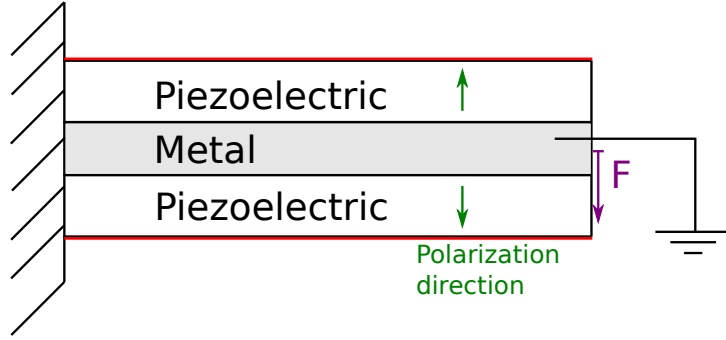


Figure 1: Two-dimensional model of the optimized bimorph harvester. The green arrows represent the piezoelectric polarization directions of the two layers. The red line is the initial position of the electrodes and the purple arrow indicates where the harmonic force is applied. The harvester is clamped in the left hand-side and the metal substrate is grounded. The harvester is optimized in open-circuit conditions.

may be due to difficulties in the production of complex piezoelectric structures, which in recent years has seen considerable improvements with advances in Additive Manufacturing (AM) techniques, and may enable the manufacturing of more sophisticated harvester designs, including the production of composite piezoelectric materials for energy harvesting^[6,7].

Thus, in this extended abstract, a piezoelectric energy harvester is modeled as a bimorph two-dimensional beam under plain strain hypothesis^[8]. The beam is composed of two piezoelectric layers of opposing polarities (series connection) and an intermediate metallic substrate, under open-circuit conditions, as shown in Fig. 1. It is subjected to a harmonic excitation in the free end. Its topology is optimized using the Bidirectional Evolutionary Structural Optimization (BESO) method^[9]. An initial optimization process is done considering no periodicity constraint. Next, the concept of cells is used for the application of the periodicity constraint^[10,11] and the results are compared to the initial one.

The FE model is shown in section 2 and the topology optimization procedure is shown in section 3. The objective function consists on minimizing the inverse ratio of the output electric energy by the input force work^[2,3]. The BESO method is then used to optimize the topology of the piezoelectric material of the harvester, considering a harmonic load on the free end of the beam and a fixed topology for the metallic substrate. The sensitivities of a minimization problem are derived, and different penalization parameters are used for each of the piezoelectric material's stiffness^[3] in order to find a better convergence. Section 4 shows the results of the topology optimization of the harvester considering no periodicity and periodicity, with 36 cells. A conclusion summarizing the results is presented in section 5.

2 MODEL FORMULATION

The piezoelectric energy harvesting device is modeled as a bimorph beam under plain-strain hypothesis, with series connection of the parallel piezoelectric layers and grounded on the substrate. Linear isoparametric four-node elements are considered for the FE analysis.

After simplifying the constitutive equations of piezoelectricity using plain-strain hypothesis from the linear Hamilton principle and knowing the linear stress-displacement and electric field-electric potential relations, the element piezoelectric and mass stiffness matrices can be obtained. After an assembly procedure, considering a harmonic excitation of amplitude F and excitation frequency ω and that the harvester is in open-circuit condition (no electric charges), the following linear equation is obtained^[12,13]:

$$\left(\begin{bmatrix} \mathbf{K}_{uu} & \mathbf{K}_{\phi u}^T \\ \mathbf{K}_{\phi u} & -\mathbf{K}_{\phi\phi} \end{bmatrix} - \omega^2 \begin{bmatrix} \mathbf{M} & \mathbf{0} \\ \mathbf{0} & \mathbf{0} \end{bmatrix} \right) \begin{Bmatrix} \mathbf{u} \\ \phi \end{Bmatrix} = \begin{Bmatrix} \mathbf{F} \\ \mathbf{0} \end{Bmatrix} \quad (1)$$

In eq. (1), \mathbf{F} , \mathbf{u} and ϕ are the nodal applied force, displacement and voltage amplitude vectors, respectively, while \mathbf{K}_{uu} , $\mathbf{K}_{\phi u}$, $\mathbf{K}_{\phi\phi}$ and \mathbf{M} are the global mechanical stiffness, piezoelectric coupling, dielectric and mass matrices, respectively. The element-wise calculation of the matrices are shown in eq. (2).

$$\begin{aligned} \mathbf{K}_{uu}^e &= \int_{\Omega^e} \mathbf{B}_u^T \mathbf{c}^E \mathbf{B}_u d\Omega^e \\ \mathbf{K}_{\phi u}^e &= \int_{\Omega^e} \mathbf{B}_\phi^T \mathbf{e} \mathbf{B}_u d\Omega^e \\ \mathbf{K}_{\phi\phi}^e &= \int_{\Omega^e} \mathbf{B}_\phi^T \boldsymbol{\epsilon}^S \mathbf{B}_\phi d\Omega^e \\ \mathbf{M}^e &= \int_{\Omega^e} \mathbf{N}^T \rho \mathbf{N} d\Omega^e \end{aligned} \quad (2)$$

In eq. (2), the superscript e indicates an element, \mathbf{N} is the matrix that contain the coefficients of the shape linear shape functions, \mathbf{B}_u and \mathbf{B}_ϕ are the first order derivative matrices of the shape functions, used to interpolate the displacements and electric potentials, respectively. The piezoelectric material properties \mathbf{c}^E , \mathbf{e} , $\boldsymbol{\epsilon}^S$ and ρ are shown in Table 1 for PZT-4. The substrate material is steel, with $E = 200 \text{ GPa}$ Young's modulus, $\nu = 0.29$ Poisson's ratio and $\rho = 7860 \text{ kg/m}^3$ specific mass.

The boundary conditions are: zero displacements in the clamped portion of the beam; zero electric potential for the piezoelectric-substrate interface; the furthest upper piezoelectric surface nodes have equal electric potential, as well as the lower ones, due to the electrodes. This coupling restriction is met by expanding eq. (1) using a Lagrange matrix $\boldsymbol{\Lambda}^{[13]}$, which contains the equipotential voltage restrictions. Simplifying eq. (1) to $\mathbf{K}_g \mathbf{u}_g = \mathbf{F}_g$, the following linear system must be solved:

Table 1: PZT-4 properties

Property	Value
Elasticity matrix \mathbf{c}^E (constant electric field)	$\begin{bmatrix} 1.390 & 0.778 & 0.743 & 0 & 0 & 0 \\ 0.778 & 1.390 & 0.743 & 0 & 0 & 0 \\ 0.743 & 0.743 & 1.154 & 0 & 0 & 0 \\ 0 & 0 & 0 & 0.256 & 0 & 0 \\ 0 & 0 & 0 & 0 & 0.256 & 0 \\ 0 & 0 & 0 & 0 & 0 & 0.306 \end{bmatrix} 10^2 GPa$
Coupling matrix \mathbf{e}	$\begin{bmatrix} 0 & 0 & -5.2 \\ 0 & 0 & -5.2 \\ 0 & 0 & 15.1 \\ 0 & 12.7 & 0 \\ 12.7 & 0 & 0 \\ 0 & 0 & 0 \end{bmatrix} C/m^2$
Dielectric matrix $\boldsymbol{\epsilon}^S$ (constant strain)	$\begin{bmatrix} 6.45 & 0 & 0 \\ 0 & 6.45 & 0 \\ 0 & 0 & 5.62 \end{bmatrix} nF/m$
Specific mass ρ	$7500 kg/m^3$

$$\begin{bmatrix} \mathbf{K}_g & \boldsymbol{\Lambda}^T \\ \boldsymbol{\Lambda} & \mathbf{0} \end{bmatrix} \begin{Bmatrix} \mathbf{u}_g \\ \mathbf{l} \end{Bmatrix} = \begin{Bmatrix} \mathbf{F}_g \\ \mathbf{0} \end{Bmatrix} \quad (3)$$

In equation (3), \mathbf{l} is a vector that when pre-multiplied by $\boldsymbol{\Lambda}^T$ represents the internal forces necessary to impose the electrode coupling constraints, and is not used for subsequent calculations.

3 TOPOLOGY OPTIMIZATION

The topology of the piezoelectric harvester is optimized using the soft-kill BESO method^[9] in order to maximize the mechanical to electric energy conversion ratio, or rather, minimize its inverse value ζ , as shown in the objective function in eq. (4)^[2,3].

The BESO method is a sensitivity based topology optimization method that uses discrete design variables. This is especially advantageous for the thickness profile optimization of piezoelectric harvesters, since the location of the electrode is easily defined by the solid-void boundaries during the optimization process. Checkerboard pattern and mesh dependency are avoided by applying a filter in each iteration.

$$\begin{aligned}
 & \text{minimize} \quad \zeta = 1 + \frac{\Pi^S}{\Pi^E} \\
 & \text{subject to} \quad \sum_i x_i V_i = V^* \\
 & \quad \quad \quad x_i = x_{\min} \text{ or } 1
 \end{aligned} \tag{4}$$

In eq. (4), Π^S and Π^E are the dynamic mechanical and electric energies, respectively, calculated as shown in eq. (5). V^* is the target volume.

$$\Pi^S = \mathbf{u}^T (\mathbf{K}_{uu} - \omega^2 \mathbf{M}) \mathbf{u} \quad \text{and} \quad \Pi^E = \boldsymbol{\phi}^T \mathbf{K}_{\phi\phi} \boldsymbol{\phi} \tag{5}$$

Furthermore, in eq. (4), x_i with $i = 1, \dots$, *number of elements* are the design variables, which are equal to 1 if the FE is solid and equal to a small value x_{\min} , close to zero, when it is void. To determine if the element should be solid or void, the element sensitivities α_i are calculated, which are equal to the derivative of the objective function with respects to the design variables x_i , as shown in equation (6).

$$\alpha_i = \frac{\partial \zeta}{\partial x_i} = \frac{1}{\Pi^S} \frac{\partial \Pi^S}{\partial x_i} - \frac{1}{\Pi^E} \frac{\partial \Pi^E}{\partial x_i} \tag{6}$$

Where the derivative of the mechanical Π^S and electric Π^E energies with respect to the i-th design variable are calculated using the adjoint method as:

$$\begin{aligned}
 \frac{\partial \Pi^S}{\partial x_i} &= \left(\frac{1}{2} \mathbf{u}^T + \boldsymbol{\lambda}_1^T \right) \left(\frac{\partial \mathbf{K}_{uu}}{\partial x_i} - \omega^2 \frac{\partial \mathbf{M}}{\partial x_i} \right) \mathbf{u} + \boldsymbol{\lambda}_1^T \frac{\partial \mathbf{K}_{\phi u}^T}{\partial x_i} \boldsymbol{\phi} + \boldsymbol{\mu}_1^T \frac{\partial \mathbf{K}_{\phi u}}{\partial x_i} \mathbf{u} - \boldsymbol{\mu}_1^T \frac{\partial \mathbf{K}_{\phi\phi}}{\partial x_i} \boldsymbol{\phi} \\
 \frac{\partial \Pi^E}{\partial x_i} &= \left(\frac{1}{2} \boldsymbol{\phi}^T - \boldsymbol{\mu}_2^T \right) \frac{\partial \mathbf{K}_{\phi\phi}}{\partial x_i} \boldsymbol{\phi} + \boldsymbol{\lambda}_2^T \left(\frac{\partial \mathbf{K}_{uu}}{\partial x_i} - \omega^2 \frac{\partial \mathbf{M}}{\partial x_i} \right) \mathbf{u} + \boldsymbol{\lambda}_2^T \frac{\partial \mathbf{K}_{\phi u}^T}{\partial x_i} \boldsymbol{\phi} + \boldsymbol{\mu}_2^T \frac{\partial \mathbf{K}_{\phi u}}{\partial x_i} \mathbf{u}
 \end{aligned} \tag{7}$$

The following linear systems are solved to find the adjoint vectors $\boldsymbol{\lambda}_1$, $\boldsymbol{\mu}_1$, $\boldsymbol{\lambda}_2$ and $\boldsymbol{\mu}_2$, respectively:

$$\begin{aligned}
 \begin{bmatrix} \mathbf{K}_{uu} - \omega^2 \mathbf{M} & \mathbf{K}_{\phi u}^T \\ \mathbf{K}_{\phi u} & -\mathbf{K}_{\phi\phi} \end{bmatrix} \begin{Bmatrix} \boldsymbol{\lambda}_1 \\ \boldsymbol{\mu}_1 \end{Bmatrix} &= \begin{Bmatrix} -(\mathbf{K}_{uu} - \omega^2 \mathbf{M}) \mathbf{u} \\ \mathbf{0} \end{Bmatrix} \\
 \begin{bmatrix} \mathbf{K}_{uu} - \omega^2 \mathbf{M} & \mathbf{K}_{\phi u}^T \\ \mathbf{K}_{\phi u} & -\mathbf{K}_{\phi\phi} \end{bmatrix} \begin{Bmatrix} \boldsymbol{\lambda}_2 \\ \boldsymbol{\mu}_2 \end{Bmatrix} &= \begin{Bmatrix} \mathbf{0} \\ -\mathbf{K}_{\phi\phi} \boldsymbol{\phi} \end{Bmatrix}
 \end{aligned} \tag{8}$$

In order to implement the sensitivity calculations shown above, the derivative of each stiffness matrix with respects to the design variables have to be defined. In this work, the SIMP material interpolation scheme is used, with a penalization factor for each of the material property. Thus, the element stiffness matrices are:

$$\mathbf{K}_{uu}^e = x^{p_1} \mathbf{K}_{uu0}^e \quad \mathbf{K}_{\phi u}^e = x^{p_2} \mathbf{K}_{\phi u0}^e \quad \mathbf{K}_{\phi\phi}^e = x^{p_3} \mathbf{K}_{\phi\phi0}^e \quad \mathbf{M}^e = x^{p_m} \mathbf{M}_0^e \tag{9}$$

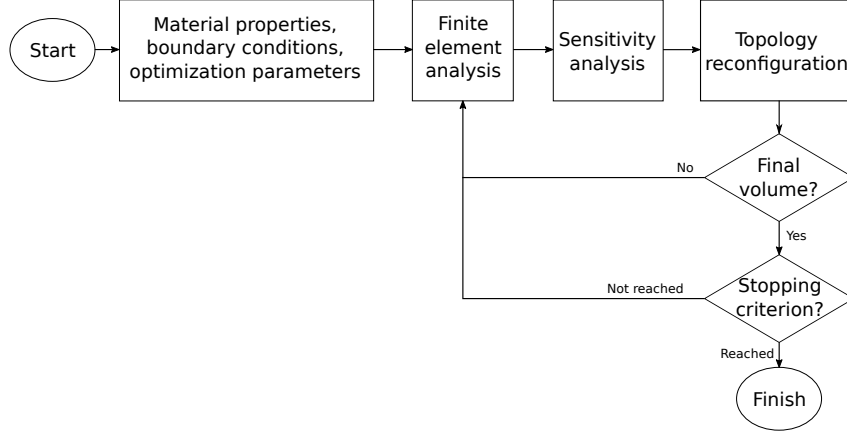


Figure 2: BESO flowchart

The subscript 0 indicates the value when the element is solid, calculated as shown in (2).

Additional weight factors w_S and w_E are used in eq. (6) to improve the algorithm's convergence stability, with $0 < w_E = 1 - w_S < 1$.

$$\alpha_i = w_S \frac{1}{\Pi^S} \frac{\partial \Pi^S}{\partial x_i} - w_E \frac{1}{\Pi^E} \frac{\partial \Pi^E}{\partial x_i} \quad (10)$$

The cellular topology is obtained by applying a periodicity constraint in the sensitivity calculation and through the subsequent step in the optimization algorithm by, in which the topology is redesigned, by adding or removing a number of elements multiple of the number of cells. In this work, the design domain consists solely on piezoelectric elements.

The initial volume of the design domain is 100%. Figure 2 shows a flowchart of the optimization procedure. After defining the material property values, the boundary constraints and the optimization parameters, the iterative procedure starts. A FE analysis is done, thus obtaining \mathbf{u} and ϕ . Next the sensitivity calculation, filtering and analysis is performed and, based on their values as well as the next iteration's volume, the topology is reconfigured (values of x_i). This loop repeats itself until the target volume is reached and a stopping criterion is met. The stopping criterion is determined by the mean value of the objective function's variation during the last 10 iterations, and has to be less than a certain value, such as $1 \cdot 10^{-7}$.

4 RESULTS

In this section results of the proposed topology optimization algorithm are shown, first considering no periodicity constraint and then with it. The problem optimizes the piezoelectric harvester shown schematically in Fig. 1, which also shows what the boundary conditions are. The applied harmonic point force has a 1 N amplitude. The harvester has a 100 mm length, a 40 mm thickness and an 8 mm thick substrate. As mentioned

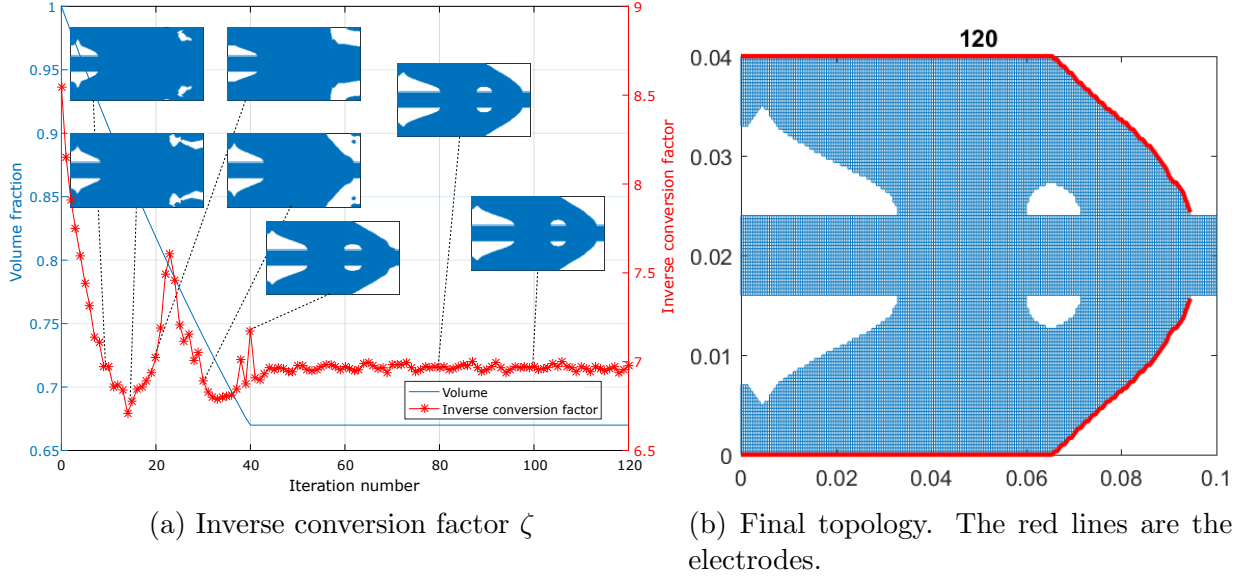


Figure 3: Results for no periodicity constraint

previously, the piezoelectric material considered for the analysis was PZT-4, with the properties shown in Table 1, and a substrate was considered steel, with $E = 200 \text{ GPa}$, $\nu = 0.29$ and $\rho = 7860 \text{ kg/m}^3$. In all cases, the harvester is optimized for low frequency excitation: $\omega = 300 \text{ Hz}$. The target volume of the piezoelectric material was 67% of its initial volume.

4.1 No periodicity constraint

The topology was optimized using a 200 by 120 (24000) element mesh. The evolutionary ratio was 1%, the maximum element addition ratio was 0.5% and the filter radius was 4 mm. The penalization factors p_1 , p_2 , p_3 and p_m were 3, 2, 1 and 1, respectively. The sensitivity weight factors were $w_S = 62\%$ and $w_E = 38\%$. The results are shown in Fig. 3.

The inverse conversion factor was successfully minimized from 8.56 to 6.95. And the electric potential difference between the upper and lower electrodes decreased from 55.95 mV to 34.15 mV.

4.2 Cellular: 36 cells

The topology was then optimized considering 6 by 6 (36) cells, with a total of 108000 elements. The evolutionary ratio was 0.5%, the maximum element addition ratio was 0.25% and the filter radius was 4 mm. The penalization factors and the sensitivity weight factors were the same as in the no periodicity case. The results are shown in Fig. 4.

The inverse conversion factor was minimized from 8.56 to 6.75. Notice that the inverse

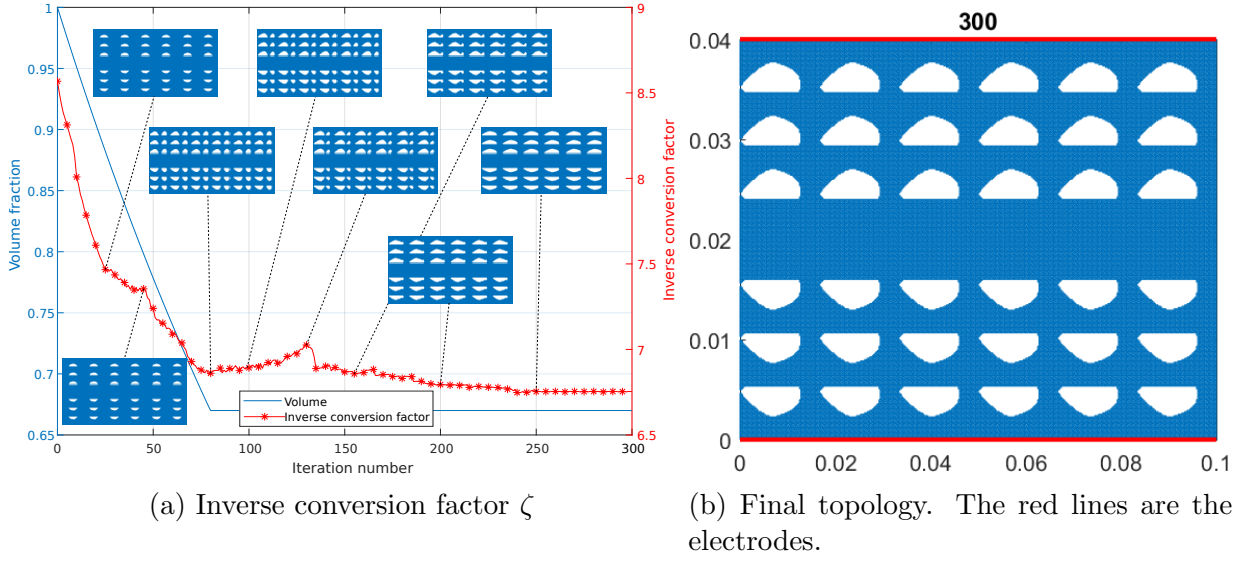


Figure 4: Results for a bimorph piezoelectric harvester with 36 cells

conversion factor's final value is smaller than the value of the optimized non-periodic case. Furthermore, the electric potential difference between the two electrodes decreased from 55.95 mV to 47.79 mV . The electric potential difference is larger than for the non-periodic case, which is more favorable, especially considering that for closed-circuits it is generally desired to maximize the electrical power output, which is directly proportional to the square of this value. It is noticeable how the convergence curve in Fig. 4 is more stable than in Fig. 3.

5 CONCLUSIONS

A two-dimensional bimorph beam-like piezoelectric energy harvesting device with series connection modeled under plain-strain hypothesis was successfully topologically optimized using a soft-kill BESO algorithm for harmonic excitation under open-circuit condition. Two main results were shown: one considering no periodicity constraint; and another with 36 cells.

The results show that the optimal topology for the periodic case yields a inverse conversion factor equal to 6.75 (a measure of mechanical to energy conversion efficiency), which is smaller than that of the optimized topology for the non-periodic case, namely 6.95. Furthermore, the electric potential voltage difference between the electrodes is larger for the cellular optimized topology, which is more desirable, with regards to electrical power output to a closed-circuit.

For future projects, damping effects can be taken into account in the harmonic analysis, base excitation can be considered as the input instead of an applied force and the periodic topology optimization can be done using the inverse homogenization method.

6 ACKNOWLEDGEMENTS

The authors are grateful to FAPESP (São Paulo Research Foundation, grant numbers 2013/08293-7 and 2018/00075-4) and CAPES (Coordination for the Improvement of Higher Education Personnel) for their financial support of this work.

REFERENCES

- [1] Erturk, A. and Inman, D.J., Piezoelectric Energy Harvesting. John Wiley & Sons, Ltd (2011).
- [2] Zheng, B., Chang, C.J. and Gea, H.C., Topology optimization of energy harvesting devices using piezoelectric materials. *Structural and Multidisciplinary Optimization* (2008)38(1):17–23.
- [3] Noh, J.Y. and Yoon, G.H., Topology optimization of piezoelectric energy harvesting devices considering static and harmonic dynamic loads. *Advances in Engineering Software* (2012)53:45 – 60.
- [4] Lin, Z.Q., Gea, H.C. and Liu, S.T., Design of piezoelectric energy harvesting devices subjected to broadband random vibrations by applying topology optimization. *Acta Mechanica Sinica* (2011)27(5):730–737.
- [5] Kiyono, C.Y., Silva, E.C.N. and Reddy, J.N., Optimal design of laminated piezocomposite energy harvesting devices considering stress constraints. *International Journal for Numerical Methods in Engineering* (2016)105(12):883–914.
- [6] Kim, K., Zhu, W., Qu, X., Aaronson, C., McCall, W.R., Chen, S. and Sirbulu, D.J., 3d optical printing of piezoelectric nanoparticle–polymer composite materials. *ACS Nano* (2014)8(10):9799–9806.
- [7] Bodkhe, S., Turcot, G., Gosselin, F.P. and Therriault, D., One-step solvent evaporation-assisted 3d printing of piezoelectric PVDF nanocomposite structures. *ACS Applied Materials & Interfaces* (2017)9(24):20833–20842.
- [8] de Almeida, B.V. and Pavanello, R., PIEZOELECTRIC HARVESTER TOPOLOGY OPTIMIZATION USING A MULTIPARAMETER MATERIAL MODEL. *Proceedings of the XXXVIII Iberian Latin American Congress on Computational Methods in Engineering, ABMEC Brazilian Association of Computational Methods in Engineering* (2017) .
- [9] Huang, X. and Xie, M., Evolutionary Topology Optimization of Continuum Structures: Methods and Applications. Wiley (2010).

- [10] Vicente, W.M., Picelli, R., Pavanello, R. and Xie, Y.M., TOPOLOGY OPTIMIZATION OF PERIODIC STRUCTURES FOR COUPLED ACOUSTIC-STRUCTURE SYSTEMS. Proceedings of the VII European Congress on Computational Methods in Applied Sciences and Engineering (ECCOMAS Congress 2016), Institute of Structural Analysis and Antiseismic Research School of Civil Engineering National Technical University of Athens (NTUA) Greece (2016) 3565–3582.
- [11] Vicente, W., Zuo, Z., Pavanello, R., Calixto, T., Picelli, R. and Xie, Y., Concurrent topology optimization for minimizing frequency responses of two-level hierarchical structures. *Computer Methods in Applied Mechanics and Engineering* (2016)301:116–136.
- [12] IEEE, IEEE Standard on piezoelectricity. ANSI/IEEE Std 176-1987 (1988).
- [13] Cook, R.D., Malkus, D.S. and Plesha, M.E., Concepts and Applications of Finite Element Analysis. Wiley (2001).

Design of a Damper for Suborbital Payloads Based on Honey Comb Structures and Additive Manufacture

Eduardo Amaro*, Fernando Velazquez**

*UNAM, **UNAM

ABSTRACT

One of the most critical phases in suborbital flights is guarantee the integrity of the payload. This can suffer severe damage during the landing because of the impact. To solve this issue dampers are implemented for dissipating kinetical energy. However, this implies add mass to the gondola, which reduces the altitude reached during the flight. In this work honey comb structures are applied to design a light damper for suborbital payloads. The main objective is to maximize the energy dissipation while mass is minimized. By changing geometric parameters several structures were proposed and studied by Finite Element Analysis to calculate the energy absorption during impact. Due to the geometric complexity of the structure additive manufacture is used for manufacturing the structure.

Topology Optimisation of Metallic Fins in Adsorbed Natural Gas Tanks

Ricardo Amigo^{*}, Robert Hewson^{**}, Emilio Silva^{***}

^{*}University of Sao Paulo, ^{**}Imperial College London, ^{***}University of Sao Paulo

ABSTRACT

Adsorption is a retention mechanism of fluid molecules on solid surfaces that is explored in gas storage applications. Adsorbed Natural Gas (ANG) tanks are constituted by porous materials which accumulates gas molecules by adsorption, reaching storing densities similar to tanks based on compression at much lower pressure. The major drawback of such tanks is the high dependency of the adsorption phenomenon on temperature, which hinders the attainment of the full storage capacity. In this work, the Topology Optimisation Method (TOM) is implemented to distribute metal in adsorbent beds to improve the heat exchange in order to maximise the total mass of gas admitted during tanks filling cycle. FEniCS is used to solve the governing equations of the adsorption problem (continuity, energy balance and adsorption kinetics) and the sensitivities are obtained via the transient adjoint method. Resulting topologies are presented and compared with tank constituted by pure adsorbent beds.

Efficient Topology Optimization with Geometric Nonlinearities Using Reanalysis-based Approaches

Oded Amir^{*}, Matti Spicer^{**}

^{*}Technion - Israel Institute of Technology, ^{**}Technion - Israel Institute of Technology

ABSTRACT

Topology optimization is a computational method for finding the optimal distribution of material in a given design domain. It is typically applied for balancing weight and stiffness, and has developed into a widespread computational design approach that is widely used in automotive and aerospace industries. Because the problem is defined and solved on a finite element discretization of the continuum domain, it inherently involves a very large number of state variables (e.g. displacements) that need to be computed in every design cycle. Several approaches have been suggested for reducing the computational effort invested in such sequences of finite element analyses, however they focus on optimization considering linear static responses. The need for efficient procedures is more evident when the underlying structural analysis is nonlinear – this is the focus of the current contribution. In this talk, we will present and discuss efficient solution procedures for nonlinear structural analysis based on reanalysis and reuse of information throughout the optimization process. First, we follow the two schemes proposed in [1]: I) The solution (i.e. displacements) of the nonlinear structural analysis corresponding to a certain design cycle is used as a starting point for the analysis in the next design cycle; II) The factorization (or preconditioner) of the tangent stiffness matrix corresponding to a certain design cycle is reused in subsequent design cycles. Second, we investigate the influence of the problem formulation: In linear static cases, it was shown that reanalysis is more effective for volume minimization than for stiffness maximization due to the advantages of “stiff preconditioning” [2]. The extension of this observation to the case of geometrically nonlinear (GNL) responses will be examined and discussed. Finally, we enhance the procedures presented in [1] by employing reanalysis in the solution of the linear adjoint problem, enabling further computational savings. Preliminary results show that significant computing time can be reduced by applying various combinations of the schemes described above. Furthermore, the effect of “stiff preconditioning” and the consequent benefit of volume minimization are shown to be valid also for the GNL case. Test cases will include the optimization of beams and columns undergoing large deformations and buckling. [1] Amir, O., 2011. Efficient reanalysis procedures in structural topology optimization (Doctoral dissertation, PhD thesis, Technical University of Denmark). [2] Amir, O., 2015. Revisiting approximate reanalysis in topology optimization: on the advantages of recycled preconditioning in a minimum weight procedure. *Structural and Multidisciplinary Optimization*, 51(1), pp.41-57.

A Redox Fuel Cell Capable of Converting Fuels to Electricity at a High Rate

Liang An*

*The Hong Kong Polytechnic University

ABSTRACT

The use of hydrogen peroxide in fuel cells has recently received increasing attention, primarily due to its several unique characteristics when compared with the use of gaseous oxygen. However, there are three issues associated with the use of hydrogen peroxide in fuel cells. Firstly, the actual cathode potential is lower than the theoretical one, which is mainly attributed to the mixed potential resulting from the simultaneous hydrogen peroxide oxidation reaction on the cathode. Secondly, the hydrogen peroxide oxidation reaction releases gaseous oxygen, leading to a two-phase mass transport. Thirdly, the reduction of hydrogen peroxide in fuel cells has to use metal catalysts, such as platinum, palladium and gold. In this work, we propose to create the cathode potential by introducing a redox couple to the cathode while to use hydrogen peroxide to chemically charge to redox ions. The redox cathode not only completely eliminates the mixed-potential problem associated with the direct reduction of hydrogen peroxide, but also enables a faster cathodic electrochemical kinetics even without noble metal catalysts. It has been demonstrated that the direct ethanol fuel cell with a redox couple of V(IV)/V(V) yields a peak power density of 450 mW cm⁻² at 60°C, which is 87.5% higher than that of the conventional cell with direct reduction of hydrogen peroxide.

Coupled Atomistics and Discrete Dislocations in 3d (CADD-3d)

Guillaume Anciaux^{*}, Jaehyun Cho^{**}, Till Junge^{***}, Max Hodapp^{****}, Jean-François Molinari^{*****},
William Curtin^{*****}

^{*}EPFL, ^{**}EPFL, ^{***}EPFL, ^{****}EPFL, ^{*****}EPFL, ^{*****}EPFL

ABSTRACT

Capturing plasticity at realistic dislocation densities with high configurational complexity requires a continuum-level discrete dislocation dynamics (DDD) description. However, many features controlling dislocation motion are inherently atomistic, such as the interaction of dislocations with solutes, precipitates, cracks, interfaces and nucleation. In two dimensions, modeling these phenomena in a multi-scale manner was possible thanks to the method Coupled Atomistic and Discrete Dislocation dynamics (CADD2d). Here, we present an approach that extends this multiscale coupling in 3d (CADD3d). The algorithm principle will be described in details, where dislocations can be described with atomistic resolution intimately coupled to a surrounding continuum domain in full 3d. In such a case, individual dislocation lines may span both domains simultaneously, therefore forming hybrid dislocations, partially represented with dislocated atoms and partially as discrete lines. Continuum dislocation properties and atomistic dislocation properties need to match closely. An implementation prototype is presented based on the DDD code Paradis and on the MD code LAMMPS, altogether interfaced with the coupling code LibMultiScale. Simulations of the dynamics of a single hybrid dislocation and of a hybrid dislocation loop will illustrate the potential and robustness of the approach for near-seamless motion of dislocations into, across, and out of the atomistic domain. Finally we present the nucleation of dislocation loops emitted from a Frank-Read source and then transformed into DD dislocations, demonstrating the possibilities of our framework.

A Higher-Order Finite Element ALE Method with Non-conforming Mesh Refinement

Robert Anderson^{*}, Veselin Dobrev^{**}, Robert Rieben^{***}, Vladimir Tomov^{****}, Jakub Cervený^{*****}, Tzanio Kolev^{*****}

^{*}LLNL, ^{**}LLNL, ^{***}LLNL, ^{****}LLNL, ^{*****}University of West Bohemia in Pilsen, ^{*****}LLNL

ABSTRACT

We present non-conforming adaptive mesh refinement extensions for a higher-order finite element ALE code and methodology that has been under development by Kolev, Dobrev, Rieben, et. al. [1][2]. The underlying ALE methodology is a Lagrange plus remap scheme, and can be characterized as a higher-order generalization of the classical staggered grid Lagrange plus remap hydrodynamics methods. The Lagrangian phase uses continuous finite elements for kinematic variables and the curvilinear mesh, and discontinuous finite elements for thermodynamic variables. The remap phase is based on a conservative, monotonic DG formulation. The AMR extension involves element-by-element, potentially anisotropic h-refinement at a fixed polynomial order. The resulting AMR systems of equations involve constraints on hanging nodes when there are continuity requirements, and in this case the system is solved through variational restriction. The hanging node constraints are specified through a prolongation matrix P , which maps "true" degrees of freedom (DOFs) to the full set of DOFs which are potentially non-conforming if no constraints are applied. The efficient construction of P in parallel is an essential component of the AMR method. Parallel partitioning of the AMR hierarchy is achieved through the use of a space-filling curve, which is then equipartitioned to distribute the elements to MPI ranks to achieve load balance. These methods have been incorporated into the finite element library MFEM, which forms the foundation of the ALE code under development. With the choice of abstractions utilized in MFEM, it is notable that adoption of AMR in the aforementioned ALE code is remarkably unintrusive. With the foundations of an AMR capability in place, we will discuss some initial verification and performance characterization results of the ALE-AMR method, and ongoing research into suitable refinement criteria and the use of dynamic regridding. [1] V. Dobrev, Tz. Kolev and R. Rieben, "High-Order Curvilinear Finite Element Methods for Lagrangian Hydrodynamics", SISC., Vol. 34, pp. B606-B641, (2012). [2] R. Anderson V. Dobrev, Tz. Kolev and R. Rieben, "Monotonicity in High-Order Curvilinear Finite Element ALE Remap," IJNMF, Vol. 77, pp. 249-273 (2014). This work was performed under the auspices of the U.S. Department of Energy by Lawrence Livermore National Laboratory under Contract DE-AC52-07NA27344.

Row-Wise Clustering for Sparse and Spatial Local Reduced-Order Bases

Spenser Anderson^{*}, Tina White^{**}, Phil Avery^{***}, Charbel Farhat^{****}

^{*}Stanford University, ^{**}Stanford University, ^{***}Stanford University, U.S. Army Research Laboratory, ^{****}Stanford University

ABSTRACT

The construction of a Projection-based Reduced-Order Model (PROM) relies on the precomputation of a Reduced-Order Basis (ROB) representing an approximation subspace that, despite having a dimension much smaller than that of the underlying High-Dimensional Model (HDM), can capture its dominant features. It is common to build this ROB by collecting many solution snapshots from the HDM and compressing them using the SVD. However, for highly nonlinear problems characterized by multiple regimes, a single ROB often needs to be prohibitively large in order to deliver the desired accuracy. This issue was recently addressed by introducing the concept of local ROB's [1]. There, the solution manifold is partitioned into subregions using a clustering algorithm applied to the columns of the snapshot matrix. Local ROB's are constructed by compressing the clustered snapshots, and are assigned to the subregions of the manifold they best represent. Although this approach has demonstrated a significant potential for achieving simultaneously good speed-ups and accuracy, it has room for improvement. To this end, this talk will describe a complementary approach for constructing local ROB's where clustering is performed row-wise or row-column-wise, instead of column-wise. More importantly, it will be shown that row clustering, which can be described as spatial clustering, is an effective approach for sparsifying a ROB and therefore accelerating online PROM simulations. It will also be shown that for problems with localized phenomena, row clustering leads to more effective PROM's than column clustering. Most importantly, row clustering can be combined with column clustering to simultaneously achieve dimensional reduction and sparsification, and therefore to maximize computational efficiency. It is also amenable to existing hyper reduction techniques such as GNAT [2] for CFD, and ECSW [3] for CSD. Finally, the talk will illustrate all stated properties of row clustering with several examples from computational mechanics. 1. D. Amsallem, M. Zahr and C. Farhat, Nonlinear Model Order Reduction Based on Local Reduced-Order Bases, *International Journal for Numerical Methods in Engineering*, Vol. 92, pp. 891-916 (2012) 2. K. Carlberg, C. Bou-Mosleh and C. Farhat, Efficient Nonlinear Model Reduction via a Least-Squares Petrov-Galerkin Projection and Compressive Tensor Approximations, *International Journal for Numerical Methods in Engineering*, Vol. 86, pp 155-181 (2011) 3. C. Farhat, T. Chapman and P. Avery, Structure-Preserving, Stability, and Accuracy Properties of the Energy-Conserving Sampling and Weighting (ECSW) Method for the Hyper Reduction of Nonlinear Finite Element Dynamic Models, *International Journal for Numerical Methods in Engineering*, Vol. 102, pp. 1077-1110 (2015)

Spanwise Surface Roughness Heterogeneity: Circulation Intensity and a Prognostic Model for Turbulent Secondary Flows

William Anderson*, Kalyan Shrestha**

*UT Dallas, **UT Dallas

ABSTRACT

Spanwise surface heterogeneity beneath high-Reynolds number, fully-rough wall turbulence is known to induce mean secondary flows in the form of counter-rotating streamwise vortices. The secondary flows are a manifestation of Prandtl's secondary flow of the second kind -- driven and sustained by spatial heterogeneity of components of the turbulent (Reynolds averaged) stress tensor. The spacing between adjacent surface heterogeneities serves as a control on the spatial extent of the counter-rotating cells, while their intensity is controlled by the spanwise gradient in imposed drag (where larger gradients associated with more dramatic transitions in roughness induce stronger cells). In this work, we have performed an order of magnitude analysis of the mean (Reynolds averaged) streamwise vorticity transport equation, revealing the scaling dependence of circulation upon spanwise spacing. The scaling arguments are supported by a simulation data. Then, we demonstrate that mean streamwise velocity can be predicted a priori via a similarity solution to the mean streamwise vorticity transport equation. A vortex forcing term was used to represent the affects of spanwise topographic heterogeneity within the flow. Efficacy of the vortex forcing term was established with large-eddy simulation cases, wherein vortex forcing model parameters were altered to capture different values of spanwise spacing.

Modeling of Organic-organic Interfaces and Mixtures for Organic Photovoltaic Applications

Denis Andrienko*

*Max Planck Institute for Polymer Research

ABSTRACT

We will discuss the role of mesoscale order, electrostatic effects, defects, and roughness for charge splitting and detrapping at organic-organic interfaces. We will show how inclusion of mesoscale order resolves the controversy between experimental and theoretical results for the energy-level profile and alignment in a variety of photovoltaic systems, with direct experimental validation [1,2]. We will show how one can predict open-circuit voltages of planar heterojunction solar cells, in excellent agreement with experimental data, based only on crystal structures and interfacial orientation. We will show how long-range molecular order and interfacial mixing generate homogeneous electrostatic forces that can drive charge separation and prevent minority carrier trapping across a donor-acceptor interphase [2]. Comparing several of small-molecule donor-fullerene combinations, we will illustrate how tuning of molecular orientation and interfacial mixing leads to a trade-off between photovoltaic gap and charge-splitting and detrapping forces, with consequences for the design of efficient photovoltaic devices. By accounting for long-range mesoscale fields, we will obtain the ionization energies in both crystalline and mesoscopically amorphous systems with high accuracy [4,5]. References: [1] C. Poelking, M. Tietze, C. Elschner, S. Olthof, D. Hertel, B. Baumeier, F. Wuerthner, K. Meerholz, K. Leo, D. Andrienko, *Nature Materials*, 14, 434, 2015 [2] C. Poelking, D. Andrienko, *J. Am. Chem. Soc.*, 137, 6320, 2015 [3] M. Schwarze, W. Tress, B. Beyer, F. Gao, R. Scholz, C. Poelking, K. Ortstein, A. A. Guenther, D. Kasemann, D. Andrienko, K. Leo, *Science*, 352, 1446, 2016 [4] P. Kordt, J. J. M. van der Holst, M. Al Helwi, W. Kowalsky, F. May, A. Badinski, C. Lennartz, and D. Andrienko, *Adv. Funct. Mater.* 25, 1955, 2015 [5] C. Poelking, D. Andrienko *J. Chem. Theory Comput.*, 12, 4516, 2016

FE Modelling of Tensile Deformation of Ductile Cast Iron Using In-Situ 3D Tomography Results as Input and Validation

Tito Andriollo*, Yubin Zhang**, Jesper Thorborg***, Jesper Hattel****

*Department of Mechanical Engineering, Technical University of Denmark, **Department of Mechanical Engineering, Technical University of Denmark, ***Department of Mechanical Engineering, Technical University of Denmark, ****Department of Mechanical Engineering, Technical University of Denmark

ABSTRACT

In key industrial sectors like transportation and energy production there is a strong demand for improving the performance of ductile cast irons, in order to optimize designs for lower weight and longer life. Consequently, research efforts are currently being made to understand quantitatively the mechanisms controlling deformation and fracture at the micro-scale. As emphasized in a recent review paper (Hütter et al. [2015]), a major challenge is represented by the complex material microstructure, which consists of graphite particles embedded in a steel matrix. Remarkably, most of the theoretical models developed so far assume that this microstructure is stress-free at room temperature. However, recent synchrotron-based studies by the present authors have demonstrated that the thermal contraction mismatch between the graphite and the matrix during manufacture leads to localized elastic and plastic deformation (Zhang et al. [2016]). Also, the residual stress field associated with the elastic strain is non-negligible and highly affected by the sub-structure of the graphite particles, which creates stress concentrations in the matrix (Andriollo et al. [2017]). The present work takes these studies to the next step by investigating how this inhomogeneous residual stress field affects the deformation mechanisms of the material at the micro-scale. First, a FE model based on a RVE obtained from micro computed tomography (CT) is developed and used to simulate manufacture and tensile loading of ductile cast iron. Then, the model results are validated by means of digital volume correlation, based on CT scans acquired in-situ during deformation. Finally, the importance of taking residual stress and 3D effects into account is discussed in relation to previous findings from the literature.

REFERENCES: Andriollo, T., Hellström, K., Sonne, M.R., Thorborg, J., Tiedje, N., and Hattel, J. 2018, “Uncovering the local inelastic interactions during manufacture of ductile cast iron: How the substructure of the graphite particles can induce residual stress concentrations in the matrix”, J. Mech. Phys. Solids, 111, 333–357. Hütter, G., Zybelle, L., and Kuna, M. 2015, “Micromechanisms of fracture in nodular cast iron: From experimental findings towards modeling strategies – A review”, Eng. Fract. Mech., 144, 118–141. Zhang, Y.B., Andriollo, T., Fæster, S., Liu, W., Hattel, J., and Barabash, R. I. 2016, “Three-dimensional local residual stress and orientation gradients near graphite nodules in ductile cast iron”, Acta Mater., 121, 173–180.

Error Estimation and Adaptivity Using Hierarchical Splines with Applications to Fracture Mechanics

Cosmin Anitescu^{*}, Somdatta Goswami^{**}, Timon Rabczuk^{***}

^{*}Leibniz Universität Hannover, ^{**}Bauhaus-Universität Weimar, ^{***}Bauhaus-Universität Weimar

ABSTRACT

We present a method for error analysis and adaptivity when the approximation space considered is that of smooth piecewise polynomials. It is well-known that higher-order and higher smoothness bases, such as the ones used in isogeometric analysis [1] provide an efficient way to approximate smooth solutions as well as compatibility with existing CAD models. Nevertheless, we focus on applications to problems with discontinuities, for which adaptivity is needed to efficiently represent the approximate solution. We introduce and compare recovery and residual-based estimators for hierarchical splines, as well as algorithms for performing h- and p- adaptivity. The problems considered involve fracture which is modeled by means of a phase field approach [2]. Several benchmark problems will be considered to demonstrate the performance of the presented method. [1] T.J.R. Hughes, J.A. Cottrell, Y. Bazilevs, Isogeometric analysis: CAD, finite elements, NURBS, exact geometry and mesh refinement, Computer Methods in Applied Mechanics and Engineering, Volume 194, Issues 39–41, 2005, Pages 4135–4195, ISSN 0045-7825, [2] C. Miehe, M. Hofacker, F. Welschinger, A phase field model for rate-independent crack propagation: Robust algorithmic implementation based on operator splits, Computer Methods in Applied Mechanics and Engineering, Volume 199, Issues 45–48, 2010, Pages 2765–2778, ISSN 0045-7825

Self-organization of Nanostructured Morphologies in Physical Vapor Deposited Phase-separating Multicomponent Alloys

Kumar Ankit*, Rahul Raghavan**

*Arizona State University, **Arizona State University

ABSTRACT

Experiments have demonstrated a rich variety of self-organized nanoscale concentration modulations in physical vapor deposited films of phase-separating alloys. However, a comprehensive model that is capable of predicting the entire spectrum of these self-organized nanostructures as a function of material and processing parameters has yet to be developed. We adopt a phase-field approach to numerically investigate the role of substrates, deposition rates, phase fraction and separation kinetics, on the morphological self-structuring in vapor-deposited alloys. Based on synergies with experimental results, we map out the processing space where the evolution of mixed morphology is favorable. We propose new strategies for morphology control based on the insights gained from our numerical study.

Isogeometric Analysis on Trimmed Volumetric Geometries

Pablo Antolin^{*}, Annalisa Buffa^{**}, Gershon Elber^{***}, Massimiliano Martinelli^{****}, Fady Massarwi^{*****}

^{*}École polytechnique fédérale de Lausanne. Switzerland, ^{**}École polytechnique fédérale de Lausanne. Switzerland / Istituto di Matematica Applicata e Tecnologie Informatiche "Enrico Magenes", IMATI - CNR. Pavia, Italy, ^{***}Technion - israel Institute of Technology, ^{****}Istituto di Matematica Applicata e Tecnologie Informatiche "Enrico Magenes", IMATI - CNR. Pavia, Italy, ^{*****}Technion - israel Institute of Technology

ABSTRACT

The idea of designing and analyzing methods able to alleviate the remeshing step by directly using the output of CAD is the challenge of Isogeometric analysis (IGA), which was proposed by T.J.R. Hughes and co-authors in 2005. In this work we propose a methodology for treating volumetric geometries (V-reps), constructed using the IRIT modeler through boolean operations and trimming. It allows to use isogeometric discretizations in a Galerkin-like context for 2D and 3D spline trimmed domains in a fully automatic way. When trying to assemble the operators of a discrete variational problem element by element, it is immediately clear that integrals for the Bézier elements affected by the boolean operations are not easily computable. Suitable quadrature formulas that consider only the part of the element inside the computational domain are required. In order to do that we split the geometry in Bézier elements. The elements not affected by trimming operations are processed in a standard way, while for trimmed Bézier elements we present two different approaches. A first approach subdivides the trimmed element into spline patches (tiles), that together are identical geometrically to trimmed Bézier element. Currently, this approach is only applicable for 2D geometries (even embedded in a 3D euclidean space). A second methodology consists in meshing "à la finite elements" every trimmed element. Thus, for every trimmed element a boundary representation (B-rep) is created, then we create a high-order mesh (in order to approximate correctly the boundary of the B-rep) of the interior using Gmsh. This approach works for both 2D and 3D geometries. In both approaches the quadrature formula of every Bézier element is composed by a set of quadrature formulas, one for every tile. In addition to compute integrals in the interior of the computational domain, this methodology allows to compute integrals on the domain boundary. The degree of the tiles is chosen accordingly to the degree of the spline functions used in the discretization of the unknown variables. We show theoretically that, by using the same degree for both the discretization of the unknowns and the tiles, the method presents optimal approximation properties for any degree. We present numerical results that support the theoretical results and examples involving complex and trimmed geometries that illustrate the potential applicability of the method. Finally, future perspectives are drawn.

Optimum Design of Thrust Bearings for Maximizing the Load Capacity

Olga Antonova*, Alexey Borovkov**, Yuri Boldyrev***, Igor Voynov****

*Peter the Great St.Petersburg Polytechnic University, **Peter the Great St.Petersburg Polytechnic University,
Peter the Great St.Petersburg Polytechnic University, *Peter the Great St.Petersburg Polytechnic University

ABSTRACT

One of the most important structural elements of the wide range of the power machines is hydrodynamic thrust bearing which perceives a major part of load. The important operational parameter that characterizes the efficiency of the bearing is the load capacity of an oil wedge, which has nonlinear dependence on gap size. However, reduction of oil film thickness leads to decreasing the bearing stability under dynamic loads. In this study we consider the lubricant layer microgeometry profiling with the aim of optimal design of the hydrodynamic bearing for ensuring the maximum load capacity. Historically the first formulation of the considered problem in one-dimensional case goes back to the work by J.W. Rayleigh published in 1918 [1]. The Rayleigh results were much ahead of his time, were repeated later by S. Y. Maday only in 1967 [2]. In 1975 one of the authors together with V.A. Troitsky considered the spatial variational problem put by Rayleigh to gain the optimal shape profile for the rectangular gap region. Here we enlarge the results of the previous works in relation to the sector thrust bearings based on advanced computing technologies. The special case for one sector of self-aligning acting bearing with profile consisted of two parts: straight line and generalized ellipse was considered. Geometrical parameters which define profile curvature were used as optimization variables during optimization procedure. Using special code IOSO the optimization problem was solved. As objective function the maximum of pressure integral over the lubricant layer surface was used. To solve the optimization problem, the CFD mesh for investigated domain was generated and hydrodynamics problem, using Navier-Stokes equations was solved on the basis of numerical approach and commercial CFD code ANSYS/CFX. The numerical simulation of the problem was carried out using the St.Petersburg Polytechnic Supercomputer Center. References [1] Lord Rayleigh. Notes on the theory of lubrication, Phil. Mag.35 (1) (1918),p. 1-12. [2] C. J. Maday A Bounded Variable Approach to the Optimum Slider Bearing, Trans. ASME. Ser. F. J. Lubr. Technol. 90(1) (1968), p. 240-242 [3] Yu.Yu. Boldyrev, V.A. Troitsky One spatial variational problem of the theory of gas lubrication, Tidings AS USSR MFG 5(1975), p.34-39

Modeling Microwave Induced Fragmentation of Heterogeneous Rocks for Mining Applications

Thomas Antretter^{*}, Michael Toifl^{**}, Philipp Hartlieb^{***}, Ronald Meisels^{****}, Friedemar Kuchar^{*****}

^{*}Institute of Mechanics, Montanuniversitaet Leoben, ^{**}Institute of Mechanics, Montanuniversitaet Leoben, ^{***}Chair of Mining Engineering and Mineral Economics, Montanuniversitaet Leoben, ^{****}Institute of Physics, Montanuniversitaet Leoben, ^{*****}Institute of Physics, Montanuniversitaet Leoben

ABSTRACT

Excavation processes in mining and tunneling are very costly, especially if the rock material is very hard. Only 1% of the invested energy is converted into the creation of new surfaces, i.e., the fragmentation of the rock while almost the entire rest is lost as frictional heat. A more economical alternative is to heat up the rock by means of microwave irradiation thereby creating thermal stresses high enough to generate cracks in the rock so that subsequent mechanical processes already cut into a partly pre-damaged and hence softer material. Quantification of the potential energy savings requires a thorough analysis of the physical phenomena coming into play. This includes a) the propagation of the electro-magnetic waves emitted by a high-power microwave source into the rock-material, b) locally varying heating due to absorption of the microwaves, c) redistribution and evolution of the temperature field due to heat conduction, d) thermal expansion of the differently heated areas followed by mechanical strains and stresses inside the rock that locally exceed the rock's strength thus leading to micro-cracks that eventually coalesce and form a dominant crack. The heterogeneous nature of natural rocks must be taken into account, because the different material properties of the individual constituents of a rock significantly amplify the temperature gradients and stresses hence accelerating the formation of cracks. The theoretical investigations were carried out by a numerical full field analysis of the coupled phenomena a) to d) enumerated above. The electrical material properties, more specifically the permittivity across a wide temperature range, were experimentally measured in a specifically designed oven. The thermal expansion properties were determined using dilatometry on thin rock samples. The numerically obtained crack patterns showed a good agreement with the ones found in full-scale microwave irradiation experiments.

Evolutionary Aseismic Design of Three-Dimensional Structures with Passive Devices

Georgios Apostolakis*, Gary Dargush**

*University of Central Florida, **SUNY at Buffalo

ABSTRACT

Current seismic codes do not incorporate a systematic and well-established methodology for the topological distribution and properties of passive devices in three-dimensional structures. The issue is further exaggerated when structures are subject to extreme events and operate well within their inelastic range. To overcome the above shortcomings, an evolutionary computational framework was developed to design tall regular and irregular three-dimensional buildings when subjected to a predefined seismic environment (Apostolakis and Dargush, 2012). The framework incorporated Mixed Lagrangian Formalism (MLF) variational principles within an evolutionary compact Cellular Automata-based Genetic Algorithm (CAGA). From the evolutionary process, the optimal placement, strength and size of hysteretic dampers throughout the height of the structures were obtained. The topological distributions of the braces throughout the height of the structure corresponded to patterns that were not seen in common practice. Furthermore, the optimization framework produced optimal designs with reduced drifts while reducing accelerations at the same time, when compared to the original base structure. In this presentation, our previous work is extended to include different type of passive devices (e.g., viscous dampers), enhanced Self-Automated based Genetic Algorithm (SAGA) incorporating deep learning technique to establish the weighted probabilistic gene-by-gene cross-over and mutation operations, and hierarchical multiscale brace architectures where brace topology patterns can span multiple bays/stories (mega-braces). The objectives will be to establish (a) a robust computational framework to yield designs based on ductility demand throughout the height of the yielded structure under seismic loading, (b) identify optimal designs with ductility demand uniformly distributed throughout the height, (c) realize novel three-dimensional multiscale mega-brace architectures, (d) require modest computational and engineering effort well within the range of typical seismic design firms. Apostolakis G, Dargush GF, Filiatrault A (2014) Computational Framework for Automated Seismic Design of Steel Frames with Self-Centering Connections, ASCE Journal of Computing in Civil Engineering, 28(2), 170-181. Apostolakis G, Dargush GF (2012) Optimal Design of Three-Dimensional Structures with Hysteretic Braces, 15th World Conference on Earthquake Engineering (WCEE), 24-28 September, Lisbon, Portugal. Apostolakis G, Dargush GF (2010) Optimal Seismic Design Of Moment-Resisting Steel Frames with Hysteretic Passive Devices, Earthquake Engineering and Structural Dynamics, 39, 355-376.

Hermite and dG Methods for Wave Equations and Their Application to Uncertain and Inverse Problems

Daniel Appelö^{*}, Thomas Hagstrom^{**}, Mohammad Motamed^{***}, Arturo Vargas^{****}, Yunan Yang^{*****}

^{*}University of Colorado, Boulder, ^{**}Southern Methodist University, ^{***}University of New Mexico, ^{****}Lawrence Livermore National Laboratory, ^{*****}University of Texas at Austin

ABSTRACT

In this talk we report on the development of high order Hermite and dG methods for wave equations in second order form and its applications to forward propagation of uncertainties and the inversion of material parameters from boundary measurements. The Hermite methods come in two flavors, dissipative and conservative. The dissipative method achieves space-time accuracy of order $(2m+1)$, while the conservative method has space-time order $(2m)$. Besides their high order of accuracy in both space and time combined, the methods have the special feature that they are stable for CFL numbers up to and including unity for all orders of accuracy. Curiously, when using CFL equal to one, the orders of both methods increase. Our spatial discontinuous Galerkin discretization of wave equations in second order form relies on a new energy based strategy featuring a direct, mesh-independent approach to defining interelement fluxes. Both energy-conserving and upwind discretizations can be devised. The method comes with optimal a priori error estimates in the energy norm for certain fluxes and we present numerical experiments showing that optimal convergence for certain fluxes. The forward propagation of uncertainties is performed by a new multi-order Monte Carlo algorithm for computing the statistics of stochastic quantities of interest. The method is a non-intrusive technique based on a high (but variable) order discretizations, as those presented. The algorithm is built upon a hierarchy of degrees of polynomial basis functions rather than a mesh hierarchy used in multi-level Monte Carlo. In addition to the convenience of working with a fixed mesh, which is desirable in many real applications with complex geometries, the multi-order method is particularly beneficial in reducing errors due to numerical dispersion in long-distance propagation of waves. To invert for P and S velocities in the elastic wave equation we extend the novel trace-by-trace quadratic Wasserstein metric (W2) technique pioneered by Yang and co-authors. We give examples comparing W2 with the standard L2 misfit.

A Lower-Triangular Mass Matrix Approach to Explicit Time Advancement for Continuous Triangular Finite Element Methods

Jay Appleton^{*}, Brian Helenbrook^{**}

^{*}Clarkson University, ^{**}Clarkson University

ABSTRACT

When using explicit time advancement with continuous high order finite elements, a mass matrix is formed which must be inverted to advance the solution in time. For the Gauss-Lobatto-Lagrange basis typically used on quadrilaterals, an accurate approximate diagonal mass matrix exists which makes explicit time stepping methods efficient while achieving p th-order spatial convergence rates. No such approach exists for triangular methods. This work introduces an alternative in the form of a lower-triangular method that achieves p th-order convergence. This specific lower-triangular method allows for computationally efficient time advancement without sacrificing spatial accuracy.

Usage of the Discrete Element Method for the Study of Concrete

Antonio Aquino*, Ruben Lopez**, Osvaldo Quintana***

*National University of Asuncion. Faculty of Engineering, **National University of Asuncion. Faculty of Engineering,
***National University of Asuncion. Faculty of Engineering

ABSTRACT

The DEM was applied for the first time to concrete by Bazant and his collaborators (Zubelewicz & Bazant, 1987; Bazant et al., 1990) based on the DEM previously proposed for the study of granular geomaterials, (Cundall & Strack, 1979). In the current literature, some models represent cement grains by equivalent spheres as an initial state prior to the hydration process (Maekawa et al., 2009). Ulm & Lemarchand (2003), sought to obtain the mechanical properties of cement paste as a function of time during the hydration process from the development of a multiscale model validating their results through experimental data obtaining a very good correlation of them. Within the area of the study of the cement hydration process there is still a limited literature that addresses this process through this numerical technique. On the other hand, in recent times with the use of mass concrete structures in civil construction has been necessary to consider the evolution of temperature in the structure to prevent the formation of cracks of thermal origin in it. This work proposes obtaining a multi-scale model that describes the phenomena associated with the hydration of concrete and applying this model to the analysis of the different types of concrete produced in Paraguay. The model is implemented through the use of the Discrete Elements Method (DEM). To calibrate the implementation of the mechanical component of the model, the Abaqus program was used. For this simulation, the strategy used to initialize the model consisted of specifying the approximate initial position of the particles with some distance between them to allow the particles that accommodate themselves in their position under the action of gravity. The element consists on an only one node element that describes the spherical particle, whose kinematics is modeled as a rigid body and where any adjustment is made in the model constituting the contact between particles. For the calibration of the implementation of the thermal component of the model, the LIGGGHTS program was used, where spherical particles were also used. The obtained results show that the method of the discrete elements is suitable to model a thermo-mechanical problem, in addition, the temperature distributions obtained are comparable with those obtained in a continuous model based on the Finite Element Method.

The Discontinuity-Enriched Finite Element Method (DE-FEM): New Developments for Fracture and Unfitted Mesh Problems

Alejandro M. Aragón*, Jian Zhang**, Sanne J. van den Boom***, Elena De Lazzari****, Dongyu Liu*****, Max van der Kolk*****, Matthijs Langelaar*****, Angelo Simone*****, Fred van Keulen*****

*Delft University of Technology, Delft, the Netherlands, **Delft University of Technology, Delft, the Netherlands, ***Delft University of Technology, Delft, the Netherlands, ****Delft University of Technology, Delft, the Netherlands, *****Delft University of Technology, Delft, the Netherlands, *****Delft University of Technology, Delft, the Netherlands, *****University of Padua, Padova, Italy, *****Delft University of Technology, Delft, the Netherlands

ABSTRACT

Weak and strong discontinuities play an important role in the analysis of a wide range of (multi-physics) problems, such as fracture or multi-phase materials. In standard Finite Element Analysis (FEA), discontinuities are explicitly taken into account by the spatial discretization, by ensuring that any material interfaces, domain boundaries, and/or cracks coincide with element sides. Creating such a matching mesh can be a challenging exercise, especially when dealing with complex 3D geometries. To make matters worse, remeshing has to take place in cases where the problem domain undergoes changes between analysis steps. This occurs, for example, in shape or topology optimization or in fluid-structure interaction. Remeshing is also an important issue in crack propagation, where a special mesh has to be created around crack fronts. The Discontinuity-Enriched Finite Element Method (DE-FEM) [1] was recently introduced as a novel enriched formulation to model weak and strong discontinuities without the need of a matching mesh. In DE-FEM, enriched degrees of freedom are placed only along discontinuities, resulting in a new modelling paradigm with several key properties. Indeed, this allows a hierarchical implementation of enrichment functions, which simplifies the analysis of arbitrary cracked configurations (e.g., n-junctions or cracks traversing material interfaces). Moreover, Dirichlet boundary conditions can be prescribed in a strong manner, which gives DE-FEM an edge over other enriched formulations such as XFEM/GFEM. In this presentation, we will demonstrate the versatility of the method in the context of fracture mechanics, granular materials, immersed domains, and fluid-structure interaction. We illustrate the method for modelling 2D and 3D cracks, and NURBS-enhanced discontinuities. Furthermore, we demonstrate DE-FEM as an immersed boundary (or embedded domain) method for problems in elasticity and in the context of fluid dynamics and fluid-structure interaction. Finally, we show the stability of the method with regards to the condition number of the resulting system matrices.

REFERENCES [1] Aragón AM, Simone A. The discontinuity-enriched finite element method. *Int J Numer Meth Engn*. 2017;112:1589–1613. <https://doi.org/10.1002/nme.5570>

Non-linear Multi-Scale Modeling of 3D Fabric-Rubber Composites

Damian Aranda-Iglesias^{*}, Gaetano Giunta^{**}, Salim Belouettar^{***}, Anne Peronnet-Paquin^{****},
Franco Sportelli^{*****}, Daniel Keniray^{*****}

^{*}Luxembourg Institute of Science and Technology, ^{**}Luxembourg Institute of Science and Technology,
^{***}Luxembourg Institute of Science and Technology, ^{****}The Goodyear Tire & Rubber Company, ^{*****}The
Goodyear Tire & Rubber Company, ^{*****}The Goodyear Tire & Rubber Company

ABSTRACT

Mechanical testing of complex 3D fabric-rubber composites considering structurally different textiles as reinforcements are expensive and time-consuming. Therefore, it is of benefit to develop mechanical models that allow a better understanding of the interaction between the constituents and of the role played by the different length scales in the complex textile micro-structure. The current study seeks to predict the behavior of 3D fabric-rubber composites using a multi-scale modelling approach. The composite structure is divided into simplified models at different scales and a finite element full field homogenization is conducted at each of these scales. The mechanical response is, then, fitted by appropriate isotropic or anisotropic hyperelastic material models connecting the information in a staggered multi-scale approach. The multi-scale based modeling approach presented in this work is intended to support the development of these new 3D fabric-rubber materials by enabling the optimization of the different constituents to obtain specific mechanical properties.

Hypersonic Spatially-developing Turbulent Boundary Layers via DNS

Guillermo Araya^{*}, Kenneth Jansen^{**}

^{*}University of Puerto Rico-Mayaguez, ^{**}University of Colorado-Boulder

ABSTRACT

DNS of compressible spatially-developing turbulent boundary layers is performed at a Mach number of 5 over an isothermal flat plate. Turbulent inflow information is generated by following the concept of the rescaling-recycling approach introduced by Lund et al. (J. Comp. Phys. 140, 233-258, 1998), although, the proposed methodology is extended to hypersonic flows. Furthermore, a dynamic approach is employed to connect the friction velocities at the inlet and recycle stations (i.e., there is no need of an empirical correlation as in Lund et al.). Additionally, the Morkovin's Strong Reynolds Analogy (SRA) is used in the rescaling process of the thermal fluctuations from the recycle plane. Low/high order flow statistics are compared with direct simulations of an incompressible isothermal ZPG boundary layer at similar Reynolds numbers and temperature regarded as a passive scalar. Focus is given to the assessment of flow compressibility on the dynamics of hydrodynamic/thermal coherent structures. Preliminary results have shown that large hydrodynamic turbulent structures are finer and less organized in compressible flow than in the incompressible regime, with less intense "gaps" of high speed fluids in between. A similar conclusion can be drawn for thermal structures. Q2 events are observed to form more elongated and voluminous zone in the incompressible case. Acknowledgement This material is based upon work supported by the Air Force Office of Scientific Research under award number FA9550-17-1-0051. An award of computer time was provided by the Innovative and Novel Computational Impact on Theory and Experiment (INCITE) program and the Theta and Aurora Early Science Programs. This research used resources of the Argonne Leadership Computing Facility, which is a DOE Office of Science User Facility supported under Contract DE-AC02-06CH11357. NSF-CBET Grant #1512393. XSEDE computational allocation #TG-CTS170006.

A Multiscale Hybrid-Mixed Method for the Stokes/Brinkman Equations

Rodolfo Araya*

*Departamento de Ingenieria Matematica, Universidad de Concepcion, Concepcion, Chile

ABSTRACT

In this work a Multiscale Hybrid-Mixed method (MHM), applied to the Stokes/Brinkman equations on heterogeneous media, is introduced and analyzed. Given a coarse partition of the domain and using a hybrid formulation, the MHM method consists of independent Stokes/Brinkman local problems brought together by a face-based weak formulation on the skeleton of the partition. The multiple scales of the media are incorporated in the basis functions which are driven by the local problems with prescribed Neumann boundary conditions. Once available (exactly or approximatively), the multiscale basis functions are used to compute the degrees of freedom from a face-based global variational problem defined on the skeleton of the partition. The numerical solution shares the important properties of the continuum as the local equilibrium with respect to external forces and local mass conservation. Several numerical tests assess the accuracy and the conservative properties of the MHM method on academic and highly heterogeneous cases.

A One-dimensional Model for Large Deformation and Materially Nonlinear Analysis of 3-D Structures

Archana Arbind*, J N Reddy**, Arun Srinivasa***

*Advanced Computational Mechanics Laboratory, Department of Mechanical Engineering, Texas A&M; University, College Station, **Advanced Computational Mechanics Laboratory, Department of Mechanical Engineering, Texas A&M; University, College Station, ***Department of Mechanical Engineering, Texas A&M; University, College Station

ABSTRACT

In this study, a general higher-order 1-D theory (i.e., rod theory) is presented to analyze the large deformation of 3-D structures, which have a space curve as their central axis (see Arbind and Reddy [1] and [2]). A general displacement field of the cross-section perpendicular to the reference curve has been considered in the form of Fourier series in the curvilinear polar cylindrical coordinate system. For the framing of the reference curve, Frenet frame (for C3 continuous regular space curve) as well as frame based on relatively parallel field or Bishop frame (see [3]) for more general C1 continuous and piece-wise regular curve are used. A nonlinear finite element formulation has been presented for linear and nonlinear material such as incompressible neo-Hookean and Mooney-Rivlin solids. The incompressibility condition is imposed via the Lagrange multiplier method and the penalty method in two separate finite element models. Also, due to the one-dimensional nature of this formulation, this theory can be easily implemented for the higher-order gradient elasticity, which requires higher-order continuous interpolation function in the finite element model; this can be easily achieved by higher-order Hermite interpolation functions in the one-dimensional analysis. Various numerical examples are presented to illustrate the application of the presented theory to analyze the curved pipe or other shell structures, which have application in bio-mechanics. The numerical results have been compared with the shell theory or 3-D finite element model of the same problems. **Keywords.** one-dimensional theory; general higher-order rod theory; Neo-Hookean material; Mooney-Rivlin material; analysis of curved pipe **References:** [1] A Arbind and JN Reddy. A one-dimensional model of 3-d structure for large deformation: a general higher-order rod theory. *Acta Mechanica*, pages 1-29, 2017. [2] A Arbind and JN Reddy. A general higher-order one-dimensional model for large deformation analysis of solid bodies. *Computer Methods in Applied Mechanics and Engineering*, 328:99-121, 2018. [3] Richard L Bishop. There is more than one way to frame a curve. *The American Mathematical Monthly*, 82(3):246-251, 1975.

General Constitutive Updating for Finite Strain Formulations Based on Assumed Strains and the Jacobian

Pedro Areias*, Timon Rabczuk**

*CERIS - Instituto Superior Técnico and Universidade de Évora, Portugal, **Bauhaus University, Weimar, Germany

ABSTRACT

Compatibility between element technology featuring assumed (finite)-strains based on least-squares and most constitutive formulations employed in elastic and inelastic contexts is a demanding task. Local frames are required for anisotropic and cohesive laws, some assumed-strain element technologies do not explicitly provide the deformation gradient, and total Lagrangian approaches are often inadequate for advanced plasticity models. Kirchhoff stress-based \mathbf{F}_e \mathbf{F}_p decompositions are also not convenient for ductile damage models. In addition, if rotational degrees-of-freedom are used, as is the case in beams and shells, the adoption of a fixed undeformed configuration entails implementation brittleness. An additional aspect to consider is remeshing by element partition, which precludes the storage of constitutive tensors in local frames, invalidating the stored quantities. Based on seven algorithmic requirements and the corresponding design solutions, we introduce a general constitutive updating algorithm based on the strain and the Jacobian provided by the element. This allows the use of virtually any constitutive law with any finite-strain element formulation while satisfying the seven requirements. In addition, Newton-Raphson convergence properties are extraordinary, at the cost of precision in the strain rate estimation. As a prototype element implementation, we present a stable hexahedron based on least-squares strains. A BFGS secant estimation is employed for the weight in the least-squares so that softening constitutive laws can be adopted without stability issues at the element level.

A Lattice Boltzmann Finite Element Methodology for 2D Fluid-structure Interaction with Moving Boundary Conditions

Marco Argenta^{*}, Sara Bueno^{**}

^{*}UFPR, ^{**}UFPR

ABSTRACT

This work proposes a methodology for solving two-dimensional incompressible fluid-structure interaction in moving and deformable boundary problems. The proposition is modeling the fluid flow by lattice Boltzmann method (LBM) using BGK formulation (Bhatnagar et al, 1954), whose principle is based on mesoscale discretization of the particles with motion on a fixed grid of probabilities, and the moving and deformed boundary using frame finite elements. The LBM has computational advantages in computational cost comparing to the conventional solution based on the Navier-Stokes equations (Guzella et al, 2016). However, even being very efficient, modeling the boundary conditions in the LBM are still a problem for numerical stability when the interactions between fluid and structure take effect, especially when the structure is flexible. In order to simulate this behavior the lattice mesh at each iteration is updated creating or destroying lattices according to fluid domain defined by the flexible boundary conditions, moreover an interpolation algorithm for lattices with immersed boundary is proposed. These informations are obtained by mapping the fluid displacements that are consequence of the geometric variation in domain. The novelty of this work is modeling the boundary using finite element method (FEM) considering one-dimensional frame elements restricted to small deformations and rotations. This version is very attractive for solving coupling problems because numerical instabilities are reduced due to the low complexity of the elements formulation with allow a better understanding of the simulation in order to rise the complexity of the model. Furthermore, using frame elements enables to obtain tensions and deformations results in the walls that hold the fluid in motion. The method is described and it is validated on well-established literature similar two-dimensional cases.

Parametric Study of a Fractal Helmholtz Resonator System

Clara Argerich Martin*, Rubén Ibanez Pinillo**, Anaïs Barasinski***, Emmanuelle
Abisset-chavanne****, Francisco Chinesta*****

*GeM, Ecole Centrale Nantes, **ICI, Ecole Centrale Nantes, ***GeM, Ecole Centrale Nantes, ****ICI, Ecole
Centrale Nantes, *****ESI Group, ENSAM Paris

ABSTRACT

The Helmholtz resonator is one of the oldest acoustic devices and has been largely exploited in literature. Different acoustic absorption systems have been designed and proposed, acoustic solutions vary from combining different resonators to adding a membrane to widen the sound absorption range, as in [1]. In this work we propose an acoustic system of connected Helmholtz Resonators following a fractal generation based on the 'Cantor Set' fractal formation, which is explained on detail in [2]. A single Helmholtz resonator is able to absorb a specific frequency depending on its geometry: the volume of the cavity and the length and diameter of the pipe. In our proposed system we start with two Helmholtz resonators connected by a pipe, and at each new generation new cavities are added whose geometry depends on the initial one. The main benefit of using a fractal sequence is that the resonance frequencies of the system depend on the initial volume, length and diameter of the pipes and the number of generations. In other words, the stiffness matrix of the dynamic system depends on the initial geometry of the problem and the number of generations, which leads to a parametric eigenvalues problem. Through a non-intrusive resolution of the parametric eigenvalue problem and the subsequent construction of a model relating geometrical parameters with eigenfrequencies, an inverse problem for attenuating certain frequencies present in the incident acoustic loading can be formulated and successfully solved. A deeper machine-learning based analysis should inform on the most relevant geometrical parameters with respect to the wished target, and more particularly the relationship between space curvatures (at the different fractal generations) and time curvatures (frequencies) that could be also put in relation using a model or deep learner. Finally the parametric acoustic problem will be solved in the frequency domain, while including selective linear or frequency-dependent damping, by combining the parametric PGD-rationale with a wavelet based approximation to regularise the solution procedure in presence of highly localized solution around the (parametric) natural frequencies. [1] A.Sanada, N. Tanaka Extension of the frequency range of resonant sound absorbers using two-degree-of-freedom Helmholtz-based resonators with a flexible panel. Applied Acoustics 74 (2013) 509–516 – 2012 [2] Mandelbrot B, The fractal geometry of Nature. New York (NY): W.H. Freeman and Company; 1983.

General Purpose Finite Element Library for Computation of High-Order Multivariable Sensitivities

Mauricio Aristizabal^{*}, Harry Millwater^{**}, Manuel Garcia^{***}

^{*}Universidad EAFIT, ^{**}University of Texas at San Antonio, ^{***}University of Texas at San Antonio

ABSTRACT

Computation of accurate sensitivities of finite element analysis is a necessity for general multiphysics problems. Among different approaches, hypercomplex algebras, i.e. algebras with one or more imaginary units, have been successfully used to compute high order derivatives due to the lack of subtraction cancellation error. This work presents a library that uses the variational formulation of the Partial Differential Equation that model multi-physics problems and computes high order sensitivities with respect to multiple variables using Order Truncated Imaginary (OTI) numbers. These variables include problem parameters, shape derivatives and boundary conditions. The library has been tested with different physical models including the Laplace/Poisson equation, linear elasticity and the stokes equation in 2D. Derivatives with respect to shape (both Lagrangian and Eulerian derivatives), spatial coordinates and/or problem parameters, such as heat transfer coefficient and modulus of elasticity were obtained. All derivatives were computed using only one finite element analysis, hence only required one assembly procedure. Results showed that similar to the solution of the state variable, derivative accuracy is dependent on the mesh discretization. Also, all computed derivatives obtained lower error than the best equivalent finite difference solution. Solution time of the system using LU factorization showed that solving each new derivative takes approximately 2.5% the time it takes to solve the real-only system of equations. As a result, the developed library using OTI algebra allows a more efficient computation of high order derivatives for multivariable sensitivities in the finite element method.

Coupling Mechanical Evolution to Electrochemical Performance in Lithium-Ion Batteries

Craig Arnold*

*Princeton University

ABSTRACT

Because of their high energy densities and high working voltages, lithium-ion batteries are the most suitable energy storage choice for a variety of applications from large scale battery electric vehicles to small scale implantable medical devices. These systems are well-known to experience both mechanical and electrochemical phenomena and in this presentation, we discuss how the evolution of internal and external mechanical stress affects the electrochemical performance over the lifetime and how the electrochemical state of the system influences its mechanical properties. Based on a detailed understanding of mechanical and electrochemical coupling, we find that spatially localized phenomena which create non-uniform ionic transport across the electrode materials have the most significant effect on system lifetime and safety. Using numerical models as well as experimental measurements, we identify the critical length scale for localization and suggest methodologies for mitigating such phenomena in real-world battery systems.

Updating Nonparametric Probabilistic Models in Structural Dynamics by Bayesian Statistical Inversion of Symmetric Positive Definite Matrices in High Dimension

Maarten Arnst^{*}, Christian Soize^{**}

^{*}University of Liège, ^{**}Université Paris-Est

ABSTRACT

This work is concerned with the updating of probabilistic models for the dynamical behavior of structures and their associated parametric and model uncertainties. Whereas much research in structural dynamics has already addressed the Bayesian statistical inversion of mechanical parameters of structural-dynamics models, the present work focuses on the Bayesian statistical inversion of reduced matrices of reduced-order models. In [1], Soize had introduced a nonparametric probabilistic modeling approach, which uses the maximum-entropy principle to construct a probability distribution capable of representing parametric and model uncertainties in reduced matrices of reduced-order models. In the present work, this probability distribution serves as the prior probability distribution, which is then updated by using Bayes' formula to accommodate data relevant to the dynamical behavior of the structure in a posterior probability distribution. This Bayesian statistical inverse problem is computationally challenging because the support of the posterior is restricted to the symmetric positive definite matrices and because it is of high dimension. In [2], Soize had introduced an Ito-SDE-based MCMC method for sampling from maximum-entropy probability distributions in high dimension. In the present work, this method serves as a basis to propose a method for sampling from the Bayesian posterior. The proposed method exploits a transformation of measure to set up the Markov chain in terms of state variables whose distribution is standard Gaussian under the prior probability distribution but non-Gaussian under the posterior probability distribution. It inherits computational efficiency from the fact that it can exploit the gradient and the Hessian of the distance that the Bayesian update uses to gauge the fit between the reduced-order model and the data. At the conference, we will present the proposed Bayesian statistical inversion, its computational aspects, and its application to an illustration from structural dynamics. [1] C. Soize. A nonparametric model of random uncertainties for reduced matrix models in structural dynamics. Probabilistic Engineering Mechanics, 15:277-294, 2000. [2] C. Soize. Construction of probability distributions in high dimension using the maximum entropy principle: Applications to stochastic processes, random fields and random matrices. International Journal for Numerical Methods in Engineering, 76:1583-1611, 2011.

Computational Approximation of Mesoscale Field Dislocation Mechanics at Finite Deformation

Rajat Arora^{*}, Amit Acharya^{**}

^{*}Carnegie Mellon University, ^{**}Carnegie Mellon University

ABSTRACT

Dislocation, being the primary carriers of plastic deformation, play a pivotal role in determining the strength and mechanical properties of engineering materials. The use of first principles to understand complex dislocation interactions occurring at extremely small spatial and temporal scales has been successful in modeling material behavior. However, the steep computational cost associated with these methods limit the system sizes and simulation times that can be achieved in practice. Hence, a continuum scale 'fundamentally accurate' model that enables a predictive understanding of dislocation-mediated deformation serves a complementary purpose. We describe finite deformation results of a Partial Differential Equation (PDE) based model, termed as Mesoscale Field Dislocation Mechanics (MFDM), to understand meso-macroscale plasticity in solids as it arises from dislocation motion / nucleation within the material. The potential and generality of MFDM are demonstrated by applying it to study some (initial) boundary value problems. We demonstrate the stress-field path followed in a body corresponding to a sequence of dislocations starting from a single dislocation to a stress-free dislocation wall constituting a grain boundary. Another example that will also be presented is to quantify the change in the volume in the body upon introduction of dislocations dating back to Toupin and Rivlin's seminal work. Size effects and development of strong in-homogeneity in the simple-shearing of physically constrained and unconstrained grains in the material up to large strains will also be demonstrated. The mechanical structure and the thermodynamical framework of MFDM provide the driving force for the dislocation velocity which has the property that the curve moves perpendicular to itself in space when the dislocation density field is localized. Adopting this as a kinematical implication, we also present a simple example demonstrating longitudinal shear band propagation through essentially the motion of its tip wherein the driving force is uncoupled to the stresses.

Modelling the Round Window Membrane of the Guinea Pig: An Experimental Characterization of Fiber Distribution Based on Microscopic Imaging

Miguel Arriaga^{*}, Daniel Arteaga^{**}, Xun Wang^{***}, Wenbin Wang^{****}, Dimitrios Fafalis^{*****}, Karen Kasza^{*****}, Anil Lalwani^{*****}, Jeffrey Kysar^{*****}

^{*}Columbia University, ^{**}Columbia University, ^{***}Columbia University, ^{****}Columbia University, ^{*****}Columbia University, ^{*****}Columbia University, ^{*****}Columbia University, ^{*****}Columbia University

ABSTRACT

The round window membrane (RWM) is a biological membrane separating the perilymph fluid-filled inner ear from the air-filled middle ear cavity, protecting the inner ear from middle ear pathology and modulating changes in perilymphatic pressure produced by the movement of the stapes. While the integrity of the RWM is essential for normal hearing, it is also the only easily accessible portal to the inner ear and therefore the ideal candidate for delivery of medicine and collection of samples for diagnosis. This access is a significant challenge for the current medical technology since the RWM is small (diameter <2mm), thin (thickness<100μm) and pre-stressed, thus easily tearing when perforated with standard surgical tools. To aid in the development of new surgical tools for a structurally safe access through the RWM, a robust modelling of the mechanical behavior of the RWM is necessary. The RWM possesses a layer of connective tissue (collagen and elastic fibers) that endows it with most of its mechanical strength and therefore characterization of the distribution and orientation of these fibers is essential. Confocal microscopy was conducted on intact RWMs isolated from Hartley guinea pigs to characterize for the first time the distribution of collagen and elastic fibers. The fibers were imaged by capturing the emitted signals due to second-harmonic-generation, auto-fluorescence and Rhodamine-B staining. A quantitative analysis of both orientation and dispersion was done such that a structure tensor approach modelling of the fibers was possible. Experimental tests of pressure bulging and micro-indentation were conducted to validate the numerical model and to estimate the hyperelastic parameters of the membrane.

Automatic Boundary Condition Model Parameterisation in Computational Haemodynamics

Christopher J Arthurs*, C Alberto Figueroa**

*King's College London, **University of Michigan; King's College London

ABSTRACT

Finding appropriate parameter values for boundary condition models remains one of the most difficult and time-consuming tasks when creating multi-scale models of haemodynamics. Typically, before any clinical or scientific questions can be addressed, a computational baseline model must first reproduce some carefully-defined target metrics, derived both from a combination of patient-specific and population data [1]. Practically and typically, this task amounts to finding appropriate values of resistances, compliances and inertances within lumped parameter network models of the vasculature beyond the boundaries of the three-dimensional portion of the model. Due to the time-consuming nature of this task, methods for automatic parameterisation by assimilation of patient data are of great interest. It has been shown how reduced-order unscented Kalman filtering (ROUKF), a sequential parameter estimation technique which makes use of an ensemble of simulation “particles” to construct a continuously-updated best estimate of a set of model parameters can be used to determine suitable parameter values for reproducing patient data [2]. However, these methods have only been applied to simple cases such as three-element Windkessel models, and cannot be directly applied to more complex boundary condition models due to the fact that such models have internal state, both present and historical, which must remain consistent with the particles. In the present work, we demonstrate how ROUKF can be applied to more complex models using a least squares approach to generate an internal boundary condition state which is consistent with the particle to which it belongs. We examine the particular case of finding the parameters of a coronary microvascular circuit in the presence of periodic extramicrovascular compression due to myocardial contraction, demonstrating that all five state parameters can be estimated from two continuous observations in the three-dimensional domain: one of pressure and one of volumetric flow. References [1] Arthurs C J, Agarwal P, John A V, Dorfman A L, Grifka R G and Figueroa C A. Reproducing Patient-Specific Hemodynamics in the Blalock–Taussig Circulation Using a Flexible Multi-Domain Simulation Framework: Applications for Optimal Shunt Design. *Front Pediatr.* 2017; 5: 78. DOI: 10.3389/fped.2017.00078 [2] Xiao, N. Simulation of 3-D Blood Flow in the Full Systemic Arterial Tree and Computational Frameworks for Efficient Parameter Estimation. PhD Thesis, Stanford University. December 2013.

Computational Swine Model for Regional Contractility in Ischemia with Left Bundle Branch Block

Jayavel Arumugam*, Lik Chuan Lee**, Ghassan Kassab***

*Michigan State University, **Michigan State University, ***California Medical Innovations Institute

ABSTRACT

Cardiac Resynchronization Therapy (CRT) non-responder rate sustains at 30% over two decades [1]. The reasons for therapy non-response remain unclear. The ability of the myocardium, with reduced myocardial perfusion and left bundle branch block (LBBB), to contract in response to the therapy is confounding [2]. We present our investigations on the interplay between ischemia and LBBB during bi-ventricular (BiV) pacing using a computational swine cardiac electro-mechanics (EM) model. The EM model accounts for signal conduction and mechanics. The signal conduction is described by the modified FitzHugh-Nagumo equations. The mechanics model comprises of a Fung-type passive constitutive model and an active stress constitutive model. Simulations are performed on a realistic biventricular geometry using the finite element method. Mechanical boundary conditions are applied using a lumped-parameter Windkessel model for systemic and pulmonic circulation. LBBB and different pacing conditions are simulated by varying the conduction velocity and applied electrical stimulus. Ischemia is simulated by decreasing contractility in the ischemic regions [3]. Pacing response and metabolic demand are quantified using cardiac output and regional fibre stress-fibre strain area, respectively. Our investigations using the computational model suggest that the metabolic demand with LBBB significantly increases in the presence of ischemia. This is consistent with previous experimental studies and clinical observations [1, 2]. Thoroughly validated refinements of the EM model are expected to be useful in predicting subject-specific CRT response during different pacing conditions. Further, extending the EM model to account for myocardial perfusion will enhance the utility of the model. [1] Kerckhoffs R.C.P., Lumens J. K., et al. Progress in Biophysics and Molecular Biology (2008) 97: 543-561. <https://doi.org/10.1016/j.pbiomolbio.2008.02.024> [2] Svendsen M., Prinzen F.W., et al. Experimental Biology and Medicine (2012) 237-6: 644-651. <https://doi.org/10.1258/ebm.2012.012023> [3] Lee L.C., Wenk J.F., et al. Journal of Biomechanical Engineering (2011) 133: 094506 1-5. doi:10.1115/1.4004995

Implementation of Probabilistic Calculation of Tsunami Hydrodynamic Force

Rafael Aránguiz*, Pedro Osvaldo Rossel**

*Universidad Catolica de la Santisima Concepción, **Universidad Catolica de la Santisima Concepción

ABSTRACT

The design of port facilities at risk of tsunami attack requires tsunami forces to be estimated. These forces can be classified as impact, hydrodynamic, buoyancy, hydrostatic, and debris-induced, among other types. In general, two approaches can be used to estimate tsunami forces, namely, deterministic and probabilistic. While the former requires few tsunami scenarios such that maximum force values are selected, the latter requires hundreds or thousands of them and the adjustment of probabilistic density functions. In the present work, the hydrodynamic forces on a single structure in a fishing port are estimated using the probabilistic approach. Since hydrodynamic force depends on both sea surface elevation and current velocity, these variables need to be properly calculated. First, a synthetic earthquake catalog was generated and then a stochastic slip distribution was defined for each earthquake scenario in order to obtain the tsunami initial condition. To run the numerical tsunami simulations, the NEOWAVE (Non-hydrostatic Evolution of Ocean WAVEs) model was utilized. This model is based on the nonlinear shallow-water equation with a vertical velocity term to account for weakly dispersive waves. The vertical velocity term facilitates modeling of tsunami generation and transfer of kinetic energy from seafloor deformation. When the kinematic source mechanism is implemented, it is possible to complement the non-hydrostatic formulation to provide an accurate description of the wave dynamics. During the 2011 Japan tsunami, tide gauges across Hawaii and an ADCP off the Honolulu coast allowed both the computed surface elevation and current velocity to be validated. Several random variables were defined for computation of tsunami scenarios such as event location, slip distribution, focal depth and rise time, while the other seismic parameters were set to be fixed according to geological configuration. Three nested grids were defined to run the simulations and the integration time steps and roughness coefficients were defined and tested in order to avoid any instability. An automatic algorithm was developed to construct the stochastic scenarios, run the simulations and extract hydrodynamic variables at the given location; thus, a synthetic database of hydrodynamic force is constructed and the probabilistic analysis is assessed. At the conference, we will show the numerical setup for tsunami simulations and preliminary results of stochastic tsunami source models.

A Physical Simulation Based Earthquake Scenario and a Multi-scale Tsunami Simulation

Mitsuteru Asai^{*}, Naoki Nakaya^{**}, Ryoichiro Agata^{***}, Takane Hori^{****}, Toshitaka Baba^{*****}

^{*}Kyushu university, ^{**}Kyushu University, ^{***}JAMSTEC, ^{****}JAMSTEC, ^{*****}Tokushima University

ABSTRACT

In our study, a multi-scale earthquake and tsunami simulation has been developed. The Level-1 tsunami simulation is the same as the practical tsunami simulation made using a two-dimensional (2D) shallow water equation, which is mainly solved by the finite difference method. The main purpose of the Level-1 tsunami simulation is to make an immediate prediction of the tsunami magnitude. The stabilized incompressible SPH (ISPH) method [Asai et al., (2012)] is used for the 3D tsunami inundation simulation as the Level-2 tsunami simulation. These 2D and 3D tsunami simulations are coupled by a virtual wave maker [Asai et al. (2015)]. The virtual wave maker generates a virtual wave in the 3D particle simulation space to smoothly connect from the pre-simulated 2D tsunami simulation result. Before we perform these multi-scale tsunami simulations, we need to estimate an earthquake scenario. Then, an earthquake scenario simulation [Hyodo and Hori (2011)] is done by using a high performance finite element code; GAMERA [Ichimura (2017)]. The physical based earthquake simulation, in which a high-fidelity heterogeneous geographical layer is assumed to make the FEM model, gives the transient crustal deformation and these simulation results become the inputs of the above tsunami simulation. The physical simulation based earthquake and tsunami simulation result is compared with an analytical solution based earthquake and tsunami simulation result. Finally, we discuss the necessity of the high fidelity earthquake scenario simulation. Reference [1] Asai, M. et al.: A Stabilized Incompressible SPH Method by Relaxing the Density Invariance Condition International Journal for Applied Mathematics, Vol.2012, Article ID 139583, 24 pages, 2012. [2] Asai, M. et al. : Coupled tsunami simulation based on a 2D shallow-water equation-based finite difference method and 3D incompressible smoothed particle hydrodynamics, Journal of Earthquake and Tsunami, Vol. 10, 2016 [3] Hyodo, M. and Hori, T. : An interpretation of crustal deformation associated with the 2011 tohoku earthquake, The seismological Society of Japan 2011 Fall Meeting, pp.2-12, 2011 [4] Ichimura, T. et al. Tsunami Analysis Method with High-Fidelity Crustal Structure and Geometry Model, Journal of Earthquake and Tsunami, Vol.11, No.5, 2017

Multiscale Modeling of Pure Nickel

Imran Aslam^{*}, Shane Brauer^{**}, Andrew Bowman^{***}, Bradley Huddleston^{****}, Justin Hughes^{*****}, Daniel Johnson^{*****}, William Lawrimore^{*****}, Luke Peterson^{*****}, William Shelton^{*****}, Mark Horstemeyer^{*****}

^{*}Mississippi State University, ^{**}Mississippi State University, ^{***}Mississippi State University, ^{****}Mississippi State University, ^{*****}Los Alamos National Laboratory, ^{*****}Mississippi State University, ^{*****}U.S. Army Engineer Research and Development Center, ^{*****}Mississippi State University, ^{*****}Louisiana State University, ^{*****}Mississippi State University

ABSTRACT

A physically-based, multiscale modeling approach has been applied, in tandem with uncertainty quantification, to simulate three-point bending of pure nickel. Downscaling requirements are driven by the complex stress state induced by the three-point bend, which is experimentally obtained as a force-displacement. Those requirements are then met by upscaling from the atomistic length scale to the macroscale. Density functional theory was utilized at the electronic principal's scale to determine the lattice parameter and equilibrium energy of nickel (Ni), which were then upscaled to the atomistic scale. At the atomistic length scale the Modified Embedded Atom Method was used to calibrate the nickel energy potential curve, which was then used to simulate the motion of a dislocation and, subsequently, to determine the dislocation velocity. The dislocation velocity was then upscaled to the microscale to evaluate the hardening constants of nickel by utilizing Multiple Dislocation Dynamics Plasticity simulations. The hardening constants are upscaled as parameters used in Crystal Plasticity simulations to obtain the stress-strain curves for the three stress states, compression, tension, and shear. The stress-strain curves are upscaled to the macroscale and calibrated using the MSU-ISV Plasticity-Damage Model. The macroscale calibration is fed into Abaqus as a user material model in order to accurately replicate the three-point bending of a thin sheet of pure nickel. Uncertainty was quantified at each length scale as well as propagated throughout the length scales. The force-displacement data obtained from Abaqus is in good agreement with the experimental result.

Numerical Modeling of Coupled Thermo-Mechanical Behavior of Ni-Ti Shape Memory Alloys for Large Deformations

Ozgur Aslan*, Vahid Rezazadeh**

*Atilim University, **Middle East Technical University

ABSTRACT

Shape memory alloys (SMAs) hold a significant importance in different areas of engineering such as aeronautics, adaptive structures, oil/gas down-hole, and high-temperature applications of automobile industry and there is a growing effort to produce mathematical models in order to imitate the related behaviors in a precise manner. This work utilizes a numerical model based on the finite strain framework of continuum mechanics to establish a thermodynamically consistent theory for SMAs. With the martensitic volume fraction as the internal variable evolving with phase transformation, the thermo-mechanically coupled theory both captures the rate and temperature dependency. The model is implemented in a commercial finite element program by writing a user-material subroutine and both isothermal and coupled simulations conducted on different 2-D and 3-D model problems are shown to demonstrate the high capability in capturing various qualitative behavior of Ni-Ti SMA such as pseudoelasticity, one-way shape memory effect and thermomechanical behavior under cyclic thermal loading together with their good agreement with the experimental findings.

Angiotensin-II infusion on ApoE-/- mice is a popular model of aortic aneurysm and dissection. We have recently demonstrated that the dissecting aneurysmal lesions in these mice start with a medial tear near the ostia of celiac and mesenteric arteries. Given the location-specific nature of the disease, we hypothesized that the local mechanical equilibrium may drive disease initiation. To this end we developed a novel computational approach to evaluate the in-vivo strain field in the abdominal aorta. Combining ex vivo synchrotron images with in vivo micro-CT, we incorporated model features such as non-uniform aortic wall thickness, non-uniform stretch field and the inclusion of small aortic side branches into our computational models and showed how these often overlooked features impact the location of hotspots in the computed strain field [1]. In this work we validate these simulations with image-guided histology in order to investigate whether regions of high strain collocate with sites of micro-structural damage. N=10 ApoE-/- mice were infused with Angiotensin-II for 3 days and underwent a contrast-enhanced micro-CT scan prior to euthanasia. The aorta was imaged ex-vivo using Phase-contrast X-Ray Microscopy (PCXTM) at 6.5 μ m isotropic resolution. The same protocol was followed for n=6 saline-infused controls. An in-house automated framework was implemented to morph the non-pressurized non-stretched ex-vivo PCXTM geometry onto the pressurized stretched in-vivo micro-CT geometry [1]. For each animal the output was a mouse-specific structural finite element simulation. Contrast agent infiltration in the aortic wall was used to detect the location of micro-ruptures in the tunica media [1] and image-guided histology in these locations was performed to validate and quantify the vascular damage. Preliminary results show good agreement between hotspots of early vascular damage and hotspots of computed maximal strain. The highest strain values occurred invariably in the vicinity of the celiac and mesenteric arteries and collocated with intramural micro-ruptures and leukocyte infiltration. Moreover, the inter-subject variability of the maximal strain locations (cranial/caudal or right/left of the ostium) corresponded qualitatively to the inter-subject variability of PCXTM-detected contrast agent leakage. We conclude that strain concentrations near side branches could partially explain the focal nature of the disease. References [1] Ferraro, M., Trachet, B., Aslanidou, L., Fehervary, H., Segers, P., and Stergiopoulos, N., &&"Should we ignore what we cannot measure? How non-uniform stretch, non-uniform wall thickness and minor side branches affect computational aortic biomechanics in mice. &&" Ann Biomed Eng (2017).

Vibroacoustics Modeling of Complex Structures with Attached Heterogeneous Noise Control Materials Using a Hybrid Finite Elements - Transfer Matrix Method

Nouredine Atalla*, Luca Alimonti**

*Université de Sherbrooke, **ESI US R&D;

ABSTRACT

This paper discusses the modeling of the vibration and acoustic responses of structures with attached sound packages, using hybrid FE-TM (Finite Elements - Transfer Matrix) methods. It consists of two parts. In the First, a general framework to calculate the absorption and transmission coefficients of a periodic representation of the structure and its sound package is presented. The approach assumes oblique plane wave excitation and accounts for fluid coupling with the excitation and receiving fluid domains. Several examples are presented to demonstrate the accuracy of the approach. A special attention is given to complex structures (e.g. sandwich composites, highly damped structures, ribbed panels, curved structures) and heterogeneous sound packages (metamaterials in particular). In the second part, the ability of the classical Transfer Matrix Method (TMM) to model these same structures is investigated. Firstly, a simple approach to derive the frequency and heading dependent transfer matrices from the periodic model of the system is presented. Next, its use within the classical TMM is presented. Finally, the range of applicability and usefulness of the presented hybrid method is discussed by a systematic comparison with the results of part 1.

The Shifted Boundary Method for Embedded Domain Computations: Application to Solid Mechanics

Nabil Atallah^{*}, Alex Main^{**}, Guglielmo Scovazzi^{***}

^{*}Duke University, ^{**}Duke University, ^{***}Duke University

ABSTRACT

Embedded/immersed boundary methods circumvent the challenge of representing complex geometries through their ease in mesh generation. On the other hand, with such a decision arises the need to integrate over the cut elements. To counter this dilemma and maximize on the advantages of embedded methods, we propose a novel approach, named "shifted boundary method". The proposed method obviates the need to integrate over the cut boundary elements by weakly imposing an equivalent boundary condition on its surrogate (formed of un-cut elements) counterpart. We start by presenting the method for the Poisson problem along with its associated Lagrangian on the surrogate domain and its corresponding boundary. We then present the method in light of elasticity problems whereby we study stability and convergence of the method with the support of a series of tests that display the robustness and accuracy of the method.

The Future for Predicting Response for Extreme Environments Using a Combination of Experimental Techniques and Numerical Simulations

Stephen Attaway*

*Sandia National Labs

ABSTRACT

Many challenges remain in the search for numerical models that are predictive for extreme events. This talk will provide some examples of extreme events that require a combined approach for modeling and simulation with tests and evaluation. Most structures are designed for a functional life that keeps their behavior in the linear elastic, small deformation range. When buildings are subjected to extreme loads from earthquakes, fires, or terrorist attacks, the tools used for structural designs often fail to provide a technical basis for risk. Using a combination of modeling and simulation with tests and evaluation can provide the technical basis for high-consequence decisions relative to system safety and performance margins. The emergence of exascale computers with millions of cores allows simulations of transient dynamics phenomena at unprecedented scales and fidelity. Even with this increase in compute power some simulations are too costly to directly model all of physics. Full scale testing for many problems is often too costly or impractical. Both modeling and simulation combined with tests and evaluation are needed to reduce uncertainty and provide a technical basis for risk acceptance in extreme events.

Meshless Methods for Manifolds: Hydrodynamics of Curved Fluid Interfaces and Related Applications

Paul Atzberger^{*}, Ben Gross^{**}, Nathan Trask^{***}

^{*}University California Santa Barbara, ^{**}University California Santa Barbara, ^{***}Sandia

ABSTRACT

We discuss recent advances in the development of meshless methods for solving partial differential equations on general manifolds. We present a discretization framework based on Generalized Moving Least Squares (GMLS) and exterior calculus formulation of the pdes. Motivated by applications arising in soft condensed matter physics and biophysics, we show how our approaches can be used to solve hydrodynamic equations on curved fluid interfaces. We also present convergence results comparing our GMLS methods with a spectral solver in the case of radial manifolds. We then show some advantages of our GMLS methods demonstrating the capability to handle quite general manifold topologies and to adapt numerical resolution. We conclude by presenting results for hydrodynamic interactions in drift-diffusion dynamics of particle inclusions within a curved fluid interfaces showing some of the important roles played by topology and geometry.

Interplay between Mechanical, Electrostatic and Electronic Nonlinearities inside a MEMS Converting Cardiac Vibrations to Electric Power with Pacemaker Applications

Denis Aubry^{*}, Bogdan Vysotskyi^{**}, Philippe Gaucher^{***}, Fabien Perrain^{****}, Elie Lefeuve^{*****}

^{*}Ecole CentraleSupélec, ^{**}MSSMat/C2N-Site d'Orsay, ^{***}MSSMat., ^{****}C2N-Site d'Orsay, ^{*****}C2N-Site d'Orsay

ABSTRACT

In this talk, we intend to present the numerical simulation of a MEMS which converts heart beating movements to electrical power and is thus able to charge the battery of a pacemaker. Mechanical nonlinearities cannot be avoided because the heart vibration spectrum is not favorable to power production and higher frequencies must be generated. Electric current comes from electrostatic charges and the deformable capacity versus current relationship is also highly non-linear. Finally energy harvesting implies the use of electronic components such as diodes whose behavior is extremely nonlinear. We show that the numerical control of these nonlinearities is mandatory and must be finely tuned and controlled to prove the efficiency of the system and its sensitivity. Comparison between the predicted and experimental power production of a newly design MEMS demonstrates the essential role of these considerations.

Tangential Adaptivity in Volume Boundary Layer Mesh Generation

Romain Aubry*

*United States Naval Research Laboratory

ABSTRACT

Boundary layer mesh generation traditionally extrudes the no-slip surfaces into the volume. While this may provide an accurate geometry, the surface curvature distorts without control the prescribed size at the surface. Even on flat surfaces, the extrusion maintains the same mesh size, while the user prescribed size may vary for thick boundary layers in the volume. This causes numerous practical issues, such as the transition between boundary layer mesh and the isotropic mesh, the collision of front of different sizes. In order to remedy these pitfalls, we propose to adapt in the tangential direction the boundary layer to maintain a size consistent with the prescribed one, as well as a seamless transition with the isotropic part.

Modelling Seabed Ploughing Using the Material Point Method

Charles Augarde*, Andrew Brennan**, William Coombs***, Michael Brown****, Michael Cortis*****, Scott Robinson*****

*Dept of Engineering, Durham University, UK, **Civil Engineering, Dundee University, UK, ***Dept of Engineering, Durham University, UK, ****Civil Engineering, Dundee University, UK, *****Dept of Engineering, Durham University, UK, *****Civil Engineering, Dundee University, UK

ABSTRACT

Ploughing is a complex process for which to devise numerical models since it involves material and geometric nonlinearity and is truly 3-dimensional. The Material Point Method (MPM) seems to be a good contender for this modelling since it decouples the deformation of the problem domain from the discretisation framework. This presentation describes recent UK research that has paired numerical modelling of ploughing using the MPM with laboratory experimentation, the latter to provide string validation to the former. Various issues that have been met with in the development of the MPM to provide the ploughing model are discussed, such as dealing with essential boundary conditions and proper implementation of plasticity models. The standard MPM is shown to be a robust choice in comparison to more complex approaches, such as the GIMP and CPDI methods, which seek to reduce the cell-crossing instability but bring additional problems or complexities.

A Computational Heart Model of Pulmonary Arterial Hypertension

Reza Avaz*, Emilio Mendiola**, Joao Soares***, Richard Dixon****, Michael Sacks*****

*University of Texas at Austin, **University of Texas at Austin, ***Virginia Commonwealth University, ****Texas Heart Institute, *****Virginia Commonwealth University

ABSTRACT

Pulmonary arterial hypertension (PAH) imposes a pressure overload on the right ventricular free wall (RVFW), leading to substantial growth of muscle cells and remodeling in fiber architecture. The effects of these alterations on the biomechanical behavior of the RVFW and the organ-level cardiac function remain largely unexplored. Recent experimental studies on the mechanical and morphological properties of normal and hypertensive RVFW myocardium suggest that myocardial wall stress is the primary mediator of RVFW growth and remodeling (G&amp;amp;R) responses. An accurate quantification of the wall stress evolution during the development of PAH is needed to determine the correlation between the wall stress and G &amp;amp;R mechanisms. To this end, there is a need to develop a detailed computational heart model that can accurately simulate the effect of PAH in the heart, and thus can be used to understand pathophysiology of RVFW remodeling, its connection to wall stress alterations, and its impact on organ-level cardiac function. We have developed a high-fidelity finite-element (FE) heart model of PAH using extensive time-course datasets from a normal rat heart and from a hypertensive rat heart simulating the pressure overload in the right ventricle (RV). We have implemented a pipeline that integrates a meshed geometry from a high-resolution image of the rat heart, detailed imaging data on the fiber structure of the same heart, and a novel compressible hyperelastic material model accounting for both passive and active behaviors of myocardium. The developed heart model offers a high performance capability for inverse problems such as fine-tuning the active properties of myocardium and characterizing shape change patterns of the RV. We used our model to investigate the correlations between the alterations in the wall stress, the remodeling of the RVFW microstructure, and the shape changes in the RV during the development of PAH. The detailed description of organ-level remodeling patterns can replace the traditional measures of RV dimensions and volume that often lead to gross and limited information on cardiac performance. Ultimately, development and implementation of our model in patient-specific organ-level simulations will allow investigation of optimal diagnosis and new individualized stem-cell interventions for PAH.

Link Shape Synthesis for Dynamic and Structural Requirements

Pedro Enrique Avila-Hernandez*, Fernando Velazquez-Villegas**, Francisco
Cuenca-Jimenez***

*Engineering Faculty, UNAM, **Engineering Faculty, UNAM, ***Engineering Faculty, UNAM

ABSTRACT

In the last three decades, different methods of link shape synthesis for balanced linkages have been proposed. However, any of them has considered the mechanical properties of links material. This paper presents for first time the shape synthesis of a four-bar mechanism link that takes into consideration the mechanical properties of its material. This method adapts through Multi-Objective Genetic Algorithm (MOGA), the optimum topologic methods Solid Isotropic Microstructure with Penalization (SIMP) and Evolutionary Structural Optimization (ESO) to determine the shape of a link that satisfies structural and dynamic (balancing) requirements. The method is able to process all the requirements in parallel to determine the link shape. The results show that a link shape that balances a mechanism can be obtained without determining its inertial parameters previously.

Finite-element Predictions of Human Aortic Root Enlargement Based on the Homogenized Constrained Mixture Model

Stephane Avril^{*}, Joan Laubrie^{**}, Jamal Mousavi^{***}

^{*}Université de Lyon, ^{**}Université de Lyon, ^{***}Université de Lyon

ABSTRACT

Recently, growth and remodeling (G & R) has been increasingly approached based on the constrained mixture theory (CMT) to predict a variety of arterial mechanobiological behaviors [1, 2]. Most of previously published work has been limited to simplified cases as isotropic growth, axisymmetric motions, mono-layer wall and/or membrane approximations. Although such models have increased our insights in vascular adaptation, a 3D anisotropic bilayer model has the potential of considering more complex cases of arterial G & R such as aortic root enlargement. Therefore, herein, a 3D numerical model based on homogenized CMT is implemented in ABAQUS through a coupled UEL to predict anisotropic G & R of arteries. At the Gauss points level, the passive behavior is assumed hyperelastic and a strain energy function (SEF) is assumed for each constituent with decoupled contributions of the purely volumetric and isochoric parts. Although the same SEF is assumed for every element across the geometry of the artery, different material properties and mass fraction can be applied at each layer. It is considered that the arterial wall is composed of a constrained mixture of elastin, collagen fibers and smooth muscle cells (SMC) and includes the in situ stresses existing in the reference configuration. Four collagen fibers with different mass fractions in media and adventitia in the axial, circumferential and angular directions are considered. The contractility of SMC and turnover of collagen fibers are assumed stress dependent. Simulations are performed on a bilayer thick-wall geometry reconstructed from the CT scan of a patient harboring an ascending thoracic aortic aneurysm (ATAA), subjected to boundary conditions in homeostatic conditions. Two different mechanisms are considered for the initiation of aneurysm enlargement, namely loss of SMC contractility and damage of elastin. Different gain parameters for collagen turnover are considered. The models are able to predict realistic aortic root enlargement as confirmed by a follow-up MRI performed on the same patient. Our findings confirm the determinant role of SMC contractility during ATAA growth. References [1] F.A. Braeu, A. Seitz, R.C. Aydin and C.J. Cyron. Holzapfel. Homogenized constrained mixture models for anisotropic volumetric growth and remodeling. *Biomech Model Mechanobiol*, 29(8): 16(3):889–906, 2017. [2] A. Valentín, J.D. Humphrey and G.A. Holzapfel. A finite element-based constrained mixture implementation for arterial growth, remodeling, and adaptation: theory and numerical verification. *Int J Numer Method Biomed Eng*, 29(8):822–49, 2013.

Thermo-mechanical Process Modelling for Selective Laser Melting

Can Ayas*, Yabin Yang**

*Delft University of Technology, **Delft University of Technology

ABSTRACT

Selective laser melting (SLM) is a powder based additive manufacturing method suitable for metallic components. In SLM the part is built utilising a laser beam which scans over the powder bed in order to selectively melt and consolidate thin sections of a solid part in a layer-by-layer fashion. Although SLM enables manufacturing of topology optimized, geometrically complex designs which cannot be realised by traditional subtractive manufacturing techniques, it suffers from distortion of the part and residual stresses induced. Distortion of the part can result in out of tolerance components and residual stresses can cause failure during the build. It is well-known that both part distortions and residual stresses are induced due to heating/cooling cycles associated with laser melting and the corresponding thermal expansion/contraction leading to displacement and stress fields. Therefore it is of great interest to identify process parameters such as laser power and scanning speed and scanning strategies that minimize the detrimental part distortion and residual stresses of a design to be built by SLM. For this purpose, we present a thermo-mechanical modelling framework that is able to predict the temperature transients and the corresponding evolution of mechanical field quantities during the build process. The former is calculated using a computationally efficient semi-analytical method where the closed form analytical solutions of line heat sources describing scanning lines are superimposed with numerically calculated image fields to enforce boundary conditions of the design at hand. The latter requires a one way coupled thermo-mechanical coupling where the temperature induced strain alongside the elastic and plastic strain is calculated leading to the stress state of the component. Temperature dependent J2 elasto-plastic material with kinematic hardening is considered. Several case studies are investigated by the proposed model. The residual stresses and part deformations are investigated as a function of different scanning strategies at different layers. The predictions of the model are compared with experimental findings and existing approximate modelling schemes available in literature.

Discrete Tangent Vector Fields and PDEs on Surfaces

Omri Azencot*, Mirela Ben Chen**

*UCLA, **Technion - Israel Institute of Technology

ABSTRACT

Tangent vector fields are widely used in computer graphics, where they are applied to various tasks such as texture generation on surfaces, and physical simulation for animation. In this talk we will describe a new discretization of tangent vector fields on triangle meshes that is inspired by the classic point of view in differential geometry, namely that vector fields are linear operators on scalar functions. Taking this approach allows us to numerically simulate various PDEs on discrete surfaces, such as function advection and fluid flow, in an efficient and stable manner, with theoretical guarantees. We will show the application of this approach to the problem of simulating thin films on curved triangle meshes. In this problem the motion is governed by a fourth-order nonlinear PDE, which involves geometric quantities such as the curvature of the underlying surface, and is therefore difficult to discretize. Inspired by a recent variational formulation for this problem on smooth surfaces, we present a corresponding model for triangle meshes. We provide a discretization for the curvature and advection operators which leads to an efficient and stable numerical scheme, requires a single sparse linear solve per time step, and exactly preserves the total volume of the fluid. We validate our method by qualitatively comparing to known results from the literature, and demonstrate various intricate effects achievable by our method, such as droplet formation, evaporation, droplet interaction and viscous fingering. The talk is based on the papers [1], [2], where [1] has received one of the three best paper awards at SCA. References: [1] Functional Thin Films on Surfaces, Omri Azencot, Orestis Vantzos, Max Wardetzky, Martin Rumpf and Mirela Ben-Chen. Proceedings of ACM Symposium on Computer Animation, Los Angeles, 2015. [2] Functional Thin Films on Surfaces. Orestis Vantzos, Omri Azencot, Max Wardetzky, Martin Rumpf and Mirela Ben-Chen. IEEE Transactions on Visualization and Computer Graphics 23(3), 2017.

A Computational Bio-Chemo-Mechanical Model of Inflammation for Tissue Engineering Vascular Grafts

Abhay B. Ramachandra*, Ramak Khosravi**, Jason Szafron***, Jay Humphrey****

*Yale University, **Yale University, ***Yale University, ****Yale University

ABSTRACT

The limited availability of autologous vessels for cardiovascular surgeries has highlighted the need for optimally engineered vessels. Tissue engineered vascular grafts (TEVGs) have shown promise as alternatives to autologous vessels, but post-operative complications remain. The complex interplay in vivo amongst biological, chemical, and mechanical factors governs the outcome of an implanted TEVG, with inflammation playing a critical role [1], and creates design challenges for polymeric scaffolds used in these applications. To gain insights into roles of inflammation in the development and failure of TEVGs, and to design of better scaffolds, we propose a bio-chemo-mechanical computational model of inflammation and tailor it for TEVGs. For illustrative purposes, we model the inflammatory response by focusing on cells and pathways most relevant to TEVGs. Specifically, the biochemical part of the inflammation model consists of inflammatory cells (e.g., Ly6C+/ Ly6C- monocytes, classically and alternately activated macrophages and tissue resident macrophages), cytokines (e.g., TGFbeta, iNOS, IL-10), cells (e.g., endothelial, inflammatory, and synthetic), extracellular matrix constituents (e.g., collagen) and proteases (e.g., MMPs). The kinetics of the inflammatory model are modeled using Michaelis-Menten kinetics. The polymer degradation, derived from experimental data, drives the inflammation while circumferential wall and shear stresses, predicted from a constrained mixture model of growth and remodeling of a TEVG [2], influence (via constitutive equations) the turnover of synthetic smooth muscle, stress mediated collagen, and TGFbeta. Thus, the proposed model is immuno-driven and mechano-mediated. The model is calibrated against existing experimental data from the literature. The complexity of the model yields an abundance of parameters. Bayesian methods and simplex optimization routines are used to estimate the parameters. We also report results of system identification for this data-poor system. The results not only help to gain insights into the role of inflammation in the development and failure of TEVGs, they also promise to help guide future experiments. [1] Roh, Jason D., et al. "Tissue-engineered vascular grafts transform into mature blood vessels via an inflammation-mediated process of vascular remodeling. " Proceedings of the National Academy of Sciences 107.10 (2010): 4669-4674. [2] Miller, Kristin S., et al. "Computational model of the in vivo development of a tissue engineered vein from an implanted polymeric construct. " Journal of Biomechanics 47.9 (2014): 2080-2087.

Enhanced Electroosmotic Flow and Ion Selectivity through a Patterned Soft Channel with pH-Regulated Uncharged Grooves

NAREN BAG*, SOMNATH BHATTACHARYYA**

*INDIAN INSTITUTE OF TECHNOLOGY KHARAGPUR, **INDIAN INSTITUTE OF TECHNOLOGY KHARAGPUR

ABSTRACT

This article deals with the modulation of electroosmotic flow (EOF) through the parallel plate soft nanochannel where the grooves are filled with polyelectrolyte layer (PEL). The PEL of the grooves containing both acidic and basic functional groups. The solid walls of the channel are assumed to be maintained at a constant surface charge density and the surface of the grooves are assumed to be a zero surface charge density. A nonlinear model based on the nonlinear Poisson-Nernst-Planck equation coupled with the Darcy-Brinkman equation is adopted. Going beyond the widely employed Debye-Huckel linearization, we adopt a sophisticated numerical tool to study the effect of pertinent parameters on the modulation of EOF through the soft periodic groove nanochannel. We have illustrated the effect of PEL and surface charge density, electrolyte concentration, softness parameter, periodic length of the groove channel and electrolyte pH. Several interesting key features, including the flow enhancement factor and occurrence of zero flow rate, are studied by regulating the charges entrapped within the PEL and the surface charge distributed along the channel walls. In addition to the flow modulation, we have also demonstrated the selectivity of the mobile ions through the soft nanochannel. The results indicate that the channel can be cation-selective, an anion-selective as well as non-selective based on the nature of the charges within the PEL and walls charge. In order to validate our numerical code, we have compared our computational average velocity in a soft nanochannel with flat walls corresponding to the analytic solution based on Poisson-Boltzmann linear model with Debye-Huckel approximation. The computed results differ from the analytic solution for thicker Debye layer when PEL is either uncharged or the charge of the PEL and walls have the same sign, while for the case of oppositely charged PEL and walls, analytic solution differs from the numerical solution when Debye layer is thinner. We have also seen that the average velocity of the present result approaches to the analytic solution for higher values of the periodic length. The present study also shows that the flow reversal and zero ion selectivity i.e., a non-selective channel for an oppositely charged PEL and walls. References 1. Wang, C. 2003 Flow over a surface with parallel grooves. *Phys. Fluids*. 15(5), 1114-1121. 2. Matin, M. H. & Ohshima, H. 2015 Combined electroosmotically and pressure driven flow in soft nanofluidics. *J. Colloid Interface Sci.* 460, 361-369.

Non-local Modeling: Macroscopic Behavior of a Randomly Voided Material and Influence of Void Morphology on the Elastic Properties Gradient

Sami BEN ELHAJ SALAH*, Carole Nadot-Martin**, Mikaël GUEGUEN***, Azdine Nait-Ali****

*Institut Pprime, ISAE-ENSMA, **Institut Pprime, ISAE-ENSMA, ***Institut Pprime, ISAE-ENSMA, ****Institut Pprime, ISAE-ENSMA

ABSTRACT

Keywords: homogenization theory, non-local theory, second gradient theory

The asymptotic expansion analysis was developed in the framework of homogenization technique, which is applicable for three-dimensional composites made up of inclusions randomly embedded within a matrix. The so-called asymptotic expansion homogenization (AEH) method was developed by Francfort [1] for the case of linear thermoelasticity in periodic structures. The AEH method has been employed to calculate the homogenized thermomechanical properties of composite materials (elastic moduli and coefficient of thermal expansion). This technique of homogenization enables to replace heterogeneous materials by a homogeneous equivalent medium including second-order displacement gradients [2]. The displacement vector and the stress tensor are considered as functions of macroscopic (x) and microscopic (y) variables. They may be expanded in a series of powers of small (material) parameter “ η ”, which is the ratio between macroscopic and microscopic scales. More precisely, the present work is devoted to linear stochastic homogenization and Gamma-convergence problems for variational functional. This Gamma-convergence allows us to study the corresponding variational problem and to prove the convergence of the minimums and of the minimizers. By combining variational convergence with ergodic theory, we study the macroscopic behavior of linear elastic heterogeneous materials. The inclusions are randomly distributed within a matrix, their size is of order “ η ”. The variational limit functional energy obtained when “ η ” tends to 0 is deterministic and non-local [3]. By including the characteristic displacement vectors, or correctors, the problem can be solved in order to evidence some links with second gradient theory. Computational results in periodic and stochastic cases will be exposed and discussed. This work shows that the asymptotic expansion homogenization method has a strong history of development in the mathematical and engineering fields and it is an accurate and efficient tool not only to predict the mechanical properties of voided materials but also as a vehicle for enabling multistate analysis. An extension of this study will be devoted to the construction of non-local damage model that consists in introducing the gradient of damage (grad α). References [1] Francfort, G., “Homogenization and linear thermoelasticity”, SIAM J Math Anal; 14(4), 696-708 (1983). [2] Forest, S., Cardona, JM., and Sievert, R., “Thermoelasticity of second-grade media”, Continuum Thermomechanics, 163-176 (2000). [3] Michaille, G., Nait-Ali, A., and Pagano, S., “Macroscopic behavior of a randomly fibered medium”, Journal of Pure and Applied Mathematics, 96(3), 230-252 (2011).

Simulation of Coupled Thermal and Mechanical Effects Induced by the Metallurgical Phase Changes in the Welding of Large Components for the Nuclear Industry

Clement BERTHINIER*

*CEA - SEMT/LM2S (Saclay, France)

ABSTRACT

Many industrial metals (such as 16MND5 steel) are subject to allotropic phase transformations during a thermal heating and cooling cycle. These thermal cycles are observed when welding large components that are the pipes of the cooling circuits in the nuclear industry. At first, the objective of this work is to achieve in Cast3M the coupling between the resolution of thermal, metallurgy and mechanics. The metallurgical phase changes proposed in this work are based on two models: the Koistinen-Marburger model and the Leblond-Devaux model. On one hand, these phase changes, have an impact on the thermal and mechanical properties of the different parts (materials properties modifications) and on the other hand induced a plasticity phase change source term. The implementation of these models in Cast3M is verified and validated by comparisons to analytical solutions and numerical solutions from other finite element software (Sysweld and Code_ASTER). In a second step, these developments are used to evaluate the stress and deformation state of two tubes after a predetermined welding sequence. The modeling carried out is in 3D. The parameters injected into the phase change models are chosen to correspond to the TRC diagram of 16MND5 steel. The effects and interest of thermal-mechanical-metallurgical coupling are discussed.

SFE Methods Applied to Nuclear Containment Buildings Behavior

David BOUHJITI*, Frédéric DUFOUR**, Benoît MASSON***, Julien BAROTH****

*Industrial chair PERENITI (3SR LAB, EDF-SEPTEN), **PERENITI Chairholder (3SR LAB, EDF-SEPTEN/DTG/CIH), ***EDF-SEPTEN, ****Univ. Grenoble Alpes, CNRS, Grenoble INP, 3SR, F-38000 Grenoble, France

ABSTRACT

The aim of this work is to investigate the pertinence of SFE methods when dealing with concrete behavior at the scale of large reinforced and prestressed structures such as Nuclear Containment Buildings. Their simulation involves the use of strongly non-linear behavior laws requiring hefty computational time and a considerable number of parameters (more than 50) affecting their response to the simultaneous Thermo-Hydro-Mechanical (THM) loads. Being a heterogeneous and multiphase material, concrete properties show intrinsically spatio-temporal variations (in addition to epistemic and ontological ones related to the mixing, casting and curing processes) affecting the aging process in terms of cracking, drying, creep and tightness. In opposition to classical deterministic approaches - which are not sufficient when dealing with random phenomena such as size effects, cracking and permeability -, the introduction of such variations in numerical models is a mandatory step for better assessment of their present behavior and accurate prediction of their future one. The main question remains: which is the most efficient strategy in order to optimize the computational time and still be able to perform an accurate sensitivity analysis (up to what order ?) and uncertainties quantification/propagation through the various THM and leakage calculation steps ? In this contribution concrete cracking patterns are defined according to a stochastic size effect law and a regularized, local and damage-based model. The spatial heterogeneity of concrete at the Representative Structural Volume scale is described using Random Fields and the aging effects on concrete 's long term behavior (uncertainties propagation) is assessed using non-intrusive methods such as: perturbation/quadrature methods and projection methods namely the polynomial chaos expansion approaches. Depending, on the output of interest (mean, coefficient of variation, n-ith statistical moment, pdf) a comparative analysis is performed for the required computational time vs. the error estimation of each output using the results from Monte Carlo approach as a reference.

A Computational Damage Approach for Localized Failure in Quasi-brittle Materials

TINH QUOC BUI*, SOHICHI HIROSE**

*TOKYO INSTITUTE OF TECHNOLOGY, **TOKYO INSTITUTE OF TECHNOLOGY

ABSTRACT

In this talk, we present a computational approach based on a novel smoothing gradient-enhanced damage model for localized failure problems in quasi-brittle materials. This approach is particularly tailored to low-order finite elements (e.g., Q4 or T3). In this model, the characteristic length is a stress level dependent parameter. The displacements and nonlocal equivalent strain fields are approximated in the framework of low-order finite elements, i.e., the same interpolation functions are used for both primary variables. A novel modified evolving gradient parameter, which heavily depends on the principal stress and equivalent strain states, serving to reduce the impact of localized deformation, is introduced. Consequently, the spurious damaged zones and stress oscillation induced by the standard gradient damage models can be overcome. Numerical examples in one- and two-dimensions with shear band analysis for quasi-brittle materials are analyzed.

Aggregated Unfitted Finite Element Methods for Large Scale Simulations on Octree Meshes

Santiago Badia^{*}, Francesc Verdugo^{**}, Alberto Martín^{***}

^{*}Universitat Politècnica de Catalunya / CIMNE, ^{**}CIMNE, ^{***}CIMNE

ABSTRACT

The use of unfitted finite element methods (FEMs) is an appealing approach for different reasons. They are interesting in coupled problems or to avoid the generation of body-fitted meshes. One of the bottlenecks of the simulation pipeline is the body-fitted mesh generation step and the unstructured mesh partition. The use of unfitted methods on background octree Cartesian meshes avoids the need to define body-fitted meshes, and can exploit efficient and scalable space-filling curve algorithms. In turn, such schemes complicate the numerical integration, imposition of Dirichlet boundary conditions, and the linear solver phase. The condition number of the resulting linear system does depend on the characteristic size of the cut elements, the so-called small cut cell problem. In this work, we will present a parallel unfitted framework that relies on adaptive octree background meshes and space-filling curve partitioners. In order to solve the small cut cell problem, we will consider a re-definition of the finite element spaces that solves this issue, leading to condition number bounds as the ones for body-fitted schemes without any kind of perturbation/stabilization of the Galerkin formulation. We will also define appropriate iterative linear solvers based on domain decomposition preconditioning that are robust and scalable.

Single Chain Polymer Nanoparticles as Building Blocks for A New Class of Polymers

Suwon Bae^{*}, Meredith Silberstein^{**}

^{*}Cornell University, ^{**}Cornell University

ABSTRACT

Incorporating intra-chain crosslinks into a single polymer chain is a powerful way to tailor the thermo-mechanical properties of the polymer chain. Intra-chain crosslinks restrict the motion of constituent monomers and modify polymer chain configuration. When induced under moderate to bad solvents these crosslinks lock the polymer chains into collapsed conformations, forming single chain polymer nanoparticles (SCPNs). The thermo-mechanical properties of individual SCPNs can be tuned by means of the crosslinking ratio. In addition to individual SCPNs, bulk polymer synthesized with SCPNs as its building blocks shows a response different than that synthesized with linear chains. Here a molecular dynamics (MD) approach is adopted to investigate the effect of intra-chain crosslinking on both individual SCPNs and bulk polymers formed from assembly of SCPNs. Firstly, we explore the mechanics of SCPNs as individual units. We use a coarse-grained model of a polyethylene-like polymer with Dreiding potential. The dependence of the properties of individual SCPNs on chain length and crosslinking ratio is studied by varying the degree of polymerization and the number of intra-chain crosslinks. While the response is almost independent of the chain length, the response does depend on the crosslinking ratio. As the crosslinking ratio is increased, the glass transition temperature increases and the motion of monomers is more restricted. When subjected to flat plate compression, all SCPNs exhibit behaviors similar to that of a foam with the stress growing rapidly after the structure was compacted. The foam effect was most pronounced in the behavior of SCPNs with the highest cross-linking ratio. We then present how intra-chain crosslinking can be used to tune the thermo-mechanical properties of a bulk polymer assembled from SCPNs. Because of the intra-chain crosslinks within each single chain polymer, only limited portions of each polymer chain interact with other chains. When subjected to uniaxial tension, the bulk with a higher crosslinking ratio shows higher strength and earlier fracture. This computational result is supported by our previous experimental work. We will discuss in detail how the kinematics and energetics of the SCPN assembly differs from those of a bulk linear polymer.

Coupled Shock-Plasticity-Damage Modeling of Explosive Welding by RKPM

Jonghyuk Baek*, Guohua Zhou**, J. S. Chen***, Michael Hillman****

*University of California at San Diego, **The Pennsylvania State University, ***University of California at San Diego,
****The Pennsylvania State University

ABSTRACT

The explosive welding (EXW) process entails shock waves, large plastic deformation, and fragmentation around the collision point, troubling the traditional mesh-based methods for reliable solution. In this work, a computational framework based on the semi-Lagrangian reproducing kernel particle method (SL-RKPM) [1] is introduced for the modeling of EXW. For modeling shocks in plastically deformed solid, a Godunov-type shock algorithm formulated under the stabilized non-conforming nodal integration (SNNI) framework [2] is employed, where the Godunov scheme is embedded in the volumetric strain energy via a purely node-based flux gradient evaluation which ensures the linear momentum conservation. The Gibbs instability is controlled through the smoothed flux divergence in SNNI. The effects of high strain-rate and high temperature on plasticity and damage in the metals are taken into consideration in the material law. The kernel stability in SL-RKPM to accurately capture excessive plastic flow and metal jetting is ensured by introducing a strain rate dependent kernel support update. Adaptive refinement strategies near the contact interface are also introduced. The jet formation, smooth to wavy interface morphologies transition, and the welding condition along the metal interface are compared to several experimental results to validate the effectiveness of the proposed methods for EXW modeling. References [1] Guan, P., Chen, J. S., Wu, Y., Teng, H., Gaidos, J., Hofstetter, K., Alsaleh, M. Semi-Lagrangian reproducing kernel formulation and application to modeling earth moving operations. *Mechanics of Materials* 2009; 41(6):670–683. [2] Zhou, G., Chen, J. S., and Hillman, M. A Godunov-type Semi-Lagrangian Galerkin Meshfree Method for Modeling Shocks in Solid and Fluid, to be submitted.

Optimal Design of RVE of Polymer Nanocomposites Based on Fourier Transform Approach: A Multiscale Homogenization Analysis

Kyungmin Baek*, Hyunseong Shin**, Maenghyo Cho***

*Seoul National University, **Korea Electronics Technology Institute, ***Seoul National University

ABSTRACT

Representative volume element (RVE) is a unit structure that represents the overall behavior of materials, and is widely used in the field of computational mechanics to characterize the physical properties of material. Polymer nanocomposites, which are composed of various nano-fillers and polymer matrix, have dependency of polymer chain state, particular agglomeration, and volume fraction of particles for determination of RVE size. While there are sufficient studies to analyze the mechanical and thermal behaviors of polymer nanocomposites by arbitrarily selecting RVE [1], it has been challenging to determine the size of RVE that can accurately describe the behaviors of nano-structured materials. Even though some experimental method have been established for woven composites [2], it cannot be applied properly to the polymer nanocomposites because of local uncertainties caused by interaction between the polymer matrix and nanoparticles. In this study, a new numerical approach-based on Fourier transform is proposed to determine optimal RVE size of polymer Nanocomposites. The space domain information for the distribution of nanoparticles is transformed to frequency domain. After that, we determine optimal design of RVE to represent overall behavior of the global structures analyzing the wave length of frequency. Furthermore, the multiscale analysis are conducted to investigate the mechanical behaviors of the polymer nanocomposites. In this study, the multiscale bridging methodology in which the molecular dynamics (MD) simulation information is up-scaled to the continuum finite element model is applied to reflect the mechanical properties of interphase zone depending on the agglomeration of nanoparticles. The mechanical properties of polymer nanocomposites can be effectively obtained by asymptotic homogenization method [3]. We expect that the proposed scheme can broaden the applicability of the computation mechanics in fields of complex materials and structures. Acknowledgements This work was supported by a grant from the National Research Foundation of Korea (NRF) funded by the Korea government (MSIP) (Grant No. 2012R1A3A20488 41). References [1] H. Shin, K. Baek, J.-G. Han, M. Cho, Compos. Sci. Technol. 2017, 138, 217-224. [2] B. Koonbor, S. Ravindran, A. Kidane, Opt. Laser. Eng. 2017, 90, 59-71. [3] M. Cho, S. Yang, S. Chang, S. Yu, Int. J. Numer. Meth. Eng. 2011, 85, 1564-1583.

Material Defect Evaluation Based on Lattice Defect Dynamics and Machine Learning

Abdollah Bagheri^{*}, Peter Chung^{**}

^{*}University of Maryland-College Park, ^{**}University of Maryland-College Park

ABSTRACT

In this paper, a computational method is presented to evaluate material defects using lattice defect dynamics and machine learning. For generating training data for machine learning, the dynamical matrix for defective lattices is calculated from the pristine lattice using linear operators which require less computational efforts; then, the phonon density of state is computed for each defect case. In training data, we assume the defect as two vacancies in a lattice with different distances between vacancies. An artificial neural network is designed and trained with the training data to predict defects from the phonon density of state. For the verification of the method, the effect of defects in the phonon density of state of Si is studied and defects are then estimated by the machine learning method.

Accurate Adaptive Eulerian Framework for Liquid-gaz-solid Interactions

Chahrazade Bahbah^{*}, Mehdi Khalloufi^{**}, Youssef Mesri^{***}, Elie Hachem^{****}

^{*}MINES ParisTech - CEMEF - CFL research group, ^{**}MINES ParisTech - CEMEF - CFL research group, ^{***}MINES ParisTech - CEMEF - CFL research group, ^{****}MINES ParisTech - CEMEF - CFL research group

ABSTRACT

We propose an accurate adaptive Eulerian framework for multiphase flows. It consists in combining an a posteriori error estimator that minimizes the interpolation error of the finite element solution followed by an interpolation with restrictions method that conserves physical properties of the field being interpolated. Momentum and mass equations have been solved using the Variational MultiScale method, coupled with an implicit treatment of the surface tension and anisotropic meshing. A convective self-reinitialization Level-Set method is used as a tool for describing the interface evolution. Several numerical examples and new benchmarks, in 2D and 3D, will be presented to illustrate the efficiency of the approach. Finally, we show that the extension of this framework to heat transfer and phase change allows simulating liquid-gaz-solid interactions and thus the complex boiling phenomena.

Homogenization and Stochastic Fracture Simulation of Quasi-brittle Materials

Bahador Bahmani^{*}, Ming Yan^{**}, Philip Clarke^{***}, Katherine A. Acton^{****}, Anand Nagarajan^{*****},
Soheil Soghrati^{*****}, Sarah C. Baxter^{*****}, Robert B. Haber^{*****}, Reza Abedi^{*****}

^{*}University of Tennessee Knoxville (UTK)/ Space Institute (UTSI), ^{**}The Ohio State University, ^{***}University of Tennessee Knoxville (UTK)/ Space Institute (UTSI), ^{****}University of St. Thomas, ^{*****}The Ohio State University, ^{*****}The Ohio State University, ^{*****}University of St. Thomas, ^{*****}University of Illinois at Urbana-Champaign, ^{*****}University of Tennessee Knoxville (UTK)/ Space Institute (UTSI)

ABSTRACT

Microstructural architecture strongly affects the response of brittle and quasi-brittle materials. Models that assume spatially uniform fracture strength do not capture the influence of microscale inhomogeneities on crack patterns and on observed values and scatter in critical macroscopic measures such as ultimate load and absorbed energy. In this work, we present stochastic models and homogenization methods that generate macroscopic fracture strength fields which incorporate the effects of microscale flaws. We use two methods to generate Statistical Volume Elements (SVEs) in this work. In the first, we use Conforming to Interface Structured Adaptive Mesh Refinement (CISAMR) [1] to generate a 2D finite element mesh from microstructure images that exactly tracks inclusion boundaries. In the second, we use a Voronoi-tessellation-based method [2] to generate SVEs that, in contrast to the first approach, are not square-shaped and do not cut through inclusion boundaries. We compare results from the two methods and discuss the effects of boundary conditions and SVE size on homogenized elastic and fracture properties. We use the statistics of the fracture strength field and the Karhunen-Loeve method to generate consistent realizations of the homogenized fracture-strength field for use in dynamic fragmentation simulations based on alternative macroscopic fracture models. In the first fracture model, an interfacial damage model explicitly represents crack nucleation from weak points in the material as well as subsequent crack propagation. The second uses a rate-dependent bulk model to represent material degradation implicitly. An asynchronous spacetime discontinuous Galerkin method [3] with advanced adaptive meshing capabilities tracks crack paths and captures sharp moving fronts in dynamic simulations based on the two fracture models. We present numerical results demonstrating the effects of loading rate, underlying SVE size, and the chosen fracture model on macroscopic measures such as fracture pattern and fracture-energy dissipation. References: [1] S. Soghrati, A. Nagarajan, and B. Liang. "Conforming to interface structured adaptive mesh refinement technique for modeling heterogeneous materials." *Computational Mechanics*, 125:24-40, 2017. [2] K.A. Acton and S.C. Baxter. "Characterization of Random Composite Properties Based on Statistical Volume Element Partitioning." *Journal of Engineering Mechanics* 144.2 (2017): 04017168. [3] R. Abedi, R.B. Haber, and P.L. Clarke. "Effect of random defects on dynamic fracture in quasi-brittle materials." *International Journal of Fracture* 208.1-2 (2017): 241-268.

Multiscale Analysis of Heterogeneous Systems with Randomly Distributed Inclusions and Defects

Mahesh Bailakanavar*

*Thornton Tomasetti, Inc.

ABSTRACT

Generation of RVE's is a vital step in the multiscale analysis of heterogeneous materials. Unlike materials with periodic microstructure, generation of morphological details of materials with randomly distributed inclusions, such as defects in ceramics, hard and soft domains in polymers and chopped fiber composites pose various challenges such as: (i) Accurate representation of the inclusion shape, size, volume fraction and spatial orientation and distribution of the inclusions to minimize geometric approximation errors (i) Generation of unit cells with packing fraction as high as 45%, typically found in industrial grade composite materials (ii) Determination of the unit cell size that constitutes a macroscopically homogeneous material (iii) Generation of unit cells in quick succession with maximum computational efficiency for utilization in a stochastic multiscale framework. A Hierarchical Random Sequential Adsorption (HRSA) based algorithm is developed with the following features (i) Robustness - can generate RVE's with volume fraction of up to 45% for aspect ratios as high as 20 (ii) Versatility - able to generate unit cells with inclusions of varying shapes and sizes (iii) Efficiency - hierarchy of algorithms with increasing computational complexity A statistical study aimed at determining the effective size of the unit cell with randomly distributed chopped fibers is conducted for two material systems, namely 35% by volume randomly distributed glass fiber microstructure and a 35% by volume randomly distributed carbon fiber microstructure geometry. The results suggest that for material system with randomly distributed inclusions the optimal size of the unit cell depends upon the relative stiffness of the phases comprising the microstructure. Next, the HRSA algorithm is used in generating the RVE of matrix phase of a CMC system consisting of process-induced defects at crossover points, matrix voids, shrinkage cracks and interlaminar separation. The computed effective matrix properties suggest that the manufacturing induced defects have the most pronounced effect on the through thickness elastic modulus of the matrix. The results suggest that accounting for the defects induced matrix anisotropy is crucial for accurately modeling the damage and failure in CMC systems.

A Coupled Multiscale Approach to Modeling Aortic Valve Leaflet Tissue

Ahmed Bakhaty^{*}, Sanjay Govindjee^{**}, Mohammad Mofrad^{***}

^{*}University of California, Berkeley, ^{**}University of California, Berkeley, ^{***}University of California, Berkeley

ABSTRACT

Cellular mechanotransduction is the process by which biological cells respond to mechanical stimuli and activate biochemical pathways. Due to the importance of the microscale behavior in biological systems, traditional biomechanical modeling is limited in its capabilities. Multiscale modeling techniques, such as computational homogenization[1] (also known as “FE²”), however, can be used to investigate the micromechanical behavior of cells in biological systems, and hence mechanotransduction. Huang[2] proposed the valvular interstitial cells (VIC) aspect ratio as a mechanical measure of cellular mechanotransduction activity and performed experiments that investigated the metric in response to physiological loading of aortic valve leaflet tissue. Numerical simulations that mimic these experiments were carried out but limited to 2D and uncoupled 3D models (i.e., no interaction between the macroscale and microscale). In this study, we apply FE² to aortic valve leaflet tissue in 3D to study the mechanical behavior of the VIC in response to organ-scale mechanical loading. The modeling scheme importantly utilizes self-consistent material models based on layer-wise experimental data from aortic valve tissue.[3] Our simulations demonstrate a viable method for fully multiscale modeling of aortic valve tissue. We find that the “apparent” VIC aspect ratio observed in experiments may not necessarily be consistent with the actual 3D deformations of the cells. [1] Kouznetsova, V., Brekelmans, W.A.M. and Baaijens, F.P.T., 2001. An approach to micro-macro modeling of heterogeneous materials. *Computational Mechanics*, 27(1). [2] Huang, H.Y.S., Liao, J. and Sacks, M.S., 2007. In-situ deformation of the aortic valve interstitial cell nucleus under diastolic loading. *Journal of biomechanical engineering*, 129(6). [3] Bakhaty, A.A., Govindjee, S. and Mofrad, M.R., 2017. Consistent trilayer biomechanical modeling of aortic valve leaflet tissue. *Journal of biomechanics*, 61, pp.1-10.

Prediction Modeling of Exergy Destruction Rates of Turboprop Engine Components by the Use of Genetic Algorithm Based Artificial Neural Networks

Tolga Baklacioglu*, Onder Turan**, Hakan Aydin***

*Anadolu University, **Anadolu University, ***Tusas Engine Industries

ABSTRACT

This study illustrates a deep learning approach supported by metaheuristic design, targeting the foremost features and parameters of artificial neural network (ANN) framework used in predicting the rate of exergy destruction attainable in various components of an experimental turboprop engine. The development of deep ANN architectures comprising of three-hidden layers, using data obtained during real experimentation considering multiple engine parameters was accomplished in this regard. The employed engine parameters included gas generator speed, torque, power, airflow, and fuel mass flow obtained through turboprop engine runs. Once the deep learning ANN frameworks were hybridized with a metaheuristic approach, such as genetic algorithms (GAs), the optimization of the features of the initial network was facilitated. The features include biases, momentum factor, step-size, and weights for the back-propagation (BP) learning model, in addition to the number of neurons that are located in the hidden layers in terms of network topology design. The analysis of errors revealed a close fit involving the predicted values of the model and references made on real data in exergy destruction rates for the engine components. The use of appropriately chosen values in preceding networks weights produced more accurate testing results (R values of 0.998986, 0.998315, 0.996497, and 0.996649 for combustor, compressor, gas turbine, and power turbine, respectively) in networks using three hidden layers compared to those using lower hidden layers. Furthermore, optimizing deep ANNs using the GAs delivers not only further improved accuracy (R values of 0.999656, 0.999641, 0.998929, and 0.999966 for the previously mentioned engine components, respectively) but also an effective utilization of time in the resulting models.

Controlling Electronic Properties of Two-dimensional Organic-inorganic Halide Perovskites

Ganesh Balasubramanian*

*Lehigh University

ABSTRACT

Organic-inorganic halide perovskites, which have sparked a substantial interest due to their excellent photovoltaic properties, have also been synthesized in stable two-dimensional forms. The reduction in dimension promises an exciting opportunity to tune the transport properties of these functional materials. Here, we share findings from first principle calculations of various engineered two-dimensional hybrid organic-inorganic halide perovskite structures. While on one hand, the structures possess excellent transport properties similar to their bulk counterparts, on the other hand, the reduced dimensionality offers the advantage of tuning the band gaps over a broad range. In addition, by employing strain engineering to these two-dimensional materials, we are able to control transport properties including electrical conductivity and Seebeck coefficient. Our efforts are directed towards employing computational sciences for engineering designer perovskites with tailored properties.

Effects of Morphology on the Mechanical Properties of Heterogeneous Polymer-grafted Nanoparticle Networks

Anna Balazs*

*University of Pittsburgh

ABSTRACT

Using computational modeling, we examine how varying the arrangement of binary mixtures of polymer grafted nanoparticles (PGNs) in a network affects the mechanical properties of the composite. The free ends of the grafted chains on the PGNs contain reactive groups that can form labile bonds with reactive ends on nearby PGNs, and thereby form extensive networks. This bond formation is reversible, with the bonds breaking and reforming at a specified rate. The two types of particles in the network differ in the strength of the labile bonds that they form with their neighbors, forming both relatively strong and weak interconnections. We examine the response of this dynamic network to tensile deformation when the binary PGNs are arranged in an alternating, layered structure or a random mixture. We determine the ultimate tensile properties (strength, toughness), the strain recovery and behavior under cyclic loading for samples with the layered and random architectures. We demonstrate that the layered structures display self-healing behavior and exhibit enhanced mechanical properties relative to the random system. Using our model, we can tune both the spatial and temporal characteristics of the hybrid material. Thus, the approach provides a useful tool for determining how to tailor these parameters to achieve superior mechanical behavior in PGN networks.

Beams with Variable Mechanical Properties: Planar Timoshenko-like Model and Numerical Solution via Iso-Geometric Collocation

Giuseppe Balduzzi^{*}, Simone Morganti^{**}, Josef Füssl^{***}, Alessandro Reali^{****}, Ferdinando Auricchio^{*****}

^{*}Institute for Mechanics of Materials and Structures (IMWS), Vienna University of Technology, Vienna, Austria,

^{**}Department of Electrical, Computer, and Biomedical Engineering, University of Pavia, Pavia, Italy, ^{***}Institute for Mechanics of Materials and Structures (IMWS), Vienna University of Technology, Vienna, Austria, ^{****}Department of Civil Engineering and Architecture (DICA), University of Pavia, Pavia, Italy, ^{*****}Department of Civil Engineering and Architecture (DICA), University of Pavia, Pavia, Italy

ABSTRACT

Beams and plates with smooth variations of mechanical properties are frequently used in several engineering fields. As an example, the presence of knots leads to non-uniform distribution of stiffness and grain direction within timber structural elements (e.g., Glued Laminated Timber (GLT) beams and Cross Laminated Timber (CLT) plates) and substantially influences the mechanical response of the structural element. First and foremost, since the structural element under analysis is made of an anisotropic material with principal directions not aligned with the beam axis, shear deformations depend on all stress components. Such a dependency is reasonable and expected considering the 2D constitutive relation of the material, while its influence on the beam's constitutive relation is less trivial and needs enhanced tools for the evaluation of the stiffness coefficients [1]. Furthermore, [2, 3] highlight that every variation of mechanical properties within the beam body leads axial internal force and bending moment to produce non-vanishing shear stresses and deformations. This contribution discusses a simple and effective Timoshenko-like planar beam that can effectively handle both the so far introduced problematics. The model turns out to be naturally represented by a mixed, explicit system of six ordinary differential equations in which both internal forces and beam's generalized displacements are the independent variables. Complexity of beam's constitutive relations and variability of its coefficients do not allow for an easy computation of the model's analytical solution, making the usage of numerical tools mandatory. Unfortunately, classical approaches like mixed finite elements might entail several issues (e.g., shear locking, ill-conditioned matrices, etc.). Conversely, the isogeometric collocation method allows an equal order approximation of all unknown fields, without affecting the stability of the solution. This makes such an approach simple, robust, and particularly suitable for solving the system of ODEs governing the proposed beam model. A rigorous comparison with highly refined 2D FE analysis will demonstrate the effectiveness of the proposed modelling strategy. REFERENCES [1] H Murakami, E Reissner, and J Yamakawa. Anisotropic beam theories with shear deformation. *Journal of Applied Mechanics*, 63(3):660-668, 1996. [2] Giuseppe Balduzzi, Mehdi Aminbaghai, Ferdinando Auricchio, and Josef Füssl. Planar Timoshenko-like model for multilayer non-prismatic beams. *International Journal of Mechanics and Materials in Design*, 2017. doi:10.1007/s10999-016-9360-3. [3] Giuseppe Balduzzi, Mehdi Aminbaghai, and Josef Füssl. Linear response of a planar FGM beam with non-linear variation of the mechanical properties. In Alfredo Güemes, Ayeche Benjeddou, José Rodellar, and Jinsong Leng, editors, *SMART 2017*, pages 1285-1294. CIMNE, 2017.

Moving-least-squares Immersed Boundary Method for Thin Rigid Structures

Rahul Bale^{*}, keiji onishi^{**}, Niclas Jansson^{***}, Amneet Pal Singh Bhalla^{****}, Makoto Tsubokura^{*****}

^{*}RIKEN AICS, ^{**}RIKEN AICS, ^{***}KTH Royal Institute of Technology, ^{****}Lawrence Berkeley National Lab,
^{*****}RIKEN AICS, KOBE University

ABSTRACT

Constraint immersed boundary (CIB) method is a fictitious domain approach for fluid-structure interaction problems in which an immersed body (IB) is represented by volumetric Lagrange multipliers (that impose rigid body constraint) in the combined momentum equation. The incompressible Navier-Stokes equation is solved on a Cartesian mesh, whereas the Lagrange multipliers are defined on a non-conforming Lagrangian mesh. The Eulerian-Lagrangian interactions, i.e., velocity interpolation and force spreading, are mediated by regularized Peskin's delta functions [1]. The CIB approach has been applied successfully to model volumetric bodies at intermediate Reynolds number flow applications in the past [2,3], in which the volumetric treatment of Lagrange multipliers ensure that there is no fluid sloshing inside the IB, and effectively making the fluid inside move with the IB velocity. Representing the IB with only a surface mesh leads to spurious flow inside the body that grows with Reynolds number. For many applications with complex geometries, this is particularly challenging for two reasons. First, in most applications CAD geometry is available in surface mesh format. Second, it may not always be possible to separate the inside region from outside region. In this work, we extend the CIB method to model thin bodies using surface mesh representation. The method requires modifying delta functions using moving-least-squares (MLS) approach by identifying the two sides of the IB surface. The weights of the delta functions are modified such that velocity interpolation and force spreading occur separately on either side of the IB surface, but they still satisfy the original moment conditions which are known to conserve energy, force, and torque during Eulerian-Lagrangian interactions. The MLS approach does not add substantially to the computational cost because the immersed body is an object of codimension-1 in the simulations. We present several cases of flow past bluff bodies showing a dramatic reduction of fluid sloshing using the new approach at intermediate to high Reynolds number. In addition, we also discuss some theoretical properties of the modified delta functions. [1] Peskin CS. The immersed boundary method. *Acta numerica*. 2002, 11:479-517. [2] Bhalla, A. P. S., Bale, R., Griffith, B. E., & Patankar, N. A. A unified mathematical framework and an adaptive numerical method for fluid-structure interaction with rigid, deforming, and elastic bodies. *Journal of Computational Physics*, (2013), 250, 446-476. [3] Kallemov B, Bhalla A, Griffith B, Donev A. An immersed boundary method for rigid bodies. *Communications in Applied Mathematics and Computational Science*. 2016, 11(1):79-141.

Scale-Resolving Simulations of Turbulent Boundary Layers with Flow Separation

Riccardo Balin^{*}, Eric Peters^{**}, John Evans^{***}, Philippe Spalart^{****}, Kenneth Jansen^{*****}

^{*}University of Colorado Boulder, ^{**}University of Colorado Boulder, ^{***}University of Colorado Boulder, ^{****}The Boeing Company, ^{*****}University of Colorado Boulder

ABSTRACT

Due to the large computational cost associated with DNS and LES, most engineering flows are currently modeled with RANS. During the stages of design, for instance, the large number of simulations required to explore the parameter space dictates the use of the less computationally intensive RANS methods. Moreover, the large Reynolds numbers in which most air and water vehicles operate put DNS and LES completely out of reach. Unfortunately, RANS models perform poorly when dealing with boundary layers affected by strong adverse pressure gradients and flow separation, plaguing the prediction and design of systems exhibiting such characteristics. Therefore, it is of great value to better understand the physics involved in separation of a turbulent boundary layer, and to gather data for such flows with the hope of improving the prediction of RANS models (and other closure models as well) through statistical approaches to turbulence modeling. To accomplish this task, scale-resolving simulations of two turbulent boundary layers affected by adverse pressure gradients and separation are carried out. In one case, the pressure gradient is designed to produce incipient separation of the layer well inside the flow domain, while in the other case full flow separation is studied. DNS, LES, wall-modeled LES, and DES of both separated boundary layers are performed, and comparisons are drawn between the different approaches, as well as with the RANS predictions of the flows. Experimental data is also used to verify the numerical results. Attention is given to the boundary layer in the region leading to and after separation ensues. In particular, the details of the Reynolds stresses, turbulent kinetic energy budget and effective eddy viscosity are reported. The Reynolds number of the boundary layer is close to the upper limit of what is practical for a DNS.

Uncertainty Propagation in a 3D Asymmetrically Pretensioned Guyed Mast

Jorge Sebastian Ballaben^{*}, Marta Beatriz Rosales^{**}, Rubens Sampaio^{***}

^{*}Universidad Nacional del Sur - CONICET, ^{**}Universidad Nacional del Sur - CONICET, ^{***}Pontificia Universidade Catolica do Rio de Janeiro

ABSTRACT

The study of the nonlinear dynamic response of a guyed mast considering the uncertainty of the guys pretension is reported in this work. The structure consists in a real life guyed mast of 20 m high and one level of three cables. The mast is represented by an equivalent beam-column with the addition of second order effect due the axial loads of the cables. The three guys behavior is described through cables with an initial pretension and only tensile capacity. The partial differential equations are discretized using the finite element method, considering Hermite elements for the mast (Bernoulli beam theory) and nonlinear cable elements for the guys. A lateral dynamic load is applied on the mast, through a cosine function with its frequency selected to avoid the natural frequencies of the system. An ad hoc software developed by the first author is employed to solve the nonlinear dynamic problem. Once the deterministic problem is stated, an uncertainty quantification is carried out. In this case, the stochastic variable is the pretension. Since the design value can be modified at the construction stage and during the service life, the pretension force is modeled as a random variable with a probability density function (PDF) derived from the Principle of Maximum Entropy (PME). In previous works of the authors, the case in which all the cables have the same pretension (though stochastic) was solved. However, a situation in which the cables do not have the same value of pretension is possible due to eventual discrepancies in the installation. Thus, a small random error is introduced to make the guys tensions different among them. The radial symmetry is thus lost. The model herein presented contributes to attain a more realistic description of the structure, mainly regarding the three-dimensional representation and the sensibility to the variability of the guy pretensions. The obtained results (natural frequencies and modes, dynamic displacements, etc.) and its interpretation through statistic tools, improve the understanding of the real dynamic properties and behavior of slender and flexible guyed structures.

Fully Resolved Cellular-scale Simulation of Blood Flow in Physiologically Realistic Microvascular Networks

Peter Balogh*, Prosenjit Bagchi**

*Rutgers University, **Rutgers University

ABSTRACT

An efficient three-dimensional computational tool [1] for simulating cellular-scale blood flow within highly complex geometries is presented. The motivation behind the development is to provide a framework capable of modeling the diverse range of interface types present in microcirculatory blood flow, thus permitting the study of such complex flows while retaining the cellular-scale details. Simultaneously modeling this diverse range of interface types, however, presents a major challenge numerically. The method must be capable of modeling deformable cell surfaces, such as red blood cells, white blood cells, or circulating tumor cells, highly complex stationary interfaces such as microvascular networks or microfluidic devices, as well as moving rigid interfaces such as inactivated platelets. To accomplish this we use immersed boundary methods (IBMs) integrated into a coupled finite-volume/spectral fluid flow solver. A sharp-interface IBM is used to model the complex stationary interfaces as well as the moving rigid interfaces. A continuous forcing front-tracking method is used in conjunction with the finite element method to model the interfaces of the deformable cells. The overall computational domain resembles a box, discretized in space by a fixed, uniform, rectangular Eulerian grid. The governing fluid flow equations are numerically solved on this grid using a projection method for the time integration, with a staggered arrangement of the flow variables. All interfaces are immersed into this computational domain. With the sharp-interface method constraints are enforced at Eulerian grid points such that a no-slip condition is achieved at the interface. With the front-tracking method, the stresses generated in the membrane due to resistance against shearing, area dilatation, and bending are computed on a Lagrangian grid. They are then coupled to the bulk fluid on the Eulerian grid with a body-force term constructed from a finite-span delta function added to the governing equations. Various validations are presented to establish the accuracy of the simulation tool. The versatility of the tool is then demonstrated by simulations of cells flowing in microfluidic devices as well as in physiologically realistic microvascular networks. The later example was the focus of our recent work [2] in which several unexpected phenomena were revealed. Overall, the methodology presented provides a viable framework for studying the flow of whole blood through highly complex physiological geometries while simultaneously capturing the cellular-scale details. References: [1] Balogh, P. & Bagchi, P., J. Comp. Phys., 2017, 334, 280-307. [2] Balogh, P. & Bagchi, P., Biophys. J., 2017, 113, 2815-2826.

Experimental and Numerical Characterization of Plastic Flow and Ductile Damage in Extruded Aluminium

Sandra Baltic^{*}, René Hammer^{**}, Julien Magnien^{***}, Thomas Antretter^{****}, Werner Ecker^{*****}

^{*}Materials Center Leoben Forschung GmbH, ^{**}Materials Center Leoben Forschung GmbH, ^{***}Materials Center Leoben Forschung GmbH, ^{****}Montanuniversität Leoben, ^{*****}Materials Center Leoben Forschung GmbH

ABSTRACT

Because of the excellent functional and structural properties, aluminium alloys have many applications: from large lightweight structures, over car bodies to the smallest electronic components. The object of this research is the ductile behaviour of aluminium alloys formed into cans by impact extrusion. The plastic flow and the fracture strain loci of two material grades have been investigated: AW-1050 and AW-6082. To precisely predict the material flow and ductile damage under complex loading, detailed material characterization is required. To this aim, miniature tensile test specimens are optimized by numerical simulations to cover a wide range of stress states for the model calibration. Final sample geometry includes dogbone, notched and shear specimens. We propose a new method, which leads to a biaxial stress state under uniaxial tensile testing. Special attention is paid to the effect of stress triaxiality and Lode angle parameter on the fracture strain under plane stress conditions (Bai and Wierzbicki, 2015). Digital Image Correlation is utilized to track the plastic flow and to identify the initiation and development of localized strain during tensile test. Sample position is planned so that the effect of anisotropy, due to the extrusion process, can be quantified. Three different angles with respect to the extrusion direction are considered: 0°, 45°, 90°. Tensile test results in different orientations allowed to calculate the anisotropy coefficients which determine the shape of the yield function. The tests are accompanied by FEM to identify the damage evolution and strain to fracture for the calibration of the damage model. Tensile testing of miniature samples with non-standard experimental setup and numerical modelling of damage evolution and failure with highly localized strain are the challenges, which have been successfully overcome by this contribution. Complete range of the Lode angle parameter and positive stress triaxialities for plane stress conditions has been covered just by making use of uniaxial tensile experiments. The calibrated model is expected to predict the mechanical response of extruded aluminium cans under complex loading and finds its application in the precise prediction of the opening pressure for safety vent design. References Bai, Y.; Wierzbicki, T.: A comparative study of three groups of ductile fracture loci in the 3D space. In: Engineering Fracture Mechanics 135 (Supplement C), S. 147–167, 2015

Quantification of the Probability of Failure in Sheet Metal Forming Problems of Advanced High Strength Steel

Daniel Balzani^{*}, Niklas Miska^{**}

^{*}Ruhr-Universitaet-Bochum, Chair of Continuum Mechanics, Germany, ^{**}Ruhr-Universitaet-Bochum, Chair of Continuum Mechanics, Germany

ABSTRACT

Numerous production processes and constructions rely on an accurate description of the material behavior and the boundary conditions to the problem. Such input variables may become uncertain and then an accurate calculation of the probability of failure is required. In particular in many modern materials, which make use of heterogeneous microstructures, such as advanced high strength steels, specific challenges arise from a significant variation of microstructure morphology leading to uncertain macroscopic material properties. Here, a new method is proposed to solve this problem. The method is based on the simulation of large sets of microscopic boundary value problems using finite elements and the subsequent homogenization of the microscopic mechanical quantities to obtain the effective macroscopic properties of the material. For each of these simulations a different microstructure is considered, which is selected such that the statistical variation of the computed microstructures is as close as possible to a variation in the real material. To assure this constraint, we exploit the concept of statistically similar representative volume elements (SSRVEs) [1]. This concept is originally formulated as minimization of a statistical least-square functional governed by distances of statistical measures describing the real material and the one of the SSRVE. Thereby, an artificial microstructure is constructed which matches best the morphology of the real microstructure in a statistical sense. Here, we consider the least-square functional as measure for the similarity of microstructure morphology and create a set of statistically similar volume elements (SSVEs) such that the variation of the least-square functional over the SSVEs follows the one of the real material. To ensure an efficient quantification of the associated uncertain macroscopic material parameters, a Multi-Level Monte-Carlo Approach is used. However, the resulting uncertain macroscopic properties may not necessarily follow specific distribution functions. Also other parameters of sheet metal forming problems as e.g. the friction coefficient may possess uncertainties which can hardly be quantified. This means that only limited data on the uncertain quantities in terms of bounds or moments of reduced order will be available, which prevents a classical uncertainty quantification procedure. In order to overcome this problem, the Optimal Uncertainty Quantification (OUQ) framework [2] can be considered to determine the sharpest bounds possible to the probability of failure in sheet metal forming problems, where the limited data is included as constraint to a global minimization/maximization principle. The proposed method is demonstrated with an example of advanced high strength steels. [1] D. Balzani, L. Scheunemann, D. Brands, and J. Schröder. Construction of two- and three-dimensional statistically similar RVEs for coupled micro-macro simulations. *Computational Mechanics*, 54(5):1269–1284, 2014. [2] H. Owhadi, T. J. Sullivan, M. McKerns, and M. Ortiz. Optimal Uncertainty Quantification. *SIAM Rev.*, 55(2):271–345, 2013

Modeling and Validating Conformational and Chemical Pathways in Macromolecular Systems

Nilesh Banavali*

*Wadsworth Center, New York State Department of Health

ABSTRACT

Enhanced Sampling Molecular Dynamics (ES-MD) simulations provide a robust route to overcome the timescale limitations of brute-force MD approaches, and understand the complex free energy landscapes that govern functional behavior of biomolecules. However, novel intermediates identified through ES-MD simulations are frequently considered speculative till experimental validation can be provided for them. Many biological systems also function through a complex combination of conformational and chemical transitions that are difficult to seamlessly model using ES-MD simulations. One underutilized source of validation of conformational transitions is the existing structural data deposited in the RCSB Protein Data Bank (PDB). This presentation will demonstrate how multi-dimensional histograms can be used to mine the structural heterogeneity in the PDB to inexpensively model conformational pathways. Unusual structural intermediates that explain important functional characteristics, and are possibly identifiable only through extensive ES-MD simulations, can be predicted using this approach at minimal computational cost. Specific features of structural intermediates separately identified through enhanced sampling MD simulations can also be validated by easy identification of similar counterparts in the PDB. A strategy called Restrained Geometries and Topology Switching (RGATS) will also be presented that can be used to model chemical reactions in complex environments using any Molecular Mechanics (MM) program, with no additional software implementation. This strategy enables application of any ES-MD method, implemented in any MM program, for elucidating conformational features of biochemical reaction pathways. In particular, this strategy allows rapid prediction of reactant, intermediate, or product state structures for any chemical reaction in any bio-molecular context, when an accurate structural model in any one of these states is available.

Understanding Deformation Capacity Variability in Ductile Fiber-reinforced Cement-based Composite Components through Numerical Simulation

Matthew Bandelt*, Mandeep Pokhrel**

*New Jersey Institute of Technology, **New Jersey Institute of Technology

ABSTRACT

Numerous applications of ductile fiber-reinforced cement-based composites have been proposed to improve the ductility, durability, and damage resistance of structures throughout the world. Experimental findings have shown that the flexural failure of reinforced beams using ductile cementitious materials is often governed by fracture of reinforcement rather than crushing of compression zone, as is commonly observed in traditional reinforced concrete structures. Experimental research has identified how certain factors, such as reinforcement ratio, influence deformation capacity; however, significantly variability in component ductility is still not well understood. This study explores the variability in deformation capacity in ductile fiber-reinforced cement-based composites containing steel reinforcement. Computational finite element models are simulations are carried out to understand the influence of mechanical properties, reinforcement ratio, boundary conditions, and structural geometry on deformation capacity. Two-dimensional continuum models were created and simulated using total strain-based models up to the point of simulated reinforcement fracture. Damage patterns in the fiber-reinforced cementitious material and reinforcement are studied at different deformation levels to identify the spread of plasticity in reinforced components. The results of this study provide a better understanding of how structural members with ductile cement-based composite behave in relation to various material and structural properties. Numerical simulations show how flexure and shear crack progression influences reinforcement strain distribution, rebar fracture, and deformation capacity. Results are compared with experimentally observed damage progression, strain localization, and deformation capacity.

Polycrystal Plasticity Modeling of High Cycle Fatigue Behavior in Ti-6Al-4V and Residual Stresses in Dissimilar Welded Ti Alloys

Ritwik Bandyopadhyay*, Michael Sangid**

*Purdue University, **Purdue University

ABSTRACT

Fatigue is one of the most common modes of failure in engineering components. Despite many studies, the physics of fatigue crack initiation is an open field of research, due to the complexities in evolving micromechanical states and diverse local microstructure in the region of crack initiation. Recently, with the advent of high performance computing, crystal plasticity (CP) models, integrated within the finite element method (FEM), are used to study this issue, by accounting for anisotropic material behavior and slip system activation. These investigations help to identify dominating physical mechanisms, especially strain localization and stress concentration, which are precursors to fatigue crack initiation. Such mechanisms, in general, depend on grain morphology, intergranular misorientation, lattice structure, macroscopic load regime, etc. In the present study, we simulate high R-ratio high cycle fatigue response in Ti-6Al-4V using a CP-FEM framework and analyze several damage indicator parameters in relation to crack initiation observed during a companion experiment. Design against high cycle fatigue crack initiation is strongly influenced by the presence and nature (tensile or compressive) of the residual stress field. In the second part of this talk, we analyze residual stress profiles across the linear friction weld joints of Ti-6Al-4V-to-Ti-6Al-4V and Ti-6Al-4V-to-Ti-5Al-5Mo-5V-3Cr alloys using energy dispersive x-ray diffraction measurements to identify the complete lattice strain tensor in the alpha and beta phases in these materials. These residual stress profiles can be suitably incorporated within polycrystal plasticity finite element framework to study the physics of fatigue crack initiation in an effective way.

Cohesive Zone Modelling on Initiation and Propagation of Fatigue Crack

Anuradha Banerjee*, Nijin I. S**, Shravan Kumar R.***

*Indian Institute of Technology Madras, Chennai, **Indian Institute of Technology Madras, Chennai, ***Indian Institute of Technology Madras, Chennai

ABSTRACT

Fatigue is one of the most critical modes of failure due to the progressive growth of micro-structural damage even under sub-critical loads. Diverse approaches using Cohesive zone law have been adopted for the better prediction of fatigue failure in the recent years [1]. These models were successful in predicting growth data of a pre-existing crack but could not be applied in prediction of initiation of crack from notch tip as there exists significant differences between the state of stress ahead of a notch-tip and a crack-tip. In the present work, a stress-state dependent cohesive model, combined with an irreversible damage parameter has been used in simulation of fatigue crack growth initiation and continued growth in a representative aluminum alloy. For simulation of realistic fatigue crack growth, from its initiation and during its continued growth till final failure, stress-state is incorporated by expressing the traction separation law of cohesive elements as a function of biaxiality ratio (?) and separation [2]. This cohesive law has an associated cohesive strength, σ_{max} , and cohesive energy, σ_o . These parameters, however, in the model are dependent on the triaxiality of the stress-state and thus, not material constants. Stress-state with higher ?, corresponds to higher triaxiality, results in higher σ_{max} and lower σ_o . Growth of damage, as per the effective stress concept of continuum damage mechanics, results in overall degradation of the process zone [3]. The model is implemented as interface elements and plane strain simulations of crack initiation and growth under cyclic loading are performed for two different load ranges. The stress-state of neighbouring continuum elements is used in the traction-separation behaviour of the cohesive elements. A combination of the fatigue damage model parameters is identified that is able to reproduce the crack growth curves in the high cycle fatigue regime observed experimentally. Further, a discussion is developed on the specific role of the stress-state on the initiation life and crack growth rates under sub-critical cyclic loading. References [1] Kuna M, Roth S. General remarks on cyclic cohesive zone models. *Int J Fract* 2016:1–21. [2] Banerjee, R. Manivasagam, Triaxiality dependent cohesive zone model, *Engineering Fracture Mechanics* 76 (12) (2009) 1761–1770. [3] K. Roe, T. Siegmund, An irreversible cohesive zone model for interface fatigue crack growth simulation, *Engineering fracture mechanics* 70 (2) (2003) 209–232.

Modeling Compressive Fracture of Haversian Bone Using Porosity Based Lattice Model

Anuradha Banerjee*, Ashwiji Mayya**, R. Rajesh***

*Indian Institute of Technology Madras, India, **Indian Institute of Technology Madras, India, ***1. The Institute of Mathematical Sciences, Chennai, India 2. Homi Bhabha National Institute, India

ABSTRACT

Cortical bone, found in the central part of long bones like femur, is known to adapt to local mechanical stresses. This adaptation has been linked with Haversian remodeling involving resorption of existing primary bone followed by laying of secondary osteonal systems. As a consequence of remodeling, both, the structure of porosity network as well as the matrix properties can be expected to evolve. Fracture process in complex heterogeneous quasi-brittle materials like bone involves multiple porosities and dissipative micro-fracture events leading to progressive loss in load bearing capacity prior to failure. Modeling such complex fracture process is vital for assessment of bone health, to design mechanically compatible implants and porous scaffolds. Also, similar models may be applicable in understanding the fracture behavior of other brittle porous materials like wood, rock etc. Here, we characterize the three dimensional porosity network of bovine Haversian bone and examine the role of the overall porosity, structure of the porosity network and the matrix properties in its vulnerability against compressive failure. Using micro-Computed Tomography, the detailed structure of porosity network is obtained pre- and post-compression testing. Based on the periodicity in the features of porosity along tangential direction, we develop a two dimensional porosity-based random spring network model (RSNM) for Haversian bone. The load bearing capacity in compression predicted using RSNM simulations is shown to be significantly lower than experiments of Haversian bone as a result of changes in structure of the porosity network and increase in mean porosity while considering matrix properties as those of primary/plexiform samples obtained from same cross-section [1]. Using EDS line scans, however, the Haversian bone matrix is shown to be less stiff than that of plexiform samples. The failure properties of Haversian bone matrix that are iteratively determined to reproduce the experimental response are shown to be consistently higher than corresponding primary/plexiform bone matrix properties. The predictions, thus, suggest that Haversian bone due to remodeling has a bone matrix that is less stiff but significantly tougher than primary/plexiform microstructure of same cross-section. The findings are consistent with the variations in properties due to differences in levels of structural hierarchy of the microstructures [2]. References 1. Mayya, A., Banerjee, A., Rajesh, R., 2017. Phys. Rev. E 96 (5), 053001. 2. Zhang, Z., Zhang, Y.-W., Gao, H., 2011. Proc. R. Soc. Lond., B, Biol. Sci. 278 (1705), 519–525.

Probabilistic Thermomechanical Material Modeling of Ductile Metals from Uncertain Test Data

Aakash Bangalore Satish*, Michael D. Shields**

*Johns Hopkins University, **Johns Hopkins University

ABSTRACT

The mechanical response of ductile metals in simulations is represented using viscoplastic material models that are calibrated using experimental data. Calibration is usually performed deterministically from a small number of test data, often from one test, and therefore does not account for natural variability in the material properties. We present a Bayesian framework for probabilistic calibration of a viscoplastic damage model for ductile metals from an ensemble of test data under differing boundary conditions (uniaxial tension to plane strain) possessing variability in its temperature dependent mechanical response. The influence of the material variability on the response of structural components is then illustrated in comparison with the response of structural components whose material model is calibrated using traditional deterministic methods. The method is specifically applied to modeling the response of aluminum 6061-T6 components, where the material is calibrated using a series of over 150 mechanical tests under two different stress states at six temperatures. A brief description of the testing program and the resulting material variability will also be presented.

A Stable and Accurate Partitioned FSI Algorithm for Incompressible Flow and Rigid Bodies

Jeffrey Banks^{*}, William Henshaw^{**}, Donald Schwendeman^{***}, Qi Tang^{****}

^{*}Rensselaer, ^{**}Rensselaer, ^{***}Rensselaer, ^{****}Rensselaer

ABSTRACT

This talk discusses our continuing study of fluid-structure interaction (FSI) problems involving incompressible fluids and rigid bodies. Such FSI problems arise in many applications of science and engineering, such as particulate flows and mechanical heart valves. We discuss the development of the an added-mass partitioned (AMP) algorithm that remains stable, without sub-iterations, for light and even zero mass rigid bodies when added-mass and viscous added-damping effects are large. The scheme is based on a generalized Robin interface condition for the fluid pressure that includes terms involving the linear and angular acceleration of the rigid body. Added mass effects are handled in the Robin condition by inclusion of a boundary integral term that depends on the pressure. Added-damping effects are treated with approximate added-damping tensors that are defined by certain integrals over the surface of the body. We begin by discussing the development and analysis of the AMP scheme for simple model geometry in two spatial dimensions. Extension of the scheme to general geometry and three dimensions is then performed using finite difference methods and overlapping grids. For our parallel implementation we employ parallel sparse linear solvers for the pressure Poisson equation, including the non-standard AMP interface condition. Stability for light solids, and second-order accuracy are demonstrated for a series of challenging benchmark problems

Multiscale Data Assimilation via Multivariate Gaussian Process Regression

David Barajas-Solano^{*}, Alexandre Tartakovsky^{**}

^{*}Pacific Northwest National Laboratory, ^{**}Pacific Northwest National Laboratory

ABSTRACT

We present a spatial interpolation approach for parameter fields incorporating measurements with two different support volumes, a point support or fine scale, and a finite support or coarse scale. The proposed approach treats the fine and coarse fields as components of a bivariate Gaussian process with a parameterized multiscale covariance model. We employ a full bivariate Matérn kernel as multiscale covariance model, with shape and smoothness hyperparameters that account for the coarsening relation between fine and coarse fields. In contrast to similar multiscale kriging approaches that assume a known coarsening relation between scales, the hyperparameters of the multiscale covariance model are estimated directly from data via pseudo-likelihood maximization. We illustrate the proposed approach with a predictive simulation application for PDEs with heterogeneous parameters. Multiscale Gaussian process regression is employed to estimate the two-dimensional parameter distribution from synthetic multiscale measurements. The resulting stochastic model for coarse saturated conductivity is employed to quantify uncertainty in pore pressure predictions.

Reduced Order Modeling via PGD for Highly Transient Thermal Evolutions in Additive Manufacturing

Andrea Barbarulo*, Bruna Favoretto**, Charles-Andre De Hillerin***, Victor Oancea****, Omar Bettinotti*****

*CentraleSupélec Université Paris-Saclay, **CentraleSupélec Université Paris-Saclay / Dassault Systèmes SIMULIA Corp, ***Dassault Systèmes SIMULIA Corp, ****Dassault Systèmes SIMULIA Corp, *****Dassault Systèmes SIMULIA Corp

ABSTRACT

Since their inception, Selective Laser Melting (SLM) and Electron Beam Melting (EBM) Powder Bed Fabrication (PBF), as prime examples in additive manufacturing (AM), proved to be a paradigm shift for manufacturing processes. They consist in selective melting of superposed layers of metal powder thanks to a machine-controlled moving high energy source. Due to their nature, these processes allow for unprecedented freedom in designing, personalizing and optimizing mechanical parts. Moreover, they are particularly suited for software-hardware integration when the desired geometry is conceived with a Computer Assisted Design (CAD) tool and directly produced by an automated process, removing all intermediate steps between designers' vision and the physical world. Nevertheless, due to the young age of AM and to the lack of a complete mastering of the process by either experimental or numerical means, the mechanical properties of the produced parts are often unpredictable, severely constraining its use in high end applications. For this reason, numerical methods capable to predict final characteristics of the part, to spot critical points during the process and to help the design process itself, seem a necessity. Unfortunately, SLM and EBM encompass complex multiphysics (thermal, mechanical, electromagnetic, metallurgic, phase change) and pose a gigantic multi-scale problem in both space and time, which requires special consideration in numerical analysis. This work focuses on highly nonlinear thermal phenomena occurring in the immediate proximity of the fast moving heat source where temperature evolution rates, phase changes and thermal gradients are the most intense, all happening on a very small scale. The idea is to provide a low-cost / high accuracy simulation of this important zone. To provide this solution, a Reduction Order Model (ROM) technique called Proper Generalized Decomposition (PGD) has been adapted for this problem to consider highly temperature dependent material properties, phase change, latent heat, a laser that moves rapidly along the path and rapidly evolving Neumann boundary conditions. This model order reduction technique allows computing a reduced base for each variable without solving the full eigenvalue problem. Thanks to this technique, computational cost is significantly reduced and variable separation is achieved enabling to deal with highly meaningful reduced bases. This work also contains an in-depth study on PGD controls (number of modes, number of iterations, etc.) and on how they can be best selected for efficient computations. This work is part of an ongoing collaboration between Dassault Systèmes and MSSMat, CentraleSupélec University.

An Active Set Type Method for 2D Hyperelastic Problems with Unilateral Contact and Coulomb's Friction

Mikaël Barboteu*, David Danan**

*University of Perpignan, France, **INSERM Rennes, France

ABSTRACT

In this work a Primal Dual Active Set (PDAS) type method is considered to solve mathematical problems which describe the frictional contact between hyperelastic bodies and a perfectly rigid obstacle. The Primal Dual Active Set type method is based on two points: first, the reformulation of frictional contact conditions as equivalent nonlinear complementarity functions and, next the use of a semismooth Newton method for the solution of the nonlinear complementarity equations, see [2,3]. This iterative method leads to consider specific boundary conditions on the contact boundary nodes belonging to active or inactive sets directly related to the status of contact and friction. Therefore, at each Newton iteration, we have to consider the solutions of problems with simple boundary conditions, such as Dirichlet, Neumann or Robin boundary condition as mentioned in [1,2,3]. This kind of method, as the well-known Stabilized or Nitsche's methods, allows more flexibility for finite element discretization (no discrete inf-sup condition, non-conforming meshes, etc.). The main trait of such method is that it does not require the use of the Lagrange multipliers both for the enforcement of the frictional contact conditions and the determination of the contact and friction stresses. As a consequence the implementation of the algorithm is facilitated, the condition number of the systems is better and the resolution is faster. Our aim is to present in detail the theoretical formulation and numerical algorithm of the PDAS method for three-dimensional problems with unilateral constraints and Tresca or Coulomb friction law. Then we derive a specific and simplified form of the frictional contact active set conditions in the case of 2D problems. In particular, we analyze this active set method and carry out qualitative theoretical and numerical comparisons with the well-known augmented Lagrangian method by considering representative contact problems for quasi-static and dynamic processes. [1] S. Abide, M. Barboteu and D. Danan, Analysis of two active set type methods for unilateral contact problems, Appl. Math. and Comput., 284 Issue C, 2016, 286-307. [2] M. Hintermuller, V. Kovtunenkov, and K. Kunish, Semismooth Newton methods for a class of unilaterally constrained variational problems, Adv. In Math. Sci. and Appl., 147, 2004, 513-535. [3] S. Hueber, G. Stadler and B.I. Wohlmuth, A primal dual active set algorithm for three-dimensional contact problems with coulomb friction, SIAM J. Sci. Comput., 30(2), 2008, 572-596.

Robust Inside-Outside Segmentation Using Generalized Winding Numbers

Gavin Barill^{*}, Neil G. Dickson^{**}, Ryan Schmidt^{***}, David Levin^{****}, Alec Jacobson^{*****}

^{*}University of Toronto, ^{**}Side Effects Software, Inc., ^{***}Gradientspace, ^{****}University of Toronto, ^{*****}University of Toronto

ABSTRACT

Solid shapes in computer graphics are often represented with boundary descriptions, e.g. triangle meshes, but animation, physically-based simulation, and geometry processing are more realistic and accurate when explicit volume representations are available. Tetrahedral meshes which exactly contain (interpolate) the input boundary description are desirable but difficult to construct for a large class of input meshes. Character meshes and CAD models are often composed of many connected components with numerous self-intersections, non-manifold pieces, and open boundaries, precluding existing meshing algorithms. We propose an automatic algorithm handling all of these issues, resulting in a compact discretization of the input's inner volume. We only require reasonably consistent orientation of the input triangle mesh. By generalizing the winding number for arbitrary triangle meshes, we define a function that is a perfect segmentation for watertight input and is well-behaved otherwise. This function guides a graphcut segmentation of a constrained Delaunay tessellation (CDT), providing a minimal description that meets the boundary exactly and may be fed as input to existing tools to achieve element quality. We highlight our robustness on a number of examples and show applications of solving PDEs, volumetric texturing and elastic simulation. Furthermore, we express the generalized winding number as a boundary integral common to electrostatics. This allows us to employ the fast multipole method to expand our algorithm to a wider variety of geometries and applications.

Joule Heating Effect of Electroosmotic Flow through Soft Nanochannel

Sirsendu Sekhar Barman*, Somnath Bhattacharyya**

*Indian Institute of Technology, Kharagpur, **Indian Institute of Technology, Kharagpur

ABSTRACT

The present study deals with thermal transport characteristics of an electrolyte solution flowing through a slit nanochannel with polyelectrolyte walls, known as soft nanochannel. The sources of the fluid flow are the electrokinetic effects that trigger an electroosmotic flow (EOF) under the impact of a uniformly applied electric field. The direction and flow rate of EOF is governed by strength of the electric field, concentration of electrolytes, temperature, pressure, viscosity etc. The thermal transport characteristics is mainly dependent on Joule heating which is generated when an electric field is applied across conductive liquids. Such Joule heating not only causes increase in temperature but also creates a temperature gradient. The change of liquid temperature and the presence of temperature gradient would have an impact on the EOF. Ion and liquid transport in polyelectrolyte-grafted soft nanochannels have been employed for various applications such as biological analysis, chemical process, developing nanofluidic and much more. The present study includes the coupling Poisson-Boltzmann equation, the modified Navier-Stokes equations, the modified Nernst-Planck equation and the modified energy equation. Governing equations along with proper boundary conditions are solved numerically through a control volume approach over a staggered grid arrangement. Discretized equations are solved through the pressure correction based iterative SIMPLE (Semi-Implicit Method for Pressure-Linked Equations) algorithm. The results are expressed in form of the average velocity, average entropy generation ((Savg)) for both step-like PEL and diffuse PEL. Solutions are obtained with a good agreement with the corresponding linear solutions of Matin, Ohshima et al.(2016) [1] for both the velocity field and temperature field. Extensive studies are carried out showing how the average velocity changes with the change of surface temperature. The average entropy generation is estimated with the solutions of Zhao et al.(2010) [2]. The average entropy generation is presented to analyse its dependency on softness parameter, bulk electrolyte concentration, PEL concentration, PEL thickness, surface charge density. The average entropy diminishes with the increase of surface temperature and it also increases with the increase of Joule heating. The average entropy decreases with the increase of decay length for diffuse PEL. References [1] M. Matin, H. Ohshima, Thermal transport characteristics of combined electroosmotic and pressure driven flow in soft nanofluidics, Journal of colloid and interface science 476 (2016) 167–176. [2] L. Zhao, L. Liu, Entropy generation analysis of electro-osmotic flow in open-end and closed-end micro-channels, International Journal of Thermal Sciences 49 (2) (2010) 418–427.

Shock Waves Produced by the Interaction of Dynamic Crack with Heterogeneities

Fabian Barras^{*}, Philippe H. Geubelle^{**}, Jean-François Molinari^{***}

^{*}École Polytechnique Fédérale de Lausanne, ^{**}University of Illinois at Urbana-Champaign, ^{***}École Polytechnique Fédérale de Lausanne

ABSTRACT

Recent experiments reveal how dynamic fracture is characterized by the interplay of the crack front with microscopic material heterogeneities (see for example [1]). Heterogeneous dynamic fracture remains a current challenge both for numerical modeling and experiments because of the associated fine time and length scales. In this work, we rely on a spectral boundary integral formulation of the elastodynamic wave equations derived in [2]. The numerical discretization focuses only along the rupture plane bounding two semi-infinite solids and allows a very fine description of the fracture process which is modeled following a cohesive approach. This work study the perturbation of dynamic crack front in presence of tougher inclusions along the rupture plane. We show numerically how shock waves are radiated from cusp emerging after large distortion of the crack front. We detail how these short-lived bursts persist far from the heterogeneity location and impact the overall rupture dynamics. Since any material presents heterogeneities at a certain scale, we further investigate how the heterogeneous interface properties (heterogeneity size, toughness contrast, crack speed) control the transition from quasi-homogeneous to heterogeneous dynamics. We finally measure the size of the fracture process zone and discuss the role of this critical length scale for heterogeneous dynamic fracture. REFERENCES [1] Guerra, C. and Scheibert, J. and Bonamy, D. and Dalmas, D. Understanding fast macroscale fracture from microcrack post mortem patterns. Proceedings of the National Academy of Sciences, Vol. 109, 390–394, 2012. [2] M. S. Breitenfeld and P. H. Geubelle. Numerical analysis of dynamic debonding under 2D in-plane and 3D loading. International Journal of Fracture, Vol. 93, 13–38, 1998. [3] F. Barras, P. H. Geubelle and J.-F. Molinari. Interplay between Process Zone and Material Heterogeneities for Dynamic Cracks. Physical Review Letters, Vol. 119, 2017.

Level-Set XFEM Sensitivity Analysis and Topology Optimization of Elastomeric Gels

Jorge Luis Barrera Cruz*, Kurt Maute**

*University of Colorado, Boulder, **University of Colorado, Boulder

ABSTRACT

Research on soft, active materials has flourished in recent years driven by a broad range of applications including actuation systems, tissue engineering, and soft robotics. These applications benefit from unique material properties such as large deformations, wide range of stimulants, and high motion complexities. Elastomeric gels are among the dominant members of this group of materials. The computational design of components/devices using these materials require not only mathematical models that accurately predict their response, but also robust optimization methods capable of handling model intricacies. This paper introduces a topology optimization approach for finding the spatial arrangement of stimuli-responsive elastomeric gels that swell upon contact with water, namely, hydrogels. The optimization approach combines a level set method for describing the material layout and a generalized version of the extended finite element method (XFEM) for predicting the response. This combination of methods yields optimization results that can be directly printed without the need for additional post-processing techniques. The highly nonlinear chemo-mechanical transient behavior of hydrogels is described by partial differential equations that advance in time through an internal state variable that represents the swelling state of the gel. A formulation for the computation of the sensitivities using the adjoint method for transient models captures the internal state variable dependencies. Computational aspects of the implementation of this approach into the level-set XFEM framework are discussed. The effect of the internal state variable on the sensitivities of problems subjected to various objectives is examined with numerical examples. Furthermore, the ability of the proposed optimization method to yield a highly resolved description of the optimized material layout is demonstrated by design studies in which initial simple configurations transform into target shapes. As the complexity of the target shape increases, the optimal spatial arrangement of the material phases becomes less intuitive, highlighting the advantages of the proposed optimization method.

Uncertainty Quantification of a Damage and Fatigue Phase Field Model

Eduardo Augusto Barros de Moraes*, Mohsen Zayernouri**, Mark Meerschaert***

*Michigan State University, **Michigan State University, ***Michigan State University

ABSTRACT

In this talk we present the uncertainty quantification of the structural damage and fatigue phase field model presented in [1]. In the non-isothermal, thermodynamically consistent model, the damage phase field is a continuous dynamical variable, and fatigue is treated as a continuous internal variable. The underlying assumptions and hypotheses involved in the modeling process may lead to gaps in the physical intuition, and uncertainties in the results from the choice of parameter values. In order to develop better models that can accurately predict failure in materials, we need to understand and identify the sources of uncertainty presented in current models. In this analysis, we consider an isothermal isotropic linear elastic material with viscous dissipation under the hypothesis of small deformations. We use the Monte Carlo and the Probabilistic Colocation methods to evaluate the expectation of the quantities of interest and measure the uncertainty with respect to the variation of several parameters. [1] JL Boldrini, EA Barros de Moraes, LR Chiarelli, FG Fumes, and ML Bittencourt. A non-isothermal thermodynamically consistent phase field framework for structural damage and fatigue. *Computer Methods and Applied Mechanics and Engineering*, 312:395-427, 2016.

A Two-scale Homogenization Approach for Fluid Saturated Porous Media Based on TPM and FE²-Method

Florian Bartel^{*}, Tim Ricken^{**}, Jörg Schröder^{***}, Joachim Bluhm^{****}

^{*}TU Dortmund University, ^{**}Stuttgart University, ^{***}Duisburg -Essen University, ^{****}Duisburg -Essen University

ABSTRACT

Thinking about the description of porous materials, e.g. metal foam, human tissue, plants or soils, we always have to take into account a global design composed of various substructures with different characteristics on a lower level. Examples of such substructures are pores which can be saturated with fluids or gases, fibers with different orientations or cells which can be influenced by chemical reactions. For the theoretical description of the behavior, enhanced continuum mechanical models give promising approaches. Up to now, due to the high complexity, it has not been possible to simulate these systems with only one design model. Hence, it is necessary to think about techniques which simplify the model but still consider the essential characteristics. It is clear, future applications will consider the discrete microstructure of materials. For example the topology can be received by CT-scanning and therefrom Representative Volume Elements (RVEs) can be designed. Therefore, we are preparing the Theory of Porous Media (TPM), see [1], for the usage in combination with the FE²-Method, cf. [2] and [3]. This contribution will present a two-scale homogenization approach for fluid saturated porous media with a reduced two-phase material model, which covers the behavior of large poro-elastic deformation. The main aspects of theoretical derivation for the weak form, the lower level boundary conditions under consideration of the Hill-Mandel homogeneity condition and the averaged macroscopic tangent moduli will be pointed out and a numerical example will be shown. Still, solving a coupled problem in FE² environment is extremely time consuming. Therefore, a parallel solution strategy is absolutely essential. Remarks on the investigation of High Performance Computation in this context will be given. Besides, model order reduction techniques lead to an impressive improvement of runtime. Hereby one has to accept approximation inaccuracy, however errors are small for engineering problems. Hence, we investigate in modified Proper Orthogonal Decomposition (POD) methods. Conceptual ideas will be discussed. References [1] R. de Boer and W. Ehlers, Theorie der Mehrkomponentenkontinua mit Anwendung auf bodenmechanische Probleme, Technical report, Teil I, Forschungsberichte aus dem Fachbereich Bauwesen, Heft 40, Universität GH-Essen, 1986. [2] C. Miehe, Computational micro-to-macro transitions for discretised micro-structures of heterogeneous materials at finite strains based on the minimization of averaged incremental energy, Computer Methods in Applied Mechanics and Engineering, 2002. [3] J. Schröder, A numerical two-scale homogenization scheme: the FE²-method, in J. Schröder, K. Hackl (editors), CISM course 550, Plasticity and Beyond, Springer, 1-64, 2014.

Gaussian Quadrature for C1 Cubic Clough-Tocher Macro-triangles

Michael Barton^{*}, Jiri Kosinka^{**}

^{*}BCAM - Basque Center for Applied Mathematics, ^{**}University of Groningen

ABSTRACT

A numerical integration rule for multivariate cubic polynomials over n -dimensional simplices was designed by Hammer and Stroud [12]. The quadrature rule requires $n + 2$ quadrature points: the barycentre of the simplex and $n + 1$ points that lie on the connecting lines between the barycentre and the vertices of the simplex. In the planar case, this particular rule belongs to a two-parameter family of quadrature rules that admit exact integration of bivariate polynomials of total degree three over triangles. We prove that this rule is exact for a larger space, namely the C1 cubic Clough-Tocher spline space over macro-triangles if and only if the split-point is the barycentre. P. C. Hammer and A. H. Stroud. Numerical integration over simplexes. Mathematical tables and other aids to computation, 10(55):137-139, 1956.

Modeling Microstructural Heterogeneity During Failure Using Coupled Porosity and Crystal Mechanics

Nathan Barton*, John Moore**

*Lawrence Livermore National Laboratory, **Lawrence Livermore National Laboratory

ABSTRACT

Porosity (i.e., microscale void fraction) is a mechanism of ductile failure that is of ongoing concern, with recent interest spurred by new additive manufactured materials where initial voids and defects occur during component fabrication. Voids are often modeled explicitly at the crystal scale or implicitly—based on homogenized porosity models—at the component scale. This work couples crystal mechanics with these homogenized porosity models to alleviating the need for mesh resolution of sub-scale voids in crystal-scale modeling. This approach allows for the study of void families of varying potency, size, and distribution and their interaction with heterogeneous microstructures. This work shows examples from both quasi-static and dynamic loading scenarios and explores the connections among porosity kinetics, microstructural realism, and materials strength. This work was performed under the auspices of the U.S. Department of Energy by Lawrence Livermore National Laboratory under Contract DE-AC52-07NA27344 (LLNL-ABS- 743444).

A Phase Field Microcracking Description Coupled with Viscoelastic Concrete Behavior

Benoit Bary^{*}, Thomas Helfer^{**}, Olivier Fandeur^{***}, Julien Yvonnet^{****}, Qi-Chang He^{*****},
Daicong Da^{*****}

^{*}CEA, Service d'Etude du Comportement des Radionucléides, France., ^{**}CEA, Service d'Etude et de Simulation du comportement des Combustibles, France., ^{***}CEA, Service d'Etudes Mécaniques et Thermiques, France.,
^{****}Université de Paris-Est Marne-La-Vallée, France., ^{*****}Université de Paris-Est Marne-La-Vallée, France.,
^{*****}Université de Paris-Est Marne-La-Vallée, France.

ABSTRACT

Concrete is an important constitutive material of nuclear power plants and waste storage structures whose main role is to ensure high level of performance regarding the required middle to long-term containment function. As such, creep and microcracking are known significant factors affecting the mechanical properties and the long term behavior of concrete, and may call into question the safety of nuclear facilities. The accurate modelling of these phenomena including their coupled effects have then to receive a special attention. We propose in this study to apply the relatively recent method making use of a phase field approach to reproduce the initiation and propagation of microcracking in concrete. This method rests on a diffuse description of the microcrack surfaces by one scalar variable whose values result from a specific balance equation. As a main contribution, it is extended here and coupled to a linear viscoelastic behavior to mimic the creep (and possibly shrinkage) of the material. A classical generalized Maxwell model is retained for modelling this viscoelastic behavior. At first, an energy-based formulation is developed to express the equations governing both viscoelastic mechanical and phase field problems. In this first attempt, only cracking due to extensions is considered. Different simple fracture criteria based on positive stresses or strains with and without threshold are applied and tested. The resulting approach is next implemented in the FE code Cast3M so as to solve both systems of equations. Applications to a homogeneous material subject to loading with various durations and intensity are then analyzed and discussed with regard to the different crack driving state functions. In a second stage, 3D simulations of heterogeneous concrete samples made up of elastic aggregates dispersed in a mortar matrix concentrating the viscoelastic behavior are performed. These numerical specimens are generated with polyhedral aggregates having various size and shapes, and which are randomly distributed in a box. The effects of the aggregate shape on the microcracking development and the macroscopic behavior of samples subject to creep loading are investigated. To this aim, different specimens are created with elongated and flattened polyhedral aggregates with given aspect ratio, and the obtained results are analyzed and confronted in particular in terms of microcrack patterns.

Multivariant Martensitic Transformations at Finite Strains and with Interfacial Stresses, and Interaction between Inclusion and Martensitic Transformations: A Phase Field Study

Anup Basak*, Valery Levitas**

*Iowa State University, **Iowa State University

ABSTRACT

A thermodynamically consistent novel multiphase phase field approach for temperature- and stress-induced martensitic transformations with N variants is developed at finite strain and taking the interfacial stresses into account. The model considers $N+1$ order parameters, where one of them describes austenite <-> martensite transformations and the others describe the variant. The free energy of the system consists of the strain energy, thermal energy for austenite <-> martensite transformations, barrier energy for all possible transformations, penalization energy for derivation of the variant-variant transformation path from a straight line and also for coexistence of three or more phases at a single material point, and penalization for the interfacial energy. Considering that N order parameters related to the variants are constrained to a plane in the order parameter space, the coupled system of Ginzburg-Landau equations are derived, the thermodynamic equilibrium conditions for homogeneous phases are obtained, and the instability criteria for homogeneous phase transformations are established. The present model resolves all the shortcomings existing in the models available in the literature. Three kinematic models (KMs) for the transformation deformation gradient are assumed: in KM-I it is a linear combination of the Bain tensors for the variants; in KM-II it is exponential of the linear combination of the natural logarithm of the Bain tensors; in KM-III it is derived using the twinning equation from crystallographic theory. Based on this model a finite element code has been developed. Several problems yielding complex microstructures are studied: (i) Evolution of microstructures with two variants in a sample under biaxial strains, and also the effect of sample size. (ii) Twinning using the generalized plane strain method, and also the sample size effect. (iii) Microstructure in a two-variant system under nanoindentation. (iv) Microstructure evolution in samples with nontransforming inclusion, where the energy of the interface between the inclusion and the surrounding phases is consistently taken into account. The influence of the ratio between the widths of the inclusion-martensite interfaces, austenite-martensite interface, and variant-variant interfaces are studied. Reference A. Basak, V.I. Levitas, Interfacial stresses within boundary between martensitic variants: Analytical and numerical finite strain solutions for three phase field models, 139 (2017) Acta Materialia, 174-187

A Damage Mechanics Theory with No Curve Fitting: Unification of Newtonian Mechanics & Thermodynamics

Cemal Basaran*

*University at Buffalo

ABSTRACT

Abstract The field of classical mechanics is based on Sir Isaac Newton's work in "The Principia," published in 1687. In this work, Newton introduced the world to three universal laws of motion, which describe the relationships of any object, the forces acting upon it and the object's resulting motion. It is these three laws that make up the foundation for classical mechanics, and all subsequent theories of mechanics are derived from them. But Newtonian mechanics still cannot account for the past, present or future of any aspect of a physical body or its governing equations. Around 1850, Rudolf Clausius and William Thomson (Kelvin) formulated both the First and Second Laws of Thermodynamics. Because the field of thermodynamics governs the past, present and future of all physical bodies, the aging process and life span of any physical body can be modeled in accordance with the thermodynamics laws. Still, thermodynamics alone cannot convey the response of a physical body under an external force at any given moment – something classical mechanics equations are able to achieve. Being able to accurately predict the life span of physical bodies, both living and non-living, has been one of humankind's eternal endeavors. Over the last 150 years, many unsuccessful attempts were made to unify the fields of classical mechanics and thermodynamics, in order to create a generalized and consistent theory of evolution of life-span of inorganic and organic systems. The objective has been to map out the aging process of a physical body using classical mechanics equilibrium equations while also predicting its life span. Most past attempts were based solely on the use of physical experiments, which would reveal the aging rate and life span of any physical body first. The experimental data is later be used to create a life-span expectancy model by curve fitting, like in the damage mechanics theory proposed by L. M. Kachanov. Authors, will report a new unified mechanics theory that can now predict the aging and life span of any physical body based purely on mathematical calculations and without the need for any prior life-span degradation testing or curve fitting phenomenological damage mechanics models.

A Computational Approach to Additive Manufacturability of Low and High Gamma Volume Fraction Nickel-Based Superalloys

Hector C. Basoalto^{*}, Chinnapat Panwisawas^{**}, Richard Turner^{***}, M. J. Anderson^{****}, B. Saunders^{*****}, J. W. Brooks^{*****}

^{*}University of Birmingham, ^{**}University of Birmingham, ^{***}University of Birmingham, ^{****}University of Birmingham, ^{*****}Rolls-Royce, PLC, ^{*****}University of Birmingham

ABSTRACT

The manufacture of engineering components for aerospace applications through the selective laser melting (SLM) process is challenging. High volume fraction nickel-based superalloys are prone to cracking during the SLM process or subsequently in hot isostatic pressing (HIP) of the SLM part. This paper presents a numerical study on the evolution of microvoid dispersions and precipitate distributions for two nickel-based superalloys representing a low (IN718) and high (CM247LC) volume fraction alloys. The proposed modelling framework explicitly takes into account chemical compositions and commercially representative powder size distributions for each alloy. Simulations of single layer depositions indicate that CM247LC has a higher propensity to form lack-of-fusion and melt-flow induced micro-voids than IN718. It is shown numerically that, for the conditions investigated and thermodynamic parameters used, these differences are largely governed by the powder size distribution and not by the thermophysical parameters of these alloys for the conditions investigated. Composition dependent properties are shown to influence the thermal gradients during solidification, with CM247LC predicted to cool at a faster rate than IN718. These differences are expected to influence the residual stress development during SLM. A coupled mean field/finite element approach has been used to predict the global precipitate evolution within a simple rectangular build as well as a subsequent HIP cycle. Unimodal and multimodal particle distributions are predicted for IN718 and CM247LC at the end of SLM, respectively. A higher volume fraction of is predicted for CM247LC at the end of the SLM process. During HIP, simulations indicate a dramatic increase in the volume fraction in CM247LC, which can result in a reduction in stress relaxation and consequently large tensile residual stress states.

Calving Glaciers and Ice Shelves: New Insight from Old Theories

Jeremy Bassis^{*}, Morgan Whitcomb^{**}, Lizz Ultee^{***}

^{*}University of Michigan, ^{**}University of Michigan, ^{***}University of Michigan

ABSTRACT

Projections of the growth and demise of ice sheets and glaciers require physical models of the processes governing flow and fracture of ice. The flow of glacier ice has been treated using increasingly sophisticated dynamical models. In contrast, fracture, the process ultimately responsible for half of the mass lost from ice sheets through iceberg calving, is often included using ad hoc parameterizations. Here we seek bridge this gap by introducing a model where ice obeys a power-law rheology appropriate for intact ice only up to a yield strength. Above the yield strength, we introduce a separate, weaker rheology that represents quasi-brittle failure along pre-existing faults and fractures—similar to Nye's unfortunately abandoned plastic approximation of glacier ice. Assuming glacier ice is unyielded allows us to bound the long term average rate of terminus advance of grounded glaciers, providing a first principles estimate of rates of retreat associated with the so-called marine ice cliff instability. Application of the model to idealized ice shelves, in contrast, shows that in the absence of strong ocean forcing, the yield strength is exceeded along the shear margins of ice shelves. If we allow the yield strength to decrease with increasing plastic strain of yielded ice, then rifts localize along the margins, in a pattern remarkably similar observations. These rifts decrease the coupling with the margin decreasing the buttressing capacity of the ice shelves, but also can extend across portions of the ice shelf, becoming the detachment boundary of ice bergs. Our approach to simulating failure of glacier ice provides a promising method of simulating the large-scale failure of glaciers and ice shelves that includes not only marine-ice-cliff instability failure, but also rifting and failure of ice shelves yet is computationally tractable enough to be included in continental ice sheet models.

STABILITY MODELING UNCERTAINTY WHEN DRILLING VERTICAL AND INCLINED WELLBORES THROUGH HETEROGENEOUS FIELD

NATHALIA A. BATALHA¹, OMAR Y. DURÁN¹, PHILIPPE R. B. DEVLOO¹,
LUIZ C. M. VIEIRA JR.¹

¹University of Campinas Av. Albert Einstein,
951 Campinas, SP – BR, 13083-852
nathalia_batalha@hotmail.com,
omaryesiduran@gmail.com,
phil@fec.unicamp.br, vieira@fec.unicamp.br.

Key words: Vertical and Inclined Wellbore, Wellbore Stability, Stochastic Field, Numerical Modeling.

Abstract. A stochastic two-dimensional geomechanical model developed by the authors and presented herein is used to predict wellbore stability in heterogeneous formations. It consists of a finite element model and assumes linear elastic and isotropic material behavior under plane strain state. The model simulates the stress state around vertical and inclined wellbores when a formation is submitted to internal drilling fluid pressure. This new state of stress may lead to rock failure, which is analyzed through a failure criteria. Since the exact variation of formation mechanical properties is not known, a spatially correlated field is used to evaluate the variability of the rock material properties. In the present model, the random variable is the formation elastic modulus. The correlation between each pair of finite elements is determined by a covariance function. A two-dimensional spatially correlated field is used to verify the correlation between the elements of a vertical wellbore. A different approach, however, is necessary to model inclined wellbores. Once the direction and inclination of a wellbore are defined, a three-dimensional spatially correlated field becomes necessary to best simulate the formation field. Simulations using the stochastic model proposed herein and considering constant elastic modulus have been compared. It is observed that when considering a constant elastic modulus, the area of the plastic zone is symmetric at the borehole wall; when using the stochastic model, however, the plastic zone area surrounding the well is not symmetric. Stochastic simulations have been carried out with different heterogeneous fields for vertical and inclined wells, and distributions of the plastic zone areas were obtained for each case. Based on the stochastic field probabilistic analysis, a distribution function is presented, which aims to best assist a decision making process to determine if a mud pressure is operationally acceptable or not.

1 INTRODUCTION

Numerical models have been developed to simulate the stress state around wellbores, in order to predict the formation behavior in drilling operations. Those models intend to define the best drilling fluid density (or mud weight) to be used. The mud weight must be designed to keep the well stable and not cause rock failure. Most models, however, assume that the mechanical properties of the rocks are constant in all the simulated domain. In fact, it is known that the formation elastic properties are not the same in all drilled layer. Thus, a heterogeneous field must be considered to obtain a more realistic analysis. Since the variation of rock mechanics is not known due to challenging wellbore locations and sample procedures, a randomic but correlated field can be assumed in order to carry out a probabilistic analysis.

The present work aims to introduce a geomechanical modeling coupled to a geostatistics model to predict heterogeneous formation behavior in drilling operations. The geomechanical model assumes linear elastic and isotropic rock material behavior with plane strain condition. An yield criterion was selected to identify the formation's failure area/plastic region around borehole wall. The geostatistics analysis was developed based on a stochastic field model. The stochastic field is based on a covariance function, which specifies the correlation between the mechanical characteristics of neighboring elements of a domain.

This stochastic analysis approach enables a more realistic evaluation of the wellbore failure. A mud weight believed to be safe, may not be indicated to a well once a stochastic analysis is carried out. The geostatistical model can help on decision-making over these issues. The model can be used for vertical, horizontal and inclined wellbores.

2 ROCK AND DRILLING FLUID: A MECHANICAL INTERACTION

A stable and well designed wellbore guarantees operation safety and prevents several issues such as stuck pipe, cavity enlargement, formation fracturing, time loss and substantial expenditures. The stability of a well depends on: the equilibrium of the rock stresses (in-situ stresses), its material properties, and the drilling fluid's density or also called, mud weight.

In-situ stresses are natural developed during a rock formation and they are a consequence of gravity interactions, tectonic process, and others. These stresses are composed by the overburden pressure σ_{ov} , defined by the weight of all rock layers over a rock element. In a response to the overburden stress (or vertical stress $\sigma_{ov} = \sigma_V$), there are the horizontal stresses, which avoid the lateral deformation induced by vertical loading. In-situ stresses are subjected to the static equilibrium equation:

$$\text{div}(\boldsymbol{\sigma}) + \mathbf{b} = 0 \quad (1)$$

The drilling process, however, changes the state of stress around the borehole wall. The drilling fluid is used in the drilling operation to avoid the borehole closure and fill the open space once occupied by the rock. The drilling fluid temporarily supports the borehole wall while drilling. The drilling fluid's density must be high enough to prevent kicks (pore pressure - PP) and wellbore

closure, but low enough to prevent hydraulic fracture, formation failure and circulation loss, [6]. Thus, the mud weight (or drilling fluid density) is responsible for keeping the wellbore walls stable.

The formation around the borehole wall experiences deformation due to the relief of stresses, once the rock is removed, and then, replaced by the drilling fluid. It is possible that the stress state change is significant, which leads to operational problems. In order to minimize these risks, geomechanical models have been used in the project and development stage of wells. Understanding the new stress state of vertical, inclined and horizontal wellbores is essential to ensure a safe operation. The stress state simulation allows the definition of the optimal drilling fluid density to be used in a certain formation.

3 METHODOLOGY

A geomechanical model was developed in order to simulate the formation behavior when mud pressure is applied to the borehole wall. The numerical model presented herein was developed using finite element method (FEM), and assumes linear elastic and isotropic material behavior under plane-strain state. The method was implemented in NeoPZ, which is an open-source library for the development of finite element simulations, [2]. A yield criterion was selected to describe the formation's plastic region at the borehole wall. The geostatistics analysis was developed based on a stochastic field model. The methodology used to implement this model is presented in this section.

3.1 The geomechanical model

Once the wellbore length is very long (kilometers long sometimes) compared to the selected domain x and y , it is assumed a plane-strain state model, considering null displacement in the z direction. The simulation is, therefore, two-dimensional, which significantly reduces computational time. As depicted in Figure 1, the finite element mesh is selected as a cross section of the wellbore. The hole cavity is the central circumference and the remaining area, refers to the original formation being drilled.

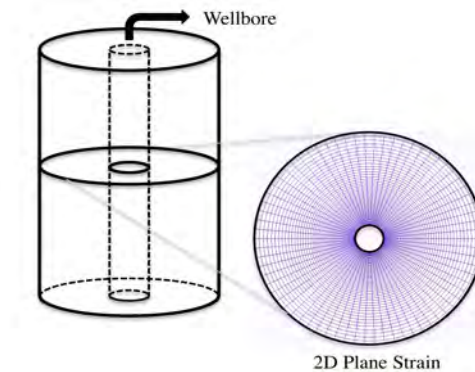


Figure 1: Two-dimensional mesh surrounding the wellbore

The FEM algorithm starts at finding the displacement $\mathbf{u}(x, y)$ from the equilibrium equation,

$$\begin{cases} \operatorname{div}(\boldsymbol{\sigma}) + \mathbf{b} = 0 \\ \mathbf{u} = \mathbf{u}_D \text{ on } \delta\Omega_D \\ \boldsymbol{\sigma} \cdot \mathbf{n} = g \text{ on } \delta\Omega_N \end{cases} \quad (2)$$

Where,

- $\boldsymbol{\sigma}$ is the stress tensor;
- \mathbf{b} is the body force vector;
- \mathbf{u} is the displacement vector;
- u_D and g are known functions;
- $\boldsymbol{\sigma} \cdot \mathbf{n}$ is the normal flux on the boundary $\delta\Omega_N$;
- Ω is the domain;
- $\delta\Omega_D$ and $\delta\Omega_N$ are the boundary conditions, Dirichlet and Neumann respectively.

The space of testing functions is defined by:

$$V(\Omega) = \{\mathbf{v} \in H^1(\Omega); \mathbf{v} = 0 \text{ on } \delta\Omega_D\} \quad (3)$$

Where,

$$H^1(\Omega) = \{\mathbf{v} \in \mathbf{L}^2(\Omega); \nabla \mathbf{v} \in \mathbf{L}^2(\Omega)\} \quad (4)$$

By multiplying the equilibrium equation by the testing function \mathbf{v} , integrating over the domain Ω , and using the divergence theorem, we have that:

$$-\int_{\Omega} \nabla \mathbf{v} \cdot \boldsymbol{\sigma} d\Omega + \int_{\delta\Omega} \mathbf{v} \cdot \boldsymbol{\sigma} \cdot \mathbf{n} ds + \int_{\Omega} \mathbf{v} \cdot \mathbf{b} d\Omega = 0 \quad (5)$$

Assuming that between the elements,

$$\int_{\Gamma} \llbracket \mathbf{v} \cdot \boldsymbol{\sigma} \cdot \mathbf{n} \rrbracket \approx 0 \quad (6)$$

and applying,

$$\boldsymbol{\sigma} \cdot \mathbf{n} = g \text{ on } \delta\Omega_N \quad (7)$$

$$\mathbf{v} = 0 \text{ on } \delta\Omega_D \quad (8)$$

The forming function can be stated as:

$$a(\mathbf{u}, \mathbf{v}) = f(\mathbf{v}) \quad \forall \mathbf{v} \in V(\Omega) \quad (9)$$

Given that:

$$a(\mathbf{u}, \mathbf{v}) = \sum_{\Omega} \int \nabla \mathbf{v} \cdot \boldsymbol{\sigma} d\Omega \quad (10)$$

$$f(\mathbf{v}) = \sum_{\Omega} \int \mathbf{v} \cdot \mathbf{b} d\Omega + \int_{\delta\Omega_N} \mathbf{v} \cdot \mathbf{g} ds \quad (11)$$

And by the stress-strain relation for linear elastic condition, we find the stress tensor

$$\boldsymbol{\sigma} = \mathbf{C} \boldsymbol{\varepsilon} + \boldsymbol{\sigma}_0 \quad (12)$$

With \mathbf{C} being the elastic constant matrix, $\boldsymbol{\sigma}_0$ the initial stress tensor and $\boldsymbol{\varepsilon}$ the strain tensor as follows:

$$\boldsymbol{\varepsilon}(x,y) = \begin{pmatrix} \frac{\partial u_x}{\partial x} & \frac{1}{2} \left(\frac{\partial u_y}{\partial x} + \frac{\partial u_x}{\partial y} \right) \\ \frac{1}{2} \left(\frac{\partial u_x}{\partial y} + \frac{\partial u_y}{\partial x} \right) & \frac{\partial u_y}{\partial y} \end{pmatrix} \quad (13)$$

DiMaggio-Sandler yield criterion was selected and implemented in the geomechanical model in order to describe the failure area/plastic region surrounding the wellbore. This failure criteria was chosen once it well describes the constitutive behavior of rocks, [1]. The failure criteria yield function Φ is composed of two functions. In the present analysis, however, only the failure surface envelope function is considered. Therefore, the envelope which limits the elastic deformation under confinement is disregarded. Failure occurs when $\Phi > 0$.

3.2 Spatially correlated field for heterogeneous formation

Heterogeneous rock mechanics properties may significantly influence the formation behavior, and as a consequence, also influence the mud weight to be used in the operation. A probabilistic evaluation of a given field allow a more realistic analysis of the rock stress state, and help, with better accuracy, selecting the best density for the drilling fluid. The pore pressure and fracture gradients are very narrow and a small change can affect wellbore stability. Therefore, this stochastic field modeling represents an important issue to be addressed in wellbore stability analysis.

Since the model is a plane model, the simulation is set for a specific layer or rock formation. In other words, it assumes one average mechanical property for the whole field. Therefore, the stochastic model is built with one layer at a time.

The finite elements mesh is built using a geometric progression, which leads to a greater mesh refinement close to the wellbore wall, where the greatest change in stress state is found. The stochastic grid follows the same geometry as the finite element mesh. Thus, each element receives a random but correlated value of Young's modulus. Following the geometric progression, there is more variation closer to the wellbore wall and less changes over the remaining domain. Nevertheless, it is also possible to not use the geometric progression and then the elements would be equally distributed and the Young's modulus would also be uniformly defined in the mesh.

A spatially correlated field is used to evaluate the variability of the formation material properties. The correlation between each pair of elements is defined by a covariance function. In this model, the random variable is the formation elastic modulus (Young's modulus). The Squared Exponential

covariance function was chosen for this model. The covariance function, also known as kernel, is as follows:

$$k = \exp^{-\gamma r^2} \quad (14)$$

The selected kernel allows the user to control the distance for which the correlation between the elastic modulus of two elements is not relevant. The control is set by the constant γ , which is associated to the spatial frequency in the field, [4]. Therefore, the scale γ defines the smoothness of the stochastic field.

The covariation function also depends on the distance between the elements centroids, defined by r . A matrix $R_{m,m}$ holds all distances between each pair of elements, calculated by their elements centroids coordinates (X) :

$$R_{ij} = \begin{pmatrix} \sqrt{(X_1 - X_1)^2} & \sqrt{(X_1 - X_2)^2} & \cdots & \sqrt{(X_1 - X_m)^2} \\ \sqrt{(X_2 - X_1)^2} & \sqrt{(X_2 - X_2)^2} & \cdots & \sqrt{(X_2 - X_m)^2} \\ \vdots & \vdots & \ddots & \vdots \\ \sqrt{(X_m - X_1)^2} & \sqrt{(X_m - X_2)^2} & \cdots & \sqrt{(X_m - X_m)^2} \end{pmatrix} \quad (15)$$

The correlation matrix $K_{m,m}$, holds the correlation between all pair of elements, and it is a function of the matrix R and the scale γ :

$$K(\gamma, R)_{ij} = \begin{pmatrix} k_{1,1} & k_{1,2} & \cdots & k_{1,m} \\ k_{2,1} & k_{2,2} & \cdots & k_{2,m} \\ \cdots & \cdots & \ddots & \vdots \\ k_{m,1} & k_{m,2} & \cdots & k_{m,m} \end{pmatrix} \quad (16)$$

Matrix K is then decomposed by the singular value decomposition method, such that $K = USV^T$. The product of the left singular vector U and the square root of the diagonal matrix S , multiplies a Gaussian random and uncorrelated vector \mathbf{d}_{rand} , generating a correlated vector \mathbf{d}_{corr} .

The random but correlated vector \mathbf{d}_{corr} is then scaled multiplying it by a standard deviation (std_E) and summed to an average Young's Modulus (E_{avg}).

$$E_{\text{StochasticField}} = \mathbf{d}_{\text{corr}} * std_E + E_{\text{avg}} \quad (17)$$

$E_{\text{StochasticField}}$ refers to a stochastic but correlated field of Young's modulus. The variable std_E is the standard deviation of the Young's modulus, and E_{avg} is the Young's modulus, both given as input.

3.3 A 3D spatially correlated field for inclined wellbores

A new approach must be considered for inclined wellbores. Inclined wellbores are obtained from drilling in a given direction and inclination angle. Inclination angle is the angle between the

wellbore axis tangent and the local gravitational vector. Therefore, a vertical wellbore has inclination angle of 0 degrees and a horizontal wellbore has inclination angle of 90 degrees. Direction angle consists of the angle between the horizontal wellbore projection and the true geographic north. This angle is commonly referred as “wellbore azimuth”. It varies from 0 degrees to 360 degrees, and is measured in the clockwise direction starting at the geographic north, [5].

Fjar et al (2008) [3] presented in his work that a transformation of the in-situ stresses to the local stress tensor of a inclined wellbore can be obtained from a rotation between the z and y axes. This operation can be represented in matrix notation as follows:

$$[\sigma^o] = [Q][\sigma_{InSitu}][Q]^T \quad (18)$$

Where,

$$Q = \begin{pmatrix} \cos[\alpha]\cos[\beta] & \sin[\alpha]\cos[\beta] & -\sin[\beta] \\ -\sin[\alpha] & \cos[\alpha] & 0 \\ \cos[\alpha]\sin[\beta] & \sin[\alpha]\sin[\beta] & \cos[\beta] \end{pmatrix} \quad \text{and,} \quad \sigma_{InSitu} = \begin{pmatrix} \sigma_H & 0 & 0 \\ 0 & \sigma_h & 0 \\ 0 & 0 & \sigma_V \end{pmatrix}$$

σ_{InSitu} : In-situ stresses

α : wellbore direction/azimuth

β : wellbore inclination

Q : rotation matrix, composed by the rotation between the z and y axis.

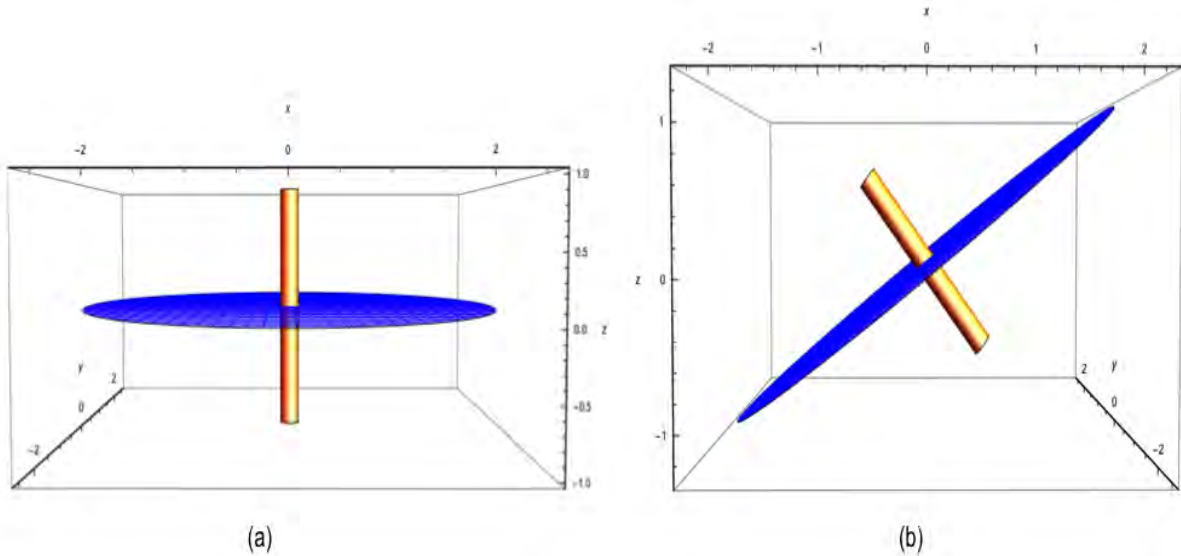


Figure 2: a) Vertical wellbore mesh (b) Inclined wellbore mesh

A two-dimensional correlated field is considered for vertical wellbores since the mesh is perpendicular to the well. Inclined wellbores' mesh is also perpendicular to the well orientation, but

embedded in the layer that the geomechanical model is being analyzed. Figure 2 illustrates the difference between the two cases.

The geomechanical model also assumes a two-dimensional approach for inclined wellbores. The simplification is possible due to the local stress tensor transformation previously described. For the stochastic analysis, however, the mesh is inclined compared to the horizontal formation layer; according to the wellbore inclination and direction. In order to evaluate the heterogeneous field of a drilled layer and determine the correlation between elements, a three-dimensional correlated field was developed.

The three-dimensional approach follows five steps: (1) definition of the height and radius of a cylindrical layer, (2) selection of two-dimensional mesh as if it had been in the vertical model, (3) selection of number of cross sections inside the cylindrical layer using the same two-dimensional mesh, (4) rotation of an extra two-dimensional mesh inside the cylindrical layer following the wellbore direction and inclination, and (5) definition of the coordinates of all elements centroids. All the steps can be seen in Figure 3. All meshes are discretized in the same way, as well as the inclined mesh.

The correlation matrix $K_{m,m}$ is therefore, calculated for all pair of elements centroids. The stochastic field over the inclined mesh (in red) is correlated with inclined neighboring elements, which allows the use of the two-dimensional geomechanical model. The methodology described herein to create three-dimensional correlated layers, allows the user to expeditiously generate drilling fields.

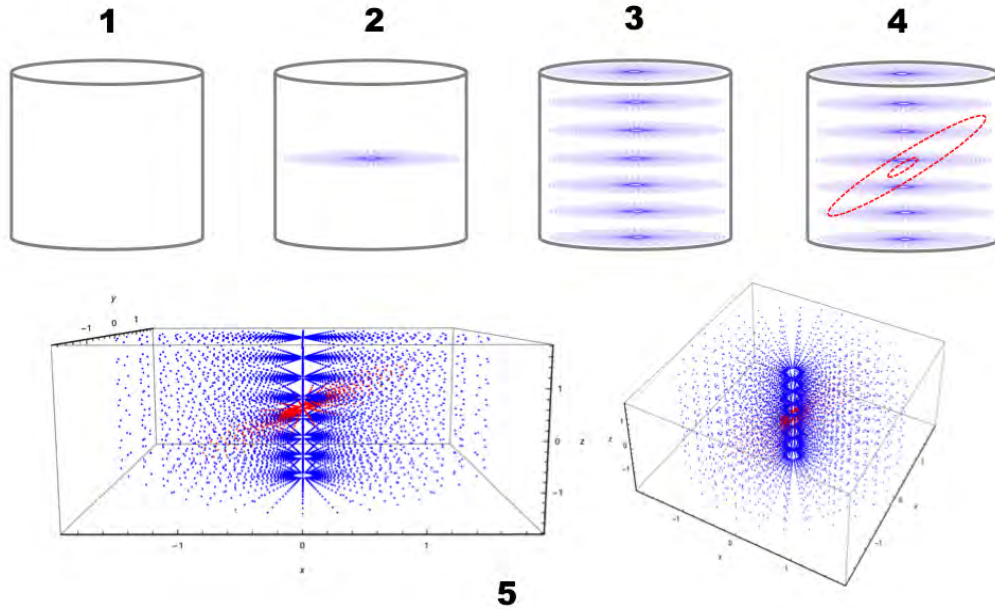


Figure 3: Five steps of the 3D spatially correlated field methodology

4 RESULTS AND DISCUSSIONS

This section presents the results of a case study carried out using the numerical model and analysis method proposed herein. The wellbore in question was a carbonatic rock, and it was already known that the selected drilling fluid pressure would induce a plastic zone at the wellbore wall. The wellbore parameters were reported in [1] as well as, the material parameters for the yield criterion. The input values used in the simulations are summarized in Table 1; the same values were used in vertical and inclined wellbores. The carbonatic material parameters for DiMaggio-Sandler criterion are A : 152.52; B : 0.0015489, and C : 146.29.

Wellbore Radius	0.10795	Meters
External Radius	3	Meters
Young's Modulus	29269	MPa
Poisson's ratio	0.203	-
Wellbore Pressure (Pw)	19.5	MPa
Vertical In-situ Stress (σ_V)	-48.2	MPa
Minor Horizontal Stress (σ_h)	-45.9	MPa
Major Horizontal Stress (σ_H)	-62.1	MPa
$\mathbf{b}(x, y)$	0	Body forces neglected

Table 1: Geomechanical model input data

4.1 Vertical wellbore homogeneous and heterogeneous field

Heterogeneous field cases were compared to a homogeneous field simulation. All models assumed the same input parameters, except for Young's modulus. Note that an homogeneous field simulation - single value of Young's modulus for the entire dominion - is common practice by petroleum engineers. The same Young's modulus value used in the homogeneous case became the mean of the stochastic field. The standard deviation considered in this study was based on a coefficient of variation of 10%. Figure 4 depicts for a homogeneous field model and for a single model of heterogeneous field simulation: Young's modulus fields, plastic zone at the borehole wall (where $F_1 = \Phi$) based on the yield criterion, and the plastic region areas plot.

The total area of the plastic zone for the homogeneous field was $13.9cm^2$, and $12cm^2$ for the heterogeneous field example case depicted in Figure 4. It can be noted that the plastic region around the wellbore for a homogeneous field was symmetric. For the heterogeneous case, however, the plastic zone surrounding the wellbore was not symmetric, presenting 56% of the total area on the top side and 44% of the total plastic zone area on the down side in Figure 4. The scale factor used in this heterogeneous case analysis was $\gamma = 4.318$, which is forty times the wellbore radius.

This asymmetry commented above may lead to operational problems while drilling. Thus, a drilling fluid density believed to be safe considering a homogeneous formation, may present higher and asymmetric plastic zone in a heterogeneous analysis. Note that, the mud properties are designed to stabilize the most vulnerable side of the well.

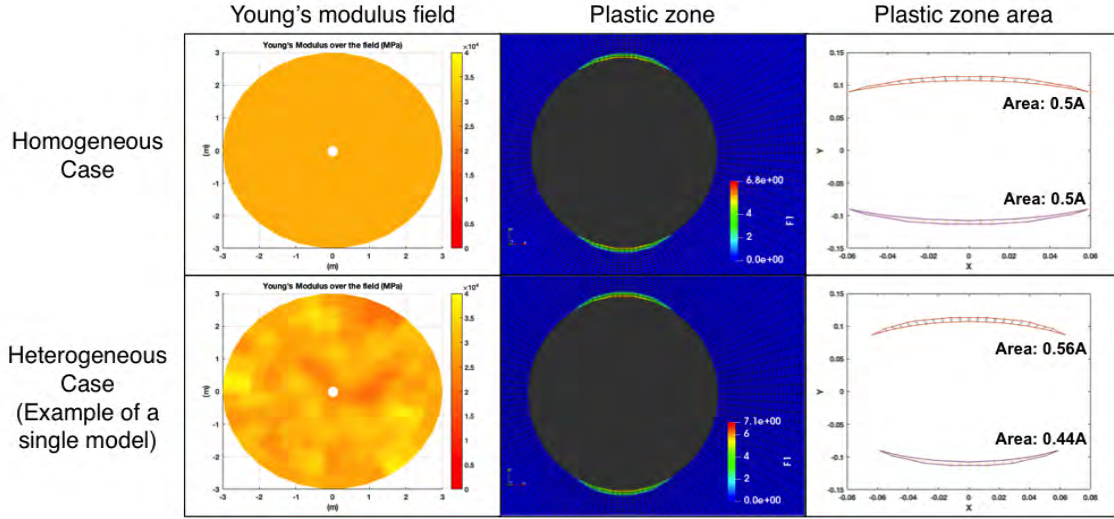


Figure 4: Plastic zone for the homogeneous and a heterogeneous case - Vertical wellbore

4.2 Inclined wellbore

An inclined wellbore analysis was carried out. The analysis assumed the same input parameters as the vertical analysis, but for this inclined study the three-dimensional stochastic field generation method was used. Therefore, a cylinder was built for the stochastic analysis. For the present case, the cylinder had eight equal cross sections and each section includes a two-dimensional and horizontal mesh, while the inclined mesh was embedded within the cylinder.

In order to reduce computational processing time, the mesh was changed to 2 meters of external radius. The number of elements and the wellbore radius were kept the same as in the vertical analysis. The space between each mesh in the cylinder was 0.5 meters and the cylinder's total height was 4 meters. The borehole had 45 degrees of inclination and azimuth/direction of 30 degrees. The scale factor used in the heterogeneous analysis for the inclined wellbore was also $\gamma = 4.318$. Similar to the vertical wellbore, the inclined wellbore heterogeneous analysis also presented asymmetric plastic regions.

4.3 Probabilistic analysis

Ten thousand simulations were carried out with different stochastic fields for vertical and inclined wellbores. The total plastic zone area distributions were obtained for both cases. Figure 5 depicts the simulations histograms. The vertical analysis presented standard deviation of $0.92cm^2$ and the total plastic region area ranged from $9.9cm^2$ to $17cm^2$ approximately. For the inclined case, the analysis presented standard deviation of $1.04cm^2$ and the total plastic region ranged from $0.57cm^2$ to $8.72cm^2$.

The mean and the total plastic zone area of the homogeneous cases are also depicted in the histograms. The histogram depicts that the total area of the plastic region for the inclined wellbore was significantly smaller than for the vertical case.

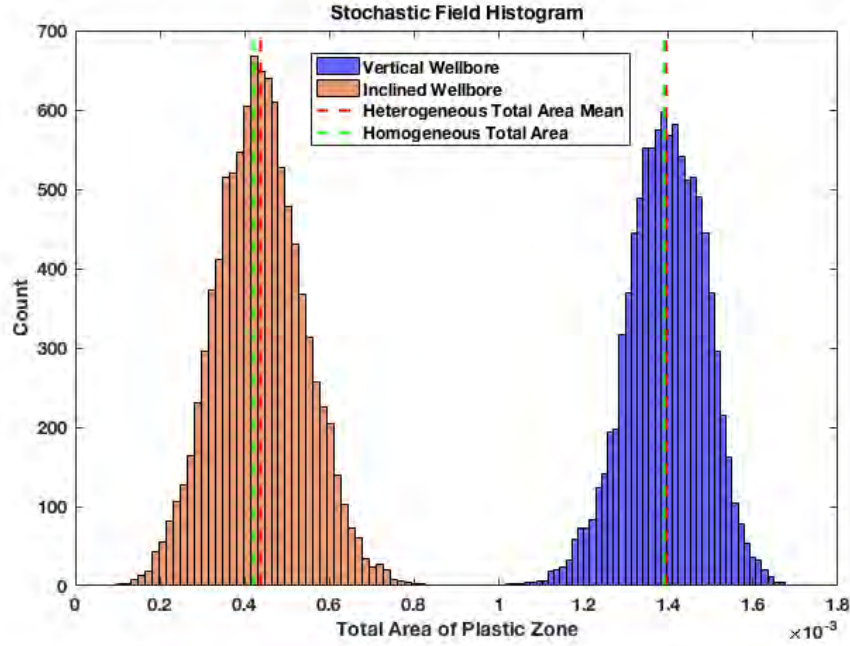


Figure 5: Stochastic Field histograms

The probabilistic analysis allows the user to verify the failure probability based on a maximum value of plastic zone area, using the simulated drilling fluid's density. If the maximum allowed area (A_y) of the plastic region at the borehole wall were a percentage of the well cavity area (A_w), the failure probability of reaching the maximum failure area could be verified by:

$$P_f = P(A_T > A_y) \quad (19)$$

Where, $A_y = p\%$ of A_w , and A_T is the total area of plastic region.

A_y	P_f - Vertical Wellbore	P_f - Inclined Wellbore
$0.1A_w$	1.8426e-134	9.4579e-210
$0.05A_w$	1.0743e-06	6.2867e-41
$0.03A_w$	0.9993	1.1642e-10
$0.01A_w$	0.9999	0.75141

Table 2: Failure Probability based on Monte-Carlo simulation of the plastic zone area

As an example, Table 2 presents the failure probability (P_f) of the vertical and inclined stochastic cases for 10%, 5%, 3%, and 1% of A_w . It was assumed normal distribution for both cases, and the probability density function was integrated from A_y to $+\infty$.

It can be noted that, for the present study, the mud pressure at the borehole wall may be safer for inclined wells than vertical wells.

5 CONCLUSIONS

A stochastic geomechanical model was developed to predict the formation behavior in drilling operations considering heterogeneous fields. The simulation method proposed herein predicted the total area of plastic region surrounding the wellbore once it is submitted to a mud/drilling fluid's pressure. The results showed that, when considering a heterogeneous field, a non-symmetric plastic region may occur. This lack of symmetry may lead to future operational problems.

A new procedure was proposed to evaluate stochastic fields of inclined wellbores; this procedure allows the modeling of thick formation layers based on two-dimensional geomechanical models.

The distributions of the total plastic zone areas determined in the stochastic analysis leads to an evaluation of the probabilistic failure and if it is still operationally accepted or not, using the considered mud pressure. The present model also allowed to assess the failure probability by setting a maximum acceptable plastic region area at the borehole wall. A mud pressure believed to be safe may not be indicated for the operation after a probabilistic analysis is carried out.

The present study intends to prevent operational issues while drilling and help on decision making process.

References

- [1] Diogo Lira Cecílio. *Modelagem Elastoplástica Aplicada à Simulação Numérica da Estabilidade de Poços de Petróleo*. PhD thesis, State University of Campinas, December 2014.
- [2] Philippe Remy Bernard Devloo. Pz: An object environment for scientific programming. *Comput. Methods Appl. Mech. Engrg.*, 150:133–153, 1997.
- [3] E. Fjar, R. M. Holt, A.M. Raaen, R. Risnes, and P. Horsrud. *Petroleum Related Rock Mechanics*. Number 978-0-444-50260-5. Elsevier, 2nd edition, 2008.
- [4] P. Graham Cranston; Mathew C.Richie; Luiz C.M. Vieira Jr. Effects of soil support on the stability of corrugated metal pipe. *Structural Stability Research Council*, March 2017.
- [5] L. A. S. Rocha, D. Aruaga, R. Andrade, J. L. B. Vieira, and O. L. A. Santos. *Perfuração Direcional*. Interciência, 2008.
- [6] Luiz Alberto Santos Rocha and Cecilia Toledo de Azevedo. *Projetos de Poços de Petróleo*. Interciência, 2nd edition, 2007.

An Isogeometric Approach to the Forward Problem of Optical Tomography: An Efficiency Comparison in Solving Radiative Transfer Equation

Vahid Bateni^{*}, Robert West^{**}

^{*}Virginia Tech, ^{**}Virginia Tech

ABSTRACT

Optical Tomography (OT) is a powerful imaging modality for medical diagnosis as well as biological tissue observations. OT is a sensitive and relatively inexpensive method of medical imaging which uses Near-Infra-Red (NIR) Light as the source, hence it is a non-invasive and non-ionizing modality compared with other x-ray based Computed Tomography (CT)-Scans. The NIR light is applied to the tissue and the output photon intensity is measure at the boundaries. OT Reconstruction is achieved through solution of an Inverse problem of object identification based on the measured photon intensity. The Inverse solution is usually performed in the form of an optimization scheme with iterative steps based on solving the forward scattering problem in the medium. The forward problem is solved in a number of methods, the most accurate of which is through numerical solution to the Radiative Transfer Equation (RTE). A simpler solution for RTE is performed through application of Diffusion Approximation (DA), and numerically solving the result, e.g. using Finite Elements Method (FEM). Recently we applied the Isogeometric Analysis (IGA) to solve this problem. However for many novel applications of OT encompassing small volumes, shallow depth or early photon scattering patterns (first few femtoseconds) the DA is not applicable. Hence more solutions are required. Previously Discontinuous Galerkin Finite Element Method (DG FEM) has been applied in parallel with the Discrete Ordinate Method (DOM) to solve the non-diffuse RTE. Also a "streamline diffusion modified Continuous Galerkin (CG) method" has also been suggested. Recently, a Blended Isogeometric Discontinuous Galerkin (BIDG) Method has also been introduced. In this paper, we apply the BIDG method in parallel with DOM to solve non-diffuse RTE. Initial results are generated and evaluated with previous methods.

CFD Simulation of Breathing in the Upper Airway of Patients with Obstructive Sleep Apnea Using Prescribed Motion from Cine MRI

Alister Bates^{*}, Andreas Schuh^{**}, Keith McConnell^{***}, Robert Fleck^{****}, Jason Woods^{*****},
Raouf Amin^{*****}, Charles Dumoulin^{*****}

^{*}Cincinnati Children's Hospital Medical Center, ^{**}Imperial College London, ^{***}Cincinnati Children's Hospital Medical Center, ^{****}Cincinnati Children's Hospital Medical Center, ^{*****}Cincinnati Children's Hospital Medical Center, ^{*****}Cincinnati Children's Hospital Medical Center, ^{*****}Cincinnati Children's Hospital Medical Center

ABSTRACT

Introduction Previous methods for computational fluid dynamics (CFD) simulation of airflow in the upper airways have been based either on static geometries, which do not account for changes in airway shape, or on fluid-structure interaction, which only predicts pressure-induced motion. Obstructive sleep apnea (OSA) is a condition where the upper airway collapses during breathing, causing the patient to wake, and long-term, leads to cardiovascular complications and, in pediatrics, developmental delay. CFD has the potential to provide regionalized diagnostic information about the causes of airway collapse and the effect this has on patients' breathing effort[1,2]. Therefore, a need exists for CFD to assess the causes of airway collapse in OSA, incorporating airway movement due internal air pressure or neuromuscular motion. **Methods** Magnetic resonance imaging (MRI) generated 3D images of the airway. This non-ionizing technique allows patients to be scanned for long periods covering many breaths, meaning breaths in which the airway collapses can be identified and analyzed. A static high-spatial-resolution scan (0.35×0.35×0.8mm) was segmented to create an accurate airway surface (ITK-snap 3.6.0). High-temporal-resolution cine-MRI then captured the airway motion through 3D images captured every 0.32s throughout breathing. Inlet breathing flowrates were captured synchronously with imaging via MRI-compatible spirometry. Airway motion was calculated from image and surface registration of the cine-MR images (MIRTK 1.1)[1]. This motion field was applied to the high-spatial-resolution airway surface, resulting in a moving airway wall throughout breathing. Large-eddy simulation CFD was performed in STAR-CCM+ 12.0.4 using the moving wall boundary condition and recorded breathing flowrates (CFD timestep=0.1ms). Meshing resulted in approximately 3 million polyhedral and prismatic cells. Control points on the airway surface moved following recorded airway motion, causing the interior mesh to morph. The work done by the airway wall on the internal flow (neuromuscular motion) and vice versa (pressure-driven motion) were calculated from the dot product of the pressure-force and airway-wall motion vectors. **Results** In a healthy volunteer and OSA patient, respectively, the airway anatomy did 25% and 37% more work on the internal airflow than the flow did on the wall. **Conclusions** In both a healthy volunteer and sedated pediatric sleep apnea patient, the majority of motion was not correlated with the pressure force on the airway wall, meaning most of the motion was neuromuscular, rather than pressure-driven and therefore fluid-structure-interaction modelling is not appropriate in OSA. **References** 1 Bates, A.J. et al. Clin. Biomech. (2017) 2 Bates, A.J. et al. J. Biomech. (2016)

Numerical Simulation of Spheres Immersed in Viscous One- and Two-fluid Flows

Laura Battaglia^{*}, Esteban A. Zamora Ramírez^{**}, Mario A. Storti^{***}, Marcela A. Cruchaga^{****},
Roberto Ortega Aguilera^{*****}

^{*}Centro de Investigación de Métodos Computacionales (CIMEC), UNL-CONICET, Predio CONICET Santa Fe "Dr. Alberto Cassano", Colectora Ruta Nac. Nro 168, Km 0, Paraje El Pozo, Santa Fe, Argentina, ^{**}Centro de Investigación de Métodos Computacionales (CIMEC), UNL-CONICET, Predio CONICET Santa Fe "Dr. Alberto Cassano", Colectora Ruta Nac. Nro 168, Km 0, Paraje El Pozo, Santa Fe, Argentina, ^{***}Centro de Investigación de Métodos Computacionales (CIMEC), UNL-CONICET, Predio CONICET Santa Fe "Dr. Alberto Cassano", Colectora Ruta Nac. Nro 168, Km 0, Paraje El Pozo, Santa Fe, Argentina, ^{****}Departamento de Ingeniería Mecánica, Universidad de Santiago de Chile (USACH). Av. Bdo. O'Higgins 3363, Santiago de Chile, Chile, ^{*****}Departamento de Ingeniería Mecánica, Universidad de Santiago de Chile (USACH). Av. Bdo. O'Higgins 3363, Santiago de Chile, Chile

ABSTRACT

The behaviour of immersed spheres moving in one and two-fluid systems is determined by the solution of two main problems, which are the fluid dynamics and the rigid body dynamics. The fluid problem is solved with a stabilized finite element method, with an interface capturing technique for the two-fluid flow cases. The body dynamics is followed with a Newton scheme, that require velocities and pressures from the flow field in order to determine the external forces over the sphere and, then, the corresponding displacements inside the domain. This multiphysics coupling strategy is applied to different analytical and experimental cases, with special emphasis on a sloshing case in a tank with a baffle.

Simulating the Effects of Microscale Heterogeneities on the Mechanical Response of Tantalum during High-Rate Loading

Corbett Battaile*, Michael Prime**, Damian Swift***, Nathan Moore****, Matthew Lane*****

*Sandia National Laboratories, **Los Alamos National Laboratory, ***Lawrence Livermore National Laboratory,
****Sandia National Laboratories, *****Sandia National Laboratories

ABSTRACT

Nearly all engineering materials contain internal heterogeneities that exist on one or more length scales, e.g. dislocations from thermomechanical processing, grains in a polycrystalline metal, voids in a pressed or additively manufactured material, or second phases in an alloy. These internal microstructures can have a strong effect on a material's properties, and are often used advantageously for just that purpose. In this paper we will focus on two types of microscale heterogeneities in tantalum: internal voids in thermally sprayed coatings, and engineered surface ripples. In the former case, voids are an unavoidable consequence of thermal spraying, but they can be used to achieve advantageous properties in certain applications. In the latter case, the Rayleigh-Taylor instability that occurs when the rippled surface is subjected to dynamic conditions can be used to study the strength of the material. We will describe micromechanics simulations using Sandia's Alegra software [1] to model "flyer plate" impact of thermally sprayed tantalum, and Rayleigh-Taylor experiments conducted on both the University of Rochester's Omega Laser [2] and Lawrence Livermore National Laboratory's National Ignition Facility (NIF) [3]. We will also discuss how we use these results to establish microstructure-properties relationships for Tantalum under high-rate loading. 1) http://www.cs.sandia.gov/ALEGRA/Alegra_Home.html; 2) http://www.lle.rochester.edu/omega_facility/; 3) <http://lasers.llnl.gov/about/what-is-nif>

A Coupled, Two-Phase Fluid-Sediment Material Model and Mixture Theory Implemented Using the Material Point Method

Aaron Baumgarten*, Ken Kamrin**

*Massachusetts Institute of Technology, **Massachusetts Institute of Technology

ABSTRACT

Dynamic fluid-sediment interactions present a challenge to traditional numerical modelling techniques. These flows can involve bulk motion of millions of sediment particles (e.g. riverbed and shoreline erosion) and therefore require intensive computational resources for modeling using discrete element methods (DEM). Other flows of interest have highly turbulent regions (e.g. the head of submerged slope avalanches) and are therefore difficult to capture in finite element methods (FEM). Recent work on modeling granular materials as continuum using the material point method (MPM) has shown promise for capturing such complex material dynamics. A numerical implementation of a new fluid-grain coupled material model in MPM is presented. Qualitative results show the breadth of problems which this model can address. Quantitative results demonstrate the accuracy of this model as compared with analytical models, results of other numerical techniques, and empirical observations.

Data-driven Computational Modeling to Link Diagnostics with Prognostics

Konstantinos Baxevanakis*, Brian Wisner**, Krzysztof Mazur***, Vignesh Perumal****, Antonios Kotsos*****

*1) Theoretical and Applied Mechanics Group, Department of Mechanical Engineering & Mechanics, Drexel University, USA and 2) Wolfson School of Mechanical, Electrical and Manufacturing Engineering, Loughborough University, LE11 3TU, UK, **Theoretical and Applied Mechanics Group, Department of Mechanical Engineering & Mechanics, Drexel University, USA, ***Theoretical and Applied Mechanics Group, Department of Mechanical Engineering & Mechanics, Drexel University, USA, ****Theoretical and Applied Mechanics Group, Department of Mechanical Engineering & Mechanics, Drexel University, USA, *****Theoretical and Applied Mechanics Group, Department of Mechanical Engineering & Mechanics, Drexel University, USA

ABSTRACT

Current damage identification in materials under operational conditions is accomplished using experimental characterization and testing methods as well as Nondestructive Testing and Evaluation (NDE&amp;T) techniques. Despite the progress in instrumentation and measuring, the estimation of the evolving material state and the reliable prediction of remaining useful life at the component and structural levels remain challenging tasks. In this context, a computational damage approach which is driven by material and NDE data is presented in this talk. The material investigated is an aerospace grade precipitate-hardened aluminum alloy. In this class of metals, damage nucleation is known to be linked with second phase particles that are inherent in the material and result from the alloying process. In this work, subsized specimens were mechanically loaded inside a Scanning Electron Microscope (SEM), while acoustic and optical methods were used to track the damage process. The experimental studies revealed a connection between the particle crystallography and stoichiometry with the location of particle fracture relative to soft and hard grains. In addition, the pronounced mismatch in stiffness between particles and neighboring grains caused strain localizations and led to fracture of these particles or crack propagation into the surrounding matrix, depending on the local microstructural features which was confirmed with both in situ and ex situ X-ray computer microtomography. To form the data-driven computational damage model, first the experimental information was used in a crystal plasticity finite element model (FEM) that predicted the location of strain localizations near the particles. This information was transferred into a continuum plasticity FEM in which the extended FEM approach coupled with specific fracture initiation criteria was used to study the particle fracture and the associated wave propagation that relates to Acoustic Emission. Then, the recorded data was post-processed using a novel machine-learning approach that combines outlier analysis with clustering to form custom damage evolution curves appropriate for both monotonic and cyclic loading cases. The derived curves were subsequently implemented in the FEM as custom damage laws. To simulate the effect of evolving damage state the plasticity FEM was coupled with a stiffness degradation approach dictated by custom subroutines that implemented the previously defined damage laws. The results highlight the effect of the data-driven damage model on the macroscopic mechanical response using different specimen and component geometries.

Hydraulic Crack Branching, Gas Permeability and Creep of Shale: Comprehensive Computational Model

Zdenek P. Bazant^{*}, Gowri Srinivasan^{**}, Hari S. Viswanathan^{***}, William Carey^{****}, Viet Tuan Chau^{*****}, Saeed Rahimi-Aghdam^{*****}, Hyunjin Lee^{*****}, Hoang Nguyen^{*****}, Cunbao Li^{*****}

^{*}Northwestern University, ^{**}Los Alamos National Laboratory, ^{***}Los Alamos National Laboratory, ^{****}Los Alamos National Laboratory, ^{*****}Northwestern University, ^{*****}Northwestern University, ^{*****}Northwestern University, ^{*****}Northwestern University, ^{*****}Northwestern University, ^{*****}Northwestern University

ABSTRACT

The talk will summarize extensive recent results at Northwestern University and Los Alamos Scientific Laboratory on the mathematical and computational modeling of hydraulic fracturing of gas shale and the problem of its preexisting permeability. Presented will be: 1) A three-phase medium model for cracking of anisotropic shale, flow of fracking fluid in cracks and diffusion of water into shale pores, 2) its computational implementation, 3) analysis of creep closing of cracks over geologic time span and 4) the problem of preexisting gas permeability of deep shale strata. Results of extensive computational simulations will be provided.

IGA: From Early Results to Recent Developments

Yuri Bazilevs*

*Brown University

ABSTRACT

This presentation honoring Prof. T.J.R. Hughes will cover the early days of IGA development, and will summarize progress made in the last decade on this subject. Achievements in several areas of computational mechanics - solids, structures, fluids, and FSI - will be highlighted, focusing on the uses of IGA that are pushing the boundaries of these disciplines. Integration with engineering design, which to this day remains the main goal of IGA, will be highlighted in the advanced applications shown.

Computational Verification of Extreme Value Probability of Fishnet Strength Model for Imbricated Lamellar Nacre-like Biomimetic Materials

Zdenek Bažant*, Wen Luo**

*Northwestern University, **Northwestern University

ABSTRACT

Similar to nacre or brick-and-mortar structures, imbricated lamellar structures can be widely found in natural and man-made materials and are of interest for biomimetics. These lamellar structures are known to be rather insensitive to defects and have a high fracture toughness. Their deterministic behavior has been intensely studied, but statistical studies have been rare and no undisputed theoretical basis exists for its probability distribution (pdf and cdf) of strength. This paper presents a numerical and theoretical study of the probability distribution of strength and of the corresponding statistical size effect of the brick-and-mortar structure. After reasonable simplifications of the shear bonds, a lamellar axially loaded lamellar shell is statistically modelled as a fishnet pulled diagonally. A finite element model with stochastic element strength is developed and used in Monte Carlo simulations of fishnet failure for over 1 million (10^6) numerical realizations. An analytical model for failure probability of the fishnet is developed and matched to the computed statistical histograms of strength for various sizes and different link strength distributions. Finally, the statistical size effect of fishnet is studied numerically and analytically.

A Numerical Investigation on Damage and Breakage of Ore Particles under Impact Loading

Lawrence Bbosa^{*}, Temitope Oladele^{**}, Dion Weatherley^{***}

^{*}Centre for Minerals Research, University of Cape Town, South Africa, ^{**}Centre for Minerals Research, University of Cape Town, South Africa, ^{***}Sustainable Minerals Institute, Julius Kruttschnitt Mineral Research Centre, The University of Queensland

ABSTRACT

Abstract Comminution is a critical stage of mineral processing, in which size reduction of mined ore is achieved by crushing and grinding in order to increase the likelihood of mineral liberation in subsequent stages. The process is well known to be energy intensive, often accounting for the highest operating cost, while also frequently being reported to be highly inefficient. Fundamental research in the area of ore fracture is the most promising means of improving or optimizing current industrial practices. In this regard, computational modelling has emerged as a valuable tool to glean new insights into the design and operation of a wide range of devices. The impact breakage of ore by grinding media falling under gravity is a common size reduction mechanism in many comminution devices. In the present work, laboratory experiments are conducted with a Short Impact Load Cell (SILC), with which a steel ball of known mass is released by a pneumatic mechanism and descends in freefall onto a particle from a fixed height. The impact response is measured with a load cell and is used to derive quantities such as force to fracture and absorbed strain energy. Numerical simulations of these tests are conducted using the Discrete Element Method (DEM). Particles are modelled as assemblies of indivisible spheres with adjacent spheres connected by cylindrical linear elastic beams. These cohesive bonds are broken when the inter-particle stress exceeds a specified limit. The results highlight the good agreement between numerical simulations and experiments, demonstrating the ability of the simulations to capture realistic physical behavior. The paper also highlights the unique insights that such simulations provide on understanding the breakage of ore particles in comminution. References [1] Bourgeois, F.S. & Banini, G.A., 2002. A portable load cell for in-situ ore impact breakage testing. *International Journal of Mineral Processing*. 65(1):31-54 [2] Napier Munn, A., Morrell, S., & Kojovic, T., 1999. *Mineral Comminution Circuits (their Operation and Optimization)*. The University of Queensland: JKMRC Monograph Series in Mining and Mineral Processing, 2. [3] Weatherley, D., Boros, V., & Hancock, W., 2011. *ESyS-particle tutorial and user's guide Version 2.1*. Earth Systems Science Computational Centre, The University of Queensland.

Direction Fields Based on Ginzburg-Landau Functional: Computing Cross and 3D Frame Fields

Pierre-Alexandre Beaufort*, Alexandre Chemin**, Christophe Geuzaine***, François Henrotte****, Jean-François Remacle*****

*Université catholique de Louvain, **Université catholique de Louvain, ***Université de Liège, ****Université catholique de Louvain, *****Université catholique de Louvain

ABSTRACT

Tensorial elements such as quadrangles and hexahedra are considered to be superior to simplices (triangles, tetrahedra). For a given number of vertices, there are much less tensorial elements than simplices: in the case of quadrangles versus triangles, it is about a factor two. Hexahedra are preferred among mechanical engineering community since they avoid the shear locking problem which tetrahedra suffer. However, meshing quadrangles or hexahedra is not a trivial task. The quality of tensorial elements is strongly related to vertex location. Indeed, the vertices have to be consistent with a grid, i.e. to be connected each other in an orthogonal way with adequate valence. This connectivity scheme may be described by a direction field: for quadrangles (hexahedra), a cross (3D frame) field (respectively). Those direction fields should be smooth, and **unit normed**. Actually, the direction field should give the mean orientation of the boundaries (if any) within the domain. However, it is not always possible to build a full unit normed (and smooth) direction field on a domain: some critical/singular points (lines) arise. In the case of direction field on closed surfaces, it is due to the topology according to the Poincaré-Hopf theorem. We propose here a PDE approach to compute those directions. The PDEs express the minimum of the Ginzburg-Landau functional. This functional has two terms: a smoothing term and a penalty term. The latter term fosters directions which are unit normed. The representation of a direction depends on its dimension: a cross field is represented by a vector field (which corresponds to a complex valued function), while a 3D frame field is modelled by a 4th order tensor field. The full consistence of using Ginzburg-Landau functional lays in its penalty factor which is parametrized by the coherence length, i.e. the characteristic length of the domain. The coherence length affects the critical points (lines) of the direction fields. In 2D, Bethuel et al. has deeply detailed its effects: the Ginzburg-Landau energy is mostly due to the squares of indices of critical points, and the logarithm distances between them. In 3D, it becomes interesting: the Dirichlet energy of singularities becomes finite. [Bethuel et al.] F. Bethuel, H. Brezis, F. Hélein, Ginzburg-Landau Vortices, volume 13, Springer Science & Business Media, 2012. [Beaufort et al.] P.-A. Beaufort, J. Lambrechts, F. Henrotte, C. Geuzaine, J. Remacle, Computing cross fields: a PDE approach based on Ginzburg-Landau theory

OPTIMUM DESIGN OF ROBUST COMPLIANT MECHANISMS WITH UNCERTAINTIES IN OUTPUT STIFFNESS

GUSTAVO A. DA SILVA[†], EDUARDO. L. CARDOSO*, AND ANDRÉ T. BECK[†]

[†]Structural Engineering Department, University of São Paulo
Av. Trabalhador São-Carlense, 400, 13566-590, São Carlos, SP, Brazil
gustavoassisdasilva@gmail.com (G. A. DA SILVA), atbeck@sc.usp.br (A. T. BECK)

*Mechanical Engineering Department, State University of Santa Catarina
89219-710, Joinville, Santa Catarina, SC, Brazil
eduardo.cardoso@udesc.br (E. L. CARDOSO)

Key words: Topology Optimization, Robust Optimization, Compliant Mechanism, Uncertain Stiffness.

Abstract. It is nowadays widely acknowledged that optimal structural design should be robust w.r.t. the uncertainties in operational parameters. Compliant mechanisms must operate under a variety of conditions; hence, the uncertainty in output stiffness is large and also determinant for the optimal design. In this paper, optimal topology of compliant mechanisms is addressed. Two approaches are considered to formulate the objective function of the robust optimization problem: a probabilistic approach, where the objective function combines the expected value and the standard deviation of the output displacement, and a possibilistic approach, where both the crisp value and the width of the uncertainty interval of the output displacement are considered. The probabilistic solutions are computed by Monte Carlo Simulation; the possibilistic solutions are computed by smart interval propagation. It is shown that both formulations lead to designs where the output displacement is less sensitive to the variations in output stiffness. The possibilistic and probabilistic solutions are compared in terms of resulting topologies and computational efficiency. As an additional benefit, it is observed that large variations in output stiffness can hinder the appearance of one-node connected hinges, usually found in the deterministic approach to compliant mechanism design.

1 INTRODUCTION

Topology optimization is an important tool widely employed in structural design. It has been employed to solve several kinds of engineering problems, from academic to industrial applications¹. Among its variety of applications, it is found the compliant mechanism design under uncertainty, main subject of this research.

A literature review revealed several papers addressing the topology design of compliant mechanisms under uncertainty. In Maute and Frangopol², reliability-based design optimization is employed to achieve optimized compliant mechanisms under boundary conditions and material property uncertainties. In Kogiso et al³, robust design is employed for solving continuum mechanisms problems under load uncertainty. In Chen et al⁴, a robust approach is proposed to take load and material property uncertainties into account in the design of compliant mechanisms. In Sigmund⁵ and Wang et al⁶, the robust approach based on erosion, intermediate and dilation operators is proposed and employed to the design of manufacturing tolerant compliant mechanisms. This approach is latter improved to take non-uniform boundary uncertainties into account⁷.

The classical topology optimization problem of compliant mechanisms consists in the maximization of the geometrical advantage given an output stiffness⁸. It is well known, that the output stiffness has a great impact over the topology of the optimized compliant mechanism. A compliant mechanism, optimized for actuating over a specific output, may not be suitable for actuating over an output with slightly different stiffness. This matter would not be an issue when working with outputs whose stiffness is certainly known. However, if there is uncertainty in the output stiffness, one has to employ an alternative technique to the traditional formulation of compliant mechanisms design, in order to properly handle this uncertainty during the optimization process.

This work aims at proposing two robust formulations to solve the problem of compliant mechanisms design considering an uncertain output stiffness, depending on how the uncertain stiffness is addressed: 1) probabilistic; and 2) possibilistic. When the uncertain output stiffness is modelled as a random variable, one can employ the probabilistic formulation, where the traditional objective function (output displacement) is replaced by a weighted sum between its expected value and standard deviation. On the other hand, when there is no sufficient information about the uncertain output stiffness, and only its maximum and minimum values are available, one can employ the possibilistic approach, where the objective function is replaced by a weighted sum between the mean value of the interval and a measure of its width.

In order to demonstrate applicability of proposed approaches (probabilistic and possibilistic), the classical inverter mechanism problem is solved. Obtained results are compared with the traditional (deterministic) result from the literature, clearly demonstrating the importance of employing such formulations when addressing topology design problems of compliant mechanisms under uncertain output stiffness.

2 TOPOLOGY OPTIMIZATION OF COMPLIANT MECHANISMS

In this work, the traditional density-based approach⁹ is employed. It consists in a layout optimization procedure of a fixed reference domain: 1) the topology optimization problem of compliant mechanisms is formulated; 2) the design domain is discretized with finite elements; 3) each finite element is associated with a relative density ρ_e (design variables of the optimization problem), that can assume values from 0 (which mimics void material) to 1 (which mimics solid material); 4) the topology optimization problem is solved by employing well established mathematical programming approaches.

In this paper, all formulations are developed based on the displacement-based Finite Element Method (FEM) under the hypotheses of linear elasticity subjected to static loads. The resulting

topology optimization problems are solved by employing the Sequential Linear Programming (SLP) approach. Sensitivities are obtained with the adjoint procedure.

The traditional linear density filter¹⁰ is employed to avoid checkerboard patterns and mesh dependency.

2.1 Deterministic formulation

In this work, we formulate the topology optimization problem of compliant mechanisms for one output only, as illustrated in Figure 1.

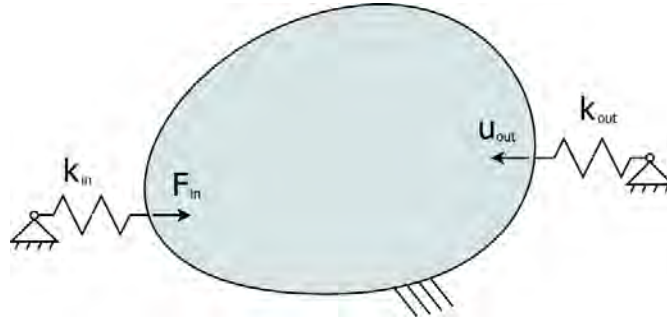


Figure 1 – Illustration of design with input stiffness k_{in} , output stiffness k_{out} , input force F_{in} and output displacement u_{out} .

The objective is the maximization of the displacement at the output port, while constraining the amount of material (volume fraction). The output displacement acts on a linear spring with stiffness k_{out} , representing the stiffness of the output medium. The mechanism is actuated by a given load coupled to a linear spring with stiffness k_{in} , in order to simulate a force transducer.

The optimization problem is written as:

$$\begin{aligned}
 & \text{Max. } u_{out}(\boldsymbol{\rho}) \\
 & \text{s. t. } \begin{aligned} & V(\boldsymbol{\rho}) \leq V_{max} \\ & \mathbf{K}(\boldsymbol{\rho})\mathbf{U}(\boldsymbol{\rho}) = \mathbf{F} \\ & 0 \leq \rho_{min} \leq \rho_e \leq 1 \end{aligned} \quad e = 1..N_e
 \end{aligned} \tag{1}$$

where the objective function, $u_{out}(\boldsymbol{\rho})$, is the displacement at the output port, $V(\boldsymbol{\rho})$ is the volume of the structure, V_{max} is the maximum admissible volume (volume constraint) defined by the designer, $\mathbf{K}(\boldsymbol{\rho})$ is the global stiffness matrix, $\mathbf{U}(\boldsymbol{\rho})$ is the global displacement vector, \mathbf{F} is the global load vector and N_e is the number of elements in the mesh. The global stiffness matrix is obtained by assembling, in the global level, all the local element stiffness matrices, $\mathbf{k}_e(\rho_e) = \mathbf{k}_e^b \rho_e^p$ (SIMP – Solid Isotropic Material with Penalization¹), and, in addition, the stiffness of input k_{in} and output k_{out} ports. We can denote this assembly symbolically as:

$$\mathbf{K}(\boldsymbol{\rho}) \leftarrow \bigcup_{e=1}^{N_e} \mathbf{k}_e(\rho_e), \bigcup k_{in}, \bigcup k_{out}, \tag{2}$$

where the minimum value of ρ_{min} is assumed for the relative densities to avoid a singular FEM problem.

The structural volume of the structure is computed as

$$V(\boldsymbol{\rho}) = \sum_{e=1}^{N_e} V_e \rho_e, \quad (3)$$

where V_e is the volume of finite element e .

The traditional formulation, Equation (1), is suitable for designing compliant mechanisms when there is no source of uncertainty related to any parameter utilized during optimization. Next subsections aim at proposing two distinct formulations for solving the compliant mechanisms problems when there is uncertainty in the output stiffness k_{out} .

2.2 Probabilistic formulation

When there is uncertainty in the output stiffness, i.e., when its value is not certainly known, formulation described in Equation (1) is no longer appropriate, since it can lead to non-optimal solutions. Considering that magnitude of the output stiffness is represented by a random variable X , as $k_{out}(X) = (1 + X) k_{out}^0$, where k_{out}^0 is the mean value of the output stiffness, one can rewrite optimization problem described in Equation (1) to take the aleatory uncertainty into account, under a robust framework, such that:

$$\begin{aligned} \text{Max.} \quad & E[u_{out}(\boldsymbol{\rho}, X)] + \beta \text{Std}[u_{out}(\boldsymbol{\rho}, X)] \\ \text{s. t.} \quad & V(\boldsymbol{\rho}) \leq V_{max} \\ & \mathbf{K}(\boldsymbol{\rho}, X) \mathbf{U}(\boldsymbol{\rho}, X) = \mathbf{F} \\ & 0 \leq \rho_{min} \leq \rho_e \leq 1 \quad e = 1..N_e \end{aligned} \quad (4)$$

where $E[u_{out}(\boldsymbol{\rho}, X)]$ is the expectation and $\text{Std}[u_{out}(\boldsymbol{\rho}, X)]$ the standard deviation of the displacement at the output port.

The main difference between the probabilistic formulation, Equation (4), and the deterministic formulation, Equation (1), is in the consideration of an additional term in the objective function, related to the standard deviation of the output displacement.

The inclusion of the standard deviation in the objective function has a great impact over the optimized designs. It works at reducing the sensitivity of the optimized result with respect to variations in the output stiffness, i.e., we can achieve robust designs which are not affected from slight variations in the output stiffness, unlike the deterministic unstable solution.

Of course it becomes a compromise relation when one has to choose the number of standard deviations, β , to be considered during optimization. For small values of β we basically recover the original deterministic formulation, Equation (1); whereas for large values of β we focus at reducing design sensitivity with respect to the uncertain output stiffness. Hence, the number of standard deviations β has an important role over the optimization problem and must be carefully chosen by the designer, depending on the application of the compliant mechanism.

In this work, evaluation of $E[u_{out}(\boldsymbol{\rho}, X)]$ and $\text{Std}[u_{out}(\boldsymbol{\rho}, X)]$ are performed through Monte Carlo Simulation¹¹.

2.3 Possibilistic formulation

When there is uncertainty in the output stiffness, but it cannot be reasonably represented through a random variable, one may employ a possibilistic approach to address the problem. In this subsection, we assume the only available information regarding the output stiffness are its minimum and maximum values, i.e., the output stiffness is represented by an unknown variable Z , as $k_{out}(Z) = (1 + Z) k_{out}^0$, with $Z \in [\underline{Z}, \bar{Z}]$.

The possibilistic version of the optimization problem is written as:

$$\begin{aligned}
 \text{Max.} \quad & \frac{\max(u) + \min(u)}{2} + \gamma \sqrt{(\max(u) - \min(u))^2} \\
 \text{s. t.} \quad & V(\boldsymbol{\rho}) \leq V_{max} \\
 & \mathbf{K}(\boldsymbol{\rho}, Z) \mathbf{U}(\boldsymbol{\rho}, Z) = \mathbf{F} \\
 & 0 \leq \rho_{min} \leq \rho_e \leq 1 \quad e = 1..N_e
 \end{aligned} \tag{5}$$

where $u = u_{out}(\boldsymbol{\rho}, Z)$. Purpose of formulation presented in Equation (5) is remarkably similar to the purpose of formulation in Equation (4). Despite presenting distinct numerical behaviors, parameter γ has the same purpose of parameter β and the term $\sqrt{(\max(u) - \min(u))^2}$, related to the width of the interval of the output displacement, has the same purpose of the standard deviation in the probabilistic approach.

Since linear analysis is employed when solving for equilibrium, minimum and maximum values of output displacement are easily obtained by evaluating for \bar{Z} and \underline{Z} , associated with maximum and minimum values of output stiffness, respectively, such that: $\min(u_{out}(\boldsymbol{\rho}, Z)) = u_{out}(\boldsymbol{\rho}, \bar{Z})$ and $\max(u_{out}(\boldsymbol{\rho}, Z)) = u_{out}(\boldsymbol{\rho}, \underline{Z})$.

3 NUMERICAL RESULTS

In this section, the inverter mechanism problem is addressed, Figure 2. Hypotheses of plane stress are adopted. Input data are: Young's Modulus of 3 GPa, Poisson's coefficient of 0.4, input force of $F_{in} = 200$ N, input stiffness of $k_{in} = 1 \times 10^5$ N/m, admissible structural volume of $V_{max} = 20\% V_{domain}$, stiffness penalization factor of $p = 3$ (SIMP), thickness of 5 mm and filter's radius of 1.5 mm. The problem is discretized with $N_e = 2000$ four-node bilinear isoparametric elements with additional deformation modes¹². The optimization problem is solved with a SLP algorithm with fixed moving limits of 5%.

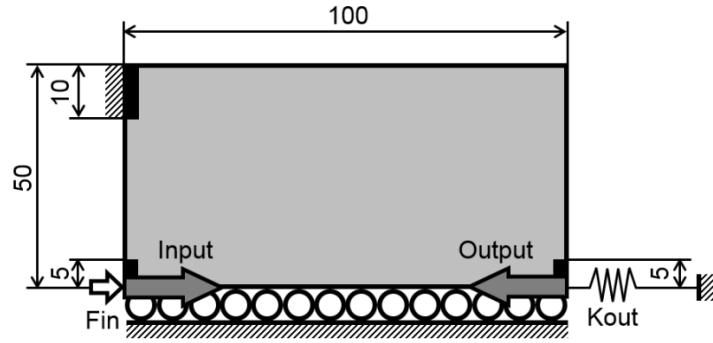


Figure 2 - Design domain for the inverter compliant mechanism. All the dimensions are in mm.

The optimization problem is solved by the three approaches presented in this work:

- 1) the traditional deterministic approach, with $k_{out} = 1 \times 10^3$ N/m;
- 2) the proposed probabilistic approach, with $k_{out}^0 = 1 \times 10^3$ N/m and $X \sim U(-0.5, 0.5)$, i.e., the output stiffness follows an uniform distribution as $k_{out}(X) \sim U(0.5 \times 10^3, 1.5 \times 10^3)$ N/m;
- 3) the proposed possibilistic approach, with $k_{out}^0 = 1 \times 10^3$ N/m and $Z \in [-0.5, 0.5]$, i.e., the output stiffness may assume any value in range $k_{out}(Z) \in [0.5 \times 10^3, 1.5 \times 10^3]$ N/m;

An important choice when solving the optimization problem under uncertain output stiffness is regarding the parameters β and γ , that governs the weight of standard deviations or width of intervals, for probabilistic and possibilistic approaches, respectively. For this study, we choose $\beta = \gamma = 20$.

Figure 3 shows optimized topologies for the three problems analyzed herein. One can clearly see the differences between deterministic solution (leftmost topology) and robust solutions (middle and rightmost topologies). The deterministic solution presents a larger number of structural members when compared with the robust solutions.

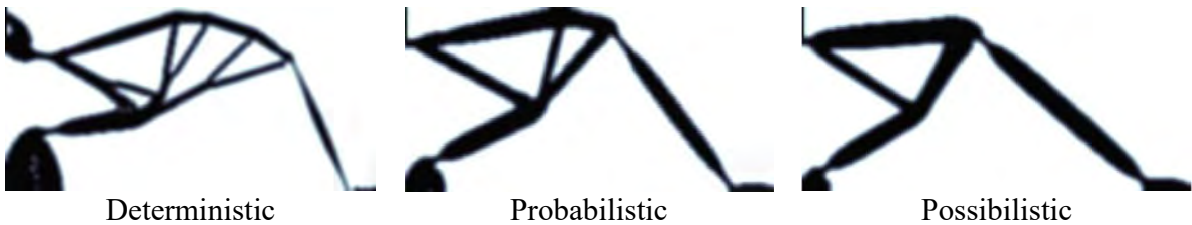


Figure 3 – Topologies optimized for the three presented approaches.

Regarding the performance of the mechanisms, one can also verify large differences between deterministic and robust solutions. In order to demonstrate the unstable behavior of the deterministic solution and, on the other hand, demonstrate the extremely small sensitivity of robust solutions with respect to changes in the output stiffness, all solutions are post-processed for minimum and maximum output stiffness considered during optimization, Figure 4.

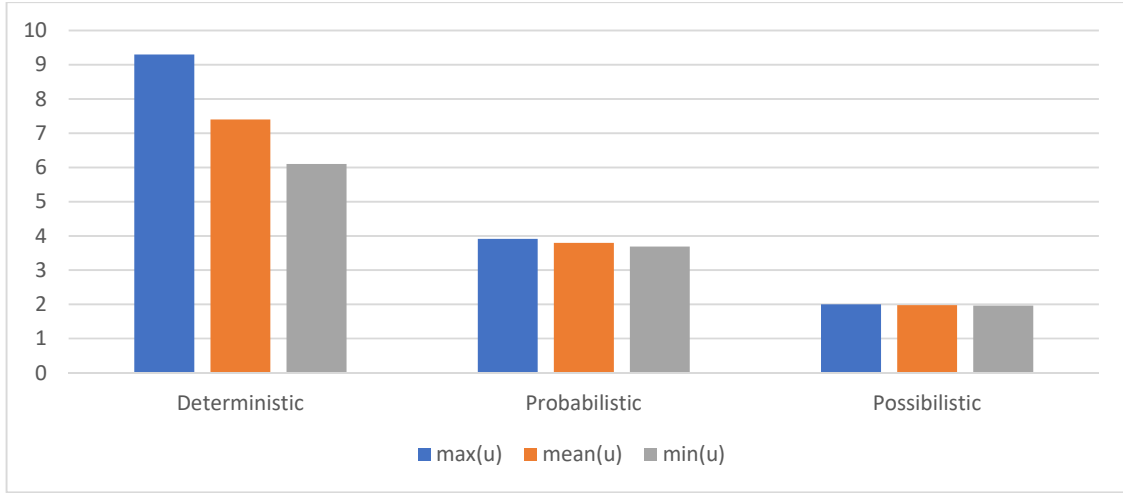


Figure 4 – Output displacements evaluated for the mean output stiffness and its extreme values. All the dimensions are in mm.

Although a larger output displacement is obtained when the deterministic design is employed, its variation with respect to a variation in the output stiffness is extremely large. Both probabilistic and possibilistic approaches work at reducing this large variation of the output displacement, however, its magnitude is also reduced. It is a compromise relation between performance and robustness, that should be taken into account by the designer, depending on the application of the compliant mechanism.

Both probabilistic and possibilistic approaches lead to robust results, but different mean performances are observed, due to different mathematical behavior of the formulation for same parameters β and γ (a smaller value of γ is necessary if the goal is obtaining equivalent result to the probabilistic approach). Both approaches are suitable if the goal is achieving a robust solution, with smaller performance sensitivity with respect to change in the output stiffness. The choice between both approaches should be done depending on how the uncertainty in the output stiffness is described. If there is sufficient information to describe the output stiffness as a random variable, the probabilistic formulation is suitable, otherwise, one can employ the possibilistic formulation.

4 CONCLUSIONS

Topology design of compliant mechanisms under uncertainty in the output stiffness was addressed. Two distinct robust formulations were proposed to handle the uncertainty in the stiffness of the output medium, depending on how the uncertain variable is described: 1) a probabilistic approach, if the output stiffness is described by a random variable; 2) a possibilistic approach, if one has only the bounds of the output stiffness.

Both approaches were employed to solve the inverter problem and compared with the traditional deterministic design. Post-processing demonstrates that the deterministic design is extremely sensitive with respect to changes in the output stiffness. It was also demonstrated that both robust approaches are suitable at greatly reducing the sensitivity of the output displacement with respect to variations in the output stiffness.

REFERENCES

- [1] Bendsøe, M.P. and Sigmund, O. *Topology Optimization: Theory, Methods and Applications*, Springer, 2003.
- [2] Maute, K. and Frangopol, D.M. (2003) Reliability-based design of mems mechanisms by topology optimization. *Comput Struct* 81(8–11):813–824. [https://doi.org/10.1016/S0045-7949\(03\)00008-7](https://doi.org/10.1016/S0045-7949(03)00008-7)
- [3] Kogiso, N., Ahn, W., Nishiwaki, S., Izui, K. and Yoshimura, M. Robust topology optimization for compliant mechanisms considering uncertainty of applied loads. *Journal of Advanced Mechanical Design, Systems, and Manufacturing*, 2(1):96–107, 2008.
- [4] Chen, S., Chen, W. and Lee, S. *Struct Multidisc Optim* (2010) 41: 507. <https://doi.org/10.1007/s00158-009-0449-2>.
- [5] Sigmund, O. Manufacturing tolerant topology optimization, *Acta Mechanica Sinica* 25 (2) (2009) 227–239. doi:10.1007/s10409-009-0240-z.
- [6] Wang, F., Lazarov, B.S. and Sigmund, O. On projection methods, convergence and robust formulations in topology optimization, *Structural and Multidisciplinary Optimization* 43 (6) (2011) 767–784. doi:10.1007/s00158-010-0602-y.
- [7] Schevenels, M., Lazarov, B.S. and Sigmund, O. Robust topology optimization accounting for spatially varying manufacturing errors. *Comput Meth Appl Mech Eng.* 2011;200(4952):3613–3627. <https://dx.doi.org/10.1016/j.cma.2011.08.006>
- [8] Sigmund, O. (2007) On the Design of Compliant Mechanisms Using Topology Optimization, *Mechanics of Structures and Machines*, 25:4, 493–524, doi: 10.1080/08905459708945415
- [9] Sigmund, O. and Maute, K. Topology optimization approaches, *Structural and Multidisciplinary Optimization* 48 (6) (2013) 1031–1055. doi:10.1007/s00158-013-0978-6.
- [10] Sigmund, O. Morphology-based black and white filters for topology optimization. *Struct Multidiscipl Optim.* 2007;33(4–5):401–424. <https://doi.org/10.1007/s00158-006-0087-x>
- [11] Melchers, R.E. and Beck, A.T. (2017) *Structural reliability analysis and prediction*, 3rd edn. Wiley, New York
- [12] Jiao, Z.-P., Pian, T.H.H. and Yong, S. A new formulation of isoparametric finite elements and the relationship between hybrid stress element and incompatible element. *International Journal for Numerical Methods in Engineering*, pages 15–27, 1997.

An Immersed Reproducing Kernel Particle Method for Modeling Inhomogeneous Media Using Nitsche's Method

Frank Beckwith*, J. S. Chen**

*University of California, San Diego, **University of California, San Diego

ABSTRACT

Many structures are constructed using reinforced concrete. The modeling of reinforced concrete at the rib-scale is difficult with conventional methods such as the finite element method (FEM) due to the conforming requirements with respect to the material interface. An immersed Reproducing Kernel Particle Method (RKPM) is proposed to model the complex reinforcement geometry using an immersed domain approach. The compatibility conditions on the material interfaces are enforced via Nitsche's method with embedded equilibrium. This approach allows independent approximations and discretizations for the background matrix and the foreground inclusion, and naturally yields strain jumps across the material interfaces. The reproducing kernel (RK) approximations and discretizations of both foreground and background domains are considered in this work due to their high continuity [1], but other approximations such as the finite element method can also be employed under this framework. Several numerical examples with application to reinforced concrete are presented to examine the effectiveness of the proposed method. The modeling of mechanical interlock and bar debonding phenomena in the reinforced concrete pull-out test by the proposed is also demonstrated. References [1] J. S. Chen, M. Hillman, and S.-W. Chi. Meshfree methods: Progress made after 20 years. *Journal of Engineering Mechanics*, 143(4):04017001, 2017.

Molecular Dynamics Simulation of Nanosize Effects in Nanoreinforced Polymers; From Interface to Macroscopic Mechanical Properties

Fahmi Bedoui^{*}, Andres Jaramillo-Botero^{**}, William A. Goddard III^{***}

^{*}Sorbonne Universités - Université de Technologie de Compiègne, ^{**}Materials and Process Simulation Center, CalTech, ^{***}Materials and Process Simulation Center, CalTech

ABSTRACT

The process-structure-property relationships are far less well understood in nanoreinforced polymers than in other materials; to the point that these are rarely of any practical or commercial utility. In addition to the microstructural complexity, nanoreinforced polymer behavior seems to be dependent on the size of the reinforcing nano structures (e.g. nanoparticles, nanowires, nanotubes, etc.) Here, we report on recent efforts to quantify and model such nanosize effects on the elastic and thermal properties of a Poly(methyl methacrylate) -PMMA polymer reinforced with spherical silica nanoparticles ranging in diameter, from 15 nm to 500 nm. Our results, confirm the nanosize effect and mechanisms that alter the experimentally observed macroscopic elastic modulus of the nanocomposite (see Blivi et al., 2016 [1]). This data allowed us to calibrate the interface characteristics that enter into an extended version of the linear homogenization model proposed by Brisard et al. [2] and Duan et al [3]. In order to provide cross quantitative validation and to tailor the experimental work, we adopted an atomistic modeling approach to help answer the main question that needs to be answered: • Do particles act through interface, interphase or both, to convey the polymer with enhanced mechanical properties (origin of size effect) at nanometric particle size? This work will present preliminary results from molecular dynamics simulations that confirm the effect of particle size on the macroscopic materials properties of silica-PMMA nanoreinforced composites made with constant volume fraction but different silica particles. We used the two-phase thermodynamic model [4] to derive the entropy distribution in the various polymer layers from the interface to the bulk. This provides new insights into the local mechanical and physical properties, that otherwise are inaccessible. References [1] A.S.Blivi, F.Benhui, J.Baib, D.Kondoc, F.Bedoui. Polymer Testing 2016;56:337. [2] Brisard S, Dormieux L, Kondo D. Computational Materials Science 2010;48 589. [3] H.L.Duan, J.Wang, Z.P.Huang, Z.Y.Luo. Mechanics of Materials 2005;37 723. [4] Lin S-T, Maiti PK, Goddard WA. The Journal of Physical Chemistry B 2010;114:8191.

Simplified Formulation for Avaliating Displacements in Beams with Moving Boundary Conditions

Thomás Bedusque Verderesi*, Marco André Argenta**

*Universidade Federal do Paraná, **Universidade Federal do Paraná

ABSTRACT

The corotational method is a powerful approach for solving non-linear finite beam elements, mostly utilized to investigate its dynamics. However, where most papers present studies in the shape functions and its derivations (to obtain mass and stiffness matrices), this work takes advantage of the cubic interpolations for solving the inertia terms, combining it to moving boundary conditions with constant velocity and acceleration. We simulated the beam as an overcomplicated n-arms pendulum. The first problem is that with more arms the less stiff it becomes. The solution is to embed nonlinear longitudinal springs for the axial stiffness and with rotational springs for its rotational and shear stiffness, containing one of each for connecting pendulum arms, then, simulating as a moving pendulum. Once described its law of motion correctly, the elements match the displacements of one another at springs with multifreedom constraints (MFC), where one displacement, velocity, and acceleration has to be constrained to another, eliminating the chaotic nature of the multi-pendular motion. We used the master-slave method, which eliminates the slaves degrees of freedom and makes the otherwise singular stiffness matrix solvable again. We simulated the beam with a concentrated force and different positions and moving boundary conditions with constant velocity at first and then with constant acceleration, in order to study the stresses and strains variations within it. The other parameter is the number of elements used to build the beam model, analyzing if the number of elements makes an analysis more accurate. We compared the model to an accepted one such as the corotational Timoshenko's beam theory, in a stationary situation, validating it for the displacements caused by an applied force and for the rigid body movement.

Solving the Linearized Stationary Quasi-Geostrophic Equations of the Ocean Using the Particle Difference Method

Andrew Beel^{*}, Tae Yeon Kim^{**}, Jeong-Hoon Song^{***}

^{*}University of Colorado Boulder, ^{**}Khalifa University of Science, Technology and Research, ^{***}University of Colorado Boulder

ABSTRACT

The development of accurate and robust numerical methods for solving higher order partial differential equations is crucial for both theoretical model validation and practical applications in many areas of science and engineering. This study explores the capability of the recently developed strong form collocation method, i.e. the particle difference method (PDM) [1] in solving the linear Stommel (the second-order PDE) and Stommel-Munk (the fourth-order PDE) models, linearized versions of the stationary quasi-geostrophic equations (SQGE) of the ocean [2]. The PDM is based on a Taylor polynomial approximation of the solution field with moving least squares approach. Numerical examples considered herein include: i) the Stommel equation on a square domain with a strong Western boundary layer, ii) the Stommel-Munk equation on a rectangular domain with and without a strong Western boundary layer, and iii) the Stommel-Munk equation on an irregular polygon representing the Mediterranean Sea. In the first example, numerical solutions from the PDM are compared with exact solutions, producing near-optimal empirical convergence results for both a quadratic and quartic polynomial approximation. In the second example, for both uniform tensor product grid and meshing software-generated random arrangements of collocation points, the PDM exhibits excellent convergence properties in both the discrete relative L^2 norm error and relative infinity norm error. For the third example, the analytical solution is unavailable, so a contour plot and qualitative comparison to numerical results from another numerical method, presented originally in [3], are presented. References [1] Y.C. Yoon and J.H. Song, "Extended particle difference method for weak and strong discontinuity problems: Part I. Derivation of the extended particle derivative approximation for the representation of weak and strong discontinuities", *Computational Mechanics*, 53 (2014), 1087-1103 (2014). [2] Tae-Yeon Kim, Traian Iliescu, Eliot Fried, "B-spline based finite-element method for the stationary quasi-geostrophic equations of the ocean", *Computer Methods in Applied Mechanics and Engineering*, 286 (2015) 168-191. [3] T.Y. Kim, E.J. Park and D.W. Shin, "A C0-discontinuous Galerkin method for the stationary quasi-geostrophic equations of the ocean", *Computer Methods in Applied Mechanics and Engineering*, 300 (2016) 225-244.

Estimating Material Parameter Distributions of Fibers with Extremely Limited Experimental Efforts

Lars Beex^{*}, Hussein Rappel^{**}, Stephane Bordas^{***}

^{*}University of Luxembourg, ^{**}University of Luxembourg, ^{***}University of Luxembourg

ABSTRACT

Numerous materials are essentially discrete networks of fibers, yarns or struts at length scales substantially smaller than the application scale. Some examples of these materials are foams, paper materials, printed lattices and textiles. Besides the possible geometrical randomness, many of these materials are characterized by the fact that each fiber, yarn or strut has its own set of material parameters. Incorporating this randomness in discrete mechanical models can substantially influence the predictions, compared to those of mechanical models in which no randomness of material parameters is included. If we assume that the material parameters of each discrete constituent are realisations from a distribution, the parameters of this probability density function (PDF) must be identified. The most conventional manner of identifying the parameters of such a PDF is to experimentally identify the material parameters of hundreds of fibers, yarns or struts and subsequently, use these material parameters to identify the parameters of the distribution. This entails an enormous amount of experimental efforts, which is the reason that hardly anybody has gone and will go through these efforts. As an alternative to testing hundreds of fibers, yarns or struts, we will present an approach that requires the testing only a few fibers. We will use Bayes' theorem for this purpose, which entails the proposition of the shape of PDF, as well as a proposition of the possible values of this PDF (albeit as distributions as well). For each set of material parameters, we then assess how likely it is that it comes from the proposed PDF including its proposed parameters and we update the PDF's proposed parameters such that the likelihood that the set is a realisation of this PDF increases. In order to explain the approach as gently as possible, we will not directly deal with the PDF's parameters as parameters that also originate from a PDF. Instead, we will first focus the PDF's parameters as deterministic variables [1]. Since our study does not deal with actual experimental results and we artificially generate our experimental data instead, we know the actual parameters we try to recover and hence, we can accurately and consistently assess the accuracy of the approach. [1] Rappel H, Beex LAA, Bordas SPA, 'Bayesian inference to identify parameters in viscoelasticity', Mechanics of Time-Dependent Materials, 2017, In press.

Unstructured Space-Time Meshes in the Context of Stabilized Finite Element Methods and Moving Boundary Problems

Marek Behr*, Violeta Karyofylli**

*Chair for Computational Analysis of Technical Systems, RWTH Aachen University, **Chair for Computational Analysis of Technical Systems, RWTH Aachen University

ABSTRACT

Moving-boundary flow simulations are an important design and analysis tool in many areas of engineering, including civil and biomedical engineering, as well as production engineering. Interface-capturing offers unmatched flexibility for complex free-surface motion, while interface-tracking approach is very attractive due to its better mass conservation properties at low resolution. We focus on these alternative approaches in the context of flow simulations based on stabilized finite element discretizations of Navier-Stokes equations, including space-time formulations that allow extra flexibility concerning grid design at the interface. Space-time approaches offer some not-yet-fully-exploited advantages when compared to standard discretizations; among them, the potential to allow some degree of unstructured space-time meshing. A method for generating simplex space-time meshes has been developed, allowing arbitrary temporal refinement in selected portions of space-time slabs. The method increases the flexibility of space-time discretizations, even in the absence of dedicated space-time mesh generation tools. The resulting tetrahedral (for 2D problems) and pentatope (for 3D problems) meshes are being used in the context of cavity filling flow simulations, such as those necessary to design injection molding processes.

Dynamic Fracture Modeling of Ductile Materials with Peridynamics

Masoud Behzadinasab^{*}, John Foster^{**}

^{*}University of Texas at Austin, ^{**}University of Texas at Austin

ABSTRACT

Prediction of crack initiation, propagation, and ductile fracture can be very challenging in metallic materials with complex geometries. Damage accumulation along the plastic loading path governs the fracture initiation in ductile materials. Over the past two decades, the peridynamic theory has been exploited for modeling dynamic problems involving fracture. Peridynamics has, however, mostly applied in modeling fracture in brittle materials, and its robustness in ductile fracture modeling has not been fully explored. Recently Foster et al. (2017) proposed a new framework to incorporate classical finite deformation material models in peridynamics. Tupek et al. (2013) has also introduced a constitutive damage modeling approach for peridynamics to take advantage of the well-established classical damage models. A material model corresponding to the finite strain elastoplasticity theory of Simo (1988) and a damage model corresponding to Johnson-Cook model (1985) have been implemented in Peridigm, an open-source massively-parallel computational peridynamics code. This framework has been applied to the Sandia Fracture Challenge 3. The model was first calibrated by the data provided by Sandia National Laboratories. Following that, a blind prediction was performed on the challenge geometry and results were compared. We demonstrate the capabilities of the new correspondence framework and possible factors behind the discrepancy between the simulation results and the experiments.

Contact of Higher-Order Elements for Explicit Dynamics

Stephen Beissel*

*Southwest Research Institute

ABSTRACT

In recent years, higher-order elements have been used to great advantage in various fields of scientific computing, but not in the dynamics of solids. There are likely multiple reasons for this. However, one of the primary reasons is probably the difficulty of accurately enforcing contact boundary conditions between the curved surfaces of higher-order elements. This difficulty is magnified by the essential role of contact in problems of practical significance. Recently, higher-order elements have been introduced for the dynamics of solids with explicit time integration. These elements have been shown to provide much greater accuracy to the analysis of wave propagation than standard first-order elements on the bases of equal mesh refinement, equal computing time, and equal allocated memory. In the first part of this presentation, a typical legacy contact algorithm is adapted to contact of the new higher-order elements. This algorithm was derived from the preservation of nodal momenta and has been used successfully for years with first-order elements. It is evaluated for higher-order elements by examining the transmission of a compressive planar wave through a flat interface. The wave is correctly transmitted across the interface only under special conditions, but not for all alignments of the elements on the opposing surfaces, and not when the elements are of differing orders. In the next part of the presentation, a new formulation of contact is derived for the higher-order elements to avoid these shortcomings, and to accommodate curved surfaces. The new formulation is derived from the weak form of the equations of motion, in a manner consistent with the derivation of the higher-order elements. As a result, the new formulation correctly transmits a compressive planar wave across a contact interface for any alignment of the opposing elements, and any combination of element orders. In the last part of the presentation, comparisons of numerical examples demonstrate the importance of modeling the curved surfaces of the elements by their n th-order polynomials, rather than decomposing them into multiple first-order facets for the legacy algorithm. The examples include sliding of surfaces with initial curvature, and contact between surfaces with deformation-induced curvature resulting from large plastic flows.

Optimisation Methods for the Design of Tall Buildings Based on Sustainability and Efficiency Factors

Laura Bellamy*, Theodoros Mourtis**, Andrew Phillips***

*Imperial College London, **Robert Bird Group, ***Imperial College London

ABSTRACT

Sustainability is an increasingly important factor in global decision-making, and provision of infrastructure is responsible for a large part of global greenhouse gas emissions [1]. Whilst efforts are made to reduce the operational carbon in the construction industry, work is still necessary to lower embodied carbon [2]. Currently, in many cases when designing a tall building, the optimisation process is largely based on engineers' experience. Whilst this experience is extremely valuable and will often reach good results, making use of the parametric tools that are now available could reach improved results and save time in the design process. This can lead to efficient designs and savings on material quantities, lowering the embodied carbon of structures. Tools are being developed, in collaboration between industry and academia, for the optimisation of tall buildings to work towards these objectives. They include slab, column and core optimisation. Rhinoceros 3D and its parametric design tool Grasshopper are used to conduct the optimisation. They allow to analyse thousands of designs in a short time, easily implement design changes and compare optimisation goals. The plug-in Karamba and the genetic algorithm component Galapagos are used for finite element analysis and optimisation. For the slab, the variables are the column locations and the number of columns on the plate; the column dimensions can be computed in the analysis, based on ultimate load capacity and axial shortening criteria. Multiple objective functions, such as net moment in the slab, strain energy or deflections, are used for the optimisation. For core optimisation, the variables include wall thicknesses both in plan and with height, lintel properties, shear wall lengths, as well as different geometrical arrangements. Possible objective functions include overall deflections, inter-storey drifts and lintel and wall stresses. The dynamic response of the structure is considered. These tools are versatile and can be used at different design stages. They can be used for the conceptual design where the outputs are trends that the engineers can use, allied to their experience, to achieve optimised, efficient designs. They can also be used later in a project when there are more constraints and the results confirm or improve the decisions made. The tools are being tested on theoretical examples and case studies and are used by industry for real projects. [1] UNEP SBCI, 2009, Buildings and Climate Change: Summary for Decision-Makers. [2] De Wolf, C., Pomponi, F., Moncaster, A., 2017, Energy and Buildings, 140, 68-80.

An Application of a Constitutive Model with Damage to a Foundation with Fiber Reinforced Soil

Juan Pablo Bellassai*, Ruben Lopez**, Antonio Aquino***, Nilo Consoli****

*National University of Asuncion, **National University of Asuncion, Faculty of Engineering, ***National University of Asuncion, Faculty of Engineering, ****Federal University of Rio Grande do Sul

ABSTRACT

The addition of fibers in the soil improves several of its mechanical properties and modify the mechanism of failure of the same. On the other hand, the Continuous Damage Mechanics can conveniently describe the beginning of microcracks to coalescence and the subsequent formation of macrocracks, to make this can be used a homogenization techniques defining the representative volume to evaluate the evolution of the damage of the material. In geotechnical engineering, the first proposals of constitutive models with continuous damages for granular soils and for cohesive soils were published. This work consists in the presentation of the numerical results of the application of an elastoplastic constitutive law with continuous damage developed recently. This developed model is based on the hypothesis of equivalent deformation and consists of a constitutive law of the type Drucker-Prager modified by introducing the damage of the material. For the integration of the model an algorithm with an implicit integration scheme was used. Even if the damage model developed was anisotropic, the model implementation was performed considering isotropic damage, predicting the necessary tests for the characterization of the material in our laboratory. The model was coded in the FORTRAN programming language and later inserted as the UMAT subroutine of ABAQUS software. To obtain the parameters and to make the calibration of the model, experimental data obtained in the CML were used, by means of a triaxial equipment under cyclic loading and unloading tests. For the validation of the model, several samples of soil with fibers were simulated and the results compared with the experimental values available in our laboratory. Subsequently, a study of a foundation was carried out in a fiber reinforced soil, submitted to a tear test. The results show the regions where it presents the highest concentration of damage and its evolution during the application of the load. Based on the results obtained it is possible to conclude that: (a) The Continuous Damage Mechanics is applicable in the study of the behavior in the elastoplastic state with damage of the fiber reinforced soils, (b) The measurement of the damage of the material based on the variation of the elastic modulus and in an elastoplastic constitutive law with damage developed based on the hypothesis of equivalent deformation between damaged and effective configurations, is adequate to model the phenomena associated with geotechnical projects

Goal-Oriented Adaptive Error Control of Stochastic Compressible System Approximations

Anca Belme^{*}, Frédéric Alauzet^{**}, Didier Lucor^{***}, Jan Van Langenhove^{****}

^{*}University Pierre and Marie Curie, Institut Jean le Rond d'Alembert, ^{**}INRIA Saclay, ^{***}LIMSI, CNRS, University Paris-Saclay, ^{****}University Pierre and Marie Curie, Institut Jean le Rond d'Alembert

ABSTRACT

The simulation of complex nonlinear engineering systems such as compressible fluid flows may be targeted to make more efficient and accurate the approximation of a specific (scalar) quantity of interest of the system. Putting aside modeling error and parametric uncertainty, this may be achieved by combining goal-oriented error estimates and adaptive anisotropic spatial mesh refinements. To this end, an elegant and efficient framework is the one of (Riemannian) metric-based adaptation where a goal-based a priori error estimation is used as indicator for adaptivity (see for example [1]). Indeed, goal-based methods have the advantage of focusing resolution where is needed, reducing thus the computational cost in computing the targeted quantity of interest. This work proposes a novel extension of the aforementioned approach based on a Riemannian metric computation to the case of systems approximations bearing a stochastic component. The adaptive approach is indeed necessary in the stochastic space since we are interested in accurately capturing singularities such as shocks known to propagate from the deterministic (spatial) to the uncertain parameters domain ([2,3]). To this end, an optimisation problem leading to the best control of the distinct sources of errors is formulated in the continuous framework of the Riemannian metric space [4]. Algorithmic developments are also presented in order to quantify and adaptively adjust the error components in the deterministic and stochastic approximation spaces. The capability of the proposed method is tested on various compressible, steady problems, including on a HyShot II scramjet configuration subjected to geometrical and operational parametric uncertainties. It is demonstrated to accurately capture discontinuous features of stochastic compressible flows impacting some quantities of interest, while balancing computational budget and refinements in both spaces. References: [1] A. Loseille, A. Dervieux, and F. Alauzet. Fully anisotropic goal-oriented mesh adaptation for 3D steady Euler equations. *J. Comp. Phys.*, 229:2866–2897, 2010. [2] C.M. Bryant, S. Prudhomme, and T. Wildey. Error decomposition and adaptivity for response surface approximations from PDEs with parametric uncertainty. *SIAM/ASA Journal on Uncertainty Quantification*, 3(1):1020–1045, 2015. [3] L. Mathelin and O. Le Maître. Dual-based a posteriori error estimate for stochastic finite element methods. *Communications in Appl. Math. and Comput. Science*, 2(1):83–115, 2007. [4] J.W. Van Langenhove. Adaptive control of deterministic and stochastic approximation errors in simulations of compressible flow. PhD thesis, University Pierre and Marie Curie (Paris VI), Paris, France, 2017.

A Computational Model for the Finite Element Analysis of Coupled Hygro-thermo-elasto-visco Plastic Behaviours: Application to Timber Structures

Salim Belouettar^{*}, Ahmed Makradi^{**}, Marc OUDJENE^{***}

^{*}Luxembourg Institute of Science and Technology, Luxembourg, ^{**}Luxembourg Institute of Science and Technology, ^{***}University of Lorraine, France

ABSTRACT

A 3-D rheological model that accounts for elastic, plastic, hygro-expansion, viscoelastic and mechano-sorption is developed. A coupled hygro-mechanical multiscale modelling is developed and implemented in a finite element commercial software via user subroutine material. The modelling considers instantaneous and time-dependent responses of material wood that include elastic, plastic, hygro-expansion, viscoelastic and Mechano-sorption deformations. The partial differential equations governing heat transfer and thermo-elasticity are solved in the three-dimensional space whereas the partial differential equation for moisture diffusion in the two dimensional domains. The model is used to analyze the response of wood structures when subjected to coupled loading such as moisture, heat and mechanical loading.

Dassault Systèmes 3DEXPERIENCE High Performance Modelling-meshing, Visualization and New SIMULIA AMG-based Iterative Solving Technology to Solve Real-world Industrial Problems of 200+ Million Degrees of Freedom

Vladimir Belsky*

*Dassault Systemes, R&D; SIMULIA

ABSTRACT

For a long time, many of our customers are looking for ways to solve super large problems but have little success due to many constraints: difficulty creating such models, inability to solve those models that could be created, and the inability to display the results of those problems that could be solved. We currently observe an “explosion” of model sizes from many customers from very different industries all over the world. 100M Degrees of Freedom implicit finite element models are becoming the reality these days. In this presentation we discuss both our experience with the state-of-art AMG-based iterative solving technology and its performance using real world industrial examples for solving ultra-big models which size can be up to 200M Degree of Freedom. During the last decade, almost all the commercial vendors of finite element software started offering both iterative and direct solver technology for solving large sparse systems of linear equations arising from finite element discretization of structural mechanical problems using an implicit time integration approach. Typically, when working with large problems, a majority of the wall clock time is spent in the linear equation solver. For blocky models the time spent in the direct sparse solver is more than 2/3 of the entire analysis time and all other processing steps are much faster. From our experience the number of floating point operations (FLOPS) required by a direct sparse solver to factorize the matrices has a quadratic grow rate with the number of degrees of freedom; and sometimes the growth rate could be even higher! This means that the direct solver technology has limitations when it comes to solving really “large” scale problems. However, “large” scale problem means not only the number of equations, but mainly the number of FLOPS required for factorization. In other words, the applicability of the direct- solution technique depends largely on how “bulky” the problem is (the power in the exponent in the relation between the number of FLOPS and the number of degrees of freedom). Alternatively, iterative solvers provide a scalable and fast solution for “large” problems. They are scalable in the problem size sense as well as parallel scaling. They provide dramatic performance improvements for suitable applications. Moreover, in many cases they act as enabling technology rather than a solver alternative. Particularly, this is true for cases where the direct solver factorization cost is prohibitively expensive. Unfortunately, iterative solver technology has inherent limitations and robustness issues. Very often in real-world industrial applications, iterative solvers fail to converge because of various modeling issues that are present in a model. The direct solver technology is much more forgiving in this aspect. There are many reasons for traditional iterative solvers having convergence problems (unphysical behavior of gasket elements, insufficient amount of contact constraints to keep all of the parts in the model from rigid body movements, highly heterogeneous materials, etc. A new AMG-based technology was recently developed and implemented in Abaqus/Standard which allows for dramatic robustness improvement of the AMG iterative procedure applied to real world industrial problems which routinely include advanced modelling features such as multipoint constraints, gaskets with highly nonlinear material properties, contact constraints, kinematic couplings, pretension sections, periodicity boundary conditions, etc. Our extensive experiments with the most complex customer models demonstrated robustness of the new equation solver which was absolutely impossible to observe with the traditional AMG procedures. We will demonstrate this claim using some of these results.

Conservative Extension of the MAC Scheme to Polyhedral Meshes

René Beltman^{*}, Martijn Anthonissen^{**}, Barry Koren^{***}

^{*}Eindhoven University of Technology, ^{**}Eindhoven University of Technology, ^{***}Eindhoven University of Technology

ABSTRACT

The MAC scheme introduced by Harlow and Welch [1] is one of the most popular methods for simulating viscous incompressible flow. The MAC scheme is a staggered Cartesian mesh method in which the incompressible Navier-Stokes equations are discretized in terms of the normal velocity components at the cell faces and the pressure variables in the cell centers. The staggered positioning of the velocity variables allows for an efficient discretization of the continuity equation that leads to exact conservation of mass and avoids pressure oscillations. Moreover, it can be shown that the method also conserves momentum, and, secondary quantities like kinetic energy (in the inviscid limit) and vorticity. In recent years, many advances have been made in the field of polytopal discretization methods. These advances allow for an extension of the MAC scheme to polytopal meshes. For the incompressible Stokes equations these extensions have been introduced in recent years (see for example [2]). However, a fully conservative extension of the discrete convective term to polytopal meshes has not been found yet. In this paper we study different extensions of the MAC scheme to polytopal meshes. We show that these extensions have many of the favorable properties of the Cartesian-mesh MAC scheme. Moreover, we focus on the convective term and discretize different formulations (conservative, rotational) of this term. We analyze them and compare their numerical efficiency. References [1] F.H. Harlow, J.E. Welch, Numerical calculation of time-dependent viscous incompressible flow of fluid with free surface, *Physics of Fluids* 8, 2182-2189, 1965. [2] J. Bonelle, A. Ern, Analysis of compatible discrete operator schemes for the Stokes equations on polyhedral meshes, *IMA Journal of Numerical Analysis* 35, 1672-1697, 2014.

Comparative Responses of the Q6 and PIPER 6YO Human Body Model in Simulated Frontal Impacts

Aditya Belwadi*, Jalaj Maheshwari**, Nhat Duong***

*The Children's Hospital of Philadelphia, **The Children's Hospital of Philadelphia, ***The Children's Hospital of Philadelphia

ABSTRACT

There has been ample evidence from real world crashes that belt-positioning booster seats reduce injury risk for children 4 through 7 years of age. Newer booster seat designs have been moving the lap-belt anterior of the anterior superior iliac spine (ASIS) potentially causing them to load the pelvis at a later time in the crash sequence. The objective of this project was to gain insight into causation of injuries sustained by children seated in newer booster seat designs in simulated frontal impacts utilizing pediatric human body finite element models. The PIPER 6-year-old human body finite element (FE) model along with a Q6 FE model was utilized. The test environment was modeled as per FMVSS 213 test conditions. Booster seat models were developed by scanning physical seats and converting them FE mesh with elastic/plastic material properties. The sled test condition was validated against physical test conditions of the instrumented Q6 restrained using a 3-point lap-shoulder belt (without a retractor/pre-tensioner). HIC36, head and chest resultant accelerations were matched to within (plus/minus 8% of maximum along with phase matching). The PIPER HBM was then positioned as per the test condition on four different booster conditions (No booster, Highback, lowback and portable) on the 213-test bench. A frontal crash pulse of 24G (Max at 80ms over 120ms) was utilized. A total of 16 simulations were carried out with the Q6 and PIPER FE models. Kinetic and kinematic measures were extracted and processed as per SAEJ211. The kinetic measures (HIC36, head and chest resultant acceleration) of the Q6 were well within FMVSS 213 IARV limits. For the newer seat designs with anterior lap-belt routing, the response of the Q6 was similar to the test condition – increased neck force (Fy) and delayed engagement with the pelvis causing the torso to arch forward. The PIPER HBM submarined as expected for the condition with a booster seat. In both the no-booster and portable seat condition the shoulder belt engaged the neck (ie; medial motion) causing excessive strain (21%) in the neck musculature. The torso arching caused higher lumbar. Booster seats are in general shown to be effective measures for restraining children safely. Newer seat designs have proved to be innovative while providing solutions to changes in mobility. The human body model provides a good measures of injury assessment for children restrained in these seats. Additional testing is needed to address other crash modes.

Extended-adaptive Computational Methodology for the Solution of Adhesive Contact Problems

Hachmi Ben Dhia^{*}, Shuimiao Du^{**}

^{*}CentraleSupélec-Université Paris-Saclay, ^{**}CentraleSupélec-Université Paris-Saclay

ABSTRACT

Adhesive contact between solids is important to many areas of applied science and technology, particularly nowadays for the design of micro and nano electronic devices. This is one of the reasons for which an important range body of research works is still devoted to adhesive contact problems (ACP) at different scales. This work is an investigation on some mathematical and computational aspects of theoretical formulations and numerical approximation methods in this topic. We present and test some new ideas that contribute to the enhancement of the reliability and efficiency of the resolution of ACP, based on the Lennard-Jones (LJ) surface potential, in the continuum framework. More precisely, to address mathematical and numerical pitfalls of the phenomenological stiff repulsive part of the LJ model, a sequence of partitions of contact models is adaptively constructed to both extend and approximate the LJ model. It is formed by a combination of the LJ model with a sequence of shifted-Signorini (or, alternatively, -Linearized-LJ) models, indexed by a shift parameter field, defined on the potential contact surface. For each model of this sequence, a weak (hybrid mixed or primal) formulation of the associated local ACP is developed. To track the critical localized areas of adhesive contact, a two-step strategy is developed: Independently of the iterations, a macroscopic contact problem, based on a macro contact model (no adhesion), is first formulated, approximated and solved once to detect contact-noncontact separation zones. In the second step and at each shift-adaptive iteration, a micro-macro ACP, based on a given shifted partition of micro-macro adhesive contact model is re-formulated within the multiscale Arlequin framework [1]-[3]; the micro-Arlequin patches being defined in the critical areas detected in the first step. This problem is consistently approximated and solved to compute accurately the solution in the adhesive contact zones, while reducing significantly the computation costs. Numerical results for classical adhesive contact tests are given. The adaptive shift-algorithm proves to be remarkably performant and the comparison of our results with available analytical and numerical results, obtained with other approaches, shows the effectiveness of our global strategy. [1] H. Ben Dhia, Multiscale mechanical problems: the Arlequin method, *Comptes Rendus Acad Sci, Paris*, 326(12), 1998, 899-904 [2] H. Ben Dhia, C. Zammali, Level-Sets fields, placement and velocity based formulations of contact-impact problems, *IJNME*, 69, 13, 2007, 2711-2735 [3] H. Ben Dhia, Further Insights by Theoretical investigations of the Multiscale Arlequin Method, *IJMCE*, 6(3), 2008, 215-232 2008

Multidisciplinary Design Optimization of Transport Aircraft Wing Using High Fidelity Modeling Process

Abdelkader Benaouali*, Stanislaw Kachel**

*Military University of Technology, **Military University of Technology

ABSTRACT

Because of its role as the primary lifting surface of an aircraft, a special attention must be drawn to the wing design by considering both structural mechanics and aerodynamics as well as the strong dependency between them. The design is no longer a trial-and-error procedure due to the introduction of numerical optimization, resulting in what is currently designated as multidisciplinary design optimization MDO in the case where several disciplines are involved. The aim to accurately model the complex wing behavior necessitates the use of high fidelity modeling techniques, namely finite element method (FEM) and computational fluid dynamics (CFD). The objective of this work is to construct an MDO framework, proposed for the design of transport aircraft wing, based on an automated environment which integrates a set of most popular and commonly used commercial modeling and simulation software. It goes through geometric modeling in SIEMENS NX, Aerodynamic meshing in ICEM CFD, flow solution using ANSYS FLUENT, Structural modeling and analysis in MSC.PATRAN/NASTRAN. The integration is made possible by means of data exchange translators available in most of computer aided tools, while the design automation is realized via respective software scripting capabilities as well as the possibility to run in batch mode. Because of the simulation cost required for evaluating the high fidelity models, especially for CFD calculations, a single run of the design framework may be very time consuming making a direct optimization on the design framework highly impractical. Therefore, an optimization strategy based on meta-modeling techniques is adopted. The improved Latin Hypercube Sampling (IHS) is used for the Design of Experiments (DoE) and the radial basis function (RBF) method is used as the surrogate model. The reliability of the proposed approach is investigated through its application for design of a transport aircraft wing considering shape and structural design variables. In order to perform an optimization that considers both structural and aerodynamic performance, the objective function must combine the wing aerodynamic and structural properties. In this work, aircraft range is chosen as it is a function of the lift-to-drag, which represents the wing aerodynamic performance, and the ratio of the initial and final cruise aircraft weights which represents the structural optimization term.

A First--Principles Approach to the Derivation of a Reduced Order Model for Vortex--Induced Structural Oscillations

H. Benaroya^{*}, S. Mottaghi^{**}

^{*}Rutgers University, ^{**}William J. Hughes Technical Center, FAA

ABSTRACT

While variational methods have proven to be very effective tools in modeling the dynamics of solid systems, there have been many challenges faced in applying them to fluid systems and fluid-structure interaction (FSI) problems. As evident from the literature, the efforts to apply Hamilton's principle and Lagrange's equations to the problems of fluid dynamics have had relative success in certain cases, mainly ideal fluids. There exist no general variational approaches for fluid-structure interactions, or for viscous fluid dynamics problems. One main challenge arises from relating the variational principles in the Lagrangian frame to the Eulerian frame. Therefore, we start by considering the Eulerian and the Lagrangian reference frames and review the relations between dynamic properties as described in these reference frames for a general control volume. Then, these relations are used to identify the difficulties faced in applying variational principles in an Eulerian frame of reference. Having identified the challenges above, Jourdain's principle (JP) is proposed as an effective tool to overcome some of those difficulties. Then, JP is extended so as to become applicable to control volumes containing Newtonian incompressible viscous fluids. In this way we derive the Navier-Stokes equations. Subsequently, JP is used to derive the energy rate equation for a general control volume containing Newtonian incompressible viscous fluids, suggesting that a correction term may need to be added to the classical energy equation. Moreover, the limitations of the classical energy equation are explored by deriving it from Hamilton's principle. This lays the theoretical foundation for utilizing JP for modeling both fluids and structures as FSI systems. The general formulation is extended so that the reduced-order modeling of FSI and VIV systems can be performed using the extended JP. By using this very general framework, we can add assumptions in order to derive well-known "flow-oscillator" models. These flow-oscillator models are generally presented following an examination of experimental results, with semi-empirical equations of motion that generally represent similar global dynamic behavior stipulated. By being able to simplify the more general equations to these flow-oscillator equations, we are able to discover some of the implicit assumptions they represent.

Modeling of Failure Propagation in High Explosive Using Dominant Crack Approach

Bart Benedikt*, Partha Rangaswamy**

*Los Alamos National Laboratory, **Los Alamos National Laboratory

ABSTRACT

Numerical simulations of systems composed of High Explosives (HE) capable of accurately predicting the state of stress and deformation during various dynamic loading scenarios require high-fidelity constitutive models of HE. In this research, a strain rate-dependent model for propagating damage under dynamic loading is presented. The constitutive model is based on the concepts of Statistical CRACK Mechanics (SCRAM) and strain rate dependent visco-elasticity. The damage evolution in HE is modelled by simulating the rate of growth also called the critical crack. Critical crack is defined as a crack that becomes unstable for a given loading conditions. In the formulation presented here the critical crack propagation is assumed to depend on the rate and history of loading rate. The numerical implementation of the constitutive model into ABAQUS/Standard implicit finite element code through a user subroutine is also presented. The developed finite element code is used to numerically simulate several tests performed on HE materials available to the authors. The results of the simulations and the comparison with the experimental work are presented and discussed. The method to calibrate the model parameters based on the testing results is discussed. In general, the numerical simulation was able to correctly predict the material regions, which were most likely to initiate the failure. In conclusion, we argue that the present approach is a considerable improvement over existing models used to simulate HE behavior [1-2] and it can be successfully used to predict the bulk response and the initiation and propagation of failure in the studied HE materials. References 1. Addessio, F. L., Johnson, J. N., 1990. A constitutive model for the dynamic response of brittle materials. *Journal of Applied Physics* 67, 3275-3286 2. Bennett, J. K., Haberman, K. S., Johnson, J. N., Assay, B. W., Henson, B. F., 1998. A constitutive model for the non-shock ignition and mechanical response of high explosives. *Journal of the Mechanics and Physics of Solids* 46, 2303-2322. LA-UR-17-31482

Improvement and Verification of Moving Particle Semi-Implicit Method for Multi-Physics Simulation of High Viscosity Fluids

Nicolas Benkemoun^{*}, Seiichi Koshizuka^{**}, Kazuya Shibata^{***}

^{*}The University of Tokyo, ^{**}The University of Tokyo, ^{***}The University of Tokyo

ABSTRACT

The MPS method was originally proposed for use for purely Newtonian fluids and is mainly used with water or oils, or fluids of similar viscosities. However, issues arise when using increasingly higher viscosities. Using the higher order terms proposed by Khayyer and Gotoh [1], we analyze the flow of highly viscous polymers. We also implement a Cross viscosity model to check the behavior of shear dependent fluids, which allows the study of more realistic behaviors. Comparison with an improved SPH scheme [2] is done to evaluate this improvement of the MPS method. A qualitative thermal analysis is also carried out for future applications to a Thermoplastic Injection Process. [1] A. Khayyer and H. Gotoh, "Enhancement of stability and accuracy of the moving particle semi-implicit method", J. Comput. Phys., 230, pp. 3093-3118, (2011) [2] J. Ren et al., "Simulation of complex filling process based on the generalized Newtonian fluid model using a corrected SPH scheme", Comput. Mech., 46, pp. 643-665, (2012)

On the Role of Structure Tensors in Large Strain Anisotropic Hyper-Elastoplasticity of Geomaterials and Drucker-Prager/Cap Plasticity

Kane Bennett^{*}, Richard Regueiro^{**}, Darby Luscher^{***}

^{*}Los Alamos National Laboratory, ^{**}University of Colorado Boulder, ^{***}Los Alamos National Laboratory

ABSTRACT

Describing anisotropic mechanical behavior of a material requires identifying preferential directions of the material, giving rise to second order structure tensors (also called fabric tensors in the context of geomechanics). Structure tensors allow the scalar valued tensor functions of hyper-elastoplasticity, namely the free-energy, plastic potential, and yield function, to be expressed as isotropic functions representing an anisotropic material response. Ensuring thermodynamic consistency of elastoplastic constitutive models for geomaterials further requires accounting for inelastic volume changes and appropriately discriminating between elastic and plastic contributions to the deformation field. The precise way that these two basic requirements are fulfilled (i.e., formulating anisotropic hyper-elastoplastic models for geomaterials) necessitates making certain assumptions and material specific constitutive choices. In this talk, large strain anisotropic hyper-elastoplasticity of geomaterials is examined, with emphasis on the role of structure tensors in formulating thermodynamically consistent constitutive equations. Formulation is carried out in terms of Mandel and Eshelby-Mandel stresses within the intermediate configuration associated with the multiplicative split of the deformation gradient. Necessary material assumptions and particular constitutive choices are identified for the development of a novel anisotropic Drucker-Prager/Cap material model. The ability of the model to capture anisotropic elastoplastic behavior is exemplified through numerical experiments and nonlinear finite element modeling of existing measurements.

Recent Developments in Isogeometric Analysis for LS-DYNA

David Benson^{*}, Liping Li^{**}, Attila Nagy^{***}, Stefan Hartmann^{****}

^{*}LSTC, ^{**}LSTC, ^{***}LSTC, ^{****}Dynamore GmbH

ABSTRACT

LS-DYNA is the first commercial code to support IGA through the implementation of generalized elements, and then through key word descriptions of patches of B-spline and NURBS elements. Three shell formulations and a solid element formulation are currently available. Additional capabilities have been recently added, including improved contact, anisotropic material modeling, spotweld modeling and support for unstructured spline capabilities through the specification of their Bezier extraction. These and other recent additions are described and demonstrated. In addition, some of the difficulties industry has encountered in moving to this new technology are discussed.

Extended Virtual Element Method for Problems with Singularities

Elena Benvenuti^{*}, Andrea Chiozzi^{**}, N. Sukumar^{***}, Gianmarco Manzini^{****}

^{*}Engineering Department, University of Ferrara, Italy, ^{**}Engineering Department, University of Ferrara, Italy, ^{***}UC Davis, USA, ^{****}Los Alamos National Laboratory, New Mexico, USA

ABSTRACT

Extended Virtual Element Method for Problems with Singularities E. Benvenuti^{1*}, A. Chiozzi¹, N. Sukumar², G. Manzini³ ¹ University of Ferrara, Ferrara, Italy ² University of California, Davis, USA ³ Los Alamos National Laboratory, New Mexico, USA E-mail: andrea.chiozzi@unife.it, elena.benvenuti@unife.it, n.sukumar@ucdavis.edu, gmanzini@lanl.gov Keywords: virtual element method; extended finite element method; singularities. The eXtended Finite Element Method (XFEM) was first proposed by Belytschko & group [1] as an innovative computational technology for dealing with discontinuities and singularities without tailored meshes. This goal is achieved by enriching the approximation space by means of additional shape functions that reproduce the non-smooth features of the expected solution. Owing to its great flexibility, XFEM has become one of the most exploited methodology for crack simulation in mechanical and structural engineering. More recently [2], an eXtended Finite Element Method exploiting polygonal basis functions has been proposed for polytopal meshes, that can be especially useful when meshing complex domains, such as those occurring in bodies with cracks and inclusions. The Virtual Element Method (VEM) is a generalization of the Finite Element Method capable of dealing with very general polytopal meshes without using polygonal basis functions[3]. The key feature of VEM relies on the introduction of a suitable projector operator to approximate the bilinear form arising in the weak formulation of the continuous problem, so that the explicit construction of the elemental basis functions can be avoided. Based on illustrative numerical examples, the presentation to be delivered at the conference aims to discuss how to extend the XFEM to polytopal meshes by exploitation of the VEM methodology in problems with singular unknown fields. References [1] Moës, N., Dolbow, J. and Belytschko, T., "A finite element method for crack growth without remeshing", International Journal for Numerical Methods in Engineering, 46, 131-150, 1999. [2] Tabarraei, A. and Sukumar, N., "Extended finite element method on polygonal and quadtree meshes", Computer Methods in Applied Mechanics and Engineering, 197, 425-438, 2008. [3] Beirão da Veiga, L., Brezzi, F., Cangiani, A., Manzini, G., Marini, L.D. and Russo, A., "Basic Principles of Virtual Element Methods", Mathematical Models and Methods in Applied Sciences, 23, 119-214, 2013.

Towards Optimal Design of Engineering Systems

Viktor Berbyuk*, Seyed Milad Mousavi Bideleh**

*Chalmers University of Technology, Gothenburg, Sweden, **VETEC AB, Mölndal, Sweden

ABSTRACT

This paper presents a review on methods, algorithms and tools available for robust optimal design of engineering systems. The focus primarily is put on methods and algorithms for global sensitivity analysis (GSA) and solution of Pareto optimization problems (POP) for multidimensional nonlinear mechanical systems. The computer code SAMO, developed at Chalmers University of Technology, is presented as an efficient toolbox for optimal design of engineering systems with different applications. At this stage, the toolbox SAMO includes two modules: SAMO-GSA and SAMO-POP. The module SAMO-GSA is developed based on the multiplicative version of the dimensional reduction method (M-DRM) [1]. In the SAMO-GSA an efficient approximation is employed to simplify the computation of variance-based sensitivity indices associated with a general function of n -random variables. The GSA results of the engineering system in question are then presented as a mapping of the design parameters and total sensitivity indices of the objective functions. These results might be used as an input to the SAMO-POP for multi-objective optimization. The module SAMO-POP works based on genetic algorithm (GA). The GA settings include lower and upper bounds for variation of the design parameters, population size, number of generations, elite count, and Pareto fraction settings. The results of SAMO-POP are presented in terms of Pareto fronts and corresponding Pareto sets for further analysis and decision making by the user. The efficiency of the proposed algorithms and developed toolbox is illustrated, first on scholar applications (thermally induced stress intensity factor and quarter car vehicle model), and second by GSA and solutions of several multi-objective optimization problems for a nonlinear multidimensional mechanical system which represents bogie suspension components of a high-speed train [2-3]. Finally, based on the literature review and the results obtained the paper presents the outlook of the future research in developing of computationally efficient algorithms for extension of the toolbox SAMO for robust optimal design of engineering systems. References 1. Zhang, X. and M. D. Pandey, (2014), An effective approximation for variance-based global sensitivity analysis, *Reliability Engineering and System Safety*, 121, 164-174. 2. Mousavi Bideleh, M.S. and V. Berbyuk, (2016), Global sensitivity analysis of bogie dynamics with respect to suspension components, *Multibody System Dynamics*, 37, No. 2, 145-174, DOI: 10.1007/s11044-015-9497-0, <http://dx.doi.org/10.1007/s11044-015-9497-0> 3. Mousavi-Bideleh, M.S., and V. Berbyuk, (2016), Multiobjective optimisation of bogie suspension to boost speed on curves, *Vehicle System Dynamics*, 54, No 1, 58-85, DOI: 10.1080/00423114.2015.1114655 <http://dx.doi.org/10.1080/00423114.2015.1114655>

A Finite Element Method for Modeling Surface Growth and Resorption of Deformable Solids

Guy Bergel*, Panayiotis Papadopoulos**

*University of California, Berkeley, **University of California, Berkeley

ABSTRACT

Surface growth and resorption occur in a variety of engineering applications and natural phenomena including the accretion of layers in tree trunks and shells, polymerization of filaments aiding locomotion of cells, additive manufacturing, and metal solidification. The deposition of mass onto the surface of a physical body generates material points whose reference configurations depend on their time of deposition. Furthermore, the removal of mass through a given surface defines an ablated boundary along a formerly interior portion of the domain. Both addition and removal of mass characterize a rate-dependent process in which the spatial representation of a given subregion in a physical body relies on an evolving reference configuration [1]. In this work, a numerical framework is developed to capture the surface growth and resorption of a solid undergoing finite deformation using a methodology which extends the classical arbitrary Lagrangian-Eulerian (ALE) finite element method [2]. To this end, an intermediate configuration is defined which tracks the evolving reference state of the body based on the position of its surface and thus provides a means for enforcing balance laws at a given time. Examples illustrating the effects of surface growth and resorption on the spatial and temporal convergence of a two-dimensional body in plane strain are discussed. Moreover, specific algorithmic procedures of growth-induced multibody interaction are introduced within the context of cell motility. References [1] G. A. Ateshian, "On the theory of reactive mixtures for modeling biological growth," *Biomechanics and Modeling in Mechanobiology*, vol. 6, pp. 423–445, Nov 2007. [2] N. Hodge and P. Papadopoulos, "A continuum theory of surface growth," *Proceedings of the Royal Society of London A: Mathematical, Physical and Engineering Sciences*, vol. 466, no. 2123, pp. 3135–3152, 2010.

ONERA Composite Material Law for Crash Simulation

Julien Berthe^{*}, Frédéric Laurin^{**}, Antoine Hurmane^{***}

^{*}ONERA, ^{**}ONERA, ^{***}ONERA

ABSTRACT

To reduce the environmental impact and the weight of the vehicles, the transportation industry is increasingly using organic matrix composite materials in structural parts. Such parts are submitted to various kinds of loading, mechanical as well as thermal, during the life cycle of an aircraft. Due to the cost of full-scale testing, advanced numerical method are more and more used to predict the response of a composite aircraft structure regarding crash loading. Various improvements of advanced simulations can be considered: material law, cohesive law, contacts modelling... In this work, an advanced material law is considered and improved in order to accurately describe the rate dependency of organic matrix composite materials. The ONERA progressive failure model which has been well ranked in the second world wild failure exercise has been considered as a starting point. Firstly, some simplifications have been done to take into account the specificities of crash simulations. Secondly, based on test results available at ONERA and/or tests available in the literature, the introduction of rate dependencies in the material law has been considered. In order to validate or justify some hypothesis, new experimental procedures have been developed or proposed. An overview of the recent experimental results and of the future experimental tests for the material law validation will also be presented in this paper.

Stabilizing DG Methods on Polygonal Meshes via Computable Dual Norms

Silvia Bertoluzza^{*}, Ilaria Perugia^{**}, Daniele Prada^{***}

^{*}Consiglio Nazionale delle Ricerche, ^{**}University of Vienna, ^{***}Consiglio Nazionale delle Ricerche

ABSTRACT

The choice of the stabilization terms (or, equivalently, of the definition of the numerical fluxes and/or traces) is a key issue in the design of DG methods. Usually, some form of penalization is somehow added, where some residual term is measured in a mesh dependent norm, designed so that it somehow mimics the norm of the dual space where the residual naturally exists. The treatment, in the analysis, of such mesh dependent norms calls for the use of direct and inverse inequalities, which, in turn, depend on some “shape regularity” assumptions on the underlying tessellation, which are not always easily satisfied in the polygonal framework. With the final aim of relaxing such requirement, we will present, in this talk, a way to design “cheap” computable norms (and scalar products) for the dual spaces where the residuals live, and of using them in designing the stabilization term for a DG type method for the Poisson equation on a polygonal mesh, in which the unknown in the polygonal elements, the fluxes and the unknown on the edges, are all, independently, approximated by polynomials of degree k .

Scalability and Portability of Large Scale Turbulent Combustion Problems

Martin Berzins*

*SCI INSTITUTE, UNIVERSITY OF UTAH

ABSTRACT

When solving large scale turbulent combustion problems using adaptive techniques, the coming of exascale computer architectures such as Argonne National Laboratory 's A21 and the presence of very different pre-exascale machines such as the fastest present machine the Tianhu SunwayLight and the DOE Summit and Sierra raises the challenge of being able to port codes across very different computer architectures. While the use of approaches based upon Asynchronous Many Task (AMT) Runtime Systems such as the Uintah framework considered here makes porting easier, the central challenge of obtaining performance from the actual loops of the adaptive code remains. In order to explore this issue this talk will examine the performance of the adaptive mesh-based radiation solver using approaches such as the Kokkos portability library within an AMT code. A successful attempt to port Uintah to the Tianhu SunwayLight will be described as a demonstrator of the overall portability approach. This is joint work with Zhang Yand iapm Beijin and Alan Humphrey, John Holmen, Damodar Shahasbarude, Brad Peterson and John Schmidt at Utah.

Hydraulic Fracturing in Naturally Fractured Reservoir Simulation Using Finite Elements with Embedded Discontinuities

Leila Beserra^{*}, Leonardo Guimarães^{**}, Osvaldo Manzoli^{***}

^{*}Federal University of Pernambuco, ^{**}Federal University of Pernambuco, ^{***}São Paulo State University

ABSTRACT

Hydraulic fractures usually propagate perpendicular to the direction of least principal stress, because this is the direction that defines the lowest work. However, modeling hydraulic fracturing in the presence of a natural fracture network is a challenging task, due to the strong coupling that exists between fluid flow and mechanical behavior, as well as the complex interactions between propagating fractures and existing natural interfaces. From the mathematical point of view it is a coupled hydro-mechanical problem, where equations for fluid flow through porous media and fractures (fluid mass balance) and medium deformation and fracture propagation (mechanical problem) have to be solved simultaneously considering the constitutive equations that describe the material behavior. When a fracture propagates through a continuous media, discontinuities in the displacement and fluid pressure fields are introduced. The selection of an appropriate fracture propagation model is a critical task in modeling of hydraulic fracturing. In this paper, a strong discontinuity approach, proposed by Manzoli and Shing (2006), to embed discontinuities into finite elements was implemented in a numerical code that performs numerical analysis of fluid flow in a deformable reservoir. The presence of natural fractures includes an additional difficulty for the modeling of hydraulic fracturing, since they may affect the fluid flow in the reservoir and the orientation of the induced fracture. In order to apply the formulation presented in this paper, the hydraulic fracturing problem in reservoirs with pre-existing fractures was simulated. A numerical tool was used to embed the natural fracture network into the finite element mesh, with respect to the geological mapping of these fractures. To model the mechanical behaviour of material, was adopted a tensile damage model proposed by Sánchez et al. (2014). The resulting numerical code was used to model hydraulic fracture propagation through naturally fractured reservoirs with relatively coarse meshes in a reasonable computational time. Furthermore, the results provided an important insight into the mechanisms that generate microseismicity that occurs during hydraulic fracture stimulation. The interpretation of microseismicity based on geomechanical analysis gives a more realistic estimation of the stimulated reservoir volume (SRV), otherwise SRV can be overestimated. REFERENCES Manzoli, O.L. and Shing, P.B. [2006] A general technique to embed non-uniform discontinuities into standard solid finite elements. *Computers & Structures*, 84, 742–757. Sánchez, M.; Manzoli, O. L.; Guimarães, L. J. N. [2014] Modeling 3-D desiccation soil crack networks using a mesh fragmentation technique. *Computers and Geotechnics*, 62, 27-39.

Data-driven Design of New Materials and Structures

Miguel Bessa*

*Delft University of Technology

ABSTRACT

A data-driven computational framework [1] combining Bayesian machine learning for imperfection sensitive quantities of interest, uncertainty quantification and multi-objective optimization is developed to analyze and design new materials and structures. This talk intends to demonstrate the generality of the proposed framework, highlighting key challenges and possible solutions illustrated by three different design problems: toughening composite materials by tuning the plastic behavior of the constituents, improving collapse behavior of ultra-thin satellite structures with uncertain ultimate buckling strength, and finding unprecedented properties by exploring a new material concept. [1] Bessa, M.A., Bostanabad, R., Liu, Z., Hu, A., Apley, D.W., Brinson, C., Chen, W., Liu, Wing Kam, "A framework for data-driven analysis of materials under uncertainty: Countering the curse of dimensionality," Computer Methods in Applied Mechanics and Engineering, 320, 633–667 (2017).

The GENERIC formalism for the thermodynamically consistent formulation and discretization of coupled thermomechanical solids

Peter Betsch*, Mark Schiebl**

*Institute of Mechanics, Karlsruhe Institute of Technology (KIT), Germany, **Institute of Mechanics, Karlsruhe Institute of Technology (KIT), Germany

ABSTRACT

GENERIC (General Equation for the Non-Equilibrium Reversible-Irreversible Coupling) is a double-generator formalism for the thermodynamically consistent formulation of problems from continuum mechanics. The GENERIC-based formulation relies on an additive decomposition of the evolution equations into a reversible part and a dissipative part. While the reversible part is generated by the total energy of the system, the irreversible part is generated by the total entropy. Originally, GENERIC has been developed in the context of complex fluids (H.C. Öttinger, *Beyond Equilibrium Thermodynamics*, Wiley, 2005). More recently, the GENERIC framework has been extended to solid mechanics. Romero (I. Romero, Thermodynamically consistent time-stepping algorithms for nonlinear thermomechanical systems, *IJNME*, 79(6): 706-732, 2009) realized soon the great potential of the GENERIC formalism for the design of structure-preserving numerical schemes and coined the notion of a thermodynamically consistent (TC) method. Alternatively, TC schemes may be termed Energy-Entropy-Momentum (EEM) schemes. These methods can be viewed as extension to dissipative systems of earlier developed Energy-Momentum (EM) schemes for conservative systems with symmetry such as large strain elastodynamics and flexible multibody dynamics (P. Betsch, editor, *Structure-preserving Integrators in Nonlinear Structural Dynamics and Flexible Multibody Dynamics*, Vol. 565 of CISM Courses and Lectures, Springer, 2016). Previously developed GENERIC-based TC methods for thermomechanically coupled solids are typically subject to serious limitations such as (i) the use of the entropy density as thermodynamical variable, and (ii) the restriction to isolated (or closed) systems in which the boundaries are neglected. In the present talk we propose a generalized GENERIC-based formulation that (i) allows for the free choice of the thermodynamical variable among either the temperature, internal energy density or entropy density, and (ii) takes into account the boundaries of the system. The new formulation lays the ground for the design of structure-preserving (e.g. TC) methods for the solution of initial boundary value problems for thermomechanically coupled solids. In the talk we focus on the dynamics of thermoelastic solids with heat conduction.

A Closed-Form Solution and Comparison for the One-Dimensional Orthorhombic Quasicrystal and Crystal Plate

Arpit Bhardwaj^{*}, Koushik Roy^{**}

^{*}Undergraduate Student, IIT BHU, ^{**}Assistant Professor, IIT Patna

ABSTRACT

Quasicrystals (QCs) are solids with a long-range quasi-periodic translational order, and a long-range orientational order was first discovered around in 1984. The work includes derivation of the exact-closed form solution for simply supported quasicrystal and crystal plates by using propagator matrix method under surface loading, free vibration, and patch loading. As a numerical example a quasicrystal and a crystal plate are considered, and after investigation, the variation of displacement and stress fields along the thickness of these two plates are presented. Further, it includes analyzing the displacement and stress fields for two plates having two different stacking arrangement, i.e., QuasiCrystal/Crystal/QuasiCrystal and Crystal/QuasiCrystal/Crystal and comparing their results. This will not only tell us the change in the behavior of displacement and stress fields in two different materials but also how these get changed after trying their different combinations. For the free vibration case, Crystal and Quasicrystal plates along with their different stacking arrangements are considered, and displacements are plotted in all directions for different Mode Shapes. At last, effect of patch loading is considered as a result of dynamic loading on multi-layered 1D plate and numerous results were obtained such as, displacement and Stress fields for different area of patch along with different normalized frequencies, displacement and Stress fields for different ratios of Phason-Phonon Coupling constant ϵ and C_{66} along the thickness direction, displacement and Stress fields variation along one of the Length's direction. The numerical results can be further used as a benchmark for investigating various properties of quasicrystals which make them different from crystals. Using the results from the stacking arrangement QuasiCrystal/Crystal/QuasiCrystal, we can use properties of Quasicrystal such as less friction coefficient and low conductivity which will lower the frictional losses in machines if we can use brittle Quasicrystal as a coating over a strong crystal axle. Keywords: Quasicrystals, Multilayered Plates, Surface Loading, Patch Loading, Free Vibration References: [1] L.-Z. Yang, Y. Gao, E. Pan, and N. Wakschanski, "An exact closed-form solution for a multilayered one-dimensional orthorhombic quasicrystal plate," *Acta Mechanica*, vol. 226, no. 11, pp. 3611–3621, 2015. [2] Wakschanski N, Pan E, Yang L, Gao Y. Free Vibration of a Multilayered One-Dimensional Quasi-Crystal Plate. *ASME. J. Vib. Acoust.* 2014;136(4):041019-041019-8. doi:10.1115/1.4027632. [3] T. Fan, *The Mathematical Elasticity of Quasicrystals and its Applications*. Springer, 2011.

Certified Model Order Reduction of an Elastic Body with Large Deformations

Ashish Bhatt*, Dennis Grunert**, Jörg Fehr***, Bernard Haasdonk****

*University of Stuttgart, **University of Stuttgart, ***University of Stuttgart, ****University of Stuttgart

ABSTRACT

Model order reduction (MOR) of nonlinear mechanical systems is a technique of reducing the computational complexity of the corresponding mathematical model by reducing associated degrees of freedom and thereby obtaining a model of reduced dimension. This reduced model can then be simulated efficiently in multi-query scenarios. The gain in simulation efficiency often comes at the cost of the low fidelity of the reduced model. Model verification or certification of the reduced method by estimating the error incurred is important to use the simulation for management decisions and engineering applications. We derive the equation of motion of an elastic body under large rigid motion in the absolute coordinate formulation (ACF) using principles of continuum mechanics. For this purpose, the motion of the elastic body is decomposed into a large rigid body displacement and a small elastic displacement with respect to some fixed inertial frame. The principle of virtual work is then used to derive a second order nonlinear differential equation, with a constant mass matrix, governing the motion of the body with respect to the inertial frame. Constraints to the elastic body are modeled with additional algebraic equations. The overall motion of the body is therefore governed by a nonlinear DAE. The parametrized equation obtained from the spatial discretization of the DAE is often very high dimensional and is therefore computationally prohibitive to solve especially in multi-query scenarios. One, therefore, needs a reduction strategy [1] to simulate the system dynamics efficiently. In the absence of rigid body motion, the resulting DAE is linear and we investigate the error incurred in such systems in [3]. We are interested in the reduction and estimation of the error incurred in the nonlinear DAE in [2].

References: [1] Benner, Peter, and Tatjana Stykel. "Model order reduction for differential-algebraic equations: a survey." Surveys in Differential-Algebraic Equations IV. Springer International Publishing, 2017. 107-160. [2] Bhatt, Ashish, and Fehr, Jörg, and Bernard Haasdonk. "Error Estimation in Model Order Reduction of an Elastic Body under large rigid motions." In A.F. Radu (Ed.) European Conference on Numerical Mathematics and Advanced Applications, submitted, 2017. [3] Fehr, Joerg, and Grunert Dennis, and Bhatt, Ashish, and Bernard Haasdonk. "A Sensitivity Study of Error Estimation in Reduced Elastic Multibody Systems." In 9th Vienna International Conference on Mathematical Modelling, submitted, 2018.

Design of Morphing Shape Memory Polymer Structures Via Topology Optimization

Anurag Bhattacharyya^{*}, Kai A. James^{**}

^{*}University of Illinois at Urbana-Champaign, ^{**}University of Illinois at Urbana-Champaign

ABSTRACT

We present a novel approach to the design of morphing structures using topology optimization, while incorporating shape memory polymers (SMPs). The thermomechanical characteristics of SMPs can be exploited to actuate structural deflection to enable morphing toward a target shape. Structures displaying multiple target shapes can be designed by leveraging SMPs with specific deformation characteristics. In the current study, topology optimization is used to optimally distribute a combination of active (SMP) and passive material phases within the design domain. In this way, we are able to tailor the nonlinear response of the structure to achieve the desired morphology. The large-scale deformation undergone by the structure is modeled using a hybrid theory that combines deformable media with a hyperelastic material model. An isoparametric finite element model is used for modeling the deformation characteristics of the structure, and the non-linear structural equilibrium equations are solved using a displacement-controlled Newton-Raphson procedure. The material distribution is parameterized using a modified multi-material SIMP formulation, and the resulting design optimization problem is solved using a gradient-based approach. The design sensitivities are derived and implemented using an adjoint sensitivity formulation. Optimization results will include two-dimensional planar structures capable of deforming into target configurations in response to controlled thermal loads.

Computational Model of Transcatheter Aortic Valve Replacement: a Patient-Specific Approach to Minimize Clinical Complications

Matteo Bianchi^{*}, Gil Marom^{**}, Ram Ghosh^{***}, Giorgia Bosi^{****}, Danny Bluestein^{*****}

^{*}Stony Brook University, ^{**}Tel Aviv University, ^{***}Stony Brook University, ^{****}University College London, ^{*****}Stony Brook University

ABSTRACT

Introduction Transcatheter aortic valve replacement (TAVR) is a minimally invasive procedure which often represents the only lifesaving solution for patients with severe calcific aortic valve (AV). Despite its promising outcomes, adverse events such prosthesis migration and peri-procedural complications such as paravalvular leakage (PVL) have been reported. New lower-profile stents have shown to exert higher mechanical compression on the conduction fibers, thus leading to cardiac conduction abnormalities (CCAs) as a result of suboptimal placement. This work focuses on a patient-specific approach to study the effect of heart beating and the correspondent risk of CCAs following TAVR. Secondly, the effect of valve positioning and balloon inflation on stent anchorage and degree of post-procedural PVL are investigated. **Methods** Refined patient-specific models were reconstructed from pre-TAVR CT scans of patients suffering from PVL and CCAs after TAVR. AV leaflets were modeled with variable thickness and calcifications were embedded in the aortic root [1]. The crimping, the catheterization process and the deployment of the stent was modeled in Abaqus Explicit. Stent anchorage was quantified in terms of contact area and pressure. Transient diastolic flow analyses were conducted in Ansys Fluent and the degree of PVL was quantified as total regurgitant flow rate during diastole. The effect of the heart beating on TAVR valve performance was studied using Simulia Living Heart Human Model (LHHM). The LHHM AV motion was applied to CCAs patient-specific models to assess the strain distribution in the region of the atrio-ventricular node. These results were compared to healthy subjects to determine a mechanical threshold predictive of CCAs. **Results** Three PVL and three CCAs cases have been reconstructed and analyzed with three positions (aortic, midway, ventricular) and two expansions (nominal and over-expansion). PVL quantities showed agreement with correspondent patients' echocardiographic data. A self-expandable Evolut R and a balloon-expandable SAPIEN stents were deployed in the heart beating for three successive cycles, with ventricular deployments and over-expansions leading to higher logarithmic strains in the region in proximity of the left bundle branch, suggesting an increased risk of CCAs. **Discussion** Our study offers a comprehensive methodology to evaluate TAVR valves' performance using patient-specific reconstructed geometries and incorporating novel aspects such as the effect of cardiac motion on the procedure outcome. This would ultimately offer the possibility to develop predictive models to reduce the impact of post-procedural complications. **Acknowledgements:** Funding ? NIH (1U01HL131052, DB). **References** [1] Bianchi, M, et al., Artif Organs, 40:E292-E304, 2016.

Synchrotron measurement and simulation of the heterogeneous internal strain state evolution during in-situ heating in commercial purity titanium with two different crystallographic textures

Thomas Bieler^{*}, Philip Eisenlohr^{**}, Darren Pagan^{***}, Armand Beaudoin^{****}, Fionn Dunne^{*****}, Benjamin Britton^{*****}, Zebang Zheng^{*****}

^{*}Michigan State University, ^{**}Michigan State University, ^{***}Cornell High Energy Synchrotron Source, ^{****}Cornell High Energy Synchrotron Source, ^{*****}Imperial College, ^{*****}Imperial College, ^{*****}Imperial College

ABSTRACT

Computational modeling of anisotropic materials such as titanium is commonly done with a starting assumption of a zero-stress state. However, most non-cubic materials have anisotropic coefficients of thermal expansion. A consequence of this is that upon cooling from a heat treatment temperature, crystals shrink at different rates with decreasing temperature, leading to buildup of elastic strains. In materials with a high yield strength, this can lead to elastic strains that are a significant fraction of the yield stress. To assess this effect, two samples of commercial purity titanium, one with near-random texture, and the other with a strong texture with a preferred c-axis orientation with about 8 x random, were heated in-situ in the CHESS beamline F-2 while collecting diffraction patterns. From averages of the $\langle \epsilon_{11} \rangle$ and $\langle \epsilon_{33} \rangle$ dimensions as a function of temperature, the expansion coefficients for the two alloys showed a similar cross over where the c-axis expansion exceeded a-axis expansion between 700 and 800°C, but the slopes were slightly different. Analysis of internal strain data indicate that some grains have internal stresses as large as 150 MPa at room temperature. The neighborhood of near-zero stress grains was compared with highly stressed grains, revealing different relationships between averages of grain neighbor misorientation vs. distance from each grain in the near-random and textured samples. Anisotropic crystal elastic and plastic simulations of the experiments using the measured microstructures (grain morphology and crystallographic orientations) and thermal history, with the experimentally characterized initial stresses, anisotropic thermal expansion, and temperature dependent elastic moduli have been carried out to compare with measurements to assist interpretation of the experiment and to assess the credibility of the microstructural models.

On the Form-Finding Problem of a New Class of Tensegrity Metamaterials

Zbigniew Bieniek^{*}, Ida Mascolo^{**}, Ada Amendola^{***}, Gianmario Benzoni^{****}, Fernando Fraternali^{*****}, Mariella De Piano^{*****}, Francesco Fabbrocino^{*****}

^{*}Rzeszów University of Technology, Poland, ^{**}University of Salerno, Italy, ^{***}University of Salerno, Italy, ^{****}University of California, USA, ^{*****}University of Salerno, Italy, ^{*****}University of Salerno, Italy, ^{*****}Pegaso University, Italy

ABSTRACT

Keywords: Metamaterials, tensegrity, soft modes The category of “extremal materials” has been introduced to define materials that simultaneously show very soft and very stiff deformation modes [1], and are called unimode, bimode, trimode, quadramode and pentamode materials, depending on the number of soft modes. Extremal materials that are receiving increasing interest are the so-called pentamode lattices, which consist of diamond-like lattices featuring five soft modes of deformation. The unit cell forming the this lattice is made of four rods meeting at a point. Previous studies show that pentamode lattices confined between stiffening plates have the ability to carry unidirectional compressive loads with sufficiently high stiffness, while behaving very soft in shear [2]. Because of their unusual mechanical features, these structures have been proposed for transformation acoustics, elasto-mechanical cloak, and seismic isolation (refer, e.g., to [2]-[3] and the references therein). This study examines the mechanical behavior of a novel class of mechanical metamaterials alternating class ? tensegrity structures [4] and stiffening plates. Analytical formulae for the vertical and bending stiffness properties are developed, and the dependence of such quantities on the main design parameters, which include the lattice constant, the solid volume fraction, the cross-section area of the rods, and the layer thickness, is studied. The potential use of the analyzed metamaterials as novel seismic-isolation devices and impact-protection equipment is highlighted. References [1] Milton, G.W., Cherkaev, A.V., “Which elasticity tensors are realizable?”, Journal of Engineering Materials and Technology, 117(4), 483-493 (1995). [2] Fraternali, F., Amendola, A., “Mechanical modeling of innovative metamaterials alternating pentamode lattices and confinement plates”, Journal of the Mechanics and Physics of Solids, 99, 259-271 (2017). [3] Bückmann, T., Thiel, M., Kadic, M., Schittny, R., Wegener, M., “An elastomechanical unfeelability cloak made of pentamode metamaterials”. Nature Communications 5:4130 (2014). [4] Bieniek, Z.W., “The self-equilibrium configurations for the class ? triangular tensegrity prism”, Proc. XXIII Aimeta Congress, 1093-1097 (2017).

High-dynamic Strengthening of Cementitious Materials: Structural Effect and Influence of Concrete Hardening

Eva Binder^{*}, Yong Yuan^{**}, Herbert Mang^{***}, Bernhard Pichler^{****}

^{*}TU Wien - Vienna University of Technology; Tongji University, ^{**}Tongji University, ^{***}TU Wien - Vienna University of Technology; Tongji University, ^{****}TU Wien - Vienna University of Technology

ABSTRACT

During the service of infrastructural facilities, spanning typically over 100 years, exceptional load cases such as explosions and traffic accidents need to be considered. Both load cases result in high-dynamic loading of the structure, herein assumed to be made out of concrete. In this contribution the focus is split. In the first part, strengthening of cementitious materials under high-dynamic loading is quantified by means of the dynamic increase factor (DIF). In the second part, the influence of hardening of concrete on the dynamic strength and the DIF is investigated. The present contribution follows the approach of Fischer et al. [1], who developed a model for the dynamic increase factor, based on the loading rate, the quasi-static strength, the Young's modulus, the shear modulus, and the crack length, which is related to the specimen size. In the first part, the model predictions are compared with experiments by Zhang et al. [2] on mortar cylinders with two different heights. In the second part, the same model for the DIF is combined with a validated multiscale model for cementitious materials to determine the influence of the hardening process on the dynamic behavior. In this context, the concrete used for the immersed tunnel of the Hong Kong-Zhuhai-Macao-Bridge is analysed, and a high-dynamic compression test is simulated, see [3]. As regards the first part, it is concluded, that strengthening of cementitious materials includes a structural effect. Concerning the second part, the results imply, that the dynamic strength of concrete increases and that the DIF decreases with progressive hardening of concrete. Acknowledgment The authors are indebted to the Austrian Science Fund for their financial support in the framework of the FWF-project "Bridging the Gap by Means of Multiscale Structural Analyses" (project number: P 281 31-N32). References [1] I. Fischer, B. Pichler, E. Lach, C. Turner, E. Barraud and F. Britz, Compressive strength of cement paste as a function of loading rate: Experiments and engineering mechanics analysis, *Cement and Concrete Research* 58 (2014) 186-200. [2] M. Zhang, H. Wu, Q. Li and H. Huang, Further investigation on the dynamic compressive strength enhancement of concrete-like materials based on split Hopkinson pressure bar tests. Part I: Experiments, *International Journal of Impact Engineering* 36 (2009) 1327-1334. [3] H. Wang, E. Binder, H. Mang, Y. Yuan and B. Pichler Multiscale structural analysis inspired by exceptional load cases concerning the immersed tunnel of the Hong Kong-Zhuhai-Macao Bridge, submitted to *Underground Space*.

Mixed Discrete-Continuum Approach for Modelling the Fracture Behaviour of Soft Collagenous Tissues

Kevin Bircher*, Alexander Edmund Ehret**, Edoardo Mazza***

*Department of Mechanical and Process Engineering, ETH Zurich, Switzerland, **Department of Mechanical and Process Engineering, ETH Zurich, Switzerland; Empa, Swiss Federal Laboratories for Materials Science and Technology, Dübendorf, Switzerland, ***Department of Mechanical and Process Engineering, ETH Zurich, Switzerland; Empa, Swiss Federal Laboratories for Materials Science and Technology, Dübendorf, Switzerland

ABSTRACT

While the deformation behaviour of soft collagenous tissues, such as the fetal membranes (FM) and the liver capsule (LC), has been investigated intensively, the mechanisms underlying their fracture are still poorly understood, despite their importance for events of tissue failure and damage. In particular, investigations regarding the defect tolerance of fetal membranes would provide valuable input for therapies to prevent their premature rupture. Based on our characterization of the multiscale deformation behaviour of collagenous membranes, we introduced a numerical tool that is capable of efficiently performing fracture-related simulations by combining a discrete fiber network model in the near-field of a crack with a continuum representation of the far field. This tool was applied to investigate the crack propagation in soft collagenous tissues for strip biaxial fracture tests and compared to corresponding experiments of bovine LC, human FM and soft elastomers (PDMS). The near field of a defect in LC and FM was also visualized with a multiphoton microscope (MPM) in order to characterize the compaction behaviour and the reorientation of fibers. With the discrete fiber network model, a fibre-level failure criterion was implemented which dictates material failure. This allowed avoiding the stress singularity present in the crack near field of a continuum model. Systematic parameter variation indicated the influence of fiber deformation and failure behaviour on tissue rupture properties. Simulations and corresponding MPM observations showed that the crack near field size is in the sub-millimeter range and therefore much shorter than for elastomers such as PDMS. Interestingly, our simulations for soft collagenous tissues show that large sample-sizes are required for the determination of the tearing energy. Thus, conventional fracture mechanical approaches are not applicable for defects of few millimeters in the tissues as typically occurring in clinically and physiologically relevant cases.

Partitioned Adaptive Parallel Multirate Methods for Coupled Stiff Systems

Philipp Birken^{*}, Peter Meisrimel^{**}, Azahar Monge^{***}

^{*}Lund University, ^{**}Lund University, ^{***}Lund University

ABSTRACT

The efficient numerical simulation of stiff multiphysics systems remains a core challenge in scientific computing. Examples are fluid structure interaction, earth system models or turbulent flames. We consider problems with the following characteristics: They are large scale, all components are stiff, possibly on different time scales and there are codes for the subproblems available. Thus, we want a partitioned numerical method, meaning that reuse of the existing codes is possible. Thereby, we assume that while we have access to the source codes, we want to edit that code as little as possible. In particular we assume that we can repeat a time step. We are then looking for numerical methods that are implicit and at least order two, time adaptive, allow the subsolvers to run in parallel and allow for different time steps in the different models. We are not aware of a method that fulfills all of these properties and suggest two methods of our own for the case of two systems being coupled. The core idea is the following: We have a time integration method of at least order two for each subproblem and assume that we can restart these with new initial data and that during time integration, information for the other solver at all times can be provided using interpolation. This continuous representation of the numerical solution is updated after each local time step. Then the solvers run in parallel over a macro time window and are free to choose their own timesteps in an adaptive way without outside interference. At the end of the macrostep, it is checked if the coupled system is fulfilled up to a tolerance, if not, the time window is repeated. Crucial questions are order of the time integration method and convergence of the time window iteration, also called waveform relaxation. This is shown numerically for representative test cases. For the specific case of two linear heat equations with different material properties coupled across an interface, we suggest to do the waveform relaxation in the form of a Neumann-Neumann coupling, known from domain decomposition. There, the choice of the relaxation parameter is crucial and previous analysis by Gander and Kwok for the semidiscrete case does not apply. We thus perform a fully discrete analysis for the case of fixed but different time steps for the subproblems. Numerical results show that this can be used for the time adaptive case as well.

3D Mapping of the Osteocyte Lacunae Network with the Adaptive Bone (Re)modeling Dynamics

Annette Birkhold^{*}, Pouyan Asgharzadeh^{**}, Lydia Farack^{***}, Sara Checa^{****}, Oliver Röhrle^{*****},
Paul Zaslansky^{*****}, Bettina Willie^{*****}

^{*}Charité - Universitätsmedizin Berlin, Germany; University of Stuttgart, Germany, ^{**}University of Stuttgart, Germany, ^{***}Charité - Universitätsmedizin Berlin, Germany, ^{****}Charité - Universitätsmedizin Berlin, Germany, ^{*****}University of Stuttgart, Germany, ^{*****}Charité - Universitätsmedizin Berlin, Germany, ^{*****}Charité - Universitätsmedizin Berlin, Germany; McGill University, Canada

ABSTRACT

Bone is a highly adaptive biomaterial that optimizes its microstructure depending on the mechanical loads placed on it. The exact mechanisms by which a network of interconnected mechanical strain-sensing cells, embedded in the bone matrix, termed osteocytes, orchestrate bone turnover and mineral homeostasis remains largely unknown. Here, we present a multimodal preclinical tomographic imaging approach to correlate the 3D osteocyte lacunar network with bone formation and resorption dynamics in a mouse tibia after in vivo mechanical loading. Using a mouse model we analyze bone (re)modeling occurring over a short period of time. Female C57Bl/6J mice were subjected to in vivo cyclic compressive loading of the left tibia (2 weeks, approx. 5 min/day; $F_{max}=11N$; $1200\ \mu?$ at the medial surface of the tibia midshaft) with the right tibia as internal control (1). Dynamic in vivo μ CT-based time-lapsed microcomputed tomography (day 0 – day 15; isotropic voxel size $10.5\ \mu m$) was used to monitor bone micro-architecture response to load. In vivo images were registered and segmented to extract formation patches and resorption cavity geometries (2). High-resolution 3D Synchrotron- μ CT imaging was performed on the same bones (isotropic voxel size $876\ nm$). SR- μ CT images were registered with in vivo images and locally segmented to extract osteocyte lacunae geometries. 3D individual osteocyte lacunar descriptors and global osteocyte lacunar network descriptors were extracted. A correlation of the 3D osteocyte cellular level network topology with the dynamic bone surface (re)modeling processes at the tissue level was performed. Our data reveals that the 1) osteocyte lacunae network changes as the tissue ages (formation ? mineralization ? maturation) and during resorption. 2) The osteocyte lacunae network influences the probability of formation and resorption processes occurring. 3) Adaptive processes, such as an earlier alignment of new osteocyte lacunae in response to loading, were identified. Our 3D-correlation imaging approach will enhance our understanding of regulation of bone remodeling and homeostasis following physiological development, pathological conditions, or pharmaceutical intervention. 1. Willie et al. Diminished response to in vivo mechanical loading in trabecular and not cortical bone in adulthood of female C57Bl/6 mice coincides with a reduction in deformation to load. Bone 55, 335–346 (2013). 2. Birkhold et al. Mineralizing surface is the main target of mechanical stimulation independent of age: 3D dynamic in vivo morphometry. Bone 66, 15–25 (2014).

Direct Volumetric Manufacturing of Composites via Addressable Joule Heating

Andrew Birnbaum^{*}, Athanasios Iliopoulos^{**}, John Steuben^{***}, John Michopoulos^{****}

^{*}US Naval Research Laboratory, ^{**}US Naval Research Laboratory, ^{***}US Naval Research Laboratory, ^{****}US Naval Research Laboratory

ABSTRACT

Despite increasing levels of acceptance in a number of niche areas, traditional additive manufacturing (AM) techniques continue to suffer from a number of fundamental drawbacks that act to limit their broad adoption. There exist a wide variety of AM methods and technologies that can be classified according to various criteria, including energy source type (e.g. laser beam, electron beam, UV lamp, etc.) power requirements and material systems. Each of these methods also tend to have added requirements such as inert atmospheres, high vacuum processing and powder handling, that represent a significant overhead and inhibit cost reduction. Furthermore, the vast majority of additive manufacturing methods rely on an ultra-serialized approach for building parts. Often described as “layer-by-layer,” in reality, these are hierarchically serial, point-by-point, path-by-path and layer-by-layer approaches. The multi-scale stratification of mass and accompanying complex thermal histories introduced by such hierarchical processes give rise to a series of deleterious consequences in terms of scaling behavior/build times, structural anisotropy, microstructural defects, mesoscopic deficiencies and macroscopic geometric deviations. This work proposes a new methodology that addresses many of these drawbacks by implementing a truly volumetric approach to additive manufacturing. That is, instead of building parts a single point at a time in a hierarchical manner, by spatially controlling the energy distribution within a three-dimensional build domain, one can build composite parts from large constituent volumes, in parallel, by addressable, resistive heating. The presented work consists of a theoretical treatment of the underlying physics, a computational approach to discretization into geometrical sub-domains, process planning via the solution of an inverse problem for implementing the proper control, and, finally, the demonstration of a preliminary prototype along with our plans for the future.

Simplified Fatigue Procedure for Analyzing the Postbuckling Behavior of a Composite Single-Stringer Specimen

Chiara Bisagni*

*Delft University of Technology

ABSTRACT

Fatigue life of postbuckled composite stiffened panels is a complex issue which remains difficult to predict due to the interaction of several damage modes and geometric nonlinearities. Composite stiffened panels are particularly used in the aerospace industry, and are capable to sustain loads that far exceed their buckling load. The skin-stringer separation is one of the most common types of damage in composite stiffened structures, and can initiate and propagate under both static and fatigue loading. Therefore, the ability to assess the fatigue mechanisms is essential for the design of aerospace structures that satisfy damage tolerance and lifetime requirements. A composite single-stringer specimen is here analyzed, as it exhibits most of the challenges that characterize the analysis of a multi-stringer panel and at the same time reduce the computational effort. The fatigue capabilities of the new Abaqus procedures are investigated to predict the life and collapse of the composite single-stringer specimen in the postbuckling field, that is highly dependent on the nonlinear mode of deformation. In particular, a simplified fatigue procedure is used [1]. It solves linear elastic fatigue crack growth problems considering a load or displacement envelope strategy instead of a cycle-by-cycle based approach. It means that the applied numerical load remains constant at the maximum value of the cyclic load and interface elements are degraded based on a discrete number of elapsed cycles after each time increment. Avoiding the need to explicitly model each individual fatigue cycle provides greater computational efficiency. The simplified fatigue procedure demonstrated to account for geometric nonlinearities and for stiffness change after buckling, and to capture the separation onset and some stages of the propagation. The numerical results are compared with test data obtained by the author in previous experimental campaigns [2-3]. Future investigation of the fatigue algorithm will consider stress ratio effects, and various mixed-mode fatigue delamination growth laws so to be able to consider changes in mixed-mode ratio during the analysis. 1. Di Memmo I. and Bisagni C., "Fatigue Simulation for Damage Propagation in Composite Structures", Proceedings American Society of Composites Conference, pages 1009-1019, 2017. 2. Dávila C.G. and Bisagni C., "Fatigue Life and Damage Tolerance of Postbuckled Composite Stiffened Structures with Initial Delamination", Composite Structures, 161:73-84, 2017. 3. Dávila C.G. and Bisagni C., "Fatigue Life and Damage Tolerance of Postbuckled Composite Stiffened Structures with Indentation Damage", Journal of Composite Materials, <https://doi.org/10.1177/0021998317715785>, 2017.

Brainware for Sciences – A Distributed HPC Competence Centre to Link Experts, Users and Computing Centres

Christian Bischof*, Dörte Carla Sternel**

*TU Darmstadt, **TU Darmstadt

ABSTRACT

The efficient use of HPC systems requires users in most instances scientist to be aware of both architecture, underlying system software and operating procedures such as scheduling. While this complexity can be masked in certain cases for well-established workflows around well-maintained community software, a university setting with its variety of application scenarios for the most part falls outside of this carefree domain. Instead, in order to make good use of expensive HPC resources, scientists using HPC resources need to be made aware of issues such as efficient programming or scheduling, and be cogniscent of the strength and weaknesses of certain computing architectures. Most scientists, however, are mainly interested (and trained) in getting their science done, and not so much in the more computer science issues mentioned before. To close this gap, the term brainware was coined to denote HPC experts that can fill this gap, and support users with their scientific codes, both hands-on and by educating them. In the German state of Hesse, such a brainware center was established with funding from the Hessian State Ministry of Higher Education, Research and the Arts. Altogether, seven scientists are funded at the five universities in Darmstadt, Frankfurt, Gießen, Kassel, and Marburg, as well as a managing director. Together, these “brainware” people are a place that every scientist with questions pertaining to the HPC systems at those sites can turn to. They are catalysts for a focussed collaboration of application scientists, computer scientists and computing centres towards an efficient use of the Hessian HPC landscape and, ultimately, for accelerating the scientific outcomes depending on simulation. The Hessian Competence Center for High Performance Computing has been in operation since 2013, and is now in its second round of funding. On the basis of this experience, we will report on the activities of the centre, the feedback we obtained from users on the topics of interest, and the social engineering challenges faced in such a distributed competence network. The results underscore the pivotal role that good software engineering practices play in HPC software stewardship, i.e. the “taking care” of program over time.

Influence of the Microstructure on the Deformation Behaviour of cp-titanium with Large Grains

Robert Bischof^{*}, Luisa Böhme^{**}, Charlotte Kuhn^{***}, Ralf Müller^{****}, Eberhard Kerscher^{*****}

^{*}Institute of Applied Mechanics, University of Kaiserslautern, ^{**}Materials Testing, University of Kaiserslautern,
^{***}Institute of Applied Mechanics, University of Kaiserslautern, ^{****}Institute of Applied Mechanics, University of
Kaiserslautern, ^{*****}Materials Testing, University of Kaiserslautern

ABSTRACT

Manufacturing processes on small scales are of high importance. Simulation techniques, such as the Finite-Element-Method (FEM), are important tools to predict the workpiece behaviour in manufacturing processes. In micro-cutting the machining tool is about the same scale as the grains of the crystalline workpiece. Thus the crystal structure has to be considered in the FEM material model. The material to be examined is commercially pure (cp-) titanium with a hexagonal-closed-packed (hcp) crystal structure. The influence of the crystalline material is modeled by a crystal plastic material model. It considers the reversible elastic behaviour through a compressible Neo-Hookean material law. The anisotropic plastic deformation is considered by specifying the slip planes and slip direction of the hcp crystal structure. One problem of elasto-plastic material models with several slip systems is the possible non-uniqueness of the set of active slip systems. To avoid this problem, a viscoplastic material formulation is used. The viscoplastic parameters are chosen such that the viscoplastic material behaviour approximates the elasto-plastic limit. Locking effects, which arise due to the volume preserving plastic deformations, are alleviated by a modified F-bar deformation gradient [1]. The results of the FEM simulations are compared with experimental data for further development and validation of the material model. Small scale tensile tests of cp-titanium are performed to investigate the material behaviour. The dimension of the specimen are small enough that the crystal structure has an influence on the material behaviour, but large enough that the material can be considered as polycrystal. The grain orientation of the specific sample is provided by electron backscatter diffraction (EBSD) investigations. The influence of the grain orientation on the micro-cutting process is shown. [1] de Souza Neto, E. A.; Peric, D.; Owen, D. R. J.: Computational Methods for Plasticity: Theory and Applications. New York: John Wiley & Sons, 2011.

A Variational Method to Avoid Locking – Independent of the Discretization Scheme

Manfred Bischoff*, Simon Bieber**, Bastian Oesterle***, Ekkehard Ramm****

*University of Stuttgart, **University of Stuttgart, ***University of Stuttgart, ****University of Stuttgart

ABSTRACT

We present a variational method for problems in solid and structural mechanics that is designed to be intrinsically free from locking when using equal order interpolation for all involved fields [1]. The method is inspired by the DSG (Discrete Strain Gap) method [2] and can be interpreted as its variational counterpart. As it involves displacement degrees of freedom as well as additional degrees of freedom obtained from integrated strains, which mostly have the physical units of displacements as well, it is denoted as Mixed Displacement (MD) method. The specific feature of the formulation is that it avoids all geometrical locking effects (i.e. locking effects related to geometric parameters, like the slenderness, as opposed to material locking effects, e.g. Poisson locking) for any type of structural or solid model, independent of the underlying discretization scheme. In the context of thin-walled structures, the most important geometric locking phenomena are transverse shear locking and membrane locking. While the former can elegantly be circumvented via hierarchic shell models [3], a similar approach to remove membrane locking has not yet been found. The possibility to employ equal order interpolation for all involved fields circumvents the task of finding particular function spaces to remove locking and avoid artificial stress oscillations. This is particularly attractive for instance for isogeometric analysis using unstructured meshes or T-splines. Comprehensive numerical tests underline the promising behavior of the proposed method for geometrically linear and non-linear problems in terms of displacements and stress resultants using standard finite elements, isogeometric finite elements and a meshless method. The method can also be applied in the context of collocation. [1] S. Bieber, B. Oesterle, E. Ramm, M. Bischoff. A variational method to avoid locking – independent of the discretization scheme, International Journal for Numerical Methods in Engineering, accepted for publication. [2] K.-U. Bletzinger, M. Bischoff, E. Ramm, A unified approach for shear-locking-free triangular and rectangular shell finite elements, Computers and Structures, 2000; 75(3); 321-334. [3] B. Oesterle, Ramm E. and Bischoff M., A shear deformable, rotation-free isogeometric shell formulation, Computer Methods in Applied Mechanics and Engineering, 2016; 307; 235-255.

Modeling Electroactive Polymers and Electromechanical Instability

Dana Bishara^{*}, Mahmood Jabareen^{**}

^{*}Technion – Israel Institute of Technology, ^{**}Technion – Israel Institute of Technology

ABSTRACT

Electroactive polymers (EAPs) are an emerging class of smart materials, which has gained a wide popularity among researchers in the last two decades. EAPs are considered promising materials due to their ability to undergo large deformations when they are subjected to external electric stimuli. Therefore, various applications have been proposed in the literature including artificial muscles, medical devices and soft robotic applications. A typical EAP based actuator consists of a thin film of dielectric elastomer, which on its major surfaces, two flexible electrodes are smeared, and an electric potential difference between the electrodes is applied. The mode of action is principally based on Coulomb forces generated by the electric field, which causes the polymer membrane to exhibit geometrical changes, i.e., contraction in the thickness direction and expansion of the surfaces. Despite the high-level of actuation performances enabled by EAPs, their extensive use is conditioned by the requirement of high driving electric fields. As a result, the applied electric field may cause an electromechanical instability or electric breakdown. Unlike gases or liquids, as the electric breakdown in solid dielectrics takes place, tubular conductive channels evolve, and they do not recover when the voltage is discharged. In this work, a computational model including the electromechanical coupling and the large deformation combined with time dependent behavior of EAPs is developed. This model has been calibrated to provide a quantitative tool for predicting the realistic behavior of the widely used dielectric elastomer VHB. Moreover, the electromechanical instability has been studied within the proposed model using a general convexity condition, from which the Hessian matrix must be positive definite at the equilibrium state.

A Review of Boundary and Interface Representations in Meshfree Solid Mechanics for Extreme-deformation Applications

Joseph Bishop*, Mike Tupek**

*Sandia National Laboratories, **Sandia National Laboratories

ABSTRACT

Meshfree methods for solid mechanics have been in development for over 25 years. Initial motivations included alleviation of the burden of mesh creation and the desire to overcome the limitations of traditional mesh-based discretizations in extreme deformation applications. One challenge for meshfree methods is maintaining an accurate representation of the domain boundary and internal interfaces during extreme deformation. Without an accurate boundary representation, it becomes difficult to implement a self-contact algorithm that avoids pathological material welding. Furthermore, it becomes challenging to update the connectivity of the meshfree discretization (semi-Lagrangian) in highly non-convex domains. Here, a review of boundary and interface representations in meshfree methods is presented. The various techniques are critically compared for several applications in extreme mechanics.

A Non-Isothermal Thermodynamically Consistent Phase Field Framework for Structural Damage and Fatigue in Plasticity

Marco Bittencourt^{*}, Geovane Haveroth^{**}, José Boldrini^{***}

^{*}University of Campinas, ^{**}University of Campinas, ^{***}University of Campinas

ABSTRACT

We present a general thermodynamically consistent non-isothermal non-local phase field framework for the evolution of damage, fatigue and fracture in plasticity under the hypothesis of small deformation. The damage phase field is considered a continuous dynamical variable whose evolution equation is obtained by the Principle of Virtual Power. The fatigue phase field is a continuous internal variable whose evolution equation is considered as a constitutive relation to be determined in a thermodynamically consistent way. In this work, we use high order finite elements for approximation and a semi-implicit scheme to perform the time integration of the equations, which allows us to decouple the variables and use larger time steps. We compare different degradation functions for the damage variable.

Influence of Deformation Induced Topological Anisotropy on Mechanical Properties of Silica Glass: An Atomistic Study

Erik Bitzek*, Sudheer Ganiseti**

*FAU Erlangen-Nürnberg, **FAU Erlangen-Nürnberg

ABSTRACT

Glasses are generally believed to be isotropic materials. However, it is well known that anisotropy can be introduced in silica glass, e.g., by wire drawing, and that the mechanical properties are subsequently anisotropic. Since topology plays an important role for the mechanical properties, it is necessary to understand the physics behind the development of topological anisotropy on the atomic scale. Here we present the results of atomistic simulations using an ab-initio based polarisable force field. Isotropic silica glass was prepared by the melt quenching method. Anisotropy was introduced at different temperatures by either elongating, compressing or shearing the glass at different rates. During load, transient anisotropy is observed, as characterized by the anisotropy factor. Significant persistent anisotropy, which remains after load removal, could only be introduced by compression and shear. The conditions favourable to the formation of persistent anisotropy, the underlying mechanisms and the relationship between transient and persistent anisotropy are analysed in detail. Samples with persistent topological anisotropy also show a pronounced anisotropy in the mechanical properties, in particular on the elastic constants and fracture strain. The results are compared to simulations on bulk metallic glasses and discussed in the framework of mesoscale and continuum models for the deformation of amorphous materials.

Homogenisation-based Modelling of Skeletal Muscle Tissue across the Scales

Christian Bleiler*, Pedro Ponte Castañeda**, Oliver Röhrle***

*University of Stuttgart, **University of Pennsylvania, ***University of Stuttgart

ABSTRACT

Like for many biological materials, the elastic properties of skeletal muscle tissue can vary quite significantly between different persons or between different muscle types of one single person. It is well known that these distinct mechanical properties are due to variations in the microstructure of the material. For skeletal muscles, especially the arrangement and the stiffness of collagen fibres in the connective tissue define the macroscopic passive stiffness, while the sarcomeres (contractile units) enable an active contractility of the muscles. Moreover, the microstructural arrangement not only influences the stiffness, but also the anisotropy of the material at the macroscale. Continuum-mechanical muscle models based on phenomenological approaches are easy to implement, but lack the ability to take microstructural properties into account in a natural way. Hence, experimental data for every desired muscle type to be modeled is required, but usually not available. To overcome this issue, we propose a novel, homogenisation-based material model, which predicts the mechanical behaviour of muscle tissue by incorporating the decisive parts of the underlying microstructure, here, (i) the connective tissue and (ii) the muscle fibres. Furthermore, instead of computationally expensive numerical homogenisation methods, like FE², we proceed from well-founded analytical methods [1] in order to get the effective material response on the macroscale. The description of the collagenous tissue is based on angular integration models [3]. Therefore, the direction-dependent properties of the macroscopic tissue are direct consequences of the arrangement and the mechanical properties of the micro-constituents, especially of the collagen fibres. The present model is able to predict the specific anisotropy (transverse isotropy) of muscle tissue as observed in experiments [2] simply by including the arrangement of the microstructure without the need of further constitutive assumptions as it would be the case for standard phenomenological models. Concluding, this study presents a novel, hyperelastic muscle model, which includes microstructural data in order to obtain the effective response of the overall muscle tissue by using analytical homogenisation methods. [1] Avazmohammadi R., Ponte Castañeda P.: Tangent Second-Order Estimates for the Large-Strain, Macroscopic Response of Particle-Reinforced Elastomers. *J Elasticity* 112:139-183, 2013. [2] Böhl M., Ehret A. E., Leichsenring K., Weichert C., Kruse R.: On the anisotropy of skeletal muscle tissue under compression. *Acta Biomater* 10:3225-3234, 2014. [3] Lanir Y.: Constitutive equations for fibrous connective tissues. *J Biomech* 16:1-12, 1983.

Phase-field Modeling of Anisotropic Brittle Fracture in Fiber-reinforced Composites

Jeremy Bleyer^{*}, Roberto Alessi^{**}

^{*}Ecole des Ponts ParisTech, Laboratoire Navier, Université Paris-Est, ^{**}SAPIENZA, University of Rome

ABSTRACT

The phase-field approach to fracture is an effective method to describe and simulate complex fracture phenomena and is therefore gaining increasing attention by the computational mechanics community. Many extensions have already been considered ranging from dynamic aspects, plasticity, fluid transport in porous media, finite deformation, etc. However, few works have dealt with anisotropic effects. In particular, these works have considered only an anisotropic fracture energy with an underlying isotropic elastic material. As a result, no work has extended yet the phase-field approach to consider fracture in anisotropic media, in particular fiber-reinforced composites. The present contribution aims at closing this gap by proposing a phase-field approach for brittle fracture in an anisotropic material. In particular, it is shown that standard models including one phase-field variable and possibly an anisotropic fracture energy are not well suited to describe complex crack paths in such materials. Instead, we propose to endow the phase-field energy functional with multiple damage mechanisms, e.g. longitudinal fiber cracking and transverse matrix cracking in the case of fiber-reinforced composites. Although, numerical examples focus on this situation, the proposed framework is sufficiently general to be also applied to all situations where different fracture mechanisms are involved within the same material such as different failure mechanism in tension and compression, fracture anisotropy depending on mode mixity, cracking of composite laminates, etc. Illustrative applications demonstrate that the proposed model is able to capture well known features of crack propagation in fiber-reinforced media such as propagation in the fiber preferential direction, straight propagation under mode II loading but also non trivial behaviors such as crack kinking, whereas a standard phase-field model, even if equipped with an anisotropic fracture energy, is not. Although our work does not focus on an exhaustive description of the complex constitutive behavior of fiber-reinforced composites, we hope that it will contribute to a decisive advance in the development of the phase-field approach for this extremely important class of materials.

Peridynamic Modeling of Corrosion Damage and Fracture

Florin Bobaru^{*}, Siavash Jafarzadeh^{**}, Jiangming Zhao^{***}

^{*}University of Nebraska-Lincoln, ^{**}University of Nebraska-Lincoln, ^{***}University of Nebraska-Lincoln

ABSTRACT

We present a peridynamic model for corrosion damage and stress-dependent fracture. We find that corrosion changes the material properties in a layer near the corrosion front [3]. The peridynamic model introduced here [1] captures the growth of corrosion pits [2] and verifies the measured properties of the embrittled layer. The corrosion process is autonomous in a peridynamic model, freeing the model from geometrical restrictions that would otherwise be present. Examples will also be shown from numerical tests spanning intergranular corrosion to uniform corrosion. The numerical examples are compared with experimental results and we observe a good match between the two. We also discuss future steps to be taken in peridynamic modeling of corrosion processes. References [1] S. Li, Z. Chen, L. Tan, F. Bobaru, "Corrosion-induced embrittlement in ZK60A Mg alloy", Materials Science & Engineering A, 713: 7-17 (2018) <https://doi.org/10.1016/j.msea.2017.12.053> [2] S. Jafarzadeh, Z. Chen, F. Bobaru, "Peridynamic modeling of repassivation in pitting corrosion of stainless steel", Corrosion (2017). <https://doi.org/10.5006/2615> [3] Shumin Li, Ziguang Chen, Fei Wang, Bai Cui, Li Tan, and F. Bobaru, "Analysis of Corrosion-Induced Diffusion Layer in ZK60A Magnesium Alloy", Journal of The Electrochemical Society, 163(13): C784-C790 (2016). doi: 10.1016/j.cma.2016.08.012

Optimization-based, Property Preserving Finite Element Methods

Pavel Bochev^{*}, Marta D'Elia^{**}, Denis Ridzal^{***}, Mauro Perego^{****}

^{*}Sandia National Laboratories, ^{**}Sandia National Laboratories, ^{***}Sandia National Laboratories, ^{****}Sandia National Laboratories

ABSTRACT

We present an optimization-based approach for the accurate, property preserving finite element solution of Partial Differential Equations (PDEs) in which the solution is obtained by solving a suitably defined constrained optimization problem. The objective is to minimize the distance to a given finite element target, computed by a formally accurate but not necessarily property preserving scheme, while physical properties such as maximum principle and/or preservation of local solution bounds define the constraints. This divide-and-conquer strategy separates solution accuracy from the preservation of the relevant physical properties and always finds a globally optimal, with respect to the given target, solution that also satisfies these properties. To illustrate the approach we consider the finite element solution of a model scalar advection-diffusion equation and present some preliminary numerical studies. The talk will also examine connections between the optimization-based property preserving solution of PDEs and algebraic flux correction techniques for the preservation of local solution bounds. This material is based upon work supported by the U.S. Department of Energy, Office of Science, Office of Advanced Scientific Computing Research. D. Ridzal also acknowledges funding by the Advanced Simulation &&& Computing (ASC) Program.

Optimal Design of Bio-inspired Multi-material Soft Robots

Narasimha Boddeti^{*}, Oliver Weeger^{**}, Pablo Valdivia y Alvarado^{***}, Martin Dunn^{****}

^{*}Singapore University of Technology and Design, ^{**}Singapore University of Technology and Design, ^{***}Singapore University of Technology and Design, ^{****}Singapore University of Technology and Design

ABSTRACT

Animals make use of biological structures with tailored distribution of materials with different properties to achieve a variety of desired functions such as fins for swimming and wings for flying. Recent advances in robotics have recognized this and moved towards realizing designs for robots with soft materials that mimic biology to achieve improved performance and versatile functionality under disparate operating conditions. Advances in additive manufacturing technologies have also aided in this by allowing arbitrary yet precise placement of desired materials in a component. Even as bio-inspired designs offer considerable performance gains over traditional robots, they are not necessarily the most optimal designs for engineering applications as biological designs are a result of evolutionary pressures and constraints while engineering applications are devoid of such constraints. With that in mind, our goal here is to develop a topology optimization based framework for design of bio-inspired structures with optimal distribution of materials (either isotropic or anisotropic) to realize desired performance criterion such as target deformation, minimum compliance and optimal power consumption while accounting for constraints imposed by the fabrication approach. We will exercise the abilities of our framework in the context of design and fabrication of an under-actuated batoid-like soft robot fabricated via multi-material 3D printing. Batoids (e.g. stingrays, manta rays) are a group of fish species that are flat bodied with enlarged pectoral fins. They make an ideal basis for autonomous underwater robotics due to their simple body kinematics with excellent maneuverability and efficient operation. We will seek optimal batoid-like designs tailored for different 3D printing techniques (viz. voxel based material jetting and embedded 3D printing) with single or multiple objectives including target dynamic deformation behavior and placement of the actuator.

Modeling Coulomb Interactions in Ionic Solids for Atomistic-to-Continuum Methods

Vishal Boddu^{*}, Denis Davydov^{**}, Bernhard Eidel^{***}, Paul Steinmann^{****}

^{*}University of Erlangen-Nuremberg, ^{**}University of Erlangen-Nuremberg, ^{***}University of Siegen, ^{****}University of Erlangen-Nuremberg

ABSTRACT

Existing atomistic-to-continuum multiscale methods, such as the quasicontinuum method, are applicable exclusively in cases where the atomic interactions are short-ranged. This restriction on the nature of atomic-level interactions for the multiscale methods exclude an extremely large class of materials, essentially--all dielectrics, polarizable solids and ionic solids, that are central to numerous scientific and industrial applications. So far there has been only one approach, to the best of our knowledge, that enables the applicability of atomistic-to-continuum methods for ionic crystals. The method involves coarse-graining of the long-range Coulomb interactions in ionic crystals [1]. In doing so, the ionic charges are expressed in terms of a charge density field defined on two different length scales, namely the length scale of atomic unit cell and the characteristic continuum length scale. However, this approach assumes complete separation of scales and for a finite atomistic system this is naturally not true. Furthermore, realizing adaptive refinement and seamless coarse-graining using this approach is not trivial. Unphysical artifacts of the direct cutoff based truncated sum to evaluate Coulomb interactions in ionic solids have been pointed out in a number of studies. However, recently it is understood that the artifacts of the direct cutoff based truncated sum can be significantly minimized if a suitable correction term is added [2]. In this work we examine whether or not such cutoff-based methods are suitable to carry out the accumulation of the Coulomb interactions within the context of atomistic-to-continuum multiscale methods. In this regard, we choose the quasicontinuum method from the existing collection of the multiscale methods for demonstration. References: [1] Marshall, J. and Dayal, K., 2014. Journal of the Mechanics and Physics of Solids 62, 137-162. [2] Fukuda, I. and Nakamura, H., 2012. Biophysical reviews, 4.3, 161-170.

Modeling Transient Aircraft Engine Operation

Christoph Bode^{*}, Jens Friedrichs^{**}, Andreas Kellersmann^{***}, Florian Herbst^{****}, Joerg Seume^{*****}

^{*}Institute of Jet Propulsion and Turbomachinery TU Braunschweig, ^{**}Institute of Jet Propulsion and Turbomachinery TU Braunschweig, ^{***}Institute of Jet Propulsion and Turbomachinery TU Braunschweig, ^{****}Institute of Turbomachinery and Fluid Dynamics Leibniz University Hannover, ^{*****}Institute of Turbomachinery and Fluid Dynamics Leibniz University Hannover

ABSTRACT

Due to the multidisciplinary design approach of large-scale and high complex capital goods there exist several different forms of operational behavior and deteriorational effects depended to the typical case of application. In case of a jet engine these effects are most often unknown or at least not accurately considered because of the large product cycles which are linked to the high costs of these goods. This means that for a jet engine a detailed understanding of the above mentioned effects for single components and for the overall system for stationary and transient operational behavior is necessary. This is even more pronounced when it comes to the interaction (amplification or reduction) of multiple components under the influence of wear as well as repair and overhaul in sense of parameters like performance as well as reliability and safety of the overall system. The Collaborative Research Center '871 "Regeneration of complex capital goods" is investigating these issues. To investigate the transient engine performance effects, the Institute of Jet Propulsion and Turbomachinery (IFAS) of Technische Universität Braunschweig is developing the simulation tool ASTOR (Aircraft Engine Simulation for Transient Operation Research) within the research center. The objective is to create an analytical simulation environment for gas turbine processes where the operational behavior of an existing gas turbine could be modeled accurately. This basic model is to be retained while arbitrary modifications to the engine are examined. These modifications could include additional bleed systems, power off take or the deterioration of engine components. Since the basic engine model is retained, this model would also be accurate in predicting the operational performance of the engine if the same modifications are applied in an experiment. The general application of the gas path analysis is difficult since every additional parameter which has to be calculated requires additional boundary conditions which affect the entire engine model. To avoid this, a system theory approach is used to establish a model which could be used similar to the model of an electric or hydraulic circuit. Circuit models consist of interconnected building blocks where each block models the behavior of an individual component. With this method it is possible to describe even the most complex circuits with sufficient accuracy and the basic circuit model could be retained and validated while additional components are added or single components modified. Thus the dedicated effects of the modification could be observed in the model.

Model Order Reduction for Additive Manufacturing Process

Brice Bognet^{*}, Olivier Desmaison^{**}, Francisco Chinesta^{***}

^{*}GeM, Ecole Centrale Nantes, ^{**}ESI Group, France, ^{***}Arts et Métiers ParisTech

ABSTRACT

Key Words: Model Reduction, Powder Bed Fusion, Separated representation Additive manufacturing (AM) processes are of increasing interest in today's industrial context. Several different technologies are getting mature, allowing the production of complex quality parts, however the simulation associated to such processes is still a challenge for the scientific community. In the present work, we focus on the simulation of residual stresses and distortion of parts produced by Powder Bed Fusion (PBF) technologies. The inherent complexity of the process, including many possible process parameters and various possible tool path, lead to a necessity of running simulations prior to the manufacturing in order to determine optimal parameters, correct for eventual process induced distortions and check the actual printability of a design. Simulation of such processes implies various difficulties, including: - multi-scale process (powder scale, heat source scale, part scale, tool-path length) - multi-physics with non-linearity (phase change, plasticity, large displacement) - geometric complexity, including supporting structures being optimized for heat dissipation and/or distortion reduction - layers thickness (issue for standard discretization techniques) All those difficulties combined together lead to failure of standard discretization based numerical strategies. In order to overcome some of those difficulties, the physics is first simplified: we consider the activation of full layers at the time in the simulation (eventually lumping several of them), ignoring the actual tool-path and filling strategy. Moreover, an equivalent shrinkage is applied directly in a mechanical simulation, ignoring the actual heat transfer problem and phase changes. Secondly, we use a specially developed model reduction approach to keep down the number of degrees of freedom. Our approach is based on the so-called Proper Generalized Decomposition, where quantities of the model are described using a separation of variables approach. When solving the elasto-plastic problems, a space variables separation is used, such that all quantities of the model are expressed as sums of products of the in-plane coordinates $\{x,y\}$ (coordinates on the bed surface), the out-of-plane coordinate $\{z\}$ (stacking direction) and the number of the domain $\{n\}$. The last discrete coordinate n being associated to a domain decomposition strategy, and representing the domain number associated to one or a group of layers depending on the layers lumping strategy. Thanks to the use of such separated representation, the 3D problem to be solved is reduced to a set of 2D and 1D sub-problems, reducing drastically the number of degrees of freedom, and therefore reducing the simulation time.

A Loosely Coupled Scheme for Fictitious Domain Approximations of Fluid-Structure Interaction Problems with Immersed Thin-Walled Structures

Ludovic Boilevin-Kayl^{*}, Miguel Ángel Fernández^{**}, Jean-Frédéric Gerbeau^{***}

^{*}a) Inria Paris, 75012 Paris, France and b) Sorbonne Universités, UPMC Université Paris 6, UMR 7598 LJLL, 75005 Paris, France, ^{**}a) Inria Paris, 75012 Paris, France and b) Sorbonne Universités, UPMC Université Paris 6, UMR 7598 LJLL, 75005 Paris, France, ^{***}a) Inria Paris, 75012 Paris, France and b) Sorbonne Universités, UPMC Université Paris 6, UMR 7598 LJLL, 75005 Paris, France

ABSTRACT

We are interested in the simulation of elastic thin-walled bodies immersed in an incompressible viscous fluid. Cardiac valves are the main motivation of the present study. To our knowledge, the coupling schemes used in this context are usually implicit or semi-implicit. This yields unconditional stability but at the price of solving a computationally demanding coupled system at every time step. The design of explicit coupling schemes – i.e. schemes that call the two solvers only once per time-step – is of major interest, especially for three-dimensional simulations. However, the major drawback of the existing approaches (e.g., [1]) is that either stability or accuracy demands severe time-step restrictions (e.g., parabolic CFL) or correction iterations. We propose a new solution that overcomes these difficulties. The fluid is modelled with the Navier–Stokes equations, in a Eulerian setting, and the valves are described by a Reissner-Mindlin shell type model in Lagrangian formulation. The interface coupling is enforced through Lagrange multipliers approximated with Dirac masses (e.g., [2]). The proposed coupling scheme is an extension of the Robin-Neumann splitting proposed in [3] to the present unfitted mesh framework. It treats implicitly the coupling of the fluid with the solid inertia and explicitly the coupling with the solid elastic effects. In addition, the choice of Dirac masses for the Lagrange multipliers, combined with a consistent lumped-mass approximation in the solid, yields a very efficient implementation in the fluid solver which makes the coupling scheme explicit. The resulting numerical method is provably stable in the energy norm. Numerical examples, including cardiac valves, will be presented. Comparisons in terms of accuracy and computational efficiency with respect to the implicit scheme will be discussed and will illustrate the benefits of the explicit scheme. This new method is very promising and outperforms the coupling schemes we are aware of. This work has been supported by the project MIVANA and the companies Kephalios and Epygon. References: [1] D. Boffi, N. Cavallini and L. Gastaldi. Finite element approach to immersed boundary method with different fluid and solid densities. *Math. Models Methods Appl. Sci.*, 21, (2011), 2523–2550. [2] N. Diniz dos Santos, J.-F. Gerbeau and J.-F. Bourgat, A partitioned fluid–structure algorithm for elastic thin valves with contact, *Comput. Methods Appl. Mech. Engrg.*, 197, (2008), 1750–1761. [3] M.A. Fernández, J. Mullaert and M. Vidrascu, Explicit Robin-Neumann schemes for the coupling of incompressible fluids with thin-walled structures, *Comput. Methods Appl. Mech. Engrg.*, 267, (2013), 566–593.

Shear Transformation Activation and Distribution in the Deformation of Amorphous Materials

Francesca Boioli^{*}, Tristan Albaret^{**}, Anne Tanguy^{***}, David Rodney^{****}

^{*}LEM UMR-104, CNRS-ONERA, Chatillon, ^{**}ILM, University of Lyon 1, ^{***}LaMCoS, INSA Lyon, ^{****}ILM, University of Lyon 1

ABSTRACT

Amorphous solids are characterized by high strength and low ductility. The latter property is a consequence of the localization of the plastic deformation in shear bands, which leads to catastrophic failure. As a consequence, understanding the localization of plastic deformation and the formation of shear bands is of utmost importance. Generally, it has been accepted that local irreversible rearrangements of small clusters of atoms, Shear Transformations (STs), are the elementary processes involved in the deformation of amorphous systems and several mesoscale models based on STs have been proposed. Still the fundamental mechanisms underlying ST occurrence and shear bands formation are not yet clear. In this context, atomistic simulations can provide significant details that would otherwise be unavailable. In this work we investigate amorphous silicon by performing quasi-static and molecular dynamics shear simulations with Stillinger-Weber type potentials. First, the analysis of the shear simulations allow to identify local plastic rearrangements. By fitting their displacement field on collections of Eshelby spherical inclusions, we characterize their size and plastic strain. This result provides atomic-scale parameters to characterize the local shear rearrangements needed to build mesoscale simulations. Second, using the Nudged Elastic Band method, we calculate the energy barriers and the activation volumes involved in the plastic rearrangements caused either by isolated STs or by cascades of interacting STs accessing the strain-rate sensitivity of glass plasticity, another important parameter for mesoscale models. Finally, we investigate the dynamic process of ST formation, determining the characteristic time involved in the development of STs and the influence of the strain rate on the STs distribution and organization.

A Thermodynamically Consistent Model for Shape-Memory Ionic Polymers

Alain Boldini^{*}, Abdolhamid Akbarzadeh Shafaroudi^{**}, Stefano Mariani^{***}

^{*}Politecnico di Milano, ^{**}McGill University, ^{***}Politecnico di Milano

ABSTRACT

Smart materials have recently attracted the attention of many researchers due to their unique multifunctional properties; however, their practical applications are still somehow limited due to the lack of constitutive models capable of accurate description of their multiphysics behavior. Dealing with ionic polymers with shape memory effects, e.g. the commercially available Nafion™, we propose a thermodynamically consistent model for the fully coupled chemo-electro-thermo-mechanical response to external stimuli. Moving from continuum thermodynamics, the relevant conservation laws are discussed. The constitutive equations are then obtained via an appropriate choice of the Helmholtz free-energy function, through the standard Coleman-Noll procedure. The free-energy function is set by properly linking recognized models for the description of electro-mechanical effects in ionic polymers on one side, and of shape memory effects in polymers on the other side. The instantaneous (elastic) and time-delayed (viscous) response of the polymer in a finite strain setting and the fixation of alternate shape configurations through a thermo-mechanical training are discussed. The obtained model is then implemented in the commercial finite element software Abaqus™ through a UEL (user element) interface. The model and its implementation are validated by comparing calculated numerical results with data obtained from tests conducted in an ad-hoc designed experimental campaign. Results are finally reported on the use of these shape-memory polymers as triggering mechanisms of folding/unfolding of an origami-inspired deployable structure.

Adaptive Discontinuous Galerkin Schemes for Unsteady Under-resolved Problems

Thomas Bolemann^{*}, Gregor Gassner^{**}

^{*}University of Cologne, University of Stuttgart, ^{**}University of Cologne

ABSTRACT

Unsteady multi-scale problems pose high requirements on the resolution, both in space and time, for appropriately covering the relevant physical phenomena. In recent years high-order methods in general and discontinuous Galerkin methods in particular have made substantial progress. Investigations have shown that these methods have highly favorable properties for multi-scale problems, such as LES in the field of fluid dynamics, due to their superior scale-resolving capabilities. It is valid to assume that practically all simulations for these problems are under-resolved due to the high resolution requirements, thus making efficient schemes a key requirement. In this work we use the discontinuous Galerkin Spectral Element Method (DGSEM), which is among the most efficient high-order schemes, due to consequent use of tensor-product operators, with split-form fluxes ensuring the stability of the scheme. Since unsteady phenomena lead to strongly varying resolution requirements, the basic scheme is combined with an octree-based adaptive mesh refinement. To avoid the global impact of small time-steps in refined areas, we utilize a local-time stepping approach based on a space-time formulation, where the time steps are linked to groups of octants. Most numerical frameworks of this complexity are implemented using statically typed low-level programming languages such as C/C++ or Fortran, mainly for performance reasons. We take another approach, using Julia a modern high-level, dynamic language. Focused on numerical computing, it provides performance on par with low-level languages. By this choice we can keep the numerical framework as compact and user-friendly as possible and retain the feasibility for rapid-prototyping complex algorithms. In the talk we will present the novel Julia-based DGSEM framework and outline the basics of the numerical method and provide details on the parallel implementation of the octree-based AMR and LTS algorithm. We will furthermore compare it to the established open-source solver Flexi (<https://www.flexi-project.org/>), a Fortran-based DGSEM framework already operating at Petascale level, developed by the same authors. We will detail on implementation differences and present benchmarks for selected model problems with a focus on fluid dynamics.

Discrete Element Modeling of Powder Spreading for Metal Additive Manufacturing

Dan Bolintineanu*, Jeremy Lechman**

*Sandia National Laboratories, **Sandia National Laboratories

ABSTRACT

Metal additive manufacturing technologies such as selective laser melting rely on layer-by-layer deposition of powder. Spreading of the powder in layers of controlled thickness forms the basis for subsequent selective laser melting or sintering. It is therefore essential to quantify and understand the relationships between powder properties, powder processing parameters and powder bed structure. We present discrete element method (DEM) simulations pertaining to the processing of metal AM powders in the context of additive manufacturing. DEM simulations can account for arbitrary variations in particle-scale properties such as size and shape distribution, as well as various aspects of interparticle contact mechanics, such as variations in friction (e.g. due to particle surface roughness) or variations in interparticle cohesion (e.g. due to chemical composition and particle surface morphology variability). We present a detailed sensitivity study relating the detailed structure of the powder bed to variations in these powder properties as well as powder processing parameters (e.g. layer thickness, spreader blade geometry and speed). In characterizing the powder bed, we examine a variety of spatial statistics, including descriptors of the powder bed surface and the spatial distribution of porosity within the bulk of the powder bed. We note significant variability on length scales relevant to the AM process (e.g. typical laser spot size and powder layer thickness). While such metrics are challenging to determine experimentally, they provide important information for uncertainty quantification efforts in the context of full AM process modeling. Both interparticle friction and cohesion are shown to have notable effects on powder bed structure. As these properties are difficult to measure experimentally, we also discuss preliminary efforts to incorporate powder rheology measurements as both input and validation for our models. Due to the particle-level detail in these simulations, we are able to explore a wide range of particle properties, and therefore provide quantitative insight into powder selection and handling decisions for additive manufacturing. Sandia National Laboratories is a multimission laboratory managed and operated by National Technology and Engineering Solutions of Sandia, LLC, a wholly owned subsidiary of Honeywell International, Inc., for the U.S. Department of Energy's National Nuclear Security Administration under contract DE-NA0003525.

Shape Identification and Optimization in Elastoplastic Boundary Value Problems Using Parametric Integral Equation System (PIES) and Particle Swarm Optimization (PSO)

Agnieszka Boltuc*

*University of Bialystok

ABSTRACT

Shape optimization (identification) is one of the stages of the design of mechanical structures. The solution of these problems is usually achieved by minimization of the objective function describing the optimization criterion. In practice, it leads to multiple solving of a direct problem with the modified geometry. Therefore, it is extremely important, especially in the case of complex elastoplastic problems, to choose the appropriate method for solving direct problems. It can be carried out using FEM or BEM, however both have a serious disadvantage – they require discretization of the boundary and the domain (at least the plastic zone). In the literature are attempts to modelling the optimized boundary by curves. It significantly reduces the number of design variables, but the numerical solution of the direct problem still requires division into elements. Considering the above, the PIES method [1] is proposed for solving direct elastoplastic problems. It is characterized by the separation of shape approximation from solutions approximation and allows for elementless modeling of the boundary (by curves) and the domain (by surface patches). Its effectiveness stems from a reduced number of design variables (only control points of curves), the lack of discretization and automatic adaptation of its mathematical formalism to the changing shape. The latter results from PIES's main feature - the shape is analytically integrated into its mathematical formula. Additionally, the area of the plastic zone is not discretized repeatedly, but is defined once by a single surface, whose shape, if coincident with the shape of the boundary, automatically adjusts to the changes. For optimization purposes the particle swarm optimization method is applied. As indicated in recent publications it is more effective than classical evolutionary algorithms, because allows for greater diversity and exploration over a single population with lower computational costs. This is especially important in elastoplastic problems solved by incremental-iterative scheme, because in inverse problems we have to deal with nested iterative processes, which significantly increases the computational effort. The proposed strategy was tested on several examples. Shape identification was performed basing on values from selected measurement points on the boundary, while shape optimization consisted in minimizing plastic deformation areas. Obtained results confirm the efficiency of the method. References: [1] A.Boltuc, Parametric integral equation system (PIES) for 2D elastoplastic analysis, Engineering Analysis with Boundary Elements, 69, 21-31, 2016. Acknowledgements: These investigations were supported by the National Science Centre, Poland (Project NCN MINIATURA no.2017/01/X/ST8/00534).

Formulation of Plasticity Models through Symbolic Regression

Geoffrey Bomarito*, Kathryn Esham**, Saikumar Yeratapally***, Jacob Hochhalter****

*National Aeronautics and Space Administration, Langley Research Center, Hampton, VA, **The Ohio State University, Columbus, OH, ***National Institute of Aerospace, Hampton, VA, ****National Aeronautics and Space Administration, Langley Research Center, Hampton, VA

ABSTRACT

Material plasticity models typically consist of an assumed functional form and fitting parameters. The functional form is often derived from a simplified analytical model. The fitting parameters exist in order to give flexibility to the model to fit many materials. In most cases, the real material deviates from the idealized analytical model and the functional form of the plasticity model is not completely accurate. Traditionally, the revision and iteration on the analytical model and functional form relies on human intuition and interaction. Production of accurate models in this way can take decades. In this work, an alternate approach is taken whereby a plasticity model is formulated based on a representative volume element (RVE) simulated with the finite element method. The approach can be seen as a method of computational homogenization. Rather than relying on an assumed functional form and tuning the parameters to match the homogenized response of the RVE, the response is used directly as an input to a symbolic regression routine. Symbolic regression is a machine learning method that fits data with an equation of arbitrary functional form. The result is a plasticity model that fits the response of the RVE, without assumption of its functional form. A verification of the method is performed showing that the Von Mises plasticity model can indeed be derived from symbolic regression of simulated response data.

LES-type Models for the Simulation of Flows Past Hydraulic Structures

Fabian Bombardelli*, Juan Pablo Toro**, Joongcheol Paik***

*Univ. of California, Davis, **Andres Bello University, Chile, ***Gangneung-Wonju National University, South Korea

ABSTRACT

Several works have been presented in recent years regarding the use of LES-type models to simulate the flow past hydraulic structures. These models serve the purpose of providing evidence on the turbulence coherent structures at a much smaller computational cost and larger Reynolds numbers than LES or DNS. These simulations have a tremendous promise in giving notable insight into the flow mechanisms. Here, we first discuss the development of a detached eddy simulation (DES) for the flow past stepped spillways, and we compare the results to those of standard Reynolds-Averaged Navier-Stokes (RANS) simulations. Comparisons not only highlight the power of the DES in terms of its prediction, but they also underscore the good agreement with data. Further, we show that the entrainment of air seems to be the consequence of well-organized thin tubes which interact with the free surface. Then, we present simulations of the flow past a gate, developed with a modified Scale-Adaptive Simulation (SAS) model and results of a simulation of flow past a bridge pier. We address the ratio between the eddy viscosity to the fluid kinematic viscosity and its impact on the first type of flow. We corroborate that the SAS has a nice property of a weak dependence on the mesh size close to the wall (obviously in relative terms), and assess its computational cost. We further obtain the coherent structures associated with both flows explaining some of the interesting features of the flow.

Automatic Quadrilateral and Hexahedral Mesh Generation via Integer-Grid Maps

David Bommes*

*RWTH Aachen University

ABSTRACT

Automatically generating quadrilateral and hexahedral meshes that smoothly align to freeform surfaces and offer a high amount of regularity and low distorted elements is a notoriously challenging task. Novel algorithms based on global optimization rely on the construction of integer-grid maps, which pull back a Cartesian grid of integer isolines from a 2D or 3D domain onto a structure aligned quadrilateral or hexahedral mesh. Such global optimization algorithms do not suffer from limitations known from local advancing front methods, as for instance a high rate of irregularity, and enable meshes comparable to manually designed ones by finding a good compromise between regularity and element distortion. In my talk, I will give an overview of the state of the art and discuss the strengths and weaknesses of available algorithms, including open challenges for hexahedral meshing. Through rapid progress in the last years, nowadays for quadrilateral meshing a high level of robustness, performance and quality is available. It is expected that such algorithms will soon conquer commercial applications and strongly relieve users from the time-consuming task of manually generating quadrilateral meshes.

A Two-Level Nested Model Reduction Framework for a Class of Optimization Problems Characterized by a High-Dimensional Parameter Space

Gabriele Boncoraglio^{*}, Spenser Anderson^{**}, Charbel Farhat^{***}

^{*}Stanford University, ^{**}Stanford University, ^{***}Stanford University

ABSTRACT

Optimization problems in computational mechanics typically involve the solution of a combination of linear and nonlinear PDEs to evaluate the objective function, and/or enforce complex constraints. Most often, they involve a large number of optimization parameters. They are usually solved using a Nested Analysis and Design approach, and therefore incurs the repeated solutions of the aforementioned PDEs at different parameter points. The computational expense of these solutions is often reduced by replacing the underlying High-Dimensional Models (HDMs) by less computationally intensive surrogate models such as a, for example, Projection-based Reduced-Order Models (PROMs). This defines the context of this talk which will describe a novel computational framework for solving PDE-constrained optimization problems using PROMs. Specifically, the focus will be set on those problems characterized by a high-dimensional design space and at least one linear and steady PDE. The framework is based on the concept of a database of local PROMs and the associated concept of interpolation on matrix manifolds [1]. To address the challenges raised by high-dimensional parameter spaces, adaptive least-squares radial basis functions [2] are first introduced to facilitate interpolation in tangent spaces to matrix manifolds. Then, the dimensionality of the parameter space itself is reduced by representing its elements using low-dimensional affine subspace approximations. This results in a two-level nested model reduction framework where first, the parameter space is restricted to a low-dimensional subspace to yield an optimization problem with fewer variables, then a constructed or interpolated PROM is used to reduce the dimensionality of the linear PDE. This framework will be illustrated with the solution of several realistic constrained optimization problems in aeronautics, including design optimization problems under flutter constraints. Its online speed, flexibility, and its enabling of multi-start approaches to global optimization will also be demonstrated. 1. D. Amsallem and C. Farhat, An Online Method for Interpolating Linear Parametric Reduced Order Models, SIAM Journal for Scientific Computing, Vol. 33, pp. 2169–2198 (2011) 2. G.E. Fasshauer, Adaptive Least squares Fitting with Radial Basis Functions on the Sphere, Mathematical Methods for Curves and Surfaces, Vanderbilt University Press, Nashville, pp. 141-150 (1995)

Flow and Mechanics in Fractured Media as Mixed-Dimensional PDEs

Wietse Boon*, Jan Nordbotten**

*University of Bergen, **University of Bergen

ABSTRACT

In the mixed-dimensional representation of fractured media, the fractures are considered as lower-dimensional manifolds. This concept is successively applied to the lines and points at the intersections between fractures leading to a hierarchical geometry of manifolds of codimension one. By imposing these modelling assumptions a priori in the continuous setting, the basis is formed for the introduction of coupled PDEs on the mixed-dimensional geometry, which we refer to as mixed-dimensional PDEs. In this work, we consider Darcy flow combined with linear elasticity on mixed-dimensional representations of fracture networks. Since the associated, governing equations are fully coupled, the systems of equations are presented using mixed-dimensional differential operators which map between the different dimensions. In turn, the resulting system of equations is considered as mixed-dimensional and is analysed as such, before the introduction of the discretization scheme. We present theoretical results related to the structure of mixed-dimensional elliptic partial differential equations from which multiple conforming discretization schemes arise using dimensionally hierarchical finite elements. Keeping later purposes such as transport problems and fracture propagation in mind, our main interest lies in obtaining accurate flux fields and stress states which respect physical conservation laws. Therefore, we employ mixed finite elements which allow for a local preservation of such laws. The symmetry of the stress tensor is imposed in a weak sense, thus leading to the use of familiar, conforming, finite elements with relatively few degrees of freedom. Results concerning convergence and stability of the mixed finite element schemes are shown. These are supported by numerical examples in two- and three-dimensional domains in which the lower-dimensional inclusions, intersection lines, and points have significantly different material properties compared to the surroundings.

An Adaptive Multi-Model Approach to Simulate the Damage of Composite Panels with Initial Defect under Compressive Loading

Eva Borakiewicz*, Vincent Chiaruttini**, Antoine Hurmane***, Frédéric Laurin****

*Airbus Operations, Université Paris Saclay, Onera - The French Aerospace Lab, **Onera - The French Aerospace Lab, ***Onera - The French Aerospace Lab, ****Onera - The French Aerospace Lab

ABSTRACT

The growing industrial interest for predictive virtual testing makes the development of advanced numerical tools essential to achieve confident and realistic complex numerical simulations. For instance, one may wonder to what extent an initial defect affects the global behavior of a slender composite structure under compressive loading. The resolution of this problem necessitates expertises in both numerical approaches and material constitutive behaviors while several non-linearities sources are arisen such as large deformation and material on-going degradation. Responding to those problematics, this work presents an adaptive multi-model method to predict the residual strength of a structure with an initial defect. Like other multiscale approaches [1], our technique attempts to put in each location of the structure just the right amount of complexity in terms of meshing and material behavior. In this respect, the structure is divided in two parts separated by a boundary that is allowed to evolve during the simulation in order to gain in overall computation time. The first part concentrates non-linearities using a complex non-linear damage constitutive law and a multi-layered mesh. An advanced mesoscale model [2] is chosen in order to take into account several material non-linearities and to correctly predict a laminate's degradation processes. The second part, which is complementary to the first one, has a simpler elastic behavior. The local area, which is at first concentrated around the defective zone, evolves according to the progression of damage during the simulation process. Such an approach induces dealing with remeshing, field transfer and coupling between models aspects which will be detailed related to our implementation within a commercial finite element solver. Various numerical assessments (from both academic and industrial applications of the aeronautical domain) will be presented in the context of composite structures to demonstrate the efficiency of this strategy. [1] Multiscale strategy for solving industrial problems, O. Allix, Computational Mechanics, pp 107-126, 2006 [2] A multiscale progressive failure approach for composite laminates based on thermodynamical viscoelastic and damage models, F. Laurin, N. Carrère, J.-F. Maire, Composites: Part A, 38, pp 198-209, 2007

Predicting Failure in High-Strength Steels Using Phase-Field Methods

Michael Borden^{*}, Pulama Bhattacharya^{**}, Michael Scott^{***}

^{*}Brigham Young University, ^{**}Brigham Young University, ^{***}Brigham Young University

ABSTRACT

In this presentation, we will describe our recent efforts to enhance phase-field methods to accurately predict failure in high-strength steels. This work will extend recent advances in phase-field models for fracture in ductile materials to include additional failure criteria, such as the Cockcroft-Latham fracture criteria. We will also describe our efforts to develop a methodology to determine the various parameters required by the models. A number of numerical results that demonstrate the performance of the models with respect to benchmark experimental results will be shown.

Weakly Intrusive Level-Set Topology Optimization for Multiphysics Problems

Felipe Bordeu^{*}, Julien Cortial^{**}

^{*}Safran SA, ^{**}Safran SA

ABSTRACT

The majority of commercial topology optimization software available on the market relies on a tightly coupled simulation package to compute the state of the system and the sensitivities at every iteration of the optimization. In general these solvers are dedicated to only one (or at best two) type(s) of physics (solid, thermal, fluid...) making the topology optimization of inherently multiphysics problems difficult, if not impossible. Also, the virtually universal use of variable density (or SIMP) methods complicates the modeling of interface phenomena and further increases the level of intrusiveness. In this work we propose a new architecture to construct topology optimization software. The approach is based on two key ideas. The first ingredient is the use of the level-set method [1] to track the optimization interface combined with a remeshing strategy [2] to maintain a body-fitted physical discretization. The use of conformal meshes enables to model the physics on the interface (i.e. interface thermal behavior, boundary layer behavior...) more accurately. Also in the case of weakly coupled problem the different physics can be solved by dedicated, highly performant solvers. The second ingredient is the separation of the equations of the optimization problem into two sets, one related to the physical problems and the other to the computation of the gradient and the shape evolution mechanism. The first set of equations can be solved by any (commercial/parallel) simulation software, ideally one that is already available and in routine use. The second set of equations, including the calculation of the next candidate (new iterate), calculation of the gradient and the manipulation of the level-set, are delegated to an independent, Python-based library. We call this approach "weakly intrusive" because even if we use a commercial code to compute the physical solution in a "black box" fashion, we still need to solve auxiliary (adjoint) problems to generate the next candidate. These auxiliary problems can be solved by the same commercial software (if supported) or by an independent finite element solver. Examples of topology optimization for parts with realistic, industrial geometries will illustrate the proposed methodology and software architecture. [1] Allaire G., Jouve F., Toader A-M, "A level-set method for shape optimization", CR Acad. Sci. Paris, Serie I, 334, 1125-1130, 2002. [2] C. Dapogny, C. Dobrzynski and P. Frey, "Three-dimensional adaptive domain remeshing, implicit domain meshing, and applications to free and moving boundary problems", J. Comput. Phys., 262, 358-378, 2014.

An Adaptive Mesh Refinement Approach for Eulerian Turbulent Fluid-Structure Interaction Computations

Raunak Borker^{*}, Sebastian Grimberg^{**}, Phil Avery^{***}, Charbel Farhat^{****}

^{*}Stanford University, ^{**}Stanford University, ^{***}Stanford University, US Army Research Laboratory, ^{****}Stanford University

ABSTRACT

Embedded Boundary Methods (EBMs) [1] for the solution of Fluid-Structure Interaction (FSI) problems are typically formulated in the Eulerian setting. This makes them more attractive than alternative computational frameworks for FSI problems where the structure undergoes large structural motions and/or deformations, or topological changes. For viscous problems however, EBMs suffer from a major drawback in that they do not track the boundary layers [2]. In principle, this disadvantage can be overcome using Adaptive Mesh Refinement (AMR). However, this approach raises several issues ranging from interpreting the concepts of anisotropy and aspect ratio in this setting, to achieving computational efficiency for a given Reynolds number. To this end, this talk presents an approach for performing AMR in Eulerian turbulent FSI computations that is based on the distance to the nearest wall boundary, which typically evolves and deforms in time. It efficiently tracks every embedded discrete surface using a fast predictor-corrector estimation algorithm and adapts the embedding mesh so that all boundary layers stay resolved at all times. It is also equipped with a Hessian-based mesh adaptation criterion for capturing solution features. In general, AMR gives rise to non-conforming mesh configurations that can complicate the semi-discretization process. The proposed AMR approach addresses this issue by explicitly enforcing mesh conformity during the mesh adaptation process, via an appropriately designed scheme for adding and deleting edges and elements. It is implemented, together with a dynamic mesh repartitioning strategy for load balancing, in the massively parallel AERO Suite for highly nonlinear FSI problems, which features the FIVER (Finite Volume method with Exact two-material Riemann solvers) [3] EBM for CFD and FSI. Its potential for enabling the efficient solution of highly nonlinear, turbulent FSI problems is demonstrated with numerous examples associated with the simulation of supersonic parachute inflation dynamic problems. 1. R. Mittal and G. Iaccarino, Immersed Boundary Methods, Annual Review of Fluid Mechanics, Vol. 37, pp. 239-261 (2005) 2. C. Farhat and V. Lakshminarayan, An ALE Formulation of Embedded Boundary Methods for Tracking Boundary Layers in Turbulent Fluid-Structure Interaction Problems, Journal of Computational Physics, Vol. 263, pp. 53-70 (2014) 3. C. Farhat, J.-F. Gerbeau and A. Rallu, FIVER: A Finite Volume Method Based on Exact Two-Phase Riemann Problems and Sparse Grids for Multi-Material Flows with Large Density Jumps, Journal of Computational Physics, Vol. 231, pp. 6360-6379 (2012)

Dislocation-Phase Boundary Interaction – a Peierls-Nabarro Finite Element Approach

Franz Bormann^{*}, Ron Peerlings^{**}, Marc Geers^{***}

^{*}Eindhoven University of Technology, ^{**}Eindhoven University of Technology, ^{***}Eindhoven University of Technology

ABSTRACT

ABSTRACT To get a better insight into the interaction of edge dislocation pile-ups with a phase boundary we perform a numerical study of a simplified two-phase continuum microstructure. The model comprises a soft Phase A that is flanked by a harder Phase B. Embedded in both phases lies a single glide plane, perpendicular to and continuous across the phase boundary. Centred within Phase A lies a dislocation source that emits dislocation dipoles under sufficiently high shear stress. On the remote boundary, a shear stress is applied that triggers dislocation nucleation and drives the dislocations towards the phase boundary. Due to the phase contrast between both phases, a natural source of dislocation obstruction is present. This leads to the formation of dislocation pile-ups. Eventually, the driving forces on the dislocations exceed a critical threshold such that i) the leading dislocation of the pile-up is transmitted into Phase B or ii) the leading dislocation is absorbed into the phase boundary inducing local decohesion. Other scenarios such as dislocation reflection or dislocation nucleation at the phase boundary are not considered. For this study we adopt the Peierls-Nabarro model [1] in a 2D plane strain finite element framework. Both phases are split into two linear elastic media that are connected by the glide plane. Along the glide plane a relative tangential displacement, or disregistry, is allowed for that is mapped to the intrinsic misfit energy. The employed potential is periodic, and thus nonconvex, to capture the effect of lattice periodicity. Along the phase boundary an exponential cohesive zone law is introduced to include decohesion. The model is discretised by finite elements and solved with the Truncated Newton method, along the lines proposed by Nash [2]. The modelling thus obtained provides a natural interplay between dislocations, external boundary conditions and the phase boundary, including the possibility of decohesion. No additional criteria for the dislocations' interaction with the phase boundary is required. The numerical solutions obtained allow us to study the interplay between dislocations and interface decohesion as a function of material properties of the two phases and the phase boundary, as well as the current internal dislocation configuration. **REFERENCES** [1] J.P. Hirth, J. Lothe, Theory of dislocations, Wiley, New York, Vol. II., 1982. [2] S.G. Nash, "A survey of truncated-Newton methods", J. Comput. Appl. Math., 124, 45-59, 2000.

Bayesian Calibration of Expensive Computer Models

Ramin Bostanabad^{*}, Weizhao Zhang^{**}, Jian Cao^{***}, Wei Chen^{****}

^{*}Northwestern University, ^{**}Northwestern University, ^{***}Northwestern University, ^{****}Northwestern University

ABSTRACT

As the role of computer models in investigating physical phenomena increases, more efficient and rigorous uncertainty quantification and propagation methods are pursued in various fields of science and engineering. This is because, regardless of the scale and purpose of the physical process under study, computer models are not perfect and differ from the reality for a variety of reasons including our lack of knowledge which result in discrepancies between the model predictions and the observed values. Additionally, computer models are often developed to be applicable to a wide range of applications. However, to use a model for prediction in a specific context, one may have to adjust some of its inputs by calibrating them against some experimental data. Lack of data is another prevalent source of uncertainty in mechanics since most computer simulations and experimental data are rather costly and time-consuming to gather. The goal of this work is to employ a modular Bayesian approach [1-3] to calibrate a high-dimensional phenomenological material law developed for modeling fiber composites in finite element simulations. Following the seminal work of Kennedy and O'Hagan [1], our goal is to (i) model the (potential) bias of the computer model by placing a Gaussian process prior on it and finding its posterior distribution, and (ii) estimate the calibration parameters. However, special care is exercised to address the identifiability issues (between the posterior of the calibration parameters and the posterior of the bias function) commonly faced in Bayesian calibration since (i) the calibration parameters of our model have distinct physical meaning, and (ii) there are certain physical constraints that the posterior of the computer model has to satisfy. Additionally, artificial simulations are added to the training dataset to enforce the physical constraints and partially address the lack of data due to considerable costs in running the computer model. 1. Kennedy, M.C. and A. O'Hagan, Bayesian calibration of computer models. *Journal of the Royal Statistical Society: Series B (Statistical Methodology)*, 2001. 63(3): p. 425-464. 2. Bayarri, M., et al., Computer model validation with functional output. *The Annals of Statistics*, 2007: p. 1874-1906. 3. Arendt, P.D., et al., Improving identifiability in model calibration using multiple responses. *Journal of Mechanical Design*, 2012. 134(10): p. 100909.

Application of a Multi-Scale Hysteresis Model to Dynamic Seal Friction

Johan Steffen Bothe^{*}, Matthias Wangenheim^{**}

^{*}Leibniz Universitaet Hannover, Institut fuer Dynamik und Schwingungen, ^{**}Leibniz Universitaet Hannover, Institut fuer Dynamik und Schwingungen

ABSTRACT

Dynamic seals prevent mass transfer across system boundaries while allowing relative motion of the corresponding sealing surfaces with minimum friction loss. For this presentation, a multi-scale analysis originally created for the simulation of hysteresis friction in tire-road contact is adapted and applied to dynamic seal friction. Adhesive, viscous and cohesive friction mechanisms are ignored. The multi-scale analysis uses viscoelastic material data in the form of prony parameters including temperature dependence. The countersurface is approximated by a set of sine waves, which have the same height-difference correlation as the original countersurface when superposed. The effect of lubrication on hysteresis friction is implemented by surface data modification. Simulation results are validated against experimental data.

A Hybrid High-Order Method for Nonlinear Elasticity on General Polyhedral Meshes

Michele Botti^{*}, Pierre Sochala^{**}, Daniele A. Di Pietro^{***}

^{*}Université de Montpellier, ^{**}Bureau de Recherches Géologique et Minières, ^{***}Université de Montpellier

ABSTRACT

We formulate and analyze a novel Hybrid High-Order discretization of a class of (linear and) nonlinear elasticity models in the small deformation regime which are of common use in solid mechanics. The proposed HHO discretization is inspired by the recent works on linear elasticity [2] and Leray--Lions operators [1]. It hinges on degrees of freedom that are discontinuous polynomials on the mesh and on the mesh skeleton. Based on these degrees of freedom, we reconstruct discrete counterparts of the strain and of the displacement by solving local linear problems inside each mesh element. These reconstruction operators are used to formulate a local contribution composed of two terms: a consistency term inspired by the weak formulation of problem and a stabilization term penalizing cleverly designed face-based residuals. The resulting method is valid in two and three space dimensions, it supports general meshes including polyhedral elements and nonmatching interfaces, enables arbitrary approximation order, and can be efficiently implemented thanks to the possibility of statically condensing a large subset of the unknowns for linearized versions of the problem. Additionally, the method satisfies a local principle of virtual work on each mesh element, with interface tractions that obey the law of action and reaction. For monotone stress-strain relations, convergence to minimal regularity solutions is proved following the ideas of [3]. Moreover, optimal error estimates hold under the additional conditions of Lipschitz continuity and strong monotonicity on the stress-strain law. The performance of the method is investigated on an extensive panel of model problems using two types of nonlinear stress-strain laws. [1] D. A. Di Pietro and J. Droniou, A Hybrid High-Order method for Leray--Lions elliptic equations on general meshes. *Math. Comp.*, 2017. [2] D. A. Di Pietro and A. Ern, A hybrid high-order locking-free method for linear elasticity on general meshes. *Comput. Meth. Appl. Mech. Engrg.* 283, pp 1--21, 2015. [3] J. Droniou and B. P. Lamichhane, Gradient Schemes for Linear and Non-linear Elasticity Equations. *Numer. Math.* 129 (2), pp 251--277, 2015.

Analysis of Local Strain in Nodular Graphite Cast Iron at the Onset of Coalescence by Means of 3D Numerical Modeling Combined with X-Ray Laminography and Digital Volume Correlation

Pierre-Olivier Bouchard*, Victor Trejo-Navas**

*Mines ParisTech, PSL-Research University, CEMEF - Centre de mise en forme des matériaux, CNRS UMR 7635, CS10207 rue Claude Daunesse 06904 Sophia Antipolis Cedex, France., **Mines ParisTech, PSL-Research University, CEMEF - Centre de mise en forme des matériaux, CNRS UMR 7635, CS10207 rue Claude Daunesse 06904 Sophia Antipolis Cedex, France.

ABSTRACT

Ductile fracture for metallic materials is generally resulting from void nucleation, growth and coalescence mechanisms. Thanks to advanced in situ Synchrotron Radiation Computed Laminography techniques [1], it is now possible to observe these mechanisms during mechanical tests with different stress states. However, in order to understand and model such mechanisms, it is necessary to assess local mechanical fields within the microstructure all along the tests. This can now be achieved thanks to Digital Volume Correlation (DVC) for displacement measurements and strain calculations in the bulk of the microstructure [2]. The work presented herein uses both techniques and describes a finite element (FE) framework in which 3D heterogeneous microstructures are meshed and studied for large plastic strains [3]. Thanks to this framework, immersed microstructures and DVC boundary conditions are considered for more realistic numerical simulations at the microscale of nodular graphite cast iron submitted to tensile loading with various stress states [4]. Equivalent strain values prior to coalescence in the intervoid ligament resulting from DVC and FE simulations are compared for different pairs of coalescing voids with either internal necking or void-sheet coalescence mechanisms. The numerical study is generalized to a bigger group of void pairs in the cast iron microstructure in order to get more representative data and to discuss the possibility of validating a strain-based coalescence criterion while taking into account the occurrence of the two aforementioned coalescence mechanisms. This work was performed within the COMINSIDE project funded by the French Agence Nationale de la Recherche (ANR-14-CE07-0034-02 grant). 1. A. Buljac, T. Taillandier-Thomas, T. F. Morgeneyer, L. Helfen, S. Roux and F. Hild. Early strain localization during flat to slant crack transition in AA 2198 T8 sheet: In situ 3D measurements. *International Journal of Fracture*, 200(1):49-62, 2015 2. T. F. Morgeneyer, T. Taillandier-Thomas, L. Helfen and F. Hild. On strain and damage interactions during tearing: 3D in situ measurements and simulations for a ductile alloy (AA2139-T3). *Journal of the Mechanics and Physics of Solids*, 96:550-571, 2016 3. A. Buljac, M. Shakoar, J. Neggers, M. Bernacki, P.-O. Bouchard, L. Helfen, T. F. Morgeneyer and F. Hild, Numerical Validation Framework for Micromechanical Simulations based on Synchrotron 3D Imaging, *Computational Mechanics*, 59(3): 419–441, 2017

Frequency Response of Assembled Structures with Identified Multi-interface Proportional Damping

Noureddine Bouhaddi*, Mohamed Krifa**, Scott Cogan***, Najib Kacem****

*Univ. Bourgogne Franche-Comté, FEMTO-ST Institute, CNRS/UFC/ENSMM/UTBM, Department of Applied Mechanics, **Univ. Bourgogne Franche-Comté, FEMTO-ST Institute, CNRS/UFC/ENSMM/UTBM, Department of Applied Mechanics, ***Univ. Bourgogne Franche-Comté, FEMTO-ST Institute, CNRS/UFC/ENSMM/UTBM, Department of Applied Mechanics, ****Univ. Bourgogne Franche-Comté, FEMTO-ST Institute, CNRS/UFC/ENSMM/UTBM, Department of Applied Mechanics

ABSTRACT

The severe dynamic environment of take-off and flight of launchers presents risks of damage and life cycle limitation of the payload. To improve the dynamic comfort of the payload, damping treatments are employed at the final stage of the launcher assemble. One well-known solution is the limitation of the vibration amplitudes by dissipating the energy at the bolted joints between the stages. To our knowledge, there is not a simple and effective method that allows an accurate damping prediction at the full structure level from the knowledge of localized dissipation between the components. Indeed, to model the damping of an assembled structure made up of several components, one carries out a 3D modeling of the interfaces [1] to have a good representation of the dissipation. The result is a damping model identified by interface, which is difficult to exploit in the prediction of the dynamic behavior of the full model. Moreover, for uniformly distributed dissipation, it is common to use the Rayleigh damping assumption to represent the damping matrix in the equivalent viscous model. In general, common methods [2] identify this matrix at a single interface. In this work, we propose a method of modeling the multi-interface Rayleigh damping which consists of the following steps: (i) calculation of the modal damping of each interface taken separately by using the modal effort method [3] or the modal displacement method developed in PERMAS finite element software; (ii) identification of the proportional damping matrix of each interface (proportionality coefficients of stiffness and mass matrices); (iii) assembly of the identified damping matrices; (iv) prediction of the dynamic response of the complete structure from the global model. The proposed method was validated on a reduced model of the ARIANE 5 launcher to calculate the dynamic responses taking into account the different types of dissipation in the interfaces for the asymmetric load case and successfully compared to the reference results. The main advantages of the proposed method are the simplicity of the numerical implementation, the reduction of the CPU, the quality of prediction and the perspective of integration in an optimization procedure of interfaces design with high damping performances. References [1] S. Bograd, P. Reuss, A. Schmidt, L. Gaul and M. Mayer, Mechanical Systems and Signal Processing, 25(8), 2801–2826, 2011. [2] S. Adhikari, 293(1), 156–170, 2006. [3] A. Caignot, P. Ladevèze, D. Néron and J. F. Durand, Engineering Computations, 27(5), 621-644, 2010.

A Model for Cellular Mechanotransduction and Contractility at Finite Strain

Nikolaos Bouklas^{*}, Selman Sakar^{**}, William Curtin^{***}

^{*}Cornell University, ^{**}EPFL, ^{***}EPFL

ABSTRACT

In this work we introduce a theoretical and computational modeling framework for the contractile response of single cells triggered by external mechanical stimuli. The structural response due to the formation and dissociation of stress fibers is modeled following isotropic anisotropic contractile phases with an orientation that evolves with time and strain. The passive and active structural components are postulated to act in parallel, and the re-orientation process drives the anisotropic phase of stress fiber orientation to align with the direction of the maximum principal stretch. A reduced form of the Hai-Murphy model is used to follow kinetics of myosin states considering the combined effect of ‘latch’- and ‘cross’-bridge states. The introduction of distinct isotropic and anisotropic activation allows modeling of the contractile intensity of each phase. Traction on the cell surface initiate bio-chemical signaling through the RhoA pathway, which in turn controls both myosin contraction and F-actin polymerization. A signaling model is introduced to effectively connect intracellular events with the traction on the cell surface. The overall model is defined by a free energy density function that couples the deformation and the activation, and associated equilibrium and kinetic models for evolution. Features of the model are highlighted via implementation in a finite element model and application to benchmark problems. The model captures the dynamic contractile responses of cells and stress fiber re-alignment under complex load histories. For example, physiologically relevant scenario such as relaxation of cells to their initial state upon removal of applied loads can be simulated.

Haemodynamic Analysis in Arterial Models in Relation to Pulmonary Valve Treatment in Adults with Congenital Heart Disease

Maria Boumpouli*, Mark Danton**, Terence Gourlay***, Asimina Kazakidi****

*University of Strathclyde, **Golden Jubilee National Hospital, ***University of Strathclyde, ****University of Strathclyde

ABSTRACT

Introduction Pulmonary artery stenting and valve replacement (PVR) are common interventions in an increasing population of adult patients with previously repaired congenital heart disease [1]. Indications for intervention include assessing regional haemodynamics and effects on right ventricular volume and function [2]. The criterion for intervention remains largely empirical and the optimal timing remains unknown. This work aims to investigate the altered haemodynamic environment of adults with congenital heart disease, pre- and post- operative PVR to establish a computational fluid dynamic (CFD) derived metric for determining the optimal requirement for PVR and stenting. In this initial work, we present CFD results in simplified geometries representing the proximal pulmonary artery and bifurcation. **Methods** Blood flow simulations were performed using an implementation of the finite volume method. The flow was assumed to be incompressible and governed by the Newtonian Navier-Stokes equations. Physiological vessel dimensions and boundary conditions were used in the models. Local velocities and wall shear stress values were evaluated numerically. **Results and Discussion** Blood flow in the pulmonary bifurcation is strongly dependent on the local geometrical characteristics and haemodynamic conditions. An increase in the flow separation is observed when the angle of the bifurcation increases. In addition, the geometry has a significant effect on the velocities and shear stresses developed on the vessel wall. Future work will involve anatomically-correct reconstructions from CT and MRI image data of adult congenital heart patients that have or are about to undergo pulmonary valve replacement. Numerical studies of these models will provide an insight into the underlying flow mechanisms of more complex 3D patient-specific geometries. **Acknowledgements** This work is funded by the University of Strathclyde Research Studentship Scheme (SRSS) Research Excellence Awards (REA), Project No 1208. **References** [1] Kogon B.E., et al (2015) Seminars in Thoracic and Cardiovascular Surgery. 27 p57 [2] Buechel, E.R.V., et al. (2005). European Heart Journal. 26 p2721

Crack Nucleation in Variational Phase Field Models of Fracture

Blaise Bourdin^{*}, Jean-Jacques Marigo^{**}, Corrado Maurini^{***}, Erwan Tanné^{****}

^{*}Department of Mathematics and Center for Computation & Technology, Louisiana State University, Baton Rouge, LA 70803, USA, ^{**}Laboratoire de Mécanique des solides, École Polytechnique, Route de Saclay, Palaiseau 91120, France, ^{***}Sorbonne Universités, UPMC Univ Paris 06, CNRS, UMR 7190, Institut Jean Le Rond d'Alembert, Paris F-75005, France, ^{****}Department of Mathematics, University of British Columbia, Vancouver, Canada

ABSTRACT

Since their inception in the mid-90's, variational phase-field models of fracture have steadily gained popularity. Part of this success is undoubtedly due to their ability to capture complex fracture behavior, including nucleation and propagation along complex unknown path in 2 and 3 dimensions without the need for ad-hoc criteria and geometric restrictions on crack path. In this talk, I will focus on crack nucleation. I will show that carefully constructed variational phase-field models can account for crack nucleation in the strength and toughness regimes, and for scale effects. I will give arguments in favor of identifying the model regularization parameter and the classical concept of a cohesive length. I will illustrate my claims with validation and verification experiments in a broad range of brittle materials and geometries.

Isogeometric Hierarchical Model Reduction for Parameter-Dependent Problems

Yves Antonio Brandes Costa Barbosa^{*}, Simona Perotto^{**}, Alessandro Veneziani^{***}

^{*}Politecnico di Milano, ^{**}Politecnico di Milano, ^{***}Emory University / IUSS Pavia

ABSTRACT

In engineering applications, numerical models have evolved to account for the demands in speed and accuracy. In particular, different model reduction techniques have been properly incorporated to compute, with a reasonable level of precision, the solution of partial differential equations in a constrained time and with a contained computational burden. In particular, our interest is for Hierarchical Model (HiMod) Reduction techniques [1], suitably combined with Isogeometric Analysis (HigaMod), according to the setting proposed in [2] and successively applied in a data assimilation context [3]. HigaMod is a reduction procedure suited to downscale models when the phenomenon at hand presents a preferential direction of flow, e.g., when modelling the blood flow in arteries or the water flow in a channel network. The method showed a significant improvement in reducing the computational power and simulation time, while giving enough information to analyze the problem at hand. In this communication, we generalize HigaMod approach to a parameter-dependent framework, setting the so-called HigaPOD formulation, which merges the computational benefits of HigaMod with the ones characterizing a Proper Orthogonal Decomposition (POD). In particular, we will refer either to linear and nonlinear problems by setting ad-hoc procedures for both the cases. The results so far obtained, although preliminary, are very promising. Thus, after introducing the basic HigaMod framework, we will focus on the HigaPOD approach by verifying the corresponding performances on some benchmark configurations. [1] S. Perotto. A survey of hierarchical model (Hi-Mod) reduction methods for elliptic problems. In Numerical Simulations of Coupled Problems in Engineering. Series: Computational Methods in Applied Sciences, Vol. 33, Springer, S.R. Idelsohn Ed. (2014), 217-241. [2] S. Perotto, A. Reali, P. Rusconi and A. Veneziani. HIGAMod: a Hierarchical IsoGeometric Approach for MODeL reduction in curved pipes. Comput. & Fluids, 142 (2017), 21-29. [3] Y. A. Brandes C. Barbosa, S. Perotto, A. Veneziani. A Kalman filtering data assimilation procedure based on Hierarchical Isogeometric Model reduction. In preparation.

Multiscale Design of Nonlinear Composites Using an Interface-Enriched Generalized FEM

David Brandyberry*, Philippe Geubelle**

*University of Illinois at Urbana-Champaign, **University of Illinois at Urbana-Champaign

ABSTRACT

Advances in manufacturing technology such as additive manufacturing are enabling the creation of new composite materials with microstructures of increasing complexity. These material microstructures can be designed to fit desired macroscopic responses by changing the geometry and constituent properties. The shape and layout of inclusions, and the properties of their interfaces can greatly affect the constitutive and failure behavior of the composite. These two microstructural parameters, i.e., the shape and properties of the inclusion/matrix interfaces, constitute the design parameters of this study. In this work, a multiscale, parallel Interface-Enriched Generalized FEM (IGFEM) solver is developed to efficiently solve large 3D structural problems involving complex internal microstructures, extract the homogenized macroscopic material properties, and compute the analytic design sensitivities to drive a gradient-based design optimization algorithm. In this study, material interfaces are represented on the highest level by simple geometric shapes which can be described by functions such as spheres and ellipsoids. Standard finite element methods are capable of modeling the constitutive response of complex microstructures. However, generalized finite element methods such as IGFEM have much greater flexibility in representing the discretized geometry without the complex and costly meshing process. Because IGFEM uses a fixed non-conforming mesh, it offers major advantages in shape optimization studies over regular FEM since large shape changes do not cause mesh distortion or require remeshing. To capture the nonlinear behavior of material interfaces, a cohesive law is introduced to govern their traction-separation behavior. A smoothed trapezoidal model provided by (Scheider & Brocks, 2003) is chosen here for its flexibility, allowing us to capture high initial stiffness of the 'intact interface' while controlling the progressive failure of the inclusion/matrix interface. Gradient-based design optimization presents a very efficient method for determining optimal microstructure shape and constituents. The optimal set of shape and cohesive interface parameters are found to match the homogenized response to a given desired macroscopic nonlinear constitutive behavior. An analytic shape and material sensitivity is derived to capture the gradients of the described nonlinear problem with respect to our design variables extremely efficiently. Scheider, I., and Brocks, W. (2003). Simulation of cup-cone fracture using the cohesive model. Engineering Fracture Mechanics, 70:14, 1943–1961.

Novel Approaches towards the Efficient Simulation of Falling Nano-Ribbons

Michael Braun^{*}, Raúl Radovitzky^{**}

^{*}Massachusetts Institute of Technology, ^{**}Massachusetts Institute of Technology

ABSTRACT

Nano-ribbons are flexible structures whose length is much larger than their width which in turn is much larger than their thickness. These different length scales equip nano-ribbons with some remarkable motion and deformation characteristics when being immersed in certain fluid flows. In this talk, we present our ongoing work towards an efficient simulation tool suitable for exploring these characteristics: We utilize our finite element code SumMIT to simulate the falling behavior of elastic nano-ribbons in an ambient viscous fluid. On the one hand, this task requires the solution of a structural dynamics problem that involves large deformations and different length scales; on the other hand, it also requires an efficient computation of the deformation-dependent viscous forces exerted by the fluid on the nano-ribbons. As for the structural part of our approach to this fluid-structure interaction problem, we model the nano-ribbons using discontinuous Galerkin shell finite elements [1] which have been shown to be effective in the thin shell limit. Regarding the fluid part, we are not aimed at discretizing the fluid domain and solving the full Navier-Stokes equations since we are primarily interested in the motion and deformation of the nano-ribbons under low Reynolds number conditions. Instead, the resulting viscous forces acting onto the nano-ribbons are computed using different fluid models that are based on the assumption of Stokes flow. They comprise a boundary element method for open surfaces [2] and the recently published slender-ribbon theory [3]. In our talk, we elaborate on the coupling of these fluid models to the structural problem, discuss their verification, and present our findings on the falling behavior of elastic nano-ribbons in air. References [1] B. Talamini and R. Radovitzky. A discontinuous Galerkin method for nonlinear shear-flexible shells. *Computer Methods in Applied Mechanics and Engineering*, 303:128–162, 2016. [2] L. Heltai, J. Kiendl, A. DeSimone, and A. Reali. A natural framework for isogeometric fluid-structure interaction based on BEM-shell coupling. *Computer Methods in Applied Mechanics and Engineering*, 316:522–546, 2017. [3] L. Koens and E. Lauga. Slender-ribbon theory. *Physics of Fluids*, 28(1):013101, 2016.

Sediment Transport over Evolutionary Bedforms by the Particle Finite Element Method

Rafael Bravo*, Pablo Becker**, Pablo Ortiz***, Sergio Idelsohn****

*University of Granada, **International Center for Numerical Methods in Engineering, ***University of Granada,
****International Center for Numerical Methods in Engineering

ABSTRACT

The numerical simulation of sediment transport coupled with evolutionary erodible bedforms is essential for the analysis of the morphodynamics of sediment structures. The erosion and evolution of a bedform is a dynamical coupled problem that must be studied with methods able to simulate the interface between the sediment flow and erodible bed. The Particle Finite Element Method (PFEM) with movable mesh was successfully applied in the past to model free surface flows problems such as the interaction of flows with boundaries, or the strong erosion of beds subjected to high velocity flows [1]. A numerical strategy based on the new version of the Particle Finite Element Method with fixed mesh (PFEM-2) is presented for the simulation of sediment flows coupled with evolutionary erodible boundaries. The present approach models in a Lagrangian frame with fixed mesh the evolution of a bed-form using an advection–diffusion equation and is solved with the explicit time integration method PFEM-2 from [2], which permits to employ intermediate-large time steps and takes advantage of its easy computer parallelization. This approach overcomes the restrictions of previous PFEM developments applied to model the erosion, see [1], that was simulated by the conversion of soil to fluid elements leading to sudden changes in the geometry. In this work flow and bedform are coupled in a staggered way. Flow is solved using an standard Finite Element fluid solver compatible with Arbitrary Lagrangian–Eulerian (ALE) techniques, which allows the deformation of the mesh at every time step. The evolution of bedform and flow is linked by the empirical sediment flux relation of Meyer-Peter-Müller. The model is able to reproduce with good agreement the lab experiments of the evolution of subaqueous small dunes under different flow conditions from [3]. This research is supported by MICIIN Grant #BIA-2015-64994-P (MINECO/FEDER) REFERENCES [1] Oñate E, Celigueta MA, Idelsohn SR (2006) Modeling bed erosion in free surface flows by the particle finite element method. *Acta Geotechnica* 1(4):237–252. [2] Bravo, R Becker P, Ortiz P (2017) Numerical simulation of evolutionary erodible bedforms using the particle finite element method. *Computational Particle Mechanics* 4(3):297–305. [3] Leclair S (2002) Preservation of cross-strata due to the migration of subaqueous dunes: an experimental investigation. *Sedimentology* 49(6):1157–1180.

Modeling of Actual-Size Organic Electronic Devices from Efficient Molecular-Scale Simulations

Jean-Luc Bredas^{*}, Haoyuan Li^{**}

^{*}Georgia Institute of Technology, ^{**}Georgia Institute of Technology

ABSTRACT

The rational development of organic electronic devices requires to gain a molecular insight into the structure-performance relationships for the organic semiconductor active layers. To this end, molecular-scale simulation techniques, such as the kinetic Monte Carlo (KMC) method, have been exploited in the modeling of organic electronic devices.[1-2] However, such simulations are computationally expensive and, as a result, limited to nanometer-size systems; this is well below the micrometer-size systems that would be needed in order to consider actual-scale morphologies and to reliably model low dopant concentrations and trap densities. An alternate molecular-scale simulation technique, the master equation (ME) approach, is in principle less computationally demanding. However, up to now, ME methodologies have been scarcely applied to device modeling because of their lesser accuracy, which mainly originates in their inability to (fully) account for the electrostatic interactions among charge carriers.[3] Here, we overcome this limitation and show that both short-range and long-range electrostatic interactions can be properly included in ME simulations. The important result is that efficient, reliable molecular-scale simulations can now be applied to systems 100 times the size of those previously accessible. In addition, by exploiting GPU acceleration, we demonstrate that ME simulations of micrometer-sized systems can be completed in a matter of hours on a desktop computer, while the estimated computational cost for an equivalent KMC simulation reaches 300 years. This quantum leap in the modeling capability has allowed us to investigate a micrometer-size diode device and to uncover, in the case of a single-component active layer, that there exist large inhomogeneities in the charge carrier distributions. In the case of a blend morphology, the charge transport in an actual-scale device is found to evolve differently as a function of applied voltage, in comparison to the case of a uniform, single-component film. By now offering the possibility of incorporating such features in the description of realistic-scale systems, our methodology represents a major step into a deeper understanding of the operation of organic electronic devices. References: [1] P. K. Watkins; A. B. Walker and G. L. B. Verschoor, *Nano Lett.*, 2005, 5, 1814. [2] M. Mesta; M. Carvelli; R. J. de Vries; et al., *Nat. Mater.*, 2013, 12, 652. [3] J. J. M. van der Holst; F. W. A. van Oost; R. Coehoorn and P. A. Bobbert, *Phys. Rev. B*, 2011, 83, 085206.

Task-based Parallelism for Finite-Element Models of Shallow Water Flows

Max Bremer^{*}, Kazbek Kazhyken^{**}, Hartmut Kaiser^{***}, Craig Michoski^{****}, Clint Dawson^{*****}

^{*}The University of Texas at Austin, ^{**}The University of Texas at Austin, ^{***}Louisiana State University, ^{****}The University of Texas at Austin, ^{*****}The University of Texas at Austin

ABSTRACT

The advent of exascale computing has introduced a massive increase in the amount of concurrency within modern supercomputers. The efficient utilization of these new architectures necessitates a change in programming models. In this talk, we present a task-based implementation of a discontinuous Galerkin finite element method for the shallow water equations. The results have been implemented within a new C++ open-source project, called dgswem-v2, which is a discontinuous Galerkin fork of ADCIRC and parallelized using High Performance ParallelX (HPX). HPX is a novel task-based C++ runtime designed to execute lightweight threads while avoiding costly synchronizations. Scaling results will be presented on the latest architectures including Intel Xeon Phi Knights Landing as well as Skylake chips. Particular emphasis will be placed on contrasting HPX's performance with a traditional MPI parallelization in order to provide practical insights.

Dynamics of Human Thoracic Aorta under Pulsatile Blood Pressure

Ivan Breslavsky*, Marco Amabili**

*McGill University, **McGill University

ABSTRACT

Introduction and Methods Deformations of a thoracic segment of the human descending aorta under static and dynamic pressure is studied. The aortic segment is modeled as a circular cylindrical shell with three layers (intima, media, and adventitia). The material of each layer is considered to be viscoelastic, hyperelastic and reinforced by two families of collagen fibers. The anisotropic hyperelastic law used in this study is the Holzapfel-Gasser-Ogden model [1]. As is well known, aortas in vivo are not stress-free even without the blood pressure load. We account for two types of residual stresses – circumferential and axial ones. The shell has spring boundary conditions that simulate the connection with the remaining parts of the aorta and it is filled with pressurized blood, simulated by potential flow theory. The material parameters are taken from the literature [2]. We compare two sets of material parameters, corresponding to middle-aged and old man. Results and Discussion Initially we applied static pressure to obtain the configuration corresponding to the average contribution of the dynamical blood pressure. Subsequently, nonlinear dynamics under physiological pulsatile pressure was analyzed with the local models method [3]. The contribution of the added masses of blood into the inertia has been taken into account, as well as the dynamic stiffening effect. It was found that for the both middle-aged and old patients the amplitude of the dynamical response increases with the heart beating rate in the physiological range. At heart beating rates higher than 100 beats per minute, the dependence of the amplitudes of the aorta response on the frequency of the pulsatile pressure is very significant. This is a strong evidence that nonlinear dynamics is important in evaluating the aorta deformations. References [1] Holzapfel, G.A., Gasser, T.C., and Ogden, R.W., “A New Constitutive Framework for Arterial Wall Mechanics and a Comparative Study of Material Models”, *J. Elasticity*, 61, pp. 1-48 (2000). [2] Weisbecker, H., Pierce, D.M., Regitnig, P., and Holzapfel, G.A., “Layer-specific damage experiments and modeling of human thoracic and abdominal aortas with non-atherosclerotic intimal thickening”, *J. Mech. Behav. Biomedical Mater.*, 12, pp. 93-106 (2012). [3] Breslavsky, I.D., Amabili, M., and Legrand, M., “Physically and Geometrically Non-Linear Vibrations of Thin Rectangular Plates”, *Int. J. Non-Linear Mech.*, 58, pp. 30-40 (2014).

Successes and Challenges from the Performance Optimisation and Productivity Centre of Excellence

Sally Bridgwater^{*}, Nick Dingle^{**}, Jonathan Boyle^{***}, Jon Gibson^{****}, Wadud Miah^{*****}

^{*}Numerical Algorithms Group Ltd, ^{**}Numerical Algorithms Group Ltd, ^{***}Numerical Algorithms Group Ltd,
^{****}Numerical Algorithms Group Ltd, ^{*****}Numerical Algorithms Group Ltd

ABSTRACT

The Performance Optimisation and Productivity (POP) Centre of Excellence in Computing Applications was funded by the European Union 's Horizon 2020 programme to help people in the EU write more efficient parallel code and thus boost their productivity. In two and a half years of operation POP has completed approximately 150 investigations of codes drawn from a wide range of scientific domains of which around one third were computational mechanics or fluid dynamics codes. This talk will look at the types of improvements that POP's users have been able to achieve because of engaging with the project. POP's success stories include a CFD code, for which the user reported a 3x performance improvement, an OpenFOAM solver which achieved a 25% performance improvement along with other computational mechanics and CFD examples. We will also draw out some common performance issues identified by the analyses relevant to computational mechanics and fluid dynamics codes as well as highlighting some of the technical and organisational challenges we have had to overcome. The methodology used within the project for analysis of parallel codes, provides a quantitative way of measuring the relative impact of the different factors inherent in parallelisation. A feature of the methodology is that it uses a hierarchy of metrics, each metric reflecting a common cause of inefficiency in parallel programs. These metrics then allow comparison of parallel performance (e.g. over a range of thread/process counts, across different machines, or at different stages of optimisation and tuning) to identify which characteristics of the code contribute to inefficiency. This provides the knowledge necessary to decide the best course of action to get performance, and determine how much effort is needed with a clear view of the potential reward via reproducible and comparable measurements of the performance. POP is a collaboration between Barcelona Supercomputer Center, High Performance Computing Center Stuttgart, Juelich Supercomputing Centre, Numerical Algorithms Group Ltd, RWTH Aachen, and TERATEC.

A Semi-automatic Method to Characterize the Mechanical Properties of Specific Patient: Application on Pelvic System

Mathias Brieu^{*}, Guillaume Dufaye^{**}, Olivier Mayeur^{***}, Jean-françois WITZ^{****}, Pauline Lecomte-Grosbras^{*****}, Laurent Patrouix^{*****}

^{*}LAMcube, Centrale Lille, France., ^{**}Satt nord, LAMcube, France., ^{***}LAMcube, Centrale Lille, France., ^{****}LAMcube, Centrale Lille, France., ^{*****}LAMcube, Centrale Lille, France., ^{*****}LAMcube, Centrale Lille, France.

ABSTRACT

Female genital prolapse represents a major problem with 60% of women over 60 years old being concerned [1]. To prevent from such problem, numerical simulation of the pelvic mobility aims to evaluate pelvic floor disorder in order to further help for pelvic floor surgery planning [2]. Such application of numerical simulation for surgical evaluation and planning will only be possible if patient-specific anatomy and mechanical properties are known [3]. The aim of the study is to introduce a semi-automatic reconstruction of the pelvic system and the characterization of the mechanical properties of a specific patient. This approach will be validated according to a physical model, based on a representative pelvic system. The Patient-Specific geometric model is obtained from images analysis on MRI allowing to generate a pelvic cavity FE model [3]. Since the principal difficulty is to estimate the intra-abdominal pressure, medical device has been developed to measure the intravaginal pressure during coughing. This probe is compatible with MRI examination to synchronise the pressure and dynamic MRI and motion tracking algorithm. The proposed inverse method is based on the minimization of the gap between Finite Element (FE) analysis and dynamic MRI observation, to finally identify the patient-specific tissue's mechanical properties of anatomical structures. To evaluate this numerical approach, we manufactured a physical model of the pelvic system, compatible with MRI techniques, where every input parameters are totally controlled (imposed pressure, material properties and geometry), in order to mimic the geometry, behaviour, pressure level and compare results. The application to the physical model allows us to quantify uncertainties of the proposed method based on MRI data treatment. The comparison between the imposed pressure and the intravaginal sensor are same with constant gap, which validate the sensor application. Results on the physical model are in range of the experimental data bank of the constitutive material (silicone rubber). This non-destructive identification approach is also validated on patient-specific geometry and works are in progress to apply this method in clinical case, with patient-specific pressure measured with our probe imposed on our FE model. [1] Samuelsson et al. American Journal of Obstetrics and Gynecology, 1999, 180 : 299-305 [2] Chen et al. Journal of Biomechanics, 2015, 48 : 238-245. [3] Mayeur et al. Annals of Biomedical Engineering, 2016, 44(1) : 202-212.

Nanomine – Polymer Nanocomposite Data Resource to Design Next Generation Materials

L. Cate Brinson^{*}, Claire Lin^{**}, Bingyin Hu^{***}, Wei Chen^{****}, Yixing Wang^{*****}, Linda Schadler^{*****}, Deborah McGuinness^{*****}, Jim McCusker^{*****}, Rui Yan^{*****}

^{*}Duke University, ^{**}Duke University, ^{***}Duke University, ^{****}Northwestern University, ^{*****}Northwestern University,
^{*****}RPI, ^{*****}RPI, ^{*****}RPI, ^{*****}RPI

ABSTRACT

Nanocomposites can exhibit significant physical property changes with very small loadings of nanofiller. However, the properties of nanocomposites can be influenced by many factors, including chemical synthesis details where small changes in the composition of the constituents can lead to unexpected large changes in resultant properties. Consequently trial-and-error iterative experiments have mainly been used to develop and study these materials. Although systematic approaches and databases have been developed in some areas for metallic alloy systems on top of the processing-structure-property (p-s-p) paradigm, the field of polymers and their composites have largely been lacking. The materials genome concept however offers compelling advantages to enhance our understanding of and design of polymer nanocomposites. In this presentation, we present the Nanomine data resource, the schema and ontology supporting the database, as well as the application of this data resource and case studies. Nanomine is a data-driven web-based infrastructure combining a database, data search and visualization tools, data-driven material analysis tools and physics-based modeling for polymer nanocomposites. Our infrastructure is developed based on the NIST Materials Data Curation System (MDCS). MDCS is inherently a No-SQL based database system and organizes the data using a user-defined XML schema. To appropriately capture the full features of possible data for nanocomposite, we designed the basic structure of the NanoMine schema and continue expanding to incorporate more features during our development. We also developed a robust ontology for polymer nanocomposites based on our XML schema that was used to support organization, search and visualization services of the material data. This ontology also formalizes relationships inherent in our XML schema and can act as a translator to accept multiple XML formats, enhancing ability to share across different data resources. Using the XML schema and the ontology, we have developed a prototype web-based system for polymer nanocomposite material data archiving, data exploration and visualization, characterization and analysis, as well as simulation and design. Current database contained over 1500 samples manually collected from over 150 papers and is continuously expanding. Nanomine aims to capture the physical properties, processing conditions and microstructure information reported in literature or individual research labs using standardized format and terminology. With sufficient data in each p-s-p domain, we are creating case studies to link processing conditions with the quantified microstructure information, interphase properties and bulk composite response by building statistical correlations coupled by image analysis and physics-based simulation tools.

AN ERROR INDICATOR BASED ON A WAVE DISPERSION ANALYSIS FOR THE VIBRATION EIGENMODES OF ANISOTROPIC ELASTIC SOLIDS DISCRETIZED BY THE ENERGY ORTHOGONAL TWENTY NODE HEXAHEDRAL FINITE ELEMENT

Francisco J. Brito

Departamento de Ingeniería Industrial, Universidad de La Laguna
Calle Méndez Núñez 67-2C
Santa Cruz de Tenerife 38001, Spain
E-mail address; fjbrito@ull.es

Key words: energy-orthogonal stiffness, numerical dispersion, vibration eigenmodes.

Summary. *This contribution studies the dispersion of the bulk elastic waves in homogeneous and anisotropic elastic media discretized by the twenty-node hexahedral finite element. The element stiffness matrix is split into basic and higher order components which are respectively related to the mean and deviatoric components of the strain field. This decomposition is applied to the elastic energy of the finite element assemblage. By a dispersion analysis the higher order energy is related to the energy error for the propagating waves. An averaged correlation is proposed to apply the higher order energy as an error indicator for vibration eigenmodes.*

1 INTRODUCTION

It is well known that the wave scattering at boundaries creates an interference field that, if composed solely of waves of frequency equal to a natural frequency of the solid, takes the form of a standing-wave field which is an eigenmode of the continuum [1]. For a homogeneous, anisotropic and linearly elastic solid this standing-wave field could be considered essentially composed of bulk quasi-longitudinal and quasi-shear waves. In this case the goal of determining the finite element mesh required to accurately represent a given number of eigenmodes could be approached by analysing the effect of the spatial discretization over the propagation of such bulk waves in unbounded media. This effect becomes apparent by observing the dispersive behavior of the waves, a phenomenon that is not present in the physical system, the analysis of which will be approached in this contribution. A recent sample of the extensive research about the subject of the wave propagation in discretized solid media can be found in reference [2].

The anisotropic elastic media considered in this research cover laminated composites with periodic layering. The oriented plies can be reduced to a unit cell geometry with repeats throughout the laminate. The unit cell is generally composed of alternating uniaxial layers in two or more directions and can also include isotropic layers [3,4], Fig. 1.

It is supposed that the wavelength of the elastic waves is much larger than the thickness of the unit cell. In this case the laminated composite could be replaced by an effective homogeneous medium with elastic properties computed by the Backus' procedure [5]. Specifically, the laminated composites considered in this research are made combining epoxy, aluminum and diverse fibers. In Table 1, the density ρ and the non-null components of the

elasticity matrix \mathbf{C}^c , relating the stresses and engineering strains components, in the material coordinate system, Fig. 1, are shown for the uniaxial basic materials [6, 7, 8, 9].

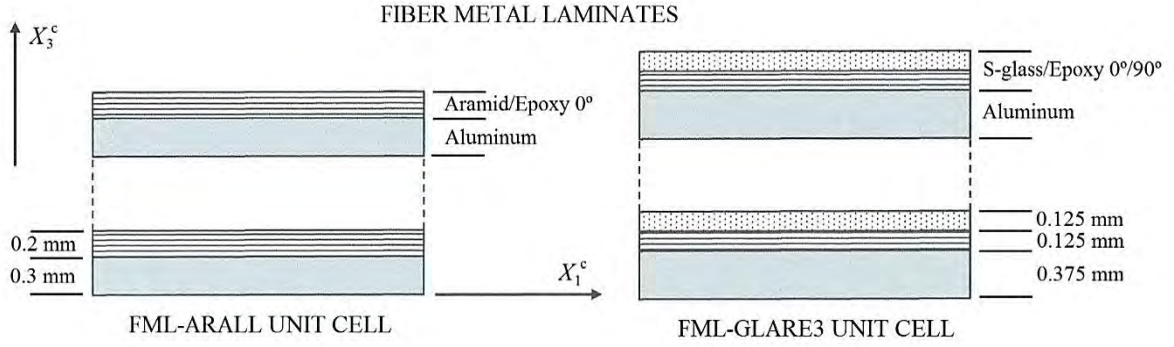


Figure 1. Laminated composites with periodic layering.

C_{IJ}^c	Uniaxial Carbon/Epoxy [6]	Uniaxial Aramid/Epoxy [6]	Uniaxial S-glass/Epoxy [8, 9]	Uniaxial Bo-Al [7]	Isotropic Aluminum [6]
11	162.00	60.00	59.52	269.07	110.00
12	11.80	1.70	8.08	58.50	56.00
13	11.80	5.00	8.08	58.50	56.00
22	17.00	5.80	20.14	188.60	110.00
23	8.20	5.00	8.72	76.34	56.00
33	17.00	8.50	20.14	188.60	110.00
44	4.40	1.80	5.71	56.13	27.00
55	8.00	2.30	7.60	60.19	27.00
66	8.00	2.10	7.60	60.19	27.00
ρ	1610.00	1600.00	2000.00	2520.00	2700.00

Table 1. Elastic properties (GPa) and density (kg/m³) of the uniaxial basic materials.

1.1 Finite element formulation

In a solid medium discretized by the finite element method the equations of equilibrium governing its linear dynamic response for time-harmonic waves with damping neglected may be cast in matrix form [10],

$$(\mathbf{K} - \omega^2 \mathbf{M}) \mathbf{\tilde{u}} = \mathbf{F}; \quad \mathbf{\tilde{u}} = \mathbf{\tilde{u}} \exp(-i\omega t), \quad \mathbf{F} = \mathbf{\tilde{F}} \exp(-i\omega t) \quad (1)$$

where: \mathbf{K} (\mathbf{M}), stiffness (mass) matrix of the finite element assemblage; $\mathbf{\tilde{u}}$ ($\mathbf{\tilde{F}}$), column matrix containing the complex amplitude of the nodal displacements (nodal external loads); $\omega = 2\pi/T$, circular frequency; T , period of wave; t , time. The elastic energy of the finite element assemblage will be

$$E = \frac{1}{2} \text{Re}[\mathbf{\tilde{u}}^T \mathbf{K} \mathbf{\tilde{u}}] \quad (2)$$

Considering the matrix \mathbf{B}^e at element level, relating the engineering strain components to the nodal values of displacement, and the elasticity matrix \mathbf{C} , the element stiffness matrix will be

$$\mathbf{K}^e = \int_{\Omega_e} (\mathbf{B}^e)^t \mathbf{C} \mathbf{B}^e dV \quad (3)$$

If the matrix \mathbf{B}^e is partitioned into mean and deviatoric components,

$$\mathbf{B}^e = \bar{\mathbf{B}}^e + \mathbf{B}_d^e; \quad \bar{\mathbf{B}}^e V^e = \int_{\Omega_e} \mathbf{B}^e dV, \quad \mathbf{B}_d^e = \mathbf{B}^e - \bar{\mathbf{B}}^e \quad (4)$$

the matrix Eq. (3) would be decomposed as addition of basic and higher order components,

$$\mathbf{K}^e = \mathbf{K}_b^e + \mathbf{K}_h^e; \quad \mathbf{K}_b^e = (\bar{\mathbf{B}}^e)^t \mathbf{C} \bar{\mathbf{B}}^e V^e, \quad \mathbf{K}_h^e = \int_{\Omega_e} (\mathbf{B}_d^e)^t \mathbf{C} \mathbf{B}_d^e dV \quad (5)$$

In this case it is said that the element stiffness matrix is formulated in energy-orthogonal form [11]. The decomposition in Eq. (5) holds for the complete model,

$$\mathbf{K} = \mathbf{K}_b + \mathbf{K}_h \quad (6)$$

For a stationary wave, the amplitude of nodal displacements $\tilde{\mathbf{u}}$ is a real-valued vector. Then, from Eq. (2), the period-averaged elastic energy for the discretized domain will be

$$\bar{E} = \frac{1}{2} \tilde{\mathbf{u}}^t \mathbf{K} \tilde{\mathbf{u}} \int_0^1 \cos^2(2\pi\tau) d\tau = \frac{1}{4} \tilde{\mathbf{u}}^t \mathbf{K} \tilde{\mathbf{u}} \quad (7)$$

where: $\tau = t/T$, $0 \leq \tau \leq 1$, dimensionless time. By introducing Eq. (6) into Eq. (7), the basic and higher order period-averaged elastic energies will be obtained. The latter component will be

$$\bar{E}_h = \frac{1}{4} \tilde{\mathbf{u}}^t \mathbf{K}_h \tilde{\mathbf{u}} \quad (8)$$

2 DISPERSION ANALYSIS

The unbounded elastic domain is discretized by a regular mesh of standard twenty-node hexahedral finite elements HE20 [10], Fig. 2. The nodal lattice formed by the finite element assemblage has four nodes per unit cell. Different meshes with the same element volume can be obtained by selecting the aspect ratio parameter, $0 < \gamma \leq 1$; and the skew angle, $0 \leq \beta < 90^\circ$. The angle of rotation α between the finite element mesh coordinate system and the material coordinate system can also be selected, Fig. 2.

For uniform plane harmonic waves, the displacement vector field will be

$$\mathbf{u} = \tilde{\mathbf{u}}(\mathbf{r}) \exp(-i\omega t), \quad \tilde{\mathbf{u}}(\mathbf{r}) = A \hat{\mathbf{a}} \exp(i\kappa \mathbf{n} \cdot \mathbf{r}) \quad (9)$$

where: A , amplitude of the wave; $\hat{\mathbf{a}}$, polarization vector, unit vector indicating the direction of the particle displacement; \mathbf{n} , wave normal, unit vector indicating the direction of the wave propagation; $\kappa = 2\pi/\lambda = \omega/c$, wave number; λ , wavelength; c , phase velocity of the continuum.

The wave normal has the components $n_1 = \cos\phi \sin\theta$, $n_2 = \sin\phi \sin\theta$ and $n_3 = \cos\theta$, where: ϕ , azimuthal angle, $0 \leq \phi \leq 360^\circ$; θ , polar angle, $0 \leq \theta \leq 180^\circ$, Fig. 2.

The polarization vectors and phase velocities are solution of the Christoffel Equation [12],

$$(l_{iK} C_{KL} l_{Lj}) \hat{a}_j = \rho c^2 \hat{a}_i, \quad i, j = 1, \dots, 3; \quad K, L = 1, \dots, 6 \quad (10)$$

where the non-null values of l_{iK} are: $l_{11} = n_1$, $l_{15} = n_3$, $l_{16} = n_2$, $l_{22} = n_2$, $l_{24} = n_3$, $l_{26} = n_1$, $l_{33} = n_3$, $l_{34} = n_2$, and $l_{35} = n_1$.

The elasticity matrix in the finite element mesh coordinate system and the one in the material coordinate system are related by the equation $C_{KL} = M_{KI}^B C_{IJ}^c M_{LJ}^B$ where \mathbf{M}^B is the Bond matrix.

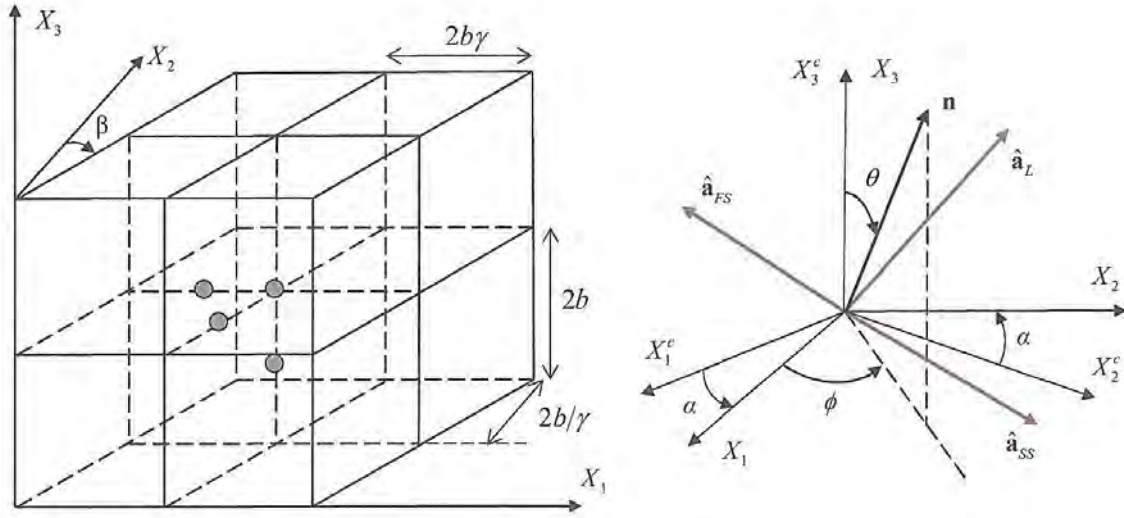


Figure 2. Elastic domain discretized by a regular mesh of HE20 elements and polarization vectors.

The three mutually orthogonal waves computed by solving the eigenproblem Eq. (10) are, Fig. 2: ($_{SS}$, c_{SS}), slow quasi-shear wave, SS; ($_{FS}$, c_{FS}), fast quasi-shear wave, FS; and ($_{L}$, c_L), quasi-longitudinal wave, L.

For a plane elastic wave Eq. (9) the density of period-averaged elastic energy can be computed by the equation [6],

$$\bar{E}_0 = \frac{1}{4} \rho \omega^2 A^2 \quad (11)$$

2.1 Characteristic equations

The characteristic equations can be found assuming harmonic waves Eq. (9) with different amplitudes in each node of the unit cell,

$$\tilde{\mathbf{u}} = A_j \hat{\mathbf{a}} \exp(i\mathbf{k}\mathbf{n} \cdot \mathbf{r}), \quad j = 1, \dots, 4 \quad (12)$$

Inserting the solutions Eq. (12) into the homogeneous part of Eq. (1), the characteristic equation for each node of the unit cell is yielded by equilibrium of nodal forces into the direction of the particle displacement [13],

$$\mathbf{F}_K \cdot \hat{\mathbf{a}} - \omega^2 \mathbf{F}_M \cdot \hat{\mathbf{a}} = 0 \quad (13)$$

where: \mathbf{F}_K , nodal force associate to the global stiffness matrix; \mathbf{F}_M , nodal force associate to the global mass matrix.

By considering Eq. (13) for each node of the unit cell, a homogeneous system of four algebraic equations is formed,

$$\mathbf{Z}\mathbf{A} = \begin{bmatrix} a_{ij}(m, \phi, \theta, \alpha, \beta, \gamma) + \varpi^2 b_{ij}(m, \phi, \theta, \alpha, \beta, \gamma) \end{bmatrix} A_j = 0, \quad i, j = 1, \dots, 4 \quad (14)$$

$$m = b\kappa/\pi = 2b/\lambda, \quad \varpi = (2b/c)\omega \quad (15)$$

where: m , dimensionless wave number, $0 < m < 1$; b , half of the element size; ϖ , dimensionless frequency of the discretized elastic domain.

In this procedure the global stiffness matrix has been expressed in a suitable form,

$$\mathbf{K} = \rho c^2 (2b) \mathbf{K}^0 \quad (16)$$

Similarly, the global mass matrix has been expressed as $\mathbf{M} = \rho(2b)^3 \mathbf{M}^0$.

2.2 Dispersion equations

The system of homogeneous algebraic equations given in Eq. (14) has a non-trivial solution only if the matrix \mathbf{Z} is singular; that is, $\det[\mathbf{Z}] = 0$. Then it is yielded the following polynomial equation which is called the characteristic frequency equation for the plane wave propagation,

$$\sum_{r=0}^4 c_r(m, \phi, \theta, \alpha, \beta, \gamma) \varpi^{2r} = 0, \quad c_4 = 1 \quad (17)$$

By computing the zeros of Eq. (17), the four dispersion equations are then yielded,

$$\varpi_k = \varpi_k(m, \phi, \theta, \alpha, \beta, \gamma), \quad k = 1, \dots, 4 \quad (18)$$

Substituting Eq. (18) into Eq. (14), the wave amplitudes corresponding to the nodes of the unit cell are yielded for each dispersion equation. The range of dimensionless wave number values where each dispersion equation represents the propagation of elastic waves in the discretized medium will be called the acoustical branch of the dispersion equation. In order to determine the acoustical branches the following constraint conditions are imposed,

$$A_1 = 1; \quad A_j(m, \phi, \theta, \alpha, \beta, \gamma) > 0, \quad j = 2, 3, 4 \quad (19)$$

$$(\partial \varpi / \partial m)_{\phi, \theta, \alpha, \beta, \gamma} > 0 \quad (20)$$

In molecular physics, condition Eq. (19) is called the restriction of the lattice spectrum to the acoustical branch [14]. The constraint condition Eq. (20) imposes that the normal component of the energy transport velocity must have the wave direction [6]. The preliminary constraint condition $\dim[\mathbf{N}(\mathbf{Z})] = 1$ over the dimension of the null space of matrix \mathbf{Z} must be imposed in order to Eq. (19) would be a meaningful constraint condition. From this point, for each dispersion equation only the acoustical branch will be considered.

From Eq. (15) the indicators of numerical dispersion for the phase velocity and the normal component of the group velocity can be expressed as

$$e_p = c_p/c = (2\pi)^{-1} \varpi/m, \quad e_{gn} = c_{gn}/c = (2\pi)^{-1} \partial \varpi / \partial m \quad (21)$$

2.3 Elastic energy at the unit cell

From Eq. (2), (15) and (16) the density of period-averaged elastic energy is computed,

$$\bar{E} = \frac{1}{2} \rho(\omega/\varpi)^2 \int_0^1 \text{Re}[\tilde{\mathbf{u}}^T \exp(-i2\pi\tau)] \text{Re}[\tilde{\mathbf{F}}^0 \exp(-i2\pi\tau)] d\tau \quad (22)$$

where: $\mathbf{F}^0 = \tilde{\mathbf{F}}^0 \exp(-i2\pi\tau)$, column matrix of forces at the nodes of the unit cell.

From the decomposition in Eq. (6), the above computed density of period-averaged elastic energy Eq. (22) can be partitioned as addition of basic and higher order components. Then, the percentage of period-averaged higher order elastic energy can be defined as

$$e_h = \bar{E}_h / \bar{E}, \quad e_h = e_h(m, \phi, \theta, \alpha, \beta, \gamma) \quad (23)$$

From Eq. (22) and (11), the percentage indicator of elastic energy error associated with the spatial discretization that is introduced by the finite element model is defined as

$$\varepsilon = (\bar{E} / \bar{E}_0) - 1, \quad \varepsilon = \varepsilon(m, \phi, \theta, \alpha, \beta, \gamma) \quad (24)$$

From Eq. (23) and (24), a mapping between the elastic energy error and the percentage of higher order elastic energy can be also computed,

$$\varepsilon = \varepsilon(e_h, \phi, \theta, \alpha, \beta, \gamma) \quad (25)$$

2.4 Numerical research

For the SS, FS and L waves, the indicators Eq. (21), (23) and (24) are computed versus dimensionless wave number for different meshes, directions of wave propagation and media. An example of the indicators Eq. (23) and (25) is shown in Fig. 3. It is observed that Eq. (23) and it is deduced that Eq. (24) both vanish as dimensionless wave number goes to zero; that is, as the mesh is refined and in the limit of long waves. It must be remarked that the behavior of the higher order elastic energy as dimensionless wave number goes to zero is a consequence that the strain field inside each element becomes uniform. That is, given the mesh, in the limit of long waves, the density of elastic energy approaches to zero more slowly than its higher order component; and, given the wavelength, as the solution converges on account of mesh refinement, the density of elastic energy is increasingly dominated by its basic component.

Investigating the relationship between the elastic energy error and the percentage of higher order elastic energy Eq. (25), it can be observed from Fig. 3 that both variables could be related by a cubic function for moderate values of the higher order elastic energy,

$$\varepsilon = (A(\phi, \theta, \alpha, \beta, \gamma) * e_h + B(\phi, \theta, \alpha, \beta, \gamma)) * e_h^2 \quad (26)$$

For each of the waves (SS, FS, and L) and media considered in this research, an averaged correlation between the elastic energy error and the percentage of higher order elastic energy is sought by computing averaged values for the coefficients A and B .

First, two reference values of the percentage of higher order elastic energy are selected. Then, by Eq. (23) and Eq. (25), the related reference values of dimensionless wave number and percentage of elastic energy error are respectively computed,

$$e_{h1} = 0.10 \quad e_{h2} = 0.20 \rightarrow m_{1,2} = f_{m1,2}(\phi, \theta, \alpha, \beta, \gamma), \quad \varepsilon_{1,2} = f_{\varepsilon1,2}(\phi, \theta, \alpha, \beta, \gamma) \quad (27)$$

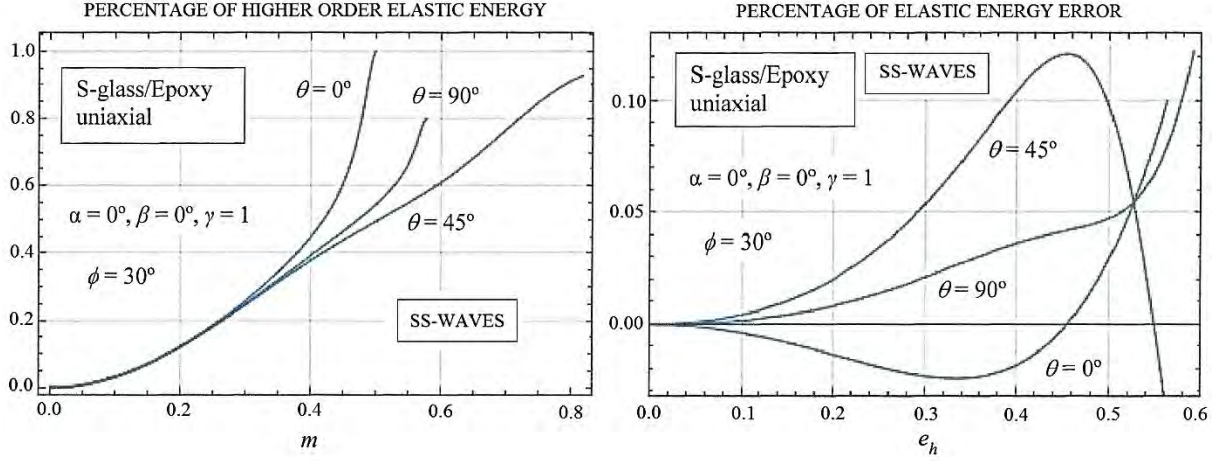


Figure 3. Higher order elastic energy versus dimensionless wave number and versus elastic energy error.

Next, the mean value of each reference dimensionless wave number and the root mean square value of each reference energy error are computed on the range of propagation angle,

$$m_{1,2}^M(\alpha, \beta, \gamma) = \frac{1}{\pi^2} \int_0^\pi \int_0^\pi m_{1,2} d\phi d\theta, \quad \varepsilon_{1,2}^{RMS}(\alpha, \beta, \gamma) = \sqrt{\frac{1}{\pi^2} \int_0^\pi \int_0^\pi \varepsilon_{1,2}^2 d\phi d\theta} \quad (28)$$

The integrals in Eq. (28) are computed by a step of $\pi/36$ for the azimuthal and polar angles. For media with cross-ply fibers, the finite element mesh coordinate system and the material one are coincident ($\alpha = 0^\circ$); however, for media with uniaxial fibers, the finite element mesh coordinate system is oriented both in the direction of the fibers ($\alpha = 0^\circ$) and perpendicular to them ($\alpha = 90^\circ$), being averaged the values of the integrals computed in each case.

Then, the mean reference values above computed are averaged by selecting three different meshes having the same element volume, Fig. 2: Q_1 , square section: $\beta = 0^\circ, \gamma = 1$; Q_2 , rectangular section with aspect ratio (1:2): $\beta = 0^\circ, \gamma = 1/\sqrt{2}$; Q_3 , skewed section: $\beta = 45^\circ, \gamma = 1$. That is,

$$\overline{m}_{1,2}^M = \frac{1}{3} [m_{1,2}^M(Q_1) + m_{1,2}^M(Q_2) + m_{1,2}^M(Q_3)], \quad \overline{\varepsilon}_{1,2}^{RMS} = \frac{1}{3} [\varepsilon_{1,2}^{RMS}(Q_1) + \varepsilon_{1,2}^{RMS}(Q_2) + \varepsilon_{1,2}^{RMS}(Q_3)] \quad (29)$$

The above computed mesh-averaged reference values Eq. (29) are shown in Tables 2 and 3 for each of the media and waves investigated. For details of ARALL and GLARE3 see Fig. 1.

Finally, by the mesh-averaged reference values of elastic energy error, the averaged values of the coefficients A and B for the cubic correlation Eq. (26) are then computed,

$$\overline{\varepsilon}_{1,2}^{RMS} = [\overline{A} * e_{h1,2} + \overline{B}] * e_{h1,2}^2 \rightarrow \varepsilon = (\overline{A} * e_h + \overline{B}) * e_h^2 \quad (30)$$

By similar procedure, the mesh-averaged reference values of the indicators of numerical dispersion for the phase velocity and the normal component of the group velocity Eq. (21) are also computed. The second mesh-averaged reference values are shown in Table 4.

		Carbon/Epoxy uniaxial	Aramid/Epoxy uniaxial	S-glass/Epoxy uniaxial	Bo-Al uniaxial	Aluminum
\overline{m}_1^M	SS	0.1755	0.1755	0.1755	0.1755	0.1755
	FS	0.1754	0.1754	0.1756	0.1755	0.1755
	L	0.1752	0.1751	0.1749	0.1749	0.1747
\overline{m}_2^M	SS	0.2570	0.2567	0.2569	0.2569	0.2569
	FS	0.2568	0.2566	0.2570	0.2570	0.2568
	L	0.2557	0.2555	0.2551	0.2548	0.2544
HOMOGENIZED						
		Carbon/Epoxy Cross-ply	Aramid/Epoxy Cross-ply	S-glass/Epoxy Cross-ply	ARALL	GLARE3
\overline{m}_1^M	SS	0.1755	0.1755	0.1755	0.1755	0.1755
	FS	0.1756	0.1757	0.1757	0.1756	0.1757
	L	0.1751	0.1751	0.1750	0.1750	0.1749
\overline{m}_2^M	SS	0.2570	0.2568	0.2568	0.2568	0.2568
	FS	0.2573	0.2576	0.2574	0.2573	0.2574
	L	0.2557	0.2554	0.2551	0.2554	0.2548

Table 2. Mesh-average of the mean values of the first and second reference dimensionless wave number.

		Carbon/Epoxy uniaxial	Aramid/Epoxy uniaxial	S-glass/Epoxy uniaxial	Bo-Al uniaxial	Aluminum
$\overline{\epsilon}_1^{RMS}$	SS	0.002755	0.002735	0.002756	0.002757	0.002781
	FS	0.003224	0.003424	0.002944	0.002831	0.002781
	L	0.003676	0.003843	0.004249	0.004426	0.004928
$\overline{\epsilon}_2^{RMS}$	SS	0.011963	0.011687	0.011995	0.011988	0.011963
	FS	0.014300	0.015536	0.012862	0.012312	0.011963
	L	0.016685	0.018174	0.020068	0.021241	0.024421
HOMOGENIZED						
		Carbon/Epoxy Cross-ply	Aramid/Epoxy Cross-ply	S-glass/Epoxy Cross-ply	ARALL	GLARE3
$\overline{\epsilon}_1^{RMS}$	SS	0.002831	0.002756	0.002797	0.002801	0.002784
	FS	0.003025	0.003046	0.002828	0.002910	0.002831
	L	0.003800	0.003906	0.004256	0.004227	0.004540
$\overline{\epsilon}_2^{RMS}$	SS	0.012340	0.011892	0.012252	0.012133	0.012201
	FS	0.012893	0.013034	0.012220	0.011945	0.012031
	L	0.016635	0.017561	0.020050	0.019338	0.021910

Table 3. Mesh-average of the rms values of the first and second reference percentage of elastic energy error.

From Table 2 it is deduced that the first and second mesh-averaged reference values of elastic energy error roughly correspond, in an averaged sense, to six and four elements per wavelength, respectively. The same conclusion can be applied to the mesh-averaged reference values of the indicators of numerical dispersion. In such averaged sense, the elastic energy error of the quasi-longitudinal waves is greater than the one of the quasi-shear waves, Table 3. The elastic energy error of the slow quasi-shear waves is weakly dependent on the elastic properties and its second

mesh-averaged reference value is slightly greater than one per cent. An opposite behavior is shown by the indicators of numerical dispersion, Table 4. In this case, the numerical dispersion of the quasi-shear waves is greater than the one of the quasi-longitudinal waves, and the indicator of numerical dispersion of the quasi-longitudinal waves is the variable weakly dependent on the elastic properties.

		Carbon/Epoxy uniaxial	Aramid/Epoxy uniaxial	S-glass/Epoxy uniaxial	Bo-Al uniaxial	Aluminum
\overline{e}_{p2}^M	SS	1.00320	1.00393	1.00317	1.00316	1.00348
	FS	1.00304	1.00275	1.00305	1.00312	1.00348
	L	1.00221	1.00225	1.00221	1.00219	1.00207
\overline{e}_{gn2}^M	SS	1.01584	1.01937	1.01570	1.01564	1.01723
	FS	1.01502	1.01366	1.01511	1.01545	1.01723
	L	1.01084	1.01104	1.01078	1.01065	1.01005
HOMOGENIZED						
		Carbon/Epoxy Cross-ply	Aramid/Epoxy Cross-ply	S-glass/Epoxy Cross-ply	ARALL	GLARE3
\overline{e}_{p2}^M	SS	1.00286	1.00309	1.00290	1.00251	1.00275
	FS	1.00303	1.00282	1.00317	1.00333	1.00357
	L	1.00219	1.00227	1.00222	1.00217	1.00215
\overline{e}_{gn2}^M	SS	1.01419	1.01539	1.01435	1.01252	1.01366
	FS	1.01502	1.01404	1.01574	1.01649	1.01768
	L	1.01075	1.01112	1.01085	1.01061	1.01046

Table 4. Second mesh-averaged reference values of the indicators of numerical dispersion.

3 MODAL ANALYSIS

As application it is explored the use of the averaged correlation Eq. (30) as a reference to apply the higher order elastic energy as an error indicator for the finite element vibration eigenmodes. These ones are the solution of the eigenproblem [10],

$$(\mathbf{K} - \omega_j^2 \mathbf{M}) \tilde{\boldsymbol{\psi}}_j = \mathbf{0}, \quad j = 1, \dots, n \quad (31)$$

where ω_j and $\tilde{\boldsymbol{\psi}}_j$ are the finite element natural frequencies and eigenvectors, respectively.

By introducing the relation of \mathbf{K} -orthogonality $\tilde{\boldsymbol{\psi}}_i^T \mathbf{K} \tilde{\boldsymbol{\psi}}_j = \delta_{ij} \omega_j^2$ into Eq. (7), the following expression for the modal elastic energy is yielded,

$$\overline{E}_j = \frac{1}{4} \omega_j^2, \quad j = 1, \dots, n \quad (32)$$

The error for the modal elastic energy computed with the discretized elastic domain is estimated by a reference model that will be obtained by dividing each element of the actual mesh into eight elements. The modal elastic energies computed with the actual model and the ones computed with the reference model will be compared by the modal elastic energy error,

$$EEE = (\overline{E} / \overline{E}^{REF}) - 1, \quad EEE = (\omega / \omega^{REF})^2 - 1 \quad (33)$$

where \overline{E} and \overline{E}^{REF} are defined by Eq. (7), and Eq. (32) has been taking into account.

The modal elastic energy error computed by mesh halving Eq. (33) will be compared with the so-defined as standard modal elastic energy error which is computed by averaging the correlation Eq. (30) for the slow and fast quasi-shear waves, and by using the higher order elastic energy computed with the actual model,

$$SEEEs(PHE) = \frac{1}{2}(\varepsilon_{SS} + \varepsilon_{FS}) \quad (34)$$

where the percentage of higher order elastic energy computed with the actual model PHE will be evaluated by Eq. (7) and (8).

In order to select the standard modal elastic energy error Eq. (34), it has been taking into account the heuristic that given the frequency both the percentage of higher order elastic energy and the spatial discretization error should be mainly influenced by the slowest waves which have the shortest wavelengths.

Two test problems have been analyzed, Fig. 4: a tapered block fixed at its base and made of cross-ply carbon/epoxy homogenized, and a cantilever thick plate made of nine unit cells of FML-GLARE3 homogenized.

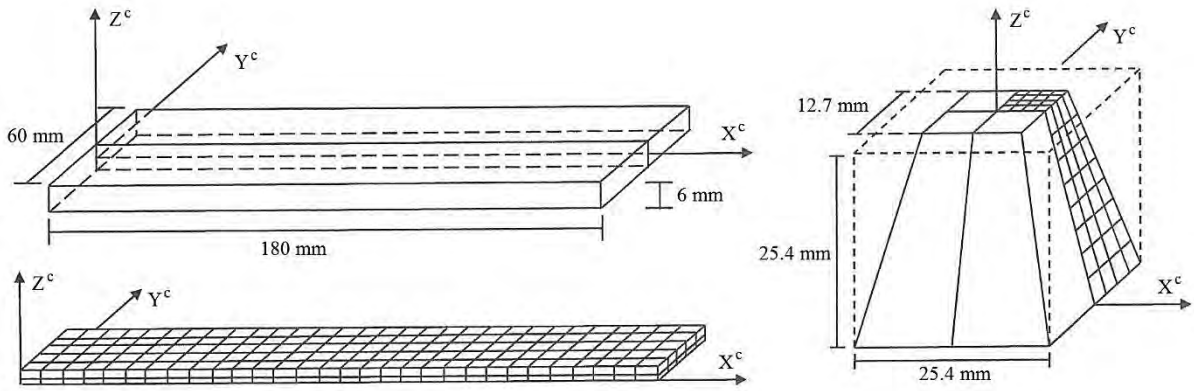


Figure 4. Tapered block fixed at its base and cantilever thick plate.

From Table 5 it is observed that the percentage of higher order energy PHE decreases as the mesh is refined for each of the eigenmodes computed. Then, this energy component behaves as a modal error indicator, which is in accordance with the numerical dispersion analysis.

From Fig. 5 it is observed that the standard modal energy error SEEEs Eq. (34) generally overestimates the modal energy error computed by mesh halving EEE Eq. (33). For the tapered block, which is a bulk solid, both indicators generally exhibit similar evolution shapes as the modal order increases. Clearly, by the standard modal energy error SEEEs the accuracy of the finite element eigenmodes could be confidently verified in order to select a cutoff modal order for values of energy error up to a neighbourhood of one per cent, an optimum upper bound to properly capture the eigenmodes from the engineering point of view.

4 CONCLUSIONS

The noteworthy conclusions of this contribution are:

#MODE	TYPE	PHE	PHE REF	#MODE	TYPE	PHE	PHE REF
1	AS	0.066156	0.017351	9	AS	0.083576	0.022333
2	AA	0.090874	0.026115	10	AS	0.076795	0.019839
3	AS	0.068166	0.017944	11	AS	0.086763	0.023320
4	AS	0.072159	0.019119	12	AA	0.103444	0.029204
5	AA	0.092516	0.026555	13	AS	0.099536	0.027649
6	AA	0.095225	0.027235	14	AS	0.094541	0.025594
7	AS	0.077795	0.020745	15	AA	0.109833	0.030844
8	AA	0.098722	0.028061	16	AS	0.112904	0.032069

Table 5. Cantilever thick plate. Percentage of higher order elastic energy computed with the actual model PHE versus the one computed by the reference model PHE REF.

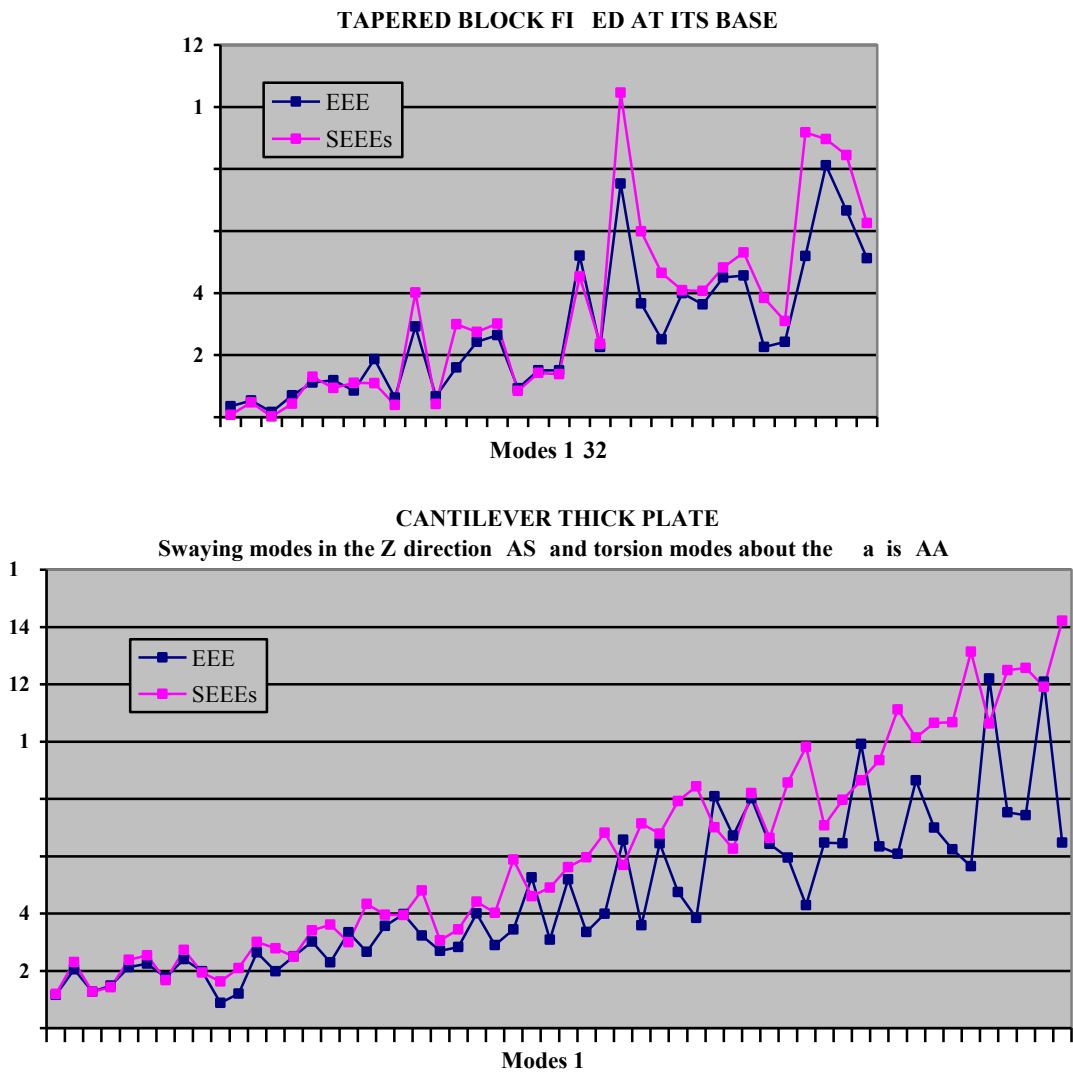


Figure 5. Standard modal elastic energy error SEEEs versus modal elastic energy error computed by mesh halving EEE for two test problems.

- - For homogeneous and anisotropic elastic media discretized by the energy-orthogonal twenty-node hexahedral finite element, by a dispersion analysis of plane harmonic waves an averaged correlation between the percentage of higher order elastic energy and the elastic energy error is yielded both for the quasi-longitudinal waves and the quasi-shear waves.
- - The use of the slow quasi-shear wave correlation and the fast quasi-shear wave correlation as reference to apply the higher order elastic energy as an error indicator for the finite element vibration eigenmodes is successfully tested.

REFERENCES

- [1] Fahy, F. Sound and structural vibration. Academic Press, (1985).
- [2] Kolman, R., Cho, S.S., Park, K.C. and Gonzalez, J.G. An explicit time scheme with local time stepping for one-dimensional wave and impact problems in layered and functionally graded materials. Proceedings COMPDYN 2017. Rhodes Island, Greece.
- [3] Vlot, A. and Gunnink, J.W. Fibre metal laminates an introduction. Kluwer Academic Publishers, (2001).
- [4] Alderliesten, R. Fatigue and fracture of fibre metal laminates. Springer, (2017).
- [5] Milton, G.W. The theory of composites. Cambridge University Press, (2002).
- [6] Rokhlin, S.I., Chimenti, D.E. and Nagy, P.B. Physical ultrasonics of composites. Oxford University Press, (2011).
- [7] Datta, S.K. and Shah, A.H. Elastic waves in composite media and structures. CRC Press, (2009).
- [8] Baker, A.A. and Scott, M.L. Composite materials for aircraft structures. American Institute of Aeronautics and Astronautics AIAA, (2016).
- [9] Kollár, L.P. and Springer, G.S. Mechanics of composite structures. Cambridge University Press, (2003).
- [10] Bathe, K.J. Finite Element Procedures. Prentice Hall, (1996).
- [11] Felippa, C.A., Haugen, B. and Militello, C. From the individual element test to finite element templates: evolution of the patch test. Int. J. Meth. Eng. (1995) 38:199-229.
- [12] Auld, B.A. Acoustic fields and waves in solids. Volume I. Krieger Publishing Company, (1990).
- [13] Okrouhlik, M. and Höschl, C. A contribution to the study of dispersive properties of one-dimensional lagrangian and hermitian elements. Computers and Structures (1993) 49:779-795.
- [14] Brillouin, L. Wave propagation in periodic structures. Dover Publications, (2003).

Virtualisation of Realistic Microstructures for 3D Crystal Plasticity Using Limited Information

Ben Britton^{*}, Simon Wyatt^{**}, Yi Cui^{***}

^{*}Imperial College London, ^{**}Imperial College London, ^{***}Imperial College London/Brunel

ABSTRACT

As material scientists and engineers, we have developed the ability to extract data-rich information that describe the evolving deformation state from the surface of 3D materials, using techniques such as high angular resolution electron backscatter diffraction (EBSD) and high spatial resolution digital image correlation (DIC). This information can be used to understand the evolution of the deformation state of the material on the surface, and this data is now coupled with physically based simulations to explore the validity, and utility, of crystal plasticity models [1]. However, we know that the 3D state of the material can be important but that it can be expensive to access with high fidelity (e.g. using destructive sectioning methods or difficult to access X-ray synchrotron experiments) and for routine samples. In this talk, we will present a new framework to utilise a combined 2D morphology, stereology derived morphology information and crystallographic texture to create representative, and useful, microstructures for input into a 3D FFT based crystal plasticity simulation (using DAMASK [2]). In this talk, we will outline the methodology and discuss how it can be used to understand the efficacy of crystal plasticity models in predicting deformation. [1] Jiang, J., Dunne, F.P.E., and Britton, T.B. "Towards predictive understanding of fatigue crack nucleation in Ni-based superalloys " JOM (2017) <http://dx.doi.org/10.1007/s11837-017-2307-9> [2] <https://damask.mpie.de>

Nonlinear System Stochastic Response Determination Under Non-white and Non-Gaussian Excitation via the Wiener Path Integral Technique

Olga Brudastova^{*}, Ioannis Kougoumtzoglou^{**}, Apostolos Psaros^{***}, Aaron Appelle^{****},
Giovanni Malara^{*****}

^{*}Columbia University, ^{**}Columbia University, ^{***}Columbia University, ^{****}Columbia University, ^{*****}University of Reggio Calabria

ABSTRACT

Uncertainty propagation in engineering mechanics and dynamics is a highly challenging problem that requires development of analytical/numerical techniques for determining the stochastic response of complex engineering systems. In this regard, although Monte Carlo simulation (MCS) has been the most versatile technique for addressing the above problem, it can become computationally daunting when faced with high-dimensional systems or with computing very low probability events. Thus, there is a demand for pursuing more computationally efficient methodologies, such as the recently developed Wiener Path Integral (WPI) technique [1-3]. In this paper, the WPI technique for determining the joint response probability density function (PDF) of nonlinear systems subject to Gaussian white noise excitation is generalized to account for non-white, non-Gaussian, and non-stationary excitation processes. Specifically, modeling the excitation process as the output of a filter equation with Gaussian white noise as its input, it is possible to define an augmented response vector process to be considered in the WPI solution technique. A significant advantage relates to the fact that the technique is still applicable even for arbitrary excitation power spectrum forms. In such cases, it is shown that the use of a filter approximation facilitates the implementation of the WPI technique in a straightforward manner, without compromising its accuracy necessarily. Several numerical examples pertaining to both single- and multi-degree-of-freedom systems are considered, while comparisons with Monte Carlo simulation (MCS) data demonstrate the accuracy of the technique. [1] H. S. Wio, Path integrals for stochastic processes: An introduction. World Scientific, 2013. [2] I. A. Kougoumtzoglou, P. D. Spanos, An analytical Wiener Path Integral technique for non-stationary response determination of nonlinear oscillators, Probabilistic Engineering Mechanics 28 (2012) 125-131. [3] I. A. Kougoumtzoglou, P. D. Spanos, Nonstationary stochastic response determination of nonlinear systems: A Wiener Path Integral formalism, Journal of Engineering Mechanics 140 (9) (2014) 04014064.

Model Reduction and A Posteriori Error Estimation in the Context of Stable Variational Formulations of Parametrized Transport Equations

Julia Brunken^{*}, Mario Ohlberger^{**}, Kathrin Smetana^{***}, Karsten Urban^{****}

^{*}University of Münster, ^{**}University of Münster, ^{***}University of Twente, ^{****}University of Ulm

ABSTRACT

Motivated by high-dimensional kinetic transport equations we consider in this talk stable variational formulations and model reduction techniques for possibly time-dependent transport equations. Kinetic equations describe densities in phase space consisting of independent space, time, and velocity variables. To tackle the high-dimensionality we employ the Reduced Basis-Hierarchical Model Reduction approach where we use a problem-adapted basis in the velocity variable to arrive at a hyperbolic system in the space-time domain [1]. In this context, stable discretizations and efficient error estimators are desirable both for the construction of the reduced basis and the validation of reduced solutions. To derive such stable variational formulations for general transport equations we use, similar to [2], an ultraweak approach to find an L^2 approximation of the solution. We introduce new pairs of optimally stable trial and test spaces: By first choosing a suitable test space and then defining the trial space by the application of the adjoint operator, we obtain optimally stable spaces with an inf-sup constant of one in the continuous as well as in the discrete case. The setting allows for an easy implementation of the solution procedure and is especially beneficial in the context of model reduction for parametrized transport equations: We apply the Reduced Basis method to parametrized equations within this framework and investigate possible a posteriori error estimators used in the construction of the reduced model. Due to the optimally inf-sup-stable setting, residual-based error estimators benefit from perfect constants, and, in contrast to previous works, no further stabilization is needed for the reduced spaces. Hence, also the reduced models can be constructed easily and efficiently. We exemplify the approach by presenting numerical results for full order and reduced order models for kinetic transport equations and compare our new framework to existing works [2, 3]. References: [1] J. Brunken, T. Leibner, M. Ohlberger, and K. Smetana. Problem adapted hierarchical model reduction for the Fokker-Planck equation. *Proceedings of the Conference Algorithm*, pages 13–22, 2016. [2] W. Dahmen, C. Huang, C. Schwab, and G. Welper. Adaptive Petrov-Galerkin methods for first order transport equations. *SIAM J. Numer. Anal.*, 50(5):2420–2445, 2012. [3] W. Dahmen, C. Plesken, and G. Welper. Double greedy algorithms: reduced basis methods for transport dominated problems. *ESAIM Math. Model. Numer. Anal.*, 48(3):623–663, 2014.

Machine Learning and Sparse Optimization to Characterize and Control Fluids

Steven Brunton*

*University of Washington

ABSTRACT

The discovery of physical laws and governing equations from data is currently undergoing a revolution, driven by the rise of big data, algorithmic advances, and increasing computational power. In complex, multi-scale systems, physical laws often remain elusive, although data are abundant. This presentation will discuss recent approaches to leverage machine learning and sparse optimization to characterize and control multi-scale systems using the following generalized pipeline: 1) identify low-dimensional patterns in high dimensional data, 2) discover dynamical systems governing the evolution of these patterns, 3) compute embeddings defined by intrinsic coordinates in which the nonlinear dynamics appear linear, 4) identify optimized sensor locations to maximally inform real-time dynamics, and 5) design controllers to manipulate system behavior. The overarching perspective taken in this work is that of parsimony and interpretability, preferring simple, compact, and efficient model representations. First, we will describe the sparse identification of nonlinear dynamics (SINDy) framework to discover the governing equations underlying a dynamical system simply from data measurements, leveraging advances in sparsity-promoting techniques and machine learning. The resulting models are parsimonious, balancing model complexity with descriptive ability while avoiding overfitting. The only assumption about the structure of the model is that there are only a few important terms that govern the dynamics, so that the equations are sparse in the space of possible functions. This perspective, combining dynamical systems with machine learning and sparse sensing, is explored with the overarching goal of real-time closed-loop feedback control of complex systems. Next, connections to the Koopman operator will be discussed. Koopman operator theory has emerged as a dominant method to represent nonlinear dynamics in terms of an infinite-dimensional linear operator. A linear representation of nonlinear dynamics has tremendous potential to enable the prediction, estimation, and control of nonlinear systems with standard textbook methods developed for linear systems. Particular emphasis will be placed on the use of data-driven Koopman theory to characterize and control high-dimensional fluid dynamic systems. This presentation will focus primarily on applications in fluid dynamics, although many pressing applications stand to benefit from these methods, such as understanding cognition from neural recordings, inferring patterns in climate, determining stability of financial markets, predicting and suppressing the spread of disease, and controlling turbulence for greener transportation and energy.

A Modified Phase Field Model for Mixed-mode Crack Propagation with Consistent Kinematic Modes

Eric Bryant^{*}, WaiChing Sun^{**}

^{*}Columbia University, ^{**}Columbia University

ABSTRACT

Cracks in brittle, isotropic, homogeneous materials often propagate such that the pure Mode I kinematic mode is maintained at the crack tip. However, numerous geo-materials, such as sedimentary rock, shale, mudstone, concrete and gypsum, the Mode I and Mode II critical fracture energies are distinct. In such cases, it is likely that secondary Mode II and mixed-mode propagation may occur. This has previously been exhibited by experiments where wing cracks and secondary cracks develop from pre-existing flaws under a combination of shear and tensile or shear and compressive loadings. To capture the mixed-mode fracture propagations, a mixed-Mode I/II fracture model that employs multiple critical energy release rates based on Shen and Stephansson, IJRMMS, 1993 is adopted in a phase field framework. Within each incremental time step, an explicit-implicit operator-split scheme is used such that a local energy minimization problem is solved such that the crack propagation direction and the corresponding kinematics modes are determined. This step is followed by the update of the phase field and that of the displacement. Several numerical examples that demonstrated the Mode II and mixed mode crack propagations in brittle materials are presented. Possible extensions of the model that captures the degradation related to shear/compressive damage commonly observed in sub-surface applications and triaxial compression tests are discussed.

Numerical Analysis of Damage and Fracture Mechanisms in Ductile Metals at Different Loading Conditions

Michael Brünig*, Steffen Gerke**, Marco Schmidt***

*Bundeswehr University Munich, **Bundeswehr University Munich, ***Bundeswehr University Munich

ABSTRACT

The presentation deals with the numerical analysis of the effect of stress state on damage and fracture behavior of ductile metals. Within the general framework of continuum thermodynamics of irreversible processes a thermodynamically consistent anisotropic damage and failure model based on kinematic definition of damage tensors is discussed. The continuum model is based on free energy functions defined in fictitious undamaged and damaged configurations, respectively, leading to elastic material laws which are affected by damage. It is well known that besides stress intensity, stress triaxiality and the Lode parameter are important factors that control initiation of plastic flow, damage and fracture. In this context, a generalized hydrostatic-stress-dependent yield condition and a non-associated flow rule are used to adequately describe the plastic behavior of ductile metals. Furthermore, a damage criterion formulated in stress space is proposed based on a series of experiments and corresponding numerical simulations. Different branches of the damage criterion are taken into account corresponding to different damage and fracture mechanisms depending on stress triaxiality and Lode parameter. To validate these criteria new experiments with different two-dimensionally loaded specimens taken from aluminum alloy sheets have been developed. Specimens' geometries and loading conditions have been proposed using numerical simulations of biaxial experiments to achieve different stress states in critical regions where damage and fracture are expected to occur. These biaxially loaded specimens will allow consideration of combined shear-tension and shear-compression stress states leading to different damage and fracture mechanisms. Numerical analysis of these tests show that they cover a wide range of stress triaxialities and Lode parameters. Numerically predicted damage and fracture modes are validated by scanning electron microscopy of fracture surfaces.

Kino-Geometric Sampling Reveals Functional Molecular Motions Across Scales

Dominik Budday^{*}, Rasmus Fonseca^{**}, Sigrid Leyendecker^{***}, Henry van den Bedem^{****}

^{*}Chair of Applied Dynamics, University of Erlangen-Nuremberg, Germany, ^{**}Department of Molecular and Cellular Physiology, Stanford University, USA; Biosciences Division, SLAC National Accelerator Laboratory, Stanford University, USA, ^{***}Chair of Applied Dynamics, University of Erlangen-Nuremberg, Germany, ^{****}Biosciences Division, SLAC National Accelerator Laboratory, Stanford University, USA

ABSTRACT

The function of macromolecules relies on fast, dynamic exchanges between three-dimensional conformations. Molecular dynamics (MD) simulations can reveal time-resolved, atomically detailed snapshots of these exchanges, but require sophisticated computational resources to overcome spatio-temporal barriers separating functional substates. By contrast, algorithms for randomized exploration of molecular conformational spaces can provide a fast, coarse-grained alternative, while still providing insight into molecular mechanisms. Here, we present our kino-geometric sampling (KGS) and modeling framework to study functional molecular motions across scales. KGS represents molecules as articulated multi-body complexes with dihedral angles as revolute degrees of freedom and selected non-covalent interactions such as hydrogen bonds as holonomic constraints [1]. The constraints define a lower-dimensional manifold in conformation space. KGS can rapidly explore the constraint manifold or model conformational transitions [2] using collision-free move sets proposed by sophisticated motion planners. Maintaining constraints along a sampling trajectory reduces expensive energy calculations and can bridge spatio-temporal scales out of reach for MD. Modeling the conformational transition of Adenylate Kinase between apo and holo states confirms that the KGS structural pathway passes known intermediate crystal structures as close as dynamic importance sampling molecular dynamics [2]. KGS revealed coupled motions between the functionally important M20 and FG-loops in Dehydrofolate Reductase, in qualitative agreement with MD [3]. Furthermore, our method suggests that a hydrogen bond network imparts a spatially resolved hierarchy of protein motions, analogous to eigenmodes from normal mode analysis. Enhancing our approach with a more sophisticated force-field may help access hidden excited states based off intermediate structures. Taken together, KGS is a versatile toolbox, capable of studying molecular flexibility and rigidity, and modeling. Our method is a supplementary, kinematic approach to generate hypotheses about functional dynamics of macromolecules. Subsequent detailed MD simulations can validate these hypotheses, and provide access to kinetics. [1] D. Budday, S. Leyendecker, and H. van den Bedem. *Journal of the Mechanics and Physics of Solids* 83, 36-47, 2015. [2] D. Budday, R. Fonseca, S. Leyendecker, and H. van den Bedem. *Proteins: Structure, Function, and Bioinformatics* 85(10), 1795-1807, 2017. [3] R. Fonseca, D. Budday, and H. van den Bedem. *Journal of Computational Chemistry*, DOI: 10.1002/jcc.25138, 2018 (in press).

Biomechanical Characterization of Brain Tissue

Silvia Budday^{*}, Gerhard Sommer^{**}, Paul Steinmann^{***}, Gerhard Holzapfel^{****}, Ellen Kuhl^{*****}

^{*}Friedrich-Alexander Universität Erlangen-Nürnberg, ^{**}Graz University of Technology, ^{***}Friedrich-Alexander Universität Erlangen-Nürnberg, ^{****}Graz University of Technology, Norwegian University of Science and Technology, ^{*****}Stanford University

ABSTRACT

Computational simulations are a powerful tool to understand the mechanical behavior of biomaterials. However, an essential prerequisite for realistic numerical predictions is the thorough experimental characterization of the material response. It is required to develop appropriate constitutive models and, equally importantly, to carefully calibrate the corresponding constitutive parameters. Biomechanical testing can be challenging for ultrasoft tissues such as brain tissue due to its high deformability and fragileness. Different test setups have led to contradictory results in the literature, not only with respect to the tissue's stiffness but also concerning directional and regional dependencies, or the influence of post-mortem time. This clearly demonstrates that the test setup has to be carefully chosen to guarantee a homogeneous deformation and to minimize boundary effects. Here, we perform finite element simulations to study effects of specimen geometry or loading modes and set the limits for maximum loadings that still allow for a homogeneous deformation state. We show that rectangular specimen dimensions can mistakenly yield a direction-dependent response. We further discuss the influence of the tissue's compressibility. Our results are valuable to design appropriate test setups and optimize testing conditions in the future.

Human Osteocyte Development during Bone Formation in a Bone-on-chip

Elisa Budyn*, Nabila Gaci**, Samantha Sanders***, Morad Bensidhoum****, Patrick Tauc*****,
Bertrand Cinquin*****, Eric Schmidt*****, Herve Petite*****

*Ecole Normale Supérieure Cachan, **Ecole Normale Supérieure Cachan, ***Ecole Normale Supérieure Cachan,
****University Paris-Diderot, *****Ecole Normale Supérieure Cachan, *****Ecole Normale Supérieure Cachan,
*****University of Illinois at Chicago, *****University Paris-Diderot

ABSTRACT

Osteocytes are long-term living cells responsible for bone mineralization and characterized by a body bearing numerous processes. Osteocytes orchestrate bone homeostasis and coordinate the interactions between the osteoclasts and mesenchymal stem cells (MSCs) during remodeling. Osteoblasts differentiate into osteocytes or bone lining cells that cover non-remodeling endosteal bone surfaces that are recruited during the activation phase to seal the site of bone formation by osteoblasts, modulate the osteoclastic resorption and further differentiate into osteoblasts. However fundamental knowledge of human bone stromal cells in situ mechanobiology is challenging to quantify in particular as the mechanical properties of their environment changes as mineralization takes place. Bones-on-chip offer the opportunity to develop in situ 3D imaging and modelling of concurrent chemo-mechanical phenomena in controlled conditions and for long-term culture. Human mesenchymal stem cells were reseeded in decellularized human bone to create bone-on-chip that were cultured for over 26 months. The application of mechanical load to live systems is known to influence the cell differentiation, matrix formation and biological response. In situ measurements of the mechanical microenvironment of the cells can be quantified numerically while the cell chemical response can be observed in vitro for human native osteocytes and stem cell derived osteocytes in either native or neo-formed ECM. The cell morphology, expressed genes, and their production of proteins and minerals using PCR, immunohistochemistry, in situ immunofluorescence and the conditioned medium analysis can monitor the cell differentiation and secretome. The cytoplasmic calcium concentration variations seemed to adapt to the expected in vivo mechanical load at the successive stages of cell differentiation in agreement with studies using fluid flow stimulation. The bone-on-chip produced after 109 days an ECM of which the strength was nearly a quarter of native bone and that contained type I collagen at 256 days and calcium minerals at 39 days. The morphology of the cells displayed organized network and the newly-formed matrix were further characterized by immuno-fluorescence under confocal microscopy at 547 days and revealed the presence of E11 and sclerostin. Different cells populations were identified and one type was organized in network and connected by long processes.

Assessing the Impact of Strength Model Parameters on Simulated Cerium Flyer Plate Behavior

Joanne Budzien^{*}, Karlene Maskaly^{**}, JeeYeon Plohr^{***}

^{*}Los Alamos National Laboratory, ^{**}Los Alamos National Laboratory, ^{***}Los Alamos National Laboratory

ABSTRACT

Cerium flyer plate experiments were simulated using the LANL Lagrangian hydrodynamics code FLAG and results were compared to experimental results. The range of experiments examined includes shocking through the cerium gamma-alpha phase transition. Several sets of parameters for the Preston-Tonks-Wallace strength model have been produced through fits to experimental Hopkinson bar data. We will present simulation results showing the effect of varying the strength parameter sets including simulations with no strength. This process may aid in differentiating the various parameter sets by testing them under conditions different from the calibration experiments.

Bone Mineral Heterogeneity as a Signature of Remodelling and Mineralisation Processes: Linking to the Cellular Scale

Pascal Buenzli^{*}, Chloé Lerebours^{**}, Paul Roschger^{***}, Andreas Roschger^{****}, Richard Weinkamer^{*****}

^{*}School of Mathematical Sciences, Queensland University of Technology, Brisbane, Australia, ^{**}School of Mathematical Sciences, Monash University, Clayton, Australia, ^{***}Ludwig Boltzmann Institute of Osteology at the Hanusch Hospital of WGKK and AUVA Trauma Centre Meidling, 1st Medical Department, Hanusch Hospital, Vienna, Austria, ^{****}Max Planck Institute of Colloids and Interfaces, Department of Biomaterials, Potsdam, Germany, ^{*****}Max Planck Institute of Colloids and Interfaces, Department of Biomaterials, Potsdam, Germany

ABSTRACT

Bone mineral density distributions (BMDDs) are frequency distributions of bone mineral density that provide measures of the mineral heterogeneity of bone samples. While BMDDs have been shown to provide signatures of bone physiology in health and disease [1], mathematical models of BMDDs are required to decrypt how dynamic parameters of bone remodelling and bone mineralisation are entangled in these measurements [2,3]. In this contribution, we will present new mathematical developments that enable us to account for the influence of microscopic resorption patterns of osteoclasts in the mineral make-up of a bone sample. We use this mathematical model to interpret differences observed in BMDD measurements of trabecular bone and femoral cortical bone [3]. Our analysis shows that it is not possible to explain these differences in BMDD measurements by accounting only for differences in turnover rate between these two skeletal sites, nor by accounting for differences in turnover rate and in osteoclast resorption patterns. We propose that the rate of mineral accumulation in bone matrix must differ as well. The BMDD properties of peak position and width in trabecular and femoral cortical BMDDs could be explained by a simple hypothesis, namely that minerals accumulate in bone matrix at a speed proportional to bone turnover rate. This suggests a primordial role of the micro-environmental availability of minerals, freed up during bone resorption, in how they become embedded in bone matrix at late stages of mineralisation. References 1. Roschger P, Paschalis EP, Fratzl P, Klaushofer K (2008) Bone 42:456 2. Ruffoni D, Fratzl P, Roschger P, Klaushofer K, Weinkamer R (2007) Bone 40:1308 3. Buenzli PR, Lerebours C, Roschger A, Roschger P, Weinkamer R (2017) Late stages of mineralisation and their signature on the bone mineral density distribution. In press, Conn. Tiss. Res.

Real-time Patient Specific Surgical Simulation using Corotational Cut Finite Element Method: Application to Needle Insertion Simulation

Huu Phuoc Bui^{*}, Satyendra Tomar^{**}, Franz Chouly^{***}, Alexei Lozinski^{****}, Stéphane P. A. Bordas^{*****}

^{*}University of Franche-Comté, ^{**}University of Luxembourg, ^{***}University of Franche-Comté, ^{****}University of Franche-Comté, ^{*****}University of Luxembourg

ABSTRACT

We present the Corotational Cut Finite Element Method for real-time surgical simulation. Users only need to provide a background mesh which is not necessarily conforming to the boundaries/interfaces of the simulated object. The details of the latter, represented by its surface or/and its internal interfaces, which can be directly obtained from binary images, are taken into account by a multilevel subelement embedding algorithm applied to elements of the background mesh that are cut by the surface/interfaces. To stabilize the system matrix when elements are cut by the surface/interfaces with very small intersections, we propose to move the background node(s) of the concerned cut elements by a distance proportional to the element size. This approach is simple but it can avoid the stability issues in such situations. Moreover, this approach does not include additional parameters as, e.g. ghost penalty method [1]. Dirichlet boundary conditions can be implicitly imposed on the surface using Lagrange multipliers, whereas traction or Neumann boundary conditions, which is/are applied on parts of the surface, can be distributed to the background nodes using shape functions. The implementation is verified by convergence studies with optimal rates. To verify the reliability of the method, it is applied to various needle insertion simulations (e.g. for biopsy or brachytherapy) into brain and liver models while considering frictional interactions between the needle and the tissue. Numerical results show that the present method can make the discretization independent from geometric description, and it can avoid the complexity of mesh generation of complex geometries while retaining the accuracy of the standard Finite Element Method. The proposed methodology is very suitable for real-time and patient specific simulations as it improves the simulation accuracy by automatically, and properly, taking the geometry of the simulated object into account. References [1] E. Burman et al, Int J Numer Meth Engg, vol. 104, no. 7, pp. 472-501, 2015.

Quantifying the Effects of Intraluminal Thrombi and Their Poroelastic Properties on Abdominal Aortic Aneurysms

Martina Bukac*, Miguel Rodriguez**, Shawn Shadden***

*University of Notre Dame, **University of California Berkeley, ***University of California Berkeley

ABSTRACT

An abdominal aortic aneurysm (AAA) occurs when weakened aortic walls bulge or dilate. Because the aorta is the primary conduit of blood to the body, a ruptured AAA can cause life-threatening bleeding. Intraluminal thrombi (ILT) are found in most of AAAs of clinically relevant size, and their influence on the wall stress and risk of rupture remains highly controversial. We will present a novel, poroelastic model for intraluminal thrombus (ILT), which captures both the flow within ILT and its deformation. The model for ILT is coupled with pulsatile blood flow and arterial wall deformation. The fully coupled model is used to study the biomechanics in a patient-specific abdominal aortic aneurysm (AAA). Using finite element analysis, numerical simulations were performed to investigate the role of ILT on the risk of AAA rupture as assessed by Peak Wall Stress (PWS). We will present a numerical study of the effects of ILT permeability on the vascular wall stress, as well as the risk of ILT embolization.

A Data-driven Approach for Stability and Control of Fluid-Structure Systems

Sandeep Reddy Bukka*, Allan Ross Magee**, Rajeev K Jaiman***

*National University of Singapore, **National University of Singapore, ***National University of Singapore

ABSTRACT

A data-driven model reduction approach for fluid-structure interaction (FSI) problem of a vibrating structure in an incompressible flow is presented. The method relies on the Eigensystem Realization algorithm (ERA) to construct the reduced-order model (ROM) in a state-space format, which provides a low-order representation of the unsteady flow dynamics in the neighborhood of the equilibrium steady state. A systematic stability analysis is performed via ERA-based ROM to obtain the eigenvalue distribution and to estimate a possible lock-in region of a coupled FSI system. A series of numerical tests on canonical configurations such as single, side-by-side and tandem cylinder arrangements in both two dimensional (low Re) and three dimensional (high Re) regimes are carried out. The proposed method is shown to produce consistent results from numerical tests when compared to full order nonlinear fluid-structure simulations in terms of predicting the lock-in regions. The motivation behind choosing such diverse test cases is to demonstrate the versatility of the proposed method. From the stability analysis, two modes are found to be dominant and contribute towards the phenomenon of VIV. The mode with the frequency close to that of wake flow behind stationary structure is termed as wake mode (WM) and the one with frequency close to the natural frequency of the structure is referred to as structure mode (SM). Shifting the eigenvalues of SM from unstable to stable region essentially manifests the mitigation of the VIV of structure. This can be achieved by using active feedback control techniques such as blowing and suction or passive control techniques. Appendages such as fairings, connected-C, helical strakes on the structure can be very effective in the suppression of VIV and are considered as passive control techniques in this study. Overall, the proposed stability analysis framework is proven to be effective in designing both active and passive control techniques by shifting the unstable eigenvalues of the SM to the stable region. [1] Yao, W., and Jaiman, R., 2017. "Model reduction and mechanism for the vortex-induced vibrations of bluff bodies". Journal of Fluid Mechanics, 827 pp. 357-393 [2] Yao, W., and Jaiman, R., 2017. "Feedback control of unstable flow and vortex-induced vibration using the eigensystem realization algorithm". Journal of Fluid Mechanics, 827, pp. 394-414 [3] Reddy, S. B., Magee, A. R., & Jaiman, R., 2018. "A Data-driven approach for stability analysis of Vortex-Induced Vibrations". In ASME 2018 37th International Conference on Ocean, Offshore and Arctic Engineering, (under review)

Numerical Investigation of Coupling Schemes for Structural Acoustics

Gregory Bunting^{*}, Scott Miller^{**}

^{*}Sandia National Laboratories, ^{**}Sandia National Laboratories

ABSTRACT

Loosely coupled schemes for structural-acoustic coupling are examined that obtain the same order of accuracy as the monolithic scheme. The coupling algorithms are implemented in Sierra-SD, a massively parallel finite element application for structural dynamics and acoustics. By adapting the predictor-corrector scheme of Farhat et al. (2006), second order time accuracy is achieved with the loosely coupled approach. Node-to-face mappings allow arbitrary discretizations of the structural-acoustic interface. Convergence rates are verified with a one dimensional piston problem with known solution. Numerical results are compared to a shock induced plate experimental benchmark. Computational times for loose and strong coupling are compared for a sphere scattering problem. Sandia National Laboratories is a multimission laboratory managed and operated by National Technology and Engineering Solutions of Sandia, LLC., a wholly owned subsidiary of Honeywell International, Inc., for the U.S. Department of Energy's National Nuclear Security Administration under contract DE-NA-0003525.

Computational Design of 2D Nano-Materials Using Two-Stage Searching Strategy Combining Molecular and Ab-initio Approaches

Tadeusz Burczynski*, Wacław Kus**, Marcin Mazdziarz***, Adam Mrozek****

*Institute of Fundamental Technological Research of Polish Academy of Sciences, Warsaw, Poland, **Silesian Technical University, Gliwice, Poland, ***Institute of Fundamental Technological Research of Polish Academy of Sciences, Warsaw, Poland, ****AGH University of Science and Technology, Kraków, Poland

ABSTRACT

New potentially 2D graphene-like materials are generated by the two-stage searching strategy combining molecular and ab-initio approaches. The two candidates X and Y are obtained from molecular calculations and the memetic base algorithm which combines the evolutionary algorithm and the conjugate-gradient optimization technique. The main goal of the optimization is to find stable arrangements of carbon atoms under certain imposed conditions (e.g. density, shape and size of the unit cell). The fitness function is formulated as the total potential energy of an atomic system. The optimized structure is considered as a discrete atomic model and interactions between atoms are modeled using the AIREBO potential, especially developed for carbon and hydrocarbon materials. The parallel approach used in computations allows significant reduction of computation time. Validation of the obtained results and examples of the models of the new 2D materials X and Y obtained using the described algorithm are presented, along with their mechanical properties [1]. In the second stage the two candidates X and Y are then in depth analysed using first-principles Density Functional Theory from the mechanical, structural, phonon and electronic properties point of view. Both proposed polymorphs of graphene X and Y are mechanically and dynamically stable and can be metallic-like [2]. Optimal searching for the new stable atomic arrangements of two-dimensional graphene-like carbon lattices with predefined mechanical properties are also considered using the described memetic method combines the evolutionary algorithm and the conjugate-gradient optimization. The main goal of the optimization is to find stable arrangements of carbon atoms placed in the unit cell with imposed periodic boundary conditions, which reveal desired mechanical properties. Two examples of the newly obtained models of the flat, carbon materials are presented. Their mechanical properties are additionally validated during the simulation of the tensile tests using molecular dynamics [3]. At present both new 2D materials with predefined mechanical properties are analysed using first-principles DFT. References [1] Mrozek A., Kus W., Burczynski T., Nano level optimization of grapheme allotropes by means of a hybrid parallel evolutionary algorithm. *Comput. Mater. Sci.*, 106, 2015, 161-169. [2] Mazdziarz M., Mrozek A., Ku? W., Burczynski T., First-principles study of new X-graphene and Y-graphene polymorphs generated by the two stage strategy. *Materials Chemistry and Physics*, 202, 2017, 7-14. [3] Mrozek A., Kus W., Burczynski T., Method for determining structures of new carbon-based 2D materials with predefined mechanical properties. *Inter. J. Multiscale Computational Engineering*, 15(5), 2017, 379-394.

Understanding the Damage Evolution of Dry Carbon Fibre Yarns in Contact with Pulleys During Textile Processing

Boris Burgarella^{*}, Louis Laberge Lebel^{**}, Alexandre Marcoux^{***}

^{*}Ecole Polytechnique de Montreal, ^{**}Ecole Polytechnique de Montreal, ^{***}Ecole Polytechnique de Montreal

ABSTRACT

Thanks to their great specific rigidities and resistances, composite materials tends to progressively replace metal in the design of high-performance structures. As an example, the last generation of airliners (Airbus A350, Boeing 787, and Bombardier CSeries) now includes up to 50% in mass of composite materials. Carbon fibers are often chosen to design parts that undergo heavy loads. These fibers are usually shipped as tows, consisting of hundreds to thousands clustered single filaments. May it be for coating, storage, braiding or weaving process, carbon tows often needs to be driven through a series of pulleys. Such a process may induce strong material loss due to filament rupture and therefore induce unwanted costs. In order to understand the cause of this rupture, carbon fiber tows behavior have been investigated through experimental and numerical analyses. Filament scale explicit dynamic calculations have been conducted and compared to experimental measurements gathered on a specifically designed test bed. The experimental and numerical data obtained with different pulley and tow architectures have then been used to determine a rupture criterion.

Modelling and Application of Viscoelastic Material Behavior with Fractional Derivatives

Michael Burgwitz^{*}, Matthias Wangenheim^{**}

^{*}Scientific Assistant, ^{**}Assistant Director

ABSTRACT

In structural dynamics the modelling of the material behavior is an important challenge. Some materials like steel can be well represented by linear constitutive laws but when dealing with viscoelastic components these relations become more complex. A common way to represent viscoelastic behavior is the so called prony series. A less known approach is the use of fractional derivatives. We apply a force-displacement based formulation incorporating fractional derivatives to model viscoelastic behavior to be able to simulate measured results: We recalculate a measured DMTA and compare its prony series and fractional representation. After that we utilize the fractional model to calculate the stick-slip behavior of a pneumatic seal. After giving a short overview regarding fractional derivatives and their numerical treatment in general, it is shown how we incorporated these into the material model. The detailed explanation of the model is followed by its application and comparison to measured results.

How to Overcome the 90 Degree Uncertainty in Collagen Fibre Orientation Evaluated Using Polarized Light Microscopy

Jiri Bursa*, Stanislav Polzer**, Kamil Novak***, Anna Polisenska****, martin Hrton*****, Petr Dvorak*****

*Brno University of Technology, Czech Republic, **VSB-Technical University of Ostrava, Czech Republic, ***TRW Automotive Czech s.r.o., Czech Republic, ****Brno University of Technology, Czech Republic, *****Brno University of Technology, Czech Republic

ABSTRACT

Although collagen fibers are responsible for distinctive mechanical response of many biological tissues such as skin, tendons, cartilages or arteries, information on their orientation and dispersion in arteries is still insufficient, ambiguous and contradictory; it is often estimated from a few manual Polarized Light Microscopy (PLM) measurements (typically $n \sim 10^1$ points per image). The automated PLM algorithm we have proposed in [1] offers an amount of information on fiber orientations which is larger by orders ($n \sim 10^4$ points per image) and operator-independent. The results are comparable with those obtained from quantitative polarized light microscopy requiring much more sophisticated and expensive equipment, such as confocal microscope with a quarter-wave plate and rotating analyzer [2]. Our algorithm was verified using artificial images with both sinus-like and straight lines mimicking the arrangement of collagen fibers in soft tissues and also validated using histological images of porcine tendons with more or less wavy fibers. Unfortunately, in the basic setup of PLM microscope (analyzer perpendicular to polarizer) our algorithm is limited by the 90° periodicity of polarized light intensity, i.e. it cannot distinguish between mutually perpendicular directions. The novelty of the presented approach is in a specific angle between the polarizer and analyzer which results in transmitting some colors (monochromatic light of specific wavelengths) with 180° periodicity. Exploitation of intensity of different colors enables us to transform histological images into histograms of directions in the full range between 0 and 180° . Although interpretation of these histograms is easy and straightforward only for tissues with straight collagen fibers or their regular periodical waviness, the method can make the automated analysis of preferred directions in fibrous tissues widely accessible and help to disclose preferential directions in any birefringent structures. In the field of arterial tissues, it has a potential to distinguish between dispersion and waviness of collagen fibers or between their local and global directions, as well as to answer the still opened question on the number of fiber families in different arterial tissues. It can be also advantageously used for calibration of another automated method based on nonpolarized light microscopy and Fast Fourier Transform [3]. Acknowledgement This work was supported by project of Czech Science Foundation No. 18-13663S. References [1] Novak K. et al., Microscopy and Microanalysis, 2015, doi:10.1017/S1431927615000586 [2] Massoumian F. et al., Quantitative polarized light microscopy, Journal of Microscopy, 2003, 10.1046/j.1365-2818.2003.01095.x [3] Polzer S. et al., Microscopy and Microanalysis, 2013, doi:10.1017/S1431927613013251

Tuning Mechanical Instabilities with Magnetoelastomers

Philip Buskohl^{*}, Vincent Chen^{**}, Carson Wiley^{***}, Abigail Juhl^{****}, Stephan Rudykh^{*****}

^{*}AFRL, ^{**}UES, Inc, ^{***}UES, Inc, ^{****}AFRL, ^{*****}Technion - Israel Institute of Technology

ABSTRACT

Magnetoelastomers are an important class of hyperelastic materials that generate a large deformation and stiffness increase in response to a magnetic field. An intrinsic mechanical response to a magnetic field is advantageous due to the fast, reversible and non-contact tuning of the material properties. Potential applications for magnetoelastomers include soft actuators, adaptive vibration dampers, mechanical filters and sensors. Previous theoretical studies have predicted that stiffness tuning of the MAE can be leveraged to tune the critical buckling strain in stiff/soft laminates of MAEs within a non-active elastomeric matrix [1,2], however experimental validation is needed. To address this issue, we fabricated the stiff/soft composite MAE laminate specimens using a commercial silicone (Sylgard 184) as the non-responsive soft matrix and a silicone loaded with carbonyl iron particles for the stiff, magnetoactive layer. The polymer matrix underwent several modifications to increase the stiffness ratio between the soft encapsulating matrix and the stiff MAE layer, including tuning of the crosslinker to polymer ratio, incorporation of hydride-terminated silicone to promote a linear network, and addition of silicone oil to further reduce crosslinking. A custom compression test jig was developed to systematically load the laminate specimen in the presence of a magnetic field. The study provides feedback on the sensitivity of the buckling strain to experimental specimen sizing/edge effects and provides broader insight on the practical integration of MAE instabilities into functional devices. [1] Rudykh, S., et al. "Multiscale instabilities in soft heterogeneous dielectric elastomers" Proceedings of the Royal Society A, Vol. 470. No. 2162, 2014 [2] Rudykh, S, and Bertoldi, K. & "Stability of anisotropic magnetorheological elastomers in finite deformations: a micromechanical approach." Journal of the Mechanics and Physics of Solids, 61.4 (2013): 949-967.

Consistent Bayesian Inference with Push-Forward Measures: Surrogate Modeling and Convergence of Solutions

Troy Butler^{*}, Tim Wildey^{**}, John Jakeman^{***}

^{*}CU Denver, ^{**}Sandia National Laboratories, ^{***}Sandia National Laboratories

ABSTRACT

Models are useful for simulating key processes and generating significant amounts of (simulated) data on quantities of interest (QoI) computed as a set of functionals from a model solution. This simulated data can be compared directly to observable data to address many important questions in scientific modeling. However, many key characteristics governing system behavior described as input parameters in the model remain hidden to direct observation. Thus, scientific inference fundamentally depends on the formulation and solution of a stochastic inverse problem (SIP) to describe sets of probable model parameters. Statistical Bayesian inference (see e.g., [1, 2]) is the most common approach solving the SIP using both data and an assumed error model on the QoI to construct posterior distributions of model inputs and model discrepancies. We have recently developed an alternative Bayesian solution to the SIP based on the measure-theoretic principles developed in [3]. We prove that this approach, which we call consistent Bayesian inference, produces a posterior distribution that is consistent in the sense that the push-forward probability density of the posterior through the QoI map will match the distribution on the observable data, i.e., the posterior is consistent with the model and the data [4]. Our approach only requires approximating the push-forward probability density of the prior, which is fundamentally a forward propagation of uncertainty. We briefly summarize the consistent Bayesian approach including existence, uniqueness, and stability of solutions. A comparison to statistical Bayesian inference is also provided. Motivated by computationally expensive models, we discuss the impact of using surrogate models to approximate the QoI on the construction of the push-forward of the prior density. We then outline the basic theoretical argument of convergence of the push-forward of the prior density using a generalized version of the Arzela-Ascoli theorem to prove a converse of Scheffé's theorem. REFERENCES [1] M. Kennedy and A. O'Hagan, "Bayesian calibration of computer models", *Journal of the Royal Statistical Society: Series B (Statistical Methodology)*, Vol. 63, pp. 425-464, (2001). [2] A. M. Stuart, "Inverse problems: A Bayesian perspective", *Acta Numerica*, Vol. 19, pp. 451-559, (2010). [3] J. Breidt, T. Butler, and D. Estep, "A computational measure theoretic approach to inverse sensitivity problems I: Basic method and analysis", *SIAM J. Numer. Analysis*, 49, pp. 1836-1859, (2012). [4] T. Butler, J. Jakeman and T. Wildey, "A consistent Bayesian formulation for stochastic inverse problems based on push-forward measures", arXiv:1704.00680, submitted and in review (2016)

On Application of the SSRVE Methodology to Phase Transformations Modelling in Steels

Krzysztof Bzowski*, Maciej Pietrzyk**, Lukasz Rauch***

*AGH University of Science and Technology, **AGH University of Science and Technology, ***AGH University of Science and Technology

ABSTRACT

Multiscale modelling of materials processing is a promising but computationally costly methodology. Therefore, an attempt to improve numerical efficiency of numerical simulation methods using material microstructures focuses mainly on two aspects: parallelization of numerical procedures and simplifying the virtual representation of the material. One of the solutions gaining popularity is the idea of statistically similar representative volume element (SSRVE) [1]. Its aim is to reduce the number of finite elements needed to discretize the volume of the microstructure. Simplification of the computational domain is achieved by transforming complex material microstructure images – often referenced as representative volume element (RVE) - into simpler, artificial cell with fewer grains and comparable statistical and rheological behaviour to its original counterpart. Application of various coefficients to design optimal SSRVE is discussed in [2]. The present paper discusses the idea of the SSRVE, material microstructures descriptions as well as generation methods of unit cell for two-phase steel microstructures. The application of the simplification procedure will be demonstrated in modelling of diffusion phase transitions in DP steels. Proposed model driven by diffusion of carbon with the moving boundary (Stefan problem) was implemented on the basis of solution of Level Set equations coupled with diffusion equation. Application of implicit method for interface evolution allow to overcome the limitations associated with the complicated shape of grains, but also in a natural way will reflect the impact of curvature of the front and influence chemical forces on the velocity of the interface. Two different phase transformations phenomena will be modeled. Austenitic – during heating, and ferritic – during cooling. Phase composition, phase volume fraction, kinetic of the process, grain size and distribution of the carbon concentration will be determined for a given parameters of a heat treatment process. Study of intercritical annealing process will be used as an example of investigation of influence of nonuniform carbon concentration to microstructure properties. Acknowledgements: Financial support of the NCN project no. 2015/17/N/ST8/01024

References 1. Scheunemann L., Schröder J., Balzani D., Brands D., Construction of Statistically Similar Representative Volume Elements – Comparative Study Regarding Different Statistical Descriptors, *Procedia Engineering*, Vol. 81, 2014, 1360-1365. 2. Rauch L., Pernach M., Bzowski K., Pietrzyk M., On application of shape coefficients to creation of the statistically similar representative element of DP steels, *Computer Methods in Materials Science*, Vol. 11, 2011, 531-541.

Towards Integration of Active Elements into Finite Element Models of Adaptive Structures

Michael Böhm^{*}, Oliver Sawodny^{**}

^{*}University of Stuttgart, ^{**}University of Stuttgart

ABSTRACT

Adaptive structures present a completely new approach in structural engineering. Actuators are included between two nodes each to control the structure's state. Different actuation principles are possible, some unknown yet. Examples for state of the art actuators include hydraulic cylinders, pneumatic actuators and even electric motors. The control input has to be modeled depending on the actuation principle. While passive structures are commonly studied using FE-analysis, where mass and stiffness matrices are calculated in the usual way that is largely automated, the input has to be included manually. Some FE-tools offer the possibility to include simple actuators, such as the LINK11 element in ANSYS. However, it is not possible to define forces depending on the actual state of the structure, i.e. including the control algorithm in the analysis. Overall, this only allows for a limited analysis of adaptive structures with active structural elements. Commonly, when working with adaptive structures, other analysis tools have to be used to manually integrate the active elements in the analysis afterwards. As a first step towards a better integration of these elements and towards a more user-friendly and seamless analysis of adaptive structures, we present here a methodology to calculate an additional input matrix automatically for active elements, simplifying the subsequent analysis. In order to do this, we present possible actuation principles and compare them with respect to their suitability for different tasks, revealing fundamental pros and cons leading to different use cases for each principle. Specifically, we will study parallel actuation and serial actuation. The former means integrating the actuator in parallel to an existing passive support element, while the latter describes an in-series-integration of the actuator into a passive support element. Combinations of these principles are also possible and considered. As a third actuation principle, we briefly discuss changing a structural element's stiffness, as well.

On the Phenomenological Modelling of History Effects in Skeletal Muscles

Markus Böl^{*}, Robert Seydewitz^{**}, Tobias Siebert^{***}

^{*}Institute of Solid Mechanics, Braunschweig, Germany, ^{**}Institute of Solid Mechanics, Braunschweig, Germany,
^{***}Institute of Sport and Motion Science, Stuttgart, Germany

ABSTRACT

Among the different types of soft tissue, skeletal muscles are able to contract and to generate active forces. A well-established experimental procedure to obtain active mechanical properties is to measure the force during isometric contraction while the positions of the muscle ends are fixed. Experimental observations revealed, however, that the amount of forces strongly depends on the elongation history. A muscle, which undergoes isometric contraction, isokinetic elongation and again isometric contraction, generates higher active forces than for pure isometric contraction at final length. This force difference is often described as force enhancement. Contrary, considering isokinetic contraction between first and second isometric contraction, forces are lower in comparison to pure isometric contraction. The drop of the active force at same length is designated as force depression. Although, experimental data about history effects such as force enhancement and depression are available and well documented, the underlying mechanism behind those effects still remains not fully understood. In that sense we present a phenomenological three-dimensional continuum-based approach to simulate the above mentioned history effects. For the identification of the model parameters experimental data of the soleus muscle were used. Further, the model was implemented in a finite element framework to analyse stress distribution in the muscle architecture during contraction.

Design of Fixed-Geometry Fluid Diodes Considering 2D-Swirl by Using Topology Optimization

Bruno C Souza^{*}, Emílio C N Silva^{**}

^{*}University of Sao Paulo, ^{**}University of Sao Paulo

ABSTRACT

The scope of this article is to propose a new methodology of designing fixed-geometry fluid diodes using Topology Optimization considering a 2d-swirl system in order to maximize its efficiency. In several applications, such as mechanical and labyrinth seals in compressors and in hydraulic systems, it is necessary to inhibit the fluid flow in one direction. For such cases, a classic labyrinth seal or a simple one-way check-valve can be applied due to the simplicity, size and cheapness, however the rotating axis in many equipment may need a 2D axisymmetric system and complex geometries obtained nowadays from topology optimization method with the 3D printing technology can produce more efficient devices. Nikola Tesla has proposed in 1920 a patent of an intuitive geometry of passive valves and Sen Lin et al (2015) has proposed another geometry using topology optimization of a 2D geometry that can be used for example in flat-plate oscillating heat pipe (Thompson et al, 2011), however not considering any rotation of inner components. Thus this work explores how the topology optimization can help designing passive valves for systems with rotating parts which is relevant for example in the design of sealing for compressors and turbines. The topology optimization is implemented, considering the energy dissipation in both direction and the rotation of rotor in respect to the stator. Different parameters of Reynolds and rotational speed has been tested and the new geometries of fixed-geometry fluid diodes are offered. Bibliography Lin, Sen, et al. & "Topology optimization of fixed-geometry fluid diodes." Journal of Mechanical Design 137.8 (2015): 081402. Thompson, S. M., H. B. Ma, and C. Wilson. & "Investigation of a flat-plate oscillating heat pipe with Tesla-type check valves." Experimental Thermal and Fluid Science 35.7 (2011): 1265-1273.

Generalized Gradient Phase-field Theories

VICTOR CALO*, Luis Espath**, Eliot Fried***

*Curitn University, **KAUST, ***OIST

ABSTRACT

We postulate a virtual power principle for second-grade materials described by phase fields. We a priori assume a lack of smoothness in arbitrary parts of the domain, by explicitly accounting for corner and edge microtractions. Subject to thermodynamic constraints, we develop a general set of balance equations, constitutive relations, and boundary conditions for a phase-field model where its free-energy includes second gradients. The resulting balance equations are general and independent of constitutive equations. The thermodynamics of the process constrain the constitutive relations through the free-energy imbalance. We then show the equivalence between the principle of virtual power for second-grade phase fields and the balance of microforces and microtorques. This framework allows us to generalize the second-grade phase-field (Swift–Hohenberg) equation and the conserved second-grade phase-field (Phase-Field Crystal) equations. Finally, we depict the configurational traction (Eshelby traction) involved in both theories.

Numerical Computation of the Forces Previously Measured in a Rigid Tube Bundle Under Turbulent Cross Flow

Jerome CARDOLACCIA*, Sofiane HOUBAR**, Ulrich BIEDER***, Philippe PITEAU****

*Den-SERVICE d'études mécaniques et thermiques (SEMT), CEA, Université Paris-Saclay, F-91191, Gif-sur-Yvette, France, **Den-SERVICE de thermo-hydraulique et de mécanique des fluides (STMF), CEA, Université Paris-Saclay, F-91191, Gif-sur-Yvette, France, ***Den-SERVICE de thermo-hydraulique et de mécanique des fluides (STMF), CEA, Université Paris-Saclay, F-91191, Gif-sur-Yvette, France, ****Den-SERVICE d'études mécaniques et thermiques (SEMT), CEA, Université Paris-Saclay, F-91191, Gif-sur-Yvette, France

ABSTRACT

In Pressurized Water Reactors (PWR), the turbo-alternator producing electric current is fed by several Steam Generators (SG). These consist of long vessels in which secondary water vaporizes throughout thousands of U-tubes containing the hot water of the primary circuit. Maintaining the integrity of the U-tubes is a top priority in order to prevent loss of coolant and contamination of the secondary flow. The Fluidelastic Instability (FEI) is a major threat in that respect : under certain conditions, some tubes may enter into uncontrollable vibrations involving wear or fatigue and thus potential failure in the long-term. Despite decades of joint effort, researchers have failed so far to provide a thorough explanation of this phenomenon. The lack of insight into how the fluid behaves in such complex systems has long been, in our very own opinion, one of the main hurdle standing in the way of a breakthrough. Indeed, while a fair quantity of experimental data has been gathered (most often on simplified bundles made of short portions of straight cylinders submitted to a cross flow), it essentially depicts tubes displacements or efforts exerted on them. It is only since the last years that numerical simulations have started to flourish, giving us more detailed knowledge about the fluid behavior. The present work is about building a numerical simulation reproducing our in-house experimental facility and trying to compare measured versus computational data. As for now, all of the 3x5 tubes will be fixed so that there is no fluid-structure interaction per se. The major obstacles concern the rather high Reynolds number (66K based on the gap velocity) combined with the extent of the domain (span-to-diameter ratio equal to 10) and the time duration required for appropriate statistics. Other difficulties arise from the treatment and confrontation of 2D versus 3D data. The TrioCFD code has been used for the resolution of the single-phase incompressible Navier-Stokes equations. In the end, we offer our humble answers to repeated questions like "Is a tube length of one diameter sufficient for the 3D simulations ?" or "How many rows of cylinders are required to get a fully turbulent flow ?".

A Random Choice Method for Modelling the Rubinstein and Stefan-like Problems

sabrina CARPY*, hélène MATHIS**, Teodor Burghilea***, Cathy CASTELAIN****, Gael CHOBLET*****, Anaïs CRESTETTO*****, Caroline DUMOULIN*****, Olivier GRASSET*****, Guy MOEBS*****, Erwan LE MENN*****, Gabriel TOBIE*****

*Planetology and Geodynamics, LPG-CNRS, Université de Nantes, France., **Mathematics, LMJL-CNRS, Université de Nantes, France., ***Thermics and Energy, LTEN-CNRS, Université de Nantes, France., ****Thermics and Energy, LTEN-CNRS, Université de Nantes, France., *****Planetology and Geodynamics, LPG-CNRS, Université de Nantes, France., *****Mathematics, LMJL-CNRS, Université de Nantes, France., *****Planetology and Geodynamics, LPG-CNRS, Université de Nantes, France., *****Planetology and Geodynamics, LPG-CNRS, Université de Nantes, France., *****Planetology and Geodynamics, LPG-CNRS, Université de Nantes, France., *****Planetology and Geodynamics, LPG-CNRS, Université de Nantes, France., *****Planetology and Geodynamics, LPG-CNRS, Université de Nantes, France.

ABSTRACT

Simulations of liquid-solid phase change are of major importance both for industrial applications (i.e. solidification of a binary alloy in metallurgical engineering), but also for investigating complex natural phenomena from microscopic to planetary scales. This work is part of a research project aimed at studying the Exchange Processes between the deep icy layers and the ocean of the giant moons around Jupiter and Saturn. By studying the properties of the moving interfaces separating the liquid and the solid phases at melting temperature, new insights into the characteristics of the deep internal structures of the giant moons might be gained. When the material is pure, the interface is at a constant melting temperature; this is the well-known two-phase Stefan problem. When a solute is present in the material, the melting temperature is no longer constant but depends on the concentration of the solute in the liquid and the solid phases that can coexist at thermodynamical equilibrium. Coupled heat and mass transfer process drive the phase transition by a jump in concentration at the melting front while the temperature remains continuous. Far from the melting front, the phase transition is modelled by phasic heat and mass diffusion equations given by the Fourier and the Fick laws [1]. In our study, we propose to define the moving interface by a Rankine-Hugoniot type jump relation of the heat fluxes at the melting free boundary. In order to capture the moving melting front, we introduce a Lagrange projection scheme based on a random sampling projection. Using a finite volume formulation, we define accurate numerical fluxes for the temperature and concentration fields that guarantee the sharp treatment of the boundary conditions at the moving front, especially the jump of the concentration according to the liquidus solidus diagram. We compare our Random Choice Method with exact solution [2] and level set method developed in [3] and provide some numerical illustrations that assess the good behavior of our method. [1] L. I. Rubinstein. The Stefan problem. American Mathematical Society, Providence, R.I., 1971. Translated from the Russian by A. D. Solomon, Translations of Mathematical Monographs, Vol. 27. [2] F. J. Vermolen, J. Vermolen, C. Vuik and S. van der Zwaag. A comparison of numerical models for one-dimensional stefan problems. J. Comput. Appl. Math., 2006 [3] S. Chen, B. Merriman, S. Osher, and P. Smereka. A simple level set method for solving stefan problems. J. Comp. Phys., 1997.

Effects of Breakaway Oxidation on the Stress Evolution and Degradation of Thermal Barrier Coatings

Yijun CHAI^{*}, Yueming LI^{**}, Kazuhiro OGAWA^{***}

^{*}Xi'an Jiaotong University, ^{Tohoku University}, ^{**}Xi'an Jiaotong University, ^{***}Tohoku University

ABSTRACT

As an inevitable process of alloy in high-temperature service, oxidation changes the composition and induces extreme large stress in the alloy, resulting in alloy degradation in such aggressive environments. The NiCrAlY BC (bond coat) of TBCs (thermal barrier coatings) is a typical alloy used in aerospace and land-based gas turbines, which functions as an oxidation and corrosion-resistance layer adhered to the superalloy component. Experiments [1-2] showed that the oxidation process of BC can be divided into several stages for how breakaway oxidation occurs, and some researches [3-4] were conducted to model the breakaway oxides growth. However, the relationship between the breakaway oxidation and stress evolution as well as the degradation mode of TBCs has not been reported. This work studies the oxide scale (including the alumina and the breakaway oxide) growth upon high-temperature oxidation, by developing an ABAQUS User-Defined Element code. The results reveal distribution and volume fraction of the evolved oxide at any given time. The stress evolutions induced by the mixed oxide growth and the non-linear behavior (combined creep-plastic) of the BC and TGO (thermally grown oxide) are investigated. The degradation mode of TBCs is finally analyzed. This work provides a convenient strategy for the understanding of how the breakaway oxidation evolves and its effects on the TBCs failure.

A New Hybrid Particle-Mesh Approach for Incompressible Fluid Dynamics

CHRIS CHARTRAND*, Blair Perot**

*Sandia National Laboratories, **University of Massachusetts Amherst

ABSTRACT

The Navier Stokes equations can be naturally divided into two parts. On the left-hand side of the equations there are the time evolution and the advection terms. These two terms make up the material derivative. On the right-hand side, there are the pressure, viscous, and other force terms. In this work, we propose using a hybrid numerical solution approach to compute incompressible fluid dynamics. The method shown here will use a static mesh to represent continuum variables, such as pressure and viscous stresses, and use particles to represent extrinsic variables such as mass and momentum. The particles are accelerated by the Eulerian pressure and viscous stress fields, and similarly particle motion is used as the sources for the viscous stress tensor and for the discrete Poisson equation that solves for the pressure. The proposed method solves for pressure and viscous forces directly at each particle location via the mesh based continuum representation. The method strives to be a mimetic particle method with attributes similar to dual mesh methods. In this formulation, the dual mesh is the particle locations. The complexity of the mimetic particle dual mesh method arises because the particle dual mesh contains no connectivity or geometric information like a classical dual mesh does. The talk explores what is required to obtain local conservation of mass, momentum, angular momentum, and kinetic energy, and second order spatial convergence for the velocity and pressure. The method has some commonality with classic PIC [1][2] and FLIP [3] methods with some notable differences. [1] D. Burgess, D. Sulsky, and J. Brackbill, "Mass matrix formulation of the flip particle-in-cell method," *Journal of Computational Physics*, vol. 103, no. 1, pp. 1–15, 1992. [2] C. Jiang, C. Schroeder, and J. Teran, "An angular momentum conserving affine-particle-in-cell method," *Journal of Computational Physics*, vol. 338, pp. 137–164, 2017. [3] J. Brackbill and H. Ruppel, "Flip: A method for adaptively zoned, particle-in-cell calculations of fluid flows in two dimensions," *Journal of Computational Physics*, vol. 65, no. 2, pp. 314–343, 1986.

Calculation of Exact Potential Energy Hessians Based on FEM

STAVROS CHATZIELEFTHERIOU*, NIKOS LAGAROS**

*Institute of Structural Analysis & Antiseismic Research, School of Civil Engineering, National Technical University of Athens, **Institute of Structural Analysis & Antiseismic Research, School of Civil Engineering, National Technical University of Athens

ABSTRACT

The potential energy of nanostructures within the molecular mechanics (dynamics) framework is usually calculated by adding bonded and nonbonded atomic energy contributions, i.e. bonds between 2 atoms, bond angles involving 3 atoms, dihedral angles involving four atoms, nonbonded terms expressing the Coulomb and Lennard-Jones interactions, etc. In this work a novel, a FE-based procedure is presented for studying the mechanical behavior of 3D nanostructures at the atomic scale. The energy gradient and Hessian matrix of such assemblies are commonly computed numerically; a potential energy FE model is proposed herein where these two components are expressed analytically. In particular, generalized finite elements are developed that express the interactions among atoms in a manner equivalent to that invoked in simulations performed based on the molecular dynamics method. Thus, the global tangent stiffness matrix for any nanostructure is formed as an assembly of the generalized finite elements and is directly equivalent to the Hessian matrix of the potential energy. The advantages of the proposed model are identified in terms of both accuracy and computational efficiency.

Recent Results in Improving the Material Point Method for Model-Based Simulation and Evaluation of the Additive Manufacturing Process

ZHEN CHEN^{*}, Jun Tao^{**}, Yu-Chen Su^{***}, Yonggang Zheng^{****}, Yong Gan^{*****}

^{*}Dalian University of Technology / University of Missouri, ^{**}Dalian University of Technology, ^{***}University of Missouri, ^{****}Dalian University of Technology, ^{*****}Zhejiang University

ABSTRACT

The multiphase (solid-fluid-gas) and multiscale (from nano to continuum) interactions in the mushy zone of additive manufacturing (AM) of metallic parts play a key role in determining the long-term performance of AM products. Based on the conservation laws of mass, momentum and energy, the generalized interpolation material point (GIMP) method is being developed for simulating and evaluating the fully coupled thermomechanical responses in the AM process. The fully coupled thermomechanical GIMP method (CTGIMP) considers the effects of both the temperature on deformation and the deformation on temperature [Tao et al., 2017]. A staggered solution scheme is designed to solve the coupled governing equations with explicit time integration. To improve the solution accuracy for multiphase interactions, the recent results [Gan et al., 2017; Lu et al., 2018] will be integrated into the CTGIMP. The improved CTGIMP representing the spatial discretization of a continuum will then be combined with molecular dynamics representing physical particles at nanoscale in order to effectively perform concurrent multiscale simulation of the AM process. Representative examples will be presented to demonstrate the proposed model-based simulation and evaluation procedure. References Gan, Y., Sun, Z., Chen, Z., Zhang, X., and Liu, Y., "Enhancement of the Material Point Method Using B-spline Basis Functions," *International Journal for Numerical Methods in Engineering*, <https://doi.org/10.1002/nme.5620>, 2017. Lu, M., Zhang, J., Zhang, H., Zheng, Y., and Chen, Z., "Time-discontinuous Material Point Method for Transient Problems," *Computer Methods in Applied Mechanics and Engineering*, Vol. 328, pp. 663-685, 2018. Tao, J., Zhang, H., Zheng, Y., and Chen, Z., "Development of Generalized Interpolation Material Point Method for Simulating Fully Coupled Thermomechanical Failure Evolution," submitted for publication in *Computer Methods in Applied Mechanics and Engineering*, 2017.

NON LINEAR ANALYSIS OF BEAMS AND FRAMES BY MEANS OF A NEW SMART DISPLACEMENT BASED (SDB) BEAM ELEMENT

B. PANTO^{*}, D. RAPICAVOLI[†], S. CADDEMI[‡] AND I. CALIO[◊]

Department of Civil Engineering and Architecture, University of Catania
Via Santa Sofia 64, 95125 - Catania, Italy

^{*}bpanto@dica.unict.it

[†]daviderapicavoli@hotmail.it

[‡]scaddemi@dica.unict.it

[◊]icalio@dica.unict.it

Key words: Beam element, Diffused plasticity, Fibre approach, Displacement based approach, Displacement shape functions.

Abstract. In this paper a new displacement based beam finite element within the framework of diffused plasticity models is proposed. The proposed element is based on the formulation of enriched adaptive displacement shape functions which, contrarily to standard approaches, are able to update in accordance to the diffusion of the plastic deformations during the analysis. In view the adaptive character of the presented displacement shape functions the element is named Smart Displacement Based (SDB) beam element. The stiffness matrix of the SDB element is provided explicitly and shown to be dependent on the displacement shape functions updating. The axial force-bending moment interaction is approached by means of a fibre discretisation suitable for the analysis of r/c frame members. The SDB element is shown to be accurate and further improved by the proposal of a procedure to verify strong equilibrium of the axial force along the beam element which is not usually accomplished by classical displacement based beam elements.

1 INTRODUCTION

The standard displacement based inelastic beam element suffers of approximations related to the inability of the cubic polynomial interpolation functions to properly describe the displacement response of the beam when exhibiting inelastic behaviour^[1]. The increase of the number of finite elements, or the use of higher order functions with additional internal degrees of freedom, are common remedies suggested to improve the approximation leading to an unavoidable reduction of the computational efficiency^[2]. Improvements in mesh refinement procedures of displacement based elements have been achieved in^[3,4] where each structural member (upgraded with quartic shape functions) is checked upon occurrences of plastic deformations and, when necessary, subjected to restricted automatic re-meshing.

Alternatively, it has been shown that the development of force based finite elements, based on the adoption of exact force shape functions, lead to more accurate results, although requiring different and more complicated iterative solution strategies^[5-8]. On the other hand, since force based beam finite elements do not rely on displacement shape functions, they are not for their nature dedicated to the reconstruction of the displacement field during the analysis which requires a double integration procedure for the above purpose^[9]. Moreover, the force based approach is not able to reproduce the linear curvature distribution appearing in the plastic zones as shown by detailed experimental analysis^[10]. A comprehensive analysis and critical discussion of the two approaches is reported in^[11] together with an extensive literature therein contained.

Within this scenario, this work proposes a new displacement beam element aiming at avoiding a re-meshing of each structural member however providing an accuracy competitive with force based procedures. Precisely, this paper proposes a new inelastic beam element, within the context of the displacement based approach, employing variable displacement shape functions denoted as Smart Displacement Shape Functions (SDSFs). The analytic expressions of the SDSFs are provided explicitly as related to the plastic deformation evolution in the beam element. The latter expressions are obtained by identifying, at each step, an equivalent tangent beam, characterised by abrupt variations of flexural stiffness, as a suitable representation of the current inelastic state of the beam. The presented approach leads to the formulation of a Smart Displacement Based (SDB) beam element whose accuracy appears to be comparable to those obtained through a force based approach but requiring a reduced implementation effort and a more straightforward approach. The term “smart” aims at emphasizing the ability of the element to upgrade the displacement field according to the current inelastic state. The proposed SDB beam element is able to incorporate a fibre approach for non linear analysis of r/c sections and it is formulated to account for the axial load-bending moment interaction. Finally, a procedure to impose strong equilibrium of the axial force along the beam element, which is not usually accomplished by classical displacement based beam elements is proposed. Precisely, within the Newton-Raphson predictor-corrector type iterative incremental procedure, a inner iteration scheme is started, after each corrector phase, by imposing a fictitious axial strain field and terminated when the axial force over the integration Gauss points is constant.

2 THE STEPPED BEAM MODEL

In the usual non linear beam elements undergoing diffused plasticity, where control cross sections are chosen at the Gauss integration points, stiffness decay due to the occurrence of plastic strains is usually supposed to be uniform over pre-defined segments of the beam. The beam element during the iterative step-by-step integration procedure develops according to a stepped beam model where both axial and flexural stiffness undergo abrupt variations along the beam axis. In this section the closed form solution of the non-uniform Euler-Bernoulli (E-B) beam model according to stepped variations of axial and flexural stiffness is proposed to lay the bases for an accurate description of the state of the beam during the evolution of the plastic strains.

The governing equations in x, z plane of a beam with abscissa x , $0 \leq x \leq L$, and with abrupt axial $\beta_{x,i}$ and flexural $\beta_{z,i}$ stiffness changes at x_i , $i = 1, \dots, n$, subjected to a static axial $p_x(x)$ and transversal $p_z(x)$ load distribution, can be written as follows:

$$\begin{aligned}
E_o A_o \left\{ \left[1 - \sum_{i=1}^n (\beta_{x,i} - \beta_{x,i-1}) U(x - x_i) \right] u'_x(x) \right\}' &= -p_x(x) \\
E_o I_o \left\{ \left[1 - \sum_{i=1}^n (\beta_{z,i} - \beta_{z,i-1}) U(x - x_i) \right] u''_z(x) \right\}'' &= p_z(x)
\end{aligned} \tag{1}$$

where the apex indicates derivative with respect to x , while E_o, A_o, I_o represent the reference values of the Young modulus, the area and the moment of inertia of the cross section, respectively, and $U(x - x_i)$ is the well know Heaviside (unit step) generalised function. Integration of Eq. (1) according to the generalised function integration rules^[12] leads to the following explicit expressions for the axial displacement and the transversal deflection functions $u_x(x), u_z(x)$, respectively:

$$\begin{aligned}
u_x(x) &= a_1 + a_2 g_2(x) + g_3(x) \\
u_z(x) &= c_1 + c_2 x + c_3 f_3(x) + c_4 f_4(x) + f_5(x)
\end{aligned} \tag{2}$$

where $a_1, a_2, c_1, c_2, c_3, c_4$ are integration constants and $p_x^{[k]}(x), p_z^{[k]}(x)$ indicate the k -th primitive functions of the relevant external load distributions $p_x(x), p_z(x)$, respectively. The functions $g_2(x), g_3(x), f_3(x), f_4(x), f_5(x)$ appearing in Eq. (2) are defined as follows:

$$\begin{aligned}
g_2(x; \beta_{x,i}^*) &= -x - \sum_{i=1}^n \beta_{x,i}^* (x - x_i) U(x - x_i) \\
g_3(x; \beta_{x,i}^*) &= -\frac{p_x^{[2]}(x)}{E_o A_o} - \sum_{i=1}^n \frac{\beta_{x,i}^*}{E_o A_o} [p_x^{[2]}(x) - p_x^{[2]}(x_i)] U(x - x_i) \\
f_3(x; \beta_{z,i}^*) &= \left[x^2 + \sum_{j=1}^n \beta_{z,i}^* (x - x_i)^2 U(x - x_i) \right] \\
f_4(x; \beta_{z,i}^*) &= x^3 + \sum_{j=1}^n \beta_{z,i}^* (x^3 - 3x_i^2 x + 2x_i^3) U(x - x_i) \\
f_5(x; \beta_{z,i}^*) &= \frac{p_z^{[4]}(x)}{E_o I_o} + \sum_{i=1}^n \frac{\beta_{z,i}^*}{E_o I_o} [p_z^{[4]}(x) - p_z^{[4]}(x_i)] U(x - x_i) - \sum_{i=1}^n \beta_{z,i}^* p_z^{[3]}(x_i) (x - x_i) U(x - x_i)
\end{aligned} \tag{3}$$

where the following new parameters $\beta_{x,i}^*, \beta_{z,i}^*$ have been defined:

$$\beta_{x,i}^* = \frac{\beta_{x,i}}{1 - \beta_{x,i}} - \frac{\beta_{x,i-1}}{1 - \beta_{x,i-1}}, \quad \beta_{z,i}^* = \frac{\beta_{z,i}}{1 - \beta_{z,i}} - \frac{\beta_{z,i-1}}{1 - \beta_{z,i-1}} \tag{4}$$

The solution in Eqs. (2)-(4) represents an explicit closed-form expression of axial and transversal displacement of an E-B beam in presence of an arbitrary number of abrupt cross-section which does not require the imposition of any continuity conditions where the discontinuities occur. The latter explicit closed-form solution is adopted in the next sections to formulate a two node non linear beam finite element able to account for diffusion of plasticity along the beam axis.

For convenience of notation the positions of the abrupt cross section variations are collected in the vector $\mathbf{x}^{EI} = \{x_1, x_2, \dots, x_i, \dots, x_n\}^T$, while the intensity of the axial and flexural stiffness are collected in the vectors $\boldsymbol{\beta}_x^* = \{\beta_{x,1}^*, \beta_{x,2}^*, \dots, \beta_{x,n}^*\}^T$, $\boldsymbol{\beta}_z^* = \{\beta_{z,1}^*, \beta_{z,2}^*, \dots, \beta_{z,n}^*\}^T$.

3 THE SMART DISPLACEMENT SHAPE FUNCTIONS

Based on the solution of the stepped beam model proposed in the previous section a beam element with nodal degrees of freedom as in Fig.1 can be conveniently introduced by formulating the shape functions of the axial $u_x(x)$ and transversal $u_z(x)$ displacements by imposing the following conditions:

$$\begin{aligned} u_x(0) &= q_1; & u_z(0) &= q_2; & \varphi(0) &= -u'_z(0) = -q_3; \\ u_x(L) &= q_4; & u_z(L) &= q_5; & \varphi(L) &= -u'_z(L) = -q_6 \end{aligned} \quad (5)$$

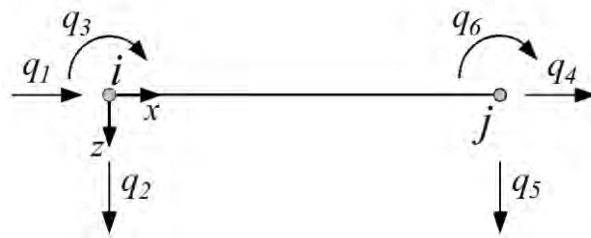


Fig. 1. The nodal degrees of freedom of the beam element.

Enforcement of Eq. (5) by using the solution in Eqs. (2)-(4) leads to the expressions of the axial and transversal deflection, collected in the vector $\mathbf{u}^T(x; \mathbf{x}^{EI}, \boldsymbol{\beta}^*) = [u_x(x; \mathbf{x}^{EI}, \boldsymbol{\beta}^*) \quad u_z(x; \mathbf{x}^{EI}, \boldsymbol{\beta}^*)]$, in terms of nodal displacement vector $\mathbf{q}_e = \{q_1, q_2, q_3, q_4, q_5, q_6\}^T$ and the external load function as follows:

$$\mathbf{u}(x; \mathbf{x}^{EI}, \boldsymbol{\beta}^*) = \mathbf{N}(x; \mathbf{x}^{EI}, \boldsymbol{\beta}^*) \cdot \mathbf{q}_e + \mathbf{u}_p(x; \mathbf{x}^{EI}, \boldsymbol{\beta}^*) \quad (6)$$

where $\mathbf{N}(x; \mathbf{x}^{EI}, \boldsymbol{\beta}^*)$ collects the relevant displacement shape functions as follows:

$$\mathbf{N}(x; \mathbf{x}^{EI}, \boldsymbol{\beta}^*) = \begin{bmatrix} N_{x,1} & 0 & 0 & N_{x,2} & 0 & 0 \\ 0 & N_{z,1} & N_{z,2} & 0 & N_{z,3} & N_{z,4} \end{bmatrix} \quad (7)$$

with

$$\begin{aligned}
N_{x,k}(x; \mathbf{x}^{EI}, \boldsymbol{\beta}^*) &= {}^k A_1 + {}^k A_2 g_2(x; \beta_{x,i}^*), \quad k=1,2 \\
N_{z,j}(x; \mathbf{x}^{EI}, \boldsymbol{\beta}^*) &= {}^j C_1 + {}^j C_2 x + {}^j C_3 f_3(x; \beta_{z,i}^*) + {}^j C_4 f_4(x; \beta_{z,i}^*), \quad j=1, \dots, 4 \\
{}^1 A_1 &= 1; \quad {}^1 A_2 = -\frac{1}{g_2(L)}; \quad {}^2 A_1 = 0; \quad {}^2 A_2 = \frac{1}{g_2(L)} \\
{}^1 C_1 &= 1; \quad {}^1 C_2 = 0; \quad {}^1 C_3 = -\frac{f_4'(L)}{w}; \quad {}^1 C_4 = \frac{f_3'(L)}{w}; \\
{}^2 C_1 &= 0; \quad {}^2 C_2 = 1; \quad {}^2 C_3 = \frac{-f_4'(L) + f_4(L)f_2'(L)}{w}; \quad {}^2 C_4 = \frac{-f_3(L) + f_3'(L)}{w}; \\
{}^3 C_1 &= 0; \quad {}^3 C_2 = 0; \quad {}^3 C_3 = \frac{f_4'(L)}{w}; \quad {}^3 C_4 = -\frac{f_3'(L)}{w}; \\
{}^4 C_1 &= 0; \quad {}^4 C_2 = 0; \quad {}^4 C_3 = -\frac{f_4(L)}{w}; \quad {}^4 C_4 = \frac{f_3(L)}{w}; \\
w &= f_3(L)f_4'(L) - f_4(L)f_3'(L)
\end{aligned} \tag{8}$$

Finally, the last vector in Eq. (6), defined as $\mathbf{u}_p^T(x; \mathbf{x}^{EI}, \boldsymbol{\beta}^*) = [u_{p_x}(x; \mathbf{x}^{EI}, \boldsymbol{\beta}^*) \quad u_{p_z}(x; \mathbf{x}^{EI}, \boldsymbol{\beta}^*)]$, providing the additional contributions of the external load distributions $p_x(x), p_z(x)$ to the axial and transversal displacements, is given as follows:

$$\begin{aligned}
u_{p_x}(x; \mathbf{x}^{EI}, \boldsymbol{\beta}^*) &= -\frac{g_3(L)}{g_2(L)} g_2(x) + g_3(x) \\
u_{p_z}(x; \mathbf{x}^{EI}, \boldsymbol{\beta}^*) &= \frac{f_4(L)f_5'(L) - f_5(L)f_4'(L)}{w} f_3(x) + \frac{f_5(L)f_3'(L) - f_3(L)f_5'(L)}{w} f_4(x) + f_5(x)
\end{aligned} \tag{9}$$

It has to be noted that the shape function matrix $\mathbf{N}(x; \mathbf{x}^{EI}, \boldsymbol{\beta}^*)$, in Eqs. (7),(8), and the load vector contribution $\mathbf{u}_p(x; \mathbf{x}^{EI}, \boldsymbol{\beta}^*)$ in Eq. (9), allow the reconstruction of the element deformed configuration once the nodal displacements are evaluated. The displacement shape functions proposed in Eqs. (7),(8) differ from the classical polynomials in view of additional distributional terms able to account for the abrupt cross section variations. For the latter reason their dependence on the vectors $\mathbf{x}^{EI}, \boldsymbol{\beta}^*$, has been highlighted throughout Eqs. (6)-(9). The distributional terms appearing in the functions $g_2(x), g_3(x), f_3(x), f_4(x), f_5(x)$, as formulated in Eq. (3), are those subjected to update at the Gauss integration points during the inelastic analysis conducted by means of a Newton-Raphson type of procedure. In fact, the parameters in the vector $\boldsymbol{\beta}^*$ change with the axial and flexural stiffness according to the chosen inelastic constitutive model. In view of the adaptive character of the proposed displacement shape function with the occurrence of plastic deformations the latter are here addressed to as Smart Displacement Shape Functions (SDSFs).

Once the SDSFs, to be updated during the evolution of non linear events, have been defined it is now possible to evaluate the vector of generalised deformation components $\mathbf{d}(x) = [\varepsilon_o(x) \quad \chi_y(x)]^T$, collecting the axial deformation $\varepsilon_o(x)$ of the beam geometrical axis

and the curvature $\chi_y(x)$ of the proposed beam element, expressed in terms of nodal displacements and distributed external forces, by accounting for the standard Euler-Bernoulli model relationships, as follows:

$$\mathbf{d}(x; \mathbf{x}^{El}, \boldsymbol{\beta}^*) = \mathbf{B}(x; \mathbf{x}^{El}, \boldsymbol{\beta}^*) \cdot \mathbf{q}_e + \tilde{\mathbf{u}}_p(x; \mathbf{x}^{El}, \boldsymbol{\beta}^*) \quad (10)$$

where the matrix $\mathbf{B}(x; \mathbf{x}^{El}, \boldsymbol{\beta}^*)$ and the vector $\tilde{\mathbf{u}}_p(x; \mathbf{x}^{El}, \boldsymbol{\beta}^*)$, also subject to updating during the iterative step-by-step inelastic analysis, contain the first and second derivatives of the SDSFs and the load dependent terms $u_{p_x}(x; \mathbf{x}^{El}, \boldsymbol{\beta}^*), u_{p_z}(x; \mathbf{x}^{El}, \boldsymbol{\beta}^*)$, respectively.

4 THE SMART DISPLACEMENT BASED BEAM ELEMENT STIFFNESS MATRIX

The formulation of the SDSFs presented in the previous sections is adopted to define a Smart Displacement Based (SDB) beam element by providing the expression of the element stiffness matrix according to the application of the principle of virtual work.

By exploiting a fibre approach^[5,6], the cross section area is discretised into n_f fibres, as depicted in Fig.4 in the form of stripes, each of them is characterised by an area A_f and a uni-axial non linear normal stress-axial strain elastic-plastic behaviour (since shear deformations and the consequent interaction with axial deformations is not taken into account). By assuming the principle of planar section conservation, the axial strain $\varepsilon_x(x)$ of each fibre is written as:

$$\varepsilon_x(x; z_f) = \varepsilon_o(x) + \chi_y(x)z_f = \begin{bmatrix} 1 & z_f \end{bmatrix} \begin{bmatrix} \varepsilon_o(x) \\ \chi_y(x) \end{bmatrix} = \boldsymbol{\alpha}(z_f) \cdot \mathbf{d}(x) \quad (11)$$

where the row vector $\boldsymbol{\alpha}(z_f) = \begin{bmatrix} 1 & z_f \end{bmatrix}$, depending on the distance z_f of the f -th fibre from the beam axis, has been introduced. The axial deformation of the f -th fibre of the cross section can be expressed in terms of nodal displacements \mathbf{q}_e for the proposed SDB beam element by replacing Eq. (10), purged of the external load contribution $\tilde{\mathbf{u}}_p(x; \mathbf{x}^{El}, \boldsymbol{\beta}^*)$, into Eq. (11) as follows:

$$\varepsilon_x(x; z_f) = \boldsymbol{\alpha}(z_f) \cdot \mathbf{B}(x; \mathbf{x}^{El}, \boldsymbol{\beta}^*) \cdot \mathbf{q}_e \quad (12)$$

The non linear uni-axial constitutive relation between the axial strain $\varepsilon_x(x; z_f)$ and the normal stress $\sigma_x(x; z_f)$ can be written as $\sigma_x(x; z_f) = E_T(x; z_f)\varepsilon_x(x; z_f)$ in terms of the tangent modulus $E_T(x; z_f)$ of the f -th fibre at cross section with abscissa x , to be evaluated according to the uni-axial constitutive model chosen for the applications.

Application of the principle of virtual displacements for the SDB beam element, in view of the fibre approach introduced in Eq. (12), writes:

$$\mathbf{Q}_e^T \cdot \delta \mathbf{q}_e = \mathbf{q}_e^T \int_0^1 \mathbf{B}^T(x; \mathbf{x}^{EI}, \boldsymbol{\beta}^*) \sum_{f=1}^{n_f} \boldsymbol{\alpha}^T(z_f) E_T(x; z_f) A_f \boldsymbol{\alpha}(z_f) \mathbf{B}(x; \mathbf{x}^{EI}, \boldsymbol{\beta}^*) dx \delta \mathbf{q}_e(x; z_f) \quad \forall \delta \mathbf{q}_e \quad (13)$$

where $\delta \mathbf{q}_e$ indicates virtual nodal displacements. Eq. (13) implies the following element stiffness matrix $\mathbf{K}_e(\mathbf{x}^{EI}, \boldsymbol{\beta}^*)$, dependent on the current state of the element by means of the plastic intensity parameter vectors $\boldsymbol{\beta}^*$ and the plastic segment extension vector \mathbf{x}^{EI} , defined as follows:

$$\mathbf{K}_e(\mathbf{x}^{EI}, \boldsymbol{\beta}^*) = \int_0^1 \mathbf{B}^T(x; \mathbf{x}^{EI}, \boldsymbol{\beta}^*) \mathbf{k}(x) \mathbf{B}(x; \mathbf{x}^{EI}, \boldsymbol{\beta}^*) dx \quad (14)$$

The inner matrix $\mathbf{k}(x)$ appearing in the integral in Eq. (14) represents the cross section stiffness matrix obtained by the adopted fibre discretisation as follows:

$$\mathbf{k}(x) = \sum_{f=1}^{n_f} \boldsymbol{\alpha}^T(z_f) E_T(x; z_f) A_f \boldsymbol{\alpha}(z_f) = \begin{bmatrix} \sum_{f=1}^{n_f} E_T(x; z_f) A_f & \sum_{f=1}^{n_f} E_T(x; z_f) A_f z_f \\ \sum_{f=1}^{n_f} E_T(x; z_f) A_f z_f & \sum_{f=1}^{n_f} E_T(x; z_f) A_f z_f^2 \end{bmatrix} \quad (15)$$

The cross section stiffness matrix given in Eq. (30) is used to retrieve the values of the discontinuity parameters collected in the vector $\boldsymbol{\beta}^*$ during the non linear analysis once the integration of the non linear constitutive equations is performed for each fibre of the cross sections. Furthermore, the expression reported in Eq. (14) shows clearly how the element stiffness matrix \mathbf{K}_e , differently from the classical displacement based approach commonly adopted in the literature, depends on the variation of the shape functions which are updated in accordance to the discontinuity parameter vector $\boldsymbol{\beta}^*$.

According to the Gauss integration scheme, the element stiffness matrix in Eq. (14) can be evaluated as follows:

$$\mathbf{K}_e(\mathbf{x}^{EI}, \boldsymbol{\beta}, \boldsymbol{\beta}^*) \approx \sum_{r=1}^n \mathbf{B}^T(x_r^G; \mathbf{x}^{EI}, \boldsymbol{\beta}^*) \mathbf{k}(x_r^G) \mathbf{B}(x_r^G; \mathbf{x}^{EI}, \boldsymbol{\beta}^*) w_r \quad (16)$$

where the matrix $\mathbf{B}(x_r^G; \mathbf{x}^{EI}, \boldsymbol{\beta}^*)$, collecting the derivatives of the displacement shape functions formulated explicitly in Eqs. (12)-(14), are evaluated at the Gauss integration cross sections (the positions of the Gauss points are indicated as x_i^G , $i=1, \dots, n$) and updated at each iteration as plastic deformations occur. The inner matrix $\mathbf{k}(x_r^G)$ in the product appearing in Eq. (16) represents the tangent stiffness matrix of the Gauss cross sections to be evaluated by means of integration of the fibre constitutive equations through the cross section according to Eq. (15).

6 AXIALLY EQUILIBRATED SDB BEAM ELEMENT

One of the problems encountered in the formulation of classical DB beam element is due to the assumption of the linear axial shape functions implying a constant axial force distribution during the analysis which does not reflect the variation of the internal axial force at the Gauss cross sections obtained by integration of the non linear constitutive laws. As a result axial equilibrium is not strictly enforced along the beam axis and it is rather verified in a weak form. The latter issue, clearly discussed in^[2], implies a low performance of the DB element and requires a dense mesh to reach an accuracy comparable to the FB approach against experimental results. The concept of DB beam element strictly satisfying axial equilibrium along the beam axis was originally introduced by Izzudin et al.^[13] for non-linear elastic problems while an interesting and appealing approach to achieve strong axially equilibrium for DB beam elements was recently proposed by Tarquini et al.^[14] with an internal iterative procedure to correct the axial strains at each Gauss point requiring the solution of a linear system of equations.

In this section the SDSFs proposed in section 3 are employed to formulate an axially equilibrated SDB beam element (SDB/ae) in a strong form. Precisely, in order to reach a constant axial load along the Gauss integration points, a point load distributions, generated by the axial force difference $N(x_i^G) - N(x_{i-1}^G)$, $i = 1, \dots, n$, between each two successive Gauss points will be exploited, defined as follows:

$$\tilde{p}_x(x) = \sum_{i=1}^{n-1} [N(x_i^G) - N(x_{i-1}^G)] \delta(x - x_i) \quad (17)$$

where $\delta(x - x_i)$ is the well know Dirac's delta distribution adopted in Eq. (17) to model a sequence of axial point loads concentrated at cross sections $x_i, i = 1, \dots, n$. The axial load distribution $\tilde{p}_x(x)$, as defined in Eq. (17), is responsible for the onset of the axial displacement increment field $\Delta u_{\tilde{p}_x}(x; \mathbf{x}^{EI}, \boldsymbol{\beta}^*)$ straightforwardly provided by the first expression in Eq. (9) as follows:

$$\Delta u_{\tilde{p}_x}(x; \mathbf{x}^{EI}, \boldsymbol{\beta}^*) = -\frac{g_3(L)}{g_2(L)} g_2(x) + g_3(x) \quad (18)$$

where $g_2(x), g_3(x)$ are evaluated by means of Eq. (3) for the axial load distribution $\tilde{p}_x(x)$ in Eq. (17).

The axial displacement increment field $\Delta u_{\tilde{p}_x}(x; \mathbf{x}^{EI}, \boldsymbol{\beta}^*)$, due to the axial point distribution $\tilde{p}_x(x)$ in Eq. (17), gives rise to a fictitious axial deformation increment $\Delta \varepsilon_{\tilde{p}_x}(x; \mathbf{x}^{EI}, \boldsymbol{\beta}^*) = \frac{d}{dx} \Delta u_{\tilde{p}_x}(x; \mathbf{x}^{EI}, \boldsymbol{\beta}^*)$ responsible of an inner iterative correction of the trial axial deformation until a constant axial force is obtained over the element delivering an axially equilibrated element.

In other words, within the standard predictor-corrector Newton-Raphson procedure, after the element state determination an internal iterative procedure is triggered by the superimposition of the axial deformation increment $\Delta \varepsilon_{\bar{p}_x}(x; \mathbf{x}^{El}, \boldsymbol{\beta}^*)$ due to the lack of axial force equilibrium in strong form. When the increment $\Delta \varepsilon_{\bar{p}_x}(x; \mathbf{x}^{El}, \boldsymbol{\beta}^*)$ is applied a new element state determination is performed to determine the updated axial force unbalance. The inner iterations are stopped when the difference of axial forces $N(x_i^G) - N(x_{i-1}^G)$, $i = 1, \dots, n$, is null, delivering a strongly axially equilibrated element.

5 APPLICATION

The reinforced concrete cantilever beam studied in^[14] by means of standard and axial equilibrated displacement elements, as well as the forced based approach is analysed in this section. The beam length is $L = 300\text{cm}$ with rectangular cross section $30 \times 40\text{cm}$ and 20mm of cover concrete. Twelve $\phi 16$ reinforcing steel bars are symmetrically disposed along the section, as reported in Fig.2a. The analyses are conducted applying a shear force F at the free end of the beam. A constant axial force $N = 75\text{kN}$, corresponding to $1,25\%$ of the axial-compression capacity of the section, is applied to the beam.

In the numerical simulations the modified Kent and Park constitutive law, according to Yassin model^[15], is adopted in compression while a linear softening behaviour is adopted in traction. The compression strength of the confined concrete is $f_{cc} = 42\text{Mpa}$, while the strength of the unconfined concrete is $f_c = 37\text{Mpa}$. The concrete strain at the peak-stress are respectively $\varepsilon_c = 0,24\%$ and $\varepsilon_{cc} = 0,28\%$ for unconfined and confined concrete which correspond to an initial Young modulus $E_c = 30\text{Gpa}$ of the Kent and Park model. The tensile strength of the concrete is assumed equal to 10% of the compression strength and the softening slope equal to $2/3 E_c$. The steel bars are modelled by the Menegotto and Pinto constitutive law^[16] with Young modulus $E_s = 200\text{Gpa}$, $f_y = 480\text{Mpa}$, hardening 0.5% , initial value of the curvature parameter 15 and curvature degradation parameters respectively $0,925$ and $0,15$.

The proposed SDB/ae model is compared to the standard DB model, the DB/ae model^[14] and the FB model. In particular, the analyses employing the SDB/ae model and the DB/ae model are performed through the software HISTRA^[17], where both models have been implemented, while the analyses on the standard DB model and the FB model are performed in OPENSEES^[18] environment employing the "Concrete02" and "Steel02" uniaxial materials. All the analyses are performed considering a single finite element, 10 Gauss-Lobatto integration points and discretising the cross section by means of 40 fibres. Figure 2b reports the capacity curves in terms of external force F versus the lateral deflection of the free end of the column $u_z(L)$.

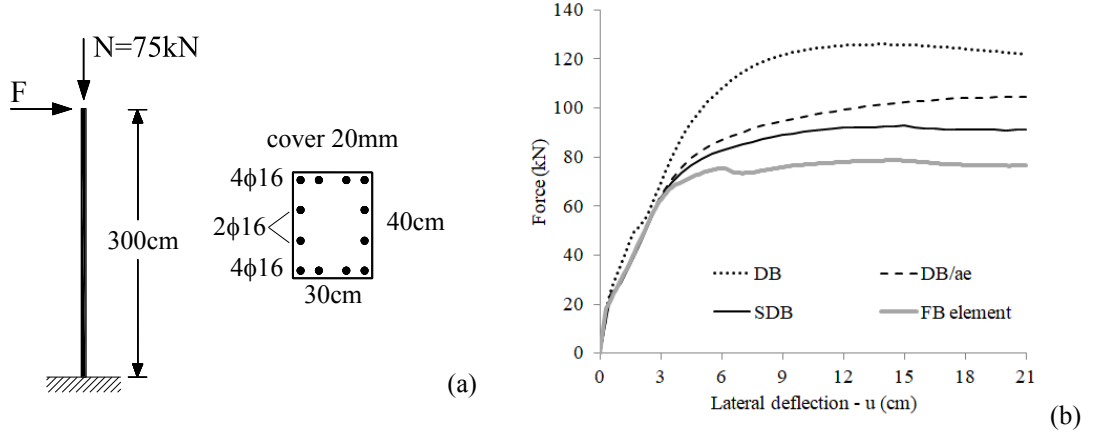


Fig.2. Cantilever geometrical layout (a) and comparison of the monotonic lateral capacity curves (b).

The maximum lateral force registered by the FB model is 78,6 kN. The standard DB model overestimates the beam lateral strength of 60,1% (126,0kN), while the error decreases to 33,2% and 18,1% by using the DB/ae model and the SDB/ae model, respectively, providing a reliable prediction of the load-carrying capacity of the beam, even though a mesh refinement of the beam is not introduced.

0 shows sensitivity of the SDB/ae model to the number of the integration points (0a) and the number of elements adopted for the beam discretisation (0b). In the same Figure 3 the lines representative of the FB and standard DB responses are also reported. A low influence on the response is observed by increasing the integration points from 5 to 20, while by increasing the number of elements the SDB/ae response converges to the FB curve.

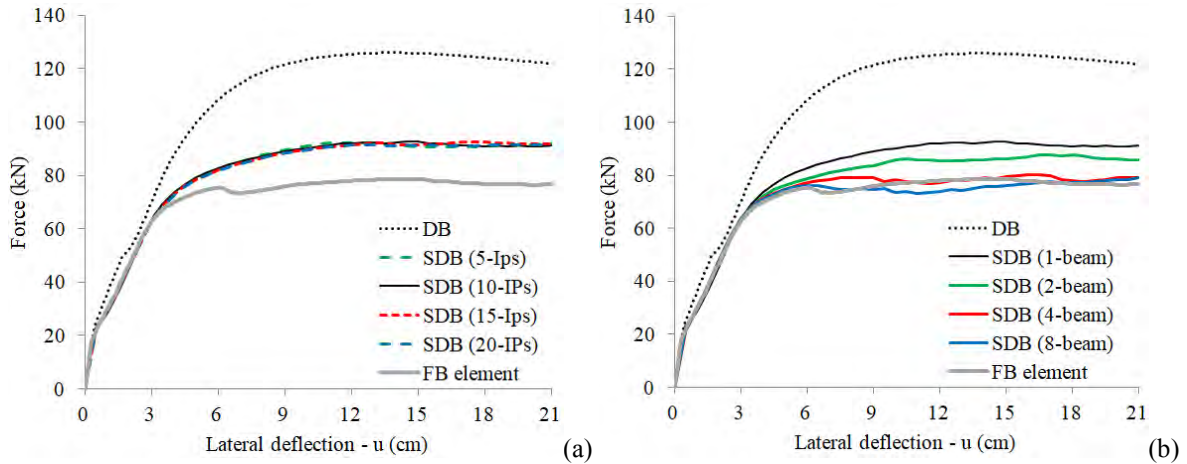


Fig.3. Influence of the number of the integration points (a), and the number of elements with 10 IPs (b) on the capacity curves for the system in Fig.2.

6 CONCLUSIONS

The shape functions, adopted by classical displacement based finite formulations for the discretisation of the beam element displacement field, are based on the adoption of Hermite polynomials which, however, are not able to capture the curvature variations due to along axis plastic deformation occurrences. The latter circumstance results in the inadequacy of such shape functions to properly represent the displacement field in presence of flexural stiffness variations implied by plastic constitutive behaviour. As a result a great computational disadvantage is related to the need of adopting refined meshes in order to converge towards a more accurate solutions which are, on the contrary, provided by force based finite elements procedures.

In order to improve the performance of displacement based beam finite elements for inelastic analysis of beam-like and frame structures in this work the concept of Smart Displacement Shape Functions (SDSFs) capable of updating during the diffusion of plastic deformations along the beam axis has been proposed. The SDSFs change during the iterative step-by-step analysis following the stiffness decay of the control cross sections according to a model of non uniform beam with stepped variations of both axial and flexural stiffness. The SDSFs updating is transferred to additional distributional terms explicitly introduced by closed form integration of the fourth order integration of the Euler-Bernoulli stepped beam.

The stiffness decay during the plastic incremental analysis is evaluated according to a fibre approach very convenient for r/c cross sections in order to account for the interaction of axial force –bending moment. The proposed beam element is formulated with six degrees of freedom at the element nodes and its smart character provides a better accuracy with respect to classical displacement based beam elements which is comparable with the alternative force based approach.

REFERENCES

- [1] Crisfield, M.A. Non-linear finite element analysis of solids and structures, John Wiley & Sons, Chichester, UK, Vol. I, (1991), Vol. II, (1997).
- [2] Calabrese, A., Almeida, J.P., Pinho, R. Numerical issues in distributed inelasticity modeling of rc frame elements for seismic analysis. *Journal of Earthquake Engineering* (2010) 14: 38-68.
- [3] Izzudin, B.A., Elnashai, A.S. Adaptive space frame analysis: part I, a plastic hinge approach. *Structures & Buildings* (1993) 99(3): 303-316.
- [4] Izzudin, B.A., Elnashai, A.S., Adaptive space frame analysis: part II, a distributed plasticity approach. *Structures & Buildings* (1993) 99(3): 317–326.
- [5] Spacone, E., Filippou, F.C., Taucer, F.F. Fiber beam-column model for non-linear analysis of r/c frames: Part I. Formulation. *Earthquake Engineering and Structural Dynamics* (1996) 25: 711–725.

- [6] Spacone, E., Filippou, F.C., Taucer, F.F. Fiber beam-column model for non-linear analysis of r/c frames: Part II. Applications. *Earthquake Engineering and Structural Dynamics* (1996) 25: 727–742.
- [7] Spacone, E., Ciampi, V., Filippou, F.C. Mixed formulation of nonlinear beam finite element. *Computers and Structures* (1996) 58(1): 71–83.
- [8] Neuenhofer, A., Filippou, F.C. Evaluation of nonlinear frame finite element models. *Journal of Structural Engineering (ASCE)* (1997) 123(7): 958–956.
- [9] Neuenhofer, A., Filippou, F.C. Geometrically nonlinear flexibility-based frame finite element. *Journal of Structural Engineering (ASCE)* (1998) 124(6): 704–711.
- [10] Goodnight, J.C., Kowalsky, M.J., Nau, J.M. Effect of load history on performance limit states of circular bridge columns. *Journal of Bridge Engineering (ASCE)* (2013) 18(12): 1383–1396.
- [11] Almeida, J.P., Tarquini, D., Beyer, K. Modelling approaches for inelastic behaviour of rc walls: Multi-level assessment and dependability of results. *Archive of Computational Methods in Engineering* (2016) 23: 69–100.
- [12] Pantò, B., Rapisavoli, D., Caddemi, S., Calìo, I. A smart displacement based (SDB) beam element with distributed plasticity. *Applied Mathematical Modelling* (2017) 44: 336–356.
- [13] Izzudin, B.A., Karayannis, C.G., Elnashai, A.S. Advanced nonlinear formulation for reinforced concrete beam-columns. *Journal of Structural Engineering (ASCE)* (1994) 120(10): 2913–2934.
- [14] Tarquini, D., Almeida, J. P., Beyer, K. Axially equilibrated displacement based beam element for simulating the cyclic inelastic behaviour of RC members. *Earthquake Engng Struct. Dyn.*, (2017) 46: 1471–1492.
- [15] Yassin, M. Nonlinear analysis of prestressed concrete structures under monotonic and cyclic loads. Ph.D. dissertation, University of California (Berkeley) (1994).
- [16] Menegotto, M., Pinto, P.E. Method of analysis of cyclically loaded RC plane frames including changes in geometry and non-elastic behavior of elements under normal force and bending. Preliminary Report IABSE (1973) vol. 13.
- [17] HiStrA (Historical Structure Analysis). HISTRA s.r.l, Catania, Italy. Release 17.2.3, April 2015. <http://www.histra.it>.
- [18] McKenna, F. OpenSees: a framework for earthquake engineering simulation. *Computing in Science & Engineering*, (2011) 13(4): 58–66.

Study of a Vibroacoustic Interior Problem with Viscoelastic Sandwich Structure Using the Asymptotic Numerical Method

jean-marc Cadou^{*}, Bertille Claude^{**}, Laetitia Duigou^{***}, Gregory Girault^{****}

^{*}IRDL - Université de Bretagne Sud - France, ^{**}IRDL - Université de Bretagne Sud - France, ^{***}IRDL - Université de Bretagne Sud - France, ^{****}IRDL - Université de Bretagne Sud - France

ABSTRACT

The aim of this study is to compute the eigenvalues of a vibroacoustic interior problem with fluid-structure coupling. A displacement-pressure formulation is chosen to modelize the problem. Then, the spatial discretisation with the finite element method leads to a non symmetric and poorly conditioned matrix system. It is proposed to solve this discretized system with the Asymptotic Numerical Method (ANM). This method associates a high order perturbation method to a continuation technique [1]. Thus, the initial nonlinear problem is linearized and a set of linear algebraic systems easier to solve is obtained. The proposed method is validated with numerical tests on a conservative problem (that is to say for an elastic structure). These tests show that the computational times required with this method are lower than those needed with an Arnoldi-based method. Moreover our method is not sensitive to poorly conditioned matrix, so there is no need to add a preconditioning step [2]. Once the conservative problem is solved, the corresponding solutions are used as initial values to solve the associated dissipative problem (that is to say a viscoelastic sandwich structure [3]). Numerical developments are ongoing to evaluate the method coupling the homotopy to the ANM, and results are expected for the conference. REFERENCES [1] L. Duigou, E. M Daya and M. Potier-Ferry, Iterative algorithms for non-linear eigenvalue problems. Application to vibrations of viscoelastic shells, Computer Methods in Applied Mechanics and Engineering, Vol. 192, pp. 1323-1335, 2003. [2] B. Claude, L. Duigou, G. Girault and J.M. Cadou, Eigensolutions to a vibroacoustic interior coupled problem with a perturbation method, Comptes Rendus Mécanique, Vol. 345, 2, pp. 130-136, 2017. [3] L. Rouleau, J.F. Deu, A. Legay and J.F. Sigrist, Vibro-acoustic study of a viscoelastic sandwich ring immersed in water, Journal of Sound and Vibration, Vol. 331, pp. 522-539, 2012.

MICRO-SCALE THERMAL SIMULATIONS OF CEMENT PASTES CONTAINING MICROENCAPSULATED PHASE CHANGE MATERIALS (MPCM)

ANTONIO CAGGIANO^{*,†}, CHRISTOPH MANKEL^{*}, AND EDUARDUS A.B.
KOENDERS^{*}

^{*} Institute of Construction and Building Materials, TU-Darmstadt, Germany
Franziska-Braun-Straße 3 (vorm. Petersenstr. 12)
Darmstadt, Germany

caggiano@wib.tu-darmstadt.de, mankel@wib.tu-darmstadt.de, koenders@wib.tu-darmstadt.de
www.wib.tu-darmstadt.de

[†]LMNI, INTECIN, CONICET, Universidad de Buenos Aires
Av. Las Heras 2214
Ciudad Autónoma de Buenos Aires, Argentina
acaggiano@fi.uba.ar

Keywords: Thermal-energy storage, Enthalpy-based method, MPCMs, Porous cementitious containers, Microscale, Hydration.

Abstract. In the last decades, the use of smart components embedded inside cementitious composites, called Phase Change Materials (PCMs), has become a more and more attractive solution for saving energy and to provide a more efficient thermal comfortability to modern buildings and constructions. This work presents the current research activities running at the Institute of Construction and Building Materials (WiB) of TU Darmstadt, and deals with the investigation of advanced coupling of two physical mechanisms represented by a heat problem and microstructural heterogeneities in cement-based composites. Particularly, the thermal response of cement pastes, along with occurring phase change phenomena, will be simulated at the microscale level. A virtual 3D porous microstructure with embedded Microencapsulated-(M)PCMs, which are created with an available hydration model, provide a fundamental basis for the analysis of the morphological influence on the effective thermal energy diffusion parameters. The current work is based on investigating the influence of the morphological effect on the thermal properties of hydrating cement paste systems by using the cement hydration and microstructure development model Hymostruc, combined with MPCMs. Laboratory characterization of MPCM-pastes were also performed using several test methods which are here briefly reported. Test thermal performances in terms of heat capacity, conductivity and temperature evolutions of cement paste systems with and without MPCMs were experimentally evaluated, and are used as benchmark for calibration purposes.

1 INTRODUCTION

Building energy consumption could be easily reduced by employing smart materials that passively control the heat flow and temperature fluctuations in residential and commercial buildings [1]. Cementitious composites containing Phase Change Materials (PCMs) have been employed in the last years as a way to enhance the energy efficiency and saving of new construction [2]. A huge Thermal Energy Storage (TES) in PCMs is available in form of latent heat by reversibly changing phase between solid-liquid and vice versa. Therefore, the inclusion of PCMs in concrete could significantly improve the thermal properties of such a material, making it greener and more eco-friendly in construction and building applications [3].

Experimental activities available in literature, at several scales of observation, aimed at reporting the main benefits in terms of thermal properties of cementitious materials containing PCMs [4]. Some contributions reviewed the effect of the PCMs on the resulting mechanical capacities of concrete [5]. Other works demonstrated that by employing PCMs in concrete allows to have a certain beneficially reduction in terms of hydration heat during the hardening process of the fresh concrete [6].

Plenty of theoretical and numerical formulations have been proposed for analyzing TESs in porous cement pastes, mortar and/or concretes containing phase change materials. The majority of these models arise from an extension of the so-called Stefan problem [7]. The solution of this latter has been classically treated in literature by means of three main methods: (i) the fixed grid method [8], (ii) the deformed grid method [9] and (iii) a combination of these two latter [10]. Simulation examples related to cementitious composites are those related to the use of the so-called Enthalpy-based Method (EM), which moves into the fixed grid solution. Then, the Apparent Calorific Capacity Method (ACCM) [11-12] and the Heat Source Method (HSM) [13-14] represent two main alternatives used for solving the EM.

Concrete and other cementitious materials are multiphase (composite) materials and, for this reason, they can be considered and modelled as homogeneous continuums at the macroscale and/or structural practice-oriented one, while, at lower levels (meso-, micro- or even nano-scale) multiphase composite approaches can be considered. Available models can be thus categorized in this matter by means of those scales of observation. Structural-scale models allow to capture the essence of heat storage phenomena at the structural (building physics) scale level [15]. Macro-scale models are based on the assumption that the schematized material acts as a continuum and homogenous medium [16]. By considering lower scales of analysis (i.e., meso- and microscale behavior of PCM composite materials), the mechanism of PCMs, affected by external thermal fluctuations, can be better understood. At these lower scales the material can be idealized by considering different phases which together constitute the composite. Thereby, the interaction among the different phases (i.e., matrix, aggregates, PCMs, hydrated products, voids, water and possible interfaces between them) is explicitly considered in these approaches [17].

This work proposes a theoretical model for simulating the thermal behavior in hardened cement pastes produced with and without Microencapsulated-PCMs. An Enthalpy-based approach formulated in the framework of the Apparent Calorific Capacity Method (ACCM) is solved to accurately analyze the above mentioned phenomena. The model has been validated at macroscale

by means of temperature curves, measured from three different cement pastes without MPCMs and with 10% and 20% in MPCM volume fraction contents. Then, microscale analysis are performed on 3D virtual PCM-cement paste microstructures. The study of Representative Element Volume (REV) of heterogeneous PCM-cement paste microstructures will be performed with the aim of defining the minimum size of a sample that must be employed for determining the corresponding effective properties of a homogenized macroscopic model.

2 EXPERIMENTAL DATA

This section briefly reports the employed materials, the considered tests and results considered as reference for the numerical activities. DSC, conductivity and temperature evolution tests were done for investigating the thermal properties of plain and MPCM-cement pastes.

2.1 Materials and Methods

Nine mixtures, made with three different w/c ratios and three amount of MPCM volume fractions, were considered. A commercial ordinary Portland cement (CEM I 42,5 R) and microencapsulated paraffin waxes (namely, Micronal® DS 5038 X by BASF [18]), in form of powder MPCM, were mixed with different volume fractions. All mixtures were prepared according to EN 196-1 [19] and following the recipes highlighted in Table 1 (the first row of the Table identifies the mixture type by reporting the corresponding label which helps to provide the key information about the amount of MPCM and the considered w/c ratio).

Table 1: Mix overview of the nine paste systems.

Labels	c 4 ref [kg/m ³]	c 4 1 [kg/m ³]	c 4 2 [kg/m ³]	c 4 ref [kg/m ³]	c 4 1 [kg/m ³]	c 4 2 [kg/m ³]	c 3 ref [kg/m ³]	c 3 1 [kg/m ³]	c 3 2 [kg/m ³]
Cement	1294.4	1129.9	977.2	1383.9	1208.2	1044.9	1606.2	1402.2	1212.7
Water	582.5	508.5	39.8	553.6	483.3	417.9	481.9	420.7	363.8
MPCM	-	90.0	80	-	90.0	180.0	-	90.0	180.0
Air content [V.-%]	1.5	2.7	4.5	1.5	2.7	4.5	1.5	2.7	4.5
w/c ratio	0.45			0.40			0.30		

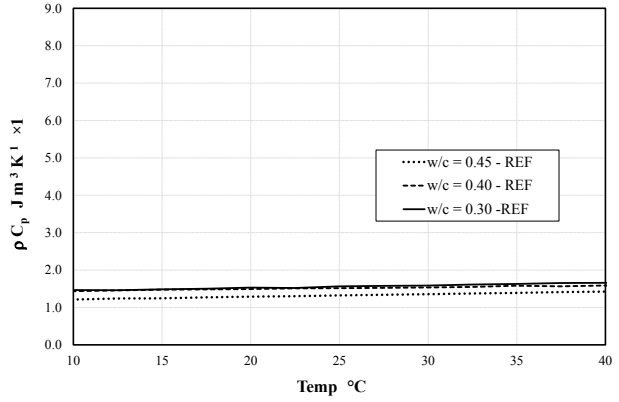
After one day of casting, all specimens were removed from the formwork and stored in a water bath at 20° C and during 28 days. Then, after the maturation, the specimens were completely dried for 42 days at 50° C until they reached a constant mass.

2.2 DSC test data

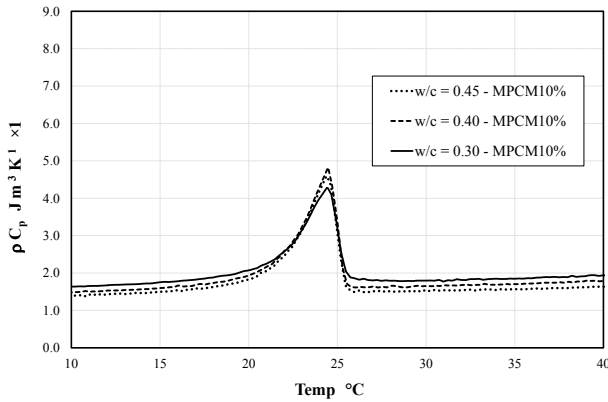
Differential scanning calorimetry (DSC) measures were performed for each one of the mixtures. Solid samples (3 per MPCM mixtures and 2 for the reference cement pastes) were prepared in aluminum DSC pans and tested (Figure 1a).



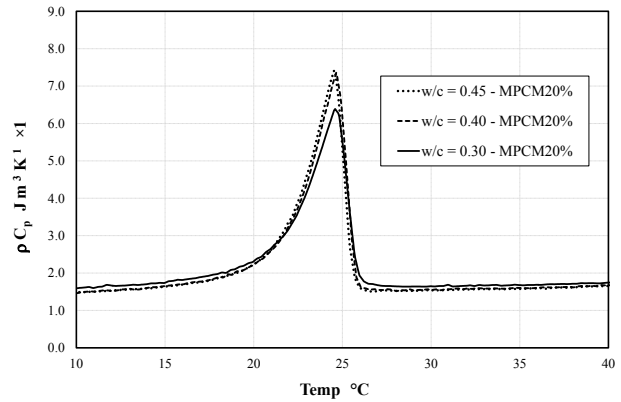
(a)



(b)



(c)



(d)

Figure 1: Results of DSC tests (obtained with a heating rate of $1 \text{ K} \times \text{min}^{-1}$) in terms of $\rho \times C_p$: (a) the used 0.6 mm pan and results with cement pastes having (b) 0%, (c) 10% and (d) 20% MPCM volume fraction.

DSC results for the reference cement pastes are shown in Figure 1b. The response of the three cement pastes is characterized by the same kind of sensible behavior, analyzed in the temperature ranges between 10 and 40 °C. As expected, the almost similar behavior characterizes each one of the cement pastes. The results also remark an almost temperature independent behavior of the $\rho \times C_p$ response.

Then, DSC thermograms of Figure 1c-d show the $\rho \times C_p - T$ response for the cases of 10% and 20% of MPCM volume fractions, respectively. They are characterized by an almost sensible behavior in the temperature ranges far from the melting point and an evident latent peak in that region close to the temperature of phase changes. Particularly, all curves are characterized by a remarkable peak which mainly represent the solid–liquid melting phase change of the MPCM stored in the

porous structure of the paste. It can be easily recognized that the latent storage capacity of the cement pastes with 20% MPCM volume fraction is strongly higher (as imaged) than the corresponding one with 10% volume fraction.

2.3 Conductivity tests

Thermal conductivity tests were performed by means of the Hot-Disk transient heat source method and using 40 mm × 40 mm × 160 mm beams. The complete test procedure is omitted in this work for the sake of brevity. However further details are available here [20].

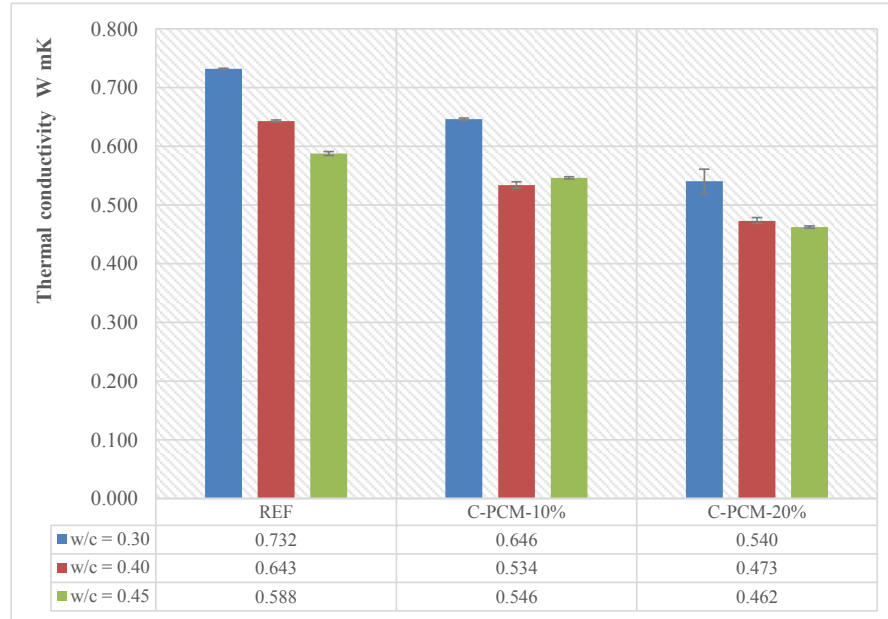


Figure 2: Thermal conductivity of the REF, C-PCM-10% and C-PCM-20% mixtures with different w/c ratios.

Figure 2 reports the results of the conductivity tests for the analyzed MPCM cement pastes. It can be observed that the thermal conductivity generally decreases when higher water-to-cement ratios are considered. Moreover, when comparing the results by focusing on the effect of MPCM replacements it can be also shown that the thermal conductivity is generally affected by the presence of MPCMs. In particular the thermal conductivity reduces when higher MPCM volume fractions are substituted in the considered matrix.

2.4 Thermal tests and mechanical tests

Temperature measurements and mechanical tests, for the complete characterization of the materials under investigation, were also done. Particularly, three spheres characterized to have a diameter of about 70 mm and produced with embedded thermocouples were cast to investigate the structural and microscale behavior of such shapes and through studying temperature evolutions under certain heating environmental conditions. The thermal experiments were accompanied by mechanical tests to observe the effect MPCMs have on the resulting strengths in both compression and bending. These results are omitted herein for the sake of the brevity, however they are fully documented in [20].

3 FIRST LAW OF THERMODYNAMICS AND ENTHALPY BASED METHOD

The basic equations, employed for predicting phase transformation phenomena in PCM cement-based systems, are described in this section.

3.1 Thermodynamics principles

The basic equation describing a heat conduction problem can be written as follows:

$$\frac{\partial Q}{\partial t} = \nabla \cdot (\lambda \nabla T) + \dot{q}_v \quad \forall \in \Omega \quad (1)$$

where Q is the heat of the system, t the time, λ the thermal conductivity of the material (depending on temperature T and position vector of the considered body Ω), \dot{q}_v is the possible source term while $\nabla \cdot$ and ∇ are the divergence and gradient tensorial operators.

In thermodynamics a small amount of heat added to a system (dQ) is defined by means of the *first law of thermodynamics* as:

$$dU = dQ - p dV \quad (2)$$

where dU is a variation of the internal energy of the system and $p dV$ the rate of the work spent, indicated as dW (under the simplified hypothesis that $dW = p dV$).

By introducing the definition of the enthalpy of a homogenous system, $H = U + p dV$, and by combining Eqs. (1) and (2), and adopting the hypothesis of a constant pressure process, the following enthalpy-based equation can be reached:

$$\frac{\partial H}{\partial t} = \nabla \cdot (\lambda \nabla T) + \dot{q}_v \quad \forall \in \Omega \quad (3)$$

which is the mostly used equation for solving phase changes in construction and building material applications, and is commonly addressed as the enthalpy-based method.

3.2 Enthalpy based and Apparent Calorific Capacity Method

The Apparent Calorific Capacity Method (ACCM) allows for describing the enthalpy evolution of a system in terms of an apparent (or sometime called effective) heat capacity during the thermal phase change.

The approach is based on following chain rule:

$$\frac{\partial H}{\partial t} = \frac{\partial H}{\partial T} \frac{\partial T}{\partial t}, \quad (4)$$

then, by introducing the so-called temperature-dependent apparent (effective) heat capacity, defined as follows:

$$\frac{\partial H}{\partial T} = \rho C_{eff}(T) \quad (5)$$

Eq. (3) modifies into the following non-linear transient heat equation:

$$\rho C_{eff}(T) \frac{dT}{dt} = \nabla \cdot (\lambda \nabla T) + \dot{q}_v \quad \forall \in \Omega \quad (6)$$

To complete the above problem statement of the ACCM approach outlined in Eq. (6), Initial Conditions (ICs) and Boundary Conditions (BCs) need to be employed.

4 MICROSCALE POROUS STRUCTURE

3D virtual PCM-cement paste microstructures were generated through the Hymostruc hydration model [24]. The generation of the microgeometries, numerically performed with the simulated hydration processes, are based on several input parameters which aim at reproducing the microscale geometries of the 9 cement pastes (with and without MPCMs) investigated in the experimental campaign (Section 2).

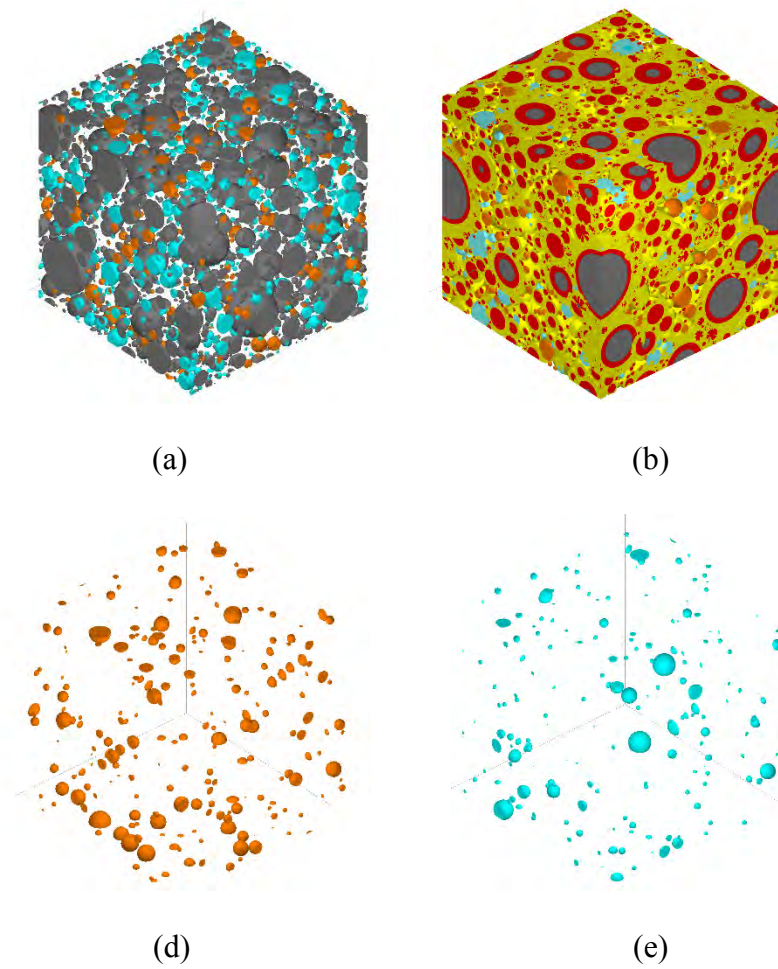


Figure 3: (a) 3D microstructure with initial anhydrated cement, (b) hydrated microstructure, (c) detail of the MPCMs and (d) air bubbles distribution. For color figures the reader could refer to the digital version of the paper.

Particle size distribution of the (anhydrated) cement, type of cement/binder, water/cement ratio, hydration age, initial mix temperature, air bubbles and MPCM particles distribution are the key input parameters which affect the final hydrated structure. They were selected following the information and measured data of the experimental campaign (i.e., cement type, water-to-cement ratio, air bubbles, MPMCs).

As example, a 3D generated geometry has been shown in Figure 3 which is characterized by a 3D virtual structure with a cubic shape with a rib size of 100 μm , a regular Portland cement with a specific surface of $400 \text{ m}^2\text{kg}^{-1}$, $w/c = 0.45$, isothermal reaction at 20°C , MPCM volume fraction of 20% with a particle distribution as highlighted in Figure 4 and air bubble contents according to Table 1. It is worth to mention that the w/c ratio is one of the key parameter that controls the morphology of the obtainable porous microstructure [25].

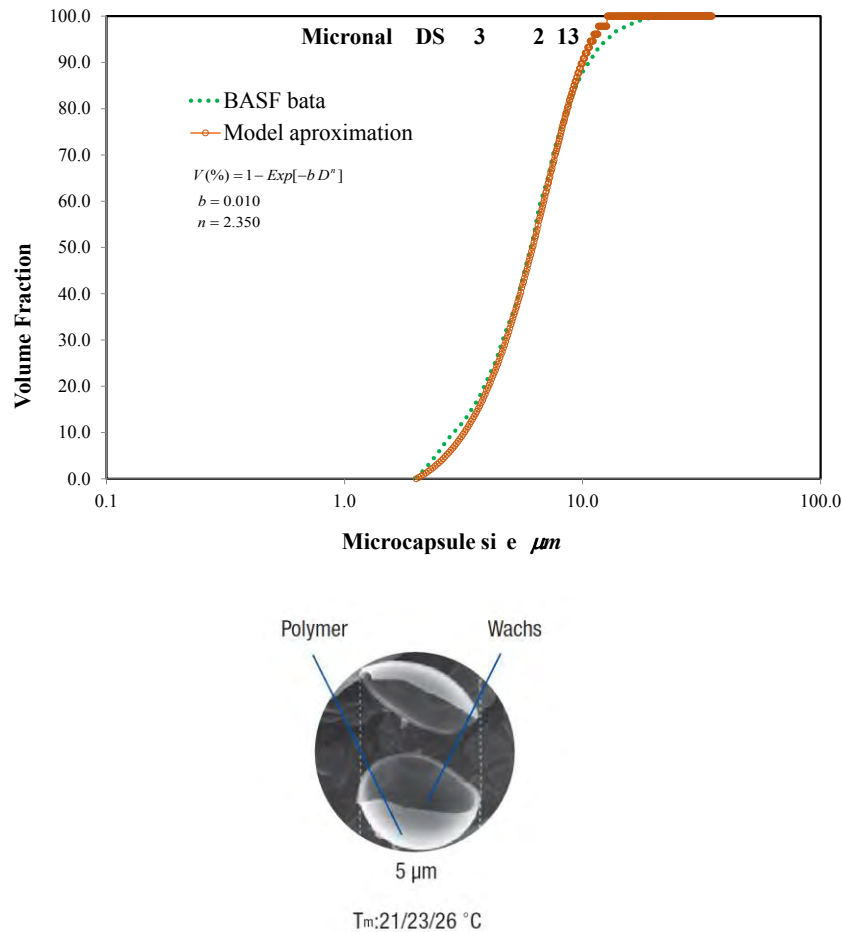


Figure 4: Grain size distribution of the employed MPCMs vs. BASF-data [18].

The initial cement particles and MPCMs are stacked based on a random selection of locations with an equal probability of occurrence. Particles allocation starts from the largest particles down to the smaller ones and the process continues until all particles in the smallest fractions have been stacked. Volume fraction and particle-size distribution follow the rule $V(\%) = 1 - \text{Exp}[-b D^n]$ which was opportunely calibrated for predicting the sheet data finished by BASF [18]. After having generated this initial particle structures, hydration algorithms are invoked for forming the 3D virtual microstructure.

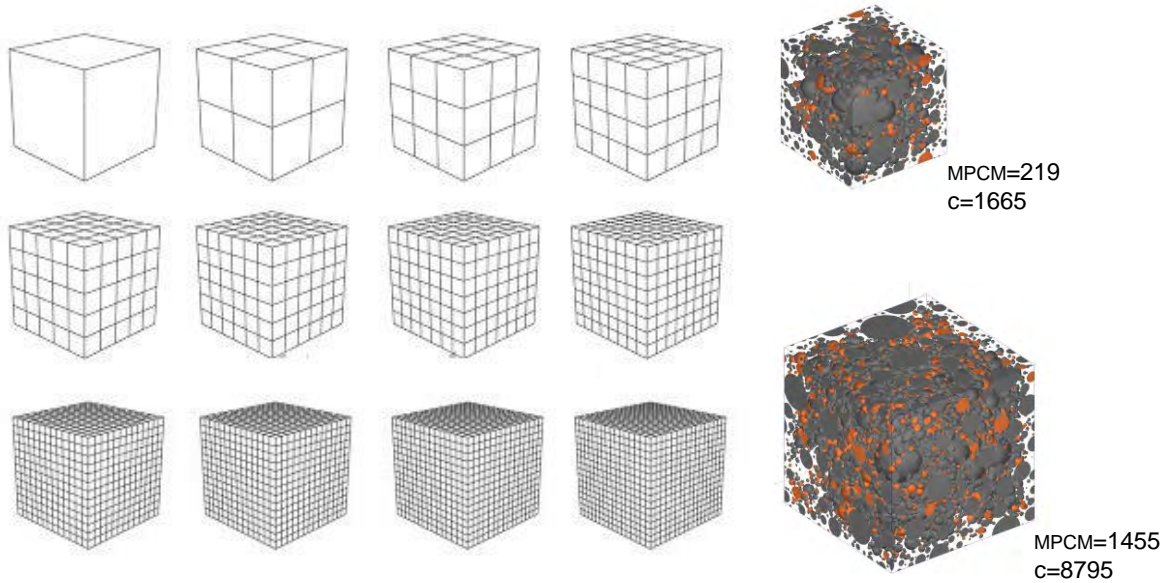


Figure 5: 3D REV microstructures with different discretization size (left) and two specimen sizes as example (e.g., 50 and 100 μm^3 on the right).

The study of the most appropriate Representative Element Volume (REV) of heterogeneous PCM-cement paste microstructures is currently ongoing and will be aimed at defining the minimum size of a sample that must be employed for determining the corresponding effective properties of the dual homogenized macroscopic model. The REV dimension should be large enough to contain the necessary information about the microstructure, thus to be representative.

An indicator proposed by Guittman et al. [23] can be estimated for each 3D microstructure to find out the most appropriate REV size and particularly to quantify the change of the calculated homogenized (effective) thermal property based on the mean value calculated for the different numerical realizations. More specifically, six different generations of the initial cement particle locations needs to be generated and used for the hydration simulation and for each different mixture type.

The following expression was proposed by Guittman et al. [23]:

$$\chi^2 = \sum_{i=1}^m (R_{\text{energy},i} - R_{\text{energy},a})^2 / R_{\text{energy},a}^2 \quad (7)$$

where $R_{\text{energy},i}$ is the investigated effective thermal energy parameter (e.g., the thermal conductivity, specific heat capacity, enthalpy), $R_{\text{energy},a}$ is the average of the investigated $R_{\text{energy},i}$, and $m=6$ the total number of numerical realizations performed with different initial cement particle and MPCM locations.

The variability of the results can be estimated with χ^2 , indicating that for smaller values of χ^2 , the closer the volume of the sample under consideration represents the expected REV. In fact, the true REV may only be obtained for a sample with an infinite volume. Nonetheless, a size of a sample can normally be used if the value of χ^2 is acceptably low. Generally, 0.1 is regarded to be an acceptable value [24].

CONCLUSIONS

This paper proposes the theoretical basis for simulating the thermal behavior of cement paste systems made with and without M-PCMs. A micro-scale based approach formulated through the use of the so-called Apparent Calorific Capacity Method (ACCM) was solved to accurately analyze the above mentioned phenomena. The model considered the experimental data measured from three different cement pastes without MPCMs and with 10% and 20% of MPCM volume fraction contents. The model validation of the proposed method dealt with simulating the experimental tests for given boundary and initial conditions and based on the adopted experimentally-based $\rho C_{\text{eff}}(T)$ curves. The proposed study was developed within the framework of the “2CENENRGY” project and will be further extended on investigating the 3D thermal-mechanical response in micro and mesoscopic structural specimens.

It may be worth to mention that although a significant research effort has already been done in the field of numerical modelling for heat transfer processes with PCM accumulations, further efforts in the field of cementitious composites embedding PCMs are certainly needed. Unambiguous knowledge on how porous microstructures, like cementitious composites or aggregates, should be built up and/or what are the critical demands that allow empty pores to serve as “closed” encapsulation cavities, is still lacking. A novel approach, combining a micro- to mesoscale poro-analysis model with a multiscale/multiphysics approach, along with a microstructural response, moisture diffusivity, phase change and thermal analysis, will be developed as next step of the current research.

ACKNOWLEDGEMENTS

The authors are grateful to the Hochschulrechenzentrum (HRZ) of TU-Darmstadt for its important support on performing calculations for this research which were partially conducted on the Lichtenberg high performance computer. The first author wishes to acknowledge the Alexander von Humboldt-Foundation for funding his position at the WiB – TU Darmstadt under the research grant ITA-1185040-HFST-P (2CENENRGY project). Finally, the support to networking activities provided by the SUPERCONCRETE Project (H2020-MSCA-RISE-2014 n 645704; <http://www.superconcrete-h2020.unisa.it/>) funded by the EU is gratefully acknowledged.

REFERENCES

- [1] Aidan, R. and Kinnane, O. The impact of thermal mass on building energy consumption, *Applied Energy* (2017) 198:108-121.
- [2] Ricklefs, A., Thiele, A. M., Falzone, G., Sant, G. and Pilon, L. Thermal conductivity of cementitious composites containing microencapsulated phase change materials. *International journal of heat and mass transfer*, (2017) 104:71-82.
- [3] Devaux, P. and Farid, M.M. Benefits of PCM underfloor heating with PCM wallboards for space heating in winter., *Applied energy*, (2017) 191:593-602.
- [4] Shadnia, R., Zhang, L. and Li, P. Experimental study of geopolymer mortar with incorporated PCM., *Construction and building materials*, (2015) 84:95-102.
- [5] Niall, D., Kinnane, O., West, R. P. and McCormack, S. Mechanical and thermal evaluation of different types of PCM–concrete composite panels., *Journal of Structural Integrity and Maintenance*, (2017) 2(2):100-108.
- [6] Kim, Y. R., Khil, B. S., Jang, S. J., Choi, W. C. and Yun, H. D. Effect of barium-based phase change material (PCM) to control the heat of hydration on the mechanical properties of mass concrete., *Thermochimica Acta*, (2015) 613:100-107.
- [7] Crank, J, *Free and Moving Boundary Problems*, (Clarendon, Oxford, 1984).
- [8] Eyres, N. R., Hartree, D. R., Ingham, J., Jackson, R., Sarjant, R. J. and Wagstaff, J. B. The calculation of variable heat flow in solids., *Philosophical Transactions of the Royal Society of London. Series A, Mathematical and Physical Sciences*, (1946) 240(813):1-57.
- [9] Lynch, D. R. and O'Neill, K. Continuously deforming finite elements for the solution of parabolic problems, with and without phase change., *International Journal for Numerical Methods in Engineering*, (1981) 17(1):81-96.
- [10] Udaykumar, H. S., Mittal, R. and Shyy, W. Computation of solid–liquid phase fronts in the sharp interface limit on fixed grids. *Journal of computational physics*, (1999) 153(2):535-574.
- [11] Šavija, B. and Schlangen, E. Use of phase change materials (PCMs) to mitigate early age thermal cracking in concrete: Theoretical considerations., *Construction and Building Materials*, (2016) 126:332-344.
- [12] Thiele, A. M., Wei, Z., Falzone, G., Young, B. A., Neithalath, N., Sant, G. and Pilon, L. Figure of merit for the thermal performance of cementitious composites containing phase change materials., *Cement and Concrete Composites*, (2016) 65:214-226.

- [13] Rostamizadeh, M., Khanlarkhani, M. and Sadrameli, S. M. Simulation of energy storage system with phase change material (PCM)., *Energy and Buildings*, (2012) 49:419-422.
- [14] Fachinotti, V. D., Cardona, A. and Huespe, A. E. A fast convergent and accurate temperature model for phase-change heat conduction., *International Journal for Numerical Methods in Engineering*, (1999) 44(12):1863-1884.
- [15] Heim, D. and Clarke, J. A. Numerical modelling and thermal simulation of PCM–gypsum composites with ESP-r., *Energy and buildings*, (2004) 36(8):795-805.
- [16] Tittlein, P., Gibout, S., Franquet, E., Johannes, K., Zalewski, L., Kuznik, F., ... and David, D. Simulation of the thermal and energy behaviour of a composite material containing encapsulated-PCM: Influence of the thermodynamical modelling., *Applied Energy*, (2015) 140:269-274.
- [17] Aguayo, M., Das, S., Castro, C., Kabay, N., Sant, G. and Neithalath, N. Porous inclusions as hosts for phase change materials in cementitious composites: Characterization, thermal performance, and analytical models., *Construction and Building Materials*, (2017) 134:574-584.
- [18] BASF, Datenblatt Micronal PCM DS 5038 X, (11/2013).
- [19] EN 196-1, Methods of Testing Cement – Part 1: Determination of Strength, (2005).
- [20] Mankel, C., Caggiano, A., Stolze, J., Guardia, C. and Koenders, E.A.B., Thermal Characterization of Porous Cement Paste Systems Containing Microencapsulated Phase Change Materials (MPCM), In RILEM-week 2018, 26-29 August 2018, Delft, the Netherlands.
- [21] Van Breugel, K. Simulation of hydration and formation of structure in hardening cement-based materials, PhD-thesis, Delft University of Technology, Delft, The Netherlands (1991).
- [22] Ukrainczyk, N. and Koenders, E.A.B., Representative elementary volumes for 3D modeling of mass transport in cementitious materials, *Modelling and Simulation in Materials Science and Engineering*, (2014) 22(3):035001.
- [23] Gitman, I.M., Gitman, M.B., and Askes H. Quantification of stochastically stable representative volumes for random heterogeneous materials. *Arch. Appl. Mech.*, (2006) 75:79-92.
- [24] Zhang, M.Z., Ye G., and van Breugel K. A numerical–statistical approach to determining the representative elementary volume (REV) of cement paste for measuring diffusivity, *Mater. de Construcc.* (2010) 300:7-20.

Analysis of Multi-crack Problems by FEM-SFBEM Coupling Method

Keming Cai^{*}, Cheng Su^{**}, Zhi Xu^{***}, Xueming Fan^{****}

^{*}South China University of Technology, ^{**}South China University of Technology, ^{***}South China University of Technology, ^{****}South China University of Technology

ABSTRACT

The computational efficiency for analysis of stress intensity factors of multi-crack problems is still an important issue in fracture mechanics. The formulation of a super element with a single crack embedded in is first developed using the spline fictitious boundary element method (SFBEM) based on the Erdogan's solutions corresponding to an infinite plane with a single crack. The super elements are then incorporated into the finite element mesh to simulate the behaviour of the multiple crack zones in a plate structure, while the other zones without cracks are modelled using the traditional finite elements. The proposed FEM-SFBEM coupling method is further applied to the analysis of stress intensity factors of multi-crack problems, in which the computational accuracy and efficiency of the present approach is demonstrated.

Hermite Spectral Method for the Homogeneous Boltzmann Equation

Zhenning Cai*, Yanli Wang**

*National University of Singapore, **Peking University

ABSTRACT

The Boltzmann equation is the fundamental mathematical model in the gas kinetic theory. However, solving Boltzmann equation numerically is expensive due to its high dimensionality and its complicated collision term. In this work, we focus on the numerical discretization of the collision term, especially for the inverse-power-law model, and we propose a Hermite spectral method to approximate it. This method can also be generalized to a modeling tool for the collision operator. Using this tool, we can generate affordable models which are much more accurate than the BGK-type models. The new models and the numerical methods keep the conservation of mass, momentum and energy exactly, and they are very efficient in capturing the lower order moments. Even for discontinuous distribution functions, the evolution of the stress tensor and the heat flux can be accurately approximated. A number of numerical experiments are carried out to verify the efficiency of this method.

Quantifying Incertitude in Astrophysical Simulation Codes

Alan Calder^{*}, Melissa Hoffman^{**}, Donald Donald^{***}, Maximilian Katz^{****}, Douglas Swesty^{*****},
Scott Ferson^{*****}

^{*}Stony Brook University, ^{**}NRAO, ^{***}Stony Brook University, ^{****}NVIDIA Corporation, ^{*****}Stony Brook University,
^{*****}University of Liverpool

ABSTRACT

We present a study addressing the treatment of incertitude, that is, epistemic uncertainty, in input parameters in astrophysical simulations. We look at the propagation of incertitude in control parameters for stellar winds in simulations performed with the MESA stellar evolution code. We apply two methods of incertitude propagation, the Cauchy Deviates method and the Quadratic Response Surface method, to quantify the output uncertainty in white dwarf stars, the endpoint of stellar evolution for low-mass stars. The methodology we apply is applicable to the problem of propagating input incertitudes through any simulation code treated as a “black box,” i.e. a code for which the algorithmic details are either inaccessible or prohibitively complicated. We have made the tools developed for this study freely available to the research community. This work was supported in part by the US Department of Energy under grant DE-FG02-87ER40317.

Modelling the Biomechanics of the Eye after Strabismus Surgery

Begoña Calvo*, Jorge Grasa**

*University of Zaragoza, **University of Zaragoza

ABSTRACT

In this work, a finite element model is presented to reach a better understanding of the eye biomechanics when subjected to strabismus surgery. During this procedure, the point of action of the extraocular muscle is changed using an adjustable suture to align properly the eyeball. Using MRI images from an animal model (New Zealand rabbit) the contours of the eyeball and muscles were segmented semi-automatically using a software application. After certain manipulation of the volumes, a 3D finite element mesh was developed and based on animal dissections, the approximate size of tendons was determined for the extraocular muscles. Active and passive behaviour of these tissues were considered using a previous muscle model with a transversely isotropic formulation in finite strains. The direction of muscle fibres that was required for the hyperelastic constitutive law was also determined from the muscle samples. The parameters needed to define both active and passive behaviour were determined experimentally using a custom made experimental protocol previously developed. Computational simulations showed how the relative position of the muscles modifies the biomechanical behaviour of the eye ball and also muscle activation levels to perform certain movements. The computational simulation could provide assistance to surgeons to decide the appropriate location of insertion points before surgery.

3D Modeling of Amoeboid Motility through Complex Environment

Eric Campbell*, Prosenjit Bagchi**

*Rutgers University, **Rutgers University

ABSTRACT

Amoeboid motility refers to a specific form of motility in which cells move by extending finger-like membrane-protrusions that are generally known as pseudopods. This form of motility is commonly observed in single-celled organisms known as amoeba. It is also observed in neutrophils, epithelial cells, embryonic cells, and in certain types of metastatic cancer cells. Amoeboid motility is a complex and multiscale process with a strong coupling between nano-scale protein biochemistry, cell deformation, and cytoplasmic and extra-cellular fluid motion. For metastatic cells, migration occurs in a 3D environment through the extra-cellular matrix (ECM) resulting in a strong interaction with the surrounding tissue. Amoeboid migration of metastatic cells, however, does not require a strong adhesion, and ECM degradation or remodeling. Instead, cells squeeze through the existing pores of the ECM. The microstructural details of the ECM as well as the deformability of the cells are expected to affect the migration behavior. To understand the coupling between cell deformability and ECM microstructure during 3D cell motility, we have developed a multiscale fully 3D computational model of amoeboid motility through complex tissue scaffolds. The methodology couples a coarse-grain model for biochemistry with cell deformation, pseudopod dynamics, cytoplasmic and extracellular flows, and ECM microstructure. We follow a continuum approach wherein the cell is modeled as a viscous liquid surrounded by viscoelastic membrane. The membrane resists deformation against area dilation, bending and shearing deformation, and the membrane stresses are obtained using a finite-element model. The intra- and extra-cellular flows are obtained following the Stokes equations that are solved by finite-volume methods. The protein biochemistry leading to the protrusive force causing pseudopod generation is coarse-grained using a dynamic pattern formation model wherein nonlinear reaction-diffusion equations are solved for activator and inhibitors using a finite-element method. The different components of the model are seamlessly integrated using the continuous forcing immersed boundary method (IBM). The microstructures of the ECM are also modeled as immersed objects, but using a sharp-interface (ghost-node) IBM. The predicted shapes of the migrating cells in unbounded medium show remarkable similarity with experimentally observed shapes of Dicty. Our simulations predict that the cell speed increases with increasing deformability, but decreases with increasing confinement. We find that the number of pseudopods increases and the pseudopods become more increasingly confined at the front of the cells with increasing deformability. This mechanism allows the cell to achieve a persistent unidirectional motion even in absence of any external cues.

Mechanics and Applications of Soft Materials -from Tunable Surfaces to Emerging Electronics to Medical Devices

Changyong Cao*

*Michigan State University

ABSTRACT

Soft materials, such as polymers, foams and hydrogels, can deform easily and to very large strains. Their shapes and sizes can vary greatly even if the applied forces are small. Different from the “hard materials” like steel and concrete, soft materials have very different and unique properties, which may have potential applications in various fields but have been much less explored. This offers people great opportunities for making breakthrough discoveries and inventions in engineering and medicine. The mechanical instabilities of hybrid (soft and hard) materials result in self-organized patterns and drastic changes in morphology, which may lead to unprecedented functions of materials, structures and devices. I will first describe how to use numerical and experimental methods to identify the instability modes and the scaling laws for generating desired tunable surface patterns. Then, I will demonstrate how to harness mechanical instabilities and large deformations from soft materials to develop stretchable supercapacitors and novel medical devices. Also, I will demonstrate how we combine the mechanics principle with additive manufacturing to fabricate robust electronics and energy-storage devices.

A Smooth Finite Element Method Based on Bivariate Simplex Splines on Triangle Configurations

Juan Cao^{*}, Zhonggui Chen^{**}, Xiaodong Wei^{***}, Yongjie (Jessica) Zhang^{****}

^{*}Xiamen University, China, ^{**}Xiamen University, China, ^{***}Carnegie Mellon University, USA, ^{****}Carnegie Mellon University, USA

ABSTRACT

Recently, a new bivariate simplex spline scheme based on triangle configurations has been introduced into the geometric computing community. It defines a complete bivariate spline space that retains many attractive theoretic properties of classical B-splines, e.g., it provides inbuilt C^{n-1} continuity across the triangle edges. In this study, we propose a framework for finite element analysis using bivariate simplex splines defined on triangle configurations and investigate its performances by conducting numerical tests on well-known benchmark cases. Within the present framework, the centroidal Voronoi tessellation method is used to generate knots on the domain. Then, knot subsets are carefully selected by a locally computed triangulation, on which shape functions are recursively computed. To achieve high-precision numerical integration, triangle faces served as background integration cells in weak formulations are obtained by triangulating the entire domain restricted to all knot-lines. Various numerical examples are carried out to numerically demonstrate the efficacy/stability and optimal convergence of the proposed method.

Stochastic Multiscale Modeling of Heterogeneous Materials

Le Cao*

*Ph.D. Student, Department of Civil Engineering, College of Engineering, University of Kentucky

ABSTRACT

Mechanical properties are varied with material heterogeneity at multiple length scales. The research aims to investigate the stochastic heterogeneous material response and progressive failure of the functionally graded lattice truss microstructures, associated with topological optimization of the fabricated architecture. Lattice truss microstructures are designed with large degrees of static indeterminacy, which may have little reserve capacity to tolerate abnormal loading conditions. Progressive failure mechanism can be triggered by the loss or reduction of the load-carrying capacity of a small portion of the entire material structure due to an applied abnormal load. Following the initial local damage, a propagation of disproportionate collapse could be spread. The colossal computation was needed traditionally to discretize the domain in finite element method, to study the heterogeneous material behavior. In multiscale modeling, the representative volume elements (RVE) at the microscale and their assembly construct the heterogeneity of a functionally graded material at the macro scale. Stochastic analysis is developed with varied microstructural member sizes and the optimal topology. The optimization is attempted in a two-dimensional domain for the cross-sections of a representative volume element (RVE). Material structure is optimized against the instability, which includes the nonlinear structural behavior. Homogenization evolution is investigated to analyze a large variety of the heterogeneous lattice truss microstructures. The results are examined with the complete structural modeling in finite element simulation. Constitutive behavior of RVE is investigated with some oscillation in both elastic and inelastic regimes. In the stochastic multiscale analysis, a probabilistic-based approach is developed in the inelastic regime, whereas the material response in the elastic regime is expected to be deterministic based on the literature in previous studies ([1], [2]). The results are mapped into a spectrum with respect to the parameters in topology optimization. Furthermore, a functionally graded material with lattice truss microstructures also likely fails due to the fracture of microstructural members. The progressive failure mechanism develops associated with internal force redistribution. The modeling technique is discussed to simulate the material failure. The effect on the failure mechanism by the uncertainty of material parameters is investigated as well.

References: [1] Graham-Brady, Lori (2017). Inelastic Homogenization of Heterogeneous Media: Case Studies for Probabilistic Analysis, Engineering Mechanics Institute (EMI) Conference 2017, ASCE, San Diego, California, June 2017 [2] Blandford, George (1996). Large Deformation Analysis of Inelastic Space Truss Structure, Journal of Structural Engineering, ASCE, vol.122, no.4, pp.407-415

Understanding the Mechanisms of Amorphous Plasticity through Molecular Simulation: Shear Flow, Slip Avalanches, and Creep

Penghui Cao^{*}, Michael Short^{**}, Sidney Yip^{***}

^{*}MIT, ^{**}MIT, ^{***}MIT

ABSTRACT

Using a meta-dynamics method of sampling activated state pathways we study three related rheological responses of a model metallic glass at experimental strain-rate levels beyond the reach of traditional molecular dynamics simulations. The problems are (1) transition from Newtonian (homogeneous) to inhomogeneous (shear localized) flow, (2) discrete stress relaxation (slip avalanches) in the onset of yielding and subsequent strain evolution, and (3) stress effects on creep rate [1]. In (1) we find an intermediate regime with characteristically strong spatial and temporal fluctuations. This points to a strain-rate mediated mechanism that acts to bridge the regime of homogeneous flow observed experimentally at low strain rates and high temperature [2] with the regime of shear-band flow probed by molecular dynamics simulation at high strain rates and low temperature [3]. In (2) we quantify the yielding response and the role of major and minor avalanches in sustaining serrated plastic deformation. In the case of deformation under a constant stress, problem (3), we demonstrate a nonlinear interplay between non-affine atomic displacement and cooperative shear transformation distortion of local atomic clusters that provides a molecular explanation of the familiar behavior of creep-rate upturn beyond a stress threshold, as well as a mechanism map delineating the effects of stress and temperature [1]. Collectively these findings lead to an understanding of the elementary processes governing deformation and flow of disordered materials and the effects of thermal and stress activations. In an overall interpretation based on the concept of potential-energy landscape, we discuss the relevance of the mechanism models of F. Spaepen and A. S. Argon, and how the present simulation results can inform and thus help unify various existing theoretical descriptions, such as the theory of shear transformation zone (STZ), extended mode-coupling theory (e-MCT), mean-field theory with weakening mechanism, and concepts of self-organized criticality for slowly driven, interaction dominated threshold systems. References: [1] P. Cao, M. P. Short, S. Yip, Proc. National Acad. Sci. 114, 13631 (2017). [2] J. Lu, G. Ravichandran, W. L. Johnson, Acta Met. 51, 3429 (2003). [3] J. Chattoraj, C. Caroli, A. Lemaitre, Phys. Rev. Lett. 105, 266001 (2010).

Coupling Effects on Cylindrical Fuel Bundles Under Axial Flow: Theory and Experiments

Roberto Capanna*, Guillaume Ricciardi**, Christophe Eloy***, Emmanuelle Sarrouy****

*CEA Cadarache, St Paul les Durance, France, **CEA Cadarache, St Paul les Durance, France;, ***Institute de Recherche sur les Phénomènes Hors Equilibre (IRPHE), Marseille, France, ****Laboratoire de Mécanique et d'Acoustique (LMA), Marseille, France

ABSTRACT

The safety of a nuclear power plant subjected to earthquakes is a major concern of the nuclear industry. Efficient modelling and accurate knowledge of the mechanical behaviour of the reactor core is therefore needed to estimate the effects of seismic excitation on a nuclear power plant. Fuel assemblies (in the reactor core) are subjected to an axial water flow, which strongly modifies the dynamical behaviour of the fuel assemblies; therefore the identification of the fluid forces is very important. In this work is presented a model for the fluid-structure interaction forces developed using the potential flow theory and considering the structure as an Euler Bernoulli beam. The flow is thus described only using one scalar function (velocity potential) instead of a vector field. This assumption strongly simplifies the fluid mechanics equations, avoiding the necessity to solve Navier-Stokes equations. The model is implemented in a Finite Element Software and pressure distribution around cylinders is solved. The empirical model is compared to reference works in literature for validation. Several simulations are run for multi-cylinder geometries in order to evaluate the influence of different parameters like the distance between cylinder, the excitation mode and the presence of symmetries in the geometry. Furthermore, in this work an experimental approach is considered. Tests are performed on an experimental mock-up made of 4 fuel assemblies (half scale) under an axial water flow. One of the fuel assemblies is excited with a hydraulic jack and the displacements on all of them are then measured. On this work we focus on the effects induced on non-excited assemblies due to the presence of water between the cylinder. The water, in fact, creates coupling between different assemblies which are not in contact each other. In the final part of this paper experimental results and numerical simulations based on the model presented before will be compared. We will outline the capability of this simple model to describe added mass effects and we will present the differences between the theoretical model and experimental results. The analysis of the discrepancies will be useful for understanding the limits of this model and to look for further improvement, as for instance adding a viscosity empirical factor into the model.

Patient-specific Simulations for Planning Treatment of Congenital Heart Diseases: A Single Centre Translational Experience

Claudio Capelli^{*}, Emilie Sauvage^{**}, Giorgia Maria Bosi^{***}, Stephane Couvreur^{****}, Benedetta Biffi^{*****}, Silvia Schievano^{*****}, Andrew Taylor^{*****}

^{*}UCL Institute of Cardiovascular Science & Great Ormond Street Hospital for Children, NHS Foundation Trust, London, UK, ^{**}UCL Institute of Cardiovascular Science & Great Ormond Street Hospital for Children, NHS Foundation Trust, London, UK, ^{***}UCL Mechanical Engineering, ^{****}UCL Institute of Cardiovascular Science & Great Ormond Street Hospital for Children, NHS Foundation Trust, London, UK, ^{*****}UCL Dept of Med Phys & Biomedical Eng, ^{*****}UCL Institute of Cardiovascular Science & Great Ormond Street Hospital for Children, NHS Foundation Trust, London, UK, ^{*****}UCL Institute of Cardiovascular Science & Great Ormond Street Hospital for Children, NHS Foundation Trust, London, UK

ABSTRACT

Patient-specific computational models have been extensively developed over the last decade and applied to investigate a wide range of the cardiovascular mechanics. Modelling can also offer support to personalized and predictive medicine. Such vision could be particularly suitable to face the wide variety of congenital heart disease (CHD). The translation of these technologies into clinical applications, however, is still far from becoming a standard of care in clinical practice and currently limited to few single cases. This study reports the experience of a single clinical and engineering centre, based in the main UK children hospital, which has been involved in the development of a modelling framework that allows the use of realistic simulations to prospectively support clinical decisions. A cohort of CHD patients (n=18) who were referred for percutaneous pulmonary valve implantation (PPVI), stenting of aortic coarctation (CoA) and repair of double outlet right ventricle (DORV) was included in this study. Image data routinely acquired for clinical assessment (MRI, CT, echocardiography, x-ray) were postprocessed to set up patient-specific models. Finite element analyses (FEA) and computational fluid-dynamics (CFD) were performed to predict structural and haemodynamic changes following the procedures. Simulations were carried out to: select the best-matching device for each anatomy; address the risks of spatial interference with surrounding structures; optimize size and positions of device; design a surgical patch. The results were presented during clinical unit's multidisciplinary meeting. Measurable clinical outcomes from the real procedures were compared with the computer model predictions. The numerical results of FEA and CFD analyses were in accordance with the delivered treatment in all cases except in one case of PPVI. When devices were implanted, the post-procedural fluoroscopy images confirmed correct sizing and positioning of the stent in PPVI and CoA cases with an average difference in the stent sizes of 1.2 and 0.8 mm, respectively. Pressure and velocity data acquired by transthoracic echocardiography showed agreement with the results calculated with CFD analyses for CoA stenting and DORV repairs with a max error less than 3 mmHg. Each computational framework process was completed within a week with no requirements for additional clinical data. The early results of using computer simulations in clinics seem to be promising in terms of reliability of the simulations, response time, and usefulness in clinical practice. The translation of these technologies is crucial as it can limit the procedural risks for treatment of CHD cases.

Uncertain Quantification for Nonlinear Structural Dynamical Systems

Evangeline Capiez-Lernout*

*Université Paris-Est

ABSTRACT

This work is devoted to a research synthesis regarding advanced computational methodologies for structural and elasto-acoustic dynamical systems. It is about improving the modeling by considering two realistic phenomena that are the nonlinear geometrical effects and the uncertainty propagation on the dynamical response. The nonlinear geometrical effects are linked to the possibility for the mechanical system to be subjected to high-amplitude vibrational motion. In this context, it is relevant to consider exceptional operating regime as out of linear range regime. Moreover, the structural complexity of industrial systems put in evidence quantified uncertainties for input parameters and also a lack of knowledge in the nature of uncertainties. A special care in the probabilistic modeling has to be taken for analyzing how uncertainty propagates through the dynamical response of the system. The consideration of both phenomena is of particular importance because the nonlinear geometrical effects act as an internal excitation outside of the excitation range, yielding unexpected resonances that can potentially be sensitive to uncertainties. Then, a supplementary methodological constraint is required. It consists in adapting the computational strategy for the case of large-scale computational models, representing complex sensitive systems that can be found in the aeronautic or aerospace context. Consequently, efficient nonlinear reduced-order models have to be constructed in order to limit the computational costs. The main theoretical steps of the present strategy are first summarized, from the construction of the stochastic nonlinear reduced-order model to its numerical resolution [1]. The nonparametric probabilistic approach is used for implementing the uncertainties [2]. Note that the explicit construction of each linear, quadratic and cubic term operators issued from the mean nonlinear reduced-order model has to be considered when uncertainty is implemented from these reduced operators. On the contrary, the stochastic nonlinear reduced internal efforts are directly constructed when uncertainty is implemented from a chosen reduced-order basis. A large panel of computational applications resulting from several academic, military and industrial collaborations is then presented. It concerns as well as the uncertain post-buckling behavior of cylindrical shells, as the intentional and unintentional turbomachinery mistuning, as the sloshing instability of the liquid surface of an aerospace tank. [1] Capiez-Lernout, E., Soize, C., Mignolet, M.-P., Computational stochastic statics of an uncertain curved structure with geometrical nonlinearity in three-dimensional elasticity, Computational Mechanics, 49(1), 87-97, 2012. [2] Soize, C., Stochastic Models of Uncertainties in Computational Mechanics, Lecture Notes in Engineering Mechanics 2, American Society of Civil Engineers, 2012.

Improving the Diffusive and Dispersive Properties of a Finite-Volume Cartesian Method in Presence of Adaptive Mesh Refinements

Francesco Capizzano*

*CIRA – Italian Aerospace Research Center 81043 Capua (CE), ITALY.

ABSTRACT

Key Words: Fluids; Finite-Volume; Cartesian method; Mesh refinement; Skew-symmetric operator. **ABSTRACT** The on-going effort aimed at developing a finite-volume Cartesian method for scale-resolving turbulent flows is described. In particular, the dissipative and dispersive properties of a discrete convective operator are investigated when applied on meshes with cell-based refinements. A skew-symmetric formulation [1, 2] is used to low the influence of numerical dissipation on the physical one especially when solving highly separated flows. The main objective is to conserve not only momentum and energy but also their quadratic forms as well as mass. In principle, this should enhance the correct evolution of the turbulent kinetic energy in the wake of bluff-bodies. Airframe noise and aero-elastic loads are typical examples in which massively separated flows play an important role. In particular, strong turbulent flows involve a wide range of spatial and temporal scales whose estimate represent a prohibitive task for methods based on Reynolds-Averaged Navier-Stokes (RANS) equations. Indeed, the latter mimic the presence of turbulent scales inside the flow field but do not resolve them. On the contrary, Large Eddy simulations (LES) resolve a significant range of turbulent scales leaving modelled only the smallest ones. The computational effort for LES simulations is, on the other hand, very high and too demanding for complex three-dimensional flows especially at high Reynolds numbers. Here, a hybrid RANS-LES Cartesian method is proposed as a reliable and robust tool for time-accurate simulations of complex flows around three-dimensional bluff-body configurations. A fully automatic and adaptive mesh refinement (AMR) strategy allows the saving of computational resources. An immersed boundary technique is coupled with a wall-model [3] in order to make affordable the study of high Reynolds number flows. Basic one- and two-dimensional studies are carried out in order to test the performance of the scheme at the interface between cells of different size. Indeed, the refined Cartesian meshes are characterized by a fixed cell-size ratio of two and accuracy issues can locally occur. A backward-facing step benchmark is carried out and the results are compared with solutions from body-conforming methods and experimental data.

REFERENCES [1] R. Verstappen, A. Veldman, Symmetry-preserving discretization of turbulent flow, *Journal of Computational Physics*, 187 (2003), 343-368. [2] J. C. Kok, A high-order low-dispersion symmetry-preserving finite-volume method for compressible flow on curvilinear grids, *Flow Turbulence Combustion*, 228 (7) (2009), 6811-6832. [3] F. Capizzano, Coupling a wall diffusion model with an immersed boundary technique, *AIAA Journal*, 54 (2) (2016), 2367-2381.

Simulation of Fretting Problems through an Enrichment-Based Approach

Raphael Cardoso^{*}, David Néron^{**}, Sylvie Pommier^{***}, José Araújo^{****}

^{*}ENS Paris-Saclay / University of Brasilia, ^{**}ENS Paris-Saclay, ^{***}ENS Paris-Saclay, ^{****}University of Brasilia

ABSTRACT

The aim of this work, in collaboration with SAFRAN Aircraft Engines, is to use an enrichment-based approach to perform fretting simulations on coarse meshes. Indeed, contact problems subjected to fretting conditions give rise to high levels of stress concentration nearby the contact surfaces, and most of the times, it requires numerical simulations carried out on relatively fine meshes in the standard FE framework, which makes some industrial applications prohibitive. The main purpose of the present work is to enrich fretting simulations performed on cylinder-on-plane contact configurations (typical use-case in the study of the fretting phenomenon) in an attempt to reduce the computational costs in such cases. The enrichment functions considered in the analysis comes from the fact that the mechanical fields distribution in the neighbourhood of the contact edges in the fretting problems analysed are similar to the ones present close to the crack tip in LEFM problems. Simulations were enriched through the X-FEM. Besides plain fretting and fretting fatigue simulations, the proposed methodology was also tested when gross slip takes place. The first results were encouraging showing that, without considerably loss of accuracy, one can work with meshes up to 10 times coarser than it should be regarding the standard FEM. The use of nonlocal intensity factors, also coming from the crack analogy approach assumed in this study, demonstrated to be good indicators of the contact status (partial/gross slip conditions), with the advantage that those intensity factors can be obtained cheaply and are not strongly sensitive to the mesh refinement. Experimental fretting fatigue tests where analytical solutions are not available were conducted in order to test the applicability of the enrichment technique proposed. In this setting, the stress solutions extracted from the enriched simulations were applied to multiaxial fatigue models in order to predict experimental observations by means of fatigue limit.

Coupling Three-Dimensional Sperm Motility and Calcium Dynamics in a Kirchhoff-Rod Model

Lucia Carichino^{*}, Sarah Olson^{**}

^{*}Worcester Polytechnic Institute, ^{**}Worcester Polytechnic Institute

ABSTRACT

Sperm are navigating in a complex three-dimensional fluid environment in order to achieve egg fertilization. Observed sperm trajectories can vary from planar to quasi-planar, and to helical, depending on the species, on the external fluid properties and on the proximity to oviductal walls. Changes in calcium concentration along the sperm flagellum regulate sperm motility and hyperactivation, characterized by an increased flagellar bend amplitude and beat asymmetry, enabling the sperm to reach and to penetrate the egg. However, the exact mechanisms of how calcium regulates the flagellar beat form are yet unknown and under investigation. We propose a fluid-structure interaction model that couples the three-dimensional motion of the flagellum in a viscous fluid with the calcium dynamics in the flagellum. The flagellum is modeled as a Kirchhoff-rod: an elastic rod where preferred intrinsic curvature and twist are imposed weakly by penalizing the energy functional. Given the low Reynolds number associated with sperm motility, the fluid surrounding the flagellum is modeled as a viscous and incompressible Newtonian fluid using Stokes equations. This fluid-structure interaction problem is solved using the method of regularized Stokeslets. The calcium dynamics are represented as a one-dimensional reaction-diffusion model on the moving flagellum, that accounts for calcium CatSper channels and calcium ATP-ase pumps in the principal piece of the sperm tail, and for a calcium store in the neck. The sperm motility and calcium dynamics are coupled assuming that the sperm flagellum preferred curvature depends on the evolving calcium concentration in time. The model is used to investigate the emergent three-dimensional waveforms and trajectories when coupling calcium and curvature, comparing three cases of preferred trajectories: planar, helical (spiral with equal amplitude in both directions), and quasi-planar (helical with smaller amplitude in one direction). The model results suggest that, given the same material properties of the sperm flagellum, the planar swimmer is faster than the three-dimensional swimmer, and clearly shows a turning motion when calcium coupling is accounted for in the model. Moreover, quasi-planar trajectories case exhibit flagelloid curves, defined as the paths followed by a fixed point on the flagellum, similar to hypotrochoid roulette with four or three singular points, depending on calcium coupling. Similar flagelloid curves have been observed experimentally.

Conservative Model Reduction for Finite-volume Models in CFD

Kevin Carlberg^{*}, Youngsoo Choi^{**}, Syuzanna Sargsyan^{***}

^{*}Sandia National Laboratories, ^{**}Lawrence Livermore National Laboratory, ^{***}HERE Technologies

ABSTRACT

We present a method for model reduction of finite-volume models that guarantees the resulting reduced-order model is conservative, thereby preserving the structure intrinsic to finite-volume discretizations [1]. The proposed reduced-order models associate with optimization problems characterized by (1) a minimum-residual objective function and (2) nonlinear equality constraints that explicitly enforce conservation over subdomains. Conservative Galerkin projection arises from formulating this optimization problem at the time-continuous level, while conservative least-squares Petrov–Galerkin (LSPG) projection associates with a time-discrete formulation. We note that other recent works have also considered ROMs that associate with constrained optimization problems [3, 2], although none are conservative. We equip these approaches with hyper-reduction techniques in the case of nonlinear flux and source terms, and also provide approaches for handling infeasibility. In addition, we perform analyses that include deriving conditions under which conservative Galerkin and conservative LSPG are equivalent, as well as deriving a posteriori error bounds. On a parameterized quasi-1D Euler equation problem, the proposed method not only conserves mass, momentum, and energy globally, but also has significantly lower state-space errors than nonconservative reduced-order models such as standard Galerkin and LSPG projection. References [1] K. Carlberg, Y. Choi, and S. Sargsyan. Conservative model reduction for finite-volume models. arXiv e-print, (1711.11550), 2017. [2] L. Fick, Y. Maday, A. T. Patera, and T. Taddei. A reduced basis technique for long-time unsteady turbulent flows. arXiv preprint arXiv:1710.03569, 2017. [3] R. Zimmermann, A. Vendl, and S. Götz. Reduced-order modeling of steady flows subject to aero- dynamic constraints. AIAA Journal, 52(2), 2014.

Proper Generalized Decomposition in Electrocardiology

Michele Giuliano Carlino^{*}, Simona Perotto^{**}, Alessandro Veneziani^{***}

^{*}University School for Advanced Studies IUSS, ^{**}MOX - Politecnico di Milano, ^{***}Emory University

ABSTRACT

Among model reduction techniques available in the literature, Proper Generalized Decomposition (PGD) [1] seems to be particularly suited to approximate parametric differential problems. In contrast to more popular model reduction techniques, such as the Reduced Basis approach, PGD builds an approximate solution without any a priori knowledge of the full solution. The basic idea of PGD is to consider the parameters of interest as additional independent variables. The consequent augmentation of the problem dimensionality is formally tackled via a classical separation of variables, that is eventually solved by an alternating direction algorithm. This approach guarantees a linear dependence of the computational complexity on the dimension of the problem, with a clear advantage for the efficiency of the procedure. In this presentation, after introducing the basics for a PGD approximation, we explore its application to the Inverse Conductivity Problem (ICP) in cardiac electrophysiology [2]. After introducing the Monodomain equations to model the polarization of the cardiac tissue cells at a macro-scale level, we show how PGD can be employed to estimate the conductivity parameters of the transmembrane electrical potential by minimizing a mismatch functional between sparse potential measures and the numerical solution. The efficient solution of the ICP is critical in clinical settings, for a factual use of computational patient-specific models. Results show that PGD is a promising option also in realistic geometries. References: [1] F. Chinesta, R. Keunings, A. Leygue, The Proper Generalized Decomposition For Advanced Numerical Simulations: A Primer. Springer Science & Business Media, 2013. [2] H. Yang, A. Veneziani, "Estimation of cardiac conductivities in ventricular tissue by a variational approach". In: Inverse Problems 31.11 (2015), p. 115001.

Simulation of Fatigue Crack Growth and Failure Using a Variational Phase-Field Model

Pietro Carrara^{*}, Marreddy Ambati^{**}, Roberto Alessi^{***}, Stefano Vidoli^{****}, Laura De Lorenzis^{*****}

^{*}Technische Universität Braunschweig, Institute of Applied Mechanics, Germany, ^{**}Technische Universität Braunschweig, Institute of Applied Mechanics, Germany, ^{***}Department of Structural and Geotechnical Engineering, SAPIENZA Università di Roma, Italy, ^{****}Department of Structural and Geotechnical Engineering, SAPIENZA Università di Roma, Italy, ^{*****}Technische Universität Braunschweig, Institute of Applied Mechanics, Germany

ABSTRACT

Fatigue is a key phenomenon in mechanics, and is largely responsible for most of structural failure. Despite the significance of the problem, most existing fatigue theories are based on empirical laws that lack of generality and predictive capabilities. Hence, the development of mathematically sound and reliable fatigue models is still an open issue. Recently, Alessi et al. [1] proposed a new variational fatigue phase-field model based on the idea that the fracture toughness is degraded as a suitable internal history variable is accumulated. Such degradation, on turn, is ruled by a suitable dissipation potential which explicitly depends on the strain history. Therein the analysis is limited to a simple case, namely: one-dimensional, linear elasticity, brittle material behavior and symmetric response in tension and compression. This work aims at extending this model to higher dimensions including the unsymmetric response in tension and compression for the evolution of both phase-field and internal history variable, on which the fatigue relies on. The tension-compression splits proposed by Amor et al. [2] and Miehe et al. [3] are adopted. Also, the use of alternative internal history variables is explored highlighting advantages and drawbacks. To show the capability of the proposed model, classical benchmark problems, such as single edge tension/shear test and compact tension (CT) specimen for cyclic loadings are investigated. The effects of load amplitude and fatigue material parameters on the fatigue life are studied. Also, for the CT specimen, the Paris' law curves relating the fatigue crack growth rate obtained numerically (da/dN) vs. the stress intensity factor (dK) deduced by available semi-empirical relationships are presented. It is shown that the model is able to describe all three typical fatigue fracture regimes, namely the fatigue fracture initiation, the stable fatigue crack propagation and the final abrupt fracture stages. [1] R. Alessi, S. Vidoli L. De Lorenzis, A phenomenological approach to fatigue with a variational phase-field model: The one-dimensional case, Engineering Fracture Mechanics, in press (2017). [2] H. Amor, J.J. Marigo, C. Maurini, Regularized formulation of the variational brittle fracture with unilateral contact: Numerical experiments, Journal of the Mechanics and Physics of Solids 57 (2009) 1209-1229. [3] C. Miehe C, F. Welschinger, M. Hofacker, Thermodynamically consistent phase-field models of fracture: variational principles and multi-field FE implementations, International Journal of Numerical Methods in Engineering 83 (2010) 1273-1311.

Thermal Simulation of Additive Manufacturing Processes Using Immersed Multi-level Isogeometric Analysis

Massimo Carraturo^{*}, Ernst Rank^{**}, Stefan Kollmannsberger^{***}, Ferdinando Auricchio^{****},
Alessandro Reali^{*****}

^{*}University Of Pavia, ^{**}Technical University of Munich, ^{***}Technical University of Munich, ^{****}University Of Pavia,
^{*****}University Of Pavia

ABSTRACT

We present the application of an advanced numerical framework, combining isogeometric analysis (IGA) and the finite cell method (FCM) [1] to the simulation of additive manufacturing (AM) processes. The different physics involved in the transient processes (phase transition from powder to liquid and solid) are treated with FCM, an immersed boundary method employing high order shape functions. The idea is to embed the solidified region within a fictitious domain which can be easily discretized by a cartesian grid, whereas the transient geometry of the physical problem is reconstructed only in the integration phase. This approach avoids the generation of a conforming mesh for the evolving domain with very complex shape. In order to exploit the local nature of the problem, in the present work FCM is combined with a multi-level implementation of IGA [2] based on the multi-level Bézier extraction technique and truncated hierarchical B-Splines (THB-splines). This method combines an efficient high order and higher continuous discretization with accurate refinement and coarsening schemes, allowing to localize the computational effort in a small region around the heat affected zone (HAZ). In fact, as shown in [3], it is favourable to choose a spatial discretization of high order together with refinement and de-refinement schemes towards the HAZ. While refinement is rather straightforward, the de-refinement procedure for high order polynomial basis is not trivial. It requires to locally project the solution from a source (fine) mesh onto a target (coarsened) mesh and, furthermore, the target discretization has to address some admissibility requirements to avoid numerical instabilities which can arise during projection. Verification and comparison with standard FEM technologies are obtained by means of analytical reference results, showing the higher approximation capabilities of the presented technology with respect to classical methodologies. Finally, validation results for the presented method are carried out using experimental data. References [1] Parvizian, J., Düster, A. and Rank, E., "Finite Cell Method" in Computational Mechanics, 41(1):121–133, (2007). [2] D'Angella, D., Kollmannsberger, S., Rank, E. and Reali, A., Multi-level Bézier extraction for hierarchical local refinement of Isogeometric Analysis, Computer Methods in Applied Mechanics and Engineering, (2017), <http://dx.doi.org/10.1016/j.cma.2017.08.017>. [3] Kollmannsberger, S., Özcan, A., Carraturo, M., Zander, N. and Rank, E., A hierarchical computational model for moving thermal loads and phase changes with applications to Selective Laser Melting, Computers & Mathematics with Applications, (2017), <https://doi.org/10.1016/j.camwa.2017.11.014>.

Understanding Spatial Adaptation in Cortical Bone and the Driving Mechanical Stimuli

Alessandra Carriero*, Andre Pereira**, Amanda Wilson***, Simone Castagno****, Behzad Javaheri*****, Andrew Pitsillides*****, Massimo Marenzana*****, Sandra Shefelbine*****

*The City College of New York, **Imperial College London, ***Imperial College London, ****Imperial College London, *****Royal Veterinary College, *****Royal Veterinary College, *****Imperial College London, *****Northeastern University

ABSTRACT

Bone is a dynamic tissue and adapts its architecture in response to biological and mechanical factors. However, we still do not understand how the process of bone adaptation is regulated. Particularly, it is still unclear how bone spatially adapts to the applied loads, and what is the mechanical stimulus for adaptation. Spatial regulation of bone mechanoadaptation has been difficult to understand for 1) the challenges to accurately investigate a spatially and temporally varying mechanical field in the bone during loading, and for 2) the difficulty to identify regions of adaptation throughout the bone, when the amount of bone formation was in the order of 10 μ m or less. Here, we use the murine tibial loading model to determine spatial relationships between the mechanical environment and bone formation in the entire tibial cortical bone. We examine both strain and fluid flow dependent stimuli in an experimentally validated finite element model. Regions of bone formation are detected with three-dimensional imaging of fluorochrome labels in a novel slice-and-view technique for cortical bone histomorphometry at high resolution (1.59 μ m). The mechanical stimuli (strain energy density or fluid velocity) are compared visually and quantitatively to regions of bone formation on the tibial endosteal and periosteal surface along the entire cortical bone length. Our results show that (i) in adult (22 weeks old) C57BL6 mouse, bone adapts to loads along its entire length on both the endosteal and periosteal surface, and that (ii) high fluid flow is able to predict formation of bone on both these surfaces, while high strain energy density can predict bone formation only periosteally. Providing clues to the biophysical stimuli to which bone responds, future studies can use this knowledge to develop loading protocols that direct bone adaptation to a specific site in osteopenic bone.

An Immersed Boundary Method and Dynamic LES Finite Element Method for Modeling Internal Combustion Engines

David Carrington*, Jiajia Waters**

*Los Alamos National Laboratory, **Los Alamos National Laboratory

ABSTRACT

A stabilized finite element mass consistent projection method has been developed for modeling turbulent reactive flow in machines with immersed moving parts. The method employs a dynamic Vreman LES where the turbulent or eddy viscosity becomes zero for laminar or fully resolved flow regions; flow regimes and regions where eddy viscosity is expected to vanish. This feature of the Vreman dynamic LES make it ideal for modeling highly unsteady wall-bounded flow. Immersed moving boundaries or moving parts either are actuated through the fluid (valves) or moving the fluid (pistons). The effect of these immersed moving boundaries on the flow is determined with immersed boundary method. A moving marker system determines the location of the immersed boundaries. The effects of these boundary motions are determined through a series of projections along the normal to a surface from the marker's location. The primitive values are determined at element nodes. On the non-fluid side of the intersected element, the primitive values are viewed as no-slip boundary values. On the fluid side of the intersected element, a normal vector is created to the moving surface from the marker's location. Then where that normal intersects neighboring fluid elements, the nearest nodal value in those neighbor fluid elements are projected orthogonally onto the normal vector and a distance to the marker is determined. With this projected value and the value on the moving surface boundary (at its current state) interpolation then provides primitive values at the intersected elements fluid nodes. A 2nd order differencing supplies the properties at these nodes. The immersed boundary method allows for an Eulerian frame for solving the physical model equations, that is, a fixed domain is being used throughout the entire simulation. Many moving boundaries surfaces can easily be simulated at once. Gridding complex systems with many parts is greatly simplified because the moving boundaries are simply represented by triangulated surfaces, in stl format. These surfaces overlay the fluid grid. Therefore, grid generation proceeds without considering the parts making a simply a convex grid for the combustion chamber and ports, something can easily be created automatically. The developed code is the 5th generation of LANL's KIVA software going by the name of KIVA-hpFE. Specifics of these methods as they pertain to the engine modeling along with their application and validation are provided.

Characterizing Slip Network Formation within a Polycrystalline Aggregate during Cyclic Loading Utilizing a Novel Formulation for Representing and Evolving Smooth Lattice Orientation Fields

Robert Carson*, Paul Dawson**

*Cornell University, **Cornell University

ABSTRACT

Cyclic loading of polycrystalline metals result in complex states of intragrain heterogeneous deformation. In cyclic loading, persistent slip bands (PSBs) have been studied since the late 1950s as a mechanism for void and crack formation in fatigued single crystals. Several models exist that offer an explanation for the formation of persistent slip bands. Of these, only a few potentially extend to polycrystalline aggregates, where the manner in which PSBs manifest is unclear [1]. From these models, however, is a recurrent ingredient which is the presence of localized slip. In this presentation, we explore how networks of localized multislip are able to traverse and evolve over a crystal and the aggregate during the first few cyclic loads of a sample. A smooth crystal lattice orientation assumption is imposed upon each crystal in order to allow for these networks to form and cross grain boundaries. First, we present the degree to which these networks are able to form not only across a crystal but also the aggregate. Next, we present how these networks can differ between an equiaxed sample and a sample instantiated from near-field high energy x-ray diffraction data. Finally, we present how various kinematic and diffraction intragrain-heterogeneous metrics [2] can present signs of network formation for a combined near-field and far-field high energy x-ray experiment. [1] J. Man, K. Obrtlík, and J. Polák. Extrusions and intrusions in fatigued metals. Part 1. State of the art and history. *Philosophical Magazine*, 89(16):1295–1336, Jun 2009. [2] Robert Carson, Mark Obstalecki, Matthew Miller, and Paul Dawson. Characterizing heterogeneous intragranular deformations in polycrystalline solids using diffraction-based and mechanics-based metrics. *Modelling and Simulation in Materials Science and Engineering*, 25(5):055008, May 2017.

Topology-Optimized Design of Ceramic Structural Elements for Civil Applications

Josephine Carstensen*, Michal Ganobjak**, Jackson Jewett***

*Massachusetts Institute of Technology, **Massachusetts Institute of Technology, ***Massachusetts Institute of Technology

ABSTRACT

Topology optimization design algorithms have in recent years become increasingly popular for mechanical engineering design; it is especially used in the automotive and aerospace industries. However, the number of gradient based algorithms for civil engineering design applications remain limited. The few existing examples include using topology optimization for conceptional structural design, outrigger-placement in dynamically loaded tall buildings and a handful of algorithms specifically for reinforced concrete design. Most of the world's civil construction makes use of concrete and other ceramic materials. These types of materials can be highly heterogeneous and typically exhibit different strength properties in tension and compression. Topology optimization algorithms have been proposed for both conventional and fiber reinforced concrete design. However, currently no designs have been fabricated and experimentally examined. In this work, we focus on numerically and experimentally examining the performance of plain concrete structures designed with existing topology optimization algorithms. The heterogeneous nature of concrete is simplified as isotropic and the strength difference in tension and compression is accounted for by (i) stress constraints [1] and (ii) neglecting the tensile capacity [2]. For civil applications, there exist many types of conventional low weight structural elements of ceramic materials, such as hollow decks, bricks or cinderblocks. With an increased focus on the energy performance of the built environment, there is renewed interest in design algorithms that can produce novel composite construction elements with combined stiffness and thermal performance. In this work, we suggest a topology optimization algorithm to design climate specific construction modules. In the algorithm, the minimum length scale is controlled through the Heaviside projection method and MMA [3] is used as the gradient-based optimizer. [1] Gaynor, A.T., Guest, J.K. and Moen, C.D. (2013), "Reinforced concrete force visualization and design using bi-linear truss-continua topology optimization", *J Struct Eng*, 139, pp 607-618. [2] Le, C., Norato, J., Bruns, T., Ha, C. and Tortorelli, D. (2010) "Stress-based topology optimization for continua", *Struct Multidisc Optim*, 41, pp 605-620. [3] Svanberg, K. (1987), "The method of moving asymptotes – A new method for structural optimization", *Int J for Numer Meth in Engrg*, 24, pp 359-373.

A Non-linear Finite Volume (NLFV) Method Coupled to a Multidimensional Optimal Order Detection Method (MOOD) for the Numerical Simulation of Oil-water Flows in Petroleum Reservoirs

Darlan Carvalho*, Fernando Licapa**, Marcio Souza***, Paulo Lyra****

*Federal University of Pernambuco, UFPE, **Federal University of Pernambuco, UFPE, ***Federal University of Paraiba, UFPB, ****Federal University of Pernambuco, UFPE

ABSTRACT

In this work, we propose a full finite volume approach to simulate two-phase flows of oil and water in heterogeneous and anisotropic petroleum reservoirs in 2-D. The pressure equation has an elliptic operator with a diffusion coefficient, which is, in general, a heterogeneous full tensor. In the context of petroleum reservoir simulation, failure to satisfy the Discrete Maximum Principle (DMP) or at least failure to produce monotone solutions leads to spurious oscillations in the pressure field that can, for instance, lead to the appearance of spurious gas in regions of the reservoir where the pressure falls erroneously below the bubble point. To solve the pressure equation, we have devised a Non-Linear Finite Volume (NLFV) method. This method provides monotone solutions and it reproduces piecewise linear solutions exactly, even for very distorted polygonal meshes and arbitrary anisotropic permeability tensors [3]. To solve the non-linear hyperbolic saturation equation, we adapt a novel method proposed by [1] called Multidimensional Optimal Order Detection (MOOD). This scheme is radically different from classical high order methods, since it is based on an “a-posteriori” limitation procedure. In short, the MOOD scheme consists in determining an optimal polynomial degree reconstruction for each control volume (CV) at each time step, satisfying some physical restriction, e.g., monotonicity. Then, the candidate solution in all control volumes are rigorously analyzed by the physical criteria. Whenever the physical criteria is violated in the control volume, the latter is marked and this solution is automatically discarded and the degree of the polynomial is decreased until the physical restriction is satisfied in the CV. The performance of the proposed full finite volume formulation is verified by solving some relevant benchmark problems. References [1] Clain, S., Diot, S., & Loubere, R., 2011. A high-order finite volume method for systems of conservation laws Multi-dimensional Optimal Order Detection (MOOD). *Journal of computational Physics* 230.10: 4028-4050. [2] Contreras, F. R. L., Lyra, P. R. M., Souza, M. R. A., & Carvalho, D. K. E., 2016. A cell-centered multipoint flux approximation method with a diamond stencil coupled with a higher order finite volume method for the simulation of oil–water displacements in heterogeneous and anisotropic petroleum reservoirs. *Computers & Fluids* 127: 1-16. [3] Queiroz, LES., Souza, MRA., Contreras, FRL., Lyra, PRM. & Carvalho, DKE. 2014. On the accuracy of a nonlinear finite volume method for the solution of diffusion problems using different interpolations strategies. *Int J Numer Meth Fl*, 74(4):270-291.

A Discontinuous Skeletal Method for Bingham Fluids

Karol Cascavita*, Jérémy Bleier**, Xavier Chateau***, Alexandre Ern****

*Université Paris-Est, CERMICS (ENPC) and INRIA Paris., **NAVIER, UMR 8205, École des Ponts, IFSTTAR, CNRS, UPE., ***NAVIER, UMR 8205, École des Ponts, IFSTTAR, CNRS, UPE., ****Université Paris-Est, CERMICS (ENPC) and INRIA Paris.

ABSTRACT

Keywords: Discontinuous Skeletal methods, Viscoplastic flows, Augmented Lagrangian methods This work is motivated by the growing interest in the simulation of yield stress fluids for civil engineering materials, blood, foams, etc. To this aim, we propose a Discontinuous Skeletal (DiSk) method for the antiplane Bingham model, inspired by the Hybrid-High Order method introduced in [1] for linear elasticity. In particular, we focus on the lowest order case, where discrete velocity unknowns are constant polynomials: one per cell and one per face, and the cells unknowns are eliminated by static condensation. The main advantages are local conservativity and the possibility to use general meshes. We consider the Augmented Lagrangian method to solve the variational inequalities resulting from the discrete Bingham problem. We introduce constant Lagrange multipliers for the velocity gradient in each cell and for its jumps at each face. In comparison to Finite Element Methods, such as the use of Taylor-Hood elements [2], a crucial advantage of DiSk methods is that polytopal meshes are supported. We can exploit their use in performing local mesh adaptation, either locally refining around liquid-solid interfaces or coarsening in the solid regions. Numerical results are presented for circular and square domains and for different Bingham numbers. We show local adaptation can be exploited and the method is shown to capture regions of sharp transition between solid- and fluid-like regimes. References [1] D.A. Di Pietro and A. Ern. A hybrid high-order locking-free method for linear elasticity on general meshes. *Comput. Methods Appl. Mech. Engrg.*, Vol. 283, pp 1-21, 2015. [2] P. Saramito and N. Roquet. An adaptive finite element method for viscoplastic fluid flows in pipes. *Comput. Meth. Appl. Mech. Eng.*, Vol. 190, pp 5391 -5412, 2001.

Some Model Order Reduction Developments at Safran

Fabien Casenave^{*}, Nissrine Akkari^{**}, Christian Rey^{***}

^{*}Safran, ^{**}Safran, ^{***}Safran

ABSTRACT

For the last two years, reduced order models have been developed at Safran on various applications. The nonlinear transient heat equation has been reduced in a context of directional solidification of turbine blades in monocrystalline alloy. The change of phase is modelled by a local maximum of the heat capacity with respect of the temperature, located around the temperature of fusion. The nonlinearity is hyperreduced using the Empirical Interpolation Method (EIM). The translation of the blade out of the oven induces an advection phenomenon in the frame of the blade, known to be poorly reducible. Local (in space) POD basis are used to recover a good speedup, and are observed to improve the stability of the EIM. Life calculation of elasto-visco-plastic materials is critical in design phases to prevent fatigue-induced deterioration of certain parts of aircraft engines. Such computations require the simulation of a large number of cycle loads on large meshes, which is currently a challenge. The POD and the EIM are used to extrapolate the behavior of the material, after some cycles have been computed using the high fidelity model. A nonintrusive model reduction platform is in development for the reduction of solid mechanics computations: starting from displacement snapshots, a mesh of the domain and the knowledge of the loading and the behavior, an in house finite element engine in python and the Zmat behavior law solver are used to carry-out the hyperreduction part of the procedure, instead of modifying the source code of the solver used to generate the snapshots. In some parts of the turbofan, the Large Eddy Simulation (LES) is computed by aircraft engine manufacturers to assess the effects of the turbulence, in particular in the combustion chamber and the injectors. The incompressible Navier-Stokes equations have been reduced using an original stabilization for the POD, based on the construction of modes for the velocity and the gradient of the velocity. To explore different local designs of injectors without recomputing the whole domain, an original procedure based on the computation of local LES and a POD correction on the rest of the domain is proposed. Finally, an original method has been proposed for the nonlinear regression of the solution of parametrized linear systems, making use of the knowledge of the (assumed affine) parametric dependence. This works aimed to add information of the underlying physics to black-box-like regression procedures.

Residual Strength Analysis of Aircraft Structures with a High Performance Computing Code

Eva Casoni^{*}, Adrià Quintanas-Corominas^{**}, Gerard Guillaumet^{***}, Jose Reinoso^{****}

^{*}CASE, Barcelona Supercomputing Center, ^{**}AMADE, University of Girona, ^{***}CASE, Barcelona Supercomputing Center, ^{****}Elasticity and Strength Material group, University of Sevilla

ABSTRACT

The use of laminated composite materials in the aircraft industry increases due to their excellent stiffness-to-weight ratios. Over the time of its service life, some parts of the aircraft are prone to damage up to the final failure. The failure from these materials involves different damage mechanisms and it is complex to predict due to anisotropy of the material. These damage mechanisms can be studied, at different length scales or even from a multi-scale point of view. In general, the mesoscale level is the most suitable and reliable for the prediction of the structural behaviour and the material degradation, but can be prohibitive for large scale structures. A 3D consistent damage model for composite laminates at the mesoscopic length scale is proposed [1]. The onset and growth of damage is based on experimental phenomenology incorporating energetic considerations into the progressive damage evolution. Additionally, the current damage model is used with continuum shell elements, that are specially formulated with the aim of reproducing the full stress state and avoid the locking pathologies inherent in solid elements [2]. The overall framework is implemented in a high-performance multi-physic parallel tool, Alya, a mechanics FE code specifically developed for large-scale massively parallel simulations [3]. The combination of continuum shell elements and the 3D damage model has been demonstrated in a simulation of stringer-stiffened composite panel test and a complex barrel fuselage, which are prone to buckle. The selected examples are a good representation of Alya applicability, because they are highly non-linear and require refined meshes in order to obtain accurate results, thus increasing the computational cost. The numerical predictions are compared to experimental results and the computational efficiency is also analysed. References [1]

A. Quintanas-Corominas, P. Maimi, E. Casoni, J. A. Mayugo, A. Turon, M. Vázquez (2017). A 3D transversally isotropic constitutive model for advanced composites implemented in a high-performance computation code. European Journal of Mechanics A/solids, (submitted) [2] J. Reinoso and A. Blázquez (2016) Application and finite element implementation of 7-parameter shell element for geometrically nonlinear analysis of layered CFRP composites. Composite Structures, 139, 263-276. [3] E. Casoni, A. Jerusalem, C. Samaniego, B. Eguzkitza, P. Lafortune, D. Tjahjanto, X. Sáez, G. Houzeaux and M. Vázquez (2015) Alya: computational solid mechanics for supercomputers. Archives of Computational methods in Engineering, 22 (4), 557-576.

Node-Based Form Finding with Shape-Dependent Target Definition

Michael Caspari^{*}, Paul Steinmann^{**}, Philipp Landkammer^{***}

^{*}Institute of Applied Mechanics, Friedrich-Alexander-Universität Erlangen-Nürnberg (FAU), ^{**}Institute of Applied Mechanics, Friedrich-Alexander-Universität Erlangen-Nürnberg (FAU), ^{***}Institute of Applied Mechanics, Friedrich-Alexander-Universität Erlangen-Nürnberg (FAU)

ABSTRACT

Metal forming processes are distinguished into sheet and bulk metal forming. This classification results from the prevailing stress state of the respective forming operation. The recent sheet-bulk metal forming (SBMF) process, presented in [1], combines the two basic processes into a single more complex process. Within this studies in particular tailored blanks are considered, i.e. semi-finished products are a priori adapted to the intended SBF process. For this purpose, our form finding algorithm is designed to optimize the shape of the semi-finished product, i.e. the material configuration in a forming process. The geometry of the semi-finished product is adapted so that the computed spatial configuration corresponds to a prescribed target spatial configuration. Differences between these two configurations are iteratively minimized. The algorithm works non-invasively, thus there is a strict separation between the form update of the finite element (FE) forming simulation. This separation allows the use of arbitrary commercial FE-solvers. Furthermore, it is possible to optimize structures of high complexity with nonlinear material behavior, contact constraints and large deformations. The basic optimization approach was first introduced by Landkammer and Steinmann [2] and various enhancements have been presented in [3]. The focus of our current work is on the further improvement of the stability and robustness of the optimization algorithm. The latest developments include two major modifications in order to enhance its applicability to real processes. The dependency of the optimized material position of individual nodes on the respective nodes in the target spatial configuration is entirely bypassed by releasing the mesh of the target spatial configuration from that of the FE forming simulation. This is realized by changing the computation of the differences between the computed spatial configuration and the target spatial configuration. In addition, a first step is made to consider manufacturability of the optimization result when manufacturing constraints must be taken into account. The constraint considered here is the available design space for the semi-finished product, which is limited by the material pre-distribution process. References: 1. Merklein, M., Allwood, J., Behrens, B.-A., Brosius, A., Hagenah, H., Kuzman, K., Mori, K., Tekkaya, A., and Weckenmann, A. (2012), „Bulk forming of sheet metal”, CIRP Annals - Manufacturing Technology, 61(2):725-745 2. Landkammer, P. and Steinmann, P. (2016), „A non-invasive heuristic approach to shape optimization in forming”, Computational Mechanics, 57(2):169-191 3. Landkammer, P., Caspari, M., and Steinmann, P. (2017), „Improvements on a non-invasive, parameter-free approach to inverse form finding”, Computational Mechanics, doi:10.1007/s00466-017-1468-2

The Divergence-Conforming Immersed Boundary Method

Hugo Casquero^{*}, Yongjie Jessica Zhang^{**}, Carles Bona-Casas^{***}, Hector Gomez^{****}

^{*}Carnegie Mellon University, ^{**}Carnegie Mellon University, ^{***}Universitat de les Illes Balears, ^{****}Purdue University

ABSTRACT

The divergence-conforming immersed boundary (DCIB) method is presented to tackle a long-standing issue of immersed boundary (IB) numerical methods for fluid-structure interaction, namely, the challenge of accurately imposing the incompressibility constraint at the discrete level [1]. IB methods deal with incompressible visco-elastic solids interacting with incompressible viscous fluids. The DCIB method follows up on our previous works [2-3], where we developed discretizations of the mathematical model proposed by the IB method based on non-uniform rational B-splines (NURBS) and T-splines, respectively. In the DCIB method, the Eulerian velocity-pressure pair is discretized using divergence-conforming B-splines, which leads to inf-sup stable, H^1 -conforming, and pointwise divergence-free Eulerian solutions. The Lagrangian displacement is discretized using NURBS, which enables to robustly handle large mesh distortions. The data transfer needed between Eulerian and Lagrangian descriptions is performed at the quadrature level by using the same spline basis functions that define the computational meshes, conducing to a fully variational formulation, sharper treatment of the fluid-solid interface, and a 0.5 increase in the convergence rate of the Eulerian velocity and the Lagrangian displacement measured in L^2 norm. By combining the generalized-alpha method and a block-iterative solution strategy, the DCIB method results in a fully-implicit discretization, which is key to impose accurately the no-penetration and no-slip conditions at the fluid-solid interface. Various two- and three-dimensional problems are solved to show all the above-mentioned properties of the DCIB method together with mesh-independence studies, comparisons with other methods from the literature, and measurement of convergence rates. The DCIB method leads to completely negligible incompressibility errors at the Eulerian level and various orders of magnitude of increased accuracy at the Lagrangian level compared to other IB methods. Finally, we use the DCIB method to answer open questions in cell-scale blood flow.

REFERENCES 1. H. Casquero, Y. J. Zhang, C. Bona-Casas, L. Dalcin, H. Gomez, Non-body-fitted fluid-structure interaction: Divergence-conforming B-splines, fully-implicit dynamics, and variational formulation, under review, 2018. 2. H. Casquero, C. Bona-Casas, H. Gomez, A NURBS-based immersed methodology for fluid-structure interaction. Computer Methods in Applied Mechanics and Engineering, 284, 943-970, 2015. 3. H. Casquero, L. Liu, C. Bona-Casas, Y. J. Zhang, H. Gomez, A hybrid variational-collocation immersed method for fluid-structure interaction using unstructured T-splines. International Journal for Numerical Methods and Engineering, 105, 855-888, 2016.

An Off-Lattice Hybrid Model for Tissue-Engineered Articular Cartilage

Simone Cassani*, Sarah Olson**

*Worcester Polytechnic Institute, **Worcester Polytechnic Institute

ABSTRACT

Articular cartilage is an avascular connective tissue that covers articular joints in the body to provide: (i) a lubricated smooth surface that allows bones to slide over each other during motion, and (ii) a shock absorbing surface that keeps bones from colliding during moderate and vigorous physical activities. Articular cartilage has a complex structure composed of a dense extracellular matrix (ECM), which includes fluid, a collagen network, and other proteins. Distributed in the matrix there are chondrocytes (cells) that synthesize the building blocks of the ECM. Nutrients and oxygen are provided via diffusion through the gel-like structure of the ECM. Pathologies such as osteoarthritis, injuries and normal wear and tear can cause the erosion and damage of articular cartilage. Due to the limited ability of cartilage to self-repair, tissue engineering represents a promising path towards the treatment of damaged cartilage. Tissue-engineered cartilage is produced in vitro to be implanted at the site of the damaged cartilage to restore its normal functionality. To guarantee a successful outcome, tissue-engineered cartilage must have specific structural and mechanical properties. In this work, a hybrid mathematical model is used to investigate the phenomena of cartilage growth in a tissue-engineered construct to elucidate and clarify the influence of different biological factors and conditions, such as scaffold porosity, nutrient distribution and cell velocity. This hybrid model couples a discrete modeling approach for the chondrocytes, with a continuous approach for the remaining components of the matrix. The chondrocytes are described using an off-lattice cellular automata model that accounts for cell movement, cell division, cell-to-cell contact inhibition and cell death. The cellular movement follows a random motion biased by the local nutrient concentration and the local porosity surrounding the cells. Cell division is modulated by the cellular cycle, and by the availability of nutrient and the level of porosity surrounding the cell. The continuous components of the model, nutrient concentration, scaffold porosity and ECM volume fraction are modeled based on physiological behaviors consistent with the literature. We use the model to investigate the influence of different scaffold properties and cell seeding on the synthesis of new ECM. The insight provided by the model will be used to elucidate some of the outcomes of laboratory experiments involving tissue-engineered articular cartilage.

Grounding System Analysis for Underground Electrical Substations Based on Boundary Element Method

Manuel Casteleiro*, Raquel Guizán**, Fermín Navarrina***, José París****, Ignasi Colominas*****

*Universidade da Coruña, **Universidade da Coruña, ***Universidade da Coruña, ****Universidade da Coruña, *****Universidade da Coruña

ABSTRACT

Electrical substations are essential elements in the electricity supply system. Traditionally, they are industrial units located above ground that require large areas of land for their electrical equipment. However, nowadays, the electricity supply system have experienced an increasing demand for power and power supply and the need to transmit electricity at high voltage levels to the bustling urban centers, since most of electricity customers live and work at cities. Consequently, the construction of new electrical substations located in urban areas, where the free surface is limited and the environmental requirements are more severe, is needed. Thus, the engineers developed the underground electrical substations, which are compact solutions where all electrical equipment is placed underground inside precast concrete enclosures. An essential element in the design of electrical substations is safety. During a fault condition, grounding systems are the devices in charge to ensure the proper functioning of the electrical equipment and the safety of people in the vicinity areas. Since the beginning of electrical substations, empirical formulas and suitable techniques are developed to calculate their parameters for uniform soil models or layered soil structures. However, underground electrical substations represent a finite heterogeneity inside the ground, and so, a specific approach that allows to model this soil structure is necessary. In this work the authors carried out a numerical approach with a realistic approximation to soil structure based on the Boundary Element Method and on the weighted residual methods of Point Collocation and Bubnov-Galerkin Method to design and analyze the grounding grid of underground electrical substations, and to calculate their main parameters, which are the ground resistance, the ground potential rise, and the step, touch and mesh voltage, as well as the voltage distributions. Finally, grounding systems analysis for real underground transformer substations has been done.

Rollover Stability Analysis of a Double-Deck Bus Under Crosswind Effects by Computational Simulation

Hugo Guillermo Castro*, Rodrigo Rafael Paz**, Facundo Del Pin***, Iñaki Caldichouri****

*Instituto de Modelado e Innovación Tecnológica (IMIT-UNNE) - CONICET - UTN Facultad Regional Resistencia,
Livermore Software Technology Corporation (LSTC) - CONICET, *Livermore Software Technology Corporation
(LSTC), ****Livermore Software Technology Corporation (LSTC)

ABSTRACT

Every road vehicle under motion experiences forces and moments caused by different sources, being the wind one of the most important. Historically, several researches (computational and experimental) have dealt with the effects of the wind over road vehicles [1]. Particularly, high sided road vehicles (e.g., double-deck buses) are highly demanded because their passenger transportation capability, being the most used mean of passenger transportation in some countries of Latin America. This type of vehicle have its centre of mass in a relatively high location so in combination with moderate velocities may give rise to rollover instabilities [2]. This scenario is further dangerous when the vehicle motion is developed along a road bend, adding lateral forces due to the centrifugal acceleration effect. In this work, as a typical application of a coupled analysis, an unsteady aerodynamics simulation of a simplified double-deck bus in windy conditions is demonstrated, and the effects of the unsteady aerodynamics on the bus motion are investigated. The obtained results are compared with the results of a conventional quasi-steady analysis. The effects of the aerodynamics clearly indicate the importance of estimating the unsteady aerodynamic forces in a vehicle motion analysis. [1] Fuller, J.; Best, M.; Garret, N.; Passmore, M.; "The importance of unsteady aerodynamics to road vehicle dynamics", Journal of Wind Engineering and Industrial Aerodynamics, 117 pp. 1-10, 2013. [2] Dorigatti, F.; Sterling, M.; Rocchi, D.; Belloli, M.; Quinn, A.D.; Baker, C.J.; Ozkan, E.; "Wind tunnel measurements of crosswind loads on high sided vehicles over long span bridges", Journal of Wind Engineering and Industrial Aerodynamics, 107-108 pp. 214 – 224, 2012.

MODELING AND IDENTIFICATION OF A STOCHASTIC MODEL OF VOCAL FOLDS FOR PRODUCING VOICE SIGNALS WITH PATHOLOGICAL CHARACTERISTICS

E. Cataldo*, C. Soize⁺ and E. Barrientos*

* Universidade Federal Fluminense, Telecommunications Engineering Department and Graduate program in Telecommunications Engineering, Rua Passo da pátria, 156, Inga, Niteroi, RJ, CEP:24210-240 , Brazil

⁺ Université Paris-Est, Laboratoire Modelisation et Simulation Multi Echelle, MSME UMR 8208 CNRS, 5 Bd Descartes, 77454 Marne-La-Vallée, France

Key words: *Voice production, stochastic model, jitter, inverse stochastic problem.*

Abstract. This paper aims to propose a stochastic model, considering three control parameters, to generate jitter based on a deterministic one-mass model for the dynamics of the vocal folds and to identify parameters from the stochastic model taking into account real voice signals experimentally obtained. To solve the corresponding stochastic inverse problem, the cost function used is based on the distance between probability density functions of the random variables associated with the fundamental frequencies obtained by the experimental voices and the simulated ones, and also on the distance between features extracted from the voice signals, simulated and experimental, to calculate jitter. The results obtained show that the model proposed is valid and some samples of voices are synthesized considering the identified parameters for normal and pathological cases.

1 INTRODUCTION

The production of a voiced sound starts when the airflow coming from the lungs is modified into the glottal signal, a quasi-periodic signal after passing through the glottis, where the vocal folds are located. The main examples of voiced sounds are the vowels and this paper is based on their production.

The acoustic pressure signal, after passing by the vocal folds, is filtered and amplified by the vocal tract and then radiated by the mouth originating the voice signal. As the vocal folds displacements are not exactly symmetric the time intervals corresponding to the air pulses of the glottal signal have random fluctuations, called jitter.

The stochastic model proposed here has the origin based on the deterministic model

created by Flanagan and Landgraf [1], known as the first model used to generate voice using a nonlinear one-mass mechanical model. More complete deterministic models were created [2;3;4;5] even considering pathological cases in the vocal folds [6] or stress situation [7] but the idea here is to show that it is possible to generate jitter and voice signal with quality from the primary model considering the stiffness as a stochastic process and, mainly, validate the model proposed identifying parameters solving an statistical inverse problem taking into account experimental normal voices and also with pathological characteristics.

2 PRIMARY DETERMINISTIC MODEL

Figure. 1 illustrates a sketch of the model.

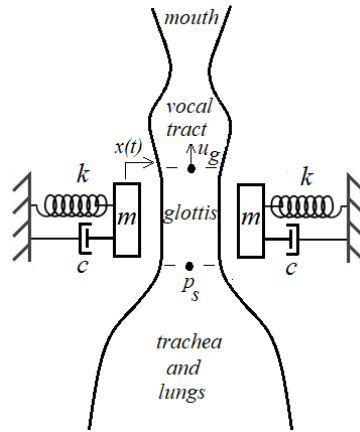


Figure 1: Sketch based on the Flanagan and Landgraf (1968) model.

Each vocal fold is represented by a nonlinear mass-stiffness-damper system and the complete model is composed by the subsystem of the vocal folds (*source*) coupled by the glottal flow to the subsystem of the vocal tract (*filter*). To generate jitter the stiffness will be considered as a stochastic process for which a model is proposed.

3 STOCHASTIC MODELING OF JITTER

The stiffness k is modeled by a stochastic process $\{K(t), t \in \mathbb{R}\}$ with values in \mathbb{R}^+ . Consequently, the dynamical position of each vocal fold will be given by a stochastic process, named $X(t)$, coupled with the stochastic process associated with the glottal flow (volume flow velocity), noted $U_g(t)$. The stochastic dynamics of the vocal folds is described by Eq. 1:

$$m \frac{d^2 X(t)}{dt^2} + \{c + c^*(X(t))\} \frac{dX(t)}{dt} + K(t) X(t) + a_1 p_B(X(t), U_g(t)) = a_2 p_s(t), \quad (1)$$

where $a_1 = 1.87 \frac{\ell d}{2}$ and $a_2 = \frac{\ell d}{2}$, with ℓ the length of each vocal fold and d the vocal fold thickness. The stochastic process $X(t)$ is the displacement of the mass m of one vocal fold, $K(t)$ is its stiffness and c is its damping coefficient when the glottis is opened; when the glottis is closed, there is an additional damping given by $c^*(X(t))$ described in the following, where the Bernoulli pressure $p_B(X(t), U_g(t))$ is also described.

The stochastic process $U_g(t)$ is the acoustic volume velocity through the glottal orifice (the glottal flow). The air pressure that comes from the lungs and forces the vocal folds is called the subglottal pressure and is denoted by $p_s(t)$. The constant parameters have been discussed in the original paper about the corresponding deterministic model¹. Some information about values can also be found in [8].

A representation of non-Gaussian stochastic process $K(t)$ can be constructed using Information Theory as explained in [9]. Following such a construction, we introduce a Gaussian second-order real-valued stochastic process, $Y = \{Y(t), t \in \mathbb{R}\}$, centered, mean-square continuous, stationary and ergodic, physically realizable. A representation of stochastic process K can then be written as

$$K(t) = k_0 + (\underline{k} - k_0)(\underline{y} + Y(t))^2, \quad \forall t \in \mathbb{R}, \quad (2)$$

in which \underline{y} is a parameter (that will be defined later) such that

$$E\{(\underline{y} + Y(t))^2\} = 1, \quad E\{(\underline{y} + Y(t))^4\} < +\infty. \quad (3)$$

The conditions defined by Eq. (3) effectively yields, for all t , $E\{K(t)\} = \underline{k}$ and $E\{K(t)^2\} < +\infty$. Let ω be the angular frequency in *rad/s* and f be the circular

frequency in *Hz* such that $\omega = 2\pi f$. The Gaussian stochastic process Y is constructed as the linear filtering, $Y = h * N_\infty$, of the centered Gaussian white noise N_∞ (generalized stochastic process) whose power spectral density function is written, for all real ω , as

$$S_N(\omega) = \frac{1}{2\pi}, \quad (4)$$

and where $h = \mathcal{F}^{-1}\{H\}$ is the inverse Fourier transform of the complex-valued frequency response function $\omega \mapsto H(\omega)$ that we defined, for all real ω , by

$$H(\omega) = \frac{a}{-\omega^2 + 2i\omega\xi b + b^2}, \quad (5)$$

in which, a , b , and ξ are three positive parameters that will be defined later.

Consequently, the power spectral density function $S_Y(\omega)$ of Gaussian stationary stochastic process Y is written, for all real ω , as

$$S_Y(\omega) = \frac{1}{2\pi} \frac{a^2}{(b^2 - \omega^2)^2 + 4\xi^2 b^2 \omega^2}, \quad a > 0, \quad b > 0, \quad \xi > 0. \quad (6)$$

From Eq. (6), it can be deduced that the mean-square derivative $\{\dot{Y}(t), t \in \mathbb{R}\}$ of stochastic process $\{Y(t), t \in \mathbb{R}\}$ is a second-order stochastic process because $\int_{\mathbb{R}} \omega^2 S_Y(\omega) d\omega < +\infty$.

Let $\{\mathbb{Z}(t) = (Y(t), \dot{Y}(t)), t \geq 0\}$ be the stochastic process with values in \mathbb{R}^2 solution of the following Itô stochastic differential equation,

$$d\mathbb{Z} = [\alpha] \mathbb{Z} dt + \beta dW(t) \quad , \quad t > 0, \quad (7)$$

with the initial condition $\mathbb{Z}(0) = (0, 0)$, in which $\{W(t), t \geq 0\}$ is the real-valued normalized Wiener stochastic process indexed by $[0, +\infty[$, where $[\alpha]$ is the (2×2) real matrix and β is the real vector such that

$$[\alpha] = \begin{bmatrix} 0 & 1 \\ -b^2 & -2\xi b \end{bmatrix} \quad , \quad \beta = \begin{bmatrix} 0 \\ a \end{bmatrix}. \quad (8)$$

It can be proved (see for instance [10]) that Eq. (7) has a unique solution $\{\mathbb{Z}(t), t \geq 0\}$ such that, for $t_0 \rightarrow +\infty$, the stochastic process $\{\mathbb{Z}(t), t \geq t_0\}$ is asymptotically stationary and tends to the stationary Gaussian stochastic process $\{(Y(t), \dot{Y}(t)), t \in \mathbb{R}\}$ in which $Y = h * N_\infty$. The first condition defined by Eq. (3) yields,

$$\underline{y}^2 + \int_{-\infty}^{+\infty} S_Y(\omega) d\omega = 1 \quad \implies \quad \underline{y}^2 = 1 - \frac{a^2}{4\xi b^3}. \quad (9)$$

Consequently, the parameters must satisfied the following conditions,

$$0 < a^2 < 4\xi b^3 \quad , \quad b > 0 \quad , \quad \xi > 0. \quad (10)$$

In order to control the bandwidth of stationary stochastic process Y , we introduce the parameter $\epsilon > 0$ [10] that is defined by

$$\epsilon = \sqrt{1 - \frac{m_2^2}{m_0 m_4}} \quad , \quad m_{2p} = \int_{\mathbb{R}} \omega^{2p} S_Y(\omega) d\omega \quad , \quad p = 0, 1, 2. \quad (11)$$

Parameter ϵ is estimated using the simulated signals and is discussed in the next section. It is important to say that the bandwidth is related to the quality of the synthesized sounds [11] and this is one of the main reasons to introduce it in this paper, discussing the relation between the presence of jitter and the quality of the voice.

4 SIMULATION

The objective of this section is to generate voice signals with jitter using the stochastic model proposed and to analyze the sensitivity of the stochastic model with respect to parameters a , b , and ξ .

As the main idea is to generate jitter, a way to measure it will also be discussed. There are different ways to analyze jitter effects [12]. At first, it is important to define the random variable associated with the duration of the glottal cycle, which is defined as

the duration between two successive times, the first one corresponding to the instant the vocal folds (glottis) opens and the second one the instant when it closes completely. The corresponding random variable will be denoted by T_{fund} . To calculate T_{fund} from $X(t)$, it was used an algorithm based on an implementation of the RAPT pitch tracker [13].

During the simulations, the values of parameters a , b , and ξ , as well as the mean of the fundamental frequency, will vary. All the other parameters will be fixed and their values are $p_s(t) = 800 \text{ Pa}$, $m = 0.24 \times 10^{-2} \text{ kg}$, $c = 346.3 \text{ m/s}$, $k_0 = 40 \text{ N/m}$, $\underline{k} = 115 \text{ N/m}$, $a_1 = 1.87 \ell d/2$ and $a_2 = \ell d/2$, with $\ell = 1.4 \times 10^{-2} \text{ m}$ and $d = 0.3 \times 10^{-2} \text{ m}$. The other parameters that are necessary to produce the sounds, including values related to the vocal tract, are given in (Cataldo and Soize, 2017). In particular, the parameter A_{g0} and the air density ρ are chosen such that $A_{g0} = 0.04 \times 10^{-2} \text{ m}^2$ and $\rho = 0.12 \text{ kg/m}^3$.

The objective of this section is to perform a sensitivity analysis of the parameters in order to better understand how to proceed to solve the inverse problem to identify parameters of the model corresponding to experimental voice which will be discussed further in the paper.

Another important objective of this section is to show that with these three parameters a , b and ξ , there are different possibilities to generate jitter, but also to control the distribution of the fundamental frequency.

Although jitter is a variation of the glottal cycle and consequently this variation is related to the random variable $F_{\text{fund}} = 1/T_{\text{fund}}$, the shape of the curve corresponding to the probability density function of F_{fund} is not so easily controlled with the variation of jitter. It means that, to identify parameters of the model, it is important to minimize the distance between measures of jitter (from simulated and experimental signals) but also distance between probability density functions of F_{fund} (simulated and experimental). So, this section will give the feeling of how to vary the parameters in order to better minimize those distances.

Thirteen cases were simulated. For each case simulated, the corresponding voice signal will be synthesized and available to be heard following the link:

<https://www.dropbox.com/sh/eo49b4usr1n4iz4/AADU8gI-JGWAeWqmxwE5u7nwa?dl=0> .

All the values of the parameters considered and also the value calculated for ε for all the simulations considered are summarized in Tab. 1.

Case	a	c_b	ξ	Relative jitter	ϵ
I	10	1	0.01	0.16%	0.43
II	200	1	0.01	0.32%	0.43
III	600	1	0.01	0.77%	0.43
IV	1200	1	0.01	3.48%	0.43
V	10	1	0.2	0.09%	0.9
VI	600	1	0.2	0.48%	0.9
VII	1800	1	0.2	1.43%	0.9
VIII	3000	1	0.2	2.51%	0.9
IX	10	1	0.5	0.09%	0.96
X	1000	1	0.5	0.80%	0.96
XI	3000	1	0.5	2.23%	0.96
XII	3000	1.5	0.5	0.90%	0.93
XIII	3000	2	0.5	0.64%	0.92

Table 1: Value of bandwidth parameter ε of stationary stochastic process Y for all the simulation cases.

As the idea is to discuss the sensitivity of the parameters with the specific objective of solving the inverse stochastic problem, some of these cases will be selected and the graphs showed and discussed and graphs of the probability density function will be constructed for some cases.

5 STATISTICAL INVERSE PROBLEM

In order to validate the model proposed, parameters a , b , and ξ are identified using experimental voice signals. This identification is carried out by introducing a cost function that is constructed writing that the probability density function associated with the simulated voice is close to the probability density function of the experimental voice and also, the jitter obtained for the simulated voice is close to the jitter of the experimental voice. The four measures of jitter are used. The cost function, denoted by $J_{\text{cost}}(a, b, \xi)$, is then defined by

$$\begin{aligned}
 J_{\text{cost}}(a, b, \xi) = & \frac{1}{2} \text{Dist}_{\text{dens}}(a, b, \xi) + \frac{1}{4} \text{JitterRel}_{\text{dist}}(a, b, \xi) \\
 & + \frac{1}{4} \text{JitterAbs}_{\text{dist}}(a, b, \xi) + \frac{1}{4} \text{JitterRAP}_{\text{dist}}(a, b, \xi) \\
 & + \frac{1}{4} \text{JitterPPQ5}_{\text{dist}}(a, b, \xi),
 \end{aligned} \tag{12}$$

in which, each quantity appearing in the right-hand side member is defined hereinafter.

(i) Let $f \mapsto f_S(f; a, b, \xi)$ be the probability density function on $[0, +\infty[$ of random variable

$F_{\text{fund}}(a, b, \xi)$ associated with the simulated voice and $f \mapsto f_R(f)$ be the probability density function on $[0, +\infty[$ of the random variable associated with the experimental voice. The distance between these two probability density functions is written as

$$Dist_{\text{dens}}(a, b, \xi) = \frac{1}{2} \int_0^{+\infty} |f_S(f; a, b) - f_R(f)| df. \quad (13)$$

The probability density functions are estimated by using the Gaussian kernel estimation method from the nonparametric statistics¹⁴. For each value of (a, b, ξ) , probability density function $f_S(\cdot; a, b, \xi)$ of $F_{\text{fund}}(a, b, \xi)$ is estimated using the realization of the stochastic process corresponding to the glottal flow computed with the stochastic model and probability density function f_R of F_{fund} is estimated using the realization of the experimental glottal signal obtained through a filtering inverse algorithm (PSIAIF) [15] of the experimental voice.

(ii) For each given value of vector (a, b, ξ) , N realizations $\{\theta_k, k = 1, \dots, N\}$ of the voice signal are computed, which allows for computing the jitter quantities. Let $Jitter_{\text{sim}}$ represent one of these four jitter quantities: $JitterRel_{\text{sim}}$, $JitterAbs_{\text{sim}}$, $JitterRAP_{\text{sim}}$, or $JitterPPQ5_{\text{sim}}$. Let $Jitter_{\text{exp}}$ be the jitter calculated with the experimental signal. Then, a distance between $Jitter_{\text{sim}}$ and $Jitter_{\text{exp}}$ can be defined by

$$Jitter_{\text{dist}} = \frac{|Jitter_{\text{sim}} - Jitter_{\text{exp}}|}{Jitter_{\text{exp}}}. \quad (14)$$

The optimal values a^{opt} , b^{opt} , and ξ^{opt} are then computed by solving the following optimization problem,

$$(a^{\text{opt}}, b^{\text{opt}}, \xi^{\text{opt}}) = \arg \min_{(a, b, \xi) \in \mathcal{C}} J_{\text{cost}}(a, b, \xi), \quad (15)$$

in which the admissible set \mathcal{C} is defined, using Eq. (10), by

$$\mathcal{C} = \{(a, b, \xi) \in \mathbb{R}^3 \text{ such that } 0 < a^2 < 4\xi b^3, \quad b > 0, \quad \xi > 0\}. \quad (16)$$

The values of the fixed parameters considered for the corresponding deterministic model are the same as considered for the simulations.

The first case to be taken into account is a voice signal from a woman producing an /e/ vowel. The parameters corresponding to the mean value \underline{k} of K is considered in a way that the mean of the random variable associated with the fundamental frequency simulated is very near of the one for the real voices. Then, the optimal values a^{opt} , b^{opt} and ξ^{opt} of parameters a , b and ξ are identified by solving the optimization problem defined by Eq. (15).

5.1 Algorithm used

- Step 1: From the experimental voice signal obtained with the vowel produced all the values corresponding to the random variable $F_{\text{fund}} = 1/T_{\text{fund}}$ are obtained using the

algorithm (Talkin, 1995) and the probability density function $f \mapsto F_R(f)$ associated is estimated. The mean value of random variable F_{fund} is calculated and is used in the other steps. From this signal, the four measures of jitter are obtained: $JitterRel_{\text{exp}}$, $JitterAbs_{\text{exp}}$, $JitterRAP_{\text{exp}}$, and $JitterPPQ5_{\text{exp}}$.

- Step 2: Using the model proposed, one signal is simulated in a way that the mean of random variable F_{fund} of this signal was near from the mean value calculated in step 1. It is not difficult to generate this signal because there are parameters in the model directly related to the fundamental frequency as, for example, f_p . However, some essays are necessary in order to obtain a mean value near the one wished. At the same time, values for a , b , and ξ have been calculated so that the estimated probability density function of random variable F_{fund} for the simulated voice signal is near from the probability density function estimated in step 1. This step 2 takes some time because it is a step of essays. Values are obtained and they will serve as start for the grid variation of the values of the fundamental frequency and also of the parameters a , b , and ξ , consequently four loops are constructed.
- Step 3: For each value of the fundamental frequency and of the triplet (a, b, ξ) , the Monte Carlo Method is used for the estimation of the probability density functions and the computation of cost function $J_{\text{cost}}(a, b, \xi)$.
- Step 4: The minimum value of the cost function estimated in Step 3 is the objective that has to be reached.

5.2 IDENTIFYING PARAMETERS

5.2.1 The first experimental voice signal considered is a female production of a vowel /e/.

After solving the inverse stochastic problem, the optimal values obtained were: $a^{\text{opt}} = 200$, $b^{\text{opt}} = (1/2)\pi f_p$, $f_p = 200 \text{ Hz}$ and $\xi^{\text{opt}} = 0.9$. Table 2 shows the values of jitter calculated for the experimental voice and for the simulated voice, after solving the inverse problem. The value obtained for the bandwidth parameter is $\epsilon = 0.98$.

Jitter	Experimental	Simulated
<i>JitterRel</i>	0.48%	0.52%
<i>JitterAbs</i>	$2.37e - 05 \text{ s}$	$2.54e - 05 \text{ s}$
<i>JitterRAP</i>	0.26%	0.30%
<i>JitterPPQ5</i>	0.29%	0.32%

Table 2: Jitter values for a female production of a vowel /a/, without pathological characteristics

As we have already discussed, not only the measures of jitter have to be taken into account but also the distance between the probability density functions $f_S(\cdot; a^{\text{opt}}, b^{\text{opt}}, \xi^{\text{opt}})$ and f_R (simulated and experimental) shown in Fig. 2.

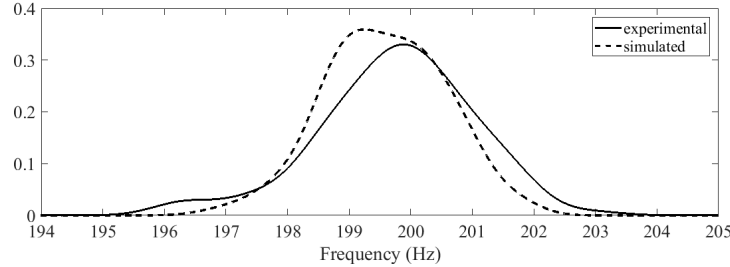


Figure 2: pdf of the random fundamental frequency corresponding to a real voice (solid line) and corresponding to the simulated for the optimal values of the parameters (dotted line) in the case without pathological characteristics.

It is important to say that if the distance between the pdfs was not taken into consideration inside the cost function, the values obtained to the jitter measures would be: $JitterRel = 0.50\%$, $JitterAbs = 2.4404e - 05 s$, $JitterRAP = 0.30\%$ and $JitterPPQ55 = 0.31\%$ and in this case the distance between the pdfs would be a little bit greater.

As a way to verify what happens when a sound is synthesized considering these optimal values of the parameters, a voice signal has been simulated with the optimal values of the parameters. The experimental signal (*exper₁.wav*) and the corresponding optimal simulated one (*simulated₁.wav*), in the same link presented before for all simulations.

5.2.2 The second case considered is a voice signal from a woman with paralysis of the vocal folds.

After solving the inverse stochastic problem, the optimal values obtained were: $a^{\text{opt}} = 1050$, $b^{\text{opt}} = (1.5\pi f_p, f_p = 226 Hz)$ and $\xi^{\text{opt}} = 0.4$. Table 3 shows the values of jitter calculated for the real voice and for the simulated voice, after solving the inverse problem. In this case, the value obtained for the bandwidth parameter is $\epsilon = 0.96$.

Jitter	Experimental	Simulated
<i>JitterRel</i>	3.24%	3.40%
<i>JitterAbs</i>	$1.44e - 04 s$	$1.42e - 04 s$
<i>JitterRAP</i>	2.03%	2.00%
<i>JitterPPQ5</i>	2.05%	2.45%

Table 3: Jitter values for a female production of a vowel /a/, with a pathology

Figure 3 shows probability density functions $f_S(\cdot; a^{\text{opt}}, b^{\text{opt}}, \xi^{\text{opt}})$ and f_R (simulated and experimental). It is important to note the difference between the values obtained for

jitter, but mainly showing that it is possible to solve the inverse stochastic problem even considering a pathological case.

In this case, the pathological one, the results are better for the distance between the values of jitter for the experimental and simulated signals than those obtained for the normal voice.

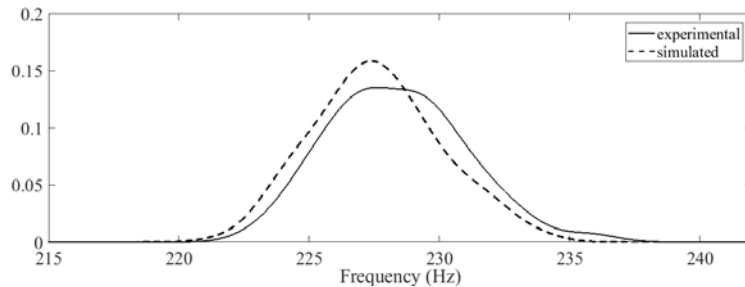


Figure 3: pdf of the random fundamental frequency corresponding to a real voice (solid line) and corresponding to the simulated for the optimal values of the parameters (dotted line) in the case without pathological characteristics.

In the normal case or in the pathological case, the value of ϵ is high. It shows that it is not directly related to the pathology, but to the quality of the synthesized sound.

6 CONCLUSIONS

A stochastic model has been proposed using three control parameters for generating jitter considering a mechanical model for producing voiced sounds. Some pathological cases have been generated and the model has been validated considering an inverse stochastic problem to identify the parameters. With three control parameters more possibilities of different sounds are obtained, including different levels of jitter and, mainly, it is possible to control the quality of the synthesized voice. The inverse stochastic problem solved to identify parameters of the model uses different measures of jitter and also the distance between probability density functions, showing that with more measured features the voices synthesized are more similar of the corresponding experimental voices. The sensitivity analysis performed before was very important to show how to change the jitter and also the distribution of frequencies in order to obtain synthesized voices near experimental voices. A pathological case caused by an unilateral paralysis of the vocal folds has been considered and, even in this case, the parameters of the model has been identified. The bandwidth parameter has been used as a measure of quality of the synthesized voice and it has also been considered when the inverse problem has been solved.

7 ACKNOWLEDGEMENTS

This work was supported by CNPq.

References

- [1] Flanagan, J. and Landgraf, L. Self-oscillating source for vocal-tract synthesizers. *IEEE Transactions on Audio and Electroacoustics* (1968) AU-16, 57–64.
- [2] Ishizaka, K. and Flanagan, J. Synthesis of voiced sounds from a two-mass model of the vocal folds. *Bell Syst. Tech. J.* (1972) 51, 1233–1268.
- [3] Avanzini, F., 2008. Simulation of vocal fold oscillation with a pseudo-one-mass physical model. *Speech Communication*, (2008) 50 (2), 95–108.
- [4] Zhang, Y. and Jiang, J. J. Nonlinear dynamic mechanism of vocal tremor from voice analysis and model simulations. *Journal of Sound and Vibration* (2008) 316 (1–5), 248–262.
- [5] Pinheiro, A. P. and Kerschen, G. Vibrational dynamics of vocal folds using nonlinear normal modes. *Medical Engineering & Physics*, (2013) 35(8), 1079–1088.
- [6] Gunter, H. E. Modeling mechanical stresses as a factor in the etiology of benign vocal fold lesions. *Journal of Biomechanics* (2004) 37 (7), 1119–1124.
- [7] Luzan, C. F., Mihaescu, J. C. M., Khosla, S.M. and Gutmark, E. Computational study of false vocal folds effects on unsteady airflows through static models of the human larynx. *Journal of Biomechanics* (2015) 48 (7), 1248–1257.
- [8] Cataldo, E., Soize, C. Voice signals produced with jitter through a stochastic one-mass mechanical model. *Journal of Voice*, (2017) 31 (1), 111e9–111e18.
- [9] Soize, C. *Uncertainty Quantification - An accelerated Course with Advanced Applications in Computational Engineering*. Interdisciplinary Applied Mathematics Series, Springer, New York, (2017).
- [10] Krée P. and Soize C. *Mathematics of Random Phenomena*. Reidel, Dordrecht, (1986).
- [11] Rabiner, L. and Schafer, R. *Theory and Application of Digital Signal Processing*. Pearson Education, (2011).
- [12] Mongia, P. K. and Sharma, R.K. Estimation and statistical analysis of human voice parameters to investigate the influence of psychological stress and to determine the vocal tract transfer function of an individual. *Journal of Computer Networks and Communications* (2014), 1–17.
- [13] A robust algorithm for pitch tracking (rapt). *Speech coding and synthesis* (1995), 495–518.
- [14] Bowman, A. W. and Azzalini, A. *Applied smoothing techniques for data analysis: The kernel approach with S-Plus illustrations*. Oxford University Press, (1997).
- [15] Glottal wave analysis with pitch synchronous iterative adaptive inverse filtering. *Speech Communication*, (1992) V. 11 (2–3) , 109–118.

A Novel OpenSees Element for FPS Bearings with Breakaway Friction

Sara Cattaneo*, Emanuele Gandelli**, Virginio Quaglini***

*Politecnico di Milano, Department of Architecture, Built Environment and Construction Engineering, **Politecnico di Milano, Department of Architecture, Built Environment and Construction Engineering, ***Politecnico di Milano, Department of Architecture, Built Environment and Construction Engineering

ABSTRACT

The increasing use of sliding bearings with curved surfaces, like the Friction Pendulum System (FPS), as seismic isolator, benefits from the improvement of numerical models that can capture their experimental performance and enhance the predictive capability of nonlinear response history analyses. Among the limits of current models, it is noted that effective implementation of the static coefficient of friction of sliding isolators in object-oriented software for structural analysis has not yet been achieved, and the use of the dynamic friction only for design is a common practice. Furthermore, specific guidance in this respect is missing. The formulation proposed in this study aims at filling this gap, by incorporating in an established numerical framework the change in the coefficient of friction occurring in the transition from the sticking, or pre-sliding phase to the dynamic sliding motion. The proposed model has been coded in the object-oriented finite element software OpenSees by modifying the standard "SingleFPSimple3d" element. The hysteretic force – displacement relationship of the FPS isolator in the horizontal direction is mathematically modelled using the theory of plasticity, while two yield conditions are introduced to switch from the static to the dynamic friction coefficient. Other features of the model are the inclusion of the dependency of the dynamic coefficient of friction on the instantaneous values of axial load and slide velocity at the interface, and the accumulated heat generated from energy dissipation. The primary assumptions in the development of the friction model and the verification of the newly developed element are validated by agreement with available data. A case study relevant to a base-isolated concrete, moment resisting frame helps to demonstrate the improved prediction capability of the new bearing element over its standard counterpart when applied to real situations, such as estimating a +50% increase in isolator displacement, superstructure drift and base shear demand under high intensity earthquakes, and possible non-activation of the sliding isolators under weak or medium intensity earthquakes.

CONTROL OF AN ACTIVE CABLE DOME USING MULTI OBJECTIVE GENETIC ALGORITHMS

STANISLAV KMET PETER CAUNER

*Technical University of Kosice, Faculty of Civil Engineering
Institute of Structural Engineering, Vysokoskolska 4
Kosice, Slovakia
stanislav.kmet@tuke.sk, peter.cauner@tuke.sk

Key words: Cable Dome, Tensegrity, Genetic Algorithm.

Abstract. Control processes of an active Levy cable dome which has the ability to adapt to current loading conditions are presented in the paper. The prototype of Levy cable dome which was developed at the Technical University of Kosice is equipped with sensors and an actuator. Theoretical models in presented numerical studies contain various loading conditions and all vertical compressed members of the studied dome are designed as actuators. The control task is stated as an optimization task where the objective is to reduce excessive displacements and stresses (forces) to acceptable levels with a minimum control effort. Active strut members of the dome can be elongated or contracted modifying internal stress distributions and nodal displacements. Relevant movements of the active struts keep the required reliability (related to serviceability and safety) of the dome subjected to changed loading effects. Multi-objective search is used to select control commands. An appropriate tool for the optimization of the control process is an application of genetic algorithm. Multi-Objective Genetic Algorithm (MOGA) used in Goal Driven Optimization (GDO) as a hybrid variant of the popular Non-dominated Sorted Genetic Algorithm-II (NSGA-II) based on controlled elitism concepts are used in these studies. Initial population, necessary to run the MOGA algorithm, consists of elongations or contractions of the active structural members.

1 INTRODUCTION

Cable domes are lightweight spatial pre-stressed structures that are increasingly investigated as structural solutions for large-span roof systems. The cable dome structures first proposed by Geiger have been developed in recent years due to their innovative forms, lightweight and deployability. They belong to a class of pre-stressed pin-jointed systems that cannot be stable without introducing prestresses to some members [1]. Cable domes are sensitive to asymmetric loads and changes in pre-stress. Active cable systems equipped with sensors and actuators provide shape-control potential that adapts the structure to changing loads and environmental conditions. Structural control is carried out by modifying the prestress state of the cable dome in order to satisfy prescribed reliability criteria due to ultimate and mainly serviceability limit states. Skelton and Sultan (1997) introduced the concept of a controllable tensegrity as a new class of smart structures capable of large displacements [2, 3, 6].

Cable domes have been developed in recent years. The names of Geiger and Levy are associated with these structures (Fig. 1). It is clear that they have been inspired by the tensegrity principle. Two kinds of compressed component can be identified: vertical struts and compressed ring. This last component is on the boundary of the system and not inside it, which excludes these systems from the tensegrity classification (by “extended” definition) [5].

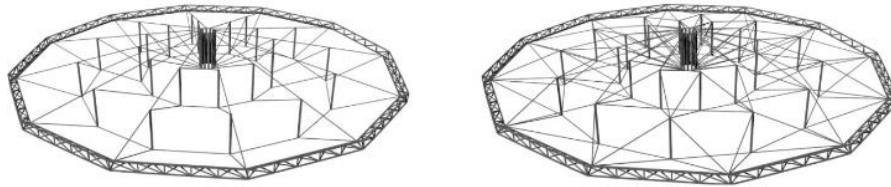


Figure 1. Geiger and Levy cable dome [7]

2 MODEL OF ACTIVE CABLE DOME IN LEVY FORM

The cable domes created of tensioned cables and compressed struts belong to hybrid tensegrity systems. A model of an active cable dome was designed and built in Laboratory of Excellent Research at the Technical University of Kosice. Prototype of cable dome is shown in Fig. 2.

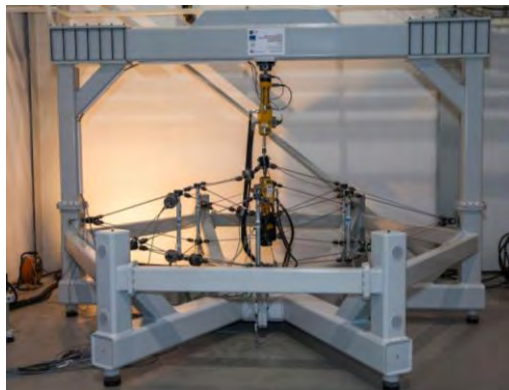


Figure 2. Prototype of Levy cable dome, Laboratory of Excellent Research TU of Kosice

The elementary shape of structure is a cable dome in Levy form with a circular base with diameter 3,0 m. Cable dome consists of 42 tension members and 7 compression members. A central compressed strut is designed as an actuator which is used to modify the geometry and pre-stress of the system. The analyzed cable dome consists of ridge cables, diagonal cables, hoop cables, vertical struts and actuator. Basic geometry of Levy cable dome is shown in Fig. 3.

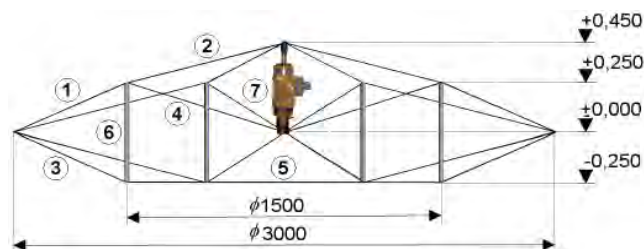


Figure 3. Section view of cable dome in Levy form with geometry and described basic structural members: (1) and (2) ridge cables, (3) and (4) diagonal cables, (5) hoop cables, (6) vertical struts and (7) actuator

Compressed struts of the cable dome are made from steel S235 with Young's modulus of elasticity $210 \cdot 10^6$ Pa and are created from circular hollow sections of 30/5 mm. The length of the struts is 500 mm. For tensile cables 1x19 wires strands with a nominal diameter of 4 mm were used. Cables were made from stainless austenitic steel 1.4401. The cross-sectional area of the cables is $9,55 \text{ mm}^2$ and Young's modulus of elasticity is $130 \cdot 10^6$ Pa. A central compressed strut is actuator which is used to modify the geometry and pre-stress of the system. The theoretical length of the actuator is 450 mm with self-weight of the actuator 16 kg and increased on the bottom point by 55 kg from connecting cylinder.

3 MULTI OBJECTIVE OPTIMIZATION METHOD

Multi-Objective Genetic Algorithm (MOGA) used in Goal Driven Optimization (GDO) as a hybrid variant of the popular Non-dominated Sorted Genetic Algorithm-II (NSGA-II) based on controlled elitism concepts are used in these studies. Concept of multi-objective optimization is based on optimization process of at least two functions to be minimized respectively maximized. In general, multi-objective criteria are defined by equations:

$$\begin{aligned} f_m(x) & \quad m = 1, 2, \dots, M \\ g_j(x) & \geq 0 \quad j = 1, 2, \dots, J \\ h_k(x) & = 0 \quad k = 1, 2, \dots, K \\ x_i^L & \leq x_i \leq x_i^U \quad i = 1, 2, \dots, n \end{aligned} \quad (1)$$

where x is vector $x = (x_1, \dots, x_n)$, g_j and h_k are boundary functions, last condition represents restriction constraint imposed on the arguments of objective function. Solution which does not satisfy condition (1) is infeasible solution. Set of solutions which satisfy condition (1) are feasible solutions. Set of possible solutions is incoherent and is created by isolated sets of feasible solutions (Pareto front) [8].

3.1 Pareto front

Pareto front is defined like set of points which represents combinations of functions $f_1 \dots f_n$, that it is not possible to reduce any value of the objective function f_i , in order to increase the value of some other function f_j . A solution is said to be optimal (Pareto optimal) if it is not dominated by any other solution in the solution space. There are non-dominant solutions on the Pareto front. Dominance of solutions is shown at the Fig. 4 [8, 9].

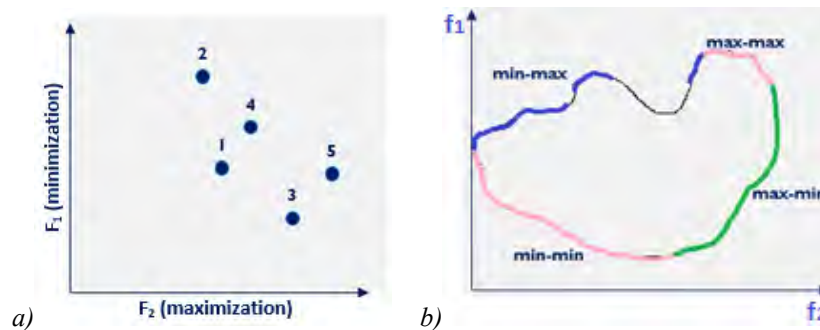


Figure 4. a) Pareto front - example of dominance b) Pareto front

If x_1 and x_2 solving problem, x_1 is dominant to x_2 , if x_1 is not worse in all objective functions $f_i(x_1)$ than x_2 and better at least in one case $f_j(x_1)$. Solutions 3 and 5 (Fig. 4) lies on Pareto front (non-dominant solutions) [8, 9].

3.2 Fitness function

The classical approach to solve a multi-objective optimization problem is to assign a weight w_i to each normalized objective function $z'_i(x)$ so that the problem is converted to a single objective problem with a scalar objective function as follows:

$$\min z = w_1 z'_1(x) + w_2 z'_2(x) + \dots + w_k z'_k(x) \quad (2)$$

where $z'_i(x)$ is the normalized objective function $z_i(x)$ and $\sum w_i = 1$. This approach is called the priori approach since the user is expected to provide the weights. Solving a problem with the objective function (2) for a given weight vector $w = \{w_1, w_2, \dots, w_k\}$ yields a single solution, and if multiple solutions are desired, the problem must be solved multiple times with different weight combinations. Let ∇ be the space of design, each of which has n runs and s factors (design variables), with each factor having q levels (samples per each design variable). Let $h(D)$ be the objective function of $D \in \nabla$. Optimised DOE (Design of experiment) for space-filling design may be generally defined by minimize an objective function $h(D)$, which maximizes the distance between design points in order to find a design $D^* \in \nabla$ and is expressed by a formulation [11]

$$h(D^*) = \min h(D), D \in \nabla. \quad (3)$$

3.3 Multi objective optimization formulation

The ultimate goal of a multi-objective optimization algorithm is to identify solutions in the Pareto optimal set. However, identifying the entire Pareto optimal set, for many multi-objective problems, is practically impossible due to its size. In addition, for many problems, especially for combinatorial optimization problems, proof of solution optimality is computationally infeasible. Therefore, a practical approach to multi-objective optimization is to investigate a set of solutions (the best-known Pareto set) that represent the Pareto optimal set as well as possible [9].

The concept of Genetic Algorithm (GA) was developed by Holland and his colleagues in the 1960s and 1970s inspired by Darwin's theory of evolution which deduces that after a natural selection and reproduction the best fittest individuals survive over the next generations. GAs implement such notion in order to solve an optimization of various single or multi-objective problems in many fields of engineering [9, 10].

In GA terminology, a solution vector $x \in X$ is called a *chromosome*. Chromosomes are made of discrete units called *genes*. Each gene controls one or more features of the chromosome. GA operate with a collection of chromosomes, called a *population*. The population is normally randomly initialized. As the search evolves, the population includes fitter and fitter solutions, and eventually it converges, meaning that it is dominated by a single solution. The procedure of a generic GA is given as follows [4, 9]:

- *First population MOGA*: Randomly generate N solutions to form the first population, P_1 . Evaluate the fitness of solutions in P_1 .

- *Crossover*: Generate an offspring population Q_t as follows:
 - Choose two solutions x and y from P_t based on the fitness values.
 - Using a crossover operator, generate offspring and add them to Q_t .
- *Mutation*: Mutate each solution $x \in Q_t$ with a predefined mutation rate.
- *Fitness assignment*: Evaluate and assign a fitness value to each solution $x \in Q_t$ based on its objective function value and infeasibility.
- *Selection*: Select N solutions from Q_t based on their fitness and copy them to P_{t+1} .
- If the *stopping criterion* is satisfied, terminate the search and return to the current population, else, set $t = t + 1$ go to Step 2 (Crossover). An operation is repeated until the final Pareto front is obtained [4, 9].

The MOGA is based on controlled elitism concepts. It supports all types of input parameters. The Pareto ranking scheme is done by a fast, non-dominated sorting method that is an order of magnitude faster than traditional Pareto ranking methods. The constraint handling uses the same non-dominance principle as the objectives, thus penalty functions and Lagrange multipliers are not needed. This also ensures that the feasible solutions are always ranked higher than the unfeasible solutions [4, 8].

Control process was carried out in the add-on Workbench module of Ansys Mechanical APDL software. The Workbench is appropriate for finding Pareto optimal (non-dominate) solutions. However, elongations of actuators generating gene of chromosome. Algorithm is shown on the Fig. 5:

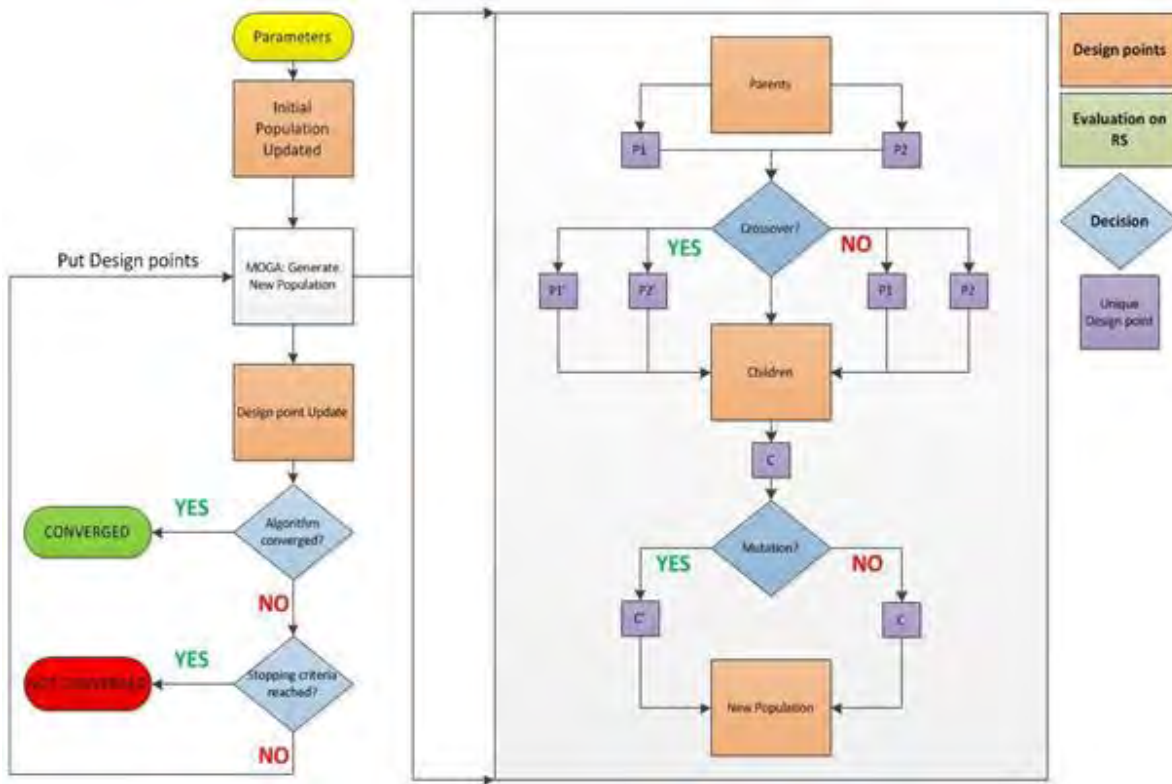


Figure . MOGA algorithm [4]

4 ANALYSIS OF CABLE DOME

Numerical analysis was carried out by Ansys Workbench software. All vertical compressed struts were created as actuators in the analysis. Paper consist of two analyses with symmetric and asymmetric load.

4.1 Symmetric load

Cable dome was loaded by maximum symmetric load. Nominal value of maximum symmetric load is 1.5 kN.m^{-2} . It leads to reach the minimal forces in cables, however, all cables were still tensioned. Axial forces under maximum symmetric load are shown in Fig. 6. Minimal force in set of ridge cables (Cable 2) is 8.26 N. If load exceeds maximum value of symmetric load, cables are not tensioned yet. It is necessary to elongate actuators to redistribute forces in the cable dome and ensure reliability criteria.

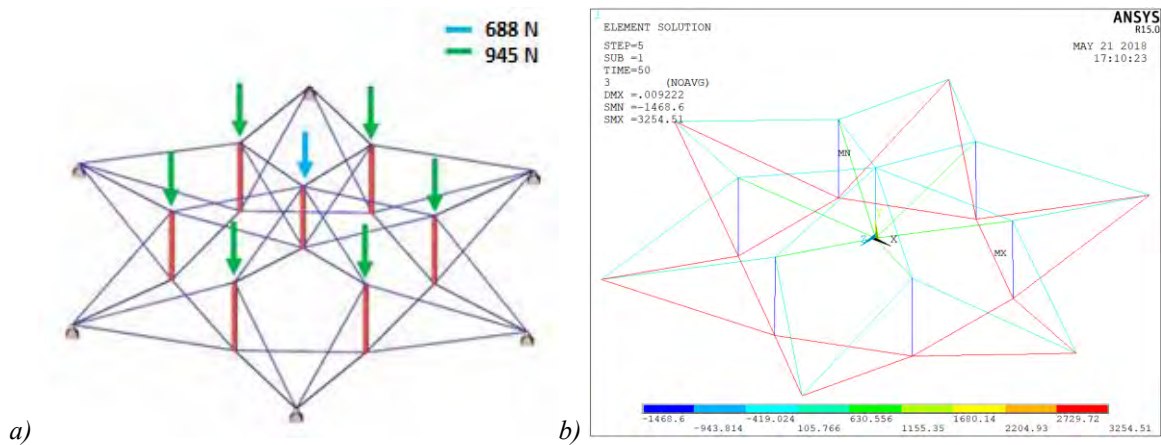


Figure . a) Maximum symmetric load (1.5 kN.m^{-2}) b) Axial forces under maximum symmetric load

Next optimization consists of finding suitable configurations of elongations of actuators which leads to satisfy prescribed reliability criteria. Obviously, ultimate and serviceability limit states are reached. Location of actuators is shown in Fig. 7.

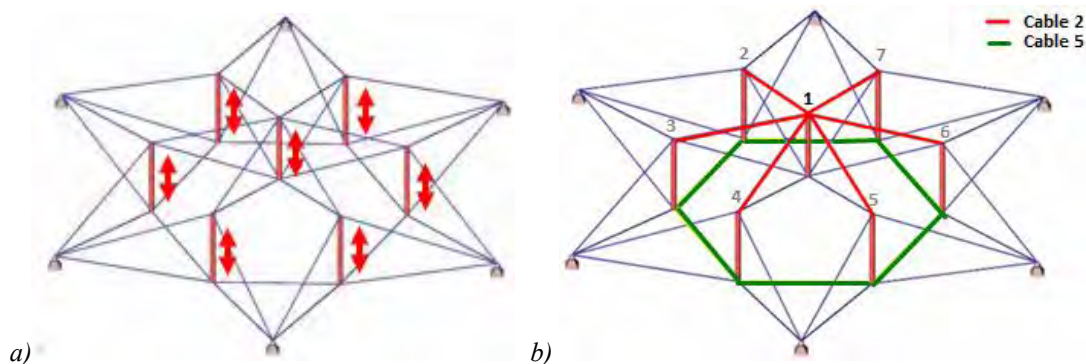


Figure . a) Actuators b) Investigated set of cables

Optimization by Multi-Objective Genetic Algorithm leads to minimize functions (4) and (5). Optimization process minimizes functions with strict constraint values of maximum forces in cable

set (Cable 5) between 4200 N and 5000 N and minimum forces in the cable set (Cable 2) greater than or equals to 400 N. Investigated sets of cables are shown in the Fig. 7. Input parameters to optimization process are elongations of actuators, which creates gene of chromosome. New population of MOGA is given by genes of these chromosomes. Step of elongations of actuators (AM - active member) is 0.001 m. Lower and upper bound of elongation is shown in Table 1.

$$F_{\min}^{Cable2} \geq 400N, (\min) \quad (4)$$

$$4200N \leq F_{\max}^{Cable5} \leq 5000N, (\min) \quad (5)$$

Table 1. Elongations of actuators

m	AM 1	AM 2	AM 3	AM 4	AM	AM	AM
Lower Bound	0.001	0.001	0.001	0.001	0.001	0.001	0.001
Upper Bound	0.015	0.01	0.01	0.01	0.01	0.01	0.01

The MOGA configuration generates 200 samples initially, 50 samples per iteration and find 5 candidates in a maximum of 20 iterations. Optimization process converged after 201 evaluations. Maximum Allowable Pareto Percentage is 70 and Convergence Stability Percentage is equal 2. One-point Type of Discrete Crossover was used in optimization. Process of minimization of functions (4) and (5) is shown in Fig. 8.

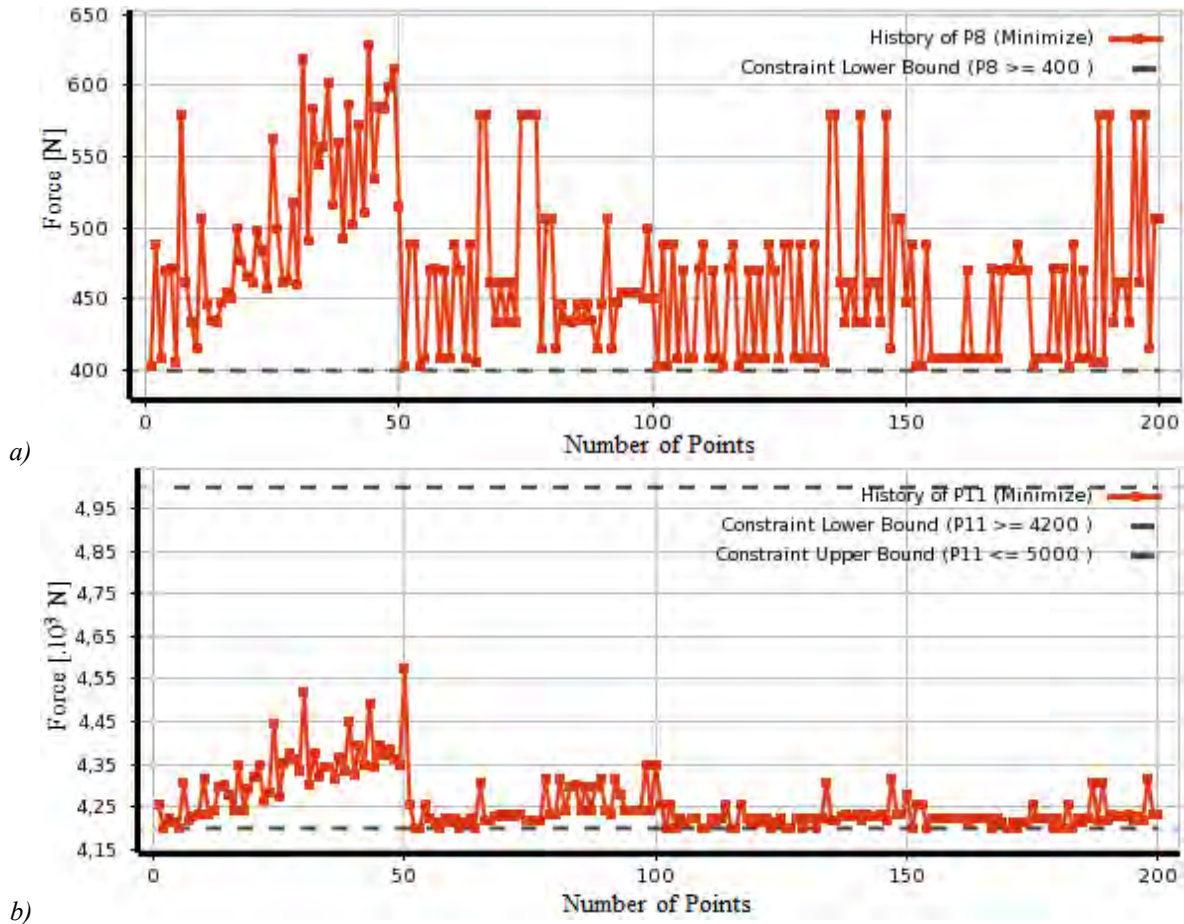


Figure . a) Minimization of function F_{\min}^{Cable2} b) Minimization of function F_{\max}^{Cable5}

Tradeoff chart, as applied to the resulting sample set, shows the Pareto dominant solutions. However, in the MOGA approach, the Pareto fronts are better articulated and most of the feasible solutions lie on the first front, as opposed to the usual results of the Screening approach where the solutions are distributed across all the Pareto fronts. Feasible solutions from Pareto fronts are shown in Fig. 9. Top 5 candidate points from Pareto fronts are in Table 2.

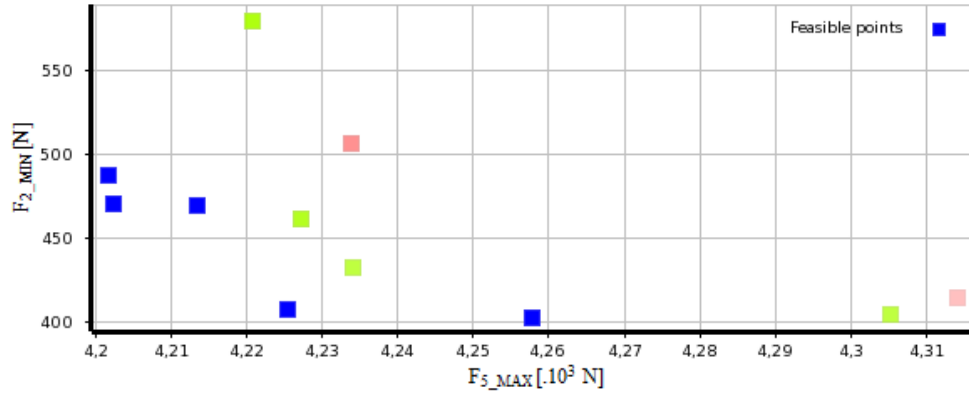


Figure 9. Feasible solutions from Pareto front

Table 2. Top 5 Candidate Points from Pareto Front

m	CP 1	CP 2	CP 3	CP 4	CP
AM1	0.004	0.006	0.002	0.002	0.003
AM2	0.002	0.004	0.006	0.006	0.006
AM3	0.005	0.007	0.001	0.001	0.007
AM4	0.002	0.003	0.009	0.009	0.001
AM	0.008	0.002	0.004	0.004	0.007
AM	0.007	0.005	0.008	0.008	0.004
AM	0.002	0.005	0.007	0.007	0.009
F₂ MIN N	408.56	471.32	433.66	433.66	488.08
F_{MA} N	4225.5	4202.3	4234.2	4234.2	4201.7

Final axial forces using elongations of actuators from Candidate Points (CP1) and (CP2) after optimization process of Levy cable dome are shown in Fig. 10.

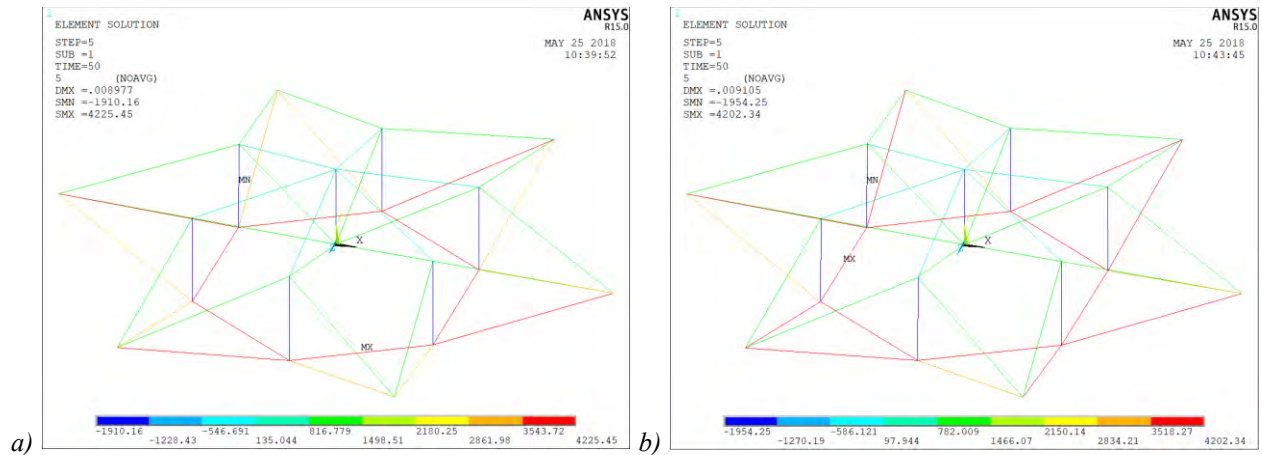


Figure 10. a) Axial forces - CP1 [N] b) Axial forces – CP2 [N]

4.2 Asymmetric load

Cable dome was loaded by maximum asymmetric load as you can see in Fig.11. Nominal value of maximum asymmetric load is 2.6 kN.m^{-2} and minimal force in set of ridge cables (Cable 2) is 1.32 N.

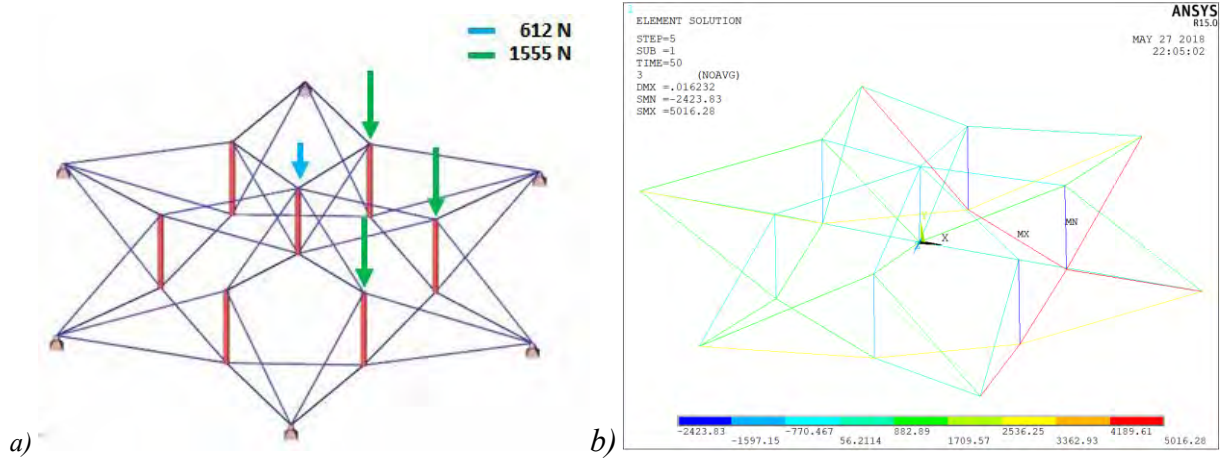


Figure 11. a) Maximum asymmetric load (2.6 kN.m^{-2}) b) Axial forces under maximum symmetric load

Optimization process leads to minimize functions (6), (7) and (8). Elongations of actuators are in Table 3. MOGA generated 200 samples initially, 50 samples per iteration and found 5 candidates in a maximum of 20 iterations. Optimization converged after 201 evaluations. Top 5 candidate points from Pareto front, as a result of best configuration of elongations of actuators in optimization process, are shown in Table 4. Top 2 CPs are shown in Fig. 12.

$$F_{\min}^{Cable 2} \geq 400N, (\min) \quad (6)$$

$$F_{\max}^{Cable 2} \leq 1000N, (\min) \quad (7)$$

$$5500N \leq F_{\max}^{Cable 6} \leq 6500N, (\min) \quad (8)$$

Table 3. Elongations of actuators

m	AM 1	AM 2	AM 3	AM 4	AM	AM	AM
Lower Bound	0.001	0.001	0.001	0.001	0.001	0.001	0.001
Upper Bound	0.01	0.01	0.01	0.01	0.01	0.01	0.01

Table 4. Top 5 Candidate Points from Pareto Front

m	CP 1	CP 2	CP 3	CP 4	CP
AM1	0.001	0.001	0.001	0.001	0.002
AM2	0.002	0.004	0.007	0.007	0.007
AM3	0.005	0.003	0.008	0.008	0.005
AM4	0.008	0.003	0.001	0.001	0.007
AM	0.006	0.009	0.007	0.007	0.009
AM	0.004	0.006	0.005	0.005	0.003
AM	0.004	0.005	0.004	0.004	0.001
F _{2 MIN} N	408.11	416.94	414.88	414.88	420.54
F _{2 MA} N	786.44	821.22	895.18	895.18	919.56
F _{MA} N	5651.5	5649.6	5579.7	5579.7	5782.4

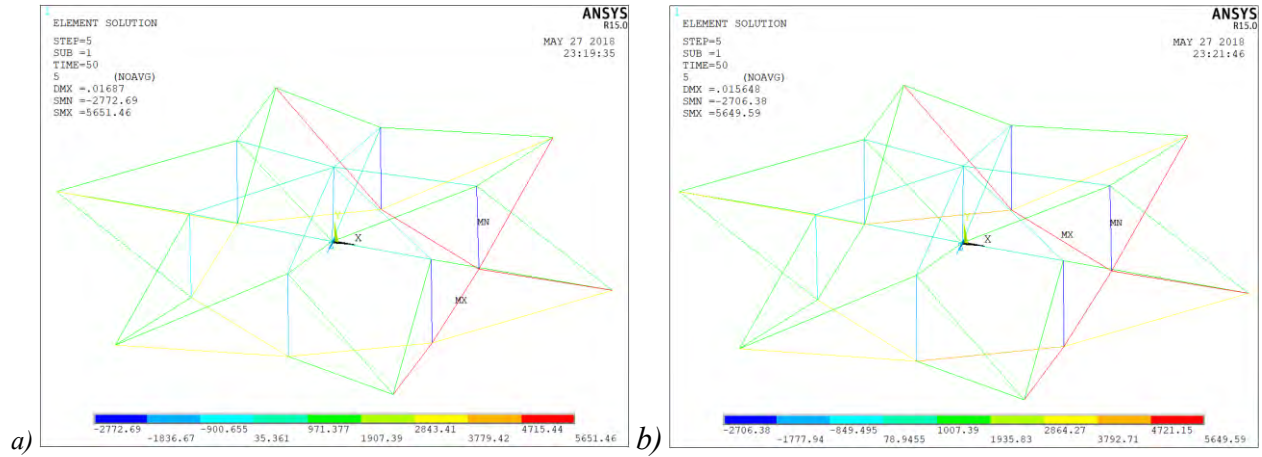


Figure 12. a) Axial forces - CP1 [N] b) Axial forces – CP2 [N]

CONCLUSIONS

Levy cable dome was analyzed by symmetric and asymmetric load. Top 3 configurations of elongations of actuators during optimization process are shown in Table 5 and Table 6. MOGA generates the best non-dominant solutions from Pareto front. Analysis of cable dome under symmetric load consists of 3 analyses.

Table . Top 3 Candidate Points from Pareto Front under symmetric load

Symmetric Load	Ma . Load			1			2		
	1. N.m ²			1. N.m ²			1. N.m ²		
m	CP 1	CP 2	CP 3	CP 1	CP 2	CP 3	CP 1	CP 2	CP 3
AM1	0.004	0.006	0.002	0.004	0.003	0.005	0.005	0.004	0.004
AM2	0.002	0.004	0.006	0.005	0.007	0.004	0.005	0.008	0.007
AM3	0.005	0.007	0.001	0.005	0.003	0.005	0.001	0.006	0.004
AM4	0.002	0.003	0.009	0.004	0.004	0.007	0.008	0.008	0.005
AM	0.008	0.002	0.004	0.007	0.002	0.004	0.007	0.003	0.005
AM	0.007	0.005	0.008	0.003	0.009	0.004	0.010	0.009	0.005
AM	0.002	0.005	0.007	0.006	0.007	0.005	0.003	0.004	0.009
F ₂ MIN N	408.56	471.32	433.66	401.27	402.89	427.3	409.78	403.35	408.06
F _{MA} N	4225.5	4202.3	4234.2	4267.3	4276.4	4279.2	4449.9	4523.1	4511.2

Table . Top 3 Candidate Points from Pareto Front under asymmetric load

Asymmetric Load	Ma . Load			1			2		
	2. N.m ²			2. N.m ²			3.12 N.m ²		
m	CP 1	CP 2	CP 3	CP 1	CP 2	CP 3	CP 1	CP 2	CP 3
AM1	0.001	0.001	0.001	0.002	0.003	0.002	0.003	0.009	0.002
AM2	0.002	0.004	0.007	0.007	0.008	0.004	0.008	0.006	0.010
AM3	0.005	0.003	0.008	0.003	0.009	0.002	0.004	0.002	0.005
AM4	0.008	0.003	0.001	0.004	0.002	0.007	0.003	0.001	0.003
AM	0.006	0.009	0.007	0.002	0.002	0.007	0.004	0.003	0.006
AM	0.004	0.006	0.005	0.009	0.003	0.007	0.007	0.006	0.009
AM	0.004	0.005	0.004	0.008	0.007	0.005	0.009	0.004	0.005
F ₂ MIN N	408.11	416.94	414.88	418.63	402.34	422.27	405.84	404.44	413.26
F ₂ MA N	786.44	821.22	895.18	765.44	825.41	793.69	803.13	833.86	877.99
F _{MA} N	5651.5	5649.6	5579.7	6007.9	5965.5	5986.9	6318.8	6241.7	6256.9

Cable dome was loaded by maximum symmetric load (1.5 kN.m^{-2}), maximum load increased by 10% (1.65 kN.m^{-2}) respectively increased by 20% (1.8 kN.m^{-2}). Optimization process of Levy cable dome under asymmetric load consists of analysis under maximum asymmetric load (2.6 kN.m^{-2}), load increased by 10% (2.86 kN.m^{-2}) and 20% (3.12 kN.m^{-2}). Axial forces of optimized Levy cable dome are shown in Fig. 13 and Fig. 14.

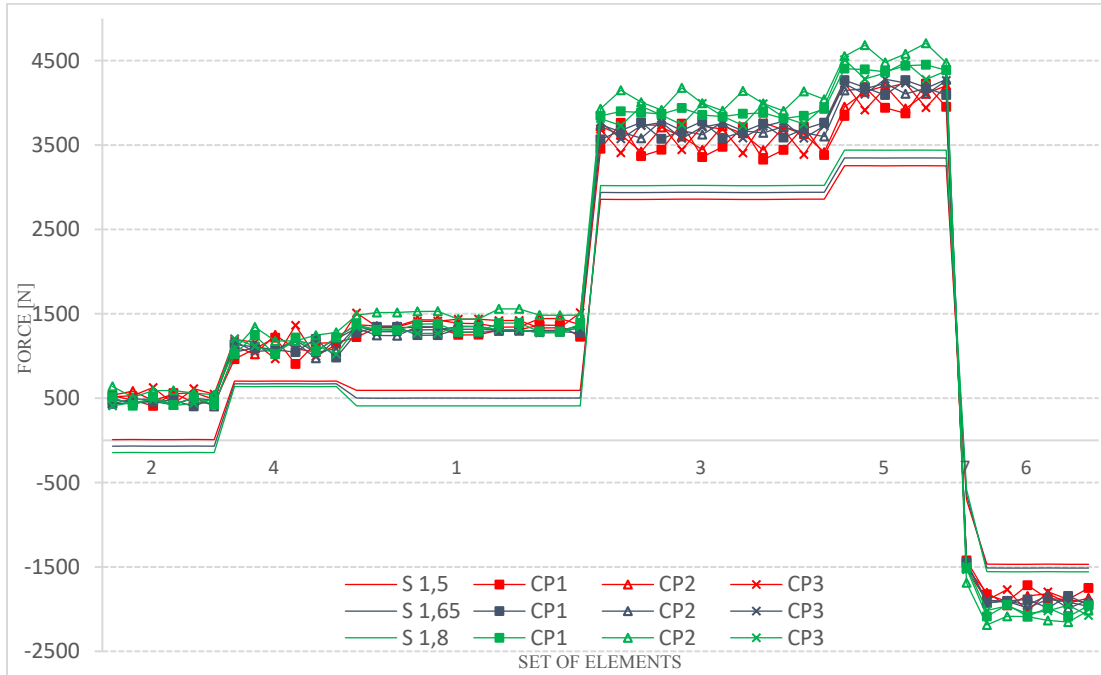


Figure 13. Axial forces – symmetric load [N]

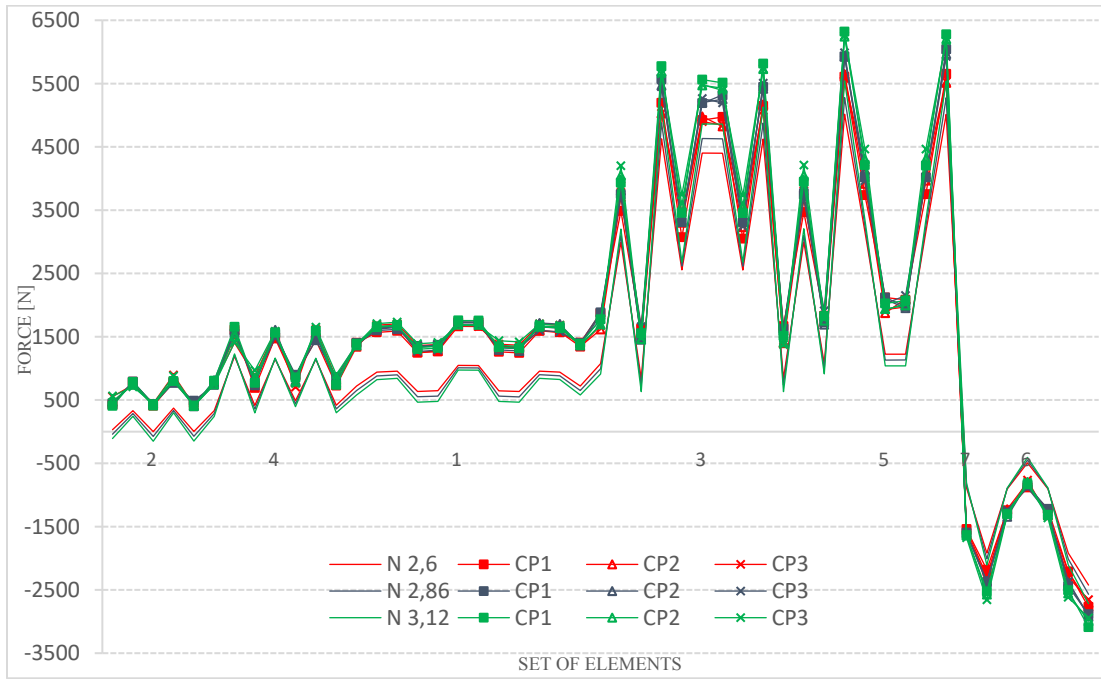


Figure 14. Axial forces – asymmetric load [N]

The objective of the NSGA algorithm (Non-Dominated Sorted Genetic Algorithm–II as a multi-criteria optimization tool MOGA) is to improve finding control commands (necessary movement of the actuators) of the cable dome. MOGA represents an effective way to find optimal solutions at Pareto front.

Ac knowledgments

This paper is the result of the Project implementation: University Science Park TECHNICOM for Innovation Applications Supported by Knowledge Technology, ITMS: 26220220182, supported by the Research & Development Operational Programme funded by the ERDF. We support research activities in Slovakia/This project is being co-financed by the European Union.

The paper is carried out within the project No. 1/0302/16, partially founded by the Science Grant Agency of the Ministry of Education of Slovak Republic and the Slovak Academy of Sciences.

REFERENCES

- [1] Kmet, S. and Mojdis, M. Time-dependend analysis of cable dome using a modified dynamic relaxation method and creep theory, *Computer and Structures*, vol. 125, September 2013, ISSN 0045-7949.
- [2] Shea, K., Fest, E. and Smith, I.F.C. Developing Intelligent Tensegrity Structures with Stochastic Search, *Advanced Engineering* 129(4), 2003, pp.515-526.
- [3] Sobek, W., Teuffel, P., Weilandt, A. and Lemaitre, C. Adaptive and lightweight, In *Proc., The Int. Conf. on Adaptable Building Structures, Eindhoven*, pages 234-245, Eindhoven, 2006.
- [4] Ansys, Inc. Release documentation of Ansys 15.0, Southpointe, 275 Technology Drive, Canonsburg, November 2013.
- [5] Motro, R. Tensegrity: Structural systems of future, *London: Kogan Page Science*, 2003. 238p. ISBN 1-903996-37-6.
- [6] Kmet, S. and Mojdis, M. Adaptive Cable Dome, *Journal of Structural Engineering*, vol. 141, Issue 9, 2015, Article number: 04014225.
- [7] Telgen, M. V. Parametric design and calculation of circular and elliptical tensegrity domes, *Master Thesis in Structural Design*. Eindhoven: Eindhoven University of Technology, Department of Architecture, Building and Planning. 2012, 211 p.
- [8] Zelinka, I. Evolutionary computing techniques – principles and applications. *Brno University of Technology, BEN – technical literature. Prague, CZ. 2009* (In Czech). 1st edition. ISBN 978-80-7300-218-3.
- [9] Konak, A., Coit, D.W. and Smith, A.E. Multi-objective optimization using genetic algorithms: A tutorial, *Reliability Engineering and System Safety*, 2006. 91(9): 992-1007.
- [10] Holland, J.H. Adaptation in ntural and artificial systems. Ann Arbor: *University of Michigan Press*; 1975.
- [11] Fang, K.T., Li, R. and Sudjianto, A. Design and Modeling for Computer Experiments. *Chapman & Hall/CRC*, Boca Raton; 2006.

A Two-scale Uncertainty Model for Transversely Fiber Reinforced Plastics

Ismail Caylak*, Eduard Penner**, Alex Dridger***, Rolf Mahnken****

*Paderborn University, **Paderborn University, ***Paderborn University, ****Paderborn University

ABSTRACT

In recent years, lightweight structures became increasingly important due to their excellent mechanical and lightweight properties. As a special component fiber reinforced plastics (FRP) become prominent. It is well known that material properties of FRP are uncertain due to the manufacturing process. In addition, there are measurement errors and missing or incomplete information on material properties. While several sources of uncertainties exist, these are often distinguished into aleatoric and epistemic uncertainty. Aleatoric uncertainty is presumed to be the intrinsic randomness of a phenomenon and is also called statistical uncertainty that can be modeled with stochastic methods based on the polynomial chaos expansion (PCE). On the other hand, epistemic uncertainty is the vagueness in a system definition due to subjectivity, simplification and incomplete knowledge that can be modeled with fuzzy methods based on the fuzzy set theory. In this presentation, we concentrate on unidirectional FRPs. Due to both constituents, fiber and matrix, composites are essentially heterogeneous, which motivates a two-scale approach. The related transversely isotropic behaviour is investigated with this approach. It takes into account the behavior of fibers and matrix separately, which renders a more realistic material behaviour of FRP. It is based on the idea to substitute the heterogeneous material with an effectively equivalent homogeneous material. As a key idea, the constitutive equations are modeled by a combination of fuzzy-stochastic methods. The stochastic material parameters are expanded with the multivariate PCE, whereas epistemic material parameters are defined as design variables and are modeled as fuzzy sets. An underlying optimization problem for the fuzzy analysis is approximated by discretization techniques, resulting into a separation of minimum and maximum problems. To become more universal, so-called quantities of interest are employed, which allow a general formulation for the target problem of interest. Experimental data of the matrix and the fibers are obtained separately. Then, in the numerical examples we investigate analytical effective properties for fuzzy-stochastic Voigt upper bounds and Reuss lower bounds. Finally, numerical results are compared with existing experimental observations.

Initial Value Problems in Nanotechnology Using Clifford Analysis

Johan Ceballos^{*}, Antonio Di Teodoro^{**}, Alexander López^{***}

^{*}Universidad De Las Américas, ^{**}Universidad San Francisco de Quito, ^{***}Universidad Politécnica del Litoral

ABSTRACT

We analyze some initial value problems using Clifford Analysis within the context of nanotechnology focusing on the possible configurations which are compatible with the symmetries of the boundaries of toy-model samples such as, quantum dots and nanoribbons in order to describe the anisotropic electronic transport in two dimensional systems, where the electrons do not obey the Schroedinger equation but the Dirac equation. This, in principle trivial difference, has quite a lot of implications in the physical behavior of new materials such as graphene and related samples. Finally, we present a matrix representation of Clifford Algebras through some algorithms.

A Combined Multiscale FEM and DPG Approach for Linear Elasticity

Witold Cecot*, Marta Oleksy**, Marek Klimczak***

*Cracow University of Technology, **Cracow University of Technology, ***Cracow University of Technology

ABSTRACT

The Multiscale Finite Element Method (MsFEM) [1] is one of the promising methods used for modeling of heterogeneous materials. It neither requires the assumption of scale separation nor periodicity of micro-structure. Moreover, it may be easily parallelized, since the essence of the MsFEM is an evaluation of special macro-scale finite element trial (approximating) shape functions that capture the micro-scale details. These functions are computed independently in appropriate patches of elements and the higher order approximation for the MsFEM has already proved to be profitable [2]. Although the method significantly reduces the computational cost, its efficiency and trustworthiness need further improvements. It may be achieved by using the ultra-weak variational formulation of the considered elasticity problem and coupling the MsFEM with the Discontinuous Petrov-Galerkin approach (DPG) [3] that is a new FEM methodology enabling computation of optimal, from the convergence point of view, test functions. Efficiency improvement is expected due to the optimal test functions offered by the DPG methodology since they enable obtaining reasonable results for a relatively small number of degrees of freedom. The ultra-weak formulation additionally simplifies, typically a cumbersome in the MsFEM, determination of boundary conditions for auxiliary, local problems and reduce the domains of the auxiliary problems to only single coarse elements. Reliability of the new version of the MsFEM is enhanced by the DPG guaranteed convergence, a built-in a'posteriori error estimate offered by this methodology and mathematically sound background of this approach. Preliminary numerical results for deformations of heterogeneous elastic bodies confirm expected profits of the proposed coupled MsFEM and DPG methodology. [1] T. Hou and X. Wu. A multiscale finite element method for elliptic problems in composite materials and porous media. *Journal of Computational Physics*, 134:169-189, 1997. [2] W. Cecot and M. Oleksy. High order FEM for multigrid homogenization. *Computers and Mathematics with Applications*, 70(7):1370-1390, 2015. [3] L. Demkowicz and J. Gopalakrishnan. A class of discontinuous Petrov-Galerkin methods. Part II. Optimal test functions. *Numerical Methods for Partial Differential Equations*, 27(1):70-105, 2011.

Triflow : Python Library for Prototyping Coupled Nonlinear PDEs. Application to Heat Transfer in Falling Films

Nicolas Cellier^{*}, Benoît Stutz^{**}, Nadia Caney^{***}, Christian Ruyer-Quil^{****}, Philippe Bandelier^{*****}

^{*}Université de Savoie Mont-Blanc, ^{**}Université de Savoie Mont-Blanc, ^{***}Université Grenoble Alpes, ^{****}Université de Savoie Mont-Blanc, ^{*****}CEA

ABSTRACT

Triflow is an open source software designed to easily implement systems of coupled non linear partial differential equations. The software appears as a python library. The library fits well with an interactive usage : this allow an effective way to test the models and explore the simulation results. It is based on the method of lines and use a mixed paradigm : the spatial derivatives are discretized and the Jacobian is computed via a symbolic engine in a first time. Then Theano, a modern framework used in deep learning algorithms, is used in order to perform on-the-fly optimisation and compilation of the schemes. High order implicit temporal schemes have been implemented. As an example of the capabilities of the Triflow library, we propose an analysis of the interaction between hydrodynamic wave regimes and heat transfer occurring on heated falling films based on an asymptotic model derived with the WRIBL method. Heat transfer across a wavy film falling on a hot plate depends not only on fluid thermal characteristics, but also on the hydrodynamic state of the flow: experimental works (Gonda, A. et al. Water falling film evaporation on a corrugated plate. Int. J. Therm. Sci. 81, 29–37 (2014).) show a non negligible impact of the hydrodynamic instabilities on transfer intensification compared to flat films. An asymptotic model based on weighted residual integrated boundary layer (WRIBL) method (1. Ruyer-Quil, C. & Manneville, P. Improved modeling of flows down inclined planes. Eur. Phys. J. B 15, 357–369 (2000).) has been written for the fluid dynamic and the heat transfer. Compared to previous attempts (1. Kalliadasis, S., Ruyer-Quil, C., Scheid, B. & Velarde, M. G. Falling Liquid Films. 176, (Springer London, 2012).), this new formulation compares satisfactorily to the solutions to the Fourier equation even at large values of the Prandtl number. Less expensive than direct numerical simulations (DNS), solving this asymptotic model allows for fast exploration of the physical parameters and their impacts on the heat flux and the interaction between hydrodynamics and heat transfer. One of the main goals is to use that tool and the comprehension of these interactions in order to improve the industrial equipments employing heated falling films. One way could be to force beneficial instabilities with the plate shape design. To this aim, we have included the effect of a corrugated plate shape in the models within a soft slope hypothesis.

Unraveling the Structure-property Relationships in Fiber-composite Materials Using Machine Learning and Global Sensitivity Analysis

David Cereceda^{*}, Raman Arora^{**}, Jessica A. Krogstad^{***}, Francisco L. Jiménez^{****}, Michael D. Shields^{*****}, Lori Graham-Brady^{*****}

^{*}Villanova University, ^{**}Johns Hopkins University, ^{***}University of Illinois at Urbana-Champaign, ^{****}University of Colorado at Boulder, ^{*****}Johns Hopkins University, ^{*****}Johns Hopkins University

ABSTRACT

The development and deployment of advanced new materials are linked to the understanding of their structure-property relationships. Physically-based approaches have extensively been used for this purpose, but they present some limitations related to their computational cost and the communication of information between the multiple hierarchical length scales involved. For their part, data models are designed to be computationally efficient, but they are not necessarily formulated with an explicit knowledge of the physical behavior of the system under study. In this work, we develop a machine-learning based model that exploits a combination of the physical knowledge of the microstructure with data-driven techniques to predict the local strain field in the material. In particular, we apply this method to extract the structure-property linkages in a two-dimensional metal matrix composite (MMC), by using a fully-connected neural network. As part of the model, global sensitivity analysis is also employed to identify the most prominent microstructural features that drive the mechanical behavior of the material.

Poroelasticity of Sedimentary Basin during Glaciation

Daniele Cerroni^{*}, Paolo Zunino^{**}, Anna Scotti^{***}, Luca Formaggia^{****}

^{*}Politecnico di Milano, ^{**}Politecnico di Milano, ^{***}Politecnico di Milano, ^{****}Politecnico di Milano

ABSTRACT

Reconstructing the stress and deformation history of a sedimentary basin is a challenging and important problem in the geosciences and a variety of applications [2]. The mechanical response of a sedimentary basin is the consequence of complex multi-physics processes involving mechanical, geochemical, thermal, geophysical and geological aspects. The strongly coupled nature of the deformation problem may be understood in terms of the feedback underlying crustal dynamics. The pore fluid pressure affects stress, stress changes can lead to fracturing, and fracturing can affect pore fluid pressure. Similarly, stress can affect mineral solubility, causing mineral dissolution which, in turn, can affect rock rheology and, therefore, stress. The basin deformation analysis requires accounting of the coupling among the many interacting reaction, transport and mechanical (RTM) processes. For the mechanical analysis at the macroscopic scale, phenomena that contribute to the compaction of sediments are purely-mechanical compaction which originates mainly from rearrangement of the solid particles during burial and mechano-chemical compaction resulting from dissolution–precipitation mechanisms, generally induced by stress (pressure - dissolution). Purely mechanical phenomena prevail in the upper layers, whereas chemical compaction dominates for deeper burial as stress and temperature increase. Moreover during the glaciation the water inside the porous rock can freeze changing the mechanical and geochemical properties of the medium. The water in the upper layers of the basin can erode and hugely modify the top layer of the basin changing its poromechanical response. In this work we assume that this surface is described by the zero value of a given function of the space. The levelset introduces a discontinuity in the solution and the Extended finite element method is used to take into account this discontinuity.

Flat-top Partition of Unity Method for Electronic Structure Calculations

Ondrej Certik^{*}, Gianmarco Manzini^{**}, Lee Collins^{***}, N. Sukumar^{****}, John Pask^{*****}, Marc Alexander Schweitzer^{*****}

^{*}Los Alamos National Laboratory, ^{**}Los Alamos National Laboratory, ^{***}Los Alamos National Laboratory, ^{****}UC Davis, ^{*****}Lawrence Livermore National Laboratory, ^{*****}University of Bonn

ABSTRACT

A flat-top partition of unity method (FT-PUM) will be presented to solve the equations of Kohn-Sham density functional theory. The partition of unity weight functions are multiplied by functions consisting of enrichment functions and polynomials that span the trial space of the standard finite element method. The enrichment functions are derived from solutions of isolated atoms. Convergence studies with the state-of-the-art planewave method will be shown, as well as with non-enriched spectral finite elements. We show that the FT-PUM formulation yields an order of magnitude reduction in the degrees of freedom required to attain chemical accuracy. The method performs similarly to the recently developed partition of unity finite element method (PUFEM), but affords the significant advantage that it produces a well conditioned standard eigenvalue problem, thus facilitating efficient, parallel solution.

Macro-mechanical Modelling of Localized Cracks in Masonry Structures Using a Tracking Algorithm

Miguel Cervera*, Luca Pelà**, Savvas Saloustros***

*UPC-BarcelonaTech/CIMNE, **UPC-BarcelonaTech/CIMNE, ***UPC-BarcelonaTech/CIMNE

ABSTRACT

Masonry refers to a wide diversity of construction techniques and composite materials, varying according to local building traditions and material availability. This variability has impeded the development of a general methodology for the analysis of masonry structures, and has motivated the proposal of different numerical approaches specifically tailored to the simulation of masonry. Despite this extensive inventory of numerical approaches, a common choice for the analysis of large masonry structures is a macro-mechanical material representation through irreducible continuum finite element models. This “macro-modelling” approach allows an easier development of the numerical model and an affordable computational cost for the analysis. Nevertheless, it commonly results in a non-realistic representation of cracking as a smeared quantity over large areas within the structure, which contradicts the localized nature of cracks and hampers the identification of local and global collapse mechanisms. Additionally, cracking tends to propagate along the directions imposed by the sides of the finite elements in a spurious way. To overcome the above limitations, this work presents a numerical model based on the classical smeared crack approach and a novel local tracking algorithm oriented to the analysis of masonry structures under monotonic and cyclic loading [1,2]. The use of the tracking algorithm enhances the crack representation compared with classical smeared crack approaches, facilitating the identification of developing damage patterns on the analyzed structure [3]. In addition to that, the tracking algorithm enhances significantly the mesh-independency of the numerical simulation. At constitutive level, masonry is represented as a homogenized material with average mechanical properties through a local continuum damage mechanics model. A simple and explicit algorithmic formulation is adopted by including the description of irreversible deformations as an additional internal variable into an orthotropic continuum damage model [2]. The proposed methodology is applied to the simulation of experimental results on in-plane loaded masonry walls available in the literature. Keywords: Macro-modelling, tracking algorithm, masonry structures, cracking, cyclic loading References [1] Saloustros S, Pelà L, Cervera M, Roca P (2016) Finite element modelling of internal and multiple localized cracks. *Comput Mech* 59:299–316. doi: 10.1007/s00466-016-1351-6 [2] Saloustros S, Cervera M, Pelà L (2017) Tracking multi-directional intersecting cracks in numerical modelling of masonry shear walls under cyclic loading. *Meccanica* (in press) . doi: 10.1007/s11012-017-0712-3 [3] Saloustros S, Pelà L, Cervera M, Roca P (2017) An Enhanced Finite Element Macro-Model for the Realistic Simulation of Localized Cracks in Masonry Structures: A Large-Scale Application. *Int J Archit Herit* (in press) . doi: 10.1080/15583058.2017.1323245

Common Implementation of Phase-field and Non-local Implicit Gradient Models for Ductile Failure

Jose Cesar de Sa^{*}, Erfan Azinpour^{**}, Joao Ferreira^{***}, Marco Parente^{****}

^{*}University of Porto, Portugal, ^{**}University of Porto, Portugal, ^{***}University of Porto, Portugal, ^{****}University of Porto, Portugal

ABSTRACT

Damage and failure in ductile materials models, with their attractive simplifications of the microstructural complexity associated with these phenomena, comprise the presence of softening at the constitutive level, which is known as a possible source of problems in their numerical implementation. To somehow restore the well-posedness of the set of partial differential equations to be solved, regularized solutions, often resorting to non-local and gradient theories with the recourse of a characteristic length associated with the size of the non-local support region definition, may be utilised. The similar nature of the mathematical coupled temperature-displacement problems and non-local implicit gradient models for material ductile failure is explored using the existing built-in thermo-mechanically coupled finite-element solutions in common commercial software. In particular the nonlocal implicit gradient of the Lemaitre damage model and the phase field model are addressed. The diffusive regularization of those material models are associated with the heat conduction equation, therefore circumventing the need of including special user subroutines to implement explicitly the weak form resultant from the coupling between momentum conservation and the evolution of the diffusive field. Using benchmarking examples, the proposed methodology, in what concerns capability to avoid mesh dependency and to predict cracked regions, is assessed.

Application of the Edge-based Gradient Smoothing Technique to Acoustic Radiation and Acoustic Scattering from Rigid and Elastic Structures in Two Dimensions

Yingbin Chai^{*}, Cong Cheng^{**}, Wei Li^{***}, Xiangyu You^{****}

^{*}Huazhong University of Science and Technology, ^{**}Huazhong University of Science and Technology,
^{***}Huazhong University of Science and Technology, ^{****}Huazhong University of Science and Technology

ABSTRACT

The acoustic scattering and acoustic radiation from underwater object is a very interesting physical phenomenon in ocean acoustics and is also often encountered in practical ocean engineering applications. Therefore, how to precisely calculate and predict the acoustic scattered field is of great importance to improve the acoustical properties of the ocean engineering structures. In general, the analytical or semi-analytical approaches are only effective for the problems with simple geometries. When it comes to more practical problems with very complicated geometries, the analytical solutions are always impossible to obtain. In these cases, we have to resort to numerical methods. As is well-known to all, the conventional finite element method (FEM) is constrained by the “numerical dispersion error” issue for solving acoustic problems at high frequencies. In this paper, the gradient smoothing technique (GST) which is based on the edges of the elements is combined with the conventional FEM to construct a novel edge-based smoothed FEM (ES-FEM) for two dimensional exterior structural-acoustic problems. In this model, the ends of elements edges are sequentially connected to the centroids of the surrounding elements to form the so-called smoothing domains (SDs). Then the smoothed gradient field can be obtained by performing the GST over these obtained SDs. The present ES-FEM is able to provide a relatively appropriate stiffness of the real system owing to the “softening effects” from the GST. Therefore, the accuracy of the solutions for acoustic radiation and acoustic scattering can be significantly improved. For the purpose of handling the exterior Helmholtz equation, the involved infinite domains are truncated by a predefined artificial boundary B and the Dirichlet-to-Neumann (DtN) map is employed on B to prevent any possible spurious reflecting acoustic waves from the far-field. Several supporting numerical examples demonstrated that the ES-FEM with DtN map was very effective for exterior structural-acoustic problems and could produce more accurate numerical results than the conventional FEM.

Periodic Unsteady Flow Simulation Using Harmonic Balance Method

Zhenxia Chai^{*}, Wei Liu^{**}, Ming Zeng^{***}, Xiaoliang Yang^{****}

^{*}National University of Defense Technology, ^{**}National University of Defense Technology, ^{***}National University of Defense Technology, ^{****}National University of Defense Technology

ABSTRACT

In recent years, Fourier-based frequency domain techniques are widely applied to significantly reduce the computational expense for analyzing unsteady periodic problems. Among the frequency domain algorithms, the harmonic balance method (HBM) proposed is computationally efficient for unsteady flow problems, especially for periodic unsteady flow. The basic principle of this method is to decompose the flow variables into a Fourier series, which transforms the unsteady flow into several steady problems coupled by a spectral time-derivative operator. The whole time history of a complete unsteady periodic flow can be reconstructed from the steady results. The present research simulates time-periodic unsteady transonic and subsonic flows around pitching airfoils via the solution of unsteady Euler equations, using HBM and compares it with the traditional time domain method (TDM) and experimental data to demonstrate the accuracy, efficiency and memory requirement of HBM. The test cases are NACA 0012 pitching airfoils with transonic and subsonic inflows. The unsteady pitching aerodynamic forces and moments are rebuilt, and the pressure coefficient distributions at different points in a pitching cycle are also reconstructed by HBM. These results are then compared with experimental data and TDM. The results show that for subsonic flow, only one harmonic is enough for HBM computation to achieve the same accuracy with TDM. Meanwhile, for strongly nonlinear unsteady transonic flow, it can be modeled to engineering accuracy with a small number of harmonics. Thus, the HBM is computationally efficient, it can reduce the computing time greatly with only about 1/10 (one-harmonic) and 1/4 (three harmonics) of that needed by the TDM. We also note that, both the computation time and memory requirement of the harmonic balance method increase linearly as the number of harmonics increases. For transonic flow, the reconstructed pressure distributions with three harmonics agree well with TDM at all points on the aerofoil except where the shock appears and moves. In this region more harmonics are needed to reconstruct the nonlinear behavior, and then the efficiency of the HBM when compared with the TDM may be lost. Thus, it is necessary to do further studies on adaptive harmonic balance method to solve highly nonlinear time-periodic flows and reduce the computational time and memory requirement.

Fast and Adaptative Boundary Element Methods for 3D Acoustic and Elastodynamic Problems

Stéphanie Chaillat^{*}, Patrick Ciarlet^{**}, Faisal Amlani^{***}, Félix Kpadanou^{****}, Adrien Loseille^{*****}

^{*}CNRS - POEMS, ^{**}ENSTA - POEMS, ^{***}ENSTA - POEMS, ^{****}ENSTA - POEMS, ^{*****}INRIA

ABSTRACT

The main advantage of the Boundary Element Method (BEM) [1] is that only the domain boundaries (and possibly interfaces) are discretized leading to a drastic reduction of the total number of degrees of freedom. In traditional BE implementation the dimensional advantage with respect to domain discretization methods is offset by the fully-populated nature of the BEM matrix, with set-up and solution times rapidly increasing with the problem size. In the last couple of years, fast BEMs have been proposed to overcome the drawback of the fully populated matrix. The Fast Multipole Method (FMM) is a fast, reliable and approximate method to compute the linear integral operator and is defined together with an iterative solver. The efficiency of the method has been demonstrated for 3D wave problems. However, the iteration count becomes the main limitation to consider realistic problems. Other accelerated BEMs are based on hierarchical matrices. When used in conjunction with an efficient rank revealing algorithm, it leads to a data-sparse and memory efficient approximation of the original matrix. Contrary to the FM-BEM it is a purely algebraic tool which does not require a priori knowledge of the closed-form expression of the fundamental solutions and it is possible to define iterative or direct solvers. Mesh adaptation is an additional technique to reduce the computational cost of the BEM. The principle is to optimize (or at least improve) the positioning of a given number of degrees of freedom on the geometry of the obstacle, in order to yield simulations with superior accuracy compared to those obtained via the use of uniform meshes. If an extensive literature is available for volume methods, much less attention has been devoted to BEMs. In this contribution, we give an overview of recent works to speed-up the solution of 3D acoustic and elastodynamic BEMs. More precisely, we will present - some preconditioning technics for iterative solvers; - iterative and direct solvers based on H-matrices [2]; - an anisotropic metric-based mesh adaptation technic [3]. [1] M. BONNET, Boundary integral equation methods for solids and fluids, John Wiley, 1995. [2] S. CHAILLAT, L. DESIDERIO, P. CIARLET, Theory and implementation of H-matrix based iterative and direct solvers for Helmholtz and elastodynamic oscillatory kernels, Journal of Computational Physics 351 (2017), pp 165-186. [3] S. CHAILLAT, S.P. GROTH, A. LOSEILLE, Metric-based anisotropic mesh adaptation for 3D acoustic boundary element methods, submitted.

PBDW: a non-intrusive Reduced Basis Data Assimilation Method and its application to Outdoor Air Quality Models

Rachida Chakir^{*}, Janell K. Hammond^{**}, Frederic Bourquin^{***}, Yvon Maday^{****}

^{*}Université Paris Est, IFSTTAR, ^{**}Université Paris Est, IFSTTAR, ^{***}Université Paris Est, IFSTTAR, ^{****}Sorbonne Université

ABSTRACT

As the population increases, cities must constantly reassess their urban planning. However, this must be done in such a way to preserve the quality of life of its inhabitants. Energy saving, sustainable water and air quality are some of the important challenges associated with growing cities. In this context, the monitoring of the different urban flows (pollution, heat) is very important. For instance data assimilation approach can be used in monitoring. These methods incorporate available measurement data and mathematical model to provide improved approximations of the physical state. The effectiveness of modeling and simulation tools is essential. Advanced physically based models could provide spatially rich small-scale solution, however the use of such models is challenging due to explosive computational times in real-world applications. Beyond computational costs, physical models are often constrained by available knowledge on the physical system. To overcome these difficulties, we resort the Parameterized-Background Data-Weak (PBDW) method introduced in [1]. The PBDW formulation combines a Reduced Basis (RB) [2] from the physically based model and the experimental observations, in order to provide a real-time and state estimate in a non-intrusive manner. The RB is used to diminish the cost of using a high-resolution model by exploiting the parametric structure of the governing equations. In addition, variational data-assimilation techniques are used to correct the model error. In this work we extend the PBDW method to the monitoring of urban air quality as an important use case but also as an example of the very generic approach that proves well suited to online monitoring of urban flows over large scales. We build a RB approximation space from a sample of solutions from air quality models based on CFD with varying meteorological conditions and pollution. The goal is to rapidly estimate online pollutant concentration around an area of interest (up to tens of hectares). In case studies presented here, the method allows to correct for unmodeled physics and treat cases of unknown parameter values, all while significantly reducing online computational time. REFERENCES [1] Y. Maday, A.T Patera, J.D. Penn and M. Yano, "A parameterized-background data-weak approach to variational data assimilation: formulation, analysis, and application to acoustics", Int. J. Numer. Meth. Engng (2014). [2] Prud'homme, C., Rovas, D. V., Veroy, K., Machiels, L., Maday, Y., Patera, A. T., & Turinici, G. (2002). "Reliable real-time solution of parametrized partial differential equations: Reduced-basis output bound methods". Journal of Fluids Engineering, 124(1), 70-80

Use of Modified Johnson-Cook Model in Simulation of Metal-ceramic Composite Cold Spraying

Rohan Chakrabarty*, Jun Song**

*McGill University, **McGill University

ABSTRACT

Owing to the low processing temperatures and subsequent minimal thermal residual stresses, cold spray (CS) process has a significant potential as a fabrication route for freeform components, thus making it a prospective additive manufacturing technology. Over the past decade or so, cold spray experiments have been accompanied with systematic computational modeling to optimize the coating deposition conditions and predict the coating properties and thereby their performance. One of the most widely used plasticity models for prediction of material behavior at high strain rate is Johnson-Cook (JC) model. However, the model's shortcomings at the strain rates experienced during cold spray lead to inaccuracies in the predictions. Still, it is predominantly used owing to its simplicity and rich material parameters database. Though other models such as Preston - Tonks - Wallace (PTW) models have been considered more suitable for the high strain-rate predictions, they require many more material constants and are complex to implement numerically than JC model. Thus, in this study, we have incorporated a modified form of JC model to the cold spray simulations, which accounts for the viscous regimes experienced at high strain rates. The predictions obtained from the modified JC model has been found to be consistent with the cold spray experimental results. This modified JC model is then used to demonstrate the building-up process of the ceramic-metal composite coating. This study contributes important mechanistic knowledge towards understanding and predicting the ceramic retention and composite coating characteristics during cold spraying.

Spatial and Temporal Scale Bridging of Atomistic-Continuum Concurrent Multiscale Models for Inelastic Modelling of Materials

Subhendu Chakraborty*, Somnath Ghosh**

*Student, **Professor

ABSTRACT

Atomistic-continuum concurrent multiscale models are widely used to assess the deformation mechanisms of material. Where only the most critical part of the domain is modelled with atomistic resolution and rest of the domain is considered as continuum. The interface region between these two subdomains works as a medium of information transfer between these two different models. Most of these multiscale models suffer from two critical limitations. First, mismatch of time-scale between atomistic and continuum domain. Second, limited capability to deal with plasticity. In this present study, both of these issues are addressed. To match the time scale between atomistic and continuum domain, a new time marching scheme is proposed. In this scheme, Strain Boost based Hyperdynamics[1] is used to accelerate the time evolution of the atomistic domain. Under each load increment both atomistic and the continuum domain is iteratively evolved until both the convergence in the solution and time match between the domains are obtained. By using this method, the lowest strain rate of 10^4 is achieved which is impossible to achieve using conventional Molecular Dynamics and within similar computational resource. The proposed method is used to study and parametrize the propagation speed of a preexisting crack in a nickel single crystal. The parameterized crack propagation relation extracted from this concurrent model is used to study the kinetics and energetics of crack evolution for much larger domain using pure continuum scale model[2]. This model is extended further to incorporate the plastic capability for both the atomistic and continuum domain. The continuum domain is modelled using density based CPFE. To transport the plastic state variables from atomistic to continuum, dislocations at the interface region are converted from their discrete representation in the atomistic domain to the density form. This incoming dislocations are considered as incoming flux for the continuum CPFE model. The model is used to study and parametrize the evolution of plastic state variables during inhomogeneous deformation of a nickel single crystal owing to the presence of defects inside the grain. Parametrized relations are used to assess the material behavior for large scale pure continuum simulations. [1] S. Chakraborty, J. Zhang and S. Ghosh. Comp. Mat. Science, 121 (2016) 23-24. [2] J. Zhang, S. Chakraborty and S. Ghosh. J. for Multiscale Comp. Engineering, 15(2): 1-21 (2017).

Control of Discretization and Model Reduction Errors in Shape Optimization Performed Using Isogeometric Analysis (IGA) and Proper Generalized Decomposition (PGD)

Ludovic Chamoin*, Phuong Thai**

*ENS Paris-Saclay, **ENS Paris-Saclay

ABSTRACT

IGA has gained much attention over the last decade, particularly due to the fact that it enables one to solve problems directly on the geometry extracted from a CAD model; it thus simplifies the link between design and analysis [1]. IGA involves, for both the geometry and analysis, smooth and high-order NURBS functions associated with control points and weights. The IGA framework can be effectively coupled with reduced-order modeling (ROM) when dealing with parametrized geometry and shape optimization. To this end, the position of control points and the value of weights become design parameters, and ROM enables to compute efficiently the solutions over the whole parameter space. Here, we focus on ROM performed by means PGD, which is a technique based on a modal decomposition with separation of variables [2]. In the present work, we propose to control error sources inherent to this coupling between IGA and PGD when conducting shape optimization. First, in order to address discretization error, we introduce an a posteriori error estimate based on duality and the Constitutive Relation Error (CRE) concept. It can be used for a large set of mechanics problems, particularly for linear or nonlinear material behaviors described by means of convex potentials (elasticity, visco-plasticity, damage, contact, etc.). To the best knowledge of the authors, it is the first a posteriori error for IGA which is generic and which provides both guaranteed and fully computable bounds. Second, we extend the estimate in order to take into account modal truncation when resorting to PGD solutions. The control of this latter error source uses tools which were primarily introduced in the FEA context [3]. The obtained error estimators and indicators then enable to conduct adaptive processes. The talk will be illustrated with several numerical experiments, for linear or nonlinear (damage) problems, and with a focus on goal-oriented error estimation and adaptivity performance. References: [1] Hughes T.J.R, Cottrell J.A, Bazilevs Y, Isogeometric analysis: CAD, finite elements, NURBS, exact geometry an mesh refinement, Computer Methods in Applied Mechanics and Engineering, 2005, 194:4135-4195 [2] Chinesta F, Keunings R, Leygue A, The Proper Generalized Decomposition for Advanced Numerical Simulations - A Primer, Springer, 2014 [3] Chamoin L, Pled F, Allier P.E, Ladevèze P, A posteriori error estimation and adaptive strategy for PGD model reduction applied to parametrized linear parabolic problems, Computer Methods in Applied Mechanics and Engineering, 2017, 327:118-146

Discretely Entropy Stable Discontinuous Galerkin Methods for Nonlinear Conservation Laws

Jesse Chan*

*Rice University

ABSTRACT

High order methods offer several advantages in the approximation of solutions to hyperbolic equations, such as improved accuracy and low numerical dispersion and dissipation. However, high order methods also tend to suffer instabilities when applied to nonlinear hyperbolic equations such as the compressible Euler equations and shallow water equations. Often, these instabilities require filtering, limiting, or artificial dissipation to ensure that the solution does not blow up. At the root of these problems is the fact that the stability of the continuous problem does not imply stability at the discrete level. This talk will show how to construct high order schemes based on summation-by-parts theory which recover a discrete statement of entropy stability, and will discuss the extension of such methods to a more general class of discontinuous Galerkin methods. We will conclude by showing numerical results in one and two dimensions which support the presented theoretical results.

Thermal Simulation of Fused Filament Fabrication with Fiber Filled Composites

Aaditya Chandrasekhar*, Behzad Rankouhi**, Krishnan Suresh***

*University of Wisconsin-Madison, **University of Wisconsin-Madison, ***University of Wisconsin-Madison

ABSTRACT

Due to recent advancements in material technology such as fiber filled matrix, fused filament fabrication (FFF) is being increasingly used to produce functional parts. The preferential orientation of the fibers, combined with the layer-wise printing leads to enhanced anisotropic material behavior. This can be utilized to obtain desired mechanical performance of the fabricated part [1]. However, studies have shown that the temperature history during the printing process can have an adverse effect on the accumulation of residual stress, delamination, and distortion of the part. In this paper, we numerically investigate the evolution of temperature during the printing of a fiber filled composite using an anisotropic model, and an assembly free finite element solver. The anisotropic orientation of each mesh element is obtained from the machine instruction for the printing process (G-code). This is combined with experimentally obtained thermal conductivity tensor [2], to study the effects of raster path and fiber infill percentage on the heat conduction of the part. The numerical results are validated using infrared thermography during fabrication of samples with commercially available carbon fiber-filled polymer. The simulation framework can be used to predict the behavior of the part during and after the fabrication process. References [1] Zhang, P., Liu, J., & To, A. C. (2017). Role of anisotropic properties on topology optimization of additive manufactured load bearing structures. *Scripta Materialia*, 135, 148–152. <https://doi.org/10.1016/j.scriptamat.2016.10.021> [2] Mulholland, T., Goris, S., Boxleitner, J., Osswald, T. A., & Rudolph, N. (2018). Fiber Orientation Effects in Fused Filament Fabrication of Air-Cooled Heat Exchangers. *JOM*, 1–5. <https://doi.org/10.1007/s11837-017-2733-8>

A General Framework for Predicting Friction in Metals

Michael Chandross^{*}, Adam Hinkle^{**}, Andrew Kustas^{***}, Nicolas Argibay^{****}

^{*}Sandia National Laboratories, ^{**}Sandia National Laboratories, ^{***}Sandia National Laboratories, ^{****}Sandia National Laboratories

ABSTRACT

While pure metals generally exhibit high friction and wear, nanocrystalline metals often show much lower friction and correspondingly low wear. We have developed and validated a model of friction in FCC metals that links the interfacial grain structure directly with the macroscopically measured friction coefficient. Recent work has shown that similarly low friction is possible in BCC metals, and we present a suite of simulations and experiments that demonstrate a general framework for connecting microstructural evolution and tribological response in both FCC and BCC metals. We show evidence that low friction is linked to grain boundary sliding as the dominant mechanism for stress accommodation. We utilize large-scale molecular dynamics simulations and targeted experiments to explore the various steady-state friction regimes of metals and alloys, with a goal of elucidating the structure-property relationships, allowing for the engineering of tribological materials and contacts based on material properties. Sandia National Laboratories is a multimission laboratory managed and operated by National Technology and Engineering Solutions of Sandia, LLC., a wholly owned subsidiary of Honeywell International, Inc., for the U.S. Department of Energy's National Nuclear Security Administration under contract DE-NA0003525.

The Study on Pseudo-elastic Effect of Ni-Ti Shape Memory Alloys

I-Ling Chang*, M.H. Tsai**

*National Cheng Kung University, **National Cheng Kung University

ABSTRACT

The shape memory properties, i.e., phase transformation induced by temperature and stress, of Ni-Ti alloy bulks are investigated using molecular dynamics simulation. First, the phase transformation behaviors of Ni-Ti alloy for various nickel composition ratios are studied under cooling and heating process. W parameter analysis is adopted for phase identification, i.e., martensite and austenite. It is noticed that the transformation temperature decreases as nickel composition ratio increases, which is consistent with experimental observation. Besides, there exists temperature hysteresis in thermal cycle for nickel composition ratio less than 51.5%. Second, the stress-assisted martensitic phase transformation is examined for 51%Ni-Ti alloy under cyclic uniaxial compression loading and unloading. It is noted that the stress needed to induce martensitic phase transformation from austenite at high temperature could become higher or lower with cycles depending on whether the previous loading causes any dislocation inside. The observation could provide an explanation for the contradictive experiment results reported in the literature.

Phase-field Modeling of Grain Growth with CSL Boundaries

Kunok Chang*

*Kyunghee University

ABSTRACT

The phase-field modeling has been actively applied to simulate grain growth phenomena in the solid-state polycrystalline materials. Even though the former works deeply contribute to enhance the fundamental understanding of the grain growth phenomena, they assumed the isotropic grain boundary energy and mobility for the simplicity. In recent years, parallel computing technology, such as GPGPU (General-Purpose computing on Graphics Processing Units) and OpenMP has developed dramatically, and anisotropic grain growth simulation can now be performed on a box-sized workstation rather than a clustered supercomputer. The stress corrosion cracking phenomenon is a long-standing challenge in the field of nuclear engineering because it poses a threat to the integrity of the Ni-based alloy in the secondary system of the nuclear power system. Also, it is well known that CSL (Coincidence Site Lattice) boundary, for example Sigma 3 boundary, play a significant role in determining stress corrosion cracking behavior in Alloy 600. Therefore, understanding of effect of CSL boundary in grain growth of Alloy 600 is highly significant to predict the integrity of the nuclear system. However, incorporating CSL in grain growth simulation requires extremely high computation resources, it has not been considered in the former computational studies of grain growth. In this study, we incorporated not only anisotropic grain boundary energy but also CSL boundary such as sigma 3 grain boundary. We quantitatively analyzed how CSL affects the microstructure evolution of Alloy 600 and the results has been compared with former experimental observations.

Study of Failure of Reinforced Concrete Material with Concrete Damaged Plastic Model

Weitze Chang*

*National Center for Research on Earthquake Engineering, Taiwan

ABSTRACT

Reinforced Concrete (RC) play an important role in modern construction industry caused of its economical, long-life, and easy-molded advantages. However, the combination of steel reinforcing bars and concrete which mixed by rock (coarse aggregates), sand, water, and various power-sized particles makes its dynamic behavior complex and not easy to be predicted, especially especially after failure occurs. Traditionally, Finite Element Analysis (FEA) is a good choice to model RC material and works well in both elastic and plastic stage, but cannot describe the post-peak part after concrete failure. In this study, the Concrete Damaged Plastic (CDP) model (Lubliner, et al., 1989; ABAQUS Inc., 2010) is introduced to model the dynamic behavior of RC column in cyclical loading test. The friction and sliding between the interface of steel reinforcing bars and concrete material is also considered. After systematic study of model simplifying, performance improving, and validation with experimental data, this paper show that the proposed simulation can be expected to applied in concrete industry in the future. Keywords: Reinforced concrete, cyclical loading test, fracture, concrete damaged plastic model Reference * Lubliner, J., Oliver, J., Oller, S., and Oñate, E. (1989). "A Plastic-Damage Model for Concrete, International Journal of Solids and Structures, 25: 299-326. * ABAQUS Inc., (2010). "Damaged Plasticity Model for Concrete and Other Quasi-brittle Materials," in Abaqus Analysis User's Manual v6.10, Section 4.5.2, 14 pages.

Projection-based Model Reduction of Nonlinear Structural Dynamics Models with Contact Surfaces

Todd Chapman*, Charbel Farhat**

*Stanford University, **Stanford University

ABSTRACT

Projection-based model order reduction (PMOR) is a potentially enabling technology for the routine analysis of full configuration structural systems through numerical methods. Relatively speaking however, PMOR is still in its infancy in the context on nonlinear analysis but significant progress has been made in the last decade especially in the area of hyper reduction. However, in many scenarios contact must be modeled in order to analyze realistic engineering configurations. Incorporating contact constraints into a projection-based reduced order model (PROM) poses a distinct difficulty since the reduced coordinates are not associated with a mesh while contact is intimately linked to locality on a mesh. Furthermore, in the case of projection-based hyper-reduced order models (HPROMs) the majority of the mesh is discarded after a sampling procedure so that determining the appropriate constraints becomes non-trivial. Enforcement of contact constraints has been addressed in the context of PMOR through the use of Lagrange multipliers for node-to-node contact. The approach requires the collection of dual snapshots which, like the compression of displacement snapshots through a truncated SVD, must be compressed under the additional constraint of nonnegativity. This leads to the construction of a dual reduced order basis (ROB) through nonnegative matrix factorization. The dual ROB associated with the fixed node-to-node contact can then be precomputed offline. However, scenarios involving kinematic nonlinearities and sliding contact in which constraints cannot be reasonably precomputed offline have not been addressed. In addition to these difficulties, the contact PROM with Lagrange Multipliers must satisfy Inf-Sup conditions for solvability which requires that the dual ROB be of a lesser dimension than the primal ROB. The dual subspace must be large enough to accurately reconstruct the contact forces but not so large that it violates solvability of the reduced system of equations. Since contact is often associated with highly concentrated forces, snapshot data will typically be sparse which poses challenges for compression due to the uncertainty principle. This talk presents a one-sided projection method (akin to the mortar method) for the reduction of contact forces arising from large deformation contact. The principle of nonnegative matrix completion is also presented in the context of efficiently compressing dual snapshot data for the construction of an appropriate nonnegative dual basis. These two components are demonstrated in constructing effective PROMs for several challenging contact problems including the underbody blast of an ARES tank.

AN ISOGEOMETRIC FORMULATION FOR LARGE DEFORMATION ANALYSIS OF SOLIDS IN BOUNDARY REPRESENTATION

MARGARITA CHASAPI* AND SVEN KLINKEL*

*Chair of Structural Analysis and Dynamics

RWTH Aachen University

Mies-van-der-Rohe Str. 1, 52074, Aachen, Germany

Email address: chasapi@lbb.rwth-aachen.de, website: <http://www.lbb.rwth-aachen.de/>

Key words: Isogeometric Analysis, NURBS Basis Functions, Nonlinear Solid Surface, Scaled Boundary Finite Element Method, Large Deformations.

Abstract. This contribution deals with geometrical nonlinear problems within the framework of the so-called scaled boundary isogeometric formulation (SB-IGA). We propose this approach for the isogeometric analysis of surfaces especially, if only a boundary description of the geometry is available. This is for example the case with solids, which are typically modeled only by their boundary surfaces in CAD. To provide a numerical approach for surfaces with arbitrary number of boundaries, we combine the merits of the isogeometric analysis and the scaled boundary finite element method. The main idea lies in the parameterization of the solid in analogy with the scaled boundary finite element method (SB-FEM). Hence, the boundary of the surface is scaled in respect to a specified scaling center inside the domain. To solve the boundary value problem, we apply the weak form of equilibrium in the circumferential direction of the boundary and the radial scaling direction in the interior of the domain. As in standard IGA, the NURBS functions that describe the geometry of the boundary also interpolate the unknown displacement field. We employ NURBS also for the approximation of the solution in radial scaling direction. This approach has shown promising results in the scope of linear elasticity and plasticity problems. Here, a formulation for geometrical nonlinear 2D problems is presented. The derived linearized operator is used within a Newton-Raphson iterative scheme. We study numerical examples in the scope of nonlinear elasticity and plasticity and assess the performance of SB-IGA by comparison to other numerical methods.

1 INTRODUCTION

In the finite element analysis (FEA) framework, Lagrange basis functions form the basis for the approximation of the geometry and the displacement response of the structure. Due to this approximation, the geometry of the analysis model differs from the original geometry of the Computer Aided Design (CAD) software. Hughes introduced the idea of Isogeometric Analysis [¹, ²], which circumvents the geometrical approximation error and provides a seamless integration of CAD and FEA software. In IGA, NURBS interpolate the geometry and the solution field.

Thus, the geometry remains *exact* throughout the entire analysis process. Currently, commercial CAD software employ the boundary representation modeling technique for the modeling of solids [3]. Thus, only the boundary surfaces of the solid are available in CAD. This observation motivates the development of a boundary-oriented formulation within the isogeometric analysis framework.

A well-known boundary-oriented method that combines the advantages of the boundary element method (BEM) and the finite element method (FEM) is the scaled boundary finite element method (SB-FEM). It is as a semi-analytical fundamental-solution-less boundary element method [4, 5]. For the parametrization of the structure interior, a radial scaling parameter and a parameter in the circumferential direction along the boundary is defined. The scaling parameter runs from a central point, the scaling center, to the boundary. The position of the scaling center is chosen so, that the total boundary of the domain is visible, which means that the domain occupied by the solid must be star-shaped. Sub-structuring of the domain is, in general, possible. In this way, the domain is covered by scaling the boundary in respect to the scaling center. In the circumferential direction, a standard finite element approach with Lagrange basis functions is employed [4]. NURBS basis functions can be used as given in [6, 7, 8, 9] for the description of the geometry and the approximation of the solution. The weak form of equilibrium is only enforced in the circumferential direction. In the scaling direction, the equilibrium is strongly applied. This results in a second order ordinary differential equation (ODE) in terms of the scaling parameter, which is the so-called scaled boundary finite element equation. For linear elasticity, a unique analytical solution exists, which can be computed with the eigenvalue method. For nonlinear problems, a linearization based on the homotopy analysis method is proposed in [10] and special shape functions based on the solution of linear problems are derived in [11, 12]. Alternatively, the Galerkin projection of the weak form in radial scaling direction allows the treatment of nonlinear problems. This approach has been investigated in [13, 14] for the solution of elasticity and plasticity problems. The performance of B-splines and NURBS for nonlinear problems has been studied e.g. in [15, 16].

This paper deals with an isogeometric formulation for large deformation analysis of surfaces, which are designed by the boundary representation modeling technique in CAD. The geometry and displacement of the boundary is interpolated by NURBS basis functions. Hence, we keep the *exact* geometry of the boundary for the analysis. We employ NURBS for the approximation in scaling direction, which allows for nonlinear behavior. The Galerkin method is applied in both the radial scaling and the circumferential direction. Due to the nonlinear deformation behavior, the iterative Newton-Raphson scheme is employed for the linearization of the solution. Finally, nonlinear problems are assessed by comparison to the isogeometric analysis

2 PARAMETRIZATION

The parametrization of the computational domains follows the idea of the scaled boundary finite element method [4, 5]. The two-dimensional domain Ω is decomposed into sectional subdomains $\partial\Omega_s$, which are parameterized in the same fashion and assembled to cover the whole domain. For the transformation of the geometry, a radial scaling parameter ξ is introduced to describe the interior of each section, as shown in Figure 1. The boundary of the solid is scaled in respect to a scaling center C , which is defined such as the total boundary of the solid is visible. This approach requires a star-shaped domain. For domains that do not fulfill this requirement, sub-structuring is

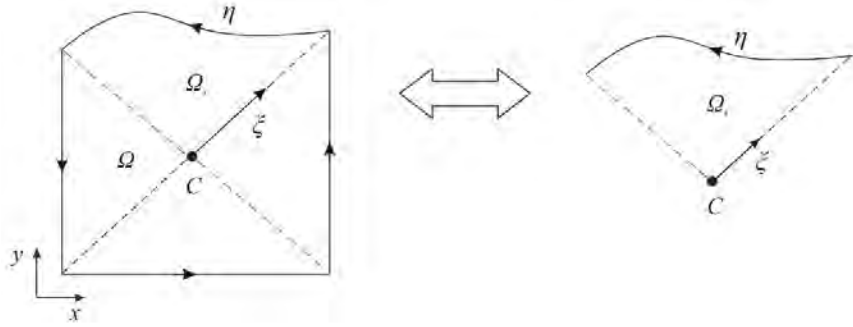


Figure 1: The scaled boundary parametrization of the domain Ω .

possible [4, 7, 12, 14]. The radial scaling parameter ξ runs from the scaling center towards the boundary, where $\xi = 0$ denotes the scaling center C and $\xi = 1$ the boundary. The circumferential direction of each section corresponds to the boundary of the domain, which is parameterized with a circumferential parameter η running from $\eta = 0$ to $\eta = 1$. The coordinates of the scaling center are denoted as \mathbf{x}_0 . Employing this parametrization, the position of a point on the boundary \mathbf{x}_s and inside the domain \mathbf{x} can be expressed as

$$\mathbf{x}_s = \mathbf{N}_b(\eta)\mathbf{X}_s \quad \text{on } \partial\Omega, \quad \mathbf{x} = \mathbf{x}_0 + \xi(\mathbf{x}_s(\eta) - \mathbf{x}_0) \quad \text{in } \Omega. \quad (1)$$

The NURBS basis functions $\mathbf{N}_b(\eta)$ are employed to describe the boundary of the surface. This fits perfectly to the boundary representation modeling technique employed in CAD. The vector \mathbf{X}_s denotes the coordinates of the control points on the boundary. The Jacobian matrix can be derived by employing the scaled boundary transformation as

$$\mathbf{J} = \begin{bmatrix} \frac{\partial x}{\partial \xi} & \frac{\partial y}{\partial \xi} \\ \frac{\partial x}{\partial \eta} & \frac{\partial y}{\partial \eta} \end{bmatrix} = \begin{bmatrix} 1 & 0 \\ 0 & \xi \end{bmatrix} \underbrace{\begin{bmatrix} x_s - x_0 & y_s - y_0 \\ \frac{\partial x_s}{\partial \eta} & \frac{\partial y_s}{\partial \eta} \end{bmatrix}}_{\bar{\mathbf{J}}(\eta)} \quad (2)$$

which results in a multiplicative decomposition with the determinant $\det \mathbf{J} = \xi \det \bar{\mathbf{J}} = \xi \bar{J}$. An area element can be transformed from the physical to the parameter space by $dA = \xi \bar{J} d\xi d\eta$. Furthermore, we define the differential operator \mathbf{D} as a function of the submatrices $\mathbf{b}_1(\eta)$, $\mathbf{b}_2(\eta)$

$$\mathbf{D} = \begin{bmatrix} \frac{\partial}{\partial x} & 0 & \frac{\partial}{\partial y} & 0 \\ 0 & \frac{\partial}{\partial y} & 0 & \frac{\partial}{\partial x} \end{bmatrix} = \frac{1}{\bar{J}} \left(\mathbf{b}_1^T(\eta) \frac{\partial}{\partial \xi} + \frac{1}{\xi} \mathbf{b}_2^T(\eta) \frac{\partial}{\partial \eta} \right), \quad (3)$$

$$\mathbf{b}_1^T(\eta) = \begin{bmatrix} y_{s,\eta} & 0 & -x_{s,\eta} & 0 \\ 0 & -x_{s,\eta} & 0 & y_{s,\eta} \end{bmatrix}, \quad \mathbf{b}_2^T(\eta) = \begin{bmatrix} y_0 - y_s & 0 & x_s - x_0 & 0 \\ 0 & x_s - x_0 & 0 & y_0 - y_s \end{bmatrix}.$$

3 GOVERNING EQUATIONS

In this section, the two-dimensional boundary value problem for nonlinear elasticity will be formulated. The domain Ω is bounded by $\partial\Omega = \partial_u\Omega \cup \partial_t\Omega$, where $\partial_u\Omega$ is the boundary with a prescribed displacement $\bar{\mathbf{u}}$ and $\partial_t\Omega$ is the boundary with a prescribed traction $\bar{\mathbf{t}}$. The derivation is restricted to bounded domains without loss of generality. The governing equation reads

$$\text{Div } \mathbf{P} + \mathbf{b} = \mathbf{0}. \quad (4)$$

Here the vector \mathbf{P} denotes the stress vector in the reference configuration and \mathbf{b} the body force. The Dirichlet and Neumann boundary condition is defined as

$$\mathbf{u} = \bar{\mathbf{u}} \quad \text{on } \partial_u\Omega, \quad \mathbf{NP} = \bar{\mathbf{t}} \quad \text{on } \partial_t\Omega. \quad (5)$$

\mathbf{N} is the normal outward vector on the reference configuration and reads

$$\mathbf{N} = \begin{bmatrix} N_x & 0 & N_y \\ 0 & N_y & N_x \end{bmatrix}. \quad (6)$$

Considering large deformation theory, the deformation gradient and right Cauchy-Green tensor are given as

$$\mathbf{F} = \text{Grad} \mathbf{x} = \mathbf{I} + \text{Grad} \mathbf{u}, \quad \mathbf{C} = \mathbf{F}^T \mathbf{F}. \quad (7)$$

We consider a hyperelastic Neo-Hooke material with the strain energy function

$$W(\mathbf{C}) = \frac{\mu}{2}(\text{tr} \mathbf{C} - 3) - \mu \ln(J) + \frac{\Lambda}{4}(J^2 - 1 - 2 \ln(J)), \quad (8)$$

where μ is the shear modulus, Λ the Lamé parameter and $J = \det \mathbf{F}$. The first and second Piola-Kichhoff stress can be expressed as

$$\mathbf{S} = 2 \frac{\partial W}{\partial \mathbf{C}}, \quad \mathbf{P} = \mathbf{FS}. \quad (9)$$

4 DISCRETIZATION WITH NURBS

In this study, we follow the idea of isogeometric analysis, thus NURBS basis functions are employed to describe the geometry of the boundary and to approximate the displacements $\mathbf{u}_b(\xi = 1)$ at the boundary of each section Ω_s . The expression for the geometry and displacement of the boundary reads

$$\mathbf{x}_s = \sum_{i=1}^{n_{bc}} R_{i,p}(\eta) \mathbf{X}_{s,i} = \mathbf{N}_b(\eta) \mathbf{X}_s, \quad \mathbf{u}_b = \sum_{i=1}^{n_{bc}} R_{i,p}(\eta) \mathbf{U}_{s,i} = \mathbf{N}_b(\eta) \mathbf{U}_s(\xi) \quad (10)$$

where i is the index of the control point along the boundary and n_{bc} the number of control points of section Ω_s . The coordinates of the boundary control points are denoted by \mathbf{X}_s and boundary NURBS by $\mathbf{N}_b(\eta)$. In order to construct NURBS, an open knot vector is introduced with $\mathbf{H} = [\eta_1, \eta_2, \dots, \eta_{n_{bc}+p+1}]$, where $\eta_i \in \mathbb{R}$ is the i th knot and i is the knot index. The B-spline basis functions are employed, which are derived by the Cox de Boor formula [17]. Considering the weighting factor w_i for the i th B-spline function $N_{i,p}$, the NURBS basis function $R_{i,p}$ with polynomial degree p reads

$$R_{i,p} = \frac{N_{i,p} w_i}{\sum_{k=1}^{n_{bc}} N_{k,p} w_k} \quad (11)$$

In the scaling direction, we employ NURBS basis functions to approximate the displacement response. Note, that straight lines represent the scaling direction. The weighting factors are set equal along a radial scaling line, i.e. we have B-splines in the scaling direction. In order to construct the basis functions in scaling direction, the knot vector $\Xi = [\xi_1, \xi_2, \dots, \xi_{n_{cp}+q+1}]$ is introduced. Here, the number of control points per radial scaling line is n_{cp} and the polynomial degree q . Note, that $\xi_1 = 0$ stands for the scaling center C and $\xi_{n_{cp}+q+1} = 1$ for the boundary. After rearranging all control point vectors $\mathbf{U}_{s,i}$ of Equation (10) in the vector \mathbf{U}_s and approximating with the basis function $R_{j,p}$ in scaling direction, the displacement for one section reads

$$\begin{aligned} \mathbf{u}_b &= \underbrace{\begin{bmatrix} R_{1,p} & 0 & R_{2,p} & 0 & \dots & R_{n_{bc},p} & 0 \\ 0 & R_{1,p} & 0 & R_{2,p} & \dots & 0 & R_{n_{bc},p} \end{bmatrix}}_{\mathbf{N}_b(\eta)} \mathbf{U}_s(\xi) \\ &= \mathbf{N}_b(\eta) \sum_{j=1}^{n_{cp}} R_{j,q}(\xi) \mathbf{U}_j = \mathbf{N}_b(\eta) \mathbf{N}_s(\xi) \mathbf{U}. \end{aligned} \quad (12)$$

Note, that for each control point two nodal degrees are assumed, so that the dimension of the displacement vector $\mathbf{U}_{s,i}$ is 2 and of the vector \mathbf{U} is $2 \cdot n_{cp}$ respectively. Figure 2 illustrates an example of the interpolation in the radial scaling and circumferential direction for a section. It is worth noting, that the stiffness matrix of a section can be alternatively derived by employing triangular patches in the framework of isogeometric analysis. In the following, we express the discretized form of the operator \mathbf{D}^h as a function of the submatrices $\mathbf{b}_1(\eta)$ and $\mathbf{b}_2(\eta)$

$$\mathbf{D}^h = \frac{1}{\bar{J}} \left(\mathbf{b}_1 \mathbf{N}_b \mathbf{N}_{s,\xi} + \frac{1}{\xi} \mathbf{b}_2 \mathbf{N}_b \mathbf{N}_s \right). \quad (13)$$

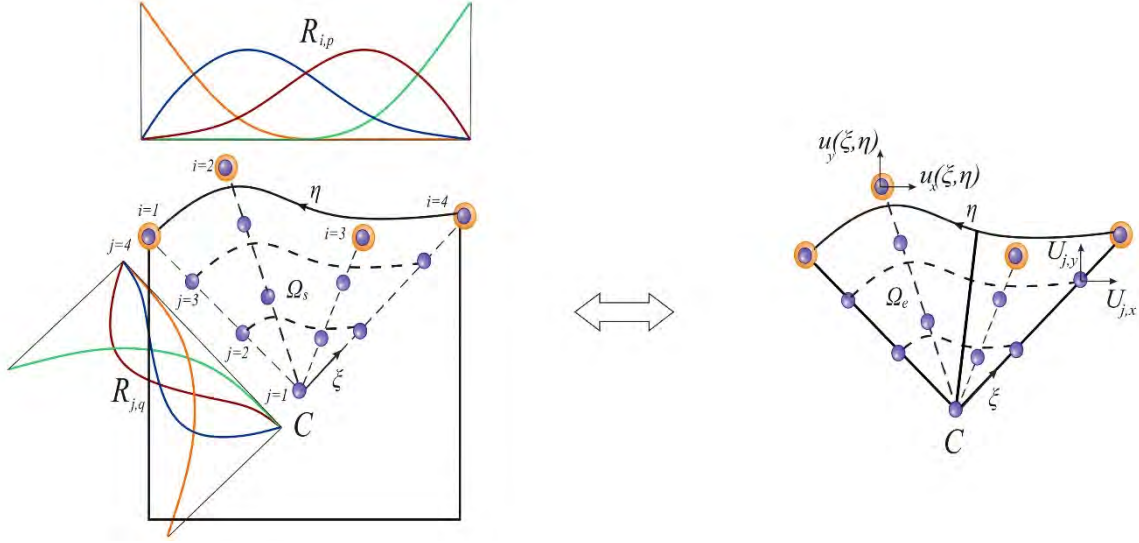


Figure 2: NURBS basis functions in parameter space of section Ω_s .

For the solution, we employ the Galerkin method. Considering Equation (4) and the boundary conditions in Equation (5) it holds

$$\sum_{s=1}^{nsec} \delta \mathbf{U}_j^T \left[\int_{\Omega_s} \xi \mathbf{D}^{h^T} \hat{\mathbf{F}}^T \mathbf{S} \bar{J} d\xi d\eta \mathbf{U}_j - \int_{\Omega_s} \xi \mathbf{N}^T \mathbf{b} \bar{J} d\xi d\eta - \int_{\partial\Omega_s} \mathbf{N}^T \mathbf{b}_2^T \hat{\mathbf{F}} \mathbf{S} l d\xi \mathbf{U}_j \right] = \mathbf{0}. \quad (14)$$

Here, the vector $\mathbf{N} = \mathbf{N}_b(\eta) \mathbf{N}_s(\xi)$ denotes the shape functions per radial scaling line and l is the integration length per radial scaling line. The vector $\hat{\mathbf{F}}$ contains the components of the deformation gradient. For the sake of simplicity, the body forces are neglected. By applying a linearization to the weak form with a displacement increment of $\Delta \mathbf{u} = \mathbf{u}^{k+1} - \mathbf{u}^k$ we derive

$$\mathbf{D} \mathbf{G}^k(\mathbf{u}^k, \delta \mathbf{u}) \Delta \mathbf{u} = \sum_{s=1}^{nsec} \delta \mathbf{U}_j^T \int_{\Omega_s} \underbrace{\xi \mathbf{D}^{h^T} (\hat{\mathbf{F}}^T \mathbb{C}_T \hat{\mathbf{F}} + \hat{\mathbf{S}}) \mathbf{D}^h \bar{J}}_{\mathbf{K}} d\xi d\eta \Delta \mathbf{U}_j \quad (15)$$

where \mathbf{K} denotes the stiffness matrix and \mathbb{C}_T the consistent tangent modulus. Moreover, $\hat{\mathbf{S}}$ contains the components of the second Piola-Kirchhoff stress. Having derived all necessary equations, we can now apply this formulation for geometrical nonlinear analysis of boundary represented surfaces.

5 NUMERICAL EXAMPLES

This section illustrates the performance of the proposed formulation by means of two numerical examples. The accuracy and efficiency of the proposed approach is evaluated by comparison to the isogeometric analysis.

5.1 Cook's membrane

The proposed formulation is employed for the nonlinear analysis of Cook's membrane. The geometry and boundary conditions are presented in Figure 3. The scaling center C is defined here as the geometric center of the domain. The computational domain is partitioned into 4 sections. The boundary and scaling direction of each section is initially defined with the polynomial degree $p = 2$ and extends to $p = 4$ and $p = 6$. Additionally, h -refinement is performed for each polynomial degree. Plain strain state is assumed. The trapezoidal plate of Figure 3 is subjected to combined bending and shear. Reference results are available in the literature for large deformation analysis [18, 19].

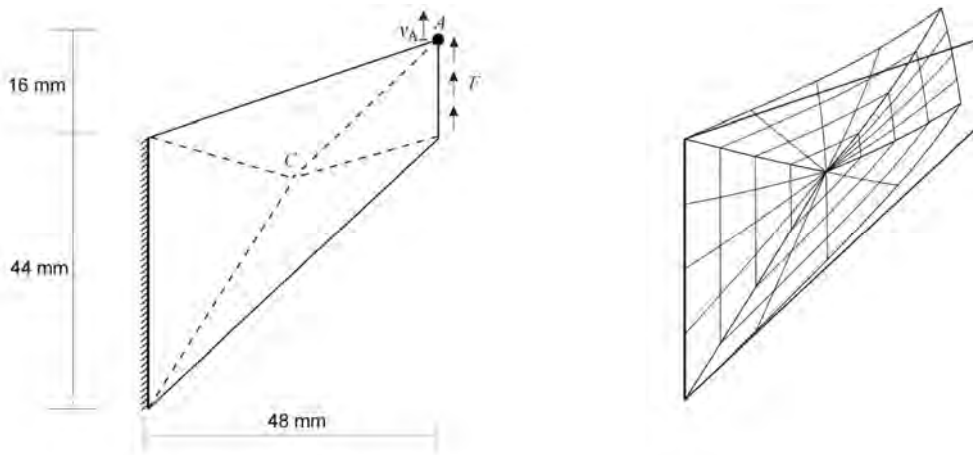


Figure 3: Problem definition and final deformed configuration.

For better illustration, we first refer to the small strain range and study the performance for nonlinear material behavior. A J_2 -plasticity model is employed for the analysis in analogy to [14]. The material properties are the elasticity modulus $E = 207$ MPa, the Poisson's ratio $\nu = 0.3$, the yield stress $\sigma_y = 0.45$ MPa and the linear isotropic hardening modulus $H = 0.12924$. The unit vertical force $F = 1.0$ N is applied per load step. In Figure 4 we observe the load deformation curve for the vertical displacement v_A . For comparison, an isogeometric computation is performed. Both solutions are computed with a mesh of sixth order shape functions and almost the same degrees of freedom. The results imply that there is a good agreement between the proposed formulation and isogeometric analysis in the small strain range. Furthermore, we consider nonlinear deformation behavior. The material properties are set according to reference studies in the literature for better comparison [19]. Here, the bulk modulus is $\kappa = 40.0942 \cdot 10^4$ MPa and the shear modulus $\mu = 80.1938$ MPa. This leads to a nearly incompressible state. The unit force $F = 1.0$ N is applied per load step in 100 load steps. The final deformed mesh can be seen in Figure 3. For comparison, we perform the computation on isogeometric k -refined meshes. The results can be observed in Figure 5. The results with quadratic polynomial degree seem to suffer from locking for both the proposed approach and IGA. The proposed formulation performs better than IGA for coarse discretizations, whereas IGA performs better for finer discretizations.

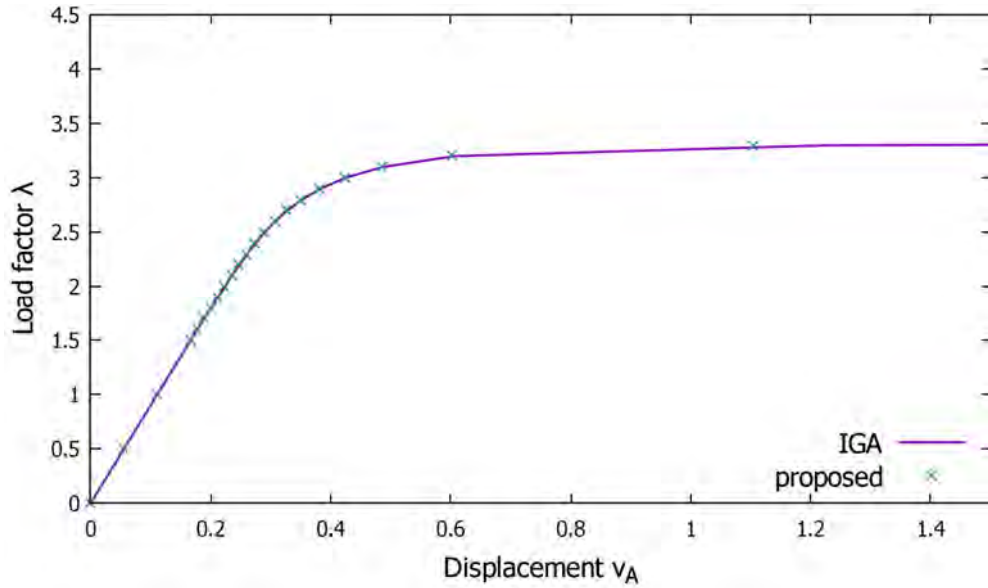


Figure 4: Load deformation curve and comparison with IGA.

Both solutions converge to the same value, which agrees very well with the reference results in the literature [19]. For higher polynomial degrees, locking is alleviated without any treatment of the incompressibility. The results indicate a very good agreement for higher polynomial degrees. It can be concluded that the proposed formulation converges for all polynomial degrees and is in general comparable to isogeometric analysis.

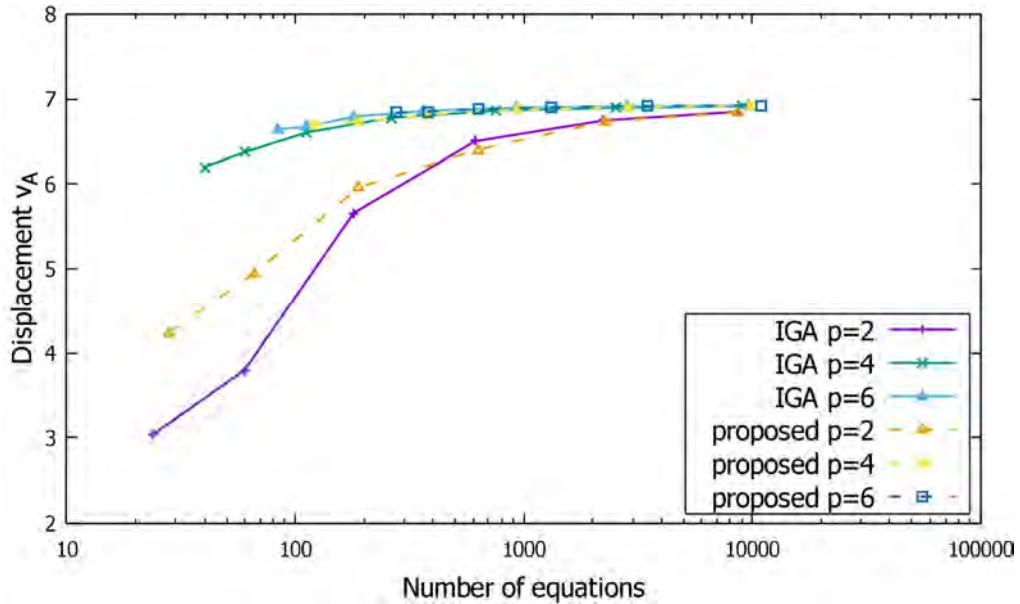


Figure 5: Convergence study and comparison with IGA.

5.2 Notched plate

The second numerical example concerns a notched plate with the geometry and boundary conditions shown in Figure 6. The objective of this test is to demonstrate the applicability of the formulation for non-convex polygonal domains with arbitrary number of boundaries. In the present study, we restrict ourselves to bounded domains. Therefore, the domain is sub-structured here in two subdomains with scaling center C_1 and C_2 respectively. Note, that an application of the formulation to unbounded domains is in principle possible. Plain strain state is assumed. The material properties are the shear modulus $\mu = 0.3422 \text{ N/mm}^2$ and the Lamé constant $\Lambda = 99.771867 \text{ N/mm}^2$. Displacement control is applied in 50 steps, with a total prescribed displacement $u = 100 \text{ mm}$ on the right edge of the plate.

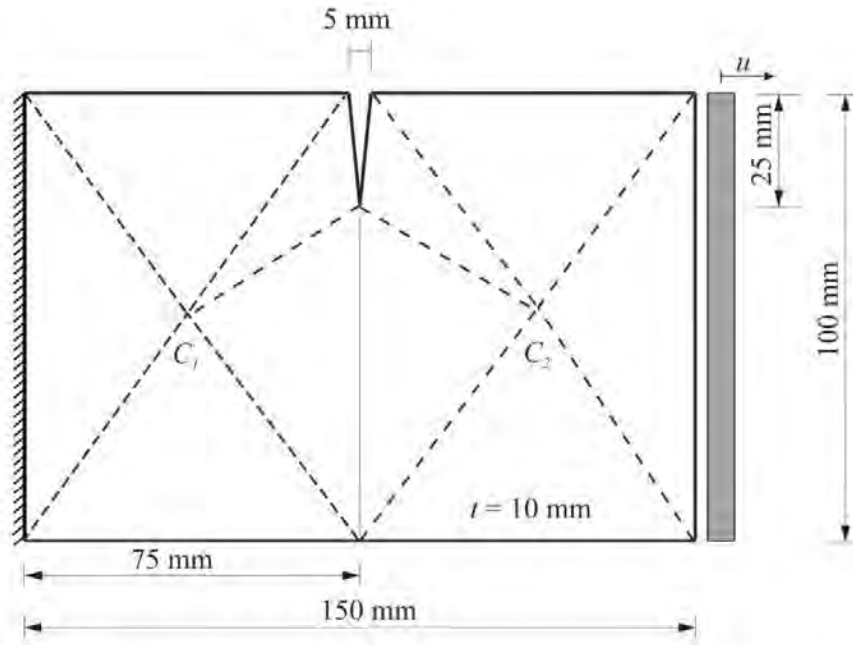


Figure 6: Problem definition and loading. ^[11]

For the computation, the polynomial degree is chosen as $p = 4$ for the boundary and the scaling direction. The horizontal reaction force of the plate is monitored. For comparison, an isogeometric mesh with polynomial degree $p = 4$ and nearly the same degrees of freedom is computed. Due to the geometry, 4 rectangular patches are employed to model the area around the notch with IGA. Figure 7 depicts the force displacement curve for both solutions. The results indicate a very good agreement. It can be concluded, that the proposed formulation seems to be a promising approach for the modeling of domains with arbitrary number of edges that does not induce any significant modeling effort.

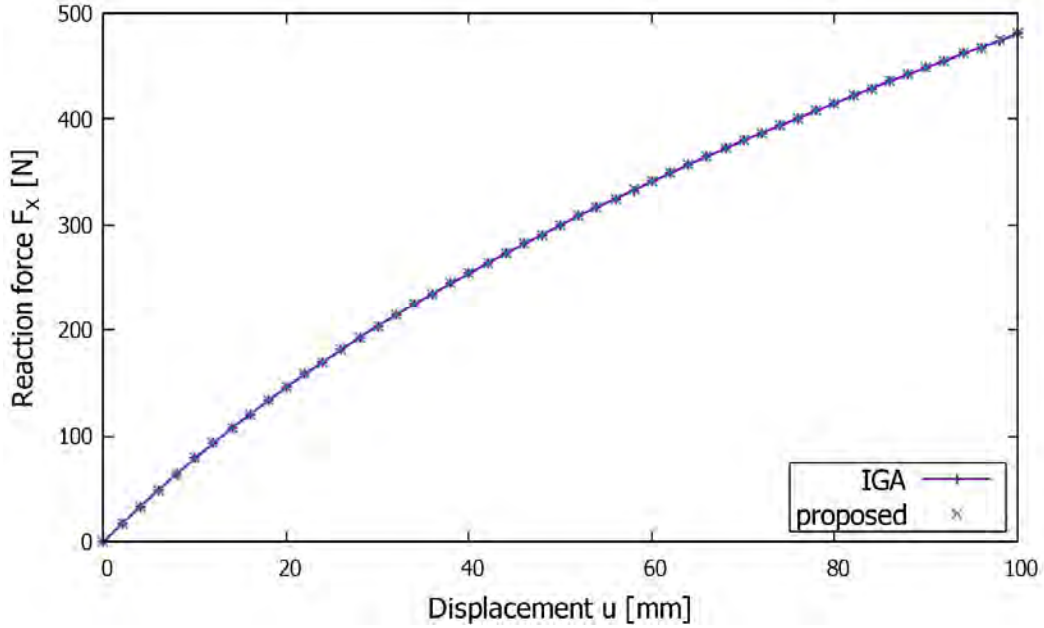


Figure 7: Reaction force displacement curve and comparison with IGA.

6 CONCLUSIONS

This paper deals with an isogeometric formulation for geometrical nonlinear analysis of boundary represented solids. The proposed approach fits perfectly the boundary representation modeling technique employed in CAD to model solids. To parameterize the boundary surfaces of the solid, the idea of the scaled boundary finite element method is employed. NURBS basis functions describe the geometry and approximate the solution. Hence, the *exact* geometry of the boundary is exploited for the analysis. For the solution, we employ the Galerkin method. The linearized operator is derived and used within an iterative Newton-Raphson scheme. We assess the formulation based on numerical examples of nonlinear elasticity and plasticity. For comparison, we employ the isogeometric analysis. The results indicate a good agreement with the isogeometric analysis. The proposed formulation is applicable to domains with arbitrary number of edges and sub-structuring is in general possible. An algorithmic framework for the optimal decomposition of arbitrary domains is a subject of future research. Finally, it can be concluded that the proposed formulation seems to be a promising alternative to isogeometric analysis, if only the geometry of the boundary is available.

ACKNOWLEDGMENTS

The first author wishes to acknowledge the support of the International Association for Computational Mechanics (IACM) for the participation at the 13th World Congress on Computational Mechanics. The financial support of the German Research Foundation (DFG) for the research is also acknowledged.

REFERENCES

- [1] Hughes, T.J.R, Cottrell, J.A. and Bazilevs, Y. Isogeometric analysis: CAD, finite elements, NURBS, exact geometry and mesh refinement. *Comput. Methods Appl. Mech. Engrg.* (2005) 194:4135-4195.
- [2] Cottrell, J.A., Hughes, T.J.R. and Bazilevs, Y. *Isogeometric Analysis: Toward Integration of CAD and FEA*. John Wiley & Sons, (2009).
- [3] Stroud, I. *Boundary Representation Modelling Techniques*. Springer, (2006).
- [4] Song, C. and Wolf, J.P. The scaled boundary finite-element method – alias consistent infinitesimal finite-element cell method – for elastodynamics. *Comput. Methods Appl. Mech. Engrg.* (1997) 147:329-355.
- [5] Song, C. A matrix function solution for the scaled boundary finite-element equation in statics. *Comput. Methods Appl. Mech. Engrg.* (2004) 193:2325-2356.
- [6] Lin, G., Zhang, Y., Hu, Z. and Zhong, H. Scaled boundary isogeometric analysis for 2D elastostatics. *Science China Physics, Mechanics and Astronomy* (2014) 57:286-300.
- [7] Natarajan, S., Wang, J.C., Song, C. and Birk, C. Isogeometric analysis enhanced by the scaled boundary finite element method. *Comput. Methods Appl. Mech. Engrg.* (2015) 283:733-762.
- [8] Klinkel, S., Chen, L. and Dornisch, W. A NURBS based hybrid collocation-Galerkin method for the analysis of boundary represented solids. *Comput. Methods Appl. Mech. Engrg.* (2015) 284:689-711.
- [9] Chen, L., Dornisch, W. and Klinkel, S. Hybrid collocation-Galerkin approach for the analysis of surface represented 3D-solids employing SB-FEM. *Comput. Methods Appl. Mech. Engrg.* (2008) 295: 268–289.
- [10] Lin, Z. and Liao, S. The scaled boundary FEM for nonlinear problems. *Commun. Nonlinear Sci. Numer. Simulat.* (2011) 16:63-75.
- [11] Behnke, R., Mundil, M., Birk, C. and Kaliske, M. A physically and geometrically nonlinear scaled-boundary-based finite element formulation for fracture in elastomers. *Internat. J. Numer. Methods Engrg.* (2014) 99:966-999.
- [12] Ooi, E., Song, C. and Tin-Loi, F. A scaled boundary polygon formulation for elastoplastic analyses. *Comput. Methods Appl. Mech. Engrg.* (2014) 268:905-937.

- [13] Chen, L., Simeon, B. and Klinkel, S. A NURBS based Galerkin approach for the analysis of solids in boundary representation. *Comput. Methods Appl. Mech. Engrg.* (2016) 305:777-805.
- [14] Chasapi, M. and Klinkel, S. A scaled boundary isogeometric formulation for the elasto-plastic analysis of solids in boundary representation. *Comput. Methods Appl. Mech. Engrg.* (2018) 333:475-496.
- [15] Breitenberger, M., Apostolatos, A., Philipp, B., Wüchner, R. and Bletzinger, K.-U. Analysis in computer aided design: Nonlinear isogeometric B-Rep analysis of shell structures. *Comput. Methods Appl. Mech. Engrg.* (2015) 284:401-457.
- [16] Schillinger, D., Ruess, M., Zander, N., Bazilevs, Y., Düster, A. and Rank, E. Small and large deformation analysis with the p - and B-spline versions of the Finite Cell Method. *Comput. Mech.* (2012) 50:445-478.
- [17] Piegl, L. and Tiller, W. The NURBS Book, in: *Monographs in Visual Communications*. Springer, (1997).
- [18] Mathisen, K., Okstad, K.M., Kvamsdal, T. and Raknes, S. Isogeometric analysis of finite deformation nearly incompressible solids. *J. Struct. Mech.* (2011) 44:260-278.
- [19] Elguedj, T., Bazilevs, Y., Calo, V. and Hughes, T. \bar{B} and \bar{F} projection methods for nearly incompressible linear and non-linear elasticity and plasticity using higher-order NURBS elements. *Comput. Methods Appl. Mech. Engrg.* (2008) 197:2732-2762.

Error Estimation for Stress Distributions in Polycrystalline Alloys

Kamalika Chatterjee*, Robert Carson**, Paul Dawson***

*Cornell University, **Cornell University, ***Cornell University

ABSTRACT

Crystal based finite element modeling is an invaluable tool for predicting stress distributions in polycrystalline structural alloys such as Ti-6Al-4V. The accuracy of the prediction depends on estimation and control of the errors associated with discretization. In the current work, the errors in the stress distribution are estimated in virtual polycrystalline samples of alpha-Titanium (hcp phase of Ti-6Al-4V). To estimate the error, the discontinuous stress field (element-by-element stresses) over a grain is smoothed by projecting the stress components to the nodes [1]. The differences between the continuous (smooth) and discontinuous stress fields, calculated at individual gauss points are utilized to estimate the L2 norm of errors for corresponding elements and grains. Error estimations are performed for different cases of microstructures and sample instantiations (using Neper [2]). Magnitudes of the errors are found to depend on microstructural features. For example, the locations of sharp orientation gradients developed through heterogeneous deformation in the polycrystal are associated with significant errors. Mesh refinement is performed at those locations based on the numerical solution obtained using a trial mesh. Simulations then are repeated using the refined mesh to reduce the errors in the problematic regions. The mesh refinement technique introduced in this work helps improve the prediction of stress distributions in polycrystalline aggregates. [1] Zienkiewicz, O. C., & Zhu, J. Z. (1987). International journal for numerical methods in engineering, 24(2), 337-357. [2] Quey, R., Dawson, P. R., & Barbe, F. (2011). Computer Methods in Applied Mechanics and Engineering, 200(17), 1729-1745.

Computing Singularly Perturbed Differential Equations and Plasticity Without Constitutive Assumptions

Sabyasachi Chatterjee*, Amit Acharya**

*Carnegie Mellon University, **Carnegie Mellon University

ABSTRACT

Obtaining coarse response of systems of ordinary differential equations (ODE) containing rapidly oscillatory response as well as fast monotonic decay without detailed information on the evolution of the original (fine) variables is an interesting, but challenging task. For a given autonomous system of ODE, we consider developing practical models for determining the slow/coarse behavior of the ODE system which reflect a measurement of the underlying dynamics. We study equations with and without apriori split into slow and fast components. When there is a vast separation of the time-scales of the coarse and the fine dynamics, computing the ordinary differential equation takes a lot of computing time and is not practical. The goal of our study is to suggest efficient computational tools that help revealing the limit behavior of such systems. We define coarse variables using modern mathematical tools like Young Measure and Practical Time Averaging (PTA) which incorporates many rigorous ideas. The computational algorithm reveals an approximation of the limit dynamics which is an approximation of the full solution. We also discuss how to determine the fine initial conditions which ensures a correct coarse response. Finally, we apply this method to develop a macroscopic model to compute the plastic strength and study the microstructure of crystalline materials at the meso-macro scale from the underlying motion of crystal defects. We couple an exact, non-closed partial differential equation based theory (Mesoscale Field Dislocation Mechanics, MFDM) representing the evolution of space-time averaged dislocation dynamics, that contains well-defined place-holders for microscopic dislocation dynamics based input. These inputs are prescribed by a carefully designed coupling, on the slow time-scale of meso-macro response, with time-averaged response of fast, local discrete Dislocation dynamics (DD) simulations. The rationale behind adopting such a coupled PDE-ODE approach instead of a completely DD based approach is primarily the vast separation in time-scales between plasticity applications that operate at quasi-static loading rates and the fundamental time scale of dislocation motion as embodied in DD which makes it impractical to reach appreciable applied strain using DD alone. The constitutive equations are replaced by inputs from Discrete Dislocation Dynamics while the associated elastic boundary value problem is solved using finite element method with a limited set of assumptions.

A Posteriori Analysis and Efficient Refinement Strategies for the Poisson-Boltzmann Equation

Jehanzeb Chaudhry*

*University of New Mexico

ABSTRACT

The Poisson-Boltzmann equation (PBE) is a second order nonlinear partial differential equation that models the electrostatic interactions of charged bodies such as molecules and proteins in an electrolyte solvent. The PBE is a challenging equation to solve numerically due to the presence of singularities, discontinuous coefficients and boundary conditions. Hence, there is often large error in the numerical solution of the PBE that needs to be quantified. The focus of this presentation is robust error estimation and refinement strategies for computing a quantity of interest (QoI), such as the solvation free energy, from the solution of the PBE. We employ adjoint based a posteriori analysis to accurately quantify the error in a QoI computed from the finite element solution of the PBE. We identify various sources of error and propose novel refinement strategies based on a posteriori error estimates.

Multifidelity Robust Optimization with Information Reuse

Anirban Chaudhuri^{*}, Karen Willcox^{**}

^{*}Massachusetts Institute of Technology, ^{**}Massachusetts Institute of Technology

ABSTRACT

This work presents a multifidelity method for optimization under uncertainty. Accounting for uncertainties during optimization ensures a robust design that is more likely to meet performance requirements. Designing robust systems can be computationally prohibitive due to the numerous evaluations of expensive high-fidelity numerical models required to estimate system level statistics at each optimization iteration. In this work, we focus on the robust optimization problem formulated as a linear combination of the mean and the standard deviation of the quantity of interest. We propose a multifidelity Monte Carlo approach combined with information reuse to estimate the mean and the variance of the system outputs using the same set of samples. The method leverages multiple low-fidelity models and the existing information from the designs visited during the prior optimization iterations. The information reuse from previously visited designs takes advantage of model autocorrelation between similar designs during the optimization. Nested control variates are used to combine the multiple fidelities and reuse the information from previous optimization iterations. We optimally allocate resources between the different fidelities that minimizes the variance in the nested control variate estimators for both the mean and the variance for a given budget. The multifidelity robust optimization method with information reuse maintains the same level of accuracy as a regular Monte Carlo estimate using only high-fidelity solves. However, the use of cheaper low-fidelity models and existing information leads to significant computational savings for the multifidelity robust optimization method as compared to a regular Monte-Carlo-sampling-based approach.

Computation of Incompressible Navier-Stokes Equations by Local Radial Basis Function Collocation Method

Bang-Fuh Chen^{*}, Bing-Han Lin^{**}, Chia-Cheng Tsai^{***}

^{*}National Sun Yat-sen University, ^{**}National Sun Yat-sen University, ^{***}National Kaohsiung Marine University

ABSTRACT

A meshless local radial-basis-function collocation method (LRBFCM) based on the multiquadric type radial basis function is used to solve incompressible Navier-Stokes equations. The projection method, sometimes called fractional-step methods, is implemented in the present study. The usage of non-uniformly distributed nodes makes the nodes generation in the computational domain become quite simple in LRBFCM. Two numerical cases are provided to verify the accuracy and the stability of the proposed numerical scheme, which include Taylor's decaying vortices and lid-driven square cavity flow. Convergence rates of pressure and velocity confirm the second-order accuracy of the algorithms. The numerical solutions of lid-driven square cavity flow were obtained for Reynolds numbers up to 1000, and very good agreements with the existing results are obtained. The success of these numerical simulations indicates the potential of the proposed numerical model in simulating incompressible flow geometrical and dynamic complexity.

On Study of Hybrid TMD and TLD System on Structure Motion Control

Bangfuh Chen*, Chih-hua Wu**

*professor, **PhD

ABSTRACT

In this paper, the hybrid tuned mass damper (TMD) and tuned liquid damper (TLD) are used to suppress the dynamic motion of a structure. The time-independent finite difference method is used to evaluate the sloshing liquids in the TLD and the Runge-Kutta method to calculate the dynamic response of TMD. The effects of TMD on base structure (BS) motion suppression are significant when the external forcing frequency is close to the resonant frequencies of the coupled system. Extensive researchers had reported suggested mass ratio, liquid ratio, tuned mass and tuned liquid frequencies. However, the precise physics explanation of the phenomenon are incomplete and rarely discussed, whereas they are clearly explained in this study. In this study, we will clarify the optimal value of the TLD frequency on structure motion reduction control is exactly equal to the exciting frequency. The addition of TLD to the system would further reduce the dynamic response of the structure when the natural frequency of the liquid tank is equal to the external forcing frequency and the out-of-phase occurs between sloshing-induced and external forces and both forces cancel each other and the resultant force acting on the structure nearly vanishes so does the structure motion. According to the numerical simulations of this study and experimental measurements of the associated study, we may suggest a practical design approach of the hybrid TMD+TLD system for a structure motion control. 1. Determine the fundamental frequency of the structure. 2. Determine the response spectrum of the possible of expected ground motion. 3. Determine the most thread exciting frequencies to the structure. 4. Select the tuning frequency of TLD according to step 3. And use to determine the tank width and water depth. 5. One also need to be noted, the smaller liquid depth ratio provides better motion response reduction. In order to avoid slamming and breaking wave occurred in the TLD, the suggested liquid depth ratio is as small as 0.1 and the tank width and liquid depth can be determined according to this number. (Chen and Yang 2017). Chen, Bangfuh and Yang Binhan, (2017) , Experimental study of a hybrid TMD and TLD on structure motion reduction, Ocean Engineering, submitted.

A Higher Order, Adaptively Integrated Cohesive Element

Boyang Chen^{*}, Raffaele Russo^{**}

^{*}TU Delft, Faculty of Aerospace Engineering, ^{**}TU Delft, Faculty of Aerospace Engineering

ABSTRACT

Cohesive Elements (CE) are known to suffer from the limitation that its size must be several times smaller than the cohesive zone length. The willingness of the authors is to present, with this paper, an adaptively integrated cohesive element which employs a higher-order interpolation of the separations. The validation of the CE has been made by simulating delamination problems chosen from already verified cases in literature (Turon, et al., 2007). For the case of a DCB problem, the cohesive zone length was estimated to be 0.8 mm. Using linear CEs would require a maximum element size of 0.25 mm in order to accurately capture the experimental curve. With 2 mm and larger linear CEs, the results would be far off from the experimental ones. The authors present here a 2D, two-node cohesive element. In addition to the usual two displacement degrees of freedom, each node contains an additional rotational degree of freedom, thereby achieving a higher-order interpolation of the separation field. While the interpolation remains unchanged during analysis (i.e., no additional partitioning or enrichment involved), the integration scheme changes with respect to the damage/failure status of the element. Comparisons with the results of the linear CE demonstrate that the proposed element is able to substantially improve the prediction accuracy of large cohesive elements (2 mm to 5 mm elements). The predicted delamination initiation load of 2.5-mm CE was 171% of the experimental value with linear CEs, and this is now improved to 104% with the proposed element. In the case of even larger CEs, 4-mm linear CE predicts 321% of the experimental initiation strength while the proposed 5-mm element's prediction is at 108%. In terms of propagation, linear 2.5-mm and 4-mm CEs' predictions are far off the experimental curve, while the proposed 2.5-mm and 5-mm elements' predictions stay relatively close to the experimental curve, with largest discrepancies of around 10% of the peak load.

Phase-Field Modeling of Dendrite Formation in Lithium Metal Batteries

Chih-Hung Chen^{*}, Chun-Wei Pao^{**}

^{*}Research Center for Applied Sciences, Academia Sinica, Taiwan, ^{**}Research Center for Applied Sciences, Academia Sinica, Taiwan

ABSTRACT

Lithium metal is widely considered to be an ideal anode material for next-generation rechargeable batteries for its high theoretical capacity (3,860 mAh/g) and low electrochemical potential (-3.04 V). However, lithium-metal-based batteries are still not commercially available due to the fact that uncontrollable lithium dendrites can easily form during battery charging and then lead to short-circuit risk and poor cycling performance. It has been known that various lithium dendritic patterns, such as needle-like, mossy, and fractal, can develop under different charging conditions. Although recent studies have found a link between the dendritic patterns and applied current density, the growth mechanism of lithium dendrites in three-dimensions remains poorly understood. In order to investigate the evolution of the electrode/electrolyte interface and its stability, we propose a multi-scale phase-field model for lithium dendrite formation. By introducing a phase order parameter to distinguish the electrode and electrolyte, this method is applicable to describe the electrolyte/electrode interface migration and microstructure evolution. The governing equations of motion for ionic concentration, electric potential and phase order parameter are variationally derived. The classical Butler-Volmer reaction kinetics is used to describe the nonlinear relationship between current density and overpotential at the electrode/electrolyte interface. By imposing relevant boundary conditions for electric potential and current density, we first demonstrate that this model is able to reproduce the sharp interface Butler-Volmer reaction kinetics in one dimension. Different dendritic patterns are observed in our preliminary thin three dimensional simulations. We perform fully three dimensional simulations to investigate the effects of applied electric potential on the dendritic patterns. In addition, recent experimental studies have shown that the lithium dendrite growth can be greatly stabilized by applying a pulse charging scheme. We apply this model to study the effect of pulse frequency on the dendritic patterns and the simulation results are compared with experimental observations.

Multiscale Non-Equilibrium Molecular Dynamics Simulation and Applications

Chuin-Shan David Chen*, Chi-Hua Yu**, Yu-Chuan Hsu***

*National Taiwan University, **National Taiwan University, ***National Taiwan University

ABSTRACT

Atomistic-based multiscale modeling theory and computational method for static problems have been successfully developed in the past decade. The advance has transformed the way we design micro and nanoscale materials for static problems. In contrast, the development of dynamic multiscale method for non-equilibrium simulations is limited, mainly due to spurious wave-reflection problems on the interface between atoms and continuum. In this talk, I will present our recent work on developing a novel multiscale non-equilibrium molecular dynamics (NEMD) simulation method based on the concept of time history kernels in real space [1]. The concept of finite-size virtual domain allows us to construct a novel multiscale NEMD. Dynamic responses of atoms in the virtual domain can be effectively constructed through a careful choice of time history kernels. The proposed method allows us to overcome the length scale limitation posed on NEMD simulations. Applications of the multiscale NEMD method for wave propagation and thermal transport will be addressed. [1] C-S Lee, Y-Y Chen, C-H Yu, Y-C Hsu, C-S Chen (2017), "Semi-analytical solution for the generalized absorbing boundary condition in molecular dynamics simulations," Computational Mechanics, 60, 23-37.

Residual Crushing Performance of Square Carbon Fiber Reinforced Plastic (CFRP) Composite Tubes after Transverse Low-Velocity Impact

Dongdong Chen^{*}, Xintao Huo^{**}, Shaowei Tong^{***}, Guangyong Sun^{****}, Xinglong Liu^{*****}

^{*}State Key Laboratory of Advanced Design and Manufacture for Vehicle Body, Hunan University, Changsha, 410082, China, ^{**}State Key Laboratory of Advanced Design and Manufacture for Vehicle Body, Hunan University, Changsha, 410082, China, ^{***}State Key Laboratory of Advanced Design and Manufacture for Vehicle Body, Hunan University, Changsha, 410082, China, ^{****}School of Aerospace, Mechanical and Mechatronic Engineering, The University of Sydney, Sydney, NSW 2006, Australia, ^{*****}State Key Laboratory of Advanced Design and Manufacture for Vehicle Body, Hunan University, Changsha, 410082, China

ABSTRACT

With the increasing demand of light-weight for vehicles, carbon fiber reinforced plastic (CFRP) composite, which has a better strength to weight ratio, has been widely used as energy absorption structures, such as crash boxes for progressive folding energy absorption under axial compressive loads. During its whole life time, various impact cases may happen, such as drop out of tools or collision of stones. While CFRP are usually rather sensitive to dynamic impact loadings and even minor, invisible damage could cause the performance reduction. However, studies existed on residual properties of CFRP tubes mainly considered the impact in axial direction, limited studies were available to evaluate the effect of transverse impact on residual axial compression characteristic. This work aims to study the residual crushing performance of square CFRP tubes after transverse low-velocity impact with experimental and numerical methods. Firstly, serials of low-velocity impact tests were conducted to examine the damage modes with the increase of impact energy. Then the quasi-static axial compression tests were carried out to characterize the degradation of residual crushing performance induced by the impact. The main damage modes are matrix cracking for lower impact energies, delamination and fiber breakage for high impact energies. Peak forces of impact force-displacement curves increase with the increase of impact energy. It is also found that the degradation of residual compression properties could be divided into different regions. Different with the progressive crushing mode seen in the un-impacted tubes, collapse and unstable local buckling were observed in the axial crushing tests. The peak load and specific energy absorption of the performed tubes were also analyzed with un-impacted tubes finally. Together with cross-section views in impact position, the performance reduction during axial compression caused by impact were explored, which showed a shear failure mode. Finally, a finite element model was established for describe the dynamic behavior of CFRP tubes and validated with experimental results with a user-defined material subroutine VUMAT.

An Efficient Computational Fluid Dynamics-based Aeroelastic Reduced Order Model for Aeroelastic Global Optimization

Gang Chen^{*}, Dongfeng Li^{**}, Yixing Wang^{***}, Andrea Da Ronch^{****}, Yueming Li^{*****}

^{*}State Key Laboratory for Strength and Vibration of Mechanical Structures, School of Aerospace, Xi'an Jiaotong University, ^{**}State Key Laboratory for Strength and Vibration of Mechanical Structures, School of Aerospace, Xi'an Jiaotong University, ^{***}State Key Laboratory for Strength and Vibration of Mechanical Structures, School of Aerospace, Xi'an Jiaotong University, ^{****}Faculty of Engineering and the Environment, University of Southampton, Southampton, ^{*****}State Key Laboratory for Strength and Vibration of Mechanical Structures, School of Aerospace, Xi'an Jiaotong University

ABSTRACT

This paper presents an aeroelastic optimization study for three dimensional wing at global level. The study employs Genetic Algorithms (GAs) as an optimization tool in combination with an efficient Computational Fluid Dynamics-based aeroelastic Reduced-Order Model (ROM). The Proper Orthogonal Decomposition (POD) method has been shown its accuracy and efficiency for aeroelastic analysis at fixed flight condition for a frozen model configuration. POD vectors generated from unsteady flow solution snapshots based on one set of structural modeshapes. In the aeroelastic optimization process, in order to keep the ROM's accuracy, a new CFD-based POD/ROM could be reconstructed when modeshapes changed, these reconstruction procedures take a considerable time, and greatly increasing the time cost of the aircraft design. In this study, the aeroelastic modeling counts for both stiffness and mass matrix variation of wing structure at global level to maximize flutter speed. Finally, the most feasible and optimal solutions were effectively obtained by the presented aeroelastic optimization.

Feature-Based Recombination Deep Neural Network for Reduce Order of Aero-elastic System

Gang Chen^{*}, Dongfeng Li^{**}, Yixing Wang^{***}

^{*}Xi'an Jiaotong University, ^{**}Xi'an Jiaotong University, ^{***}Xi'an Jiaotong University

ABSTRACT

A recombination DNN (Deep Neural Networks) model based features of flow field to reduce order of aero-elastic system is carried out in this paper. NN (Neural Networks) is an efficient model for reducing order of flow and aero-elastic system. However, traditional NN models are actually system identification methods. Different from these, the proposed DNN model improve the accuracy and generalization capability through using convolutional neural network to extract the information of flow field in each time step. In order to synthesize different kinds of input variables, a novel serial network is also introduced. Of particular interest about NN is to determine the weights of neuron. The synthesized network with an improved Back-Propagation (BP) algorithm is employed to ascertain parameters of NN model through deep learning process. Using NACA0012 2D aero-elastic model, the DNN is fed by the basic variables at every coarse grid of flow field as the input and the aerodynamic forces as the target data, which is computed by the full order Euler computations. The DNN is iteratively trained using the proposed improved BP algorithm to predict the aerodynamic forces in different time steps and the results are compared with the full-order computations which show good consistence. At last, combining the proposed DNN with the structural motion equations, a Reduced Order Model (ROM) for aero-elastic system is obtained. Using the ROM, we do a flutter analysis for NACA0012. And a sensitivity study is performed to identify the hyper-parameters of DNN for predicting flow field such as the number of neurons, the number of layers and the kernel size of convolutional neural network, and so on. Within the error threshold, the proposed DNN model has reduced nearly four orders of magnitude about the degree of freedom compared the full order computation and significantly cuts down the consumed computational resources. We also try to transfer the form of Euler equation to explore why DNN can predict so good results. Some useful theoretical conclusions about predicting flow with DNN are found. The proposed feature-based recombination DNN has an important and wide significance to the design and control of aircraft, especially when unsteady or aero-elastic effect is prominent.

Fully Implicit, Conservative, Multidimensional Electromagnetic Particle-In-Cell Algorithms for Multiscale Kinetic Plasma Simulation on Curvilinear Meshes

Guangye Chen^{*}, Luis Chacon^{**}

^{*}LANL, ^{**}LANL

ABSTRACT

Particle-in-cell (PIC) simulation techniques are widely used for first-principles simulations of plasma dynamics. Classical PIC employs an explicit approach (e.g. leap-frog) to advance the Vlasov-Maxwell/Poisson system using particles coupled to a grid. Explicit PIC is subject to both temporal (CFL) and spatial (aliasing) stability constraints, challenging system-scale kinetic simulations, even with modern super-computers. Implicit algorithms can potentially eliminate these stability constraints, thus holding promise for significant speedups. Implicit PIC algorithms have been explored since the late 1970's, but have suffered from various ailments originating in the lack of non-linear consistency and of strict conservation properties. In this presentation, we discuss a multi-dimensional, nonlinearly implicit, conservative electromagnetic PIC algorithm [1,2]. The approach delivers both accuracy and efficiency for multi-scale plasma kinetic simulations, and extends previous proof-of-principle 1D studies [3]. To avoid noise issues associated with numerical Cherenkov radiation for large implicit timesteps, we consider the Darwin approximation to Maxwell's equations, which projects out the light wave analytically. The formulation conserves exactly total energy, local charge, canonical momentum in the ignorable directions, and preserves the Coulomb gauge. Linear momentum is not exactly conserved, but errors are controlled by an adaptive particle sub-stepping orbit integrator. Key to the performance of the algorithm is a moment-based preconditioner, featuring the correct asymptotic limits. The formulation has been extended to curvilinear meshes [2], which opens the possibility of accurate body-fitted and/or spatially adaptive PIC simulations. The superior accuracy and efficiency properties of the scheme will be demonstrated with various numerical examples. [1] G. Chen, L. Chacón, *Comput. Phys. Commun.* 197, 73-87 (2015). [2] L. Chacón and G. Chen, *J. Comput. Phys.*, 316, 578–597 (2016) [3] G. Chen, L. Chacón, and D.C. Barnes, *J. Comput. Phys.*, 230 (18), 7018-7036 (2011).

A Self-stabilized Peridynamic Correspondence Material Model

Hailong Chen^{*}, Benjamin Spencer^{**}

^{*}Idaho National Laboratory, ^{**}Idaho National Laboratory

ABSTRACT

Non-Ordinary State-based Peridynamic (NOSPD) correspondence models are very useful in applying classical continuum material constitutive models to peridynamics but suffer from some practical difficulties, such as non-invertibility. This non-invertibility can be understood as existence of many possible deformations of a family that result in the same force state. As a consequence there would be many possible deformation states of the entire body for a given loading history. This has the practical effect in computations of resulting in zero-energy modes of deformation in the numerical mesh that need to be suppressed. Various remedies for zero-energy modes control are available in the literature, and these methods can be categorized into two groups: fictitious spring-force based methods and stabilized field state based methods. Although can be used to alleviate the instability due to existence of zero-energy modes, these methods do not provide resolution to the fundamental problem in correspondence formulation. Issues such as adjustment of control parameters based on material model and discretization scheme and strain/stress oscillations still exist in these stabilization schemes. In this presentation, we will present a Self-stabilized Non-Ordinary State-based Peridynamic (SNOSPD) correspondence material model based on the concept of bond-oriented reduced deformation gradient to better solve material instability issues. The proposed bond-oriented reduced deformation gradient is formulated for the purpose of accurate calculation of force state within each individual bond. The content of this presentation will be organized as follows: we will first briefly review some details on continuous deformation gradient in Continuum Theory and how the conventional peridynamic nodal deformation gradient is deduced from deformation states of a family. Following this, review of the conventional correspondence material model will be presented. Existence of zero-energy modes in NOSPD will be analytical examined. After that, details on formulation of the proposed bond-oriented reduced deformation gradient and derivation of force state will be discussed. Numerical results on various problems will be presented to establish the validity and accuracy of the proposed formulation. Discussions and conclusions are made based on comparison with other control schemes.

Numerical Investigation of Air-gun Bubble Dynamics Based on FEM

Hailong Chen^{*}, Xiugang Lu^{**}, Shuai Zhang^{***}, Shiping Wang^{****}

^{*}Harbin Engineering University, ^{**}Harbin Engineering University, ^{***}Harbin Engineering University, ^{****}Harbin Engineering University

ABSTRACT

In this paper, a high pressure bubble model is built with ABAQUS software based on finite element method (FEM) to simplify the excitation process of seismic air-gun. This model is validated by comparing its predictions with the air-gun experiments in an open top tank. Numerical simulation of the air-gun bubble subjected to various boundary conditions and at different depths is carried out and discussed. The relationships between initial gas pressure and the first maximum bubble radius as well as the first period of oscillation are studied. Meanwhile, the jet dynamics and the migrating behaviors of the bubble under the effect of buoyancy are carefully investigated. This paper provides a basic understanding of the pressure field and shockwave of seismic air-gun bubble which is widely applied to ocean seabed geophysical exploration and the shock testing of naval vessels. Keywords: Seismic air-gun, Bubble dynamics, Pressure field, Finite element method, ABAQUS

Identification of Transient Boundary Conditions with Improved Cuckoo Search Algorithm and Polynomial Approximation

Haolong Chen^{*}, Bo Yu^{**}, Huanlin Zhou^{***}, Zeng Meng^{****}

^{*}School of Civil Engineering, Hefei University of Technology, Hefei, P.R.China, ^{**}School of Civil Engineering, Hefei University of Technology, Hefei, P.R.China, ^{***}School of Civil Engineering, Hefei University of Technology, Hefei, P.R.China, ^{****}School of Civil Engineering, Hefei University of Technology, Hefei, P.R.China

ABSTRACT

The cuckoo search (CS) algorithm combined with Broyden-Fletcher-Goldfarb-Shanno (BFGS) algorithm (CS-BFGS) is proposed to identify time-dependent boundary conditions for 2-D transient heat conduction problems in functionally gradient materials. Firstly the nonlinear partial differential equation is linearized by the analog equation method. The dual reciprocity boundary element method (DRBEM) is used to solve the direct problem. Then taking the unknown boundary conditions as a polynomial function of coordinates with time-dependent coefficients, the CS-BFGS is applied to obtain the unknown coefficients of the polynomial function. As a result, the time-dependent boundary conditions are evaluated. The convergence speed of the improved CS algorithm is faster than the CS algorithm. What's more, the effect of the polynomial degree is discussed. As the polynomial degree increases, the inverse results are more accurate but the iterative number and computation time also increase. Finally, the influences of the position and number of measurement points, and random errors on the inverse results are investigated. With the measurement points closer to the boundary, with the increase of measurement point number and with the decrease of measurement errors, the results are more accurate.

Artificial Neural Network Potential for Methylammonium Lead Iodide and Lead Iodide

Hsin-An Chen*, Chun-Wei Pao**

*Research Center for Applied Sciences, Academia Sinica, Taipei, Taiwan, **Research Center for Applied Sciences, Academia Sinica, Taipei, Taiwan

ABSTRACT

Recently, organic-inorganic metal halide perovskite solar cell has attracted great attentions because of its high absorption coefficient, high power conversion efficiency ($>20\%$, increasing rapidly), easy processing and low cost in fabrications. The most notable light-harvesting material used in the perovskite solar cell is methylammonium lead iodide (MAPbI₃), which is typically synthesized from lead iodide (PbI₂) and methylammonium iodide (MAI). Among all factors influencing performance of the perovskite solar cell, the surface morphology and the grain size of perovskite MAPbI₃ in the cell are the most important ones, which govern the power conversion efficiency. However, the reaction mechanism for the synthesis of perovskite MAPbI₃ from PbI₂ is still not concluded. To elucidate the detail of the reaction mechanism, atomistic molecular simulations of the formation of MAPbI₃ within PbI₂ is required. However, ab initio molecular simulations are extremely time and resource-consuming and therefore not suitable for studying the MAPbI₃ reaction pathways or microstructures. In the present study, we demonstrate that by utilizing tens of thousand MAPbI₃ and PbI₂ structures and energies from ab initio calculations as training sets, we are able to train an artificial neural network (ANN) model potential for classical molecular simulations of PbI₂ and MAPbI₃ perovskite systems. This ANN model potential provides good predictions in system energetics and can be used for large-scale simulations well beyond the reach of conventional ab initio calculations for studying the microstructure evolution of MAPbI₃ perovskite crystals.

Performance Comparison of Nodally Integrated Galerkin Meshfree Methods and Nodally Collocated Strong Form Meshfree Methods

J. S. Chen^{*}, Mike Hillman^{**}

^{*}University of California, San Diego, ^{**}The Pennsylvania State University

ABSTRACT

For a truly meshfree technique, Galerkin meshfree methods rely chiefly on nodal integration of the weak form [1]. In the case of Strong Form Collocation meshfree methods, direct collocation at the nodes can be employed [2]. In this paper, performance of these node-based Galerkin and collocation meshfree methods is compared in terms of accuracy, efficiency, and stability [3]. Considering both accuracy and efficiency, the overall effectiveness in terms of CPU time versus error is also assessed. Based on the numerical experiments, the Galerkin meshfree methods with smoothed gradients and variationally consistent integration yield the most effective solution technique, while direct collocation of the strong form at nodal locations has comparable effectiveness. References 1. Chen, J. S., Hillman, M., Rüter, M., "An Arbitrary Order Variationally Consistent Integration Method for Galerkin Meshfree Methods," International Journal for Numerical Methods in Engineering, Vol. 95, pp. 387–418, 2013. 2. Hu, H. Y., Chen, J. S., and Hu, W., "Weighted Radial Basis Collocation Method for Boundary Value Problems," International Journal for Numerical Methods in Engineering, Vol. 69, pp. 2736-2757, 2007. 3. Hillman, M. and Chen, J. S., Performance Comparison of Nodally Integrated Galerkin Meshfree Methods and Nodally Collocated Strong Form Meshfree Methods. Advances in Computational Plasticity, [Ed. Onate, E.], Springer, pp. 145-164, 2018.

Implicit Gradient for Numerical Solution of PDEs

J. S. Chen^{*}, Mike Hillman^{**}

^{*}University of California, San Diego, ^{**}The Pennsylvania State University

ABSTRACT

Implicit gradient (IG) is expressed in an integral equation with embedded gradient consistency without explicit derivatives. It offers a paradigm for constructing approximation of function derivatives for the numerical solution of PDEs, either by using strong forms or weak forms. A straightforward application of IG is for the gradient typed regularization of ill-posed problems, such as the strain localization problems. GI can also be used to construct stabilization of convection dominated problems and as the stabilization of nodally integrated Galerkin equation. Without the need of taking derivatives of approximation functions, GI also offers computational efficiency for Meshfree based numerical solution of PDEs. This talk will introduce continuous and discrete GI for approximation of derivatives, discuss the gradient consistency of GI and its convergence properties in solving PDEs, and demonstrate its applications to strain localization, convection dominated problems, and modeling of damage and fracture processes in solids subjected to extreme loadings.

Wave Amplification in an Array of Open Caissons

Jiahn-Horng Chen^{*}, Yan-Xiang Lin^{**}, Da-Wei Chen^{***}

^{*}National Taiwan Ocean University, ^{**}National Taiwan Ocean University, ^{***}National Taiwan Ocean University

ABSTRACT

Harbour resonance provides a possible way to amplify wave energy for wave energy converters (WEC) operating in regions of medium wave energy density. In the present paper, we conducted a computational study on the amplification effect for an array of cylindrical caissons with an opening of angle θ . The parameters include the distance between two adjacent caissons, the angle of caisson opening, and the amplitude and period of the incident waves. The open source code OpenFOAM was employed for all computations. The volume of fluid (VOF) method was used to capture the free surface. Both linear and nonlinear incident waves were used for upstream boundary conditions. The results show that proper combinations of these parameters can result in significant wave amplifications in the caisson. Meanwhile, the wave outside the caisson can be significantly reduced after it passes the array.

Strong-Form Formulated Generalized Displacement Control Method for Nonlinear Analysis

Jian-Yu Chen^{*}, Judy Yang^{**}

^{*}National Chiao Tung University, ^{**}National Chiao Tung University

ABSTRACT

In the traditional analysis of geometric nonlinearity, the most popular method is formulated on the basis of weak-form such as the finite element method. Due to the element nature, its application is limited by the numerical integration in the governing equation and the quality control of deformed mesh. The meshfree methods have been developed and become one leading research topic in the field of computational mechanics since 1990s. In particular, the strong form collocation methods require no additional efforts to deal with numerical integration and impose Dirichlet boundary conditions, thereby making the collocation methods computationally efficient. Concerning geometric nonlinearity, how to accurately reflect the change in the slope of the load-deflection curve of the structure and remain numerically stable are of major concerns in the incremental-iterative process. As a result, we propose a strong-form formulated generalized displacement control method to analyze geometrically nonlinear problems, where the radial basis collocation method is adopted. The numerical examples demonstrate the ability of the proposed method for large deformation analysis.

Biomechanical Assessment of Femoral Neck Convex Deformity Using Patient-Specific FE Analysis

Junning Chen^{*}, Matthew Wilson^{**}, Tengteng Tang^{***}, Christopher Smith^{****}, Peter Fratzl^{*****},
Richard Weinkamer^{*****}, Rizhi Wang^{*****}

^{*}Department of Engineering, University of Exeter, Exeter, United Kingdom, ^{**}Exeter Hip Unit, Royal Devon & Exeter NHS Foundation Trust, Exeter, United Kingdom, ^{***}Department of Materials Engineering, University of British Columbia, Vancouver, BC, Canada, ^{****}Department of Engineering, University of Exeter, Exeter, United Kingdom, ^{*****}Department of Biomaterials, Max Planck Institute of Colloids and Interfaces, 14476 Potsdam, Germany, ^{*****}Department of Biomaterials, Max Planck Institute of Colloids and Interfaces, 14476 Potsdam, Germany, ^{*****}Department of Materials Engineering, University of British Columbia, Vancouver, BC, Canada

ABSTRACT

Femoral neck convex deformity has been known as the cam type impingement in the hip joint, and has a very high prevalence in elder population. Recent research on cam-impingement has shown increasing evidence in active young adults [1]. The morphological changes near the femoral head and neck junction lead to severe pain during movement and a reduced range of motion; in the long term, it will result in osteoarthritis [1]. There has also been rising concern for its association with the increasing risk of hip fracture [2]. Hip arthroplasty was one of the most common and successful surgical procedures to provide sufficient clearance in the joint by shaving down the bony bump at the deformity, therefore improving the range of motion and reducing pain. Despite a growing interest in diagnosing and treating hip impingement, little has yet been revealed on the biomechanical effects of either deformity or surgical intervention to proximal femur integrity and fracture risk. This study aims 1) to establish a numerical framework to quantitatively assess its biomechanical changes, by combining ex vivo high resolution peripheral quantitative computed tomography (HR-pQCT) and in silico finite element analysis (FEA); and 2) to evaluate the potential surgical effects after hip arthroplasty by using patient-specific modelling technique to virtually simulate surgery outcomes. Two proximal femora were used in this study, one freshly frozen human cadaveric femur diagnosed with impingement and one control with no observed abnormality. Both samples were scanned with HR-pQCT with a voxel size of 41 μm^3 . The obtained images were segmented in ScanIP Ver. 7. Two patient-specific geometric models were created by an inverse engineering approach with non-uniform rational basis splines (NURBS). On the pathological model, three different extents of tissue removal were virtually performed to simulate the surgical procedure, providing three post-surgical models on the same patient profile. All five models were imported to ABAQUS Ver. 6.14 for voxel-based heterogeneous micro-FEA. Our results suggested that the convex deformity led to severe stress concentration in the local region compared to the control, indicating raised risk of fracture under impact, and a balanced surgical plan is preferred to provide the minimal joint clearance without significantly increasing the fracture risk. References [1] E. Dickenson, et al. (2015) Prevalence of Cam Hip Shape Morphology: a Systematic Review. *Osteoarthritis and Cartilage*. 24(6): pp. 949-961. [2] K.L. Bell, et al. (1999) Structure of the Femoral Neck in Hip Fracture: Cortical Bone Loss in the Inferoanterior to Superoposterior Axis. *Journal of Bone Mineral Research*. 14: pp. 111-9.

Seismic Study of a Transition Tunnel by Using Numerical Simulations

Juntao Chen^{*}, Haitao Yu^{**}, Yong Yuan^{***}

^{*}Tongji University, ^{**}Tongji University, ^{***}Tongji University

ABSTRACT

Tunnels can be constructed by immersed, TBM, drill-and-blast, cut-and-cover, or combination of aforementioned methods. Thus, the cross-section of tunnel constructed by means of different tunneling methods is generally different. When this is the case of TBM connected with drill-and-blast directly, a transition portion is needed to accommodate the shapes of cross-section formed by the two types of tunneling methods. This paper is focused to study the seismic response of the transition tunnel connecting TBM segmental lined tunnel and drill-and-blast tunnel by conducting numerical simulations. The transition tunnel is composed of four portions including segmental lined tunnel section, segmental lined tunnel with inner, multi-lined tunnel section and drill-and-blast tunnel section. In addition, during the numerical simulation, strong earthquake motions are considered to study the damage mechanism of the tunnel structure. Based on results, the ovaling deformation and stress distribution for each tunnel section is first compared and studied; then, the influence of the change of tunnel cross-section and stiffness on the seismic response of tunnel is full analyzed; at last, the damage model of the transition tunnel under strong earthquake is discussed.

Powell–Sabin B-splines for Cohesive Fracture Analysis

Lin Chen*, René de Borst**

*University of Sheffield, **University of Sheffield

ABSTRACT

The numerical simulation of fracture is a technically relevant and scientifically challenging issue, and has been a focal point of attention since the early simulations in the 1960s. From the very beginning, two different approaches have been pursued, discrete methods in which cracks are treated as geometric discontinuities, leading to topological changes, and the distributed, or smeared approach, in which discontinuity is modelled by distributing it over a small, but finite band. For the discrete method, the cohesive zone model is often used to model fracture processes in many quasi-brittle and ductile materials, in particular when the size of the fracture process zone is non-negligible compared to the structural dimensions. It can easily be incorporated in finite element formulations (FEM), especially when the crack path is pre-defined. Over the past decades, various FEM technologies have been proposed which can achieve this, such as interface elements and embedded discontinuities. Recently, isogeometric analysis (IGA) has also been used for crack propagation [1, 2]. The crack segment is represented by the NURBS or T-spline basis functions. IGA can accurately predict the local stress field. However, NURBS and T-splines have some limitations when modelling (cohesive) fracture, and a discrete representation of a crack fails in some situations. This restriction is due to the crack segment insertion in the parameter domain and the reparameterization in the physical domain [2]. In this contribution, we employ the Powell–Sabin B-splines, which are based on triangles, to model cohesive crack propagation. The crack is introduced directly in the physical domain. Due to the use of triangles, re-meshing is more straightforward. To implement the proposed method in existing finite element programs, Bézier extraction is employed. It is ideal for adopting an element-wise point of view for crack propagation and extension. The accuracy of the approach to model free crack propagation is demonstrated by several numerical examples, including an L-shaped beam, a SEN beam, and the Nooru-Mohamed concrete panel. References [1] Verhoosel, C.V., Scott, M.A., de Borst, R., and Hughes, T.J.R. An isogeometric approach to cohesive zone modeling. *International Journal for Numerical Methods in Engineering* 87: 175 (2011): 336-360. [2] Chen, L., Verhoosel, C.V., de Borst, R.. An isogeometric method for cohesive fracture analysis. *International Journal for Numerical Methods in Engineering*, submitted.

Life-time Based Design of Transmission Mechanism of Micro-positioning Stage

Min Chen^{*}, Shunqi Zhang^{**}, Xiang Wang^{***}, Derrick Tate^{****}

^{*}Xi'an Jiaotong-Liverpool University, ^{**}Shanghai University, ^{***}Xi'an Jiaotong-Liverpool University, ^{****}Xi'an Jiaotong-Liverpool University

ABSTRACT

The micro-positioning driven by piezoelectric actuator is a key technology used in a broad variety of applications, like the precision manufacture, optical measurement and microsurgery. The output accuracy is mainly determined by two factors, the actuator and the transmission flexure hinges. The flexure hinges perform their function through local deformation, which tends to lead to stress concentration and fatigue failure. This paper presents a general numerical approach, namely limit and shakedown analysis, to predict the safety state of smart structures made of heterogeneous materials under unknown cyclic loadings. With the homogenization theory and finite element approach, the shakedown problem is converted to a large-scale nonlinear optimization programming. Furthermore, a general platform in with the combination of FEM and interior-point-algorithm based optimization tool is developed, which make the practical application possible.

Scan Pattern Integrated Structural Topology Optimization for Laser Powder Bed Fusion Process Based on Inherent Strain Theory

Qian Chen^{*}, Jikai Liu^{**}, Xuan Liang^{***}, Albert To^{****}

^{*}Department of Mechanical Engineering and Material Science, University of Pittsburgh, ^{**}Department of Mechanical Engineering and Material Science, University of Pittsburgh, ^{***}Department of Mechanical Engineering and Material Science, University of Pittsburgh, ^{****}Department of Mechanical Engineering and Material Science, University of Pittsburgh

ABSTRACT

Inherent strain theory based fast method has recently been proposed for additive manufacturing(AM) process simulation. Inherent strain theory based topology optimization, which can significantly reduce simulation time, is now possible and has been actively explored to reduce the thermal process induced defects, such as residual distortion and stress. On the other hand, the laser sintering path dependency issue has not been considered in these optimization issues. More specifically, the extracted inherent strain for laser powder bed fusion process is sintering path dependent, which is generally larger in the raster direction than transverse direction. In fact, Optimizing the laser sintering path is an alternative solution to further reduce these thermal process induced defects. Hence, to fill the gap, a laser scan pattern integrated structural topology optimization method is proposed to address two critical problems.: 1) Scan pattern optimization for fixed geometry to minimize residual stress, and 2) Concurrent structural topology and scan pattern optimization for the same optimization purpose. The scan pattern is optimized instead of the sintering path since the EOS M290 is a closed system which has the embedded scan pattern that can only be parametrically altered. To fit the cyclic characteristic of topology optimization, full-body inherent strain method will be utilized to replace the more accurate layer-by-layer approach, and a less time-consuming one-step static analysis will be performed in each optimization loop. Anisotropic thermal expansion coefficients will be applied to activate the inherent strain. Effectiveness of the proposed method will be proved by several numerical cases and experimental validation.

Resolving Large-scale Geophysical Flows over Unstructured Meshes: a Class of New Vorticity-Divergence Based Numerical Schemes

Qingshan Chen^{*}, Lili Ju^{**}, Roger Temam^{***}

^{*}Clemson University, ^{**}University of South Carolina, ^{***}Indiana University Bloomington

ABSTRACT

Unstructured meshes have been gaining popularity in recent years, because they are almost free of polar singularities, and remain highly scalable even at eddy resolving resolutions. However, to unleash the full potential of these meshes, new schemes are needed. The classical C-grid scheme, which is widely popular on structured meshes, has serious issues concerning the reconstruction of the tangential velocity component. This talk presents new numerical schemes based on an old idea, namely the collocated vorticity-divergence formulation (so-called Z-grid), for large-scale geophysical flows on unstructured centroidal Voronoi meshes. Using the finite-volume discretization technique, the schemes conserve the mass and the absolute vorticity locally, and the potential enstrophy globally. It is also shown that, in an area-averaged sense, the schemes reproduce the Lagrangian transport property for potential vorticity, which is fundamental to the understanding of the dynamics of large-scale geophysical flows. A major challenge of vorticity-divergence based numerical schemes is the specification of the boundary conditions for the PDEs. The current project adopts a hybrid approach that combines explicit and implicit implementations of the boundary conditions on the streamfunction and the velocity potential. This talk will go over the analytical and practical aspects of the schemes, and finish with some high-resolution numerical results.

Dynamic Analysis for Parallel Stabilized Platform

Qunkai Chen^{*}, Chenliang Li^{**}, Yuefa Zhou^{***}

^{*}College of Aerospace Engineering and Civil Engineering, Harbin Engineering University, Room 2035, Building 11, No.145, Nantong Street, Nan gang District, 150001 Harbin, Heilongjiang Province, P.R. China, ^{**}College of Aerospace Engineering and Civil Engineering, Harbin Engineering University, Room 2035, Building 11, No.145, Nantong Street, Nan gang District, 150001 Harbin, Heilongjiang Province, P.R. China, ^{***}College of Aerospace Engineering and Civil Engineering, Harbin Engineering University, Room 2035, Building 11, No.145, Nantong Street, Nan gang District, 150001 Harbin, Heilongjiang Province, P.R. China

ABSTRACT

This paper studies on the multi-degree of freedom electro –hydraulic hybrid stabilized platform, which is consisting of up platform and lower platform. Both of them are the six-DOF parallel platform supported by six extensible links (Stewart platform). The function of lower platform is to simulate yawing, rolling and pitching motions, and the function of up platform can be utilized as stabilized platform to isolate the disturbance, to keep parallel to the horizontal plane or track certain target. Kinematics and dynamics of this structure are analyzed. The inverse kinematics of multi-degree of freedom electro –hydraulic hybrid stabilized platform are analyzed in this paper, and the inverse dynamics equation of multi-degree of freedom electro –hydraulic hybrid stabilized platform are studied by Kane formulation. ; using the software program of MATLAB to the motion model for motion simulation and dynamic simulation and draw simulation graphs, and through analyzing and summarizing, draw conclusions. Meanwhile the driving forces-time results from MATLAB are compared with the results form ADAMS software, which verify the correctness of this approach. The results obtained would be useful for the design and analysis of practical manufacture.

Implementation of Anisotropic Cam Clay Model into Abaqus and Its Application to Cavity Expansion Problem

Shengli Chen^{*}, Kai Liu^{**}

^{*}LOUISIANA STATE UNIVERSITY, ^{**}LOUISIANA STATE UNIVERSITY

ABSTRACT

Dafalias' (1987) anisotropic Cam Clay model, based strictly on the critical state concept, is one of the most widely used anisotropic elastoplastic constitutive models for clays, attributed mainly to its relative simplicity, yet still capable of capturing the essential features of the anisotropic soil behaviour. This paper develops an implicit integration algorithm for the anisotropic Cam Clay soil model, using the standard return mapping approach (elastic predictor-plastic corrector), to obtain the updated stresses for the given strain increments. It is found that the formulation of the constitutive integration involves essentially 19 simultaneous equations, which contains 6 stresses σ_{ij} , 6 plastic strain increments $d\epsilon_{ij}^p$, and 7 state variables ϵ_{ij} and p_c as the unknowns to be solved for. The integration algorithm for the anisotropic Cam Clay model is implemented into the finite element analysis commercial program, ABAQUS, through the material interface of UMAT (user defined material subroutine), and then used for the analysis of the fundamental cavity expansion problem. The predictions from the ABAQUS simulations are generally in excellent agreement with the available analytical solutions, thus demonstrating the accuracy and robustness of the proposed integration scheme.

A Discontinuous Galerkin/Cohesive Zone Approach for Impact Failure Analyses of Automotive Laminated Glass

Shunhua Chen^{*}, Naoto Mitsume^{**}, Wei Gao^{***}, Tomonori Yamada^{****}, Mengyan Zang^{*****},
Shinobu Yoshimura^{*****}

^{*}The University of Tokyo, ^{**}The University of Tokyo, ^{***}Guangdong University of Technology, ^{****}The University of Tokyo, ^{*****}South China University of Technology, ^{*****}The University of Tokyo

ABSTRACT

Automotive laminated glass is a simple sandwiched composite structure, which is comprised of two soda-lime glass sheets bonded by one plastic interlayer, polyvinyl butyral (PVB). It is considered to be a safety component of a vehicle because of its excellent performance in absorbing impact energy and bonding glass fragments. Meanwhile, the impact failure patterns of an automotive windshield glazing contribute to traffic accident reconstruction. The purpose of this work is to develop a discontinuous Galerkin(DG)/cohesive zone approach for the impact failure, including glass cracking and possible debonding, of laminated glass. This approach models inter-element failure by switching the interface constraints from a DG formulation to an extrinsic cohesive expression, which is able to get rid of the so-called artificial compliance and time discontinuity problems existing in cohesive zone models, while being quite scalable for parallel computing. A laminated glass finite element model is proposed, which allows for the use of non-matching finite element meshes for adhesion modeling between glass and PVB, and gradual coarsening glass meshes for the areas away from the impact zone, and thus to reduce computational cost. In order to better capture the impact force history, the cohesive strengths in the impact zone are determined by a glass strength distribution considering initial flaws[1]. However, for the other areas where the crack behaviors have relatively small influences on the impact force history, the cohesive strengths are artificially adjusted so as to satisfy the minimum mesh size requirements in the context of cohesive zone modeling. Finally, the impact fracture behavior of a laminated glass plate is simulated. The effectiveness of the developed computational approach is validated by comparing the numerical results with the experimental ones[2] in terms of crack velocity history and cracking sequence. The impact cracking mechanism of a laminated glass plate is thoroughly discussed as well. Reference: [1] Alter, Christian, Stefan Kolling, and Jens Schneider. "An enhanced non-local failure criterion for laminated glass under low velocity impact." *International Journal of Impact Engineering* 109 (2017): 342-353. [2] Xiaoqing Xu, Jun Xu, Jingjing Chen et al. "Investigation of dynamic multi-cracking behavior in PVB laminated glass plates." *International Journal of Impact Engineering* 100 (2017): 62-74.

Efficient Meshfree Method for Additive Manufacturing Process

Songtao Chen^{*}, Qinglin Duan^{**}, Yining Wang^{***}, Shuhui Li^{****}

^{*}Department of Engineering Mechanics, Dalian University of Technology, ^{**}Department of Engineering Mechanics, Dalian University of Technology, ^{***}Department of Engineering Mechanics, Dalian University of Technology, ^{****}Department of Engineering Mechanics, Dalian University of Technology

ABSTRACT

Additive manufacturing (AM) is an advanced model-free manufacturing technology by means of the layered deposition of materials and in recent years it attracts intensive attentions. The metal additive manufacturing process induced high temperature gradient due to the non-uniform heat input which would detrimentally affect the microstructure, material properties, residual stress, and distortion. Therefore, the thermal history of metal additive manufacturing is significant in predicting the quality of component. Recently, many FEM models have been established to investigate thermal behavior during AM. For example, Denlinger et al. [1] developed a three-dimensional finite element model for the prediction of temperature, residual stress, and distortion in multi-layer Laser Powder-Bed Fusion builds. However, the temperature gradient around the molten pool is very high and fluctuates violently and FEM (usually only linear approximation is employed) is difficult to describe such high gradients accurately. Furthermore, the size of heat affected zone (only several tens of microns) is very small compared to the entire component. However, FEM is inconvenient to implement local refinement whereas uniform grids lead to high computational cost. Meshfree methods, such as the element-free Galerkin (EFG) method [2], possess apparent advantages in constructing high order approximation and adaptive refinement (or coarsening) since construction of meshfree approximation is only dependent on a set of scattered nodes, instead of a mesh. Especially, Duan et al. [3] developed an improved EFG method by correcting nodal derivatives at quadrature points based on the Hu-Washizu three-field variational principle. This method remarkably reduces the number of quadrature points for high order approximation and significantly improves computational efficiency. It is named as consistent element-free Galerkin (CEFG) method since it is able to exactly pass patch tests in a consistent manner. In this work, application of the CEFG method to simulate additive manufacturing process is presented. By making full use of the merit of meshfree approximation, “mesh” coarsening is conveniently and adaptively employed in regions far from current manufacturing layer. This reduces the scale of the computation and accelerates the simulation tremendously. Numerical results also demonstrate that the proposed method is able to simulate the evolution of the thermal fields in additive manufacturing process.

Topology Optimization for Twist Chirality of Materials Induced by Axial Strain

Wei Chen^{*}, Xiaodong Huang^{**}

^{*}Swinburne University of Technology, ^{**}Swinburne University of Technology

ABSTRACT

An object or system is chiral if it is distinguishable from its mirror image. The chirality is widely observed in biological materials and structures. Artificial chiral structures inspired by natural materials have also demonstrated significant applications in industry. With growing interest in chiral material design, most of the research work follows the traditional trial-and-error approach. To achieve the chirality of materials, a systematic design method, e.g., utilizing topology optimization technique, has never been reported. In this paper we propose a systematic topology optimization method on designing materials of tubes or beams exhibiting the twist chirality under the axial strain. Such a twist chirality of the structure has many potential applications. The optimization objective is to maximize the twist angle of a structure constructed by optimally designing microstructures of cellular or composite materials. The proposed two-scale topology optimization problem is solved by the extended bi-directional evolutionary structural optimization (BESO) method. The results show that various topological patterns of microstructures are achieved and the resulting structures exhibit the desirable twist chirality. However, the twist chirality of the structure somewhat depend on the size of the material unit cell. Numerical analysis indicates that, with the decrease of the unit cell size, the twist angle of structures gradually increases or decreases and finally approaches its bound, which corresponds to the one obtained by the proposed topology optimization.

Design Optimization of Underwater Acoustic Anechoic Layers Under Set Frequency Bands

Wenjiong Chen^{*}, Chenjing Ren^{**}, Shutian Liu^{***}

^{*}Dalian University of Technology, ^{**}Dalian University of Technology, ^{***}Dalian University of Technology

ABSTRACT

Thin rubber layers with air-filled cavities can be used as anechoic submarine coatings. The size and shape of the air-filled cavity (i.e the hole structure) are have greatly influence upon the acoustic performance of the underwater sound absorption coatings. In this paper, a methodology is proposed for designing the hole structure for maximizing the acoustic absorption of the underwater acoustic anechoic layers under set frequency bands. The acoustic cavity structure is separated into several cylindrical channel structures with gradient inner diameters. Therefore, based on the one-dimensional physical model of uniform cylindrical channel, the equivalent parameters (equivalent density and equivalent modulus) each sound absorption layer can be obtained. Then, the sound absorption performance of composite-gradient absorptive coating is calculated by the transfer matrix method. Moreover, the influence of structural parameters and material parameters on the sound absorption performance of the coating is discussed. Finally, the genetic algorithm is employed to optimize the hole structure for maximizing the sound absorption coefficient in specific frequency bands. Utilizing the constructed optimization model, the parameters of hole structure are derived with optimal sound absorption under the set frequency bands, which is a helpful guidance on the design of anechoic coatings.

Numerical Simulation of Water Entry of Three-dimensional Oblique Cylinder by MPSGPU-SJTU

Xiang Chen*, Decheng Wan**

*Shanghai Jiao Tong University, **Shanghai Jiao Tong University

ABSTRACT

Water entry is a very complex flow problem in the naval architecture and ocean engineering, which always accompanies with the slamming, the large deformation of free surface and moving boundary. Thus, numerically simulating water entry is a challenging task of researchers. In the present work, the moving particle semi-implicit method (MPS), a fully Lagrangian particle method for incompressible fluid, is used to simulate this problem. However, most previous researches of our group focus on two-dimensional water entry problems because of huge computation time on CPU. GPU parallel acceleration technique widely used in scientific calculations is applied to improve computational efficiency of MPS. In addition, the motion function of multi-degree of freedom (multi-DOF) is developed for real three-dimensional water entry problem. In this paper, the cylinder model with an oblique angle of 35° is the same as experimental model by Sun et al. in 2015. The cylinder vertically enters the still water with an initial velocity of 1.92 m/s. The motions of surge, heave and pitch are free. The simulation of whole process is carried out by our in-house solver MPSGPU-SJTU, which is developed on improved MPS and GPU acceleration technique. In the previous work by Tang et al. in 2016, only half of computational domain is simulated due to the symmetry of this problem. Because of the improvement of computational efficiency, the whole computational domain is built to capture more details of fluid field in this work. By GPU calculation, the motions of cylinder are accurately predicted. And details of pressure field and free surface deformation can be observed by GPU simulation. The numerical results show a good agreement with the corresponding experimental data and SPH results. In addition, the computation times of one hundred steps between GPU and CPU is compared. These comparisons show that MPS method coupling with GPU acceleration technique is feasible and faster for the direct numerical study of multi-DOF three-dimensional water entry problem.

Fully Implicit NS Solver for Thermo-Chemical Non-equilibrium Flow Using GMRES Algorithm

Xianliang Chen^{*}, Song Fu^{**}

^{*}School of Aerospace Engineering, Tsinghua University, Beijing, 100084, China, ^{**}School of Aerospace Engineering, Tsinghua University, Beijing, 100084, China

ABSTRACT

A significant characteristic of hypersonic flow is the steeply rising temperature within field as Mach number increases. Extremely high temperature of air will excite vibrational energy internally within molecules and cause dissociation and even ionization within the gas[1], leading to considerable deviations from conventional calorically-perfect gas assumption. Meanwhile, thermal and chemical equilibrium of air cannot be reached everywhere, especially behind shocks, due to the finite rate of energy relaxation and reaction, thus a wide variety of non-equilibrium models are developed in the pursuit of more appropriate simulations of hypersonic flow. The increase of complexity in models and difficulty in numerical treatment results in greatly increased computing time and memory, therefore efficient non-equilibrium solver is expected. In this paper, iterative method GMRES(Generalized Minimum RESidual) is introduced as time-stepping method in thermo-chemical non-equilibrium flow, leading to a fast, robust Navier-Stokes solver. LUSGS(Lower-Upper Symmetric Gauss-Seidel) method is used as preconditioner to utilize the advantage of its robustness and low-memory requirement[2]. The numerical results obtained indicate that the efficiency of implicit stepping outperforms explicit counterparts in orders because of the great numerical stiffness of vibrational and chemical source terms. Within implicit methods, the combination of GMRES and LUSGS still results in acceleration of convergence compared to LUSGS alone. Key words: Non-equilibrium Flow, GMRES REFERENCE [1] Anderson J D. Hypersonic and High-Temperature Gas Dynamics, Second Edition[M]. McGraw-Hill, 2006. [2] Hong L, Baum J D, Löhner R. A Fast, Matrix-free Implicit Method for Compressible Flows on Unstructured Grids[J]. Journal of Computational Physics, 1998, 146(2):73-78.

Numerical Analysis on the Buckling, Postbuckling and Delamination Growth of Variable Angle Tow Composite Plates with Delamination Using Cohesive Zone Model

Xiaodong Chen^{*}, Zhangming Wu^{**}, Guojun Nie^{***}, Wuxiang Liu^{****}

^{*}Tongji University, ^{**}Cardiff University, ^{***}Tongji University, ^{****}Tongji University

ABSTRACT

Variable angle tow (VAT) composite plates have been made possible by using advanced automated fibre placement (AFP) technology. Such designs have shown considerable freedom in stiffness tailoring to exploit the enhanced performance for lightweight composite plates or structures. Unfortunately, VAT composite plates are not immune to the occurrence of delamination, which may lead to the undesirable loss of both stiffness and strength. In the present study, the compressive behavior of VAT composite plates with delamination damage was numerically evaluated to explore the complex mechanisms of interaction between postbuckling and delamination growth. Both through-the-width and embedded delaminations involved in composite laminates are constructed in the numerical simulation. A three-dimensional solid element is employed to discretize the VAT composite plate, and the bonded interface where delamination is expected to propagate is modelled by using an in-house cohesive element available in Abaqus software. The cohesive element has a bilinear constitutive relationship in terms of traction and separation, which allows modelling of progressive damage and failure in cohesive layers. Within the framework based on the continuum damage mechanics, both delamination initiation and growth occurred in VAT composite plates are predicted. Numerical results obtained using FEA incorporated with the progressive damage model are compared with those in existing literatures and a good agreement between them is found. Effects of the pre-existing delamination and varying fibre orientation angles on the buckling, postbuckling and delamination growth of VAT composite plates are thoroughly investigated in numerical examples. It is shown that the compressive strength of delaminated composite plates is significantly affected by the delamination growth during the postbuckling process. The numerical study also shows that the residual buckling resistance of delaminated composite plates can be significantly improved through using the VAT design concept. In addition, the mechanism of taking advantages of VAT laminates to improve both buckling and postbuckling properties of delaminated composite plates is studied in details. This research provides preliminary fundamentals for the designers to perform the damage tolerance design of VAT composite structures.

Development of an Integrated 1D-0D Simulation System with Functions of 3D Modeling &&&&& Visualization

Yan Chen^{*}, Masaharu Kobayashi^{**}, Changyoung Yuhn^{***}, Hao Zhang^{****}, Marie Oshima^{*****}

^{*}Graduate School of Interdisciplinary Information Studies, The University of Tokyo, ^{**}Graduate School of Interdisciplinary Information Studies, The University of Tokyo, ^{***}Department of Mechanical Engineering, The University of Tokyo, ^{****}Department of Mechanical Engineering, The University of Tokyo, ^{*****}Institute of Industrial Science / Graduate School of Interdisciplinary Information Studies, The University of Tokyo

ABSTRACT

To evaluate the effects of surgery and predict changes in the flow distribution afterwards, we have been developing a patient-specific 1D-0D blood flow simulation system. When the postoperative effects are examined, the global circulatory system must be considered in order to emulate alteration of blood flow after surgery [1]. Although a 3D simulation can provide information about local blood flow, the 1D-0D simulation reflects the changes in the global cardiovascular system with much more reasonable costs than the 3D simulation. On the contrary, since there is no 3D geometry information presented in 1D-0D simulation, it is difficult to grasp the 3 dimensional behavior of blood flow. Therefore, we developed modules for geometric modeling and visualization based on V-modeler [2], which is in-house 3D-modeling and visualization system in order to visualize the blood flow by dynamically mapping the simulation results onto a 3D surface model of large arteries in the cardiovascular system. To construct the visualization module, we used both patient-specific geometry data, which are acquired from patient-specific medical images, and statistic geometry data. We applied a method of deformable model so as to connect 1D simulation results of patient-specific parts with 0D ones of statistic parts in order to represent the physiological characteristics of global blood flow. In addition, we have also developed a method to change geometry interactively to mimic a surgery such as CAS (Carotid artery stenting). For instance, it enables users to create new geometry by changing the radii of vessel geometry, and send the information on the new geometry as input data to the simulation. As the result, the present methods on 3D modeling and visualization enables the 1D-0D simulation to be displayed with dynamic 3D information. Reference [1] Zhang, H., N. Fujiwara, M. Kobayashi, S. Yamada, F. Liang, S. Takagi, and M. Oshima. Development of a Numerical Method for Patient-Specific Cerebral Circulation Using 1D-0D Simulation of the Entire Cardiovascular System with SPECT Data. 44:2363, 2016. [2] Kobayashi, M., K. Hoshina, S. Yamamoto, Y. Nemoto, T. Akai, K. Shigematsu, T. Watanabe, M. Oshima. Development of an Image-Based Modeling System to Investigate Evolutional Geometric Changes of a Stent Graft in an Abdominal Aortic Aneurysm. Circulation advpub, 2015.

Mechanics of Cancer Cell Cluster Passage Through Micro-constrictions

Yeng-Long Chen*

*Academia Sinica

ABSTRACT

Cancer cells and clusters may be able to enter and exit through micro-constrictions in the blood vessels during the metastatic stage. The constrictions could be more than an order of magnitude smaller than the clusters, which begs the question of how the passage occurs. The extravasation process involves severe cell deformation and sufficiently strong inter-cell adhesion during the contraction flow. Using advanced modeling that couples fluid flow, cell mechanics, and inter-cell adhesion, we investigated the mechanics of how cell clusters are able to traverse a much smaller capillary. We found that depending on the inter-cellular adhesion, the cluster could become stuck, pass through intact, or break up during passage [1]. The model predictions capture the qualitative behavior of cancer cell cluster passage through microfluidic constrictions, suggesting possible pathway for future treatments. [1] S.H. Au, B.D. Storey, J.C. Moore, Q. Tang, Y.L. Chen, S. Javaid, A.F. Sarioglu, R. J. Sullivan, M.W. Madden, R. O'Keefe, D.M. Lengenau, D.A. Haber, S. Maheswaran, S.L. Stott and M. Toner* (2016) Clusters of circulating tumor cells traverse capillary-sized vessels, Proc. Natl. Acad. Sci. U.S.A. 113, 4947

Full Atomic Modeling of the Parathyroid Hormone/parathyroid Hormone-related Protein Type 1 Receptor and Its Ligand Binding

Yi-Hsiang Chen*, Shu-Wei Chang**, Chuin-Shan Chen***

*National Taiwan University, **National Taiwan University, ***National Taiwan University

ABSTRACT

Parathyroid hormone/parathyroid hormone-related protein type 1 receptor, known as PTHR1, is a class B G protein-coupled receptor. It has been considered as a drug target for bone-related diseases, such as Eiken syndrome, Hypoparathyroidism and Osteoporosis. Binding of the PTHR1 and its ligands, parathyroid hormone (PTH) and parathyroid hormone-related protein (PTHrP), leads to the conformational change of PTHR1 transferring the signal for crucial biochemical reactions such as blood calcium ion balance, bone turnover regulation and skeletal development. The abnormal PTHR1, mutated in certain critical sequences, results in many diseases, such as Blomstrand's lethal chondroplasia, Ollier's disease, Jansen's metaphyseal chondroplasia and Brachydactyl type E. However, the structure of the transmembrane domain of PTHR1 and how the ligand alters the structure of PTHR1 are still unclear. Understanding these molecular mechanisms will help enable possible treatments for the receptor/hormone related diseases. In this study, we combine homology modeling and molecular dynamics simulations to investigate the structure of full length PTHR1. We use the crystal structures of glucagon receptor and corticotropin-releasing factor receptor 1 as templates to create the homology model of PTHR1. The full atomistic model of the PTHR1 is compared with the class A receptors and two available class B receptors. The intramolecular interactions and structural features of the PTHR1 are analyzed to provide fundamental insights into the structure of the PTHR1. Furthermore, we use molecular dynamics simulations to investigate the interactions between the PTHR1 and the native ligands including PTH and PTHrP. The intermolecular hydrogen bonds, binding sites, binding affinity, and conformational changes of PTHR1 are analyzed. In the last part, we investigate the effects of three types of mutations which have been found on PTHR1/PTHrP, including (a) extracellular domain mutations: P132L (Blomstrand's lethal Chondroplasia and Familial primary failure of tooth eruption), R150C (Ollier's disease) and R174C (Familial primary failure of tooth eruption); (b) transmembrane domain mutations: H223R, T410P and I458R (all related to Jansen's metaphyseal chondroplasia); (c) PTHrP mutations, L8P and L24P (both related to Brachydactyl type E). This study provides an effective framework to understand the structure of class B G-Protein coupled receptors. The model is in a good agreement with previous experimental studies. The results of the structure of PTHR1, the binding mechanism of its ligands and the molecular origin of receptor related mutations provide molecular insights into receptor-related diseases and could enable the design of novel drugs.

Stiffness Thresholds of Carbon Nanotube Networks

Yuli Chen^{*}, Fei Pan^{**}

^{*}Institute of Solid Mechanics, Beihang University, ^{**}Institute of Solid Mechanics, Beihang University

ABSTRACT

For carbon nanotube (CNT) networks (CNTNs), with increasing network density, there may be sudden changes in the properties, such as the sudden change in electrical conductivity at the electrical percolation threshold. In this work, the stiffness of CNTNs is studied and especially the existence of stiffness thresholds are revealed. Two critical network densities divide the stiffness behavior into three stages: zero stiffness, bending dominated and stretching dominated stages. The first critical network density is a criterion to judge whether or not the network is capable of carrying load, defined as the stiffness threshold. The second critical network density is a criterion to measure whether or not most of the CNTs in network are utilized effectively to carry load, defined as bending-stretching transitional threshold. Both thresholds are found to be intrinsic features of CNTNs, independent of loading conditions. Based on the geometric probability analysis, a theoretical methodology is developed to predict the two thresholds and explain their underlying mechanisms, and a simple piecewise expression is summarized to describe the stiffness of CNT networks, in which the relative stiffness of networks depends only on the relative network density and the CNT aspect ratio. Based on the two stiffness thresholds, the out-of-plane bending of film-like CNTNs is studied. The pure bending of CNTNs consists of two types of deformation, the out-of-plane deformation and the in-plane deformation, which both contribute to the bending stiffness. The bending stiffness presents a four-stage regime with the network density, which is divided by the electrical percolation threshold and two stiffness thresholds. Using the energy theorems and superposition method, a simple piecewise analytical expression for bending stiffness is proposed. This work provides a solid theoretical foundation for the design and property prediction of CNTNs, and the method and results can also be extended to other networks constructed by nanotubes and nanowires. Reference [1] Chen Y, Pan F, Guo Z, et al. Stiffness threshold of randomly distributed carbon nanotube networks [J]. J Mech Phys Solids, 2015, 84.395-423. [2] Pan F, Chen Y, Qin Q. Stiffness thresholds of buckypapers under arbitrary loads [J]. Mech Mater, 2016, 96. 151-68. [3] Pan F, Chen Y, Liu Y, et al. Out-of-plane bending of carbon nanotube films [J]. Int J Solids Struct, 2017, 106-107: 183-199.

Adaptive Time-stepping Algorithm for Simulating Snap-through Instability in Bistable Structures

Zi Chen^{*}, Yin Liu^{**}, Guangchao Wan^{***}

^{*}Thayer School of Engineering, Dartmouth College, Hanover, NH 03755, USA, ^{**}Thayer School of Engineering, Dartmouth College, Hanover, NH 03755, USA, ^{***}Thayer School of Engineering, Dartmouth College, Hanover, NH 03755, USA

ABSTRACT

Snap-through instability, typically featuring a rapid shape transition, has been found useful in a wide range of natural and engineered structures, such as the Venus flytrap and bistable composites. The snap-through behaviors have a common feature in that the time scale of the deformation is much smaller than that in other deformation stages, which brings challenges for numerical simulations, such as intensive computation induced by the usage of extremely small size of time step and numerical divergence arising from large shape change in a very short time. In this talk, we will introduce nonlinear dynamical finite element (FE) computational framework for efficiently capturing the shape evolution of structures with snap-through instability. The nonlinear dynamical FE equations are first discretized in the time domain based on the Newmark scheme. Next, unlike the traditional time-stepping scheme where a fixed value (or the range) of time step is required before simulation, both the displacement and time increments are introduced as unknowns in the incremental FE formulations, and an arc-length equation, related to the total displacement increment is introduced to complete the equation system. In the algorithm, the time-step size can be automatically adjusted based on the prescribed arc-length and the displacement increment, which permits the usage of large time-step sizes for slow deformation and small time-step sizes for fast deformation. Furthermore, we will introduce several numerical examples involving snap-through instability, including a 2D simply-supported pre-buckled beam and a 3D bistable trilayer composite shell, which demonstrate that the algorithm can efficiently simulate dynamical snap-through behaviors with automatic adjustment of the time-step size.

3D Numerical Simulation of the Chip Geometry during Machining

Kévin Chenegrin^{*}, Eric Feulvarch^{**}, Habib Karaoui^{***}, Mathieu Girinon^{****}, Frédéric Valiorgue^{*****}

^{*}Univ. Lyon, ENISE, LTDS, UMR 5513 CNRS - SAFRAN Tech, ^{**}Univ. Lyon, ENISE, LTDS, UMR 5513 CNRS, ^{***}SAFRAN Tech, ^{****}CETIM, ^{*****}Univ. Lyon, ENISE, LTDS, UMR 5513 CNRS

ABSTRACT

This work focuses on the development of a 3D finite element model simulating a turning operation in the thermal and mechanical steady state. It is based on the work of Girinon et al. [1] which proposed an approach based on a Eulerian formulation which allows representing the material flow without the need for simulating the transient step (chip formation and element damaging). This modelling makes it possible to know temperature distribution in the chip, the machined part, the tool and tool-holder. This numerical simulation has been successfully applied for the computation of residual stresses during a drilling operation [2]. Unfortunately, such an approach needs to know the geometry of the chip that can be obtained from experimental Quick Stop Tests (QST). The objective of this communication is to propose a numerical technique avoiding experiments by computing the quasi-stationary geometry of the chip in 3D in a Eulerian Framework with the software SYSWELD. The chip geometry is compared to experimental observations for a turning operation. [1] M. Girinon, F. Valiorgue, V. Robin, and E. Feulvarch, 3D stationary simulation of a turning operation with an Eulerian approach, Appl. Therm. Eng., vol. 76, pp. 134-146, (2015). [2] M. Girinon, F. Valiorgue, H. Karaoui, and E. Feulvarch, 3D numerical simulation of drilling residual stresses, Comptes Rendus Mecanique, in press, (2018).

FEM-Cluster Based Reduction Method for Efficient Numerical Prediction of Effective Properties of Heterogeneous Materials

Gengdong Cheng^{*}, Xikui Li^{**}, Yinghao Nie^{***}, Hengyang Li^{****}

^{*}Dalian University of Technology, ^{**}Dalian University of Technology, ^{***}Dalian University of Technology, ^{****}Dalian University of Technology

ABSTRACT

A novel FEM-Cluster reduced order method which enables efficient numerical prediction of effective properties of heterogeneous material in nonlinear range is proposed. The cluster concept initially presented in the work by WK Liu et al [1] is introduced and extended to derive a full FEM multi-scale formulation of the Representative Unit Cell (RUC) to circumvent the heavy computational burden required for a direct numerical simulation (DNS) of the high-fidelity RUC. The proposed method is formulated in a consistent framework of finite element method. It provides a two-phases, comprising the offline and the online phases, numerical algorithm for predicting effective nonlinear mechanical properties of heterogeneous materials. The basic theory of RUC is introduced and the finite element implementation of the RUC subjected to given periodic homogeneous displacement boundary condition and the uniformly distributed eigen-strain over the RUC is described. The reduced order model is built up at the offline phase. It consists of clustering process and construction of the cluster-interaction matrix under the assumption of the linear elasticity. In the clustering process, the RUC is divided into a number of the clusters according to values of elemental strain concentration factors, which are obtained from full FEM analysis of the high-fidelity RUC. The RUC is subjected to periodic homogeneous boundary condition and one component of the uniformly distributed eigen-strain vector over the RUC one by one in turn, by k-means clustering. The cluster interaction matrix is constructed with numerical results of the DNS subjected to uniform eigen-strain for each cluster in turn. It represents the interactions between each two arbitrary clusters in the RUC in terms of the uniformly distributed eigen-strain over one cluster and the average stress over another cluster. Its mathematical structures and physical properties are discussed. The online elasto-plastic phase of the reduced order model is performed by the incremental non-linear FE analysis using the constant cluster-interaction matrix, which plays a role in the present work conceptually similar to the initial elastic modular matrix used in the "initial stiffness method" for the traditional incremental elasto-plastic analysis. By doing so, accurate and efficient numerical prediction of effective properties of heterogeneous material in nonlinear range are fulfilled in a consistent way. The performances of the proposed reduced order model and its numerical implementation are studied and demonstrated by several numerical examples. Reference [1] Zeliang Liu, M.A. Bessa, Wing Kam Liu. Comput. Methods Appl. Mech. Engrg. 306 (2016) 319–341.

Efficient Numerical Ice Sheet Simulations over Long Time Spans

Gong Cheng^{*}, Lina von Sydow^{**}, Per Lötstedt^{***}

^{*}Uppsala University, ^{**}Uppsala University, ^{***}Uppsala University

ABSTRACT

The full-Stokes models to palaeo-ice sheet simulations have previously been highly impractical due to the requirement on the mesh resolution close to the grounding-line. We propose and implement a new sub-grid method for grounding-line migration in full Stokes equations with equidistant mesh. The beauty of this work is to avoid remeshing when the grounding-line moves from one steady state to another. A new boundary condition is introduced to accommodate the discontinuity in the physical and numerical model. The method is implemented in Elmer/ICE that solves the full Stokes equation with the finite element method. The convergence of the sub-grid method is examined as the mesh is refining and the results are compared with MISIMP benchmark.

Multiscale Mechanical Modeling of Damage Behavior in Drilling of Unidirectional CFRP with Thermo-mechanical Coupling

Hui Cheng*, KunPeng Du**

*Northwestern Polytechnical University, **AVIC Xi'an Aircraft Industry (Group) Company LTD

ABSTRACT

Drilling is one of the most common machining methods for unidirectional carbon fiber-reinforced polymer (UD CFRP) structure, which is a complex thermal-mechanically coupled process. To reveal the deformation mechanism and damage behavior in UD CFRP drilling, a multiscale mechanical modeling for UD CFRP drilling with thermal-mechanical coupling is demonstrated in this paper. which captures the failure modes for fibers, matrix and the interface based on a micro-level RVE and the delamination between different layers in macro-level simulation. Failure models for the fiber, matrix and interface region are applied depending on the material properties of each of these three phases in micro-scale. A modified cohesive element model which can avoid the excessive element distortion in dynamic simulation and propagate the heat is also developed to represent the delamination in macro-scale. Numerical simulations based on the above model with different fiber orientations were performed to predict the damage behaviors. Drilling tests with the conditions as considered in the simulations were carried out to validate the multiscale mechanical modeling. Drilling force get by sensors and damage model measured by scanning electron microscope can match well with the simulation.

Ultrasonic Properties of Polymer Composites with Particle Inclusions

Jian Cheng^{*}, Zhanli Liu^{**}, Zhuo Zhuang^{***}

^{*}Tsinghua University, ^{**}Tsinghua University, ^{***}Tsinghua University

ABSTRACT

Glass particles / polyurea composites have great anti-ultrasonic performance and improve a lot at high strain rate / frequency. In order to simulate high strain rate / frequency conditions, many researchers use ultrasonic technology to determine the properties of composite materials, which can easily achieve high-frequency input. In this study, the dynamic mechanical properties of glass particles / polyurea composites were systematically studied by means of ultrasonic test platform, and the glass microspheres were changed to SiO₂ nano-particles to observe the performance changes. In addition, a computational model based on random distribution inclusions was established to calculate the mechanical properties of the corresponding composites. The main contributions were as follows: (1) The high-frequency ultrasonic attenuation performance test platform of composite materials was established; (2) The ultrasonic attention properties of glass particles / polyurea composites and SiO₂ nano-inclusions / polyurea composites were measured at different frequencies; (3) A computational model for predicting the dynamic mechanical properties of glass inclusions / polyurea composites was established. The experimental platform and calculation model for ultrasonic attenuation performance analysis were established, and several samples were tested and calculated. It can be found that the attenuation coefficient of the polyurea and composites increased rapidly with the increase of the input frequency, and the attenuation performance with the glass inclusions was better than that of the composites with nano-particles. The attenuation performance of the composites with glass inclusions can be increased by 10% (2.5MHz) to 14% (1.5MHz), compared to pure polyurea. The complex modulus also behaved the same law, and the loss modulus was sensitive to the frequency change, and the storage modulus was kept constant. In the calculation, we also found that for the specific sample and input frequency, the composites with higher volume fraction of glass microspheres and the larger inclusion diameter have the better attenuation performance.

Delayed Unstable Expansion of a Gel Balloon

Jian Cheng^{*}, Zheng Jia^{**}, Teng Li^{***}

^{*}University of Maryland College Park, ^{**}Zhejiang University, ^{***}University of Maryland College Park

ABSTRACT

The loss of stability, i.e. the burst is commonly observed during the inflation of a rubber balloon. The sudden change in size happens instantaneously once the applied pressure reaches a critical value. However, the inflation of a hydrogel balloon deviates from its better-understood rubber counterpart. In this paper, we demonstrate that when a gel balloon is subject to a pressure even less than the critical value for instantaneous burst, solvent molecules diffuse into the gel network, dilute, and effectively weaken the polymeric network. A hydrogel balloon undergoes a slow and continuous evolution of swollen states. Depending on the material properties and applied pressure the swelling process may either carry the gel balloon to a final equilibrium state, or continues infinitely and eventually results in a sudden burst. We further provide a phase diagram which divides the response of a gel balloon into 3 categories: instantaneous burst, delayed burst, and steady growth, based on the given material properties and applied pressure.

Open Source Package of High Performance Immersed Finite Element Method (IFEM) for Fluid-Structure Interactions

Jie Cheng^{*}, Lucy Zhang^{**}

^{*}Rensselaer Polytechnic Institute, ^{**}Rensselaer Polytechnic Institute

ABSTRACT

In this talk, we present a successful refactoring of our existing code, the immersed finite element method (IFEM) and its derivatives, the modified IFEM (mIFEM) for fluid-structure interaction analysis. The algorithm is originally based on the immersed concept, i.e., solid mesh is immersed in the fluid, and the interaction between fluid and solid relies on interpolation between grids. The mIFEM takes advantage of the immersed concept of no-remeshing for the computational domain, and further develops on a volumetric weak form basis where the fluid and the solid solvers can function and evaluate their own dynamics independently. In this work, we utilize open source packages intensively for both the fluid and the solid solvers: the standard finite element ingredients are handled by deal.II, the parallel linear algebra is dealt with by PETSc, the mesh partition relies on p4est, the building process is generated by CMake for cross-platform, and the documentation is done by Doxygen. The source code is written in the object-oriented fashion, automated unit tests and regression tests are deployed. Version-control, peer review and data preservation are carried out. After the refactoring, the number of lines in the code decreases significantly and the performance gain is remarkable. More importantly, with a modern software framework facilitated by open source software, the maintenance is much easier than before, and the life time of the software is expected to last longer. We welcome contributions, including various features to treat interface interpolation, solid material types, fluid solvers for compressible fluid, turbulent flows, etc. from the computational mechanics community.

Fast Process Modeling Based Support Structure Design Optimization for Minimizing Residual Stress and Distortion in Metal Additive Manufacturing

Lin Cheng^{*}, Xuan Liang^{**}, Albert To^{***}

^{*}University of Pittsburgh, ^{**}University of Pittsburgh, ^{***}University of Pittsburgh

ABSTRACT

Metal additive manufacturing (AM) as a revolutionary manufacturing technique has been gradually accepted by engineers and applied for rapid manufacturing of functional end-use components. However, there are two key physical phenomena preventing its broad applications, namely the residual stress and large deformation inherent in the melting and solidification processes. These phenomena cause delamination and cracking during the manufacturing process, which can stop the recoater blade from spreading the powder, as well as lead to part warpage after removing from the building tray. To address these issues, a novel design optimization methodology based on fast process modeling is proposed for the design of support structure, in order to reduce residual stress and distortion and ensure manufacturability. First, a modified inherent strain method is proposed and employed for fast prediction of the stress and deformation. It is based on thermo-mechanical modeling at mesoscale and implemented as a one-time static mechanical analysis. Thus, the process modeling can be significantly accelerated and compatible with structural design. Second, a projection scheme is proposed to map the domain of support structure for a given solid component, in which the minimum support area is found for the next step. Third, lattice structure topology optimization is applied to minimize the mass consumption of support structure subjected to yield stress constraint. This not only prevent failure of the AM build by limiting the residual stress below the yield strength, but also reduce material required for support structure. Moreover, the self-support nature of lattice structure, and its ability to provide accurately mechanical representation, makes it a natural design tool for support structure design. Several examples are performed and manufactured to demonstrate the efficiency of the proposed algorithm. Both numerical simulation and experiments prove that the proposed method can significantly reduce residual stress and guarantee the success of metal AM fabrication.

Research on Anti-water Pressure Capability of Railway Tunnel Lining by CDEM (Continuous-Discontinuous Element Method)

Pengda Cheng^{*}, Ping Lu^{**}, Liangtian Peng^{***}, Gang Zhou^{****}, Li Ming Zhang^{*****}, Guo Jun Wang^{*****}, Bao Lin Liu^{*****}, Tian Yang^{*****}

^{*}Institute of Mechanics, Chinese Academy of Sciences, Beijing 100190, China, ^{**}Sichuan Xu Da Railway Co., Ltd. Luzhou, 646000, China, ^{***}Sichuan Xu Da Railway Co., Ltd. Luzhou, 646000, China, ^{****}Sichuan Provincial Railway Construction Co., Ltd, Chengdu, 610031, China, ^{*****}Sichuan Provincial Railway Construction Co., Ltd, Chengdu, 610031, China, ^{*****}China Railway Eryuan Engineering Group Co., Ltd(Chongqing), Chongqing 400023, China, ^{*****}China Railway Eryuan Engineering Group Co., Ltd(Chongqing), Chongqing 400023, China, ^{*****}University of Chinese Academy of sciences, Beijing 100049, China; Institute of Mechanics, Chinese Academy of Sciences, Beijing 100190, China

ABSTRACT

Abstract: The hydrogeological conditions are complex in southwest China, and the anti-water pressure capability of railway tunnel lining is widely regarded in the transportation project. When the drainage conditions are limited, high external water pressure may cause the lining cracking, which is the serious threat to the tunnel safety. Scientifically and rationally assessing the anti-water pressure capability of the lining is very important to the design of the lining structure. In this paper, the research method combine the theoretical analysis and the numerical simulation, the numerical calculation model is established by using the continuous-discontinuous element method (CDEM). Based on that model, the destruction process of tunnel lining under different water pressure conditions is simulated, the stress and strain changes of the initial support, steel-concrete lining and waterproofing board are analyzed. Finally, the development of the cracks and the fracture degree in tunnel lining can be obtained under different water pressure conditions, meanwhile the assessment method can be proposed by using the fracture degree. That has the important practical application value for optimizing the design parameters of the tunnel anti-water lining.

References [1] Li SH, Wang JG, Liu BS, et al. Analysis of critical excavation depth for a jointed rock slope by face-to-face discrete element method. Rock Mechanics and Rock Engineering, 2007, 40(4): 331-348 [2] Itasca Consulting Group Inc. FLAC-3D (Fast Lagrangian Analysis of Continua in 3 Dimensions), Version 3. 0, User&amp;amp;amp;amp;apos;s Manual. USA: Itasca Consulting Group Inc, 2005 [3] LI Shihai ZHOU Dong LIU Tianping. Risk analysis method of accumulated landslide based on fracture degree[J]. Chinese Journal of Rock Mechanics and Engineering, 2013, 32:3909-3917.

Turbulence Spectra in the Stable Atmospheric Boundary Layer

Yu Cheng^{*}, Qi Li^{**}, Stefania Argentini^{***}, Pierre Gentine^{****}

^{*}Department of Earth and Environmental Engineering, Columbia University, New York, NY 10027, USA,

^{**}Department of Earth and Environmental Engineering, Columbia University, New York, NY 10027, USA,

^{***}Institute of Atmospheric Sciences and Climate, CNR, Rome, Italy, ^{****}Department of Earth and Environmental Engineering, Columbia University, New York, NY 10027, USA

ABSTRACT

Stratification causes turbulence spectra to deviate from Kolmogorov's isotropic $-5/3$ power-law scaling in the universal equilibrium range at high Reynolds number. However, a consensus has not been reached with regard to the exact shape of the spectra. Here we propose a theoretically-derived shape of the TKE and temperature spectra that consists of three regimes at small Froude number: the buoyancy subrange, a transition region and isotropic inertial subrange separated by the buoyancy scale and Ozmidov scale through derivation. These regimes are confirmed by various observations in the atmospheric boundary layer. We also show that DNS may not apply in the study of very stable boundary layers as they cannot correctly represent the observed spectral regimes seen in actual boundary layers because of the lack of scale separation. In addition, the spectrum in the transition regime explains why Monin-Obukhov similarity theory cannot entirely describe the behavior of the stable atmospheric boundary.

Controlling of Wave Propagation in Composite with Spherical Inclusions in Meso-scale

Luo Chengcheng*, Liu Zhanli**

*+86-15201522105, **18811584467

ABSTRACT

Control of wave of wave propagation is always a hot spot in scientific research, which has also so many applications such as noise reduction and blast wave protection. According to previous studies, the Bragg scattering and resonant oscillations are two main principles to control the elastic wave. Based on their theories, we developed a finite element to see the wave propagation in composite particled with spherical inclusions. The distribution of inclusions can be both periodic and casual. By changing the size and volume ratio in composite, we can find the case which gains the most decrease of the wave. The model is generated by abaqus using python and the preprocess and the postprocess can be all automatic. The shape of the particle and the properties of materials can be modified in later research.

An Improved Contact Detection Algorithm for Dynamic Finite Element Analysis

Chen Chengjun^{*}, Chen Xiaowei^{**}, Liu Ming^{***}

^{*}Institute of Systems Engineering, CAEP, ^{**}Frontier Science Research Institute of Beijing Institute of Technology,
^{***}Institute of Systems Engineering, CAEP

ABSTRACT

Contact detection has a significant effect on the efficiency and accuracy of finite element analysis for dynamic contact problems. In this paper, a new contact-pair detection algorithm for dynamic contact simulation in the finite element has been developed and implemented in the transient dynamic finite element code PANDA-IMPACT. The newly developed contact detection strategy composed of: (1) a global search strategy based on the octree algorithm that is used to efficiently find out all the possible candidates for contact and, (2) a robust local search algorithm derived based on the geometric position relationship between the slave segments and the corresponding master segments to determine the actual contact pairs. In the new algorithm, the centroid of the contact segment and its characteristic length (one kind of mean length of contact segment) are employed to represent the segment's true geometry. As a consequence, the contact segments are reduced to a series of discrete points, and the building and updating processes of the octree are very straightforward. The cost of the new global searching is of the order of $O(N \log 8M)$, where N is the number of the slave nodes, M is the number of master segments. In local searching phase, contact point is evaluated analytically based on the principles of force-equivalence and moment-equivalence, and a reverse mapping algorithm. Difficulties associated with the conventional contact algorithms, such as stability and blind zone problems, are resolved. Several numerical simulations of typical benchmarks and physical engineering problems demonstrate that the proposed contact determination strategy is effective and robust, and has good applicability.

Development of an Adaptive Material Point Method Coupled with a Phase Field Model for Analyzing Damage Process and Crack Propagation

Young-Jo Cheon^{*}, Hyun-Gyu Kim^{**}

^{*}Seoul National University of Science and Technology, ^{**}Seoul National University of Science and Technology

ABSTRACT

In this study, a new method is developed by combining material point method and phase field method for the analysis of damage evolution and crack propagation in materials. In the conventional finite element method, it is difficult to simulate damage evolution and crack propagation due to meshing a new geometry and the effect of element shape on crack propagation. A background grid of material particles is adaptively refined based on the material damage which is evaluated by solving a phase field model. The characteristic length of material damage and crack propagation is applied to multiscale adaptive material point method and phase field method. The proposed approach is verified through numerical examples of several crack propagation problems.

Dispersive Effective Behaviour of High-contrast Periodic Media

Kirill Cherednichenko^{*}, Alexander Kiselev^{**}, Yulia Ershova^{***}

^{*}University of Bath, ^{**}Dragomanov National Pedagogical University, ^{***}University of Bath

ABSTRACT

We prove sharp operator-norm asymptotic equivalence estimates between a family of periodic quantum graphs with rapidly oscillating high-contrast weights and ‘‘homogenised’’ models with energy-dependent interface conditions. The asymptotic analysis is carried out ‘‘on the spectrum’’, i.e. it includes order-sharp asymptotic estimates for the eigenfunctions of the mentioned operator families. We show that the above asymptotically equivalent models are equivalent to models for the so-called time-dispersive media, which in the time domain involve memory, and we characterise the corresponding time convolution kernel explicitly.

Statistical Learning Methods and Reduced Order Model for Random Fluid-structure Interaction Problems

Mathilde Chevreuil^{*}, Anthony Nouy^{**}, Erwan Grelier^{***}

^{*}GeM - Université de Nantes, France, ^{**}LMJL - Centrale Nantes, France, ^{***}GeM - Centrale Nantes, France

ABSTRACT

The robust design of structures in a fluid environment may involve numerous sources of uncertainties in the model in order to predict their impact on the response. It reveals necessary to develop reliable and efficient tools for the prediction of such responses and in this framework, functional approaches for uncertainty quantification suffer from the highly nonlinear behaviour of the response to the input uncertainties. In order to tackle such problems, we consider statistical learning methods based on least squares minimization for high dimensional problems where the output is approximated in suitable low-rank tensor formats [1]. The storage complexity of these formats grows linearly with the dimension which makes possible the construction of an approximation using only few samples [2]. However the rank of the approximation of the stochastic dynamic response may be high and the method thus loses its efficiency. The key is to propose a suitable functional representation and an adapted parametrization with a new set of variables for the computation of the response so to obtain structured approximations with low complexity. The latter parametrization is determined automatically by coupling a projection pursuit method [2] and low rank approximation. [1] W. Hackbusch. Tensor Spaces and Numerical Tensor Calculus. Springer Berlin Heidelberg, 2012. [2] M. Chevreuil, R. Lebrun, A. Nouy, and P. Rai. A least-squares method for sparse low rank approximation of multivariate functions. SIAM/ASA JUQ, 3(1):897–921, 2015. [3] J. H. Friedman and W. Stuetzle. Projection pursuit regression. Journal of the American statistical Association, 76(376):817–823, 1981.

Stretch-induced Softening and Rupture of DNA

Qingjia Chi^{*}, Xin Lai^{**}, Lisheng Liu^{***}

^{*}Department of Mechanics and Engineering Structure, Wuhan University of Technology, China, ^{**}Department of Mechanics and Engineering Structure, Wuhan University of Technology, China, ^{***}Department of Mechanics and Engineering Structure, Wuhan University of Technology, China

ABSTRACT

The mechanical properties of DNA play an important role in its participation in the replication, transcription, recombination and other biological behaviors. But the vast majority of investigations have focused on its biochemical properties based on base sequence. And there are fewer studies on DNA's biomechanical properties, leading to insufficient understanding of some of its mechanical properties. Using unified ideal chain model to investigate force-induced deformations of DNA, we evaluate the softening behavior of DNA. The model can solve the mismatch problem between the models describing force-extension of double-stranded and single-stranded DNA, and can cover the whole force regime. A crossover force is obtained for dsDNA using unified ideal chain model. Moreover, we present results of stretch-induced rupture obtained from peridynamics. Peridynamics provides a reformulation of continuum elasticity theory which is better-suited to model rupture of biopolymers. The governing equation of peridynamics is integral rather than differential, and particles are connected in a non-local manner. Peridynamics can be regarded as an upscaling of molecular dynamics. The application of peridynamics to the investigation of biopolymers is novel and may provide a new inquiry method.

Gradient Reproducing Kernel Collocation Method for High Order PDEs

Sheng-Wei Chi*, Ashkan Mahdavi**

*University of Illinois at Chicago, **University of Illinois at Chicago

ABSTRACT

The Reproducing Kernel approximation in conjunction with the Collocation Method (RKCM)[1] was introduced for solutions of PDEs and engineering problems for some time. Although it offers only algebraic convergence, being less sensitive to the nodal distribution and of compact structure, thus better conditioning, make it an attractive method for engineering applications. However, taking direct derivatives of the reproducing kernel approximation is computationally expensive, in comparison to other commonly used approximations for collocation methods, such as RBFs. In this work, we address the high computational cost in the RKCM while achieving optimal convergence by adopting gradient reproduction kernel approximations for all derivatives involved in a PDE. In contrast to the earlier work in [2], both first order and second order derivatives involved in the approximation for a second order PDE are expressed by gradient reproducing kernels in the present method. We show that the same number of collocation points and source points can be used in the G-RKCM for optimal convergence. The present method is further introduced for problems governed by 4th order PDEs, such as Kirchhoff plate problems and 4th order phase-field model for fracture [3]. The numerical studies show that the present method is much faster and more robust than the RKCM. [1] H. Y. Hu, J. S. Chen, and W. Hu, Weighted radial basis collocation method for boundary value problems, *International Journal for Numerical Methods in Engineering* 69, p.2736-2757, 2007. [2] S.W. Chi, J.S. Chen, H.Y. Hu, and J.P. Yang, A gradient reproducing kernel collocation method for boundary value problems, *International Journal for Numerical Methods in Engineering* 93(13), p.1381-1402, 2013. [3] M.J. Borden, T. J.R. Hughes, C. M. Landis, C. V. Verhoosel, A Higher-Order Phase-Field Model for Brittle Fracture: Formulation and Analysis within the Isogeometric Analysis framework, *Computer Methods in Applied Mechanics and Engineering*, 273, p. 100-118, 2014.

Developing Effective Guidelines Towards Robust Design of Passenger Vehicle Front-ends with Respect to Pedestrian Lower Leg Impact for Early Development Phases

Stefano Chiapedi*, Andreas Koukal**, Fabian Duddeck***

*Technische Universität München, Munich, Germany, **AUDI AG, Ingolstadt, Germany, ***Technische Universität München, Munich, Germany and Queen Mary University of London, UK

ABSTRACT

Pedestrian Protection has gathered lots of attention in academia and industry over the last two decades, aimed at reducing the likelihood of injuries to pedestrians in the event of impact with a car. Research into this discipline has been promoted by the quick evolution of consumer tests requirements, especially in the European market, and has led to a significant redesign of passenger vehicle front-ends. The pedestrian lower leg impact test underwent recently a major consumer test change, as a new legform impactor, the so-called Flexible Pedestrian Legform Impactor (FlexPLI), was introduced [2]. The injury criteria associated with this impactor present a complex link with both geometry and stiffness of the vehicle front-end. Nevertheless, these are usually settled at different design stages, further raising the challenges to be faced in such a cost- and time-consuming product development process. Moreover, practical structural modifications at late stages, such as changes in size and thickness, have limited influence on the injury criteria [1], pointing out the need for early decisions. Effective guidelines towards robust designs, on both geometry and stiffness, delivered in early design stages, are therefore very valuable. CAE tools play an essential role in the vehicle development process. Detailed, high-fidelity FE models of the car front-end enable accurate predictions of the structural response under a great variety of load cases. Nevertheless, the computational effort and the complexity associated with those models are often incompatible with structural optimization methods. In cases where a particular load case, such as the FlexPLI impact, is of interest, simplified, low-fidelity FE models can be derived [3], whose range of validity is restricted to a specific operating region, yet simulation speed and parametrization flexibility are significantly enhanced, thus favoring the application of optimization techniques. In the current work, a method is presented to develop guidelines for early design stages of passenger vehicles concerning requirements for the pedestrian lower leg impact, exploiting the advantages of low-fidelity FE models. References [1] Stefano Chiapedi, Andreas Koukal, and Fabian Duddeck. Sensitivity Analysis for Pedestrian Lower Leg Impact. In 7th GACM Colloquium on Computational Mechanics, pages 408–412. University of Stuttgart, Germany, 2017. [2] Euro NCAP. Pedestrian Testing Protocol. Technical Report 7.1.1, 2014. [3] Simon Mößner, Tim Rudolph, and Fabian Duddeck. Surface Modelling of Vehicle Frontends for Pedestrian Safety with the FlexPLI. International Journal of Crashworthiness, 22(3):243–259, 2017.

An Adaptive Remeshing Method for Crack Initiation and Propagation Using Cohesive Zone Model

Vincent Chiaruttini^{*}, Eva Borakiewicz^{**}, Noémie Rakotomalala^{***}

^{*}Onera, Université Paris-Saclay, ^{**}Onera, Université Paris-Saclay, ^{***}Safran Tech

ABSTRACT

Over the last several decades, a wide range of numerical methods have been developed to efficiently simulate 3D crack propagation: for instance X-FEM, GFEM, BEM or FEM with adaptive remeshing. These approaches have been successful in many situations, yet many issues are still encountered when dealing with complex aspects such as crack lips contact in finite strain, highly non-linear elastic-plastic material behaviors, dealing with both crack initiation and propagation stages... Recent developments have been carried out to address these issues: variational formulation of fracture, phase-field, thick level-set, are some promising strategies to deal with the complete damage to failure problem. Our approach is focused on the capability to mix very complex highly non-linear elastic-plastic material models (for ductile or thermo-mechanical-fatigue failure) with a numerical strategy suitable to simulate a complete scenario from the finite strain plastic deformation of a structure through damage, crack initiation, propagation and up to complete failure. Concerning the material behavior part, a wide range of models can be used, depending on the context (fatigue or critical failure). An important point to remember is the formulation must be independent of the mesh size and orientation as a many adaptive remeshing operations will be performed in order to adapt the computational cost in the zones where non-linearities occur. Thus, in the case of finite strain ductile failure, a regularized formulation of the constitutive model can be required. Sharing some aspects with a previously developed technique [1], we perform local remeshing in identified critical zones where the material dissipation is maximal, and a specific mesh transfer algorithm is applied to ensure further calculation. However, in order to deal with both damage and failure aspects, this new approach aims to insert, in the identified damage zones, a cohesive surface whose size and orientation will be dynamically controlled, in order to satisfy a maximal dissipation during the failure process (using some algorithms previously presented in [2]). To highlight the performance and robustness of this method, various numerical assessments will be presented. This work was performed within the SEMAFOR project funded by the French Agence Nationale de la Recherche ANR-14-CE07-0037 grant). References [1] A new marching ridges algorithm for crack path tracking in regularized media, S Feld-Payet, V Chiaruttini, J Besson, F Feyel, IJSS, 71, 2015, 57-69. [2] An adaptive algorithm for cohesive zone model and arbitrary crack propagation, V Chiaruttini, D Geoffroy, V Riolo, M Bonnet, EJCM/REM, 21, 3-6, 2012, 208-218.

Superiority of the Bottom Geometry of Surfboard from the Viewpoint of Drag Performance

Kazuhisa Chiba^{*}, Shin-nosuke Ishikawa^{**}

^{*}The University of Electro-Communications, ^{**}The University of Electro-Communications

ABSTRACT

We aim at quantitatively clarifying the superiority of the bottom geometry of surfboard which has never been implemented. The bottom geometry of surfboards is an important factor to derive the ability of surfers. Various designs such as flat, vee, and concave have been developed so far, but its performance is decided by the sense of shapers and surfers; it has not been quantitatively evaluated. In this research, we have quantitatively evaluated the performance of the bottom geometry using gas-liquid two-phase flow analysis via the drag value of surfboards as an index when paddling and riding. The drag should be lower at paddling as well as it should be higher at riding; we need the tradeoff performance at between paddling and riding. We prepare three-types bottom geometry: flat, single concave, and double concave (we will focus on long-board, so vee geometry is omitted here). As a result, we confirmed that a single concave geometry has better performance under both paddling and riding conditions with respect to drag and it turned out that there was no tradeoff between those conditions. Moreover, a large amount of curvature (the depth of concave) is better performance, and its physical reasons. When paddling, since the board is positioned parallel to the uniform flow, the deeper concave increases the wetting area and the drag increases. By contrast, when riding, a surfboard has a yaw-angle against uniform flow, so the flow accelerates on the side of the surfboard and the drag drops. We consequently clarified the difference between the depth of concave and the drag value on yaw-angle against uniform flow of surfboard.

Cohesive Polytopal Finite Element Methods for Simulating Dynamic Fracture

Eric Chin^{*}, Joseph Bishop^{**}, Rao Garimella^{***}, N. Sukumar^{****}

^{*}UC Davis, ^{**}Sandia National Laboratories, ^{***}Los Alamos National Laboratory, ^{****}UC Davis

ABSTRACT

We present dynamic fracture simulations using cohesive surfaces inserted on inter-element surfaces on polytopal meshes. Cohesive finite elements provide a natural means for modeling nucleating and extending cracks in solids. However, a sufficient network of possible internal crack surfaces is required to insert cohesive elements. An optimal network would both have no preferential direction and be able to accurately follow arbitrary paths. To meet these criteria, we use polytopal elements generated from a maximal Poisson-disk sampled domain. Maximal Poisson-disk sampling provides a means to robustly and rapidly generate a geometry conforming mesh with an optimal fracture network. Elements are convex and can be modified to have good element quality for finite element analysis, while still maintaining an optimal fracture network. Wachspress and maximum entropy basis functions are used to form a finite element basis over the polytopes. Cohesive zone elements are dynamically inserted at facets between the polytopes in the mesh. As the analysis progresses, we track and update the evolving mesh topology using a graph-based approach, which allows mesh operations to be completed robustly and rapidly. Contact is enforced through a penalty method which is applied to both closed cohesive surfaces and general interpenetration of two polytopal elements. Several numerical examples are presented which illustrate the capabilities of the method (capturing large deformation effects, branching cracks, self-contact) and demonstrate convergence of solutions.

Data, Information and Knowledge: A Multiscale Framework

Francisco Chinesta^{*}, Emmanuelle Abisset^{**}, Elias Cueto^{***}

^{*}ENSAM ParisTech, ^{**}ECN, ^{***}University of Zaragoza

ABSTRACT

Data-based modeling and simulation appears nowadays as a new pillar of the XXI century engineering. However, making the parallel with the atomic theory, one could expect that data (as atoms) even being at the foundation of the information theory, represent in general a too fine scale for most engineering applications. In mechanics the different scales were addressed using the appropriate representations and models, and all these scales were inter-connected using adequate bridges. Such a multi-scale representation, in the field of data-sciences, could constitute a major accomplishment, and very certainly a real change of paradigm, in data-based science and technology. In this work some proposals concerning the dynamics of data, information and knowledge, covering the micro, meso and macro scales will be discussed, and important questions addressed: which data, when and where for increasing at maximum the knowledge gain. Dynamics of information will be compared with Liouville dynamics and finally the question of probabilistic versus deterministic (with internal variables) dynamics discussed from two very different perspectives, the classical probability theory (Bayes) and its quantum counterpart (where superposition applies), the last opening the possibility of encountering surprising events. This last point is extremely important when putting the human in the loop for creating cognition models to be used for assimilating data (driver assistants or augmented engineers).

Multiphysic and Multiscale Modeling of Additive Manufacturing Processes by Metal Deposition

Michele Chiumenti^{*}, Emilio Salsi^{**}, Miguel Cervera^{***}, Eric Neiva^{****}, Santiago Badia^{*****}

^{*}International Center for Numerical Methods in Engineering (CIMNE), Universidad Polit cnica de Catalu a, Campus Norte UPC, 08034 Barcelona, Spain, ^{**}International Center for Numerical Methods in Engineering (CIMNE) Universidad Polit cnica de Catalu a, Campus Norte UPC, 08034 Barcelona, Spain, ^{***}International Center for Numerical Methods in Engineering (CIMNE), Universidad Polit cnica de Catalu a, Campus Norte UPC, 08034 Barcelona, Spain, ^{****}International Center for Numerical Methods in Engineering (CIMNE), Universidad Polit cnica de Catalu a, Campus Norte UPC, 08034 Barcelona, Spain, ^{*****}International Center for Numerical Methods in Engineering (CIMNE), Universidad Polit cnica de Catalu a, Campus Norte UPC, 08034 Barcelona, Spain

ABSTRACT

In this work the framework for the numerical simulation of the Additive Manufacturing (AM) process by Metal Deposition is presented. A fully coupled thermo-mechanical analysis is performed following the actual scanning sequence of the AM machine [1-2]. Hence, the high-fidelity simulation of the fabrication process is achieved, accounting for both precise power source input and the heat loss by convection and radiation mechanisms. The computed thermal field has been proven a remarkable matching with the temperature evolution recorded at different thermocouple locations. Hence, this temperature evolution is used to feed a mesoscale model suitable for computing the kinetics of the microstructure formations. Focusing on Ti64 alloy, the solid state transformations is described by the $\gamma \rightarrow \beta$ diffusion-controlled transformation through JMAK equations, while, in case of faster cooling rates, the martensitic phase is modeled using the empirical Koistinen-Marburger law. During the re-heating phase, the dissolution of the martensitic phase is described by JMAK equation, while the transformation from β to γ phase is modeled as instantaneous transformation. The predicted microstructure is compared with the experimental evidence

POD-ROM for Nonlinear Structural Analysis Based on Co-rotational Finite Element and Parallelized Domain Decomposition

Haeseong Cho^{*}, Haedong Kim^{**}, SangJoon Shin^{***}

^{*}Seoul National University, ^{**}Sejong University, ^{***}Seoul National University

ABSTRACT

In this paper, a nonlinear structural analysis based on the reduced-order modeling and proper orthogonal decomposition (POD-ROM) is developed. A procedure for POD-ROM is divided into two stages: offline and online. In the offline stage, a reduced dynamic system is constructed using POD modes [1]. The resulting ROMs are constructed by Galerkin projection of the extracted POD modes into the structural governing equations. In the online stage, the relevant analysis is performed using reduced structural governing equations. However, the computational cost in the offline stage may become significant especially when large-size structural analysis is required. And, the nonlinear analysis may become cumbersome to define accurate ROM due to the linearized characteristics in the ROM based on Galerkin projection. As a result, additional computing algorithm may be required and it is required to be efficient. Hence, relevant computational algorithm is proposed. First, the parallel computing algorithm is proposed to ensure efficiency in the offline stage. In order for parallel computation, domain decomposition using METIS algorithm [2] is used and the parallelized finite element matrix assembling technique is developed. Then, the ROM for nonlinear analysis is developed. In order for that, co-rotational finite elements are developed [3]. And, the ROM is constructed at every iteration of Newton-Raphson solver. Also, the present parallel computing algorithm is employed in each constructing procedure. Without the parallelization of the ROM, it is found that the computational efficiency in the online stage will be improved up to 68% when compared to that of the FOM. In the future, examinations will be conducted by using the present parallelized POD-ROM. [1] Sirovich L., "Turbulence and the dynamics of coherent structures," Quarterly of Applied Mathematics, Vol. 45, 1987, pp. 561–590. [2] Karypis, G., "METIS: A software package for partitioning unstructured graphs, partitioning meshes, and computing fill-reducing orderings of sparse matrices ver. 5.1.0," <http://glaros.dtc.umn.edu/gkhome/metis/metis/overview>, 2013. [3] Cho, H. S., Kim, H.D., and Shin, S.J., "Geometrically nonlinear dynamic formulation for three-dimensional co-rotational solid elements," Computer Methods in Applied Mechanics and Engineering, Vol. 328, 2018, pp. 301–320.

Modelling of Polycrystalline Materials Using the Dislocation Dynamics Method

Jaehyun Cho^{*}, Sylvie Aubry^{**}, Athanasios Arsenlis^{***}

^{*}Lawrence Livermore National Laboratory, ^{**}Lawrence Livermore National Laboratory, ^{***}Lawrence Livermore National Laboratory

ABSTRACT

The dislocation dynamics method aims at predicting the strength of metals and alloys by modelling the interaction and evolution of dislocations lines. Nearly all dislocation dynamics methods focus on single crystalline materials despite the fact that most engineering materials are polycrystalline and grain boundaries are known to influence plastic behavior. Grain boundary modelling is often neglected because of their complexity. Accurate prediction of the strength of metals and alloys depends on the understanding of the complex interaction between grain boundaries and dislocations that composes their microstructure. In this presentation, we extend the dislocation dynamics method to polycrystalline materials. Grain boundaries are represented by planes from which dislocations can emit. The emission process is accurately modelled through topological operations and is based on a power dissipation criterion. Upon meeting a grain boundary, a dislocation can transmit, reflect, and/or leave a residual dislocation in the grain boundary plane. Several examples of dislocation emission will be presented to illustrate the method.

Multiscale Modeling of Photoresist Fabrication in EUV Lithography Process

Maenghyo Cho^{*}, Muyoung Kim^{**}, Junghwan Moon^{***}, Joonmyung Choi^{****}, Byunghoon Lee^{*****}

^{*}Seoul National University, ^{**}Seoul National University, ^{***}Seoul National University, ^{****}SAMSUNG ELECTRONIC CO., LTD, ^{*****}SAMSUNG ELECTRONIC CO., LTD

ABSTRACT

Size of wafer has been decreased for improving performance and productivity in semiconductor manufacturing industry, and Extreme Ultraviolet (EUV) light source is one of the most promising candidates to achieve the downsizing. Even though experimental- and theoretical approaches have been suggested to investigate physical mechanism of photoresist (PR) fabrication, technical huddles resulting from complex photochemistry hinder full-description of multiphysics problem such as chemical reaction by electron attachment or diffusion of reactant. From this point of view, we constructed multiscale model having sequential framework of density functional theory (DFT)-molecular dynamics (MD)- finite difference method (FDM). Our newly-developed model provides rigorous description of photo-triggered chemical reaction (acid activation by electron attachment and acid diffusion-deprotection evolution) and also quantification of sub-10 nm PR morphology in atomistic level. This achievement will be the cornerstone of theoretical research which facilitates fundamental understanding on important factors for EUV performance and rational design of the next-generation PR.

Multi-disciplinary Design Optimization for Structure, Dynamic and Flow Characteristic in Subsea By-pass Valve

Su-gil Cho^{*}, Jaewon Oh^{**}, Sanghyun Park^{***}, Cheonhong Min^{****}, Jeonghee Lee^{*****},
Hyungwoo Kim^{*****}, Tae Hee Lee^{*****}

^{*}Korea Research Institute of Ship and Ocean Engineering, ^{**}Korea Research Institute of Ship and Ocean Engineering, ^{***}Korea Research Institute of Ship and Ocean Engineering, ^{****}Korea Research Institute of Ship and Ocean Engineering, ^{*****}Korea Research Institute of Ship and Ocean Engineering, ^{*****}Korea Research Institute of Ship and Ocean Engineering, ^{*****}Hanyang University

ABSTRACT

A bypass valve, which is used for the safe lifting of mineral resources in deep-sea mining, functions as preventing reverse flow at emergency case. The valve has a simple mechanism, but its design is very difficult because it must guarantee not only structural safety even emergency case but also flow performance at normal operation condition. This equipment should also operate under sludge flow with a mixture of seawater and manganese nodules. Since deep-sea mining system has not been commercialized, the valve is a new attempt and there are many design parameters to consider for design, such as by-pass valve type or size, volume flow rate, leakage hole size, leakage hole position, block type, block shape so on. In this study, fluid dynamics, multi-body dynamics, structure analysis of valves are performed using commercial CAE software. Furthermore, these CAE softwares are linked to the optimization program and multi-disciplinary design optimization is performed for valve design. Finally, a prototype valve was produced and the lab scale valve tests are performed for validation.

Two- and Three-dimensional Crack Path Prediction for Mixed-mode Cohesive Fracture by Using Cohesive Zone Modeling

Habeun Choi^{*}, Moon Kyum Kim^{**}, Kyoungsoo Park^{***}

^{*}Yonsei University, ^{**}Yonsei University, ^{***}Yonsei University

ABSTRACT

Cohesive zone models have been one of the most effective tool for representing nonlinear fracture behaviors of materials. For accurate modeling of a displacement discontinuity under mixed-mode conditions, an element splitting scheme [1] is proposed in conjunction with crack initiation criteria, i.e., the maximum strain energy release rate [2]. When the strain energy release rate at a crack tip exceeds the cohesive fracture energy, a continuum element is split and a cohesive surface element is adaptively inserted. Crack propagation direction is identical to an angle which maximizes the strain energy release rate. To accurately approximate strain energy release rate at a crack tip, a virtual mesh grid is generated around a crack tip. The topology-based data structure (TopS) [3] is utilized to update local element connectivities when elements split. A bilinear softening model is used for the constitutive relationship of cohesive concrete fracture. The proposed computational framework is verified and validated by illustrating mixed-mode fracture examples. In a two-dimensional case, four-point shear test and double-edge-notched fracture test in plain concrete are simulated. And also a single edge notched tension test is simulated for a material with microstructure. Multiple crack initiations, crack branching and coalescences are represented using the proposed framework. In three-dimensional case, a mode I crack propagation problem is illustrated to verify the consistency of the element splitting scheme. Then, non-planar crack surface is represented by using the proposed scheme. References [1] H. Choi, K. Park. Removing mesh bias in mixed-mode cohesive fracture simulation using element split and stress recovery. in preparation [2] Bouchard, P. O., Bay, F., & Chastel, Y. (2003). Numerical modelling of crack propagation: automatic remeshing and comparison of different criteria. *Computer methods in applied mechanics and engineering*, 192(35), 3887-3908. [3] Celes, W., Paulino, G. H., & Espinha, R. (2005). A compact adjacency-based topological data structure for finite element mesh representation. *International journal for numerical methods in engineering*, 64(11), 1529-1556.

An ICME Approach for Predicting the Ductility of Thin-Walled High Pressure Die Casting Magnesium

Kyoo Sil Choi^{*}, Erin Barker^{**}, Xin Sun^{***}, Mei Li^{****}, John Allison^{*****}

^{*}Pacific Northwest National Laboratory, ^{**}Pacific Northwest National Laboratory, ^{***}Oak Ridge National Laboratory,
^{****}Ford Motor Company, ^{*****}University of Michigan, Ann Arbor

ABSTRACT

Mg castings have found increasing applications in lightweight vehicles because magnesium and its alloys are the lightest metallic structure materials. However, a critical technical hurdle hindering the wider applications of Mg castings in vehicle applications is its limited ductility. The factors limiting their ductility can be categorized into two types: intrinsic and extrinsic. Intrinsic factors include features intrinsic to the specific Mg alloy such as the phase composition, grain size, morphology, volume fraction and mechanical properties of its constituent phases. Extrinsic factors come from the external processes applied to the alloy such as casting and heat treatment processes, and they include porosity, segregation, incomplete fill, hot tear and cold shut, etc. In our study, as an integrated computational materials engineering (ICME) approach, we examined the influence of both factors on the ductility of high pressure die castings (HPDC) of Mg alloys based on microstructure-based finite element modeling method. Two different modeling approaches (i.e., intrinsic modeling and extrinsic modeling) were adopted. The lower-length scale intrinsic modeling is to predict the matrix properties based on the grain size-level microstructures and its phase properties extracted from nanoindentation test. The matrix properties predicted from intrinsic modeling can be used as the input properties for the upper-length scale extrinsic modeling. The extrinsic modeling, which is more focused in this presentation, is to predict the macroscopic ductility of the Mg casting which mainly depends on the porosity distributions. For the extrinsic modeling, three-dimensional (3D) microstructure-based finite element models were developed based on actual porosity distributions of some cast Mg samples, measured with CT scanning. The results show that the ductility and fracture locations predicted from simulations agree well with the experimental results. This indicates that the developed 3D extrinsic modeling method may be used to examine the influence of various aspects of pore sizes/distributions as well as intrinsic properties (i.e., matrix properties) on the ductility/fracture of Mg castings.

Isogeometric Optimal Design of Lattice Metamaterials

Myung-Jin Choi^{*}, Hong-Yeon Jung^{**}, Seonho Cho^{***}, Sehyun Kang^{****}, Myung-hoon Oh^{*****}

^{*}Seoul National University, ^{**}Seoul National University, ^{***}Seoul National University, ^{****}Seoul National University,
^{*****}Seoul National University

ABSTRACT

This paper presents a systematic synthesis of three-dimensional lattice metamaterials having the engineered properties of extremal negative Poisson's ratio and phononic band-gap size. Along the way, we study several significant issues on the deformation analysis and the design sensitivity analysis (DSA). On the finite deformation of the geometrically exact spatial beams, we discuss the invariance property of spatially discretized problems in the isogeometric analysis (IGA) framework. On the other hand, in the configuration and sizing DSA formulation, the design variations can be expressed by exploiting the kinematics of the beam model, whose material derivatives yield the configuration DSA expressions, and the sizing design of cross-section considers both of the thickness and orientation designs. Importantly, for lattice structures on curved surfaces, like medical stents, the lattice needs to be located on a specified surface, which results in huge number of nonlinear equality constraints and difficulty in parameterization of design variables. To overcome this, lattice structures and their design variables are defined on planar rectangular domains, and the concept of free-form deformation and global curve interpolation are employed to obtain the analytical expressions for the control net of lattice structure on curved surfaces. The material derivative of the analytical expressions eventually leads to design velocity field. The considered applications of design optimizations using the developed methods are two folds: first, synthesis of auxetic structures achieving target Poisson's ratio in both of tensile and compressive loadings. Configuration and sizing designs are simultaneously performed during design optimization in order to sufficiently reduce error between target and actual Poisson's ratio in finite deformations. The optimal design is manufactured using 3-D printing technology and verified through tension and compression experiments. Second, we find optimal designs of lattice structures for maximizing the phononic band-gap size at low frequency. In the wave propagation analysis, the Bloch theorem is utilized for periodic boundary conditions, and the effects of pre-loading is investigated.

Finite Difference Method for a Conservative Allen-Cahn Equation on Non-flat Surfaces

Yongho Choi^{*}, Darae Jeong^{**}, Seong-Deog Yang^{***}, Junseok Kim^{****}

^{*}Korea University, ^{**}Korea University, ^{***}Korea University, ^{****}Korea University

ABSTRACT

We present an efficient numerical scheme for the conservative Allen-Cahn equation on various surfaces embedded in a narrow band domain in the three-dimensional space. We apply a quasi-Neumann boundary condition on the narrow band domain boundary using the closest point method. This boundary treatment allows us to use the standard Cartesian Laplacian operator instead of the Laplace-Beltrami operator. We apply a hybrid operator splitting method for solving the CAC equation. First, we use an explicit Euler method to solve the diffusion term. Second, we solve the nonlinear term by using a closed form solution. Third, we apply a space-time dependent Lagrange multiplier to conserve the total mass. The overall scheme is explicit in time and does not need iterative step; therefore, it is fast. A series of numerical experiments demonstrate the accuracy and efficiency of the proposed hybrid scheme.

Reduced Order Models and Adaptive Mesh Refinement in Multiple Stress Topology Optimization

Youngsoo Choi^{*}, Daniel Tortorelli^{**}, Cosmin Petra^{***}, Miguel Salazar De Troya^{****}, Daniel White^{*****}

^{*}Lawrence Livermore National Laboratory, ^{**}Lawrence Livermore National Laboratory, ^{***}Lawrence Livermore National Laboratory, ^{****}Lawrence Livermore National Laboratory, ^{*****}Lawrence Livermore National Laboratory

ABSTRACT

A classical compliance topology optimization problem can result in an optimal solution with stress concentration regions. For more preventive design, stress quantity must be included in topology optimization formulations. Stress topology optimization requires a fine mesh to accurately represent stress quantities, which makes the optimization process slow. To relax the computational burden, but maintain the high accuracy of the stress computation, Adaptive Mesh Refinement (AMR) is useful. Although AMR contributes to relax the computational burden of stress topology optimization process by only refining the part where necessary, a success of AMR heavily depends on error estimates/indicators. There are geometric error indicators and residual-based error estimates (e.g., bounds). Another issue with AMR is that AMR changes mesh resolution throughout the optimization process. This implies that linear solver at each optimization iteration can be affected by potential ill-conditioning due to mesh changes. Additionally, the optimization process cannot avoid multiple expensive physics simulations in design process. Therefore, to further accelerate the procedure without losing much accuracy in stress computations, reduced representation of decision variables is desirable. There are two types of reduced representation: 1. a priori representation and 2. a posteriori representation. A priori reduced representation includes Fourier representation. A posteriori representation includes a data-driven (e.g., POD-based) representation. Data-driven representation performs better than a priori reduced representations in terms of accuracy and speed up. However, a data-driven method requires an offline phase to train data and the performance greatly depends on the quality of data. Additionally, the offline phase can be computationally expensive although it must be done only once. On the other hand, a priori representation does not require any expensive offline phase. We will introduce both approaches and present advantages and disadvantages of each method in terms of accuracy and speed up with multiple-objective stress topology optimization problems.

Unified modeling framework for brittle, quasi-brittle, and ductile failures of pressure-sensitive rocks

Jinhyun Choo^{*}, WaiChing Sun^{**}

^{*}The University of Hong Kong, ^{**}Columbia University

ABSTRACT

Rocks display a wide range of failure modes depending on the confining pressure. The failure mode is localized and brittle fracture under a low confining pressure, but it increasingly becomes more diffuse and ductile as the confining pressure increases. Moreover, it has been shown that a rock under tensile loading can show a hybrid fracture mode in which tensile and shear fracture modes are mixed. Nevertheless, existing computational models usually focus on one of these failure modes. This talk will introduce a recently developed computational framework for unified modeling of these different failure modes under a wide range of confining pressure [1]. The framework couples a phase-field approach to fracture and pressure-sensitive plasticity. By doing so, it can capture the brittle failure mode using a phase-field approach, whereas it can simulate the ductile failure mode by plasticity. The coupling of phase-field and plasticity also allows for simulating quasi-brittle shear fracture and hybrid fracture as observed from experiments. The key ideas of this new coupling, such as the use of phase-field effective stress, will be discussed. Reference: [1] Choo, J. and Sun, W. C. (2018). Coupled phase-field and plasticity modeling of geological materials: From brittle fracture to ductile flow. *Computer Methods in Applied Mechanics and Engineering*, 330, 1–32.

Nitsche-based Approximation of Contact for Explicit Integration of Elastodynamic Problems

Franz Chouly^{*}, Yves Renard^{**}

^{*}Université Bourgogne Franche Comté, ^{**}INSA Lyon

ABSTRACT

The dynamic of deformable solids with impact can be approximated numerically using an explicit time-marching scheme. This topic has already been the object of an important literature: explicit schemes for penalized contact, Moreau's NSCD schemes (non-smooth contact dynamics), Paoli-Schatzman scheme, mass redistribution method [3], etc. However, all the difficulties have not been overcome to obtain a method with satisfying properties of stability, monotonicity, accuracy and energy conservation, in the sense that, generally, at least one of these characteristics has a degraded behavior. The purpose of this presentation will be to explore further the properties of the Nitsche-based approximation of contact condition, presented in [1,2] (for the static case and implicit schemes respectively) when it is associated with an explicit time-marching scheme. For this, comparisons will be provided with the aforementioned methods in terms of energy conservation, convergence and occurrence of spurious oscillations. [1] F. Chouly, P. Hild, Y. Renard. Symmetric and non-symmetric variants of Nitsche's method for contact problems in elasticity: theory and numerical experiments. *Math. Comp.*, 84:1089--1112, 2015 [2] F. Chouly, P. Hild, Y. Renard. A Nitsche finite element method for dynamic contact: 1. Semi-discrete problem analysis and time-marching schemes. *ESAIM Math. Model. Numer. Anal.*, 49:481--502, 2015 [3] H. Khenous, P. Laborde, Y. Renard. Mass redistribution method for finite element contact problems in elastodynamics. *Eur. J. Mech., A/Solids*, 27(5):918--932, 2008

A Peridynamic Model of Crevice Corrosion

Bufan Chu^{*}, Qiwen Liu^{**}, Lisheng Liu^{***}

^{*}Department of Mechanics and Engineering Structure, Wuhan University of Technology, ^{**}Department of Mechanics and Engineering Structure, Wuhan University of Technology, ^{***}State Key Laboratory of Advanced Technology for Materials Synthesis and Processing Wuhan University of Technology

ABSTRACT

A new Peridynamic (PD) model of crevice corrosion is proposed by taking the ion migration and ion diffusion into account based on the dilute solution theory and Nernst-Planck equation. The 304 stainless steel square sample containing a crevice in NaCl solution is studied. Based on the classical diffusion governing equation, the PD formulation is established. Then based on the established PD model, the distribution of metal ion concentration during crevice corrosion was simulated. And the characteristics of the material point are described in terms of its own concentration, the diffusion bond is introduced to describe the connection between the material points. Through the diffusion bond, ions diffuse from the material points with high concentration to that with low concentration. The influences of different solid diffusion coefficients and crevice width on crevice corrosion damage are also analyzed. Finally, the results of the sample simulations and the model verification to other simulations are presented.

Study the Dynamic Elastic-Plastic Fracture of Metals Under Strong Shock Loading

Dongyang Chu^{*}, Xiang Li^{**}, Zhanli Liu^{***}

^{*}Department of Engineering Mechanics, Tsinghua University, ^{**}Department of Engineering Mechanics, Tsinghua University, ^{***}Department of Engineering Mechanics, Tsinghua University

ABSTRACT

The elastic-plastic fracture mechanism of metals under strong shock loading is quite different from which under quasi-static loading, and the study about it has proven difficult. Under the strong shock loading, the metals undergo complex physical processes such as large deformation and elastic-plastic fracture. These physical processes also have complex coupling with the propagation of strong shock waves and strong sparse waves. In this paper, a computational model has been established based on the framework of thermodynamics to simulate the dynamic fracture of metals with large deformation under strong shock loading. The fracture of material is described based on phase field method. Therefore, this elastic-plastic phase field dynamic fracture model can realize the simulation of the whole process of material failure and crack propagation, and it can also simulate various fracture modes accurately under the propagation of shock wave and sparse wave. We study the dynamic deformation and fracture of a cylindrical steel plate under internal blast loading, and the numerical results is consistent with the experimental results. By simulating, the mechanism of energy transformation and elastic-plastic fracture for steel plate under strong shock loading are studied. This study may contribute to further understanding on the design of explosion containment vessels and can be applied to the engineering field. References: 1 Michael J. Borden et al. (2016), Computer Methods in Applied Mechanics and Engineering. 312: 130–166. 2, Qi Dong et al. (2016), Journal of Pressure Vessel Technology, 138 (6).

The Mechanical Property and Microstructure of Scaffolds Regulate Differentiation of Annulus Fibrosus-Derived Stem Cells

Genglei Chu^{*}, Bin Li^{**}

^{*}Soochow University, ^{**}Soochow University

ABSTRACT

Introduction The current engineered bionic disc tissue is considered as a potential way for treating intervertebral disc degeneration disease, which yet still remains challenging due to the complex radial gradient of natural annulus fibrosus (AF) tissue in cell phenotype, biochemical composition, microstructures, and mechanical properties. Previously, we have found that the differentiation of annulus fibrosus-derived stem cells (AFSCs) could be regulated by the elasticity of scaffold [1]. In this study, we attempted to examine the combined effect of both mechanical and microstructural features on the gene expression of AFSCs. **Method** AFSCs were cultured on four types of poly(ether carbonate urethane) urea (PECUU) scaffolds with controlled elasticity and fiber diameter: soft, small diameter; stiff, small diameter; soft, large diameter and stiff, large diameter, then incubated for 7 days. **Results** AFSCs were almost uniformly oriented along the fiber direction of scaffolds. AFSCs on the scaffolds of small diameter were round, while they were spindle-shaped on scaffolds of large diameter regardless of substrate elasticity. Mature focal adhesions were clustered around the periphery of cells on large diameter scaffolds, especially on stiff scaffolds. On the small diameter scaffolds, immature focal adhesions were distributed in a much diffused manner. Western Blot, immunofluorescence and q-PCR results revealed that when the diameter of scaffold was kept constant, the expression of collagen-I in AFSCs increased with scaffold elasticity, while the expression of collagen-II and aggrecan genes showed an opposite trend. Moreover, when scaffold elasticity was controlled, the gene expression of collagen-I in AFSCs increased with fiber diameter. In contrast, the expression of collagen-II and aggrecan decreased. Such substrate elasticity and microstructure dependent changes of AFSCs were similar to the gradient characteristics of native AF tissue. In addition, increasing elasticity and fiber diameter of scaffolds promoted YAP activation and its nuclear translocation. **Discussion** The results illustrate that the mechanical property is a potent regulator of AFSCs differentiation. Moreover, we reveal that microstructure of scaffold affects spreading area, focal adhesion and differentiation of AFSCs. Therefore, both mechanical property and microstructure of scaffold regulate AFSCs differentiation, possibly through a YAP-dependent mechanotransduction mechanism, thus providing a solid foundation for the tissue engineering applications of AFSCs. **Reference** [1] Zhu C, Li J, Liu C, Zhou P, Yang H, Li B. Modulation of the gene expression of annulus fibrosus-derived stem cells using poly(ether carbonate urethane)urea scaffolds of tunable elasticity. *Acta biomaterialia*. 2016;29:228-38.

The Derivation of Heat Conduction Models with Fluctuations

Weiqi Chu^{*}, Xiantao Li^{**}

^{*}Pennsylvania State University, ^{**}Pennsylvania State University

ABSTRACT

During the past two decades, there has been rapidly growing interest in modeling heat transport at the microscopic scale. As the size of electrical and mechanical devices is decreased to the micron and sub-micron scales, they often exhibit heat conduction properties that are quite different from the observations familiar at macroscopic level, e.g., Fourier Law. At such scale, the observable quantities also carry substantial fluctuations. In this talk, heat conduction models are derived directly from the many-particle system as a coarse-grained description. By selecting the local averaged energy as the coarse-grained variables, we apply different projection formalisms to derive the reduced models. In sharp contrast to conventional energy transport models, this derivation yields stochastic dynamics models, whose solutions converge to mild solutions of continuous SPDEs as the spacing goes to zero. The model also exhibits non-locality in space and time. We discuss the approximation of the non-local term to ensure the correct statistics of the solution.

Modeling High-strain-rate Responses Brittle Porous Media with Fracture Opening and Closure

Chukwudi Chukwudozie^{*}, SeonHong Na^{**}, WaiChing Sun^{***}

^{*}Columbia University, ^{**}Columbia University, ^{***}Columbia University

ABSTRACT

In engineering applications that involves impacts, earthquake, and explosion, geomaterials are subjected to unusually high strain rate loading. This high strain rate leads to material responses significantly different than the quasi-static counterpart. The competition between elastic wave propagation and fracture propagation often leads to complex features, such as multiple fracture branches, coalescence, and closure. These mechanisms in return affect the two-way hydro-mechanical coupling between the fractured solid skeleton and the pore fluid. In this work, we use an implicit function to approximate cracks to dynamic crack growth and closure in brittle porous materials under high-strain-rate loading. To model the crack opening, closing, and slip behaviors under the dynamic conditions, we introduce a homogenization procedure to convert interface plasticity for strong discontinuity to a regularized anisotropic plasticity model with nonlocal plastic flow aligned with the gradient of the phase field. Both the two-field u-p and the three-field u-w-p and u-U-p formulations are implemented. The results are compared in numerical experiments.

Application of Refined Polygon Wall Boundary Model in PNU-MPS Method

Soh-Myung Chung*, Jong-Chun Park**

*Pusan National University, **Pusan National University

ABSTRACT

In order to analyse or solve Engineering problems engaged with fluid flow such as slamming, impact force induced by wave, and sloshing, two methods have been widely used in Computational Fluid Dynamics. One is a grid-based method and the other is a particle-based method. Chiefly, in simulation using particle method, there are several advantages. Since particle method thoroughly meets conservation of mass, it is possible to carry out long-time simulation. Furthermore, it is advantageous to express the motion of a fluid as a movement of particles without making the grid or re-meshing. Even though particle method is good at solving mentioned problems, flow instability issue has been appreciated as being a major obstacle to taking the merits of particle method in simulation. In the present study, in order to impose more precise boundary conditions and suppress the pressure instability derived from imprecise boundary condition including the free-surface, the polygon wall boundary model [1] is employed to the PNU-MPS (Pusan-National-University-modified Moving Particle Semi-implicit) method [2]. The enhanced and refined simulation method called as PNU-MPS-POLY is applied to solve the hydrostatic pressure problems for verifying through the comparison with analytic solution and other simulation result [1]. Moreover, the intensified treatment in boundaries is confirmed for sloshing problem [3] in a rectangular tank and applied to simulate sloshing phenomena in a glass of wine.

Transport Phenomena in Confined Granular Systems with Applications to Pharmaceutical Solids

Pedro Henrique Cidreiro Marints*, Payam Poorsolhjoui**, Marcial Gonzalez***

*Purdue University, **Purdue University, ***Purdue University

ABSTRACT

Imbibition and drainage of water through the pore spaces of granular media play a crucial role in all aspects of their behavior. For example, granular infrastructure materials that experience cycles of rain-freeze-thaw undergo considerable damage to their structural integrity. Of relevance to this presentation, pharmaceutical tablets rely on the process of imbibition into their pore structure for drug dissolution and release processes. In the present study, a three dimensional pore-network model capable of capturing the intricate microstructure of highly confined granular systems, with desired level of accuracy is presented. The model solves mass-transport of wetting and non-wetting fluids through the pore space in a computationally feasible manner. It assumes the two fluids to be incompressible and immiscible. The granular bed microstructure is represented by a random polydisperse packing of spherical particles. The pore space between particles is decomposed into throats that are connected to each other at volumeless pores. Two-phase Poiseuille flow is assumed inside the pore structure and conservation of mass is solved at all throats at every time step calculating the movement of the interfaces between wetting and non-wetting fluids. Entrapment of disconnected phases within the pore-space is allowed by implementing specific rules on interface displacements—these rules use a pore binary status, i.e., whether it is predominantly occupied by the wetting or non-wetting fluid, which is assigned based on the mass flux of incoming pore flows. The hysteresis movement of the interface is captured by using two different values for advancing and receding contact angles between wetting fluid and particles. Finally, a predictor-corrector approach based on flow direction and mass conservation is used in order to derive interface locations at the end of each time step-fixed time steps are used to improve stability and contain the computational cost. The pore structure is decomposed into throats and volumeless pores using a Radical Voronoi tessellation of the poly-disperse. In addition, a Constructive Solid Geometry (CSG) algorithm is used to define the hydraulic parameters of the interconnected throats. Validation of the model with experimental observations of penetration of a sessile drop deposited on a slightly compressed powder bed made of β -lactose monohydrate, a typical excipient found in pharmaceutical formulations, shows that the developed algorithm captures the behavior of wetting fluids in vicinity of granular media with feasible amount of computational demand with low computational cost, compared to direct numerical simulation of the Navier Stokes equation in the exact pore space geometry.

Isogeometric Manifold Basis Functions with Prescribed Sharp Features and Cracks

Fehmi Cirak*, Qiaoling Zhang**

*University of Cambridge, **University of Cambridge

ABSTRACT

Manifold-based surface construction techniques are well known in geometric modelling and a number of variants exist. Common to all is the concept of constructing a smooth surface by blending together overlapping patches (or, charts) as in differential geometry description of manifolds. We combine manifold techniques with conformal parameterisations and the partition-of-unity method to derive basis functions on unstructured quadrilateral meshes. The obtained basis functions correspond to the vertices of the mesh and have arbitrary prescribed smoothness and approximation order. Each patch on the manifold consists of several elements and has a corresponding planar patch with a smooth one-to-one mapping onto the manifold. On the collection of conformally parameterised planar patches the partition-of-unity method is used for approximation. The smooth partition-of-unity, or blending, functions are assembled from tensor-product b-spline segments defined on a unit square. Polynomials with prescribed degree and continuity are used as local approximants on each patch. Sharp features and cracks are represented with suitably chosen C^0 -continuous and discontinuous local polynomials, respectively. As will be demonstrated, the new manifold basis functions have to be carefully constructed in order to be suitable for both geometric modelling and analysis. This is achieved by considering several affine and conformal mappings depending on the local connectivity of the mesh and arrangement of sharp features and cracks. Our numerical simulations indicate the optimal convergence of the resulting approximation scheme for Poisson problems and near optimal convergence for thin-plate and thin-shell problems discretised with structured and unstructured quadrilateral meshes. References: Majeed, M. and Cirak, F. Isogeometric analysis using manifold-based smooth basis functions. *Computer Methods in Applied Mechanics and Engineering* (2017) 316:547--567. Zhang, Q. and Cirak, F. Manifold-based isogeometric analysis basis functions with sharp features and cracks. Preprint (2018).

Heat Transfer over Super-Hydrophobic and Liquid Infused Surfaces

Umberto Ciri*, Stefano Leonardi**

*The University of Texas at Dallas, **The University of Texas at Dallas

ABSTRACT

Turbulent flows are involved in several engineering fields, such as energy or transport. In many applications, the objective is to reduce the drag that is associated with turbulent motion in order, for instance, to increase the efficiency of air or marine vehicles or oil transport in ducts. In other cases, the strong turbulent mixing is exploited to enhance heat transfer for various applications. In general, heat transfer and drag are closely related in turbulent flows ("Reynolds analogy"), as they are driven by the same physical mechanisms. Recently, super-hydrophobic (SHSs) and liquid-infused surfaces (LISs) have been studied as a means of reducing drag in turbulent flows. These surfaces consist of a micro-texture of posts and cavities, filled with a second fluid, which create a mixed interface solid-fluid with the primary fluid. SHS features have a thin-film hydrophobic coating, that increments the motion of water drops by reducing their contact-angle hysteresis and traps air in the cavities. In LISs, a second liquid (immiscible with the primary fluid) replaces the air pockets in the surface features. Conceptually, the flow over LIS and SHS reproduces a two-layer configuration over a rough surface, where the roughness elements are constituted by the surface textures. Turbulent drag reduction is possible because the second fluid (air trapped in the textures for SHS, and lubricant liquid for LIS) creates a slip interface with the primary fluid, thus reducing friction drag. Experimental and numerical studies have shown great potential for these methods. However, relatively less attention has been dedicated to the heat transfer process over these surfaces. The objective of the present study is to investigate how heat transfer is affected in these configurations, where several factors are at play: the surface texture geometry, the thermodynamic properties of the fluids, as well as the interfacial dynamics. A parametric study will be conducted using direct numerical simulations of turbulent flow and heat transfer over LIS and SHS. The numerical code resolves the dynamics of both fluids with an energy-conserving finite difference scheme. The textures are modeled with the immersed boundary method, and the two-fluid interface is tracked with a level-set method. The simulations will provide data to assess whether LIS/SHS can also be employed in heat transfer enhancement applications, besides drag reduction.

On the Coupling of Spectral Element Method with Discontinuous Galerkin Approximation for Elasto-Acoustic Problems

Aurélien Citrain^{*}, Hélène Barucq^{**}, Henri Calandra^{***}, Julien Diaz^{****}, Christian Gout^{*****}

^{*}INSA Rouen-Normandie Université LMI EA 3226, Team Project Magique3D (INRIA.UPPA.CNRS), ^{**}Team Project Magique3D (INRIA.UPPA.CNRS), ^{***}TOTAL SA, ^{****}Team Project Magique3D (INRIA.UPPA.CNRS), ^{*****}INSA Rouen-Normandie Université LMI EA 3226

ABSTRACT

Obtain accurate images of the underground is today the topic of a lot of studies. To do this, the simulations of elasto-acoustic waves has shown is efficiency and several numerical methods have been developed with the aim of a gain of accuracy and reducing at best the computational costs. Among them, Discontinuous Galerkin Method (DGM) has demonstrated is efficiency when the use of unstructured grid is necessary to approach complicated geometries. When it comes to structured meshes, Spectral Element Method (SEM) is preferred in particular because it's require a lower computational burden. In this work, we propose to couple these two methods when the propagation media is represented by an hybrid mesh composed of unstructured and structured cells, with the aim of reducing the computational costs. For example, when the medium include a layer of water and the use of unstructured grid is not necessary. Here, we're interested with time-dependent problem, so we have a need of doing stability analysis in order to find the optimal CFL condition. In this presentation, we will describe the methodology of coupling DG-SEM and establish the stability of the method using various time scheme. Then, some numerical results will be presented to show the efficiency of the method in particular we will made a comparison of the computational costs between the ones of DG-SEM and those of DGM and SEM.

Migrating a Production Multiphysics Finite Element Code to Next-generation and Heterogeneous Architectures Using the Kokkos Abstraction Layer

Jonathan Clausen^{*}, Victor Brunini^{**}, Mark Hoemmen^{***}, David Noble^{****}, Christian Trott^{*****}

^{*}Sandia National Laboratories, ^{**}Sandia National Laboratories, ^{***}Sandia National Laboratories, ^{****}Sandia National Laboratories, ^{*****}Sandia National Laboratories

ABSTRACT

High-performance computer architectures have increasingly fine-grained and heterogeneous forms of parallelism. This makes the traditional approach to parallelism in scientific applications, using the Message Passing Interface (MPI) for coarse-grained distributed-memory parallelism with no threads within MPI processes, may no longer give best performance on many future computers. The SIERRA Aria thermal/fluid application has a large, complex production codebase developed in C++ over the past few decades. Aria's core computational kernels rely on C++ features like dynamic polymorphism, which are good for software productivity, but take some care to work correctly and perform well on some computer architectures. Key to managing the complexities associated with programming for many-core and heterogeneous architectures is the use of Kokkos (<http://github.com/kokkos/kokkos>), an abstraction layer for shared-memory parallel programming and thread-scalable data structures that supports a variety of back ends including openMP and CUDA. In this talk, we discuss the strategies used to provide portable performance on newer architectures while maintaining a clean, sustainable codebase in the Aria production code. "Portable performance" means we can write computation kernels once and have these kernels run efficiently on different architectures. Accordingly, we present work on the use of Kokkos data structures and parallel constructs, Single Instruction Multiple Data (SIMD) instructions, as well as other code structures within prototype and production applications to demonstrate their impact. Application performance when running on CPU architectures such as Intel Sandy Bridge, Haswell and Knights Landing processors, as well as GPU-based architectures is shown. Also, the relative merits of threading, hyperthreading, and SIMD vectorization on Intel platforms are discussed. Sandia National Laboratories is a multimission laboratory managed and operated by National Technology and Engineering Solutions of Sandia LLC, a wholly owned subsidiary of Honeywell International Inc. for the U.S. Department of Energy's National Nuclear Security Administration under contract DE-NA0003525.

Tailoring VMS-based FEM for Different Boundary Value Problems

Ramon Codina*

*Universitat Politècnica de Catalunya

ABSTRACT

The Galerkin finite element approximation of many boundary value problems may suffer instabilities arising from different origins. The main two groups are those appearing in singularly perturbed problems, such as plates with small thickness or convection-diffusion problems with small diffusion, and those in which there is a compatibility condition in the interpolation spaces for the unknowns, such as the Stokes or the Darcy problems. Furthermore, instabilities may arise for a given problem just by changing the space where the solution is sought. The power of the VMS approach is demonstrated by the fact that it has served us to design stabilized finite element methods in all cases we have tried, ranging from flow problems (incompressible, compressible, low Mach, viscoelasticity) to solid mechanics problems (damage, plasticity, plates) and waves and electromagnetism. There are of course many aspects that deserve improvement, the most important being the design of the stabilization parameters, but definitely experience has shown that VMS is certainly a paradigm in computational mechanics.

Immersed Boundary Hierarchical B-spline Method for the Numerical Simulation of Nano-Scale Electromechanical Transduction

David Codony*, Onofre Marco**, Sonia Fernández-Méndez***, Irene Arias****

*Universitat Politècnica de Catalunya, **Universitat Politècnica de Catalunya, ***Universitat Politècnica de Catalunya, ****Universitat Politècnica de Catalunya

ABSTRACT

Continuum modeling of physical phenomena at the micron- and sub-micron scales requires high-order continuum theories in order to take into account size or length-scale effects. This is the case of relevant micronscale electromechanical transduction mechanisms such as flexoelectricity: a two-way electromechanical coupling between strain-gradient and electric polarization fields. To this end, we consider the generalized continuum model in [1], which describes the flexoelectric coupling as a fourth order partial differential equation, with displacements and electric potential as the only mechanical and electrical unknowns. The high-order nature of the PDE requires C^1 -continuous solutions, so the standard Finite Element Method (FEM) is not suitable, and advanced discretization methods are required such as the Meshfree Method [1] and the Mixed FEM [2]. These methods are relatively expensive, the former uses C^∞ smooth basis functions with expensive evaluation and integration, whereas the latter increases the number of unknowns to circumvent the smoothness requirement. Here, we propose an alternative numerical method based on an Immersed Boundary HB-spline approach. (Hierarchical) B-spline basis functions provide high-order continuity of the original unknowns and are efficiently evaluated and integrated. Since they are globally defined on a Cartesian parametric space, we consider a regular Cartesian mesh and make use of the Immersed Boundary concept to permit simulations on arbitrary domain shapes, which can be exactly represented. High-order numerical integration is specifically performed on each cut cell [3]. Boundary and interface conditions are weakly enforced by means of the Nitsche's method. This high-order method is particularly attractive, since it can capture the exact geometry of the domain, can easily handle material inclusions and interfaces, considers spatial resolution adaptivity, can be easily extended to shape optimization and permits parallel computation. We present the particularization of the Nitsche's method to the formulation in [1] and show numerical examples of electromechanical transduction at small scales, including conductive inclusions and multi-material setups of particular engineering interest. References [1] A. Abdollahi, D. Millán, C. Peco, M. Arroyo, and I. Arias. Phys. Rev. B, 91:104103 (2015) [2] S. Mao, P. K. Purohit, and N. Aravas, Proceedings of the Royal Society of London A: Mathematical, Physical and Engineering Sciences, 472(2190) (2016) [3] O. Marco, R. Sevilla, Y. Zhang, J. J. Ródenas, and M. Tur, International Journal for Numerical Methods in Engineering, 103(6): 445468 (2015)

Strength-oriented Design of Periodic Microstructures Using Topology Optimization

Pedro Coelho^{*}, José Guedes^{**}, Hélder Rodrigues^{***}, João Cardoso^{****}

^{*}UNIDEMI-UNL Portugal, ^{**}IDMEC Portugal, ^{***}IDMEC Portugal, ^{****}UNIDEMI-UNL Portugal

ABSTRACT

Topology optimization problems with stress based criteria are of special interest in engineering practice because they provide not only very efficient designs but also ones where the material strength is not compromised [1]. However, contributions from topology optimization in material microstructure design with stress criteria have been scarce. The present work addresses topology optimization of a material unit-cell mixing void and solid phases taking into account and controlling the induced stress distribution. The optimal topology is defined on the top of a finite element mesh with the help of density based design variables. However, due to the highly non-linear stress distribution verified in most cases it is required an appropriate finite element discretization. With that purpose one pursues here the h-refinement method. Finally, a level of mesh discretization is selected balancing stress predictions accuracy with computational time cost. The stress-design singularity problem in topology optimization with stress constraints is solved through relaxation techniques such as the epon-approach and the qp-approach [2]. The local nature of the stress constraint implies that the optimization problem number of constraints is the same order of the total number of the problem design variables. The computational cost of this "point-wise" control of stresses is then significant but softened in the scope of the present work through the application of parallel computing techniques. The topology optimization problem is formulated as the material volume minimization on the density variables subject to stiffness and stress constraints. The unit-cell response to an external applied load is obtained through homogenization [3]. Simple load cases (biaxial and shear) are considered leading to symmetries both in density and stress distributions. The obtained strength-oriented optimal lay-outs are compared to results published in the literature for validation.

Acknowledgements: This work was partially supported by the Portuguese Foundation for Science and Technology, FCT-Portugal, through the projects UID/EMS/00667/2013, UID/EMS/50022/2013 and PTDC/EMS-PRO/4732/2014. [1] Duysinx P, Bendsøe MP (1998) Topology optimization of continuum structures with local stress constraints. Int J for Num Meth in Engng 43(8): 1453-1478 [2] Bruggi M, Duysinx P (2012) Topology optimization for minimum weight with compliance and stress constraints. Struct Multidisc Optim 46: 369-384 [3] Guedes JM, Kikuchi N (1990) Preprocessing and postprocessing for materials based on the homogenization method with adaptive finite element method. Comput Meth Appl Mech Engng 83: 143-198

Impacts of Topology Optimization Method Choice on Designing for Prescribed Structural Frequency Response

Peter Coffin*, Tyler Schoenherr**

*Sandia National Lab, **Sandia National Lab

ABSTRACT

Density methods for topology optimization typically rely on the interplay between objective and constraints that are penalized differently to minimize intermediate material. This presentation will discuss fundamental method choices as applied to the problem of fixture design, where the objective is to generate fixture geometry that has structural frequency response matching that of a prescribed next level assembly. In this design problem, a volume or mass constraint may not be desired or active, impacting the effectiveness of common density methods. The Solid Isotropic Material with Penalization (SIMP) density method and an explicit Level-Set Conformal Decomposition Finite Element Method (LS-CDFEM) will be compared for this design problem. Additionally, regularization via quantities such as static response and common geometric measures will be investigated. The advantages and disadvantages of these different methods will be discussed regarding generating the most useful and physically realizable designs.

Sensitivity Analysis and Uncertainty Quantification of a 1D Fluids Model of the Pulmonary Circulation

Mitchel Colebank^{*}, Mette Olufsen^{**}, M. Umar Qureshi^{***}, Naomi Chesler^{****}, Dirk Huismeier^{*****}

^{*}Biomathematics Graduate Program, North Carolina State University, Raleigh, NC, USA, 27695-8205,

^{**}Department of Mathematics, North Carolina State University, Raleigh, NC, USA, 27695-8205, ^{***}Department of Mathematics, North Carolina State University, Raleigh, NC, USA, 27695-8205, ^{****}Department of Biomedical Engineering and Madison, University of Wisconsin at Madison, WI, 53706-1609 USA, ^{*****}School of Mathematics & Statistics, University of Glasgow, Glasgow, G12 8QQ, U.K.

ABSTRACT

For decades fluid dynamics models have been used to predict flow and pressure wave propagation in the cardiovascular system [1]. More recently focus has shifted to fitting these measured waveforms to data and on obtaining geometries from imaging [2]. However, little work has been done to understand how error in image segmentation impacts fluid dynamics. This is of particular importance in network models, since at each bifurcation the vessel dimensions change significantly. In the pulmonary vasculature, networks branch rapidly and hence the dimensions of each vessel change in concert. While vascular networks are similar from organism to organism, connectivity of the vessels may vary drastically. This study addresses uncertainty in blood flow and pressure predictions from 1D networks extracted from micro-CT images together with flow and pressure measurements from control mice. 1D Networks are extracted from micro-CT images from C57BL6/J mice (Jackson Laboratory, Bar Harbor, ME) using global thresholding techniques, where smoothness and lower threshold limits in the network segmentation are varied. To obtain the rendered networks, we fix the number of steps for a semi-automated contour evolution algorithm. The 1D network is obtained by calculating centerlines, connected at the barycenter of each junction. All vessel segments are assumed straight with a radius defined as the mean over the vessel, calculated away from the junction. Fluid dynamic predictions are obtained by solving the 1D Navier-Stokes equations combined with a linear constitutive equation relating pressure and area [2-4]. At junctions, pressure is assumed continuous and flow is conserved. A measured flow profile is applied at the inlet and a three element Windkessel boundary condition is attached at each terminal vessel. Similar to previous studies [3] nominal parameter values were calculated using imaging data and available flow and pressure data. Each simulation is computed using a variable geometry, where the variance of each vessel's dimensions comes from 20 a priori segmentations of one micro-CT image. Since a measured inflow is attached at the inlet, the main variations are associated with predictions of pressure and vessel area. Results reveal significant variation within the network, emphasizing model sensitivity to geometric parameters. Uncertainty is also associated with outflow boundary conditions, vessel stiffness, and the inflow profile [4]. [1] van de Vosse et al. (2011) *Annu Rev Fluid Mech*, 43:p467 [2] Qureshi et al, (2014) *Biomech Model Mechanobiol* 13: p1137 [3] Qureshi et al. (2017) arXiv:1712.01699 [physics.flu-dyn] [4] Paun et al. (2017) *Stat Neerl*, in press.

Nonreciprocal Elastodynamical Waves Using Programmable Metacomposite

Manuel Collet*, Sami Karkar**, Kaijun Yi***

*LTDS, CNRS, Ecole Centrale de Lyon, **LTDS, CNRS, Ecole Centrale de Lyon, ***LTDS, CNRS, Ecole Centrale de Lyon

ABSTRACT

Research activities in smart materials and adaptive structures are of a great interest for many years. In order to implement new vibroacoustic functionalities inside complex coupled metacomposite, new technologies are now available which allow integration of dense and distributed set of smart materials, electronics, chip sets and power supply systems for implementing distributed control strategies. It is also possible to develop the next generation of smart “composite” structures also called adaptive metacomposite. By using such an integrated distributed set of electromechanical transducers, one can imagine to control vibroacoustic flow in a large frequency band and implement unconventional behavior such as non-reciprocal wave propagation. Time-space modulated structures (or dynamic structures) possess properties modulated both in time and space that can be program inside adaptive metacomposite with suitable technologies. This contribution gives a comprehensive understanding of the behaviors induced by dynamic structures and proposes some technological implementations. Reflection and transmission of elastic waves incident on dynamic structures are numerically studied using a specific using of multiple scattering theory. It is shown that the scattering matrix directly describes all the unconventional wave propagation phenomena induced by time-space modulated metacomposite in specific situations. Results show that multiple Bloch modes are stimulated in dynamic structures by incident harmonics, these modes lead to the observed unusual wave conversion phenomena. Practical implementations are also discussed and mechanical diodes are proposed.

Mesoscale Multiphysics Modeling of Ablation in Composite Thermal Protection System Materials Using the Conformal Decomposition Finite Element Method

Lincoln Collins^{*}, Scott Roberts^{**}

^{*}Sandia National Laboratories, ^{**}Sandia National Laboratories

ABSTRACT

Thermal protection systems (TPS) for aerospace applications are commonly used to protect vehicles from intense heat fluxes experienced during flight. These TPS materials are typically comprised of a fibrous fabric encompassed in a phenolic resin. When exposed to the heat fluxes of atmospheric re-entry, heat is dissipated through the ablation of the resin by pyrolysis, causing its recession through the fiber matrix and the release of products that react with the remaining charred porous material. The performance of these systems is dictated by the microstructural features of the composite governing its behavior in a complex multi-physical system coupling thermal transport, reactive fluid transport, mechanical stress formation, and re-radiation. At the mesoscale, modeling the ablation requires an accurate description of surface recession and tracking the changing interface of the resin phase coupled with the gas-phase transport of product gases. Using a simplified description of the resin decomposition chemistry, we focus on the mesoscale modeling of this process. Multiple level-set formulations are used to describe the various phases: a stationary background mesh generated using either analytical parameterizations or tomographic data describes a representative woven fabric, and a dynamic, conformal mesh describes the receding resin domain. The Conformal Decomposition Finite Element Method (CDFEM) is used to dynamically decompose a background tetrahedral mesh into conformal material domains. This conformal interface treatment is required to characterize the pyrolysis surface chemistry. Effective thermal-mechanical properties and ablation rates are calculated for the domain as a function of recession. Sandia National Laboratories is a multi-mission laboratory managed and operated by National Technology and Engineering Solutions of Sandia, LLC., a wholly owned subsidiary of Honeywell International, Inc., for the U.S. Department of Energy 's National Nuclear Security Administration under contract DE-NA0003525.

Simulation of Geomechanical Processes Using Viscoelastoplastic Models for Solid Mechanics with Large Deformations

Oriol Colomés*, Guglielmo Scovazzi**, Nabil Abboud***, Nabil Atallah****

*Duke University, **Duke University, ***Duke University, ****Duke University

ABSTRACT

In this work we propose a quasi-static formulation for the solid mechanics problem to simulate buoyant instabilities of salt layers under rock formations. We consider visco-elasto-plastic constitutive models to characterize the mechanical properties of the rock and salt formations. Our approach enables the characterization of materials with different constitutive models, one for each layer. A variational multiscale (VMS) approach is used to stabilize the numerical instabilities that appear when incompressible materials are considered. With this method, simple linear tetrahedral Finite Elements can be used. To accurately characterize large deformations of the soil, an Arbitrary Lagrangian-Eulerian (ALE) formulation is used, together with a remeshing strategy. The different layers of the salt and rock are modelled using an embedded approach with explicit interfaces, in which the layer surfaces are embedded in a background mesh, avoiding the need of generating meshes of complex geometries. The interfaces between different materials are defined by a given surface mesh, which is then advected according to the material motion. With the explicit treatment of the interfaces, less numerical dissipation is introduced, having a more accurate definition of the interface position than, for instance, level set methods.

On Characterizing the Viscous and Porous Effects in Human Brain Tissue

Ester Comellas*, Silvia Budday**, Jean-Paul Pelteret***, Paul Steinmann****

*University of Erlangen-Nuremberg (FAU), **University of Erlangen-Nuremberg (FAU), ***University of Erlangen-Nuremberg (FAU), ****University of Erlangen-Nuremberg (FAU)

ABSTRACT

Adequate characterization of human brain tissue rheology is crucial to obtaining meaningful computational predictions within a clinical context. Experimental evidence shows that the essential features of brain tissue are nonlinearity, preconditioning, hysteresis, and tension-compression asymmetry [1]. Past work in our group has characterized brain tissue using a finite viscoelastic material model [2]. The obtained results support the hypothesis that brain tissue behaviour is characterized by at least two different time scales. Herein, the longer time scale seems to be associated with the poroelastic interaction of fluid flowing within the solid network of cells and extracellular matrix in the tissue. The shorter one seems to be attributed to the viscoelastic nature of the solid skeleton itself, primarily due to fluid flow inside the cells. The monophasic viscoelastic model can only implicitly capture the porous effects of the longer time scale. To address this shortcoming, we have developed a biphasic nonlinear poro-viscoelastic model to further explore the role of viscous and porous effects in human brain tissue. Within the framework of the theory of porous media, we treat the material as an immiscible aggregate of a nonlinear viscoelastic solid skeleton saturated with pore fluid. Using the deal.II finite element library [3], the governing equations are linearised with automatic differentiation techniques, and a monolithic scheme is used to solve for the unknown solid displacements and fluid pore pressure values. Numerical examples are presented to verify and validate our results with the experimental data available. Our work serves to further elucidate the rheology of brain tissue. We anticipate the insights gained in the characterization of the poro-viscoelastic behaviour of brain tissue will contribute to the future development of clinically relevant predictive and preventive computational approaches to treat trauma-related brain pathologies. References [1] S. Budday, G. Sommer, J. Haybaeck, P. Steinmann, G.A. Holzapfel and E. Kuhl, Rheological Characterization of Human Brain Tissue. *Acta Biomater.*, 60:315–329, 2017. [2] S. Budday, G. Sommer, G.A. Holzapfel, P. Steinmann and E. Kuhl, Viscoelastic parameter identification of human brain tissue. *J. Mech. Behav. Biomed. Mater.*, 74:463–476, 2017. [3] D. Arndt, W. Bangerth, D. Davydov, T. Heister, L. Heltai, M. Kronbichler, M. Maier, J.-P. Pelteret, B. Turcksin and D. Wells, The deal.II Library, Version 8.. *J. Numer. Math.*, 25(3):137–146, 2017.

Improvements for Structural Model Interfacing between Non-conforming Meshes

Simone Coniglio^{*}, Christian Gogu^{**}, Joseph Morlier^{***}

^{*}Airbus\ISAE\Université de toulouse, ^{**}UPS\Université de Toulouse, ^{***}ISAE\Université de Toulouse

ABSTRACT

The interfacing of non-conforming meshes arises in several practical situations in both structural and multi-disciplinary finite element analysis. In Structural finite element analysis this communication can pose some difficulties. In fact using a simple collocation scheme (i.e. imposing the kinematic continuity between interface surfaces through interpolation [1]) artificial interface stiffening, gap openings or stress concentrations localized near the interface arise eventually. Hence in literature several methods were developed to alleviate these problems, for instance, by imposing kinematic continuity in an integral or weak. The mortar approach [2] is maybe one of the most popular approaches in this context. Nevertheless its computational burden and implementation complexity can be a limit for practical implementation. In the Fluid-Structure Interaction field a new approach, the Internodes [3], was proposed to achieve accuracy similar to Mortar, on the other hand reducing implementation and computational effort. This promising technique has been studied from a theoretical point of view and tested on patch tests and Fluid-Structure Interaction applications. This work will first compare on academic benchmark problems several approaches for interfacing non-conforming meshes, including the Mortar and Internodes approach. These approaches are compared according to several metrics: balance of forces and moments, displacement field error and displacements continuity, stress field error. Moreover a new approach that tries to achieve similar performance to Mortar but is simpler to implement is presented. Finally we note that most existing techniques can have issues with the non-satisfaction of Moment equilibrium at the interface. This problem is enhanced and quantified through several numerical experiences on the benchmark problems. A further contribution is proposed to satisfy “a priori” the mechanical moment equilibrium equation at non-conforming interface. This technique consists in a correction that can be applied to every technique tested in this work. After the proposed moment correction all techniques show better performance at a very small computational cost.

2. REFERENCES [1] Barlow John. Constraint relationships in linear and nonlinear finite element analyses. International Journal for Numerical Methods in Engineering. 1982;18(4):521–533. [2] Bernardi, Christine. "A new nonconforming approach to domain decomposition: the mortar element method. " Nonlinear partial equations and their applications (1989). [3] Deparis Simone and Forti. INTERNODES: an accurate interpolation-based method for coupling the Galerkin solutions of PDEs on subdomains featuring non-conforming interfaces. Computers & Fluids. 2016;141:22–41.

Higher-Order Asynchronous Coupling for Fluid-Fluid Interaction

Jeffrey Connors*

*University of Connecticut

ABSTRACT

The distribution of energy across space and time scales is quite different between the atmosphere and ocean. Therefore, codes for air-sea interaction are constructed by coupling together atmosphere and ocean components, each highly optimized using different numerical methods, by passing fluxes of conserved quantities between the components in the form of boundary conditions at the air-sea interface. For efficiency, the fluxes are usually asynchronous, meaning they are calculated using data extrapolated from previous times for at least one component. Moreover, these extrapolations are low-order accurate in terms of the time step size associated with the coupling interval. The accuracy may be improved via iteration, but this is expensive. In some cases, higher-order extrapolation in time may suffice to improve accuracy and circumvent or reduce iteration costs, but then stability considerations arise. For a simplified, model problem of fluid-fluid interaction, a rigorous stability analysis is performed for higher-order extrapolation of fluxes. A scaling analysis provides some intuition regarding the use of high-order extrapolation methods for climate or regional forecasting applications. Some computations are provided to illustrate different coupling configurations; that is, using low- versus high-order extrapolations and with or without iterations to tighten the coupling.

Quadrilateral Bi-cubic Conforming Finite Elements for Plates and Shells

Loredana Contrafatto^{*}, Leopoldo Greco^{**}, Massimo Cuomo^{***}

^{*}University of Catania - Italy, ^{**}University of Catania - Italy, ^{***}University of Catania - Italy

ABSTRACT

In this work, we present a new formulation for a class of quadrilateral conforming finite elements for pure bending Kirchhoff plate problems and its extension to general shells. The rational enrichment of the cubic Bezier's basis, proposed by J. Gregory in 1974 for obtaining G1 continuous surfaces, is the starting point of the formulation. The element presents 20 degrees of freedom and can be generalized in the context of isogeometric analysis including the knot insertion operation and polynomial degrees different than 3. The rational interpolation is modified in order to obtain a formulation able to reproduce states of constant curvature that pass the patch test. Examples demonstrate that the proposed element presents optimal rate of convergence and presents high robustness with respect to mesh distortion even when non-structured meshes are considered.

Biomolecular Electrostatics Calculations Using Polarizable Force Fields in a Continuum Ionic Solvent, with Algorithmic and Hardware Acceleration

Christopher D Cooper*

*Universidad Técnica Federico Santa María

ABSTRACT

Rather than treating the solvent degrees of freedom explicitly, implicit-solvent models use continuum electrostatic theory to compute the mean-field potential in biomolecular systems. This yields a coupled system of partial differential equations, with the Poisson equation in the protein region (enclosed by the molecular surface), and the Poisson-Boltzmann equation in the exterior domain. The charge distribution inside the protein, due to the atomic charges, is modeled by force fields that usually place fixed point charges at the locations of the atoms. However, more elaborate force fields have emerged lately, which consider higher order multipoles, and polarizability. One popular force field of this type is AMOEBA, which describes the charge distribution with permanent point monopoles, dipoles, and quadrupoles, and allows for the dipole component to react to an external field. In this work, we present an implementation of the Poisson-Boltzmann solver PyGBe, that is compatible with the AMOEBA force field. PyGBe uses a boundary integral formulation of the system of partial differential equations, and solves it numerically with a boundary element method. Moreover, it uses a treecode algorithm to accelerate a quadratically scaling matrix-vector product to $O(N\log N)$, and offloads the most computationally intensive parts to a GPU card. To account for polarizability, we solve for the electrostatic potential with self-consistent iterations, so that the induced dipole component converges. The boundary integral formulation treats the point multipoles inside the protein analytically, which is an important advantage compared to volumetric solvers, where the multipolar charge distribution needs to be interpolated to a mesh. Furthermore, preliminary results show that the multipolar representation of the protein has a small effect on the mesh sizes required to correctly resolve the electrostatic potential, making a boundary integral formulation ideal for implicit-solvent calculations using AMOEBA. For the conference, we will present details of our implementation in PyGBe, and validation results using analytical expressions and small molecules. Also, we will show calculations with larger biomolecules, assessing the performance of the boundary integral formulation in a polarizable and multipolar description of the charge distribution.

Adaptive Simulation of Plates and Shells with Hierarchical B-Splines

Luca Coradello*, Annalisa Buffa**, Rafael Vázquez***

*École Polytechnique Fédérale de Lausanne, **École Polytechnique Fédérale de Lausanne, ***École Polytechnique Fédérale de Lausanne

ABSTRACT

The novel paradigm of Isogeometric Analysis (IGA) [1] applied to the Finite Element Method (FEM) has been a thriving area of research in recent years, aiming at closing the gap between design and analysis. In Computer Aided Design (CAD) the standard representation of shapes is obtained via the so-called Boundary Representation (B-rep), which eases the integration between CAD and dimensionally-reduced models such as plates and shells. Additionally, thanks to the higher inter-element regularity achievable with B-Splines compared to standard finite elements, fourth-order Partial Differential Equations (PDEs) (i.e. the governing equations of plates and shells) can be discretized in a straight-forward manner without the need of additional degrees of freedom. However, due to the tensor product nature of IGA, local refinement is a pivotal area of research in the IGA community. Moreover, how to properly capture sharp features in the solution and how to trigger an adaptive algorithm to resolve those features, are still wide open questions in mechanical problems.[2] In this work, we propose a new a-posteriori error estimator for plates and shells, which is computationally cheap and does not require the evaluation of the residual in a strong form. This is a crucial advantage, since the evaluation of the residual requires the computation of derivatives of shape functions up to order four (on a surface in case of a shell). Specifically, starting from the work of [3], we develop an adaptive algorithm for fourth-order PDEs, which is simple and performs well in steering adaptive simulations. Through several numerical examples on both smooth and singular benchmarks we show the reliability and efficiency of the proposed method. References: [1] Hughes, T.J.R., Cottrell, J.A. and Bazilevs, Y. "Isogeometric analysis: CAD, finite elements, NURBS, exact geometry and mesh refinement", *Computer methods in applied mechanics and engineering*, page 4135-4195, (2005) [2] Buffa, A. and Giannelli, C. "Adaptive isogeometric methods with hierarchical splines: error estimator and convergence", *Mathematical Models and Methods in Applied Sciences*, page 1-25 (2017). [3] Bank, R.E. and Kent Smith, R. "A Posteriori Error Estimates Based on Hierarchical Bases", *Society for Industrial and Applied Mathematics*, page 921-935 (1993).

Evaluation of Residual-based Turbulence Models on the Drag and Lift Computations of Risers with Helical Strakes

Adriano M. A. Cortes*, Erb F. Lins**, Paula A. Sesini***, Renato N. Elias****, Alvaro L. G. A. Coutinho*****

*Federal University of Rio de Janeiro, **Federal University of Para, ***Federal University of Rio de Janeiro, ****Federal University of Rio de Janeiro, *****Federal University of Rio de Janeiro

ABSTRACT

Risers are one of the most critical structures in the offshore production of Oil and Gas. Due to hydrodynamics loads and Vortex-induced vibrations (VIV) caused by sea currents, they suffer intense material fatigue, possibly implying severe damage to them. To avoid this setback, different strategies have been applied by the O&G industry to reduce such vibrations (VIV). One of those strategies, classified as passive VIV suppressors, consists of attaching helical strakes to the riser surface. To evaluate the efficiency of the strakes addition becomes mandatory to estimate and predict the drag and lift forces. Besides experimental investigations, for example [1], numerical simulations are successful tools to tackle such challenge. An additional issue regarding the numerical investigations, in this case, is the turbulent regime of the flow. To address this matter, we used the residual-based variational multiscale (RB-VMS) framework, an implicit LES scheme with a scale separation given a priori by a proper decomposition of the fields & spaces [2,3]. Based on the considerations in [2] we investigate different eddy viscosities within the RB-VMS framework and evaluate their influence in the drag and lift forces computations. The simulations are done with our in-house incompressible flow solver, EdgeCFD [3], a hybrid MPI+OpenMP parallel edge-based implementation of the RB-VMS method. [1] Y. Gao, J. Yang, Y. Xiong, M. Wang and G. Peng, Experimental investigation of the effects of the coverage of helical strakes on the vortex-induced vibration response of a flexible riser. Applied Ocean Research, 2016. [2] A. A. Oberai and T. J. R. Hughes, A palette of fine-scale eddy viscosity and residual-based models for variational multiscale formulations of turbulence. Computational Mechanics, 2016. [3] E. F. Lins, R. N. Elias, G. M. Guerra, F. A. Rochinha and A. L. G. A. Coutinho, Edge-based finite element implementation of the residual-based variational multiscale method. Int. J. Numer. Meth. Fluids, 2009.

An HDG Formulation for the Two-phase Flow through Porous Media Simulations

Albert Costa-Solé*, Eloi Ruiz-Gironés**, Josep Sarrate***

*Universitat Politècnica de Catalunya, **Barcelona Supercomputing Center - BSC, ***Universitat Politècnica de Catalunya

ABSTRACT

Two-phase flow through porous media problems are commonly solved in petroleum reservoir simulation, specifically, during the secondary phase of the oil recovery process. This stage starts when the natural pressure difference between the reservoir and the surface is not high enough to move the hydrocarbons upward. In order to mobilize the oil (non-wetting phase) to the production wells and to keep the flow rate, water (wetting phase) is injected through the reservoir, [1]. We assume that both phases and the rock are incompressible and phases are immiscible and occupy the reservoir porosity. The governing equations are obtained from combining, for each phase, mass conservation with Darcy's law, leading to a coupled non-linear system of transient PDE's, [2]. Oil companies are interested in using unstructured meshes to obtain a better representation of the reservoir geometry complexity and also to obtain high-accuracy solutions, [2]. All of these requirements are achieved by high-order continuous Galerkin formulations. Nevertheless, local mass conservation can also be achieved by using a discontinuous and hybridizable Galerkin formulation (HDG) [3]. One of the main advantages of this method, is that when a time integration algorithm of order $p+1$ is used in conjunction with element-wise polynomials of degree $p \geq 0$, the scalar unknowns and their fluxes converge with order $p+1$ in the L_2 -norm, [3]. Moreover, the scalar unknowns can be post-processed in order to obtain a convergence rate of $p+2$ in the L_2 -norm. We present a novel high-order HDG formulation to solve the two-phase flow problem in a heterogeneous porous media, taking into account all the mentioned assumptions. In particular, we apply a high-order HDG formulation in the spatial discretization, combined with a DIRK method for the time discretization. This leads to an implicit scheme for both the pressure and the saturation unknowns. Finally, we assess the efficiency and the main features of the proposed HDG formulation showing several 2D and 3D simulations with homogeneous and heterogeneous material properties. [1] Z. Chen, G. Huan and Y. Ma, Computational methods for multiphase flows in porous media, Siam, Vol. II, 2006. [2] Y. Epshteyn, B. Rivière, Fully implicit discontinuous finite element methods for two-phase flow, Appl. Numer. Math. 57 (2007), no. 4, 383–401. [3] N.C. Nguyen, J. Peraire and B. Cockburn, An implicit high-order hybridizable discontinuous Galerkin method for nonlinear convection-diffusion equations, J. Comput. Phys. 228 (2009), no. 23, 8841–8855.

Influence of Material Heterogeneity on the Stability of Explicit High-Order Spectral Element Methods

Regis Cottereau^{*}, Ruben Sevilla^{**}

^{*}CNRS, CentraleSupélec, Université Paris-Saclay, ^{**}Swansea University

ABSTRACT

Summary: The paper proposes several stability estimates for wave propagation in random heterogeneous media with high-order spectral elements, generalizing classical CFL conditions. This talk [1] describes precisely the influence of material heterogeneity on the stability of explicit time marching schemes for the high-order spectral element discretisation of wave propagation problems. Two different types of heterogeneity are considered. In a first part, it consists in a periodic fluctuation of the density and stiffness parameters, whose period is related to the characteristic element size of the mesh. A new stability criterion is derived analytically for quadratic and cubic one dimensional spectral elements in heterogeneous materials, which may in some situations replace the current rule of thumb. The analysis presented reveals the origin of instabilities that are often observed when the stability limit derived for homogeneous materials [2] is adapted by simply changing the velocity of the wave to account for the material heterogeneity. In a second part, a more complete heterogeneity is considered and precise stability estimates are obtained based on Irons and Trehan theorem [3] and general eigenvalue bounds. Finally, in a third part, very simple estimates are obtained for rapidly fluctuating media. Several extensions of the results are discussed, including higher order approximations, higher dimensions and random media. Extensive numerical results demonstrate the validity of the new stability estimates. REFERENCES [1] R. Sevilla and R. Cottereau, Influence of material heterogeneity on the stability of explicit high-order spectral element methods. Submitted for publication in Comput. Phys., 2017. [2] G. Cohen, Higher-order numerical methods for transient wave equations, Springer, 2001. [3] A. J. Wathen. An analysis of some element-by-element techniques. Comput. Meth. Appl. Mech. Engr. 74, pp. 271-287, 1989.

Structural Optimization of Jackets for Offshore Wind Turbines under Dynamic Loading

Iván Couceiro*, Raquel Guizán**, José París***, Fermín Navarrina****, Xesús Nogueira*****,
Ignasi Colominas*****, Manuel Casteleiro*****

*Universidade da Coruña, **Universidade da Coruña, ***Universidade da Coruña, ****Universidade da Coruña,
*****Universidade da Coruña, *****Universidade da Coruña, *****Universidade da Coruña

ABSTRACT

The design of bottom fixed steel substructures as supports for offshore wind turbines is a very demanding task in terms of computational resources. The analysis of the structural behavior is not straightforward nor conventional and also hard to be assessed with the required accuracy. And the complexity of the problem rises to a much higher level when the optimization of the structure is simultaneously addressed. For this reason, most of the approaches that have been proposed so far require important simplifications of the structural model, the loading conditions or the dynamic response, what gives rise to a significant loss of accuracy in the results. In this work we present a methodology for the dynamic response shape and sizing optimization of offshore jackets under Ultimate Limit Stress, Fatigue Limit State and frequency constraints. The structural analysis takes into account the rotation of the blades, and the whole structure -including the jacket, the tower, the rotor-nacelle assembly and the blades- is modeled as a whole, in order to capture the coupled dynamic behavior. Time integration is based on the Non-Linear Newmark algorithm. Wave and wind loading are considered and fatigue damage is assessed in terms of S-N curves [1] by means of the Palmgren-Miner rule and the Rainflow algorithm for counting stress cycles. The optimization process is addressed by means of a Sequential Linear Programming type algorithm, which requires performing the first order full sensitivity analysis. The sensitivities are obtained through Direct Differentiation, which is clearly more efficient than the Adjoint State Method in this case [2]. The optimization results show fair robustness of the algorithm when facing different problems, and substantial reductions in the weight of the steel jackets are obtained. The optimized designs are strongly conditioned by all the types of imposed constraints. As a general rule, the structural sizing is mostly determined by the fatigue constraints, while the frequency constraints have a major impact on the final shape and how the design is driven through the optimization process. [1] DNV-RP-C203 Fatigue design of offshore steel structures. Det Norske Veritas, 2011. [2] F. Navarrina, S. López-Fontán, I. Colominas, E. Bendito, M. Casteleiro, High order shape design sensitivity: a unified approach. Computer Methods in Applied Mechanics and Engineering, 188: 681-696, 2000.

Implicit Boundary and Anisotropic Mesh Adaptation, Immersed Method and Stabilized Finite Element for Multiphase Flow Simulation

Thierry Coupez^{*}, Elie Hachem^{**}, Hugues Digonnet^{***}, Luisa Rocha Da Silva^{****}

^{*}MINES ParisTech, ^{**}Mines ParisTech, ^{***}Ecole Centrale de Nantes, ^{****}Ecole Centrale de Nantes

ABSTRACT

A wider use of numerical simulation is still depending on meshing and adaptive meshing capabilities when complex geometry, multi-domain, moving interface and multiphase flow are involved. This task becomes more and more difficult when it is combined with a posteriori adaptive meshing or/and dealing with moving interfaces and boundary layers and also when running on massively parallel computers. In order to overcome the lack of flexibility of the common body fitted method, the alternative proposed here, is based on an implicit representation of the interfaces by a local distance function using a hyperbolic tangent filter. Therefore, the geometries can be interpolated and contribute to the numerical error which is detected by an a posteriori error estimator technique. This approach favors the full usage of anisotropic adaptive meshing techniques providing an optimal capture of the interfaces within the volume mesh, whatever is the complexity of the geometry involved. From the flow solver side, unstructured meshes with highly distorted elements (however solution aligned) need to rely on a robust solution framework. The interface condition transfer is enforced by following the immersed boundary/volume (IVM) methodologies for fluid/fluid and or fluid/structure interaction. The proposed multiphase flow solver, including a related local level set technique is based on a stabilized finite element method (VMS) that can afford with anisotropic meshing with high aspect ratio elements. For transient flow a complete stabilization approach including the interface stabilization term and the dynamic of the subscales will be proposed with a quasi-optimal calculation of the stabilization parameter. The error estimation and the metric calculation will be presented and various application examples will be proposed. [1] T. Coupez, E. Hachem, "Solution of high Reynolds Incompressible Flow with Stabilized Finite Element and Adaptive Anisotropic Meshing", *Comp. Meth. in App. Mech. and Engng* Vol. 267, pp. 65-85, (2013) [2] T. Coupez, L. Silva, E. Hachem, *Implicit boundary and adaptive anisotropic meshing*, SEMA SIMAI Springer Series, Vol. 5, pp. 1-18, (2014) [3] L Silva, T Coupez, H Digonnet, *Massively parallel mesh adaptation and linear system solution for multiphase flows*, *International Journal of Computational Fluid Dynamics* 30 (6), 431-436, (2016) [4] E Hachem, S Feghali, T Coupez, R Codina 2015 'A three-field stabilized finite element method for fluid-structure interaction: elastic solid and rigid body limit', *International Journal for Numerical Methods in Engineering* 104 (7), 566-584

Integrating In-Situ Data Analysis and Visualization on libMesh Library

Alvaro Coutinho^{*}, Patrick Valduriez^{**}, Jose Camata^{***}, Vitor Silva^{****}, Daniel de Oliveira^{*****},
Marta Mattoso^{*****}

^{*}COPPE/UFRJ - Brazil, ^{**}Inria and LIRMM - France, ^{***}DCC/UFJF - Brazil, ^{****}COPPE/UFRJ - Brazil, ^{*****}IC/UFF -
Brazil, ^{*****}COPPE/UFRJ - Brazil

ABSTRACT

In situ data analysis and visualization have been used successfully in large-scale computational simulations to extract and visualize scientific data of interest. Such data are obtained from partial (or final) simulation results, and typically stored in raw data files. However, existing In Situ Data Analysis and Visualization (ISAV) solutions have limited online query processing and no support for dataflow analysis. The latter is a challenge for exploratory raw data analysis. In this work, we propose a solution that integrates a dataflow analysis tool, DfAnalyzer, with ParaView Catalyst for performing ISAV and monitoring dataflow from simulation runs. DfAnalyzer contributes with dataflow analyses to monitor the simulation evolution by grouping parameters, associating input data and parameters to solver convergence data, all coupled to ParaView visualizations. We validate our approach solving particle-laden flows using an adaptive mesh refinement and coarsening (AMR/C) solver built on top of the libMesh library. The model involves solving the Navier-Stokes equations coupled to a transport equation for the sediment concentration. The Navier-Stokes equations are discretized by a finite element residual-based variational multiscale formulation, while the transport equation uses a stabilized finite element formulation with discontinuity capturing. The online dataflow query support helps to investigate the effects on the physics of the problem when exploring different input parameter values. Queries can track the sediment concentration (e.g. should be less or equal to 1) at different time steps. This analysis requires relating them to the input parameters, such as time adaptivity control method, AMR/C parameters and the nonlinear tolerance for the flow and sediments solvers. Another example is monitoring the flow and transport sedimentation solver convergence (final linear and nonlinear residuals), and relate them to the images generated by Catalyst visualization pipeline for each time step. Our experimental results show that our approach yields a rich data analysis support with negligible overhead.

Numerical Simulation of Pipeline Flotation in Liquefied Sand

Massimiliano Cremonesi*, Federico Pisanò**, Gabriele Della Vecchia***

*Politecnico di Milano, Italy, **TU Delft, Netherlands, ***Politecnico di Milano, Italy

ABSTRACT

Submarine pipelines are widely employed to transport hydrocarbons through the ocean from wells to production and distribution plants. Pipelines are usually laid in trenches, either left open or filled with sand. Pipelines in trenches are typically exposed to soil liquefaction. This phenomenon can be triggered by wave action, earthquakes or tidal fluctuations leading to very large pipeline displacements. The present work aims to present a numerical technique to analyze the pipeline flotation and sinking in liquefied sand. The Particle Finite Element Method has been adapted and extended to tackle this kind of problems [1,2]. The approach is based on the assumption of soil fully liquefied at the inception of pipeline flotation, which justifies the use of a one-phase fluid model [2]. A non-Newtonian Bingham-like constitutive law has been calibrated to describe the liquefied soil behavior. A simplified, soil mechanics based approach has been also introduced to include reconsolidation effects[3]. Soil-pipe interaction is reproduced via a staggered scheme. The numerical approach has been validated against experimental tests to show the effectiveness and robustness of the proposed techniques. [1] Cremonesi M., Frangi A., Perego U. (2010) A lagrangian finite element approach for the analysis of fluid-structure interaction problems. International journal for numerical methods in engineering 84, No. 5, 610-630 [2] Della Vecchia G., Cremonesi M., Viti A., Pisanò F. (2018) On the use of the dam breaking test for the rheological characterisation of liquefied sands. Géotechnique Letters, submitted for publication. [3] Pisanò F., Cremonesi M., Bortolotto F., Della Vecchia G. (2018) Feeding soil mechanics into the CFD analysis of pipeline flotation in liquefied sand Géotechnique, submitted for publication.

Modeling Size Effects in the Strength Statistics of Nanoindentation

Joshua Crone^{*}, Jaroslaw Knap^{**}

^{*}US Army Research Laboratory, ^{**}US Army Research Laboratory

ABSTRACT

Nanoindentation experiments reveal that the onset of plastic deformation occurs over a wide range of indenter loads when the indenter size approaches the mean dislocation spacing. Under these conditions, it has been shown that plastic deformation is due to the activation of pre-existing dislocations, rather than homogeneous dislocation nucleation. Quantifying the effect of dislocation density on the mean and variance of the critical indenter force has remained a challenge with current experimental capabilities. In the present work, we use discrete dislocation dynamics (DDD) simulations of indentation to quantify the effect of dislocation density and indenter size on the mean and variance of the critical force to induce plasticity. Furthermore, we employ DDD to identify the underlying dislocation mechanisms that lead to the onset of plastic deformation and pop-in. To include free surface effects and the highly varying stress field induced by the indenter, we couple the bulk DDD simulator, ParaDiS, with a parallel finite element solver. Simulations are carried out for multiple randomly seeded dislocation configurations at several dislocation densities in order to obtain a statistically relevant measure on both the mean and standard deviation of the critical force. Our results suggest a power law scaling for both the mean and standard deviation with respect to the dislocation density, which is in good agreement with the limited experimental work on quantifying this effect.

Multiscale Designer: Efficient Multiscale Simulation at the Structural Scale with Minimal Testing

Robert Crouch^{*}, John Kytasty^{**}, Jacob Fish^{***}

^{*}Altair Engineering, ^{**}Altair Engineering, ^{***}Columbia University

ABSTRACT

Development of accurate computational models for composite materials presents two challenges for industry practitioners. Challenge one: the computational expense of homogenization based multiscale models make simulation at structural scales infeasible, often even when high performance computing capabilities are used. Multiscale Designer addresses this difficulty with a unique multiscale, reduced order modelling technique that maintains the physically meaningful parameters of multiscale models based on computational homogenization, while greatly reducing the computational burden. Challenge two: the input parameters of a multiscale models for a composite material are the properties of the constituent materials, e.g. carbon fiber and epoxy, and it is often not possible to fully characterize a complex constituent material such as carbon fiber by performing experiments on the constituent in isolation. Even if such experiments are possible, manufacturing processes often result in different in situ properties. Multiscale Designer addresses these difficulties by providing a multiscale calibration procedure that requires a minimum number of experimental tests to specify the material parameters. This approach to determining the parameters is based on rigorous inverse calibration, and within Multiscale Designer, this inverse calibration is automated and highly accessible to practicing engineers. In particular, stochastic approaches provide crucial insight into the reliability of the inverse solution, and can inform the analyst when the lack of a particular experimental observation negatively impacts the solution. The salient features of Multiscale Designer are: (i) arbitrary numbers of spatial scales, (ii) a unique model reduction scheme that reduces the computational cost of complex n-scale material systems, (iii) stochastic reverse engineering procedures that reliably identify material properties at multiple spatial scales, and (iv) seamless integration in major commercial finite element codes. We demonstrate the capabilities of Multiscale Designer by showing how to calibrate the constituent material parameters for a non-crimp fabric used in the automotive industry and then validating the model on structural scale component subjected to bending. The calibration and validation experiments were performed at General Motors, and the validation simulations were conducted using the Multiscale Designer plugin for the explicit finite element code Radioss.

Valve-Seat Contact Analysis in Internal Combustion Engine in Order to Predict and Reduce the Wear Level

Martial Crozet*, Benyebka Bou-Saïd**, Yves Berthier***, David Jones****, Mark Fowell*****

*INSA de Lyon/LaMCoS/Volvo, **INSA de Lyon/LaMCoS, ***INSA de Lyon/LaMCoS/CNRS, ****Volvo, *****Volvo

ABSTRACT

The valve / valve seat contact plays a significant role in determining the sealing of the combustion chamber as well as the flow of intake and the exhaust of gases, in an internal combustion engine. Any changes of this contact may lead to a reduction in engine performance and an increase in emissions, which can lead to increased maintenance cost and therefore reduced freight efficiency. Due to the continuous requirement to increase engine performance (i.e. increased cylinder pressure, reduce pollutant content and increased durability), the valve / valve seat contact may become a significant factor in future engine development. The aim of the current work is to improve the understanding of the factors affecting the wear of the valve / valve set contact and to enable better optimization of the system at the design stage, using both computational modelling and experimental measurements. To achieve this, a rigid body dynamic model coupled with finite element analysis has been developed in order to assess, the global valve motion as a function of the engine operating conditions, the vibration response of the system, and the local contact conditions at the valve / valve seat interface. Four distinct phases of relative valve / valve seat motion have been identified: 1. Impact between the valve and the seat. Impact speed is supposed to be controlled by the camshaft geometry. However, in the current study using measured camshaft geometry the impact velocity was shown to be underestimated by currently used industrial tools; 2. Macro scale sliding of valve in valve seat. Due to any geometrical misalignment, the valve can slide against the seat insert creating interfacial shear stress which may cause plastic deformation and 3rd body transformation; 3. Valve vibration during steady state, which can induce a fretting motion within the contact area; 4. Elastic deformation of the valve due to combustion pressure, resulting in sliding at the valve / valve seat contact interface. From this work, it has been possible to identify and correlate wear behaviour observed using SEM, with each of these distinct phases. From this it has been possible to highlight geometric parameters which may be adapted in the design process to reduce the severity of the contact conditions while maintaining a sufficient gas seal.

An Adaptive Fixed-Mesh ALE Formulation for Free Surface Problems: Numerical Model and Experimental Validation

Marcela Cruchaga^{*}, Ernesto Castillo^{**}, José Flores^{***}, Joan Baiges^{****}

^{*}Departamento de Ingeniería Mecánica, Universidad de Santiago de Chile, ^{**}Departamento de Ingeniería Mecánica, Universidad de Santiago de Chile, ^{***}Departamento de Ingeniería Mecánica, Universidad de Santiago de Chile, ^{****}Departamento de Ingeniería Civil y Ambiental, Universidad Politécnica de Cataluña

ABSTRACT

A free surface flow formulation is presented and applied to model a proposed experiment of an oil sloshing problem. The numerical technique encompasses an adaptive remeshing technique and an arbitrary Lagrangian-Eulerian stabilized fixed mesh finite element methodology. A level set approach is used to capture the moving interface. A sloshing experiment is reported with the aim to provide valuable data to validate the numerical model. The experiment consists of a rectangular tank filled with vegetable oil subjected to controlled vibrating motions. The free surface evolution is captured using a motion capturing technique. The study includes different filling depths and motion conditions, i.e., amplitudes and frequencies. The numerical results obtained with the proposed model are satisfactorily compared with experimental data.

A Finite Viscoelasticity Model in Curvilinear Coordinates for the Nonlinear Dynamic Analysis of Cable Structures

Miquel Crusells-Girona*, Filip Filippou**, Robert Taylor***

*University of California, Berkeley, **University of California, Berkeley, ***University of California, Berkeley

ABSTRACT

This paper presents the formulation and validation of a finite viscoelastic material model in curvilinear coordinates that is suitable for the nonlinear dynamic analysis of cable structures under large displacements. The formulation is based on a general multiplicative decomposition of the deformation gradient in multiple viscous strains, and uses a quadratic evolution law in terms of the Kirchhoff axial force and of the Lie derivative of the left Cauchy-Green strains [1]. This material model is used with a mixed variational formulation of the catenary problem that allows a continuous and a discontinuous axial force distribution, and is thus capable of representing the axial force jump under concentrated forces [2]. The proposed finite viscoelastic material model is first used to represent the physical internal mechanisms and the air resistance that dissipate the high-frequency compression waves in flexible cables with different sag-to-span ratios [3]. The analyses of three simply-supported cables from the literature under large-amplitude free vibration [3] and one simply-supported cable under earthquake excitation show that a small relaxation time is effective in removing the undesired high-frequency contributions to the dynamic response. A model with multiple viscoelastic strains and large relaxation times is implemented in the mixed element to model the overall decay of the dynamic cable response. The same examples show that, for small displacements, results reduce to the infinitesimal approximation, while the nonlinear inelastic components account for the more general decaying behavior of the response with phase transitions and 3d coupling. In conclusion, the proposed viscoelastic material model and its numerical implementation constitute a generalization of existing cable formulations to curvilinear coordinates and large displacements. The resulting element and its numerical implementation are characterized by consistency, accuracy and numerical robustness. [1] S. Reese and S. Govindjee, "A theory of finite viscoelasticity and numerical aspects", *International Journal of Solids and Structures*, 35, 3455-3482 (2013). [2] M. Crusells-Girona, F.C. Filippou and R.L. Taylor, "A mixed formulation for nonlinear analysis of cable structures", *Computers & Structures*, 186, 50-61 (2017). [3] M. Crusells-Girona, F.C. Filippou and R.L. Taylor, "Nonlinear static and dynamic analysis of mixed cable elements", *Proceedings of the 14th International Conference on Computational Plasticity – Fundamentals and Applications*. Barcelona, 2017.

Parametric Numerical Modelling of Thermally-bonded Nonwovens: Effect of Manufacturing Parameters

Vincenzo Cucumazzo^{*}, Emrah Demirci^{**}, Memis Acar^{***}, Behnam Pourdeyhimi^{****}, Vadim Silberschmidt^{*****}

^{*}Loughborough University, ^{**}Loughborough University, ^{***}Loughborough University, ^{****}North Carolina State University, ^{*****}Loughborough University

ABSTRACT

Nonwovens are engineered polymer-based materials with a microstructure made of randomly distributed fibres bonded together with mechanical, thermal or chemical techniques. Due to an anisotropic and nonlinear nature of their mechanical behaviour, modelling their mechanical performance is challenging. This becomes particularly complex for thermally-bonded nonwovens, since their mechanical response is not only influenced by material properties, but also by manufacturing parameters (e.g. shape, orientation and pattern of bond points and calendering temperature). In order to account for these effects, a novel subroutine-based parametric finite-element (FE) model was proposed in this research. Such a method allows automated modelling of nonwoven materials considering variability of their material and design parameters. The FE modelling approach was conducted within a continuous domain and incorporated an elastic-plastic constitutive material model to capture strain-hardening effects, large deformations and rotations. The obtained numerical results of these simulations were compared with experimental data obtained from tensile tests performed in various loading directions, namely, machine and cross directions. The developed numerical scheme will be improved further to include a damage model capable of describing various damage scenarios.

Thermodynamically Sound Data-driven Computational Mechanics

Elías Cueto^{*}, David González^{**}, Francisco Chinesta^{***}

^{*}Universidad de Zaragoza, ^{**}Universidad de Zaragoza, ^{***}ENSAM ParisTech

ABSTRACT

In the paradigm of data-intensive science, automated, unsupervised discovering of governing equations for a given physical phenomenon has attracted a lot of attention in several branches of applied sciences. In this work we propose a method able to avoid the identification of the constitutive equations of complex systems, and rather work in a purely numerical manner by employing experimental data. In sharp contrast to most existing techniques, this method does not rely on the assumption on any particular form for the model (other than some fundamental restrictions placed by classical physics such as the second law of thermodynamics, for instance) nor forces the algorithm to find among a pre-defined set of operators those whose predictions fit best to the available data. Instead, the method is able to identify both the Hamiltonian (conservative) and dissipative parts of the dynamics while satisfying fundamental laws such as energy conservation or positive production of entropy, for instance. The proposed method is tested for some examples of discrete as well as continuum mechanics, whose accuracy demonstrate the validity of the proposed approach.

A Perspective on New Generation Stent-graft by Metamaterial Design and Computational Optimization

Fangsen Cui^{*}, Yucheng Zhong^{**}, Gideon Praveen Kumar^{***}, Gongfa Chen^{****}, Jackie Pei Ho^{*****}, Hwa Liang Leo^{*****}, Chang Shu^{*****}

^{*}Institute of High Performance Computing, A*STAR, ^{**}Institute of High Performance Computing, A*STAR, ^{***}Institute of High Performance Computing, A*STAR, ^{****}Guangdong University of Technology, ^{*****}National University of Singapore, ^{*****}National University of Singapore, ^{*****}Fuwai Hospital, Chinese Academy of Medical Sciences

ABSTRACT

Aortic pathologies such as aneurysm and dissection can be treated by less invasive method – the endovascular aortic repair (EVAR). It provides a lower operative mortality and morbidity solution compared to conventional open surgery repair. The key medical device used for EVAR is called stent-graft (SG) and has been successfully used for abdominal aortic aneurysm repair as well as straight thoracic aorta. For aortic arch with sharp curve variations, it is challenging to minimize complications such as endoleaks with thoracic endovascular aortic repair (TEVAR). The other challenging issue with the aortic arch is to preserve the three supra-aortic branches blood flow which usually requires hybrid repair, chimney repair, and even custom-made fenestrated or branched devices with high morbidity and cost. To design new generation stent-graft, the new design concept such as origami structure and auxetic materials can play a key role in improving the performance and minimizing complications. However, such metamaterial stent-graft must be well tailored so its mechanical performance can be better utilized. In addition, computational solid mechanics, computational fluid dynamics, and multi-objective optimization can be used for the development of new generation stent-graft. In this paper, first we review recent progress on developing metamaterial stent-graft. The benefits of such design incorporated with our previous proposed design are then discussed. Furthermore, simulations on the evaluation of mechanical performance of stent-graft are presented. The optimization methodology of stent-graft design is also discussed. References 1. W Wu, X Song, J Liang, et al. Mechanical properties of anti-tetrachiral auxetic stents, Composite Structures, online Nov 20, 2017 2. Z You, Folding structures out of plate materials, Science 2014;345(6197):623-645 3. G. Alaimo F. Auricchio M.Conti, M. Zingales, Multi-objective optimization of nitinol stent design, Medical Engineering & Physics, Volume 47, September 2017, Pages 13-24

New Insights in Dislocation Behaviors under Shock Loading

Yinan Cui^{*}, Giacomo Po^{**}, Nasr Ghoniem^{***}

^{*}UCLA, ^{**}UCLA, ^{***}UCLA

ABSTRACT

Understanding the mechanical behavior of metallic solids under extreme conditions of high strain rate is of great interest to engineering applications. However, until recently little understanding of the effect of the elastodynamic stress field emission by dislocations on dislocation behaviors has been achieved. In all the available three dimensional discrete dislocation dynamics (DDD) method, dislocations are treated in a quasi-statically way, even though the time-dependent nature is found to be very important when the strain rate is higher than $10^6/s$. This work presents the first 3D DDD method, based on a fully time-dependent elastodynamic description of the elastic fields of discrete dislocations. The fundamental time-dependent solutions and its numerical implementation are presented. New insights on dislocation interactions during shock loading are revealed.

A Novel Fatigue Strength Prediction Method for Optical Fibers with Initial Flaws

Yuxuan Cui^{*}, Yunxia Chen^{**}, Jingjing He^{***}

^{*}Beihang University, ^{**}Beihang University, ^{***}Beihang University

ABSTRACT

The dynamic fatigue behavior of optical fiber is strongly affected by the surface defects generated during manufacture and handling. Crack initiation and propagation due to stress concentration would result in catastrophic failure of optical fibers. In this work a physics-based model is presented to quantify the effect of initial flaws. Artificial triangle indentations are introduced with indentation method to represent the natural flaws of optical fiber caused by material uncertainties or manufacture procedure. Two geometry parameters, the diametrical length of the indentation impression and the diametrical flaw length, are chosen to describe the influence of initial flaws. Both cases for indentation with or without radial cracks are included in this study. Experimental studies are used to validate the proposed method and a good agreement is observed between the model predictions and experimental data.

Uncertainty Quantification in the Brazilian Outbreak of Zika Virus

Americo Cunha Jr*, Eber Dantas**, Michel Tosin***

*Universidade do Estado do Rio de Janeiro, **Universidade do Estado do Rio de Janeiro, ***Universidade do Estado do Rio de Janeiro

ABSTRACT

Several instances of Zika virus epidemic have been reported around the world in the last 20 years, causing Zika fever to become a disease of international concern. The use of mathematical models for epidemics in this context is very important, once they are useful tools to predict the outbreaks underlying numbers, and allow one to test the effectiveness of different strategies to combat associated diseases. This work deals with the development and calibration of an epidemic model to describe the Zika virus outbreak in Brazil. The modeling and quantification of the initial conditions uncertainties is also of interest. In order to calibrate the model, two inverse problems (one deterministic and another one stochastic) are formulated and solved. A consistent stochastic model of uncertainties is constructed by means of a parametric probabilistic approach, which employs Monte Carlo method to compute the propagation of uncertainties.

Continuum Damage and Plasticity Model for Higher Gradient Materials

Massimo Cuomo^{*}, Loredana Contrafatto^{**}, Leopoldo Greco^{***}

^{*}University of Catania, ^{**}University of Catania, ^{***}University of Catania

ABSTRACT

Continuum Damage and Plasticity Model for Higher Gradient Materials M. Cuomo, L. Contrafatto, L. Greco
Department of Civil Engineering and Architecture University of Catania - ITALY
Complex materials, among which those usually referred to as metamaterials, exhibit different, often independent, mechanisms for the evolution of anelastic phenomena at the micro- and at the macro-scale. Gradient plasticity, originally introduced for geomaterials, has been extended to a large variety of non local materials, see e.g. [1]. Similarly, continuum damage has been extended to micromorphic and higher gradient models, introducing internal damage variables and their gradient. Damage evolution is determined by rate equations depending upon the thermodynamic conjugate forces, related to the local value of the damage variables and to its gradient. An additional field differential equation is then obtained for damage compatibility, that has to be solved simultaneously with the equilibrium equations. In this work is proposed a new continuum damage model for strain gradient materials characterized by two independent damage internal variables, each evolving with its own law. In this way no additional field equation for the damage variable is needed. The derivation has been obtained within a thermodynamic framework, introducing suitable functionals for the internal energy and for the rate of dissipation. Specific objectives of the work are: - to present a damage model for strain gradient materials that does not need the solution of additional differential equations; - to analyze a simpler version of the model, in order to compare it with local damage models - to study whether also in this case, similarly to what has been found by the author with non local softening plasticity models, the presence of strain gradients is able to avoid strain localization and consequently mesh dependency in the numerical simulations. Numerical simulations of a strain gradient mode with damage, eventually couple with plasticity, will be discussed. [1] Forest, S., Micromorphic Approach for Gradient Elasticity, Viscoplasticity, and Damage, Journal of Engineering Mechanics ASCE, 2009, vol. 135, 3, 117-131.

Dislocation Cross-slip in FCC Metal Alloys

William Curtin*, W.G. Noehring**

*EPFL, **EPFL

ABSTRACT

Cross-slip of screw dislocations is the thermally-activated dislocation process that influences dislocation structuring, work hardening, fatigue, and ductility. Cross-slip has been widely studied in elemental fcc alloys, where the cross-slip energy barrier scales inversely with the stacking fault energy. This thermally-activated phenomenon has been incorporated into various studies of mesoscale plasticity using discrete dislocation dynamics to demonstrate its role in plasticity. Most engineering materials are alloys with some elements in solid solution, yet the cross-slip in alloys has typically been considered to depend only on the stacking fault energy of the alloy. Here, we report on atomistic studies of the cross-slip process in a wide range of fcc random solid solution alloys and demonstrate that the cross-slip energy barrier itself is statistically distributed so that the stacking fault alone does not reflect the operative barriers in a real alloy. The standard deviation of the distribution of cross-slip barriers can be computed knowing only the solute/dislocation and solute/solute interaction energies. The cross-slip of long dislocation segments typical of real materials (1000b or larger) then involves both nucleation at locally favorable (low activation energy) regions of solutes and propagation (lateral extension) that is driven by either Escaig or Schmid stresses. A random walk model in the presence of local fluctuations in cross-slip energy difference is developed to predict the operative distribution of energy barriers as a function of solute concentration, dislocation length, and applied stress levels, with excellent quantitative success. These results demonstrate that the cross-slip barriers in alloys are much smaller than those in the pure metals, making cross-slip much more frequent in alloys. The resulting models are suitable for incorporation into dislocation-level models and may inform crystal plasticity models, while the consequence on various macroscopic plasticity phenomena are discussed.

Computational Mechanics Intelligence: How to Teach Continuum Mechanics to an Artificial Intelligence Using Computer Simulations

Christian Cyron*, Roland Aydin**

*Hamburg University of Technology, **Technical University of Munich

ABSTRACT

Over the last years, we have witnessed several groundbreaking advances in artificial intelligence (AI) that were based on a simple strategy: a virtual training environment was created by setting up some general rules. Subsequently, an AI, typically represented by an artificial neural network (ANN), was placed in this training environment and allowed to practice a certain kind of activity until it reached a superhuman level of mastery. The rules of the training environment were, for example, the rules of the board game Go in the AlphaGo project. Other research projects rely on virtual environments as used in computer games in order to train an AI to perform intelligent actions within such environments or solve certain problems. All this research has in common so far that it uses training environments defined by rules whose complexity is far below the one of real physics. With physically more realistic training environments one could train AIs to solve problems, for example, from mechanical engineering that require so far intense human interactions. Creating physically realistic models of systems and processes in mechanical engineering is the main objective of computational mechanics. It is thus natural to combine computational mechanics and machine learning to create what one may refer to as “computational mechanics intelligence”, that is, a kind of artificial/computational intelligence that is endowed with an accurate understanding of a certain mechanical problem and which is trained in a virtual environment created by methods from computational mechanics. In this talk we will discuss fundamental aspects of the idea of computational mechanics intelligence. We will discuss how to combine ANNs with finite element simulations in order to provide physically realistic and accurate training environments to ANNs. In particular we will address a key question: how can one achieve an acceptable computational cost of such a set-up for AI training despite the necessity of numerous computational simulations, each of which can be associated with a substantial computational cost when trying to model a complex physical system accurately. The strategy is based on a smart coupling of the learning progress of the AI with the resolution of the computational models that provide the training environment for the AI. We demonstrate advantages of our strategy using some simple examples from continuum mechanics in one and higher dimensions.

Shock Structure in Porous Metals: The Interplay of Material Strain Rate Dependency with Micro-inertia Effects

Christophe Czarnota^{*}, Sébastien Mercier^{**}, Alain Molinari^{***}

^{*}LEM3 - UMR CNRS 7239, Université de Lorraine - 7 rue Félix Savart BP 15082 - 57073 METZ Cedex 03 - FRANCE, ^{**}LEM3 - UMR CNRS 7239, Université de Lorraine - 7 rue Félix Savart BP 15082 - 57073 METZ Cedex 03 - FRANCE, ^{***}LEM3 - UMR CNRS 7239, Université de Lorraine - 7 rue Félix Savart BP 15082 - 57073 METZ Cedex 03 - FRANCE

ABSTRACT

The present work proposes to examine the combined influence of micro-inertia and material rate dependency on the shock structure in porous metals. Porosity is assumed to be moderate and voids are not connected. Beyond some propagation distance from the shock initiation site (few times the effective plastic shock width), steady plastic shock waves are formed. As the shock wave is traveling in the porous medium, voids are facing a rapid collapse. Material particles located in the vicinity of voids are subjected to very high acceleration. Owing to the mass density of the matrix, the local acceleration induces local inertia effects, called micro-inertia. Micro-inertia effects are embedded in the overall constitutive response of the porous material following the work of [Molinari and Mercier, 2001] and [Czarnota et al., 2017]. The overall response of porous materials is obtained by a dynamic homogenization approach where the static part is determined from a GTN viscoplastic flow potential. The present talk will enlighten the influence of the material strain rate sensitivity on the shock structure and the interplay between the material viscosity and micro-inertia effects. One of the major finding of the present study concerning shock wave structures is the relationship connecting the plastic strain rate within the shock to the shock amplitude. The [Swegle and Grady, 1985] power law relationship will thus be revisited for porous metals. Acknowledgement: The research leading to these results has received funding from the European Union's Horizon2020 Programme (Excellent Science, Marie-Sklodowska-Curie Actions) under REA grant agreement 675602 (Project OUTCOME). REFERENCES: Czarnota, C., Molinari, A., and Mercier, S., 2017, "The structure of steady shock waves in porous metals ", to appear in J. Mech. Phys. Solids. Molinari, A. and Mercier, S., 2001, "Micromechanical modelling of porous materials under dynamic loading ", J. Mech. Phys. Solids 49, 1497–1516. Swegle, J. W. and Grady, D. E., 1985, "Shock viscosity and the prediction of shock wave rise times", J. Appl. Phys., 58(2), 692-701.

Determination of Effective Cross-Section Properties by Chemo-Mechanical Simulations

Lisa-Marie Czernuschka^{*}, Ioannis Boumakis^{**}, Jan Vorel^{***}, Marco Marcon^{****}, Roman Wan-Wendner^{*****}

^{*}Christian Doppler Laboratory LiCRoFast, Institute of Structural Engineering, University of Natural Resources and Life Sciences, Vienna, Austria, ^{**}Christian Doppler Laboratory LiCRoFast, Institute of Structural Engineering, University of Natural Resources and Life Sciences, Vienna, Austria, ^{***}Christian Doppler Laboratory LiCRoFast, Institute of Structural Engineering, University of Natural Resources and Life Sciences, Vienna, Austria, ^{****}Christian Doppler Laboratory LiCRoFast, Institute of Structural Engineering, University of Natural Resources and Life Sciences, Vienna, Austria, ^{*****}Christian Doppler Laboratory LiCRoFast, Institute of Structural Engineering, University of Natural Resources and Life Sciences, Vienna, Austria

ABSTRACT

The safety and sustainability of state of the art bridge structures is a crucial task in modern civil engineering practice. The long-term behavior of concrete is complex and influenced by many different phenomena such as aging, shrinkage, creep and their interactions. As widely known, the main source of these phenomena is the hydration of concrete, which is strongly influenced by the boundary conditions, the mix design, as well as the geometry of the structure. Hence, careful consideration of these effects is required especially for large concrete structures. The latter show significant spatial gradients in reaction degree, temperature and humidity, consequently also being visible in material properties. In order to be able to capture the behavior as accurately as possible, a strong numerical tool is of great importance. This study presents the determination of effective cross-section properties by utilization of chemo-hygro-thermal simulations coupled with mechanical analysis in a multi-physics framework [1,2]. This framework is calibrated and validated based on an extensive experimental campaign, comprising temperature and humidity evolution measurements, as well as calorimeter, shrinkage and modulus data. Specifically, effective cross section properties of different practically relevant types under different boundary conditions are derived. Influences of environmental boundary conditions and cross-section characteristics on thermal strains, shrinkage and their interaction with creep are analyzed and discussed in detail. [1] Di Luzio, G. and Cusatis, G., Hygro-thermo-chemical modeling of high performance concrete - I: Theory, Cement and Concrete Composites, 2009; 31:301-308. [2] Di Luzio, G. and Cusatis, G., Hygro-thermo-chemical modeling of high performance concrete - II: Numerical implementation, calibration and validation, Cement and Concrete Composites, 2009; 31:309-324.

Enhancing Alya Multiphysics Code with WSMP Solver and Solving Large Scale Ill-Conditioned Problems

Paula Córdoba*, Guillaume Houzeaux**, Seid Koric***, Anshul Gupta****

*Barcelona Supercomputing Center, **Barcelona Supercomputing Center, ***National Center for Supercomputing Applications & University of Illinois, ****IBM Watson Research Center

ABSTRACT

The discretization of partial differential equations of complex physical problems involves solving linear systems of equations with a great number of unknowns. The resultant matrix obtained from this discretization is often sparse and ill-conditioned. In many cases problems are solved in fine structured meshes with irregular geometries yielding ill-conditioned matrices, where using implicit methods together with preconditioned iterative solvers often diverge or the preconditioned system can be computationally more expensive than using direct methods. This work aims at improving the parallel scalability and robustness of the hybrid MPI/OpenMP high performance computational code Alya developed at BSC-CNS by using the parallel linear solver WSMP solver from IBM Watson. In this framework WSMP, a direct linear solver developed at IBM Watson has been integrated into Alya code to study and improve the performance of such problems. To do so, Alya's parallel structure and matrix format has been adapted to the one required by WSMP and WSMP has been integrated into Alya workflow for symbolic and numerical factorization as well as solution steps. Finally WSMP has been validated and compared with Alya's internal solvers performing scalability and convergence studies on several real life cases of heat transfer and solid mechanic problems. The results of this collaboration will improve Alya's numerical robustness and open the door for the high-fidelity multiphysics modeling of complex processing real scale. M. Vázquez, G. Houzeaux and S. Koric et al., Alya: Multiphysics engineering simulation toward exascale, Journal of Computational Science, 2016, In Press, doi:10.1016/j.jocs.2015.12.007 S. Koric and A. Gupta, "Sparse Matrix Factorization in the Implicit Finite Element Method on Petascale Architecture, " Computer Methods in Applied Mechanics and Engineering, 2016 v.32,281-292, 2016

Locally Refined Isogeometric Analysis of Trimmed Shells

Davide D'Angella*, Luca Coradello**, Massimo Carraturo***, László Kudela****, Stefan Kollmannsberger*****, Ernst Rank*****, Alessandro Reali*****

*Technische Universität München, TUM Institute for Advanced Study, **École polytechnique fédérale de Lausanne,
Università degli Studi di Pavia, *Technische Universität München, *****Technische Universität München,
*****Technische Universität München, TUM Institute for Advanced Study, *****Università degli Studi di Pavia,
TUM Institute for Advanced Study

ABSTRACT

The Isogeometric B-Rep analysis of shells allows to perform computations on the exact geometry, reducing the gap between analysis and design [1]. However, how to properly handle trimmed surfaces is still a frequently discussed question. Moreover, small geometric features or localized mechanical responses demand for higher accuracy in selected areas. In this work we present how different techniques can be successfully combined to perform efficient Kirchhoff-Love shell analysis. In particular, we present how the trimming can be dealt with at the integration level by means of an immersed boundary method like the Finite Cell Method (FCM) [2]. Conforming integration domains are adaptively produced to accurately capture the geometry [3], while the element shape is kept regular and not distorted. This is used together with local hierarchical refinement to efficiently adapt the mesh locally. In conclusion, we show how these methodologies can create a powerful tool for the integration of design and analysis of B-Rep shell models. [1] Breitenberger, M., et al. "Analysis in computer aided design: Nonlinear isogeometric B-Rep analysis of shell structures," Computer Methods in Applied Mechanics and Engineering, 284, 2015. [2] Rank, E., et al. A. "Geometric modeling, isogeometric analysis and the finite cell method," Computer Methods in Applied Mechanics and Engineering, 249-252, 2012. [3] Kudela, L., et al. "Efficient and accurate numerical quadrature for immersed boundary methods," Advanced Modeling and Simulation in Engineering Sciences, 2: 10, 2015.

A Optimization-based Coupling Strategy for Local and Nonlocal Elasticity Problems

Marta D'Elia^{*}, Pavel Bochev^{**}, Mauro Perego^{***}, David Littlewood^{****}

^{*}Sandia National Lab.s, ^{**}Sandia National Lab.s, ^{***}Sandia National Lab.s, ^{****}Sandia National Lab.s

ABSTRACT

Nonlocal continuum theories such as peridynamics and nonlocal elasticity can capture strong nonlocal effects due to long-range forces at the mesoscale or microscale. For problems where these effects cannot be neglected, nonlocal models are more accurate than classical Partial Differential Equations (PDEs) that only consider interactions due to contact. However, the improved accuracy of nonlocal models comes at the price of a computational cost that is significantly higher than that of PDEs. The goal of Local-to-Nonlocal (LtN) coupling methods is to combine the computational efficiency of PDEs with the accuracy of nonlocal models. LtN couplings are imperative when the size of the computational domain or the extent of the nonlocal interactions are such that the nonlocal solution becomes prohibitively expensive to compute, yet the nonlocal model is required to accurately resolve small scale features. We propose an optimization-based coupling strategy for the solution of a nonlocal elasticity problem. Our approach formulates the coupling as a control problem where the states are the solutions of the nonlocal and local equations, the objective is to minimize their mismatch on the overlap of the nonlocal and local domains, and the controls are virtual volume constraints and boundary conditions. We present the implementation of our coupling strategy using Sandia's agile software components toolkit, which provides the groundwork for the development of engineering analysis tools. We show that our method passes linear and quadratic patch tests and we present numerical convergence studies. Using three-dimensional geometries, we also show that our approach can be successfully applied to challenging, realistic, problems.

Fast Helmholtz Solvers on Multi-Threaded Architectures

Ruiyang DAI^{*}, Jean-François Remacle^{**}, Christophe Geuzaine^{***}

^{*}Université catholique de Louvain (UCL), ^{**}Université catholique de Louvain (UCL), ^{***}Université de Liège

ABSTRACT

Solving the Helmholtz equation in the high frequency regime is a notoriously difficult problem. In this paper, we aim at solving Helmholtz problem in heterogeneous media in the frequency domain. A high order continuous finite elements is thus used. Because of the high frequency, a large number of unknowns is required to obtain accurate solutions of the problem (typically 4 elements per wavelength for a polynomial order of 4). Linear systems arising at high frequency are indefinite and iterative methods fail to converge. The large number of unknowns forbids to use direct methods as well. Thus, a Domain Decomposition Method (DDM) with a double sweep preconditionner has been developed and implemented in parallel on modern Intel Knight's landing architectures. Both the assembly of the system and the resolution have been parallelized with reasonable success. We will discuss optimal strategies that are specific to the KNL: fast finite element assemblies using AVX512 extensions, size and number of sub-domains, multiple right hand sides, efficiency of linear solves... Extension to hybrid parallelism i.e. using several KNL's will be discussed as well.

Seismic Assessment of Existing Structures: Contribution of In-Situ Measurements by Ambient Vibrations in the Design of Numerical Models

Cedric DESPREZ*

*IFSTTAR, Université Paris-Est Marne-la-Vallée 14-20 bd Newton, cité Descartes, 77447 Marne la vallée

ABSTRACT

Seismic assessment of existing structures is a major issue of civil engineering. Indeed, many constructions built before seismic requirement codes are located in moderate or important seismic areas. Expectations are high regarding the preservation of human life, strategic installations, economic activities and cultural heritage. The numerical modeling is often used to perform an advanced vulnerability assessment. In this context, the level of precision sought highly depends on the knowledge got on the considered construction; this knowledge being often lacunars. Based on several case-studies, this paper highlights the value of structural measurements by ambient vibrations in the design of a numerical mock-up and the resulting analysis. The first case study concerns a reinforced concrete building built in the 1960s for which a vulnerability analysis was carried out on the basis of a multifibre beam finite element model. The second case concerns the evaluation of a hydroelectric concrete gravity dam before and after retrofitting work. The modeling was carried out with finite three-dimensional elements. The third case focuses on the application of this type of measures in the context of the simplified modeling of masonry heritage monuments. For each of these cases, datas obtained from the in-situ measurements were particularly interesting since they notably allow accessing the modal characteristics of the structures or sub-structures; high value factor in the response of a structure. The application of this technology to various typologies of constructions demonstrates its robustness and the associated perspectives in terms of representativeness in numerical modeling.

A New Solid-shell Finite Element Dedicated to Non-linear Thin-to-thick Structures - Application to Energy Production Facilities and Safety Structures

Mouhamadou DIA*, Nahiene Hamila**, Anthony Gravouil***, Dzifa Kudawoo****

*Energie de France (EDF), **Univ Lyon, INSA Lyon, CNRS, Lamcos 5259, France, ***Univ Lyon, INSA Lyon, CNRS, Lamcos 5259, France, ****Energie de France (EDF)

ABSTRACT

Thin or thick shell like structures are naturally present in most industrial structures and particularly in nuclear power plants such as pipes, tanks, reactor-buildings, to name just a few. Their mechanical modeling imply to describe properly shell kinematics and to capture accurately through-thickness phenomena, as the calculations to be carry out can be highly non-linear. To satisfy those requirements, solid-shell elements are a good option. In the present contribution the solid-shell element initially formulated in small deformation [1] is extended to large deformations adapted for modeling non-linear effects combined with contact and elastic-plastic behavior. This solid-shell element has nine nodes: eight located at the vertex and the ninth placed at the element center. The middle-node is endowed with only one degree of freedom, in the thickness direction, allowing the assumption of a quadratic interpolation of the transverse displacement. Unlike solid-shell finites elements reported previously in the literature [2] and formulated under the hypothesis of plane stress, the new solid-shell element here mentioned uses a complete three-dimensional constitutive law [3], thanks to the middle-node. Moreover, to handle the various locking problems that usually arise on solid-shell formulation, the reduced integration technique is used as well as the assumed shear strain method. Finally to assess the effectiveness and performance of this new formulation, we will investigate a set of popular benchmark problems, involving geometric non-linear analysis as well as elastic-plastic behavior. [1] Bassa, B., Sabourin, F., & Brunet, M. (2012). A new nine-node solid-shell finite element using complete 3D constitutive laws. *International Journal for Numerical Methods in Engineering*, 92(7), 589-636. [2] Abed-Meraim, F., & Combescure, A. (2001, June). SHB8PS a new intelligent assumed strain continuum mechanics shell element for impact analysis on a rotating body. In 1st MIT Conference. [3] Sansalone, M., Sabourin, F., & Brunet, M. (2011). A new shell formulation using complete 3D constitutive laws. *International Journal for Numerical Methods in Engineering*, 86(6), 688-716.

Simulation of a Dam Behaviour with a Damage Model

Sébastien DOMITILE*, Romain TAJETTI**

*EDF - CIH, **EDF - CIH

ABSTRACT

The Brévières dam is located in French Alps and at immediate downstream of Tignes dam. It represents one of the closure structures of Malgovert water intake. This dam is a movable weir made in concrete and masonry of 24 meters height and 17 meters wide above the foundation. It's composed of three passes equipped with gates and bounded by four piles put on concrete slab. The foundation on dam lies on rock on its sides and on a breach made of crushed materials in the center. Displacements of the rock sides cause valley tightening bringing important displacements of dam and significant forces. This situation led to dam collapse mechanisms reflected by very important cracks. The dam has been auscultated by topography since 1994. The dam behavior is characterized by a shortening of bank in bank and an elevation of right bank compared to the left. The set of these phenomena are involved to the difficulties to operate gates for flood releases. Number of studies have been developed to understand tightening mechanisms and to find solutions to ensure the operation of the spillways without success in the long term. Thus, we have decided to model the dam and its surrounding to simulate its passed behavior until 2016 and predict its evolution with the aim to integrate some reparation solutions in the model to evaluate them and to ensure efficiency at long term. The works were modelled with a hexahedral volumetric mesh through Nx V9 and performed with ASTER. The movements of foundation are traduced by imposed displacements of nodes. A first model was based on linear elastic approach coupled with contact law. It showed a good representation between the model and auscultations. Stresses analysis explained the disorders observed on dam. Nevertheless the range of actual stresses couldn't ensure the validity of elastic model for predicting behavior of dam. We have decided to use a damage model to simulate future behavior in relation to the solutions for remedial works. The constitutive law used is the damage concrete law developed by EDF-CIH and LMDC of Toulouse University. The results of this simulation were better in comparison with elastic model. They gave predicting displacements of fixed supports of gates for different scenarios of civil works. This study provides an example of damage models use to improve decision aid.

Multiscale Topological Design of Heterogeneous Materials and Structures without Scale Separation

Daicong Da^{*}, Julien Yvonnet^{**}, Liang Xia^{***}, Min Vuong Le^{****}, Guangyao Li^{*****}

^{*}Université Paris-Est, ^{**}Université Paris-Est, ^{***}Huazhong University of Science and Technology, ^{****}Université Paris-Est, ^{*****}Hunan University

ABSTRACT

Most existing literature on multiscale topology optimization, e.g. tailoring the topology of material microstructures for the concurrently designed macrostructures in terms of structural stiffness, using the classical homogenization method to bridge the microscopic and macroscopic scales. However, the classical homogenization method assumes separation between two scales, i.e., the material microstructures are assumed to be infinite small, resulting the optimally designed microscopic structures by this scheme can't be manufactured. To this end, this work put forward a new multiscale topology optimization framework in a context of non-separated scales to obtain the optimal material microstructures with manufacturable details. A nonlocal filter-based homogenization approach capable of dealing with the heterogeneous materials and structures without scale separation is adopted to perform the multiscale computations. The constitutive relationship at the higher scale is derived by a fully microscopically-based framework to account the heterogeneous details, and the effective local fields can be reproduced by solving the structural problem at higher scale on a coarse mesh only, resulting the degree of freedom greatly reduced. On the other hand, a computationally efficient sensitivity formulation with all information of local fields is derived to perform the topology optimization design. Finally, several numerical benchmark examples are presented to demonstrate the effectiveness of the proposed method. The presented work then provides a very promising tool to design manufacturable microscopic structures within multiscale topology optimization framework. [1] J. Yvonnet, G. Bonnet, A consistent nonlocal scheme based on filters for the homogenization of heterogeneous linear materials with non-separated scales, *Int. J. Solids. Struct.* (2014) [2] A. Tognevi, M. Guerich and J. Yvonnet, A multi-scale modeling method for heterogeneous structures without scale separation using a filter-based homogenization filter, *Int. J. Numer. Meth. Engng* (2016)

Virtual Manufacturing and Performance Coupling for Endless Fibre Reinforced Plastics – A General Concept

Patrick Da Luca^{*}, André Berger^{**}

^{*}ESI Group, ^{**}Dr.

ABSTRACT

Due to their superior strength to density ratio fibre reinforced plastics (FRP) provide a high performance for energy dissipating parts and are consequently ideal for lightweight design for crashworthiness. However, due to the complex inner structure of FRP parts the prediction of the mechanical behaviour in simulation under crash loading is still challenging. Using multi-scale approaches taking into account different level of information, like micro-scale and meso-scale offer new possibilities but also provide new challenges. How to get a proper virtual model of the complex fibre architecture on meso-scale? How to identify predictive mechanical properties on micro-scale? Therefore, this presentation will demonstrate a general modular concept for the derivation of the complex inner fibre structure of FRP based on manufacturing simulation and the determination of fracture curves using virtual testing on micro-scale. The latter is subsequently used to determine the parameters of PUCK's law for inter-fibre fracture. Finally, the two approaches are combined to demonstrate the potential of a multi-scale-approach for a filament wound tube under axial crash loading by comparing the results obtained by simulation with experimental data. In addition, it will be shown how the approach can be used to represent various manufacturing processes i.e. braiding or different base materials.

Adaptive Inexact Semismooth Newton Methods for the Contact Problem between Two Membranes

Jad Dabaghi^{*}, Martin Vohralik^{**}, Vincent Martin^{***}

^{*}Inria Paris & CERMICS (ENPC), ^{**}Inria Paris & CERMICS (ENPC), ^{***}Université technologie de Compiègne (UTC)

ABSTRACT

We propose an adaptive inexact version of a class of semi-smooth Newton methods. As a model problem, we consider the system of variational inequalities describing the contact between two membranes and its conforming finite element discretization. Any iterative linearization algorithm like the Newton-min, Newton-Fisher Burmeister is taken into account, as well as any iterative linear algebraic solver. We prove an a posteriori error estimate between the exact solution and the approximate solution which is valid on any step of the linearization and algebraic resolution. Our estimate is based on flux reconstructions in discrete subspace of $\text{H}^{-1}(\text{div}; \Omega)$ and on potential reconstructions on discrete subspaces of $H^1(\Omega)$ satisfying the constraints. The estimate distinguishes the discretization, linearization, and algebraic components of the error and allows us to formulate adaptive stopping criteria for both solvers. Under these criteria, the local efficiency of our estimates is also established. Numerical experiments for the semi-smooth Newton-min algorithm in combination with the GMRES solver confirm the efficiency of the method.

High Order FEA of Proximal Humeri – Mechanical Response and Yield Prediction Validated by Experiments

Gal Dahan*, Zohar Yosibash**

*Tel Aviv University, **Tel Aviv University

ABSTRACT

While a major part of proximal humerus fractures are classified as non-displaced and can be treated non-operatively, the management of the displaced fractures remains a controversial matter. In such cases, the orthopedic surgeon is required to assess the fracture's stability, to determine if surgical intervention is needed. Nowadays, such clinical diagnoses are based on X-ray examination of the fracture and surgeon's personal experience. With the high incidence of proximal humerus fractures in the elderly, and the growing incidence of surgically treated fractures and revision surgeries [1], there is a need for a biomechanical-based quantitative tool that can assist the surgeons in the clinical decision-making process and in particular, in stability assessment. The first step towards this solution is obtaining a verified and validated high order FE (p-FE) model, compared to experimental observations of the mechanical response and fracture of proximal humeri. In [2] verified and validated p-FE models of humeri were presented, using empirical-based isotropic inhomogeneous material properties derived originally for the femur. In the in-vitro experiments used for validation, the humeri were also loaded to obtain fracture, and yield loads were compared to p-FE predictions using a maximum strain criterion. Since bone is known to be anisotropic, the p-FE models are enhanced to include orthotropic material properties. According to [3], based on voxel average rules for X-ray attenuation coefficient, and representing the bone by means of continuum micromechanics (MM), the orthotropic effective stiffness tensor can be calculated and a failure criterion at the trabecular level may be considered. REFERENCES [1] Bell J., Leung B.C., Spratt K.F., Koval K.J., Weinstein J.D., Goodman D.C. and Tosteson A. "Trends and Variation in Incidence, Surgical Treatment, and Repeat Surgery of Proximal Humeral Fractures in the Elderly". The Journal of Bone and Joint Surgery-American Volume, 93, 121–131, 2011. [2] Dahan G., Trabelsi N., Safran O. and Yosibash Z., "Verified and validated finite element analyses of humeri", Journal of Biomechanics, 49,1094-1102, 2016. [3] Hellmich C., Kober C., and Erdmann B. "Micromechanics-based conversion of CT data into anisotropic elasticity tensors, applied to FE simulations of a mandible". Annals of Biomedical Engineering, 36:1, 108-122, 2008.

Calibration and Factor Analysis of Particle Sandpile Process for Additive Manufacturing via Discrete Element Simulation

Ling Dai*

*Scientist

ABSTRACT

For modern additive manufacture, particle pouring and piling process at micron size scale is the fundamental procedure. Traditionally, at macro scale, the particle sandpile has been calibrated via measuring the bulk properties, such as repose angle, mechanical test, etc. Nowadays, the discrete element simulation tool shows strong power to provide deep understanding for the process and mechanism, significantly help to enhance our understandings for the modern additive manufacture technology. Here, we carried out a serial of discrete element simulations to model the particle dynamic process from pouring to sandpile formation under various conditions of friction, material property, damping and particle size. The results were calibrated with the sandpile geometry and packing density, aiming to the functional performance for additive manufacture. Through our investigation, we found that in order to obtain satisfactory piling morphology for following additive manufacturing process, we need to dominantly control both the sliding friction and rolling friction. The material property and damping conditions didn't much affect the pile morphology, but led to some side effects on the cost of computational aspects. The distribution of particle size presented charming mechanism, based on which extraordinary packing density could be achieved, which was significantly beneficial to the functional performance. In summary, our works provides an overall understanding of process and mechanism for particle pouring and piling procedure, which makes the fundamental contribution to the modern additive manufacture.

Application of the Haar Wavelet Method to Dynamic Stability Analysis of Truncated Conical Shells

Qiyi Dai^{*}, Qingjie Cao^{**}

^{*}Harbin Institute of Technology, ^{**}Harbin Institute of Technology

ABSTRACT

In this paper, the Haar wavelet method is employed to analyze the parametric instability of truncated conical shells under static and time dependent periodic axial loads. The present work is based on the Love first-approximation theory for classical thin shells. The displacement field is expressed as the Haar wavelet series in the axial direction and trigonometric functions in the circumferential direction. Then the partial differential equations are reduced into a system of coupled Mathieu-type ordinary differential equations describing dynamic instability behavior of the shell. Using Bolotin's method, the first-order and second-order approximations of principal instability regions are determined. The correctness of present method is examined by comparing the results with those in the literature and very good agreement is observed. The difference between the first-order and second-order approximations of principal instability regions for tensile and compressive loads is also investigated. Finally, numerical results are presented to bring out the influences of various parameters like static load factors, boundary conditions and shell geometrical characteristics on the domains of parametric instability of conical shells.

Implications of Mode of Control and Loading Rate on the Determination of Concrete Fracture Properties

Gilda Daissè*, Christian Carloni**, Roman Wan-Wendner***

*University of Natural Resources and Life Sciences, Vienna, Austria, **University of Bologna, Bologna, Italy,

***University of Natural Resources and Life Sciences, Vienna, Austria

ABSTRACT

Among all the parameters that characterize the concrete behavior, the fracture energy is one of the most crucial for the (numerical) investigation of damage propagation and failure in reinforced concrete members. Currently no standards exist that provide guidance to the characterization of concrete fracture properties. The experimental evaluation of fracture energy is influenced by different laboratory limitations, such as specimens' size [1] and mode of control during the fracture test. In order to investigate the differences between specimen geometries and evaluate the effect of mode of control on the fracture test, a numerical analysis supported by an experimental campaign and digital image correlation (DIC) is presented. The Lattice Discrete Particle Model (LDPM) [2] has been used to simulate concrete and to provide realistic crack patterns and crack widths. In the first part of the study the relationship between load point displacement rate, opening rate at the position of a surface-mounted extensometer, and actual strain rate at the crack tip are established for a number of specimen geometries and sizes by means of calibrated numerical simulations. For this purpose, the position of the crack tip is identified through an energetic approach. It is well-known that concrete is a visco-elastic material with strain-rate dependent fracture properties [3]. The potential influence of differences in loading rate on the determined fracture energy owing to these two phenomena is investigated in the second part, based on simulated three-point bending tests of differently sized specimens with two notch depths, loaded at different rates. The simulations are supported by an experimental campaign including Digital Image Correlation (DIC) data of the ligament area of beams loaded at different rates. The latter study has relevance both for the determination of a recommended loading rate and for permitting an acceleration range in the post-peak to shorten the test duration. References: [1] Bazant Z. and Kazemi M: Size dependence of concrete fracture energy determined by RILEM work-of-fracture method, *International Journal of Fracture*, 1991; 51(2):121-138. [2] Cusatis, G.; Pelessone, D.; Mencarelli, A. Lattice Discrete Particle Model (LDPM) for failure behavior of concrete. I: Theory. *Cem. Concr. Compos.* 2011,33, 881–890. [3] F. P. Zhou (1992). Time dependent crack growth and fracture in concrete. Ph.D thesis, Lund Univ. of Technology, Lund, Sweden.

A Nonlinear Mechanical Model for Soft Robot Arms

Francesco Dal Corso^{*}, Costanza Armanini^{**}, Diego Misseroni^{***}, Davide Bigoni^{****}

^{*}University of Trento, ^{**}University of Trento, ^{***}University of Trento, ^{****}University of Trento

ABSTRACT

The key to the mechanical design of soft structures lies in the development and use of nonlinear models, among which, the Kirchhoff rod which allows for the description of large deflection of elastic one dimensional structures. With reference to a planar setting, a basic model of soft robot arm is presented as a cantilever beam, with its free end subject to a dead load, and constrained by a continuously rotating clamp. The problem is addressed through new theoretical, numerical, and experimental developments providing design principles to be exploited towards the achievement of targeted positions for the load and the realization of snap mechanisms. More specifically, the considered system behaves as an elastica compass, so that smooth transitions of the deformed shape are observed and the free end traces a closed curve, which approaches a circle as the stiffness of the rod is increased. Differently, when the load is higher than that leading to buckling, an unstable configuration is reached at a specific value of the clamp angle and the rod displays a snap back instability. An analytical model is developed to predict the critical clamp angle for which the snap back occurs, while the subsequent dynamic motion is simulated through a specific numerical model. The reliability of the theoretical predictions is finally validated through experimental tests performed on physical models. Acknowledgements: Support from the ERC Advanced Grant Instabilities and non-local multiscale modelling of materials 340561-FP7-PEOPLE-IDEAS-ERC-2013-AdG (2014-2019) is gratefully acknowledged.

Multi-body Moving Mesh Approach to Efficiently Handle Large Displacements of Immersed Complex Geometries

Wafa Daldoul^{*}, Elie Hachem^{**}, Youssef Mesri^{***}

^{*}MINES ParisTech - CEMEF - CFL research group, ^{**}MINES ParisTech - CEMEF - CFL research group, ^{***}MINES ParisTech - CEMEF - CFL research group

ABSTRACT

The CFD simulations involving moving bodies undergoing large displacements represent a real challenge. These simulations, which combine the difficulties, related to instability, meshing and Fluid-Structure Interaction are generally difficult to perform and have a high computational cost. In this work we propose an efficient "r-to-h" adaptation algorithm for moving boundaries problems using only vertex displacements and local h-adaptation operations. It is based on the Inverse Distance Weighting (IDW) interpolation method combined with a selective h-adaptation. It involves local mesh modifications such as edge flipping, local refinement and local coarsening for only badly-shaped elements. The developed approach is tested and validated on multi-body simulations with turbulent flows interactions.

Patient-Specific Bicuspid Aortic Valve Finite-Element Models with Raphe

Jérémy Dallard^{*}, Michel Labrosse^{**}, Benjamin Sohmer^{***}, Carsten Beller^{****}, Munir Boodhwani^{*****}

^{*}Department of Mechanical Engineering, University of Ottawa, Canada, ^{**}Department of Mechanical Engineering, University of Ottawa, Canada, ^{***}Division of Cardiac Anesthesiology, University of Ottawa Heart Institute, Canada, ^{****}Department of Cardiac Surgery, University of Heidelberg, Germany, ^{*****}Division of Cardiac Surgery, University of Ottawa Heart Institute, Canada

ABSTRACT

Introduction: The aortic valve is normally composed of three cusps. However, in one common lesion, two cusps are fused together, generating closure malfunction and back-flow. In such bicuspid aortic valves (BAV), the conjoined area of the fused cusps is termed raphe. There is a need to better understand BAV biomechanics, with direct applications in surgery. However, the geometry and material properties of the raphe, and the mechanical influence of the raphe on BAV function have not been studied, nor has the patient-specific modeling of BAV been considered [1,2]. The present study aims to propose improvements on both aspects. **Methods:** Three patient-specific FE models of BAVs (average age 60 yrs) were created based on measurements obtained from 3D trans-esophageal echocardiography and assuming age-dependent material properties [3]. The FE models were run assuming that the raphe material properties were identical to the cusps's. The unpressurized valve geometry was determined by an iterative shrink-pressurize algorithm to minimize the error between seven measured vs. computed geometrical parameters [3]. Two levels of model validation were used: 1) the pressurized computed geometry of the BAV was compared to that observed from medical imaging (anatomical validation); 2) measured vs. computed geometric parameters used in clinical routine were compared to validate the BAV function in terms of its dynamics and pathology mechanism (functional validation). Finally, rigid raphe were also tried to assess the impact of the raphe's stiffness on the cusps's motion. **Results:** The pathology was successfully reproduced in the FE models of all three patients. The combined average errors for the three cases were 1.5% for the anatomical validation, 11.6% for the functional validation of cusps motion based on 12 different measurements, and 34.5% for the functional validation based on the quantification of the valve opening area. Mechanical stress transmission from the fused cusps to the aortic wall was observed through the raphe. As measured from geometric parameters used in clinical routine, a rigid raphe decreased cusp motion along the valves axis by 77% and was not consistent with observations from medical imaging. **Conclusion:** The first age-dependent BAV patient-specific models with raphe were created and analyzed. The findings support the use of material properties for the raphe that are identical to the cusps's. **References:** [1] Conti CA et al. (2010) The Journal of thoracic and cardiovascular surgery 140(4):890-896. [2] Fedak PW et al. (2002) Circulation 106(8):900-904. [3] Labrosse MR et al. (2015) Medical image analysis 20(1):162-172.

A Mathematical Model of Extravascular Platelet Aggregation

Nicholas Danes*, Karin Leiderman**

*Colorado School of Mines, **Colorado School of Mines

ABSTRACT

Platelet aggregation is an essential part of hemostasis, the process to stop bleeding in response to a vascular injury. The local hemodynamics and the nature of the injury can affect size, structure and formation time of a platelet aggregate. Our previous models were restricted to study intravascular clot formation, which is confined to the interior of a single vessel. Here, we develop a mathematical model of extravascular platelet aggregation that has been iteratively developed with an experimental microfluidic device. Our previous model of platelet aggregation is extended to include a transiently bound platelet species and a new description for the limited transport of platelet densities using the finite element method. The setup includes two channels in parallel, a blood and a wash channel, connected by an “extravascular” injury channel. Separate flow rates are imposed at the inlets of the two parallel channels to force blood through the injury channel and exit through the outlet of the wash channel. The injury channel is coated with small proteins that initiate platelet aggregation. Under various shear rates, hematocrits and platelet counts, computational estimates of occlusion times, flow fields, and platelet aggregate porosities are compared to experimental measurements. We find that the timing and spatial distribution of extravascular platelet aggregates are sensitive to these variations.

An Adaptive hp-Refinement Strategy with Inexact Solvers and Computable Guaranteed Bound on the Error Reduction Factor

Patrik Daniel^{*}, Alexandre Ern^{**}, Martin Vohralík^{***}

^{*}Inria Paris & Université Paris-Est, CERMICS (ENPC), ^{**}Université Paris-Est, CERMICS (ENPC) & Inria Paris,

^{***}Inria Paris & Université Paris-Est, CERMICS (ENPC)

ABSTRACT

In this work we extend our recently proposed adaptive refinement strategy for hp-finite element approximations of elliptic problems by taking into account an inexact algebraic solver. Namely, on each level of refinement and on each iteration of an (arbitrary) iterative algebraic solver, we compute guaranteed a posteriori error bounds on the algebraic and the total errors in energy norm. For the algebraic error upper bound, we crucially exploit the nested hierarchy of hp-finite element spaces created throughout the adaptive algorithm, whereas the total error bound is computed using the finest space only. These error bounds allow us to formulate adaptive stopping criteria for the algebraic solver ensuring that the algebraic error does not significantly contribute to the total error. Next, we use the total error bound to mark mesh vertices for refinement via Dörfler's bulk-chasing criterion. On patches associated with marked vertices only, we solve two separate primal finite element problems with homogeneous Dirichlet boundary conditions, which serve to decide between h-, p-, or hp-refinement. Altogether, we show that these ingredients lead to a computable guaranteed bound on the ratio of the total errors of the inexact approximations between successive refinements (the error reduction factor), when the stopping criteria are satisfied. Finally, in a series of numerical experiments, we investigate the practicality of the proposed adaptive solver and the accuracy of our bound on the reduction factor.

High-Order Finite Element Methods for Efficient High-Rate Lumped-Mass Explicit Modeling

Kent Danielson^{*}, Mark Adley^{**}, Neil Williams^{***}, Eric Lynd^{****}

^{*}Geotechnical & Structures Laboratory, U.S. Army Engineer Research and Development Center, ^{**}Geotechnical & Structures Laboratory, U.S. Army Engineer Research and Development Center, ^{***}Geotechnical & Structures Laboratory, U.S. Army Engineer Research and Development Center, ^{****}Geotechnical & Structures Laboratory, U.S. Army Engineer Research and Development Center

ABSTRACT

This presentation discusses the recent advances in higher-order finite elements for lumped-mass explicit approaches typically needed for high-rate weapons effects modeling. Topics include benefits of 2nd order tetrahedral, wedge, and hexahedral element formulations for both compressible and nearly incompressible materials as well as at higher orders, superconvergence and variable extraction, and efficient explicit time solution methods. These technologies are included in ERDC-GSL in-house meshing (ProMesher), parallel analysis (ParaAble), and visualization (PenView) codes as well as implementations into popular meshing (Cubit), parallel analysis (EPIC), and visualization (ParaView) software freely and readily available to DoD and other government agencies. These elements have also been linked with several integration schemes to the ERDC-GSL PENCURV cavity expansion-based penetration resistance functions for deformable penetrator trajectory simulation within both the ParaAble and EPIC codes. These capabilities are also incorporated into comprehensive and seamless modeling capabilities, computed serially or by launching massively parallel Linux/Unix jobs, all within the PENCURV+ Windows GUI and framework. The benefits for shape optimization and large tradespace analyses are also demonstrated.

Tunable Seat Belt Behavior in Nanocomposite Interfaces Inspired from Bacterial Adhesion Pili

Kerim Dansuk*, Sinan Keten**

*Northwestern University, **Northwestern University

ABSTRACT

A challenging problem in designing nanocomposites is to engineer nanoparticle interfaces that have tunable cohesive strength and rate-responsive behavior, for which inspiration can be taken from biological systems. An exemplary bio-interface is the Chaperone-Usher (CU) pili, such as type 1 expressed by bacteria *Escherichia coli*. The pili have unique biomechanical properties that enhance the ability of bacteria to sustain attachment to surfaces under large stresses, such as constant force extensibility, logarithmic velocity-uncoiling force dependence, and adhesive tips with catch bond behavior that exhibit longer bond life-times at greater force levels. Although biophysics of the pili under strain/stress is well-studied for anti-infective applications that aim to compromise pili adhesion, utilizing the biomechanical properties of the pili in material design applications is yet to be explored. In this work, we have modeled the elongation of a single CU pilus with catch bond tip adhesin and examined its toughness response using Monte Carlo simulations. We showed that the pilus can act as a “molecular seat belt” that exhibits low toughness when pulled slowly and high toughness when pulled rapidly. Furthermore, we found that systematically varying the catch bond and shaft parameters leads to tunable seat belt behavior at the interface, where the sharpness of the transition from the low toughness to the high toughness regime and the velocity at the start of the transition can be dictated by molecular design parameters. Lastly, we test the performance of CU pilus in slowing down a fast particle, and reveal that pili can effectively stop micron size projectiles with high initial velocities. The molecular seat belt mechanism presented here provides insight into how nanocomposite interfaces can be engineered to create molecular networks with linkers that switch on or off depending on strain rate.

Modeling Uncertainty and Propagation of Data in Rigid Musculoskeletal Simulation: Unavoidable Best Practice for Translating Models to Clinical Routine Practice

Tien Tuan Dao*, Marie Christine Ho Ba Tho**

*Université de technologie de Compiègne, France, **Université de technologie de Compiègne, France

ABSTRACT

Rigid musculoskeletal simulations have been intensively investigated to estimate joint kinematics, loading, and muscle forces for clinical decision support [1]. However, the use of these simulation outcomes in clinical routine practice remains a challenging issue. Data uncertainty due to human variabilities, differences in experimental protocols and measuring techniques is one of the possible causes affecting on the reliability of simulation outcomes. In this talk, current knowledge, limitations and future challenges related to this important issue will be presented. In particular, we will present recent achievements from our group using precise and imprecise probabilities to model data uncertainties related to segmental and muscle properties [2]. Advanced data fusion has been also developed to reduce data uncertainties [3]. Data uncertainty of dependent parameters has been taken into consideration using copulas. Model uncertainty has been also quantified. Demonstrations of developed methodologies will be focused on rigid musculoskeletal models of the lower limbs. Propagation of data uncertainties on the joint loading and muscle force estimation will be also presented. In fact, accounting data and model uncertainties become unavoidable best practice for translating the developed models and associated simulation outcomes into clinical routine in the framework of in silico medicine. Keywords: Data uncertainty, model uncertainty, uncertainty modeling, uncertainty propagation, rigid musculoskeletal modeling, reliable simulation outcomes. Acknowledgements This work was carried out in the framework of the Labex MS2T, which is funded by the French Government. References [1] TT Dao, F Marin, P Pouletaut, P Aufaure, F Charleux, M C Ho Ba Tho (2012). Estimation of Accuracy of Patient Specific Musculoskeletal Modeling: Case Study on a Post Polio Residual Paralysis Subject. *Computer Method in Biomechanics and Biomedical Engineering* 15 (7): 745-751. [2] TT Dao, MC Ho Ba Tho (2015). Assessment of Parameter Uncertainty in Rigid Musculoskeletal Simulation using a Probabilistic Approach. *Journal of Musculoskeletal Research*, Vol. 18, No. 3 (2015) 1550013. [3] TT Dao, MC Ho Ba Tho (2017). A Consistent Data Fusion Approach for Uncertainty Quantification in Rigid Musculoskeletal Simulation. *Journal of Mechanics in Medicine and Biology*. 17(4), 1750062

Simulation of Dynamic Damage Evolution due to Micro-cracking in Quasi-brittle Materials

Nitin Daphalapurkar^{*}, Darby Luscher^{**}, Daniele Versino^{***}

^{*}Los Alamos National Laboratory, ^{**}Los Alamos National Laboratory, ^{***}Los Alamos National Laboratory

ABSTRACT

Simulations incorporating micro-cracking-based damage model are used to elucidate dynamic compressive response of a quasi-brittle material permeated by spatially evolving wing-cracks. Effective elastic compliance considers mechanism of wing-crack activation from pre-existing flaws, which are characteristic of flaw-sensitive quasi-brittle materials (e.g. energetic and geological materials). Increment in macroscale compliance due to growth of a single planar wing-crack is used for calculation of damage strain. Constitutive model incorporates evolution of effective compliance and tensorial damage, which is in turn driven by the growth of planar wing-cracks. Model is demonstrated by comparing results predicted from simulations with measurements from high-rate experiments.

Scattering Problem at an Interface Using Bloch Wave Theory: Application to Seismic Metamaterials

Michaël Darche^{*}, Denis Aubry^{**}, Fernando Lopez-Caballero^{***}, Bing Tie^{****}

^{*}CentraleSupélec, Paris-Saclay University, ^{**}CentraleSupélec, Paris-Saclay University, ^{***}CentraleSupélec, Paris-Saclay University, ^{****}CentraleSupélec, Paris-Saclay University

ABSTRACT

To assure the stability of constructions to a seismic perturbation or vibration, there are a lot of different types of waves that should be suppressed or at least reduced, for example the surface waves induced by a railway. Instead of the traditional systems installed on existing construction, there is an increasing interest for para-seismic protections modifying the soil around the area where the waves have to be attenuate with barrier or periodic inclusions. Different methods have been used to study these problems (e.g. finite elements, Floquet theory, etc.). We want to propose an alternative approach based on Bloch wave theory. This approach uses the periodicity of a physical lattice to give periodic transformed responses on Bloch mode from any solution. Contrary to a fully simulation using finite element among others, we need only to identify the eigenvalues and the eigenmodes on a primitive cell to evaluate the behavior on the whole lattice due to its periodicity. It allows to reduce considerably the size of the numerical model. With the analysis of the dispersion curves, some frequency bandgaps could appear depending on the lattice parameters and the medias properties. These gaps provide informations on the diffraction of the wave through the inclusions. Moreover the scattering problem which appears at the boundary between the periodic media and the homogeneous one has also been treated as well because Bloch theorem usually works for infinite medias. On account of the complexity of this part, the problem is applied to acoustic wave propagation through a plane interface between the semi-infinite medias. Analytical results are shown considering some basic arrays. To validate the model, some cases will be tested and compared with existing numerical and experimental results. A parametric study concerning the effect of the number of inclusions and the contrast of rigidity between the soil and the inclusion on the bandgaps apparition is done.

Convolved Action Principles and Space-Time Finite Element Methods for Elastodynamics

Gary Dargush*, Georgios Apostolakis**

*University at Buffalo, SUNY, **University of Central Florida

ABSTRACT

The appearance of temporal convolutions in the reciprocal theorem for dynamical problems leads naturally to the development of mixed convolved action principles (Dargush and Kim, 2012), as an extension of work by Gurtin, Tonti and Oden and Reddy (1984). For linear continuum elastodynamics, the governing equations written in terms of displacements and stress impulses display an elegant symmetry that can lead to the formulation of stationary action principles, similar to those associated with Hamilton, except using temporal convolution rather than an inner product over the time interval. As a result, the issues with Hamilton's principle relating to end point constraints and dissipative phenomena are resolved. Remarkably, the stationarity of the mixed convolved action provides not only the governing partial differential equations, but also the specified boundary and initial conditions, as its Euler–Lagrange equations. Thus, the entire elastodynamic initial/boundary value problem is encapsulated in a scalar mixed convolved action functional written in terms of displacements and stress impulses. Furthermore, the convolved action provides the foundation for the development of true space-time finite element methods (Dargush et al., 2015). In this presentation, our previous work is extended to formulate a minimum principle for the discretized convolved action, along with an interesting maximum principle for discretized complementary convolved action. New finite element methods are developed for each of these two principles and several prototype examples are examined and compared. Oden JT, Reddy JN (1983) Variational Methods in Theoretical Mechanics. Springer, Berlin. Dargush GF, Kim J (2012) Mixed Convolved Action. Phys. Rev. E 85, 066606. Dargush GF, Darrall BT, Kim J, Apostolakis G (2015) Mixed Convolved Action Principles in Linear Continuum Dynamics, Acta Mechanica, 226(12), 4111-4137.

Goal-Oriented hp-Adaptivity Using Unconventional Error Representations

Vincent Darrigrand^{*}, David Pardo^{**}, Théophile Chaumont-Frelet^{***}, Ignacio Muga^{****}, Serge Prudhomme^{*****}

^{*}Basque Center for Applied Mathematics (BCAM), ^{**}University of the Basque Country (UPV-EHU), ^{***}Basque Center for Applied Mathematics (BCAM), ^{****}Pontificia Universidad Católica de Valparaíso (UPCV), ^{*****}École Polytechnique de Montréal

ABSTRACT

An increasing number of engineering applications require a good accuracy of a given quantity of interest. The design of a mesh that provides the desired precision is therefore crucial. Goal-oriented adaptive methods provide such meshes. To represent the error in the quantity of interest with local and computable indicators, one computes the influence function by solving the adjoint problem with the (continuous linear) quantity of interest as the source. Errors in the primal and adjoint solutions applied to the adjoint operator provide the error representation. We introduced in [1, 2, 3] an alternative error representation with the use of an alternative operator that allows us to compute a Riesz representation of the error of the adjoint problem. If the alternative operator is selected as the original operator of the adjoint problem, we recover the classical method. This method can be applied to a wide range of problems of any dimension. While we previously studied a purely p-adaptive process, the topic of this presentation will focus on applying the alternative error representation to h- and hp-adaptive processes. Mesh coarsening will also be considered during the adaptive process. Numerical examples will be drawn from multi-dimensional (2D) problems such as the Helmholtz or convection-dominated diffusion problems. References: [1] V. Darrigrand, D. Pardo, and I. Muga. Goal-oriented adaptivity using unconventional error representations for the 1D Helmholtz equation. *Computers & Mathematics with Applications*, 69(9):964–979, 2015. [2] V. Darrigrand, A. Rodríguez-Rozas, I. Muga, D. Pardo, A. Romkes, and S. Prudhomme. Goal-oriented adaptivity using unconventional error representations for the multi-dimensional Helmholtz equation. *International Journal for Numerical Methods in Engineering*, 113(1):22–42, 2018. [3] V. Darrigrand, A. Rodríguez-Rozas, D. Pardo, and I. Muga. Goal-oriented p-adaptivity using unconventional error representations for a 1D steady-state convection-diffusion problem. *Procedia Computer Science*, 108:848–856, 2017. International Conference on Computational Science, ICCS 2017, 12-14 June 2017, Zurich, Switzerland.

Real-space Electronic Structure Studies on the Energetics of Dislocations in Al-Mg Materials System and Its Connection to Mesoscale Models

Sambit Das*, Vikram Gavini**

*University of Michigan, **University of Michigan

ABSTRACT

We study the dislocation core in Aluminum and Magnesium using a local real-space formulation of orbital-free density functional theory, implemented using finite-element discretization. The framework enables direct calculation of isolated dislocation core energetics. So far our studies on edge [1,2] and screw [3] dislocations in Aluminum, and ongoing studies in Magnesium, suggest that the core size—region with significant contribution of electronic effects to dislocation energetics—is around seven to ten times the magnitude of the Burgers vector. This is in stark contrast to estimates based on atomic displacements. Interestingly, our study further indicates that the core-energy of the dislocations are strongly dependent on external macroscopic strains. Role of such core-energetics behaviour towards the low ductility of Magnesium in the c-axis is currently being investigated. Next, we use the electronic structure core energetics information to inform higher scale models. In particular, we develop a continuum energetics model for a discrete dislocation network, which accounts for the core energy dependence on macroscopic deformations, and from the variations of the core energy with respect to the nodal positions of the network, we obtain the nodal core force [3] which can directly be incorporated into discrete dislocation dynamics frameworks. This nodal core force includes contributions that are not accounted for in currently used discrete dislocation dynamics models which assume the core energy to be a constant excepting for its dependence on the dislocation line orientation. Using static case studies involving simple dislocation structures, we demonstrate that these additional contributions can be significant in comparison to the elastic Peach-Koehler force even up to distances of 10-15 nm between dislocation structures. Furthermore, we have incorporated the nodal core force into a 3-D dislocation dynamics implementation, where we are investigating the influence of core effects on elementary mechanisms of dislocation enabled hardening in Aluminum such as structure and strength of various dislocation junctions, critical passing stress around obstacles etc. [1] Iyer, M., Radhakrishnan, B., Gavini, V., 2015. Electronic-structure study of an edge dislocation in Aluminum and the role of macroscopic deformations on its energetics. J. Mech. Phys. Solids 76, 260–275. [2] Das, S., Iyer, M., Radhakrishnan, B., Gavini, V., 2016. Corrigendum to [1]. J. Mech. Phys. Solids 95, 428–429. [3] Das, S., and Gavini, V., 2017. Electronic-structure study of a screw dislocation in Aluminum and the role of macroscopic deformations on its energetics. J. Mech. Phys. Solids 104, 115–143.

Finite-Strain Homogenization Models for Multi-Scale Porous Viscoplastic Polycrystals and Applications

Shuvrangs Das*, Dawei Song**, Pedro Ponte Castañeda***

*University of Pennsylvania, **University of Pennsylvania, ***University of Pennsylvania

ABSTRACT

We formulate constitutive models for the finite-strain macroscopic response of porous viscoplastic polycrystals using the recently developed iterated second-order homogenization method [1]. The model is then used to estimate the effective behavior under various types of loadings, with special attention to simple shear and pure shear strain loadings. The porous polycrystal is modeled as a two-scale composite, where large voids are distributed randomly in a fine-grained polycrystalline matrix with the grains described by single-crystal viscoplasticity. The method constructs a linear comparison composite (LCC) with material properties chosen via a suitable variational statement and the same sub-structure as the actual nonlinear composite. In turn, the macroscopic response of the two-scale LCC is derived by means of a sequential homogenization procedure, utilizing the self-consistent estimates for the effective behavior of the polycrystalline matrix and the Willis estimates for the effective behavior of the porous composite. The iterated homogenization improves over the non-iterated estimates, especially at low porosities, high nonlinearities and high triaxialities, by allowing a finer “discretization” of the matrix and, thereby reproducing the matrix behavior accurately. In addition, consistent homogenization estimates for the average strain rate and spin fields in the voids and grains are used to develop evolution laws for the sub-structural variables, including the porosity, void shape and orientation, as well as the “crystallographic” and “morphological” textures of the underlying matrix. The model then is used to generate estimates for both the instantaneous effective response and the evolution of the microstructure for porous FCC and HCP polycrystals under simple shear and pure shear strain loadings. The effect of macroscopic vorticity is deduced by comparing the evolutions of sub-structural variables and macroscopic response for simple shear with corresponding results for pure shear loading (no macroscopic rotation). The effects of textures on the effective behavior are demonstrated by comparing with the effective response of porous isotropic materials. The textures have hardening effects and the vorticity has softening effects on the macroscopic response, and their interactions result in complex behavior of the effective response. In addition, more general loading conditions, involving combined tension and shear, are considered to explore the effect of the stress triaxiality on the macroscopic hardening or softening for the porous polycrystals. Reference: [1] Song, D. and Ponte Castañeda, P., 2017. A finite-strain homogenization model for viscoplastic porous single crystals: I—Theory. *Journal of the Mechanics and Physics of Solids*, 107, pp.560-579.

New Bounds on Tangential Constitutive Elasticity Matrix for Non-Linear Elastic Materials: A Multiscale Approach

Sonjoy Das^{*}, Sourish Chakravarty^{**}

^{*}University at Buffalo, ^{**}Massachusetts Institute of Technology

ABSTRACT

A novel multiscale framework is proposed in this work to determine two matrix-valued bounds on the macroscopic tangential constitutive elasticity matrix for nonlinear elastic materials. The two bounds reflect the effects of underlying heterogeneous microstructures and are obtained by considering a small mesoscopic material volume element that is smaller than the classical representative volume element. This small mesoscopic material volume element not only includes multiple phases of materials but may also contain multiple microcracks which can be potentially dangerous and lead to catastrophic structural calamities or poor structural performance if not detected in time since they merge together to form macro-level cracks. The theoretical argument given in a previous work [1] for small deformation linear elasticity theory is extended in the present work. Two special uniform incremental boundary value problems on the small mesoscopic material volume element, that is finitely deformed and assumed to be in a state of uniform macroscale deformation gradient, are proposed to construct the matrix-valued bounds on the macroscopic tangential constitutive elasticity matrix. Micromechanical analyses based numerical procedure is outlined to evaluate the matrix-valued bounds for the macroscopic material property. The proposed method is demonstrated by the evaluating the bounds for a small material volume element with nonlinear elastic microstructures and several microcracks that induce heterogeneity and anisotropy in the macroscopic tangential constitutive elasticity matrix. It will be useful to characterize the heterogeneous nonlinear elastic materials such as metals, composites, and polymers that may include microcracks. Bibliography [1]. Huet, C., 1990. Application of variational concepts to size effects in elastic heterogeneous bodies. J. Mech. Phys. Solids 38 (6), 813–841.

Computationally Effective Lubrication Theory Based Modeling of Cerebrospinal Fluid in Brain Mechanics during Impact on Head

Sonjoy Das*, Abhishek Venketeswaran**

*University at Buffalo, **University at Buffalo

ABSTRACT

Finite element head models (FEHM) are increasingly used to gain insights into the mechanisms of traumatic brain injury (TBI). An important component in this context is the realistic modeling of the flow of cerebrospinal fluid (CSF) at the interface of the skull and brain. The CSF is contained in a chamber known as sub-arachnoid space (SAC). One vital function of the CSF is to absorb some energy during head impact and protect the brain inside the skull. Existing FEHM in the literature characterizes the CSF as a nearly incompressible solid with low shear modulus, to bypass the challenges and computational cost associated with the coupling between a solid mechanics solver (for skull and brain) and a fluid mechanics solver (for CSF). The present work develops a theoretical framework to characterize the CSF flow and the dynamics of the brain and skull motion resulting from an impact to the skull. A simplified geometry of the head is adopted, constituting of the brain, CSF and skull, each being represented by spheres of their representative diameters. The CSF flow in the SAC (thickness is about less than 3 mm) is modeled as a flow through thin gap using the lubrication theory. The inertial component of the Navier-Stokes equation, which is typically ignored in classical lubrication model, is retained in the present formulation. The velocity flow field of the CSF is represented by relying on stream functions. The resulting governing equation for the CSF flow turns out to be a fourth order linear partial differential equation (PDE) [1]. It has been experimentally reported in literature [2] that both the brain and skull solely undergo rigid body motions during the time duration of the impact (~10-2 s). Accordingly, the brain and skull are modeled as rigid bodies during this duration of the impact. The rigid body dynamics of the brain is found to be governed by an integro-differential equation (IDE) in terms of the CSF pressure, skull and brain accelerations. The IDE and the PDE form the governing equations for the fluid structure interactions. These equations are solved numerically using the finite element (FE) approach and the associated computational scheme is found to be superior and more effective than the simulation of the fluid structure interaction based full-scale FE model. The result of CSF flow is validated against the predictions from the fluid structure interaction module of Abaqus® (v 6.14-5). References [1]. Exact and approximate solutions for transient squeezing flow. Lang, Ji, Santhanam, Sridhar and & Wu, Qianhong. 10, 2017, Physics of Fluids, Vol. 29, p. 103606. [2]. Separating brain motion into rigid body displacement and deformation under low-severity impacts. Zou, Hong, Schmiedeler, James P and & Hardy, Warren N. 6, 2007, Journal of Biomechanics, Vol. 40, pp. 1183-1191.

New Positive-Definite Random Matrix Ensembles and their Applications in Mechanics

Sonjoy Das*

*University at Buffalo

ABSTRACT

The scientific community has seen an increasing surge of applications of positive-definite random matrix ensembles in the fields of mechanics and multiscale mechanics in recent years. These ensembles are employed to directly model several positive-definite matrix-valued objects, e.g., mass matrices, stiffness matrices, small-deformation constitutive elasto-plasticity tensor, finite-deformation constitutive non-linear elasticity tensor, etc. Matrix variate distributions, e.g., Wishart/Gamma distribution, Beta Type 1 distribution, Kummer-Beta distribution, or distributions derived from them, are currently used for this modeling purpose. These distributions are, however, parameterized such that they induce specific mean and covariance structures that do not allow sufficient flexibility in modeling high level of uncertainties. The current work will discuss two new positive-definite random matrix ensembles that are likely to provide more flexibility in modeling high level of uncertainties. Applications of the new ensembles will be illustrated through examples from mechanics.

Two-scale Modeling of Thermo-mechanical Dynamic Damage in Brittle Solids

Cristian Dascalu*, Kokouvi Gbetchi**

*Université de Lorraine, Laboratoire d'Etude des Microstructures et de Mécanique des Matériaux, Metz, France,

**Université de Lorraine, Laboratoire d'Etude des Microstructures et de Mécanique des Matériaux, Metz, France

ABSTRACT

Under impact mechanical loadings or thermal shocks, structural components made of brittle materials may be exposed to dynamic failure. The appropriate modeling of the failure mechanisms at different scales of observation and the prediction of the corresponding thermo-mechanical damage evolution in such materials are essential for structural reliability predictions. Over the last decades, it has been established that thermo-mechanical coupling plays an important role in the proper description of the dynamic fracture. Although the thermo-elastic coupling has been often neglected in the dynamic fracture studies, it was shown experimentally that these effects are not negligible under transient conditions. For instance, Rittel (1999) reported experiments showing significant temperature drops at the crack tip during the initiation phase of mode I dynamic fracture in PMMA samples. The aim of the present contribution is to show that the observed thermo-elastic effects associated with the rapid failure can be successfully predicted using a two-scale dynamic damage model. For this, a new theoretical model able to assess the interplay between micro-cracking and thermo-mechanical evolutions during dynamic fracture processes is proposed. In the last years, we developed a two-scale damage model (Keita et al. 2014, Dascalu 2018) for the dynamic failure of brittle materials. In the present context, the model is extended to account for the thermo-elastic coupling at microscopic and macroscopic scales. The evolution law for damage is deduced using asymptotic developments homogenization from small-scale descriptions of mode I dynamic propagation of micro-cracks. The crack-tip heating process and the bulk thermo-elasticity are considered at the micro scale. The resulting homogenized model is sensitive to the size of the microstructure through a length parameter present in the damage law. Finite Elements simulations have been performed to characterize local and structural responses predicted by the new model. In particular, the impact test on compact compression PMMA specimens was reproduced and the obtained results are in good agreement with those reported in the experiments (Rittel, 1999). Keywords: Micro-cracks, two-scale damage model, dynamic brittle failure, thermo-mechanical coupling, microstructural size effects, finite-element simulations. References: Rittel, D. 1999. Thermomechanical aspects of dynamic crack initiation. *Int. J. Fracture*. 99, 199-209. Keita O., Dascalu, C., Francois B., 2014. A two-scale model for dynamic damage evolution. *J. Mech. Phys. Solids*. 64, 170-183. Dascalu, C., 2018. Multiscale modeling of rapid failure in brittle solids: Branching instabilities. *Mechanics of Materials*. 116, 77-89.

Computational Modeling of 2D Materials and their Heterostructures for Sustainable Energy Storage: Opportunities and Challenges

Dibakar Datta^{*}, Vidushi Sharma^{**}, Kamalika Ghatak^{***}

^{*}New Jersey Institute of Technology (NJIT), ^{**}New Jersey Institute of Technology (NJIT), ^{***}New Jersey Institute of Technology (NJIT)

ABSTRACT

Because of the low gravimetric capacity of conventional graphite anode (theoretical value of 372 mAh/g), and massive structural changes and volume expansion of silicon anode (on the order of 300%) extensive research has been carried out during last few decades to develop anode materials that can yield much higher capacity. We, therefore, examined the possibility of 2D materials for application of high-capacity anode materials. By first-principle calculations based on density functional theory (DFT), we investigated the adsorption of lithium (Li), sodium (Na), and calcium (Ca) on graphene with divacancy and Stone-Wales defects. We find that with controlled defect topology, we can achieve a maximum storage capacity of approximately 1675, 1450 and 2900 mAh/g for Li-, Na-, and Ca-ion batteries respectively. Our results indicate a new paradigm of 2D materials based energy storage. However, despite enormous opportunities, we need to concern about several challenges such as adatom trapping at the defect sites, the effect of defects on adatoms diffusivity, microstructural changes, e.g., mechanical degradation at defect sites, etc. Besides graphene, several other 2D materials such as graphene allotropes, Transition Metal Dichalcogenides (TMD), etc. Moreover, by building heterostructures made by stacking of different 2D materials, it is possible to combine the advantage and eliminate the disadvantages of the individual materials. However, we need a computational genome to identify the optimal heterostructures for the energy storage. In this talk, we will provide a detailed overview of opportunities and challenges of modeling of 2D materials and its heterostructures for sustainable energy storage applications.

ROBUST TARGET DESIGN FOR COMPLEX SYSTEMS USING MULTI-OBJECTIVE OPTIMIZATION

MARCO DAUB* AND FABIAN DUDDECK*,†

* Technische Universität München
Arcisstraße 21, 80333 Munich, Germany
e-mail: {marco.daub, duddeck}@tum.de

† Queen Mary University of London
Mile End Road, London E1 4NS, UK

Keywords: Robust design, interval uncertainties, lack of knowledge, complex systems, multi-objective optimization.

Abstract. *During complex systems development, various uncertainties occur. Designs chosen at an early stage often turn out to be non-permissible at a later stage because of uncertain or currently unknown conditions. Therefore, a specific type of robust design is desirable which is insensitive to such conditions. Though, a challenge is that many uncertainties are not quantifiable at an early stage of development due to lack of knowledge. To overcome this, Hendrix et al. (1996) proposed to target the “most interior” design in the region of permissible designs which is then called a “robust design”. This design centering method mainly addresses errors in manufacturing. However, other sources of uncertainties like changing operation conditions or model uncertainties, compare (Beyer, Sendhoff, 2007), are not considered with this approach. Hence, the method proposed in this work includes these uncertainties by using multi-objective optimization. Here, an optimal or robust design maximizes both tolerances in (controllable) design variables, tolerances in uncontrollable model parameters, and distances between the system performances and their threshold values.*

1 INTRODUCTION

In complex system design, uncertainties can be classified according to where they occur and how they are modeled mathematically. Depending on this classification, an overview is given in [1], how a robust design which is resistant to the uncertainties that are considered can be calculated. However, in real-world applications the information on the uncertainties is often limited, especially at an early design phase. This is due to imprecise or incomplete knowledge which is also referred to as epistemic uncertainties in literature. To overcome this problem, a method to find robust designs was proposed in [3] where maximal possible deviations of the design variables are sought by still satisfying all requirements. In [4] and [5] the method was slightly adapted and applications to complex systems design were given. Nevertheless, all considerations focused only on uncertainties in the controllable design variables.

In this work, the method of [3] is generalized by including uncertainties in uncontrollable parameters, the system responses and its threshold values in order to account for a non-reducible lack-of-knowledge situation in early design phase. Here, robust target designs are obtained by using multi-objective optimization. In chapter 2, definitions and uncertainties that occur in complex system design are considered before an enhanced method to calculate robust target designs is introduced. In chapter 3, the method is then applied to a simple crash design problem and results are visualized.

2 METHODOLOGY

2.1 Definitions

For complex systems, the goal is to find a suitable design. The corresponding design variables $x_i \in \mathbb{R}$, $i = 1, \dots, d$ are collected in a d -dimensional vector $x \in \mathbb{R}^d$ with $x = (x_1, \dots, x_d)$. Each design variable is lower bounded by $x_{ds,i}^l \in \mathbb{R}$ and upper bounded by $x_{ds,i}^u \in \mathbb{R}$, i.e. $x_{ds,i}^l \leq x_i \leq x_{ds,i}^u$ or $x_i \in [x_{ds,i}^l, x_{ds,i}^u]$ for $i = 1, \dots, d$. As the design variables can be chosen by a decision maker within these bounds, they are also called controllable variables. The Cartesian product of the intervals $[x_{ds,i}^l, x_{ds,i}^u]$ form the design space Ω_{ds} with $\Omega_{ds} \subset \mathbb{R}^d$.

In complex systems design, there are also quantities that cannot be controlled. These are the uncontrollable parameters $p_l \in \mathbb{R}$, $l = 1, \dots, q$ which are collected in a q -dimensional vector $p \in \mathbb{R}^q$. For given x and p , the responses of the system can be determined uniquely. The responses $z_j \in \mathbb{R}$, $j = 1, \dots, m$ are collected in a m -dimensional vector $z \in \mathbb{R}^m$. The relationship between x , p and z can be expressed by using a system performance function $f : \mathbb{R}^d \times \mathbb{R}^q \rightarrow \mathbb{R}^m$ with

$$z = f(x, p). \quad (1)$$

In general, there are requirements in complex systems design that bound the system responses. Without loss of generalization, only upper thresholds $f_c(p) \in \mathbb{R}^m$ are considered in the following as a multiplication of an inequality with lower thresholds will yield upper thresholds. Together with the restrictions of the design space, these requirements form a set of permissible

designs which is

$$\Omega_c = \{x \in \Omega_{ds} : f_j(x, p) \leq f_{c,j}(p), j = 1, \dots, m\}. \quad (2)$$

It shall be remarked that x and p can be responses of subsystems, and their values depend on lower level design variables or parameters. Here, this is included by the uncertainty consideration.

2.2 Uncertainties

In reality, the values of the selected design variables, the uncontrollable parameters, the system responses and their thresholds are usually uncertain, compare [1]. Inaccurate manufacturing or uncertainties propagated from a lower system level can affect the values of design variables or a priori chosen uncontrollable parameters for example. The values of uncontrollable parameters can also depend on changing environmental or operating conditions. Approximation errors inherent to the chosen model give rise to uncertainties in the system responses including their thresholds.

In early phase of complex systems design, there is only limited data about the uncertainties due to imprecise or incomplete knowledge. This complicates a proper mathematical quantification. In the following, it is assumed that the real values are symmetrically distributed around nominal values. Furthermore, they can be found within intervals where the interval bounds are unknown and only tolerance bands for the real values are given. The nominal values are marked with a check and express the selected variables in the case of design variables. It holds

$$x_i \in [\check{x}_i - \delta, \check{x}_i + \delta] \quad (3)$$

for $\delta \geq 0$, $\check{x}_i - \delta \geq x_{ds,i}^l$, $\check{x}_i + \delta \leq x_{ds,i}^u$, $i = 1, \dots, d$,

$$p_l \in [\check{p}_l - \gamma, \check{p}_l + \gamma] \quad (4)$$

for $\gamma \geq 0$, $l = 1, \dots, q$, and

$$f_j(x, p) - f_{c,j}(p) \in [(\check{f}_j(x, p) - \check{f}_{c,j}(p)) - \varepsilon, (\check{f}_j(x, p) - \check{f}_{c,j}(p)) + \varepsilon] \quad (5)$$

for $\varepsilon_j \geq 0$, $x \in \Omega_{ds}$, $p \in \mathbb{R}^q$, $j = 1, \dots, m$ where δ , γ , and ε are the maximal tolerances.

2.3 Robust target design

In [3], a design is said to be robust, if possible deviations do not lead to a non-permissible design, i.e. $x \notin \Omega_c$. A method is proposed how the tolerances for the design variables can be maximized by allowing only permissible designs. This is a design centering problem, see [2]. However uncertainties in uncontrollable parameters, the system responses and its thresholds, are not incorporated. Thus, a method which generalizes the one in [3] is proposed here that

maximizes all tolerances by using multi-objective optimization. For given nominal values of the uncontrollable parameters, the problem statement reads

$$\begin{aligned}
 & \underset{\check{x}, \delta, \gamma, \varepsilon}{\text{maximize}} && (\delta, \gamma, \varepsilon) \\
 & \text{subject to} && \delta, \gamma, \varepsilon \geq 0, \\
 & && x_{\text{ds},i}^l \leq x_i \leq x_{\text{ds},i}^u, \quad i = 1, \dots, m, \\
 & && \check{f}_j(x, p) + \varepsilon \leq \check{f}_{c,j}(p), \quad j = 1, \dots, m \\
 & && \forall x_i \in [\check{x}_i - \delta, \check{x}_i + \delta], \quad i = 1, \dots, d, \\
 & && \forall p_l \in [\check{p}_l - \gamma, \check{p}_l + \gamma], \quad l = 1, \dots, q.
 \end{aligned} \tag{6}$$

Problem (6) is a multi-objective optimization problem with three objective functions. The nominal values for the design variables as part of a Pareto optimal solution are called a robust target design which considers various uncertainties. Pareto optimal solutions are solutions where it is impossible to improve in any of the objectives without degrading in another one.

In general, it is not easy to obtain Pareto optimal solutions of problem (6) because the optimization constraints must be satisfied for all possible x and p . In chapter 3, it is shown how problem (6) can be solved for a simple crash design problem.

3 APPLICATION TO CRASH DESIGN

3.1 A simple problem

An example of a complex system that must fulfill requirements is a vehicle. Regarding crash tests like the USNCAP crash load case where the vehicle is driven against a rigid wall with a velocity v_0 , specific requirements can be set. The maximal acceleration, the energy absorption, and the order of deformation of the relevant components are system responses which have to be bounded. They can be calculated from the force-deformation characteristics of the components where their degrees of freedom are the design variables. In general, force-deformation characteristics cannot be designed as they are responses of the components' lower level design variables. Therefore, this selection must follow a second step, which is not part of this paper.

In figure 1, a simple example for a vehicle front structure which is modeled as two components is shown, see [5]. It shall be remarked that this example only illustrates the approach and a focus on more complex examples will be put in subsequent papers.

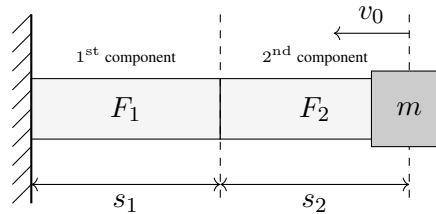


Figure 1: Simple crash problem for a vehicle front structure with two components, compare [5]

In every component, the force-deformation characteristics are modeled as constant. Hence, both components have one degree of freedom and the design variables are F_1 and F_2 with $F = (F_1, F_2)$. The lower bounds of the design variables are given by $F_{\text{ds},i}^l = 0$ kN and the upper bounds by $F_{\text{ds},i}^u = 500$ kN, $i = 1, 2$.

Furthermore, the nominal values of the system responses and their thresholds are

$$\check{f}_1(F, p) - \check{f}_{c,1}(p) = F_1 - ma_c, \quad (7)$$

$$\check{f}_2(F, p) - \check{f}_{c,2}(p) = F_2 - ma_c, \quad (8)$$

$$\check{f}_3(F, p) - \check{f}_{c,3}(p) = -s_1 F_1 - s_2 F_2 + \frac{1}{2} m (v_0)^2, \quad (9)$$

$$\check{f}_4(F, p) - \check{f}_{c,4}(p) = F_1 - F_2, \quad (10)$$

compare [5]. The equations (7)-(8) relate to the maximal acceleration, equation (9) to the energy absorption and equation (10) to the order of deformation of the two components. The section lengths s_1, s_2 , the mass m , the initial velocity of the vehicle v_0 , and the critical acceleration a_c are uncontrollable parameters and are collected in the vector $p = (s_1, s_2, m, v_0, a_c) \in \mathbb{R}^5$. Here, the given nominal values are $\check{s}_1 = 0.30$ m, $\check{s}_2 = 0.30$ m, $\check{m} = 1500$ kg, $\check{v}_0 = 15.6 \frac{\text{m}}{\text{s}}$, and $\check{a}_c = 300 \frac{\text{m}}{\text{s}^2}$.

To get the nominal values of a robust design, the tolerances that are considered must be maximized. In order to account for the applicability of problem (6) to this specific system, the tolerances are transformed into relative tolerances with

$$\delta = \frac{F_{\text{ds},i}^u - F_{\text{ds},i}^l}{2} \bar{\delta}, \quad i = 1, \dots, m \quad (11)$$

$$\gamma = \check{p}_l \bar{\gamma}, \quad l = 1, \dots, q \quad (12)$$

$$\varepsilon = \max\{\check{f}_{c,j}(\check{p}) - \check{f}_j(F, \check{p}) : F \in \Omega_{\text{ds}}\} \bar{\varepsilon}, \quad j = 1, \dots, m \quad (13)$$

and $0 \leq \bar{\delta}, \bar{\gamma}, \bar{\varepsilon} \leq 1$.

3.2 Results for robust target design

As the constraint corresponding to equation (7) is redundant as well as the constraints on the design space, the optimization constraints for the simple crash design problem reduce to

$$\check{F}_2 + 250\text{kN}\bar{\delta} + 450\text{kN}\bar{\varepsilon} \leq 450\text{kN}(1 - \bar{\gamma})^2, \quad (14)$$

$$-0.3\text{m}(1 - \bar{\gamma})(\check{F}_1 + \check{F}_2) + 150\text{kJ}(1 - \bar{\gamma})\bar{\delta} + 117.48\text{kJ}\bar{\varepsilon} \leq -182.52\text{kJ}(1 + \bar{\gamma})^3, \quad (15)$$

$$\check{F}_1 - \check{F}_2 + 500\text{kN}\bar{\delta} + 500\text{kN}\bar{\varepsilon} \leq 0, \quad (16)$$

and $-\bar{\delta}, -\bar{\gamma}, -\bar{\varepsilon} \leq 0$. This can be obtained as the maxima of $\check{f}_j(F, p) - \check{f}_{c,j}(p)$, $j = 1, \dots, m$, are always adopted at the border of the intervals for x and p . In Figure 2, it is shown how increasing $\bar{\delta}$, $\bar{\gamma}$, or $\bar{\varepsilon}$ affect the set of permissible nominal values for \check{F}_1 and \check{F}_2 .

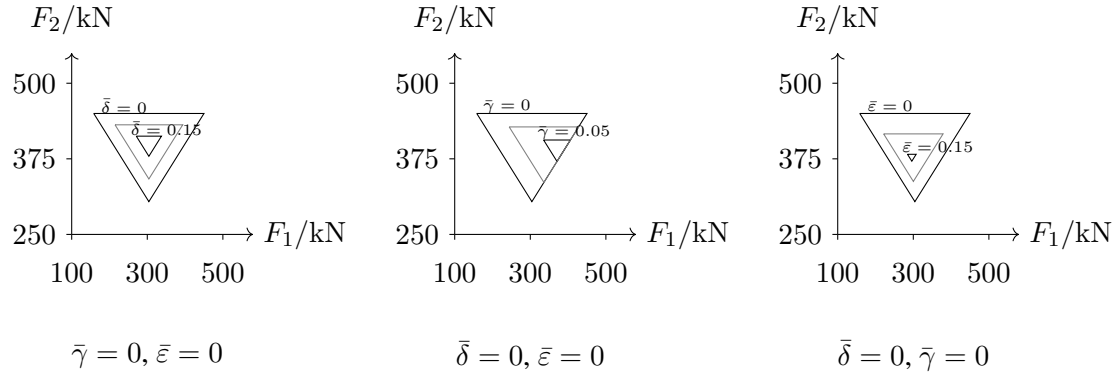


Figure 2: Set of permissible nominal values for \check{F}_1 and \check{F}_2 , depending on $\bar{\delta}$, $\bar{\gamma}$, and $\bar{\varepsilon}$

The location of the set varies, depending on which one of $\bar{\delta}$, $\bar{\gamma}$, and $\bar{\varepsilon}$ is increased. This already gives an idea of the Pareto optimal solutions of the simple crash design problem and their corresponding robust target designs. Some of them are visualized in Figure 3.

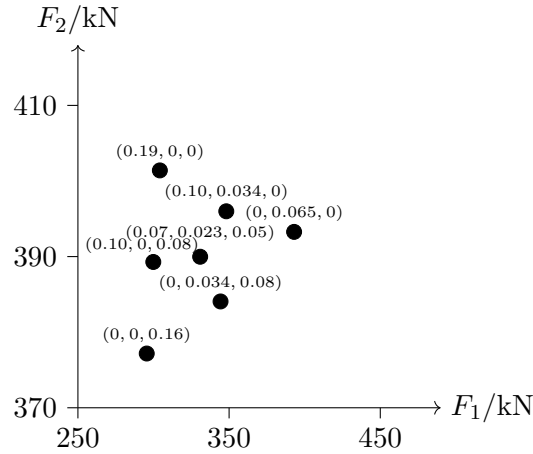


Figure 3: Selected robust target designs for the simple crash design problem together with their tolerances stated in $(\bar{\delta}, \bar{\gamma}, \bar{\varepsilon})$

Here, the dependency of the robust target design values on $\bar{\delta}$, $\bar{\gamma}$, and $\bar{\varepsilon}$ is emphasized. This does not mean that there is no other possible combination of $(\bar{\delta}, \bar{\gamma}, \bar{\varepsilon})$ for any robust target design, but changing this combination leads to a solution which is not Pareto optimal. Given the Pareto optimal solutions, it is the choice of the decision maker to balance the different objectives in order to select the most suitable nominal values for the design variables \check{F}_1 and \check{F}_2 .

4 CONCLUSIONS

In this work, it was introduced how a robust target design for complex systems design that considers various uncertainties can be found by maximizing tolerances (intervals) for the uncertainties. This helps to handle the lack-of-knowledge situation in early development phase. Uncertainties in controllable design variables, uncontrollable parameters, the system responses and their threshold values are considered separately by using multi-objective optimization. If the real values of these uncertainties can be found within the optimized intervals, the complex system always satisfies the given requirements. For a simple crash design problem, Pareto optimal solutions could be calculated and the dependency of the robust target designs on the maximal tolerances for the different uncertainties could be shown. For further research, a general algorithm to solve the proposed problem statement is recommended.

ACKNOWLEDGMENTS

This work was supported by the SPP 1886 "Polymorphic uncertainty modelling for the numerical design of structures" of the German Research Foundation, DFG.

REFERENCES

- [1] BEYER, H.-G., AND SENDHOFF, B. Robust optimization – A comprehensive survey. *Computer Methods in Applied Mechanics and Engineering* 196, 33-34 (2007), 3190–3218.
- [2] HARWOOD, S. M., AND BARTON, P. I. How to solve a design centering problem. *Mathematical Methods of Operations Research* 86, 1 (2017), 215–254.
- [3] HENDRIX, E. M., MECKING, C. J., AND HENDRIKS, T. H. Finding robust solutions for product design problems. *European Journal of Operational Research* 92, 1 (1996), 28–36.
- [4] ROCCO, C. M., MORENO, J. A., AND CARRASQUERO, N. Robust design using a hybrid-cellular-evolutionary and interval-arithmetic approach: A reliability application. *Reliability Engineering & System Safety* 79, 2 (2003), 149–159.
- [5] ZIMMERMANN, M., AND VON HOESSLE, J. E. Computing solution spaces for robust design. *International Journal for Numerical Methods in Engineering* 94, 3 (2013), 290–307.

Forecasting and Predictive Simulation for Coastal Ocean Processes

Clint Dawson*

*University of Texas at Austin

ABSTRACT

Coastal ocean models are used for many different applications, including environmental studies, modeling of tsunamis and hurricane storm surge modeling. Recent extreme events have pointed to the need to extend current modeling capabilities by including additional physics at multiple spatial and temporal scales, improving algorithms and concurrently enhancing computational speed through high performance computing. In this talk, we will describe recent advances in multi-physics couplings, new algorithmic advances in modeling using discontinuous Galerkin methods, and improvements in high performance computing through the use of High Performance ParallelX (HPX). We will discuss applications to recent hurricanes, and outline needs for future research.

ALGORITHM FOR EXTRACTION OF LOCAL PANELS FROM SURFACE FINITE ELEMENT MODEL AND APPLICATION IN WING DESIGN

SHUVODEEP DE^{*}, RAKESH K. KAPANIA[‡]

^{*}Postdoctoral Research Associate

Kevin T. Crofton Department of Aerospace and Ocean Engineering
Virginia Polytechnic Institute and State University, Blacksburg, VA, 24061-0203
Email: shuvode@vt.edu

[‡]Norris and Wendy Mitchell Endowed Professor

Kevin T. Crofton Department of Aerospace and Ocean Engineering
Virginia Polytechnic Institute and State University, Blacksburg, VA, 24061-0203
Email: rkapania@vt.edu

Keywords: Finite-element Model, Mesh, Local-panels, Algorithm,

Abstract. Multi-disciplinary optimization (MDO) of structures is gaining popularity due to exponential increase in computational power. It is a common practice to solve problems involving highly complex systems where the system is decomposed into multiple smaller components to make it feasible to use parallel computation to reduce the overall time of optimization. In this work a new algorithm is developed to create local panels from two dimensional (surface) finite element models comprising of triangular element. The algorithm is based on applying set algebra on the connectivity data of the finite element model and is independent of nodal coordinates. The first step is to determine the nodes and the elements on the outer edge of the panel, the second to find the elements except the elements on the boundary that share one of the internal nodes. The elements ids are stored in a vector. Now the elements which share at least one node with the elements listed are found and their ids are stored in the same vector. This step is repeated till the vector do not change and it would contain the elements defining the local panel. The main advantage of this algorithm is that it can be used to create local panels of any shape and size and can be applied used for a wide range of structures including the aero-foil skin of aircraft wing, the cylindrical fuselage of the aircraft or the hull of a submarine. The study also includes creation of stiffeners on the local panels and finding the proper elements for the stiffeners. Once the local panels are determined, the structure is ready for global-local optimization. The algorithm is first demonstrated by dividing a rectangular surface using a family of curves of different orientations. Then it is used to divide the upper and lower skin of the NASA CRM Wing using intersection of curvilinear spars and ribs (*SpaRibs*) of different curvatures and orientation. This algorithm has been integrated to the EBF3GLWingOpt framework which is being developed by Kapania et al. at Virginia Tech to perform global local optimization of wide range of aircraft wing having *SpaRibs*.

1 INTRODUCTION

One of the most important concern while designing vehicles is to reduce structural weight, which can directly lead to reduction in fuel consumption. During the era when computers were expensive and not so powerful, structural design was mostly done by hand calculation on simplified mathematical models. However, since the seventies, due to rapid increase in computational power numerical solution techniques like Finite Element Analysis (FEA) have gained immense popularity. Not only the details and the complexity of the system can be included in the analysis, but multiple disciplines can now be considered while setting up a structural optimization problem. This avenue of research where several disciplines are incorporated into the optimization problem is known as Multidisciplinary Design Optimization (MDO). The major advantage of solving such a problem arise when relevant disciplines are not independent of each other, in other words, the disciplines interact with each other. Application of MDO for structural design can be traced back to work of Schmit [1] [2] [3]. In his work, finite element methods and algorithms for numerical optimization are used. In subsequent years, Haftka [4] [5] [6], Fulton [7] designed aircraft wings considering constraints on strength, stability and flutter velocity. MDO rapidly gained popularity in aerospace engineering and soon problems were solved involving complete model of aircraft [8] [9] [10] [11] [12]. The processes followed in MDO have either monolithic or distributed architectures [13]. In any MDO, the first step is almost always to describe the system using a set of design variables. The goal is to find the best values for the design variables that minimizes (or maximizes) the objective function while satisfying constraints in several disciplines. For example, in problems involving structural design, the size, shape or topology of the structure are described by a set of design variables. By applying appropriate numerical optimization algorithms, the problem is solved for a set of design variables that gives minimum weight or maximum compliance while satisfying constraint like maximum von Mises stress, minimum buckling factor, maximum displacement etc. In a monolithic architecture, all the design variables and constraints are considered in a single optimization process. This process, commonly known as All-at-Once optimization [14], although simple to implement is computationally expensive when the number of design variables is large. Such problems involving large number of design variables are often solved using the other process of MDO i.e. distributed architecture. The distributed MDO architectures involves the decomposition of a complex systems into multiple smaller components which are then described by a lower number of design variables and optimized independently. The process is usually implemented using parallel computation which can reduce wall clock time by several times. This process of decomposition of a system into simple sub-system is often known as global/local design optimization.

The aircraft wing is a complex structure consisting of the outer aerofoil shell known as the wing-skin, and internal stiffening elements: the ribs and spars. The global/local optimization process as described above has been used by several research groups including Cimpa *et al.* [15]. Even though the availability of computational power makes the exploration of large design space feasible, there has always been concern in the industry about manufacturing limitations. It is often very expensive to produce unconventional designs using conventional manufacturing processed. However, with invention of 3D printing techniques, the manufacturing industry is likely to be revolutionized over the next few decades. A new additive manufacturing technique known as Electron Beam Free Form Fabrication or EBF3 in short has recently been developed by Taminger and Hafley [16] at

NASA Langley Research Center to fabricate metallic structures of complex shapes, which now can be printed with significant precision. This technology inspired Kapania et al. at Virginia Tech [17] [18] [19] to propose the use of curvilinear stiffening elements to reduce structural weight and achieve desirable aeroelastic properties for aircrafts. The EBF3GLWingOpt is one of the several optimization frameworks that is being developed at Virginia Tech to optimize aircraft structures using curvilinear spars and ribs (*SpaRibs*). It performs global/local optimization of high aspect ratio cantilever transport aircraft wing for multiple constraints including stress, buckling and crippling. The wing geometry and mesh are generated using commercial software, MSC.PATRAN and MSC.NASTRAN is used for static and buckling analysis. The framework is written in Python environment and it enables use of parallel processing.

In the original version of **EBF3GLWingOpt**, written by Liu et al., the Linked-shape method proposed by Locatelli et al. [18] is used to create *SpaRibs* in each of the wing-boxes using limited number of design variables (which specified the shape of the *SpaRibs*). The upper and the lower skin of the wing are divided into local panels using the intersection of the *SpaRibs* and the stiffeners are attached to on each of the panels. The thickness of each of the local panels, the stiffener height and thickness are considered as design variables. The optimization framework could only explore limited design space where *SpaRibs* could start at the leading-edge spar and end at the trailing-edge spar. In order to overcome this limitation, De et. al. [20] proposed the *Extended-space method* to create *SpaRibs*. By this method not only the constraint on the starting and ending point of the *SpaRibs* was removed but also *SpaRibs* crossing the junction of the inner and outer wing-box can be created. In addition, the algorithm to extract local panel from the finite element model as used the original version of **EBF3GLWingOpt** framework was dependent on nodal coordinate coordinates of the nodes and could extract only panels with four edges from the finite element model. Moreover, the idea of dividing a surface into local panels and assigning a thickness design variable to each of the panels is very generalized and can be applied not only to aircraft wings but different other structures including automobile, ships, buildings etc. Thus, the need was felt to develop a generalized algorithm to break a finite element model into local panels. In the following work, such an algorithm to divide a surface mesh (consisting of triangular elements) has been discussed. The process can be implemented on the CRM wing for any *SpaRibs* configuration as well as other shell-structures like the fuselage or automobile frame with minor modifications. This algorithm is not dependent on nodal coordinates and is purely based on set operations performed on the element connectivity matrix.

The article is organized into seven sections. Section 2 mention the Mesh-continuity algorithm by which element and nodes interior to the local panel can be found. Section 3 mention the order in which the panels are numbered. To make the Mesh-continuity algorithm work, the elements interior to the local panel and along the outer edge need to be determined at first. Section 4 discuss the process of determining these elements. Section 5 demonstrate the algorithm on a simple problem. Section 6 and Section 7 discuss the integration of the algorithm with **EBF3GLWingOpt** framework and demonstrates its effectiveness for range of *SpaRibs* profiles with example.

2 MESH CONTINUITY ALGORITHM

The goal is to come up with an algorithm to extract local panels from the finite element mesh of a larger structure given its boundary nodes. To do so, the elements interior to the local panel along its outer edge i.e., which share the boundary nodes need to be determined. Once these boundary nodes are determined it is a straightforward process to determine all nodes and elements interior to the local panel using the connectivity matrix information, following the steps given in Figure 1.

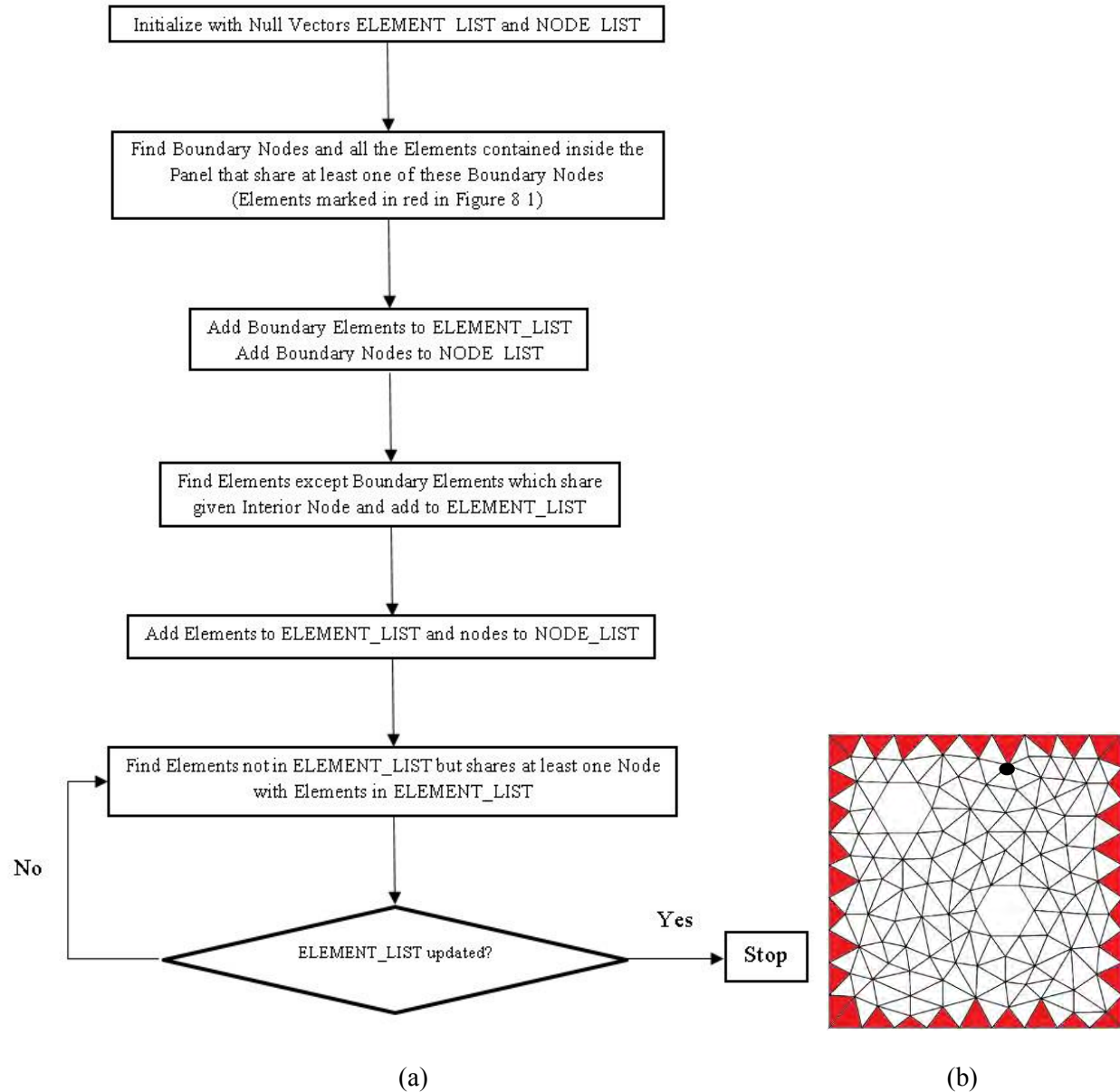


Figure 1: a Mesh Continuity Algorithm to find Elements inside Local Panel b Determining Panel Elements by Boundary Elements red and an Interior Node black

3 NUMBERING OF THE LOCAL PANEL

In this method, the finite element model of the wing skin is first sliced using the set of curvilinear ribs and then each slice is again divided using the curvilinear spar. The numbering process of the local panels is shown in Figure 2.

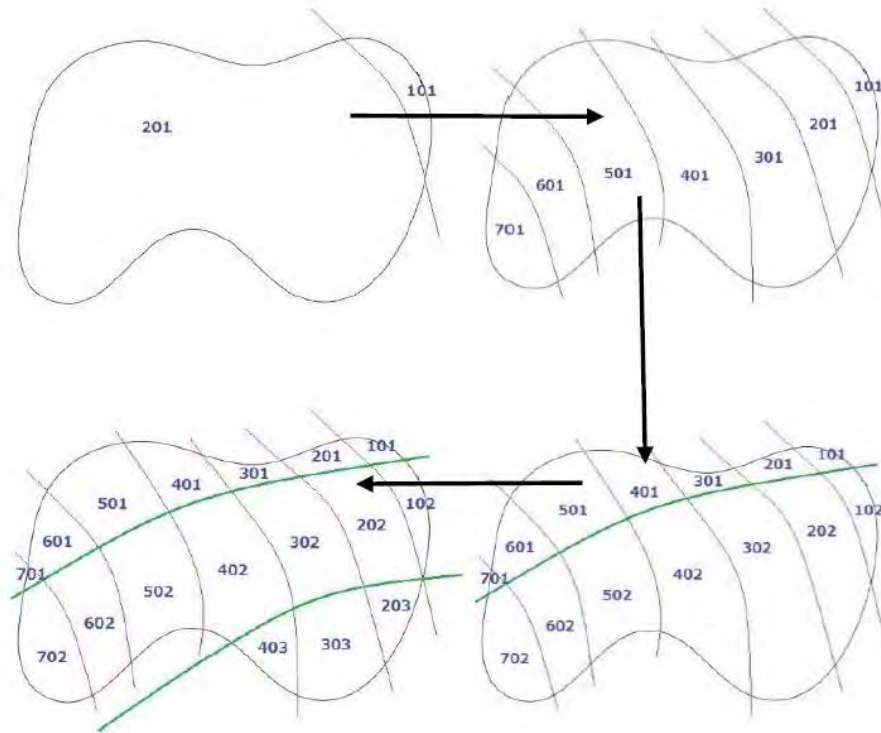


Figure 2: Numbering the Local Panels

4 ALGORITHM TO DETERMINE THE BOUNDARY ELEMENTS

The Mesh-continuity algorithm is easy to apply once the elements along the outer boundary of the panel is determined. The general process to find this boundary elements is a bit complicated and will be discussed in detail this section with a simple example where the objective is to split a rectangular plate (with holes) meshed with triangular elements into two panels. The process consists of two steps. The first step is to determine all elements along the free boundary that is part of one of the panels. The second step is to determine the elements with edges along the dividing curve which are interior to the panel.

4.1 To determine elements along free boundary:

The plate shown in Figure 3 (b) is needed to be split along Curve 2 (Curve 3 is the next curve in the family, Curve 1 is the previous one). First elements along the free edge of the panels will be

found. In the algorithms described in this section, CHECKPOINT_NODE refers to the node with respect to which the positions of other nodes are determined. ELEMENT_LIST_1 and ELEMENT_LIST_2 are vector containing [Element ID, Connectivity Nodes] while NODE_LIST_1 and NODE_LIST_2 are list of Nodes. All of them are initialized as null sets.

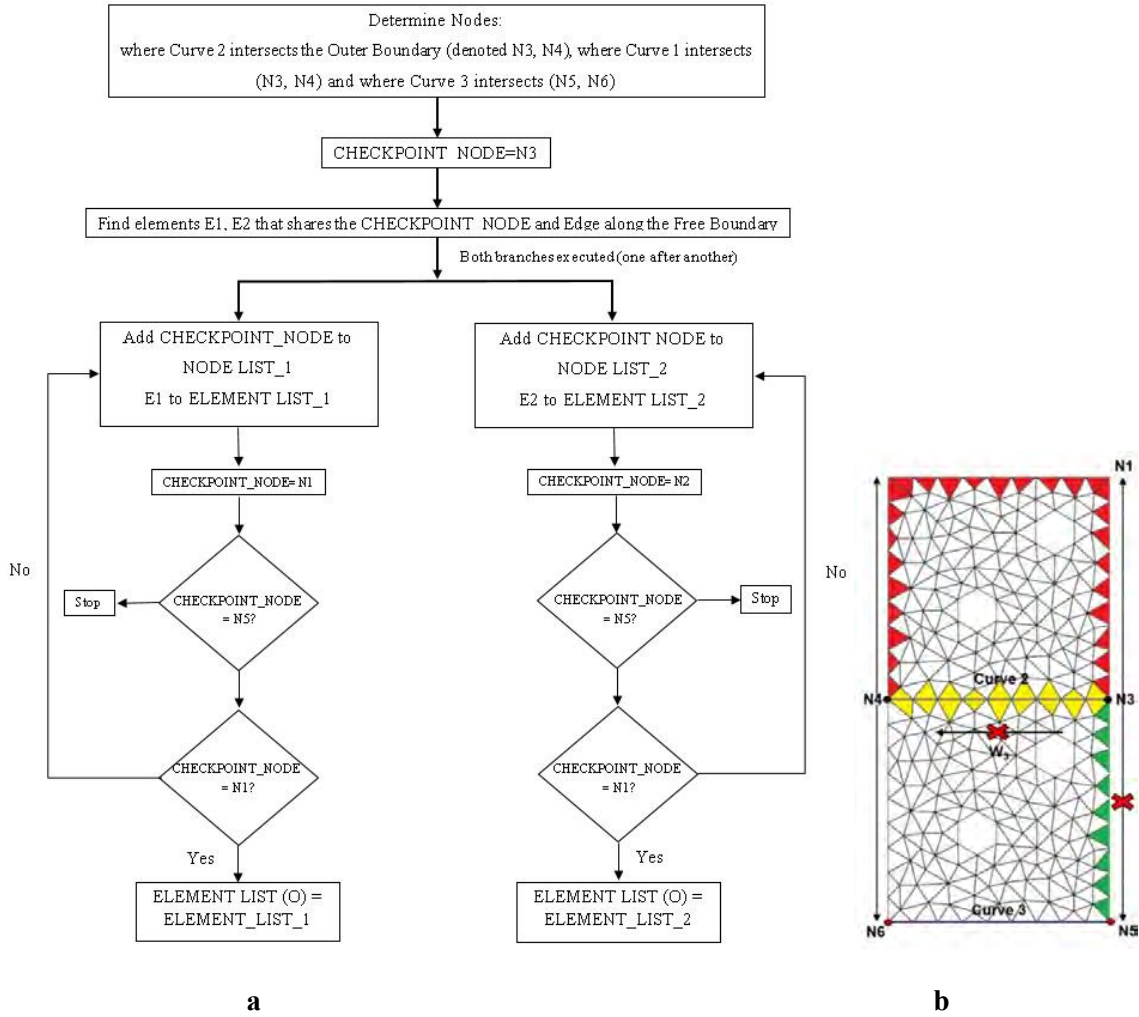


Figure 3: a Plate are Split by Three Non Intersecting Curves b Algorithm to determine Elements along the Outer free Boundary

The nodes along Curve_1 is already known. Thus, finding the elements along this curve is very simple. All it need is to find the elements that has at least two nodes along Curve_1. The elements in ELEMENT_LIST (O) and those along Curve_1 are marked in red.

The algorithm described in Figure 3 is not applicable to find the elements interior to the local panel with edges along Curve_2, as will include elements outside the local panel as well (elements shown in Yellow in Figure 4 b). This is because all those elements have edges along the curve. To find the elements only interior to the panels another algorithm has been developed. To do this, another algorithm has been developed, which is named Middle Element Algorithm (MEA).

4.2 Middle Element Algorithm MEA :

Here the objective is to determine elements on the left/right side of a curve C (red) in Figure 4 (a).

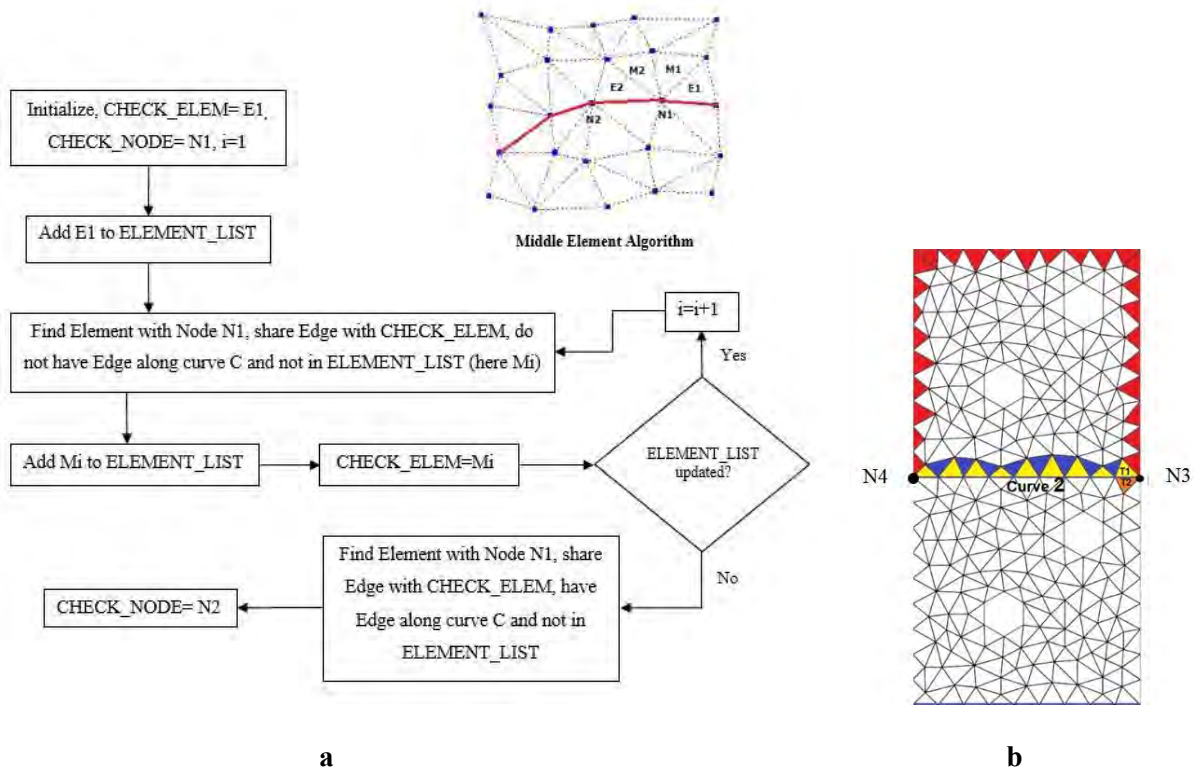


Figure 4: a Middle Element Algorithm b Using Middle Element Algorithm to find Elements in Local Panel

The elements contained in the vector ELEMENT_LIST consists of elements only above Curve 2 (marked by yellow and blue in

Figure 4. The elements contained in ELEMENT_LIST (O) and ELEMENT_LIST forms the outer boundary of the panel above the Curve 2. Once these elements along the outer boundary are determined, the mesh Continuity Algorithm can be used to find all the elements belonging to the panel.

E AMPL WITH SIMPLE PROBLEM

The algorithm is demonstrated first on a simple example. The rear wing-box of Boeing HSCT N+2 Wing containing 7 *SpaRibs* in the span-wise direction and 8 *SpaRibs* in the chord-wise direction is constructed in MSC.PATRAN as shown in Figure 5.

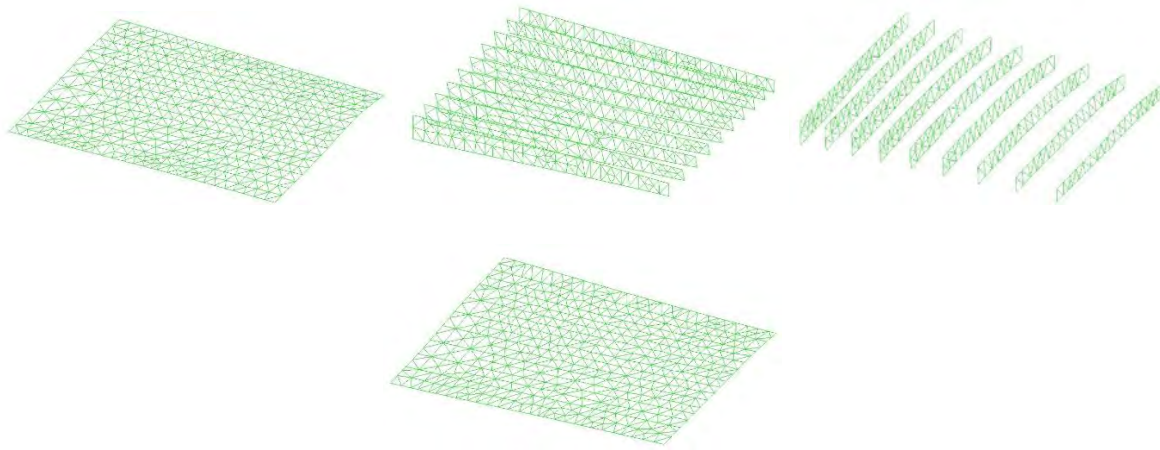


Figure 5 : a Geometry of Rear Wing box of Boeing HSCT N 2 Wing using Linear shape Method b Mesh using Triangular Elements

Figure 6 shows a local panel from the top skin from the wing-box using *SpaRibs* intersection created using the algorithm.

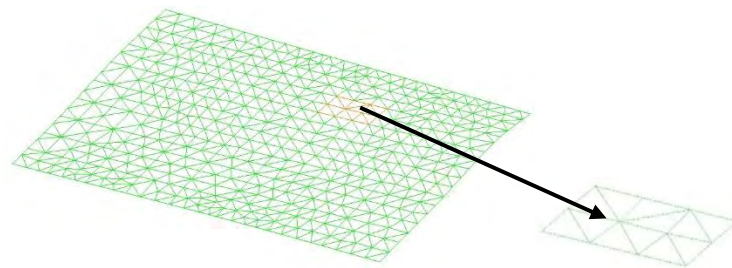


Figure 6 : Local Panel from Upper Skin of Boeing N 2 HSCT Wing box

INTEGRATION OF ALGORITHM WITH EBF3GLWINGOPT

The algorithm as discussed is integrated with **EBF3GLWingOpt** framework to create local panel on the upper and lower skin of the NASA CRM Wing (high-aspect ratio transport aircraft wing) for a range of *SpaRibs* configurations possible using the *Extended-space Method*. The wing-skin is first divided by the set of *SpaRibs* which replace the ribs. Each of the sections is then divided by the family of *SpaRibs* that replace the spars. The boundary nodes are the nodes common to the wing-skin and the *SpaRibs*, thus bounding the local panel. Since the algorithm is completely based on set operations performed on the connectivity matrix and independent of nodal coordinates, the algorithm can be used in a variety of problems requiring generation of local panels. The process is

also independent of the element ids and it works no matter in whatever order the elements are distributed. Depending on the shape of the bounding *SpaRibs* the panel can have any number of edges starting from three and up. Another advantage of this method is that the boundary nodes of each of the local panels is already determined and the information is stored to be used to impose boundary conditions during the optimization process.

In case of irregular panels, it is more difficult to determine the order in which the edges are numbered in MSC.PATRAN. Further a panel can have any number of edges. This makes it a challenging to develop a generalized parameterization method to create stiffener on panels. An alternative approach is developed where stiffeners are laid down on the global model and are meshed with the quad elements. The element size is chosen to be larger than the height of the stiffeners to ensure that the stiffeners are represented by a chain of quad elements with each elements sharing two common nodes with the skin. The nodes belonging to each of the local panels is already known by the method of creating local panels using the Mesh Continuity Algorithm. The MSC.NASTRAN .bdf file for the stiffeners are generated and read to find the quad elements with nodes common with the nodes of each of the local panels. These elements form the stiffeners for respective local panels. An example of such a stiffened panel is shown in Figure 7.

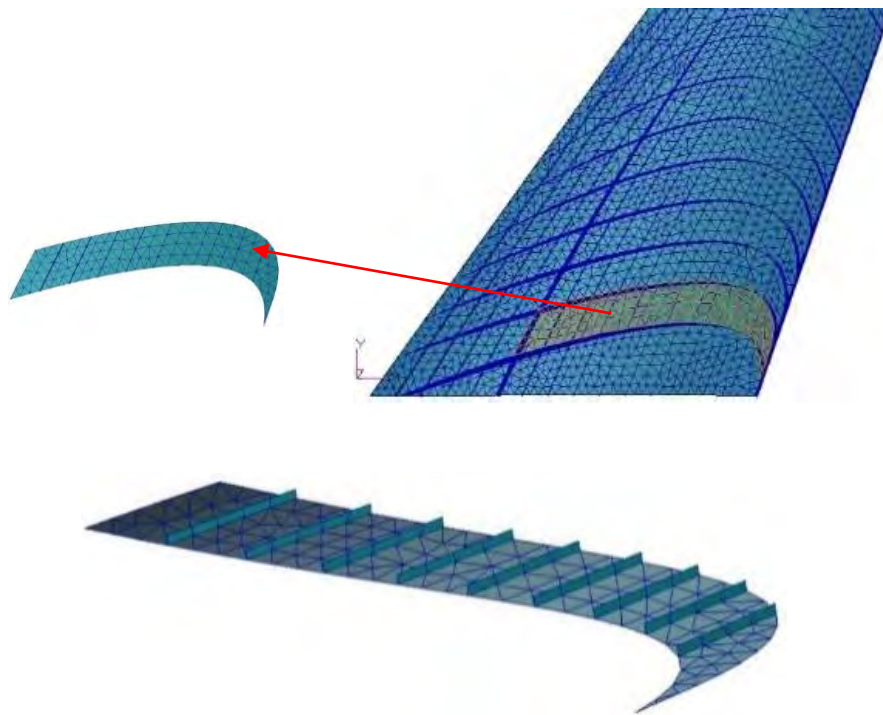
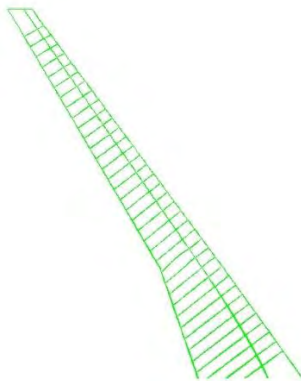

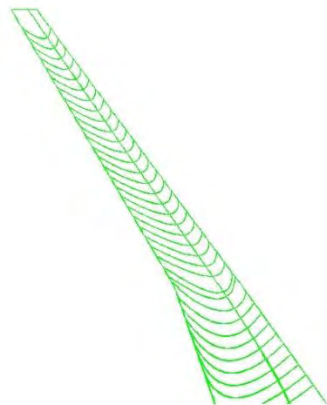
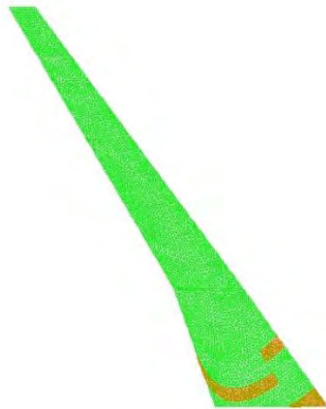
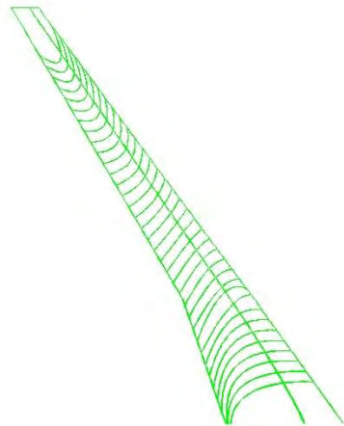
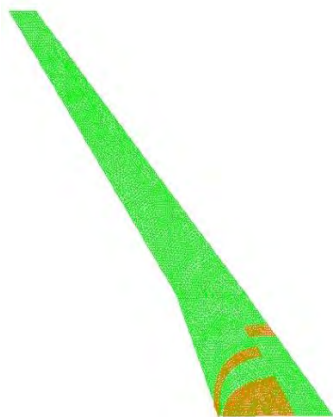


Figure 7 : Local Panel with Stiffeners formed by quad Elements

E AMPLES OF APPLICATION

The proposed algorithm has been implemented on wings with different *SpaRibs* profile and is found to be effective for *SpaRibs* of different orientation and curvature. Table 1 shows some of the examples.

Table 1: Creation of Local Panels from NASA CRM Wing using SpaRibs intersection

SpaRibs Profile	E ample of Local Panels
	
	
	

CONCLUSIONS

This paper gives a detailed description of a new algorithm to create stiffened local panels from the finite element model of the wing. The algorithm used in the original **EBF3GLWingOpt** framework to create local panels fails for many of the *SpaRibs* configurations possible to be created using the new method of parameterization as it was limited to the creation of four-edged panels only with two edges along adjacent spars. The new algorithm is based on performing set operations on the connectivity data of the wing finite element model and is independent of nodal coordinate. It can be used to create local panels of any shape and size and can be used for structures other than the NASA CRM wing. Elements of the stiffeners attached with each of the local panels are found and stiffened panels are created. Once the local panels are determined, the structure is ready for global-local optimization.

REFERENCES

- [1] L. A. Schmit and R. K. Ramanathan. Multilevel Approach to Minimum Weight Design Including Buckling Constraints. *AIAA Journal* (1978) 16:97–104
- [2] L. A. Schmit. Structural Synthesis: Its Genesis and Development. *AIAA Journal* (1981) p. 1249–1263,
- [3] L. A. Schmit. Structural Design by Systematic Synthesis. Pittsburg (1960)
- [4] R. T. Haftka. Optimization of Flexible Wing Structures Subject to Strength and Induced Drag Constraints. (1977) 15:1101-1106
- [5] J. H. Starnes Jr. and R. T. Haftka. Preliminary Design of Composite Wings for Buckling, Strength, and Displacement Constraints. *Journal of Aircraft* (1979) 16:564–570
- [6] R. T. Haftka, J. H. Starnes Jr., F. W. Barton and S. C. Dixon. Comparison of Two Types of Optimization Procedures for Flutter Requirements. *AIAA Journal*. (1975) 13:1333–1339
- [7] R. E. Fulton, J. Sobieszczanski, O. Storaasli, E. J. Landrum and D. Loendor. Application of Computer-Aided Aircraft Design in a Multidisciplinary Environment. *Journal of Aircraft*, (1974) 11:369–370
- [8] I. Kroo, S. Altus, R. Braun, P. Gage and I. Sobieski. Multidisciplinary Optimization Methods for Aircraft Preliminary Design. 5th AIAA Symposium on Multidisciplinary Analysis and Optimization (1994)
- [9] V. M. Manning. Large-scale design of supersonic aircraft via collaborative Optimization, PhD Thesis, Stanford University. (1999)
- [10] N. E. Antoine and I. M. Kroo. Framework for aircraft conceptual design and environmental performance studies. *AIAA Journal*. (2005) 43:2100-2109
- [11] R. P. Henderson, J. Martins and R. E. Perez. Aircraft Conceptual Design for Optimal Environmental Performance. *Aeronautical Journal* (2012) 116:1
- [12] J. J. Alonso and M. R. Colonno. Multidisciplinary optimization with applications to sonic-boom minimization. *Annual Review of Fluid Mechanics*. (2012) 44:505-526
- [13] J. R. R. A. Martins and A. B. Lambe. Multidisciplinary Design Optimization: A Survey of Architectures. *AIAA Journal*. (2013) 51:2049-2075

- [14] J. Sobieszczanski-Sobieski and R. T. Haftka. Multidisciplinary Aerospace Design Optimization: Survey of Recent Developments. *Structural Optimization*. (1997) 14:1-23
- [15] P. D. Ciampa and B. Nagel. Global Local Structural Optimization of Transportation Aircraft Wings. 51st AIAA/ASME/ASCE/AHS/ASC Structures, Structural Dynamics, and Materials Conference, Orlando, Florida. (2010)
- [16] K. M. Taminger and R. A. Hafley. Electron Beam Freeform Fabrication for Cost Effective Near-Net Shape Manufacturing," in , VA: NATO/RTOAVT-139 specialists' meeting on cost effective manufacture via net shape processing. Amsterdam (The Netherlands): NATO (2006) Hampton (2006)
- [17] D. Locatelli, S. B. Mulani and R. K. Kapania. Wing-Box Weight Optimization Using Curvilinear Spars and Ribs (SpaRibs). *Journal of Aircraft*. (2011) 48:1671-1684
- [18] D. Locatelli, A. Y. Tamijani, S. B. Mulani and R. K. Kapania. Multidisciplinary Optimization of Supersonic Wing Structures Using Curvilinear Spars and Ribs (SpaRibs). 54th AIAA/ASME/ASCE/AHS/ASC Structures, Structural Dynamics, and Materials Conference, Structures, Structural Dynamics, and Materials and Co-located Conferences, Boston, Massachusetts. (2013) AIAA 2013-1931.
- [19] M. Jrad, S. De and R. K. Kapania. Global-Local Aeroelastic Optimization of Internal Structure of Transport Aircraft Wing. 18th AIAA/ISSMO Multidisciplinary Analysis and Optimization Conference, Denver, Colorado. (2017)
- [20] S. De, M. Jrad, D. Locatelli, R. K. Kapania and M. Baker. SpaRibs Geometry Parameterization for Wings with Multiple Sections using Single Design Space. 58th AIAA/ASCE/AHS/ASC Structures, Structural Dynamics, and Materials, Dallas. (2017)
- [21] K. Singh, W. Zhao and R. K. Kapania. Optimal Design of Curvilinearly Stiffened Shells. 58th AIAA/ASCE/AHS/ASC Structures, Structural Dynamics, and Materials Conference, Washington DC. (2017)
- [22] I. Sobieski and I. Kroo. Aircraft Design Using Collaborative Optimization. 34th Aerospace Sciences Meeting and Exhibit. (1996) AIAA-96-0715
- [23] R. Braun, P. Cage, I. Kroo and I. Sobieski. Implementation and Performance issues in Collaborative Optimization. 6th AIAA/NASA/ISSMO Symposium on Multidisciplinary. (1996). AIAA-96-4017
- [24] J. Sobieszczanski-Sobieski, B. B. James and A. R. Dovi. Structural Optimization by Multilevel Decomposition. *AIAA Journal*. (1985) 23: 1775–1782
- [25] J. Sobieszczanski-Sobieski. Optimization by Decomposition: A Step from Hierarchic to Non-Hierarchic Systems. NASA Langley Research Center TR-CP-3031, Hampton, VA (1988)
- [26] Q. Liu, M. Jrad, S. B. Mulani and R. K. Kapania. Global/Local Optimization of Aircraft Wing Using Parallel Processing. *AIAA Journal*. (2016) 54: 3338-3348

An Efficient Solution Approach for Multiphysics Modeling of Electrosurgery

Suvranu De^{*}, Rahul .^{**}, Zhongqing Han^{***}

^{*}Rensselaer Polytechnic Institute, ^{**}Rensselaer Polytechnic Institute, ^{***}Rensselaer Polytechnic Institute

ABSTRACT

Instruments that utilize radiofrequency (RF) alternating current are increasingly being utilized to perform a variety of surgical and other therapeutic procedures. Modeling of such procedures considering coupled electro-thermo-mechanical multiphysics and multiscale interactions with high degree of realism is challenging. Current best practices for the efficient solution of such multiphysics problems are based almost exclusively on multigrid methods and preconditioned Krylov subspace methods [1]. However, design of efficient application specific monolithic multiphysics multigrid solvers or preconditioners for the Krylov solvers is challenging [2]. We have developed a multi-physics model to investigate the effects of cellular level mechanisms on the electro-thermo-mechanical response of hydrated soft tissues with radiofrequency (RF) activation. A level set method is used to capture the interfacial evolution of tissue damage with the level set evolution equation derived from the second law of thermodynamics. We propose a coupled scheme to solve the resulting algebraic set of equations for the electric charge conservation, linear momentum balance, and temperature evolution equation. The coupled systems of equations are solved simultaneously using a Krylov subspace based iterative solver (e.g. GMRES) with an efficient block preconditioner. The block preconditioning technique effectively deflates the spectrum of the system matrix by clustering eigenvalues of system matrix around suitably chosen parameters [3]. This results in exponential convergence of the Arnoldi iterations with linear increase in the computational cost with increasing number of degrees of freedom when compared to the well-known block Jacobi and an algebraic multigrid (AMG) based preconditioners. Example problems illustrate the computational accuracy and efficiency of the technique. References [1] Keyes, D.E., McInnes, L.C., Woodward, C., et al., 2013. Multiphysics simulations: Challenges and opportunities. *Int. J. High Perform. Comput. Appl.* 27, 4-83. [2] Verdugo, F., Wall, W.A., 2016. Unified computational framework for the efficient solution of n-field coupled problems with monolithic schemes. *Comput. Methods Appl. Mech. Eng.*, 310, 335-366. [3] Rahul, De, S., 2011. An efficient block preconditioner for Jacobian-free global-local multiscale methods. *Int. J. Numer. Methods Eng.*, 87, 639-663.

Micropolar Asymptotic Homogenization for Periodic Cauchy Materials

Maria Laura De Bellis*, Andrea Bacigalupo**, Giorgio Zavarise***

*University of Salento, **IMT Lucca, ***Polytechnic University of Turin

ABSTRACT

We present a micropolar-based asymptotic homogenization approach [1,2] for the analysis of composite materials with periodic microstructure. The up-scaling relations are inspired by those originally proposed by [3] in the framework of the computational homogenization, expressing the local displacement field as a function of a cubic polynomial kinematic map depending on first, second and third order homogeneous tensors directly related to the classical and micropolar 2D deformation modes [4,5,6]. The local displacement field is described as superposition of the macroscopic driven kinematic map and local periodic perturbation fields. These perturbation functions are inherently related to the heterogeneous nature of the composite medium and are derived from the solution of recursive cell problems. The down-scaling relations are derived from a newly proposed third order asymptotic expansion of the local displacement field in terms of the macroscopic displacement and its first, second and third order gradients. The overall micropolar elastic tensors derive from a properly conceived energy equivalence between the macroscopic point and a representative portion of the heterogeneous material at the microscopic scale. Different applications to bi-phase orthotropic layered material to are proposed in order to exploit the capabilities of the proposed approach. [1] Smyshlyaev V. and Cherednichenko K. On rigorous derivation of strain gradient effects in the overall behaviour of periodic heterogeneous media. *Journal of the Mechanics and Physics of Solids*, 48(6):1325-1357, (2000). [2] Bacigalupo, A., Second-order homogenization of periodic materials based on asymptotic approximation of the strain energy: formulation and validity limits *Meccanica*, (49), 1407-1425 (2014). [3] Forest, S., Sab, K., Cosserat overall modelling of heterogeneous materials. *Mech. Res. Commun.* 25, 449-454 (1998). [4] Addessi, D., De Bellis, M. L. and Sacco, E. Micromechanical analysis of heterogeneous materials subjected to overall Cosserat strains. *Mechanics Research Communications*, 54:27-34, (2013). [5] Addessi, D., De Bellis, M. L. and Sacco, E. A micromechanical approach for the Cosserat modeling of composites. *Meccanica*, 51(3):569-592, (2016). [6] Bacigalupo, A. and Gambarotta, L. Computational two-scale homogenization of periodic masonry: Characteristic lengths and dispersive waves. *Computer Methods in Applied Mechanics and Engineering* 213:16-28, (2012).

Mechanical and Structural Multi-scale Modelling of Bone Material

Paolino De Falco^{*}, Li Xi^{**}, Wolfgang Wagermaier^{***}, Richard Weinkamer^{****}, Peter Fratzl^{*****},
Himadri Shikhar Gupta^{*****}

^{*}(1) School of Engineering and Material Sciences, Queen Mary University of London, (2) Max Planck Institute of Colloids and Interfaces, Department of Biomaterials, ^{**}(1) School of Engineering and Material Sciences, Queen Mary University of London, (3) Department of Nuclear Engineering, North Carolina State University, ^{***}(2) Max Planck Institute of Colloids and Interfaces, Department of Biomaterials, ^{****}(2) Max Planck Institute of Colloids and Interfaces, Department of Biomaterials, ^{*****}(2) Max Planck Institute of Colloids and Interfaces, Department of Biomaterials, ^{*****}(1) School of Engineering and Material Sciences, Queen Mary University of London

ABSTRACT

To enhance the predictive power of mechanical models of bone, not only do the models have to be improved, but also new experimental data matched to model predictions at multiple hierarchical levels. At the level of the mineralized bone matrix, relatively few computational studies exist linking the structural parameters and mechanical properties at different length scales. Here, we propose a two dimensional and two-level hierarchical model of the bone matrix (mineralized fibril and lamella) to predict fibrillar mechanical response as a function of architectural parameters of the mineralized matrix. Specifically, we built a modified version of the laminate theory to predict the Young's modulus of bone as a function of the aspect ratio of mineral platelets [1] and degree of orientation. Our model shows that lowered mineralization combined with altered mineral nanostructure leads to lowered mechanical competence in bone. Our approach was also applied to fit experimental data obtained by small angle X-ray scattering (SAXS) on models of healthy and glucocorticoid induced osteoporotic bone showing how the reduced mineral volume fraction, reduced degree of alignment and aspect ratio are responsible for reduced mechanical properties in osteoporotic bone. In an attempt to expand scattering experiments for structural investigations of the bone mineral nanostructure to three dimensions, we also present first results on a new approach based on 3D SAXS experiments and Computed Tomography algorithms. These investigations can be used as tool for the diagnosis of bone diseases and the prediction of mechanical consequences of structural changes.

A COMPUTATIONAL GEOMETRY BASED ALGORITHM FOR SOLVING THE YIELD-LINE PROBLEM

M. DE FILIPPO*, J. S. KUANG†

*The Hong Kong University of Science and Technology
Clear Water Bay, Kowloon, Hong Kong
mdefilippo@connect.ust.hk

† The Hong Kong University of Science and Technology
Clear Water Bay, Kowloon, Hong Kong
cejkuang@ust.hk

Keywords: Collapse Mechanism, Computational Geometry, Computational Mechanics, Reinforced Concrete Slabs, Yield-line.

Abstract. Horizontal Reinforced Concrete (RC) slabs are commonly used in civil engineering industry for the construction of floors, ceilings, and more importantly bridges. The adoption of Finite Element Method (FEM) in industry has become massive to an extent to which engineers are starting to blindly rely on such analyses. However, the usage of FEM is not proper for every structural problem or purpose. For the case of structural assessment of flat RC slabs due to transverse load, plastic methods represent a more valid alternative and suitable approach. The plastic analysis involving the problem of assessing their strength and researching the most critical collapse mechanism due to flexure is well-known in literature as yield-line problem. Throughout the last century, many researchers have attempted to solve such problem. For simple geometries and boundary conditions, exact solutions were found, but they have showed lack of general applicability. Several techniques of approximated upper and lower bound methods have then been proposed, however nowadays the problem yet remains only partially solved. This paper aims at targeting the problem of collapse mechanism detection, and proposes an algorithm based on the solution of a set of computational geometry problems. The input is given by a plastically admissible moment field, which can be obtained through whatever method, and a fully automated technique is built according to the location of each yielded and next-to-yield moment triad in the physical domain. The results are shown along with the method of solution for the typical case of square simply supported slab under transverse distributed load.

1 INTRODUCTION

The yield-line method of analysis is a long-established hand method for evaluating the maximum carrying capacity of a slab, and its linked collapse mechanism. In the early ages of last century, the first version of such method has been proposed. In 1923, Ingerslev¹ was the first to coin the term 'yield-line', which describes subsequent locations along which yielding conditions are fulfilled. The estimation of such yield-line patterns gives an approximate evaluation of the collapse mechanism of the slab. As introduced, an analysis of the assessment of a slab is then subdivided into two parts, namely, estimation of maximum sustainable load, and detection of collapse mechanism. This paper will focus on this last aspect of the problem. In the past decades, this field of research has attracted the interest of many researchers. Middleton² developed a computer program for the assessment of RC slabs, famous nowadays in the UK, called COBRAS³. The software is based on a library of potential crack patterns. He has observed several recurrent collapse mechanisms that may occur when analyzing square slabs under different boundary and load conditions. He has then implemented them in an experience-based software. Chan⁴, Munro et al.⁵, and Balasubramanyam⁶ also proposed several techniques for the identification of the most critical layout of yield-lines. Many of the proposed methods of solution involve the implementation of optimization techniques through either Linear Programming (LP) or Conic Programming (CP), according to the degree of the imposed constraints. Given the complex fractural behavior of RC slabs, the problem is mathematically and geometrically hard to solve. Many attempts turned to be successful, but only on specific cases. Nowadays, there is still lack of fully automated yield-line analysis tools able to properly detect the collapse mechanism of RC slabs due to bending. This paper aims at presenting an easy-to-compute technique for the detection of a layout of yield-lines linked to the collapse of slabs, implemented through the usage of simple computational geometry algorithms. The simple case of a square simply supported slab under uniform transverse load has been taken as sample, and the overall procedure along with obtained results are shown throughout this paper.

2 ASSUMPTIONS

The method of detection of collapse mechanisms for RC slabs to be introduced in the next section is based on the following assumptions:

- The problem is restricted to static plate bending due to transverse loading conditions.
- Collapse mechanisms are solely associated with bending. The effects of shear are not taken into account by any mean. Shear failure is also disregarded.
- It is assumed that ductility of the slab is adequate enough for brittle failure to not occur.
- A plastically admissible field of moments has to be provided as input. Bending moments in the two directions of the slab, twisting moment, and principal moments are required. They can have been evaluated through different tools, such as a Non-linear FE analysis including the effects of plasticity in both concrete and steel.

In the case to be shown, the field of moments has been computed through the so-called Pseudo-Lower Bound Method for RC Slabs⁷.

3 YIELD CHECK

Given the definition of Yield-line, it is imperative to perform a check on whether yielding conditions are fulfilled by triads of moments, $\mathbf{m}^{e(i,j)} := \{M_x^{e(i,j)}, M_y^{e(i,j)}, M_{xy}^{e(i,j)}\}$, individually associated to a certain element e at the i -th row and j -th column in the mesh. The detection of physical locations in the slab where yielding is reached is of critical importance for the identification of a collapse mechanism. A bi-conical linearized version of Nielsen's criterion^{8,9}, as shown in a 3-dimensional $M_x - M_y - M_{xy}$ space in Fig. 1(a), is used as reference yield criterion, and it is referred to as f . Such figure also shows a sample configuration of moment triads with reference to the mentioned criterion. Yielded moments and non-yielded moments are marked accordingly. Fig. 1(b) illustrates the location of such yielded moments in the physical domain of the slab.

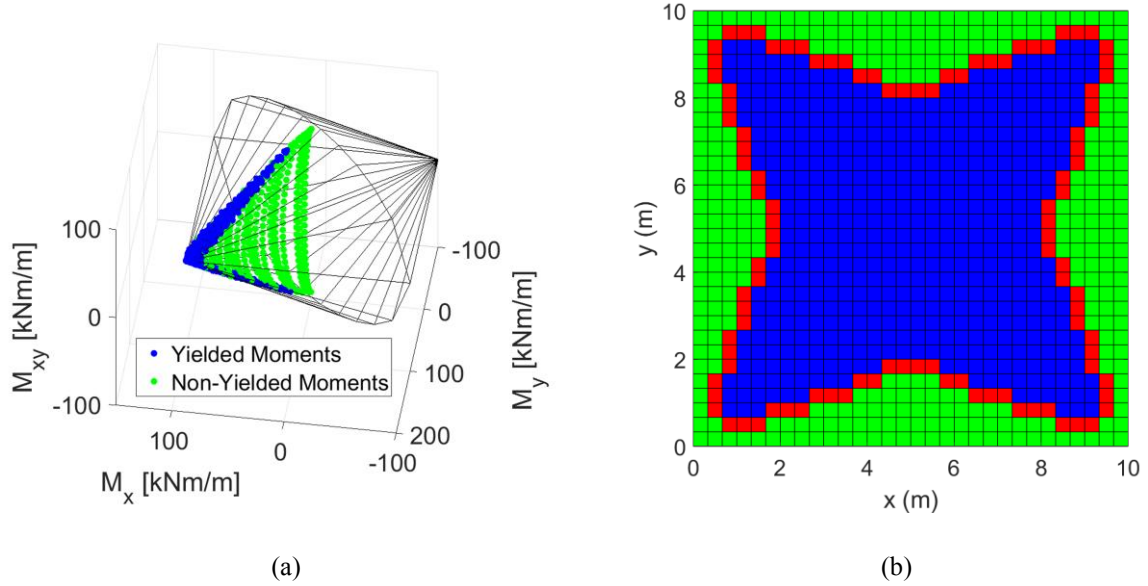


Figure 1: Moments Configuration: (a) Location of yielded and non-yielded moment triads in the moments space. (b) Location of yielded and non-yielded moments on the slab, respectively, in blue and green elements. Non-yielded neighbors of yielded elements (next-to-yield) are depicted in red.

A yield-check is performed according to the yielding condition given in the following Eq.

$$\mathbf{m}^{e(i,j)} := \{M_x^{e(i,j)}, M_y^{e(i,j)}, M_{xy}^{e(i,j)}\} \mid f(\mathbf{m}^{e(i,j)}) = 0 \quad (1)$$

4 METHODOLOGY

4.1 Mechanism triggering criterion

The moment triads have been located, respectively, in the slab, and in the moment space. Given the configurations shown in Fig. 1, it has to be defined whether yielding in the slab is triggering a collapse mechanism or not. In order to do so, a criterion has to be established for automatically evaluate the eventual occurrence of a collapse. Such criterion is formulated as it follows:

“Collapse of an slab under transverse load, due to flexure, is occurring if and only if at least a set of yield lines can be traced from the center of load to all constrained edges, creating a convex closed polygon composed by triangular facets.”

Hence, the problem of detection of the collapse mechanism can mathematically be expressed as it follows.

Given the physical domain of the slab, composed by the set Λ of all elements $e(i, j)$ constituting the mesh, the subset Ψ of yielded elements is defined by the elements satisfying the condition given in Eq. (1), hence it follows that

$$\mathbf{m}^{e(i,j)} := \{M_x^{e(i,j)}, M_y^{e(i,j)}, M_{xy}^{e(i,j)}\} \mid f(\mathbf{m}^{e(i,j)}) = 0 \vdash e(i, j) \in \Psi \quad (2)$$

The subset Ω of non-yielded elements $e(i, j)$ having $e(i \pm 1, j)$, left- or right-neighbor, or $e(i, j \pm 1)$, bottom- or top-neighbor, as yielded element, hence satisfying at least one of Eq. (3) and (4), are classified as non-yielded neighbors of yielded elements, or more simply as next-to-yield elements.

$$\{\mathbf{m}^{e(i,j)} \mid f(\mathbf{m}^{e(i,j)}) < 0, f(\mathbf{m}^{e(i \pm 1, j)}) = 0\} \vdash e(i, j) \in \Omega \quad (3)$$

$$\{\mathbf{m}^{e(i,j)} \mid f(\mathbf{m}^{e(i,j)}) < 0, f(\mathbf{m}^{e(i, j \pm 1)}) = 0\} \vdash e(i, j) \in \Omega \quad (4)$$

A representation of their location in the slab is given in Fig. 1(b). Yield line patterns have to be searched within the subset $\Upsilon := \Psi \cup \Omega \subseteq \Lambda$ of yielded and next-to-yield elements. The subset of elements in Ω are hence conservatively considered to have the same residual capacity of a yielded element. Their exclusion from Υ would provide an additive reserve of bearing capacity.

Given the set of all vertices in the slab, $\mathbf{V} = \{v_1, v_2, \dots\}$, the subset of yielded and next-to-yield vertices is then defined as given in the following

$$\forall e(i, j) \subseteq \Upsilon, \Upsilon := \{v_1, v_2, \dots\} \in e(i, j) \subseteq \Upsilon \quad (5)$$

By defining edges as connections of geographically subsequent vertices in Υ , and their weights d , as the distances from one vertex to another, an undirected graph is created. A representation of such graph, according to the location of yielded and next-to-yield elements is given in Fig. 2.

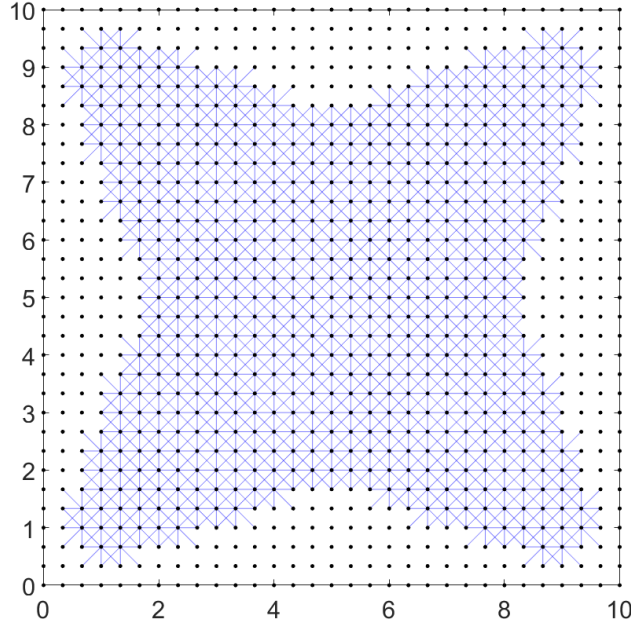


Figure 4 Undirected graph obtained through vertices \mathbf{Y} , according to the configuration given in Fig. 3.

Let $\mathbf{B} := \{b_1, b_2, \dots\}$ be the set of vertices along the constrained boundaries, as displayed in Eq. (6), Φ is defined as the subset of yielded vertices at the boundaries, and as consequence it follows that $\Phi \subseteq \mathbf{B}$, $\Phi \subseteq \mathbf{Y}$.

$$\forall b \in \mathbf{B} \mid b \in \mathbf{Y} \therefore b \in \Phi \quad (6)$$

If the boundary conditions at the vertex b do not constrain the bending moments, M_x and M_y , hence in case at least one of Eq. (7) or Eq. (8) is satisfied, then such vertices will also be included in \mathbf{Y} , and hence in Φ .

$$\forall b \in \mathbf{B} \mid M_x^b = 0 \vdash b \in \mathbf{Y} \therefore b \in \Phi \quad (7)$$

$$\forall b \in \mathbf{B} \mid M_y^b = 0 \vdash b \in \mathbf{Y} \therefore b \in \Phi \quad (8)$$

As consequence of the aforementioned definition of mechanism triggering criterion, a set of paths has to be found from the center of load c to at least two yielded vertices at each constrained boundary $b \in \Phi$.

4.2 Yield-line tree

A set of feasible yield-lines can be found by solving a set of Shortest Path Problems (SPP) from the center of load to the subset of yielded and next-to-yield vertices in Φ at each constrained boundary. As shown in the above figure, no path exists connecting the vertex

located at the center of load c (corresponding to the center of the slab in the current case of uniformly distributed load) and any vertex $b \in \Phi$, because $\Phi := \emptyset$ hence a collapse mechanism cannot be triggered. An example in which, instead, a feasible solution to the SPP problem exists, is illustrated in Fig. 3.

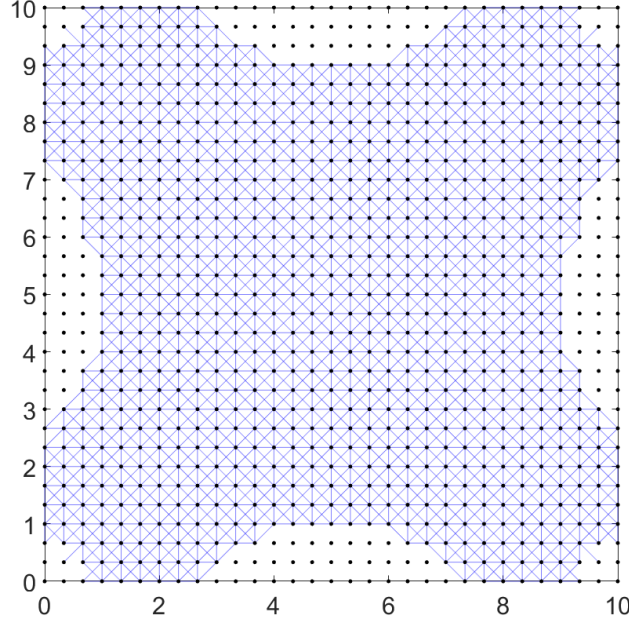


Figure Undirected graph obtained through vertices \mathbf{Y} , according to a moment configuration corresponding to a higher load intensity than the one shown in Fig. .

The SPP returns m sets of paths \mathbf{P} , composed by vertices $v \in \mathbf{Y}$, ending in each reachable vertex $b \in \Phi$ at each constrained boundary, with different weights $d(\mathbf{P})$. They are all feasible solutions for triggering a collapse mechanism. In accordance with the mechanism criterion, the set of non-coincident paths \mathbf{S} with minimum $d(\mathbf{P})$, hence the shortest (two per each boundary), are chosen to be the most critical. Eq. (9) summarizes the above-mentioned concept, and Fig. 4 displays a sample yield-line tree found for the undirected graph of yielded and next-to-yield vertices and edges illustrated in Fig. 3.

$$\mathbf{S} := \{c, \dots, v, \dots, b\} \mid \min_{v \in \mathbf{Y}, b \in \Phi} d(\mathbf{P}_k) \quad (9)$$

<p>with $\mathbf{P}_k := \{c, \dots, v, \dots, b\}$ $b \in \Phi \subseteq \mathbf{B}$ $k = \{1, \dots, m\}$</p>	<p>sample k-th shortest paths from c to b a yielded or next-to-yield vertex at the boundary index of found path</p>
--	--

m amount of feasible paths from c to each reachable vertex $b \in \Phi$ for a single constrained edge

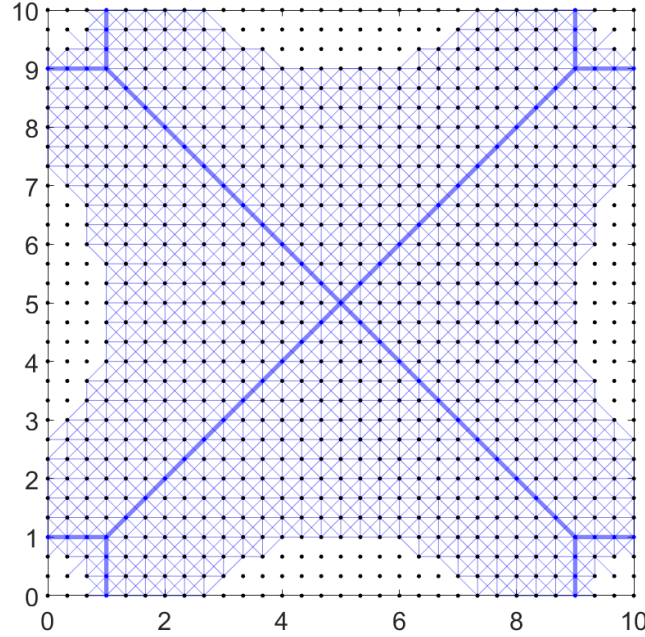


Figure 4.3 Undirected graph obtained through vertices \mathbf{Y} for a moment configuration for which a yield line tree, representing the cracking patterns, can be detected. Each set of yield lines is highlighted with blue lines.

4.3 Axes of rotation

The last requirement enounced in the mechanism triggering criterion for the occurrence of collapse, is the creation of a convex closed path connecting the end points of the set of paths \mathbf{S} such that triangular facets can be created. The yield-lines constituting such paths are commonly referred in literature as axes of rotation or hogging yield-lines. A collapse mechanism is expected to occur within the closed path, with the triangular facets rotating with respect to each other around yield-lines, and rotating around the axes of rotation. The parts of the slab falling outside the closed path constituted by axes of rotation are expected to remain intact, hence they do not participate in the collapse mechanism. The rotation around the axes of rotation requires yielding to occur due to a hogging moment, therefore the solution is contained within a subset $\mathbf{Y}^- = \mathbf{\Psi}^- \cup \mathbf{\Omega}^- \subseteq \mathbf{\Lambda}$. The subset $\mathbf{\Psi}^-$ defines yielded hogging elements, so that Eq. (10) is satisfied. The subset $\mathbf{\Omega}^-$ of non-yielded elements $e(i, j)$ for which at least one of Eq. (11) and (12) is satisfied, are classified as non-yielded neighbors of yielded hogging elements, or more simply as next-to-yield hogging elements.

$$\left\{ \mathbf{m}^{e(i,j)} \mid M_1^{e(i,j)} < 0, f(\mathbf{m}^{e(i,j)}) = 0 \right\} \vdash e(i,j) \in \mathbf{\Psi}^- \quad (10)$$

$$\left\{ \mathbf{m}^{e(i,j)} \mid M_1^{e(i,j)} < 0, f(\mathbf{m}^{e(i,j)}) < 0, f(\mathbf{m}^{e(i\pm 1,j)}) = 0 \right\} \vdash e(i,j) \in \Omega^- \quad (11)$$

$$\left\{ \mathbf{m}^{e(i,j)} \mid M_1^{e(i,j)} < 0, f(\mathbf{m}^{e(i,j)}) < 0, f(\mathbf{m}^{e(i,j\pm 1)}) = 0 \right\} \vdash e(i,j) \in \Omega^- \quad (12)$$

with $\left| M_1^{e(i,j)} \right| > \left| M_2^{e(i,j)} \right|$ hogging principal moments greater in absolute value than other principal moments at the same location

The subset of yielded and next-to-yield hogging vertices is then defined as

$$\forall e(i,j) \subseteq \mathbf{Y}^-, \mathbf{Y}^- := \{v_1, v_2, \dots\} \in e(i,j) \subseteq \mathbf{Y}^- \quad (13)$$

Similarly as previously done for \mathbf{Y} , again edges are defined as connections of geographically subsequent vertices in \mathbf{Y}^- , and their weights d , as the distances from one vertex to another. An undirected graph composed of such edges and vertices is created. A representation of such graph, according to the locations of yielded hogging elements, is illustrated in Fig. 5.

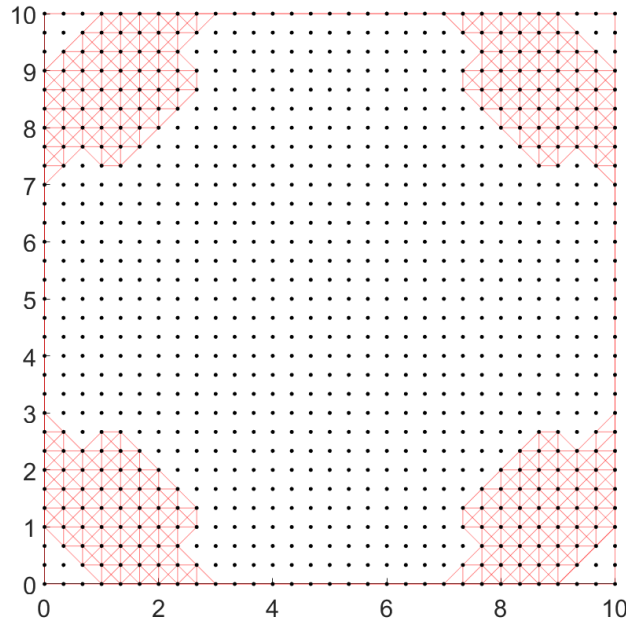


Figure Undirected graph obtained through vertices \mathbf{Y}^- .

The path \mathbf{R} is obtained through the junction of all the n shortest paths \mathbf{P} , composed by vertices $v \in \mathbf{Y}^-$, passing through all the end vertices $b \in \mathbf{S}$. Such path is found by the individual assessment of SPPs between subsequent end vertices in the paths \mathbf{S} . The above-mentioned concept is summarized in Eq. (14). The paths can be evaluated according to subsequent vertices either clockwise or counterclockwise.

$$\mathbf{R} := \{b_1, \dots, v, \dots, b_2\} \cup \dots \cup \{b_n, \dots, v, \dots, b_1\} \mid \min_{v \in \mathbf{Y}^-, b \in \mathbf{S}} d(\mathbf{P}_r) \quad (14)$$

with $\mathbf{P}_r := \{b_l, \dots, b_{l+1}\}$ sample r-th shortest path from b_l to b_{l+1}
 l generic index
 $r = \{1, \dots, n\}$ index of found path
 n amount of paths necessary to connect all the geographically subsequent vertices $b \in \mathbf{S}$

The path \mathbf{R} defining the axes of rotation, is superposed to the yield-line tree (shown in Fig. 4) obtaining as result the collapse mechanism displayed in Fig. 6. Axes of rotation and yield-line tree are respectively depicted in red and blue lines.

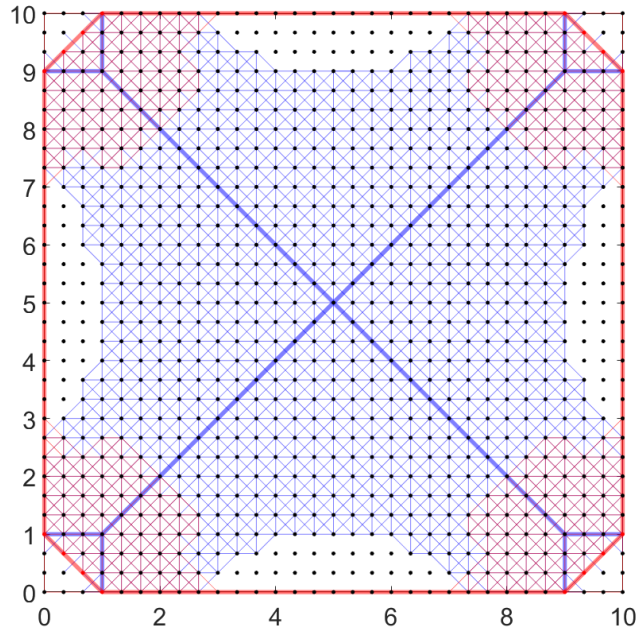


Figure 6 collapse Mechanism composed by yield line tree (blue line) and axes of rotation (red line), respectively lying in the undirected graphs defined by vertices in \mathbf{Y} and \mathbf{Y}^- .

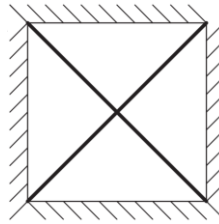


Figure 7 Exact analytical solution of the case of simply supported slab under uniform transverse load.

A close match between the results obtained through the above-shown methodology and the collapse mechanism of RC slabs is found. The exact analytical solution of the analyzed case of simply supported slab under uniform transverse load is given in Fig. 7.

DISCUSSION

From the comparison of Fig. 6 and 7, it can be noticed that the obtained solution fits well the collapse mechanism of the slab. It can immediately be observed that the crack patterns differ at the corners. When approaching the corners, the yield-line tree tends to split into two ends at the two boundaries. Among the assumptions at the basis of this study, failure in the slab is solely associated with bending, hence the effect of shear is not considered. The input of the proposed method is provided by a plastically admissible moment field. At a free or a simply supported boundary, both bending moments are theoretically null. Hence, it is obvious that, in the results of the algorithm, cracks tend to turn to region of the slab where yielding is already reached or is next to be reached, and moments are higher. In Fig. 4, it is clearly illustrated that the undirected graph created from \mathbf{Y} does not include the vertices close to the corners, therefore it is impossible for the algorithm to detect a yield-line ending at the corner. Moreover, as shown in Fig. 5, regions approaching the corners are not included in \mathbf{Y}^- neither. A test carried out by Nilson et al.¹⁰, displayed in Fig. 8, shows experimental evidence of such phenomenon for a simply supported slab under uniform transverse load.

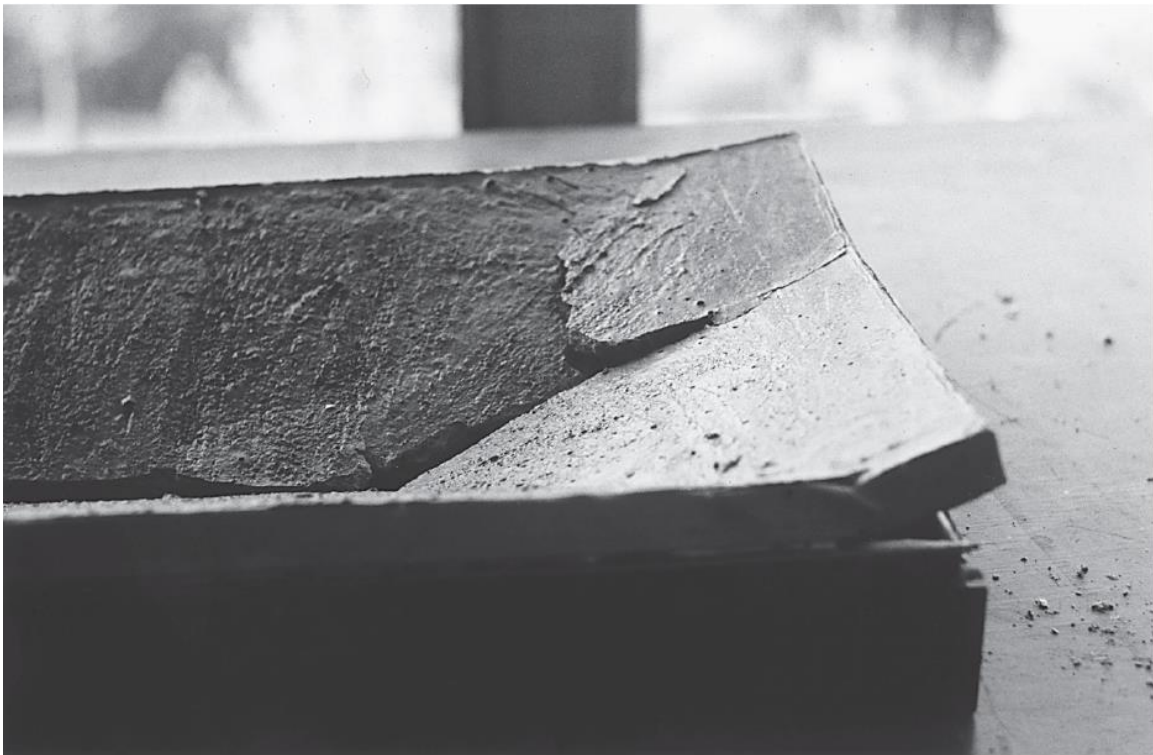


Figure 8 Corner crack of a simply supported beam under uniform transverse load.¹⁰

CONCLUSIONS

A simple algorithm based on computational geometry problems has been presented as attempt of solving the yield-line problem for RC slabs. The evaluation of ultimate load capacity has not been carried out. The focus of the present study is the identification of the most critical collapse mechanism. It has been demonstrated that the problem of identifying critical yield-line patterns leading to collapse of a slab can be formulated through a junction of well-known simple computational geometry problems. The development of a fully reliable method for the automated obtention of crack patterns leading to the collapse mechanism of slabs has not been achieved yet. For many decades several researchers have proposed hand- and automated-based techniques of upper and lower bound limit analyses, with the intention of returning the yield-lines configuration as output. Automated methods mainly involve the usage of non-linear mathematical optimization procedures with either linear or quadratic constraints. The hardness of implementation of such optimization procedures, its computational cost, and the lack of evidence of full reliability, leave the problem yet unsolved. Through the proposed technique, the complexity of the problem has been considerably reduced. The shown analogy gives evidence of a pragmatic match with the desired collapse mechanism obtained with a very low computational cost. The main aim is to overturn the hard belief that recourse to complex mathematical optimization procedures is always necessary when facing this type of problems. SPP is a computational geometry problem for which its solution is largely validated since decades. The analogy of obtained results with collapse mechanisms shows a base of foundation for a more global adaptability. Given the mathematical reliability of the results obtained through SPP, the mentioned analogy is hence founded on a solid basis of geometrical trustworthiness. The method of solution has been tested for the shown simple case, hence its application to more cases remains yet to be investigated. However, the methodology has been thought observing the behavior of RC slabs for several load and boundary condition cases. General applicability and adoption is the biggest challenge in this field of research. The development of a fully reliable technique may potentially be achieved through the involvement of several case-based machine learning algorithms. The ongoing research is focused on the development of a lower bounded solution for the assessment of RC slabs, including both evaluation of load-carrying capacity and detection of collapse mechanism.

REFERENCES

- [1] Ingerslev Å. The strength of rectangular slabs. *ournal of the Institution of tructural Engineers*. 1923;1(1):3-14.
- [2] Middleton CR. Concrete bridge assessment. *ridge urveyor onference*. Mar 24, 1998.
- [3] Middleton CR, Cambridge Enterprise Limited University of Cambridge. Cobras. 2014.

- [4] Chan H. The collapse load of reinforced concrete plate. *International Journal of Numerical Methods in Engineering*. 1972;5(1):57-64.
- [5] Munro J, Da Fonseca A. Yield line method by finite elements and linear programming. *Structural Engineering*. 1978;56B:37-44.
- [6] Balasubramanyam KV, Kalyanaraman V. Yield-Line analysis by linear programming. *Structural Engineering*, ASCE, 1988;114(6):1431-1437.
- [7] De Filippo M, Kuang JS. Concept of a pseudo-lower bound solution for reinforced concrete slabs. *International Journal of Civil and Environmental Engineering*. 2018;12(3):349-353.
- [8] Nielsen MP, Hoang LC. Limit analysis and concrete plasticity. CRC press; 2016.
- [9] Nielsen MP. Yield criteria for reinforced concrete slabs. *flydebetingelser for ernbetonplader. (translated from) nordisk betong, (), 1963.*
- [10] Nilson AH, Darwin D, Dolan CW. *Design of concrete structures*. 15th ed. McGraw-Hill Education (India) Pvt Limited; 2012.

Optimization of Piezoelectric Actuator Polarization and Topology: A Simultaneous Approach Based on the Controllability Gramian

Daniel De Leon^{*}, Juliano Gonçalves^{**}, Eduardo Perondi^{***}

^{*}Federal University of Rio Grande do Sul (UFRGS), ^{**}Federal University of Rio Grande do Sul (UFRGS), ^{***}Federal University of Rio Grande do Sul (UFRGS)

ABSTRACT

This article addresses the problem of piezoelectric actuator design for active structural vibration control using the topology optimization method and a simultaneous approach for the optimization problem with respect to piezoelectric actuator topology and polarization profile is investigated. The optimization problem is written in terms of the controllability Gramian which is a measure that describes the ability of the actuator input to move the system states from an initial condition to a desired final state, at rest for instance, in a finite time interval. A coupled finite element model of the structure with embedded in-plane actuators is derived assuming a two-phase material, and this structural model is written into the state-space representation considering modal displacements and velocities as state variables. Then, the optimization procedure aims to determine the distribution of piezoelectric material and polarization which maximizes the controllability for a given vibration mode. In order to achieve this goal, the material interpolation scheme is carried out by means of the Piezoelectric Material with Penalization and Polarization (PEMAP-P) model [1] and both the optimum actuator layout and polarization profile are obtained simultaneously. The derivatives with respect to the polarization and design variables are calculated analytically. Numerical examples are presented considering the control of bending vibration modes in beams for a couple of boundary conditions and different target vibration modes are taken into account in the optimization problem to show the efficiency of the proposed formulation. A Linear-Quadratic Regulator (LQR) is synthesized for each case of controlled structure in order to compare the influence of the polarization profile on the displacement responses with active damping and we can observe that the simultaneous optimization approach presents an improvement in the control performance for all analyzed cases. The results are also compared to a formulation that does not take into account the electrode polarity in the optimization problem, i.e., the polarization profile is stated a priori and positive and negative regions are insulated of each other by means of null-polarity areas. Moreover, this approach allows the synthesis of a simple control system with only one input channel which is more suitable for practical applications. Therefore, the formulation presented in this work is an initial study towards a single formulation considering several aspects of the actuator topology design problem based on controllability. [1]~Silva ECN, Kikuchi N (1999) Design of piezoelectric transducers using topology optimization. Smart Materials and Structures 8(3):350-364.

Recent Progress on Isogeometric Reduced Quadrature Techniques

Laura De Lorenzis^{*}, Frederik Fahrendorf^{**}, Hector Gomez^{***}

^{*}TU Braunschweig, ^{**}TU Braunschweig, ^{***}Purdue University

ABSTRACT

An efficient implementation of isogeometric analysis (IGA) requires non-standard quadrature techniques. Standard Gaussian rules are not well-suited for IGA, since they do not take advantage of the higher continuity of the shape functions. Therefore different quadrature strategies have been investigated. Bringing the concept of reduced quadrature to the extreme, collocation methods have been proposed and have recently gained increasing attention for linear as well as non-linear problems. A recent important development in isogeometric collocation and, more generally, reduced quadrature techniques has emerged in the context of the so-called variational collocation method. The idea is that for isogeometric basis functions there exists a set of points, termed Cauchy-Galerkin points, such that collocation at these points reproduces the Galerkin solution exactly. Good estimates of these points have been found by means of superconvergence theory. In this talk, we report on recent advancements made possible by the concept of variational collocation both in isogeometric collocation methods and in reduced quadrature rules for Galerkin schemes. In the former, significant advantages are obtained over classical collocation schemes in terms of spatial convergence rates. In the latter, new schemes can be proposed which can be seen as intermediate between the Galerkin variational formulation and the direct evaluation of the strong form in collocation approaches. The potential of the new methods in several research directions is also outlined.

Modelling Thermo-osmosis within Elastic-plastic Porous Media Undergoing Finite Strains

Nico De Marchi^{*}, Valentina Salomoni^{**}

^{*}University of Padova, ^{**}University of Padova

ABSTRACT

Thermo-osmotic processes have been observed in clay-rich materials. Thermal and even chemical osmotic flows are in fact two of the main coupled flows caused by heat and ion transport in clay-rich media (Roshan and Rahman, 2011); the overall direction of water flow by thermo-osmosis depends on the entropy difference between water in the clay pores and that of water trapped in the diffuse interface layer or clay interlayers. Particularly, by assembling the most exhaustive data including the parameters necessary for the analysis on thermo-osmosis available in literature, Gonçalves et al. (2012) confirmed that thermo-osmosis may prevail over the classical Darcy flow driven by pressure gradients, in clay-rich formations under natural or artificial thermal gradients. A coupled three-dimensional THM model in finite strains within the framework of the modified mixture theory is here presented, developed from a previous HM version (Spiezia et al., 2016) for saturated porous media. The upgraded model accounts for a permeability tensor dependent on deformation of the solid skeleton and thermo-osmosis, as well as a mixed three-dimensional finite element is implemented for ensuring stability requirements of the adopted formulation. References: 1. Roshan, H., Rahman, S.S., 2011. A fully coupled chemo-poroelastic analysis of pore pressure and stress distribution around a wellbore in water active rocks. *Rock Mech. Rock Eng.* 44(2): 199-210. 2. Gonçalves, J., de Marsily G., Tremosa, J., 2012. Importance of thermo-osmosis for fluid flow and transport in clay formations hosting a nuclear waste repository. *Earth Planet. Sci. Lett.* 339-340: 1-10. 3. Spiezia, N., Salomoni, V.A., Majorana, C.E., 2016. Plasticity and strain localization around a horizontal wellbore drilled through a porous rock formation. *Int. J. Plasticity* 78: 114-144.

Strengthening Optimization in Curved Masonry Structures by Tensegrity Modelling

Mariella De Piano^{*}, Valentino Paolo Berardi^{**}, Rosa Penna^{***}, Luciano Feo^{****}, Raffaele Miranda^{*****}

^{*}University of Salerno, Italy, ^{**}University of Salerno, Italy, ^{***}University of Salerno, Italy, ^{****}University of Salerno, Italy, ^{*****}University of Salerno, Italy

ABSTRACT

A tensegrity procedure is used to design to the minimal mass of tensile reinforcements of masonry structures with arbitrary shapes [1]-[2]. The proposed strengthening methodology allows for the design of minimal mass resisting mechanisms of systems formed by a network of masonry rods, mainly working in compression, and grids of tensile reinforcements. It creates a minimal mass output of the strengthened model, which can be observed as lumped stress network and connect model of the examined structures [3]-[4]. Assuming a perfectly plastic response by each member, the existence of such resisting mechanisms ensures that the reinforced structure is stable under the examined loading conditions, due to the safe theorem of the limit analysis of elastic-plastic bodies. The approach includes an explicit determination of the state of pre-stress to be applied to tensile reinforcements, in order that they are effective under pre-existing loading conditions. Different numerical examples show the potential of the proposed approach in designing minimal mass FRP/FRCM reinforcements of masonry vaults and domes, which are aimed at preserving sufficient 'cracking-adaptation' capacity of the reinforced structure. References [1] Fraternali, F., Carpentieri, G., Modano, M., Fabbrocino, F., Skelton R.E., "A tensegrity approach to the optimal reinforcement of masonry domes and vaults through fiber-reinforced composite materials", *Composite Structures*; 134, 247–254 (2015). [2] Fabbrocino, F., Farina, I., Berardi, V.P., Ferreira, A.J.M., Fraternali, F., "On the thrust surface of unreinforced and FRP-/FRCM-reinforced masonry domes". *Composites. Part B, Engineering*, 83, 297-305, (2015). [3] Fraternali, F., "A Thrust Network Approach to the Equilibrium Problem of Unreinforced Masonry Vaults via Polyhedral Stress Functions". *Mechanics Research Communications*; 37, 198-204, (2010). [4] Berardi, V.P., Chiozzi, A., Fraternali, F., Grillanda, N., De Piano, M., Milani, G., Tralli A., "A numerical approach to the evaluation of collapse load multiplier of masonry curved structures" *Proc. XXIII Aimeta Congress*, 1515-1525 (2017).

FE Investigation of Bond Behaviour of PBO-FRCM Composite for the Strengthening of Masonry Structures

Mario De Stefano^{*}, Valerio Alecci^{**}, Luisa Rovero^{***}, Giulia Misseri^{****}, Gianfranco Stipo^{*****}

^{*}Università di Firenze, ^{**}Università di Firenze, ^{***}Università di Firenze, ^{****}Università di Firenze, ^{*****}Università di Firenze

ABSTRACT

Protection and safeguarding of existing masonry structures, especially those classified as cultural heritage, require to define sustainable and compatible intervention technologies, material acceptance standards and, more importantly, adequate design tools. Innovative intervention strategies pivoting on the use of fibre-reinforced composites have increasingly proliferated in the last years, and have enabled the development of specific applications for existing masonry, using organic-modified cement-based matrixes associated to either organic or inorganic fibre nets characterised by loose weft-warp layouts. In particular, from an engineer-conservationist angle, Fibre Reinforced Cementitious Matrix (FRCM) solutions have overcome major drawbacks of FRPs, such as deterioration of the substrate layer (i.e. ancient masonry to be preserved) due to the well-known debonding phenomena, capacity cutback for high operating temperatures and low breathability, [1-2]. However, results already available in the literature need further investigation especially devoted to the development of reliable safety assessment and design tools, [3]. In this investigation, the response of a poly-benzoxazole (PBO) FRCM system experimentally tested on both its standalone constituents and on composite layout adhered to bricks, i.e. double-shear test (DST), is FE modelled. The mechanical properties of materials were refined on experimental evidences of the composite constituents to fit the response of the composite system FEM model to the experimented DST equilibrium path. In particular, assuming a plane strain model, the substrate, i.e. a clay brick, and the PBO fibre are considered as linear elastic, with elastic stiffness retrieved from experimental tests. Then, the cement-based matrix is discretised in 2D-quadratic elements with total strain smeared-crack failure criterion, assuming a multilinear tension softening law, calibrated on dedicated three-point bending tests. Furthermore, fibre-matrix interface is lumped at 0D elements on which normal and shear elastic stiffness as well as non-linear bond-slip law have been refined to fit outcomes of the experimental DST global behaviour. FEM outcomes agree well with the DST experimental behaviour, which revealed an undisturbed substrate and a failure mechanism at fibre matrix interface. Moreover, FEM non-linear analyses adequately represents the phenomenology of the DST response, i.e. a first linear branch, loss of stiffness due to crack increase, and final softening branch with matrix-fibre slippage. In conclusion, experimental results confirmed the efficacy of FRCM systems for repair and strengthening historical buildings, given the increase in ductility and load carrying capacity that they can provide. Besides, FEM outcomes showed that, in this framework, further investigation is necessary for other constituent materials, systems and test layouts. [1] Alecci, V., De Stefano, M., Luciano, R., Rovero, L., Stipo, G., 2015. Journal of Composites for Construction 04015041. [2] Alecci, V., Focacci, F., Rovero, L., Stipo, G., De Stefano, M., 2016. Composite Structures 149, 184–196. [3] D’Ambrisi, A., Feo, L., Focacci, F., 2013. Composites Part B: Engineering 46, 15–20.

Extended Numerical Modelling of Structural Adhesive Joints

Stijn Debruyne^{*}, Mathias Creyf^{**}, Korneel Van Massenhove^{***}

^{*}KU Leuven, Mechanical Engineering @ Bruges campus, ^{**}KU Leuven, Mechanical Engineering @ Bruges campus, ^{***}KU Leuven, Mechanical Engineering @ Bruges campus

ABSTRACT

Abstract: This work presents a novel approach of modelling structural adhesive joints in a finite element context. On the one hand it focuses on modelling time-evolving mechanical characteristics of adhesive joints. In adhesive bonding, ageing phenomena affect the adhesive bulk material and the adhesive-adherent interface characteristics differently. Both zones of an adhesive joint are thus to be modelled adequately to capture structural ageing effects. In this work, the adhesive bulk material is represented by a 3D mesh applying a nonlinear material model which allows element rupture. This is based on unidirectional tensile, compressive and shear curves. The adhesive-adherent interface is modelled by cohesive zone elements and seeded with mode I & II interface fracture toughness data. This approach allows for the simulation of cohesive, adhesive and mixed cohesive-adhesive failure of the adhesive joint. Through-thickness effects (e.g. due to moisture diffusion into the adhesive bulk material) are taken into account by dynamically updating the element material properties corresponding to the applied ageing conditions and duration. On the other hand, the presence of defects and voids makes the mechanical behavior of adhesive joints even more complex to analyse and predict. Therefore, this work presents the results of an extensive uncertainty quantification which analyses the effects of heterogeneities in adhesive joints on their static and dynamic stiffness. The work concludes with a summary of ongoing research work and prospects to further related challenges in structural adhesive joining. References: Banea M, da Silva L.F.M, Campilho R. Mode I fracture toughness of adhesively bonded joints as a function of temperature: Experimental and numerical study. International Journal of Adhesion and Adhesives, 2011, 31, p. 273-279. Chaves F.J.P, da Silva L.F.M, de Moura M.F.S.F, Dillard D.A, Esteves V.H.C. Fracture Mechanics Tests in Adhesively Bonded Joints: A Literature Review. The Journal of Adhesion, 2014, 90, p. 955-992. Datla N.V, Ulicny J, Carlson B, Papini M, Spelt J.K. Mixed-mode fatigue behavior of degraded toughened epoxy adhesive joints. International Journal of Adhesion and Adhesives, 2011, 31, p. 88-96.

Computational Methods for the Dynamic Analysis of Conventional and Innovative Railway Tracks

Kris Decroos*, Patrick Vanhonacker**

*D2S International, **APT

ABSTRACT

In this paper a computational method for the efficiency determination of different source related mitigation measures for railway induced vibrations is presented. Comparison between the dynamic behaviour of railway vehicles (passenger/freight) on ladder tracks (a proposed mitigation system) is compared to the behaviour on a conventional ballasted concrete sleeper (tie) track using a combined finite element and multibody model. A numerical method for the comparison between ground-borne vibrations propagation on ladder track and concrete sleeper (tie) track under quasi static and dynamic loads is presented. Besides the impact of vehicle speed and suspension stiffness, several types of excitation and their impact on the dynamic behaviour are investigated: rail roughness, geometric track deviation, corrugation, wheel flats ...

The Effect of Imperfectly Known Local Subsoil Conditions on The Response of Buildings to Ground Vibration

Geert Degrande^{*}, Manthos Papadopoulos^{**}, Stijn François^{***}, Geert Lombaert^{****}

^{*}KU Leuven, ^{**}KU Leuven, ^{***}KU Leuven, ^{****}KU Leuven

ABSTRACT

Dynamic soil-structure interaction plays a crucial role in the response of buildings to ground vibration. Ground vibration in the built environment are produced by earthquakes or environmental sources like road and railway traffic or construction and industrial activities. Geotechnical investigations suggest that the soil properties exhibit considerable spatial variability even within apparently homogeneous soil deposits. As the soil immediately below a building may have a dominant role in the structural response, the aim of this paper is to assess the influence of imperfectly known local subsoil conditions on the response of buildings to ground vibration in the frequency range between 1 Hz and 80 Hz which is of interest for environmental induced vibration. A probabilistic finite element-perfectly matched layers model is developed for the analysis of the stochastic dynamic soil-structure interaction problem where the shear modulus of the soil in the vicinity of a building is modeled as a conditional random field. A subdomain formulation is employed to impose loading by an external incident wave field in the model. The uncertainty on the subsoil properties is propagated to the response of the building by means of Monte Carlo simulation. A case study is considered to investigate the influence of the spatial correlation length of the random field representing the shear modulus of the subsoil, and the foundation type of the building. A building with raft foundation and a building with individual foundation footings are studied. The buildings are excited by the wave field generated by a remote vertical point load at the soil's surface. The uncertainty on the response of the buildings varies over frequency bands but as a general trend increases with frequency. The foundation type is a crucial parameter determining the structural response and the associated uncertainty bounds.

Calculation of a Steady Water Surface Using Deforming Grids and Fluid-structure Interaction Techniques

Joris Degroote*, Toon Demeester**, Harald van Brummelen***, Jan Vierendeels****

*Ghent University, Flanders Make, **Ghent University, ***Eindhoven University of Technology, ****Ghent University, Flanders Make

ABSTRACT

Steady water surfaces are present around ships moving at a constant speed in open waters or in straight canals, but also in confluences of rivers or canals. Numerical simulation of these steady free surfaces can be performed with a fitting or a capturing method. While capturing methods use a stationary grid and some marker to indicate the presence of water, fitting methods deform the grid such that the water surface corresponds with the top of the grid. Several fitting methods involve a (pseudo) time stepping process with limited step size for stability and are consequently not efficient in cases where steady state is only reached after a long physical time. By contrast, the technique developed by van Brummelen et al. (JCP, 2001) is truly steady, but requires a coupled solver where the pressure gradient and vertical velocity can be combined implicitly in a boundary condition. The goal of this research is to develop a new fitting method for steady free surface flow using a general-purpose steady CFD solver. To support this development, an analysis of a simplified test case has been performed, namely two-dimensional, incompressible and inviscid flow over a flat bottom, with a specified mean flow velocity and water depth. The relation between a sinusoidal perturbation of the free surface and the resulting perturbation of the pressure in the flow at the top of the domain has been calculated for different ratios of the water depth to wave number and water depth to flow velocity (Froude number). With the insight from this stability analysis, different iterative schemes are investigated. Quasi-Newton techniques can deal with unstable modes and modes which converge slowly, but the latter increase in number as the mesh is refined, requiring multi-grid or other techniques.

Emerging Applications of Earthquake Simulations for Performance-Based Risk Assessment and Decision Making

Gregory Deierlein*, Nenad Bijelic**, Ting Lin***, Frank McKenna****

*Stanford University, **Stanford University, ***Marquette University, ****University of California

ABSTRACT

Technologies to computationally simulate earthquakes and their effects on the built environment are advancing to the stage of providing meaningful data for engineering applications for design and policy development. This presentation will review developments in a number of areas, including validation of earthquake simulations and development of computational workflows to facilitate their practical applications. Physics-based earthquake simulations, conducted by researchers associated with the Southern California Earthquake Center (SCEC) and other organizations, are providing data to more realistically characterize the effects of local and regional geology (basin effects, etc.) on earthquake ground motions. Data from SCEC's Cybershake simulations are now being used to improve regional hazard maps for the Los Angeles Basin and undertake risk assessments of buildings and other infrastructure (<https://scec.usc.edu/scecpedia/CyberShake>). Studies of building collapse risk with simulated seismograms offer new opportunities to apply machine learning techniques to deaggregate risk to identify causal earthquake faults and features. The Natural Hazards Engineering Research Infrastructure (NHERI) SimCenter is developing computational workflow tools to integrate a broad array of simulation software with high-performance computing platforms and data repositories to facilitate these applications. For example, a recent testbed application by the SimCenter involves simulating the response of 1.8 million buildings to a simulated M7.0 Scenario earthquake in the San Francisco Bay Area (<https://simcenter.designsafe-ci.org/framework/>). By integrating earthquake simulation and urban planning tools, these computational workflows offer important opportunities to incorporate earthquake risk into decision making for public policies and planning. However, in as much as these applications offer tremendous promise, they also raise many research challenges, ranging from needs to (1) streamline workflows to optimize computational resources and data management, (2) devise scalable approaches to characterizing uncertainties in input data and models, and (3) plan simulations and organize the resulting data in ways that can effectively inform decision making.

An Immersed Interface Approach for Fluid Structure Interaction Using Discontinuous Shape Functions

Facundo Del Pin^{*}, Iñaki Çaldichoury^{**}, Rodrigo Paz^{***}, Chien-Jung Huang^{****}

^{*}Livermore Software Technology Corporation, ^{**}Livermore Software Technology Corporation, ^{***}Livermore Software Technology Corporation, ^{****}Livermore Software Technology Corporation

ABSTRACT

It is of general knowledge that the pre-processing of complex geometries used in engineering applications is a major burden in Finite Element analysis of fluid problems. There are many situations where a detailed high quality mesh is preferred and possible mandatory. Such is the case for problems where shear stresses are an important component of the total force, i.e. ground vehicle aerodynamics, aircraft drag prediction and some bio-mechanics applications where the stresses in the endothelium are need to predict the development of some diseases. There are many other applications though where pressure forces are enough in terms of accuracy or where rapid prototyping of engineering parts do not need the accuracy required in the final stages of engineering design. In these cases the geometry could be simplified by approximating the domain walls immersing them inside a much simpler domain. This simplification becomes even more appealing in the presence of an internal structure that interacts with the fluid. In the current work the sub-element interfaces of the geometry will be approximated by level set distance functions. The walls could be part of a flexible structure or they could be rigid. The pressure discontinuity across the wall (in the case of shell structural elements) will be approximated by discontinuous shape functions as described in [1]. One of the main advantages of this approach is that it is easily adapted to an existing solver since no additional degrees of freedom need to be added. The presentation will include details of the additions that the existing solver needed such as: 1) boundary recognition; 2) level set representation; 3) sub-element splitting; 4) computation of the new interpolation functions and integration; 5) assembly and solution.

[1] R.F. Ausas, F.S. Sousa, G.C. Buscaglia, An improved finite element space for discontinuous pressures, Comput. Methods Appl. Mech. Engrg. (2009), doi: 10.1016/j.cma.2009.11.011

Error-driven Reduction and Optimization of Chemical Kinetic Mechanisms

Aurelie Delaroque^{*}, Patrick da Costa^{**}, Alexis Matynia^{***}

^{*}Sorbonne Université, ^{**}Sorbonne Université, ^{***}Sorbonne Université

ABSTRACT

With the stiffening of environmental regulations, pollutants emission calculations are crucial in the conception and optimization of engine combustion chambers. To ensure precision of the computed species profiles, a detailed chemical kinetic mechanism must be used. For complex fuels, such model can contain up to a thousand species, each of them adding a new equation to the system describing the reactive flow. Therefore, an efficient way to reduce computational cost is to reduce the number of species. Reduction methods for kinetic mechanisms are based upon chemical and/or mathematical properties of the system. In this work, the Directed Relation Graph [1] and Sensitivity Analysis reduction methods were used for an automatic reduction in perfectly stirred reactors (0D configuration) and freely propagating flames (1D configuration). An optimization using genetic algorithm [2] can then be performed to compensate the reduction induced error. This error was evaluated in two ways: comparison of the profiles integrals and through quantities of interest inspired by the work of Selim et al.[3]. The algorithm enables the user to choose several species of interest with different error tolerances. An iterative reduction is performed, each of the targets having an adaptive cut-off threshold scaled on the error of the reduced model. Independent thresholds allows the reduction procedure to carry on separate branches of the directed graph or different parts of the sensitivities matrices when one target reaches the maximal error allowed. The ability of the algorithm to reduce combustion kinetic mechanisms is assessed for different configurations and operating conditions (equivalence ratio, pressure, etc.). The importance of the error evaluation criteria is assessed and the tool performances are presented. Summary of the presentation : • Numerical combustion: origin of the computational cost and how to reduce it • Reduction with error-driven adaptive threshold • Post reduction model optimization References : [1] T. Lu, C. K. Law : A directed relation graph method for mechanism reduction. Proceedings of the Combustion Institute, 2005. [2] L. Elliott, D.B. Ingham, A.G. Kyne, N.S. Mera, M. Pourkashanian, C.W. Wilson : Genetic algorithms for optimization of chemical kinetics reaction mechanisms. Progress in Energy and Combustion Science, 2004 [3] H. Selim, S.Y. Mohamed, A.E. Dawood, S. Mani Sarahy : Understanding premixed flame chemistry of gasoline fuels by comparing quantities of interest. Proceedings of the Combustion Institute, 2016

A DPG Approach to Raman Gain in Optical Fiber Amplifiers

Leszek Demkowicz^{*}, Sriram Nagaraj^{**}, Jacob Grosek^{***}, Socratis Petrides^{****}

^{*}ICES, UT Austin, ^{**}ICES, UT Austin, ^{***}AFRL, ^{****}ICES, UT Austin

ABSTRACT

This talk will focus on the use of the DPG methodology in the modelling and simulation of optical fiber laser amplifiers with nonlinear Raman gain. Specifically, we study the operation of an optical fiber as an amplifier, i.e., a mechanism to convert pump light into signal light. The signal and pump fields are governed by two weakly coupled nonlinear time harmonic Maxwell equations to be solved using curvilinear 3 dimensional elements. Our model for the Raman gain is novel, and reflects the third order nature of the non linearity. We consider an ultra weak DPG formulation for the discretization of two systems of equations and the non linearity is handled by using fixed point (simple) iterations between the two systems. We use a DPG implementation of perfectly matched layer (PML) at the exit end of the fiber. Our results verify the Raman gain model and indeed show that the signal field gains power along the fiber with an expected efficiency. In addition, our results pave the way for the study of additional thermal effects modelled by coupling the electromagnetic phenomena with the heat equation. These thermal effects lead to detrimental modal instabilities in the fiber called transverse mode instability (TMI). Along the way, we show how the desirable properties of DPG, namely, mesh-independent uniform stability, and a computable error indicator leading to automatic adaptivity are useful in this application. To the authors' best knowledge, this is the first comprehensive fully vectorial 3-dimensional DPG model of this problem.

Topology Optimization of Hyperelastic Lattice Structures that Exhibit Negative Stiffness Behavior

Hao Deng^{*}, Lin Cheng^{**}, Albert C To^{***}, Devlin Hayduke^{****}

^{*}University of Pittsburgh, ^{**}University of Pittsburgh, ^{***}University of Pittsburgh, ^{****}Materials Sciences Corporation

ABSTRACT

Lattice materials that exhibit negative stiffness, also known as phase transformation, is characterized by a long serrated loading and unloading plateaus, making these materials suitable for energy absorption and damping applications. Instead of exploiting plastic deformation, these materials are designed to be hyperelastic in the negative stiffness regime and hence their deformation is fully recoverable. Topology optimization, such as material distribution-based methods, has become a popular approach to design high-performance structures and is employed in this work to design negative stiffness lattices. Design of hyperelastic materials incorporates both geometric and material nonlinearity due to large deformations. An appropriate method is adopted here to avoid mesh excessive distortion in low density area to stabilize numerical simulations. The topology optimization of lattice structures that exhibit negative stiffness contains nonlinear stability optimization and material failure constraints. The lattice structure, which shows snap-through behavior, usually presents damping properties, which is closely related to multiple stable configurations and the transformations between these phases. Therefore, to some extent, if stable phase can be optimized through topology optimization, this will open the door to optimize energy dissipation of lattice structure. Meanwhile, hyperelastic material failure constraint should be taken into consideration to make our structures fully recoverable, which is a distinct difference with other energy absorption material such as metal. Thus, our goal in this paper is to optimize lattice structures stable phase with material failure constraints so that our objective of energy dissipation ability will greatly increase, which will make this lattice structure be an ideal material for damping and energy absorption application.

Computational Modeling of Bronchial Airway Narrowing Mechanics for Elucidation of Respiratory Airflow Limitation in Health and Disease

Linhong Deng^{*}, Xiaohao Shi^{**}, Linlin Zhu^{***}, Che Zhao^{****}, Shengye Zhou^{*****}

^{*}Institute of Biomedical Engineering and Health Sciences, Changzhou University, Changzhou, Jiangsu, China,

^{**}Institute of Biomedical Engineering and Health Sciences, Changzhou University, Changzhou, Jiangsu, China,

^{***}Institute of Biomedical Engineering and Health Sciences, Changzhou University, Changzhou, Jiangsu, China,

^{****}Institute of Biomedical Engineering and Health Sciences, Changzhou University, Changzhou, Jiangsu, China,

^{*****}Institute of Biomedical Engineering and Health Sciences, Changzhou University, Changzhou, Jiangsu, China

ABSTRACT

Introduction: Although it is important to explore potential treatment of chronic obstructive airway diseases such as asthma, as well as to discover interesting biophysical phenomena in airway system, the research of biomechanical models of airway narrowing remains a both appealing and challenging field. Here we report some of the most recent work, in particular, that emphasize on asthmatic airway narrowing behavior. More specifically, we focus on the modeling of individual airway behaviors as well as interactions due to coupling between airways and their surrounding structures. This includes interesting phenomena involving the airways and the airway smooth muscle (ASM) layer embedded within the airway wall. The airway wall was modeled as a composite tubular structure embedded with ASM layer that was characterized by the volume, Young's modulus and orientation of ASM in either healthy or diseased state (e.g. asthma). **Methods and Materials:** CT scan images of airway tree from an adult male was obtained, from which a digital geometrical model of human airway tree from 0 to 5/6 level was reconstructed. Subsequently, a finite element model (FEM) of the airway tree was established, which incorporated ASM hyperplasia and hypertrophy by changing the volume of ASM layer, and ASM orientation by changing the effective modulus on the relevant direction. Using FEM analysis, the airflow-ASM interactions under different ventilation patterns were simulated via computational fluid dynamics (CFD) methods. The characteristic volume, Young's modulus of the ASM were measured using fresh airway tissues from pig lungs cut at 0°, 15°, 30°, 45°, 60°, and 75° to the longitudinal and transverse direction and stained. **Results:** ASM layer thickness and mechanical properties in the airway wall were highly nonlinear, and hyperelastic. The experimental results of the airway wall mechanical properties was able to be fitted by the Holzapfel strain-energy density function. We found that as ASM layer became thicker under the same ventilation condition, the shear stress on the airway wall and airflow velocity increased; whereas increase of the angle between ASM and horizontal plane would reduce the stress on the circumferential direction, but the shear stress was greater for the same breath pattern and airway thickness. **Conclusions:** With computational modeling method, we were able to simulate in situ airflow-ASM interactions during ASM contraction, in the absence or presence of pathological condition relevant to asthma including hyperplasia and hypertrophy, structural reorganization, and hopefully elucidate the connection between airway hyperresponsiveness (AHR) and abnormal ASM contraction patterns.

Rapid Computation of Inversion Heat Conduction Problems with Reduced Order Models

Brian Dennis*, Ashkan Akbaryeh**

*University of Texas at Arlington, **University of Texas at Arlington

ABSTRACT

Many inverse problems in heat conduction, such as determination of unknown boundary conditions or unknown shapes, require the solution of a parametric optimization problem. Typically this involves the coupling of a numerical optimization routine with a thermal analysis model based on a numerical method such as the finite element method. Since many of these problems are ill-conditioned, many calls to the analysis routine may be required by the optimizer to find an accurate minimum of the objective function. If the analysis model is large due to complex geometry, the computational time may be on the order of hours using a computer cluster. Many researchers make use of meta models to reduce the computing cost of optimization problems with expensive analysis calls. This involves making a predictive regression model to accelerate the objective function evaluation. Response surface modeling is the most common statistical tool used for meta modeling but artificial neural networks and kriging have also been used. However, if the analysis model is based on a finite element discretization of a partial differential equations, then a Galerkin method utilizing a reduced order basis could produce a rapidly computable meta-model based on the original differential equation. The basis functions are determined using proper orthogonal decomposition (POD) based on training data generated by the finite element model. Typically POD is applied to time vary data, but we show that it can also be successfully applied to data varying in parametric space as well. In our case the POD is applied to data generated by the finite element models that are evaluated over a range of parameter values. In this work we compared the performance of reduced order modeling (ROM) to response surface methods (RSM) and demonstrated that ROMs are more accurate and require a smaller set of training data. In addition, the resulting computational model, once trained, is so rapidly computed that it can be used in real time systems, such as model predictive control applications. We present applications to the inverse determination of unknown boundary conditions and the inverse determination of unknown shapes in steady and unsteady heat conduction. These examples involve finite element models with hundreds of thousands of degrees of freedom but the resulting ROM-based inverse problem can be solved in real time on a modest notebook computer.

Long-Duration Blast Response of Steel Columns: The Influence of Section Orientation

Jack Denny*, Simon Clubley**

*University of Southampton, **University of Southampton

ABSTRACT

Explosive blast loading has potential to exert forces on structural columns far higher than their capacity, causing permanent deformation. Recent large-scale industrial accidents such as the 2005 Buncefield disaster, the 2013 West Texas fertiliser factory explosion and the 2015 Tianjin disaster have highlighted a growing need to understand the response of structures to long-duration blasts. Typically defined by positive pressure durations over 100ms, long-duration blasts develop in the later stages of propagation i.e. in the 'far field' from the source of detonation. Such blasts are extremely powerful, generating substantial impulse and dynamic pressures (blast winds) capable of exerting damaging drag loads on columns. In reality, structures and their constituent column elements may be subjected to blast loads from various angles of incidence (section orientation) depending on the detonation location. Characterising such blast loading on columns can be complex, typically requiring approximation using drag coefficients for which there is limited availability or understanding, particularly when concerning different section orientations. Blast resistant design manuals and simplified predictive methods are generally limited to considering orthogonal axes, with no prior studies or guidance pertaining to the structural response of columns at different section orientations. Representing part of a broader experimental programme, six full-scale long-duration blast trials were conducted to investigate and quantify the influence of column section orientation on loading, transient dynamic response and final damage state. Nine steel square hollow section (SHS) columns were tested at orientations of 0, 30 or 45 degrees to the direction of blast propagation. Specimens were instrumented with surface pressure transducers, permitting calculation of column blast loading as a function of section orientation. High-speed video and high-fidelity laser topology quantified column transient dynamic response and permanent deformation respectively. Columns at oblique section orientations measured higher loading than orthogonal or symmetric orientations, resulting in larger permanent deflections. Analysis showed that column orientation greatly influenced loading and structural response due to varying projected area, aerodynamics and section mechanical properties. Importantly, results demonstrate that section orientation is non-trivial and has potential to cause considerably different final damage states. Results of this study provide new understanding of direct relevance to both engineering design practitioners and researchers.

Non Parametric Probabilistic Modeling for the Problem of Scattering Waves by a Solid with a Random Geometry into an External Acoustics Fluids

Christophe Desceliers*

*Université Paris-Est

ABSTRACT

A random computational model for the scattering of acoustical waves by a solid with an uncertain geometry into an acoustic external fluid is presented. The construction of a parametric probabilistic model for such a random geometry involves an important number of random variables. Since the stochastic dimension of such probabilistic model can be important, then the solving of the inverse statistical problem of random geometry can be very computationally tricky. This is the reason why a new nonparametric probabilistic model is developed. Nevertheless, It should be noted that the random acoustic impedance matrix which is a frequency-dependent random matrix is such that its real and imaginary parts must verify the Kramer-Kronig relations which implies its analyticity in the complex upper half-plane in order to get the causality of the random physical system [1, 2]. Consequently, it is necessary to take into account the Kramer-Kronig relations for the construction of the probabilistic model of the random impedance matrix. The strategy for constructing of the probabilistic model of the random impedance matrix consists in constructing the probabilistic model of its frequency-dependent real part and then to obtain the probabilistic model of the frequency-dependent imaginary part in using a Hilbert transform such that the Kramer-Kronig relations are verified. The theory of information is used to construct the probabilistic model of the real part of the random impedance acoustic matrix by taking into account the available information that is the positivity of the real part, its mean values and that the random frequency-response of the random computational model is a second-order random vector. A numerical example is presented which corresponds to the scattering of an incident wave by a solid for which the geometry is random. A parametric probabilistic model of the geometry is constructed and compared with the proposed nonparametric probabilistic model. [1] Christian Soize, Igor E. Poloskov. Time-domain formulation in computational dynamics for linear viscoelastic media with model uncertainties and stochastic excitation. Computers and Mathematics with Applications, Elsevier, 2012, 64 (11), pp.3594-3612. [2] Rémi Capillon, Christophe Desceliers, Christian Soize. Uncertainty quantification in computational linear structural dynamics for viscoelastic composite structures. Computer Methods in Applied Mechanics and Engineering, Elsevier, 2016, 305, pp.154-172.

Towards Predicting Instabilities of Lipid Monolayers: A Benchmark Problem

Luca Deseri^{*}, Massimiliano Fraldi^{**}, Giuseppe Mensitieri^{***}, Stefania Palumbo^{****}, Valentina Piccolo^{*****}, Luka Pocivavsek^{*****}

^{*}University of Trento (Italy), University of Pittsburgh (USA), ^{**}University of Napoli-Federico II (Italy), ^{***}University of Napoli-Federico II (Italy), ^{****}University of Trento (Italy), ^{*****}University of Trento (Italy), ^{*****}University of Pittsburgh Medical Center

ABSTRACT

Surfactants at air/water interfaces in lungs are subject to cyclic dynamical straining during breathing. Often time, in-plane and out-of-plane rearrangements of the lipid structures coating lungs alveoli are exhibited in pathological situations, eventually leading to their collapse. Similar, although more controllable, situations are observed in planar lipid monolayers set up in the laboratory, where uniaxial squeezing is induced to test the response of such systems. Preliminary studies towards an understanding of the collapse mechanisms exhibited by such structures are presented through the analysis of a benchmark problem. There, the stress relaxation in the out-of-plane mode turns out to be characterized by a scaling law between the wavelength at the onset of instability and the geometrical and constitutive parameters. Given the findings on the wavelength mentioned above, the current predictions based on Molecular Dynamics do not relate collapse through bending at the observed experimental scales. Henceforth, a predictive strategy that can provide the right scaling and modes is still missing. A platform owing to the first insights on the length scales involved in such phenomena is envisioned based on the preliminary results of the analytical and experimental of thin films mimicking the lipid monolayer on a viscous substrate.

Applying the Multiscale Hybrid Mixed Method to the Numerical Simulation of Discrete Fracture Networks

Philippe Devloo^{*}, Chen-Song Zhang^{**}, Wenchao Teng^{***}

^{*}FEC/UNICAMP, ^{**}NCMIS & LSEC, Academy of Mathematics and System Sciences, ^{***}School of Engineering, Peking University

ABSTRACT

The multiscale hybrid mixed method (MHM) is applied to the numerical approximation of two-dimensional fluid flow in porous media with fractures. The two-dimensional fluid flow in the reservoir and the one-dimensional flow in the discrete fractures are approximated using mixed finite elements. The coupling of the two-dimensional flow with the one-dimensional fracture flow is enforced using the pressure of the one-dimensional flow as a Lagrange multiplier to express the conservation of fluid transfer between the fracture flow and the divergence of the one-dimensional fracture flux. A zero-dimensional pressure (point element) is used to express conservation of mass where fractures intersect. The issuing simulation is then reduced using the MHM method leading to surprisingly accurate results with a very reduced number of global equations. A general system was developed where fracture geometries and conductivities are specified in an input file and meshes are generated using the public domain GMsh software. Several test cases illustrate the effectiveness of the proposed approach comparing the multiscale results with direct simulations.

On Geometry-based High-order Unstructured Methods for Structural-acoustics

Saikat Dey*

*US NRL

ABSTRACT

We discuss recent developments in high-order finite and infinite element based approaches for accurate solution of problems in structural acoustics. We present several applications related to vibratory and scattering response of elastic structures excited by mechanical and/or acoustic sources. We identify and highlight the importance of high-order discretizations and the role of geometry for accurate solution of such wave-dominated problems.

Quasi-Static and Dynamic Finite Element Analysis of Hydroelastic Problems Considering Structural Geometric Nonlinearities

Jean-François Deü^{*}, Christophe Hoareau^{**}, Roger Ohayon^{***}

^{*}Conservatoire national des arts et métiers, Paris, France, ^{**}Conservatoire national des arts et métiers, Paris, France, ^{***}Conservatoire national des arts et métiers, Paris, France

ABSTRACT

This work concerns the nonlinear modeling of elastic structures containing internal liquids with free surface. This kind of hydroelastic problem is still the subject of active researches, e.g. for the design of flexible tanks in aeronautical or space industry, in which linearized approaches can be questioned [1, 2]. The objective of this work is therefore to take into account geometrical nonlinearities in the structural part of fluid-structure interaction problems for quasi-static solution and vibration prediction. Firstly, we propose to address the quasi-static equilibrium state of the nonlinear coupled system by using the finite element method. The effect of the incompressible internal fluid on the structure is modeled by hydrostatic follower forces without meshing the internal fluid domain. In order to take into account the evolution of the wetted surface during the non-linear deformation of the structure (by considering the fluid volume conservation) a level-set approach is adapted to the fluid-structure interface elements, thus avoiding any remeshing [3]. In a second part, we study the linearized vibrations of the fluid-structure coupled problem around this prestressed state. We show that the structural vibrations are not only influenced by the presence of the liquid (added mass effect) but also by the initial stress state of the structure, both effects can play in an opposite direction. Reduced order models, based on both Modal Superposition and Proper Orthogonal Decomposition approaches will be finally proposed to perform parametric studies on the influence of structural nonlinearities on the vibrations of the coupled system. Several numerical examples will be also presented to illustrate the effectiveness of the developed approaches. [1] J.-S. Schotté, R. Ohayon, Linearized formulation for fluid-structure interaction: Application to the linear dynamic response of a pressurized elastic structure containing a fluid with a free surface, *Journal of Sound and Vibration*, 332 (10), 2396-2414, 2013. [2] R. Ohayon, C. Soize, Nonlinear model reduction for computational vibration analysis of structures with weak geometrical nonlinearity coupled with linear acoustic liquids in the presence of linear sloshing and capillarity, *Computers & Fluids*, 141, 82-89, 2016. [3] C. Hoareau, J.-F. Deü. Non-linear finite element analysis of an elastic structure loaded by hydrostatic following forces, *Proceedings of EURO-DYN 2017*, *Procedia Engineering*, 199, 1302-1307, 2017.

A Computational Method for Moving Particles on Thin Deformable Shells: Application to Surface Tessellation

Sanjay Dharmavaram*, Robijn Bruinsma**, Luigi Perotti***

*Department of Physics and Astronomy, UCLA, **Department of Physics and Astronomy and Department of Chemistry, ***Department of Radiological Sciences and Department of Bioengineering

ABSTRACT

Many problems in softmatter and membrane biophysics, such as finding equilibrium configurations of protein clusters on cell-membranes, highly defect ridden structure of Gag polyproteins in immature HIV capsids, and the unusual fluid-like state of Archaeal viruses [1] can all be understood as systems of interacting particles (typically representing proteins or protein capsomers) on deformable surfaces. The coupled interactions between the particles and the underlying elastic medium to which they are constrained pose significant computational challenges. For example, finite element methods typically: 1) impose expensive constraints to anchor particles to the surface; 2) use multi-step minimizations by sequentially moving particles on a rigid surface and subsequently updating the surface to accommodate the new particle configuration; or 3) restrict particles to the nodes of the underlying mesh (of the surface) giving a coarse approximation of the equilibrium state. In this study, we propose a new variational formulation to circumvent these challenges. Our method is based on a Lagrangian description of particle positions where instead of treating the particle positions on the current surface as the degrees-of-freedom, we treat the particle positions on the reference configuration (the “pull-back” '') as the degrees-of-freedom. The advantage of this method is that particles automatically lie on the surface and no multi-step minimizations or additional constraints are necessary, and since the particles are not restricted to lie at the nodes of the mesh, they are free to explore all possible equilibrium configurations. We demonstrate the efficacy of this method by applying it to three benchmark problems in different dimensions and show that the theoretical convergence rates in energy and displacement norms are realized. We also apply this method to particles moving on deformable unduloid surfaces as model for Archaeal viruses. In this application, we show how the proposed method can be applied to compute the tessellation of a deformable surface with positive and negative Gauss curvature and therefore its optimal tiling in terms of basic pentamers, hexamers, and heptamers. [1] Useful scars: Physics of the capsids of archaeal viruses, L.E. Perotti et. al, Phys Rev E 94 (2016).

A New Joint Element for the Modeling of Contact Interaction and Damage in SFR Fuel Assemblies

François Di Paola^{*}, Bertrand Leturcq^{**}, Jean-Baptiste Minne^{***}

^{*}Atomic Energy Commission (CEA), ^{**}Atomic Energy Commission (CEA), ^{***}Communication et Systèmes (CS-SI)

ABSTRACT

The fuel assembly of a sodium fast nuclear reactor (SFR) is a hexagonal tube containing around 200 fuel pins made of steel. In order to avoid overheating and damage on the assembly, a helical steel wire is wound around each pin. This wire maintains a suitable distance between pins and ensures a proper mixing of the sodium. Nevertheless, the intense fast neutron irradiation induces a significant isotropic swelling and creeping of the pins. This progressively leads to contact closure, helical bowing of the pins, and a strong ovalisation of the cladding sections. At such an interaction level, there is a possibility of cladding damage due to thermal creep accumulation. Modeling such a structure is a numerical challenge: around 10 000 contact areas, highly nonlinear material behavior laws, high mesh density needed for damage location. Thus, a simplified approach is developed: the two components are modeled by classical finite elements with a low mesh density: the hexagonal tube by shell elements, the fuel pins by beam elements. In addition, we have developed a new joint element dedicated to the contact interaction between components and the radial crushing of the pins. This element, with only two nodes, connects the neutral fiber of neighboring beams (or the mid-surface of shells). It takes into account: - the gap and the contact between two pins (or a pin and the tube), - the thermal expansion and the irradiation swelling of the pin cross sections (including heterogeneity of temperature), - the radius increase by creeping under internal pressure loading, - the elastic rigidity of the pin crushing (locally pinching a short section of a tube), - the contact force, altered by the two creeping behaviors, when pinching this 3D tube section, - the counter ovalisation force due to internal pressure on the deformed shape of the pins, - the hot point stress and strain tensors on the internal skin (strain concentration), - the hot point damage accumulation due to thermal creeping only. This connecting element has been implemented in the Cast3M finite element code (<http://www-cast3m.cea.fr>). Eventually, the model validation is made: - on the joint element, and compared to detailed 3D solid calculations, - on the global fuel assembly model, and compared to a few relevant assembly experiments, which were conducted in the PHENIX French SFR. It shows good agreement to the measurements and a very significant CPU performance gain compared to 3D solid models.

Aftershock Fragility and Residual Capacity Assessment of Infilled Frames Using an IDA Based Framework

Fabio Di Trapani^{*}, Gabriele Bertagnoli^{**}, Marzia Malavisi^{***}

^{*}Politecnico di Torino (Italy), ^{**}Politecnico di Torino (Italy), ^{***}Politecnico di Torino (Italy)

ABSTRACT

Seismic sequences frequently occurred in many regions of the world. The initial event (mainshock) is followed by a number of secondary shakings (aftershocks) which may lead structures to collapse because of progressive damage accumulation [1]. Reinforced concrete frame structures are generally infilled with masonry walls, and it is well known that these strongly interact with primary structures during seismic events. Infills significantly increase overall strength and stiffness, and also modify collapse modalities. The paper investigates seismic response of bare and infilled frames subject to mainshock/aftershock sequences. Aftershock fragility curves are obtained making use of a new specific assessment framework, based on a double Incremental Dynamic Analysis (IDA) [2]. Ground motions are in fact obtained combining mainshocks at fixed intensities with increasing intensity aftershocks. OpenSees [3] software platform is used to perform analyses of a reference prototype structure. The adopted double-IDA procedure, allows defining residual capacity diagrams, showing reduction of average collapse PGA as a function of mainshock intensity. Results show that masonry infills provide noticeable additional capacity seismic to resist aftershock shakings in comparison with bare frame structures, but only if local shear failure of reinforced concrete members is avoided. References [1] Hosseinpour F, Abdelnaby AE. Effect of different aspects of multiple earthquakes on the nonlinear behavior of RC structures. *Soil Dyn Earthq Eng* 2017;92:706–25. [2] Vamvatsikos, D., Cornell, A.C., 2002, Incremental dynamic analysis, *Earthquake Engineering and Structural Dynamics*, 31(3), 491–514. [3] McKenna, F., Fenves, G.L., Scott, M.H., 2000. Open system for earthquake engineering simulation, University of California, Berkeley, CA.

A Probability Density Function for Polycrystalline Two-dimensional Materials

Christopher S. DiMarco*, James Hone**, Jeffrey W. Kysar***

*Columbia University, **Columbia University, ***Columbia University

ABSTRACT

We examine the intergranular failure of polycrystalline two-dimensional materials by calculating a probability density function (PDF) based on a multiscale model and validated against nanoindentation experiments. Two-dimensional materials are of particular research interest due to their low defect density, which results in fracture strengths approaching their theoretical limits. Since scalable synthesis methods results in a polycrystalline structure, an understanding of the mechanics of their grain boundaries is necessary. Nanoindentation experiments on free-standing circular membranes reveal these materials have a non-Gaussian distribution in their critical failure load. First, we consider the transition in failure mechanisms through simulations of the nanoindentation experiments using the finite element method (FEM). The model admits two modes of failure: (1) within the grain boundary due to void nucleation and (2) within the grain due to a structural instability. A membrane-based cohesive zone model (CZM) is formulated based on molecular dynamic simulations to model the grain boundary behavior and a 5th order nonlinear anisotropic elastic constitutive relation describes the material behavior within each grain. The material properties of graphene are applied for these initial investigations. A simplified domain containing a single straight grain boundary is considered to develop a force-distance relationship between the critical failure load and the grain boundary distance from the indenter tip. Second, the force-distance relationship is fit with a piecewise continuous function and utilized to calculate a PDF. Initially, a periodic, hexagonal grain structure is considered as motivation. Then, a more realistic grain structure is considered by using a randomly generated Voronoi Tessellation. Finally, the resulting PDF is compared against the nanoindentation experiments in an effort to validate the material properties of the grain boundary.

Critical Analysis of the Drucker-Prager/Cap (DPC) Model When Modeling Pharmaceutical Die Compaction Process

Harona Diarra*, Vincent Mazel**, Pierre Tchoreloff***

*Université de Bordeaux/ Université Paris Sud, **Université de Bordeaux, ***Université de Bordeaux

ABSTRACT

The numerical simulation with DPC model requires the characterization of the model parameters. Depending on the method used, the instrumentation of the devices or the accuracy of the measures, the data obtained from experiments for the characterization of the model parameters may vary from a study to another. In this work, the influence of the elastic and plastic parameters on the numerical results during the compression cycle is discussed. Variations of $\pm 20\%$ on the values of Young's modulus E and Poisson's ratio obtained from the literature were applied. The variation of E has no influence on the final tablet thickness and the radial transmission curve. The distributions of the density, the axial and radial stresses do not change when E varies. A small Poisson's ratio gives high residual die wall pressures and low tablet thickness and vice versa. The stress distribution is completely dependent on Poisson's ratio. For numerical study with DPC model, a better characterization of Poisson's ratio is capital. The failure surface of the DPC model consists of two principal parts: the failure line and the cap surface. The failure line parameters are the cohesion d and the friction angle b . The cap parameters (hydrostatic pressure p_a , eccentricity R and hydrostatic yield pressures p_b) are calculated from d and b . Thus the variation of R , p_a and p_b is due to the variation of d and b . The parameters d and b are obtained from failure strengths s_d and s_u . In this work, variations of $\pm 53\%$ were applied to s_d and s_u and the corresponding values of b and d were calculated. The numerical representation of the compression curves shows that the curves obtained from the variation of d and b are superimposed. Thus, the variations of the failure line have no consequence on the compression and decompression results. An alternative model without failure line (modified Cam-Clay (MC-C) model) is introduced to simulate the powder behavior during die compaction process. This model is simple to use and requires less experimental tests for the parameter characterization. The axial stress-tablet thickness curves obtained from the two models are superimposed. The radial transmission curve obtained from MC-C model is identical to that obtained from DPC model. The stress and the density distributions are the same for the two models. This shows that the MC-C model is able to predict the powder behavior during the compression as well as the DPC model.

Overview of Brazilian Scientific Production in Engineering Areas

Patricia Dias^{*}, Tales Moreira^{**}, Thiago Dias^{***}, Gray Moita^{****}

^{*}CEFET-MG, ^{**}CEFET-MG, ^{***}CEFET-MG, ^{****}CEFET-MG

ABSTRACT

From the access and extraction of data sources of large-scale scientific publications, several studies are possible to obtain information about the published works, besides the possibility of categorization and visualization of them. In this study, data are used for the scientific production of the Brazilian researchers who work in the area of Engineering. Therefore, the data are obtained through a data extraction and processing framework responsible for obtaining the Lattes Platform curricula. With the extraction of all the curricula of the selected set it is possible to characterize the individuals as well as describe a panorama of their scientific production using bibliometric analyzes to quantify how these individuals have divulged their researches.

A Temporary Analysis of the Main Topics of Engineering Research in Brazil

Thiago Dias^{*}, Jether Oliveira^{**}, Gray Moita^{***}

^{*}CEFET-MG, ^{**}CEFET-MG, ^{***}CEFET-MG

ABSTRACT

The Internet and its services are fundamental factors that have boosted the significant growth in the dissemination of scientific articles in recent decades. Consequently, there is an overall increase in researchers from all areas of knowledge interested in understanding scientific development. Since this understanding can provide important inputs to assist different types of decision making, such as assisting researchers in choosing new research themes, making researchers more productive, and also serving as a basis for research. scientific policies aiming at new advances in science. Thus, this paper aims to identify and analyze the main topics investigated between 1962 and 2016 by Brazilian doctors who work in the areas of engineering. For this, bibliometric studies are carried out on the whole set of keywords of the scientific articles referring to the great area of ??engineering, published in proceedings of congresses and in journals by the Brazilian doctors.

DAMASK - The Düsseldorf Advanced Material Simulation Kit for Modeling Multi-Physics Crystal Plasticity, Thermal, and Damage Phenomena

Martin Diehl^{*}, Pratheek Shanthraj^{**}, Philip Eisenlohr^{***}, Franz Roters^{****}, Dierk Raabe^{*****}

^{*}Max-Planck-Institut für Eisenforschung GmbH, Max-Planck-Straße 1, 40237 Düsseldorf, Germany,

^{**}Max-Planck-Institut für Eisenforschung GmbH, Max-Planck-Straße 1, 40237 Düsseldorf, Germany, ^{***}Chemical Engineering and Materials Science, Michigan State University, East Lansing, MI 48824, USA,

^{****}Max-Planck-Institut für Eisenforschung GmbH, Max-Planck-Straße 1, 40237 Düsseldorf, Germany,

^{*****}Max-Planck-Institut für Eisenforschung GmbH, Max-Planck-Straße 1, 40237 Düsseldorf, Germany

ABSTRACT

Crystal plasticity modeling is a powerful computational materials science approach for the investigation of mechanical structure-property relations in metals and has been successfully applied to study diverse micromechanical phenomena ranging from strain hardening in single crystals to texture evolution in polycrystals. However, when considering the increasingly complex microstructural composition of modern alloys and their exposure to - often harsh - environmental conditions, the focus in materials design has shifted towards incorporating more constitutive and internal variable details of the process history and environmental factors into these structure-property relations. A number of niche tools, containing multi-physics extensions of the crystal plasticity method, have been developed to address such topics. Such implementations, while being very useful from a scientific standpoint, are, however, designed for specific applications and substantial efforts are required to extend them into flexible multi-purpose tools that enable a general end-user community to implement custom-made constitutive solutions for particular applications. With DAMASK we, therefore, undertake the effort to provide an open, flexible, and easy to use implementation to the scientific community that is highly modular and allows the use and straightforward implementation of different types of constitutive laws and numerical solvers. The internal modular structure of DAMASK follows directly from the hierarchy inherent to the employed continuum description. The highest level handles the partitioning of the prescribed field values on a material point between its underlying microstructural constituents and the subsequent homogenization of the constitutive response of each constituent. The response of each microstructural constituent is determined, at the intermediate level, from the time integration of the underlying constitutive laws for elasticity, plasticity, damage, phase transformation, and heat generation. A number of selected examples are shown to demonstrate the capabilities of DAMASK to predict structure-property relations in different material classes.

A PGD Arithmetic Toolbox: Explicit Solution of the Discrete Version of Parametric Problems

Pedro Diez^{*}, Antonio Huerta^{**}, Sergio Zlotnik^{***}

^{*}Universitat Politècnica de Catalunya, BarcelonaTech, ^{**}Universitat Politècnica de Catalunya, BarcelonaTech,

^{***}Universitat Politècnica de Catalunya, BarcelonaTech

ABSTRACT

Separable approximations efficiently deal with high-dimensional data. In particular, the Proper Generalized Decomposition (PGD) provides separable functions as solutions of boundary value problems. The general PGD framework contains a large family of methodologies, all of them providing solutions in for of separable objects, that is a sum of terms, being each term a product of 1D functions (or arrays). Some of the PGD methodologies have been conceived to tackle nonlinear problems. We present a general methodology to perform basic operations (sum, product, division, exponentiation...) for this type of objects. The idea is based on the principle of the PGD compression, that is a separable least squares approximation of any multidimensional function. The PGD compression is extensively used in practice to compact the separable solution in less terms without loss of accuracy. Here, this concept is applied to both algebraic tensor structures and functions in multidimensional Cartesian domains. Moreover, a straightforward extension of this concept is devised to operate with multidimensional objects stored in the separable format. That allows creating a toolbox of PGD arithmetic operators. Thus, the toolbox is used to perform elemental operations with PGD type objects. This is of particular interest to solve nonlinear problems with PGD techniques by simply replicating the iterative algebraic solvers that are used in the standard Finite Element framework.

Spherical Indentation on Biological Films with Surface Energy

Yue Ding^{*}, Wei-Ke Yuan^{**}, Gang-Feng Wang^{***}

^{*}Department of Engineering Mechanics, Xi'an Jiaotong University, ^{**}Department of Engineering Mechanics, Xi'an Jiaotong University, ^{***}Department of Engineering Mechanics, Xi'an Jiaotong University

ABSTRACT

Micro-/nano-indentations have been widely used to measure the mechanical properties of biological cells and tissues, but the direct application of classical Hertzian contact model would lead to overestimation of elastic modulus due to the influence of finite thickness and surface energy. In this work, we analyze spherical indentation of biological films considering both large deformation and surface energy. The hyperelastic behavior of biological films is characterized by neo-Hookean model, and the influence of surface energy is addressed through finite element simulation. Based on dimensional analysis, the explicit expressions of load-depth relation accounting for film thickness, large deformation and surface energy are achieved for bonded or non-bonded films. Under a specific load, the consideration of large deformation increases the indent depth, while the finite thickness of films tends to decrease the indent depth, compared to the linear elastic Hertzian solution. More importantly, surface energy evidently alters the load-depth relation for micro-/nano-indentations, which reduces the indent depth and makes the films seemingly stiffer. These results provide a fundamental relationship to accurately extract the mechanical properties of biological films from indentation tests.

Dislocation Dynamics Based Continuum Model for FCC and BCC Metals under Shock Loading

Nenad Djordjevic*, Rade Vignjevic**, Lewis Kleely***, Simon Case****

*Brunel University London, UK, **Brunel University London, UK, ***Brunel University London, UK, ****Atomic Weapon Establishment, UK

ABSTRACT

Recent experimental data has revealed that, over a short time (nanoseconds scale) at the beginning of the shock loading of metals, the precursor amplitude greatly exceeds Hugoniot Elastic Limit (HEL), before decaying to the level of the HEL. To capture this aspect of material behaviour at the continuum scale, physical effects related to high rate dislocation mechanics have to be taken into consideration [1,2]. The dislocation mechanics approach used here is described by three microscale state variables: density of mobile dislocations, density of immobile dislocations and velocity of dislocations (each calculated per slip system). Mobile dislocation density and dislocation velocity are incorporated at the continuum level by using the generalised Orowan relation, whilst the immobile dislocation density controls the yield strength of the material. The density evolutions of mobile and immobile dislocations are controlled by dislocation kinetic equations, which account for the generation of new dislocations, immobilisation of mobile dislocations at the barriers and annihilation of mobile dislocations with other mobile dislocations and of mobile dislocations and immobile dislocations. Dislocation velocity is determined by integration of the equations of motion for the dislocations. The dislocation mechanics model combined with the continuum scale material model [3] was implemented in the LLNL Dyna3d, together with the vector shock equation of state, which was developed for modelling the response of orthotropic metals to high strain rate loading including the shock loading. Model validation was done by comparison of numerical results with experimental data for plate impact tests (1D strain state) for FCC (aluminium and copper) and BCC (tantalum) single crystal structures. The difference between the experimental and numerical values of the compared parameters (longitudinal stress, pulse length, elastic precursor relaxation time) was within 10%. Notably the plate impact tests show that over the first 50ns after impact the pre-cursor wave has an amplitude similar to the stress levels behind the shock wave, relaxing to HEL with time (wave propagation). 1. A.E. Mayer, K.V. Khishchenko, P.R. Levashov, P.N. Mayer, Modelling of plasticity and fracture of metals at shock loading, *Journal of Applied Physics*, 113(19), 2013. 2. V. Krasnikov, A. Mayer and A. Yalovets, Dislocation based high-rate plasticity model and its application to plate-impact and ultra short electron irradiation simulation, *International Journal of Plasticity*, 27, 1294-1308, 2011. 3. R. Vignjevic, N. Djordjevic, V. Panov, Modelling of Dynamic Behaviour of Orthotropic Metals Including Damage and Failure, *International Journal of Plasticity*, 38, 47-85, 2012.

Finite Element Analysis of Abdominal Aortic Aneurysm - Benefits of EVAR Procedure and Predictions of Post-operative Complications

Smiljana Djorovic*, Igor Koncar**, Lazar Davidovic***, Nenad Filipovic****

*Faculty of Engineering, University of Kragujevac, Kragujevac, Serbia; Bioengineering Research and Development Center (BioIRC), Kragujevac, Serbia, **Clinic for Vascular and Endovascular Surgery, Serbian Clinical Center, Belgrade, Serbia, ***Clinic for Vascular and Endovascular Surgery, Serbian Clinical Center, Belgrade, Serbia, ****Faculty of Engineering, University of Kragujevac, Kragujevac, Serbia; Bioengineering Research and Development Center (BioIRC), Kragujevac, Serbia

ABSTRACT

Abdominal aortic aneurysm (AAA) requires endovascular aneurysm repair (EVAR) procedure in case of high-risk patients. Last years, computational modeling and analysis of AAA and implanted stent grafts (SGs) have become useful methods to define the present state of the patient and predict risk of post-operative complications [1, 2]. With that aim, this study analyzed the patient-specific AAA after EVAR procedure and SG implantation and determined biomechanical parameters which cannot be measured in vivo, such as the Von Mises stress and displacements of SG and aortic wall, as well as the velocity field of blood. The study included computational simulation of blood flow through implanted SG and interaction between SG, intraluminal thrombus (ILT) and aortic wall. The fluid-solid interaction was solved using the finite element (FE) method. Every domain of the patient-specific geometrical model was created on the basis of computed tomography (CT) scan images and consisted of a 3D finite element mesh. The computational simulation of cardiac cycle was performed for an average blood properties and parabolic blood flow, which was considered incompressible, viscous and laminar. Solid domains (aortic wall, SG and ILT) were modeled under the assumption of linearly-elastic isotropic material, whereby aortic wall and SG had constant thickness. Considering the difficulties in SG reconstruction, simplified SG was modeled, with material characteristics of equivalent composite material. As result, at the peak systolic moment aortic wall displacements and Von Mises stress in the aortic wall were decreased and in normal range, which indicated that EVAR procedure reduced risk of AAA growth and rupture. On the other hand, SG was under the high Von Mises stress, especially at the SG bifurcation where jet of blood, created during systole provided high velocity, which may cause SG migration and endoleaks. In summary, the results showed that EVAR procedure was beneficial for AAA, but in needs the follow-up, by means of biomechanical parameters determination, in order to predict post-operative complications. [1] Z. Li, C. Kleinstreuer, "Blood flow and structure interactions in a stented abdominal aortic aneurysm model", Medical Engineering & Physics, 27(5), pp. 369-382, June 2005. [2] D.S. Molony, A. Callanan, E.G. Kavanagh, M.T. Walsh, T.?. McGloughlin, "Fluid-structure interaction of a patient-specific abdominal aortic aneurysm treated with an endovascular stent-graft," BioMed Eng OnLine, vol. 8, October 2009.

Multi-scale Topological Optimization of Innovative Materials Using Computational Vadamecum

Tristan Djourackovitch^{*}, Nawfal Blal^{**}, Nahiene Hamila^{***}, Anthony Gravouil^{****}

^{*}Univ Lyon, INSA-Lyon, CNRS UMR5259, LaMCoS, F-69621, France, ^{**}Univ Lyon, INSA-Lyon, CNRS UMR5259, LaMCoS, F-69621, France, ^{***}Univ Lyon, INSA-Lyon, CNRS UMR5259, LaMCoS, F-69621, France, ^{****}Univ Lyon, INSA-Lyon, CNRS UMR5259, LaMCoS, F-69621, France

ABSTRACT

Topological optimization is a key issue to reduce structure weight while preserving suitable mechanical properties. The latest developments of 3D printing techniques make it possible nowadays to design more innovative materials with suitable optimized micro-architectures. This needs connect the topological optimization of both the structure (under given boundary conditions and external loadings) and the micro-architecture. In order to go through the different scales of the design process (from the micro-designed material to the optimal macro-structure), computational homogenization approaches [1] provide a suitable framework to achieve multi-scale topological optimization. However, the prohibitive memory and computational costs of such methods still remain an open issue for engineering applications. In order to highly decrease the expensive costs, we propose a reduced order strategy based on an offline/online approach. At the offline stage, the effective behavior at the scale of the microstructure is optimized taking into account the viabilities of the underlying parameters. This step is done once for all using a multi-scale topological optimization solver. Two methods are then compared: 1) the SIMP (Solid Isotropic Material with Penalization) method [2] based on the introduction of a density parameter as the design variable, and 2) the level set method which consists in moving interfaces between material and voids using shape derivative. The offline step allows the constructions of parametric computational vadamecums of optimized microarchitectures. These latter can be used at the online phase to perform the optimization of the structure [3]. [1] M. Geers, V. Kouznetsova, W. Brekelmans, Multi-scale computational homogenization: trends and challenges, J. Comput. Appl. Math. 234 (7) (2010) 2175–2182. [2] O.Sigmund. Materials with Prescribed Constitutive Parameters: an inverse Homogenization Problem. Int. J. Solids Structures, 1994.? [3] Ferrer, A., Oliver, J., Cante, J. C., Lloberas-Valls, O., 2016. Vadamecum-based approach to multi-scale topological material design. Adv. Model. and Simul. in Eng. Sci. , 3 – 23

Energy-based Modeling of the Non-local Damage Behavior in the Adhesive Interface of FRP-Metal Hybrid Material Systems

Michael Dlugosch*, Jens Fritsch**, Stefan Hiermaier***

*Fraunhofer-Institute for High-Speed Dynamics, Ernst-Mach-Institut, EMI, **Fraunhofer-Institute for High-Speed Dynamics, Ernst-Mach-Institut, EMI, ***Fraunhofer-Institute for High-Speed Dynamics, Ernst-Mach-Institut, EMI

ABSTRACT

Motivated by efficiency goals and upcoming strict EU-regulations for CO₂-emissions, lightweight design plays an increasingly important role in automotive engineering. Novel hybrid material systems combining advanced composite materials (such as CFRP and GFRP) with conventional body-in-white steels are one way to reduce the vehicle weight while simultaneously meeting the growingly stringent crash safety requirements. While various previous studies were able to document the general potentials of such hybrid material systems for crash structural applications [1, 2], defining efficient modeling techniques for numerical crash simulations in the early vehicle concept development phase poses a great challenge to engineers and researchers alike [3]. Next to the development of material models and model complexity issues (such as the number of shell elements used to model a laminate), finding a technique to efficiently model the adhesive interface's binary behavior under crash conditions is critical. The exploration of strongly simplified rigid tie connections – with respect to cohesive zone modeling approaches - on a structural subsystem level leads to the identification of a very particular damage phenomenon and to the revelation of a significant drawback of existing techniques. This study introduces the experimental investigation of this phenomenon, which comprises the non-local damage behavior of the adhesive interface within a hybrid material system upon FRP-fracture under tension. A new energy-based analytical model including a hybrid specific modification of the BK cohesive zone fracture model is able to accurately predict the damaged interface area upon FRP-fracture and may thus be used to enhance strongly simplified and efficient interface modeling techniques for vehicle subsystem concept structures under crash loading. The presentation will include the results of the experimental procedures to analyze the special damage phenomenon as well as the stepwise derivation of the energy-based model and a discussion of results and further implementation strategies

References [1] Bambach, M. R. 2013. Fibre composite strengthening of thin-walled steel vehicle crush tubes for frontal collision energy absorption. *Thin-Walled Structures* 66, 15–22. [2] Dlugosch, M., Lukaszewicz, D., Fritsch, J., and Hiermaier, S. 2016. Experimental investigation of hybrid material systems consisting of advanced composites and sheet metal. *Composite Structures*, 152, 840–849. [3] Mildner, C. 2013. Numerische und experimentelle Untersuchungen des Crashverhaltens von FVK-verstärkten Metallstrukturbauteilen. Dissertation, Technische Universität München.

An XFEM Enriched Computational Model Generation Library for Multi-material and Multi-physics Applications

Keenan Doble^{*}, Kurt Maute^{**}, David Noble^{***}, Miguel Aguiló^{****}

^{*}University of Colorado Boulder, ^{**}University of Colorado Boulder, ^{***}Sandia National Laboratories, ^{****}Sandia National Laboratories

ABSTRACT

In this work, an eXtended Finite Element Method (XFEM) model generation library is presented. The library's core functionality will be discussed and its numerical performance analyzed. The library's interface with a geometry engine is abstracted to accommodate many types of geometry descriptions including analytic, discrete distance fields and surface meshes. The geometry model is then immersed in the computational domain and the library computes an XFEM discretization. The result is a geometry conforming pseudo-mesh. This pseudo-mesh separates the computational domain by material which enables integration of the weak form of the governing equations for each material phase individually. This is useful for multi-physics and multi-material applications. To support phase change problems and shape optimization, the pseudo-mesh contains interface node and side sets that store information about how their positions change as the interface geometry is perturbed. The interface side sets are double sided which allows for weak enforcement of interface conditions. Additionally, the conformal pseudo-mesh stores enrichment information which is crucial for consistent interpolation of the solution fields. A discussion of this enrichment strategy is provided. Since the library is aimed to be used on exa/petascale problems, the method of generating a conformal and parallel consistent XFEM model has been developed with minimizing parallel communication in mind. The decomposition method and a study of the library's scalability in the number of CPU's will be provided. The library recursively handles geometry models allowing for an arbitrary number of materials in the computational domain. The scalability regarding the number of materials will be demonstrated. Two examples are to be shown. The first example is the XFEM model generation of a femur using CT scan data to show the robustness of the library in handling complex geometry configurations. The second is a composite fiber example where each fiber is a different material to show the library's ability to handle multiple materials.

Experimental and Numerical Analysis of the Surface Properties of the PC/ABS

T. Doca^{*}, F.M. Andrade Pires^{**}

^{*}University of Brasília, ^{**}University of Porto

ABSTRACT

The constant improvement of additive manufacture [1] creates several interesting opportunities for the enhancement of mechanical components. For instance, the engineering of new materials from the combination of others while keeping the best properties of each one of them. In this work, we present the experimental and numerical analysis of an effective combination of two polymers [2]: Polycarbonate (PC) and Acrylonitrile Butadiene Styrene (ABS). This combined material has high impact strength, high stiffness, heat resistance and is very easy to process. It is employed in the manufacture of car parts, portable hand-held devices, gas tanks and structural components in general. The study aims the investigation of surface properties [3], such as coefficient of friction, roughness, hardness, wear resistance and wear morphology. Moreover, an analysis of these parameters is used to verify the potential of the PC/ABS as protective coatings. Simulations of the wear process [4] are also conducted in order to evaluate the challenges of modelling such complex material. References [1] I. Gibson, D. Rosen, B. Stucker. Additive Manufacturing Technologies. Second edition, Springer, New York, (2015). [2] B. S. Lombardo, H. Keskkula, D. R. Paul. Influence of ABS type on morphology and mechanical properties of PC/ABS blends. Journal of Applied Polymer Science, 54, 1697–1720 (1994). [3] B. Bhushan. Modern tribology handbook. CRC Press, Boca Raton, Florida, (1999). [4] T. Doca, F.M. Andrade Pires. Finite element modeling of wear using the dissipated energy method coupled with a dual mortar contact formulation. Computers and Structures 191, 62–79 (2017).

An Interface-based Approach for Segmentation of Multiphase Microstructure Images

Gunay Dogan*

*Theiss Research, NIST

ABSTRACT

Image segmentation is the problem of identifying homogeneous regions or phases and their interfaces/boundaries in given images. It is a fundamental step for quantitative analysis of microstructure images. It is also a necessary step for finite element (FE) simulations of microstructure physics using of OOF, because the FE simulations require a mesh that conforms to the phases and interfaces encoded in the microstructure image. Unfortunately, the multiphase image segmentation problem is NP-hard, namely, a globally optimal algorithm to find an unknown number of phases to delineate them in a given image is computationally impractical. However, effective heuristic algorithms exist, and in this talk, we present one that focuses on the interfaces between the phases. Identifying the interfaces in a given microstructure image effectively segments the image partitioning the image domain into the distinct regions or phases. In this approach, instead of categorizing or labeling each pixel, we start with an initial set of candidate interfaces (or boundary curves in 2d images), and evolve them gradually to find and fit the real interfaces in the given image. The initial interfaces can be provided by the users or an automated initialization routine. The interfaces are usually represented very compactly with a much smaller number of unknowns than the number of pixels in the image, reducing the memory requirements and running times dramatically. The interface evolution itself is guided by a segmentation energy that is minimized when the interfaces partition the image into phases, each of which can be approximated by an average value (of image intensity, orientation, or other image characteristic). The interface evolution is essentially a gradient descent process. To improve convergence of the algorithm and to further reduce running times, we incorporate second order sensitivity of the segmentation energy, and realize an accelerated descent in the form of a shape-Newton algorithm. This improved descent procedure increases the robustness of the segmentation with respect to imaging conditions as well. We demonstrate the effectiveness of our algorithm with several examples.

Nonlinear Multiscale Modeling of Porous and Composite Materials Under Small and Large Deformations

Issam Doghri^{*}, Marieme El Ghezal^{**}, Ludovic Noels^{***}, Ling Wu^{****}

^{*}Université catholique de Louvain, ^{**}Université catholique de Louvain, ^{***}Université de Liège, ^{****}Université de Liège

ABSTRACT

Multiscale models are proposed for plastic matrix materials in which multiple cavities or solid inclusions are embedded. Semi-analytical micromechanical models are proposed based on mean-field homogenization (MFH) and verified against full-field finite element (FE) analyses on representative volume elements (RVEs). For composites, two finite strain MFH formulations are proposed. For both, local constitutive equations of each solid phase are based on a multiplicative decomposition of the deformation gradient onto elastic and inelastic parts and hyperelastic-plastic stress-strain relations. The first MFH formulation is an incremental-tangent one [1] based on relating the macroscopic rate values of the nominal stress (transpose of first Piola-Kirchhoff) and the deformation gradient. The second MFH formulation is an incremental-secant one [2]. It is based on unloading the composite material to zero macroscopic stress and taking into account per-phase residual strains and stresses in each phase. The formulation uses Cauchy and Kirchhoff stresses and logarithmic strains in each phase. Finally, we propose an original micromechanical formulation for a rigid plastic matrix containing multiple spherical inclusions [3]. It is based on coupling Gurson's single cavity solution with a generalized self-consistent (GSC) model at the RVE level. A secant formulation of GSC using second statistical moments in each phase is proposed. For all three contributions, numerical algorithms were developed and implemented. The MFH predictions were extensively tested against direct FE simulations of RVEs or unit cells, for several heterogeneous microstructures under various loadings. [1] Doghri, I., M.I. El Ghezal, L. Adam, 2016. « Finite strain mean-field homogenization of composite materials with hyperelastic-plastic constituents », *International Journal of Plasticity*, 81, 40-62, 2016. [2] El Ghezal, M.I., L. Wu, L. I. Doghri, L. Noels, 2017. "Finite strain extension of the incremental-secant homogenization formulation for elasto-plastic composites", submitted. [3] El Ghezal, M.I., I. Doghri, 2017. "Porous plasticity: predictive second moment homogenization models coupled with Gurson's solution", submitted.

Design of System to Control the Fall of a Suborbital Payload

Diego Domínguez*, Fernando Velázquez**

*UNAM, **UNAM

ABSTRACT

One of the most important problems in suborbital flights is the recovery of the payload. Avoiding difficult access areas (mountains, forests, lakes, lagoons, rivers, etc.) or dangerous areas (populated areas, vehicle ways, etc.) is very convenient. In this work, a mechatronic system to control the fall of a suborbital payload is proposed, considering the use of a paraglider. The simulation of the paraglider movement controller is shown, considering wing flight techniques. The air disturbances common in this type of missions, dynamic model and the prohibited areas of landing are also considered to design the controller. The results obtained from the simulation will be compared with the results that will be obtained after the implementation of the mechatronic system in suborbital flights of the CSM-UNAM (Mexican Service Load UNAM).

A Reduction-Consistent and Thermodynamically-Consistent Formulation and Associated Algorithm for Multiphase Flows of N Immiscible Incompressible Fluids

Suchuan Dong*

*Purdue University

ABSTRACT

In this talk we focus on the dynamics of an isothermal system of N ($N \geq 2$) immiscible incompressible fluids with different physical properties (e.g. densities, viscosities, and pair-wise surface tensions). These problems are characterized by multiple types of fluid interfaces and pairwise surface tensions, multiple types of three-phase lines, density contrasts and viscosity contrasts among multiple fluids, and multiple types of moving contact lines and multiple contact angles when solid walls are present. We present a reduction-consistent and thermodynamically consistent formulation and an associated numerical algorithm for simulating such N -phase problems. By reduction consistency we refer to the property that if only a set of M ($1 \leq M \leq N-1$) fluids are present in the system (while the other fluid components are absent) then the N -phase governing equations and boundary conditions will exactly reduce to those for the corresponding M -phase system. By thermodynamic consistency we refer to the property that the formulation honors the thermodynamic principles and rigorously satisfies the mass conservation, momentum conservation, second law of thermodynamics, and the Galilean invariance principle. Our N -phase formulation is based on a more general method that allows for the systematic construction of reduction-consistent formulations, and the method suggests the existence of many possible forms of reduction-consistent and thermodynamically consistent N -phase formulations. An efficient numerical algorithm for simulating N -phase problems based on this formulation are developed. Extensive numerical experiments will be presented for several multiphase flow problems involving multiple fluid components and large density ratios and large viscosity ratios, and simulation results are compared with the physical theories or the available physical solutions. These comparisons demonstrate that our method produces physically accurate results for this class of problems. References: 1. S. Dong, "Wall-bounded multiphase flows of N immiscible incompressible fluids: Consistency and contact-angle boundary condition", *Journal of Computational Physics*, 338, 21-67, 2017. 2. S. Dong, "Physical formulation and numerical algorithm for simulating N immiscible incompressible fluids involving general order parameters", *Journal of Computational Physics*, 283, 98-128, 2015. 3. S. Dong, "Multiphase flows of N immiscible incompressible fluids: A reduction-consistent and thermodynamically consistent formulation and associated algorithm", arXiv:1707.09023, 2017.

A Fully Lagrangian SPH-based Method for Simulation of Abrasive Waterjet Impacting on Metallic Surface

Xiangwei Dong*, Zengliang Li**

*College of Mechanical and Electronic Engineering, China University of Petroleum(East China), **College of Mechanical and Electronic Engineering, China University of Petroleum(East China)

ABSTRACT

A lagrangian model for the numerical simulation of the impact of abrasive waterjet on metallic surface is proposed in this paper. In the method both fluid (water) and solid phases (target) are described by smoothing particle hydrodynamics (SPH). Waterjet is modeled as a viscous fluid with weak compressibility, metallic target is modeled as an elastic-plastic material. Abrasive particles, which are explicitly included in the waterjet, are modeled as rigid bodies and are initially surrounded by the water. The interactions between fluid and solid, between abrasive and solid, and between abrasive and fluid, are modeled through suitable terms that are commonly used in the SPH. Simulation tests of impact of abrasive-water-jet are carried out as challenging examples to verify the applicability of the proposed model. The result demonstrates the attractiveness of this new approach in relevant applications such as abrasive waterjet (AWJ) cutting and solid particle erosion (SPE). Advantages of the method are robustness, conceptual simplicity and relative ease of incorporating new physics.

Long Term Integration of Burgers Equation with Rough Noise

Yuchen Dong^{*}, Zhongqiang Zhang^{**}

^{*}WPI, ^{**}WPI

ABSTRACT

We propose a restarted stochastic collocation methods for Burgers equation driven by white noise. The standard stochastic collocation methods suffer from the curse of dimensionality. To reduce the dimensionality in random space, we apply independent component analysis to reconstruct the computed solutions every few time steps. After such a reconstruction, we then match in time and compute solutions with appropriate stochastic collocation methods and repeat the aforementioned procedure until desired integration time instant. Numerical results and some basic analysis of the proposed methodology will be presented. Reference: [1] Z. Zhang, M. V. Tretyakov, B. Rozovskii, and G. E. Karniadakis. A recursive sparse grid collocation method for differential equations with white noise. SIAM J. Sci. Comput., 36(4): A1652-A1677, 2014. [2] H. Cagan Ozen, Guillaume Bal. Dynamical polynomial chaos expansions and long time evolution of differential equations with random forcing. SIAM/ASA J. Uncertain. Quantif., 4(1):609-635,2016. [3] A. Hyvärinen, J. Karhunen, E.Oja. Independent Component Analysis. John Wiley & Sons, New York, 2001.

Atomic Scale Modeling of Structural Response of 2D Materials to Mechanical and Chemical Environments

Avinash Dongare^{*}, Jin Wang^{**}

^{*}University of Connecticut, ^{**}University of Connecticut

ABSTRACT

Transition metal dichalcogenides (TMDs), such as molybdenum disulfide (MoS₂), have attracted attention for applicability in next-generation electronic materials and energy storage technologies. This talk highlights the current understanding of the atomic scale structural response of these layered materials when subjected to strains as well as solid-state reactions during intercalation and de-intercalation. The strain response is investigated for chemical vapor deposition (CVD) grown flakes few layered MoS₂ that are either free standing or supported on to a substrate using classical molecular dynamics (MD) simulations. The chemical response is investigated for the structural transformations during solid-state reactions related to intercalation and de-intercalation reactions using density functional theory calculations. The mechanisms of strain relaxation and the energetics of intercalation-induced transformations at the atomic scales will be presented.

Uncertainty Quantification Using Low-fidelity Data

Alireza Doostan^{*}, Jerrad Hampton^{**}, Hillary Fairbanks^{***}, Akil Narayan^{****}

^{*}CU Boulder, ^{**}CU Boulder, ^{***}CU Boulder, ^{****}University of Utah

ABSTRACT

The use of model reduction has become widespread as a means to reduce computational cost for uncertainty quantification of PDE systems. In this work, we present a model reduction technique that exploits the low-rank structure of the solution of interest, when exists, for fast propagation of high-dimensional uncertainties. To construct this low-rank approximation, the proposed method utilizes models with lower fidelities (hence cheaper to simulate) than the intended high-fidelity model. After obtaining realizations to the lower fidelity models, a set of reduced basis and an interpolation rule are identified and applied to a small set of high-fidelity realizations to obtain this low-rank, bi-fidelity approximation. In addition to the construction of this bi-fidelity approximation, we present convergence analysis and numerical results. This is a joint work with Hillary Fairbanks (CU Boulder), Jerrad Hampton (CU Boulder), and Akil Narayan (U of Utah).

Isogeometric Dual Mortar Coupling for Complex NURBS Surface Patch Models

Wolfgang Dornisch*, Joachim Stöckler**, Ralf Müller***

*University of Kaiserslautern, **TU Dortmund University, ***University of Kaiserslautern

ABSTRACT

Isogeometric analysis fosters a further integration of design and analysis by using the geometry description of the CAD system also for the numerical analysis. Hereby, the use of Non-Uniform Rational B-splines (NURBS) surfaces is common, but entails the need for a coupling of non-conforming patches in order to avoid unnecessary refinement for complex multi-patch models. The use of mortar methods [1] allows a coupling which requires neither additional variables nor empirical parameters. The use of mortar methods in the style of [1] for the coupling of two NURBS surface patches has been proposed in [2]. A more efficient dual mortar method with local support along the interfaces has been proposed in [3]. An arbitrary number of patches can be coupled, but additional treatment for intersecting interfaces is required. Within this contribution, an improved class of dual basis functions is presented, which allows a complete decoupling of the individual interfaces. This is of high relevance for the sparsity and condition of the global stiffness matrix, as well as for the efficiency of the computations and the accuracy of the solution. Numerical examples show the influence of the chosen concept for the dual basis functions on the aforementioned criteria. A comparison to computations with conforming meshes shows that both accuracy and efficiency of the proposed mortar method are highly competitive to standard conforming computations. [1] C. Bernardi, Y. Maday, A. T. Patera, Domain Decomposition by the Mortar Element Method, in: H. G. Kaper, M. Garbey, G. W. Pieper (Eds.), Asymptotic and Numerical Methods for Partial Differential Equations with Critical Parameters, Springer Netherlands, Dordrecht, pp. 269-286, 1993. [2] W. Dornisch, G. Vitucci, S. Klinkel, The weak substitution method – An application of the mortar method for patch coupling in NURBS-based isogeometric analysis, Int. J. Numer. Meth. Engng. 103, 205-234, 2015. [3] W. Dornisch, J. Stöckler, R. Müller. Dual and approximate dual basis functions for B-splines and NURBS – Comparison and application for an efficient coupling of patches with the isogeometric mortar method. Comput. Methods Appl. Mech. Engrg. 316, 449-496, 2017.

ROTATIONS OF THE PARAMETRIC N -PENDULUM WITH A VIEW ON ENERGY HARVESTING FROM OCEAN WAVES

FRANCO E. DOTTI*, FLORENCIA REGUERA[†], AND SEBASTIÁN P. MACHADO*

*Grupo de Investigación en Multifísica Aplicada, Facultad Regional Bahía Blanca, Universidad Tecnológica Nacional. Consejo Nacional de Investigaciones Científicas y Técnicas.

11 de Abril 461

B8000LMI Bahía Blanca, Buenos Aires, Argentina

fdotti@frbb.utn.edu.ar; smachado@frbb.utn.edu.ar

[†]Area Hidráulica, Departamento de Ingeniería, Universidad Nacional del Sur. Grupo de Investigación en Multifísica Aplicada, Facultad Regional Bahía Blanca, Universidad Tecnológica Nacional.

Av. Alem 1253

B8000LMI Bahía Blanca, Buenos Aires, Argentina

florencia.reguera@uns.edu.ar

Key words: Parametric N -pendulum, Wave Energy, Nonlinear Dynamics.

Abstract. In this article, we expand the knowledge on the dynamics of the parametric N -pendulum, as a universe of non-linear behavior is unveiled. With the final purpose of extracting energy from the ocean waves, we focus on rotational motion which is the most energetic steady state. The existence of rotating attractors is explored, for different configurations of the N -pendulum. The nonlinear parametric dynamics is explored by means of numerical simulations in order to comprehend the behavior of the N -pendulum and to establish the best conditions for energy harvesting. Results are presented through control spaces, bifurcation diagrams and basins of attraction.

1 INTRODUCTION

Among the large number of designs aimed at wave energy harvesting, pendulum wave energy converters (WECs) are attractive due to the simplicity of the mechanisms involved, in combination with the high kinetic energy available in its rotational motion. The concept is very simple and intuitive: a pendulum on a floating platform, to which the sea waves impose a vertical motion at a certain (predominant) frequency. If stable rotational motion of the pendulum is achieved, part of the kinetic energy of rotations can be converted into electrical energy by a generator attached to the pendulum axis¹. Now, given the low frequencies of the sea waves, it is impractical to consider a simple pendulum since the length required to achieve parametric

resonance results to be prohibitively large. A pendulum of multiple concentric masses, i.e. a N -pendulum, comes to solve this problem as low natural frequencies can be achieved with a relatively small size of the WEC².

Rotations are not uncommon in the dynamics of the parametric pendulum, although most of the times they coexist with other responses. Steady rotations are classified in four categories³: pure rotations, oscillating rotations, straddling rotations and large amplitude rotations. Pure rotations have a significant attribute in terms of energy harvesting: the angular velocity always maintains the same sign. This ensures that there is no change in the direction of rotation, implying no oscillatory motion of any kind. In other words: being the parametric pendulum a potential well system, pure rotations always ensure a “walk out of the well”, thus being the most energetic motion of the pendulum⁴. Given the symmetry of the system, pure rotations exist in conjugate pairs: if a clockwise rotation orbit exists, then an equivalent anticlockwise orbit must also exist⁵. In this article, pure rotations are regarded as synonymous of *rotations*, while the other categories are regarded merely as *oscillations*. Rotations can also be categorized according to their period, n . The most energetic are period-1 ($n = 1$), i.e, one rotation per load cycle. Rotations with $n = 2$ (one rotation per two load cycles) or higher are slower and thus less energetic. Period-1 rotations are pursued for energy harvesting purposes. However, rotations of period two or more are not negligible in terms of energy extraction.

By means of numerical simulations, we address in this article the nonlinear dynamics of a parametric N -pendulum system with the purpose of establishing the best conditions for energy harvesting. The article is organized as follows. After this introduction, we introduce the mathematical model (Section 2). Then, in Section 3, the nonlinear dynamics of the system is addressed by means of numerical simulations. Finally, the results of the study are presented and discussed (Section 4).

2 MATHEMATICAL MODEL

Figure 1 shows a schematic N -pendulum, which is contained in the xy plane. Each of the N masses are separated by a fixed angular distance $\psi = 2\pi/N$, and arranged concentrically around a pivot axis. Length l_1 is assumed to be greater than or equal to any of the other lengths (l_2, l_3, \dots, l_N), and the same assumption is made for mass m_1 with respect to m_2, m_3, \dots, m_N . Both l_1 and m_1 constitute the *main arm*, as pointed. The angle θ is measured with respect to the main arm and denotes the angular position relative to the vertical direction. A time-dependent external motion $Y(t)$ is imposed to the pivot axis. The center of mass of the system is located at the point C .

From classic mechanics of systems of particles⁶, kinetic, potential and dissipative energy terms can be derived respectively as

$$\begin{aligned} T &= \frac{1}{2} M \left\{ \left[Y' + l_c \theta' \sin(\theta + \varphi) \right]^2 + \left[l_c \theta' \cos(\theta + \varphi) \right]^2 \right\} + \frac{1}{2} K_0 (\theta')^2, \\ V &= gM \left[l_1 - l_c \cos(\theta + \varphi) \right], \\ D &= \frac{1}{2} b (\theta')^2 \sum_{i=1}^N l_i^2, \end{aligned} \tag{1}$$

where g is the gravity, φ is the phase shift of the center of mass with respect to the main arm and l_C is the distance from C to the origin. These are given by

$$\varphi = \arctan \left[(x_C / y_C) \Big|_{\theta=0} \right], \quad l_C = \left(\sqrt{x_C^2 + y_C^2} \right) \Big|_{\theta=0}, \quad (2)$$

where x_C and y_C are the coordinates of the point C , given by

$$\begin{aligned} x_C &= \frac{1}{M} \sum_{i=1}^N m_i l_i \sin [\theta + (i-1)\psi], \\ y_C &= l_1 - \frac{1}{M} \sum_{i=1}^N m_i \{ l_1 - l_i \cos [\theta + (i-1)\psi] \}, \end{aligned} \quad (3)$$

and $M = \sum_{i=1}^N m_i$. The factor K_0 in (1) is associated to the kinetic energy relative to the center of mass, and it is given by

$$K_0 = \sum_{i=1}^N \left\{ m_i \left\{ l_i^2 + l_C^2 - 2l_i l_C \cos [(i-1)\psi - \varphi] \right\} \right\}. \quad (4)$$

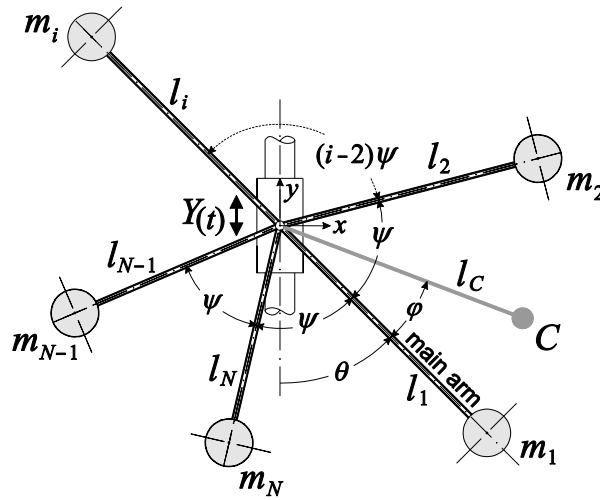


Figure 1. Scheme of the vertical parametric N -pendulum.

The viscous friction coefficient b in (1) is defined as independent of mass shapes, since bobs are very similar one to each other. By introducing (1) into Lagrange equation for one degree of freedom non-conservative systems, the equation of motion for an arbitrary vertical forcing $Y(t)$ is obtained as

$$I\theta'' + b\theta' \sum_{i=1}^N l_i^2 + M l_C (Y'' + g) \sin(\theta + \varphi) = 0, \quad (5)$$

where the inertia of the system is defined as $I = K_0 + M l_C^2$. Now, if a sinusoidal motion of the form $Y(t) = -H_S \cos \Omega_S t$ is considered as external forcing, (5) can be written as

$$I\theta'' + b\theta' \sum_{i=1}^N l_i^2 + M l_C (H_S \Omega_S^2 \cos \Omega_S t + g) \sin(\theta + \varphi) = 0. \quad (6)$$

Now, in order to gain in generality, (6) can be expressed in its dimensionless form as

$$\ddot{\theta} + \beta \dot{\theta} + (R \cos \omega \tau + 1) \sin(\theta + \varphi) = 0, \quad (7)$$

where the superimposed dots over some symbols indicate derivation with respect to the dimensionless time $\tau = \omega_0 t$. The dimensionless forcing parameters ω and R are defined as

$$\omega = \Omega / \omega_0, \quad R = H_s \omega^2 M l_c / I, \quad (8)$$

and the natural frequency of the system corresponds to

$$\omega_0 = \sqrt{g M l_c / I}. \quad (9)$$

Finally, a viscous friction parameter β is also defined in (7), as

$$\beta = I^{-1} \omega_0^{-1} b \sum_{i=1}^N l_i^2. \quad (10)$$

By means of (7), the dynamics of the system of Fig. 1 can be addressed from a general viewpoint, regardless of the physical constants of each particular system. The steady response of the system depends on parameters ω , R and β , which in turn depend on the magnitudes of masses and lengths and also on the number of arms N .

3 NUMERICAL SIMULATIONS

The dynamics of pendulum systems governed by (7) is explored. Such equation is solved numerically by means of a classic Runge-Kutta method implemented in *Wolfram Mathematica*. As a general rule, a dimensionless simulation time of $t_s = 2500$, with the purpose of ensure steady state responses. To avoid transients, the first $t_d = 2300$ are discarded in the construction of all the diagrams.

To study the topology of the responses of (7), a good choice is to fix β and φ and see what happens while varying the forcing parameters R y ω , as presented in the control space Fig. 2. This choice is not arbitrary: it is demonstrated⁷ that a variation of the damping parameter only shifts the multidimensional control space upwards or downwards. Meanwhile, φ is just a phase angle which does not alter the dynamics, except for a shift in the rest position of the pendulum. Thus, nothing too interesting happens while varying β and φ . Figure 2 clearly shows that topology may change dramatically as R and/or ω are varied. The coexistence of stable periodic and chaotic solutions is possible, depending on initial conditions. The map of Fig. 2 is constructed as follows: for each fixed pair (R, ω) , several simulations are performed with different initial conditions; the topology of each steady state is computed to give the color classification of the corresponding point (R, ω) in the control space. One can observe that, if the excitation amplitude is sufficiently low (low R), the rest position is the only possible stable solution and the system behaves as a linear one. As R increases, oscillations, rotations and tumbling chaos⁵ appear, unveiling a rich nonlinear dynamics. In the construction of Fig. 2, steps

of $1/100$ were employed for R and ω , while 63 initial states were considered for each pair (R, ω) , producing a total of $5.67 \cdot 10^6$ simulations.

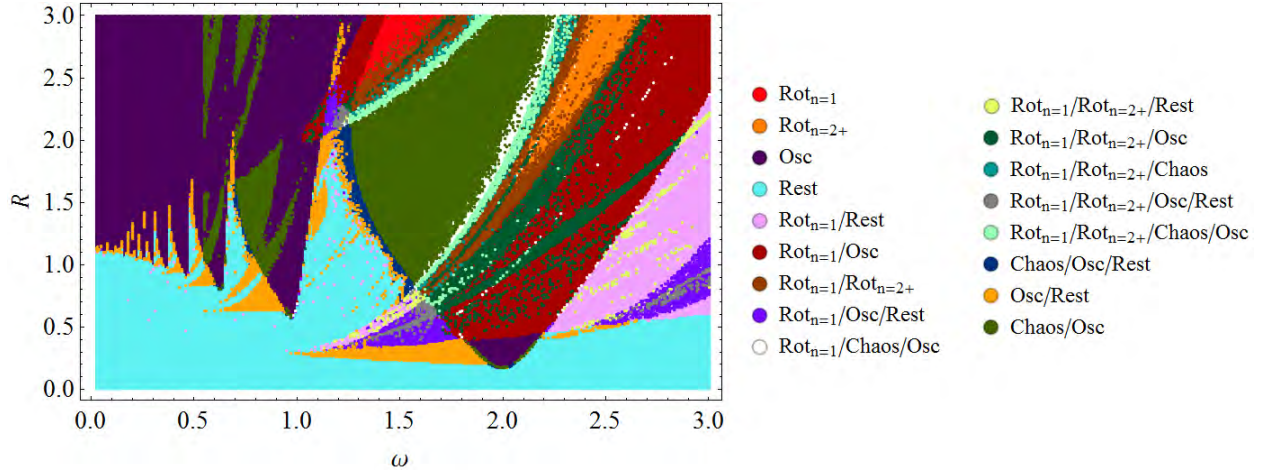


Figure 2. Control space R - ω showing the most significant physical responses of a system with $\beta = 0.1$ and $\varphi = 0$. $\text{Rot}_{n=1}$ means “pure rotations of period 1” while $\text{Rot}_{n=2+}$ means “pure rotations of period 2 or higher”.

The rest position is always a solution of (7), either stable or unstable. Contours of Fig. 3 indicate the probability of occurrence of a stable rest solution. The resonance zones are those regions of the control space inside which the rest position is unstable (i.e. probability is zero in Fig. 3, since unstable solutions are not captured by numerical simulations). Resonance zones are represented by the blue “tongues” in Fig. 3, centered around $\omega = 2/p$, being p a positive integer. The largest resonance zone lies around $\omega = 2$ ($p = 1$) and is called the *main resonance zone*. For energy harvesting purposes, it is convenient to lie inside the resonance zones since the rest solution is the less energetic state (recall that the parametric pendulum is a potential well system).

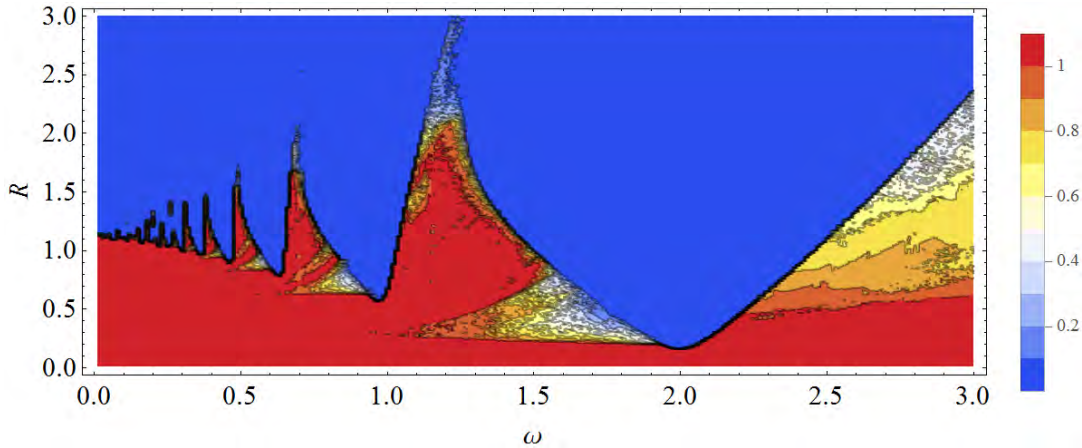


Figure 3. Stability diagram showing the resonance zones (blue tongues). Contours indicate the probability of occurrence of a stable rest solution. $\beta = 0.1$ and $\varphi = 0$.

As stated in the Introduction, period-1 rotations are desired since they are the most energetic motion of a parametric pendulum. Contours of Fig. 4 show the probability of occurrence of

stable period-1 rotations, given a random initial state. Such magnitude represents a measure of the robustness of rotations since it quantifies the ease of a trajectory to stick to the rotating attractor (blue: low robustness; red: high robustness). In practical terms, rotational motion cannot take place for $\omega < 1$. Moreover, there is a wide range of the control space where rotations are not possible, irrespective of the initial conditions (blue areas). On the other hand, the red area located at $R > 2.1$ and $1.2 < \omega < 1.7$ means that all initial states produce rotations. This implies that rotation is the only stable steady state. Consequently, a design of a pendulum WEC with such settings of R and ω would not require an external control to reach and maintain rotations, thus strongly simplifying energy extraction. Sadly, such high values of R cannot be reached by the forcing of the sea waves^{8,9}. However, a suitable design of a WEC can be obtained in the vicinity of the main resonance zone, where rotation is also a common response, as can be checked from Fig. 3. Comparing Fig. 4 and Fig. 5, one can verify the increase in the probability of obtaining stable rotations when the period-1 restriction is removed.

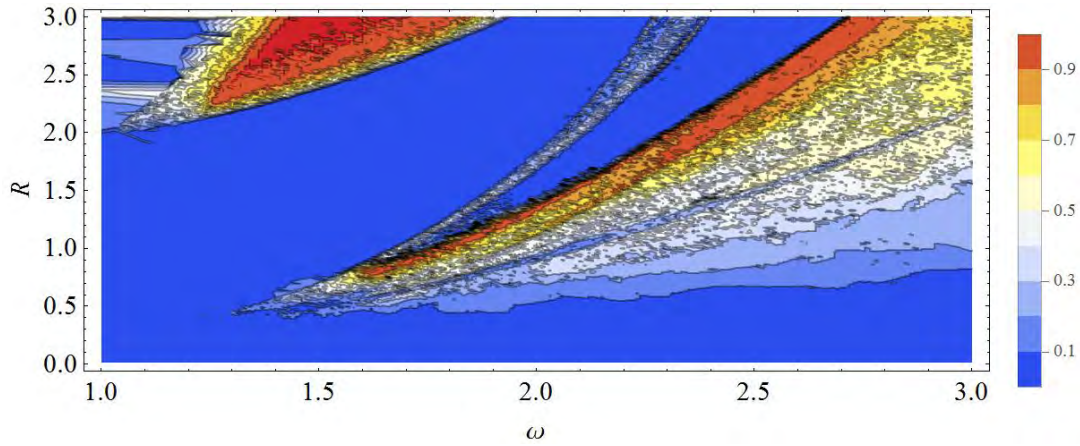


Figure 4. Period-1 rotation zones in the control space. $\beta = 0.1$ and $\varphi = 0$.

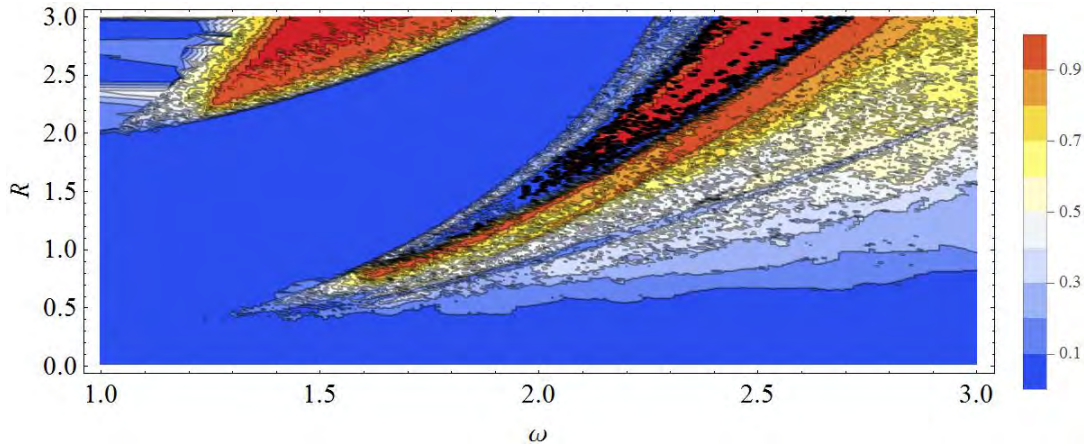


Figure 5. Rotation zones in the control space, regardless of the period. $\beta = 0.1$ and $\varphi = 0$.

The topology of the response for $\omega = 2$ can be studied by means of a bifurcation diagram, as the one presented in Fig. 6. The first qualitative observation is that rotations can be obtained for a wide range of R : they suddenly appear at $R = 0.450$ by a fold (or saddle-node) bifurcation, and

vanishes by a crisis at $R = 1.810$ after a period-doubling cascade. The values of R must be taken as indicative, since they can shift with a modification of damping. Nevertheless, the topology does not change. Period-1 rotating attractors always coexist with oscillatory attractors. This implies that initial conditions and robustness play an important role in order to reach a stable rotation.

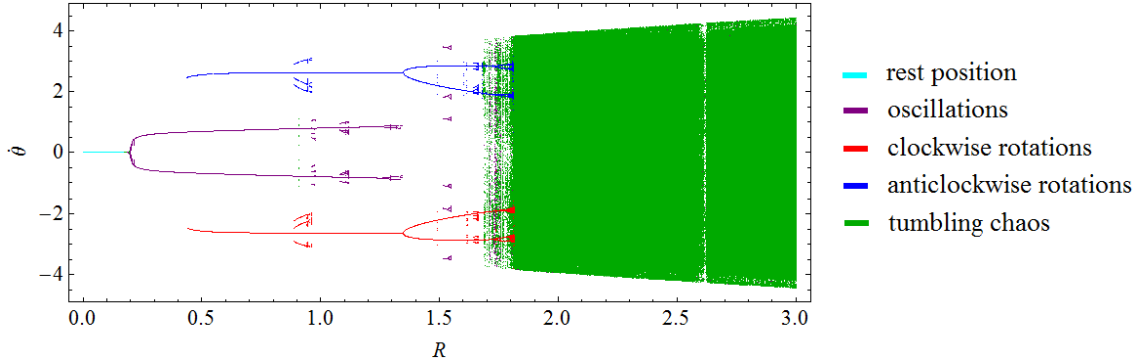


Figure 6. Bifurcation diagram of $\dot{\theta}$ for the main parametric resonance ($\omega = 2$), $\beta = 0.1$, $\varphi = 0$.

Fig. 7 presents a sequence of rotational responses in the phase plane as R is varied, with transients included. These phase planes are associated to the bifurcation diagram of Fig. 6. The sequence shows the topological evolution of the period-1 rotating attractors in the phase plane, from their birth at $R = 0.450$ until their disappearance at $R \approx 1.810$, as well as its interaction with other attractors. Fig. 7a shows the situation previous to the birth of the stable rotating attractor: an oscillation is the only possible response, since the rest position has just lost stability by means of a supercritical Hopf bifurcation (at $R = 0.196$). Fig. 7b shows how the stable branches of both symmetric period-1 rotating attractors suddenly appear, by a fold bifurcation. From $R = 0.450$ up to $R = 0.900$, period-1 rotations and period-2 oscillations coexist, being Fig. 7b the phase portrait of the system. From $R = 0.900$ (Fig. 7c), a pair of period-3 rotating attractors attempt against robustness of period-1 rotations. This is because all initial states captured by the period-3 attractors are *stolen* from period-1 attractors. This is also evidenced in the control space of Fig. 3, as a blue stripe extended approximately from $(R, \omega) = (0.5, 1.5)$ to $(R, \omega) = (2.3, 3.0)$. This pair of period-3 attractors run into cascade by a supercritical flip (period doubling) bifurcation at $R = 0.945$ (Fig. 7d) and finally vanish in a crisis at $R = 0.960$. From this point on, the topological structure of Fig. 7b is recovered, as period-1 rotations and period-2 oscillations are the only possible steady states. Up to $R = 1.350$, rotatory responses remain unchanged and only oscillatory responses undergo topological changes. As an example, Fig. 7e shows how the period-2 oscillating attractor has doubled its period. An interesting event takes place between $R = 1.331$ and $R = 1.350$: the oscillatory attractor has suddenly vanished after a rapid cascade and period-1 rotation is the only possible steady state (Fig. 7f). This is of course an ideal scenario for energy harvesting, as all initial conditions produce stable rotations. Sadly (again) the interval of R is too short, being practically impossible to tune, especially if the external forcing presents variations as in the case of the sea waves. At $R = 1.350$ a flip bifurcation occurs, doubling the period of the rotating attractor (Fig. 7g). Period-2 rotations take place, thus initiating the inevitable Feigenbaum cascade. Phase plane of Fig. 7h is associated to the period-6 oscillating motion that can be clearly observed in Fig. 6 at $R = 1.550$. This attractor appears briefly as R is varied, and corresponds to an oscillating rotation (in the sense of Garira and Bishop³), as can be

checked from Fig. 7h. Finally, Fig. 7i shows the rotating attractor at the edge of the crisis that will trigger its disappearance. A high periodic rotation can be obtained after very long transients, but most of the initial conditions give rotating chaos: an unpredictable aperiodic rotation. After $R = 1.810$, no periodic solution survives, being tumbling chaos the only possible response of the system.

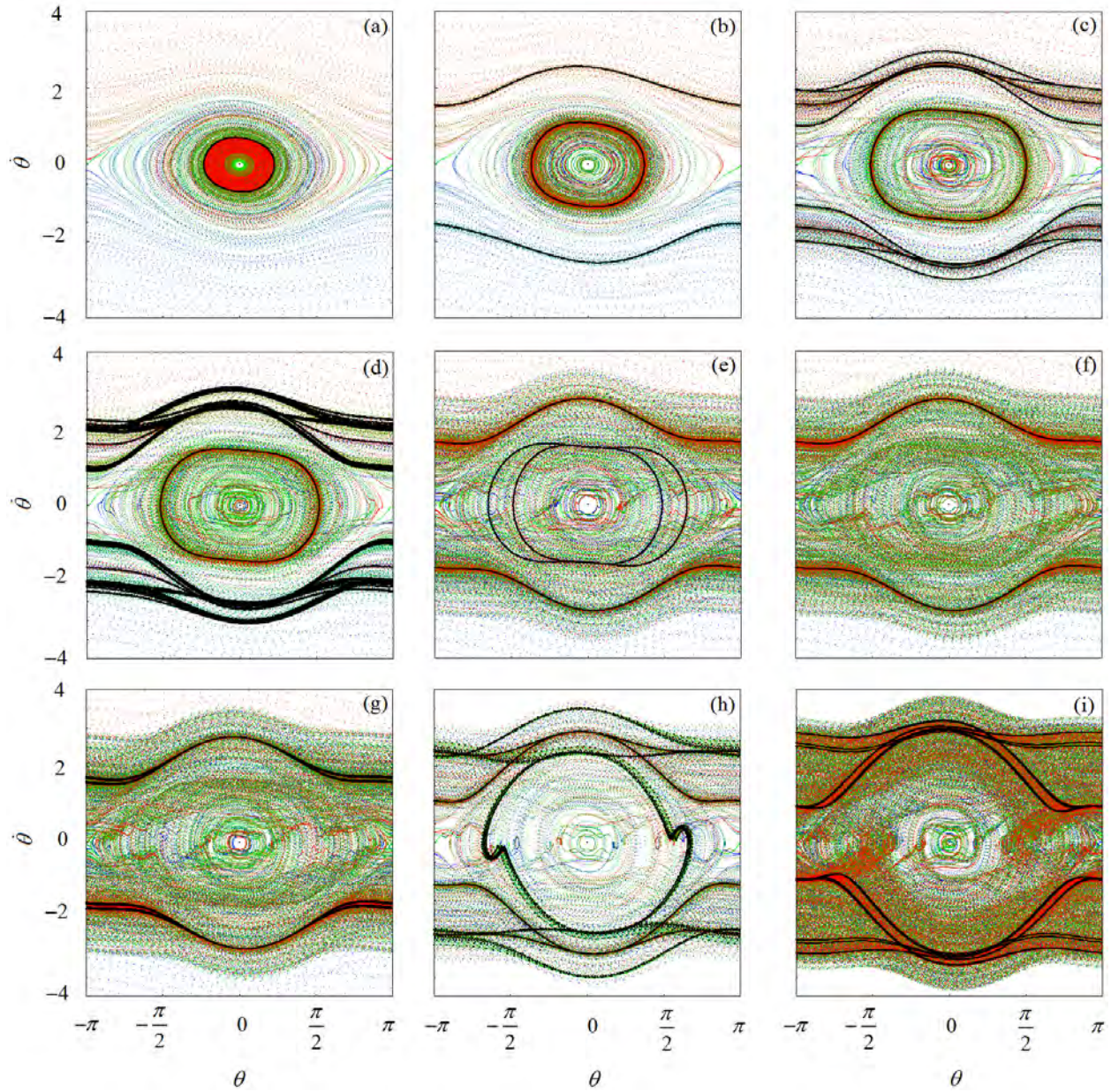


Figure 7. Sequence of the rotational responses, for $\omega = 2$, $\beta = 0.1$ and $\varphi = 0$. (a) $R = 0.250$; (b) $R = 0.450$; (c) $R = 0.900$; (d) $R = 0.945$; (e) $R = 1.329$; (f) $R = 1.331$; (g) $R = 1.350$; (h) $R = 1.550$; (i) $R = 1.750$;

It is worth noting that, between $R = 1.331$ and $R = 1.810$, and except for some small interference, rotations represent the only possible response of the pendulum.

4 CONCLUSIONS

This article aims to contribute to the development of pendulum systems for energy extraction from ocean waves. By means of numerical simulations, the dynamics of a parametric pendulum with multiple concentric masses, i.e. a N -pendulum, is addressed. The importance of such configuration lies in the need of reaching very low natural frequencies of the system, to mate with the excitation frequencies of the sea waves. The study is focused on how to achieve and maintain rotating motions of the N -pendulum, as period-1 rotations represent the most energetic motion of a pendulum.

A main conclusion of this work is that with a correct configuration of non-dimensional excitation and damping parameters, steady rotations can be easily reached and predicted. Such parameters are closely related to an adequate design of the pendulum harvester. Although damping parameters can be estimated in a relatively easy way, forcing parameters depend on sea wave motion and only can be bounded between certain limits, and statistically known. However, with an adequate design of the harvester, period-1 rotating attractors are robust against changes in excitation. In addition, for some specific combinations of the parameters, all initial conditions produce the most energetic rotating motion: a period-1 rotation. This is very interesting for energy harvesting because, theoretically, no external control action would be needed to reach rotating motion.

Energy harvesting by means of pendulum rotations is a very attractive idea because high amounts of energy could be recovered with simple and relatively small devices. The present work contributes to the knowledge on the field, but it is only a step aiming to understand the dynamics of the mechanical system in a simplified way. Further research is needed, including: active control of rotations to cope with variations of external forcing, optimization of the harvester devices for a maximum energy extraction, development of a suitable generator for the conversion of kinetic to electric energy, influence of the proper generator dynamics, influence of the synchronization phenomenon, and several others.

REFERENCES

- [1] Wiercigroch, M., A new concept of energy extraction from waves via parametric pendulum. UK Patent Application, 2010.
- [2] Yurchenko, D. y Alevras, P., Dynamics of the N -pendulum and its application to a wave energy converter concept. *International Journal of Dynamics and Control*, 1:290–299, 2013.
- [3] Garira, W. y Bishop, S.R., Rotating solutions of the parametrically excited pendulum. *Journal of Sound and Vibration*, 263:233–239, 2007.
- [4] Thompson, J., Stewart, H., *Nonlinear dynamics and chaos*. John Wiley & Sons, 2002.
- [5] Clifford, M. y Bishop, S., Rotating periodic orbits of the parametrically excited pendulum. *Physics Letters A*, 201:191–196, 1995.

- [6] Chow, T., Classical mechanics. John Wiley & Sons, 1995.
- [7] Leven, R., Pompe, B., Wilke, C. y Koch, B., Experiments on periodic and chaotic motions of a parametrically forced pendulum. *Physica D*, 16:371–384, 1985.
- [8] LeMéhauté, B., An introduction to hydrodynamics and water waves. Springer, 1976.
- [9] Reguera, F., Dotti, F., Sosa, M. and Machado, S., Applicability of parametric *N*-pendulum wave energy converters in the Argentine Sea. To appear in *Renewable Energy*, 2019.

On the Connection between Possibility Theory and Probability-box Theory in Structural Mechanics

Alex Dridger*, Ismail Caylak**, Rolf Mahnken***, Eduard Penner****

*Chair of Engineering Mechanics, Paderborn University, North rhine westphalia, Germany, **Chair of Engineering Mechanics, Paderborn University, North rhine westphalia, Germany, ***Chair of Engineering Mechanics, Paderborn University, North rhine westphalia, Germany, ****Chair of Engineering Mechanics, Paderborn University, North rhine westphalia, Germany

ABSTRACT

In many engineering applications the uncertainty quantification has become important in order to obtain authentic results. In general physical parameters are influenced by different types of uncertainty, where basically aleatory and epistemic types are distinguished. The first type is of intrinsic nature and may be described by stochastic methods based on randomness. The epistemic uncertainty, as the second type, arises due to a lack of knowledge. In practice, e.g. a safety assessment in the engineering sector both types of uncertainty occur simultaneously. Thus, in order to describe the corresponding uncertainty characteristic referred to as "imprecise probability"; different techniques were introduced [1]. A commonly used approach in structural mechanics is called the probability-box (p-box) ansatz [2] using probability bound analysis capturing uncertain information with pairs of lower and upper distribution functions. Moreover, a possibilistic approach [3] based on the fuzzy set theory may be used in order to describe imprecise probability using alpha-level discretization techniques. Compared to the first approach, the second one is rarely applied in structural mechanics. Furthermore, advocates of the p-box approach are criticizing the possibilistic approach and vice versa. This work examines both approaches in structural mechanics. For this, due to sparse available information, material parameters are characterized by imprecise probability. To this end, a p-box defined by two cumulative distribution functions and a possibility distribution comprising a family of probability distributions are generated. The probability bound analysis and the alpha-level discretization technique, respectively, are used to calculate a quantity of interest considering the sparse information of input material parameters. We investigate the relation between both approaches, e.g. that a p-box can be encoded by a pair of possibility distributions. Furthermore, the advantages and disadvantages are discussed extensively in order to understand why especially the possibility theory is rarely applied in the engineering sciences in contrast to, e.g. the computer sciences. Finally, our results are clarified in a numerical example. [1] Coolen F, Troffaes M, Augustin T. Imprecise probability 2011 (pp. 645-648), International encyclopedia of statistical science: Springer. [2] Traffaes M, Miranda E, Destercke S. On the connection between probability boxes and possibility measures. Information Sciences. 2013;224(Supplement C):88-108. [3] Dubois D, Prade H. Possibility theory and its applications: Where do we stand?. In: Kacprzyk J, Pedrycz W, eds. Springer handbook of computational intelligence. Berlin Heidelberg: Springer 2015 (pp. 31-60).

Thermo-mechanical Behaviour of Fire Protected Steel Structures Using Coupled Multiphysics Finite Element Analysis

Georgios Drosopoulos*, Iksha Singh**, Siphesihle Motsa***, Georgios Stavroulakis****

*Structural Engineering and Computational Mechanics Group (SECM), University of KwaZulu-Natal, Durban, South Africa, **Structural Engineering and Computational Mechanics Group (SECM), University of KwaZulu-Natal, Durban, South Africa, ***Structural Engineering and Computational Mechanics Group (SECM), University of KwaZulu-Natal, Durban, South Africa, ****Computational Mechanics and Optimization Institute (COMECO), Technical University of Crete, Chania, Greece

ABSTRACT

A numerical modelling approach is proposed for the simulation of the structural performance of steel structures in fire conditions. Coupled, transient, temperature-displacement non-linear finite element analysis is used to describe the steel structure and passive fire protection (concrete/gypsum boards), under both thermal and mechanical loading. The main concept, which is under investigation in this work, is the consideration of the gradual damage of the passive fire protection due to fire conditions, on the evaluation of the structural performance of the steel structure. Both concrete and gypsum boards, are expected to develop cracks and fail at elevated temperatures, after a duration of the fire event. Delamination between boards and the structure may also appear. Then, their contribution to the fire protection is reduced or totally vanished. This work proposes a simple finite element modelling and analysis scheme, to take into account this gradual damage of the fire protection. Principles taken from contact mechanics are applied to the steel - protection interface, to account for thermal and mechanical contact. A standard fire (temperature – time) curve is considered to be the thermal loading of the structures under investigation. Mechanical loads varying linearly over the time, are considered simultaneously to thermal loads. Applications to simple structural elements (steel column-beam) and more complex systems (steel connection) are presented. Force-displacement diagrams are used to quantify the strength of the systems and compare the unprotected and the protected structures. Yielding of the considered structures, after each loading scenario and fire protection configuration, is recorded. Among the main concepts under investigation, are mentioned here the consideration of bi-axial loads and the application of fire loading in one or more surfaces of the unprotected and fire protected steel structures. The gradual loss of the fire protection under a fire event results in the drastic reduction of the strength of steel structures. This is quantified in the presented research. References 1. Arablouei, A., and Kodur, V. (2016a). "Effect of fire insulation delamination on structural performance of steel structures during fire following an earthquake or an explosion." *Fire Safety Journal*, 84, 40-49. 2. Zografopoulou, K., and Mistakidis E. (2017). Numerical simulation of the behaviour of steel members with damaged SFRM fire protection coatings at elevated temperatures, EUROSTEEL 2017, September 13–15, Copenhagen, Denmark.

An Accurate and Effective Local Average Contact Method

Guillaume Drouet^{*}, Patrick Hild^{**}, Mickaël Abbas^{***}

^{*}Electricité De France R&D; ^{**}Mathematical Institute of Toulouse, Paul Sabatier University, ^{***}Electricité De France R&D;

ABSTRACT

Finite element methods are often used to approximate the unilateral contact problems. Such problems show a nonlinear boundary condition, which roughly speaking requires that the solution u is non-positive on a part of the boundary of the domain Ω . This nonlinearity leads to a weak formulation written as a variational inequality which admits a unique solution and the regularity of the solution shows limitations whatever the regularity of the data is. A consequence is that only finite element methods of order one and of order two are of interest. In this work we are interested in contact problems of two bodies whose respective meshes not coincide on the contact interface using finite element methods of order one and two in two and three space dimensions. In this case it is now known that the local node-on-segment contact conditions are not satisfactory in comparison with more global approaches inspired from the mortar domain decomposition method adapted to contact problems. But, these more global approaches are most of the time complicated to implement in a generic way in an industrial FEM software. The goal of this work is to define a local and developer-friendly method that is as efficient as standard mortar approaches, the Local Average Contact (LAC) method. This approach handles in a local way the contact constraint by averaging locally on some well defined patches the jump of the normal displacement independently of the space dimension and of the degree and type of the finite elements. The LAC method can be seen as a Lagrange method in which the multiplier representing the contact pressure is piecewise constant independently of the degree (one or two) of the finite elements chosen for the displacements, this method then satisfies the inf-sup condition thanks to the definition of the local patches. In this work we show that the method provides optimal convergence results in the energy norm in the general case of non-matching meshes and therefore combines both the advantages of locality and accuracy and is as efficient as the original mortar approach. The locality is a key point to implement efficiently in a generic way on all elements the method on the targeted FEM software. We exhibit several numerical experiments, both academics and industrials, the results are obtained with the official implementation of the method in the open-source FEM software code_aster. The extension of the method to the contact-friction case is in progress.

A Comparative Study of B-Spline- and Lagrange- FEM in Solving Acoustic Scattering Problems

Shaima Magdaline Dsouza^{*}, Tahsin Khajah^{**}, Stéphane P.A. Bordas^{***}, Sundararajan Natarajan^{****}

^{*}Indian Institute of Technology Madras, Chennai, India, ^{**}University of Texas at Tyler, ^{***}University of Luxembourg, Luxembourg, ^{****}Indian Institute of Technology Madras, Chennai, India

ABSTRACT

We compare the performance of B-Spline- and Lagrange- Finite Element Methods in solving acoustic problems. The space truncation error is artificially excluded from the numerical solution by modifying the exact solutions. Hence, the numerical error is reflecting the pollution, and discretization errors and therefore a true indicator of the numerical performance. The comparison is performed based on the error per degree of freedom in low and high order analysis. The pollution error is studied by comparing the evolution of the numerical error for increasing frequencies in both methods. Then, the structure and the condition number of the resulted linear systems are compared to clarify the strength and weakness of each method.

Multiphysics Topology Optimization Using DCT-based Compression

Jianbin Du^{*}, Pingzhang Zhou^{**}, Zhenhua Lv^{***}

^{*}Tsinghua University, ^{**}Tsinghua University, ^{***}Tsinghua University

ABSTRACT

Abstract Traditional topology optimization methods often need to deal with a large number of design variables equivalent to the number of finite elements analyzed, the quantity could be from a number of thousands to even hundreds of millions. The latter normally means that in order to obtain an effective design with enough details, a lot of computing resources need to be consumed [1], which increases to a great extent the cost of topology optimization in large-scale engineering applications. In this work, we developed a novel topology optimization method based on DCT (Discrete Cosine Transform) compression technique [2], which can greatly reduce the number of both the design variables and the computational scale of finite element analysis in topology optimization under the premise of maintaining a certain accuracy of optimization design. As one of the most popular transform technique in digital image compression, the DCT may effectively filter the high frequency components in a set of spatially distributed data without (or with very less) loss of the main characteristics of the data, which provides the solid foundation of the present method. Numerical examples on multiphysics designs including static, dynamic and thermal structural topology optimization are performed to validate the proposed method and show its advantage in improvement of computational efficiency of large scale designs. Interesting features of the present method and further possible development of the method in the future are discussed. **Keywords:** Multiphysics topology design; Discrete cosine transform; Computational efficiency; Finite element; High frequency filter; Acknowledgement The research is supported by NSFC (11772170, 11372154) which is gratefully acknowledged by the authors. **References** [1] Niels Aage, Erik Andreassen, Boyan S. Lazarov & Ole Sigmund, Giga-voxel computational morphogenesis for structural design, *Nature*. 2017, 550: 84–86. [2] P. Zhou, J. Du, Z. Lu, Highly efficient density-based topology optimization using DCT-based digital image compression, *Structural and Multidisciplinary Optimization*. 2018, 57: 463-467.

Comparison between Truncation and Stabilizing Error in Multiphase Moving Particle Semi-implicit Method Based on Corrective Matrix

Guangtao Duan^{*}, Seiichi Koshizuka^{**}, Akifumi Yamaji^{***}, Bin Chen^{****}

^{*}Department of Systems Innovation, The University of Tokyo, 7-3-1, Hongo, Bunkyo-ku, Tokyo 113-8656, Japan,

^{**}Department of Systems Innovation, The University of Tokyo, 7-3-1, Hongo, Bunkyo-ku, Tokyo 113-8656, Japan,

^{***}Cooperative Major in Nuclear Energy, Graduate School of Advanced Science and Engineering, Waseda University, Tokyo 169-8555, Japan, ^{****}State Key Laboratory of Multiphase Flow in Power Engineering, Xi'an Jiaotong University, Xi'an 710049, PR China

ABSTRACT

The moving particle semi-implicit (MPS) method has great advantages in simulating free surface, multiphase and fluid-solid interaction flows owing to its Lagrangian nature. However, the Lagrangian motion of particles also brings two challenges: the anisotropic particle distribution and the particle clumping. The former can decrease the accuracy of original MPS models and cause some random discretization error. The corrective matrix is effective to reduce such error to the level of truncation error. The latter can trigger instability easily due to particles' continuous approaching and thus some adjustment strategies for stability have to be adopted, thereby resulting in stabilizing error. The purpose of this paper is to compare the relative magnitude of the truncation and stabilizing error, which is of great significance to understand the reliability as well as capability of particle methods and further to compensate discrepancy. Due to the difficulty in separating different kinds of error from total error in dynamic simulations, an indirect approach is developed for the comparison. The basic idea is to check whether significant decline of the total error takes place after the truncation error is further reduced by high-order schemes. First, new discretization schemes based on second order corrective matrix (SCM) are proposed for MPS to reduce the truncation error further. Second, the SCM schemes are coupled with the our previous MMPS methods and stabilizing strategies. Then, various typical free-surface/multiphase flows, including Taylor-Green vortex, excited pressure oscillation flow, elliptical drop deformation and bubble rising flow, are simulated to test the variance of total error between using the FCM (first order corrective matrix) and SCM schemes. It is found that the SCM schemes did not remarkably reduce the total error, implying that the stabilizing error is dominant compared to the truncation error. Therefore, reducing the error due to stabilizing strategies is of more significance to reduce the total error.

Consistent Element-free Galerkin Method for Crack Growth

Qinglin Duan^{*}, Xin Gao^{**}, Zeyang Feng^{***}, Xikui Li^{****}

^{*}Dalian University of Technology, ^{**}Dalian University of Technology, ^{***}Dalian University of Technology, ^{****}Dalian University of Technology

ABSTRACT

Prediction of material failure by fracture is of major concern in many engineering problems. In the past decades, several types of computational methods have been developed to model fracture. Among them, the element-free Galerkin (EFG) method [1] is one of the major methods developed for this purpose at the earliest stage. In comparison with the traditional finite element method, EFG is more convenient to construct high order approximation and to implement h-adaptive computations. This provides certain advantages in numerical modelling of cracks. However, the EFG method is computationally inefficient since a large number of integration points is required and even worse, it is not able to exactly pass patch tests. In recent years, Duan et al. [2] developed an improved EFG method by correcting nodal derivatives at quadrature points based on the Hu-Washizu three-field variational principle. The number of integration points is significantly reduced, whereas the solution accuracy and convergence are greatly improved. This leads to a significant increase in computational efficiency. In particular, the method is able to exactly pass patch tests in a consistent manner and thus it is named as consistent element-free Galerkin (CEFG) method. In addition, the method can obtain very accurate stress fields. This work extends the CEFG method to crack problems in which the accuracy of stress solutions is crucial. Background integration mesh is used to describe cracks geometrically. The description of the discontinuity in displacement at cracks is based on the phantom node method [3] which does not need to add additional nodal degrees of freedom. The algorithm to introduce the phantom nodes and the method to evaluate the domain integral in cracked “element” are proposed. Numerical results show that the developed method is able to exactly pass the discontinuous patch test and to accurately predict crack paths. Adaptive refinement at the tip of extending cracks is also presented. References 1. Belytschko T, Lu YY, Gu L. Element-free Galerkin methods. *International Journal for Numerical Methods in Engineering* 1994; 37:229–256. 2. Duan QL, Gao X, Wang BB et.al. Consistent element-free Galerkin method. *International Journal for Numerical Methods in Engineering* 2014; 99:79–101. 3. Song JH, Areias Pedro M. A. and Belytschko T. A method for dynamic crack and shear band propagation with phantom nodes. *International Journal for Numerical Methods in Engineering* 2006; 67:868–893.

A Hierarchical Non-Intrusive Algorithm for the Generalized Finite Element Method

Armando Duarte^{*}, Travis Fillmore^{**}

^{*}University of Illinois at Urbana-Champaign, ^{**}University of Illinois at Urbana-Champaign

ABSTRACT

An algorithm for non-intrusively coupling a commercial finite element software with a research code implementing a hierarchical enrichment of finite element spaces is presented. Examples of hierarchical methods supported by the algorithm are the Generalized or eXtended FEM (GFEM), the scale-bridging GFEM with numerically defined enrichment functions (GFEMgl), and the p-version of the FEM. The proposed Hierarchical Non-Intrusive Algorithm (HNA) combines the vast library of classical elements available in commercial FEM platforms with the ability of the GFEMgl to analyze localized phenomena like cracks and spot welds, on coarse meshes. The algorithm does not require iterations between the standard and Generalized FEM platforms and is simple to implement. Examples showing the application of the HNA to the coupling of Abaqus with a 3-D GFEMgl software are presented. They also demonstrate the benefits of combining finite elements available only in a commercial platform with a GFEM.

Framework Design Methodology and Experience with FLASH

Anshu Dubey*

*Argonne National Laboratory

ABSTRACT

Scientific software used for simulation of complex multiphysics phenomena has many characteristics that make it uniquely challenging to architect and maintain. The models being computed have multiple operators which can have diverse requirements from the system hardware and software. Often the operator requirements are at cross-purpose with one another, where what is good for one is bad for another. Similarly, data structures and data layout that are optimal for one operator need not be the best for another. Additionally, there exists a positive feedback loop between scientific understanding and more demands on both simulation software and system resources needed to run the simulations. Greater understanding leads to higher fidelity models that usually imply greater diversity in methods and solvers used, and/or greater resolution, which implies more resources being utilized. The key framework design elements in face of such complexity are separation of concerns, and a collection of encapsulated building blocks that interoperate with one another through well defined interfaces. These two basic elements of design philosophy have been deployed in most successful multiphysics codes such as FLASH, Uintah, Amber, NWChem and many others. These codes have served their respective scientific communities for a decade or more, and have even branched out to serve other communities. We use FLASH as an example to illustrate how these basic design principles have resulted in an extensible framework that has been exploited by several research communities to adopt FLASH for their own use. FLASH is a composable, multiphysics, multiscale simulation software with a large and varied international user base in several research communities. FLASH was originally developed for simulating thermonuclear runaways in astrophysics. It has undergone three major version revisions, and a fourth one is underway to prepare the code for the forthcoming heterogeneity in platforms. This presentation will highlight the challenges in maintaining separation of concerns during various revisions to the code all the way to the current ongoing revision, and the corresponding variations in our approach to framework design.

On the Performance of the Numerical Manifold-based Mass Lumping Scheme in Comparison to Standard Diagonalization Methods

Sascha Duczek^{*}, Hauke Gravenkamp^{**}

^{*}Otto von Guericke University Magdeburg, ^{**}University of Duisburg-Essen

ABSTRACT

The application of explicit time integration schemes is an indispensable prerequisite for solving highly dynamic problems such as wave propagation or impact events. However, to fully harness the advantages of explicit time stepping algorithms, the mass matrix needs to be in diagonal form. This can be achieved by a variety of different methods known as mass lumping techniques [1]. The row sum technique is an intuitive procedure where all components of a row of the mass matrix are summed, and the result is placed on the main diagonal. In the context of Serendipity-type finite elements, this approach is unfortunately only viable for nodal-based linear shape functions. Otherwise negative components arise which have detrimental effects on the solution of transient problems. Here, an impaired convergence or even a divergence of the results is observed. Another heuristic approach proposed by Hinton, Rock, and Zienkiewicz is the HRZ method (diagonal scaling) [2]. This technique guarantees positive entries on the main diagonal of the mass matrix but is still only applicable to (higher order) nodal-based shape functions. A mathematically appealing approach to mass lumping is the so-called nodal quadrature technique also referred to as optimal lumping [1]. This method can be deployed in connection with tensor product shape functions defined on Gauß-Lobatto-Legendre (GLL) or Chebyshev-Gauß-Lobatto (CGL) points. Considering a trunk space formulation (Serendipity-type finite elements) of higher order finite elements, the optimal lumping scheme is not applicable as it is generally not possible to construct an integration rule of the required accuracy that guarantees positive weighting. Therefore, a different mass lumping scheme based on the numerical manifold method has recently been proposed. It is important to note that also in this case mass lumping is only applicable to nodal shape functions. Considering modal or hierarchic shape functions, a diagonal mass matrix is physically meaningless and leads to an impaired convergence of the results. In the present contribution, all properties of this method are discussed and its performance is compared to the aforementioned conventional mass lumping methods. Guidelines on the recommended use of each method are then derived from the numerical results. References [1] Cook, R. D.; Malkus, D. S. & Plesha, M. E. Concepts and Applications of Finite Element Analysis, John Wiley & Sons, 1989 [2] Hinton, E.; Rock, T. & Zienkiewicz, O. C. A Note on Mass Lumping and Related Processes in the Finite Element Method, Earthquake Engineering and Structural Dynamics, 1976, 4, 245-249

DIRECT COMPUTATION OF ABSORBING BOUNDARY CONDITIONS AT THE DISCRETE LEVEL

D. DUHAMEL*

*Laboratoire Navier, Ecole des Ponts ParisTech,
IFSTTAR, CNRS, UPE, UMR 8205, Champs-sur-Marne, France

Key words: Finite Element, absorbing boundary, wave, Helmholtz equation, discrete method

Abstract. The calculation of wave radiation in exterior domains by finite element methods can lead to large computations. A large part of the exterior domain is meshed and this computational domain is truncated at some distance where local or global boundary conditions are imposed at this artificial boundary. These conditions at finite distance must simulate as closely as possible the exact radiation condition at infinity and are generally obtained by discretizing an operator on the boundary.

Here, we propose a different approach, still based on the finite element method. Instead of finding an absorbing operator and then discretizing it, we will estimate the absorbing operator directly at the discrete level and build a sparse matrix approximating the absorbing condition. This discrete absorbing matrix is added to the dynamic stiffness matrix of the problem which is then solved in a classical way. The problem is considered for acoustics in the frequency domain and is described by the Helmholtz equation. The coefficients of the absorbing matrix are found from the solutions of small size linear systems for each node on the radiating boundary. This is done using a set of radiating functions for which a boundary condition is written. The precision of the method is estimated from the number of functions in the test set and from the number of coefficients allowed in the sparse matrix. Finally, some examples are computed to validate the method.

1 INTRODUCTION

Solving the Helmholtz equation in unbounded domains is important in many problems of mechanics and physics, for instance for the acoustic radiation or the diffraction around a body immersed in a fluid. Using the finite element method to solve the problem, one has to define a finite truncated domain on which the solution should be as close as possible to the solution on the unbounded domain. For this, it is necessary to define a boundary condition at the exterior of this truncated domain. These conditions at finite distance must simulate as closely as possible the exact radiation condition at infinity. This boundary condition could be global or local depending if all the degrees of freedom on the boundary are connected or if a given node is only coupled to a limited number of nodes around it. Among the global approaches we find the Dirichlet to Neumann (DtN)

proposed by [1, 2], or the boundary element method described in many classical textbooks like [3, 4, 5]. Both methods lead to full matrices and generate heavy computations.

In local methods, on the contrary, the condition at a boundary node involves only a limited number of neighbouring nodes. They can be classified into mainly three sets: those involving only the degrees of freedom of the domain, those with additional degrees of freedom at nodes on the boundary and those with an additional domain. Concerning the absorption conditions which do not involve additional variables or domains, a first possibility is using infinite elements as proposed by [6, 7, 8, 9]. These are elements extending at infinity and satisfying the Sommerfeld radiation condition. However, it needs the development of special elements based on functions with outwarding propagation wave-like behaviour in the radial direction. Other absorbing boundary conditions involving differential operators of different orders on the boundary were proposed by different authors [10, 11, 12]. These relations were improved by Bayliss and Turkel [13, 14] using sequences of local non-reflecting boundary conditions in spherical and cylindrical coordinates. However, all these conditions are difficult to implement above the second order because of the high order derivatives involved in their formulations. More efficient boundary conditions can be obtained by the addition of variables on the exterior surface such as in [15, 16]. They involve only second derivatives of the auxiliary variables and so can be efficiently implemented. Surrounding the computational domain by absorbing layers was also proposed by [17, 18] with the perfectly matched layer in which the wave equation is analytically continued into complex coordinates. This however can add a non negligible number of degrees of freedom to the problem and the optimal parameters in the absorbing layer are not so easy to find.

Most of the previous absorbing boundary conditions are written at the continuous level, but it can be interesting to write them at the discrete level. For instance, boundary conditions at the discrete level using the properties of periodic media were proposed by [19]. In [20] boundary conditions based on the PLM were written after discretisation of the equations and were found to be more efficient than their continuous versions. Such a discrete approach is used in this paper. The following section presents the problem formulation and the building of the discrete absorbing matrix. Then some examples are presented before the conclusion.

2 PROBLEM FORMULATION

2.1 Helmholtz equation

We consider the two-dimensional acoustic equation in the frequency domain in the exterior Ω_e of a bounded domain Ω_i of boundary Γ_i , see Fig.1. The Helmholtz equation with a Neumann boundary condition on Γ_i and a radiation condition at infinity is

$$\begin{aligned} \Delta p + k^2 p &= f \text{ on } \Omega_e \\ \frac{\partial p}{\partial n} &= g \text{ on } \Gamma_i \\ \frac{\partial p}{\partial r} - ikp &= o\left(\frac{1}{\sqrt{r}}\right) \text{ when } r \rightarrow \infty \end{aligned} \tag{1}$$

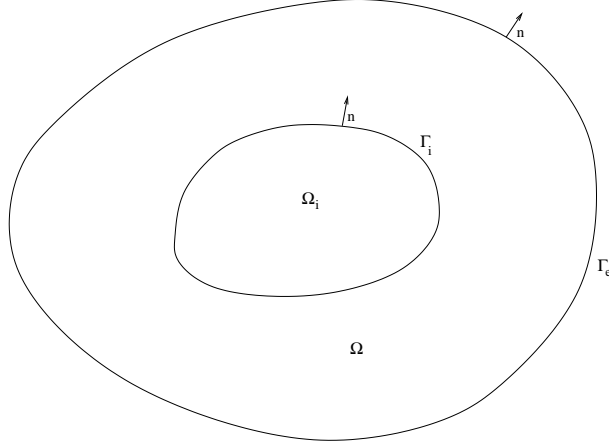


Figure 1: Exterior domain.

with f and g given functions representing the sources in the domain and at the boundary. The domain Ω_e is truncated at some finite distance by the boundary Γ_e and the discrete problem is posed on the bounded domain Ω located between the surfaces Γ_e and Γ_i . Its variational formulation is

$$\int_{\Omega} (\Delta p + k^2 p) q dx = \int_{\Omega} f q dx \quad (2)$$

$$- \int_{\Gamma_i} \frac{\partial p}{\partial n} q ds + \int_{\Gamma_e} \frac{\partial p}{\partial n} q ds + \int_{\Omega} (-\nabla p \cdot \nabla q + k^2 p q) dx = \int_{\Omega} f q dx \quad (3)$$

with q a test function and the exterior normals n on surfaces Γ_i and Γ_e . One assumes that the absorbing boundary condition can be written on the surface Γ_e as

$$\frac{\partial p}{\partial n} = A p \quad (4)$$

where A is an operator acting on the pressure p inside Ω . So the variational formulation is now

$$\int_{\Gamma_e} (A p) q ds + \int_{\Omega} (-\nabla p \cdot \nabla q + k^2 p q) dx = \int_{\Omega} f q dx + \int_{\Gamma_i} \frac{\partial p}{\partial n} q ds \quad (5)$$

2.2 Discretisation of the absorbing operator

The absorbing operator is such that

$$\begin{aligned} \int_{\Gamma_e} \frac{\partial p}{\partial n}(s) q(s) ds &= \int_{\Gamma_e} (A p)(s) q(s) ds \\ &= \int_{\Gamma_e} \int_{\Omega} A(s, x) p(x) q(s) dx ds \end{aligned} \quad (6)$$

The discrete form can be written as

$$\mathbf{M}^s \mathbf{q} = \mathbf{M}^s \mathbf{A} \mathbf{M}^v \mathbf{p} \quad (7)$$

with

$$\begin{aligned} M_{lj}^s &= \int_{\Gamma_e} N_l^s(s) N_j^s(s) ds \\ M_{im}^v &= \int_{\Omega} N_i^v(x) N_m^v(x) dx \end{aligned} \quad (8)$$

\mathbf{q} is the vector of the normal derivatives of the pressure at the nodes of Γ_e and \mathbf{p} the vector of the pressures at nodes in Ω . N^s and N^v are the usual interpolation functions on the boundary and in Ω respectively. Finally the vectors \mathbf{p} and \mathbf{q} are linked by

$$\mathbf{q} = \mathbf{A} \mathbf{M}^v \mathbf{p} \quad (9)$$

and one has to identify the matrix $\mathbf{A} \mathbf{M}^v$.

2.3 Determination of the absorbing matrix

The solution of the problem can be expanded as

$$p(r, \theta) = \sum_{-\infty}^{+\infty} a_n H_n(kr) e^{in\theta} \quad (10)$$

The completeness of the expansion on the boundary was proved by [21, 22, 23]. One now has to find an approximation of the matrix $\tilde{\mathbf{A}} = \mathbf{A} \mathbf{M}^v$. One looks for a discrete operator acting on the pressure at nodes inside Ω such that the matrix $\tilde{\mathbf{A}}$ is sparse and the relation (9) is satisfied for outgoing waves.

For a node i at point \mathbf{x}_i on the boundary, one considers nodes i_j at points \mathbf{x}_{i_j} in Ω with $j = 1 \dots n_i$ in the neighborhood of \mathbf{x}_i and such that $\mathbf{x}_{i_1} = \mathbf{x}_i$. So the line i of the matrix $\tilde{\mathbf{A}}$ will have non zero coefficients only at nodes i_j . To find these coefficients, one writes equation (9) for Hankel functions of different orders n . Choosing a point \mathbf{o} interior to Ω_i , one should have

$$\frac{\partial}{\partial n_i} (H_n(k|\mathbf{x}_i - \mathbf{o}|) e^{in\theta_i}) = \sum_{j=1 \dots n_i} a_j^i (H_n(k|\mathbf{x}_{i_j} - \mathbf{o}|) e^{in\theta_{i_j}}) \quad (11)$$

for $-N \leq n \leq N$ and n_i the exterior normal at node i . Denoting the vectors

$$\mathbf{f}_i = \begin{bmatrix} \frac{\partial}{\partial n_i} (H_{-N}(k|\mathbf{x}_i - \mathbf{o}|) e^{-iN\theta_i}) \\ \dots \\ \frac{\partial}{\partial n_i} (H_0(k|\mathbf{x}_i - \mathbf{o}|)) \\ \dots \\ \frac{\partial}{\partial n_i} (H_N(k|\mathbf{x}_i - \mathbf{o}|) e^{iN\theta_i}) \end{bmatrix} \quad \text{and} \quad \mathbf{a}_i = \begin{bmatrix} a_{i_1}^i \\ \dots \\ a_{i_{n_i}}^i \end{bmatrix} \quad (12)$$

and the matrix

$$\mathbf{H}_i = \begin{bmatrix} H_{-N}(k|\mathbf{x}_{i_1} - \mathbf{o}|) e^{-iN\theta_{i_1}} & \dots & H_{-N}(k|\mathbf{x}_{i_{n_i}} - \mathbf{o}|) e^{-iN\theta_{i_{n_i}}} \\ \dots & \dots & \dots \\ H_0(k|\mathbf{x}_{i_1} - \mathbf{o}|) & \dots & H_0(k|\mathbf{x}_{i_{n_i}} - \mathbf{o}|) \\ \dots & \dots & \dots \\ H_N(k|\mathbf{x}_{i_1} - \mathbf{o}|) e^{iN\theta_{i_1}} & \dots & H_N(k|\mathbf{x}_{i_{n_i}} - \mathbf{o}|) e^{iN\theta_{i_{n_i}}} \end{bmatrix} \quad (13)$$

Relation (11) can be put under the form

$$\mathbf{f}_i = \mathbf{H}_i \mathbf{a}_i \quad (14)$$

Its solution is

$$\mathbf{a}_i = (\mathbf{H}_i^* \mathbf{H}_i)^{-1} \mathbf{H}_i^* \mathbf{f}_i \quad (15)$$

with $*$ denoting the hermitian transpose of a matrix. The vector \mathbf{a}_i gives the i th line of the matrix $\tilde{\mathbf{A}}$. Considering these relations for all nodes at the boundary, one gets the sparse matrix $\tilde{\mathbf{A}}$ describing an approximate absorbing boundary condition on Γ_e .

The discretisation of the other parts of the variation formulation (5) leads to the final discrete equation.

$$(\mathbf{K} - \tilde{\mathbf{A}} - k^2 \mathbf{M}) \mathbf{p} = \mathbf{f} \quad (16)$$

which can be solved by classical solvers.

3 NUMERICAL EXAMPLES

3.1 Test problem

As example we consider an annular domain limited by an interior circle of radius $0.15m$ and an exterior circle of radius $0.3m$ (see Fig.2). The sound velocity is $c = 340m/s$. A boundary condition is defined at the interior circle as the normal derivative of the sound pressure generated by a point source located at point $\mathbf{x}_s = (0.1, 0)$ and is given by

$$q(\mathbf{x}) = -\frac{ik}{4} \frac{\mathbf{n} \cdot (\mathbf{x} - \mathbf{x}_s)}{|\mathbf{x} - \mathbf{x}_s|} H_1(k|\mathbf{x} - \mathbf{x}_s|) \quad (17)$$

with \mathbf{x} the position of a node on the interior boundary and \mathbf{x}_s the position of the point source. The analytical solution is given by

$$p(\mathbf{x}) = \frac{i}{4} H_0(k|\mathbf{x} - \mathbf{x}_s|) \quad (18)$$

and will be compared to various numerical solutions.

We define the errors e_g on the whole domain Ω and e_b on the exterior boundary Γ_e by

$$\begin{aligned} e_g^2 &= \frac{\sum_{i \text{ node on } \Omega} |p_i^{num} - p_i^{ana}|^2}{\sum_{i \text{ node on } \Omega} |p_i^{ana}|^2} \\ e_b^2 &= \frac{\sum_{i \text{ node on } \Gamma_e} |p_i^{num} - p_i^{ana}|^2}{\sum_{i \text{ node on } \Gamma_e} |p_i^{ana}|^2} \end{aligned} \quad (19)$$

with the superscripts *ana* and *num* denoting respectively the analytical and numerical solutions.

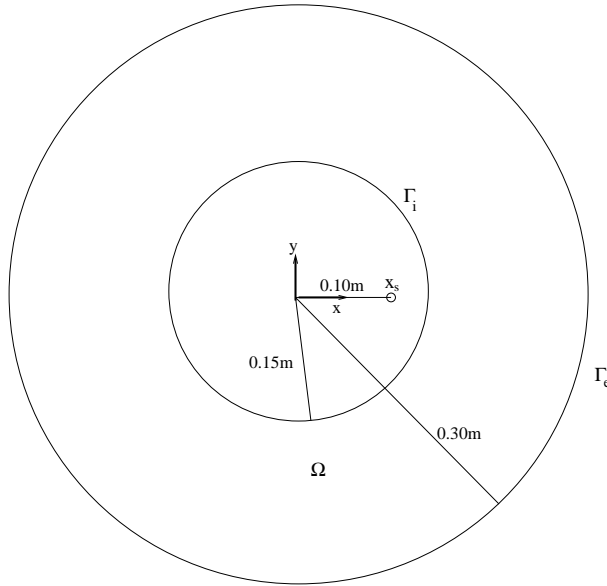


Figure 2: Annular domain.

3.2 Influence of different parameters

We begin by estimating the influence of the truncation order N on the error. In Fig.3 four solutions are plotted. The first one is obtained with the crude boundary condition $\frac{\partial p}{\partial n} = ikp$ (denoted as the ik solution), two solutions are obtained by the present method with respectively $N = 0$ and $N = 1$ and the last one is the analytical solution for the frequency $100Hz$. These solutions are obtained by taking $n_i = 20$ coefficients for each boundary node in the building of the matrix \tilde{A} . As can be seen the ik solution leads to large errors while the solutions with the present method lead to rather good solutions even for the simplest one with $N = 0$. The numerical errors are given in table 1 with similar conclusions.

condition	global error	boundary error
ik	0.837	0.956
N=0	0.059	0.078
N=1	0.003	0.005

Table 1: Errors for the different boundary condition at 100Hz

In Fig.4 the solution is plotted versus the number of points n_i used to build \tilde{A} with $N = 1$. Using $n_i = 2$ is clearly not enough. However, one can see that $n_i = 5$ gives a rather good solution which is still improved by using more points. Numerical values are given in table 2.

Finally Fig.5 compares the analytical solutions and the numerical ones for different frequencies. Only $n_i = 2$ points are used which leads to crude estimates. While the

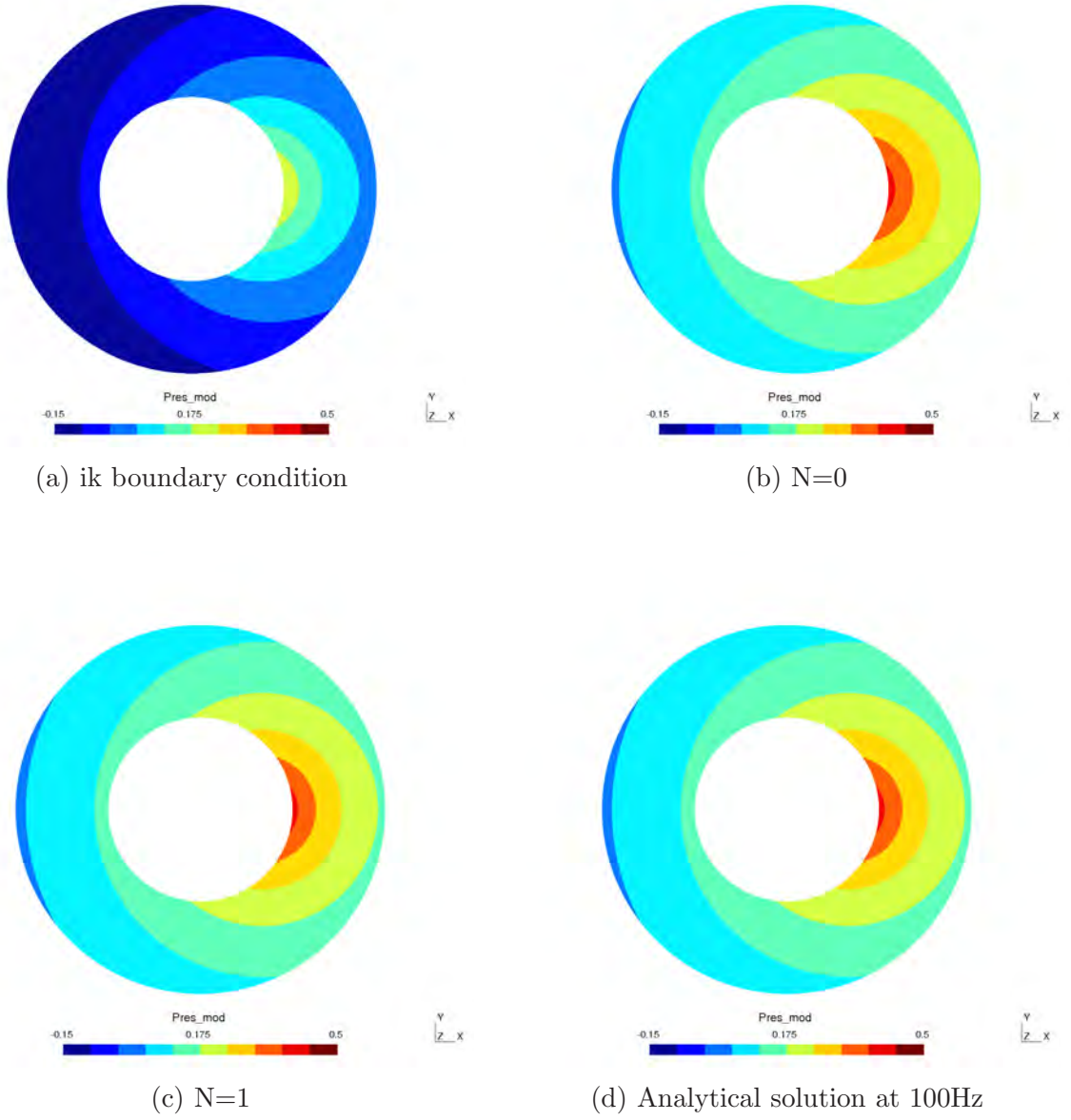


Figure 3: Comparison of solutions at 100Hz

solution at $100Hz$ shows important errors, the results at $300Hz$ and $1000Hz$ are much better. This shows that the condition is more efficient as the frequency increases as for other absorbing boundary conditions.

4 CONCLUSION

A new numerical method has been presented for computing absorbing boundary conditions for the Helmholtz equation. It builds a discrete absorbing matrix directly from

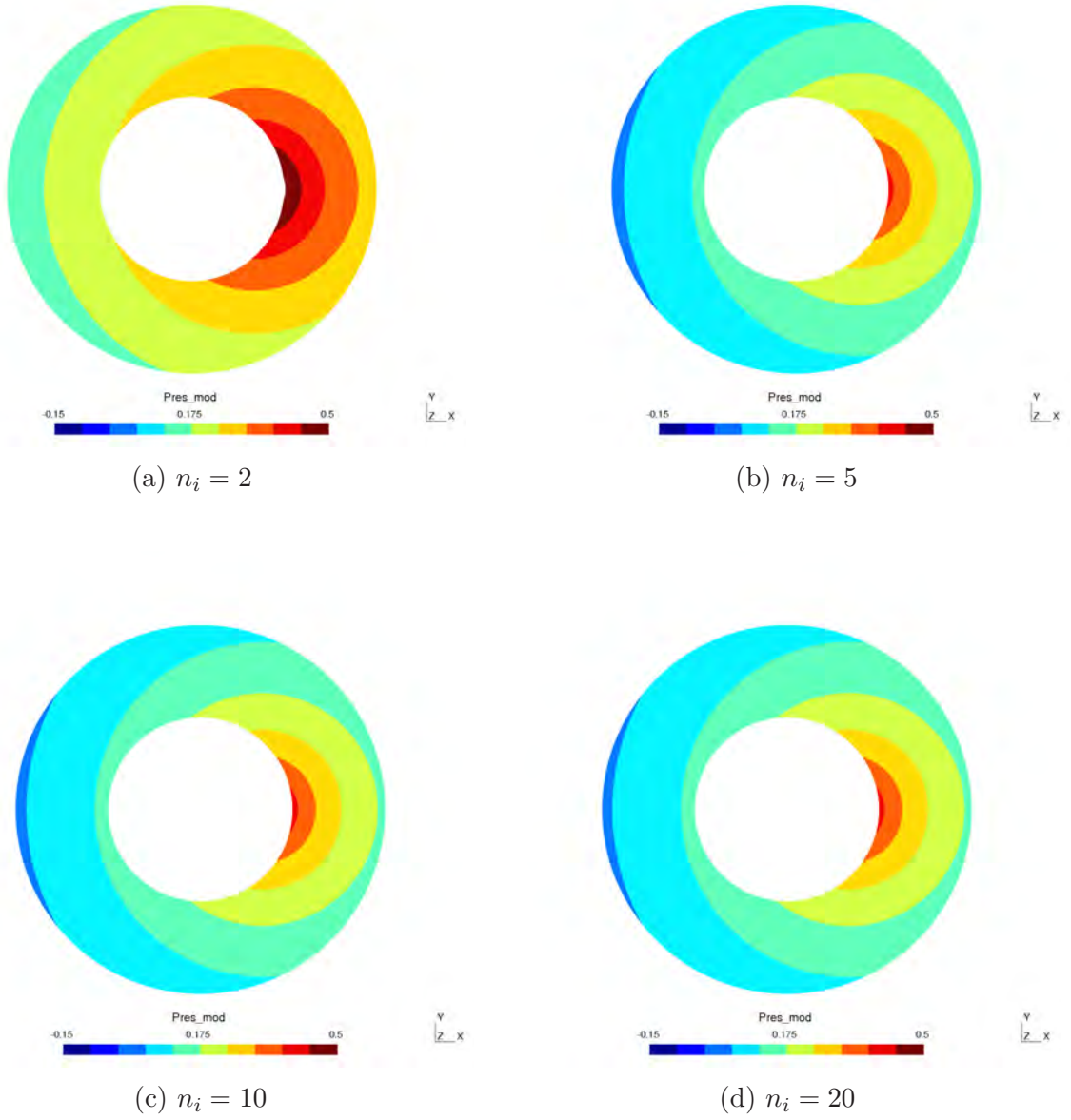


Figure 4: Solutions for different numbers of nodes used to define the matrix \tilde{A}

the finite element discretisation of the problem. This can be applied to any shape and does not require additional variables or additional domains. So the number of degrees of freedom is the same as for the problem without absorbing boundary conditions. Examples show the accuracy of the method. Similar approaches could be used for other wave propagation problems such as for the propagation of elastic waves. Future works will include comparisons with other classical absorbing boundary conditions and the consideration of more complex domains such as domains with corners.

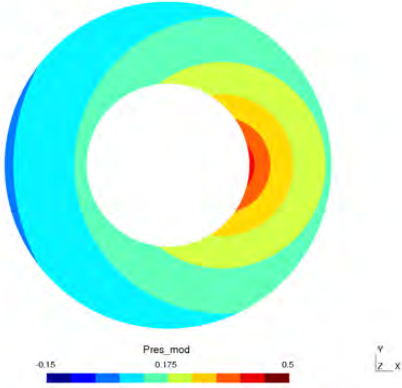
Number of nodes	global error	boundary error
$n_i = 2$	0.459	0.522
$n_i = 5$	0.010	0.013
$n_i = 10$	0.005	0.006
$n_i = 20$	0.003	0.005

Table 2: Error for different numbers of nodes used to build the matrix \tilde{A}

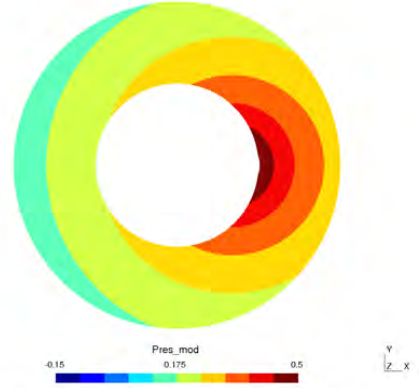
REFERENCES

- [1] J.B. Keller and D. Givoli. Exact non-reflecting boundary conditions. *Journal of computational physics*, 82(1):172–192, 1989.
- [2] D. Givoli and J.B. Keller. A finite element method for large domains. *Computer Methods in Applied Mechanics and Engineering*, 76(1):41–66, 1989.
- [3] C.A. Brebbia and S. Walker. *Boundary Element Techniques in Engineering*. Newnes-Butterworths, 1980.
- [4] R.D. Ciskowski and C.A. Brebbia. In *Boundary element methods in acoustics*. Computational mechanics publications, Elsevier Applied Sciences, 1991.
- [5] M. Bonnet. *Boundary Integral Equation Methods for Solids and Fluids*. John Wiley and Sons, 1995.
- [6] P. Bettess. Infinite elements. *International Journal for Numerical Methods in Engineering*, 11(1):53–64, 1977.
- [7] P. Bettess. *Infinite Elements*. Penshaw Press, 1992.
- [8] D.S. Burnett. A three-dimensional acoustic infinite element based on a prolate spheroidal multipole expansion. *Journal of the Acoustical Society of America*, 96:2798–2816, 1994.
- [9] R.J. Astley. Infinite elements for wave problems: a review of current formulations and an assessment of accuracy. *International Journal for Numerical Methods in Engineering*, 49(7):951–976, 2000.
- [10] B. Engquist and A. Majda. Absorbing boundary conditions for numerical simulation of waves. *Proceedings of the National Academy of Sciences*, 74(5):1765–1766, 1977.
- [11] R. Clayton and B. Engquist. Absorbing boundary conditions for acoustic and elastic wave equations. *Bulletin of the Seismological Society of America*, 67(6):1529–1540, 1977.
- [12] A. C. Reynolds. Boundary conditions for the numerical solution of wave propagation problems. *Geophysics*, 43(6):1099–1110, 1978.

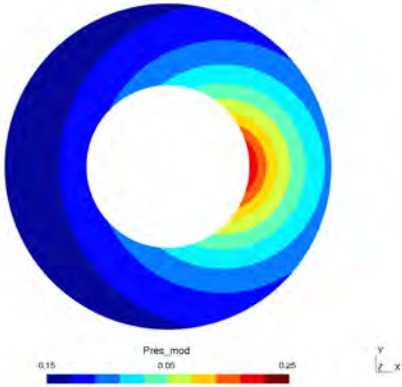
- [13] A. Bayliss and E. Turkel. Radiation boundary conditions for wave-like equations. *Communications on Pure and Applied Mathematics*, 33(6):707–725, 1980.
- [14] A. Bayliss, M. Gunzburger, and E. Turkel. Boundary conditions for the numerical solution of elliptic equations in exterior regions. *SIAM Journal on Applied Mathematics*, 42(2):430–451, 1982.
- [15] F. Collino. High-order absorbing boundary conditions for wave propagation models. straight line boundary and corner cases. In *Proc. 2nd Int. Conf. on Mathematical & Numerical Aspects of Wave Propagation*, R. Kleinman et al. SIAM, pages 161–171, Delaware, USA, 1993.
- [16] T. Hagstrom and S.I. Hariharan. A formulation of asymptotic and exact boundary conditions using local operators. *Applied Numerical Mathematics*, 27(4):403 – 416, 1998.
- [17] J.P. Berenger. A perfectly matched layer for the absorption of electromagnetic waves. *Journal of computational physics*, 114(2):185–200, 1994.
- [18] J.P. Berenger. Three-dimensional perfectly matched layer for the absorption of electromagnetic waves. *Journal of computational physics*, 127(2):363–379, 1996.
- [19] D. Duhamel and T.M. Nguyen. Finite element computation of absorbing boundary conditions for time-harmonic wave problems. *Computer Methods in Applied Mechanics and Engineering*, 198(37):3006–3019, 2009.
- [20] S. Thirunavukkarasu and M.N. Guddati. Absorbing boundary conditions for time harmonic wave propagation in discretized domains. *Computer Methods in Applied Mechanics and Engineering*, 200(33):2483 – 2497, 2011.
- [21] D. Colton. Runge's theorem and far field patterns for the impedance boundary value problem in acoustic wave propagation. *SIAM Journal on Mathematical Analysis*, 13(6):970–977, 1982.
- [22] R.F. Millar. On the completeness of sets of solutions to the helmholtz equation. *IMA Journal of Applied Mathematics*, 30(1):27–37, 1983.
- [23] Y. Liu and J.S. Bolton. On the completeness and the linear dependence of the cartesian multipole series in representing the solution to the helmholtz equation. *The Journal of the Acoustical Society of America*, 140(2):EL149–EL153, 2016.



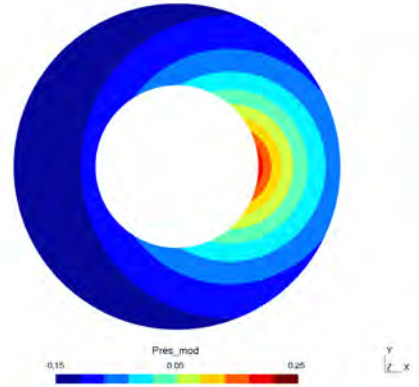
(a) Analytical solution 100Hz



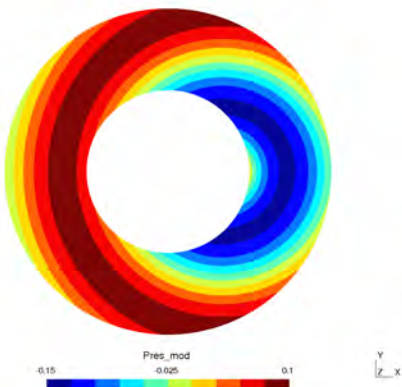
(b) Numerical solution 100 Hz



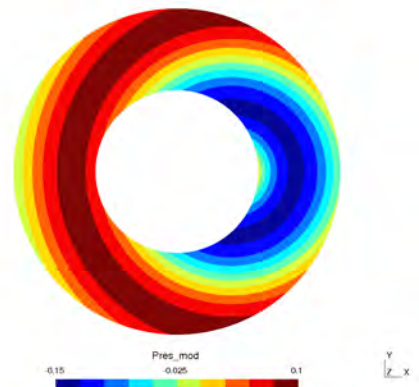
(c) Analytical solution 300Hz



(d) Numerical solution 300 Hz



(e) Analytical solution 1000Hz



(f) Numerical solution 1000 Hz

Figure 5: Solutions for different frequencies

Microstructural Origins of Fatigue Crack Nucleation

Fionn Dunne*, Bo Chen**, Jun Jiang***

*Imperial College, **Imperial College, ***Imperial College

ABSTRACT

An integrated experimental, characterization and computational crystal plasticity study of cyclic plastic beam loading has been carried out for nickel single crystal (CMSX4), oligocrystal (MAR002) and polycrystal alloys in order to assess quantitatively the mechanistic drivers for fatigue crack nucleation. The experimentally validated modelling provides knowledge of key microstructural quantities (accumulated slip, stress and GND density [1]) at experimentally observed fatigue crack nucleation sites and it is shown that while each of these quantities is potentially important in crack nucleation, none of them in its own right is sufficient to be predictive. However, the local (elastic) stored energy density, measured over a length scale determined by the density of GNDs, has been shown to predict crack nucleation sites in the single and oligocrystal tests. In addition, once primary nucleated cracks develop and are represented in the crystal model, the stored energy correctly identifies where secondary fatigue cracks are observed to nucleate in experiments [2]. This (Griffith-Stroh type) quantity also correctly differentiates and explains intergranular and transgranular fatigue crack nucleation. Further, for the polycrystal containing an oxide agglomerate, multiple crack nucleations occurred at the nickel matrix-inclusion interface and both nucleation and growth were found to be crystallographic with highest slip system activation driving crack direction. Local slip accumulation was found to be a necessary condition for crack nucleation, and that in addition, local stress and density of geometrically necessary dislocations are involved. Fatemi-Socie and dissipated energy were also assessed against the experimental data, showing generally good, but not complete agreement. However, the local stored energy density (of a Griffith-Stroh kind) identified all the crack nucleation sites as those giving the highest magnitudes of stored energy. [1] Yongjun Guan, Bo Chen, Jinwen Zhou, Ben Britton, Jun Jiang, Fionn Dunne. Crystal Plasticity Modelling and HR-DIC Measurement of Slip Activation and Strain Localisation in Single and Oligo-crystal Ni Alloys under Fatigue. Intl. Jnl. Plasticity. 88, 70-88, 2017. [2] Bo Chen, Jun Jiang, Fionn Dunne. Microstructurally-sensitive fatigue crack nucleation in Ni-based single and oligo crystals. Jnl. Mech. Phys. Solids. 106, 15-33, 2017. [3] Bo Chen, Jun Jiang, Fionn Dunne. Is Stored Energy Density the Primary Meso-scale Mechanistic Driver for Fatigue Crack Nucleation? Intl. Jnl. Plas. 101, 213-229, 2018.

Data-Driven and Reduced Order Modeling : An Attempt at a Taxonomy of Problems and Approaches

Karthik Duraisamy*

*University of Michigan, Ann Arbor

ABSTRACT

With the growing interest in data-driven and reduced order modeling approaches, there is a pressing need to classify different problem formulations and approaches using a consistent language. Since this field is inherently multi-disciplinary, even the use of basic terms tend to be confusing and often misused. In this talk, an attempt is made at establishing a taxonomy of approaches in data-driven and reduced order modeling. Different classes of problems that are addressed by these approaches will also be categorized and examples from literature will be provided. The intent of this talk is to set the stage for the use of a common terminology such that the community can - in the future - efficiently navigate literature and more easily exchange ideas.

A Multi-scale Method for a Three-Phase Reservoir Simulator Considering Gravity Effects

Omar Y. Duran Triana^{*}, Philippe Devloo^{**}, Sonia M. Gomes^{***}

^{*}Researcher, ^{**}Professor, ^{***}Professor

ABSTRACT

The scope of this work is to develop and implement a fast integration point mixed finite element -- finite volume scheme, that can solve fine detailed geological realizations by the use of a new multi--scale approach- that allows the fast generation of computational reservoir models taking in account gravity effects. The strong formulation being considered is the weighted pressure formulation for the black--oil model. Using a integration point mixed finite element -- finite volume discretization scheme, that stores all the required data at integration points and the multi--scale hybrid mixed method MHM with local mass conservation at any scale, it is possible to solve efficiently conservative fluxes on both coarse and fine scales. Once theses fluxes are determined, they are used to solve the transport equations of the flowing phases. The nonlinearities associated with black--oil model are treated with a segregated multi--physics solver. We present how to account the buoyancy effects, as well evaluations for computational efficiency and accuracy on a series of full and corresponding multi-scale reservoir models with a high degree of realism, highly heterogeneous rock properties distributed in an representative domain considering complex reservoir and wells geometric descriptions. The multi-scale simulation with integration point mixed finite element method allow us to compute every simulation states in a reasonable time, and it represents a robust and fast approach that enable us to simulate a detailed geological realizations not allowed be possible with current upscaling methods.

A General Mesh Smoothing Approach for Finite Elements

Raul Durand*

*University of Brasilia

ABSTRACT

The elements geometry in finite element meshes can be enhanced by means of smoothing procedures. This paper presents a smoothing technique based on ideal shapes and the use of finite element deformation analyses. Initially, it is assumed that the ideal shape for a particular element corresponds to a regular shape, e.g. polygon or polyhedron with the highest quality metric, with the same area or volume. Based on the initial element coordinates and thanks to the singular value decomposition (SVD) properties, a desired location for the ideal shape is found. Assuming a given mechanical stiffness, the nodal forces required to transform an element into its ideal version is calculated. Once the corresponding nodal forces for all elements are found, a deformation analysis is carried out aiming to transform the elements geometry into the desired ones. The solution provides a deformed mesh with elements with improved quality. The whole process can be applied iteratively to get better improvements. In practice, just few iterations (e.g. two or three) are enough to obtain significant enhancements. The method is applicable to improve finite element meshes constituted by linear and quadratic elements in two and three dimensions.

Energy Stable Discontinuous Galerkin Approximations of the Perfectly Matched Layer for Linear Wave Equations

Kenneth Duru^{*}, Alice-Agnes Gabriel^{**}, Gunilla Kreiss^{***}, Leonhard Rannabauer^{****}

^{*}Munich University, Germany, ^{**}Munich University, Germany, ^{***}Uppsala University, ^{****}Technical University of Munich

ABSTRACT

Computational procedures based on discontinuous Galerkin (dG) schemes can be flexible, high order accurate, provably stable, and well-suited for complex large scale wave propagation problems. However, real world wave propagation problems are often formulated in large or unbounded domains. An effective and reliable domain truncation scheme becomes essential, since it enables efficient and high fidelity numerical simulations. The perfectly matched layer (PML) has emerged as an efficient and robust technology to simulate the absorption of waves in many applications. However, previous attempts to effectively include the PML in many modern numerical methods, such as the dG method, proved to be a nightmare for practitioners. Exponential and/or linear growth is often seen in numerical simulations. We present a provably energy-stable dG approximation of the perfectly matched layer (PML) for the three and two space dimensional (3D and 2D) linear wave equations, in first order form. Our approach is rooted in a rigorous mathematical analysis, beginning from the continuous model down to the discrete problem. We derive continuous energy estimates for the 3D PML in the Laplace space. By emulating the energy estimate in the discrete setting we construct asymptotically stable dG approximation of the PML for the wave equation. The analysis will focus on the 3D linear acoustics wave equation. But, we will demonstrate extensions of our method to the 3D linear elasto-dynamic equations. These have been implemented in the dG code, ExaHyPE, a simulation engine for hyperbolic PDEs on adaptive Cartesian meshes, for exascale supercomputers. Finally, we present a large scale numerical simulation of a geophysical wave propagation problem, involving the scattering and interactions of acousto-elastic waves, in a complicated Earth model, with geologically constrained complex free-surface topography.

Towards Exa-scale Multi-physics Simulations of Earthquakes

Kenneth C. Duru^{*}, Alice-Agnes Gabriel^{**}, Leonhard Rannabauer^{***}, Michael Bader^{****}

^{*}LMU Munich, ^{**}LMU Munich, ^{***}TUM, ^{****}TUM

ABSTRACT

Realistic earthquake scenarios combine spontaneous dynamic rupture propagation on pre-existing fault interfaces according to non-linear friction laws with seismic wave propagation. The up-to-date largest (1500 km of faults) and longest (500 s) dynamic rupture simulation is modeling the 2004 Sumatra-Andaman earthquake on the curved mega-thrust and a system of splay faults validated by geodetic, seismological and tsunami observations. Such dynamic earthquake sources can be readily coupled to tsunami simulations to analyse tsunami generation and propagation. Whereas these earthquake simulations are based on the Discontinuous Galerkin method exploiting unstructured meshes to account for complex geometries (e.g. high resolution topography and bathymetry, 3D subsurface structure, and fault networks) feature preserving meshing poses limitations for large-scale problems. We present a first application scenario of the ExaHyPE engine, an hyperbolic PDE engine designed to enable exascale (10^{18} FLOPs/sec) simulations for conservation laws on future supercomputers without manual meshing.

High-Order Finite Element Methods for Acoustics

Fabian Duvigneau*, Ulrich Gabbert**, Sascha Duczek***

*Otto von Guericke University Magdeburg, **Otto von Guericke University Magdeburg, ***Otto von Guericke University Magdeburg

ABSTRACT

The acoustic behavior of structures has lately been in the focus of industrial applications, due to the fact that the acoustic emission of a product is one major parameter which significantly influences the customer perception with respect to comfort and functionality. In this context, the numerical simulation of vibroacoustic problems needs to provide reliable information in order to be able to evaluate the acoustic behavior of new products already in an early stage of the product development process. With the help of a suitable simulation model expensive experimental studies can be reduced and acoustically improved designs can be developed. However, there are already commercial software tools available which offer the opportunity to solve coupled vibroacoustic problems. These tools are typically based on conventional low-order finite element methods (h-FEM) for solving the governing partial differential equations (PDEs) of the problem. In this contribution the advantages of high-order finite element methods (p-FEM), such as a possibly exponential convergence rate [1], will be exploited. In such an approach the same accuracy can be obtained by using significantly less degrees of freedom (dof) compared to classical h-FEM simulations. Consequently, the required computational time required for the analysis can be significantly reduced for a given target accuracy. This property is of special importance when complex structures of practical relevance are under investigation. Even today the overall efficiency of the simulation process is still an issue, despite the ever growing computational power. To exploit the described advantages, high-order FEMs have to be extended to acoustical problems. In the current contribution the vibration analysis and the fluid-structure-interaction are also taken into account. The advantage of high-order methods has been demonstrated by the authors in previous studies, e.g. in the context of wave propagation analysis [2] and multi-physics applications such as piezoelectricity [3]. In this contribution the developed high-order simulation approach is discussed and the received results are compared both with commercial finite element solutions as well as with measurements. Here, the focus is placed on the accuracy and the required computational effort of the different methods. References [1] Szabó, B. & Babuška, I.: "Finite Element Analysis", John Wiley and Sons, 1991 [2] Willberg, C.; Duczek, S.; Vivar Perez, J. M.; Schmicker, D. & Gabbert, U.: "Comparison of Different Higher Order Finite Element Schemes for the Simulation of Lamb Waves", Computer Methods in Applied Mechanics and Engineering, 2012, Vol. 241-244, pp. 246-261 [3] Duczek, S. & Gabbert, U.: "Anisotropic Hierarchic Finite Elements for the Simulation of Piezoelectric Smart Structures", Engineering Computations, 2013, Vol. 30, pp. 682-706

Contact Pressure Solution Deformation in Phase Field Models

Branislav Dzepina^{*}, Daniele Dini^{**}, Daniel Balint^{***}

^{*}Imperial College London, ^{**}Imperial College London, ^{***}Imperial College London

ABSTRACT

Pressure solution is a deformation mechanism experienced by non-hydrostatically stressed elastic bodies whose primary mode of material transport is diffusive mass transfer. Although originally investigated within the geology community to describe the enhanced compaction of rock and soil particles, the pressure solution mechanism is also applicable to the high pressure sintering of advanced metals and ceramics. During the ultra-high pressure liquid phase sintering of diamond grains, which is the focus of the study, it is estimated that inter-particle contact pressures can approach 100 GPa at some of the contacts. Within the vicinity of such contacts, significant elastic strain energy is stored in the material. As a result of diffusive transfer through the liquid phase, material is transported along energy gradients from the centre of the contact to the lesser-stressed surrounding particle surface. Tracking of the particle interfaces due to this deformation mechanism is not trivial, especially when other processes such as bonding are considered. Thus a phase field model for this process is justified. Elastic energy in phase field models have previously been reported in literature, however, these models are usually concerned with the strain energy resulting from elastic mismatch at the interfaces, phase transformation or strain fields applied to the entire simulation domain. The presented work is an extension of the advection-diffusion sintering phase field model initially proposed by Wang [1]. The original sintering model is modified by the incorporation of contact mechanics and an elastic strain energy term in the free energy functional. The particles are initiated by scalar fields which represent their concentration within the simulation domain. Given a starting configuration, the diffuse interfaces of the particles are allowed to evolve in time in order to minimise the energy of the system. Contact pressure distribution within the contact is approximated by the overlap of the scalar fields that represent the respective particles. Rigid particle motion by advection velocity fields is used to maintain contact between the deforming particles. The effect of pressure solution deformation on the shape of a single particle pressed onto a non-interacting wall is presented. The proposed model is also applied to the demonstration of high pressure sintering between two particles and finally to a cluster of several interacting particles. [1] Yu U. Wang, Computer modeling and simulation of solid-state sintering: A phase field approach, Acta Materialia, Volume 54, Issue 4, 2006, Pages 953-961

A Coupled Phase-field/Diffusion/Deformation Model for Upper and Lower Bainitic Transformation

Martin Düsing*, Rolf Mahnken**

*Paderborn University, **Paderborn University

ABSTRACT

The bainitic transformation in steel leads to two different morphologies, upper and lower bainite, which distinguish due to different carbon diffusion mechanisms [1]. The constant temperature during the displacive transformation from austenite to bainitic ferrite influences the mobility of the carbon during the subsequent diffusion. The movement of the carbon determines the location of the carbides, which precipitate at accumulations of carbon. In upper bainite the carbon atoms succeed in leaving the supersaturated bainitic ferrite by diffusing across the interface while in lower bainite most of the carbon stays within the bainitic ferrite and accumulate there [1]. In this contribution we present a new model simulating the above described phase transformation. A phase-field method is applied to govern the three phases austenite, bainitic ferrite and carbide while an elaborate diffusion model considers the separation of carbon within the supersaturated bainitic ferrite and the diffusion across the interface. It is based on a Cahn-Hilliard diffusion equation. To describe the slim shape of the bainitic ferrite phase the model is coupled with deformations. The simulation is based on a thermodynamic framework of generalized stresses as introduced by Gurtin [2] for a two phase Ginzburg-Landau system and a Cahn-Hilliard equation. We extend this framework for multiphase-field models coupled to a viscous Cahn-Hilliard equation and deformations. The framework distinguishes between basic balance laws which are universal and constitutive equations which depend on the specific material. The Clausius-Duhem inequality is used to impose restrictions to the constitutive equations. The numerical examples show the transformation from austenite to bainitic ferrite, the subsequent diffusion and the precipitation of carbides [3]. Depending on the constant temperature the different diffusion mechanisms are weighted. For low temperatures most of the carbon starts to separate within the bainitic ferrite while only a minor part succeed in leaving the supersaturated phase. Subsequently carbides precipitate at accumulations of carbon. For higher temperatures the carbon diffuses across the interface into the austenite phase. In the example one can see how the concentration within the austenite between two phases of bainitic ferrite grows until carbides precipitate. [1] Bhadeshia, H. K. D. H. Bainite in steels, Cambridge, Second Edition (2001). [2] Gurtin, M. E., Physica D: Nonlinear Phenomena (1996) 92:178–192. [3] Düsing, M. and Mahnken, R., Int J Solids Struct (2017) doi:10.1016/j.ijsolstr.2017.11.018

VoroCrust: Conforming Polyhedral Meshing without Clipping

Mohamed Ebeida*

*Sandia National Laboratories

ABSTRACT

We present VoroCrust: a novel approach to polyhedral meshing that simultaneously generates a quality mesh of the surface of a Piecewise Linear Complex (PLC) model and decomposes the enclosed volume by unweighted Voronoi cells with good aspect ratios conforming to the surface mesh, without clipping or bad normals. Up to our knowledge, our method is the first to solve this open problem. VoroCrust also outputs an approximation of the medial axis of the input model and provides a fast technique for in/out point classification. To design our solution, we introduce new definitions of the medial axis and the local feature size that cater to PLC models. To further ensure enough protection around sharp features of the input model, we also present the concept of Maximal-Poisson Disk Sampling (MPS) with extended coverage, and provide a solution method. We experimentally illustrate the robustness and output quality of VoroCrust through a collection of models of varying complexity, successfully preserving sharp features if any. In this talk we also present the recently released VoroCrust software and discuss its performance in practice.

Atomistic Fracture Analysis of Silica Glass Based on its Network Topology

Firaz Ebrahim^{*}, Franz Bamer^{**}, Bernd Markert^{***}

^{*}RWTH Aachen University, Germany, ^{**}RWTH Aachen University, Germany, ^{***}RWTH Aachen University, Germany

ABSTRACT

The nanostructural arrangement of amorphous silica glass can be described based on its short and medium-range order. The latter is represented by rings of various sizes composed of corner-sharing tetrahedra [1,2]. In this study, we perform classical molecular dynamics simulations to investigate the quenching rate influence on the deformation and fracture behaviour depending on the medium-range order. For this purpose, we use a two- and three-body interaction potential [3] to prepare several samples with statistically different amorphous states by quenching molten silica to ambient temperature considering different quenching rates. All samples are subjected to tensile loadings and it is shown that the mechanical behaviour depends on the associated ring statistics. [1] Rino JP, Ebbsj\"o I, Kalia RK, Nakano A, Vashishta P (1993) Structure of rings in vitreous SiO\$_2\$. Physical Review B 47:3053-3062. [2] Hobbs LW, Jesurum CE, Pulim V, Berger B (1998) Local topology of silica networks. Philosophical Magazine A 78:679-711. [3] Vashishta P, Kalia RK, Rino JP, Ebbsj\"o I (1990) Interaction potential for SiO\$_2\$: A molecular-dynamics study of structural correlations. Physical Review B 41:12197-12210.

Nonconforming Finite Element Approximations of the Phase Field Model of Lipid Membranes

Faezeh Ebrahimi^{*}, Arzhang Angoshtari^{**}

^{*}The George Washington University, ^{**}The George Washington University

ABSTRACT

Boundaries of living cells and vesicles are lipid membranes composed of amphiphilic lipid molecules which form a bilayer-structure of only a few nanometers thickness. It is well-known that the phase field approach provides a powerful framework for approximating configurations of lipid membranes. In this approach, the governing equation for obtaining equilibrium configuration of lipid membranes is a fourth order PDE in terms of the phase field function. In this talk, we introduce nonconforming finite element approximations of the governing equation by using several finite elements including the Hermite tetrahedron and the Morley element.

Mechanics of Bio-inspired 1D Metamaterial Scale Covered Structure under Torsional Load

Hossein Ebrahimi^{*}, Hessein Ali^{**}, Ranajay Ghosh^{***}

^{*}University of Central Florida, ^{**}University of Central Florida, ^{***}University of Central Florida

ABSTRACT

A metamaterial is a material designed and engineered to obtain some mechanical or physical properties, which cannot be observed in nature or real materials. Metamaterials can be made of assemblies of multiple components and usually have repeating patterns may be inspired from bio-structures. Properties of metamaterials are more affected from their geometrical design, patterns, orientations or structures rather than the properties of the main material or other constituents. One of the bio-structures that there are a lot of efforts on mimicking them as metamaterials to design flexible dermal armor is structure of fish or reptile scales due to high stiffness performance under bending, twisting and indentation. These biomaterials have good geometrical design and mechanical properties, which provide flexibility, mobility, durability in failure and protection against predators. In this work, the behavior of one-dimensional scale covered structure will be discussed under twisting load. To this end, an analytical model is derived by establishing the geometrical relation depends on length, width and distance between the scales. The results compared with numerical model which obtained by ABAQUS. It is concluded that three different regimes exist, which include linear operation phase before scales engagement, high nonlinear phase due to relatively rigid scales engagement and rigid phase after achieving to the derived kinematic locking condition. In addition, the mechanics of the system will be discussed by considering the scales as some torsional springs, which affect the deformation of elastic substrate. Finally, it will be demonstrated how designing and analysis of fish scales covered structures can be helpful to achieving stiffness, rigidity and protection besides flexibility and lightweight which are not available in regular materials.

Polynomial Chaos Approximation Using B-Splines

Christoph Eckert^{*}, Michael Beer^{**}

^{*}Leibniz Universität Hannover - Institute for Risk and Reliability, ^{**}Leibniz Universität Hannover - Institute for Risk and Reliability

ABSTRACT

Random variables can be approximated by the Polynomial Chaos (PC) representation by truncating the series expansion. Ordinarily, the basis of these series are Hermite polynomials. In this study the representation is based on B-Spline functions, which are commonly used in the area of computer aided design (CAD). Hughes et. al. established the Isogeometric Analysis (IGA) which extends the finite element method through the usage of B-Spline, or its extensions non-uniform rational B-Splines (NURBS). The features and limitations of polynomial chaos with Hermite polynomials are reviewed and the approximation by B-Splines of a Gaussian random variable is investigated.

Particle-size Segregation Theory Applied to the Erosion-deposition Dynamics of Granular Avalanches

Andrew Edwards*, Nico Gray**

*University of Manchester, **University of Manchester

ABSTRACT

Almost all geophysical events involving granular materials - such as snow avalanches, debris flows and pyroclastic flows - exhibit a continuous exchange of particles between a depositional flow and the erodible substrate that it propagates on. The balance between erosion and deposition can have a great influence on the flow duration and runout distance, which are important factors to consider for hazard risk assessment and mitigation. A perfect balance between erosion and deposition is even possible in certain conditions (Edwards, Viroulet, Kokelaar & Gray, 2017), resulting in a flow that propagates steadily downslope whilst maintaining a constant shape and velocity. By releasing a small amount of yellow sand onto an erodible bed of the the same material, but instead coloured red, it is shown that the erosion-deposition process in a steady avalanche eventually results in the the flowing material consisting entirely of particles that have been eroded from the substrate layer. Furthermore, different steady state regimes are possible for a given slope inclination angle depending on the amount of sand released. The experiments are simulated using a depth-averaged avalanche model and a friction law that allows dynamic, static and intermediate flow regimes for angular materials (Edwards et al., 2017). This model is augmented with the large-particle transport equation (Gray & Kokelaar, 2010) for the evolution of an inversely graded shock interface between an instantaneously and sharply segregated layer of large particles above a layer of small particles in a bidisperse flow. The inclusion of a segregation equation here allows the tracking of the interface between the two different coloured sands and therefore the redistribution of grains due to erosion and deposition. By plotting the colour of the sand according to the depth-averaged yellow concentration at each position, it is shown that all of the key experimental features are qualitatively reproduced by the numerics.

A Scaled Boundary Multiscale Approach to Crack Propagation via Hybrid Balanced Quadrees

Adrian Egger^{*}, Savvas Triantafyllou^{**}, Eleni Chatzi^{***}

^{*}ETH Zurich, ^{**}University of Nottingham, ^{***}ETH Zurich

ABSTRACT

The modelling of crack propagation by means of the finite element method is a highly challenging task. The extended finite element method (XFEM) has been proposed to mitigate the need for remeshing while accurately representing the singular stress field around the crack tip, using additional enrichment terms. Unfortunately, these enrichment terms must be specified prior to analysis, which impedes fully automated and general crack propagation schemes utilizing stress intensity factors (SIFs). Damage related phenomena within the context of linear elastic fracture mechanics (LEFM) can be elegantly and efficiently accounted for via the scaled boundary finite element method (SBFEM) [1]. A significant advantage of SBFEM lies in its semi-analytical nature, which permits the direct extraction of the SIFs, based on their formal definition without any a priori knowledge, and computation at negligible computational cost. This is achieved by introducing a scaling centre in the domain, effectively transforming the cartesian reference system to one resembling polar coordinates and reducing the computational dimension by one in the process. The resulting arbitrary polygons must be star convex, which is exploited for use with hybrid balanced quadrees [2] to elegantly reduce computational cost via precomputation of most stiffness matrices, while eliminating issues commonly associated with hanging nodes. While SBFEM significantly accelerates LEFM-related computations, the simulation of more involved problems still poses a considerable challenge. One possible way to mitigate such issues is by utilizing multiscale methods. In this work, the extended multiscale finite element method (EMsFEM) [3] is harnessed to define a coarse mesh, where the governing equations of the problem are solved, while exploiting SBFEM for modelling crack propagation on the fine mesh. Computational gains are achieved by only resolving for those representative volume elements (RVEs) that are affected by crack propagation. References: [1] J.P. Wolf, The scaled boundary finite element method, Wiley, 2003. [2] Ooi, E., Man, H., Natarajan, S., & Song, C. (2015). Adaptation of quadtree meshes in the scaled boundary finite element method for crack propagation modelling. Engineering Fracture Mechanics, 144, 101-117. [3] H.W. Zhang, J.K. Wu, Z.D. Fu, Extended multiscale finite element method for elasto-plastic analysis of 2D periodic lattice truss materials. Computational Mechanics, 45, 623-635, 2010.

Micro-Scale Modeling of Cell-Extracellular Matrix Interactions

Jonas Eichinger*, Roland Aydin**, Jay Humphrey***, Christian Cyron****

*Technical University of Munich, **Technical University of Munich, ***Yale University, ****Technical University of Munich

ABSTRACT

The extracellular matrix consists of a network of diverse filamentous proteins, glycoproteins, and glycosaminoglycans, which together provide mechanical support and biological cues to the resident cells. Importantly, mechanical cell-matrix interactions play crucial roles in tissue health and disease. Changes in matrix properties affect, for example, cell migration and differentiation. At the same time, cells actively sense and regulate their surrounding extracellular matrix, presumably to establish or maintain a preferred (so-called homeostatic) state. Integrin linker proteins connect the actin cytoskeleton inside the cells through the cell membrane to the extracellular filaments and form the cornerstone for this two-way feedback loop consisting of mechanosensation and mechanoregulation [1]. This talk introduces a novel computational framework for modeling extracellular matrix mechanics on the micro-scale, including cell-matrix interactions in three dimensions. Individual matrix fibers as well as cross-linker proteins are modeled explicitly and discretized by finite elements to capture their micromechanical properties such as bending and extensional stiffness. Dynamic inter-fiber cross-linking is considered by linker types that can bind fibers with a certain probability and unbind with a force dependent off rate [2], respectively. Other linker types, following a force dependent catch-slip-bond behavior [3] and endowed with the ability to contract, are used to link cells to discrete binding sites on matrix filaments. Using finite elements for the cells also enables us to model a two-way coupling between cells and matrix. Contact between different fibers in the extracellular matrix is captured in our computational model to account for effects of physical entanglements. In this talk, we will first introduce our general computational model and then we will show simulation results and compare them with data collected from experiments for cell seeded tissue equivalents within a biaxial bioreactor. References [1] Humphrey JD, Dufresne ER, Schwartz MA. Mechanotransduction and extracellular matrix homeostasis. *Nature reviews Molecular cell biology*. 2014;15(12):802-812. [2] Kim J, Feng J, Jones CAR, et al. Stress-induced plasticity of dynamic collagen networks. *Nature Communications*. 2017;8:842. [3] Weng S, Shao Y, Chen W, Fu J. Mechanosensitive subcellular rheostasis drives emergent single-cell mechanical homeostasis. *Nature materials*. 2016;15(9):961-967.

Finite Element Implementation of a Phase Mixture Model for Tempered Martensitic Steels

Johanna Eisenträger*, Konstantin Naumenko**, Yevgen Kostenko***, Holm Altenbach****

*Otto-von-Guericke-Universität Magdeburg, Institute of Mechanics, Universitätsplatz 2, 39106 Magdeburg, Germany, **Otto-von-Guericke-Universität Magdeburg, Institute of Mechanics, Universitätsplatz 2, 39106 Magdeburg, Germany, ***Siemens AG, Power and Gas Division, Rheinstr. 100, 45478 Muelheim an der Ruhr, Germany, ****Otto-von-Guericke-Universität Magdeburg, Institute of Mechanics, Universitätsplatz 2, 39106 Magdeburg, Germany

ABSTRACT

Tempered martensitic steels with high chromium content are often used for power plant components under complex thermo-mechanical loads. These components are subjected to frequent start-ups and shut-downs in combination with long holding times at high temperatures. These loading conditions induce both creep and fatigue issues in the structure. Consequently, martensitic steels are a viable choice as they feature excellent properties, such as high creep strength and corrosion resistance, to withstand these conditions. On the other hand, these alloys suffer from softening due to microstructural changes, what should be taken into account by a constitutive model. This contribution presents a unified phase mixture model for rate-dependent inelasticity of a 12% Cr heat-resistant steel and demonstrates the implementation of the model into the finite element method. In a first step, the multi-axial phase mixture model is introduced. The phase mixture model distinguishes two phases, i.e. a hard and a soft phase, which are connected via an iso-strain approach. A backstress and a softening variable are introduced as internal variables, thus allowing for the consideration of non-linear kinematic hardening as well as softening effects. The model results in a coupled system of three evolution equations with respect to the inelastic strain, the backstress, and the softening variable. The model is implemented into the commercial finite element code ABAQUS with a user material subroutine. In order to update the stress and the two internal variables, the backward Euler method is used in combination with a Newton-Raphson iteration. Furthermore, the consistent tangent operator is introduced for the phase mixture model. A wide range of benchmarks for uni-axial as well as multi-axial stress states is taken into account in order to verify the implementation. The numerical results are compared to experimental measurements for high temperature tensile tests. Finally, an idealized steam turbine rotor is analyzed using the proposed model. In a first step, the temperature fields are computed in a transient heat transfer analysis, taking varying steam temperatures and heat transfer coefficients into account. The temperature fields serve as input for the subsequent structural analysis, which additionally considers a time-dependent steam pressure and rotational frequency. The structural analysis provides stress-strain hystereses for different kinds of start-ups and shut-downs, which can be used for further fatigue and damage assessment.

Multi-scale, Multi-axial Failure Modelling for Composites

Bassam El Said*, Stephen Hallett**

*University of Bristol, **University of Bristol

ABSTRACT

Recent advances in composite manufacturing and design have encouraged engineers to introduce composites to more complex structures. The usage of composites in energy, marine, automotive and aerospace applications leads to the design and manufacturing of thicker composite structures for load critical applications. Consequently, the need has arisen for modelling of more complex structures with integrated geometric features such as changes in thickness, curvature and connectors. In addition to these features, the load levels mandate considerably thicker composite structures, which brings a new set of challenges. Damage models in composites have largely been focused at the micro and ply-scale. Understanding the ply and inter-ply damage modes is valuable since these damage mechanism control the failure at the structural scale. For a thin layup, it is possible to construct a ply-by-ply model, even at feature scale e.g. open holes. However, for thick composite structures where the ply count can be in the hundreds, these high-fidelity models are no longer a viable option. Consequently, there is a pressing need to develop homogenized failure models which operate on the structure scale without having to describe the composite ply orientations explicitly. In this paper, the challenges associated with this homogenised modelling approach will be detailed, developed and verified against experimental results. The proposed numerical framework starts from a set of high fidelity Representative Volume Element (RVE) meso-scale models under periodic boundary conditions. The RVE models include the phenomenological damage models such as matrix cracking, delamination and fibre failure. A set of RVE models is solved under various combinations of loads representing different stress states. A dedicated computational homogenization module generates effective stress strain curves for each RVE model. These curves are generated for all six stress components (3 axial + 3 shear). The effective stress / strain curves are then used to generate sets of damage surfaces that are used to construct a combined failure surface including the contribution of all the macro-scale stress components. In a macro-scale model, a virtual RVE is constructed around each integration point. The underlying ply-orientation is known for each virtual RVE but not modelled explicitly. Next, the simulation interacts with the combined damage surface by providing a stress-state and receiving a fourth order tangential stiffness tensor for each integration point. The proposed model was shown to accurately predict damage initiation and progression for a set of experimental benchmark problems.

Adaptive Mesh Refinement and Coarsening Strategies for Hurricane Sensitive Regions

Omar El-Khoury^{*}, Ethan Kubatko^{**}, Dylan Wood^{***}

^{*}The Ohio State University, ^{**}The Ohio State University, ^{***}The Ohio State University

ABSTRACT

In this study, we will present the development and implementation of adaptive mesh refinement and coarsening algorithms into a Discontinuous Galerkin Shallow Water Equation Model (DG-SWEM), commonly used for simulating hurricane storm surge [1]. The application of these algorithms aims to significantly reduce the computational cost of a storm surge simulation while preserving the desired accuracy. The process of the adaptive algorithms includes three stages: (1) detecting localized regions to refine based on a defined cone of uncertainty associated with the predicted hurricane storm track; (2) refining the elements within these localized regions, while maintaining a 1-irregular mesh; and (3) updating the associated bathymetry in these areas by interpolating from an underlying high-resolution bathymetry set constructed from a moving least squares approximation [2]. Some of the challenges encountered include maintaining load balance in parallel computation and conserving mass and momentum during the refinement process. Preliminary numerical results will be presented, comparing the efficiency of the approach to the Advanced Circulation (ADCIRC) Model. Ultimately, the proposed methodology aims to help design more efficient early warning systems for hurricanes, which can help reduce the consequences of coastal hazards. References [1] Dawson, C., Kubatko, E.J., Westerink, J.J., Trahana C., Mirabito, C., Michoskia C., Panda, N., Discontinuous Galerkin methods for modeling hurricane storm surge, *Advances in Water Resources*, 34, pp. 1165-1176, 2011. [2] Brus, S. R. (2017). Efficiency Improvements for Modeling Coastal Hydrodynamics through the Application of High-Order Discontinuous Galerkin Solutions to the Shallow Water Equations (Doctoral dissertation, University of Notre Dame).

Tongue Kinematics during Infant Feeding

David Elad^{*}, Andrew Laine^{**}, Catherine Genna^{***}

^{*}Tel Aviv University, Israel, ^{**}Columbia University, New York, USA, ^{***}Lactation Consultant, IBCLC, New York, USA

ABSTRACT

The tongue is an important organ that has a pivotal role in the process of swallowing and speech. In neonates and infants optimal performance of the tongue is crucial for proper nutritive sucking and swallowing. Successful breastfeeding requires dynamic synchronization between the infant mandible oscillation, rhythmic motility of its tongue, and the breast milk ejection reflex that drives maternal milk towards the nipple outlet. During suckling, the infant compresses the areola-nipple region with its gums and generates sub-atmospheric oral pressures via the oscillating mandible and pulsating tongue. The tongue muscle plays a key functional role in the regulation of intra-oral pressures which are required for latch-on, extraction of human milk from the breast and swallowing. We developed an objective methodology to extract quantitative information of tongue kinematics from submental ultrasound video clips that were recorded during infant feeding on the breast or artificial bottle nipples. The method is based on efficient detection of the palate and upper tongue outlines in successive frames of the recorded ultrasound images. This was followed by registration with respect to the hard palate and computation of the special tongue motility about polar coordinates with an origin below the chin. We analyzed the tongue kinematics during breast feeding of healthy infants, as well as tongue-tied infants before and after surgical intervention (i.e., frenotomy) to improve tongue mobility. In addition we also analyzed the tongue kinematics of infants feeding on bottle nipples. Using FFT algorithms we computed the spatial dominant frequencies of tongue motility in the different cases. We also employed wavelet algorithms to explore differences between healthy breastfeeding and restricted feeding with a tied tongue, as well as bottle feeding. The results revealed that this methodology can be utilized for diagnostic and post-intervention in problematic cases of infant feeding.

Simulating Earthquake Rupture on Frictional Interfaces Using an Asynchronous Space-time Discontinuous Galerkin Method

Ahmed Elbanna^{*}, Amit Madhukar^{**}, Robert Haber^{***}, Reza Abedi^{****}

^{*}University of Illinois Urbana Champaign, ^{**}University of Illinois Urbana Champaign, ^{***}University of Illinois Urbana Champaign, ^{****}University of Tennessee at Knoxville

ABSTRACT

Earthquakes are among the most destructive natural hazards to mankind with losses exceeding thousands of lives and billions of US dollars annually. An outstanding challenge is to accurately model earthquake nucleation, propagation, and arrest alongside with the stress-accumulation patterns during the seismic cycle to develop physics-based seismic hazard models for informed risk analysis and policy making. A critical barrier for the application of conventional numerical analysis techniques, such as time-marching finite element or finite difference methods on non-adaptive meshes, is the wide range of length and time scales (from sub-millimeter to kilometers and from milli-seconds to centuries) involved in the earthquake processes. This multi-scale character makes the problem computationally intractable even on state-of-the-art supercomputing platforms. We overcome this challenge by using an asynchronous space-time Discontinuous-Galerkin (aSDG) method with dynamic adaptive meshing that enables variations of spatial and temporal resolution over several orders of magnitude across the solution domain. To illustrate our method, we apply the aSDG method to the earthquake benchmark problem TPV205-2D provided by the Southern California Earthquake Center (SCEC). The problem setup includes a planar slip-weakening frictional interface embedded in a two-dimensional linear elastic domain. The rupture is initiated by overstressing a localized patch on the fault surface beyond its static frictional strength. The rupture propagates bilaterally and interacts with areas of inhomogeneous stress and frictional properties. The aSDG method accurately resolves the different phases of rupture growth and arrest as well as the radiation fields associated with the non-uniform propagation. With dynamic adaptivity, the method provides unprecedented resolution of the crack process zone and the elastodynamic fields outperforming other methods, such as conventional finite elements, with respect to run time, memory requirements, and accuracy. We discuss the potential of the aSDG to provide a unique computational pathway to efficient multiscale dynamic rupture simulations in seismology and a critical missing link for transitioning between physics-based simulation and societal risk management.

Isogeometric Analysis for Primary Shaping Manufacturing Processes

Stefanie Elgeti^{*}, Florian Zwicke^{**}, Sebastian Eusterholz^{***}, Daniel Hilger^{****}

^{*}RWTH Aachen University, ^{**}RWTH Aachen University, ^{***}RWTH Aachen University, ^{****}RWTH Aachen University

ABSTRACT

Using a mold or die, primary shaping manufacturing processes form material from an initially unshaped state (usually melt) into a desired shape. All of these processes have in common that the exact design of the mold cannot be determined directly and intuitively from the product shape. This is due to the non-linear behavior of the material regarding the flow and solidification processes. Consequently, shape optimization as a means of numerical design can be a useful tool in mold development. The core of our optimization tool [1] is the in-house flow solver XNS, which combines a space-time method with either polynomial or isogeometric shape functions with a GLS stabilization. XNS is able to exploit the common communication interfaces for distributed-memory systems. The flow solver has been coupled with the open-source optimization frameworks NLOPT and Dakota. For geometry representation, no matter the function representation, we utilize an in-house spline library which supports both NURBS and T-splines. Spline representations are very natural in engineering design, as they allow the shape optimization result to be easily transferred back into the CAD-based design process. Furthermore, they require a low number of optimization parameters and allow the incorporation of manufacturing constraints. Obviously, isogeometric analysis aligns well with this type of shape optimization. Topics discussed will be our approach to shape optimization as well as methods for simulating the flow through, in and behind the mold/die. Furthermore, advances in the topics of solidification and free-surface flows with boundary-conforming isogeometric methods will be shown [2]. [1] S. Elgeti, M. Probst, C. Windeck, M. Behr, W. Michaeli, and Ch. Hopmann, "Numerical shape optimization as an approach to extrusion die design", Finite Elements in Analysis and Design, Vol. 48, pp. 35-43, 2012. [2] F. Zwicke, S. Eusterholz, S. Elgeti, "Boundary-Conforming Free-Surface Flow Computations: Interface Tracking for Linear, Higher-Order and Isogeometric Finite Elements", Computer Methods in Applied Mechanics and Engineering, Vol. 326C, pp. 175-192, 2017.

Automatic Isogeometric Analysis Suitable Trivariate Models Generation from Standard B-REP Models

Thomas Elguedj^{*}, Tristan MAQUART^{**}, Michel Rochette^{***}, Anthony Gravouil^{****}

^{*}Université de Lyon, CNRS, INSA-Lyon, LaMCoS UMR5259, France, ^{**}Université de Lyon, CNRS, INSA-Lyon, LaMCoS UMR5259, France; ANSYS Research & Development, France, ^{***}ANSYS Research & Development, France, ^{****}Université de Lyon, CNRS, INSA-Lyon, LaMCoS UMR5259, France

ABSTRACT

Key Words: Isogeometric Analysis, NURBS, Global Parameterization, Cross Fields, Cuboid Decomposition. We present an effective method to automatically construct trivariate B-spline models of complicated geometry and arbitrary topology. Our method takes as input a B-rep solid model defined by its triangulated boundary. Using cuboid decomposition [1,2], an initial polycube approximating the input boundary mesh is built. The polycube can be used to approximate very roughly the geometry of a model while faithfully replicating its topology. Due to its highly regular and trivariate structure, the polycube is suitable for serving as the canonical domain of the volume parameterization required for trivariate NURBS construction. The polycube's nodes and arcs decompose the input model locally into quadrangular patches, and globally into hexahedral domains. Using cross fields and aligned global parameterization [3], the position of the polycube nodes and arcs are optimized across the surface in a way to achieve low overall patch distortion, and alignment to principal curvature directions and sharp features. Based on the optimized polycube and parameterization, compatible B-spline boundary surfaces are reconstructed. Finally, the interior volumetric parameterization is computed using Coon's interpolation and the B-spline surfaces as boundary conditions. The efficiency and the robustness of the proposed approach are illustrated by some examples. **REFERENCES** [1] H. Al-Akhras, T. Elguedj, A. Gravouil, and M. Rochette, "3D Isogeometric Analysis Suitable Trivariate NURBS Models from Standard B-Rep CAD", *Computer Methods in Applied Mechanics and Engineering*, doi:10.1016/j.cma.2016.04.028, 2016. [2] Bo Li, Xin Li, Kexiang Wang, and Hong Qin. "Surface mesh to volumetric spline conversion with generalized poly-cubes". *IEEE Transactions on Visualization and Computer Graphics*, 99(PrePrints):1, 2013. [3] Marcel Campen and Leif Kobbelt. "Quad layout embedding via aligned parameterization". In *Computer Graphics Forum*, volume 33, pages 69-81. Wiley Online Library, 2014.

Micromechanical Cohesive Zone Modeling of Creep Fracture

Elsiddig Elmukashfi*, Alan Cocks**

*Department of Engineering Science, University of Oxford, Park Road, OX1 3PJ Oxford, UK, **Department of Engineering Science, University of Oxford, Park Road, OX1 3PJ Oxford, UK

ABSTRACT

In many polycrystalline materials, under creep conditions, failure due to the nucleation, growth and coalescence of voids. In many engineering alloys cavitation occurs primarily on the grain boundaries, and their growth is controlled by grain-boundary and surface diffusion and/or power-law creep. In the context of fracture mechanics, in the vicinity of a macroscopic primary crack tip, secondary micro-cracks are formed as a result of the intensive void growth and coalescence. These secondary cracks propagate and coalesce creating the new crack surfaces and allowing the primary macroscopic crack to advance along an interface or interconnected grain-boundaries. This localized cavitation process and its influence on crack propagation is commonly modelled as a continuum process. Another modelling method is through the use of interface damage zone models where the damage development is described by a traction/separation-rate law. In this study, we propose a micromechanically motivated mixed-mode traction/separation-rate law. This model is based on the grain-boundary cavitation model of Cocks and Ashby [1]. In particular, we follow the approach described by Yalcinkaya and Cocks [2] and its extension to the creep fracture case described in Elmukashfi and Cocks [3]. In order to derive closed form analytical constitutive models, the cavitated zone is represented by an array of pores idealized as cylinders. Deformation within the cavitated zone is constrained in the plane of the zone by the undamaged material either side of the interface. This constraint changes as the cavities grow. A rate potential is identified from which the interface zone response can be derived under applied normal and tangential tractions, which take into account the evolving local constraint and changing aspect ratio of the pores. The interface model is implemented using the Finite Element method. We adopt the surface-like cohesive formulation such that a cohesive/interface element consists of two surface elements which coincide in the reference configuration. The utility of the model is illustrated through studies of creep crack growth under mixed mode loading conditions in 3-D cracked bodies of advanced engineering alloys and dissimilar metal welds. We explore the conditions under which classical fracture mechanics parameters, such as the creep J-integral C^* can be used to describe the macroscopic crack growth behavior. Keywords: cohesive zone, traction/separation-rate, micromechanics, crack propagation, creep [1] Cocks, A.C., Ashby, M., 1980. Metal science 14, 395–402. [3] Yalcinkaya, T., Cocks, A.C., 2015. In: Key Engineering Materials, 993–999. [4] Elmukashfi, E. and Cocks, A.C., 2017. Int J Fracture, 208, 145-170.

Numerical Approaches for Speedup of Simulations Regarding the Monodomain Reaction-Diffusion Equation in Neuro-Muscular System

Nehzat Emamy*, Pascal Litty**, Thomas Klotz***, Oliver Röhrle****, Miriam Mehl*****

*Institute for Parallel and Distributed Systems, University of Stuttgart, **Institute for Parallel and Distributed Systems, University of Stuttgart, ***Institute of Applied Mechanics (CE), SimTech Research Group on Continuum Biomechanics and Mechanobiology, University of Stuttgart, ****Institute of Applied Mechanics (CE), SimTech Research Group on Continuum Biomechanics and Mechanobiology, University of Stuttgart, *****Institute for Parallel and Distributed Systems, University of Stuttgart

ABSTRACT

We present various numerical improvements in time stepping and iterative solvers in order to speed up the simulation of chemo-electromechanical processes in muscle fibers. The fiber simulation is embedded in a three-dimensional muscle model. Increasing the efficiency of the fiber simulation is crucial to be able to achieve realistic results for the whole three-dimensional muscle. The chemo-electromechanical models as proposed by Röhrle et al. [1] and Heidlauf and Röhrle [2] are particularly well-suited to incorporate many structural and functional features of skeletal muscles. The desired degree of detail and complexity within these models requires the coupling of different physical phenomena on different temporal and spatial scales. This is realized by linking multiple sub-models, which account for the main mechanical and electro-physiological properties. Using the above mentioned models, realistic simulations are extremely computationally demanding. Therefore, we consider different possibilities and approaches to speedup our simulations while maintaining the required details and accuracy. We focus on one computationally challenging part of the model, which is the monodomain reaction-diffusion equation. The equation comprises microscopic reactions existing at the cell membrane (0D sub-model) and diffusion of the action potentials along muscle fibers (1D sub-model). Currently, we use different discretizations, i. e., time-step size for the 0D and 1D sub-models to reduce the computational costs. However, there could be still more potential to reduce the computational time by using adaptive time stepping for the monodomain equation or skip solving the 1D sub-model at the times that only the 0D sub-model is active to generate force. The other approach which we study to reduce the computational costs is applying model order reduction techniques (MOR) to the monodomain equation. Applying the proper orthogonal decomposition (POD) to reduce the monodomain equation saves us a factor of 2 in the computation time. Further speedup is expected by using the Greedy-POD and discrete empirical interpolation method (DEIM) for approximating the nonlinear reaction terms of the 0D sub-model. References: Röhrle, O., Davidson, J. B., and Pullan, A. J. (2012). A physiologically based, multi-scale model of skeletal muscle structure and function. *Frontiers in Physiology* 3, 358. Heidlauf, T. and Röhrle, O. (2013). Modeling the Chemo-electromechanical Behavior of Skeletal Muscle Using the Parallel Open-Source Software Library OpenCMISS. *Computational and Mathematical Methods in Medicine* 2013, 1-14.

Yaw-Angle Dependence of Vortex Generator Installed on Flat Plate upon Heat Transfer Enhancement Effect

Shihoko Endo*, Kaoru Iwamoto**, Akira Murata***

*Tokyo University of Agriculture and Technology, **Tokyo University of Agriculture and Technology, ***Tokyo University of Agriculture and Technology

ABSTRACT

Heat transfer enhancement is of great importance in various fields of engineering. In this study, the heat transfer enhancement effect by vortex generators (VGs) installed on a flat plate in a boundary layer was verified by direct numerical simulation. The main objective is to confirm the influence of their yaw angle on heat transfer performance. The governing equations are incompressible continuity, Navier-Stokes and energy equations. A periodic boundary condition is imposed in the spanwise direction. Free-slip condition is imposed on an upper boundary, and non-slip and constant temperature conditions are imposed on a lower wall. The initial field and the inlet flow are laminar boundary layer distribution. Convective outflow condition is imposed on the outlet. VGs are expressed on the lower wall by an immersed boundary method. The shapes of VGs are hemispherical, delta-shaped and V-shaped with the height of the boundary layer thickness at the inlet. As for the case of zero yaw angle, the averaged Nusselt numbers in the downstream of the hemispherical, the delta-shaped and the V-shaped VGs were 2.6, 2.9, and 4.5 times as much as that of the flat surface, respectively. In addition, in order to investigate the influence of the yaw angle on the heat transfer performance, the yaw angle was changed from 0 degree to 180 degrees in increments of 30 degrees. For instance of the results, the delta-shaped VG is a triangle when viewed from the top and is shaped such that the height decreases from one vertex to the others. As for 0 degree, the highest apex of the triangle is positioned most upstream, and the height becomes lower toward the flow direction. In this case, a vortex pair approaches the wall as it goes to the downstream and develops in the spanwise direction away from the mid-plane of the VG. When VG has a yaw angle of 180 degrees, the lowest two apexes in the triangle are positioned on the most upstream, and the height increases toward the flow direction. In this case, averaged Nusselt numbers in the downstream of delta-shaped VG decreases by 54%. This might be caused by the vortex pair moving away from the wall as it goes to the downstream and approaching the mid-plane of the VG. In consequence, it is confirmed that the difference in the generation process of the vortex pair due to the yaw angle affected the heat transfer performance.

GENERALISED PRIMAL-DUAL GRIDS FOR UNSTRUCTURED CO-VOLUME SCHEMES

DARREN ENGWIRDA¹

¹Center for Climate Systems Research, Columbia University
2880 Broadway, New York City, NY 10025, USA

`darren.engwirda@columbia.edu; dengwirda.github.io`

Keywords Mesh generation and optimisation; Power diagrams; Voronoi diagrams

Summary *The generation of high-quality staggered unstructured grids is considered, leading to the development of a new optimisation scheme designed to construct weighted ‘Regular-Power’ tessellations. The generation of these grids is motivated by the desire to improve the performance and accuracy of numerical methods based on unstructured co-volume type schemes, including various staggered grid techniques for the simulation of fluid dynamics and hyperbolic transport. In this study, a hybrid optimisation strategy is used to optimise the geometry, topology and weights associated with general, two-dimensional Regular-Power tessellations using a combination of gradient-ascent and energy-based techniques. The performance of the new method is tested experimentally, with a range of complex, multi-resolution primal-dual grids generated for various coastal and regional ocean modelling applications.*

1. INTRODUCTION

The development of co-volume schemes on general unstructured meshes leads to a challenging grid generation problem, requiring the construction of a compatible *primal-dual pair* $(\mathcal{T}, \mathcal{D})$ that tessellates a given domain $\Omega \subset \mathbb{R}^d$ into a set of discrete elements. The pair $(\mathcal{T}, \mathcal{D})$ is required to be a dual structure; a tessellation of the points $\mathbf{X} \in \mathbb{R}^d$ into a primal *simplicial triangulation* \mathcal{T} and its dual *polyhedral complex* \mathcal{D} . Here, duality is expressed as a relationship between the faces of the triangulation and its dual, such that each d -simplex is associated with a dual vertex (a 0-cell), each $(d-1)$ -simplex is associated with a dual edge (a 1-cell) spanning between the two dual vertices associated with the adjacent d -simplexes, and so on, as per^[1]. Such structures are also typically required to satisfy a number of additional conditions: preserving *orthogonality* between adjacent faces in \mathcal{T} and \mathcal{D} , conforming to general, user-defined constraints on *grid-spacing*, and consisting of *optimally-shaped* grid-cells, designed to minimise the error associated with discrete numerical operators.

2. CONSTRAINTS ON CO-VOLUME GRIDS

The ‘TRSK’ formulation of Ringler et al^[2,3,5] and Thurburn et al^[4] is a mimetic finite-

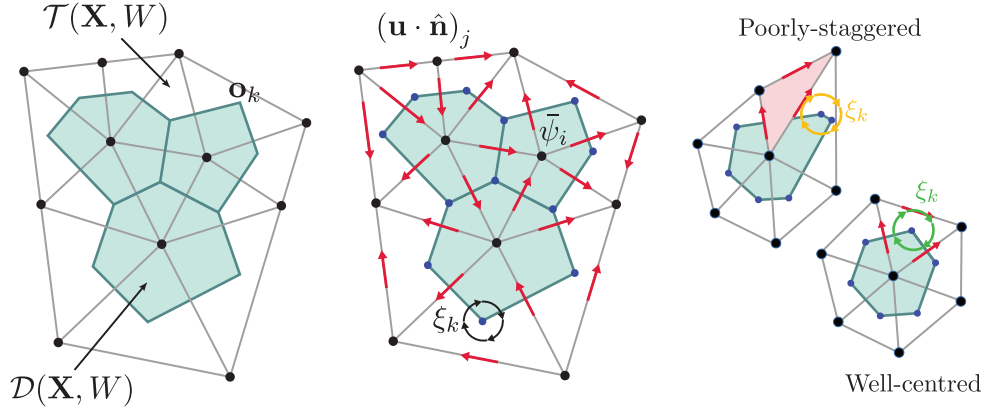


Figure 1: Anatomy of an unstructured co-volume scheme for geophysical fluid dynamics, illustrating: (a) locally-orthogonal primal-dual grid staggering, (b) the mimetic finite-difference/volume formulation of Ringler et al^[2,3], and (c) a comparison of *well-centred* and *poorly-staggered* configurations. In (a), polygonal cells in the dual grid are formed by joining the orthocentres \mathbf{o}_k associated with adjacent primal triangles. In (b), the unstructured TRSK scheme employs conservative *cell-centred* tracer quantities $\bar{\psi}_i$, *edge-centred* normal velocity components $(\mathbf{u} \cdot \hat{\mathbf{n}})_j$, and auxiliary *vertex-centred* vorticity variables ξ_k . In (c), the *well-centred* (lower) and *poorly-staggered* (upper) configurations differ in the relationship between dual vertices and primal triangles. In the well-centred configuration, all dual vertices are *interior* to their parent triangles. In the poorly-staggered configuration, a dual vertex is *exterior* to its associated triangle (shaded). Note that adjacent primal/dual edges do not intersect in the poorly-staggered configuration.

difference/volume scheme for the solution of geophysical flow problems on unstructured grids. Fluid pressure, depth, and density degrees of freedom are located within the dual polygonal control volumes, and a set of orthogonal velocity vectors are positioned along the primal grid edges. Additional vorticity degrees of freedom are placed at the vertices of the dual grid cells. Such an arrangement facilitates the construction of a standard conservative finite-volume type scheme for the transport of cell-centred fluid properties, and a mimetic finite-difference formulation for the evolution of velocity components. Vorticity is computed by considering the discrete circulation of velocity about primal triangles. See Figure 1 for details. The TRSK scheme is currently employed in the Model for Prediction Across Scales (MPAS) for both atmospheric and oceanic modelling^[5,2,3].

Despite its unstructured nature, such a formulation is not applicable to general unstructured tessellations; requiring that a number of auxiliary geometrical constraints also be satisfied. Specifically, such schemes necessitate the use of grids that are not only staggered and pair-wise orthogonal but also *well-centred* and *centroidal*. These additional conditions are constraints on the geometry of the underlying primal triangles and their dual polygons; requiring, firstly, that all dual vertices lie within the interior of their associated primal triangles, and, secondly, that all primal and dual vertices be positioned at the centroids of their associated staggered grid cells. Such structures can be used to construct compact spatial discretisation schemes that exhibit optimal numerical performance. The unstructured TRSK scheme described previously is known to

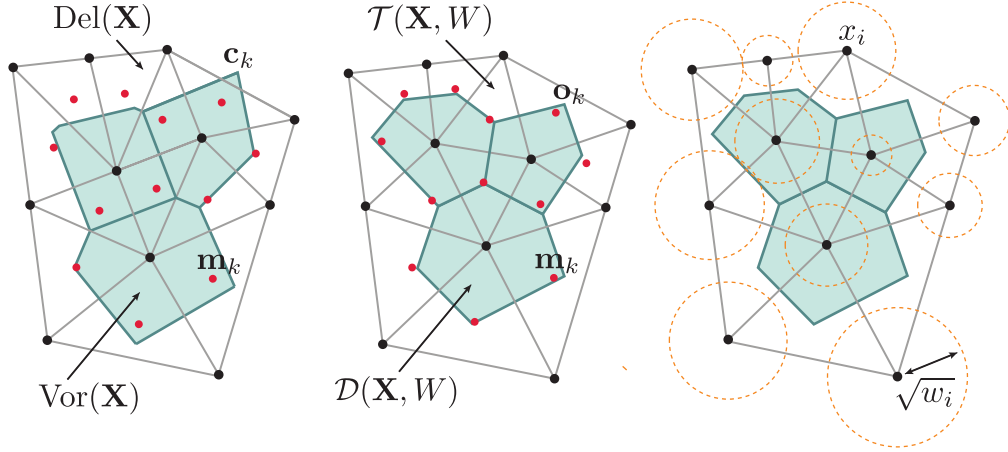


Figure 2: A comparison of various unstructured primal-dual pairs, showing: (a) a standard Delaunay-Voronoi tessellation, (b) an optimised Regular-Power structure, and (c) the distribution of vertex weights employed in (b). The position of triangle centroids and poorly-staggered elements is highlighted in (a) and (b), demonstrating that the weighted Regular-Power grid is both more centroidal and better self-centred than the corresponding Delaunay-Voronoi mesh. Note that though the underlying Delaunay triangulation is of high quality and is approximately centroidal, its corresponding Voronoi dual incorporates a range of undesirable features, including short edge-segments and non-optimal staggering.

achieve second-order accurate convergence on uniform primal-dual grids that are well-centred, centroidal and pair-wise orthogonal^[2].

3. REGULAR TRIANGULATIONS & POWER DIAGRAMS

Before describing the new primal-dual grid generation algorithm in full, several concepts associated with the construction of *regular triangulations* and their associated dual *power diagrams* are presented. These structures can be viewed as a weighted generalisation of the conventional Delaunay tessellation and its dual Voronoi complex. Such structures are also sometimes referred to as *Laguerre diagrams* or *Dirichlet cell complexes* (see, for example^[7]).

Definition 1 (Weighted points & power distance). A *weighted* point set is defined as a pair $(\mathbf{X}, W) = \{(\mathbf{x}_1, w_1), (\mathbf{x}_2, w_2), \dots, (\mathbf{x}_n, w_n)\}$, where $\{\mathbf{x}_i\} \subset \mathbb{R}^d$ are a set of points embedded in d -dimensional Euclidean space and $\{w_i\} \subset \mathbb{R}$ are an associated set of scalar weights. The *power distance*^[7], herein denoted $\pi_i(\mathbf{x})$, between an unweighted point $\mathbf{x} \in \mathbb{R}^d$ and a weighted point (\mathbf{x}_i, w_i) is defined as $\pi_i(\mathbf{x}) = \|\mathbf{x} - \mathbf{x}_i\|^2 - w_i$, where $\|\cdot\|$ is the standard Euclidean distance operator.

Definition 2 (Regular-Power complex). Given a weighted point set (\mathbf{X}, W) , the *power complex*^[7] $\mathcal{D}(\mathbf{X}, W)$ is the union of cells $\{D_i\}$, where each $D_i = \{\mathbf{x} \in \mathbb{R}^d \mid \pi_i(\mathbf{x}) < \pi_j(\mathbf{x}), \forall j \neq i\}$. The associated primal complex $\mathcal{T}(\mathbf{X}, W)$ is a simplicial triangulation of the weighted points (\mathbf{X}, W) , consisting of the union of simplexes $\{\tau_k\}$, where each τ_k contains the vertices $\{\mathbf{x}_1, \mathbf{x}_2, \dots, \mathbf{x}_k\} \in \mathbf{X}$ iff $\bigcap_{j=1}^{j=k} D_j \neq \emptyset$ ^[8]. The primal complex is

known as a *regular triangulation* of the weighted points (\mathbf{X}, W) .

The power complex is a Voronoi-like subdivision of space, where each cell $D_i \in \mathcal{D}$ defines a convex region $\mathbf{x} \subseteq \mathbb{R}^d$ for which the weighted point (\mathbf{x}_i, w_i) is *closer*, in a weighted sense, than all other points in (\mathbf{X}, W) . Such structures, along with their dual regular triangulations, offer a generalised framework for the construction of meshes for co-volume schemes^[1,8,9]; providing a family of compatible, pair-wise orthogonal primal-dual structures parameterised by the set of scalar weights W . In this work, the selection of an *optimal* set of weights is sought; tuning the geometry of the power cells to construct a primal-dual structure with optimal characteristics. The proposed approach is related to recent work on weighted tessellations by Mullen et al^[8,9] and Walton et al^[10,11]. See Figure 2 for details.

Given a weighted point set (\mathbf{X}, W) , the associated Regular-Power tessellation is fully specified by determination of the position of vertices associated with the polyhedral dual. These points are known as *orthocentres*, and can be viewed as a weighted generalisation of the circumcentres associated with the standard Delaunay-Voronoi structure.

3.1 Weighted ‘edge’ orthocentres

Given a triangle τ_i in the weighted primal mesh $\mathcal{T}(\mathbf{X}, W)$, the *orthocentre* associated with the edge $\{(\mathbf{x}_i, w_i), (\mathbf{x}_j, w_j)\} \in \tau_i$ is the point \mathbf{o}_e of equal power distance to the endpoints

$$\|\mathbf{x}_i - \mathbf{o}_e\|^2 - w_i = \|\mathbf{x}_j - \mathbf{o}_e\|^2 - w_j. \quad (1)$$

Constraining the point \mathbf{o}_e to the edge vector, and solving for the associated line parameter $t \in \mathbb{R}$ leads to an expression for \mathbf{o}_e , such that

$$\mathbf{o}_e = \mathbf{x}_i + t(\mathbf{x}_j - \mathbf{x}_i), \quad 0 \leq t \leq 1, \quad (2)$$

$$t = \frac{1}{2} \left(\frac{w_i - w_j + \|\mathbf{x}_i - \mathbf{x}_j\|^2}{\|\mathbf{x}_i - \mathbf{x}_j\|^2} \right). \quad (3)$$

Note that in unweighted configurations with $w_i = w_j = 0$, the expression for \mathbf{o}_e reduces to a simple equation for the edge midpoint \mathbf{m}_e , with $t = \frac{1}{2}$, as expected. Note also that \mathbf{o}_e is sensitive to the *difference* in the weights w_i and w_j rather than their magnitude, with equally weighted configurations $w_i = w_j = \beta \in \mathbb{R}$ again recovering $\mathbf{o}_e = \mathbf{m}_e$.

3.2 Weighted ‘face’ orthocentres

Given a triangle τ_i in the weighted primal mesh $\mathcal{T}(\mathbf{X}, W)$, the *orthocentre* associated with the face $\{(\mathbf{x}_i, w_i), (\mathbf{x}_j, w_j), (\mathbf{x}_k, w_k)\} \in \tau_i$ is the point \mathbf{o}_f of equal power distance to the three corner vertices

$$\|\mathbf{x}_i - \mathbf{o}_f\|^2 - w_i = \|\mathbf{x}_j - \mathbf{o}_f\|^2 - w_j = \|\mathbf{x}_k - \mathbf{o}_f\|^2 - w_k. \quad (4)$$

Following suitable algebraic manipulation, these expressions lead to the following system of linear equations for the point \mathbf{o}_f

$$\begin{bmatrix} \delta x_{ij} & \delta y_{ij} \\ \delta x_{ik} & \delta y_{ik} \end{bmatrix} \begin{bmatrix} \Delta x \\ \Delta y \end{bmatrix} = \frac{1}{2} \begin{bmatrix} \delta x_{ij}^2 + \delta y_{ij}^2 - \delta w_{ij} \\ \delta x_{ik}^2 + \delta y_{ik}^2 - \delta w_{ik} \end{bmatrix}, \quad (5)$$

$$\mathbf{o}_f = \mathbf{x}_i + (\Delta x, \Delta y), \quad (6)$$

where $\delta(\cdot)_{ij}$ denotes the difference $(\cdot)_j - (\cdot)_i$. Note that in unweighted configurations with $w_i = w_j = w_k = 0$, the point \mathbf{o}_f is equivalent to the centre of the circumscribing ball \mathbf{c}_f associated with τ_i . Noting again that the expression for \mathbf{o}_f is a function of the local weight differences δw_{ij} , δw_{ik} , equally-weighted triangles with $w_i = w_j = \beta \in \mathbb{R}$ reduce to $\mathbf{o}_f = \mathbf{c}_f$. Such considerations demonstrate that Regular-Power structures differ from conventional Delaunay-Voronoi pairs only in cases where there is a non-uniform distribution of weights throughout the grid.

4. OPTIMISATION OF PRIMAL-DUAL GRIDS

The full primal-dual grid generation algorithm seeks a set of vertex positions \mathbf{X} and associated vertex weights W that induce a primal-dual pair with optimal geometrical and topological characteristics. The grid generation task is cast as an optimisation problem; seeking to maximise a pair of primal-dual grid quality metrics. All primal and dual optimisation operations are designed to be *quality-preserving*; ensuring that the local, worst-case incident grid quality metrics $\mathcal{Q}^T(\mathbf{X})$ and/or $\mathcal{Q}^D(\mathbf{X}, W)$ are non-decreasing.

4.1 A primal grid quality metric

Given a triangle τ_i in the weighted primal mesh $\mathcal{T}(\mathbf{X}, W)$, the *area-length* ratio^[12] is employed as a local primal grid quality metric $\mathcal{Q}_i^T(\mathbf{X})$; designed to measure the relative distortion and irregularity of the primal grid cells.

$$\mathcal{Q}_i^T(\mathbf{X}) = \frac{4\sqrt{3}}{3} \frac{A_i}{\|\mathbf{e}\|_{\text{rms}}^2}. \quad (7)$$

Here, A_i is the signed area of the triangle τ_i and $\|\mathbf{e}\|_{\text{rms}}$ is the associated root-mean-square edge length. The area-length ratio is a robust, scalar measure of triangle shape quality, and is normalised to achieve a score of +1 for ideal elements. The area-length ratio decreases with increasing cell distortion, achieving a score of +0 for degenerate elements and -1 for ‘tangled’ elements with reversed orientation.

4.2 A dual grid quality metric

Given a triangle τ_i in the weighted primal mesh $\mathcal{T}(\mathbf{X}, W)$, a local dual grid quality metric $\mathcal{Q}_i^D(\mathbf{X}, W)$ is proposed; designed to measure the relative geometrical *defect* between polygonal

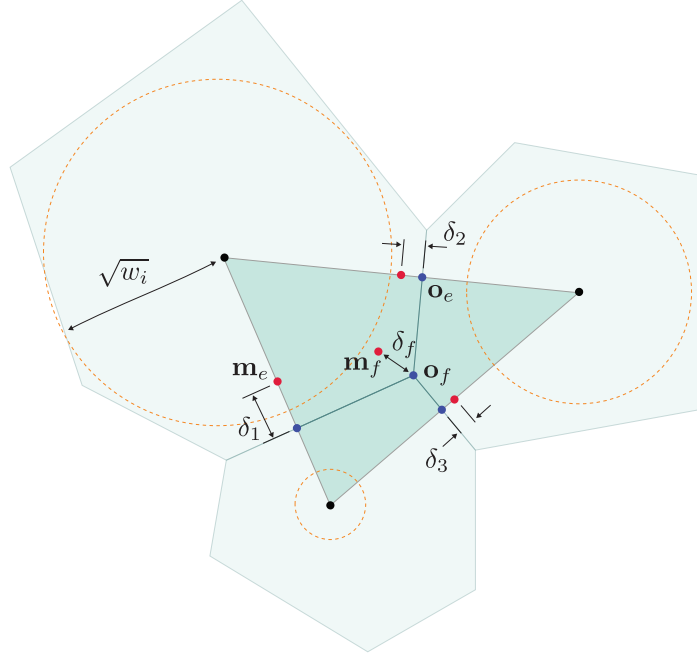


Figure 3: Anatomy of the dual cost metric (8), showing the contributions to $\mathcal{Q}_i^{\mathcal{D}}(\mathbf{X}, W)$ for a single triangle $\tau_i \in \mathcal{T}(\mathbf{X}, W)$. Here, the triangle and edge centroids \mathbf{m}_f and \mathbf{m}_e are drawn in red, and the associated weighted orthocentres \mathbf{o}_f and \mathbf{o}_e are drawn in blue. Non-uniform vertex weights w_i are applied at the vertices of τ_i . The dual quality metric is a function of the local face- and edge-centred defects $\delta_f = \|\mathbf{m}_f - \mathbf{o}_f\|$ and $\delta_e = \|\mathbf{m}_e - \mathbf{o}_e\|$; representing the geometrical offset between adjacent faces in the generalised pair $(\mathcal{T}, \mathcal{D})$.

cells in the orthogonal dual $\mathcal{D}(\mathbf{X}, W)$ and an ideal centroidal configuration

$$\mathcal{Q}_i^{\mathcal{D}}(\mathbf{X}, W) = \underbrace{\beta_f \left(1 - \left(\frac{\delta_f}{\bar{l}_f} \right)^2 \right)}_{\text{'defect' at face}} + \underbrace{\beta_e \left(\frac{1}{3} \sum_{e=1}^3 1 - \left(\frac{\delta_e}{\bar{l}_e} \right)^2 \right)}_{\text{mean 'defect' at edges}}, \quad (8)$$

$$\text{with } \delta_f = \|\mathbf{o}_f - \mathbf{m}_f\|, \quad \delta_{1,2,3} = \|\mathbf{o}_{1,2,3} - \mathbf{m}_{1,2,3}\|. \quad (9)$$

Here, $\mathbf{o}_f, \mathbf{o}_e$ are the weighted orthocentres associated with the face and edge segments of the triangle τ_i , the points $\mathbf{m}_f, \mathbf{m}_e$ are the corresponding face and edge centroids, and $\bar{l}_f = \frac{1}{3} \sum l_e$ is a local characteristic length, taken as the mean of the incident edge lengths l_e . Such a scaling serves to non-dimensionalise the various defect terms in (8), and results in a metric $\mathcal{Q}_i^{\mathcal{D}}(\mathbf{X}, W)$ that is *scale-invariant*. The linear coefficients β_f and β_e weight the face- and edge-centred contributions to $\mathcal{Q}_i^{\mathcal{D}}(\mathbf{X}, W)$. In this study, a simple average is employed, with $\beta_f = \beta_e = \frac{1}{2}$, indicating that equal ‘importance’ is assigned to both face- and edge-centred defects. See Figure 3 for additional detail.

The metric $\mathcal{Q}_i^{\mathcal{D}}(\mathbf{X}, W)$ is a smooth function of the geometry of the triangle τ_i and the weights centred at its vertices. A maximum value $\mathcal{Q}_i^{\mathcal{D}}(\mathbf{X}, W) = 1$ is attained when the dual

cell is optimally staggered with respect to the triangle τ_i ; spanning between its centroid and edge midpoints, such that $\mathbf{o}_f = \mathbf{m}_f$ and $\mathbf{o}_e = \mathbf{m}_e$. Conversely, $\mathcal{Q}_i^{\mathcal{D}}(\mathbf{X}, W) \rightarrow 0$ as the relative face- and/or edge-centred defects increase as the local primal-dual staggering becomes less centroidal. The function $\mathcal{Q}_i^{\mathcal{D}}(\mathbf{X}, W)$ aims to provide a combined measure of the quality of the staggering between primal and dual grid cells, with the first term in (8) accounting for the defect between the dual grid vertices and triangle centroids, δ_f , and the second term the mean defect between dual grid edges and triangle edge midpoints, δ_e . Such considerations are designed to minimise the numerical error of the model co-volume discretisation scheme described previously, where a mutually centroidal staggering between the primal and dual grid cells, vertices and edges is optimal.

4.3 Selection of locally-optimal weights

Given a weighted primal triangulation $\mathcal{T}(\mathbf{X}, W)$, the task of constructing a high-quality orthogonal dual $\mathcal{D}(\mathbf{X}, W)$ can be cast as an optimisation problem

$$\text{find } W \subset \mathbb{R}, \text{ such that } \min \mathcal{Q}_i^{\mathcal{D}}(\mathbf{X}, W) \forall \tau_i \in \mathcal{T}(\mathbf{X}, W) \text{ is maximised.} \quad (10)$$

In general, (10) is a global, non-convex optimisation problem, with the weight at each vertex $w_i \in \mathcal{T}(\mathbf{X}, W)$ contributing to the non-linear metric $\mathcal{Q}_k^{\mathcal{D}}(\mathbf{X}, W)$ for all adjacent triangles $\tau_k \in \mathcal{T}(\mathbf{X}, W)$. Rather than attempting to solve this global problem directly, a simpler, locally-optimal approach is pursued; seeking the solution of a sequence of local, decoupled problems. Noting that each weight w_i has local influence, contributing to the metrics $\mathcal{Q}_k^{\mathcal{D}}(\mathbf{X}, W)$ for the triangles $\tau_k \in \mathcal{T}(\mathbf{X}, W)$ adjacent to \mathbf{x}_i only, a steepest-ascent type update is employed, with

$$w_i^{n+1} = w_i^n + \Delta_i^m v_i^n, \quad (11)$$

where

$$v_i^n = \frac{d}{dw_i} \mathcal{Q}_j^{\mathcal{D}}(\mathbf{X}, W) \quad \text{and} \quad j = \operatorname{argmin}_k \mathcal{Q}_k^{\mathcal{D}}(\mathbf{X}, W) \forall \text{adj. } \tau_k \in \mathcal{T}(\mathbf{X}, W). \quad (12)$$

Here, the index k is taken as a loop over the primal triangles $\tau_k \in \mathcal{T}(\mathbf{x}, w)$ incident to \mathbf{x}_i . The scalar step length $\Delta_i^m \in \mathbb{R}^+$ is computed via a line search along the gradient ascent vector v_i and, in this study, is taken as the first value that leads to an improvement in the worst-case incident-quality metric $\mathcal{Q}_j^{\mathcal{D}}(\mathbf{X}, W)$. Note that the ascent vector v_i^n is taken as the gradient of the *worst* incident quality metric, rather than some mean measure, and that the scheme is biased toward providing updates in a *worst-first* manner as a result.

4.4 Selection of locally-optimal vertex positions

Considering the *geometrical* optimality of the primal grid $\mathcal{T}(\mathbf{X}, W)$, a *mesh-smoothing* procedure is undertaken; seeking to reposition vertices to improve both the primal grid quality metrics $\mathcal{Q}^{\mathcal{T}}(\mathbf{X})$ and conformance to a user-defined mesh-spacing function $\bar{h}(\mathbf{x}) : \mathbb{R}^2 \rightarrow \mathbb{R}^+$. A

hybrid, two-pass strategy is pursued; employing a variation of the Optimal Delaunay Triangulation (ODT) scheme of Chen et al^[13,14] as a first-pass update, and falling back to a constrained, gradient-ascent type approach when required.

4.4.1 ‘Optimal’ weighted triangulations

Given a vertex \mathbf{x}_i in the primal mesh $\mathcal{T}(\mathbf{X}, W)$, an update is attempted using a variation on the ODT strategy of Chen et al^[13,14]. In the conventional formulation, primal vertices are repositioned to the weighted mean of adjacent triangle circumcentres. In the current work, this strategy is modified to incorporate the weighted Regular-Power structure pursued here; replacing the triangle circumcentres with the associated element orthocentres. Primal vertex positions are thus updated as a weighted sum of the adjacent dual vertex coordinates. Adapting the ODT-style update strategy of Chen and Holst^[14], primal vertices are repositioned such that

$$\mathbf{x}_i^{n+1} = (1 - \Delta_i^m) \mathbf{x}_i^n + \Delta_i^m \sum_{\tau_j \in *_{\bar{i}}} \frac{|\tau_j|_{\bar{h}}}{|*_{\bar{i}}|_{\bar{h}}} \mathbf{o}_j. \quad (13)$$

Here, $*_{\bar{i}}$ denotes the *star* of \mathbf{x}_i — the local set of elements $\tau_j \in \mathcal{T}(\mathbf{X}, W)$ adjacent to \mathbf{x}_i . $|\tau_j|_{\bar{h}}$ denotes the *spacing-weighted* area of the triangle τ_j , and $|*_{\bar{i}}|_{\bar{h}}$ the summation of such terms over the set $*_{\bar{i}}$. The points \mathbf{o}_j are the orthocentres associated with the triangles τ_j and Δ_i^m is a relaxation factor, computed via a local line search.

4.4.2 Direct gradient-ascent

While the ODT-type iteration is effective in improving the quality and mesh-spacing conformance of a grid on average, it is not guaranteed to improve the metrics in all cases. Therefore, an additional gradient-ascent type strategy is pursued^[15,16,17], in which vertex positions are adjusted based on the local gradients of incident element-quality functions $\mathcal{Q}^T(\mathbf{X})$. Specifically, a given vertex $\mathbf{x}_i \in \mathcal{T}(\mathbf{X}, W)$ is repositioned along a local *steepest-ascent* vector, chosen to improve the quality of the worst incident element

$$\mathbf{x}_i^{n+1} = \mathbf{x}_i^n + \Delta_i^m \mathbf{v}_i^n, \quad (14)$$

where

$$\mathbf{v}_i^n = \frac{\partial}{\partial \mathbf{x}_i} \mathcal{Q}_j^T(\mathbf{X}) \quad \text{and} \quad j = \operatorname{argmin}_k \mathcal{Q}_k^T(\mathbf{X}) \quad \forall \text{ adj. } \tau_k \in \mathcal{T}(\mathbf{X}, W). \quad (15)$$

The index k is taken as a loop over the primal triangles $\tau_k \in \mathcal{T}(\mathbf{X}, W)$ incident to the vertex \mathbf{x}_i , $\Delta_i^m \in \mathbb{R}^+$ is a scalar step-length, and the ascent vector \mathbf{v}_i^n is taken as the gradient of the *worst* incident quality metric.

4.5 Incremental updates to mesh topology

Given a pair of adjacent triangles $\{\tau_i, \tau_j\} \in \mathcal{T}(\mathbf{X}, W)$ a local re-triangulation can be achieved by *flipping* the local connectivity about the shared edge $\{x_i, x_j\}$, forming a new edge between

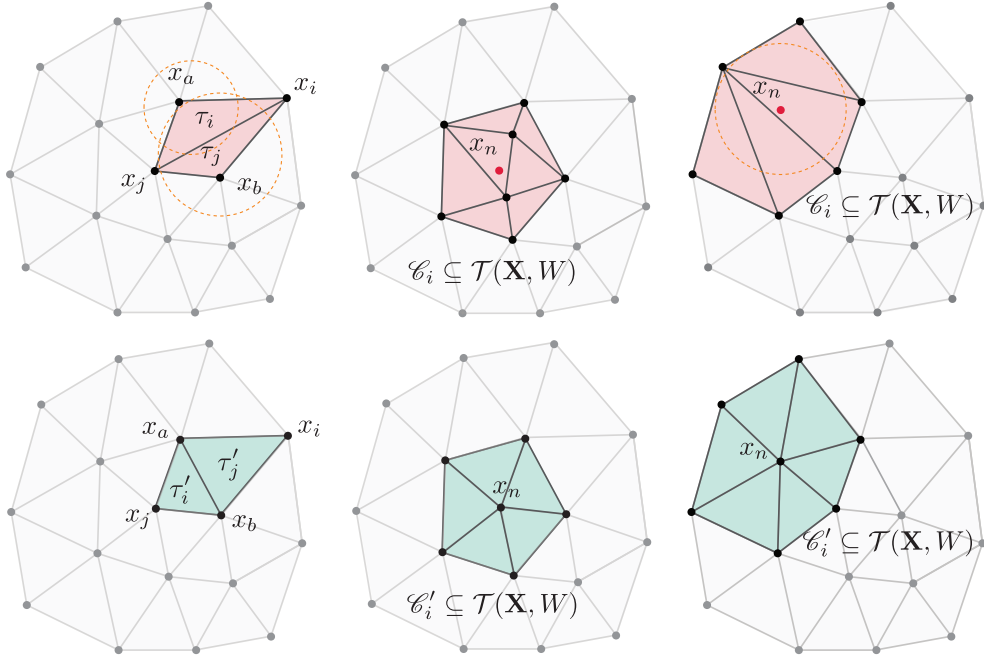


Figure 4: Topological operations for primal grid optimisation, showing (left) an edge-flip, (middle) an edge-collapse, and (right) an edge-refinement operation. Grid configurations before and after each update are shown in the upper and lower panels, respectively.

the opposing vertices $\{x_a, x_b\}$. This operation replaces the existing triangle pair $\{\tau_i, \tau_j\}$ with a new set $\{\tau'_i, \tau'_j\}$. See Figure 4a for details. In the present work, the iterative application of such edge-flipping operations is used to incrementally transform the topology of the primal triangulation. Specifically, given a general triangulation $\mathcal{G}(\mathbf{X}, W)$, possibly violating the local weighting criterion, a cascade of edge-flips are employed to transform $\mathcal{G}(\mathbf{X}, W)$ into a valid regular triangulation $\mathcal{T}(\mathbf{X}, W)$. For each adjacent pair $\{\tau_i, \tau_j\} \in \mathcal{G}(\mathbf{X}, W)$, a flip is enacted if a local violation of the weighted criterion is detected. New triangles created by successful edge flips are subsequently re-examined until no further modifications are required.

4.6 Refinement & edge collapse

In addition to updates to the bulk geometry and topology of the grid, mesh quality and mesh spacing conformance can often be further improved through the addition and/or removal of vertices. In the present work, such behaviour is achieved through a set of *edge-refinement* and *edge-collapse* operations, generalising the methodology presented by the author in^[17] to handle general weighted primal-dual tessellations.

4.7 A coupled optimisation schedule

The full primal-dual grid optimisation procedure is realised as a combination of the various

geometrical and topological operations described previously; organised into a particular iterative optimisation schedule. Each outer iteration consists of a fixed set of operations: eight sweeps to update vertex positions and weights, an iterative edge-flipping scan to restore the local ‘weighted’ triangulation criterion, and, finally, a single pass of edge refinement/collapse operations.

5. RESULTS & DISCUSSIONS

A set of optimised primal-dual pairs are presented in Figure 5, showing: (a) the geometry of the test problem, (b) the primal triangulation $\mathcal{T}(\mathbf{X}, W)$, (c) contours of the target grid-spacing function $\bar{h}(\mathbf{x})$, and (d) detail of the associated dual structure $\mathcal{D}(\mathbf{X}, W)$. Results are shown after the application of the primal-dual optimisation procedure. Dual cells are coloured by their relative power W_r , showing the distribution of vertex weights throughout the grid. These results show that the new algorithm is successful in generating very high-quality unstructured Regular-Power grids that conform to complex boundaries and grid-spacing constraints. Comparisons with a conventional Delaunay-Voronoi optimisation scheme^[17,6] shows that the new methods result in grids that are more centroidal and are better self-centred. Future work will seek to analyse the impact of these optimised Regular-Power grids on the numerical performance of staggered unstructured numerical schemes (i.e. MPAS-O^[3,5,18]), and to extend the grid generation framework to higher-dimensional configurations, including surface and volumetric meshing problems.

CODE AVAILABILITY

The JIGSAW mesh generation package is available online: <https://github.com/dengwirda/jigsaw-geo-matlab>.

REFERENCES

- [1] P. Memari, P. Mullen, M. Desbrun, Parametrization of generalized primal-dual triangulations, in: Proceedings of the 20th International Meshing Roundtable, Springer, 2011, pp. 237–253.
- [2] T. Ringler, J. Thuburn, J. Klemp, W. Skamarock, A unified approach to energy conservation and potential vorticity dynamics for arbitrarily-structured C-grids, *Journal of Computational Physics* 229 (9) (2010) 3065–3090.
- [3] T. Ringler, M. Petersen, R. Higdon, D. Jacobsen, P. Jones, M. Maltrud, A multi-resolution approach to global ocean modeling, *Ocean Modelling* 69 (2013) 211–232.
- [4] J. Thuburn, T. Ringler, W. Skamarock, J. Klemp, Numerical representation of geostrophic modes on arbitrarily structured C-grids, *Journal of Computational Physics* 228 (22) (2009) 8321 – 8335.
- [5] W. C. Skamarock, J. B. Klemp, M. G. Duda, L. D. Fowler, S.-H. Park, T. D. Ringler, A multiscale nonhydrostatic atmospheric model using centroidal Voronoi tessellations and C-grid staggering, *Monthly Weather Review* 140 (9) (2012) 3090–3105.
- [6] D. Jacobsen, M. Gunzburger, T. Ringler, J. Burkardt, J. Peterson, Parallel algorithms for planar and spherical Delaunay construction with an application to centroidal Voronoi tessellations, *Geoscientific Model Development* 6 (4) (2013) 1353–1365.

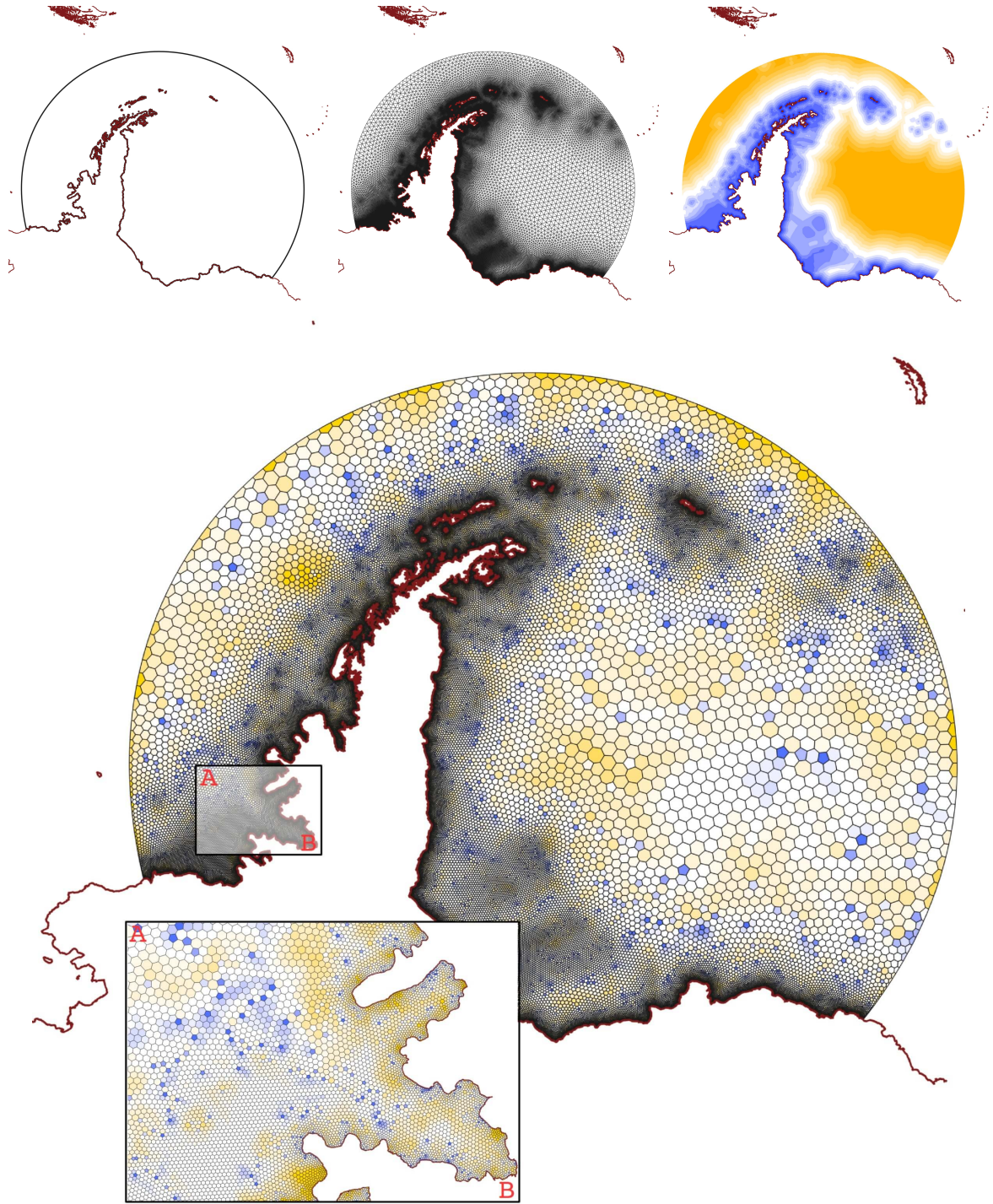


Figure 5: An optimised primal-dual grid for the Antarctic test-case, showing (clockwise from top-left): (a) the coastal geometry and open-boundary definition, (b) the weighted triangulation $\mathcal{T}(\mathbf{X}, W)$ (c) contours of the mesh spacing function $\bar{h}(\mathbf{x})$, and (d) the dual power diagram $\mathcal{D}(\mathbf{X}, W)$. Here, dual cells are coloured by their *relative power*, with blue tones indicating negative values, orange tones positive values, and white tones associated with values approaching zero.

- [7] F. Aurenhammer, Power diagrams: properties, algorithms and applications, *SIAM Journal on Computing* 16 (1) (1987) 78–96.
- [8] P. Mullen, P. Memari, F. de Goes, M. Desbrun, HOT: Hodge-optimized triangulations, *ACM Transactions on Graphics (TOG)* 30 (4) (2011) 103.
- [9] F. d. Goes, P. Memari, P. Mullen, M. Desbrun, Weighted triangulations for geometry processing, *ACM Transactions on Graphics (TOG)* 33 (3) (2014) 28.
- [10] S. Walton, O. Hassan, K. Morgan, Advances in co-volume mesh generation and mesh optimisation techniques, *Computers & Structures* 181 (2017) 70–88.
- [11] S. Walton, O. Hassan, K. Morgan, Reduced order mesh optimisation using proper orthogonal decomposition and a modified cuckoo search, *International Journal for Numerical Methods in Engineering* 93 (5) (2013) 527–550.
- [12] V. N. Parthasarathy, C. M. Graichen, A. F. Hathaway, A Comparison of Tetrahedron Quality Measures, *Finite Elements in Analysis and Design* 15 (3) (1994) 255–261.
- [13] L. Chen, J.-C. Xu, Optimal Delaunay triangulations, *Journal of Computational Mathematics* (2004) 299–308.
- [14] L. Chen, M. Holst, Efficient mesh optimization schemes based on optimal Delaunay triangulations, *Computer Methods in Applied Mechanics and Engineering* 200 (9) (2011) 967–984.
- [15] L. A. Freitag, C. Ollivier-Gooch, Tetrahedral mesh improvement using swapping and smoothing, *International Journal for Numerical Methods in Engineering* 40 (21) (1997) 3979–4002.
- [16] B. M. Klingner, J. R. Shewchuk, Aggressive tetrahedral mesh improvement, in: *Proceedings of the 16th international meshing roundtable*, Springer, 2008, pp. 3–23.
- [17] D. Engwirda, JIGSAW-GEO (1.0): locally orthogonal staggered unstructured grid generation for general circulation modelling on the sphere, *Geoscientific Model Development* 10 (6) (2017) 2117.
- [18] P. S. Peixoto, Accuracy analysis of mimetic finite volume operators on geodesic grids and a consistent alternative, *Journal of Computational Physics* 310 (2016) 127–160.

As-manufactured Simulation of Short Fiber Filled Injection Molded Plastics

Jaesung Eom*

*Autodesk

ABSTRACT

This talk shows how the integration of nonlinear structural simulation with multiscale material model and injection molded simulation work together for As-manufactured simulation of short fiber filled injection molded plastics. Injection molding simulation can predict the distribution of fiber orientation throughout a part, in addition to the warped shape of the ejected, room-temperature part. To connect subsequent nonlinear (progressive failure) structural simulation of the short fiber filled part, Autodesk has developed new software to seamlessly link the results of injection molding simulation with nonlinear structural response simulation that features a multiscale progressive failure model for short fiber filled plastics. This solution for Digital Prototyping, provides fast, accurate and flexible tools for enhanced FEA of composite structures, including progressive failure analysis to help reduce testing and shorten design cycles by identifying potentially unforeseen design/material deficiencies.

Creating and Fracturing Polymer Matrix Composites with Complex Fiber Architectures

Randall Erb*

*Northeastern University

ABSTRACT

In this presentation, I will explore our recent work creating and fracturing polymer matrix composites with complex fiber architectures. To generate these architectures, we rely on 3D Magnetic Printing a technique that we developed which combines real-time magnetic assembly processes to orient reinforcing particles within a polymer during conventional SLA or FDM 3D Printing. Our produced fiber architectures have resolutions down to 50 microns, making them the highest resolution of fiber reinforced composite to-date. After generating these complex composites, we proceed to break them. We observe fracture behavior within these complex architectures and establish structure-property relationships. We discuss when cracks will deflect, and when tortuous crack paths can be related to increased toughness. The principle system considered in this presentation is alumina reinforced acrylate, however, these techniques and findings are material non-specific.

Observing Fracture in Composite Fiber Architectures Generated from Mathematical Formulas

Robert Zando¹, Philip Buskohl², Randall M. Erb³

¹Northeastern University
360 Huntington Ave
Boston, MA, 02115
zando.r@husky.neu.edu

² Air Force Research Laboratory
AFRL/RXAS, 2179 12th Street
Wright-Patterson AFB, OH 45433-7718
philip.buskohl.1@us.af.mil

³Northeastern University
360 Huntington Ave
Boston, MA, 02115
r.erb@neu.edu

Introduction

Fiber-reinforcement in composite polymer materials has a tremendous potential to improve the specific strength and toughness of a given structure. Additionally though, it is a well-observed phenomenon that these strengthening characteristics have a high degree of anisotropy, which limits their utility to specific directions of applied loading. However, we hope to take advantage of this anisotropy, in order to control to some degree the exact mode of failure of materials composed of this material, via the engineering of specific filler paths within a given material. Such an achievement would not only

allow for the design of materials with predictive modes of failure for specific applications, but also the creation of extended paths for the propagation of a fracture, effectively boosting the total continuum surface energy.

In order to explore these applications, a series of samples with different alignment paths were produced to be fractured using an Instron Tension testing machine to compare the crack propagation paths against the function used to create the alignment fields. Samples were manufactured using two-dimensional magnetic alignment to produce the carbon fiber fracture paths and polymerized in sections using a UV projector.

Fracture Mechanics within Composite Polymers

The study of the formation and propagation of fractures through a material is one of intense interest in the field of materials science, both as a means of qualitatively measuring the mechanical properties of the material and determining the most likely modes of failure for structures. However, despite a wide body of work into the nature of crack formation and expansion, there exists few known methods of directly manipulating the physical characteristics of fractures within a given material. The field of composite materials, most notably composite polymers, offers the potential to change this. Using a combination of modern photopolymer materials, combined with new techniques for directly aligning filler materials within a bulk polymer matrix, it is now possible to engineer specific paths for fractures to follow.

Composite polymers are, most broadly, any combination of known filler materials (fibers, platelets, etc.) suspended within a matrix of bulk polymer, offering enhanced strengthening characteristics. In the case of fibrous filler material, this strengthening effect is most pronounced along the lengthwise direction of the polymer due to the decreased instance of potential surface flaws due to the small cross-sectional area. The orientation of the fiber also has a strong influence on the propagation mechanics of a fracture. As the fracture sunders atomic bonds between molecules within the sample matrix, it is inclined to directions with the lowest surface energy (i.e., lowest bond strength). In the case of a carbon fiber composite polymer, this would be parallel to the direction of fiber orientation, since this would require breaking the bonds between fiber interface and the bulk polymer interface (weaker secondary bonds) versus the bonds connecting the carbon atoms of the fiber (stronger covalent bonds). Due to this phenomenon, it should be possible to control the direction of crack propagation within a given material using pre-engineered alignment paths.³

Magnetic Alignment

In order to achieve the desired fracture propagation paths, it was necessary to align the individual fibers within the bulk matrix with a high degree of resolution. To produce this alignment, the most effective technique was to directly align the fibers using an external magnetic field. The composite, suspended in a resin bath, could then be cross-linked via exposure to specific images of UV-light, forming a solid structure composed of the bulk resin and filler carbon fiber

(Figure 1). However, as the carbon fiber is itself only weakly responsive to magnetic fields, it was first necessary to artificially magnetize the carbon fiber filler material.

Magnetization of the carbon fiber was achieved via the doping of iron oxide nanoparticles onto the surface of the carbon fiber.¹ In order to accomplish this, a mixture of 37.5 microliters of EMG 605 Ferrofluid per 1 gram of carbon fiber were mixed together using a rotating magnet field and stir-bar for ~1.5 days. This coating of super paramagnetic nanoparticles upon the surface of the carbon fiber rods ensures that the rods experience the effect of an ultra-high magnetic response effect (an extreme sensitivity to external magnetic fields), and are therefore able to align along the direction of the applied magnetic field.

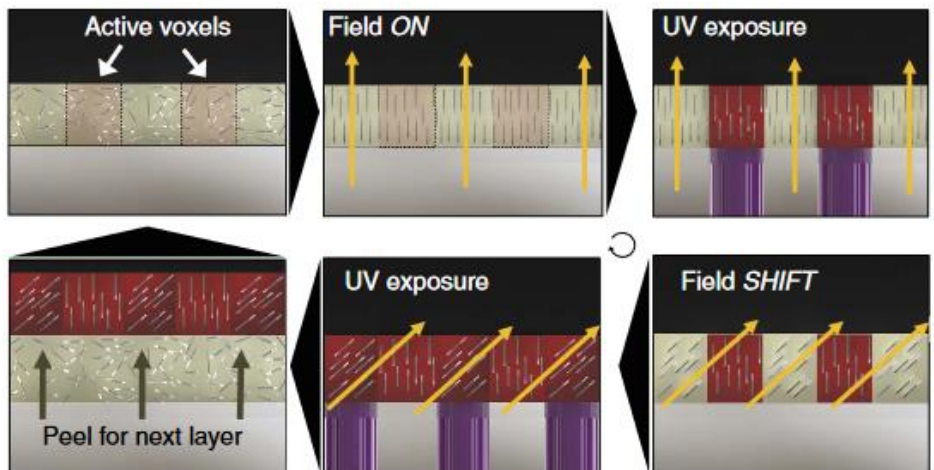


Figure 1: The magnetic alignment and UV exposure process²

Prior efforts to produce the required external field focused on the use of a series of iron-core solenoids. However, despite the high amount of resolution the solenoids were capable of producing, the flux density of the field was found to be insufficiently high to align the fibers within a high-viscosity polymer resin within a reasonable amount of time (usually averaging ~250 Gauss). Fortunately, the experiment required only single layer samples, so less sophisticated methods of printing could be employed to produce the alignment for the test structures. Ultimately, this issue was overcome using a rare-earth magnet placed directly over the printing area (propped up on a small, custom printed platform). When situated sufficiently close to the resin bath, the fibers were able to align parallel to the direction the magnet was facing, and were exposed to a field of sufficiently high flux density (500+ Gauss) to allow the fibers to align within a reasonable amount of time. The magnet was manually rotated for each alignment direction, trading the extreme (and time-consuming) resolution of the solenoid system for a simpler (and substantially faster) magnetic alignment technique.

Printing and Testing the Fracture Samples

To print the samples with the aligned fiber directions, it is necessary to divide the print into different sections, each section containing a specific alignment angle. This was achieved by writing a Matlab program designed to take a specific function and convert sections of it into different angles

based on how changes to the slope of the function at different points of the x-boundary. By first creating a mesh grid, then applying a function to it, it was possible to calculate the angle of the function to be printed at every point along the x-axis. In order to reduce the print times to reasonable levels, the alignment angles are rounded to the nearest increment of 20, though future testing will vary the angle resolution to determine its effect on fracture path. This resulted in a filled contour map representing all of the different alignment angles of the function that would be applied to different sections of the sample under test (Figure 2).

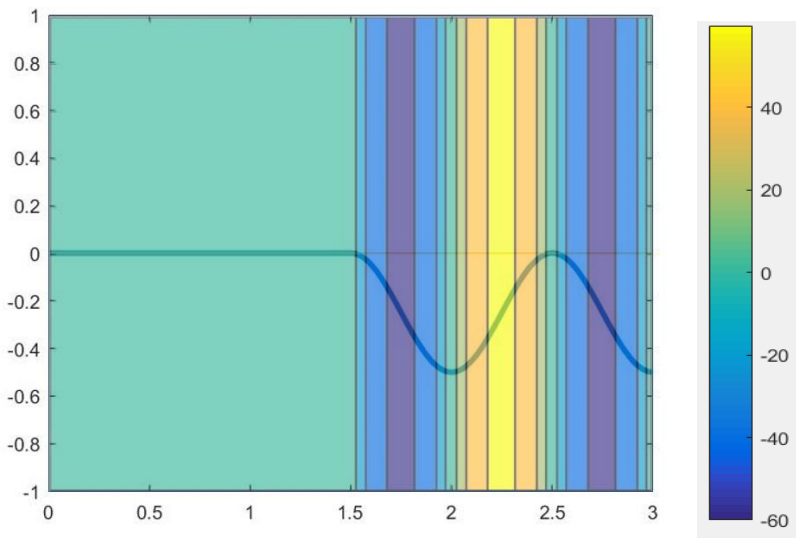


Figure 2: Example of a sinusoid wave converted into a set of alignment angles

The next step for the printing process was to convert these different “angle sections” into a format which could be read using the UV projector. This was accomplished by changing the different alignment angle sections (increments of 20) into a series of arrays, wherein each section to be printed at a given time had a value of 1, while the surrounding area was assigned a value of 0. This allowed the different arrays to be converted into a set of bitmap files (monochrome images where each pixel had a value of either 0 or 1) which could then be placed into a Power Point slide (see Figure 3). Each slide was projected onto the UV sensitive resin for 30 seconds after several minutes of magnetic alignment in the necessary direction, eventually curing all of the alignment sections into a single piece, with a final unaligned image of the total structure projected to ensure that the interfaces of the different sections were properly crosslinked together, limiting their potential effect on the mechanical properties of the samples under test.



Figure 3: The sample and one of its constituent alignment angles (-60 degree sections from the Fig.1 sinusoid)

The end result was a single 25mm x 50mm sample, with a thickness of ~0.3mm sample of photo-cured composite polymer resin (Figure 4). The sample was then post-processed

to ensure uniformity of sample properties in terms of resin cross-linking and mechanical strength. It was first exposed to a bath sonicator to remove any residual, uncured or partially cured resin on the surface of the sample, making it safe for users to handle during fracture testing and removing any additional particulates that may have become attached to the sample surface during the printing or removal process. This step was immediately followed by a 15 minute exposure to a UV-radiation source within a custom-built chamber to finalize any incomplete cross-links. Once the additional UV exposure was completed, an additional notch was added to the sample, extending 1mm from the end of the printed notch to act as a point of stress concentration, ensuring the fracture initiates in the same location for all tests. Finally, the post-processing was completed by placing the sample in an oven at 90C for two hours.

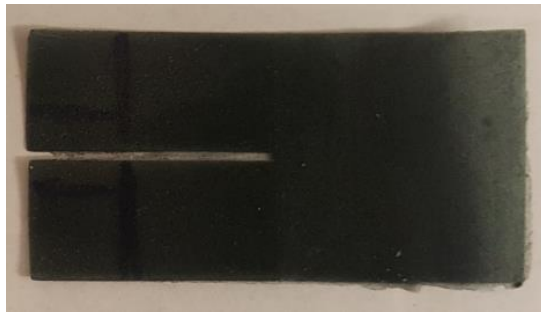


Figure 4: Completed fracture sample

Following printing and post-processing, the sample was fractured using an Instron Tension Testing machine to

determine crack path and material surface energy. The sample is gripped at both the top and bottom portions separated by the pre-printed sample notch and strained at a rate of 2mm/min, initiating the crack and propagating the fracture until two completely new surfaces are created. The resulting stress-strain curve was used to estimate the surface energy of the sample and the fracture path was compared against the function used to produce the alignment angles.

Results

Fractures showed a strong dependence on the alignment path of the carbon fibers within the composite matrix. Samples printed using sinusoidal wave patterns or more unique functions like the Lotka-Volterra predator-prey model produced fracture paths with a high degree of qualitative similarity to the alignment fields of the printed functions. This works suggests mechanistic routes for controlling fracture within fiber reinforced composites are possible, as well as an exciting new technique for using mechanical fracture to predict lowest energy or increasing the overall surface energy of a composite structure.

References

- [1] Erb, R. M., Libanori, R., Rothfuchs, N., & Studart, A. R. (2012). Composites Reinforced in Three Dimensions by Using Low Magnetic Fields. *science*, (6065), 199-204.
doi:10.1126/science.1210822
- [2] Martin, J. J., Fiore, B. E., & Erb, R. M. (2015). Designing bioinspired composite reinforcement architectures via 3D magnetic printing. *nature communications*, , 8641.
doi:10.1038/ncomms9641
- [3] BD, Agarwal, and Broutman LJ. *analysis and performance of Fiber composites*. 2nd ed., John Wiley & Sons, Inc, 1990.

Optimization of Reinforced Concrete Structures Using an Innovative DMPSO Algorithm

Mohammadjavad Esfandiari*, Girum Urgessa**

*George Mason University, **George Mason University

ABSTRACT

Numerous evolutionary objective optimization algorithms have been developed all around the world and widely used for solving optimization problems in engineering. However, in the realm of optimization of reinforced concrete (RC) structures, these algorithms tend to be less effective because of the substantial number of design variables, enormous size of the search space, and availability of design constraints. As a result, RC structures are typically designed by using the traditional trial-and-error approach. On the contrary, this paper presents an innovative algorithm combining multi-criterion decision-making (DM) and Particle Swarm Optimization (PSO) for accelerating convergence towards optimum design solutions in reinforced concrete (RC) structures. The DM-PSO algorithm leads to feasible optimal designs, while also taking advantage of infeasible designs during the optimization procedure. All practical and architectural requirements are considered for obtaining directly constructible designs that will need no further modifications. The effectiveness of the proposed algorithm is illustrated in optimization of a 3D RC structure subjected to seismic forces. The results obtained confirm the ability of the proposed DM-PSO algorithm to find optimal solutions efficiently for RC optimization problems. Based on the findings of this research, the DM-PSO algorithm is deemed to model practical design problems that consider the variations in cross-sectional dimensions of concrete structures, the variation in detailing and the variations in placement of reinforcement bars.

Thermodynamically Consistent Multiscale Homogenization Based on Virtual FE for Concrete Failure Analyses

Guillermo Etse^{*}, Felipe Lopez Rivarola^{**}, Matias Benedetto^{***}

^{*}University of Tucuman, Argentina, ^{**}University of Buenos Aires, ^{***}University of Buenos Aires

ABSTRACT

The recent evolution of multi-scale analysis based on homogenization processes has increased the demand of mesoscopic evaluations to provide the appropriate and sufficient information for the macroscopic response of concrete boundary value problems. In this context, it is desired that the thermodynamical features of the fine scale are preserved during the homogenization procedure that injects the mechanical responses in the macro scale. This shall involve the free energy density and the dissipation which may be decoupled in different components depending on the multiphysical characteristics of the failure process under development in cementitious material-based mixtures like concrete. One of the most severe shortcomings of mesoscopic Finite Element Analysis of cement-based composites is the intrinsic geometrical complexity that arises when considering real aggregate, mortar distributions and aggregate-mortar interactions. A mesh that is insufficiently representative of the actual geometry imposes unrealistic constraints and boundary conditions that strongly affect the numerical solution and the related accuracy. In this work, a thermodynamically consistent semi-concurrent multiscale approach [1] for modeling the thermo-poro-plastic failure behavior of concrete materials is considered to account for the mesoscopic cracking and mechanical degradation phenomena in the macroscopic level of observation. Thereby, and to overpass the difficulties involved in the mesoscopic meshing of concrete materials, the recently developed Virtual Element Method (VEM) [2], [3] is used, which allows discretizations of the domain into arbitrary polygons. In the first part of this work, the fundamental equations describing the homogenizations of the thermodynamical variables, the dissipation and the free energy, as well as the constitutive models are described. Then, the basis of the VEM technology and the proposed procedure for concrete-mesoscopic meshing are outlined. Finally, numerical analyses are presented involving stress paths and failure behavior under tensile and compressive conditions that shows the potential and efficiency of the VEM for complex discretizations such as those required in concrete mesoscale analysis and for both, localized and diffuse failure modes, in the framework of thermodynamically consistent multiscale homogenization schemes. REFERENCES [1] F. Lopez Rivarola, G. Etse and P. Folino, "On thermodynamic consistency of homogenisation-based multiscale theories". Submitted to Journal of Engineering Materials and Technology, ASME. 2016. [2] Applications of the virtual element method for cracking analysis of cement-based composites using interface elements. M. Benedetto, A. Caggiano, G. Etse. ENIEF 2016, Argentinean Conference on Computational Mechanics. Cordoba, Nov 2016. [3] Brezzi F., Beirão da Veiga L., Marini L.D. Virtual elements for linear elasticity problems. SIAM Journal on Numerical Analysis, 51(2):794–812, 2013.

Easily Computable Metrics for Assessing the Quality of High-Order Finite Element and Isogeometric Meshes

John Evans^{*}, Luke Engvall^{**}

^{*}University of Colorado Boulder, ^{**}University of Colorado Boulder

ABSTRACT

High-order finite element and isogeometric methods have become immensely popular recently for the numerical solution of systems of partial differential equations. However, while significant effort has been dedicated toward the development of quality metrics for straight-sided simplicial and tensor-product meshes, there has been relatively little research devoted toward the development of quality metrics for curvilinear meshes. In fact, state-of-the-art quality metrics such as the scaled Jacobian cannot even be employed to answer the question: Does a given sequence of curvilinear meshes exhibit optimal convergence rates? In this talk, we present a new family of quality metrics for high-order finite element and isogeometric meshes which overcome the limitations of state-of-the-art metrics. The new metrics are motivated by classical interpolation theory, and they rely on the use of a Bernstein-Bezier polynomial or rational basis to represent the geometric mapping over each element [1,2]. The metrics are also easily computable in that they only involve the computation of finite-difference-like stencils of the Bernstein-Bezier control net, and they can be employed to arrive at sufficient and computable conditions for guaranteeing a sequence of curvilinear meshes exhibits asymptotically optimal convergence rates. The metrics can be applied to curvilinear simplicial, tensor-product, or mixed finite element meshes as well as B-spline, Non-Uniform Rational B-splines (NURBS), T-spline, or hierarchical B-spline isogeometric meshes. A number of examples are provided illustrating the limitations of state-of-the-art quality metrics and the promise of the proposed quality metrics. [1] L. Engvall and J.A. Evans, "Isogeometric triangular Bernstein-Bezier discretizations: Automatic mesh generation and geometrically exact finite element analysis." *Computer Methods in Applied Mechanics and Engineering*, 304:378-407, 2016. [2] L. Engvall and J.A. Evans, "Isogeometric unstructured tetrahedral and mixed-element Bernstein-Bezier discretizations." *Computer Methods in Applied Mechanics and Engineering*, 319:83-123, 2017.

A Phase-Field Description of Brittle Crack Propagation in Nuclear Fuels

Olivier FANDEUR*, Thomas HELFER**

*CEA Paris Saclay, **CEA Cadarache

ABSTRACT

The fuel element of most Pressurized Water Reactors are made of a stack of uranium dioxide pellets where heat-generating nuclear fission reactions take place and a zirconium alloy cladding which constitutes a guarantee against dispersion of fissile material and fission products. Modelling the in-reactor behaviour of such fuel elements is made complex by the myriad of coupled, nonlinear, chemical, mechanical, thermal and microstructural changes that take place within the fuel. From the mechanical point of view alone, various contributions must be taken into account, such as brittle fracture of the fuel pellets at reactor start-up, thermally and radiation induced viscoplasticity, swelling due to fission products, pellet-cladding mechanical interaction (PCMI), etc. The cracking of pressurised water reactor fuel pellets has the two main consequences on the macroscopic mechanical behaviour of the fuel rod: firstly, to relieve the stress in the pellet, upon which the majority of the mechanical and physico-chemical phenomena are dependent, and secondly, to lead to pellet fragmentation. Taking fuel cracking into account is therefore necessary to adequately predict the mechanical loading of the cladding during the course of an irradiation. Simulating these phenomena is challenging both from a numerical standpoint and from the point of view of the physical phenomena involved. As a result of this, advanced and robust numerical techniques are necessary, especially in large-scale fuel performance. Our presentation will focus on the treatment of the fuel cracking through a phase-field approach using the finite element solver Cast3M, developed by CEA, and also the first steps to deal with unstable crack propagation in a quasi-static point of view

Mode Jumping in Post Buckling of Simply Supported Thin Plates Using Exact Strip Method

CAROL FEATHERSTON*, DAVID KENNEDY**, MUTHANA AL-SAYMAREE***

*Cardiff University, **Cardiff University, ***Cardiff University

ABSTRACT

This work investigates the post buckling behaviour of thin plates including the mode jumping phenomenon. This phenomenon occurs when the initial post buckling equilibrium path becomes unstable, and the jump to a more stable path is characterised by a sudden change in mode shape. Its occurrence depends on the plate aspect ratio and boundary conditions. Two different approaches are introduced to predict the jumping point along the post buckling equilibrium path. Analysis is performed using the exact strip software VICONOPT [1], and numerical results are validated against finite element analysis. The first approach is based on Koiter's effective width theory [2] for the post buckling of simply supported plates in longitudinal compression. Stress is redistributed towards the plate edges until only a small amount of load is carried in the central region. The theory assumes that two strips at the plate edges will carry a uniform load and the centre of the plate is unloaded. The edge strips each have SSSF boundary conditions and their effective width decreases as the applied load is increased. Thus their critical buckling loads increase, and their associated mode shapes have increasing numbers of half-waves along the plate length. The second approach considers the strain energy of different equilibrium paths. A jump can occur from the initial equilibrium path to a secondary path when the energy of the latter becomes lower than that of the former. Strain energies are calculated by integrating the load-end shortening curves, either analytically by approximating them as cubic polynomials or numerically by the trapezoidal rule. Mode jumping predictions using the energy approach show good agreement with finite element analysis for all aspect ratios considered. The effective width approach predicts a relatively late mode jump for plates whose aspect ratios indicate a jump is likely to occur soon after critical buckling. [1] Kennedy D, Featherston CA, 2010. Exact strip analysis and optimum design of aerospace structures. *Aeronautical Journal*, 114(1158):505-512. [2] Koiter, WT, 1943. The effective width of flat plates for various longitudinal edge conditions at loads far beyond the buckling load. NLL Report S287, Amsterdam, pp. 365-374.

ACCOUSTIC OPTIMIAZATION OF GEAR BOX STRUCTURE

GUOBAO FENG*, XIAOYAN TENG[†], HETAO ZHAO[†], DONGYAN SHI[†]

*Harbin Engeering University

[†]Harbin Engeering University, China

Harbin, Heilongjiang Province, P.R.China

Key words: Boundary Element, Gear box, stiffener; damping layer;

Abstract.

In this paper, the acoustic response of gearbox structure is optimized and analyzed. Firstly, the boundary element method is used to calculate the contribution of the acoustic response part of the gearbox structure, and the contribution of the acoustic radiation response of each part is obtained. The upper cover is focused in this paper. Secondly, the topology optimization aiming at maximizing the first frequency is performed to obtain the optimal material distribution of the upper cover. In the end, the upper cover is treated with reinforcement, and is attached with constrained damp where is topological position and maximum amplitude of vibration. The result reveals that the reinforcement can restrain the sound pressure level of the first frequency, but it increases the response peak of the high frequency. Whereas the effect of two kinds of constraint damping treatment is not as obvious as that of the reinforcement at first frequency, but it can better suppress the high frequency response.

1.INTRODUCTION

The gearbox structure is an important transmission device, and its vibration and noise will directly affect the overall equipment noise level. At present, the acoustical optimization of the gearbox structure is mainly focused on the gear transmission part, and the acoustic response of the box structure is less optimized^[1]. The internal shaft vibration of the gear box is transmitted to the gear box body to stimulate the vibration of the box body to radiate noise. Most of the vibration noise is radiated from the surface of the structure, and the radiation area of the gear box body is relatively large relative to the wheel train. Therefore, The noise reduction design of the gear box structure is necessary.

2. GEAR BOX STRUCTURE MODEL

2.1.GEAR BOX STRUCTURE GEOMERTY MODEL ESTABLISHMENT

3D modeling software is used to perform 3D solid modeling of the gearbox structure. A good model is shown in Figure 1.1. It includes the upper box and the lower box. The upper box box has a

wall thickness of 10mm, and the lower box adopts dual compartments. The plate supports the wall structure. The middle of the two plates is connected by ribs. As shown in Figure 1.1(b), the wall thickness is 10mm. The upper box is mainly used for dust prevention and noise isolation, while the lower box is mainly used for supporting. Therefore, the above structural design is adopted^[2].

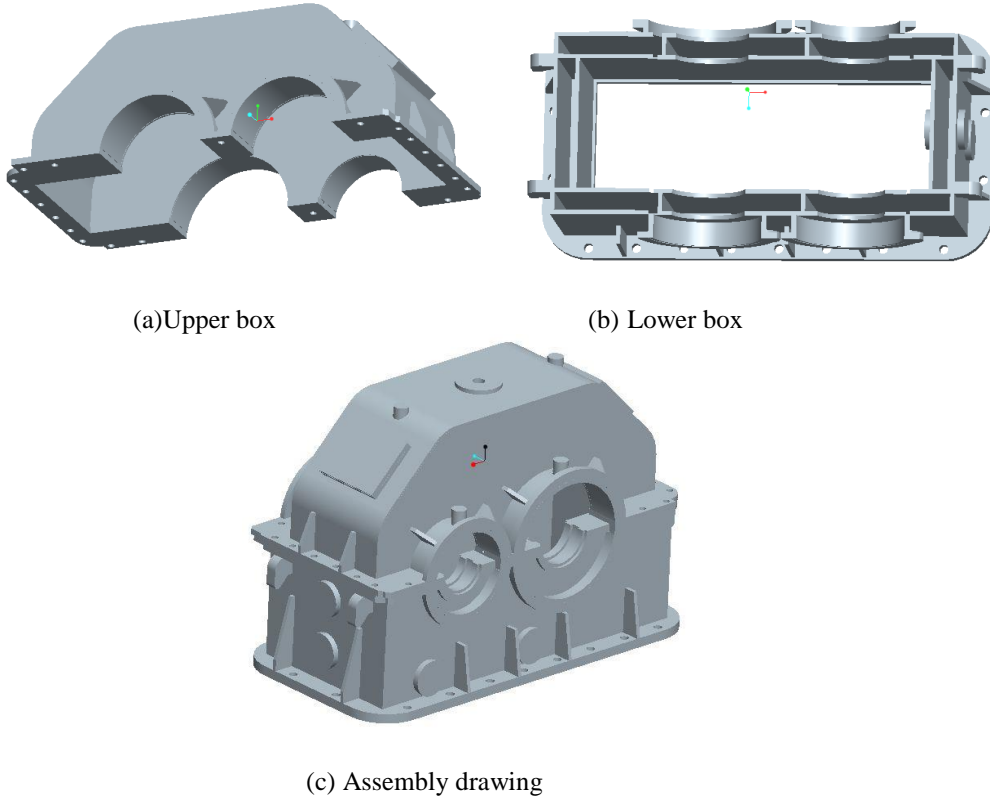


Figure 1.1. Gear box body model

2.2.Gear Box Dody Finite ELEMENT MODLE ESTABLISHMENT

To divide a finite element mesh on a structural geometric model, the first step is to simplify the established geometric model. Since the established geometric model is built according to the actual structure, there are many small features, such as small rounds, oil paths. Holes and so on. When establishing the finite element model, if you want to divide the mesh at these small structures, you must divide the mesh very small, you need to increase a lot of calculation time, and have little effect on the calculation result, so you have to do this structure. Simplify^[3]. However, it is not possible to determine the simplified criterion completely based on the size of the structure, because the stress concentration phenomenon may occur in some small areas. This type of area must be encrypted in order to increase the calculation accuracy.

In this paper, hypermesh is used to perform finite element meshing. Before the partitioning, the geometry of the structure must be cleaned to eliminate the defects such as surface crevices, free edges, and overlaps caused by the software import problem. After the geometric cleanup, the structure can be more suitable for the network. The division of the grid and improve the quality of grid division^[4].

In this paper, C3D8 unit is used, that is, an 8-node hexahedral linear full integration unit, when

the unit shape is more regular. The number of Gaussian integration points used by the full integration method is sufficient to accurately integrate the polynomials in the element stiffness matrix. In some areas that are not particularly regular, a combination of hexahedron and pentahedron is used for meshing to better simulate model boundaries. According to the experience grid size usually choose 1% of the size of the structure. The box structure finite element model is shown in Figure 1.2. It has a total of 54077 units and 92862 nodes^[4].

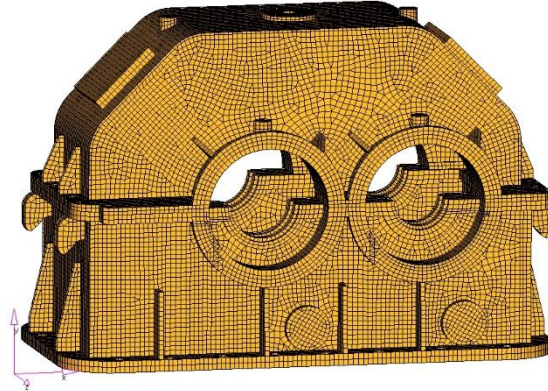
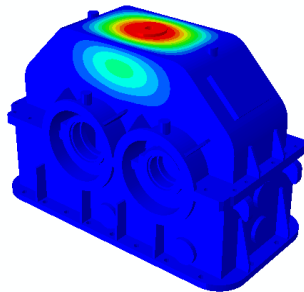
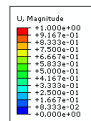


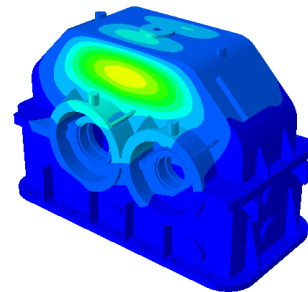
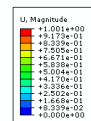
Figure 1.2 Gear box box finite element model

3.GEAR BOXSTRUCTUREMODAL CALCULATION

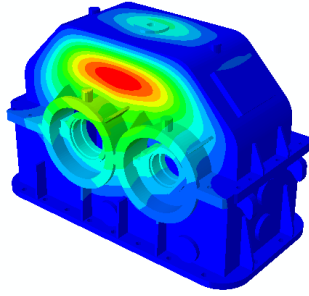
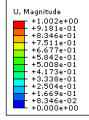
The modal analysis of the structure is the basis of the dynamic analysis. Through the modal analysis, the vibration of the structure can be understood and the resonance frequency of the structure can be known, which provides theoretical support for other dynamic analysis. The lower end of the gear box structure is fixedly restrained, and the upper and lower boxes are connected by a tie constraint to simulate the bolt connection. The first ten modal vibration modes are calculated as shown in Figure1.3, and the natural frequency and vibration modes of each mode are shown in Table 1.1. From the calculation structure, it can be seen that the first ten modal vibrations are mainly concentrated on the upper box body. This is mainly because the upper box structure has a smaller wall thickness and a smaller structural rigidity, and can be the first to reach the resonant frequency of the structure. The lower box adopts a double-separator design, which greatly increases the rigidity and stability of the structure^[5].



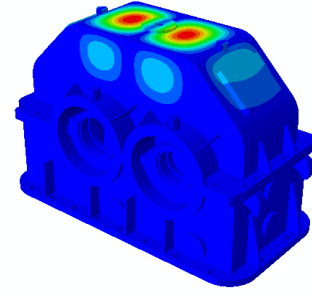
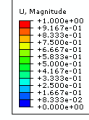
The first-order vibration mode frequency



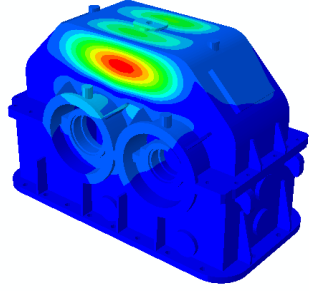
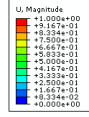
The second-order vibration mode frequency



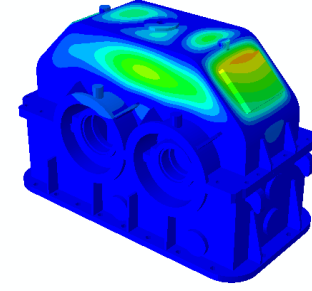
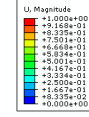
The third-order vibration mode frequency



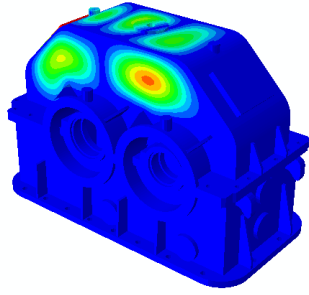
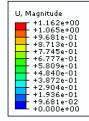
The fourth-order vibration mode frequency



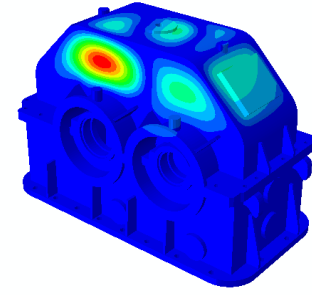
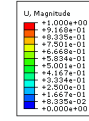
The fifth-order vibration mode frequency



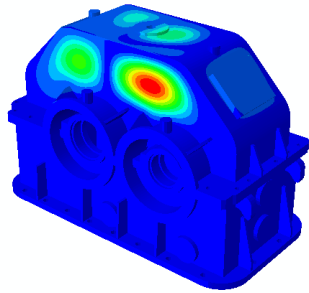
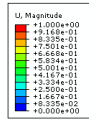
The sixth-order vibration mode frequency



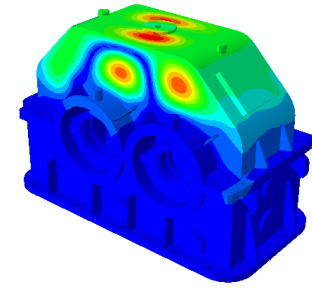
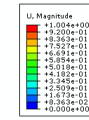
The seventh-order vibration mode frequency



The eighth-order vibration mode frequency



The ninth-order vibration mode frequency



The tenth-order vibration mode frequency

Figure1.3 The first 10 modes of the box**Table 1.1 Natural frequencies and mode shapes**

Modal order	Natural frequency (Hz)	Vibration mode	Modal order	Natural frequency (Hz)	Vibration mode
1	196.08	Vent hole up and down vibration	2	216.02	Swing in Z direction
3	277.28	Expansion and contraction deformation	4	285.75	Twisted top of box
5	315.72	Upper case Z movement	6	389.12	Box shrinkage deformation
7	401.81	Extrusion deformation	8	409.61	Upper cabinet sidewall distortion
9	477.16	Distortion of sidewalls and top	10	492.16	Twist and Z swing

4. CALCULATION OF ACOUSTIC RESPONSE PLATEe CONTRIBUTION OF GEAR BOX STRUCTURE

4.1. Acoustic plate contribution

The boundary element method is used to calculate the contribution of the acoustic plate. The boundary element grid is defined as a number of plates. The volume of sound pressure caused by each plate is calculated, and the proportion of the sound volume in the whole is analyzed. Which plate is the total sound is analyzed. The pressure exerts the greatest influence, starting with positive or negative effects^[6].

When calculating the contribution of the gear box structure plate, the acoustic transfer vector ATV (Acoustic Transfer Vector) is used. In the case of small pressure, the acoustic equation can be considered linear, so a linear relationship can be established between the input (vibration at the surface of the structure) and the output (the sound pressure somewhere in the sound field) [56] if The surface of the structure is discrete into a finite number of units so that the sound pressure at a point in the sound field is:

$$p = \{ATV(\omega)\}^T \{v_n(\omega)\} \quad (1-1)$$

In formula (1-1):p- sound pressure vector in the sound field.

ATV - acoustic transfer vectors;

v_n -Vibration velocity in the direction of the normal to the surface of the structure;

ω -Angular frequency.

To analyze the contribution of the plate, the boundary element mesh is divided into different plates. At this time, the sound pressure contribution of each plate to a certain point in the sound field is the sum of the contributions of all the elements contained in the plate, ie:

$$P_c = \sum p_{e,j}(\omega) \quad (1-2)$$

$$P_{e,j}(\omega) = ATV_i(\omega) \cdot v_{e,j}(\omega) \quad (1-3)$$

in(1-3): $P_{e,j}(\omega)$ -Sound pressure contribution of the unit.

$v_{e,j}(\omega)$ - Unit i normal speed.

The optimization of the acoustic response of the structure is to improve some parts of the structure and finally achieve the purpose of vibration reduction and noise reduction. The primary goal of noise reduction design is to determine where to optimize and improve. The calculation of the contribution of the acoustic plate is to find the position that needs to be optimized^[7,8].

4.2 Calculation of Contribution of Acoustic Plates in Gearbox Structures

Before the calculation of the acoustic response of the gear box structure, the harmonic response of the gear box structure is calculated, and the vibration response of the gear box structure is changed with the frequency. The processing of the boundary conditions is the same as in the modal calculation, and a sinusoidal load is applied at the bolt hole position to simulate the bearing pressure distribution. The load size is taken as 500N. The calculated frequency range is selected as 150-550Hz, which includes the first ten modal frequency ranges of the vibration of the gearbox structure.

The block that divides the grid of the gear box structure into 10 meshes is shown in Figure 1.4. The specific positions of the plates are shown in Table 1.2. The reference sound pressure point is located at a position 1 m directly above the gear box and the sound pressure response cloud diagram of the overall sound field is shown in Figure 1.5. The sound pressure frequency response curve of the reference point is shown in Figure 1.6. It can be seen from the curve that the first peak of the sound pressure level appears at 195 Hz, and the two larger peaks after that appear at 315 Hz and 512 Hz. The sound pressure level response at three frequencies extracts the plate contribution to the reference point, as shown in Figure 1.7-1.9:

Table 1.1 Boundary element location

plate	position	plate	position
1	Upper box upper cover	2	Lower box rear wall
3	Lower right wall panel	4	Upper rear wall panel
5	Upper box front wall	6	Lower box front wall
7	Lower box left wall	8	Front bearing cap
9	Rear bearing cap		

It can be seen from the figure that at 195Hz and 315Hz, the contribution of plate 1,4,5 is the largest, that is, the upper and lower wall and upper cover on the upper box contribute the most to the sound pressure level, and these two places The frequency is exactly the first-order and fifth-order modal frequencies of the vibration of the gearbox structure. It can be seen from Fig. 5.3 that the vibrations of the box on the gearbox at these two-order modal frequencies are very violent, and thus produce larger The sound pressure level contributes, and produces a peak in the sound pressure level. At the frequency of 512Hz, the sound pressure contributions of plates 1, 2, 4, 5, and 6 are relatively large. However, due to the phase difference, the resulting sound pressure level is closer to 315Hz. At this time, the structural frequency is lower. The high excitation of the vibration of the box structure results in a large contribution of the various blocks of the gear box to the sound pressure level of the field point. Because the frequency of the external load subjected to the structure is from low to high, the low-frequency phase must pass through. Therefore, the low-order frequency is more important for the structure, so this paper focuses on the gear box structure at 195

Hz. The structural acoustic response at 315 Hz is the optimization of the acoustic response of the upper box structure.

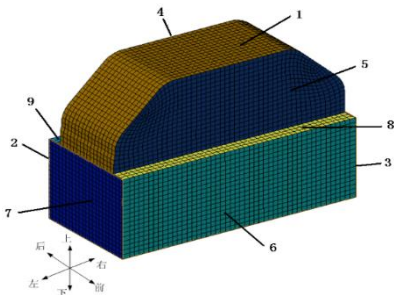


Figure 1.4 Gear box boundary element grid division

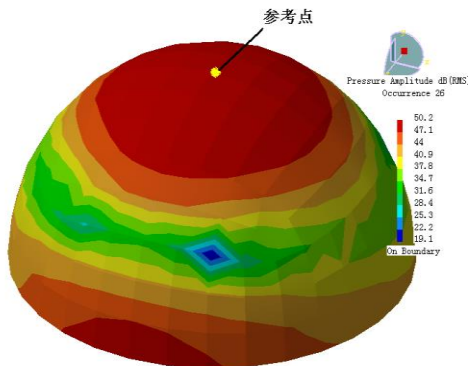


Figure 5.5 Sound pressure response cloud diagram of sound field outside gear box

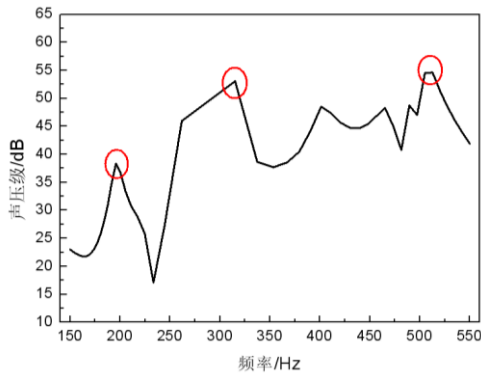


Figure 1.6Acoustic pressure frequency response curve of sound field reference point outside gearbox

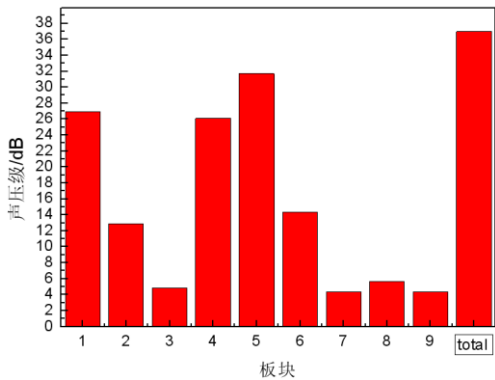


Figure 1.7 Plate contribution at frequency195Hz

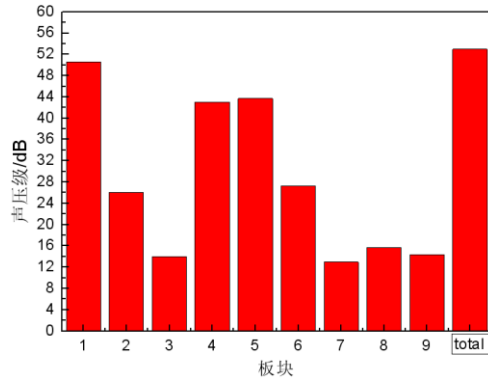


Figure 1.8 Plate contribution at frequency 315 Hz

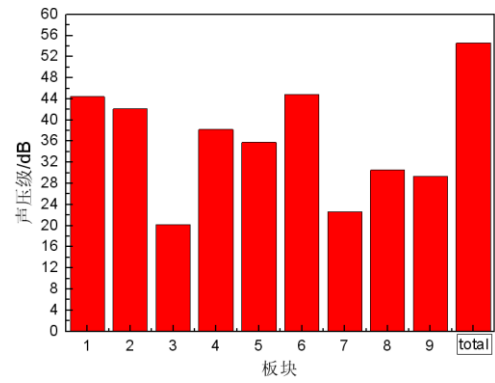


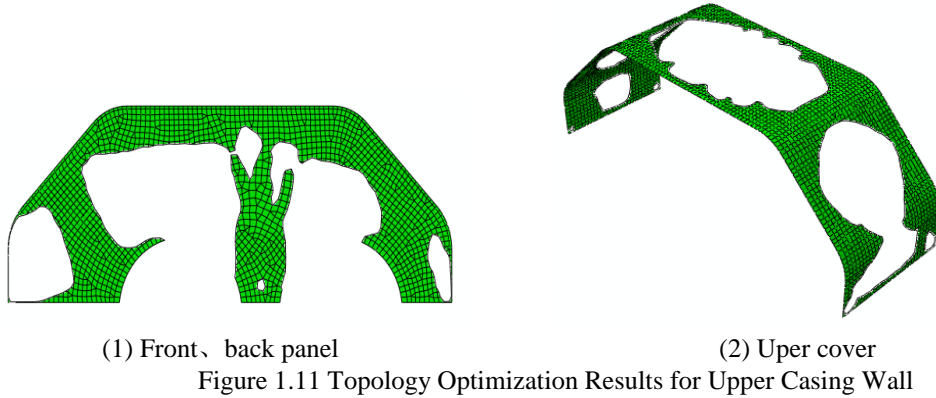
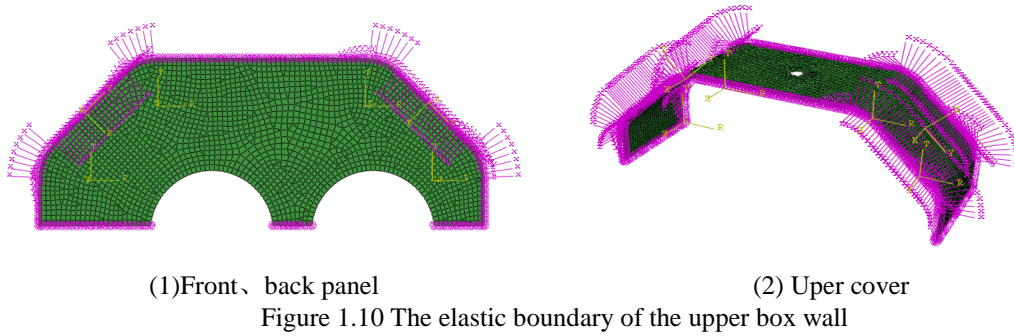
Figure 1.9 Plate contribution at frequency 512 Hz

5 TOPLOGICAL OPTIMIZATION OF ELASTIC BOUNDARY OF BOX WALL ON GEAR BOX

5.1 Topological Optimization of Elastic Boundary of Box Wall on Gearbox

From the above calculations, it can be seen that the front and rear wall panels and the upper cover of the upper box body have the largest contribution to the acoustic response and are the locations that need to be optimized. Because the upper box wall of the gear box body is relatively thin, it occupies a small part of the weight of the entire box body. If the entire box body is optimized, the material at the upper box wall must be almost deleted, leaving Higher-quality parts (such as bearing seats) can greatly improve the stiffness of the structure, but such topological forms do not provide a valuable reference for structural improvement. Moreover, optimizing the entire box structure also consumes computational resources. Therefore, in this paper, the front and rear walls of the upper box and the upper cover are separately proposed. The coil spring is arranged on the wall board to simulate the elastic boundary in the gear box. The layout of the coil spring is shown in Figure 1.10. In the transition of the arc and the position of the hypotenuse, a local coordinate system needs to be established, so as to ensure the correctness of the stiffness direction of the coil spring. As for the knot stiffness K_j of the coil spring, it is 50,000 for the convenience of loading. From the previous research, we can see that with the increase of the boundary stiffness, the optimized material will tend to be distributed toward the boundary. In fact, as long as a relatively moderate stiffness value is obtained between the boundary freeness and the boundary fixed branch, the results from the topology optimization In the middle, we can roughly infer the topological form of the other boundary stiffness, so the node stiffness of the coil spring is taken as 50000 enough to meet the requirements of the structural topology optimization of the elastic boundary topology^[8].

Taking the maximization of the first-order modal frequency of the structure as the optimization goal, from the viewpoint of improving the structural rigidity, at least 50% of the material of the structure is removed, and the optimized structure is shown in Figure 1.11. It can be seen from the optimized results. In order to maximize the stiffness of the structure, materials will be distributed in more rigid locations. With the first-order vibration mode of the gear box structure, it can be seen that most of the material in the first-order mode vibration is removed. This design for vibration reduction and noise reduction provides a trend of material distribution modification.



5.2. Topology Optimization Form Distribution Ribs

In order to improve the stiffness of the gear box structure to increase its natural frequency, the arrangement of stiffeners is adopted in the topology optimized form, and the stiffener section is selected as L type. From the previous studies, it is known that the L-shaped ribs have the best vibration resistance. Noise reduction effect. The side wall of the upper box after the ribs are arranged is shown in Figure 1.12.

In order to test its noise reduction effect, the acoustic response of the entire gearbox structure was calculated. Similarly, the reference point 1m directly above the gearbox was used as the basis for assessing the sound pressure level. The frequency response curve of the sound pressure level was shown in Figure 1.13. Show. It can be seen that with the stiffener structure, the first-order sound pressure response peak is flattened, and the sound pressure level response peak value is reduced from the original 38.34dB to 25.86dB, which is reduced by 12.48dB. It can be seen that the arrangement of stiffeners according to the topology optimization method has obvious effects on the suppression of the first-order mode vibration modes. In addition, the sound pressure level frequency response curve has a tendency to move to a high frequency as a whole, and the sound pressure level response at a high frequency band tends to increase, mainly because additional stiffeners change the stiffness of the structure and change the local quality of the structure. The distribution then generates new vibration peaks. Therefore, if certain structures are only operating at a specific frequency, consider using additional stiffeners to reduce vibration noise. Because the topology optimization is for the first-order frequency of the structure, the results of the sound pressure level response at the first-order modal frequency fully verify the effectiveness of topology optimization in vibration reduction and noise reduction.

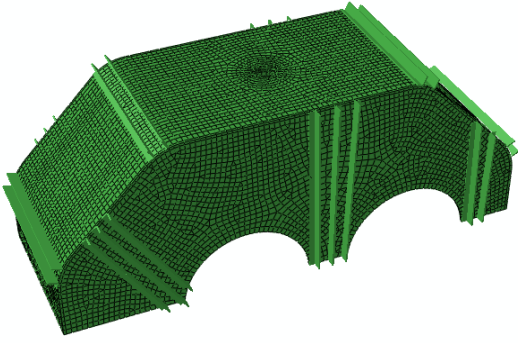


Figure 1.12 Upper shell wall stiffener layout

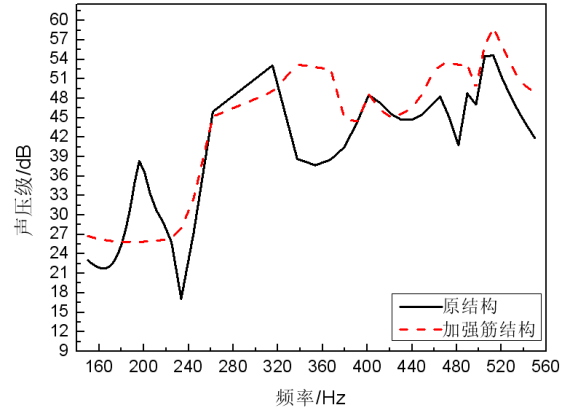


Fig. 1.13 Comparison of sound pressure level response after stiffening the upper box wall

5.3. Topology optimization form distribution constrained damping layer

The arrangement of the constrained damping layer for the topology-optimized structure is shown in Figure 5.14. Select the damping layer thickness of 5mm, the material is SA-3, the constrained layer thickness is 2mm, and the material is Al6061. This selection can maximize the advantages of vibration damping materials. The acoustic response of the gear box structure is calculated, and the sound pressure frequency response curve obtained from the reference point is shown in Figure 5.15. From the curve, it can be seen that after the constrained damping layer is added, the response curve of the sound pressure response curve and the original structure is basically the same. Consistently, the sound pressure levels at the three peaks all decreased. The most significant reduction at the first peak was reduced from 38.34 dB to 31.72 dB, which was a decrease of 6.62 dB, and the second peak at 53.07 was reduced to 52.02 dB, which was reduced. At 1.05 dB, the structure of the constrained damping layer near the third peak produces a new peak in the sound pressure level response. The vibration of the structure is mainly complicated at high frequencies. The damping layer arranged for low-order vibration is at high frequencies. Due to the added mass effect, a new peak in the sound pressure level response was generated.

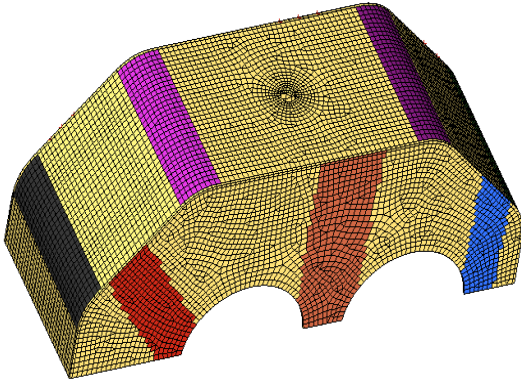


Figure1.14 Upper Casing Wall Additional

Topology Form Constrained Damping Layer

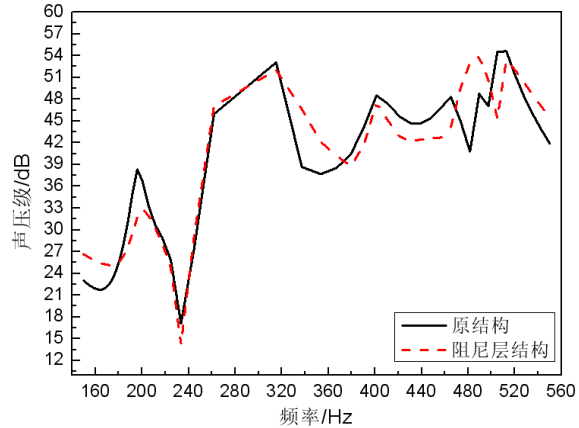


Figure 1.15 Topographically Formed Constrained Damping Layer Reference Point Sound Pressure Frequency Response Curve

For the first-order mode shape of the gear box structure, constrained damping layers are

arranged at large amplitudes. The area of the damping layer is the same as that of the topological layout, as shown in Figure1.16. Similarly, the sound pressure level frequency response at the sound field reference point outside the gear box structure is calculated, as shown in Figure1.17. It can be seen that after the constrained damping layer is added, the three sound pressure level response peaks are all significantly reduced. The decrease at the peak is most obvious from 38.34dB to 31.21dB, which is a decrease of 7.13dB, the second peak is reduced from 53.07 to 46.29dB, which is a decrease of 6.78dB, and the third peak is decreased from 54.62 to 52.84dB, which is a decrease of 1.78. dB, visible in the three peaks of the sound pressure level drop is significantly greater than the topological form of the damping, and the sound pressure level of the frequency response function curve and the original structure of the frequency response curve is in good agreement, additional sound pressure level response peak almost Did not appear to achieve a good noise reduction effect.

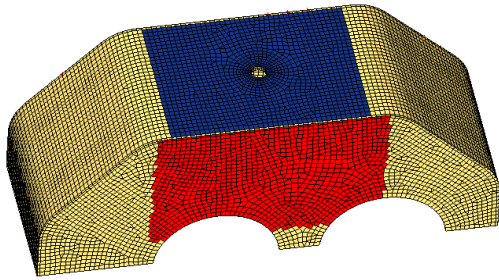


Fig 1.16 The upper box wall is attached to a Constrained damping layer for large displacements of vibration

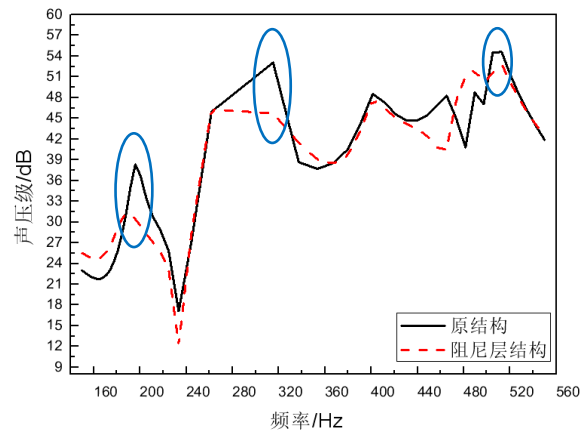


Figure1.17 Acoustic Pressure Response Curve of Reference Point for Additional Constrained Damping Layers for Large Vibration Displacement

From the above calculations, it can be seen that arranging the damping layer in topological form can significantly reduce the peak value of the sound pressure level response, but the effect of the reduction does not have a good effect of arranging the damping at the maximum amplitude location. The use of an additional damping layer results in less peaks in the additional sound pressure level generated by the structure. Therefore, machines operating under wide-band conditions will have better noise reduction performance in the form of additional damping.

Summarizing the optimization results of the gear box structure, as shown in Table 1.3, it can be seen from the table that the most obvious suppression of the first-order sound pressure level peak suppression in the three optimized forms is to add the structure of the reinforcement according to the topology, and At the second peak, this arrangement has no noise reduction effect, but it will move the sound pressure level response curve towards high frequencies. At the second peak, the structure with the damping layer at the maximum amplitude has the best noise reduction effect. It can be seen that the form of additional damping can achieve the effect of noise reduction over a wide range of frequencies, and the form of additional stiffeners can only be in relatively narrow frequency bands, and the noise reduction effect is more obvious.

Table 5.2 Comparison of the optimization results of the gearbox structure

structure type	The first peak	Decline	The second peak	Decline
----------------	----------------	---------	-----------------	---------

	sound pressure level		sound pressure level	
Original structure	38.34	0	53.07	0
Additional stiffeners in topological form	25.86	12.48	53.10	-0.3
Topological form additional damping layer	31.72	6.62	52.02	1.05
Amplitude layer with maximum amplitude	31.21	7.13	46.29	6.78

6. CONCLUSION

Based on the calculation results of the acoustic plate contribution of the gear box structure, the elastic boundary topology optimization was performed on the front and rear wall panels of the upper box and the upper box cover. The reinforcement ribs and the damping layer were arranged according to the optimization results, and the gear box acoustics were obtained. Optimize the structure. The box structure with reinforced ribs has a very significant suppression effect on the sound pressure level at the first-order modal frequency, but the sound pressure level response increases at high frequencies. Arranging the damping layers in topological form can significantly reduce the peak value of the sound pressure level response, but the effect of the reduction is not as obvious as the effect of damping at the maximum amplitude location, and the sound pressure level response curve and the unresponsive sound pressure level response of the damping layer are arranged. The curves are very similar, resulting in fewer peaks in the extra SPL.

ACKNOWLEDGEMENTS

This research is supported by the National Natural Science Foundation, of China (Grant NO.51505096), and National Natural Science Foundation of Heilongjiang Province of China (Grant NO.2016056, E2016024). The authors are thankful to Harbin Engineering University for English correction of the manuscript. This paper is funded by the International Exchange Program of Harbin Engineering University for Innovation-oriented Talents Cultivation.

REFERENCES

- [1] Greeves.C.S. Gear noise. Noise Control and Vibration Reduction.1974,5 (4):163-166P.
- [2] R.H.Badgley. Gearbox noise reduction: prediction and measurement of mesh-frequency vibrations within an operating helicopter rotor-drive gearbox. J. Eng. for Industry. 1974,96(2):11-22P.
- [3] Coltrona.M.L.,Stone.B.J..The torsional vibration of gearbox with backlash. Multi-Body Dynamics: Monitoring and Simulation Techniques. 2004,(3): 287- 297P.
- [4] Rongfang Li. Gearbox vibration and noise experimental research. Mechanical design and research. 2003, 19(5):63-65P
- [5] Jianming Zhong. The impact of the gearbox structure design on noise. Mechanical transmission. 1992,S1:23-24P
- [6] Liming YU. Research on Damping and Damping of Gearboxes. Master of Harbin Engineering University. .2010:61-64P
- [7] Yuting Lu. Vibration damping design and optimization of marine gearboxes. Master of Harbin Engineering University. 2011:17-20P
- [8] Huang X,Xie Y M. Evolutionary Topology Optimization of Continuum Structures:Methods and Applications:United Kingdom:John Wiley & Sons Limited,2010:17-38

Multi-scale Analysis of Stretched Plates by a Boundary Element Formulation

GABRIELA R FERNANDES*, Maria Júlia M. Silva**, Jordana F. Vieira***, Caio F. Gonçalves****

*Federal University of Goiás (UFG) – Regional Catalão, Brazil, **Federal University of Goiás (UFG) – Regional Catalão, Brazil, ***Federal University of Goiás (UFG) – Regional Catalão, Brazil, ****Federal University of Goiás (UFG) – Regional Catalão, Brazil

ABSTRACT

In this paper multi-scale analyses of stretched plates composed of heterogeneous materials are performed. The Boundary Element Method is adopted to model both the macro-continuum, represented by the plate, and the micro-scale, denoted as RVE (Representative Volume Element). Voids and inclusions can be defined inside the microstructure matrix, where different elastic properties and constitutive models can be assumed for each phase. The RVE is modelled considering the sub-regions technique, where the dissipative forces are approximated over the domain using cells. Besides, the in-plane displacements have also to be approximated over the domain if different Poisson's ratios are considered for the RVE phases. Initially, the macro-continuum strain is imposed to the microstructure (or RVE) boundary and the elastic forces computed. From these forces a strain field can be obtained and the microstructure equilibrium problem solved what requires an iterative procedure to find the displacement fluctuations field that auto-equilibrates the microstructure stress field, according to the constitutive models assumed for the phases and to the boundary conditions in terms of displacements fluctuations. The multi-scale modelling is based on the framework presented in the paper "Peric D., de Souza Neto E. A., Feijóo R., Partovi M., Molina A.C., On Micro-to-Macro Transitions for Multiscale Analysis of Heterogeneous Materials: Unified Variational Basis and Finite Element Implementation, Int. J. Numer. Methods Engrg. (2011) 87: 149-170." After solving the equilibrium problem of the RVE, the micro-to-macro transition is made by applying the volume averaging hypothesis of strain and stress tensors in order to obtain the material constitutive response and return to the macro-continuum problem. The BEM formulation adopted to model the macro-continuum is detailed in the work "Fernandes GR and de Souza Neto EA. Self-consistent linearization of non-linear BEM formulations with quadratic convergence. Computational Mechanics v.52, p.1125 - 1139, 2013." Some numerical examples are then analyzed to show that the proposed formulation compares very well to the finite element model, being a suitable tool for the analysis of stretched plates composed of heterogeneous materials.

An Augmented Lagrange Formulation of Large Deformation Frictional Contact Using IsoGeometric Analysis

Mathieu Fabre^{*}, Annalisa Buffa^{**}, Pablo Antolin^{***}

^{*}EPFL - École polytechnique fédérale de Lausanne, ^{**}EPFL - École polytechnique fédérale de Lausanne, ^{***}EPFL - École polytechnique fédérale de Lausanne

ABSTRACT

In the present work, we consider an isogeometric method for solving rigid-deformable frictional contact problems in small and large deformations. The contact constraints are treated with a mortar like approach combined with a interpolation of gap (to see [1] on a second order elliptic equations and [3] using a augmented Lagrangian method). These constraints are satisfied with an augmented Lagrangian formulation to impose both the Signorini contact conditions and the Coulomb's conditions. An Active Set Strategy [4] ensures these conditions. For the discretization, we used NURBS of degree p for the displacement and B-Splines of degree $p + 2$ for the Lagrange multiplier. Indeed, an inf-sup stability and an optimal a priori error estimate without assumption on the unknown contact set are proved for mixed formulation of frictionless contact to ensure a good property of the method using these elements. Some numerical results will be presented showing the good convergence properties of our algorithms on numerical tests in two and three dimensions in small and large deformation. [1] E. Brivadis, A. Buffa, B. Wohlmuth, and L. Wunderlich, Isogeometric mortar methods. Comput. Methods in Appl. Mech. Eng. 284:292-319, 2015. [2] T. J. R. Hughes, J. A. Cottrell and Y. Bazilevs, Isogeometric analysis: CAD, finite elements, NURBS, exact geometry and mesh refinement. Comput. Methods in Appl. Mech. Eng. 194:4135- 4195, 2005. [3] L. DeLorenzis, P. Wriggers and G.Z. avarise, A mortar formulation for 3d large deformation contact using nurbs-based isogeometric analysis and the augmented Lagrangian method. Springer-Verlag 49:1-20, 2012. [4] A. E. Maliki, M. Fortin, J. Deteix, and A. Fortin, Preconditioned iteration for saddle-point systems with bound constraints arising in contact problems. Comput. Methods in Appl. Mech. Eng. 254:114- 125, 2013.

Unified Formulation and Analysis of Discontinuous Galerkin Methods for Flows in Fractured Porous Media on Polygonal and Polyhedral Grids

Chiara Facciola^{*}, Marco Verani^{**}, Paola Francesca Antonietti^{***}

^{*}MOX, Politecnico di Milano, ^{**}MOX, Politecnico di Milano, ^{***}MOX, Politecnico di Milano

ABSTRACT

We propose a formulation based on discontinuous Galerkin (DG) methods in their generalization to polytopic grids for the simulation of flows in fractured porous media. Our method is very flexible from the geometrical point of view, being able to handle meshes made of arbitrarily shaped elements, with edges/faces that may be in arbitrary number (potentially unlimited) and whose measure may be arbitrarily small [1], cf. also [3]. Our approach is very well suited to tame the geometrical complexity featured by most of applications in the computational geoscience field. More precisely, we adopt a model for single-phase flows that considers the case of a single fracture, treated as a $(d-1)$ -dimensional interface between two d -dimensional subdomains, $d = 2, 3$. In the model, the flow in the porous medium (bulk) is assumed to be governed by Darcy's law and a suitable reduced version of the law is formulated on the surface modelling the fracture. The two problems are then coupled through physically consistent conditions. We focus on the numerical approximation of the coupled bulk-fracture problem and present and analyze, in the unified setting of [2], all the possible combinations of primal-primal, mixed-primal, primal-mixed and mixed-mixed formulations for the bulk and fracture problems, respectively. In particular, the primal discretizations are obtained using the Symmetric Interior Penalty DG method, and the mixed discretizations using the Local DG method, both in their generalization to polytopic grids. We perform a unified analysis of all the derived combinations of DG discretizations for the bulk-fracture problem. We prove their well-posedness and derive optimal a priori hp-version error estimates in a suitable (mesh-dependent) energy norm. Finally, we present numerical experiments assessing the validity of the theoretical error estimates. [1] P. F. Antonietti, C. Facciola, A. Russo, and M. Verani. Discontinuous Galerkin approximation of flows in fractured porous media on polytopic grids. Submitted, 2017. [2] D. N. Arnold, F. Brezzi, B. Cockburn, and L. D. Marini. Unified analysis of discontinuous Galerkin methods for elliptic problems. SIAM J. Numer. Anal., 39(5):1749--1779, 2001/02. [3] A. Cangiani, Z. Dong, and E. H. Georgoulis. hp-version space-time discontinuous Galerkin methods for parabolic problems on prismatic meshes. SIAM J. Sci. Comput., 39(4):A1251--A1279, 2017.

Mesoscale Modeling of Damage in Woven Composite Materials: From Experimental Characterization to Numerical Analysis

Christian Fagiano*, Aurelien Doitrand**, Vincent Chiaruttini***, Martin Hirsekorn****

*ONERA - The French Aerospace Lab, **ONERA - The French Aerospace Lab, ***ONERA - The French Aerospace Lab, ****ONERA - The French Aerospace Lab

ABSTRACT

Damage onset and evolution in composites made of a woven reinforcement embedded in a polymer matrix is driven by the multi-scale nature of the material. It starts at the micro-scale with fiber-matrix debonding and plastic stretching of the polymer matrix. The micro-damages then coalesce to form transverse yarn cracks, which are coupled with decohesions between crossing yarns around the yarn crack tips. The meso-scale architecture of the woven reinforcement has a strong influence on the local strain distributions and thus on yarn crack and decohesion initiation and evolution. In order to take into account the influence of the fiber reinforcement architecture on the mechanical behavior of the studied materials, a realistic description of the meso-scale geometry obtained by modeling the preforming step of the dry fabric is necessary. In the proposed approach, the damage mechanisms observed experimentally in a woven polymer matrix composite are modeled at the mesoscopic scale [1]. A realistic geometry of the composite is obtained at the mesoscopic scale by taking into account the relative shifts between the fabric layers and the preforming of the dry reinforcement before resin injection. The quality of the consistent mesh of the Representative Unit Cell (RUC) is ensured using both geometry- and energy-based error indicators. The effects of mesoscopic damage on the macroscopic mechanical properties, obtained by periodic homogenization, are evaluated by inserting discrete cracks in the FE meshes. A criterion coupling stress and energy conditions is used to determine intra yarn damage onset [2]. An algorithm for the simulation of damage evolution is also presented [3]. The predicted damage locations as well as the evolution of the homogenized properties are similar to the experimental observations. References [1] A. Doitrand et al. (2015) Experimental characterization and numerical modeling of damage at the mesoscopic scale of woven polymer matrix composites under quasi-static tensile. *Composites Science and Technology*, 119, 1-11 [2] A. Doitrand et al. (2017) Damage onset modeling in woven composites based on a coupled stress and energy criterion. *Engineering Fracture Mechanics*, 169, 189-200. [3] A. Doitrand et al. (2017) Mesoscale analysis of damage growth in woven composites. *Composites Part A: Applied Science and Manufacturing*, 96, 77-88.

Patient-specific Nonlinear Computational Modeling of Metastatic Femurs: Influence of the Bone-metastasis Interaction on Femur Strength

Cristina Falcinelli*, Alessio Gizzi**, Giuseppe Vairo***, Alberto Di Martino****

*Campus Bio-Medico University of Rome, **Campus Bio-Medico University of Rome, ***University of Rome "Tor Vergata", ****Campus Bio-Medico University of Rome

ABSTRACT

The assessment of fracture risk in patients with femoral metastases is essential to find the best treatment to prevent a pathological fracture. Mirel's scoring was proposed for clinical fracture risk assessment, but it was demonstrated as characterized by a low predictive power (specificity around 35%). As such, ascertaining the fracture risk and identifying treatment requirements are still challenging issues. In this framework, patient-specific computed tomography (CT)-based finite element (FE) models can be successfully used to characterize the mechanical behavior of metastatic bones and thus they can be adopted for a more accurate assessment of fracture risk. Computational studies, defined via CT-based FE modeling approaches, were validated against experimental measurements of femur fracture load in the case of in-vitro metastatic lesions [1]. However, several limitations exist: i) metastases were usually artificially created and modelled as voids; ii) available FE models overestimate experimental fracture loads, and iii) the interaction between bone and metastasis, as well as changes in bone material properties due to metastatic disease, were generally not accounted for [2]. It is well known that healthy bone undergoes continuous adaptation and self-repair by resorption and formation (remodeling process) and it tends to optimize its internal structure as a result of stimuli induced by loading processes. Accordingly, the presence of the lesion can potentially lead to a local dysregulation of such a bone remodeling, thereby producing deep changes in bone structure adjacent to the metastasis. As such, an altered mechanical response is expected from the surrounding healthy bone, inducing a modification in ultimate strength features. This work aims to apply a nonlinear CT-based FE modeling approach to clinical scenarios characterized by femoral metastases. In particular, a novel coupling strategy is proposed with a description of the metastasis based on different material model formulations [3]. Strain and stress fields are evaluated, and a novel stress/strain-based risk indicator is defined and compared with available clinical scoring methods. Proposed computational approach highlights that a refined description of the metastasis and of the bone constitutive response around the lesion allows improving the assessment of the mechanical behavior of a metastatic femur. As such, this strategy opens to the possibility of enhancing predictability power towards the definition of accurate fracture risk assessment. 1. Yosibash et al., Bone, 69:180-190, 2014 2. Goodheart et al., J Orthop Res, 33:1226-1234, 2015 3. Whyne et al., J Biomech, 34:1317-1324, 2001

Insights from Concurrent Constitutive Modeling and Atomistic Simulation of Strain Localization in Metallic Glass

Michael Falk^{*}, Adam Hinkle^{**}, Chris Rycroft^{***}, Michael Shields^{****}

^{*}Johns Hopkins University, ^{**}Sandia National Laboratory, ^{***}Harvard University, ^{****}Johns Hopkins University

ABSTRACT

Atomistic simulation methods can provide some insight regarding the mechanisms of plastic deformation and methods for quantitatively predicting strain localization, a limiting failure process in high-strength metallic glasses and other amorphous materials. We utilize such atomistic calculations to parameterize the effective-temperature shear transformation zone theory. We then directly cross-compare molecular dynamics simulations and continuum representations of these same materials in order to test and validate our constitutive theories. The role of coarse graining in the linkage of continuum and atomistic methods is crucial, and convergence only arises above a critical length scale on the order of tens of angstroms. The investigation makes clear the need to separate out the relevant fluctuations in material structure from the shorter wavelength fluctuations that serve to obscure them. It is, in the end, the interactions between these larger-scale fluctuations via the material's mechanical response that controls the failure process during strain localization.

A Multiscale Method Capturing Dynamic Wave Propagation in High Meso-scales

Jinghong Fan^{*}, Ross Stewart^{**}

^{*}Kazuo Inamori School of Engineering, Alfred University, NY, ^{**}Corning, Inc.

ABSTRACT

A refinement in the Generalized Particle (GP) Multiscale Method has been made that captures dynamic wave propagation in high meso-scopic particle scales. Through the use of interpolating the 3D displacement field to map onto the implicit atoms that are lumped to form the particles, the atomic scale's interatomic pair potentials can be used to calculate the appropriate forces on the generalized particles yielding an accurate material response with a fraction of the degree of freedom required for molecular dynamics simulations.

3D Phase Field Simulation of Fusion and Void Formation of Triplet Metallic Powders

Tai-Hsi Fan^{*}, Ji-Qin Li^{**}

^{*}Department of Mechanical Engineering, University of Connecticut, ^{**}Department of Mechanical Engineering,
University of Connecticut

ABSTRACT

Laser-based additive manufacturing (AM) processes using metallic powders are important in aerospace and biomedical applications on producing shape-complicated and functional parts. However, achieving superior quality and liability of AM-produced parts remains a great challenge because the geometric accuracy and surface quality are often inferior to conventionally machined parts due to the formation of voids or defects. The defects such as voids, notches, or even cracks are often caused by incomplete melting of powders, lapping, gas entrapment or precipitation during the process. As a result, although near-net-shape production is a significant advantage, the as-manufactured parts or specimen usually have rough surface and are subjected to crack initiation and propagation, which may lead to early fracture of the parts. Motivated by this challenge, a 3D phase field model is developed to simulate the incomplete melting and fusion of triplet powders during laser heating. The conceptual study focuses on the morphology change, phase transition dynamics and the void formation from triplet powders with various shapes and arrangements in space. The void formation is quantified according to the packing density, characteristic dimension of the spheroid powders, the symmetry of their arrangement, and laser beam parameters. The fully coupled phase field, energy, and Navier-Stokes-Korteweg momentum equations are solved by Fourier spectral method with periodic boundary conditions and pseudo-spectral approximation for the nonlinear effects. Without the complication of evaporation and powder-substrate interaction, we present the essential interfacial evolution dynamics, the interplay of multiple solid-liquid melting interfaces, and the deformable free surfaces subjected to thermal capillary effect in a 3D space. Various arrangements of powders and laser control parameters are applied to characterize the void formation between powders upon resolidification. The basic understanding and quantitative information provided by this primitive model are relevant to remediation strategies on reducing or possibly removal of the surface defects.

Dynamic Impact Characteristics of Defective Functionally Graded Honeycombs

Tao Fan*

*Harbin Engineering University

ABSTRACT

With the characteristics of light weight, good shock absorption capability and ease of fabrication, the honeycomb structures have drawn a lot of attention [1-3]. In this paper, the in-plane impact properties of functional graded honeycombs are studied with the consideration of defects. On the one hand, defects exist inevitably in the production of honeycomb structures and the defects are introduced by missing some cell walls randomly. The influences of the defect locations and the defect ratios on the dynamic crushing characteristics of the honeycombs are discussed. The dependences of the deformation modes and the energy absorption abilities on the defects are discussed of the honeycomb structures. On the other hand, the functionally graded properties are introduced by changing the cell wall thicknesses, which leads to the varieties of density gradient. It should be noted that the positive density gradient means the thickness of the cell wall decreases along the impact direction and the negative density gradient denotes the thickness of the cell wall increases along that direction. Based on a given relative density, the dynamic deformation modes and energy absorption of the honeycombs with different density gradients are investigated. The results show that the energy absorption abilities for the honeycombs with the negative density gradient are much stronger than those with the positive ones. In general, both density gradient and defect property have significant influences on energy absorption ability. Furthermore, the influences of impact velocities are analyzed. The dynamic crushing behaviors are not sensitive to the impact directions at the lower velocities. With the increasing of the impact velocities, the energy absorption abilities of the honeycombs can be improved. At last, the coupling effects of the defects and functionally graded properties are discussed, which should be considered in the design and analysis of the mechanical characteristics of light-weight structures. This paper is helpful for the design and analysis of the mechanical characteristics of the honeycomb materials and structures. References [1] Fleck, N.A., Deshpande, V.S., Ashby, M.F., 2010. Micro-architected materials: past, present and future. *Proceedings of the Royal Society A* 466, 2495–2516. [2] Ajdari, A., Nayeb-Hashemi, H., Vaziri, A., 2011. Dynamic crushing and energy absorption of regular, irregular and functionally graded cellular structures. *International Journal of Solids and Structures* 48, 506–516. [3] Liu, Y., Zhang, X.C., 2009. The influence of cell micro-topology on the in-plane dynamic crushing of honeycombs. *International Journal of Impact Engineering* 36, 98–109.

Modeling, Calibration and Validation of Residual Stress in Injection Molded Thermoplastics

Zhiliang Fan^{*}, Russell Speight^{**}, Paul Brincat^{***}, Chris Friedl^{****}

^{*}Autodesk Australia Pty Ltd, ^{**}Autodesk Australia Pty Ltd, ^{***}Autodesk Australia Pty Ltd, ^{****}Autodesk Australia Pty Ltd

ABSTRACT

Residual stress distribution in thermoplastic injection molding is largely determined by the varying pressure history, coupled with the frozen layer growth. A realistic simulation of residual stress at different stages of the injection molding process is critical to the accurate prediction of shrinkage and warpage [1,2,3,4,5]. As the injection molding process involves highly complex multi-physics phenomena, such as a fast cooling rate, high pressure, phase change, crystallization and morphology, fiber orientation, stress relaxation and time-varying boundary conditions, many assumptions in mathematical modeling have to be used to make the simulation feasible. In this paper, a range of commonly-used theoretical shrinkage models are discussed, including the generic shrinkage model, anisotropic thermo-viscous-elastic residual stress model and anisotropic thermo-viscoelastic residual stress model. It is shown that these theoretical models can generally provide acceptable results which help engineers to optimize the processing condition and mold and part design. On the other hand, the lack of a complete set of characterization data for materials in the range of process variables of interest for injection molding and approximations in the assumptions of mathematical modeling influence the simulation accuracy more or less. An effective way to improve accuracy further is to calibrate the theoretical models based on measured shrinkage data which is collected from the real processing system in actual injection molding. The methodology and significance of calibration and validation of the residual stress models are explored. The performance of calibrated models in real-world industrial applications is evaluated. References [1] R. Zheng, R.I.Tanner and X.J.Fan, Injection Molding: Integration of Theory and Modelling Methods, Springer, 2011. [2] Z. Fan, B. Lin, F. Costa, X. Jin, R. Zheng and P. Kennedy, Three-Dimensional Warpage Simulation for Injection Molding, Soc. Plastics. Eng. Proc. of Annual Technical Conference (ANTEC), Chicago, USA, 2004. [3] P. Kennedy, R. Zheng, High accuracy shrinkage and warpage prediction for injection molding. Soc. Plastics. Eng. Proc. of Annual Technical Conference (ANTEC), San Francisco, 2002, [4] Z. Fan, H. Yu, Z. Zuo, R. Speight. Anisotropic Thermo-viscous-elastic Residual Stress Model for Warpage Simulation of Injection Molded Parts, Soc. Plastics. Eng. Proc. of Annual Technical Conference (ANTEC), Anaheim, 2017 [5] Z. Fan, R. Speight. Effect of Stress Relaxation on Shrinkage and Warpage of Injection Molded Parts. Soc. Plastics. Eng. Proc. of Annual Technical Conference (ANTEC), Florida 2018

Robust Topology Optimization of Additive Manufacturing Structures with Consideration of Manufacturing Tolerance and Boundary Layer Defects

HuiruShutian FanLiu*, Huiru Fan**

*Dalian University of Technology, **Dalian University of Technology

ABSTRACT

Additive manufacturing technologies have provided new opportunities for fabricating structure with high geometrical complexity. However, thermal deformation, powder adhesion and nebulizing often occur in the printing process, which will leads to uneven distribution of material in the outer boundary layer of the structure. Therefore, the material of the boundary layer is weaker than the inner material, and the structural performance can't reach the expected target. In this paper, we present a new robust topology optimization method for additive manufacture structures with consideration of the manufacturing tolerance and boundary layer defect. The boundary layer defect is modeled as a lower stiffness coated layer, and is described based on the filter and projection of relative density field and its gradient. The manufacturing tolerance and the thickness of the coated layer are assumed as uncertain parameters, and determined by the filter radius and threshold of projection. We assume that the uncertainties are small and the influence of uncertain variables on the system response is evaluated by the perturbation method. In order to describe the robustness, we study the selection rules of weighted coefficients based on the weighted objective function of compliance expectations and standard deviations. We propose a performance index named as "coefficient of variation for compliance" which indicates the effects of the expectation and standard deviation with appropriate weights. Thus, the robust topology optimization is formulated as minimizing coefficient of variation. Numerical examples show the correctness of the proposed method, which can effectively reduce the variation coefficient of compliance and improve the robustness of the structure.

Adaptive DDES of a Vertical Tail/Rudder Assembly with Active Flow Control

Jun Fang^{*}, Riccardo Balin^{**}, Michel Rasquin^{***}, Ramesh Balakrishnan^{****}, Kenneth Jansen^{*****}

^{*}Argonne National Laboratory, ^{**}University of Colorado Boulder, ^{***}Cenaero, ^{****}Argonne National Laboratory,
^{*****}University of Colorado Boulder

ABSTRACT

As the dawn of exascale computing approaches, unprecedented computing power is reshaping the ways researchers cope with challenging engineering flow problems. Large-scale massively parallel simulations have now become a complementary source of knowledge to experiments and provide unique opportunities to advance our understanding of turbulent flows and better inform engineering designs. Successful experimental validation of active flow control has been previously achieved at a Reynolds number of $3.5e5$ matching a 1/19th scale vertical tail/rudder assembly of a Boeing 767 model tested in the Rensselaer Polytechnic Institute wind tunnel at a speed of 20 m/s. In the current study, continued simulations are carried out for more sophisticated geometries and even higher Reynolds numbers. A highly scalable implicit flow solver, PHASTA, which has demonstrated excellent scalability on all 786,432 cores (over 3 M processes) of the Blue Gene/Q (Mira) at Argonne, has been employed in our study. The superior scaling, coupled with anisotropic adaptive meshing procedures, has made PHASTA an ideal tool for simulating challenging engineering flow problems involving flows at high Reynolds numbers with complex anisotropic solution features, and complicated geometries. The simulations we perform are aimed at matching the experimental conditions of the CalTech wind tunnel where a 1/9th scale vertical tail/rudder assembly was tested with a zero side-slip angle applied to the main vertical tail and a 30° deflection angle applied to the rudder. Two flow control devices are considered herein: the first one includes 24 synthetic jets, and the other 24 sweeping jets. The simulations adopt a hybrid delayed detached eddy simulation (DDES) turbulence model for both geometry configurations. The DDES is particularly well suited for this application where flow separation occurs near the junction between the stabilizer and the rudder. Specifically, the DDES model applies the RANS model on the stabilizer where the flow is fully attached for the considered zero side-slip angle. Meanwhile, the LES model is automatically triggered in the plume of jets and above most of the rudder, downstream of the hinge line where flow separation occurs due to the high rudder deflection angle. With the access to state-of-the-art HPC, the intended study will be the first DDES of sweeping jets compared to synthetic jets on a full aerodynamic configuration. It will provide a complementary and detailed view of the flow interactions, and in turn produce the much-needed insight to understand and exploit the underlying physical mechanisms related to active flow control.

Response of an Infinite Beam on a Locally Inhomogeneous and Non-linear Winkler Foundation Excited by a Constant Moving Load

Andrei B. Faragau*, Karel N. van Dalen**

*Delft University of Technology, **Delft University of Technology

ABSTRACT

Transition radiation is emitted when a source moves along a straight line with constant velocity and acts on or near an inhomogeneous medium [1,2]. Transition radiation occurs, for example, when a train crosses an inhomogeneity in the railway track, such as a transition in foundation stiffness. As the velocity of the trains becomes closer to the wave velocity in the subsoil, wave radiation is amplified and may cause plastic deformation in the transition zone. Studies of transition radiation in finite one-dimensional systems with non-linear foundation behaviour are available in the literature. However, studies that properly account for the infinite extent of the system are not. To this end, the system composed of an infinite beam resting on a locally inhomogeneous and non-linear Winkler foundation, and subjected to a constant moving load is analysed in this paper. The Winkler foundation is assumed to be piecewise linear, and the system thus behaves linearly between non-linear events. Therefore, the solution can be obtained using a mixed time-frequency method [3]. The use of the Finite Difference Method for the spatial discretization combined with derived non-reflective boundary conditions enables us to simulate the behaviour of an infinite system; the computational domain covers the area with the transition in foundation stiffness. Results show that the plastic deformation in the transition zone is a consequence of constructive interference of the excited free waves and the so-called eigenfield that moves with the load. Increasing the load velocity, decreasing the transition length (i.e., smoothness) and/or increasing the foundation stiffness dissimilarity leads to amplified free wave excitation, and consequently to stronger constructive interference and larger plastic deformation. The model and solution method presented in this paper can be used for preliminary design of transition zones. Given the stiffness jump and the maximum train velocity, the optimum length of the transition zone can be obtained such that minimum damage results in the railway track. REFERENCES [1] A.I. Vesnitskii and A.V. Metrikin, Transition radiation in mechanics. *Physics-Uspekhi* 39, pp. 983-1007, 1996. [2] K.N. van Dalen, A. Tsouvalas, A.V. Metrikine, and J.S. Hoving. Transition radiation excited by a surface load that moves over the interface of two elastic layers. *International Journal of Solids and Structures* 73-74, pp. 99–112, 2015. [3] J.S. Hoving and A.V. Metrikine. A mixed time-frequency domain method to describe the dynamic behaviour of a discrete medium bounded by a linear continuum. *APM Proceedings*, St. Petersburg, Russia, 2015.

Ratcheting and Mean Stress Relaxation in Polycrystalline Aggregates - a Mesoscopic Perspective

Harris Farooq^{*}, Samuel Forest^{**}, David Ryckelynck^{***}, Georges Cailletaud^{****}

^{*}Centre des Matériaux Mines ParisTech, ^{**}Centre des Matériaux Mines ParisTech, ^{***}Centre des Matériaux Mines ParisTech, ^{****}Centre des Matériaux Mines ParisTech

ABSTRACT

When a geometry is cyclically loaded under a mean stress or strain, ratcheting as well as mean stress relaxation are observed. Classical macroscopic models produce both quantities in excess as opposed to experimental findings [1]. Purely phenomenological solutions have been proposed in the framework of macroscopic plasticity models, and studies have been devoted to the intragranular behaviour, but little attention has been paid to model such phenomena using polycrystal aggregates especially going up to the regime of cyclic mechanical stability. It is shown that the interaction between different grains is enough to cater for such complex phenomena using crystal plasticity for FCC crystals. Light will be shed on how different grains accommodate each other and how the classical definition of constant rate ratcheting is nearly impossible in a virtual polycrystal. More importantly, a detailed study will allow us to show that, for a prescribed stress loading, the absence of ratcheting on a macroscopic level does not mean that local steady state is achieved [2]. Analytic diagrams will also be built to give an insight on how to stay in the ratcheting regime or to switch to elastic-plastic accommodation. With regards to mean stress relaxation, a start will be taken from a single crystal model depicting different relaxed stable regimes. Then a transition from a single to a representative polycrystal will be presented focusing on the capacity of the polycrystal model to reproduce experimental behaviour. Different mean stress relaxed hysteresis regimes will be depicted and attention will be paid to the local evolution of plasticity. To go up to asymptotic values, for a large range of loading parameters, model reduction techniques as well as strictly rate-independent models will also be incorporated [3]. References: [1] J. L. Chaboche, D. Nouailhas, Constitutive modeling of Ratchetting effects - Part I: experimental facts and properties of the classical models, J. Eng. Mater. Technol. 111, 384 – 392, 1989 [2] Y. Guilhem, S. Basseville, F. Curtit, J-M. Stephan, and G. Cailletaud. Investigation of the effect of grain clusters on fatigue crack initiation in polycrystals. International Journal of Fatigue, 32(11):1748 – 1763, 2010 [3] D. Ryckelynck, D. M. Benziane, A. Musienko, and G. Cailletaud. Toward “green” mechanical simulations in materials science. European Journal of Computational Mechanics, 19(4):365–388, 2010.

From Fibre Reinforced Concrete Lined Tunnels to Catalysts for Hydrogen Production: Applications of FEMDEM Technology

Ado Farsi^{*}, John-Paul Latham^{**}

^{*}Imperial College London, ^{**}Imperial College London

ABSTRACT

Algorithms for FEMDEM simulations started to be proposed from the 90s. Extensive developments and applications of the FEMDEM method have been carried out after the release of the open source Y-code by Munjiza in 2004, and different versions have been released, including the code developed from the collaboration between Queen Mary University and Los Alamos National Laboratory, the Y-Geo and Y-GUI software that have been developed by the Geomechanics Group led by Giovanni Grasselli at Toronto University, and VGeST (Virtual Geoscience Simulation Tools) released by the Applied Modelling and Computation Group (AMCG) at Imperial College London. Recently the AMCG has upgraded and renamed VGeST as 'Solidity'. A commercial FEMDEM code developed by Geomechanica (www.geomechanica.com), has also been released in Canada, although its application has been limited to modelling geomaterials. While the first Y-code employed finite strain elasticity coupled with a smeared crack model to capture deformation, rotation, contact interaction and fragmentation, the AMCG at Imperial College has greatly improved the code, implementing a range of constitutive models in 3D, thermal coupling, parallelisation and a faster contact detection algorithm. Two applications of FEMDEM will be presented in this talk: One is that to the simulation of fracture propagation in fibre-reinforced-sprayed-concrete (FRSC) lined tunnels, which has been the object of recent research. Since this was the first attempt at using FEMDEM to simulate fracture in FRSC structures, a new joint-element constitutive model for fibre-reinforced concrete has been implemented and validated with three-point bending experimental data. The code has also been applied to a practical tunnel design case study to better understand the post-crack behaviour of FRSC linings. The ultimate objective is to reach a better understanding of the fracture mechanics and crack propagation behaviour of FRSC tunnels. The second application is that to the simulation of packing and pellet fragmentation. Numerical simulations have been validated and used to describe the pellet packing structure in fixed-bed reactors and the fragility of the pellets against applied loads. The ultimate objective of this research is to provide a satisfactory description of how the shape of pellets influences their packing density and the structural integrity of the pack.

Personalized Electromechanical Modeling of Pathophysiological Left Atrial Function

Thomas Fastl^{*}, Christoph Augustin^{**}, John Whitaker^{***}, Ronak Rajani^{****}, Mark O'Neil^{*****}, Gernot Plank^{*****}, Martin Bishop^{*****}, Steven Niederer^{*****}

^{*}King's College London, ^{**}University of California, Berkeley, ^{***}King's College London, ^{****}King's College London, ^{*****}King's College London, ^{*****}Medical University of Graz, ^{*****}King's College London, ^{*****}King's College London

ABSTRACT

Atrial fibrillation (AF) is a supraventricular tachyarrhythmia characterized by uncoordinated atrial activation with consequent deterioration of mechanical function and associated with increased morbidity and mortality. The complex interactions between electrics and mechanics in combination with the underlying anatomy provide multiple potential pathways through which an altered electromechanical environment adversely affects atrial physiology and function. Personalized computational modeling provides a novel framework for integrating and interpreting the combined role of atrial electrophysiology and biomechanics in AF development and sustenance. Personalized computational models were generated from high-resolution coronary computed tomography angiography (CTA) data and discretized into high-resolution tetrahedral finite element meshes. The complex left atrial myofiber architecture was estimated using an automated approach informed by anatomical and morphological images and based on local solutions of Laplace's equation. Cellular electrophysiology was represented using a biophysically-based human atrial cell model, while the propagation of the electrical activity was described by the monodomain model. Experimental biaxial mechanical tension test data of human atrial tissue were reinterpreted using a microstructurally-based anisotropic strain-energy function and represented the mechanical response of the left atrial myocardium. The coupling between electrophysiology and biomechanics was achieved using a biophysically-based active contraction model adapted to human atrial cell measurements. The hemodynamic response at the pulmonary veins and the mitral valve was governed by a phase-dependent Windkessel model, while the effect of the ventricles was incorporated using displacement trajectories. Personalized computational models generated from high-resolution coronary CTA data included the heterogeneous thickness distribution of the left atrial myocardium and qualitatively reflected the complex left atrial myofiber architecture. The specific impact of an altered electromechanical environment, i.e., changes in myocardial stiffness, blood pressure, and ventricular deformation, on left atrial function over the individual phases of the cardiac cycle were quantified. This allows the comparison between healthy controls and patients with different pathological conditions to quantitatively investigate the link between electrophysiology and biomechanics and identify the capacity of the atria to sustain AF.

Recent Improvements in the ADvanced CIRCulation (ADCIRC) Model for Cross-scale Unstructured Finite Element Baroclinic Simulations

Arash Fathi^{*}, Ali Samii^{**}, Casey Dietrich^{***}, Clint Dawson^{****}, Kendra Dresback^{*****}, Rosemary Cyriac^{*****}, Cheryl Ann Blain^{*****}

^{*}Institute for Computational Engineering and Sciences, ^{**}University of Texas at Austin, ^{***}North Carolina State University, ^{****}University of Texas at Austin, ^{*****}University of Oklahoma, ^{*****}North Carolina State University, ^{*****}Naval Research Laboratory

ABSTRACT

We discuss a series of improvements that we have made in ADCIRC in order to improve the quality of baroclinic simulations for cross-scale ocean models. We show how each of these improvements provides more accurate results for a series of test models. Next, we show how these improvements enhance the quality of simulation results for a Gulf of Mexico model. ADCIRC utilizes an unstructured grid, which allows it to accurately capture high-resolution bathymetry. Due to the unstructured nature of the grid, higher mesh resolution can be used in regions of interest, or near the mouth of the rivers where fresh water gets mixed with saline water, or in areas where solution gradient is large. Our improvements include systematic smoothing of bathymetry in regions where the bathymetry is steep, but mesh resolution is not adequate. We also discuss a scheme for the accurate computation of the baroclinic pressure gradients. Since our unstructured grid encompasses a wide range of spatial scales, we use biharmonic horizontal diffusion and viscosity operators to avoid over-smoothing. We present an adaptive filtering strategy, and show how it can be used to eliminate noise from the computed quantities when needed. We will show simulation results of realistic situations and report encouraging results.

A Review of FSI Techniques for Heavy Fluids - Focus on a Generic Adaptive Framework for Flows with Interfaces Interacting with Failing Structures Applied to Failing Tanks under Impact

Vincent Faucher*

*French Energy Commission (CEA)

ABSTRACT

The present contribution is first dedicated to the review of some industrial fluid-structure situations of interest involving heavy fluids (i.e. water, liquid metals or oil for instance), classically imposing a fully coupled solution of the FSI problem, and the associated modeling and solving techniques. Situations like flow in rod bundles, with potential additional mechanical excitation, sloshing in tanks, explosion in pools with immersed structures, impact on pipes... are considered, in an effort to categorize the phenomena and exhibit some relevant and general principles to deal with their numerical representation with accuracy, robustness and efficiency. Many of the situations discussed above shall be addressed in the course of the corresponding Mini-Symposium. The second part of the contribution thus consists in a focus on the particular, yet common in the field of safety for industrial installations, case of fast transient interaction between flows with interfaces and structures under large deformations potentially leading to failure. The main goal of the proposed research is then to introduce a generic adaptive framework to provide high-resolution solutions with an automatic tracking of wave fronts and physical interfaces through a set of fully combinable mesh refinement indicators.

Hybrid Hyper-reduction Method Applied to Contact Mechanics with Non-linear Material Behavior

Jules Fauque^{*}, David Ryckelynck^{**}, Isabelle Ramière^{***}

^{*}MINES ParisTech, PSL research university, Centre des Matériaux, CNRS UMR 7633 — CEA Cadarache,

^{**}MINES ParisTech, PSL research university, Centre des Matériaux, CNRS UMR 7633, ^{***}CEA Cadarache

ABSTRACT

The model reduction of mechanical problems involving contact remains an important issue in computational solid mechanics. We propose an extension of the classical hyper-reduction method based on a reduced integration domain [1] to frictionless contact problems written by a mixed formulation and numerically solved using Lagrange multipliers that physically represent the contact forces. As the potential contact zone is naturally reduced through the reduced mesh involved in hyper-reduced equations, the dual reduced basis is chosen as the restriction of the dual full-order model basis. Indeed, only the contacts in the RID are treated but with a local high fidelity. We then obtain a hybrid hyper-reduced model combining empirical modes for primal variables with finite element approximation for dual variables. If necessary, the inf-sup condition of this hybrid saddle-point problem can be enforced by extending the hybrid approximation to the primal variables. This leads to a hybrid hyper-reduced/full-order model strategy. By this way, a better approximation on the potential contact zone is furthermore obtained. As for the classical hyper-reduction method, the primal solution is obtained on the whole domain thanks to the related reduced basis. The contact forces can be reconstructed, if needed, on the potential contact zone by post-processing the HR predictions. In [2], the proposed hybrid hyper-reduction strategy has been successfully applied to a one-dimensional static obstacle problem and also to a three-dimensional contact problem between two linearly elastic bodies. The method gives a good approximation of the contact forces, especially compared to other existing model order reduction approach [3]. The hybrid hyper-reduced method is currently extended to deal with non-linear material behavior. The first results confirm the efficiency of the proposed approach in terms of precision and speed-up. [1] D. Ryckelynck [2009]: "Hyper reduction of mechanical models involving internal variables". International Journal for Numerical Methods in Engineering, 77(1):75–89 [2] J. Fauque, I. Ramière and D. Ryckelynck [2017]: "Hybrid hyper-reduced modeling for contact mechanics problems". Submitted [3] M. Balajewicz, D. Amsallem and C. Farhat [2015]: "Projection-based model reduction for contact problems". International Journal for Numerical Methods in Engineering, 106(8):644–663

CONTINUUM FINITE DEFORMATION HYDRODYNAMICS OF GRANULAR FLOWS

ALOMIR H. FAVERO NETO*, RONALDO I. BORJA[†]

Stanford University
473 Via Ortega
Stanford, CA, USA

*alomir@stanford.edu, [†]borja@stanford.edu

Key words: Granular flows, Hydrodynamics, SPH method, Finite deformation, Plasticity.

Abstract. Simulation of granular flows finds applications in many engineering, computational and industrial problems. One problem in particular is of special interest here: the simulation of sediment flows, like debris-flows, mudflows and landslides. These phenomena are among the most threatening to lives and property as the recent (2018) mudflow events in California highlight. In order to evaluate these phenomena quantitatively, we present a Lagrangian formulation for simulating the continuum hydrodynamics of granular flows. Our formulation is based on the multiplicative elasto-plasticity theory for finite deformations. We use the family of smoothed particle hydrodynamics (SPH) methods to implement our formulation, which has some advantages over the traditional Eulerian formulations usually applied within the SPH method. We also propose a variant of the conventional dynamic boundary conditions to simulate the solid boundary in our simulations. To validate our implementation, we perform a set of benchmark plane strain simulations of laboratory-scale collapse tests of dry sand columns. Results from these simulations suggest that the formulation is robust enough to model the continuum hydrodynamics of granular flows in a laboratory-scale setting. The boundary condition proposed is capable of imposing a non-penetration and (partial) no-slip boundary condition without resorting to complicated contact algorithms or determining boundary planes and their normal vectors. Furthermore, the finite deformation formulation does not require the time integration of strain or stress rates, bypassing the necessity of determining objective rates, and hence, satisfying objectivity naturally. Finally, since in our formulation the only variables updated at each time step are the velocities and positions, the computational implementation is simpler and more efficient. The potential of the technique for modeling more complex field-scale scenarios characterized by complex geometries and multi-physical processes is evident and is the next goal for the research.

1 INTRODUCTION

The recent events (2018) in Santa Barbara county, California, are a reminder of the serious treat mudslides and debris-flows pose to property and life. There has been significant progress on the numerical simulation of granular flows, as we moved on from rudimentary slope stability analysis, based on static equilibrium of homogeneous bodies, to complex physical models able to account for the coupled effects of heterogeneous sediment deformation and ground-water flow. Many such models for landslide triggering rely on a mesh discretization of the physical domain [3, 6-8, 13, 22, 25, 29] which is limited to small deformations due to mesh connectivity. More recently, the literature has seen the development of a class of continuum particle methods capable of handling the large deformations involved in granular flows. Examples of such methods are the *Material Point Method* [2,16], *peridynamics* [23], *reproducing kernel particle Method* [36], and the *smoothed particle hydrodynamics* (SPH) method [18,31]. In particular, the SPH method (our method of choice) has been applied to investigate slope stability problems using plasticity theory [10,11,14,30] and solid-fluid interaction [9,12], as well as implementations considering hypoplastic model [20,33] and granular inertia effects [32].

Common to all the works mentioned is the usage of kernel calculations based on the current position of particles (Eulerian kernel) and the tensorial quantities of interest are represented in their Eulerian form. Furthermore, they all apply the Jaumann [34] stress rate to try obtaining objectivity for finite deformation calculations. Apart from the lack of uniqueness of such stress rates, the use of Eulerian kernels is known to produce numerical issues for materials with tensile strength, the so-called tensile instability [19].

In this work, we adopt a different approach, and explore a Lagrangian finite deformation formulation. The constitutive model is a hyperelasto-plastic one, based on the multiplicative split of the deformation gradient tensor. The advantages of such an approach are manifold and include bypassing the issue of the rate form of constitutive models [35], and the absence of tensile instability and lower computational costs for the total Lagrangian scheme. On top of these advantages, since SPH accuracy and stability are directly related to the particle's arrangement (or disorder), an updated or total Lagrangian approach relies on a more stable configuration of particles which improves these characteristics of the method. The use of hyperelasticity and multiplicative plasticity enables the state of stress to be uniquely determined from the current state of elastic strain, which depends only on the update of the particles' positions, hence reducing the integration error associated with an additional integration of strain and stress rate equations. Finally, all the standard constitutive update algorithms for infinitesimal deformation plasticity remain unchanged and can be applied directly [34].

The sequence of presentation is as follows: Section 2 presents a brief introduction to the finite deformation continuum formulation and constitutive framework; Section 3 presents the implementation aspects to the SPH method; Section 4 presents the results of our numerical simulations and their comparison with experimental data; and Section 5 presents the conclusions and ideas for further work.

2 CONTINUUM FORMULATION AND CONSTITUTIVE FRAMEWORK

Following Lee's theory [24], consider an elementary volume with reference position vector, \mathbf{X} , that has moved to a new position in the current configuration $\mathbf{x}(\mathbf{X}, t) = \mathbf{X} + \mathbf{u}(\mathbf{X}, t)$, where $\mathbf{u}(\mathbf{X}, t)$ is the displacement vector relative to the reference configuration. We define the deformation gradient \mathbf{F} as:

$$\mathbf{F} = \frac{\partial \mathbf{x}}{\partial \mathbf{X}} = \mathbf{1} + \frac{\partial \mathbf{u}}{\partial \mathbf{X}}, \quad (1)$$

where $\mathbf{1}$ is the second order identity tensor. The deformation gradient tensor can be multiplicatively decomposed into an elastic, \mathbf{F}^e , and a plastic, \mathbf{F}^p , parts:

$$\mathbf{F} = \mathbf{F}^e \cdot \mathbf{F}^p. \quad (2)$$

We can now write the elastic left, and plastic right, Cauchy-Green tensors as follows:

$$\mathbf{b}^e = \mathbf{F}^e \cdot \mathbf{F}^{eT}, \quad \mathbf{c}^p = \mathbf{F}^{pT} \cdot \mathbf{F}^p. \quad (3)$$

Furthermore, we can determine the stress state through a hyperelastic equation of the form:

$$\boldsymbol{\tau} = J\boldsymbol{\sigma} = 2 \frac{\partial \Psi}{\partial \mathbf{b}^e} \cdot \mathbf{b}^e, \quad (4)$$

where $J = \det(\mathbf{F})$, $\boldsymbol{\sigma}$ is the Cauchy stress tensor, $\boldsymbol{\tau}$ is the Kirchhoff stress tensor, and $\Psi = \Psi(\mathbf{b}^e)$ is the elastic stored energy function. We only consider here elastically isotropic materials, which alongside material frame invariance suggests rewriting Equation (4) as a function of the principal values of \mathbf{b}^e , b_A^e ($A = 1, 2, 3$). Following [34], we can write $\Psi = \Psi(\varepsilon_1^e, \varepsilon_2^e, \varepsilon_3^e)$, where ε_A^e are the principal elastic logarithmic stretches, $\varepsilon_A^e = \ln(\lambda_A^e)$, with $\lambda_A^e = \sqrt{b_A^e}$. Finally, the elastic constitutive equation (4) takes the form:

$$\tau_A = \frac{\partial \Psi}{\partial \varepsilon_A^e}, \quad (5)$$

where τ_A are the principal values of $\boldsymbol{\tau}$.

To complement our constitutive model, we consider a rate-independent plastic response characterized by a yield condition of the form:

$$\mathcal{F} = \mathcal{F}(\tau_1, \tau_2, \tau_3, k) = 0, \quad (6)$$

where k is a plastic internal variable that determines the size of the elastic region. If the flow rule is non-associative, we have $\dot{Q} \neq \dot{\mathcal{F}}$, where Q is a plastic potential. The flow rule is given by

$$-\frac{1}{2} \mathcal{L}_v \mathbf{b}^e = \dot{\gamma} \frac{\partial Q}{\partial \boldsymbol{\tau}} \cdot \mathbf{b}^e, \quad (7)$$

where $\mathcal{L}_v \mathbf{b}^e$ is the Lie derivative of \mathbf{b}^e , and $\dot{\gamma}$ is the consistency parameter rate. Without further detail (the reader is referred to [35] for the complete derivation), one can show that the standard form of the elastic strain update from infinitesimal formulation is recovered as follows in principal component space

$$\varepsilon_{A,n+1}^e = \varepsilon_{A,n+1}^{e,tr} - \Delta\gamma_{n+1} \frac{\partial Q}{\partial \tau_{A,n+1}}, \quad (8)$$

where the subscript $n + 1$ refers to the values at the end of a typical time interval $[t_n, t_{n+1}]$. Equation (8) is obtained through the usual elastic predictor-plastic corrector scheme, where if the updated state of stress lies within the yield surface, $\mathcal{F} \leq 0$, the step is elastic, and the new state of stress is determined directly from Equation (5) and $\Delta\gamma_{n+1} = 0$.

If the step is not elastic, Equation (8) is solved alongside the yield function (6) for the three elastic logarithmic stretches plus the consistency parameter $\Delta\gamma$. This system is usually non-linear and requires a local Newton-Raphson iteration [5,35]. In SPH, this is performed at each particle for both updated and total Lagrangian schemes. The next section presents the SPH basic formulation and some implementation aspects.

3 SPH IMPLEMENTATION

The SPH method is a continuum method applicable to boundary value problems. The dynamic equation of equilibrium in the reference configuration (Lagrangian form) has the strong form:

$$\mathbf{a} := \frac{d\mathbf{v}}{dt} = \frac{1}{\rho_0} \text{DIV}(\mathbf{P}) + \mathbf{g}, \quad (9)$$

where \mathbf{P} is the first Piola-Kirchhoff stress tensor, ρ_0 is the reference density, \mathbf{g} is the body force per unit of mass (gravity), and $\text{DIV}(\cdot)$ is the divergence operator with respect to the reference coordinates. This dynamic balance is subject to boundary and initial conditions as well. The reader is directed to [17,26,28,38-40] for more information about the SPH method and implementation details.

We adopt an updated Lagrangian scheme in this work [4,40] in which the reference configuration is updated at each time step, thus, the reference configuration is the one at time t_n , and the current configuration is the one at time t_{n+1} . Deformation is driven by the relative displacement $\Delta\mathbf{u}_{n+1} = \mathbf{u}_{n+1} - \mathbf{u}_n$ and the relative deformation gradient, now denoted \mathbf{f}_{n+1} , which assumes the role of the deformation gradient \mathbf{F}_{n+1} . Given that at time t_n all necessary variables are known for a given particle i , the only update equations we need to solve are for velocity and position,

$$\mathbf{v}_{i,n+1} = \mathbf{v}_{i,n} + \mathbf{a}_{i,n} \Delta t, \quad (10)$$

$$\mathbf{x}_{i,n+1} = \mathbf{x}_{i,n} + \mathbf{v}_{i,n+1} \Delta t. \quad (11)$$

The time step Δt must obey the Courant-Friedrich-Lewy (CFL) condition [26] for stability, which is given by

$$\Delta t = \alpha \frac{h}{c_v}, \quad (12)$$

where $\alpha \leq 1$ is a scalar, $h = 1.5\Delta$ is the smoothing length, Δ is the initial interparticle distance, and c_v is a numerical sound speed for the material defined as

$$c_{v,i} = \max \left(\sqrt{\frac{E_0}{\rho_{i,0}}}, \sqrt{\frac{K_0}{\rho_{i,0}}} \right), \quad (13)$$

where E_0 and K_0 are the initial tangent and bulk elastic modulus of the material.

The relative deformation gradient is calculated with the Lagrangian kernel gradient, defined by the particle arrangement at time t_n as follows

$$\langle \mathbf{F}_i \rangle_{n+1} = \sum_{j=1}^N \frac{m_j}{\rho_{j,n}} (\Delta \mathbf{u}_{j,n+1} - \Delta \mathbf{u}_{i,n+1}) \otimes \nabla_n W_{ij}, \quad (14)$$

where W is the kernel function, and $\nabla_n W_{ij} = \nabla W(\|\mathbf{x}_{i,n} - \mathbf{x}_{j,n}\|, h)$. The balance of linear momentum, Equation (9) in SPH has the form

$$\langle \mathbf{a}_i \rangle_{n+1} := \sum_{j=1}^N m_j \frac{(\mathbf{P}_{i,n+1} + \mathbf{P}_{j,n+1})}{\rho_{i,n} \rho_{j,n}} \cdot \nabla_n W_{ij} + \mathbf{g}_i. \quad (15)$$

Finally, the balance of mass in Lagrangian form is obtained by updating the mass density through the following kinematic relationship

$$\rho_{n+1} = \frac{\rho_n}{J_{n+1}}, \quad (16)$$

where J_{n+1} is the determinant of the relative deformation gradient tensor, Equation (14). In all our simulations, we used the Wendland C6 kernel [15].

The last aspect of implementation is the imposition of solid wall boundaries, meaning that soil particles should not penetrate them, and an approximate no-slip condition should be attained. We adapt the formulation of Adami et al. [1]. In this approach, the stress of soil particles near a solid boundary are extrapolated to the boundary particles, which enter the calculation through Equation (15). The boundary particles are also accounted for when calculating the deformation gradient of soil particles. Given a boundary particle, b , the stress associated with it is given as:

$$\mathbf{P}_b = \sum_{s=1}^{N_s} \frac{m_s}{\rho_s} [\mathbf{P}_s + \rho_s \mathbf{g}_s \otimes (\mathbf{x}_s - \mathbf{x}_b)] \tilde{W}_{bs}, \quad (17)$$

where s refers to neighboring soil particles, and \tilde{W}_{bs} is the normalized kernel given by

$$\tilde{W}_{bs} = \frac{W_{bs}}{\sum_{s=1}^{N_s} \frac{m_s}{\rho_s} W_{bs}}. \quad (18)$$

The use of the normalized kernel ensures that a homogeneous state of stress is represented exactly. Based on numerical evidence, this formulation yields better geostatic stresses and for the range of simulations performed here, and no boundary penetration was observed. Furthermore, a no-slip boundary condition can be approximately achieved.

4 LABORATORY SCALE TESTS

We implemented this formulation into a Python/Cython-based SPH code. Usage of Cython written modules allows us to keep the dynamic testing capabilities and syntax friendliness of Python, while achieving nearly C-speed with our code. In all the simulations described herein, we adopted an updated Lagrangian scheme, with updates of the reference configuration performed at every time step. This avoids instability problems arising from total Lagrangian schemes [38]. The code structure is very simple, with one main loop that marshals the simulation in time, and one inner loop for the constitutive update, required in the Newton-Raphson solver.

In terms of constitutive models, we specifically utilized a hyperelastic-perfectly plastic model with a Drucker-Prager (DP) yield criterion. The elastic stored energy function chosen is known as the Henky model, given by

$$\Psi = \frac{1}{2} K \ln(J_e)^2 + G \|\mathbf{e}^e\|^2, \quad (19)$$

where K and G are the elastic bulk and shear modulus of the soil respectively, J_e is the Jacobian of the elastic part of the deformation gradient, and \mathbf{e}^e is the deviatoric part of the principal elastic logarithmic stretches.

The DP yield criterion is given by

$$\mathcal{F} = \sqrt{3J_2} + \alpha_\phi p - k \leq 0, \quad (20)$$

where $J_2 = \frac{1}{2} \mathbf{S} : \mathbf{S}$, and \mathbf{S} is the deviatoric part of the Kirchhoff stress tensor. α_ϕ and k are material parameters related to the Mohr-Coulomb parameters, ϕ and c , and are given for the plane strain case by

$$\alpha_\phi = \frac{3\sqrt{3}\tan(\phi)}{\sqrt{9 + 12\tan^2(\phi)}}, \quad (21)$$

$$k = \frac{3\sqrt{3}c}{\sqrt{9 + 12\tan^2(\phi)}}. \quad (22)$$

The plastic potential \mathcal{Q} for the non-associative flow rule is similar to the yield function and is given by

$$Q = \sqrt{3J_2} + \alpha_\psi p, \quad (23)$$

where α_ψ is calculated the same way as Equation (21), substituting the internal friction angle ϕ , by the dilation angle of the soil, ψ .

4.1 Plane strain collapse of dry sand columns

In this set of simulations, our goal was to reproduce the experimental results of [27] to validate our proposed approach and implementation. The experiments consisted of laterally contained sand in a rectangular channel that is instantly allowed to flow laterally. Lube et al. [27] determined that the final runout distance, d_∞ , and final height, h_∞ , of the samples were only functions of a characteristic initial geometric parameter $a = \frac{h_0}{d_0}$. Figure 1 shows a schematic setup of the samples, and the geometric variable of interest.

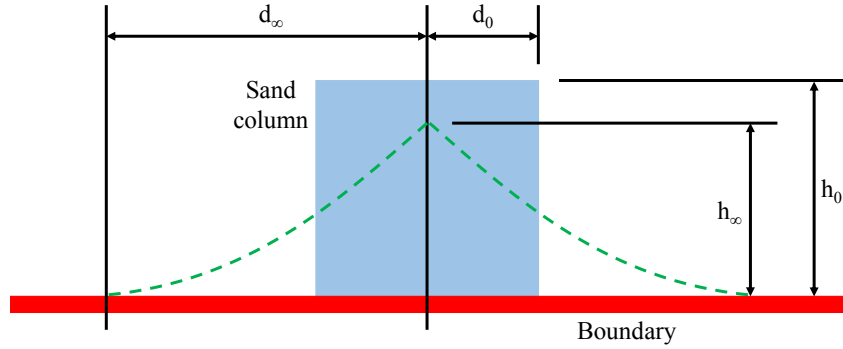
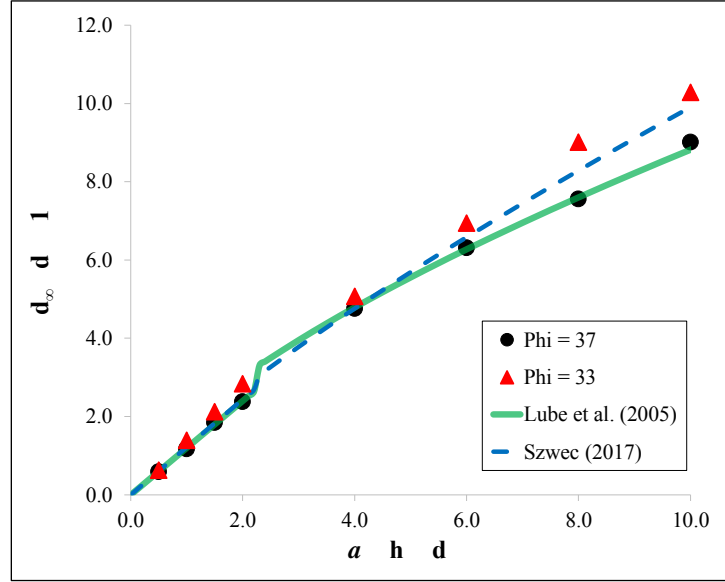


Figure 1: Plane strain sand column collapse: shaded area represents the initial column, and dashed curve represents the final geometry.

We varied the ratio a in our simulations from 0.5 to 10, and used two values of friction angle, $\phi = 33^\circ$, and $\phi = 37^\circ$. These values are similar to the ones used in other works [14,32,37] and serve as a good basis for comparison. The sand was considered cohesionless and in the critical state, $\psi = 0$, consistent with other authors [11,21,30,33]. For all simulations, the initial interparticle distance was chosen equal to 0.02 m, tangent elastic modulus $E = 20.16$ MPa, Poisson ratio $\nu = 0.3$, and time step $\Delta t = 5 \times 10^{-5}$ s. All simulations ran for about 1.5 s. Due to the absence of cohesion, no artificial stress was introduced into the formulation. We also did not use any artificial viscosity or damping term to treat stress oscillation. Figure 2 below shows the simulation results on top of the prediction curves determined experimentally by Lube et al. [27], and numerically obtained with the SPH method by Szewc [37].


 Figure 2: Non-dimensional runout distance versus initial geometric ratio a .

Based on our scatterplot, a least squares curve was adjusted, yielding the following relationship between the runout distance and the geometric ratio, a , for $\phi = 37^\circ$:

$$\left(\frac{d_\infty}{d_0}\right) = \begin{cases} 1 + 1.2a & (0 \leq a \leq 2.3), \\ 1 + 1.83a^{0.69} & (a > 2.3). \end{cases} \quad (24)$$

The results agree very well with those reported in [27]. The median error between curves is approximately 1.45%, with a standard deviation of 0.71%. Even for $\phi = 33^\circ$, and $a > 8.0$, the maximum error is approximately 12%. Figure 3 shows the same plot for the final height of the column.

Once again, a least squares curve was fit to the scattered data of $\phi = 37^\circ$ as follows:

$$\left(\frac{h_\infty}{d_0}\right) = \begin{cases} 0.98a & (0 \leq a \leq 1.15), \\ 1.03a^{0.69} & (a > 1.15). \end{cases} \quad (25)$$

Similar to the runout distance, the results agree very well with the equations proposed in [27]. The error in the linear range is 2.0%, while for the non-linear range it's less than 7.0%.

4.2 Analysis of the results

There is a discrepancy between the numerical and experimental results. While experimental data show an invariance of the kinematics of flow with respect to the internal friction angle, the same is not true for the numerical model. This result is also observed by other authors [21,27,33,37]. The continuum representation with constant material parameters is not capable of recovering discrete effects, like the so-called granular inertia, and more sophisticated constitutive models and new physics must be added to recover such effects (see [32] for example).

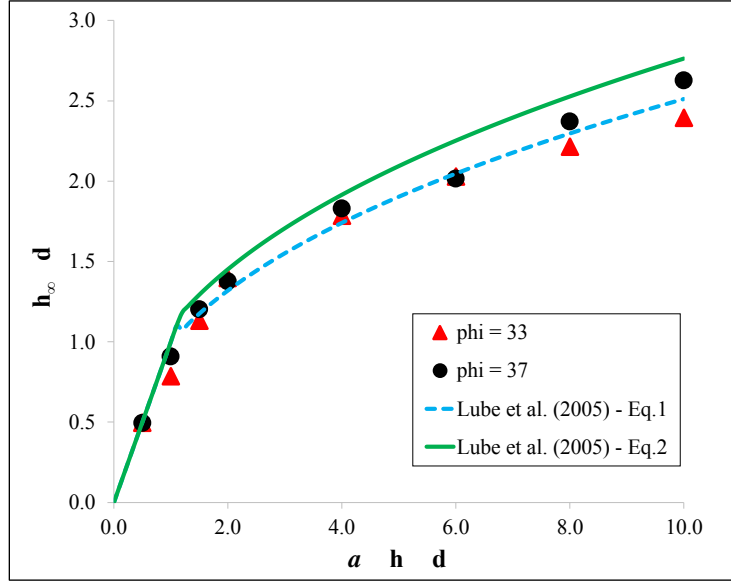


Figure 3: Non-dimensional final height versus initial geometric ratio a . Solid curve is the same as the dashed one for the non-linear part, multiplied by a factor of 1.10.

It is worth mentioning another aspect not presented here due to page limitations; that is, the matter of stress oscillation, very common to the SPH method. In our simulations, we did not include the traditional artificial viscosity term, or any other damping term. We did observe the same type of stress oscillation presented elsewhere [20,21]. Despite this oscillation, it is known that SPH (fortunately) can predict the kinematics of the flow fairly accurately despite such numerical phenomenon. We are currently investigating the use of different damping terms and solution techniques that could reduce stress oscillation within the context of finite deformations. When we simply adopted the standard artificial viscosity, we were able to obtain smoother stress fields. However, the typical checkerboard pattern persisted in the highly strained areas.

CONCLUSION

We presented a Lagrangian, finite deformation implementation of the SPH method. At the formulation's core is the multiplicative split of the deformation gradient [24]. To the knowledge of the authors, this is the first time such a formulation has been applied to granular flows in the context of the SPH method. The advantages of this formulation are numerous, and include: (a) bypassing rate equations for stress and strain, and the choice of an objective stress rate; (b) elimination of the so-called tensile instability if a total Lagrangian scheme is applicable; and (c) reduction of computational costs associated with neighbor searching algorithms for the total Lagrangian or updated Lagrangian schemes (the latter if the update is not performed at every time step), since the neighbor search algorithm can be performed only every certain number of steps, or only once for the total Lagrangian approach.

A boundary formulation adapted from the work of [1] and cast into the finite deformation framework was also proposed. This formulation is extremely simple and straightforward to incorporate into any SPH code. In all our tests, no penetration was allowed by this formulation and an approximate no-slip condition was attained.

The finite deformation and boundary formulations were tested with great success by simulating laboratory-scale experiments with dry sand. Our results agreed very well with experimental data and peer-related papers. We were able to capture the overall kinematic behavior of the sediment, like the runout distance, final height and geometry of the final deposit. These are promising results that encourage future use of such an approach to field-scale problems like mudflows and debris-flows. Moving forward we are exploring new constitutive models, and techniques to reduce stress oscillation, as well as simulations of field-scale problems.

REFERENCES

- [1] Adami, S., Hu, X.Y., Adams, N.A. A generalized wall boundary condition for smoothed particle hydrodynamics. *Journal of Computational Physics*. (2012) 231:7057-7075.
- [2] Bandara, S., Ferrari, A., Laloui, L. Modelling landslides in unsaturated slopes subjected to rainfall infiltration using material point method. *Int J Num Analyt Meths Geomech*. (2016) 40(9):1358-1380.
- [3] Becker, P.A., Idelsohn, S.R. A multiresolution strategy for solving landslides using the Particle Finite Element Method. *Acta Geotechnica*. (2016) 11:643-657.
- [4] Bonet, J., Lok, T.S.L. Variational and momentum preservation aspects of Smooth Particle Hydrodynamic formulations. *Comput Methods Appl Mech Engrg*. (1999) 180:97-115.
- [5] Borja, R.I. *Plasticity Modeling and Computation*. Springer, Berlin-Heidelberg (2013).
- [6] Borja, R.I., Liu, X., White, J.A. Multiphysics hillslope processes triggering landslides. *Acta Geotechnica* (2012) 7(4):261-269.
- [7] Borja, R.I., White, J.A., Liu, X., Wu, W. Factor of safety in a partially saturated slope inferred from hydro-mechanical continuum modeling. *Int J Num Analyt Meths Geomech*. (2012) 38(2):236-248.
- [8] Borja, R.I., White, J.A. Continuum deformation and stability analyses of a steep hillside slope under rainfall infiltration. *Acta Geotechnica*. (2010) 5(1):1-14.
- [9] Bui, H.H., Fukugawa, R. An improved SPH method for saturated soils and its application to investigate the mechanisms of embankment failure: Case of hydrostatic pore-water pressure. *Int J Numer Anal Methods Geomech*. (2013) 37:31-50.
- [10] Bui, H.H., Fukugawa, R., Sako, K., Wells, C. Slope stability analysis and discontinuous slope failure simulation by elasto-plastic smoothed particle hydrodynamics (SPH). *Geotechnique*. (2011) 361(7):565-574.
- [11] Bui, H.H., Fukugawa, R., Sako, K., Ohno, S. Lagrangian meshfree particles method (SPH) for large deformation and failure flows of geomaterial using elastic-plastic soil constitutive model. *Int J Numer Anal Methods Geomech*. (2008) 32:1537-1570.

- [12] Bui, H.H., Sako, K., Fukugawa, R. Numerical simulation of soil-water interaction using smoothed particle hydrodynamics (SPH) method. *Journal of Terramechanics*. (2007) 44:339-346.
- [13] Camargo, J., Quadros Velloso, R., Vargas, E.A. Jr. Numerical limit analysis of three-dimensional slope stability problems in catchment areas. *Acta Geotechnica*. (2016) 11(6):1369-1383.
- [14] Chen, W., Qiu, T. Numerical Simulations of Granular Materials using Smoothed Particle Hydrodynamics Method. *Geotechnical Special Publication ASCE*. (2011) 217:157-164
- [15] Dehnen, W., Aly, H. Improving convergence in smoothed particle hydrodynamics simulations without pairing instability. *Mon Not R Astron Soc*. (2012) 425:1068-1082.
- [16] Fern, E.J., Soga, K. The role of constitutive models in MPM simulations of granular column collapses. *Acta Geotechnica*. (2015) 11(3):659-678.
- [17] Monaghan, J.J., Gingold, R.A. Smoothed particle hydrodynamics: theory and application to non-spherical stars. *Mon Not R Astron Soc*. (1977) 181:375-389.
- [18] Gholami Khorzani, M., Galindo-Torres, S.A., Scheuermann, A., Williams, D.J. SPH approach for simulating hydro-mechanical processes with large deformations and variable permeabilities. *Acta Geotechnica*. (2017)
<https://doi.org/10.1007/s11440-017-0610-9>.
- [19] Gray, J.P., Monaghan, J.J., Swift, R.P. SPH elastic dynamics. *Comput Methods Appl Mech Engrg*. (2001) 190:6641-6662.
- [20] Guo, X., Peng, C., Wu, W., Wang, Y. A hypoplastic constitutive model for debris materials. *Acta Geotechnica*. (2016) 11:1217-1229.
- [21] He, X., Liang, D. Study of the Runout of Granular Columns with SPH Methods. *Int J Offshore Polar Engrg*. (2015) 25(4):281-287.
- [22] Kakogiannou, E., Sanavia, L., Nicot, F., Darve, F., Schreer, B.A. A porous media _nite element approach for soil instability including the second-order work criterion. *Acta Geotechnica*. (2016) 11(4): 805-825.
- [23] Lai, X., Ren, B., Fan, H., Li, S., Wu, C.T., Regueiro, R.A., Liu, L. Peridynamics simulations of geomaterial fragmentation by impulse loads. *Int J Num Analyt Meths Geomech*. (2015) 39(12):1304-1330.
- [24] Lee, E.H. Elastic-plastic deformation at _nite strains. *J Appl Mech*. (1969) 36:1-6
- [25] Lei, X., Yang, Z., He, S., Liu, E., Wong, H., Li, X. Numerical investigation of rainfall-induced fines migration and its influences on slope stability. *Acta Geotechnica*. (2017) 12(6):1431-1446.
- [26] Liu, G.R., Liu, M.B. Smoothed particle hydrodynamics: a meshfree particle methods. World Scientific, Singapore. (2003).
- [27] Lube, G., Huppert, H.E., Stephen, R., Sparks, J., Freundt, A. Collapses of two-dimensional granular columns. *Physical Review E*. (2005) 72(4).
- [28] Lucy, L.B. A numerical approach to the testing of the fission hypothesis. *The Astronomical Journal*. (1977) 82(12):1013-1024.

- [29] Meng, X., Wang, Y., Wang, C., Fischer, J.-T. Modeling of unsaturated granular flows by a two-layer approach. *Acta Geotechnica*. (2017) 12(3):677-701.
- [30] Nonoyama, H., Moriguchi, S., Sawada, K., Yashima, A. Slope stability analysis using smoothed particle hydrodynamics (SPH) method. *Soils and Foundations*. (2015) 55(2):458-470.
- [31] Pastor, M., Yague, A., Stickley, M.M., Manzanal, D., Mira, P. A two-phase SPH model for debris flow propagation. *Int J Num Analyt Meth Geomech*. (2018) 42(3):418-448.
- [32] Peng, C., Guo, X., Wu, W., Wang, Y. Unified modelling of granular media with Smoothed Particle Hydrodynamics. *Acta Geotechnica*. (2016) 11:1231-1247.
- [33] Peng, C., Wu, W., Yu, H.S., Wang, C. A SPH approach for large deformation analysis with hypoplastic constitutive model. *Acta Geotechnica*. (2015) 10:703-717.
- [34] Simo, J.C. Algorithms for static and dynamic multiplicative plasticity that preserve the classical return mapping schemes of the infinitesimal theory. *Comput Methods Appl Mech Engrg*. (1992) 99:61-112.
- [35] Simo, J.C., Hughes, T.J.R. *Computational Inelasticity*. Springer, New York. (1998).
- [36] Siriakorn, T., Chi, S.-W., Foster, C., Mahdavi, A. u-p semi-Lagrangian reproducing kernel formulation for landslide modeling. *Int J Num Analyt Meths Geomech*. (2018) 42(2):231-255.
- [37] Szewc, K. Smoothed particle hydrodynamics modeling of granular column collapse. *Granular Matter*. (2017) 19(3).
- [38] Vidal, Y., Bonet, J., Huerta, A. Stabilized updated Lagrangian corrected SPH for explicit dynamic problems. *Int J Numer Meth Engrg*. (2007) 69:2687-2710.
- [39] Vignjevic, R., Reveles, J.R., Campbell, J. SPH in a Total Lagrangian Formalism. *Comp Modeling Engrg Sciences*. (2006) 14(3):181-198.
- [40] Violeau, D. *Fluid mechanics and the SPH method: theory and applications*. Oxford University Press, UK. (2012).

Seismic Attenuation in Realistic Fracture Networks

Marco Favino^{*}, Jürg Hunziker^{**}, Klaus Holliger^{***}, Rolf Krause^{****}

^{*}Institute of computational science, Università della Svizzera italiana, ^{**}Institute of Earth Sciences, University of Lausanne, ^{***}Institute of Earth Sciences, University of Lausanne, ^{****}Institute of computational science, Università della Svizzera italiana

ABSTRACT

Seismic imaging of fractures has important applications in geothermal and hydrocarbon exploration, nuclear waste disposal and CO₂ storage. However, direct imaging is generally not possible, because typical seismic wavelengths are much larger than the fracture thickness. Conversely, indirect imaging might be possible, as seismic waves undergo strong attenuation in fractured media due to Fluid Pressure Diffusion (FPD). To better understand FPD in fractured media, we perform numerical upscaling experiments on realistic samples. We model fractures as highly compliant and highly porous features, while the background material is much stiffer and much less porous. In the case of P-waves, an undrained compressibility test is applied to a representative sample of the fractured region of interest. The rectangular sample is compressed by applying a harmonically oscillating vertical displacement along its upper boundary. At the other boundaries no normal displacements of the solid phase are allowed. By solving the quasi-static poroelastic equations in the space-frequency domain, we obtain through numerical upscaling the frequency-dependent and complex-valued stress-strain relations of the probed sample, which then allow for inferring the P-wave velocity dispersion and attenuation. For S-waves, shear tests are used in a similar manner. Due to numerical limitations, such studies were so far limited to simplistic models of fractured media. In this study, we use a newly developed finite-element code to consider fracture networks of realistic complexity and to investigate FPD in relation to fracture connectivity and effective storativity. Computationally efficient and fully “hands-off” adaptive meshing independent of the fracture geometry makes it feasible to run simulations on a large number of stochastically generated realistic fracture networks.

Effective Elastic Properties of Materials with High-Density Cracks

Piotr Fedelinski*, Mateusz Holek**

*Institute of Computational Mechanics and Engineering, Silesian University of Technology, Gliwice, Poland,

**Silesian University of Technology, Gliwice, Poland

ABSTRACT

One of the most important aims of micromechanical modeling is the determination of effective properties of materials containing cracks. Cracks can reduce significantly stiffness and strength of materials. Therefore, it is very important to know the influence of cracks on the overall material properties. Additionally, knowledge about the effective properties can be used to estimate density of defects. Theoretical methods usually give accurate results for low densities of cracks having simple geometry. More general cases can be considered using numerical methods. The aim of the work is analysis of effective elastic properties (Young modulus and Poisson ratio) of plates containing high-density cracks. Materials with branched and intersecting cracks regularly or randomly distributed and oriented are considered. A possible contact of crack surfaces is taken into account. The effective properties are calculated using representative volume elements (RVE) with a large number of cracks. The RVEs can contain cracks in the interior or cracks intersecting boundaries. Many RVEs are analyzed in order to obtain statistically representative results. The RVEs are modeled by using the boundary element method (BEM). The BEM allows simple generation of RVEs with cracks and gives very accurate results [1]. Average strains and stresses in the RVEs are computed using boundary displacements and tractions, which are directly obtained by the BEM. In order to compute effective properties different boundary conditions are imposed on the RVEs: displacements, tractions and mixed conditions. The effect of the size of RVEs on accuracy is studied. An influence of density and orientation of cracks on effective properties are analyzed. Additionally stress intensity factors (SIF) are computed using the path independent J-integral. The maximal and average SIFs in the RVEs are calculated. The computed overall properties are compared with theoretical predictions and available numerical results presented in the literature. Materials with high-density cracks have small Young moduli, however there is no direct quantitative correlation between the stiffness and fracture. Local positions of cracks have strong influence on stress intensity factors while the effective modulus, which is a volume average quantity, is less sensitive to such distributions. 1. Fedelinski P., Analysis of representative volume elements with random microcracks, Chapter 17, Computational Modelling and Advanced Simulation, Eds Murin J. et al., Computational Methods in Applied Sciences 24, Springer Science+Business Media B.V., pp. 333-341 (2011). Acknowledgement: The scientific research is financed by National Science Centre, Poland in years 2016-2019, grant no. 2015/19/B/ST8/02629.

Thermal Buckling Analysis of Composite Laminates with Variable Angle Tows Based on the Three Order Shear Deformation Theory

Li Fei*, Nie Guojun**

*Tongji University, **Tongji University

ABSTRACT

Thermal buckling analysis of composite laminates with variable angle tows is presented in this study. Three order shear deformation plate theory, in conjunction with Chebyshev-Ritz method, is employed in the current formulation. It is assumed that fibre angle of each layer varies linearly along the length of composite laminate and the critical thermal buckling loads of composite laminates with variable angle tows under different boundary conditions and uniform temperature rise are solved. Numerical results are compared with those existed in references and the accuracy of the solutions is validated. Moreover, the effect of different fibre paths and boundary conditions on the critical thermal buckling loads is discussed in numerical examples. It is found that the critical thermal buckling loads of laminate plates with variable angle tows can be improved by selecting proper fibre paths. The numerical results show the critical thermal buckling loads of variable angle tows composite plates under boundary conditions considered can be greatly improved compared with traditional laminates with linear fibers. The results obtained here can provide a reference for the design of this new kind of variable stiffness structures.

Simulating Multiaxial Ratcheting Using Directional Distortional Hardening Models

Heid Feigenbaum*, Christine Welling**, Rene Marek***

*Northern Arizona University, **Northern Arizona University, ***Institute of Thermomechanics Academy of Sciences of the Czech Republic

ABSTRACT

Ratcheting is defined as the accumulation of plastic strains during cyclic plastic loading. Simulating ratcheting is extremely difficult because any small error in plastic strain during a single cycle will add to become a large error after many cycles. Multiaxial ratcheting is particularly difficult to simulate, because not only must the amount of plastic strain be predicted, but also the direction of the plastic strain. Most constitutive models for metals use the associative flow rule which states that the plastic strain increment is in the direction normal to the yield surface. With the associative flow rule, it is imperative to have the shape of the yield surface predicted accurately because relatively small deviations in shape may result in significant deviations in the normal to the yield surface and thus the plastic strain increment. These deviations in the normal the yield surface can accumulate over many cycles to give large errors in the overall ratcheting strain. In order to improve predictions of multiaxial ratcheting, we use constitutive models that include the evolution of the shape of the yield surface. In particular, we present several recent models that include directional distortional hardening (DDH). Directional distortion is the change of shape of the yield surface such that a region of high curvature develops approximately in the direction of loading and a region of flattening develops approximately opposite to the direction of loading. DDH has been observed on a wide variety of metals when a sensitive enough definition of yield is used. The models also include advanced kinematic hardening (KH) rules that have been specifically developed to improve ratcheting predictions. In this work, we compare the simulations using DDH models to those with KH alone and experimental data for multiaxial ratcheting from the literature. Furthermore, we compare results using different step-sizes and numerical schemes to ensure convergence of these models in the simulations. Results suggest that directional distortional hardening can improve ratcheting predictions, however the addition of directional distortional hardening yields relatively small improvements compared to kinematic hardening alone. This strongly suggests the need for additional modeling developments in order accurately predict ratcheting strains under a wide variety of cyclic plastic loadings.

Insights on Constitutive Modeling of Magnetic Shape Memory Alloys

Heidi Feigenbaum^{*}, J. Lance Eberle^{**}, Constantin Ciocanel^{***}, Glen Dsilva^{****}

^{*}Northern Arizona University, ^{**}Northern Arizona University, ^{***}Northern Arizona University, ^{****}Northern Arizona University

ABSTRACT

Magnetic shape memory alloys (MSMAs) are interesting materials because they exhibit large recoverable strain (up to 10%), in response to magnetic or mechanical loading, and fast response time (higher than 1 kilohertz). These characteristics of the MSMAs make them potentially suitable for development of actuators, sensors, and power harvesters. The macroscopic behavior of MSMAs is explained by the fact that the material's martensitic phase comprised of tetragonal unit cells at room-temperature. The different configurations of these tetragonal unit cells are considered different variants of the micro-structure. When no external field is present, the short side of the tetragonal unit cell is approximately parallel with the easy axis for the internal magnetization vector intrinsic to each cell. To minimize magnetic energy, this internal magnetization vector tends to align with external fields. However, in MSMAs, it is easier to achieve this alignment through variant reorientation than by rotating the internal magnetization vectors away from the easy axis. Thus, in the presence of a magnetic field, variant reorientation often occurs. The variants may also reorient in order to align the short side of the unit cell with an applied compressive stress. Variant reorientation leads to mechanical strain and an overall change in the material's magnetization, which can be used for actuation and sensors and power harvesters, respectively. In this work, we explore several constitutive models for the macro-scale behavior of MSMAs. All models are thermodynamics based and ensure that dissipation is positive during any type of loading. However, the discussed models make different assumptions relative to the relevant energy terms and/or the micro-mechanics of MSMAs. For example, we consider models with and without demagnetization included in the Gibbs free energy, and models with and without the rotation of the magnetization vector away from the easy axis. Comparison of these models' predictions facilitate the understanding of the features that are most important for the formulation of a robust constitutive model for MSMAs. In addition to comparing all these models to each other, they are calibrated and validated with experimental results. For calibration, only the material response under mechanical loading is considered, while for validation, model predictions of material's global strain under various magnetic and mechanical loadings is considered. Care is taken to ensure that the model's magnetic inputs correctly correlate to experimental conditions, given the lack of clarity in the literature on the difference between applied and effective magnetic field.

Progressive Failure of Woven Composites at High Strain Rates

Nicolas Feld*, Fabien Coussa**, Benoit Delattre***

*Safran, **Groupe PSA, ***Groupe PSA

ABSTRACT

The high speed progressive failure of woven composites is investigated for automotive crash applications. The material of interest is a 2x2 twill glass fabric embedded in a polyamide 6,6 matrix, designed specifically to address the needs of this industry. A constitutive model is proposed to take into account the influence of strain rates between 0.0001 and 100 /s, which are commonly observed in high speed automotive impacts. The originality of the model lies in its modular formulation, where rate effects are introduced as a supplementary mechanism to an otherwise rate-independent damage elastic-plastic model [1]. As well, a dedicated identification procedure allows all rate effect parameters to be independently identified. Concerning the dynamic simulation of composite structures, such a model may cause a loss of uniqueness of the response if softening regularization is not properly introduced. In this work, a bounded rate damage model is used solely for regularization [2]. It is not used to take into account any physical damage rate effects, related to the speed of Rayleigh waves, which occur at much smaller characteristic times. Several key points related to the use of bounded rate models for regularization purposes are presented. First, bounded rate models enforce a strict upper bound for damage rate. Effectively the damage flow law is affected progressively and does become rate-dependent. We will see how a few precautions in the material parameters and a strict separation of the rate effects – those of interest for the simulation and those used for softening regularization – allow keeping the damage law rate-independent for the considered range. In a second part, the identification of the remaining parameters of the bounded rate model and the effectiveness of the regularization are examined. It will be shown how time and space convergence must be achieved, using time step and mesh refinement respectively, in order for the bounded rate model to prevent loss of uniqueness. As long as the physical rate effects of damage are not sought, an ideal relation between material parameters and time step may also be prescribed in order to limit refinement to the strict necessary minimum, while ensuring regularization. [1] Feld et al. A novel approach for the strain rate dependent modelling of woven composites. Composites Structures, under review. [2] Allix. The bounded rate concept: A framework to deal with objective failure predictions in dynamic within a local constitutive model, IJDM 22 (6), 2013.

Measuring the Plate to Rod Transition during Osteoporosis Progression Independent of Bone Mass

Alessandro Felder^{*}, Richard Domander^{**}, Phil Salmon^{***}, Michael Doube^{****}

^{*}Royal Veterinary College, ^{**}Royal Veterinary College, ^{***}Bruker micro-CT, ^{****}Royal Veterinary College

ABSTRACT

Structure model index (SMI) has been the de facto standard to measure the plate to rod transition during progression of the bone disease osteoporosis (and its animal models) since the 1990s. Studies based on SMI suggest that an initially more plate-like trabecular bone geometry becomes more rod-like during bone mass loss. SMI, however, is seriously biased by bone mass [1]. It is therefore unclear whether reducing bone mass is accompanied by an independent change in geometry. We implemented Ellipsoid Factor (EF) [2] to quantify plates and rods within three-dimensional images in BoneJ2, a plugin collection for ImageJ2, and applied it to images of trabecular bone from bone-loss series. EF relies on axis ratios of ellipsoids that are inscribed within the trabecular bone, and is therefore necessarily unbiased by bone mass, measured as volume fraction (BV/TV). We performed finite element simulations with FEniCS using a validated elastic-plastic constitutive law [3] on the same trabecular bone volumes to explain how rod-plate changes, if they exist at all, influence the apparent modulus, apparent yield strength and, ultimately, fracture risk. [1] Salmon, P. L. et al. (2015) 'Structure Model Index Does Not Measure Rods and Plates in Trabecular Bone', *Frontiers in Endocrinology*, 6. doi: 0.3389/fendo.2015.00162. [2] Doube, M. (2015) 'The Ellipsoid Factor for Quantification of Rods, Plates, and Intermediate Forms in 3D Geometries', *Frontiers in Endocrinology*, 6. doi: 10.3389/fendo.2015.00015. [3] Schwiedrzik, J. et al. (2016) 'Experimental validation of a nonlinear FE model based on cohesive-frictional plasticity for trabecular bone', *International Journal for Numerical Methods in Biomedical Engineering*, 32(4), doi: 10.1002/cnm.2739.

Unification of Geometrically Nonlinear Finite Element Analysis of Solids and Structures

Carlos Felippa*, Carlos Melo**

*Department of Aerospace Engineering Sciences, University of Colorado Boulder, **Department of Aerospace Engineering Sciences, University of Colorado Boulder

ABSTRACT

Geometrically nonlinear structural FEM was introduced in 1960 in an article by Turner, Dill, Martin and Melosh. It evolved rapidly over the next 25 years. The three Lagrangian kinematic descriptions (LKD) in use today: Total Lagrangian (TL), Updated Lagrangian (UL) and Corotational (CR) appeared over the period 1965-1985, and eventually found their way into production FEM codes. Yet none of the three can be viewed as universally applicable because they display strengths and weaknesses that limit their application range. For example, TL finds it hard to cope with very large rotations, whereas CR is hampered by truly large, flow-like deformations. To increase the range, some commercial FEM codes are trying to implement two LKD. But this can be an expensive undertaking since it involves recoding the entire FEM library, which may involve millions of code lines. Can a unified kinematic description be implemented in a single library? The idea is that the user would pick the one that best fits the target problem, like flipping a three-way switch. The presentation describes research in progress that attacks that problem. The basic tool is use of a finite strain measure originally proposed by Seth in 1964 for 1D and extended to 3D tensorial form by Hill in 1981. The Seth-Hill (SH) family has a parameter m called the SH index that varies from 2 to -2. It embodies several well known Lagrangian measures, e.g. Green-Lagrange for $m=2$, Biot for $m=1$, and Almansi-Hamel for $m=-2$. Their Eulerian counterparts can be obtained by switching tensors in the polar decomposition. While offering a nonlinear FEM course, the first author discovered that the nonlinear bar element in 3D could be universally formulated within the SH framework, with the TL, CR and UL forms of the residual and stiffness equations emerging for three m values. Thus a bar element module equipped with the SH index as argument, could produce the three standard descriptions, as well as an infinity of other ones, without need of extensive recoding. E.g., setting $m=0$ would give the Hencky or logarithmic measure, which is preferred by many workers for modeling finite strain elastoplasticity. Extension to the 3-node triangle in 3D is being investigated, using "natural stretch gages" -- an extension of the "strain node" concept developed by the first author in his 1966 thesis, which later evolved into the assumed natural strain (ANS) formulation. Preliminary results appear encouraging.

Continuous Discontinuous Element Method and Its Application to Rock Blasting Process Simulation

Chun Feng^{*}, Shihai Li^{**}

^{*}Key Laboratory for Mechanics in Fluid Solid Coupling Systems, Institute of Mechanics, Chinese Academy of Sciences, ^{**}Key Laboratory for Mechanics in Fluid Solid Coupling Systems, Institute of Mechanics, Chinese Academy of Sciences

ABSTRACT

Continuous discontinuous element method (CDEM) is an explicit numerical method, which is based on generalized Lagrangian equation. According to combining the algorithms of continuous media and discontinuous media together, and by way of element fracturing and edge fracturing, the progressive failure process of rock mass could be simulated well. Rock blasting is a complicated process, involving explosive detonation, stress wave propagation, detonation gas flowing, rock fragmentation, fragments flying and accumulation. To obtain a reasonable numerical result, Landau firing explosive model is adopted to precisely calculate the blasting effect, gas flow model based on crack channel is introduced to simulate rock fracturing under detonation gas, elastic-damage-fracture constitutive law is used to describe the damage and fracture process of rock, and semi-spring & semi-edge combined contact model is introduced to efficiently calculate the flying, collision and accumulation process of large number of fragments. The numerical simulation of explosion crater test is carried out. Flying velocity of fragments, size distribution of fragments and crater volume obtained by numerical simulation are more or less the same as those obtained by experiment, which demonstrates that CDEM and corresponding models is good at simulating rock blasting process. Based on the blasting technology in south region in Anqian open-pit mine in China, a generalized three-dimensional bench blasting model with 3 rows and 21 bore holes is set up, and the complete process from explosive detonation to muckpile formation is carried out. Numerical results show that, except the tensile crack behind the blasting area, the muckpile shape and heaving degree obtained by numerical simulation are accordant with the ones obtained by field test to some extent, which demonstrates the feasibility to simulate the three-dimensional bench blasting by CDEM.

The Research of Effect of Abrasive Properties on Abrasive Water Jet Cutting Based on SPH

Long Feng^{*}, Zengliang Li^{**}, Xiangwei Dong^{***}, Mingchao Du^{****}

^{*}China University of Petroleum, ^{**}China University of Petroleum, ^{***}China University of Petroleum, ^{****}China University of Petroleum

ABSTRACT

The smooth particle hydrodynamics (SPH) method is a Lagrangian method, which is widely used to solve the problem of high velocity impact. Therefore, the study of abrasive water jet cutting with SPH method also has its unique advantages. At present, when using the SPH method to study the problem of abrasive water jet, the following methods are mainly used: Basing on the volumetric flow rates of the two materials, the volume percentages of water and abrasive can be achieved. Then the randomized algorithm is utilized to realize the percentage of two kinds of SPH particle numbers and their distribution. This simplified model neglects the shape parameters of abrasive particles. Therefore, it is impossible to study the effect of different shapes and sizes of abrasive particles on the cutting performance. The model of coupled SPH-FEM is used to simulate the cutting process of abrasive jet. With appropriate material models, it is capable to simulate the relevant damage phenomena in AWJ impact process. However, abrasive particles usually have irregular shape with angularity. Impacts of such particles can cause large plastic deformation or even material removal, which may result in the heavily distorted elements leading to poor accuracy. It is known that most the element-based methods have the similar difficulties. Based on the reasons above, a new calculation model is proposed to study the effect of abrasive particle parameters on cutting performance in this paper. In the method, both fluid and solid are described by SPH, in which water is modeled as viscous fluid with weak compressibility, and metallic target is modeled as elastic-plastic material. Abrasive particles are explicitly included inside the water jet flow and modeled as rigid bodies with specific shape. The interactions among fluid, solid, and abrasive, are modeled using suitable techniques that are commonly used in SPH. With the help of this model, the following work has been completed: The effects of different shapes of abrasive particles on the cutting performance during the cutting process are simulated. The simulation results show that the efficiency of the angular abrasive particle cutting is higher than that of the spherical abrasive particles, but in the process of removing the target material, the shape of the exfoliating material is irregular, indicating that the tangent surface of the angular abrasive particles is worse than the spherical particles. At the same time, the interaction between the abrasive particles can also be obtained.

Multiscale Modeling of the Primary Cilium

Zhe Feng^{*}, Zhangli Peng^{**}

^{*}University of Notre Dame, ^{**}University of Notre Dame

ABSTRACT

We develop a multiscale modeling method to predict the stress and mechanical behavior of a cell with a primary cilium during the thermal fluctuation or deformation under fluid flow. The primary cilium is a microtubule-based organelle that extends from the surface of most vertebrate cells. The cilium has been shown to play important roles in both biophysical and biochemical changes in the extracellular environment. As a fluid sensor, the mechanical and structural properties of the cilium and how these properties contribute to the mechanical sensing channels opening are still incompletely known. Our model shows the response of different parts of the cilium cell in mesoscale level. In our model, dissipative particle dynamics (DPD) method is used for both fluid flow and cell particles. Microtubules, centrosome, membrane, nucleus and other important organelles are included and analyzed in our whole cell model. During the thermal fluctuation and deformation in fluid flow, the rotational spring of the centrosome and the bending stiffness of cilium compete with each other to control this process. In our simulation, we study the effects of microtubules bending rigidity, bilayer bending stiffness and actin cortex shear stiffness in this competition. We provide detailed deformation and stress of the cilium at the mesoscale level in fluid flow and thermal fluctuations with or without the optical trap.

Progress and Challenges with Part-scale Modeling of Powder Bed Fusion Metal Additive Manufacturing

Robert Ferencz^{*}, Rishi Ganeriwala^{**}, Ryan Vignes^{***}, Neil Hodge^{****}

^{*}Lawrence Livermore National Laboratory, ^{**}Lawrence Livermore National Laboratory, ^{***}Lawrence Livermore
National Laboratory, ^{****}Lawrence Livermore National Laboratory

ABSTRACT

Many researchers are exploring thermomechanical modeling of the laser powder bed fusion (PBF) process to gain insights into residual stresses and distortions arising during this metal additive manufacturing process. This is a challenging problem due to the range of scales: temporally from milliseconds for local material transformation to hours and days for overall part fabrication; spatially from 100 microns for the local melt pool versus overall part dimensions. Various approaches are being pursued to identify and implement abstractions rendering the problem computationally tractable while still yielding results providing meaningful insights. We are adapting a general purpose, nonlinear thermal-mechanical finite element code to model the PBF process. First touching upon some of our earlier successes modeling PBF for a stainless steel [1], we then survey challenges we have encountered as we attempt to model more general configurations and material systems. These difficulties have motivated reexamination of our assumptions and approaches, pointing the way toward more general and robust modeling. This work was performed under the auspices of the U.S. Department of Energy by Lawrence Livermore National Laboratory under Contract DE-AC52-07NA27344. LLNL-ABS-744404.

Powder Bed Fusion Metal Additive Manufacturing: Challenges and Progress with Part-scale Modeling

Robert Ferencz*

*Lawrence Livermore National Laboratory

ABSTRACT

Many researchers are exploring thermomechanical modeling of the laser powder bed fusion (PBF) process to gain insights into residual stresses and distortions arising during this metal additive manufacturing process. This is a challenging problem due to the range of scales: temporally from milliseconds for local material transformation to hours and days for overall part fabrication; spatially from 100 microns for the local melt pool versus overall part dimensions. Various approaches are being pursued to identify and implement abstractions rendering the problem computationally tractable while still yielding results providing meaningful insights. We are adapting a general purpose, nonlinear thermal-mechanical finite element code to model the PBF process. First touching upon some of our earlier successes modeling PBF for a stainless steel, we then survey challenges we have encountered as we attempt to model more general configurations and material systems. These difficulties have motivated reexamination of our assumptions and approaches, pointing the way toward more general and robust modeling. We will conclude this talk with some reminiscences of fulfilling years spent studying under and working with Thomas J.R. Hughes. This work was performed under the auspices of the U.S. Department of Energy by Lawrence Livermore National Laboratory under Contract DE-AC52-07NA27344. LLNL-ABS-744404.

A Computational Model of Ballistic Cranial Soft Tissue Wounding Using Smoothed Particle Hydrodynamics: Towards a Forensics Tool

Justin Fernandez*, Eryn Kwon**, Simon Bickerton***, Michael Taylor****

*University of Auckland, New Zealand, **University of Auckland, New Zealand, ***University of Auckland, New Zealand, ****Institute of Environmental Science and Research, New Zealand

ABSTRACT

Introduction: Computational and biomechanical modelling of cranial ballistic wounding can inform the forensic process. One particular type of evidence from a cranial ballistic impact is called 'backspatter'. Backspatter is fluid and brain particle spatter originating from the entry site and travelling against the direction of the bullet, towards the shooter. The reverse directionality of the backspatter has specific evidential value, as it may establish a link between the victim and the shooter via transfer of biological matter as well as positions of the persons involved [1]. Currently, animal and physical models are used to model cranial ballistic wounding and backspatter. However, these models are of high cost and require long manufacturing and setup time. More recently, high performance computing has been used to overcome many ethical and practical costs associated with ballistic research. This study presents an accurate computational model, representing highly complex human anatomy and material properties, to be used as a surrogate cranial model to study gunshots, with specific interest to the 'backspatter' problem. **Methods:** A computational model of a human cranium geometry based on a live female MRI scan was developed consisting of three layers of scalp-skull-brain geometry. The ballistic event was computationally simulated using smooth particle hydrodynamics (SPH) [2], a meshless particle based method, for a projectile shot from a distance of 1 m. The simulation result was validated against a ballistic experimental result of a matching physical model which had equivalent geometry and simulant materials. A high speed video was sampled at the same frame rate as the time steps of the SPH simulation. **Results and Discussion:** The computational model qualitatively reproduced the forward and backspatter particle spray pattern observed in the experiment. Quantitative evaluation of speed, timing and quantity of particles were also consistent. The blowout shape associated with the ballistic event also compared well to the experiment. The tail splash and temporary cavitation mechanisms were both observed and confirmed as major backspatter mechanisms when the subcutaneous gas pocket mechanism was eliminated. The model can be used to evaluate simulant material selection, projectile type and speed impact as well as reveal 'backspatter' patterns relative to the projectile conditions to support forensic evaluation. **References:** 1. Karger B et al, Forensic Pathology Reviews, Totowa, United States, p. 139-172, 2008. 2. Gingold RA and Monaghan JJ, Monthly notices of the Royal Astronomical Society. 181:375-389, 1977.

Multi-model Arlequin Method for Fast Transient Dynamics with Fluid-structure Interaction

Alexandre Fernier^{*}, Vincent Faucher^{**}, Olivier Jamond^{***}

^{*}French alternative energies & atomic energy commission, ^{**}French alternative energies & atomic energy commission, ^{***}French alternative energies & atomic energy commission

ABSTRACT

The simulation of industrial applications — such as crashes, impacts, and explosions — is a real challenge both from a numerical and industrial point of view. Explicit time integrators are widely used in order to treat them, and though they are conditionally stable, they do not require any iterations to deal with non-linearities. Another difficulty is the generation of large meshes. In many industrial applications, such as nuclear safety simulations, it is necessary to locally modify the geometry or physical properties of the model to allow for different settings to be tested. In this paper we propose a multi-model approach for local changes in the geometry of a problem. A first mesh, called the substrate, represents the main geometry, while a second one, called the 'patch', locally improves the modeling of the problem. The patch is independently meshed and superimposed using the Arlequin framework: the kinematic quantities are weakly set equal on a coupling zone and weight parameters are used to represent the relative significance of each model. In this paper we treat the explicit integration (central difference scheme) of the interaction between a fluid (ideal gas), modeled by the Euler equations, and an elastodynamic structure. For both the fluid and structure the momentum equation is considered in non-conservative form and treated using the FEM. The mass and energy conservation are considered in their conservative form and treated in FV. The weight parameters are used to compute the mass matrix and the forces. Thus, they strongly impact the stability of the system and the time step can drop to zero. We present diagonalizing techniques to circumvent this issue. Also, for the momentum equations, the choice of weight parameters is critical. They need to be constant within each element in the coupling zone, and are, therefore, discontinuous across models. In the equilibrium equation for the fluid the pressure forces are weighted so that a force between two elements having the same pressure but different weight arises. Our study quantifies the impact of these ghost forces and proposes to filter them by enriching the coupling. For both the mass and energy conservation equations, either the Arlequin method or a Chimera-like approach can be used. When using the Arlequin framework the use of continuous weight parameters simplifies the computation of boundary conditions. Both approaches are tested and compared with a full chimera approach for the fluid on relevant cases.

Numerical Methods for Fluid-structure Interaction with Immersed Thin-walled Solids

Miguel A. Fernández*, Jean-Frédéric Gerbeau**, Ludovic Boilevin-Kayl***

*Inria Paris, **Inria Paris, ***Inria Paris

ABSTRACT

The numerical methods for the simulation of elastic thin-walled bodies immersed in an incompressible viscous fluid typically fall into one of the following two categories: fitted mesh and unfitted mesh methods. Fitted mesh methods are known to deliver optimal accuracy for moderate interface displacements, but they become cumbersome or lose efficiency in presence of topological changes (e.g., due to contacting solids). Unfitted mesh methods, such as the Immersed Boundary/Fictitious Domain methods, allow for arbitrary interface displacements. Nevertheless, this flexibility comes at a price: the mismatch between the fluid and solid meshes complicates the interface coupling (e.g., introduction of Lagrange multipliers). Among these unfitted mesh alternatives, we mention the Fictitious Domain (FD) method [1] and the recently proposed Nitsche-XFEM method [2]. The FD method with Dirac Lagrange multipliers [1] is relatively simple to implement (only interpolation between meshes are required). Nevertheless, it is known to yield suboptimal accuracy in space and potential interfacial mass loss due to the continuous nature of the pressure approximations across the interface. The Nitsche-XFEM method [3] combines an overlapping mesh treatment of the discrete interfacial discontinuities with a fully consistent enforcement of the interface coupling (Lagrange multipliers free) which guarantees optimal accuracy. However, this requires a specific track of the interface intersections and the integration over cut elements which demands a much more involved implementation. In this work, we provide a comparison of these two approaches on several FSI benchmarks involving moving interfaces and topology changes, which illustrate their respective performances in terms of accuracy. This work has been supported by the start-up companies KephaliOS and Epygon through the MIVANA project. References: [1] N. Diniz dos Santos, J.-F. Gerbeau, J.-F. Bourgat. A partitioned fluid–structure algorithm for elastic thin valves with contact, *Comput. Methods Appl. Mech. Engrg.*, 197, (2008), 1750-1761. [2] F. Alauzet, B. Fabrèges, M.A. Fernández, M. Landajuela. Nitsche-XFEM for the coupling of an incompressible fluid with immersed thin-walled structures, *Comput. Methods Appl. Mech. Engrg.*, 301, (2016), 300–335.

Coupled Electrochemistry and Mechanics in Mesoscale Simulation of Lithium-Ion Cathodes

Mark Ferraro^{*}, Bradley Trembacki^{**}, Victor Brunini^{***}, David Noble^{****}, Scott Roberts^{*****}

^{*}Sandia National Laboratories, ^{**}Sandia National Laboratories, ^{***}Sandia National Laboratories, ^{****}Sandia National Laboratories, ^{*****}Sandia National Laboratories

ABSTRACT

Analysis of lithium-ion battery performance and degradation presents many multi-physics challenges as we look to understand the plethora of coupled mechanisms occurring within a single electrode. Electrochemical reactions in the active material introduce mechanical stresses as cathode particles swell upon lithium intercalation. The presence of a secondary conductive binder phase additionally complicates these mechanisms, altering ionic and electronic conduction pathways, masking available surface area for reaction, and buffering mechanical contacts. Furthermore, mechanical strain in this polymeric phase affects the material's electrical conductivity. These phenomena result in an inextricable electrochemical/mechanical coupling which must be carefully addressed in any computational simulation. This talk will cover complications arising from these coupled physics as well as the mesh characteristics required for accurate mesosstructure reconstruction and system convergence. The conformal mesoscale meshes of particle, conductive binder, and electrolyte phases are generated by the Conformal Decomposition Finite Element Method (CDFEM) algorithm, derived directly from 3D computed tomography data of Li-ion cathodes. Here, we will discuss the effect of mesh resolution on key electrochemical properties and behavior of the half-cell during discharge, the impact of dimensionality on convergence, and computational scalability from a simple two-particle model to a full-thickness cathode reconstruction. Sandia National Laboratories is a multi-mission laboratory managed and operated by National Technology and Engineering Solutions of Sandia, LLC., a wholly owned subsidiary of Honeywell International, Inc., for the U.S. Department of Energy's National Nuclear Security Administration under contract DE-NA0003525.

Vectorization of Riemann Solvers for the Shallow Water Equations with One and Two Layers

Chaulio Ferreira*, Kyle T. Mandli**, Michael Bader***

*Technical University of Munich, **Columbia University, ***Technical University of Munich

ABSTRACT

We evaluate the benefits of applying vectorization to the numerical routines of GeoClaw, a software designed for simulation of depth-averaged geophysical flows. GeoClaw provides a framework for simulations with Finite Volume Methods including Adaptive Mesh Refinement based on layered Cartesian patches and shared memory parallelization (OpenMP). In this work, we considered two different numerical models currently implemented in GeoClaw. The first one is based on plain Shallow Water Equations with a single layer, while the second one uses Shallow Water Equations with two vertical layers, as described in [1]. Our prime focus was to vectorize the Riemann solvers used in the simulations, because they represent the majority of the computational costs in both numerical models. That was accomplished by reorganizing the application data structures such as to make them suitable for vectorization and by adding compiler directives where necessary. Since we rely on auto-vectorization by the compiler, our implementation is portable across various architectures with different SIMD instruction sets. As experimental platform, we use two modern architectures with considerable SIMD vector width: Intel Xeon (Haswell architecture) and Intel Xeon Phi (Knights Landing architecture - KNL). The Haswell processor uses the AVX2 instruction set (256-bit), which is supported by various recent processors; and the KNL uses the AVX-512 instruction set (512-bit), which is supported by the most modern Intel processors and is expected to be supported by the next generations of Intel processors [2]. On the KNL processor, our performance experiments have shown improvements ranging from 2.9 to 5.7 times in the efficiency of the solver subroutines. On the Haswell processor, we have experienced more modest improvements, ranging from 1.5 to 2.1 times. References: [1] Mandli, K.T., 2013. A numerical method for the two layer shallow water equations with dry states. *Ocean Modelling*, 72, pp.80-91. [2] Intel, 2017. Instruction Set Extensions and Future Features - Programming Reference. Available at: <https://software.intel.com/sites/default/files/managed/c5/15/architecture-instruction-set-extensions-programming-reference.pdf>

Multiaxial Fatigue Life Estimation Using an Improved Lemaitre's Continuous Damage Model

Guilherme Ferreira^{*}, Lucival Malcher^{**}, Raniere Neves^{***}

^{*}University of Brasília, ^{**}University of Brasília, ^{***}University of Brasília

ABSTRACT

ABSTRACT Multiaxial fatigue is a phenomenon responsible for the failure of several types of mechanical components. Traditionally, models such as Smith-Watson-Topper and Fatemi-Socie, e.g., are successfully used in predicting fatigue life in proportional multiaxial loads under constant amplitude. However, such models usually fail to adequately predict failures in cases where variable amplitudes and/or non-proportional multiaxial loads are employed. Thus, alternative approaches (continuous damage mechanics [1] and micromechanics of voids, e.g.) have been used to predict fatigue life under complex loads. An improved Lemaitre's model with the function of damage denominator dependent from the level of triaxiality, normalized third invariant and two calibrations points (one axial and other torsional) was successfully used by Malcher and Mamiya [2] as a way of improving the results obtained in monotonic loads under different levels of triaxiality. In the present work the improved Lemaitre's model [2] was used to predict lives in multiaxial fatigue for SAE 1045 steel specimens [3]. The kinematic hardening effect was modeled according to Chaboche's model with 3 backstress terms (2 non-linear and 1 linear). Additionally, an interpolator function was used to determine the damage denominators under axial and torsional conditions. The techniques adopted produced satisfactory results in the analyzed cases. **REFERENCES** [1] Lemaitre, J., Desmorat, R., 2005. Engineering Damage Mechanics: Ductile, Creep, Fatigue and Brittle Failures. Berlin: Springer. [2] Malcher, L., Mamiya, E.N., 2014. An improved damage evolution law based on continuum damage mechanics and its dependence on both stress triaxiality and the third invariant. Int. J. Plast. 56, 232-261. [3] Leese, G.E., Socie, D., 1989. Multiaxial Fatigue: Analysis and Experiments. Advances in Engineering, AE-14. Society of Automotive Engineers.

Out-of-the-Box and Ready-to-Print Optimized Structures in Additive Manufacturing Processes

Nicola Ferro*, Stefano Micheletti**, Simona Perotto***

*Politecnico di Milano, **Politecnico di Milano, ***Politecnico di Milano

ABSTRACT

The recent spread of Additive Manufacturing (AM) techniques has undoubtedly raised interest in a deeper knowledge of production processes and of their potentialities. From an engineering point of view, there is a strong concern in understanding the actual benefits brought by AM, with respect to traditional (subtractive) techniques, still massively exploited. In particular, it is widely agreed that, to take advantage of the peculiar features of AM processes, structures have to be conceived via new paradigms, free from the standard constraints of subtractive procedures. In this respect, topology optimization (TO) provides a relevant mathematical tool for the design of geometries characterized by completely new shapes and features. SIMP (Solid Isotropic Material with Penalization) method represents one of the approaches to TO most frequently investigated in the literature [1]. In more detail, SIMP identifies the optimal material distribution inside an assigned design domain and under certain constraints on the final configuration. Nevertheless, variants of SIMP have been proposed in the literature to overcome some issues arising from the basic procedure and to increase the quality of the resulting structures. In this presentation, we focus on two distinct design objectives, namely, a) a ready-to-print and b) an out-of-the-box optimization. In the first case, we aim at designing structures which are almost ready for the industrial production, containing any post-processing (e.g., smoothing) technique as much as possible. For this purpose, we propose to enrich SIMP algorithm with the employment of computational meshes strictly customized to the optimization procedure [2]. Objective b) is pursued by properly combining a shape [3] with a topology optimization procedure, with an additional benefit on the objective functional to be minimized. For both goals a) and b), after introducing the background mathematical setting, we provide the implemented algorithms assessed on benchmarks as well as on more challenging structure configurations. [1] M. P. Bendsoe and O. Sigmund, *Topology optimization: theory, methods, and applications*, Springer Science & Business Media, 2013. [2] S. Micheletti, S. Perotto, L. Soli, *Ottimizzazione topologica adattativa per la fabbricazione stratificata additiva*, Italian patent application No. 102016000118131, filed on November 22, 2016 and International patent application PCT (No. PCT/IB2017/057323), 2017. [3] G. Allaire, F. Jouve, and A. M. Toader, A level-set method for shape optimization, *Comptes Rendus Mathematique*, Vol. 334, pp. 1125-1130, 2002.

Goal-Oriented Adaptive Verification of Unsteady Chaotic Flows

Krzysztof Fidkowski*

*University of Michigan, USA

ABSTRACT

Automated and rigorous error estimation and mesh adaptation techniques have already dramatically improved the robustness and reduced the cost of simulating complex steady and deterministic unsteady flows. Yet the applicability of these methods to chaotic flows, such as large-eddy simulations (LES), remains a challenge due to: (1) the non-deterministic nature of the physics, which stifles state-of-the art output-based error estimation methods; (2) pollution of statistical outputs by sampling errors due to finite-time integration; and (3) the wide range of length scales requiring resolution, which demands meshes that tax computational resources even on today's high-performance machines. The present work addresses these challenges through output-based approaches, which offer a mathematical framework for high accuracy and robustness by focusing discretization attention on only those regions that are important for the prediction of a specified quantity of interest. We demonstrate the robustness and efficiency of novel verification, adaptation, and optimization techniques for practical compressible Navier-Stokes simulations of engineering interest. We show that existing output-based error estimation and adaptation methods can be modified to simulate flow problems that exhibit small-scale unsteadiness, such as small-amplitude vortex shedding off an airfoil at moderate Reynolds numbers. On the other hand, for more challenging problems, in which unsteady, non-periodic flow features consume more of the computational domain, traditional output-based verification methods fail due to adjoint instabilities. Formal adjoint regularization techniques, such as least squares shadowing (LSS), address this problem but at a steep computational cost. We therefore combine LSS with reduced-order modeling to improve efficiency of error estimates, which then drive mesh adaptation. Results with prototypical chaotic systems and the compressible Navier-Stokes equations demonstrate the applicability of these methods for verification of statistical outputs of engineering interest.

Computational Methods for Subject-Specific Blood Flow Modeling

C. Alberto Figueroa*

*University of Michigan

ABSTRACT

Advances in computational methods and three-dimensional imaging techniques have enabled the quantification of cardiovascular mechanics in subject-specific anatomic and physiologic models. Research efforts have been focused mainly on the following key areas: i) pathogenesis of vascular disease, ii) development and optimization of medical devices, iii) virtual surgical planning, and iv) non-invasive diagnostics. However, despite great initial promise, the actual use of patient-specific computer modelling in the clinic has been very limited. Clinical diagnosis still relies on traditional methods based on imaging and invasive measurements. Invasive trial-and-error paradigms are often seen in vascular disease research, where animal models are used profusely to quantify simple metrics that could be evaluated via non-invasive computer modelling techniques. Lastly, medical device manufacturers rely mostly on in-vitro models to investigate the anatomic variations, arterial deformations, and biomechanical forces needed for the design of medical devices. Our research team has been developing a set of tools for simulation of image-based hemodynamics (CRIMSON) that aims to bridge the gap between the research world and the clinic. The main features of the CRIMSON simulation environment are: i) A parallel blood flow solver with Fluid-Structure Interaction capabilities and Multi-scale inflow and outflow boundary conditions. ii) A modern GUI for medical image data segmentation based on the Medical Imaging Interaction Toolkit (MITK). iii) Libraries for automatic estimation of parameters required for boundary and material parameter specification. These parameter estimation routines are based on Kalman-filtering theory. iv) Routines to enable the automatic simulation of transitional cardiovascular stages. These routines mimic the action of key cardiovascular functions such as the baroreflex, and local auto-regulations such as those in the coronary and cerebral circulations. In this talk, we will provide an overview of the most novel features for the software, specifically the functions for parameter estimation and simulation of transitional stages, and highlight a series of future developments for the project.

Modeling Hemodynamics and Homeostatic Conditions in a Multiscale Fluid-Solid Growth Model of the Pulmonary Arterial Tree

Vasilina Filonova^{*}, C. Alberto Figueroa^{**}, Hamidreza Gharahi^{***}, Seungik Baek^{****}

^{*}University of Michigan, ^{**}University of Michigan, ^{***}Michigan State University, ^{****}Michigan State University

ABSTRACT

Coupling hemodynamics with growth and remodeling of pulmonary arterial vessels is crucial for understanding the progress of incurable diseases such as pulmonary arterial hypertension. Progressive thickening and/or stiffening of distal pulmonary vessels yield to an increase in pulmonary arterial pressure which can lead to fatal right heart failure. In this work, we extend a fluid-solid growth formulation [] for modeling stress-mediated tissue growth and remodeling in pulmonary arterial tree. Key components that must be incorporated in the modeling effort include: a fractal tree model of blood flow in the distal pulmonary arterial tree; a high-resolution, image-based 3D hemodynamic model; appropriate characterization of the model parameters; and, most importantly, growth and remodeling formulations to describe the disease progression in proximal and distal vessels. The present work is the first step, which focuses on developing a multiscale hemodynamic model of the cardiopulmonary circulation. This model will enable defining homeostatic baseline states for the subsequent growth and remodeling studies. The presented problem has both spatial and temporal multiscale phenomena. The spatial multiscale (multi-resolution) represents the fluid dynamics problem in the distal vasculature tree via impedance boundary conditions assigned at the outflows of the image-based 3D model. We use a coupled-momentum method [] for modeling fluid-solid interactions, and a coupled multidomain approach for defining outflow impedance boundary conditions utilizing a Dirichlet-to-Neumann framework. The impedance boundary condition is calculated from analytical solutions utilizing Womersley's theory of pulsatile flow in deformable vessels []. The temporal multiscale phenomena must characterize two separate time scales: a fast scale associated to the pulsatile flow and a slow scale associated to the tissue growth and remodeling. Here we present a formal temporal multiscale analysis applied to this framework to justify and enrich the formulation presented in [1].

References [1]. C. A. Figueroa et al., Comput. Methods Appl. Mech. Engrg., 198 (2009), 3583-3602. [2]. C. A. Figueroa et al., Comput. Methods Appl. Mech. Engrg., 195 (2006), 5685-5706. [3]. M. S. Olufsen et al., Ann. Biomed. Eng., 28 (2000), 1281-1299.

Deep Convolutional Neural Networks for Eigenvalue Problems in Mechanics

David Finol^{*}, Yan Lu^{**}, Vijay Mahadevan^{***}, Ankit Srivastava^{****}

^{*}Illinois Institute of Technology, ^{**}Illinois Institute of Technology, ^{***}Amazon AWS AI Group, ^{****}Illinois Institute of Technology

ABSTRACT

In this paper we show that deep convolutional neural networks (CNN) can massively outperform traditional densely connected neural networks (both deep or shallow) in predicting eigenvalue problems in mechanics. In this sense, we strike out in a novel direction in mechanics computations with strongly predictive neural networks whose success depends not only in neural architectures being deep, but also in being fundamentally different from traditional neural architectures which have been used in mechanics until now. To show this, we consider a model problem: predicting the eigenvalues of a 1-D phononic crystal. However, the general observations pertaining to the predictive superiority of CNNs over fully-connected multi-layer perceptrons (MLP) should extend to other problems in mechanics as well. In the present problem, the optimal CNN architecture reaches 98% accuracy level on unseen data when optimized with just 40,000 training samples. Fully-connected MLPs - typically the network of choice in mechanics research - on the other hand, does not improve beyond 85% accuracy even with 100,000 training samples. We also show that even with a relatively small amount of training data, CNNs have the capability to generalize well for our problems and that they automatically learn deep symmetry operations such as translation invariance. Most importantly, however, we show how CNNs can naturally represent mechanical material tensors and that the convolution operation of CNNs has the ability to serve as local receptive fields, which is a natural representation of mechanical response. Strategies proposed here may be used for other problems of mechanics and may, in the future, be used to completely sidestep certain cumbersome algorithms with a purely data driven approach based upon deep architectures of modern neural networks such as deep CNNs.

Towards Multifield Discrete Element Modeling of Concrete Structures

Christian Flack^{*}, Felix Ockelmann^{**}, Dieter Dinkler^{***}

^{*}TU Braunschweig, ^{**}TU Braunschweig, ^{***}TU Braunschweig

ABSTRACT

Concrete structures are affected by many external and internal influences during their lifetime. Thus deep knowledge and subsequently mathematical modeling of the different coupled underlying mechanical, physical and chemical processes is extremely important to predict the behavior of materials and structures. The presented modeling concept is based on discrete-element methods. The heterogeneous structure of concrete is modeled by a three-dimensional bonded contact model[1], derived from the model of CUNDALL [2] for granular assemblies. The aim of the approach is to directly capture the significant processes taking place in the microstructure. Therefore a given domain is discretized with rigid spherical particles, representing the aggregates according to a grading curve regarding stress-deformation behavior. The cementitious contact zone is represented by a spring-damper system between two particles. The micromechanical parameters can be adapted to fulfill the global Young's modulus and Poisson's ratio at macro scale. The "empty" space between the aggregates filled up with cement paste is exploited by a voronoi diagram. In addition the temperature distribution is computed using a network of thermal links between the particle centers. Furthermore there are many chemical reactions taking place inside during the whole lifetime of a concrete structure. The hydration process e.g. determines strength and durability at a very early stage. Later on different chemical reactions can destroy or strengthen the structure. There, the goal is to consider any arbitrary chemical reaction which has been defined before. Therefore a process zone between two particles is introduced, where all the chemical processes are evaluated. Needed information about water content e.g. is provided by a discrete pore network model using the voronoi diagram. Changes in substrates concentration lead to variations in the contact stiffnesses due to coupling of processes. This way a microstructure-related chemo-thermo-mechanical model is developed which may be applied to macro scale constructions. [1] F. Ockelmann, D. Dinkler, A discrete element model for the investigation of the geometrically nonlinear behaviour of solids, Computational Particle Mechanics, 2017 [2] P.A. Cundall, O.D. Strack, A discrete numerical model for granular assemblies, Geotechnique 29(1), 47-65, (1979).

Semi-Automatic Computational Strategies for the Prediction of TPVR Outcomes

Vittoria Flamini^{*}, Hannah Tredway^{**}, Doff Mcelhinney^{***}, Puneet Bhatla^{****}

^{*}NYU Tandon School of Engineering, ^{**}NYU Langone Medical Center, ^{***}Stanford University Medical Center,
^{****}NYU Langone Medical Center

ABSTRACT

Transcatheter pulmonary valve replacement (TPVR) is an alternative to open-heart surgery and is frequently considered in patients with RVOT conduit obstruction and/or regurgitation. In patients with a surgical RVOT conduit, the conduit often passes over or is adjacent to a proximal coronary artery (CA) branch, carrying a risk of CA compression with conduit stenting. In large multicenter trials, approximately 5% of TPVR candidates were excluded by performing a pre-TPVR balloon angioplasty, but even when this dynamic CA compression testing is performed, CA compromise with catastrophic outcome occurs occasionally. Therefore, the development of a noninvasive tool to identify patients who are good candidates for TPVR would reduce the inadvertent risks and exposure to unnecessary invasive procedures and hence improve the overall health and well-being of this patient population, who is already burdened with multiple open heart surgeries. In this work, we developed a framework to generate patient-specific, non-invasive, semi-automatic, biomechanical simulations of TPVR procedure on RVOT conduits for CA compression prediction. This semi-automatic framework was created by analyzing retrospectively the routine clinical images of patients who underwent this procedure at NYU Medical School. In all the analyses, the implementation of the computer simulations was blinded, i.e. the investigator was unaware of the outcome of the pre-TPVR interventions. For each patient medical images were collected and segmented, resulting in a three-dimensional, personalized model of the RVOT conduit, aortic root and proximal coronary arteries. This model was then imported into a finite element software and computational simulations of the TPVR procedure implemented. The results of the semi-automatic framework, in which the orientation of the model, the placement of the balloon, and the simulations parameters are defined automatically via numerical analyses based on differential geometry, were compared against the results of the cath-lab. Simultaneously, the same patient geometries were analyzed and pre-processed via a more traditional, manual approach and the results of these finite element simulations used for further validation of the semi-automatic approach. Finally, the semi-automatic framework for CA compression prediction was further tested by including patient data, imaging studies, and cath-lab outcomes collected across several children hospitals. When compared with cath-lab outcomes, the simulations of pre-TPVR angioplasty were successful in predicting adverse events. There was minimal difference in the outcomes predicted by the two computational approaches considered. However, the semi-automatic approach reduced pre-processing times in half, thus demonstrating feasibility for the translational application of this computational approach in the clinical setting.

Imaging Nanoscale Elastic Strain-Wave Dynamics with Ultrafast Electron Microscopy

David Flannigan*, Daniel Cremons**, Daniel Du***, Dayne Plemmons****, Spencer Reisbick*****

*Department of Chemical Engineering and Materials Science, University of Minnesota, 421 Washington Avenue SE, Minneapolis, MN 55455, **Department of Chemical Engineering and Materials Science, University of Minnesota, 421 Washington Avenue SE, Minneapolis, MN 55455, ***Department of Chemical Engineering and Materials Science, University of Minnesota, 421 Washington Avenue SE, Minneapolis, MN 55455, ****Department of Chemical Engineering and Materials Science, University of Minnesota, 421 Washington Avenue SE, Minneapolis, MN 55455, *****Department of Chemical Engineering and Materials Science, University of Minnesota, 421 Washington Avenue SE, Minneapolis, MN 55455

ABSTRACT

Conventional transmission electron microscopy (TEM) has become an indispensable tool for comprehensive atomic and nanoscale materials characterization. While TEM spatial and energy resolutions have reached half-angstrom and few-meV levels, respectively, state-of-the-art detectors are able to resolve dynamics occurring only on the order of milliseconds. Such temporal resolutions are insufficient for studying a wealth of charge-carrier, structural, and magnetic dynamic behaviors. To overcome this, stroboscopic pump/probe approaches have been developed by interfacing a conventional TEM with short-pulsed lasers. In this way, temporal resolutions can be improved by 10 orders of magnitude to sub-picosecond timescales. In this talk, I will describe our work on the development and the application of this approach – ultrafast electron microscopy (UEM) [1]. I will begin by providing a brief overview of the UEM methodology and technology specific to our lab. Following this, I will describe a selection of our results on resolving the influence of nanoscale structural discontinuities (e.g., interfaces and crystal terraces) on coherent, elastic strain-wave dynamics in thin crystalline materials [2,3]. Among other behaviors, we find that wave-train emergence occurs at extended discontinuities, with propagation directions oriented normal to the interface, independent of in-plane crystallographic direction. Properties of the wave trains (GHz frequencies, speed-of-sound velocities, and single in-plane wave directions) suggest the generation of a single acoustic-phonon mode following photoexcitation, with observable interference effects occurring at vacuum/crystal interfaces. For example, in thin wedges of undoped germanium, we have directly imaged the formation and propagation of hypersonic acoustic-phonon wavefronts along distinct in-plane directions of residual shear strain, independent of crystallographic orientation. We also find that the nucleation period of the phonon wavetrains is well-matched by Auger recombination times in highly photoexcited germanium, thus indicating a spatially-resolved link between charge-carrier and lattice dynamics, likely via scattering processes. I will conclude by briefly describing a simple time-dependent finite element model that captures the general experimentally-observed behaviors. [1] D. A. Plemmons, P. K. Suri, and D. J. Flannigan, Chem. Mater. 27, 3178 (2015). [2] D. R. Cremons, D. A. Plemmons, and D. J. Flannigan, Nature Commun. 7, 11230 (2016). [3] D. R. Cremons, D. X. Du, and D. J. Flannigan, Phys. Rev. Materials 1, 073801 (2017).

Multi-fidelity Uncertainty Quantification for Healthy and Diseased Cardiovascular Models

Casey Fleeter^{*}, Gianluca Geraci^{**}, Daniele Schiavazzi^{***}, Andrew Kahn^{****}, Alison Marsden^{*****}

^{*}Stanford University, ^{**}Sandia National Laboratories, ^{***}University of Notre Dame, ^{****}University of California San Diego, ^{*****}Stanford University

ABSTRACT

Hemodynamic cardiovascular models provide non-invasive estimates of important clinical indicators. Although the use of hemodynamic models is increasing, difficulties in quantifying the effects of uncertainty stemming from multiple sources hinders widespread adoption in the clinic. The desire for clinically relevant and useable results motivates the transition to a stochastic framework for uncertainty quantification (UQ). However, in the cardiovascular modeling context, standard approaches for UQ face significant challenges due to the large number of uncertain inputs and the significant computational cost of realistic three-dimensional simulations. We propose a stochastic framework that leverages three cardiovascular model fidelities, with varying temporal and spatial mesh levels, to rigorously quantify the variability in hemodynamic outputs while, at the same time, keeping the computational cost reasonable. Using the SimVascular open-source platform, 3D anatomic models are constructed from medical image data, followed by the solution of incompressible Navier-Stokes equations governing blood flow in elastically deformable vessels [1,2]. Simplifying assumptions generate lower-fidelity models. 1D models consist of a simplified geometry automatically extracted from the 3D model, while 0D models are obtained from equivalent circuit representations of blood flow in deformable vessels. Multi-level and multi-fidelity (MLMF) estimators [3] implemented in Sandia's DAKOTA toolkit are leveraged to reduce the variance in our output quantities of interest (QoIs) while maintaining reasonable computational cost. We demonstrate this framework on healthy and diseased models of aortic and coronary anatomies. We simulate both steady and pulsatile input flow waveforms for all models. Uncertainties in the parameters defining the material properties of the vessels and fluid, as well as the lumped parameter RCR (aortic model) and coronary (coronary model) outlet boundary conditions are investigated after first tuning these parameters to produce realistic output hemodynamic values. The performance of the MLMF estimators is measured by the computational cost to obtain a given accuracy of global and local hemodynamic QoIs as compared to traditional UQ methods. We see significant, on the order of 10 to 100 times, reduction in total computational cost. As expected, global quantities, including pressure and flow waveform properties, show larger reductions with the MLMF estimators than local quantities, such as those relating to wall shear stress, as the latter rely more heavily on the highest fidelity model evaluations. [1] Updegrove, A. et al., Ann. Biomed. Eng., 2016. [2] Figueroa, A. et al., Comput. Methods in Appl. Mech. Eng., 2006. [3] Geraci, G. et al., 19th AIAA Non-Deterministic Approaches Conference, 2017.

A Cracked Hinge based Meso-Scale Formulation for RC Beams with Fibre Reinforced Concrete

Paula Folino*, Antonio Caggiano**, Enzo Martinelli***

*1Universidad de Buenos Aires, Fac. de Ingeniera, INTECIN - CONICET, Argentina., **1Universidad de Buenos Aires, Fac. de Ingeniera, INTECIN - CONICET, Argentina. 2AvH Stipendiat, TU Darmstadt, Institute für Werkstoffe im Bauwesen, Deutschland., ***3University of Salerno, Fisciano, SA Italy

ABSTRACT

This paper aims to analyse the post-cracking behaviour of real scale RC beams made of Fibre-Reinforced concrete (FRC) and tested in four-point-bending. Specifically, it proposes a model based on combining an appropriate fracture-based stress-crack opening relationship for the plain concrete matrix with proper constitutive laws aimed at capturing the crack-bridging effect of macro-fibres. An original meso-scale approach is followed for reproducing the complex influence of fibres on the overall response depending on the cracking onset and evolution. Particularly, explicit mechanisms, such as pull-out and dowel actions [1], are explicitly modelled, taking into account fibre type, geometry and spatial distribution: the presence of different types of fibres in FRC is also covered by the model. Moreover, the mechanical contribution of steel reinforcing bars is also taken into consideration. Numerical analyses demonstrate the accuracy of the proposed model, as their output are in very good agreement with a set of experimental results on RC beams recently tested at the University of Buenos Aires. The theoretical modelling activity presented in this paper stem out of the “SUPERCONCRETE” (H2020-MSCA-RISE-2014 n 645704) project, funded by the European Union as part of the H2020 Framework Programme. REFERENCES [1] Caggiano, A., Etse, G., & Martinelli, E. (2012). Zero-thickness interface model formulation for failure behavior of fiber-reinforced cementitious composites. Computers & Structures, 98, 23-32.

Finite Element Method Uncertainty Analysis, Asymptotic Solution, and a New Approach to Accuracy Assessment (*)

Jeffrey Fong*, Pedro Marcal**, Robert Rainsberger***, Li Ma****, Alan Heckert*****
Filliben*****

*U. S. National Institute of Standards and Technology., **MPACT Corporation, ***XYZ Scientific Applications, Inc.,
****U. S. National Institute of Standards and Technology, *****U. S. National Institute of Standards and Technology,
*****U. S. National Institute of Standards and Technology

ABSTRACT

Errors and uncertainties in finite element method (FEM) computing can come from the following eight sources, the first four being FEM-method-specific, and the second four, model-specific: (1) Computing platform such as ABAQUS, ANSYS, COMSOL, LS-DYNA, etc.; (2) choice of element types in designing a mesh; (3) choice of mean element density or degrees of freedom (DOF) in the same mesh design; (4) choice of a relative percent error (RPE) or the Rate of RPE per DOF on a log-log plot to assure solution convergence; (5) uncertainty in geometric parameters of the model; (6) uncertainty in physical and material property parameters of the model; (7) uncertainty in loading parameters of the model, and (8) uncertainty in the choice of the model. By considering every FEM solution as the result of a numerical experiment for a fixed model, a purely mathematical problem, i.e., solution verification, can be addressed by first quantifying the errors and uncertainties due to the first four of the eight sources listed above, and then developing numerical algorithms and easy-to-use metrics to assess the solution accuracy of all candidate solutions. In this paper, we present a new approach to FEM verification by applying three mathematical methods and formulating three metrics for solution accuracy assessment. The three methods are: (1) A 4-parameter logistic function to find an asymptotic solution of FEM simulations; (2) the nonlinear least squares method in combination with the logistic function to find an estimate of the 95 % confidence bounds of the asymptotic solution; and (3) the definition of the Jacobian of a single finite element in order to compute the Jacobians of all elements in a FEM mesh. Using those three methods, we develop numerical tools to estimate (a) the uncertainty of a FEM solution at one billion DOF, (b) the gain in the rate of RPE per DOE as the asymptotic solution approaches very large DOE&amp;amp;apos;s, and (c) the standard deviation of the Jacobian distribution (sd-J) of a given mesh design. Those three quantities are shown to be useful metrics to assess the accuracy of candidate solutions in order to arrive at a so-called &amp;amp;quot;best&amp;amp;quot; estimate with uncertainty quantification. Our results include calibration of those three metrics using problems of known analytical solutions and the application of the metrics to sample problems, of which no theoretical solution is known to exist. (*) Contribution of National Institute of Standards and Technology. Not subject to copyright.

A Goal-Oriented, Inverse Decision-Based Design Computational Framework for the Robust Design of an American Football Helmet

Tate Fonville*, Anand Nellippallil**, Mark Horstemeyer***, Farrokh Mistree****

*Mississippi State University, **University of Oklahoma, ***Mississippi State University, ****University of Oklahoma

ABSTRACT

Much has been written about brain damage to athletes who participate in contact sports in general and American football in particular. Essentially, helmet equipment has not been historically designed with the metrics directly related to the brain. By using brain damage as a performance metric, we are developing a goal-oriented, inverse decision-based design method with the end performance goal of total energy absorption so as to mitigate the possibility of brain damage to athletes. The helmet system is partitioned into three subassemblies, namely, the helmet shell, the stress wave damper, and the helmet liner. In the shell subassembly, thickness of the paint and outer/inner shells are treated as variables. The stress wave damper is fixed to the shell and specifications (for example, base radius, length, volume, etc.) for the complex geometry are treated as variables. The liner subassembly consists of Velcro, TPU foam wrap, and the foam material with thickness and area ratio being treated as variables. Each of the subassemblies is linked via an information chain (consisting of variables and goals) beginning with the paint and ending with the liner foam. Considering the end goal of zero energy at the head, we define the forward process as an energy transfer from the external paint to the helmet liner. We solve for subassembly specifications in an inverse manner beginning with the foam liner and working backwards towards the paint. The mathematics underlying our proposed goal-oriented, inverse decision-based design method is embodied in the Concept Exploration Framework (CEF). We plan to garner the data from finite element analysis using Abaqus (explicit) in which an Internal State Variable (ISV) elastic-viscoplastic material model will be used to accurately capture the constitutive behavior of the helmet shell, the stress wave damper, and the helmet liner. The boundary conditions will include a normal load and a transverse load with velocities appropriated by the NOCSAE standard for American Football Helmets. In keeping with the theme of the conference, namely, Computational Mechanics in Complex Product Development, in our paper we plan to present the salient features a. of the partitioning of a complex design problem (a football helmet); b. of the computational mechanics to support design decision making (modeling the behavior of the helmet shell, the stress wave damper, and the helmet liner); c. of the Concept Exploration Framework.

Extended Finite Elements Applied to Poroelasticity in Faulted Porous Media

Luca Formaggia^{*}, Anna Scottio^{**}, Daqing Liu^{***}

^{*}Politecnico di Milano, ^{**}Politecnico di Milano, ^{***}Politecnico di Milano

ABSTRACT

In several applications related, for instance, to the exploitation of oil and geothermal reservoirs and CO₂ sequestration activities, the injection or extraction of fluids can alter the stress field in the reservoir and induce preexisting faults to reactivate. Simulation of this type of phenomena requires to couple the poroelastic equations with a model of the hydraulic and mechanical behavior of the fault. In this context, the eXtended Finite Element Method (XFEM) can be of interest to account for discontinuities in the flow and displacement fields. In this work, the fault is defined by a one-codimensional interface and we have implemented the coupling conditions describing the frictional contact by a Nitsche approach. This is an alternative to the augmented Lagrangian formulations more commonly used for this type of problem. A fixed-stress splitting strategy, extended to this type of problem, has been used to decouple the computation of pressure and displacement. Mixed formulation has been used for the flow field, giving rise to a three field formulation. In this presentation we will illustrate some preliminary results of this procedure.

Coupling FEM and Meshfree Peridynamics for Efficient Simulation of Hydraulic Fracturing

John Foster^{*}, Jason York^{**}

^{*}The University of Texas at Austin, ^{**}The University of Texas at Austin

ABSTRACT

In the effort to create new technology to enhance our ability to retrieve usable hydrocarbons, the technique of hydraulic fracturing has shown to be extremely beneficial. This involves pumping fluids at high pressures to induce and propagate fractures near the wellbore to stimulate production in otherwise low permeability reservoirs. To better understand the physical processes involved, several models have been proposed for numeric simulation. This work expands on the nonlocal hydraulic fracturing model based on the theory of peridynamics, detailed in Ouchi et al. (2015). As the model continues to develop complex capabilities, such as fully coupled poromechanics and inelasticity, computational expense continues to be an ever-growing concern. In the work by Galvanetto et al. (2016), a method is introduced for coupling nonlocal bond-based peridynamic grids with local finite element meshes. This coupling method demonstrated applicability to static equilibrium problems, while introducing negligible errors in displacements. In this work, the coupling method is implemented with the nonlocal hydraulic fracturing model, using peridynamics near existent and propagating fractures, as well as a standard Galerkin finite element formulation away from fractures. To increase computational efficiency, adaptive meshing techniques are introduced with the capability of converting finite element nodes to meshfree peridynamic nodes. This presentation will include a discussion of the model and techniques implemented, as well as their impact on simulation capabilities and performance. References: Ouchi, H., Katiyar, A., York, J., Foster, J.T., and Sharma, M.M. (2015). A fully coupled porous flow and geomechanics model for fluid driven cracks: a peridynamics approach. *Computational Mechanics*, 55(3), 561-576. Galvanetto, U., Mudric, T., Shojaei, A., and Zaccariotto, M. (2016). An effective way to couple FEM meshes and Peridynamics grids for the solution of static equilibrium problems. *Mechanics Research Communications*, 76, 41-47.

On the Behavior of a Roller Bearing Seismic Isolator

Dora Foti^{*}, Nicola Menga^{**}, Giuseppe Carbone^{***}

^{*}Polytechnic University of Bari, ^{**}Polytechnic University of Bari, ^{***}Polytechnic University of Bari

ABSTRACT

Abstract In this paper, we focus on the behavior of an innovative seismic rolling isolator in light to provide a passive protection to light structures from earthquakes damages. The specific isolation system belongs to the class of Rubber Layer Rolling Bearings (RLRB), and consists of steel cylinders interposed between steel plates padded with viscoelastic layers (rubber). Due to the geometry of the RLRB system, a partial motion decoupling is introduced between the ground and the superstructure. Moreover, the high-damping viscoelastic material employed in the system partially dissipate the seismic energy, thus reducing the relative displacement between the base and the building. In this work, we provide a deep insight into the viscoelastic behavior of such a isolation system. We specifically address the contact problem between the rigid cylinders and the viscoelastic layers, exploiting specific contact mechanics techniques to correctly model the effect of the layers finite thickness on the results. The theoretical model provides useful guidelines for a design optimization aiming at producing high energy dissipation with low force transmissibility. Further, in view of an extension to the case of multi-layer rubber system, we investigate the effect of different boundary conditions on the viscoelastic layers involved in the RLRB isolator, such as: (i) a rigid constraint; (ii) a uniformly distributed pressure. These, represent the two limiting cases of a layered system in which the external layer stiffness is infinitely high and vanishing, respectively. References D. Foti, A. Catalan Goni, S. Vacca. On the dynamic response of rolling base isolation systems. *Structural Control and Health Monitoring*, 2013, 20(4), 639-648. ISSN: 1545-2255. DOI: 10.1002/stc.1538. Menga, N., Foti, D., & Carbone, G. (2017). Viscoelastic frictional properties of rubber-layer roller bearings (RLRB) seismic isolators. *Meccanica*, 52(11-12), 2807-2817. Menga, N., Afferrante, L., & Carbone, G. (2016). Effect of thickness and boundary conditions on the behavior of viscoelastic layers in sliding contact with wavy profiles. *Journal of the Mechanics and Physics of Solids*, 95, 517-529.

On Non-Uniform Torsion in FGM Beam Structures and the Extraction of Relevant Stiffness Quantities based on SAFE

Peter Fotiu*, Justin Murin**, Stephan Kugler***

*University of Applied Sciences Wiener Neustadt, Austria, **Slovak University of Technology in Bratislava,

***University of Applied Sciences Wiener Neustadt, Austria

ABSTRACT

Beam structures made of a Functionally Graded Materials (FGMs) show location dependent material parameters throughout their arbitrarily shaped cross-section. The load case of torsion introduces warping of the cross-section and a non-uniform theory of torsion has to be applied to achieve accurate solutions using one-dimensional finite elements. Starting with a suitable kinematic assumption where the cross-section rotates rigidly in its projection plane pivoting at the shear or drill center, the axial motion of a generic point is quantified based on an unknown warping function (depending on the cross-section coordinates) multiplied with an axial field quantifying the amount of warping. The well-known and frequently applied Vlasov's theory of torsion uses the first derivative of torsion angle ϕ to quantify warping axially. This leads to two independent stiffness quantities (torsion stiffness and warping stiffness) which have to be identified using SAFE in connection with one fourth order ODE. Such a strategy delivers shear stress distributions due to torsion only and not based on warping. The resultant torsional moment is separated artificially into a primary part (due to torsion) and into a secondary part due to warping. Alternatively, if the axial distribution of warping may be related to a yet unknown independent field rather than to the rate of twist, resulting in two coupled second order ODEs and four stiffness quantities. Such a calculation strategy is similar to the rarely applied Benscoter theory of torsion and does not require any artificial separation of section resultants since the shear stress distributions are related to both torsion and warping. Additionally, it can be shown by example that this theory of warping torsion leads to more accurate results in relation to three dimensional continuum solutions compared to Vlasov's theory especially for thick shafts. While analytical evaluations regarding a set of two coupled ODEs are somewhat more involved very efficient finite beam elements can be derived based on linear shape functions. The evaluations of the related stiffness quantities can be carried out using a reference beam problem of arbitrary length in connection with three dimensional elasticity solutions where semi-analytical finite elements (SAFE) are applied. Due to SAFE and a specialized load case for the reference problem a true dimension reduction is achieved and stress distributions, relevant cross-section parameters and stiffness quantities are accessible based on discretization of the cross-section only.

Recent developments in a 10-Node Composite Tetrahedral Finite Element for Solid Mechanics

James Foulk III^{*}, Jakob Ostien^{**}, Nathan Crane^{***}, Brandon Talamini^{****}, Alejandro Mota^{*****},
Michael Veilleux^{*****}, Kendall Pierson^{*****}

^{*}Sandia National Laboratories, ^{**}Sandia National Laboratories, ^{***}Sandia National Laboratories, ^{****}Sandia National Laboratories, ^{*****}Sandia National Laboratories, ^{*****}Sandia National Laboratories, ^{*****}Sandia National Laboratories

ABSTRACT

The adoption of tetrahedral elements in solid mechanics hinges on field resolution under finite deformations, inelasticity, contact, and transient dynamics. In this work, we present new developments in a recently reformulated, 10-node composite tetrahedral element [1]. We specifically illustrate a new integration scheme for the gradient operator that accounts for curved or “kinked” edges in which the mid-edge node is not located at the midpoint of adjacent, parent nodes. In addition, we also develop a new methodology for the stress projection and the rendering of the forces. Examples of increasing complexity in both quasi-statics and explicit transient dynamics will attempt to illustrate the benefits of the new formulation in the context of a larger workflow to reduce the time from design to analysis. Sandia National Laboratories is a multimission laboratory managed and operated by National Technology and Engineering Solutions of Sandia, LLC, a wholly owned subsidiary of Honeywell International, Inc., for the U.S. Department of Energy’s National Nuclear Security Administration under contract DE-NA0003525. [1] Ostien, J.T., Foulk III, J.W., Mota, A., Veilleux, M. (2016) A 10-Node Composite Tetrahedral Finite Element for Solid Mechanics, International Journal for Numerical Methods in Engineering 107: 1145-1170.

Towards a New Paradigm of Growth and Remodeling of Biological Tissues

Massimiliano Fraldi^{*}, Angelo Rosario Carotenuto^{**}, Stefania Palumbo^{***}, Arsenio Cutolo^{****},
Massimiliano Zingales^{*****}, Luca Deseri^{*****}

^{*}University of Napoli Federico II, ^{**}University of Napoli Federico II, ^{***}University of Trento, ^{****}University of Napoli Federico II, ^{*****}University of Palermo, ^{*****}University of Trento

ABSTRACT

Since the work of Fung (see reference 1) there has been a clear need of new generation models capable to bridge together the scales at which multiphysics phenomena govern growth and remodeling of biological tissues. In this work, the authors propose an experimentally informed multiscale methodology based on Structured Deformations (see reference 2), delivering effective fields characterizing the geometrical changes of bodies at multiple scales. Structured Deformations intrinsically can account for microstructural changes at various length scales, including formation and coalescence of voids and rearrangements of the material. Unlike traditional, yet phenomenological, local multiplicative decomposition of the deformation gradient widely used in growing media, the fields arising in Structured Deformations allow for describing the kinematics of the whole body, including both growth and remodeling. This arises through precise bottom-up characterizations, owing the submacroscopic structure of the material to bear trace macroscopically. In order to extract effective constitutive properties of tissues undergoing growth and remodeling, a novel multiscale targeted bottom-up approach is proposed to find the (Helmholtz) energetics governing the multiphysics involved in such processes. The approach can be relevant to follow structural and morphological reorganization of a number of biological tissues where growth and remodeling are crucial issues and could be easily coupled with cells competition occurring at micro-scale level to include selected bio-chemical dynamics (see reference 3). 1) Y.C. Fung, Biomechanics: Mechanical Properties of Living Tissues, Springer-Verlag New York, 1993. 2) L. Deseri, D.R.Owen (2015). Stable Disarrangement Phases Arising from Expansion/Contraction or from Simple Shearing of a Model Granular Medium, Int. J.Eng. Sciences 96 111-130 3) M.Fraldi, A. R. Carotenuto (2018). Cells competition in tumor growth poroelasticity. J Mech. Physics Solids 112, 345-367.

PFEM Formulation for FSI Problems Involving Newtonian and Non-Newtonian Fluids

Alessandro Franci^{*}, Xue Zhang^{**}, Miguel Angel Celigueta^{***}, Eugenio Oñate^{****}

^{*}CIMNE (International Center for Numerical Methods in Engineering), ^{**}CIMNE (International Center for Numerical Methods in Engineering), ^{***}CIMNE (International Center for Numerical Methods in Engineering), ^{****}CIMNE (International Center for Numerical Methods in Engineering)

ABSTRACT

The aim of the talk is to present a purely Lagrangian method to simulate free-surface Bingham fluids and their interaction with structures, also accounting for the 3D effects. The Particle Finite Element Method (PFEM) [1] is used to deal with bodies that are suffering from huge deformations. A Papanastasiou model has been implemented into a stabilized PFEM strategy [2] with the aim of modeling both Newtonian and Non-Newtonian fluid flows. The possibility of coupling the PFEM model with a Discrete Element Method (DEM) formulation is also investigated. On the other hand, to compute the solid objects and structures that interact with the fluid flow, the standard Finite Element Method (FEM) and a hypoelastic constitutive model are used. The fluid-solid coupling is modeled via a monolithic approach for fluid-structure interaction (FSI), called Unified formulation [3]. Several 2D and 3D numerical examples are presented. The numerical tests include the simulation of fresh concrete slump tests, a mud flow over an inclined plane receiving the impact of a solid object, and dam break of Bingham fluids against an elastic membrane. The numerical simulations are validated against the results of laboratory tests or those available in the literature. [1] S.R. Idelsohn, E. Oñate, and F. Del Pin. The particle finite element method: a powerful tool to solve incompressible flows with free-surfaces and breaking waves. *International Journal for Numerical Methods in Engineering*, 61, 964-989, 2004. [2] E. Oñate, A. Franci, and J.M. Carbonell. Lagrangian formulation for finite element analysis of quasi-incompressible fluids with reduced mass losses. *International Journal for Numerical Methods in Fluids*, 74 (10), 699-731, 2014. [3] A. Franci, E. Oñate, and J.M. Carbonell. Unified Lagrangian formulation for solid and fluid mechanics and fsi problems. *Computer Methods in Applied Mechanics and Engineering*, 298, 520-547, 2016.

Constitutive Models and their Application to Predict Geomaterial Failure Resulting from Embedded Detonations

Andy Frank^{*}, Jessica Fulk^{**}, Jason Roth^{***}, Michael Hammons^{****}

^{*}U.S. Army Engineer Research and Development Center, ^{**}U.S. Army Engineer Research and Development Center, ^{***}U.S. Army Engineer Research and Development Center, ^{****}U.S. Army Engineer Research and Development Center

ABSTRACT

Modeling highly impulsive extreme loading events is of significant interest to government, industry, and academia. Some areas of U.S. Army interest include the study of events like projectile penetration, shaped-charge penetration, and close-in explosive detonation, which involve a spectrum of challenging material behaviors and failure modes. Material behaviors resulting from the high-rate impulsive loading, large deformations and material damage, fracture, and failure must be accurately represented; accurate representation of material geometry and interfaces is also essential. Other key elements include capturing material compressibility in the high pressure environment and the damping of different materials under explosive loading. Lagrangian hydrocodes are preferred for simulation of structural response dominated events, but this presents additional challenges with computational cost for some embedded detonation problems where the spatial and temporal domains can be very large. The ability to accurately model these essential mechanisms of embedded detonation problems pose challenges from the perspectives of 1) developing efficient and effective material models that go beyond basic phenomenological formulations, and 2) experimental characterization to accurately quantify the material response and subsequently enable model enhancement. The U.S. Army Engineer Research and Development Center (ERDC) has specific interests in this class of problems and in tools for modeling embedded detonation effects. Accordingly, ERDC has developed constitutive models to work towards developing improved capabilities that address these geomaterial response modeling challenges [1,2]. These models are three-invariant plasticity models that simulate non-linear elastic behavior, irreversible hydrostatic crushing, material yielding, plastic flow, and damage. They contain unique features to simulate the rate-dependent response of geomaterials, including rate-dependent behavior in cohesive strength, frictional strength, hydrostatic crushing, and material damage. Here we will provide an overview of the models and include benchmark experiments used in model validation. Example simulations of embedded detonations in layered geomaterials and the material failure mechanisms produced will also be discussed.

REFERENCES [1] A.O. Frank, An elastic-plastic material model for concrete under high rate impulsive loads: modeling, implementation, and testing of the high rate brittle (HRB) concrete model. ERDC/GSL TR-12-10, 2012. [2] M.D. Adley, K.T. Danielson and A.O. Frank, Virtual material laboratory (VML), Version 1.0: Applications to Advanced Fundamental Concrete (AFC) model. ERDC/GSL TR-13-09, 2013.

Energy-momentum Consistent Time Integration Schemes for Multi-field Problems

Marlon Franke^{*}, Alexander Janz^{**}, Rogelio Ortigosa^{***}, Mark Schiebl^{****}, Peter Betsch^{*****}

^{*}Institute of Mechanics, Karlsruhe Institute of Technology (KIT), Germany, ^{**}Institute of Mechanics, Karlsruhe Institute of Technology (KIT), Germany, ^{***}Zienkiewicz Centre for Computational Engineering, Zienkiewicz Centre for Computational Engineering, ^{****}Institute of Mechanics, Karlsruhe Institute of Technology (KIT), Germany, ^{*****}Institute of Mechanics, Karlsruhe Institute of Technology (KIT), Germany

ABSTRACT

A new approach for the design of energy-momentum (EM) consistent time integrators for nonlinear coupled problems is proposed. Polyconvexity inspired internal or Helmholtz free energy functionals are obtained by using the rediscovered tensor cross product which is basically applied on the cofactor and the Jacobian of the right Cauchy-Green strain tensor and greatly simplifies the algebra, see Betsch, Janz and Hesch (submitted to Comput. Methods Appl. Mech. Engrg., 2017). On this basis multi-field problems concerning non-linear thermo-elastodynamics, see Franke, Janz, Schiebl, Betsch (submitted to Int. J. Numer. Meth. Engng., 2017) and electro-elastodynamics, see Ortigosa, Franke, Janz, Gil and Betsch (submitted to Comput. Methods Appl. Mech. Engrg., 2017), are considered. For the former a temperature based weak form is employed which facilitates the design of a structure-preserving time-stepping scheme for coupled thermo-elastic problems. For the latter a three-field internal energy-based formulation is applied. In both cases, the polyconvexity-based framework facilitates the design of EM consistent time integrators. In particular algorithmic stress formulas are employed which show a remarkably simple structure when compared to traditional, elaborate projection-based formulas. The spatial discretization relies on finite element interpolations for the unknown fields. Eventually, the superior performance of the proposed formulations is shown in several numerical examples.

Inverse Problem Coupled with the Genetic Algorithm Procedure in Modeling of Biomaterials Behavior

Marina Franulovic*, Kristina Markovic**, Stjepan Pilicic***

*Faculty of Engineering, University of Rijeka, **Faculty of Engineering, University of Rijeka, ***Faculty of Engineering, University of Rijeka

ABSTRACT

Modeling of material behavior and consequently its simulation in the operating conditions is an important step in understanding the consequences of the loading impact on various systems. This refers to the material behavior of different conventional and synthetic materials with the application on the assembly constituents' mechanical design, but also on biomaterials modeling for the simulation of the biomechanical systems. The biomaterials behavior modeling is based on the recorded stretch-stress response of the specimens isolated from the biomechanical test subjects and experimented on, together with the chosen material model appropriate for description of the phenomena that appear in material during loading. In order to make possible inverse modeling in the process of material behavior simulation, the definition of physical interdependence among unknown variables, here known as material parameters, and material response during loading, is necessary. The data sets acquired from the experimental procedures represent the probing signal for the inverse setup in the material parameter identification process. The inverse modeling here is coupled with the genetic algorithm procedure to make possible fast convergence to as accurate as possible results in presented highly non-linear material behavior. Genetic algorithm procedure has thus been developed here to identify parameters for the behavior modeling of ligaments of the human cervical spine. The procedure consists of three main parts: system characterization where influential parameters are defined, forward modeling where mechanical principles are proposed and inverse or backward modeling where objective function for the problem is set. The material characterization based on coupling inverse problem within the genetic algorithm procedure has so far proved to be applicable for parameters identification of materials with different microstructure and mechanical properties. Since it exhibited flexibility and robustness, besides for the modeling of the biomaterials, it might also be applicable to behavior characterization of other non-conventional and innovative materials. This work has been supported by Croatian Science Foundation under the project number IP-2014-09-4982 and also by the University of Rijeka under the projects number (13.09.1.2.09) and (13.09.2.2.18).

Meshfree Contact Algorithm with Provisions for Solid State Joining – Application to the Additive Friction Stir Process

Kirk Fraser^{*}, George Stubblefield^{**}, Robert Escobar^{***}, Paul Allison^{****}, Brian Jordon^{*****}

^{*}National Research Council Canada, ^{**}University of Alabama, ^{***}University of Alabama, ^{****}University of Alabama,
^{*****}University of Alabama

ABSTRACT

The additive friction stir (AFS) process is a new additive manufacturing (AM) approach where a consumable probe is deposited onto a work piece using a friction stir tool. The probe is pushed through a hole in the tool, friction between the tool/probe and the work piece causes heat to be generated. The deposited probe material forms a solid-state bond with the work piece, leading to excellent mechanical properties of the AM part. Certainly, AFS shows great promise as a high value AM process. However, significant efforts to understand better the process will be needed in the near future. Various parameters such as tool rpm, advancing speed, and probe federate (to name a few) need to be selected to have good quality AM parts. To facilitate this task, a meshfree coupled thermo-mechanical simulation code, SPHriction-3D [1], can be used. The code is ideally suited for the simulation of large plastic deformation processes such as AFS. An advanced parallelization scheme is employed on the GPU, which permits robust and efficient calculations for complex multi-physics problems in a reasonable time frame. In this work, a new meshfree joining contact algorithm is developed to take into account the intricate interaction of the work piece and the consumable probe material. Initially, the meshfree material points used to discretize the probe and the work piece are treated as two distinct and separate entities. At this point, their interactions are through a penalty based thermo-mechanical contact algorithm. Once a material point at the work piece/probe interface attains a threshold energy level, the material point is considered to be joined and interacts through the meshfree kernel. The new contact algorithm allows the SPHriction-3D code to simulate aspects of the AFS process such as material deposition, heat generation, work piece/probe mixing, as well as defect prediction. References [1] K. Fraser, "Robust and efficient meshfree solid thermo-mechanics simulation of friction stir welding," Ph.D., Applied Sciences, University of Quebec at Chicoutimi, Saguenay, Quebec, Canada, 2017.

Optimization with Polymorphic Uncertainty Models for the Design of Durable Reinforced Concrete Structures

Steffen Freitag^{*}, Philipp Edler^{**}, Katharina Kremer^{***}, Günther Meschke^{****}

^{*}Ruhr University Bochum, ^{**}Ruhr University Bochum, ^{***}Ruhr University Bochum, ^{****}Ruhr University Bochum

ABSTRACT

The lifetime oriented design of reinforced concrete (RC) structures requires to consider the expected service loads and the long-term behavior of RC. The durability of RC structures is dominated by steel reinforcement corrosion, which is driven by load induced cracking and the transport of corrosive substances into the structure. The crack width at the reinforcement layers is mainly influencing the lifetime of RC structures. In addition to a precise physical modelling of the structural behavior, it is also important to consider uncertainties of the structural loading and the material resistance within the design process. Here, finite element models are applied together with polymorphic uncertainty models within an optimization approach to improve the design of RC structures with respect to durability. In contrast to pure stochastic models, where all uncertain parameters are described by stochastic distributions, polymorphic uncertainty models allow to consider both, aleatoric and epistemic sources of uncertainty by combining stochastic and non-stochastic approaches such as intervals and fuzzy numbers. Within an optimization problem, polymorphic uncertain parameters can either be a priori parameters or design parameters to be optimized. In both cases, a surrogate problem has to be formulated to solve the optimization task, e.g. minimizing mean values, variances or quantile values in case of stochastic a priori or design parameters and e.g. worst case optimization in case of interval a priori or design parameters. To consider polymorphic uncertain design and a priori parameters, existing optimization strategies, such as the particle swarm optimization approach, are extended and modified in a way, that Monte-Carlo simulations are performed together with interval analyses for each realization of the design parameters. The new optimization strategies are applied to optimize the reinforcement layout (number and diameter of reinforcement bars and the corresponding concrete cover) of an RC bridge structure. Whereas the number and diameter of the reinforcement bars are discrete deterministic design parameters, the concrete covers are modeled as interval design parameters, with midpoints to be optimized and given radiuses taking construction imprecisions into account. The service load and the most sensitive concrete material parameters are considered as stochastic a priori parameters within the optimization. The mean value and variance of the crack width at the reinforcement layer are used as optimization objective to be minimized and the structural reliability is treated as a constraint in terms of the accepted failure probability with respect to the load bearing capacity.

Error Modeling for Approximate Solutions to Parameterized Systems of Nonlinear Equations Using Machine Learning

Brian Freno^{*}, Kevin Carlberg^{**}

^{*}Sandia National Laboratories, ^{**}Sandia National Laboratories

ABSTRACT

Decision-making applications in computational science and engineering typically require repeated evaluations of a parameterized model. Often, these models consist of nonlinear partial differential equations that are cast algebraically. For large-scale models, the computational cost associated with this many-query setting is prohibitive; therefore, solutions approximations must be employed for tractability. Examples of solutions approximations include those that arise from reduced-order models, coarse-mesh solutions, and unconverged iterations. While such approximations reduce the computational burden, often by orders of magnitude, they incur error with respect to the high-fidelity model that should be accounted for in the ultimate decision-making application. We present an approach to quantify the error introduced by these solution approximations. This is accomplished by (1) engineering features that are informative of the error, and (2) applying machine learning regression techniques (e.g., artificial neural networks, random forests, support vector machines) to construct a statistical model of the error from these features. We consider both (signed) errors in quantities of interest, as well as global state-space error norms. We present several examples to demonstrate the effectiveness of the proposed approach compared to more conventional feature and regression choices. In each of the examples, including a problem characterized by more than a quarter million degrees of freedom, the predicted errors have a coefficient of determination (R squared) value of at least 0.998.

A Kinematic Evolution Equation for the Dynamic Contact Angle and some Consequences

Mathis Fricke^{*}, Dieter Bothe^{**}, Matthias Köhne^{***}

^{*}TU Darmstadt, Germany, ^{**}TU Darmstadt, Germany, ^{***}HHU Düsseldorf, Germany

ABSTRACT

We address the moving contact line problem for two-phase incompressible flows by a kinematic (or geometrical) approach. The key idea is to derive an evolution equation for the contact angle if the transporting velocity field is given. It turns out that the resulting equation has a simple structure and expresses the time derivative of the contact angle in terms of the gradient of the velocity field at the solid wall. This result can be used to test the ability of a numerical method to correctly transport the contact angle. The imposed boundary conditions provide some information about the velocity gradient. Using this information, the kinematic evolution equation is a tool to analyze the contact angle evolution. In this paper we consider the Navier slip boundary condition, which is frequently used for the modeling of moving contact lines. Exploiting the interfacial transmission condition for the viscous stress, we derive an explicit form of the contact angle evolution for a large class of models which only involves the contact line velocity and the slip length from the Navier condition. From this equation we can read off the qualitative behavior of the contact angle evolution for smooth solutions to this class of models, which turns out to be unphysical. In particular, if the contact angle is directly related to the contact line velocity, the contact angle is a monotonically increasing or decreasing function. We discuss consequences from this observation, possible generalizations of the model as well as implications for numerical methods. **ACKNOWLEDGEMENTS** We kindly acknowledge the financial support by the German Research Foundation (DFG) within the Collaborative Research Centre 1194 "Interaction of Transport and Wetting Processes", Project B01.

HIGHER-ORDER APPROXIMATIONS OF INCOMPRESSIBLE NAVIER-STOKES FLOWS ON CURVED MANIFOLDS

THOMAS-PETER FRIES*

*Graz University of Technology
Institute of Structural Analysis
Lessingsstr. 25/II, 8010 Graz, Austria
fries@tugraz.at; www.ifb.tugraz.at

Key words: Stokes, Navier-Stokes, higher-order FEM, surface FEM, surface PDEs, manifold

Abstract. A mixed, stabilized, higher-order accurate surface finite element method is considered for stationary and instationary Stokes and Navier-Stokes flows on curved, two-dimensional manifolds. Individual element orders are employed for the velocities, pressure, and Lagrange multiplier to enforce tangential velocities. Stream-line upwind stabilization is used for flows at high Reynolds numbers. Numerical test cases are proposed and higher-order convergence rates confirmed.

1 INTRODUCTION

Flows on curved surfaces in three dimensions are important in transport processes on interfaces, e.g., in foams, biomembranes and bubble surfaces. Models for incompressible flows on two-dimensional manifolds are found, e.g., in¹⁻⁴. Herein, the surface FEM⁵⁻⁷ is employed for the approximation of stationary and instationary (Navier-)Stokes flows on general, yet fix surfaces. The involved fields are approximated using different orders of the shape functions, namely for the velocities, pressure, and Lagrange multiplier to enforce tangential velocities. The well-known Babuška-Brezzi condition applies for the resulting mixed FEM^{8,9}. Streamline-upwind Petrov-Galerkin (SUPG) stabilization is recommended for Navier-Stokes flows at large Reynolds numbers^{10,11}. For the case of the instationary Navier-Stokes equations, the Crank-Nicolson time stepping scheme is employed for the semi-discrete sytem of equations resulting from using the surface FEM in space. This work is a revision of^{12,13} proposing new test cases. The numerical results show that higher-order convergence rates are achieved provided that the finite element spaces are properly chosen.

The paper is organized as follows: In Section 2, the governing equations for (i) Stokes flow, (ii) stationary, and (iii) instationary Navier-Stokes flows on two-dimensional manifolds are given in strong form and weak form according to the surface FEM. Numerical results are

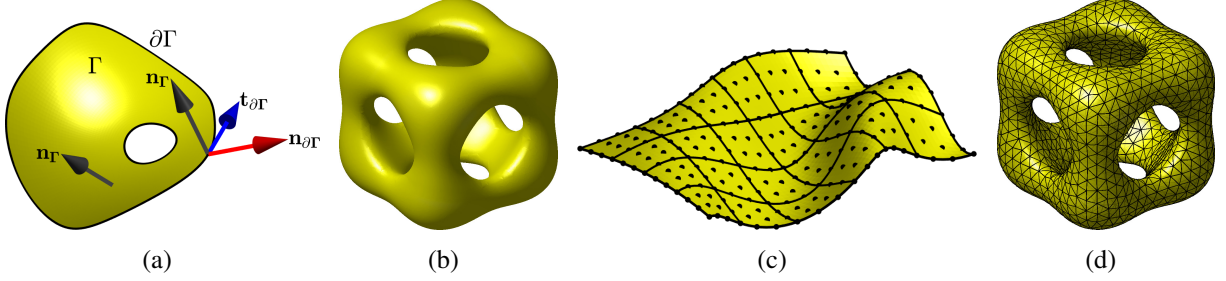


Figure 1: (a) Generic surface with normal and tangential vectors, (b) compact surface, (c) and (d) surface meshes.

presented in Section 3 and confirm higher-order accuracy. Finally, conclusions are given in Section 4.

2 GOVERNING EQUATIONS

A curved, smooth, orientable, connected surface Γ which is fixed in space over time and features a finite area is considered. There is a unit normal vector $\mathbf{n}_\Gamma \in \mathbb{R}^3$ on Γ . The surface may feature a boundary $\partial\Gamma$ with tangential vector $\mathbf{t}_{\partial\Gamma}$ pointing in direction of $\partial\Gamma$ and a co-normal vector $\mathbf{n}_{\partial\Gamma} = \mathbf{n}_\Gamma \times \mathbf{t}_{\partial\Gamma}$, see Fig. 1(a). The surface may also be compact, then, $\partial\Gamma = \emptyset$, see Fig. 1(b) and it may be given in parametrized form or implied, e.g., based on the level-set method. For the equivalence of these two cases and more mathematical details, see, e.g.,⁷. The manifold is discretized by suitable meshes of different orders and types (triangular or quadrilateral elements), see Figs. 1(c) and (d).

2.1 Surface gradients and divergence

On the manifold Γ , the tangential projector $\mathbf{P}(\mathbf{x}) \in \mathbb{R}^{3 \times 3}$ is defined by the normal vector as

$$\mathbf{P}(\mathbf{x}) = \mathbf{I} - \mathbf{n}_\Gamma(\mathbf{x}) \otimes \mathbf{n}_\Gamma(\mathbf{x}).$$

with $\mathbf{P} \cdot \mathbf{n}_\Gamma = 0$, $\mathbf{P} = \mathbf{P}^T$, and $\mathbf{P} \cdot \mathbf{P} = \mathbf{P}$.

The tangential gradient operator ∇_Γ of a differentiable *scalar* function $u : \Gamma \rightarrow \mathbb{R}$ on the manifold is given by

$$\nabla_\Gamma u(\mathbf{x}) = \mathbf{P}(\mathbf{x}) \cdot \nabla \tilde{u}(\mathbf{x}), \quad \mathbf{x} \in \Gamma, \quad (1)$$

where ∇ is the standard gradient operator, and \tilde{u} is a smooth extension of u in a neighborhood \mathcal{U} of the manifold Γ . For parametrized surfaces defined by the map $\mathbf{x}(\mathbf{r}) : \mathbb{R}^2 \rightarrow \mathbb{R}^3$, and a given scalar function $u(\mathbf{r}) : \mathbb{R}^2 \rightarrow \mathbb{R}$, the tangential gradient may be determined without explicitly computing an extension \tilde{u} using

$$\nabla_\Gamma u(\mathbf{x}(\mathbf{r})) = \mathbf{J}(\mathbf{r}) \cdot \mathbf{G}^{-1}(\mathbf{r}) \cdot \nabla_{\mathbf{r}} u(\mathbf{r}), \quad (2)$$

with $\mathbf{J} = \partial \mathbf{x} / \partial \mathbf{r}$ being the (3×2) -Jacobi matrix and $\mathbf{G} = \mathbf{J}^T \cdot \mathbf{J}$ being the metric tensor (first fundamental form). This is relevant in the context of the surface FEM, where $u(\mathbf{r})$ are the shape functions in the reference element and tangential gradients are to be determined in the physical surface elements. It is noteworthy that $\nabla_\Gamma u$ is in the tangent space of Γ and, thus, $\mathbf{P} \cdot \nabla_\Gamma u = \nabla_\Gamma u$ and $\nabla_\Gamma u \cdot \mathbf{n}_\Gamma = 0$. It is straightforward to determine second order derivatives of scalar functions, see, e.g.,¹⁴. This is important here in the context of stabilization terms in the governing equations.

When surface gradients of *vector* functions $\mathbf{u}(\mathbf{x}) : \Gamma \rightarrow \mathbb{R}^3$ are considered, it is important to distinguish directional and covariant gradients:

$$\begin{aligned} \nabla_\Gamma^{\text{dir}} \mathbf{u}(\mathbf{x}) &= \nabla_\Gamma^{\text{dir}} \begin{bmatrix} u(\mathbf{x}) \\ v(\mathbf{x}) \\ w(\mathbf{x}) \end{bmatrix} = \begin{bmatrix} (\nabla_\Gamma^{\text{dir}} u)^T \\ (\nabla_\Gamma^{\text{dir}} v)^T \\ (\nabla_\Gamma^{\text{dir}} w)^T \end{bmatrix} = \nabla \tilde{\mathbf{u}} \cdot \mathbf{P}, \\ \nabla_\Gamma^{\text{cov}} \mathbf{u}(\mathbf{x}) &= \mathbf{P} \cdot \nabla_\Gamma^{\text{dir}} \mathbf{u}(\mathbf{x}) = \mathbf{P} \cdot \nabla \tilde{\mathbf{u}} \cdot \mathbf{P}. \end{aligned}$$

Concerning the surface divergence of vector functions $\mathbf{u}(\mathbf{x}) : \Gamma \rightarrow \mathbb{R}^3$ and tensor functions $\mathbf{A}(\mathbf{x}) : \Gamma \rightarrow \mathbb{R}^{3 \times 3}$, there holds

$$\begin{aligned} \text{div}_\Gamma \mathbf{u}(\mathbf{x}) &= \text{tr}(\nabla_\Gamma^{\text{dir}} \mathbf{u}) = \text{tr}(\nabla_\Gamma^{\text{cov}} \mathbf{u}) =: \nabla_\Gamma \cdot \mathbf{u}, \\ \text{div}_\Gamma \mathbf{A}(\mathbf{x}) &= \begin{bmatrix} \text{div}_\Gamma(A_{11}, A_{12}, A_{13}) \\ \text{div}_\Gamma(A_{21}, A_{22}, A_{23}) \\ \text{div}_\Gamma(A_{31}, A_{32}, A_{33}) \end{bmatrix} =: \nabla_\Gamma \cdot \mathbf{A}. \end{aligned}$$

To derive the weak form of the governing equations, the following divergence theorem on manifolds is needed^{14,15},

$$\int_\Gamma \mathbf{u} \cdot \text{div}_\Gamma \mathbf{A} \, dA = - \int_\Gamma \nabla_\Gamma^{\text{dir}} \mathbf{u} : \mathbf{A} \, dA + \int_\Gamma \kappa \cdot \mathbf{u} \cdot \mathbf{A} \cdot \mathbf{n}_\Gamma \, dA + \int_{\partial\Gamma} \mathbf{u} \cdot \mathbf{A} \cdot \mathbf{n}_{\partial\Gamma} \, ds, \quad (3)$$

where $\nabla_\Gamma^{\text{dir}} \mathbf{u} : \mathbf{A} = \text{tr}(\nabla_\Gamma^{\text{dir}} \mathbf{u} \cdot \mathbf{A}^T)$. For *tangential* tensor functions with $\mathbf{A} = \mathbf{P} \cdot \mathbf{A} \cdot \mathbf{P}$, the term involving the curvature κ vanishes and one finds $\nabla_\Gamma^{\text{dir}} \mathbf{u} : \mathbf{A} = \nabla_\Gamma^{\text{cov}} \mathbf{u} : \mathbf{A}$.

2.2 Flow models in strong forms

The governing equations for incompressible flows on manifolds are found, e.g., in¹⁻³ among others. The outline here closely follows¹².

2.2.1 Stationary Stokes flow

Stationary Stokes flow on a manifold is considered first. Let $\mathbf{u}(\mathbf{x}) \in C^2(\Gamma)$ be the three-dimensional velocity field on the surface Γ , $p(\mathbf{x}) \in C^1(\Gamma)$ a pressure field, and $\mathbf{f}_t(\mathbf{x})$ a tan-

gential body force. The governing field equations to be fulfilled $\forall \mathbf{x} \in \Gamma$ are

$$-\mathbf{P} \cdot \operatorname{div}_{\Gamma} \boldsymbol{\sigma}(\mathbf{u}, p) = \mathbf{f}_t, \quad (4)$$

$$\operatorname{div}_{\Gamma} \mathbf{u} = 0, \quad (5)$$

$$\mathbf{u} \cdot \mathbf{n}_{\Gamma} = 0. \quad (6)$$

Equation (4) expands to three momentum equations, equation (5) is the incompressibility constraint and equation (6) represents the tangential velocity constraint that restricts the velocities to the tangent space of Γ . Two different strain tensors are introduced,

$$\boldsymbol{\varepsilon}^{\operatorname{dir}}(\mathbf{u}) = \frac{1}{2} \cdot \left(\nabla_{\Gamma}^{\operatorname{dir}} \mathbf{u} + \left(\nabla_{\Gamma}^{\operatorname{dir}} \mathbf{u} \right)^{\operatorname{T}} \right), \quad \boldsymbol{\varepsilon}^{\operatorname{cov}}(\mathbf{u}) = \frac{1}{2} \cdot \left(\nabla_{\Gamma}^{\operatorname{cov}} \mathbf{u} + \left(\nabla_{\Gamma}^{\operatorname{cov}} \mathbf{u} \right)^{\operatorname{T}} \right),$$

which are related to each other as $\boldsymbol{\varepsilon}^{\operatorname{cov}}(\mathbf{u}) = \mathbf{P} \cdot \boldsymbol{\varepsilon}^{\operatorname{dir}}(\mathbf{u}) \cdot \mathbf{P}$. The stress tensor is then defined as

$$\boldsymbol{\sigma}(\mathbf{u}, p) = -p \cdot \mathbf{P} + 2\mu \cdot \boldsymbol{\varepsilon}^{\operatorname{cov}}(\mathbf{u})$$

where $\mu \in \mathbb{R}^+$ is the (constant) dynamic viscosity. Dirichlet and Neumann boundary conditions on $\partial\Gamma_{\operatorname{D}}$ and $\partial\Gamma_{\operatorname{N}}$, respectively, are a straightforward extension from the flat case and are omitted here for brevity.

2.2.2 Stationary Navier-Stokes flow

For stationary *Navier-Stokes* flow, a non-linear advection term is added to equation (4) resulting into

$$\varrho \cdot (\mathbf{u} \cdot \nabla_{\Gamma}^{\operatorname{cov}}) \mathbf{u} - \mathbf{P} \cdot \operatorname{div}_{\Gamma} \boldsymbol{\sigma}(\mathbf{x}) = \mathbf{f}_t(\mathbf{x}), \quad (7)$$

where $\varrho \in \mathbb{R}^+$ is the (constant) fluid density and $(\mathbf{u} \cdot \nabla_{\Gamma}^{\operatorname{cov}}) \mathbf{u} := (\nabla_{\Gamma}^{\operatorname{cov}} \mathbf{u}) \cdot \mathbf{u}$. One may also write the body force as $\mathbf{f}_t(\mathbf{x}) = \varrho \cdot \mathbf{g}_t(\mathbf{x})$ where \mathbf{g}_t may, e.g., consider gravity. The remaining equations (5) and (6) and the boundary conditions remain unchanged.

2.2.3 Instationary Navier-Stokes flow

For *instationary* Navier-Stokes flow, the momentum equation (4) changes to

$$\varrho \cdot (\partial_t \mathbf{u}(\mathbf{x}, t) + (\mathbf{u} \cdot \nabla_{\Gamma}^{\operatorname{cov}}) \mathbf{u} - \mathbf{g}_t(\mathbf{x}, t)) - \mathbf{P} \cdot \operatorname{div}_{\Gamma} \boldsymbol{\sigma}(\mathbf{x}, t) = \mathbf{0}. \quad (8)$$

The functions representing the physical fields live in space (on Γ) *and* time, i.e., in the time interval $\tau = [0, T]$. Therefore, Eqs. (8), (5), and (6) have to be solved in the space-time domain $\Gamma \times \tau$. Herein, we restrict ourselves to spatially fixed manifolds Γ . The boundary conditions also extend in time dimension. Furthermore, an initial condition $\mathbf{u}_0(\mathbf{x}) = \mathbf{u}(\mathbf{x}, 0)$ is needed, which fulfills $\operatorname{div}_{\Gamma} \mathbf{u}_0 = 0$ and $\mathbf{u}_0 \cdot \mathbf{n}_{\Gamma} = 0$.

2.3 Flow models in weak forms

The standard procedure to obtain weak forms of the governing equations from above is applied: Suitable test and trial function spaces are introduced, the equations in strong form are multiplied by test functions and the divergence theorem on manifolds is applied. It is noted that the surface FEM is used for the discretization of the weak forms. A mixed FEM is used where individual orders for the geometry, k_{geom} , the velocities, k_u , the pressure, k_p , and the Lagrange multiplier for enforcing the tangential velocity constraint, k_λ , are employed. All shape functions are mapped to the same geometry mesh defining the discrete manifold Γ^h . All quantities introduced above such as the normal vector, projector, and surface operators now refer to Γ^h rather than Γ .

Assume the following suitable discrete test and trial function spaces, resp.,

$$\mathcal{S}_u^h = \left\{ \mathbf{u}^h \in [\mathcal{Q}_{k_u}^h]^3, \mathbf{u}^h = \hat{\mathbf{u}}^h \text{ on } \partial\Gamma_D^h \right\}, \quad (9)$$

$$\mathcal{V}_u^h = \left\{ \mathbf{w}_u^h \in [\mathcal{Q}_{k_u}^h]^3, \mathbf{w}_u^h = \mathbf{0} \text{ on } \partial\Gamma_D^h \right\}, \quad (10)$$

$$\mathcal{S}_p^h = \mathcal{V}_p^h = \mathcal{Q}_{k_p}^h, \quad (11)$$

$$\mathcal{S}_\lambda^h = \mathcal{V}_\lambda^h = \mathcal{Q}_{k_\lambda}^h. \quad (12)$$

\mathcal{Q}_k^h is a general finite element space of order k , i.e., the set of k -th order shape functions mapped to the geometry mesh.

2.3.1 Stationary Stokes flow

The discrete weak form of the Stokes problem reads: Given viscosity $\mu \in \mathbb{R}^+$, body force $\mathbf{f}^h(\mathbf{x})$ in Γ^h , and traction $\hat{\mathbf{t}}^h(\mathbf{x})$ on $\partial\Gamma_N^h$, find the velocity field $\mathbf{u}^h(\mathbf{x}) \in \mathcal{S}_u^h$, pressure field $p^h(\mathbf{x}) \in \mathcal{S}_p^h$, and Lagrange multiplier field $\lambda^h(\mathbf{x}) \in \mathcal{S}_\lambda^h$ such that for all test functions $(\mathbf{w}_u^h, w_p^h, w_\lambda^h) \in \mathcal{V}_u^h \times \mathcal{V}_p^h \times \mathcal{V}_\lambda^h$, there holds in Γ^h

$$\int_\Gamma \nabla_\Gamma^{\text{dir}} \mathbf{w}_u^h : \boldsymbol{\sigma}(\mathbf{u}^h, p^h) \, dA + \int_\Gamma \lambda^h \cdot (\mathbf{w}_u^h \cdot \mathbf{n}_\Gamma^h) \, dA = \int_\Gamma \mathbf{w}_u^h \cdot \mathbf{f}^h \, dA + \int_{\partial\Gamma_N^h} \mathbf{w}_u^h \cdot \hat{\mathbf{t}}^h \, dA, \quad (13)$$

$$\int_\Gamma w_p^h \cdot \text{div}_\Gamma \mathbf{u}^h \, dA = 0, \quad (14)$$

$$\int_\Gamma w_\lambda^h \cdot (\mathbf{u}^h \cdot \mathbf{n}_\Gamma^h) \, dA = 0. \quad (15)$$

The usual element assembly yields a linear system of equations with a saddle point structure as expected in the context of Lagrange multipliers. The well-known Babuška-Brezzi condition^{8,9} must be fulfilled to obtain useful solutions for all involved fields. This indicates that all involved element orders must be chosen carefully to meet these requirements.

2.3.2 Stationary Navier-Stokes flow

The discrete weak form of the stationary Navier-Stokes problem reads: Given density $\varrho \in \mathbb{R}^+$, viscosity $\mu \in \mathbb{R}^+$, body force $\varrho \cdot \mathbf{g}^h(\mathbf{x})$ in Γ^h , and traction $\hat{\mathbf{t}}^h(\mathbf{x})$ on $\partial\Gamma_N^h$, find the velocity field $\mathbf{u}^h(\mathbf{x}) \in \mathcal{S}_u^h$, pressure field $p^h(\mathbf{x}) \in \mathcal{S}_p^h$, and Lagrange multiplier field $\lambda^h(\mathbf{x}) \in \mathcal{S}_\lambda^h$ such that for all test functions $(\mathbf{w}_u^h, w_p^h, w_\lambda^h) \in \mathcal{V}_u^h \times \mathcal{V}_p^h \times \mathcal{V}_\lambda^h$, there holds in Γ^h

$$\begin{aligned} & \varrho \cdot \int_{\Gamma} \mathbf{w}_u^h \cdot \left((\mathbf{u}^h \cdot \nabla_{\Gamma}^{\text{cov}}) \mathbf{u}^h - \mathbf{g}^h \right) dA + \int_{\Gamma} \nabla_{\Gamma}^{\text{dir}} \mathbf{w}_u^h : \boldsymbol{\sigma}(\mathbf{u}^h, p^h) dA + \int_{\Gamma} \lambda^h \cdot (\mathbf{w}_u^h \cdot \mathbf{n}_{\Gamma}^h) dA \\ & - \int_{\partial\Gamma_N} \mathbf{w}_u^h \cdot \hat{\mathbf{t}}^h ds + \int_{\Gamma} w_p^h \cdot \text{div}_{\Gamma} \mathbf{u}^h dA + \int_{\Gamma} w_{\lambda}^h \cdot (\mathbf{u}^h \cdot \mathbf{n}_{\Gamma}^h) dA \\ & + \sum_{e=1}^{n_{\text{el}}} \int_{\Gamma_e} \tau_{\text{SUPG}} \left((\mathbf{u}^h \cdot \nabla_{\Gamma}^{\text{cov}}) \mathbf{w}_u^h \right) \cdot \left[\varrho \cdot \left((\mathbf{u}^h \cdot \nabla_{\Gamma}^{\text{cov}}) \mathbf{u}^h - \mathbf{g}^h \right) - \text{div}_{\Gamma} \boldsymbol{\sigma}(\mathbf{u}^h, p^h) \right] = 0. \end{aligned}$$

The equations related to the different field equations were added up for brevity. The last row adds a stabilization term which is needed to obtain stable solutions for flows at high Reynolds numbers^{16,17}. In particular, the streamline upwind Petrov-Galerkin (SUPG) method is used for the stabilization. Different definitions of the stabilization parameter τ_{SUPG} are found^{11,18} and $\tau_{\text{SUPG}} = 0$ is used when no stabilization is needed. In the stabilization term, second-order derivatives appear in the element interiors.

2.3.3 Instationary Navier-Stokes flow

The discrete weak form of the instationary Navier-Stokes problem is: Given density $\varrho \in \mathbb{R}^+$, viscosity $\mu \in \mathbb{R}^+$, body force $\varrho \cdot \mathbf{g}^h(\mathbf{x}, t)$ in $\Gamma^h \times \tau$, traction $\hat{\mathbf{t}}^h(\mathbf{x}, t)$ on $\partial\Gamma_N^h \times \tau$, and initial condition $\mathbf{u}_0^h(\mathbf{x})$ on Γ^h at $t = 0$, find the velocity field $\mathbf{u}^h(\mathbf{x}, t) \in L_2(\tau; \mathcal{S}_u^h)$, pressure field $p^h(\mathbf{x}, t) \in L_2(\tau; \mathcal{S}_p^h)$, and Lagrange multiplier field $\lambda^h(\mathbf{x}, t) \in L_2(\tau; \mathcal{S}_\lambda^h)$ such that for all test functions $(\mathbf{w}_u^h, w_p^h, w_\lambda^h) \in \mathcal{V}_u^h \times \mathcal{V}_p^h \times \mathcal{V}_\lambda^h$, there holds in $\Gamma^h \times \tau$

$$\begin{aligned} & \varrho \cdot \int_{\Gamma} \mathbf{w}_u^h \cdot \left(\partial_t \mathbf{u}^h + (\mathbf{u}^h \cdot \nabla_{\Gamma}^{\text{cov}}) \mathbf{u}^h - \mathbf{g}^h \right) dA + \int_{\Gamma} \nabla_{\Gamma}^{\text{dir}} \mathbf{w}_u^h : \boldsymbol{\sigma}(\mathbf{u}^h, p^h) dA + \int_{\Gamma} \lambda^h \cdot (\mathbf{w}_u^h \cdot \mathbf{n}_{\Gamma}^h) dA \\ & - \int_{\partial\Gamma_N} \mathbf{w}_u^h \cdot \hat{\mathbf{t}}^h ds + \int_{\Gamma} w_p^h \cdot \text{div}_{\Gamma} \mathbf{u}^h dA + \int_{\Gamma} w_{\lambda}^h \cdot (\mathbf{u}^h \cdot \mathbf{n}_{\Gamma}^h) dA \\ & + \sum_{e=1}^{n_{\text{el}}} \int_{\Gamma_e} \tau_{\text{SUPG}} \left((\mathbf{u}^h \cdot \nabla_{\Gamma}^{\text{cov}}) \mathbf{w}_u^h \right) \cdot \left[\varrho \cdot \left(\partial_t \mathbf{u}^h + (\mathbf{u}^h \cdot \nabla_{\Gamma}^{\text{cov}}) \mathbf{u}^h - \mathbf{g}^h \right) - \text{div}_{\Gamma} \boldsymbol{\sigma}(\mathbf{u}^h, p^h) \right] = 0. \end{aligned}$$

This yields a system of non-linear semi-discrete equations with initial condition $\mathbf{u}(0)$. This system may be advanced in time by using finite difference schemes and the Crank-Nicolson method is employed herein.

3 NUMERICAL RESULTS

A number of test cases have already been proposed in¹². Herein, two more test cases are suggested and even higher element orders are used for the approximations.

Because analytic solutions are hardly available in the context of flows on curved surfaces, we find it useful to study the error in the strong form of the governing equations as given in Section 2.2. Of course, due to the C_0 -continuity of the FE shape functions, those equations involving second-order derivatives may only be integrated over element interiors (just as the stabilization terms from above). For the example of stationary Stokes flow, the corresponding residual errors are defined as

$$\varepsilon_{\text{mom}} = \sqrt{\sum_{e=1}^{n_{\text{el}}} \int_{\Gamma_e} \left(\mathbf{P} \cdot \text{div}_{\Gamma} \boldsymbol{\sigma}(\mathbf{u}^h, p^h) + \mathbf{f}^h \right)^2 dA} \quad (16)$$

and

$$\varepsilon_{\text{cont}} = \sqrt{\int_{\Gamma} \left(\text{div}_{\Gamma} \mathbf{u}^h \right)^2 dA}, \quad \varepsilon_{\text{tang}} = \sqrt{\int_{\Gamma} \left(\mathbf{u}^h \cdot \mathbf{n}_{\Gamma}^h \right)^2 dA}. \quad (17)$$

This can be easily extended to the case of Navier-Stokes flows where the advection term is added to the integrand in (16).

3.1 Stationary flow on a deformed ring

A flow is considered on a deformed ring as shown in Fig. 2(a). The domain is generated using an annulus with inner radius $R_{\text{in}} = 0.5$ and outer radius $R_{\text{out}} = 1.0$ as a starting point, that is, $\Omega_r = \{\mathbf{r} \in \mathbb{R}^2 : R_{\text{in}} \leq \|\mathbf{r}\| \leq R_{\text{out}}\} \subset \mathbb{R}^2$. This annulus is associated with a third dimension using the coordinate

$$t(\mathbf{r}) = 1 - \frac{\exp\left(-1/2 \left(\frac{\|\mathbf{r}\| - \mu}{\sigma}\right)^2\right)}{\sqrt{2\pi\sigma}}, \quad \text{with } \mu = 3/4 \text{ and } \sigma = 1/4.$$

This yields a manifold Γ_r in the three-dimensional coordinate system (r, s, t) which is further deformed with a map $\mathbf{x}(\mathbf{r})$ as

$$\begin{aligned} x(\mathbf{r}) &= \tilde{r} + \tilde{r}^2 + 1/10 \cdot \sin(\tilde{r}) - 3, \\ y(\mathbf{r}) &= \tilde{s} + 1/2 \cdot \tilde{s}^2 + 1/10 \cdot \cos(\tilde{s}) - 2, \\ z(\mathbf{r}) &= t + 1/5 \cdot \sin(x(\mathbf{r}) \cdot y(\mathbf{r})), \end{aligned}$$

with $\tilde{r} = 1.2 + r$ and $\tilde{s} = 1.2 + s$. A rigid body rotation by 30° around the z -axis yields the manifold of interest Γ .

It is simple to generate meshes with the desired number of elements in radial and circumferential direction. Examples for meshes composed of quadrilateral and triangular elements are seen in Figs. 2(b) and (c).

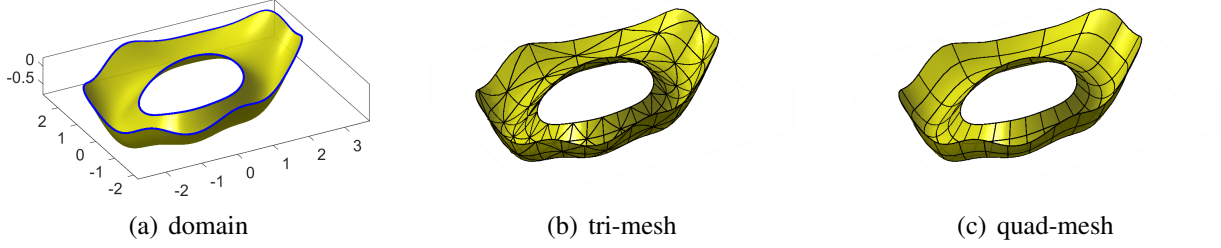


Figure 2: Ring test case: (a) domain, and meshes composed by (b) triangular and (c) quadrilateral elements.

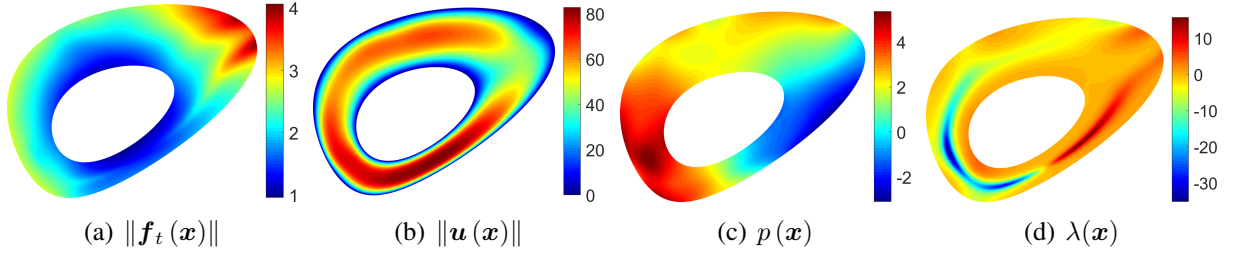


Figure 3: Ring test case from top view: (a) acceleration magnitude, (b) velocity magnitude, (c) pressure, and (d) Lagrange multiplier field.

The density and viscosity are set to $\varrho = 1$ and $\mu = 0.01$, respectively. No-slip boundary conditions are applied at *all* boundaries. This is because inflow and outflow boundary conditions may render the generation of higher order accurate results difficult. The flow is driven by an acceleration field

$$\mathbf{g}(\mathbf{x}) = \begin{bmatrix} g_x \\ g_y \\ g_z \end{bmatrix} = \begin{bmatrix} -y \\ x \\ 0 \end{bmatrix} \Rightarrow \mathbf{f}_t(\mathbf{x}) = \varrho \cdot \mathbf{P}(\mathbf{x}) \cdot \mathbf{g}(\mathbf{x}).$$

A graphical representation of the driving forces \mathbf{f}_t , and the resulting solutions for the velocity magnitude, the pressure and the Lagrange multiplier are seen in Fig. 3 (when looking in z -direction on the manifold).

For the convergence studies, finite element approximations are carried out on various meshes composed by triangular or quadrilateral Lagrange elements of different orders. Meshes with $n_R = \{4, 6, 10, 14, 20, 30, 40, 60, 80, 100\}$ elements in radial direction and $n_\theta = 4 \cdot n_R$ elements in circumferential direction are used. The individual element orders used for the convergence studies are indicated by a 4-tuple $\{k_{\text{geom}}, k_u, k_p, k_\lambda\}$. To be precise, this tuple summarizes the employed orders for the geometry, k_{geom} , the velocities, k_u , the pressure, k_p , and the Lagrange multiplier for enforcing the tangential velocity constraint, k_λ . For each tuple, meshes with different resolutions (given by n_R and n_θ) are considered and errors calculated, each time resulting

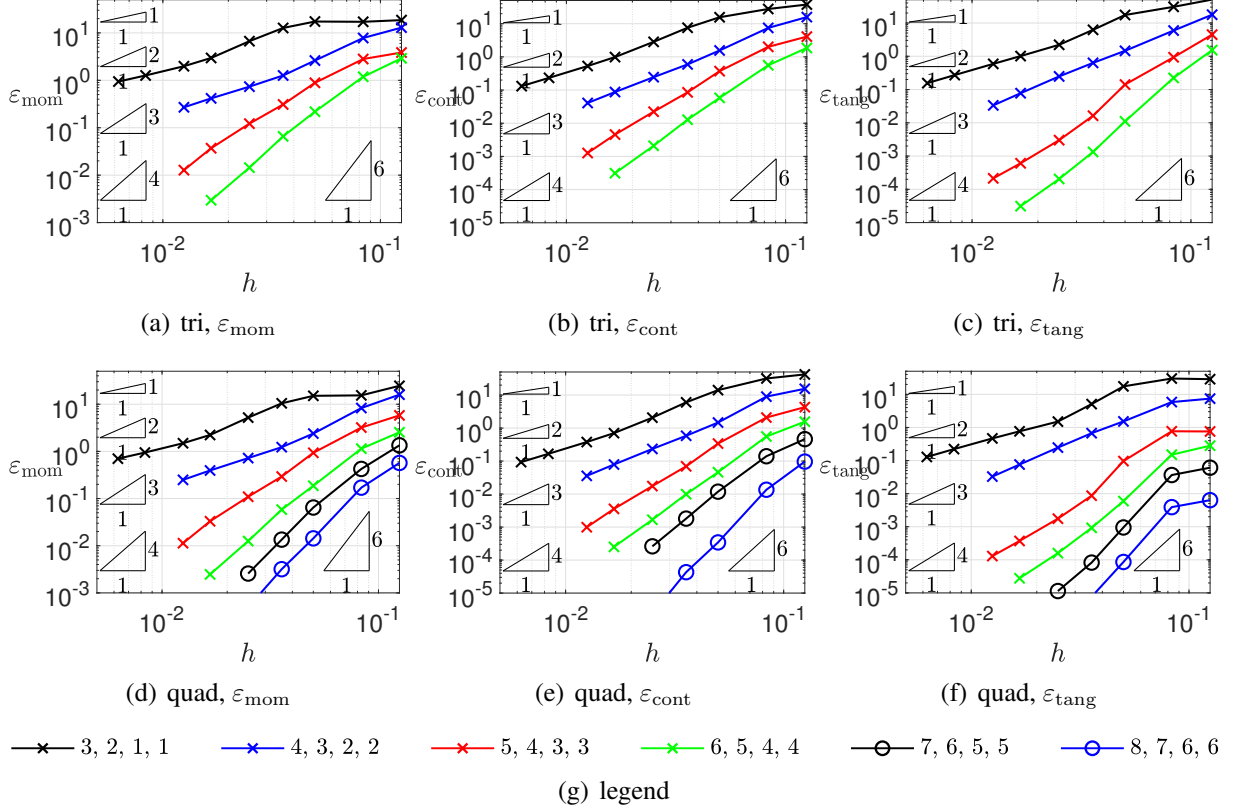


Figure 4: Convergence results in ε_{mom} , $\varepsilon_{\text{cont}}$, and $\varepsilon_{\text{tang}}$ for the ring test case, (a) to (c) for triangular elements, (d) to (f) for quadrilateral elements. The legend in (g) decodes the orders $\{k_{\text{geom}}, k_u, k_p, k_\lambda\}$ of the meshes.

in one curve in the convergence plots as indicated in the legends. The preferred setting, as already suggested in^{12,13}, is to choose $k_{\text{geom}} = k_u + 1$ and $k_p = k_\lambda = k_u - 1$ for some given k_u . With respect to the orders of the velocities compared to the pressure, this is a Taylor-Hood element¹⁹.

Convergence results are seen in Fig. 4. Triangular elements are considered with $2 \leq k_u \leq 5$ and are seen in Figs. 4(a) to (c). Quadrilateral elements are investigated with $2 \leq k_u \leq 7$ and results shown in Figs. 4(d) to (f). It is clearly seen that higher-order convergence rates in ε_{mom} , $\varepsilon_{\text{cont}}$, and $\varepsilon_{\text{tang}}$ are achieved. Because second order derivatives are involved in the computation of ε_{mom} , the convergence rates are (up to) one order less than for $\varepsilon_{\text{cont}}$ and $\varepsilon_{\text{tang}}$.

3.2 Instationary cylinder ring flow

The next example is an instationary Navier-Stokes flow on a ring-like surface with a cylindrical hole, see Fig. 5(a). An example mesh is seen in Fig. 5(b) and elements are refined to resolve the boundary layers. The density and viscosity are prescribed as $\varrho = 1.0$ and $\mu = 0.001$. The

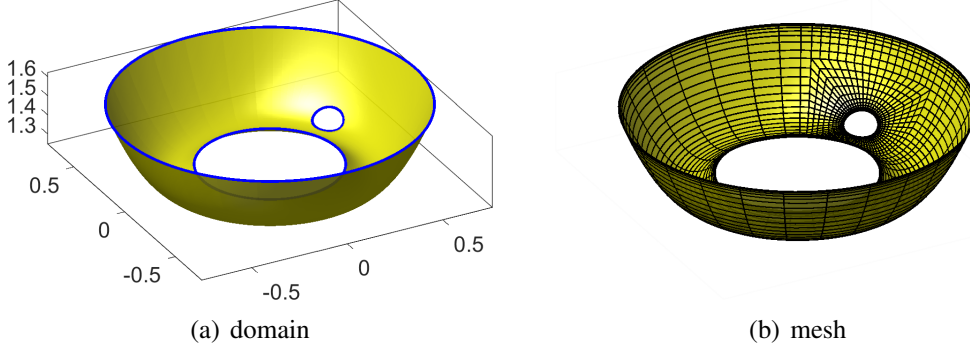


Figure 5: Cylinder test case: (a) domain and (b) mesh.

starting point to generate the curved manifold is the flat two-dimensional cylinder flow according to²⁰. The geometry is first described in 2D based on the coordinates (a, b) , labelled Ω_a , and later on mapped to obtain the curved surface Γ in 3D. In 2D, the cylinder with a diameter of 0.1 is placed slightly unsymmetrically in y -direction of the channel in $[0, 2.20] \times [0, 0.41]$. The curved manifold is then obtained using the following map,

$$\begin{aligned} x(\mathbf{a}) &= \cos(\alpha) \cdot (b + 7/20), \\ y(\mathbf{a}) &= \sin(\alpha) \cdot (b + 7/20), \\ z(\mathbf{a}) &= 2 + 1/2 \cdot d(x, y) - \sin(3 \cdot d(x, y)), \end{aligned}$$

with $\alpha = 10/11 \cdot \pi \cdot a$ and $d(x, y) = \sqrt{x^2 + y^2}$.

The flow is driven by a rotational acceleration field,

$$\mathbf{g}(\mathbf{x}) = \begin{bmatrix} g_x \\ g_y \\ g_z \end{bmatrix} = \begin{bmatrix} -y \\ x \\ 0 \end{bmatrix} \cdot g^*,$$

scaled by the parameter $g^* = \{0.15, 0.175, 0.2, 0.225\}$. The situation is observed in the time interval $t \in [0, 40]$. For $g^* = 0.15$ and at time $t = 40$, the resulting velocity magnitude, pressure, and vorticity are shown in Fig. 6. It is clearly seen that periodic flow patterns known as the Kármán vortex street are observed behind the cylinder.

Element orders of $k_{\text{geom}} = 4$, $k_u = 3$, $k_p = 2$ and $k_\lambda = 2$ are chosen in the numerical studies. 4000 time steps are employed in the Crank Nicolson method. Higher orders or more time steps achieved virtually indistinguishable results for the quantities shown below. To make the results more quantitative, the stresses at the cylinder wall are summed up to obtain a force resultant $F(t) = \|\mathbf{F}(t)\|$ in 3D. This is the equivalent of the lift and drag coefficients for the flat 2D case. Furthermore, the pressure difference between the front and back position of the cylinder (in Ω_{2D} , mapped to three dimensions) is computed, i.e., $\Delta p(t) = p_{\text{front}}(t) - p_{\text{back}}(t)$. Results are shown in Fig. 7 for the different values of g^* scaling the acceleration field. Choosing

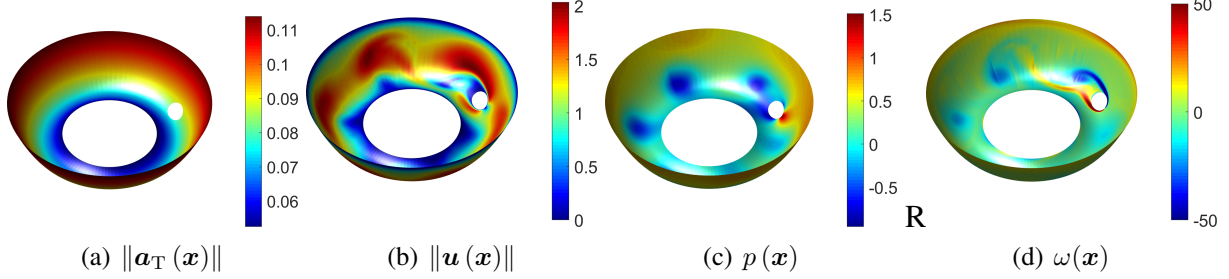


Figure 6: Cylinder test case for $g^* = 0.15$ at time $t = 40$: (a) acceleration magnitude, (b) velocity magnitude, (c) pressure, and (d) vorticity.

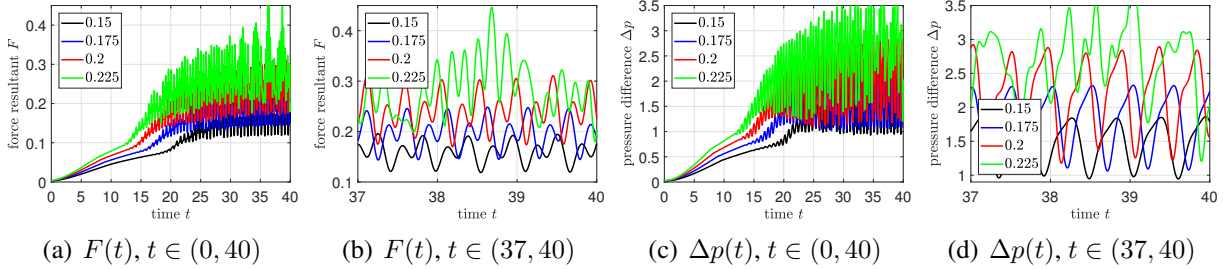


Figure 7: Force resultant $F(t)$ and pressure difference $\Delta p(t)$ obtained for the cylinder flow test case.

higher values for g^* may no longer lead to periodic but rather chaotic results. It is seen that the acceleration field has to act for about 15 seconds until the flow field changes from steady to periodic flow patterns. For $t \geq 35$, the flow patterns are fully established for $g^* \leq 2$.

4 CONCLUSIONS

A mixed, stabilized, higher-order accurate surface finite element method is considered for stationary and instationary Stokes and Navier-Stokes flows on curved surfaces in three dimensions. It is found that when the orders of the involved fields are suitably chosen, higher-order convergence rates are achieved. A particularly useful combination for a given k_u is $k_{\text{geom}} = k_u + 1$ and $k_p = k_\lambda = k_u - 1$. Future works shall investigate different stabilization methods and approaches to enforce the tangential velocity constraint. It is found that flows on manifolds have a strong potential for fundamental research in mathematics, physics, and engineering.

REFERENCES

- [1] D. Bothe, J. Prüss, On the two-phase Navier-Stokes equations with Boussinesq-Scriven surface fluid. *J. math. fluid mech.*, 12, 133–150, 2010.
- [2] T. Jankuhn, M. Olshanskii, A. Reusken, Incompressible fluid problems on embedded surfaces: Modeling and variational formulations. *arXiv:1702.02989*, 2017.

- [3] H. Koba, C. Liu, Y. Giga, Energetic variational approaches for incompressible fluid systems on an evolving surface. *Quart. Appl. Math.*, 75, 359–389, 2017.
- [4] I. Nitschke, A. Voigt, J. Wensch, A finite element approach to incompressible two-phase flow on manifolds. *Journal of Fluid Mechanics*, 708, 418–438, 2012.
- [5] A. Demlow, Higher-order finite element methods and pointwise error estimates for elliptic problems on surfaces. *SIAM J. Numer. Anal.*, 47, 805–827, 2009.
- [6] G. Dziuk. *Finite elements for the Beltrami operator on arbitrary surfaces*, chapter 6, 142–155. Springer Berlin Heidelberg, Berlin, Heidelberg, 1988.
- [7] G. Dziuk, C. Elliott, Finite element methods for surface PDEs. *Acta Numerica*, 22, 289–396, 2013.
- [8] I. Babuška, Error-bounds for finite element method. *Numer. Math.*, 16, 322–333, 1971.
- [9] F. Brezzi, On the existence, uniqueness and approximation of saddle-point problems arising from Lagrange multipliers. *RAIRO Anal. Numér.*, R-2, 129–151, 1974.
- [10] A. Brooks, T. Hughes, Streamline upwind/Petrov-Galerkin formulations for convection dominated flows with particular emphasis on the incompressible Navier-Stokes equations. *Comp. Methods Appl. Mech. Engrg.*, 32, 199–259, 1982.
- [11] T. Tezduyar, S. Sathe, Stabilization parameters in SUPG and PSPG formulations. *J. Comput. Appl. Math.*, 4, 71–88, 2003.
- [12] T. Fries, Higher-order surface FEM for incompressible Navier-Stokes flows on manifolds. *Int. J. Numer. Methods Fluids*, doi:10.1002/fld.4510, accepted, 2018.
- [13] T. Fries, Higher-order surface FEM for incompressible Navier-Stokes flows on manifolds. *arXiv: 1712.02520*, 2017.
- [14] M. Delfour, J. Zolésio, *Shapes and geometries—metrics, analysis, differential calculus, and optimization*. SIAM, Philadelphia, PA, 2011.
- [15] M. Delfour, J. Zolésio, Tangential differential equations for dynamical thin-shallow shells. *Journal of Differential Equations*, 128, 125–167, 1996.
- [16] J. Donea, A. Huerta, *Finite element methods for flow problems*. John Wiley & Sons, Chichester, 2003.
- [17] P. Gresho, R. Sani, *Incompressible flow and the finite element method*, Vol. 1+2. John Wiley & Sons, Chichester, 2000.
- [18] F. Shakib, T. Hughes, Z. Johan, A new finite element formulation for computational fluid dynamics: X. The compressible Euler and Navier-Stokes equations. *Comp. Methods Appl. Mech. Engrg.*, 89, 141–219, 1991.
- [19] C. Taylor, P. Hood, A numerical solution of the navier-stokes equations using the finite element technique. *Computers & Fluids*, 1, 73–100, 1973.
- [20] M. Schäfer, S. Turek, Benchmark computations of laminar flow around a cylinder. In E. Hirschel, editor, *Flow Simulation with High-Performance Computers II*. Vieweg Verlag, Braunschweig, 1996.

Poroelastic Assessment of Interstitial Fluid Flow Around Osteocytes in Osteoporotic Conditions

Susannah Fritton*, Vittorio Gatti**, Evan Azoulay***, Michelle Gelbs****, Michael Gerber*****

*The City College of New York, **The City College of New York, ***The City College of New York, ****The City College of New York, *****The City College of New York

ABSTRACT

The objective of this work was to assess whether interstitial fluid flow, which is critical for bone's mechanosensory system, is compromised in osteoporotic bone. Using poroelastic finite element modeling, we investigated whether changes in bone's microporosity, including the vascular and lacunar-canalicular porosities, can affect interstitial fluid flow. Two pre-clinical models were assessed: a rat ovariectomy model of postmenopausal osteoporosis, and a rat muscle-paralysis model of disuse osteoporosis. Animal-specific finite element models were created from high-resolution micro-CT scans of rat tibiae for estrogen-deficient (n=12) and disuse (n=16) experiments. The results demonstrate that increased vascular porosity due to either estrogen deficiency or disuse decreases interstitial fluid flow around osteocytes embedded in the bone cortex. By comparing the results of the two modeling studies we conclude that changes in the lacunar-canalicular fluid velocity are proportional to the increase in vascular porosity (or decrease in vascular pore separation). While vascular porosity negatively influenced bone fluid flow, it was more difficult to elucidate potential effects of changes in the lacunar-canalicular porosity for both the estrogen deficiency and disuse conditions. In the disuse study, we were able to improve the animal-specific modeling approach by representing the osteocytic lacunar network within the micro-CT derived finite element models. The rats subjected to muscle paralysis demonstrated a reduced lacunar density, but the results of the numerical analysis revealed no correlation of the reduced lacunar density with the average fluid velocity near the lacunae. An important improvement of the finite element modeling approach with the disuse project was the possibility of predicting fluid flow around a large number of osteocyte lacunae. Advancement in the imaging and computational methods allowed the quantification of the fluid flow around 500-1000 osteocyte lacunae, contained in relatively large volumes of bone cortex. This method can provide a significant advantage in describing bone's mechanosensory system at a multiscale level: from the single osteocyte response to the macroscopic whole-bone changes, including a mesoscale level, where a group of osteocytes (100-1000) can locally respond in a concerted way. Our modeling approach led to the important observation that fluid velocity around osteocytes depends largely on their specific position in the cortex. This could explain the variability of the morphology and function of the osteocytic network. In future studies, we can use this modeling approach to compare fluid flow around osteocytes with their specific biological activity, helping to bridge the gap between different scales of functional adaptation mechanisms.

Validating the Tsunami Propagation Model Geoclaw, Based on the 1995, Mw7.2 Nuweiba Earthquake

Eran Frucht^{*}, Amos Salamon^{**}, Rachamim Shem Tov^{***}, Hanan Ginat^{****}, Erez Gal^{*****}

^{*}Department of Structural Eng., Ben-Gurion University, ^{**}Geological Survey of Israel, ^{***}The Dead Sea-Arava Science Center (DSASC), ^{****}The Dead Sea-Arava Science Center (DSASC), ^{*****}Department of Structural Eng., Ben-Gurion University

ABSTRACT

The tsunami reported after the strong Mw7.2 1995 Nuweiba earthquake, together with prehistoric tsunamites found along the head of the Gulf of Elat-Aqaba (GOA) and the adjacent Red Sea, emphasize the natural hazard there. The Gulf is located along the southern part of the Dead Sea Transform, which is an active system that generates frequent strong and destructive earthquakes. The presence of a water body inside the Gulf produces potential for a tsunami by submarine earthquakes and landslides. Here we investigate the 1995 Nuweiba tsunami and validate our numerical model, as part of the preliminary evaluation of tsunami hazard along the Head of the Gulf. First, we constructed the bathymetry and topography grid of the Gulf. Next, we adopted the GeoClaw tsunami modeling program, which can solve 2D depth-averaged shallow water equations, simulate wave propagation and compute tsunami wave heights and inundation. We then simulated the 1995 Nuweiba tsunami and produced time series of the expected wave height in several artificial gauges along the northern part of the Gulf. Based on various models of the source parameters of the 1995 Nuweiba earthquake, four different scenarios were simulated. The results were then compared with field evidence, eyewitness reports and the recorded mareogram, as well as with the numerical model proposed by Abril et al. (2017). Overall, the results show relatively small waves, in the order of and in accordance with the field observations, the recorded mareogram and the numerical model of Abril et al. The findings provide profound validation of the GeoClaw model. The methodology and outcomes of this work lay down the foundation for a thorough and systematic evaluation of the tsunami hazard in this area.

Conceptual Design of a Soft Material Linear Switched Reluctance Motor for Soft Robotic Applications

Arian Fröhlich^{*}, Christoph Thon^{**}, Franz Dietrich^{***}, Carsten Schilde^{****}

^{*}Institute of Machine Tools and Production Technology, Technische Universität Braunschweig, ^{**}Institute for Particle Technology, Technische Universität Braunschweig, ^{***}Institute of Machine Tools and Production Technology, Technische Universität Braunschweig, ^{****}Institute for Particle Technology, Technische Universität Braunschweig

ABSTRACT

Common actuation principles in soft material robotics require rigid components in their chain of energy conversion devices, for example fluid pumps or tendon winding motors. In a strict sense, their embodiment in a robot, can hardly be called structurally “soft”. There are other actuation principles that use elastic or pseudo-elastic materials to transform electrical power into motion in “soft” structures directly, for example shape memory alloys and electro-active polymers. Nevertheless, power limits or travel range limits, performance quality, short material life time, electrical hazards or further practical difficulties may inhibit their deployment. This need for soft actuation principles with high power density, large travel ranges, manufacturable design, robustness, and simple systems integration is the motivation for this approach. In order to establish all-soft actuators, this approach strives for direct conversion of electrical power into motion by electro-magnetism. It is the objective to elaborate the fundamentals of electro-magnetic actuators which consist of highly elastic materials so that, ultimately, such devices can be embedded into soft robot structures without disturbing the robot’s structural softness. Among the electro-magnetic motor principles, the switched reluctance motor is identified as the research subject of highest priority, because the realization of effective elastic magnetic flux guidance therein is a preliminary technology for the other, more complex electromagnetic motor principles. In order to yield the actuation force, such an actuator requires a set of coil-driven magnetic circuits, which change their inductances when the mover travels. It is proposed to realize the magnetic circuit, which has to guide the magnetic flux through the coil and the mover, by an elastic material filled with ferro-magnetic particles. Hereby, the main technical target is to maximize the amplitude change of the magnet circuit’s inductance. The key to an effective actuator design addressed by this approach lies hence in a combination of particle embedding technology in complex shapes for effective magnetic flux geometries and model-based systems engineering that considers the cross-domain complexity of such actuators. Both are supported by function- and manufacturing-oriented simulations, such as a coupled DEM simulation for particle-filled flux guidance geometries.

Superconvergence HDG Methods on Polygonal Meshes

Guosheng Fu^{*}, Bernardo Cockburn^{**}

^{*}Brown University, ^{**}University of Minnesota

ABSTRACT

We present a new technique called M-decompositions to construct superconvergent HDG methods for diffusion problem on polygonal meshes. With the help of M-decompositions, new high-order H^1 and $H(\text{div})$ conforming finite elements are discovered.

Two Scale Topology Optimization of Shell-infill Structures Using Level Set Method

Junjian Fu^{*}, Liang Gao^{**}, Hao Li^{***}, Mi Xiao^{****}

^{*}State Key Lab of Digital Manufacturing Equipment and Technology, Huazhong University of Science and Technology, China, ^{**}State Key Lab of Digital Manufacturing Equipment and Technology, Huazhong University of Science and Technology, China, ^{***}State Key Lab of Digital Manufacturing Equipment and Technology, Huazhong University of Science and Technology, China, ^{****}State Key Lab of Digital Manufacturing Equipment and Technology, Huazhong University of Science and Technology, China

ABSTRACT

This paper proposed a two scale topology optimization method for shell-infill structures based on level set method. Two level set functions are utilized to represent the structural boundaries of macro shell and the micro infill, respectively. In the macroscopic, the design of the shell structure is defined as a compliance minimization problem. The macro shell is captured by the contour area between the zero and the k level set. The value of k is equal to the thickness of the shell. A reinitialization scheme is imposed on the macro level set function to guarantee a uniform thickness of the shell. In the microscopic, the infill is designed by periodic microstructures with the same configuration. Viewing the compliance of macro structure as the objective function, these microstructures are optimized based on level set method. The numerical homogenization method is applied to evaluate the effective elasticity tensor of the microstructure, which bridges the connection between the microstructure and the macro material property. Both 2D and 3D numerical examples are investigated to demonstrate the effectiveness of the proposed method. Results indicate that this method is of great potential in the design of bio-inspired and additive manufacturing oriented structures. Keywords: Topology optimization, Shell-infill structures, Level set method

References [1] Clausen A, Aage N, Sigmund O. Topology optimization of coated structures and material interface problems[J]. Computer Methods in Applied Mechanics and Engineering, 2015, 290: 524-541. [2] Wu J, Clausen A, Sigmund O. Minimum compliance topology optimization of shell-infill composites for additive manufacturing[J]. Computer Methods in Applied Mechanics and Engineering, 2017, 326. [3] Wang Y, Kang Z. A level set method for shape and topology optimization of coated structures[J]. Computer Methods in Applied Mechanics & Engineering, 2018, 329:553-574.

High-order Targeted ENO Scheme for Turbulence Simulations

Lin Fu^{*}, Nikolaus A. Adams^{**}

^{*}Center for Turbulence Research, Stanford University, ^{**}Chair of Aerodynamics and Fluid mechanics, Technical University of Munich

ABSTRACT

In this paper, we present a high-order targeted ENO scheme, which shows exceptional performance in conventional compressible gas dynamics, extreme simulations (Mach number of 2000), incompressible and compressible turbulence reproduction. For conventional compressible gas dynamics, the TENO scheme is robust, and shows low numerical dissipation in resolving high-wavenumber physical fluctuations while capturing the discontinuities sharply. For the extreme simulations, the proposed scheme is numerically stable and preserves the ENO property. In terms of turbulence simulations, it can faithfully predict the energy transfer for incompressible flows, resolve the vorticity, entropy and acoustic models for compressible flows. A set of benchmark simulations will be computed to validate the performance of proposed scheme.

Variational Approach of Coarse-grained Lipid Dynamics Based on Potential for Amphiphilic Molecules

Szu-Pei Fu^{*}, Rolf Ryham^{**}, Yuan-Nan Young^{***}

^{*}Fordham University, ^{**}Fordham University, ^{***}New Jersey Institute of Technology

ABSTRACT

In macroscopic models, the well-known Helfrich Hamiltonian membrane model has been extensively used to capture macroscopic physical properties of a lipid bilayer membrane. Some phenomena such as membrane fusion and micelle formation are, however, challenging to described using a macroscopic framework, and including all the molecular details has its challenges, from a numerical simulation perspective. Therefore, in order to include the salient molecular details in a coarse-grained manner, we study the dynamics of lipid bilayer membrane using Janus-type particle configurations to represent collections of lipids. These coarse-grained lipid molecules interact through an action field that measures water activity due to the presence of nearby hydrophobic surfaces, leading to specific boundary conditions on each Janus particle. We adopt two numerical frameworks to investigate the particle dynamics: (1) the finite element method (FEM); (2) the quadrature by expansion method. We also examine the numerical accuracy and qualitative comparisons for large system simulations, and compare with other potential-theoretic methods.

3D Numerical Simulation on the Interaction between Hydraulic Fractures and Natural Fractures with Spatially-Variied Properties

Wei Fu^{*}, Alexei Savitski^{**}, Branko Damjanac^{***}, Andrew P. Bunger^{****}

^{*}University of Pittsburgh, ^{**}Shell, ^{***}Itasca Consulting, ^{****}University of Pittsburgh

ABSTRACT

The estimation of hydraulic fracture (HF) propagation in fractured unconventional reservoirs is important for the reservoir stimulation design. Previous studies typically assume that natural fractures (NFs) have uniform properties and persist through the full height of the reservoir/HF, which lead to 2D views. Recent field and experimental observations, on the other hand, demonstrate that the spatial variation of NF properties can strongly influence the HF propagation patterns. In this study, a lattice model that fully couples fluid flow with rock matrix represented by quasi-randomly distributed nodes (discrete masses) and springs is employed to simulate the 3D interaction between HFs and NFs with non-uniform properties. The numerical simulations capture the strong dependence of HF propagation patterns on the NF heterogeneities, characterized by different cementation strength, cemented proportions and/or height. In a parametric study of NF properties, the simulations are observed to match an experimentally verified 3D analytical criterion well for cases with varying mechanical and/or geometrical NF properties. The simulation results also reveal that 3D interactions between HFs and NFs are not only related to localized interaction behaviors determined by local interface conditions as considered in 2D crossing criteria, but also global interaction behaviors that are influenced by the overall properties of encountered NFs.

Art of Balancing and Conforming in Discrete Elements of Continuum

XiangRong Fu^{*}, Pu Chen^{**}, MingWu Yuan^{***}

^{*}Department of Civil Engineering?China Agricultural University, ^{**}Department of Mechanics and Engineering Science, PeKing University, ^{***}Department of Mechanics and Engineering Science, PeKing University

ABSTRACT

A review on the basic theories of the finite element method or the associated computational method are presented in the paper. Some classic theories of discrete elements are studied, and some novel models of discrete elements are presented. In the view of balancing, the analytical trial functions which satisfy equilibrium equations are used to construct the stress field in the novel discrete elements. In the view of conforming, the isoparametric elements, the non-conforming elements and the super conforming elements are compared with each other in two-dimension problems . Following different theories of balancing or conforming, every kind of discrete elements forms the basic theory of the finite element method or the associated computational method. The benchmark tests show that the discrete elements combining two characters who can satisfy the equilibrium equation in the element and take into the conforming boundary condition around the element can give better perform.

Phase-field Modeling of Microstructure Evolution in Selective Laser Melting Process through a Multiscale Scheme

Yao Fu*

*University of Cincinnati

ABSTRACT

Designing novel structural materials with complex shape and geometry is enabled with the advancement of additive manufacturing processes, to meet specific performance requirements that are not imaginable with traditional subtractive manufacturing techniques. The microstructure evolution during the repeated heating/cooling process determines the various properties of manufactured products. Modeling and simulation can advance our fundamental understanding of the underlying physical processes and capability to quantify the influence of process variables on resulting component properties. Therefore, it plays an increasingly crucial role for the design and optimization of components and materials. In this study, the prediction of microstructural evolution during the additive manufacturing process is realized through the phase field modeling at the meso and micro length scale. Coupled with heat conduction equation where the latent heat of fusion is considered, the temporal and spatial evolution of the melting pool is simulated at the mesoscale with the Kim-Kim-Suzuki (KKS) model. The temperature history provides input for the microscale model, where the microstructural evolution such as dendritic growth can be predicted during the laser-materials interaction via the multiphase KKS model.

Parallelization of Microscopic Traffic Simulator and Its Load Balancing

Hideki Fujii^{*}, Yuta Ushimaru^{**}, Tomonori Yamada^{***}, Shinobu Yoshimura^{****}

^{*}The University of Tokyo, ^{**}The University of Tokyo, ^{***}The University of Tokyo, ^{****}The University of Tokyo

ABSTRACT

In order to evaluate transportation policies quantitatively, virtual social experiments using traffic simulators are adequate. It is because experiments in the real road environment are impracticable for predicting traffic phenomena as complex systems, and even small changes in conditions can affect to wide area significantly. In particular, simulators with features of both precision and scalability are preferable for applications to real-world traffic issues. In this research, we tried to parallelize a multi-agent-based traffic simulator [1, 2] using a graph partitioning approach. Cars are modeled as autonomous agents in the simulator. A car agent acquires information from its circumference (other cars, traffic signals, etc.), makes a decision autonomously, and acts accordingly. The precision is accomplished by employing a multi-agent system and realistic car behavior models, and the scalability is advanced by parallelization in this approach. Since the perceptions of the determinants for decision making of a car agent being driven are limited locally, it is reasonable to decompose road network to subnetworks. We utilized METIS [3] as a graph-partitioning tool to minimize edge cuts. The computational cost of a subnetwork in the simulation depends on the number of agents on the subnetwork and the numbers are not constant among each subnetwork. That causes load imbalance. We tested to give weights to edges to improve the imbalance. We show the result of graph partitioning approach and its parallelization performance in the presentation. Our approach contributes to import the methods that have been discussed in the field of computational mechanics to the new field of social simulation. [1] S. Yoshimura, "MATES: Multi-Agent Based Traffic and Environment Simulator - Theory, Implementation and Practical Application", CMES: Computer Modeling in Engineering and Sciences, vol. 11, no. 1, pp. 17--25, 2006. [2] H. Fujii, H. Uchida, S. Yoshimura: "Agent-based Simulation Framework for Mixed Traffic of Cars, Pedestrians and Trams", Transportation Research Part C: Emerging Technologies, vol. 85, pp. 234-248, 2017. [3] G. Karypis, V. Kumar: "A Fast and Highly Quality Multilevel Scheme for Partitioning Irregular Graphs", SIAM Journal on Scientific Computing, vol. 20, no. 1, pp. 359--392, 1999.

Detailed Finite Element Analysis of Concrete-filled-tube Column under Cyclic Loading

Jun Fujiwara^{*}, Makoto Ohsaki^{**}, Hiroyuki Tagawa^{***}, Takuzo Yamashita^{****}, Tomoshi Miyamura^{*****}

^{*}National Research Institute for Earth Science and Disaster Resilience, ^{**}Kyoto University, ^{***}Mukogawa Women's University, ^{****}National Research Institute for Earth Science and Disaster Resilience, ^{*****}Nihon University

ABSTRACT

Concrete-filled-tubes (CFTs) are used as columns of architectural and civil engineering structures. CFTs usually have large deformation capacity due to lateral constraints from steel tubes providing ductility. In some of existing studies on numerical analysis of CFTs, constraint effect such as lateral pressure between steel and concrete is obtained from experiments and considered in analysis as additional forces, etc. However, to the best of authors' knowledge, no numerical analysis method, which can simulate behaviors of CFTs under cycling loading, has been proposed. The authors have been developing a detailed finite element analysis system called E-Simulator[1,2]. In this research project, we simulate structural behavior only by combining detailed solid finite element model and material constitutive laws, which can represent damages and fractures of materials. By using E-Simulator, we can consider interaction between filled concrete and steel tube without any additional constraint effects. In this study, a detailed finite element analysis of a CFT column is conducted to simulate collapse behavior under lateral cyclic loading. In our analysis, concrete is modeled as an elastoplastic material with extended Drucker-Prager yield condition that has a smooth yield surface in tension. Softening behavior in compression is formulated based on simple damage criteria. A piecewise linear isotropic-kinematic hardening model[3] is applied to steel. We simulate a cyclic shear-bending loading experiment of a CFT column. The height is 1440 mm and the section is a 240?240 mm square tube. A pseudo-static cyclic lateral displacement with increasing amplitude is given at the top of the column under vertical load. According to the comparison of load-deformation relations obtained from the experimental and numerical results, analysis result corresponds fairly well to the experimental one. The progress of damage in the filled concrete and the steel-concrete interaction is visually illustrated in the numerical result, while it is difficult to quantify in experiments. References [1] M. Ohsaki, T. Miyamura, M. Kohiyama, M. Hori, H. Noguchi, H. Akiba, K. Kajiwara and T. Ine, High-precision finite element analysis of elastoplastic dynamic responses of super-high-rise steel frames, *Earthquake Eng. Struct. Dyn.*, Vol. 38, pp. 635-654, 2009. [2] T. Yamashita, M. Hori and K. Kajiwara, Petascale computation for earthquake engineering, *Computing in Science and Engineering*, Vol.13(4), pp. 44-49, 2011. [3] M. Ohsaki, T. Miyamura and J. Y. Zhang, A piecewise linear isotropic-kinematic hardening model with semi-implicit rules for cyclic loading and its parameter identification, *Computer Modeling and Engineering*, Vol. 111(4), pp. 303-333, 2016.

Simulation-based Assessment of Railway Dynamic Gauge for the Conception of New Trains

Christine Funfschilling*, Guillaume Perrin**

*SNCF, **CEA/DAM/DIF

ABSTRACT

In order to ensure the safety of a railway circulation, it is necessary to estimate the railway gauge to verify that the rolling stock will not run too close to the infrastructure or to another train running on an adjacent track. Currently, in France, the railway gauge is assessed thanks to an empirical deterministic approach stemming from extended experimental work. The vehicle-track system is however complex and contains several sources of uncertainties: the track irregularities, the wheel-rail contact shape and the friction coefficient, the mechanical suspension properties, the wind gusts and so on. The use of multi body simulation coupled with a probabilistic approach could thus present several advantages ; for a given train and a given railway network, we will focus here on the assessment of the risk that the dynamic gauge may not be in accordance with the certification rules. In this work, we thus propose a method to evaluate the envelope of the position of the train. To take into account the uncertainties that are inherent to the system, a probabilistic approach is developed, leading to a random envelope of the train. A three step method is adopted to evaluate the probability that the certification criteria may not be fulfilled. The first step consists in sampling a set of realistic track irregularities with a stochastic generator. This latter is based on a high dimensional non-Gaussian random field that has been identified on a large set of measurements. A Monte Carlo algorithm is used for the sampling. Railway dynamic simulations are then achieved in parallel with the commercial software Vampire. Finally the obtained displacements are processed to estimate the desired random envelope. Since very low probabilities are of interest, dedicated methods are needed for the evaluation of the final probability. A Moving Particle algorithm coupled with a Markov Chain Monte Carlo procedure is considered here, which is a particularly efficient subset method for the estimation of the probability of rare events. This is particularly important here, as the computational cost of each evaluation of the railway software is relatively high.

Materials Genomics and the Future of Structural Alloy Design and Application

David Furrer*

*Pratt & Whitney

ABSTRACT

Computational materials engineering has evolved through parallel advancement of materials characterization, physics-based understanding of materials behavior, computational modeling methods, informatics and computational methods. These linked advancements have been significant steps toward the application of Integrated Computational Materials Science and Engineering (ICMSE). Formalized materials genomics activities are increasing the rate of new material development for future, unique requirements. Materials genomics and computational materials methods have been advanced to a point where they are being substantially accepted by industry and the larger interdisciplinary engineering community. This talk will review major enabling materials genomics technologies relative to industrial applications for the design and development of next generation materials.

Numerical Simulation of Antiplane Wave Scattering by a Hydrate Inclusion Using a BEM

Akira Furukawa^{*}, Takahiro Saitoh^{**}, Sohichi Hirose^{***}

^{*}Tokyo Institute of Technology, ^{**}Gunma University, ^{***}Tokyo Institute of Technology

ABSTRACT

Frozen porous media consist of solid skeleton, pore fluid, and ice matrix. This mechanical model has been proposed by Leclaire et al [1] and well known as an extended model based on the fluid-saturated porous media proposed by Biot [2]. Recently, the frozen porous media attract a great deal of attention from researchers in the field of the geophysical exploration because this model is adequate to describe the dynamic behavior of seabed layer involving methane hydrate. Body waves in the frozen porous media propagate with dispersion and dissipation in the same manner as waves in the fluid-saturated porous media. In addition, antiplane shear wave has two propagation modes, i.e. S1- and S2-modes [3]. Therefore, it is important to consider the interaction among three phases for the evaluation of wave scattering properties of the frozen porous media. However, there are few reports with regard to the development of numerical computation methods for wave scattering by an inclusion which involves highly concentrated hydrate. This study presents a numerical simulation to understand the characteristics of wave scattering by a hydrate inclusion in the seabed layer. The problem is formulated by a boundary element method (BEM) which can deal with the antiplane shear waves in the frozen porous media. Several numerical examples are shown to provide the validity of our proposed method and scattering properties resulting from the numerical simulation. [1] Ph. Leclaire, F. Cohen-Tenoudji and J. Aguirre-Puente, Extension of Biot's theory of wave propagation to frozen porous media, J. Acoust. Soc. Am., Vol. 96, No. 6, pp. 3753-3768, 1994. [2] M. A. Biot, Theory of propagation of elastic waves in a fluid-saturated porous solid. I. Low-frequency range, J. Acoust. Soc. Am., Vol. 28, No. 2, pp. 168-178, 1956. [3] J. M. Carcione, J. E. Santos, C. L. Ravazzoli and H. B. Helle, Wave simulation in partially frozen porous media with fractal freezing conditions, J. Appl. Phys., Vol. 94, No. 12, pp. 7839-7847, 2003.

Structural Optimization of Thermoelectric Nanomaterials Using the Level Set Method

Kozo Furuta^{*}, Ayami Sato^{**}, Kazuhiro Izui^{***}, Takayuki Yamada^{****}, Mitsuhiro Matsumoto^{*****},
Shinji Nishiwaki^{*****}

^{*}Kyoto University, ^{**}Kyoto University, ^{***}Kyoto University, ^{****}Kyoto University, ^{*****}Kyoto University, ^{*****}Kyoto University

ABSTRACT

Thermoelectric devices are unique in that they can convert thermal energy to electric energy and vice versa. When a temperature gradient between two different points exists on a thermoelectric device, a voltage is generated. Conversely, when a voltage is applied between two different points on a thermoelectric device, a thermal gradient is produced. The former effect is called the Seebeck effect and is exploited in power generation systems. The latter is called the Peltier effect and is employed in cooling devices and temperature-control systems. The advantages of thermoelectric devices are compactness, lack of moving parts, maintenance-free operation, longevity, and ability to be precisely controlled, properties that have led to their broad use in various fields. Despite their utility, however, thermoelectric devices are typically deployed only in niche applications due to their comparatively low the efficiency of energy conversion, only 5% in conventional commercial modules. In recent years, dramatic improvements in nano-fabrication techniques have enabled the design of materials and devices that take nanoscale phenomena into account. Manipulating such nanostructures can enable only decrease the thermal conductivity by utilizing the phonon reflections in material interfaces, and provide novel material properties for thermoelectric materials [1]. However, little research has focused on design methods for nanoscale thermoelectric devices, since this requires consideration of properties that are discontinuous on material interfaces. Here, we propose a structural optimization method for nanoscale heat conduction problems based on a level-set method. First, we define the optimization problem using the phonon Boltzmann transport equation that can model temperature discontinuities on material interfaces when dealing with heat conduction at the nanoscale. The shape sensitivity is then computed with an adjoint method that considers discontinuous properties on material interfaces [2]. A Hamilton-Jacobi equation is applied when updating the level-set function that represents the structure [3]. Finally, numerical examples confirm the validity of our proposed structural optimization method. [1] J. Yu, S. Mitrovic, D. Tham, J. Varghese and J. Heath, ``Reduction of thermal conductivity in phononic nanomesh structures.&amp;amp;apos;&amp;amp;apos; Nature nanotechnology, Vol.5, No.10 (2010) pp. 718 - 721. [2] K. Furuta, A. Sato, K. Izui, M. Matsumoto, T. Yamada and S. Nishiwaki, ``Shape sensitivity for a two-phase heat conduction problem considering nanoscale effects.&amp;amp;apos;&amp;amp;apos; Journal of Advanced Mechanical Design, Systems, and Manufacturing, (Accepted). [3] G. Allaire and F. Jouve, ``Structural optimization using sensitivity analysis and a level-set method.&amp;amp;apos;&amp;amp;apos; Journal of Computational Physics, Vol.194 (2004) pp. 363–393.

On the DPG Method for Signorini Problems

Thomas Führer^{*}, Norbert Heuer^{**}, Ernst P. Stephan^{***}

^{*}Pontificia Universidad Católica de Chile, Santiago, Chile, ^{**}Pontificia Universidad Católica de Chile, Santiago, Chile, ^{***}Leibniz Universität Hannover, Hannover, Germany

ABSTRACT

We present results of our recent work [1], where we derive and analyse discontinuous Petrov–Galerkin methods with optimal test functions for Signorini-type problems as a prototype of a variational inequality of the first kind. We present different symmetric and nonsymmetric formulations, where optimal test functions are used only for the partial differential equation part of the problem, not the boundary conditions. For the symmetric case and lowest-order approximations, we provide a simple a posteriori error estimate. Moreover, we apply our technique to the singularly perturbed case of reaction-dominated diffusion. Numerical results show the performance of our method and, in particular, its robustness in the singularly perturbed case. References: [1] T. Führer, N. Heuer, E.P. Stephan, On the DPG method for Signorini problems, IMA J. Numer. Anal. (2017), in print.

Bipenalty Stabilized Explicit Finite Element Algorithm for Contact-impact Problems: Two-Dimensional Case

Dusan Gabriel*, Jan Kopacka**, Radek Kolman***, José A. González****, Anton Tkachuk*****,
Jiri Plesek*****

*Czech Academy of Sciences, Institute of Thermomechanics, Czech Republic, **Czech Academy of Sciences, Institute of Thermomechanics, Czech Republic, ***Czech Academy of Sciences, Institute of Thermomechanics, Czech Republic, ****University of Seville, Spain, *****University of Stuttgart, Germany, *****Czech Academy of Sciences, Institute of Thermomechanics, Czech Republic

ABSTRACT

In dynamic transient analysis, recent comprehensive studies have shown that using mass penalty together with standard stiffness penalty, the so-called bipenalty technique, preserves the critical time step in conditionally stable time integration schemes. In Reference [1] the stability and reflection-transmission analysis of the bipenalty method has been studied for one-dimensional contact-impact problems. The main attention has been paid on an upper bound estimation of the stable Courant number for the bipenalty method with respect to stiffness penalty and mass penalty parameters. This analysis has been carried out for several basic one-dimensional contact problems. In this work, the bipenalty technique is applied for the solution of two-dimensional contact-impact problems. The bipenalty method is implemented to an explicit contact algorithm based on the symmetry preserving penalty formulation [2]. The attention is focused on the stability properties of this algorithm using the derived upper bound of the stable Courant number. Next, the estimation of the stiffness and mass penalty parameters ensuring non-oscillating behavior is investigated. Several numerical examples are presented including the longitudinal impact of two thick plates/cylindrical rods, for which an analytical solutions are available. In all the cases the superiority of the bipenalty method over the standard stiffness penalty method is demonstrated. Acknowledgements to projects: MEYS CZ.02.1.01/0.0/0.0/15_003/0000493 (Gabriel, Kolman), CSF 16-03823S (Kopacka) and CSF 17-12925S (Plesek) under AV0Z20760514. The work was also supported by the Projekt-ID 57219898 funded via DAAD from Federal Ministry of Education and Research. References [1] Kopacka J., Tkachuk A., Gabriel D., Kolman R., Bischoff M., Plesek J. (2017) On stability and reflection-transmission analysis of the bipenalty method in contact-impact problems: a one-dimensional, homogeneous case study. *Int. J. Numer. Meth. Engng.*, 1–23. <https://doi.org/10.1002/nme.5712> [2] Gabriel, D., Plesek, J. and Ulbin, M. (2004), Symmetry preserving algorithm for large displacement frictionless contact by the pre-discretization penalty method. *Int. J. Numer. Meth. Engng.*, 61: 2615–2638. <https://doi.org/10.1002/nme.1173>

A Novel Framework for Joint Task and Manufacturing Optimization of Multi-Material Soft Robots

Felix Gabriel*, Franz Dietrich**, Klaus Dröder***

*TU Braunschweig, Institute of Machine Tools and Production Technology, Germany, **TU Braunschweig, Institute of Machine Tools and Production Technology, Germany, ***TU Braunschweig, Institute of Machine Tools and Production Technology, Germany

ABSTRACT

Research on soft material robotic systems has recently increased, since soft robots offer a rich potential for application in human-robot collaboration, surgical applications or search-and-rescue operations. In contrast to rigid robots, the task-specific design of soft robots highly depends on the available materials, actuation control and manufacturability. There is a significant body of work about mathematical representations of the robot motion and control, in order to determine task-optimized designs. The manufacturing of such designs is mostly considered in a subsequent stage, so that a sequential methodology evolves. This sequential procedure causes that function is prioritized over manufacturability. It is the intention to equalize this asymmetry in order to access previously unconsidered yet competitive design structures. This challenge is approached by the aggregation of a joint task-oriented and manufacturing-oriented design methodology. In such an aggregated methodology, it is straightforward to include monolithic material, gradient material and multi-material manufacturing processes. The multi-material concept is particularly attractive if the manufacturing sequence comprises the incremental application of pre-produced elements. This significantly reduces the manufacturing effort, even if the functional structure is complex. In order to elaborate a generic solution, this concept schedules finite element modeling such multi-material manufacturing processes and contributes methods to transform these models into function-oriented models for a joint development methodology. The proposed framework comprises the elaboration of two distinct methodology aggregations and their competitive comparison. Both methodologies are parameterized by a user-defined task specification towards which their function and manufacturing optimization algorithms iterate the robot design and its manufacturing plan. The goal is to implement a fully automated development framework, which connects evolutionary optimization algorithms to finite element simulations that represents both material and geometry as well as applied manufacturing procedures. In further research, a case study is intended to be carried out, where robots for a feeding task in a production scenario are developed, manufactured and characterized experimentally. For this case study, a novel design and binary actuation concept for soft robot is proposed, which is distinguished by separation of an actuated internal structure and a passive outer shell. The findings of this case study are then fed back to refine the joint development methodologies. This case study is used for the methodology comparison and to derive practical implications. Ultimately, this supports a decision about the superior methodology to be deployed further in the future.

Analysis of the Relationship between a Morphology of a Human Vertebra and its Stiffness

Aneta Gadek-Moszczak*, Justyna Borkowska**, Jacek Pietraszek***

*Institute of Applied Informatics, Cracow University of Technology, 31-864 Cracow, al Jana Pawła II 37, Poland,

**Institute of Applied Informatics, Cracow University of Technology, 31-864 Cracow, al Jana Pawła II 37, Poland,

***Institute of Applied Informatics, Cracow University of Technology, 31-864 Cracow, al Jana Pawła II 37, Poland

ABSTRACT

Osteoporotic changes lead to future low-energy fractures. The early detection of them may allow to introduce the treatment preventing many potential patients from fractures. The development of new diagnostic methods for osteoporotic changes, providing supplementary information to the routine screening tests like densitometry, would improve the accuracy of a diagnosis by more effective prediction of bone strength properties. Osteoporosis caused destruction of the trabeculae in the cancellous part of the vertebra body. Numerous researches shown the strong relation between the trabeculae architecture and the bone strength [1-2]. These reports explain the cause of a bone destruction in osteoporotic fractures, but due to a low spatial resolution of the clinical computed tomography (CT), it is not possible to implement the trabecula quantitative description as a method of a diagnosis for the osteoporotic changes. Presented study attempted to evaluate the impact of a shape of a vertebra body and the thickness of a cortical wall of the vertebra body on its stiffness. The cortical wall visible on clinical CT images that may be used for the analysis by physicians thus it is considered as a potential complementary feature for the diagnostic purpose. The performed study was based on the image of a three-dimensional human vertebra obtained from a X-ray computed microtomographic (μCT) study, clinical CT and the compression test of the vertebra. Histomorphological features of the trabeculae structure were calculated from the μCT. Clinical CT images of vertebrae were used to design simplified geometrical model for a simulation of the compressive test employing the finite elements method (FEM). The simulation of the compression test with different materials characteristic and properties, using the material characteristic of healthy bone, osteoporotic bone, and compare the result to the experimental data were performed. Obtained results of simulation were compared to the results from the real experimental compression tests of vertebrae. Finally, statistical analysis were performed, to identify the impact of all considered parameters on the stiffness. References 1. Hahn M, Vogel M, Pompesius-Kempa M, Delling G.: Trabecular bone pattern factor – a new parameter for simple quantification of bone microarchitecture. Bone, 13, 327-330 (1992). 2. Odgaard A, Gundersen HJG.: Quantification of Connectivity in Cancellous Bone, with Special Emphasis on 3-D Reconstructions. Bone, 14, 173-182, (1993)

Multi-scale Modelling of the Mechanics of Concrete Based on the Cement Paste Properties

Erez Gal^{*}, Gili Sherzer^{**}

^{*}Department of Structural Eng., Ben-Gurion University, ^{**}Department of Structural Eng., Ben-Gurion University

ABSTRACT

The mechanical response of concrete is complex and as other composite materials, multiscale modelling has the potential for modeling its macroscopic behavior. This paper presents an upscaling methodology for the modeling of the concrete mechanical properties. The suggested formulation starts from a known chemical and mechanical set of parameters of the cement paste, which are used to evaluate the mechanical properties of the LDPM (Lattice Discrete Particle Model) concrete mechanical parameters. The parameters are divided to groups, which are related to different damage modes such as: pore collapse and material compaction, cohesive behavior, and shear behavior. For each group of parameters a set of microscopic simulations are performed to complete the up-scaling methodology.

ON THE USE OF THE ADJOINT METHOD TO EVALUATE SENSITIVITIES IN ADSORBED NATURAL GAS STORAGE SYSTEMS

BRUNO G. CHIEREGATTI JO O S. BRASIL LIMA ERNANI V. VOLPE
MARCELO T. HAYASHI

¹Research Centre for Gas Innovation (RCGI)
Polytechnic School of University of São Paulo
Av. Prof. Mello Moraes, 2231 05508-000
São Paulo, SP, Brazil

bchieregatti@usp.br; www.rcgi.poli.usp.br

²Mauá Institute of Technology
Mechanical Engineering Department
Praça Mauá, 01, São Caetano do Sul, SP, Brazil
09580-900

³Federal University of ABC
Center for Engineering, Modeling and Applied Social Sciences
Rua Frei Caneca, Vila São Pedro, Santo André, SP, Brazil
09210-170

Key Words: Porous Media, Adsorption, Adjoint, Sensitivities.

Abstract. *Recently, the adsorbed natural gas (ANG) has been identified as the most promising low pressure alternative for storing natural gas. However, not attaining the capacity found in liquefied natural gas (LNG), but this technology provides a method of storing gas at substantially higher concentration than can be achieved with simple compression (SCV) and dismiss the use of refrigeration. Due to the physics of the process, the temperature of the gas increases during the adsorption, hence it decreases the adhesion of molecules in the adsorbent. The same occurs on desorption process when the temperature of the gas decreases turning it more difficult the release of the gas. Under such circumstances, it seems substantially advantageous to investigate optimum solutions to those systems, but to find them, it is necessary to evaluate sensitivities of the control parameters. In particular, on making use of so called Adjoint Method, it combines shape and parametric optimization capabilities one could potentially tackle the full breadth of the problem. Over the years, this method has proven to be a powerful tool for find sensitivities in complex systems, where a high fidelity representation of the physics is essential. It has shown to be particularly suitable to tackle problems with large numbers of control parameters, and several possibilities of optimum criteria. To explore the method's potential, numerical transient axisymmetric simulations will be carried out by using a finite element platform FreeFEM considering that the flow is governed by Navier Stokes equations ruled by Darcy's law. The Adjoint equations, which were derived from the flow physics, were also implemented in the same platform. The presentation of the article will consist in a description of Adjoint Method, followed by the mathematical model and validation tests, showing the reduction of the computation cost to evaluate sensitivities. Then, the conclusion of the work and the next steps of the research.*

1 INTRODUCTION

Worldwide, the energy market is going through a phase of intense research and development efforts. In several countries, the energy matrices are undergoing progressive changes, so as to adapt to more stringent environmental laws and to the global economy instabilities. In this scenario, the Natural Gas appears as a source of energy of growing relevance, owing to both its direct uses and to the possibilities, it offers regarding the process of gas reform, for hydrogen production and carbon capture. The growth of its share of the energy market prompts the need to optimize the chain of production, processing and storage of Natural Gas. The search for optimal solutions should allow significant savings.

Amongst the most relevant approaches to optimization, the Adjoint Method stands out as it allows an exceptional reduction in the computational costs of design sensitivity derivatives, requirement to optimization methods. The method is also attractive for its high fidelity to the flow physics, and for the great diversity of its applications. This article presents the use the Adjoint Method to find non-geometric sensitivities in Natural Gas Adsorption Systems for storage, known by the abbreviation ANG.

2 PROBLEM DESCRIPTION

2.1 Adsorption

The Adsorption is defined as the adhesion of molecules in an extremely thin layer (as of gases, solutes or liquids) to the surfaces of solid bodies or liquids with which they are in contact. It can be classified either as physical adsorption or as chemical adsorption depending on the occurrence of reactions. In this work, we are only interested in the physical adsorption phenomenon, particularly in a gas-solid interaction. Physical adsorption is caused mainly by the van der Waals force and electrostatic forces between adsorbate (gas) molecules and the atoms which compose the adsorbent (solid) surface [1,2].

2.2 ANG Technology

The ANG systems consists in a simple tank (cylindrical or not), filled by an adsorbent (activated carbon, for example). A basic scheme of the ANG tank is presented below:

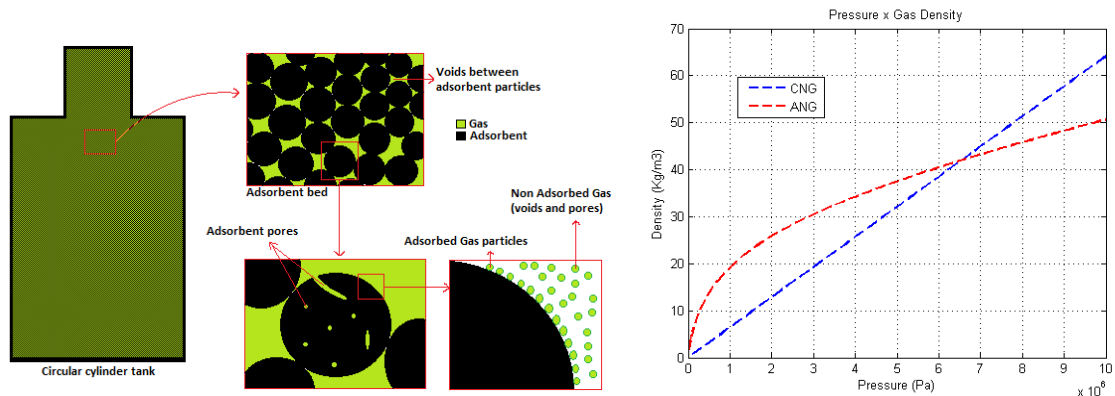


Figure 2. Left: Scheme of ANG Tank. Right: Density comparison between CNG and ANG systems at 300 K

Observing the fig.2 on the left, during the filling process, the gas can be stored in two places: i) In the spaces between the adsorbent particles and in the pores spaces, that they are considered in mathematical model only as “voids” and ii) Close to the adsorbent surfaces, that it considered as “adsorbed gas”.

As mentioned in the Introduction, the method provides a means of storing gas at substantially higher concentration than can be achieved with CNG at the same pressure [3]. Using a quantitative example, the fig. 2 on the right presents a simple comparison between the gas density (using a standard activated carbon as adsorbent) for different pressures. Also in this figure, it is clear that for a certain range of pressures, the ANG systems could store more gas than CNG at the same pressure, considering the isothermal process. In this example, using a particular adsorbent, the differences achieve 44% at 3.5MPa and exceed 100% at low pressures, close to 1.5 MPa. However, above to 6.5 MPa, the density in CNG system overtakes that ANG with standard activated carbon adsorbent.

3 FLOW PHYSICS

The governing equations are presented below, where the main assumptions are: Pure NG (100% Methane as ideal gas); properties of the adsorbent bed are constant and the bed is considered isotropic with spherical particles and homogenous pores distribution [4]. The equations were nondimensionalized, to avoid bad conditioning of matrices that are used to solve the flow equations numerically. The nondimension state equation $p = \rho_g \cdot T$ were plug in the equations and the result is presented as follows:

$$\epsilon_t \left(\frac{1}{T} \cdot \frac{\partial p}{\partial t} + \frac{p}{T^2} \cdot \frac{\partial T}{\partial t} \right) + \rho_b \frac{\partial q}{\partial t} + \nabla \cdot \vec{G} = 0 \quad (1)$$

$$\vec{G} + N_p \rho_g \nabla p = 0 \quad (2)$$

$$C_{eff} \frac{\partial T}{\partial t} - \epsilon_t \left(\frac{\gamma-1}{\gamma} \right) \frac{\partial p}{\partial t} + \nabla \cdot (\vec{G} \cdot T) - \frac{1}{P_e} \nabla^2 T - \frac{\rho_b \Delta H}{M_g} \cdot \frac{\partial q}{\partial t} = 0 \quad (3)$$

$$q = \rho_{ads} \cdot W_0 \cdot \exp \left[- \left(\frac{A}{\beta E_0} \right)^n \right] \quad (4)$$

Eq.(1) is the continuity equation where ϵ_t is the total porosity of adsorbent bed (non-dimensional); ρ_b is the density of adsorbent bed; q is defined as the density of adsorption, eq. (4), $\vec{G} = \rho_g \vec{u}$ is the specific mass flux vector, where ρ_g is the free gas density (located in the voids between particles and in the respective pores) [5].

Eq.(2) are the momentum equation with Darcy law simplifications, where ∇p is the pressure gradient; $N_p = \frac{K \rho_\infty}{\mu l_{ref} v_\infty}$ is the pressure number, defined in terms of μ (gas viscosity), K (permeability of the adsorbent bed, [4]), and the reference values of adimensionalization, ρ_∞ , l_{ref} and v_∞ .

Eq. (3) is the Energy equation, where $C_{eff} = (\epsilon_t \rho_g + \rho_b q) C_{pg} + \rho_b C_{ps}$, which C_{pg} and C_{ps} represents the specifics heat of gas and adsorbent respectively; $P_e = \frac{\rho_\infty C_{pg} v_\infty l_{ref}}{\lambda_{ref}}$ is the Péclet number; $\lambda_{eff} = \epsilon_t \cdot \lambda_g + (1 - \epsilon_t) \lambda_s$ is the effective thermal conductivity in terms of porosity and thermal conductivity of gas (λ_g) and adsorbent (λ_s), ΔH is the heat of adsorption which is assumed constant and M_g is the molar mass of the gas.

Finally, eq. (4) is the Dubinin-Astakov (DA) model [4,5], where ρ_{ads} is the adsorbed gas density, defined by: $\rho_{ads} = \frac{\overline{\rho_{ads}}}{\exp[\alpha_e(T-T_b)]}$, where $\overline{\rho_{ads}}$ is the density of liquid phase of the adsorbed fluid in the saturation region, T_b is the gas boiler temperature and α_e is the mean value of the thermal expansion of the liquefied gas. W_0 is the microporous volume per unit mass of adsorbent, β is the coefficient related to the gas-solid interaction, E_0 is the characteristic adsorption energy, and n is the DA exponent which is related to the pore size dispersion. $A = RT \ln \left(\frac{P_s}{P} \right)$ is the so-called as Polany adsorption potential: where $P_s = P_{cr} \left(\frac{T}{T_{cr}} \right)^2$.

4 NUMERICAL IMPLEMENTATION

The equations were implemented in *FreeFEM* platform [7]. This software is a high level integrated development environment for numerically solving partial differential equations in 2 and 3 dimensions. To simulate the previous equations, it is necessary to define geometry, mesh and a set of boundary conditions:

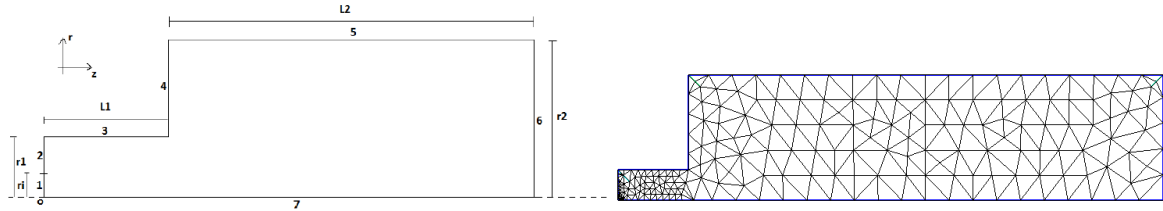


Figure 3. Left: Schematic of a 2D axis-symmetric ANG Storage System – The point “o” represents the origin of coordinate system. Right: Mesh implemented by FREEFEM++ platform

Boundary	Conditions
Inflow (1): Parabolic mass flux in the axial direction. t_{ac} is the time when the nominal mass flux is achieved.	$G_z = \begin{cases} 2\rho_0 u_{in} \left(1 - \frac{r^2}{r_i^2}\right) \left(\frac{t}{t_{ac}}\right), & \text{if } t < t_{ac} \\ 2\rho_0 u_{in} \left(1 - \frac{r^2}{r_i^2}\right), & \text{if } t \geq t_{ac} \end{cases},$ $G_r = 0, T = T_{in}$
Wall (2 - 6): No slip boundary condition with heat transfer	$G_z = 0, G_r = 0,$ $-n \cdot \nabla T = N_u (T - T_{ext})$
Symmetry (7): Since the symmetry axis is parallel to z axis, the condition, $\vec{G} \cdot \vec{n} = 0$ reduces to $G_r = 0$.	$G_r = 0$ $n \cdot \nabla T = 0$

Table 1 – Set of Boundary Conditions

Where ρ_0 is the gas density in the inlet; u_{in} is the velocity based on volumetric flow rate at STP; T_{ext} is the ambient temperature and N_u is the Nusselt number defined as $N_u = \frac{h \cdot l_{ref}}{\lambda_{eff}}$. The studies of mesh sensitivity, validation tests and exploratory simulations were published in previous works [7,8] and the following figures shows some results as example. This test verified the influence of the heat transfer coefficient at the tank walls. The Nusselt number affected directly the density of gas adsorbed and the understanding the sensitivity of this parameter could be essential to increase the tank capacity. The Adjoint method presented in the next section were implemented to find the sensitivity of this parameter.

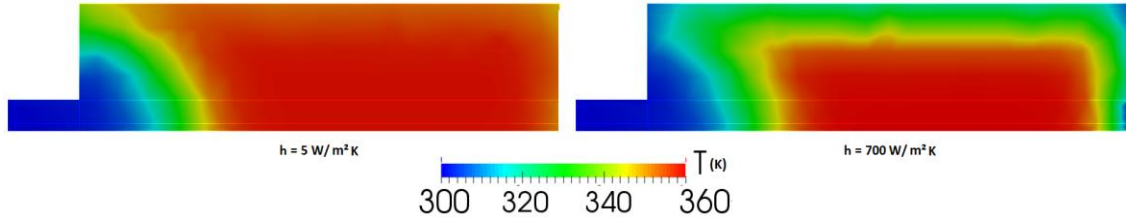


Figure 4. Temperature distribution in the end of filling process. Left: Natural Convection in tank walls. Right: Forced Convection in the tank walls ^[7,8].

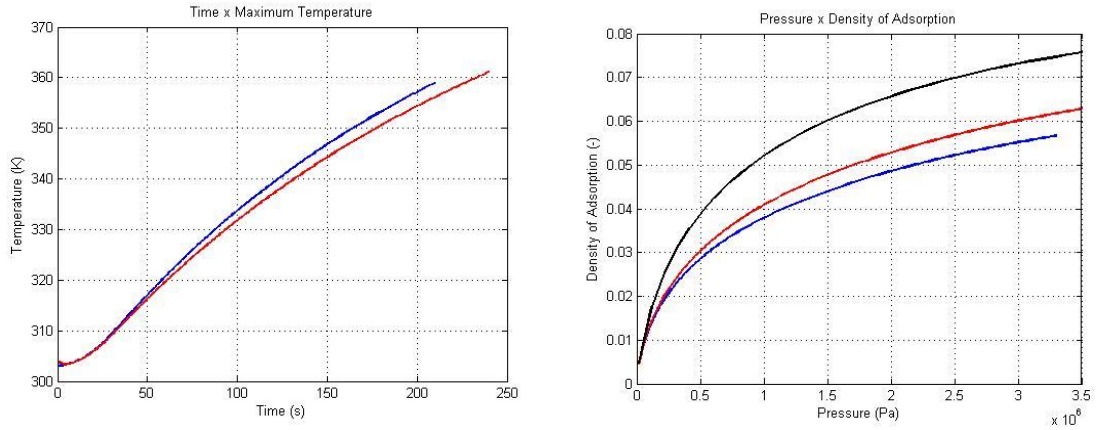


Figure 5. Left: Maximum Temperature inside the tank during the filling process. Right: Evolution of Density of Adsorption (q) during the filling process. Black: Isothermal process (ideal); Blue: Natural Convection in tank walls; Red: Forced Convection in the tank walls ^[7,8].

INTRODUCTION TO THE ADJOINT METHOD

Historically, the Adjoint Method has evolved into two distinct approaches: discrete and continuous. In the former, a discrete Adjoint operator is obtained on the basis of already discretized flow governing equations. Whereas in the latter case, the Adjoint equations are derived analytically from the equations that govern the physics, and only then, they are discretized ^[9]. Comparisons between the two approaches have also been drawn in the literature ^[10,11,12], and they do not indicate any sizable differences between them.

This article adopted the so-called continuous formulation of the Adjoint method as it is more directly in line with our approach to the Adjoint boundary problem. As an additional result of this choice, the numerical methods that were used to integrate the primal problem (flow physics) are independent of those that are applied to the dual (Adjoint), thereby making the flow and Adjoint solvers fully independent, as well.

In essence, the Adjoint method is a powerful tool to compute the sensitivity of a given measure of merit, with respect to any number of parameters that control the boundary conditions of a physical system. That system is assumed to be governed by a set of Partial Differential Equations, and the measure of merit is taken to be an objective functional. In any case, the integration boundaries, and the boundary conditions, themselves, are controlled by a set of design parameters. Under these circumstances, a natural means of estimating the sensitivity of

a functional to changes in flow parameters, would be to perturb each one of them individually, and then to compute the sensitivity gradient by central finite differences.

The procedure clearly requires two converged flow solution for each parameter variation. As the number of design parameters increases, the computational cost is bound to become prohibitive. Alternatively, by imposing the flow equations as constraints to the optimization of objective function, one precludes unrealizable solutions. That, in turn, eliminates the need for additional simulations. That is the essence of the Adjoint Method which sensitivity gradient need only 2 solutions, independently of the number of design parameters.

THE ADJOINT METHOD APPLIED IN FLOWS THOUGH POROUS MEDIA

This section is dedicated to the Adjoint problem, as it applies to the particular class of flows that is the interest in this work. It discusses the derivation of the Adjoint equations, along with their boundary and time conditions. Throughout the deduction, the references which guided the results were mentioned and it is recommended to read to deepen the theoretical basis of the method. We start by considering a measure of merit of a given physical system:

$$R[X, \alpha] = \frac{1}{T} \int_0^T \int_D F[X, \alpha] dV dt \quad (5)$$

Where F could be any function of the state vector $X = (\rho, \vec{u}, T)$ and the project parameters $\alpha = (\alpha_1, \alpha_2, \dots, \alpha_n)$. The first Gateaux variation [16] of the functional yields the expression:

$$\delta R = \langle F'_x, \delta X \rangle + \langle F'_\alpha, \delta \alpha \rangle \quad (6)$$

Where $\langle a(v), b(v) \rangle = \frac{1}{T} \int_0^T \int_D a(v) \cdot b(v) dV dt$ represents the inner product defined in the phase space and on the appropriate boundaries of the domain. In general, the term $\langle F'_\alpha, \delta \alpha \rangle$ is known in closed form and, thus, the variation can be evaluated analytically. The greatest difficulty in estimating δR lies in δX in the first term, $\langle F'_x, \delta X \rangle$, instead. To eliminate the necessity of additional converged solutions to estimate $\langle F'_x, \delta X \rangle$, the governed equations were imposed as constrains, using Lagrange multipliers, defining, the augmented functional:

$$G[X, \alpha] = R[X, \alpha] - \langle \Phi, L \rangle - \langle \beta, B \rangle_s - \langle a, \alpha - \alpha_0 \rangle_s \quad (7)$$

Where $\Phi = (\omega, \vec{\Psi}, \theta)$ are the Lagrange multipliers. L represents a operator vector which components are the eqs. (1-3). β is the multiplier for the set of the Boundary conditions and a is the constraint that ensures that the control parameters take on a given set of prescribed values $\alpha = \alpha_0$, which corresponds to a baseline configuration. Computing the variations and make a suitable combination, the first variation of augmented functional δG is [8]:

$$\delta G[X, \alpha] = -\langle \delta \Phi, L \rangle - \langle \delta \beta, B \rangle_s - \langle \delta a, \alpha - \alpha_0 \rangle_s + \langle L^* \Phi + F'_x, \delta X \rangle - \langle \beta, B'_x \delta X \rangle_s - \langle P_1(\Phi), B'_x \delta X \rangle_s - \langle B^*(\Phi), A \delta X \rangle_s + \langle F'_\alpha, \delta \alpha \rangle - \langle a, \delta \alpha \rangle - \langle \beta, B'_\alpha \delta \alpha \rangle \quad (8)$$

Where the eq.(6) has been replaced in eq.(8). The Gauss's theorem is used to transfer differential operators from the state vector X to the Lagrange multipliers:

$$\langle \Phi, L \delta X \rangle = P[\Phi, \delta X]_s - \langle L^* \Phi, \delta X \rangle \quad (9)$$

Where the term $P[\Phi, \delta X]_s = [\langle P_1(\Phi), B'_x \delta X \rangle_s + \langle B^*(\Phi), A \delta X \rangle_s]$ is the bilinear concomitant [14]. The augmented functional G realizes extrema upon the condition that eq. (8) vanishes for arbitrary, albeit realizable, variations of its parameters:

$$\delta G = 0 \forall \{\delta X, \delta \alpha, \delta \Phi, \delta \beta, \delta a\} \in \{\text{locus of realizability}\}$$

That, in turn, requires that the following conditions be met [14]:

- The equations that govern the physics (1-4) and their respective boundary conditions (table 1) are satisfied. In addition, the control parameters should take on the prescribed baseline values ($\alpha = \alpha_0$). These requirements imply that first three terms of eq. (12) are identically zero.
- On imposing the condition: $\beta = -P_1(\Phi)$, one drives to zero the sum of the fifth and sixth terms of eq. (8).
- The vector Φ must satisfy the Adjoint equation, $L^*\Phi + F'_x \delta X = 0$, as it appears in the fourth term of eq.(8). The corresponding boundary conditions are given by the operator: $B^*(\Phi) = 0$, which comes from the seventh term in that equation. This equation should determine the Φ at the boundaries, along with β thereof.
- The vector \mathbf{a} is specified by the following condition: $\langle \mathbf{a}, \delta \alpha \rangle = \langle F'_\alpha, \delta \alpha \rangle + \langle \Phi, S \delta \alpha \rangle - \langle \beta, B'_\alpha \delta \alpha \rangle = \langle F'_\alpha, \delta \alpha \rangle + \langle P_1(\Phi), B'_\alpha \delta \alpha \rangle$, which collects all the remaining terms when $\delta G = 0$. In fact, this is the realizable part of the gradient, δR [8]:

$$\delta R = \langle F'_\alpha, \delta \alpha \rangle + \langle P_1(\Phi), B'_\alpha \delta \alpha \rangle \quad (10)$$

ADJOINT EQUATIONS

This section is dedicated to applying the flow governing equations in the fourth term of eq. (8). Using the independence between the primal and dual problem, we make of the simplest form of the governing equations. It yields:

$$\begin{aligned} \langle \Phi, LX \rangle = & \langle \omega, \epsilon_t \partial_0 \rho + \rho_b \partial_0 q + \nabla \rho \vec{u} \rangle + \langle \vec{\Psi}, \vec{u} + N_p \nabla p \rangle \\ & + \langle \theta, \partial_0 \left[C_{eff} T - \epsilon_t \left(\frac{\gamma-1}{\gamma} \right) P \right] + \nabla \rho \vec{u} T - \frac{1}{Pe} \nabla^2 T - \frac{\rho_b \Delta H}{M} \partial_0 q \rangle \end{aligned} \quad (11)$$

Where $\partial_0 = \frac{\partial}{\partial t}$. Computing the Gateaux variations:

$$\begin{aligned} \langle \Phi, L \delta X \rangle = & \langle \omega, \epsilon_t \partial_0 \delta \rho + \rho_b \partial_0 \delta q + \nabla(\delta \rho \vec{u} + \rho \delta \vec{u}) \rangle + \langle \vec{\Psi}, \delta \vec{u} + N_p \nabla \delta p \rangle \\ & + \langle \theta, \partial_0 \left[\delta C_{eff} T + C_{eff} \delta T - \epsilon_t \left(\frac{\gamma-1}{\gamma} \right) \delta P \right] + \nabla(\delta \rho \vec{u} T + \rho \delta \vec{u} T + \rho \vec{u} \delta T) \\ & - \frac{1}{Pe} \nabla^2 \delta T - \frac{\rho_b \Delta H}{M} \partial_0 \delta q \rangle \end{aligned} \quad (12)$$

Now, it is necessary to transfer the time and differential operators. To the first, we make use of the rule for differentiating a product. The terms of mass and energy equations become:

$$\langle \omega, \epsilon_t \partial_0 \delta \rho + \rho_b \partial_0 \delta q \rangle = \left[\frac{1}{T} \oint \omega (\epsilon_t \delta \rho + \rho_b \delta q) dV \right]_0^T - \langle \partial_0 \omega, \epsilon_t \delta \rho + \rho_b \delta q \rangle \quad (13)$$

$$\begin{aligned} \langle \theta, \partial_0 \left[\delta C_{eff} T + C_{eff} \delta T - \epsilon_t \left(\frac{\gamma-1}{\gamma} \right) \delta P - \frac{\rho_b \Delta H}{M} \delta q \right] \rangle = & \left[\frac{1}{T} \oint \theta \left(\delta C_{eff} T + C_{eff} \delta T - \right. \right. \\ & \left. \left. \epsilon_t \left(\frac{\gamma-1}{\gamma} \right) \delta P - \frac{\rho_b \Delta H}{M} \delta q \right) dV \right]_0^T - \langle \partial_0 \theta, \left[\delta C_{eff} T + C_{eff} \delta T - \epsilon_t \left(\frac{\gamma-1}{\gamma} \right) \delta P - \frac{\rho_b \Delta H}{M} \delta q \right] \rangle \end{aligned} \quad (14)$$

The terms $\left[\frac{1}{T} \oint (\dots) \right]_0^T$ were driven to zero because at $t = 0$, the flow solution is known and its variations δX are zero. Additionally, we impose a final condition of the Adjoint problem, by imposing that they vanish ($\omega = \theta = 0$ and $\vec{\Psi} = \vec{0}$) at $t = T$ [14]. To transfer the differential

operators, the Gauss's theorem was applied in convective terms, gradient pressure and diffusive term of the energy equation as follows:

$$\langle \omega, \nabla(\delta \rho \vec{u} + \rho \delta \vec{u}) \rangle = \langle \omega, (\delta \rho \vec{u} + \rho \delta \vec{u}) \cdot \vec{n} \rangle_s - \langle \nabla \omega, (\delta \rho \vec{u} + \rho \delta \vec{u}) \rangle \quad (15)$$

$$\langle \theta, \nabla(\delta \rho \vec{u} T + \rho \delta \vec{u} T + \rho \vec{u} \delta T) \rangle = \langle \theta, (\delta \rho \vec{u} T + \rho \delta \vec{u} T + \rho \vec{u} \delta T) \cdot \vec{n} \rangle_s - \langle \nabla \theta, \nabla(\delta \rho \vec{u} T + \rho \delta \vec{u} T + \rho \vec{u} \delta T) \rangle \quad (16)$$

$$\langle \vec{\Psi}, N_p \nabla \delta p \rangle = \langle \vec{\Psi} \cdot \vec{n}, N_p \delta p \rangle_s - \langle \nabla \cdot \vec{\Psi}^i, N_p \delta p \rangle \quad (17)$$

$$\langle \theta, -\frac{1}{Pe} \nabla^2 \delta T \rangle = \langle \theta, -\frac{1}{Pe} \nabla \delta T \cdot \vec{n} \rangle_s - \langle \nabla \theta, -\frac{1}{Pe} \nabla \delta T \rangle = \langle \theta, -\frac{1}{Pe} \nabla \delta T \cdot \vec{n} \rangle_s - \langle \nabla \theta \cdot \vec{n}, -\frac{1}{Pe} \delta T \rangle + \langle \nabla^2 \theta, -\frac{1}{Pe} \delta T \rangle \quad (18)$$

The four terms with subscript "s" form the bilinear concomitant. Using the relations: $\delta p = \delta \rho T + \rho \delta T$, $\delta q = A_\rho \delta \rho + A_T \delta T$, $\delta C_{eff} = (\epsilon_t + \rho_b A_\rho) \delta \rho + (\rho_b A_T) \delta T$, $\sigma = \omega - \theta T$ and combine the terms, the Adjoint equations yield:

$$\langle \delta \rho, \Gamma_{11} \partial_0 \sigma + \Gamma_{12} \partial_0 \theta + \Gamma_{13} \nabla \sigma + \Gamma_{14} \nabla \cdot \vec{\Psi} + \Gamma_{15} \theta \rangle = \langle F'_\rho \delta \rho \rangle \quad (19)$$

$$\langle \delta \vec{u}, \Gamma_{21} \vec{\Psi} + \Gamma_{22} \nabla \sigma + \Gamma_{23} \theta \rangle = \langle F'_{\vec{u}}, \delta \vec{u} \rangle \quad (20)$$

$$\langle \delta T, \Gamma_{31} \partial_0 \sigma + \Gamma_{32} \partial_0 \theta + \Gamma_{33} \nabla \theta + \Gamma_{34} \nabla \cdot \vec{\Psi} + \Gamma_{35} \theta + \Gamma_{36} \nabla^2 \theta \rangle = \langle F'_T \delta T \rangle \quad (21)$$

Where:

$\Gamma_{11} = (\epsilon_t + \rho_b A_\rho)$	$\Gamma_{12} = \left[-\epsilon_t \left(\frac{\gamma - 1}{\gamma} \right) T - \frac{\Delta H}{M} \rho_b A_\rho \right]$	$\Gamma_{13} = \vec{u}$
$\Gamma_{14} = N_p T$	$\Gamma_{15} = -[(\epsilon_t + \rho_b A_\rho) \partial_0 T + \vec{u} \nabla T]$	
$\Gamma_{21} = -1$	$\Gamma_{22} = \rho$	$\Gamma_{23} = -\rho \nabla T$
$\Gamma_{31} = \rho_b A_T$	$\Gamma_{32} = \left[C_{eff} - \epsilon_t \left(\frac{\gamma - 1}{\gamma} \right) \rho - \frac{\Delta H}{M} \rho_b A_T \right]$	$\Gamma_{33} = \rho \vec{u}$
$\Gamma_{34} = N_p \rho$	$\Gamma_{35} = -(\rho_b A_T) \partial_0 T$	$\Gamma_{36} = -\frac{1}{Pe}$
$A_\rho = -\frac{q D_1 T}{\rho}$	$A_T = q[D_1(D_2 + 1) - \alpha_e]$	$D_1 = C_2 n (T D_2)^{n-1}$
$D_2 = \left[\ln \left(\frac{C_3 T^2}{p} \right) \right]$	$C_2 = -\left(\frac{R}{\beta E_0} \right)^n$	$C_3 = \frac{p_{cr}}{T_{cr}^2}$

Table 2 – Coefficients of Adjoint Equations

The bilinear concomitant becomes:

$$P[\Phi, \delta X]_s = \langle \sigma, (\delta \rho \vec{u} + \rho \delta \vec{u}) \cdot \vec{n} \rangle_s + \langle \vec{\Psi} \cdot \vec{n}, (\delta \rho T + \rho \delta T) \rangle_s + \langle \theta, \left(\rho \delta T \vec{u} \cdot \vec{n} - \frac{\nabla \delta T \cdot \vec{n}}{Pe} \right) \rangle_s + \langle \nabla \theta \cdot \vec{n}, \frac{\delta T}{Pe} \rangle_s \quad (22)$$

Where the terms were divided into 2 parts, where $P_1(\Phi)$ are related to linearized boundary conditions, $B'_x \delta X$ and $B^*(\Phi)$ which represents the Adjoint Boundary conditions:

BC	Flow	Flow Linearized	Adjoint
Inlet	$\rho \vec{u} - f(X, t, G_m) = 0$ $T - T_{in} = 0$	$(\delta \rho \vec{u} + \rho \delta \vec{u}) - \frac{\partial f}{\partial G_m} \delta G_m - \frac{\partial f}{\partial t_{ac}} \delta t_{ac} = 0$ $\delta T - \delta T_{in} = 0$	$\vec{\Psi} \cdot \vec{n} = 0$ $\theta = 0$
Outflow	$P - P_{out} = 0$	$(\delta \rho T + \rho \delta T) - \delta P_{out} = 0$	$\sigma = 0$

			$\nabla\theta \cdot \vec{n}$ $= -(Pe\rho\vec{u} \cdot \vec{n})\theta$
Wall	$\rho\vec{u} = 0$ $-\nabla T \cdot \vec{n} = Nu(T - T_{ext})$	$(\delta\rho\vec{u} + \rho\delta\vec{u}) = 0$ $-\nabla\delta T \cdot \vec{n} = \delta Nu(T - T_{ext}) + Nu\delta T - Nu\delta T_{ext} = 0$	$\vec{\Psi} \cdot \vec{n} = 0$ $\nabla\theta \cdot \vec{n} = Nu\theta$
Sym.	$\rho\vec{u} \cdot \vec{n} = 0$ $\nabla T \cdot \vec{n} = 0$	$(\delta\rho\vec{u} + \rho\delta\vec{u})\vec{n} = 0$ $\nabla\delta T \cdot \vec{n} = 0$	$\vec{\Psi} \cdot \vec{n} = 0$ $\nabla\theta \cdot \vec{n} = 0$

Table 3 – Flow and Adjoint Boundary Conditions

Where $G_m = \rho_0 u_{in}$, T_{in} , Nu and T_{ext} represents the average mass flux vector, inlet temperature, Nusselt number and ambient temperature respectively. These terms can be used as design parameters in the validation tests. The outflow pressure, P_{out} was not tested because the status of the research archived only the process of the filling in ANG tanks.

VALIDATION TESTS

The objective of the validation tests was to prove the reduction of the computational cost if the Adjoint Method is used to estimate the sensibility gradient. As previously mentioned, the centered finite differences was used as reference, considering it as the simplest method to evaluate sensitives. The expression of this method is presented below:

$$\frac{\partial R}{\partial \alpha_p} = \frac{R(\alpha_1, \alpha_2, \dots, \alpha_p + \delta\alpha_p, \dots, \alpha_n) - R(\alpha_1, \alpha_2, \dots, \alpha_p - \delta\alpha_p, \dots, \alpha_n)}{2\delta\alpha_p} \quad (23)$$

Where $R(\alpha_1, \alpha_2, \dots, \alpha_p + \delta\alpha_p, \dots, \alpha_n)$ and $R(\alpha_1, \alpha_2, \dots, \alpha_p - \delta\alpha_p, \dots, \alpha_n)$ are the measure of merit (objective function) evaluated for a positive ($+\delta\alpha_p$) and negative ($-\delta\alpha_p$) perturbation of design parameter α_p . These terms were evaluated using a respective numeric solution of the flow governing equations (1-4). The tests were done using two objective functions: Volumetric Average Pressure and Volumetric Average Temperature. The design parameters were four G_m , t_{ac} , Nu and T_{ext} .

9.1 Volumetric Average Pressure

Using this variable as objective function, the eqs (5-6) were determined. Using the non dimensional ideal gas state equation ($p = \rho T$):

$$R[(\rho, \vec{u}, T), (G_m, Nu, T_{ext})] = \frac{1}{T} \int_0^T \int_D \frac{p}{V_t} dV dt \quad (24)$$

$$\delta R[(\rho, \vec{u}, T), (G_m, Nu, T_{ext})] = \langle \frac{T}{V_t}, \delta\rho \rangle + \langle \frac{\rho}{V_t}, \delta T \rangle \quad (25)$$

Where V_t is the geometric volume of the tank, $\langle F'_\rho \delta\rho \rangle = \langle \frac{T}{V_t}, \delta\rho \rangle$, $\langle F'_u \delta\vec{u} \rangle = 0$, $\langle F'_T \delta T \rangle = \langle \frac{\rho}{V_t}, \delta T \rangle$ and $\langle F'_\alpha, \delta G_m \rangle = \langle F'_\alpha, \delta Nu \rangle = \langle F'_\alpha, \delta T_{ext} \rangle = 0$. With the solutions of the Flow and Adjoint equations and collecting the remaining terms of the bilinear concomitant, the sensitivity gradient yields:

$$\delta R = \begin{cases} 2\sigma \left(1 - \frac{r^2}{r_i^2}\right) \left(\frac{t}{t_{ac}}\right) \cdot \vec{n}, & \text{if } t < t_{ac} \\ 2\sigma \left(1 - \frac{r^2}{r_i^2}\right) \cdot \vec{n} & , \text{if } t \geq t_{ac} \end{cases}, \delta G_m \rangle + \begin{cases} 2\sigma \rho_0 u_{in} \left(1 - \frac{r^2}{r_i^2}\right) \left(-\frac{t}{t_{ac}^2}\right) \cdot \vec{n} & , \text{if } t < t_{ac} \\ 0 & , \text{if } t \geq t_{ac} \end{cases}, \delta t_{ac} \rangle + \left\langle \frac{\theta(T-T_{ext})}{Pe}, \delta Nu \right\rangle + \left\langle -\frac{\theta Nu}{Pe}, \delta T_{ext} \right\rangle \quad (26)$$

The four terms of δR represent the components of the sensitivity gradient, each one in terms of the respective control parameter. The tests were performed simulating a filling process, with volumetric flow of 15 LPM at STP. The geometric and adsorbent parameters were the same of the presented in [4]. The total physical time was 210s and the sensitivity gradient were estimated in three points (90, 150 and 210s). The results are presented as follows:

$\frac{\partial R}{\partial G_m}$	Adjoint	Finite Difference	Dif. (%)	$\frac{\partial R}{\partial t_{ac}}$	Adjoint	Finite Difference	Dif. (%)
s	9.561e-02	9.737e-02	-1.81%	s	-9.019e-03	-9.134e-03	-1.25%
1 s	2.892e-01	2.916e-01	-0.81%	1 s	-1.482e-02	-1.481e-02	+0.09%
21 s	6.056e-01	6.058e-01	-0.05%	21 s	-2.107e-02	-2.080e-02	+1.34%

Table 4 – Results for two sensitivity gradient components for average pressure, G_m and t_{ac}

$\frac{\partial R}{\partial Nu}$	Adjoint	Finite Difference	Dif. (%)	$\frac{\partial R}{\partial T_{ext}}$	Adjoint	Finite Difference	Dif. (%)
s	-1.967e-04	-1.962e-04	0.28%	s	2.097e-01	2.091e-01	0.28%
1 s	-9.103e-04	-9.061e-04	0.47%	1 s	6.329e-01	6.300e-01	0.45%
21 s	-2.510e-03	-2.495e-03	0.58%	21 s	1.324e+00	1.317e+00	0.59%

Table 5 – Results for two sensitivity gradient components for average pressure, Nu and T_{ext}

The differences between Adjoint and Finite Differences were very low, corroborating the consistency of the Adjoint equations, boundary conditions and gradient expressions. The components in terms of Adjoint variable θ (Nu, T_{ext}), obtained small differences than components in terms of σ (G_m, t_{ac}).

Moreover, the computational cost reduced dramatically using the Adjoint Method. Considering a comparison using the results at $t = 210s$, the cost of one numeric flow simulation, using an ordinary computer was approximately 45 minutes. For each component of gradient estimated by Finite Difference Method, the cost was 2 flow simulations, or 1,5h. Then, for estimated the values $\left(\frac{\partial R}{\partial G_m}, \frac{\partial R}{\partial t_{ac}}, \frac{\partial R}{\partial Nu}, \frac{\partial R}{\partial T_{ext}}\right) = (6.058.e - 01, -2.080e - 02, -2.495e - 03, 1.317e + 00)$ which represents the values extracted from the tables 4 and 5, the computational cost was $4 \times 1.5 = 6h$.

On the other hand, using the Adjoint Method, only two simulations were needed: The primal problem, or the base flow, with the same computational cost of a flow solution (45 minutes), and the dual problem, or the Adjoint solution, which was expected that the cost was approximately the same of the physics problem. However, the results showed a time of

processing in 1 hour and 10 minutes, 55% greater than a simple numeric flow solution. Then, the total cost of Adjoint Method was 1 hour and 55 minutes.

In the other words, to estimate the values $\left(\frac{\partial R}{\partial G_m}, \frac{\partial R}{\partial t_{ac}}, \frac{\partial R}{\partial Nu}, \frac{\partial R}{\partial T_{ext}}\right) = (6.056e - 01, -2.107e - 02, -2.510e - 03, 1.324e + 00)$, extracted from tables 4 and 5, there was necessary 32% of the computational cost in comparison between the values estimated by Finite Difference Method.

9.2 Volumetric Average Temperature

Using the volumetric Average Temperature as Objective function, keeping the same control parameters, eq.(30) at previous section, the only changes was in components of $\langle F'_X \delta X \rangle$:

$$R[(\rho, \vec{u}, T), (G_m, Nu, T_{ext})] = \frac{1}{T} \int_0^T \int_D \frac{T}{V_t} dV dt \quad (27)$$

$$\delta R[(\rho, \vec{u}, T), (G_m, Nu, T_{ext})] = \left\langle \frac{1}{V_t}, \delta T \right\rangle \quad (28)$$

Where V_t is the geometric volume of the tank, $\langle F'_\rho \delta \rho \rangle = 0$, $\langle F'_{\vec{u}} \delta \vec{u} \rangle = 0$, $\langle F'_T \delta T \rangle = \left\langle \frac{1}{V_t}, \delta T \right\rangle$ and $\langle F'_\alpha, \delta G_m \rangle = \langle F'_\alpha, \delta Nu \rangle = \langle F'_\alpha, \delta T_{ext} \rangle = 0$. The results are presented as follows:

$\frac{\partial R}{\partial G_m}$	ADJ	DF	Dif. (%)	$\frac{\partial R}{\partial t_{ac}}$	ADJ	DF	Dif. (%)
s	2.309e-03	2.229e-03	3.59%	s	-2.528e-04	-2.416e-04	4.64%
1 s	4.079e-03	3.841e-03	6.18%	1 s	-2.671e-04	-2.461e-04	8.59%
21 s	5.532e-03	5.093e-03	8.61%	21 s	-2.636e-04	-2.346e-04	12.37%

Table 6 – Results for two sensitivity gradient components for average temperature, G_m and t_{ac}

$\frac{\partial R}{\partial Nu}$	ADJ	DF	Dif. (%)	$\frac{\partial R}{\partial T_{ext}}$	ADJ	DF	Dif. (%)
s	-2.4093e-05	-2.407e-05	0.09%	s	2.838e-02	2.836e-02	0.02%
1 s	-5.599e-05	-5.589e-05	0.19%	1 s	4.421e-02	4.419e-02	0.04%
21 s	-9.644e-05	-9.626e-05	0.19%	21 s	5.830e-02	5.824e-02	0.10%

Table 7 – Results for two sensitivity gradient components for average temperature, Nu and T_{ext}

For the components in terms of σ , the results worsened in comparison between the previous result with the pressure as the objective function. On the other hand, the results of components in terms of θ kept suitable regarding the Finite Difference Method. The computational cost had the same advantages of the result with pressure as measure of merit. The cost was 33% of the Finite Difference Method.

1 CONCLUSIONS

This article represents a part of the big project, which objective is to develop a optimization loop to find best solutions of ANG systems, varying not only geometric parameters, but also operational conditions for filling and deflation process, in the other words, a non-geometric parameters. The deduction of Adjoint Method applied in flows through porous media with

adsorption was a success, reducing dramatically the computational cost and make viable the optimization using a great quantity of parameters. There were other results, using different objective functions and control parameters that will be presented in the future.

When the optimization loop is finished, the software will be able to make optimal solutions for geometry, filling/deflation time dependent curves, heat transfer using internal and external heat exchanges and others, using only a base flow solution and an Adjoint solution. For conceptual designs, this tool could help the designer to study a great quantity of configurations in a viable time, ensuring a larger probability to find an optimal solution.

REFERENCES

- [1] SUZUKI, M. Adsorption Engineering. New York: El Sevier, 1990.
- [2] SOLAR C; BLANCO,A.G; VALLONE,A; SAPAG,K; Adsorption of methane in porous materials as the basis for the storage of natural gas. In-tech, Laboratorio de Sólidos Porosos – Instituto de Física Aplicada – CONICET – Universidad de San Luis – Argentina, 2010.
- [3] JUDD, R. W; GLADDDING, D.T.M; HODRIEN, R.C; BATES, D.R; INGRAM, J.P;ALLEN, M. The use of adsorbed natural gas technology for large-scale storage. BG Technology, Gas research and Technology Centre., 1998.
- [4] SAHOO, P.K; JOHN, M; NEWALKAR,B.L; CHOUDHARY,N.V; AYAPPA,K.G; Filling characteristics for an activated carbon based adsorbed natural gas storage system. I & EC research, 2011.
- [5] MOTA, J; SAATDJIAN,E; TONDEUR,D; A simulation model of high capacity methane adsorptive storage system. Adsorption 1, 1995.
- [6] HECHT, F.; New development in FreeFem++. Journal of Numerical Mathematics, 2012, no 3-4, 251-265
- [7] CHIEREGATTI,B.G;LIMA, J.S.B;VOLPE,E.V; HAYASHI, M.T; On the use of heat exchange's devices in order to improve adsorption and desorption process of ANG tanks. 24th ABCM International Congress of Mechanical Engineering (COBEM), Curitiba, PR, Brazil, 2017.
- [8] CHIEREGATTI,B.G;LIMA, J.S.B;VOLPE,E.V; HAYASHI, M.T; Optimization based on the Adjoint Method for Natural Gas Storage Systems. Research Centre for Gas Innovation, RCGI, project #6, Scientific Report, 2018.
- [9] GILES, M., PIERCE, N; Adjoint equations in CFD: Duality, boundary conditions and solution behavior. AIAA Paper 97-1850, 1997
- [10] JAMESON, A., SRIRAM, A., MARTINELLI, L; A continuous Adjoint method for unstructured grids, AIAA Computational Fluid Dynamics Conference, AIAA 2003-3955,2003.
- [11] NADARAJAH, S. K., JAMESON, A; A comparison of the continuous and discrete adjoint approach to automatic aerodynamic optimization, AIAA 38th Aerospace Sciences Meeting and Exhibit, AIAA 2000-0667,2000.
- [12] KIM, S., ALONSO, J., JAMESON, A; A gradient accuracy study for the Adjoint-based Navier-Stokes design method, AIAA Computational Fluid Dynamics Conference, 1999.
- [13] LUSTERNICK, L., SOBOLEV, V; Elements of Functional Analysis, Hindustan Pub. Co., Delhi, 1961.
- [14] CACUCI, D. G; WEBER,F.C.M.O.E; MARABLE, J.H; Sensitivity theory for general systems on non linear equations. Nuclear Science and Engineering, V.75, p.88-110, 1980.

Elastic Instabilities and Shear Waves in Soft Composites with Periodic Arrays of Fibers

Pavel Galich*, Viacheslav Slesarenko**, Stephan Rudykh***

*Technion – Israel Institute of Technology, **Technion – Israel Institute of Technology, ***Technion – Israel Institute of Technology

ABSTRACT

Soft fiber composites (FCs), characterized by light weight, high strength and flexibility are widespread in nature. However, natural materials may also carry undesirable properties, such as biodegradability, poor resistance to moisture and/or ultraviolet radiation; hence, manmade composites hold a prominent place in industry. An advantage of nonlinear (soft) composites over linear (hard) composites is high elasticity, allowing significant reversible geometry changes, including buckling; consequently, their effective properties can be tuned by deformation. Specifically, elastic waves in soft composites can be manipulated by deformation (1, 2). It is worth mentioning also that fibrous microstructures are common for various soft biological tissues, which can experience large deformations due to growth or damage, for example. Hence, investigation of elastic wave propagation in deformed FCs can be beneficial for biomedical ultrasound testing, for instance. In this work, we investigate propagation of small amplitude shear waves in marginally stable periodic FCs with rectangular arrays of cylindrical fibers. By utilizing the Bloch-Floquet analysis superimposed on finite macroscopically applied deformations (2, 3), we determine the critical stretches and wavelengths corresponding to the onset of elastic instability in the FCs with rectangular arrays of fibers. In particular, we show that the critical strains for FCs with rectangular arrays of fibers are bounded by the corresponding critical values for 3D laminates and FCs with square arrays of fibers. Next, we investigate shear wave propagation along the fibers in these FCs deformed close to the instability point. Remarkably, analysis of shear wave polarizations can provide us with useful insights on the expected buckling shapes of the fibers. Thus, we find that fiber distribution in periodic FCs strongly influences buckling shapes of the fibers. 1. Galich PI, Fang NX, Boyce MC, Rudykh S (2017) Elastic wave propagation in finitely deformed layered materials. *J Mech Phys Solids* 98:390–410. 2. Galich PI, Slesarenko V, Rudykh S (2017) Shear wave propagation in finitely deformed 3D fiber-reinforced composites. *Int J Solids Struct* 110–111:294–304. 3. Slesarenko V, Rudykh S (2017) Microscopic and macroscopic instabilities in hyperelastic fiber composites. *J Mech Phys Solids* 99:471–482.

THE ELECTRO-THERMAL LINK FINITE ELEMENT WITH 3D SPATIAL FUNCTIONALLY GRADED MATERIAL PROPERTIES AND THERMOELECTRIC EFFECTS

JURAJ PAULECH*, GABRIEL GÁLIK*, JUSTÍN MURÍN*, VLADIMÍR KUTIŠ*,
JURAJ HRABOVSKÝ*

*Faculty of Electrical Engineering and Information Technology,
Slovak University of Technology in Bratislava
Ilkovičova 3
Bratislava, Slovakia
juraj.paulech@stuba.sk; www.stuba.sk

Key words: 3D change of material properties, Thermoelectric analysis, FGM link finite element, ANSYS.

Summary. *The contribution presents new electro-thermal link finite element for FEM analyses. This link element is suitable for modelling electro-thermal structures made of Functionally Graded Material (FGM) where 3D spatial variation of material properties is utilized. Moreover, thermoelectric effects, like Seebeck and Peltier effects are supported by the element. Semi-analytical method is used for derivation process of element matrices such electro-thermal link element. Spatial variation of material properties of the considered system is transformed to equivalent longitudinal-only variation of material properties using homogenization techniques based on volume fractions of individual material components. Because thermoelectric properties cannot be homogenized such way, these properties are directly set as longitudinal functional change in the link element. Representative numerical experiment of FGM electro-thermal structure where results from the new link element are compared with model prepared using standard finite elements in SW ANSYS are shown in the contribution. Accuracy and effectiveness of the link element is discussed and evaluated.*

1 INTRODUCTION

Nowadays, new materials are necessary for sophisticated structures like MEMS systems, advanced electronic devices, etc. Computer modelling of such complex systems, like structures with spatial variation of material properties (e.g. FGM) are, using commercial FEM code with classic elements, needs remarkable effort during preparation phase and sufficient computer equipment for solution phase because of necessity the numbers of elements and material models.

Finite elements for electric-thermal analyses of FGM materials considering Joule heat have been developed in [1]. This paper deals with derivation of new link finite element for two-way coupled static thermoelectric analyses considering Joule heat and also thermoelectric effects like Seebeck and Peltier effects. These effects describe direct conversion of thermal energy into electric energy (Seebeck effect) and conversion of electric energy into the temperature difference within the system (Peltier effect).

Let us consider straight link conductor, the conductor is a slender construction. Let the conductor is made of a mixture of two or more materials so its thermal, electric and thermoelectric material properties change according to chosen function. Under these conditions, we can consider one-dimensional system of differential equations and original method further explained in [2] for solving the differential equations for thermoelectric coupled analysis.

2 HOMOGENIZATION OF MATERIAL PROPERTIES

Let us consider a bar with circular cross-section according to Fig. 1. Its length is L [m] and diameter d [m] (cross section area A [m²]). Let the FGM bar consists of two material components – matrix (denoted by index m) and fibre (index f) where fractions of individual constituents through the volume of the bar are functionally graded. We can consider matrix volume fraction $v_m(x, y, z)$ and fibre volume fraction $v_f(x, y, z)$ for every point (x, y, z) of the bar, so the change of material properties is 3D change. Moreover, let this change has polynomial character in every main direction $v_f(x, y, z) = \sum \varepsilon_u x^n y^m z^h$; $u = \max(r, s, l)$, $n = \{0; r\}$, $m = \{0; s\}$ and $h = \{0; l\}$ at which $v_m(x, y, z) = 1 - v_f(x, y, z)$, where grades of the polynomial changes r , s and l are for longitudinal and radial directions and through the individual circle's sectors of the bar, respectively (ε_u represents constant coefficients for individual coefficients of the polynomial). Fig. 1 also shows change of fibre volume fraction through the radial direction ($d = 6.67$ mm) and length ($L = 200$ mm) of the bar, where change through the circle's sectors of the bar is shown using parametric plot of surfaces (only 6 of total 12 surfaces – sectors – are shown). Thick lines in this Fig. 1 represent fibre volume fraction in chosen layers and sublayers (described in further sections of this contribution) of the bar that are necessary for calculation of homogenized material properties for electric and thermal fields.

The process of homogenization using division of the bar into layers (in radial direction) and sublayers (for chosen circle's sectors) according to extended mixture rule [3] and laminate theory [4] is shown in Fig. 2. The result of such homogenization process is equivalent homogenized material property (electric and thermal conductivity) with polynomial change only in longitudinal direction (through the other main directions of the bar the material property has constant value derived from longitudinal change). For steady-state electro-thermal analysis, the homogenization process need to be performed separately for final homogenized electric conductivity of the bar and for final homogenized thermal conductivity of the bar (both based on electric or thermal conductivities of fibre and matrix constituents of the FGM material, respectively).

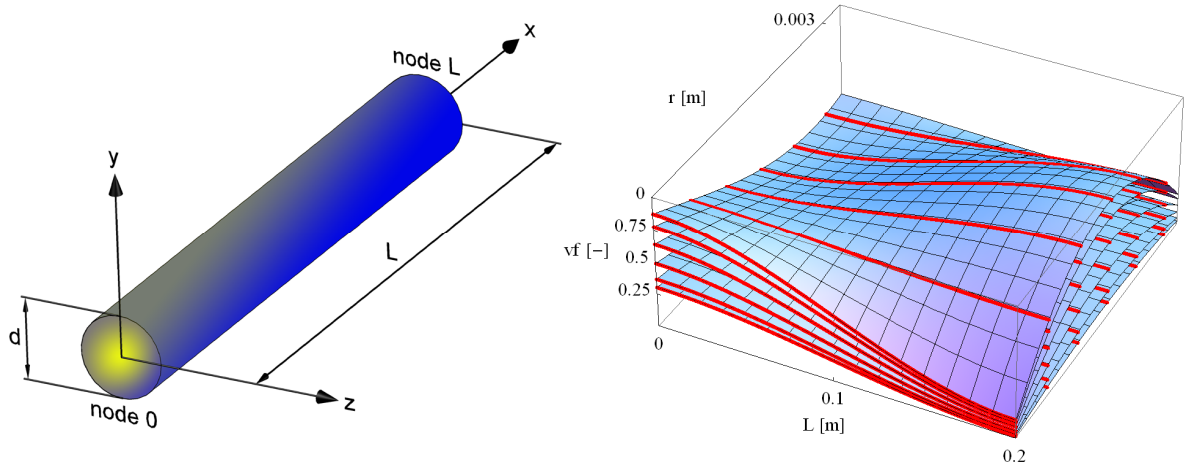


Fig. 1: FGM bar with spatial change of material properties (left), change of fibre volume fraction through the length, radial direction and circle's sections of the bar (right)

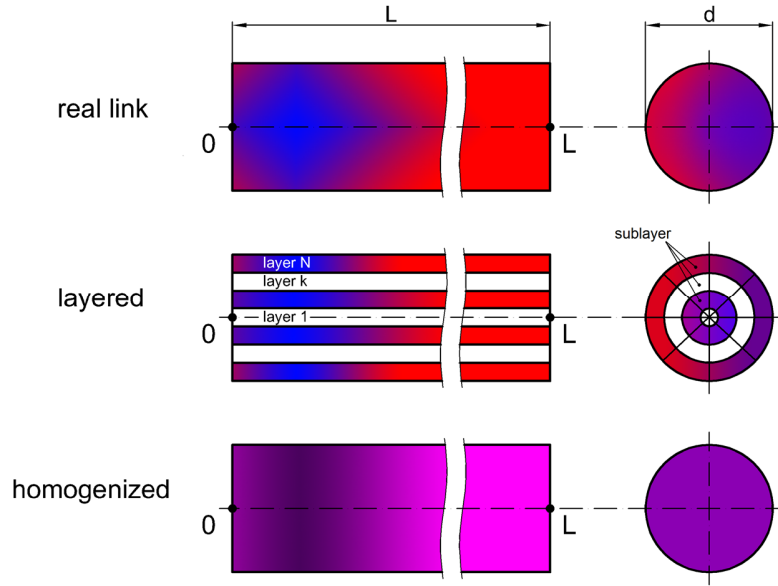


Fig. 2: Graphic representation of the homogenization process

For thermoelectric coupling that results in Seebeck and Peltier effects, Seebeck coefficient $\alpha(x, y)$ of the whole conductor needs to be known. This material property cannot be calculated according to the homogenization process based on extended mixture rule and laminate theory, because this material property is not given according to volume fractions of individual material components (except the Joule heat, thermoelectric effects are significant especially for semiconductor materials and the behaviour of the semiconductors is given according to atomic structure, not according to volume fraction of individual admixtures). Moreover, the value of Seebeck coefficient can also be negative number. The determination of final Seebeck coefficient

according to material properties of individual components is beyond the scope of this article. For our model case the final Seebeck coefficient will be chosen directly as a polynomial function $\alpha(x)$ for longitudinal direction of the homogenized conductor.

3 MATHEMATICAL BACKGROUND FOR TWO-WAY COUPLED THERMOELECTRIC ANALYSIS

Thermoelectric and electric-thermal effects like Joule heat, Seebeck, Peltier and Thomson effects are described by set of two thermoelectric constitutive equations (static analysis) [5]:

$$\begin{aligned}\mathbf{q} &= [\Pi] \cdot \mathbf{J} - [\lambda] \cdot \nabla T \\ \mathbf{J} &= [\sigma] \cdot (\mathbf{E} - [\alpha] \cdot \nabla T)\end{aligned}\quad (1)$$

where \mathbf{q} [Wm^{-2}] is heat flux vector, \mathbf{J} [Am^{-2}] is electric current density vector, $[\Pi]$ [V] is Peltier coefficient matrix, $[\lambda]$ [$\text{Wm}^{-1}\text{K}^{-1}$] is thermal conductivity matrix, T [K] is absolute temperature, \mathbf{E} [Vm^{-1}] is electric field intensity vector, $[\sigma]$ [Sm^{-1}] is electric conductivity matrix and $[\alpha]$ [VK^{-1}] is Seebeck coefficient matrix.

These constitutive equations are coupled by set of governing equations for static thermal and electric fields:

$$\begin{aligned}\nabla \cdot \mathbf{q} &= P \\ \nabla \cdot \mathbf{J} &= 0\end{aligned}\quad (2)$$

where P [Wm^{-3}] is heat generation per volume unit.

In general, we can write for electric field intensity, Peltier coefficient and heat generation:

$$\begin{aligned}\mathbf{E} &= -\nabla\varphi & P &= P_J + P_{aux} \\ [\Pi] &= T[\alpha] & P_J &= [\sigma]^{-1} \mathbf{J}^2\end{aligned}\quad (3)$$

where φ [V] is electric potential, P_J [Wm^{-3}] is Joule heat per volume unit and P_{aux} [Wm^{-3}] is auxiliary heat generation per volume unit.

Applying (1) and (3) into (2) we can write for 1D system (longitudinal direction x):

$$\begin{aligned}\frac{d}{dx} [T(x)\alpha(x)J(x)] - \frac{d}{dx} \left[\lambda(x) \frac{dT(x)}{dx} \right] &= \frac{J^2(x)}{\sigma(x)} + P_{aux}(x) \\ \frac{d}{dx} \left[\sigma(x) \frac{d\varphi(x)}{dx} \right] + \frac{d}{dx} \left[\sigma(x)\alpha(x) \frac{dT(x)}{dx} \right] &= 0\end{aligned}\quad (4)$$

4 FEM EQUATIONS FOR FGM LINK CONDUCTOR USING SEMI-ANALYTICAL METHOD FOR SOLUTION OF LINEAR DIFFERENTIAL EQUATIONS WITH VARIABLE COEFFICIENTS AND RIGHT-HAND SIDE

Procedure for solving differential equations with variable coefficients and right-hand side, which is presented in [2] is described in this chapter. General formula of such differential equation is:

$$\sum_{u=0}^m \eta_u(x) y^{(u)}(x) = \sum_{j=0}^g q_j a_j(x), \quad (5)$$

where:

- m – order of the differential equation
- $y(x)$ – unknown function of independent variable x
- $y^{(u)}(x)$ – u^{th} derivative of the unknown function
- $\eta_u(x)$ – polynomial variable coefficient for u^{th} derivative on the left-hand side of the differential equation
- g – order of a polynomial on the right-hand side of the differential equation
- q_j – constant coefficient for j^{th} power of the right-hand side polynomial
- $a_j(x) = \frac{x^j}{j!}$ – auxiliary function for the right-hand side polynomial formulation

at which $x \in \langle 0; L \rangle$, where L is the length of considered interval of unknown solution.

The solution of the differential equation with variable coefficients has the form according to [2]:

$$y^{(u)}(x) = \sum_{i=0}^{m-1} y_0^{(i)} c_i^{(u)}(x) + \sum_{j=0}^g q_j b_{j+m}^{(u)}(x), \quad (6)$$

The solution of the differential equation (5) lies in determining the transfer functions generally labelled $c(x)$ and $b(x)$ that appear in the solution. First, the functions $b_{j+m}^{(u)}(x)$ are calculated using power series and recursive process, considering $u = \{0; m\}$ and $j = \{0; g\}$. It is necessary to guarantee the convergence of the series for a given interval $x \in \langle 0; L \rangle$ for successful calculation of these functions. This is always true only for constant coefficients η_u of the differential equation. It is often necessary to divide the interval of x into the shorter sections (in our case the independent variable is geometric variable, for example $x = L$ is the length of the bar) for variable coefficients $\eta_u(x)$, and thus determine the solution also for inner region of the bar (where $x \in (0; L)$). Calculation of the transfer functions and also automatic division of the interval for non-convergence behaviour of the series is included in a computer code and listed in [2].

The differential equations suitable for presented semi-analytical solution method must fulfil the following requirements:

- one independent variable of the function
- polynomial variable coefficients of the differential equation
- polynomial character of the right-hand side of the differential equation
- known interval of the independent variable where the solution of the differential equation needs to be determined

The order of the differential equation and the order of the right-hand side are arbitrary.

The described procedure of calculation such differential equations is suitable for calculation of electric and / or thermal field within the bar (1D task with only one independent variable), where change of material properties (electric and / or thermal conductivity and / or thermoelectric Seebeck coefficient) has polynomial (therefore variable) character.

Figure 3 shows geometry and physical quantities for thermoelectric analysis considering bar structure for which final FEM equations for such coupled analysis are presented.

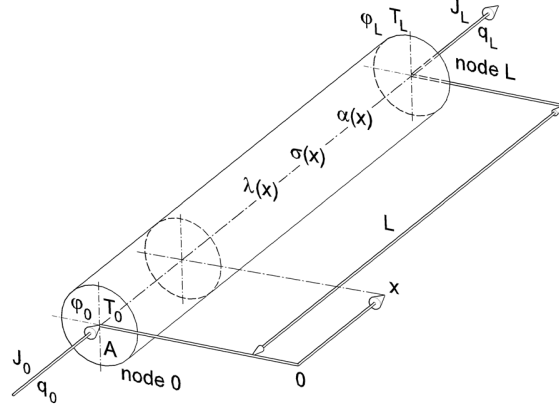


Fig. 3: Two-nodal conductor for thermoelectric analysis

Considering abovementioned semi-analytical method, the system of FEM equations for thermal field in the conductor can be expressed as:

$$\begin{bmatrix} c_0(L) + \frac{\alpha_0 J_0}{\lambda_0} c_1(L) & -1 \\ c_0(L) - \frac{c_1(L) c'_0(L)}{c'_1(L)} & \frac{c_1(L) \alpha_L J_L}{c'_1(L) \lambda_L} - 1 \end{bmatrix} \begin{bmatrix} T_0 \\ T_L \end{bmatrix} = \begin{bmatrix} \frac{c_1(L)}{\lambda_0} q_0 - \sum_{j=0}^g \varepsilon_j b_{j+2}(L) \\ \frac{c_1(L)}{c'_1(L)} \left(\frac{-q_L}{\lambda_L} + \sum_{j=0}^g \varepsilon_j b'_{j+2}(L) \right) - \sum_{j=0}^g \varepsilon_j b_{j+2}(L) \end{bmatrix} \quad (7)$$

The temperature within the range of the conductor is then:

$$T(x) = c_0(x) T_0 + c_1(x) \frac{T_0 \alpha_0 J_0 - q_0}{\lambda_0} + \sum_{j=0}^g \varepsilon_j b_{j+2}(x) \quad (8)$$

FEM equations for electric field are:

$$= \begin{bmatrix} -c_0(L) & 1 \\ -c_0(L) + \frac{c_1(L)c'_0(L)}{c'_1(L)} & 1 \end{bmatrix} \begin{bmatrix} \varphi_0 \\ \varphi_L \end{bmatrix} \\ = \begin{bmatrix} -\frac{c_1(L)}{\sigma_0} J_0 - c_1(L) \alpha_0 T'_0 + \sum_{j=0}^g \varepsilon_j b_{j+2}(L) \\ -\frac{c_1(L)}{c'_1(L)} \left(\frac{-J_L}{\sigma_L} + \alpha_L T'_L + \sum_{j=0}^g \varepsilon_j b'_{j+2}(L) \right) + \sum_{j=0}^g \varepsilon_j b_{j+2}(L) \end{bmatrix} \quad (9)$$

And the electric potential within the range of the conductor:

$$\varphi(x) = c_0(x)\varphi_0 - c_1(x) \left(\frac{J_0}{\sigma_0} + \alpha_0 T'_0 \right) + \sum_{j=0}^g \varepsilon_j b_{j+2}(x) \quad (10)$$

FEM equations for two-way coupled thermoelectric analysis need to be solved using iterative algorithm. During iteration process it is necessary to find substitutional functions for results obtained from FEM equations (results of these FEM equations are not continuous functions but only sets of discrete values) and also it is necessary to convert non-polynomials into polynomials.

5 THERMOELECTRIC ANALYSIS OF FGM LINK CONDUCTOR - NUMERICAL EXPERIMENT

In this chapter there will be one academic example of thermoelectric analysis of given FGM link conductor presented. The task will be solved using our new approach, by commercial FEM code ANSYS and also by numerical solution of differential equations in software Mathematica due to comparison reasons.

Let us consider electric conductor with circular cross-section according to Fig. 1. Its length is $L = 200$ [mm] and diameter $d = 6.67$ [mm]. Let the conductor consists of mixture of two component materials – matrix (index m) with constant electric conductivity $\sigma_m(x, y) = 1.429 \times 10^6$ [Sm⁻¹] and thermal conductivity $\lambda_m(x, y) = 1.333$ [Wm⁻¹K⁻¹], and fibre (index f) with electric conductivity $\sigma_f(x, y) = 1.111 \times 10^7$ [Sm⁻¹] and thermal conductivity $\lambda_m(x, y) = 450$ [Wm⁻¹K⁻¹]. Volume fraction of individual components is functionally changed according to chosen polynomial, graphically shown in Fig. 1.

Using extended mixture rule for chosen number of layers ($N = 6$) and 12 sublayers – segmentation of the circular cross-section, we get longitudinal variation of effective electric and thermal conductivities for individual layers and using laminate theory we can calculate also homogenized electric and thermal conductivities of FGM conductor. The equations of homogenized electric and thermal conductivities are:

$$\sigma^H(x) = 3.912 \times 10^6 + 1.035 \times 10^8 x^2 - 3.451 \times 10^8 x^3 \text{ [Sm}^{-1}\text{]} \\ \lambda^H(x) = 116.401 + 4797.41 x^2 - 15\,991.4 x^3 \text{ [Wm}^{-1}\text{K}^{-1}\text{]}$$

Let us consider final Seebeck coefficient for whole conductor according to chosen polynomial function (academic example, without considering homogenization process based on mixture of the components):

$$\alpha(x) = 2 \times 10^{-4} - 5 \times 10^{-3}x^2 \text{ [VK}^{-1}\text{]}$$

We assume static state for thermoelectric analysis. In nodes 0 and L there are electric potential, temperature, current density and heat flux specified, so the boundary conditions (see Fig. 4) are:

$$\begin{aligned} \varphi(0) &= 0 \text{ [V];} & T(0) &= 273 \text{ [K]} \\ J(L) &= 1.121 \times 10^6 \text{ [Am}^{-2}\text{];} & q(L) &= 14\,154.2 \text{ [Wm}^{-2}\text{]} \end{aligned}$$

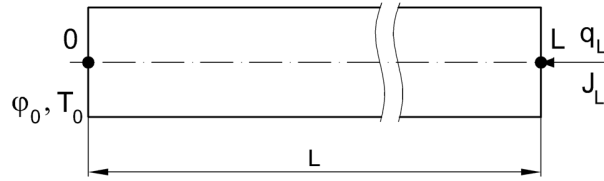


Fig. 4: Boundary conditions of the model

We also created 3D model in code ANSYS [6], we used 21 000 SOLID226 elements (20 node brick-elements). The task was also solved in software Mathematica [7], where the differential equations (5) with specified boundary conditions and homogenized material properties were numerically solved using iterative algorithm. Finally, the task was also solved by only one our new developed two-nodal link element using FEM equations (7) and (9) for nodal points of the link and with equations (8) and (10) for chosen points within the link. In Fig. 5 and Fig. 7 we can see calculated longitudinal distribution of the electric potential and temperature in the conductor, respectively. In Fig. 6 and Fig. 8 there are shown distributions of the electric current densities and heat fluxes for chosen layers (2nd, 4th and 6th layer) within the 2nd sublayer, respectively.

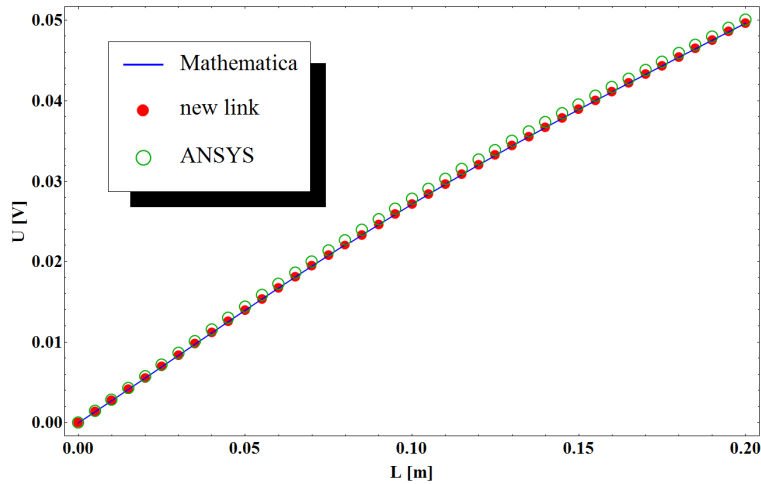


Fig. 5: Distribution of the electric potential through the length of the conductor

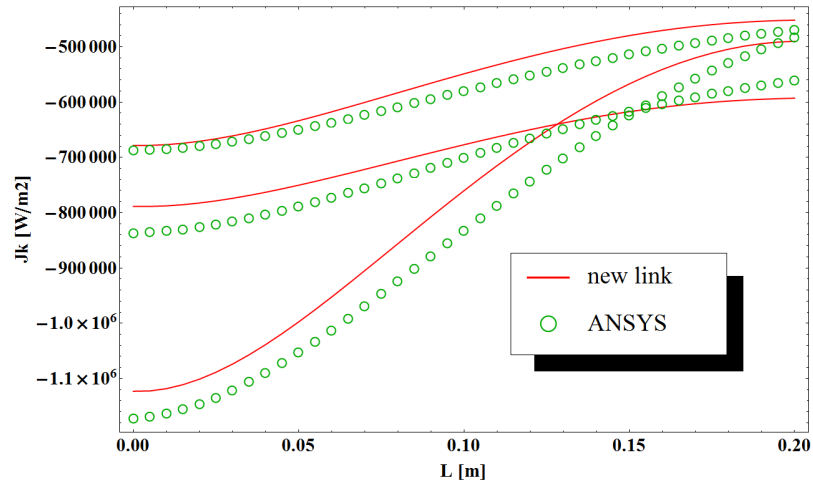


Fig. 6: Longitudinal distribution of the current densities in the chosen layers of one sublayer of the conductor

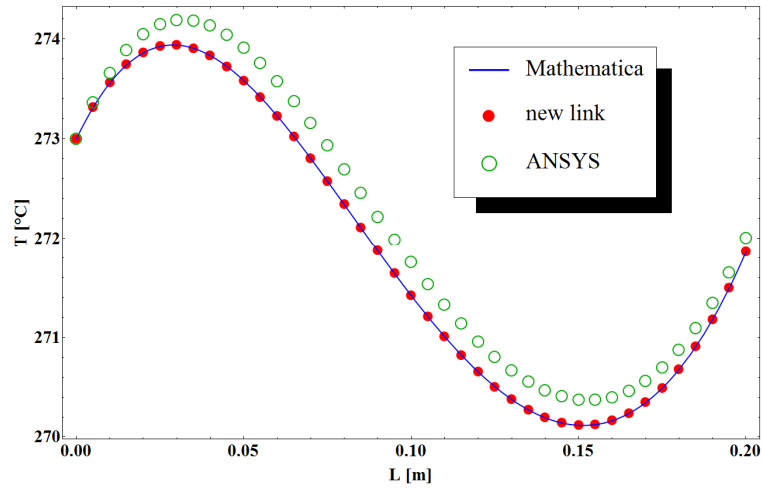


Fig. 7: Distribution of the temperature through the length of the conductor

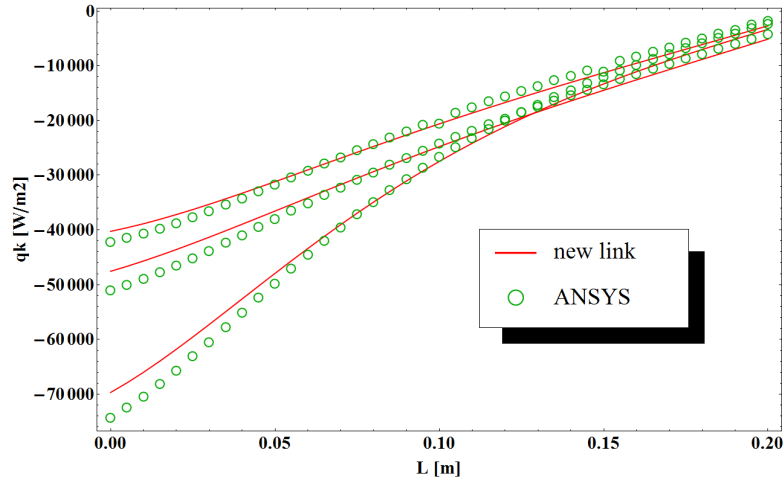


Fig. 8: Longitudinal distribution of the heat fluxes in the chosen layers of one sublayer of the conductor

In Fig. 7 it can be seen the cooled zone within one part of the model. This is due to Peltier effect based on different Seebeck coefficients applied in individual parts of the model and electric current passing through the conductor.

There is small difference in the results between ANSYS solution and calculation using the new approach because of substitutional functions used for conversion non-polynomials into polynomials during iterative process. Another differences in the results are due to fact that our approach is based on reduction of the real 3D system into 1D problem. But we can see from Fig. 5 – Fig. 8 that obtained results correspond to ANSYS 3D simulation very well.

6 CONCLUSIONS

New finite link element for two-way coupled static thermoelectric analyses for FGM with 3D spatial change of material properties has been developed in this contribution. New FEM equations with consideration Joule heat, and thermoelectric effects, like Seebeck and Peltier effects, were derived. Numerical example with good agreement between calculations with just only one new link element and commercial FEM code that uses numbers of classic elements have been presented. The new approach fully agrees with numerical solution for 1D differential equation of thermal and electric fields calculated using iterative algorithm. So, effectiveness and accuracy of the new developed link element for these analyses are at a high level.

ACKNOWLEDGMENTS

This work was supported by the Slovak Research and Development Agency under the contracts No. APVV-14-0613 and APVV-0246-12, by Grant Agency VEGA, grant No. 1/0102/18 and 1/0081/18. Authors are also grateful to the HPC Centre at the Slovak University of Technology in Bratislava, which is a part of the Slovak Infrastructure of High Performance

Computing (SIVVP project, ITMS code 26230120002, funded by the European Regional Development Funds), for the computational time and resources made available.

REFERENCES

- [1] Murín, J. et al.: Electric-Thermal Link Finite Element Made of a FGM with Spatial Variation of Material Properties. *In: Composites Part B: Engineering*. ISSN 1359-8368. Vol. 42 (2011), p. 1966-1979.
- [2] Rubin, H.: Analytische Lösung linearer Differentialgleichungen mit veränderlichen Koeffizienten und baustatische Anwendung. *Bautechnik* 76. (1999).
- [3] Murín, J., Kutíš, V.: Improved mixture rules for the composite (FGM's) sandwich beam finite element. *In: Computational Plasticity IX. Fundamentals and Applications*. Barcelona. (2007), p. 647-650.
- [4] Altenbach, H. et al.: Mechanics of composite structural elements. *Springer-Verlag*. Berlin. (2003), 468 p.
- [5] Antonova, E., Looman, D.: Finite Elements for Thermoelectric Device Analysis in ASNYS. *In: ICT International Conference*. Clemson SC USA. (2005), p. 215-218.
- [6] ANSYS Swanson Analysis System, Inc., 201 Johnson Road, Houston, PA 15342/1300, USA.
- [7] S. Wolfram MATHEMATICA 5, Wolfram research, Inc., (2003).

Models and Software for Free Energy-Based Virtual Drug Screening

Emilio Gallicchio*

*Brooklyn College and Graduate Center of CUNY

ABSTRACT

We will describe recent progress on the development of a single-decoupling alchemical binding free energy model, its efficient implementation on graphical processing units (GPUs), and applications to large-scale virtual drug screening campaigns. The free energy of binding provides a complete description of the likelihood of association between molecules because it includes from first principles entropic and conformational reorganization effects which are neglected, or only empirically estimated, by simpler models. We will present illustrative cases in which, for example, compounds with favorable energetic interactions do not bind strongly the target receptor because to do so they incur intramolecular strain and entropic penalties. By screening out such cases, free energy models can lead to higher drug screening accuracy than currently achievable with docking and scoring protocols. However, due to perceived barriers to entry, complex setup and high computational requirements, free energy models of molecular binding are still not widely adopted in academic and industrial research. To address these challenges, we have developed a streamlined and automated single-decoupling version of the well-known double-decoupling method used in drug optimization and we have implemented it on massively parallel graphical processing units (GPUs). The single-decoupling method, together with parallel Hamiltonian hopping conformational sampling, speeds up by orders of magnitude the convergence of binding free energy estimates. The GPU implementation as part of the OpenMM library is up to 100 times faster than optimized CPU implementations. We will present results of the deployment this computational framework protocol on GPU farms illustrating the advantages as well as the conceptual and technical challenges of the methodology. 1. Baofeng Zhang, Denise Kilburg, Peter Eastman, Vijay S. Pande, Emilio Gallicchio. Efficient Gaussian Density Formulation of Volume and Surface Areas of Macromolecules on Graphical Processing Units. *J. Comp. Chem.*, 38, 740-752 (2017). 2. Emilio Gallicchio, Junchao Xia, William F Flynn, Baofeng Zhang, Sade Samlalsingh, Ahmet Montes, Ronald M Levy. Asynchronous Replica Exchange Software for Grid and Heterogeneous Computing. *Computer Physics Communications*, 196, 236–246 (2015). 3. Emilio Gallicchio, Nanjie Deng, Peng He, Lauren Wickstrom, Alexander L. Perryman, Daniel N. Santiago, Stefano Forli, Arthur J. Olson and Ronald M. Levy. Virtual Screening of Integrase Inhibitors by Large Scale Binding Free Energy Calculations: the SAMPL4 Challenge. *J Comp Aided Mol Design*, 28, 475-490 (2014).

Quasi-static Crack Propagation Problems in PD-FEM Coupled Models

Ugo Galvanetto*, Mirco Zaccariotto**, Tao Ni***

*University of Padova, Italy, **University of Padova, Italy, ***Hohai University?, China

ABSTRACT

Peridynamics (PD) is a family of non-local continuum theories proposed in a series of papers since the year 2000 [1], which, by adopting an integral formulation, does not make use of spatial derivatives. For that reason, PD based computational methods are successfully used to study problems with crack propagation, in particular they have been applied to the solution of dynamic crack propagation in brittle materials. However there are crack propagation problems in which the dynamic effects are negligible, such as those associated to fatigue phenomena. It is necessary to equip PD based computational tools with static solvers. The most popular approach adopted to solve non-linear problems is the Newton-Raphson algorithm which cannot be easily used in computational tools based on PD because most PD codes work on fragile fracture adopting the prototype microelastic brittle material (PMB) which assumes that the relation between bond stretch and bond force is linear up to a maximum stretch value, beyond which the bond force drops to zero (elasto-brittle material). The discontinuous definition of the PMB model prevents a straightforward application of standard Newton-Raphson algorithms. Therefore, its use in implicit static codes is problematic. This might be one of the reasons why static crack propagation phenomena are not commonly addressed when using PD-based numerical methods. We introduce a simple and accurate way to perform an implicit solution of static problems in which the usual PMB model is adopted: the sequentially linear approach [2]. Moreover we use it in conjunction with the FEM-PD coupling technique shown in [3]. In this manner we obtain a way to increase efficiency and flexibility of PD-based codes. The paper will demonstrate the potentialities of the proposed method by studying crack propagation phenomena in 2D systems. The effects of the presence of holes and initial cracks under static load conditions will be analysed. Results will be evaluated taking into account different horizon dimensions, grid sizes, initial crack lengths and crack orientations. References [1] S. A. Silling, Reformulation of elasticity theory for discontinuities and long-range forces, *J Mech Phys Solids*, Vol. 48, pp 175-209, (2000). [2] J.R. Roots, Sequentially linear continuum model for concrete fracture, in *Fracture Mechanics of Concrete Structures*, de Borst et al (eds), Swets & Zeitlinger, Usse, pp. 831-839, (2001). [3] M. Zaccariotto, T. Mudric, D. Tomasi, A. Shojaei, U. Galvanetto, Coupling of FEM meshes with Peridynamic grids, *Comput. Methods Appl. Mech. Engrg.* 330, 471–497, (2018).

Ultrafast Laser-excited Acoustic Vibrations of Single Gold Nanorods

Yong Gan^{*}, Zheng Sun^{**}, Yonggang Shen^{***}

^{*}Zhejiang University, ^{**}Zhejiang University, ^{***}Zhejiang University

ABSTRACT

The acoustic vibrations of single gold nanorods are important for their applications in ultrasensitive sensing and nanooptics. Ultrafast laser irradiation has been a commonly used method to excite the vibrations of gold nanorods. The atomistic simulations for the vibrations of individual single-crystal and penta-twinned gold nanorods by femtosecond laser excitation have been performed [Gan et al., 2015a, 2015b, 2016], using a method that couples molecular dynamics (MD) with the two temperature model (TTM). The frequencies for the excited extensional and breathing modes of gold nanorods are obtained via the simulated nanorod responses, and then used to determine the elastic modulus of gold nanorods, in combination with continuum elasticity. With the decrease of nanorod width, the modulus of single-crystal gold nanorods decreases while the twinned nanorods become stiffer. It is shown that the elasticity theory based on the long-wavelength limit could fairly well describe the extensional periods of nanorods with an aspect ratio as small as ≈ 2.4 . The breathing mode of single-crystal nanorods characterized by the motion at the vertices is observed. For twinned nanorods, two breathing modes with the motions at the vertices and edges of the pentagonal cross-section are illustrated. It is demonstrated that the breathing periods of nanorods with an aspect ratio down to ≈ 2.5 could be well predicted by the continuum elastic model in the limit of an infinitely long rod, with the use of bulk elastic constants. In addition, we find that the breathing vibrations of the penta-twinned nanorods are more affected by the crystal structure effect than those of single-crystal nanorods. Keywords: gold nanorods; acoustic vibration; mechanical properties; size effect; continuum elasticity. References Gan, Y., Wang, C., and Chen, Z., Ultrafast laser-excited vibration and elastic modulus of individual gold nanorods, Optics Letters, 40, 340-343, 2015a. Gan, Y., Sun, Z., and Chen, Z., Extensional vibration and size-dependent mechanical properties of single-crystal gold nanorods, Journal of Applied Physics, 118, 164304 2015b. Gan, Y., Sun, Z., and Chen, Z., Breathing mode vibrations and elastic properties of single-crystal and penta-twinned gold nanorods, Physical Chemistry Chemical Physics, 18, 22590-22598, 2016.

Symbolic Time Series Analysis of the Strain Time History of Plate Structures Using Self-Powered Energy Harvesting Sensors for Monitoring of Damage Propagation in Materials

Amir H. Gandomi^{*}, Mohsen Mousavimirkalaei^{**}, Damien Holloway^{***}, JC Olivier^{****}, David G. Belanger^{*****}, Mirjam Fürth^{*****}

^{*}Stevens Institute of Technology, Hoboken, NJ 07030, USA, ^{**}School of Engineering and ICT, Univ. of Tasmania, Hobart, TAS 7001, Australia, ^{***}School of Engineering and ICT, Univ. of Tasmania, Hobart, TAS 7001, Australia, ^{****}School of Engineering and ICT, Univ. of Tasmania, Hobart, TAS 7001, Australia, ^{*****}Stevens Institute of Technology, Hoboken, NJ 07030, USA, ^{*****}Stevens Institute of Technology, Hoboken, NJ 07030, USA

ABSTRACT

Recently, a new self-powered energy-harvesting sensor has been invented at the Michigan State University, [1, 2]. The mentioned sensor has floating gates, which can be set at some threshold voltages. When the voltage induced in the piezoelectric material of the sensor exceeds one of the specified thresholds the time counter is triggered. The symbolic dynamic analysis is used in order to find the effective thresholds for the maximum detectability of the change due to any damage based on Shannon entropy. For this, a baseline needs to be constructed using the undamaged plate case to set the thresholds based on the strain time history of the plate. Hence, some tests on a pristine plate subjected to a harmonic force has been conducted. Then, the time series on the strain event is sorted and discretized into equally populated subspaces by specifying relevant thresholds. Once the sensors have been set to these thresholds, the posterior state of the structure is monitored based on the accumulated time that each sensor exceeds its specified threshold. These accumulated times will show how much the system deviated from the initial condition. This can be done by finding the distance between the cumulative probability distribution function of the damaged plate and comparing it to the uniform distribution of the strain time history of the pristine condition. The outcomes demonstrate the capability of the method for monitoring damage propagation in similar structures. Keywords: structural health monitoring, Symbolic Dynamic Analysis, Damage, signal processing, Strain, Probability Distribution Function [1] A. H. Alavi, H. Hasni, N. Lajnef, K. Chatti, Damage growth detection in steel plates: Numerical and experimental studies, Engineering Structures 128 (2016) 124–138. [2] H. Hasni, A. H. Alavi, N. Lajnef, M. Abdelbarr, S. F. Masri, S. Chakrabartty, Self-powered piezo-floating-gate sensors for health monitoring of steel plates, Engineering Structures 148 (2017) 584–601.

Residual Stress Simulations and Comparison against Experimental Measurements for Additively Manufactured Ti-6Al-4V Bridge Specimens

Rishi Ganeriwala^{*}, Neil Hodge^{**}, Donald Brown^{***}, Lyle Levine^{****}, Bjorn Clausen^{*****}, Maria Strantza^{*****}, Thien Phan^{*****}, Wayne King^{*****}

^{*}Lawrence Livermore National Laboratory, ^{**}Lawrence Livermore National Laboratory, ^{***}Los Alamos National Laboratory, ^{****}National Institute of Standards and Technology, ^{*****}Los Alamos National Laboratory, ^{*****}Los Alamos National Laboratory, ^{*****}National Institute of Standards and Technology, ^{*****}Lawrence Livermore National Laboratory

ABSTRACT

The production of metal parts via laser powder bed fusion (L-PBF) additive manufacturing is rapidly growing. However, in order for components produced via L-PBF to be used in critical applications, a high degree of confidence is required in their quality. An essential piece for such qualification is the ability to accurately know the stress state within a part. Since experimental measurement is often not feasible, having a validated model capable of reliably simulating these stresses would be extremely valuable. In this work, four Ti-6Al-4V arch-bridge shaped specimens were built via L-PBF using four different scan strategies: continuous scan aligned with the x-axis, continuous scan at 45 degrees to the x-axis, island scan aligned with the x-axis, and island scan at 45 degrees to the x-axis. A 90-degree rotation in scan orientation was performed after each layer for all four cases. The post-build residual stress in these components was determined by using x-ray diffraction to measure the strains present within the bridges, both while still attached to the base plate and after one leg had been cut off the base plate. Thermo-mechanical simulations of the bridge builds were performed using the parallelized multiphysics code Diablo. As the large range of time and length scales involved in the process prohibit simulation at the physical process scale, an agglomeration/lumping strategy was employed to estimate the residual stress in a reasonable time frame. The layer size was agglomerated such that many physical layers were lumped into one larger computational layer. Similarly, the beam size was computationally enlarged. A material model was used which captures the strain rate dependence of Ti-6Al-4V at elevated temperatures and allows for complete stress and plastic strain relaxation near melt. Parameter studies were performed to investigate different agglomeration approaches for both accuracy and computational expense. Results from the simulations exhibited good qualitative agreement with the measured strains in the bridges. However, the x-ray diffraction measurements actually showed increased strains present in the bridges built via the island scan strategies, particularly near the edges of the parts. This increase in strains for the island scan strategies was not captured in the simulations, which predicted similar residual stress profiles for all four parts. A discussion of potential reasons for both the experimental and computational findings will be presented.

Multiscale Topology Optimization for Integrated Design of the Structure and Materials

Jie Gao*, Zhen Luo**, Hao Li***, Liang Gao****

*School of Mechanical and Mechatronic Engineering, The University of Technology Sydney, 15 Broadway, Ultimo, NSW 2007, Australia, **School of Mechanical and Mechatronic Engineering, The University of Technology Sydney, 15 Broadway, Ultimo, NSW 2007, Australia, ***State Key Lab of Digital Manufacturing Equipment and Technology Huazhong University of Science and Technology, 1037 Luoyu Road, Wuhan, Hubei 430074, China, ****State Key Lab of Digital Manufacturing Equipment and Technology Huazhong University of Science and Technology, 1037 Luoyu Road, Wuhan, Hubei 430074, China

ABSTRACT

Multiscale design has become a promising research topic in recent years since some pioneering works. In order to pursue the much higher structural performance within an acceptable computational cost, this current work proposes a new multiscale topology optimization method for integrated design of the macrostructure and multiple kinds of material cells by considering three basic design elements, namely the distribution of material cells as well as the topologies of both the macrostructure and material cells. Two stages are mainly involved, including the distribution optimization and the concurrent optimization. At the first stage, a classic SIMP-based method combined with a defined post-processing mechanism is formulated to enable a multi-piece layout of the element densities, which works as the distribution of multiple kinds of material cells over the macro design domain based on the positive correlation between the element densities and material effective properties. The macrostructure would be divided into some kinds of sub regions and each sub region is featured with a kind of material effective property. At the second stage, the topologies of the macrostructure and material cells are optimized synchronously by the parametric level set method under the distribution of material cells, where the numerical homogenization method is applied to evaluate material effective properties. Several examples in 2D and 3D are provided to display the effectiveness of the proposed multiscale design method. Results indicate that the structural performance of the optimized multiscale structure can be further enhanced within an acceptable computational cost.

Development of a Finite Element/ Discontinuous Galerkin/ Level Set Method for the Simulation of the Polymer Filling Process

Puyang Gao*, Jie Ouyang**, Wen Zhou***

*Northwestern Polytechnical University, Xi'an, China, **Northwestern Polytechnical University, Xi'an, China,

***Northwestern Polytechnical University, Xi'an, China

ABSTRACT

The filling process in the injection molding always involves the polymer melt and air with different flow characteristics, large density/viscosity ratios and the transient free surface, which is treated as a challenging viscoelastic-Newtonian two phase flow problem especially on the irregular domains. In this study, the complex filling process for the irregular cavity is simulated via a combined finite element (FEM)/discontinuous Galerkin (DG)/level set method with application to the socket with five inserts, which has been rarely investigated. The rheological behavior of the viscoelastic fluid is predicted according to the eXtended Pom-Pom (XPP) constitutive model, which is suitable to describe the viscoelastic behavior of the branched polymer melt. The division and fusion of the evolving melt front in the filling stage is captured by the simple and efficient level set method. In the computational framework, we mainly need to solve the Navier-Stokes equations to get velocity field and pressure, deal with the XPP constitutive equation to update the stress values and handle the level set equation to renew the location and profile of the interface. The splitting scheme is first utilized to decouple the viscoelastic incompressible Navier-Stokes equations to get three sub-equations and makes it possible to choose the equal order interpolation function pair. And then DG is employed to deal with the non-linear hyperbolic equation and FEM is used to solve the Poisson and Helmholtz equations. In addition, the second order Runge Kutta Discontinuous Galerkin (RKDG) method is employed to handle the XPP constitutive equation and the level set equation due to their hyperbolic nature. This combined algorithm is convenient to directly cope with the irregular region of the cavity and there is no need of any stabilization terms. We first investigate the filling process of the rectangular cavity without and with a diamond insert, and compare with other numerical and experimental results to illustrate the validity of the coupled method. Moreover, as an application case, we consider the cavity of the socket with five inserts in China and analyze the influences of the inlet velocity and elasticity on the physical quantities such as stresses, stretch etc., and the simulation results could provide some numerical predictions for the polymer industry. To the best of our knowledge, this is the first attempt to simulate the polymer filling process in the irregular cavity with several inserts based on the XPP constitutive model via the combined finite element/discontinuous Galerkin/level set method.

An Efficient and Accurate Method for the Transient Heat Conduction in 2D Periodic Structures

Qiang Gao^{*}, Haichao Cui^{**}, Ying Feng^{***}

^{*}State Key Laboratory of Structural Analysis for Industrial Equipment, Department of Engineering Mechanics, Dalian University of Technology, ^{**}State Key Laboratory of Structural Analysis for Industrial Equipment, Department of Engineering Mechanics, Dalian University of Technology, ^{***}State Key Laboratory of Structural Analysis for Industrial Equipment, Department of Engineering Mechanics, Dalian University of Technology

ABSTRACT

An efficient and accurate method is developed to solve the transient heat conduction problems in two-dimensional (2D) periodic structures. For a 2D periodic structure, according to the physical feature of the transient heat conduction, the periodic property of the structure, and the physical meaning of the matrix exponential, it is demonstrated that the matrix exponential for a reasonable time step is a sparse matrix containing many identical elements. Next, based on the superposition principle of linear systems and the algebraic structure of the matrix exponential, computation of the response of the original 2D periodic structure is transformed into computation of the responses of the small-scale models with several unit cells. Finally, the precise integration method (PIM) is used to compute the temperature responses of the small-scale models. The proposed method not only inherits the accuracy and stability of the PIM but also achieves significantly improved computational efficiency in terms of both computation time and storage requirements. A series of numerical examples demonstrate that the proposed method is more efficient than the Crank-Nicholson method and can obtain highly precise solutions even with a larger time step.

Topology and Shape Optimization Based Method for Miniaturization Design of Metallic Antenna

Renjing Gao*, Chuan Liu**, Qi Wang***, Shutian Liu****

*Dalian University of Technology, **Dalian University of Technology, ***Dalian University of Technology, ****Dalian University of Technology

ABSTRACT

To meet the stronger and stronger requirement of miniaturization and integration of the wireless communication system, the antennas are expected to be miniaturized correspondingly and should be carefully designed. As a rule, miniaturization of antenna can be achieved by designing the antenna operating at a lower frequency band. Among various design methods of miniaturized antenna proposed in the literature, topology optimization attracts intense interests due to its ability of flexibly distributing the metallic materials. But it is shown that the antenna performance is extremely sensitive to the grey elements remained in the topology optimization results. To overcome this kind of sensitive issue, this work presents a topology and shape optimization based method for metallic antenna's miniaturization design. The concept configuration of antenna is obtained through topology optimization firstly. The above sensitive issue is well illustrated through a typical example, and the mechanism of this sensitive issue is thoroughly analyzed and explained. Then a shape optimization scheme is built by describing the key boundary of the antenna with Bessel curves. By adjusting the location of points of the Bessel curves, the shape of the antenna can be flexibly optimized. A new configuration of miniaturized antenna is obtained with the proposed design method. The miniaturization index of the designed antenna is demonstrated better than any result obtained with dimension optimization. Compared to the original result obtained by topology optimization, both the return loss and the frequency bandwidth of the design are improved. In addition, the boundary of the design is more smooth to ensure the antenna can be easily fabricated. The proposed type of design method can also be extended to the optimization of other metallic devices.

Numerically Efficient Microstructure-based Calculation of Internal Stresses in Superalloys

Siwen Gao^{*}, Umaaran Gogilan^{**}, Anxin Ma^{***}, Alexander Hartmaier^{****}

^{*}Interdisciplinary Centre for Advanced Materials Simulation, Ruhr-University Bochum, ^{**}Interdisciplinary Centre for Advanced Materials Simulation, Ruhr-University Bochum, ^{***}Interdisciplinary Centre for Advanced Materials Simulation, Ruhr-University Bochum, ^{****}Interdisciplinary Centre for Advanced Materials Simulation, Ruhr-University Bochum

ABSTRACT

According to the classical Eshelby inclusion problem, we introduce a new linear relation to calculate internal stresses in μm microstructures of superalloys via an effective stiffness method. To accomplish this, we identify regions with almost uniform deformation behavior within the microstructure. Assigning different eigenstrains to these regions results in a characteristic internal stress state. The linear relation between eigenstrains and internal stresses, as proposed by Eshelby for simpler geometries, is shown to be a valid approximation to the solution for complex microstructures. The Fast Fourier Transformation method is chosen as a very efficient numerical solver to determine the effective stiffness matrix. Numerical validation shows that this generalized method with the effective stiffness matrix is efficient to obtain appropriate internal stresses and that it can be easily used in the crystal plasticity finite element model to consider the influence of internal stresses on plasticity and creep kinetics in superalloys.

Multiscale Simulation on Mechanics of 2D Graphene Oxide Membranes

Wei Gao*

*University of Texas at San Antonio

ABSTRACT

Graphene oxide (GO) is an attractive building blocks in the design of advanced nanocomposite materials due to their reactive surface chemistry, which can enhance interfacial interactions while providing good in-plane mechanical properties. The mechanical properties of GO are of great importance for such applications. In this presentation, we present a multiscale simulation approach, including first principle based calculation, classical molecular dynamics simulation and continuum modeling, to study the deformation and failure of GO. Our findings demonstrate that GO should be treated as a versatile, tunable material that may be engineered by controlling chemical composition, rather than as a single, archetypical material.

Multiphysics Modeling on Fracture of Core-Shell Structured Si Nanoparticles During Charging/Discharging Cycling

Xiang Gao^{*}, Chunhao Yuan^{**}, Jun Xu^{***}

^{*}Beihang University, ^{**}Beihang University, ^{***}Beihang University

ABSTRACT

Silicon is one kind of promising electrode materials for Lithium-ion batteries in the near future because of its high electrical capacity. But the mechanical fracture and electrical degradation due to large volume expansion/contraction of Si during lithiation/delithiation cycling have been the main barrier of its broad application. In order to reduce the impact of this volume change, many managements have been proposed in the Si electrode. Core-shell structure is a typical configuration in stress management of Si and some experimental and numerical studies have been carried out on this structure. Nonetheless, studies about the fracture of core-shell structured (CSS) Si nanoparticles when they are in touch with each other during charging/discharging process are still lacking. The Multiphysics coupling behavior of the CSS Si nanoparticle during electrochemical cycling were modeled in a finite element software and the mechanical fracture and corresponding electrical degradation were then analyzed. A core-shell-structured model that contained a Si nanoparticle wrapped with amorphous carbon was established. The system containing two contacting CSS Si nanoparticles were charged and discharged under constant voltages with different rate of charge. The volume change and associated stress simulated by the model were compared with the experiment data and matched well. The effects of the amorphous carbon with different thicknesses on the volume change, stress evolution and the corresponding mechanical fracture and electrical degradation of the particles were calculated. The present study showed a best combination of charge/discharge strategy and the thickness of wrapping layer and illustrate the failure behavior of different CSS configurations, which would give guidance for the Si based battery design and help to understand the macro failure mechanism of such a CCS particle.

A New Numerical Method -- Free Element Collocation Method (FECM)

Xiao-Wei Gao^{*}, Hua-Yu Liu^{**}, Lan-Fang Gao^{***}

^{*}Dalian University of Technology, ^{**}Dalian University of Technology, ^{***}Dalian University of Technology

ABSTRACT

In this paper, a new numerical method, named as the Free Element Collocation Method (FECM), is proposed for solving general engineering problems governed by the second order partial differential equations (PDEs). The method belongs to the group of the collocation method, but the spatial partial derivatives of physical quantities are computed based on the isoparametric elements as used in FEM [1, 2]. The key point of the method is that the isoparametric elements used can be freely formed by the nodes around the collocation node. The analytical expressions for computing the global spatial partial derivatives of shape functions for the freely formed isoparametric elements are borrowed from the element differential method [3, 4]. To achieve a narrow bandwidth of the final system of equations, elements with a central node is recommended in the FECM. For this purpose a new 21-node quadratic element for 3D problems is constructed in this paper for the first time. Attributed to the use of the isoparametric elements which can guarantee the variation of physical variables consistent through all the elemental nodes, FECM can result in higher stable results than the traditional collocation method. In addition, the elements can be freely formed by local nodes, FECM has the advantage of mesh-free methods [5-7] to fit complicated geometries of engineering problems. A number of numerical examples of 2D and 3D thermal and mechanical problems are given to demonstrate the correctness and efficiency of the proposed method. Keywords: free element collocation method, element differential method, finite element method, mesh free method, thermal-mechanical problem.

Modeling the Ductile Damage Process in Commercially Pure Titanium

Xiaosheng Gao^{*}, Jinyuan Zhai^{**}, Tuo Luo^{***}

^{*}The University of Akron, ^{**}The University of Akron, ^{***}The University of Akron

ABSTRACT

In this talk we present a constitutive model, which combines the models proposed by Stewart and Cazacu [1] and Zhou et al. [2], to describe the ductile damage process in a commercially pure titanium plate and to simulate its mechanical response. In particular, a Gurson-type porous material model is modified by coupling two damage parameters, accounting for the void damage and the shear damage respectively, into the yield function and the flow potential. The plastic anisotropy and tension-compression asymmetry exhibited by the commercially pure titanium plate are accounted for by a plasticity model based on the linear transformation of the stress deviator. The theoretical model is implemented in the general purpose finite element software ABAQUS via a user defined subroutine and calibrated using experimental data. Good comparisons are observed between model predictions and experimental results for a series of specimens in different orientations and experiencing a wide range of stress states. The model is shown to capture the effect of stress state and the change of fracture mechanism. The results also reveal the important effect of the plastic anisotropy and tension-compression asymmetry on the ductile damage process. [1] Stewart, J.B., Cazacu, O., 2011; Analytical yield criterion for anisotropic material containing spherical voids and exhibiting tension-compression asymmetry. *Int. J. Solids Struct.* 48:357-373. [2] Zhou, J., Gao, X., Sobotka, J.C., Webler, B.A., Brian V. Cockeram, B.V., 2014; On the extension of the Gurson-type porous plasticity models for prediction of ductile fracture under shear-dominated conditions. *Int. J. Solids Struct.* 51: 3273–3291.

An Overview of Hypercomplex Algebras for Sensitivity Analysis in the Finite Element Method

Manuel Garcia^{*}, Mauricio Aristizabal^{**}, Harry Millwater^{***}, Daniel Ramirez^{****}, Arturo Montoya^{*****}

^{*}U, ^{**}Universidad EAFIT, ^{***}Uni, ^{****}Univer, ^{*****}Univer

ABSTRACT

Complex Taylor series expansion is a well known sensitivity computation method that lacks subtraction cancellation error and has been successfully implemented for computation of first order single variable sensitivities in many fields including fracture mechanics, fluid mechanics and heat transfer. Dual numbers are a close relative of complex numbers and are step-size independent. Both methods have been extended to multiple imaginary directions, forming new algebras capable of computing high order sensitivities of multivariable functions. Multicomplex and Multidual (hyperdual) algebras have also been successfully used in engineering applications. All mentioned algebras belong to a broader set named Hypercomplex number system that contains other algebras such as doubles, quaternions, octonions, other Cayley-Dickson and Order Truncated Imaginary (OTI) algebras. This work shows that computation of sensitivities can be generally extended to any member of the Hypercomplex number system, where the algebra and method of implementation determines the influence of the step size in the derivative computation. Complex, MultiComplex, HyperDual, Quaternion, Octonion and OTI algebras were integrated into the finite element method, for applications in fracture mechanics and heat transfer problems. A performance comparison of the different methods was accomplished. It was observed that dual, multidual and OTI algebras are stepsize independent. Complex and multicomplex algebras show quadratic convergence and Cayley-Dickson algebras show linear convergence. However, the convergence is dependent on the method of implementation. A common factor is that all algebras can be implemented so that results are free of subtraction cancellation error.

Understanding Fetal Cardiovascular Changes and the Role of Modelling

Patricia Garcia-Canadilla*, Bart Bijnens**

*DTIC, Universitat Pompeu Fabra, Barcelona, Spain, **DTIC, Universitat Pompeu Fabra, Barcelona, Spain. ICREA, Barcelona, Spain

ABSTRACT

Circulatory and haemodynamic remodeling occurs in many fetal conditions such as intrauterine growth restriction (IUGR), diabetic mothers, as well as in congenital heart disease (CHD) like aortic coarctation or univentricular hearts, and is likely to influence growth, organ development and postnatal outcome. Therefore, it would be very important and clinically relevant to better understand the mechanisms of cardiovascular remodeling in these fetal pathologies and how this reflects in cardiac structure and (clinically easily accessible) Doppler signals of the fetal circulation. This would allow us to find new biomarkers and therapeutic strategies and therefore improve future cardiovascular health of these fetuses. However, interpreting the fetal hemodynamic status in clinical practice is quite challenging, and some of the parameters, like blood pressures and organ resistances are not measurable. Computational models have proven to be a powerful tool to recreate and better understand hemodynamic changes, both under healthy and pathological conditions [1-5]. For example, model-based placenta resistance and compliance, assessed from 0D lumped models, were increased and brain resistance decreased in IUGR fetuses compared to normal ones, and adding these model-based parameters to the conventional Doppler parameters improve the detection of fetuses with adverse perinatal outcome. For more detailed modelling of the fetal cardiovascular systems, knowing the microstructure of the cardiac tissue is essential. For this, synchrotron-based phase-contrast X-ray imaging opens new perspectives. In conclusion, patient-specific computational models of the fetal circulation seem to be a good approach to assess hemodynamic and placental parameters than cannot be measured non-invasively in clinical practice, thus improving our understanding as well as the detection of fetuses with altered hemodynamics. References: [1] Garcia-Canadilla P et al. A computational model of the fetal circulation to quantify blood redistribution in intrauterine growth restriction. *PLoS Comput Biol.* 2014 Jun 12;10(6):e1003667. [2] Garcia-Canadilla P et al. Patient-specific estimates of vascular and placental properties in growth-restricted fetuses based on a model of the fetal circulation. *Placenta.* 2015 Sep;36(9):981-9 [3] Garcia-Canadilla P et al. Understanding the Aortic Isthmus Doppler Profile and Its Changes with Gestational Age Using a Lumped Model of the Fetal Circulation. *Fetal Diagn Ther.* 2017;41(1):41-50. [4] Gimenez-Minguez P et al. Assessment of Haemodynamic Remodeling in Fetal Aortic Coarctation Using a Lumped Model of the Circulation. *FIMH 2017. Lecture Notes in Computer Science*, vol 10263. Springer, Cham, p471-480, 2017. [5] Kulkarni A, et al. Remodeling of the cardiovascular circulation in Fetuses of Diabetic Mothers: A Fetal Computational Model Analysis. *Placenta.* 2017

Advances in the Simulation of Ship Navigation in Brash Ice

Julio García-Espinosa*, Borja Servan-Camas**, Jonathan Colom-Cobb***, Eugenio Oñate****

*International Center for Numerical Methods in Engineering, **International Center for Numerical Methods in Engineering, ***International Center for Numerical Methods in Engineering, ****International Center for Numerical Methods in Engineering

ABSTRACT

Abstract Brash ice is the accumulation of floating ice made up of blocks no larger than two meters across. Navigation in brash ice is becoming more usual as new navigation routes are being opened in the Arctic regions. This navigation brings new concerns regarding the interaction of ice blocks with the ship. Developments are presented towards the simulation of this navigation condition including the interaction among the ship and the ice blocks. This work presents the advances in the development of a computational tool able to simulate this problem, based on the coupling of a Semi-Lagrangian Particle Finite Element Method (SL-PFEM) with a multi rigid-body dynamics tool. The Particle Finite Element Method [1] is a versatile framework for the analysis of fluid-structure interaction problems. The PFEM combines Lagrangian particle-based techniques with the advantage of the integral formulation of the Finite Element Method (FEM). It has been shown [1][2] to successfully simulate a wide variety of complex engineering problems, e.g. free-surface/multi-fluid flows with violent interface motions, multi-fluid mixing and buoyancy-driven segregation problems etc. The latest development within the framework of the PFEM is the X-IVAS (eXplicit Integration along the Velocity and Acceleration Streamlines) scheme [2][3]. It is a semi-implicit scheme built over a Semi-Lagrangian (SL) formulation of the PFEM. In this work, the SL-PFEM model has been coupled with a multibody dynamics solver, able to handle the interactions between thousands of bodies, representing the different ice blocks. The interaction between the fluid flow and the ice blocks is performed by enriching the finite element space at the boundaries of the different blocks. This work is part of the research project NICESHIP sponsored by the U.S. Office of Naval Research under Grant N62909-16-1-2236. References [1] Idelsohn, S., Oñate, E., Del Pin, F. "The particle finite element method: a powerful tool to solve incompressible flows with free surfaces and breaking waves". International journal for numerical methods in engineering, vol. 61-7, pp. 964-989, 2004. [2] Nadukandi, P., Servan-Camas, B., Becker, P.A., Garcia-Espinosa, J. "Seakeeping with the semi-Lagrangian particle finite element method". Computational Particle Mechanics 4 (3), 321-329, 2016. [3] Idelsohn, S.R., Marti, J., Becker, P., Oñate, E.: Analysis of multifluid flows with large time steps using the particle finite element method. International Journal for Numerical Methods in Fluids, Vol. 75, No 9, 2014, pp. 621–644.

A Chimera Method Based on Dirichlet-Dirichlet Coupling Applied to Moving Boundary Problems

Luciano Garelli*, Bruno Storti**, Mario Storti***, Jorge D'Elia****

*Centro de Investigación de Métodos Computacionales (CONICET-UNL), **Centro de Investigación de Métodos Computacionales (CONICET-UNL), ***Centro de Investigación de Métodos Computacionales (CONICET-UNL),
****Centro de Investigación de Métodos Computacionales (CONICET-UNL)

ABSTRACT

The main idea of the Chimera method is to generate independent and optimized meshes for the objects present in a computational domain and then using a coupling strategy, link all these objects in order to obtain the solution of the system. The method has appealing characteristics that are convenient for applications like simplified mesh generation, moving components or boundaries, local refinement, etc. In this work a Chimera method is presented and validated in the finite element context for structured and unstructured meshes by solving the system iteratively with BiCGStab (BiConjugate Gradient Stabilized method). A Dirichlet-Dirichlet coupling imposes the continuity of the unknown on overlapping sub domains and to transfer these values between the multiples domains, a third-order interpolation method is used in conjunction with a "pasting" penalization operator. Several numerical examples are shown in order to validate the solution and assessing the precision and computational cost of the method. Also, a convergence rate analysis is carried out for the proposed interpolation method. Finally, an advection-diffusion problem involving multiple moving boundaries is solved in order to show the potential of the presented scheme. The selected benchmark problems are well documented, both experimentally and numerically.

A Reduced Order Modeling Approach to Crack Propagation in Elastic Media and its Application to Hydraulic Fracturing Models

Hasini Garikapati^{*}, Sergio Zlotnik^{**}, Clemens Verhoosel^{***}, Pedro Díez^{****}, Harald Brummelen, van^{*****}

^{*}Multi-scale Engineering Fluid Dynamics , Eindhoven University of Technology, Eindhoven, The Netherlands & Laboratori de Calcul Numèric , Universitat Politècnica de Catalunya, Barcelona, Spain, ^{**}Laboratori de Calcul Numèric , Universitat Politècnica de Catalunya, Barcelona, Spain, ^{***}Multi-scale Engineering Fluid Dynamics , Eindhoven University of Technology, Eindhoven, The Netherlands, ^{****}Laboratori de Calcul Numèric , Universitat Politècnica de Catalunya, Barcelona, Spain, ^{*****}Multi-scale Engineering Fluid Dynamics , Eindhoven University of Technology, Eindhoven, The Netherlands

ABSTRACT

Hydraulic fracturing is a challenging process to simulate, as it involves the coupling of various models: a solid model which describes the deformation of the rock induced by the fluid; a fluid flow model within the fracture, including a model for the representation of fluid leak-off to the rock formation; and a fracture propagation model. Besides, the input of the hydraulic fracturing model is affected by uncertainty. Many parameters involved in the process cannot be directly measured such as properties of the rock formations, whereas other process observables such as well pressures and seismic data can be obtained. In order to infer uncertain properties such as rock characteristics, an inversion problem has to be solved. Typically this means that one solves the forward problem many times. In this context, we make use of reduced order modeling to solve the forward problem at an affordable computational cost. More specifically, a Proper Generalized Decomposition (PGD), which provides an explicit parametric solution, is in our case used for a linear elastic solid model. In this contribution, we focus on the PGD formulation that efficiently deals with the solid problem in hydraulic fracturing, which parameterizes the stochastic material properties and geometric parameters. Furthermore, the way in which the explicit parametric solution is obtained and used to recover the solution of the forward problem is explained and considered in a hydraulic fracturing context.

Patterning and Morphogenesis of Seashells: Studies Based on the Coupling of Surface and Volume Growth with Nonlinear Elasticity

Krishna Garikipati^{*}, Shiva Rudraraju^{**}, Derek Moulton^{***}, Alain Goriely^{****}

^{*}University of Michigan, ^{**}University of Wisconsin, ^{***}University of Oxford, ^{****}University of Oxford

ABSTRACT

Seashells are an important model system for understanding mechano-morphological basis of the evolution of exoskeleton in invertebrates. Mantle tissue located at the growth front extracellularly secretes proteins and minerals and the calcification of these secretions leads to incremental growth of the exoskeleton. Most of the existing literature on the study of the complex forms (size, shape and ornamentations) in gastropods is descriptive. The mathematical understanding of the underlying mechano-morphology is at a nascent stage, primarily limited to reduced geometric representations or linear analysis of growth induced deformation modes of the mantle. In this work, we lay down the formulation for coupling of surface and volume growth that is essential to three-dimensional studies of the dynamics of seashell growth. We present a number of numerical studies of the evolving morphology driven by coupled surface and volume growth, which drive the form-defining nonlinear elastic deformation of the mantle. The focus is on understanding the effect of mantle geometry, growth rate and calcification rate on the resulting modes of deformation. Connections are made to a variety of antimarginal and commarginal ornamentations, including complex patterns such as hierarchical buckling and folding.

A Model to Predict the Progression of Abdominal Aortic Aneurysms over Time

T. Christian Gasser*, Christopher Miller**

*Department of Solid Mechanics, School of Engineering Sciences, KTH Royal Institute of Technology, Stockholm, Sweden. Faculty of Health Sciences, University of Southern Denmark, Odense, Denmark, **Department of Solid Mechanics, School of Engineering Sciences, KTH Royal Institute of Technology, Stockholm, Sweden

ABSTRACT

Background. External (mechanical) stimuli influences cell function at the level of gene expression and thereby contributes to the overall control of vascular tissue structure and function. As with other biological tissues, vascular tissue seems to adapt towards stable homeostatic mechanical conditions, and failure of reaching homeostasis may result in pathologies. Computational biomechanical modelling presents as a critical tool towards the evaluation of the underlying mechanisms associated with tissue adaptation. Tissue adaptation has to obey basic physical principles, and even within these constraints, a large number of adaptation models have been proposed [1]. Such models are able to integrate the tissue's microstructure and directly address the differing length scales of individual tissue constituents, which in turn allows for the linking of biomechanical and biochemical adaptation aspects. **Method.** Here we consider a multi-scale microstructural constitutive description of vascular tissue that accounts for temporal tissue adaption, towards its impact upon the macroscopic stress state in patient-specific Abdominal Aortic Aneurysm (AAA) geometries [2]. The present work builds upon the aforementioned model through a series of further constitutive refinements. The formulations have been implemented at the Gauss point-level of a mixed finite element formulation (FEAP, University of California at Berkeley) and test cases reflect patient-specific AAA geometries that were reconstructed from Computed-Tomography Angiography images (A4clinics Research Edition, VASCOPS GmbH). Mass turnover of vessel wall constituents is described by rate equations, which directly control the time step of the non-linear FE calculations. **Results and Discussion.** The outlined approach allows for the effective solution of the non-linear numerical problem and as such, the simulation of patient-specific AAA progression. Our results show good correlation with clinical follow-up data [3]. However, due to the scarcity of relevant experiment data, key modeling steps are based on ad hoc assumptions. Consequently, much more interdisciplinary experimental work is required to validate our modeling activities. [1] T.C. Gasser, A. Grytsan. Biomechanical modeling the adaptation of soft biological tissue. *Current Opinion in Biomedical Engineering* 1, 71-77, 2017. [2] G. Martufi and T.C Gasser. Turnover of fibrillar collagen in soft biological tissue with application to the expansion of abdominal aortic aneurysms. *Journal of The Royal Society Interface* 9 (77), 3366-3377, 2012. [3] G. Martufi, M. Lindquist Liljeqvist, N. Sakalihasan, G. Panuccio, R. Hultgren, J. Roy, T.C. Gasser, Local Diameter, Wall Stress and Thrombus Thickness Influence the Local Growth of Abdominal Aortic Aneurysms, *Journal of Endovascular Therapy*, 23(6) 957–966, 2016.

An HP-Hierarchical Framework for the Finite Element Exterior Calculus with Applications to Elasticity Problems

Robert Lee Gates^{*}, Maximilian Rüdiger Bittens^{**}, Udo Nackenhorst^{***}

^{*}Leibniz Universität Hannover, ^{**}Leibniz Universität Hannover, ^{***}Leibniz Universität Hannover

ABSTRACT

The finite element exterior calculus (FEEC) [1] is a general framework for constructing and analyzing stable mixed finite element formulations, such as the locking-free discretization of the elasticity equations. The present work introduces a dimension-independent hp-hierarchical construction of the FEEC basis on the simplex together with a suitable simplicial mesh-structure, allowing for inhomogeneous p-adaptivity and local h-refinement. The h-hierarchy of the basis and the mesh-structure are closely linked, owing to the duality between the Whitney forms and simplicial cochains. By appropriately modifying the refinement equation [2], for the discrete approximation of differential 0-forms (Lagrange elements), the proposed construction yields the well-known hierarchical Schauder basis [3], while for differential forms of higher degree, an extended form of the Haar-wavelet basis is obtained. For certain problems, the lowest-order coefficients of the proposed bases can be interpreted as an a posteriori error indicator, guiding adaptivity. We apply the developed hp-adaptive framework to various mixed problems. As the canonical choice for verifying the method, we compute adaptive solutions to the different weak formulations of the Hodge Laplacian, elaborating on cases where traditional Lagrange finite elements would fail to provide the correct solution. Furthermore, we verify the numerical reproduction of the de Rham theorem by computing the cohomology classes of selected topologies. Finally, we compute benchmark problems from the field of solid mechanics in the incompressible limit. [1] D.N. Arnold, R.S. Falk, and R. Winther. Finite element exterior calculus, homological techniques, and applications, Acta Numerica 15: 1-155, 2006. [2] E. Grinsprun. The Basis Refinement Method, PhD thesis, California Institute of Technology, 2003. [3] H. Yserentant. Hierarchical bases of finite-element spaces in the discretization of nonsymmetric elliptic boundary value problems, Computing 35(1): 39-49, 1985.

Investigation of Plastic Deformation at Micro- and Nano-scale: Modelling and Comparison with Experimental Results

Riccardo Gatti*

*LEM, UMR 104 CNRS-ONERA

ABSTRACT

Modelling plastic deformation at the micro and nanoscale is a puzzling problem in material science. The presence of free surfaces and interfaces reduce the mean free path of dislocations and change the mechanical properties of materials. This change of properties cannot be taken into account neither in continuum plasticity models, because the discrete nature of plastic deformation cannot be neglected, nor in atomistic simulations, because the simulated volume is too small and the accessible time scale is limited. A reliable tool to model crystal plasticity at such scales is the Discrete-Continuum Model (DCM). The DCM is based on a coupling between 3D Dislocation Dynamics (DD) simulations and Finite Element (FE) method. The DD simulation code is in charge of the dislocation microstructure evolution, handling the discrete nature of dislocations, while displacement field and boundary conditions are handled by the FE simulation code. In particular, in the DCM framework, not only the interaction of dislocations with free surfaces and interfaces is recovered, but also plastic incompatibilities are naturally taken into account and complex loading, close to the experimental conditions, can be imposed to the simulated object. Here, the main features of the DCM are briefly presented, emphasizing the capability of studying the plastic deformation in nano-object using anisotropic elasticity. Then the mechanical behavior of single- and bi-crystalline Ni micro-samples is investigated, comparing the result of DCM simulations with experimental data. Finally, the intriguing possibility of computing X-ray diffraction maps, post processing simulation outputs, is highlighted.

Non-intrusive Analysis of Damaged Zone of Concrete Structures for Real Cracks Description

Fabrice Gatuingt*, Rana Akiki**, Cédric Giry***

*LMT, ENS Cachan, CNRS, Université Paris-Saclay, 94235 Cachan, France, **LMT, ENS Cachan, CNRS, Université Paris-Saclay, 94235 Cachan, France, ***LMT, ENS Cachan, CNRS, Université Paris-Saclay, 94235 Cachan, France

ABSTRACT

The analysis and prediction of the degradation process and cracking of concrete structures with numerical models is an important issue in the field of civil engineering. In order to describe the global behavior of a structure composed of quasi-brittle material as well as local fields, a continuous approach using nonlinear constitutive law (e.g. damage, plasticity,...) remains the most efficient one regarding the computational time. However, one has to consider additional tools to extract discrete information about cracks like spacing and openings from these computations. The objective of this research is to propose tools capable of extracting local information such as cracking using two post-treatment methods of a global finite element analysis. First, in the proposed method, a global non-linear finite element analysis of the whole structure is performed. This analysis reveals the zones of degradation that are to be reanalyzed via a local analysis using two post-treatment methods. The first method combines a topological search method used to locate cracks developed by Bottoni et al. [1] and a continuous/discontinuous approach used to compute the crack opening initially proposed by Dufour et al. [2]. It consists in comparing the computed strain fields, with the analytical one derived from the displacement profile described as a strong discontinuity. Both strain fields are regularized using a Gaussian function. The crack opening can then be adjusted so as to reduce the gap between the regularized strain field and the regularized strong discontinuity strain field. Furthermore, a general formulation of these tools for 2D and 3D problem is proposed in this work. The direction of the mode I crack at a point is determined as the one which maximizes the crack opening along the associated 1D profile. The second method is a non-intrusive reanalysis at the local scale performed with a discrete model in order to extract fine information about crack opening. A region of interest (ROI) corresponding to the damaged area obtained from the global analysis is defined. Then, the loading steps corresponding to the steps of reanalysis are determined, where boundary conditions are extracted from the continuous displacement field and applied on the non-free surfaces of the ROI. The material is described with a discrete element approach based on an assembly of polyhedral particles linked by Euler-Bernoulli beams with brittle behaviour. Further details concerning the discrete model used at the local scale can be found in [3]. The displacement fields obtained from the FE analysis are compared to the experimental data provided from the post-processing of the actual test in order to analyze the concordance of the results on the global scale. References [1] M. Bottoni, F. Dufour, and C. Giry. Topological search of the crack pattern from a continuum mechanical computation, *Engineering Structures*. 2015 ; 99:346-359. [2] F. Dufour, G. Legrain, G. Pijaudier-Cabot, and H. Antonio. Estimation of crack opening from a two-dimensional continuum-based finite element computation, *International Journal for Numerical and Analytical Methods in Geomechanics*. 2012 ; 36:1813-1830. [3] C. Oliver-Leblond, A. Delaplace, F. Ragueneau, and B. Richard. Non-intrusive global/local analysis for the study of fine cracking, *International Journal for Numerical and Analytical Methods in Geomechanics*. 2013 ; 37:973-992.

Application of Exponential Time Integration Methods in Numerical Weather Prediction Models

Stéphane Gaudreault^{*}, Michel Desgagné^{**}, Greg Rainwater^{***}, Valentin Dallerit^{****}, Mayya Tokman^{*****}

^{*}Environment and Climate Change Canada, ^{**}Environment and Climate Change Canada, ^{***}California State University, Monterey Bay, ^{****}University of California, Merced, ^{*****}University of California, Merced

ABSTRACT

A new dynamical core suitable for numerical weather prediction over a wide range of length scales is under development at Environment and Climate Change Canada. As it is well-known, the stiffness due to the presence of rapidly propagating waves in the atmosphere renders traditional explicit methods impractical. The aim of our research is to explore an emerging class of exponential integration methods. These schemes have seen limited use in geophysical fluid dynamics due to efficiency issues. In order to circumvent some of these limitations, we recently introduced a new algorithm KIOPS for computing linear combinations of phi-functions that appear in exponential integrators. Theoretical analysis of the method and numerical simulations in a number of experimental frameworks demonstrates that KIOPS outperforms the current state-of-the-art adaptive Krylov algorithm PHIPM.

Large-scale Real-space Electronic Structure Calculations

Vikram Gavini^{*}, Phani Motamarri^{**}, Bikash Kanungo^{***}

^{*}University of Michigan, ^{**}University of Michigan, ^{***}University of Michigan

ABSTRACT

Defects play a crucial role in influencing the macroscopic properties of solids—examples include the role of dislocations in plastic deformation, dopants in semiconductor properties, and domain walls in ferroelectric properties. These defects are present in very small concentrations (few parts per million), yet, produce a significant macroscopic effect on the materials behavior through the long-ranged elastic and electrostatic fields they generate. The strength and nature of these fields, as well as other critical aspects of the defect-core are all determined by the electronic structure of the material at the quantum-mechanical length-scale. Hence, there is a wide range of interacting length-scales, from electronic structure to continuum, that need to be resolved to accurately describe defects in materials and their influence on the macroscopic properties of materials. This has remained a significant challenge in multi-scale modeling, and a solution to this problem holds the key for predictive modeling of complex materials systems. In this talk, we present some key methodological developments that have enabled large-scale electronic structure calculations—as large as explicitly treating 10,000 atom Kohn-Sham density functional theory (DFT) calculations—taking us closer to addressing this significant challenge. In particular, the development of a real-space formulation for Kohn-Sham DFT and a finite-element discretization of this formulation [1,2], which can handle arbitrary boundary conditions and is amenable to adaptive coarse-graining, will be presented. The accuracy afforded by using higher-order and enriched finite-element discretizations, and the efficiency and scalability of the Chebyshev filtering algorithm in pseudopotential and all-electron Kohn-Sham DFT calculations will be demonstrated. Further, the development of a subquadratic-scaling approach (in the number of electrons) based on a subspace projection and Fermi-operator expansion will be discussed [3,4], which will be the basis for the future development of coarse-graining techniques for Kohn-Sham DFT that can enable accurate electronic structure calculations at macroscopic scales. [1] P. Motamarri, M.R. Nowak, K. Leiter, J. Knap, V. Gavini, Higher-order adaptive finite-element methods for Kohn-Sham density functional theory, *J. Comp. Phys.* 253, 308-343 (2013). [2] B. Kanungo, V. Gavini, Large-scale all-electron density functional theory calculations using an enriched finite element basis, *Phys. Rev. B* 95, 035112 (2017). [3] P. Motamarri, V. Gavini, A subquadratic-scaling subspace projection method for large-scale Kohn-Sham DFT calculations using spectral finite-element discretization, *Phys. Rev. B* 90, 115127 (2014). [4] P. Motamarri, K. Bhattacharya, M. Ortiz, V. Gavini, Spectrum-splitting approach for Fermi-operator expansion in all-electron Kohn-Sham DFT calculations, *Phys. Rev. B* 95, 035111 (2017).

GPU-based Topology Optimization for Thermoelastic Problems

Stefan Gavranovic*, Dirk Hartmann**, Utz Wever***

*Technical University of Munich, **Siemens AG, ***Siemens AG

ABSTRACT

Additive Manufacturing is not only revolutionizing manufacturing but also the way engineers create new designs. It provides opportunities to explore much larger design spaces. This opens the possibility to reduce design weight and increase its performance to so far unreachable levels. Topology Optimization [1] as a tool helps to obtain such optimal designs, however, today it is mostly limited to CAE users. Making corresponding design tools accessible to non-expert CAE users is a key for creativity and to efficiently exploit the opportunities promised by Additive Manufacturing [2]. Key to this challenge are interactivity and enhanced user experience. In order to enable nearly interactive Topology Optimization in 3D, we implemented an efficient geometric multi-grid method [3] on structured hexahedral meshes utilizing GPU computing capabilities for performing linear structural analyses. To circumvent boundary treatment issues which arise when using non-conformal hexahedral meshes we use a cut-cell approach alongside with augmenting weak formulation of equations by means of Nitsche method. In this way, we are able to achieve desired numerical accuracy of FEM solver which is an essential building block and the most time consuming part of the Topology Optimization process. Additionally, inspired by the nature of Additive Manufacturing process, we consider influence of thermal loads in the optimization process. User experience is enhanced by integrating our tool within CAD system, thus simplifying pre-processing stage for a simulation and ultimately making the topology optimization tool accessible to non-experts. The concept has been made available to a selected user base validating the approach. References: [1] Bendsoe, Martin Philip, and Ole Sigmund. Topology optimization: theory, methods, and applications. Springer Science & Business Media, 2013. [2] S. Gavranovic, D. Hartmann, P. Stelzig (2017): Accurate Interactive Engineering Simulations Accelerated by GPU. NAFEMS World Congress 2017 [3] Dick, Christian, Joachim Georgii, and Rüdiger Westermann. "A real-time multigrid finite hexahedra method for elasticity simulation using CUDA." Simulation Modelling Practice and Theory 19.2 (2011): 801-816.

Comparison between Master-Master and Master-Slave Contact Formulations

Alfredo Gay Neto*, Peter Wriggers**, Debora Higa***

*University of São Paulo, **Leibniz Universität-Hannover, ***University of São Paulo

ABSTRACT

Computational contact models considering pointwise interactions are very useful. On this context, the master-slave contact formulation is known for its versatility in a finite element model. The election of nodes as slave points in a surface mesh together with the other surface parameterization (master) is the basis of the method. Then, slave points' movement are tracked along master surface. This constitutes the kinematic basis for the contact mechanical constraint enforcement, which is done in a pointwise manner. On the other hand, the master-master approach to account for contact [1] does not need the prior election of slave points. Both surfaces are treated as masters. They are re-parameterized along the model evolution. At each configuration, a pointwise interaction is searched. During the model evolution, the material points where contact takes place in both surfaces may change significantly. The advantage is to capture all such changes within a single contact pair search. Typically, one may find examples of this nature on rolling contact of non-conformal geometric profiles. In this context, the present work presents a comparative approach of master-slave and master-master contact formulations. The methods are compared with respect to both versatility and mathematical basis. Pros/cons of each technique are emphasized. We show that, mathematically, master-slave is a particular case of master-master contact formulation, coming from degeneration of two convective coordinates on a given surface, chosen a priori to be a slave point. A particular discussion is given to cases where overall contact may be well represented by a single pointwise interaction. Particularly, the enhanced master-slave presented in [2] is shown as a mid-step between master-slave and master-master, for the particular case on which each slave point is upgraded to a spherical surface. This shows to be useful in some applications involving spherical particles in contact with surfaces. Numerical examples will be given to support discussions. Particularly, beam-to-beam contact is taken as base-problem. [1] GAY NETO, A.; PIMENTA, P. M.; WRIGGERS, P. A Master-surface to Master-surface Formulation for Beam to Beam Contact. Part I: Frictionless Interaction. *Comput. Methods Appl. Mech. Engrg.*, v. 303, p. 400-429, 2016. [2] GAY NETO, A.; PIMENTA, P. M.; WRIGGERS, P. Contact between spheres and general surfaces. *Comput. Methods Appl. Mech. Engrg.*, v. 328, p. 686-716, 2018.

Longitudinal Impact into Viscoelastic Media

George Gazonas*, Raymond Wildman**, David Hopkins***, Michael Scheidler****

*US Army Research Laboratory, **US Army Research Laboratory, ***US Army Research Laboratory, ****US Army Research Laboratory

ABSTRACT

We consider several one-dimensional impact problems involving finite or semi-infinite, linear elastic flyers that collide with and adhere to a finite stationary linear viscoelastic target backed by a semi-infinite linear elastic half-space [1]. The impact generates a shock wave in the target which undergoes multiple reflections from the target boundaries. Laplace transforms with respect to time, together with impact boundary conditions derived in our previous work [2], are used to derive explicit closed-form solutions for the stress and particle velocity in the Laplace transform domain at any point in the target. For several stress relaxation functions of the Wiechert (Prony series) type, a modified Dubner-Abate-Crump (DAC) algorithm [3] is used to numerically invert those solutions to the time domain. These solutions compare well with numerical solutions obtained using both a finite-difference method and the commercial finite element code, COMSOL Multiphysics. The Final Value Theorem is used to show that the asymptotic (long observation time) stress and particle velocity is independent of target properties in linearly viscoelastic media with non-zero long-term equilibrium moduli, but depend only on the elastic properties of the flyer and half-space backing material. Alternatively, viscoelastic targets in which the long-term equilibrium modulus is zero, also exhibit both target length and viscosity dependent asymptotic stress; the asymptotic particle velocity is also position dependent in such targets. These results are useful for verification of viscoelastic impact simulations taken to long observation times. References: [1] Gazonas GA, Wildman RA, Hopkins DA, Scheidler MJ, Longitudinal impact into viscoelastic media, submitted. [2] Gazonas GA, Scheidler MJ, Velo AP. Exact analytical solutions for elastodynamic impact. *Int. J. Solids and Struct.* 2015; 75–76: 172–187. [3] Gazonas GA, Wildman RA, Hopkins DA, Scheidler MJ. Longitudinal impact of piezoelectric media. *Arch. Appl. Mech.* 2016; 86:497–515.

A Methodology for In Silico EVAR of Abdominal Aortic Aneurysms

Michael Gee*, André Hemmler**

*TU Munich, **TU Munich

ABSTRACT

Endovascular aneurysm repair (EVAR) is a widely used and well established technique to intervene before rupture of abdominal aortic aneurysms (AAA) occurs. However, EVAR can involve some unfavorable complications such as endoleaks or stent-graft (SG) migration. Such complications, resulting from the complex mechanical interaction of vascular tissue, SG and blood flow or incompatibility of SG design and AAA geometry, are difficult to predict. Finite element simulations can be a predictive tool for the selection, sizing and placement process of SGs depending on the patient-specific AAA geometry and hence reduce the risk of potential complications after EVAR [1]. In this contribution, we present a new virtual SG deployment methodology [5] to reproduce the final state of the deployed SG after intervention. We aim to find the final SG position in a patient-specific AAA geometry and evaluate the mechanical state of AAA and SG, such as contact forces or wall stresses. Three different constituents of the aneurysmatic tissue are considered: diseased aneurysmatic wall, intraluminal thrombus and calcifications [4]. Furthermore, the anisotropic mechanical behavior [2] of the aortic wall in the proximal and distal fixation zones of the SG are taken into account. The simulation process consists of two main steps. In a first step the SG is crimped, bent and moved by a tailor-made morphing algorithm to position the SG inside the AAA. Afterwards, the SG is released inside the AAA where it unfolds and makes contact with the luminal surface of the patient-specific vascular model. We consider mortar based frictional contact [3] between a sophisticated, finite deformation AAA and a SG composed of a parameterized, product specific (Cook Zenith Flex®) graft shell and stent wire frame that can undergo finite deformations. The simulation results of three patient-specific cases are compared to the geometry of the deployed SG taken from postinterventional CT scans. [1] F. Auricchio, M. Conti, S. Marconi, A. Reali, J. L. Tolenaar, and S. Trimarchi. Patient-specific aortic endografting simulation: From diagnosis to prediction. *Computers in Biology and Medicine*, 43(4):386 – 394, 2013. [2] G. A. Holzapfel and R. W. Ogden. Constitutive modelling of arteries. In *Proceedings of the Royal Society of London A: Mathematical, Physical and Engineering Sciences*, volume 466, pages 1551–1597. The Royal Society, 2010. [3] A. Popp, M. Gitterle, M. W. Gee, and W. A. Wall. A dual mortar approach for 3d finite deformation contact with consistent linearization. *International Journal for Numerical Methods in Engineering*, 83(11):1428–1465, 2010. [4] C. Reeps, A. Maier, J. Pelisek, F. Härtl, V. Grabher-Meier, W. A. Wall, M. Essler, H.-H. Eckstein, and M. W. Gee. Measuring and modeling patient-specific distributions of material properties in abdominal aortic aneurysm wall. *Biomechanics and modeling in mechanobiology*, 12(4):717–733, 2013. [5] Hemmler, A., Lutz, B., Kalender, G., Reeps, C., Gee, M.W. (2018) A methodology for in silico stent-graft repair of abdominal aortic aneurysms, in prep.

A New Phase-Field Formulation for Cohesive Fracture

Rudy Geelen^{*}, Yingjie Liu^{**}, John Dolbow^{***}, Michael Tupek^{****}

^{*}Duke University, ^{**}Duke University, ^{***}Duke University, ^{****}Sandia National Laboratories

ABSTRACT

Recently, phase-field models have been proposed to regularize sharp crack fronts. These fracture models have gained popularity in no small part due to their ability to handle complex failure topologies, such as crack branching and coalescence, even in three-dimensional settings. In the phase-field community, the emphasis has been on a Griffith description of brittle fracture. However, most engineering materials are not perfectly brittle in the Griffith sense, but display ductility after reaching a critical strength. Often, there exists a fracture process zone ahead of the crack tip in which micro-crack and void initiation, growth and coalescence, as well as small-scale yielding, take place. If this zone is relatively large compared to the structural dimensions, one has to rely on cohesive fracture mechanics based strategies such as the cohesive zone approach. In this work, an attempt was made to outline a framework for dealing with cohesive fracture in a phase-field setting. The development of a phase-field model for cohesive fracture is a non-trivial extension of the model available for brittle fracture. Miehe and coworkers [1] were among the first to postulate a phase-field formulation with a threshold that exhibits a linear elastic response prior to strain softening. We build on this effort by deriving a free-energy functional that is consistent with the kinetics of cohesive fracture. The governing equations are formulated in terms of a macro and micro-force balance. The latter naturally handles the irreversibility of crack growth by means of a viscous regularization. The model employs a stress-based criterion as the crack driving force, in contrast to the conventional strain-based approach [2]. In addition, the use of a novel strain energy density function is proposed, allowing for the extension to fracture in anisotropic media. The resulting free-energy expression shares some similarities with earlier work in the field of gradient-damage modeling, in particular that of Lorentz et al. [3] The proposed approach is distinctly attractive as the regularization length is shown to have virtually no effect on the constitutive response, merely acting as a numerical parameter controlling the regularization of the fracture surface. Several benchmark problems are presented to demonstrate the features of the proposed phase-field model. Keywords: phase-field, cohesive fracture, gradient-damage, finite elements [1] Miehe, C., Schänzel, L. M., & Ulmer, H. (2015). CMAME, 294, 449-485 [2] Miehe, C., Hofacker, M., & Welschinger, F. (2010). CMAME, 199(45), 2765-2778 [3] Lorentz, E., & Godard, V. (2011). CMAME, 200(21), 1927-1944

A simple linear actuator model and its application to optimization of adaptive structures

Florian Geiger^{*}, Jan Gade^{**}, Malte von Scheven^{***}, Manfred Bischoff^{****}

^{*}Institute for Structural Mechanics, University of Stuttgart, ^{**}Institute for Structural Mechanics, University of Stuttgart, ^{***}Institute for Structural Mechanics, University of Stuttgart, ^{****}Institute for Structural Mechanics, University of Stuttgart

ABSTRACT

In simulation of adaptive structures, often a model of the passive structure is created using commercial finite element software and the system matrices are then exported for further manipulation. Actuation and adaptivity are considered afterwards by introducing additional load cases or boundary conditions. Including effects like nonlinear behaviour of the structural response or system changes then causes great effort. We present a simple finite element for linear actuators that is derived with a constrained variational principle and includes the effect of actuation. The element offers the possibility to assemble the system matrices of the adaptive system directly in order to save effort when the structure is changed or nonlinear effects are included. Another important aspect is the additional insight into the structural behaviour of adaptive structures that can be won. Examples of simple truss structures using the presented element are conducted to exhibit potentials of adaptivity. The differences between including adaptivity before structural optimization and including adaptivity in the optimized passive structure are shown.

A Discontinuous Galerkin Immersed Boundary Solver for Compressible Flows: Efficient Time Integration for Artificial Viscosity Based Shock-Capturing

Markus Geisenhofer*, Björn Müller**, Florian Kummer***

*Graduate School CE, Technische Universität Darmstadt, Germany/Chair of Fluid Dynamics, Technische Universität Darmstadt, Germany, **Graduate School CE, Technische Universität Darmstadt, Germany/Chair of Fluid Dynamics, Technische Universität Darmstadt, Germany, ***Chair of Fluid Dynamics, Technische Universität Darmstadt, Germany

ABSTRACT

In this talk, we study unsteady high Mach number flows in the context of the Euler and Navier-Stokes equations. We use a Discontinuous Galerkin (DG) solver [1] that was extended to immersed boundaries where the considered geometry is represented by the zero iso-contour of a level set function. We apply cell-agglomeration that averts problems with small and ill-shaped cut cells. In order to obtain a stable and accurate solution, discontinuous flow phenomena such as shocks have to be resolved properly. Particularly, we use a shock-capturing approach based on artificial viscosity. Recently, we coupled both approaches in order to reuse the geometrical flexibility of immersed boundaries. For shock-capturing, we follow the two-step strategy presented in [2]. First, a shock sensor that is based on the modal decay of the DG coefficients detects troubled cells. Second, artificial viscosity is applied to these cells in order to smooth the solution. To advance the solution in time, we use an explicit time integration scheme. In the aforementioned setting, a severe time step restriction is caused by the additional diffusive term that leads to a drastic reduction of computational efficiency. We tackle this problem by using a local time stepping (LTS) approach [3] that partitions the grid into cell clusters. These cell clusters are updated continuously according to their local time step restriction, which is beneficial for transient simulation runs. Meeting all these challenges, we present current results of a new efficient DG immersed boundary solver for compressible flows by combining a shock-capturing scheme with an adaptive LTS method. Moreover, we show first results of the successful combination with a dynamic load balancing strategy that enables a performant parallelization based on the LTS cell clusters. [1] Müller, B., Krämer-Eis, S., Kummer, F., Oberlack, M., 2016. A high-order discontinuous Galerkin method for compressible flows with immersed boundaries. *Int J Numer Methods Eng.* [2] Persson, P.-O., Peraire, J., 2006. Sub-Cell Shock Capturing for Discontinuous Galerkin Methods, in: *Proceedings of the 44th AIAA Aerospace Sciences Meeting and Exhibit*. [3] Winters, A.R., Kopriva, D.A., 2014. High-Order Local Time Stepping on Moving DG Spectral Element Meshes. *J Sci Comput* 58, 176–202. The work of M. Geisenhofer is supported by the Excellence Initiative of the German Federal and State Governments and the Graduate School of Computational Engineering at Technische Universität Darmstadt. The work of F. Kummer is supported by the German DFG through Collaborative Research Centre 1194/B06.

3D Image Based Inspection and Finite Element (FE) Simulation of Additive Manufactured (AM) Parts

Kerim Genc*, Nicholas Brinkhoff**, Timothy Williams***, Tim Pawlak****, Lin Cheng*****, Albert To*****, Steve Pilz*****, Ronald Gull*****, Philippe Young*****

*Synopsys Inc., **North Star Imaging Inc., ***Synopsys Inc., ****ANSYS Inc., *****University of Pittsburgh,
*****University of Pittsburgh, *****ANSYS Inc., *****Synopsys Inc., *****Synopsys Inc.

ABSTRACT

Additive Manufacturing (AM) of metal parts is becoming more common as an alternative approach to traditional methods because it has many benefits, not the least of which is the tremendous design freedom that it affords designers. However, the uncertainties of AM parts in terms of accuracy, quality, strength and reliability are still relatively high and therefore troubling to manufacturers of critical components or systems. Simulation techniques are now being incorporated into the design process to help improve the quality of the AM design process, reduce weight and ensure a high probability of successful builds. Despite these efforts, however, there is still uncertainty in the differences between as-designed versus as-built AM parts, which leads manufacturers to ask the following question: "What are the differences between my design and the part that is actually manufactured and how will these differences affect performance in reality?" Companies are already spending a significant amount on 3D imaging technology like industrial Computed Tomography (CT) scanners for inspection, non-destructive evaluation and reverse engineering of Additive Manufactured (AM) parts. From CT scans, users can typically quantify porosity, crack/defect size, deviations from design etc. However, information, in and of itself, do not provide an understanding of how these defects and deviations from the desired design will affect performance in the real world. We will describe how the three domains of CT-imaging, AM and FE simulation are just now starting to connect because of a need to better understand the performance of the real as-manufactured part, not just a CAD design ideal. Typically, due to the knowledge gap between these domains, the adoption of this workflow from the 3D scan to a realistic FE simulation can be tortuous with engineers and technicians using a mix of open source, in-house and/or commercial tools to create an inefficient, unrepeatable workflow that can be an expensive drain on internal time and resources. We will demonstrate a proof of concept workflow where a lightweight bracket is designed/optimized to reduce weight and then built using the laser powder bed AM in a titanium alloy (Ti6Al4V). This bracket is then scanned via CT and then image based tools are used to inspect the geometry and generate an FE mesh, which is exported for simulation of the as built part. This workflow allows users to close the design loop and truly understand how defects and deviations in the manufactured part can affect performance in the real world.

Multilevel and Multifidelity Approaches for Uncertainty Quantification

Gianluca Geraci^{*}, Alex Gorodetsky^{**}, Michael Eldred^{***}, John Jakeman^{****}

^{*}Sandia National Laboratories, ^{**}University of Michigan, ^{***}Sandia National Laboratories, ^{****}Sandia National Laboratories

ABSTRACT

Uncertainty Quantification (UQ) plays a fundamental role in the design and analysis of complex and realistic engineering systems that rely heavily on numerical simulations. While advancements have improved the efficiency of UQ algorithms in the last two decades, UQ remains challenging in the presence of high-fidelity numerical models. State of the art UQ algorithms require multiple evaluations of a complex computer code and the number of required simulations generally increases rapidly with the number of random parameters. As a result, performing UQ for high-fidelity models is hampered by the high computational cost of each realization. Multilevel and multifidelity algorithms have recently been introduced to overcome this limitation [1,2]. Their main idea is to gather realizations of different fidelities and/or discretization levels in order to accelerate the convergence of high-fidelity model statistics, and their key strategy is to achieve a variance reduction for the statistical estimator. In this talk we cover two main aspects of these techniques. First, we discuss relation between multilevel and control variate algorithms with respect to the properties of the system under analysis. Next, we compare and interpret both multilevel and control variate approaches within a new Bayesian multifidelity model management approach [3]. Numerical results for several test cases are presented and discussed to highlight the relevant features of the different approaches. [1] M.B. Giles. "Multilevel Monte Carlo methods". Acta Numerica, 24:259-328, 2015. [2] G. Geraci, M.S. Eldred and G. Iaccarino. "A multifidelity multilevel Monte Carlo method for uncertainty propagation in aerospace applications". 19th AIAA Non-Deterministic Approaches Conference, AIAA SciTech Forum, (AIAA 2017-1951). 2017. [3] A. Gorodetsky, G. Geraci, M.S. Eldred and J. Jakeman. "Multifidelity model management using latent variable Bayesian networks". 13th World Congress in Computational Mechanics. 2018 (submitted).

Benchmark Calculations of Shear-banding Polymer Solutions

Natalie Germann*, Soroush Hooshyar**

*Technical University of Munich, **Technical University of Munich

ABSTRACT

Many soft materials such as polymer solutions develop banded velocity and concentration profiles if the shearing deformation is large enough. Concentration gradients formed during processing can have a great impact on the final texture of a product. Using the generalized bracket approach of nonequilibrium thermodynamics, we developed a new two-fluid model for semi-dilute entangled polymer solutions to study the phenomenon of shear banding [1]. We included the Giesekus relaxation to account for the overshoot of the shear stress during the start-up of a simple shear flow. In addition, we included a second nonlinear relaxation term to capture the upturn of the flow curve at high shear rates. This term is similar to the term used in the Rolie-Poly model that accounts for convective constraint release and chain stretch, with the exception of being now thermodynamically consistent. Finally, a new nonlocal stress-diffusion term was added to the time evolution equation of the polymer conformation to have smooth and unique profiles. The behavior of the new model was analyzed in three different benchmark geometries [1-2]. For the circular Couette and pressure-driven channel flow problems, we employed a pseudospectral collocation method. The 4:1 contraction case was solved using finite volumes. The results show that the steady-state solution is unique with respect to different initial conditions, the applied deformation history, and the diffusivity appearing in the equation for the differential velocity. The polymer concentration is not uniform in the flow field, since the polymer constituents are subjected to Fickian diffusion and stress-induced migration, the latter mechanism being responsible for the shear band formation. The total velocity develops a plug-like profile in the channel, with a low shear rate band near the center and a high shear rate band near the walls. In agreement with experiments [3], the flow rate exhibits a spurt at a critical pressure gradient. We will present first results on the impact of shear banding on the vortices in the contraction zone. As our model is relatively simple, it is a good candidate for more complex industrial flows. References: [1] S. Hooshyar, N. Germann, Phys. Fluids, 28 (6) (2016) 063104. [2] S. Hooshyar, N. Germann, J. Non-Newt. Fluid Mech. 242 (2017) 1-10. [3] E. B. Bagley, I. M. Cabott, D. C. West, J. Appl. Phys. 29 (1958) 109-110.

A Track Model for the Prediction of Ground-borne Vibration due to a Transition Zone

Matthias Germonpré^{*}, Geert Lombaert^{**}, Geert Degrande^{***}

^{*}KU Leuven, ^{**}KU Leuven, ^{***}KU Leuven

ABSTRACT

Currently, several numerical models are available to predict ground-borne vibration due to railway traffic. Full 3D coupled finite element-boundary element models allow for a very detailed representation of the track and the soil. However, they require high computation time and modelling effort. Therefore, much research is done on developing computationally efficient methods which exploit the regularity of the problem geometry in the direction along the track. In a 2.5D approach, the track geometry is invariant in the longitudinal direction. This approach is computationally very efficient, but does not allow to include the periodic support of the rails by sleepers and the stress distribution under the sleepers is not correctly predicted. To overcome these restrictions, the track can be assumed to be periodic. Such models are still computationally efficient and allow to include parametric excitation due to the discrete rail support. However, they cannot include other types of track stiffness variations in the longitudinal direction such as transition zones, hanging sleepers or random track stiffness variations. Alternatively, more general track models have been developed that model the soil by a series of masses, springs and dampers. Despite their efficiency, these models don't allow for a direct prediction of the vibration transfer to the free field. In this presentation, a track model based on a wave analysis technique for multi-coupled periodic structures is presented [1]. The track is divided into periodic cells, corresponding to the sleeper bays. Each sleeper bay can be modelled differently. Part of the soil is modeled by finite elements and the waves in the soil travelling in the x- and z-directions are absorbed by perfectly matched layers [2]. This method is computationally much more efficient than full 3D models and it can be used to model any type of track stiffness variation. This approach is used to model different designs of a transition zone between a ballasted track and a slab track. The resulting train-track interaction forces and free field vibrations are compared. References [1] D. Mead. The forced vibration of one-dimensional multi-coupled periodic structures: An application to finite element analysis. *Journal of Sound and Vibration*, 319:282–304, 2009. [2] S. François, M. Schevenels, G. Lombaert and G. Degrande. A two-and-a-half-dimensional displacement-based PML for elastodynamic wave propagation. *International Journal for numerical methods in engineering*, 90:819-837, 2012.

Finite Element Approximation for Thermal Electro Hydrodynamical Boussinesq Equations

Philippe Gerstner^{*}, Vincent Heuveline^{**}, Martin Baumann^{***}

^{*}University Heidelberg, ^{**}University of Heidelberg, ^{***}University of Heidelberg

ABSTRACT

We consider the hydrodynamical behavior of dielectric fluids contained in a vertical cylinder annulus under applied voltage and temperature gradient between inner and outer wall. This setting gives rise to a body force, that is a superposition of buoyancy and dielectrophoretic force (DEP). The situation can be modeled by means of the thermal electro hydrodynamical Boussinesq equations (TEHD) which are based on the standard Boussinesq approximation for natural convection, augmented by DEP force and Gauss's law for describing the electric field inside the fluid as a function of temperature. Our method for approximately solving this set of equations is based on the Finite Element Method for discretization in both, space and time. For the spatial part, we make use of stable Taylor-Hood elements, whereas temporal discretization is implemented by a Petrov-Galerkin formulation with continuous trial and discontinuous test functions. In this way, the resulting discretized problem can be solved in a time-stepping manner, with an arising set of nonlinear algebraic equations for each time step which are solved by Newton's method. Here, the main computational effort lies in the solution of large-scale linear systems whose dimensions are in the order of several millions of variables when using a reasonable spatial resolution in 3D. To cope with these systems, we developed a parallel linear preconditioner which is based on a Schur complement approach for splitting the complete system into several subsystems according to the underlying physics of the model. These subsystems correspond to discretized elliptic problems, which are well suited for being solved with highly scalable methods. We make use of the Algebraic Multigrid Method and construct the way of solving the subsequent subsystems such that the overall solution process exhibits good parallel efficiency. In our talk, we present a computational study over the range of 384 to 4096 computing cores to demonstrate parallel efficiency of our method. Moreover, we present simulation results for different temperature gradients, leading to varying classical and electric Rayleigh numbers in the order of 10^3 to 10^4 . The numerical solutions show a transition of a varying number of azimuthally to axially oriented vortices, where the latter are present in the final state of the dynamic system. Due to these vortices, radial heat transfer is enhanced as an increase of the corresponding Nusselt numbers show.

Column Collapse for Dense Granular Flows using the $\mu(I)$ -Rheology

Linda Gesenhues*, Fernando A. Rochinha**, José J. Camata***, Alvaro L.G.A. Coutinho****

*High Performance Computing Center and Department of Civil Engineering, Federal University of Rio de Janeiro, Brazil, **Mechanical Engineering Department, Federal University of Rio de Janeiro, Brazil, ***Computer Science Department, Federal University of Juiz de Fora, Brazil, ****High Performance Computing Center and Department of Civil Engineering, Federal University of Rio de Janeiro, Brazil

ABSTRACT

Non-Newtonian fluid behavior is typical for dense granular flow, as the particle concentration rises above a certain amount. Several rheology models can be used to cover this characteristic of the flow, which often happens to be viscoplastic. A model focusing on the viscosity description of dense granular flows is the so-called $\mu(I)$ -rheology. The $\mu(I)$ -rheology is based on the Coulomb friction, which states that normal stresses are proportional to the tangential stresses. Thus, the viscosity is related with a friction coefficient to the pressure. As a result of this, the friction coefficient is depending on the macroscopic and microscopic timescales of the particle rearrangement. This complex viscosity dependence on the friction coefficient results in a non-conventional viscoplastic shear-thinning behavior depending on the shear rate and the pressure. The models complexity leads to high nonlinearities and thus to oscillations, divergence and a high sensibility to input parameters. As a consequence, an appropriate regularization strategy, an adequate mesh and stabilization methods are inalienable. In this study, a 2D column collapse is simulated to analyze regularization and input parameters and their influence on the results. This parametric sensitivity study is conducted using the technique of design of experiments. We apply a Navier-Stokes solver coupled with a transport solver employing the volume-of-fluid method to describe the interface of the dense and light fluids (usually air). We use for the implementations libMesh, a C++ library that supports adaptive mesh refinement and coarsening and also interfaces with Petsc. The finite element formulation is the residual-based variational multiscale method. With libMesh, simulations are easily extended to three-dimensions. Experiences and challenges of the 3D simulation model are analyzed and discussed regarding the $\mu(I)$ -rheology. POULIQUEN, O., &amp; FORTERRE, Y. (2002). Friction law for dense granular flows: Application to the motion of a mass down a rough inclined plane. *Journal of Fluid Mechanics*, 453, 133-151. doi:10.1017/S0022112001006796 JOP, P., &amp; FORTERRE, Y. (2006). A constitutive law for dense granular flows. *Nature*, 441, 727-730. doi:10.1038/nature04801

Gradient-Based Computational Design of Microvascular Composites Based on an Interface-Enriched Generalized Finite Element Method

Philippe Geubelle^{*}, Marcus Tan^{**}, Stephen Pety^{***}, Ahmad Najafi^{****}, Scott White^{*****}

^{*}University of Illinois, ^{**}University of Illinois, ^{***}University of Illinois, ^{****}Drexel University, ^{*****}University of Illinois

ABSTRACT

Inspired from many living organisms, microvascular composites form a new class of fiber-reinforced polymeric matrix composites that contain a circulatory system made of an embedded network of microchannels. Based on the choice of the fluid circulating in the microvascular network, a wide range of multi-functionalities are being considered for these materials, including autonomic healing of internal damage, switching embedded antennas, and active cooling for high temperature applications. A recent development in the manufacturing of this class of composites, based on specially treated sacrificial fibers that are woven in the original fabric, undergo the composite cure cycle before undergoing a vaporization process, has led to the creation of microvascular networks that are integrated directly into the composite microstructure. This technology is being considered for a variety of active cooling applications, including skin materials for hypersonic aircrafts, actively cooling of car batteries and radiative cooling of nanosatellites. This new manufacturing process provides a lot of flexibility in the configuration of the embedded network. To assist with the material design process, a novel numerical tool based on an interface-based generalized finite element method (IGFEM) has been developed to model accurately and efficiently the impact of the coolant flowing through the microchannels on the thermal field in the composite. A gradient-based shape optimization scheme is then used together with the IGFEM solver to optimize the configuration of the embedded microchannel network based on a variety of objective functions and constraints. A key advantage of the IGFEM/gradient-based optimization scheme resides in the stationary nature of the non-conforming finite element mesh, which allows for the capture of evolving network shapes without facing the mesh distortion issues associated with classical FE-based shape optimization methods. Various 2D and 3D configurations of the microchannels are investigated and compared, based on their thermal and flow efficiency and on their impact on the structural integrity of the composite. We also optimize the microchannel network for redundancy. The predicted thermal impact of the optimized microvascular networks is compared with experimental observations obtained using infrared measurements. Tan, M. H. Y., Najafi, A. R., Pety, S. J., White, S. R., and Geubelle, P. H. (2016) "Gradient-based design of actively-cooled microvascular composite panels." *International Journal of Heat and Mass Transfer*, 103, 594-606. Tan, M., and Geubelle, P. H. (2017) "3D dimensionally reduced modeling and gradient-based optimization of microchannel cooling networks." *Computational Methods in Applied Mechanics and Engineering*, 323, 230–249.

Machine Learning for Efficient Sampling in UQ

Roger Ghanem*, Christian Soize**

*University of Southern California, **Univesite Paris-Est

ABSTRACT

Uncertainty quantification is about relating the credibility of a decision to relevant available information. In the realm of mechanics, information is typically described in the form of constraints, such as conservation laws or boundary/initial conditions, and data. For settings where the associated physical processes evolve over several time or spatial scales, numerical treatments can become necessary which, when compounded with a probabilistic formalism for uncertainty quantification, become rapidly prohibitive. Recent methods of probabilistic learning developed by Soize and Ghanem, mine statistical information from data very efficiently, so much so that constraints can be delineated with only a handful of data points, or simulation runs. The procedure builds on diffusion manifolds, extracting an algebraic basis that localizes the data in an ambient space. A projected Ito equation is then used to sample on this manifold with an invariant measure synthesized from available data. Applications in many areas of science and engineering will be demonstrated.

Modeling Hemodynamics and Homeostatic Conditions in a Multiscale Fluid-Solid Growth Model of the Pulmonary Arterial Tree (Part II)

Hamidreza Gharahi^{*}, Seungik Baek^{**}, Vasilina Filonova^{***}, C. Alberto Figueroa^{****}

^{*}Michigan State University, ^{**}Michigan State University, ^{***}University of Michigan, ^{****}University of Michigan

ABSTRACT

Pulmonary arterial hypertension (PAH) is a complex vascular disease associated with elevated pulmonary arterial pressure. PAH is a multi-factorial phenomenon in which the onset and early progression of the disease can be traced to permanent changes in vessel composition, geometry, and/or stiffness of the distal vasculature tree. Although clinical catheterization pressure measurements and high resolution medical images are typically readily available, current medical imaging modalities are unable to provide insight on the disease progression in the downstream vasculature. Therefore, any modeling effort must account for the role of the distal arterial tree geometry on global pulmonary hemodynamics and vascular growth and remodeling. Moreover, a key component of fluid-solid growth formulations [1] is the establishment of homeostatic (e.g. equilibrium) baseline states. The objective of the present work is to derive a methodology to define homeostatic states in the distal pulmonary arterial tree based on an extension of Murray's law and steady state hemodynamics. We constructed a multi-scale model of the pulmonary arterial tree, whereby each vessel was modeled as a 0D segment endowed with a bio-chemo-mechanical growth and remodeling model. Using an extension of Murray's law [2], each vessel radius and wall compositions were determined as a target state via a minimization problem involving the metabolic cost of maintaining the blood volume, the power needed to overcome viscous drag by the blood flow, and the metabolic cost of the vessel wall constituents under the constraint of mechanical equilibrium. The minimization problem was coupled with a steady state hemodynamic description of the arterial tree. The coupled problem produced the composition of the arteries in the arterial tree as well as their geometry. Using the small on large theory [3], the stiffness of each individual blood vessel can then be calculated from their composition. References [] C. A. Figueroa et al., *Comput. Methods Appl. Mech. Engrg.*, 198 (2009), 3583-3602. [2] S. B. Lindström et al. *Biomech. Model. Mechanobiol.*, 14 (2015), 83-91. [3] S. Baek et al., *Comput. Methods Appl. Mech. Engrg.* 196 (2007), 3070-3078.

Computational Modeling of the Orientation Controlled Two-Step Epitaxial Growth of WS₂-WS₂ Homobilayer and WS₂-WSe₂ Heterobilayer

Kamalika Ghatak^{*}, Kyunghnam Kang^{**}, Shichen Fu^{***}, Xiaotian Wang^{****}, Siwei Chen^{*****},
Eui-Hyeok Yang^{*****}, Dibakar Datta^{*****}

^{*}New jersey Institute of Technology, ^{**}Stevens Institute of Technology, ^{***}Stevens Institute of Technology,
^{****}Stevens Institute of Technology, ^{*****}Stevens Institute of Technology, ^{*****}Stevens Institute of Technology,
^{*****}New jersey Institute of Technology

ABSTRACT

Two-dimensional Van der Waals (vdW) bilayers are emerging class of materials for their unique opto-electronic and mechanical behavior. Bilayer stacking takes place through the mixing and matching in between semimetals (e.g., Graphene), semiconductors (e.g. transition metal dichalcogenides (TMDs)), and insulators (e.g., hexagonal boron nitride; h-BN). TMD bilayers are most popular due to their practical applications in electronics. TMDs possess a wide variety of tunable opto-electronic properties such as the position of band gap, indirect-direct band gap crossover, harmonic generation, valley pseudospin effects. In addition, lattice mismatch in two different monolayers ensures the possibility of its use as transistors and diodes. Among several existing growth techniques, epitaxial growth mechanism is the most preferred one due to its technological advantages such as reduction of defect density, consistency in the overall growth, growth products with sharper interfaces, the perseverance of in-plane electrical conductivity via the introduction of mirror twin grain boundaries, and simultaneous reduction of tilt grain boundaries. Our experimental group developed a new two-step epitaxial growth technique in order to generate WS₂-WS₂ homobilayer. In their current technique, first step is the formation and isolation of the orientation controlled (metal terminated or chalcogenide terminated) WS₂ monolayer followed by the second step involving orientation dependent second layer growth. Therefore, it is important to perform computational analysis in order to shed light towards this orientation controlled two-step epitaxial growth mechanism. Density Functional Theory (DFT) approach has been implemented in order to gain knowledge on the structural and electronic properties of WS₂ homobilayer and WS₂-WSe₂ heterobilayer. At first, we computed equilibrium interlayer distances and verified with the experimental data. In order to investigate the nature and strength of the interlayer interactions, various combinations of AA, AA', AB and AB' stacking are considered and the most stable combination is chosen based on formation energy. Analysis of charge transfer, Density of States (DOS) provide insight into the nature of bonding. Moreover, possible presence of dangling bonds around the edge is predicted from the charge distribution. Significant in-plane strains and out-of-plane displacements are introduced in WS₂-WSe₂ heterobilayer due to interlayer interactions. Various alignments of WS₂-WS₂ and WS₂-WSe₂ bilayer structures are studied in terms of different degree of relative rotation angle between the layers. Our results provide guidelines for experimental design of the two-step epitaxial growth technique to synthesize TMD homobilayers and heterobilayers.

Optimization Under Uncertainty for Complex PDE Models in High Dimensions

Omar Ghattas^{*}, Peng Chen^{**}, Umberto Villa^{***}

^{*}The University of Texas at Austin, ^{**}The University of Texas at Austin, ^{***}The University of Texas at Austin

ABSTRACT

We consider optimization problems governed by PDEs with infinite dimensional random parameter fields. Such problems arise in numerous applications: optimal design/control of systems with stochastic forcing or uncertain material properties or geometry; inverse problems governed by stochastic forward problems; or Bayesian optimal experimental design problems with the goal of minimizing the uncertainty or maximizing the information gain in the inferred parameters. Standard Monte Carlo evaluation of the objective results in a number of PDE constraints equal to the number of samples. The resulting many-PDE-constrained optimization problem, while deterministic, is nevertheless prohibitive to solve, especially when the PDEs are “complex” (large-scale or nonlinear or coupled) and when the parameter space is high-dimensional (as occurs after discretization of an infinite-dimensional field). We present high-order derivative-based approximations of the parameter-to-objective maps that—in combination with randomized rank-capturing algorithms—exploit the structure of these maps (geometry, smoothness, low effective dimensionality). Their use as a basis for variance reduction is demonstrated to significantly speed up Monte Carlo sampling, leading to scalable solution of several stochastic optimization problems governed by turbulent flow and wave scattering with up to $O(10^6)$ uncertain parameters. 1. P. Chen, U. Villa, and O. Ghattas, Taylor Approximation and Variance Reduction for PDE-constrained Optimal Control under Uncertainty, submitted. 2. A. Alexanderian, N. Petra, G. Stadler, and O. Ghattas, Mean-variance risk-averse optimal control of systems governed by PDEs with random parameter fields using quadratic approximations, *SIAM/ASA Journal on Uncertainty Quantification*, 5(1):1166--1192, 2017. <https://doi.org/10.1137/16M106306X> 3. A. Alexanderian, N. Petra, G. Stadler, and O. Ghattas, A fast and scalable method for A-optimal design of experiments for infinite-dimensional Bayesian nonlinear inverse problems, *SIAM Journal on Scientific Computing*, 38(1):A243--A272, 2016. <http://dx.doi.org/10.1137/140992564>

Probabilistic Learning and Sampling for Integrated Manufacturing and Performance of Composites

Ziad Ghauch^{*}, Venkat Aiharaju^{**}, Roger Ghanem^{***}, Loujaine Mehrez^{****}, Praveen Palussetti^{*****}, William Rodgers^{*****}, Arnaud Dereims^{*****}

^{*}University of Southern California, ^{**}General Motors Research Center, ^{***}University of Southern California, ^{****}University of Southern California, ^{*****}ESI Group, ^{*****}General Motors Research Center, ^{*****}ESI Group

ABSTRACT

Composites are complex material systems that exhibit physical behavior simultaneously on multiple time and spatial scales. The serviceability and failure properties of devices made out of composites exhibit a range of variability that reflects this complexity and their dependence on the details of the manufacturing process. Prognostics and efficient design of these devices requires reliance on computational tools capable of coupling across physical phenomena as well as across space and time scales. Additional requirements often add the need for a probabilistic analysis that further exacerbates the computational burden, often rendering it prohibitive. In this talk, we will demonstrate the application of new methodologies for probabilistic learning that serve to distill intrinsic structure from a handful of numerical simulations and sample additional realizations, as needed, that are consistent both with this structure and the statistics of the few initial samples. This methodology was recently developed by Soize and Ghanem and is applied in the present context to an integrated multiscale and multi physics simulation setting. The procedure begins by discovering the intrinsic structure using the method of diffusion manifolds. Following that, a stochastic Ito equation is developed that samples on this manifold, producing, at minimal cost, additional samples that are consistent with the initial set.

Robust Optimization in Training Neural Networks

Amir Gholami^{*}, Zhewei Yao^{**}, Kurt Kuetzer^{***}, Michael Mahoney^{****}

^{*}University of California, Berkeley, ^{**}University of California, Berkeley, ^{***}University of California, Berkeley,
^{****}University of California, Berkeley

ABSTRACT

There has been renewed efforts in using machine learning to tackle engineering problems. However, the training algorithms used to learn a representation of the problem is often times susceptible to adversarial perturbation. Solutions to these, require analysis and modification of the state-of-the-art optimization algorithms, along with designing robust models. In a typical machine learning task, one is given a set of input data \mathbf{x} with the corresponding response y , drawn from an unknown distribution \mathcal{P} . In practice, we only observe a set of discrete, noisy examples drawn from this distribution. Then the model is trained, often times with stochastic gradient descent, to learn this distribution. An open question is how much, if at all any, has the model learned from the distribution after the training is finished, and what is the uncertainty associated with that? This is an important aspect that has to be analyzed before these methods could be used for solving physical problems, or aid in modeling. In practice, it has to been shown to be trivial to create adversarial perturbation to the inputs of a neural network so that it produces wrong results with very high confidence. This adversarial perturbation can even be performed on models that have very high accuracy and using more training data often times does not help either, which underscores the importance to design new optimization methods to make the model more robust. One approach to address this problem is to use robust optimization instead of minimizing for the average case. In this method, one optimizes for the worst case at every iteration of the optimization. This essentially changes the minimization to a min-max problem. It can be shown that robust optimization reduces both the bias as well as the variance in the generalization error. In this work, we perform a Hessian based analysis of the adversarial training and analyze how the landscape of the objective functional changes when the network is solved with robust optimization vs when it is solved with vanilla stochastic gradient descent.

Numerical Simulation of Counterstreaming Plasma Interactions Using a Multifluid Model

Debojyoti Ghosh^{*}, Christos Kavouklis^{**}, Thomas Chapman^{***}, Richard Berger^{****}, Genia Vogman^{*****}

^{*}Lawrence Livermore National Laboratory, ^{**}Lawrence Livermore National Laboratory, ^{***}Lawrence Livermore National Laboratory, ^{****}Lawrence Livermore National Laboratory, ^{*****}Lawrence Livermore National Laboratory

ABSTRACT

Counterstreaming plasma interactions are an important phenomenon in inertial confinement fusion, where irradiation of the hohlraum with laser beams results in plasmas ablating off the hohlraum surfaces and the fuel capsules and interacting with each other. Related high-energy density physics experiments involve interactions of plasmas ablating off discs irradiated by lasers. Simulating such flows with multispecies hydrodynamic codes [1] can result in unphysical solutions due to the use of a single velocity field. Kinetic approaches [2], on the other hand, are prohibitively expensive for experimental-scale simulations. In this talk, we report on the development of EUCLID (Eulerian Code for pLasma Interaction Dynamics) based on a multifluid approach. The Euler equations are solved for each ion species and the electrons. The species interact through electrostatic forces, friction, and thermal equilibration. This model allows for distinct flows for each species through their separate velocity fields. The electrostatic potential is obtained from the charge densities using the Poisson equation. The equations are discretized on a three-dimensional Cartesian grid using a conservative finite-difference formulation, and the interface fluxes are computed using the 5th order WENO scheme. The Poisson equation is solved using a 6th order method. In addition, adaptive refinement of the mesh around regions of strong interactions is implemented using Chombo [3], a library for solving PDEs on block-structured AMR grids. The disparate masses of electrons and ions result in a stiff system of semi-discrete ordinary differential equations in time. We use the semi-implicit additive Runge-Kutta methods for time integration, where the electron acoustic modes are integrated implicitly in time, while the remaining terms in the ions and electron equations are integrated explicitly. We present the verification of EUCLID for several benchmark test cases, as well as the simulation of counterstreaming plasmas. In particular, we show that our approach is able to accurately capture plasma interpenetration when frictional forces are small, and the fluids do not converge to a single fluid within experimental time scales. [1] M. M. Marinak et al., Physics of Plasmas 5, 1125 (1998). [2] A. Kemp and L. Divol, LLNL Kinetic workshop 2016. [3] M. Adams, et al., LBNL-6616E This work was performed under the auspices of the U.S. Department of Energy by Lawrence Livermore National Laboratory under Contract No. DE-AC52-07NA27344 and funded by the LDRD Program at LLNL under project tracking code 17-ERD-081.

Fluid-Structure Interaction Simulation of Transcatheter Aortic Valve Performance in Living Heart Human Model

Ram Ghosh^{*}, Matteo Bianchi^{**}, Gil Marom^{***}, Vladimir Kashirin^{****}, Praveen Sridhar^{*****}, Karl D'souza^{*****}, Wojtek Zietak^{*****}, Danny Bluestein^{*****}

^{*}Stony Brook University, ^{**}Stony Brook University, USA, ^{***}Tel Aviv University, Israel, ^{****}Capvidia, Russia, ^{*****}Dassault Systemès, Simulia, Germany, ^{*****}Dassault Systemès, Simulia, USA, ^{*****}Capvidia, Belgium, ^{*****}Stony Brook University, USA

ABSTRACT

Introduction: Transcatheter Aortic Valve Replacement (TAVR) has emerged as a life-saving solution for inoperable elderly patients with calcific aortic valve (AV) disease, often as their only life-saving treatment [1]. However, failed delivery due to tortuous aortic geometry, valve migration, and paravalvular leaks (PVL) lead to increased stroke risk, increasing the overall morbidity and mortality post-TAVR. There are numerical studies that attempted to address these complications, but the focus was only to deploy the TAVR valves, thus neglecting their post-deployment performances during heart beating. This study proposes a fluid-structure interaction (FSI) simulation to evaluate a TAVR valve's performance by comparing its hemodynamics, PVL, and thrombogenicity with healthy and diseased aortic valves in Simulia Living Heart Human Model (LHHM). Methods: LHHM is an electro-mechanical model of heart function in which a self-expandable TAVR valve crimping and deployment procedures were simulated using finite element (FE) method. The FE solver was Abaqus Explicit. The TAVR stent equipped with the prosthetic leaflets in the deployed configuration was then used for FSI analysis. Specifically, the LHHM inner ventricular surface contraction was implemented as boundary condition. A body-fitted sub-grid geometry resolution (SGGR) method was chosen during the FSI fluid solution. The SGGR approach starts with a cartesian grid from which a geometry is subtracted to maintain a curvilinear boundary, hence ensuring body-fitted mesh. The deployed valve's structural mechanics and blood flow were modeled in Abaqus Explicit and FlowVision respectively. A 2-way strong implicit coupling was used between these two partitioned solvers using FlowVision Multi-Physics Manager. Thrombogenic potentials were calculated from probability density function of flow stress accumulation (SA) along multiple platelet trajectories [2]. Platelet motion was modeled using a transient two-phase flow simulation in ANSYS Fluent Discrete Phase Model, where the spherical particles mimic platelets. Results: The surrounding tissue stress and strain values were lowest when the stent was deployed more towards ventricular side, hence determining the optimal implantation zone. The FSI simulations of a TAVR valve in LHHM along with a healthy and diseased AV allowed us to compare their hemodynamic and thrombogenic performances. Discussions: TAVR valve structural performances during successive cycles of beating heart were successfully evaluated. The suggested numerical methodologies can ultimately pave the way for minimizing the risk of clinical complications by enhancing pre-procedural planning. Acknowledgements: Funding provided by NIH (1U01HL131052, DB). References: [1] Sedrakyan, A, et al.; JAMA Internal Medicine; 2016; 177:2. [2] Girdhar G. et al.; PLoS One; 2012; 7: e32463.

Mechanical Instability of Multilayer Molybdenum Disulfide

Susanta Ghosh^{*}, Upendra Yadav^{**}, Dibakar Datta^{***}

^{*}Department of Mechanical Engineering-Engineering Mechanics, Michigan Technological University, ^{**}Department of Mechanical Engineering-Engineering Mechanics, Michigan Technological University, ^{***}Department of Mechanical and Industrial Engineering, New Jersey Institute of Technology

ABSTRACT

Two-dimensional (2D) materials are monolayer crystals and only one atom or a few atoms thick. Two-dimensional multilayer materials (2DMMs) are made of a parallel stack of 2D materials and their mechanics are the main focus of this work. Mono- and multi-layer 2D materials possess exceptional and coupled mechanical, electrical, and thermal properties. Due to their ultra-thin membrane-like geometries and a high degree of crystalline arrangements they show rich nonlinear elasticity and elastic-buckling. The promise of 2D materials has fostered intense research leading to an expansion of this family of materials. Like graphene, other single layer 2D materials, such as Molybdenum disulfide, also behave like the thinnest nonlinear-elastic membranes having stiff in-plane and ultra-weak bending rigidity, leading to distributed buckles like wrinkles, ripples, or folds. 2DMMs have another level of complexity due to weak van der Waals interactions between neighboring layers, which interplays with the rigidity of individual layers resulting in complex deformation morphologies. Ripples and wrinkles and the ensuing elastic strain in monolayer and multilayer Molybdenum disulfide can alter their electronic properties and can also yield other properties like tunable surface leading to various high-impact applications. Therefore, understanding and predicting the mechanical instabilities of multilayer Molybdenum disulfide is a crucially important problem. Herein a continuum model is utilized to quantitatively predict the deformation mechanism, the onset of mechanical instabilities and transition between different complex periodic buckled shapes for Molybdenum disulfide (MoS₂). Further, the role of van der Waals interaction and the role of interlayer slide are also investigated. The computational results obtained in this work show very good agreement with the available experimental results.

Mathematical Modelling of Water-flooding Techniques in Heterogeneous Hydrocarbon Reservoirs

Tufan Ghosh^{*}, G. P. Raja Sekhar^{**}, Debasis Deb^{***}

^{*}Indian Institute of Technology Kharagpur, ^{**}Indian Institute of Technology Kharagpur, ^{***}Indian Institute of Technology Kharagpur

ABSTRACT

Fractured carbonate reservoirs are potential resources for crude oil and natural gas. These reservoirs are composed of matrix block with interconnected network of fractures. Oil or gas recovery from such low porosity and low permeability reservoirs are important because a large amount of such hydrocarbon fluids are trapped inside those reservoir formulations. Water-flooding or more specifically spontaneous imbibition is most effective recovery mechanism to increase the production from fractured reservoirs. However, the performance of water-flooding mainly depends on the wettability of the reservoirs. In co-current imbibition, the wetting phase displaces the non-wetting phase in such a way that the non-wetting phase moves in the same direction of the wetting phase. Hence the corresponding mathematical model requires a total flux condition. This study deals with the mathematical modeling of co-current spontaneous imbibition for heterogeneous porous reservoirs. We assume that the flow is governed by the multi-phase extension of Darcy equation, where the saturation of the local wetting phase satisfies a diffusion type of equation with an additional term from the counter-current phenomena. The study assumes that the wetting and non-wetting phases flow in the same direction, and hence the sum of Darcy's velocities (i.e. net flux) is assumed to be non-vanishing. The model is used to identify the difference in the recovery fraction between homogeneous and heterogeneous reservoir formulation. The resulting governing equations are highly non-linear in nature and have been solved numerically. We have used different porosity variation models based on the existing literature, say, exponential and inverse-linear. It has been shown that the co-current imbibition recovery is very much sensitive to the viscosity ratio, porosity variation models and the wettability of the reservoir. Effect of the viscosity ratio on the water saturation gradient and the end point mobility ratio is also studied. In addition the consequences of the nature of heterogeneity and wettability of the medium on the sweeping efficiency of co-current imbibition are investigated.

Non-Linear Crack Propagation Using X-FEM Coupled with Adaptive Mesh Refinement

Gael Gibert^{*}, Anthony Gravouil^{**}, Benoit Prabel^{***}, Clémentine Jacquemoud^{****}

^{*}Den-SERVICE d'Etudes Mécaniques et Thermiques (SEMT), CEA, Université Paris-Saclay, F-91191, Gif-sur-Yvette, France, ^{**}LAMCOS / UMR CNRS5259 / INSA de Lyon 18-20, rue des Sciences 696, ^{***}Den-SERVICE d'Etudes Mécaniques et Thermiques (SEMT), CEA, Université Paris-Saclay, F-91191, Gif-sur-Yvette, France, ^{****}Den-SERVICE d'Etudes Mécaniques et Thermiques (SEMT), CEA, Université Paris-Saclay, F-91191, Gif-sur-Yvette, France

ABSTRACT

The eXtended Finite Element Method (XFEM) [1] has been used in Cast3m [2] to simulate static and dynamic problems of crack propagation in elastic and elastic-plastic materials. In this method, the decoupling of the crack description and structure mesh is particularly adapted to incremental propagation strategy when the crack path is not known a priori. As a first point and in the context of non-linear behaviour, over-integrated elements are used [3]. As a second point the use of local propagation criteria implies an accurate description of physical quantities (stress, strain, internal variables ...) in a limited area around the crack front. Hence a priori ignorance of the propagation path forces us to use a very fine mesh of enriched elements in a rather large zone. As a consequence of these two points, the cost of this method increases drastically for engineer-sized problems. Thus we decided to develop a hierarchical Adaptive Mesh Refinement tool (AMR), to ensure that the mesh is always sufficiently fine at vicinity of the crack front during the propagation. This tool was demonstrated to work well with the X-FEM method and limits the calculation time by restraining the number of fine enriched elements to a small area. In this paper the algorithmic procedure used to simulate a crack propagation with the X-FEM method coupled with an AMR tool in Cast3m is described in detail. More particularly the presentation focuses on two important steps of this procedure: 1) the refinement algorithm for standard and enriched elements, 2) and the method used to transfer the mechanical fields from one mesh to another between two steps of propagation, especially when those fields are described with an enriched discretization. The efficiency of the method is illustrated by application cases of crack propagation in elastic-plastic media in 2 and 3 dimensions. First results fit experimental data. [1] J.C. PASSIEUX, J. RETHORE, A. GRAVOUIL, M.C. BAIETTO. Local/global non-intrusive crack propagation simulation using a multigrid X-FEM solver. Computational Mechanics, 52:1381 to 1393, 2013 [2] B. PRABEL, A. COMBESURE, A. GRAVOUIL and S. MARIE. Levelset non-matching meshes : Application to dynamic crack propagation in elastic-plastic media. International Journal for Numerical Methods in Engineering, 69 :1553 to 1569, 2007 [3] Cast3M. Finite Element software developed by the french Atomic Energy Center (CEA) www-cast3m.cea.fr, 2017

Accelerating Rational Design of Advanced Composites The Role of Modelling in Understanding Dispersed and Helicoidal Cellulose Nanocrystal Composite Properties, and Composite Damage Revealed by Fluorophores

Jeffrey Gilman^{*}, Robert Sinko^{**}, Frederick Phelan^{***}, beatriz Pazmino-Betancourt^{****}, caglar emiroglu^{*****}, Ketan Khare^{*****}, E. Johan Foster^{*****}, Sinan Keten^{*****}, Ryan Beams^{*****}, Douglas Fox^{*****}, Jack Douglas^{*****}, Christoph Weder^{*****}, Bharath Natarajan^{*****}, Jan Obrzut^{*****}, Stephan Stranick^{*****}

^{*}Materials Measurement Laboratory, National Institute of Standards and Technology, 100 Bureau Dr., Gaithersburg, MD 20899, ^{**}Department of Civil and Environmental Engineering and Department of Mechanical Engineering, Northwestern University, Evanston, Illinois 60208, ^{***}Materials Measurement Laboratory, National Institute of Standards and Technology, 100 Bureau Dr., Gaithersburg, MD 20899, ^{****}Materials Measurement Laboratory, National Institute of Standards and Technology, 100 Bureau Dr., Gaithersburg, MD 20899, ^{*****}Materials Measurement Laboratory, National Institute of Standards and Technology, 100 Bureau Dr., Gaithersburg, MD 20899, and Department of Physics, Georgetown University, Washington DC 20057, ^{*****}Materials Measurement Laboratory, National Institute of Standards and Technology, 100 Bureau Dr., Gaithersburg, MD 20899, and Department of Physics, Georgetown University, Washington DC 20057, ^{*****}Material Science and Engineering Department, Virginia Tech, Blacksburg, VA 24061, ^{*****}Department of Civil and Environmental Engineering and Department of Mechanical Engineering, Northwestern University, Evanston, Illinois 60208, ^{*****}Materials Measurement Laboratory, National Institute of Standards and Technology, 100 Bureau Dr., Gaithersburg, MD 20899, ^{*****}Department of Chemistry, American University, Washington DC 20016, ^{*****}Materials Measurement Laboratory, National Institute of Standards and Technology, 100 Bureau Dr., Gaithersburg, MD 20899, ^{*****}Adolphe Merkle Institute, University of Fribourg, Chemin des Verdiers 4, CH-1700 Fribourg, Switzerland, ^{*****}Materials Measurement Laboratory, National Institute of Standards and Technology, 100 Bureau Dr., Gaithersburg, MD 20899, and Department of Physics, Georgetown University, Washington DC 20057, ^{*****}Materials Measurement Laboratory, National Institute of Standards and Technology, 100 Bureau Dr., Gaithersburg, MD 20899, ^{*****}Materials Measurement Laboratory, National Institute of Standards and Technology, 100 Bureau Dr., Gaithersburg, MD 20899

ABSTRACT

Polymer composites are currently used in a variety of applications, such as aerospace, electronics, recreation, infrastructure, light-weight vehicles, and alternative energy generation. The rational design of advanced composites for these applications requires that data, models and measurements be used together toward specific composites performance goals, such as manufacturability, multi-functionality, environmental durability, and toughness. This presentation will cover three examples where such an integrated approach has accelerated and advanced the understanding of fundamental issues that drive the rational design of advanced composites. First, our recent advancements in the use of modelling to understand the role of surface chemistry on the properties of nanocellulose polymer composites will be reviewed; second, the modelling of mechanochemistry for understanding the interfacial damage reported by fluorescent probes will be summarized; and finally, we will report on our investigation of the novel mechanical properties of self-assembled cellulose nanocrystals (CNCs) in the helicoidal, or Bouligand structure. Such materials possess high mechanical strength and toughness, similar to bone, the mantis shrimp dactyl club or ivory, and are toughened by a combination of soft, energy-dissipating polymer and the Bouligand ordered-fiber structures. In this presentation, we will report additional simultaneous enhancements in the in-plane modulus, strength, elongation, toughness and out-of-plane flexibility of the Bouligand films by including small amounts of a longer CNC material. The mechanical properties we report in the blended films are some of the best reported for self-assembled CNC materials thus far. Using coarse grained molecular dynamics simulations of binary CNC systems we identify the role of the high aspect ratio CNC phase to be to enhance interaction strengths by maximizing CNC-CNC overlap lengths.

Analysis of Three-Dimensional Transient Channel Flow at Moderate Reynolds Numbers

Marco Giometto^{*}, Parviz Moin^{**}, George Park^{***}, Adrian Lozano-Duran^{****}

^{*}Columbia University, ^{**}Stanford University, ^{***}University of Pennsylvania, ^{****}Stanford University

ABSTRACT

The law-of-the-wall, scaling laws, and reduced-order models established largely for equilibrium turbulent boundary layers should not be assumed to be directly applicable to non-canonical wall-bounded flows. Turbulent boundary layers with mean-flow three dimensionality are one class of such non-canonical flows, with particular relevance to external aerodynamics and hydrodynamics. In these flows, the mean flow direction changes continuously across the shear-layer thickness due to the cross-stream pressure gradient induced by the geometry of the immersed body. Fundamental questions remain unanswered with regard to changes of wall-turbulence structure with the imposition of additional rates of mean strain. Using direct numerical simulation, we study temporally developing three dimensional turbulent boundary layers in a planar channel at friction Reynolds numbers from 186 up to 934 subjected to a range of spanwise forcing. This flow is well suited for the study of non-equilibrium effects due to its simple geometry. We propose an inner and outer scaling of the problem that well collapses turbulent statistics across the range of considered Reynolds numbers. We also show how rapid pressure perturbations reduce wall-normal velocity variance via pressure strain effects, yielding the observed Reynolds stress deficit during the initial transient. An analysis of the effects of variable spanwise forcing magnitude on the Reynolds stresses will also be proposed and interpreted in light of predictions from rapid-distortion theory.

A Monolithic Coupled Solver for Large Scale Simulations of Hydraulic Fracture

Bianca Giovanardi^{*}, Anwar Koshakji^{**}, Raul Radovitzky^{***}

^{*}Massachusetts Institute of Technology, ^{**}Massachusetts Institute of Technology, ^{***}Massachusetts Institute of Technology

ABSTRACT

Hydraulic fracturing of rock by the injection of a pressurized fluid is a common technique used to release formerly inaccessible hydrocarbons. 3D simulations of realistic scenarios need to tackle the complexity arising from the nonlinear hydro-mechanical coupling and from the large scale of oil reservoirs. A suitable simulation algorithm must then exhibit massively parallel scalability in order to conduct analysis with the necessary resolution in a reasonable time. We present a computational framework for the coupling of the fractured rock's mechanics with the fluid flow in the cracks, governed by Reynolds lubrication equation. The discretization consists of a hybrid discontinuous Galerkin finite element formulation for the rock, which enables the description of the crack opening between adjacent mesh elements explicitly, and a continuous Galerkin finite elements discretization for the fluid problem, formulated on mesh interfaces. After showing that a naïve staggered attempt to treat the coupling is unstable under inflow boundary conditions for the fluid, we present a robust monolithic iterative algorithm. The resulting system of strongly nonlinearly coupled equations is assembled and solved in parallel, exploiting the iterative solvers implemented in the open source library PETSc. Results in good agreement with well-known semi-analytic solutions available in literature are discussed, with particular focus on performance in terms of accuracy and scalability.

Uncertainty Quantification for Complex Systems in High Dimensions Using Grassmann Manifold Variations and Machine Learning

Dimitris Giovanis^{*}, Michael Shields^{**}

^{*} Johns Hopkins University, ^{**} Johns Hopkins University

ABSTRACT

This paper proposes a novel adaptive method for performing uncertainty quantification of high-dimensional (input and output) stochastic systems. This method addresses the limitation of the recently proposed method [1] used for uncertainty quantification of systems with high-dimensional responses, where the Delaunay triangulation limits the method to problems of modest stochastic dimension (less than about 6). In this paper, we abandon the multi-element nature of the aforementioned method by eliminating the need for discretizing the input parameter space. This is achieved by using spectral clustering [2] which, refers to a class of machine learning techniques that utilizes the eigen-structure of a similarity matrix to partition data into disjoint clusters based on the similarity of the points, in order to effectively identify areas of the parameter space where sharp changes of the solution field are resolved. In order to do this, we derive a similarity matrix based on the pairwise distances between the high-dimensional solutions of the stochastic system projected onto the Grassmann manifold. The distances are calculated using appropriately defined metrics and the similarity matrix is used in order to cluster the data based on their similarity. For each cluster, the points that are most far apart between all the points of the cluster are used as seeds and new samples are generated at their proximity which is defined based on statistical properties of the cluster. This way we populate with samples areas of the parameter space where sharp changes of the response field are resolved.

Numerical Predictions of Orthotropic Elastic Behaviour of Thin Woven Composites Used in High Frequency Printed Circuit Boards, Consequence on the Predictions of the Board Reliability

Gautier Girard^{*}, Marion Martiny^{**}, Sébastien Mercier^{***}, Mohamad Jrad^{****}, Slim Bahi^{*****},
Laurent Bodin^{*****}, François Lechleiter^{*****}, David Nevo^{*****}, Sophie Dareys^{*****}

^{*}LEM3 - Laboratoire d'Etude des Microstructures et de Mécanique des Matériaux, Université de Lorraine, UMR CNRS 7239, Ile du Saulcy, 57045 Metz, France, ^{**}LEM3 - Laboratoire d'Etude des Microstructures et de Mécanique des Matériaux, Université de Lorraine, UMR CNRS 7239, Ile du Saulcy, 57045 Metz, France, ^{***}LEM3 - Laboratoire d'Etude des Microstructures et de Mécanique des Matériaux, Université de Lorraine, UMR CNRS 7239, Ile du Saulcy, 57045 Metz, France, ^{****}LEM3 - Laboratoire d'Etude des Microstructures et de Mécanique des Matériaux, Université de Lorraine, UMR CNRS 7239, Ile du Saulcy, 57045 Metz, France, ^{*****}LEM3 - Laboratoire d'Etude des Microstructures et de Mécanique des Matériaux, Université de Lorraine, UMR CNRS 7239, Ile du Saulcy, 57045 Metz, France, ^{*****}CIMULEC, ZI Les Jonquières, 57365 Ennery, France, ^{*****}CIMULEC, ZI Les Jonquières, 57365 Ennery, France, ^{*****}Thales Alenia Space, 26 avenue Jean François Champollion 31100 Toulouse, France, ^{*****}CNES, Centre spatial de Toulouse 18 avenue Edouard Belin 31401 Toulouse cedex 9, France

ABSTRACT

Reliability of electronic devices is still a main concern for aeronautics, military and space industries. In any electronic device, the bare Printed Circuit Board (PCB) is considered as a carrier which provides interconnection between components. During the last decades, PCB technologies have strongly evolved to fulfil increased manufacturers requirements. Nowadays, OEM, PCB manufacturers and research laboratories are closely collaborating to assess PCB reliability and lifetime. To achieve that goal, it is fundamental to characterize precisely base materials in order to anticipate failure. With precise models, it is expected that finite element calculations will be able to reproduce PCB aging under environmental constraints for example... In the present work, we focus on the numerical predictions of the elastic behaviour of thin woven composites. The microstructure characterization, mechanical tests and numerical models were performed on the real material used for PCB, so it is expected that the combined experimental and numerical strategy will provide accurate predictions. The in-plane properties are measured by carrying out classical uniaxial testing. Strains are evaluated with digital image correlation. Nevertheless, the out-of-plane elastic properties cannot be captured due to the thickness of the laminate (a few hundred of microns). From the literature, it is well established that the knowledge of the out-of-plane properties is fundamental to investigate the lifetime of high density printed circuit boards. A two stage homogenization method is developed to obtain the overall elastic orthotropic behaviour of a woven composite. Inputs as internal structure and measured in-plane elastic properties are needed. A first homogenization focuses on the behaviour predictions of the yarns. In a second stage, a representative volume element is reproduced in Abaqus software. For high frequency applications, the matrix is made of a resin filled with a large volume content of ceramic inclusions. Since the behaviour of the matrix phase is unknown, an inverse method is proposed. The methodology has been applied at different temperatures in the range [-55°C; +125°C]. Finally, numerical simulations of a plated through hole in a double sided PCB will be presented. By considering the material properties obtained from datasheet or deduced from the present work, it is shown the major importance of the temperature dependency of out-of-plane properties on the lifetime of a printed circuit board. Acknowledgements: The support of the French ANR agency through the Labcom program ANR-14-LAB7-0003-01, support of CNES, Thales Alenia Space and Cimulec are acknowledged.

Optimal Truncation of Unbounded Anisotropic Elastic Computational Domains

Dan Givoli*

*Technion - Israel Institute of Technology

ABSTRACT

A common procedure for solving wave problems in unbounded elastic domains (such as problems in geophysics) is to truncate the unbounded domain via an artificial boundary, and impose an Absorbing Boundary Condition (ABC) on that boundary, with the hope of generating as little as possible spurious reflection. In this study, an optimal low-order ABC is proposed for time-dependent waves in anisotropic elastic media. This ABC enjoys the following advantages: (a) it is fully compatible with the standard finite element displacement formulation, (b) it yields a symmetric finite element formulation, (c) it is easy to implement, (d) it is proved to be strongly (energy-) stable for all anisotropic media, even for those that give rise to "inverse modes", in which the phase and group velocities have opposite signs, and (e) in typical cases it is more accurate than the well-known Lysmer-Kuhlemeyer ABC (except for isotropic media, where LK is optimal among first-order ABCs). The objective function associated with the optimal ABC is the energy-rate reflection coefficient, which is always less than unity for all media and all types of propagating waves. The success of the new ABC is demonstrated via numerical examples.

Results from DoD HPCMP CREATE(TM)-AV Kestrel for the 3rd AIAA High Lift Prediction Workshop

Ryan Glasby^{*}, J. Taylor Erwin^{**}, Douglas Stefanski^{***}, Steve Karman^{****}, Kevin Holst^{*****}

^{*}University of Tennessee, ^{**}University of Tennessee, ^{***}University of Tennessee, ^{****}Pointwise, Inc., ^{*****}University of Tennessee

ABSTRACT

HPCMP CREATETM-AV Kestrel computational fluid dynamics (CFD) component COFFE is applied to Tasks 1 – 3 of the 3rd AIAA High Lift Prediction workshop. In task 1, a series of P2 tetrahedral meshes for the NASA High-Lift Common Research Model were used to carry out flow-field versus mesh size studies at various angles of attack. In Task 2, P2 fully tetrahedral medium-fidelity meshes for the JAXA Standard Model with and without the nacelle/pylon were used to evaluate the accuracy of computed aerodynamic output as compared to experimental data for an angle of attack sweep. In Task 3, a series of P1 quadrilateral meshes was utilized to obtain the mesh convergence properties for a DSMA661 (MODEL A) airfoil at a fixed angle of attack, subsonic, high Reynolds number condition. A variety of turbulence models were employed for these computations, and the CFD solver in conjunction with the higher order meshes demonstrated the capability to accurately predict the flow-field surrounding a commercial aircraft in a high-lift configuration.

High-Order Accurate Time Integration Methods for Inductive Heating Analysis

Tobias Gleim^{*}, Detlef Kuhl^{**}

^{*}University of Kassel, ^{**}University of Kassel

ABSTRACT

An important concept in metal forming processes is local heat treatment and cooling that influence local material properties, such as ductility, hardness, yield strength, or impact resistance, see K. Steinhoff, U. Weidig and N. Saba (Functionally Graded Materials in Industrial Mass Production, 35-52, 2009). Cold forming methods by means of electromagnetic forces are also of great scientific interest, in order to obtain special shapes and product properties. To make these techniques more effective in industry, or to optimize its application, corresponding numerical simulation tools are needed. One of the main topics of these manufacturing processes is characterized by the electromagnetic-thermal influence. The inductive heating of a metal shaft is influenced by an alternating current inducing a high frequency electromagnetic field, which causes a temperature increase due to the resulting eddy currents. In order to examine this process, the fully coupled electromagnetic Maxwell equations are combined with the temperature field in a monolithic approach. Due to the high frequencies of the applied current and the strongly temperature dependent material parameters, the investigated set of temporal and spatial second order differential equations are strongly non-linear. Thus, adequate material models as well as proper numerical schemes have to be established. Therein, the focus will be on the application of high-order accurate numerical schemes in combination with appropriate error estimators, see T. Gleim (Universität Kassel, Ph.D. Thesis, 2016). These electromagnetic-thermal equations are numerically solved using the finite element method in space, time integrations schemes and Newton-Raphson method. The main focus of the talk is the high-order accurate time integration of the semidiscrete, second order ordinary differential equation. Therefore, high-order accurate Runge-Kutta schemes, see J. C. Butcher (Mathematics of Computation, Vol. 18, 50-64, 1964), and discontinuous and continuous Galerkin schemes, see T.J.R. Hughes and G.M. Hulbert (Computer Methods in Applied Mechanics and Engineering, 339-363, 1988), T. Gleim (Universität Kassel, Ph.D. Thesis, 2016), with a controllable order of accuracy are investigated. Representative examples demonstrate the numerical properties, advantages and disadvantages of the studied integration schemes.

Design and Optimization of Tubular Chassis for a Competition Vehicle

Dany Godinez*, Fernando Velazquez**

*Unam, **Unam

ABSTRACT

This research is about the use of topology optimization method applying in a chassis design for student's competitions but not limited to this; it can apply in small commercial vehicles which are based in tubular chassis. The initial body is modeled using plane surfaces, which are modified via topological optimization to define the best material distribution in the body, which satisfies the needs of the competition. Some surfaces are restricted as no design surfaces to keep critical parts of the structure. It has been proposed four load cases assuming of chassis behavior along the road and considering dynamical load factors. The optimization objective is to maximize structural stiffness, while volume is reduced until 10% of the original volume. Symmetry and thickness of the optimized surfaces are controlled, looking for well-defined geometries instead of ambiguous material paths. After this a tubular structure is designed using the optimal structure as guide. Finally, the new structure is evaluated via FEA to verify its performance.

Adjoint Topology Optimization of Mold Cavity Cooling Channels

Stephan Goeke^{*}, Olaf Wunsch^{**}

^{*}University of Kassel, ^{**}University of Kassel

ABSTRACT

Many industrial tools, like mold cavities, need internal channels with cooling fluids to remove excess heat. The achievable temperature change, or the amount of heat that can be removed, depend on several factors. The geometric influence to the performance consists on the one hand on their relative position to the surface under thermal load and on the other on the overall shape of the cooling channels. The performance of the shape does depend on contributions from both conduction and convection. Fluid flow and heat transfer in the solid must hence be solved in a coupled fashion to ensure the local fluid flow is accurately incorporated into the optimization. The aim of this contribution is to showcase a method to apply topology optimization to this problem. The optimality is gauged by a uniformity objective function for the temperature at a surface heated by a constant heat flux. A uniform surface temperature leads to a prolonged tool life since thermal stresses due to temperature differences are minimized. Due to the complex conjugate system a gradient based approach in form of the continuous adjoint method is chosen and implemented into the Software OpenFOAM. The adjoint equations for topology optimization of conjugate heat transfer systems are shown and the resulting gradients validated for both modes of transport. A level-set is used to differentiate between the different regions. The method is illustrated for pure conduction problems of filling a design space with two materials of different thermal properties. In addition the combination with fluid flow and the resulting convection dominated heat transfer system is analysed. Here the optimization highly depends on the treatment of the pressure loss. Different methods for handling this multi objective optimization problem are presented. Karpouzas, Georgios & De Villiers, Eugene. (2014). Level-Set based Topology Optimization using the Continuous Adjoint Method. OPT-i 2014 - 1st International Conference on Engineering and Applied Sciences Optimization, Proceedings.

From Macroscale to Microscale: Inferring 3D Model Parameter Distribution Using Digital Cameras and Inverse Algorithms

Sevan Goenezen^{*}, Yue Mei^{**}

^{*}Texas A&M; University, Mechanical Engineering Department, College Station, TX, ^{**}Texas A&M; University, Mechanical Engineering Department, College Station, TX

ABSTRACT

Additive manufacturing has recently regained attention and benefits from dramatic increases in computational resources and performance that was not available in its early developmental stages. In this presentation, we will make use of supercomputing resources to solve inverse problems in elasticity, and in particular to solve for model parameter variability throughout the sample that are likely to occur in additive manufacturing. In the first part of the talk, we will focus on macro-scale mechanics at scales ranging from orders of millimeters to meters. We will show for the first time that it is feasible to infer information about the interior model parameter distribution in three dimensional space for a given constitutive model, knowing solely displacements on the surface of the specimen. No assumptions will be made about the interior of the specimen and the model parameters will be assumed to be unknowns on the finite element mesh nodes and linearly interpolated throughout the domain using tetrahedral finite elements. Our problem domain will have several hundreds of thousands of unknown model parameters. The inverse problem is posed as a constrained minimization problem, where measured displacement data is correlated to computed surface displacement data under the influence of a regularization term that stabilizes the model parameter distribution due to measurement noise. The computed displacement data depends on the model parameter distribution and satisfies the equations of equilibrium, solved using in-house written finite element methods. Despite of the fact that the minimization problem is solved using an adjoint scheme that reduces computational cost drastically, OpenMP platforms together with MPI computations are introduced in an effective approach to obtain computational results in a reasonable time. Surface displacements can be conveniently determined from digital image correlation or other optical techniques using regular digital cameras. Knowing the model parameters will provide information about the additive manufacturing process and help optimize process parameters. In the second part of this talk, we will analyze feasibility to recover the crystallographic orientation of grains and their anisotropic mechanical property distribution using displacement fields obtained from digital camera images.

A Linear Solver Framework for Oil Reservoir Simulation

Paulo Goldfeld^{*}, Douglas Augusto^{**}, Luiz Carvalho^{***}, Cesar Conopoima^{****}, Leonardo Gasparini^{*****}, José Rodrigues^{*****}, Michael Souza^{*****}

^{*}UFRJ, ^{**}Fiocruz, ^{***}UERJ, ^{****}UFJF, ^{*****}Petrobras, ^{*****}Petrobras, ^{*****}UFC

ABSTRACT

As with many other applications, the need for high-performance computing in Oil Reservoir Simulation is driven by ever more refined meshes and by the necessity of multiple simulations in the context of optimization and/or uncertainty quantification. The single most costly computational task and the most difficult one to parallelize is the solution of the large linear systems arising in the Newton iteration at each time step. Despite the large selection of freely available parallel linear solvers, we found that reservoir simulation software presents enough specificities as to justify the development of a dedicated solver. One such example is a block matrix format that allows for non-homogeneous block sizes. Such a matrix arises, for instance, when using AIM (adaptive implicit method), and is not supported by standard libraries such as PETSc or Trilinos. As design baselines, we opted for hybrid MPI/OpenMP parallelism and our plan, as future developments, is to use OpenACC to take advantage of accelerators. Another interesting feature of our software is a framework for the implementation of parallel algorithms using data flow concepts, which hides much of the complexity related with communication. We will present some key aspects of the solver development and discuss numerical results obtained with matrices from real simulations of multiphase flow and geomechanics, focusing on performance and scalability.

Finite Element Modeling of Micropolar Based Phononic Crystals

Juan Gomez^{*}, Gary Dargush^{**}, Ali R. Hadjesfandiari^{***}, Nicolás Guarín-Zapata^{****}

^{*}Universidad EAFIT, ^{**}The State University of New York at Buffalo, ^{***}The State University of New York at Buffalo,
^{****}Universidad EAFIT

ABSTRACT

We address numerical simulation aspects of dispersive periodic media, where dispersion is introduced by micro-scattering effects. Instead of explicitly modeling the micro-scatters into the unit cell we make use of a micropolar (Cosserat) continuum with independent micro-rotational degrees of freedom directly translating into additional wave modes responsible for the dispersive response. We formulate—in a finite element sense— a wave propagation problem for the micropolar media and determine the dispersion relationships for a unit cell. This characterization is possible after assuming spatial periodicity and studying a single cell with the aid of Bloch-Floquet theorem to impose suitable boundary conditions at extreme faces of the cell. The resulting implementation is later used to find the dispersion curves for homogeneous and porous micro-polar solids. The introduction of kinematic variables and in particular, the addition of micro-rotations, results in additional propagation modes in the form of micro-rotational waves. At the same time, the micro-rotations also cause classical shear waves to propagate dispersively and to couple with the new micro-rotational waves. In this talk we focus in simulation aspects related to wave propagation problems in such a periodic micro-polar medium. First we derive general finite element equilibrium equations yielding discrete equilibrium relations for forces and moments. The general formulation is then implemented to address micropolar cellular materials making use of the theory of phononic crystals. Our presentation is organized as follows: - Fundamentals of Bloch analysis in periodic media. - Review of the micropolar model. - Bloch analysis for the micropolar model. - Results: numerically obtained dispersion curves for several microstructures. The study of wave propagation and dispersion relations for phononic crystals where the constituents are Cosserat solids is of interest in the study of cloaking elastodynamics. While the equations are invariant for electromagnetic waves , it has been shown that in the case of elastic bodies the equations are not invariant. Additional requirements, related with micro rotations, exist in this case, and the equations that satisfy the invariance are termed Willis equations. These can be expressed as Cosserat elasticity under some assumptions.

A Reduced Order Approach to Augmented and Mixed Reality

David González*, Alberto Badías**, Iciar Alfaro***, Francisco Chinesta****, Elías Cueto*****

*I3A, Universidad de Zaragoza, Zaragoza, Spain, **I3A, Universidad de Zaragoza, Zaragoza, Spain, ***I3A, Universidad de Zaragoza, Zaragoza, Spain, ****ESI Chair at ENSAM ParisTech, Paris, France, *****I3A, Universidad de Zaragoza, Zaragoza, Spain

ABSTRACT

In this work we explore the possibilities of reduced order modeling for augmented reality applications. We consider parametric reduced order models based upon separate (affine) parametric dependence so as to speedup the associated data assimilation problems, which involve in a natural manner the minimization of a distance functional. The employ of reduced order methods allows for an important reduction in computational cost, thus allowing to comply with the stringent real time constraints of video streams, i.e., around 30 Hz. Examples are included that show the potential of the proposed technique in different situations.

Variational Derivation of Reciprocal Mass Matrices for Isogeometrical Analysis via Localized Lagrange Multipliers

José A. González^{*}, K. C. Park^{**}, Ján Kopacka^{***}, Radek Kolman^{****}, Sang-Soon Cho^{*****}

^{*}Universidad de Sevilla, ^{**}University of Colorado Boulder, ^{***}Institute of Thermomechanics, Czech Academy of Sciences, ^{****}Institute of Thermomechanics, Czech Academy of Sciences, ^{*****}Korea Atomic Energy Research Institute

ABSTRACT

The authors proposed in a previous work [1] a variationally consistent method for the derivation of reciprocal mass matrices for FEM formulations in structural dynamics. The approximation was based on a judicious combination of the variational form of Hamilton's principle with a parametrized consistent-lumped structural mass matrix and the enforcement of interface constraints with localized Lagrange multipliers. High accuracy and efficiency of the obtained reciprocal mass matrices was demonstrated for structural transient and vibration problems. This new contribution constitutes an extension of our previous work to the field of Isogeometrical analysis, adapting the techniques used to derive reciprocal mass matrices in FEM to the particularities of B-spline and NURBS-based methods. In particular, two isogeometric methods are investigated: classical B-spline approximation and Bézier extraction techniques. Furthermore, dispersion analysis is the tool adopted to tune the parametrized reciprocal mass matrices for optimal accuracy. Finally, the reciprocal mass matrices are incorporated into explicit time integration schemes to solve classical benchmark problems and evaluate the efficiency and precision of these new isogeometrical approximations of the inverse mass matrix. References [1] González José A., Kolman R., Cho S. S., Felippa C. A., Park K. C. Inverse Mass Matrix via the Method of Localized Lagrange Multipliers. International Journal for Numerical Methods in Engineering. 2017;113(2):277–295.

Error Indicator for Polygonal Finite Element Meshes in 2D and 3D

Octavio Andrés González-Estrada*, Sundararajan Natarajan**, Juan José Ródenas***

*Universidad Industrial de Santander, **Indian Institute of Technology – Madras, ***Universitat Politècnica de València

ABSTRACT

Introduction: Arbitrary polygonal meshes in finite element approximations provide advantages in terms of meshing flexibility and accuracy, compared to traditional finite element formulations. They relax mesh conditions related to mesh distortion, and easily manage transition elements. However, as any numerical approximation, they exhibit an error which should be controlled in order to validate the numerical results in practical applications. In this work, we present strategies to quantify the discretization error in polygonal meshes, in 2D and 3D, using the Zienkiewicz-Zhu error indicator. Methods: The accuracy of recovery-based error indicators is strongly related to the quality of the recovered stress field used to evaluate the error energy norm. To recover the stress field, we propose different strategies: nodal averaging and moving least squares smoothing. It is also possible to further improve the quality of the recovered stresses by imposing equilibrium conditions. The proposed technique is applicable to smooth and singular problems by means of stress field splitting. Results and conclusions: The error estimator has been tested with smooth and singular problems having exact solution. The results in the 2D and 3D benchmark problems show a highly accurate recovered stress field, with a performance of the indicators comparable to standard finite elements. The convergence of the error indicates that the proposed error indicator is asymptotically exact and can be used to perform h-adaptivity in polygonal meshes. References [1] O. A. González-Estrada, S. Natarajan, and C. Graciano, "Reconstrucción de tensiones para el método de elementos finitos con mallas poligonales," *Rev. UIS Ing.*, vol. 16, no. 1, pp. 23–34, 2017. [2] Y. Jin, O. A. González-Estrada, O. Pierard, and S. P. A. Bordas, "Error-controlled adaptive extended finite element method for 3D linear elastic crack propagation," *Comput. Methods Appl. Mech. Eng.*, vol. 318, pp. 319–348, 2017. [3] O. A. González-Estrada, S. Natarajan, J. J. Ródenas, S. P. A. Bordas, and C. Heaney, "Recovery-Based Error Estimation for the Polygonal Finite Element Method for Smooth and Singular Linear Elasticity," in *11th World Congress on Computational Mechanics*, 2014, no. WCCM XI, pp. 1–2.

Progressive Damage Failure Analysis (PDFA) for Compression Strength After Impact (CSAI) Simulations Using an Enriched Shell Element

Tyler Goode*, Mark McElroy**, Mark Pankow***

*North Carolina State University, **NASA Johnson Space Center, ***North Carolina State University

ABSTRACT

Composites are becoming pervasive in many aerospace and automotive applications for their higher relative performance. One major challenge with using composite materials in these applications is their susceptibility to damage resulting from transverse loads such as low-velocity impact (LVI). Historically, certification of composite parts has relied heavily on experimental testing, but recent advancement in progressive damage failure analysis (PDFA) for composites has demonstrated damage models with suitable accuracy [1]. The major drawback of using these state-of-the-art models is the need for a high-fidelity mesh resulting in excessively long simulation times. To mitigate this problem, a novel shell element enriched with the Floating Node Method (FNM) and a damage algorithm based on the Virtual Crack Closure Technique (VCCT) has been developed that captures complex damage mechanisms such as delamination propagation and transverse matrix cracks while exhibiting runtimes up to two orders of magnitude faster than existing high-fidelity models [2]. In this work we will model the multi-step process of LVI and compression strength after impact (CSAI) using this enriched shell element [2]. The two-step process will be simulated to ensure that the damage is transferred correctly from one step (LVI) to the next (CSAI) correctly. The computational model will be verified and validated against existing computational data by AFRL [3]. The models are investigated for various energies and laminate stacking sequences. Finally, it will be correlated against an existing high-fidelity PDFA model to understand how the response compares in both prediction and in computational time. This work will enable efficient large-scale simulations of full structures with accurate estimations of damage and strength predictions. [1] S. B. Clay and S. P. Engelstad, "Benchmarking of composite progressive damage analysis methods: The background," *J. Compos. Mater.*, vol. 51, no. 10, pp. 1325–1331, 2017. [2] M. W. McElroy, R. Gutkin, and M. Pankow, "Interaction of delaminations and matrix cracks in a CFRP plate, Part II: Simulation using an enriched shell finite element model," *Compos. Part A Appl. Sci. Manuf.*, vol. 103, pp. 252–262, 2017. [3] S. Joglekar, M. Pankow, and V. Ranatunga, "Simulation of BVID and CAI strength of Carbon Fiber Reinforced Composite Laminates," in *Proceedings for the American Society for Composites Technical Conference*, 2016.

Approximating Eigenvalue Clusters Using Filtered Subspace Iterations

Jay Gopalakrishnan^{*}, Luka Grubisic^{**}, Jeffrey Oval^{***}

^{*}Portland State University, ^{**}University of Zagreb, ^{***}Portland State University

ABSTRACT

The FEAST algorithm is a popular eigenvalue solver in numerical linear algebra, known for its multiple layers of parallelism. The algorithm targets a cluster of eigenvalues enclosed within a contour. It can be viewed as a subspace iteration applied to an operator-valued contour integral. When used to approximate a part of the spectrum of an unbounded differential operator, it is typical to discretize the operator. When the algorithm uses the discretized operator, several basic questions arise: Does it converge? If so, does the limit subspace approximate the true eigenspace of the unbounded operator? When a higher order discretization is used, does the error in eigenvalues decrease at correspondingly higher orders? In this talk, we present a framework that allows us to answer these questions. Conclusions are drawn under a resolvent approximation condition. We then verify this assumption for the Discontinuous Petrov Galerkin (DPG) method. The new convergence results will be illustrated through numerical examples.

Some Observations on Parameter Estimation in Strongly Coupled Fluid-Structure Interaction Problems

Peter Goransson^{*}, Jacques Cuenca^{**}, Timo Lahivaara^{***}

^{*}KTH Royal Institute of Technology, ^{**}Siemens Industry Software, ^{***}University of Eastern Finland

ABSTRACT

We study the problem of inverse estimation of model parameters in resonant, acoustic fluid-structure interaction (FSI) problems over a wide frequency range 1-1000 Hz. These problems are subjected to local minima, which represents a major obstacle in the field of parameter identification. The acoustic fluid as well as the solid are modelled using the 1D wave equation, and the parameters used in the estimation are their respective speeds of sound and loss factors. The type of cost functions studied are based on the frequency response, of a field variable or a quantity derived from these. In the current work the L2-norm between a target and a model solution is used, and in order to capture the FSI effects, the power radiated into the acoustic fluid from the vibrating solid is used. The estimation is performed through different methods including gradient based optimisation, Bayesian Markov chain Monte-Carlo, and non-linear least squares. The occurrence and the background of local minima are discussed, and the performance of the different solution methods evaluated for different strengths of the coupling between the solid and the fluid. In addition, the influence of the amount of damping present in the two media will be illustrated. The correlation between different model parameters is analysed and shown how these correlations control the local minima. In the presentation, various approaches to finding the global minimum, i.e. the true model parameters, will be discussed and their effectiveness will be evaluated.

A Fokker-Planck Expansion of Jump Processes

Hossein Gorji*

*MCSS, Mathematics Department, EPF Lausanne

ABSTRACT

The dynamics of a Markovian system can be described in general by jump and diffusion processes. The aim of this talk is to discuss how a jump process governed by the Master equation can be reduced to a Fokker-Planck operator describing a diffusion process, consistently. In particular, we focus on the Fokker-Planck approximation of the Boltzmann equation for a monatomic gas. Therefore in the resulting diffusion process, the state of the particles evolve along continuous stochastic paths. That brings computationally favourable characteristics, since here no collision is performed and thus relatively coarse spatio-temporal resolutions may be employed. In fact, the effect of collisions on the dynamics of the distribution is projected to continuous stochastic forces acting as drift and diffusion. The drift and diffusion coefficients are then closed through the velocity moments of the Boltzmann operator, together with the H-theorem. The convergence of the devised Fokker-Planck approach is studied for the case of the BGK approximation of the Boltzmann equation. Furthermore, practical results for the case of reentry flows together with plume setups are presented.

Multifidelity Model Management Using Latent Variable Bayesian Networks

Alex Gorodetsky^{*}, Gianluca Geraci^{**}, Michael Eldred^{***}, John Jakeman^{****}

^{*}University of Michigan, ^{**}Sandia National Laboratories, ^{***}Sandia National Laboratories, ^{****}Sandia National Laboratories

ABSTRACT

We consider the problem of propagating uncertainty through computational simulation models of varying fidelities. Our goal is to estimate, or predict, certain quantities of interest from a specified high-fidelity model when only a limited number of simulations are available. To aid in this task, lower fidelity models can be used to reduce the uncertainty of the high-fidelity predictions. We propose to frame this problem as learning a latent variable network structure for the statistical independence relationships between the models from available simulation data. First a latent variable model is posed for each simulation model under consideration, then a network structure between the models is learned, and finally predictions are made for the output of the highest fidelity model. We demonstrate how existing techniques, such as control variate Monte Carlo and recursive co-kriging, can be interpreted as particular realizations of this framework. Furthermore, we consider both the tasks of learning the graph structure and parameters of the conditional probability distributions. Finally, we describe an experimental design procedure targeted towards reducing the uncertainty of our predictions. Examples are provided for both synthetic and physics-based simulations.

Effective Control and Computer Simulation of Large-Scale Stochastic Dynamic Systems for Reduction in Probability of Extreme Failures

Kundan Goswami^{*}, Sonjoy Das^{**}, Biswa Nath Datta^{***}

^{*}University at Buffalo, ^{**}University at Buffalo, ^{***}Northern Illinois University

ABSTRACT

Vibrating systems may encounter catastrophic failure due to resonance or flutter induced by time-varying disturbances and loading. To ensure safety and proper functionality, several vibration control techniques are available to mitigate or suppress these phenomena. In this work, an active vibration control (AVC) technique is adopted. The most popular AVC techniques developed in the recent years are the state-space based linear quadratic regulator (LQR) and H-infinity control techniques. These techniques, however, become simply ineffective for large-scale systems. To address this computational bottleneck, the physical-space based robust and minimum norm quadratic partial eigenvalue assignment (RQPEVA and MNQPEVA) techniques are proposed in the literature. In contrast with the most popular state-space based AVC techniques, the RQPEVA and MNQPEVA techniques work exclusively on the second-order model obtained by applying the finite element method on the vibrating systems. Furthermore, the RQPEVA and MNQPEVA techniques suppress only the problematic/resonant modes of vibration and guarantee the no-spillover property of the remaining large number of modes. In this work, a brief review of the LQR, H-infinity, and MNQPEVA techniques, with an emphasis on their relative computational advantages/drawbacks, is presented first. A comparative study of the three control techniques with respect to their computational effectiveness and applicability. Next, comparative study in terms of economic efficiency is presented for three systems: a small-scale (2 degree of freedom), a medium-scale (900 degree of freedom), and a large-scale (1 million degree of freedom), which are representative of various structural systems, and are subjected to a recorded data from the 1986 San Salvador earthquake. It is observed that, for large-scale systems, the MNQPEVA technique is computational more effective and economic as compared to the LQR and H-infinity techniques. In the second part of this work, we consider the effects of uncertainties that are invariably present in practice in the external disturbances and the damped natural frequencies of vibrating structures, especially of large-scale dynamic systems. Based on MNQPEVA technique and an optimization under uncertainty (OUU) scheme, a computationally efficient control methodology for large-scale systems is presented. The proposed scheme will be useful for economic design and to significantly lessen the probability of extreme failures with catastrophic consequences. A novel scheme based on hierarchical clustering and importance sampling is developed for accurate and efficient estimation of the probability of failure which is an essential ingredient in successful implementation of the proposed OUU scheme. A numerical example is included to illustrate the proposed approach.

Statistical Analysis of the Void Structure of Bi₂Sr₂CaCu₂O_x Multifilamentary Superconducting Wires and Its Effect on the Critical Current Density

Xiaofan Gou^{*}, Xinxin Zhou^{**}

^{*}Hohai University, ^{**}HOhai University

ABSTRACT

High temperature multifilamentary composites Bi₂Sr₂CaCu₂O_x/Ag/Ag-alloy (Bi2212) are the only round wires (RWs) for a potential candidate with sufficient critical current density (J_c) for fabricating high field magnet. Very complex microstructures of Bi2212 RWs, especially a large number of voids or gas bubbles in Bi2212 superconducting filaments, is believed to have strong impacts on the current-carrying and thermal diffusion of whole wires. In this article, we first statistically analyzed the size and distribution of voids in filaments using the reported microscopic data, obtaining the essential statistical regularities. An electrical model was further developed to predict the J_c of multifilamentary wires while taking into account of the current limiting mechanisms of the void structure in filaments, and the current sharing roles of filament to filament bridges. Our model predicts the quantitative dependence of J_c on the number of Bi2212 filaments in each bundle of a double-restack wire and porosity. Our results are useful optimizing design and fabrication of Bi2212 multifilamentary wires.

A Research for the Mechanics Characteristics of Bubbles and Mural Face Coupling based on the Lattice Boltzmann Method

Shi Dongyan*, Gou Yuxin[†], Wang Zhikai[‡]

*College of Mechanical and Electrical Engineering, Harbin Engineering University
Harbin, Heilongjiang, China
shidongyan@hrbeu.edu.cn

[†]College of Mechanical and Electrical Engineering, Harbin Engineering University
Harbin, Heilongjiang, China
gouyvxin@gmail.com

[‡] College of Shipbuilding Engineering, Harbin Engineering University
Harbin, Heilongjiang, China
Zhikai.wa@gmail.com

Key words: LBM, Bubbles, Mural Boundary, Interaction

Abstract. *Complex interaction force is produced due to the effect of the coupling between the bubbles and mural face. In this paper, a three dimensional gas-liquid-solid coupling dynamics model is adopted, and the optimized block-grid technology is applied to this model. Based on the viscous fluid theory, the lattice boltzmann equation to describe the movement of gas-liquid is built, at the same time the half-way bounce back model in LBM and the combination of finite difference is adopted to deal with the solid wall boundary. First, verify the correctness of the model using the classical Laplace's law. Then, the coupling characteristics of the single bubble and the solid wall and the surface solid wall are studied respectively. The solid wall boundary condition has obvious law to the surrounding pressure and the velocity field. Then studied Eo and Mo 's impact on the results under the condition of $\gamma = 1.0$.*

1 INTRODUCTION

The interaction between solid wall and bubbles has extensive engineering application background and significance to scientific research. Whether to the studies to the cavitation bubble on the propeller [1, 2], the explosion bubble near the ship [3, 4], and atmospheric pressure air bubble [5] in the piping, all need air bubble in a flow field detailed understanding and grasp of the dynamic characteristics of. Due to this problem involves many and strong nonlinear coupling effect, it becomes the research hotspot and difficulty in related field. Although, there are a lot of experimental studies on bubble dynamics. 1978 Clift [6], such as review of gravity using within the scope of different fluid properties under the buoyancy of the shape of the bubble. Bhaga etc. [7] in 1980 studied the different number of Morton (Mo) and Reynolds number (Re) under the condition of air bubbles in the process of floating shape, drafting and speed of change. Duineveld [8] and Zhang [9] studied through experiments respectively within bubbles and bubbles, and the coupling phenomenon of bubbles and free surface. But limited by the fluid properties the complex dynamics (such as viscosity, surface tension, etc.), it is unable to carry on the accurate control, resulting in many air bubbles under the condition of the research cannot be done through experiment. But it did not stop the footsteps of people continue to explore the bubble movement characteristics, with the development of computational fluid dynamics (CFD), the researchers found that by combining experimental research and numerical study way can solve this problem very well. And with a variety of excellent numerical algorithm is proposed, and the emergence of high performance computer, numerical simulation in the study of dynamics of bubble has played a more and more obvious role. Gas-liquid, gas-solid or liquid-solid research has made many significant achievements, but the study of gas- liquid-solid three phase coupling is relatively less, and mainly focused on the coupling of bubble and infinite solid wall and the coupling effect of bubbles and tiny particles. In 2001, Popinet etc. [15] studied the bubble pulsation and jet near the tablet process. In 2006, Yang, etc. [16] made the review of the coupling of liquid, bubbles, and the particles in the mixed solution. In 2011, Hassan, Amaya and Ghosh, [17-19] studied the single and multiple bubbles movement characteristics under the conditions of the different diameter and Angle of long tube. The two types of research is a common feature of bubble size and the size of the border is not in the same scale, which ignores the boundary and the boundary between the complex coupling phenomenon.

In this paper, using the lattice Boltzmann method based on free energy model, established the viscous flow field in the bubbles with scales coupling model of complicated boundary. To achieve the accuracy of capturing the gas liquid two phase boundary, two groups was introduced to the model in the Boltzmann equation, through multi-scale, which can respectively Navier - Stokes equations of second order accuracy and Cahn Hilliard equation. Rigid boundary flow processing used the previous work [20] of lattice Boltzmann complex boundary processing method. On this basis, this paper studies single bubbles with different characteristics than with boundary and the interaction characteristics of surface boundary edges and corners in the same scales, including velocity field and pressure field

around the bubble. Respectively according to the above two kinds of solid wall boundary, the calculation and analysis of the different fluid properties Mo, Eo condition for coupling characteristics are studied.

2 THEORY

2.1 Governing Equation

Based on viscous fluid mechanics theory, for a Newtonian fluid in constant temperature, and incompressible flow field, the dynamic characteristics of air bubbles can be described through a set of Navier - Stokes (navier-stokes) equations and Cahn Hilliard equation:

$$\partial \rho / \partial t + \nabla \cdot (\rho \mathbf{u}) = 0 \quad (1)$$

$$\partial (\rho \mathbf{u}) / \partial t + \nabla \cdot (\rho \mathbf{u} \mathbf{u}) = -\nabla \cdot P + \mu \nabla^2 \mathbf{u} + \mathbf{F} \quad (2)$$

$$\partial \theta / \partial t + \nabla^2 \cdot (\theta \mathbf{u}) = \varpi \nabla^2 \psi \theta \quad (3)$$

Among them, the first two equations represents the traditional navier-stokes equation and ρ , \mathbf{u} , represent the density of fluid in the flow field velocity vector and fluid viscosity, \mathbf{F} is the body force, including gravity, P for thermodynamic pressure for an ideal system, P_0 can calculate including a state equation:

$$P_0 = \nabla \cdot (\rho c_s^2) \quad (4)$$

In the equation, c_s is the sound velocity of grid, $c_s = 1 / \sqrt{3}$. In the ideal gas system, equation (4) can be revised to:

$$P = P_0 + \theta \nabla \cdot \psi_\theta = \nabla \cdot (\rho c_s^2) + \theta \nabla \cdot \psi_\theta \quad (5)$$

θ is for tracking interface defined by the order parameter, its evolution process, such as equation (3), namely Cahn Hilliard equation, including ϖ is diffusion coefficient. Based on the free energy of lattice Boltzmann model, bits of theta is thickness of border with gas liquid two phase (W), surface tension coefficient (σ), the order parameter (θ), as well as the free energy density function related parameters of the chemical potential^[22]:

$$\psi \theta = \frac{12\sigma\theta^3}{W\theta^{*4}} - \frac{3\sigma}{W\theta^{*2}} (4\theta + \frac{W^2}{2} \nabla^2 \theta) \quad (6)$$

And the $\theta^* = \frac{(\rho_L - \rho_G)}{2}$, ρ_L , ρ_G respectively the density of the liquid and the gas phases.

2.2 Lattice Boltzmann Method

According to Lee, the research into ^[23], LBM can be used to discrete the Navier - Stokes equations :

Shi Dongyan, Gou yuxin and Wang zhikai

$$f_i(\mathbf{x} + \mathbf{c}_i \delta_t, t + \delta_t) = f_i(\mathbf{x}, t) + \frac{1}{\tau_n} (f_i^{(eq)}(\mathbf{x}, t) - f_i(\mathbf{x}, t)) + \mathbf{F} \quad (7)$$

Among them, i said discrete grid direction, this paper adopts D3Q19 model, $i=0-18$. The \mathbf{c}_i , $f_i(\mathbf{x}, t)$ respects discrete grid speed and discrete volume force. Said δt time step, τ_n is relaxation coefficient. $f_i^{(eq)}(\mathbf{x}, t)$ is to meet maxwell distribution. The equilibrium state of the particle distribution function for ideal fluid without considering $f_i(\mathbf{x}, t)$, by choosing suitable $f_i^{(eq)}(\mathbf{x}, t)$, through multi-scale expansion operation, and meet the following constraints [24],

$$\sum_i f_i^{(eq)}(\mathbf{x}, t) = \sum_i f_i(\mathbf{x}, t) = \rho \quad (8)$$

$$\sum_i f_i^{(eq)}(\mathbf{x}, t) \mathbf{c}_i = \sum_i f_i(\mathbf{x}, t) \mathbf{c}_i = \rho \mathbf{u} \quad (9)$$

$$\sum_i f_i^{(eq)}(\mathbf{x}, t) \mathbf{c}_{i\alpha} \mathbf{c}_{i\beta} = (\theta \psi_\theta + c_s^2 \rho) \delta_{\alpha\beta} + \rho \mathbf{u}_\alpha \mathbf{u}_\beta \quad (10)$$

By (8) can meet the second-order precision degree to [25] the navier-stokes equations,

$$f_i^{(eq)} = \omega_i \cdot \left[\frac{P_0}{c_s^2} + \rho \left(\frac{\mathbf{c}_i \cdot \mathbf{u}}{c_s^2} + \frac{(\mathbf{c}_i \cdot \mathbf{u})^2}{2c_s^4} \right) - \frac{\mathbf{u}^2}{2c_s^2} \right] \quad (11)$$

Among them, the ω_i is the weight coefficient of particle distribution along the direction of discrete grid, $\omega_0 = 1/3, \omega_{1,6} = 1/18, \omega_{7,18} = 1/36$. P_0 can be obtained by (4). For gas liquid two phase flow system, due to considering the effect of boundary effect, Shu [22, 24] to (11) on the right side of the first revised and perfected. If $\omega_i \cdot \frac{P_0}{c_s^2} = \omega_i \cdot A_i$, is for the revised A_i ,

$$A_0 = 3\rho(1 - 2c_s^2) - 6\theta\psi_\theta \quad (12)$$

$$A_{1,18} = 3(\theta\psi_\theta + c_s^2 \rho) \quad (13)$$

3 MODEL

In this paper, the implementation of the process, the gas-liquid-solid system is divided into gas-liquid gas boundary and solid-liquid boundary of these two subsystems. Unified the lattice Boltzmann unit system, namely the $\delta_t = 1, \delta_l = 1$.

3.1 Solid-Liquid Boundary

Boundary processing method based on rebound has second order accuracy of model,

building a virtual boundary layer in the fluid-structure interaction. Combined with shi' extrapolation method get accurate macroscopic velocity on the virtual boundary. In this method, fluid particles near the border of rebound in the virtual boundary. And formula system of speed is no longer used by the actual speed of the solid wall boundary, it is the speed of the virtual boundary. In this way, it can ensure that the occurrence of collision point with the speed to collect in the same position.

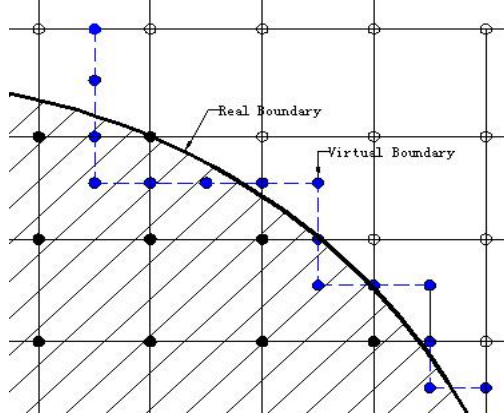


Figure1-the sketch of the curved boundary condition

In this model, the border of fluid particles specific migration process is shown in Figure 1. In Figure 1 heavy line is the location of the actual solid wall boundary, in the connection of 1/2 in virtual node structure, in turn, connect the virtual node, constitute the virtual boundary in Figure 1.

$$f_i(\mathbf{x}_f, t + \delta_t) = f_i^{(eq)}(\mathbf{x}_f, t) - 6\omega_i \rho(c_i \cdot \mathbf{u}_{mid}) \quad (14)$$

\mathbf{x}_f is closest to the solid wall of the fluid particle position, i for direction in the opposite direction of \mathbf{I} , it indicates that the rebound in the aftermath of the particles collide with the wall. \mathbf{u}_{mid} said \mathbf{x}_f with its most adjacent solid particle position \mathbf{x}_s connection speed of the center.

3.2 Gas-Liquid Boundary

By building another set of lattice Boltzmann equation can be solved by Cahn Hilliard equation, tracked the gas-liquid boundary. Compared with the traditional sense of the structure of the lattice Boltzmann equation, namely, regardless of volume force (7), in 2002, Succi etc. [27] put forward a consideration of particle transfer efficiency between adjacent lattice fixed format.

$$g_i(\mathbf{x} + c_i \delta_t, t + \delta_t) = q \cdot g_i(\mathbf{x}, t) + (1 - q) \cdot g_i(\mathbf{x} + c_i \delta_t, t) + \frac{g_i^{(eq)}(\mathbf{x}, t) - g_i(\mathbf{x}, t)}{\tau_\theta} \quad (15)$$

Shi Dongyan, Gou yuxin and Wang zhikai

Among them, the $g_i(\mathbf{x}, t)$ also said the particle number density distribution function, and $f_i(x, t)$, at the same time the macroscopic variables of the order parameter theta. Tau theta is the coefficient of relaxation in the lattice Boltzmann equation, q is control of particle transfer efficiency between lattice parameters. $q = \frac{2}{1 + 2\tau_\theta}$

When $q = 1$, (14) can be converted into traditional lattice Boltzmann equation.

4 RESULTS AND DISCUSSION

4.1 Veritfy the model

First of all, using classical Laplace's law to verify the correctness of the bubble dynamics model is established in this paper. For the unified description of fluid properties, this paper defines three dimensionless parameters of Eo and Mo, Re [22].

$$Eo = \frac{4g(\rho_L - \rho_G)R^2}{\sigma} \quad (16)$$

$$Mo = \frac{g(\rho_L - \rho_G)\mu_L^4}{\rho_L^2\sigma^3} \quad (17)$$

$$Re = \frac{2\rho_L V_{end} R}{\mu_L} \quad (18)$$

μ_L is the liquid viscosity coefficient, R is bubble radius, V_{end} is the ultimate speed of floatation bubble is smooth, the other parameters to ensure consistent with defined on.

Relevant calculation parameters for: computational domain size is $120 * 120 * 120$, bubble radius $R = 20$, $\tau_\rho = 0.6$, $\tau_\theta = 0.75$, the gas bubble wall thickness $W = 5.0$, $\Gamma = 100$, $Eo = 15.984$, $Mo = 0.03083$. According to the law of Laplace, balance when the surface tension and the internal and external pressure difference of bubble:

$$\Delta P = |P_{in} - P_{out}| = \frac{2\sigma}{R} \quad (19)$$

Shi Dongyan, Gou yuxin and Wang zhikai

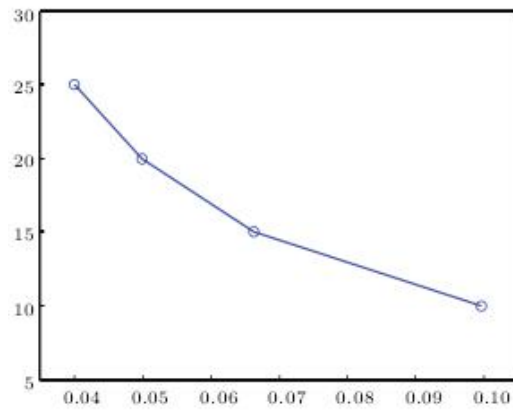


Fig.2 Under the condition of different Mo , numerical validation of the pressure difference inside and outside ΔP and R

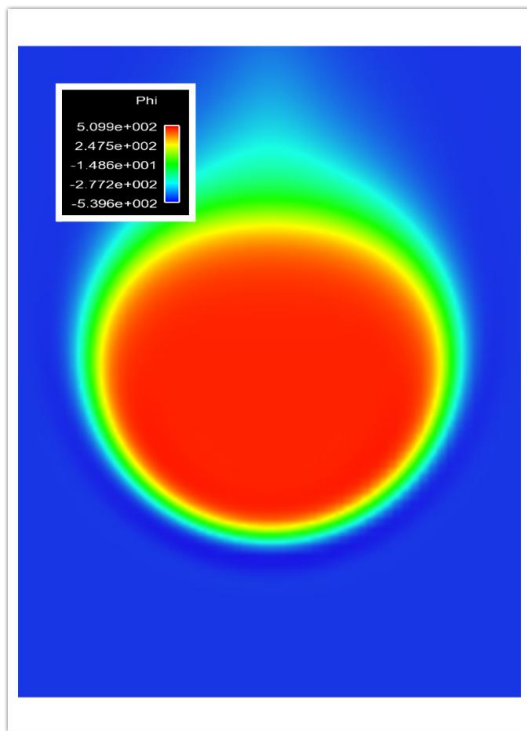


Fig.3 the density for the rising bubble

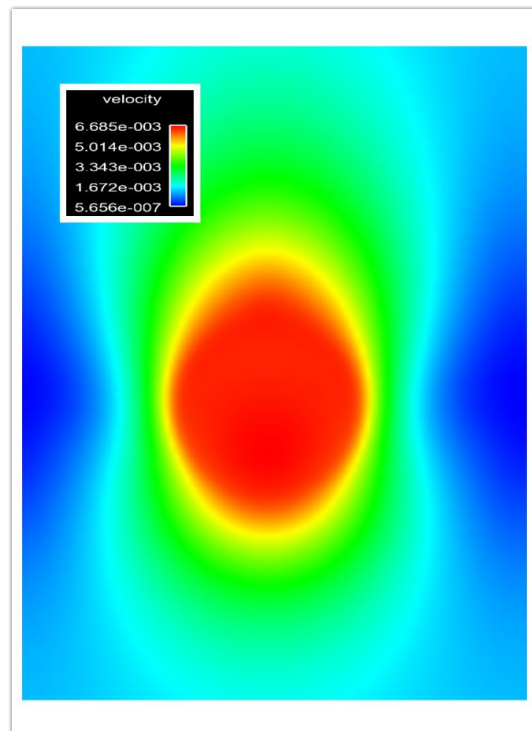


Fig.4 the velocity for the rising bubble

To verify this model is matched with the theoretical value, the paper respectively simulation experiment under the condition of the $Eo = 15.984$, $R = 10, 15, 20, 25$, the corresponding $Mo = 0.1973, 0.0877, 0.0493, 0.0316$ when bubbles as the pressure difference between the inside and outside the ΔP , as shown in figure 2. Can be found from the figure 2, measurements from this model were in good with the theoretical value, further verified the model's ability to capture gas-liquid boundary.

4.2 The interaction between the boundary and the bubble

In the process of calculainfluence on the results, and then, studied, Eo and Mo 's impact on the results under the condition of $\gamma=1.0$.

Figure 5 records the bubbles in the jet flow field around throughout throughout $t = 30000$ steps before and after $t = 40000$ steps two typical moments of stress field distribution. The black thick lines in the graph said bubble contour line in the cross section. In figure 5 (a) can be clearly observed that the bubble is formed between the solid wall of high pressure water cavity, and due to drainage phenomenon on the edge of the bubble formation of the low pressure area. Figure 5 (b) not only shows the jet through after the initial stage of the flow field of pressure distribution and the gradient direction, and can be observed after the reconstruction of smooth surface bubbles.

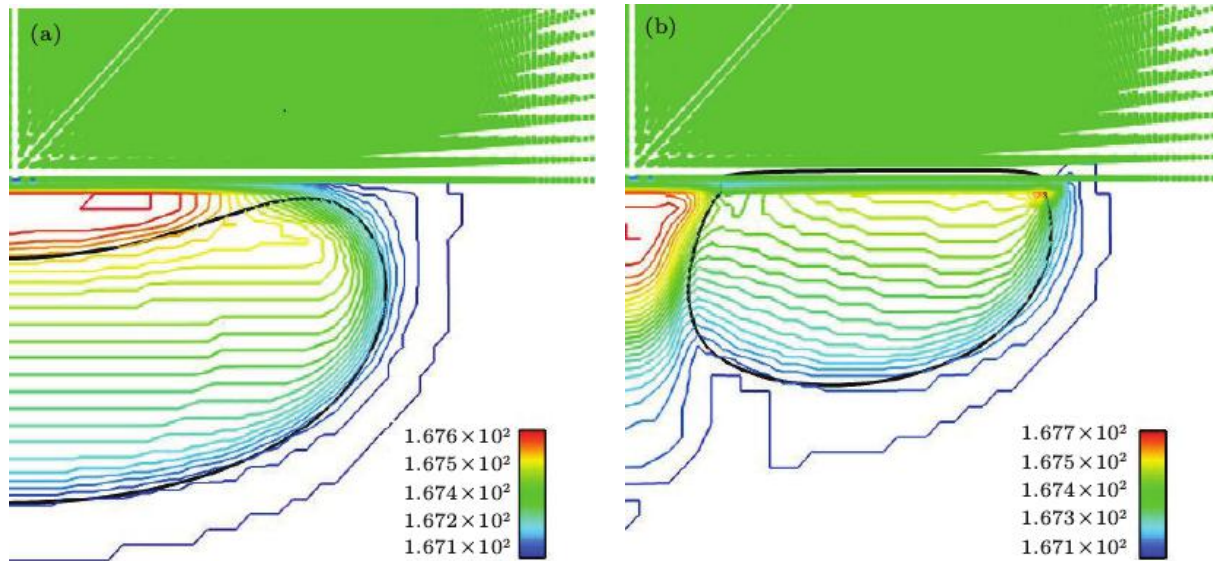


Figure5 (a) the pressure profile Bubble around flow field Bubble ($t=30000$ steps)

Figure5 (b) the pressure profile Bubble around flow field Bubble ($t=40000$ steps)

Figure 6 records the stress field distribution surrounding bubble ,the before and the after from being the circular bubble. The heavy line said bubble contour lines, thin lines for pressure equipotential line, the cloud picture for stress nephogram.From figure 6 (a) that can be observed in the bubbles on the surface to form a high, at the edge of the high produce obvious phenomenon of pressure drop, this is mainly due to the water cavity fluid in the outside, and cause the local pressure drop. On both sides of the bubble below the partial form symmetrical low pressure area, this is mainly due to the buoyancy bubbles driven flow field around the movement caused by the formation of the vortex ring [7].From figure 6 (b), the formation of circular bubble around the floating process of the spherical structure, the inside of the solid wall adjacent position relative to other higher pressure. The existence of the pressure on the one hand, will squeeze the bubble inside, cause its flat, on the other hand caused the increase of bubble ring inside diameter on the ways to level, ensure the bubble ring would be able to bypass the spherical structure.

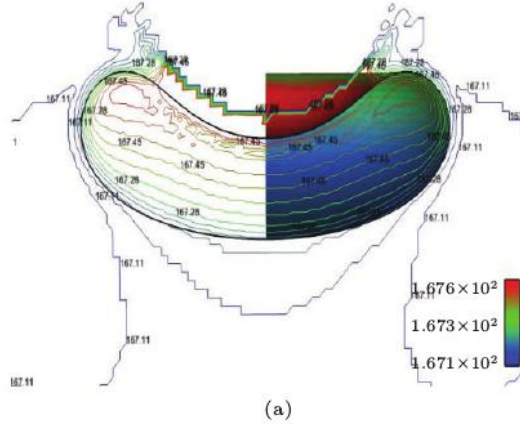


Figure6 (a) bubble surrounding pressure field distribution, before and after a circular bubble (t=15000steps)

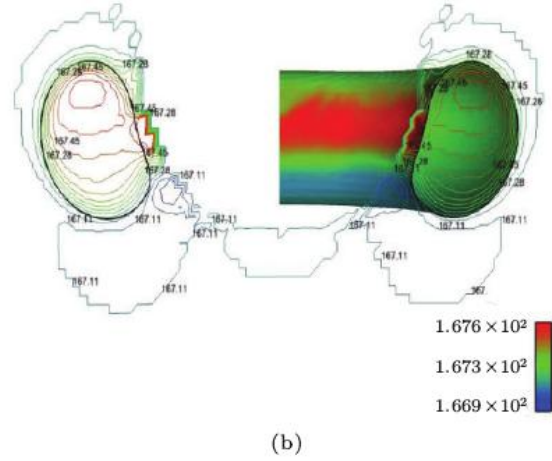


Figure6 (b) bubble surrounding pressure field distribution, before and after a circular bubble (t=20000steps)

4.3 The influence of Mo , Eo

In order to further study the effects of fluid properties on coupling rule, keep the feature sizes than $\gamma = 1.0$, $\rho_L = 1000.0$, $\rho_G = 1.0$, $\tau_\theta = 0.75$, the section to calculate the different Eo , Mo under the condition of air bubbles movement characteristics, specific parameter values are shown in table 1.

Table1 Fluid property parameter values

τ_θ	τ_n	σ	Mo	EO
0.75	0.7	2.0	0.49328	15.985
	0.75	2.0	1.20237	15.985
	0.8	2.0	2.49723	15.985
	0.61892	1.0	0.49328	31.970
	0.64865	1.0	1.20237	31.970
	0.67838	1.0	2.49723	31.970

5 DISSION

- -Based on the early stage of the solid boundary, gas-liquid convection boundary treatment, on the basis of the lattice Boltzmann research will be improved model of gas liquid two phase flow of 2 d to 3 d, and combined with complicated boundary grid Boltzmann processing method, studies the same scales bubbles with considering the effect of edge plane and solid wall surface coupling properties of the solid wall.
- -In feature sizes than certain cases, the surface tension coefficient and fluid property parameters on the coupling process between bubble and curved wall also has an important influence.
- -More research about the multi-bubbles need to be studied.

Acknowledgement

This paper is funded by the International Exchange Program of Harbin Engineering University for Innovation-oriented Talents Cultivation.

REFERENCES

- [1] Chen X P, Zhong C W, Yuan X L 2011 Comput. Math.Appl. 61 3577
- [2] Ji B, Luo X W, Wu Y L, Xu H Y 2012 Chin. Phys. Lett.29 076401
- [3] Liu Y L, Zhang A M, Wang S P, Tian Z L 2012 ActaPhys. Sin. 61 224702 (in Chinese)
- [4] Zhang A M, Yang W S, Huang C, Ming F R 2012 Com-put. Fluids 71 169
- [5] Fujiwara A, Minato D, Hishida K 2004 Int. J. Heat Fluid Fl. 25 481
- [6] Clift R, Grace J R, Weber M E 2005 Bubbles, drops, and particles (1st Ed.) (New York: Academic Press) p23
- [7] Bhaga D, Weber M E 1980 J. Fluid Mech. 105 61
- [8] Duineveld P C 1998 Appl. Sci. Res. 58 409
- [9] Zhang A M, Yao X L, Feng L H 2009 Ocean Eng. 36295
- [10] Zhang A M, Yao X L 2008 Chinese Phys. B 17 0927

Shi Dongyan, Gou yuxin and Wang zhikai

- [11] Unverdi S O, Tryggvason G 1992 J. Comput. Phys. 10025
- [12] Takahira H, Horiuchi T, Banerjee S 2004 J. Fluid Eng. 126 578
- [13] Yu Z, Yang H, Fan L S 2011 Chem. Eng. Sci. 66 3441
- [14] Delnoij E, Kuipers J A M, Swaaij W P M 1998 Third International Conference on Multiphase Flow Lydon, France, June 8–12
- [15] Popinet S, Zaleski S 2002 J. Fluid Mech. 464 137
- [16] Yang G Q, Du B, Fan L S 2007 Chem. Eng. Sci. 62 2
- [17] Hassan Y A, Ortiz-Villafuerte J, Schmidl W D 2001 Int.J. Multiphas. Flow 21 817
- [18] Amaya B L, Lee T 2011 Chem. Eng. Sci. 66 935
- [19] Ghosh S, Patil P, Mishra S C, Das A K, Das P K 2012 Eng. Appl. Comp. Fluid 6 383174701
- [20] Shi D Y, Wang Z K, Zhang A M 2014 Acta Phys. Sin.
- [21] Jacqmin D 1999 J. Comput. Phys. 155 96
- [22] Zheng H W, Shu C, Chew Y T 2006 J. Comput. Phys. 218 353
- [23] Lee T, Lin C L 2005 J. Comput. Phys. 206 16
- [24] Huang H B, Zheng H W, Lu X Y, Shu C 2010 Int. J. Numer. Meth. Fl. 63 1193
- [25] He X Y, Luo L S 1997 J. Stat. Phys. 88 927
- [26] Guo Z L, Zheng C G, Shi B C 2002 Phys. Rev. E 65 046308
- [27] Lamura A, Succi S 2003 Int. J. Mod. Phys. B 17 145

Nonlinear Simulations and Global Stability Analysis for Fluid-Structure Interaction, With Application to Flag Flapping

Andres Goza^{*}, Tim Colonius^{**}, Erick Salcedo^{***}, Phillipé Tosi^{****}

^{*}Princeton University, ^{**}California Institute of Technology, ^{***}California institute of Technology, ^{****}California Institute of Technology

ABSTRACT

Immersed boundary and interface methods do not require fluid meshes that conform to the structural domain, and are therefore promising candidates for simulating fluid-structure interaction (FSI) problems where the structure has a non-canonical geometry or is undergoing large-amplitude motion. These methods lead to a large nonlinear system of equations to enforce the fluid-structure coupling. These nonlinear equations are typically solved iteratively with either a block Gauss-Seidel procedure or a Newton-Raphson method, and there are challenges to implementing either approach efficiently: the former leads to inexpensive evaluation of a single iteration but can require dozens of iterations to converge, whereas the latter converges in a small number of iterations but has a large cost per iteration. We discuss an immersed-boundary (IB) method that inherits the fast convergence behavior of a Newton-Raphson method while retaining the small computational complexity of a block Gauss-Seidel procedure. This IB method is strongly coupled, and accounts for nonlinearities in the fluid, the structure, and the coupling between them. We also describe a global linear stability solver for FSI systems. Whereas global stability techniques are frequently used to deduce instability-driving mechanisms in fluid flows involving rigid stationary bodies, their use in FSI systems is less pervasive due to the challenges in addressing the multi-physics nature of these systems. Our global stability solver accounts for the fluid, the structure, and the coupling between them, and can therefore be used to understand physical mechanisms of the fully-coupled system. Finally, we use these numerical methods to study flapping-flag FSI systems that are promising candidates for flow energy harvesting. Compared with the conventional flag system in which the flag is placed in an unconfined flow and pinned or clamped at its leading edge, systems where the flag is either confined or where the boundary condition is placed on the trailing edge can exhibit larger flapping amplitudes and therefore generate more power. We explore the dynamics and energy conversion in these devices using the aforementioned numerical techniques.

Simulation of Gear-excited Vibrations in Wind Turbine Drivetrains with a Hybrid Numerical-Analytical Approach

Thomas Graetsch*, Frank Ihlenburg**, Marc Zarnekow***

*Hamburg University of Applied Sciences, **Hamburg University of Applied Sciences, ***Hamburg University of Applied Sciences

ABSTRACT

Gear vibrations due to varying mesh stiffness are a major source of tonal noise radiated from wind turbines. We present a hybrid approach for gear modeling that combines a detailed finite element analysis of meshing configurations with analytical models for the transient dynamics of helical gears. In a first step, the angle-dependent mesh stiffness of the gears is obtained from a sequence of static FE analyses that cover a complete meshing cycle. A comparison with results from the literature shows excellent agreement for spur gears. We also present numerical results for helical gears which so far have not been extensively studied. The results from the FE analyses are then used in the second step of the hybrid approach, where the transient dynamics of the gear system are simulated using two different analytical models. The first model describes the gears as rigid bodies with two rotational degrees of freedom. The bodies are connected via a linear spring-damper. An ordinary differential equation (ODE) of second order is obtained for the calculation of the commonly used Transmission Error (TE). The second model includes also the radial displacement along the line-of-action of the gears, which in turn can be used for the calculation of the dynamic bearing forces. The analytical models are solved numerically with a Runge-Kutta scheme. The frequency spectra of the dynamic gear vibration are obtained from the transient simulation by standard FFT. The hybrid approach was applied to the analysis of a wind turbine gearbox. The calculated TE frequency spectrum is in sound qualitative agreement with frequency response graphs of noise radiation, as obtained from acoustic field measurements. Over an analysis spectrum of several KHz, the peak frequencies in both spectra are matching exactly, while the deviation in peak amplitude characteristics is less than 5%. It can be concluded that the hybrid approach predicts well the gear vibration excitation of drivetrains, both for spur and helical gear configurations. We will also present numerical results for submodels of the drivetrain that are obtained by integrating the simulation of parameter-excited gear box vibrations into the vibroacoustic FE analysis of several drivetrain components. As the hybrid excitation model shall be used ultimately in large-scale computational analyses of complete drivetrains, reduction methods are employed that shall allow the FE analysis of large models in reasonable runtime.

Structural Dynamics and Design with Polymorphic Uncertain Data

Wolfgang Graf*

*TU Dresden

ABSTRACT

The analysis and design of structures is one of the major tasks for structural engineers [1]. The objectives of numerical analysis and design, computing robust and reliable structures, can be realized by means of analyzing different variants, application of optimization tasks, or solving inverse problems. The method of choice depends on the aim of design and the problem. But common for all is that the uncertainty of the input parameters (design parameters and other parameters) has to be taken into account, in order to investigate a realistic computational model. Numerical structural design should be robust with respect to the polymorphic nature and characteristic of the available information. Uncertainties are inherently present in resistance of structural materials, environmental and man-imposed loads, boundary conditions, physical and numerical models, and to other types of intrinsic and epistemic uncertainties. Generally, the availability of information in engineering practice is limited. Incomplete, fragmentary, diffuse, and frequently expert specified knowledge leads to imprecision in data [2]. In addition, engineers have to cope with the objective variability and fluctuations in material, geometry and loading. This contribution presents approaches for design tasks analysed with optimization or solving the inverse problem. The advantages and disadvantages of each concept are pointed out. The solution of the inverse problem, suitable in early design stages to detect permissible design spaces is one of the main points of this contribution [3]. Especially for early design stages it's necessary to take polymorphic uncertainty into account due to a lack in information. This incorporation yields to increasing numerical effort. One possibility to solve the design task in appropriate time is to apply surrogate models. This surrogate model generates a meta-model to reproduce the deterministic objective function. In this contribution, the improvement in efficiency is demonstrated by the sophisticated meta-model, Extreme Learning Machine. The applicability of the different approaches is demonstrated by means of engineering examples. References [1] Beck, J.; Graf, W.; Soize, C. (guest editors) Computational Intelligence in Structural Engineering and Mechanics, Internat. Journal of Computer-Aided Civil and Infrastructure Engineering (CACIE), special issue Vol. 30 (2015), Issue 5 [2] Graf, W.; Götz, M.; Kaliske, M. Analysis of dynamical processes under consideration of polymorphic uncertainty, Structural Safety, Vol. 52 Part B (2015), pp. 194-201 [3] Graf, W.; Götz, M.; Kaliske, M. Computing permissible design spaces under consideration of functional responses, Advances in Engineering Software (2017), online available

A Multiscale Model to Analyze the Cost of Force Production in Skeletal Muscle Tissue

Jorge Grasa*, Silvia Blemker**

*Universidad de Zaragoza, **University of Virginia

ABSTRACT

The estimation of the total energy (thermal plus mechanical) liberated during a determined activity would be useful for a more complete understanding of the energetics of human movement [1]. In this work, a new multi-scale model is proposed to evaluate the energy release rate of skeletal muscle tissue in 3D models during active contractions. This model is based on the finite element method where the cross-bridge dynamics and the total rate of energy production is considered in the material constitutive law. The shortening/lengthening velocity of the sliding filaments allows determining the liberation of heat using a classic approximation [2]. The formulation was implemented into a hyperelastic transversally isotropic constitutive model as a user dynamic library in FEBio software [3]. The computational model predicts the heat liberation rate of the tissue and other mechanical variables such as stresses and strains under different active contraction conditions. Considering this novel approach, concepts like cost of force production and efficiency can be analysed in the model not only for the global tissue but also for different specific regions. The results provided by the model have been validated according to different outcomes obtained from the literature [4] that involve in vitro experimental tests of muscles subjected to different imposed strain and stimulation patterns. The computational tool developed can provide more insights into the form and function of muscles that could help for improving clinical treatments in related diseases. References 1. B. R. Umberger, K. G. Gerritsen and P. E. Martin. A model of human muscle energy expenditure. *Comput. Methods. Biomech. Biomed. Engin.* 6(2), 99-111, 2003. 2. A. F. Huxley. Muscle structure and theories of contraction, *Prog. Biophys. Biophys. Chem.* 7, 255-318, 1957. 3. S. A. Maas, B. J. Ellis, G. A. Ateshian and J. A. Weiss. "FEBio: Finite elements for biomechanics", *J. Biomech. Eng.* 134(1):011005 (2012) 4. N. C. Holt, T. J. Roberts and G. N. Askew, The energetic benefits of tendon springs in running: is the reduction of muscle work important? *J. Exp. Biol.*, 217, 4365-4371, 2014.

A NOVEL UNCERTAINTY ACOUSTIC MODEL FOR AUTONOMOUS ROBOTICS USING CLUSTERING TECHNIQUES

M. MANZANARES, Y. BOLEA AND A. GRAU

Technical University of Catalonia
Pau Gargallo, 5, 08028 Barcelona
Email: antoni.grau@upc.edu

Key words: LPV modeling, indoor robot localization, audio, sewage system.

Abstract. The objective of the design of novel simplified acoustic model is to use it in order to locate autonomous robots in industrial environments. The acoustics of an industrial space is characterized by a non-linear dynamic. So far, in this kind of applications and for the sake of simplicity all the models are linear and this fact does not allow a suitable and accurate use. To consider all the information of the room and an improvement in the robot location a linear acoustic model with uncertainty is proposed in this research. The new contributed model is obtained by the convergence of existing methods, that is, between statistical models and the classical (and complex) wave model. Audio analysis requires the treatment of a huge amount of data which, obviously, cannot be achieved for real-time purposes. Therefore, the working range of frequencies are around Schroeder frequencies and a limited number of modes is selected using a suitable filter. This innovative model has been validated with real data through significant experiments in different rooms with an autonomous robot.

1. INTRODUCTION

Indoor robot localization is an important issue in the field of robotics. So far, usually for this purpose overall odometer, camera, infrared sensor, ultra sonic sensor, mechanical wave and laser are mainly used. Nowadays the role of acoustic perception in autonomous robots, intelligent buildings and industrial environments is increasingly important and in the literature there are different works^{1,2}.

It is very interesting the use of audio sensors according on the application. In industrial, man-made environments this type of sensors offers its main advantages: they are cheaper than other type of sensors, they hold a reach greater than the ultrasound sensors and they can cover a large area of exploration (with low directivity), they are not sensitive in front of changing light conditions, like cameras. Although audio sensors present low resolution to detect obstacles this fact is not too much relevant in industrial environments.

In an industrial plant to establish the transmission characteristics of a sound between a stationary audio source and a microphone in closed environment there are different study models: 1) the beam theory applied to the propagation of the direct audio waves and reflected audio waves in the room; 2) the development of a lumped parameters model similar to the model used to explain the propagation of the electromagnetic waves in the transmission lines and the study of the solutions given by the wave equation¹¹. Other authors propose a transfer function of a

room, denoted RTF (Room Transfer Function) that carries out to industrial plant applied sound model^{3, 9, 10}. In these works, the complexity to achieve the RFTs is evident as well as the need of a high number of parameters to model the complete acoustic response for a specific frequency range, even with almost ideal conditions.

In reference¹³ authors presented a first approximation to a theoretical model set-up which modeled the RTF in an industrial plant in order to locate mobile robots in such environments. In the present work, this model will be studied in depth as well as the features in the proposed RTF that are more suitable to be used by a mobile robot to navigate in an industrial plant; we have simplified the methodology and our goal is to determinate the x-y coordinates of the robot. In such a case, the obtained RFT will not present a complete acoustic response, but will be powerful enough to determine the robot's position.

The acoustic response of an industrial plant depends mainly on its dimensions, but also on the different absorption coefficients of the materials that form the walls, the floor and the ceiling of the plant. This work is focused in the audio waves that are generated by rotary engines present in industrial environments. Those engines generate typically a reverberant field due to the successive reflections of the waves with the environment bounds. In order to simplify the establishment of a theoretical model as well as the obtaining of the experimental model by identification, a filtering step is introduced. In this phase, the most important harmonic component in the emitted signal spectrum will be selected.

In authors' previous works^{7, 8, 12} the navigation system was presented. Those works investigated the feasibility of using sound features in the space domain for robot localization (in x-y plane) as well as robot's orientation detection. A robust sound-based indoor robot's pose (x, y, θ) detection system was proposed utilizing two microphones. For this reason, in this present work the navigation system will be skipped and the work will be focused in obtaining a more general model for rooms/closed environments through audio features. This model is LPV (linear parameters varying)¹⁴ because the parameters of the model vary along the robot's navigation. Besides, this is a simplified model with the objective to obtain a low computational time in the robot self-localization process. The calibration of these parameters is carried out by physical equations and experimentation altogether. This new model is validated through significant experiments in a real and hazardous environment with a real robot: the sewage system in Barcelona city.

2. SOUND MODEL IN A CLOSED ROOM

2.1. Theoretical model

The acoustical response of a closed room (with rectangular shape), where the dependence with the pressure in a point respect to the defined (x,y,z) position is represented by the following wave equation:

$$Lx \frac{\partial^2 p}{\partial x^2} + Ly \frac{\partial^2 p}{\partial y^2} + Lz \frac{\partial^2 p}{\partial z^2} + k^2 p = 0 \quad (1)$$

Lx , Ly and Lz denote the dimensions of the length, width and height of the room with ideally rigid walls where the waves are reflected without loss, Eq. (1) is rewritten⁶ as:

$$p(x, y, z) = p_1(x)p_2(y)p_3(z) \quad (2)$$

when the evolution of the pressure according to the time is not taken into account.

Then (2) is replaced in (1), and three differential equations can be derived and it is the same for the boundary condition. For example, p_1 must satisfy the equation:

$$\frac{d^2 p_1}{dx^2} + k_x^2 p_1 = 0 \quad (3)$$

with boundary conditions in $x = 0$ and $x = L_x$:

$$\frac{dp_1}{dx} = 0$$

k_x , k_y and k_z constants are related by the following expression:

$$k_x^2 + k_y^2 + k_z^2 = k^2 \quad (4)$$

Equation (3) has as general solution:

$$p_1(x) = A_1 \cos(k_x x) + B_1 \sin(k_x x) \quad (5)$$

Through (3) and limiting this solution to the boundary conditions, constants in (5) take the following values:

$$k_x = \frac{n_x \pi}{L_x}; \quad k_y = \frac{n_y \pi}{L_y} \quad \text{and} \quad k_z = \frac{n_z \pi}{L_z}$$

being n_x , n_y and n_z positive integers. Replacing these values in (5) the wave equation eigenvalues are obtained:

$$k_{n_x n_y n_z} = \pi \left[\left(\frac{n_x}{L_x} \right)^2 + \left(\frac{n_y}{L_y} \right)^2 + \left(\frac{n_z}{L_z} \right)^2 \right]^{1/2} \quad (6)$$

The eigenfunctions or normal modes associated with these eigenvalues are expressed by:

$$p_{n_x n_y n_z}(x, y, z) = C_1 \cdot \cos\left(\frac{n_x \pi x}{L_x}\right) \cdot \cos\left(\frac{n_y \pi y}{L_y}\right) \cdot \cos\left(\frac{n_z \pi z}{L_z}\right) \cdot e^{j\omega t} \quad (7)$$

being C_1 an arbitrary constant and introducing the variation of pressure in function of the time by the factor $e^{j\omega t}$. This expression represents a three dimensional stationary waves space in the room. For the eigenfrequencies corresponding to (6), the eigenvalues can be expressed by:

$$f_{n_x n_y n_z} = \frac{c}{2\pi} k_{n_x n_y n_z}, \quad f_{n_x n_y n_z} = \sqrt{f_{n_x}^2 + f_{n_y}^2 + f_{n_z}^2} \quad \text{and} \quad f_{n_x n_y n_z} = \sqrt{\left(\frac{n_x c}{2L_x}\right)^2 + \left(\frac{n_y c}{2L_y}\right)^2 + \left(\frac{n_z c}{2L_z}\right)^2}, \quad (8)$$

where c is the sound speed. Therefore, the acoustic response of any close room presents resonance frequencies (eigenfrequencies) where the response of a sound source emitted in the room

at these frequencies is maximum. The eigenfrequencies depend on the geometry of the room and also depend on the materials reflection coefficients, among other factors.

In our case, the transform function f_T (that relates the distance between feature space coefficients of each signal vs. source signal (see ref¹³) with the distance between the points (x,y) in the space domain) is represented by (7), considering that the pressure is the square of the amplitude of sound signals (S_j) for an specific time. The solution of this equation is real because imaginary numbers are neglected, and represented as:

$$S_j(x, y) = C_2 \cdot \cos\left(\frac{n_{d_{xy}} \pi d_{xy}}{L_{d_{xy}}}\right) \quad (9)$$

where C_2 is an arbitrary constant.

The corresponding resonant frequencies that are obtained are indicated in Table 1. Specifically, in this Table the resonant frequency corresponding to the propagation mode (3, 0, 2) can be observed. This frequency is close to 100Hz that is selected from the signal spectrum when the climatic chamber is used as sound source.

Table 1. Resonant frequencies in the experiment.

n_x	n_y	n_z	f_{nx}	f_{ny}	f_{nz}	$f(\text{Hz})$
3	2	1	49,1	68,3	43,1	94,54
4	2	0	65,5	68,3	0,0	94,62
2	1	2	32,7	34,2	86,3	98,37
3	0	2	49,1	0,0	86,3	99,25
0	3	0	0,0	102,5	0,0	102,48
1	3	0	16,4	102,5	0,0	103,77
4	2	1	65,5	68,3	43,1	103,98

For mode (3, 0, 2), this equation indicates the acoustic pressure in the rooms depending on the x-y robot's position, and this is:

$$p_{n_x n_y n_z}(x, y) = C_1 \cdot \cos\left(\frac{3\pi x}{10,54}\right) \cdot \cos\left(\frac{1,4\pi}{4}\right) \quad (10)$$

With these ideal conditions, for an ideal value for constant $C_1 = 2$ and for an ideal room without audio losses, the theoretic acoustic response in the rooms for this absolute value of pressure, and for this propagation mode.

2.2. Transfer function

Since the dimensions of industrial plants will be comparable to the wavelength of audio signals presents in the environment, distributed constant models can be used in order to model the audio waves propagation, in a similar way to those proposed for electromagnetic signals transmission lines.

In ref⁴ a model based in the sum of second order transfer functions is proposed; these functions have been build between a sound source located in a position d_s emitting an audio signal

with a specific acoustic pressure P_s and a microphone located in dm which receives a signal of pressure P_m with a time delay t_{rm} ; each function represents the system response in front to a propagation mode.

The first contribution of this work is to introduce an initial variation to this model considering that the sound source has a fixed location, and then this model can be expressed as:

$$\frac{P_m(s)}{P_s(s)} = \sum_{n=1}^M \frac{K_m s e^{t_{rm}s}}{s^2 + 2\xi_n \omega_n s + \omega_n^2} \quad (11)$$

Because our objective is not to obtain a complete model of the acoustic response of the industrial plant, it will not be necessary to consider all the propagation modes in the room and we will try to simplify the problem for this specific application without the need to work with models of higher order.

To implement this experiment, the first step is to select the frequency of interest by a previous analysis of the audio signal frequency spectrum emitted by the considered sound source (an industrial machine). Those frequencies components with a significant acoustic power will be considered with the only requirement that they are close to one of the resonant frequencies of the environment. The way to select those frequencies will be through a band-pass digital filter centered in the frequency of interest. Right now, the term M in the sum of our model will have the value N , being this new value the propagation modes resulting from the filtering process.

3. PROPOSED LPV MODEL IN A CLOSED ENVIRONMENT

For a concrete propagation mode, the variation that a stationary audio signal receives at different robot's position can be modeled, this signal can be smoothed by the variation of the absorption coefficient of the different materials that conform the objects in the room; those parameters are named K_{nm} and ξ_{nm} , and (12) results:

$$H(s, d_m) = \frac{P_m(d_m, s)}{P_s(s)} = \sum_{n=1}^N \frac{K_{nm}(d_m) s e^{t_{rm}s}}{s^2 + 2\xi_{nm}(d_m) \omega_n(d_m) s + \omega_n^2(d_m)} \quad (12)$$

where the subscript n indicates the natural frequency associated to the considered propagation mode (ω_n) and the subscript m indicates the distance of the microphone to the sound source (d_m). This natural frequency (ω_n) of the transfer function room depends on the room characteristics: L_x , L_y and L_z resulting in an LPV indoor model.

The distance (d_m) from the robot to the sound source is given by the expression:

$$d_m = \sqrt{(x_r - x_s)^2 + (y_r - y_s)^2 + (z_r - z_s)^2} \quad (13)$$

where (x_r, y_r, z_r) are the robot location coordinates and (x_s, y_s, z_s) are the sound source coordinates.

Using (12) the module of the closed room in a specific transmission mode ω_n is:

$$|H(j\omega_{nm}, d_m)| = \frac{K_{nm}}{2\xi_{nm}\omega_n} \quad (14)$$

Assuming that the audio source only emits a frequency ω_1 with an amplitude P_s the room response in the propagation mode ω_n for a specific coordinate (x, y, z) of the room is:

$$|H| = \left| \frac{P_m}{P_s} \right|_{n_x, n_y, n_z} = \left| C_1 \cos\left(\frac{n_x \pi x}{L_x}\right) \cos\left(\frac{n_y \pi y}{L_y}\right) \cos\left(\frac{n_z \pi z}{L_z}\right) \right| \quad (15)$$

being z the height of the microphone from the floor, and with

$$f_n = \sqrt{f_x^2 + f_y^2 + f_z^2} \text{ and } \omega_n = 2\pi f_n.$$

For instance, if a one-dimensional environment is considered where the three modes are propagated, as it can be seen in Fig. 1, and the observer is located at a distance $d_m = 2$ m, the values of maximum pressure in this point are A_1 , A_2 and A_3 . The total pressure received in this point is the sum of the partial pressures given by each mode.

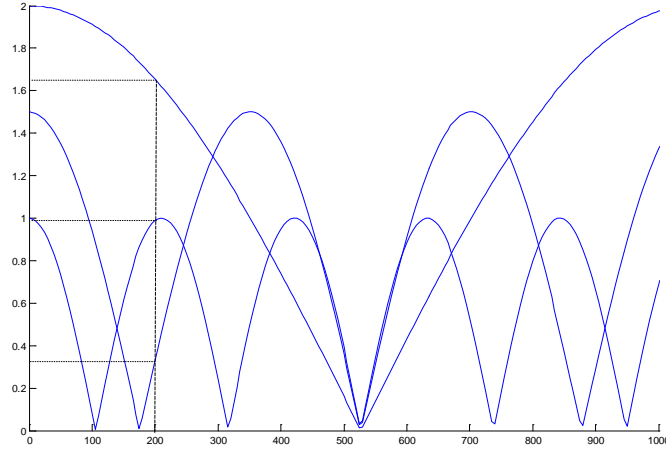


Figure. 1. Response in the one-dimensional case.

For a specific mode and location, the system behaves as a pass band filter, presenting a maximum response at the resonant frequency for the considered mode and a lower response when the signal frequency moves away from the resonant frequency.

Taking into account these considerations, equaling (14) and (15), it results:

$$\xi_{nm} = \frac{K_{nm}}{2\omega_n C_1 \left| \cos\left(\frac{n_x \pi x}{L_x}\right) \cos\left(\frac{n_y \pi y}{L_y}\right) \cos\left(\frac{n_z \pi z}{L_z}\right) \right|} \quad (16)$$

If the filter is non ideal then more than one transmission mode could be considered and therefore the following expression is obtained for a robot position d_m and a resonant frequency ω_n given by the propagation mode n_x, n_y and n_z :

$$\sum_{l=1}^n \frac{K_{nm}}{2\xi_{nm}\omega_n} = \sum_{l=1}^n C_1 \left| \cos\left(\frac{n_x \pi x}{L_x}\right) \cos\left(\frac{n_y \pi y}{L_y}\right) \cos\left(\frac{n_z \pi z}{L_z}\right) \right| \quad (17)$$

If the emitted signal power by the sound sources is constant and the audio signal power acquired with the microphones varies along the robot's position, then the pole positions in the s plane,

for the considered propagation mode, will vary in the different robot's positions and their values will be:

$$s_{1nm} = -\xi_{nm}\omega_n + \omega_n\sqrt{1-(\xi_{nm})^2} \quad (18)$$

$$s_{2nm} = -\xi_{nm}\omega_n - \omega_n\sqrt{1-(\xi_{nm})^2} \quad (19)$$

This is an LPV grey-box model where the damping factor and the natural frequency can be determined by theoretical laws and the parameter K_{nm} is calibrated through experimentation.

4. EXPERIMENTAL RESULTS

Authors have been tested an autonomous mobile robot in a very hazardous environment: the sewage system in Barcelona city.

The methodology applied to determine the robot's position is the following:

- 1) Initially a real source of sound is located in the environment. In this case an electrical is used, generating a real sound with many frequencies with its spectrum.
- 2) The robot acquires an audio signal in its current position and performs a LPV modeling process taking as input signal the filtered sound source signal and as output signal the acquired and filtered signal. The parameters corresponding to the obtained poles in this identification process will be the features components for further steps.
- 3) The Euclidean distances in the feature space are calculated between the current position and the different labeled samples.
- 4) The two first samples are chosen and the distance between them and the robot's position are then calculated. Through a transformation function f_T (see ref¹³) the distance in the feature domain is converted to a distance in the space domain. These two distances in the space domain give two possible positions by the crossing circles of distances.
- 5) To discriminate between both possible solutions, the angle between each one and the platform containing the microphone array (which contains a compass) are calculated, and the closest one to the platform angle will be chosen as discriminatory variable to select the current robot's position.
- 6) Steps 4 and 5 are repeated with the remaining labeled samples, and the solution is chosen among the closest angle to the robot's platform.

For an accurate explanation of the algorithm, the microphone array and the robot used in the experiments see ref¹³.

The acoustic response of the environment is very directional, and this fact leads to consider some uncertainty in the determination of the transformation function which relates the distance in the feature space and the domain space.

The robot, in order to determine its location, will perform the identification process between the emitted sound signal by the sound sources and the acquired signal by the microphone. Furthermore, the robot incorporates a rotary platform allowing orientating the microphone to the audio source, determining this orientation angle accurately.

As it can be seen in Fig. 2, the robot follows the trajectory indicated by the arrows. In the figure is shown the airborne picture of the city, showing the path followed by the robot beneath the street, that is, in the sewers. There are two kind of audio samples: learning and recognition samples. For the collection of learning samples, a set of audio samples have been acquired along the path with known position, authors have measured which is the exact position of such samples, that is, knowing the ground truth. Because many of these samples have been collected they are not shown in the map. In the other hand, the recognition samples are those that once collected the robot has to calculate its position based on the above system and with the information given by the previous samples in the learning phase. Those samples are labelled as P1...P8.

Figure 4 shows the hazardous environment that robots finds in the sewers, and the operative to enter the robot to the sewage by a manhole.

The acquired signal in the sewer will be used in the identification process, See Fig. 5. This signal is time-continuous and, initially, non-stationary; but because the signal is generated by revolving electrical machines it has some degree of stationarity when a high number of samples is used, in this case, 50,000 samples (1.13 seconds). The fundamental frequency is located at 100Hz, and there are also some significant harmonics above and below it. In the filtering step, in order to simplify the identification process only the fundamental frequency at 100Hz and its closer harmonics will be taken into account, specifically those corresponding to the frequencies 178, 147.6, 89 and 66.8 Hz, that get involved due to the non-ideality of the implemented filter.

The sampling frequency is 44,100Hz. Other lower frequencies could be used instead, avoiding working with a high number of samples, but this frequency has been chosen because in a near future a voice recognition system will be implemented aboard the robot and it will be shared with this audio localization system. To facilitate the plant identification process centering its response in the 100Hz component, the input and output signals will be filtered and, consequently, the input-output relationship in linear systems is an ARX model.



Figure 3. Robot environment: path followed by the robot. In red: test path; in blue path: real path with labels P1...P8 where recognition samples are collected.



Figure 4. View seen from the robot in the sewers, and some workers lowering the robot by a manhole.

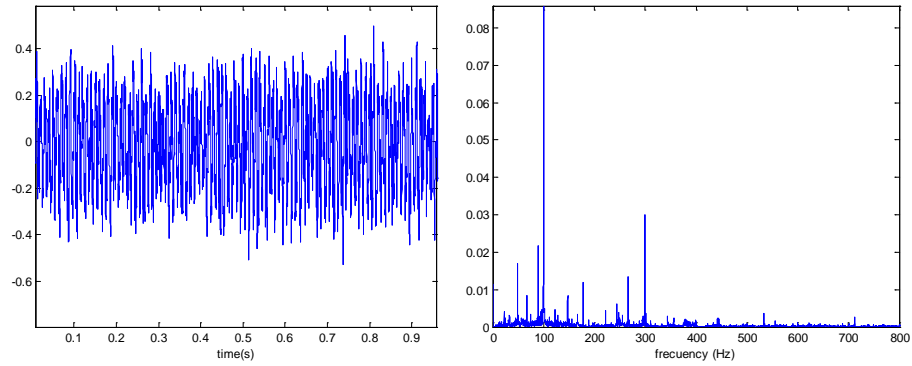


Figure 5. Source signal and its frequency spectrum.

To do that, a band-pass filter is applied to the acquired sound signals by the robot, specifically a 6th-order digital Cauer filter. Fig. 6 shows the results of the filter for the input signal in, for instance, robot position R_4 in the climatic chamber.

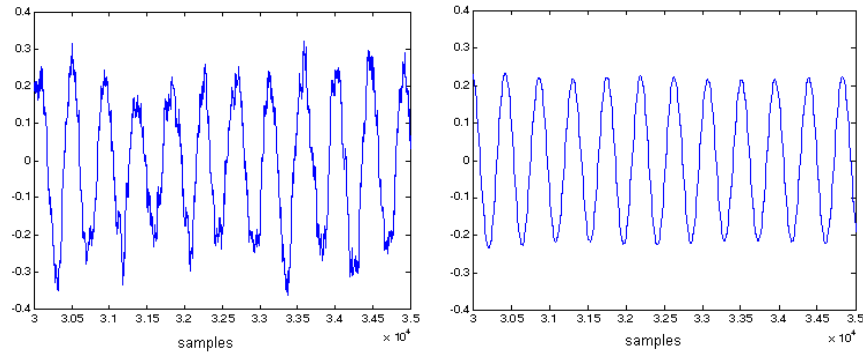


Figure 6. P3 sound signal (left) and its filtered signal (right).

The propagation modes closer to the frequency of 100Hz and its harmonics considered in the filtering process are indicated in Table 2.

Table 2. Considered propagation modes.

n_x	n_y	n_z	f_{nx}	f_{ny}	f_{nz}	$f(\text{Hz})$
4	0	0	65,5	0,0	0,0	65,46
1	0	2	16,4	0,0	86,3	87,79
3	0	2	49,1	0,0	86,3	99,25
1	2	3	16,4	68,3	129,4	147,22
2	1	4	32,7	34,2	172,5	178,87

From the proposed theoretical model, the damping coefficient for these frequencies is function of gain K and the considered robot's position (x,y,z) .

$$\xi_{nm} = \frac{K_{nm}}{2\omega_n C_1 \left| \cos\left(\frac{n_x \pi x}{L_x}\right) \cos\left(\frac{n_y \pi y}{L_y}\right) \cos\left(\frac{n_z \pi z}{L_z}\right) \right|} \quad (20)$$

In this model the acoustic energy dissipation has not been modeled and it is considered by gain K in the model and the constant C_1 that appears in the wave equation (with a value of 2, as it has been aforementioned) for a signal frequency considered in a specific robot's position. The acoustic energy is degraded into thermal energy due to the losses in reflection that will depend on the materials mainly. It is important to consider that the presence of obstacles will introduce a new loss factor that will depend on the position and size of the obstacle and the material that form it. The following expression can be used to model those effects:

$$\frac{K_{nm}}{C_1} = K_2 e^{-mf} \quad (21)$$

Then (20) can be written as follows

$$\xi_{nm} = \frac{K_2 e^{-mf}}{2\omega_n \left| \cos\left(\frac{n_x \pi x}{L_x}\right) \cos\left(\frac{n_y \pi y}{L_y}\right) \cos\left(\frac{n_z \pi z}{L_z}\right) \right|} \quad (22)$$

indicating that the higher the frequency the higher the damping ratio. From the experimental measurements in the plant, the parameters K_2 and m can be determined in (21) which quantify the different losses in the acoustic signals considered in the environment. Good results are obtained for $K_2 = 50$ and $m = 0.015$, resulting

$$\frac{K_{nm}}{C_1} = 50 e^{-0.015 f} \quad (23)$$

The LPV model is obtained from the theoretical laws and the experimental data acquired in labeled samples. The damping factor and the natural frequency are obtained by the expressions explained in the Section 3 and the previous equations (21)-(23). The amplitude constant K_{nm} is calibrated by experimentation through the least square method⁴. This procedure is carried out for those 5 models. They have been validated with the error criteria of FPE (Function Prediction Error) and MSE (Mean Square Error), yielding values about 10e-10 and 3% respectively using 3000 for this validation. Besides, for the whole estimated models the residuals autocorrelation

and cross-correlation between the inputs and residuals are uncorrelated, indicating the goodness of the models.

Table 3. Results of experiments.

Robot's position	Abs. Error X(%)	Abs. Error Y(%)
P1	1.24	0.34
P2	3.43	2.54
P3	2.04	1.23
P4	0.45	1.98
P5	3.54	3.06
P6	5.43	6.96
P7	6.43	6.12
P8	2.34	0.89

There exists another uncertainty of about ± 7.5 degrees in the angle determination due to the rotary platform in the robot that contains the microphones. Finally, to determine the current robot's position the solution that provides the closest angle to the robot's platform will be chosen. The results of our experiments are shown in Table 3. The robot made the same path up to 10 times, and the samples P1...P8 have been acquired at every run. The result is the average error for the 10 runs. The average error in absolute value for the X axis is 3.11% and in the Y axis is 2.89% providing estimated x-y positions good enough and robust.

5. CONCLUSIONS

In this article a new simplified LPV theoretical model has been presented which corresponds to the acoustic response. The aim of the model is to locate mobile robots in such environments. In this work authors presented a methodology to be applied in order to simplify the identification process in industrial plants using the acoustic signals generated by typical engines in those environments.

Because the model will be used by a mobile robot to navigate in an industrial plant, the methodology has been simplified and the goal is to determinate the x-y coordinates of the robot. In such a case, the obtained RFT will not present a complete acoustic response, but it has been demonstrated that the results are very good. The obtained feature space is related with the space domain through a general approach with acoustical meaning. The validation of this novel approach is tested in a real environment, in this case a section of a sewage system obtaining promising results. The results keep being very good when the uncertainty is incorporated in the transformation function.

ACKNOWLEDGMENT

This research has been funded with Project "ColRobTransp" MINECO ref. DPI2016-78957-R.

REFERENCES

- [1] Mumolo, E., Nolic, M., Vercelli, G. Algorithms for acoustic localization based on microphone array in service robotics, *Robotics and Autonomous Systems*. 2003, vol. 42, pp.69-88.
- [2] Csyzewski, A. Automatic identification of sound source position employing neural networks and rough sets, *Pattern Recognition Letters*. 2003, vol.24, pp.921-933.
- [3] Haneda, Y., Makino, S., Kaneda, Y. Modeling of a Room Transfer Function Using Common Acoustical Poles, *IEEE Int Conf on Acoustics, Speech, and Signal Processing, ICASSP-92*.1992, vol.2, pp. 213–216.
- [4] Ljung, L. *System identification: Theory for the user*, Ed. Prentice-Hall, 1987.
- [5] Charbonnier, R., Barlaud, M., Alengrin, G., Menez, J. Results on AR-modeling of nonstationary signals, *IEEE Trans. Signal Processing*. 1987, vol 12, no. 2, pp. 143-151.
- [6] Kayhan, A.S., Ei-Jaroudi, A., Chaparro, L.F. Evolutionary periodogram for nonstationary signals, *IEEE Trans. Signal Processing*. 1994, vol. 42. no. 6, pp. 1527-1536.
- [7] Grau, A., Bolea, Y., Manzanares, M. Robust Industrial Machine Sounds Identification Based on Frequency Spectrum Analysis, *12th Iberoamerican Congress on Pattern Recognition, CIARP 2007*, Ed. Lectures Notes in Computer Science, LNCS 4756, Santiago de Chile, 14-17 Novembre, 2007, pp. 71-77.
- [8] Bolea, Y., Manzanares, M. Grau, A. Robust robot localization using non-speech sound in industrial environments, *IEEE Int Sym on Industrial Electronics, ISIE 2008*, Cambridge, UK, 30 June- 2 July 2008.
- [9] Haneda, Y., Kaneda, Y., Kitawaki, N. Common-Acoustical-Pole and Residue Model and Its Application to Spatial Interpolation and Extrapolation of a Room Transfer Function, *IEEE Transactions on Speech and Audio Processing*. November 1999, vol. 7, no. 6.
- [10] Gustaffson, T., Pota, H.R., Vance, J., Rao, B.D., Trivedi, M.M., Estimation of Acoustical Room Transfer Functions, *Proc of the 39th IEEE Conf. on Decision and Control*, Sydney, Australia, Dec. 2000.
- [11] Kuttruff, H. *Room Acoustics*, Ed. Applied Science Publishers Ltd. 1979.
- [12] Manzanares, M., Guerra, E., Bolea, Y., Grau A. Robot Localization Method by Acoustical Signal Identification, *IEEE Emerging Tech and Factory Automation, ETFA'09*, Mallorca, Spain, 2009.
- [13] Manzanares, M., Bolea, Y., Grau, A., An Identified LPV Model for Mobile Robots Navigation with Audio Features, *36th Annual Conference of the IEEE Industrial Electronics Society IECON2010*. 7-10 November 2010, Glendale, Arizona, USA, 1064-1069.
- [14] Guiarré, L., Bauso, D., Falugi, P., “LPV model identification for gain scheduling control: An application to rotating stall and surge control problem”, *Control Eng Practice*, 2006, vol. 14(4), 351-361.

Residual-Based Variational Multiscale Simulation of Sediment Transport With Morphological Changes

Malú Grave*, José Jerônimo Camata**, Alvaro Coutinho***

*Federal University of Rio de Janeiro, **DCC/UFJF, ***Federal University of Rio de Janeiro

ABSTRACT

Sediment transport induced by fluid flows is a field of great importance in engineering applications because there are a lot of projects strongly affected by moving sediments. The transport of sediments in fluids encompasses the suspended load, where turbulence carries the sediment particles, and the bedload, where the particles near the bottom are moved sliding, rolling or by saltation, because of the shear stress on this region. The bed load transport implies bed morphological changes which are also induced by the erosion as a consequence of sediment entrainment into suspension. In this work, we implement all these phenomena as numerical models in libMesh, an open finite element library that provides a framework for multiphysics. Here, the mathematical model results from the incompressible Navier-Stokes equations combined with an advection-diffusion transport equation for suspended sediments. The Navier-Stokes equations are treated with the residual-based variational multiscale finite element formulation while the advection-diffusion transport equation uses a stabilized method with discontinuity capturing. Empirical models are used to represent the entrainment and the bedload transport rate of sediments. Special boundary conditions at the bottom are introduced to take into account sediments entrainment, as well as deposition. After each time step, we update the mesh according to the morphological changes at the bottom due the bed load transport and erosion, and an avalanching mechanism is applied in a way to avoid elevations higher than the sediment angle of repose. We validate the suspended load transport model and the boundary conditions simulating two well-documented test cases where experimental data are available. After that, we employ the full model, including bedload transport, in another test case, and the results obtained from our model are promising. Both flow field and scour pattern are similar to available experimental data.

A Class of Polygonal Spectral Elements with Adaptive p-Refinement for the Efficient Simulation of Wave Propagation Problems

Hauke Gravenkamp*

*University of Duisburg-Essen

ABSTRACT

This contribution presents a novel approach to constructing polynomial shape functions of arbitrary order on triangles and star-convex polygons. Each element is defined in local scaled boundary coordinates with the origin positioned within the kernel of the polygonal domain. Two independent sets of one-dimensional shape functions are defined along both local coordinates, i.e., the circumferential and radial direction, respectively. The two-dimensional shape functions are constructed as the tensor product of the one-dimensional polynomials similar to conventional spectral elements. This procedure allows choosing the element order independently not only for each edge but also along the radial direction. Consequently, highly flexible local refinement schemes can be applied where this element type enables the straightforward transition between subdomains subject to different meshing requirements or an elevation of the element order in the vicinity of stress concentrations. In particular, this approach is beneficial for the simulation of wave propagation phenomena, where the required nodal density is mainly predetermined by the local wavelength at the frequency of interest, rather than the geometrical complexity. The proposed polygonal element exhibits all advantages of conventional (quadrilateral) spectral elements, namely high-order completeness, partition of unity, the 'Kronecker-delta-property', as well as a straightforward construction of shape functions. In addition to the advantages that come with the extension to polygonal discretizations, computational costs for the integration of the coefficient matrices are reduced since the proposed shape functions can be integrated along both local coordinates separately, hence requiring only one-dimensional quadrature rules. Despite the fact that these elements allow local p-refinement in a highly flexible manner, the mass matrix can be lumped without loss of accuracy - two features which are usually considered to be mutually exclusive.

An Efficient Blended Mixed B-spline Formulation for Non-polar Thin Structural Models

Leopoldo Greco*, Massimo Cuomo**, Loredana Contrafatto***, Salvatore Gazzo****

*university of study of Catania, **university of study of Catania, ***university of study of Catania, ****Université de Lyon

ABSTRACT

Mixed formulations of the \bar{B} type, when applied to B-spline representations, bear significant computational cost and lead to a full stiffness matrix. In this work we present an efficient mixed formulation for avoiding membrane locking of curved non-polar thin structural models, i.e. plane Kirchhoff rod and Kirchhoff-Love shell models, in the context of isogeometric analysis. An efficient spline reconstruction of the assumed axial strains obtained by means of a local projection at the element level is performed using the method proposed by Thomas et al. in [1] for the reconstruction of the geometry. In this way a much smaller bandwidth of the stiffness matrix is obtained with respect to the non local \bar{B} -formulation, with significant reduction of the computational cost. The blended mixed formulation splits in two steps: in the first step the local \bar{B} operators are defined at the element level via projection of the strain measure (both L2- projection and discrete collocation approaches are considered). Successively, by means of the spline reconstruction algorithm, the global projection of the strain measures at the patch level is defined. Numerical experiments show that the proposed method, in addition to completely remove membrane locking, yields the same accuracy and rate of convergence as the non local \bar{B} -method.

Analysis of Forces through the Seated Pelvis during Under Body Blasts

Preston Greenhalgh*, Matthew Panzer**, Edward Spratley***, Robert Salzar****

*University of Virginia, **University of Virginia, ***University of Virginia, ****University of Virginia

ABSTRACT

Injury mitigation techniques for mounted soldiers, such as seat padding and mounting, have been implemented in mine-resistant ambush protected (MRAP) vehicles, but numerous pelvic injuries still occur within these vehicles during under body blast (UBB) events. To better prevent pelvic injuries during UBB events, a better understanding of how force is transmitted into the pelvis at very high load rates is imperative. To that end, a biofidelic finite element (FE) model of the pelvis can be a powerful tool to explore UBB response because of its low cost and ease of use in comparison to expensive and difficult high-energy cadaveric tests. Fourteen (14) bilateral gluteal soft tissue specimens were tested in axial compression using a custom drop tower. Each specimen included gluteal muscle, adipose tissue, and skin. The specimens were laid flat on a substrate attached to a load cell. A 22.7kg weight was dropped onto the specimens at 10 m/s, while a linear potentiometer was used to measure displacement of the indenter. An inverse finite element (IFE) method was used to calculate the material properties of the tissue from the drop tower data. The time-displacement data from the test was prescribed to the FE indenter. The force output from the simulation was exported to a custom program that iteratively compared the force output from the FE model to that of the experimental load cell, and selected new material coefficients based on a quasi-linear viscoelastic (QLV) material model until the force responses converged. A component pelvis FE model was made by modifying the GHBM automotive FE model, matching the boundary and input conditions of previous experimental pelvis tests performed at the University of Virginia. The pelvis was potted at S1 attached to a load cell, and a plate acting as the seat impacted the pelvis. The pelvis soft tissue material in the FE model was updated using the QLV constitutive model found in the high rate material tests. Forces and moments from the sacrum load cell in the FE model were compared to the experimental data with the original and updated soft tissue model. From preliminary analysis, greater than 30% of the applied seat platen force was transmitted through the soft tissue of the posterior pelvis, while 70% was transmitted through the skeleton. This soft tissue contribution changes the location of the seat platen center of percussion posteriorly, and may contribute significantly to the observed injury distributions seen in theater.

Cardiac Fluid-Structure Interaction by a Hyperelastic Immersed Boundary-Finite Element Method

Boyce Eugene Griffith^{*}, Charles Edward Puelz^{**}, Simone Rossi^{***}, Margaret Anne Smith^{****}

^{*}UNC, ^{**}UNC, ^{***}UNC, ^{****}UNC

ABSTRACT

During each cardiac cycle, muscle contraction and relaxation drive the blood flow through the four chambers of the heart and to the vascular system. The heart chambers – the ventricles and the atria – are separated by valves that ensure a unidirectional flow, from the right to the left heart and from the left heart to the vascular system. As the main purpose of the heart is to pump blood to the vascular system, the characterization of the cardiac blood flow is important to understand the impact of blood flow in health and disease. For this reason we have built a fluid-structure interaction model of the heart, which includes the 4 heart chambers, the valves and the main vessels. To handle the large deformations and complex geometries of the beating heart, we use the immersed boundary method to simulate the fluid-structure interaction problem. In particular, the momentum equation is solved “in a box” using the finite difference method, while the solid forces are computed on a finite element mesh. The heart muscle is assumed to be viscoelastic: the elastic stress is derived from an orthotropic strain-energy density function, while the viscous stress is inherited from the underlying Newtonian fluid. The contraction of the muscle is modeled by means of an active stress formulation driven by a simplified model for the intracellular Calcium transient. The active stress acts only in the fiber direction, which have been defined in the whole heart using simple Poisson interpolation methods. We’ll discuss the construction of the whole heart model including the creation of the geometrical models, the generation of the fiber field in the 4 heart chambers and the hyperelastic immersed-boundary finite element method.

A Bayesian Encoder-Decoder Model Order Reduction Approach for Problems in Random Heterogeneous Media

Constantin Grigo*, Phaedon-Stelios Koutsourelakis**

*Technical University of Munich, **Technical University of Munich

ABSTRACT

The macroscopic behavior of random heterogeneous media is fully determined by its microstructural properties. However, due to computational complexity, it is often barely feasible to simulate problems directly on their microscale. Reduced order modeling (ROM) techniques aim at alleviating this computational burden by only retaining most relevant fine scale material properties. We develop a fully probabilistic (semi-)supervised learning approach based on only a few tens of forward model runs which maps high-dimensional random material microstructures onto a much lower dimensional latent space (encoding) using macroscopic feature information such as porosity, correlation length or interface conditions. These latent variables then serve as the input to a less accurate, though much cheaper reduced order model (potentially based on different constitutive behavior) which emulates the expensive fine scale problem. Finally, the ROM output is used to probabilistically reconstruct the fine-grained model response (decoding), leading to sharp predictive distributions centered around the true solution field. By making use of information-theoretic criteria, the model is capable to automatically adapt the ROM emulator complexity until a user-specified level of accuracy/efficiency is met. We apply the discussed method to different problems in random heterogeneous media and show possible applications in stochastic optimization-, inverse- or control problems.

Sample Generation of Vector-valued Gaussian Functions with Prescribed Accuracy

Mircea Grigoriu*

*Cornell University

ABSTRACT

The generation of samples of Gaussian random functions is based on approximate representations which depend on finite families of random variables and converge in some sense to target Gaussian functions, e.g., truncated Karhunen-Loève (KL) series. The theory of KL series is well-established but their properties for vector-valued random functions have not been examined systematically. The common selection of truncation levels based global errors results in representations whose components may have very different accuracies. To address this potential limitation, we propose the following two-step algorithm. First, truncation levels $\{m_i\}$ are selected for the KL representations of the components $\{Z_i(x)\}$ of a target vector-valued Gaussian function $Z(x)$ such that they meet specified accuracies. This selection involves one dimensional processes. Second, the levels $\{m_i\}$ are accepted or increased if the accuracies of resulting cross correlation functions of $Z(x)$ satisfy or violate preset constraints. The algorithm is based on the facts that (i) the products of eigenfunctions of the correlation functions of components of $Z(x)$ provide an orthonormal basis for the cross correlation functions of $Z(x)$ and (ii) the correlations of the random coefficients of KL representations result from projections of the cross correlation functions of $Z(x)$ on the orthonormal bases obtained from the eigenfunctions of the correlation functions of $\{Z_i(x)\}$. Numerical examples are presented to illustrate the implementation of the proposed Monte Carlo algorithm and demonstrate its performance.

The Embedded Unit Cell (EUC): Nonlinear Material Response

Marina Grigorovitch*, Erez Gal**

*Department of Structural Eng., Ben-Gurion University of the Negev, **Department of Structural Eng., Ben-Gurion University of the Negev

ABSTRACT

In this research, the multiscale modeling ability of coupling between the macroscale structure and microscale material is extended by mean of the presented formulation that called "Embedded Unit Cell (EUC)". The embedded unit cell (EUC) approach is a concept designed to facilitate homogenization and multi scale analysis of composite materials/domains in cases where the classical theory of homogenization is not valid due to lack of periodic microscopic response. The EUC approach is based on microscopic solution of unit cell restricted by non-periodic boundary conditions and continuum domain surrounding the unit cell in order to describe the mechanical relations between various scales. The proposed methodology relies on mathematical formulation, multi-scale analysis procedure and generalized theory of homogenization, and is intended to widen the applicability of the analysis to the zones, where classical formulation cannot be applied because the required periodicity assumption is not valid. Up to now, this method was challenged by solution of several types of problems. The linear response of homogenization problems at boundary zones, which are not periodic with the rest of the structure, was successfully evaluated by the developed EUC procedure by eventually reducing the model complexity and computing resources demand. Following that, the stress concentration problems were analyzed at both elastic and elastic-plastic type of response. Such problems are characterized by homogeneous structure and shape, with exception of small-size zones with local non-periodicity relating to the rest of the structure. These small domains represent stress concentration zones, which response is evaluated by complex FE models and characterized by very demanding computing resources. The non-linear problems with elastic-plastic type of response are difficult to be solved using classical homogenization methods, because periodic assumption is hardly valid. The pair of microscopic and macroscopic problems has to be solved more than once upon incremental loading and instantly changing equivalent material properties, in contrast with single solution in the case of the linear elastic problems. Sequential information passing between the scales has to be replaced by consecutive information passing, causing enormous effect on the complexity of the numerical algorithm, so that the implementation of the evaluation procedure has been involved with advanced reprogramming of complicated finite elements software. A numerical verification study shows that the suggested approach provides appropriate and accurate approximation, compared to the reference solutions of displacement field and micro-scale stress fields.

Fast Evaluation of the Distance to the Wall in Eulerian Fluid-Structure Interaction Computations

Sebastian Grimberg^{*}, Charbel Farhat^{**}

^{*}Stanford University, ^{**}Stanford University

ABSTRACT

Highly nonlinear, turbulent, dynamic, Fluid-Structure Interaction (FSI) problems characterized by high Reynolds number flows, large structural displacements and deformations, as well as self-contact and topological changes are encountered in many applications including the study of supersonic parachute inflation dynamics [1]. For this class of FSI problems, the Eulerian computational framework, which often implies an Embedded (or immersed) Boundary Method (EBM) for CFD that is robust for viscous flows [2], is often the most appropriate one. In many circumstances, this framework requires the computation of the time-dependent distance to the wall — that is, the distance from each active mesh node of the embedding mesh to the nearest embedded discrete surface, which evolves in time and with the motion/deformation of this surface. Such circumstances include, for example, modeling turbulence using the Spalart-Allmaras or DES turbulence model, and performing Adaptive Mesh Refinement (AMR) in order to track the boundary layers. In the context of explicit-explicit fluid-structure time-integration schemes, which are often required to resolve the physics of the aforementioned class of FSI problems, evaluating at each time-step the distance to the wall is computationally prohibitive. For this reason, this talk presents two complementary approaches for reducing this computational cost. The first one recognizes that many quantities depending on the wall distance are relatively insensitive to its inaccurate evaluation in the far field. Therefore, it simplifies a state-of-the-art algorithm for computing the distance to the wall accordingly. The second approach relies on an effective distance error estimator to update the evaluation of the distance function only when otherwise a quantity of interest that depends on it would become tainted by an unacceptable level of error. The talk will also highlight the potential of combining both approaches for dramatically accelerating the solution of highly nonlinear, turbulent, FSI problems by reporting on the performance of the simulation of the inflation of a disk-gap-band parachute system in a supersonic airstream. 1. Z. Huang, P. Avery, C. Farhat, J. Rabinovitch, D. Derkevorkian and L. D. Peterson, Simulation of Parachute Inflation Dynamics Using an Eulerian Computational Framework for Fluid-Structure Interfaces Evolving in High-Speed Turbulent Flows, AIAA-2018-1540, AIAA SciTech 2018, Kissimmee, Florida, January 8-12 (2017) 2. J. Rabinovitch, Z. Huang, P. Avery, C. Farhat, A. Derkevorkian and L. D. Peterson, Preliminary Verification and Validation Test Suite for the CFD Component of Supersonic Parachute Deployment FSI Simulations, AIAA-2018-1542, AIAA SciTech 2018, Kissimmee, Florida, January 8-12 (2017)

Coupling of Incompressible Fluid Features to Mechanical and Thermal Features of LSDYNA

Roger Grimes^{*}, Facundo Del Pin^{**}, Inaki Caldichoury^{***}, Rodrigo Paz^{****}

^{*}Livermore Software Technology Corporation, ^{**}Livermore Software Technology, ^{***}Livermore Software Technology, ^{****}Livermore Software Technology

ABSTRACT

LSDYNA has evolved from a Finite Element Package for Mechanical Simulation to a Multi-Physics Simulation Package. Initially that meant the inclusion of Thermal capabilities for the Mechanical Capabilities. But LSDYNA now has features for Electromagnetics, Incompressible Fluid Flow and Compressible Fluid Flow. Over a decade ago LSTC (Livermore Software Technology) started the development of Incompressible Fluid (ICFD) Flow Features which required integration with the existing mechanical and thermal capabilities. This talk will present how we implemented this coupling for - ICFD with Mechanical Explicit Time Integration - ICFD with Mechanical Implicit Time Integration - ICFD Conjugate Heat Transfer with Mechanical Thermal Computations We will highlight the coupling of features with examples.

Controlling the Solution Transfer Error in Multi-physics Coupling for Climate Problems

Iulian Grindeanu^{*}, Vijay Mahadevan^{**}, Robert Jacob^{***}

^{*}ANL, ^{**}ANL, ^{***}ANL

ABSTRACT

It is well known that operator decomposition and unresolved solution of coupled atmosphere and ocean models, or physics and dynamics components of an atmosphere, can lead to large numerical approximation errors that can also cause stability issues. In this context, one of the components contributing to the spatiotemporal accuracy is due to the mapping between different discretizations of the sphere, to resolve spatial scales of interest in the various coupled model components. In some atmospheric and ocean model solvers, consistent and conservative remapping strategies strongly determine the propagation of discretization accuracy between models. This could also become an issue in atmosphere models where physics and dynamics are on different grids. Tracer advection done by remapping is also subject to these errors. Understanding and controlling all sources of errors in a coupled system dynamically will be key to achieving predictable and verifiable results on future architectures. We will compare several conservative and non-conservative solution transfer and remapping methods implemented within the framework of TempestRemap and MOAB in comparison to the state-of-the-art methods implemented within ESMF, and discuss the implications on numerical accuracy and computational efficiency for representative coupled model problems.

Computed Tomography Characterization of Voids in Ordinary and Ultra-High Performance Concrete

Andrew Groeneveld*, Charles Burchfield**

*US Army Engineer Research and Development Center, **US Army Engineer Research and Development Center

ABSTRACT

Ongoing research on multiscale modelling of concrete materials requires accurate characterization of the structure of the material at lower length scales. In order to characterize these materials at these scales, void sizes and spacing should be investigated along with matrix constituents and any aggregates or fibers present. This work investigates the volume and spacing of voids in two concretes, SAM-35 and Cor-Tuf Baseline. X-ray computed tomography was used to image the internal structure of concrete cylinders. Volume element (voxel) sizes in the reconstructed 3D images ranged from 32 to 57 μm . Voids were identified using an x-ray attenuation threshold and connected component analysis. The void volume and inter-void spacing (based on Delaunay triangulation between centroids) were determined. Distribution fitting was performed to generate probability density functions for use in modelling.

Protein Transport in Curved Lipid Bilayer Membranes: An Extended Saffman-Delbruck Approach Incorporating Hydrodynamics in Curved Fluid Interfaces

Ben Gross^{*}, Paul Atzberger^{**}, Misha Padidar^{***}

^{*}University California Santa Barbara, ^{**}University California Santa Barbara, ^{***}University California Santa Barbara

ABSTRACT

We develop fluctuating hydrodynamics approaches to extend Saffman-Delbruck theory to capture the collective drift-diffusion dynamics of proteins within curved lipid bilayer membranes. Our approach is at the level of fluid interfaces having any curved radial manifold shape. We take into account the two dimensional hydrodynamics of the two curved leaflets of the bilayer coupled with the three dimensional hydrodynamics of the surrounding bulk fluid. Using analytic and computational approaches, we show how Gaussian curvature can significantly impact dissipation within the curved two dimensional membrane fluid to augment the collective drift-diffusion dynamics of protein inclusions. We further show for the self-assembly of protein clusters that these effects contribute significant kinetic contributions giving differences with widely used non-hydrodynamic theories. We also present general results on the collective drift-diffusion dynamics when heterogeneous curved structures are present in the membrane geometry showing how these local Gaussian curvature effects influence hydrodynamic coupling in some interesting ways.

Algorithms for the Simulation of Curvilinear and Axisymmetric Hydraulic Fractures with Lag

Benjamin Grossman-Ponemon*, Adrian Lew**

*Stanford University, **Stanford University

ABSTRACT

Hydraulically-driven fractures are ubiquitous in nature as magma-filled dykes around volcanos or water-filled cracks which drive the calving ice sheets in the arctic. They are best known by their commercial use in fracking treatments by the oil and natural gas industry, leading an energy boom in the United States and abroad. Deeper understanding of these processes drive the need for robust simulation of hydraulic fractures. However, simulation of the evolution of fluid-filled fractures is difficult due to the need to track changing crack geometry, advance the fluid inside the crack, and compute a functional over the singular stress fields around the crack tip to determine the crack path. The recently-developed technique of Universal Meshes (UM)[1] offers a solution to these problems. By snapping only nearby nodes of a background mesh to the crack, the geometry of the problem may be resolved exactly, and a suitable domain on which to solve for the evolution of the fluid is generated. From UM, an algorithm to simulate fluid-filled fractures with lag is developed. Examples in plane-strain and axisymmetry are considered. [1] Rangarajan, R., Chiaramonte, M.M., Hunsweck, M.J., Shen, Y. and Lew, A.J., 2015. Simulating curvilinear crack propagation in two dimensions with universal meshes. *International Journal for Numerical Methods in Engineering*, 102(3-4), pp.632-670.

Application and Numerical Solution of 14-Moment Maximum-Entropy-Based Moment Closures for Describing Non-Equilibrium Gaseous Flows with Shocks

Clinton Groth^{*}, Lucie Freret^{**}

^{*}University of Toronto, ^{**}University of Toronto

ABSTRACT

The development and application of novel 14-moment maximum-entropy-based moment closures are explored for prediction of non-equilibrium gaseous flows with shocks. Closure formulations based on both an interpolative approach as well as that based on a bi-Gaussian approximation for the distribution function are considered. Both closure strategies possess or mimic many of the desirable mathematical and computational features of closures following maximum-entropy principles on which they are based. However, in contrast to closures based directly on maximum-entropy concepts, the proposed interpolative and bi-Gaussian closures afford closed-form expressions for the closing moment fluxes and thereby avoid costly numerical solution procedures commonly associated with the latter. A Godunov-type finite-volume scheme with block-based anisotropic adaptive mesh refinement (AMR) is also described for the efficient solution of the resulting moment equations on multi-block body-fitted hexahedral mesh and the suitability and accuracy of the 14-moment systems for describing non-equilibrium gaseous flows with shocks is demonstrated by considering several canonical flow problems, including planar shock structure.

Dynamic Models in Molecular Dynamics

Roman Gruzdev*, Arkadiy Soloviev**

*Southern Federal University, Rostov-on-Don, Russia, **Don State University, Rostov-on-Don, Russia

ABSTRACT

This work is devoted to the research of dynamic models of graphene based materials with molecular dynamics (MD) simulation. Our goal is to develop new methods for sample building and analysis and include those to the ACELAN-COMPOS software. Material of interest in current research – graphene – was chosen due to its unique physical properties. Main points of computer experiment are: to build molecular model of the sample; to investigate the model with LAMMPS software; to prove correctness of the results with ACELAN software. LAMMPS package was chosen as open-source up-to-date MD software with good computational potential and ACELAN with its ACELAN-COMPOS module is finite element analysis software developed at the Department of Mathematical Modeling of Southern Federal University. In MD simulation we apply specific loadings to the sample to perform amplitude-frequency analysis. After this step we perform the same analysis in ACELAN-COMPOS, thus we obtained 2 sets of frequencies. By applying statistical analysis we concluded that results are correct and in correspondence with other works.

Investigating the Effect of Local Vision-Guided Scleral Remodeling on the Development of the Eye

Rafael Grytz*, Mustapha El Hamdaoui**, Keyur Savla***

*University of Alabama at Birmingham, **University of Alabama at Birmingham, ***University of Alabama at Birmingham

ABSTRACT

It is thought that the retina can detect defocus and alter scleral remodeling to match the eye's size to its optics during development, producing eyes with good focus (emmetropia). Extensive evidence from animal studies shows that this emmetropization mechanism can adapt the eye's size to an experimentally altered focal plane using a powered lens. Clinical trials have attempted to use this mechanism for myopia control by prescribing lenses that are less powerful than needed to correct for the existing myopia. A myopic eye is too long for its own optics. Instead of slowing the myopia, the undercorrection of children's vision accelerated myopia progression. We propose that species-specific differences in the peripheral defocus underlie this species-dependent response. We have further developed our multi-scale model of the tree shrew eye [1] based on the assumptions that scleral growth is globally controlled by genetic factors while scleral remodeling is locally controlled by genetic factors and local refractive error. We estimated the focal surface from refractive and biometric measurements of three eyes. The peripheral defocus (35 degrees off-axis) showed a myopic shift of -4.13 (1.40D STDEV) compared to the central axis. Unlike tree shrews, humans often show a hyperopic shift in the periphery. We computed the local refractive error at the anterior surface of the sclera and transferred it to each scleral finite element using a mesh free approach. We simulated the emmetropization process from 24 to 180 days of visual experience (DVE). The simulation replicated the normal development of a tree shrew eye in good agreement with experiments. When the overall defocus was changed by using a negative powered lens, the eye adapted its size to precisely match the new focal surface. Inducing a hyperopic shift in the periphery by increasing the width of the focal surface by 50% at 24 DVE lead to -3.3D myopia at 180 DVE. Undercorrecting for the peripheral defocus-induced myopia by using a -2D lens (starting at 90DVE) increased the final myopia to -4.9D at 180DVE. Our results suggest that eyes with a myopic shift in the periphery (such as tree shrews) emmetropize well even if the overall defocus is altered. Eyes with a hyperopic peripheral shift (such as humans) tend to become myopic and undercorrection can lead to more myopia. This is the first model that provides a plausible explanation for this species-dependent response of the emmetropization process. [1] R Grytz, M El Hamdaoui. J Elast 2017;129:171-195.

Assessment of Wall Stresses and Internal Mechanical Heart Power in the Left Ventricle

Matthias Gsell*, Gernot Plank**

*Medical University of Graz, **Medical University of Graz

ABSTRACT

Introduction: Aortic valve disease (AVD) causes pressure and volume overload of the left ventricle (LV) which may trigger adverse remodeling and precipitate progression towards heart failure (HF). As myocardial energetics can be impaired during AVD, LV wall stresses and mechanical heart power provide a complementary view on LV performance which may aid in better assessing the state of disease. Objectives: Using a high resolution electro-mechanical (EM) in silico model of the LV as a reference, we evaluate clinically feasible Laplace-based methods for assessing LV wall stresses and mechanical heart power. Methods: We used N=4 in silico finite element (FE) EM models of LV and aorta of patients suffering from AVD. All models were personalized with clinical datasets under pre-treatment conditions. LV wall stresses and mechanical power were computed accurately from FE kinematic data and compared with clinically feasible estimation methods which were applied to the same FE model data. Results and Conclusion: Simulation results showed fundamental discrepancies between Laplace stress and internal mechanical power with the corresponding FE-based analogues, but Laplace-analysis provided sufficiently accurate estimates of mechanical peak power for clinical application. Further, external hydrodynamic power computed from synchronously recorded pressure-volume (PV) data in the LV cavity and internal mechanical power computed from LV deformation yielded essentially identical results since power expenditure during isovolumic phases was small. Thus both approaches either based on PV or Laplace analysis, are suitable for estimating peak mechanical power of the LV non-invasively, given that sufficiently accurate estimates of LV peak pressure are available.

Peridynamic Analysis of Impact Failure for Concrete Gravity Dam

Xin Gu^{*}, Qing Zhang^{**}, Erdogan Madenci^{***}

^{*}Hohai University; University of Arizona, ^{**}Hohai University, ^{***}University of Arizona

ABSTRACT

Peridynamics (PD) is an alternative approach to the classical continuum mechanics. It is based on nonlocal interactions. The PD form of the equation of motion appears as an integral-differential equation instead of partial differential equations [1]. Especially the bond-based peridynamics (BB PD) has proven robust in analyzing crack growth and progressive failure of structures under extreme loads. However, the BB PD has the fixed Poisson's ratio restriction, which is fixed to 1/4 in three-dimensional problems and plane strain problems, and 1/3 in plane stress problems. The conjugate BB PD model introduced by Wang et al. [2] is one of extensions of the traditional BB PD to overcome this limitation. In the conjugate BB PD, the nonlocal interaction forces are not only related to normal stretch of bonds, but also related to rotation bond angles of a pair of conjugate bonds. In present study, we will further develop the conjugate BB PD model to analyze the projectile impact failure and penetration problems of concrete gravity dam. Description of damage and failure process of dams under projectile impact and blast-impact objectively is a significant but difficult issue [3]. A dam suffers from the effects of gravity and hydrostatic pressure when the reservoir is full. The process of a projectile impact on the dam at different positions will be simulated after static deformation analysis. The improved conjugate BB PD is found to be effective for simulating the projectile impact failure process of dams, which involves the crack nucleation, crack propagation, final fracture and local failure. References [1] Silling SA. Reformulation of elasticity theory for discontinuities and long-range forces. *Journal of the Mechanics and Physics of Solids*. 2000, 48:175-209. [2] Wang Y, Zhou X, Shou Y. The modeling of crack propagation and coalescence in rocks under uniaxial compression using the novel conjugated bond-based peridynamics. *International Journal of Mechanical Sciences*, 2017,128-129:614-643. [3] Gu Xin, Zhang Qing. Progress in Numerical Simulation of Dam failure under Blast Loading. *Journal of Hohai University (Natural Sciences)*. 2017,45:45-55. (in Chinese).

Rate-dependent Fluid Behavior and Superficial Collagen as Protective Mechanisms of Kangaroo Shoulder Cartilage at High Strain-rates

Yuantong Gu^{*}, Namal Thibbotuwawa^{**}

^{*}Queensland University of Technology, ^{**}The University of Adelaide

ABSTRACT

Articular cartilage exhibits complex mechanical behaviors such as strain-rate-dependency under external loading. It is believed that the interplay and interaction of cartilage constituents, i.e. proteoglycans, collagen and tissue fluid is the key reason for such complex behavior in cartilage tissues. In this study, we use the kangaroo as an animal model. Through integrating with experimental studies using kangaroo cartilage, a porohyperelastic numerical model with a strain rate-dependent permeability function is developed to understand the contribution of fluid on the strain-rate dependent indentation behavior. Comparison of the porohyperelastic models with constant, strain-dependent and strain-rate-dependent permeability models indicates a statistically significant contribution of rate-dependent fluid flow to the mechanical behavior, especially at high strain-rates. However magnitude of the contribution of the rate-dependent fluid behavior was small. Therefore it is hypothesized that superficial collagen of shoulder cartilage to have a higher contribution to its mechanical behavior. Mechanical properties extracted by calibrating a newly developed indentation equation on the experimental results of sequential enzymatic degraded proteoglycan and superficial collagen indicated that superficial collagen plays a more significant role than proteoglycans in facilitating the strain-rate-dependent behavior of shoulder cartilage. Contrary to the results in studies on knee cartilage, the superficial collagen is found to equally contribute to shoulder cartilage behaviour at all strain-rates, thus affirming its significance in the mechanical behavior of shoulder cartilage. Based on the results of the investigation, it has been concluded that, although fluid affects the tissue behavior at high strain-rates, mechanical indentation behavior is dominated by the contribution of the superficial collagen. However, stain limiting superficial layer in combination with rate-dependent fluid behavior can be attributed to protective mechanisms that reduces excessive deformation of the cartilage at large strain-rates.

Bio-inspired Scaffolds for Bone Grafting

Yucong Gu^{*}, Arun Nair^{**}

^{*}University of Arkansas, ^{**}University of Arkansas

ABSTRACT

Ceramic implants are widely used in bone replacement and repairing the bone fracture. Every month, thousands of people need to undergo a surgical procedure called bone grafting to place an implant in their bones. It is a very complex surgical procedure, without a proper ceramic implant, it will pose significant health risks to the patient, or fail to heal properly. A good ceramic implant needs to have high porosity and large pore size to allow new bone cells to grow. However, a scaffold with higher porosity and larger pore size tends to reduce the mechanical strength. Thus, it is important to find a structural design, which allow the implant to have a high porosity and large pore size while retaining high strength. In this talk, computational models of bio-inspired scaffold are developed along with other common scaffolds and are subject to different loading conditions. The different geometries are tested under bending and compression loads to find the maximum stress and stress distribution. We predict the material properties based on density functional theory calculations, the effect of porosity in the material properties are modeled based on empirical relation by utilizing the density as the scaling factor. Our results show that the bio-inspired scaffold has relatively low stress levels when compared to other common scaffold structures. We also extend the study to test the bio-inspired scaffold with varying anionic and cationic substitutions occurring in the bone at the nanoscale. This study will provide an insight into a better scaffold design from bio-inspired structures and also the effect of substitutions on scaffolds.

On the Interplay Between Macroscopic Localization and Void Coalescence for Strain Rate Sensitive Materials

Vadillo Guadalupe^{*}, Reboul Javier^{**}, José Antonio Rodríguez-Martínez^{***}, Shmuel Osovski^{****}

^{*}University Carlos III of Madrid, ^{**}University Carlos III of Madrid, ^{***}University Carlos III of Madrid, ^{****}Technion,
Israel Institute of Technology

ABSTRACT

Significant progresses have been made in the last decades on the understanding and modeling of the micromechanics that govern the ductile fracture phenomena in porous metallic materials subjected to complex stress states. Two modes of plastic flow localization commonly occur in the failure of ductile materials. The first is the so-called “macroscopic localization” and occurs when the deformation becomes highly non-uniform and localizes into a thin band. The second one is the so-called “coalescence” and occurs when nearby microscopic voids interact and merge, leading to the formation of macroscopic cracks. The question addressed in the present work is whether macroscopic localization occurs prior or after the void coalescence. For that purpose, we have developed an original numerical methodology, based on 3D unitary-cell computations in ABAQUS/Standard, to simulate the evolution of a spherical void subjected to complex stress states: predefined Triaxiality and Lode parameters which remain fixed during loading. The key and original feature of our investigation, which is based on a previous work of Tekoğlu et al., (2014), is to consider the strain rate dependence on the flow behavior of the material. We have identified that the viscosity of the material plays a crucial role on both localization modes. Nevertheless, irrespective of the material properties considered, our numerical results have shown that “macroscopic localization” occurs always earlier than “coalescence”. The implications and consequences of such behavior will be exposed and discussed.

A New Closed-form Method for the Inertia Force and Moment Calculation in Reciprocating Piston Engine Design

Nanxiang Guan^{*}, Quanyong Xu^{**}, Ming Zhou^{***}, Zhifeng Xie^{****}

^{*}Tsinghua University, ^{**}Tsinghua University, ^{***}Tsinghua University, ^{****}Tsinghua University

ABSTRACT

The piston crank mechanism is an important component of the reciprocating piston engine, and it is an inherent vibration system. The calculation of the unbalance quantity is a critical procedure in the balancing mechanism design, which is adopted to balance the inertia loading. The traditional method usually used Taylor series expansion with crank-conrod ratio, then Fourier transform with the crank angle. The influence on the calculations resulting from the high order terms was generally ignored in Taylor expansion. However, the high order terms of Taylor expansion will also contribute to the low order terms in the Fourier series. This will induce poor precision in the inertia loading calculation, especially in the high crank-conrod ratio engine. This paper proposes a new closed-form method, which only adopts Fourier transformation. The coefficients of the Fourier transformation terms contain the contributions of all order terms of the crank-conrod ratio. Therefore, we name it as a closed-form method. Compared with the traditional method, the closed-form method could improve the numerical accuracy of the secondary reciprocating inertia force by 1.5% ~ 4%, when the crank-conrod ratio varies from 0.25 to 0.4. Using this new closed-form method to design a balancing mechanism, the primary and secondary reciprocating inertia forces can be completely balanced. For the engine, which the primary and secondary inertia forces are balanced, the ratio of the residual inertia force to the total force with the traditional method is 1.5%, while the ratio decreases to 0.5% with the closed-form method. The closed-form method is independent of the engine configurations?including centric engines and eccentric engine, single and multi-cylinder engines. This paper gives the applications in some cases as well.

Modeling of Ship-Wave Interaction Using Isogeometric Analysis Method

Pai-Chen Guan*, On Lei Annie Kwok**, Keng-Wei Chang***, Yang-Ling Lu****

*National Taiwan Ocean University, **National Taiwan University, ***National Taiwan Ocean University,
****National Taiwan Ocean University

ABSTRACT

The purpose of this study is to develop a numerical method that can solve the fluid-structure interaction (FSI) for near coastal ship behavior. The general structural response of ships is described by Mindlin plate theory and wave behavior is modeled by the shallow water equation. We propose the unified spatial discretization by using the Isogeometric analysis method (IGA) for both structure and fluid. The ship structure IGA method is the standard approach follows Galerkin weak form. And the IGA method for solving shallow water equation is using strong form collocation method with special discretization procedure. First, we place the collocation points at the maximum of each shape function on the parent domain to avoid the local rank deficiency. Then we introduce the non-conservative form of shallow water with flux splitting algorithm. A quasi-upwind scheme is developed to maintain the stability and regain the high order accuracy of NURBS shape functions. The proposed method is also proofed to have TVD characteristics by numerical experiment. The developed algorithm is applied to the standard sub-critical, hyper-critical flow for verification purposes. The IGA method shows robust behavior and high accuracy in those tests. Then, we test the numerical tank with ship structure floating and observe the ship motion and stress distribution.

Novel Fatigue S-N Models for Steel Reinforcing Bars with Pitting Corrosion

Xuefei Guan^{*}, Jie Chen^{**}, Jingjing He^{***}

^{*}Chinese Academy of Engineering Physics, ^{**}Beihang University, ^{***}Beihang University

ABSTRACT

Abstract: Fatigue resistance of corroded steel reinforcing bars plays an important role in the safety of reinforced concrete bridges subjected to fatigue load and corrosive environment. This paper is concerned with modelling and estimating uncertainties in fatigue life of corroded steel reinforcing bars under constant amplitude loading. Novel S-N model formats incorporating the effect of corrosion degree ρ (ρ -S-N models) are proposed based on linear elastic fracture mechanics. The proposed ρ -S-N models consider the corrosion effect on fatigue life of steel reinforcing bar in a rational background of fatigue crack propagation. The performances of the proposed ρ -S-N models are compared with the existing models in the literatures by Akaike Information Criterion (AIC), Bayesian Information Criterion (BIC), and Bayes factors. In addition, the applicability and selection of different models are discussed.

Advances in the Study of the Influence of a Rheological Law on a Numerical Model for Sediment-loaded Turbulent Flow Transport

Gabriel Guerra^{*}, Souleymane Zio^{**}, Henrique Costa^{***}, José Camata^{****}, Renato Elias^{*****},
Paulo Paraizo^{*****}, Alvaro Coutinho^{*****}, Fernando Rochinha^{*****}

^{*}Mechanical Engineering Department, Federal University of Rio de Janeiro, Brazil, ^{**}Mechanical Engineering Department, Federal University of Rio de Janeiro, Brazil, ^{***}Mechanical Engineering Department, Federal University of Rio de Janeiro, Brazil, ^{****}High Performance Computing Center, Federal University of Rio de Janeiro Brazil, ^{*****}High Performance Computing Center, Federal University of Rio de Janeiro Brazil, ^{*****}Petrobras UO-SEAL Sergipe Operational Unity, Aracaju, Sergipe, Brazil, ^{*****}High Performance Computing Center, Federal University of Rio de Janeiro Brazil, ^{*****}Mechanical Engineering Department, Federal University of Rio de Janeiro, Brazil

ABSTRACT

Numerical models can help to push forward the knowledge about complex dynamic physical systems. Turbidity currents are a kind of particle-laden flows that are a very complex natural phenomenon. Simply, they are turbulent driven flows generated between fluids with small density differences carrying particles. They also are one mechanism responsible for the deposition of sediments on the seabed. A detailed understanding of this phenomenon may offer new insight to help geologists to understand reservoir formation, a strategic knowledge in oil exploration. We present a finite element residual-based variational multiscale formulation applied to the numerical simulation of particle-laden flows in a Eulerian-Eulerian framework. Thus, the mathematical model results from the incompressible Navier-Stokes equation combined with an advection-diffusion transport equation. When sediment concentrations are high enough, empirical rheological relations close the model, describing how sediment concentrations influence the mixture viscosity. The central issue addressed here is to investigate, by computational simulations, the effects on the flow dynamics of one representative empirical rheological model. Two numerical setups, inspired by complex laboratory tests, are used for the analysis. The first is a tank with a lock-exchange configuration and the second employs a channel with a sustained current. Our findings suggest how turbulent structures and sediment deposition are affected by this empirical rheological law.

Adaptive Algorithm with Different Error Representations in Goal-Oriented Error Estimation

Diane Guignard^{*}, Serge Prudhomme^{**}, Vincent Darrigrand^{***}, David Pardo^{****}, Kenan Kergrene^{*****}

^{*}Texas A&M; University, ^{**}Ecole Polytechnique de Montréal, ^{***}Basque Center for Applied Mathematics,
^{****}Basque Center for Applied Mathematics, ^{*****}Ecole Polytechnique de Montréal

ABSTRACT

Goal-oriented error estimation is used when we are interested in a specific quantity of interest (QoI), say a linear functional of the solution of some partial differential equation, the so-called primal problem. Introducing its adjoint problem, with the QoI as right-hand side, the error in the QoI can be represented through the error of both the primal and the adjoint solutions. In practice, since these errors are unknown, a computable a posteriori goal-oriented error estimate can be obtained using for instance the solutions on a finer mesh. To be useful for adaptive strategies, the error estimate needs to be broken into local contributions and this decomposition is not unique. Even though the various error representations yield the same result globally, i.e. when summing all the local contributions, the local error indicators vary from one representation to another. Therefore, adaptive algorithms will perform differently depending upon the selected representation. The goal of this presentation is first to introduce different local error indicators for an abstract problem and then to compare their performance, when used in adaptive mesh refinement, through several numerical examples.

Stochastic Modeling and Sampling of Anisotropic Stored Energy Functions on Complex Geometries

Johann Guilleminot^{*}, Brian Staber^{**}

^{*}Duke University, ^{**}Universite Paris-Est

ABSTRACT

This talk is concerned with the construction and efficient sampling of stochastic models for spatially dependent anisotropic stored energy functions. An information-theoretic formulation is first proposed to account for theoretical constraints related, for instance, to the mathematical analysis of the nonlinear stochastic boundary value problem. A sampling algorithm is subsequently constructed and relies on solving a set of stochastic partial differential equations. These equations depend explicitly on key geometrical features inherited from the manifolds defining the boundaries of the domain. Various applications on vascular tissues are finally presented to assess the relevance of the stochastic computational framework.

Micromechanical Analysis of Damage Events in Long Fibre Reinforced Composites (LFRCs) Using the Phase Field Approach of Fracture

Teresa Guillén^{*}, Marco Paggi^{**}, José Antonio Reinoso^{***}

^{*}PhD student, ^{**}full professor, ^{***}associate professor

ABSTRACT

The design of composite structures in different engineering sectors requires the understanding of the different failure mechanisms that usually take place in long fibre reinforced composites (LFRCs). Specifically, inter-fibre (matrix) failure is one of the principal failure mechanisms of such materials at the micromechanical level. The initiation of this physical phenomenon is generally located at the fiber-matrix interface and subsequently migrates into the matrix region. The coalescence of these fracture events is responsible for macroscopic failure, which generally provokes the reduction of the stiffness properties at the structural level. In this contribution, we investigate the onset and propagation of fibre-matrix decohesion and subsequent migration into the matrix by means of the novel numerical framework combining the Phase Field approach of fracture, for the bulk failure, and the Cohesive Zone model, for the fibre-matrix interface failure, as proposed in [1]. One of the central aspects of the current methodology regards its easy integration into any FE code using a fully-implicit solution scheme. The obtained numerical predictions prove the robustness and versatility of the proposed numerical method, which allows the accurate prediction of fracture events from different signature in heterogeneous media to be performed. These results show an excellent accuracy with respect to experimental observations. Finally, these current simulations can be seen as a point of departure to construct a multiscale numerical framework within the context of the phase field approach of fracture for fibrous heterogeneous materials. References [1] Paggi, M., & Reinoso, J. (2017). Revisiting the problem of a crack impinging on an interface: a modeling framework for the interaction between the phase field approach for brittle fracture and the interface cohesive zone model. *Computer Methods in Applied Mechanics and Engineering*, 321, 145-172.

Non-intrusive Implicit/implicit Coupling &&& ABAQUS Co-simulation

Stéphane Guinard*, Omar Bettinotti**, Robin Bouclier***, Jean-Charles Passieux****

*Airbus SAS, **Dassault Systèmes SIMULIA, ***Institut de Mathématiques de Toulouse, Université de Toulouse,
****Institut Clément Ader, Université de Toulouse

ABSTRACT

Non-Intrusive Coupling Techniques (NICT) open the field to a variety of new analysis capabilities (non-intrusive domain decomposition [1], 2D-1D/3D coupling [2], determinist/stochastic analysis). In particular, NICT may meet the challenges of industrial multi-scale analysis of large aero-structures: it allows investigating local structural non-linearities, while avoiding any human intervention on existing global models. This is a significant step beyond when compared to existing numerical technologies, which may already afford the coupling of different structural models (sub-modeling), but remain penalizing in terms of operability; or which are valid only within limited domains where local non-linearities do not affect the global behavior significantly. Significant industrialization efforts and dissemination towards AIRBUS stress analysis community will be reported here: implementation of NICT as a global to local, implicit to implicit coupling engine into ABAQUS was managed, relying on co-simulation and adapted meshing strategy. Specific needs of civil aircraft structural engineering have been addressed: global shell to local solid modeling, linear orthotropic elasticity at global scale to damage and failure of composite materials at local scale. Attention was paid to consider models actually representative of day-to-day stress analysis exercises, which involve geometrical complexity, large number of dofs, mixture of element types (shell, connectors &&& solid), assembly of parts through imposed kinematical constraints. Critical sources of local non-linearity have been considered in local models: contact, damage and failure of composites, captured through adapted solid meshes (discretization at meso-constituents scale, plies &&& interfaces) and relevant constitutive models. The advent of NICT capabilities into FEM industrial software lays the path to future evolution of industrial design &&& certification processes. State-of-the-art series of models, from global rough representations to local critical details, are usually processed through top-down analysis paths, with restrained capability of bottom-up updates: outcomes from detail simulations are not leveraged properly at global level. Both local and global models could now be processed jointly, bridging different levels of abstraction together, and enabling real-time forwards and backwards analysis. Such intended &"multi-level structural analysis process&" will be exemplified by re-exploring design &&& sizing exercises practiced on representative aero-structures. [1] &"Non-intrusive Coupling: Recent Advances and Scalable Nonlinear Domain Decomposition&", M. Duval, J.-C. Passieux, M. Salaün and S. Guinard, Archives of Computational Methods in Engineering, 23(1):17-38, 2016 [2] &"On the computation of plate assemblies using realistic {3D} joint model: a non-intrusive approach&", G. Guguin, O. Allix, P. Gosselet and S. Guinard, Advanced Modeling and Simulation in Engineering Sciences, 3(16), 2016

Adaptive Immersed Method for Turbulent Flows with Boundary Layers

Ghalia Guiza^{*}, Alexandre Boilley^{**}, Philippe Meliga^{***}, Elie Hachem^{****}, Youssef Mesri^{*****}

^{*}MINES ParisTech - CEMEF - CFL research group, ^{**}Transvalor, ^{***}Centrale Marseille, M2P2, ^{****}MINES ParisTech - CEMEF - CFL research group, ^{*****}MINES ParisTech - CEMEF - CFL research group

ABSTRACT

Fluid structure interactions with complex geometries are simulated using a finite element formulation coupled with several numerical techniques to ensure stability and accuracy. First, an edge based error estimator for anisotropic mesh adaptation is used to detect automatically all flow features and boundary layers. A Variational MultiScale stabilized finite element method is employed to solve the Navier-Stokes equations. Finally, an immersed volume method is proposed to deal with fluid-structure interactions. This paper is meant to show that the combination of anisotropic meshing with stabilized finite element methods provides an adequate framework for solving turbulent flows past immersed complex geometries at high Reynolds numbers. Several 3D challenging test cases and comparisons are proposed, such as flow past an airship, a drone and a flying car.

Near-Structure Air Blast Simulations Using Zapotec, A Coupling of CTH and Sierra/SM

Arne Gullerud*, Dave Hensinger**, Tim Shelton***, Edmundo Corona****

*Sandia National Laboratories, **Sandia National Laboratories, ***Sandia National Laboratories, ****Sandia National Laboratories

ABSTRACT

The ability to conduct simulations for air-blasts and their subsequent interaction with structures is vital in the study of a range of security and safety concerns. For significant stand-offs between the blast and the structure, a range of analytic/simplified simulation techniques can provide suitable results, e.g. conwep [1] for simple geometries. However, for blasts which originate close to the structure or with complex geometries, the interaction of the explosive products, air shock, structure geometry, and material failure necessitate the use of more complex computational frameworks. Zapotec [2], an Euler-Lagrange code which couples the hydrocode CTH with the structural transient-dynamics finite element code Sierra/SM, provides such a framework. This presentation includes a short overview of the Zapotec code methodology, and then compares Zapotec simulations to two simple test series which investigate structural response to explosive detonations with small standoffs where analytic/simplified simulation techniques can fail. The Zapotec simulations compare well to the experimental results in both cases, giving confidence in the use of Zapotec for near-structure air-blast scenarios. The presentation concludes with a demonstration simulation of explosive blast on a large-scale structure. Sandia National Laboratories is a multimission laboratory managed and operated by National Technology and Engineering Solutions of Sandia, LLC., a wholly owned subsidiary of Honeywell International, Inc., for the U.S. Department of Energy's National Nuclear Security Administration under contract DE-NA0003525. Sandia document reference number: SAND2017-13775 A. [1] Hyde DW. (1988). User's Guide for Microcomputer Programs CONWEP and FUNPRO. US Army Corps of Engineers. Report AD-A195 867. [2] Bessette G, et. al. Zapotec: A Coupled Eulerian-Lagrangian Computer Code, Methodology and User Manual, Version 3.0. Sandia National Laboratories. Report SAND2016-11223.

Analytical Solution of Torsional Vibration of Uniform Circular Shaft with Multiple Concentrated Inertias

Jing Guo*

*Department of Engineering Mechanics, College of Aerospace Engineering and Civil Engineering, Harbin Engineering University

ABSTRACT

In the existing literature, many methods have been proposed to obtain the natural frequencies and modes of the vibration of uniform circular shaft with multiple concentrated elements. The torsional vibration problem was solved by using the Holzer method decades years ago. This problem was tackled by transfer matrix method and the finite element method after the rapid development of computer technology. The methods mentioned above are approximate solutions, their results are not accurate. Until 1975 (and 1979), Gorman (and Blevins) presented a new method to obtain the exact expressions of the natural frequencies and mode shapes of a uniform shaft carrying a single rotary inertia or torsional spring. In 1988, Rao gave the exact expressions for the torsional frequencies and mode shapes of the generally constrained shafts and piping with two disks. Ref. studied the torsional vibration problem of beam containing lumped elements under cantilever boundary conditions and fixed boundary conditions. As for the exact solutions of the torsional vibration of uniform shafts carrying multiple concentrated, the information concerned is rare. Only Chen presented an exact solution for free torsional vibration of a uniform circular shaft carrying multiple concentrated elements adopting the numerical assembly method, but it is still a approximate approach. In this paper, A new analytical method (AM) was used to perform the torsional vibration analysis of a uniform circular shaft carrying multiple concentrated elements (rotary inertias) with arbitrary magnitudes and locations. Three boundary conditions were studied: free-free, clamped-free and clamped-clamped. Several general rules were obtained, and the cause of the explanation was given. And it has been found that the agreement between the present results and the lumped mass method (LMM) results is good. Compared with existing method, the presented AM may be one of the simplest tools for studying the title problem.

Numerical Simulation Method Study for Inconel 718 Plate Penetration

Weiguo Guo^{*}, Xueming Tan^{**}, Longyang Chen^{***}, Tuo Wang^{****}, Yanping Li^{*****}

^{*}School of Aeronautics, Northwestern Polytechnical University, ^{**}School of Aeronautics, Northwestern Polytechnical University, ^{***}School of Aeronautics, Northwestern Polytechnical University, ^{****}School of Aeronautics, Northwestern Polytechnical University, ^{*****}School of Aeronautics, Northwestern Polytechnical University

ABSTRACT

Abstract: In modern aeroengine, the aviation regulatory agency require that all commercial turbine jet engine must include a strong blade containment system. This containment system usually consists of a thin metal casing designed to safely contain debris in the event of engine blade fragmentation. Inconel 718 nickel base superalloy is widely used in the manufacture of aeroengine casing. In the present study, to obtain real Johnson-Cook constitutive model and failure criteria parameters, a series of uniaxial compression and tensile tests of this material over a wide range of strain rate and temperature are carried out firstly. Then, with the help of Abaqus commercial software, the ball projectile and the Inconel 718 Plate are optimized for reasonable Hypermesh design, and then the parameters of Johnson-Cook constitutive model and failure criteria from experiments are employed to simulate different penetration conditions. To analyze and valuate the simulation accuracy and calculation methodology, a lot of the ballistic impact tests on Inconel718 target plates are also conducted. Moreover, the deformation and damage of the impact samples are Macro and micro analyzed by optical microscope and SEM. The numerical results of different simulation conditions (i.e. failure criteria, mesh qualities and boundary conditions) are compared with test results on ballistic impact. An ideal and higher precision results are obtained by elaborating adjustment for simulation process. Based on these results, it can conclude that, the combination of ductile fracture criterion and shear fracture criterion is better than the single Johnson-Cook failure criterion to obtain better simulation results; the fine mesh size (0.35mm) can better reflect the failure mode around the penetration hole than the coarse ones, and completely fixed boundary has a better performance than which partial fixed on predicting the overall deformation. Keywords: Penetration, Constitutive model, Failure criteria, Mesh quality, Simulation Reference [1] Silva M A G, Cisma?iu C, Chiorean C G. Numerical simulation of ballistic impact on composite laminates[J]. International Journal of Impact Engineering, 2005, 31(3):289-306. [2] Wang Y, Chen X, Young R, et al. Finite element simulation of ballistic impact on woven fabric assemblies[J]. Finite Element Analysis, 2010.

Moving Morphable Component (MMC)-based Explicit Topology Optimization-some New Developments

Xu Guo*, Weisheng Zhang**

*Dalian University of Technology, **Dalian University of Technology

ABSTRACT

Moving Morphable Components (MMC) method, which does topology optimization in an explicit and geometrical way, is a new computational framework for structural topology optimization. Unlike traditional solution frameworks, where topology optimization is achieved by eliminating unnecessary materials from the design domain or evolving the structural boundaries, a set of morphable components are used as building blocks of topology optimization in the MMC framework and optimal structural topology is obtained by optimizing the shapes, lengths, thicknesses, orientations and layout (connectivity) of morphable structural components. The advantages of the method are that 1) it can integrate the size, shape, and topology optimization in CAD modeling systems seamlessly. 2) The method can combine both the advantages of explicit and implicit geometry descriptions for topology optimization. 3) It also has the great potential to reduce the computational burden associated with topology optimization. The proposed work introduces some new developments of the MMC-based method, including solving large-scale three-dimensional topology optimization problem efficiently, additive manufacturing oriented design (self-supporting structure design, minimum length scale control and graded lattice structure design), topology optimization with multiple materials, explicit control of structural complexity, kirigami pattern design of complex 3D structure and so on. Some representative examples are presented to illustrate the effectiveness of the proposed method.

Moving Morphable Component (MMC)-based Explicit Topology Optimization-some New Developments

Xu Guo*

*Dalian University of Technology

ABSTRACT

Moving Morphable Components (MMC) method, which does topology optimization in an explicit and geometrical way, is a new computational framework for structural topology optimization. Unlike traditional solution frameworks, where topology optimization is achieved by eliminating unnecessary materials from the design domain or evolving the structural boundaries, a set of morphable components are used as building blocks of topology optimization in the MMC framework and optimal structural topology is obtained by optimizing the shapes, lengths, thicknesses, orientations and layout (connectivity) of morphable structural components. The advantages of the method are that 1) it can integrate the size, shape, and topology optimization in CAD modeling systems seamlessly. 2) The method can combine both the advantages of explicit and implicit geometry descriptions for topology optimization. 3) It also has the great potential to reduce the computational burden associated with topology optimization. The proposed work introduces some new developments of the MMC-based method, including solving large-scale three-dimensional topology optimization problem efficiently, additive manufacturing oriented design (self-supporting structure design, minimum length scale control and graded lattice structure design), topology optimization with multiple materials, explicit control of structural complexity, kirigami pattern design of complex 3D structure and so on. Some representative examples are presented to illustrate the effectiveness of the proposed method.

Discrete Element Modeling of Flexible Fiber Flow and Heat Transfer in a Rotating Drum

Yu Guo^{*}, Fan Yang^{**}, Hanhui Jin^{***}

^{*}Department of Engineering Mechanics, Zhejiang University, Hangzhou, China, ^{**}Department of Engineering Mechanics, Zhejiang University, Hangzhou, China, ^{***}Department of Engineering Mechanics, Zhejiang University, Hangzhou, China

ABSTRACT

Rotating drums have been frequently used to dry granular materials. The rotation of horizontally-arranged cylindrical drum about its major axis drives the materials inside it to flow and mix, facilitating the contacts and heat transfer between particles and drum wall surface. A flexible fiber model incorporated with heat transfer models has been developed for the studies of flow and heat transfer of flexible fibers in a rotating drum, which are much less understood than those of rigid spheres. In the simulations of rotating drum with flexible fibers, we look at contact number per fiber (coordination number), fiber movement trajectory, velocity distribution, temperature distribution, and heat transfer rate. The effects of some important fiber properties, such as fiber bending elastic modulus, fiber aspect ratio, fiber-fiber friction coefficient, and fiber-drum friction coefficient, on the fiber flow and heat transfer are explored. The knowledge obtained from the computational simulation studies is expected to guide the design and optimization of a rotating drum device for drying the flexible fibrous materials, such as textile and biomass materials.

Parameterized Grillage Model and Computational Method of Steel-concrete Composite Waffle Floor Systems Based on Numerical Simulation

Yu-Tao Guo^{*}, Mu-Xuan Tao^{**}, Xin Nie^{***}, Jian-Sheng Fan^{****}

^{*}Key Lab. of Civil Engineering Safety and Durability of China Education Ministry, Dept. of Civil Engineering, Tsinghua University, Beijing, China 100084, ^{**}Associate Professor, Key Lab. of Civil Engineering Safety and Durability of China Education Ministry, Dept. of Civil Engineering, Tsinghua University, Beijing, China 100084, ^{***}Key Laboratory of Civil Engineering Safety and Durability of China Education Ministry, Dept. of Civil Engineering, Tsinghua University, Beijing, China 100084, ^{****}Beijing Engineering Research Center of Steel and Concrete Composite Structures, Dept. of Civil Engineering, Tsinghua University, Beijing, China 100084

ABSTRACT

A steel-concrete composite waffle floor system (SCCWFS) that consists of orthogonal steel beams and a flat RC slab has potential applications in long-span building floors because of its large loading capacity, low depth-to-span ratio, and excellent ductility, as demonstrated by a previous experimental program. According to the test results, the spatial composite effect between the orthogonal steel beams and concrete slab significantly influences the performance of the SCCWFS. However, the complexity of the spatial composite effect in the SCCWFS makes it much more difficult to determine the rigidity and the internal force distribution in a routine design practice than the one-way steel-concrete composite floor or the RC waffle slab. To address this problem, a parameterized grillage model is developed in which intrinsic factors are defined to describe the critical properties of the deformation pattern, the reaction force and moment distribution of the SCCWFS; relation factors are defined to relate these properties of the SCCWFS to that of its corresponding steel grillage. Based on the parameterized grillage model, parametric analyses are conducted using a beam-shell mixed finite-element (FE) model and the influence of various parameters on intrinsic and relation factors is investigated, in which the beam height, slab thickness, length-to-width ratio, and so on are shown to be of importance. Based on the batching modelling technique developed in this paper, the data of a total of 5190 numerical models associated with seven parameters covering almost all the practical cases are then obtained. A step-shaving method is then proposed to derive formulas, which is based on the method of analysis of regression and could act as a powerful tool to deal with models that are influenced by multiple variables and the analytical form could not be directly obtained. Based on the parameterized grillage model and the step-shaving method, computational formulas to predict the vertical displacements, reaction force and moment distribution of the SCCWFS are derived and verified. Finally, design procedures, recommendations and simplified forms of the formulas are proposed, in which the formulas are proved to have an error of approximately 10%.

Seamless Integration of Isogeometric Trimmed Shell Analysis at Large Deformations, Based on the STEP Exchange Format

Yujie Guo^{*}, Jason Heller^{**}, Thomas J.R. Hughes^{***}, Martin Ruess^{****}, Dominik Schillinger^{*****}

^{*}Nanjing University of Aeronautics and Astronautics, PR China, ^{**}Faircad3d, LLC, Santa Fe, NM, USA, ^{***}ICES, The University of Texas at Austin, USA, ^{****}School of Engineering, University of Glasgow, UK, ^{*****}University of Minnesota, USA

ABSTRACT

ABSTRACT Following a series of recent innovations, isogeometric analysis for trimmed thin shell surfaces is currently developing into an accurate, efficient and mature design-through-analysis methodology. Based on a series of recent publications on the topic, we identify four key components for establishing a successful isogeometric methodology for trimmed shell analysis: (1) an efficient and accurate isogeometric shell technology, (2) methods to enforce boundary and coupling conditions at non-matching trimming curves, (3) quadrature methods for the integration of stiffness and residual forms in trimmed elements and along surface-to-surface intersection curves, (4) and the ability to query accurate geometric information related to trimmed surfaces and surface-to-surface intersection curves from CAD data structures. The first three components have profited from significant progress in both isogeometric and embedded domain finite element methods in recent years. The fourth component, the interaction of trimmed shell analysis with CAD data structures, is essential for demonstrating the competitiveness for complex real-world trimmed objects. This work contributes to this emerging technology with respect to the following aspects. On the analysis side, we present a robust variationally consistent Nitsche-type formulation for thin shells at large deformations that weakly enforces coupling constraints at trimming curves. On the geometry side, we present a set of algorithms that enable automatic interaction of trimmed shell analysis with CAD data structures based on the STEP exchange format. We integrate these methodologies in a comprehensive framework for isogeometric trimmed shell analysis. We demonstrate that our framework is able to seamlessly perform large-deformation stress analysis of an industry-scale 76-patch surface model of a Dodge RAM hood, while delivering comparable accuracy with respect to Simulia's commercial software package Abaqus. **REFERENCES** [1] Y. Guo, M. Ruess, D. Schillinger, "A parameter-free variational coupling approach for trimmed isogeometric thin shells", *Comp. Mech.*, Vol. 59, pp. 693-715, (2017). [2] Y. Guo, M. Ruess, "Nitsche's Method for a Coupling of Isogeometric Thin Shells and Blended Shell Structures", *Comput. Meth. Appl. Mech. Engrg.*, Vol. 284, pp. 881-905, (2014). [3] M. Ruess, D. Schillinger, A.I. Özcan, E. Rank, "Weak coupling for isogeometric analysis of non-matching and trimmed multi-patch geometries", *Comput. Meth. Appl. Mech. Engrg.*, Vol. 269, pp. 46-71, (2014).

Simulation of Lipid Membrane Rupture via Cellular Automation

Abhay Gupta*, Irep Gozen**, Michael Taylor***

*Santa Clara University, Department of Mechanical Engineering, **University of Oslo, Centre for Molecular Medicine Norway, ***Santa Clara University, Department of Mechanical Engineering

ABSTRACT

Biological cell membranes consist of many organized phospholipid molecules. Rupture, i.e. the forceful opening of large area pores, in these membranes is a common form of cell damage, and irreversible rupture has been implicated in disease, e.g. muscular dystrophy. Understanding and perhaps controlling membrane pore formation would be promising not only in disease treatment and prevention, but also in applications such as gene therapy and drug delivery. Previously, only circular pores were known to form in biological membranes. However, recent experimental study of model bi-layer lipid membranes spreading on solid supports has led to the discovery of two new rupture modes: fractal and floral [1]. These modes share at least a qualitative similarity to the interaction of immiscible fluids in porous media (e.g., viscous fingering and invasion percolation). What is poorly understood are the reasons a membrane might prefer to form one type of fracture pattern rather than another. It is hypothesized that heterogeneous mechanical pinning (i.e., adhesion) between lipid bilayers governs this preference. Unfortunately, the very small fluid volume entrapped between the layers, as well as the difficulty in controlling the number of pinning sites, poses limits on the experimental investigation of rupturing. To investigate these different rupture morphologies, we developed a numerical model based on cellular automation (CA). A cellular automation consists of a grid of that are assigned a specific state (e.g., a 0 or 1). These states evolve through the application of a few very simple rules. Despite their simplicity, CA are able to capture a range of complex behavior, even emergent behavior, in the areas of growth, aggregation, segregation, and percolation [2]. While CA have been of particular interest to, for example, the geological science and spatial simulation communities, its application to lipid rupture mechanics is novel. Our new CA incorporates rules from both standard percolation models and particle-based fracture methods. We demonstrate the CA via simulations of circular, floral, and fractal morphologies and show how these can be obtained through simple alterations of pinning density and behavior. REFERENCES [1] Gözen, I. et al. Fractal avalanche ruptures in biological membranes. *Nature Materials* 9, 908-912 (2010). [2] O'Sullivan, D. and Perry, G.L.W., *Spatial Simulation: Exploring Pattern and Process*, Wiley-Blackwell, 2013.

An Integrated Computational Modeling Approach to Predict Joint Properties Obtained in Solid-state Joining of Dissimilar Materials

Varun Gupta^{*}, Erin Barker^{**}, Kyoo Sil Choi^{***}

^{*}Pacific Northwest National Laboratory, ^{**}Pacific Northwest National Laboratory, ^{***}Pacific Northwest National
Laboratory

ABSTRACT

Multi-material assemblies hold the key to achieve light weighting, enhanced performance, and functionality in automobiles, aircraft, and other manufacturing applications. The desired product performance is achieved by collectively utilizing the favorable properties of different materials. Joining of such materials using conventional welding techniques, however, poses a significant challenge owing to the large differences in the physical properties of the constituent components. In dissimilar metallic systems such as Steel-Aluminum or Magnesium-Steel, the traditional fusion based welding processes can lead to undesirable large and continuous intermetallic phases, due to difference in melting points of the two metal alloys being welded. Solid-state joining techniques like friction stir welding and high velocity impact welding provide a viable approach to join such dissimilar materials. The process of determining optimal welding process parameters that lead to a robust solid-state joint using a purely experimental approach is time-consuming and expensive. Computational tools play a key role in developing a predictive understanding of the resultant joint properties. We present an integrated finite element method based computational approach with experimental support to quantitatively describe process-structure-property relationships for solid-state joints. Such a scientific framework can help accelerate the development and deployment of these solid-state joining techniques for manufacturing applications.

Probabilistic Assessment of Aircraft Structural Reliability: Major Challenges and Opportunities

Mark Gurvich*

*United Technologies Research Center

ABSTRACT

This work is aimed to review major challenges associated with probabilistic assessment of structural integrity specifically for aircraft applications and suggest most promising ways for their mitigation. The review and corresponding analysis are based on publically available sources and experience covering a broad range of aircraft and rotorcraft primary load-bearing structures in uncertain conditions. Challenges of both fundamental general solutions and practical engineering implementations are considered and prioritized. Also, challenges of different natures, such as computational (e.g., numerical efficiency), physical (e.g., methodologies to predict random damage), and practical (e.g., limited statistical information on input data) are discussed and listed. Among down-selected major challenges are issues associated with a) assessment of structural integrity with very low probabilities of failure; b) efficient modeling of random load, usage and environmental conditions; c) stochastic fatigue modeling of aircraft structures; d) impact/ballistic modeling of aircraft structures as random phenomena; e) multi-scale methods developed specifically for probabilistic assessment; f) integration of probabilistic modeling with statistical input characterization; g) simplified "engineering" methods of probabilistic analysis and assessment; and so on. For the down-selected challenges, potential solutions critically assessed for either direct implementation or additional enhancement or as an opportunity for future consideration. Finally, major observations and conclusions are summarized in form of practical recommendations.

Numerical Modelling, Simulation and Validation of Icing on a Wind Turbine Blade

Gustaf Gustafsson*, Simon Larsson**

*Luleå university of technology, **Luleå university of technology

ABSTRACT

Today there is a strong development of wind power in northern Sweden, where risk for icing conditions is present. Icing of the blades leads to changing load conditions, production loss and risk of overloading the machine components. When the ice loose from the blades, the ice throw can lead to both physical damage and personal injury. Uncertainties around these issues threaten the planned expansion in the northernmost regions. Prediction of loads and production losses are of great importance for the durability and economy of wind power plants [1]. A thrust worthy numerical model of ice loads on wind turbines will be a valuable tool for minimizing the costs due to damage and production losses caused by icing. This work presents a numerical model for simulating ice accretion on a wind turbine blade in lab-scale. It is a multi-physic model with interaction of three phases: the air, the water droplets and the wind turbine blade. The air flow is modelled with incompressible fluid dynamics (ICFD), the water droplets in the air is modelled with the discrete element method (DEM) and the wind turbine blade is modelled with the finite element method (FEM). A two way coupling is used for the interaction between the air and the water droplets and between the air and the wind turbine blade. A freezing condition controls the ice accretion when the water droplets hits the wing profile. The simulation is compared with a lab-scale experiment of ice accretion of a wind turbine profile in a wind tunnel found in literature [2]. The experiment is well documented with well defined parameters such as: temperature, wind velocity, water content in the air, size of the water droplets, wing profile and angle of attack. Two simulations were done for two different angles of attack and validated by comparing ice profiles on the blades numerically and experimentally for the two cases. Similar ice profiles were found numerically and experimentally. [1] IEA Wind Recommended Practice 13: Wind Energy in Cold Climates, 2012. [2] C. Hochart et. al., "Wind Turbine Performance under Icing Conditions", Wind Energy, 11, 319-333 (2008)

Reduced Models for Uncertainty Quantification in the Cardiovascular Network via Domain Decomposition

Sofia Guzzetti^{*}, Luis A. Mansilla Alvarez^{**}, Pablo J. Blanco^{***}, Kevin T. Carlberg^{****}, Alessandro Veneziani^{*****}

^{*}Emory University, ^{**}Laboratório Nacional de Computação Científica, ^{***}Laboratório Nacional de Computação Científica, ^{****}Sandia National Laboratories, ^{*****}Emory University

ABSTRACT

The parameters that characterize reduced 1D models of the cardiovascular system (CVS) feature variability both between patients and within a single individual, depending on physiological conditions. Characterizing this variability via uncertainty quantification (UQ) studies on the CVS entails two major challenges: (i) the computational resources required by full 3D models may not be easily accessible by users (e.g., hospitals) due to practical limitations, privacy concerns, or time constraints; (ii) Reduced 1D models may be inaccurate in capturing anomalies of the physiology in the presence of cardiovascular pathologies like stenoses or aneurysms. This introduces additional (epistemic) uncertainty that should also be characterized. The objectives of this study are (I) to design UQ solvers tailored to the CVS that promote parallelism and scalability, and (II) to enhance the accuracy of 1D reduced models without incurring computational cost. The Domain Decomposition Uncertainty Quantification (DDUQ) approach [1] performs UQ at the subsystem level, and propagates uncertainty information encoded as polynomial chaos coefficients via overlapping DD techniques, allowing for a reduction of the computational time. The local cross-sectional dynamics discarded by 1D models can be retrieved via educated reduced models such as the Transversally Enriched Pipe Element Method (TEPEM) [2], or HiMod methods [3]. The main stream dynamics and the transverse components are solved by the Finite Element Method (FEM) and by Spectral Methods, respectively, to guarantee high accuracy at low computational cost. Preliminary results show that (i) The computational cost of UQ in the CVS can be drastically reduced by promoting the independence of the subsystems and avoiding full-system simulations; (ii) The solver is scalable; (iii) Educated reduced models improve the accuracy of any 1D solver, at approximately the same computational cost. Acknowledgements CNPq, FAPERJ, NSF grant DMS 1419060. Sandia National Laboratories is a multimission laboratory managed and operated by National Technology and Engineering Solutions of Sandia, LLC., a wholly owned subsidiary of Honeywell International, Inc., for the U.S. Department of Energy's National Nuclear Security Administration under contract DE-NA-0003525. References 1. K. Carlberg, M. Khalil, K. Sargsyan, and S. Guzzetti. Uncertainty propagation in large-scale networks via Domain Decomposition. In preparation, 2017. 2. L. Mansilla Alvarez, P. Blanco, C. Bulant, E. Dari, A. Veneziani, and R. Feijóo. Transversally enriched pipe element method (TEPEM): An effective numerical approach for blood flow modeling. IJNMBE, 33(4), 2017. 3. Guzzetti S, Perotto S, Veneziani A. Hierarchical Model Reduction for Incompressible Fluids in Pipes. IJNME. 2017.

A Stabilized Cut Discontinuous Galerkin Framework (cutDG): I. Boundary Value and Interface Problems

Ceren Gürkan*, Andre Massing**

*MSc., **Dr.

ABSTRACT

ABSTRACT We develop both theoretically and implementationwise a novel cut Discontinuous Galerkin framework (cutDG) by combining stabilization techniques from the cut finite element method [1] with the interior penalty discontinuous Galerkin methods (DG) for elliptic [2] and hyperbolic problems [3]. The domain of interest is embedded into a background mesh and can cut through it in an arbitrary fashion. The discrete discontinuous Galerkin related bilinear forms are only integrated those parts of the mesh entities which are inside the physical domain of interest. In contrast to the classical cell-merging/agglomeration approach, we augment the discrete bilinear forms by properly designed stabilization to guarantee optimal convergence and condition number estimates independent of the particular cut situation. We show that the stabilization terms have to satisfy only a few abstract assumptions and we discuss possible realizations. The theoretical properties are illustrated by a number of numerical experiments including convergence and condition number tests for elliptic boundary and interface problems as well as pure advection-reaction problems. **REFERENCES** [1] E. Burman, S. Claus, P. Hansbo, M. G. Larson, and A. Massing. CutFEM: discretizing geometry and partial differential equations. *Internat. J. Numer. Meth. Engrg.*, 104(7):472- 501, November 2015. [2] D.N. Arnold. An interior penalty finite element method with discontinuous elements. *SIAM J. Num. Anal.*, 19(4):742-760, 1982. [3] F. Brezzi, L. D. Marini, and E. Süli, *Math. Models Methods Appl. Sci.* 14(12):1893-1903, 2004.

High Precision Imposition of Essential Boundary Conditions in Isogeometric Analysis by a Generalized NURBS Representation

Alireza H. Taheri*, Krishnan Suresh**

*University of Wisconsin, Madison, **University of Wisconsin, Madison

ABSTRACT

Due to the non-interpolatory behavior of spline basis functions, treatment of non-homogeneous essential boundary conditions in isogeometric analysis (IGA) is non-trivial. Several techniques including weak imposition via variational methods, or strong imposition via fitting algorithms have been proposed e.g. [1,2]. However, since splines are inherently poor in capturing rapidly varying functions, these methods result in significant error for non-smooth or discontinuous boundary conditions. In this paper, we propose a new method for the imposition of non-homogeneous essential boundary conditions in IGA by the introduction of an extension of NURBS representation. The proposed generalization is obtained by decoupling the weights associated with the control points, along both physical and parametric coordinates. This brings the possibility of treating the out-of-plane weights of boundary control points in the appropriate parametric direction as extra design variables to better approximate the boundary condition, while maintaining the underlying geometry and its parameterization intact. A global approximation technique is then introduced by setting up a nonlinear least square optimization problem whose design variables are the out-of-plane coordinates and weights of boundary control points. Subsequently, the optimization problem is solved by employing the Levenberg-Marquardt algorithm, and the obtained optimal results are imposed strongly on the problem. As the numerical results demonstrate, this procedure dramatically improves the accuracy of imposition of essential boundary conditions. In particular, unlike the existing NURBS-based methods, the proposed algorithm is able to capture sharp variations and discontinuities in the boundary conditions close to machine precision even with a coarse discretization, and without increasing the multiplicity of knots, thereby maintaining higher order continuity of the solution over the whole computational domain. Several numerical examples are presented to demonstrate substantial superiority of the suggested approach compared to existing methods. [1] Wang D, Xuan J. An improved NURBS-based isogeometric analysis with enhanced treatment of essential boundary conditions. *Comput Methods Appl Mech Eng* 2010; 199:2425–36. [2] Chen T, Mo R, Gong ZW. Imposing Essential Boundary Conditions in Isogeometric Analysis with Nitsche's Method. *Appl Mech Mater* 2011; 121–126:2779–83.

Deep Mechanical Treatment Simulations of Engineering Surfaces

Hedi HAMDI^{*}, Anis RAMI^{**}, Sawsen YOUSSEF^{***}, Achref KALLEL^{****}, Tarek MABROUKI^{*****},
Salem SGHAIER^{*****}

^{*}LTDS, University of Lyon, France, ^{**}LGM, University of Monastir, Tunisia, ^{***}LGM, University of Monastir, Tunisia,
^{****}LTDS, University of Lyon, France, ^{*****}LMAI, University of Tunis El Manar, Tunisia, ^{*****}LGM, University of
Monastir, Tunisia

ABSTRACT

In many contact application involving high pressure like the case of integrated bearing track for aeronautical applications, surface hardening are necessary to ensure wear resistance. Chemical treatment such as nitriding and carburizing are often chosen and performed. The hardening depth can reach 700 μ m and need grinding, tribo-finishing or other manufacturing processes to give the engineering surface the good surface states in relation with the finale application. In this paper, a FEM simulation of a combined turning burnishing (CoTuB) process is proposed in order to explain how and why, when rough turning and ball burnishing processes proceed simultaneously they can lead to a very high hardening level and a hardening depth two or three times higher than those obtained after nitriding or carburizing. Three-dimensional simulations of the turning process by an improved thermo-mechanical moving loading, and simultaneously the burnishing simulation by a rigid ball, allowed having a great idea of the heating and cooling history of elementary volumes on the surface and beneath it, related to the several revolutions. These information combined with the mechanicals actions imposed by the ball, can explain how the strain hardening occurs in those special thermodynamics conditions. They can also explain the physical mechanisms that are activated and why the hardening depth is increased after each revolution depending on the temperature dependence of the material behavior, the recovering rate of the ball and the process parameters. Residual stress state can also be determined by the propose FEM multiphysics simulations. They allow understanding how from a revolution to another, tensile residual stress, very close to the extreme surface, induced by turning process became progressively compressive when the ball burnishing proceeds. The final simulated residual stress profiles beneath the surface are then compared to those obtained by experimentations. Results are very surprising and very interesting. Till now, induced phenomena are well known for turning process and ball burnishing process when they are used separately. Surface integrity of the engineering surface in terms of hardening level and depth, residual stress, and so on, is very improve when those two well-known processes act together and simultaneously. This combination has surely a great future for very high accurate surface engineering applications with an increased lifetime of security mechanical parts among others.

Data Pruning of Tomographic Data for the Calibration of Constitutive Models: Application to a Resin-bonded Sand

William HILTH*, David Ryckelynck**

*Mines ParisTech, **Mines ParisTech

ABSTRACT

With the development and the generalization of digital image correlation (DIC) and digital volume correlation (DVC) techniques, the volume of data acquired has drastically increased. This raises new challenges, such as data storage, data mining or the development of relevant experiments-simulations dialog methods such as model validation and model calibration. Data pruning of the experimental results is a relevant solution, focusing on meaningful data while saving time and storage. We developed an objective method to reduce drastically the amount of data thanks to model reduction techniques. From experimental snapshots, containing the values of a given field (displacement, strain...) in all the sample at all time steps, and image correlation error maps, we can extract reduced basis and coordinates of the full experiment. These basis are used to build an experimental Reduced Domain (RD) where the data is actually needed or relevant with a modified hyper-reduction method. This RD can be completed with a chosen Zone Of Interest (ZOI), enabling to decide to keep the data where it seems worthwhile. The RID can only be 10% or 25% of the complete sample. Then, in order to simplify data exploitation and storage, we can only focus on the RD and the projection of the reduced basis on this new geometry, reducing drastically the amount of data stored. Moreover, keeping only the pruned experimental data still enables model calibration. They can be directly imposed as Dirichlet boundary conditions, with the use of an hybrid FEM/hyper-reduction method. The hybrid method calculations are 10 to 70 times quicker than full field FEM calculations. The method is applied for a model validation and calibration of a polyurethane resin-bonded sand sample studied in in situ X-Ray CT. The experimental RD was determined thanks to computed displacement field and its uncertainty. Two elastoplastic constitutive models of gradual complexity were assessed. The procedure showed that the simpler approach failed to model correctly the complex behavior of the bonded sand and motivated the development of more sophisticated constitutive equations. This new model was successfully validated and calibrated.

Numerical Simulation Study on Failure Mechanism of Octet Architected Nanolattices Subjected to Bending Load

WEI HUANG*, PING LIU**

*School of Aeronautics, Northwestern Polytechnical University, 127 Youyi West Road, Xi'an 710072, Shaanxi, P.R.China, **Institute of High Performance Computing, 1 Fusionopolis Way, #16-16 Connexis, Singapore 138632, Singapore

ABSTRACT

Abstract: With the development in high-precision lithography and thin film sputter deposition techniques, the fabrication of large-scale metamaterials has enabled to implement. Nanolattices are fabricated in creating lightweight, strong, and damage-tolerant structural metamaterials which are made up of microscale tubes with nanoscale thickness [1]. Existing studies have found that the failure behaviour of metallic glass can occur brittle-to-ductile transition by reducing the sample size to the nanoscale [2]. For nano-architected metallic glass, it can take advantage of both structural and material size effects. Hence, the bending stiffness and failure behaviour of the metallic glass nanolattices with octet unit cells were investigated by using numerical simulations for 3-point bending test in this work. The force-deflection response curves of the nanolattices with crisscrossed hollow tubes related to different cross-section shapes, different wall thicknesses and different tube aspect ratios are obtained, respectively. The simulation results reveal that the mechanical properties of the nano architected metamaterial could be controlled by the structural configuration as well as the wall thickness, cross-section shape and aspect ratio of hollow tubes. It is seen that the thickness and cross-section shape of hollow tube have strong influence on the flexural strength and failure modes of the nanolattices subjected to bending load. By changing the thickness and ellipticity of hollow tubes, it's possible to control the failure behavior (buckling, material yield and fracture) of the nanolattices. When the tube thickness is thick or the cross-section shape is prone to a circle, the nanolattices tend to fail due to the material yield failure and fracture. When the tube thickness is thin or the cross-section shape is prone to a squashed ellipse, the buckling of hollow tubes is more likely to happen in the nanolattices before the plastic damage occurred. The mechanical response of the nanolattices exhibit significantly ductility by reducing the aspect ratio of hollow tubes. The conclusions from the numerical simulations could provide the guideline for the optimization design of the nanolattices. Reference [1] Meza LR, Das S, Greer JR. Strong, lightweight, and recoverable three-dimensional ceramic nanolattices. *Science*, 2014, 345(6202): 1322-1326. [2] Lionta R, Greer JR. 3D nano-architected metallic glass: Size effect suppresses catastrophic failure. *Acta Material*, 2017, 133: 393-407. [3] Montemayor LC, Wong WH, Zhang YW, Greer JR. Insensitivity to Flaws Leads to Damage Tolerance in Brittle Architected Meta-Materials. *Scientific Reports*, 2016, 6: 20570.

Numerical Simulation Study on the Influence of Welding Induce Residual Stress to the Fatigue Crack Propagation Behavior

WEI HUANG*, Yu-E MA**

*School of Aeronautics, Northwestern Polytechnical University, 127 Youyi West Road, Xi'an 710072, Shaanxi, P.R.China, **School of Aeronautics, Northwestern Polytechnical University, 127 Youyi West Road, Xi'an 710072, Shaanxi, P.R.China

ABSTRACT

Abstract: Welding is a fundamental process in manufacturing marine structures. Welding induced residual stress and deformation is, however, inevitable due to non-uniform distribution of temperature and plastic yielding during welding process. Fatigue has been always a highly challenging and complex engineering issue which is faced by the maritime and offshore industry worldwide. However, the reported 3-D fatigue crack propagation results in welded joint obtained from finite element technique are scarce. In this work, a procedure to numerical simulation for the propagation behaviour of fatigue cracks in a 3-dimensional welded structure subjected to welding induced residual stress and fatigue loads was developed. Firstly, sequentially 3-D coupled thermo-mechanical finite element analyses were performed for the simulation of welding process to predict the temperature and residual stress distribution field in a complex welded component by using double ellipsoidal heat source model and the element birth and death technique. And then, a numerical approach based on the cohesive elements, modified Paris-Erdogan law and nodal release method was proposed to simulate 3-D fatigue crack growth process, in which the stress intensity factor at crack tip was calculated with the consideration of plasticity induced crack closure and the cohesive element model is employed to the formation of new crack propagation surface. The effects of welding parameters (including welding velocity, heat input and welding sequence) to the residual stress distribution in a 3D welded joint were investigated and the influences of welding residual stress to fatigue crack propagation behaviour and life were analysed based on numerical simulation. The simulation results reveal that the residual stress induced by welding significantly affected the fatigue life of the welded joint. The residual stress has a degradation effect on the fatigue cracks which are located at the interface zone of weld material and base material. It is seen that the fatigue crack propagation life of the welded joint significantly decreases by around 50% for the same fatigue loading when the residual stress is taken into account. This work can help estimate the fatigue life and structural integrity of complex welded structures in the marine and offshore industry. Reference [1] Fricke W. Fatigue analysis of weld joints: state of development. *Marine Structures*, 2003, 16:185-200. [2] Zhu X.K, Chao Y.J. Effects of temperature-dependent material properties on welding simulation. *Computers and Structures*, 2002, 80:967-976.

A Conservative, Entropic Multispecies BGK Model

Jeff Haack^{*}, Michael S. Murillo^{**}, Cory Hauck^{***}

^{*}Los Alamos National Laboratory, ^{**}Michigan State University, ^{***}Oak Ridge National Laboratory

ABSTRACT

In this talk we present a conservative multispecies BGK model that follows the spirit of the original, single species BGK model by making the specific choice to conserve species masses, total momentum, and total kinetic energy and to satisfy Boltzmann's H-Theorem. We apply this model to the case of mixtures in dense plasmas where one of the species is electrons, which requires a quantum treatment of the collision model to take degeneracy effects into account. We also develop a complete hydrodynamic closure for the ionic case via the Chapman-Enskog expansion, including a general procedure to generate symmetric diffusion coefficients based on this model. We numerically investigate velocity and temperature relaxation in dense plasmas and compare the model with previous multispecies BGK models, and discuss the trade-offs that are made in defining and using them.

Numerical Analysis of the Flow and Heat Transfer in a Circular Pipe Fitted with Flexible Vortex Generators

Charbel Habchi^{*}, Samer Ali^{**}, Sebastien Menanteau^{***}, Thierry Lemenand^{****}, Jean-Luc Harion^{*****}

^{*}Notre Dame University - Louaize, ^{**}Lebanese International University, ^{***}ICAM Lille, ^{****}University of Angers, ^{*****}IMT Lille Douai

ABSTRACT

Vortex generators are widely used for heat and mass transfer enhancement in multifunctional heat exchangers/reactors. Most of the studies focus on rigid vortex generators which generate a complex flow structure consisting mainly of streamwise vortices and hairpin like structures. It was shown that these vortices enhance the mixing process between the different flow regions as well as the heat transfer. In this paper, numerical simulations are used to study laminar flow in a circular pipe fitted with several arrays of flexible vortex generators. Five arrays of four equally spaced trapezoidal vortex generators are inserted in a circular pipe and inclined in a reversed position opposite to the flow direction with a certain angle of attack. A periodic rotation of 45 degrees is applied to the tabs arrays. The vortex generators are flexible and can deform due to the periodic fluid forces applied on the surfaces of vortex generators. The tabs oscillate without the addition of any external source of energy except that of the flow itself. The flow structures are analyzed using the proper orthogonal decomposition (POD) technique and the effect of tabs oscillation on vortices creation, suppression and dislocation is analyzed in details. Heat transfer is also analyzed and quantified by taking into consideration the additional pressure losses caused by the tabs oscillations. It is shown that the Nusselt number was increased by about 118% in the flexible vortex generators case relative to the rigid tabs case.

Parallel-Adaptive Implementation of Asynchronous Spacetime Discontinuous Galerkin Methods

Robert Haber^{*}, Amit Madhukar^{**}, Volodymyr Kindratenko^{***}, Reza Abedi^{****}

^{*}University of Illinois at Urbana-Champaign, ^{**}University of Illinois at Urbana-Champaign, ^{***}University of Illinois at Urbana-Champaign, ^{****}University of Tennessee Knoxville (UTK) / Space Institute (UTSI)

ABSTRACT

We present a new parallel-adaptive implementation for asynchronous spacetime discontinuous Galerkin method for hyperbolic problems; see for example [1]. In order to circumvent synchronous bottlenecks that might prevent efficient use of next-generation exascale platforms, we set aside established techniques and abstractions of parallel computation, such as the domain decomposition method (DDM) and the bulk synchronous parallel (synchronous time marching) model, and replace them with a scalable, barrier-free asynchronous solution scheme and localized fine-grain spacetime adaptive meshing. We use the Tent Pitcher algorithm [2] to generate fully unstructured spacetime meshes that satisfy a causality constraint to enable locally implicit aSDG solutions. These involve local Galerkin projections on a sequence of spacetime patches (small clusters of spacetime finite elements) that inherit the stability of implicit solvers while the overall solution exhibits the linear computational complexity reminiscent of explicit methods. The duration of each patch is determined independently and is not restricted by the order of the local basis. The processes of constructing and solving patches are interleaved and naturally share the same granularity. Locality and shared granularity render most of the algorithm embarrassingly parallel. Advancing a conforming space-like front mesh through the spacetime analysis domain is central to the Tent Pitcher algorithm. We maintain the front mesh as a global data structure to avoid DDM load balancing, a major synchronous bottleneck. Aside from querying and updating the front mesh, the algorithm is embarrassingly parallel. Adaptive meshing is implemented via modifications of the front mesh that govern refinement and coarsening of spacetime patches. However, because we must maintain the conforming property of the front mesh, these adaptive modifications are not naturally local. We present a Lazy Refinement method, first proposed but not implemented in [2], that localizes adaptive updates to the front mesh. Thus, adaptive front modifications, spacetime patch generation, and patch solutions share a common granularity and are embarrassingly parallel. We describe a software architecture that implements this scheme and present numerical results that demonstrate excellent scalability on a shared-memory host. Progress toward a distributed implementation and meshing in three spatial dimensions and time will also be discussed. References: [1] R. Abedi, B. Petracovici, and R. B. Haber. "A spacetime discontinuous Galerkin method for linearized elastodynamics with element-wise momentum balance. *Comp. Methods Appl. Mech. Engng.* 195(25-28), 3247–3273 (2006). [2] Shripad Thite. *Spacetime Meshing for Discontinuous Galerkin Methods*. Ph.D. thesis, Dept. Computer Science, Univ. Illinois Urbana-Champaign, August (2005).

Finite Element Framework for Simulating Two and Three-dimensional Viscoplastic Collapses

Elie Hachem^{*}, Luca Sardo^{**}, Anselmo Pereira^{***}, Rudy Valette^{****}

^{*}MINES ParisTech - CEMEF - CFL research group, ^{**}MINES ParisTech - CEMEF - CFL research group, ^{***}MINES ParisTech - CEMEF - CFL research group, ^{****}MINES ParisTech - CEMEF - CFL research group

ABSTRACT

We propose a stabilized finite element framework able to compute two and three-dimensional free surface flows of highly viscoplastic fluids. We chose to focus on two kinds of viscoplastic flow models: the Bingham model, corresponding to the most usual one, and the $\mu(I)$ model, that was introduced to predict dense granular rheology. Momentum and mass equations have been solved by using the Variational MultiScale method, coupled with a regularization technique and anisotropic mesh adaptation. A convective self-reinitialization Level-Set method has been used as a multiphase tool for describing the interface evolution. The obtained results on viscoplastic column collapses show good agreement with literature results in two-dimensional flows, and we provide new three-dimensional flows results.

High-Accuracy Phase-Specified Strain Measurement for Heterogeneous Matter in Digital Image Correlation Using Strain Gradient: Second-Order Displacement Gradient Application

Youssef A. F. Hafiz*, Adrian Lowe**, Zbigniew Stachurski***, Shankar Kalyanasundaram****

*Ph.D. candidate, Australian National University, **Senior Lecturer, Australian National University, ***Professor, Australian National University, ****Professor, Australian National University

ABSTRACT

To obtain high-accuracy phase-specified strain field in Digital Image Correlation (DIC), a novel technique was developed using strain gradient calculation and numerical phase separation. This technique is introduced and verified to fulfill the need of a higher accuracy strain fields in heterogeneous or discontinuous matter especially in micro-scale mechanics. In this paper, the second-order displacement gradient application is performed using Lu et. al. procedure [1] to present the peak accuracy of the technique and its application in heterogeneous matter. In addition, this exercise is performed to highlight the importance of second-order displacement gradient in heterogeneous applications. For verification purpose, the strain field resulted from second-order displacement gradient using strain gradient and phase separation technique was compared to its correspondences; first, first-order displacement gradient; second, first and second-order before applying the technique; third, strain field resulted from Finite Element Analysis (FEA) and its images were used as input for all DIC results as a bench mark for the comparison. The resulted strain from the second-order displacement gradient after applying the technique showed closer values to the FEA compared to first-order. Highlights about the differences in heterogeneous application are presented and discussed. In addition, the resulted strain from first-order displacement gradient after applying the technique showed closer results to the FEA than second-order displacement gradient before applying the technique. This shows the effect of applying the strain gradient and phase separation technique on the resulted strain field in heterogeneous matter. This will allow micro-mechanics researchers to study a full Representative Volume Element using DIC in a high accuracy to verify their models. In addition, this is the only technique, according to the author's knowledge, that results a full strain field including high-accuracy strain values at interfaces using DIC. Therefore, the interface mechanics researchers will be able to verify their models using DIC as well. [1] H. Lu; P.D. Cary, "Deformation measurement by digital image correlation: Implementation of second-order displacement gradient," Experimental Mechanics, vol. 40, no. 4, pp. 393-400, 2000.

Behavior and Structural Analyses of Floating Structures Using Smoothed Particle Hydrodynamics Method

Seiya Hagihara^{*}, Chihiro Kai^{**}, Takenaka Daiki^{***}, Shinya Taketomi^{****}, Yuichi Tadano^{*****},
Satoyuki Tanaka^{*****}

^{*}Department of Mechanical Engineering, Saga University, ^{**}Graduate School of Science and Engineering, Saga University, ^{***}Graduate School of Science and Engineering, Saga University, ^{****}Department of Mechanical Engineering, Saga University, ^{*****}Department of Mechanical Engineering, Saga University, ^{*****}Department of Transportation and Environmental Systems, Hiroshima University

ABSTRACT

The floating/fixed ocean structures such as wind power plants and other structures on offshore have to be taken account of safety in rough sea and tsunami. It is necessary to predict behaviors for both structures and fluid. The structures in the ocean are subjected to forces from the fluid. Particle methods of fluid dynamics have advantages for safe analyses to defend from natural disasters which are tsunami etc. than other numerical methods. The smoothed particle hydrodynamics (SPH) method [1] which is one of the particle methods is applied to some problems of fluid dynamics and solid mechanics. The SPH methods are mainly utilized to a number of problems for the fluid dynamics. If the structures in the ocean will be subjected to the large deformation from the waves, the stress may exceed the yield stress in the structures. The elastic-plastic effects have to be taken into account for the behavior of the structures. In the present study, the behavior of the floating or fixed structures in the ocean are calculated by using the SPH method and the computational elastic-plastic calculation for structural analysis which is appropriate to the SPH method are presented. [1] Lucy LB (1977) A numerical approach to the testing of the fission hypothesis The Astronomical Journal 82, 1013-1024.

Surface-only Physics-based Animation of Fluids and Fractures

David Hahn^{*}, Fang Da^{**}, Christopher Batty^{***}, Chris Wojtan^{****}, Eitan Grinspun^{*****}

^{*}ETH Zürich, ^{**}Columbia University, NY, ^{***}Waterloo University, ON, ^{****}IST Austria, ^{*****}Columbia University, NY

ABSTRACT

In this talk we present two recent applications of boundary element methods in computer graphics, in particular in the area of physics-based animation. Surface-only simulation techniques can achieve high efficiency and favorable scaling with increasing resolution by eschewing volumetric discretization and performing computations solely on the surface of the physical domain. At present however, three-dimensional liquid phenomena are simulated with volumetric solvers largely due to numerical challenges introduced by the nonlinearity of the governing fluid equations and the high density ratio between liquid and air. In the first part of this talk, we present a surface-only technique for simulating incompressible, uniform-density liquids in three dimensions. The liquid surface is captured by a triangle mesh on which a Lagrangian velocity field is stored. Because advection of the velocity field may violate the incompressibility condition, we describe an orthogonal projection technique to remove the divergence, while requiring the evaluation of only two boundary integrals. The forces of surface tension, gravity, and solid contact are all treated by a boundary element solver, allowing us to perform detailed simulations of a wide range of liquid phenomena, including waterbells, droplet and jet collisions, fluid chains, and crown splashes. In the second part of this talk, we present a boundary element based method for fast simulation of brittle fracture. By introducing simplifying assumptions that allow us to quickly estimate stress intensities and opening displacements during crack propagation, we build a fracture algorithm where the cost of each time step scales linearly with the length of the crack-front. The transition from a full boundary element method to our faster variant is possible at the beginning of any time step. This allows us to build a hybrid method, which uses the expensive but more accurate BEM while the number of degrees of freedom is low, and uses the fast method once that number exceeds a given threshold as the crack geometry becomes more complicated. We show that our method produces physically reasonable results in standard test cases and is capable of dealing with complex scenes faster than previous finite- or boundary-element approaches. We believe that both of our contributions advance the applicability of boundary element based techniques to physics-based animation and visual effects productions.

Industrial Methods for G-equation Combustion Model on a 3D Polyhedron Mesh

Jooyoung Hahn^{*}, Karol Mikula^{**}, Peter Frolkovič^{***}, Branislav Basara^{****}

^{*}Advanced Simulation Technologies, AVL LIST GmbH, Austria, ^{**}Slovak University of Technology, Slovakia,
^{***}Slovak University of Technology, Slovakia, ^{****}Advanced Simulation Technologies, AVL LIST GmbH, Austria

ABSTRACT

In this presentation, we propose industrially optimized numerical schemes to solve the G-equation model in premixed turbulent combustion on a 3D polyhedron mesh. The governing equations are described by the Favre mean (G-equation) and the fluctuation (G-variance equation) of flame represented by a zero level set of continuous implicit function. The turbulent flame surface equations and the turbulent flame speed formulations make a closure of G equation and G-variance equation. The G-equation is a standard level set equation containing the advection, surface normal flow, and mean curvature terms. The proposed scheme has mainly three advantages. The first is that it numerically shows higher order of convergence on very limited unknown variables in 3D polyhedron mesh. The second is that it can be easily applicable to the 1-ring face neighborhood structure for a parallel computation which is the simplest decomposed domain. The third is that a time step restriction caused by the CFL condition is practically reduced by the proposed semi-implicit scheme. The first and second advantages are also shown in a propagation in normal direction [1]. In case of the G-equation, an extension of algorithm in [1] is presented with the advection and mean curvature terms on a polyhedron mesh. The G-variance equation does not allow turbulent diffusion normal to the mean flame front. From the conventional method in [2], an approximation of a tangential diffusion term is used. We compare the difference between the original tangential diffusion and the method in [2] mainly used in the combustion community. In premixed turbulent combustion engines, we would like to present a practical difference between a higher order method and a typical upwind method of solving the G-equation and G-variance equation. Standard numerical results of each velocity term in the G-equation are also illustrated. [1] J. Hahn, K. Mikula, P. Frolkovic, B. Basara, Inflow-Based Gradient Finite Volume Method for a Propagation in a Normal Direction in a Polyhedron Mesh, Journal of Scientific Computing (2017) 1–24. DOI: 10.1007/s10915-017-0364-4. [2] N. Peters, Turbulent Combustion, Cambridge University Press (2000).

The Parametric HFGMC Micromechanics for Damage Analysis of Composite Materials and Structures

Rami Haj-Ali*, Jacob Aboudi**

*Tel-Aviv University, **Tel-Aviv University

ABSTRACT

A nonlinear formulation of the parametric high fidelity generalized method of cells (HFGMC) is offered for the micromechanical analysis 2D and 3D multiphase periodic composites (Haj-Ali and Aboudi, 2013) with evolving damage. The new analytical formulation and computational implementation of the parametric HFGMC is performed (Haj-Ali and Aboudi, 2016) with consideration for efficient nonlinear multi-scale computations. An average virtual work integral form is proposed for the HFGMC method which allows for the definition of a generalized internal resisting force vector along with its corresponding symmetric stiffness matrix. Unlike the nodal displacement-based finite element (FE), the HFGMC and its weak form are cast in terms of the work-conjugate average displacement and traction vectors, defined on the surfaces (faces) of the discretized volumes (subcells or elements). The HFGMC micromechanics is shown to be well suited for integrating the microplane theory for the fiber-matrix spatial and local nonlinear and damage fields. Another implementation of the parametric HFGMC will be demonstrated for the multi-scale and damage analysis of laminated composite structures. To that end, a refined hexagonal-array repeating unit-cell (RUC) HFGMC micromodel for the unidirectional composite is used. Local fiber and matrix damage approaches are examined. The accuracy of the developed nonlinear multiscale approach is demonstrated by a comparison with experimental results available in the literature of notched laminated composite structures

Structural Optimization of Efficient Thin Film Solar Cells Using Surrogate Models

Shima Hajimirza*

*Texas A&M; University

ABSTRACT

This work uses surrogate modeling for efficient optimization and design of nano-scale thin film solar cell structures with enhanced opto-electrical characteristics. Study of thin film structures that selectively respond to input irradiance requires solving complex electromagnetic and quantum level first principle simulations. These simulations are intense and time-consuming. Therefore design of efficient sub-wavelength thin film structures is a complex optimization of a function with extremely high computational cost. Surrogate modeling can be invoked to alleviate the computational burden of design by approximating the wavelength-dependent opto-electrical characteristics of nano-scale geometries using selected sampling data and learning. We demonstrate that this approach can be reliably used to design several thin film solar cells with enhanced conversion efficiency in times significantly shorter than conventional optimization techniques offer. We study multi-layer silicon-based solar cells as well as organic thin film cells infused with nano-particles. The studied structures all benefit from surface texturing which is a commonly used technique for increasing the optical depth of a semiconductor without increasing the physical depth, therefore increasing the overall photon absorption and carrier collection. The underlying mechanisms responsible for such modifications (e.g. surface plasmonic excitation) are complex and geometry dependent. We demonstrate that Artificial Neural Networks can be used to learn these mechanisms as a function of geometry and wavelength. The surrogate model can then be used reliably for consequent optimization and analysis.

Recent Efforts on Curved Element Mesh Adaptation

Morteza Hakimi Siboni^{*}, Kazem Kamran^{**}, Onkar Sahni^{***}, Mark Shephard^{****}

^{*}Rensselaer Polytechnic Institute, ^{**}Rensselaer Polytechnic Institute, ^{***}Rensselaer Polytechnic Institute,
^{****}Rensselaer Polytechnic Institute

ABSTRACT

To maintain the rate of convergence of high-order methods in simulations over curved domains the mesh entities must be curved to the boundary with a sufficient order of geometric approximation. The application of high-order methods to problems with complex geometric domains requires the tool for the creation and adaptation of curved meshes. Building on previous efforts that focused on supporting quadratic curved element mesh adaptation [1], this presentation will overview efforts to extend those procedures to higher-order mesh geometry and improve curved anisotropic mesh adaptation. The most commonly used approach to create curved meshes is to employ the available straight-sided or linear mesh generation tools for the initial mesh and then apply operations to upgrade that mesh to the desired higher-order curved mesh. However, there are now mesh generation tools that generate at least quadratic curved meshes (e.g., [2]). A tool has been created that can accept a mesh with either straight-sided/linear or curved/quadratic elements and upgrade that mesh to a higher-order curved mesh. Note that the current procedure is limited to meshes for which curved boundaries are being approximated by triangular faces. In addition to curving mesh entities classified on the domain boundaries, this procedure includes identifying and fixing poorly shaped and invalid internal entities that are created as a result of curving the boundary entities. Poorly shaped or invalid entities are fixed by applying appropriate split, swap, collapse, and interior mesh entity curving operations. The same sets of operations are used in the mesh adaptation procedure that is driven by an anisotropic mesh metric field. Bezier mesh geometry is used internally in these procedures due to its ability to more effectively control the mesh geometry as well as to provide efficient algorithms and computation. These procedures are easily linked with high-order analysis codes, for example, ACE3P code that is used to model complex particle accelerator geometries and MFEM code that is used to simulate plasma heating in a tokamak device using complex antenna arrangements. [1] Lu, Q., Shephard, M.S., Tendulkar, S. and Beall, M.W., 2014. Parallel mesh adaptation for high-order finite element methods with curved element geometry. *Engineering with Computers*, 30(2), pp.271-286. [2] Simmetrix web page, www.simmetrix.com.

On Asymptotic and Pre-asymptotic Convergence Rates of Higher Order FE Methods

Harri Hakula^{*}, Ivo Babuska^{**}

^{*}Aalto University, ^{**}University of Texas at Austin

ABSTRACT

The pointwise convergence of the Legendre expansion is of interest both theoretically through the application of the p-version of FEM. The known results in 1D and higher dimensions are asymptotic in nature, that is, concerned with p approaching infinity. In many cases, however, it is meaningful to consider pre-asymptotic behaviour where a well-defined convergence rate exists but is different from the eventual asymptotic one. In particular this is relevant in the context of engineering applications where the polynomial orders can be far from the asymptotic range. Our work is based on Wahlbin [1] and Saff and Totik [2]. Adaptive hp-method solvers must be able to make local changes both in the mesh (h) and the local polynomial order (p). Sobolev regularity estimation [3] is often used in determination of the local p . Sobolev regularity estimation is based on certain asymptotics of the Legendre expansion and thus may lead to ambiguous results if the local polynomial order is in the pre-asymptotic range. We illustrate this using benchmark problems including engineering application, thin shells of revolution and show the ultimate validity of the theorems. Computing hp-FEM simulations at very high polynomial orders requires non-standard solver technology. Our solver, based on Mathematica, supports integration using long floating point formats and in the case of constant coefficient problems also exact integration. We rely on Mathematica's builtin solvers for linear algebra. In this talk we emphasize the need for further work both in theory and construction of modern solvers supporting very high polynomial orders if the applications so require. [1]Wahlbin, L.B. A comparison of the local behavior of spline L_2 -projections, Fourier series and Legendre series. In *Singularities and Constructive Methods for Their Treatment*, volume 1121 of *Lecture Notes in Mathematics*, pages 319–346. Springer, 1985. [2] Saff, E.B and Totik,V. *Polynomial-Approximation Of Piecewise Analytic-Functions*, *Journal of the London Mathematical Society--Second Series*, 39, 1989, 487-498. [3] Houston, P. and Suli, E. A note on the design of hp-adaptive finite element methods for elliptic partial differential equations, *CMAME*, 194, 2005, 229-243.

Importance of Plasma Amino Acid Profile for Induction of Hepatic Steatosis under Protein Malnutrition

Fumihiko Hakuno^{*}, Hiroki Nishi^{**}, Masato Masuda^{***}, Daisuke Yamanaka^{****}, Shin-Ichiro Takahashi^{*****}, Ryuji Shioya^{*****}, Yasushi Nakabayashi^{*****}

^{*}The University of Tokyo, ^{**}The University of Tokyo, ^{***}Toyo University, ^{****}The University of Tokyo, ^{*****}The University of Tokyo, ^{*****}Toyo University, ^{*****}Toyo University

ABSTRACT

We previously reported that a low-protein or a low-amino acid diet caused animals to develop fatty liver containing a high level of triglycerides (TG), similar to the human nutritional disorder “kwashiorkor”. Only a dietary arginine or threonine deficiency was sufficient to induce hepatic TG accumulation. However, supplementation of a low-amino acid diet with arginine or threonine failed to reverse it. In addition, we could not find any correlation between serum amino acid concentrations and liver TG level in terms of a single amino acid. So we dealt with individual data sets of serum amino acid concentrations as multi-dimensional vector data to conduct a comprehensive in silico analysis using machine learning programs. As an input data, we took data from a total of 135 rats which were fed various diets supplemented with 20 kinds of single amino acids. We carried out the Self-Organizing Map (SOM) analysis using only serum amino acid concentrations as input data which did not include the data on liver TG. By this analysis, we obtained a square map on which rats with similar serum amino acid profiles were successfully put near each other. Surprisingly, even though the classification was made only based on the data on serum amino acid concentrations, liver TG level was also smoothly classified, suggesting that the liver TG level was correlated well with a serum amino acid profile. Next, we applied another machine learning algorithm, multi-layer perceptron (MLP). We took serum amino acid concentrations of each rat as input data, and liver TG as output data. For learning, we made several MLPs whose numbers of mid-layers were 3, 4 and 5. After learning was completed, the serum amino acid concentrations of “unlearned” rats were put into each algorithm to obtain their output liver TG values. Then the obtained liver TG values were compared with measured actual liver TG values, and differences and error rates were calculated. As a result, higher number of mid-layers exhibited a lower error rate and individual hepatic TG accumulation levels could be predicted using just a data set of serum amino acid concentrations with good accuracy. In silico analysis succeeded in predicting liver TG level from the serum amino acid profile. Based on these results, we conclude that serum amino acid profile, which is sensed by hepatocytes, defined the hepatic TG levels.

Quantification of Multiscale Second-order Flow Structures in the Wake of a Square Wall-mounted Cylinder under Two Inflow Scenarios

Charlotte Haley^{*}, Mihai Anitescu^{**}, Christopher Geoga^{***}

^{*}Argonne National Laboratory, ^{**}Argonne National Laboratory, ^{***}Argonne National Laboratory

ABSTRACT

Widely used methods for quantification of flow structures in turbulence such as proper orthogonal decomposition or dynamic mode decomposition provide an incomplete description of fully spatiotemporal flow dynamics, since they ignore the coupling between spatial and temporal oscillatory modes. Additionally, it is difficult to verify and validate the result of a simulation or compare with another simulation by looking at the modes alone. We propose a fully spatiotemporal approach to the problem of identifying spatially varying modes of oscillation in fluid dynamics simulation output by means of multitaper frequency-wavenumber spectral analysis. Two-dimensional spectrum estimation allows one to extract velocities of traveling waves and phase angles of standing waves in a section of data composed of one spatial dimension and one time dimension. Additionally, these estimates are accompanied by confidence intervals which allow one to assign significance in the direct comparison of two simulations' output in wavenumber-frequency space. This analysis applied to data obtained from simulation of a square wall-mounted cylinder under laminar and turbulent inflow conditions reveals widely different flow characteristics. Laminar inflow case data has a strong traveling wave in wavenumber-frequency space while turbulent spectra show more diffuse behavior with power in frequency-wavenumber space concentrated along a line corresponding to a turbulent energy cascade with velocity 0.95 nondimensional units.

Influence of Microstructure and Surface Roughness on Fatigue Initiation in Extruded Aluminum

Håkan Hallberg^{*}, Sigmund Kyrre Ås^{**}, Bjørn Skallerud^{***}

^{*}Lund University, Sweden, ^{**}Norwegian University of Science and Technology, Norway, ^{***}Norwegian University of Science and Technology, Norway

ABSTRACT

Comprehensive experimental data on the fatigue properties of extruded Al6082-T6 is used together with crystal plasticity simulations to investigate the microstructure and surface roughness influence on fatigue initiation. The surface roughness of the specimens used in the experiments was mapped with White Light Interferometry (WLI) and the location of the fatigue initiation sites was identified and characterized in each sample. With surface geometries based on the WLI scans, densely meshed non-linear FE models were used to identify the locations of the highest macroscopic stress concentrations. A somewhat surprising outcome of the experimental study is that the majority of fatigue failures were initiated at surface irregularities that did not correspond to the most significant macroscopic stress concentration. Since the depths of the surface irregularities are comparable to microstructure features - such as the grain size - the present study explores to what extent microstructure variations can be a cause for the observed material behavior. The numerical investigation is performed by using crystal plasticity simulations and simulation models which are based on the actual surface geometries and material microstructures encountered in the experiments. Grain structure and texture are taken into account and the simulations reveal that variations in the microstructure can indeed make initiation of fatigue more likely to occur near surface notches that have macroscopic stress concentrations lower than maximum. Different frequently employed fatigue initiation parameters (FIP) are investigated and it is shown that a FIP based on a modified Fatemi-Socie criterion adds valuable information on local slip activity. The predictions obtained by using this criterion are to some extent conflicting with the results based on other FIPs, for example based on accumulated plastic strain or stored energy. A key observation is that macroscopic stress concentrations alone are insufficient and crystal plasticity simulations provide a competent additional tool in analyzing fatigue initiation mechanisms in polycrystalline samples. Not only the magnitude of stress concentrations, but also the stress gradients near surface irregularities appear as important aspects to consider when analyzing fatigue initiation. In addition, highly misoriented grain interfaces, which constitute significant barriers to plastic slip, provide internal domains in the material where initiation of fatigue damage appears more likely to occur than at the stress concentrations that are due to the surface roughness. The present investigation clearly highlights the importance of considering the influence of microstructure heterogeneities on fatigue properties in polycrystals.

Numerical Implementation of Viscoelastic Constitutive Models with Phase Evolution

Craig Hamel^{*}, Jerry Qi^{**}

^{*}Georgia Institute of Technology, ^{**}Georgia Institute of Technology

ABSTRACT

Polymeric materials exhibit the phenomenon that new structures (such as crosslinking, crystal formation, or reformation of chains, etc.) are formed in a stress-free state. This aspect of these materials adds great complexity when deformation and polymerization occur simultaneously which is the case in many active polymeric material systems. We refer to this notion as phase evolution and view this idea as a cornerstone for the formulation of accurate constitutive models that capture the behavior of soft active materials. Previous literature regarding the mechanics of materials exhibiting phase evolution has been limited to hyperelastic constitutive models and has not included dissipative effects. This work examines the implementation aspects of numerically integrating a large deformation material model which exhibits viscoelastic properties as well as phase evolution. Due to the ever-increasing demand of efficient simulation based design this has limited the application of certain materials with complex multi-physical behavior such as shape memory systems. An efficient method for implementing such models would further the presence of active materials within industry. The major challenge is efficiently accounting for individual phases possessing different reference configurations and being able to track this complex mechanical response when the material is subjected to large deformations. To account for this material behavior a continuum based approach will be used to formulate a general finite strain framework that captures the coupling of the viscoelastic response with phase evolution. A naïve implementation of such a model proves to be computationally cost prohibitive as the number of phases and viscous state variables increases. This necessitates the development of a viscoelastic effective phase model (VEPM) to account for the effect the combined deformation histories have on the mechanical response. The VEPM reduces the number of state variables to a constant number for an arbitrary number of phases allowing for an efficient implementation in commercial FEM software. Both the naïve and VEPM implementation of the model will be compared for simple mechanical boundary value problems to verify the accuracy as well as a rudimentary convergence and running time studies. Finally, exemplary 3D finite strain simulations will be presented and compared to experimental results to verify the method.

A hysteretic constitutive model for dry woven composite fabric under large strain.

Nahiene Hamila^{*}, Yvan Denis^{**}, Eduardo Guzman-Maldonado^{***}, Fabrice Morestin^{****}

^{*}INSA Lyon, ^{**}INSA Lyon, ^{***}IRT Jules Verne, ^{****}INSA Lyon

ABSTRACT

Draping composite reinforcement on non-developable shapes necessarily leads to deformations in the plane generating large shears between warp and weft. Sliding between fibers and between yarns creates friction that dissipates energy. This paper presents a constitutive model describing the dissipative behavior of 2D composite textile reinforcements under large strain. The model is based on two innovative points. First, the additive decomposition of Green - Naghdi is considered, which leads to write the yield function and the plastic law in a conventional manner. This is very uncommon for anisotropic fields. Secondly, nested surfaces according with Mroz Theory define the strong non-linearity of the problem. The use of these two points allows to define a flexible dissipative model for numerical simulations. The dissipation process driven by fibres friction is exclusively associated with the in-plane shear deformation mode. As a result, the material parameters are calibrated using standard methods, like the Picture Frame.

Direct Numerical Simulation of Turbulence Eddy Shocklets: Dependence of Small-Scale Statistics and Numerical Stability on Forcing Functions and Physical Configuration

Peter Hamlington^{*}, Colin Towery^{**}, Alexei Poludnenko^{***}

^{*}University of Colorado Boulder, ^{**}University of Colorado Boulder, ^{***}Texas A&M; University

ABSTRACT

Eddy shocklets arise in compressible turbulent flows where turbulent velocity fluctuations become locally supersonic and lead to the formation of small-scale, weak, and unconfined shock-like structures. In practice, eddy shocklets can be expected to occur in high-speed compressible flows, such as exist inside scramjet engines, and are strongly moderated by viscous diffusion. As a result, the thickness of these eddy shocklets is of the same order as the Kolmogorov microscale of the flow. This is in distinct contrast to strong, confined shockwaves generated by the mean flow configuration, whose thicknesses scale with the local molecular mean free path. Despite being very weak shockwaves that can notionally be resolved by standard direct numerical simulation techniques, eddy shocklets represent a distinct challenge to the numerical stability and accuracy of monotonic and non-oscillatory numerical methods, including mature and popular shock-capturing schemes such as the Godunov finite volume method of corner transport upwinding with piecewise-parabolic reconstruction (CTU-PPM). In this talk, we present findings from several sets of three-dimensional direct numerical simulations (3D DNS) conducted to evaluate the effects of various kinetic and thermal energy forcing techniques to sustain compressible homogenous turbulence in an adiabatic domain, as well as to determine the required spatial, temporal, and statistical resolution to study eddy shocklets using the CTU-PPM reacting flow code Athena-RFX. We find that different large-scale kinetic energy forcing schemes can result in substantially different Mach number scaling and small-scale statistics of dilatational fluctuations generally, and eddy shocklets in particular. In agreement with previous literature, we find that the use of negative thermal energy forcing, which ensures statistical stationarity in an adiabatic domain, also leads to significant quantitative differences in dilatational dynamics. Finally, we compare results from simulations with different physical configurations, including different caloric equations of state, bulk viscosities, and Prandtl numbers.

Multi-Level Spectral Deferred Correction Scheme for the Shallow-Water Equations on the Sphere

Francois Hamon^{*}, Martin Schreiber^{**}, Michael Minion^{***}

^{*}Lawrence Berkeley National Laboratory, ^{**}University of Exeter, ^{***}Lawrence Berkeley National Laboratory

ABSTRACT

The numerical modeling of global atmospheric processes is a challenging scientific application and requires accurate time integration methods for the discretized governing partial differential equations. These complex processes operate on a wide range of time scales, and often have to be simulated over long periods of time – up to a hundred years for long-term paleoclimate studies –, which constitutes a challenge for the design of stable and efficient integration schemes. We propose an efficient and high-order accurate implicit-explicit numerical scheme combining Multi-Level Spectral Deferred Corrections (MLSDC) with a spatial discretization based on the Spherical Harmonics (SH) transform to solve the shallow-water equations on the sphere. In MLSDC, a sequence of low-order corrections is applied iteratively to a provisional solution to achieve high-order temporal accuracy. The corrections are performed on a hierarchy of coupled space-time levels to shift the computational work to the coarse levels and reduce the cost of the integration. Our MLSDC scheme fully takes advantage of the features of the SH transform in the construction of accurate transfer functions between space-time levels as well as in the design of efficient solvers for the implicit systems. Using numerical examples, we show that our implicit-explicit MLSDC numerical scheme is stable for large time steps, and achieves up to eighth-order temporal accuracy. We also compare its computational cost to that of existing single-level implicit-explicit time integration methods.

A Hybrid Local/Nonlocal Continuum Model for Wave Propagation in Linear Elastic Solid

Fei Han^{*}, Gilles Lubineau^{**}

^{*}Dalian University of Technology, ^{**}King Abdullah University of Science and Technology

ABSTRACT

In this paper, we apply a hybrid local/nonlocal continuum model to study wave propagations in the linear elastic solid. Through this hybrid model, the peridynamic model, which is a nonlocal continuum model, is applied to the key domain of a structure, where damage and fracture exists to cause the wave dispersions. In the rest of the structure, the classical continuum model is used to describe wave propagations without dispersions. The wave speeds of plane waves for low- and high-frequency are derived in different domains described by the pure local, pure nonlocal and hybrid models, respectively. The wave dispersions are plotted through the analytical and numerical solutions. The discrete formulation of the hybrid equations of motion is also described. Two-dimensional numerical examples illustrate the validity and accuracy of the proposed model. It is shown that the hybrid local/nonlocal continuum model can be successfully applied to simulate wave propagations in the linear elastic solid with a crack.

Effect of Microstructural Resolution in Virtual Samples on Property Evaluation of Cement Paste Using Crack Phase Field Model

Tong-Seok Han*, Ji-Su Kim**

*Yonsei University, **Yonsei University

ABSTRACT

Virtual specimens with complex random microstructures can be obtained from micro-CT. Depending on the length characteristics of the microstructural features, the detailed description of the microstructural features in the generated virtual specimens are influenced by the resolution or voxel size of the samples. When the virtual samples are evaluated using virtual loading tools, the maximum number of voxels in the virtual samples should be within the limit of plausible computation effort. Due to this limitation and to guarantee the representative volume of the evaluated samples, the degree of detailed microstructural description can be affected. This, in turn, can also affect the evaluated properties. In this study, effect of void microstructure resolution of cement pastes on the characterization and property evaluation is investigated. The virtual samples are prepared from the synchrotron micro-CT images, and the same data set with different resolutions are characterized and evaluated using the crack phase field model [1]. Through the analysis, the effect of resolution change on the microstructural characteristics and material responses (stiffness and tensile strength) is evaluated, and the characterization and the properties are correlated. The issue of selecting modeling input parameters for the crack phase field model is addressed, and the selected parameters are applied to cementitious materials with additional distinct microstructural features, i.e., cement paste embedded with glass beads. The modeling parameter selection process for virtual specimens, where distinct void microstructural features with different scales are present, is discussed. [1] C. Miehe, L.-M. Schänzel, H. Ulmer, Phase field modeling of fracture in multi-physics problems. Part I: Balance of crack surface and failure criteria for brittle crack propagation in thermo-elastic solids, *Comput. Meth. Appl. Mech. Eng.* 294 (2015) 449–485.

DNS of Particle-laden Turbulent Channel Flow in Transitional Regime

Masaki Hanabusa^{*}, Takahiro Tsukahara^{**}

^{*}Tokyo University of Science, ^{**}Tokyo University of Science

ABSTRACT

It is known that intermittent localized turbulence in a channel flow sustains in the form of oblique bands, so-called turbulent stripe [1]. The stripe pattern forms obliquely against the mainstream with an interval much larger than the channel gap and sustains steadily. Studies of such large-scale intermittent structures are important for understanding the subcritical transition process, but the robustness of the structure in multiphase flows has not been investigated. Pan & Banerjee [2] showed that small particles suppress sweep motions and large particles enhance them in the particle-laden turbulent flow. In the former case, another study also reported a particle-induced drag reduction [3]. However, it is still unclear whether the turbulent stripe would be formed or not in flows with small particles. In this study, we investigate the subcritical transition process in particle-laden channel flows with focusing on the stripe formation. We performed direct numerical simulations of pressure-driven plane channel flows with point particles, in which particle-particle interactions were not considered. The volume fraction of particles we tested here was low sufficiently to neglect the interactions. The particle motion was described by the Basset-Boussinesq-Ossen equation. Force on particles was considered as drag force to calculate the particle-fluid interaction. We investigated the effect of particles on the turbulent stripe, varying the Stokes number at a fixed volume fraction. In the one-way coupling simulation, we found that particle distribution was rather homogeneous in the wall-parallel direction even with the turbulent stripe. On the other hand, heavier particles accumulate near the wall even without gravity. In the two-way coupling, the stripe appeared to be disturbed and broken temporarily for the heavier particles. This result might be caused by particles accumulating near the wall. In the full paper, we would discuss the influence of interaction force on the fine-scale eddies in the turbulent stripe. References [1] T. Tsukahara, Y. Seki, H. Kawamura and D. Tochio, DNS of turbulent channel flow at very low Reynolds numbers, In Proc. 4th Intl Symp. on Turbulence and Shear Flow Phenomena, 2005. [2] Y. Pan and S. Banerjee, Numerical simulation of particle interactions with wall turbulence, Phys. Fluids, 8, 2733, 1996. [3] L. H. Zhao, H. I. Andersson, and J. J. J. Gillissen, Turbulence modulation and drag reduction by spherical particles, Phys. Fluids, 22, 081702, 2010.

Microstructural Finite Element Modeling of Discontinuous Fiber Reinforced Composites

Imad Hanhan^{*}, Ronald Agyei^{**}, Michael D. Sangid^{***}

^{*}Purdue University, ^{**}Purdue University, ^{***}Purdue University

ABSTRACT

Fiber reinforced polymer composites are light weight and high strength materials, making their development desirable especially for the aerospace industry. However, their implementation hinges on large scale testing programs, which require thousands of specimen level experimental tests to qualify their mechanical properties. Combined with the fact that composite materials still have many unknown behaviors and failure mechanisms, it can be very complicated to certify the use of a composite material and model its mechanical behavior. A common practice for composite modeling is to homogenize the material properties for macro-scale applications, and use their predicted elastic properties – coupled with an internal damage parameter – to represent the mechanical response of the material. For discontinuous fiber composites, homogenization becomes even more complicated, due to extreme spatial heterogeneity in the microstructure. This work aims to model the behavior, including the damage evolution, of discontinuous fiber reinforced composites at the microstructural level. While not homogenizing the material increases the computational cost, it allows for identifying and modeling the heterogeneous deformation mechanisms and helps build confidence in the model's predictions. Preliminary work in this study is to instantiate the exact geometry of the microstructure from X-ray computed tomography (XCT) reconstructions, as well as to conduct linear elastic models of the exact microstructure. The model's prediction of deformation is directly compared to companion results from in situ XCT studies. This work aims to accelerate the qualification of fiber reinforced composite materials by developing enhanced predictive capabilities of the strength and failure mechanisms at the microstructural level. Overall, the results expand the current understanding of composite mechanical performance, and provide a methodology for multi-scale composite material modeling.

Numerical Solution for Nonlinear Random Vibrations of Beams with Fractional Derivative Elements

Zhaopeng Hao*, zhongqiang zhang**

*Department of Mathematics, Worcester Polytechnic Institute, **Department of Mathematics, Worcester Polytechnic Institute

ABSTRACT

In this work, we will talk about the numerical solution for nonlinear beam model under uncertainty with nonlocal damping. Specifically, we consider a stochastic beam equation with additive space-time noise with a time-fractional derivative modelling a damping effect. However, solving such an equation numerically is usually prohibitively expensive, even in one dimension. The main challenges are high cost of Monte Carlo simulation for realizations in random space and a large amount of storage due to the nature of the fractional derivative. To alleviate the difficulties, we develop a fast deterministic solver for the nonlinear stochastic beam model with reasonable computational cost and low memory storage. More precisely, we adopt an implicit-explicit scheme in time so that the nonlinear term is treated explicitly. With the time discretization scheme, we use a Fourier spectral method in physical space which leads to fully decoupled stochastic ODEs. Thus the resulting scheme can be embarrassingly parallelized. Moreover, we approximate the fractional derivative by a fast L1 scheme with a low storage. Numerical example will be given to show the efficiency and accuracy of the numerical solution.

Spectral Behavior of Nitsche's Method

Isaac Harari^{*}, Uri Albocher^{**}

^{*}Tel Aviv University, ^{**}Tel Aviv University, Afeka College

ABSTRACT

Incompatible discretization methods provide added flexibility in computation by allowing meshes to be unaligned with geometric features and easily accommodating non-interpolatory approximations. Such formulations that are based on Nitsche's approach to enforce surface constraints weakly, which shares features with stabilized methods, combine conceptual simplicity and computational efficiency with robust performance. The basic workings of the method are well understood, in terms of a bound on the parameter. However, its spectral behavior has not been explored in depth. In addition to the physical eigenpairs which approximate the exact ones, as in the standard formulation, Nitsche's method gives rise to mesh-dependent eigenpairs associated with weak enforcement of boundary or interface constraints. The dependence of the eigenvalues on the Nitsche parameter is related to a boundary quotient of the eigenfunctions (reminiscent of the Rayleigh quotient). Numerical studies show that, for the most part, the constraint eigenvalues exhibit essentially linear growth with the parameter, whereas the physical eigenvalues are virtually constant, in line with the values of the corresponding boundary quotients. This behavior sheds light on the role of the stabilization parameter in attaining coercivity for the Nitsche method. Departures from this behavior occur in specific veering zones, in which the eigenpairs lack clear type. Eigenvalue veering does not impair the performance of the method. The spectrum of a reduced system obtained by algebraic elimination contains only physical eigenpairs, and is free of veering. The favorable features of the reduced system warrant its use in the solution of boundary-value problems. To date, incompatible discretizations are rarely used for eigenvalue problems in engineering applications, possibly due to the potential presence of mesh-dependent constraint eigenpairs. Removing the added degrees of freedom on the boundaries addressed by the Nitsche approach by Irons-Guyan reduction is a relatively inexpensive procedure that preserves the essential structure of the underlying formulation, and yields a system that contains only physical eigenpairs. As such, the spectrum is virtually insensitive to stabilization beyond the threshold required for coercivity, preserving the conditioning of the standard formulation. Being free of the constraint eigenpairs, the Irons-Guyan reduced Nitsche formulation of the eigenvalue problem may be solved by any conventional eigenvalue solver. This procedure facilitates the use of Nitsche's method for formulating eigenvalue problems, and justifies its use in explicit dynamics.

Shear Transformation Zone Dynamics Simulations of Nanomechanical Experiments

Thomas Hardin*, Christopher Schuh**

*MIT, **MIT

ABSTRACT

Shear Transformation Zone Dynamics (STZD) simulations treat plastic deformation of metallic glass as a series of thermally activated, localized, discrete shear events. In STZD, shear events interact and their effects propagate on a continuum level, often modeled by the Finite Element Method. The shear events are controlled using Transition State Theory and the kinetic Monte Carlo method, enabling STZD simulations to cover experimentally relevant time scales. However, past STZD simulations have modeled samples of only a few tens of nanometers in any dimension, precluding side-by-side comparison with actual nanomechanical experiments. This talk presents STZD simulations on experimentally relevant length and time scales, and discusses the methods used to achieve such large sample sizes. Also, the role of free volume as a simulation state variable is discussed, with particular focus on tension-compression asymmetry. Finally, the challenges and opportunities in pairing STZD simulations side-by-side with experiments are discussed.

Multiresolution Adaptive Wavelet Solver for Nonlinear Partial Differential Equations with Error Control

Cale Harnish^{*}, Karel Matouš^{**}, Daniel Livescu^{***}

^{*}University of Notre Dame, ^{**}University of Notre Dame, ^{***}Los Alamos National Laboratory

ABSTRACT

Simulations of practical engineering applications must solve coupled systems of nonlinear partial differential equations (PDEs), with features evolving on a wide range of spatial and temporal scales. This multiscale and multiphysics nature is a challenge for classical computational methods and may impose prohibitive computational requirements. To overcome these challenges, we have developed a novel multiresolution wavelet based algorithm to solve PDEs with significant data compression and explicit error control. Our proposed numerical method exploits the features of the biorthogonal interpolating wavelet family of basis functions, and second generation wavelets, to solve initial-boundary value problems on finite domains. We maximize the traditional data compression ability of wavelets by creating a unique multiresolution representation for each field, and using the minimum number of collocation points to define the coarsest resolution. Moreover, we compute spatial derivatives by operating directly on the wavelet bases. We provide a priori error estimates for the wavelet representation of fields, their derivatives, and the aliasing errors associated with the nonlinear terms in a PDE. Then, our estimates are used to construct a sparse multiresolution spatial discretization that guarantees the prescribed accuracy for each unknown. Our algorithm includes a predictor-corrector procedure within the time advancement loop to dynamically adapt the computational grid and maintain the prescribed accuracy of the solution of the PDE as it evolves. Furthermore, we present a simplified index notation for the wavelet operations to facilitate their matrix-free computational implementation. Our highly adaptive algorithm has been verified on a variety of nonlinear problems including Burgers's equation and the Navier-Stokes equations. Convergence to the analytical solutions is achieved at a rate which is in agreement with a priori estimates. Our algorithm provides accurate solutions to coupled systems of nonlinear PDEs with explicit error control, significant data compression, and fine scale features are well resolved with no spurious numerical oscillations.

Compressible Flow and Conjugate Heat Transfer Using Blended RBF Interpolation

Michael Harris^{*}, Alain Kassab^{**}, Eduardo Divo^{***}

^{*}University of Central Florida, Mechanical and Aerospace Engineering Dept., Orlando, FL USA, ^{**}University of Central Florida, Mechanical and Aerospace Engineering Dept., Orlando, FL USA, ^{***}Embry-Riddle Aeronautical University, Department of Mechanical Engineering, Daytona Beach, FL USA

ABSTRACT

A meshless blended radial basis function (RBF) methodology is developed to solve conjugate heat transfer problems with convection to viscous compressible flow coupled with conducting solids. The radial basis function interpolation uses Hardy Multiquadrics which depends on a shape parameter and the shape parameter is typically chosen to be a large value rendering the RBF flat. The approach of choosing a large shape parameter tends to interpolate smooth data very well providing spectral accuracy in cases, although this approach tends to fail for steep gradients requiring the shape parameter to be lowered to capture the shock and prevent oscillations. The blended radial basis function method uses low shape parameter interpolation when shocks or steep gradients are detected and then switches to high value shape parameter RBF interpolation where the data is smooth. The blended RBF approach has proven to show stability and accuracy in many test cases. Numerical examples are presented to validate the approach of solving viscous compressible flow with conjugate heat transfer using the blended RBF methodology.

The Influence of Sacrificial Bonds on the Mechanical Properties of Soft Tissue

Markus Hartmann*, Huzaifa Shabbir**

*Computational Physics Group, Faculty of Physics, University of Vienna, Austria, **Computational Physics Group, Faculty of Physics, University of Vienna, Austria

ABSTRACT

Biological materials, like bone, wood, silk or the mussel byssus, often tailor their mechanical properties using reversible cross-links. These cross-links are weaker than the covalent backbone of the structures and, thus, normally fail before the backbone ruptures when the structure is loaded. This rupture of cross-links may expose some – previously shielded – part of the molecule to loading. This interplay of cross-link rupture and revealing of hidden length provides a very efficient energy dissipation mechanism leading to an elevated toughness of the structure. Because the cross-links “sacrifice” themselves for the overall mechanical performance of the structure, they are also called “sacrificial bonds”. The reversibility of bonds means that sacrificial bonds may reform after the load is released. This mechanism ensures that the system recovers its original mechanical properties with time, providing some self-healing capabilities. In my talk I will present a computational model to study the influence of sacrificial bonds on the mechanical behavior of fibrous systems. We model linear polymer chains using atomistic bead-spring models. Some of these beads are defined as “sticky” and may form additional cross-links. Using Monte Carlo methods, computational load displacement curves are obtained and analysed. I will discuss how the density of sticky sites, their arrangement, topology and coordination influences the mechanical behavior of a single polymer chain or of a chain bundle. In particular, it will be shown that temperature and entropy reduce the efficacy of these bonds significantly, although the cross-links are relatively strong with a binding energy of approximately 50 kBT [1]. It will be discussed how the topology of formed cross-links influences the most basic mechanical parameters of the system like elastic modulus, work to fracture and strength. I will show that compared to non-cross-linked fibers the strength in chain bundles may even be reduced when cross-links are introduced in the system [2]. Finally, the influence of the coordination of cross-links on the mechanics of fibrous systems will be discussed. Motivated by metal coordination bonds that may form cross-links between more than two monomers, it will be shown that a higher coordination changes the mechanics of the system drastically [3]. [1] Nabavi, Harrington, Paris, Fratzl & Hartmann, New J. Phys. 16, 013003 (2014) [2] Nabavi & Hartmann, Soft Matter 12, 2047 (2016) [3] Shabbir & Hartmann, New J. Phys. 19, 093024 (2017)

Enhanced Beam-Theory Derived Shear Stress Distributions in Tramway Rails

Patricia Hasslinger*, Aleš Kurfürst**, Edgar Fischmeister***, Thomas Hammer****, Christian Hellmich*****, Stefan Scheiner*****

*Institute for Mechanics of Materials and Structures, TU Wien - Vienna University of Technology, Vienna, Austria,

**Institute for Mechanics of Materials and Structures, TU Wien - Vienna University of Technology, Vienna, Austria,

Wiener Linien GmbH & Co KG, Vienna, Austria, *Wiener Linien GmbH & Co KG, Vienna, Austria, *****Institute for Mechanics of Materials and Structures, TU Wien - Vienna University of Technology, Vienna, Austria,

*****Institute for Mechanics of Materials and Structures, TU Wien - Vienna University of Technology, Vienna, Austria

ABSTRACT

In many urban areas, tramways are the backbone of the local public transport system imposing high requirements on its reliability. During service, rail fractures and material degradation due to wear or environmental influences are the main causes of disruptions. Rail fractures occur if the loads acting onto the rails induce stress states which exceed the strength of the steels the rails are made of. In the case of rail transport, these loads, resulting predominantly from the rail car axles, are not only extraordinary high, but also concentrated on small contact areas between the rail car wheels and the rails. In this study, the fracture tendency of tramway rails is investigated by employing a novel shear-compliant beam theory, considering normal and shear forces, bending moments as well as primary and secondary torsional moments. Our main interest lies in shear stress distributions throughout the cross sections of grooved rails. Interestingly, the locations of maximum shear stresses arising from discontinuities in shear forces, as encountered with abrupt changes in the embedment conditions, agree remarkably well with fracture patterns observed in real life. This marks a new level of advanced computational mechanics entering railway engineering.

Prediction of Thermoelastic Behavior of Porous Media Using a Multiscale Asymptotic Expansion Homogenization Method

Mohammad Hatami*, Alireza Sarvestani**, David Bayless***

*PhD Student, **Assistant Professor, ***Professor

ABSTRACT

Mineralogical compositions, such as shale, are modeled as multiphase porous materials with mechanical properties that are mainly influenced by mineral grains, pores, pore networks, and their permeability. Asymptotic expansion homogenization (AEH) is a multiscale computational methodology primarily used for determination of stress and deformation in heterogeneous materials. By decoupling the local (micro) and a global (macro) length scales, this method is proved to be a computationally efficient tool to evaluate the continuum field quantities in a localized region of interest. In this research, an AEH scheme is built into a finite element model to study the thermo-elasticity of heterogeneous porous media. A stochastic method based on Gaussian function distributions is used to generate realistic random microstructures within the matrix, with different porosities. Based on the proposed AEH method, homogenized material properties, namely thermal conductivity, Young's modulus, and thermal expansion coefficient of the porous media are determined. Consequently, the effect of pore size and porosity on distribution of stress and deformation in a cylindrical shale sample placed in a gas permeability chamber is studied. The effect of gas pressure gradient coupled with other microstructural variables on the evolution of stress and deformation at microscales are studied.

Modelling Selective Laser Melting with Focus on Optimizing the Scanning Path for Minimizing Final Distortions

Jesper Hattel*, Sankhya Mohanty**

*Technical University of Denmark, DTU, **Technical University of Denmark, DTU

ABSTRACT

Residual stresses and deformations continue to remain one of the primary challenges towards expanding the application of selective laser melting (SLM) as an industrial scale manufacturing process. The process continues to suffer from these challenges due to the localized heating, rapid cooling and high temperature gradients that occur during the process. To address these issues, numerical model based process optimization strategies for laser-scanning paths are presented and discussed. Various reduced order models simulating the thermal, mechanical and thermo-mechanical phenomena during SLM, which have been developed by combining commercial software with in-house codes, are demonstrated. A multilevel optimization strategy is adopted using a customized genetic algorithm developed for optimizing cellular scanning strategy for selective laser melting, with the objective of reducing residual stresses and deformations. The resulting thermo-mechanically optimized cellular scanning strategies are compared with standard scanning strategies and have been used to manufacture standard samples. The optimization results show how model-based process optimization can reduce the geometrical irregularities and ensure dimensional tolerances. Keywords: Additive Manufacturing, 3D printing, thermomechanical modelling, distortions, optimization

AN INTERPRETATION OF THE BOUNDARY CONDITION FOR PRESSURE POISSON PARTIAL DIFFERENTIAL EQUATION IN MOVING PARTICLE SEMI-IMPLICIT METHOD

MOTOFUMI HATTORI 1) and SEIICHI KOSHIZUKA 2)

1) Kanagawa Institute of Technology, Department of Information Media
hattori@ic.kanagawa-it.ac.jp
1030 Shimo-ogino Atsugi-city Kanagawa-prefecture Zip 243-0292, Japan

2) The University of Tokyo,
School of Engineering, Department of Systems Innovation
koshizuka@sys.t.u-tokyo.ac.jp
7-3-1 Hongo Bunkyo-ku Tokyo Zip 113-8654, Japan

Key words : Moving particle semi-implicit method, Moving particle simulation,
Pressure Poisson equation, Non-homogeneous Neumann boundary condition

Abstract. The non-homogeneous boundary condition for the pressure Poisson partial differential equation in MPS are transformed to the source term of the pressure Poisson partial differential equation.

1 INTRODUCTION

When Koshizuka et al. [3] developed the Moving Particle Semi-implicit method, they computed pressure by solving the Poisson partial differential equation with the “homogeneous” Neumann boundary condition. Later, Asai [5] , Tamai [6] and other researchers solved the Poisson partial differential equation with the “non-homogeneous” Neumann boundary condition.

By the mathematics theory about partial differential equation, non-homogeneous boundary condition can be transformed to the source term of the partial differential equation by using Dirac delta functions [1].

In this presentation, the authors applies this mathematics theory to the problem how to compute pressure by solving the Poisson partial differential equation. The non-homogeneous Neumann boundary condition will be transformed to the source term of the Poisson partial differential equation with the homogeneous Neumann boundary condition. This source term corresponds to the particle number density feedback of the Moving Particle Semi-implicit method.

2. FLUID PARTICLES

Let $\Omega(t)$ be the liquid's fluid domain at time t . Let $\partial\Omega(t)$ be the boundary of the fluid domain $\Omega(t)$. The boundary $\partial\Omega(t)$ consists of the free surface $\partial\Omega(t)_{\text{Dirichlet}}$ of the liquid and the wall $\partial\Omega_{\text{Neumann}}$ of the waterway. That is

$$\partial\Omega(t) = \partial\Omega(t)_{\text{Dirichlet}} \cup \partial\Omega_{\text{Neumann}} \quad (1)$$

We assume that the wall of the waterway does not move and $\partial\Omega_{\text{Neumann}}$ does not change as the time t goes on. .

For the position $\mathbf{r} = (r_x, r_y, r_z) \in \Omega(t)$ and the time t , let $\mathbf{a}(t, \mathbf{r})$ be the acceleration of the fluid particle \mathbf{r} , let $\mathbf{v}(t, \mathbf{r})$ be the velocity of the fluid particle \mathbf{r} , let $P(t, \mathbf{r})$ be the pressure around the fluid particle \mathbf{r} , and let $\rho(t, \mathbf{r})$ be the mass density around the fluid particle \mathbf{r} . Let

$$\frac{\partial}{\partial \mathbf{r}} = \left(\frac{\partial}{\partial r_x}, \frac{\partial}{\partial r_y}, \frac{\partial}{\partial r_z} \right) \quad (2)$$

be the spatial partial differential operator. Then the Laplace partial differential operator (which is positive definite) is expressed as

$$(-1) \frac{\partial}{\partial \mathbf{r}} \cdot \frac{\partial}{\partial \mathbf{r}} = (-1) \frac{\partial}{\partial r_x} \frac{\partial}{\partial r_x} + (-1) \frac{\partial}{\partial r_y} \frac{\partial}{\partial r_y} + (-1) \frac{\partial}{\partial r_z} \frac{\partial}{\partial r_z} \quad (3)$$

3. NAVIER-STOKES PARTIAL DIFFERENTIAL EQUATION

The dynamics of the fluid particle \mathbf{r} is governed by the following Navier-Stokes partial differential equation

$$\frac{D\mathbf{r}}{Dt} = \mathbf{v}(t, \mathbf{r}) \quad \text{for } \mathbf{r} \in \text{Int } \Omega(t) \quad (4)$$

$$\rho \mathbf{a}(t, \mathbf{r}) = \rho \frac{D\mathbf{v}}{Dt} = (-1) \frac{\partial P}{\partial r} + \mu \frac{\partial}{\partial r} \cdot \frac{\partial}{\partial r} \mathbf{v}(t, \mathbf{r}) + \rho \mathbf{g} \quad \text{for } \mathbf{r} \in \text{Int } \Omega(t) \quad (5)$$

and the boundary conditions

$$0 = \mathbf{v}(t, \mathbf{r}) \quad \text{for } \mathbf{r} \in \partial\Omega_{\text{Neumann}} \quad (6)$$

$$0 = \mathbf{a}(t, \mathbf{r}) \quad \text{for } \mathbf{r} \in \partial\Omega_{\text{Neumann}} \quad (7)$$

$$0 = \mathbf{v}(t, \mathbf{r}) \cdot \mathbf{n}(\mathbf{r}) \quad \text{for } \mathbf{r} \in \partial\Omega_{\text{Neumann}} \quad (8)$$

$$0 = \mathbf{a}(t, \mathbf{r}) \cdot \mathbf{n}(\mathbf{r}) \quad \text{for } \mathbf{r} \in \partial\Omega_{\text{Neumann}} \quad (9)$$

Here, $\mathbf{g} = (0, 0, -9.81[\text{m/s}^2])$ is the gravity acceleration. $\mathbf{n}(\mathbf{r})$ is the “inner” normal vector at position $\mathbf{r} \in \partial\Omega_{\text{Neumann}}$.

Since we consider the case that the fluid’s velocity is sufficiently smaller than the sound velocity, we assume the flow’s incompressibility

$$\frac{\partial}{\partial r} \cdot \mathbf{v}(t, \mathbf{r}) = 0 \quad \text{for } \mathbf{r} \in \text{Int } \Omega(t) \quad (10)$$

4. PRESSURE POISSON PARTIAL DIFFERENTIAL EQUATION AND BOUNDARY CONDITION

Applying $\partial/\partial \mathbf{r}$ to the both sides of the Navier-Stokes partial differential equation (5) and considering the incompressibility (10), one obtain the following Poisson partial differential equation

$$\rho \frac{\partial}{\partial r} \cdot \mathbf{a}(t, \mathbf{r}) = (-1) \frac{\partial}{\partial r} \cdot \frac{\partial}{\partial r} P(t, \mathbf{r}) + 0 + 0 \quad \text{for } \mathbf{r} \in \text{Int } \Omega(t) \quad (11)$$

id est

$$(-1) \frac{\partial}{\partial r} \cdot \frac{\partial}{\partial r} P(t, \mathbf{r}) = f(t, \mathbf{r}) = \rho \frac{\partial}{\partial r} \cdot \mathbf{a}(t, \mathbf{r}) \quad \text{for } \mathbf{r} \in \text{Int } \Omega(t) \quad (12)$$

Let $\mathbf{n}(\mathbf{q})$ be the “inner” normal vector at position $\mathbf{q} \in \partial\Omega_{\text{Neumann}}$. The spatial partial derivative along the “inner” normal vector and the spatial partial derivative along the “outer” normal vector may not equal. The spatial partial derivative along the “inner” normal vector can be computed by physical quantities in the fluid domain $\Omega(t)$, although the spatial partial derivative along the “outer” normal vector cannot be computed by physical quantities in the fluid domain $\Omega(t)$.

Taking the inner product between the inner normal vector $\mathbf{n}(\mathbf{q})$ and the both sides of the Navier-Stokes partial differential equation (5), one obtain the

Neumann boundary condition

$$\rho \mathbf{a} \cdot \mathbf{n} = (-1) \frac{\partial P}{\partial \mathbf{n}} + \left(\mu \frac{\partial}{\partial \mathbf{r}} \cdot \frac{\partial}{\partial \mathbf{r}} \mathbf{v} \right) \cdot \mathbf{n} + \mathbf{g} \cdot \mathbf{n} \text{ for } \mathbf{q} \in \partial\Omega_{\text{Neumann}} \quad (13)$$

id est

$$\frac{\partial P(t, \mathbf{q})}{\partial \mathbf{n}(\mathbf{q})} = h(\mathbf{q}) = \mathbf{g} \cdot \mathbf{n} + (-1) \rho \mathbf{a} \cdot \mathbf{n} + \left(\mu \frac{\partial}{\partial \mathbf{r}} \cdot \frac{\partial}{\partial \mathbf{r}} \mathbf{v} \right) \cdot \mathbf{n} \quad (14)$$

$$= \mathbf{g} \cdot \mathbf{n} + 0 + 0 \quad (15)$$

because the boundary condition (8) and (9) at the wall $\partial\Omega_{\text{Neumann}}$.

At time t and the position $\mathbf{q} \in \partial\Omega(t)_{\text{Dirichlet}}$ on the free surface, the pressure satisfies the Dirichlet boundary condition

$$P(t, \mathbf{q}) = 0 \text{ for } \mathbf{q} \in \partial\Omega(t)_{\text{Dirichlet}} \quad (16)$$

5. GREEN FUNCTION FOR HOMOGENEOUS BOUNDARY CONDITION

Let $K(\mathbf{r}, \mathbf{q})$ be the Green function of the Poisson partial differential equation and the homogeneous boundary condition [2]. The Green function $K(\mathbf{r}, \mathbf{q})$ satisfies the Poisson partial differential equation

$$\delta(\mathbf{r} - \mathbf{q}) = (-1) \frac{\partial}{\partial \mathbf{r}} \cdot \frac{\partial}{\partial \mathbf{r}} K(\mathbf{r}, \mathbf{q}) \text{ for } \mathbf{r}, \mathbf{q} \in \text{Int } \Omega(t) \quad (17)$$

with the source term $\delta(\mathbf{r} - \mathbf{q})$, the homogeneous Neumann boundary condition

$$\frac{\partial}{\partial \mathbf{n}(\mathbf{r})} K(\mathbf{r}, \mathbf{q}) = 0 \text{ for } \mathbf{r} \in \partial\Omega(t)_{\text{Neumann}} \text{ for } \mathbf{q} \in \text{Int } \Omega(t) \quad (18)$$

and the homogeneous Dirichlet boundary condition

$$K(\mathbf{r}, \mathbf{q}) = 0 \text{ for } \mathbf{r} \in \partial\Omega(t)_{\text{Dirichlet}} \text{ and for } \mathbf{q} \in \text{Int } \Omega(t) \quad (19)$$

6. NON-HOMOGENEOUS BOUNDARY CONDITION IS TRANSFORMED TO THE SOURCE TERM OF THE POISSON PARTIAL DIFFERENTIAL EQUATION

The solution $P(\mathbf{r})$ of the pressure Poisson partial differential equation (12) and the boundary conditions (14) (16) is expressed by the following integral

$$P(t, \mathbf{r}) = \int_{\mathbf{q} \in \Omega(t)} K(\mathbf{r}, \mathbf{q}) f(t, \mathbf{q}) d\mathbf{q} + \int_{\mathbf{q} \in \partial\Omega_{\text{Neumann}}} K(\mathbf{r}, \mathbf{q}) h(\mathbf{q}) d\sigma(\mathbf{q}) \quad (20)$$

Let $\delta(\mathbf{q})$ be the delta function whose support is $\partial\Omega_{\text{Neumann}}$.

$$P(t, \mathbf{r}) = \int_{\mathbf{q} \in \Omega(t)} K(\mathbf{r}, \mathbf{q}) f(t, \mathbf{q}) d\mathbf{q} + \int_{\mathbf{q} \in \Omega(t)} K(\mathbf{r}, \mathbf{q}) h(\mathbf{q}) \delta(\mathbf{q}) d\mathbf{q} \quad (21)$$

$$= \int_{\mathbf{q} \in \Omega(t)} K(\mathbf{r}, \mathbf{q}) (f(t, \mathbf{q}) + h(\mathbf{q}) \delta(\mathbf{q})) d\mathbf{q} \quad (22)$$

Then the pressure $P(t, \mathbf{r})$ is also be computed by the following Poisson partial differential equation

$$(-1) \frac{\partial}{\partial \mathbf{r}} \cdot \frac{\partial}{\partial \mathbf{r}} P(t, \mathbf{r}) = f(t, \mathbf{r}) + h(\mathbf{r}) \delta(\mathbf{r}) \quad \text{for } \mathbf{r} \in \text{Int } \Omega(t) \quad (23)$$

with the source term $f(t, \mathbf{r}) + h(\mathbf{r}) \delta(\mathbf{r})$ and the homogeneous B.C.

$$\frac{\partial P(t, \mathbf{q})}{\partial \mathbf{n}(\mathbf{q})} = 0 \quad \text{for } \mathbf{q} \in \partial\Omega_{\text{Neumann}} \quad (24)$$

$$P(t, \mathbf{q}) = 0 \quad \text{for } \mathbf{q} \in \partial\Omega(t)_{\text{Dirichlet}} \quad (25)$$

7. PARTICLE NUMBER DENSITY FEEDBACK IN MPS

Tanaka and Masunaga [4] computed the pressure by solving the following Poisson partial differential equation

$$\left(\frac{-1}{\rho_0} \right) \frac{\partial}{\partial \mathbf{r}} \cdot \frac{\partial}{\partial \mathbf{r}} P(t, \mathbf{r}) = (1 - \alpha) \frac{\partial}{\partial \mathbf{r}} \cdot \frac{0 - \mathbf{v}(t - \Delta t, \mathbf{r})}{\Delta t} + \alpha \frac{n(t, \mathbf{r}) - n_0}{\Delta t \Delta t} \quad (26)$$

$$= (1 - \alpha) \frac{\partial}{\partial \mathbf{r}} \cdot \frac{\mathbf{v}(t, \mathbf{r}) - \mathbf{v}(t - \Delta t, \mathbf{r})}{\Delta t} + \alpha \frac{n(t, \mathbf{r}) - n_0}{\Delta t \Delta t} \quad (27)$$

$$= (1 - \alpha) \frac{\partial}{\partial \mathbf{r}} \cdot \mathbf{a}(t, \mathbf{r}) + \alpha \frac{n(t, \mathbf{r}) - n_0}{\Delta t \Delta t} \quad \text{for } \mathbf{r} \in \text{Int } \Omega(t) \quad (28)$$

with homogeneous boundary conditions. Here, $n(t, \mathbf{r})$ is the particle number density at time t , n_0 is the true value of the particle number density, ρ_0 is the true value of the mass density of the fluid, and $0 \leq \alpha \leq 1$ is the weight coefficient for the feedback of the particle number density.

By considering that the fluid particles always collides the bottom of the wall $\partial\Omega_{\text{Neumann}}$ the waterway, the equation (23) corresponds to the equation (28).

8 CONCLUSIONS

The pressure Poisson partial differential equation with the non-homogeneous boundary condition is transformed to the pressure Poisson partial differential equation with homogeneous boundary condition whose source term is the mass density feedback which was introduced by Moving Particle Semi-implicit method .

ACKNOWLEDGEMENT

The authors would like to express their thanks to Prof. Yoshihiro SHIBATA (Waseda University) for discussing about the derivation for the Neumann boundary condition for the pressure Poisson partial differential equation. Also they would like to express their thanks to Dr. Tasuku TAMAI (The University of Tokyo) for discussing about the importance of the Neumann boundary condition for the pressure Poisson partial differential equation in Moving Particle Simulation [6].

REFERENCES

- [1] Yoshiyuki Sakawa, "Optimum Systems Control Theory", chapter 11, Corona publishing, (1972), in Japanese
- [2] Seizo Ito, "Diffusion partial differential equation", Kinokuniya publishing,(1979), chapter 4, in Japanese
- [3] Seiichi Koshizuka, "Particle method", Maruzen publishing, (2005), in Japanese
- [4] Masayuki Tanaka and Takayuki Masunaga, "Stabilization and smoothing of pressure in MPS method by Quasi-Compressibility", Journal of Computational Physics, Volume 229 Issue 11, (2010), pp 4279-4290
- [5] Mitsuteru Asai, "Tsunami analysis by SPH and boundary condition in particle methods", Lectures at Takeda Hall in The University of Tokyo, 4 March (2013)
- [6] Tasuku Tamai, "Development of Least Squares Moving Particle Semi-implicit method ", Master Thesis of The University of Tokyo, March (2014) in Japanese

Using Modeling and Machine Learning to Accelerate High-Throughput Experimental Materials Discovery

Jason Hattrick-Simpers^{*}, Fang Ren^{**}, Logan Ward^{***}, Travis Williams^{****}, Kevin Laws^{*****},
Christopher Wolverton^{*****}, Apurva Mehta^{*****}

^{*}NIST, ^{**}SLAC National Accelerator Laboratory, ^{***}University of Chicago, ^{****}University of South Carolina,
^{*****}University of New South Wales, ^{*****}Northwestern University, ^{*****}SLAC National Accelerator Laboratory

ABSTRACT

Over the past 10 years there has been a resurgent interest in the development of novel metallic alloys, both as multiple principle component solid solution alloys, so-called high entropy alloys (HEA) as well as amorphous metallic glasses. Although a number of empirical rules have been proposed for the prediction of potential alloy compositions, calculating their stability and quantifying their properties of interest at operating temperatures from first principles represents a significant challenge. In fact, even high-throughput experimental studies struggle to effectively explore such large composition-processing-property parameter spaces efficiently. Here, I will discuss an approach that seeks to address the rational experimental exploration of such alloys by combining theory, experiment and data science. Our approach is to use insights from the literature, theory, and/or data mining to identify the regions of parameter space most likely to yield interesting materials. We then employ computationally guided high-throughput synthesis techniques to strategically probe composition and processing space. In situ synchrotron diffraction studies yield tens of thousands of data sets describing the evolution of the alloy phase and corrosion products. The data are evaluated using automated knowledge extraction techniques, enabling us to assess our experiments, update the models used to generate the initial lead materials, and plan the next material system to study. In this talk, I will emphasize our recent work using these techniques to investigate phase stability in metallic glasses.

Title: A Collision-Based Hybrid Method for Linear Transport

Cory Hauck*

*Oak Ridge National Laboratory

ABSTRACT

We present a hybrid method for simulating kinetic equations with multiscale phenomena in the context of linear transport. The method consists of (i) partitioning the kinetic equation into collisional and non-collisional components; (ii) applying a different numerical method to each component; and (iii) re-partitioning the kinetic distribution after each time step in the algorithm. Preliminary results show that, for a wide range of test problems, the combination of a low-order method for the collisional component and a high-order method for the non-collisional component provides a level of accuracy that is comparable to a uniform high-order treatment of the entire system. We also investigate the use of integral-deferred correction techniques to increase the temporal accuracy of the individual components of the hybrid method and assess the benefits in overall efficiency.

Homogenization and Design Optimization for a Periodic Heterogeneous Plate with Frame Structure under a Given Constraint

Michael Hauck^{*}, Julia Orlik^{**}, Stephan Wackerle^{***}

^{*}Fraunhofer ITWM, ^{**}Fraunhofer ITWM, ^{***}Fraunhofer ITWM

ABSTRACT

The design optimization problems for heterogeneous elastic plates with frame structure as shown in [1] arise in many different applications, for instance in filters under local bending or analysis of textiles. We consider a plate with an in-plane periodic structure under a local point-bending moment or force. We employ basic homogenization techniques for linear periodic heterogeneous plates and pass to the anisotropic Kirchhoff-Love plate in the limit, where the effective bending coefficients were obtained from the auxiliary bending unit experiments on the periodicity cell by averaging of the local moments of outer-plane stresses. Since the plate structure is made of beam, we use the beam-FE method for solving the cell-problems. We homogenize the plate and then find an analytic solution under the local bending perturbation. Our further aim is to minimize the deflection caused by a localized load in the effective anisotropic plate. For that case we need to define a design space as in [2], which takes into account the constraint of anisotropy. We provide a particular example, where we can show how the design parameters influence the maximal plate deflection. References: [1] Hauck, M., Klar, A., & Orlik, J. (2017). Design optimization in periodic structural plates under the constraint of anisotropy. ZAMM?Journal of Applied Mathematics and Mechanics/Zeitschrift für Angewandte Mathematik und Mechanik. [2] Orlik, J., Panasenko, G., & Shiryayev, V. (2016). Optimization of Textile-Like Materials via Homogenization and Beam Approximations. Multiscale Modeling & Simulation, 14(2), 637-667.

VMS A Posteriori Error Estimation for the Incompressible NS Equations

Guillermo Hauke*, Diego Irisarri**

*EINA - Zaragoza, **EINA - Zaragoza

ABSTRACT

The genesis of stabilized methods was established in [1] from the standpoint of the variational multiscale theory (VMS). By splitting the solution into resolved and unresolved scales, it was shown that stabilized methods take into account an approximation of the unresolved scales into the finite element solution. Recent works have shown that these unresolved scales contain fairly accurate error information that can be exploited to formulate explicit a posteriori error estimators which are consistent with the assumptions inherent to stabilized methods [2,3]. In this presentation new highlights will be given about global and local a posteriori estimation for the incompressible Navier-Stokes equations using the VMS error time-scales. References: [1] T.J.R. Hughes, Multiscale phenomena: Green's functions, the Dirichlet-to-Neumann formulation, subgrid scale models, bubbles and the origins of stabilized methods. *Comput. Meth. Appl. Mech. Engrg.* 127, 387-401, (1995). [2] G. Hauke, D. Fuster and M.H. Doweidar, Variational Multiscale a-Posteriori Error Estimation for Multi-dimensional Transport Problems. *Comput. Meth. Appl. Mech. Engrg.* 197, 2701-2718, (2008) [3] G. Hauke, D. Fuster, F. Lizarraga, Variational Multiscale a-Posteriori Error Estimation for Systems: The Euler and Navier-Stokes Equations. *Comput. Meth. Appl. Mech. Engrg.* 283, 1493-1524, (2015)

A Review of VMS for A Posteriori Error Estimation

Guillermo Hauke*

*EINA - Zaragoza

ABSTRACT

The variational multiscale theory (VMS) was proposed in [1] to explain and unify various fundamental problems in computational mechanics including the origin of stabilized methods. By splitting the solution into resolved and unresolved scales, it was shown that stabilized methods take into account an approximation of the unresolved scales into the finite element solution. These unresolved scales contain important subgrid information, that has been used up for providing accurate turbulence models for LES [2]. Recent works have also shown that the unresolved scales can be used to formulate explicit and implicit a posteriori error estimators which are consistent with the assumptions inherent to stabilized methods [3]. In this presentation we will summarize the achievements of VMS and the error-time scales to estimate the numerical error and its potential to adapt the meshes. [1] T.J.R. Hughes, Multiscale phenomena: Green's functions, the Dirichlet-to-Neumann formulation, subgrid scale models, bubbles and the origins of stabilized methods. *Comput. Meth. Appl. Mech. Engrg.* 127, 387--401, (1995). [2] Y. Bazilevs, V.M. Calo, J.A. Cottrell, T.J.R. Hughes, A. Reali, G. Scovazzi, Variational multiscale residual-based turbulence modeling for large eddy simulation of incompressible flows. *Comput. Meth. Appl. Mech. Engrg.* 197, 173--201, (2007) [3] G. Hauke, D. Fuster, F. Lizarraga, Variational Multiscale a-Posteriori Error Estimation for Systems: The Euler and Navier-Stokes Equations. *Comput. Meth. Appl. Mech. Engrg.* 283, 1493--1524, (2015)

Uncertainty Quantification in Finite Element Models: Application to Soft Tissue Biomechanics

Paul Hauseux^{*}, Jack S. Hale^{**}, Raphaël Bulle^{***}, Franz Chouly^{****}, Alexei Lozinski^{*****},
Stéphane P.A. Bordas^{*****}

^{*}University of Luxembourg, ^{**}University of Luxembourg, ^{***}University of Luxembourg, ^{****}Bourgogne Franche Comté University, ^{*****}Bourgogne Franche Comté University, ^{*****}University of Luxembourg and Cardiff University

ABSTRACT

We present probabilistic approaches aiming at the selection of the best constitutive model and to identify their parameters from experimental data. These parameters are always associated with some degree of uncertainty. It is therefore important to study how this statistical uncertainty in parameters propagates to a safety-critical quantity of interest in the output of a model. Efficient Monte Carlo methods based on variance reduction techniques (Sensitivity Derivatives Monte Carlo methods [Hauseux et al. 2017] and MultiLevel Monte Carlo [Giles 2015] methods) are employed to propagate this uncertainty for both random variables and random fields. Inverse and forward problems are strongly connected. In a bayesian setting [Matthies et al. 2017], developing methods that reduce the number of evaluations of the forward model to an absolute minimum to achieve convergence is crucial for tractable computations. Numerical results in the context of soft tissue biomechanics are presented and discussed.

A Plate Element Formulation for Modeling Progressive Damage and Residual Strength of Laminates

Devlin Hayduke*

*Materials Sciences Corporation

ABSTRACT

Advanced composite material systems are vital to the development of lightweight, multi-functional aerospace structures. In addition to reducing the weight of the structure, these material systems provide the ability to expand the function of the structure by tailoring stiffness and strength characteristics for numerous applications. Consequently, carbon fiber-reinforced epoxy structures have become very attractive for airframe applications. It is normally accepted that a limiting characteristic of laminated composite structures of this nature is the response of the impacted material to compressive loads, e.g. buckling. It is also well documented that delamination is the predominant damage mode in composite materials subjected to impact damage. Consequently, novel advanced composite material design and analysis approaches are sought to minimize the risk of damage from low-energy impacts resulting from operations and maintenance impact accidents. An analysis tool that contains novel mathematical/physical approaches for accurately assessing the residual compressive strength in impact-damaged composite structures is desired. In response to this need, a user element (UEL) subroutine for use with commercially available analysis codes has been developed by Materials Sciences Corporation. In particular, an enhanced plate formulation element that offers advantages in both the economy and reliability of computations has been realized. The formulation integrates a nonlinear material model to evaluate progressive damage and failure of composite materials on a ply-by-ply basis while incorporating a shear correction model that accurately predicts the nonlinear transverse response of impacted composite structures. A brief overview of the theoretical formulation of the element and embedded nonlinear material model will be provided. Followed by examples of standard characterization tests and the corresponding data reduction methodology required to determine model parameters for a commonly used intermediate modulus carbon fiber reinforced epoxy material system. In addition, an example of the residual strength predictions for a standard test specimen that exhibits progressive damage due to transverse shear will be reviewed. Finally, results of analysis models, e.g., dynamic and quasi-static, that were used to predict residual strength of an impacted laminated panel will be compared to experimental results.

Investigation of Fluid-Driven Fracture in Porous Medium Using Diffusive Phase-Field Fracture Approach

Bang He^{*}, Pania Newell^{**}, Mary Wheeler^{***}

^{*}The University of Utah, ^{**}The University of Utah, ^{***}The University of Texas at Austin

ABSTRACT

The fluid-driven fracture exists in many porous mediums, including but not limited to, geological subsurface media, biological organs, chemical reactant, etc. The fracture in porous matrix is usually a primary concern, because it often relates to the failure of entire material system. Therefore, understating the mechanism of fluid-driven fracture in porous medium is an important task in many scientific and engineering applications. However, because of the complex coupled physics of the intertwining interaction among fluid flow, porous medium, and fracture propagation, as well as the stress singularity at the crack tip, it is usually challenging to numerically investigate it. Some recent works on the phase-field modeling have constructed the generalized free energy equation for saturated porous medium by taking the pressure term and phase-field free energy into account, where the phase-field method is extended to the fully coupled fluid-driven fracture problems in porous medium. With this method, it is feasible for us to take a closer look at the essential characteristics of the fluid-driven fracture in porous medium and circumvent the discontinuity problem in numerical simulation. Therefore, we conducted two comprehensive investigation of the fluid-driven fracture in porous medium based on the penny crack model, considering that penny crack is massively investigated in published literature and there are lots of data available to validate our numerical result through comparison. The first part will focus on the influence of fluid injection pressure on fracture growth pattern for a given porous medium. With this work, the relation between fracture propagation and fluid injection can be established. Moreover, we anticipate that the underlined porosity (e.g. shape, size, and distribution) will also impact the fracture growth. Therefore, aside from the injection pressure-fracture relation, we will also present an endeavor to explore the porosity and pore size effect on fracture growth by using the multi-scale phase-field modeling method for fractured porous structure. In this study, the contribution of porosity and pore size to fracture will be studied by considering their continuous effect on the permeability and Biot's coefficient. Furthermore, at the pore-scale, the fracture growth along the variation of porosity and pore size will also be examined by modeling the pore with micro element and carrying over the micro element response to macro models. Through this investigation, we can extend our understanding on how

An Evaluation Approach of Dynamic Brittle Fracture Using Limited Sensor Data

Jingjing He^{*}, Yibin Zhou^{**}, Yongxiang Wang^{***}, Haim Waisman^{****}, Rilin Shen^{*****}

^{*}Beihang University, ^{**}Beihang University, ^{***}Columbia University, ^{****}Columbia University, ^{*****}Harbin Institute of Technology

ABSTRACT

The prevention of fracture-induced failure is a major challenge in engineering designs, as a consequence, a wide variety of numerical simulations of fracture processes have been studied over decades. In this work, we propose a simulation approach for brittle fracture to the dynamic case combined with dynamic responses reconstruction method and phase-field model. In contrast to discrete descriptions of fracture, phase-field descriptions do not require numerical tracking of discontinuities in the displacement field. The fracture surface is approximated by a field, which smoothes the boundary of the crack over a small region. The evolution of fracture surfaces follows from the solution of a coupled system of partial differential equations, which greatly reduces implementation complexity. The previous work named as REMD (reconstruction based on empirical mode decomposition) is extended to accurately obtain the structural displacement responses in time domain. One of the advantages of the REMD is to provide accurate dynamic response information for fracture crack simulation using sparse and remote strain gauges installed in the structure. For the mode shape information will change as the stiffness of cracked elements decrease in the fracture process, we present a step calculation scheme to update the exact mode shape included crack evolution information. Then, the behavior of the dynamic model is studied by performing a number of numerical cases. These cases show that the combination of the phase-field model and REMD provides an effective method for simulating fracture process in two dimensions.

A Decomposed Subspace Reduction for Fracture Mechanics Based on ISBFM Galerkin Meshfree Method

Qizhi He^{*}, J. S. Chen^{**}, Camille Marodon^{***}

^{*}University of California, San Diego, ^{**}University of California, San Diego, ^{***}OptimaRH Consulting

ABSTRACT

Repeated simulations of fracture in materials under various conditions are important in many applications but are computationally unaffordable. A decomposed subspace reduction (DSR) method is proposed for fracture mechanics modeled by a Galerkin meshfree method, where the meshfree approximation is based on a smooth reproducing kernel approximation enriched by non-smooth near-tip basis functions. The Galerkin formulation is formulated via the integrated singular basis function method (ISBFM) [1, 2] to avoid the need of high-order quadrature scheme for domain integration near the crack tip, and consequently yields a sparser discrete system for effective model order reduction (MOR) procedures. The DSR method is proposed for the ISBFM discrete system, such that the low-rank representation of the smooth subspace is obtained while the non-smooth subspace is optimally preserved. Compared with the standard model reduction based on a modal projection, DSR better represents the singularity and discontinuity properties of fracture problem in its low-dimensional reduced-order approximation. Numerical examples are given to validate the effectiveness of the proposed MOR method for fracture mechanics. References [1] Georgiou, G. C., Olson L, Smyrlis Y. S., A singular function boundary integral method for the Laplace equation, Communications in Numerical Methods in Engineering, 12(2), pp. 127–134. 1996. [2] Chen, J. S., Marodon, C., Hu, H. Y., Model order reduction for meshfree solution of Poisson singularity problems. International Journal for Numerical Methods in Engineering, 102(5), pp.1211–1237, 2015.

Adaptive Reduction of the Dimensionality of Multiscale Models in Solid Mechanics and Structural Dynamics

Wanli He^{*}, Charbel Farhat^{**}

^{*}Stanford University, ^{**}Stanford University

ABSTRACT

Heterogeneous materials are often encountered in solid mechanics and structural dynamics problems. The brute force Finite Element (FE) solution of such problems usually requires extremely fine meshes and leads to prohibitively expensive numerical simulations. For this reason, alternative approaches such as the multiscale FE2 have been developed. Typically, these assume that the material configuration is homogeneous at the macroscale but heterogeneous at the smallest represented scale, and couple the sequence of scales using localization and homogenization procedures. For many problems however, they remain computationally unaffordable as at each but the finest scale, they require the solution of a unit cell problem at each quadrature point of the associated FE mesh. For this reason, a model reduction framework was recently presented in [1] for dramatically accelerating the solution of nonlinear dynamic multiscale problems. In this framework, the dimensionality of the governing equations is reduced using the POD method, and computational efficiency is achieved for the evaluation of the nonlinear reduced-order terms using the Energy Conserving Sampling and Weighting method. Training is performed in two steps. First, a microscale hyper reduced-order model is constructed in-situ in order to achieve significant speedups even in non-parametric settings. Next, a classical offline-online training approach is performed to build a parametric hyper reduced-order macroscale model. A notable feature of this approach is the minimization, at the macroscale level, of the cost of the training using the in-situ hyper reduced-order microscale model to accelerate snapshot acquisition. A weak spot however is the in-situ training itself which, for sufficiently large macroscale models, requires an adaptive reduction process to keep the global ROB accurate and economical at all times. This talk will present such an adaptive process based on the concept of a database of local ROBs that is constructed and updated on-the-fly. This process treats the deformation gradient as a vector parameter domain, which enables it to locate each unit cell problem in the database and assign to it online the most appropriate local ROB. Its accuracy is optimized by collecting new snapshots as needed and updating accordingly the local ROBs. The resulting adaptive nonlinear model reduction framework is illustrated with the fast solution of several nonlinear dynamic multiscale problems. 1. M. J. Zahr, P. Avery, and C. Farhat, A Multilevel Projection-based Model Order Reduction Framework for Nonlinear Dynamic Multiscale Problems in Structural and Solid Mechanics, International Journal for Numerical Methods in Engineering, Vol. 112, pp. 885-881 (2017)

Beam Damage Localization Using Indirectly Identified Mode Shapes

Wen-Yu He^{*}, Jian He^{**}, Wei-Xin Ren^{***}, Songye Zhu^{****}

^{*}Hefei University of Technology, ^{**}Hefei University of Technology, ^{***}Hefei University of Technology, ^{****}The Hong Kong Polytechnic University

ABSTRACT

This paper presents a damage localization method for beam structures by using the indirectly identified mode shapes without reference data. Mode shapes with high spatial resolution in a damaged state is extracted from the moving vehicle response via Hilbert transform (HT). To avoid the low anti-noise ability of the central difference method, regional mode shape curvature (RMSC) in the damaged state is defined to replace the traditional mode shape curvature. Subsequently the RMSC in an undamaged state is estimated by using the RMSC in a damaged state and the polynomial approximation that assumes RMSC in an undamaged state has smooth surface. Finally the RMSC change is used to localize damage in beam structures. Numerical studies are carried out to investigate the feasibility and efficiency of the proposed damage localization index (DLI). The results indicate that the proposed method can effectively overcome the disadvantages of traditional mode shape based damage localization methods, such as the requirement for high spatial resolution and reference mode shapes, and the central difference method induced low anti-noise ability.

Numerical Simulation for the Fracture Behaviour of Carbon Nanotubes

Xiaoqiao He*

*City University of Hong Kong

ABSTRACT

An atomic-based cellular automata algorithm (ACAA) is presented for the atomic-scale simulation of carbon nanotubes (CNTs). The ACAA employs the inter-atomic potential to account for multi-body interactions. Thus, the ACAA method is as accurate as the molecular dynamic (MD) method and much faster than MD simulations. The stress-strain response from elastic deformation to fracture of CNTs is simulated by using the ACAA method. The effect of a vacancy defect is examined on the tension characteristic of CNTs. The numerical results show that the ACAA is a effective method for the simulation of large system of CNTs.

The Effect of Marangoni Instabilities on Horizontal Ribbon Growth

Brian Helenbrook*

*Clarkson University

ABSTRACT

An arbitrary-Lagrangian-Eulerian hp finite element is used to study the dynamics of single-crystal horizontal ribbon growth of silicon. Solidification kinetics are included to model the non-isotropic growth of solid silicon. This study focuses on the fluid dynamics of the process in particular examining how Marangoni flows affect the final grown crystal. It is shown that depending on the chosen magnitude of the derivative of surface tension coefficient with temperature, marangoni stresses can cause a chaotic flow to develop. This flow leads to fluctuations in the free-surface height, which in turn create irregularities on the surface of the grown crystal. The amplitude and wavelength of the irregularities predicted by the model are compared to those seen in experiments performed at Applied Materials using the floating silicon method (a variant of horizontal ribbon growth).

Fast, Robust and Portable Implementations of Complex Mechanical Behaviours with the MFront Code Generator

Thomas Helfer*

*CEA, DEN, DEC, SESC

ABSTRACT

The PLEIADES software environment is devoted to the thermomechanical simulation of nuclear fuel elements behaviour under irradiation. This platform is co-developed in the framework of a research cooperative program between Électricité de France (EDF), AREVA and the French Atomic Energy Commission (CEA). Within this platform, a unified software environment for capitalisation of material knowledge has been developed and released as an open-source project: the MFront code generator [2,3]. This code generator provides several high level domain specific languages that allow the user to express the constitutive equations in a form closed to their mathematical expression. Those domain specific languages use a mathematical library based on advanced programming techniques provided by the C++ language (template meta-programming, static polymorphism, expression templates, loop unrolling, etc..) which allow the compiler to highly optimize the generated code. This talk will focus on mechanical behaviours which are by essence complex and may have significant impact on the numerical performances of mechanical simulations. MFront users can describe all kinds of mechanical phenomena, such as viscoplasticity, plasticity and damage, for various types of mechanical behaviour (small strain or finite strain behaviour, cohesive zone models). MFront provides various interfaces to finite element solvers which allow the same implementation to be used in many finite element solvers, such as: Abaqus/Standard and Abaqus/Explicit, Ansys APL, CalculiX, Code_Aster, Cast3M, etc. Several benchmarks show that the generated mechanical behaviours are computationally efficient and have performances on par with native build-in implementations in Code_Aster, Cast3M, Abaqus/Standard, etc. This talk will provide: - an overview of the MFront code generator. - an example of the implementation of complex plastic behaviour at finite strain with an implicit scheme and the impact of the algorithms used to solve the implicit system on the robustness and numerical performances: those algorithms range from simple physically motivated modifications to the standard Newton-Raphson algorithm to advanced trust-region algorithms (Powell DogLeg, Levenberg-Marquart). [1] David Plancq et al. PLEIADES: a unified environment for multi-dimensional fuel performance modeling. In International meeting on LWR fuel performance, Florida, 2004. [2] <http://tfel.sourceforge.net> [3] Thomas Helfer et al. Introducing the open-source mfront code generator : Application to mechanical behaviours and material knowledge management within the PLEIADES fuel element modelling platform. Computers & Mathematics with Applications, 70(5) :994–1023, September 2015.

Biofidelic FEMs for Assessing Hip Fracture Risk in Elderly Women

Benedikt Helgason^{*}, William S. Enns-Bray^{**}, Hassan Bahaloo^{***}, Ingmar Fleps^{****}, Yves Pauchard^{*****}, Elham Taghizadeh^{*****}, Sigurdur Sigurdsson^{*****}, Philippe Büchler^{*****}, Thor Aspelund^{*****}, Vilmundur Gudnason^{*****}, Stephen J. Ferguson^{*****}, Halldor Palsson^{*****}

^{*}Institute for Biomechanics, ETH Zürich, Zürich Switzerland and School of science and Engineering, Reykjavik University, Reykjavik Iceland, ^{**}Institute for Biomechanics, ETH Zürich, Zürich Switzerland, ^{***}School of Engineering and Natural Sciences, University of Iceland, Reykjavik, Iceland, ^{****}Institute for Biomechanics, ETH Zürich, Zürich Switzerland, ^{*****}McCaig institute for Bone and Joint health, Cumming school of medicine, University of Calgary, Calgary Canada, ^{*****}Institute for Surgical Technology and Biomechanics, University of Bern, Switzerland, ^{*****}The Icelandic Heart Association Research Institute, Kopavogur, Iceland, ^{*****}Institute for Surgical Technology and Biomechanics (ISTB), University of Bern, Switzerland, ^{*****}The Icelandic Heart Association Research Institute, Kopavogur, Iceland, ^{*****}The Icelandic Heart Association Research Institute, Kopavogur, Iceland, ^{*****}Institute for Biomechanics, ETH Zürich, Zürich Switzerland, ^{*****}School of Engineering and Natural Sciences, University of Iceland, Reykjavik, Iceland

ABSTRACT

Introduction FEM based prediction of hip fracture risk has in the past focused on the sensitivity of quasi-static femoral strength as a fracture risk indicator. The load that the femur is subjected to as a result of impact, which is the cause of most hip fractures, has sparsely been investigated. This study aimed to develop a high throughput pipeline for generating biofidelic FEMs that simulate impact loading resulting from sideways falling and assess their fracture classification accuracy. Methods Whole pelvic FEMs were generated from baseline CT scans for 254 females from the AGES-Reykjavik cohort. The femur on the impacted side was segmented from the CT data and corresponding FEM generated with heterogeneous, visco-plastic material properties mapped to it [1]. Models of soft tissue and other skeletal structures, not fully visible in the CT data, were generated with a combination of morphing and statistical shape modelling techniques. The FEMs were subject to sideways fall impact at 3 m/s. Fragility ratio (FR) was defined as the ratio between peak forces of paired biofidelic models, one with fully elastic and the other with non-linear material properties for the proximal femur. An expected end-point value (EEV) was defined as the FR weighted by the probability of falling assessed based on self-reported fall frequency at baseline. Bone tissue tensile damage and change in maximum volumetric strain (?MVS) were also assessed based on the FEM results. Fracture classification was quantified in terms of area under the receiver-operator curve (AUC). Results Age-adjusted AUC was highest for ?MVS (0.72), followed by FR (0.71), aBMD (0.70), and EEV (0.68). Partial-AUC corresponding to an osteoporotic threshold (aBMD of 0.57g/cm³) was highest for FR (0.043), followed by EEV (0.042), ?MVS (0.033), and aBMD (0.028). Maximum elastic femur force was correlated with femoral head radius, pelvis width, and soft tissue thickness (R²=0.79; RMSE=0.46 kN; p<0.005). Discussion The marginal improvement in FE-based AUC values compared to aBMD was similar to previous studies [2], however larger differences were observed for partial-AUC. The addition of fall frequency information did not significantly improve the sensitivity of hip fracture classification, suggesting that an improved assessment of fall probability is necessary for accurately identifying individuals predisposed to fracture. A novel estimate of peak femoral impact force as a function of subject biometrics provides valuable information for future studies simulating subject-specific impact loads. References [1] Enns-Bray et al., JMBBM, 78:196-205, 2018. [2] Kopperdahl et al., JBMR, 29:570-580 2014.

Multi-Scale Fracture Mechanics Approach to Simulate Crack Propagation in Repaired Sensitized Aluminum

Bozhi Heng^{*}, Stephanie TerMaath^{**}

^{*}University of Tennessee, Knoxville, ^{**}University of Tennessee

ABSTRACT

Stress corrosion cracking (SCC) is one of the main failure modes of Al-Mg (5xxx series) alloys used in marine structures. The precipitation of Al₂Mg₃ β -phase along grain boundaries takes place when Al-Mg alloys are exposed to elevated temperature over a prolonged time, which is defined as sensitization. The combination of marine environment and sensitization makes the alloys more susceptible to SCC due to the dissolution of the β -phase in salt water. Fiber reinforced composite patches have been demonstrated as an effective approach to prevent and slow crack growth in ship structures. Characterization of crack repair performance will allow for use of composite patches as an alternative to traditional repair techniques as a permanent repair. The goal of this research is to develop high-fidelity multi-scale computational models to predict and investigate crack growth in sensitized aluminum repaired with composite patches. The main challenge of this research is the lack of conclusive experimental data and the current incomplete knowledge of the complex mechanism for SCC. Therefore, the main objective is to develop mathematical models to describe the mechanisms of crack growth in sensitized aluminum through experimentation and multi-scale modeling. Then the mathematical models will be applied to investigate the effects of composite patches on crack propagation in sensitized aluminum. The greatest advantage of the proposed multi-scale modeling is its ability to cover micro factors of material microstructure in SCC such as β -phase distribution and grain orientation. However, this makes it difficult to homogenize models from a low-level scale to a high-level scale model. A developed probabilistic approach will be used for the homogenization process. Multiple cracks and branching crack growth is another reason for the complication of SCC analysis. A 3D model based on extended finite element method (XFEM) will be developed to simulate stress corrosion crack propagation with complex crack surfaces and crack paths.

Discretization of Weak and Strong Discontinuities in Non-Conformal Meshes

Paul Hennig^{*}, Arne Claus Hansen-Dörr^{**}, Markus Kästner^{***}

^{*}TU Dresden, Germany, ^{**}TU Dresden, Germany, ^{***}TU Dresden, Germany

ABSTRACT

In the numerical analysis of heterogeneous materials, weak and strong discontinuities arise in the field variables due to rapidly changing mechanical properties at material interfaces or due to propagation of cracks if a specific failure load is exceeded. Details about the local topology of heterogeneous microstructures are typically taken from imaging methods or are given in terms of random distributions. To reduce the time for costly meshing processes, different non-standard discretization techniques have been developed to discretize these heterogeneities in non-conforming meshes. These include polygonal or extended FEM, the hp-d-adaptive finite cell method, or its hp-adaptive B-spline version [1]. While good convergence rates can be achieved for the latter two, stress oscillations may occur because sharp material interfaces are modeled in terms of a continuous basis. Here, we incorporate material interfaces into a non-conforming discretization using a regularized interface representation. Adaptive, local h-refinement based on THB-splines [2] is applied to provide an hr-adaptive refinement strategy, where element size h and regularization length r are reduced simultaneously. In combination with specific homogenization assumptions across the interface, good convergence rates and local stresses are obtained. To account for local damage and failure, the modeling of the heterogeneous material structure is extended by a phase-field model for bulk and interface cracks. In this way, the cumbersome topological updates of the analysis mesh to track the crack path, are avoided. Crack initiation and propagation is controlled by solving an additional scalar field problem that is coupled to the mechanical one [3]. To model interface failure between two materials we combine the phase field approach with a local reduction of the critical fracture energy in the area of the regularized material interface. The method considers possible interactions between the regularization of the interface and the phase-field and ensures crack propagation with the experimentally observed fracture toughness of the interface. Finally we demonstrate the proposed modeling approach in numerical examples for crack propagation in heterogeneous materials using non-conformal meshes. [1] D. Schillinger and E. Rank. An unfitted hp-adaptive finite element method based on hierarchical B-splines for interface problems of complex geometry. CMAME, 2011. [2] P. Hennig, S. Müller and M. Kästner. Bezier extraction and adaptive refinement of truncated hierarchical NURBS. CMAME, 2016. [3] B. Bourdin, G.A. Francfort, and J-J. Marigo. Numerical experiments in revisited brittle fracture. JMPS, 2000.

Polymorphic Uncertainty Quantification for Stability Analysis of Fluid Saturated Soil and Earth Structures

Carla Henning*, Tim Ricken**

*University of Stuttgart, **University of Stuttgart

ABSTRACT

Nowadays, numerical simulations enable the description of mechanical problems in many application fields, e.g. in soil or solid mechanics. During the process of physical and computational modelling, a lot of theoretical model approaches and geometrical approximations are sources of errors. These can be distinguished into aleatoric (e.g. model parameters) and epistemic (e.g. numerical approximation) uncertainties. In order to get access to a risk assessment, these uncertainties and errors must be captured and quantified. In the framework of the priority program SPP 1886 of the DFG, in the present subproject (sp12) the focus is driven on quantification and assessment of polymorphic uncertainties in computational simulations of earth structures, especially for fluid-saturated soils. To describe the strongly coupled and non-linear solid-fluid response behavior, the theory of porous media (TPM) will be used [1]. To capture the impacts of different uncertainties on computational results, two promising approaches of analytical and stochastic sensitivity analysis will enhance the deterministic structural analysis [2, 3]. A simple consolidation problem already provided a high sensitivity in the computational results towards variation of material parameters and initial values. The variational sensitivities are used as a tool for optimization procedures and capture the impact of different parameters as continuous functions. An advantage is the accurate approximation of the solution space and the efficient computation time as well as the consistent and simultaneous development of the TPM model and its sensitivity expressions. A disadvantage lies in the complex analytical derivation and algorithmic implementation. In contrast to this access, the probabilistic sensitivity analysis from the field of statistics provides methods that indeed are combined with high computational costs, but have a great applicability and comparably low realisation effort. The overall objective is to figure out the respective strengths to develop more efficient methods and tools for the reliable and economic sizing of earth structures in the long-run. [1] W. Ehlers and J. Bluhm: Foundations of multiphasic and porous materials, Porous Media: Theory, Experiments and Numerical Applications, pages 3-86., Springer-Verlag, 2002. [2] J. Stieghan: Variationelle Sensitivitätsanalyse in der Theorie poröser Medien Technische Universität Carolo-Wilhelmina zu Braunschweig, 2008. [3] J. E. Oakley and A. O'Hagan: Probabilistic sensitivity analysis of complex models: a Bayesian approach, J. R. Statist. Soc. B, 66(3):751-769, 2004.

Appropriate Inlet Boundary Conditions for Scale-Resolving Simulations of Turbomachinery Configurations

Florian Herbst*, Christoph Mueller-Schindewolf***, Felix Schwarzbach***, Mark Ziesse****, Christoph Bode*****

*Institute of Turbomachinery and Fluid Dynamics, Leibniz Universitaet Hannover, Germany, **Institute of Turbomachinery and Fluid Dynamics, Leibniz Universitaet Hannover, Germany, ***Institute of Turbomachinery and Fluid Dynamics, Leibniz Universitaet Hannover, Germany, ****Institute of Turbomachinery and Fluid Dynamics, Leibniz Universitaet Hannover, Germany, *****Institute of Jet Propulsion and Turbomachinery, University of Braunschweig, Germany

ABSTRACT

Turbomachinery designer e.g. of jet engines constantly strive for maximizing the machine's power-to-weight ratio and efficiency, reducing noise emissions, and ensuring structural health. Achieving these objectives requires a thorough understanding of the flow physics as well as a precise prediction of the machine's characteristics in the design process. Turbomachinery flows cover a wide range of Reynolds and Mach numbers ranging from incompressible to compressible flow, incorporating laminar, transitional, and fully turbulent boundary layers. These effects as well as three-dimensional vortical flow structures, periodic-unsteady wake interactions, and multistage flow effects interact and determine the machine's characteristics. In the design process reduced-order models (e.g. RANS methods) of such flows are and will be for some time prime due to their computational efficiency. However, scale-resolving methods provide a powerful tool for the further development of reduced-order models as they provide spatially and temporal highly-resolved insight into these complex flow physics of realistic configurations. Against this background and with this motivation the authors applied and developed scale-resolving methods for complex turbomachinery applications in recent years [1,2]. Basis is an implicit finite-volume approach providing second order accuracy in time and space which has been applied either for LES (implicit and explicit modeling) or for hybrid computations. The current presentation focusses on the prescription of exact inflow conditions typical for turbomachinery configurations by means of a LES of a low-pressure turbine cascade. Those inflow conditions can either be generated by resource-intensive precursor simulations of three-dimensional periodic boxes or by synthetic boundary conditions, whereas the latter are cheaper and much more flexible. A modified synthetic-eddy-method will be presented which suits the demands and specifications of the application to turbomachinery. The approach provides interfaces for the prescription of steady and unsteady shear-layers, such as wakes, by temporally changing velocities, Reynolds-stresses, and turbulent length-scales. Furthermore, it will be extended to compressible flows by adding a mechanism to uncouple acoustic waves. The precision of the method will be shown by verification and experimental validation. Moreover, the relevance of such a flexible inlet boundary condition method for accurately simulating turbomachinery configurations with scale-resolving methods will be demonstrated. [1] Müller-Schindewolf; Baier; Seume; Herbst (2017): Direct Numerical Simulation Based Analysis of RANS Predictions of a Low-Pressure Turbine Cascade. ASME J. Turbomachinery, 139(8). [2] Mimic; Jätz; Herbst (2017): Correlation between Total Pressure Losses of Annular Diffusers and Integral Stage Design Parameters. Proc. of Global Power and Propulsion Forum, Shanghai, China.

Elastic and Dynamic Properties of Membrane Phase-field Models: the Viscosity of Blood and the Bending Rigidity of Red Blood Cells

Aurora Hernandez-Machado*

*University of Barcelona, Spain

ABSTRACT

Phase-field models have been extensively used to study interfacial phenomena, from solidification to vesicle dynamics. We will analyze a phase-field model that captures the relevant physical features that characterize biological membranes [1]. We will show that the Helfrich theory of elasticity of membranes can be applied to phase-field models, allowing to derive the expressions of the stress tensor, lateral stress profile and elastic moduli. We will discuss the relevance and interpretations of these magnitudes from a phase-field perspective. Taking the sharp-interface limit we will show that the membrane macroscopic equilibrium equation can be derived from the equilibrium condition of the phase-field interface. As an application, we will study a dynamic phase-field model that describes the behavior of red blood cell membranes [2]. The rheological properties of blood depend highly on the concentration and membrane elasticity of its red blood cells. These properties affect the viscosity of blood, as well as, its non-linear rheological (shear thinning) behavior. In some cases these effects are related to diseases, such as typical anemia or alpha-thalassemia. By mean of the analysis of the front advancement of blood in a microchannel, we will determine experimentally the viscosity of different samples of blood and we will relate the viscosity with the bending rigidity of its red blood cells. [1] G. R. Lazaro, I. Pagonabarraga, A. Hernandez-Machado, Eur. Phys. J. E 40, 77 (2017) [2] C. Trejo-Soto, G. R. Lazaro, I. Pagonabarraga, A. Hernandez-Machado, (Preprint, 2018)

IDENTIFICATION OF DAMAGE IN FRAMES BASED ON THE CURVATURE MATRIX OF THE FRF.

JUAN C. HERRERA

Civil & Industrial Engineering Department
Faculty of Engineering
Pontificia Universidad Javeriana
Calle 18 No. 118-250, Cali, Colombia
E-mail:juancherrera@javerianacali.edu.co

Key words: damage identification, FRF, Timoshenko beam, structural health monitoring.

Summary. In this paper a method for damage identification in frame structures based on the curvature-matrix of the Frequency Response Function (FRF) is proposed. Two new indices to predict the damage location and to estimate the severity of the damage in a structure are formulated. To evaluate the effectiveness of the method, numerical simulations are performed in different damage scenarios simulated in a one-story, one-bay frame using the classic Timoshenko beam theory. The structural damage is simulated by reducing the shear and flexural stiffness of selected elements of the frame using Finite Element modelling. The FRF for the undamaged and damaged frame is obtained with the frequencies and mode shapes of the lower modes and the curvature of the FRF is numerically calculated by using a centered finite-difference based on the Taylor series expansion. The results indicate that the proposed method can localize and estimate the damage severity in simple frames.

1 INTRODUCTION

The structural condition assessment of existing civil infrastructures such as buildings and highway bridges is decisive to prevent probable catastrophic events and for planning the potential investments in repair, rehabilitation of this critical infrastructure. Structural damage identification through changes in dynamic characteristics, provide a global way to evaluate the structural condition. When damage occurs in a structure there is a change in one or more of its dynamic properties and these changes in the stiffness or flexibility of structure will cause changes in the modal properties.

In the last two decades a variety of methods based on Frequency Response Function (FRF) data have been proposed in the technical literature¹⁻⁴. The use of FRFs for damage detection have definite advantages over the traditional methods using modal analysis data⁵. One significant advantage lies in the fact that FRF data provide abundant information on the dynamic behavior of a structure. Additionally, the FRFs are less contaminated because they are directly measured from structures.

In this paper, a methodology for structural damage identification based on the FRF-Curvature is formulated. First, the concept of FRF-Curvature matrix is formulated. Next, two new damage indices based on the variations of this matrix over the structure are proposed. The damage indices are conceived to indicate the damage location and to estimate the severity of the damage in a structure directly from the measured FRF-Receptance. Finally, numerical simulations are performed to evaluate the effectiveness of the proposed damage indices to localize and quantify the severity of damage in a one-story, one-bay frame.

2 THE FREQUENCY RESPONSE FUNCTION

The general mathematical representation of a single degree of freedom (SDOF) system can be expressed by

$$m\ddot{x}(t) + c\dot{x}(t) + kx(t) = F(t) \quad (1)$$

Assuming that the forcing function is harmonic of the form $F(t) = F_0 e^{i\Omega t}$ and the damping is linear and viscous, the Frequency Response Function (FRF) can be defined by

$$H(\Omega) = \frac{1}{1 - \left(\frac{\Omega}{\omega_n}\right)^2 + i2\xi\left(\frac{\Omega}{\omega_n}\right)} \quad (2)$$

where ω_n and ξ are, respectively, the natural frequency and the damping ratio.

For multiple degree of freedom (MDOF) systems with classic damping, the Frequency Response Function (FRF) between the degrees of freedom r and s is defined as

$$H_{rs}(\Omega) = \sum_{j=1}^n \frac{\phi_{rj}\phi_{sj}}{\omega_j^2 - \Omega^2 + 2\xi_j\omega_j\Omega i} \quad (3)$$

where, ϕ_{ij} is the row “ i ” of the vibration mode “ j ”; ω_j y ξ_j are the natural frequency and the damping ratio of the “ j ” mode, respectively.

$H_{rs}(\Omega)$ is the response of the DOF r due to a single harmonic force excitation of unit amplitude applied at the DOF s . This particular FRF where the response or output is described in terms of the displacement and the input is a force is known as the Receptance function.

3 FORMULATION

In this work, a damage index based on the FRF-Curvature matrix is proposed. The index was conceived to predict the damage location and to estimate the severity of the damage in a structure directly from the measured FRF-Receptance. The damage indices are based on the change of the FRF-Curvature at the elements of the structure for a given excitation frequency.

The functions $H_{rs}(\Omega)$ defined by the Equation (3) can be arranged in matrix form. This leads to a Receptance Matrix defined as

$$[H(\Omega)] = \begin{bmatrix} H_{11} & H_{12} & \cdots & H_{1n} \\ H_{21} & H_{22} & \cdots & H_{2n} \\ \vdots & \vdots & \ddots & \vdots \\ H_{n1} & H_{n2} & \cdots & H_{nn} \end{bmatrix} \quad (4)$$

The curvature matrix of the FRF-Receptance $[H''(\Omega)]$ is defined as:

$$[H''(\Omega)] = \begin{bmatrix} H''_{11} & H''_{12} & \cdots & H''_{1n} \\ H''_{21} & H''_{22} & \cdots & H''_{2n} \\ \vdots & \vdots & \ddots & \vdots \\ H''_{n1} & H''_{n2} & \cdots & H''_{nn} \end{bmatrix} \quad (5)$$

The matrix for damage identification based on the Receptance curvature, is defined by

$$[\Theta]_{n \times n} = [H''(\Omega)]_{n \times p} [H''(\Omega)]_{p \times n}^T \quad (6)$$

where,

$[H''(\Omega)]$: curvature matrix of the FRF-*Receptance* for a frequency Ω .

n : number of points where the FRF is obtained

p : number of points where the input force is applied.

If the input force is applied at a single point “ k ”, the diagonal of $[\Theta]$ is defined as

$$\{\theta\} = \{(H''_{1,k})^2 \quad (H''_{2,k})^2 \quad \cdots \quad (H''_{n,k})^2\} \quad (7)$$

The Receptance-curvature for each frequency can be calculated numerically by using a central finite-divided difference based on an expansion of the Taylor series. For the Receptance FRF measured at location j due to a excitation force at position k , the curvature of the Receptance $H_{j,k}(\Omega)$ can be calculated by:

$$H''_{jk}(\Omega) = \frac{|H_{j+1,k}(\Omega)| - 2|H_{j,k}(\Omega)| + |H_{j-1,k}(\Omega)|}{h^2} \quad (8)$$

where h is the distance between two consecutive measurement points: (j) and $(j+1)$.

For the damaged structure, the FRF curvature matrix is defined by

$$[\Theta_*]_{n \times n} = [H_*''(\Omega)]_{n \times p} [H_*''(\Omega)]_{p \times n}^T \quad (9)$$

where $H_*''(\Omega)$ is the curvature of the FRF-*Receptance* for the damaged structure.

If the input force is applied at a point “ k ”, the diagonal of $[\Theta_*]$ is defined as

$$\{\theta_*\} = \{(H_{*1,k}'')^2 \quad (H_{*2,k}'')^2 \quad \cdots \quad (H_{*n,k}'')^2\} \quad (10)$$

In terms of the FRF curvature matrices, the index for damage location expresses the relationship between the states of a structure element with damage and without damage, defined by:

$$\{\chi\} = \{\theta_*\} ./ \{\theta\} \quad (11)$$

In the Equation (11) the symbol ($./$) is used to indicate that the division of the vectors is done element by element.

The proposed damage severity index is defined by

$$\{\Gamma\} = \eta [1 - \{\varphi\} ./ \{\varphi_*\}] \quad (12)$$

where,

$$\eta = \frac{\sum_{i=1}^n H_{ik}''}{\sum_{i=1}^n H_{*i,k}''} \quad (13)$$

After the damage index Γ_j is computed, the value of the indicator is normalized according to the rule formulated by Kim and Stubbs⁶:

$$Z_j = \frac{\Gamma_j - \mu}{\sigma} \quad (14)$$

where μ and σ are, respectively, the mean value and the standard deviation of the damage index Γ_j .

The damage is assigned to the elements by using a statistical-pattern-recognition technique that utilizes hypothesis testing⁶: The null hypothesis, referred to as H_0 , corresponds to the structure *not* damaged at the element j and the alternate hypothesis, denoted as H_1 , means that the structure *is* damaged at the element j . To assign damage to a specific location, the following decision rule is used: (a) select H_0 if $Z_j < 1,9$ or (b) select the alternate H_1 if $Z_j \geq 1,9$. This test corresponds to a confidence level of 97 %.

4 NUMERICAL SIMUATIONS

To demonstrate the effectiveness of the proposed damage indices to locate and estimate the structural damage, the one-storey frame shown in Figure 1 is considered. Four damage scenarios are analyzed. The FRF and the FRF-curvature of the damaged and undamaged structures were generated numerically. The FRF-curvature was obtained numerically with Equation (8).

The following dimensions and material properties are used for the frame: span length $L = 2.5$ m, height of the frame $H = 2.5$ m, height of the cross section $h = 0.125$ m, width of the cross section $b = 0.05$ m, elastic modulus $E = 200000$ MPa and mass density $\rho = 20.21$ kg/m³. For the numerical simulation the beam was divided into 20 finite elements of equal length. Four damage scenarios were studied and are listed in Table 1. The structural damage is simulated by reducing the flexural stiffness (EI) and the shear stiffness (GA) of an element near the beam's mid-span.

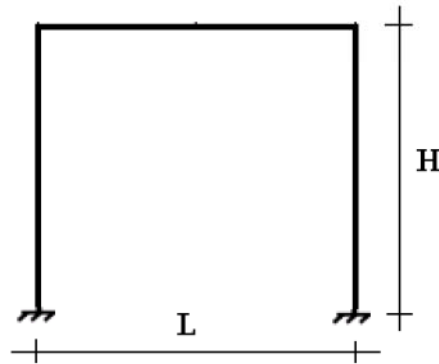


Figure 1. One-bay frame.

Damage scenario	Location	E,G reduction (%)
D1	0.5L	50
D2	0.5L	40
D3	0.5L	30
D4	0.5L	25

Table 1. Damage scenarios.

To calculate the proposed indices, the values of the Receptance-FRF were obtained at 19 locations equally spaced along the longitudinal axis of the beam. The Receptance-FRF was calculated with Equation (3) for the first three mode shapes and was assumed that the modal damping ratio ξ_j was constant for all the modes and equal to 0.05. Using the values of the Receptance FRF, the FRF-curvatures were generated numerically via a central difference approximation by using Equation (6).

The damage location index is shown in Figure 2. The indices were calculated for a frequency of 220 rad/s. The estimated location of damage and damage severity index values are shown in Figures 3 to 6. The estimated severity of damage is listed in Table 2. As can be seen, for the damage scenarios analyzed, the proposed indices are able to indicate the location of the damaged regions of the frame's beam and the severity of the defects.

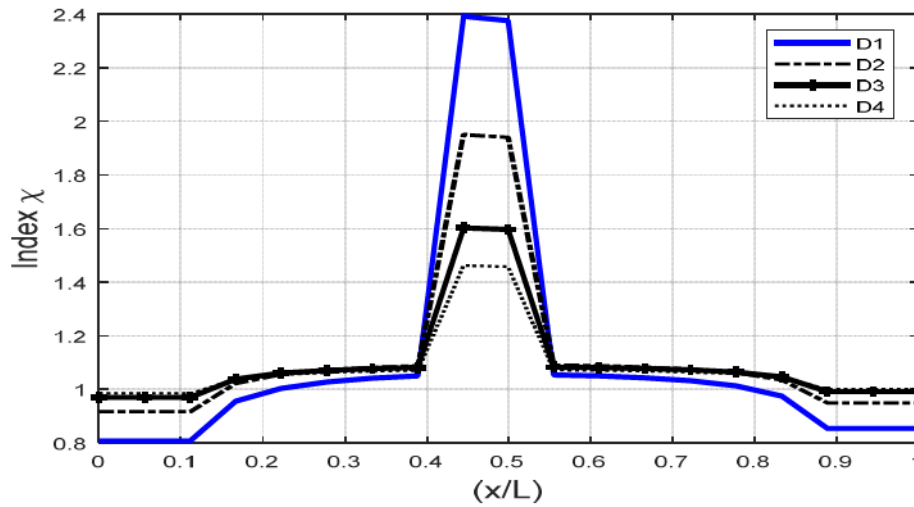


Figure 2. Damage location.

Damage Scenario	Simulated Damage (%)	Estimated Damage (%)	Error (%)
D1	50	52,0	4
D2	40	42,0	5
D3	30	35,0	17
D4	25	30,0	20

Table 2. Damage severity.

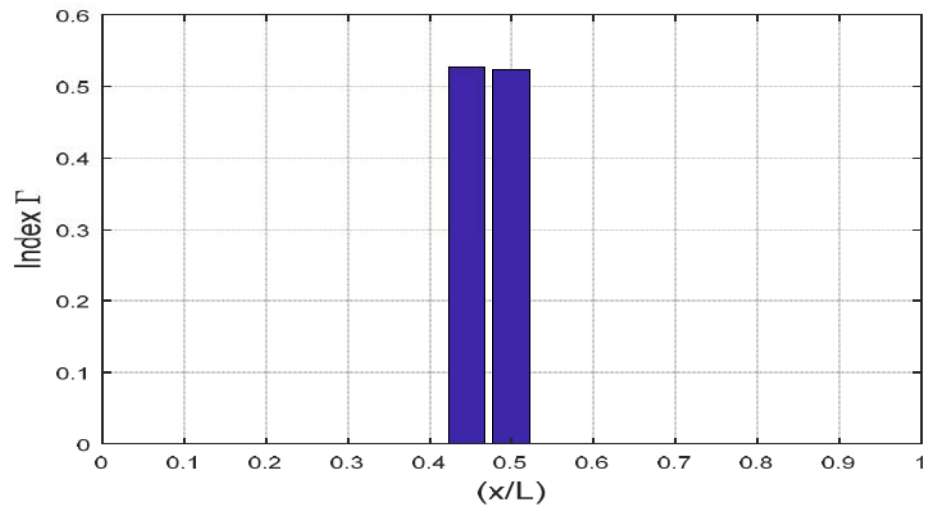


Figure 3. Damage severity index - scenario D1.

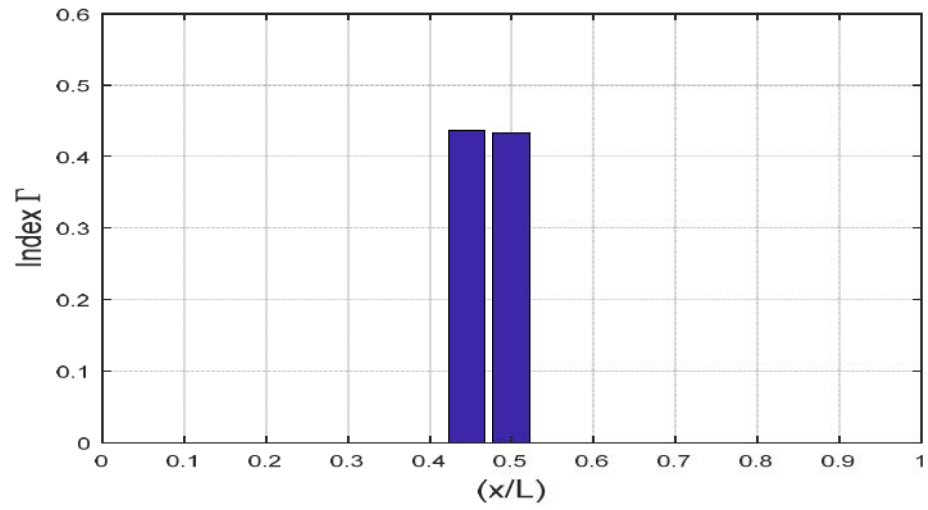


Figure 4. Damage severity index - scenario D2.

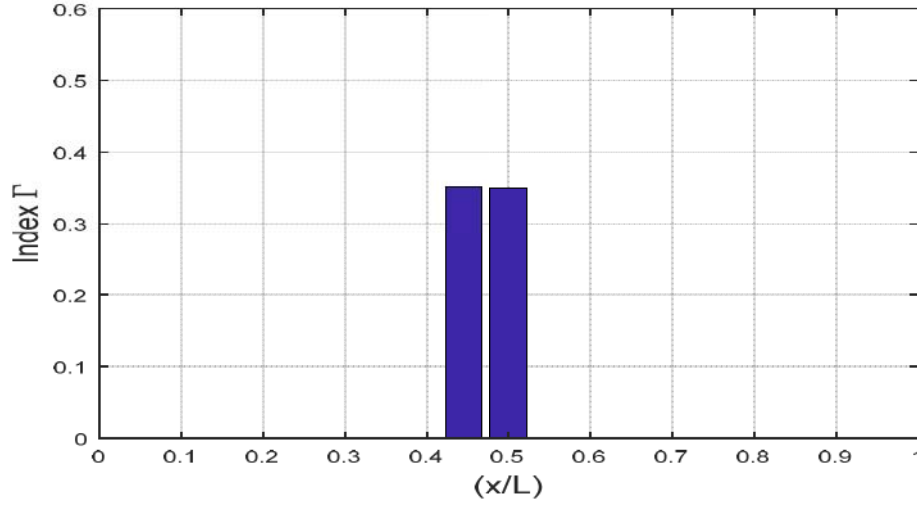


Figure 5. Damage severity index - scenario D3.

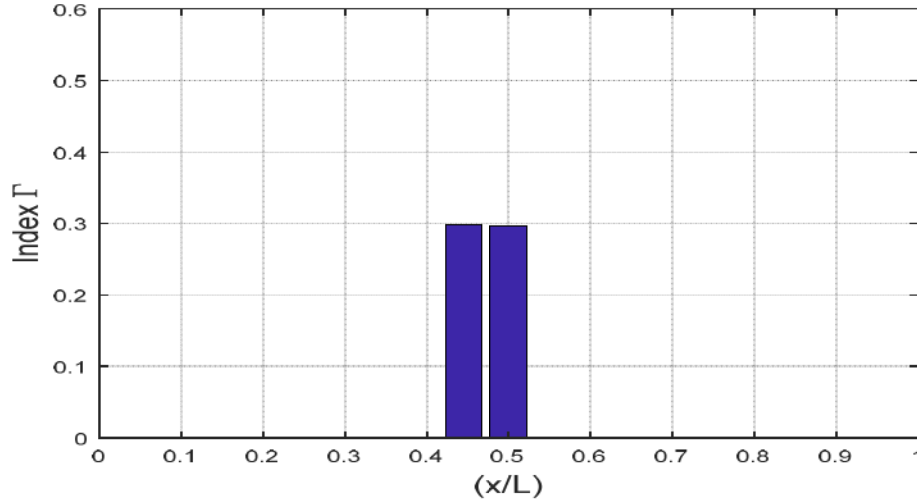


Figure 6. Damage severity index - scenario D4.

5 CONCLUSIONS

This article presents the theoretical formulation of two indices to locate and quantify the severity of the damage in a structure directly from the Frequency Response Function, based on the matrix of FRF-Receptance curvatures. The indices were evaluated for different damage scenarios, varying the severity of the damage in a one-bay frame beam using Timoshenko's beam theory. The results obtained from the numerical simulations indicate that the proposed indexes can locate and estimate the damage severity for single damage scenarios in the analyzed frame. Although errors in the quantification of damage severity were obtained, for practical engineering purposes these could be acceptable. The proposed damage indices could serve as an alternative to the traditional techniques of structural damage identification through modal analysis.

REFERENCES

- [1] Thyagarajan, S.K., Schulz, M.J., and Pai, P.F. Detecting structural damage using frequency response functions. *Journal of Sound and Vibration*, (1998) 210:162–70.
- [2] Sampaio, R. P., Maia, N. M. and Silva, J. M. Damage detection using the frequency-response-function curvature method. *Journal of Sound and Vibration*. (1999) 226:1029-1042.
- [3] Lee, U. and Shin, J. A frequency response function-based structural damage identification method. *Computers & Structures*. (2002) 80:117-132.
- [4] Esfandiari, A., Bakhtiari-Nejad, F., Rahai A. and Sanayei, M. Structural model updating using frequency response function and quasi-linear sensitivity equation. *Journal of Sound and Vibration*. (2009) 326:557-573.
- [5] He, J. Damage detection and evaluation. In: “Modal analysis and testing.” Eds. Silva, J. and Maia, N., Kluwer, Dordrecht. pp. 325-344, (1999).
- [6] Kim, J.T. and Stubbs, N. Model uncertainty and damage detection accuracy in plate-girder bridges. *Journal of Structural Engineering*. (1995) 121:1409–1417.

An Axiomatic Formulation for a Class of Multiphysical Systems

Ismael Herrera-Revilla*

*UNAM

ABSTRACT

Axiomatic formulations are very effective for achieving three fundamental paradigms of mathematical and scientific thinking: generality, clarity and simplicity (Herrera and Pinder, 2012). Generality yields an enormous economy of effort in the study and discussion of many subjects; in research, it is invaluable because models possessing it anticipate results for many unforeseen situations. Clarity yields certainty of knowledge. As for simplicity: simplifying ideas permit transforming complicated systems and phenomena into simple ones, which in turn upgrades efficiency and the level of complexity of systems amenable to treatment. For microscopic physical systems Schrödinger equation constitutes a formulation of this kind. Regarding macroscopic systems, it is well known that the groundwork for establishing axiomatic approaches to continuum mechanics was done at the second half of the XX Century by a group of scholars and researchers some of whose most conspicuous leaders were Clifford Truesdell and Walter Noll. The author had the privilege of participating in some of such developments. Based on their results the author has introduced a novel axiomatic formulation that, for macroscopic physical systems, constitutes a counterpart of Schrödinger equation. In this talk, the basic axiomatic formulation of continuous systems is presented and taking it as starting point is extended to a class of multiphysical systems. Then, I present some of the most important applications thus far made. REFERENCES Herrera-Revilla, I. & Pinder, G.F. "Mathematical Modelling in Science and Engineering: An axiomatic approach", John Wiley, 243p., 2012. Herrera-Revilla, I. "A Systematic Formulation of Multiphysical Systems and Its Application to Boundary-Layers and Shock-Profiles". International Journal for Multiscale Computational Engineering, 14(2): 135-148, 2016.

Three-Dimensional Simulations of Failure by Shear Band Formation

Josh Herrington^{*}, Nithin Thomas^{**}, Amine Benzerga^{***}

^{*}Texas A&M; University, ^{**}Texas A&M; University, ^{***}Texas A&M; University

ABSTRACT

Analyses of ductile failure by shear banding versus cumulative damage growth by void growth to coalescence are carried out using a coupled plasticity and damage formulation. The constitutive porous metal plasticity relations account for void shape effects, void rotation, plastic anisotropy and void coalescence. The latter is modelled using a separate effective yield function with associated evolution equations of the internal parameters. The resulting model is a hybrid two-surface pressure-sensitive and dilatant plasticity model. The same model is employed to study (i) the effect of plastic anisotropy on crack initiation in round notched bars; (ii) the conditions under which failure occurs subsequent to shear band formation as opposed to void-coalescence induced crack initiation. In particular, an important distinction is made between shear failure and failure in shear. The results obtained show that plastic anisotropy is sufficient to trigger shear band formation in initially round bars.

Site-specific Property Maps of Additively Manufactured Metals Using a Mesoscale, Multi-Physics Modeling Framework

Carl Herriott*, Nadia Kouraytem**, Xuxiao Li***, Wenda Tan****, Vahid Tari*****, Anthony Rollett*****, Ashley Spear*****

*University of Utah, **University of Utah, ***University of Utah, ****University of Utah, *****Carnegie Mellon University, *****Carnegie Mellon University, *****University of Utah

ABSTRACT

The microstructure of additively manufactured (AM) metals has been shown to be quite heterogeneous and exotic when compared to conventionally manufactured metals. Consequently, the effective mechanical properties of AM metal parts are expected to vary both within and among different builds due to the laser interaction with the melt pool and solidification characteristics. This work presents a multiphysics modeling framework for simulating the process, microstructure, and properties of AM metal volumes. The framework is entirely automated, from the generation of the microstructure to the resulting spatial-property maps. The framework uses a 3D solidification and nucleation model to simulate a grain-resolved build domain created by a multi-pass, multi-layer, Directed Laser Deposition (DLD) process. The entire build domain is automatically divided into discrete sub-volumes to interrogate site-specific effective mechanical properties. Each sub-volume is first passed into DREAM.3D, where microstructural statistics are recorded, and an input file is written out to simulate mechanical testing on the sub-volume using a parallelized elasto-viscoplastic fast Fourier Transform (EVP-FFT) model. The effective stress-strain response of each sub-volume is analyzed automatically to extract the effective mechanical properties. The Young's modulus is found by applying a Hough transform to the stress-strain response to identify the elastic region. Based on the Young's modulus, a 0.2% yield offset is applied to approximate the yield strength of each sub-volume. Once these effective mechanical properties are found, they are then used to generate heat maps showing how these properties vary spatially throughout the simulated-build domain. As a demonstration, the framework is applied to DLD SS316L volumes with microstructures ranging from fully columnar to fully equiaxed. In this demonstration, we investigate three orthogonal planes (and multiple locations of each plane) throughout each build volume. The first plane, the transverse-direction – build-direction plane, highlights the impact of successive build layers on resulting mechanical properties. The next plane, the transverse-direction - laser-scanning direction plane, highlights variability of the mechanical properties across the build plane at three specific build layers: just above the substrate, mid-build height, and the top of the build volume. Finally, the scanning-direction - build-direction plane, sampled on the center of the track and between two successive tracks, looks at the variability between successive laser tracks. Site-specific property maps are generated for each case to compare the range of properties both within and among each of the build domains. The multiphysics framework and property maps could provide a path toward design and qualification of AM metal parts.

A Multiphase-field Model for Anisotropic Brittle and Ductile Crack Propagation in Cast Iron Brake Discs

Christoph Herrmann^{*}, Felix Schwab^{**}, Ephraim Schoof^{***}, Daniel Schneider^{****}, Britta Nestler^{*****}

^{*}Institute of Digital Materials Science (IDM), Karlsruhe University of Applied Science, Germany, ^{**}Institute of Applied Materials - Computational Materials Science (IAM-CMS), Karlsruhe Institute of Technology, Germany, ^{***}Institute of Digital Materials Science (IDM), Karlsruhe University of Applied Science, Germany, ^{****}Institute of Applied Materials - Computational Materials Science (IAM-CMS), Karlsruhe Institute of Technology, Germany, ^{*****}Institute of Applied Materials - Computational Materials Science (IAM-CMS), Karlsruhe Institute of Technology, Germany

ABSTRACT

In trucks, brake discs made of cast iron are often used, which, in order to ensure the safety of road users, must satisfy the highest mechanical demands. To calculate the service life of brake discs, it is particularly important to consider crack growth. The material considered in the presentation is cast iron with lamellar graphite and a pearlitic matrix. The pearlitic matrix is assumed to be isotropic and ductile, whereas the graphite lamellae are considered to be brittle with an elliptical anisotropy. The phase-field model for crack propagation in multiphase systems by Schneider et al. [1] was extended in order to simulate cracking in the examined material. For the purpose of the model extension, a directional and plasticity dependent crack resistance was introduced. Validation examples of ductile and brittle anisotropic crack propagation are presented. By means of an exemplary cast iron structure, the applicability of the presented model to a multiphase system will be demonstrated. [1] D. Schneider, E. Schoof, Y. Huang, M. Selzer, B., Nestler (2016). Phase-field modeling of crack propagation in multiphase systems. Computer Methods in Applied Mechanics and Engineering, 312, 186-195.

A Micromechanical Damage Model for Brittle Failure of Short Fiber Reinforced Thermoplastics

Patrick Arthur Hessman*, Fabian Welschinger**, Kurt Hornberger***, Thomas Böhlke****

*Karlsruhe Institute of Technology (KIT), Robert Bosch GmbH, **Robert Bosch GmbH, ***Robert Bosch GmbH,
****Karlsruhe Institute of Technology (KIT)

ABSTRACT

Short fiber reinforced thermoplastics (SFRT) have been of great interest to both research and industry due to their high specific stiffness and strength as well as their cost-effective application in semi-structural parts. During the injection-molding process the fibers tend to align with the shear flow in the cavity, resulting in heterogeneous and complex fiber orientation states that significantly influence the mechanical behavior of the finished part. Mean field homogenization models are an attractive class of methods that can be applied to composite materials in order to include the effects of the phase properties, orientation and volume fractions on the effective material behavior and phase stresses and strains. In this work, the Two-Step [1] and Mori-Tanaka [2] homogenization schemes are employed to model the mechanical properties of a dry polyamide 6.6 thermoplastic polymer with a short glass fibers mass fraction of 35% (PA66-GF35). Its microstructural morphology, including the fiber orientation and length distributions, is resolved by means of x-ray micro-computed tomography scans and a single fiber segmentation and analysis procedure. An efficient numerical scheme is applied to include this information in the microstructural model. For the given class of materials and restricting ourselves to monotonic loading, damage and failure is mainly governed by two mechanisms: Initial interfacial debonding and subsequent matrix rupture. The presented approach captures the former by means of a probabilistic interfacial damage model based on the concept of effective inclusions [3] and assuming the interfacial strength to be Weibull-distributed. Matrix rupture is described similarly by an isotropic progressive damage law. Coupled with the mean field schemes, the modeling approach is capable of describing the orientation-dependent progressive failure of the material at hand, which is highlighted by a comparison with experimental data from tensile tests on specimens cut out of injection-molded plates. [1] Pierard, O., Friebel, C., and Doghri, I. (2004). Mean-field homogenization of multi-phase thermo-elastic composites: a general framework and its validation. *Composites Science and Technology* 64, 1587–1603 [2] Benveniste, Y. (1987). A new approach to the application of Mori-Tanaka's theory in composite materials. *Mechanics of Materials* 6, 147–157 [3] Fitoussi, J., Bourgeois, N., Guo, G., and Baptiste, D. (1996). Prediction of the anisotropic damaged behavior of composite materials: introduction of multilocal failure criteria in a micro-macro relationship. *Computational Materials Science* 5, 87–100.

Numerical Simulation of Debris Flow on General Topography with Pore Pressure Evolution and Hypoplastic Granular Material Behavior

Julian Heß^{*}, Yih-Chin Tai^{**}, Yongqi Wang^{***}

^{*}Technische Universität Darmstadt, ^{**}National Cheng Kung University, ^{***}Technische Universität Darmstadt

ABSTRACT

In debris flows, consisting of granular particles and an interstitial fluid, the pore-pressure feedback and the internal contact stress of the grains are mechanisms of importance. These two characteristics play a crucial role and significantly affect the dynamic behaviors: the pore pressure feedback, which reduces the intergranular friction and, hence, enhances the mobility of the whole mixture, and the internal contact stress, which accounts for the non-linear deformational behavior of granular materials. In this work, we present a continuum-mechanical model for debris flows, including two additional internal variables, the extra pore-pressure and the hypoplastic stress, the latter depicting internal friction. These variables are described by a pressure diffusion equation and a transport equation related to the hypoplastic material, respectively. The thermodynamically consistent model is scaled, depth-integrated and embedded in terrain-following coordinates, adapting the concept of general topography in combination with unified coordinates, allowing for the numerically favorable treatment of flows over complex topography. Numerical simulations are performed with this model, applying a shock-capturing non-oscillatory numerical scheme. Parameter studies are performed on the properties of the proposed model, complemented by comparison with experimental data. The results are presented and show that, in comparison to classical debris flow approaches, the proposed model provides a phenomenological insight into the crucial roles and the impact of the pore-pressure feedback and hypoplastic intergranular friction in the flow dynamics.

Acoustic Emissions Damage Detection in Musical Instrument Strings

Mason Hickman*, Prodyot Basu**

*Vanderbilt University, **Vanderbilt University

ABSTRACT

Composite metal strings are used exclusively in amplified instruments such as the electric guitar, which use electromagnetic pickups to transmit the vibration of strings to an output signal. Instrument strings undergo damage from mechanical and environmental wear during their design life. Mechanical wear is caused by low-stress abrasion of the strings on the neck. Over time, the cross section of the strings in the neck region is reduced in area from being repeatedly pressed against the fret wires. When strings are subject to fatigue from continued use, the frequency response characteristics change leading to eventual failure of the string. For this reason, musicians and instrument technicians who make regular use of stringed instruments incur significant costs changing strings on a regular basis. There is a lack of published literature on the behavior of strings with different geometries and material properties subject to this type of tension and fatigue applied over the life of the string. The development of a method to optimize string geometries to obtain a desired frequency response and design life is of great interest to the players of the instrument as well as manufacturers seeking to modernize their production process. As no recognized method currently exists for damage identification and prognosis in instrument strings, the strings are often replaced routinely on an arbitrary basis, irrespective of the actual condition of the strings. The purpose of this research is to develop a tool capable of accurately predicting failure by monitoring and parameterizing transients in the frequency domain. Existing technology can determine the fundamental frequency of the signal for tuning purposes, but neglects the higher-order harmonics in the signal that define the instrument's tonal quality. As the strings are fatigued, the amplitude and frequency of the harmonics present in the signal are shifted and scaled resulting from the damage. This research takes advantage of existing passive sensing and pitch detection technology, but seeks to use the information obtained from sampling the signal more intelligently. The proposed approach uses the available high-frequency information in the signal to characterize damage in the instrument strings. When the instrument is retuned during the life of the strings, the difference between the new signal and the original calibrated signal is measured and used to characterize damage using digital signal processing techniques and empirically trained statistical models. A machine learning approach is used to explore design space and identify combinations of material phases that will optimize the performance of the strings.

Fast Formation and Assembly in Isogeometric Analysis with Applications in Linear Elasticity

Rene Hiemstra^{*}, Francesco Calabro^{**}, Thomas Hughes^{***}, Mattia Tani^{****}, Giancarlo Sangalli^{*****}

^{*}University of Texas at Austin, ^{**}Universita degli Studi di Cassino e del Lazio Meridionale, ^{***}University of Texas at Austin, ^{****}Universita di Pavia, Dipartimento di Matematica, ^{*****}Universita di Pavia, Dipartimento di Matematica

ABSTRACT

Recently a new formation and assembly strategy was proposed in [1], which resulted in significant speedups in the formation and assembly time of the Galerkin mass matrix in isogeometric analysis. The strategy relies on two key ideas: 1) assembly row by row, instead of element by element; and 2) an efficient formation strategy based on weighted quadrature and sum factorization that is applied to each specific row of the matrix. The resulting computational effort is proportional to the number of degrees of freedom of the trial space. Consequently, this type of formation and assembly scales favorably with polynomial degree, which opens the way for high order isogeometric analysis employing k-refinement. In this work we discuss various important details for the practical implementation of the weighted row-wise formation strategy proposed in [1]. Specifically, we extend the weighted quadrature scheme to accurately integrate the elements of the stiffness matrix in linear elasticity, we propose a new selection of quadrature points that works in the general setting of mixed continuity non-uniform isogeometric spaces and we propose an algorithm for the computation of a corresponding set of quadrature weights. Finally, we show that the row-wise formation strategy allows for the direct construction of the system matrix in the sparse matrix data structure, yielding significant savings in memory operations with respect to standard assembly approaches. Several numerical benchmarks will be shown to illustrate the efficiency and efficacy of the proposed methodology. [1] F. Calabro, G. Sangalli, M. Tani, Fast formation of isogeometric Galerkin matrices by weighted quadrature, *Computer Methods in Applied Mechanics and Engineering* (2017) 316:606-622.

Discontinuous Galerkin Methods for Layered Ocean Models: Thin Layers and Well-Balanced Forcing

Robert Higdon*

*Oregon State University

ABSTRACT

In a layered ocean model, the vertical coordinate is a quantity related to density, and in a vertical discretization the fluid can be represented as a stack of layers of constant density. Depending on the dynamics of the flow, one or more of these layers can be reduced to near-zero thickness in certain regions. In a DG algorithm, this situation requires a suitable use of limiters and a suitable implementation of horizontal viscosity. In the present work, the viscosity is implemented via the local DG method, as adapted to a barotropic-baroclinic time splitting that is used to address the multiple time scales (external and internal) that are present in ocean dynamics. Another issue in a layered model is the representation of the horizontal pressure forcing. The present work uses a weak Galerkin form of the pressure forcing that is automatically well-balanced in the case of the constant-density, single-layer shallow water equations. In the multi-layer case, this Galerkin form can be implemented using ideas related to the barotropic-baroclinic splitting mentioned above.

Development of Mesh-free Simulation Tool for the Prediction of Microcracks in Composites with Various Fiber Shapes

Ryo Higuchi^{*}, Tomohiro Yokozeki^{**}, Toshio Nagashima^{***}, Tomonaga Okabe^{****}, Takahira Aoki^{*****}

^{*}The University of Tokyo, ^{**}The University of Tokyo, ^{***}Sophia University, ^{****}Tohoku University, ^{*****}The University of Tokyo

ABSTRACT

Recently, the manufacturing technology of various shapes and diameters of carbon fibers has been developed. Therefore, freedom in design of composite microstructure has been improved. In other words, numerous candidates of composite microstructure should be investigated toward the microscopic optimization of composite. To this end, experimental approach, analytical approach, and conventional numerical approach such as finite element method (FEM) are not useful. Experimental approach is costly and time-consuming. Analytical approach cannot be applied to complicated fiber shape such as 2-lobed fiber shape. Conventional FEM is able to handle complicated fiber shape. However, element edge should be aligned with fiber shape and remeshing is inevitable when the microstructure is changed. This limitation makes it difficult to conduct comprehensive numerical investigation. In fact, only a few kinds of fiber shape have been investigated in previous numerical study which utilized the conventional FEM. Consequently, the authors believe that mesh-free microscale simulation tool is required to easily investigate various composite microstructure and to accomplish the microscopic optimization of composite. This study proposes the mesh-free microscale simulation tool which consists of two computational techniques; extended finite element method (XFEM) [1] and the homogenization method using key degree of freedom (DoF) [2]. Firstly, the XFEM with ramp enrichment function [3] was implemented for an efficient simulation of enormous composite microstructures. In this method, the composite microstructure can be modeled independently of the mesh. Secondly, homogenization method was introduced to evaluate an effect of microstructure on the macroscopic material and fracture properties. Here, a key DoF method was incorporated to simply handle the periodic boundary conditions. The validity of the proposed tool was examined by comparing the results against conventional FEM and experiment. Finally, the 3D periodic unit cell simulations of various fiber shapes (circular, elliptical, and 2-lobed) were performed to investigate an effect of fiber shape on the macroscopic material and fracture properties. Reference 1. N. Moës et al., *Int. J. Numer. Meth. Eng.* 46, pp. 131-150, (1999). 2. S. Li et al., *Compos. Part A-Appl. S.*, 42 (7), pp. 801-811, (2011). 3. N. Moës et al., *Comput. Methods Appl. Mech. Eng.*, 192, pp. 3163-3177, (2003).

A Computationally Efficient Variable Kinematics Continuum Shell Element for 3D Stress Field Analysis in Layered Shell Structures

Aewis Hii*, Sergio Minera**, Rainer Groh***, Alberto Pirrera****, Luiz Kawashita*****

*Bristol Composites Institute (ACCIS), University of Bristol, **Bristol Composites Institute (ACCIS), University of Bristol, ***Bristol Composites Institute (ACCIS), University of Bristol, ****Bristol Composites Institute (ACCIS), University of Bristol, *****Bristol Composites Institute (ACCIS), University of Bristol

ABSTRACT

Structural analysis by means of the finite element method (FEM) has become an integral part of the design cycle of shell structures, for buckling, vibration and 3D stress fields analyses. Despite the advances in computational power, these analyses are still being conducted separately with different topologies of structural elements, for instance 2D elements for stability and vibration; and 3D elements for the analyses of detailed stresses. This disparity is largely due to the high computational costs associated with using 3D elements, and inability of 2D elements to capture 3D stress fields, especially in layered structures where through-thickness distortions inform the overall structural behaviour and localised failure initiations. The motive behind our work is to utilise recent advances in computational power and computational mechanics, to derive a hierarchical 2D formulation that can accurately capture both global and local behaviour in shell structures. In doing so, global stiffness and buckling, as well as detailed stress analyses can be performed in a single model. This work presents a new geometrically nonlinear variable kinematics continuum shell (VKCS) formulation based on Carrera's Unified Formulation (CUF), offering capabilities to model shell structures of any geometry with hierarchical axiomatic expansions. The governing equations are derived from the Principle of Virtual Displacements and solved using the finite element method. The shell domain is discretised with charts based on an isoparametric map with no simplifying assumptions made about the geometry. The displacement field is written in a unified formulation, allowing the axiomatic fidelity in the through-thickness direction to be refined in a straightforward and integrated manner. In a linear analysis, the formulation yields excellent, indeed asymptotically correct 3D stresses when compared with 3D-FEM at locations close to the free edges and boundaries, where stresses are inherently three-dimensional in nature. VKCS elements do not require shear correction factors nor 3D stress recovery procedures for accurate stresses. The low computational costs required to achieve converged 3D stress fields with VKCS element makes it an economical alternative to classical 3D-FEM for the analysis of thick and layered shell structures. Finally, we show that numerical results from VKCS in analyses involving geometrical non-linearity are in excellent agreement with benchmarks available in the literature.

Generalized Reproducing Kernel Peridynamics

Michael Hillman^{*}, Guohua Zhou^{**}

^{*}The Pennsylvania State University, ^{**}The Pennsylvania State University

ABSTRACT

Peridynamics is a reformulation of the governing equations of solid mechanics into integral equations such that discontinuities are directly admitted in the solution. Typically the implementation is based on satisfaction of the strong form with nodal integration, yielding a meshfree technique. Recently, some initial insights into the relationship between the state-based peridynamic meshfree implementation [1] with the meshfree reproducing kernel particle method [2] have been established for uniform discretizations [3]. This work expands on these efforts by establishing commonality between the two methods in a general, arbitrary setting, and it is shown that the derivative approximations employed in the two methods can be cast into a single framework. Leveraging these new-found relationships, a higher-order peridynamic meshfree method is proposed where optimal convergence can be attained up to arbitrary order, and can also correct deficiencies in the original implementation of state-based peridynamics to ensure linear accuracy. Several numerical examples are given to demonstrate the effectiveness of the proposed formulation. References: [1] S.A. Silling, M.A. Epton, O. Weckner, J. Xu, E. Askari, "Peridynamic states and constitutive modeling," J. Elast. (88) 2, 151–184, 2007. [2] W.K. Liu, S. Jun, Y.F. Zhang, "Reproducing kernel particle methods," Int. J. Numer. Methods Fluids. (20) 8–9, 1081–1106, 1995. [3] M.A. Bessa, J.T. Foster, T. Belytschko, W.K. Liu, "A meshfree unification: Reproducing kernel peridynamics," Comput. Mech. (53) 6, 1251–1264, 2014.

FLUXO: A High Order Parallel 3D Discontinuous Galerkin Framework for Stable Non-linear Resistive MHD Simulations

Florian Hindenlang*, Gregor Gassner**, Eric Sonnendrücker***

*Max Planck Institute of Plasma Physics, Garching, Germany, **Mathematical Institute, University of Cologne, Germany, ***Max Planck Institute of Plasma Physics, Garching, Germany

ABSTRACT

In fusion devices, plasma is confined by strong torus-shaped magnetic fields. Two main designs are distinguished, the Tokamak with an axisymmetric field and the Stellarator with a fully 3D field. Physical plasma instabilities, triggered by the interaction between the inhomogeneous magnetic field and strong density and temperature gradients, can change, deteriorate or even break the confinement [1]. A valid model to study the linear growth and the non-linear interaction of plasma instabilities are the resistive full MHD equations. The numerical simulation of these problems exhibits substantial resolution requirements, demanding for highly accurate schemes and for parallelization and strong scaling of the MHD solver. In addition, with the current Wendelstein 7-X Stellarator experiments at IPP Greifswald, numerical tools being able to simulate fully three-dimensional, non-axisymmetric configurations are necessary. The MHD simulation starts from a non-trivial steady state of the ideal MHD equations, representing an equilibrium between gas pressure and magnetic pressure. Then the equilibrium is disturbed and instabilities grow and interact. The equilibrium is computed by specifically designed equilibrium solvers, e.g. VMEC [2]. First, we will discuss the generation of three-dimensional high order meshes for Tokamak and Stellarator configurations. The open-source tool HOPR (github.com/fhindenlang/hopr) uses VMEC equilibrium data to generate the mesh, consisting of unstructured and curved hexahedral elements. For the 3D simulations, we employ the highly efficient Discontinuous Galerkin Spectral Element Method [3] implemented in parallel in the open-source FLUXO solver (github.com/project-fluxo) [4], originally developed at IAG in Stuttgart and extended at IPP in Garching and at MI in Cologne. The solver exhibits high parallel efficiency both for weak and strong scaling. We will discuss some details of the implementation and also show benchmark simulations of MHD instabilities. In addition, we discuss recent advances on the formulation and implementation of entropy-stable DGSEM for resistive MHD [5]. [1] J.P. Freidberg, *Ideal MHD*, Cambridge University Press, 2014 [2] S.P. Hirshman, W.I. van Rij and P. Merkel, *Comp. Phys. Comm.* 43, 143 (1986) [3] K. Black, *Kybernetika* 35, 1 (1999) [4] F. Hindenlang, G. Gassner, C. Altmann, A. Beck, M. Staudenmaier and C.-D. Munz, *Computers & Fluids* 61 (2012) [5] M. Böhm, A. Winters, D. Derigs, G. Gassner, S. Walch, J. Saur, submitted to *Computers & Fluids* (2017)

CFD Simulations for Full-scale Performance Predictions of Ships

Takanori Hino^{*}, Natsumi Murakami^{**}, Tetsuro Mlyaji^{***}

^{*}Yokohama National University, ^{**}Yokohama National University, ^{***}Yokohama National University

ABSTRACT

Although ship flow CFD methods have reached the stage on which they are routinely used in practical ship hull form design works, most of current applications are for model-scale performance predictions. This is mainly because the conventional ship hull form design is based on the performance of models and CFD simulations are used as alternative to model tests. On the other hand, along with the rapid development of computing power, the demands for full-scale performance predictions by CFD are increasing year by year. The full-scale simulations are expected to give rational propulsive power estimations and wake distributions in ship-scale. However, the full-scale CFD applications are not considered as practical as the model-scale counterparts, since the validation of full-scale computations is not sufficiently accomplished due to the lack of full-scale validation data. The objective of the present paper is to assess the capability of the up-to-date CFD methods for full-scale ship flow simulations. 'Workshop on Ship Scale Hydrodynamic Computer Simulation' organized by Lloyd's Register in 2016 offered the validation data of the full-scale ship. The first test case is taken from this workshop data. The geometries of a ship hull and a propeller and the sea trials records were provided in the workshop. CFD simulations are performed using the up-to-date Navier-Stokes solver. Overset grid capability of the solver is used to cope with the complex geometries of an actual ship. The numerical results are compared with the sea trials data and the level of simulation accuracy is discussed. The second test case is Japan Bulk Carrier (JBC) which was designed for the validation of a ship flow with an energy saving duct and adopted as one of the test cases of CFD Workshop Tokyo 2015. One of the anticipations for full-scale CFD simulations is performance prediction of energy saving devices (ESDs) since the interaction of turbulent wake and ESDs is the most vital factor with a strong scale effect. Although the validation data is available only for model-scale, the full-scale performance predictions are compared with the results of the conventional procedure of extrapolation from model to ship and the scale effect on the ESD performance is assessed. From two test cases above, the present status of full-scale ship flow simulations are reviewed and the future development strategy is discussed.

Construction of the Remote Robot Programming Environment

Shinji Hioki*

*Tezukayama University

ABSTRACT

In order to maintain learner's motivation, we propose the use of "Robots" as efficient educational PSE tools. When we do the robot programming, we need the robots in our laboratory. In this research, we will construct the remote environment in which we can do the robot programming without the robots in our laboratory. By using this environment, anyone who wants to do robot programming can make his research.

Defining Extended CAE Technology toward the Integration of CAE and AI

Tohru Hirano*

*Daikin Information Systems

ABSTRACT

Computer Aided Engineering (CAE) Technology is widely utilized for Innovative Design in the Enterprises in Japan [1]. Recently, Digital Technologies such as IoT and AI are evolving and expanding rapidly to the conventional Industries, and the Design and Development of those products are required drastically changed to adapt to those environment. Here, Extended CAE Technology is defined so as to include not only the Synthesis and Optimization Approach but also the IoT and AI Technology. At first, the history and current range of CAE Technology are reviewed. Then, recent progress of AI Technology is summarized especially on Deep Learning, Reinforcement Learning and Transfer Learning. Concerning to IoT Technology, the key architecture of IoT, that is, Cyber Physical Systems, is described in view of Connected Products and Services as well as Data Assimilation which combines Experiment and Simulation. Finally, Extended CAE Technology is proposed for the Design and Development of Connected Products and Services. [1] T. Hirano, Leaveraging CAE Technology for Innovative Design in the Enterprise, July 2016, WCCM2016 MS915, Paper No.150062

EXPLICIT NON-DIFFERENTIABLE ENERGY MINIMIZATION ALGORITHM FOR DYNAMIC RIGID-COHESIVE FRACTURE

M. Reza Hirmand* and Katerina D. Papoulia^{†*}

*Department of Mechanical and Mechatronics Engineering
University of Waterloo
Waterloo, Ontario, Canada
mhirmand@uwaterloo.ca

[†] Department of Applied Mathematics
University of Waterloo
Waterloo, Ontario, Canada
papoulia@uwaterloo.ca

Key words: cohesive fracture, initially rigid, non-differentiable energy minimization, sub-gradient, staggered iteration

Abstract. A dynamic crack propagation algorithm is proposed that relies on the minimization of a non-differentiable potential using a staggered iteration strategy. The solution of each time step entails an iterative two-step scheme, in which the openings are first computed at each interface point through solving a local non-convex optimization problem and then used to update the deformation of the body. Potential crack paths are postulated at inter-element boundaries and cracks are treated as separate entities from the bulk by introducing the crack opening and bulk deformation as independent variables. Using the Nitsche method, the constrained objective potential is written without the need of introducing Lagrange multipliers as additional unknowns. The non-differentiability is treated by exploiting the sub-gradient of the interface potential which allows to relate the interface traction to its opening at the non-differentiability point (i.e. zero opening). Thanks to the non-differentiability, activation happens automatically when a certain level of energy is reached in the body; thus, the method sidesteps the complexities of introducing an extrinsic activation criterion encountered in conventional formulations. Numerical results are presented for the fragmentation of a thick cylinder under impulsive internal pressure in order to show the robustness of the proposed algorithm in modelling complicated dynamic crack propagation problems involving branching and fragmentation.

1 INTRODUCTION

Rigid-cohesive fracture is a versatile tool for fracture analysis in a domain of homogeneous material, in which potential crack paths are not known *a priori* and may include branching and fragmentation. In these models, the transition from the undamaged to the damaged state happens upon satisfaction of an external stress criterion and no displacement jump (opening) occurs prior to activation of the cracks. This is conventionally achieved by adaptively inserting interface elements (or enrichment degrees of freedom in an extended FEM setting) during the course of the simulation whenever and wherever they are needed,¹⁻⁵ or, alternatively, through enforcing a zero opening constraint at the interface elements in a Discontinuous Galerkin setting.⁶

It was pointed out^{7,8} that in conventional finite element models of rigid-cohesive fracture, the vector of nodal forces is a discontinuous function of the deformation at the time of activation of an interface. As standard finite difference schemes are not developed to deal with discontinuous problems, numerical integration of these models in time presents a number of difficulties. In explicit time stepping computations, it often leads to nonphysical shocks, lack of convergence in the error norm as the time step is refined, over-activation of interfaces and unphysical velocity fields.⁷⁻⁹ The use of rigid-cohesive models in implicit calculations is also an issue since nonlinear Newton solvers are typically designed for continuous equations and will present difficulties if the equations are discontinuous in their unknowns.

Recently, an energy approach to rigid-cohesive fracture was proposed by Papoulia¹⁰ based on a non-differentiable cohesive potential. The non-differentiability of the cohesive potential is the core of the method and gives the interfaces the property that they do not open until a certain level of stress (or energy) that is encoded in the functional is reached; thus, the method entirely bypasses the activation criterion and its associated difficulties. The approach is distinct from regularized energy formulations such as phase-field¹¹ and eigenfracture approaches¹² in that it represents cracks as strong discontinuities rather than as smeared cracks. A discontinuous Galerkin implementation of the method was presented by Hirmand and Papoulia.⁹ In both works, minimization of the non-differentiable non-convex potential was handled by making use of a continuation strategy along with the trust region minimization algorithm. The present work proposes a new computational algorithm for the minimization of the non-differentiable functional based on a partitioned (staggered) solution strategy and the use of the *sub-gradient*¹³ of the interface potential at the non-differentiability point. The method simplifies the implementation of the energy approach of Papoulia¹⁰, making the proposed method well suited for tackling complicated dynamic crack propagation problems involving branching and fragmentation.

2 FORMULATION OF THE ENERGY APPROACH

We follow the formulation of the energy approach proposed by Papoulia¹⁰ and Hirmand and Papoulia.⁹ A solid body $\Omega \subset \mathbb{R}^{n_{\text{dim}}}$ ($n_{\text{dim}} = 2, 3$) is considered, which is bounded externally by $\partial\Omega$ and contains an evolving internal discontinuity boundary $\Gamma_d \subset \mathbb{R}^{n_{\text{dim}}-1}$ representing cracks, as shown in Figure 1. The external boundary $\partial\Omega$, whose unit outward normal is denoted \mathbf{n} , consists of disjoint parts $\partial_u\Omega$ and $\partial_t\Omega$, on which displacement and traction boundary conditions are

prescribed, respectively. We describe the complete state of deformation of the body by a displacement field $\mathbf{u}(\mathbf{x}, t): \Omega \rightarrow \mathbb{R}^{n_{\text{dim}}} \times [0, T)$ and a discontinuity opening field $\boldsymbol{\delta}(\mathbf{x}, t): \Gamma_d \rightarrow \mathbb{R}^{n_{\text{dim}}} \times [0, T)$ and require that

$$[[\mathbf{u}(\mathbf{x}, t)]] - \boldsymbol{\delta}(\mathbf{x}, t) = \mathbf{0} \quad \text{on } \Gamma_d, \quad (1)$$

where $[[\mathbf{u}(\mathbf{x}, t)]]$ is a jump discontinuity of the displacement field on Γ_d . The normal and sliding components of the jump are defined as $[[u_n]] = [[\mathbf{u}]] \cdot \mathbf{n}_d$ and $[[\mathbf{u}_s]] = [[\mathbf{u}]] - [[u_n]]\mathbf{n}_d$, respectively, where \mathbf{n}_d is the unit normal to the discontinuity. Similarly, $\delta_n = \boldsymbol{\delta} \cdot \mathbf{n}_d$ and $\boldsymbol{\delta}_s = \boldsymbol{\delta} - \delta_n \mathbf{n}_d$. Defining the opening $\boldsymbol{\delta}$ and deformation \mathbf{u} as independent variables enables the formulation to treat the crack as an entity separate from the bulk and, therefore, the energy formulation to model the bulk and interface potentials with a certain amount of independence.

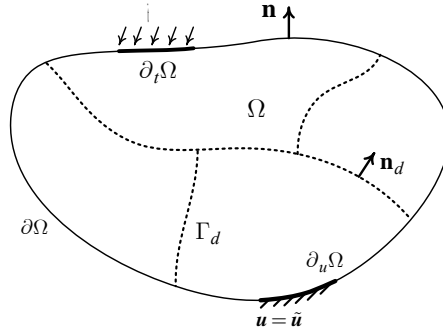


Figure 1. Schematic of a solid body Ω with internal discontinuity boundaries Γ_d .

The potential energy of the elastic body is expressed as the sum of the energy due to the bulk deformation, $\pi_{\text{bulk}}(\mathbf{u})$, the energy stored in the interfaces, $\pi_{\text{intf}}(\boldsymbol{\delta})$, the dynamic energy due to inertia, $\pi_{\text{dyn}}(\mathbf{u})$, and the energy due to the work of external forces, $W_{\text{ext}}(\mathbf{u})$,

$$\pi(\mathbf{u}, \boldsymbol{\delta}) = \pi_{\text{bulk}}(\mathbf{u}) + \pi_{\text{intf}}(\boldsymbol{\delta}) + \pi_{\text{dyn}}(\mathbf{u}) - W_{\text{ext}}(\mathbf{u}), \quad (2)$$

where

$$\begin{aligned} \pi_{\text{bulk}}(\mathbf{u}) &= \int_{\Omega \setminus \Gamma_d} \psi(\boldsymbol{\varepsilon}(\mathbf{u})) dV, \\ \pi_{\text{intf}}(\boldsymbol{\delta}) &= \int_{\Gamma_d} (\phi(\boldsymbol{\delta}) + \theta(\delta_n)) dS, \\ W_{\text{ext}}(\mathbf{u}) &= \int_{\Omega \setminus \Gamma_d} \mathbf{u} \cdot \mathbf{b} dV + \int_{\partial_t \Omega} \mathbf{u} \cdot \tilde{\mathbf{t}} dS. \end{aligned} \quad (3)$$

We consider linear elasticity and infinitesimal deformation, for which the strain energy density function ψ in π_{bulk} is

$$\psi(\boldsymbol{\varepsilon}(\mathbf{u})) = \frac{1}{2} \boldsymbol{\varepsilon}(\mathbf{u}) : \mathbf{D} : \boldsymbol{\varepsilon}(\mathbf{u}), \quad (4)$$

in which \mathbf{D} is the elasticity constitutive tensor and $\boldsymbol{\varepsilon}(\mathbf{u}) = \nabla^s \mathbf{u} \in \mathbb{R}^{n_{\text{dim}}} \times \mathbb{R}^{n_{\text{dim}}}$ is the symmetric part of the displacement gradient. In the definition of $W_{\text{ext}}(\mathbf{u})$, \mathbf{b} is the body force per unit volume and $\tilde{\mathbf{t}}$ is a prescribed traction vector on $\partial_t \Omega$. The precise form of $\pi_{\text{dyn}}(\mathbf{u})$ depends on the particular time stepping scheme employed for temporal discretization.^{9,10} In the present work, we have employed the dynamic potential proposed by Hirmand and Papoulia⁹ corresponding to the Generalized Newmark scheme. For further details in regards to $\pi_{\text{dyn}}(\mathbf{u})$, the reader is referred to the works of Papoulia¹⁰ and Hirmand and Papoulia.⁹

The initially-rigid cohesive energy function ϕ and the interpenetration penalty function θ in π_{intf} are functions of $\boldsymbol{\delta}$ and of $\delta_n = \boldsymbol{\delta} \cdot \mathbf{n}_d$, respectively, and are both non-differentiable at their origins ($\boldsymbol{\delta} = \mathbf{0}$ and $\delta_n = 0$, respectively). This is the crucial mathematical property that keeps the interfaces closed until a certain level of stress/elastic energy is reached in the body (i.e., initially-rigid behavior), see the discussion by Papoulia.¹⁰ A general class of cohesive models proposed by Ortiz and Pandolfi¹ is considered in which the cohesive potential $\phi(\boldsymbol{\delta})$ is expressed as a function of a scalar effective opening displacement δ , defined as $\delta(\delta_n, \boldsymbol{\delta}_s) = \sqrt{(\delta_n^+)^2 + \beta^2 |\boldsymbol{\delta}_s|^2}$, where $\delta_n^+ = \max(\delta_n, 0)$ and β is a material constant that weights the normal and tangential components of the displacement vector. In the present work, the potential employed corresponds to a linear softening behavior similar to the one used by Hirmand and Papoulia.⁹ The interpenetration penalty potential $\theta(\delta_n)$ is taken to be the indicator function $I_{\mathbb{R}^+}(\delta_n)$.⁹

The equilibrium of the body is characterized by the solution of the following constrained minimization problem that must be solved at each time step:

$$\text{Find } (\mathbf{u}^*, \boldsymbol{\delta}^*) \in \mathcal{U} \times \mathcal{D} \text{ minimizing } \pi(\mathbf{u}, \boldsymbol{\delta}) \text{ subject to } \mathbf{g}(\mathbf{u}, \boldsymbol{\delta}) = \mathbf{0}, \quad (5)$$

where \mathcal{U} and \mathcal{D} are spaces of admissible solutions which depend on the particular finite element implementation and

$$\mathbf{g}(\mathbf{u}, \boldsymbol{\delta}) = \llbracket \mathbf{u}(x, t) \rrbracket - \boldsymbol{\delta}(x, t) \quad (6)$$

is a linear constraint function. The Lagrangian for the constrained optimization problem (5) is⁹

$$\mathcal{L}(\mathbf{u}, \boldsymbol{\delta}, \boldsymbol{\lambda}) = \pi(\mathbf{u}, \boldsymbol{\delta}) + \int_{\Gamma_d} \boldsymbol{\lambda} \cdot \mathbf{g} dS, \quad (7)$$

where $\boldsymbol{\lambda}$ is the Lagrange multiplier field. A saddle point of the above Lagrangian corresponds to a solution $(\mathbf{u}^*, \boldsymbol{\delta}^*)$ of (5).

3.1 SPATIAL DISCRETIZATION AND THE FINITE DIMENSIONAL PROBLEM

It is noted that taking the derivative of (7) to arrive at a weak form through a variational formulation is not a valid approach in the present setting because the interface potential π_{intf} in (2) is not globally differentiable.^{9,10} The finite element discretization is, therefore, directly applied to the

energy functional (7) to arrive at a finite-dimensional, non-differentiable energy minimization problem. In such approach, activation happens automatically when a certain level of energy that is encoded in $\phi(\delta)$ is reached.^{9,10} The method sidesteps the time-discontinuity and traction lacking issues observed in the literature.^{7,8}

We follow Hirmand and Papoulia⁹ for the finite element discretization of \mathbf{u} and δ . A discontinuous Galerkin discretization is used for the approximation of \mathbf{u} , whereas a piecewise constant approximation is considered for the approximation of δ . The discontinuous Galerkin discretization \mathbf{u}_h is achieved by requiring the neighboring finite elements to not share nodal points and edges, allowing for jump discontinuities $[[\mathbf{u}_h]]$ at inter-element boundaries (Figure 2). The union of inter-element boundaries constitutes the discretized discontinuity boundary $\Gamma_{d,h}$ where the cracks can form. The piecewise constant approximation δ_h is constructed by introducing M nodal points with coordinates $\xi_I \in \Gamma_{d,h}$, $I = 1, 2, \dots, M$ on the interface (see Figure 2). The location of the nodal points holding opening degrees of freedom is chosen to be the Gauss quadrature points of the interface elements emplaced at the inter-element boundaries of the bulk mesh. As such, each Gauss point of the interface holds an interface opening degree of freedom.

The Lagrange multiplier λ is then replaced by a numerical flux due to Nitsche that is only a function of primal variables: $\lambda_h^{DG} = \langle \sigma_h \rangle \mathbf{n}_d + \frac{1}{2} \eta \mathbf{g}_h$, where σ_h is the Cauchy stress tensor computed strongly from \mathbf{u}_h , η is a sufficiently large penalty number and $\langle * \rangle = \frac{1}{2}(*^+ + *^-)$.

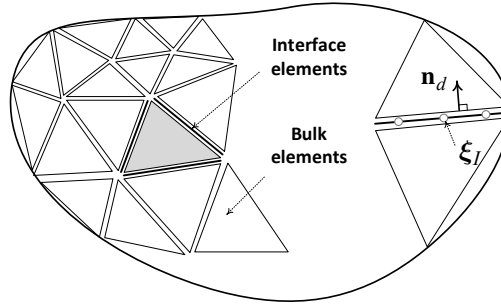


Figure 2. Schematic of the DG discretization Ω_h of the domain and related definitions

Inserting Discontinuous Galerkin approximations \mathbf{u}_h , δ_h and the numerical flux $\lambda_h^{DG}(\mathbf{u}_h, \delta_h)$ to the minimization problem (7), the finite-dimensional problem that must be solved at each time step reads:

$$\min_{(\bar{\mathbf{u}}, \bar{\delta})} \mathcal{L}^{DG}(\bar{\mathbf{u}}, \bar{\delta}) = \pi(\mathbf{u}_h, \delta_h) + \int_{\Gamma_d} \langle \sigma_h \rangle \mathbf{n}_d \cdot \mathbf{g}_h dS + \frac{1}{2} \int_{\Gamma_d} \eta \mathbf{g}_h \cdot \mathbf{g}_h dS, \quad (8)$$

where $\bar{\mathbf{u}}$ and $\bar{\delta}$ denote the global vector of nodal unknowns corresponding to \mathbf{u}_h and δ_h , respectively.

3 STAGGERED MINIMIZATION ALGORITHM

The proposed staggered minimization algorithm relies on the general partitioning approach widely used in the solution of coupled mechanical problems.¹⁴ In such approaches, systems are spatially decomposed into partitions and the solution is advanced in time through solving each partition separately within an iterative solution strategy. Accordingly, we construct a staggered iteration loop in which the minimization problem (7) is solved for $\bar{\mathbf{u}}$ and $\bar{\boldsymbol{\delta}}$ independently until convergence is achieved for the coupled problem within the iterations. Minimization with respect to $\bar{\mathbf{u}}$ is straightforward since the objective function in (7) is quadratic in and differentiable with respect to $\bar{\mathbf{u}}$ everywhere. However, a direct minimization with respect to $\bar{\boldsymbol{\delta}}$ is out of reach due to non-differentiability of ϕ and θ in π_{intf} at their origins with respect to the unknown opening $\bar{\boldsymbol{\delta}}$. We make use of the sub-gradients of ϕ and θ , denoted $\partial\phi$ and $\partial\theta$, respectively, to treat non-differentiability at the non-differentiability points.¹³ A brief description of the sub-gradients $\partial\phi$ and $\partial\theta$ is as follows.

As presented by Lorentz,¹³ the definition of the sub-gradient of a function coincides with its gradients anywhere it is differentiable. Given that the interface potentials ϕ and θ are differentiable everywhere except at their origins, the points that require special attention are $\boldsymbol{\delta} = \mathbf{0}$ for ϕ and $\delta_n = 0$ for θ . A sub-gradient of ϕ at $\boldsymbol{\delta} = \mathbf{0}$ is given by¹³

$$\partial\phi = \{\mathbf{t}_{\text{cohs}} \in \mathbb{R}^{n_{\text{dim}}} \mid t_{\text{cohs}} \leq \sigma_c\}, \quad (9)$$

in which t_{cohs} is an effective norm of \mathbf{t}_{cohs} defined as

$$t_{\text{cohs}} = \sqrt{(t_{\text{cohs},n}^+)^2 + \beta^{-2}|\mathbf{t}_{\text{cohs},s}|^2}, \quad (10)$$

where $t_{\text{cohs},n}$ and $\mathbf{t}_{\text{cohs},s}$ are the normal and sliding components of \mathbf{t}_{cohs} , respectively, and σ_c is the material strength of the cohesive model. The sub-gradient of θ at $\delta_n = 0$ is given by¹³

$$\partial\theta = \{t_{\text{cont}}\mathbf{n}_d \mid t_{\text{cont}} \leq 0, \delta_n \geq 0, t_{\text{cont}} \cdot \delta_n = 0\}. \quad (11)$$

At all other points, the sub-gradients $\partial\phi$ and $\partial\theta$ coincide with gradients $\nabla_{\boldsymbol{\delta}}\phi$ and $\nabla_{\boldsymbol{\delta}}\theta$, respectively, that is, $\partial\phi = \{\nabla_{\boldsymbol{\delta}}\phi\}$ for $\boldsymbol{\delta} \neq \mathbf{0}$ and $\partial\theta = \{\nabla_{\boldsymbol{\delta}}\theta\}$ for $\delta_n \neq 0$. The two problems to be solved sequentially within the staggered iterations within each time step can be expressed as

$$\min_{\bar{\mathbf{u}}} \left\{ \pi_{\text{bulk}}(\mathbf{u}_h) + \pi_{\text{dyn}}(\mathbf{u}_h) - W_{\text{ext}}(\mathbf{u}_h) + \int_{\Gamma_d} \boldsymbol{\lambda}_h^{\text{DG}} \cdot \mathbf{g}_h dS \right\}, \quad (12\text{-a})$$

$$\min_{\bar{\boldsymbol{\delta}}_I} \{ \phi(\bar{\boldsymbol{\delta}}_I) + \theta(\bar{\delta}_{n,I}) + \boldsymbol{\lambda}_{h,I}^{\text{DG}} \cdot \mathbf{g}_{h,I} \} \quad \forall \boldsymbol{\xi}_I \in \Gamma_{d,h}, \quad (12\text{-b})$$

for which the first order minimality conditions are obtained as

$$\mathbf{M}\bar{\ddot{\mathbf{u}}} + \mathbf{K}_{uu}\bar{\mathbf{u}} + \mathbf{K}_{u\boldsymbol{\delta}}\bar{\boldsymbol{\delta}} - \mathbf{F}_{\text{ext}} = \mathbf{0}, \quad (13\text{-a})$$

$$\mathbf{p}_h - \eta\bar{\boldsymbol{\delta}}_I \in \partial\phi(\bar{\boldsymbol{\delta}}_I) \cup \partial\theta(\bar{\delta}_{n,I}) \quad \forall \boldsymbol{\xi}_I \in \Gamma_{d,h}, \quad (13\text{-b})$$

with \mathbf{M} (mass matrix), \mathbf{K}_{uu} and $\mathbf{K}_{u\delta}$ coefficient matrices obtained after taking the gradient of the discretized potential (7), and $\mathbf{p}_h = \langle \boldsymbol{\sigma}_h \rangle \cdot \mathbf{n}_d + \eta \llbracket \mathbf{u}_h \rrbracket$.

We note that the particular discretization scheme employed for δ_h makes the potential of the interfaces separable in each nodal unknown $\bar{\delta}_I$. This leads to independent local minimization problems with respect to $\bar{\delta}_I$ at each Gauss point ξ_I of the interface, see equations (12-b) and (13-b). When the interface potentials are differentiable, solution of the local problem (12-b) is rather straightforward as the gradients of the potentials ϕ and θ are uniquely defined. In this case, equation (13-b) simplifies to $\mathbf{p}_h - \eta \bar{\delta}_I = \nabla_{\delta_I} \phi + \nabla_{\delta_I} \theta \quad \forall \xi_I \in \Gamma_{d,h}$ and a minimization algorithm such as the trust region method¹⁵ can be readily used to minimize the objective function (12-b). Note that the choice of a trust-region algorithm is necessary as the objective function in (12-b) is generally not convex in its unknown $\bar{\delta}_I$. Prior to the activation of interfaces, however, or when an activated interface undergoes contact, the minimal solution has to be obtained by exploiting the definition of the sub-gradients equations (9) and (11) at the non-differentiability points. This leads to the following scheme for the treatment of the local minimization problem (12-b) at each interface Gauss point $\xi_I \in \Gamma_{d,h}$:

IF $\delta_{max} = 0$ and $t_{cohs} \leq \sigma_c$, THEN $\bar{\delta}_I = \mathbf{0}$ (pre-activation conditions).

ELSE, solve the minimization problem (12-b) for $\bar{\delta}_I \neq \mathbf{0}$. If $p_{h,n} < 0$, set $\bar{\delta}_{n,I} = 0$ and solve for $\bar{\delta}_{s,I}$ only.

In the above, δ_{max} is defined as the maximum effective opening attained up until the current time step; that is, at time t_{i+1} , $\delta_{max,i+1} = \max_{t' \in \{t_0, \dots, t_i\}} \delta(t')$.

Remark 1. The staggered minimization algorithm presented here can be used with both explicit and implicit time stepping schemes. For an explicit time stepping scheme, however, the minimization algorithm requires only one staggered iteration to achieve the solution of the next time step. This is because the predictor of the displacement unknowns at the first staggered iteration readily gives the final solution of the time step with no need to correct in subsequent staggered iterations.

Remark 2. In our experience, minimization of the local problem (12-b) normally takes less than ten trust-region iterations to converge when a proper initial estimate is used for the initiation of the trust region minimization algorithm.

4 NUMERICAL SIMULATION RESULTS

We consider the fragmentation of a thick cylinder subjected to impulsive internal pressure in order to demonstrate the robustness of the proposed algorithm in modeling multiple crack growth problems. The problem set-up, material properties and time history of the applied pressure are shown in Figure 3. The internal pressure decays exponentially by time as $p(t) = p_0 e^{-t/t_0}$, where $p_0 = 400 \text{ MPa}$ and $t_0 = 100 \mu\text{s}$. The problem considered here has been previously studied by Song and Belytschko¹⁶ and Hirmand and Papoulia.⁹

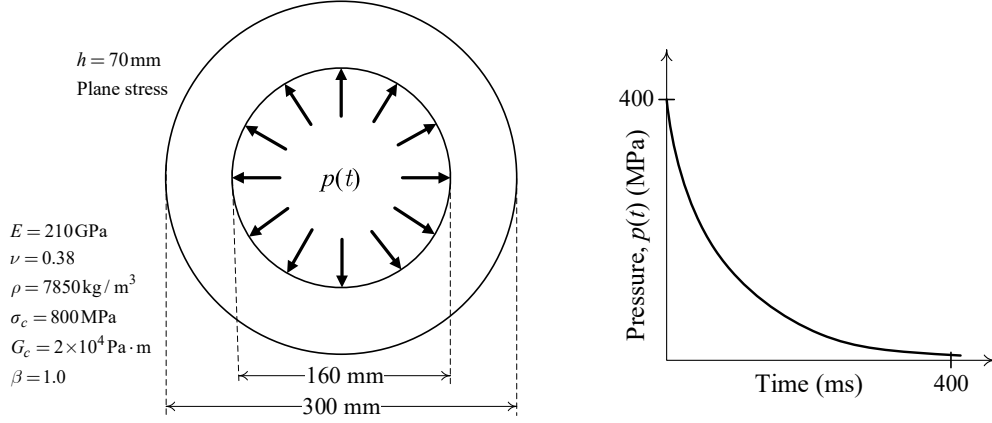


Figure 3. Fragmentation of a thick cylinder; problem definition and relevant properties.

The mesh used consists of 1692 bulk elements, 2394 interface elements and a total of 17334 nodal points (displacement + opening). The dilatational wave speed in the material is $v_d = 5591 \text{ m/s}$.⁹ An explicit time step would be limited by $\Delta t_{cr} = h_{min}/v_d$, where $h_{min} = 1.2 \text{ mm}$ is the minimum element size. We performed the simulations using both explicit and implicit time stepping schemes for a total time of $T = 78 \mu\text{s}$. For the explicit time stepping solution, we used $\Delta t = 0.9 \Delta t_{cr}$ to ensure stability of the time stepping algorithm. For the implicit time stepping solution, we used $\Delta t = 2 \Delta t_{cr}$ and considered two different convergence criteria in order to investigate the effect of the number of staggered iterations on the accuracy of the simulation results. In the first case, a sufficiently small tolerance was defined and convergence of the staggered iterations was determined based on the variation of unknown variables $\bar{\mathbf{u}}$ and $\bar{\delta}$ in successive iterations. Staggered iterations were allowed to continue until convergence to this pre-determined tolerance was achieved. In the second case, the number of staggered iterations was limited to a maximum of 3 iterations, irrespective of the magnitude of the terminal errors. The final deformed configurations and the activation patterns obtained in different simulations are shown in Figures 4 and 5, respectively. Results obtained by different schemes show good agreement. In addition, results are comparable to those reported in the literature by Hirmand and Papoulia⁹ and Song and Belytschko.¹⁶

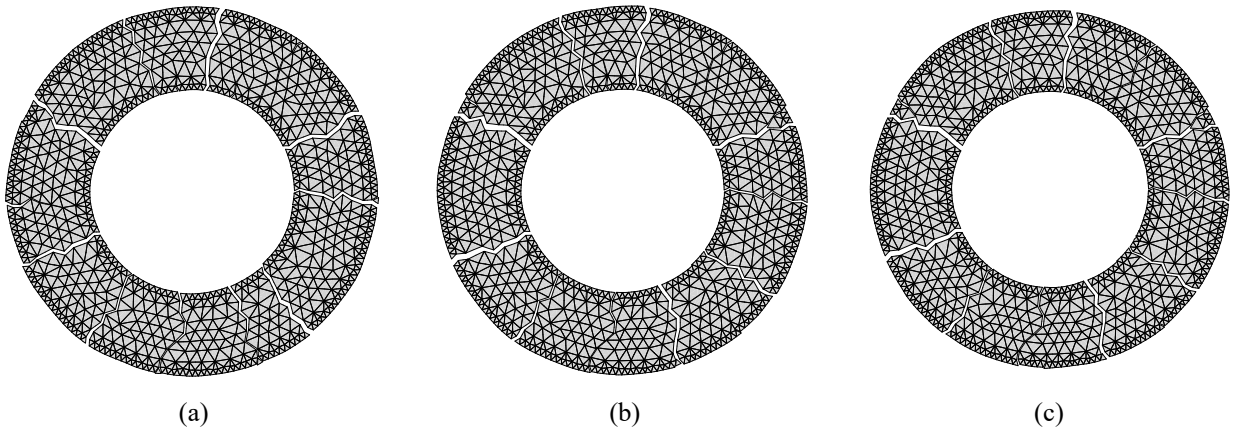


Figure 4. Fragmentation of a thick cylinder; final deformed meshes (magnified 10 times) obtained by (a) explicit time stepping (b) implicit time stepping until convergence and (c) implicit time stepping, three iterations

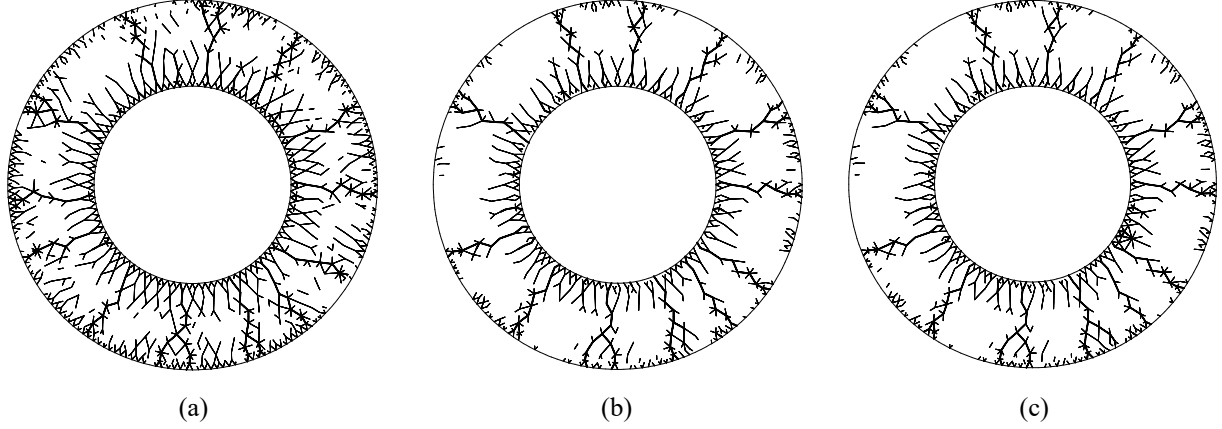


Figure 5. Fragmentation of a thick cylinder; interface activation patterns obtained by (a) explicit time stepping (b) implicit time stepping until convergence and (c) implicit time stepping, three iterations.

Finally, the convergence profile of the converged staggered iterations is shown in Figure 6 at three representative time steps corresponding to post failure of the interfaces (prior to failure of the interfaces, the staggering scheme converge in one iteration since the equations are linear). The convergence profiles show stable behavior indicative of the robustness of the proposed staggered solution strategy.

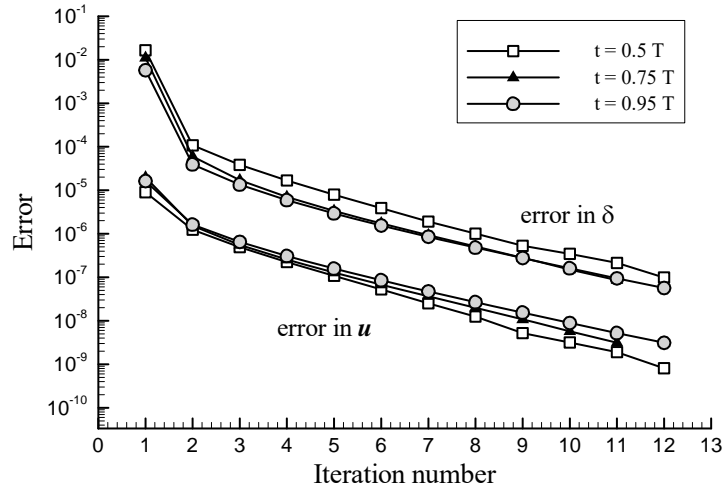


Figure 6. Convergence profile of the staggered iterations in implicit calculations.

5 CONCLUSION

A new computational algorithm was presented for rigid-cohesive fracture on the basis of non-differentiable energy minimization. The method entails a staggered solution strategy in which minimization is performed with respect to the bulk deformation and with respect to crack opening unknowns independently. The method offers several advantages over a monolithic approach as the differentiable, convex part and the non-differentiable, non-convex part of the problem are solved separately. The use of the sub-gradient concept for treatment of the non-differentiability, together

with the particular discretization scheme employed for the interface openings, simplifies minimization of the non-differentiable, non-convex part of the potential significantly. In addition, the partitioned solution strategy offers desirable flexibility from a computer programming perspective: the method can be implemented within an existing solid mechanics finite element code with minimal effort.

REFERENCE

- [1] M. Ortiz, A. Pandolfi, Finite-deformation irreversible cohesive elements for three-dimensional crack-propagation analysis, *Int. J. Numer. Methods Eng.* 44 (1999) 1267–1282.
- [2] G.T. Camacho, M. Ortiz, Computational modelling of impact damage in brittle materials, *Int. J. Solids Struct.* 33 (1996) 2899–2938.
- [3] J. Dolbow, T. Belytschko, A finite element method for crack growth without remeshing, *Int. J. Numer. Methods Eng.* 46 (1999) 131–150.
- [4] A.R. Khoei, M. Vahab, M. Hirmand, An enriched-FEM technique for numerical simulation of interacting discontinuities in naturally fractured porous media, *Comput. Methods Appl. Mech. Eng.* 331 (2018) 197–231.
- [5] A.R. Khoei, M. Hirmand, M. Vahab, M. Bazargan, An enriched FEM technique for modeling hydraulically driven cohesive fracture propagation in impermeable media with frictional natural faults: Numerical and experimental investigations, *Int. J. Numer. Methods Eng.* 104 (2015) 439–468.
- [6] R. Radovitzky, A. Seagraves, M. Tupek, L. Noels, A scalable 3D fracture and fragmentation algorithm based on a hybrid, discontinuous Galerkin, cohesive element method, *Comput. Methods Appl. Mech. Eng.* 200 (2011) 326–344.
- [7] K.D. Papoulia, C. Sam, S.A. Vavasis, Time continuity in cohesive finite element modeling, *Int. J. Numer. Methods Eng.* 58 (2003) 679–701.
- [8] C.-H. Sam, K.D. Papoulia, S.A. Vavasis, Obtaining initially rigid cohesive finite element models that are temporally convergent, *Eng. Fract. Mech.* 72 (2005) 2247–2267.
- [9] M.R. Hirmand, K.D. Papoulia, A continuation method for rigid-cohesive fracture in a discontinuous Galerkin finite element setting, *Int. J. Numer. Methods Eng.* (2018) 1–24. doi:<https://doi.org/10.1002/nme.5819>.
- [10] K.D. Papoulia, Non-differentiable energy minimization for cohesive fracture, *Int. J. Fract.* 204 (2017) 143–158.
- [11] B. Bourdin, G.A. Francfort, J.-J. Marigo, Numerical experiments in revisited brittle fracture, *J. Mech. Phys. Solids.* 48 (2000) 797–826.
- [12] B. Schmidt, F. Fraternali, M. Ortiz, Eigenfracture: an eigendeformation approach to variational fracture, *Multiscale Model. Simul.* 7 (2009) 1237–1266.
- [13] E. Lorentz, A mixed interface finite element for cohesive zone models, *Comput. Methods Appl. Mech. Eng.* 198 (2008) 302–317.
- [14] C.A. Felippa, K.C. Park, C. Farhat, Partitioned analysis of coupled mechanical systems, *Comput. Methods Appl. Mech. Eng.* 190 (2001) 3247–3270.
- [15] S.J. Wright, J. Nocedal, Numerical optimization, Springer Sci. 35 (1999) 7.
- [16] J. Song, T. Belytschko, Cracking node method for dynamic fracture with finite elements, *Int. J. Numer. Methods Eng.* 77 (2009) 360–385.

Numerical Analysis of Crack Propagation in Tempered Glass Plate

Sayako Hirobe^{*}, Kenji Oguni^{**}, Yasumasa Kato^{***}, Kazushige Yoda^{****}

^{*}Keio University, ^{**}Keio University, ^{***}Asahi Glass Co., Ltd. (AGC), Production Technology Division, ^{****}Asahi Glass Co., Ltd. (AGC), Automotive Company

ABSTRACT

The fracture of the thermally tempered glass results in the complex crack patterns with a large number of small fragments. The prediction of the shape of the fragments in fractured tempered glass is required for the product safety, because sharp edge brings harmful risk to users. However, no effective numerical method for the estimate of crack paths in tempered glass has been proposed so far. This research presents the numerical analysis method to simulate the dynamic fracture process in thermally tempered glass plate. The tempered glass has the spatial distribution of the residual stress in both in-plane and cross-section direction resulting from the thermal tempering process. The crack paths and the shape of the fragments change depending on the residual stress distribution. This implies that the residual stress pattern plays a significant role for the fracture behavior in the tempered glass. Particle Discretization Scheme Finite Element Method (PDS-FEM) is one of the fracture analysis methods for the solid continuum. PDS-FEM applies the particle discretization to the field variables by using discontinuous and non-overlapping shape functions defined on the conjugate geometries: Delaunay tessellation and Voronoi tessellations. We implement the treatment of the residual stress field to PDS-FEM. In the framework PDS-FEM, the solid continuum is expressed by the set of the Voronoi particles. According to the particle discretization, PDS-FEM can define the Hamiltonian of the system to provide the time evolution of the dynamic behavior of the linearly elastic body. Also, this discretization scheme can evaluate the displacement field expressed by the translational motion of the rigid body particles with the same accuracy as the ordinary FEM. These advantages of PDS-FEM enable us to evaluate the release and the re-distribution of the residual stress in the process of the dynamic crack propagation. We could demonstrate that the crack patterns and the crack propagation process obtained from the preliminary numerical analysis are analogous to those typically observed in the fracture of the thermally tempered glass. This ensures that the proposed numerical analysis method successfully captures the fundamental mechanism for the dynamic crack propagation in the thermally tempered glass.

Finite Element Modeling and Simulation of Failure in Heterogeneous Composite-Metal Layers

Franz Hirsch*, Markus Kästner**

*Technische Universität Dresden, Institute of Solid Mechanics, Germany, **Technische Universität Dresden, Institute of Solid Mechanics, Germany

ABSTRACT

Modern lightweight structures, e.g. in automotive and aircraft applications, exploit their full potential utilizing a multi-material design. Hence, it is convenient to apply isotropic lightweight metals in regions with a complex three-dimensional stress state and fiber-reinforced polymers (FRP) in regions with determined loading directions. These design approaches require suitable joining strategies. Next to common joining technologies based on bolts and rivets or bonding agents, intrinsic interlocking joints are a promising solution [1]. On the microscale, such connections can be achieved with defined surface structures of the metal component, so that the polymer matrix fills the gaps and form a contour joint. The comprehension of the damage process is valuable during the design process and often hard to determine experimentally, where numerical investigations are suitable means. In this contribution, a finite element model of a representative boundary layer [2] between a metal component and an FRP is presented, to study the complex failure behavior and damage mechanisms under mechanical loading. We distinguish adhesive failure of the metal-polymer and the fiber-polymer interface and cohesive failure of the polymer material. The behavior of the polymer is described by an elastic-plastic damage model at large strains with a regularization to avoid the typical mesh dependence of softening material models. Local adhesive failure is modeled by a cohesive zone approach based on a traction-separation formulation. The application of a homogenization scheme for adhesive layers [3] enables the extraction of effective traction-separations relations and the determination characteristic interface properties. The numerical studies show, that rough or structured metal-polymer interfaces shift the dominant damage mechanism from pure adhesive to cohesive failure of the polymer and therefore to an increased effective strength of the boundary layer. This effect occurs especially under shear loading, which correspond to the typical observations of higher shear strengths compared to the values in tension direction. References [1] R. Kießling, J. Ihlemann, M. Pohl, M. Stommel, C. Dammann, R. Mahnken, M. Bobbert, G. Meschut, F. Hirsch, M. Kästner (2016) On the Design, Characterization and Simulation of Hybrid Metal-Composite Interfaces. *Applied Composite Materials*, 23, 1-19. [2] F. Hirsch, M. Kästner (2017) Microscale simulation of adhesive and cohesive failure in rough interfaces. *Engineering Fracture Mechanics* 178, 416–432. [3] M.V.C. Alfaro, A.S.J. Suiker, C.V. Verhoosel, R. de Borst (2010) Numerical homogenization of cracking processes in thin fibre-epoxy layers. *European Journal of Mechanics - A/Solids* 29, 119-131.

Isogeometric Shape Optimization for Innovative Design of Stiffened Structures

Thibaut Hirschler*, Robin Bouclier**, Arnaud Duval***, Thomas Elguedj****, Joseph Morlier*****

*Univ Lyon, INSA-Lyon, CNRS, LaMCoS UMR5259, 27 Avenue Jean Capelle, F69621 Villeurbanne Cedex, France, **Université de Toulouse, INSA-Toulouse, CNRS, IMT UMR5219, 135 Avenue de Rangueil, F31077 Toulouse Cedex 04, France, ***Univ Lyon, INSA-Lyon, CNRS, LaMCoS UMR5259, 27 Avenue Jean Capelle, F69621 Villeurbanne Cedex, France, ****Univ Lyon, INSA-Lyon, CNRS, LaMCoS UMR5259, 27 Avenue Jean Capelle, F69621 Villeurbanne Cedex, France, *****Université de Toulouse, ISAE Supaero, CNRS, ICA UMR5312, 10 Avenue Edouard Belin, F31055 Toulouse Cedex 04, France

ABSTRACT

Structural optimization requires a suitable mix of an accurate geometric description and an efficient analysis model. Isogeometric Analysis (IGA) fills this need, as it reconciles computer-aided design (CAD) with structural analysis by using spline functions as finite element bases. Since CAD uses the boundary representation (B-rep), IGA is especially suitable for analyzing structures whose geometry is easily derived from a surface, as is the case for shells. Therefore, the efficiency of IGA-based shape optimization of shells has been observed [1-2] and capable algorithms have been proposed. However, its applicability to complex structures as skin stiffened aerostructures is not yet proven. Non-conforming interface [3] between the stiffeners and the skin is needed in order to get an attractive design space. The simplicity and the efficiency of the coupling depends on the chosen shell formulation. We explore and compare the use of two formulations: the Kirchhoff-Love formulation for thin shells and a solid-shell model for thicker shells. Starting from numerical examples involving simple stiffened panels, the final goal is to propose a general framework for optimizing the buckling behavior of large and complex aeronautical structures. [1] J. Kiendl, R. Schmidt, R. Wüchner and K.-U. Bletzinger, Isogeometric shape optimization of shells using semi-analytical sensitivity analysis and sensitivity weighting, *Comput. Methods Appl. Mech. Eng.*, Vol. 274, pp. 148--167, 2014. [2] A.P. Nagy, S.T. Ijsselmuiden and M.M. Abdalla, Isogeometric design of anisotropic shells: Optimal form and material distribution, *Comput. Methods Appl. Mech. Eng.*, Vol. 264, pp. 145--162, 2013. [3] R. Bouclier, J.-C. Passieur and M. Salaün, Local enrichment of NURBS patches using a non-intrusive coupling strategy: Geometric details, local refinement, inclusion, fracture, *Comput. Methods Appl. Mech. Eng.*, Vol. 300, pp. 1--26, 2016.

Adapting Precision in Scientific Simulations

Jeffrey Hittinger^{*}, Peter Lindstrom^{**}, Alyson Fox^{***}, Daniel Osei-Kuffuor^{****}, Geoffrey Sanders^{*****}, G. Scott Lloyd^{*****}, James Diffenderfer^{*****}, Janica Gordon^{*****}

^{*}Lawrence Livermore National Laboratory, ^{**}Lawrence Livermore National Laboratory, ^{***}Lawrence Livermore National Laboratory, ^{****}Lawrence Livermore National Laboratory, ^{*****}Lawrence Livermore National Laboratory, ^{*****}Lawrence Livermore National Laboratory, ^{*****}University of Florida, ^{*****}Southern University of New Orleans

ABSTRACT

Decades ago, when memory was a scarce resource, computational scientists routinely worked in single precision and were more sophisticated in dealing with the pitfalls finite-precision arithmetic. Today, however, we typically compute and store results in 64-bit double precision by default even when very few significant digits are required. Many of these bits are representing errors – truncation, iteration, roundoff – instead of useful information about the solution. This over-allocation of resources is wasteful of power, bandwidth, storage, and FLOPs; we communicate and compute on many meaningless bits and do not take full advantage of the computer hardware we purchase. Because of the growing disparity of FLOPs to memory bandwidth in modern computer systems and the rise of General-Purpose GPU computing – which has better peak performance in single precision – there has been renewed interest in mixed precision computing, where tasks are identified that can be accomplished in single precision in conjunction with double precision. Such static optimizations reduce data movement and FLOPs, but why stop there? We often adapt mesh size, order, and models when simulating to focus the greatest effort only where needed. Why not do the same with precision? At LLNL, we are developing the methods and tools that will enable the routine use of dynamically adjustable precision at a per-bit level depending on the needs of the task at hand. Just as adaptive mesh resolution frameworks adapt spatial grid resolution to the needs of the underlying solution, our goal is to provide more or less precision as needed locally. We will discuss a new technique based on local, adaptive floating-point compression to address the data bandwidth problem within simulations and repurpose a defect correction technique that can adaptively reduce the cost of floating point operations. This work was performed under the auspices of the U.S. Department of Energy by Lawrence Livermore National Laboratory under Contract DE-AC52-07NA27344.

A Development of Polygonal Finite Shell Element and Its Application to Coupling Non-matching Meshes

Thuan Ho Nguyen Tan*, Hyun-Gyu Kim**

*Seoul National University of Science and Technology, **Seoul National University of Science and Technology

ABSTRACT

In this work, a polygonal shell formulation on arbitrary polygonal meshes is developed for shell analysis. Assumed natural strains in the form of the mixed interpolation of tensorial components (MITC) approach are employed to avoid the transverse shear locking when the thickness of shell tends to zeros. In addition, an assumed membrane strain field is constructed to alleviate the membrane locking by a linear combination of the tying membrane strains. The non-matching meshes can be effectively connected by the polygonal shell elements at non-matching interfaces. Several basic tests and practical examples are performed to verify the present method. [1] P.-S. Lee, K.-J. Bathe, Development of MITC isotropic triangular shell finite elements, *Comput. Struct.* 82 (2004) 945–962. [2] K.-J. Bathe, E.N. Dvorkin, A formulation of general shell elements—the use of mixed interpolation of tensorial components, *Int. J. Numer. Methods Eng.* 22 (1986) 697–722. [3] Y. Ko, P.-S. Lee, K.-J. Bathe, The MITC4+ shell element and its performance, *Comput. Struct.* 169 (2016) 57–68.

Domain Decomposition Least-squares Petrov--Galerkin (DD-LSPG) for Nonlinear Model Reduction

Chi Hoang*, Kevin Carlberg**

*Sandia National Laboratories, **Sandia National Laboratories

ABSTRACT

Many tasks in computational science and engineering are *many query* in nature: they require the repeated simulation of a parameterized computational model. Model reduction has become a popular approach to make such tasks tractable. Such techniques first perform an *offline* training stage during which the computational model is simulated for multiple parameter instances. Then, during an *online* deployed stage, these techniques reduce the dimensionality and complexity of the original computational model at arbitrary parameter instances by performing a projection process onto a low-dimensional subspace. While such reduced-order models (ROMs) have demonstrated success in many applications, challenges arise when applying model reduction either to *extreme-scale models* or to *decomposable systems*, i.e., systems composed of well-defined components. In the former case, the extreme-scale nature of the original computational model renders the offline training simulations infeasible. In the latter case, the many-query task often involves design, wherein components are swapped or their interconnecting topology is modified; in this case, the original computational model changes between queries, rendering training simulations (which assume a fixed original computational model) challenging. To address these problems, we propose a domain-decomposition least-squares Petrov--Galerkin (DD-LSPG) model-reduction method. Rather than constructing a low-dimensional subspace for *the entire state space*, low-dimensional subspaces are constructed for different subdomains or components characterizing the original model. During the offline stage, only *subdomain training simulations* are needed in the case of extreme-scale models, and only *component training simulations* are required in the case of decomposable systems. During the online stage, the approach constructs a LSPG model for each subdomain/component (including hyper-reduction in the case of nonlinearities), and enforces (weak) compatibility on the *ports* connecting them. Mathematically, the resulting ROM corresponds to a nonlinear least-squares problem with linear equality constraints. We propose several different strategies for defining the ingredients characterizing the methodology: (i) three different ways to construct basis functions on the interface/ports of subdomains (which imply different offline training strategies), (ii) different methods for enforcing compatibility (iii) four different solvers that expose different levels of concurrency and intrusiveness. Numerical results performed on problems in heat transfer and fluid dynamics demonstrate that the proposed method outperforms typical model-reduction techniques in terms of both accuracy and (parallel) computational time.

WAVE FINITE ELEMENT METHOD AND MOVING LOADS FOR THE DYNAMIC ANALYSIS OF RAILWAY TRACKS

T. HOANG*, D. DUHAMEL*, G. FORET*,
J.L. POCHET† AND F. SABATIER†

*Laboratoire Navier, UMR 8205, Ecole des Ponts ParisTech,
IFSTTAR, CNRS, UPE, Champs-sur-Marne, France
tien.hoang@enpc.fr, denis.duhamel@enpc.fr, gilles.foret@enpc.fr

†Eurotunnel Group, Coquelles, France
jean-luc.pochet@eurotunnel.com, francis.sabatier@eurotunnel.com

Key words: Wave Finite Element, Railway Dynamics, Periodic Structure, Waveguide, Computing Methods.

Abstract. Based on the finite element method, the wave finite element method (WFE) permits to analyze the dynamics of a periodic structure by using a wave decomposition on one period. This method reduces the number of DOF and it has advantages in calculation time. However, it cannot be applied easily to a railway track because this structure is subjected to moving loads which are not considered in a classical WFE. In this article, we present a technique to deal with moving loads applying in a railway track where the track components are modeled by 3D continuous media. By using the classical WFE for one track period in frequency domain, we can rewrite the vector of DOF and loads in a wave base. Then, we can calculate the wave amplitudes of the moving loads from their representation in this base. Thereafter, we apply the wave analyze of WFE to the hold structure. The result shows that the moving loads lead to a sum of wave amplitudes. Finally, we apply this method for a railway track subjected to constant moving loads with numerical application. The new technique permits to analyze the dynamic of railway tracks by considering only one track period.

1 INTRODUCTION

The dynamic of railway track has been studied with different methods. The analytical methods permit to calculate very fast track responses for different types of tracks [1-6]. These methods base on the model of beams supported by a viscoelastic foundation or the model of periodically supported beams [6]. The numerical methods have been developed by using the finite element method (FEM). The advantage of this method is to give a complete analysis. However, it can not take easily the whole length of the railway track and the calculation time is long. Some reduced techniques have been developed for the FEM. Recently, the wave finite element method [7-10] has been applied to the railway track analysis. This method is based on the wave decomposition of one track period then

using the wave analysis to compute the response of the whole track. However, the classical WFE can not take into account the moving loads of a train applied to the rail and this article deals with this problem.

By rewriting the dynamic equation of one period (a substructure) of the railway track subjected to a load in the frequency domain, we obtain a relation for the vector of DOF and nodal loads at the left and right boundary of the substructure and this relation is including the moving loads. Then, we use the WFE technique to rewrite the expression of the track response. On the other side, we present a bounded limit for an infinite periodic railway track which leads to a simple expression of the response. The applications have been developed then for a normal railway track and ones with a defect zone or a transition zone.

1.1 Dynamic equation

Consider a railway track with a periodic interval as shown in Figure 1. This interval is represented by one period (a substructure) with all components of the tracks (rails, pads, supports, foundations...). The track is subjected to dynamic loads of a train and we consider that all loads are given.

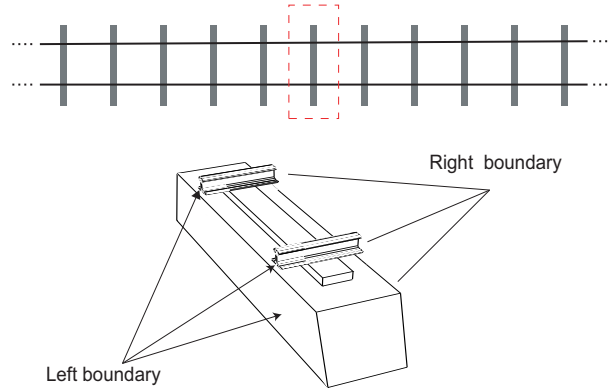


Figure 1: Periodic railway track represented by a substructure

By using the finite element method for a substructure, the dynamic equation can be written as follows

$$\mathbf{D}_{tot}\mathbf{q} = \mathbf{F} \quad (1)$$

where $\mathbf{D}_{tot} = \mathbf{K} + j\omega\mathbf{C} - \omega^2\mathbf{M}$ is the dynamic stiffness matrix (DSM) of the substructure. We note that the aforementioned equation holds for all type of modeling (beam, 2D or 3D). Then, we can rewrite the DSM as follows

$$\begin{bmatrix} \tilde{\mathbf{D}}_{II} & \tilde{\mathbf{D}}_{IL} & \tilde{\mathbf{D}}_{IR} \\ \tilde{\mathbf{D}}_{LI} & \tilde{\mathbf{D}}_{LL} & \tilde{\mathbf{D}}_{LR} \\ \tilde{\mathbf{D}}_{RI} & \tilde{\mathbf{D}}_{RL} & \tilde{\mathbf{D}}_{RR} \end{bmatrix} \begin{bmatrix} \mathbf{q}_I \\ \mathbf{q}_L \\ \mathbf{q}_R \end{bmatrix} = \begin{bmatrix} \mathbf{F}_I \\ \mathbf{F}_L \\ \mathbf{F}_R \end{bmatrix} \quad (2)$$

where L, R and I denote for the left, right boundaries and inner nodes of the substructure as shown in Figure 1. Then, we can reduce the inner nodes \mathbf{q}_I of the cell from the first

row of equation (2) and we obtain

$$\begin{bmatrix} \mathbf{D}_{LI}\mathbf{F}_I \\ \mathbf{D}_{RI}\mathbf{F}_I \end{bmatrix} + \begin{bmatrix} \mathbf{D}_{LL} & \mathbf{D}_{LR} \\ \mathbf{D}_{RL} & \mathbf{D}_{RR} \end{bmatrix} \begin{bmatrix} \mathbf{q}_L \\ \mathbf{q}_R \end{bmatrix} = \begin{bmatrix} \mathbf{F}_L \\ \mathbf{F}_R \end{bmatrix} \quad (3)$$

where

$$\begin{aligned} \mathbf{D}_{LL} &= \tilde{\mathbf{D}}_{LL} - \tilde{\mathbf{D}}_{LI}\tilde{\mathbf{D}}_{II}^{-1}\tilde{\mathbf{D}}_{IL} & \mathbf{D}_{LR} &= \tilde{\mathbf{D}}_{LR} - \tilde{\mathbf{D}}_{LI}\tilde{\mathbf{D}}_{II}^{-1}\tilde{\mathbf{D}}_{IR} \\ \mathbf{D}_{RL} &= \tilde{\mathbf{D}}_{RL} - \tilde{\mathbf{D}}_{RI}\tilde{\mathbf{D}}_{II}^{-1}\tilde{\mathbf{D}}_{IL} & \mathbf{D}_{RR} &= \tilde{\mathbf{D}}_{RR} - \tilde{\mathbf{D}}_{RI}\tilde{\mathbf{D}}_{II}^{-1}\tilde{\mathbf{D}}_{IR} \\ \mathbf{D}_{LI} &= \tilde{\mathbf{D}}_{LI}\tilde{\mathbf{D}}_{II}^{-1} & \mathbf{D}_{RI} &= \tilde{\mathbf{D}}_{RI}\tilde{\mathbf{D}}_{II}^{-1} \end{aligned} \quad (4)$$

We see that equation (3) presents a relation between the loads and displacements at the left and right boundaries of a cell. This equation contains a term of \mathbf{F}_I which is zero when the substructure has non external loads.

1.2 Boundary conditions

We denote (n) for the substructure number n in the track interval. For the two consecutive substructures, the right boundary of (n) is the left boundary of $(n+1)$. Therefore, we have

$$\begin{aligned} \mathbf{q}_R^{(n)} &= \mathbf{q}_L^{(n+1)} \\ \mathbf{F}_R^{(n)} + \mathbf{F}_L^{(n+1)} &= \mathbf{F}_{\partial R}^{(n)} \end{aligned} \quad (5)$$

where $\mathbf{F}_{\partial R}^{(n)}$ is the external load at the right boundary R of the substructure (n) . By combining equations (3) and (5), we obtain

$$\begin{bmatrix} \mathbf{q}_L^{(n+1)} \\ -\mathbf{F}_L^{(n+1)} \end{bmatrix} = \begin{bmatrix} \mathbf{D}_{qI}\mathbf{F}_I^{(n)} \\ \mathbf{D}_{fI}\mathbf{F}_I^{(n)} - \mathbf{F}_{\partial R}^{(n)} \end{bmatrix} + \mathbf{S} \begin{bmatrix} \mathbf{q}_L^{(n)} \\ -\mathbf{F}_L^{(n)} \end{bmatrix} \quad (6)$$

where

$$\mathbf{S} = \begin{bmatrix} -\mathbf{D}_{LR}^{-1}\mathbf{D}_{LL} & -\mathbf{D}_{LR}^{-1} \\ \mathbf{D}_{RL} - \mathbf{D}_{RR}\mathbf{D}_{LR}^{-1}\mathbf{D}_{LL} & -\mathbf{D}_{RR}\mathbf{D}_{LR}^{-1} \end{bmatrix}, \quad (7)$$

and

$$\begin{bmatrix} \mathbf{D}_{qI} \\ \mathbf{D}_{fI} \end{bmatrix} = \begin{bmatrix} -\mathbf{D}_{LR}^{-1}\mathbf{D}_{LI} \\ \mathbf{D}_{RI} - \mathbf{D}_{RR}\mathbf{D}_{LR}^{-1}\mathbf{D}_{LI} \end{bmatrix} \quad (8)$$

We can rewrite equation (6) as follows

$$\mathbf{u}^{(n+1)} = \mathbf{S}\mathbf{u}^{(n)} + \mathbf{b}^{(n)} \quad (9)$$

where

$$\mathbf{u}^{(n)} = \begin{bmatrix} \mathbf{q}_L^{(n)} \\ -\mathbf{F}_L^{(n)} \end{bmatrix}, \quad \mathbf{b}^{(n)} = \begin{bmatrix} \mathbf{D}_{qI}\mathbf{F}_I^{(n)} \\ \mathbf{D}_{fI}\mathbf{F}_I^{(n)} - \mathbf{F}_{\partial R}^{(n)} \end{bmatrix} \quad (10)$$

Equation (9) presents a relation between DOF (displacements and loads) of a substructure (n) and its next substructures $(n+1)$. Here $\mathbf{b}^{(n)}$ presents the external loads on the substructure (n) (hence, when the substructure is free, $\mathbf{b}^{(n)} = 0$). For a series

of substructures, this equation presents a geometric series which can be reduced to the following results

$$\mathbf{u}^{(n)} = \mathbf{S}^n \mathbf{u}^{(0)} + \sum_{k=1}^n \mathbf{S}^{n-k} \mathbf{b}^{(k-1)} \quad (11)$$

$$\mathbf{u}^{(0)} = \mathbf{S}^n \mathbf{u}^{(-n)} + \sum_{k=0}^{n-1} \mathbf{S}^k \mathbf{b}^{(-k)} \quad (12)$$

Equations (11) and (12) give the relations of the responses at the substructure (n) and $(-n)$ respectively, and the response at the reference origin. Note that the origin can be placed at any substructure because the railway track is periodic.

1.3 Load of a train

The load of a train applying on one period (n) of the track is presented by a dynamic force $f_n(x, t)$ with x is local position and t is the time. In the frequency domain, when using the finite element method, the nodal load on the rail at the period n in the moving reference is presented by $\mathbf{f}_n(\omega)$. In the fixed reference, the load on the period (n) is presented by $f_n(x, t + \frac{nl}{v})$ with l is the length of one period and v is the train speed. Thus, the nodal load in the frequency domain is given by

$$\mathbf{F}_*^{(n)}(\omega) = e^{i\omega \frac{nl}{v}} \mathbf{f}_*^{(n)}(\omega) \quad (13)$$

where \mathbf{F}_* can be \mathbf{F}_I or $\mathbf{F}_{\partial R}$. We see that when the train load is stable, $\mathbf{f}_*^{(n)}(\omega)$ does not depend on n and the load on all period has the same spectrum but different phases given by the first term $e^{i\omega \frac{nl}{v}}$.

Bounded conditions: We suppose that the train move on an limited interval of the track and therefore, the track response at infinity are bounded

$$\lim_{n \rightarrow \pm\infty} \{\mathbf{q}^{(n)}, \mathbf{F}^{(n)}\} \text{ are bounded} \quad (14)$$

2 WAVE DECOMPOSITION

2.1 Calculation of wave base

We will now calculate the eigenvalues and eigenvectors $\{\mu_j, \phi_j\}_j$ of the matrix \mathbf{S} given by equation (9). By definition, we have

$$\mathbf{S}\phi_j = \mu_j \phi_j \quad (15)$$

Due to the symplectic nature of the matrix \mathbf{S} , we consider the eigenproblem of the transformation $\mathbf{S} + \mathbf{S}^{-1}$ which yields eigenvalues of the form $\lambda_j = \mu_j + 1/\mu_j$ given by [9]

$$\left[\left(\mathbf{N}' \mathbf{J} \mathbf{L}'^T + \mathbf{L}' \mathbf{J} \mathbf{N}'^T \right) - \lambda_j \mathbf{L}' \mathbf{J} \mathbf{L}'^T \right] \mathbf{z}_j = 0 \quad (16)$$

where

$$\mathbf{L}' = \begin{bmatrix} \mathbf{0} & \mathbf{I}_n \\ \mathbf{D}_{LR} & \mathbf{0} \end{bmatrix}, \quad \mathbf{N}' = \begin{bmatrix} \mathbf{D}_{RL} & \mathbf{0} \\ -(\mathbf{D}_{LL} + \mathbf{D}_{RR}) & -\mathbf{I}_n \end{bmatrix}, \quad \mathbf{J} = \begin{bmatrix} \mathbf{0} & \mathbf{I}_n \\ -\mathbf{I}_n & \mathbf{0} \end{bmatrix} \quad (17)$$

Thereafter, each pair of eigenvalues (μ_j, μ_j^*) can be computed analytically by the quadratic equation $(x^2 - \lambda_j x + 1 = 0)$. Also, the eigenvectors corresponding to these eigenvalues are computed by the closed-form expressions

$$\phi_j = \begin{bmatrix} \mathbf{I}_n & \mathbf{0} \\ \mathbf{D}_{RR} & \mathbf{I}_n \end{bmatrix} \mathbf{w}'_j, \quad \phi_j^* = \begin{bmatrix} \mathbf{I}_n & \mathbf{0} \\ \mathbf{D}_{RR} & \mathbf{I}_n \end{bmatrix} \mathbf{w}'_{j^*} \quad (18)$$

where $\mathbf{w}'_j = \mathbf{J}(\mathbf{L}'^T - \mu_j^* \mathbf{N}'^T) \mathbf{z}_j$ and $\mathbf{w}'_{j^*} = \mathbf{J}(\mathbf{L}'^T - \mu_j \mathbf{N}'^T) \mathbf{z}_j$.

If we note $\Phi = [\phi_1 \cdots \phi_n]$ and $\Phi^* = [\phi_1^* \cdots \phi_n^*]$, we have a wave base $\{\Phi, \Phi^*\}$ of the transformation \mathbf{S} . We can also separate the components of the wave base corresponding to \mathbf{q}, \mathbf{F} as follows

$$\Phi = \begin{bmatrix} \Phi_q \\ \Phi_F \end{bmatrix}, \quad \Phi^* = \begin{bmatrix} \Phi_q^* \\ \Phi_F^* \end{bmatrix} \quad (19)$$

Orthogonality and normalisation: the wave base is symplectic orthogonal in the meaning of $\phi_j^T \mathbf{J} \phi_i = \phi_j^{*T} \mathbf{J} \phi_i^* = 0$ ($\forall i, j$) and $\phi_j^{*T} \mathbf{J} \phi_i = \phi_j^T \mathbf{J} \phi_i^* = 0$ ($\forall i \neq j$) (see [9]). However, the base is not normalized automatically after computation of the eigenproblem. We can calculate the weighting matrix as follows

$$\begin{aligned} \Psi &= \Phi^{*T} \mathbf{J} \Phi = \Phi_q^{*T} \Phi_F - \Phi_F^{*T} \Phi_q \\ \Psi^* &= \Phi^T \mathbf{J} \Phi^* = \Phi_q^T \Phi_F^* - \Phi_F^T \Phi_q^* \end{aligned} \quad (20)$$

The matrices Ψ, Ψ^* are diagonal and satisfying $\Psi^* = -\Psi^T$. Thus, we can normalize the wave base by calculating a matrix $\mathbf{T} = \Psi^{1/2}$ where \mathbf{T} is a diagonal matrix with the diagonal equals to the square root of the diagonal of Ψ . The normalized wave base is presented by $\Phi \mathbf{T}$ and $\Phi^* \mathbf{T}$.

2.2 Wave decomposition

We can decompose each vector of equation (9) in this wave base as follows

$$\begin{aligned} \mathbf{u}^{(n)} &= \Phi \mathbf{Q}^{(n)} - \Phi^* \mathbf{Q}^{*(n)} \\ \mathbf{b}^{(n)} &= \Phi \mathbf{Q}_E^{(n)} - \Phi^* \mathbf{Q}_E^{*(n)} \end{aligned} \quad (21)$$

where $\mathbf{Q}^{(n)}, \mathbf{Q}^{*(n)}$ are the wave amplitudes of $\mathbf{u}^{(n)}$ and $\mathbf{Q}_E^{(k)}, \mathbf{Q}_E^{*(k)}$ are the wave amplitudes of the external loads on the intermediate substructures $\mathbf{b}^{(n)}$.

Remark: the wave decomposition in equation (21) is different to usual expression for WFE by the minus sign on the right to left waves. The advantage of this expression is that we can calculate directly the wave amplitudes by using the symplectic orthogonality of the wave base as the following

$$\begin{aligned} \mathbf{Q}^{(n)} &= \Phi^{*T} \mathbf{J} \mathbf{u}^{(n)}, & \mathbf{Q}^{*(n)} &= \Phi^T \mathbf{J} \mathbf{u}^{(n)} \\ \mathbf{Q}_E^{(n)} &= \Phi^{*T} \mathbf{J} \mathbf{b}^{(n)}, & \mathbf{Q}_E^{*(n)} &= \Phi^T \mathbf{J} \mathbf{b}^{(n)} \end{aligned} \quad (22)$$

By substituting equation (10) into equation (22), we obtain

$$\begin{aligned}\Phi^{*T} \mathbf{J} \mathbf{b}^{(n)} &= (\Phi_q^{*T} \mathbf{D}_{fI} - \Phi_F^{*T} \mathbf{D}_{qI}) \mathbf{F}_I^{(k)} - \Phi_q^{*T} \mathbf{F}_{\partial R}^{(k)} \\ \Phi^T \mathbf{J} \mathbf{b}^{(n)} &= (\Phi_q^T \mathbf{D}_{fI} - \Phi_F^T \mathbf{D}_{qI}) \mathbf{F}_I^{(k)} - \Phi_q^T \mathbf{F}_{\partial R}^{(k)}\end{aligned}\quad (23)$$

In addition, we have the relation between the Φ_q and Φ_F as follows (see [?])

$$\begin{aligned}\Phi_F &= \mathbf{D}_{RR} \Phi_q + \mathbf{D}_{RL} \Phi_q \mu^* = -(\mathbf{D}_{LL} \Phi_q + \mathbf{D}_{LR} \Phi_q \mu) \\ \Phi_F^* &= \mathbf{D}_{RR} \Phi_q^* + \mathbf{D}_{RL} \Phi_q^* \mu = -(\mathbf{D}_{LL} \Phi_q^* + \mathbf{D}_{LR} \Phi_q^* \mu^*)\end{aligned}\quad (24)$$

By combining equations (22) and (23) into equation (24), we obtain

$$\begin{aligned}\mathbf{Q}_E^{(k)} &= \left[(\mu \Phi_q^{*T} \mathbf{D}_{LI} + \Phi_q^{*T} \mathbf{D}_{RI}) \mathbf{F}_I^{(k)} - \Phi_q^{*T} \mathbf{F}_{\partial R}^{(k)} \right] \\ \mathbf{Q}_E^{*(k)} &= \left[(\mu^* \Phi_q^T \mathbf{D}_{LI} + \Phi_q^T \mathbf{D}_{RI}) \mathbf{F}_I^{(k)} - \Phi_q^T \mathbf{F}_{\partial R}^{(k)} \right]\end{aligned}\quad (25)$$

Equation (25) show that the wave amplitude of external loads on one substructure can be calculated directly from its loads and it does not depend on the other substructures.

Now we will calculate the amplitude from the wave amplitudes $\{\mathbf{Q}^{(n)}, \mathbf{Q}^{*(n)}\}$. By replacing equation (21) with $n = 0$ into equation (11), we obtain

$$\mathbf{u}^{(n)} = \Phi \mathbf{Q}^{(n)} - \Phi^* \mathbf{Q}^{*(n)} = \Phi \mu^n \mathbf{Q} - \Phi^* \mu^{*n} \mathbf{Q}^* + \sum_{k=1}^n \Phi \mu^{n-k} \mathbf{Q}_E^{(k)} - \Phi^* \mu^{*n-k} \mathbf{Q}_E^{*(k)} \quad (26)$$

Then, by substituting equation (22) into the aforementioned equation, we obtain

$$\begin{aligned}\mathbf{Q}^{(n)} &= \mu^n \left(\mathbf{Q} + \sum_{k=1}^n \mu^{*k} \mathbf{Q}_E^{(k)} \right) \\ \mathbf{Q}^{*(n)} &= \mu^{*n} \left(\mathbf{Q}^* + \sum_{k=1}^n \mu^k \mathbf{Q}_E^{*(k)} \right)\end{aligned}\quad (27)$$

In a similar way, by combining equations (21) into equation (12), we obtain the following result

$$\begin{aligned}\mathbf{Q}^{(-n)} &= \mu^{*n} \left(\mathbf{Q} - \sum_{k=0}^{n-1} \mu^k \mathbf{Q}_E^{(-k)} \right) \\ \mathbf{Q}^{*(-n)} &= \mu^n \left(\mathbf{Q}^* - \sum_{k=0}^{n-1} \mu^{*k} \mathbf{Q}_E^{*(-k)} \right)\end{aligned}\quad (28)$$

Equations (27) and (28) present the relations between the wave amplitudes of the external loads and the amplitudes $\{\mathbf{Q}, \mathbf{Q}^*\}$ of $\mathbf{u}^{(0)}$. In the next section, we will develop the wave analysis by using this result and the boundary condition for an infinite periodic track.

3 ANALYSIS OF A COMPLETE RAILWAY TRACK

3.1 Response of an infinite periodic railway track

We consider a railway without defects as show in Figure 1. The track is an infinite periodic structure subjected to moving dynamic loads which can be different from one period to another. We will find the response by using the bounded condition.

By substituting equations (27) and (28) into equation (21), we obtain

$$\begin{aligned} \mathbf{u}^{(n)} &= \Phi \boldsymbol{\mu}^n \left(\mathbf{Q} + \sum_{k=1}^n \boldsymbol{\mu}^{*k} \mathbf{Q}_E^{(k)} \right) - \Phi^* \boldsymbol{\mu}^{*n} \left(\mathbf{Q}^* + \sum_{k=1}^n \boldsymbol{\mu}^k \mathbf{Q}_E^{*(k)} \right) \\ \mathbf{u}^{(-n)} &= \Phi \boldsymbol{\mu}^{*n} \left(\mathbf{Q} - \sum_{k=0}^{n-1} \boldsymbol{\mu}^k \mathbf{Q}_E^{(-k)} \right) - \Phi^* \boldsymbol{\mu}^n \left(\mathbf{Q}^* - \sum_{k=0}^{n-1} \boldsymbol{\mu}^{*k} \mathbf{Q}_E^{*(-k)} \right) \end{aligned} \quad (29)$$

For a damped structure, $\|\boldsymbol{\mu}\| < 1$ and $\|\boldsymbol{\mu}^*\| > 1$ (see [8]). Therefore, we have $\boldsymbol{\mu}^n \rightarrow 0$ and $\boldsymbol{\mu}^{*n} \rightarrow \infty$ when n tends to infinity. Therefore, in order to get $\mathbf{u}^{(n)}$ and $\mathbf{u}^{(-n)}$ in equation (29) satisfying the bounded condition (14), the coefficients corresponding to $\boldsymbol{\mu}^{*n}$ must tend to zeros when $n \rightarrow \infty$. That means

$$\mathbf{Q} = \sum_{k=0}^{\infty} \boldsymbol{\mu}^k \mathbf{Q}_E^{(-k)}, \quad \mathbf{Q}^* = - \sum_{k=1}^{\infty} \boldsymbol{\mu}^k \mathbf{Q}_E^{*(k)} \quad (30)$$

By substituting the aforementioned equation into equation (21) with $n = 0$, we obtain

$$\begin{aligned} \mathbf{q}^{(0)} &= \Phi_q \sum_{k=0}^{\infty} \boldsymbol{\mu}^k \mathbf{Q}_E^{(-k)} + \Phi_q^* \sum_{k=1}^{\infty} \boldsymbol{\mu}^k \mathbf{Q}_E^{*(k)} \\ \mathbf{F}^{(0)} &= \Phi_F \sum_{k=0}^{\infty} \boldsymbol{\mu}^k \mathbf{Q}_E^{(-k)} + \Phi_F^* \sum_{k=1}^{\infty} \boldsymbol{\mu}^k \mathbf{Q}_E^{*(k)} \end{aligned} \quad (31)$$

Equation (31) is the expression of the response of the substructure at $n = 0$. For the others substructures $n \neq 0$, we can calculate the response by using equation (29). There is another way to calculate the responses $\mathbf{u}^{(n)}$ by translating the reference origin and using again the formulation (31).

3.2 Remarks

- We see that the response $\mathbf{u}^{(0)}$ is the combination of two terms corresponding to the sum of left and right waves generated by the external forces from the two sides. If the structure is subjected by an external load at only one side of a period, the expressions in equation (31) have only one term and the eigenvalue $\boldsymbol{\mu}$ is exactly the rate of the wave amplitudes between the left and right boundary of one period. Therefore, the eigenvalues $\boldsymbol{\mu}$ plays a role as a **structural damping factor** of a periodic structure.

Table 1: Parameters of a periodically supported beam

Rail section mass (ρS)	kg/m	60
Rail stiffness (EI)	MNm ²	6.3
Distance of sleepers (l)	m	0.6
Block mass (M)	kg	100
Damping factor of rail pad (η_1)	MNsm ⁻¹	1.97
Stiffness of rail pad (k_1)	MNm ⁻¹	192
Damping coeff. under support (η_2)	MNsm ⁻¹	0.17
Stiffness under support (k_2)	MNm ⁻¹	26.4

- This method does not need to inverse any matrix, the responses can be calculated directly from the wave decompositions. Therefore, we have reduced the DOF of all structure to only one substructure.
- When the moving load is the same for all substructure, by combining equations (13) and (25) we obtain

$$\mathbf{Q}_E^{*(n)} = e^{i\omega \frac{nl}{v}} \mathbf{Q}_E^{*(0)}, \quad \mathbf{Q}_E^{(k)} = e^{i\omega \frac{nl}{v}} \mathbf{Q}_E^{(0)} \quad \forall n \quad (32)$$

In addition, $\boldsymbol{\mu}$ is a diagonal matrix, we can use a formula of the geometric series $\sum_{k=0}^{\infty} (a\boldsymbol{\mu})^k = \frac{1}{1-a\boldsymbol{\mu}}$ provided that $\|a\boldsymbol{\mu}\| < 1$ (this is a diagonal matrix with the values calculated by the formulas in the expression). Therefore, we can rewritten equation (31) as follows

$$\begin{aligned} \mathbf{q}^{(0)} &= \Phi_q \frac{1}{1 - \boldsymbol{\mu} e^{-i\omega \frac{l}{v}}} \mathbf{Q}_E^{(0)} + \Phi_q^* \frac{\boldsymbol{\mu} e^{i\omega \frac{l}{v}}}{1 - \boldsymbol{\mu} e^{i\omega \frac{l}{v}}} \mathbf{Q}_E^{*(0)} \\ \mathbf{F}^{(0)} &= \Phi_F \frac{1}{1 - \boldsymbol{\mu} e^{-i\omega \frac{l}{v}}} \mathbf{Q}_E^{(0)} + \Phi_F^* \frac{\boldsymbol{\mu} e^{i\omega \frac{l}{v}}}{1 - \boldsymbol{\mu} e^{i\omega \frac{l}{v}}} \mathbf{Q}_E^{*(0)} \end{aligned} \quad (33)$$

- We can decompose the real loads of a train into dynamic and statique loads. Because the statique loads are constant, we can apply the formula (33) for this term and then apply the formula (31) for the dynamic loads.

4 NUMERICAL APPLICATIONS

Consider a periodically supported beam subjected to a constant moving load as shown in Figure 2, where the rail is modeled by Euler-Bernoulli beam and the support systems are the mass-springs. The beam is subjected to a constant moving load $Q = 100kN$. The parameters of the railway track are given in Table 1. Now we will compare the analytic solution [6] and the numerical method. From the finite element method with element type B21 in Abaqus, we obtain the dynamic stiffness matrix of the beam for one period of length l . In order to take into account the supports, we add the support dynamic stiffness into the beam stiffness matrix at the term in the diagonal corresponding to the DOF of the contact point between the beam and the spring-mass. Figure 3 shows a comparison

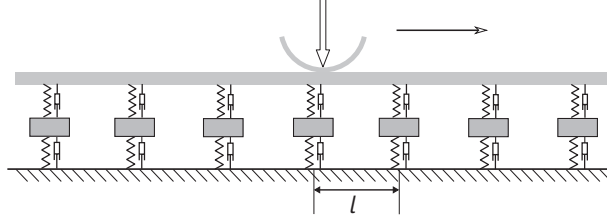


Figure 2: Periodically supported beam subjected to a moving load

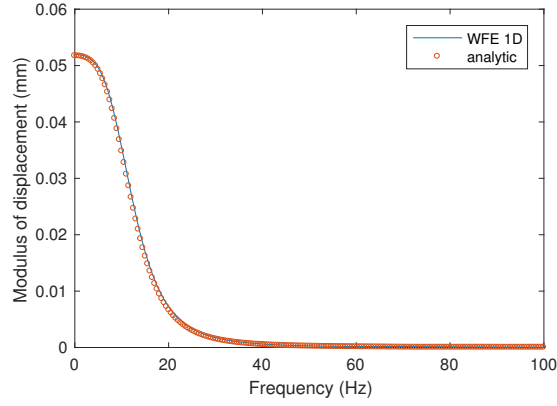


Figure 3: Response of the periodically supported beam by the analytical and numerical methods

of the analytic and numerical results with element B21 of size 1cm in Abaqus. In this example, the calculation times of the numerical method is almost the same time of the analytical method. We note that this result is for an infinite beam for the both two methods and it does not exist for the classical FEM. In addition, Figure 4 presents the structural damping factor μ .

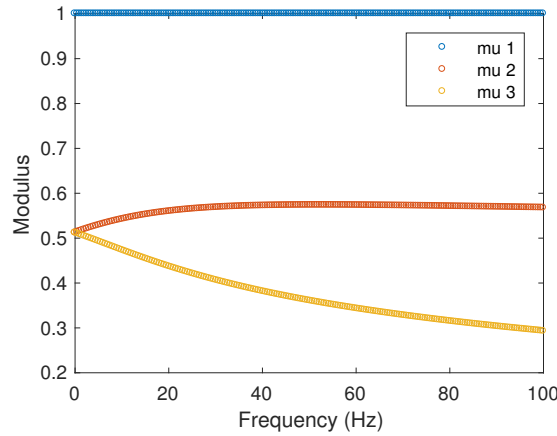


Figure 4: Structural damping factor of a railway track

Moreover, the numerical method permits to calculate the response of the track subjected to dynamic forces as shown in Figure 5. Here we consider a random dynamic force occurs at one point on the track with an amplitude $Q_{dyna} = 100\text{kN}$ in an frequency bandwidth $[25 - 50]\text{Hz}$. The track response is the sum of the response to the static load calculated by equation (33) and the dynamic load calculated by equation (31).

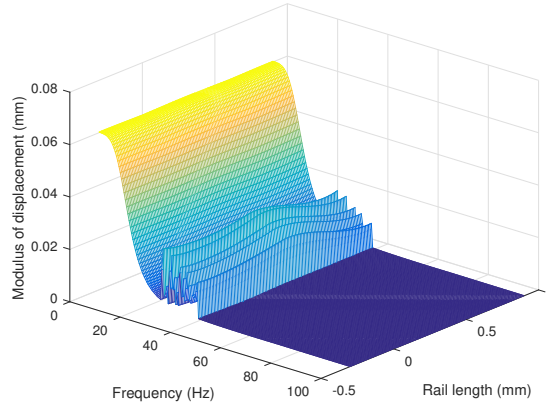


Figure 5: Response of the track to a dynamic load

Now we consider an example of a non-ballasted railway track where the supports contains a rail pad, a concrete block and an elastic pad under the block. All the component of the support and the concrete slab are simulated by the element finit method with the mesh shown in Figure 6. In this model, we have 16.075 elements C3D8R. The base of the slab is fixed and the track is subjected by moving force $Q = 100\text{kN}$ at a row of nodes on the rail.

Figure 7 presents the response of the loaded point by WFE for beam and 3D models and the analytic result. The calculation time for 3D model is 21.6h and for other model is about 0.2s. We see that the responses by different methods are coherent. The 3D model response has noise because it cause by the error of the eigenvalue calculation.

5 CONCLUSION

By using the wave finite element method, we demonstrate that the wave amplitude at the boundary of one period of the track can be represented by a sum of the wave amplitude which corresponds to the moving loads. This characteristics comes from the bounded condition of the infinite periodic structure. This method permits to reduce the DOF of the railway track to only one track period while remaining all the dynamic load.

REFERENCES

- [1] D.J. Mead, Free wave propagation in periodically supported, infinite beams, J. Sound Vib. 11 (2) (1970) 181–197.

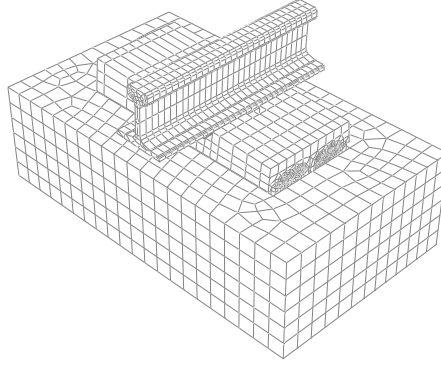


Figure 6: Example of a non-ballasted railway track

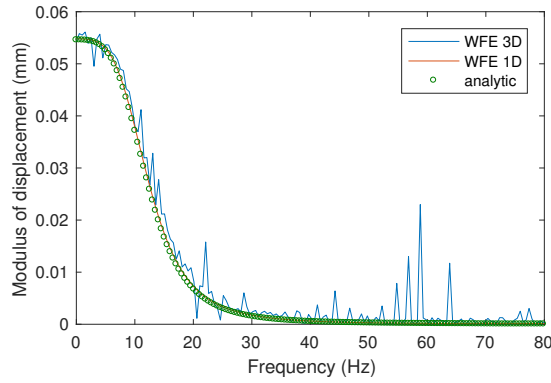


Figure 7: Response of the track subjected to a dynamic load

- [2] D.J. Mead, Wave propagation in continuous periodic structures: research contributions from Southampton, *J. Sound Vib.* 190 (3) (1996) 495–524.
- [3] A.V. Metrikine, K. Popp, Vibration of a periodically supported beam on an elastic half-space, *Eur. J. Mech. A/Solid* 18 (1999) 679–701.
- [4] A.V. Vostroukhov, A. Metrikine, Periodically supported beam on a visco-elastic layer as a model for dynamic analysis of a high-speed railway track, *Int. J. Solids Struct.* 40 (2003) 5723–5752.
- [5] P.M. Belotserkovskiy, On the oscillation of infinite periodic beams subjected to a moving concentrated force, *J. Sound Vib.* 193 (3) (1996) 705–712.
- [6] Hoang, T. and Duhamel, D. and Foret, G. and Yin, H. P. and Joyez, P. and Caby, R., Calculation of force distribution for a periodically supported beam subjected to moving loads, *Journal of Sound and Vibration* (2017), 388, 327–338,
- [7] Zhong W.X and Willians F. W. On the direct solution of wave propagation for repetitive structures, *J Sound Vib.* (1995), 181(3):485–501.

- [8] Duhamel D., Mace B.R., Brennan M.J. Finite element analysis of the vibrations of waveguides and periodic structures. *J Sound Vib.* (2006), 294(1–2):205–20.
- [9] Mencik J-M, Duhamel D. A wave finite element-based approach for the modeling of periodic structures with local perturbations. *Finite Elem Anal Des* (2016) 121:40–51.
- [10] Mencik J-M, Duhamel D. A wave-based model reduction technique for the description of the dynamic behavior of periodic structures involving arbitrary-shaped substructures and large-sized finite element models. *Finite Elem Anal Des* (2015) 101:1–14.

A Lattice Green Function Method for Atomistic/Continuum Coupling: Theory and Data Sparse Implementation

Max Hodapp^{*}, Guillaume Anciaux^{**}, William Curtin^{***}, Jean-François Molinari^{****}

^{*}Ecole polytechnique fédérale de Lausanne (EPFL), ^{**}Ecole polytechnique fédérale de Lausanne (EPFL), ^{***}Ecole polytechnique fédérale de Lausanne (EPFL), ^{****}Ecole polytechnique fédérale de Lausanne (EPFL)

ABSTRACT

Treating atoms individually in material science applications comes along with high computational cost with increasing simulation size. However, many problems require atomic scale resolution only in small parts of the computational domain to resolve the nonlinear behavior of isolated defects, e.g. crack tips, dislocations, voids etc. Commonly these problems are treated using homogeneous Dirichlet conditions on the outer boundary (or the elastic field of the defect). However, if the Green function of the defect is long range, the problem sample has to be sufficiently large to reach a desired accuracy. In the 1970's Sinclair and co-workers proposed so-called flexible boundary conditions which minimize inhomogeneous forces appearing in the pad domain after each atomistic relaxation by means of lattice Green functions [1]. In its original form the method is of $O(NM)$, where N and M are the number of pad and real atoms, respectively, which becomes quickly unfeasible with increasing problem size. Here, we show that Sinclair's incremental update equation can be shown to be equivalent to a gradient descent iteration with respect to a weighted inner product space which converges to a discrete boundary method (DBM) analog to the boundary integral equation for exterior PDE's. In order to overcome the bottleneck of memory consumption we exploit the fact that the boundary matrices can be represented as hierarchical matrices [2]. Starting from the coupled atomistic/DBM problem we construct a fast and memory efficient monolithic solver which we have integrated into the open source atomistic code LAMMPS. We outline the efficiency of the proposed method for various test cases. We have recently proposed a simplified solution procedure for a novel coupled atomistic and discrete dislocation method in 3d by detecting dislocations in the entire atomistic system and subsequently using the displacement field of the complete dislocation network as a boundary condition for the atomistic problem [3]. While being accurate and simple to implement, this method is impracticable for general problems involving other types of defects. With our new DBM it becomes possible to embed moderately large atomistic domains in infinite continua. We present numerical examples for a hybrid dislocation bow-out in an (effectively) infinite medium. References [1] Sinclair, J. E. et al.: Flexible boundary conditions and nonlinear geometric effects in atomic dislocation modeling. JAP, 1978 [2] Bebendorf, M.: Hierarchical matrices. Springer, 2009 [3] Hodapp, M. et al.: Coupled atomistic/discrete dislocation method in 3D part II: Validation of the method. JMPS (submitted), 2017

Forecasting Sea Ice Movement in the Arctic Basin Using the Discrete Element Method

Taylor Hodgdon^{*}, Arnold Song^{**}, Matthew Parno^{***}, Brendan West^{****}, Devin O'Connor^{*****}

^{*}Cold Regions Research & Engineering Laboratory, ^{**}Cold Regions Research & Engineering Laboratory, ^{***}Cold Regions Research & Engineering Laboratory, ^{****}Cold Regions Research & Engineering Laboratory, ^{*****}Cold Regions Research & Engineering Laboratory

ABSTRACT

The global climate is rapidly changing and is especially amplified in the Arctic due to the diminishing sea ice cover. As the Arctic warms and conditions change, the assumptions and mechanical models that govern the forecast tools are also changing. The majority of current sea ice models use a continuum approach that typically use constitutive models that homogenize and parameterize processes that occur over relatively short length scales. For example, pressure ridges and fractures typically have widths on the order of tens of meters, in contrast to grid length scales on the order of kilometers in most sea ice models. We present work that uses the discrete element method (DEM) to examine mechanical processes, such as pressure ridging, at appropriate length scales using realistic floe geometries with spatially varying mechanical properties. This model, coupled with a workflow to assimilate remotely sensed data allows us to better estimate sea ice parameters and improve larger scale model parameterizations.

Continued Evolution of a Part-scale Finite Element Model for Selective Laser Melting at LLNL

Neil Hodge^{*}, Rishi Ganeriwala^{**}, Robert Ferencz^{***}

^{*}Lawrence Livermore National Laboratory, ^{**}Lawrence Livermore National Laboratory, ^{***}Lawrence Livermore National Laboratory

ABSTRACT

Selective Laser Melting (SLM) is a manufacturing process which can realize significant benefits over traditional manufacturing processes, including significantly shortened time between design and manufacture of parts, and the ability to create parts with much more geometric complexity than has previously been tenable, or in some cases, even possible. However, the extreme sensitivity of the results to input parameters results in a process that is difficult to predict, and thus control. Indeed, it is not uncommon for the resulting parts to vary significantly from the desired geometry, and have associated residual stresses, due to the influence of extreme and inhomogeneous thermal gradients. The SLM process is difficult to model for several reasons, including the complex, dynamic physical phenomena, as well as its severely multiscale character. The current presentation will describe ongoing work within the parallel, implicit finite element code Diablo, toward several goals: (1) addition of new, and improvement of existing, physics, and (2) improvement of the throughput of simulations, while simultaneously keeping degradation of the solution accuracy to a minimum.

A New Class of Generalized Finite Element Spaces for Problems with Immersed Interfaces

Susanne Hoellbacher*, Gabriel Wittum**

*ECRC, King Abdullah University of Science and Technology, **ECRC, King Abdullah University of Science and Technology

ABSTRACT

For applications like multiphase flow, free surface flow or diffusion problems with discontinuous density, interface forces or fluxes arise on free boundaries and the location of the boundary changes in time. Instead of mesh adaptation or the introduction of artificial forces we follow the idea of adapted finite element spaces on elements cut by the immersed interface. The proposed spaces generalize the idea of balancing fluxes along a surface which essentially characterizes and constitutes a finite volume formulation. The derivation of the generalized spaces is inspired by the Petrov-Galerkin weak formulation of the finite volume method. Within a finite volume formulation the boundary fluxes naturally arise. As a consequence, the derived spaces similarly take the shape of the boundaries directly into account and the proposed spaces are well suited for the imposition of boundary conditions on immersed boundaries. Furthermore, the generalized finite element spaces get employed to the usual continuous Galerkin formulation. Therefore, the discrete system is symmetric and intrinsically stable. In particular, unlike in most DG formulations, there is no need for interior penalization in order to guarantee stability. Finally, we will show that the spaces obey even local conservation laws due to their relation to the finite volume formulation. As numerical examples, we consider diffusion problems and multiphase flow problems such as particle-fluid and gas-fluid mixtures. Regarding the special case of particle-fluid flow, a typical issue are spurious oscillations due to a bad approximation of the pressure near the interface. Our computations show, that the spurious pressure oscillations were eliminated by the new method without having to introduce interior penalty terms. The results therefore demonstrate that the adapted spaces describe the physics of the discrete interface appropriately.

Direct Finite Element Simulation of Turbulence and Unified Continuum Fluid-Structure Interaction

Johan Hoffman^{*}, Johan Jansson^{**}, Niclas Jansson^{***}, Frida Svelander^{****}, Van Dang Nguyen^{*****}, Massimiliano Leoni^{*****}, Niyazi Cem Degirmenci^{*****}, Ezhilmathi Krishnasamy^{*****}

^{*}KTH, ^{**}KTH/BCAM, ^{***}KTH, ^{****}KTH, ^{*****}KTH, ^{*****}KTH/BCAM, ^{*****}KTH/BCAM, ^{*****}BCAM

ABSTRACT

We present recent advances in methodology and applications of our framework for simulation of turbulent flow and fluid-structure interaction. On the foundation of stabilized finite element methods and a posteriori error estimation, we have developed an approach to turbulence simulation where no model resolution is set a priori and unresolved scales are not explicitly modelled, but instead the resolution of the model is determined as part of the simulation by adaptive mesh refinement and the finite element approximation converges to a weak solution of the Navier-Stokes equations with respect to selected functionals, such as lift and drag in an application of aerodynamics, for example [1]. In this talk we present new developments with regards to the underlying mathematical theory, a posteriori error estimation, and the mesh adaption algorithms, in particular with respect to high performance computing. We also present recent advances of the monolithic approach to fluid-structure interaction we have developed, where the fundamental conservation laws are formulated for the unified continuum of all phases in the problem, which leads to a robust method for fluid-structure interaction, including contact mechanics. The methods are implemented in the open source software FEniCS-HPC [2], and we present new results from applications in flight aerodynamics, wind turbines, and patient-specific heart simulations [3]. References [1] J. Hoffman, J. Jansson, N. Jansson, R. Vilela De Abreu, Towards a parameter-free method for high Reynolds number turbulent flow simulation based on adaptive finite element approximation, *Comput. Meth. Appl. Mech. Engrg.*, Vol.288, pp.60-74, 2015. [2] J.Hoffman, J.Jansson, N.C.Degirmenci, J.H.Spühler, R.V.De Abreu, N.Jansson, A.Larcher, FEniCS-HPC: Coupled Multiphysics in Computational Fluid Dynamics, Jülich Aachen Research Alliance (JARA) High-Performance Computing Symposium, Springer, pp.58—69, 2016. [3] D.Larsson, J.Hiromi Spühler, S.Petersson, T.Nordenfur, M.Colarieti-Tosti, J.Hoffman, R.Winter, M.Larsson, Patient-specific left ventricular flow simulations from transthoracic echocardiography: robustness evaluation and validation against Ultrasound Doppler and Magnetic Resonance Imaging, *IEEE Trans Med Imaging*, 2017.

Physiological and Pathological Cortical Thickness Variations

Maria Holland^{*}, Antonio Hardan^{**}, Alain Goriely^{***}, Ellen Kuhl^{****}

^{*}University of Notre Dame, ^{**}Stanford University, ^{***}University of Oxford, ^{****}Stanford University

ABSTRACT

The brains of humans and many other mammals are characterized by deep wrinkles and folds in the surface layer, the cortex. The thickness of this cortical layer is an important biomarker for a wide variety of neurological disorders, and alterations in cortical thickness have been associated with neurodevelopmental disorders including epilepsy, schizophrenia, and Autism Spectrum Disorders (ASD) [1]. However, cortical thickness is significantly heterogeneous throughout the brain, featuring a marked regional asymmetry, with thicker peaks (called gyri) and thinner valleys (called sulci). It has been suggested that this is the result of localized heterogeneities in growth, but our findings [2] indicate that this thickness difference appears in non-growing materials as well. Here we show that a simple homogeneous bilayered system of a growing layer on an elastic substrate universally bifurcates into a spatially heterogeneous system with thicker peaks and thinner valleys. We present a combined experimental, computational, and analytical approach that illustrates the origin and evolution of this pattern as a consistent instability phenomenon in soft materials, likely related to the strong dependency on boundary conditions and loading in the instability behavior of soft materials [3]. In light of this finding, we use the regional gyral-sulcal cortical thickness ratio as a tool to investigate atypical cortical folding and structure in individuals on the ASD spectrum. Using medical imaging data from the Autism Brain Imaging Data Exchange as well as a study of twins with and without ASD, we analyze differences in cortical thickness variation between diagnosis groups and explore potential biomechanical explanations for the evolution of these patterns. Our findings support previous work suggesting that mechanics plays an important role in the development of the brain, showing that this characteristic pattern of thickness variation in the cortex can be explained at least partly by forces arising during cortical folding. [1] Hardan AY, Muddasani S, Vemulapalli M, Keshavan M, Minshew N (2006) An MRI study of increased cortical thickness in autism. *Am J Psychiatry* 163:1290-1292. [2] Holland MA, Budday S, Li G, Shen D, Goriely A, Kuhl E (2018) Symmetry breaking in the developing brain: Cortical thickness variations emerge from folding. Submitted. [3] Holland MA, Li B, Feng XQ, Kuhl E (2017) Instabilities of soft films on compliant substrates. *J Mech Phys Solids* 98:350-365.

Evaluation of Mesh-Control Techniques for FSI Analysis Handling Large Deformation in Structural and Fluid Domains

Giwon Hong^{*}, Tomonori Yamada^{**}, Naoto Mitsume^{***}, Shinobu Yoshimura^{****}

^{*}The University of Tokyo, ^{**}The University of Tokyo, ^{***}The University of Tokyo, ^{****}The University of Tokyo

ABSTRACT

Fluid-structure interaction (FSI) analysis has been used to clarify design variables related to FSI phenomena. One application is the analysis of flapping motions to improve flapping wing aerodynamics and to design optimized models for micro air vehicles (MAVs) in morphology and kinematics. A flexible wing is deformed nonlinearly during flapping cycles, so it is important to track its surface properly and to get its aerodynamic data accurately in terms of FSI analysis. We have developed the three-dimensional FSI analysis system employing partitioned iterative coupling methods [1], which utilize existing solvers: a parallel FEM flow solver FrontFlow/blue and a parallel FEM structure solver ADVENTURE_Solid. The system successfully analyzed simple flapping motions. To handle a flexible structure is still a challenging issue in FSI analysis, since the large deformation in both structural and fluid domains follows when the structure moves excessively. Consequently, mesh distortion occurs and the degenerated shape of the domains makes FSI analysis failed. Some way such as remeshing might be a good option to continue the analysis. However, we have researched on the analysis depending on initial data in order to maximize the efficiency of parallel computing. In this research, we focus on the way to deal with the deformation of a fluid domain. We aim to make FSI analysis progress by controlling a mesh in a proper way, even if the large deformation and mesh distortion follow. In order to improve the distortion, fluid meshes are partitioned in different ways, and mesh-control techniques such as SEMMT [2] are examined to control those meshes. We also intend to keep the mesh resolution near the interface between two domains. Then, we evaluate the difference of analyses that each mesh-control technique is applied for. Finally, we propose improved mesh-control techniques to contribute the stability of FSI analysis. References [1] T. Yamada, G. Hong, S. Kataoka, S. Yoshimura. Parallel partitioned coupling analysis system for large-scale incompressible viscous fluid-structure interaction problems. *Computers & Fluids*, 141, pp. 259–268, 2016. [2] K. Stein, T.E. Tezduyar, R. Benney. Automatic mesh update with the solid-extension mesh moving technique. *Computer Methods in Applied Mechanics and Engineering*, 193, pp. 2019–2032, 2004.

A HYDROELASTIC ANALYSIS OF A BEAM-CONNECTED MULTI-BODY FLOATING STRUCTURE FOR SOLAR POWER PLANT IN WAVES

SA YOUNG HONG ¹ BYOUNG WAN KIM ² AND HYUN SUNG KIM ³

* Korea Research Institute of Ships & Ocean Engineering (KRISO)
1312-32 Yuseong-daero, Daejeon 34103, South Korea
University of Science & Technology (UST)
217 Gajeong-ro, Daejeon 34113, South Korea
¹sayhong@krios.re.kr; www.kriso.re.kr
²kimbw@krios.re.kr; www.kriso.re.kr
³eegys_zz@krios.re.kr; www.kriso.re.kr

Key words: solar power plant, floating body, connector beam, hydroelastic analysis, frequency-domain analysis, time-domain analysis

Abstract. The hydrodynamic performance of a floating solar energy converter system in waves is analyzed considering elastic behaviors of connector structures in this study. The converter system is composed of hundreds of floating concrete blocks to support photovoltaic modules. The slender elastic connector structure combines the floaters into a large unit system. The floating solar power converter system keeps its position by using mooring system. To assure structural integrity as well as operability of the system in waves, both the frequency-domain and time-domain approaches are adopted to analyze hydroelastic behaviors of the system. In numerical formulation, HOBEM (Higher Order Boundary Element Method) is applied to floating body part and FEM (Finite Element Method) was applied to connector beams and mooring lines. HOBEM is a highly accurate and efficient method in analysis of multi-body hydrodynamic interactions. The frequency domain analysis is powerful in parametric design stage because it provides relatively simple and fast calculations. In specific cases, time domain analysis is required to see the results in detail for transient behavior coupled with mooring lines, and for nonlinear large amplitude and low frequency motion responses due wave drift forces under harsh environments. In the present study, the frequency-domain analysis is implemented which is useful for structural optimization design process while the time domain analyses is implemented useful for extreme structural and mooring responses. In addition to discussions on structural safety of the system, an efficient algorithm for reduction of computational burden considering a few thousand floaters of multiple MW class floating solar power plants is discussed by comparison with a fully direct FEM formulation and Guyan reduction scheme for connector structures as well.

1. INTRODUCTION

Due to recent global climate change, a number of Asian and North American countries are focusing on increasing renewable energy portion for sustainable development of electric power and reduction of CO₂ to suppress global warming. Solar electric power has been emerging as a dominating position, competing with an existing crown chair of wind energy. Both energy resources require a huge area to obtain commercially viable large-scale production. Ironically, those resources induce unwanted environmental pollutions such as noise, views, shade and reflections of sun light, which result in negative effects on the ecology of human and animal worlds. The first simple solution to resolve this problem was to place those facilities at remote area, far from the place with high population of human beings, even though the negative impacts on animal still exist. For photovoltaic electric power generation, the portion of floating solar power generation has been increasing since 2007 due to its advantages coming from using void space. Using void space reduced legal conflicts with nearby residents in view of sociology and enhanced efficiency is possible by virtue of uniformly flat area and cooling effect thanks to surrounding cooling water in terms of technology. There still exists some considerations associated with technical challenge for extension to sea areas beyond inland water surface, in terms of cost down and assurance of safety. Such an advantage is more effective in countries with limited flat and void space such as Korea and Japan. A preliminary study on floating solar power system by Hong et al. (2017) showed positive perspectives on a large scale floating solar power system in the sea region by adopting hydroelastic approach in design and analysis of floaters and supporting frame structures.

Most of ocean renewable energy is affordable only when an appropriate structure is provided for assurance of safety as well as economic efficiency considering characteristics of ocean renewable energy source and environmental conditions of the site.

The floating solar power system can be modelled as a mass-spring-damper system for design and analysis purpose. The system is composed of multiple floaters supporting photovoltaic cells, grillage structures combining multiple floaters into one large unit structure, and mooring system providing restoring forces to keep the position of floating structures within a target location. For huge floating structures, the design concept adopting hydroelasticity is useful for finding an optimal structural solution for assurance of safety under harsh environment as well as economy.

In design of floating solar power system, in many cases, engineers calculate hydrodynamic responses of unit modules for simplicity. However, Hong et al.(2017) found that total module need to be analyzed to get more reliable results because the responses are different as shown in Fig. 1 which was referred from Hong's previous research [1]. As seen in the figure, the response curves show different peak locations and stress levels because the two different sized structure have different mass and spring, which resulted in different natural frequencies and resonant behaviors. This result clearly demonstrated why the whole structure should be analyzed because the analysis result for a small unit gives more conservative estimation than that of the whole structure.

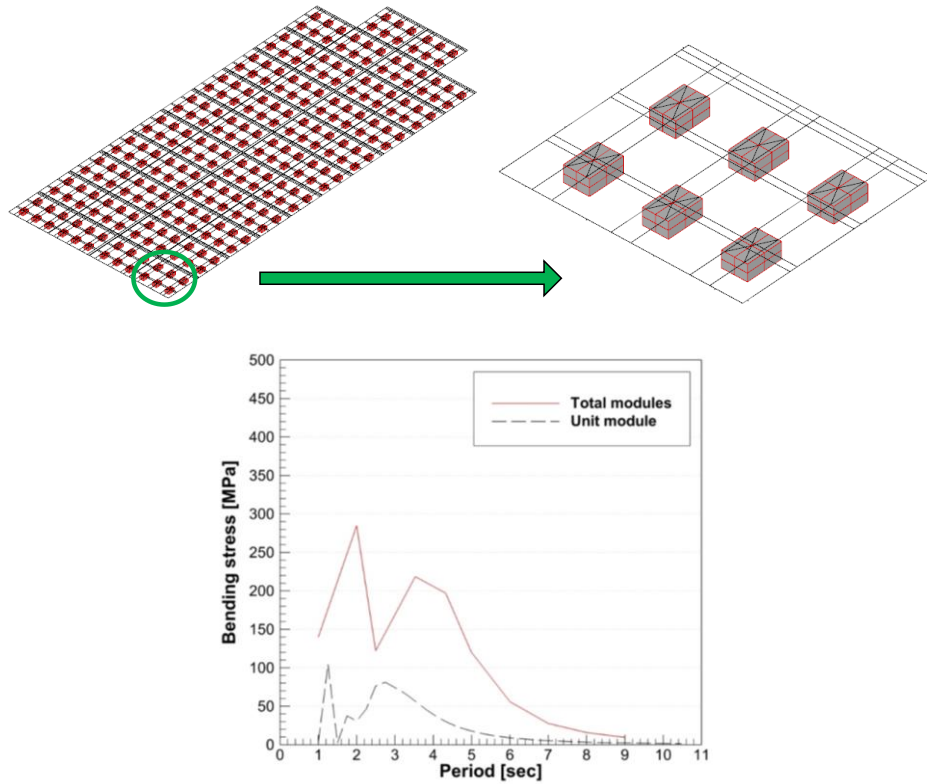


Fig. 1 Comparison of total module and unit module in hydrodynamic responses of floating solar power plant

In the present study, the hydroelastic behaviors of a floating solar energy converter system in waves is analyzed. The converter system is composed of hundreds of floating concrete blocks to support photovoltaic modules. The slender elastic connector structure combines the floaters into a large unit system. Both the frequency-domain and time-domain approaches are implemented in hydroelastic analysis. The frequency domain analysis is powerful in parametric design stage because it provides relatively simple and fast calculations. In specific cases, time domain analysis is required to see the results in detail for transient behavior coupled with mooring lines, and for nonlinear large amplitude and low frequency motion responses due wave drift forces under harsh environments. In this study, frequency-domain and time domain analyses results were compared with each other to verify both results and investigate transient effects and nonlinearity. In addition to discussions on structural safety of the system, an efficient algorithm for reduction of computational burden considering a few thousand floaters of multiple MW class floating solar power plants is discussed by comparison with a fully direct FEM formulation and Guyan reduction scheme for connector structures as well.

2. FLOATING SOLAR POWER PLANT

The developed solar power plant system is comprised of multiple floating bodies and connectors. Floating bodies were made of concrete blocks and they support solar energy generation system on topside. The blocks were connected with steel profile beams and mooring lines are attached to the beams to keep the position. Fig. 2 shows geometric layout of the plant system. Shape of one concrete block and the section shape of the connector beams are shown in Fig. 3. The mechanical properties of floaters, connectors and mooring lines were summarized in Table 1.

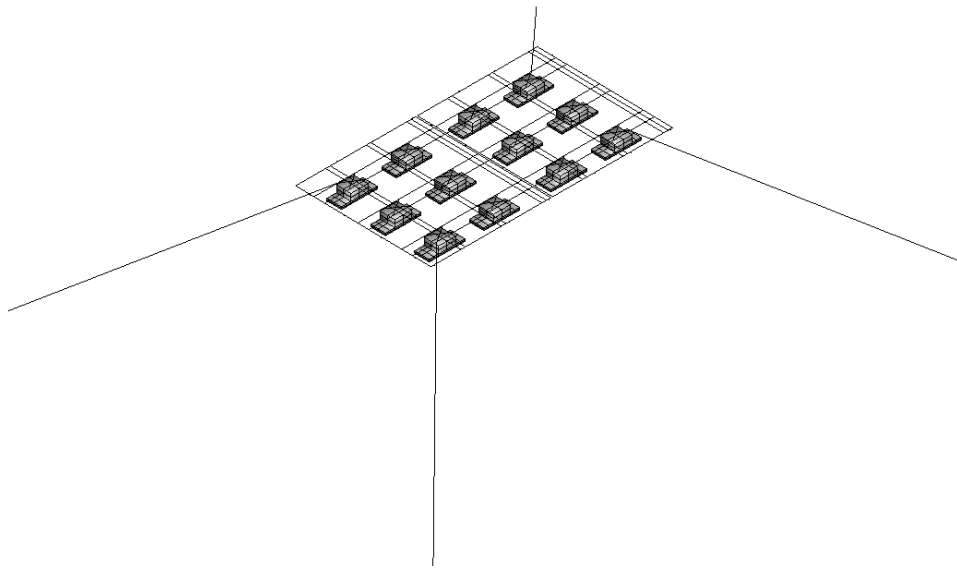


Fig. 2 Layout of floating solar power plant system

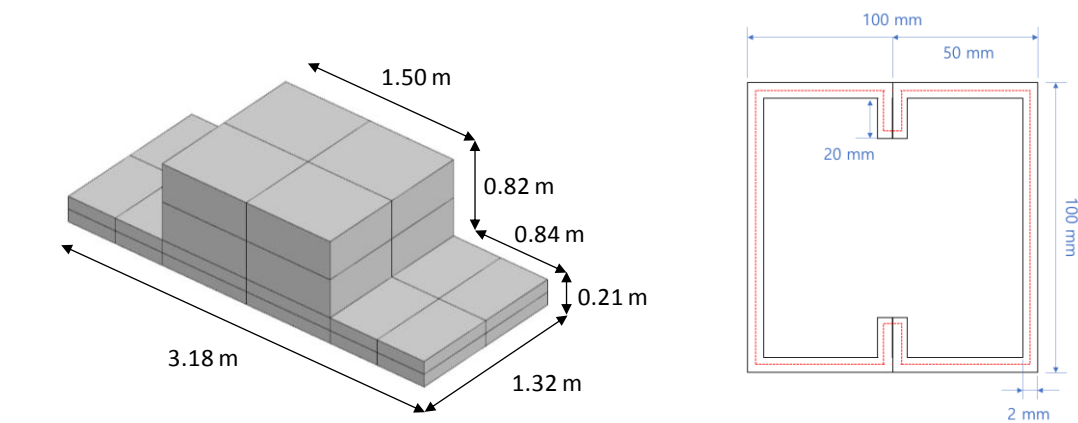


Fig. 3 Floating concrete block and section profile of connector beam

Table 1 Particulars of floater and connector

Part	Property	
Floating bodies	Type	Concrete block
	Breadth×Length×Depth×Draft	1.32m×3.18m×1.03m×0.84m
	Displacement	2.128896 ton
Connectors	Type	Steel profile beam
	Axial stiffness (EA)	1.869×10 ⁸ N
	Bending stiffness (EI)	294,580 N-m ²
	Torsion stiffness (GJ)	121,810 N-m ²
	Mass per length (m)	7.12 kg/m
Mooring lines	Type	Steel spring
	Spring constant (K)	849.166 N/m

Water depth of the target site is set to be 10 m. Waves and drifts effects were considered for main environmental forces. Wave frequencies of $0.05 \sim 2\pi$ rad/s were considered and wave height(H) was assumed to be $\lambda/10$ but not greater than 0.5 m. Heading angle of wave, β is considered for 0, 45 and 90 deg.

3. EQUATION OF MOTION

Hydroelastic equation of motions should be formulated and solved to analyze coupled responses of floaters, connectors and mooring lines in waves. Coupled equation can be expressed by (1) in frequency domain.

$$(-\omega^2[M_b + M_c] - i\omega[C_b + C_c] + [K_b + K_c])\{u(\omega)\} = \{f_w(\omega)\} \quad (1)$$

where $[M_b]$ is mass matrix for floating bodies including added mass effect, $[C_b]$ is hydrodynamic damping matrix, $[K_b]$ is restoring stiffness matrix of floating bodies, $\{f_w(\omega)\}$ is wave force vector, $\{u(\omega)\}$ is displacement vector for bodies, connectors and mooring lines. ω is wave frequency. This study applied HOBEM [2,3] to obtain added mass, hydrodynamic damping and wave forces because it provides highly accurate and efficient solution in the analysis of multi-body interactions. In (1), $[M_c]$ is mass matrix for connector beams and mooring lines, $[C_c]$ is damping matrix, $[K_c]$ is stiffness matrix and FEM [4] was applied to formulating connector beams and mooring lines. Frequency domain analysis is very fast because it calculates only steady-state amplitude of responses. It is also useful to see the responses versus frequencies rapidly. So it is usually employed in predesign stage. However, frequency analysis cannot review the transient responses including natural mode components. It neither can see the responses in mixed frequency forces such as drift force. In that case, time domain analysis is required and the equation of motions takes the form by (2).

$$[M_b + M_c]\{\ddot{u}(t)\} + [C_b + C_c]\{\dot{u}(t)\} + [K_b + K_c]\{u(t)\} = \{f_w(t) + f_d(t)\} \quad (2)$$

where $\{f_d(t)\}$ is force vector due to drift forces. This paper applied the method by Choi et al. [1] to calculate drift forces. Time domain analysis can review the transient or mixed components of responses. But, it is time consuming because it calculates time series of responses. Numerically stable time marching should be chosen in time domain analysis. This study applied the modified Newmark algorithm [5] in time marching.

If floating body part alone is a main concern in the analysis, simpler equation can be formulated by using Guyan reduction [6]. It takes the form.

$$(-\omega^2[M_b] - i\omega[C_b] + [K_b + K_c])\{u_b(\omega)\} = \{f_w(\omega)\} \quad (3)$$

where $\{u_b(\omega)\}$ is displacement for floating bodies and $[K_c]$ is reduced stiffness matrix due to effect by connectors and mooring lines. If stiffness matrix of connectors and mooring lines are partitioned with part B where floating bodies are attached and part A for otherwise

$$[K_c] = \begin{bmatrix} \text{---} & \text{---} \\ \text{---} & \text{---} \end{bmatrix} \quad (4)$$

the equivalent reduced stiffness matrix is obtained by

$$[K_c] = [K_c] - [K_c] [K_A]^{-1} [K_c] \quad (5)$$

Eq. (3) is simpler than (1) or (2). However, it cannot investigate responses in connectors or mooring lines. If stresses in connectors are main design concerns, (1) or (2) should be solved.

4. NUMERICAL ANALYSES AND DISCUSSIONS

The floating solar power system was analyzed by HOBEM and FEM described in section 3. Total HOBEM nodes for floating bodies are 888 and number of FEM nodes for connector beams are 664. Displacements at the floating body and stresses in connector beams were investigated and the results were compared for frequency and time domain analyses. Displacements at floating body no. 1 and stresses at connector element no. 35 in $\beta=45$ deg were compared because the maximum responses were observed at the condition. Their locations are shown in Fig. 4.

Analysis results are summarized in Figs. 5~15. Fig. 5 compares frequency domain analysis with Guyan reduction (Eq. (3)) and time domain analyses (Eq. (2)) for floating body motions. Transient responses due to long period drift motions are well shown in time domain analysis but it cannot be shown in frequency domain analysis. However, steady state responses are well agreed. Eq. (3) is applicable if floating body motions alone are main design parameters. However, connector stresses as well as floating body motions are key design factors in the floating system in this study. So, body-connector coupled analysis are required. Therefore, Eqs.

(1) and (2) were mainly applied in this study and the other figures are comparing Eqs. (1) and (2). Fig. 6 shows steady-state amplitude of connector stress versus wave period. Bigger stresses are shown at two peaks. The first peak is related with natural bending period of connector beam. It is 1.18 sec. The second peak is due to natural heave period of floating body. It is 3.22 sec. It is shown that frequency and time domain results agree well. Frequency domain analysis is faster than time domain analysis because it only calculates amplitude and phase of responses. For example, cpu time was 52.656 sec in time domain analysis of one frequency case in this example study with simulation time=400 sec with time step=0.1 sec. While, cpu time was merely 0.098 sec for one frequency case in frequency domain analysis. So, the frequency responses curve like Fig. 6 is easily obtained from frequency domain analysis. Figs. 7~9 compare time series of connector stresses for frequency and time domain analyses. Some differences are shown in transient part between frequency and time domain analyses because the effect by natural bending mode or drift force are included in the transient part. Time domain analysis can describe the transient behavior but frequency domain cannot. However, good agreements are shown in the steady-state stresses because transient components are damped out in the steady-state part.

Fig. 10 summarizes displacements at floating body versus wave period. The peak values in x, y and z displacements are related with natural periods of surge, sway, heave, respectively. They are 27.06 sec, 27.06 sec and 3.22 sec. Figs. 11~13 compare time series of displacements at floating body for frequency and time domain analyses. Slowly varying displacements due to drift forces or transient displacements due to natural modes can be investigated in time domain analyses but they cannot be in frequency domain analysis. However, steady-state amplitude are well agreed between time domain and frequency domain analyses.

Higher wave was analyzed to see the variation of connector stress and mooring line tension versus wave heights. Figs. 15 and 16 are the results. It is shown that connector stress and mooring line tension linearly increase for wave heights due to negligible drift effects at that wave period

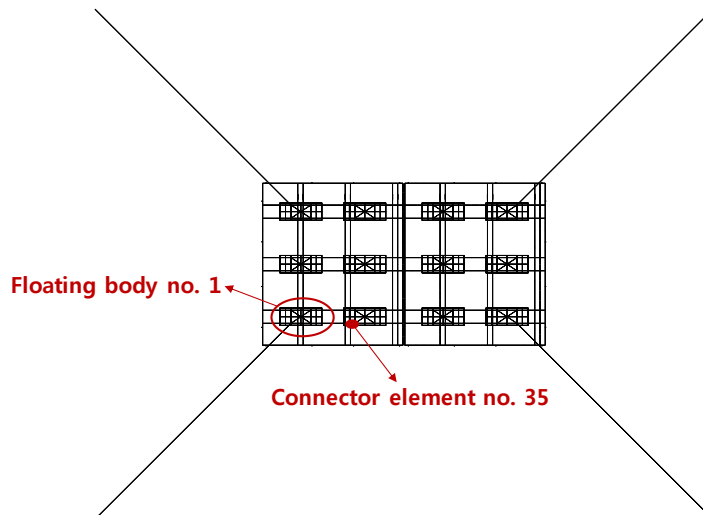
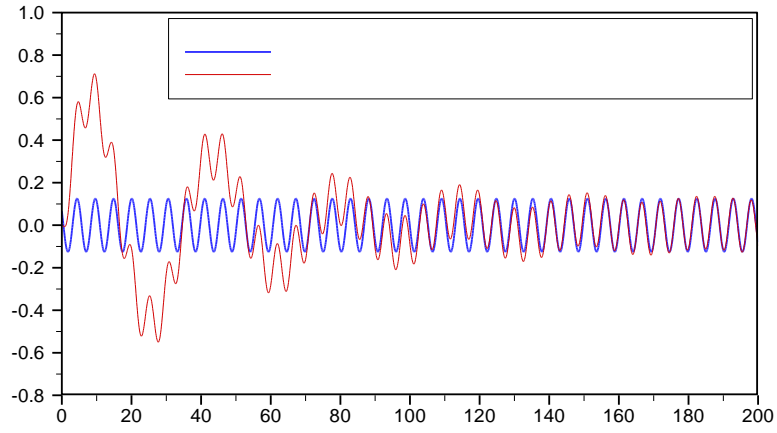
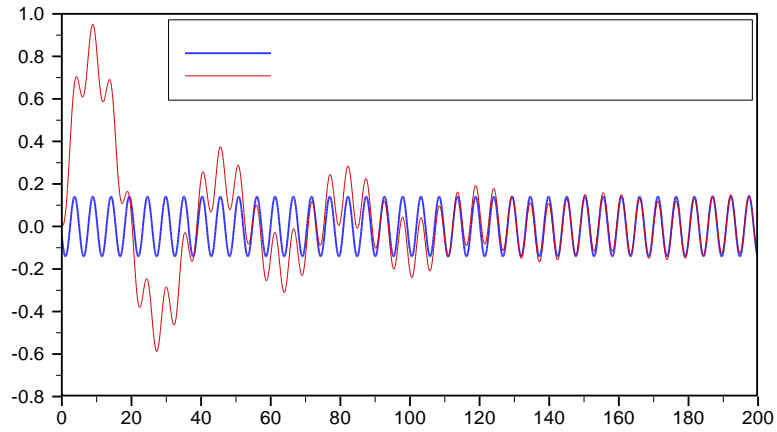


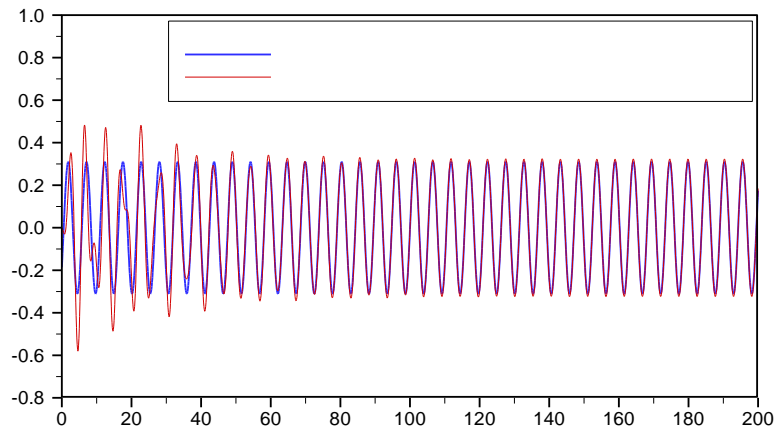
Fig. 4 Locations for maximum responses



(a) x-direction



(b) y-direction



(c) z-direction

Fig. 5 Comparison of Guyan reduction and time domain analysis for floating body displacements ($T=5.236$ sec, $\beta=45$ deg, body 1)

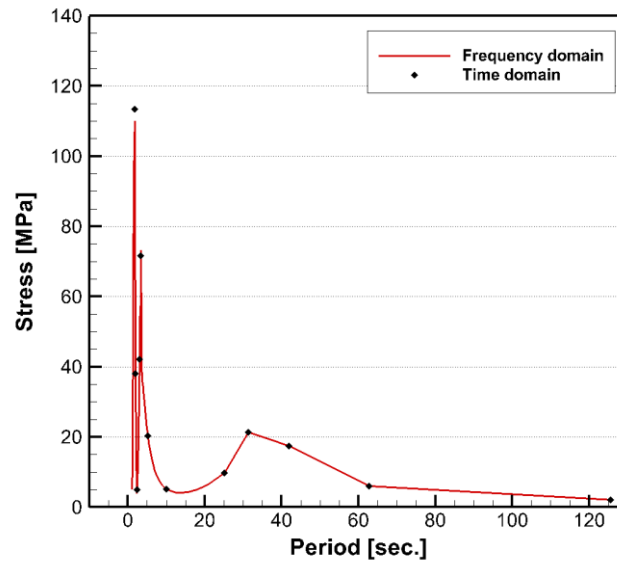
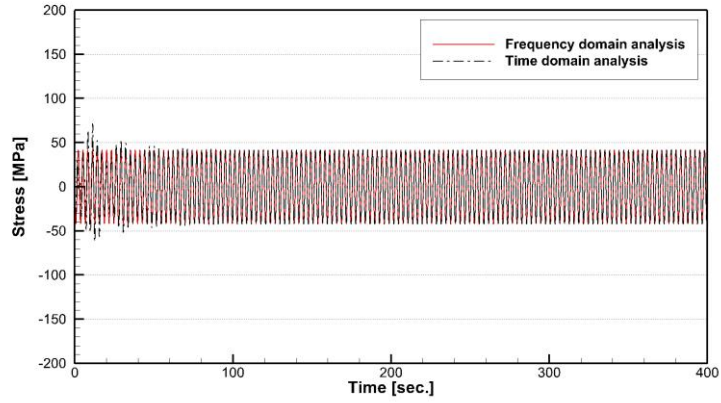
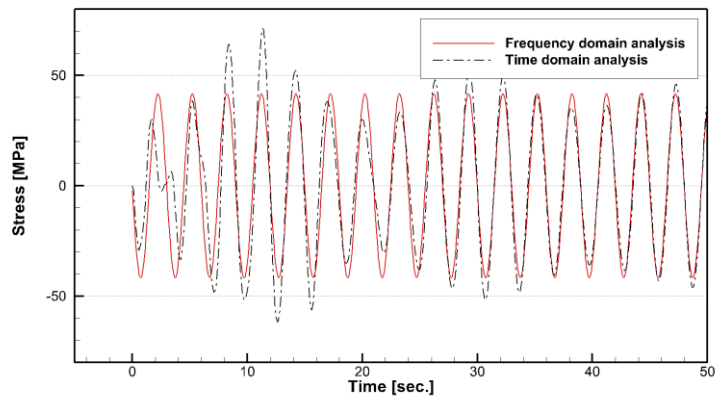


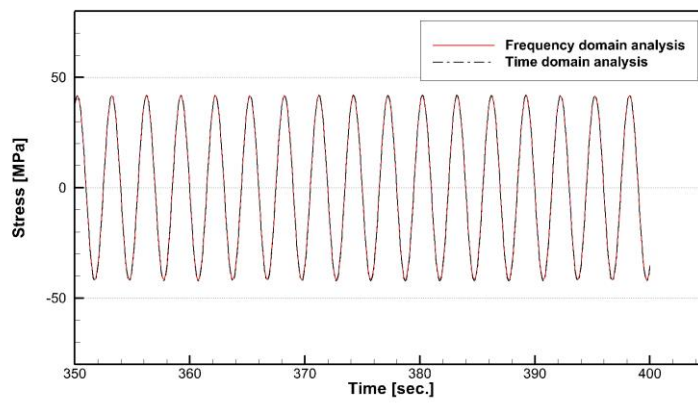
Fig. 6 Connector stress curve versus wave period ($\beta=45$ deg, Element no. 35)



(a) Full time view

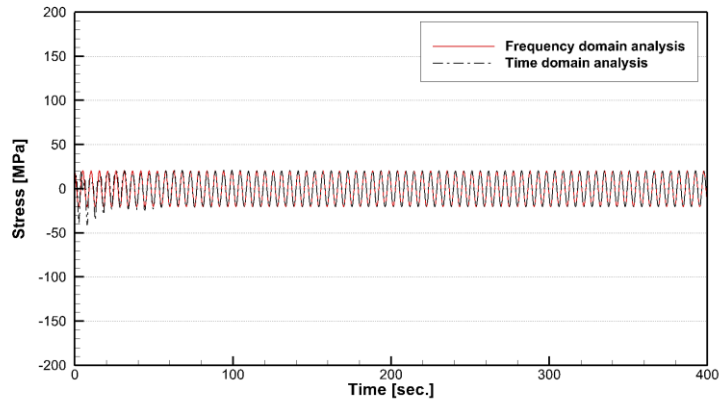


(b) Zoom view (transient part)

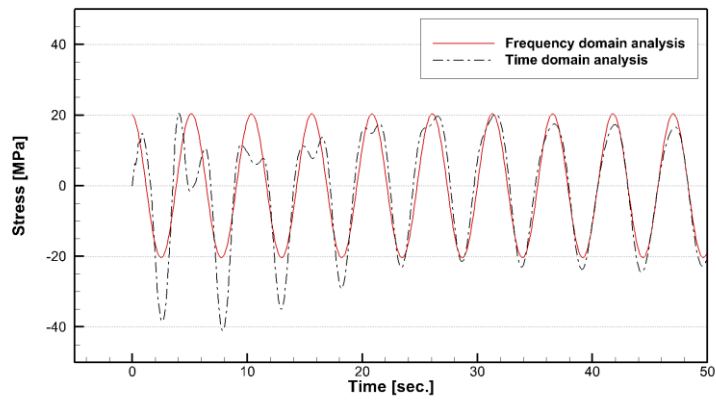


(c) Zoom view (steady-state part)

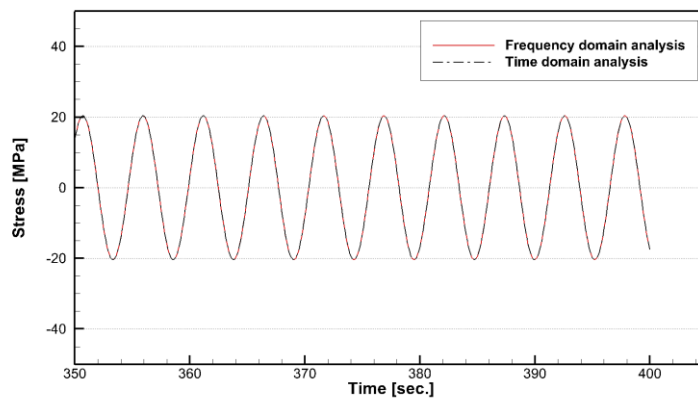
Fig. 7 Time series of connector stress ($T=3.000$ sec, $\beta=45$ deg, Element no. 35)



(a) Full time view

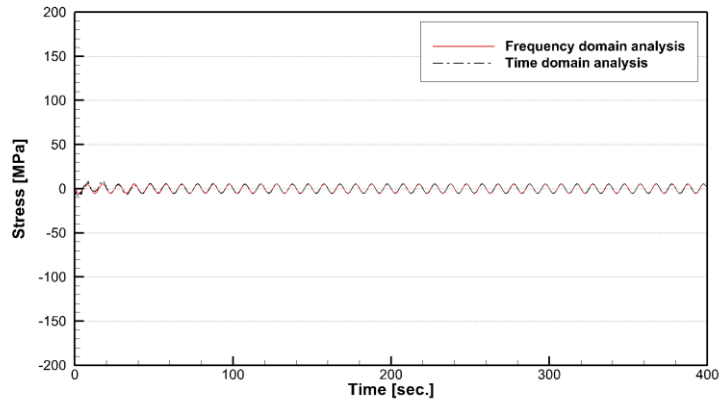


(b) Zoom view (transient part)

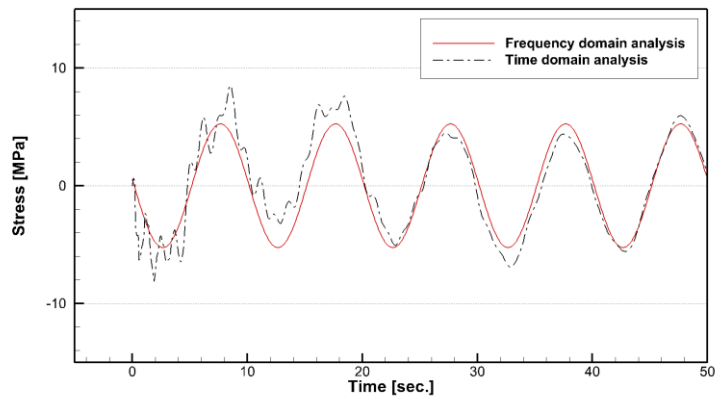


(c) Zoom view (steady-state part)

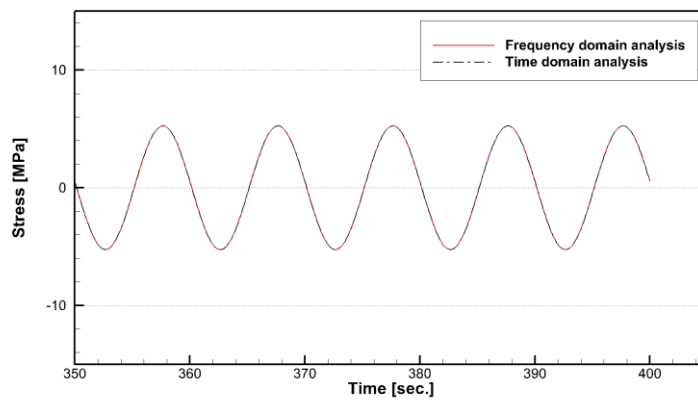
Fig. 8 Time series of connector stress ($T=5.236$ sec, $\beta=45$ deg, Element no. 35)



(a) Full time view

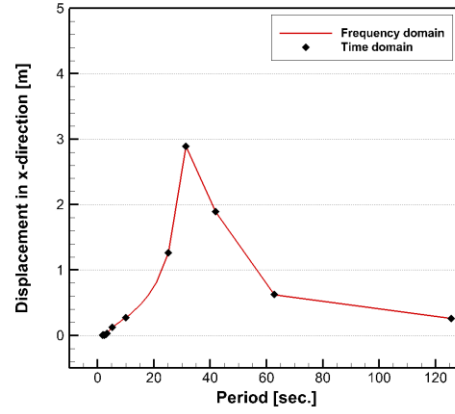


(b) Zoom view (transient part)

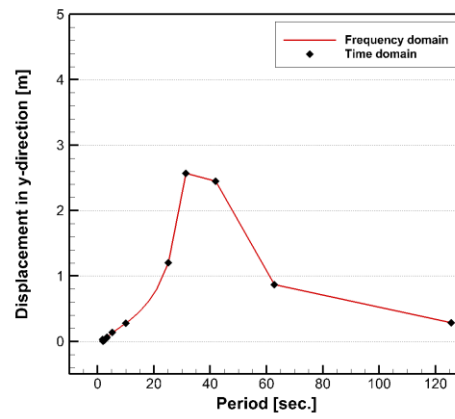


(c) Zoom view (steady-state part)

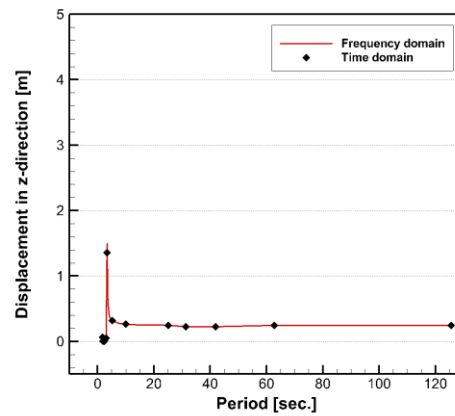
Fig. 9 Time series of connector stress ($T=10.000$ sec, $\beta=45$ deg, Element no. 35)



(a) x-direction

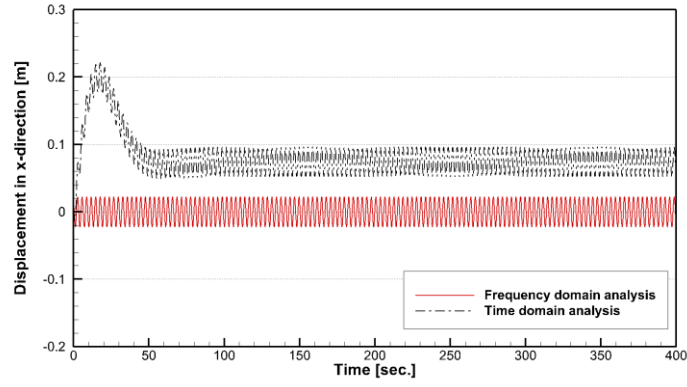


(b) y-direction

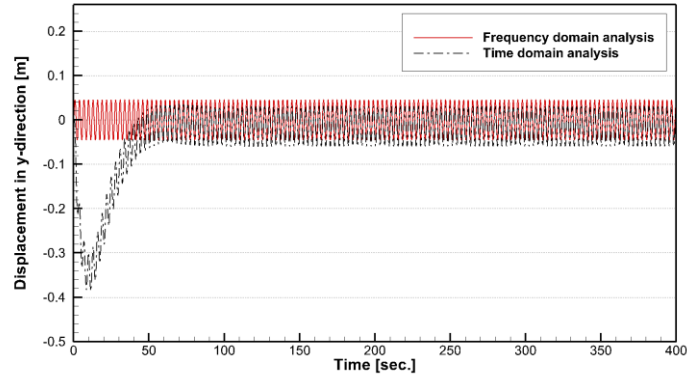


(c) z-direction

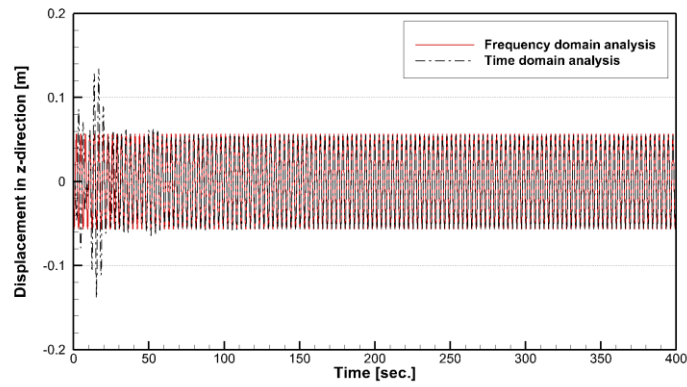
Fig. 10 Floating body displacement curve versus wave period ($\beta=45$ deg, Body 1)



(a) x-direction

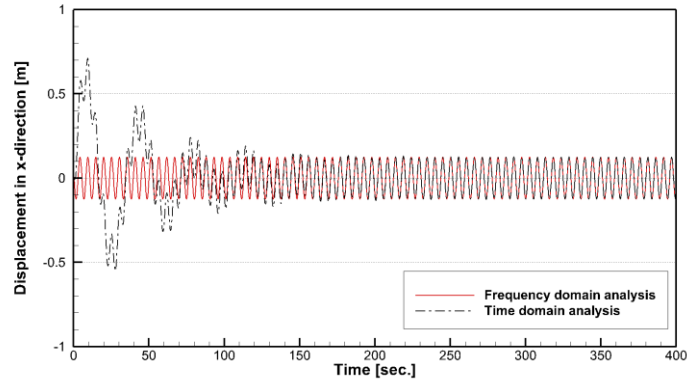


(b) y-direction

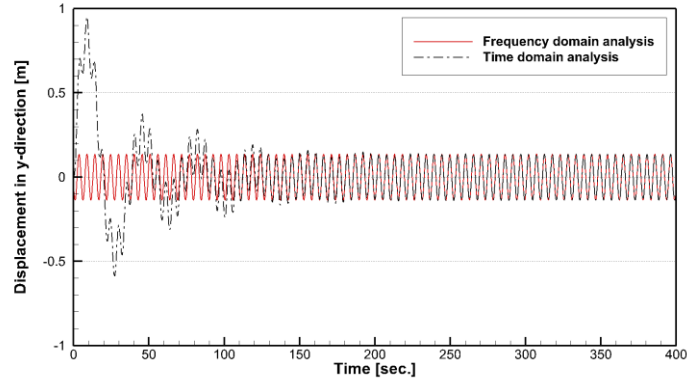


(c) z-direction

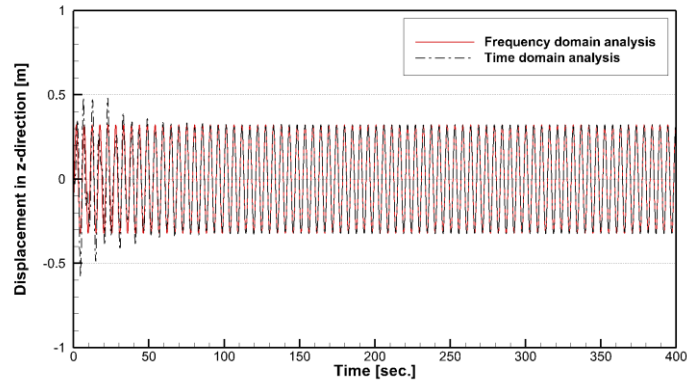
Fig.11 Time series of floating body displacement ($T=3.000$ sec, $\beta=45$ deg, Body 1)



(a) x-direction

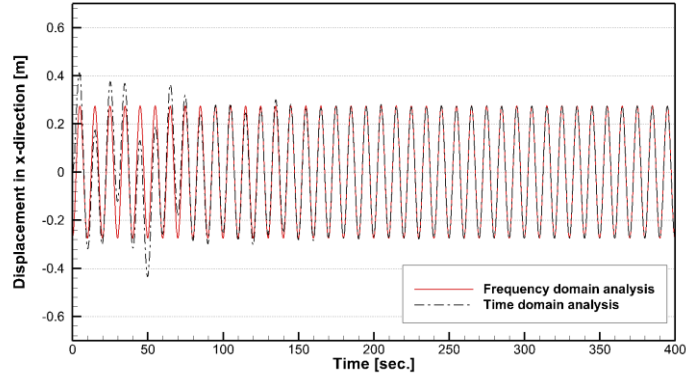


(b) y-direction

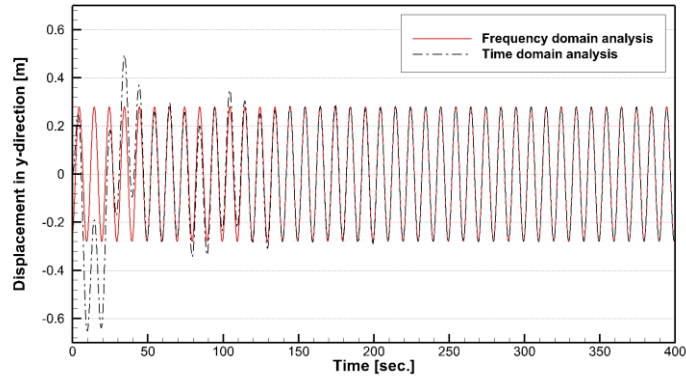


(c) z-direction

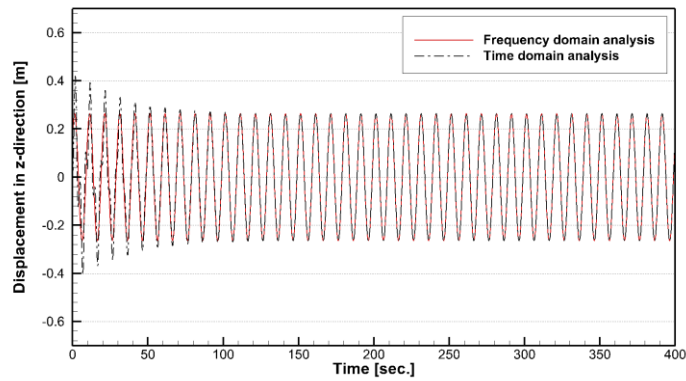
Fig. 12 Time series of floating body displacement ($T=5.236$ sec, $\beta=45$ deg, Body 1)



(a) x-direction



(b) y-direction



(c) z-direction

Fig. 13 Time series of floating body displacement ($T=10.000$ sec, $\beta=45$ deg, Body 1)

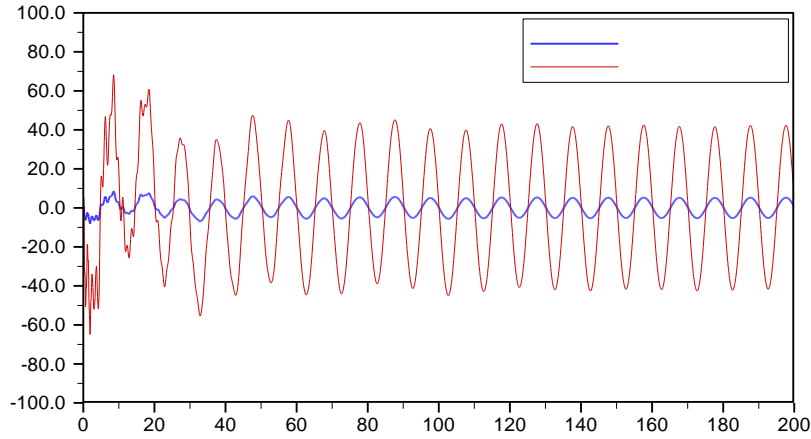


Fig. 14 Comparison of connector stresses for wave heights ($T=10.000$ sec, $\beta=45$ deg, Element no. 35)

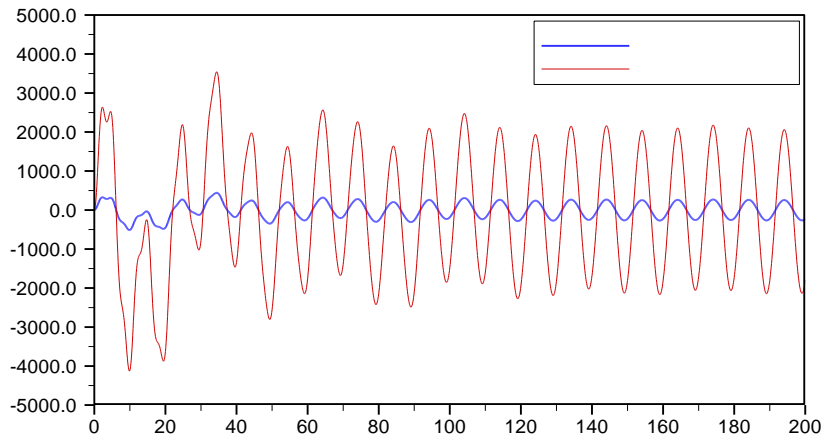


Fig. 15 Comparison of mooring line tensions for wave heights ($T=10.000$ sec, $\beta=45$ deg)

5. CONCLUSIONS

The hydroelastic behaviors of a floating solar energy converter system in waves has been analyzed both in frequency-domain and time-domain. Guyan reduction scheme for connector structures also has been implemented for application to huge structures which can cover tens of MW structures. From a series of systematic numerical investigations of the results from three different approaches, the following conclusions are drawn.

- The results of frequency-domain analysis were verified by those of time-domain analysis. The motion RAO and stress RAO from both the frequency-domain analysis and time-domain analysis showed equivalent results in steady state while the time-domain results showed transient effect and drift motion effect as well. It was confirmed that the frequency domain

analysis results provide a variety of beam natural mode response as well. The computational time of the frequency-domain analysis was more than 500 times than the time-domain when the simulation time set to be 400sec. in full scale, which corresponds to 40 cycles when wave period is assumed to be 10 seconds.

- However, frequency domain analysis cannot review transient or slowly varying responses due to natural mode behavior or drift forces. They can be observed by time domain analysis.
- It was confirmed that Guyan reduction results gave same motion response as the frequency-domain analysis results. This implies Guyan reduction approach can give first screening information of a very huge structures because vertical mode motion correlates very well with stress RAO curves. But, we should be careful for using the Guyan reduction approach as the first screening tool because the Guyan reduction results cannot resolve beam natural model response.
- Further numerical analysis for a real huge floating solar power system is needed for final decision of the present three steps approach for analysis of the floating solar power plant.

REFERENCES

- [1] Hong, S.Y. Preliminary Study on a Floating Solar Power Plant in Sea Area. Europe-Korea Conference on Science and Technology 2017 (EKC 2017), July 2017, Stockholm, Sweden.
- [2] Choi, Y.R., Hong, S.Y. and Choi, H.S. An analysis of second-order wave forces on floating bodies by using a higher-order boundary element method. *Ocean Engineering* (2000) 28:117-138.
- [3] Hong, S.Y., Kim, J.H., Cho, S.K., Choi, Y.R. and Kim, Y.S. Numerical and experimental study on hydrodynamic interaction of side-by-side moored multiple vessels. *Ocean Engineering* (2005) 32:783-801.
- [4] Kim, B.W., Sung, H.G., Kim, J.H. and Hong, S.Y. Comparison of linear spring and nonlinear FEM methods in dynamic coupled analysis of floating structure and mooring system. *Journal of Fluids and Structures* (2013) 42:205-227.
- [5] Chung, J. and Hulbert, G.M. A time integration algorithm for structural dynamics with improved numerical dissipation : The generalized α -method. *Journal of Applied Mechanics* (1993) 60:371-375.
- [6] Guyan, R.J. Reduction of stiffness and mass matrices. *AIAA Journal* (1965) 3:380.

A Modification of the Multi-step Optimisation of Variable Stiffness Laminates for Manufacturable Design

Zhi Hong^{*}, Sergio Turteltaub^{**}, Daniël Peeters^{***}

^{*}Delft University of Technology, ^{**}Delft University of Technology, ^{***}University of Limerick

ABSTRACT

A commonly-used method for the optimisation of variable stiffness laminates involves a three-step procedure, namely (1) optimising the laminate in terms of lamination parameters, (2) retrieving the fiber angles and (3) constructing the fiber path, sequentially[1]. To control the fiber steering in each layer of the laminate, manufacturing constraints, which control the maximum curvature of the fiber angles, need to be considered[2]. Traditionally, manufacturing constraints have been imposed at the second step in terms of controlling the fiber path curvature. In that case, the constraints affect the design, which typically results in a loss of performance between the optimal results from the first and the second step. In the present work, we propose a scheme to include the manufacturing constraints directly at the first step by taking gradient constraints on the lamination parameters and perform a comparative analysis between the present and the previous method. We test our method in several numerical cases to minimize the compliance of variable stiffness laminate with in-plane loads and compare the results from the existing design method. The initial numerical results show that our method can generate manufacturable designs and bridge the gaps of the performance loss between the first and second steps. Furthermore, the computational performance can also be enhanced simultaneously due to the reduced number of gradient constraints. One limitation of the proposed scheme is that the maximum curvature of the fiber angle is not controlled precisely, which may result in a higher compliance. Therefore, there should be a trade-off when making a decision between enforcing the constraints a priori or a posteriori. Keywords: variable stiffness laminate, lamination parameter, manufacturable design, structural optimisation [1] IJsselmuiden S T. Optimal design of variable stiffness composite structures using lamination parameters[J]. PhD Thesis, 2011. [2] Peeters D M J, Hesse S, Abdalla M M. Stacking sequence optimisation of variable stiffness laminates with manufacturing constraints[J]. Composite Structures, 2015, 125: 596-604.

Computer Simulation of Glasses under Shear: From the Onset of Flow to Shear Banding

Juergen Horbach^{*}, Gaurav Shrivastav^{**}, Pinaki Chaudhuri^{***}, Mehrdad Golkia^{****}

^{*}University of Duesseldorf, Germany, ^{**}TU Berlin, Germany, ^{***}The Institute of Mathematical Sciences, Chennai, India, ^{****}University of Duesseldorf, Germany

ABSTRACT

The response of glasses to mechanical loading often leads to the formation of inhomogeneous flow patterns that may strongly affect the materials properties. Among them, shear bands, associated with strain localization in form of band-like structures, are ubiquitous in a wide variety of materials, ranging from soft matter systems to metallic alloys. Molecular dynamics simulations of the Kob-Andersen Lennard-Jones mixture are performed to investigate the onset of flow and the subsequent formation of shear bands. Deeply supercooled systems as well as systems far below the glass transition temperature are sheared, using a planar Couette flow geometry. Shear is imposed via the boundaries, using Lees-Edwards boundary conditions at a constant strain rate. We show that the onset of flow is marked by a directed percolation transition of mobile regions [1]. Shear banding is observed at sufficiently low strain rates. We analyze the nucleation of the shear-banded structures as well as the mechanical properties of the deformed glasses. [1] G. P. Shrivastav, P. Chaudhuri, and J. Horbach, Yielding of glass under shear: a directed percolation transition precedes shear-band formation, Phys. Rev. E 94, 042605 (2016).

Integrated Earthquake Simulation for Estimation of Earthquake and Tsunami Hazard and Disaster Using HPC

Muneo Hori^{*}, Takamasa Iryo^{**}, Takane Hori^{***}

^{*}The University of Tokyo, ^{**}Kobe University, ^{***}JAMSTEC

ABSTRACT

Integrated earthquake simulation (IES) is aimed at computing whole processes of earthquake hazard and disaster. The core idea of IES is seamlessly combining various numerical analysis methods such as earthquake generation analysis, structural seismic response analysis and social disaster recovery analysis. IES has implemented a few analysis methods in it which use HPC so that a larger urban area is computed considering various earthquake scenario. A smart platform that automatically construct suitable analysis models for implemented analysis methods is developed. This platform uses various data resources such as 3D maps and local government inventory. In this presentation, the current state of developing IES is explained, and a few examples of integrated simulations of earthquake hazard and disaster estimation in actual cities in Japan are presented.

A Proposal of Monitoring and Forecasting Method for Crustal Activity in and Around Japan with 3D Heterogeneous Medium Using a Large-Scale High-Fidelity Finite Element Simulation

Takane Hori^{*}, Tsuyoshi Ichimura^{**}, Kohei Fujita^{***}, Ryoichiro Agata^{****}, Takuma Yamaguchi^{*****}

^{*}Japan Agency for Marine-Earth Science and Technology, ^{**}Earthquake Research Institute, The University of Tokyo, ^{***}Earthquake Research Institute, The University of Tokyo, ^{****}Japan Agency for Marine-Earth Science and Technology, ^{*****}Earthquake Research Institute, The University of Tokyo

ABSTRACT

Recently, we can obtain continuous dense surface deformation data on land and partly on the sea floor. The obtained data are not fully utilized for monitoring and forecasting of crustal activity, such as spatio-temporal variation in slip velocity on the plate interface including earthquakes, seismic wave propagation, and crustal deformation. For construct a system for monitoring and forecasting, it is necessary to develop a physics-based data analysis system including (1) a structural model with the 3D geometry of the plate interface and the material property such as elasticity and viscosity, (2) calculation code for crustal deformation and seismic wave propagation using (1), (3) inverse analysis or data assimilation code both for structure and fault slip using (1) & (2). To accomplish this, it is at least necessary to develop highly reliable large-scale simulation code to calculate crustal deformation and seismic wave propagation for 3D heterogeneous structure. Unstructured FE non-linear seismic wave simulation code has been developed. This achieved physics-based urban earthquake simulation enhanced by 1.08 T DOF x 6.6 K time-step. A high fidelity FEM simulation code with mesh generator has also been developed to calculate crustal deformation in and around Japan with complicated surface topography and subducting plate geometry for 1km mesh. This code has been improved the code for crustal deformation and achieved 2.05 T-DOF with 45m resolution on the plate interface. This high-resolution analysis enables computation of change of stress acting on the plate interface. Further, for inverse analyses, waveform inversion code for modeling 3D crustal structure has been developed, and the high-fidelity FEM code has been improved to apply an adjoint method for estimating fault slip and asthenosphere viscosity. Hence, we have large-scale simulation and analysis tools for monitoring. We are developing the methods for forecasting the slip velocity variation on the plate interface. Although the prototype is for elastic half space model, we are applying it for 3D heterogeneous structure with the high-fidelity FE model. Furthermore, large-scale simulation codes for monitoring are being implemented on the GPU clusters and analysis tools are developing to include other functions such as examination in model errors.

A Simple Direct-Forcing Immersed Boundary Projection Method with Prediction-Correction for Fluid-Solid Interaction Problems

Tzyy-Leng Horng*, Po-Wen Hsieh**, Suh-Yuh Yang***, Cheng-Shu You****

*Feng Chia University, **National Chung Hsing University, ***National Central University, ****National Central University

ABSTRACT

In this paper, we propose a simple and novel direct-forcing immersed boundary (IB) projection method in conjunction with a prediction-correction (PC) process for simulating the dynamics of fluid-solid interaction problems, in which each immersed solid object can be stationary or moving in the fluid with a prescribed velocity. The method is mainly based on the introduction of a virtual force which is distributed only on the immersed solid bodies and appended to the fluid momentum equations to accommodate the internal boundary conditions at the immersed solid boundaries. More specifically, we first predict the virtual force on the immersed solid domain by using the difference between the prescribed solid velocity and the computed velocity, which is obtained by applying the Choi-Moin projection scheme to the incompressible Navier-Stokes equations on the entire domain including the portion occupied by the solid bodies. The predicted virtual force is then added to the fluid momentum equations as an additional forcing term and we employ the same projection scheme again to correct the velocity field, pressure and virtual force. Although this method is a two-stage approach, the computational cost of the correction stage is rather cheap, since the associated discrete linear systems need to be solved in the correction stage are same with that in the prediction stage, except the right-hand side data terms. Such a PC procedure can be iterated to form a more general method, if necessary. The current two-stage direct-forcing IB projection method has the advantage over traditional one-stage direct-forcing IB projection methods, consisting of the prediction step only, by allowing much larger time step, since traditional methods generally request quite small time step for flow field relaxed and adjusted to the solid body movement even using implicit scheme. Numerical experiments of several benchmark problems are performed to illustrate the simplicity and efficient performance of the newly proposed method. Convergence tests show that the accuracy of the velocity field is super-linear in space in all the 1-norm, 2-norm, and maximum norm. We also find that our numerical results are in very good agreement with the previous works in the literature and one correction at each time step appears to be good enough for the proposed PC procedure. Keywords: incompressible Navier-Stokes equations, fluid-solid interaction, immersed boundary method, projection scheme, direct-forcing method, prediction-correction

Pointwise Divergence-free Higher Order Space-time Hybridizable and Embedded Discontinuous Galerkin Methods for Incompressible Flows

Tamas Horvath^{*}, Sander Rhebergen^{**}

^{*}University of Waterloo, ^{**}University of Waterloo

ABSTRACT

The Space-time Discontinuous Galerkin (ST-DG) method is an excellent method to discretize problems on deforming domains. This method uses DG to discretize both in the spatial and temporal directions, allowing for an arbitrarily high order approximation in space and time. Furthermore, this method automatically satisfies the geometric conservation law which is essential for accurate solutions on time dependent domains. We present a higher-order accurate Hybridizable or Embedded Discontinuous Galerkin (DG-H or DG-E) method for incompressible flows. This discretization guarantees a pointwise divergence-free velocity field on simplicial meshes.

Topology Optimization for Elastoplastic Large Deformation Considering Various Hardening Behavior with Multiplicative Decomposition

Hiroya Hoshiba^{*}, Junji Kato^{**}, Takashi Kyoya^{***}

^{*}Tohoku University, ^{**}Tohoku University, ^{***}Tohoku University

ABSTRACT

The present study proposes an advanced topology optimization method for elastoplastic large deformation. This method includes description of finite strain kinematic hardening and can be applied exactly to optimal design of structures subjected to historical loading. Regarding topology optimization considering finite elastoplasticity, a previous work by [1] introduces sensitivity analysis based on the so-called transient adjoint method. However, kinematic hardening behavior in addition to finite strain theory has yet to be considered. On the other hand, a conditional sensitivity analysis for elastoplastic composites has been proposed by [2] and low-cost and accurate sensitivity analysis is achieved. In this study, we extend the conditional approach and incorporate the advanced elastoplastic material model into the conventional topology optimization framework. In formulating finite strain elastoplastic model including kinematic hardening law, all deformations are decomposed in a multiplying manner according to their meanings. Hence elastoplastic constitutive equations are described with reference to two different plastic intermediate configurations. Based on this special property, new sensitivity analysis is precisely formulated and sensitivity is analytically derived to carry out gradient-based optimization algorithm. Finally, several numerical examples will be shown to discuss practical concerns, e.g. accuracy in sensitivity, computational costs and its numerical convergence. REFERENCES: [1] M. Wallin, V. Jönsson, E. Wingren: Topology optimization based on finite strain plasticity, *Struct. Multidisc. Optim.* 54: 783-793 (2016) [2] J. Kato, H. Hoshiba, S. Takase, K. Terada, T. Kyoya: Analytical sensitivity in topology optimization for elastoplastic composites, *Struct. Multidisc. Optim.* 52: 507-526 (2015)

On Thermo-electro-mechanics of Electro-active Polymers

Mokarram Hossain*

*Zienkiewicz Centre for Computational Engineering, Swansea University, UK

ABSTRACT

Electro-active polymers (EAPs) draw considerable attention thanks to large actuation mechanisms. EAPs are nowadays well-known and promising candidates for producing sensors, actuators and energy harvesters. In general, polymeric materials are sensitive to differential temperature histories. Moreover, it is a non-trivial task to maintain a prescribed temperature during experimental characterizations of EAPs under electro-mechanically coupled loads. Such difficulties to maintain constant temperature is not only because of an external differential temperature history but also because of the changes in internal temperature caused by the application of high electric loads. In this contribution, a thermo-electro-mechanically coupled constitutive framework is proposed based on the total energy approach. Departing from relevant laws of thermodynamics, thermodynamically consistent constitutive equations are formulated. To demonstrate the performance of the proposed thermo-electro-mechanically coupled framework, several non-homogeneous boundary-value problems will be solved. The results illustrate the influence of various thermo-electro-mechanical couplings [1, 2, 3]. 1. M. Mehnert, M. Hossain, P. Steinmann, On nonlinear thermo-electro-elasticity, *Proc. R. Soc. A* 472 (2190), 20160170, 2016 2. M. Mehnert, M. Hossain, P. Steinmann, Towards a thermo-magneto-mechanical coupling framework for magneto-rheological elastomers, *International Journal of Solids and Structures*, 117-132:128, 2017 3. M. Hossain, P. Steinmann, Modelling electro-active polymers with a dispersion-type anisotropy, *Smart Materials and Structures*, <https://doi.org/10.1088/1361-665X/aa9f88>

CAD-integrated Template-based Patient-Specific Vascular Modeling for Isogeometric Analysis

Shaolie Hossain*, Benjamin Urick**, Travis Sanders***, Jessica Zhang****, Thomas Hughes*****

*The University of Texas at Austin, **The University of Texas at Austin, ***The University of Texas at Austin,
****Carnegie Mellon University, *****The University of Texas at Austin

ABSTRACT

Patient-specific vascular modeling typically involves three fundamental steps: image processing, analysis suitable model generation, and computational analysis. Analysis suitable model generation techniques that are currently utilized suffer from several difficulties and complications, which often necessitate manual intervention and crude approximations. Because the modeling pipeline spans multiple disciplines, the benefits of integrating a computer-aided design (CAD) component that offers a robust, intuitive, and highly customizable framework for the geometric modeling tasks has been largely overlooked. In this work, we present a CAD-integrated template-based modeling framework that streamlines the construction of solid NURBS (non-uniform rational B-spline) vascular models for performing isogeometric finite element analysis. Examples of arterial models for mouse and human circles of Willis and a porcine coronary tree are presented. The benefits of the presented approach, such as quicker processing time and more accurate reconstruction of complex models, are also highlighted.

Mixed-mode Fracture Analysis in Brittle and Quasi-brittle Materials Based on the Generalized Maximum Energy Release Rate Criterion

Cheng Hou^{*}, Xueling Fan^{**}

^{*}Xi'an Jiaotong University, ^{**}Xi'an Jiaotong University

ABSTRACT

In this paper, a modified mixed-mode fracture model called generalized maximum energy release rate criterion is proposed, which simultaneously involves the effects of the mixed-mode I/II stress intensity factors and the T-stress. This model can be used to predict the mixed-mode I/II crack initiation angles and fracture resistances in brittle and quasi-brittle materials. The results show that the T-stress plays an important role on the mixed-mode fracture analysis when an energy-based criterion is employed. Moreover, a series of mixed-mode fracture prediction curves are compared with the experimental results in literatures for semi-circular bend specimens made of PMMA and central cracked Brazilian disk specimens of Neiriz marble. Comparison results show that the modified criterion proposed in this work performs better in predicting the crack initiation angles and the fracture resistances than the conventional maximum energy release rate criterion. Key words: maximum energy release rate criterion; mixed mode; T-stress; crack initiation angle; fracture resistance

Dynamic Meshing Analysis of Spur Gear Based on the Modified Vector Form Intrinsic Finite Element (VFIFE) Method

Xiangying Hou^{*}, Zongde Fang^{**}, Jinke Jiang^{***}

^{*}Northwestern Polytechnical University, ^{**}Northwestern Polytechnical University, ^{***}Chang'an University

ABSTRACT

Lumped-mass method and dynamic equations are the most commonly used methods in the dynamic analysis due to its less computation amount than finite element method. However, the lumped-mass method has its own problems: limited accuracy, strong subjectivity and unable to display stress and displacement distribution. To solve dynamic non-linear problems, we proposed the modified vector form intrinsic finite element (VFIFE) method, which reduce computational complexity compared to the traditional VFIFE method [1]. Even though explicit difference is adopted, the advantages of good convergence and simple algorithm make it suitable for high-speed problems. In this paper, we combined contact algorithm and the modified VFIFE method to simulate spur gear dynamics and also rewrote the central difference equation considering Rayleigh damping. Taking a specific gear pair for example, we could obtain the transmission error response as well as the stress distribution, contact pattern and contact force to guide design. We could obtain rather precise results with a coarse mesh and the numerical results show the effectiveness and accuracy of the proposed method [2-4]. In addition, this method is not limited to gear analysis, but suitable for high-speed non-linear problems in engineering fields. [1] X. Hou, Z. Fang, Solid structure analysis with large deformation of eight-node hexahedral element using vector form intrinsic finite element, *Advances in Structural Engineering*, Published online. [2] T.Y. Wu, J.J. Lee, E.C. Ting, Motion analysis of structures (MAS) for flexible multibody systems: planar motion of solids, *Multibody System Dynamics*, 20 (2008) 197-221. [3] H.H. Lee, P.Y. Chang, J.W.Z. Lu, A.Y.T. Leung, V.P. lu, K.M. Mok, Development on A New Plate Element of Vector Form Intrinsic Finite Element, (2010) 1512-1517. [4] X. Hou, Z. Fang, Static Meshing Analysis of Spiral Bevel Gears Based on Vector Form Intrinsic Finite Element Method, *Journal of Xi'an Jiaotong University* 51 (2017) 85-92.

Simulations of Suspension Flows with a Meshless Moving Least Squares Scheme

Amanda Howard^{*}, Martin Maxey^{**}

^{*}Brown University, ^{**}Brown University

ABSTRACT

This talk will focus on a meshfree method for simulations of neutrally buoyant, non-Brownian particles in Stokes flow. We will discuss a meshless scheme using Moving Least Squares polynomial reconstructions to provide a computationally efficient method with higher order accuracy for use with general boundary conditions and arbitrary polynomial shapes while maintaining stability. In finite difference schemes for Stokes flow, satisfying an inf-sup condition is necessary to control spurious pressure modes. Without a mesh, this framework is not applicable. Here, a finite difference-like staggered discretization is used to couple a divergence-free velocity and pressure reconstruction, resulting in a stable meshless scheme for Stokes flow that can be coupled with the motion of particles suspended in the flow [1]. The emphasis will be on applications to dense suspensions of particles, especially particles with polydispersed sizes and non-spherical shapes. The presentation here will discuss the implementation in 3D with multiple particles and how the results can be used to benchmark other lower fidelity methods such as the Force Coupling Method. In meshless methods, the boundaries of the particles are sharply defined, allowing for sharp resolution for problems such as heat conduction. [1] Nathaniel Trask, Martin Maxey, Xiaozhe Hu, A compatible high-order meshless method for the Stokes equations with applications to suspension flows, In Journal of Computational Physics, Volume 355, 2018, Pages 310-326.

Variably Thermalized Soft Glassy Rheology

Robert Hoy*

*Physics, University of South Florida

ABSTRACT

We present a version of soft glassy rheology that includes thermalized strain degrees of freedom. It fully specifies systems' strain-history-dependent positions on their energy landscapes and therefore allows for quantitative analysis of their heterogeneous yielding dynamics and nonequilibrium deformation thermodynamics. We first illustrate the very different characteristics of thermal and athermal plasticity by contrasting systems' evolution under thermalized vs. nonthermalized plastic flow rules. Then we present a generalized flow rule that continuously interpolates between thermalized and nonthermalized flow, and use it to analyze more realistic scenarios wherein flow is partially thermalized.

Fluid-Structure Interaction Analysis of Transcatheter Heart Valves

Ming-Chen Hsu^{*}, Michael C.H. Wu^{**}

^{*}Iowa State University, ^{**}Iowa State University

ABSTRACT

Transcatheter heart valves (THVs) have emerged as a minimally invasive alternative to surgical bioprosthetic heart valves therapy. THVs offer advantages such as less postoperative pain, faster rehabilitation, and better pressure gradients. However, issues such as paravalvular leakage, leaflet fatigue, and valve migration limit the widespread use of THV in the younger population, especially due to the lack of data concerning its long-term performance and durability. In this work, we develop and apply a biomechanically rigorous and physiologically realistic computational fluid-structure interaction framework based on immersogeometric analysis to study the combined effect of leaflet geometry, biomaterial property, and blood flow pattern on valve performance.

Automated, Component-based Mesh Morphing for Parametric Finite Element Human Modeling

Jingwen Hu*, Abeselom Fanta**, Kai Zhang***, Byoung-Keon Park****, Katelyn Hunter*****,
Mathew Reed*****

*University of Michigan Transportation Research Institute, Ann Arbor, MI, USA; Department of Mechanical Engineering, University of Michigan, Ann Arbor, MI, USA, **University of Michigan Transportation Research Institute, Ann Arbor, MI, USA; Department of Mechanical Engineering, University of Michigan, Ann Arbor, MI, USA, ***State Key Laboratory of Advanced Design and Manufacturing for Vehicle Body, Hunan University, Changsha, Hunan, China, ****University of Michigan Transportation Research Institute, Ann Arbor, MI, USA, *****Altair Engineering, Troy, MI, USA, *****University of Michigan Transportation Research Institute, Ann Arbor, MI, USA; Center for Ergonomics, Industrial and Operations Engineering, University of Michigan, Ann Arbor, MI, USA

ABSTRACT

Among the whole population, small, obese, and/or older occupants are at increased risk of death and serious injury in motor-vehicle crashes compared with mid-size young men. Current adult finite element (FE) human body models (HBM) have been developed in a few body sizes (large male, midsize male, and small female) with reference body dimensions similar to those of the available physical anthropomorphic test devices (ATDs). The limited number of body sizes available has resulted in part because the time needed to develop an FE HBM using typical methods is measured in months or even years. In this study, we developed an automated component-based mesh morphing method that can sequentially morph the component geometries of the Global Human Body Model Consortium (GHBMC) mid-size male model into target geometries for a diverse population predicted by a set of statistical geometry models for ribcage, pelvis, femur, tibia, and external body surface. We also included a system to automatically correct/smooth highly distorted mesh in the models. Using the new method, twelve models were developed representing seated occupants with a wide range of stature (175 cm and 188 cm), body-mass index (BMI) (25, 30 and 35) and age (30 and 70 years old). The newly generated human body models showed similar mesh quality compared to the original GHBMC model and. They also displayed no significant changes in BMI from target values. The component-based mesh morphing method was also found to be relatively faster and more efficient than the previous region-based mesh morphing method due to landmark reduction in each morphing step. The morphed models were subjected to six regional impact simulations, including abdominal bar impact, oblique abdominal hub impact, frontal thorax hub impact, lateral shoulder impact, impact to the pelvis, and lateral thorax impacts. The simulation boundary conditions were set based on those reported in the PMHS tests. The simulation results were then compared to the PMHS test corridors. Overall, the simulation results displayed large variations among the 12 morphed models and strong correlations between human characteristics and human impact responses. However, age, height, and BMI showed different trends depending on the type of impact, which were generally consistent with the literature. This study demonstrated the robustness of the component-based mesh morphing method to generate reliable human models for a diverse population and effectively use these models for impact simulations. ? References Bouquet, R., Ramet, M., Bermond, F., Caire, Y., Talantikite, Y., Robin, S., Voiglio, E., Year Pelvis human response to lateral impact. In The 16th International Technical Conference on the Enhanced Safety of Vehicles (ESV). Windsor, ON, Canada. Hardy, W.N., Schneider, L.W., Rouhana, S.W., 2001. Abdominal impact response to rigid-bar, seatbelt, and airbag loading. Stapp Car Crash Journal 45, 1-32. Hu, J., Fanta, A., Neal, M., Reed, M., Wang, J., Year Vehicle Crash Simulations with Morphed GHBMC Human Models of Different Stature, BMI, and Age. In The 4th International Digital Human Modeling Symposium (DHM2016). Montréal, Québec, Canada. Hu, J., Rupp, J., Reed, M., 2012. Focusing on vulnerable populations in crashes: recent advances in finite element human models for injury biomechanics research. Journal of Automotive Safety and Energy 3, 295-307. Hu, J., Zhang, K., Fanta, A., Hwang, E., Reed, M.P., Year Effects of Male Stature and Body Shape on Thoracic Impact Response Using Parametric Finite Element Human Modeling. In 25th International Technical Conference on the Enhanced Safety of Vehicles (ESV). Detroit, MI. Hwang, E., Hallman, J., Klein, K., Rupp, J., Reed, M., Hu, J., 2016a. Rapid Development of Diverse Human Body Models for Crash Simulations through Mesh Morphing. SAE Technical Paper 2016-01-1491. Hwang, E., Hu, J., Chen, C., Klein, K., Miller, C., Reed, M., Rupp, J., Hallman, J., 2016b. Development, Evaluation, and Sensitivity Analysis of Parametric Finite Element Whole-Body Human Models in Side Impacts. Stapp Car Crash Journal 60, 473-508. Kemper, A.R., McNally, C., Kennedy, E.A., Manoogian, S.J., Duma, S.M., 2008. The influence of arm position on thoracic

response in side impacts. *Stapp Car Crash Journal* 52, 379-420. Klein, K.F., 2015. Use of Parametric Finite Element Models to Investigate Effects of Occupant Characteristics on Lower-Extremity Injuries in Frontal Crashes PhD Dissertation University of Michigan. Klein, K.F., Hu, J., Reed, M.P., Hoff, C.N., Rupp, J.D., 2015. Development and Validation of Statistical Models of Femur Geometry for Use with Parametric Finite Element Models. *Annals of biomedical engineering* 43, 2503-2514. Koh, S.W., Cavanaugh, J.M., Mason, M.J., Petersen, S.A., Marth, D.R., Rouhana, S.W., Bolte, J.H.t., 2005. Shoulder injury and response due to lateral glenohumeral joint impact: an analysis of combined data. *Stapp Car Crash Journal* 49, 291-322. Lebarbé, M., Petit, P., Year New biofidelity targets for the thorax of a 50th percentile adult male in frontal impact. In 2012 IRCOBI Conference. Neathery, R.F., 1974. Analysis of chest impact response data and scaled performance recommendations. *SAE Technical Papers*. Park, J., Reed, M.P., Hallman, J.J., 2016. Statistical models for predicting automobile driving postures for men and women including effects of age. *Human Factors* 58, 261-278. Reed, M.P., Manary, M.A., Flannagan, C.A., Schneider, L.W., 2000. Effects of vehicle interior geometry and anthropometric variables on automobile driving posture. *Hum Factors* 42, 541-552. Reed, M.P., Manary, M.A., Flannagan, C.A., Schneider, L.W., 2002. A statistical method for predicting automobile driving posture. *Hum Factors* 44, 557-568. Reed, M.P., Parkinson, M.B., 2008. Modeling Variability in Torso Shape for Chair and Seat Design, *ASME International Design Engineering Technical Conferences*, New York, NY, pp. 1-9. Shi, X., Cao, L., Reed, M.P., Rupp, J.D., Hoff, C.N., Hu, J., 2014. A statistical human rib cage geometry model accounting for variations by age, sex, stature and body mass index. *J Biomech* 47, 2277-2285. Shi, X., Cao, L., Reed, M.P., Rupp, J.D., Hu, J., 2015. Effects of obesity on occupant responses in frontal crashes: a simulation analysis using human body models. *Computer methods in biomechanics and biomedical engineering* 18, 1280-1292. Vavalle, N.A., Davis, M.L., Stitzel, J.D., Gayzik, F.S., 2015. Quantitative Validation of a Human Body Finite Element Model Using Rigid Body Impacts. *Annals of biomedical engineering* 43, 2163-2174. Viano, D.C., 1989. Biomechanical responses and injuries in blunt lateral impact. *Stapp Car Crash Journal* 33, 113-142. Wang, Y., Bai, Z., Cao, L., Reed, M.P., Fischer, K., Adler, A., Hu, J., 2015. A simulation study on the efficacy of advanced belt restraints to mitigate the effects of obesity for rear-seat occupant protection in frontal crashes. *Traffic injury prevention* 16, S75-S83. Wang, Y., Cao, L., Bai, Z., Reed, M.P., Rupp, J.D., Hoff, C.N., Hu, J., 2016. A parametric ribcage geometry model accounting for variations among the adult population. *J Biomech*. Zhang, K., Cao, L., Fanta, A., Reed, M.P., Neal, M., Wang, J.T., Lin, C.H., Hu, J., 2017. An automated method to morph finite element whole-body human models with a wide range of stature and body shape for both men and women. *Journal of biomechanics*.

A Progressive Bearing Damage and Failure Model for Composite Interference-fit Joints

Junshan Hu^{*}, Hailin Li^{**}, Kaifu Zhang^{***}

^{*}Northwestern Polytechnical University, ^{**}Northwestern Polytechnical University, ^{***}Northwestern Polytechnical University

ABSTRACT

The interference-fit joint is widely used for thin-walled composite sheets assembly in aviation field. Understanding the damage and failure mechanism of such joint structures has great importance for optimal design of composite joining. Therefore, an evaluation method for the initial and progressive failure of composite interference-fit joints was proposed based on the Hashin type criteria and damage mechanics. In the model, the initial failure (crack initiation in the fiber and/or matrix) and progressive failure (crack growth in the fiber and/or matrix) were evaluated using the separate fiber- and matrix-dependent damage variables, respectively. The user-defined subroutine UMAT was developed based on coupling theories of the failure criterion and damage mechanics in order to efficiently analyze the progressive failure phenomenon in the bearing region of the composite joints. In addition, a technique based on viscous regularization, a characteristic element length and fracture energies of fiber and matrix are used in the model to alleviate mesh-dependence and improve convergence. The influence of interference-fit size, clamping force and applied external loading on damage evolution and failure are considered and good agreements are observed in experimental results.

Skew-symmetric Nitsche's Formulation and Applications in Isogeometric Analysis

Qingyuan Hu^{*}, Franz Chouly^{**}, Stéphane Bordas^{***}, Ping Hu^{****}, Gengdong Cheng^{*****}

^{*}Dalian University of Technology, ^{**}Université Bourgogne Franche-Comté, ^{***}University of Luxembourg, ^{****}Dalian University of Technology, ^{*****}Dalian University of Technology

ABSTRACT

An universal and simple skew-symmetric Nitsche's formulation is introduced into isogeometric analysis (IGA). The derivation of the skew-symmetric Nitsche's formulation is straightforward if one starts from the standard symmetric Nitsche's formulation, and the obtained Nitsche terms are skew-symmetric. Variants of presented formulation are suitable for essential applications in IGA: (displacement or rotational) boundary conditions imposing, patch coupling, and moreover contact problems for the first time in IGA to our knowledge. For boundary conditions imposing, an important advantage of the skew-symmetric Nitsche's formulation is that there is no need to deal with the stabilization parameter as in the standard symmetric Nitsche's formulation. Numerical tests showed that the Nitsche's formulation could impose boundary conditions successfully in a weak sense. For patch coupling, the skew-symmetric Nitsche's formulation is also parameter-free. Through numerical studies it is observed that the condition number of the stiffness matrix by the skew-symmetric Nitsche's formulation is much smaller than the standard symmetric one. In cases of free vibration, the coupling process introduces "outlier" frequencies and corresponding eigenmodes, which are highly localized at these coupled interfaces. The Nitsche's contact formulation is able to theoretically recover the contact (KKT) conditions, it depends much less on the stabilization parameter than the penalty method, and does not introduce extra degrees of freedom as the Lagrange multiplier method. Numerical tests illustrated that the skew-symmetric Nitsche contact formulation can predict the contact pressure distribution to some extent, in addition it behaves more robustly with respect to the stabilization parameter, the element length ratio on contact boundary, and the order of adopted shape functions than the standard one.

Smoothed Particle Galerkin Method with a Second-order Accurate Momentum-Consistent Algorithm for Simulating Thermal-Mechanical Flow Drill Screw Processes

Wei Hu^{*}, C.T. Wu^{**}, Xiaofei Pan^{***}

^{*}Livermore Software Technology Corporation, ^{**}Livermore Software Technology Corporation, ^{***}Livermore Software Technology Corporation

ABSTRACT

In this paper, we present a stabilized Galerkin approximation in a meshfree framework [1] for the simulation of metal threading in the three-dimensional Flow Drill Screw (FDS) process. A second-order accurate momentum-consistent smoothing algorithm is proposed for the desired stability and accuracy in the meshfree structural analysis using the particle integration. A staggered explicit time integration scheme is employed to couple thermal and mechanical systems of equations. To avoid the tension instability in the nonlinear structural analysis, an adaptive anisotropic Lagrangian kernel [2] is considered in the formulation which makes it possible to handle the severe deformation problem in simulating the thread forming phenomena. A bond-based material failure criterion [3] is adopted to prevent the excessive straining due to the assumption of continuous approximation of displacement field in meshfree Galerkin approach. Finally, a three-dimensional FDS problem is analyzed to demonstrate the effectiveness of the present meshfree numerical procedure. [1] C.T. Wu, M. Koishi, W. Hu, A displacement smoothing induced strain gradient stabilization for the meshfree Galerkin nodal integration method, *Comput. Mech.* 56 (2015) 19-37. [2] C.T. Wu, S.W. Chi, M. Koishi, Y. Wu, Strain gradient stabilization with dual stress points for the meshfree nodal integration method in inelastic analysis, *Int. J. Numer. Methods Engrg.* 107 (2016) 3-30. [3] C.T. Wu, Y. Wu, J.E. Crawford, J.M. Magallanes, Three-dimensional concrete impact and penetration simulations using the smoothed particle Galerkin method, *Int. J. Impact Engrg.* 106 (2017) 1-17.

A Symplectic Analytical Singular Element for Thermal Conduction with Singularities in Anisotropic Material

Xiaofei Hu^{*}, Weian yao^{**}

^{*}Dalian University of Technology, ^{**}Dalian University of Technology

ABSTRACT

Thermal conduction problem with singularity in anisotropic materials is still challenging. This is mainly because the thermal conductivity coefficients become functions of the angular coordinate under the polar coordinate system. The analytical study become extremely complex especially when multiple bounded materials are involved in the problem. In order to solve this problem, a sub-field method is first introduced to divide the material around crack tip into several fields in which the material properties are assumed constants under the polar coordinate system. For each sub-field, the symplectic dual approach is then applied to find the general solution of eigen solution. The relationship among the eigen solution of the sub-fields are constructed through the compatibility conditions at the interface between adjacent sub-fields. Then, a symplectic analytical singular element (SASE) is constructed of which the displacement and stress fields are defined by the obtained eigen solutions. The SASE contains rich information of the analytical eigen solution of the boundary value problem and hence is very accurate and efficient for the discussed problem. The general intensity factors can be solved directly without any post-processing. A few numerical examples are worked out to demonstrate the proposed method.

Atomistic Dislocation Core Energies and the Calibration of Discrete Dislocation Dynamics

Yi Hu^{*}, W. A. Curtin^{**}

^{*}LAMMM, EPFL, ^{**}LAMMM, EPFL

ABSTRACT

The method of Discrete Dislocation Dynamics (DDD) [1] has emerged as a valuable tool for modeling the collective behavior of dislocations at the mesoscale, providing insights into a range of plasticity phenomena. DDD uses a continuum line description of the dislocation, with various phenomena controlled by atomistic aspects, such as the Peierls stress, mobility, and core energy, introduced as parameters. To achieve quantitative predictive capability, reflecting real materials, the DDD method can benefit from various improvements, such as anisotropic elasticity [2], partial dislocations for fcc and hcp crystals, and accurate core or self energies. Some phenomena require atomistic resolution, and hence the calibration of DDD to specific atomistic behavior is valuable. Here, we use molecular statics simulations to accurately determine the total dislocation energy in fcc crystals, from which we derive core energies necessary to represent the total energy within anisotropic elasticity. The variation in core energy versus dislocation character deviates significantly from the results obtained by continuum linear elastic dislocation theory. We then examine the use of the derived core energy in established DDD methods for predicting dislocation line tension in a simple bow-out problem. We are unable to reach agreement between such DDD simulations and fully atomistic simulations of the bow-out process in fcc Al [3]. Since fcc dislocations dissociate into two partial dislocations separated by a stacking fault, the analysis is extended to extract the core energies of partial dislocations as a function of dislocation character. Results are also compared to other recent studies of atomistic core energies. The prospects for quantitative linking of atomistic and DDD descriptions of dislocations are discussed in light of our findings. [1] A. Arsenlis, W. Cai, M. Tang, M. Rhee, T. Oppelstrup, G. Hommes, T. G. Pierce, and V. V. Bulatov. Enabling strain hardening simulations with dislocation dynamics. *Modelling and Simulation in Materials Science and Engineering*, 15(6):553, 2007. [2] S. Aubry and A. Arsenlis. Use of spherical harmonics for dislocation dynamics in anisotropic elastic media. *Modelling and Simulation in Materials Science and Engineering*, 21(6):065013, 2013. [3] B. A. Szajewski, F. Pavia, and W. A. Curtin. Robust atomistic calculation of dislocation line tension. *Modelling and Simulation in Materials Science and Engineering*, 23(8):085008, December 2015.

A Coupled Kinetic Monte Carlo-Finite Element Method Mesoscale Modeling In Metallic Glass Matrix

Chang-Wei Huang*, Yu-Cheng Chen**, Pierre Hamm***, Yu-Chieh Lo****

*Department of Civil Engineering, Chung Yuan Christian University, Taoyuan, 32023, Taiwan, **Department of Materials Science and Engineering, National Chiao Tung University, Hsinchu, 30010, Taiwan, ***Department of Materials Science and Engineering, National Chiao Tung University, Hsinchu, 30010, Taiwan, ****Department of Materials Science and Engineering, National Chiao Tung University, Hsinchu, 30010, Taiwan

ABSTRACT

Metallic glasses (MGs) have exhibited many promising properties such as high yield strength, low friction coefficient and high resistance to corrosion, oxidation and wear. However, the localized deformation and poor ductility due to shear bands prohibit the further applications of MGs. In this study, a mesoscale model combining the kinetic Monte Carlo algorithm and the finite element method is developed to investigate the deformation behaviors of MGs. The shear transformation zone (STZ) is viewed as the fundamental deformation unit and each nanoscale volume element in the MGs is considered as a potential STZ. The mesoscale modeling is capable of simulating MGs processing and deformation on time and length scales greater than those by atomistic modeling. The proposed computational framework is firstly verified by a sanity check and then applied to simulate uniaxial tension test. Simulations of the uniaxial tension demonstrate the key factor of the shear band formation is the strain-induced softening.

A Non-ordinary State-based Peridynamic Modeling for Hydraulic Fracture

Dan Huang^{*}, Yubin Zhang^{**}, Yepeng Xu^{***}

^{*}Hohai University, ^{**}Hohai University, ^{***}Hohai University

ABSTRACT

A coupled fluid-structure interaction model based on the peridynamic theory has been proposed and applied to hydraulic fracture problems. A nonlocal constitutive model which can describe the mechanical behavior and fracture characteristics of rock and concrete-like quasi-brittle materials is proposed based on the non-ordinary state-based peridynamic theory. An equivalent hydraulic pressure term coupled with flow equation was embedded in the peridynamic model to describe the fluid flow and track the hydraulic pressure on the new-born crack surfaces. Considering the contact between surfaces of cracks, a short-range repulsive force between material points was implemented and corresponding contact algorithms were developed. The proposed model and algorithms were validated through simulating the hydraulic fracture of typical concrete gravity dams in different loading cases, and comparing the numerical results with experimental observations and other numerical results. Key words: hydraulic fracture; crack propagation; state-based peridynamics; contact

*Acknowledgement: The support of the National Natural Science Foundation of China (No. 51679077) and the Fundamental Research Funds for the Central Universities in China (Nos. 2015B18314, 2017B13014) is gratefully acknowledged. [1] Silling S A, Epton M, Weckner O, et al. Peridynamic states and constitutive modeling[J]. Journal of Elasticity, 2007,88(2): 151-184. [2] Warren T L, Silling S A, Askari A, et al. A non-ordinary state-based peridynamic method to model solid material deformation and fracture[J]. International Journal of Solids and Structures, 2009,46(5): 1186-1195. [3] Katiyar A, Foster J T, Ouchi H, et al. A peridynamic formulation of pressure driven convective fluid transport in porous media[J] Journal of Computational Physics, 2014,261(3):209-229

A Family of Non-Oscillatory Embedded Boundary Methods for Viscous Flow and Fluid-Structure Interaction Problems

Daniel Huang*, Charbel Farhat**

*Stanford, **Stanford

ABSTRACT

The second-order Finite Volume method with Exact two-material Riemann Problems (FIVER) [1] is both a computational framework for multi-material flows characterized by large density jumps, and an Embedded Boundary Method (EBM) for CFD and highly nonlinear Fluid-Structure Interaction (FSI) problems [2]. For FSI problems, this EBM has demonstrated the ability to address viscous effects along wall boundaries [3], and large deformations and topological changes of such boundaries [2]. However, like for most EBMs, its performance in the vicinity of a wall boundary can be sensitive with respect to the position and orientation of this boundary relative to the embedding mesh. This is due to ill-conditioning issues that arise when an embedded discrete surface becomes too close to a node of the embedding mesh, which may lead to spurious oscillations in the computed solution gradients at the wall boundary. These issues are resolved here by introducing an alternative definition of the active/inactive status of a mesh node that removes all sources of ill-conditioning. Two additional contributions are presented. The first one is a new procedure for constructing the fluid-structure half Riemann problem underlying the semi-discretization by FIVER of the convective fluxes that replaces one extrapolation by an interpolation. The second contribution is a post-processing algorithm for computing quantities of interest at the wall that achieves smoothness in the computed solution and its gradients. Lessons learned from these enhancements are then generalized to eliminate from the original version of FIVER its aforementioned sensitivities while maintaining the original definition of the status of a mesh node. This leads to a family of second-generation, second-order FIVER methods whose performance is illustrated in this talk for a challenging flow problem over a bird wing characterized by a feather-induced surface roughness, and a complex flexible flapping wing problem for which experimental data is available. 1. A. Main, X. Zeng, P. Avery and C. Farhat, An Enhanced FIVER Method for Multi-Material Flow Problems with Second-Order Convergence Rate, *Journal of Computational Physics*, Vol. 329, pp. 141-172 (2017) 2. K.G. Wang, P. Lea and C. Farhat, A Computational Framework for the Simulation of High-Speed Multi-Material Fluid-Structure Interaction Problems with Dynamic Fracture, *International Journal for Numerical Methods in Engineering*, Vol. 104, pp. 585-623 (2015) 3. V. Lakshminarayan, C. Farhat and A. Main, An Embedded Boundary Framework for Compressible Turbulent Flow and Fluid-Structure Computations on Structured and Unstructured Grids, *International Journal for Numerical Methods in Fluids*, Vol. 76, pp. 366-395 (2014)

High Performance Computing of Distortion and Stresses in Welded and Additive Manufactured Structures

Hui Huang^{*}, Chen Jian^{**}, Zhili Feng^{***}

^{*}Oak Ridge National Laboratory, ^{**}Oak Ridge National Laboratory, ^{***}Oak Ridge National Laboratory

ABSTRACT

Numerical simulation is an efficient way to better understand the thermal and mechanical evolution during welding and additive manufacturing (AM) processes and to design and optimize the processes. However, with today's computational tools, thermal-mechanical simulation of the continuous metal depositing process is extremely time-consuming. As a result, many simulation models proposed so far are based on simplification that either the continuous manufacturing pass is lumped, or the dimension of model is decreased. For example, residual stress simulation of multipass girth welds are mostly performed using two-dimensional (2D) axisymmetric models. In this study, a new finite element code recently developed in house at Oak Ridge National Lab was used for simulation of both welding and additive manufacturing. Our new code effectively utilizes GPU based high-performance computers to allow for realistic simulation of the transient thermal and mechanical response of materials during arc based manufacturing process. Our code further accelerates based on the consideration of unique physics associated with manufacturing processes that are characterized by steep temperature gradient and a moving heat source. It is capable of modeling large-scale problems that cannot be easily handled by the existing commercial simulation tools. To demonstrate the accuracy and efficiency, our in-house code was compared with the commercial modeling tools by simulating a single pass pipe girth weld. Our code achieved comparable solution accuracy with respect to the commercial one but with over 100 times less on computational cost. Moreover, a multi-pass girth weld model with over 1 million elements and 180 thousand time-steps was successfully analyzed in 3.2 days. The 3D analysis demonstrated more realistic stress distribution that is not necessarily axisymmetric along the hoop direction. A benchmark study on a cylinder model by selective laser melting was also carried out and compared to the experimental measurements. Distortion shape was well reproduced by the new code and computational time was drastically reduced relative to that by commercial model. Effects of layer-by-layer activation and element-by-element activation scheme on distortion and stress accuracy was clarified by the efficient numerical model.

Non-reciprocal Wave Propagation in Time-varying Modulated Lattices

Jiahui Huang^{*}, Yuchen Zhao^{**}, Xiaoming Zhou^{***}

^{*}Key Laboratory of Dynamics and Control of Flight Vehicle, Ministry of Education and School of Aerospace Engineering, Beijing Institute of Technology, Beijing 100081, China, ^{**}Key Laboratory of Dynamics and Control of Flight Vehicle, Ministry of Education and School of Aerospace Engineering, Beijing Institute of Technology, Beijing 100081, China, ^{***}Key Laboratory of Dynamics and Control of Flight Vehicle, Ministry of Education and School of Aerospace Engineering, Beijing Institute of Technology, Beijing 100081, China

ABSTRACT

The modulated mediums are materials whose properties could vary periodically in both the space and time. Non-reciprocal wave propagation can be acquired in the modulated medium, and is expected to bring new technological concepts to wave-control engineering. In this work, we study an infinite space-time lattice structure composed of the time-varying mass and the spring of constant stiffness. The Bloch-based theoretical method is developed for the computation of the dispersion diagrams of the modulated lattice system. It is found that the asymmetric band of the fundamental branch emerges if the spatiotemporal modulation of inertial mass constitutes a travelling-wave field pattern, which behaves like a biasing field that breaks the time-reversal symmetry. Asymmetric bandgaps are opened due to the modulation-induced mode interaction of different orders. A purely unidirectional bandgap can be available when the super cell involves over three time-varying elements, and the phase difference of time-varying mass between adjacent elements is the same. The effect of modulating frequency and amplitude of time-varying mass is analyzed. It is found that the modulating frequency affects primarily the frequency position of the asymmetric bandgap, while the modulating amplitude determines its frequency bandwidth. We also study the non-reciprocal wave phenomenon in modulated lattices involving simultaneous time-driven mass and stiffness. Adding the space-time modulation over stiffness leads to the wider asymmetric bandgap and the flexible control on the gap position. Finally, we will present some possible designs of structured elements with time-varying mass and/or time-varying stiffness. The modulated lattice structure is expected to open a new avenue in the unprecedented control over sounds and vibrations. Reference: Trainiti, G., Ruzzene, M., 2016. Non-reciprocal elastic wave propagation in spatiotemporal periodic structures. *New J. Phys.* 18, 083047. Vila, J., Pal, R.K., Ruzzene, M., Trainiti, G., 2017. A Bloch-based procedure for dispersion analysis of lattices with periodic time-varying properties. *J. Sound Vib.* 406, 363-377.

On the Accurate and Efficient Simulation of Ferrofluids

Libo Huang*

*KAUST

ABSTRACT

Ferrofluid, due to its peculiar behavior in the magnetic field, has drawn the attention from various disciplines. In contrast to its wide applications, its large-scale simulation is less addressed. Previous simulations are mesh-based, while we present a method tackling the problem on a particle basis. The core idea is to treat each particle as a distribution (e.g. symmetric truncated Gaussian) of fluid. The aggregation of all particles forms the spatial distribution of the ferrofluid. In the external field, the ferrofluid acts as a soft magnetizable material, and the total magnetic field is the sum of the external field and the field generated by the ferrofluid itself, called the demagnetization field. The magnetization relationship is nonlinear, but the total demagnetization field is a linear combination of the field generated by each particle (distribution). Since each particle after magnetization would affect other particles, an optimization method is used to get the final magnetic field, minimizing the difference between the demagnetization field influencing the particles, and the demagnetization field generated by the particles. With the final magnetic field, various force models can be used, either classical Kelvin forces or modern forces derived from thermodynamics. Combining the force term and surface tension with existing Navier-Stokes solvers, either pure Lagrangian, for example, the Smooth Particle Hydrodynamics (SPH) method, or mixed Eulerian and Lagrangian for example the (A) Particle In Cell ((A)PIC) method, one can obtain both accurate and efficient large-scale simulations of ferrofluids.

Numerical Investigation on Dynamic Contact Angles of Nano-Scale CO₂-Water-Silica Systems

Pengyu Huang^{*}, Luming Shen^{**}, Yixiang Gan^{***}, Federico Maggi^{****}, Abbas El-Zein^{*****}

^{*}The University of Sydney, ^{**}The University of Sydney, ^{***}The University of Sydney, ^{****}The University of Sydney, ^{*****}The University of Sydney

ABSTRACT

CO₂ geosequestration into deep saline aquifers may be a viable strategy for reducing greenhouse gas emissions and mitigating anthropogenic climate change. In CO₂ geosequestration, the CO₂ is commonly compressed into supercritical CO₂ and injected into the aquifers for long-term storage. The structural and residual trapping capacities of the aquifers depend on CO₂-brine interfacial tension and contact angle in CO₂-brine-mineral geophysical systems. While earlier molecular dynamics (MD) simulations have been used to study the CO₂-brine interfacial tension and the static contact angles of CO₂-brine-mineral systems at different temperatures and pressures, we study in this work the dynamic contact angles of CO₂-water-silica systems during supercritical CO₂ injections at different injection rates with MD. The supercritical CO₂ flow induced by a moving piston is injected into water between two parallel silica plates; the simple point charge (SPC) water model (Teleman, Jönsson, &&&& Engström, 1987), the elementary physical model (EPM2) for CO₂ molecules (Nieto-Draghi, de Bruin, Pérez-Pellitero, Bonet Avalos, &&&& Mackie, 2007) and the silica surface model developed by (Emami et al., 2014) are used in these simulations. Both intramolecular and intermolecular degrees of freedom are considered in the simulations. The interaction parameters between dissimilar atoms are computed using Lorentz-Berthelot combining rules. Scenarios with different area densities of the silanol groups on the silica surfaces are also considered to reproduce hydrophilic and hydrophobic surfaces. The preliminary results show the dependence of dynamic contact angles on injection rates. This study will help us better understand and predict the mechanism of CO₂ injections and the storage capacities in deep saline aquifers. References Emami, F. S., Puddu, V., Berry, R. J., Varshney, V., Patwardhan, S. V., Perry, C. C., &&&& Heinz, H. (2014). Force field and a surface model database for silica to simulate interfacial properties in atomic resolution. *Chemistry of Materials*, 26(8), 2647-2658. Nieto-Draghi, C., de Bruin, T., Pérez-Pellitero, J., Bonet Avalos, J., &&&& Mackie, A. D. (2007). Thermodynamic and transport properties of carbon dioxide from molecular simulation. *The Journal of Chemical Physics*, 126(6), 064509. Teleman, O., Jönsson, B., &&&& Engström, S. (1987). A molecular dynamics simulation of a water model with intramolecular degrees of freedom. *Molecular Physics*, 60(1), 193-203.

Interface Structure Dependent Incipient Plasticity of Graphene/Cu Nanomultilayers

Ping Huang^{*}, Shuang Zhang^{**}, Fei Wang^{***}

^{*}State Key Laboratory for Mechanical Behavior of Material, School of Materials Science and Engineering, Xi'an Jiaotong University, ^{**}State Key Laboratory for Mechanical Behavior of Material, School of Materials Science and Engineering, Xi'an Jiaotong University, ^{***}State Key Laboratory for Strength and Vibration of Mechanical Structures, School of Aerospace, Xi'an Jiaotong University

ABSTRACT

Even though graphene possesses extremely high strength and elastic modulus, it is still a challenge to use it as structural materials due to its extrinsic dimension limit. Then, composite structure combined graphene and proper metals, i.e., graphene/metal nanocomposites, was proposed to be a possible way recently to achieve diverse properties that cannot be provided by single constituent material. For nanocomposites, interface structure generally played a significant role in determining mechanical properties as individual layer thickness of the constituent layers decreases to less than tens of nanometers, such as interface structure transition, acting as sources for nucleating dislocations. Unlike the well documented metal/metal composites, the mechanisms and how interface structure evolve upon plastic deformation in the graphene/metal composites are still unclear and under intense debate. In the present study, molecular dynamics simulations were used to explore the interface structure and the inception of plasticity of graphene/Cu nano-multilayers. Specific attention was paid on how the graphene/Cu interface structural features affect the strength of the nano-multilayers. After relaxation, the strain distribution along graphene/Cu interface was non-uniform. The role of the interface structure in the plastic deformation of graphene/Cu nano-multilayers was studied under two loading axes, and it was found (i) preferential slip systems within Cu layers all followed the Schmid factors and regular nucleation sites were from interface where the local strain is the highest, which behavior is different from other metal/metal system, and (ii) dislocations propagated in two {111} slip planes with the partial dislocation $\frac{1}{6}\langle 112 \rangle$ along the specific directions in which the strain is higher. In addition, incipient plastic deformation originated from the graphene/Cu interface could effectively enhance the strength and elastic modulus of the graphene/Cu nano-multilayers compared with nanocrystalline Cu. It was concluded the interface strain changes the nucleating behavior and graphene acting as a constrained layer leads to the strengthening effect.

A Fractional Viscoelastic Model for Shape Memory Polymers

Rong Huang^{*}, Zhouzhou Pan^{**}, Zishun Liu^{***}

^{*}International Center for Applied Mechanics, State Key Laboratory for Strength and Vibration of Mechanical Structures, Xi'an Jiaotong University, ^{**}International Center for Applied Mechanics, State Key Laboratory for Strength and Vibration of Mechanical Structures, Xi'an Jiaotong University, ^{***}International Center for Applied Mechanics, State Key Laboratory for Strength and Vibration of Mechanical Structures, Xi'an Jiaotong University

ABSTRACT

Shape memory polymers (SMPs) have been widely studied because they can recover from a deformed shape to their original shape by a certain external stimulus. In order to investigate this interesting process and predict this kind of deformation behavior, many researchers have generated constitutive models from different aspects of views. However, most of the proposed constitutive models include a great amount of parameters and these parameters must be carefully selected and verified by a large amount of experiments. This complex process not only generate extra work for data processing but also limits the application and development of the constitutive models. Therefore, it is indispensable to develop a new constitutive model which can take into account both the accuracy and the simplicity. From the experiment observations, we found that the majority of shape memory polymers show a power-law type relaxation behavior instead of an exponential type correlations curve between relaxation modulus and time. Considering this phenomenon, we propose a fractional viscoelastic constitutive model with less parameters for SMP which give good agreement with the experimental thermomechanical behavior of SMPs and also reduces the workload of parameters fitting. The article draw up to match through frequency and time sweep curve fitting form previous SMP experiments to establish the mathematics model. Then we applied the model to calculate the SMP behavior during uniaxial tension and free recovery process under different loading cases. Both the mathematical model and the real experiment results give good consistency. In addition, the comparison between an integral and fractional viscoelastic models of SMP are discussed in our study. We hope the proposed model in our researches could provide some new ideas in designing and optimizing potential SMP applications.

Steady-State Crack Growth in Polymer Gels by Linear and Nonlinear Poroelastic Models

Rui Huang^{*}, Yalin Yu^{**}, Chad Landis^{***}

^{*}University of Texas at Austin, ^{**}University of Texas at Austin, ^{***}University of Texas at Austin

ABSTRACT

Large deformation and solvent migration are coupled during fracture of polymer gels. We developed a nonlinear finite element method to simulate steady-state crack growth in polymer gels, with which we calculated the J-integral as a function of the crack speed. To understand the numerical results, we developed an analytical solution for the asymptotic crack tip fields based on a linear poroelastic formulation. A strip with a semi-infinite crack in steady state was studied in details by both the linear and nonlinear models. The crack-tip fields predicted by the asymptotic solution are confirmed by the numerical results. It is found that, due to the poroelastic effect, the crack-tip stress intensity factor is generally smaller than the stress intensity factor predicted by linear elasticity model. The size of the poroelastic crack-tip field is characterized by a diffusion length scale that depends on the crack speed. For relatively fast crack growth, the diffusion length is small compared to the strip thickness, and the crack-tip field transitions to the elastic K-field at a distance proportional to the diffusion length. In this case, the energy release rate by a modified J-integral decreases with increasing crack velocity. For relatively slow crack growth, the diffusion length is comparable to or greater than the strip thickness, and the crack-tip field is confined by the strip thickness and transitions to a one-dimensional diffusion zone ahead of the crack tip. In this case, the energy release rate increases with increasing crack speed. Surprisingly, the energy release rate approaches the same limit for both fast and slow crack growth, but with a peak in between. These results suggest that, if the intrinsic fracture toughness of the gel is independent of the crack speed, the apparent fracture toughness including the energy dissipation due to solvent diffusion would be considerably greater than the intrinsic toughness and depends non-monotonically on the crack speed or the strip thickness.

Eulerian Reproducing Kernel Particle Method for Shock Modeling

Tsung-Hui Huang*, J. S. Chen**

*University of California, San Diego, **University of California, San Diego

ABSTRACT

The following issues be properly addressed in modeling shock wave propagation in hydrodynamical systems: (1) correct representation of essential shock physics, (2) stabilization of Gibbs phenomenon at discontinuity, and (3) capturing shock front with minimal smearing of moving discontinuity. In this work, we introduce a stabilized Eulerian reproducing kernel particle method (RKPM) for shock modeling. RKPM is considered herein due to its versatility in adaptive refinement and in adjusting smoothness independently to the order of completeness in the approximation. A stabilized conforming nodal integration (SCNI) is constructed with locally enriched Riemann flux, such that the essential shock physics, Rankine-Hugoniot jump condition and Lax entropy condition, are satisfied. The oscillation control is provided through the smoothed flux divergence in the SCNI framework. Furthermore, to increase the accuracy at shock front, a Monotonic Upstream-Centered Scheme for Conservation Laws (MUSCL) type flux reconstruction is introduced to achieve higher order spatial accuracy. Several numerical examples are analyzed to verify the effectiveness of the proposed framework.

A Consistent Damage Model for Structural Components of Different Materials

Wei Huang*, Zhi Zhou**

*Department of Mechanics and Engineering Structure (Wuhan University of Technology), **State Key Laboratory of Disaster Reduction in Civil Engineering (Tongji University)

ABSTRACT

Owing to the existence of varied structural components with different materials in the hybrid structures, the seismic damage failure performance and mechanisms of each component are quite different, consequently resulting in the need for a unified standard for its performance assessment. Based on the widely-used Park-Ang damage model, a consistent modification form which is suitable for structural components of different materials is proposed in the paper. The experiment statistics of various components of different materials are collected and analyzed to study the combination coefficient of the consistent damage model. Despite that the specific limit values are all calculated by the consistent damage model at the same performance levels, obvious difference exists between components of different materials. In order to build the correlation between the consistent damage model and the damage performance for components of different materials, normalized corresponding parameters are introduced to the unified damage model to specify the damage limit values at each performance level for components of different materials.

An Immersed Boundary Projection Method for Fluid-Flexible Body Interaction

Wei-Xi Huang^{*}, Luo-Hao Wang^{**}, Chun-Mei Xie^{***}

^{*}Tsinghua University, ^{**}Tsinghua University, ^{***}Tsinghua University

ABSTRACT

An immersed boundary projection method with primitive variables is proposed for simulation of fluid-flexible body interaction. Two types of flexible bodies are considered, i.e., the 2D filament and the 3D flag. The filament's motion is constrained with the inextensible condition (while the flag is in-plane inextensible), and its interaction with the incompressible fluid flow is counted by the additional momentum forcing. In the present formulation, the pressure, the momentum forcing and the tension of the filament are uniformly considered as Lagrange multipliers, which act to satisfy the divergence-free condition, the no-slip condition on the immersed boundary and the inextensibility constraint of the filament, respectively. The whole system is solved within the framework of the projection approach. For numerical implementation, a three-step approximate factorization process is proposed to decouple the tension, the momentum forcing and the pressure sequentially from the velocity fields, thus significantly reducing the computational cost. The proposed method is validated by comparing the flow-induced flapping motion with the previous studies. Both the temporal and spatial accuracies are verified and the computational cost is also measured. Results have shown good coherence with the previous studies as well as significant reduction in computational cost.

Numerical Study of Upper Airway with Obstructive Sleep Apnoea/hypopnoea Syndrome Using Large Eddy Simulation

Xiao-Wen Huang*, Ming-Jyh Chern**, Hung-Ta Hsiao***

*National Taiwan University of Science and Technology, **National Taiwan University of Science and Technology,
***National Tsing Hua University

ABSTRACT

Obstructive sleep apnoea/hypopnoea syndrome (OSAHS) is a common disorder of adult, which is caused by repeated obstruction the upper airway during sleep. The effects of OSAHS are not only the sleep quality but also the occurrence of disease such as hypertension, stroke and myocardial infarction. Apnoea-hypopnoea index (AHI) is an acceptable measure for the severity of OSAHS. Most of treatments are continuous positive airway pressure (CPAP) which is considered to be the standard treatment for patients with moderate-to-severe. The alternative way to prevent life-long CPAP treatment is a surgical technique. In the present study, the pre-operative and post-operative CT scan of upper airway by patients were re-constructed and converted to in vitro three-dimensional models. The transitional/turbulent flow simulations during inspiration and expiration were studied using Large Eddy Simulation (LES) in the in vitro 3D models of upper airway with a 0D lumped parameter model. Furthermore, the results show that the pressure drop of upper airway was significantly reduced after surgery and this model may be further applied for clinical evaluation in future.

Numerical Analysis of Tower Effects on Wake Flows of Floating Offshore Wind Turbine

Yang Huang^{*}, Decheng Wan^{**}

^{*}Shanghai Jiao Tong University, ^{**}Shanghai Jiao Tong University

ABSTRACT

The floating offshore wind turbine (FOWT), consisting of wind turbine, floating support platform and mooring system, is quite a complex floating structure system. Accurate prediction of FOWT's coupled aerodynamic responses is of great challenge. The tower effects are usually not taken into consideration in the simulations of wind turbine aerodynamics using an actuator line model. However, it has been suggested by other researchers that including the tower effects is important in better predicting the near wake and unsteady power output. To study the influence of tower effects on coupled aero-hydrodynamic responses of FOWTs, the tower is modeled within an unsteady actuator line model in fully coupled simulations of FOWTs under variable wind and wave conditions. In the present study, the unsteady actuator line model (UALM) is embedded into in-house CFD solver naoe-FOAM-SJTU to establish a fully coupled CFD analysis tool named FOWT-UALM-SJTU for simulations of FOWTs. The blades and the tower of the wind turbine are represented by actuator lines, and the body forces applied to the flow field are calculated according to two-dimensional airfoil data. Coupled aero-hydrodynamic simulations of OC3 Hywindspar FOWT model under shear wind and regular wave conditions are conducted. The unsteady aerodynamics of wind turbines and tower effects are predicted by the UALM, and the hydrodynamic responses of floating platforms and mooring tensions can be obtained by naoe-FOAM-SJTU. From the simulations, unsteady aerodynamic characteristics including the rotor power, thrust, and detailed wake flow information are available. To better understand tower effects, the numerical results considering the tower effects are compared with previous results that the tower effects are ignored. Furthermore, both the wake flow and the aerodynamic loads are analyzed to study the influence of tower effects on coupled dynamic responses of the FOWTs. It can be found that the use of a tower model with unsteady actuator line model can improve near wake prediction accuracy. And considering the tower effects helps in more precisely predicting transient aerodynamic loads of the FOWTs.

An Innovative Fluid-Structure Computational Framework for Supersonic Parachute Inflation Dynamics

Zhengyu Huang*, Charbel Farhat**, Phil Avery***

*Stanford University, **Stanford University, ***US Army Research Laboratory, Stanford University

ABSTRACT

There is significant evidence today that the supersonic flow regime has a profound effect on the performance of a parachute [1]. Causes for even greater concern are the canopy failures observed during the inflation process in flight tests conducted by NASA for Mars landing, and the limited number of tests that can be performed for developing a better understanding of how to avoid such failures. Yet, most if not all relevant computational efforts have focused so far on developing CFD and Fluid-Structure Interaction (FSI) parachute models for the much easier to simulate post-inflation regime. To this effect, this talk will begin with a short presentation on the development of an Eulerian computational framework for evolving fluid-structure interfaces in high-speed turbulent flows, whose design is motivated by the need to simulate parachute inflation dynamics. The framework is built around an Eulerian computational model for FSI that has proven itself for the simulation of the failure analysis of submerged structures subjected to explosions and implosions [2]. It incorporates in the computations a suitable material failure model, captures the effects of strain rate and temperature, and accounts for the various interactions between the fluid subsystem. It resolves all self-contact effects of the parachute during its inflation, and tracks and resolves all evolving boundary layers using a tailored adaptive mesh refinement approach [3]. Next, the talk will proceed with the discussion of a set of preliminary simulations of a parachute's opening process performed using this computational framework, initiating from a folded state of the parachute pre-inflation to the fully inflated state. Finally, the talk will conclude with an original idea about modeling different folding patterns to predict the influence of the folding pattern on the inflation process and initial, intermediate, and final stress state of the fabric when the parachute survives the inflation dynamics. 1. S. Lingard, Supersonic Parachutes, Parachutes Systems Technology Short Course, U.S. Army Yuma Proving Ground, Yuma, Arizona, May 17-21, 2010. 2. K. Wang, P. Lea and C. Farhat, A Computational Framework for the Simulation of High-Speed Multi-Material Fluid-Structure Interaction Problems with Dynamic Fracture, International Journal for Numerical Methods in Engineering, Vol. 104, pp. 585-623 (2015) 3. R. Borker, S. Grimberg, P. Avery, C. Farhat and J. Rabinovitch, An Adaptive Mesh Refinement Concept for Viscous Fluid-Structure Computations Using Eulerian Vertex-Based Finite Volume Methods, AIAA-2018-1072, AIAA SciTech 2018, Kissimmee, Florida, January 8-12 (2017)

Hybridizable Discontinuous Galerkin from Low to High Order

Antonio Huerta^{*}, Ruben Sevilla^{**}, Matteo Giacomini^{***}

^{*}Universitat Politecnica de Catalunya, ^{**}Swansea University, ^{***}Universitat Politecnica de Catalunya

ABSTRACT

Consistent stabilization of convection dominated problems is based in the seminal work by Hughes and coworkers. Hybridizable Discontinuous Galerkin has in recent years demonstrated its ability to solve a wide range of engineering problems. The HDG method is able to provide the optimal approximation properties that are characteristic of mixed methods, including the possibility to build a superconvergent solution, whilst retaining the advantages of DG methods. In addition, HDG methods are known to reduce the globally coupled degrees of freedom, when compared to other DG methods. Moreover, HDG is competitive compared to the traditional continuous Galerkin (CG) method and has comparable costs (in terms of floating point operations) to CG [1]. Other advantages of HDG, such as block structured information and element-by-element operations must be exploited to improve its performance compared to CG because parallelism and memory access are crucial for the final runtime. When high-order approximations are competitive, HDG can be combined with NURBS-enhanced finite element method (NEFEM) [2] to design a superior and reliable strategy where degree adaption allows to attain the desired accuracy. Moreover, in the context of computational mechanics, an alternative formulation to impose physical natural boundary conditions and strongly the symmetry of the strain tensor is proposed by means of the well-known Voigt notation for symmetric tensors. Optimal convergence of the mixed variable is retrieved for low-order elements and a novel local post-process procedure leading to a superconvergent velocity field is advanced. Other scenarios are however more suited for low-order approximations. Under this perspective, a new finite volume paradigm is presented [3]. It is called face-centered finite volume (FCFV) and is based on an HDG method with constant degree of approximation. First order convergence on both the solution and its gradient is obtained without a reconstruction of the gradients. Therefore, contrary to other finite volume methodologies, the accuracy of the FCFV method is not compromised in the presence of highly stretched or distorted elements. [1] A. Huerta, A. Angeloski, X. Roca, and J. Peraire. "Efficiency of high-order elements for continuous and discontinuous Galerkin methods." Int. J. Numer. Methods Eng., 96(9):529–560, 2013. [3] R. Sevilla, and A. Huerta. "HDG-NEFEM with degree adaptivity for Stokes flows," to appear in Journal of Scientific Computing (2018). [3] R. Sevilla, M. Giacomini, and A. Huerta. "A face-centred finite volume method for second-order elliptic problems." arXiv:1712.06173 (2017).

High-Performance Model Order Reduction Techniques for Geometrical Non-linear Problems: Application to Multi-scale Material Homogenization Problems

Alfredo Huespe*, Manuel Caicedo**, Javier Mroginski***, Sebastian Toro****, Javier Oliver*****

*CONICET, Argentine Council for Science and Technology, Argentina, **CIMNE – Internacional Center for Numerical Methods in Engineering, ***Applied Mechanical Dept., Universidad Nacional del Nordeste, Argentina, ****CONICET, Argentine Council for Science and Technology, Argentina, *****CIMNE – Internacional Center for Numerical Methods in Engineering

ABSTRACT

The purpose of this work is to generalize a version of the High Performance Reduced-Order Model (HPROM) technique, previously presented by the authors in [1], in the context of hierarchical multiscale models for heterogeneous non-linear-materials undergoing infinitesimal strains, is generalized to deal with a different range of applications. Typically, large elasto-plastic deformation problems subjected to small rotation regimes, observed in multiscale homogenization problems arising in a wide range of material modeling applications. The proposed HPROM technique uses a Proper Orthogonal Decomposition (POD) procedure to build a reduced basis of the primary kinematical variable of the micro-scale problem, defined in terms of the micro-deformation gradient fluctuations. Then a Galerkin-projection, onto this reduced basis, is utilized to reduce the dimensionality of the micro-force balance equation, the stress homogenization equation and the equivalent macro-constitutive tangent tensor equation. Finally, a reduced goal-oriented cubature rule is introduced to compute the non-affine terms of these equations [2]. The work is focused on the numerical assessment of the HPROM technique. The numerical experiments are performed on a micro-cell simulating a randomly distributed set of elastic inclusions embedded into an elasto-plastic matrix. This micro-structure is representative of a typical ductile metallic alloy. The HPROM technique applied to this type of problem displays high computational speed-ups, increasing with the complexity of the finite element model. We conclude that this technology is adequate for applications in material modeling involving two length scales, using full 3D cells with refined micro-structural details. [1] J. Oliver, M. Caicedo, A.E. Huespe, J.A. Hernández, E. Roubin, Reduced order modeling strategies for computational multiscale fracture Comput. Meth. App. Mech. Eng. 313, 560-595 (2017) [2] J.A. Hernández, J. Oliver, A.E. Huespe, M.A. Caicedo, J.C. Cante, High-performance model reduction techniques in computational multiscale homogenization, Comput. Meth. App. Mech. Eng., 276, 149-189 (2014)

Probing Mechanics at the Scales of Cells and Tissue via Optical Coherence Tomography

Nicholas Hugenberg*, Assad Oberai**, Li Dong***

*Rensselaer Polytechnic Institute, **University of Southern California, ***University of Texas at Austin

ABSTRACT

In this talk we will describe new developments from the field of Optical Coherence Elastography (OCE) that have enabled the mapping of the mechanical properties of cells, clusters of cells, and tissue. OCE affords a spatial resolution of about 10-20 microns, and a field of view of about 2-5 millimeters. This makes it ideal for quantifying the mechanical microenvironment for diseases like cancer and atherosclerosis. We will focus on new computational methods within OCE that have made this possible. These include new adaptive grid methods for solving inverse problems, and methods for solving the nonlinear inverse elasticity problem.

From (HHT)-Alpha to Omega?

Gregory Hulbert*

*University of Michigan

ABSTRACT

It has been more than 40 years since the HHT-alpha time integration method was published in one of the early volumes of Earthquake Engineering and Structural Dynamics. It is, without doubt, the most cited method for structural dynamics, with the possible exception of Newmark's seminal work in the 1950's. In this presentation, we will articulate why the HHT-alpha has maintained its prominence. We will also propose a lingua franca, using the works Tom Hughes as inspiration, for researchers who endeavor to introduce new time integration methods, so that such contributions to the time integration field can be correctly classified, categorized and recognized.

Modeling Thrombus Formation in Abdominal Aortic Aneurysms

Jay Humphrey*, Druv Bhagavan**, Paolo Di Achille***

*Yale University, **Yale University, ***Yale University

ABSTRACT

Over 75% of abdominal aortic aneurysms develop an intraluminal thrombus, that is, a blood clot. Although there is controversy surrounding the potential roles of thrombus in the natural history of aneurysms, increasing evidence suggests that a thrombus releases biomolecules can contribute to degradation of the aneurysmal wall, thus leading to continued enlargement and increased risk of rupture. There is, therefore, strong motivation to predict where and when a thrombus might form in particular patients [1]. We suggest that thrombus initiates when two hemodynamic factors co-localize in space and time. First, the endothelial cell layer that lines the inner surface of the aorta and the aneurysm must be rendered susceptible to platelet attachment. Second, this susceptible region must be presented with activated platelets that can attach and aggregate. We suggest further that once a thrombus initiates, it will continue to grow within the flow field until hemodynamic forces become sufficient to prevent any further platelet attachment or protein adsorption. We use open source software, SimVascular, to solve the requisite Navier-Stokes equations and a custom Lagrangian particle tracking code to estimate platelet motions. Based on our computational findings, we propose two scalar hemodynamic metrics to predict both thrombus formation and deposition in patient-specific models of abdominal aortic aneurysms and show that predictions compare favorably with results obtained from medical imaging [2,3]. Finally, we consider hemodynamics within a host of idealized model aneurysms and use kriging to explore parametrically the effect of five different morphological features of the infrarenal aorta and associated aneurysm on thrombus formation and identify potential clinical predictors of future thrombus accumulation. [1]. Wilson J.S. et al. (2013) J Biomech Engr 135:021011. [2] Di Achille P. et al. (2014) Proceed R Soc A 470:20140163. [3]. Di Achille P. et al. (2017) Int J Num Meth Biomed Eng 33:e02828

Construction of Simplified Models for Crack Propagation in Random Heterogeneous Media

Darith Hun^{*}, Johann Guilleminot^{**}, Julien Yvonnet^{***}, Michel Bornert^{****}

^{*}Laboratoire Modélisation Simulation Multi Echelle (MSME), ^{**}CEE, Duke University, ^{***}Laboratoire Modélisation Simulation Multi Echelle (MSME), ^{****}Laboratoire Navier

ABSTRACT

In this work, a method is proposed to describe cracks in random heterogeneous media. To avoid describing all heterogeneities, we propose a simplified model which takes into account local fluctuations due to both elasticity and damage parameters variability through a filter-based technique. First, we develop a filter-based homogenization technique using moving windows to construct a simplified model where heterogeneities are described with a larger wavelength than the fully described model. For elastic parameters, the local elastic properties are directly provided by the filter method, while the damage parameters are obtained by inverse approach of crack propagation in the simplified model with respect to the direct numerical simulation in the heterogeneous medium. The phase field method [1,2] is employed for initiation and crack propagation simulations. A stochastic model is constructed to generate realizations of the simplified model which is able to reproduce statistically both mechanical response and crack paths. The random elastic characteristics of the simplified model can be identified by a stochastic descriptor based on the maximum entropy principle introduced in [3], and used for generating the local elastic properties of the simplified model over arbitrary meshes, which can be locally refined in the neighborhood of the crack path. Regarding damage parameters, an optimization problem is solved, ensuring that the statistical mechanical response is consistent with the direct numerical simulations in the heterogeneous medium. The technique is illustrated through problems involving crack propagation in fiber-reinforced composites. Keywords: Crack propagation, heterogeneous media, multi-scale, Numerical homogenization, phase field methods, stochastic model, Maximum Entropy Principle. [1] G. Francfort, J.-J. Marigo, Revisiting brittle fracture as an energy minimization problem, *Journal of the Mechanics and Physics of Solids* (8) (1998) 1319–1342. [2] B. Bourdin, G.A Francfort, J-J Marigo, Numerical experiments in revisited brittle fracture, *Journal of the Mechanics and Physics of Solids* 48 (2000) 797-826. [3] Jaynes ET. Information theory and statistical mechanics, *Physical Review* (1957), 106, 620.

Non-conforming Finite-element Method for Cardiac Electrophysiology Simulations

Daniel Hurtado*, Javiera Jilberto**

*Pontificia Universidad Católica de Chile, **Pontificia Universidad Católica de Chile

ABSTRACT

The study of cardiac disease in the human heart has greatly benefitted from computational tools in the last decade. In particular, the field of computational electrophysiology has enabled in-silico studies of arrhythmogenesis, cardiac failure and therapy design that are otherwise impossible to perform in-vivo. Despite these advances, the computational effort associated to whole heart simulations remains prohibitively high, as accuracy of such simulations impose strict discretization demands both in space and time. For example, in order to recover accurate conduction velocities and wavefront shapes in cardiac simulations, the mesh size in Q1 finite-element formulations cannot exceed 0.1 mm [1]. Here we propose a novel non-conforming finite-element scheme for solving the cardiac electrophysiology equations, suitable for arbitrary cardiac domains [2]. We show that the proposed spatial interpolation scheme results in more accurate wavefront shapes and lower mesh-dependence in the conduction velocity than traditional Q1 formulations, while retaining the same number of global degrees of freedom. As a result, coarser discretizations of cardiac domains can be employed in simulations without significant loss of accuracy, thus reducing the overall computational effort. We demonstrate the applicability of the proposed scheme in the study of cardiac arrhythmogenesis by simulating the generation of spirals in cardiac tissue and heart biventricular domains, and the effect of non-conforming schemes in improving the accuracy-efficiency trade-off of cardiac simulations. References [1] Pezzuto, S., Hake, J., & Sundnes, J. (2016). Space-discretization error analysis and stabilization schemes for conduction velocity in cardiac electrophysiology. *International Journal for Numerical Methods in Biomedical Engineering*. [2] Hurtado, D. E., & Rojas, G. Non-conforming finite-element formulation for cardiac electrophysiology: an effective approach to reduce the computation time of heart simulations without compromising accuracy. *Computational Mechanics*, in press.

Disbonding of Sandwich Panels Exhibiting Fiber Bridging Accounting for Mode Mixity

Daniel Höwer^{*}, Bradley A. Lerch^{**}, Brett A. Bednarczyk^{***}, Evan J. Pineda^{****}, Stefanie Reese^{*****}, Jaan-Willem Simon^{*****}

^{*}Institute of Applied Mechanics, RWTH Aachen University, 52074 Aachen, Germany, ^{**}NASA Glenn Research Center, Cleveland, OH 44135, USA, ^{***}NASA Glenn Research Center, Cleveland, OH 44135, USA, ^{****}NASA Glenn Research Center, Cleveland, OH 44135, USA, ^{*****}Institute of Applied Mechanics, RWTH Aachen University, 52074 Aachen, Germany, ^{*****}Institute of Applied Mechanics, RWTH Aachen University, 52074 Aachen, Germany

ABSTRACT

Due to their very high stiffness to weight ratio, sandwich panels with honeycomb core and carbon fiber reinforced plastic facesheets are becoming increasingly popular in aerospace applications. However, the honeycomb topology also provides modelling challenges when the disbonding between facesheet and sandwich core is to be modelled [1] [2]. The authors have previously shown that the disbonding between the facesheet and the honeycomb core of said sandwich panels cannot be accurately described by established cohesive zone formulations and a novel formulation was developed [3]. The formulation requires a number of parameters which can be extracted from experiments by combining load displacement data on the one hand and digital image correlation strain data on the other hand. The parameter set was obtained for the interface between IM7/8552-1 prepreg tape and Hexcel 5052 aluminum honeycomb core bonded with FM 300K film adhesive, which constitutes the baseline design of the cargo fairing of the NASA Space Launch System (SLS). The novel formulation is comprised of two cohesive components, one of which is related to the initial interface traction while the other one is related to the bridging tractions in the wake of the crack tip. So far, this formulation has only been used to describe the mode I dominated disbonding of single cantilever beam specimens. Subsequently, the formulation has been extended to account for mixed-mode disbonding through a potential-based approach. Results obtained with the mixed-mode formulation are presented herein. Bibliography [1] P. Davidson, A. M. Waas and C. S. Yerramalli, "Experimental determination of validated, critical interfacial modes I and II," Composite Structures, vol. 94, pp. 477-483, 2012. [2] A. Ural, A. T. Zehnder and A. R. Ingraffea, "Fracture mechanics approach to facesheet delamination in honeycomb: measurement of energy release rate of the adhesive bond," Engineering Fracture Mechanics, vol. 70, pp. 93-103, 2003. [3] D. Höwer, B. A. Lerch, B. A. Bednarczyk, E. J. Pineda, S. Reese and J.-W. Simon, "Cohesive zone modeling for mode I facesheet to core delamination of," Composite Structures, vol. 183, pp. 568-581, 2018.

IMPACT ANALYSIS OF ALUMINUM WHEEL WITH INFLATED TIRE

SATOSHI ISHIKAWA*, TOMOYUKI ITOH[†]

*IDAJ Co., Ltd.
7-1-1 Onoe-dori, Chuo-ku
Kobe, Hyogo, Japan
ishikawa.satoshi@idaj.co.jp

[†]BBS Japan Co., Ltd.
525, Fukutarokke
Takaoka, Toyama, Japan

Key words: Aluminum wheel, Inflated tire, Dynamics, Impact.

Abstract. The design process of aluminum wheels has become one of the critical matters in order to improve convenience and safety in an automobile vehicle. Since the impact test has been one of the most important subjects for the strength requirements of the aluminum wheel, the 13 degree lateral impact test was regulated as standard test by SAE. Furthermore, automobile makers compel the 90 degree vertical impact test in recent years. Hence, wheel product makers have executed not only 13 degree impact test but also 90 degree test. While these impact tests caused the large amount of costs and human resources, the necessity of preliminary investigation was highly demanded on the design stage. Therefore, it is needed to analyze the wheel impact test by using CAE technology. Also, it is demanded for development of accurate analysis results with comparing to experimental data. In this paper, we explored the use of Abaqus/Standard and Explicit for impact analysis of aluminum wheel with inflated tire. The analysis model consisted of an aluminum wheel and complicated tire structure. The process of inflation of tire was executed by Abaqus/Standard as an implicit method, subsequently the inflation conditions were imported to Abaqus/Explicit dynamic analysis for impact tests. The results of impact analyses were compared with the empirical results; the performance and accuracy were examined. In addition, we investigated the incompressible effect of tire material with Poisson's ratio. Our proposed method provides new structural designs that prove the potential of the concept to improve the strength and durability of the aluminum wheel.

1 INTRODUCTION

To improve convenience and safety of automobile vehicles, impact tests for Aluminum wheel

have been required for the guarantee of safety condition. SAE (SAE, 2003) regulates the 13degree lateral impact test which is shown in Figure 1. This test aims for side contact to a curbstone. The target is the lateral stiffness of total tire system.

But in recent years, Automobile manufacturers require more critical test which is 90 degree vertical impact test shown in Figure 2. The target is the vertical stiffness of total tire system. By contrast, those impact experiments require high cost including human resources.

To achieve a higher level of design, the practical use of CAE system is significant. In this paper, we discussed the application of impact analysis of aluminum wheel. The analysis model was composed of aluminum wheel and tire structure. The tire structure model was naturally inflated with pressure load by Abaqus/Standard, and the results of implicit analysis were imported to Abaqus/Explicit for the dynamical impact analysis afterward. Both results of 13 and 90 degree impact analyses were compared with the experimental data; the performance and accuracy were examined.

Moreover we investigated the effect of Poisson's ratio, the incompressibility is important issue not only rubber tire quality but also the total stiffness of tire and wheel. The differences of Poisson's ratio caused severe results of permanent deformation of the wheel.

We emphasize that our proposal analysis methods can help us design more robust and sophisticated Aluminum Wheel.



Figure 1. 13 degree falling test is regulated by SAE.



Figure 2. 90 degree falling test.

2 FE MODEL

2.1 13 degree model

To meet the SAE standard requirements shown in Figure 3, FEA model was assembled with four parts in our modeling study. Figure 4 shows the 13 degree impact test model. The model consisted of Aluminum wheel, test jig, rigid striker and tire.

This analysis model was formed with two steps. In the first step, the tire was statically inflated to regulated 200kPa pressure; this process was analyzed by Abaqus/Standard. In the second step, the impact dynamic analysis was executed by Abaqus/Explicit. Naturally, the first step static results were imported to the second dynamic analysis as an initial condition.

In the first simulation, the inflation step was performed on the half model of three dimensional tire. Figure 5 shows the detailed structure of tire. The main part of tire was modeled with three dimensional hexahedron solid elements which were applied to the simple Neo hookean hyperelastic material. The belts and carcass were modeled by reinforced bar of surface elements embedded in continuum elements. Furthermore, the steel bead was modeled with three dimensional solid elements. The most important wheel model was generated as 10nodes modified tetrahedron solid element. The sample test piece for the stress-strain behavior was cut out from the formed wheel.

In order to set clear boundary and loading conditions in the dynamic procedure, the FE model involved test jig part as Figure 4. In addition, the test jig model was supported by connector elements which figured the rubber inelastic behavior. The initial velocity which was assumed the free dropping above 230mm height was applied to the striker. This height is regulated by SAE.

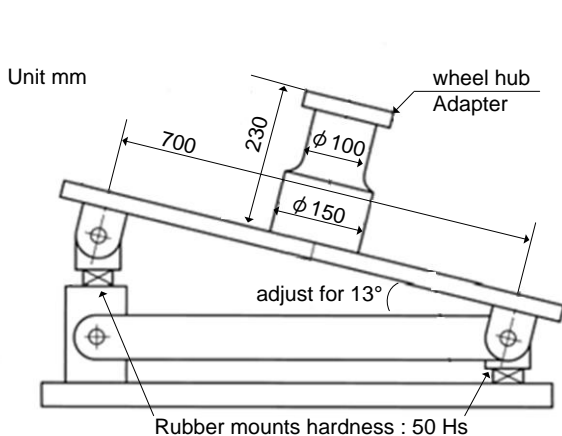


Figure 3. 13 degree falling test apparatus.

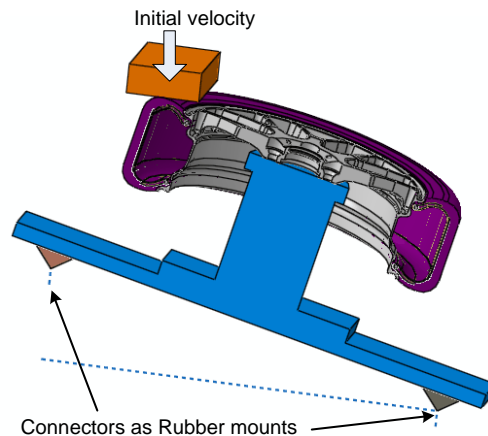


Figure 4. 13 degree FE analysis model.

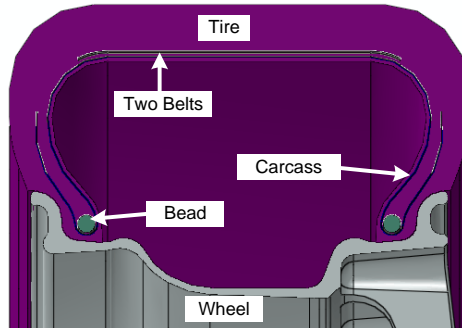


Figure 5. Section structure of tire.

2.2 90 degree model

Figure 6 shows the 90 degree analysis model. This model was formed with two steps as same as 13 degree analysis model. The first step was tire inflation analysis by Abaqus/Standard, following, the impact dynamic analysis was executed by Abaqus/Explicit at the second step. The tire pressure varied with the size of wheel in the actual test. In this analysis, the tire pressure was applied to 260kPa.

The tire structure and the material of wheel were same as 13 degree model. The entire fixed boundary condition was applied on the center face of the wheel. The initial velocity which was assumed the free dropping above 101.6mm height was applied to the striker under the explicit dynamic analysis.

The contact conditions with friction phenomena were invoked between tire and wheel, and also between striker and tire. While another contact condition was applied to whole area such as tire's self-contact condition in different coefficient of friction.

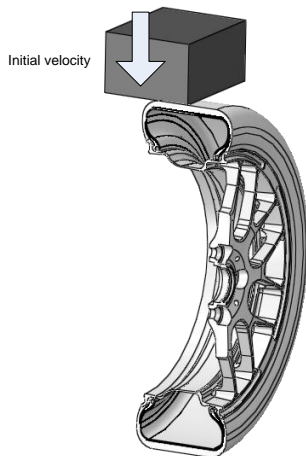


Table 1. Model size

Part	Element type	Number of nodes	Number of elements
Wheel	C3D10M	150249	86465
Tire	C3D8R	10080	6958
Bead	C3D8R	1188	520
Belt	SFM3D4R	2040	1848
Carcass	SFM3D4R	2880	2769
Base (13 degree model only)	C3D10M	59455	38968

Figure 6. 90 degree FE analysis model.

2.3 Model size

Table 1 shows the typical model size and element types of each parts. The material of wheel was Aluminum alloy which was composed from Al-Mg-Si. The wheel was modeled with quadratic tetrahedron element (C3D10M).

The tire was modeled as a slightly compressible hyperelastic material with reduced integration linear hexahedral element (C3D8R).

The fiber reinforcement was modeled as a linear elastic material at the parts of belts and carcass with surface element (SFM3D4R) embedded into the tire part.

The base part used in only 13 degree analysis was modeled as ordinary steel with quadratic tetrahedron solid element. The material was just linear elastic.

3 RESULTS

3.1 13 degree model

In order to examine our proposal model, two analyses were performed. One analysis was with tire model, and the other was without tire model. The section outlines of original shape and deformed configurations are shown in Figure 7. The thin line shows the original shape, the black solid line shows the deformed shape which is real experimental result, the coincided blue line indicates the result of FEA model with inflated tire, and the last red line which is depicted at the lowest position indicates the result without tire. The result of FEA model with inflated tire coincided with the experimental result. On the other hand, if the tire model was omitted, the permanent displacement result was calculated larger than it with tire model. These results insist that even in the 13 degree analysis case the tire model is essential.

Figure 8 shows the principal strain contour of dynamic implicit analysis, while Figure 9 shows the real experimental result which had the crack on the side of spoke. In this investigation, we adopted the trial wheel model for reducing weight. As Figure 8 describes, the analysis model was able to estimate the actual crack area.

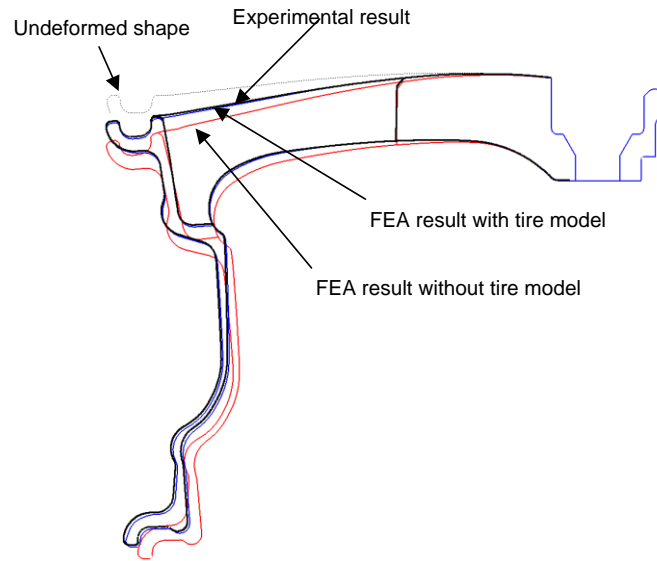


Figure 7. Comparison of deformed section outlines.

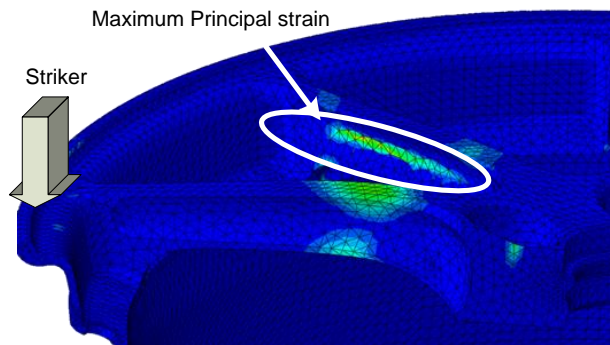


Figure 8. Maximum principal strain at thin spoke wheel model.

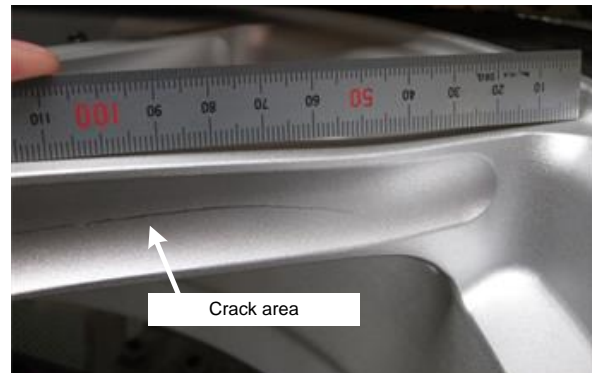


Figure 9. Crack line at thin shaped wheel on experimental test.

3.2 90 degree model

3.2.1 Deformation

Figure 10 and 11 show the deformation both tire and wheel. This frame illustrates the maximum displacement at instance. Because of incompressibility of rubber material, the wheel suffered from large plastic deformation.

Figure 12 shows the mirror deformation configuration, while Figure 13 shows the deformation of experimental test. The analysis acquired the same amount of deformation and figure.

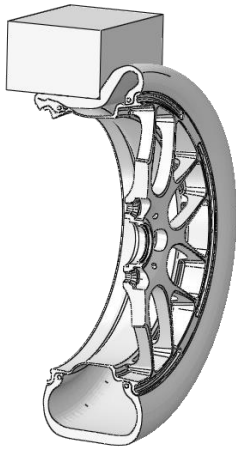


Figure 10. Whole deformation figure.

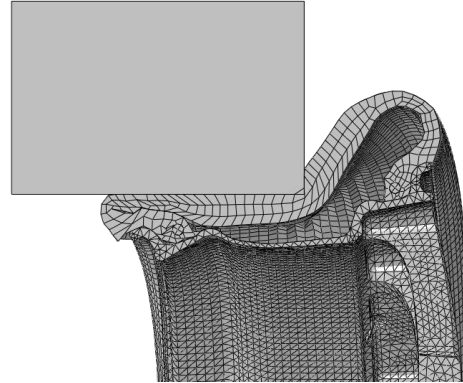


Figure 11. Maximum deformation of tire and wheel.

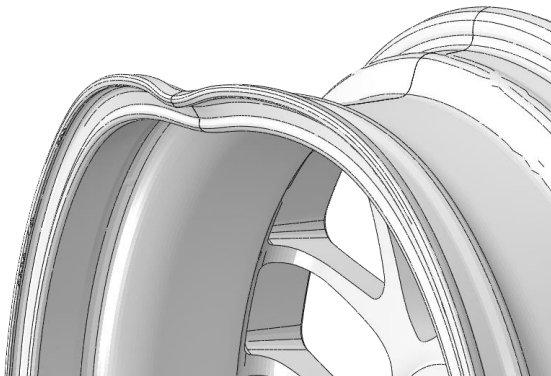


Figure 12. Mirror deformation configuration.



Figure 13. Result of experimental test.

3.2.2 Poisson's effect

Figure 11 revealed the compressive stiffness is the most significant for the 90 degree drop analysis. Therefore we investigated the effect of Poisson's ratio. Table 2 shows the analysis results with various Poisson's ratio. If Poisson's ratio became nearly incompressible behavior, the large permanent displacement was invoked as shown in Figure 14.

If we apply the nearly incompressible material on the Explicit analysis, the time step will be smaller than normal condition in expectations because of the Courant condition. Nevertheless Table 2 showed that all of the calculation time was about same order. It was thought that the reason was because the mesh size of the wheel was much smaller than rubber.

Table 2. Classification of Poisson's ratio. Maximum displacement of wheel and calculation time.

Case	Poisson's ratio	Maximum displacement[mm]	Wall time [hh:mm]
1	0.499	36.36	33:01
2	0.49	31.89	21:44
3	0.48	29.90	32:47
4	0.47	28.84	32:39

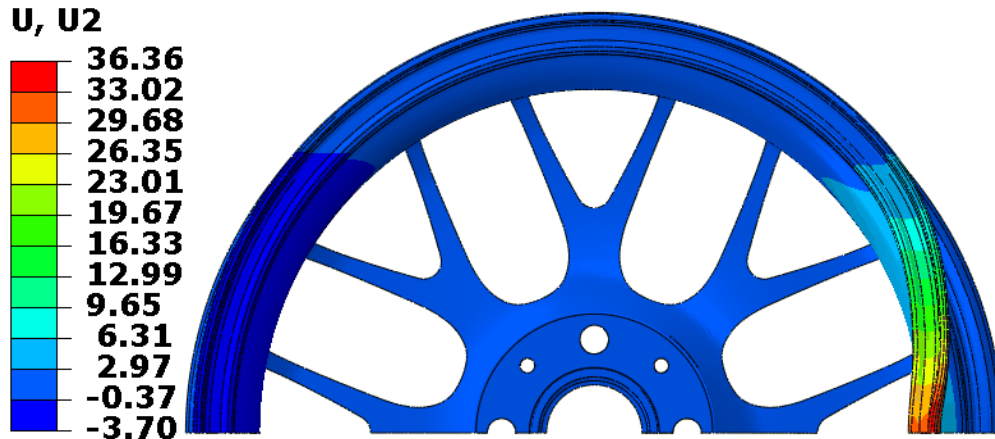


Figure 14. Contour plot of deformed wheel which was applied Poisson's ratio as 0.499.

4 CONCLUSION

We established the FE analysis model for 13 and 90 degree Aluminum impact test with inflated tire. Abaqus has the seamless connection between implicit and explicit procedures. This function is substantial for integrating impact analysis with inflated tire.

The study of 13 degree model argued the need for modeling of tire. The analysis result showed large displacement of wheel without tire model.

The result of 90 degree model depicted same amount of deformation and shape for a real examination. Furthermore, the Poisson's ratio indicated the importance of incompressibility of tire material.

REFERENCES

- [1] SAE J 175, 2003. Wheel – Impact Test Procedure – Road Vehicle
- [2] Abaqus User's Manual, Version 6.12, 2013. Dassault Systèmes Simulia Corp., Providence, RI.

Rx-FEM Prediction of Delamination Migration in Multilayered Tapered Composite Beam Specimens under Fatigue Loading

Endel larve^{*}, Hari Adluru^{**}, Kevin Hoos^{***}

^{*}University of Texas at Arlington, ^{**}University of Texas at Arlington Research Institute, ^{***}University of Texas at Arlington Research Institute

ABSTRACT

Multilayered Clamped Tapered Beam Specimen (CTBS) designed by Advanced Composite Project Team at NASA Langley Research Center (LaRC) in Hampton, VA [1] is considered. This specimen contains a ply tapering feature characteristic of aerospace applications and allows studying the matrix crack initiation from pristine condition as well as delamination initiation and evolution including migration from one interface to another. Discrete Damage Modeling (DDM) method termed Regularized Extended Finite Element Method (Rx-FEM) described in Ref. [2] was used in the present work. The Rx-FEM allows modeling the displacement discontinuity associated with individual matrix cracks in individual plies of a composite without regard to mesh orientation by inserting additional degrees of freedom in the process of the simulation. A regularized crack surface Heaviside step function is used in finite elements, which are duplicated along the crack path. The propagation of the mesh independent crack is then performed by using cohesive zone method where the displacement jump is computed as spatial separation of the duplicated elements and the crack surface energy obtained through volume integration by using the gradient of the crack surface Heaviside step function. The methodology has been extensively applied to strength prediction of coupon and subelement level composite structures under tensile, compressive and more recently fatigue loading in Ref [3]. The CTBS simulations were performed simultaneously with experiments conducted by NASA LaRC. The static peak load predicted by using the transverse strength value obtained from the three point bend test method was in good correlation with the experiment whereas the peak load predicted by using values resulting from tensile testing of 900 coupons was lower than experiment. Two load amplitude levels of 0.9 and 0.79 of the static peak strength were selected for R=0.2 constant amplitude fatigue loading. The delamination migration location and cycle count were predicted and compared with experimental data. References [1] Ratcliffe, J., Deobald, L., Mabson, G. and Carvalho, N., NASA-TM-2017-219623, July 2017 [2] larve, E. V., Gurvich, M. R., Mollenhauer, D. H., Rose, C. A. and Da'vila, C. G., (2011), "Mesh-Independent Matrix Cracking and Delamination Modeling in Laminated Composites," Int. J. Numer. Meth. Eng, 88(80), pp. 749-773 [3] E. V. larve , K. Hoos, M. Braginsky, E. Zhou, and D. H. Mollenhauer, Progressive failure simulation in laminated composites under fatigue loading by using discrete damage modeling, Journal of Composite Materials, Vol 51, Issue 15, 2017, pp. 2143-2161

Quantifying the Size Effect in Localized Failure of Composite Structures through Coupled Probability-Multiscale-Mechanics Computations

Adnan Ibrahimbegovic*, Xuan-Nam Do**, Emir Karavelic***, Mijo Nikolic****

*University of Technology Compiegne, France, **University of Technology Compiegne, France, ***University of Technology Compiegne, France, ****University of Technology Compiegne, France

ABSTRACT

This paper deals with important challenge on quantifying durability, life-time integrity and safety against failure of massive composite structures under extreme conditions. The illustrative applications come from the area of energy production systems, with both currently dominant nuclear (nuclear power plant) or renewable energy sources (wind turbines and hydro-turbines). Special attention is given to costly massive structures with 'irreplaceable' components, which are characterized by a number of different failure modes that require the most detailed description and interaction across the scales. We would like to significantly improve the currently dominant experimental approach, and thus accelerate innovations in this domain. The main objective is development of novel Heterogeneous2 Multiscale Method capable of representing strain field heterogeneities induced by evolution (and interaction) of localized failure mechanisms in massive structure, pertaining to micro scale (FPZ-fracture process zone), macro scale including softening (macro cracks) and non-local macro scale (bond-slip for long fiber reinforcement). The objective of Heterogeneous2 Multiscale Method is also to provide capabilities for quantifying the risk of premature localized failure through probability description of initial defects (microstructure heterogeneity) and uncertainty propagation through scales. The novel scientific concept to be explored pertains to multiscale formulation and solution of coupled nonlinear mechanics-probability problem replacing the standard homogenization approach that can only provide average (deterministic) properties of heterogeneous composites. This concept is of interdisciplinary nature with Mechanics (defining probability distribution) and Applied Mathematics (providing uncertainty propagation) combined in order to capture the influence of heterogeneities and fine scale defects on premature failure. The most important challenge concerns the ability to provide the sound, probability-based explanation of size effect (with different failure modes observed for different size specimens and real structure built of the same composite materials). The biggest potential gain concerns changing the validation procedures for massive structures that are beyond the size suitable for testing at present. The scientific gains concern providing the Heterogeneous2 Multiscale Method that connects computations with design studies (optimization), testing (identification) and safety verification (monitoring) of massive composite structures. The scientific gains also concern further placing the proposed method within multiphysics framework, along with the original use of goal oriented error estimates to provide sufficiently reliable interpretation of extreme conditions (e.g. fluid or heat flow) and the code-coupling software implementation to quickly integrate existing simulation codes within such a framework.

Advances on Hybrid-PGD

Rubén Ibáñez Pinillo*, Emmanuelle Abisset-Chavanne**, Elias Cueto***, Francisco Chinesta****

*École Centrale de Nantes, ICI High Performance Computing, 1 Rue de la Noë, 44000, Nantes, France, **École Centrale de Nantes, ICI High Performance Computing, 1 Rue de la Noë, 44000, Nantes, France, ***Universidad de Zaragoza, Edificio Betancourt, Maria de Luna, s/n, 50018, Zaragoza, Spain, ****ENSAM ParisTech, PIMM ESI-Group Chair, Boulevard de l'Hôpital 151, F-75013, Paris, France

ABSTRACT

Model order reduction techniques are an appealing tool to alleviate prohibitive computational efforts. Indeed, POD-like methods, where a set of snapshots are used to construct an a posteriori reduced basis, are proved to be effective when only few modes are carrying most part of the information. PGD-like methods can be highlighted as a priori method, where a specific tensorial separated representation is used. By means of the last technique, parametric solutions are obtained in a very efficient way, just like the possibility of uncoupling spatial dimensions i.e. in-plane-out-of-plane separated representation. Even though a priori model order reduction methods are a very powerful tool, the number of modes required to represent accurately a given solution could increase drastically depending on the structure of the tensorial separated representation. For instance, a transient heat problem with a spatial moving source is not optimal when space and time are separated independently. Therefore, several ideas are tested in the present work. Firstly, PGD will be used as a tool to provide a local enrichment of a global polynomial approximation, always under the constraints of the partition of the unity. Secondly, the direction of the modes can be introduced as a extra coordinate. Hence, the solution becomes more separable, requiring less number of modes, by properly selecting the direction of the separated representation. However, if the solution is highly non linear, the best direction will not be the same everywhere, requiring a different axis rotation locally. Thus, techniques to select the best local direction just like interpolation of non-cartesian domains are studied.

Development of Meshfree Particle Method for Solid Mechanics

Masakazu Ichimiya^{*}, Nobuki Yamagata^{**}, Pedro Marcal^{***}

^{*}Advanced Creative Technology Co., Ltd., ^{**}Advanced Creative Technology Co., Ltd., ^{***}MPACT Corp.

ABSTRACT

Development of Meshfree Particle Method for Solid Mechanics Masakazu Ichimiya¹, Nobuki Yamagata¹, and Pedro V. Marcal² ¹ Advanced Creative Technology Co., Ltd., ² MPACT Corp. Key Words: MeshFree Particle Method, SSPH, Solid Mechanics, Elastostatic. The meshfree method has developed greatly as a solution to partial differential equations. Among them, the Meshfree particle methods, such as SPH were successfully applied mainly to hydrodynamics. Considering coupling of solid with fluid dynamics, etc., it is important to apply the meshfree particle method to solid mechanics as well. Thus, the meshfree particle method was applied to solid mechanics. 1. Although the conventional SPH is a dynamic analysis method and applied to impact destruction and the like, there were some difficulties in application to static analyses which account for most structural problems. Therefore, the SSPH method was selected as a meshfree particle method applicable to solid mechanics, and it was formulated by incorporating material and geometrical nonlinearities in addition to elastic mechanics. 2. In order to evaluate its applicabilities, the objects to be analyzed were general such as bending of beam, bending of flat plate, and stress concentration problem such as plate including circular hole. Also, thermal stress analysis was performed. 3. As a result, it was found that the mesh free particle method SSPH can be applied with high accuracy on the solid mechanics including elastostatic.

Implicit Finite Element Solver with HPC towards HQC of Earthquakes

Tsuyoshi Ichimura^{*}, Kohei Fujita^{**}, Takuma Yamaguchi^{***}, Muneo Hori^{****}, Lalith Wijerathne^{*****}

^{*}The University of Tokyo, ^{**}The University of Tokyo, ^{***}The University of Tokyo, ^{****}The University of Tokyo, ^{*****}The University of Tokyo

ABSTRACT

Extensive usage of numerical simulations is desirable for estimating responses of sophisticated heterogeneous models in earthquake problems. As the boundary conditions and geometric shape have strong effects on numerical results, use of finite element analysis methods is desirable. However, because the domain size is huge and the required resolution high, degrees of freedom are in the order of 10^{8-12} ; it is difficult to conduct finite element analysis using such large models. Thus, unfortunately, simplified models are conventionally used. To realize finite element analysis with such large models, researches enhanced by HPC have been conducted. Our developed algorithm enhances computational capability and enables us to conduct nonlinear wave finite element analysis with 1 trillion degrees of freedom, and static linear finite element analysis with 2 trillion degrees of freedom. Further improvement is conducted towards HQC in earthquakes with GPU and AI (e.g. multiple analysis for huge models, considering the uncertainty of the model/scenario).

A Particle Method with Second Order Approximation in Space-Time

Sergio R. Idelsohn*, Juan M. Gimenez**, Horacio J. Aguerre***, Norberto M. Nigro****

*Centro de Investigaciones en Métodos Computacionales, (CIMEC) and Centro Internacional de Métodos Numéricos en Ingeniería, (CIMNE), **Centro de Investigaciones en Métodos Computacionales, (CIMEC), ***Centro de Investigaciones en Métodos Computacionales, (CIMEC), ****Centro de Investigaciones en Métodos Computacionales, (CIMEC)

ABSTRACT

Lagrangian-based methods using particles are established methodologies which rely on the goodness of particles for solving the convective term of transport equations. Despite having shown impressive results for some particular applications and presenting promissory potential for parallel architectures, the efficiency of particle-based methods solving the incompressible Navier-Stokes equations currently does not justify its massive use in replace of classical Eulerian methodologies. Strategies such as PFEM-2 [1] have decreased the huge computational cost of particle methods, but mainly because of the low order schemes employed. This work presents the first proposal of a second order accurate particle method in both time and space for solving incompressible flows equations within a Lagrangian formulation. This methodology consists on reinterpreting the convective term of any transport equation as a source term estimated with particles. An updated version of the eXplicit Integration Following the Acceleration and Streamlines (X-IVAS) method [2] is used and a second order projection scheme is employed to transfer data from the particles to the mesh. In the case of incompressible flows, the modified momentum equation is used as velocity predictor without modifying the original rate of convergence of the Eulerian solution but improving the numerical approximation of the convective term. With the aim of presenting the methodology and particle-mesh interaction, firstly the solution of scalar transport equations is shown. Then, incompressible flow problems are solved where the rate of convergence of the method is assessed experimentally and the need of iterating the X-IVAS during velocity-pressure coupling is revealed. The implementation on the open source platform OpenFOAM allows employing general polyhedral meshes and obtaining reliable computing times comparisons. Results reveals that, for the analyzed cases, the current method is able to obtain the same or lower level of error than a fast Eulerian alternative, but saving considerably total computing time. [1] "Lagrangian versus Eulerian integration errors"; Sergio Idelsohn, Eugenio Oñate, Norberto Nigro, Pablo Becker, Juan Gimenez; Comput. Methods Appl. Mech. Engrg. 293, 15,191–206. [2] "Analysis of multi-fluid flows with large time steps using the Particle Finite Element Method"; Sergio Idelsohn, Julio Marti, Pablo Becker, Eugenio Oñate. Int. Journal for Num. Methods in Fluids, 75, 621-644.

A New Numerical Approach to the Solution of Partial Differential Equations with Optimal Accuracy on Irregular Domains and Embedded Uniform Meshes.

Alexander Idesman*

*Texas Tech University

ABSTRACT

A new numerical approach based on the minimization of the local truncation error is suggested for the solution of partial differential equations. Uniform Cartesian meshes are currently used for the space discretization. Similar to the finite difference method, the form and the width of the stencil equations are assumed in advance. A discrete system of equations includes regular uniform stencils for internal points and non-uniform cut stencils for the nodes located close to the boundary. The unknown coefficients of the discrete system are calculated by the minimization of the order of the local truncation error. The main advantages of the new approach are a high accuracy and the simplicity of the formation of a discrete (semi-discrete) system of equations for irregular domains. For the regular uniform stencils, the stencil coefficients can be found analytically. For non-uniform cut stencils, the stencil coefficients are numerically calculated by the solution of a small system of linear algebraic equations (10-20 algebraic equations). In contrast to the finite elements, there is no necessity to calculate by integration the elemental mass and stiffness matrices that is time consuming for high-order elements. As a mesh, the grid points of a uniform rectangular (square) mesh as well as the points of the intersection of the boundary of a complex irregular domain with the horizontal, vertical and diagonal lines of the uniform mesh are used; i.e., in contrast to the finite element meshes, a trivial mesh is used with the new approach. Changing the width of the stencil equations, different high-order numerical techniques can be developed with the new approach. Currently the new technique is applied to the solution of the time dependent wave and heat equations and the time independent Laplace equation. The theoretical and numerical results show that for the width of the stencil equations equal to that for the linear quadrilateral finite elements, the new technique yields the fourth order of accuracy of the numerical results on irregular domains for the considered partial differential equations (it is much more accurate compared with the linear and even quadratic finite elements at the same number of degrees of freedom).

Computational Challenges Towards Exascale Fusion Plasma Turbulence Simulations

Yasuhiro Idomura*

*Japan Atomic Energy Agency

ABSTRACT

Turbulent transport is one of key issues in fusion science. To address this issue via a five dimensional (5D) gyrokinetic model, the Gyrokinetic Toroidal 5D full-f Eulerian code GT5D has been developed. On the K-computer, inter-node parallelization techniques such as multi-dimensional/-layer domain decomposition and communication-computation overlap were developed, and strong scaling of GT5D was improved up to 73,728 nodes [Idomura et al., Int. J. HPC Appl. (2014)]. This computing power enabled us to study ITER relevant issues such as the plasma size scaling of turbulent transport. However, extensions of GT5D towards burning plasmas including kinetic electrons and multi-species ions require exascale computing. Under the post-K project (Japanese exascale computing project), we have developed computing techniques for the next generation computing platforms based on many core processors. In this talk, we discuss computational challenges related to complicated intra-processor memory hierarchy and limited inter-node communication performance compared with accelerated computation. The former issue is addressed by optimizing data access patterns of a stencil kernel on each many core architecture, and high performance gains are obtained on several many core architectures [Asahi et al., IEEE-TPDS (2017)]. The latter issue is resolved by using advanced communication-avoiding Krylov methods, which enables an order of magnitude reduction of collective communications [Idomura et al., ScalA17@SC17]. By applying these novel computing techniques, the performance of GT5D is dramatically improved on the Oakforest-PACS, which consists of 8,208 KNLs.

Performance Evaluation of Stabilized F-bar Aided Edge-based Smoothed Finite Element Method with Four-node Tetrahedral Elements (SymF-barES-FEM-T4) for Contact Problem

Ryoya Iida^{*}, Yuki Onishi^{**}, Kenji Amaya^{***}

^{*}Tokyo Institute of Technology, ^{**}Tokyo Institute of Technology, ^{***}Tokyo Institute of Technology

ABSTRACT

Tetrahedral elements are widely used in many practical finite element (FE) analysis because complex shapes cannot be meshed into high-quality hexahedral meshes. However, classical tetrahedral elements have issues in accuracy, robustness and stability especially for nearly incompressible materials. Although the u/p hybrid formulation with tetrahedral elements are typically chosen as general methods for nearly incompressible materials, they cannot be directly applied to explicit dynamics. Therefore, highly accurate explicit dynamics for complex shapes of nearly incompressible materials are still open problems. Recently, smoothed finite element methods (S-FEMs), which are known as the highly accurate four-node tetrahedral (T4) formulations, have been proposed and gather attention. S-FEMs are purely displacement-based formulation unlike u/p hybrid formulation, and thus can be easily extended to the explicit dynamics. Onishi et.al. have proposed an advanced S-FEM called F-bar aided edge-based smoothed finite element method with T4 element (F-barES-FEM-T4) to realize stable and accurate FE analysis for nearly incompressible materials. F-barES-FEM-T4 shows the excellent accuracy without locking and pressure checkerboarding in the large deformation static and quasi-static implicit analysis. Meanwhile, in dynamic analysis, it is reported that F-barES-FEM-T4 has unstable deformation mode and causes energy divergence. The authors have proposed an stabilized F-barES-FEM-T4 in dynamic analysis called SymF-barES-FEM-T4. SymF-barES-FEM-T4 achieves removing instability and realizing accurate long-term dynamic analysis only by modifying the definition of B-matrix of internal force vector. However, the performance evaluations were restricted to too simple or unpractical scenarios without contact analysis and more practical evaluations are still needed. The aim of this research is to evaluate the performance of SymF-barES-FEM-T4 in contact-included scenario. Some examples reveal that SymF-barES-FEM-T4 realize stable contact analysis without any issues such as contact force oscillation.

Investigation of Elastoplastic Deformation Behavior of Polycarbonate Using Molecular Dynamics Simulation

Daiki Ikeshima^{*}, Kazunori Miyamoto^{**}, Akio Yonezu^{***}

^{*}Chuo University, ^{**}Chuo University, ^{***}Chuo University

ABSTRACT

Polycarbonate (PC) is an important engineering polymer that has been used as the structural material in a wide range of applications. In polymer materials, the molecular structure is very crucial for their macroscopic mechanical properties. This study investigated the elastoplastic deformation mechanism at molecular structural level during uni-axial tensile loading and nano indentation by using molecular dynamics (MD) simulation. In this study, to drastically improve computational efficiency, coarse-grained (CG) approach for MD simulation is newly established. In other words, a new CG force field is developed for PC based on full-atom MD simulations [1]. In this approach, the four functional groups (phenylene, isopropylidene, phenylene and carbonate) in a molecular chains are recognized to be four coarse grained particles. First, uni-axial tensile deformation is performed using the newly developed force field. During uni-axial tensile deformation, the polymer chains undergo elastic deformation, and are followed by plastic deformation. The deformation mechanism at molecular structural level (molecular topology) is investigated. Especially, it is found that changes in the bond stretch, bending angle and torsional angle of molecular chains during uni-axial tensile deformation are quantitatively examined. It is found that their potential energy significantly changes with respected to the applied tensile strain. Based on the variation of potential energy, we discussed mechanism of yielding onset and plastic deformation. Especially, change of potential energy of bending angle is raised at yielding. Next, nano indentation test is performed in MD simulation. During a loading process, reaction force (which comes from the interaction force between indenter probe and polymer surface) shows increasing with respected to the penetration depth. Energy variations associated with bond stretching, bending and torsion are further investigated to obtain useful insights of the deformation mechanism. It is found that their potential energy significantly changes with respected to the penetration depth. Based on the variation of potential energy, the mechanism of yielding onset and plastic deformation during AFM nano indentation test is also discussed. Reference [1] D. Ikeshima et al., Molecular origins of elastoplastic behavior of polycarbonate under tension: A coarse-grained molecular dynamics approach, Computational Materials Science 145 (2018), 306-318.

Powder Jet Additive Manufacturing Modeling for Residual Deformation and Stress Prediction

Athanasios Iliopoulos^{*}, John Michopoulos^{**}, John Steuben^{***}, Andrew Birnbaum^{****}

^{*}U.S. Naval Research Laboratory, ^{**}U.S. Naval Research Laboratory, ^{***}U.S. Naval Research Laboratory, ^{****}U.S. Naval Research Laboratory

ABSTRACT

The rapid interest in Additive Manufacturing (AM), alongside the undesired effects it introduces on the fabricated parts, have motivated the need to develop tools for the prediction and correction of such effects. In the rush to accommodate the pace the end users and the industry dictate in their eagerness to adopt AM, most of the tools developed have been designed using semi-empirical simulation approaches and in many cases are dependent on non-deterministic adjustment requirements against inconsistencies between the predicted and fabricated parts qualities. In this talk we present a new approach that is based on an accurate point-by-point energy and mass deposition model, that closely follows the process in powder jet technologies. The computational methodology is implemented using a pre-defined mesh, that follows the powder jet g-code program, and enables mass and thermal energy deposition using spatiotemporally dependent properties by properly activating material property transitions. The model fully couples thermal physics and structural mechanics. An implementation of the proposed computational infrastructure is presented for the COMSOL Multiphysics finite element analysis software. The process is demonstrated for a thin walled square box geometry that was also manufactured using a powder jet system. The results of the simulations are evaluated against their ability to predict deformation and residual stresses, alongside thermocouple data that was captured during the fabrication of the part.

ACOUSTIC SIMULATION SYSTEM BASED ON ACOUSTIC WAVE THEORY CONSIDERING ACOUSTIC IMPEDANCE

KEITA IMAI¹⁾, MASAKI TANIGAWA²⁾, TORU YOSHIMACHI³⁾,
AND KAZUO KASHIYAMA⁴⁾

1) Graduate student, Graduate School of Science and Engineering
1-13-27, Kasuga, Bunkyo-ku,
Tokyo, 112-8551, Japan
Email address; a13.apg4@g.chuo-u.ac.jp

2) Center for Social System Engineering, Simizu Co.
3-4-17, Etchujima, Koto-ku,
Tokyo, 135-8530, Japan
Email address; tanigawa@shimz.co.jp

3) Department of Engineering Business, JSOL Co.
2-5-24, Harumi, Chuo-ku,
Tokyo, 104-0053, Japan
Email address; toru.yoshimachi@gmail.com

4) Professor, Faculty of Science and Engineering
1-13-27, Kasuga, Bunkyo-ku
Tokyo, 112-8551, Japan
Email address; kaz@civil.chuo-u.ac.jp

Key words: AMR Method, Impulse Response , Acoustic Impedance

Abstract. This paper presents an impulse response analysis method considering acoustic impedance for reproducing arbitrary reflection and a transmission condition. The CIP method using adaptive mesh refinements (AMR) is employed the discretization of wave equation. The pseudo impulse wave is employed for the impulse response analysis. The present analysis method is expected to be a useful method to plan and design for noise barrier or various construction works in urban area, and also help make a consensus between the constructor and the local residents.

1 INTRODUCTION

In our previous research [1], in order to perform sound field analysis efficiently, an impulse response analysis method based on wave acoustic theory using AMR (Adaptive Mesh Refinement) and CIP method and auralization system has been developed in order to perform sound field analysis efficiently. The method has only been assumed only complete reflection. However the real sound wave have attenuation with a reflection and a transmission by road surface or noise barrier effect. Since the noise prediction without any attenuation was low

accuracy, it can not be applied to the practical designing or planning. In order to improve the applicability of the method, the acoustic impedance which is the characteristic value of the medium acting as a resistance are considered. Reflection and transmission occur in the portion where the acoustic impedance extremely changes. The boundary condition with acoustic impedance was introduced into our analysis procedure. The following three assumptions are considered, (1) no dependence of reflection and transmission on frequencies, (2) no phase difference between reflected wave and transmitted wave, (3) no energy loss on the boundary. As the result of computational analysis, a method to express simply reflection and transmission phenomenon is proposed. This method is applied to a benchmark problem and the validity of its numerical result is examined by comparing with the theoretical solution. Also, effects of convolution and auralization are investigated.

2. CIP METHOD

2.1 Governing equations and Characteristic curves

The one-dimensional wave propagation in the air can be expressed by the equation of motion and the equation of continuity as

$$\rho \frac{\partial u}{\partial t} + \frac{\partial p}{\partial x} = 0 \quad (1)$$

$$\frac{\partial p}{\partial t} + \rho c^2 \frac{\partial u}{\partial x} = 0 \quad (2)$$

where p [Pa] is the sound pressure, u [m/s] is the particle velocity, ρ [kg/m³] is the density of air, and c [m/s] is the sound velocity. Equations (3) and (4) are obtained by multiplying equation (1) by c and adding to or subtracting from equation (2):

$$\frac{\partial}{\partial t} f_x^+ + c \frac{\partial}{\partial x} f_x^+ = 0 \quad (3)$$

$$\frac{\partial}{\partial t} f_x^- - c \frac{\partial}{\partial x} f_x^- = 0 \quad (4)$$

where f_x^+ is defined as $f_x^+ = \rho c u + p$, f_x^- is defined as $f_x^- = \rho c u - p$. Equation (3) and (4) represent the positive propagation of f_x^+ and the negative propagation of f_x^- by the speed c . The physical values at the next time step $n+1$ are obtained by advecting those values at the current time step n along the characteristic curves as shown in **Fig.1**. As a result, the sound

pressure p and the particle velocity u can be derived as follows

$$p = \frac{f_x^+ - f_x^-}{2} \quad (5)$$

$$u = \frac{f_x^+ + f_x^-}{2\rho c} \quad (6)$$

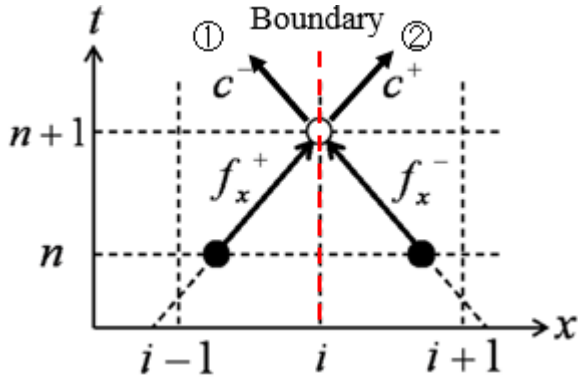


Fig.1 Advection on characteristic

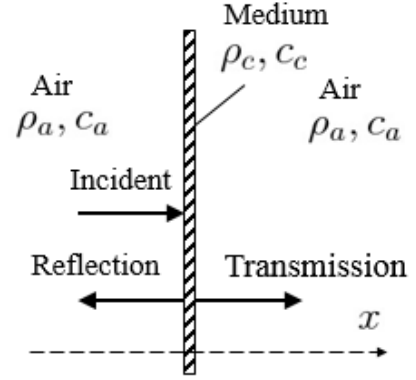


Fig.2 Reflection and transmission with acoustic impedance

2.2 CIP Interpolation

The CIP (Constrained Interpolation Profile) method [2] is a highly accurate differential solution method for advection equations that move physical quantities along characteristic curves. When obtaining the physical quantity to be advected, the CIP interpolation that interpolates from the physical quantity and the derivative value at the lattice point by using a cubic polynomial is performed, thereby the profile of the exact solution is relatively well maintained. The multidimensional problem extends the one-dimensional CIP method to each coordinate axis direction. In the case of three dimensions, it is obtained by solving advection equations for y direction and z direction in addition to equations (3) and (4). The CIP method realizing this multidimensional advection includes the M type CIP method and the C type CIP method. In this research, the C type CIP method which enables high accurate analysis is used [3].

2.3 Acoustic impedance

In this research, acoustic impedance is introduced to ensure the accuracy of the noise prediction result by considering attenuation due to reflection and transmission. The acoustic impedance is the characteristic value of the medium acting as a resistance. Reflection and transmission are generated in the portion where the acoustic impedance extremely changes as shown in **Fig.2**. The boundary condition considering the acoustic impedance is introduced. The following three assumptions are considered, (1) no dependence of reflection and transmission on frequencies, (2) no phase difference between reflected wave and transmitted wave, (3) no energy loss on the boundary. Then, the reflection and transmission phenomenon can be simply treated analysis method. The acoustic impedance on the boundary is expressed by the following formula.

$$Z_c = \rho_c c_c = -\frac{p_c}{u_c} \quad (7)$$

Z_c is the impedance, ρ_c is the density, c_c is the sound speed, p_c is the sound pressure, u_c is the particle velocity in the assumed boundary. Sound pressure and particle velocity according to (5), (6) are substituted to this equation on the boundary. Then the following formula is derived.

$$f_x^+ = \frac{Z_c - Z_a}{Z_c + Z_a} f_x^- \quad (8)$$

Z_a is impedance of the air. Similarly, regarding the transmission direction,

$$\frac{2Z_a}{Z_c + Z_a} f_x^+ \quad (9)$$

Then, assuming that there is no energy loss at the boundary, coefficients of the formulas (8) and (9) are determined so that the reflection and the transmission together become 1.

3. INCIDENT WAVE CONDITION USING IMPULSE RESPONSE

3.1 Impulse response

Impulse response is obtained at a sound receiving point when a very short wave signal is input to a certain space. By convolving the impulse response obtained by analyzing in advance and

the input waveform, it can be easily obtained the output waveform at the sound receiving point. When a sound data is used as an input wave , auralization can be realized.

3.2 Pseudo impulse

The Dirac delta function with a flat frequency characteristic is suitable for the impulse response analysis. However, since the real impulse has a steep shape, it is difficult to calculate with high accuracy using the discretization method. For this reason, a pseudo is approximate discretization is used. In this study, a pseudo impulse based on convolution integral method proposed by Lubich which is expressed by the following equation [4].

$$p_n \Delta t \cong \frac{R^{-n}}{L} \sum_{L=0}^{L-1} \left(\frac{1}{4\pi r} e^{\frac{-sr}{c}} \right) e^{(-2\pi i \frac{nl}{L})} \quad (10)$$

Fig.3 illustrates the waveform and frequency characteristic of Lubich pseudo impulse response with $r = 0.2$ m and $\Delta t = 0.01026$ ms in the equation (10). A constant spectrum up to 3500 Hz and a rapid decrease in higher frequency range can be seen in **Fig.3**.

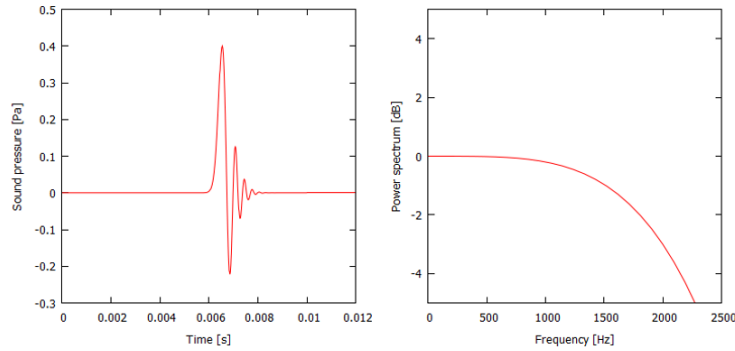


Fig.3 Waveform and frequency characteristic of Lubich pseudo impulse response

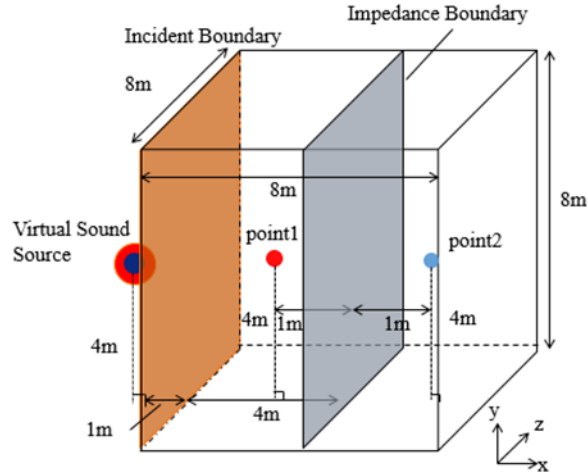


Fig.4 Computational domain (1)

4. NUMERICAL TEST EXAMPLE

4.1 Numerical Conditions

The computational domain is shown in **Fig.4**, and analysis with a minimum space discretization width of 0.015625 m and a time discretization width of 0.020525 ms ($CFL = 0.45$) was carried out. The distance between the virtual sound source and the incident boundary was set to 1 m, an impedance boundary was set at 4 m from the incident boundary, and sound receiving points were set 1 m front and 1 m backward from the impedance boundary (1 m front: point1, 1 m backward: point2) [5]. $Z_c = 1224 \text{ Pa} \cdot \text{s} / \text{m}$ and $Z_a = 408 \text{ Pa} \cdot \text{s} / \text{m}$ were set as values of acoustic impedance. Z_c is a virtual acoustic impedance and is set to a value such that the sound pressure peak theoretically becomes 0.5 times as compared with the perfect reflection or complete transmission. Acoustic impedance $Z_c = 1224 \text{ Pa} \cdot \text{s} / \text{m}$, $Z_c = \infty \text{ Pa} \cdot \text{s} / \text{m}$, and $Z_c = 408 \text{ Pa} \cdot \text{s} / \text{m}$ correspond to case1, case2 (perfect reflection) and case3 (perfect transmission), respectively.

4.2 Numerical Results

Fig. shows the sound pressure distribution and mesh idealization for each case in x-y section (z axis is 4 m height). **Fig.** shows the time history of sound pressure at receiving points. At point1, the primary wave is a direct wave and the secondary wave is a reflected wave. The solid line is the case1, the dotted line is the case2 analysis result. From **Tab.1**, the peak ratio of sound pressures is close to 0.5, which is in a good agreement with the theoretical value.

Similarly, the time history of sound pressure at point2 is shown on **Fig. .** When the solid line is the case1, the dotted line is the case3 analysis result. From **Tab.2**, the peak ratio of these sound pressures is also close to the theoretical value.

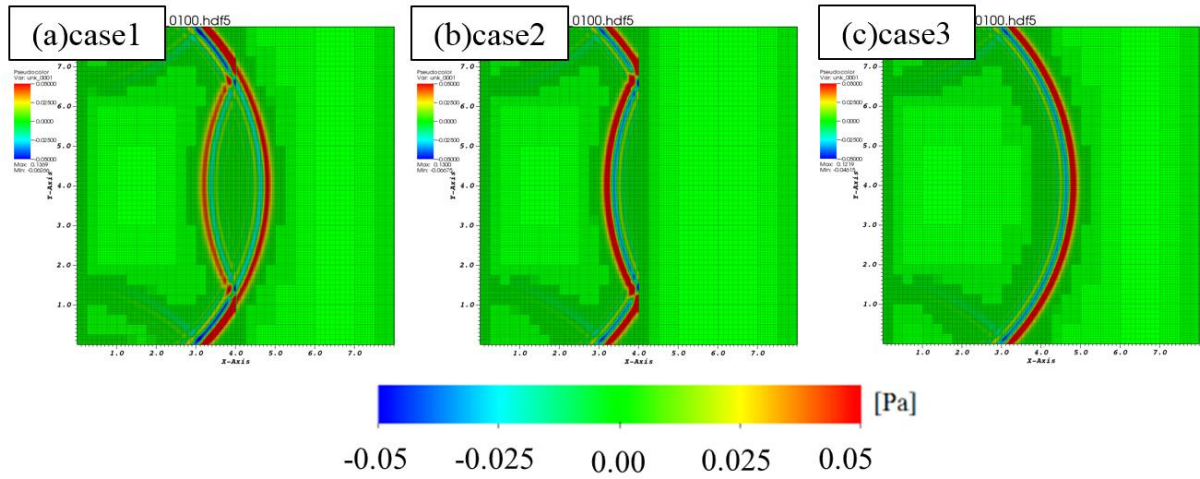


Fig. Sound pressure distribution and mesh idealization for each case

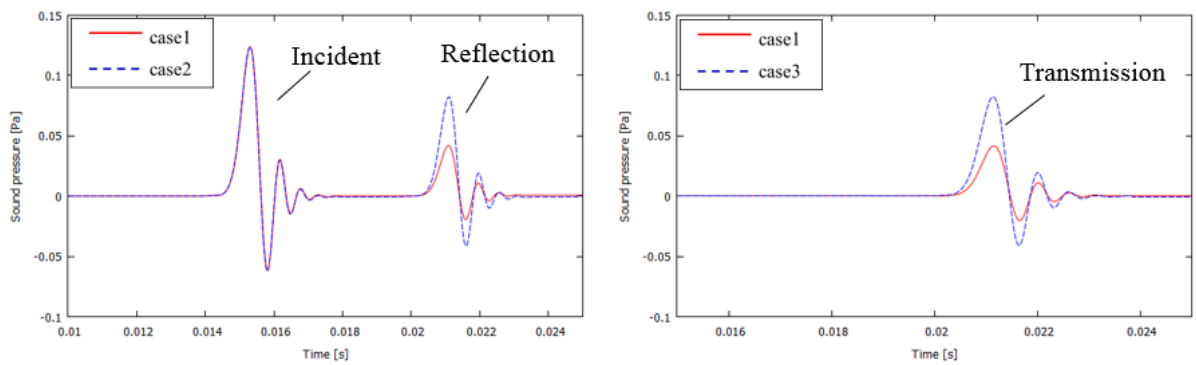


Fig. The time history : point1 (left) and point2 (right)

Tab.1 Comparison of peak values at point1

	case 1	case2	Ratio
point1	0.04198	0.08222	0.51

Tab.2 Comparison of peak values at point2

	case 1	case3	Ratio
point2	0.04173	0.08246	0.51

5. AURALIZATION EXAMPLE

Auralization is realized by converting the output result (numerical data) obtained at the sound receiving point to sound WAV data. The converted WAV data is auralized using a speaker in the VR device. In our previous research, a system that can simultaneously provide the visual information and auditory information was developed [6]. In this system, a stereophonic sound presentation method based on Ambisonics is adopted [7].

The auralization setting is shown in **Fig. .** The analysis conditions are the same as the example in section 4. The distance between the virtual sound source and the incident boundary was set to 1 m, impedance boundary (noise barrier) was set at 4 m from the incident boundary, the barrier is 4m height, and sound receiving points were set 1 m backward from the impedance boundary.

The convolution results of sound source data and impulse response in each case are shown in **Fig. .** Breaking noise is adopted as sound data for convolution. As a result, the sound pressure lowering can be confirmed by considering the acoustic impedance. **Fig. .** shows the state of projection by VR device. The actual auralization sound will be indicated at the presentation.

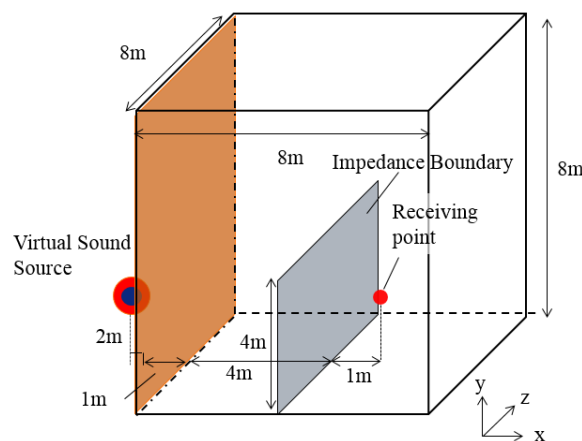


Fig. Computational domain (2)

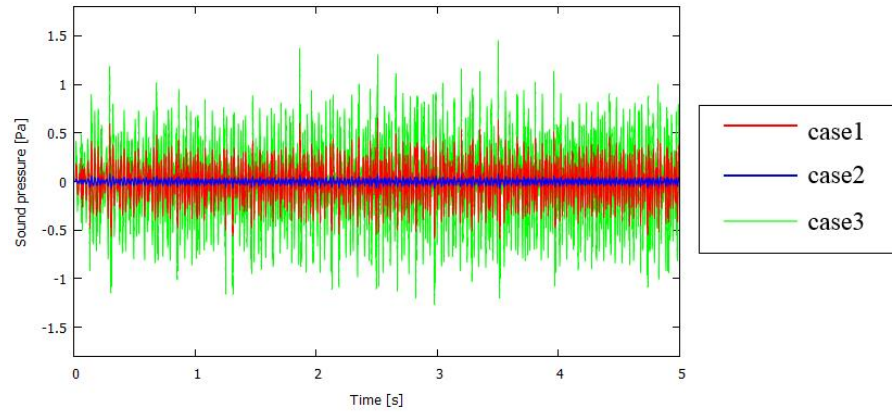


Fig. Convolution results for each cases



Fig. Projection by VR device

6. CONCLUSION

In this research, this method has been applied to the benchmark problem and the validity of its numerical result has been examined by the comparison with the theoretical solution. The conclusions are as follows:

- By considering the acoustic impedance, the sound pressure peak ratio of simulated result to both perfect reflection and complete transmission showed good agreement with the theoretical value. As the results, the usefulness of the presented analysis method could be confirmed.
- In the auralization examination, the attenuation of the sound waveform could be well expressed.

In the future work, this method will be applied to models assuming actual noise barrier and residential environment.

REFERENCES

- [1] Toru Yoshimachi, Masanori Tanigawa and Kazuo Kashiya : Development of the noise prediction method based on the pseudo impulse response and it's auralization using VR technology, Journal of Civil Engineering A2 (Applied Mechanics) vol.72 No.2 pp.207-216 2016.
- [2] H.Takewaki, A.Nishiguchi and T.Yabe : Cubic interpolated pseudo-particle method (CIP) for solving hyperbolic type equations, J. Comput.Phys.61 , pp. 261-268 1985.
- [3] Yuki Tachioka, Yosuke Yasuda and Tetsuya Sakuma : Time domain sound field analysis by CIP method - comparison with FDTD method -, Acoustic Society of Japan, pp.979-982,2007.
- [4] Lubich,C. : Convolution quadrature and discretized operational calculus.I Numer Math.52, pp.129-145, 1988.
- [5] Toru Yoshimachi, Masaki Tanigawa, and Kazuo Kashiya : Imitation Impulse Response for Acoustic Wave Analysis, Journal of Civil Engineering A2 (Applied Mechanics) vol.71 No.2 pp.349-357 2015.
- [6] Masaki Tanigawa, Kou Ejima, Kazuo Kashiya and Masayuki Simura : Development of Mixed Traffic Noise Evaluation System Using VR and acoustic Spatialization Technology, Journal of Civil Engineering A2 (Applied Mechanics)Vol.70,No.2,I 195-I 202, 2014.
- [7] Ward, D.B. and Abhayapala, T.D.: Reproduction of Aplane-wave Sound Field using an Array of Loudspeakers, Speech and Audio Processing, IEEE Transactions on, vol.9 pp.697-707, 2001.

Macro-element Strategy Based upon Spectral Finite Elements for Transient Wave Propagation. Application to Ultrasonic Inspection of Composite Structures

Alexandre Imperiale*, Edouard Demaldent**

*CEA LIST, **CEA LIST

ABSTRACT

Modelling high-frequency wave propagation is a major asset in numerous advanced industrial fields. However, proposing a numerical solution of these problems require complex and expensive computational procedures. Furthermore, it is often expected from numerical solvers to support parametric variations, imposing efficient management of batches of configurations. In order to address both difficulties, we propose a modelling strategy relying on a reciprocity relation [1] based upon the distinction of incident and diffracted fields. This separation enables to isolate the varying part of the configurations in a localized area, so that the overall computational load is significantly reduced. Concerning the numerical solver itself, we propose a numerical computation strategy based on a domain decomposition approach. The topology of each subdomain is obtained from the deformation of a reference hexahedron, thus allowing the construction of a dedicated mesh data structure supporting high-order finite element spaces [2] and leading to optimized unassembled finite element operations. Upon the assumption of conform interfaces, the transmission between these macro-elements can be carried out naturally by gathering contributions at interfaces, or in more complex cases, e.g. fluid-structure interactions, using the mortar element method [3]. We apply this approach to ultrasonic inspections of 3D plate-like carbon fiber reinforced composite structures. In this context, traditional homogenization procedures lead to stratified anisotropic material properties, whose anisotropic orientations depend on the geometric deformation of the specimen (e.g. from flat to curved media). To that end, we introduce two coordinate systems representing the specimen prior to and after its deformation, and passing from one system to another enables on-the-fly reconstruction of local fiber orientation. Splitting directions typically used in absorbing layer formulations are deduced in the same manner. [1] B. A. Auld. General electromechanical reciprocity relations applied to the calculation of elastic wave scattering coefficients. *Wave Motion*, 1(1): 3 – 10, 1979. [2] G. Cohen. *Higher-Order Numerical Methods for Transient Wave Equations*. Scientific Computation, Springer, 2002. [3] F. Ben Belgacem, The Mortar finite element method with Lagrange multipliers. *Numerische Mathematik*, 84(12): 173 – 197, 1999.

Optimal Design of Thermoplastic Composite Quilted Stratum Process Manufactured Parts

Francois-xavier Irisarri^{*}, Cédric Julien^{**}, Terence Macquart^{***}, Denis Espinassou^{****}

^{*}ONERA, Châtillon, France, ^{**}ONERA, Châtillon, France, ^{***}University of Bristol, United Kingdom, ^{****}CETIM, Nantes, France

ABSTRACT

A novel framework for the optimization of composite structures manufactured using the recently developed Quilted Stratum Process (QSP®) is presented in this paper. Over the last decades, the excellent mechanical properties of composites over their metallic counterpart have resulted in the growing use of composite materials in aerospace industries. However, applications to other industries have been limited due to their higher costs and long processing times. The QSP® consists in the stamping of an assembly of thermoplastic composite patches having unidirectional or woven reinforcement. As such, QSP® is suitable for the cost-effective and automated high speed production of composite parts. It encompasses the continuous production of composite bands as well as its automated cutting, positioning and stamping. Despite the potential cost and time benefits associated with this new manufacturing process, there is currently no method available for the design of composite parts associated with QSP®. In this research, we develop the first design and optimization method adapted to the composite parts manufactured by QSP®: the so-called Quilted Stratum Design (QSD®). QSD® is based on a two-level optimization strategy. At the first level, a continuous structural optimization problem is solved using lamination parameters as design variables. The optimal solution obtained gives an idealized target defining the best achievable mechanical performances and the corresponding stiffness and thickness distributions over the structure. The second optimization step aims at retrieving a manufacturable structure that matches the target solution. A typical QSP® part is built from a net-shape preform, which is assembled from patches of different size, thickness and material. Thus, in the present work, the QSP® part is encoded using two sets of indices. The first one refers to a user-defined material library while the second one refers to a library of available patches. This patch library is determined based on the clustering of the target stiffness and thickness distributions in order to bring out areas of uniform stiffness properties and thickness. Consequently, a patch is defined as a shape, size and position on the flattened form of the part. Furthermore, in order to minimize the material waste and cost, patch shapes are restricted to trapezoids cut in the full width of a band. Hence, the basis of the trapezoid defines the material orientation of the patch. This description of the QSP® part lends itself nicely to be implemented in an evolutionary optimizer, which is thus used to solve this second optimization step.

Simulating Traffic Congestions in a City after a Major Earthquake Using a Large Number of Demand Patterns

Takamasa Iryo^{*}, Junji Urata^{**}, Kazuki Fukuda^{***}, Riki Kawase^{****}, Genaro Peque Jr.^{*****}, Lalith Wijerathne^{*****}, Wasuwat Petprakob^{*****}

^{*}Kobe University, ^{**}Kobe University, ^{***}Kobe University, ^{****}Kobe University, ^{*****}Kobe University, ^{*****}University of Tokyo, ^{*****}University of Tokyo

ABSTRACT

A road network is likely to be severely congested after a major earthquake. Damages on infrastructure and buildings significantly reduces capacity of a road network. The deterioration of a road transport system will delay a lot of travels including essential ones such as rescues of victims and interfere a recovery from a disaster. Assessing congestion of a road network in a recovery process from a disaster is essential to maintain disaster resilience of a city and country. Simulating a traffic flow by a computer is a popular approach to assess road congestion. However, existing ones basically intend to simulate a normal situation with a fixed traffic demand pattern given. Estimating a single demand pattern after a major earthquake before it happens is virtually impossible. We construct a stochastic model describing how the demand is generated. Then, various demand patterns that are likely to happen are sampled by a Monte Carlo simulation. A large number of demand patterns generated by the stochastic model should be similar to each other. This property would be useful to reduce total calculation time of simulations for all demand patterns. However, this is not a trivial task owing to the time-dependency of traffic congestions. We developed an efficient algorithm for different demand patterns that are similar to each other by HPC (high-performance computer). In the algorithm, a traffic flow is regarded as a continuous flow like a fluid flow. Dynamics of a traffic flow is described by a partial differential equation system called LWR (Lighthill-Whitham-Richards) model. A traffic flow pattern of each link is independently calculated by the LWR model. To parallelise the calculation, a road network is divided into a number of sub-networks and they are assigned to each CPU. Inconsistency of traffic flow patterns between links are likely to happen owing to the calculations ignoring interdependency of a traffic flow across links. This inconsistency is corrected by repeating the process that transmits information of traffic flow patterns between links and updates a traffic flow pattern in each link. The traffic simulator is designed to handle a network of Tokyo and surrounding area in Japan including about 400 thousand links and 26 million vehicle trips. In the session, we present case studies of this network, as well as details of the simulation.

Phase-field Simulation of Diffusional-displacive Transformation and Stress-strain Response in Ti-Nb-O Alloys

Yuya Ishiguro^{*}, Yuhki Tsukada^{**}, Toshiyuki Koyama^{***}

^{*}Nagoya University, ^{**}Nagoya University, ^{***}Nagoya University

ABSTRACT

Beta-type Ti-Nb alloys exhibit shape memory and superelasticity properties due to the martensitic transformation (MT) from beta phase (parent phase) to alpha" phase (martensite phase) and are assumed to be promising materials for biomedical applications [1]. When oxygen is added to Ti-Nb alloys, the stress-strain hysteresis of the alloys becomes slim as the oxygen content increases. This unique property has been considered to be related to the nanoscale minute martensite, which is called nanodomain [2]. In this study, we focus on the spinodal decomposition of beta phase at 1073 K and its effect on the stress-strain response at room temperature. The spinodal decomposition of beta phase in Ti-Nb-O alloys was simulated by the phase-field method using thermodynamic parameters of equilibrium phase diagram. Simulation results show that the oxygen addition induces the spinodal decomposition, and the beta phase separates into nanoscale beta1 and beta2 phases; the beta1 is O-rich, Ti-rich and Nb-lean phase and the beta2 is Nb-rich, O-lean and Ti-lean phase. Thermodynamic analyses have revealed that the increase in oxygen content in Ti-Nb-O alloys increases the driving force for the spinodal decomposition. The external tensile stress was applied to the calculated (beta1 + beta2) microstructure to simulate the MT and the stress-strain response at room temperature. It has been shown that the beta1 phase preferentially transforms to the alpha" phase when the external stress exceeds a critical value but the beta2 phase acts as a local barrier against the MT. As a result, the long-range MT is suppressed and the minute alpha" phase is formed reflecting the nanoscale beta1 phase. However, the beta2 phase also transforms into the alpha" phase when the magnitude of external stress is increased. The Gibbs free energy calculation has revealed that the difference of the driving force for the MT (Gibbs free energy difference between the beta and alpha" phases) between the beta1 and beta2 phases is attributable to the niobium concentration difference between the two phases. It is assumed that the formation of nanodomain and the unique stress-strain response in oxygen added Ti-Nb alloys are closely related to the nanoscale heterogeneity of the niobium concentration derived from the oxygen induced spinodal decomposition at high temperatures. References: [1] S. Miyazaki et al., Mater. Sci. Eng. A 438-440 (2006) 18-24. [2] M. Tahara et al., Acta Mater. 59 (2011) 6208-6218.

Finite Element Modeling of Fluid Migration through Wellbore Interface Crack

Mohammad Islam^{*}, Nicolas Huerta^{**}, Robert Dilmore^{***}, Mehrdad Massoudi^{****}

^{*}US Department of Energy, National Energy Technology Laboratory (NETL), Pittsburgh, PA 15236, USA, ^{**}US Department of Energy, National Energy Technology Laboratory (NETL), Pittsburgh, PA 15236, USA, ^{***}US Department of Energy, National Energy Technology Laboratory (NETL), Pittsburgh, PA 15236, USA, ^{****}US Department of Energy, National Energy Technology Laboratory (NETL), Pittsburgh, PA 15236, USA

ABSTRACT

Carbon capture, utilization, and storage (CCUS) describes a set of technically viable processes to separate carbon dioxide (CO₂) from industrial byproduct streams and inject it into deep geologic formations to store it from the atmosphere and/or improve hydrocarbon recovery. Behavior of such engineered geologic systems is complex, and involves coupled interactions of various natural and man-made components that can significantly impact system performance. Legacy wells located within the spatial domain of new injection and production activities represent potential pathways for unwanted fluid migration, and understanding their response to those activities is needed to ensure hydrodynamic isolation of targeted intervals. Finite element (FE) method numerical techniques represent a useful tool to simulate those multi-phase and multi-component interactions. The potential presence of cracks in the cemented well annulus can open a pathway to allow unwanted vertical migration of fluid (i.e., CO₂, and aqueous-phase) and create conditions for further crack propagation due to hydraulically induced stresses. In this study, a single-casing composite well system is considered, composed of steel casing, cemented annulus, and rock formation with a partial microannulus formed at the interface of the steel casing and the cement sheath. Using an open-source code [1], a coupled FE analysis is conducted. The flow is assumed to be isothermal and the effects of temperature are ignored. To account for the flow of CO₂ phase and the aqueous phase, a two-phase flow [2] approach is applied in to describe flow and stress response in the interfacial crack. Furthermore, the porous solid media (cement and rock) are modeled using the elastic-plastic Mohr-Coulomb criterion. The solid steel is modeled as a linear elastic material. To illustrate the gas-phase and liquid-phase transition, the van Genuchten model [3] is used. In this paper, the effects of interfacial crack width and length on the predicted mechanical stress distribution and fluid flow are investigated. References: [1] Kolditz, O., et al. (2012). "OpenGeoSys: an open-source initiative for numerical simulation of thermo-hydro-mechanical/chemical (THM/C) processes in porous media." *Environmental Earth Sciences* 67(2): 589-599. [2] Bear, J. and Y. Bachmat (1990). *Introduction to Modeling of Transport Phenomena in Porous Media*. London, Kluwer Academic Publishers. [3] van Genuchten, M. T. (1980). "A closed form equation for predicting the hydraulic conductivity of unsaturated soils." *Soil Science Society of America Journal* 44(5): 892-898.

Progressive Collapse Analysis of Buildings and Its Risk Estimation Using Key Element Index

Daigoro Isobe*, Kota Azuma**

*University of Tsukuba, **University of Tsukuba

ABSTRACT

In case of emergency such as intense fire or collision of some objects to buildings, there is a risk of progressive collapse; a phenomenon which occurred to the World Trade Center (WTC) towers during the 9.11 terrorist attacks. The official statements released by the Federal Emergency Management Agency (FEMA) in 2002, and also by the National Institute of Standards and Technology (NIST) in 2005 and 2008, concluded that the details of the failure process after the decisive initial trigger that sets the upper part in motion were very complicated and their clarification would require large computer simulations. In this study, the collapse behaviors of steel framed buildings are simulated using the Adaptively Shifted Integration (ASI) - Gauss code to investigate the relation between a key element index, which indicates the contribution of a structural column to the vertical capacity of the structure, and the scale of progressive collapse. Collapse was initiated by removing specific columns from the models designed based upon different axial force ratios. Some patterns of removed columns, of which the locations were restricted to a single floor, were investigated. The total potential energy values of structural members after the collapse were used to estimate the collapse scale of the buildings. By evaluating the numerical results using the key element index, it was found that the larger the integrated value of key element index the higher the risk of progressive collapse; however, some peculiar tendencies were observed in the cases of removed columns with extremely symmetrical or asymmetrical locations. The critical integrated values of key element index to cause a large-scale progressive collapse tend to depend on the strengths of buildings, and they cannot be uniquely decided. This is due to the fact that the key element index is a parameter which does not relate to the strength of the building itself, and it cannot be compared relatively between buildings with different strengths. Therefore, the key element index may be used to predict and compare the risks of progressive collapse, only in the same building, but even when the locations of removed columns are variously assumed. References Isobe D. An Analysis Code and a Planning Tool Based on a Key Element Index for Controlled Explosive Demolition. International Journal of High-Rise Buildings 2014; 3(4), 243-254. Isobe D. Progressive Collapse Analysis of Structures: Numerical Codes and Applications, Elsevier, eBook ISBN: 9780128130421, Paperback ISBN: 9780128129753, 2017.

Numerical Simulation of Electro-Thermal Ice Protection Systems

Emiliano Iuliano*, Michele Ferraiuolo**

*CIRA, the Italian Aerospace Research Center, **CIRA, the Italian Aerospace Research Center

ABSTRACT

Aircraft in-flight icing represents a major threat for aviation safety. Along the flight path, an aircraft component may encounter a cloud with super-cooled water droplets that, due to their unstable status, may freeze upon impact. The formation of a thin layer of ice can significantly alter the aerodynamic performance, thus leading to drag increase, lift reduction, loss of control, engine flow distortion and compressor blades structural damage (if ice blocks are ingested within the engine inlet). In order to avoid such issues, ice protection systems are usually installed on critical components like wings, tails, probes, engines. These systems can be classified into de-icing and anti-icing systems. The former aims at breaking the bond of already formed ice with the solid substrate (expulsive or heated types); the latter, instead, are activated prior or during the icing process to prevent any ice formation (heated types, coatings). With reference to anti-icing, the focus of the present investigation is on electro-thermal systems. In this case, the solid substrate consists of a multi-layered structure with heater elements (resistors) embedded at interfaces between layers. The aim is to increase the surface temperature above the freezing point, allowing the caught water mass to flow downstream (running-wet anti-icing) or to evaporate (evaporative anti-icing). The role of numerical simulation is crucial in designing such systems and in reducing the experimental testing burden. The current practice is to size it by evaluating the most critical icing conditions through ice accretion simulation, identifying the regions where ice is expected to grow and, finally, estimating the heating power. Here, a coupled methodology to simulate and optimize the performance of an electro-thermal anti-icing system is proposed in an integrated fashion. The classical tool chain of icing simulation (aerodynamics, water catch and impact, mass and energy surface balance) is coupled to the heat conduction analysis through the multi-layered substrate. Steady and unsteady coupling approaches have been implemented: the first is computationally lighter while the latter is mandatory when heaters are switched on with predefined temporal laws. A thorough comparison between the two methods will be shown. Validation results obtained on benchmark test cases, drawn from NASA database, will be detailed as well as comparison with numerical results from literature.

A Moment Method for Polydisperse Flows Resulting from a Radiological Dispersal Device

Lucian Ivan^{*}, Francois Forgues^{**}, James McDonald^{***}

^{*}Canadian Nuclear Laboratories, ^{**}University of Ottawa, ^{***}University of Ottawa

ABSTRACT

Accurate prediction of the dispersal of particles resulting from the detonation of a radiological dispersal device (RDD) presents many modelling and numerical challenges, especially when urban environments are considered. Certain modelling challenges occur due to the presence of a range of particle sizes generated in the fragmentation process and the associated fireball. Furthermore, radioactive particles in such flow situations transition from a granular-phase regime near the explosion site to a dilute-phase farther away. The particulate phase at locations within each regime will likely display a range of velocities and particle sizes. This talk presents a moment model designed to accurately treat these effects while remaining computationally affordable for large-scale practical calculations. The proposed model is an extension of the well-known maximum-entropy ten-moment model from rarefied gas dynamics with an addition for the treatment of a range of particle diameters. This model allows for anisotropic variance of particle velocities in the phase space and directly treats correlations between particle diameter and velocity. The resulting system comprises fifteen first-order hyperbolic balance laws that are quite simple mathematically. For example, the flux Jacobian possesses an eigenstructure that can be expressed entirely in closed form, and consequently, it allows in-depth analysis of the system's behaviour. This talk presents a derivation of the model and an analysis of the eigenstructure of the system, which characterizes the fifteen waves that are present. For simple diameter-dependent particle-drag models, such as Stokes flow, a dispersion analysis is presented that quantifies the behaviour of the model from the free-flight, drag-free regime all the way to low-Stokes-number, drag-dominated flows. This demonstrates the stability of the partial differential equations describing the model and shows how the apparent waves, present in solutions, are affected by the regime in which a flow exists. A numerical implementation for one- and two-dimensional problems is presented. Numerical solutions for simple problems, for which analytic solutions are available, as well as large-scale computations that are more typical of real-world situations are shown to illustrate the predictive capabilities of the model. It is shown that the new model offers clear advantages in terms of accuracy when compared to traditional Eulerian models for multi-phase flows.

Topology Optimization of Nonlinear Periodic Microstructures with Viscoplastic Material Properties

Niklas Ivarsson^{*}, Daniel Tortorelli^{**}, Mathias Wallin^{***}

^{*}Lund University, ^{**}Lawrence Livermore National Laboratory, ^{***}Lund University

ABSTRACT

In this talk we discuss a framework for generating optimal topologies of periodic microstructures with viscoplastic constitutive behavior. Finite deformation is considered and materials with tailored macroscopic mechanical properties are designed. We evaluate effective material properties by performing numerical tensile and shear deformation tests of a single unit cell, as opposed to standard homogenization approaches, and also incorporate irreversible material effects. The constitutive model that we employ was proposed by [1] and is based on finite strain isotropic hardening viscoplasticity. The mechanical balance laws are formulated in a total Lagrangian setting and solved using the Newton-Raphson algorithm together with an adaptive time-stepping scheme. The optimization problem is regularized by introducing a periodic version of the Helmholtz' partial differential equation filter and iteratively solved using the method of moving asymptotes (MMA) which is based on the gradients of the cost and constraint functions. Since the material model is path-dependent the sensitivity will be so too. Sensitivities needed for each design update are obtained from the adjoint sensitivity scheme presented in [2] which for plasticity will be a terminal value problem. In the numerical examples we consider several objectives: 1) tailored specific stress-strain response, achieved by minimizing the error between actual end prescribed target response, 2) design of microstructures for maximum energy dissipation. Near black and white solutions are obtained through the use of Heaviside thresholding technique and penalization of intermediate designs. The applicability of the algorithm is demonstrated by several numerical examples of optimized three-dimensional plane strain continuum structures exposed to multiple load cases over a wide macroscopic strain range. This work was partially performed under the auspices of the U.S. Department of Energy by Lawrence Livermore Laboratory under contract DE-AC52-07NA27344, cf. ref number LLNL-CONF-717640. The financial support from the Swedish research council (grant ngb. 2015-05134) is gratefully acknowledged. The authors would also like to thank Professor Krister Svanberg for providing the MMA code. 1. Simo JC, Miehe C. Associative coupled thermoplasticity at finite strains: Formulation, numerical analysis and implementation. *Computer Methods in Applied Mechanics and Engineering* 1992; 98:41–104. 2. Michaleris P, Tortorelli DA, Vidal CA. Tangent operators and design sensitivity formulations for transient non-linear coupled problems with applications to elastoplasticity. *International Journal for Numerical Methods in Engineering* 1994; 37(14):2471–2499.

Masonry Micromodels Using High Order 3D Elements

Salvador Ivorra^{*}, J.I. Gisbert^{**}, D. Bru^{***}, F.J. Baeza^{****}

^{*}University of Alicante, ^{**}University of Alicante, ^{***}University of Alicante, ^{****}University of Alicante

ABSTRACT

The main objective of this paper is the use of high order 3D elements in the numerical modelling of masonry structures. For this purpose, FE models corresponding to standard tests were made and calibrated using results of experimental tests. In particular, this document will analyze the resistant behavior to uniaxial and diagonal compression walls made with brick. The numerical micromodel has been developed using the ANSYS code with non-linear hexaedrical 8 and 20 nodes tridimensional elements to represent brick and mortar, such as solid185 and solid186, in contrast to traditional FE models which use element solid65 as finite element to represent masonry behavior. Drucker-Prager and Rankine models have been used to study the compression-tension failure surface, adding a linear hardening-softening-dilatation behavior. Moreover, fracture-energies based cohesive zones have been added to contacts between mortar and bricks, in order to allow debonding failure between these two materials. These modelling method prove to be a valid technique to simulate brick masonry behavior according to experimental results, and will be used as a base to develop FEM analysis to study the effect of Textile Reinforced Mortars (TRM) to reinforce masonry specimens.

PRACTICAL STEPS TOWARDS PERFORMANCE STEWARDSHIP FOR COMPUTATIONAL SCIENTISTS

C. Iwainsky, and D.C. Sternel

Hessisches Kompetenzzentrum für Hochleistungsrechnen¹
Technische Universität Darmstadt
Alexanderstraße 2, 64289 Darmstadt, Germany
e-mail: [iwainsky,sterne]@hpc-hessen.de;
web page: <http://www.hkhlr.de/>

Key words: Performance Engineering, Active Performance Documentation, Performance Stewardship

Abstract. Achieving high performance has been in the focus in the past, but sustaining achieved performance remains an open topic. Performance degradation, if not actively monitored for, can creep in and severely diminish the productivity of codes and their operating scientists' research. The current state of the art to detect such a creeping performance loss is performance analysis. A performance analysis is a considerable investment in resources to generate the necessary data and to subsequently analyze it. The resulting insight is only directly applicable to the specific analyzed software variant and data set. Each code variant and configurations must be, in principle, separately analyzed to ensure the absence of performance bugs. Therefore, frequently repeated performance analysis is not sustainable for every program execution during the long lifespan of a code. We present, how so called "active performance documentation" can be used to achieve resilience against performance loss from creeping code deterioration or configuration errors. Such an active documentation consists of small code augmentations placed at critical points in the program that monitor specific performance indicators, and validate those against specifications of acceptable performance. Thus, developers and users of a code using active performance documentation will be aware, when and if the performance of their code deteriorates, at which point appropriate counter-measures can be undertaken. With the use of active performance documentation, users and developers of computational code will be able to react to performance problems, instead of having to proactively scan for potential issues.

¹The "Hessisches Kompetenzzentrum für Hochleistungsrechnen" is funded by the Hessian State Ministry of Higher Education, Research and the Arts.

1 Introduction

Performance is an important aspect of many scientific applications, as computational solutions require typically a large invest of High Performance Computing (HPC) resources. Here, performance is defined as the ability to utilize a given amount of computational resources to produce as much meaningful work as possible. While achieving performance has been in the focus in the past, resulting in a plethora of technological and methodological techniques, the issue of sustaining performance achieved remains an open topic.

The performance is limited by the constraints of the specific hardware used and by the capability of the used software to make efficient use of these resources. Examples for hardware constraints are network performance, CPU performance, available memory, storage performance, or the maximum up-time of a system; examples for software constraints are the data-set size or the precision required of the result. A good performance is all too often a trade-off between user-requirements and available resources. To preserve good long term performance, an achieved performance must be monitored and maintained to account for changes in constraints and requirements.

While changes in hardware are rare and obvious, changes in the software or its run-time configuration and their effects are subtle and frequently remain unnoticed. This is especially the case in an academic environment, where software is actively worked on to keep up with advances in domain knowledge and methodology or applied to substantially different scenarios than it was originally intended for. This, in combination with the loss of usage-experience due to frequently changing developer and user base caused by academic life-cycles and project driven development, creates an environment where the performance of a software can decrease without being noticed, if not actively monitored for.

Performance Stewardship (PS) describes the holistic approach where the performance of a software is not a simple byproduct, but a primary concern on the same level as software features or correctness. It follows, that the performance of a software is something to be actively preserved and maintained in all phases of its life-cycle. One important aspect of PS is the monitoring of program executions and evaluation of the resulting information to detect degrading performance. The current state of the art relies entirely on the user to use performance models or to conduct a performance analysis:

1. Performance models parameterized by the software configuration traits and hardware parameters are used to predict values of observable metrics, such as the wall-time of the application. If the observed metric matches with the predicted value, then the performance is considered to be OK, and if not, a performance problem must have occurred.
2. For performance analysis, dedicated measurement runs are used to generate performance data that is analyzed for performance deficiencies. This analysis is substantially based on experience of the analyst and uses usually an implicit and abstract performance model of the machine used and software executed.

Both techniques have their challenges. The precise performance models with predictive qualities required for the first approach are rare, and the creation of such models requires substantial expertise and considerable effort. Current research, such as the ExtraP-project [2], aims to make performance models more accessible, but still requires considerable expertise to use. The performance analysis approach is expert driven and resource-intensive in nature, as separate experiments must be conducted for the sole purpose of generating measurement data. Additionally, the measurement overheads incurred with current methods require a tailored measurement setup [4], which is configuration specific and often a result of multiple refinements of the measurement infrastructure. While performance analysis may lead to considerable insight in an applications runtime behavior, it is unfeasible to perform an user-driven analysis for every execution as the overheads of such an approach, be it runtime overheads or human time invested, would in most cases surpass the potential benefits in detecting performance creep.

Therefore, a more accessible method is necessary that can be used easily by developers and domain scientists to achieve performance stewardship of their codes.

2 Performance Mistakes

From years of experience advising and supporting users of different HPC systems², we identified three reoccurring performance issues: load balancing, over-parallelization and performance critical component misconceptions.

Load balancing, or the issue of unbalanced workloads, is a considerable challenge for scientific applications, both for multi-processing and multi-threading [3]. Simply stated, the principal issue is that, due to synchronization of imbalanced workloads, not all computational entities contribute evenly to the outcome. In consequence, some of the allocated resources are wasted and the performance of the program decreases. The underlying root-cause is case specific. Examples are imbalanced domain partitioning or software with adaptive refinement. Also external sources, such as intermittent network congestion or temperature based CPU over- or under-clocking, will effect the work balance of a parallel application. While users and developers are, in principle, aware of the work-balancing issue, countermeasures are challenging in both implementation and usage. On the one hand, runtime load-balancing methods are difficult to implement, incur additional overhead and are often not available in existing code-bases. On the other hand, static work-balancing, i.e. balancing the workload before each execution, requires prior information, a very good understanding of the input parameter and knowledge of resulting runtime behavior such as a performance model. For this reason, in everyday HPC usage, application users are rarely aware of their codes actual workload distribution.

Runtime **over-parallelization** is yet an other issue that users often struggle with. Over-parallelization describes the effect that with increasing parallelism the performance

²The authors currently support HPC users from all Hessian universities, such as user of the Lichtenberg HPC system at TU Darmstadt.

gains drop, to the point, where an additional degree of parallelism actually increases the runtime. Possible root causes are, for example, increasing communication-costs, as observed in previous work [5], or domain partitioning to the point at which each parallel entity has only a few elements to process; this can even culminate in each parallel entity having only a single element to process.

The following case study exemplifies this issue: A given code was used for parameter studies for material structure calculations, with hundreds of experiments to be conducted. The code was benchmarked by the user to assess its fastest configuration, which was determined to be at 72 MPI processes on three 24 core machines. However, the user did not realize that even though there was a continued speedup up to 72 processes, the efficiency had substantially dropped. In this case, the efficiency dropped from above 69.9% at 16 processes, to 35% at 32 cores down to 25% efficiency at 72 cores. As many of the planned experiments were independent from each other, the best performance for the user was to run 3 experiments at 16 cores, instead of one experiment at 72 cores. This provided a net-speedup for the desired work of 3x without any code modification. Had a mechanisms been available in the code to notify the user of a low efficiency, this situation would have been rectified much earlier than it was.

Performance critical component misconceptions (PCCM) is a collective term for performance issues originating from development practice. A PCCM is a performance issue caused by a code region or kernel that is considered by the developers of the code to be non-critical or where the developer is unaware of its existence. The problem of such a misconception is, that without explicit profiling, such expensive code regions are likely to remain unnoticed and therefore never addressed in tuning and optimization. The reasons for such PCCM are manifold.

For example, developers of parallel software aim to optimize their codes, but due to time constraints focus on perceived performance critical components and ignore less critical components. This is even further emphasized by the fact, that their intent is to implement new mathematical solvers or physical simulation capabilities to their code. Understandably, their development effort is spent to optimizing these regions. While focusing on critical code is important for good performance, it is easy to neglect tuning and optimizing the other aspects of a code, such as the I/O components before and after the computation intensive regions, or the management routines used for check-pointing or data-structure management. Such a PCCM, for example, was discovered by Calotoiu et al.[2] in a widely used weather simulation package, where an I/O related section had a so far unknown performance issue.

An other example for PCCM can be observed in codes with continued development. Here, the addition of new functionality, restructuring of code or inclusion of new methods can easily shift the location of computation heavy aspects. This, by itself, is not an issue, but optimizations made for the previous code version might no longer apply. Also a human element plays a problematic role: past experience with the code is frequently used without checking its validity for the new code version, thus creating possibilities for

PCCM and in conclusion to performance problems

Simple profiling, and other performance analysis methods, can and will detect such changes and shifts in performance critical regions and prevent PCCM. However, this requires the users and developers to use such tools in their daily development process. And even if such methods are known, the fact that such analyzes require explicit and additional after-development steps results in developers often simply neglecting this crucial step, as their actual goal is to conduct their computational experiments.

These three issues are a tiny sub-set of all potential performance issues. The three described, however, occur easily by mistake, even by experts, and are, in our experience, not too uncommon in the bulk of engineering applications run in HPC centers. Measurements of codes with production configurations are the only way to guard against such mistakes. The likeliness of such mistakes is unfortunately further amplified by the proliferation of ready-to-use packages, such as OpenFOAM, Wien2K or VASP, as a larger experience and knowledge gap exists between the original developers, who are typically aware of these issues, and "end-users" that have to learn to use the software as well as cope with all the peculiarities of good performance.

3 Active Performance Documentation

HPC users and code developers require an approach to automate the monitoring and analysis aspects, and the means to integrate this in their applications in order to mitigate the performance mistakes described earlier.

3.1 Method

To provide a practical mechanism in support of PS, we propose the following approach:

- In a first step, the application is augmented with permanent measurement and analysis facilities in combination with developer defined performance criteria. Ideally the performance checks and validation are integrated directly into the code-base itself, but also external specifications and measurement facilities are possible.
- The resulting software is then used as is, allowing for unchanged application workflows without the need of interleaved explicit profiling and validation runs. As the added measurement and analysis system evaluates every execution, a creeping or accidental performance loss can not remain unnoticed and appropriate countermeasures can be applied.

We call this concept *active performance documentation* (APD), as the mechanisms in the code document the expected performance behaviour.

Such APDs provide, on the one hand, a confidence and ease of mind into the scientific software, as it will "notify" the user when the software is running deficient. Also, performance experts, such as members of the many performance engineering groups at HPC centers, can focus their effort on known deficient codes, instead of having to proactively

trriage all codes for their performance. On the other hand, the run-time measurement and validation of complex performance models will add overhead, which must be controlled for.

3.2 Performance Model Simplifications

Active performance documentation is at its core a hybrid of both performance models and measurement-based performance analysis. It therefore requires aspects from both methods: a sufficiently precise performance model, which is, as described earlier, difficult to come by, and a low-overhead measurement system, which is also challenging to integrate into arbitrary codes. This would be too complex for most domain experts and engineers to apply to their codes. Fortunately, for the three specific performance mistakes described earlier, i.e. load-imbalances, over-parallelization and performance critical component misconceptions, simplifications can be applied that eliminate the need for an explicit mathematical performance model³ and that have, in comparison, lower and easier controlled measurement costs.

To derive these simplifications, we first define the performance issues and demonstrate how the complexity of performance models can be substituted by far more easily implemented runtime measurements:

A load imbalance is defined as follows: Assuming that the target metric is the runtime t and the (performance) model $\mathcal{T}(\mathbf{R}, \dots)$ describes the runtime of a parallel computing entity⁴ P_n for a specific region \mathbf{R} of code, then a load imbalance is defined by $\mathcal{T}(P_a, \mathbf{R}, \dots) < \mathcal{T}(P_b, \mathbf{R}, \dots)$. The ellipsis here is a placeholder for the many additional arguments required, such as machine specific parameters like memory bandwidth or networking latency, and input parameters like the domain size used. To assess, if this comparison is true for a given program for all configurations, a performance model replicate all aspects of the code, which is very complex. However, as active performance documentations do not intend to argue this equation for all executions, but only for a specific execution, the model of a specific region can be substituted by a runtime measurement. Therefore, it is not necessary compute the runtime of the different computation entities from parameters, but the desired metric, i.e. runtime, can be simply measured, communicated and compared on a global level.

Similarly, for over-parallelization, the local workload can be compared to the various overheads. Here, performance models, (see [1]), describe the time spent in the CPU and other components as sums of partial models, each modeling specific aspects of the program, such as communication, I/O and other activities. To ensure that a specific component, such as the computation, remains the dominant part, the individual terms of the model can be separated and compared to each other. Assuming that the runtime model \mathcal{T} can be split into the component models for CPU time $\mathcal{T}_{\text{cpu}}(\mathbf{R}, \dots)$ and commu-

³An example and its derivation for such a model can be found in Bauer et al.[1].

⁴A parallel computing entity can be a process or thread, with the number n used as means for identification.


```

1 for (time_step < end) {
2     while(not_converged) {
3         exchange_local_boundaries(...);
4         compute_local_solution(...);
5         communication_error(...);
6     }
7     compute_global_contribution(...);
8     communicate_global_contribution(...);
9 }

```

Listing 1: Demonstrator Pseudocode

This pseudo-code mimics the a compute and communication structure found in some fluid dynamics codes. Compute only regions are highlighted in green color, and communication and synchronization in red color.

nication time $\mathcal{T}_{\text{comm}}(\mathbf{R}, \dots)$, then a comparison between both terms can be used to ensure proper compute to overhead-ratio. For example, $\mathcal{T}_{\text{cpu}}(\mathbf{R}, \dots) > 9 * \mathcal{T}_{\text{comm}}(\mathbf{R}, \dots)$ states that the time spend in communication should not exceed 10% of the runtime of that region ($\mathcal{T}_{\text{cpu}} + \mathcal{T}_{\text{comm}}$). Again, moving from a generic model to a specific execution instance, the modeled components can be replaced with measurements of the specific components from that region.

Performance critical component misconceptions correspond to the developer relying on a partial model \mathcal{T}' describing a subset of the full, but unknown, model \mathcal{T} . This model, while not 100% correct, sufficiently approximates the full model, if the error $\mathcal{E}_t = \mathcal{T} - \mathcal{T}'$ is small enough, i.e. $\mathcal{E}(\mathbf{R}, \dots) \ll \mathcal{T}(\mathbf{R}, \dots)$. For a specific execution the generic model can be substituted with the measurements.

The metric used so far, was the time spent in specific components of the code, i.e. compute and communication. While a plethora of possible metrics exists on current hardware platforms, such as hardware performance counters counting the number of floating-point operations, or memory accesses, their precise interpretation is often hardware-specific, compiler depended and requires considerable expertise. This does not imply, that these more detailed metrics should not be used, but we consider them too complex for this step towards active performance documentation. This is especially the case, as the runtime of specific components, if measurable, can function as a stand in for these more precise metrics. On today's HPC systems three principal components can be considered as measurable: The CPU with its compute units, the network components, and the I/O system. Time measurements of these three components aggregate to the total runtime of a specific application run, and therefore can be used to describe the full application behavior.

3.3 Active Documentation Example

Using these simplifications, it is possible to express the desired performance checks directly in the program. To demonstrate this, we use the pseudo-code of Listing 1 as a

```

1  for (time_step < end) {
2      #pragma apd balanced( $t_{\text{cpu}}$ ,0.1,NEXT_STATEMENT)
3      while(not_converged) {
4          exchange_local_boundaries(...);
5          compute_local_solution(...);
6          communication_error(...);
7      }
8      #pragma apd balanced( $t_{\text{cpu}}$ ,0.1,NEXT_STATEMENT)
9      compute_global_contribution(...);
10     communicate_global_contribution(...);
11 }

```

Listing 2: Demonstrator Pseudocode with Work-balance APD

This pseudo-code is augmented with two APDs defining the expected work-balance. Computations are highlighted in green color, communication and synchronization in red color, and APD code is highlighted in blue. `NEXT_STATEMENT` specifies, that the APD operates only on the next statement, and sub-elements.

demonstrator. Listing 1 mimics the work-flow of typical fluid-dynamics applications, and depicts a simple boundary-region based parallelization of a solver with local computations (line #3-4), global convergence check (line #5) and global operations (line #7-8).

For this example, a lack of **load balancing** implies, that one of the computational entities must compute more than the others. This entity, either a thread or a process, will spend more time in the routines of line #4 and #7 of Listing 1. To state for this example, that the workload must be balanced, one could either specify that the loop body of the while-loop, that the whole while-loop or that the global computation must be balanced. The granularity of the scope chosen will effect the overhead. In this case, either option is viable, as the loop contains a call to a communication routine, which are typically more expensive than a local measurement and comparison. Therefore, the cost of tracking the runtime and exchanging it will be in the worst case on the same order of magnitude as the loop body, but will in most situations be masked by the communication and actual computation overhead. The same consideration applies to the second communication routine of line #8. Borrowing from the C-pragmas, the pseudo-code syntax **apd balanced(metric,deviation,region)**⁵ describes that for the designated region, e.g. the next statement, a computation entity, i.e. a tread of process, may only deviate up to 10% from the slowest in terms of the given metric. Listing 2 offers an example for such an active performance documentation using the CPU time metric t_{cpu} .

In the case of **over parallelization**, the computational aspects shrink, e.g. in the case of strong scaling due to constant domain partitioning with increasing number of processes. The ratio of work, i.e. the time spent using the CPU, shifts from the computation code, lines #5 and #9 in Listing 1, to the communication code in lines #4, #6 and #10. In general, as

⁵The pragma is used in lieu of an actual implementation using a domain specific language or other programming constructs native to the host language.

```

1  #pragma apd cold( $t_{comm}$ , 0.1, NEXT_STATEMENT)
2  for (time_step < end) {
3      #pragma apd balanced( $t_{cpu}$ , 0.1, NEXT_STATEMENT)
4      while(not_converged) {
5          exchange_local_boundaries(...);
6          #pragma apd hot( $t_{cpu}$ , 0.98, CURRENT_SCOPE)
7          compute_local_solution(..);
8          communication_error(...);
9      }
10     #pragma apd balanced( $t_{cpu}$ , 0.1, NEXT_STATEMENT)
11     compute_global_contribution(...);
12     communicate_global_contribution(...);
13 }

```

Listing 3: Demonstrator Pseudo-code with Work-balance APD

This pseudo-code is augmented with a hot- and cold-spot APD defining the expected ratio of compute to communication. Computations are highlighted in green color, communication and synchronization in red color, and APD code is highlighted in blue. `CURRENT_SCOPE` expands the APD to cover all elements of the current scope.

long as the computation dominates, this is considered acceptable to a certain degree, but at the latest when communication dominates, the CPU no longer contributes effectively to the computational solution. The precise communication to compute ratio is depended of the specific situation. A guard against such behavior is the measurement of time spent computing (t_{cpu}) and communicating (t_{comm}) and a comparison between both times. Without further evidence, it is for $t_{cpu} \gg t_{comm}$ safe to assume, that the compute to communication efficiency of the monitored code aspect is sound. Rephrased, the fraction CPU-time to the wall-time of the region must be much larger than 50%. This is more commonly known as a *hot-spot*; in this case it is a hot-spot of CPU usage.

Thus, by stating that for the given region a CPU-time hot-spot exists, a clear and measurable definition of its behavior is specified. As a side effect, a developer reading the APD in the source-code with APD will be able to understand the intended behavior. In a complementary fashion, the same behavior could be defined by a communication *cold-spot*, stating that communication should not exceed a specific fraction of work.

For example, using hot- and cold-spots in Listing 2, it is possible to specify good computational efficiency. Using the pseudo-code syntax **apd hot(metric, deviation, region)**, a computation hotspot is defined with a 98% hotness, i.e. 98% of this regions runtime must be spent in computation. In absence of other contributors, this also implicitly defines a communication cold-spot of 2%. The APD in line #1 of Listing 3 states, that for the whole example the communication time should at maximum consume 10% of runtime. If the code is executed with twice the number of processes, the local domain will only contain half the number of elements to compute, cutting the runtime of the computation in half. Assuming the communication time remains constant, the remaining computa-

```

1 #pragma coverage( $t_{\text{cpu}}$ ,0.9,CURRENT_SCOPE)
2 main(...) {
3     startup(...)
4     #pragma apd cold( $t_{\text{comm}}$ ,0.1,NEXT_STATEMENT)
5     for (time_step < end) {
6         #pragma apd balanced( $t_{\text{cpu}}$ ,0.1,NEXT_STATEMENT)
7         while(not_converged) {
8             exchange_local_boundaries(...);
9             #pragma apd hot( $t_{\text{cpu}}$ ,0.98,CURRENT_SCOPE)
10            compute_local_solution(...);
11            communicate_error(...);
12        }
13        #pragma apd balanced( $t_{\text{cpu}}$ ,0.1,NEXT_STATEMENT)
14        compute_global_contribution(...);
15        communicate_global_contribution(...);
16        output_timestep(time_step,...)
17    }
18    shutdown(...)
19 }

```

Listing 4: Demonstrator Pseudo-code for APD guarding against PCCM

This pseudo-code is augmented with a single APD defining the global coverage of all APDs in the code. Computations are highlighted in green color, communication and synchronization in red color, and APD code is highlighted in blue.

tion time must be 18 times the communication time to pass the criterion. Double that number for each doubling of the number parallel processes. It is obvious, that eventually the communication time will outclass the runtime, and thus fail the comparison. Thus, by focusing on the simple concept of "hot-" and "cold-spots" in combination with metrics representing the critical components of HPC systems, i.e. networking, I/O, memory, or CPU performance, users can define active performance documentation that prevents issues, such as over-parallelization.

The pseudo-code of Listing 1 is too simple possible to demonstrate a guard against performance critical component misconceptions. We extend the pseudo-code (see Listing 4), with a startup-routine, an output-routine at the end of the time-step loop body, and a shutdown routine at the end. Here, the APD **apd coverage(metric, percentage, region)** describes the coverage of all other APD in the code of the corresponding region. If, as in this case, a coverage of 90% is specified, then this states that for the given metric 90% must be covered by other APD. For Listing 4, this means that 90% of all runtime must be spent in the hotspot (line #10). If, for example, the start-up routine were to become computational expensive and would consume 15% of t_{cpu} , then the coverage APD would fail and notify the user of one ore more undiscovered computational intensive regions.

```

1 // #pragma apd balanced(tcpu, 0.1, NEXT_STMT)
2 double local_start_time=get_wtime();
3 compute_global_contribution(...);
4 double delta_t=get_wtime()-local_start_time;
5 double global_max_time;
6 MPI_Allreduce(&delta_t,&max_t,1,MPI_DOUBLE,MPI_MAX,APD_COMM);
7 if (delta_t<(1-0.1)*max_t) perror("APD failed");
8 communicate_global_contribution(...);

```

Listing 5: APD to native code transformations example

This pseudo-code showcases the transformation of a work-balance APD to native code. Computations are highlighted in green color, communication and synchronization in red color, and APD code is highlighted in blue.

3.4 Implementation Aspects

So far, we used pseudo-code pragmas to specify and anchor an APD in the source code. Such a transformation can be implemented in a compiler, such as the LLVM compiler.

However, the concepts that the pragmas represent, can also manually be implemented in the source code, using the native programming language. For example, the APD for load-balancing requires for each process two measurements of the required metric, e.g. CPU-time, and a communication call to exchange the locally measured data. Listing 5 shows a possible implementation. In line #2 the walltime before the monitored regions is acquired. Line line #4 measures the walltime after the region and computes the time spent in the `compute_global_contribution` section of the code. Lines line #5-7 declare a variable to store the global maximum, which is then obtained via an `MPI-Allreduce` call. In this case, we use a unique communicator to isolate the communication calls from the APD system from the rest of the program to avoid communication problems. Line line #7 implements the check against the given criterion and prints an error message, if it fails.

4 Conclusion

Performance of software, especially parallel software, is challenging to obtain and difficult to maintain. *Performance Stewardship*, i.e. the methodical approach for maintaining performance, is becoming an important aspect of scientific software. *Active performance documentation* (APD) offers a shift from a proactive monitoring approach, where one actively looks for performance issues, to a reactive approach, where one only has to react to occurring issues. We propose the concept of augmenting the code with measurement facilities and automated analysis capability to automatically track all executions of the software. However, generic APD is complex and subject of research. But for reoccurring mistakes that can seriously hamper performance, simplifications can be applied that make APD viable. We demonstrate the use of such APD on a demonstrator pseudo-code for *load imbalances*, *over-parallelization* and *performance critical component misconceptions*.

Even though the concept of APD is subject of current ongoing research, we demonstrate that the concept can already be applied to codes, although not yet with automated support by compilers or tools.

In conclusion, it is critical, according to the popular wisdom "knowing of the existence of a problem is the first step in solving it", to detect performance issues in every execution of a code to mitigate problems as soon as possible. APDs offers exactly this knowledge, if properly implemented, and provides the necessary support for *Performance Stewardship*.

REFERENCES

- [1] Greg Bauer, Steven Gottlieb, and Torsten Hoeffler. Performance modeling and comparative analysis of the MILC lattice QCD application su3_rmd. In *Cluster, Cloud and Grid Computing (CCGrid), 2012 12th IEEE/ACM International Symposium on*, pages 652–659. IEEE, May 2012.
- [2] Alexandru Calotoiu, Torsten Hoeffler, Marius Poke, and Felix Wolf. Using automated performance modeling to find scalability bugs in complex codes. In *Proceedings of the International Conference on High Performance Computing, Networking, Storage and Analysis*, SC '13, pages 45:1–45:12, New York, NY, USA, 2013. ACM.
- [3] Florina M. Ciorba, Christian Iwainsky, and Patrick Buder. Openmp loop scheduling revisited: Making a case for more schedules. In *Proceedings of 14th International Workshop on OpenMP, IWOMP 2017*, Stony Brook, NY, USA, To appear 2018.
- [4] Christian Iwainsky and Christian Bischof. Calltree-controlled instrumentation for low-overhead survey measurements. In *Parallel and Distributed Processing Symposium Workshops, 2016 IEEE International*, pages 1668–1677. IEEE, 2016.
- [5] Christian Iwainsky, Samuel Sarholz, Dieter an Mey, and Ralph Altenfeld. Leveraging multicore cluster nodes by adding OpenMP to flow solvers parallelized with MPI. In Douglas Mewhort, Natalie Cann, Gary Slater, and Thomas Naughton, editors, *High Performance Computing Systems and Applications*, volume 5976 of *Lecture Notes in Computer Science*, pages 62–69. Springer, June 2010.

Comprehensive Grid Resolution Study of WALE Model for Large Eddy Simulation of Turbulent Pipe Flow

Daiki Iwasa^{*}, Yusuke Nabae^{**}, Koji Fukagata^{***}

^{*}Keio University, ^{**}Keio University, ^{***}Keio University

ABSTRACT

In recent years, reduction of CO₂ emission has become an urgent issue in order to mitigate the global warming. It is said that three quarters of CO₂ emission out of transport is from the road sector. The Cross-ministerial Strategic Innovation Promotion Program (SIP) in Japan aims at improving the thermal efficiency of IC engines up to 50 percent, where an IC engine simulator, named HINOCA, is being developed so as to enable prediction and improvement of IC engines. This simulator consists of different physical models of IC engines, such as turbulent flow, ignition, and combustion. As for the turbulence simulation, the wall-adapting local eddy-viscosity (WALE) model is adopted for the subgrid-scale model in large-eddy simulation (LES). However, for HINOCA to complete a simulation within a realistic computational time, it is inevitable to choose the grid spacings much coarser than that is well accepted. Therefore, we need to assess the accuracy of WALE model in the case where the computational grid is very coarse. In the present study, we perform a comprehensive grid resolution study of the WALE model in a turbulent pipe flow. The LES is performed under the constant flow rate at the bulk Reynolds number of 5300. The computational grid is uniform in the streamwise (longitudinal) and spanwise (azimuthal) directions while non-uniform in the wall-normal (radial) direction. A top-hat filter is used for the spatial filter. The results show that the turbulent statistics such as the mean velocity profiles and the second order moments significantly depend on the spanwise grid resolution, while less sensitive to the streamwise grid resolution. The coarsest streamwise and spanwise grid resolutions producing reasonable statistics are found to be about 56 and 18 wall units, which is in accordance with conventional LES studies. The sensitivity to the wall-normal grid spacing is found to be much less than what is usually believed. Surprisingly, the statistics are reasonably well reproduced using only 6 computational points in the radial direction if only the first computational point is located within 5 wall units from the wall.

A Variational Multiscale Method for Dynamic Viscoelasticity and Quasi-static Elasto-plasticity Using Linear Tetrahedral Elements

nabil abboud^{*}, guglielmo scovazzi^{**}, oriol colomes^{***}

^{*}duke university, ^{**}duke university, ^{***}duke university

ABSTRACT

We propose an extension of the dynamic variational multiscale stabilization (D-VMS) to nearly/fully incompressible viscoelastic materials using quadrilateral/tetrahedral finite elements. We test the approach on two different viscous constitutive laws, namely, models based on Prony series and models based on the multiplicative decomposition of the deformation gradient. In addition, we propose a new variational multiscale approach for quasi-static elasto-plasticity. The main features of this method are the definition of an effective shear modulus as well as the use of fine-scale pressure. Our method is based on a mixed formulation, in which the momentum equation is complemented by a pressure equation in rate form for viscoelasticity and static form for elasto-plasticity. The unknowns are approximated with piecewise linear, continuous finite element functions. For viscoelasticity, in order to prevent spurious oscillations, the pressure equation is augmented with a stabilization operator specifically designed for viscoelastic problems, in that it depends on the viscoelastic dissipation.

Modeling of Light Aircraft Landing Gears: Convenient Damping Settings According to Runway Type

nadia arif^{*}, Frédéric lebon^{**}, Hélène ELIAS-BIREMBAUX^{***}, iulian rosu^{****}

^{*}Aix-Marseille Univ., CNRS, Centrale Marseille, LMA, Marseille, France, ^{**}Aix-Marseille Univ., CNRS, Centrale Marseille, LMA, Marseille, France, ^{***}Aix-Marseille Univ., CNRS, Centrale Marseille, LMA, Marseille, France, ^{****}Aix-Marseille Univ., CNRS, Centrale Marseille, LMA, Marseille, France

ABSTRACT

Light aircrafts are designed to be used in both developed and undeveloped areas of a country. Hard landing conditions such as shocks and rebounds may occur on irregular terrains. The main role of the landing gear is to dissipate the energy of the landing impact. Although, a part of shock energies is absorbed by under-inflated tires. The aim of this work is to study light aircraft landing gears, and suggest convenient damping settings according to runway type. The study is carried out through three steps. Firstly, Bush tire are modeled with finite elements taking into account tire geometry and materials specifications. The tire-runway contact is modeled using hard contact and friction coefficients are determined experimentally. Secondly, three different landing gear systems are modeled: a classical spring steel landing gear, a landing gear with bungee cords and a recent landing gear equipped with a real damper. Traditionally, landing gear numerical simulations have been carried out with Multi-body Dynamics (MBD) software. In this study, finite elements are used combined with connectors, mass concentrations, springs/dampers and rigid elements. Thus, stress, deformation and energy within landing gears components are obtained, taking into account the nonlinearities of the system. Finally, aircraft dynamic rolling simulations are conducted. The systems' transient dynamic responses on rolling over obstacles are evaluated, as well as efforts and rebound amplitudes submitted to the aircraft body. An efficiency comparative study between the landing gears is conducted. On the other hand, the damper's stiffness and damping laws are investigated. The influence of these parameters on the landing gear dynamic performance in different rolling conditions is highlighted. Thus, aircraft rolling simulations on different types of runways (by introducing variable friction coefficients and runway shapes) are conducted. These simulations allow settings' adjustment based on the landing gear dissipation efficiency for each case.

A 2D Finite Element Model for the Common Carotid Artery and its Surrounding Anatomy: Effects on Arterial Stiffness Assessment

adriaan campo*, joris dirckx**

*Laboratory of Biophysics and BioMedical Physics (BIMEF); University of Antwerp; Antwerp; Belgium, **Laboratory of Biophysics and BioMedical Physics (BIMEF); University of Antwerp; Antwerp; Belgium

ABSTRACT

Introduction: Cardiovascular disease (CVD) is the most common cause of death worldwide, and its prevalence is increasing [1]. Research indicates that the onset of CVD can be slowed down or even prevented when detected in an early stage. An early indicator for CVD is increased stiffness of the large elastic arteries such as the aorta and the common carotid artery (CCA). Therefore, arterial stiffness detection is being developed as screening method through various methodologies such as carotid-femoral pulse wave velocity (PWV) detection using tonometry and distensibility coefficient (DC) detection using ultrasound (US), amongst other methods [2]. Using US, DC is often estimated by imaging a 2D, longitudinal cross-section of the CCA. The position of the upper and lower CCA wall is measured during diastole and systole. Assuming radial distension of the CCA, with the CCA maintaining its circular cross-section throughout the heart-cycle, the relative change in arterial cross-sectional area for a given pressure change can be readily estimated, or an indicator for arterial stiffness: the DC [3]. Since the stiffness of the CCA is much higher than the stiffness of the bulk surrounding tissue, a steady circular cross-section throughout the heart-cycle can be assumed. However, the influence of nearby structures with different stiffness than the CCA cannot be ignored. In this study, the influence of a realistic measurement situation on a US DC measurement is evaluated. Methods: A 2D static finite element model (FEM) of the CCA and its surrounding anatomy is constructed, based on 3 cross-sections of the left and right CCA of 10 healthy volunteers, resulting in 60 data-points with significantly different anatomical features. DC as estimated with US, is then compared with the “ground-truth” DC as based on the true area change. Hereby, the influence of nearby structures with different stiffness than the CCA is included, as well as the pressure of the US probe. Results and conclusion: Stiffness is overestimated using US in the majority of the cases as compared to the “ground-truth” stiffness. However, the detected difference is smaller than 5% which is not relevant for medical applications [4]. Therefore, we conclude that our results do not show contraindications for the use of US for DC detection. [1] World health organisation n.d. <http://www.who.int/en/>. [2] Laurent S et al. Hypertension 2001;37:1236–41. [3] Nichols et al. McDonald’s Blood Flow in Arteries: Theoretical, Experimental and Clinical Principles. Hodder Arnold Publishers; 2011. [4] Laurent S et al. Stroke 2006;2588–605.

Indentation Response of Freestanding Two-dimensional Materials with an Adhesive Boundary Condition

guoxin cao*

*Tongji University

ABSTRACT

The mechanical behavior of freestanding (FS) two-dimensional (2D) materials is commonly investigated through indentation tests performed via atomic force microscopy (AFM), where a 2D-material is placed on a substrate with a cylindrical hole and indentation is performed over the FS region of the 2D-material over the hole. Here, we perform theoretical and finite element analyses to show that the conventional assumption of a clamped boundary condition in existing models of such tests is inappropriate and should be replaced with an adhesive boundary condition in which the 2D-material can be partially detached from the substrate. A new analytical model which accounts for the adhesive boundary condition is then developed and shown capable of describing the indentation response of FS 2D-materials.

New Rortex Based Omega Method

Sita charkrit^{*}, Chaoqun Liu^{**}, Xiangrui Dong^{***}, Yisheng Gao^{****}

^{*}University of Texas at Arlington, ^{**}University of Texas at Arlington, ^{***}University of Texas at Arlington,
^{****}University of Texas at Arlington

ABSTRACT

In this paper, a new vortex identification method named Rortex-Omega method is introduced based on the Rortex, which is a mathematical definition proposed by our group. The basic idea of this new Omega is the normalization of Rortex. The new Omega is defined as a ratio of the rotation square over the sum of rotation square and anti-symmetric shear square. Compared with other vortex identification methods, this method has several advantages: it can capture both strong and weak vortex structures in turbulence and transition flow to be a case independent and a normalized method; It can be further used in studying the turbulence vortex structures, turbulence modeling and correlation analysis as a physical quantity just like pressure, density, etc.

Staggered Multi-material ALE Code for Large-deformation Problems with Changing-topology Interfaces

junxia cheng^{*}, Heng Yong^{**}, Shuanghu Wang^{***}, Liang Pan^{****}

^{*}Institute of Applied Physics and Computational Mathematics, ^{**}Institute of Applied Physics and Computational Mathematics, ^{***}Institute of Applied Physics and Computational Mathematics, ^{****}Institute of Applied Physics and Computational Mathematics

ABSTRACT

The Arbitrary Lagrangian-Eulerian(ALE) Formulation has been the research hotspot since the work of Hirt etc., which emerged to alleviate the drawbacks of traditional Eulerian and Lagrangian formulations. The algorithm described by Hirt etc. couldn't rezone across material interfaces, which was called simple ALE (SALE). A powerful extension to SALE is to incorporate VOF(volume of fluid) or MOF(moment of fluid) capability into the mixed cells containing multiple materials, which was called multi-material ALE(MMALE)[1]. Staggered Lagrangian schemes have been extensively used in the simulations of elastic-plastic multi-material problems since the numerical simulation emerged, but Lagrangian schemes couldn't tackle the problems of changing-topology interfaces. So, Multi-material ALE method, which is effective to the large-deformation problems with changing-topology interfaces, has been the trend of computational mechanics in recent years. Aiming to meet the need of numerical simulations of multi-material large-deformation problems, we develop the staggered multiple-material ALE code. We use MOF interface reconstruction method [3], the equivalent strain closure model for mixed cells (containing multiple materials) and conservative flux-based multi-material remapping method [2] to develop the staggered multi-material ALE code. Numerical results of shock tube, Rayleigh Taylor incompressible instability problem and interaction problem of a shock wave with Helium bubble, prove that our multi-material ALE code is valid in the multi-material large-deformation problems with changing-topology interfaces. Our MMALE code will be a useful tool in the large-deformation numerical simulation field. The Multi-material ALE scheme can treat the multi-material problems with the views of Lagrangian, Eulerian or ALE flexibly, so it is booming all over the world in recent years, but there are still some difficulties in the development of MMALE, especially the closure model is a challenge for the materials with absolutely different properties. In the future, we will study the closure models to extend the applications of MMALE. Key words: large-deformation problems, multi-material ALE, MOF reconstruction method

References [1]A. J. Barlow, P. H. Maire, W. J. Rider, R. N. Rieben, M. J. Shashkov, Arbitrary Lagrangian-Eulerian Methods for Modeling High-Speed Compressible Multimaterial Flow, Journal of Compressible Physics, 322, 603-665, 2016. [2]Milan Kucharik, Mikhail Shashkov, Conservative Multi-Material Remap for Staggered Multi-Material Arbitrary Lagrangian-Eulerian Methods, Journal of Computational Physics, 258, 268-304, 2014. [3]V. Dyadechko, M. Shashkov, Moment-of-Fluid Interface Reconstruction, LA-UR-05-7571, 2005.

Computational Methods for Fracture in Fluid-Saturated Porous Media

Rene de Borst*

*University of Sheffield, Department of Civil and Structural Engineering

ABSTRACT

Since the pioneering work of Terzaghi and Biot, the flow of fluids in deforming porous media has been given considerable attention. Nevertheless, flow in fractured or fracturing porous media has received less attention, although the physics of the flow within such discontinuities can be very different from that of the interstitial fluid in the surrounding deforming bulk, and in spite of its technological and societal importance as in energy and environmental issues. Herein we develop a general model for flow in progressively fracturing porous media. Since the cross-sectional dimension of the fracture is small compared to its length, the flow in the crack can be averaged over the width. A two-scale model results, including momentum and mass couplings between the subgrid scale and the macroscopic scale. Numerically, the two-scale model imposes some requirements on the interpolation of the displacement and pressure fields. Moreover, it will be shown that the interpolation of the pressure across the crack has implications for the physics that can be accommodated [1]. Discretisation methods are needed to model a crack, which is essentially an internal free boundary. Interface elements are an option, but have restrictions in terms of flexibility. Exploiting the partition-of-unity property allows the crack path to be decoupled from the underlying discretisation. Another possibility is isogeometric analysis. We develop an isogeometric formulation for porous media, including stationary and propagating cracks, such that it is possible to have fluid transport in the cracks. Within this framework crack initiation and propagation can be modelled in two ways: either via lowering the order of the interpolation [2], or by using isogeometric interface elements [3]. [1] R. de Borst, Computational Methods for Fracture in Porous Media, Elsevier, New York, pp. 206, 2018. [2] C.V. Verhoosel, M.A. Scott, R. de Borst, T.J.R. Hughes, An isogeometric approach to cohesive zone modelling, International Journal for Numerical Methods in Engineering, 87, 336 – 360, 2011. [3] J. Vignollet, S. May, R. de Borst, Isogeometric analysis of fluid-saturated porous media including flow in the cracks, International Journal for Numerical Methods in Engineering 108, 990 – 1006, 2016.

Modelling and Numerical Analysis of Sloshing in LNG Containment Tanks

Rien de Böck*, Arris Tijsseling**, Barry Koren***

*Eindhoven University of Technology, **Eindhoven University of Technology, ***Eindhoven University of Technology

ABSTRACT

Assessment of the impact loads of sloshing liquefied natural gas (LNG) on containment tanks of seagoing LNG carriers is a major structural design challenge. Especially breaking LNG waves can cause severe damage. A lot of research into this is currently being done, using (scaled) experiments and numerical studies. Due to the many physical parameters involved: liquid compressibility, gas compressibility, the ratio of the densities of the phases, phase transition and more, it is impossible to scale the entire process in a unified way. To study these parameters separately we perform numerical modelling and analysis of multiphase compressible fluid-flow problems. To start with, a five-equation two-fluid flow model [1] is discretized in space with an innovative higher-order accurate finite-volume method. The higher-order model is obtained through spatial reconstruction with a limiter function, for which latter some novel formulations are presented. We study the one-dimensional case of a liquid column impacting a gas pocket entrapped at a solid wall. This is known as the generalized Bagnold model [2]. It mimics the impact of a breaking wave in an LNG containment system, where the gas pocket is entrapped below the wave crest and the tank wall. Furthermore, the impact of a shock wave on a gas bubble immersed in air is simulated, in two dimensions, and compared to experimental results from [3]. Two cases are considered, one where the bubble gas is heavier (R22), and one where it is lighter (Helium) than the ambient air. The bubble deforms and surface instabilities form and develop. The computational results obtained have a good resemblance to the references. The correct wave speeds are computed and the surface instabilities are qualitatively similar. References 1. A.K. Kapila, R. Menikoff, J.B. Bdzil, and D.S.S.F. Son. Two-phase modeling of deflagration-to- detonation transition in granular materials: Reduced equations. *Physics of Fluids*, 13, 2001, pp. 3002-3024. 2. L. Brosset, J-M. Ghidaglia, P-M. Guilcher, and L. le Tarnec. Generalized Bagnold model. ISOPE, 2013. 3. J.F. Haas and B. Sturtevant. Interaction of weak shock waves with cylindrical and spherical gas inhomogeneities. *Journal of Fluid Mechanics*, 81, 1987, pp. 41-76.

A Geometric Nonlinear iFEM Approach Using Solid Elements

Cornelis de Mooij^{*}, Marcias Martinez^{**}, Rinze Benedictus^{***}

^{*}Delft University of Technology, ^{**}Clarkson University, ^{***}Delft University of Technology

ABSTRACT

A Geometric Nonlinear iFEM Approach Using Solid Elements Cornelis de Mooij¹, Marcias Martinez^{2,1} and Rinze Benedictus¹ ¹ Delft University of Technology ² Clarkson University Abstract. Structural Health Monitoring (SHM) is a growing field of research, as it has the potential to simultaneously improve the reliability of structures and reduce their maintenance cost. SHM requires accurate stress and strain information, preferably for the entire structure. Unfortunately, it is often infeasible to instrument every part of the structure, making it necessary to estimate the stress and strain fields based on data from a limited number of sensors. One promising technique for making this estimate is the Inverse Finite Element Method (iFEM), which can be applied to any combination geometry and loading conditions. It can also process several different types of sensor data. For this study, an iFEM algorithm was developed that uses solid elements and is capable of geometrically nonlinear analyses. These capabilities are both novel and necessary for aircraft wings and wind turbine blades. These structures often have thick regions and experience large deflections and rotations. Solid elements are more appropriate for modelling thick regions than shell elements, which are used in most of the iFEM literature. Geometric nonlinearity is necessary to accurately model large deflections and rotations. As a proof-of-concept, the strain and displacement distributions were determined numerically for several geometrically nonlinear benchmark tests from the literature, using a FEM code that was developed in-house and verified using Abaqus CAE. A varying number of virtual sensors were simulated based on the finite element results, in lieu of experimental data. The data from these sensors were used as input for the iFEM algorithm, which was also developed in-house. It was shown that the iFEM results match the literature values for geometric nonlinear conditions, even when only a limited number of virtual sensors were used.

Numerical Analysis of Residual Stresses of SS304L on Selective Laser Melting

Diego de Moraes*, Madhukar Somireddy**, Aleksander Czekanski***

*York University, **York University, ***York University

ABSTRACT

Residual stress is one of the most noticeable issues found in Additive Manufacturing components, especially when working with metal powder alloys, which will need high temperature in order to build the part. For this reason, several testing procedures are necessary to be implemented in order to validate a new alloy use in Metal Powder Bed Processes. The usual tests are minimum wall thickness assessment, cracking and warping analysis, process parameter optimization and melt pool analysis. The testing procedures usually demands long-term development and planning, for this reason Numerical Models are being implemented in numerous scales nowadays, from Discrete Element Modeling of powder to Thermal and Mechanical modeling, to minimize the range of parameters used in testing and optimize the process. These simulations are important either for the pre-analysis and for evaluation of parameter selection utilizing the selected new alloy, thus the objective of this study is to evaluate the effectiveness of this approach. The model proposed is a thermomechanical simulation of Selective Laser Melting process (SLM) to obtain the residual stresses when scanning a single track through the powder bed. The material selected is the Stainless Steel 304L, which is not commercially available on SLM manufacturers yet and it is a promising alloy to be largely used for Additive Manufacturing technology due its low cost along with the SS316L. The laser is modeled using the heat flux formulation based in a Gaussian profile described by Goldak et al, utilizing a double ellipsoid shape to effectively match the shape of the moving heat source present in SLM process. Close attention is required when inputting the powder properties, especially emissivity and thermal conductivity which has to be conditioned given parameters like chamber pressure, thermal gas conductivity, powder diameter, porosity and initial temperature. A Fortran subroutine is implemented and linked to the FEM solver to account for all the X-Y orientations as well the heat source input parameters. The validation is performed by literature, especially with the study of Simsom et al and Yakout et al, who performed experimental measurements of the residual stresses through XRD. The results are presented for 3 power different power inputs (100W, 200W and 400W), in order to analyse the impact on the final residual stresses on commercially available equipment.

Numerical and Experimental Aspects of Modeling and Fabricating Soft Robots

Kristin de Payrebrune*

*TU Kaiserslautern

ABSTRACT

The recent interest in soft robots arises from their adaptability, versatility and flexibility, which is very beneficial for new applications of human-robot interaction, healthcare or field exploration. Many prototypes have already proven the feasibility of soft robots to grasp indistinct objects, to walk on uneven surfaces, or to interact with humans. Additional research on mathematical models of these continuous deformable robots are in progress to predict their performance in real live and operating situations. At the Institute of Applied Structural Mechanics, pneumatic actuated and tendon driven soft robots have been fabricated and analyzed, and a rod model has been developed to describe the robot under loading and walking conditions. For a quadruped soft robot, we will present design aspects to optimize the performance of the soft robot and results of the experimental analyses. Furthermore, a simple rod model will be presented with which the deformation of the soft material structures can be described under pressurization. To parameterize the rod model, special experiments are conducted and will be discussed. Beside the research on soft robots, a tendon driven robot has been developed that moves autonomously on a horizontal or inclined surface. Via servomotors, the three segments of the robot can be controlled such that the robot is able to walk straight forward or on a circular path. The capability to walk on an inclined surface was tested on several surface materials and the results will be presented and related to the friction coefficient between surface and contacting limb.

Preconditioned Iterative Solvers for Immersed Finite Element Methods with Application to Flow Problems

Frits de Prenter^{*}, Clemens Verhoosel^{**}, Joseph Benzaken^{***}, John Evans^{****}, Harald van Brummelen^{*****}

^{*}Eindhoven University of Technology - University of Colorado Boulder, ^{**}Eindhoven University of Technology, ^{***}University of Colorado Boulder, ^{****}University of Colorado Boulder, ^{*****}Eindhoven university of Technology

ABSTRACT

Immersed methods are useful tools to preclude expensive (re-)meshing operations for flow problems around complex objects, flow problems on scanned domains, and fluid-structure interaction problems with large deformations. A common pitfall of immersed techniques is, however, ill-conditioning of the linear system [1]. This impedes the convergence of iterative solvers, and often compels researchers to resort to direct solvers. This hinders the efficient and inexpensive computation of solutions of large sparse systems, as the computational cost of direct solvers does not scale well with the size of the linear system, making them unsuitable for the increasingly large problems being solved by immersed methods, e.g. [2]. In [1] we have analyzed the fundamental cause of ill-conditioning of immersed finite element methods and, based on this analysis, in [3] we have developed a preconditioner that is tailored to immersed flow problems. We demonstrate that this preconditioner brings the condition number down to that of standard, mesh-fitting, finite elements, such that the linear system can be solved iteratively. Like standard finite elements, the conditioning of this preconditioned system still depends on the grid size however. In this contribution we shortly describe the cause of the conditioning problems and the developed preconditioner, and extend this approach to investigate possibilities to apply the preconditioner as a smoother in a multigrid cycle to develop a scalable solver that is robust to both the grid size and how elements are cut. [1] F. de Prenter, C.V. Verhoosel, G.J. van Zwieten and E.H. van Brummelen. Condition number analysis and preconditioning of the finite cell method. *Comp. Meth. App. Mech. Engng.* 2017. [2] F. Xu, D. Schillinger, D. Kamensky, V. Varduhn, C. Wang and M.-C. Hsu. The tetrahedral finite cell method for fluids: Immersogeometric analysis of turbulent flow around complex geometries. *Computers & Fluids*. 2016. [3] F. de Prenter, C.V. Verhoosel and E.H. van Brummelen. Preconditioning immersed isogeometric finite element methods with application to flow problems. *arXiv preprint*. 2017.

A Physical Multifield Model Predicts the Development of Volume and Structure in the Human Brain

Rijk de Rooij*, Ellen Kuhl**

*Stanford University, **Stanford University

ABSTRACT

The human brain, amongst that of most other mammalian brains, assumes a highly folded structure throughout its development after being initially smooth. This folded structure offers the great benefit of allowing more surface area for a given brain volume. Indeed, the cortical layer at the brain surface accommodates the cell bodies of the nerve cells that provide the brain with its processing capabilities. Several pathologies in neurodevelopment have been associated with abnormalities in cortical folding and behavioral disorders. A thorough understanding of neurodevelopment is therefore critical towards understanding and, potentially, treating such disorders. The prenatal development of the human brain is characterized by a rapid increase in brain volume and a development of a highly folded cortex. At the cellular level, these events are enabled by symmetric and asymmetric cell division in the ventricular regions of the brain followed by an outwards cell migration towards the peripheral regions [1]. The role of mechanics during brain development has been suggested and acknowledged in past decades, but remains insufficiently understood. Here we propose a mechanistic model that couples cell division, cell migration, and brain volume growth to accurately model the developing brain between weeks 10 and 29 of gestation [2]. Our model accurately predicts a 160-fold volume increase from 1.5cm³ at week 10 to 235cm³ at week 29 of gestation. In agreement with human brain development, the cortex begins to form around week 22 and accounts for about 30% of the total brain volume at week 29. Our results show that cell division and coupling between cell density and volume growth are essential to accurately model brain volume development, whereas cell migration and diffusion contribute mainly to the development of the cortex. We demonstrate that complex folding patterns, including sinusoidal folds and creases, emerge naturally as the cortex develops, even for low stiffness contrasts between the cortex and subcortex. References: [1] S. Budday, P. Steinmann, E. Kuhl, 2015, Physical biology of human brain development, *Frontiers in Cellular Neuroscience* 9 (2015) 257. [2] R. de Rooij and E. Kuhl, 2018, A physical multifield model predicts the development of volume and structure in the human brain, *Journal of the Mechanics and Physics of Solids*, (accepted)

RF Signal Compression Using Multiresolution Wavelet Decomposition for Efficient Piecewise Pulse Wave Imaging

Ketson dos Santos*, Iason Apostolakis**, Elisa Konofagou***, Ioannis Kouglioumtzoglou****

*Columbia University, **Columbia University, ***Columbia University, ****Columbia University

ABSTRACT

During the contraction-relaxation cycle the heart produces pressure pulses, also known as pulse waves, which travel through the vessel wall with a certain velocity. This Pulse Wave Velocity (PWV) can be estimated by the piecewise Pulse Wave Imaging (pPWI) technique based on a high frame-per-second (FPS) (e.g., 8000 fps) ultrasound imaging [1]. In this regard, one can map the localized arterial wall stiffness in vivo aiming at the detection and monitoring of localized vascular diseases. Nevertheless, certain limitations exist related to data transfer and storage capacity due to the high FPS adopted in the data acquisition step. Therefore, large time-varying RF-frames in the order of gigabytes and containing only a dozen milliseconds of data are inevitably produced in one single clinical evaluation. To circumvent such big data limitations a data compression technique based on a multiresolution 1-D wavelet analysis [2] is proposed considering the strong correlation of the RF-frames in the time domain. A numerical example involving real data is considered, while the signal-to-noise ratio (SNR) and the achieved compression ratio are adopted as performance measures. [1] I. Z. Apostolakis, S. D. Nandlall, and E. E. Konofagou, "Piecewise pulse wave imaging (ppwi) for detection and monitoring of focal vascular disease in murine aortas and carotids in vivo," IEEE Transactions on Medical Imaging, vol. 35, no. 1, pp. 13–28, Jan 2016. [2] S. G. Mallat, "A theory for multiresolution signal decomposition: the wavelet representation," IEEE Transactions on Pattern Analysis and Machine Intelligence, vol. 11, no. 7, pp. 674–693, Jul 1989.

Accuracy Verification of Sensitivity Analysis for Topology Optimization Problems Considering Dynamic Structural Behavior

takuma endo^{*}, junji kato^{**}, takashi kyoya^{***}

^{*}Tohoku University, ^{**}Tohoku University, ^{***}Tohoku University

ABSTRACT

For topology optimization problems considering dynamic structural behavior, the accuracy of sensitivity is very important. It is suggested that there is a possibility that an error may occur in the design sensitivity in the dynamic problem. However, details such as specific parameters that can cause errors are still not clear. The purpose of this study is to investigate errors in the sensitivity of the objective function to design variables. Here, we verify the accuracy of the design sensitivity from the two viewpoints, the time discretization method and the dynamic governing equation terms. Regarding the time discretization method: central difference method (explicit method) and the Newmark γ method (implicit method) are used for numerical analysis. We examine how influence the choice of explicit method and implicit method has on design sensitivity. Regarding the governing equation: inertia term and viscosity term can be considered a cause of errors. We show concrete numerical calculation example and confirm the influence on the design sensitivity when considering these terms.

Data-Driven Macro-Micro Modeling of Process-Structure Linkages in Directed Energy Deposition of Ni-based Superalloy

zhengtao.gan^{*}, yanping.lian^{**}, wing.kam.liu^{***}

^{*}Northwestern University, ^{**}Northwestern University, ^{***}Northwestern University

ABSTRACT

Additive manufacturing (AM) is of tremendous interest in engineered structural materials. However, multi-scale complicated physical phenomena simultaneously occur during the process and result in complex microstructure forming spatially and an-isotropic mechanical properties within the build. The relationships between multi-physics processes, solidified microstructure and mechanical properties in AM have not been thoroughly understood. For addressing this need, a multi-scale modeling framework for process-structure relationships is proposed. (1) A part-scale thermal-CFD module considering heat transfer, fluid flow (Marangoni effect) and mass addition is proposed. (2) A Meso/Micro-scale grain/dendrite structure evolution module is proposed to simulation grain nucleation, epitaxial growth, and columnar to equiaxed transformation (CET). The temperature history, liquid metal velocity in the melt pool, columnar to equiaxed transformation, and size/morphology of dendrite during AM of Ni-based superalloy can be predicted and validated by experimental results.

Dynamic Analysis of Stewart Stabilized Platform by Newton Euler Method

xiaoxu guo*, yue fa zhou**

*College of Aerospace Engineering and Civil Engineering, Harbin Engineering University, China, **College of Aerospace Engineering and Civil Engineering, Harbin Engineering University, China

ABSTRACT

Stewart parallel mechanism is characterized by its important research and application value. In the decades after being presented, many scholars have done a great deal of work¹⁻³. In this thesis, we mainly study the dynamics parts in the application of stabilized platform, deriving a dynamic equation based on Newton Euler method with the pods' qualities and inertia tensors are taken into account in the formulation. For verifying the theoretical results, formulation has been implemented in a program written in MATLAB compared to the ADAMS simulation results, then plotting the driving force diagrams under the several different motion forms. From the final results, it can conclude that the simulation results coincide with the actual driving force of the stabilized platform, and we also analyse the reason of driving force when it's easy to go wrong, which provides a theoretical basis for the dynamic control of the stabilized platform. The disturbance motion state of the lower platform for which is provided by the motion simulator fixed with it. Keywords: Stewart stabilized platform, Newton-Euler method, Dynamics, Matlab, Adams

Numerical Simulation of Steady States Associated with Thermomechanical Processes - Application to Welding and Rolling

Yabo JIA^{*}, Rémi Lacroix^{**}, Jean-Christophe Roux^{***}, Eric Feulvarch^{****}, Jean-Michel Bergheau^{*****}

^{*}University Lyon, ENISE, CNRS, UMR 5513, Laboratoire de Tribologie et Dynamique des Systèmes, 58 rue Jean Parot, 42023 Saint-Etienne Cedex 02, France, ^{**}ESI Group 70 Rue Robert, 69006 Lyon, France, ^{***}University Lyon, ENISE, CNRS, UMR 5513, Laboratoire de Tribologie et Dynamique des Systèmes, 58 rue Jean Parot, 42023 Saint-Etienne Cedex 02, France, ^{****}University Lyon, ENISE, CNRS, UMR 5513, Laboratoire de Tribologie et Dynamique des Systèmes, 58 rue Jean Parot, 42023 Saint-Etienne Cedex 02, France, ^{*****}University Lyon, ENISE, CNRS, UMR 5513, Laboratoire de Tribologie et Dynamique des Systèmes, 58 rue Jean Parot, 42023 Saint-Etienne Cedex 02, France

ABSTRACT

The numerical simulation of thermo-mechanical processes is based on the modeling of the couplings between several physical phenomena such as heat transfer, metallurgy and mechanics. The classical time-stepping methods enable accurate predictions of the physical variables but are generally time consuming because these processes often involve moving loadings leading to fast evolutions and high gradients of the physical variables, and consequently to the choice of very small time steps. For simulations of thermomechanical forming processes like welding, the thermal, mechanical and metallurgical fields associated with moving loadings can reach steady states. Several authors have therefore proposed eulerian or mixed lagrangian-eulerian computation methods to determine directly or incrementally the steady states ([1][2][3]). In this paper, an eulerian approach with nodal integration is presented. Using nodal integration, the transfers are still necessary but may be performed in a more rigorous way, and this method permits to use standard linear tetrahedral elements in plasticity. In order to demonstrate the performance of eulerian approach with nodal integration, we propose first to compare this method with an incremental approach of calculation of the steady states associated to the welding process. Then, a simulation of the steady state with an application to rolling is presented and discussed in relation to existing arbitrary lagrangian-eulerian approaches ([4] [5]).

REFERENCES [1] J. Huetink, P.T. Vreede, J. Van der Lugt, Progress in mixed eulerian-lagrangian finite element simulation of forming processes, Int. J. for Numer. Meth. Engng 1990, Vol. 30, 1441-1457. [2] J.-M. Bergheau, D. Pont and J.-B. Leblond, « Three-dimensional simulation of a LASER surface treatment through steady state computation in the heat source comoving frame », Mechanical Effects of Welding, IUTAM Symposium Lulea (Sweden), 1991, edited by L. Karlsson, L.-E. Lindgren, M. Jonsson, 1992, Springer-Verlag, Berlin Heidelberg, pp. 85-92. [3] J.Y. Shanghvi and P. Michaleris, « Thermo-elasto-plastic finite element analysis of quasi-state processes in Eulerian reference frames », Int. J. Numer. Meth. Engng 2002 Volume 53, pages 1533-1556 [4] J.M BERGHEAU, J.B LEBLOND, 'A nouvel finite element method based on a nodal integration technique for nonlinear problems of solid mechanics', complas 2017, 5 -7 September 2017, Barcelona, Spain. [5] Y. Crutzen, R.Boman, L. Papeleux, J.P Ponthot, 'Arbitrary Lagrangian Eulerian simulations cold roll forming processes including inline welding' complas 2017, 5 -7 September 2017, Barcelona, Spain.

The Cosserat Point Element (CPE) for Modeling Static and Dynamic Response of Structures at Finite Deformations

Mahmood Jabareen*

*Technion - Israel Institute of Technology

ABSTRACT

The theory of a Cosserat point has been used to develop a 3D brick Cosserat point element (CPE) for the static and dynamic numerical solutions of elastic structures that undergo finite deformations. The Cosserat approach postulates an average form of the deformation measure and connects the kinetic quantities to derivatives of a strain energy function. Once this strain energy has been specified, the procedure for obtaining the kinetic quantities needs no integration over the element region and it ensures that the response of the CPE is hyperelastic. Also, the constitutive equations of the CPE were designed to analytically satisfy a nonlinear form of the patch test. Specifically, the strain energy function is additively decomposed into two parts: one controlling the homogeneous deformations and the other controlling the inhomogeneous deformations. Developing a functional form for the strain energy of the inhomogeneous deformations has proven to be challenging. Recently, a functional form of the inhomogeneous strain energy function was developed, which causes the CPE to be a truly user friendly element that can be used with confidence for problems with finite deformation. It was observed that the three-dimensional brick CPE is a robust, an accurate element that can be used to accurately predict the response of thin plates and shells with only one element through the thickness. Also, the CPE does not exhibit unphysical locking or hourglassing for thin structures or nearly incompressible material response.

Urban Flow Simulations Using LES Lattice Boltzmann Method

Jerome Jacob^{*}, Pierre Sagaut^{**}

^{*}Aix Marseille Univ, CNRS, Centrale Marseille, M2P2, Marseille, France, ^{**}Aix Marseille Univ, CNRS, Centrale Marseille, M2P2, Marseille, France

ABSTRACT

Urban flow simulation on full scale configurations are widely used in the literature to assess pedestrian wind comfort, pollutant dispersion and thermal comfort inside cities. Urban flows are very complex three dimensional turbulent flows with several physical processes such as building wake interaction or channeling mechanisms. Most of these simulations have been performed using Reynolds Average Navier-Stokes (RANS) approach due to reasonable computational cost whereas Large Eddy Simulation (LES) are mainly used for simplified areas such as isolated buildings or street canyon. In this work we propose the use of lattice Boltzmann method[1] (LBM) based on the resolution of Boltzmann equation which describes the evolution of particle distribution function instead of Navier Stokes equations. This method is a very efficient method for massively parallel simulation due to local and linear algorithm. Furthermore the use of immersed boundary conditions and embedded uniform meshes with a ratio of 2 for the grid step between two successive refinement levels permit to mesh complex areas such as city more easily that make LBM a very interesting method for urban flow simulation. In this work the Boltzmann equation is discretized on a D3Q19 lattice and a single relaxation time regularized collision operator[2] is used to ensure the stability of the model. Some properties of this regularized collision operator have been used to perform implicit and explicit wall modeled LES simulations inside the Shinjuku area, a 1 km² part of Tokyo city center. These simulations are compared with several RANS simulation available in the literature and validated by comparisons with wind tunnel and in-situ measurements provided by the Architectural Institute of Japan. [1] X. He, L.-S. Luo, Theory of the lattice Boltzmann method: From the Boltzmann equation to the lattice Boltzmann equation, Physical Review E 56 (6) (1997) 6811-6817 [2] O. Malaspinas, Increasing stability and accuracy of the lattice Boltzmann scheme: recursivity and regularization. ArXiv, pages 1-31, 2015

Modeling the Biomechanics of a Four Chamber Cardiac Model with Myocardial Infarction

Arian Jafari^{*}, Edward Pszczolkowski^{**}, Adarsh Krishnamurthy^{***}

^{*}Iowa State University, ^{**}Iowa State University, ^{***}Iowa State University

ABSTRACT

Abstract: Cubic-Hermite finite element meshes are widely used for simulating cardiac biomechanics due to their superior convergence characteristics and their ability to capture smooth geometries compactly compared to linear tetrahedral meshes. However, such meshes have previously been used only with simple ventricular geometries with non-physiological boundary conditions due to challenges associated with creating cubic-Hermite meshes of the complex heart geometry. The complex geometry of the heart, especially near atrial regions and valves necessitates the appearance of extraordinary nodes (nodes with 3 or ≥ 5 adjacent elements in 2D) in the mesh. Extraordinary nodes allow the mesh to capture the geometric characteristics of the heart accurately and apply physiologically accurate boundary conditions. However, consistently interpolating the finite element fields in the presence of extraordinary nodes requires additional mathematical formulation. In this work, we created a four-chamber cardiac model utilizing cubic-Hermite elements and simulated a full cardiac cycle by coupling the 3D finite element model with a lumped circulation model. The G_1 continuity of the finite-element fields in the neighborhood of extraordinary nodes were maintained using an ensemble coordinate system with a linear global-to-local transformation. The myocardial fiber orientations were interpolated within the mesh using the Log-Euclidean method to overcome the singularity associated with interpolation of orthogonal matrices. Physiologically accurate boundary conditions were applied to the nodes along the valve plane. We then simulated a complete cardiac cycle of a healthy heart and of a heart with myocardial infarction. We compared the pumping function of the heart for both cases by calculating the work done by the ventricle (area enclosed inside the left ventricular Pressure-Volume (P-V) loop) and the base-apex shortening. We observed a 12% reduction in work done by the heart after myocardial infarction and a corresponding reduction in the base-apex shortening. The displacement of the infarcted region and the corresponding region in a healthy heart was also compared to understand the influence of myocardial infarction on the local displacements of the myocardium. The myocardial wall displacements obtained from the four-chamber cardiac model are comparable to actual patient data without requiring complicated non-physiological boundary conditions usually required in truncated ventricular heart models. References: 1) Adarsh Krishnamurthy, Matthew J. Gonzales, Gregory Sturgeon, W. Paul Segars, Andrew D. McCulloch, Biomechanics simulations using cubic Hermite meshes with extraordinary nodes for isogeometric cardiac modeling, In Computer Aided Geometric Design, Volume 43, 2016, Pages 27-38, ISSN 0167-8396.

An Isogeometric Collocation Method for Karhunen-Loeve Discretization of Random Fields

Ramin Jahanbin^{*}, Sharif Rahman^{**}

^{*}The University of Iowa, ^{**}The University of Iowa

ABSTRACT

Many uncertainty quantification problems in engineering and applied sciences require modeling spatial variability of random input parameters. For instance, the tensile and fracture toughness properties of engineering materials, the size and shape characteristics of mechanical components, and the wind and snow loads in structural systems all exhibit randomness that varies not only from sample to sample, but also from point to point in their respective domains. Therefore, random field treatment of spatial varying randomness is a vital ingredient in computational analysis. Loosely speaking, a random field represents a random quantity at each point of the domain and, therefore, engenders an infinite number of random variables. In practice, though, the number of random variables must be finite and manageable but also large enough to ensure an optimal or accurate approximation of the original random field. This process is often referred to as random field discretization. This paper presents an isogeometric collocation method for solving a Fredholm integral eigenvalue problem, leading to random field discretization by the Karhunen-Loeve expansion. The method involves a projection onto finite-dimensional a subspace of a Hilbert space, basis splines (B-splines) and non-uniform rational B-splines (NURBS) spanning the subspace, and standard methods of eigensolutions. Like the existing isogeometric Galerkin method [1], the NURBS-based collocation method also preserves exact geometrical representation of the physical or computational domain and exploits regularity of basis functions delivering globally smooth eigensolutions. However, in the collocation method, the construction of the system matrices for a d-dimensional eigenvalue problem requires at most d-dimensional domain integrations, as compared with 2d-dimensional integrations in the Galerkin method. Therefore, the introduction of the isogeometric collocation method for random field discretization offers a huge computational advantage over the existing Galerkin methods. Numerical examples illustrate the accuracy, efficiency, and convergence properties of the proposed isogeometric method for obtaining eigensolutions. [1] Rahman, S. "A Galerkin Isogeometric Method for Karhunen-Loeve Approximation of Random Fields," submitted to Computer Methods in Applied Mechanics and Engineering, 2017.

Using Deep Neural Networks for Data-Driven Inverse Modeling of Turbulent Wake Dynamics

Rajeev Jaiman^{*}, Tharindu Miyanawala^{**}

^{*}National University of Singapore, ^{**}National University of Singapore

ABSTRACT

An efficient deep learning technique for the model reduction of the Navier-Stokes equations for unsteady flow problems is proposed. The proposed technique relies on the Convolutional Neural Network (CNN) and the stochastic gradient descent method. Of particular interest is to predict the unsteady fluid forces for different bluff body shapes for 3D high-Reynolds number flows. The discrete convolution process with a non-linear rectification is employed to approximate the mapping between the bluff-body shape and the fluid forces. The deep neural network is fed by the Euclidean distance function as the input and the target data generated by the full-order Navier-Stokes computations for primitive bluff body shapes. The convolutional networks are iteratively trained using the stochastic gradient descent method with the momentum term [1] to predict the fluid force coefficients of different geometries and the results are compared with the full-order computations. We attempt to provide a physical analogy of the stochastic gradient method with the momentum term with the simplified form of the incompressible Navier-Stokes momentum equation. We also construct a direct relationship between the CNN-based deep learning and the Mori-Zwanzig formalism [2] for the model reduction of dynamical system. A systematic convergence and sensitivity study is performed to identify the effective dimensions of the deep-learned CNN process such as the convolution kernel size, the number of kernels and the convolution layers. We perform the CNN predictions initially for low Re (laminar wake) and then for high Re (turbulent wake) flows. Within the error threshold, the prediction based on our deep convolutional network has a speed-up nearly four-orders of magnitude for the low Re and five-orders of magnitude for the high Re compared to the full-order results. The CNN only consumes a very small fraction of computational resources as well. The proposed CNN-based approximation procedure enables to perform the parametric design of bluff bodies on personal computers and devices. Overall, this method has a profound effect on design space exploration and the feedback control of separated flows. References: [1] D. E. Rumelhart, G. E. Hinton, and R. J. Williams, "Learning representations by back-propagating errors", Cognitive modeling, vol. 5, no. 3, pp. 1-4, 1988. [2] Tharindu P. Miyanawala and Rajeev K. Jaiman, "An Efficient Deep Learning Technique for the Navier-Stokes Equations: Application to Unsteady Wake Flow Dynamics", arXiv preprint arXiv:1710.09099, 2017.

Construction of Basis Functions for Algebraic Dual Space

Varun Jain^{*}, Yi Zhang^{**}, Artur Palha^{***}, Marc Gerritsma^{****}

^{*}Delft University of Technology, ^{**}Delft University of Technology, ^{***}Eindhoven University of Technology, ^{****}Delft University of Technology

ABSTRACT

In this work we develop a discretization method that explicitly uses functions from the algebraic dual space. Duality pairing between functions from the primal space and the dual space can be done in terms of the degrees of freedom only and do not (directly) depend on the basis functions, [2]. First, we prove the duality of these basis functions using the two examples from [1]. We prove the equivalence at discrete level between i) a pair of Dirichlet-Neumann problem in $H(\text{div}, K)$, and ii) a pair of Dirichlet-Neumann problem in $H(\text{curl}, K)$. We corroborate these proofs with numerical tests. Second, we demonstrate the application of these basis functions for two model constraint problems: i) scalar Laplacian, and ii) vector Laplacian. In both the applications we observe that the discretization of the constraint eq. is purely topological and is independent of grid shape and grid size. The corresponding matrix block consists of 1, -1 and 0 only, and is extremely sparse. Consequently, the condition number for the system is very low. The method is inf-sup stable. The error shows exponential convergence for both the applications. [1] C. Carstensen, L. Demkowicz, J. Gopalakrishnan, Breaking spaces and forms for the DPG method and applications including Maxwell equations, *Computers and Mathematics with Applications* 72 (2016) 494–522. [2] V. Jain, Y. Zhang, A. Palha and M. Gerritsma, Construction and application of algebraic dual polynomial representations for finite element methods, arXiv1712.09472, 2017.

Taking into Account Thermal Constraints in Topology Optimization of Structures Built by Additive Manufacturing

Lukas Jakabcin*, Grégoire Allaire**

*Ecole Polytechnique, France, **Ecole Polytechnique, France

ABSTRACT

In this talk, we introduce a model and several constraints for shape and topology optimization of structures, built by additive manufacturing techniques. The goal of these constraints is to take into account the thermal residual stresses or the thermal deformations, generated by processes like Selective Laser Melting, right from the beginning of the structural design optimization. In other words, the structure is optimized concurrently for its final use and for its behavior during the layer by layer production process. It is well known that metallic additive manufacturing generates very high temperatures and heat fluxes, which in turn yield thermal deformations that may prevent the coating of a new powder layer, or thermal residual stresses that may hinder the mechanical properties of the final design. Our proposed constraints are targeted to avoid these undesired effects. Shape derivatives are computed by an adjoint method and are incorporated into a level set numerical optimization algorithm. Several 2-d and 3-d numerical examples demonstrate the interest and effectiveness of our approach. References: G. Allaire, L. Jakabcin, Taking into account thermal residual stresses in topology optimization of structures built by additive manufacturing, submitted. HAL preprint: hal-01666081 (2017).

Space-Time Discretization for the Enhanced Velocity Mixed Finite Element Method: Applications to Modeling Fractures in Large Scale Reservoir Simulators

Mohamad Jammoul^{*}, Benjamin Ganis^{**}, Gurpreet Singh^{***}, Ivan Yotov^{****}, Mary Wheeler^{*****}, Sanghyun Lee^{*****}

^{*}University of Texas at Austin, ^{**}University of Texas at Austin, ^{***}University of Texas at Austin, ^{****}University of Pittsburgh, ^{*****}University of Texas at Austin, ^{*****}Florida State University

ABSTRACT

Hydraulic fracturing is a widely used technology to stimulate tight and unconventional reservoirs and increase their ultimate recovery. Fractures are propagated in the rock matrix to create a fracture network and enhance the flow of hydrocarbons from the reservoir into the wellbore. The numerical simulation of hydraulic fracturing involves multiple multiphysics phenomena including: (1) fractures propagation, (2) fluid flow in the fractures and the reservoir, and (3) the accompanying mechanical deformations. Various computational models have been developed to simulate these coupled processes, yet many hydraulic fracture models focus on the near wellbore effects and fail to represent the holistic reservoir behavior. In this work, we develop a numerical framework to integrate non-planar fractures in large scale reservoir simulator (IPARS). The fracture permeability and geometry are obtained using the phase field fracture propagation method (IPACS). Fractures are then represented in the reservoir as small subdomains with high permeability coupled to the surrounding permeable formation. This configuration allows the simulation of the fluid flow in the reservoir and the fractures, yet restricts the time step. This means that fractured reservoir on the scale of kilometers would need to have its time steps governed by flow through fractures with apertures on the scale of millimeters. A space-time discretization is thus adopted, where the spatial domain is decomposed into overlapping or non-overlapping subdomains and a space-time variational formulation is employed. The flow in the reservoir is discretized using an Enhanced Velocity Mixed Finite Element Method. EVFEM adds additional velocity degrees of freedom on non-matching spatial and temporal interfaces to ensure the continuity of the flux. Numerical results are presented to show the impact of the induced fractures on the overall reservoir productivity.

Numerical and Experimental Investigation on Fracture Characteristics of Multilayer Graphene

Bongkyun Jang*, Byungwoon Kim**, Jae-Hyun Kim***, Hak-Joo Lee****

*Korea Institute of Machinery and Materials, **Korea Institute of Machinery and Materials, ***Korea Institute of Machinery and Materials, ****Korea Institute of Machinery and Materials

ABSTRACT

Graphene is 2-dimensional carbon layer with sp²-bondings like carbon nanotube and fullerene, and shows outstanding electrical, thermal, optical, and mechanical properties. Its excellent physical properties have been utilized for the various applications such as transparent conductor and, high-performance energy harvester and storage. Among them, extraordinary mechanical properties of graphene attract the attention to many fundamental researchers [1]. For fracture behavior of single crystalline and polycrystalline graphene, several experimental and analytical researches are performed, until now [2]. However, fracture mechanisms of multilayer graphene have not been fully studied, yet. In this study, we investigated fracture characteristics of multilayer graphene with experimental and numerical methods. For the fracture experiments, multilayer graphene specimens are fabricated by mechanical exfoliation from natural graphite and transferred onto tensile jigs, which can realize precise alignment and accurate application of loads to the specimens. In addition, narrow notches are fabricated with focused ion beam on the edges of the graphene specimens. Using these specimens, in situ fracture tests are performed under the scanning electron microscope. Load-displacement curves measured in the fracture experiments, and fracture load is obtained for each fracture specimen. Under the consideration of the shapes of the fracture specimens, we construct finite element models. By comparing the experimental results and the load-displacement curves calculated by finite element analyses, Young's modulus of multilayer graphene is estimated. In addition, the stress distribution near the crack tip of the specimen can be calculated by the analysis. At the failure load, singular stress fields near the crack tip imply the intensified stress at the crack propagation, and the fracture toughness can be derived from them. Based on the experiments and finite element analysis, the fracture toughness of multilayer graphene is enhanced compared to the monolayer. From in situ observation of the fracture surface, interlayer slippages occur near the crack tip and fracture surface at the fracture. To elucidate the fracture mechanisms of multilayer graphene, molecular dynamics simulation is performed on the multilayer graphene specimens with single edge crack. The numerical simulation helps to explain how the fracture of multilayer graphene occurs when a uniaxial load applied. The experimental and numerical research on fracture of multilayer graphene can contribute to developing graphene-based electronic devices, and enhance the reliability of them. References [1] Lee, C., Wei, X., Kysar, J. W. & Hone, J. Science 321, 385-388 (2008). [2] Jang, B., et al. Nanoscale 9, 17325 (2017)

Topology Optimization for Three-dimensional Ultrasonic Acoustic Lens Design

Gang-Won Jang*, Quang Dat Tran**

*Sejong University, Republic of Korea, **Sejong University, Republic of Korea

ABSTRACT

For topology optimization of acoustic problems, the use of the finite element method (FEM) is limited to low or mid frequency applications because of considerable computational efforts especially in three-dimensional problems. To resolve this, a new method for efficiently solving topology optimization of high-frequency ultrasonic acoustic problems is proposed by combining the edge-based smoothed finite element method (ES-FEM) [1] and the wave based method (WBM) [2]. The ES-FEM is formulated by incorporating the gradient smoothing techniques of mesh free methods into the FEM. The ES-FEM is very suitable for acoustic problems due to the proper softening effect provided by the edge-based gradient smoothing operation. Because a close-to-exact stiffness of the system can be obtained in the ES-FEM, the dispersion error can be effectively suppressed in high frequency problems. Meanwhile, the WBM can give very accurate solutions with small number of degrees of freedom when applied to problems with simple geometries because it employs exact solutions of the governing equation as field variables. Through the hybrid use of the ES-FEM and WBM, great efficiency in the reduction of computational effort for high-frequency acoustic problems can be expected while retaining high analysis accuracy. The primary objective of this study is to develop shape and topology optimization of high-frequency acoustic problems based on the combined use of the ES-FEM and WBM. In the present paper, the entire domain is separated into design and non-design domains; the ES-FEM is applied to the design domain while the WBM is applied to the non-design domain. The interface tracking phase field approach in [3] is employed to implicitly parameterize the boundaries of acoustic lenses, which move according to design sensitivities during optimization. The effectiveness of the proposed hybrid method of the ES-FEM and WBM is verified by solving three-dimensional acoustic topology optimization problems with high frequency range (0.5-1MHz). Keywords: Acoustic topology optimization, Phase field method, Edge-based smoothed finite element method, Wave based method, Ultrasonic acoustic waves

References [1] Liu GR, Nguyen TT (2010) Smoothed Finite Element Methods, CRC Press, ISBN 978-1-4398-2027-8. [2] Desmet W (1998) A Wave Based Prediction Technique for Coupled Vibro-acoustic Analysis (Ph.D. thesis), KULeuven. [3] Takezawa A, Nishiwaki S, Kitamura M (2010) Shape and topology optimization based on the phase field method and sensitivity analysis. Journal of Computational Physics 229(7):2697-2718.

Linear Smoothed eXtended Finite Element Method for Hyperelastic Materials

Chintan Jansari^{*}, Sundararajan Natarajan^{**}, Krishna Kannan^{***}

^{*}Indian Institute of Technology Madras, ^{**}Indian Institute of Technology Madras, ^{***}Indian Institute of Technology Madras

ABSTRACT

In this talk, we propose the Linear Smoothed eXtended Finite Element Method for large deformation problems of hyperelasticity, with material interfaces in plane strain approximation. The eXtended Finite Element Method (XFEM) allows for the interior discontinuities to be represented independent of the underlying discretization. This is done by augmenting the conventional approximation space with suitable ansatz that carries the information of the local behaviour. However, this leads to difficulties in the numerical integration of the weak form and poor convergence properties due to the blending elements. The difficulty with the numerical integration is alleviated by employing the strain smoothing technique. And the stable XFEM is used to suppress the blending issues. Some numerical examples are solved and verified with the conventional FEM based on conforming mesh.

Immersive Simulation at Extreme Scale

Kenneth Jansen^{*}, John Evans^{**}, Alireza Doostan^{***}, Kurt Maute^{****}, Felix Newberry^{*****}, Corey Nelson^{*****}

^{*}University of Colorado Boulder, ^{**}University of Colorado Boulder, ^{***}University of Colorado Boulder, ^{****}University of Colorado Boulder, ^{*****}University of Colorado Boulder, ^{*****}University of Colorado Boulder

ABSTRACT

Parallel computing now delivers simulations in a time scale that could change the paradigm of how scientists, engineers, and other practitioners address discovery and design questions. Tools have been developed to precisely define a specific, complex simulation which can then be executed in seconds on computers. However, for discovery and design questions where the next variant of the problem requires change to the problem definition, the time to redefine the problem takes much longer. This delay interrupts intuition and learning about how the change in problem definition relates to a change in solution. To realize this innovative paradigm shift, referred to here as immersive simulation, requires the development of new approaches to problem definition editing that allow practitioners to interact with the simulations (visual model iteration) in a manner where they can dynamically experience (via in situ visualization that employs massive data reduction) the influence of parameter variations. In this talk we will describe our research efforts to advance state of the art tools into more generic components that, when integrated, will make the following capabilities available to any partial differential equation (PDE) solver: i) live, reconfigurable visualization of ongoing simulations, ii) live, reconfigurable problem definition to allow the dynamic solution insight to guide the choice of key problem parameters, iii) real-time parameter sensitivity feedback, iv) error estimation and adaptivity, and v) integration and demonstration of reliable, immersive simulation. This research will not only drive several of its science components in innovative and new directions, but, once integrated, will provide the field of simulation (and the science community that has developed an increasing dependence on it) with the ability to intuitively explore the behavior of the system. Furthermore, this research will allow interactively redefining the geometry, boundary conditions, and other parameters, to experience the science, and thereby greatly accelerate discovery and innovation.

Time-resolved Adaptive Direct FEM Simulation Prediction of Flow Separation

Johan Jansson*

*KTH Royal Institute of Technology

ABSTRACT

We present an adaptive finite element method for time-resolved simulation of aerodynamics without any turbulence model parameters, which is applied to a benchmark problem from the HiLiftPW-3 workshop to compute the flow past a JAXA Standard Model (JSM) aircraft model at realistic Reynolds number. The mesh is automatically constructed by the method as part of an adaptive algorithm based on a posteriori error estimation using adjoint techniques. No explicit turbulence model is used, and the effect of unresolved turbulent boundary layers is modeled by a simple parametrization of the wall shear stress in terms of a skin friction. In the case of very high Reynolds numbers we approximate the small skin friction by zero skin friction, corresponding to a free slip boundary condition, which results in a computational model without any model parameter to be tuned, and without the need for costly boundary layer resolution. We introduce a numerical tripping noise term to act as a seed for growth of perturbations, the results support that this triggers the correct physical separation at stall, and has no significant effect pre-stall. We show that the methodology quantitatively and qualitatively captures the main features of the JSM experiment - aerodynamic forces and the stall mechanism - with a much coarser mesh resolution and lower computational cost than the state of the art methods in the field, with convergence under mesh refinement by the adaptive method. Thus, the simulation methodology appears to be a possible answer to the challenge of reliably predicting turbulent-separated flows, for a complete air vehicle. We also present recent comparison against leading high-order frameworks in connection to the 5th International Workshop on High Order CFD Methods, showing that adaptivity and large timesteps enables high computational efficiency. The methodology is further extended to fluid-structure interaction with an embedded discontinuity in the phase interface by doubling the solution field, and we show a snapshot of the development. [1] J. Hoffman, J. Jansson, N. Jansson, R. V. de Abreu, and C. Johnson. Computability and Adaptivity in CFD. Encyclopedia of Computational Mechanics (Ed. E. Stein, R. de Borst and T.J.R. Hughes), John Wiley and Sons, (2017). [2] J. Jansson, E. Krishnasamy, M. Leoni, N. Jansson, and J. Hoffman. Time-resolved adaptive direct fem simulation of high-lift aircraft configurations. Springer Brief: Numerical simulation of the aerodynamics of high-lift configurations, 2017.

A Mixed Variational Framework for Structure-preserving Space-time Discretization for Non-linear Electro-elastodynamics

Alexander Janz^{*}, Peter Betsch^{**}, Marlon Franke^{***}, Rogelio Ortigosa^{****}

^{*}Institute of Mechanics, Karlsruhe Institute of Technology (KIT), Germany, ^{**}Institute of Mechanics, Karlsruhe Institute of Technology (KIT), Germany, ^{***}Institute of Mechanics, Karlsruhe Institute of Technology (KIT), Germany, ^{****}Zienkiewicz Centre for Computational Engineering, Swansea University, Wales

ABSTRACT

The present talk deals with a new approach to the design of energy and momentum (EM) consistent integration schemes in the field of non-linear electro-elastodynamics, see Ortigosa, Franke, Janz, Gil and Betsch (submitted in Comput. Methods Appl. Mech. Engrg., 2017). The importance of electro-active polymers (EAPs) in different applications such as actors and sensors, soft robotics or artificial muscles requires advanced simulation techniques to prognosticate the behavior of such smart materials. Typically, these materials are described as electro-static but nevertheless the consistent time-integration of the electro-mechanical model plays an important role concerning the numerical stability and accuracy. In this talk we present a new approach to the design of energy-momentum consistent algorithms motivated by the structure of polyconvex stored energy functions and tailor-made for the consistent space-time discretization of EAPs. The presented time-integrator is based on the internal energy of the system, which is in accordance with the concept of polyconvexity for nonlinear electro-mechanics, see Gil and Ortigosa (Comput. Methods Appl. Mech. Engrg., 302: 293-328, 2016). Based on a Hu-Washizu-type mixed variational framework with a novel cascade form of kinematic constraints a new algorithmic stress formula is proposed, see Betsch, Janz and Hesch (accepted in Comput. Methods Appl. Mech. Engrg., 2017), which is a typical feature of energy-momentum methods. Furthermore, a tensor-cross product operator for second order tensors is used, which greatly simplifies the algebraic formulation. In addition, the time-discrete weak form of the Gauss's law and Faraday's law along with the concept of partitioned discrete derivatives leads to an implicit one-step time integrator which consistently approximates the linear momentum, the angular momentum as well as the total energy. The resulting structure-preserving integrator shows superior numerical stability and robustness compared to alternative formulations. Moreover, the mixed variational framework makes possible a wide variety of alternative finite element formulations. Along with an appropriate combination of the interpolation spaces high performance finite elements can be generated. Several numerical examples dealing with large strains and electric fields are shown. These examples demonstrate the advantageous properties of the newly developed structure-preserving discretization scheme.

A Reliability Based Design Optimization Method for MASH TL-3 Concrete Barriers under Vehicle Crashes

Erica Jarosch^{*}, Qian Wang^{**}, Hongbing Fang^{***}, Hangfeng Yin^{****}

^{*}Manhattan College, ^{**}Manhattan College, ^{***}The University of North Carolina at Charlotte, ^{****}Hunan University

ABSTRACT

Concrete barriers are commonly adopted on state highways to redirect impacting vehicles and reduce occupant injury risks. Due to the rigidity of a concrete barrier compared to other types of traffic barriers, its performance primarily depends on its cross-sectional shape. Besides physical crash tests, numerical simulations based on high-fidelity finite element (FE) analyses can be conducted to assess the performance of traffic barriers. This research work focused on the development of a reliability based design optimization (RBDO) method for concrete barriers subjected to vehicle impacts. The concrete barriers met the test level-3 (TL-3) requirements specified in the Manual for Assessing Safety Hardware (MASH). The proposed design optimization method started with nonlinear FE simulations at certain sample points so that crash responses could be used to evaluate barrier performance. A successive metamodeling technique developed using augmented radial basis functions (RBFs) was applied to create approximate functions of implicit crash responses. Once the RBF metamodels were created to approximate crash simulation results, the design constraints that included reliability calculations were evaluated using any sampling method such as Monte Carlo simulations (MCS). Finally, a genetic algorithm (GA) was adopted to optimize the objective function subjected to all the design constraints. The RBDO method integrated FE simulations, metamodels, MCS, and GA, and provided a useful tool for the design of roadside barriers. A concrete barrier example was solved and numerical results were presented to demonstrate the effectiveness of the design optimization method.

Error Estimation in Discontinuous Galerkin Method with Polygonal Finite Elements

Jan Jaskowiec*

*Cracow University of Technology, Institute for Computational Civil Engineering, Poland

ABSTRACT

In the paper three methods for error estimation in the two-dimensional (2D) discontinuous Galerkin method (DGM) are presented. The applied DGM version uses arbitrary polygonal finite elements [1,2]. The Chebyshev basis functions are used for approximation. They are constructed recursively which makes the method very efficient and flexible. It is then quite easy to calculate higher order derivatives of the basis functions on the polygonal finite elements. In the first error estimation method, the residual error from the strong form can be obtained directly from the approximate solution. The residual error is discontinuous, so the Zienkiewicz-Zhu smoothing procedure is employed for the continuous error distribution. In the DGM the recursive basis functions are utilized. In this case, it is very easy to obtain a low order solution of the considered problem in a situation when the higher order solution is already calculated. It is because the stiffness matrix has hierarchical construction, and so the lower order stiffness matrix is just a part of the primary stiffness matrix. In the second method, the error is estimated by comparison of two approximate solutions. The two solutions are of different orders and the lower-order solution is calculated with marginal cost. In the third method, a special boundary value problem (PVB) is constructed to estimate the error. The error PVB is obtained and solved with low computational costs due to some special properties of the DGM utilized in this method. The quality of the error estimation is very high in the last method. The paper is illustrated with two-dimensional benchmark examples where the standard scalar Poisson's boundary value problems are considered. In the examples the correctness and flexibility of the proposed error estimation methods are shown. The two-dimensional examples of linear elasticity are also presented, in which the errors are estimated in situations when stress concentrations occur in the final solution. [1] E. B. Chin, J. B. Lasserre, and N. Sukumar (2015) Numerical integration of homogeneous functions on convex and nonconvex polygons and polyhedra. *Computational Mechanics*, 56(6):967–981 [2] J. Jaskowiec, P. Plucinski and A. Stankiewicz (2016) Discontinuous Galerkin method with arbitrary polygonal finite elements *Finite Elements in Analysis and Design* 120:1–17

Higher Order Multipoint Meshless FDM for Two-scale Analysis of Heterogeneous Materials

Irena Jaworska*

*Cracow University of Technology

ABSTRACT

The paper focuses on application of the Multipoint solution approach – the higher order extension of the Meshless Finite Difference Method (MFDM) to the numerical homogenization of the heterogeneous material with periodic structure. The Finite Element Method (FEM) has been the most commonly applied method of computer modeling for the multiscale problem. However, this fact does not mean that one should not search for the alternative, perhaps more efficient approaches, especially based on the meshless technique which uses only a set of nodes for discretization of the continuum and therefore leads to greater flexibility. Recently developed Multipoint meshless method is discussed here for this purpose. The higher order Multipoint approach is followed the original Collatz [1] concept and the essential idea of the MFDM [2] – the moving weighted least squares approximation, using the arbitrarily irregular cloud of nodes as well as various formulations of b.v. problem. The higher order approximation, applied in the Multipoint method, is based on the additional degrees of freedom at all stencil nodes, taking into account e.g. the right hand side of considered differential equation. It improves obtained solution without necessity of providing additional unknowns to both – the mesh and the MFD operator, and also may be used e.g. for high quality a posteriori error estimation of the results. The higher order Multipoint meshless method, like the MFDM solution approach [3], may be used at both – the macro and the micro levels in the two-scale analysis of heterogeneous materials based on the single RVE. The analysis of the convergence results of the effective material parameters for the set of meshes with increasing number of nodes as well as comparison with FEM was conducted. The error analysis done at the micro level confirm the high quality of the Multipoint solution, which may be used as the improved reference solution instead of the true analytical one for the a posteriori error estimation. Further research is planned. 1. L. Collatz, *Numerische Behandlung von Differential-gleichungen*, Springer-Verlag, Berlin, 1955. 2. J. Orkisz, *Finite Difference Method (Part III)*, in *Handbook of Computational Solid Mechanics*, ed. M. Kleiber, Springer-Verlag, Berlin, 336–431, 1998. 3. I. Jaworska, *On some aspects of the meshless FDM application for the heterogeneous materials*, *International Journal for Multiscale Computational Engineering*, 15(4):359–378, 2017.

MACROSCOPIC INELASTIC BEHAVIORS SIMULATED BY A STOCHASTIC MULTI-SCALE NUMERICAL MODEL FOR HETEROGENEOUS MATERIALS

PIERRE JEHEL

Laboratory MSSMat-UMR 8579 (CentraleSupélec/CNRS)
Université Paris-Saclay, CentraleSupélec, 3 rue Joliot-Curie, 91190 Gif-sur-Yvette, France
E-mail: pierre.jehel[at]centralesupelec.fr

Key words: Random heterogenous material; Inelastic cyclic behavior; Uncertainty quantification; Global sensitivity analysis; Variance decomposition.

Abstract. *The uncertainty and the sensitivity of the response of a nonlinear stochastic multi-scale numerical model for randomly heterogenous material is investigated. 9 input parameters and 10 descriptors of the time-dependent output response are considered. The material model has been presented elsewhere and is introduced as a 'black box function' in the present paper, parameterized so that the model is deterministic and that variability in the outputs only comes from the variability introduced in the inputs. The objective is twofolds: (i) surveying the variety of macroscopic behaviors the material model considered is capable of representing, and (ii) assessing the relative importance of the model inputs in the model outputs to, for instance, define efficient parameters identification protocols. A preliminary analysis of the linear dependency between the output descriptors is presented and a reduced set of 6 descriptors is eventually selected. Then, the influence of the model input parameters on each of these model response descriptors is investigated using a global sensitivity analysis technique based on the functional decomposition of their respective total variance.*

1 INTRODUCTION

The mechanical behavior of a wide range of natural or manufactured materials is characterized by macroscopic engineering parameters that depend on phenomena at heterogeneous smaller scales (concrete, nano-engineered materials [12]). On the one hand, experimental devices and techniques allow characterizing the spatial distribution of material properties at micro-scales as for instance the combination of atomic force microscope imaging and quantitative nanomechanical property mapping techniques employed in [14] for a study of Young's modulus distribution in the so-called interfacial transition zone in concrete material. On the other hand, computational material models allow carrying out numerical experiments that have the potential of investigating the material behavior in a range of configurations that can be difficult to reach with sole experimental investigation. There is therefore a need for developing such numerical material models that can simulate engineering properties at macro-scale from relevant

information coming from lower scales. This has been a topic of continuing research in the field of computational mechanics for decades.

The development of the inelastic stochastic multi-scale numerical model investigated in the present work (see [5] and [6]) was initially motivated by the need for a concrete model that is capable of representing the contribution of material damping to the overall structural damping in the seismic analysis of civil engineering assets. In earthquake engineering, structural damping is indeed commonly introduced in numerical simulations using ad hoc damping models such as the pervasive so-called Rayleigh damping model. Unfortunately, as nonlinear structural analysis is performed, resorting to such ad hoc approach potentially results in large uncertainties when assessing structural seismic performance.

This concrete model [5, 6] is based on a meso-scale where the heterogeneous structure is represented by random vector fields. Local behavior at meso-scale is nonlinear and can be seen as the homogenized response of other mechanisms at lower scales when explicit construction of smaller scales is not possible. The model is constructed with a set of parameters that describes the structure of the random vector fields (correlation coefficients, correlation lengths and functions); a set of parameters that characterizes the mean, variance and distribution of physical parameters at meso-scale (initial stiffness, yield stress and stiffness degradation ratio); and a set of parameters for spatial discretization of the material domain (finite element method) and of the random fields (spectral representation method [11]). A representative volume element (RVE) can be retrieved with the ability to represent salient features of the concrete uniaxial cyclic compressive response that are not explicitly represented at meso-scale, like for instance the hysteresis loops experimentally observed in unloading-reloading cycles.

The objective of this paper is twofolds: (i) surveying the variety of macroscopic behaviors this numerical inelastic stochastic multi-scale material model is capable of representing, and (ii) assessing the relative importance of the model inputs in the model outputs to, for instance, define efficient parameters identification protocols. Next section is focussed on introducing the model input parameters. Then, a probabilistic framework is set in section 3 for uncertainty and global sensitivity analysis. In section 4, the results of an application are presented and, finally, a list of conclusions closes the paper.

2 THE MATERIAL MODEL AND ITS INPUT PARAMETERS

The material model used in this paper has been developed to represent the restoring force $f(t)$ of a 1D nonlinear material in a given cyclic quasi-static loading displacement time history $u(t)$ where t is the pseudo-time (Fig. 1). This material model is referred to as \mathcal{M} , it takes t along with a set of parameters \mathbf{x} as inputs, and yields the restoring force history $f(t)$ as output.

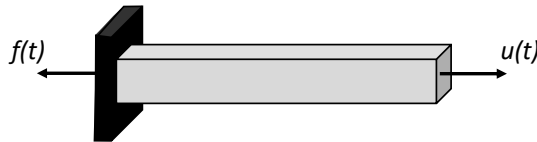


Figure 1: The experiment: bar with quasi-static displacement $u(t)$ imposed at one end, with other end fixed where reaction $f(t)$ develops; it is assumed that the experiment is such that the strain field is homogeneous in the bar.

The material model \mathcal{M} that is used in this work has been presented in [5, 6]. Therefore, we only introduce here its main characteristics along with the list of input parameters that will be used for uncertainty and sensitivity analyses hereafter. Also, for the sake of illustrating, we

consider that the modeled material is concrete; but any other random heterogeneous material described by 3 scales as introduced in Tab. 1 and Fig. 2 could fit this setting.

Scale	Observations	Modeling assumptions
Micro	Physical and chemical mechanisms occur	Internal variables are considered in the framework of continuum thermodynamics [1, 8] to convey information from this scale to the meso-scale (see Fig. 3).
Meso	Aggregates and the cement paste are observable and build an heterogeneous material structure	The heterogeneity at this scale is represented using random fields rather than an explicit representation of the structure.
Macro	Homogeneous quantities are retrieved for engineering purposes	Classical homogenization technique in the framework of the Finite Element Method is used [9, 10].

Table 1: The 3 scales introduced in the model \mathcal{M} . Concrete material is considered here as an illustrating example.

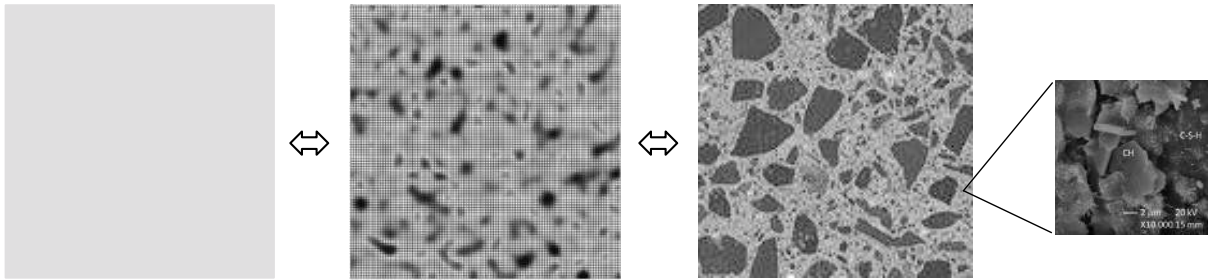


Figure 2: From left to right: [a] equivalent homogeneous concrete (macro-scale), [b] representation of the heterogeneous concrete at meso-scale (5 cm \times 5 cm-square), [c] actual heterogeneous concrete (5 cm \times 5 cm-square), and [d] zoom on the underlying microstructure in the cement paste (20 μ m \times 20 μ m-square observed through Scanning Electron Microscope, courtesy A.P.M. Trigo [13]).

The model uses stochastic fields to represent spatial variations – that is random heterogeneity – in the material properties at meso-scale. The actual meso-scale shown in Fig. 2[c] is replaced by random vector fields as shown in Fig. 2[b]. In the particular case of a 1D material behavior, which this work is limited to, three parameters are represented as spatially variable as illustrated in Fig. 3: the initial stiffness $C(\mathbf{p}, \omega)$ (or Young’s modulus at meso-scale), the yield stress $\sigma_y(\mathbf{p}, \omega)$, and the stiffness degradation ratio $r(\mathbf{p}, \omega) \in [0, 1]$, where \mathbf{p} is a position in the material and ω recalls the randomness in the quantity. The three quantities are correlated and the same correlation coefficient ρ is considered for any pair of parameters. The parameters \mathbf{x} of model \mathcal{M} are listed in Tab. 2.

The model \mathcal{M} can be stochastic: same input parameters \mathbf{x} and imposed displacement history $u(t)$ can yield different outputs. Nevertheless, it has been shown in [5, 6] that the model can also be deterministic: same input parameters \mathbf{x} and loading history $u(t)$ would yield same output. In other words, it is possible to parameter the model in such a way that a material Representative Volume Element (RVE) is simulated. This can be achieved using particular set of spatial parameters ($N = 16$, $M = 32$, $M_f = 96$, $L_0/\ell = 0.1$, $\epsilon_R = 0.01$ using the same notations as in [5]). This parameterization is used in this paper so that uncertainty observed in the output parameters \mathbf{y} would only come from uncertain input parameters \mathbf{x} .

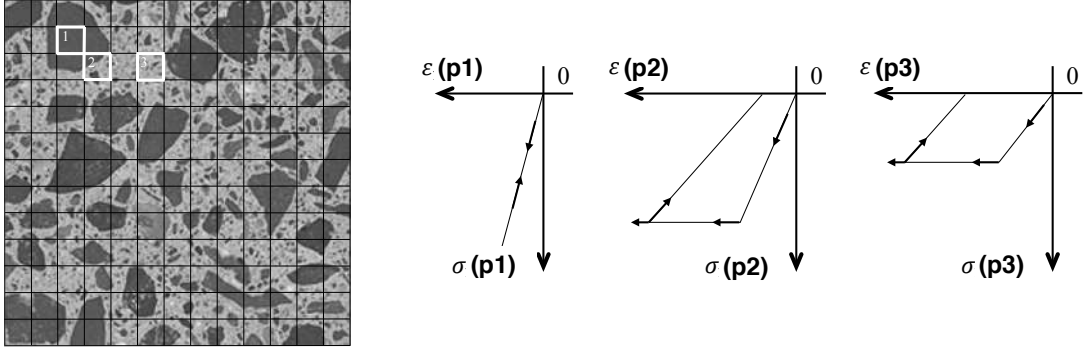


Figure 3: Behavior law at meso-scale depends on the position \mathbf{p} in the heterogeneous material. Initial stiffness, yield stress, and stiffness degradation ratio at any point \mathbf{p} are modeled as random variables.

\mathbf{x}	Description
$x_1 = law_C$	Initial stiffness C distribution (log-normal or uniform)
$x_2 = a_C$	Mean of law_C
$x_3 = b_C$	Variance of law_C
$x_4 = law_{\sigma_y}$	Yield stress σ_y distribution (log-normal or uniform)
$x_5 = a_{\sigma_y}$	Mean of law_{σ_y}
$x_6 = b_{\sigma_y}$	Variance of law_{σ_y}
$x_7 = a_r$	Mean of the stiffness degradation ratio uniform distribution law_r
$x_8 = b_r$	Variance of law_r
$x_9 = \rho$	Correlation coefficient between $(C$ and $\sigma_y)$, $(C$ and $r)$, or $(\sigma_y$ and $r)$

Table 2: List of the $N^x = 9$ model input parameters $x_j, j = 1 \dots N^x$ considered in this work.

3 UNCERTAINTY AND SENSITIVITY ANALYSES OF THE MODEL OUTPUT

Let introduce the probability space (Θ, \mathcal{S}, P) with sample space Θ , collection of events \mathcal{S} , and probability measure P . To introduce a certain degree of belief in the set \mathbf{x} of the model input parameters, we consider them as random variables $\mathbf{X} : \theta \in \Theta \mapsto \mathbf{X}(\theta)$. Consequently, the model output $f(t)$ also is a random variable $F(t) : \theta \mapsto F(t, \theta)$ for all $t \in [0, T]$ and we have the deterministic model \mathcal{M} that is the mapping

$$\mathcal{M} : (\theta, t) \mapsto F(t) = \mathcal{M}(\mathbf{X}, t) \quad (1)$$

3.1 Uncertainty analysis

The uncertainty in the model output can be analyzed computing quantities such as the mean, variance, and cumulated density function for all $t \in [0, T]$:

$$E[F(t)] = \int_{\Theta} \mathcal{M}(\mathbf{X}(\theta), t) dP(\theta) \quad (2)$$

$$V[F(t)] = \int_{\Theta} (E[F(t)] - \mathcal{M}(\mathbf{X}(\theta), t))^2 dP(\theta) \quad (3)$$

$$\Pr[F(t) \leq f(t)] = \int_{\Theta} \delta_{f(t)}[\mathcal{M}(\mathbf{X}(\theta), t)] dP(\theta) \quad \text{with} \quad \delta_{f(t)}[\cdot] = \begin{cases} 1 & \text{if } \cdot \leq f(t) \\ 0 & \text{if } \cdot > f(t) \end{cases} \quad (4)$$

This requires computing integrals over the sample space Θ . To this purpose, Monte Carlo simulations are performed from a Latin hypercube sample (LHS) of size N^s . LHS is adopted here for its efficiency compared to random sampling [3, 7] with the N^x input random variables in \mathbf{X} assumed as mutually independent.

3.2 Sensitivity analysis

For the analysis of the sensitivity of the model output to the inputs, the approach adopted in this work is based on a functional decomposition of the variance (see e.g. [4]), $\forall t \in [0, T]$, as:

$$V[F(t)] = \sum_{j=1}^{N^x} D_j[F(t)] + \sum_{1 \leq j < k \leq N^x} D_{jk}[F(t)] + \dots + D_{12\dots N^x}[F(t)] \quad (5)$$

where $D_j[F(t)] = V[E[F(t)|X_j]]$, $D_{jk}[F(t)] = V[E[F(t)|X_j, X_k]] - D_j[F(t)] - D_k[F(t)]$ and so on. Then, the following first-order and total indices are computed from $(N^x + 2) \times N^s$ computations of the model response as:

$$s_j = \frac{D_j[F(t)]}{V[F(t)]} \quad (6)$$

$$s_{jT} = s_j + \frac{\sum_{k=1, k \neq j}^{N^x} D_{jk} + \sum_{1 \leq k \neq j < l \neq j}^{N^x} D_{jkl} + \dots + D_{12\dots N^x}}{V[F(t)]} \quad (7)$$

where s_j , respectively s_{jT} , is the portion of $V[F(t)]$ due to input x_j alone, respectively to x_j and all the interactions of x_j with the other input variables.

4 APPLICATION

4.1 Uncertainty in the model input parameters

The distributions selected for the uncertain input parameters are introduced in Tab. 3.

$\mathbf{X}(\theta)$	Distribution: $law(mean, variance)$	
$X_1 = LAW_C$	$\mathcal{B}_{0.5}$: either $\mathcal{U}(a_C, b_C)$ or $\mathcal{L}(a_C, b_C)$	with probability 0.5 each
$X_2 = A_C$ [MPa]	$\mathcal{U}(\tilde{a}_C = 30e3, 0.04 \tilde{a}_C^2)$	such that $C \geq 0$
$X_3 = B_C$ [MPa ²]	$\mathcal{U}(\tilde{b}_C = 15e3, 0.04 \tilde{b}_C^2)$	such that $C \geq 0$
$X_4 = LAW_{\sigma_y}$	$\mathcal{B}_{0.5}$: either $\mathcal{U}(a_{\sigma_y}, b_{\sigma_y})$ or $\mathcal{L}(a_{\sigma_y}, b_{\sigma_y})$	with probability 0.5 each
$X_5 = A_{\sigma_y}$ [MPa]	$\mathcal{U}(\tilde{a}_{\sigma_y} = 35, 0.04 \tilde{a}_{\sigma_y}^2)$	such that $\sigma_y \geq 0$
$X_6 = B_{\sigma_y}$ [MPa ²]	$\mathcal{U}(\tilde{b}_{\sigma_y} = 20, 0.04 \tilde{b}_{\sigma_y}^2)$	such that $\sigma_y \geq 0$
$X_7 = A_r$	$\mathcal{U}(\tilde{a}_r = 0.5, 0.04 \tilde{a}_r^2)$	such that $r \in [0, 1]$
$X_8 = B_r$	$\mathcal{U}(\tilde{b}_r = 0.02, 0.04 \tilde{b}_r^2)$	such that $r \in [0, 1]$
$X_9 = Rho$	$\mathcal{U}(0.5, 1/12)$	(support is $[0, 1]$)

Table 3: Random variables and there distributions characterized by their mean and variance. \mathcal{B} , \mathcal{U} , and \mathcal{L} are Bernoulli, uniform, and log-normal distributions. How to find the support of a uniform distribution from its mean and variance is shown in the Annex. Quantities with superimposed tilde $\tilde{\cdot}$ are some nominal mean values; a coefficient of variation of 20% is considered to calculate the variance associated to these nominal mean values.

4.2 Model response descriptors

We start by simulating the material response in one symmetric loading cycle with macroscopic strain amplitude $E = 3.5e^{-3}$. $N^s = 500$ simulations are run and model responses are plot in Fig. 4. From the observation of this figure we choose a series of N^y model response descriptors as introduced in Fig. 5, gathered in vector \mathbf{y} . Then, we seek possible linear dependencies – other types of dependencies could of course be sought too – and build Fig. 6. From Fig. 6, it is observed that model response after point D is strongly correlated to model response between points O and D. Accordingly, only the following $N^y = 6$ model response descriptors will be considered thereafter: $y_1 = C_O$, $y_2 = C_B$, $y_3 = \Sigma_A$, $y_4 = \Sigma_B$, $y_5 = \Sigma_D$, and $y_6 = E_C$.

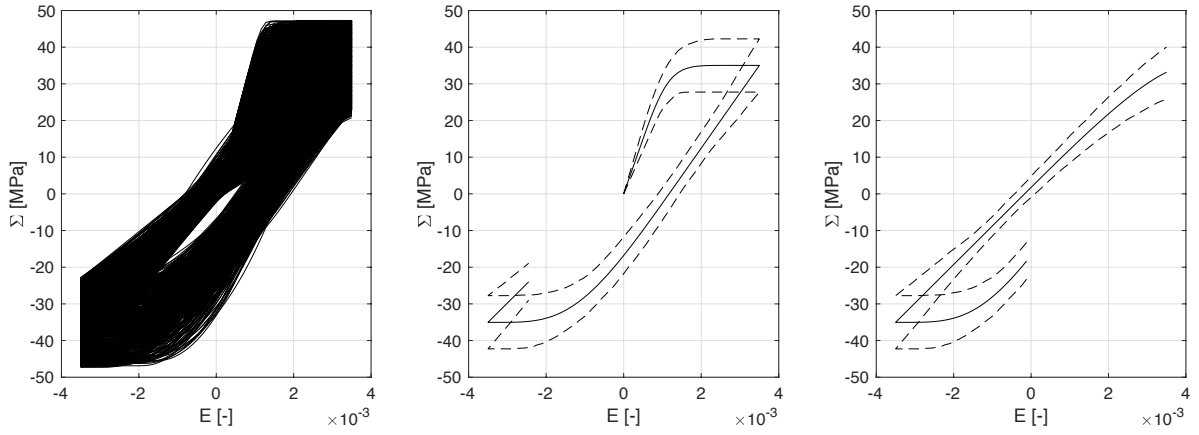


Figure 4: [left] $N^s = 500$ model response curves. [middle] and [left] Sample mean along with the 10% and 90% percentiles (dashed line); response curves are split into two parts for better readability.

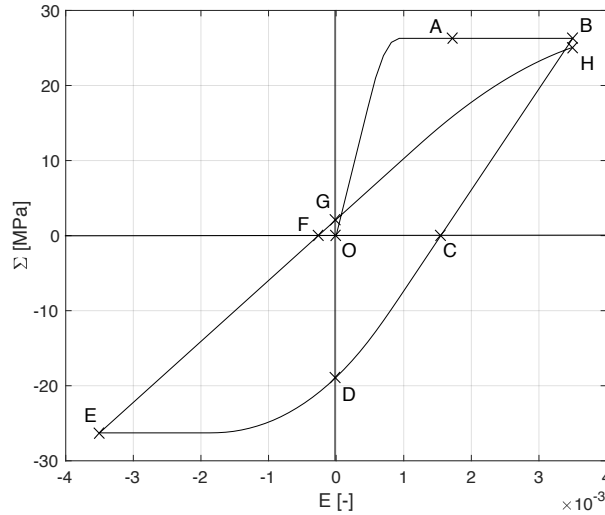


Figure 5: Model response descriptors: initial tangent modulus C_O and unloading tangent modulus at point B C_B ; stresses Σ_A ($E = 1.75e^{-3}$), Σ_B , Σ_D , Σ_E , Σ_G , and Σ_H ; strains E_C and E_F .

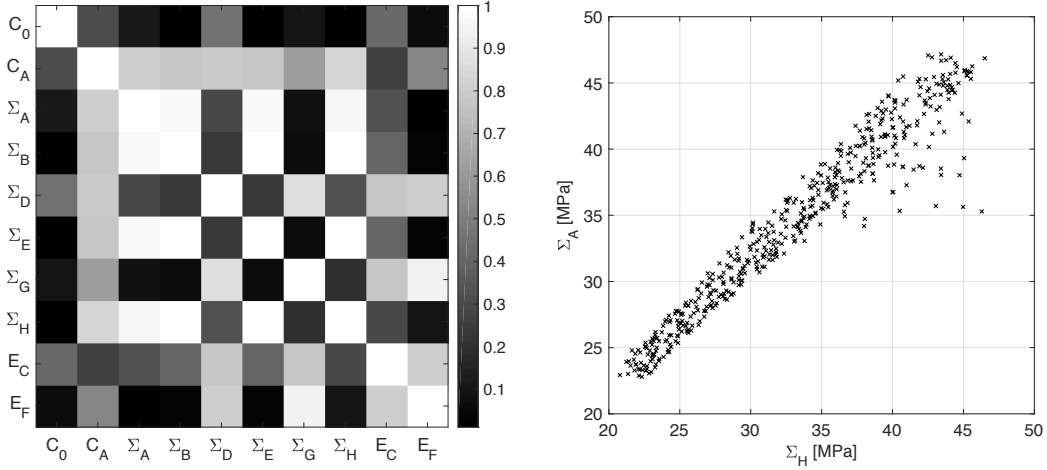


Figure 6: [left] Absolute value of the sample Pearson correlation coefficients between model response descriptors y_k , $k = 1 \dots N^y$; [right] scatterplot of Σ_A versus Σ_H showing strong linear correlation.

4.3 Uncertainty and sensitivity estimators

To estimate global sensitivity of the model outputs \mathbf{y} to the inputs \mathbf{x} , the method detailed in [2] (Sect. 6.13) has been implemented. Accordingly:

1. A first LHS $[x_{ij}]$, $i \in [0, N^s]$ and $j \in [0, N^x]$, is generated and the model response $\mathbf{y}_i(t) = \mathcal{M}(\mathbf{x}_i, t)$ is computed for each set of input parameters $\mathbf{x}_i = [x_{i1} \dots x_{iN^x}]$. From these quantities, estimators of the mean and variance in Eqs. (2) and (3) are computed $\forall k \in [1 \dots N^y]$ as:

$$\hat{E}[Y_k] = \frac{1}{N^s} \sum_{i=1}^{N^s} y_{k,i}(t) \quad ; \quad \hat{V}[Y_k] = (\hat{\sigma}[Y_k])^2 = \frac{1}{N^s} \sum_{i=1}^{N^s} (\hat{E}[Y_k] - y_{k,i}(t))^2 \quad (8)$$

2. Another sample $[\bar{x}_{I,j}] = [p(\mathbf{x}_1) \dots p(\mathbf{x}_{N^s})]$, $I \in [0, N^s]$, is built, where $p(\mathbf{x}_j)$ is a random permutation without replacement of the N^s elements of the j -th column of $[x_{ij}]$. The model response $\bar{\mathbf{y}}_I(t) = \mathcal{M}(\bar{\mathbf{x}}_I, t)$ is computed for each $\bar{\mathbf{x}}_I = [\bar{x}_{I1} \dots \bar{x}_{IN^x}]$. Then, N^x samples of N^s model responses are obtained by reordering the computed $\bar{\mathbf{y}}_I(t)$'s as follows: $\bar{\mathbf{y}}_i^{(j)}(t) = \mathcal{M}([\bar{x}_{I1} \dots \bar{x}_{Ij} = x_{ij} \dots \bar{x}_{IN^x}], t)$, $j \in [0, N^x]$.
3. A last LHS $[\check{x}_{ij}]$, $i \in [0, N^s]$ and $j \in [0, N^x]$, is generated and N^x samples of N^s model responses are computed as $\bar{\mathbf{y}}_i^{(j)} = \mathcal{M}(\bar{\mathbf{x}}_i^{(j)}, t)$, $\bar{\mathbf{x}}_i^{(j)} = [\bar{x}_{i1}^{(j)} \dots \bar{x}_{iN^x}^{(j)}]$, with $\bar{x}_{iJ}^{(j)} = x_{iJ}$ for $J \in [0, N^x]$ except for $J = j$ where $\bar{x}_{iJ}^{(j)} = \check{x}_{ij}$.

Estimators for the sensitivity indices are then computed, $\forall k \in [1 \dots N^y]$, as:

$$\hat{s}_{k,j} = \frac{1}{\hat{V}[Y_k]} \left(\frac{1}{N^s} \sum_{i=1}^{N^s} y_{k,i}(t) \times \bar{y}_{k,i}^{(j)}(t) - \hat{E}[Y_k]^2 \right) \quad (9)$$

$$\hat{s}_{k,jT} = \frac{1}{N^s \times \hat{V}[Y_k]} \sum_{i=1}^{N^s} y_{k,i} \left(y_{k,i} - \bar{y}_{k,i}^{(j)} \right) \quad (10)$$

Altogether, the model has to be run $(2 + N^x) \times N^s$ times. In the present work, $N^x = 9$, $N^s = 300, 400$, or $1,000$, and computing one model response takes less than 2 seconds. The calculated estimations are shown in Tab. 4.

	N^s	$y_1 = C_0$	$y_2 = C_B$	$y_3 = \Sigma_A$	$y_4 = \Sigma_B$	$y_5 = \Sigma_D$	$y_6 = E_C$
$\hat{E}[Y_k]$	300	29,998 MPa	15,034 MPa	34.470 MPa	35.034 MPa	-16.801 MPa	1.156e-3
	600	29,997 MPa	15,040 MPa	34.441 MPa	35.035 MPa	-16.776 MPa	1.155e-3
	1,000	29,997 MPa	15,008 MPa	34.344 MPa	35.030 MPa	-16.700 MPa	1.152e-3
$\hat{\sigma}[Y_k]$	300	6,001 MPa	2,822 MPa	6.565 MPa	7.007 MPa	5.509 MPa	3.06e-4
	600	6,000 MPa	2,848 MPa	6.507 MPa	7.000 MPa	5.561 MPa	3.09e-4
	1,000	6,000 MPa	2,835 MPa	6.413 MPa	7.006 MPa	5.494 MPa	3.04e-4
$\hat{s}_1 (x_1 = law_C)$	300	0.012	0.058	0.112	0.056	-0.012	0.058
	600	-0.074	-0.021	-0.003	-0.029	-0.050	-0.068
	1,000	0.003	-0.006	0.119	-0.011	0.046	0.075
$\hat{s}_2 (x_2 = a_C)$	300	1.000	0.070	-0.018	-0.104	0.256	0.269
	600	1.000	0.127	0.068	0.016	0.268	0.225
	1,000	1.000	0.159	0.137	-0.018	0.294	0.204
$\hat{s}_3 (x_3 = b_C)$	300	0.077	0.087	-0.004	-0.081	0.083	0.062
	600	-0.015	0.013	0.022	-0.021	-0.003	-0.039
	1,000	0.008	0.029	0.157	0.017	-0.028	-0.034
$\hat{s}_4 (x_4 = law_{\sigma_y})$	300	-0.024	0.167	0.135	0.048	0.112	0.144
	600	-0.056	0.028	-0.004	-0.038	0.063	0.025
	1,000	-0.011	0.056	0.149	0.017	0.076	0.072
$\hat{s}_5 (x_5 = a_{\sigma_y})$	300	-0.042	0.626	1.032	1.002	0.023	0.218
	600	-0.034	0.573	0.994	1.000	0.014	0.131
	1,000	-0.014	0.614	1.103	1.003	0.046	0.187
$\hat{s}_6 (x_6 = b_{\sigma_y})$	300	-0.078	0.030	0.035	-0.014	-0.034	0.022
	600	0.003	0.042	0.054	-0.016	-0.017	-0.114
	1,000	0.004	0.017	0.106	-0.018	0.016	0.012
$\hat{s}_7 (x_7 = a_r)$	300	-0.070	0.331	0.097	0.049	0.679	0.709
	600	0.011	0.300	0.040	0.030	0.644	0.595
	1,000	0.029	0.335	0.130	0.002	0.697	0.618
$\hat{s}_8 (x_8 = b_r)$	300	-0.066	-0.004	0.074	0.016	-0.034	0.073
	600	0.026	0.000	-0.012	-0.049	-0.003	-0.075
	1,000	0.011	0.088	0.173	0.042	0.076	0.058
$\hat{s}_9 (x_9 = \rho)$	300	-0.021	0.066	0.102	0.019	-0.053	-0.041
	600	-0.007	0.006	0.063	0.015	-0.007	0.008
	1,000	-0.074	0.010	0.115	-0.001	0.011	0.034
$\hat{s}_{1T} (x_1 = law_C)$	300	0.000	0.000	-0.001	0.000	0.002	-0.002
	600	0.000	-0.002	0.002	0.002	-0.003	0.004
	1,000	0.000	0.000	0.000	-0.000	0.001	-0.001
$\hat{s}_{2T} (x_2 = a_C)$	300	1.020	0.038	0.017	-0.002	0.212	0.179
	600	0.914	0.230	0.046	0.002	0.374	0.297
	1,000	0.945	0.067	-0.083	-0.001	0.246	0.202
$\hat{s}_{3T} (x_3 = b_C)$	300	0.000	0.001	0.000	0.000	0.004	-0.002
	600	0.000	0.000	0.001	0.001	-0.001	0.000
	1,000	0.000	-0.001	0.000	0.000	-0.003	-0.001
$\hat{s}_{4T} (x_4 = law_{\sigma_y})$	300	0.000	0.000	-0.005	-0.002	0.019	-0.001
	600	0.000	0.002	-0.004	-0.001	0.008	-0.004
	1,000	0.000	0.000	-0.003	-0.002	0.001	-0.001
$\hat{s}_{5T} (x_5 = a_{\sigma_y})$	300	0.000	0.581	0.894	0.939	0.111	0.180
	600	0.000	0.547	0.920	1.005	0.049	0.223
	1,000	0.000	0.565	0.893	1.023	0.078	0.171
$\hat{s}_{6T} (x_6 = b_{\sigma_y})$	300	0.000	-0.002	0.007	-0.004	0.006	0.001
	600	0.000	-0.003	0.004	0.001	-0.003	-0.004
	1,000	0.000	-0.001	0.000	-0.000	-0.002	-0.001
$\hat{s}_{7T} (x_7 = a_r)$	300	0.000	0.174	-0.003	-0.003	0.572	0.554
	600	0.000	0.316	0.000	0.000	0.619	0.566
	1,000	0.000	0.343	-0.004	-0.003	0.721	0.607
$\hat{s}_{8T} (x_8 = b_r)$	300	0.000	-0.008	-0.001	0.000	0.002	-0.008
	600	0.000	-0.006	0.002	0.002	0.001	-0.007
	1,000	0.000	-0.004	-0.001	-0.000	-0.004	-0.003
$\hat{s}_{9T} (x_9 = \rho)$	300	0.000	0.000	0.000	0.000	-0.001	0.002
	600	0.000	0.007	0.003	0.005	0.012	0.007
	1,000	0.000	0.009	-0.004	-0.004	-0.005	0.021

Table 4: Estimates $\hat{E}[Y_k]$ and $\hat{\sigma}[Y_k]$ for expected value and standard deviation of the model response descriptors y_k with $k = 1 \dots N^y$; estimates \hat{s}_j for the contribution of each input x_j with $j = 1 \dots N^x$; estimates \hat{s}_{jT} for the contribution of each input x_j and all its interactions with the other inputs x_p with $p = 1 \dots N^x$ and $p \neq j$.

5 CONCLUSIONS

In the particular case of the experiment shown in Fig. 1, and from the above presented work, the following conclusions can be drawn about the inelastic stochastic multi-scale numerical model for random heterogeneous materials developed in [5] and [6]:

- Fig. 4: The model simulates macroscopic behaviors of analogous shapes for all the sets of input parameters considered.
- Tab. 4: Clear trends regarding the relative importance of the model input parameters on the outputs can be observed with a relatively small number of simulations.
- Tab. 4: 3 out of 9 input parameters are key to control the simulated macroscopic response, namely the means of the random fields at meso-scale: a_C , a_{σ_y} , and a_r .
- Tab. 4: Combined actions of two or more input parameters on the model outputs are very limited ($\hat{s}_{k,j} \approx \hat{s}_{k,jT}$, $\forall (j, k) \in [1, N^x] \times [1, N^y]$).
- Tab. 4: Initial stiffness C_O at macro-scale solely depends on the mean a_C of the initial stiffness marginal distribution at meso-scale (see Fig. 4). This is in accordance with the way the model is built: by definition $C_O = \langle C(\mathbf{p}, \omega) \rangle$ with $\langle C(\mathbf{p}, \omega) \rangle$ the spatial mean of the initial stiffness field over the material RVE, and, consequently to ergodicity properties of the random vector field at meso-scale $a_C = \langle C(\mathbf{p}, \omega) \rangle$; accordingly: $C_O = a_C$.

ACKNOWLEDGEMENT

Part of this work has been developed while visiting the Department of Civil Engineering and Engineering Mechanics at Columbia University in the City of New York.

REFERENCES

- [1] Germain P., Nguyen Q.S., Suquet P. Continuum thermodynamics. ASME Journal of Applied Mechanics (1983) 50:1010–1020.
- [2] Helton J.C., Johnson J.D., Sallaberry C.J., Storlie C.B. Survey of sampling-based methods for uncertainty and sensitivity analysis. Reliability Engineering & System Safety (2006) 91:1175–1209.
- [3] Helton J.C., Davis F.J. Latin hypercube sampling and the propagation of uncertainty in analyses of complex systems. Reliability Engineering & System Safety (2003) 81:23–69.
- [4] Iooss B., Lemaître P. *A review on global sensitivity analysis methods*. In: Meloni C. and Dellino G. (Eds.) Uncertainty management in Simulation-Optimization of Complex Systems: Algorithms and Applications, Springer, 2015.
- [5] Jehel P. A Stochastic Multi-scale Approach for Numerical Modeling of Complex Materials – Application to Uniaxial Cyclic Response of Concrete. In: Ibrahimbegovic A. (ed.), Computational Methods for Solids and Fluids. Springer, pp. 123–160 (2016).
- [6] Jehel P., Cottureau R. On damping created by heterogeneous yielding in the numerical analysis of nonlinear reinforced concrete frame elements. Computers and Structures (2015) 154:192–203.

- [7] Mc Kay M.D., Conover W.J., Beckman, R.J. A comparison of three methods for selecting values of input variables in the analysis of output from a computer code. *Technometrics* (1979) 21:239–245.
- [8] Maugin G. The thermodynamics of nonlinear irreversible behaviors: An introduction. World Scientific, Singapore (1999).
- [9] Miehe C., Koch A. Computational micro-to-macro transitions of discretized microstructures undergoing small strains. *Archive of Applied Mechanics* (2002) 72:300–317.
- [10] Nemat-Nasser S., Hori M. Micromechanics: Overall properties of heterogenous materials. Elsevier Science Publishers B.V., Amsterdam, The Netherlands (1993).
- [11] Popescu R., Deodatis G., Prevost J.H. Simulation of homogeneous nonGaussian stochastic vector fields. *Probabilistic Engineering Mechanics* (1998) 13(1):1–13.
- [12] Savvas D., Stefanou G., Papadopoulos V., Papadrakakis M. Effect of waviness and orientation of carbon nanotubes on random apparent material properties and RVE size of CNT reinforced composites. *Composite Structures* (2016) 152:870–882.
- [13] Trigo A.P.M., Liborio J.B.L. Doping technique in the interfacial transition zone between paste and lateritic aggregate for the production of structural concretes. *Materials Research* (2014) 17(1):16–22.
- [14] Zhu X., Gao Y., Dai Z., Corr D.J., Shah S.P. Effect of interfacial transition zone on the Young's modulus of carbon nanofiber reinforced cement concrete. *Cement and Concrete Research* (2018) 107:49–63.

ANNEX - Support of a uniform distribution with know mean and variance

Let $\mathcal{U}(a, b)$ be a uniform distribution over the range $[x; y]$ ($x < y$) with mean a and variance $b^2 > 0$. In this annex, we show how to calculate x and y from a and b . By definition, the following nonlinear system has to be solved:

$$\begin{cases} x + y = 2a \\ (y - x)^2 = 12b^2 \end{cases} \quad (11)$$

Introducing $C^2 = 4a^2$ and $D^2 = 12b^2$, Eqs. (11) implies that:

$$\begin{cases} (x + y)^2 = C^2 \\ (x - y)^2 = D^2 \end{cases} \quad \Rightarrow \quad \begin{cases} x + y = \pm C \\ x - y = \pm D \end{cases} \quad (12)$$

Consequently, we have the following four possible couples of solutions:

$$\begin{aligned} (x_1, y_1) &= ((C + D)/2, (C - D)/2) \\ (x_2, y_2) &= ((C - D)/2, (C + D)/2) \\ (x_3, y_3) &= ((-C + D)/2, (-C - D)/2) \\ (x_4, y_4) &= ((-C - D)/2, (-C + D)/2) \end{aligned} \quad (13)$$

From Eqs. (13), the following table can be built:

i	$(x_i + y_i)/2$	$x_i - y_i$	$(C, D) = (2a, \sqrt{12}b)$	$(C, D) = (2a, -\sqrt{12}b)$	$(C, D) = (-2a, \sqrt{12}b)$	$(C, D) = (-2a, -\sqrt{12}b)$
1	$C/2$	D	<i>No</i>	<i>Yes</i>	<i>No</i>	<i>No</i>
2	$C/2$	$-D$	<i>Yes</i>	<i>No</i>	<i>No</i>	<i>No</i>
3	$-C/2$	D	<i>No</i>	<i>No</i>	<i>No</i>	<i>Yes</i>
4	$-C/2$	$-D$	<i>No</i>	<i>No</i>	<i>Yes</i>	<i>No</i>

A *Yes* means that both conditions $(x_i + y_i)/2 = a$ and $x_i < y_i$ are true for the corresponding values of C and D , while a *No* is indicated otherwise. Because there is always one and only one *Yes* for each value of i , this table shows the intuitive fact that x and y are uniquely determined from a and b . Besides, if for instance we consider that $(x, y) = (x_2, y_2)$ in Eqs. (13) with $C = 2a$ and $D = \sqrt{12}b$ (corresponding to a *Yes*), we have:

$$x = a - \sqrt{3}b \quad \text{and} \quad y = a + \sqrt{3}b \quad (14)$$

As a direct application of Eqs. (14), it is for instance straightforward to guarantee that $[x, y] \subset [0, 1]$ if, for any $a \in [0, 1]$, b is calculated as

$$\begin{cases} a - \sqrt{3}b \geq 0 \\ a + \sqrt{3}b \leq 1 \end{cases} \Rightarrow b \leq \min \left(a/\sqrt{3} ; (1 - a)/\sqrt{3} \right) \quad (15)$$

Acoustic Black Holes: from Generalization to Realization

Wonju Jeon*

*KAIST

ABSTRACT

This study starts with a simple question: can we efficiently reduce the vibration of plates or beams using a lightweight structure that occupies a small space? As an efficient technique to dampen vibration, we adopted the concept of an Acoustic Black Hole (ABH) with a simple modification of the geometry. The original shape of an ABH has a straight wedge-type profile with power-law thickness, with the reduction of vibration in beams or plates increasing as the length of the ABH increases. However, in real-world applications, there exists an upper bound of the length of an ABH due to space limitations. Therefore, in this study, the authors propose a curvilinear shaped ABH using the simple mathematical geometry of an Archimedean spiral, which allows a uniform gap distance between adjacent baselines of the spiral. In numerical simulations, the damping performance increases as the spiral length of the Archimedean spiral increases regardless of the curvature of the spiral in the mid- and high-frequency ranges. Adding the damping material to the ABH could strongly enhance the damping performance while not significantly increasing the weight. In addition, the authors experimentally investigate the effect of curvatures of the curved ABH on the vibration damping performance. The curved ABHs studied in this work are divided into two cases: (1) the curved ABH with the baseline of constant curvatures which has a circular arc shape, (2) the curved ABH with the baseline of varying curvatures. After manufacturing the spiral ABH with high precision, the authors perform experiments to investigate the effect of curvatures on the damping performance of the circular arc shaped ABHs. An Archimedean spiral ABH, a particular form of the curved ABH of slowly varying curvatures is also investigated experimentally in order to create the possibility of using the spiral ABH as a new and efficient method of damping vibration in real-world problems.

Identification of Elastic Moduli and Length Scale Parameter for Strain Gradient Theory from Full-field Measurements

Iksu Jeong*, Euiyoung Kim**, Maenghyo Cho***

*Department of Mechanical and Aerospace Engineering, Seoul National University, Seoul, Republic of Korea, **4th Industrial Revolution R & D Center, Korea Institute of Machinery & Materials, Daejeon, Republic of Korea,

***Department of Mechanical and Aerospace Engineering, Seoul National University, Seoul, Republic of Korea

ABSTRACT

Classical continuum solid mechanics have been widely used in various fields for decades, but cannot demonstrate some phenomena such as size effects and deformation of micro- and nano-scale structures. To overcome these limitations, many researchers have developed the strain gradient theory in which the classical theory is enriched by adding first derivatives of macroscopic strains, i.e. second derivatives of displacements, to the constitutive equations. Additional parameters called length scale parameters need to be introduced for the higher order terms and it is necessary to experimentally measure the exact value of the parameters for the practical application of the strain gradient theory. Recent advances in optical devices and image processing have led to the development of methodologies such as digital image correlation which can measure full-field displacements of structures. Full-field measurements make it possible to identify more accurate and realistic material parameters compared to the traditional method especially when the stresses and strains are not uniform. Furthermore, identification methods based on full-field measurement can extract the parameters from a relatively small number of experiments even though the material has heterogeneous or nonlinear constitutive properties. In this research, constitutive parameters for gradient elasticity including length scale parameter are identified from full-field displacements by minimizing the gap between measured and numerical quantities. For the numerical analysis, finite element method with staggered gradient elasticity based on Ru-Aifantis theorem is used since it only need C0-continuous interpolation functions. Finite element analysis of the strain gradient theory basically requires C1-continuity due to the higher order terms, but staggered gradient elasticity divides the solution process into two step so that C0 elements suffice. The accuracy and robustness of the proposed method are verified in a couple of numerical examples. Keywords: Identification, Full-field measurement, Gradient elasticity, Length scale parameter References [1] H. Askes, I. Morata, E.C. Aifantis, Finite element analysis with staggered gradient elasticity, Computers and Structures, 2008, Vol. 86, pp. 1266-1279 [2] S. Avril et al., Overview of identification methods of mechanical parameters based on full-field measurements, 2008, Exp. Mech., Vol. 48, pp. 381-402 Acknowledgement This work was supported by the National Research Foundation of Korea(NRF) grant funded by the Korea government(MSIP) (No. 2012R1A3A2048841

Calculation of Surface Energy Barriers of Droplet Adhesion to Textured Solid Surface in Cassie-Baxter Wetting Mode by Using Numerical Modeling

Minsoo Jeong^{*}, Seunghwa Ryu^{**}, Keonwook Kang^{***}

^{*}Department of Mechanical Engineering, Yonsei University, Republic of Korea, ^{**}Department of Mechanical Engineering, KAIST, Republic of Korea, ^{***}Department of Mechanical Engineering, Yonsei University, Republic of Korea

ABSTRACT

The phenomenon that particles stick to the solid surface is called particle surface adhesion. The wettability of a particle on the surface can be tuned by changing the topology of the surface. In this work, we developed a line tension model to understand the surface adhesion phenomenon of a deformable body to solid surface. Our model is validated by comparing with analytical solutions of D. Kim et al.(2016)[1] and Young et al.(1805)[2] which calculate the surface energy and contact angle of water droplet adhered to the solid surface in Cassie-Baxter wetting mode. The model produces consistent result that the wettability of the patterned solid surface is lower than that of flat surface. Besides, the unrealistic non-smooth droplet shape is avoided in our numerical modeling. In addition, the surface energy barriers that are generated when the contact angle changes in the Cassie-Baxter wetting mode are calculated. [1] Kim et al., "Wetting theory for small droplets on textured solid surfaces", Scientific Reports, 6:, 37813 (2016) [2] Young et al., "An Essay on the Cohesion of Fluids", Phil. Trans. R. Soc. Lond., 95:, 65–87 (1805)

High Fidelity Modeling and Simulation of Earthquake Soil Structure Interaction Effects for Infrastructure Objects

Boris Jeremic*, Yuan Feng**, Han Yang***, Hexiang Wang****, Francis McKenna*****, David McCallen*****

*UCD, LBNL, **UCD, ***UCD, ****UCD, *****LBNL, *****LBNL

ABSTRACT

Interaction of dynamics of three components: (1) an earthquake, (2) soil/rock and (3) the structure, control the response of structures during earthquakes. It is postulated that this interaction, called Earthquake Soil Structure Interaction (ESSI) can sometimes be beneficial and sometimes detrimental to dynamic response of infrastructure objects. Accurate modeling of ESSI effects is possible when modeling uncertainties, that are introduced in results when modeling simplifications are made, are controlled and that their influence on results is known. A hierarchy of models, from simpler toward more sophisticated, is used to estimate influence of modeling uncertainties. Higher modeling sophistication models require high performance computing (HPC) approach to simulations. Presented here is our approach to modeling ESSI effects for dynamic behavior of buildings and other safety related structures (bridges, dams, etc.). Approach is based on a notion of availability of a hierarchy of modeling and simulation tools, from low to high fidelity, that allow for deterministic and probabilistic models to be used in the analysis. Effects of modeling simplifications on ESSI modeling and simulation results are tested through the use of multiple levels of sophistication for models, from simple 1D elastic stick models, to sophisticated 3D inelastic solid, contact, shell, beam models. In addition, accurate following of seismic energy, as it propagates through the soil structure system, is used to improve safety and economy of infrastructure objects. HPC approach to modeling and simulation of ESSI effects is presented on both fine and coarse grained levels. Fine grain level HPC is based on application of Small Linear Algebra (SLA) to tensor computations on the constitutive and finite element level. Coarse grained level HPC is based on massively parallel computations using Ring Buffer (RB) dynamic load balancing that is applicable to local clusters, to Cloud Computing (Amazon Web Services (AWS) for example) as well as to large national supercomputers (EDISON and CORI at LBNL for example). A number of examples will illustrate aspects of modeling and simulation of ESSI behavior using HPC approach. All simulations are performed using the Real ESSI Simulator system (<http://real-essi.info/>).

Free Damage Propagation with Memory

Prashant Jha^{*}, Robert Lipton^{**}

^{*}Department of Mathematics Louisiana State University, ^{**}Center for Computation and Technology and
Mathematics Louisiana State University

ABSTRACT

We introduce a simple model for free damage propagation based on non-local potentials. The model is developed using a state based peridynamic formulation. The resulting evolution is shown to be well posed. At each instant of the evolution we identify the damage set. On this set the local strain has exceeded critical values either for tensile or hydrostatic strain and damage has occurred. For this model the damage set is nondecreasing with time and associated with damage variables defined at each point in the body. We show that energy balance holds for this evolution. For differentiable displacements away from the damage set we show that the nonlocal model converges to the linear elastic model. We provide several numerical examples modeling fatigue and fracture.

Dynamics of Thin Liquid Films on Vertical Cylindrical Fibers

Hangjie Ji^{*}, Claudia Falcon^{**}, Abolfazl Sadeghpour^{***}, Zezhi Zeng^{****}, Andrea Bertozzi^{*****},
Sungtaek Ju^{*****}

^{*}University of California, Los Angeles, ^{**}University of California, Los Angeles, ^{***}University of California, Los Angeles, ^{****}University of California, Los Angeles, ^{*****}University of California, Los Angeles, ^{*****}University of California, Los Angeles

ABSTRACT

Viscous thin liquid films flowing down vertical fibers can exhibit interesting dynamics via the formation of droplets driven by a Rayleigh mechanism with the presence of gravity. Motivated by experimental results on the effects of nozzle geometry on the dynamics of these viscous droplets by Sadeghpour et al. (2017), we further study a thin film model for the gravity-driven flow in the Rayleigh-Plateau Regime. The governing equation is a fourth-order nonlinear parabolic PDE for the film thickness that takes into consideration hydrodynamic boundary conditions, surface tension, intermolecular forces, and gravity. Time-dependent computations of the spatial evolution of the film reveal a strong influence of inlet boundary conditions that characterize different nozzle geometry. Numerical solutions of traveling wave solutions also yield information on the profile and propagation velocity of fluid beads, which are compared to experiments.

Buffering Capacity of Non-spherical Granular Materials Based on DEM Simulations with Super-quadric Elements

Shunying Ji^{*}, Ying Yan^{**}, Siqiang Wang^{***}

^{*}State Key Laboratory of Structural Analysis for Industrial Equipment, Dalian University of Technology, Dalian 116023, China, ^{**}School of civil and Safety Engineering, Dalian Jiaotong University, Dalian, 116028, China,

^{***}State Key Laboratory of Structural Analysis for Industrial Equipment, Dalian University of Technology, Dalian 116023, China

ABSTRACT

Granular systems commonly encountered in industry or nature are comprised of non-spherical grains. Compared to spherical particles, high discretization and interlocking among particles can dissipate effectively the system energy and improve the buffer capacity. The superquadric element based on continuous function representation can construct the geometric shape of irregular particles accurately, and then its contact detection between particles can be calculated easily. In this paper we study the buffer capacity of non-spherical particles under impact load by the discrete element method (DEM). To examine the validity of the algorithms and this model, we compare with the analytical results for a single cylinder impacting a flat wall and the previous experimental result for spherical granular material under impact load, and this method is verified by the good agreement between the simulated results and the previous experiments. Furthermore, the influences of granular thickness and particle shapes on the buffer capacity are discussed. The results show that a critical thickness H_c is obtained for different particle shapes. The buffer capacity is improved for increasing the granular thickness when $H < H_c$, but is independent of the granular thickness and particle shapes when $H > H_c$. Moreover, decreasing the particle blockiness and increasing or decreasing the aspect ratio of cylinder-like particles and box-like particles have more effective buffer capacity for the non-spherical particle systems.

An Accurate Weakly Compressible SPH Method for Simulating Interfacial Multiphase Fluid Flow Involving Complex Geometries and Motions

Zhe Ji^{*}, Michael Gestrich^{**}, Milos Stanic^{***}, Thomas Indinger^{****}

^{*}FluiDyna GmbH, ^{**}FluiDyna GmbH, ^{***}FluiDyna GmbH, ^{****}FluiDyna GmbH

ABSTRACT

Numerical simulations of interfacial multiphase fluid flow have a wide range of applications across engineering fields. Simulations of oil distribution in transmission systems regularly involve complex geometries and high-speed motions. Robust and accurate handling of multiple material phases and the interaction with complex moving geometries is a challenging problem for any numerical method. As a particle-based method, Smoothed Particle Hydrodynamics (SPH) conserves mass and momentum. The sharp interface condition is inherently satisfied and characterized by particles carrying distinct material properties, which is the main advantage over the grid-based methods. Nonetheless, regarding to multiphase simulations, traditional SPH suffers from several numerical difficulties and extra treatments are required in order to maintain stability and sharpness of the interface. In this work, an accurate weakly compressible SPH method is developed to simulate interfacial multiphase flow involving complex geometries and rigid-body motions. In order to decrease numerical oscillation of the pressure field, the pair-wised particle interaction is calculated by solving a one-dimensional Riemann problem. An extended HLLC Riemann solver [1] is tailored to handle interactions between different materials with general equations of state and large density ratio. For continuous region within one phase, a modified Riemann solver [2] is employed to decrease the intrinsic numerical dissipation. In addition, a generalized wall boundary condition, based on solving a one-side Riemann problem, is extended to multiphase situation to handle interactions regarding to complex moving geometries with the existence of triple points. Moreover, to go beyond 1st order of accuracy and overcome some well-known difficulties of the traditional SPH method, a second-order gradient estimator as well as the MUSCL-Hancock scheme are utilized. Lastly, to avoid the disorder of particle positions and creation of void regions, the transport velocity formulation is embedded as well. The proposed SPH method is implemented in a high performance multi-GPU code developed by FluiDyna GmbH. Extensive numerical tests including academic and industrial benchmarks are carried out in the end to validate the accuracy of proposed numerical method. The results exhibit significant improvement over traditional SPH. More physically plausible results are observed by producing better-resolved fluid structures and a more accurate pressure field. [1] C. Zhang, X. Hu, N. Adams, Journal of Computational Physics 335 (2017) 605–620. [2] X. Hu, N. Adams, G. Iaccarino, Journal of Computational Physics 228 (2009) 6572–6589.

An Adaptive IGA Collocation Method with a Recovery-based Error Estimator

Yue Jia^{*}, Cosmin Anitescu^{**}, Yongjie Zhang^{***}, Timon Rabczuk^{****}

^{*}Northwestern Polytechnical University, Xi'an, China, ^{**}Institute of Structure Mechanics, Bauhaus University Weimar, Germany, ^{***}Carnegie Mellon University, Pittsburgh, USA, ^{****}Institute of Structure Mechanics, Bauhaus University Weimar, Germany

ABSTRACT

Abstract The current work presents an enhanced isogeometric analysis (IGA) [1] collocation method, where the collocation points are different from the usual Greville-abscissae. It is well known that the location of the collocation points plays an important role in the accuracy and stability of IGA collocation methods. This is particularly true for non-uniform meshes and domains generated from multi-patch geometries. We propose a collocation method based on Gaussian points [2], which has improved accuracy as compared to using C1 splines and a recovery-based error estimator can be derived by sampling the solution at particular points in the domain. Adaptivity is implemented using a hierarchical spline basis [3], which satisfies the C1 continuity requirement. The proposed approach is demonstrated for arbitrary polynomial degrees and has been tested by several benchmark problems, including multipatch domains and geometries with re-entrant corners. **Key words:** IGA collocation method; Gaussian-collocation points; PHT-Spline; linear elasticity; error estimation **References** [1] Hughes T J R, Cottrell J A, Bazilevs Y. Isogeometric analysis: CAD, finite elements, NURBS, exact geometry and mesh refinement [J]. Computer Methods in Applied Mechanics and Engineering, 2005, 194(39-41): 4135-4195 [2] De Boor C, Swartz B. Collocation at Gaussian Points [J]. SIAM Journal on Numerical Analysis, 1973, 10(4): 582-606 [3] Deng J S, Chen F, Li X, et al. Polynomial splines over hierarchical T-meshes[J]. Journal Graphical Models, 2008, 70(4): 76-86

Quasi-nonlocal Coupling of State-based Peridynamics Model with Classical Continuum Mechanics Model

Feng Jiang*, Yongxing Shen**

*University of Michigan-Shanghai Jiao Tong University Joint Institute, Shanghai Jiao Tong University, **University of Michigan-Shanghai Jiao Tong University Joint Institute, Shanghai Jiao Tong University

ABSTRACT

The peridynamics and continuum models of elasticity have their pros and cons. The peridynamics model can be naturally applied to a region where a crack propagates or damage emerges, while the continuum mechanics model is most cost efficient and easier to enforce boundary conditions. Coupling of these models provides a way to fully take advantage of their merits. However, the energy based coupling schemes usually suffer from the spurious “ghost force” effect. To relieve this issue, in this work, a quasi-nonlocal coupling technique has been developed to couple the state-based peridynamics model with continuum mechanics model. The essential idea of the coupling is that the transition region interacts with the peridynamics region in a nonlocal way while it interacts with the continuum region in a local way. In the transition region, the stiffness tensor and the influence function are modified so that both the force patch test and the energy patch test are passed at the nodal points. Since there are more equations than parameters, the parameters are determined with l^1 -minimization. Numerical examples demonstrating the accuracy and efficiency of the coupling model are presented. [1] S.A. Silling et al., Peridynamic states and constitutive modeling, J. Elasticity, 88:151-184, 2007. [2] C. Ortner, L. Zhang, Energy based atomistic-to-continuum coupling without ghost forces, Comput. Methods Appl. Mech. Engrg., 279:29-45, 2014. [3] X. H. Li and J. Lu, Quasi-nonlocal coupling of nonlocal diffusions. SIAM J. Numer. Anal., 55 (5):2394-2415, 2017.

Offline-Enhanced Reduced Basis Method through Adaptive Construction of the Surrogate Training Set

Jiahua Jiang^{*}, Yanlai Chen^{**}, Akil Narayan^{***}

^{*}University of Massachusetts Dartmouth, ^{**}University of Massachusetts Dartmouth, ^{***}University of Utah

ABSTRACT

The Reduced Basis Method (RBM) is a popular certified model reduction approach for solving parametrized partial differential equations. It has been combined with many multiscale methods such as domain decomposition. One critical stage of the offline portion of the algorithm is a greedy algorithm, requiring maximization of an error estimate over parameter space. In practice this maximization is usually performed by replacing the parameter domain continuum with a discrete ‘‘training’’ set. When the dimension of parameter space is large, it is necessary to significantly increase the size of this training set in order to effectively search parameter space. Large training sets diminish the attractiveness of RBM algorithms since this proportionally increases the cost of the offline phase. However, the large size of parameter inputs leads to high computational costs in offline stage. In this work we propose novel strategies for offline RBM algorithms that mitigate the computational difficulty of maximizing error estimates over a training set. The main idea is to identify a subset of the training set, a ‘‘Surrogate Training Set’’ (STS), on which to perform greedy algorithms. The STSs we construct are much smaller in size than the full training set, yet our examples suggest that they are accurate enough to induce the solution manifold of interest at the current offline RBM iteration. We propose two algorithms to construct the STS: Our first algorithm, the Successive Maximization Method (SMM) method, is inspired by inverse transform sampling for non-standard univariate probability distributions. The second constructs an STS by identifying pivots in the Cholesky Decomposition of an approximate error correlation matrix. We demonstrate the algorithm through numerical experiments, showing that it is capable of accelerating offline RBM procedures without degrading accuracy, assuming that the solution manifold has rapidly decaying Kolmogorov width.

A Multi-Material Structural Topology Optimization Based on Parametric Level Set Approach Using Cardinal Basis Functions

Long Jiang*, Shikui Chen**

*Department of Mechanical Engineering, State University of New York at Stony Brook, **Department of Mechanical Engineering, State University of New York at Stony Brook

ABSTRACT

As a further development of the conventional level set methods, the parametric level set method is an improvement over its predecessor in the topology optimization area. By parameterizing the level set function, the topology optimization not only can preserve clear design result boundaries but also can avoid some undesired deficiencies in the conventional level set approach, such as the reinitialization scheme. Integrated with mathematical programming, the parametric level set approach can achieve higher numerical robustness and better handling of multiple constraints. To get an accurate material property interpolation from the level set model to the physical model, the level set function is preferred to be maintained as a signed distance function (SDF). In this research, this feature is realized by introducing a distance regularization energy functional. With this energy functional minimized, the level set function around the design boundary will be maintained as a signed distance function. At the same time, the level set function can be kept flat at the locations away from the design boundaries. Overall, this type of level set function is referred as the distance-regularized level set function. By being flat at areas away from the design boundaries, the level set function can penetrate the zero level easier, improving the design robustness by creating new holes. When extended to the multi-material structure designing, different level set functions are utilized to represent different material phases, and the overlapping areas are reconciled via the Merriman-Bence-Osher (MBO) operator. However, the distance-regularized-shape level set function may cause numerical issues while applying this operator. A sub-optimization scheme is introduced to reshape the level set function before and after the MBO operation to ensure its success. Conventionally, the parametric level set approach uses radial basis function (RBF) in the parameterization. However, due to the overlapping of the neighboring RBFs, the range of the corresponding weights, to be used as the optimization design variable, cannot be explicitly determined. In this research, a newly-constructed cardinal basis function (CBF) is utilized to parameterize the level set function. This CBF is equal to one at the selected node and is equal to zero elsewhere. By using this CBF in the parameterization, the design variable range can be explicitly determined, as the range of the level set function itself.

Effects of grain size and shape on the plasticity of FCC polycrystals : A Dislocation Dynamics Study

Maoyuan Jiang^{*}, Benoit Devincre^{**}, Ghiath Monnet^{***}

^{*}EDF R&D, Department MMC, France, ^{**}Laboratoire d'Etude des Microstructures, CNRS-ONERA, France, ^{***}EDF R&D, Department MMC, France

ABSTRACT

From the seminal work of Hall and Petch (HP), the effect of grain size on the mechanical properties of polycrystal is well known. Nevertheless, the elementary properties responsible for the HP effect are still matter of debate. Besides, theoretical and experimental investigations are today essentially focused on polycrystals made of equiaxial grains. However, industrial materials are usually formed with grains having non-equiaxed shapes (perlite, matensite, bainite etc.). In this work, Dislocation Dynamics (DD) simulation is used to identify the elementary mechanisms controlling the HP effect at the dislocations scale. In addition, the influence of grain shape is explored by considering simple periodic polycrystalline aggregates made of grains with cube, plate or needle shapes. First, simulations have been made with a very simple periodic model of aggregates. Grain boundaries (GBs) are considered impenetrable to the dislocation gliding inside the grains. Results show that the HP effect is globally obeyed and the interaction with GBs is strongly affected by the number of active slip systems. Secondly, we designed simulations to test the influence of grain shape on the HP effect. We show that the HP effect is strongly affected by the grain shapes. A simple model based on the calculation of the dislocation mean free path is proposed to account for the influence of the grains morphology. In the context of strain gradient plasticity, the HP effect is explained by the presence of a back-stress inside the grains that emerges from strain incompatibility between grains in a deformed polycrystal. In other words, geometrically necessary dislocations (GNDs) must accumulate at GBs to accommodate the different distortion field imposed to the grains during plasticity. By virtue of the Nye's tensor, the above property can be directly tested and quantified in DD simulations. For the simplest simulation geometry, the computed back-stress as function of the distance to the GB interface can be compared with theoretical models. Essentially, a crystal plasticity field model is found to correctly calculate the back-stress amplitude close to the GB interface while the DD simulation results exhibit a decay trend for the stress components. A twist subgrain calculation accounting for the finite size of the GND microstructure gives much better agreement with the DD simulation results.

A Coupled Finite Volume Methods and Extended Finite Element Methods for the Dynamic Crack Propagation Modelling with the Pressurized Crack Surfaces

Shouyan Jiang^{*}, Chengbin Du^{**}

^{*}Department of Engineering Mechanics, Hohai University, Nanjing 210098, China, ^{**}Department of Engineering Mechanics, Hohai University, Nanjing 210098, China

ABSTRACT

In this paper, we model the fluid flow within the crack as one-dimensional flow and assume that the flow is laminar, the fluid is incompressible, and accounts for the time-dependent rate of crack opening. Here, we discretise the flow equation by finite volume methods. The extended finite element methods are used for solving solid medium with crack under dynamic loads. Having constructed the approximation of dynamic extended finite element methods, the derivation of governing equation for dynamic extended finite element methods are presented. The implicit time algorithm is elaborated for the time discretization of dominant equation. In addition, the interaction integral method is given for evaluating stress intensity factors. Then, the coupling model for modelling hydraulic fracture can be established by the extended finite element methods and the finite volume methods. We compare our present numerical results with our experimental results for verifying the proposed model. Finally, we investigate the water pressure distribution along crack surface and the effect of water pressure distribution on the fracture property.

3D Multi-scale Modeling of Microstructure Dependent Inter-granular Fracture in UO₂ Using a Phase-field Approach

Wen Jiang^{*}, Larry Aagesen^{**}

^{*}Idaho National Laboratory, ^{**}Idaho National Laboratory

ABSTRACT

The brittle fracture behavior of UO₂ fuels is strongly influenced by the porosity and grain size distributions in the underlying microstructure. In service, there is significant evolution of these microstructural features, which can alter the fracture properties and subsequently the thermo-physical-mechanical behavior of the nuclear fuels. To incorporate these microstructural effects on the fracture behavior, a three-dimensional multi-scale modeling framework is developed in the present work. Within this framework, the grain-boundary fracture properties obtained from molecular dynamics simulations are utilized in a phase-field fracture model to investigate the inter-granular brittle crack propagation in this material. The fission gas bubble formation model is coupled with fracture to study their interaction and influence on the fracture properties. Subsequently, the parameters of an engineering scale fracture model are obtained by fitting the stress-strain evolution obtained from the phase-field simulations. This framework provides a hierarchical coupling of properties evaluated at the atomistic scale to perform more realistic engineering level predictions of fracture in nuclear fuel pellets.

Evaluation of the Benefit of Strengthening Shield Tunnels by Epoxy-bonded Filament Wound Profiles by Means of a Parametric Study Based on Multiscale Analysis

Zijie Jiang^{*}, Xian Liu^{**}, Lele Zhang^{***}, Yong Yuan^{****}, Herbert A. Mang^{*****}

^{*}Department of Geotechnical Engineering, Tongji University, China, ^{**}Department of Geotechnical Engineering, Tongji University, China, ^{***}Department of Geotechnical Engineering, Tongji University, China, ^{****}Department of Geotechnical Engineering, Tongji University, China, ^{*****}Institute for Mechanics of Materials and Structures, Vienna University of Technology, Austria

ABSTRACT

Large deformations of shield tunnels may be the consequence of a long period of operation or of nearby pit construction. Epoxy-bonded filament wound profiles (FWP) have been employed more recently to strengthen the deformed segmental tunnel linings. Full-scale tests were performed to prove the effectiveness of this method. The present paper contains a report on a macroscopic numerical model, which has been validated by comparing numerical results with experimental results. Multiscale analysis is an important ingredient of the modeling process, aimed at improving computational efficiency and fidelity. In this model, the reinforced concrete segments and the strengthening material, i.e. FWP, are simulated by means of beam elements. The joints which connect adjacent reinforced concrete segments are modeled by a group of nonlinear spring elements. Previous research has shown that the behavior of the joints may have significant influence on the mechanical behavior of the overall structure. Based on the developed numerical model, a comprehensive parametric study of the influence of several design parameters, such as, for example, Young's modulus of the FWP and the mechanical properties of the bond between the FWP and a segment of the tunnel, on the increase of both the load-carrying capacity and the overall stiffness of the structure was performed. Based on the results from this study, an optimal combination of design parameters for strengthening of shield tunnels by FWP is proposed. Moreover, the influence of the geometric dimensions of the strengthened structure and of the soil environment on the overall benefit of this strengthening was obtained. The soil environment is intergraded into the model by means of a specific scheme of loading. It is shown that this influence is smaller than the one of the geometric dimensions of the lining, which is itself relatively small.

A Link between Multiplicative Hyper-Elasto-Plasticity and Additive Hypo-Elasto-Plasticity Models: the Kinetic Logarithmic Stress Rate

Yang Jiao*, Jacob Fish**

*Columbia University, **Columbia University

ABSTRACT

Plasticity is one of the most common energy dissipation mechanisms featuring large strain in solids. Geometric nonlinearity is therefore often involved in constitutive models adopted for numerical simulation of plastic behavior of solids. Such constitutive models are usually developed through extension of the corresponding infinitesimal-deformation models into the large strain regime. Distinct large-strain plasticity models, however, can be obtained as large-strain generalizations of the same classical infinitesimal-deformation model. Understanding of the relation between these different models for the same purpose is thus of crucial importance for ensuring reliability of the computational approaches to studying plasticity. In the present study, two well-recognized categories of large-strain elastoplasticity models, i.e. the multiplicative hyper-elasto-plasticity and additive hypo-elasto-plasticity models, are analyzed with relation between them revealed. At first, the well-known additive hypo-elasto-plasticity models, which are based on additive decomposition of the rate of deformation into elastic and plastic parts, are critically examined. Through an unloading stress ratchetting obstacle test, it is shown that even a relatively recent, self-consistency-oriented variant of such models, which features the logarithmic stress rate, exhibits physical inconsistency (nonphysical energy dissipation) in an unloading process. A remedy is accordingly proposed through a simple modification to the logarithmic stress rate employed by the model. It is demonstrated that the resulting objective stress rate, termed the kinetic logarithmic rate due to its dependency on stress, renders the corresponding additive models capable of representing energy dissipation-free elastic response whenever plastic flow is absent. The multiplicative hyper-elasto-plasticity models, which are usually considered to be distinct from the additive ones in that they assume multiplicative decomposition of the deformation gradient into elastic and plastic parts, are then analyzed. It is proved that for isotropic materials the multiplicative models coincide with the additive ones if a newly discovered objective stress rate is employed by the later. This objective stress rate, termed the modified kinetic logarithmic rate, reduces to the kinetic logarithmic rate in the absence of strain-induced anisotropy. Such equivalence between the two categories of elastoplasticity models is illustrated through numerical model problems which consider homogeneous deformation along with J2 plasticity with associative plastic flow rule. It is also demonstrated in these problems that other well-known additive models, such as those based on the Jaumann and logarithmic rates, may considerably deviate from the multiplicative models.

Multi-Phase-Field Simulation of Eutectic Solidification of Binary Alloys Using a Thermodynamically Consistent Model

Peter Jimack*, Peter Bollada**, Andrew Mullis***

*University of Leeds, **University of Leeds, ***University of Leeds

ABSTRACT

This presentation will introduce the derivation of a consistent temperature equation for phase-field models of non-isothermal alloy solidification, and demonstrate its application in two dimensions for the eutectic solidification of a binary alloy based upon an appropriate multi-phase-field model. This non-isothermal model is derived using a formulation based upon the dissipative bracket of Beris and Edwards [1]. Originally designed for modelling complex fluids, the dissipative bracket has ready application in phase field modelling. In outline, we design the bracket to return the phase and alloy concentration field equations, and then use the mechanism of the bracket to automatically return the entropy field, which in turn, using generalised standard thermodynamic identities, gives the thermal field [2]. Our numerical scheme for solving the resulting system is based upon the use of spatial adaptivity and implicit time-stepping via a nonlinear multigrid scheme (the Full Approximation Scheme, FAS). The core components of this implementation will be described, including parallelization based upon a domain decomposition approach. We will illustrate both the quantitative and the qualitative importance of the non-isothermal model by contrasting numerical results against isothermal runs for a range of multiphase solidification problems, including eutectic solidification of a binary alloy, where multiple solid phases grow simultaneously in a cooperative manner. [1] A.N. Beris, B.J. Edwards, *Thermodynamics of Flowing Systems: With Internal Microstructure*, Oxford Engineering Science Series, OUP, USA, 1994. [2] P.C. Bollada, P.K. Jimack, A.M. Mullis, Bracket formalism applied to phase field models of alloy solidification, *Computational Materials Science* 126:426–437, 2017.

Estimation of Bridge Frequency from Traversing Vehicle by Short-time Stochastic Subspace Identification

Nan Jin^{*}, Themelina S. Paraskeva^{**}, Elias G. Dimitrakopoulos^{***}, Lambros S. Katafygiotis^{****}

^{*}Hong Kong University of Science and Technology, Department of Civil and Environmental Engineering, Clear Water Bay, Kowloon, Hong Kong, ^{**}Hong Kong University of Science and Technology, Department of Civil and Environmental Engineering, Clear Water Bay, Kowloon, Hong Kong, ^{***}Hong Kong University of Science and Technology, Department of Civil and Environmental Engineering, Clear Water Bay, Kowloon, Hong Kong, ^{****}Hong Kong University of Science and Technology, Department of Civil and Environmental Engineering, Clear Water Bay, Kowloon, Hong Kong

ABSTRACT

The eigenfrequencies of the bridge are important for various engineering applications, such as the health monitoring and the damage detection of the bridge. Over the past decade, there is a growing interest in an “indirect” approach to extract the bridge dynamic properties from vibration of the traversing vehicles. Compared with the traditional technique of installing sensors at multiple locations on the bridge, this approach is more economical, time-saving, portable and most importantly, applicable to every bridge. The traversing vehicle plays the role of a “vibration shaker” exciting the bridge, and at the same time is also a “receiver” collecting information from the bridge. Thus, it is feasible to extract modal parameters of the bridge by processing the vibration response of the vehicle. In general, the frequencies of the bridge and the traversing vehicle are not strictly constant, if the interaction between the two sub-systems and the mass of the vehicle is non-ignorable. However, their time variations are by far longer than their dynamics. For such a time-variant system, the Short-time Stochastic Subspace Identification (ST-SSI) method is proposed to extract the bridge frequencies from the vibration response and the dynamic characteristics of the traversing vehicle. Specifically, the present study assesses the accuracy and the effectiveness of the ST-SSI method that is used to identify the frequencies of a straight reinforced concrete bridge, from the vibration response of a traversing vehicle. As a proof of concept, herein the response of the vehicle is estimated from the vehicle-bridge interaction dynamic analysis. The dynamic characteristics of the vehicle are assumed known. For the needs of the ST-SSI method, the equations of motion for the vehicle and the bridge are discretized in state space, and then transformed to a series vectors by separating the known vehicle-related parameters from the unknown parameters. Finally, the observability matrix containing the bridge dynamic properties is derived by linear algebra techniques, including the Hankel matrix, LQ decomposition, orthogonal projection and singular value decomposition. The bridge frequencies identified with the proposed ST-SSI method are validated against the theoretically correct values, and conclusions regarding the feasibility of the method are drawn.

Bending Analysis of Multilayered Composite Beams in Terms of a New Mixed Global-local Higher-order Theory

Qilin Jin^{*}, Weian Yao^{**}, Xiaofei Hu^{***}

^{*}Dalian University of Technology, Dalian, China, ^{**}Dalian University of Technology, Dalian, China, ^{***}Dalian University of Technology, Dalian, China

ABSTRACT

Accurately predicting of the transverse shear stresses for multilayered composite structure based on the equivalent single-layer theory is still challenging. In the existing method, the complex post-processing procedure based on three dimensional (3D) equilibrium equation was used. Thus, an improved equivalent single-layer theory which describe transverse shear stresses of multilayered composites accurately is expected. In this study, an accurate and computationally attractive mixed-form global-local higher-order theory (MGLHT) is developed for the bending analysis of multilayered composite beams. The theory is derived using the kinematic assumptions of global-local higher-order theory (GLHT) and employs the Reissner mixed variational theorem (RMVT). Moreover, the MGLHT retains a fixed number of displacement variables regardless of the number of layers. The benefit of the proposed MGLHT over the GLHT is that no post-processing approach is needed to accurately calculate the transverse shear stresses. The equilibrium equations and analytical solution of the present model can be obtained based on the Reissner mixed variational equation. The effects of transverse shear stress on the displacements and in-plane stress have been investigated in detail. Numerical results show that the transverse shear stresses can be accurately determined from the proposed model. In addition, the transverse shear stresses derived from the RMVT have a slight effect on displacements and in-plane stress for symmetric beams. For antisymmetric beams, such effect on transverse displacement and in-plane stress is slight, but it is significant on in-plane displacement.

A Comparative Study of Modeling Shear Band Propagation via Embedded Weak Discontinuity with Global, Local and No-tracking Strategies in Three Dimensions

Tao Jin^{*}, Hashem Mourad^{**}, Curt Bronkhorst^{***}

^{*}Los Alamos National Laboratory, ^{**}Los Alamos National Laboratory, ^{***}Los Alamos National Laboratory

ABSTRACT

A tracking strategy has been proposed by Oliver et al. [1] to ensure the continuous propagation of discontinuity surfaces in three dimensions (3D). The basic idea of this strategy is to solve a heat-conduction type boundary value problem for a family of isosurfaces of a scalar level set function as the potential discontinuity surface in the same discretized domain of the mechanical problem. In literature, this strategy has been implemented locally (the local tracking) [2] and globally (the global tracking) [3] to model Mode I fracture via the embedded strong discontinuity. In this research, for the first time we manage to integrate the tracking strategy with the embedded weak discontinuity approach to model shear band propagation that mimics Mode II fracture in the context of explicit finite element formulation. The algorithmic and implementation details regarding the global and local tracking strategies are provided. By comparing the numerical results obtained from simulations using the global, local and no-tracking strategies with the experimental results of the split-Hopkinson pressure bar test, we demonstrate the necessity of ensuring the continuity of the shear band surface to treat shear band propagation. Moreover, we discuss the suitability and the computational cost related to the global and local tracking strategies through several numerical examples. [1]. Oliver, J., Huespe, A.E., Samaniego, E., Chaves, E.W.V., 2002. On strategies for tracking strong discontinuities in computational failure mechanics. Proceedings of the Fifth World Congress on Computational Mechanics (WCCM V), July 7-12, 2002, Vienna, Austria Mang HA, Rammerstorfer FG, Eberhardsteiner J (eds). [2]. Armero, F., Kim, J., 2012. Three-dimensional finite elements with embedded strong discontinuities to model material failure in the infinitesimal range. Int. J. Numer. Methods Eng. 91, 1291–1330. [3]. Linder, C., Zhang, X., 2013. A marching cubes based failure surface propagation concept for three-dimensional finite elements with non-planar embedded strong discontinuities of higher-order kinematics. Int. J. Numer. Methods Eng. 96, 339–372.

Simulation of the Cutting Process in Softening and Hardening Soils

Zhefei Jin^{*}, James Hambleton^{**}

^{*}Northwestern University, ^{**}Northwestern University

ABSTRACT

Ploughing and cutting processes in soils are difficult and inefficient to simulate using conventional approaches, such as the finite element method and discrete element method, due to the occurrence of extremely large, potentially discontinuous plastic deformation. Recently, a numerical technique for modeling this process in sands was proposed by Kashizadeh and Hambleton [1] and Hambleton et al.[2]. This approach is based on incremental plastic analysis, which has high efficiency and stability to capture the essential physics and features of the problem. The present study refines this technique in two key respects. Firstly, a shear band with finite thickness is incorporated in the new model, thus introducing a key length scale and parameter that influences the predicted deformed shape. Secondly, and more importantly, a more sophisticated material law is implemented. The effects of hardening and softening, as well as the dilatancy and compaction within the shear band, are introduced. With the modified model, it is observed in the case of hardening (compaction) that the occurrence of multiple successive shear bands appearing at variable locations gives the impression of continuous shearing. This is markedly different from the previously predicted response in the case of softening (dilatancy). In that case, the shear bands appear at distinct locations, and the transition from one location to the next is reflected in distinct peaks in the force-displacement history [1,2]. In the more general case, where an initial hardening phase is followed by softening, only one peak force is obtained in the modified model. The computational results are compared with some preliminary experimental data obtained in the Soil-Structure and Soil-Machine Interaction Laboratory at Northwestern University, which utilizes a six-axis robot for actuation and data acquisition. [1] Kashizadeh, E., Hambleton, J.P., and Stanier, S.A. (2014). A numerical approach for modelling the ploughing process in sands. Proc. 14th International Conference of the International Association for Computer Methods and Advances in Geomechanics, Kyoto, Japan, Sept. 22-25, pp. 159-164. [2] Hambleton, J.P., Stanier, S.A., White, D.J., and Sloan SW. (2014). Modelling ploughing and cutting processes in soils. Australian Geomechanics, 49(4), 147-156.

Eigenspace-Based Characterization of Structural Uncertainty in Large-Eddy Simulation Closures

Lluís Jofre^{*}, Stefan Domino^{**}, Gianluca Iaccarino^{***}

^{*}Stanford University, ^{**}Sandia National Laboratories, ^{***}Stanford University

ABSTRACT

Large-eddy simulation (LES) has gained significant importance as a high-fidelity technique for the numerical resolution of complex turbulent flow. In comparison to direct numerical simulation (DNS), LES approaches reduce the computational cost of solving turbulent flow by removing small-scale information from the conservation equations via low-pass filtering. However, the effects of the small scales on the resolved flow field are not negligible, and therefore their contribution in the form of subgrid-scale (SGS) stresses needs to be modeled. As a consequence, the assumptions introduced in the closure formulations result in potential sources of structural uncertainty that can affect the quantities of interest (QoI). Therefore, the aim of this work is to characterize their model-form uncertainty and its impact on the QoIs by means of recently developed eigenspace-based strategies [1,2,3] that decompose the SGS stress tensor in terms of magnitude (trace), shape (eigenvalues) and orientation (eigenvectors) to facilitate the analysis. In the presentation, the strategy will be described in detail and investigations based on filtered DNS and LES of turbulent free shear flow will be discussed. [1] L. Jofre, S. P. Domino, and G. Iaccarino. A framework for characterizing structural uncertainty in large-eddy simulation closures. *Flow Turbulence and Combustion*, 1-23, 2017. [2] G. Iaccarino, A. A. Mishra, and S. Ghili. Eigenspace perturbations for uncertainty estimation of single-point turbulence closures. *Physical Review Fluids* 2, 024605. [3] M. Emory, J. Larsson, and G. Iaccarino. Modeling of structural uncertainties in Reynolds-averaged Navier-Stokes closures. *Physics of Fluids* 25, 110822, 2013.

Multimesh: Finite Element Methods on Arbitrarily Many Intersecting Meshes

August Johansson*, Mats Larson**, Anders Logg***, Benjamin Kehlet****

*Simula Research Laboratory, **Umea University, ***Chalmers University of Technology, ****Simula Research Laboratory

ABSTRACT

We will present a framework for expressing finite element methods on arbitrarily many intersecting meshes: multimesh finite element methods [1]. The framework enables the use of separate meshes to discretize parts of a computational domain, such as the components of an engine, the domains of a multiphysics problem, or solid bodies interacting under the influence of forces from surrounding fluids or other physical fields. Multimesh finite element methods are particularly well suited to problems in which the computational domain undergoes large deformations as a result of the relative motion of the separate components of a multi-body system. This is a challenging situation if one would use a single mesh. The key feature of the framework is that arbitrarily many (but finite) meshes are allowed to intersect. To make this possible, accurate quadrature rules for performing the necessary volume and boundary integrals are crucial. We will in this talk present a novel procedure to systematically construct quadrature rules with appropriate positive and negative weights using a basic result from combinatorics. Furthermore, suitable stabilization are needed to ensure an optimal method also for elements of high order. Here we follow [2]. The condition at the interface (continuity) is enforced weakly by the Nitsche method. In the presentation, we formulate the multimesh finite element method for the Poisson equation and show that it is optimal and stable. We also present numerical examples to demonstrate the optimal order convergence also for high order elements, optimal conditioning of the linear system, the numerical robustness of the formulation and implementation, as well as the applicability of the methodology. [1] Johansson, A., Larson, M.\ G., Logg, A and Kehlet, B. \textit{MultiMesh: Finite Elements on Arbitrarily Many Intersecting Meshes}. In preparation, 2017. [2] Johansson, A., Larson, M.\ G., and Logg, A. \textit{High order cut finite element methods for the Stokes problem}. Advanced Modeling and Simulation in Engineering Sciences, Vol.\ \textbf{2}, 2015.

On the Modelling of Technical Rubber Regarding Multiphysical Environmental Conditions

Michael Johlitz*, Alexander Lion**

*Institute of Mechanics, Bundeswehr University Munich, Germany, **Institute of Mechanics, Bundeswehr University Munich, Germany

ABSTRACT

In more or less all thinkable applications, polymer parts are thermomechanically loaded and exposed to different environmental media. In the most general case, the loadings are time-dependent and nonstationary and the composition of the media can change. An example is a hydraulic tube of a dredge which consists of fibre reinforced elastomers. The outer side of the tube is surrounded by water, dry or by humid air with a time-dependent temperature and its inner side is in contact with hydraulic oil whose temperature and pressure are time-dependent too. The outer side is also commonly also exposed to electromagnetic radiation like UV. The combination of all these influences leads to diffusion, dissolution, physicochemical reactions and changing material properties of the polymer. In order to simulate such phenomena with numerical methods, it is necessary to combine the theory of continuum mechanics with thermodynamics, chemistry and material transport. Due to the complex nature of these problems, it is impracticable to formulate one single model that can take all possible phenomena into account. As a good starting point, the thermomechanical balance equations are formulated for an open system which consists of only two materials: a deformable solid and a liquid. The liquid can diffuse into and out of the solid and can react with it. The diffusion is accompanied by reversible or irreversible swelling and changing material properties of the solid. Based on the structure of the balance relations and motivated by experience, a constitutive model for a suitable thermodynamic potential is developed and evaluated. For simplification, the dry solid is assumed to be nonlinearly elastic and the liquid to be non-viscous. The talk closes with the discussion of the final set of equations and some numerical simulations.

Predicting Baseplate Preheating Effects on Residual Stress and Microstructure in LENS Parts

Kyle Johnson^{*}, Theron Rodgers^{**}, Shaun Whetten^{***}, Joseph Bishop^{****}, Phillip Reu^{*****}, Kurtis Ford^{*****}, Michael Stender^{*****}, Lauren Beghini^{*****}

^{*}Sandia National Laboratories, ^{**}Sandia National Laboratories, ^{***}Sandia National Laboratories, ^{****}Sandia National Laboratories, ^{*****}Sandia National Laboratories, ^{*****}Sandia National Laboratories, ^{*****}Sandia National Laboratories, ^{*****}Sandia National Laboratories

ABSTRACT

Additive Manufacturing (AM) has many potential benefits as a manufacturing technique such as complex shape production, rapid prototyping capability, and cost reduction. However, barriers to widespread adoption still exist in the form of detrimental effects like high residual stresses and non-uniform grain microstructures. Both of these effects are highly dependent on the extreme thermal gradients and high cooling rates found in the AM process. Prediction of the resulting residual stress profile and microstructure opens up many options for process optimization in order to tailor microstructure and stress profiles. This work presents methods of predicting the thermal, residual stress, and resultant microstructure for 304L stainless steel cylinders using the Laser Engineered Net Shape (LENS) AM process. The spatial and temporal evolutions of thermal history are first modeled using the Sierra finite element code. The thermal history is then used as input into a solid mechanics simulation in which material is deposited and builds residual stress upon cooling due to thermal strain. The material constitutive behavior is modeled using the Bammann-Chiesa-Johnson temperature and history-dependent viscoplastic internal state variable model. In addition to room temperature, four additional baseplate preheat temperatures up to 450°C were then modeled to investigate the effect on residual stress. Corresponding builds were produced and relaxation-based residual-stress measurement techniques were used to compare results to those predicted by the simulations. Finally, the thermal model is used in a Potts Kinetic Monte Carlo simulation using the SPPARKS code suite. Grain formation and solid-state evolution is predicting by using a cubic lattice of sites with grain “spins” that switch to neighboring spins based on a temperature-dependent grain mobility. Rapid grain growth occurs in the high thermal gradients near the melt pool and decreases with distance. The microstructure predictions for each preheat temperature are presented, along with experimental results. Sandia National Laboratories is a multitechnology laboratory managed and operated by National Technology and Engineering Solutions of Sandia LLC, a wholly owned subsidiary of Honeywell International Inc. for the U.S. Department of Energy’s National Nuclear Security Administration under contract DE-NA0003525.

Peridynamics Modelling of Weibull-Type Behaviour in Ceramic Nuclear Fuel Pellets

Lloyd Jones*, Glyn Rossiter**, Mark Wenman***

*Imperial College London, **National Nuclear Laboratory (UK), ***Imperial College London

ABSTRACT

During operation, nuclear fuel experiences large temperature changes, with a steep thermal gradient from the hot centre to the cooler surface. Some information may be gleaned from in situ measurements at test reactors, and some from studying fuel once it is removed from service. Both of these options are expensive and limited. Computer models potentially allow for much greater insight into the processes that damage fuel, and those that allow it to function properly. Since uranium dioxide (UO₂) fuel is ceramic, its fracture behaviour should be well described by Weibull theory, also known as weakest link theory. Weibull theory posits that ceramic fracture is caused by cracks nucleating on microscopic flaws. Since these flaws are of a distribution of sizes, the fracture strength of ceramics follow a similar distribution. Peridynamics is well suited to modelling this problem due to its strengths in handling discontinuities. Randomisation of bond strengths is common in peridynamics(1). In this work, a link is made between the random properties of ceramics and the random strengths of the peridynamics bonds. The problems with simple randomisation methods are discussed, and a method for recreating Weibull characteristics in peridynamics simulations is presented. REFERENCES 1. Oterkus S, Madenci E. Peridynamic modeling of fuel pellet cracking. Eng Fract Mech. 2017 May 1;176:23–37. ?

Modeling Material Variability with Uncertainty Quantification and Machine Learning Techniques

Reese Jones^{*}, Francesco Rizzi^{**}, Jeremy Templeton^{***}, Jake Ostien^{****}, Coleman Alleman^{*****}, Moe Khalil^{*****}, Ari Frankel^{*****}

^{*}Sandia, ^{**}Sandia, ^{***}Sandia, ^{****}Sandia, ^{*****}Sandia, ^{*****}Sandia, ^{*****}Sandia

ABSTRACT

Material variability originating from heterogeneous microstructural features, such as grain and pore morphologies, can have significant effects on component behavior and creates uncertainty around performance. Current engineering material models typically do not incorporate microstructural variability explicitly, rather functional forms are chosen based on intuition and parameters are selected to reflect mean behavior. Conversely, mesoscale models that capture the microstructural physics, and inherent variability, are impractical to utilize at the engineering scale. An enhanced design methodology must be developed for materials with significant variability, such as current additively manufactured metals. To address these challenges we have developed a method based on the Embedded Uncertainty formulation of Sargsyan, Najm, and Ghanem (2015) to calibrate distributions of material parameters from high-throughput experimental data. With this method, material variability is directly associated with commonly-used material parameters using a chosen nominal model. One of the benefits of this approach is that expert knowledge can be extended to interpret the effect of (hidden) microstructure on variable mechanical response. In a complementary effort, we are also developing machine learning techniques to handle the large volume of data from high-throughput methods. The focus of this aspect of the work is on adapting common machine learning models, such as neural networks, to obey the same exact properties and symmetries as traditional constitutive models while representing features in the data in a flexible, bias-less manner. Sandia National Laboratories is a multi-mission laboratory managed and operated by National Technology and Engineering Solutions of Sandia, LLC., a wholly owned subsidiary of Honeywell International, Inc., for the U.S. Department of Energy's National Nuclear Security Administration under contract DE-NA-0003525

A Particle Based Modelling Approach for Predicting Charge Dynamics in Tumbling Ball Mills

Pär Jonsén*, Simon Larsson**, Bertil Pålsson***, Samuel Hammarberg****, Göran Lindkvist*****

*Division of Mechanics of Solid Materials, Luleå University of Technology, Sweden, **Division of Mechanics of Solid Materials, Luleå University of Technology, Sweden, ***Minerals and Metallurgical Engineering, Luleå University of Technology, Sweden, ****Division of Mechanics of Solid Materials, Luleå University of Technology, Sweden, *****Division of Mechanics of Solid Materials, Luleå University of Technology, Sweden

ABSTRACT

Wet grinding of minerals in tumbling mills is a highly important process in the mining industry. During grinding in tumbling mills, lifters submerge into the charge and create motions in the ball charge, the lifters is exposed for impacts and shear loads that will wear down the lifters. Increased loading can accelerate the wear and the lining has to be replaced. Replacing the lining is an expensive and time consuming operation that is preferred to be done within planned maintenance stops. Prediction of the charge motion and wear rate for different grinding operations and linings are therefore desirable to predict the lining life. Modelling of wet grinding in tumbling mills that include pulp fluid and its interaction with both the grinding balls and the mill structure is an interesting challenge and some different approaches have been suggested, see [1-2]. For an effective and successful prediction, the numerical model has to be able to handle the pulp fluid and its simultaneous interactions with both the ball charge and the mill structure, in a computationally efficient approach. In this work, the pulp fluids are modelled with a Lagrange based method called incompressible computational fluid dynamics, (ICFD), which gives the opportunity to model free surface flow. This method gives robustness and stability to the fluid model and is efficient as it gives possibility to use larger time steps than the conventional CFD. The ICFD solver can be coupled to other solvers as in this case the finite element method, (FEM) solver for the mill structure and the discrete element method (DEM) solver for the ball charge. The combined ICFD-DEM-FEM model can predict both charge motion and responses from the mill structure, as well as the pulp liquid flow and pressure. The numerical grinding case presented here is validated against experimentally measured driving torque signatures from an instrumented small-scale batch ball mill, see [3]. This approach opens up the possible to predict the volume of the high-energy zone and optimise lifter design and operating conditions. The ICFD solver show improve efficiency and robustness for studying tumbling mill systems and can predict the charge dynamics in such systems. [1] Jonsén, P. et al., Minerals Engineering. Accepted publication [2] Jonsén, P., Stener, J.F., Pålsson, B.I. and Häggblad, H.-Å., Min. Eng., Vol. 73, 77–84, 2015. [3] Jonsén, P. Stener, J. F. Pålsson, B. I. and Häggblad, H.-Å., Minerals and Metallurgical Processing, vol. 30, No. 4, 220-225, 2013.

Mixed Nonlinear Localization: Two-Scale Approximation of the Robin Parameter

Hinojosa Jorge*, Saavedra Karin**

*Universidad de Talca, Chile., **Universidad de Talca, Chile.

ABSTRACT

Performing nonlinear analysis of large structures at fine scale is one of the industrial challenges of our times. The post-buckling analysis of aeronautical structures is a typical example. During the structural tests for certification achieved on complete fuselages of aircraft, local buckling of the skin between stiffeners occurs. For increasing loads, these nonlinear areas can expand and provoke redistributions of stresses in the structures. For workloads usually met in service, these phenomena are reversible, the material remaining in the elastic domain. However, they can provoke stress concentrations at the bases of stiffeners and may be at the origin of local damages leading to global failure. The idea of the nonlinear localization strategy [1, 2, 3] is the treatment of the localized nonlinearities at the subdomain level, avoiding dealing with a high number of different local buckling modes, improving the robustness of the method. The other point on this strategy is to use a mixed domain decomposition scheme in order to favour neither the displacement continuity, which is a too stiff condition, nor the interface equilibrium, but a combination of both (a Robin-like condition). This mixed scheme shares similar features with continuation methods to control the algorithm convergence. In previous works [1] was shown that the decomposition choice could lead to different equilibrium paths depending on the followed “numerical” path. When a subdomain that buckles is decomposed into two subdomains its behaviour could be modified leading to a different solution. In [1] it also has been shown the convergence equilibrium of a stiffened panel when skin buckling occurs, showing a 5-lobes buckling for the non-subdivided subdomain and 4-lobes for the subdivided subdomain. Also, the equilibrium path are consequently different and the global buckling deformed shape are different as well as the global compressive behaviour, reducing the final load in 30%. In this work, we focus on the choice of dedicated Robin operator for common industrial features. A two-scale approximation [2] is implemented. [1] Hinojosa J, Allix O, Guidault P-A, Cresta P. “Domain decomposition methods with nonlinear localization for the buckling and post-buckling analyses of large structures”. *Advances in Engineering Software*. 2014;70:13-24 [2] Gendre L, Allix O, Gosselet P. “A two-scale approximation of the Schur complement and its use for non-intrusive coupling”. *International Journal for Numerical Methods in Engineering*. 2011;87(9):889-905.

Coarse-grained Twinning Characteristics for Crystal Plasticity Gleaned from Atomistic Simulations

Shailendra Joshi*

*University of Houston

ABSTRACT

We employ molecular dynamics (MD) simulations to investigate the evolution of extension twinning in magnesium single crystals under a range of multi-axial loading. The objective is to understand the evolution of variant twin volume fraction and number of twins, which enable describing the evolution of the twinning at the coarser, crystal plasticity length-scales. We investigate the role of stress state in the activation and interaction between different twin variants through signatures of nucleation, growth, coalescence and detwinning. Significant dislocation plasticity occurs on basal and prismatic $\langle a \rangle$ slip systems during and after twinning. Prior to coalescence phase, twinning volume fraction exhibits an exponentially decaying distribution. We propose phenomenological formulae for the evolution of volume fraction and number of twins, which should serve as a starting point for constructing improved coarse-grained crystal plasticity models for twinning.

Gradient Crystal Plasticity Modeling of Twin Boundary Migration Effects on Deformation Stability in Nanotwinned Metals

Shailendra Joshi*

*University of Houston

ABSTRACT

Our ongoing work is to understand the role of twin boundaries (TBs) in the deformation and failure characteristics of nanotwinned (NT) materials. To that end, we implemented a gradient crystal plasticity model within a finite element framework, which accounts for slip and slip rate gradients that are intrinsically coupled to TB migration. Using this framework, we extract intricate coupling between TB migration and twin size, load orientation and the energy barrier of dislocation-TB interactions. The resulting kinetic relation is then adopted in probing the size-dependent stress-strain responses and microstructural instabilities in polycrystalline NT materials without explicitly modeling twins.

A 3D Partitioned Coupled Variational Formulation for Multifield and Multiphase Modeling

Vaibhav Joshi^{*}, Rajeev K. Jaiman^{**}, Pardha S. Gurugubelli^{***}

^{*}National University of Singapore, ^{**}National University of Singapore, ^{***}National University of Singapore

ABSTRACT

A 3D coupled variational framework has been proposed to solve a nonlinear dynamical multifield problem of multiphase turbulent fluid flow interacting with a flexible multibody dynamic system. The proposed coupled solver is motivated by the modeling of offshore vessel-riser system which is exposed to harsh environmental conditions, viz, free-surface ocean waves and high velocity ocean currents. The dynamical response of such offshore system can be quite challenging due to strong two-way interaction of the vortex-induced vibration of riser and the wave-induced motion of vessel. We address three key numerical challenges in the proposed variational coupled formulation: (i) stable and robust coupling of incompressible turbulent flow with a system of nonlinear elastic bodies described in a co-rotated frame, (ii) a conservative and positivity preserving two-phase coupling based on the phase-field approach, and (iii) the stable integration of phase-field solver with fluid-flexible multibody solver involving moving boundaries. In the proposed formulation, the modeling of the air-water interface is accomplished by the positivity preserving variational method [1] applied to the conservative Allen-Cahn phase-field equation [2] and the turbulence is modeled by Delayed Detached Eddy Simulation [3]. The structural domain consisting of multibodies is solved using a nonlinear co-rotational method, whereas the fluid domain is solved by the Petrov-Galerkin variational method. The flow, turbulence and two-phase equations are written in an arbitrary Lagrangian-Eulerian (ALE) framework which takes into effect the moving boundaries of the structure. This multifield formulation consisting of fluid, structure, turbulence, two-phase and ALE, is solved in a partitioned iterative implicit manner. The partitioned scheme utilizes the nonlinear iterative force correction at the fluid-structure interface for stability at low structure-to-fluid mass ratios typically found in the offshore systems. We verify accuracy and robustness of our formulation on simple and reproducible academic examples and applicability to large-scale scenario of offshore vessel-riser system interacting with ocean waves and current flow. References: [1] Joshi, V. and Jaiman, R.K., A positivity preserving variational method for multi-dimensional convection-diffusion-reaction equation. *Journal of Computational Physics*, 339, Pg. 247-284 (2017). [2] Joshi, V. and Jaiman, R.K., A positivity preserving and conservative variational scheme for phase-field modeling of two-phase flows. *Journal of Computational Physics*, Accepted for publication (2018). [3] Joshi, V. and Jaiman, R.K., A variationally bounded scheme for delayed detached eddy simulation: Application to vortex-induced vibration of offshore riser. *Computers and Fluids*, 157, Pg. 84-111 (2017).

Goal-oriented Adaptivity for Micromorphic Problems Based on Duality Techniques

Xiaozhe Ju^{*}, Rolf Mahnken^{**}

^{*}University of Paderborn, ^{**}University of Paderborn

ABSTRACT

It is well-known that the classical Cauchy-Boltzmann continuum, in spite of its simplicity, has its limitations, e.g. on the simulation of strain localization phenomena or size effects. For a remedy, one may resort to the so-called generalized continuum theories, see e.g. [1] and references therein. Amongst others, we consider a class of higher order continua, namely the micromorphic continua, where the kinematics is enriched by means of a microstructure undergoing an affine micro deformation. The increasing number of the degrees of freedom in such a theory clearly motivates an application of adaptive methods. In this contribution, we present a general framework of goal-oriented adaptivity for such kind of problems. To this end, we derive a goal-oriented error estimator, leading to an effective adaptive method for controlling the discretization errors of the finite element method. For illustration, we address both elasticity and plasticity problems. For linear elastic micromorphic problems, we show the consistency of the resulted dual problem, ensuring an optimal convergence order, see [2]. For plasticity (time-dependent) problems, as shown in [3], we construct a specific dual problem tracking backwards in time to account for the accumulation of errors over time. Additionally, numerical examples are shown. References: [1] T. Dillard, S. Forest, P. Ienny: Micromorphic continuum modelling of the deformation and fracture behaviour of nickel foams, *European Journal of Mechanics A/Solids* 25, 526-549 (2006). [2] X. Ju, R. Mahnken: Goal-oriented adaptivity for linear elastic micromorphic continua based on primal and adjoint consistency analysis, *Int. J. Numer. Meth. Engng.* 112, 1017-1039 (2017). [3] M. Schmich, B. Vexler: Adaptivity with dynamic meshes for space-time finite element discretizations of parabolic equations, *SIAM J. Sci. Comput.* 30(1), 369-393 (2008).

Towards Efficient Isogeometric Matrix Assembly: Partial Tensor Decomposition and Numerical Quadrature Rules for Trimmed Domains

Bert Juettler^{*}, Angelos Mantzaflaris^{**}, Felix Scholz^{***}

^{*}Johannes Kepler University, Linz, ^{**}Johannes Kepler University, Linz, ^{***}RICAM, Austrian Academy of Sciences

ABSTRACT

The efficient assembly of matrix elements for isogeometric simulations poses many challenging problems. On the one hand, the high polynomial degrees and the large overlap of the basis functions motivates the use of new approaches to achieve computational efficiency. Among the various approaches to address this issue, we mention the use of special numerical integration techniques for spline functions [1]. On the other hand, the use of trimming operations increases the geometric complexity of the domains. Consequently, there is a need to develop suitable techniques for numerical integration. More information is provided in the survey article [2]. The talk reports on two recent developments to address these two issues. First, we describe the method of partial tensor decomposition, which allows to increase the efficiency of numerical quadrature by systematically exploiting the tensor-product structure of isogeometric discretizations, thereby reducing the dimension of the occurring integrals. Compared to the full decomposition approach, which has been established in [3], it is easier to implement, since it relies entirely on standard techniques from numerical linear algebra. It also provides a further reduction of the computational costs when used in connection with h-refinement. Second, we show how to derive special quadrature rules for trimmed domains by considering the implicit representation of the trimming curves and surfaces. This representation can be obtained via (exact or approximate) implicitization. Based on the implicit form, we use linearization to simplify the trimmed elements. Our quadrature rules combine integration over the simplified trimmed element with an integration of an auxiliary function over the linearized cutting curve or surface. The latter integration gives a correction term that restores the required order of convergence. This approach allows us to perform numerical quadrature on trimmed domains without having to compute intersections explicitly. Both methods have been implemented in the G+Smo C++ library [4].

References [1] R.R. Hiemstra, F. Calabro, D. Schillinger, T.J.R. Hughes: Optimal and reduced quadrature rules for tensor product and hierarchically refined splines in isogeometric analysis, *Comp. Meth. Appl. Mech. Engrg.* 316 (2017), 966-1004. [2] B. Marussig, T.J.R. Hughes: A Review of Trimming in Isogeometric Analysis: Challenges, Data Exchange and Simulation Aspects, *Archives of Computational Methods in Engineering*, in press (2017), doi 10.1007/s11831-017-9220-9. [3] A. Mantzaflaris, B. Juettler, B.N. Khoromskij, U. Langer: Low-rank tensor methods in Galerkin-based isogeometric analysis, *Comp. Meth. Appl. Mech. Engrg.* 316 (2017), 1062-1085. [4] Geometry + Simulation Modules, gs.jku.at/gismo.

Architected Piezoelectrics for Dynamic Control of Mechanical Wave Propagation

Abigail Juhl^{*}, Carson Willey^{**}, Vincent Chen^{***}, Phillip Buskohl^{****}

^{*}Air Force Research Laboratory, ^{**}Air Force Research Laboratory, ^{***}Air Force Research Laboratory, ^{****}Air Force Research Laboratory

ABSTRACT

Periodically repeating resonant substructures are the building blocks of many acoustic metamaterials and phononic crystals. The usefulness of a component made from such an array of unit cells is that the vibratory, or wave propagation behavior can be engineered to create frequency bands in which mechanical motion is forbidden, or highly attenuated, termed bandgaps. One major drawback of producing bandgaps through structural design is that the bandgap is fixed once the structure is decided upon leaving no opportunity for bandgap reconfiguration. In order to create a tunable bandgap structure some portion of the locally resonant unit cells must be variable and controllable by outside, preferably remote, stimulus. An approach for tuning a structure experiencing forces or practical origin and magnitude is the use of piezoelectric elements acting as electrically tunable stiffness and damper elements. Due to the difficulty in fabricating complex architectures in piezoelectric materials and integrating electrodes, research in this area has been mostly theoretical, or limited to 1D plates or patches of piezoelectrics. This talk will focus on steps made towards simulating structures augmented by the addition of shunted piezoelectric patches for the suppression of particular structural mode shapes.

Fast Spectral Solvers without Linear Reference Medium

Till Junge*

*École polytechnique fédérale de Lausanne

ABSTRACT

In the field of computational homogenization of periodic representative volume elements (RVE), over the last two decades, fast Fourier transform (FFT)-based spectral solvers have emerged as a promising alternative to the finite element method (FE). Most of these spectral methods are based on the work of Moulinec and Suquet [1] and split an RVE's mechanical response into the response of a linear reference medium and a periodic fluctuation due to heterogeneities. The main advantage of this formulation over FE is that it can be both significantly faster and have a much smaller memory-footprint. The two main problems are 1) the choice of the linear reference medium, which is typically based on heuristics, is not trivial and has a strong impact on the method's convergence (A bad choice can render the method non-convergent), and 2) a high-frequency numerical artifact (Gibbs ringing) around areas of sharp phase contrast due to non-uniformly converging Fourier series coefficients. Numerous studies have suggested mitigations to both of these problems (e.g. [2]), but they have remained substantial disadvantages compared to the more expensive, but also more robust FE. Recent work by Zeman et al. [3] proposes a new formulation for spectral solvers which dispenses with the linear reference problem and converges unconditionally. We present μ Spectre, an open implementation of this novel method and use it to show that the new approach is frequently more computationally efficient than its linear reference medium-based predecessors, converges in the presence of arbitrary phase contrast - including porosity - and eliminates or drastically reduces Gibbs ringing. [1] H. Moulinec and P. Suquet. A numerical method for computing the overall response of nonlinear composites with complex microstructure. *Computer Methods in Applied Mechanics and Engineering*, 157(1):69–94, 1998 [2] M. Kabel, T. Böhlke, and M. Schneider. Efficient fixed point and Newton-Krylov solvers for FFT-based homogenization of elasticity at large deformations. *Computational Mechanics*, 54:1497–1514, 2014 [3] J. Zeman, T. W. J. de Geus, J. Vondřejc, R. H. J. Peerlings, and M. G. D. Geers. A finite element perspective on non-linear FFT-based micromechanical simulations. *International Journal for Numerical Methods in Engineering*, 2016

IGA-BEM for Lifting Flows

PANAGIOTIS KAKLIS*, SOTIRIOS CHOULIARAS**, CONSTANTINOS POLITIS***,
ALEXANDROS-ALVERTOS GINNIS****, KONSTANTINOS KOSTAS*****

*UNIVERSITY OF STRATHCLYDE, GLASGOW (UK), **UNIVERSITY OF STRATHCLYDE, GLASGOW (UK),
TECHNOLOGICAL EDUCATIONAL INSTITUTE OF ATHENS (GR), *NATIONAL TECHNICAL UNIVERSITY
OF ATHENS (GR), *****NAZARBAYEV UNIVERSITY, ASTANA (KZ)

ABSTRACT

Combining Iso-Geometric analysis (IGA) with Boundary Element Methods (BEM) for inviscid lifting flows imposes a number of difficulties. Firstly, an IGABEM collocation scheme has to take into account the tangent-plane discontinuity occurring along the trailing edge (TE). More important, the scheme has to handle the non-linear Kutta condition, securing continuity of the normal velocity and pressure through the a-priori unknown wake, a force-free boundary surface emanating from TE. In this presentation we shall review the status of our work towards developing a pair of IGABEM collocation schemes for computing steady lifting flows around 2D and 3D bodies , e.g., hydrofoils, marine propellers; [1,2]. In the latter case, the ansatz functions are inherited from T-spline representations which are free from singularities occurring, e.g., at the tip of a propeller blade, when NURBS are used. [1] Kostas, K.V., Ginnis, A.-A. I., Politis, C.G., Kaklis, P.D, "Shape-optimization of 2D hydrofoils using an Isogeometric BEM solver", Computer-Aided Design, vol. 82, pp. 79-87, (2017). [2] Chouliaras, S.P., Kaklis, P.D., Ginnis, A.-A.I., Kostas, K.V., Politis, C.G., "An IGA-BEM method for the open-water marine propeller flow problem", International Conference on Isogeometric Analysis, Pavia (IT), 11-13 September 2017.

Topology Optimization for Shape-Memory Alloys

ZILIANG KANG*, Kai James**

*University of Illinois at Urbana-Champaign, Department of Aerospace Engineering, **University of Illinois at Urbana-Champaign, Department of Aerospace Engineering

ABSTRACT

Shape-memory alloys are a unique class of active materials, as some of them exhibit a bidirectional shape-memory effect. This effect enables shape memory alloys to deform and recover under a prescribed temperature cycle, which makes shape memory alloys an ideal material for use in self-actuated morphing applications. However, the most widely used titanium-based shape memory alloys have large electrical resistance when using joule heating from electrical current as a source of actuation. By contrast copper-based shape-memory alloys are efficient electrical conductors but they have poor deformation caused by the shape memory effect. Therefore, we present a novel method for the design of shape-memory activated structures based on a multimaterial topology optimization method, which aims to create structures that are manufacturable via 3D printing, and also exhibit desirable shape-memory effects. Assuming isotropy throughout the structure, we consider a two-dimensional stress-free problem in which we optimize the distribution of several distinct candidate materials plus a void phase to get optimal strain caused by the shape-memory effect, under a predetermined temperature cycle caused by joule heating. The thermomechanical response of the structures is modeled using nonlinear, multi-physics finite element analysis. The electrical conductivity and shape-memory transformation temperature of each finite element within the discretized structure are represented via a series of coefficient functions that implicitly define the material distribution. The design task is carried out using gradient-based optimization, with the design sensitivities obtained via adjoint sensitivity analysis. We demonstrate the proposed design framework using a series of two-dimensional thermomechanical benchmark problems. Keywords: shape-memory alloys, topology optimization, multimaterial optimization, multi-physics design

The Contact Problem of a Two Deformable Orthotropic Elastic Solids

Aysegül KUCUKSUCU*

*Unfortunately, Bursa Orhangazi University, which was the university I worked, closed after 15th July 2016 coup attempt in Turkey. So, I could not write the name of the university.

ABSTRACT

In this study, the contact problem of two deformable orthotropic solids is considered. The problem is solved by using analytical method. The Poisson's ratio of the cylinders are assumed to be constant and the contact is frictional, obeying the Coulomb law of dry friction with constant friction coefficient and the contact is assumed to be the Hertzian. In the formulation of the contact problem, it is assumed that the principal axes of orthotropy are parallel and perpendicular to the contact. Four independent engineering constants are replaced by a stiffness parameter, a stiffness ratio, a shear parameter, and an effective Poisson's ratio, Cauchy-type singular integral equations of the mixed-boundary value contact problem are prevailed using Fourier transform and solved numerically to obtain contact pressure and in-plane stress distribution. The analytical solution of the study presents correlation between contact stress and in-plane stress distributions and orthotropic material parameters, length parameters and the coefficient of friction.

Modelling and Simulation of Engineered Cementitious Composites with Shape Memory Alloy Fibres

Mieczysław KUCZMA*

*Poznan University of Technology, Institute of Structural Engineering

ABSTRACT

A thermodynamically consistent model for cementitious composites reinforced with shape memory fibres is considered. Cementitious composites, including concrete being the most used structural material, possess some inherent shortcomings. They are very weak in tension in comparison to their compressive strengths and are brittle materials with low ductility which results from development of micro-cracks. The addition of shape memory alloy fibres to cementitious composites will enhance their ductility and damping capacity. Shape memory alloys exhibit very large (up to 8-10%) recoverable strains, as a result of stress and temperature induced transformations between austenite and martensite phases. The SMA are smart materials which demonstrate unusual phenomena: the shape memory effect, and pseudoelasticity (superelasticity) with characteristic flag-shaped hysteresis loops in loading/unloading cycles. For cementitious matrix of the composite a constitutive model for concrete with progressive damage is used, whereas for the monolithic shape memory alloy fibre a constitutive model is applied that accounts for occurrence of three phases (austenite and two variants of martensite). The evolution law for volume fractions of martensite variants is derived from the second law of thermodynamics in Clausius-Duhem inequality form. From the computational point of view, the deformation process of the cementitious composite with shape memory fibres is discretized in space by the FEM and solved incrementally in time as an implicit strain driven problem (sequence of complementarity problems). Results of numerical simulations will illustrate the observed influence of shape memory alloy fiber reinforcement on the response of the cementitious composite.

Modelling and Simulation of Dynamic Fracture of Polycrystalline TiAl Alloys under High Velocity Particle Impact

Mohammad Rizviul Kabir*

*German Aerospace Center

ABSTRACT

Multi-phase polycrystalline TiAl alloys show complex fracture behaviour under high velocity particle impact (HVPI). The front-side damage and back-side crack networks are found to be microstructure sensitive, which implies that the local microstructure variations of this alloy may lead to unwanted blade failure during operation. Therefore, it is important to know how these microstructures influence crack initiation and crack propagation. To this aim in the present work a numerical modelling approach has been proposed that takes into account the microstructural statistics via polycrystal modelling and a combined damage and fracture ansatz for impact fracture behaviour. The polycrystal models were generated using Voronoi cells considering grain aspect ratio and texture. The grain boundaries were modelled applying thin cohesive layers between grains. Two types of microstructures have been studied; one with the globular grains and the other with elongated grains. The material data were obtained from detail experimental work [1]. The proposed approach allows a quantitative prediction of crack networks as observed by the experiments for different TiAl microstructures. Under dynamic impact, cracks mainly propagate through grain boundaries which have been captured using cohesive damage model. It was found that for globular grains star-shaped crack network was formed and for the elongated grains the crack extends longitudinally. The length of the crack branches can be studied for varying damage parameters at the grain boundaries. This information is useful for further analysis of fatigue life and durability of the TiAl alloy. [1] S. Gebhard, Partikel-Impact an α -Titanaluminid-Legierungen. PhD Thesis, University of Stuttgart, Germany, 2011

Phase Field Modeling of Fission Gas Bubble Growth in Nuclear Fuels

Amy Kaczmarowski^{*}, Dane Morgan^{**}, Shiva Rudraraju^{***}

^{*}Sandia National Laboratories, ^{**}University of Wisconsin Madison, ^{***}University of Wisconsin Madison

ABSTRACT

Fission gas bubble growth is critical to the behavior of nuclear fuels in fission nuclear reactors. Bubbles can induce fuel swelling that could lead to fuel-cladding contact, generate increased stresses on the cladding and lead to undesired fuel-cladding chemical interactions. In addition, the bubbles also decrease the thermal conductivity of the fuel and thus effect the performance of the nuclear reactors. In this talk, we present a novel coupled phase field formulation for tracking bubble growth and the resulting deformation of the surrounding matrix material. The model demonstrates the application of moving Neumann conditions corresponding to the gas pressure from the equation of state, and its relative advantage over other relevant interface tracking methods. Numerical examples will demonstrate the evolution of mechanics and stress concentrations in single bubble and multiple bubble growth scenarios.

NONLINEAR PHENOMENA OF SHORT AND LONG WAVELENGTH RAIL DEFECTS ON VEHICLE-TRACK INTERACTION

CHATPONG CHIENGSON*, SAKDIRAT KAEWUNRUEN*, AND AKIRA AIKAWA[†]

*School of Engineering, The University of Birmingham
52 Pritchatts Road
Edgbaston B152TT United Kingdom

Email addresses: c.chiengson@gmail.com (C. Chiengson); s.kaewunruen@bham.ac.uk (S. Kaewunruen)

[†]Railway Dynamics Division, Railway Technical Research Institute
Hikari-cho, Kokubunji
Tokyo 185-8540 Japan
Email address: aikawa.akira.11@rtri.or.jp

Key words: Dynamic interaction, Coupling vehicle-track modeling, short wavelength defect, long wavelength defect, coupled rail surface defects.

Abstract. Every day, over 100 million of train traffics are being operated globally. The first priority in train operation management is ‘*safety*’. During each operation, the dynamic interactions between vehicle and track usually impose vibrations and acoustic radiations and become a moving source of vibroacoustics along the railway network. Especially when there is imperfection of either wheel or rail, the dynamic amplification of loading conditions and reflected vibration effects on infrastructure and rolling stocks is significantly higher. In practice, imperfection of rail tracks is inevitable and can be classified into short wave length and long wave length defects. The imperfections can statistically induce high-intensity impact loadings up to 25% of *annual* track loading conditions. The short wavelength defects include high-frequency related rail surface defects such as dipped joint rails, rail squats, rolling contact fatigues (RCFs), rail gabs and crossing noses. The long wavelength defects are those associated with low frequency vibrations such as differential track settlement, mud pumping, bridge ends, stiffness transition zone, etc. Most previous studies into vehicle-track interactions were concerned only to a single one of the defect separately. This study is the world first to evaluate the coupling dynamic vehicle-track interactions over coupled short and long wavelength rail defects. The vehicle model has adopted multi degrees of freedom coupling with a discrete supported track model using Herizian contact theory. This paper highlights the nonlinear dynamic impact load factors experienced by railway track components due to wheel/rail contacts. The insight into the nonlinear phenomena will enable predictive track maintenance and risk-based track inspection planning adaptation to enhance public safety and reduce unplanned maintenance costs.

1 INTRODUCTION

There are two types of modern railway tracks suitable for various purposes of railway operations. A selection of trackform (ballasted vs ballastedless track) is commonly based on capital cost, lifecycle cost, asset management and operations (e.g. train speeds, axle load, and ride quality). For over 200 years, railway tracks have evolved. Considering the whole life cycle values, modern ballasted railway tracks have become the most efficient and effective infrastructure for the railway industry operating *below* 250 km/h of train speed for over centuries. The ballasted tracks have been tailored and optimised over and over; and they are often used in light rail tracks, metro networks, suburban rail network and intercity rail lines since they are relatively inexpensive and quite superior in terms of maintainability and constructability [1-4]. In contrast, ballastless tracks or concrete slab tracks are often utilised for highspeed rail lines (with train speed over 250 km/h) to reduce maintenance costs due to highspeed related swift degradation of traditional track components (e.g. accelerated densification and dilation of ballast, poor ride comfort due to differential track settlement/stiffness, ground-borne noise and vibration problems, etc.) [1, 5-9]. In practice, railway maintainers and operators are suffering from many of rail surface defects that lead to increased maintenance (either planned or unplanned), operational downtime and delay, more frequent monitoring and track patrol, and possibly the broken rails leading to train derailments [10-12].

Commonly, urban rail operators experience social problems of ground-borne, structure-borne noise and vibration induced by short and long wavelength rail defects. For instance, extra level of noise excited by rail squats (short wavelength type) was observed by residents near Woolloomooloo viaduct in Sydney, Australia [13-14]. Reportedly, the cost of rail replacement due to rail squats and studs has become a major part of the whole track maintenance cost in European countries [15]. Note that the rail squats and studs are typically classified as the growth of any cracks that has grown longitudinally through the subsurface. The subsurface lamination crack later results in a depression of rail surface sometimes called ‘dark spot’ [16]. There are two initiation types of the rail surface defects. Such rail defects are commonly referred to as ‘squats’ when they were initiated from rolling contact fatigue (RCF) cracks, and as ‘studs’ when they were associated with white etching layer due to wheel slips or excessive tractive effort [16].

Moreover, with heavier and faster trains, the dynamic load transferring on to track and its components such rails, sleepers, ballast and formations is higher and amplified by the traffic speeds and rail surface defects. These dynamic impact loading conditions often damage the track support and cause initial differential settlement and plastic deformation. The track issue does not stop here. Such the plastic deformation and initial differential settlement further form and couple with short wavelength defects (if any) to exponentially aggravate the dynamic loading condition [17-19]. Therefore, it is highly important to understand the coupled dynamic effect of rail defects on the rail infrastructure so that rail operators and maintainers can develop suitable cost-effective strategies for operations and maintenance. An example of strategies is to carry out preventative track maintenance (such as re-tamping, re-grinding and ballast cleaning when early sign of damage is inspected). In many regional railways (such as freight services), speed restrictions have been adopted to delay the maintenance regime when the rail defects exist. Note that these strategies are often called ‘Base Operating Conditions (BOCs)’ in railway industry practices. The BOCs have been developed from internal R&D activities and extensive empirical experience in

the rail industry over the centuries. On this ground, the established railway authorities of course do not lack of expertise and best practices. However, they might lose sight of nonlinear combined effects and might lead to inefficient and ineffective track maintenance if such effects are not being investigated or inspected timely. This current study will fill this gap by establishing a new insight into nonlinear phenomena of combined short and long wavelength rail defects so that the *safety-critical* track inspection regime can be effectively adapted.

Initially, the detailed modelling of rail track dynamic and wheel-rail interaction was studied in 1992 while D-track program for dynamic simulation also have been created by Cai for his PhD's thesis of Queen's University in Canada [20]. Afterward, Iwnick has done a benchmark, which was called Manchester Benchmarks in 1998 [21]. In 2005; Steffens [22] has adopted the parameter of Manchester Benchmarks to compare performance of vary dynamic simulation programs and also developed the user-interface of D-track. On the other hand, D-track had still an issue of lower result than others and then the owner has revised the program after this benchmark. Subsequently, Leong has done the Benchmark II with the revised version of D-Track in 2007 [23].

In this present study, the dynamic simulation concept by Cai [20] has been adopted as seen in Figure 1 since the track model has included Timoshenko beam theory for rail and sleepers, which enable a more accurate behaviours of tracks. Note that rail cross section and sleeper pre-stressing are among the key influences on shear and rotational rigidities of Timoshenko beam behaviors in numerical modelling of railway tracks [24-27]. The irregularity of wheel and rail will cause higher dynamic impact force that the design condition level or serviceability limit state. The exceeding magnitude of the force generated by wheel and rail irregularities will damage track components and impair ride quality [28]. This study thus is the first to present the wheel-rail dynamic forces over both single defects and coupled defects. The dynamic amplification factor will be highlighted to identify the effect of train speeds. The scope of this study will be focused on ballasted railway tracks. The commonly used 106t freight wagons will be modeled and coupled with the discrete supported track model. The track model will be based on a standard rail gauge (1.435m). The outcome of this study will help railway organization in improving the predictive maintenance and inspection regimes.

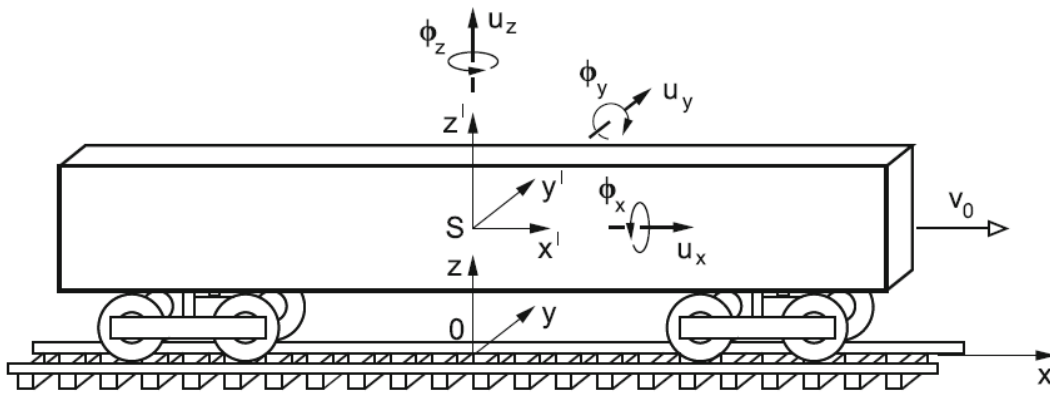


Figure 1: Coupling vehicle-track model [22]

2 DYNAMIC BEHAVIOURS

To design a ballasted railway track, it is important to assure safety and satisfy all the requirements of various stakeholders. The variety of dynamic loads from vehicle-track interaction and different environments make the rail infrastructure design highly complicated.

2.1 Dynamic wheel load

The dynamic loads induced by the vehicle moving on track structure will be considered as quasi-static force (equivalent to a static load times a factor) when the loads contain typically less than 10 Hz and is used to study behaviour of vehicle and design of the track foundation. In many cases, the perfect rail and wheel surfaces will be used to calculate of contact force and a factor (dynamic factor) to apply to the static wheel load and give a result for quasi static wheel load. The low-frequency load from a vehicle will apply to track geometry at a few cycles per second (up to 20 Hz).

In Australia, the most common method for calculation is presented by the Railway of Australia (ROA) manual or called “A Review of Track Design Procedures” or the “Blue Book”. The Dynamic Impact Factor (DIF) from this method ignores vertical track elasticity. The dynamic vertical wheel load (PD) is expressed empirically as a function of the static wheel load (P_s) where \emptyset is the Dynamic impact factor (always ≥ 1). For example, $PD = \emptyset P_s$.

2.2 Eisenmann' Classical Formula

The Eisenmann formula is the most common method used for calculation the dynamic impact factor, used in a general track design. At the same time, the Eisenmann formula is modified by ROA and is used internationally. The Eisenmann formula (Eq. 1) and modified Eisenmann (Eq. 2) are shown respectively.

$$P_D = (1 + \delta\eta t) \cdot P_s \quad (1)$$

$$P_D = (1 + \delta\beta\eta t) \cdot P_s \quad (2)$$

where δ = Track condition factor; η = Speed factor, where $\eta = 1$ for speed (v) < 60 km/h and $\eta = 1 + [(v-60)/140]$ for $v > 60$ km/h; t = Upper confidence level (UCL) factor; $\beta = 1$ for loaded vehicles; and 2 for unloaded vehicles.

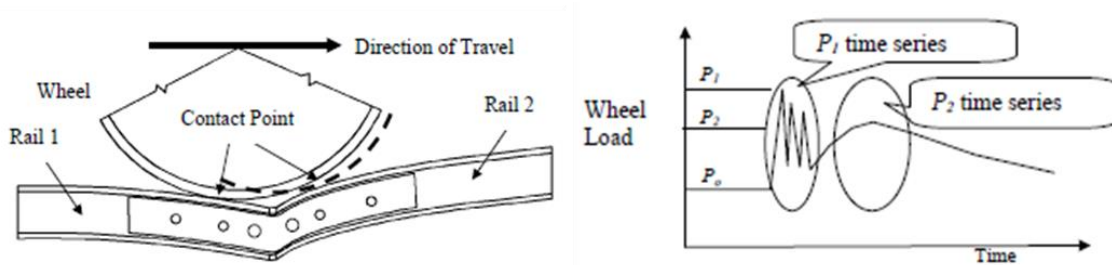


Figure 2: Impact force of wheel/rail contact at dipped rail joint [13]

2.3 Wheel trajectory over short wavelength rail defect

Dipped rail joint is termed to define the sum of an angle of dipped trajectory between each rail and the horizontal (in milli-radians). The two components of this angle consist of permanent deformation of the rail ends and the deflection of the joint under load. Jenkins et al. [29] described that the wheel travelling across a dipped rail joint creates the force peak as P1 and P2. The shape of the irregularity and characteristics of the vehicle create impact loading which the force at dipped joint increases almost linearly with the speed and angle of the dip. When the trains travelling at high speed approach a rail joint, the wheel lose will lose contact with the railhead of rail and land on the connected rail that generate the high dynamic impact force as illustrated in Figure 2.

The P1 force is a very high frequency ($\cong 200$ Hz -1000Hz) that is less than 0.5 millisecond in length (0.25 - 0.5 millisecond after crossing the joint). The compression of contact zone between wheel and rail create the inertia of rail and sleepers which does not directly transform to ballast or subgrade settlement. However, it has a significant effect on wheel/rail contact force. The P2 is occurred at a lower frequency range ($\cong 50$ Hz -200Hz) than P1 occurring much later at typically 6 – 8 milliseconds. The unsprung mass and the rail/sleeper mass are moving down together influencing the compression of the ballast below the sleeper. P2 forces therefore increase the contact stresses and also induce the loads on sleepers and ballast. P2 force will be considered mostly by the track design engineer. Jenkins et al. [29] provided a method of calculation as follows:

$$P_1 = P_0 + (2\alpha v) \cdot \sqrt{\frac{k_H m_e}{1 + \frac{m_e}{m_u}}} \quad (3)$$

$$P_2 = P_0 + (2\alpha v) \cdot \sqrt{\frac{M_u}{M_u + M_t}} \times \left[1 - \frac{\pi C_t}{4\sqrt{K_t(M_u + M_t)}} \right] \times \sqrt{K_t M_u} \quad (4)$$

where: P_1 and P_2 = dynamic rail force (kN); P_0 = vehicle static single wheel load (kN); k_H = a chord stiffness to the Hertzian contact stiffness; m_e = the effective track mass (kg); m_u = the vehicle unsprung mass (kg); 2α = Total joint angle (rad); v = speed of vehicle (m/s); K_t = equivalent track stiffness (MN/m); M_t = equivalent track mass (kg); and C_t = Equivalent track damping (kNs/m).

2.4 Track settlement

Track settlement can cause the train passing the track with higher dynamic load increasing high-frequency variations to the ballast and subgrade. It will then cause non-elastic or plastic deformations with permanent setting. In normal situation, the track will generally not return to the same position but to the very close point (accumulated deformation). As time passes, all of non-elastic deformations will create a new track position and this phenomenon becomes

differential track settlement. The track alignment and surface level of track also change due to the accumulated non-elastic deformations. The irregularity of track will increase low-frequency oscillation of vehicle. However, the track settlement often takes place at the transition area to a bridge. In addition, the quality of ballast, sub-ballast and the subgrade are also the factor inducing permanent deformation [30-31].

Track settlements typically consist of two phases. The first phase is after tamping that the gap between ballast particles is reduced quickly and so this layer is consolidated. The second phase is slower while the densification and inelastic behaviour of the ballast and subgrade materials are concerned as the two majors parameters influencing the ballast settlement that are the deviatoric stress, vibrations, degradation and subgrade stiffness. The empirical settlement equation for the substructure is shown below. It does only consider the ballast settlement not including subgrade settlement:

$$Z_{iN} = Z_{i0} + f(\log N, \sigma_{be}, I_{dyn}, I_{dec}, I_{Esub}) \quad (5)$$

This equation describes the settlement of ballast below the sleeper I where: Z_{i0} = the given void amplitude; N = Number of load cycles; σ_{be} = the vertical equivalent stress in the ballast layer; I_{dyn} = the dynamic factor; I_{dec} = the degradation factor; and I_{Esub} = the subgrade stiffness factor.

3 COUPLING VEHICLE-TRACK MODELLING

The track model (D-Track) is simulated on Winkler foundation principal which only cross-section of track dynamic responses is considered symmetrically. Rail and sleeper were represented on elastic beam of either the Timoshenko type. The sleepers also support the rail as discrete rigid masses. Free-body diagram of track model are shown in the Figure 3(a) where $P(t)$ is a moving wheel force at constant speed (v). Figure 3 (b) represents the force from rail to sleeper through the rail seat (i^{th}) and reaction force $k_s z_i(y, t)$ per unit length.

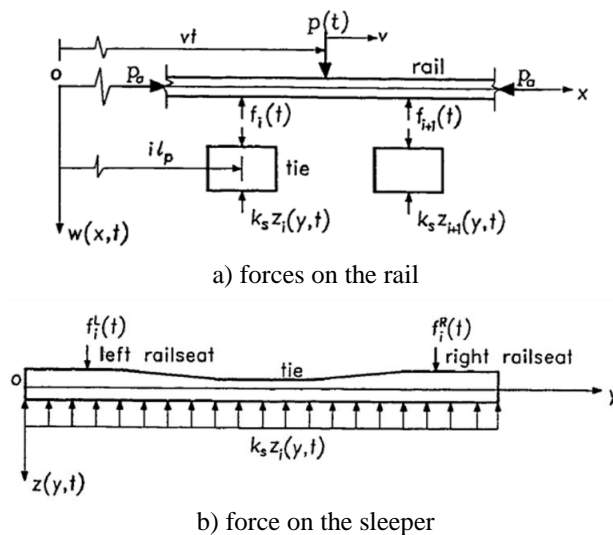


Figure 3: Free-body diagram of track model [22]

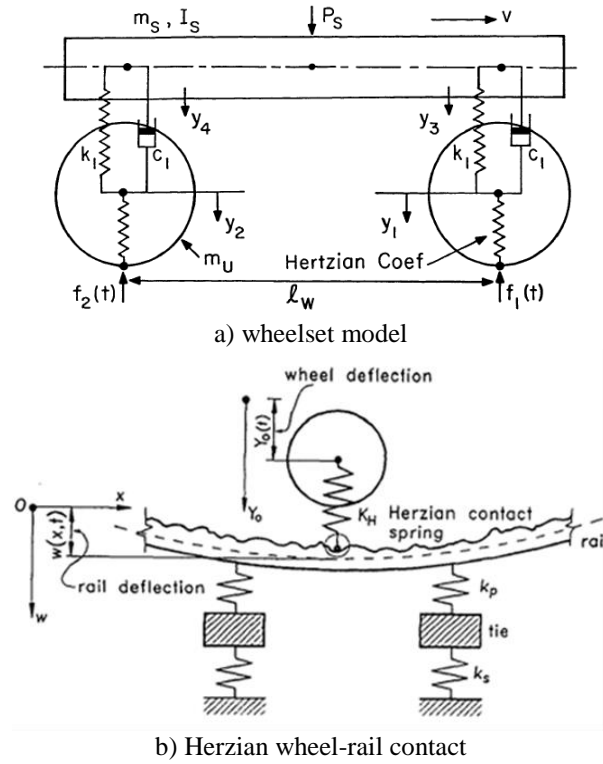


Figure 4: Free-body diagram of vehicle-track model [22]

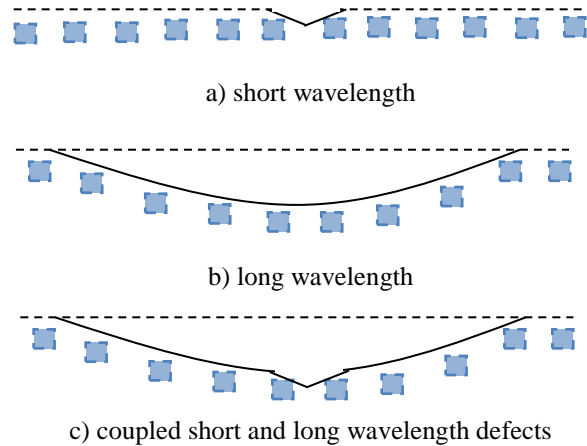


Figure 5: Rail irregularity models

The wheelset model in this modelling consists of a four-degree of freedom which include of one bogie with two-axle, rail and track. The wheelset model uses the unsprung masses (m_u) and the sideframe mass (m_s, I_s) to calculate on one rail through the primary suspension (k_1, c_1) as shown in Figure 4(a). The components of vehicles are demonstrated as a spring load by using Hertzian contact model. Moreover, the equations of motion in this model used the principles of Newton's law and beam vibration to apply. Integration between wheelset and track equations can be calculated by the non-linear Hertzian wheel-rail interaction model as illustrated in Figure 4 (b). The D-Track model has been benchmarked by [23, 24] in order to assess the accuracy and

verify the precision of numerical results. D-Track is thus adopted for this study. Rail surface profile irregularities can be estimated as inverse half-sinusoidal curve as shown in Figure 5(a). For track settlement, the study focus on a long span defect (such as large mud pumping tracks) with a wavelength of 10m as shown in Figure 5(b).

4 RESULTS AND DISCUSSIONS

The numerical simulations have been carried out using 106t freight wagon with wheel radius of 0.46m and Hertzian spring constant of $0.87 \times 10^{11} \text{ N/m}^{3/2}$. The dynamic wheel/rail contact forces can be seen in Figure 6.

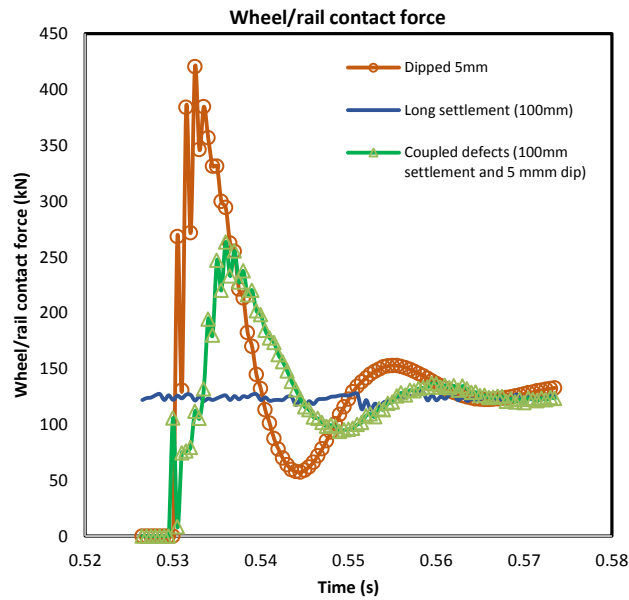


Figure 6: Wheel/rail contact force

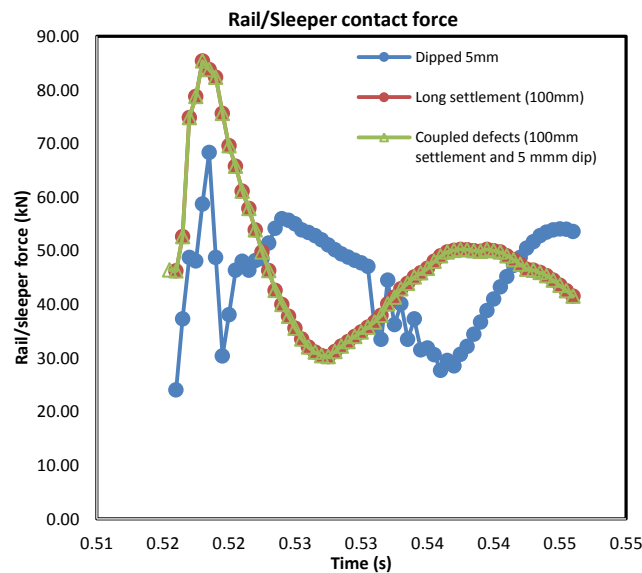


Figure7: Rail/sleeper contact force

Short wavelength defects have significant effects on the wheel/rail contact force in comparison with long wavelength defects. In contrast, surprisingly, it is apparent that long wavelength defect plays higher influence on the dynamic railseat loads (rail/sleeper contact) as shown in Figure 7.

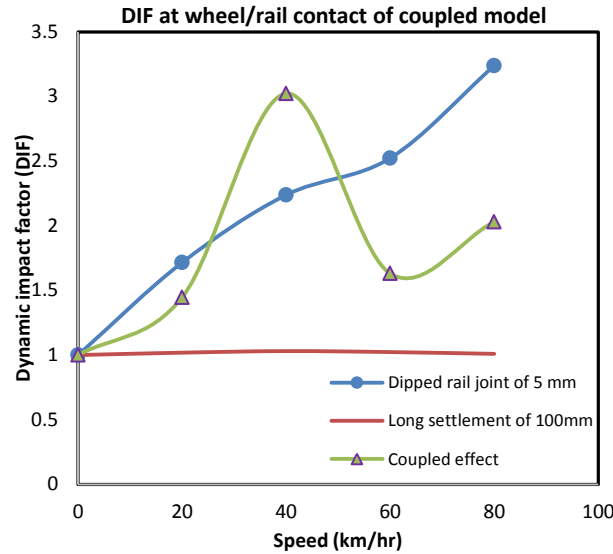


Figure 8: DIF at wheel/rail contact force

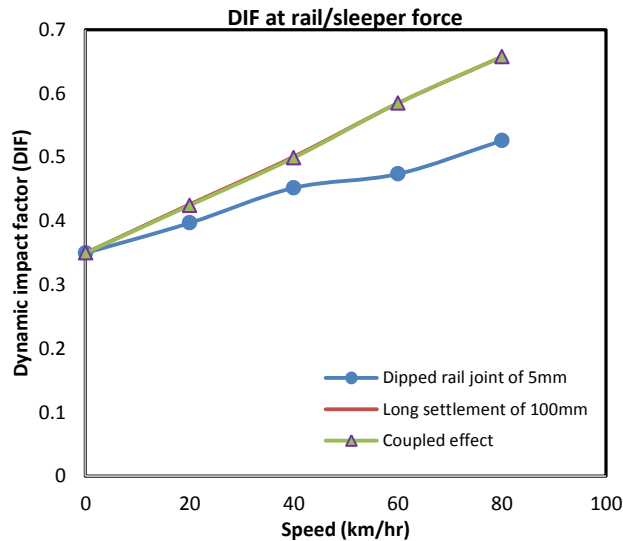


Figure 9: DIF at rail/sleeper contact force

The dynamic impact factor (DIF) can be evaluated from dynamic over static wheel force ratio. Figures 8 and 9 demonstrate the coupling dynamic vehicle-track interaction on contact forces and railseat loading conditions. It is clear that the coupling wheel/rail contact force is nonlinear (Figure 8) whilst rather linear relationships can be observed on the load sharing (Figure 9). It is clear that the individual short rail surface defects influence significantly the high frequency force at wheel/rail contact. However, the coupled short and long wavelength defects does not seem to play a strong influence on wheel/rail contact, but instead influence how the load is distribute on the sleepers.

5 CONCLUSION

This paper presents the nonlinear dynamic interactions between vehicle and track, which can cause vibrations and acoustic radiations to railway neighborhood. The nonlinear effects of coupled short and long wavelength rail defects on vehicle-track interaction have been highlighted. It is the first to evaluate the coupling dynamic vehicle-track interactions over coupled short and long wavelength rail defects. The results show that the coupled effect plays a key role on magnifying the rail/sleeper contact forces (railseat loads). The insight implies that sleepers will experience excessive dynamic loads and they can deteriorate and abrade at a relatively faster rate. More results on parametric effects of short and long wavelength as well as the effect of defect severity will appear elsewhere in the near future. This understanding into the nonlinear phenomena will help track engineers to manage and operate infrastructure assets more effectively.

ACKNOWLEDGEMENT

The second author wishes to thank the Australian Academy of Science and Japan Society for the Promotion of Sciences for his Invitation Research Fellowship (Long term), Grant No. JSPS-L15701 at the Railway Technical Research Institute and The University of Tokyo, Tokyo Japan. The authors wish to gratefully acknowledge the financial support from European Commission for H2020-MSCA-RISE Project No. 691135 “RISEN: Rail Infrastructure Systems Engineering Network,” which enables a global research network that tackles the grand challenges [32] in railway infrastructure resilience and advanced sensing under extreme events (www.risen2rail.eu). This project is also financially sponsored by H2020-S2R Project No. 730849 “S-CODE: Switch and Crossing Optimal Design and Evaluation”.

REFERENCES

- [1] Esveld, C., *Modern Railway Track*, The Netherlands MRT Press, (2001).
- [2] Remennikov, A.M., Kaewunruen, S., A review on loading conditions for railway track structures due to wheel and rail vertical interactions. *Structural Control and Health Monitoring*, 15(2): 207-234, (2008).
- [3] Thompson, D.J., *Railway Noise and Vibration*. Elsevier, Amsterdam, The Netherlands, (2010).
- [4] Indraratna, B, Salim, W and Rujikiatkamjorn, C, *Advanced Rail Geotechnology - Ballasted Track*, The Netherlands: CRC Press/Balkema, (2011).
- [5] Griffin, D.W.P., Mirza, O., Kwok, K., and Kaewunruen, S., “Composite slabs for railway construction and maintenance: A mechanistic review”, *IES Journal of Civil and Structural Engineering*, 7(4): 243-262, (2014).
- [6] Griffin, D.W.P., Mirza, O., Kwok, K., and Kaewunruen, S., “Finite element modelling of modular precast composites for railway track support structure: A battle to save Sydney Harbour Bridge”, *Australian Journal of Structural Engineering* 16 (2), 150-168, (2014).

- [7] Binti Sa'adin, S. L., Kaewunruen, S., and Jaroszweski, D. "Risks of Climate Change with Respect to the Singapore-Malaysia High Speed Rail System". *Climate* 4, 65, (2016).
- [8] Binti Sa'adin, S. L., Kaewunruen, S., Jaroszweski, D., "Operational readiness for climate change of Malaysia high-speed rail", *Proceedings of the Institution of Civil Engineers – Transport*, 169 (5), 308-320, (2016).
- [9] Binti Sa'adin, S. L., Kaewunruen, S., and Jaroszweski, D. Heavy rainfall and flood vulnerability of Singapore-Malaysia high speed rail system. *Australian Journal of Civil Engineering*, 14(2): 123-131, (2016). doi:10.1080/14488353.2017.1336895
- [10] Kaewunruen, S., Sussman, J. M., and Einstein, H. H. "Strategic framework to achieve carbon-efficient construction and maintenance of railway infrastructure systems." *Frontiers in Environmental Sciences*, 3:6, (2015), doi:10.3389/fenvs.2015.00006
- [11] Setsobhonkul S, Kaewunruen S and Sussman JM, "Lifecycle assessments of railway bridge transitions exposed to extreme climate events". *Frontiers in Built Environments*, 3:35, (2017), doi: 10.3389/fbuil.2017.00035
- [12] Kaewunruen, S., Ishida, M., Marich, S., "Dynamic wheel–rail interaction over rail squat defects", *Acoustics Australia*, 43(1): 97-107, (2015).
- [13] Sun, Y.Q., Cole, C., McClanachan, M., Wilson, A., Kaewunruen, S. and Kerr, M.B., "Rail short-wavelength irregularity identification based on wheel-rail impact response measurements and simulations", *Proceedings of the 9th International Heavy Haul Conference*, June 21-23, Shanghai, China, (2009).
- [14] Kaewunruen, S. and Remennikov, A.M., "Current state of practice in railway track vibration isolation: an Australian overview", *Australian Journal of Civil Engineering* 14 (1), 63-71, (2016).
- [15] Tuler, M.V., Kaewunruen, S., "Life cycle analysis of mitigation methodologies for railway rolling noise and groundbourne vibration", *Journal of Environmental Management* 191, 75-82, (2017).
- [16] Wilson, A., Kerr, M., Marich, S., and Kaewunruen, S. "Wheel/rail conditions and squat development on moderately curved tracks". in: *CORE 2012: Global Perspectives; Conference on railway engineering*, 10-12 September 2012, Brisbane, Australia. Barton, A.C.T.: Engineers Australia, 2012: 223-230, (2012).
- [17] Kaewunruen, S. and Remennikov, A.M., "Dynamic properties of railway track and its components: Recent finding and future research directions." *Insight - Non-Destructive Testing and Condition Monitoring*, 52(1): 20-22, (2010).
- [18] Kaewunruen, S., Ishida, M., "Field monitoring of rail squats using 3D ultrasonic mapping technique," *Journal of the Canadian Institute for Non-Destructive Evaluation*, 35(6): 5-11, (2014) (invited).
- [19] Kaewunruen, S., Remennikov, A.M., "Field trials for dynamic characteristics of railway track and its components using impact excitation technique," *NDT & E International* 40 (7), 510-519, (2007).
- [20] Cai, Z. Modelling of rail track dynamics and wheel/rail interaction. PhD Theses, Queen's University, Canada, (1992).

- [21] Iwnicki, S. Manchester Benchmarks for Rail Vehicle Simulation, *Vehicle System Dynamics*, 30 (3-4): 295-313, (1998).
- [22] Steffens, D. M. Identification and development of a model of railway track dynamic behavior. MEng Thesis, Queensland University of Technology, Australia (2005).
- [23] Leong, J. Development of Limit State Design of Methodology for Railway Track. MEng Thesis, Queensland University of Technology, Australia (2007).
- [24] Kaewunruen, S. and Remennikov, A.M., "Experimental determination of the effect of wet/dry ballast on dynamic sleeper/ballast interaction." *ASTM J of Testing and Evaluation*, 36(4): 412-415, (2008).
- [25] Kaewunruen, S. and Remennikov, A.M., "Sensitivity analysis of free vibration characteristics of an in-situ railway concrete sleeper to variations of rail pad parameters." *Journal of Sound and Vibration*, 298(1-2), 453-461, (2006).
- [26] Kaewunruen, S. and Remennikov, A.M., "Experimental determination of the effect of wet/dry ballast on dynamic sleeper/ballast interaction." *ASTM J of Testing and Evaluation*, 36(4): 412-415, (2008).
- [27] Remennikov, A. and Kaewunruen, S., "Determination of dynamic properties of rail pads using instrumented hammer impact technique," *Acoustics Australia*, 33(2): 63-67. (2005).
- [28] Kaewunruen, S. Lewandowski, T., Chamniprasart, K. "Dynamic responses of interspersed railway tracks to moving train loads", *International Journal of Structural Stability and Dynamics*, 18(1): 1850011, (2018).
- [29] Jenkins, H.H., Stephenson, J.E., Clayton, G.A. The effect of track and vehicle parameters on wheel/rail vertical dynamic force. *Rail engineering Journal*, 2-16, 1974.
- [30] Kaewunruen, S., Minoura, S., Papaelias, M., Remennikov, A.M., [Asymmetrical influences on nonlinear dynamics of railway turnout bearers](#), The 24th International Congress on Sound and Vibration, London, U.K., 23-27 July (2017).
- [31] Kaewunruen, S., Ngamkhanong, C., Janeliukstis, R., You, R., Influences of surface abrasions on dynamic behaviours of railway concrete sleepers, The 24th International Congress on Sound and Vibration, London, U.K., 23-27 July (2017).
- [32] Kaewunruen, S., Sussman, J. M., and Matsumoto, A. Grand challenges in transportation and transit systems. *Frontiers in Built Environments*, 2:4, (2016) doi:10.3389/fbuil.2016.00004

Phase Field Material Point Method for Impact Induced Fracture

Emmanouil Kakouris*, Savvas Triantafyllou**

*Centre for Structural Engineering and Informatics, The University of Nottingham, **Centre for Structural Engineering and Informatics, The University of Nottingham

ABSTRACT

Predictive modelling of impact induced fracture is of extreme interest to the engineering community as it pertains to various applications, e.g., projectile impact and rocking of deformable medium. Dynamic failure mechanisms in brittle solids are governed by complex fracture phenomena such as crack initiation, multiple crack branching, or crack arrest. Mesh distortion errors that are inevitable in large displacement FEA hinder the fidelity of dynamic impact simulations where the deformability of the contact surfaces significantly affects the resulting contact forces and corresponding failure surfaces. Material point methods provide high fidelity solutions for large displacement and large deformation problems [1]. Rather than relying on the notion of a deforming mesh, material point methods introduce a particle based approximation for the deformable body that move within a non-deforming mesh. This introduces a considerable advantage as opposed to purely particle based methods as the continuum approximation is preserved thus releasing the requirement for high particle densities. To this point, material point implementations for brittle fracture have proven efficient in tackling quasi-static crack propagation in terms of computational simplicity and robustness. Phase Field Material Point Method (PF-MPM) has been successfully introduced [2] for quasi-static brittle fracture problems. In this, the phase field is resolved at material points and mapped onto grid nodes where the phase field governing equations are solved. PF-MPM has further been extended to account for surface energy densities with strongly anisotropy [3]. In this work, the PF-MPM is originally extended to account for dynamic brittle fracture within an anisotropic regime. Furthermore, a frictional contact framework is adopted to accurately capture the intriguing effects governing impact fracture problems. The phase field governing equations are solved independently for each contact body employing a predictor-corrector algorithm. The merits of the proposed scheme in tackling impact dynamics are investigated through a set of benchmark cases. [1] Sulsky D., Chen Z. and Schreyer H.L. (1994). A particle method for history-dependent materials. *Computer Methods in Applied Mechanics and Engineering*, 118 (1-2), pp. 179-196 [2] Kakouris, E. G., and Triantafyllou, S. P. (2017) Phase-Field Material Point Method for Brittle Fracture, *International Journal for Numerical Methods in Engineering* 112 (12), pp. 1750 -1776. [3] Kakouris, E.G., and Triantafyllou, S. P., (2017). Material point method for crack propagation in anisotropic media: a phase field approach, *Archive of Applied Mechanics*, DOI: <https://doi.org/10.1007/s00419>.

Particle-based Flow Simulations for Complicated Viscous Fluid

Kazuhiko Kakuda^{*}, Wataru Okaniwa^{**}, Ituki Nishino^{***}, Shinichiro Miura^{****}

^{*}Nihon University, ^{**}Nihon University, ^{***}Nihon University, ^{****}Nihon University

ABSTRACT

The numerical simulations of three-dimensional (3D) viscous fluid flows including multi-scale/physics and moving boundary/obstacle are indispensable in science and engineering fields from a practical point of view. Numerical difficulties have been experienced in the solution of the Navier-Stokes equations at higher Reynolds numbers. In particular, it is well known that the centered finite difference and standard Galerkin finite element formulations lead to spurious oscillatory solutions for flow problem at high Reynolds number regimes. To overcome such spurious oscillations, various upwind/upstream-based schemes have been significantly presented by many researchers in both frameworks. On the other hand, there are various gridless/meshless-based particle methods, such as SPH (Smoothed Particle Hydrodynamics) method[1], MPS (Moving Particle Semi-implicit) one[2], and PFEM (Particle Finite Element Method)[3] to simulate effectively such complicated flow problems. Recently, the physics-based computer simulations on the GPU (Graphics Processing Units) have increasingly become an important strategy for solving efficiently various problems, such as fluid dynamics, solid dynamics, and so forth. The purpose of this paper is to present the application of the GPU-based SPH/MPS method to 3D complicated fluid flow problems, namely the dam-breaking flow problem and the droplet-falling with surface tension. As the surface tension model, we adopt the inter-particle potential force with a potential coefficient. The problems of the dam-breaking flow and the droplet-falling with surface tension have been widely used to verify the applicability and validity of the numerical methods. The GPU-implementation consists mainly of the search for neighboring particles in the local grid cell using hash function for both methods. The MPS scheme is also applied to solve implicitly the Poisson equation with respect to the pressure fields by using GPU-based SCG (Scaled Conjugate Gradient) method. The workability and validity of the present approaches are compared with experimental data and other numerical ones. References [1] Gingold, R.A. and Monaghan, J.J., Smoothed Particle Hydrodynamics: Theory and Application to Non-spherical Stars, Mon. Not. R. astr. Soc., Vol.181, 1977, pp.375-389, 1977. [2] Koshizuka, S. and Oka, Y., Moving-particle Semi-implicit Method for Fragmentation of Incompressible Fluid, Nucl. Sci. Eng., Vol.123, pp.421-434, 1996. [3] Idelsohn, S.R., Onate, E. and Pin, F.Del, The Particle Finite Element Method: A Powerful Tool to Solve Incompressible Flows with Free-surfaces and Breaking Waves, Int. J. Numer. Meth. Engng., Vol.61, pp.964-989, 2004.

Data Analytics for Mining Process-Structure-Property Linkages for Hierarchical Materials

Surya Kalidindi*

*Georgia Tech

ABSTRACT

A majority of the materials employed in advanced technologies exhibit hierarchical internal structures with rich details at multiple length and/or structure scales (spanning from atomic to macroscale). Collectively, these features of the material internal structure are here referred to as the material structure, and constitute the central consideration in the development of new/improved hierarchical materials. Although the core connections between the material's structure, its evolution through various manufacturing processes, and its macroscale properties (or performance characteristics) in service are widely acknowledged to exist, establishing this fundamental knowledge base has proven effort-intensive, slow, and very expensive for most material systems being explored for advanced technology applications. The main impediment arises from lack of a broadly accepted framework for a rigorous quantification of the material's structure, and objective (automated) identification of the salient features that control the properties of interest. This presentation focuses on the development of data science algorithms and computationally efficient protocols capable of mining the essential linkages from large ensembles of materials datasets (both experimental and modeling), and building robust knowledge systems that can be readily accessed, searched, and shared by the broader community. The methods employed in this novel framework are based on digital representation of material's hierarchical internal structure, rigorous quantification of the material structure using n-point spatial correlations, objective (data-driven) dimensionality reduction of the material structure representation using data science approaches (e.g., principal component analyses), and formulation of reliable and robust process-structure-property linkages using various machine learning techniques. This new framework is illustrated through a number of case studies.

Modeling and Simulation of Magnetorheological Elastomers Filled with Magnetically Hard Particles

Karl Alexander Kalina*, Jörg Brummund**, Philipp Metsch***, Markus Kästner****

*Institute of Solid Mechanics, TU Dresden, Germany, **Institute of Solid Mechanics, TU Dresden, Germany,
Institute of Solid Mechanics, TU Dresden, Germany, *Institute of Solid Mechanics, TU Dresden, Germany

ABSTRACT

Magnetorheological elastomers (MREs) are a class of active composites which can alter their macroscopic properties if an external magnetic field is applied. Typically, these materials consist of a polymer matrix filled with micron-sized magnetically soft particles such as carbonyl iron. Another type of fillers are magnetically hard particles as NdFeB which exhibit significant magnetic hystereses effects. MREs with this kind of composition have features as field dependent coercivity and remanent magnetization which are typical for conventional magnetically hard materials. Recently published experiments [1, 2] indicate a significant influence of the effective hysteresis loops on the matrix stiffness in such MREs. In this contribution we investigate the microstructural causes of this effect by the use of a computational modeling approach. The analyzed MREs are described by a microscopic model [2], i. e. the heterogeneous microstructure consisting of magnetizable inclusions embedded into a polymer matrix is taken into account explicitly. The constitutive models for the magnetizable particles and the polymer matrix are formulated separately. In order to describe the irreversible magnetic behavior of the NdFeB particles a thermodynamically consistent vector-hysteresis model based on [3] is used. The governing equations of the coupled magneto-mechanical problem are solved by a nonlinear finite element formulation [2]. Therein, the evolution equation of the hysteresis model is solved by means of an implicit integration scheme. In order to connect the macroscopic and the microscopic magnetic and mechanical quantities, a suitable computational homogenization scheme is applied [2]. The presented simulations indicate a rotation of the particles within the soft polymer matrix material. Due to this effect, the effective hystereses of the MRE are significantly smaller than the hystereses of pure NdFeB. The presented computational results are qualitatively in good agreement with the experiments discussed in [1]. References [1] J. M. Linke, D. Yu. Borin, S. Odenbach, First-order reversal curve analysis of magnetoactive elastomers, *RSC Adv.*, 6, pp. 100407-100416, (2016). [2] K. A. Kalina, J. Brummund, P. Metsch, M. Kästner, D. Yu. Borin, J. M. Linke, S. Odenbach, Modeling of magnetic hystereses in soft MREs filled with NdFeB particles, *Smart Mater. Struct.*, 26, pp. 105019-105031, (2017). [3] A. Bergqvist, Magnetic vector hysteresis model with dry friction-like pinning, *Physica B*, 233, pp. 342-347 (1997).

Efficient and Reliable Simulation of Failure of Reinforced Concrete Structures under Impact (RTG 2250: Mineral-bonded Composites for Enhanced Structural Impact Safety)

Michael Kaliske^{*}, Viktor Mechtcherine^{**}, Aurel Qina^{***}, Alexander Fuchs^{****}

^{*}Institute for Structural Analysis, TU Dresden, ^{**}Institute of Construction Materials, TU Dresden, ^{***}Institute for Structural Analysis, TU Dresden, ^{****}Institute for Structural Analysis, TU Dresden

ABSTRACT

Existing concrete or reinforced concrete structures feature, as a rule, a relatively low resistance to various sorts of impact loading, such as shock, collision or explosion. The primary goal of Research Training Group 2250 (RTG 2250) is to bring substantial improvements in the impact-resistance of existing buildings by applying thin layers of strengthening material. By using innovative, mineral-bonded composites, public safety and the reliability of vitally important infrastructure should be significantly enhanced. The scientific basis to be developed will additionally enable to build new, impact-resistant structures economically and ecologically. In order to elaborate a deep understanding of the specific structural behavior under impact loading, theoretical and numerical models extending far beyond current knowledge have to be developed. An important role is played by the simulation of the bond between the fibers and the matrix under very high strain rates as well as the development of relevant constitutive laws. For a realistic description of the macroscopic structural failure of strengthened concrete structures under impact by an extended microplane model and by the discrete implementation of local damage by the eigenstrain approach, a large number of detail developments (material description at impact with microplane model for reinforced concrete and reinforcement layer, effective nonlocal description of extended inelasticity, formulation of eigenstrain for inelasticity) needs to be taken into account. Moreover, challenges in the combination of the methods (e.g. description of the wave propagation for the selected modelling) have to be overcome. The contribution introduces the RTG generally and elaborates on the simulation of structural behavior of this class of structures and loading cases.

Investigation of the Properties of Dislocation Structures by XRD and HR-EBSD Experiments Coupled with 2D DDD Simulations

Szilvia Kalácska^{*}, Péter Dusán Ispánovity^{**}, István Groma^{***}

^{*}Eötvös Loránd University (ELTE), ^{**}Eötvös Loránd University (ELTE), ^{***}Eötvös Loránd University (ELTE)

ABSTRACT

X-ray diffraction (XRD) is a well-established experimental method for determining the dislocation density values in materials science, that helped developing basic models of crystal plasticity. To evaluate the X-ray line profiles measured on bulk samples the so called “strain broadening” setup is applied and the asymptotic properties of the X-ray intensity distributions are investigated with the momentum method [1]. The recently developed technique for investigating the statistical properties of dislocation structures by high resolution electron backscatter diffraction (HR-EBSD) enables us to calculate and examine the internal stress distribution in deformed crystalline materials. The application of the momentum method to HR-EBSD is a novel way to determine the total dislocation density [2]. The comparison of the two methods will be shown in the presentation to corroborate the results measured on copper single crystals. To explore the relevance and potential of the HR-EBSD-based evaluation method a 2D discrete dislocation dynamics simulation is applied [3]. The model establishes the understanding of the unexpected behaviour observed in the calculated HR-EBSD moments. It is also shown that the dislocation arrangement does not affect the tail of the probability distribution of the internal stress. The availability of spatially resolved stress maps opens further perspectives for the evaluation of correlation properties and mesoscale parameters of heterogeneous dislocation structures. [1] I. Groma, X-ray line broadening due to an inhomogeneous dislocation distribution. *Physical Review B* 57, 7535 (1998). [2] Sz. Kalácska, I. Groma, A. Borbély and P.D. Ispánovity, Comparison of the dislocation density obtained by HR-EBSD and X-ray profile analysis. *Applied Physics Letters* 110, 091912 (2017). [3] P.D. Ispánovity, I. Groma, G. Györgyi, F.F. Csikor and D. Weygand, Submicron plasticity: yield stress, dislocation avalanches, and velocity distribution. *Physical Review Letters* 105, 085503 (2010).

Variational Sea Ice Mechanics in the Regional Arctic System Model

Samy Kamal^{*}, Andrew Roberts^{**}, Elizabeth Hunke^{***}, William Lipscomb^{****}, Wieslaw Maslowski^{*****}

^{*}Naval Postgraduate School, ^{**}Naval Postgraduate School, ^{***}Los Alamos National Laboratory, ^{****}National Center or Atmospheric Research, ^{*****}Naval Postgraduate School

ABSTRACT

Since the 1970s, large-scale sea ice models have approximated compressive ice strength and mechanical thickening using empirical functions that modify the areal ice thickness distribution, $g(h)$, under horizontal compression and shear. Yet, observational and modeling research since the 1980s has demonstrated that these empirical functions are flawed: compressive strength approximations that parameterize constant frictional loss relative to potential energy gain during ridging may perform no better than simple and unphysical estimates of ice strength. $g(h)$ is itself a scale-dependent representation of sea ice thickness that should not be applied to models with resolution less than 10 km and it is missing the critical dimension of macro-porosity associated with fracture and fragmentation of individual ridges just a few meters across. Most importantly, empirical redistribution of $g(h)$ overlooks the principle of stationary action as applied to non-conservative systems. Without considering the variational principles of ice mechanics, it is difficult to derive well-posed physics to represent ridging within the grid cells or elements of Eulerian or Lagrangian sea ice models, respectively, for horizontal resolutions of less than 1km to more than 50km. This work presents the first known application of variational sea ice ridging to a basin-scale coupled model – the Regional Arctic System Model (RASM) – that rectifies the problems highlighted above. Ridging statistics are computed by coarse-graining the degrees of freedom associated with individual ridge formation. Equations governing sea ice momentum and mass conservation have been derived using variational principles upwards from the scale of individual ridges, and therefore do not require empirical functions for sub-grid redistribution of sea ice thickness in our 9km model. Instead, the principle of virtual work determines the prevalence, shape, and porosity of ridges of different sizes that in turn ascertain the compressive strength of the pack within each model grid cell. This is achieved using an expanded state-space for the thickness distribution that includes macro-porosity. Results presented are objectively assessed against previous RASM simulations using both isotropic (EVP) and anisotropic (EAP) rheologies using freeboard skill scores obtained with an ICESat emulator.

Fast Level Set Topology Optimization by Means of a Sparse Hierarchical Data Structure

Sandilya Kambampati^{*}, Carolina Jauregui^{**}, Ken Museth^{***}, Hyunsun Alica Kim^{****}

^{*}University of California San Diego, ^{**}University of California San Diego, ^{***}Voxel Tech Inc., ^{****}University of California San Diego

ABSTRACT

The application of level set methods for topology optimization offers several advantages, such as being able to handle complex topological changes and having an implicit definition of the dynamic boundary. However, a common criticism is that they tend to suffer in terms of computational efficiency when compared to the traditional topology optimization based on material distribution. We note that common level set topology optimization methods utilize dense (vs sparse) grid data structures, which significantly limits the memory efficiency and hence the available resolution of the dynamic interface. Another common numerical technique in the level set methods is the Fast Marching Method, which is an inherently a serial algorithm with a time complexity of $O(N \log N)$ and does not easily parallelize. In this paper we demonstrate how the efficiency of level set methods for topology optimization can be substantially improved by employing the sparse data structure VDB [1], which is a hierarchical data structure that shares some of the performance characteristics of B+ trees traditionally used for high-performance file systems and relation data bases. As such VDB offers fast grid data access (average $O(1)$) and high grid resolutions with low memory footprints. We also employ more modern algorithms like the Fast Sweeping Methods, that has recently been parallelized for sparse grids and offers a superior time complexity of (N) [2]. Specifically we present benchmark studies of level set topology optimization. This includes discussions of the computational times and memory footprints of topology optimization based on the sparse VDB data structure as well as a reference implementation based on a dense grid. The efficiency and scalability of advection schemes used to update the level set method such as the inverse square distance interpolation, Fast Marching Method, and Fast Sweeping Method, will also be discussed. References: [1] K. Museth, "VDB: High-Resolution Sparse Volumes With Dynamic Topology". ACM Transactions on Graphics, Volume 32, Issue 3, Pages 27:1-27:22, June 2013. [2] K. Museth, "Novel Algorithm for Sparse and Parallel Fast Sweeping: Efficient Computation of Sparse Signed Distance Fields, ACM SIGGRAPH 2017 Talks, Pages 74:1--74:2, July 2017.

Crack Progress Analysis of Plain Concrete Using Prescribed Displacement Based on Hybrid-type Penalty Method

Atsushi Kambayashi*, Norio Takeuchi**, Yoshihiro Fujiwara***, Tadahiko Shiomi****

*Graduate School of Engineering and Design, Hosei University, **Graduate School of Engineering and Design, Hosei University, ***Mind Inc., ****Mind Inc.

ABSTRACT

Crack progress analysis of plain concrete using prescribed displacement based on hybrid-type penalty method Atsushi Kambayashi / Norio Takeuchi Graduate School of Engineering and Design, Hosei University Yoshihiro Fujiwara / Tadahiko Shiomi Mind Inc. We studied a new function of a crack opening utilizing the hybrid-type penalty method (HPM) developed by Takeuchi [1] to analyze the strength characteristics of the structural members of reinforced concrete structures. In fracture analysis, the measurement of crack mouth opening displacement (CMOD) is important because it is directly related to the fracture energy, G_f . The HPM can accurately assess the CMOD in discrete cracks at intersection boundaries between the subdomains of the HPM, thereby reflecting accurate fracture energy of the discrete cracks. Using the HPM, we simulated experimental tests conducted for a concrete structure and showed good qualitative and quantitative agreements between the simulated and the experimental results. [2]. Although most of analyses were conducted using load control method and satisfactory results were obtained only the region from continua to discontinua, deformation control method used to obtain further analysis such as softening phenomena. In this work, we introduced a new function for a prescribed displacement control with the HPM. This involved introducing an algorithm for the prescribed displacement in the rmin method [3], which is an incremental load method. The rmin method can accurately track tensile cracking and compressive failure in concrete structure. To validate the accuracy of the displacement control analysis with the new function, we conducted several analyses using uniform triangular mesh and Delaunay triangular mesh. And , we also simulated the three-point bending test for notched beams, which is a standard test of the plain concrete. Finally, we discuss the load-displacement relationship between the experimental tests and numerical results. References [1] N. Takeuchi, Elasto-plastic analysis in soil and rock mechanics by using hybrid-type penalty method, Proc. of International Conference dedicated to the 95th Anniversary of Academician Nagush Kh. Arutyunyan, Institute of Mechanics National Academy of Sciences of Armenia, Yerevan-2007, pp.492–496. [2] Y. Fujiwara, N. Takeuchi, T. Shiomi, and A. Kambayashi, Discrete Crack Modeling of RC Structure Using Hybrid-Type Penalty Method, Int. J. Aerospace and Lightweight Structures, 3(2), 2013, pp. 263–275. [3] Y. Yamada, Y., N. Yoshimura and T. Sakurai, Plastic stress–strain matrix and its application for the solution of elasto-plastic problem by a finite element method, Int. J. Mechanical Sciences, 10, 1968, pp. 343–354.

Partially-Averaged Navier-Stokes Formulation of Two-Layer Turbulence Model

Chetna Kamble*, Sharath Girimaji**

*Texas A&M; University, **Texas A&M; University

ABSTRACT

Seamless transition between the Reynolds-Averaged Navier-Stokes (RANS) and Direct Numerical Simulation (DNS) is achieved by the Partially-Averaged Navier-Stokes (PANS) bridging strategy. In PANS, the physical resolution is controlled by filter widths which quantify the extent of partial averaging via the unresolved to total kinetic energy and dissipation ratios. This scale-resolving simulation method offers resolution of large scale turbulent structures at reasonable computational costs. In the present study, the PANS closure modeling is applied to a two-layer turbulence model which couples the standard k-epsilon model in the outer layer with a one-equation model in the near wall region. In RANS context, this turbulence model exhibits a superior near wall behavior compared to other near wall treatments. The PANS modified two-layer model aims to improve upon the near wall predictions by resolving the unsteady flow features of turbulence. The outer region in the PANS two-layer turbulence model is a PANS modified k-epsilon turbulence model, whereas, the inner layer comprises of a PANS modified one equation model of unresolved kinetic energy. The unresolved eddy viscosity and dissipation in the inner layer are specified in terms of unresolved kinetic energy and length scales. The effectiveness of the proposed PANS modified two-layer turbulence model is studied by a detailed comparison with a PANS k-omega turbulence model for a three-dimensional Channel flow for frictional Reynolds number, $Re_{\tau} = 180$ and $Re_{\tau} = 590$. The proposed model is assessed on the performance in reproducing the mean statistics, the turbulent flow quantities and the resolution of the turbulent flow structures. The PANS modified two-layer model displays improved accuracy in capturing the turbulent flow physics and thereby solidifying the effectiveness of the two-layer PANS scheme in the near wall region.

Isogeometric Analysis Using FEniCS

David Kamensky*, Yuri Bazilevs**

*University of California, San Diego, **University of California, San Diego

ABSTRACT

This talk introduces recent work on implementing extraction-based isogeometric analysis (IGA) [1] on top of the FEniCS open source finite element (FE) software project [2], while retaining many of the powerful features that make the latter an attractive analysis platform. We hopefully dispel the sentiment that FEniCS and IGA present conflicting visions for automating numerical solution of partial differential equations (PDEs). Several aspects of our implementation differ from the algorithms for Bézier extraction put forward by Borden et al. [3] in 2011, and our alternative approach may be useful for retrofitting other FE codes as well. A collection of object-oriented abstractions separate PDE solution from generation of extraction operators and thereby permit the use of a wide variety of spline types. We cover, as illustrative examples, the discretization of various PDEs that benefit from IGA and the use of T-splines imported from CAD software. We conclude by discussing possible future directions, and welcome input from the FE(niCS) and IGA communities. References: [1] <https://doi.org/10.1016/j.cma.2004.10.008> [2] <https://doi.org/10.1007/978-3-642-23099-8> [3] <https://doi.org/10.1002/nme.2968>

High-Order Meshes for the 3D Simulation of Electro-Magnetic-Induced Fusion

Kazem Kamran^{*}, Mark S. Shephard^{**}, Cameron W. Smith^{***}, Tzanio Kolev^{****}, Syun'ichi Shiraiwa^{*****}, Mark L. Stowell^{*****}

^{*}Rensselaer Polytechnic Institute, ^{**}Rensselaer Polytechnic Institute, ^{***}Rensselaer Polytechnic Institute, ^{****}Lawrence Livermore National Laboratory, ^{*****}Massachusetts Institute of Technology, ^{*****}Lawrence Livermore National Laboratory

ABSTRACT

Fusion reactors have sophisticated detailed 3D geometries, especially in the SOL/antenna region, which their inclusion is crucial for a reliable simulation of fusion process. In this work, a fully automated parallel mesh infrastructure, PUMI1, that generates adapted curved meshes classified on the CAD model, is integrated in to a state-of-the-art plasma simulation solver2. This 3D edge plasma wave solver is implemented in the MFEM3 open source scalable C++ library that supports elements of different type i.e. H1 to L2 and order. To demonstrate the effect of the high-order geometry representation, a realistic detailed 3D CAD model of the antenna placed in the fusion chamber is chosen and the effect of the adapted curve mesh on the quality of the RF wave solution is studied. [1] D.A. Ibanez, E.S. Seol, C.W. Smith and M.S. Shephard, "PUMI: Parallel unstructured mesh infrastructure." ACM Transactions on Mathematical Software (TOMS) 42.3 (2016): 17. [2] S. Shiraiwa, J.C. Wright, P.T. Bonoli, T. Kolev, and M. Stowell, "RF wave simulation for cold edge plasmas using the MFEM library." EPJ Web of Conferences. Vol. 157. EDP Sciences, 2017. [3] <http://ceed.exascaleproject.org/mfem/>

Efficient Numerical Solution of the Hydraulic Fracture Problem for Planar Cracks

Sergey Kanaun*

*Tecnológico de Monterrey, México

ABSTRACT

Efficient Numerical Solution of the Hydraulic Fracture Problem for Planar Cracks S. Kanaun Tecnológico de Monterrey, México An infinite elastic medium with a planar crack is considered. The crack is subjected to pressure of fluid injected inside the crack at a point of its surface. Description of the crack growth is based on the lubrication equation (local balance of the injected fluid and the crack volume), the elasticity equation for crack opening caused by fluid pressure, Poiseuille equation related the fluid flux with crack opening and the pressure gradient, and the criterion of crack propagation of linear fracture mechanics. The crack growth is simulated by a series of discrete steps. Each step consists of three stages: increasing the crack volume by a constant crack size, crack jump to a new size defined by the fracture criterion, and filling the new crack configuration by the fluid presented in the crack [1]. The problem is ill-posed and requires specific methods for numerical solution. The proposed method is based on an appropriate class of approximating functions for fluid pressure distributions on the crack surface and the theory of solution of ill-posed problems. It is shown that for small fluid viscosity, the three-parameter model of pressure distribution on the crack surface can be used [2]. The model allows one to satisfy the condition at the point of fluid injection, the balance equation of the volume of injected fluid and the crack volume, and fracture criterion at the crack edge. The analysis of evolution of the crack boundary is based on an original method of fast numerical solution of the integral equations of the crack problem of elasticity. The method allows constructing the crack boundary at discrete time moments for media with varying elastic properties and fracture toughness [3]. Evolution of the crack boundary in the process of fluid injection, time dependence of pressure distributions and crack openings are presented for examples of hydraulic fracture crack growth in layered heterogeneous media. [1] Kanaun S, Discrete model of hydraulic fracture crack propagation in homogeneous isotropic elastic media, International Journal of Engineering Sciences,10:1-14, 2017. [2] Kanaun S, Hydraulic fracture crack propagation in an elastic medium with varying fracture toughness, International Journal of Engineering Sciences,120:15-30, 2017. [3] Kanaun S, Markov A, Discrete and Three-Parameter Models of Hydraulic Fracture Crack Growth, WSEAS Transactions on Applied and Theoretical Mechanics, 12:147-156, 2017.

Constraints Handling in Multi-Objective Evolutionary Algorithm by Two-Stage Non-Dominated Sorting Using Direct/ Neighborhood Mating for Multi-Disciplinary Optimization

Masahiro Kanazaki^{*}, Minami Miyakawa^{**}, Hiroyuki Sato^{***}

^{*}Tokyo Metropolitan University, ^{**}Hosei University, ^{***}The University of Electro-Communications

ABSTRACT

A non-dominated sorting and dieted mating (TNSDM) is an operator to handle the constraint in evolutionary algorithms and authors have shown its applicability to real-world multi-disciplinary design problems with difficult-constraints. In original two-stage non-dominated sorting and dieted mating, parents are selected by non-dominated sorting based on constraint violation values and objective functions sequentially. NSGA-II with original TNSDM has achieved better performance than the well-known existent method. Extreme Pareto solutions, which are the end of the Pareto front and are equivalent to the optimum solution of the single objective problem, could not be acquired well only by the TNSDM. To overcome this problem, we developed a new method by introducing local mating in identical ranks in the TNSDM. We propose the expansion of TNSDM by adding neighborhood mating in identical ranks, and this is decided by non-dominated sorting. The proposed constrained handling method is employed in NSGA-II. We investigated the proposed approach by solving a test function and hybrid rocket design problem, a real-world problem. Each problem has six constraints. These problems are solved by the constrained NSGA-II, which is based on the simple penalty method, and the original TNSDM based NSGA-II. According to investigations, the proposed approach and TNSDM based optimizations acquire better Pareto front than the simple penalty based method does. In addition, the proposed method can acquire not only compromised solutions but also extreme Pareto solutions in good agreement with the TNSDM method. Comparing convergence history via hypervolume, the best performance also can be observed by the proposed method.

Dynamic Behaviour of Different Pulmonary Monocusp Valve Designs

Harkamaljot Kandail*, Marcelle Uiterwijk**, Jolanda Kluin***, Frans van de Vosse****, Carlijn Bouten*****, Anthal Smits*****, Sandra Loerakker*****

*Eindhoven University of Technology, Netherlands, **Academic Medical Centre, University of Amsterdam, Netherlands, ***Academic Medical Centre, University of Amsterdam, Netherlands, ****Eindhoven University of Technology, Netherlands, *****Eindhoven University of Technology, Netherlands, *****Eindhoven University of Technology, Netherlands

ABSTRACT

Purpose: Right ventricular outflow tract in children with congenital heart diseases is often reconstructed with a transannular patch and a monocusp valve. However, there are no set standards for the monocusp valve design and as such, these designs vary from clinic to clinic. The aim of this investigation is to propose an optimal pulmonary monocusp valve design with physiologic opening and closing behaviour, good coaptation and minimal aortic regurgitation. **Methods:** Dynamics of a pulmonary monocusp valve which is currently under pre-clinical evaluation within 1Valve program, hereinafter referred to as PMV-1 valve, were simulated using finite element (FE) methods to optimise the monocusp design. A second hypothetical valve design was then proposed to overcome the limitations of PMV-1 valve and its dynamic behaviour was also simulated using FE methods. The native pulmonary artery was modelled as an anisotropic material using a Holzapfel-Gasser-Ogden model while the monocusp valves and transannular patches were modelled as isotropic Neo-Hookean hyperelastic materials. Valve dynamics were simulated by imposing the pressure difference between the right ventricle and the pulmonary artery on the ventricular side of the respective monocusp valve designs and all simulations were performed for three cardiac cycles. **Results:** Dynamics of PMV-1 valve from the FE model were compared with dynamics from an ex-vivo heart model and a good agreement between the numerical and experimental results was observed. PMV-1 valve was implanted in the pulmonary artery in the closed position and its free-edge was prone to folding when the monocusp valve opened during systole. During diastole, only an edge-based coaptation between the free-edge of PMV-1 valve and pulmonary artery was observed. Unlike the initial design, the proposed design of the second monocusp valve is meant to be implanted in the open position. FE results for the second monocusp valve predicted that the free-edge of this valve design does not fold during the entire cardiac cycle. Also, better coaptation was seen for this valve design as the coaptation length between the free-edge and pulmonary artery was approximately 2.1 mm. **Conclusion and future work:** FE results from this investigation suggest that it is desirable to implant the pulmonary monocusp valve in the open instead of the closed position to achieve physiologic valve dynamics. This is an ongoing research project and fluid-structure interaction simulations are currently being performed to quantify aortic regurgitation and the risk of thrombosis associated with each valve design.

Spectral Element Solutions for Heat Transfer Augmentation

Kento Kaneko*, Paul Fischer**

*UCIC, **UCIC

ABSTRACT

We consider spectral element based simulations of thermal transport to study heat transfer augmentation in pipe flow with wire coil inserts, which induce turbulence and a rotational mode. We compare our numerical results with available experimental data for three distinct coil geometries and several Reynolds numbers. Several additional simulations were run to determine the change in the Nusselt number when the rotational mode is completely removed. Three cases have geometries with equally-spaced tori whose distance corresponds to the pitch in the coil cases and a fourth case has a meandering coil with no net helicity. We present Nusselt number vs. Reynolds number results for all of these cases and analyze the effectiveness of gradient-diffusion based models for prediction of mean thermal transport in these configurations.

Modeling of Locked Particle Behavior in Magnetic Separation Using DEM and FEM

Masanori Kaneko^{*}, Yuki Tsunazawa^{**}, Takuma Tokoro^{***}, Giuseppe Granata^{****}, Chiharu Tokoro^{*****}

^{*}Graduate School of Creative Science and Engineering, Waseda University, ^{**}National Institute of Advanced Industrial Science and Technology, ^{***}Graduate School of Creative Science and Engineering, Waseda University, ^{****}Faculty of Science and Engineering, Waseda University, ^{*****}Faculty of Science and Engineering, Waseda University

ABSTRACT

Magnetic separation is one of the mineral processing technology. Its technology utilizes magnetic susceptibility of different substances to separate them. In conventional magnetic separation studies, a particle was assumed as a free particle composed of one component. On the other hand, in actual operations, feed particles usually consist of locked particles composed of some components. The efficiency of magnetic separation was affected by locked particles. To achieve high efficiency, it is necessary that locked particles are appropriately controlled in the magnetic separation. However, there has not been little knowledge about the magnetic force acting on locked particles and the behavior of the locked particles in magnetic separators. Therefore, it is important to model the magnetic force acting on locked particles in magnetic field. This study modeled the magnetic force acting on locked particles by the magnetic field analysis. This study assumed that locked particles composed of two components with different magnetic susceptibilities. The finite element method (FEM) was used to calculate the magnetic force acting on a locked particle. According to the FEM analysis on the different composition ratio of locked particles, it was introduced that the model formula of the relationship between the magnetic susceptibility and the composition ratio of locked particles in the magnetic field. The FEM analysis suggested that this model formula depended on distribution of components within particles. Based on the FEM analysis results, magnetic separation incorporating locked particles model was simulated. In this simulation, the behavior of locked particles was calculated by the discrete element method (DEM), and the magnetic field in a magnetic separator was calculated by the FEM. Using this simulation, it was analyzed that the relationship between the applied magnetic field and the efficiency of magnetic separation. Furthermore, the simulation result was compared with the experimental results. In the case of particles consisting of only free particles, the simulation results qualitatively agreed with the experimental result. However, there was some quantitative difference between the simulation and experimental results. In the case of particles containing locked particles, the difference between the simulation and experimental results became smaller. As a result, it was suggested that the behavior of locked particles could be appropriately simulated by the locked particle model.

Development of a Stable Structure-fluid-electrostatic Analysis System

Shigeki Kaneko^{*}, Tomonori Yamada^{**}, Shinobu Yoshimura^{***}, Giwon Hong^{****}, Naoto Mitsume^{*****}

^{*}The University of Tokyo, ^{**}The University of Tokyo, ^{***}The University of Tokyo, ^{****}The University of Tokyo, ^{*****}The University of Tokyo

ABSTRACT

Fluid-structure interaction (FSI) is an important phenomenon in engineering because it often causes unexpected mechanical vibration and sometimes brings the structural destruction. Numerical simulation is effective for the research on the control of FSI because numerical simulation is proper for parametric study and can cut the cost of experiments. In our previous study [1], we proposed FSI analysis with active control, where both fluid and structural analyses were performed in detail, but specific models of actuators and sensors were not considered. It was assumed that the mass and volume of the actuators and sensors could be neglected and arbitrary control force could be given. It is necessary to introduce a specific model in order to put the previous analysis to practical use. For reducing the vibration caused by FSI, piezoelectric actuators and sensors are widely used because it has excellent electromechanical properties. For examples, flutter phenomenon which causes undesired vibration to the aircraft is diminished by using piezoelectric materials. In this study, we implement the model of piezoelectric materials to our previous system. In order to analyze strictly all the physics of piezoelectric materials, the host structure, and the surrounding fluid, we develop a general-purpose structure-fluid-electrostatic analysis system by integrating electrostatic analysis and partitioned iterative FSI analysis of the previous system. To find an optimal balance between accuracy and computational cost, we propose and verify three coupling approaches. In the first approach, structure-fluid-electrostatic analysis is split into electrostatic analysis and FSI analysis. The second approach splits into fluid analysis and structure-electrostatic analysis. The structure-electrostatic is solved by monolithic approach. In the third approach, electrostatic analysis is inserted into FSI iteration. In the present study, we investigate the stability of each system by simulating various control of FSI, and we compare three systems in the viewpoint of stability. References [1] S.Kaneko, G.Hong, N.Mitsume, T.Yamada, S.Yoshimura, Partitioned-coupling FSI analysis with active control, Computational Mechanics, Vol.60, Nos.4, pp.549-558, 2017.

A Study on Accuracy Improvement of Decomposed Surrogate Model with Random Samples for High Dimension Problem

Kyeonghwan Kang*, Ikjin Lee**

*KAIST (Korea Advanced Institute of Science and Technology), **KAIST (Korea Advanced Institute of Science and Technology)

ABSTRACT

Surrogate model has been widely used to solve engineering problems with heavy computation, and there have been many studies to generate surrogate model with limited samples due to the computation cost. However, practical surrogate model generating method dealing with high dimensional design space are still challenging. Among the approaches dealing with high dimensional surrogate model, decomposition is one of popular approach for its efficiency and flexibility. There are various approaches of decomposition, but accurate decomposition results require to generate samples not in the decomposed design space. Furthermore, there can exist random samples in practice engineering problem, but these samples are also difficult to be utilized in the decomposed surrogate model. In this study, the potential accuracy improvement method using the samples not in the decomposed design space is proposed. Previously unused samples are considered for approximation using Gaussian process and variable screening, and virtual samples are generated to improve the accuracy of each decomposed surrogate model. Numerical examples and engineering problem are used to check the performance of proposed method, and it is shown that the accuracy of the surrogate model is surely improved with random samples.

Topology Optimization with Manufacturing-related Constraints Expressed by Domain Integral of Level Set Function

Zhan Kang^{*}, Yaguang Wang^{**}, Pai Liu^{***}

^{*}Dalian University of Technology, China, ^{**}Dalian University of Technology, China, ^{***}Dalian University of Technology, China

ABSTRACT

In topology optimization of continuum structures, certain geometrical constraints and interfacial behaviors, as well as uncertain geometrical manufacturing imperfections, are often of great importance to ensure the manufacturability or integrity of the structures. This talk will present some of our new developments on the study of manufacturing-related topology optimization problems in the level set function-based framework. The level set, as an implicit geometrical model, offers a natural description of shape and topology evolution and thus can be suitably used for representation of some geometrical constraints [1]. In our previous work, we proposed a unified integral-form constraint to avoid overlaps, to control the distances among the embedded objects in the topology optimization of multi-component structures [2]. Now we extend the idea of integral-form constraints to expression of other geometrical constraints to ensure the manufacturability of topology optimization results, including the casting constraint, the overhang angle constraint in additive manufacturing, and the shell-infill configuration description. All these constraints have explicit domain-integral forms, facilitating their sensitivity analysis with respect to shape variations. This approach inherits the properties of easier geometric information extraction of the implicit level set model. We also propose a level set-based implicit description model for modeling geometrical uncertainties arising from manufacturing errors. In particular, this model can mimic topological defects often exhibited by micro-size fabrication, which may result in breakage of load transmission paths of the optimized designs. Such a model is then combined with the uncertainty quantification techniques and employed in robust topology optimization considering random manufacturing errors. Keywords: topology optimization, level set, manufacturing constraint, geometrical constraints, geometrical uncertainty References 1. G. Allaire, F. Jouve, G. Michailidis, Thickness control in structural optimization via a level set method, *Struct. Multidiscip. Optim.* 53 (2016) 1349-1382. 2. Z. Kang, Y. Wang, Y. Wang, Structural topology optimization with minimum distance control of multiphase embedded components by level set method, *Comput. Methods Appl. Mech.* 306 (2016) 299-318.

Exchange-correlation Potentials from Electron Densities Using a Complete Basis

Bikash Kanungo*, Vikram Gavini**

*Mechanical Engineering, University of Michigan, Ann Arbor, MI, **Mechanical Engineering, University of Michigan, Ann Arbor, MI

ABSTRACT

Exchange-correlation (xc) functionals, the cornerstone of the success of density functional theory (DFT), encapsulate the quantum many-electron interactions in terms of a mean-field. Although known to be unique functionals of the ground-state electronic charge density, $n(r)$, the exact form of these functionals - expressed either as energy ($\text{Exc}[n(r)]$) or potential ($\text{Vxc}[n(r)]$) - are unknown, necessitating the use of approximate functionals. The existing xc functionals, despite their success in predicting wide range of materials properties, exhibit notable failures - under-predicted bandgaps, incorrect bond-dissociation curves, wrong charge-transfer excitations, to name a few. Typically, these approximations are constructed through semi-empirical parameter fitting in model systems, thereby making systematic improvement and conformity to certain known exact conditions difficult. We attempt to address this through data-driven modeling of xc functionals. This involves, generating a training data set comprising of $n(r)$ to $\text{Vxc}(r)$ map, and then, use of machine learning algorithms to learn the functional form of $\text{Vxc}[n(r)]$ (and $\text{Exc}[n(r)]$), conforming to the exact conditions. In this work, we tackle the first step of generating the training data. To elaborate, it involves generating accurate $n(r)$ from wavefunction-based calculations (e.g., quantum Monte-Carlo, full Configuration-Interaction), and then inverting the Kohn-Sham (KS) eigenvalue problem to obtain the $\text{Vxc}(r)$ that yields the same $n(r)$. We perform the inversion by posing it as a PDE-constrained optimization problem with $\text{Vxc}(r)$ as the control variable and the KS eigenvalue problem as the PDE-constraint. We note that all previous attempts at this inverse problem have suffered from non-unique solutions or spurious oscillations in $\text{Vxc}(r)$, both of which are attributed to the incompleteness of the Gaussian basis that was employed in the inversion. We resolve them by using spectral finite-elements - a complete basis - to discretize the problem. We employ limited-memory BFGS (a quasi-Newton solver) to solve the nonlinear optimization problem. Additionally, we make use of appropriate weights for the objective function to expedite convergence as well as to avoid ill-conditioning in the low density region. We validate the algorithm, to an accuracy of ≤ 1 mHa, for cases where the densities are obtained from known xc functionals (LDA and GGA). Next, we demonstrate the capability of the algorithm for densities obtained from wavefunction-based calculations. Time permitting, we demonstrate preliminary results from simple regression techniques, that can faithfully generate bond-dissociation curves, using a few data points, thereby holding promise for future machine learning algorithms on the training data.

Genetic Algorithm for Optimizing an Airfoil Shape of Wind Turbine by Direct-forcing Immersed Boundary Modeling

Chao-Ching Kao*, Ming-Jyh Chern**, Tzyy-Leng Horng***, Nima Vaziri****

*National Taiwan University of Science and Technology, **National Taiwan University of Science and Technology,
Feng-Chia University, *Islamic Azad University Karaj Branch

ABSTRACT

Renewable energy is a popular topic nowadays due to energy shortage. Especially wind energy converted by a wind turbine receives more attentions. In the present study, the blade design of the wind turbine using a couple method with computational fluid dynamics (CFD) and genetic algorithm (GA) is discussed. The blade shape is the most significant effective parameter in the wind energy conversion. Hence, we dedicated to utilizing an optimal method for the cross-sectional shape of blade, i.e., an airfoil, in order to get the better efficiency for producing the higher lift and lower drag to drive the wind turbine. According to the previous study, the Genetic Algorithm (GA) is known to be the robust method in the optimal design area. The Real-coded Genetic algorithm is considered because it can solve the defect of binary code. That is, the chromosomes length is too long to code. While the PARSEC parameterization method is used to represent the shape of airfoil through the eleven parameters as the control variables. Furthermore, a direct-forcing immersed boundary (DFIB) method is employed for simulations of interaction of rotating blades in a flow field at moderate low Reynolds number. Numerical results reveal that the shape of airfoil can be optimized and the proposed DFIB model coupled with GA successfully simulates the moving blade in flow field for obtaining the high lift-drag ratio.

Investigating Strain Localization in Additively Manufactured Ti-alloys Using Detailed Material Characterization, Crystal Plasticity Finite Element Modeling and High Resolution Digital Image Correlation

Kartik Kapoor*, Todd Book**, Michael Sangid***

*Purdue University, **Purdue University, ***Purdue University

ABSTRACT

Titanium alloys, produced via additive manufacturing techniques, offer tremendous benefits over conventional manufacturing processes such as reduction in production lead time and increased geometrical flexibility. However, there is inherent uncertainty associated with their material properties, often stemming from the variability in the manufacturing process itself along with the presence of residual stresses in the material, which prevents their use as critical components. The current work investigates Ti-6Al-4V, a dual phase Titanium alloy produced via direct metal laser sintering by carrying out crystal plasticity finite element (CPFE) simulations which models both the alpha and beta phases of the material explicitly and high-resolution digital image correlation (HR-DIC) on samples subject to cyclic loading. This is preceded by detailed material characterization using electron backscatter diffraction and back-scattered electron imaging whose results are utilized to create a realistic finite element microstructural mesh with spatial and crystallographic information about both the alpha and beta phases of the material. In addition, results from TEM studies, informing about distribution of the total dislocation density are utilized to inform the CPFE model itself. A method to incorporate the effect of grain-level residual stresses via geometrically necessary dislocations (GNDs) is developed and implemented within the CPFE framework. Using this approach, grain level information about residual stresses, in the form of GND densities obtained spatially over the region of interest, directly from the experimental material characterization, is utilized as an input to the model. Results indicate that the simulation strain maps show good match with those obtained using HR-DIC. In addition, possible sites for damage nucleation are identified, which correspond to regions of high plastic strain accumulation and occur near prior beta boundaries suggesting that prior beta boundaries play a critical role in strain localization. Further, a more robust method to incorporate residual stresses that involves modifying the elastic-plastic decomposition of the deformation gradient is proposed and implemented within the CPFE model. This is then tested with an available dataset of High-Energy Diffraction Microscopy experiments performed on Ti-alloys.

Fibrous Materials Characterization through a 3-D Fiber Network Model

Alp Karakoc^{*}, Jouni Paltakari^{**}, Eero Hiltunen^{***}

^{*}Aalto University, ^{**}Aalto University, ^{***}Aalto University

ABSTRACT

The current work presents a 3-D fiber network model mimicking fibrous materials such as non-woven felt, paper and paperboards [1]. The objective is to investigate the effects of geometric properties and interactions of fibers on the overall stiffness and strength characteristics. In consideration to the objective, a stochastic micro-mechanical approach using random sequential adsorption was implemented to generate fiber geometries, alignments and positions in a confined space. Thereafter, material properties were assigned to each fibers and cohesive properties on the surface of each fiber intersection. Dirichlet boundary conditions were applied on the confined space and the problem was solved in explicit time integration scheme to determine the fiber network characteristics. [1] Karakoç A., Hiltunen E., Paltakari J. Geometrical and spatial effects on fiber network connectivity. Composite Structures, 2017; 168: 335-344.

The Elusive Granular Length Scale: Continuum vs Discrete

Konstantinos Karapiperis*, Jose Andrade**

*California Institute of Technology, **California Institute of Technology

ABSTRACT

Classical Cauchy continuum theories are known to be ill-posed after the onset of shear banding instability in granular materials. More elaborate continuum descriptions have provided a remedy by introducing a length scale, but have not enjoyed general acceptance due to the lack of a sound micromechanical basis. The renewed interest in such theories is largely due to grain-scale observations providing partial justification of the underlying assumptions. In this work, we provide a critical assessment of micropolar plasticity by comparing continuum predictions with grain-scale measurements in virtual triaxial experiments of real sands. Particularly, we employ the recently developed 3D Level-Set Discrete Element Method to shed light into the kinematics (rotational vortices) and kinetics (force chain buckling, couple stress) of shear bands obtained by means of advanced homogenization schemes. Upon identifying the major limitations of current theoretical models, we propose elements of an alternative framework possessing a direct physical interpretation of the granular length scale, towards the final goal of developing an enhanced multiscale theory.

PARALLEL PARTITIONED FINITE ELEMENT SOLVERS WITH NON-MATCHING TIME-STEPS

SAEID KARIMI
FullRank Software LLC
3139 W. Holcombe Blvd. #325
Houston, TX 77025, USA
skarimi@fullranksoftware.com; www.fullranksoftware.com

Key words: multi-time-step, time-integration methods, structural dynamics, domain decomposition, differential-algebraic equations.

1. INTRODUCTION AND MOTIVATION

Computational methods play an increasingly important role in modern engineering and scientific practice. Availability of high-performance computers along with the advanced (and easy-to-use) software, has enabled practitioners to successfully model complex physical, chemical and biological processes. For instance, fluid-structure interaction problems are some of the most challenging to efficiently model [1]. Irrespective of the problem, any large real-world computer modeling of engineering or scientific applications typically relies on partitioning (domain decomposition) of computational domain and parallel computing.

Domain partitioning (or domain decomposition) algorithms have become a popular approach to develop fast parallel solvers for various problems [2; 3]. In these algorithms, the spatial computational domain is split into a number of subdomains. This allows distribution of the computation among a pool of processors (CPUs and GPUs) available [4]. Obviously, such algorithms need some information (either primal or dual quantities) to be transferred across to adjacent subdomains. The domain partitioning can be either overlapping or non-overlapping. In general, the interface variables and compatibility of solution near the interface are defined implicitly.

In addition to work distribution among parallel processors, domain partitioning algorithms have other advantages. One can use different numerical formulations in different subdomains. Therefore, based on the nature of the process occurring at a particular subdomain, a suitable numerical formulation can be implemented to approximate the solution in the desired subdomain. A class of methods that offers such flexibility in terms of time-stepping (i.e., with different time-steps in different subdomains) is labeled *multi-time-step* or *sub-cycling* methods [6; 7]. Under this class of methods, the user can choose non-matching time-steps for time-integration in different subdomains. This feature is particularly of interest when a mix of implicit and explicit time-integration algorithms are used in different

subdomains [8; 9; 10]. In light of domain partitioning algorithms, multi-time-step methods can be of strong or weak types.

Weak multi-time-step algorithms rely on iterative approximation of variables in subdomains and their respective interfaces. These updated quantities are then used to advance the solution in other subdomains in time, which will in turn be used to update interface quantities. This iteration continues until desired convergence criteria are satisfied. This type of algorithm is extremely popular and forms the basis for many partitioned and multi-physics simulations. One of the main reasons why such algorithms are common is that the available (or legacy) solvers can be easily adopted in this approach, hence, accelerating the development phase. Some (but not all) of successful applications of weak algorithms can be found in [10; 11; 12]. Despite the attractive concept, weak partitioned algorithms are prone to numerical instability, especially in time-dependent problems. An alternative approach to multi-time-step simulation is to use strong coupling [13]. Unlike the weak algorithms, strong partitioning algorithms update the subdomain variables and the interface conditions monolithically. This means that iterations from one subdomain to another are not needed. These algorithms have better properties with respect to numerical stability. However, these algorithms are not as popular as the weak type. The reason being that development of software based on strong algorithms needs major modification to the existing computer codes. This hurdle translates into longer and more complicated development process. This drawback, however, has not stopped researchers to investigate strong multi-time-step algorithms. Some results in this area can be found in [14; 15; 16; 17].

This article is devoted to an overview of strong partitioning algorithms with non-matching time-steps. The theory and other aspects of these algorithms will be outlined. For the sake of presentation, we will limit our scope to elastodynamics problems. The rest of this paper is organized as follows: Section 2 is devoted to the theory and numerical formulation, Section 3 presents some numerical examples to demonstrate the discussed algorithms, and the conclusions are drawn in Section 4.

2. MATHEMATICAL MODELS AND NUMERICAL ALGORITHMS

2.1. Governing equations. Consider an open domain $\Omega \subset \mathbb{R}^{nd}$ and $\Gamma_D \cup \Gamma_N = \partial\Omega$. Boundary subsets Γ_D and Γ_N are mutually exclusive. The time-interval of interest is $\mathcal{I} = [0, T)$. The displacement field of the solid body, \mathbf{u} defined in Ω , evolves according to conservation of linear momentum. We take the density of the solid to be ρ and the specific body force to be \mathbf{b} . The governing PDE can hence be written as:

$$\rho \frac{\partial^2 \mathbf{u}}{\partial t^2} = \text{div} [\mathbf{T}] + \rho \mathbf{b} \quad \mathbf{x} \in \Omega, t \in \mathcal{I} \quad (2.1a)$$

$$\mathbf{u} = \mathbf{u}_p \quad \mathbf{x} \in \Gamma_D, t \in \mathcal{I} \quad (2.1b)$$

$$\mathbf{T} \hat{\mathbf{n}} = \mathbf{t}_p \quad \mathbf{x} \in \Gamma_N, t \in \mathcal{I} \quad (2.1c)$$

$$\mathbf{u} = \mathbf{u}_0 \quad \mathbf{x} \in \Omega, t = 0 \quad (2.1d)$$

$$\frac{\partial \mathbf{u}}{\partial t} = \mathbf{v}_0 \quad \mathbf{x} \in \Omega, t = 0 \quad (2.1e)$$

where \mathbf{u}_p and \mathbf{t}_p are prescribed values for displacement and traction on boundary. The initial displacement and velocity are shown as \mathbf{u}_0 and \mathbf{v}_0 . The stress tensor is denoted by \mathbf{T} and $\text{div}[\cdot]$ is the divergence operator. The stress tensor is related to the displacement field

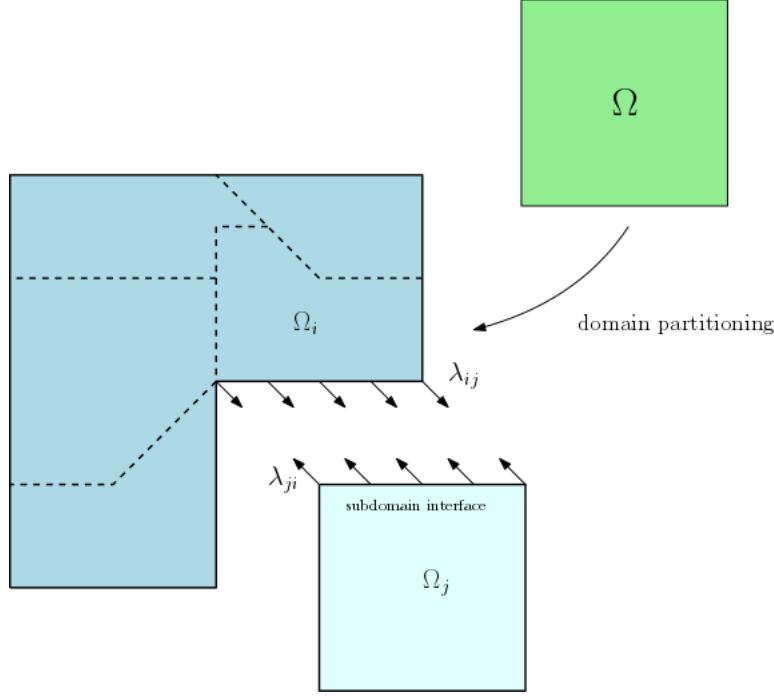


FIGURE 1. Domain partitioning of initial domain Ω into an arbitrary number of subdomains is shown (dashed lines show the interfaces between subdomains). Subdomains Ω_i and Ω_j share an interface (subdomain interface in the figure), where the Lagrange multipliers $\lambda_{ij} = -\lambda_{ji}$ are used to enforce compatibility of solution.

through a constitutive relation. For a more detailed account of constitutive models for solids and their finite element treatment, the reader can consult [18] and references therein.

In this paper, we are concerned with solving coupled PDEs of the form given in (2.1) on multiple subdomains that share interface with one another. Hence, in addition to the typical initial and boundary conditions given in (2.1), one needs constraints to ensure compatibility of the displacement fields at the interface of subdomains. As shown in figure 1, we will use Lagrange multipliers defined on subdomain interfaces to enforce an algebraic constraint of form

$$\mathbf{u}_i - \mathbf{u}_j = \mathbf{0} \quad (2.2)$$

on the interface of Ω_i and Ω_j (and all other neighboring subdomains). Subindices i and j indicate the respective subdomains. This equation, in addition to the conservation equation in (2.1) for each subdomain, completes the formulation of the problem on a partitioned domain. One can derive a weak form using a desired formalism (e.g., Galerkin) and discretize using the finite element methods.

2.2. Finite element discretization. Consider domain Ω partitioned into \mathcal{S} non-overlapping subdomains. The boundary of each subdomain Ω_i is comprised of $\partial\Omega_i \cap \Gamma_D$, $\partial\Omega_i \cap \Gamma_N$ and $\tilde{\Gamma}_i$. The part of boundary that is shared with other subdomains' boundaries is denoted by

$\tilde{\Gamma}_i$. The function spaces needed for a FEM discretization of the problem at hand include

$$\mathcal{U}_i = \left\{ \mathbf{u}_i \in (H^1(\Omega_i))^{nd} \mid \mathbf{u}_i = \mathbf{u}_p \text{ on } \mathbf{x} \in \Gamma_D \cap \partial\Omega_i, \frac{\partial \mathbf{u}_i}{\partial t} \in (L^2(\Omega_i))^{nd}, \frac{\partial^2 \mathbf{u}_i}{\partial t^2} \in (L^2(\Omega_i))^{nd} \right\} \quad (2.3a)$$

$$\mathcal{W}_i = \left\{ \mathbf{w}_i \in (H^1(\Omega_i))^{nd} \mid \mathbf{w}_i = \mathbf{0} \text{ on } \mathbf{x} \in \Gamma_D \cap \partial\Omega_i \right\} \quad (2.3b)$$

for all subdomains $i = 1, \dots, \mathcal{S}$. In addition, trace operators are needed that are defined on the subdomain interfaces

$$\mathcal{M} = \left\{ \boldsymbol{\mu} \in \left(H^{-1/2} \left(\bigcup_{i=1}^{\mathcal{S}} \tilde{\Gamma}_i \right) \right)^{nd} \right\}. \quad (2.4)$$

Furthermore, the inner product on any subset K of Ω is defined as

$$(a, b)_K = \int_K a \cdot b \, d\Omega, \quad (2.5)$$

with $a \in \mathcal{W}_i$ and $b \in \mathcal{U}_i$. Given these definitions, a weak form for the partitioned can be written on finite element e belonging to the triangulation (mesh) on subdomain i (i.e., $\forall \Omega_e \subset \mathcal{T}(\Omega_i)$, $i = 1, \dots, \mathcal{S}$) as: find $\mathbf{u}_i \in \mathcal{U}_i$ and $\boldsymbol{\lambda} \in \mathcal{M}$, such that

$$\left(\mathbf{w}, \rho \frac{\partial^2 \mathbf{u}_i}{\partial t^2} \right)_{\Omega_e} = (\mathbf{w}, \mathbf{t}_p)_{\partial\Omega_e \cap \Gamma_N} + (\mathbf{w}, \text{Sign}[\tilde{\Gamma}_i] \boldsymbol{\lambda})_{\partial\Omega_e \cap \tilde{\Gamma}_i} - (\text{grad}[\mathbf{w}^T], \mathbf{T})_{\Omega_e} + (\mathbf{w}, \rho \mathbf{b})_{\Omega_e} \quad \forall \mathbf{w} \in \mathcal{W}_i \quad (2.6a)$$

$$(\boldsymbol{\mu}, \mathbf{u}_i - \mathbf{u}_j)_{\tilde{\Gamma}_i \cap \tilde{\Gamma}_j} = 0 \quad i, j = 1, \dots, \mathcal{S}, \quad i \neq j \text{ and } \tilde{\Gamma}_i \cap \tilde{\Gamma}_j \neq \emptyset \quad \forall \boldsymbol{\mu} \in \mathcal{M} \quad (2.6b)$$

where $\text{Sign}[\Gamma_i]$ is an arbitrary sign of +1 or -1 assigned to the subdomain interfaces such that

$$\text{Sign}[\tilde{\Gamma}_i \cap \tilde{\Gamma}_j] = -\text{Sign}[\tilde{\Gamma}_j \cap \tilde{\Gamma}_i]. \quad (2.7)$$

It should be noted that proper inf-sup conditions [19] need to be satisfied to ensure stability of this discretization. Finite element discretization results in a differential/algebraic equation [20] in terms of the nodal displacement values and the Lagrange multipliers as given below:

$$\mathbf{M}_i \ddot{\mathbf{u}}_i = \mathbf{f}(\dot{\mathbf{u}}_i, \mathbf{u}_i; t) + \mathbf{C}_i^T \boldsymbol{\Lambda} \quad i = 1, \dots, \mathcal{S} \quad (2.8a)$$

$$\sum_{i=1}^{\mathcal{S}} \mathbf{C}_i \mathbf{u}_i = \mathbf{0} \quad (2.8b)$$

where \mathbf{M}_i and \mathbf{u}_i are the mass matrix and nodal displacements, respectively. The vector of nodal Lagrange multipliers is denoted by $\boldsymbol{\Lambda}$ and \mathbf{C}_i are the signed Boolean matrices (discretized trace operators). The superposed dots show differentiation with respect to time. Equation (2.8) is a differential/algebraic equation of index 3. This equation can be solved in a multitude of ways.

2.3. Algebraic interface constraint. Note that in a time-continuous setup, the algebraic constraint can be replaced by its derivatives given below

$$\sum_{i=1}^{\mathcal{S}} \mathbf{C}_i \mathbf{u}_i = \mathbf{0}, \quad \sum_{i=1}^{\mathcal{S}} \mathbf{C}_i \dot{\mathbf{u}}_i = \mathbf{0}, \quad \sum_{i=1}^{\mathcal{S}} \mathbf{C}_i \ddot{\mathbf{u}}_i = \mathbf{0} \quad (2.9)$$

However, the time discretization of equations (2.8) with either of the constraints given in (2.9) will indeed yield different numerical values (as it is expected). Also, enforcing one type of interface constraint (e.g., displacements or velocities) does not imply compatibility of the other kinematic variables at the subdomain interface [21]. This phenomena is known as *drift-off*, which refers to deviation of the numerical solution from the constraints manifold [20]. Hence, one of the main difficulties in developing numerical algorithms for differential/algebraic equations compared to purely differential equations is recognizing the drift-off in the numerical solution. Drift-off is usually not avoidable. Hence, various numerical methodologies for controlling this effect have been developed [22; 23].

A method for controlling the drift-off was proposed by Baumgarte in [24]. The motivation behind using the Baumgarte stabilization method is to control drift-off from the displacement, velocity and acceleration constraints. The Baumgarte stabilization method for the current problem reads as follows:

$$\sum_{i=1}^S \mathbf{C}_i \ddot{\mathbf{u}}_i + \alpha_1 \sum_{i=1}^S \mathbf{C}_i \dot{\mathbf{u}}_i + \alpha_2 \sum_{i=1}^S \mathbf{C}_i \mathbf{u}_i = \mathbf{0} \quad (2.10)$$

where α_1 and α_2 are user-defined constants that control (supress) the values of drift-off. Note that the Baumgarte stabilization method is an efficient way of controlling the drift-off, as only one algebraic constraint (as a result only one Lagrange multiplier) is used. For comparison, the Gear-Gupta-Leimkuhler (GGL) methodology [21; 25; 26] requires more than one algebraic constraint (and consequently more than one Lagrange multiplier). Hence, the size of the problem is smaller and more suitable for computer simulations, especially in practical problems with a large number of subdomains. However, GGL method often provides better accuracy because the extra interface constraints are directly enforced.

In this article, Newmark time-integration methods will be used. Time discretization using the Newmark method [27] can be written as:

$$\mathbf{v}^{(n+1)} = \mathbf{v}^{(n)} + (1 - \gamma)\Delta t \mathbf{a}^{(n)} + \gamma \Delta t \mathbf{a}^{(n+1)} \quad (2.11a)$$

$$\mathbf{d}^{(n+1)} = \mathbf{d}^{(n)} + \Delta t \mathbf{v}^{(n)} + \Delta t^2 \left(\frac{1}{2} - \beta \right) \mathbf{a}^{(n)} + \Delta t^2 \beta \mathbf{a}^{(n+1)} \quad (2.11b)$$

where Δt is the time-step, β and γ are time-integration parameters. The time-discretized values of displacement, velocity and acceleration are denoted by \mathbf{d} , \mathbf{v} and \mathbf{a} , respectively. Note that with domain partitioning one can choose subdomain-specific time-steps and integration parameters. Having subdomain-specific parameters give the user the freedom to choose different members of the Newmark time-stepping family of algorithms for different subdomains. An important application of this feature is the implicit-explicit time-integration. The Newmark time-stepping algorithms (and its descendants) are well studies in numerical solution of second-order differential equations. Application of this class of methods to solution of differential algebraic equations (such as in equation (2.8)) is studied to a lesser extent. In the following section, we will explore the differences in the outcome of numerical simulations based on the type of interface constraint utilized.

3. NUMERICAL EXAMPLE

Consider a unit square domain agitated by a time-dependent force applied at the point $(0,0)$ described as:

$$f(t) = e^{-t} \sin(t) \quad t \in [0, 5]. \quad (3.1)$$

The boundaries on $x = 1$ and $y = 1$ are non-absorbing (Dirichlet-type) and the rest of the boundary is free. We will model propagation of a scalar wave over the domain by splitting it into three non-overlapping subdomains. In figure 2 the domain decomposition is shown. We will use linear triangular elements for finite element discretization. The speed of propagation in this medium is set to be $c_0 = 0.1$. The time-integration parameters in all subdomains will be $\beta = 1/4$ and $\gamma = 1/2$ (see (2.11)). The subdomain time-steps are set to $\Delta t_1 = 0.02$, $\Delta t_2 = 0.002$ and $\Delta t_3 = 0.002$. The system time-step is $\Delta t = 0.02$.

The interface compatibility criteria of interest will be the v-continuity method and the Baumgarte stabilization methods. In the v-continuity method, we will only enforce continuity of velocities near the interface. Constraints on compatibility of displacements and accelerations will not be enforced. In the Baumgarte stabilization method, as given in equation (2.10), a linear combination of displacement, velocity and acceleration values at the interface is set to zero. In this numerical illustration, we will choose $\alpha_1 = 2/\Delta t$ and $\alpha_2 = \sqrt{2}/\Delta t^2$.

The numerical values at time $t = 15$ are shown in figure 3. It can be seen that the difference in the two numerical results is about 0.1% of the values. In both cases of v-continuity and Baumgarte stabilization methods, the time-stepping parameters are exactly the same. Hence, the difference shown is only a result of interface compatibility conditions. Notably, the two methods give different values in energy as well. Figure 4 shows this quantity against time. This difference in energy, ΔE , at every time-step is defined as

$$\Delta E^n = |E_{\text{v-continuity}}^{(n)} - E_{\text{Baumgarte}}^{(n)}| \quad \forall n \quad (3.2)$$

which is the difference in energy based on the v-continuity and the Baumgarte stabilization method. As a result, one can conclude that the two methods have different numerical energy dissipation properties as well. This numerical example shows that the interface condition alone causes a deviation in the resulting numerical values.

4. CONCLUSION

With growing accessibility to computational capacity (such as cloud services, etc.) development of numerical algorithms designed to take full advantage of this architecture is more necessitated than ever before. A popular approach to distribution of work among a cluster of processors is the domain decomposition (domain partitioning) method. In this class of methods, the computational domain is split into several subdomains and the arrays associated with each subdomain can be manipulated by a few of the processors available, independently. The interface variables are used to enforce compatibility of numerical solution, and need to be transferred to other processors.

In this article, we overviewed the non-overlapping domain partitioning approach for a simple structural dynamics model. We looked into the mathematical theory of partitioned finite element discretization which results in differential/algebraic equations. Through a numerical example, two popular interface compatibility methods for partitioned algorithms were compared. Multi-time-step and strongly coupled time-integration algorithm was used

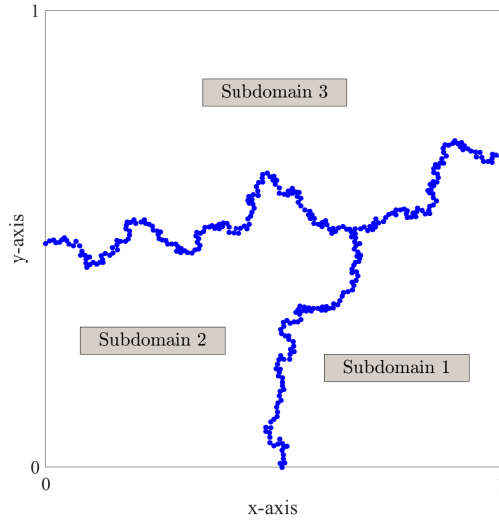


FIGURE 2. Partitioning of the computation domain into three non-overlapping subdomains.

to show how different subdomain interface conditions can affect the final numerical values. It was also shown that interface conditions lead to particular numerical energy dissipation characteristics. Based on the application, the user needs to identify the proper subdomain interface constraints to be used.

REFERENCES

- [1] Y. Bazilevs, K. Takizawa, and T. E. Tezduyar. *Computational Fluid-Structure Interaction: Methods and Applications*. John Wiley & Sons, 2013.
- [2] V. Dolean, P. Jolivet, and F. Nataf. *An Introduction to Domain Decomposition Methods: Algorithms, Theory, and Parallel Implementation*. SIAM, 2015.
- [3] A. Toselli and O. Widlund. *Domain Decomposition Methods: Algorithms and Theory*. Springer Science & Business Media, 2006.
- [4] M. Papadrakakis, G. Stavroulakis, and A. Karatarakis. A new era in scientific computing: Domain decomposition methods in hybrid CPU–GPU architectures. *Computer Methods in Applied Mechanics and Engineering*, 200:1490–1508, 2011.
- [5] K. B. Nakshatrala, A. Prakash, and K. D. Hjelmstad. On dual Schur domain decomposition method for linear first-order transient problems. *Journal of Computational Physics*, 228:7957–7985, 2009.
- [6] S. Karimi and K. B. Nakshatrala. On multi-time-step monolithic coupling algorithms for elastodynamics. *Journal of Computational Physics*, 273:671–705, 2014.
- [7] S. Karimi and K. B. Nakshatrala. A monolithic multi-time-step computational framework for first-order transient systems with disparate scales. *Computer Methods in Applied Mechanics and Engineering*, 283:419–453, 2015.
- [8] T. J. R. Hughes and W. K. Liu. Implicit-explicit finite elements in transient analysis: Stability theory. *Journal of Applied Mechanics*, 45(2):371–374, 1978.

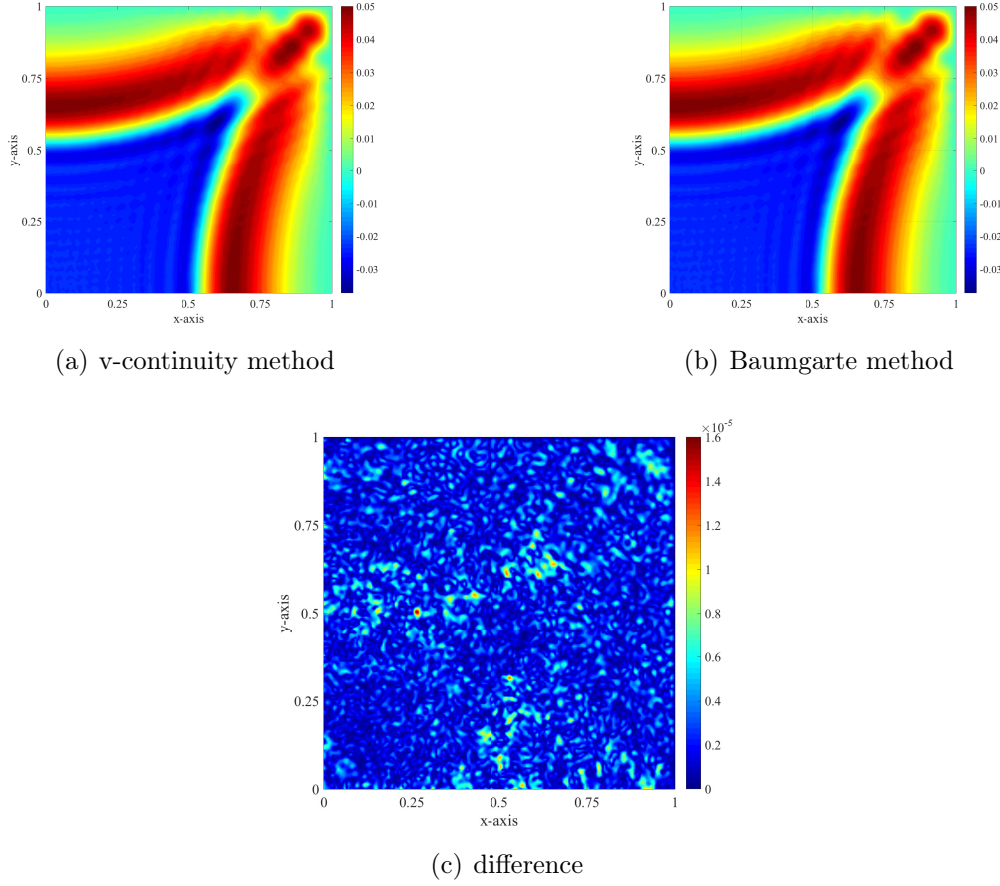


FIGURE 3. In this figure, the value of displacements at time $t = 15$ using both the v-continuity and Baumgarte stabilization methods is shown. The difference from the two solutions is also shown.

- [9] T. Belytschko and R. Mullen. Stability of explicit-implicit mesh partitions in time integration. *International Journal for Numerical Methods in Engineering*, 12(10):1575–1586, 1978.
- [10] C. Farhat, M. Lesoinne, and N. Maman. Mixed explicit/implicit time integration of coupled aeroelastic problems: Three-field formulation, geometric conservation and distributed solution. *International Journal for Numerical Methods in Fluids*, 21(10):807–835, 1995.
- [11] C. Farhat, M. Lesoinne, P. LeTallec, K. Pierson, and D. Rixen. FETI-DP: a dual-primal unified FETI method–Part I: A faster alternative to the two-level FETI method. *International Journal for Numerical Methods in Engineering*, 50(7):1523–1544, 2001.
- [12] S. Piperno and C. Farhat. Partitioned procedures for the transient solution of coupled aeroelastic problems–Part II: Energy transfer analysis and three-dimensional applications. *Computer Methods in Applied Mechanics and Engineering*, 190(24-25):3147–3170, 2001.
- [13] A. Gravouil and A. Combescure. Multi-time-step explicit–implicit method for non-linear structural dynamics. *International Journal for Numerical Methods in Engineering*,

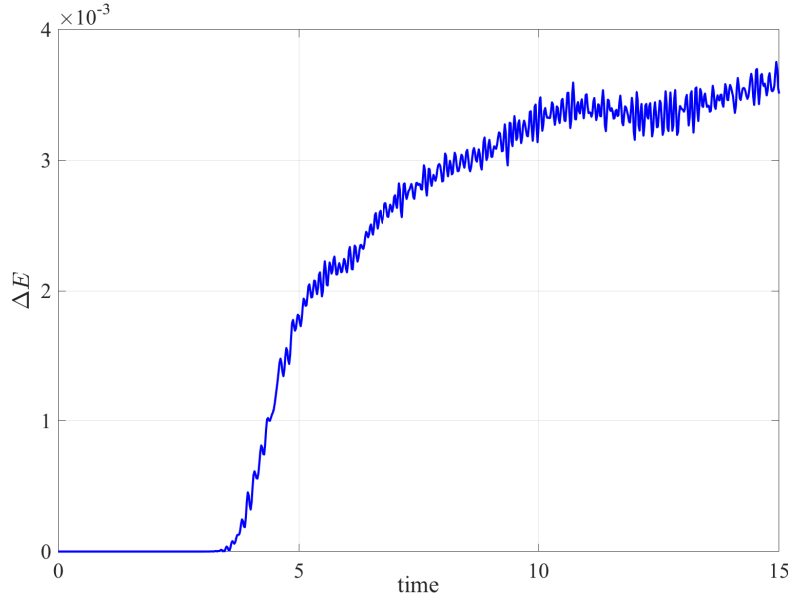


FIGURE 4. The difference in the calculated value of the energy from the v-continuity and the Baumgarte methods is shown.

- 50(1):199–225, 2001.
- [14] M. W. Gee, U. Küttler, and W. A. Wall. Truly monolithic algebraic multigrid for fluid–structure interaction. *International Journal for Numerical Methods in Engineering*, 85(8):987–1016, 2011.
 - [15] N. Mahjoubi, A. Gravouil, A. Combescure, and N. Greffet. A monolithic energy conserving method to couple heterogeneous time integrators with incompatible time steps in structural dynamics. *Computer Methods in Applied Mechanics and Engineering*, 200(9–12):1069–1086, 2011.
 - [16] O. S. Bursi, Z. Wang, C. Jia, and B. Wu. Monolithic and partitioned time integration methods for real-time heterogeneous simulations. *Computational Mechanics*, 52(1):99–119, 2013.
 - [17] M. Beneš. Convergence and stability analysis of heterogeneous time step coupling schemes for parabolic problems. *Applied Numerical Mathematics*, 121:198–222, 2017.
 - [18] P. Wriggers. *Nonlinear Finite Element Methods*. Springer, 2008.
 - [19] F. Magoulès and F. X. Roux. Lagrangian formulation of domain decomposition methods: A unified theory. *Applied Mathematical Modeling*, 30(7):593–615, 2006.
 - [20] G. Wanner and E. Hairer. *Solving Ordinary Differential Equations II: Stiff and Differential–Algebraic Problems*. Springer, 1991.
 - [21] O. Brüls, V. Acary, and A. Cardona. Simultaneous enforcement of constraints at position and velocity levels in the nonsmooth generalized- α scheme. *Computer Methods in Applied Mechanics and Engineering*, 281:131–161, 2014.
 - [22] W. Blajer. Methods for constraint violation suppression in the numerical simulation of constrained multibody systems—A comparative study. *Computer Methods in Applied Mechanics and Engineering*, 200(13–16):1568–1576, 2011.

- [23] P. Flores, M. Machado, E. Seabra, and M. T. da Silva. A parametric study on the Baumgarte stabilization method for forward dynamics of constrained multibody systems. *Journal of Computational and Nonlinear Dynamics*, 6(1):011019, 2011.
- [24] J. Baumgarte. Stabilization of constraints and integrals of motion in dynamical systems. *Computer Methods in Applied Mechanics and Engineering*, 1(1):1–16, 1972.
- [25] C. W. Gear, B. Leimkuhler, and G. K. Gupta. Automatic integration of Euler–Lagrange equations with constraints. *Journal of Computational and Applied Mathematics*, 12:77–90, 1985.
- [26] C. Lunk and B. Simeon. Solving constrained mechanical systems by the family of Newmark and α -methods. *ZAMM-Journal of Applied Mathematics and Mechanics*, 86(10):772–784, 2006.
- [27] N. M. Newmark. A method of computation for structural dynamics. *Journal of the Engineering Mechanics*, 85(3):67–94, 1959.

Squeeze-film Flow in the Presence of a Thin Anisotropic Porous Bed: an Application to Knee Joint

Timir Karmakar*, Raja Sekhar G. P.**

*Indian Institute of Technology Kharagpur, India, **Indian Institute of Technology Kharagpur, India

ABSTRACT

We consider a theoretical model of squeeze-film flow in the presence of a thin porous bed. It is assumed that a flat bearing is approaching towards the porous bed. The gap between the porous bed and the bearing is assumed to be filled with a Newtonian fluid. The liquid porous interface is assumed to be flat. Assuming that the fluid is Newtonian, we use Navier-Stokes equation in the fluid region and Darcy equation in the fluid saturated porous region. Lubrication approximation is used to the hydrodynamic equation of motion in the gap and in the porous region. We use Beavers & Joseph (1967) and Le Bars & Worster (2006) conditions at the liquid-porous interface and present a detailed analysis on the corresponding impact. We assume that the porous bed is anisotropic in nature with permeabilities K_2 and K_1 along the principal axes. Accordingly, the anisotropic angle θ is taken as the angle between the horizontal direction and the principal axis with permeability K_2 . We show that the anisotropic permeability ratio and the anisotropic angle make a significant influence on contact time, flux, velocity etc. The analysis is presented when a bearing approaches the porous bed for a given constant velocity or a given constant load is presented. We present some important findings relevant to knee joint based on the anisotropic of the human cartilage. The permeability of the articular cartilage depends on the proteoglycan matrix especially glycosaminoglycan (GAG) chains and the properties are influenced by the arrangement of the collagen fibres in different directions which form an anisotropic network of the human cartilage. In case of constant load, we have estimated the time duration a healthy human knee remains fluid lubricated. While in case of a constant velocity, we have estimated the load a human knee can sustain. 1. Beavers G S, Joseph D D, Boundary conditions at a naturally permeable wall, Journal of fluid mechanics, 30, pp. 197-207, 1967. 2. Le Bars M, Worster M G, Interfacial conditions between a pure fluid and a porous medium: implications for binary alloy solidification, Journal of fluid mechanics, 550, pp. 149-173, 2006. 3. Knox D J, Wilson S K, Duffy B R, McKee S, Porous squeeze-film flow, IMA Journal of applied mathematics, 80, pp. 376-409, 2013

Physics Informed Deep Learning

George Karniadakis*

*Brown University

ABSTRACT

For more than two centuries, solutions of partial differential equations (PDEs) have been obtained either analytically or numerically based on well-behaved forcing and boundary conditions for well-posed problems. However, in real-life applications the available input data are often incomplete, noisy, and of variable fidelity, rendering existing computational methods ineffective. Moreover, despite the availability of big data in many domains, high-fidelity scientific data are small and expensive to obtain. We are changing this paradigm in a fundamental way by establishing an interface between probabilistic machine learning and PDEs that express known physical laws and constraints. We develop data-driven algorithms for general nonlinear PDEs using Gaussian processes and deep neural networks tailored to the corresponding integro-differential operators. The only observables are scarce and noisy multi-fidelity data for the forcing/solution, which could be scattered anywhere in the domain. We refer to these smart systems that encode the proper physical laws in their description as Physics-Informed Learning Machines (PILM). This work is based on work of Maziar Raissi and Paris Perdikaris.

On Nonlocal Theories: Mathematical Models and Computational Approaches

Anssi Karttunen^{*}, J.N. Reddy^{**}

^{*}Aalto, ^{**}Texas A&M; University

ABSTRACT

Structural continuum theories require a proper treatment of the kinematic, kinetic, and constitutive issues accounting for possible sources of non-local and non-classical continuum mechanics concepts and solving associated boundary value problems. There is a wide range of theories, from higher gradient to truly nonlocal. These include, for example, strain gradient theories [1, 2], couple stress theories, Eringen's stress gradient theories [3], and micropolar theories [4] (the micropolar theory of elasticity includes an independent microrotation), and thermodynamically consistent structural theories. In this lecture, an overview of recent research on strain gradient, stress gradient, couple stress, micropolar, and thermodynamically consistent theories in developing the governing equations beams, plates, and sandwich structures will be presented and their computational aspects will be discussed. In addition, a graph-based finite element framework (GraFEA) suitable for the study of damage in brittle materials will be discussed [5]. Acknowledgements: The author is pleased to acknowledge the collaboration on non-local and non-classical mechanics with Arun Srinivasa (TAMU), and Karan Surana (KU), and Debasish Roy (IISc). References 1. R.D. Mindlin, Influence of couple-stresses on stress concentrations. *Experimental Mechanics*, 3(1), 1-7, 1963. 2. A.R. Srinivasa and J.N. Reddy, *Journal of Mech Phys Solids*, 61(3), 873-885, 2013. 3. A.C. Eringen, *International Journal of Engineering Science*, 10, p. 1, 1972. 4. A.T. Karttunen, J.N. Reddy, and J. Romanoff, *Composite Structures*, 185, 656-664, 2018. 5. Parisa Khodabakhshi, J.N. Reddy, and Arun Srinivasa, *Meccanica*, 51(12), 3129-3147, Dec 2016

Simulation and Auralization for Noise Using Virtual Reality Technology

Kazuo Kashiya*

*Chuo University

ABSTRACT

The evaluation of noise is very important for planning and designing of various construction works in urban area. There have been presented a number of evaluation methods for noise simulation. Based on the frame of reference used, those methods can be classified into two categories: 1) Methods based on the geometrical acoustic theory and 2) Methods based on acoustic wave theory. Both methods have advantages and disadvantages. For the methods based on the geometrical acoustic theory, the CPU time is very short but the numerical accuracy is low comparing with the methods based on the acoustic wave theory. On the other hand, the method based on the acoustic wave theory gives accurate solutions but the simulation becomes a large scale simulation. In the conventional studies, the computed noise level is described by the visualization using computer graphic such as iso-surface. Although the visualization is a powerful tool to understand the distribution of noise, it is difficult to recognize the noise level intuitively. This paper presents noise evaluation systems based on acoustic wave theory using virtual reality technology. The system exposes to users the computed noise level with both the auditory information using sound source signal and the visual information using CG image. The CIP method using AMR and FEM are employed for the discretization of wave equation. The ambisonics based on the spherical surface function expansion is employed to realize the stereoscopic sound field using computational results and sound source data. We performed the observation to obtain the sound source data for the auralization. The present system is shown to be a useful tool for planning and designing tool for various construction works in urban area, and also for consensus building for designers and the local residents.

The Effect of Water on the Wrinkling Formation in Graphene, and the Interlayer Shear between Graphene Bilayers

Jatin Kashyap^{*}, Dibakar Datta^{**}

^{*}New Jersey Institute of Technology, ^{**}New Jersey Institute of Technology

ABSTRACT

Graphene, a two-dimensional material, is the cynosure in nanotechnology with wide ranges of applications. Wrinkling, a ubiquitous phenomenon in graphene, severely weakens its performance. In some cases, however, wrinkling is advantageous such as hydrophobic surface, energy storage. Whether beneficial or not, it is crucial to understand the wrinkles formation mechanism in graphene. Experimental investigations suggest that during the growth process, because of the humid environment in the growth chamber, water diffuses into graphene and substrate and plays a significant role in the wrinkle formation in graphene. There is no systematic computation investigation at all to address this critical issue. We, therefore, performed molecular dynamics simulation to analyze this important phenomenon by considering a simplistic model with graphene on graphene substrate and diffused water inside. First, we consider the absence of water inside and observe the formation of bigger wrinkle due to the coalescence of initial small wrinkles. However, if the initial wrinkles have a very high angle, the final wrinkle formed after coalescence is too high to maintain its stability and collapses to form multifold graphene structure. Next, we consider the humidity effect. The configuration of final wrinkle structure is governed by the competition between bending energy of wrinkled graphene and the van der Waals (vdW) energy between graphene, substrate, and water in-between. At low initial angle (e.g., 6 degrees), condensation of diffused water dominates the final wrinkle structure. At the intermediate initial angle (e.g., 11 degrees), when only one water layer is present, the bending energy dominates. However, with the increase in water density, i.e., more water layer inside, condensation of water droplet governs the final structure. At higher initial angle (e.g., 21 degrees), bending energy dominates and regulates the final wrinkle configuration. With the increase in initial wrinkle angle, the width of the final wrinkle formed after coalescence decreases while the final height shows a reverse trend. We further investigated the effect of water in the interlayer shear of graphene bilayer. We notice when the water is absent in between the layers, the interlayer shear shows a symmetric trend and the maximum shear is around 60 MPa. However, the presence of water droplet significantly reduces the maximum shear. Our systematic computational analysis provides a deeper insight into the role of water in the wrinkling formation in graphene and the interlayer shear between graphene bilayers.

Material Design of Elastoplastic Media with Decoupling Multi-scale Analysis

Junji Kato^{*}, Shun Ogawa^{**}, Hiroya Hoshiba^{***}, Takashi Kyoya^{****}

^{*}Tohoku University, ^{**}Tohoku University, ^{***}Tohoku University, ^{****}Tohoku University

ABSTRACT

The present study proposes material design of elastoplastic media in the framework of a decoupling multi-scale analysis. The objective function is to maximize the energy absorption capacity of macrostructure with a prescribed material volume in the microstructure. Isotropic von Mises elastoplastic material model is employed for the constituents of microstructure and the anisotropic Hill plasticity model is used for the macroscopic constitutive law. In the framework of the decoupling multi-scale analysis, material parameters in the Hill's material model are identified by solving the microscopic boundary value problems based on the finite element analysis. This process is called numerical material testing. In the topology optimization of microstructure, conventional SIMP approach is utilized and gradient-based method is employed. In this study, the methodology to obtain the accurate sensitivity with low computational costs is proposed, where the sensitivity of the incremental strain with respect to design variables can be eliminated using the return mapping algorithms. It is verified by a series of numerical examples that the proposed method has a great potential to design elastoplastic media, especially advanced materials such as functional materials.

Strain Shielding in Femurs with an Implant

Yekutiel Katz*, Zohar Yosibash**

*Tel Aviv University, **Tel Aviv University

ABSTRACT

More than half a million hip replacement surgeries are performed annually in the US, and similarly in Europe. The inserted metallic prosthesis in these surgeries changes the femur's natural loading conditions, leading to bone remodeling and resorption. This phenomenon, commonly known as "stress shielding", leads to reduction of implant's mechanical stability and increases the risk of periprosthetic femoral fracture. Thirteen percent of hip replacement surgeries undergo a revision surgery within ten years [1]. Orthopedic surgeons usually choose a prosthesis based on clinical outcome reports, statistical data and their personal experience. No scientific tool exists that may assist surgeons to determine the biomechanically optimal prosthesis for a specific patient. Finite element analyses may be used as such a tool. The first essential step must be their verification and experimental validation. Intact femurs mechanical response had already been shown to be well predicted by high-order finite element models based on patient-specific QCT scans [2]. The generation of finite element models representing implanted femurs followed by their experimental validation will be presented. The experiments were conducted on fresh frozen cadaver femurs, loaded in different configurations. Measurements were performed using the 'gold standard' strain gauges, and also novel methods as digital image correlation. Once the models were validated, they were used to compare the mechanical behavior before and after the implantation. To quantify the implant's performance, comparison of the strain fields was performed. Strains were addressed rather than stresses due to their stimulation of the biological remodeling mechanism [3]. Norms to quantify strain shielding will be suggested. Such norms may assist orthopedic surgeons to choose an optimal implant for the specific patient, from the vast available variety of implants. [1] G. Labek, M. Thaler, W. Janda, M. Agreiter, and B. Stockl, "Revision rates after total joint replacement: Cumulative results from worldwide joint register datasets", Bone Joint J., vol. 93-B, no. 3, pp. 293–297, 2011. [2] N. Trabelsi, Z. Yosibash, C. Wutte, P. Augat, and S. Eberle, "Patient-specific finite element analysis of the human femur-A double-blinded biomechanical validation," J. Biomech., vol. 44, no. 9, pp. 1666–1672, 2011. [3] E. H. Burger and J. Klein-Nulend, "Mechanotransduction in bone - role of the lacuno-canalicular network," FASEB J., vol. 13, no. 9001, pp. S101–S112, 1999.

An Overset Mesh Framework Applied to the Hybridizable Discontinuous Galerkin Finite Element Method for Dynamic Meshes

Justin Kauffman^{*}, Jonathan Pitt^{**}

^{*}The Pennsylvania State University, ^{**}The Pennsylvania State University

ABSTRACT

Fluid-structure interaction simulations where the solid bodies are undergoing larger deformations require special handling of the mesh motion for Arbitrarily Lagrangian-Eulerian (ALE) formulations. Such formulations are necessary when body-fitted meshes with certain characteristics, such as boundary layer resolution, are required to properly resolve the problem. This work presents an overset mesh method to accommodate such problems in which flexible bodies undergo large deformations, or where rigid translation modes of motion are present as well. To accommodate these motions of the bodies through the computational domain, an overset mesh enabled ALE formulation for fluid flow is discretized with the hybridizable discontinuous Galerkin (HDG) finite element method. The overset mesh framework applied to the HDG method enables the deforming and translating dynamics meshes to maintain mesh quality without re-meshing. Verification and validation are presented along with an example calculation.

A Hybrid Quasicontinuum Method

Aditya Kavalur*, Woo Kyun Kim**

*University of Cincinnati, **University of Cincinnati

ABSTRACT

Quasicontinuum (QC) is a spatial multiscale method which approximates the potential energy of an atomistic system with reduced computational cost. Like other partitioned-domain approaches, QC divides the simulation domain into atomistic and continuum regions. A full-atomistic description is restricted only to the atomistic region with the continuum region adopting a finite element method-based coarse-graining scheme and a continuum constitutive relation called the Cauchy-Born (CB) rule. While the CB rule can capture the full-nonlinearity of the strain energy density in the continuum region, its computational cost is one order of magnitude higher than the linear elastic (LE) constitutive relation, which is adopted by other partitioned-domain methods. In this study we propose a novel hybrid QC method where CB and LE are combined to increase the efficiency of the original QC method. The extension consists of two main steps. First, the continuum region is further divided into sub-domains such that the CB rule is applied only to those sub-regions adjoining the atomistic region with the energy of the remaining continuum region being approximated using the linear elastic constitutive relation. Second, a corrective force term is added as dead load to the nodes in the LE region in order to retain the higher order accuracy. Two test examples of Lomer dislocations and nanoindentation are employed to validate the proposed method. The simulation results reveal that the hybrid method is numerically more efficient than the original QC method while maintaining virtually the same accuracy.

Design of Cultivation Environment Scenario of *Oryza sativa* L.

E. Kawabe^{*}, S. Nishiuchi^{**}, E. Kita^{***}

^{*}Nagoya University, ^{**}Nagoya University, ^{***}Nagoya University

ABSTRACT

While Japanese agriculture is high productivity, farmers are aging. Once the skillful farmers are retired, their knowledge should be lost. The aim of this study is to design the cultivation environment scenario of *Oryza sativa* L. "Koshihikari". If the optimized scenario is obtained, the newcomers can do like the skillful farmers. The yield and the quality data in the rice cultivation and the environment scenario are collected by Agricultural Research Center of each prefecture and Japan Meteorological Agency, respectively. The prediction models of the yield and the quality of the *Oryza sativa* L. are defined by the multiple regression analysis or neural network analysis of the rice cultivation data (yield and quality) and the environment scenario such as average temperature, maximum temperature, minimum temperature, precipitation, hours of sunlight and diurnal temperature range. The objective function of the optimization problem is defined so as to maximize the yield and the quality of the *Oryza sativa* L. Design variables are composed of the part of the environment scenario variables such as maximum and minimum temperatures. Constraint conditions for the design variables are the upper and the lower bounds of the temperatures. Optimization problem is solved by L-BFGS-B method. The initial temperature fluctuation is the average year temperature in Nagoya. The optimized year temperature is considerably lower and then, very similar to that in Tadami. References [1] L. Taiz, E. Zeiger, Plant Physiology. Fifth Edition, 2010. [2] S. Yoshida, Fundamentals of Rice Crop Science. The International Rice Research Institute, 1981. [3] T. Mitchell, Machine Learning. McGraw-Hill, 1997.

Subdomain Local FE Solver Design for DDM on Many-core Architectures

Hiroshi Kawai^{*}, Masao Ogino^{**}, Ryuji Shioya^{***}, Tomonori Yamada^{****}, Shinobu Yoshimura^{*****}

^{*}Toyo University, ^{**}Nagoya University, ^{***}Toyo University, ^{****}The University of Tokyo, ^{*****}The University of Tokyo

ABSTRACT

Exa-scale supercomputers will appear around 2020–2022. To obtain high intra-node performance, efficient utilization of processor cache memory should be considered. The traditional memory access-intensive approach, which prefers less computing and more storage on main memory, might not be effective for supercomputers in near future. The Domain Decomposition Method (DDM) is one of the effective parallel finite element schemes. We have been developing an FE-based parallel structural analysis code, ADVENTURE Solid, based on DDM, with the Balancing Domain Decomposition (BDD) pre-conditioners. The re-design of the subdomain local FE solver part, which is a performance sensitive kernel in the DDM code, is required. Here in this work, an “on-cache” iterative solver based on the DDM framework is developed. The subdomain local FE solver of the DDM code is implemented using CG solvers with element-by-element matrix storage-free approaches. These iterative solvers are parallelized using OpenMP, so that each subdomain can be solved by multiple cores. By adjusting the subdomain size so that the footprint fits within the last-level cache of a processor, this DDM code can be considered as a kind of an “on-cache” iterative solver”. Performance benchmark results are shown on various kinds of HPC platform having many core scalar processors, such as Skylake Xeon, Knights Landing and Fujitsu PRIMEHPC FX100.

Effect of Strain Path on Microstructure and Texture Inhomogeneity during Accumulative Angular Drawing Process of Ti-6Al-4V

Jakub Kawalko^{*}, Krzysztof Muszka^{**}, Piotr Bala^{***}, Marcin Kwiecien^{****}, Paulina Lisiecka-Graca^{*****}, Maciej Szymula^{*****}

^{*}AGH University of Science and Technology, Academic Centre for Materials and Nanotechnology, ^{**}AGH University of Science and Technology, Faculty of Metals Engineering and Industrial Computer Science, ^{***}AGH University of Science and Technology, Academic Centre for Materials and Nanotechnology, ^{****}AGH University of Science and Technology, Faculty of Metals Engineering and Industrial Computer Science, ^{*****}AGH University of Science and Technology, Faculty of Metals Engineering and Industrial Computer Science, ^{*****}AGH University of Science and Technology, Faculty of Metals Engineering and Industrial Computer Science

ABSTRACT

Accumulative Angular Drawing (AAD) process is a novel method used to produce wires with controlled inhomogeneity of microstructure and properties. Similarly to Severe Plastic Deformation (SPD) processes, it introduces high accumulation of deformation energy in the cross-section of the drawn wire and enables activation of additional deformation mechanisms compared to conventional drawing processes. In the current work, AAD process will be applied to produce wires made of Ti-6Al-4V alloy. This alloy is characterized by a limited ductility at room temperature due to hexagonal closed packed (HCP) structure. During AAD process strain path changes occur, what besides reduction of the cross-section area, introduces additional bending, shearing, burnishing and torsion to the deformed wires, and thanks to that, activates additional slip planes allowing successful realization of deformation process. In the present work, level of inhomogeneity of microstructure, texture and properties resulting from applied strain path history will be assessed. Conclusions regarding interrelationships between deformation history and resulting microstructural changes will be drawn in the light of possible texture mechanisms that are activated during AAD process. Due to a number of process parameters that affect the microstructural inhomogeneity, acquired data can be used for the numerical modeling. Understanding of the AAD of Ti alloys with the aid from computer simulation will enable optimization of the process towards better control of microstructure and texture inhomogeneity what, in turn, will allow production of titanium wires with controlled gradual changes in their microstructure and properties.

SEISMIC RESPONSE CONTROL FOR EQUIPMENT WITH CASTERS USING SWITCHING WHEEL LOCK CONDITIONS

YOSUKE KAWANISHI*, MASAYUKI KOHIYAMA*

*Graduate School of Science and Technology, Keio University
3-14-1 Hiyoshi, Kohoku-ku, Yokohama 223-8522, Japan
yosuke.kawanishi@keio.jp

Key words: Seismic Response Control, Caster Wagon, Furniture, Rocking, Sliding,
Numerical Analysis

Abstract. When an earthquake occurs, the people in and/or contents of buildings may suffer damage due to the sliding or overturning of furniture and equipment or the falling of objects even if the structure of the building experiences no damage. In this study, using numerical analyses, we investigate a model of effective equipment caster wheel control to reduce damage caused by the moving and overturning of equipment during earthquakes and propose a control method to switch the lock and free conditions of the caster wheel. In the numerical analyses, a simulator library of three-dimensional rigid body dynamics is used and two-direction earthquake ground motion is input into a model of a 10-story steel frame building. The horizontal displacement and the falling down of the equipment model are expressed depending on the caster lock condition.

1 INTRODUCTION

In an earthquake event, to protect people in a building, we need to consider not only the damage to a building's structure but also the damage caused by furniture in the building. When an earthquake occurs, furniture in a building and/or their contents may hit people or may overturn and hinder evacuations, as reported in the 2011 Great East Japan Earthquake. In particular, the seismic resistance of medical equipment is important because it affects whether medical activities can be performed following an earthquake. Most medical equipment are equipped with casters for convenience, and in the case of the 1995 Hyogo-ken Nanbu Earthquake, it was reported that medical equipment with high centers of gravity overturned when the casters were locked and moved around and collided with other equipment and the walls when the casters were not locked. Nikfar and Konstantinidis ^[1] estimated the seismic responses of hospital equipment supported by casters. They determined the frictional resistance of the casters, evaluated the seismic response of the equipment, and performed shaking table experiments. Kamada et al. ^[2] proposed an earthquake response control of caster-supported wagons using an ER, variable-type brake and demonstrate its effectiveness via simulations and excitation

experiments. In past studies of furniture earthquake response analyses, it has been common to use a spring–mass model; however, this model does not consider the shape of the structure. Saomoto and Yoshimi ^[3] analyzed furniture earthquake responses using a physics engine, the Open Dynamics Engine (ODE) and performed numerical analyses considering the shape of the furniture. Masatsuki and Midorikawa ^[4] quantitatively examined the fluctuations of large displacements considering the collisions of multiple pieces of furniture and walls using a physical simulator, Springhead2. Isobe et al. ^[5] developed an effective numerical code based on the adaptively shifted integration (ASI)–Gauss technique for analyzing the motion of furniture subjected to seismic excitations.

In this study, using an ODE numerical analysis, we investigate effective caster wheel control to reduce damage due to equipment moving and overturning during earthquakes and propose a control method to switch the lock and free conditions of the caster wheels.

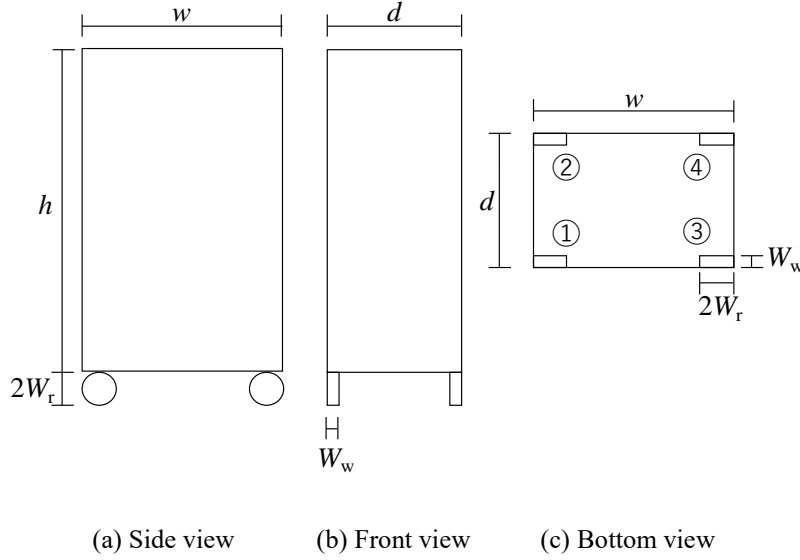
2 OUTLINE OF THE SIMULATION AND CASTER CONTROL METHOD

In the numerical analysis, we use ODE, which is a simulator library of three-dimensional rigid body dynamics. The modeled equipment with casters consists of a box and four wheels. The width, depth, height, and mass of the model are 0.45 m, 0.30 m, 0.80 m, and 10 kg, respectively. First, we input the two-direction earthquake ground motion (NS and EW) into a model of a 10-story steel frame building with a first natural period of 0.8 s and obtained the acceleration response time history on the top (9th) floor. We assumed that the equipment is placed on the top floor of the building and input the response acceleration waves to the floor slab to obtain the response time history of the equipment model. We compared the responses for the following three caster conditions: (1) setting the casters as locked, (2) setting the casters as free, and (3) switching the casters between locked and free at constant time intervals.

2.1 THE EQUIPMENT MODEL

In this study, we consider the equipment model shown in Figure 1 and define the variables as shown in Table 1. The value obtained in the experiment conducted by Saito et al. ^[6] is used as the friction coefficient.

We name the casters as shown in Figure 1(c). In addition, for the sake of simplicity, the caster swivels do not rotate and are fixed at the position shown in Figure 1.

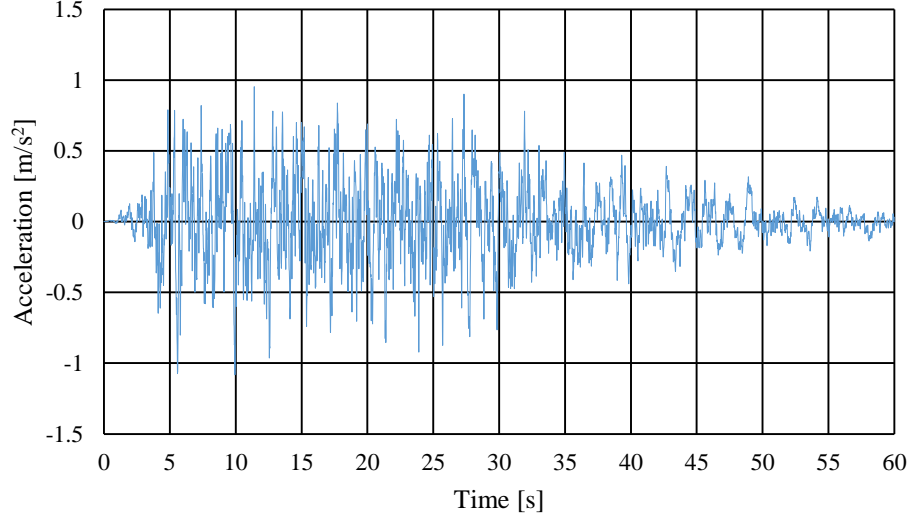
**Figure 1.** The equipment model.**Table 1.** Parameters of the equipment with casters.

Specification	Variable	Value
Equipment width	w	0.40 m
Equipment depth	d	0.30 m
Equipment height	h	0.80 m
Equipment mass	M	10 kg
Caster mass	M_c	0.05 kg
Caster wheel radius	W_r	0.0375 m
Caster wheel width	W_w	0.75 m
Friction coefficient when the casters are locked	μ_0	0.3
Static friction coefficient	μ_s	0.4
Friction coefficient when the casters are released	μ_{free}	0.02

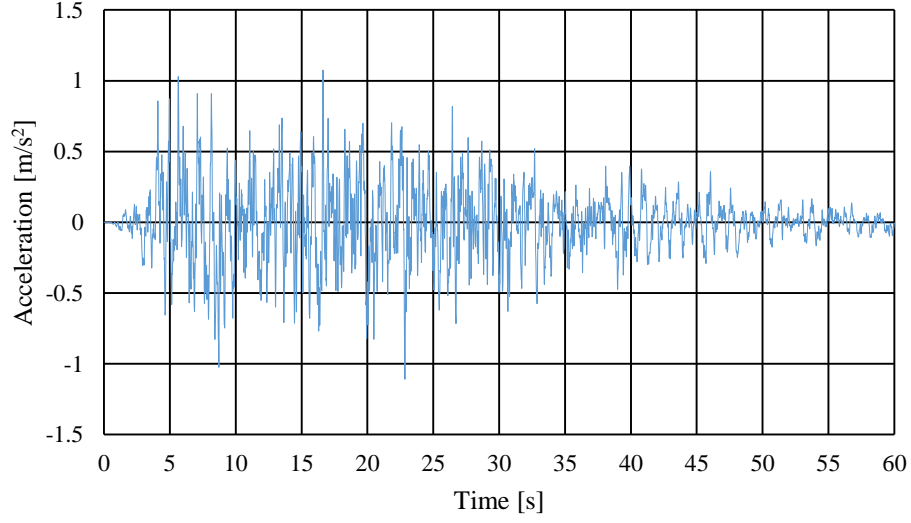
2.2 DYNAMIC ANALYSIS OF A BUILDING MODEL

With respect to the input ground motions, we use simulated ground motions of “rare earthquake ground motion” at an outcrop engineering bedrock with random phase components, as prescribed in Notification No. 1461 of the Ministry of Construction, Japan, May 31, 2000. The ground motions correspond to a return period of approximately 50 years. Figure 2 shows the

time history of the input ground acceleration, and Figure 3 shows the target acceleration spectrum and acceleration response spectra of the input waves.



(a) EW direction



(b) NS direction

Figure 2. Time history of the ground acceleration input to a 10-story building model.

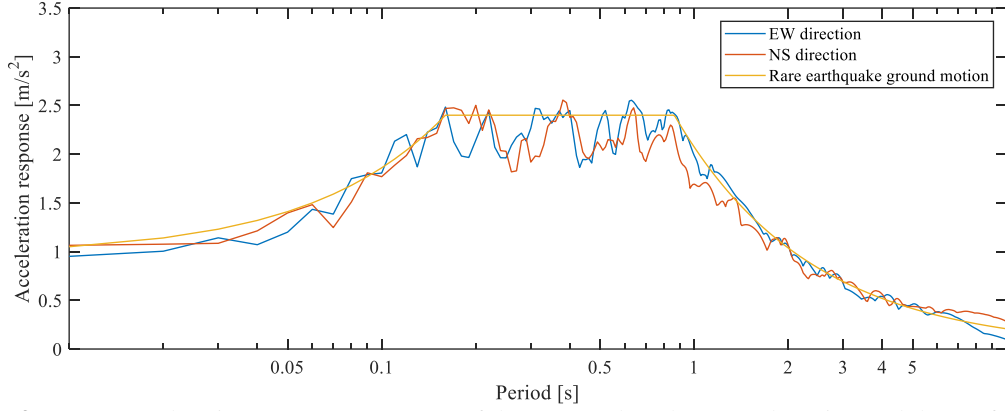


Figure 3. Target acceleration response spectrum of the rare earthquake ground motion and those of the input waves (5% damping).

We enter these input acceleration waves into the building model and obtained the acceleration response for each floor. We use the Newmark β method for the time history response analysis. With respect to the behavior of the specimen from a previous study by Purvance et al. ^[7], we consider the influence of the input wave in the vertical direction to be small. Therefore, in this analysis, we only input the horizontal acceleration waves and obtained the horizontal acceleration response of the building. The results of the time history response analysis for the 9th floor are shown in Figure 4, and Figure 5 shows the floor response spectrum on the 9th floor.

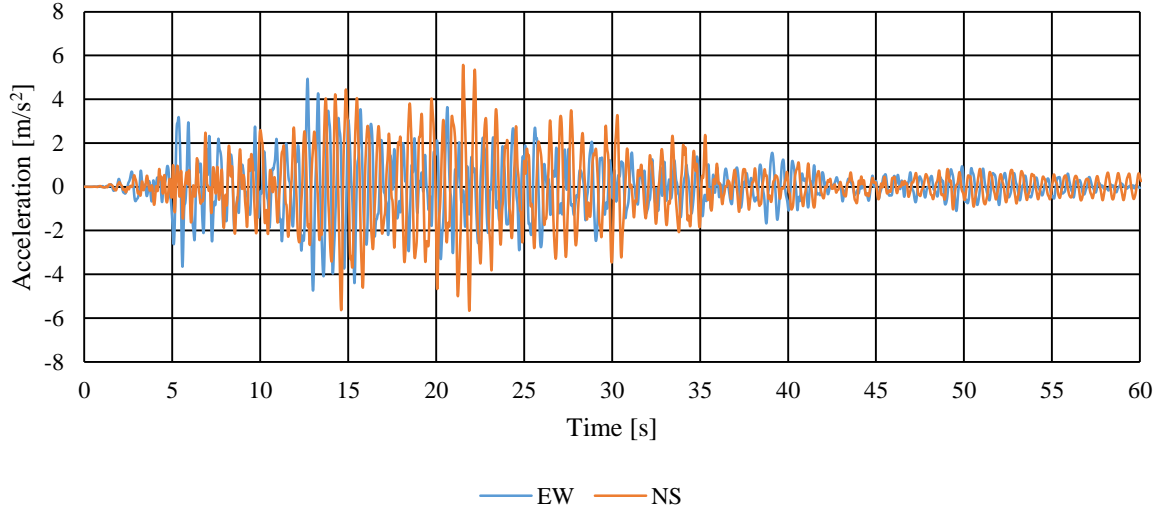


Figure 4. The results of the time history acceleration response analysis for the 9th floor of the building model.

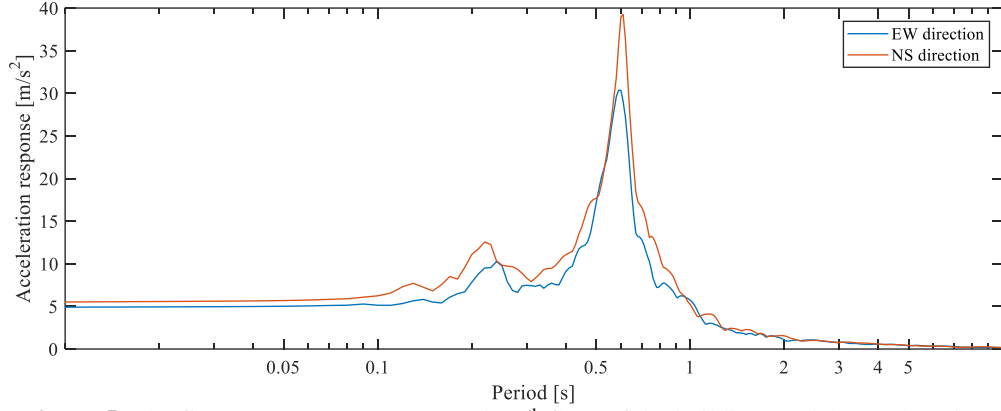


Figure 5. The floor response spectrum on the 9th floor of the building model (5% damping).

3 NUMERICAL ANALYSIS OF THE EQUIPMENT RESPONSE

3.1 ANALYSIS CONDITIONS

In the numerical analysis of equipment response, we set the time step to 0.01 s and the number of analysis steps to 6000. When a floor responds to the earthquake and the equipment model vibrates, the position and posture of the equipment change. Therefore, we consider the following 10 patterns for the possible posture of the equipment as shown in Table 2.

Table 2. The posture of the equipment.

Case	Condition
(a)	The case when all casters touch the floor.
(b1)	The case when casters 1 and 2 touch the floor.
(b2)	The case when casters 3 and 4 touch the floor.
(b3)	The case when casters 1 and 3 touch the floor.
(b4)	The case when casters 2 and 4 touch the floor.
(c1)	The case when only caster 1 touches the floor.
(c2)	The case when only caster 2 touches the floor.
(c3)	The case when only caster 3 touches the floor.
(c4)	The case when only caster 4 touches the floor.
(d)	The case when the equipment jumps and none of the casters touch the floor.

For the sake of simplicity, we assume the following.

- Only the inertial force and the frictional force are applied to the equipment.

- The inertial force is applied to the center of gravity of the equipment box model and the four casters of the equipment model.
- The equipment model is a rigid body and the casters do not swing or roll.
- After the equipment model falls down, we assume that the equipment does not move anymore.
- We consider the equipment model to have fallen when part of the upper surface of the equipment model touches the ground.
- We consider both static and dynamic friction forces.
- The angular velocity and angular acceleration are obtained from the rotation angle via the finite difference method.
- We assume that the normal forces of each caster wheel are equal. They are actually different; however, what matters is the resultant of the normal forces. There is no difference in the movement of the equipment model if these forces are assumed to be equal.

First, we consider the case when the caster i is locked. The frictional force vector $\mathbf{F}_{\text{frc},i}$ is defined as

$$\mathbf{F}_{\text{frc},i} = \begin{pmatrix} -\mathbf{F} & \left(|\mathbf{F}| < \sum_{i=1}^4 F_{s,i} \wedge \dot{\mathbf{x}}_i = 0 \right) \\ -\mu_0 N_i \times \left(\frac{\dot{\mathbf{x}}_i}{|\dot{\mathbf{x}}_i|} \right) & \left(\left(|\mathbf{F}| \geq \sum_{i=1}^4 F_{s,i} \wedge \dot{\mathbf{x}}_i = 0 \right) \vee \dot{\mathbf{x}}_i \neq 0 \right) \end{pmatrix}, \quad (1)$$

$$F_{s,i} = \mu_s N_i, \quad (2)$$

where \mathbf{F} is the inertial force vector applied at the center of gravity of an equipment model, $F_{s,i}$ is the maximum static friction force calculated at the caster i , μ_0 is the static frictional coefficient, μ_s is the dynamic friction coefficient, N_i is the normal force at the wheel of caster i , \mathbf{x}_i is the displacement of caster i , and $\dot{\mathbf{x}}_i$ is the velocity of caster i . The friction force is applied to the position where the casters touch the ground.

Di Egidio and Contento^[8] defined the normal force N_i using a formula balancing the horizontal direction, the vertical direction, and rotation such that

$$N_i = m(g + b'_1 \ddot{\theta} - h'_1 \dot{\theta}^2), \quad (3)$$

where m is the mass of the equipment model and g is the gravitational acceleration. Suppose ϕ is defined by the angle between the yaw axis of a rigid body and the horizontal vector perpendicular to its rotating axis, then θ is calculated such that $\theta = \frac{\pi}{2} - \phi$. b'_1 is the distance between the projected point of the center of gravity on xy -plane and the position where the casters touch the floor, and h'_1 is the height of the center of gravity of the equipment model. In the cases (b1) and (b2), b'_1 and h'_1 are shown in Figure 6 and are described as

$$b'_1 = h_1 \cos \theta - b_1 \sin \theta + W_r \cos \theta, \quad (4)$$

$$h'_1 = h_1 \sin \theta + b_1 \cos \theta + W_r(1 + \sin \theta). \quad (5)$$

where b_1 is the difference between a half of the equipment width w and the caster wheel radius W_r , and h_1 is a half height of the equipment height h .

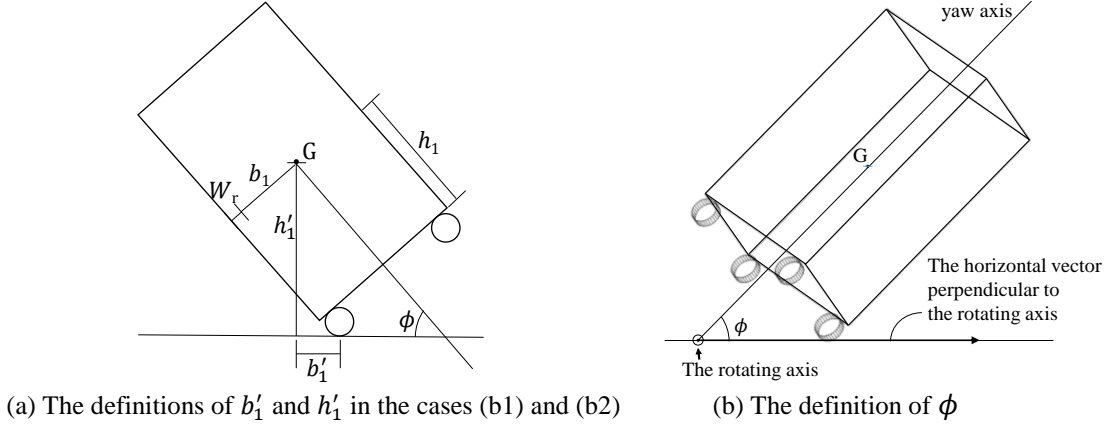


Figure 6. The definitions of parameters

Next, we consider the case when the casters are released. In addition to the friction force when the casters are locked, we apply an external force vector \mathbf{F}_{free} , which is equivalent to the casters rolling and is expressed as

$$\mathbf{F}_{\text{free}} = (\mu_0 - \mu_{\text{free}})N\mathbf{r}, \quad (6)$$

where μ_{free} is the dynamic friction coefficient when the casters are rolling and \mathbf{r} is the direction in which the casters are rolling. When θ is greater than $\frac{\pi}{4}$, the caster wheel rolls inward, and when θ is smaller than $\frac{\pi}{4}$, the caster wheel rolls outward. As with the friction force, the external force vector \mathbf{F}_{free} is applied to the position where casters touch the ground.

3.2 FLOW DIAGRAM OF THE NUMERICAL ANALYSIS

A flow diagram of the numerical analysis is shown in Figure 7; the variables are defined in Table 3.

Table 3. The variables for the flow diagram in Figure 7.

Parameter	Explanation
t	The current step number
Δt	The time step width (= 0.01 s)
Flg _{fd}	If 1, the equipment model has fallen down, and if 0, it has not.
flg _{lk}	If 1, the caster wheels are locked, and if 0, they are not.

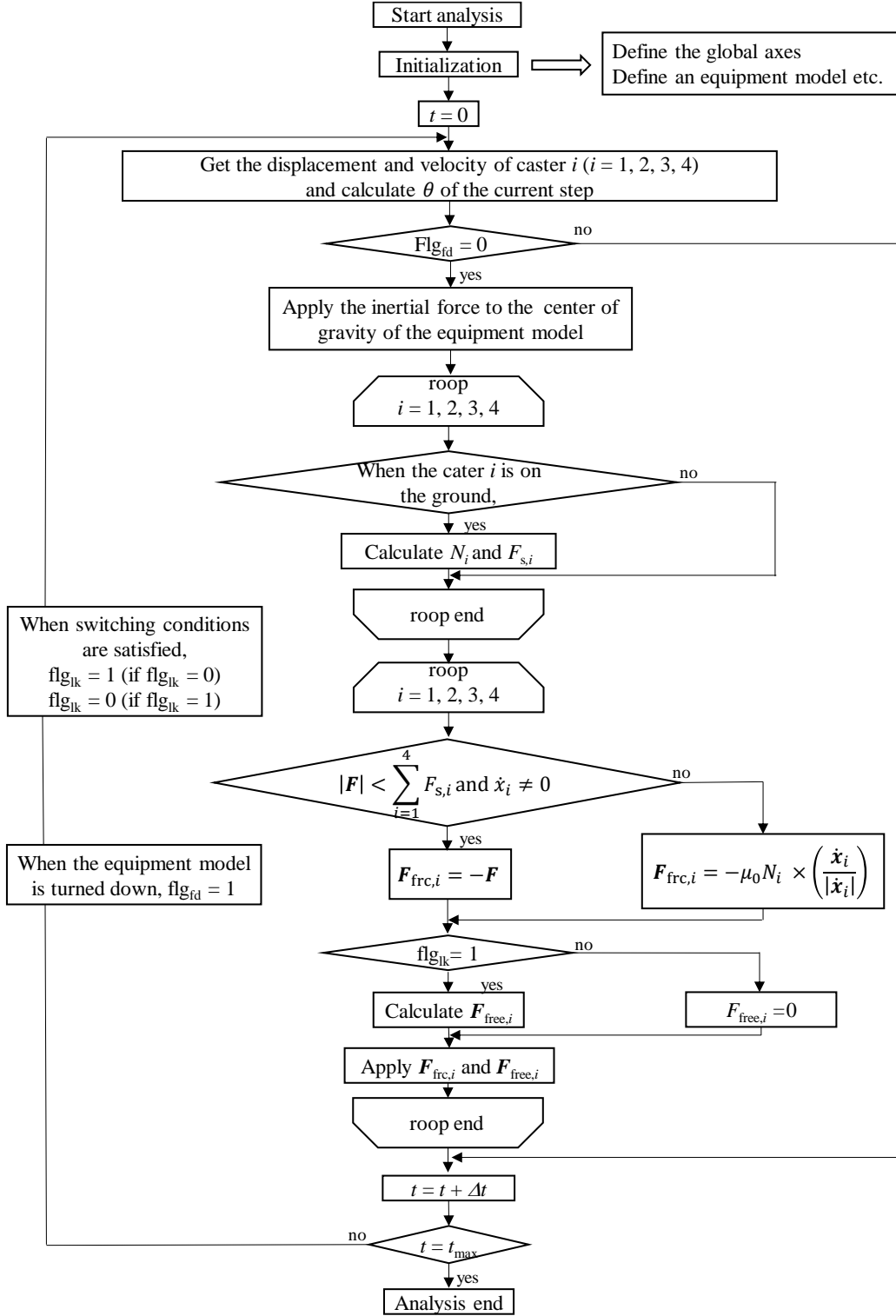


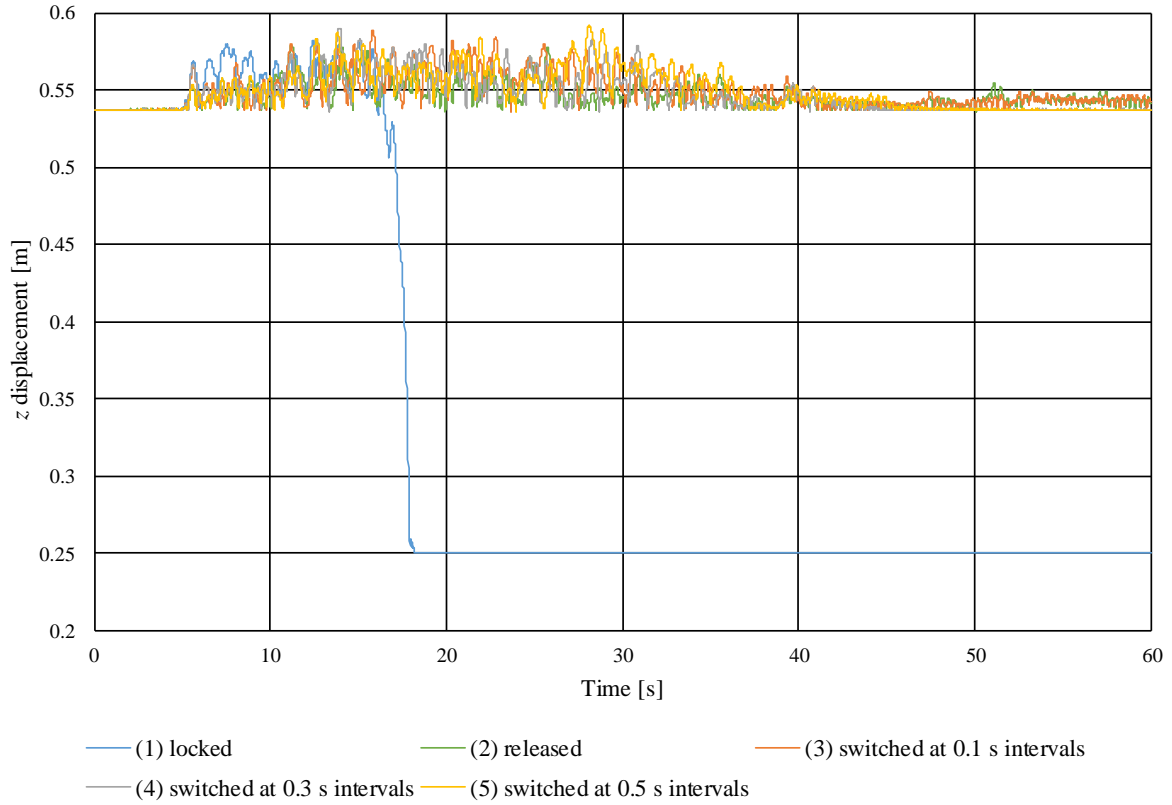
Figure 7. Flow of the numerical analysis.

3.3 CONTROL OF THE CASTERS

We consider the following five conditions to control the casters.

- (1) All casters locked.
- (2) All casters released.
- (3) All casters switched between locked and released at 0.1 s intervals.
- (4) All casters switched between locked and released at 0.3 s intervals.
- (5) All casters switched between locked and released at 0.5 s intervals.

The results of the equipment time history response analysis with control patterns (1)–(5) are shown in Figure 8.



(a) z displacement of the center of gravity of the equipment model

Figure 8. The results of the equipment time history response analysis for the five control patterns.

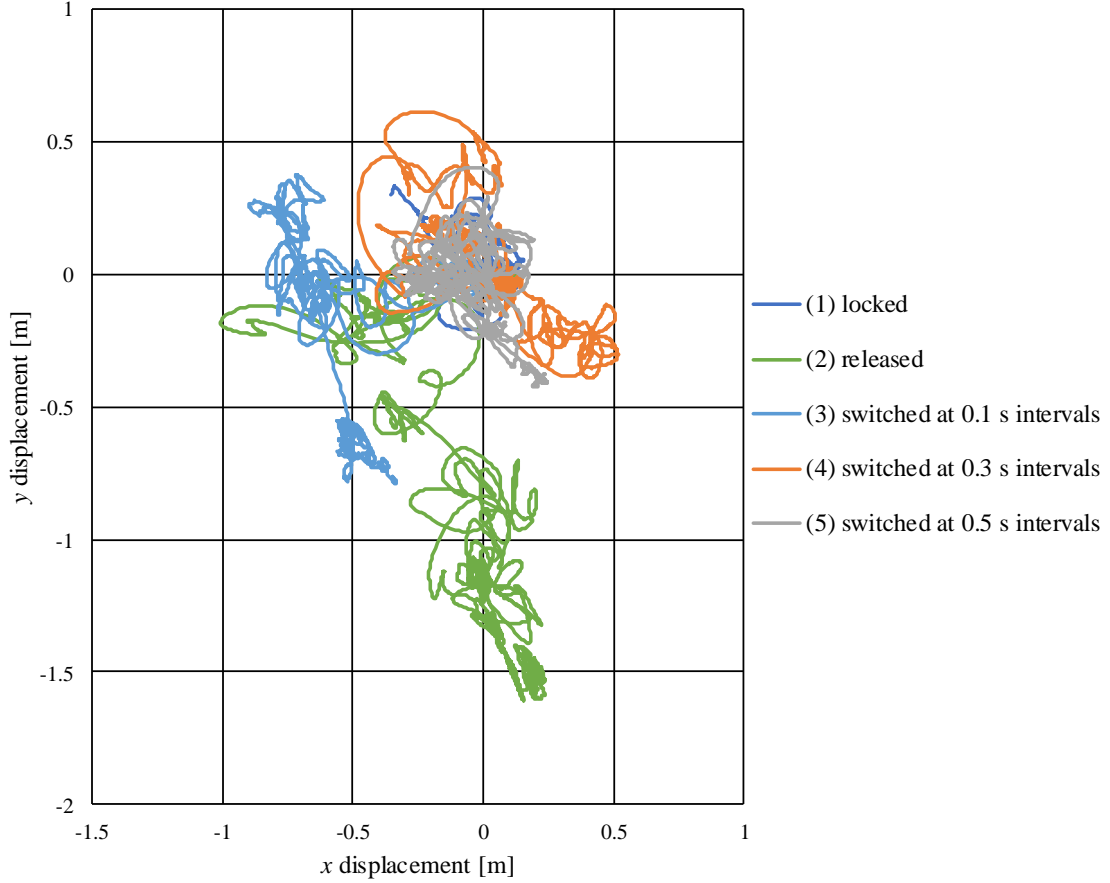


Figure 8. The results of the equipment time history response analysis for the five control patterns (continued).

From the z displacement of the center of gravity of the equipment model in Figure 8(a), the equipment model fell down only for condition (5), and from the x and y displacement of the center of gravity of the equipment in Figure 8(b), the equipment model moved to the farthest for condition (5) and moved the least for condition (4). Condition (3) resulted in a pattern where the displacement was small and the equipment did not fall down. We found that the caster switching control affects the behavior of the equipment model during seismic excitation. Therefore, caster switching control could reduce the damage in a building. However, more precise control methods need to be investigated.

4 CONCLUSIONS

We developed a simulation code to analyze the behavior of equipment with casters in a building and analyzed the motion of such equipment subjected to earthquake excitation. As a result of the numerical analysis, we confirmed that the proposed switching control could reduce the displacement and the probability of the equipment overturning. In a future study, we will derive

the overturning condition of furniture with casters from large amounts of damping control data, we will propose an optimal fixed/non-fixed switching control based on that condition, and we will perform shaking table experiments to validate our simulation results.

ACKNOWLEDGEMENTS

This work was supported by JSPS KAKENHI Grant Number 16H04455. The authors acknowledge Ms. Arisa Sugimoto for her contribution to fundamental formulation of control scheme.

REFERENCES

- [1] Nikfar, F. and Konstantinidis, D. Shake table investigation on the seismic performance of hospital equipment supported on wheels/casters. *Earthq. Eng. Struct. Dyn.* (2017) 46:243–266.
- [2] Kamada, T., Ogata, Y., Sato, E., and Takehi, A. Seismic response mitigation of medical wagon with casters by ER brake. *Proceedings of the 10th International Conference on Motion and Vibration Control* (2010) 2C35-1–2C35-9.
- [3] Saomoto, H. and Yoshimi, M. Seismic response simulation of furniture: Rational input including shape effect of building. *Journal of Japan Society of Civil Engineers, Ser. A1* (2013) 69: I_1642–I_1649.
- [4] Masatsuki, T. and Midorikawa, S. Simulation of seismic behavior of furniture in high-rise residential building due to long-period ground motion. *Journal of Japan Association for Earthquake Engineering* (2015) 15:6_1–6_11.
- [5] Isobe, D., Yamashita, T., Tagawa, H., Kaneko, M., Takahashi, T., and Motoyui, S. Motion analysis of furniture under seismic excitation using the finite element method. *Japan Architectural Review* (2018) 1: 44–45.
- [6] Saito, T., Takahashi, T., Hasegawa, R., Morita, K., Azuhata, T., and Noguchi, K. Shaking table test on indoor seismic safety of highrise buildings (Part II. Movement of furniture under long period earthquake ground motion), *Proceedings of the 14th World Conference on Earthquake Engineering* (2008) S10–014.
- [7] Purvance, D.M., Anoshehpour, A., and Brune, J.N. Freestanding block overturning fragilities: Numerical simulation and experimental validation. *Earthq. Eng. Struct. Dyn.* (2008) 37:791–808.
- [8] Di Egidio, A. and Contento, A. Base isolation of slide-rocking non-symmetric rigid blocks under impulsive and seismic excitations. *Engineering Structures* (2009) 31:2723–2734.

PROBLEM-SOLVING ENVIRONMENT (PSE) IN COMPUTATIONAL ENGINEERING AND SCIENCE

SHIGEO KAWATA*

* Graduate School of Eng., Utsunomiya University
Yohtoh 7-1-2, Utsunomiya 321-8585, Japan
kwt@cc.utsunomiya-u.ac.jp

Key Words: Problem Solving Environment, Computer assisted computations, Scientific simulation, e-Science, PSE, Uncertainty in scientific computing.

Abstract. In this paper a review is presented on the PSE (Problem Solving Environment) concept in computational engineering and science. In the PSE concept, human concentrates on target problems and works out solutions, and a part of application of solutions, which can be solved mechanically, is performed by computers or machines or software. PSE provides integrated human friendly innovative computational services and facilities for easy incorporation of novel solution methods to solve a target class of problems. PSE is an innovative concept to enrich our e-Science, e-Life, e-Engineering, e-Production, e-Commerce, e-Home, etc. The PSE-relating studies were started in 1970's to provide a higher-level programming language than Fortran, etc. in scientific computations. The trend at that time was natural to deliver more human-friendly programming environment, and was resulting in PSE, CAE (Computer Assisted Engineering), libraries, etc. At present PSE covers a rather wide area, for example, program generation support PSEs, education support PSEs, CAE software learning support PSEs, Grid/Cloud computing support PSEs, job execution support PSEs, e-Learning support PSEs, etc. This review paper includes the PSE definition, a brief history of PSE, example PSE study activities, uncertainty management PSE and a future research directions in PSE.

1 INTRODUCTION

Problem Solving Environment (PSE) concept provides integrated human-friendly innovative computational services and facilities for easy incorporation of novel solution methods to solve a target class of problems. For example, a PSE generates a computer program automatically to solve differential equations^[1-12]. Now the PSE concept covers rather wide areas in our society. PSE is an innovative concept to enrich science, human life, engineering, production and our society toward a programming-free environment in computing science. In the PSE concept, human concentrates on his/her target problems and works on solutions, and a part of application of solution, which can be solved mechanically, is performed by computers or machines or software. At present many kinds of computer-assisted problem solving environments are found everywhere in our life and in our society.

On the other hand, even today human power still contributes greatly to develop and write new softwares. For example, in scientific researches scientific discoveries are supported by theory, experiments and computer simulations. New researches tend to require new computer programs to simulate phenomena concerned. In another example, in developing new products engineers would also need new computer programs to develop the products cost-effectively. They may have to develop the new programs or learn how to use the programs for the product development. New services may also need new software systems. Therefore, the researchers and engineers may write or develop the new computer programs or learn how to use the programs. They do not like to develop nor learn the computer programs to solve their problems, but they like to devote their efforts to solve their target problems themselves.

In addition, computer simulations became the third important method after theoretical and experimental methods in science and engineering. Computer assisted problem solving is one of key methods to promote innovations in science and engineering, and contributes to enrich our society and our life from scientific and engineering sides.

The PSEs have provided the new directions to support users, engineers and scientists for

developing new services and new softwares, and also for solving their target problems based on computer systems.

The PSE-relating studies were started in 1970's to provide a higher-level programming language than Fortran, COBOL, ALGOL, PL/I and others in scientific computations. The trend at the time was reasonable to deliver more human-friendly programming environment beyond the higher-level languages shown above. Then the PSE research activity was started as well as activities of Computer Assisted Engineering (CAE) and software libraries. After the intensive developments in computer hardware and also in computer algorithms, researchers and engineers had expected an innovation in program writing and developing power. However, the enhancement in the programming power was relatively slow and weak compared with the enormous evolutions in the present hardware and algorithm power enhancements.

At present PSE covers a rather wide area, for example, program generation support PSE, education support PSE, CAE software learning support PSE, grid/cloud computing support PSE, job execution support PSE, learning support PSE, uncertainty management in scientific computing, PSE for PSE generation support (PSE for PSE), etc.

The paper includes a brief history of PSE, example PSE study activities and a future of PSE, including uncertainty management in scientific computing.

2 COMPUTER-ASSISTED PROBLEM SOLVING ENVIRONMENT (PSE)

PSE is defined as follows: "A system that provides all the computational facilities necessary to solve a target class of problems. It uses the language of the target class and users need not have specialized knowledge of the underlying hardware or software"^[6]. PSE provides integrated human-friendly innovative computational services and facilities to enrich science, life, engineering, production, commerce and our society. Based on the PSEs, human concentrates on target problems themselves, and a part of solution is performed mechanically by computers or machines or software.

In computing sciences, we need the computer power, the excellent algorithms and the programming power in order to solve scientific problems leading to scientific discoveries and development of innovative new products and services. So far, the computer power and the computing algorithms have been developed incredibly, and have provided enormous contributions to sciences, productions and services. On the other hand, the programming power has not been developed well. The concept of PSE was proposed to support the programming power in science and engineering, and has been explored for decades.

In 1985, IFIP (International Federation for Information Processing) WG2.5 (Numerical Software)^[16] organized a working conference on PSE and published the proceedings^[17]. In 1991, a working conference on Programming Environments for High-Level Scientific Problem Solving was held^[18]. In addition, a book on PSE was also published^[19]. In 2007, a working conference on Grid-Based Problem Solving Environments was held^[20]. A working conference on Uncertainty Quantification in Scientific Computing was held in 2012^[21]. The PSE activity including scientific computing environments is one of research projects in IFIP WG2.5^[16]. In these decades, international conferences tend to include the topic of PSE as one of standard topics in scientific computing. It has been recognized that PSE is an important research area in scientific computation and high-performance computing. In parallel, the PSE activities have started in several societies, scientific groups and countries. For example, in Japan, the PSE research group started in 1998 based on the previous individual PSE study activities, and the Japan Society for Computational Engineering and Science (JSCES) started in 1995, including the Study Group on PSE^[22, 23].

The PSE studies have been extensively explored over the past few decades. The explorations have been supported by the reinforced computer power and algorithm power. PSE has boosted the programming power, and have enriched problem solving methods in science and engineering to bring us innovations.

One of PSE studies^[1-12] has been extensively explored in order to support engineers and

scientists to compute or solve their own problems based on for partial differential equations (PDEs), for example. One of the major objectives in PSE researches is to help users compute or solve their problems without heavy tasks, for example, without complete knowledge for computations^[24] and/or the programs used. In this sense, the PSE provides an infrastructure for software for computational engineering and sciences.

One of typical PSEs for PDEs-based problems is ELLPACK^[8, 24]. ELLPACK is a high level system for solving elliptic boundary value problems. One can solve routine problems by simply writing them down and naming the methods to be used. The ELLPACK high-level language can reduce the programming effort for a "routine" elliptic problem.

Another typical PSE for PDEs-based problems is DEQSOL^[7, 10, 11]. DEQSOL was designed to develop an easy-to-use system for problem solving of PDE-based problems by finite difference method and finite element method. DEQSOL creates optimal Fortran codes oriented to the Hitachi vector processors.

Another PSE system of NCAS^[1, 2, 4, 9] inputs a problem information including PDEs, initial and boundary conditions, and discretization and computation schemes, and outputs a program flow graph, a C-language source code for the problem and also a document for the program and for the problem (see Fig. 1). On a host computer a user inputs his/her problem, and NCAS guides the user to solve the problem. The distributed PSE for PDEs consists of several modules: problem description, discretization, equation manipulation, program design, program generation, documentation support, module liaison and job execution service. Each module is distributed on distributed computers. Each distributed module communicates with the host module, so that outputs from each module are visualized. Independent modules, which are developed by other engineers or users for one of the functions specified above can also be used after adjustments to the distributed PSE interface^[25], if necessary. The module liaison module generates an adapter module for the distributed PSE modules. The adapter module generated by the module liaison system inputs output data from preceding modules and/or external modules, and connects the data to the input data for the next module. The PSE contains all the information of the problem, PDEs, discretization scheme, mesh information, equation manipulation results, program design structure, variables and constant definitions and program itself. Therefore, the documentation support module also generates a document for the program generated together with the problem itself in the PSE^[26].

A PSE module in NCAS also helps users generate MPI-based parallel simulation programs based on PDEs^[4]. The NCAS capability explores possibilities to visualize and steer the parallel program design process. At present NCAS supports a domain decomposition in a design of a parallel numerical simulation program, and the domain decomposition is designed or steered by users through a visualization window. After designing the domain decomposition, the parallel program itself is also designed and generated in NCAS, and the designed parallel program is visualized and steered by a Problem Analysis Diagram (PAD). In NCAS, MPI functions^[27] are employed for message passing, and a single program multiple data (SPMD) model is

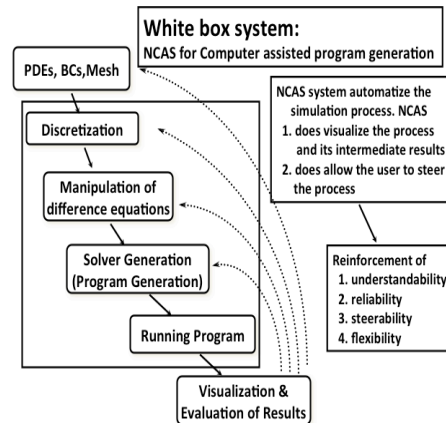


Fig. 1 An example PSE for computer assisted scientific program generation support: NCAS. NCAS inputs partial differential equations (PDEs), initial and boundary conditions, discretization method and algorithm, and outputs a C language program. The PDEs are automatically discretized and the program is generated mechanically. NCAS is a white box system, in which users can see and steer all the processes of program generation. NCAS system contains all the information for program generation, including basic equations, discretization schemes, discretized equations, boundary and initial conditions, mesh structure, program structure, and definitions of variables and constants. Therefore, a document for the corresponding program is also generated together with the program itself.

supported. The visualization and steering capabilities provide users a flexible design possibility of parallel programming.

Some PSEs provide a job execution support service on cloud or grid^[28, 29]. It is difficult for users to submit jobs to distributed computers and to retrieve calculation data from them in scientific computing. A robust job execution service system was also developed in a closed distributed computer system^[28]. The job execution service system consists of dynamic system management servers, execution servers and data servers. The dynamic system management server is duplicated in order to keep the system robust, and has an assistant management server. The dynamic system management server has a function of the job execution system management, including software deployment, program compilation, job execution, job status retrieval and computing data retrieval. This system does not require special middleware such as Globus^[30] or UNICORE^[31] or so. Users access the WWW page on the dynamic system management server, and the clients submit jobs. After the submitted job finishes, the dynamic system management server collects the information from other distributed computers. The dynamic management server and its assistant server move dynamically to new servers, if the present servers become busy. The dynamic system management server also demands the execution server to transfer the result data to the optimal data server. The dynamic system management server copies the computing data and sends the compressed computing data to another optimal data server in order for a robust data storage system. The clients can deploy their programs, execute jobs and retrieve the result data by accessing only the WWW page in the job execution service system. This job execution management server also has a function of automatic system construction, so that the users can manage the setup of the job execution management system easily on their closed distributed computers.

Another remarkable example of PSE is an education support PSE^[32]. Network-based learning has been taking an important role in education as helpful education tools. However, it is difficult for teachers to retrieve education data from students or to obtain data from the student activities. Therefore, a problem solving environment (PSE) for the education and learning support: TSUNA-TASTE^[32] was developed. The TSUNA-TASTE system collects the system-usage statistics, the information for the windows used and the operation situation of the mouse and key board of all students. The data, which the system TSUNA-TASTE collects, are stored in a database on the TSUNA-TASTE system server. Based on the data collected, teachers can have the learning status data for each student, and can guide the students in a better way.

Another research issue in PSE is validation, verification and uncertainty control in scientific simulations. When a software gives incorrect results for users, it may cause some difficulties, errors and accidents, depending on target problems^[21, 33-37]. The validation and verification mechanism is essentially important in scientific computing. This point was also pointed out by E. Houstis, J. Rice and his colleagues^[38]. Standardization and benchmark problems in each field may help to perform the validation and verification. In addition, uncertainty management must be addressed intensively in order to avoid serious accidents and disasters in our society. PSE is one of candidates to manage the uncertainty in a relatively easy way^[39]. The topic on the uncertainty is also discussed in this paper. There are many PSE examples studied so far. In the references of [17-20] and [25] one can also find the example PSEs. In the next section typical example PSEs are introduced.

3 PSE EXAMPLES

3.1 A program generation support PSE

PSE studies [2-14] for partial differential equation (PDE) based problems have been extensively explored in order to support engineers and scientists to compute or simulate their problems and products on computers in e-Sciences and e-Productions. One of the major objectives in PSE researches is to help users compute or simulate their problems without heavy tasks, for example, without complete knowledge [11, 12] for computations or without a full programming [2-13].

In this subsection a program generation support PSE, called NCAS is presented. NCAS inputs partial differential equations (PDEs), the initial and boundary conditions, the discretization method and the algorithm, and outputs a C language program for the problem. The PDEs are automatically discretized and the program is generated mechanically. NCAS is a white box system, in which users can see and steer all the processes of the program generation. NCAS contains all the information for program generation, including the basic equations, the discretization schemes, the discretized equations, the boundaries and the initial conditions, the mesh structure, the program structure, and the definitions of all the variables and the constants. Therefore, a document for the corresponding program is also generated together with the program itself. In PSE for PDEs problems, one of problems, which should be addressed, is to develop huge PSE systems, including reusability of legacy PSE software. In order to solve this problem, a module-based PSE is proposed^[9, 40]; each PSE module solves a part of PSE tasks, for example, a problem description interface, a discretization module, a scheme suggestion module, a program flow designer, a program generator, a data analyzer, a visualizer, and so on. If each module can be developed independently and works cooperatively and smoothly to solve one PSE job, the heavy work of PSE development may be drastically relaxed. In this subsection a distributed PSE, called NCAS, is introduced, which supports users to generate computer programs^[1-4, 9, 26, 40].

The PSE system of NCAS inputs a problem information including discretization and computation schemes, and outputs a program flow graph, a C language source code for the problem and also a document for the program and for the problem. On a host computer a user inputs his/her problem, and the host guides the user to solve the problem. The distributed PSE for PDEs consists of several modules: a problem description, a discretization, an equation manipulation, a program design, a program generation, documentation support, a module liaison and a job execution service. Each module is distributed on distributed computers, and all the information is described by the Extensible Markup Language (XML) including the Mathematical Markup Language (MathML). Each distributed module communicates with the host module by using XML documents, so that outputs from each module are visualized. Independent modules, which are developed by other engineers or users for one of the

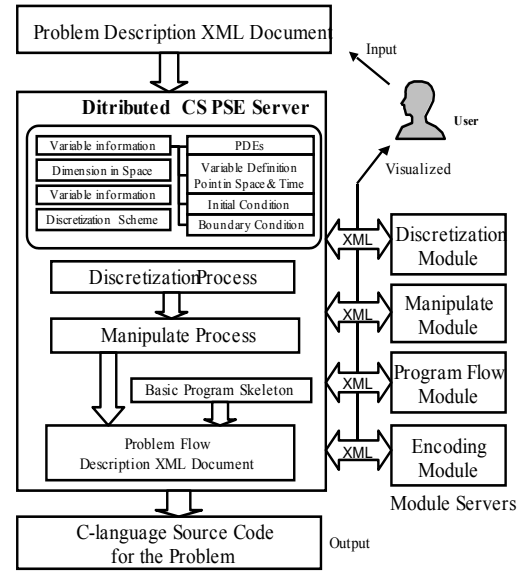


Fig. 2 Distributed-PSE: NCAS workflow.

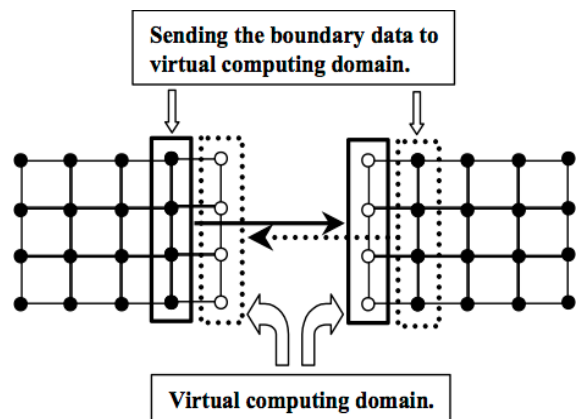


Fig. 3 Boundary data are communicated by the MPI functions in NCAS among domains decomposed. The MPI functions are automatically inserted into the program designed and generated in NCAS. The Finite Difference method (FDM) is employed in this example.

functions specified above can be also used after adjustments to the distributed PSE interface, if necessary. Therefore, the concept of the distributed PSE extends the potential of conventional PSE systems. The PSE contains all the information of the problem, PDEs, discretization scheme, mesh information, equation manipulation results, program design structure, variables and constant definitions and program itself. Therefore, the documentation support module also generates a document for the program generated and the problem itself in the PSE. The module liaison module generates an adapter module for the distributed PSE modules. The adapter module generated by the module liaison system inputs output data from preceding modules and/or external modules, and connects the data to the input data for the next module. The program generation PSE module provides a workflow shown in Fig. 2, and the user follows the workflow navigation for a problem generation.

The NCAS modules also help users generate MPI based parallel simulation programs based on partial differential equations (PDEs). The NCAS capability explores possibilities to visualize and steer the parallel program design process. At present NCAS supports a domain decomposition in a design of a parallel numerical simulation program, and the domain decomposition is designed or steered by users through a visualization window. After designing the domain decomposition, the parallel program itself is also designed and generated in NCAS, and the designed parallel program is visualized and steered by a PAD diagram. In NCAS, MPI functions are employed for message passing, and a SPMD (single program multiple data) model is supported. The visualization and steering capabilities provide users a flexible design possibility of parallel programming.

In the parallel program generation support in NCAS, for the data communication among the processors, the MPI functions are used. At least the boundary data for each domain decomposed are required to complete the computation in the adjacent processor (see Fig. 3). In NCAS the MPI functions are also automatically inserted to complete the parallel data communication programming. After specifying the domain decomposition information in NCAS, the parallel program is generated and provided to the users.

Figure 4 presents an example description of an input problem information, and Fig. 5 shows an example domain decomposition information. Through the NCAS visualization windows, for examples, shown in Figs. 4 and 5, one can check all the information and can also edit the information. In NCAS, after setting all the information for the problem description, the discretization information

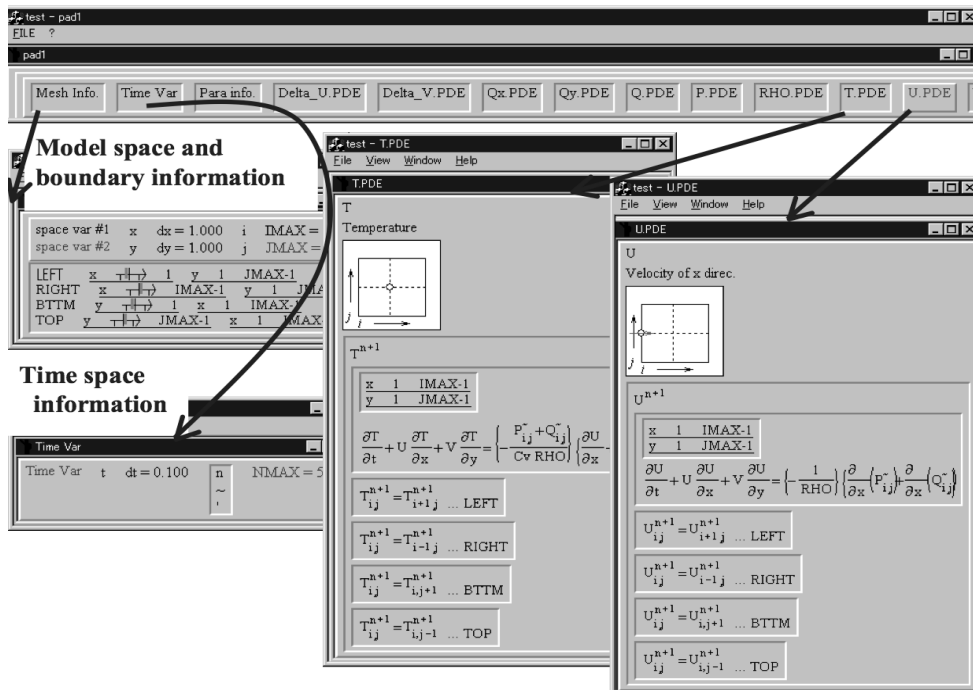


Fig. 4 An example PDE-problem description in NCAS. On each window users can edit the input description.

and the parallelization information through the NCAS windows, all the information is visualized to the users and the users can edit all the information through the windows. The discretization of each PDE is also performed automatically; depending on the discretization information which users input through the NCAS windows, the PDEs are discretized and manipulated appropriately according to the PDEs solving scheme. Then NCAS designs the parallel program for the problem, and outputs the parallel program and the corresponding document. Figure 6 shows an example MPI program automatically generated in NCAS.

In order to check the dynamic load balance function automatically generated by NCAS, during the computation an additional load was applied as shown in Fig. 7 (the left graph): by the additional load the computation time increases much in this specific case, if the static load balancing is used. When the dynamic load balancing method is selected in this example case, NCAS generates the functions, which measure the load balance of each machine dynamically, and according to the measured result each domain size is changed and adjusted dynamically to minimize the computation time. The right graph in Fig. 7 demonstrates the viability of the dynamic load balancing functions generated in NCAS, and the computation time reduction is significant in this case.

In the distributed PSE all the modules are distributed on network-linked computers. The information for the distributed modules and the computers are registered in a host computer. Newly developed modules by some users or scientists or so can be also registered in the host PSE server. The distributed PSE host server has the registered information for the modules oriented to one specific purpose, and users can obtain the information for each module and can select one of the modules to perform one task in all the PSE process.

The communication is accomplished through an interface using WWW server and Applet. The PSE server sends information described by XML to a module, and the module performs the task. The module sends the result based on the input XML information back to the PSE server. The result is visualized so that the user can check if the result is appropriate. After the successive processes, finally the NCAS generates a designed program flow and then a C program.

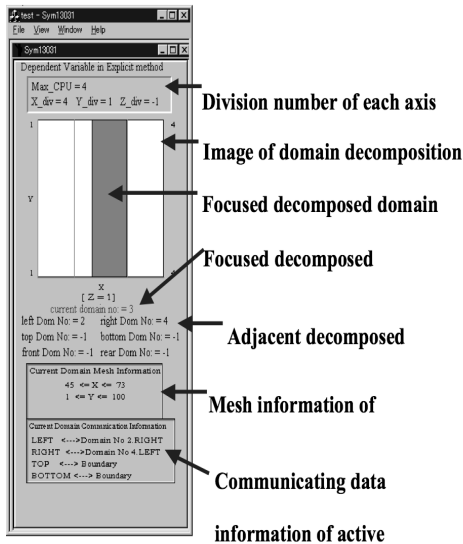


Fig. 5 Input and visualization of domain decomposition information.

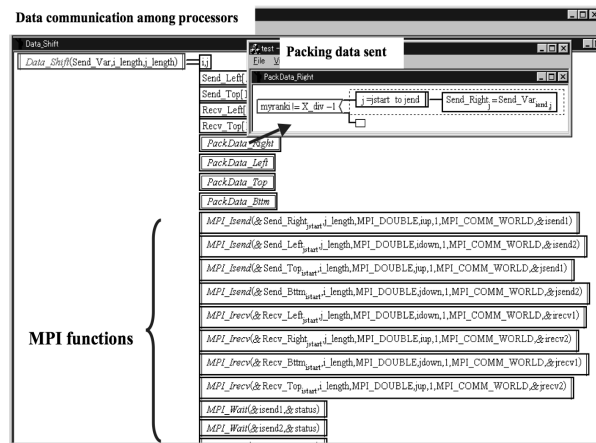


Fig. 6 Visualization of MPI functions designed for a domain decomposition information in NCAS.

3.2 An education support PSE

Network-based e-Learning is one of important education ways. In addition, the network-connected personal computers have become popular to schools and homes widely. In the network-based e-Learning, each learner can access education contents through the network anytime and anywhere. In an actual education, a network-based e-Learning system becomes popular in a long-distant learning and at the same time in a class-room education. Even inside class rooms, each computer is connected and can be used as a detecting device for the learners' progress and status. An e-Learning server may have facilities such as a user identification method or a file sharing tool in the network-based environment.

It would be difficult for teachers to know the learning state of students through each personal computer connected by a network. Without the detailed information of the students' achievement, it is difficult for the teachers to perform an appropriate guidance and education depending on the students' learning level. Therefore, the state of the students is important and required for the suitable guidance. The education-support PSE system, which provides teachers the student-achievement information, helps them in their teaching planning or the appropriate guidance.

The PSE concept was proposed to support the programming activity and also to provide integrated human-friendly computational facilities in e-Sciences and e-Productions^[1-19]. In this subsection, an education and learning support PSE system: TSUNA-TASTE is introduced^[32].

The network education support system (TSUNA - TASTE) consists of four parts (see Fig. 8). The first part is an agent of student (Fig. 8(a)). It is a software, which always works on each personal computer of the student. The agent obtains the operation information of each student. The data are obtained from the operation information of the student through the OS with a resident software working on the personal computer of each student. The second part (Fig. 8(b)) is the education support server, that collects the data, which each student agent obtains via the network. The third part (Fig. 8(c)) is the database system. The database system stores the student profile data, the student personal data, the curriculum data and the teacher's personal data. The fourth part (Fig. 8(d)) is the WWW server displaying the information stored in the database. The WWW server (Servlet system) provides an interface to the TSUNA-TASTE handling.

The agent for each student resides on the memory of the personal computer of the student and performs the following three operations. Firstly the agent exchanges the messages with the education support server. The education support server transmits the messages to each agent. The student agent analyzes the messages, and obtains the process priority and the start time of the process described in the messages. The agent stores the message data in its task table. Secondly the agent

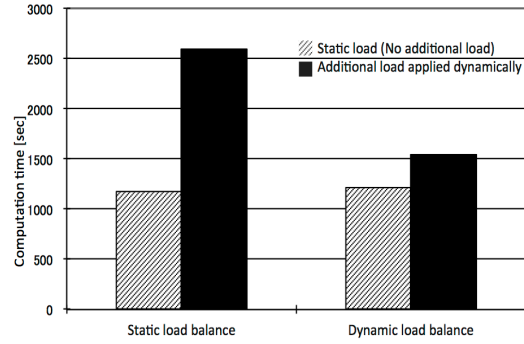


Fig. 7 A performance test result for a dynamic load balance. An additional load was applied during the computation, so that the computation time increases as shown in the left graph. When the dynamic load balancing function generated automatically by NCAS is used to this specific case, the domain size changes automatically depending on the machine load during the computation, and the result of the dynamic load balancing in the right graph shows the viability of

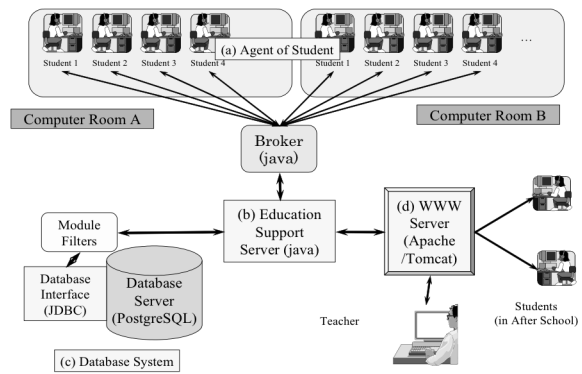


Fig. 8 Outline of the Computer assisted education support PSE: TSUNA-TASTE system.

manages the module program execution based on the task table. The module programs are small-size programs, which retrieve and output the student personal data from the student computers. The student personal data includes the achievement data, the operation data, the active window names and the process names. The third operation is a job to send back the data, which each module program collects, to the education support server. The module programs obtain the information of the student personal data from the OS of the student PCs. The module programs are implemented in the C++ language.

The module collects information about the student, however it does not store the raw data for security. It converts the raw data into statistics data. The transmission data are encoded and transferred. Furthermore, the personal information is not included in the data transmitted to the server. Thus, this system is robust for the electronic eavesdropping of data.

The education support server receives the operation data of the students through the student agent, and transmits the teacher's instructions to the students through the student agent. The education support server marks the students' absence, and identifies the students and their PCs. The education support server sends the messages of the data process demand to the agent of the student, and transmits the student personal data to the database server. The education support server also retrieves the student personal data requested by the teachers through the WWW server, and sends them back to the WWW server (see Fig. 8(d)) in the TSUNA-TASTE. The education support server is built using the Java language.

The data, which the education support server receives, are stored in the database. The database includes the private information of each student and teacher. The data contains the private information such as college student registration numbers, mail addresses and so on. These unchanged data are stored in the database together with the temporal data like the site of the student PCs. The server can receive the data from about 120 personal computers at the same time.

The WWW server system provides the user interface of the TSUNA-TASTE system. The teachers can obtain the state data of the students from the WWW system. The WWW server system presents the student achievement data, the learning progress and error occurrences situation during the programming exercises. The WWW system also provides an input interface to control the action of the TSUNA-TASTE: Through the WWW system, teachers can send a data gathering command, monitor the students' present usage of applications, and kill the unnecessary application processes on the students' PCs. The TSUNA-TASTE may open a new helpful e-Learning world.

3.3 Job execution support PSE on GRID

It is difficult for users to submit jobs to distributed computers on Cloud /Grid and to retrieve calculation data from them in scientific computing. In this subsection, a robust job execution service system is introduced in a closed distributed computer system^[28, 29, 41]. The job execution service system consists of a dynamic system management servers, execution servers and data servers as shown in Fig. 9. The dynamic system management server is duplicated in order to keep the system robust, and has an assistant management server. The dynamic system management server has a function of the job execution system management, including software deployment, program compilation, job execution, job status retrieval and computing data retrieval. This system does not require special middleware for Cloud /Grid. Users access the WWW page on the dynamic system management server, and the clients submit jobs.

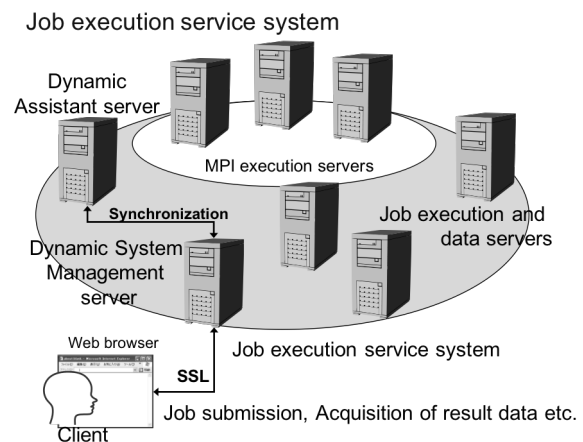


Fig. 9 Job execution service on distributed computers n Cloud / Grid.

After the submitted job finishes, the dynamic system management server collects the information from other distributed computers. When the present servers become busy, the dynamic management server and its assistant server move dynamically to new servers. The dynamic system management server also demands the execution server to transfer the result data to the optimal data server. The dynamic system management server copies the computing data and sends the compressed computing data to another optimal data server in order for a robust data storage system. The clients can deploy their programs, execute jobs and retrieve the result data by accessing only the WWW page in the job execution service system. This job execution management server also has a function of automatic system construction, so that the users can manage the setup of the job execution management system easily on their closed distributed computers.

Users access the WWW page on the dynamic system management server, and the clients submit jobs. After the submitted job finishes, the dynamic system management server collects the information from other distributed computers on Cloud / Grid. The clients can deploy their programs, execute jobs and retrieve the result data by accessing only the WWW page in the dynamic system management server.

The job execution service system acquires necessary resource information for servers for job execution and for data retrieval and storage. The resource information contains CPU architecture name, CPU operation frequency, total memory, memory in use, unused memory, load average and unused capacity of hard disk. The system sorts the resources in order for effective job execution. The users can find the resource information on the job execution service system WWW page.

Clients access the dynamic system management server through the WWW page of the system, and perform computing. Through the WWW page, the clients can up-load source files or executables to the dynamic system management server, select computing servers from among resources recommended by the system, and set execution environment. When two or more files are required for one job, the client should compress those files. When MPI jobs are executed, computing servers, on which MPI is installed, are recommended to the clients.

The compilation command, the execution method, the comment and the server name for job execution are specified by clients. The clients can also specify the storage location of the result data of the job. When the clients do not especially specify the storage data server, the system forwards the result data to the best data server. When input information is not sufficient, the job execution service system displays an error message, and advises to input the required input data. The clients can select the execution methods, or make scripts for the execution on the WWW page in a compressed file format.

When the job setting ends, the job execution service system forwards the job to a pertinent server or a server set based on the setting information. The setting file is described in XML, and contains the computing server information, the compilation command, the execution information and the data storage server information. When a compressed file, which contains source files/binaries and a make file, is sent to the computing servers, the compressed file is decompressed and the decompressed information is sent to the dynamic system management server, so that the clients can check if the file decompression is succeeded. When the compilation or the execution errors appear, the computing server notifies them to the dynamic management server. When the execution server specified is occupied by another job, the job is scheduled by the dynamic system management server.

When a job ends, the job execution server forwards the result data to a pertinent server based on the setting information. In addition, its compressed result data is stored in another data server. The result data duplication makes the data server robust and fault tolerant. When no data server is specified in the setting information, the computing server asks the dynamic system management server about the data storage servers. Based on the unused hard disk capacity, the better two data storage servers are selected from among the servers, on which no jobs run. One is for the result data uncompressed and the other is for the compressed backup data. When the result data is stored on the data servers specified, the data server locations are notified to the dynamic system management server. The client can refer to and can download the data from the WWW page on the dynamic

system management server.

4 CONCLUSIONS

The PSE has been extensively explored over the past few decades. The explorations have been supported by the reinforced computer power and algorithm power. PSE will boost up the programming power, and will enrich our e-Life and e-Science. In the near future of the PSE development we should consider how to create a PSE. To build up a PSE is a very hard task and needs huge human efforts. Therefore, PSE researchers have still been meeting this difficulty. In this research issue meta PSE or PSE for PSE may play an important role to build up service-oriented PSEs. One example of the meta PSE is a PSE Park^[39], in which many modules, developed by PSE researchers / developers, are distributed. Each module has one function or may be a one PSE, and is developed by many independent researchers and developers. By connecting the modules, PSE researchers or users can construct a single-purpose PSE or so. The interface should be opened, so that each PSE connector can be easily developed by each user or researcher or developer. The module mediator / connector may come into play there. The module base PSE may open a new PSE World.

Another research issue in PSE is validation, validity and uncertainty. When a PSE gives a wrong result for users, it may cause some difficulties, errors and accidents, depending on target problems. The validation and verification mechanisms are essentially important as usual software.

ACKNOWLEDGEMENTS

This work was supported partly by JSPS, MEXT and Japan Society of Computational Engineering and Science. The authors would like to extend their appreciations to Prof. J. Rice, Prof. E. Houstis, friends in IFIP WG2.5, and friends in the PSE research group in Japan including Prof. S. Hioki, Dr. Y. Miyahara, Prof. D. S. Han, Dr. S. W. Hwang, Prof. T. Teramoto, Dr. H. Usami, Dr. T. Maeda, Dr. Y. Manabe, Dr. H. Kobashi, Dr. Y. Hayase and our former students and friends contributed to the works relating to the paper.

REFERENCES

- [1] Boonmee, C. and Kawata, S., Computer-Assisted Simulation Environment for Partial-Differential-Equation Problem: 2. Visualization and Steering of Problem Solving Process, *Trans. of the Japan Society for Computational Engineering and Science*, Paper No. 19980002, (1998).
- [2] Boonmee, C., Kawata, S., Fujii, S., Manabe, Y. and Tago, Y., Visual Steering of the Simulation Process in a Scientific Numerical Simulation Environment - NCAS -, in print, *Enabling Technologies for Computational Science*, edited by E.Houstis and J.Rice, Kluwer Academic Pub., (2000).
- [3] Fujio, H., & Doi, S. (1998). Finite Element Description System as a Mid-Layer of PSE. *Proceedings of Conference on Computation Engineering and Science*, 3(2), (pp. 441-444).
- [4] Fujita, A., Teramoto, T., Nakamura, T., Boonmee, C. and Kawata, S. (2000). Computer-Assisted Parallel Program Generation System P-NCAS from Mathematical Model-Visualization and Steering of Parallel Program Generation Process-. *Transaction of the Japan Society for Computational Engineering and Science*, Paper No. 20000037.
- [5] Gallopoulos, E., Houstis, E. and Rice, J.R., Future Research Directions in Problem Solving Environments for Computational Science, Technical Report CSRD Report No. 1259, *Report of a workshop on Research Direction in Integrating Numerical Analysis, Symbolic Computer, Computational Geometry, and Artificial Intelligence for Computational Science*, Washington DC, April 11-12, (1991).
- [6] Gallopoulos, E., Houstis, E. and Rice, J. R. (1994). Computer as Thinker/Doer: Problem-Solving Environments for Computational Science. *IEEE Computational Science and Engineering*, 1(2), 1-23.
- [7] Hirayama, Y., Ishida, J., Ota, T., Igai, M., Kubo, S. and Yamaga, S. (1988). Physical Simulation using Numerical Simulation Tool PSILAB, *Proc. 1st Problem Solving Environment Workshop*, pp. 1-7.
- [8] Houstis, E. N. and Rice, J. R., Parallel ELLPACK, a development environment and problem solving environment for high performance computing machines, edited by In P. Gaffney and E. N. Houstis, *Programming Environments for High-Level Scientific Problem Solving*, North-Holland, Amsterdam, (1992), pp. 229-241.
- [9] Kawata, S., Boonmee, C., Fujita, A., Nakamura, T., Teramoto, T., Hayase, Y., Manabe, Y., Tago, Y. and Matsumoto, M., *Visual Steering of the Simulation Process in a Scientific Numerical Simulation Environment -NCAS-*, *Enabling Technologies for Computational Science*, E. N. Houstis and J. Rice (Ed.), Kluwer, (2000), pp. 291-300.
- [10] Okochi, T., Konno, C. and Igai, M., High Level Numerical Simulation Language DEQSOL for Parallel Computers. *Trans. of Information Processing Society of Japan*, 35(6), (1994), 977-985.
- [11] Umetani, Y., DEQSOL A numerical Simulation Language for Vector/Parallel Processors, *Proc. IFIP TC2/WG22*, 5, (1985), pp. 147-164.
- [12] Rice, J. R. and Boisvert, R. F., *Springer Series in Computational Mathematics 2, Solving Elliptic Problems Using ELLPACK*,

- Springer-Verlag, New York, (1984).
- [13] Kawata, S., Computer Assisted Problem Solving Environment (PSE), *Encyclopedia of Information Science and Technology, Third Edition*, ed. Mehdi Khosrow-Pour, Chapter 119, (2014), pp. 1251-1260, IGI Global, Hershey, PA, USA.
 - [14] Kawata, S., Computer Assisted Parallel Program Generation, *Encyclopedia of Information Science and Technology, Fourth Edition*, ed. Mehdi Khosrow-Pour, Chapter 398, (2017), IGI Global, Hershey, PA, USA.
 - [15] Kawata, S. Review of PSE (Problem Solving Environment) Study, *J. Convergence Information Tech.*, 5 2010, pp. 204-215.
 - [16] IFIP WG2.5 (International Federation for Information Processing, Working Group 2.5), IFIP WG2.5 homepage retrieved on June 12, (2017), <http://www.ifip.org/wg-2.5>
 - [17] Ford, B. and Chatelin, F. (Ed.), *Problem Solving Environments for Scientific Computing*, North-Holland, (1987).
 - [18] Gaffney, P. W., and Houstis, E. N. (Ed.), *Programming Environments for High-Level Scientific Problem Solving*, North-Holland, (1992).
 - [19] Houstis, E. N., Rice, J. R., Gallopoulos, E. and Bramley, R. (Ed.), *Enabling Technologies for Computational Science, Framework, Middleware and Environments*, Kluwer Academic Publishers, (2000).
 - [20] Gaffney, P. W. and Pool, J. C. T. (Ed.), *Grid-Based Problem Solving Environments*, Springer, (2007).
 - [21] Dienstfrey, A. and Boisvert, R. (Ed.), *Uncertainty Quantification in Scientific Computing*, Springer, (2012).
 - [22] JSCES (The Japan Society for Computational Engineering and Science), JSCES homepage retrieved on June 12, (2017), <http://www.jscs.org/>.
 - [23] PSE Research Group in Japan, homepage retrieved on June 12, 2017, <http://www.jscs.org/activity/research/pse/>.
 - [24] Rice, J. R. and Boisvert, R. F., *Solving Elliptic Problems Using ELLPACK*, Springer Series in Computational Mathematics 2, Springer, (1984).
 - [25] Kawata, S., Tago, Y., Umetani, Y. and Minami, K. (Ed.), *PSE Book: Computer assisted Problem Solving Environment in computing science (Basic & Advanced) (in Japanese)*, Tokyo: Baifukan, (2005).
 - [26] Inaba, M., Fujii, H., Kitamuki, R., Kawata, S. and Kikuchi, T., Computer-Assisted Documentation in a Problem Solving Environment (PSE) for Partial Differential Equation Based Problems, *Trans. of the Japan Society for Computational Engineering and Science*, 20040025, 2004.
 - [27] Message Passing Interface Forum, MPI: A Message-Passing Interface Standard, *Technical Report*, University of Tennessee, Knoxville, Tennessee, (1994).
 - [28] Fujii, H., Kawata, S., Sugiura, H., Saitoh, Y., Usami, H., Yamada, M., Miyahara, Y., Kikuchi, T., Kanazawa, H. and Hayase, Y., Scientific Simulation Execution Support on a Closed Distributed Computer Environment, *2nd IEEE International Conference on e-Science and Grid Computing*, (2006), 27340112.
 - [29] Kanazawa, H., Itou, Y., Yamada, M., Miyahara, Y., Hayase, Y., Kawata, S. and Usami, H., Design and Implementation of NAREGI Problem Solving Environment for Large-Scale Science Grid, *2nd IEEE International Conference on e-Science and Grid Computing*, (2006), 27340105.
 - [30] Globus, Globus Online. Retrieved June 12, (2017), <http://www.globus.org/>
 - [31] UNICORE, UNICORE. Retrieved June, (2017), <http://www.unicore.eu/>
 - [32] Teramoto, T., Okada, T., and Kawata, S., A Distributed Education-Support PSE System, *3rd IEEE International Conference on e-Science and Grid Computing*, (2007), pp. 516-520.
 - [33] CMFVVUQ (Committee on Mathematical Foundations of Verification, Validation, and Uncertainty Quantification), *Assessing the Reliability of Complex Models: Mathematical and Statistical Foundations of Verification, Validation, and Uncertainty Quantification*, The National Academies Press, (2012).
 - [34] Johnson, C. R., Top Scientific Visualization Research Problems. *IEEE Computer Graphics and Applications: Visualization Viewpoints*, 24(4), (2004), pp. 13-17.
 - [35] Kahan, W., Desparately Needed remedies for the Undebuggability of Large Floating-point Computations in Science and Engineering, *paper presented at IFIP Working Conference on Uncertainty Quantification in Scientific Computing*, retrieved on June 12, (2017), <http://www.eecs.berkeley.edu/~wkahan/Boulder.pdf>
 - [36] Rump, S. M., Verification methods: Rigorous results using floating point arithmetic. *Acta Numerica*, 19, (2010), 287-449.
 - [37] Weimer, W. R., *Exceptional Situation and Program Reliability*, PhD Thesis, University of California, Berkeley, (2005).
 - [38] Houstis, E. N., Gallopoulos, E., Bramley, E. and Rice, J. R., Problem-Solving Environment in Computational Science. *IEEE Computational Science & Engineering*, 4, (1997), pp. 18-21.
 - [39] Kawata, S., Kobashi, H., Ishihara, T., Manabe, Y., Matsumoto, M., Barada, D., Hayase, Y., Teramoto, T. and Usami, H., *Scientific Simulation Support Meta-System: PSE Park - with Uncertainty Feature Information -*, *International Journal of Intelligent Information Processing*, 3, (2012), 66-76.
 - [40] Teramoto T., Nakamura, T., Kawata, S., Matide, S., Hayasaka, K., Nonaka, H., Sasaki, E. and Sanada, Y., A Distributed Problem Solving Environment (PSE) for Partial Differential Equation Based Problems, *Trans. Jpn. Soc. Comp. Sci. Eng.*, Paper No. 20010018, (2001).
 - [41] Kawata, S., Usami, H., Hayase, Y., Miyahara, Y., Yamada, M., Fujisaki, M., Numata, Y., Nakamura, S., Ohi, N., Matsumoto, M., Teramoto, T., Inaba, M., Kitamuki, R., Fujii, H., Senda, Y., Tago, Y. and Umetani, Y., A Problem Solving Environment (PSE) for Distributed Computing, *Int. J. High Performance Computing and Network*, Vol. 1, No.4, (2004), pp. 223-230.

A Computational Fluid Dynamic Investigation of the Obesity-altered Hemodynamics in Children and Adolescents

Asimina Kazakidi*

*University of Strathclyde

ABSTRACT

Childhood obesity has become one of the major challenges of our century, taking epidemic proportions. Obesity, mainly a dietary disease, is known to advance endothelial dysfunction [1], an early sign of atherosclerotic lesions underlying most cardiovascular diseases. Endothelial damage in high-risk paediatric patients can be clinically assessed with measurements of the aortic and carotid intima-media thickness (IMT), and flow-mediated dilatation (FMD) of the brachial, radial, and femoral arteries [2]. However, it is not yet clear how the haemodynamic environment is altered in this particular group of patients and which flow-related mechanisms contribute to early vascular changes. This work will discuss a computational model of an arterial conduit with compliant walls during FDM that attempts to clarify some of these aspects. Solutions to the time-dependent, incompressible Navier-Stokes equations are based on high-fidelity finite volume and hybrid Cartesian/immersed-boundary (HCIB) methods [3] that overcome several of the shortcomings of conventional computational fluid dynamic methods and provide increased spatial flow analysis. The codes have previously been validated and used extensively in various applications. Implementation of wall motion is particularly easy with HCIB methods, which are inherently capable of handling arbitrarily large body motions and allow for effective solutions of wall configuration. The model provides an evaluation of the haemodynamic shear stresses, a common indicator of early atherosclerotic lesion localisation. Future work will include multi-scale modelling that combines high-resolution 3D blood flow computations, with macroscopic and microscopic features of the vascular environment. Further haemodynamic metrics, such as the time-averaged wall shear stress (TAWSS), the oscillatory shear index (OSI), and the transverse WSS will also be assessed, in conjunction with patient data. Acknowledgements: This project has received funding from the European Union's Horizon 2020 research and innovation programme under the Marie Skłodowska-Curie grant agreement No 749185. References [1] Cali, A.M.G. et al. (2008). Clin Endocrinol Metab 93(11) pS31 [2] Meyer AA et al. (2006) Pediatrics 117 p1560 [3] Kazakidi A et al. (2015) Comp Fluids 115 p54

Computational Mechanics in Pediatric Medicine

Asimina Kazakidi*, Vittoria Flamini**

*Strathmore, **NYU

ABSTRACT

Introduction to the topic of Computational Mechanics in Pediatric Medicine

Stress-Based Topology Optimization of Multi-Material Truss Lattice Structures

Hesaneh Kazemi^{*}, Ashkan Vaziri^{**}, Julián Norato^{***}

^{*}University of Connecticut, ^{**}Northeastern University, ^{***}University of Connecticut

ABSTRACT

We present a framework for the stress-based topology optimization of truss lattice structures made of multiple materials for desired bulk properties. Each strut in the lattice can be made of one of several available materials. We aim to solve lattice design problems subject to stress constraints, such as maximizing the lattice bulk modulus subject to stress constraints under an applied far-field traction. We employ the geometry projection method to map the geometry of each strut smoothly onto a continuous density field over a fixed finite element grid for analysis. Following recent work by our group, we adapt strategies used in density-based topology optimization to the geometry projection framework. These strategies address known challenges in stress-based topology optimization, namely the onset of singular optima and the large number of constraints. These strategies include the definition of a suitable relaxed stress, the use of aggregation functions to condense elemental stress constraints into a single optimization constraint, and the use of adaptive constraint scaling to ensure the desired stress limit is tightly satisfied. To accommodate multiple materials, we employ a novel aggregation scheme to perform the union of struts made of different materials. A size variable per material is ascribed to each strut in the lattice. Subsequently, an effective density per material is defined at each point, and the effective properties at that point are thus a function of the properties of the multiple available materials. To define the weights that determine the contribution of each strut to the effective density of a material, we adapt the Discrete Material Optimization (DMO) method. A size variable of unity indicates that the strut is made of the corresponding material. Furthermore, all size variables can be zero for a strut, allowing the optimizer to remove the strut altogether from the lattice. To avoid intermediate size variables in the optimal design, we penalize the size variables so that they are either 0 or 1. As opposed to DMO method, which enforces the penalization directly through the weighting factors, we penalize the size variables via an inequality constraint in the optimization (a 'discreteness constraint'). Moreover, each strut should be made of at most one material. Therefore, we impose another optimization constraint to ensure each strut has no more than one size variable of unity (a 'mutual material exclusion' constraint). We demonstrate the effectiveness of our method via several numerical examples.

Ductile Fracture Modelling Using Local Approaches, Application to Steel Welded Joints in Nuclear Components

Safwane Kebiri*, Myriam Bourgeois**, François Di Paola***, Habibou Maitournam****

*DEN - Service d'Etudes Mécaniques et Thermiques (SEMT), CEA, Université Paris-Saclay, F-91191, Gif-sur-Yvette, France, **DEN - Service d'Etudes Mécaniques et Thermiques (SEMT), CEA, Université Paris-Saclay, F-91191, Gif-sur-Yvette, France, ***DEN - Service d'Etudes Mécaniques et Thermiques (SEMT), CEA, Université Paris-Saclay, F-91191, Gif-sur-Yvette, France, ****IMSIA - UMR 9219 - Institut des Sciences de la mécanique et Applications industrielles

ABSTRACT

The simulation of crack propagation in ductile materials using the finite element method requires appropriate models for describing the nucleation, growth and coalescence of voids in a robust way. Local models, such as Rousselier and Gurson-Tvergaard-Needleman are now available in the finite element softwares as Cast3m [3]. A large number of models of this kind can be found in the literature, but they suffer from numerical drawbacks. First, they often show a marked mesh dependency of the solution. Second, volumetric locking of the elements is common in elastoplastic damage models in near-incompressible conditions. These two major issues must be solved in order to insure the robustness of such approaches. Our goal is to propose a model which will be able to handle these two problems. The mesh dependency can be solved by using regularization techniques, such as implicit gradient enrichment of an internal variable [1]. The locking can be treated, either using selective integration techniques, or a mixed formulation [2], which adds the volume variation as a new variable in addition to the displacement. The proposed models, based on the existing Rousselier and GTN models in Cast3m [3], address both issues using an implicit-enriched gradient of damage, and include a mixed formulation in the local models to ensure the desired robustness. In this presentation, the new models and the implementation of the new models are first presented. In a second part, simulations of crack propagation using the proposed models for axisymmetric and compact-tensile specimens in 2D using the Cast3m finite element software [3] are used to illustrate the relevancy of the approach. References [1] Samal, M. K.; Seidenfuss, M.; Roos, E.; Dutta, B. K. & Kushwaha, H. S. Finite element formulation of a new nonlocal damage model *Finite Elements in Analysis and Design*, 2008 , 44 , 358-371 [2] Lorentz, E.; Besson, J. & Cano, V., Numerical simulation of ductile fracture with the Rousselier constitutive law, *Computer Methods in Applied Mechanics and Engineering*, 2008 , 197 , 1965-1982 [3] Cast3M. Finite Element software developed by the French Atomic Energy Center (CEA) www-cast3m.cea.fr, 2017

Comparison of Immersed, Embedded, and Moving Domain Approaches for Coupled Air/Water/Granular Dynamics

Chris Kees^{*}, Yong Yang^{**}, Milad Rakhsha^{***}, Leo Nouveau^{****}, Guglielmo Scovazzi^{*****}

^{*}US Army ERDC-CHL, ^{**}US Army ERDC-CHL, ^{***}University of Wisconsin, ^{****}Duke University, ^{*****}Duke University

ABSTRACT

There is a compelling need for accurate, efficient, and robust computational models of granular media dynamics with tight coupling to multiphase air/water flow. Understanding riverine and coastal bank, dune, and sediment dynamics are just a few areas where fundamental science can be advanced with a computational laboratory representing, among other things, granular collisions and friction, air/water/solid surface tension forces, and high-Reynolds number incompressible flow. Having already invested heavily in development of conservative level set finite element methods for multiphase flow, a natural extension of our existing tools is the application of level-set-based approximations of the Nitsche approach to weak enforcement of fluid/solid Dirichlet boundary conditions [4]. The need to represent large-scale floating structures and vessels, however, also drove the development of boundary-fitted arbitrary Lagrangian-Eulerian formulations [1]. In this work we present an inter-comparison of several level-set approaches to the fluid-solid moving boundary, including the recently developed shifted boundary method [5], with a more traditional boundary-fitted deforming domain method [1]. We compare these methods in the context of modeling rigid particles interacting with air/water flow. These approaches, though recent, are not in principle new. Indeed, coupling the Discrete Element Method for granular materials to Finite Element Method has been addressed by many (e.g. [2,3]). The novel aspects of the current work are the coupling of air/water multiphase flow, higher-order FEM with immersed and embedded methods, and the opportunity for learning from inter-comparison of existing methods. [1] Ido Akkerman, Y Bazilevs, DJ Benson, MW Farthing, and CE Kees. Free-Surface Flow and Fluid-Object Interaction Modeling with Emphasis on Ship Hydrodynamics. *Journal of Applied Mechanics*, 79(1):010905, 2012. [2] B Avci and P Wriggers. A DEM-FEM Coupling Approach for the Direct Numerical Simulation of 3D Particulate Flows. *Journal of Applied Mechanics*, 79(1):010901, 2012. [3] Marcus VS Casagrande, Jose LD Alves, Carlos E Silva, Fabio T Alves, Renato N Elias, and Alvaro LGA Coutinho. A Hybrid FEM-DEM Approach to the Simulation of Fluid Flow Laden with Many Particles. *Computational Particle Mechanics*, 4(2):213{227, 2017. [4] C.E. Kees, I. Akkerman, M.W. Farthing, and Y. Bazilevs. A Conservative Level Set Method Suitable for Variable-Order Approximations and Unstructured Meshes. *Journal of Computational Physics*, 230(12):4536{4558, 2011. [5] A. Main and G. Scovazzi. The Shifted Boundary Method for Embedded Domain Computations. Part I: Poisson and Stokes Problems. *Journal of Computational Physics*, 2017.

Multiscale Computational Stability Analysis of Active Elastomers across Scales

Marc-Andre Keip^{*}, Daniel Vallicotti^{**}, Elten Polukhov^{***}

^{*}Institute of Applied Mechanics (CE), University of Stuttgart, ^{**}Institute of Applied Mechanics (CE), University of Stuttgart, ^{***}Institute of Applied Mechanics (CE), University of Stuttgart

ABSTRACT

We discuss aspects of the microscopic and the macroscopic stability of coupled, active elastomers with periodic microstructure based on a computational approach. The effective properties of the microstructured materials are determined via finite-element based computational homogenization of representative volume elements [1,2]. In the framework of the computational approach, localization-type macroscopic instabilities are detected by checking the strong ellipticity of homogenized moduli [3]. At the microscopic level, we determine bifurcation-type instabilities by means of a finite-element based Bloch-Floquet analysis [4]. The latter allows us to find altered periodicities of microstructures as well as critical macroscopic loading points [5]. Representative numerical examples will demonstrate the applicability of the proposed scheme to the detection of multiscale instabilities occurring in active elastomers. References: [1] K. Danas, Effective response of classical, auxetic and chiral magnetoelastic materials by use of a new variational principle, *J. Mech. Phys. Solids* 105:25-53, 2017. [2] M.-A. Keip and M. Rambauser, Computational and analytical investigations of shape effects in the experimental characterization of magnetorheological elastomers, *Int. J. Solids Struct.* 121:1-20, 2017. [3] A. Goshkoderia and S. Rudykh, Stability of magnetoactive composites with periodic microstructures undergoing finite strains in the presence of a magnetic field, *Comp. B Eng.*, 128:19-29, 2017. [4] K. Bertoldi and M. Gei, Instabilities in multilayered soft dielectrics, *J. Mech. Phys. Solids* 59:18-42, 2011. [5] E. Polukhov, D. Vallicotti and M.-A. Keip, Computational stability analysis of periodic electroactive polymer composites across scales, *Comput. Mech. Appl. Mech. Eng.*, submitted, 2017.

Reflections on DPG Methods

Brendan Keith*

*The Institute for Computational Engineering and Sciences

ABSTRACT

I will speak on several notable developments of the DPG methodology which I have contributed to over the past few years. Topics will include duality, DPG* methods, a posteriori error estimation, and connections to weighted least-squares problems.

Plastic Instability of Rate-Dependent Materials - Consideration of Isothermal and Adiabatic Conditions in Dynamic Tensile Tests -

Christian Keller*, Uwe Herbrich**

*Bundesanstalt für Materialforschung und –prüfung (BAM), Unter den Eichen 87, 12205 Berlin, Germany,

**Bundesanstalt für Materialforschung und –prüfung (BAM), Unter den Eichen 87, 12205 Berlin, Germany

ABSTRACT

During dynamic processes, a certain range of strain rates is often observed along loaded structures and components. For precise numerical simulations, it is necessary to determine rate-dependent properties in dynamic tests and to describe the material behavior correctly within an appropriate domain of strain rates including adiabatic heating effects at higher strain rates, typically higher than 10 s^{-1} . In principle, numerical simulations are compared to experimental results to verify the applied material models. For dynamic tensile tests considering ductile materials and large plastic deformation beyond uniform elongation, it is challenging to obtain comparable results due to plastic instability and necking of the specimen, e.g., [1]. Based on the strain gradient in a general tensile specimen, a theoretical criterion was derived describing the plastic instability in rate-dependent materials under isothermal conditions in [2]. It was applied to different multiplicative and additive constitutive relations and the analytical onset of necking was compared to results from numerical calculations of quasi-static and dynamic tensile tests. The simulations of a sheet-metal specimen with rectangular cross-section were carried out using the Finite Element Method and it was found that the numerical calculated and the theoretical predicted onset of plastic instability agree very good. The analytical criterion for instability holds even for specimens without geometrical or material imperfections and confirms that the onset of plastic instability must be considered a material characteristic. However, real dynamic problems with higher strain rates are not isothermal, the heat generated by plastic work is not dissipated to the surrounding and the temperature of the material increases significantly. Adiabatic heating and thermal softening must be considered within the constitutive relations of rate-dependent materials and the discussion of plastic instability. In this paper, an enhanced and more generalized approach for the description of the condition for stability is discussed and applied to phenomenological as well as more physical constitutive relations from the literature. This allows an individual assessment of the accuracy and verification of rate-dependent material models with respect to plastic instability. [1] Böhm, R. ; Feucht, M. ; Andrade, F. ; Du Bois, P. ; Haufe, A.: Prediction of dynamic material failure – Part I: Strain rate dependent plastic yielding. In: 10th European LS-DYNA Conference (Proceedings). Würzburg, Germany, 2015 [2] Keller, C. ; Herbrich, U.: Plastic Instability of Rate-Dependent Materials - A Theoretical Approach in Comparison to FE-Analyses. In: 11th European LS-DYNA Conference (Proceedings). Salzburg, Austria, 2017

Towards Airframe Static Stress Requirements Improvement Using Probabilistic Analyses

Martin Kempeneers*

*AIRBUS France

ABSTRACT

The sizing by analysis approach is the most commonly used mean to demonstrate the structural integrity of an airframe component. Such an approach requires to account for the effect of all the physical parameters having a significant impact on the static strength of the part. These parameters can be for example: the mechanical loads, the material properties, the thermal environment, the built stresses... For static justification, the usual sizing by analysis approach used is of the deterministic type supported by probabilities. It means that it consists in considering a priori selected values for the parameters driving the static strength in order to assess the latter in a simple deterministic allowable vs applied load comparison check. The selection of the deterministic values is then based on probabilistic conditions. For the most important parameters (i.e. the mechanical load level and the material properties), the acceptable probability of occurrence to be considered are clearly specified in the certification regulations. Each of the other additional parameters to be taken into account in the analyses has also its own statistical distribution and an associated probability of occurrence. Most of the time, for these parameters, the selection of the deterministic values is based on engineering judgement and a low probability event (or even sometimes the worst case) is selected without further analysis (no detailed analysis of the effect of the parameters on the static strength). The reasons for doing so are most of the time for the sake of simplicity or because of a lack of method and/or data to do it better. This can result in the combination of very penalizing and unrealistic conditions in sizing analyses, and consequently taking into account scenarios beyond what needs to be reasonably considered. Rationalization can be done by using probabilistic assessments. This is the purpose of the present communication which defines a general approach to build probabilistic analyses intended to support the definition of improved static stress requirements reducing the accumulated conservatism.

Time Discretization Bi-Fidelity Modeling

Vahid Keshavarzzadeh^{*}, Mike Kirby^{**}, Akil Narayan^{***}

^{*}University of Utah, ^{**}University of Utah, ^{***}University of Utah

ABSTRACT

For many practical simulation scenarios, modification of the time-step (large versus small) provides a simple low versus high fidelity scenario in terms of accuracy versus computational cost. Multifidelity approaches attempt to construct a bi-fidelity model having an accuracy comparable with the high-fidelity model and computational cost comparable with the low-fidelity model. In this talk, we present a bi-fidelity framework defined by the time discretization parameter that relies on the low-rank structure of the map between model parameters/uncertain inputs and the solution of interest. We show how this framework behaves on canonical examples, and we show real-world (practical) extensions of our methodology to molecular dynamics simulations.

Topology Optimization under Uncertainty with Multi-Resolution Finite Element Models

Vahid Keshavarzzadeh^{*}, Robert Kirby^{**}, Akil Narayan^{***}

^{*}University of Utah, ^{**}University of Utah, ^{***}University of Utah

ABSTRACT

Abstract We present a computational framework for parametric topology optimization with multi-resolution finite element (FE) models. We use our framework in a bi-fidelity setting where a coarse and a fine mesh corresponding to low- and high-resolution models are available [1]. The inexpensive low-resolution model is used to explore the parameter space and approximate the parameterized high-resolution model and its sensitivity where parameters are considered in both structural load and stiffness. Our analysis provides computable error estimates for the bi-fidelity FE approximation and its sensitivity at each design iterate. We demonstrate our approach on benchmark density-based compliance minimization problems where we show significant reduction in computational cost i.e. the number of fine-resolution simulations for expensive problems such as topology optimization under manufacturing (geometric) variability while generating almost identical designs to those obtained with single resolution mesh [2]. To show the effectiveness of our bi-fidelity approach in estimating challenging quantities we compute the parametric Von-Mises stresses for the generated designs and compare them with standard Monte Carlo simulations. References [1] Narayan A, Gittelsohn C, Xiu D. A Stochastic Collocation Algorithm with Multifidelity Models. SIAM Journal on Scientific Computing. 2014;36(2):495–521. [2] Keshavarzzadeh V, Fernandez F, Tortorelli DA. Topology optimization under uncertainty via non-intrusive polynomial chaos expansion. Computer Methods in Applied Mechanics and Engineering. 2017;318:120–147.

Parallel Adaptive Implicit Extrapolation Methods

David Ketcheson*

*KAUST

ABSTRACT

Implicit extrapolation methods were developed extensively in the last two decades of the 20th century, including several codes based on serial implementations. We investigate the efficiency of a parallel high-order adaptive implicit extrapolation solver for stiff problems.

Computational Design of Nanocellulose Materials for Better Mechanical Performance

Sinan Keten*

*Northwestern University

ABSTRACT

Natural and engineered structural (load-bearing) nanocomposites often try to exploit microstructural configurations that lead to achieve remarkable mechanical properties such as damage tolerance. However, the mechanical properties of these materials depend strongly on both the chemistry of the interfaces and the microstructure of the material system, which complicates their design. In this talk, a new computational materials-by-design approach based on coarse-grained molecular simulations for understanding physical phenomena occurring at such disparate scales will be presented. I will discuss several cases where the coupling between nanostructure and chemical structure will lead to intriguing features, specifically focusing on nanocellulose neat films and nanocomposites. Drawing an analogy between thin films and nanocomposites, I will illustrate how understanding thin film simulations help us design better load-bearing nanocomposites with nanocellulose fillers. I will conclude with an outlook on impact tolerant polymer nanocomposites and tough interfaces inspired from biological systems.

A Novel Combination of Isogeometric Analysis with Far-field Expansion Absorbing Boundary Conditions for Exterior Acoustic Problems

Tahsin Khajah*, Vianey Villamizar**

*University of Texas at Tyler, **Brigham Young University

ABSTRACT

We have devised a new method combining Isogeometric Finite Element Method (IGA-FEM) with Far-field Expansion Absorbing Boundary Conditions (FEABC) for time-harmonic exterior acoustic problems. The FEABC has been recently developed [1]. It constitutes an arbitrary accurate representation of the outgoing waves on a conveniently chosen artificial boundary. First, we derive a weak formulation of the corresponding boundary value problem that includes the FEABC in the FEM context. The construction of the FEABC is based on truncated series of the well-known Wilcox and Karp farfield expansions which are used for an exact representation of the outgoing waves in the exterior. As a result, the error of the combined method IGA with FEABC can be made as small as the error made in the interior of the computational domain by increasing the number of terms in the Karp's and Wilcox's expansions. Hence, it is possible to obtain extremely accurate numerical solutions with rather low discretization densities. Both the pollution and truncation errors are well controlled even for high frequency regimes. In fact, the accuracy of the solution on the artificial boundary and the farfield is limited by the computational resources. We will present some numerical experiments for moderate and high frequencies to show the effectiveness of our novel method. [1] Vianey Villamizar, Sebastian Acosta, Blake Dastrup, High order local absorbing boundary conditions for acoustic waves in terms of farfield expansions, Journal of Computational Physics, Volume 333, 2017, Pages 331-351, ISSN 0021-9991, <https://doi.org/10.1016/j.jcp.2016.12.048>. (<http://www.sciencedirect.com/science/article/pii/S0021999116307124>)

Computational Tools for Data-driven Design of Soft Robots

Mohammad Khalid Jawed*

*University of California, Los Angeles

ABSTRACT

We report a numerical simulation framework for the mechanics of soft robots comprised of slender structures, for application in data-driven structural design, material selection, and adaptive control. Owing to prohibitive computational cost, soft robots are often designed solely based on empirical laws through a tedious trial-and-error process with no quantitative guideline. Inspired by fast and efficient modeling of hair and clothes in the animation industry, we adapt algorithms for physically-based simulations from computer graphics. We extend the Discrete Elastic Rods method to develop a simulator for a wide class of robots comprised of multiple slender structures (rods or shells) with compliant joints. In parallel with computation, we perform experiments with biomimetic robots composed of soft thermal actuators and confirm the validity of the simulation tool. Given the large number of parameters and high degree of nonlinearity associated with the performance and functionality of soft robots, emergent machine learning techniques offer a promising avenue for their computational design and optimization. The robustness and speed of our simulation can enable data-driven analysis of a broad range of smart programmable structures beyond soft robots.

High Fidelity Anisotropic Adaptive Finite Element Method for Multiphase Flows with Phase Change

Mehdi Khalloufi*, Rudy Valette**, Elie Hachem***

*MINES ParisTech, PSL - Research University - Computing and Fluids Research Group, **MINES ParisTech, PSL - Research University - Computing and Fluids Research Group, ***MINES ParisTech, PSL - Research University - Computing and Fluids Research Group

ABSTRACT

We propose in this work a novel numerical framework, which allows dealing with the cooling of an immersed 3D solid surrounded by turbulent boiling flows with evaporation at the liquid-gas interfaces. Indeed, while standard numerical methods may not be able to deal with these heat transfer interactions simultaneously: gas-liquid-solid interfaces, vapor formations and dynamics, and 3D cooling of a heated solid, therefore, we propose in this paper a novel Eulerian method to achieve this challenging task. The key-points to achieve these difficult simulations are the development of an adaptive Eulerian framework. It uses a Level Set method to separate each state and to track each phase. A Variational Multiscale solver for the Navier-Stokes equations, which can deal with turbulent multiphase flows, is extended with implicit treatment of the surface tension. The phase change is performed using the balance of heat fluxes at the interface without the use of conforming mesh. Instead, the use of an a posteriori error estimate leading to highly stretched anisotropic elements at the interface enables to drastically reduce the interface thickness. This avoids the need of interface reconstruction or interpolation procedure. Finally, in the numerical results section, a series of 2-D and 3-D problems are solved to verify the efficiency and accuracy of the proposed framework. The cooling of an immersed solid is also presented and shows good agreement with the experimental results.

Determining the Parameters of Constitutive Laws of XFEM and CZM for Modeling Premature Failures in Plated RC Beams

Mohammad Arsalan Khan*

*Dept. of Civil Engineering, Z.H. College of Engineering and Technology, Aligarh Muslim University,
Aligarh-202002, India

ABSTRACT

Structures are strengthened with FRP or steel plates through external retrofitting. This technique has been in practice mainly for two reasons: ease of implementation and minimal aesthetic change in the structural component. However, RC beams strengthened with this technique suffer from premature failure(s); that is, a beam failing in undesirable modes of failure which are unpredictable and against which the beam is not initially designed. One critical mode of such failure is peeling, leading to a catastrophic failure by ripping off of the coverconcrete along the rebars and thereby further leaving the rebars exposed. Peeling usually starts from the end of the plate and propagates further depending on wide range of geometrical and material parameters. Debonding, which may also start from plate-end, has a different failure mechanism to peeling and so the defining parameters. However, in literature, both types of failure have largely been put in one category as a failure from plate-end; and solutions to the existing problem are largely limited to the mode-II debonding behaviour. This may be attributed to the complex nature of material behaviour, combined with geometrical non-uniformities under mixed-mode loading. Current study shows the suitability of XFEM and Cohesive Zone Model (CZM) models to respectively predict peeling and debonding failures in plated RC beams subjected to 4-point loading condition. XFEM model is utilised along with Concrete Damaged Plasticity model (CDP). Beams have been selectively picked from literature to cover a wide range of material and geometrical variables and the ones that are failing in peeling or debonding. NA series of numerical simulations are performed for different combinations of bond parameters and verified against experimental data to identify parameters of traction-separation constitutive models, defining peeling and debonding, in terms of key material properties. Considering a level of non-uniformity of result patterns associated with this problem, multiple regression analysis is performed to reach desired relations of bond parameters. Suitability of different bond-slip curves are then evaluated for CZM, where bilinear law is found to be a closest match with experimental observations. Suitability of the bond parameters, thus arrived, is demonstrated against the experimental data consisting of strain distribution, plate-end displacement, number of cracks, and load and mode of failure.

Scale Transition from Discrete to Continuous Models for Drying of Capillary Porous Media

Abdolreza Kharaghani*, Xiang Lu**, Evangelos Tsotsas***

*Otto von Guericke University Magdeburg, **Otto von Guericke University Magdeburg, ***Otto von Guericke University Magdeburg

ABSTRACT

Drying of porous media is a central process in many environmental and engineering applications. The physical processes involved are two-phase flow in porous media as well as phase transition. Two main approaches have been used to derive mathematical models for the drying process: The first approach considers the partially saturated porous medium as a continuum and partial differential equations are used to describe the mass, momentum and energy balances of the fluid phases. The continuum-scale models obtained by this approach involve constitutive laws which require effective material properties, such as the permeability, diffusivity, and thermal conductivity which are often determined by laborious experiments. The second approach considers the material at the pore scale, where the void space is represented by a network of pores. Micro- or nanofluidics models used in each pore give rise to a large system of ordinary differential equations with degrees of freedom at each node of the pore network. The characteristic length scale of the pore network models is several orders of magnitude smaller than the practically relevant length scale. A straightforward upscaling of the micro-scale models by using large pore networks is computationally costly, but it can be used to assess the quality of any chosen continuum-scale model as well as to estimate the effective parameters. When reliable estimates for these parameters have been obtained as functions of the pore size distribution and other material properties, the computationally much cheaper continuum-scale model may be used in future simulations without the need for further micro-scale simulations or experimental measurements. In this work, we demonstrate this scale transition with a three-dimensional pore network model at the micro scale and with the one-dimensional moisture diffusion model at the continuum scale. This is a quasilinear parabolic partial differential equation for the moisture content in the porous medium, where the effective moisture diffusion coefficient depends on the moisture content. We estimate this effective parameter from the post-processing of the (isothermal) micro-scale simulation results for multiple realizations of the pore space geometry from a given probability distribution.

On Relaxed Energy Potentials in Magnetomechanics

Bjoern Kiefer*, Thorsten Bartel**

*TU Bergakademie Freiberg, Institute of Mechanics and Fluid Dynamics, **TU Dortmund, Institute of Mechanics

ABSTRACT

The prediction of the effective macroscopic behaviors of micro-heterogeneous materials by means of adequate homogenization concepts is a classical problem in solid mechanics. Such analysis relies on the knowledge of geometrical, distributional and constitutive properties of the involved phases. It is well-known that standard homogenization schemes in micromechanics, such as the Taylor/Voigt and Reuss/Sachs assumptions, can also be interpreted as energetic bounds. Furthermore, energy relaxation concepts have been established that determine stable effective material responses based on appropriate convex, quasi-convex and rank-one convex energy hulls for multi-phase materials characterized by non-convex energy landscapes, see [2,3], and the references therein. In this contribution we propose analogous relaxation-based homogenization approaches for magnetizable solids---in extension of variational methods of magnetomechanics established in prior work, cf. [1-3]. In particular, we introduce novel scalar and vector-valued magnetic potential perturbation schemes. These yield relaxed effective free energy/enthalpy densities which simultaneously satisfy magnetic induction and magnetic field strength compatibility requirements---i.e.~the magnetostatic Maxwell equations---at phase boundaries. It is shown that the relaxed vector potential scheme requires the additional setting of gauge conditions to avoid spurious solutions and thereby improve its convergence behavior. In this context, we also propose adequate choices of thermodynamic potentials and their implications on the theoretical framework for constitutive modeling as well as corresponding numerical treatments. Furthermore, the challenges of implementing homogenization schemes based on potentials that are simultaneously relaxed with respect to mechanical and magnetic degrees of freedom are discussed as part of on-going work. Finally, it must be emphasized that the established variational relaxation schemes are equally applicable to the modeling of multi-phase solids exhibiting electromechanical coupling. References [1] Miehe, C., Kiefer, B., Rosato, D., An incremental variational formulation of dissipative magnetostriction at the macroscopic continuum level, *International Journal of Solids and Structures*, 48(13):1846–1866, 2011. [2] Bartel, T., Menzel, A., Svendsen, B., Thermodynamic and Relaxation-based Modeling of the Interaction Between Martensitic Phase Transformations and Plasticity, *Journal of the Mechanics and Physics of Solids*, 59(5):1004-1019, 2011. [3] Kiefer, B., Buckmann, K., Bartel, T., Numerical Energy Relaxation to Model Microstructure Evolution in Functional Magnetic Materials, *GAMM-Mitteilungen*, 38(1): 171–196, 2015.

Isogeometric Phase-field Description of Brittle Fracture in Plates and Shells

Josef Kiendl^{*}, Davide Proserpio^{**}, Marreddy Ambati^{***}, Laura De Lorenzis^{****}

^{*}Norwegian University of Science and Technology, ^{**}Norwegian University of Science and Technology, ^{***}TU Braunschweig, ^{****}TU Braunschweig

ABSTRACT

Phase-field modeling of brittle fracture is a modern promising approach that enables a unified description of complicated failure processes, including crack initiation, propagation, branching, and merging, as well as its efficient numerical treatment [1]. In this work, we apply the phase-field fracture approach to shell structures, describing both the structure and the phase field by surface models. For avoiding fracture in compression, we split of the deformation tensor in tension and compression terms as proposed in [1]. We show that this requires special attention in structural models like plates and shells, where bending deformation typically induces both tension and compression at opposite sides of the structure. We propose a new approach [2], which allows for a varying degradation through the thickness while the phase field is represented as a single two-dimensional field on the shell's middle surface. The numerical implementation is based on isogeometric analysis with a rotation-free Kirchhoff-Love shell formulation for structural analysis. We extended the NURBS-based implementation to locally refinable LR-NURBS enabling local and adaptive mesh refinement, which is a crucial aspect for computational efficiency considering that the phase-field approach requires very fine mesh resolution locally in the cracked areas. References: [1] C. Miehe, M. Hofacker, F. Welschinger. A phase field model for rate-independent crack propagation: robust algorithmic implementation based on operator splits. CMAME (2010). [2] J. Kiendl, M. Ambati, L. De Lorenzis, H. Gomez, A. Reali. Phase-field description of brittle fracture in plates and shells. CMAME (2016).

A High-order Local Discontinuous Galerkin Scheme for Viscoelastic Oldroyd B Fluid Flow

Anne Kikker*, Florian Kummer**

*Graduate School CE, Technische Universität Darmstadt, Germany/Chair of Fluid Dynamics, Technische Universität Darmstadt, Germany, **Chair of Fluid Dynamics, Technische Universität Darmstadt, Germany

ABSTRACT

In numerical simulations of viscoelastic flow a breakdown in convergence often occurs for different computational approaches at critically high values of the Weissenberg number. This is due to two major problems concerning stability in the discretization. First, we have a mixed hyperbolic-elliptic problem weighted by a ratio parameter between retardation and relaxation time of viscoelastic fluid. Second, we have a convection-dominated convection-diffusion problem in the constitutive equations. We introduce a solver for viscoelastic Oldroyd B flow with an exclusively high-order Discontinuous Galerkin (DG) scheme for all equations using a local DG formulation with penalized fluxes in order to solve the hyperbolic constitutive equations [1] and using a streamline upwinding formulation for the convective fluxes of the constitutive equations [2]. While the saddle point problem of the Navier-Stokes system is of elliptic type, the constitutive equations modelling the viscoelastic behaviour are hyperbolic. The viscous parts of the momentum equations and of the constitutive equations are weighted by a ratio parameter. So depending on that parameter a change of type from elliptic to hyperbolic can occur and the numerical solution becomes unstable [2]. We use a local DG formulation following [1] to stabilize the system of equations including the constitutive equations for Oldroyd B fluid. The DG method allows jumps in the boundary conditions and preconditioning at the elemental level, appropriate flux functions for the edges can be chosen and additional velocity-stress compatibility conditions can be easily satisfied [2]. So the DG method is a promising method for convection dominated problems and is often used in combination with streamline upwinding for the convective terms of the constitutive equations of viscoelastic flow whereas the other terms are discretized using a Finite Elements ansatz. The successful implementation of both schemes is presented in an hp convergence study and first results are shown for various benchmark problems for viscoelastic flow. References: [1] Owens, R. G., Phillips, T. N.: Computational Rheology. Imperial College Press, London, River Edge, NJ (2002). [2] Cockburn, B., Kanschat, G., Schötzau, D., Schwab, C.: Local Discontinuous Galerkin Methods for the Stokes System. SIAM J. Numer. Anal. 40 (1), 319-343 (2002). The work of A. Kikker is supported by the Excellence Initiative of the German Federal and State Governments and the Graduate School of Computational Engineering at Technische Universität Darmstadt. The work of F. Kummer is supported by the German DFG through Collaborative Research Centre 1194/B06.

Viscoelastic behavior of natural rubber with coarse-grained molecular dynamics

Byungjo Kim^{*}, Junghwan Moon^{**}, Maenghyo Cho^{***}

^{*}Seoul National University, ^{**}Seoul National University, ^{***}Seoul National University

ABSTRACT

In this work, the viscoelastic properties of natural rubber are thoroughly investigated using a coarse-grained (CG) molecular dynamics (MD) simulation method. Due to the limitation of time and length scales in the MD simulation environment, it is challenging to assess the nature of viscoelastic of polymer materials with a computational approach. In that regards, CG MD offers an equivalent system with reduced degree of freedom by replacing a group of atoms with a corresponding bead particle. To describe the interactions between beads consisting of the system, the iterative Boltzmann inversion (IBI) is used for obtaining bonded and non-bonded potential. Herein, the time dependent shear relaxation modulus is calculated using the stress autocorrelation, and dynamic modulus (storage and loss modulus) is further calculated with the Fourier transformation in a complex domain. The viscoelastic behavior of natural rubber is studied considering a chain length effect. Plus, the influence of vulcanization of rubber is taken into account. To investigate more detailed viscoelastic nature of rubber, a wide range of temperature is considered for the present study. With the present work, the viscoelastic nature of rubber is understood by employing CG MD simulations which can enhance the scale of computation in terms of length and time. Further, this work can be extended to examine more complex polymeric system regarding the long-term physical nature or thermodynamic property. **Keywords:** Coarse-grained molecular dynamics, Rubber, Viscoelastic behavior. **Acknowledgement** This work was supported by a grant from the National Research Foundation of Korea (NRF) funded by the Korea government (MSIP) (No. 2012R1A3A2048841)

Development of Electricity-harvesting Piezoelectric Polymer Beams Vibrating in a Wind Flow Around Running Electric Vehicles Using Topology Optimization

Cheol Kim^{*}, Changmin Park^{**}, Jin-Young Yoon^{***}

^{*}Kyungpook National University, ^{**}Kyungpook National University, ^{***}Hyundai Motor Company

ABSTRACT

An electric energy harvesting system that is installed on the surface of a vehicle has been developed in order to supply auxiliary electric power for EV (electric vehicles). The system consists of several thin piezoelectric polymer beams that are fixed at both ends and vibrating in an air stream around the running electric vehicle. The fluctuation of airflows around the harvesting beams attached to a car is analysed by using a CFD program. The characteristics of beam vibration and resulting generation of electricity are computed by using FEM. To maximize the amount of electricity generation from harvesting beams, the cross-sectional curvature and shape of a piezoelectric harvesting beam are optimized by the shape and topology optimization method. The structural vibration in a turbulent flow is considered during the optimization process simultaneously. For optimization, we develop a new electro-mechanical coupling coefficient and cost function for piezoelectric polymer. As results of analysis, a reasonable amount of electric power can be successfully harvested from passing airflow around a vehicle. The harvesting beam is fabricated and is installed on a car for validation tests. Real car driving tests for the harvesting system give good agreements with numerical predictions.

Tailoring the Stiffness of Tubular Structures through Auxetic Patterns

Do-Nyun Kim^{*}, Kwang Je Lee^{**}, Dongsik Seo^{***}, Jeong Min Hur^{****}

^{*}Seoul National University, ^{**}Seoul National University, ^{***}Seoul National University, ^{****}Seoul National University

ABSTRACT

Auxetic materials are emerging mechanical metamaterials showing a negative Poisson's ratio that may have interesting geometrical and mechanical properties such as synclastic curvature in bending, high impact and indentation resistance, and tuneable dynamic properties for vibration isolation and wave control. While various deformation mechanisms and patterns have been proposed to achieve a negative Poisson's ratio, little attention has been paid to its link to the fundamental mechanical properties of structures such as the stiffness. Here, we present a novel method to tailor the bending and torsional stiffness values of tubular structures by imposing auxetic cutting patterns on the tube. It is demonstrated that rational design of these patterns enables us to obtain a wide range of bending and torsional stiffness values without changing the cross-sectional shape, the size, and the material used. To illustrate, auxetic patterns based on the rigid-rotating-unit mechanism are employed and implemented on a cylindrical hollow tube by engraving alternating slits that divide the tube into rigid-rotating-unit-like and hinge-like sub-domains. Parametric studies for the geometric parameters of these patterns performed using the finite element method reveal the primary geometric parameters governing the tube stiffness. We also measure the tube stiffness experimentally for a set of patterned tubes, validating the simulation results and our design principles for stiffness control.

Auto Parameter Tuning in Topology Optimization Using Deep Reinforcement Learning

Dongjin Kim^{*}, Jaewook Lee^{**}

^{*}Gwangju Institute of Science and Technology, ^{**}Gwangju Institute of Science and Technology

ABSTRACT

In this research, a basic auto parameter tuner has been developed to generate the target number of holes in topology optimization results using deep reinforcement learning [1]. This work aims to support engineers who suffer from parameter decision in topology optimization using deep learning techniques. In topology optimization problems, the unique solution is not guaranteed. To relieve numerical instability problems, various techniques have been proposed [2]. These techniques require careful control of many parameters. If improper parameters are used, it is difficult to get satisfactory optimization results. The parameters have been determined heuristically by designer's intuition till now. Therefore, this work proposes an auto parameter tuner constructed using deep reinforcement learning [1]. The deep reinforcement learning can be used for improving a quantified performance without the supervision [1]. In this research, the quantified performance is declared as a difference between the target and designed number of holes in the result of topology optimization. Here, the number of holes are calculated by the connected-component labeling [3]. For constructing the auto parameter tuner, a python code is developed. As a result, the developed parameter tuner generates the optimization result satisfying target number of holes. [1] Minh, V., et al, Nature(2015) 518: 529. [2] Sigmund, O. & Maute, K. Struct Multidisc Optim (2013) 48: 1031. [3] Wu, K., Otoo, E. & Suzuki, K. Pattern Anal Applic (2009) 12: 117.

Quantitative phase-field simulations for solidification microstructure with different preferred growth direction

Geunwoo Kim^{*}, Munekazu Ohno^{**}, Kiyotaka Matsuura^{***}, Tomohiro Takaki^{****}

^{*}Hokkaido University, ^{**}Hokkaido University, ^{***}Hokkaido University, ^{****}Kyoto Institute of Technology

ABSTRACT

Preferred growth direction of metallic materials is one of important factors that have a great influence on solidification structures since it determines growth direction of dendritic structures. It has been understood and/or supposed, in general, that the preferred growth direction is exclusively determined by type of crystal structure. For instance, as the preferred growth direction in cubic crystals such as fcc and bcc is $\langle 100 \rangle$. In recent years, however, it was revealed that the preferred growth direction of fcc alloy (Al-Zn binary alloy) changes from $\langle 100 \rangle$ to $\langle 110 \rangle$ by increasing concentration of the solute element.[1] The preferred growth direction of crystal is entirely determined by anisotropy of solid-liquid interfacial energy. The anisotropy of interfacial energy is described by two kinds of anisotropy strength, e_1 and e_2 that characterize $\langle 100 \rangle$ growth and $\langle 110 \rangle$ growth, respectively. The transition of preferred growth direction with alloy concentration indicates that e_1 and e_2 depend on the alloy concentration.[1] It is very important to understand the dependence of size and morphology of solidification microstructure on these parameters. However, details of morphological change and dependence on solidification conditions and alloy systems have not been clarified yet. Therefore, in this study, we investigated the morphological change of the isothermally- and directionally-solidified dendritic structures associated with transition phenomenon of the preferred growth direction. In this study, the simulation of isothermal and directional solidification in fcc binary alloys was conducted by using quantitative phase-field model[2] which can predict solidification structure with high accuracy. And the morphological change was investigated by changing e_1 and e_2 systematically. Effects of several parameters such as supersaturation, cooling rate, temperature gradient and alloy system, on the morphology were also investigated. [1] T. Haxhimali, A. Karma, F. Gonzales, and M. Rappaz, Nat. Mater., 5(2006), 660 [2] M. Ohno and K. Matsuura, Phys. Rev. E 79, 031603(2009).

Crack Self-healing During the Relaxation

Hokun Kim^{*}, Sung Youb Kim^{**}

^{*}UNIST, ^{**}UNIST

ABSTRACT

Unexpected behaviors of materials are critical for designing the structures which can lead to undesirable results. Hence, it is important to understand the behaviors of materials. However, the mechanical responses of nanomaterials are different from those of bulk counterparts causing unexpected behavior. For examples, nanomaterial becomes flaw insensitive under the critical size [1], small enough nanowire undergoes a phase transformation [2], and the surface stress affects the instability of nanomaterials [3]. Therefore, identifying the unique behavior of nanomaterial is significant for nanotechnology. Using molecular dynamics simulations with embedded atom method (EAM), we observed that cracks are self-healed during the relaxation of surfaces. Crack surfaces are closed (re-bonded) without any external force applied, leaving crack tip as a dislocation. Centered and edged cracks were investigated with different sizes and aspect ratios with various materials that have different amount of surface properties. Other unexpected behaviors of nanoscale cracks are discussed specially emphasized on the effect of surface relaxation. 1. Gao, H., Ji, B., Jager, I. L., Arzt, E. & Fratzl, P. Materials become insensitive to flaws at nanoscale: lessons from nature. *Proc. Natl. Acad. Sci. U. S. A.* 100, 5597–5600 (2003). 2. Diao, J., Gall, K. & Dunn, M. L. Surface-stress-induced phase transformation in metal nanowires. *Nat. Mater.* 2, 656–660 (2003). 3. Ho, D. T., Park, S.-D., Kwon, S.-Y., Park, K. & Kim, S. Y. Negative Poisson's ratios in metal nanoplates. *Nat. Commun.* 5, 3255 (2014).

Level-set Based Shape Optimization Using Polyhedral Elements

Hyun-Gyu Kim*, Son Nguyen-Hoang**

*Seoul National University of Science and Technology, **Seoul National University of Science and Technology

ABSTRACT

In the level-set based shape optimization, the structural boundary is implicitly represented by the zero-level set of an level set function and a velocity field is computed based on a shape sensitivity analysis to iteratively update the new shape of the structures by mathematically solving the Hamilton-Jacobi equation. Most of level-set based shape optimization methods utilize a fixed regular mesh for both of the level set function evolution process and the structural domain analyses. Due to the inexactitude of a mesh for the structural model, the finite element method cannot be implemented directly for the structural analyses. In this study, the evolution of geometric shapes based on level-set based shape optimization is obtained by cutting a background hexahedral mesh. The zero isosurface of a level set function split a background hexahedral mesh. Polyhedral elements are generated at the boundaries of the split domains by the marching cube algorithm. The trimmed hexahedral meshes are partitioned into an interior domain with negative level set values and an exterior domain with positive level set values. In the level-set based shape optimization using trimmed hexahedral meshes, polyhedral elements at their boundaries play an important role for capturing the structural domain. We recently proposed an efficient scheme for constructing shape functions on polyhedral domains with non-planar faces by using MLS approximation. The polyhedral shape functions satisfy the required properties of conventional finite element method such as continuity within elements, partition of unity, linear completeness, inter-element compatibility and the Kronecker-delta property. The trimmed hexahedral meshes can provide an efficient and effective tool for level-set based shape optimization problems.

Finding Nearest Helpers for Cardiopulmonary Resuscitation Using Defibrillators

Jaewon Kim^{*}, Dongsoo Han^{**}

^{*}KAIST, ^{**}KAIST

ABSTRACT

If patients in heart attack are fell down and unable to move by themselves, they should be rescued in a hurry. The brains of the heart-attacked patients are damaged unless appropriate action is taken within 5 minutes. To help the fast rescue activity, hundreds of thousands of defibrillators have been deployed in many places these days. Nevertheless, taking first-aid measures for cardiopulmonary resuscitation for heart-attacked patients within 5 minutes is not a simple task. This paper proposes a technique to rescue heart-attacked patient using nearby defibrillators. This paper assumes that a heart-attacked patient asks a rescue service to a remote service center which is located far away from the patient. The patient usually loses consciousness immediately after the rescue request. Then the remote service center has to identify nearby people or rescue service members to help the hear-attacked patient. First, it estimates the patient's location and requests nearby special purpose access points (APs) to capture probing signals from smartphones. Then a server fetches the captured probing signals and identifies devices with the probing signals. The server determines a person who can rescue the patient and sends a message to help the patient. An experiment performed on the 7th floor, N1 building, KAIST with ten specially purpose APs. The experiment revealed that the scenario could be effective if the special purpose APs were properly installed in a service area.

Stress Based Creep Life Evaluation of Super304H Using Small Punch Creep Test

Jeong Hwan Kim^{*}, Uijeong Ro^{**}, Moon ki Kim^{***}

^{*}sungkyunkwan university, ^{**}sungkyunkwan university, ^{***}sungkyunkwan university

ABSTRACT

Ultra-supercritical power plant operating at high pressure and high temperature has advantage of high-efficiency. The super-heater and the re-heater must endure such harsh operating conditions. Metals exposed to high temperature usually fail by creep. Therefore, it is important to understand the creep to design a safe power plant. Creep phenomenon shows a plastic deformation of material in time even when it is subjected to a low stress below macroscopic yield stress. The conventional uniaxial creep test was mainly used to evaluate the creep life of the material. However, it has shortcomings that a specimen cannot be taken from a plant in-service without damage. And also, it usually takes a long test time. Small punch creep test overcomes these shortcomings by using a small sheet of specimen which is 1/200 in size compared with uniaxial creep test specimens. For this reason, the specimen can be sampled from an in-service power plant. Also, it consumes relatively less time than the uniaxial creep test. However, it was neglected in the industrial field because it is difficult to evaluate the creep life using small punch creep test than uniaxial creep test. This is because conventional life evaluation method of small punch creep test must be preceded by uniaxial creep test. Considering the aforementioned advantages, a creep life evaluation method using only small punch creep test is needed in order to reduce cost and time. In this study, a creep life evaluation method of small punch creep test was proposed. Stress based creep life evaluation method can evaluate creep life only using small punch creep test result without uniaxial creep test. Super304H which is one of the main material of ultra-supercritical power plant was used as the test specimen. And small punch creep test was performed at 650 degrees of Celsius. Finally, the suggested method is verified through Larson-Miller model.

Modeling of 3D Printed Carbon Nanotube-Thermoplastic Polyurethane Composites for Piezoresistive Pressure Sensors

Ji Hoon Kim^{*}, Jaebong Jung^{**}, Myoung-Seok Kim^{***}, Dae-Hyeong Kim^{****}

^{*}Pusan National University, ^{**}Pusan National University, ^{***}Pusan National University, ^{****}Seoul National University

ABSTRACT

In order to design flexible pressure sensors with high sensitivity, a multi-physics computational model for piezoresistivity was developed. The anisotropic change of piezoresistivity upon deformation was analyzed experimentally and numerically using a 3D resistive network model. Then a phenomenological piezoresistivity model was developed to represent the piezoresistive behavior of conductive polymer composites. Carbon nanotube-thermoplastic polyurethane (CNT-TPU) composites were produced using 3D printing and used for validation of the proposed model. The effect of processing conditions and heat treatment on sensitivity was analyzed.

Correlation Between Microstructural Characteristics and Properties of Cement Paste with Variable Void Distributions

Ji-Su Kim^{*}, Tong-Seok Han^{**}

^{*}Yonsei University, ^{**}Yonsei University

ABSTRACT

Concrete is composed of void and solid phase with hydration products [1]. Porous material generally has a material response related to its porosity. For instance, the strength of concrete is well known for being proportional to cube of gel-space ratio (e.g., Powers' model). Microstructural characteristics of cement paste include connectivity and continuity of voids as well as the porosity, and the continuity of voids has a relation to the response of materials. In this study, the material properties are described as a function of porosity and void distribution of cement paste. The correlation between microstructural characteristics and material properties is investigated using cement paste specimens with various water/cement ratio. To prepare the specimens, five water cement ratios (w/c) of cement paste are designed as 0.3, 0.4, 0.5, 0.6, and 0.7. Each specimen has a different microstructural characteristic, e.g., porosity and void continuity. In order to characterize the microstructure of the material, micro-CT images are taken and binarized into voids and solid phases [2]. A three-dimensional finite element model is generated from CT images, and a lineal-path function is used to characterize the void continuity among low-order probability functions [3]. The area of the lineal-path function is used as a quantified parameter of the void continuity. The material properties of cement paste are evaluated for strength and stiffness through compression test and nanoindentation. The crack phase field model with input parameters obtained from the experiments is performed. From this study, the relations between microstructural characteristics and material responses of cement paste are suggested in a simple functional form. [1] Mindess, S., Young, J. F., & Darwin, D. (2003). Concrete. Prentice Hall. [2] Chung, S. Y., Han, T. S., & Kim, S. Y. (2015). Reconstruction and evaluation of the air permeability of a cement paste specimen with a void distribution gradient using CT images and numerical methods. Construction and Building Materials, 87, 45-53. [3] Torquato, S. (2013). Random heterogeneous materials: microstructure and macroscopic properties (Vol. 16). Springer Science & Business Media.

Design of a Honeycomb Panel for Protection of a Steel Columns Subjected to Vehicle Collision

Jinkoo Kim^{*}, Hyungoo Kang^{**}

^{*}Sungkyunkwan University, ^{**}Sungkyunkwan University

ABSTRACT

ABSTRACT This study investigates the performance of aluminum honeycomb panels attached to the face of a steel column for reducing local damage caused by automobile collision. A method for estimating the dynamic plateau stress of honeycomb was proposed based on mass and velocity of the vehicle. In addition, the stress-strain histories were linearized to easily estimate the amount of energy absorbable by the honeycomb structure. To verify the impact energy absorption capability of the honeycomb panel designed with the proposed method, a vehicle collision analysis was carried out using an 8-ton truck. According to the analysis results, the honeycomb panel could be effective in decreasing the displacement of the structure due to vehicle collision. It was also shown that the energy absorption capacity of the honeycomb panel estimated by the proposed method was found to be quite similar to the value obtained from the collision analysis. Key words : Vehicle impact, FE analysis, Honeycomb panel
Acknowledgement This research was supported by Basic Science Research Program through the National Research Foundation of Korea(NRF) funded by the Ministry of Education(NRF-2016R1D1A1B03932880)

Free Vibration of Thin-Walled Beams with Discontinuously Varying Cross-Sections

Jun-Sik Kim^{*}, Gijun Lee^{**}

^{*}Kumoh National Institute of Technology, ^{**}Kumoh National Institute of Technology

ABSTRACT

We investigate the frequency variation due to the interface in thin-walled beams. In order to properly consider the interface effect, we calculate the warping functions of the interface by employing the constrained cross-sectional eigenvalue analysis. The formulation starts with an asymptotic formulation which is applied to the Koiter-Sanders' shell theory built upon the general tensor-based coordinate system. One-dimensional finite element analysis for the cross-section of thin-walled beams is set up first, and then it is extended to the interface between two different cross-sections. The formulation takes the form of an eigenvalue problem with Lagrange's multipliers that are used to enforce the displacement continuity, rigid-body constraint, and orthogonality conditions to the fundamental warping functions. The results obtained will be compared to those of commercial software and will be discussed in terms of the importance of interface warping functions.

Numerical Simulation of Butt-welding Considering Metallic Phase Transformation

Kyu Won Kim^{*}, Moon Kyum Kim^{**}, Woo Yeon Cho^{***}

^{*}Yonsei University, ^{**}Yonsei University, ^{***}POSCO

ABSTRACT

Residual stresses may occur the deterioration of steel structure, buckling strength and fatigue strength, and these may cause damage to the integrity of the structure. In addition, tensile residual stress occurred at the centerline of the welding part increases the crack propagation force and decreases the resistance of the structure to brittle failure. It greatly affects the fracture behavior of the welded structure. Therefore, the prediction and the evaluation of the residual strain and residual stress due to the welding are very important for the quality and life prediction of the steel structure. The distribution of residual stresses due to welding was affected by various factors such as welding parameters, types, sequence, component type, component materials and component size. The temperature variation of metallic material in the welding process causes a phase transformation of the metal. The martensitic transformation such as volumetric changes of austenitic and martensitic that caused by rapid cooling to room temperature causes significant volume changes and yield stress changes. This paper presents a coupled three-dimensional (3-D) thermal-mechanical finite element analysis to simulate residual stresses due to butt welding considering metallic phase transformation. The heat of the welding arc is modeled by a body heat flux with a double ellipsoidal distribution proposed by Goldak and Akhlagi (2012), and the moving heat source is implemented by the ABAQUS subroutine DFLUX model. In the numerical model, phase transformation plasticity is also taken into account.

Universal Meshes for Domains with Piecewise C2-regular Boundaries

Kyuwon Kim^{*}, Adrian Lew^{**}

^{*}Stanford University, ^{**}Stanford University

ABSTRACT

The idea of a universal mesh is that a background mesh can be used to achieve conforming meshes for a family of domains, which allows it to be applicable for domains with evolving boundaries. Rangarajan introduced an algorithm to achieve conforming meshes for domains with C2-regular boundaries under certain conditions, but its application on domains with more general boundaries, such as with corners, has not been studied yet. One necessary condition to achieve a valid mesh is that the projection of positive edges onto the boundary must be guaranteed to be a homeomorphism. We introduce an algorithm to select positive edges for domains with piecewise C2-regular boundaries in a manner that their projection is a homeomorphism. We introduce a theorem which assures that the projection of positive edges is sure a homeomorphism, when certain restrictions are given on the mesh. In our approach, we use the closest point projection and focus on how to choose an appropriate set of positive edges. Instead of selecting positive edges for the whole curve, the boundary is divided into a finite number of C2-continuous curves and treated separately. The positive side and positive edges are chosen individually for each curve to guarantee the projection to be a homeomorphism. Given the local maximum curvature of the curve and the maximum angle of the mesh, we also introduce an upper bound for the meshsize to guarantee the algorithm to work for domains with piecewise C2-regular boundaries.

Development of Particle Growth Model in a Taylor-Couette Crystallizer Using Immersed Boundary Method

Moon Ki Kim^{*}, Tae-Rin Lee^{**}, Jang Gyun Lim^{***}

^{*}SAINT, School of Mechanical Engineering, Sungkyunkwan Univ., Republic of Korea, ^{**}Advanced Institutes of Convergence Technology, Seoul nat. Univ., Republic of Korea, ^{***}SKKU Advanced Institute of Nano Technology (SAINT), Sungkyunkwan Univ., Republic of Korea

ABSTRACT

Lithium ion battery has led the secondary battery market. It is also expected to be widely used from portable IT devices to high capacity applications such as energy storage system and electric vehicles in the near future. To satisfy future demands, Ni_{1/3}Co_{1/3}Mn_{1/3}O₂ (NCM) has been suggested as an alternative anode material because of its high rate of discharge/charge and stability. Electrochemical performance of NCM is determined by small size with a narrow particle size distribution (PSD) and spherical morphology. Taylor-couette crystallizer (TCC) is a highly effective manufacturing device to prepare uniform NCM particles using Taylor vortex. However, controlling the quality of a product is still ambiguous because of a short reaction time and complex interactions between hydrodynamics and manufacturing parameters. To overcome this obstacle, computational fluid dynamics is employed based on population balance equations. The coupled numerical problem has been solved by standard method of moments, discretized population balance, Monte Carlo simulation, and quadrature method of moments. Each previous study is limited by size-independent coefficients, a lot of class requirement, difficulty in applying to a real reactor, and a monotonous PSD. In this paper, a new numerical approach for agglomeration/deagglomeration is introduced to predict the change of PSD with an individual particle in TCC. Firstly, based on immersed boundary method, a unit cell is prepared as a Taylor vortex to implement core mechanisms for particle growth. In the unit cell, each particle is transported by Brownian motion or shear flow resulting in collisions. Then, the state of each particle is determined by collision efficiency [1], maximum agglomerates diameter [2], and breakage potential function for the next increment. These coefficients are updated by taking into account hydrodynamic and particle characteristics. After that, multiple cases of average particle size are tried to predict final average size and PSD. As a result, the average particle size and PSD is obtained for various input cases. A growth rate induced by the change of average size indicates whether the dominant phenomenon of the system is agglomeration or deagglomeration. A positive value of the growth rate implies an increase of average particle size and vice versa. By finding the size with a growth rate of zero, the final particle size is predicted. This prediction result shows a good agreement with the experimental data. 1. Balakin B. et al., Chem. Eng. Sci. 68, 305, (2012). 2. Kim, J. M. et al., W.S., Colloid. and Surf. 385, 31, (2011).

Statistical model calibration for multivariate responses of piezoelectric energy harvester

Saekyeol Kim^{*}, Tae Hee Lee^{**}, Tae Hyun Sung^{***}, Yewon Song^{****}, Jihoon Kim^{*****}, Taehyeok Choi^{*****}

^{*}Hanyang University, Seoul, Korea, ^{**}Hanyang University, Seoul, Korea, ^{***}Hanyang University, Seoul, Korea,
^{****}Hanyang University, Seoul, Korea, ^{*****}Hanyang University, Seoul, Korea, ^{*****}Hanyang University, Seoul,
Korea

ABSTRACT

The use of computational model for predicting the performance of engineering products has been largely increased due to the fast growth in computing power. The accuracy of computational results from high-fidelity model is now a great concern for engineers. In order to improve the accuracy of computational models, uncertainty in various material properties has to be considered. To address such issues, statistical model calibration has been developed[1], which increases the predictive capability of computational models by identifying and determining the uncertainty of material properties based on the results from both the experiments and the computational models. This method, has been recently employed to improve the high-fidelity electromechanical model of piezoelectric energy harvester[2]. To the best of our knowledge, however, the multivariate responses in the statistical model calibration has never been considered, which can be an important factor to improve the accuracy of the computational model. This paper proposes a statistical model calibration method, which considers multivariate responses of piezoelectric energy harvester: natural frequency and output voltage. The proposed method is used to perform a probabilistic design of piezoelectric energy harvester and the results are compared with the results from the previous statistical model calibration.

Construction of ITZ Specimens with Functionally Graded Microstructure by Extended Stochastic Optimization and Evaluation of its Properties

Se-Yun Kim*, Tong-Seok Han**

*Yonsei University, **Yonsei University

ABSTRACT

Concrete can be divided into three phases which are aggregates, bulk cement paste and interfacial transition zone (ITZ). The ITZ is located between the aggregates and the bulk cement paste. The void phase of the ITZ has a gradient distribution depending on the distance away from the aggregate, which means the ITZ is not only a functionally graded material but also a critical section to determine properties of concrete. However, information on the ITZ microstructure is difficult to obtain compared with bulk cement paste microstructure. In this study, three kinds of the bulk cement paste are used to construct virtual ITZ specimens. The low-order probability functions are used to quantify the characteristics of the void distributions over the bulk cement paste specimens in three orthogonal directions [1]. The characteristic of the microstructure is subdivided into clustering, continuity and connectivity of void clusters, and all of the characteristics are used as resources to construct the virtual ITZ specimens using a stochastic optimization. The stochastic optimization is extended to incorporate the information of the void gradient, and the iteration process in the stochastic optimization is modified to minimize the computational resources. Using the microstructures reconstructed from the extended stochastic optimization method, the properties of the ITZ in concrete can be evaluated a virtual loading tool, e.g., a finite element method. The evaluated elastic modulus, heat conductivity and permeability in three orthogonal directions show the anisotropy of the ITZ and a good correlation between the properties and the void distribution gradient. [1] Torquato, S. (2013). Random heterogeneous materials: microstructure and macroscopic properties (Vol. 16). Springer Science & Business Media.

Towards an Integrated Model Reduction Algorithm of Component Mode Synthesis

Soo Min Kim^{*}, In Seob Chung^{**}, Jin-Gyun Kim^{***}, K. C. Park^{****}, Soo-Won Chae^{*****}

^{*}Department of Mechanical Engineering, Korea University, ^{**}Department of Mechanical Engineering, Korea University, ^{***}Mechanical Systems Safety Research Division, Korea Institute of Machinery and Materials, ^{****}Department of Aerospace Engineering Sciences and Center for Aerospace Structures, University of Colorado, ^{*****}Department of Mechanical Engineering, Korea University

ABSTRACT

In the computational approach, efficiency and accuracy are the main aims of reduced-order modeling (ROM). Numerous techniques have been studied for the last several decades, but those are still main issues. Based on the motivation, we here suggest an integrated model reduction algorithm of Craig-Bampton (CB) component mode synthesis (CMS) method [1], which is one of the widely used ROM techniques in structural dynamics society. The proposed algorithm consists of three phases: important mode selection, CB based model reduction and a posteriori error estimation. In this work, we use a priori mode selection scheme [2], which was recently developed to precisely rank dominant substructural modes. The mode selection scheme was derived by using a moment-matching approach and a consistent perturbation expansion [2]. To evaluate the accuracy of a reduced model, a posteriori error estimator recently developed by Kim et al. is also employed, which can accurately predict relative eigenvalue errors of a reduced model without any information of reference eigenvalues [3]. Combining the techniques, we propose an integrated model reduction algorithm, and demonstrate its feasibility through several numerical examples. [1]. Craig, R., & Bampton, M. (1968). Coupling of substructures for dynamic analyses. AIAA journal, 6(7), 1313-1319. [2]. Kim, S. M., Kim, J. G., Park, K. C., & Chae, S. W. (2018). A component mode selection method based on a consistent perturbation expansion of interface displacement. Computer Methods in Applied Mechanics and Engineering. 330, 578-597 [3]. Kim, J. G., Lee, K. H., & Lee, P. S. (2014). Estimating relative eigenvalue errors in the Craig-Bampton method. Computers & Structures, 139, 54-64.

Drag Effect on the Motions of Dislocations and Grain Boundaries in Nanoscale

Soon Kim^{*}, Jaehyung Hong^{**}, Sung Youb Kim^{***}

^{*}Ulsan National Institute of Science and Technology, ^{**}Ulsan National Institute of Science and Technology,

^{***}Ulsan National Institute of Science and Technology

ABSTRACT

It is well known that plastic behaviors of materials are governed by collective motion of dislocations and interactions of them with other defects. A mobility and reaction properties of the dislocation are decided by its core structure. The core makes the dislocation have nonlinear properties, which cannot be explained by classical linear elasticity theory. Furthermore, it has been reported that the core induces unexpected behaviors in nanoscale [1]. To understand the fundamentals of material plasticity, thus, it is necessary to characterize behaviors of the dislocation core by priority. Especially, in case of metallic materials, the motion of dislocations is significantly disturbed by grain boundaries, and their interactions increase ductility of the materials. In a sense that most metals used in industry are polycrystalline, the influence of grain boundaries on material plasticity must be emphasized. Despite of the importance of the grain boundaries, however, the researches of the grain boundary have been focused on phenomenological approaches rather than systematic analysis due to difficulty caused by large degree of freedom to define the grain boundaries. In this work, we employ both atomistic simulation and theoretical approach to describe motion of various low angle grain boundaries by expanding dislocation theory in nanoscale. Firstly, we observed unusual behavior that externally applied stress is reduced inside of nanoscale materials while single dislocation is in motion, which is defined stress-drop behavior [1]. By developing simple analytic equation based on discrete lattice dynamics theory, we can explain this unusual behavior. Furthermore, we also observed that the stress-drop behavior appears during motion of the grain boundaries under external stress. Unlike single dislocation, however, not only the stress-drop but also curvature of grain boundaries were observed during their motions. And our result proves that the curvature is maintained by phonon drag induced by scattering of external loading and interaction between dislocations which consist the grain boundary during its motion.

Comparison between Various Approximations for Free Energy Calculation in Partitioned-Domain Methods

Woo Kyun Kim*, Ellad Tadmor**

*University of Cincinnati, **University of Minnesota

ABSTRACT

Partitioned-domain methods are multiscale approaches that divide a system into an atomistic region where full-atomistic resolution is retained, and a continuum region represented by a coarse-grained finite element model with local constitutive relations. At finite temperature, the constitutive relation corresponds to the Helmholtz free energy of a strained infinite crystal. This study examines several approximation methods for free energy calculations used in variations of the quasicontinuum (QC) method: (1) The quasi-harmonic (QH) approximation in which the potential energy is expanded to second order and the free energy is integrated analytically; (2) the local-Harmonic (LH) approximation, which is similar to QH but with off-diagonal terms in the Hessian matrix neglected; (3) the maximum entropy (max-ent) formalism based on ideas from information theory. To test the accuracy of these methods, all three have been implemented within a single framework. The results for various problems including thermal expansion, simple shear, and a Lomer dislocation dipole will be presented. In addition, the effect of "ghost forces" (numerical artifacts appearing at the continuum-atomistic interface) in a hot-QC simulation is investigated. For static QC, ghost forces can be addressed using a dead-load correction. The effectiveness of this approach in hot-QC is tested.

Multiscale Indentation and Bending Simulations of Mono-layered Graphene in Elastic Regime

Yongwoo Kim^{*}, Keonwook Kang^{**}

^{*}Department of Mechanical Engineering, Yonsei University, Republic of Korea, ^{**}Department of Mechanical Engineering, Yonsei University, Republic of Korea

ABSTRACT

In this study, we investigated mechanical behaviors of mono-layered graphene under indentation [1] and bending using molecular statics (MS) simulations and finite element analysis (FEA). We tested circular graphene sheet with the Adaptive Intermolecular Reactive Empirical Bond Order potential (AIREBO) [2]. Changing thickness of graphene in FEA, the force-indentation depth curve was compared with that in MS. And we found an effective thickness where both results match in elastic regime. Additionally, deflection curve and induced Cauchy stress in graphene sheet were compared, too. Presented results demonstrate that the proposed method could provide a valuable tool for studying the mechanical behavior of mono-layered graphene sheet using FEA. [1] Lee, C., Wei, X., Kysar, J. W., & Hone, J. (2008). Measurement of the elastic properties and intrinsic strength of monolayer graphene. *science*, 321(5887), 385-388. [2] Stuart, S. J., Tutein, A. B., & Harrison, J. A. (2000). A reactive potential for hydrocarbons with intermolecular interactions. *The Journal of chemical physics*, 112(14), 6472-6486.

Rigid-body Mechanism Synthesis by SBM (Spring-connected Rigid Block Model) Based Topology Optimization

Yoon Young Kim*, Seok Won Kang**

*Department of Mechanical and Aerospace Engineering, Seoul National University, **Department of Mechanical and Aerospace Engineering, Seoul National University

ABSTRACT

In spite of great success of the topology optimization in designing load-carrying structures, its use in synthesizing motion-generating rigid-body mechanisms is less active. There are several issues to be resolved to advance the topology optimization based mechanism synthesis, but in this presentation, we will be focused mainly on the ground modeling issue. Especially for numerically efficient gradient-based topology optimization based synthesis, there are two ground models available, the revolute joint-connected link model and the zero-length spring-connected rigid block model (SBM). Unlike the link ground model only allowing revolute joints, we will show that the SBM developed in [1,2] allows the presentation of revolute, prismatic, and other types of joints when the spring stiffness takes on its upper or lower bound value. Because the stiffness can be interpolated as a function of a real design variable, the use of a gradient-based optimizer is readily possible. After the underlying concept of the SBM suitable to represent only revolute joints, an alternative model method called, the double-spring connected rigid block model (D-SBM) will be presented in order to represent general joints. Also, a method to deal with revolute and prismatic joints only is presented and its successful application in the design of a robotic rehabilitation device by the SBM-based topology optimization method will be presented. [1] Y.Y. Kim, G.W. Jang, J.H. Park, J.S. Hyun, S.J. Nam, Automatic synthesis of a planar linkage mechanism with revolute joints by using spring-connected rigid block models, J. Mech. Des. 129 (2007) 930–940. [2] S.W. Kang, S. I. Kim, Y. Y. Kim, Topology optimization of planar linkage systems involving general joint types, Mechanism and Machine Theory 104 (2016) 130-160.

Extended Analytic Model of Staggered Platelet Structure and Its Application to 3D Printing Technology

Youngsoo Kim*, Seunghwa Ryu**

*Department of Mechanical Engineering, Korea Advanced Institute of Science and Technology (KAIST),

**Department of Mechanical Engineering, Korea Advanced Institute of Science and Technology (KAIST)

ABSTRACT

There have been many studies to understand and utilize the superior mechanical properties of nacre with moderate stiffness and high toughness. The load transfer mechanism in the unique 'brick and mortar' structure of the nacre has been intensively analyzed and its structural features has been mimicked by various manufacturing methods such as 3D printing. However, due to the limited applicability of most analytical models and the limitation in the 3D printers, it has been difficult to theoretically predict and design the propertyed 3D printed structures. In this study, we improve the analytic models to predict the effective elastic properties of the 'brick and mortar' structure for a wide range of constituent materials and geometric ratios by correctly accounting volume (Area for 2D) average concept. In addition, we also reveal the effect of the printing direction and thickness on the 3D printed composite materials. We show that our extended analytic model accurately predict the properties of 3D printed composite when using the manufacturing-condition-dependent material properties as input. Furthermore, we suggest a new possible design to increase the toughness of composites. Our studies reveals the origin of discrepancy between theory and 3D printed structures and enable a rational design of nacre-inspired structures.

Strain-rate Dependent Microplane Constitutive Model for Dynamic Fracturing and Comminution of Concrete during Projectile Impact

Kedar Kirane^{*}, Zdenek Bazant^{**}

^{*}Stony Brook University, ^{**}Northwestern University

ABSTRACT

While numerous studies have dealt with dynamic crack propagation in concrete, they have not led to a macroscopic continuum model usable in FE analysis. Such a model was recently developed and is presented here. The model is based on the recently developed theory of comminution according to which comminution of concrete under high-rate impact loading is driven by the release of the local kinetic energy (rather than the strain energy) of the shear strain rate field. This theory yields expressions to calculate the particle size and the additional kinetic energy density that must be dissipated in finite-element codes. In previous research, it was dissipated by additional viscosity, in a model partly analogous to turbulence theory. Here it is dissipated by scaling up the material strength. Microplane model M7 is used and its stress-strain boundaries are scaled up by factors proportional to the $\sqrt[4]{3}$ power of the effective deviatoric strain rate and its time derivative. The crack band model with a random tetrahedral mesh is used and all the artificial damping is eliminated. The scaled M7 model is seen to predict correctly the crater shapes and exit velocities of projectiles penetrating concrete walls of different thicknesses. The choice of the finite strain threshold for element deletion criterion, which can have a big effect, is also studied.

Efficient Simplicial Finite Elements Via Bernstein Polynomials

Robert Kirby*

*Baylor University

ABSTRACT

The mathematical power offered by high-order finite element methods is all-too often realized at a high computational cost, especially on simplicial meshes where basis functions lack tensor product structure. However, recent work on Bernstein polynomials has led to efficient algorithms for many fundamental finite element kernels. Algorithms that evaluate load vectors and the (action of) finite element matrices with optimal complexity are now known, including for $H(\text{div})$ and $H(\text{curl})$ spaces. Additionally, optimal algorithms for interpolation and polynomial projection in the Bernstein basis, which are also required at various stages, can be given in terms of block-structured linear algebra. This structure depends intricately on the details of Bernstein polynomials. Finally, the nonnegativity of the Bernstein basis has been suggested as a pathway to enforce positivity for higher-order bases in transport or other applications with hard constraints. This talk will summarize the state of the art for Bernstein polynomials and include numerical examples.

NO_x Prediction of a Natural Gas and Hydrogen Mixed-combustion-type Gas Turbine Combustor

Ryosuke Kishine^{*}, Nobuyuki Oshima^{**}, Kohshi Hirano^{***}, Takeo Oda^{****}

^{*}Hokkaido University, ^{**}Hokkaido University, ^{***}Kawasaki Heavy Industries, Ltd., ^{****}Kawasaki Heavy Industries, Ltd.

ABSTRACT

In pursuit of a reduction in environmental loading, gas turbine combustors that use a hydrogen-enriched fuel instead of pure natural gas have entered practical service. In such a new attempt, numerical simulation is very effective for more efficient development because it can easily perform parametric studies. In our previous study [1], a numerical analysis was performed on a natural gas and hydrogen mixed-combustion-type gas turbine combustor using large-eddy simulation and a multi-scalar flamelet approach. Three conditions were analyzed with different introduction amount of hydrogen, and the tendencies of the simulation results qualitatively agreed with the knowledge in the experiments. In the current study, we aim to investigate an applicability of the numerical method for the turbulent mixed-combustion field by comparing the simulation results of NO_x emission with the experimental ones as a next step. The calculation object was the combustor of an L30A-DLE gas turbine, developed by Kawasaki Heavy Industries, Ltd. This combustor has a diffusion pilot burner, a premixed main burner, as well as a premixed supplemental burner and cooling air inlets. In order to conduct a quantitative evaluation, the reproducibility of the shape for the burners and the other parts was improved compared to our previous research. The number of elements therefore increased from about 20 million to 30 million. Calculations were conducted under two different operating conditions of the same load. The design fuel ratio of the two-type premixed burners were different in each case. Because NO_x is considered as a passive scalar in combustion calculations, it can be predicted separately from combustion calculation by LES. This idea about NO_x prediction is very effective in decreasing the calculation cost. The simulated distributions of the NO_x production rate well captured the difference between the two conditions. These results suggest that by setting the higher fuel ratio of the supplemental burner, NO_x emissions are reduced along with the decrease in the high temperature region. In our presentation, we will show the quantitative comparison results of simulated values and experimental ones about NO_x emissions. At the same time, we are planning to examine the validity of this NO_x prediction method by comparing it with the results of the normal prediction method. [1]Kishine, R., et al., 2017, "Application of Large-eddy Simulation and the Multi-scalar Flamelet Approach to a Methane-hydrogen Mixed-combustion-type Industrial Gas-turbine Combustor," Proceedings of the ASME 2017 Power and Energy Conference, PowerEnergy2017-3247.

The Influence of Binder Mobility to the Viral Entry Driven by the Receptor Diffusion

Sandra Klinge^{*}, Tillmann Wiegold^{**}, Gerhard A. Holzapfel^{***}

^{*}TU Dortmund University, ^{**}TU Dortmund University, ^{***}Graz University of Technology, Norwegian University of Science and Technology

ABSTRACT

The current presentation deals with the simulation of the viral entry into a cell. There are two dominant mechanisms typical of this process: the endocytosis und the fusion with the cellular membrane. However, we only focus on the first scenario. To this end, we consider a virus as a substrate with a constant concentration of receptors on the surface. Differently, the concentration of receptors of the host cell varies and these receptors are free to move over the membrane. When the contact with the cell surface has been achieved, the receptors start to diffuse to the contact (adhesion) zone. The membrane in this zone inflects and forms an envelope around the surface of the virus. This is the way the newly formed vesicle imports its cargo into the cell. In order to simulate the process described, we assume that the differential equation typical of the heat transport is suitable to simulate the diffusion of receptors. Additionally, we formulate two boundary conditions: First, we consider the balance of fluxes on the front of the adhesion zone. Here, it is supposed that the velocity is proportional to the gradient of the chemical potential. The second subsidiary condition is the energy balance equation depending on four different contributions: the energy of binding receptors, the free energy of the membrane, the energy due to the curvature of the membrane and the kinetic energy due to the motion of the front. The differential equation itself along with two boundary conditions forms a well-posed problem which can be solved by applying a direct method, for example the finite difference method. The talk also includes numerical examples showing the distribution of receptors over the membrane as well as the motion of the front of the adhesion surface. In particular, the influence of the mobility of receptors has been studied.

A Computational Framework for Scale-bridging in Multiscale Simulations and Its Applications to Modeling of Energetic Materials

Jaroslav Knap^{*}, Kenneth W. Leiter^{**}, Richard Becker^{***}, Brian C. Barnes^{****}

^{*}U.S. Army Research laboratory, ^{**}U.S. Army Research laboratory, ^{***}U.S. Army Research laboratory, ^{****}U.S. Army Research laboratory

ABSTRACT

Over the last few decades, multiscale modeling has become a dominant paradigm in materials modeling and simulation. The practical impact of multiscale modeling depends, to a great extent, on its ability to utilize modern large-scale computing platforms. However, since there are no general numerical and computational frameworks for multiscale modeling, the vast majority of multiscale material models or simulations are developed on a case-by-case basis. We seek to formulate an adaptive computational framework for multiscale modeling. We do not intend to develop a specific method for multiscale simulations, but instead, aim to develop a broad and flexible computational framework for designing and developing such simulations. Our focus is primarily on new scalable numerical algorithms applicable to a wide range of multiscale modeling applications and, more specifically, to scale-bridging. These algorithms fall into one of the three areas: i) adaptive computational strategies for multiscale modeling, ii) algorithms for scale-bridging in multiscale modeling, and iii) algorithms for development of surrogate models to reduce the computational cost associated with multiscale models. We present a formulation of our computational framework and describe our progress towards development of a two-scale model of an energetic material utilizing it.

Modeling Intragranular Misorientation, Grain Fragmentation, and Associated Effects on Mechanical Fields and Texture Evolution in Polycrystals Using the Viscoplastic Self-Consistent Framework

Marko Knezevic*, Rodney McCabe**, Miroslav Zecevic***, Ricardo Lebensohn****

*University of New Hampshire, **Los Alamos National Laboratory, ***University of New Hampshire, ****Los Alamos National Laboratory

ABSTRACT

In recent works, we reported the methodology to calculate intragranular fluctuations of the instantaneous lattice rotation rates (Lebensohn et al., 2016) and associated misorientation distributions developing inside each grain representing a polycrystalline aggregate within the mean-field viscoplastic self-consistent (VPSC) homogenization (Zecevic et al., 2017). The methodology is based on the second moment of intragranular stresses calculated by the VPSC model. This paper advances the methodology to incorporate the effect of the intragranular misorientations on stress fluctuations. Furthermore, the fluctuations of plastic spin are defined as a function of not only the stress fluctuations but also the intragranular misorientations. These advances facilitated the development of a grain fragmentation (GF) model within VPSC, which is conceived within the crystal orientation space. The overall model is termed GF-VPSC. Case studies including simple tension and plane-strain compression of face-centered cubic polycrystal deformed to large strains are used to illustrate the utility of the developed model. The predictions of intragranular misorientation distributions and texture evolution are compared with full-field calculations and experiments. Good agreement is obtained for the intragranular misorientation distributions and, as a result, more accurate modeling of texture evolution is facilitated by the new model relative to the standard VPSC. Since the developed intragranular misorientations act as driving forces for recrystallization, the novel GF-VPSC is shown to enable coupled modeling of microstructure evolution during deformation and recrystallization in a computationally efficient manner. Lebensohn, R.A., Zecevic, M., Knezevic, M., McCabe, R.J., 2016. Average intragranular misorientation trends in polycrystalline materials predicted by a viscoplastic self-consistent approach. *Acta. Mater.* 104, 228-236. Zecevic, M., Pantleon, W., Lebensohn, R.A., McCabe, R.J., Knezevic, M., 2017. Predicting intragranular misorientation distributions in polycrystalline metals using the viscoplastic self-consistent formulation. *Acta. Mater.* 140, 398-410.

Butterflies in Layered Media

Nicholas Knight^{*}, Michael O'Neil^{**}

^{*}NYU-Courant, ^{**}NYU-Courant

ABSTRACT

We present an algorithm for electromagnetic scattering calculations in layered media by use of butterfly-accelerated Sommerfeld integrals. In the time-harmonic setting, representing electromagnetic fields by generalized Debye sources (and their Fourier transforms) along layered media interfaces efficiently decouples several unknowns, and leads to a representation whose evaluation is amenable to acceleration via a butterfly algorithm. When coupled with an iterative solver, the corresponding integral equation formulation can be efficiently solved.

A Shell Model with Variationally Embedded Interlaminar Stresses for the Calculation of Layered Composite Structures and Delamination Effects

Gregor Knust^{*}, Friedrich Gruttmann^{**}

^{*}Solid Mechanics, Darmstadt University of Technology, Frankziska-Braun-Str. 7, 64287 Darmstadt, Germany,

^{**}Solid Mechanics, Darmstadt University of Technology, Frankziska-Braun-Str. 7, 64287 Darmstadt, Germany

ABSTRACT

The computation of interlaminar stresses is essential for the design of layered composite structures. While solid elements are able to compute these stress states, they represent a numerically expensive approach. This work deals with layered shells subjected to static loading for prediction of interlaminar stresses. The underlying shell theory is based on the Reissner-Mindlin kinematics with an inextensible director field. Additional degrees of freedom for in-plane warping and relative displacements in thickness direction are introduced. These displacements are interpolated with layerwise cubic functions, which are constant within one element and discontinuously over its boundaries. The resulting shell element is applicable for geometrically and physically nonlinear problems. Further a multifield functional based on the Hu-Washizu functional is introduced. Here the associated Euler-Lagrange equations include the usual global shell equations in terms of stress resultants, the local equilibrium in terms of stresses, the geometric field equations and the constitutive equations. In addition the functional contains a constraint, which enforces the correct shape of the warping function through the thickness [1]. The finite element formulation is based on the isoparametric concept for four-node quadrilateral shell elements. The elimination of independent stresses, warping and Lagrange parameters on element level leads to a mixed hybrid shell element with the standard 5 or 6 degrees of freedom per node. This is a fundamental characteristic, since it is possible to use standard geometrical boundary conditions. Therefore the element can be applied to complex geometrical problems. The transverse stresses are continuous at layer boundaries for linear elastic problems. An interface to three-dimensional material laws is part of the element formulation, too [2]. This allows together with the determination of thickness normal stresses the computation of delamination effects of layered laminates. Results of several examples will be shown and compared to reference solutions. Here geometrically nonlinearity, as well as physically nonlinear material behavior is considered. In comparison to 3d models, the present shell element needs only a fractional amount of computing time. References: [1] F. Gruttmann, W. Wagner, G. Knust (2016) A Coupled Global-Local Shell Model with Continuous Interlaminar Shear Stresses. *Computational Mechanics* 57:237-255. [2] F. Gruttmann, G. Knust, and W. Wagner (2017) Theory and numerics of layered shells with variationally embedded interlaminar stresses. *Computer Methods in Applied Mechanics and Engineering* 326:713-738

Three-dimensional Geometrical Characterization of Aneurysmal Location and Surface

Masaharu Kobayashi^{*}, Marie Oshima^{**}, Katsuyuki Hoshina^{***}, Shu Takagi^{****}, Masaaki Shojima^{*****}

^{*}the Graduate School of Interdisciplinary Information Studies, The University of Tokyo, ^{**}Interfaculty in Information Studies/Institute of Industrial Science, The University of Tokyo, ^{***}Division of Vascular Surgery, Department of Surgery, Graduate School of Medicine, The University of Tokyo, ^{****}Department of Mechanical Engineering, The University of Tokyo, ^{*****}Department of Neurosurgery, The University of Tokyo Hospital

ABSTRACT

Rupture of a cerebral aneurysm often leads to a devastating event with high mortality and long term disability. In the abdominal artery, celiac trunk stenosis tends to generate multiple pancreaticoduodenal arcade aneurysms. Hemodynamic factors play an important role in aneurysmal formation, growth, and rupture. Hemodynamic simulations with patient-specific arterial geometry have been performed to calculate hemodynamic forces such as wall shear stress (WSS) and WSS gradient. The three-dimensional (3D) arterial bend can be characterized as curvature and torsion along arterial centerline. Lauric et al. [1] investigated the relationship between the curvature along internal carotid artery (ICA) with aneurysm and hemodynamic forces. On the other hand, concavity and convexity on aneurysmal surface can be characterized as Gaussian and mean curvatures. The purpose of this study is to characterize both vascular geometry of peri-aneurysmal environment and aneurysmal geometry. We have been developing an image-based 3D geometrical modeling system, V-Modeler [2], to investigate quantification of arterial morphological changes. The modeling system consists of five functions: 1) segmentation of arterial lumen; 2) extraction of arterial centerlines; 3) surface reconstruction; 4) calculation of geometric parameters; and 5) tracking of arterial geometry. The centerline and surface are represented as spline functions in order to remove influence of noise in medical images. Curvature and torsion along the centerline are calculated from the spline function. In addition, we develop a spline surface fitting method using correspondence between arterial centerline and surface. The method consists of: - Triangular spline surface representation [3] considering topological changes in arterial bifurcation and aneurysm, - Construction of 1-to-N index corresponding table between centerline and surface based on boundary representation, - Arterial surface smoothing based on triangular spline surface fitting with the corresponding table, - Calculation of Gaussian and mean curvatures based on spline surface function. The method is applied to arterial geometries extracted from medical images with pancreaticoduodenal arcade and ICA aneurysms. [1] A. Lauric et al., "Curvature effect on hemodynamic conditions at the inner bend of the carotid siphon and its relation to aneurysm formation." J Biomech. 2014 Sep 22;47(12):3018-27. [2] M. Kobayashi et al., "Development of an image-based modeling system to investigate evolutionary geometric changes of a stent graft in an abdominal aortic aneurysm," Circ. J., vol.79, no.7, pp. 1534-1541, 2015. [3] S. Harmann et al, "Triangular G1 interpolation by 4-splitting domain triangles", Computer Aided Geometric Design, Elsevier, vol. 17, pp. 731-757, 2000

Computational Generation of High Quality Quad Layouts

Leif Kobbelt*

*RWTH Aachen University

ABSTRACT

The conversion of raw geometric data (that typically comes in the form of unstructured triangle meshes) to high quality quad meshes is an important and challenging task. The complexity of the task results from the fact that quad mesh topologies are subject to global consistency requirements which cannot be dealt with by local constructions. This is why recent quad meshing techniques formulate the mesh generation process as a global optimization problem. By adding hard and soft constraints to this optimization, many desired properties such as structural simplicity, principal direction alignment, as well as injectivity can be guaranteed by construction. An even more challenging problem is the computation of quad layouts, where a coarse segmentation of the input surface into essentially rectangular patches is sought which also satisfies global consistency and shape quality requirements. While being structurally related, both problems need to be addressed by fundamentally different approaches. In my talk I will present some of these approaches and demonstrate that they can generate high quality quad meshes and quad layouts with a high degree of automation but that they also allow the user to interactively control the results by setting boundary conditions accordingly.

Instability Problems of Implicit FEM Solution Procedures for Fast Rotating Structures – Instability Sources and Solutions

Markus Kober^{*}, Arnold Kühhorn^{**}, Akin Keskin^{***}

^{*}Brandenburg University of Technology Cottbus - Senftenberg, ^{**}Brandenburg University of Technology Cottbus - Senftenberg, ^{***}Rolls-Royce plc

ABSTRACT

For the solution of dynamic FEM problems in the time domain in general two possibilities exist. The first one is to solve the equations of motion with an explicit time-integration scheme, which has the advantage of being very fast but on the other hand the time-steps have to be very small for stability reasons. The second possibility is to use an implicit time-integration scheme in combination with a Newton or Quasi-Newton algorithm, which is computationally more expensive but allows for much bigger time-steps. It is well known that implicit solution procedures tend to become instable for the simulation of elastic rotating structures [1,2]. But if the simulation time of complex real-world structures is bigger than a few milliseconds explicit time-integration is too inefficient due to the small time-steps and an implicit time-integration scheme has to be used. We will demonstrate the appearance of instabilities during the implicit FE simulation of elastic rotating structures at the example of simple academic problems. If the time-step size is small enough to consider the boundary value problem to be linear in one time-step, stability maps for the time-integration algorithm can be computed [3]. Surprisingly, the described instabilities appear although the time-integration algorithm (e.g. Newmark scheme) is unconditionally stable with respect to the stability map. With the help of a simple elastic rotating pendulum we will derive the sources of the instabilities and discuss this problem in detail. It will be shown that the Newton algorithm for the solution of the nonlinear system of equations and especially the models stiffness and the used time-step size have a direct impact to the stability. These results are then transferred to the presented FE examples and a general solution for the described problems is presented. Finally, results of the transient implicit simulation of a realistic aero-engine model, rotating at 10.000 rpm and using the derived concept for stability, are shown. References [1] D. Kuhl and M.A. Crisfield, Energy-conserving and Decaying Algorithms in Non-linear Structural Dynamics, International Journal for Numerical Methods in Engineering, 1999, 45, pp. 569-599. [2] K.J. Bathe and M.M.I. Baig, On a composite implicit time integration procedure for nonlinear dynamics, Computers and Structures, 2005, 83, pp. 2513–2524. [3] K.J. Bathe and E.L. Wilson, Stability and Accuracy Analysis of Direct Integration Methods, Earthquake Engineering and Structural Dynamics, 1973, 1, pp. 283-291.

A Coupled FEM-SPH Approach for Investigating the Influence of a Fluid on the Vibration Behavior of an Oil Pan

Sebastian Koch^{*}, Sascha Duczek^{**}, Elmar Woschke^{***}

^{*}Otto-von-Guericke-University Magdeburg, ^{**}Otto-von-Guericke-University Magdeburg,

^{***}Otto-von-Guericke-University Magdeburg

ABSTRACT

Already in an early stage of the design process the manufacturer has to be enabled to estimate the performance of new products. Thus, the design of the first draft can be favorably adjusted in order to reach specific goals. Furthermore, expensive prototypes are only required for the final testing. The aim of this contribution is to improve a previously developed holistic simulation approach for the evaluation of the acoustic behavior. Here, a combustion engine is used as an automotive example [1]. An experimental investigation on an engine test bench shows significant differences between the measured and predicted results in the area of the oil pan. These differences can be traced back to the oil, which leads to a frequency shift and smaller amplitudes. Until now the oil was only taken into account as an additional mass. To improve the results, a particle-based approach is coupled with the Finite Element Method (FEM). For this a higher order FEM code [2] and the open source Smoothed Particle Hydrodynamic (SPH) program SPHysics are used. Initially, a co-simulation is performed and validated with typical benchmark examples. The interface region coincides with the surface of the solid structure and features FE nodes as well as the first row of SPH boundary particles. The pressure of the fluid particles is applied to the FE structure as an external load, which causes a deformation of the solid and consequently leads to displacements and velocities of the boundary particles. The coupling nodes and particles do not need to be conformal, as the required displacement and velocity values can be computed at any point in the interface by means of the shape functions. In a last step, the proposed method for the acoustical simulation of an oil pan is validated based on a 2D academic benchmark test. The influence of the fluid in the oil pan is quantified by a transient simulation and an inspection of the frequency spectrum computed by Fourier transformation of the results. For future applications more sophisticated coupling techniques are implemented to further improve the quality of the numerical simulation. [1] F. Duvigneau, S. Nitzschke, E. Woschke, U. Gabbert, "A holistic approach for the vibration and acoustic analysis of combustion engines including hydrodynamic interactions", *Archive of Applied Mechanics*, 86, (2016). [2] S. Duczek, *Higher Order Finite Elements and the Fictitious Domain Concept for Wave Propagation Analysis*, VDI-Verlag, VDI-Fortschritt-Berichte Reihe 20 Nr 458, (2014), url: <http://edoc2.bibliothek.uni-halle.de/hs/content/titleinfo/39725>.

Multiscale Thermomechanical Analysis of Composites Containing Phase Change Materials

Kossi-Mensah Kodjo^{*}, Julien Yvonnet^{**}, Karam Sab^{***}, Mustapha Karkri^{****}

^{*}Université Paris-Est, Laboratoire Modélisation et Simulation Multi Échelle, MSME UMR 8208 CNRS., ^{**}Université Paris-Est, Laboratoire Modélisation et Simulation Multi Échelle, MSME UMR 8208 CNRS., ^{***}Université Paris-Est, Laboratoire Navier, CNRS UMR 8205, ENPC, IFSTTAR., ^{****}Université Paris Est, Centre d'Études et de Recherche en Thermique, Environnement et Systèmes, CERTES - EA 3481.

ABSTRACT

This work presents a concurrent multiscale method for thermomechanical properties of composite structures containing Phase Change Materials (PCM) particles at microscale. The PCM inclusions change from solid to liquid phase and lead to significant modifications of the macroscopic thermal behavior. The FE2 method [1] is extended to take into account phase change effects on the macroscale thermal heat conduction. For the mechanical behavior, a classical homogenization is performed on the same Representative Volume Element used in the FE2 procedure. The thermal behavior with phase change at microscale is strongly nonlinear and involves coupling with fluid flow in the liquid phase. An apparent heat capacity method proposed in [2] is used to model the thermal phase change in the inclusions. Thermal phase changes occur at almost constant temperature and the latent heat stored (or released) is largely higher than the energy exchanged by temperature variation. Thus, PCMs with phase change in range of room temperature have a great potential in building applications: improvement of thermal inertia of civil engineering constructions and reduction of energy consumption due to air conditioning. The method is applied to concrete including encapsulated paraffin wax. The results show that the macroscale temperature's fluctuations are smoothed as compared to concrete alone. In addition, the macroscopic temperature peaks are delayed in time. Furthermore, a comparison with a direct Finite Element analysis shows the ability of the proposed strategy to predict accurately the fully nonlinear thermal behavior of PCM based composites. Keywords: Phase Change Material, Heat conduction, Computational homogenization, Multi-scale modeling, FE2 method. References [1] F. Feyel. Multiscale FE2 elastoviscoplastic analysis of composite structures, Computational Materials Science, (1999) 16(1-4):344—354. [2] M. Aadmi, M. Karkri, M. E. Hammouti. Heat transfer characteristics of thermal energy storage of a composite phase change materials: Numerical and experimental investigations, Energy, Volume, (2014), (72):381 – 392.

Composite Crashworthiness Prediction for Bumper and Crush Can Assembly

Ravi Kodwani^{*}, John Brink^{**}, Rogerio Nakano^{***}

^{*}Mr., ^{**}Mr., ^{***}Mr

ABSTRACT

The United States Automotive Materials Partnership (USAMP) approached Altair with the goal of predicting the automotive crash behavior of composite laminates subjected to 6 different test configurations. Coupon and generic component level test data were supplied to help with the development of material models. Material characterization process and determination of failure parameters using DOE are detailed in the presentation. Final correlation was to a series of “blind” sled tests completed on a woven ply composite bumper with SMC over-molded ribs and woven ply crush cans. Altair submitted the RADIOSS predictions to USAMP and USAMP shared the test data shared after that. Apart from this prediction, presentation also discusses delamination failure criteria using macro shell models and comparison with and without them.

System and Parameter Identification via Correlated Multifield Analysis.

Carsten Koenke^{*}, Long Nguyen-Tuan^{**}, Tom Lahmer^{***}, Volker Bettzieche^{****}

^{*}Institute off STructiral Mechanics, Bauhaus-Universität Weimar, ^{**}Institute off STructiral Mechanics, Bauhaus-Universität Weimar, ^{***}Institute off STructiral Mechanics, Bauhaus-Universität Weimar, ^{****}Ruhrverband Essen

ABSTRACT

System and parameter identification using methods of inverse analysis is a common problem in several engineering disciplines. In civil engineering applications the safety assessment of existing structures which often is the base for life-time predictions need system and parameter estimations for the investigated existing structures. Therefore inverse techniques are applied using sensor data from different physical fields, e.g. deformation data or temperature data. Usually only data from one physical field is used for the identification of system parameters at one time. Therewith the interaction effects between different physical fields are usually not taken into account. As an example for this interaction effects the correlation between pores, damage and cracks driven by mechanical or temperature loading and the permeability of solids can be seen. Using data from deformation measurements and superimposing this data with measurements from the hydraulic head field leads to improved identification results for the material parameters and their distribution in the domain for both fields. Inverse analysis based on correlated multifield data allows a much more robust identification of essential system parameters. The paper will present an approach in which a thermo-mechanical-hydraulic analysis will be used for the material parameter identification in masonry dam structures, i.e. to identify regions of local damage in large scale structures. Uncertainty of measured data is taken into account and leads to an information about the probability distribution of the damage zone. Issues such as correlation parameters and influence of noisy measurement data will be discussed in the presentation. The presented approach has been applied for parameter identification of existing masonry dam structures in Germany, which are in operation for already 100 years.

The Conforming Reproducing Kernel Method for an Agile Design-to-Simulation Process

Jacob Koester^{*}, J.S. Chen^{**}, Michael Tupek^{***}, Scott Mitchell^{****}, Joe Bishop^{*****}

^{*}Sandia National Laboratories and the University of California, San Diego, ^{**}University of California, San Diego,
^{***}Sandia National Laboratories, ^{****}Sandia National Laboratories, ^{*****}Sandia National Laboratories

ABSTRACT

Efficient model development for complex systems remains a challenge. Generating a mesh of sufficient quality for the Finite Element Method (FEM) can take months [1]. Research in agile design-to-simulation processes seeks to alleviate this bottleneck by taking on the difficult task of pairing automatic discretization techniques with numerical methods that are capable of producing satisfactory results. In this work, we present the Conforming Reproducing Kernel (CRK) numerical method. In this new approach, approximation functions are constructed using the reproducing kernel method with kernel functions created using Bernstein-Bezier splines on local geometry subdivisions. Meshfree methods, such as the Reproducing Kernel Particle Method (RKPM) [2], have an advantage over FEM as a high-quality mesh is not required. However, this flexibility in the construction of shape functions does present new challenges. Domain integration must be reformulated in order to maintain high accuracy and efficiency [3]. Concave geometries require special consideration so concavities are preserved. Material interfaces call for special attention so that weak discontinuities can be captured. Unlike traditional meshfree methods, CRK uses subdivisions to guide the construction of approximation functions. This allows CRK to better represent domain boundaries, especially nonconvex geometries. Also, the underlying reproducing kernel method gives CRK the flexibility to blend approximations over low quality subdivisions or handle non-contiguous meshes, making it compatible with automatic discretization processes that produce may produce low quality meshes. Previous work focused on developing the concept in two dimensions using C^1 splines on triangulations. In this presentation, the method is extended to three dimensions and kernels are constructed using tetrahedral subdivisions. Examples utilizing the conforming kernels are shown and results are compared to predictions using FEM and RKPM. [1] M. Hardwick, R. Clay, P. Boggs, E. Walsh, A. Larzelere and A. Altshuler, DART system analysis, SAND2005-4647, Sandia National Laboratories, Albuquerque, NM, 2005. [2] W.K. Liu, S. Jun and Y.F. Zhang, Reproducing kernel particle methods, International Journal for Numerical Methods in Fluids, 20, 1081-1106, 1995. [3] J.S. Chen, M. Hillman and M. Rüter, An arbitrary order variationally consistent integration for Galerkin meshfree methods, International Journal for Numerical Methods in Engineering, 95, 387-418, 2013. ^{*}Sandia National Laboratories is a multimission laboratory managed and operated by National Technology and Engineering Solutions of Sandia, LLC., a wholly owned subsidiary of Honeywell International, Inc., for the U.S. Department of Energy's National Nuclear Security Administration under contract DE-NA-0003525.

Modification of Response Surface Single Loop Method in Reliability-Based Optimization

Nozomu Kogiso*, Hiroaki Tanaka**

*Osaka Prefecture University, **Osaka Prefecture University

ABSTRACT

This study proposes an improvement method of the response surface single loop method (RSSL) [1] for the reliability-based optimization. The RSSL achieves computational efficiency with high approximation accuracy by directly evaluating the failure probability using the Hermite polynomial and the second-order approximated limit state function. Since the method does not require the most probable point (MPP) searching, the single loop reliability-based optimization is achieved, once the second-order approximation of the limit state function is established. However, we found from our experiment of application to several example problems that the RSSL method does not always have a sufficient accuracy. Especially when the approximation point of the limit state function is apart from the MPP, the approximate accuracy is deteriorated. While, the accuracy is sufficient, if the approximation point is closed to the MPP. For the purpose, we introduce an approximation point updating process in the optimization loop that utilizes an idea of the Single Loop Single Vector (SLSV) method [2] and the modified SLSV method [3]. It means that the second-order approximation point of the limit state function is updated to the approximated MPP by the SLSV method in each optimization step. Since the RSSL does not require the MPP to evaluate the failure probability, the failure probability approximation accuracy is sufficient for roughly approximated MPP. Through several numerical examples, the validity of the proposed method is illustrated by comparing between the proposed method, the original RSSL and also the SLSV. [Reference] 1. R. Mansour and M. Olsson, Response surface single loop reliability-based design optimization with higher-order reliability assessment, *Str. Multidiscip. Opt.*, 54 (2016), 63-79. 2. X. Chen, et al., Reliability based structural design optimization for practical applications, (1997), AIAA-97-1403. [3] N. Kogiso, et al., Modified single-loop-single-vector method for efficient reliability-based design optimization, *J. Adv. Mech. Des. Sys. Manuf.*, 6(7) (2012), pp. 1206-1221.

Characteristics of Singular Electric Displacement Fields at the Vertex of Interface in Piezoelectric Joints

Hideo Koguchi*, Hiromi Sato**

*Niigata Institute of Technology, **Tsugami Corporation

ABSTRACT

Singular fields of stress and electric displacement occur at the vertex of interface in piezoelectric joints under an external loading and the input of voltage¹⁾. Until now, singular stress fields are intensively investigated for relating to the reliability of joints. It can be expected that concentrated electric displacements causes large electric fields in an adjacent space (air) and electric potential will be induced on the surface of electrode when the electrode approaches to the electric field. In the present paper, a piezoelectric joint which four blocks of piezoelectric material are bonded using an insulated resin is analyzed. In this joint, singular fields occur around a center gathering four vertexes in blocks and the intensity of singularity in electric displacements around the center of cross section in the joint may be four times larger. The intensity of singularity in electric displacements is numerically investigated using a conservative integral method to pursue the possibility of application of the singular fields. It is shown that when piezoelectric materials with large piezoelectric constant are used, electric displacements are amplified. Electric fields in air near the vertex of interface have also a singularity. In this study, a singular field of electricity in air is investigated using a commercial finite element program. The order of singularity in air is a little bit different from that in the joints. The influence of thickness of resin on the electric field in air is investigated. When the thickness of the resin increases, the intensity of singularity also increases. However, when the resin becomes thick, the singular fields do not influence on electric fields at the center region of cross section in the joint. Hence, a suitable thickness of the resin exists for amplifying the electric field in air. Next, a generated voltage in the joints and in a single phase piezoelectric material for loading on the side surface is investigated in experiment. Voltage in the joints is 1.5 times as large as that in the single phase material. It is supposed that this is attributed to the singular fields in electric displacement. Reference 1) H. Koguchi, H. Sato, T. Maekawa and C. Luangarpa, Investigation on singular fields in piezoelectric joints and its application, Trans. JSME (in Japanese), Vol. 83, No. 853, 2017, DOI: 10.1299/transjsme.17-00198.

Numerical Simulation of Multi-Pass Electron Beam (EB) Scanning Process for Controlling Microstructure of Alloy 718 in EB-Powder Bed Fusion (EB-PBF)

Yuichiro Koizumi^{*}, Xiao Ding^{**}, Kenta Yamanaka^{***}, Kenta Aoyage^{****}, Yufang Zhao^{*****},
Akihiko Chiba^{*****}

^{*}Tohoku University, ^{**}Tohoku University, ^{***}Tohoku University, ^{****}Tohoku University, ^{*****}Tohoku University,
^{*****}Tohoku University

ABSTRACT

Electron beam melting (EBM) is a powder bed fusion (PBF) -type additive manufacturing (AM) process using electron beam (EB) as power source for fusing metal powder particle to fabricate metal parts. The most characteristic aspects of EBM process, compared with other metal AM process, such as selective laser melting (SLM) laser beam-PBF, are the high beam power and high scanning speed of electron beam (EB). These characteristics are believed to be beneficial for controlling the solidification condition and resultant microstructure with a large degree of freedom since they allow us to control temperature distribution variously. In this study, multi pass EB scanning process under various process conditions have been investigated by finite element method (FEM) using surface Gaussian heat source. Temperature gradient (G) and solidification rate (R) were calculated from the temporal change of simulated temperature distribution, and they were plotted on solidification map to predict microstructure. The predicted microstructures were compared to the experimentally observed microstructure to examine the validity of the scheme for predicting the microstructure of EBM-built parts. Simulated melt pool size is consistent with experimental results. With increasing heat input, predicted microstructures change from columnar to equiaxed grains. The columnar-to-equiaxed transition (CET) established for casting process is not applicable for EBM process. Peak temperature increases as pass number increases, and it will be kept constant after several passes. Melt pool width and depth increased at first and then reach stable status. Finally, a large melt pool of trapezoidal shape forms. Temperature gradient, solidification rate and cooling rate all decrease with increasing pass number. This suggests that the high scanning speed of EB can be utilized to control solidification condition precisely by controlling the local temperature gradient and solidification dynamically to obtain desired properties.

Bi-penalty Stabilized Explicit Finite Element Algorithm for Contact-impact Problems: One Dimensional Case

Radek Kolman^{*}, Jose Gonzalez^{**}, Sang Soon Cho^{***}, K.C. Park^{****}, Jan Kopacka^{*****}, Anton Tkachuk^{*****}, Dusan Gabriel^{*****}

^{*}Institute of Thermomechanics, Czech Academy of Sciences, ^{**}Universidad de Sevilla, ^{***}Korea Atomic Energy Research Institute, ^{****}University of Colorado Boulder, ^{*****}Institute of Thermomechanics, Czech Academy of Sciences, ^{*****}University of Stuttgart, ^{*****}Institute of Thermomechanics, Czech Academy of Sciences

ABSTRACT

An explicit time integration scheme for finite element solution of contact-impact problems with stabilization of contact forces using a bi-penalty formulation in finite element method for one dimensional case is presented [1]. The penalty approach for enforcing of contact constraints can be applied not only to the stiffness term but also to the inertia of the contact boundary condition. This technique is known as the bipenalty method [2]. By means of adding the bi-penalty terms (additional mass and stiffness terms concurrently) into the equations of motion corresponding to the contact pairs, we obtain a modified local dynamic system. In principle, we attune a frequency character of these equations of motion corresponding to the nodes for which contact conditions apply. The stability limit for an un-penalized/contact-free system is preserved by a special choice of mass and stiffness penalty parameter ratio. For time integration, the explicit time integration scheme is based on splitting of bulk and contact accelerations [3]. Dynamic situation in a bar without respecting contact forces is computed by pull-back time integration [4] with the critical time step size. Moreover, the time stepping process produces stable results for a large range of the stiffness penalty parameter. Behavior of the presented method is shown on impact problems of heterogeneous bars. The special attention is paid to study spurious oscillations of contact forces in one-dimensional contact-impact problem of bars. Acknowledgements to projects: CSF 17- 12925S (Kolman), CSF 16-03823S (Kopa?ka) and MEYS CZ.02.1.01/0.0/0.0/15_003/0000493 (Gabriel) under AV0Z20760514. References [1] KOLMAN, R. - KOPA?KA, J. - TKACHUK, A. - GABRIEL, D. - GONZALEZ, J. A robust explicit finite element algorithm with bipenalty stabilization for contact-impact problems, International Journal for Numerical Methods in Engineering, in preparation, 2018. [2] KOPA?KA, J. - Tkachuk, A. - Gabriel, D. - Kolman, R. - Bischoff, M. - Plešek, J. On stability and reflection-transmission analysis of the bipenalty method in impact-contact problems: a one-dimensional, homogeneous case study, International Journal for Numerical Methods in Engineering, online, 2017, DOI: 10.1002/nme.5712. [3] S. R. Wu. A priori error estimates for explicit finite element for linear elasto-dynamics by Galerkin method and central difference method. Computer Methods in Applied Mechanics and Engineering, 192(51), p. 5329 -5353, 2003. [4] KOLMAN, R. - CHO, S.S. - PARK, K.C. Efficient implementation of an explicit partitioned shear and longitudinal wave propagation algorithm, International Journal for Numerical Methods in Engineering, 2016, vol. 107, no. 7, p. 543-579.

Phase-field Simulation of the Formation of Plate-like Precipitates on Basal Plane and its Effect on the Critical Resolved Shear Stress in Magnesium-based Alloys

Kentaro Komiya^{*}, Yuhki Tsukada^{**}, Toshiyuki Koyama^{***}

^{*}Nagoya University, ^{**}Nagoya University, ^{***}Nagoya University

ABSTRACT

The Mg-Ca binary alloys microalloyed with Al and Zn show precipitation hardening by aging because plate-like precipitates (or Guinier-Preston zones) are formed on the (0001) plane (basal plane). Furthermore, an indium addition is effective for enhancing age hardening behavior because it changes the habit plane of precipitates from the basal plane to {01-10} or {2-1-10} planes (prismatic planes) [1]. Fundamental knowledge on the formation process of precipitates and the relationship between the microstructure and mechanical properties is essential for microstructure design of Mg-based alloys. In this study, the formation process of plate-like precipitates on the basal plane is simulated by three-dimensional (3D) phase field simulations, where the elastic strain energy derived from the precipitation is explicitly considered based on the phase-field microelasticity theory. It has been simulated that the volume fraction of precipitates increases with time while the number density of precipitates decreases with time. Furthermore, by using the simulated 3D two-phase microstructure, the motion of a dislocation on the (0001) slip plane is simulated under an external shear stress in order to elucidate the influence of precipitates on the dislocation dynamics. Simulation results show that the existence of precipitates delays the dislocation motion even if the dislocation does not encounter any precipitates. It has been found that the dislocation motion is influenced by the elastic interaction between the dislocation and precipitates. The dislocation dynamics simulations are performed with varying the magnitude of external shear stress and the value of critical resolved shear stress (CRSS) is estimated. It has been simulated that during the aging process, the value of CRSS increases with time in the initial stage of precipitation while the value of CRSS decreases with time in the later stage of precipitation. The simulated change in the CRSS value with time is assumed to correspond to the precipitation hardening curve. It has been shown that plate-like precipitates on the basal plane are effective for precipitation hardening, and the elastic interaction between a dislocation and precipitates has a great influence on the mechanical properties of magnesium alloys. Reference: [1] C.L. Mendis et al., Metall. Mater. Trans. A 43 (2012) 3978-3987.

Effects of Turbulence on Ignition of Fully Premixed Mixtures with Hydrocarbon Fuels

Takahiro Konagamitsu^{*}, Masayasu Shimura^{**}, Yuki Minamoto^{***}, Mamoru Tanahashi^{****}

^{*}Tokyo Institute of Technology, ^{**}Tokyo Institute of Technology, ^{***}Tokyo Institute of Technology, ^{****}Tokyo Institute of Technology

ABSTRACT

In order to realize a highly efficient spark ignition engine, establishment of combustion technology using low equivalent ratio, high turbulence intensity, high exhaust recirculation rate and the like is required. Under such conditions of combustion, however, ignition is difficult and the ignition characteristics are unknown, so it is necessary to clarify ignition characteristics such as the ignition criteria and ignition delay time. In this study, to determine the ignition criteria and effects of turbulence on the localized ignition delay time, direct numerical simulations (DNS) of forced ignition of lean fully premixed mixtures have been performed for hydrocarbon fuels such as methane and n-heptane with a high exhaust gas recirculation rate at high pressure. In the present DNS, the domain is initially filled with a fully premixed mixture at a uniform preheated temperature. As combustion conditions, equivalence ratio of the mixture, initial pressure, initial exhaust gas recirculation rate and uniform preheated temperature are set to be 0.5, 1.0 MPa, 20 % and 700 K for all fuels cases. A high-temperature kernel is used as an initial ignition kernel, and one-dimensional DNS are preliminary performed to determine the ignition criteria in terms of the ignition source energy and the thermal conduction from the ignition kernel during the induction period. Subsequently, two-dimensional DNS are performed with an initial kernel size and temperature which yields successful ignition for the one-dimensional laminar cases, to clarify the influence of the turbulent strain rate on the ignition delay time. It is found that the turbulent strain rate in the high-temperature region influences the ignition delay time. The ignition delay time increases proportionally to the square of strain rate averaged in the high concentration region of intermediate species during the induction period. This suggests that the ignition in a turbulent field is based on the balance between the influence of the local strain rate in the preheating region and the chemical time scale. Based on these observations, a simple relationship for the ignition delay time was considered based on the mean strain rate in the high concentration region of intermediate species during the induction period. The local ignition delay times predicted by this relationship, normalized using a corresponding laminar flame speed, flame thermal thickness and laminar ignition delay time, yields similar ignition trends for different fuels considered.

Gas-liquid Two-phase Flow Calculation Using Moving Particle Full-Implicit (MPFI) Method

Masahiro Kondo*

*University of Tokyo

ABSTRACT

Gas-liquid two phase flow emerges in various industrial processes like boiling, mixing, washing, bubble behavior and so on. To calculate gas-liquid two phase flow, numerical stability is very important because the large density ratio of the two fluid may easily result in instability. It is also the case in particle methods, and empirical relaxations were taken to avoid instability such as particle scattering. To achieve the numerical stability, MPFI (Moving Particle Full-Implicit) method took the approach based on the analytical mechanics, where the monotonic decrease of mechanical energy is assured. Therefore it is thought that the instability like particle scattering does not occur even in a gas-liquid system. In this study, gas-liquid two phase calculations are tested using the MPFI method to check the ability to run the calculations stably.

A Numeric Algorithm for Solving Kinetic Equations Across All Flow Regimes

Bo Kong^{*}, Rodney Fox^{**}

^{*}Ames Lab-USDOE, ^{**}Department of Biological and Chemical Engineering , Iowa State University

ABSTRACT

In nature and many engineering applications, the particle volume fraction in fluid-particle flows often exhibits large variations. In other words, the particles can be closely packed in some locations, and very dilute in other locations at the same time, such as in circulating fluidized bed reactors. Traditionally, a hydrodynamic description of particle phase is often used to simulate fluid-particle flows, which has been shown to be inaccurate for dilute flow regions when particle-particle collisions are infrequent. On the other hand, quadrature-based moment methods (QBMM), which use Gauss quadrature to approximate particle velocity distribution, have been shown to be able to provide accurate solutions for the kinetic equation. However, in dense regions, the explicit nature of QBMM makes it highly inefficient compared to hydrodynamic solvers, in which the implicit methods can be used for spatial fluxes. To accurately simulate all fluid-particle flow regions, a novel algorithm, based on splitting the kinetic flux dynamically and locally in the flow, is proposed in this work. In it, a traditional hydrodynamic solver is employed in the dense region, while in dilute to very dilute regions a kinetic-based finite-volume QBMM solver is used. This algorithm was implemented in OpenFOAM, an open-source CFD package, for particle velocity moments up to second order. Three different flow conditions, fluidized bed, wall-bound channel flow, and homogeneous cluster-induced turbulence flow, are used to test the accuracy and robustness of the proposed flux-splitting algorithm. By varying the average particle volume fraction in the flow domain, it is demonstrated that this algorithm can handle seamlessly all flow regimes present in any particular application. In this talk, we will also briefly introduce a new algorithm for simulating polydispersed dense particle flows based on QBMM.

Structural Optimization for Mechanical Structure under Linear and Nonlinear Geometry by Using Topological Technique

Suphanut Kongwat*, Hiroshi Hasegawa**

*Shibauara Institute of Technology, Japan, **Shibauara Institute of Technology, Japan

ABSTRACT

Structural optimization is a one technique to determine an optimal value which becomes a powerful technique for engineering design problem. There are three main types of structural optimization methods i.e. size optimization, shape optimization and topology optimization. According to the best outcome, the topology optimization is considered as a complex method. This is because the optimal size and shape of the initial layout are not taken into consideration. Almost of topology optimization problems are concerned to linear behavior of material by assuming a small displacement for structure. However, when the external load is applied to the structure and causes large deformation, this case is necessary to consider the problem into nonlinearity. The nonlinearities of mechanical structure are related to three main types of problem include behavior of the material, geometry and contact and friction. So, the aim of this research is to investigate the difference of optimal layout between linear and nonlinear material geometry for mechanical structure by employing the topology optimization method. For performing an optimization problem, pre-processing and post-processing of the finite element method (FEM) are required to support the optimization processes. The problem is defined into the simple mechanical structure which created in three-dimensional model (3D) by Salome-Meca. A topology optimization is formulated based on Simplified Isotropic Material with Penalization method (SIMP). The objective for optimization process is to minimize the compliance of structure by corresponding to volume fraction constraint. As the Salome-Meca is open source software, user has to write python script for any problem which is more complicated than the common feature of this software. Absolutely, the optimization process is more complicated than the common feature of Salome-Meca, all of optimization algorithm has to be written with python script by user and combine to the software for computation process. For linear optimization, this is a simple computation by requiring material properties into elasticity, boundary conditions and optimization algorithm. The optimization under nonlinear geometry is more complex than linear optimization by requiring stress-strain relation in plasticity. Moreover, time-step control is also required under nonlinear optimization to control a convergence of results. Finally, the optimal layout of optimization process under linear and nonlinear conditions is obtained and the comparison results of the optimal shape between two cases are completely different. So, the effect of nonlinearities should be concerned into optimization process for suitable results of nonlinear problem.

A Recursive Multilevel Trust Region Method for Phase-field Models of Fracture

Alena Kopanicakova*, Rolf Krause**

*Università della Svizzera italiana, **Università della Svizzera italiana

ABSTRACT

A state of the art strategy for predicting crack propagation, nucleation and interaction is the phase-field approach. In this approach a damage variable is introduced, which characterizes the state of the material between the unbroken and the broken state. However, phase-field methods require the solution of strongly nonlinear coupled systems of equations at each time-step. This is computationally challenging due to huge number of unknowns and the ill conditioning caused by local changes in the damage variable. As a consequence, the design of efficient solution methods becomes an important task. Two popular solution strategies are monolithic and staggered schemes. In the monolithic approach a fully-coupled non-linear system is solved in each loading step/ time-step, whereas in the staggered approach the evolution operator is split algorithmically into the phase field and the displacement field. Then, in each time step, it is successively solved for both quantities. Numerical evidence shows that the staggered approach is more robust than the monolithic one, but it often underestimates the speed of the crack evolution. For this reason, small time-steps are usually required. On the other hand, the monolithic approach allows for bigger time-steps, but it results in highly ill-conditioned coupled system of equations to be solved. In this work, we employ a recursive multilevel trust region (RMTR) algorithm for the monolithic approach. The method tackles the nonlinearity directly on each level. This is done by introducing level dependent nonlinear objective functions, whose minimization can yield good coarse level corrections for the fine level problem. In contrast to the standard approaches, our approach makes use of both the monolithic and the operator splitting approach. On the fine level, the RMTR solution strategy operates directly on the coupled systems of equations. On the coarse levels, the models are built by using operator splitting techniques. The numerical examples will show that presented optimization technique leads to highly efficient solution strategy. The efficiency will be demonstrated by analyzing convergence behaviour and performing comparison to the commonly used nonlinear solvers.

A Fully Compressible Multiphase SPH Scheme for Hypervelocity Impacts

Barry Koren^{*}, Iason Zisis^{**}, Bas van der Linden^{***}

^{*}Eindhoven University of Technology, The Netherlands, ^{**}Praxis Software, Greece, ^{***}LIME B.V, The Netherlands

ABSTRACT

In Smoothed Particle Hydrodynamics (SPH) for weakly compressible flows, particles of unequal masses are typically employed. In this approach, the mass ratio of the particles determines the density ratio of the different phases. For fully compressible flows, particles of equal masses are advised [1], where the smoothing length needs to adapt to large variations in density. Here, the ratio of initial densities dictates the discretization length per phase, which implies computational and geometrical restrictions [2,3]. Schemes based on number-density can accommodate particles of unequal masses and can offer a robust alternative. The present study presents and validates a number-density SPH scheme, using particles of unequal masses. Test cases considered are: (i) a one-dimensional gas-liquid shock-tube problem with known analytical solution, (ii) two classical two-phase shock-bubble-interaction experiments, and (iii) an aluminum-lead hypervelocity impact experiment, in which the aluminum and lead objects are subjected to plastic deformation, liquefaction and even sublimation. It is found that the above scheme can accurately simulate the propagation of shocks and yields improved results in the simulation of hypervelocity impacts of solids. 1. D.J. Price. Smoothed Particle Hydrodynamics and magnetohydrodynamics. *Journal of Computational Physics*, 231:759–794, 2012. 2. I. Zisis, B. van der Linden, B. Koren, and C. Giannopapa. On the derivation of SPH schemes for shocks through inhomogeneous media. *International Journal of Multiphysics*, 9:83–99, 2015. 3. I. Zisis, R. Messahel, B. van der Linden, A. Boudlal, and B. Koren. Validation of robust SPH schemes for fully compressible multiphase flows. *International Journal of Multiphysics*, 9:225–234, 2015.

Higher Order Total Variation for Regularizing Partial Differential Equations

Adeline Kornelus^{*}, Rodrigo Platte^{**}

^{*}Arizona State University, ^{**}Arizona State University

ABSTRACT

One of the main difficulties in solving the incompressible Navier-Stokes equations in fluid dynamics is the transfer of kinetic energy from coarse spatial scale to finer spatial scale, resulting in finite time singularities in the solution. In Fourier analysis, this phenomenon is described by the energy cascade from low modes to high modes. When these equations are discretized, the energy in high modes are usually lost, and as a result, spurious oscillations appear near discontinuities. In this talk, we propose using regularization techniques such as higher order total variation (HOTV), often used in image processing, to improve the numerical solution of such problems. We illustrate the accuracy of the proposed schemes using Burgers's and Euler's equations. The main idea is to penalize spurious oscillations using the polynomial annihilation and L1 minimization techniques. We treat the partial differential equation residual as the fidelity term. In particular, we show these regularized methods lead to better stability and accuracy. We apply HOTV regularization to numerical methods such as Fourier, Finite Differences and Discontinuous Galerkin. We observe that regularization properties of the solution on large scale and small scale depend on the numerical method used to discretize the equations. We also show how different number of elements and/or order of the method affects the quality of the solution. Finally, comparisons with other smoothing techniques such as entropy viscosity and essentially non-oscillatory methods are also provided.

Fluid-Structure Interaction Framework for Compressible and Incompressible Flows: Application to Aerospace and Marine Engineering

Artem Korobenko*

*University of Calgary

ABSTRACT

A Fluid-Structure Interaction (FSI) framework for compressible and incompressible flows is presented. The framework is composed of stabilized methods for fluid mechanics and thin-shell structural mechanics formulation. The key constituents of the framework are presented, including the coupling strategies, in a context of various aerospace and marine engineering applications.

From Images to Material Characterization of Additively Manufactured Micro-architected Structures

Nina Korshunova^{*}, Alexander Düster^{**}, Daniel Reznik^{***}, Stefan Kollmannsberger^{****}, Ernst Rank^{*****}, John Jomo^{*****}

^{*}Chair for Computation in Engineering, Technical University of Munich, ^{**}Numerical Structural Analysis with Application in Ship Technology (M-10), Hamburg University of Technology, ^{***}Research and Technology Center, Siemens AG, Corporate Technology, ^{****}Chair for Computation in Engineering, Technical University of Munich, ^{*****}Chair for Computation in Engineering, Technical University of Munich, ^{*****}Chair for Computation in Engineering, Technical University of Munich

ABSTRACT

Key words: Additive manufacturing, CT Scans, Numerical homogenization, Window method Recent developments in additive manufacturing have provided a unique possibility to create complex structures with porosity on micro- and meso-structural levels. Such designs can outperform conventional materials in specific industrial applications, e.g. turbine blades with a transpiration cooling. However, the high flexibility of the input parameters for the 3D printers, such as the laser diameter, hatch distance etc., challenges a reliable estimation of the mechanical behavior of the final parts. Moreover, a high variation of porosity in all of the material directions limits the application of analytical bounds based on the void fraction ratio. Numerical homogenization is an efficient and robust alternative to perform a non-destructive evaluation of the material characteristics based on high-resolution 3D images of produced specimens. The conventional Finite Element Method applied to numerical homogenization leads to a labor-intensive meshing procedure to extract the representative volume elements that makes it impractical from the industrial point of view. Furthermore, non-symmetric micro-architected structures make it difficult to apply correct boundary conditions for the solution of the microstructural boundary value problem. To address these issues, in the scope of the presented work the Finite Cell Method [1] is employed in combination with the window method [2],[3]. A road map is presented for the automatized numerical computation of the homogenized elasticity tensor of additively manufactured steel structures using 3D images. The computational results are verified with the direct finite cell computation of a given produced specimen. Validation of the proposed model is performed comparing the numerical results with the results stemming from experimental tests. REFERENCES [1] Düster, A., Parvizian, J., Yang, Z. and Rank, E. The finite cell method for three-dimensional problems of solid mechanics. *Computer Methods in Applied Mechanics and Engineering*, 197(4548):3768 – 3782, (2008). [2] Heinze, S., Jouliaian, M. and Düster, A. Numerical homogenization of hybrid metal foams using the finite cell method. *Computers & Mathematics with Applications*, 70(7):1501 – 1517, (2015). [3] Hain, M. and Wriggers, P. Numerical homogenization of hardened cement paste. *Computational Mechanics*, 42(2):197 – 212, (2008).

Solution of PDE Constrained Inverse Problems from a Machine Learning Perspective

Maximilian Koschade^{*}, Phaedon-Stelios Koutsourelakis^{**}

^{*}Technical University of Munich, ^{**}Technical University of Munich

ABSTRACT

The increasing interest in probabilistic methods for uncertainty quantification as well as PDE constrained problems typically relies on deterministic black-box solvers embedded within iterative algorithms such as Markov Chain Monte Carlo. While enabling the utilization of well-established and capable algorithms such as for instance the Finite Element Method, this approach obscures the underlying physical laws and state variables from the machinery of probabilistic inference. We advocate for an intrusive, fully probabilistic approach which constructs a probability distribution over all state variables of the PDE, which are constrained or mutually entangled by underlying physical laws. As such this method foregoes the explicit solution of the forward-model in a conventional sense and yields what can be considered a probabilistic white-box model, where forward solution and probabilistic inference no longer exist as decoupled entities. We demonstrate the applicability of this approach for the adjoint-free solution of a nonlinear, elliptic PDE constrained inverse problem, where we exploit the cheap availability of curvature information inherited from the Finite Element Method to conduct second order inference on our joint posterior over all state variables and unknown quantities simultaneously.

Condition Assessment and Prognosis in Fluid-Structure Interaction through a Data-Driven Proxy Model Inversion Framework

Justyna Kosianka^{*}, Christopher Earls^{**}

^{*}Cornell University, ^{**}Cornell University

ABSTRACT

It is essential to identify damage within a structure as early as possible in order to propose corrective measures to prevent mechanical failure – ultimately extending service life. Such damage detection can be effected through non-destructive means that employ the updating of a physics model describing the system of interest. The resulting inverse problem is concerned with locating and characterizing the damage, by considering the structural dynamic response, before and after the onset of damage. Such model-based approaches also afford prognosis potential; as a calibrated physics model is subsequently available for the damaged system. In this work, a partitioned fluid-structure forward modeling capability is developed from combining an open source CFD tool (OpenFOAM) with an open source CSD solver (CU-BEN) in a tightly coupled framework that affords stable solutions. However, such high fidelity, coupled-physics forward modeling is prohibitive for use in solving model-based inverse problems, where the forward model must be called repeatedly; thus necessitating the consideration of reduced-order modeling methods. Within the context of inversion, the high-fidelity FSI forward model is evaluated on a series of plausible (physically inspired) “damaged” states to create an offline library of modeled damaged responses. These responses are expressed in compressed form through proper orthogonal bases (e.g. obtained via proper orthogonal decomposition) and subsequently represented as points on a certain Riemannian manifold. From this off-line library of compressed response representations from the FSI model, a proxy model is constructed, by “manifold interpolation,” on the nonlinear Riemannian manifold to “fill in the gaps” for damage contexts not explicitly contained within the library, but required as part of the inversion. This subsequent online inversion is effected as a non-convex optimization problem, employing a genetic algorithm to arrive at a plausible reduced order modeling instance that conforms to observations within some prescribed limits. An exploration of spatial decomposition methods (e.g. POD vs DMD) and data sampling schemes is presented for a simple test problem of an elastic cantilever oscillating in a bluff body flow with simulated erosion damage. The framework is scaled up for use on a marine structural element, such as propellers and basic ship hull components.

Dynamic Failure of High Energy Materials

Marisol Koslowski^{*}, Nicolo Grilli^{**}, Camilo Duarte Cordon^{***}

^{*}Purdue University, ^{**}Purdue University, ^{***}Purdue University

ABSTRACT

Polymer bonded explosives consist of high energy particles in a polymeric binder. When these composites are subjected to heat, impact, or other stimulus they undergo a rapid chemical change. The sensitivity to initiation depends on the amount of energy available in the system and on the rate at which it is released. This process is controlled by the formation of high temperature localized regions known as "hot spots". The mechanisms of hot spot nucleation are controlled by the microstructure, for example in the same sample some particles ignite while others do not. Finite element simulations that explicitly describe particles, are performed to study the sensitivity of the microstructure to initiation and to identify the mechanisms of hot spot formation under a range of mechanical stimulus. The finite element model incorporates plasticity, fracture and heat transport using a phase field approach. Different microstructures with initial defects, including cracks, debonding and voids are analyzed. Our work suggests that heat generated by friction at preexisting microcracks and at particle binder interfaces are of key importance for hot-spot formation.

A Spatial Correlation Analysis of Tsunami Risk among Multiple Coastal Cities

Takuma Kotani^{*}, Shuji Moriguchi^{**}, Shinsuke Takase^{***}, Kenjiro Terada^{****}, Yu Otake^{*****}, Yo Fukutani^{*****}, Masaaki Sakuraba^{*****}, Kazuya Nojima^{*****}

^{*}Tohoku University, ^{**}Tohoku University, ^{***}Hachinohe Institute of Technology, ^{****}Tohoku University, ^{*****}Niigata University, ^{*****}Kanto Gakuin University, ^{*****}Nippon Koei Co., Ltd., ^{*****}Nippon Koei Co., Ltd.

ABSTRACT

This study presents a framework to evaluate the spatial correlation of tsunami risks among multiple coastal cities. The proposed framework consists of the three processes. First, response surfaces of the tsunami heights at selected multiple coastal cities are obtained from a series of numerical simulations in consideration of conceivable uncertainties of a tsunami hazard. Here, highly developed numerical simulations are extensively and efficiently utilized to obtain reliable data of tsunami heights under a certain scenario. Second, the statistical data sets of the tsunami height are calculated from the obtained response surfaces with the help of the Monte-Carlo simulation (MCS) [1]. Here, the use of the response surfaces, which are regarded as surrogate models, allows us to significantly reduce the calculation costs, as well as to study tendencies of simulated results against input parameters and calculation conditions [2]. In this procedure, a probability density distribution of the tsunami height is also analyzed to characterize the variability in each city. Third, the principal component analysis (PCA) is performed using the covariance matrix that can be obtained from the results of the MCS. Finally, the low risk correlation of the tsunami heights among the selected coastal cities is analyzed based on the result of PCA. Selecting the 2011 off the Pacific coast of Tohoku Earthquake as a target scenario for our tsunami risk evaluation, we present a numerical example to assess the appropriateness of the suggested framework. In specific variabilities of a few fault parameters are considered in this numerical example, and the modeling error of the numerical scheme is also considered as one of the uncertainties. Response surfaces of the coastal cities in Tohoku area are obtained from the results of several sets of tsunami simulations, then spatial correlation among the cities is analyzed. Based on the obtained results, the effectiveness and potential in providing against forthcoming tsunami hazards are discussed, and a characteristic of tsunami risk in Tohoku area is also mentioned. References [1] Honjo, Y., "Challenges in Geotechnical Reliability Based Design", proceedings of 3rd International Symposium on Geotechnical Safety and Risk, pp.11-27, 2011. [2] T. Kotani, S. Takase, S. Moriguchi, K. Terada, Y. Fukutani, Y. Otake, K. Nojima, M. Sakuraba: Numerical-analysis-aided probabilistic tsunami hazard evaluation using response surface, Journal of Japan Society of Civil Engineers, Ser. A2, Vol. 72, No. 1, pp. 58-69, 2016 (in Japanese).

A Nitsche Based Extended Finite Element (XFEM) Approach to Embedded Contact Interfaces

Hardik Kothari^{*}, Rolf Krause^{**}

^{*}Università della Svizzera italiana, ^{**}Università della Svizzera italiana

ABSTRACT

Interface problems occur in many applications in physics. For these problems, it is important to capture discontinuous behavior in order to obtain a good approximation. The extended finite element method (XFEM) allows us to model the evolution of an interface without remeshing as the interface evolves. The XFEM approach captures the discontinuities along interfaces by enriching the standard finite element solution space. The interfaces are represented, implicitly in this case, using Heaviside functions. In the case of fracture mechanics, after the initial crack propagation the newly created surfaces could also come in contact, which would give rise to self contact. The XFEM framework is well suited to model interfaces, but it becomes complicated to model contact interfaces. This is due to the fact that the contact boundaries are not explicitly represented by the nodes or the element edges. In this work, we employ Nitsche's method to weakly compute the contact constraints over these implicit interfaces. Thus, we present a unified framework for fracture and contact mechanics problems, where crack propagations and contact problems are solved on the same mesh. As a crack propagates through the mesh, it is quite likely that the newly created crack passes very close to the nodes or the element edges. Due to this, some elements are fragmented into very small and into very large fractions, which gives rise to a highly ill-conditioned linear system. Such ill-conditioned systems require special solvers and preconditioners. In our work we present a variation of a multigrid method, known as a semigeometric multigrid as a technique to reduce computational complexity. This method uses pseudo-L2 projection based prolongation and restriction operators to transfer the information between the non-nested mesh hierarchies. We demonstrate the robustness and the efficiency of this method as a solver and as a preconditioner in a series of numerical examples. [1] R. Becker, P. Hansbo and R. Stenberg. A finite element method for domain decomposition with non-matching grids, ESAIM-MMNA, 37 (2), 209-226 (2003) [2] P. Krause and P. Zulian. A parallel approach to the variational transfer of discrete fields between arbitrarily distributed unstructured finite element meshes, SIAM Journal on Scientific Computing, 38(3), C307-C333 (2016) [3] A. Hansbo and P. Hansbo. An unfitted finite element method, based on Nitsches method, for elliptic interface problems, Computer methods in applied mechanics and engineering, 191 (47), 5537-5552 (2002) [4] T. Dickopf and R. Krause. Evaluating local approximations of the L2 orthogonal projections between non-nested finite element spaces, Numerical Mathematics, 7(03), 288-316 (2014)

Stochastic Response Determination of Nonlinear Systems with Singular Diffusion Matrices via a Wiener Path Integral Based Technique

Ioannis A. Kougioumtzoglou*, Apostolos F. Psaros**, Ioannis Petromichelakis***

*Columbia University, **Columbia University, ***Columbia University

ABSTRACT

In many random vibration problems including stochastically excited multi-degree-of-freedom (MDOF) systems subjected to forces applied to only few of the DOFs, as well as a certain class of coupled electro-mechanical energy harvesters, the solution of a system of Stochastic Differential Equations (SDEs) involving singular diffusion matrices is required. This problem can be viewed, alternatively, as a set of SDEs, in conjunction with a set of homogeneous ODEs. In the present work, the Wiener Path Integral (WPI) technique, developed in \cite{koug2} to treat systems with non-singular diffusion matrices, is extended to account for coupled SDEs with singular diffusion matrices. Specifically, the WPI technique determines the response transition PDF of a system of SDEs, based on a variational argument and the solution of the corresponding variational problem. For the herein considered problem, the set of homogeneous ODEs is identified as a set of constraints imposed on the response of the SDEs; thus, leading to a constrained variational problem. Next, relying on \textit{Calculus of Variations} tools, two distinct solution methodologies are proposed. The first, more general one, treats the constraints by utilizing the Lagrange multiplier technique, while the second, which is limited to problems where the set of ODEs forms a linear system (linear constraints), takes advantage of the direct Ritz method and the properties of the nullspace of the constraint matrix, similarly to \cite{antoniou2017}. In this manner, the constrained variational problem is reduced to an unconstrained optimization problem. It is noted that the proposed framework can readily account for additional, physically imposed constraints as well, and thus, address constrained dynamics problems also. The versatility of the technique is demonstrated through diverse numerical examples, while its accuracy is validated by comparisons with pertinent Monte Carlo simulation (MCS) data.

Collapse Resilience of Reinforced Masonry Structures Under Seismic Loads

Andreas Koutras*, P. Benson Shing**

*University of California San Diego, **University of California San Diego

ABSTRACT

Reinforced masonry is widely used for low-rise construction in North America, including regions of high seismicity. Under extreme seismic forces, reinforced masonry buildings designed to comply with current codes are expected to have a low probability of collapse. Nevertheless, prior studies using simplified analytical models have shown that low-rise short-period buildings, including those constructed of reinforced masonry might not meet this expectation of the codes. This could be largely attributed to the overly conservative simplified models that were used for such analyses. To provide a more realistic assessment of the collapse potential, this paper presents a refined finite-element analysis scheme to model the inelastic behavior of reinforced masonry structures. In this scheme, smeared-crack shell elements are combined with cohesive discrete crack interface elements to model the compressive crushing and tensile fracture of masonry. The cohesive interface elements allow for a more precise representation of crack opening and closing as well as shear sliding across cracks. Reinforcing bars are modeled with beam elements that have geometric and material nonlinearities to capture bar buckling and fracture. The bar elements are connected to the masonry elements through interface elements to represent the bond-slip and dowel-action behaviors. To enhance the robustness and accuracy of the numerical solution, an element removal scheme is introduced so that the weakly restrained nodes and associated elements resulting from bar fracture or masonry crushing are removed. The material models and the interface elements have been implemented in the commercial software LS-DYNA. The modeling scheme is validated with data from quasi-static cyclic tests performed on flexure- and shear-dominated reinforced masonry walls, as well as with results of shake-table tests of reinforced masonry building systems with earthquake ground motions. Furthermore, the modeling scheme is applied to the time-history analyses of several reinforced masonry building archetypes that have been designed according to current code provisions. The buildings are subjected to bi-directional base excitation to evaluate their seismic performance through collapse.

Physics-constrained, Data-driven Discovery of Coarse-grained Dynamics

Phaedon-Stelios Koutsourelakis*, Lukas Felsberger**

*Technical University of Munich, **Technical University of Munich

ABSTRACT

This paper is concerned with the discovery of data-driven, dynamic, stochastic coarse-grained models from fine-scale simulations with a view of advancing multiscale modeling. Many problems in science and engineering are modeled by high-dimensional systems of deterministic or stochastic, (non)linear, microscopic evolution laws (e.g. ODEs). Their solution is generally dominated by the smaller time scales involved even though the outputs of interest might pertain to time scales that are greater by several orders of magnitude. The combination of high-dimensionality and disparity of time scales has motivated the development of coarse-grained (CG) formulations. These aim at constructing a much lower-dimensional model that is practical to integrate in time and can adequately predict the outputs of interest over the time scales of interest. The Mori-Zwanzig (MZ) formalism provides a rigorous mathematical foundation for constructing such an effective model. Apart from the largely unsolved computational challenges associated with finding the terms in the Generalized Langevin Equation (GLE) prescribed by MZ, it does not address the issue of finding a good set of CG state variables. Furthermore, even if the evolution equations for the variables selected were perfectly known, it is difficult (without additional assumptions such as the prescription of a lifting operator) to reconstruct or infer the evolution of the full, fine-scale system. Hence if the observables one is interested in predicting, do not exclusively depend on the coarse variables selected, the CG model constructed is not useful. In this paper, we treat the CG process with a probabilistic state-space model where the transition law dictates the evolution of the CG state variables and the emission law the coarse-to-fine map. The directed probabilistic graphical model implied, suggests that given values for the FG variables, probabilistic inference tools must be employed to identify the corresponding values for the CG states and to that end, we employ Stochastic Variational Inference. Naturally, one of the most critical questions pertains to the form of the CG evolution law which poses a formidable model selection issue. We advocate a sparse Bayesian learning perspective based on Automatic Relevance Determination (ARD) which induces sparsity in the solutions identified, avoids overfitting and reveals qualitative features of the CG evolution. The formulation advocated enables the quantification of a crucial, and often neglected, component in the CG process, i.e. the predictive uncertainty due to information loss that unavoidably takes place and manifests itself in uncertainty in the predictions.

Multi-scale Modelling of Linear and Non-linear Locally Resonant Metamaterials

Varvara Kouznetsova^{*}, Ashwin Sridhar^{**}, Priscilla Silva^{***}, Tim van Nuland^{****}, Marc Geers^{*****}

^{*}Eindhoven University of Technology, ^{**}Eindhoven University of Technology, ^{***}Eindhoven University of Technology, ^{****}Eindhoven University of Technology, ^{*****}Eindhoven University of Technology

ABSTRACT

Locally resonant metamaterials are a relatively new class of metamaterials targeting manipulation of acoustic (and more generally mechanical) waves at subwavelength frequencies. The microstructure of these metamaterials is specifically designed to provoke interaction between propagating mechanical waves and fine scale micro-inertia mechanisms, leading to exotic emerging phenomena, such as band gaps, i.e. frequency ranges in which waves do not propagate or highly attenuated, negative refraction index etc. Pushing the material behavior into a non-linear regime opens even more possible applications, e.g. tunable waveguides, adaptive passive vibration control, superdamping, acoustic diodes, cloaking, noise insulation and (vibro-acoustic) energy harvesting. The development and design of such materials and devices made thereof, requires advanced modelling techniques, capable, on one hand, to deal with complex geometries, boundary conditions and excitations, and on the other hand be computationally more efficient than direct numerical simulations. In this work, a novel computational homogenization approach will be presented for multi-scale modelling of locally resonant materials. Originating from the classical computational homogenization technique, well established for quasi-static problems, an extension to transient problems has recently been developed [1]. For linear problems, the static-dynamic decomposition can be used to derive the closed form homogenized equations representing an enriched micromorphic continuum, in which additional kinematic degrees of freedom emerge to account for micro-inertia effects [2]. In non-linear case, fully coupled two scale transient computational homogenization is used to study the wave dispersion in finite size macroscopic structures, demonstrating various phenomena emerging due to the presence of non-linearities, e.g. amplitude dependent attenuation response and higher-order harmonics generation. A new design of a vibro-diode, allowing wave propagation in one direction only, has been proposed based on the combination of the linear and non-linear local resonators. Acknowledgements: The research leading to these results has received funding from the European Research Council under the European Union's Seventh Framework Programme (FP7/2007-2013) / ERC grant agreement n°[339392]. The support from 4TU Research Center High Tech Materials (4TU.HTM) is also gratefully acknowledged. References: [1] Pham, N.K.H., Kouznetsova, V.G. and Geers, M.G.D. Transient computational homogenization for heterogeneous materials under dynamic excitation. *Journal of the Mechanics and Physics of Solids* (2013) 6: 2125-2146. [2] Sridhar, A., Kouznetsova, V.G., and Geers, M.G.D. Homogenization of locally resonant acoustic metamaterials towards an emergent enriched continuum. *Computational Mechanics* (2016) 57: 423-435.

Microstructure-Property Analysis Accelerated by Machine Learning Technique with Phase-field Method and Image-based Property Calculations

Toshiyuki Koyama*, Yuhki Tsukada**

*Nagoya University, **Nagoya University

ABSTRACT

Recently, the phase-field (PF) method has been becoming the de facto standard simulation method for calculating various types of phase transformations and microstructure developments in real materials. Since the inhomogeneous microstructure data are available from the simulation, the materials properties are estimated based on the image-based calculation in which the inhomogeneous microstructure data obtained from PF simulation is utilized as a boundary condition for calculation. In this study, we focus on the mechanical property, i.e., the stress-strain (S-S) curve of dual-phase steels. Firstly, various morphologies of microstructure observed during spheroidization process from lamella structure are prepared by conventional PF method. Secondly, the S-S curves corresponding to each calculated microstructure are evaluated by the modified secant method [1], where the matrix and inclusion phases are assumed to be ferrite and martensite, respectively. As a consequence, the dataset composed of "microstructure data" and "S-S curve" is generated. From the microstructure data, we extract the following feature amount: volume fraction, interfacial area, genus, connectivity, variance of mean curvature and variance of Gaussian curvature. In order to understand the quantitative relationship between the S-S curves and the microstructure morphologies, the neural network machine learning technique is employed. Input data to the neural network are not only the feature amount above mentioned but also the true strain in the S-S curve, on the other hand, the output data for neural network training is the true stress only. In the current work, 145 pairs of "microstructure data" and "S-S curve" were applied to optimize the neural network system, then the trained neural network which can describe the relation between microstructure and mechanical property was constructed. By using the trained neural network, the sensitivity of each feature amount to S-S curve was estimated, and the following conclusions were obtained: The final stress level of S-S curve is determined mainly by the volume fraction. It is quite interesting that the stress level at the initial rise up stage of S-S curve depends strongly on the connectivity parameter. The connectivity means the spatial continuity of martensite phase. Therefore, the optimization of martensite morphology is a key point for improving the mechanical property of dual-phase steels. [1] T. Koyama, ISIJ International, 52 (2012) 723-728.

Primary Blast Loading Effects on Axonal Deformation

Reuben Kraft^{*}, Harsha Garimella^{**}, Andrzej Przekwas^{***}

^{*}Penn State University, ^{**}CFDRC, Inc., ^{***}CFDRC, Inc.

ABSTRACT

Subject-specific computer models (male and female) of the human head were used to investigate the possible axonal deformation resulting from the primary phase blast-induced skull flexures. The corresponding axonal tractography was explicitly incorporated into these finite element models using a recently developed technique based on the embedded finite element method. These models were subjected to extensive verification against experimental studies which examined their pressure and displacement response under a wide range of loading conditions. Once verified, a parametric study was developed to investigate the axonal deformation for a wide range of loading overpressures and directions as well as varying cerebrospinal fluid (CSF) material models. This study focuses on early times during a blast event, just as the shock transverses the skull (< 5 milliseconds). Corresponding boundary conditions were applied to eliminate the rotation effects and the corresponding axonal deformation. A total of 138 simulations were developed - 128 simulations for studying the different loading scenarios and 10 simulations for studying the effects of CSF material model variance - leading to a total of 10,702 simulation core hours. Extreme strains and strain rates along each of the fiber tracts in each of these scenarios were documented and presented here. The results suggest that the blast-induced skull flexures result in strain rates as high as 150-378 s⁻¹. This rapid deformation of the axonal fiber tracts, caused by flexural displacement of the skull, suggests the possibility of rate-dependent micro-structural axonal damage according to the published experimental studies.

Stabilization of Reduced-order Flow Models through Learning-based Closure Modeling

Boris Kramer^{*}, Mouhacine Benosman^{**}, Omer San^{***}, Jeff Borggaard^{****}

^{*}Massachusetts Institute of Technology, ^{**}Mitsubishi Electric Research Labs, ^{***}Oklahoma State University,
^{****}Virginia Tech

ABSTRACT

In this talk, we present a learning-based method for stabilization of reduced-order models (ROMs) for thermal fluids, which are challenging multi-physics systems. The stabilization of the reduced-order model is achieved by using Lyapunov robust control theory to design a new closure model. Furthermore, the design parameters in the proposed ROM stabilization method are optimized using a data-driven multi-parametric extremum seeking (MES) algorithm. We show the advantages of the proposed method on numerically challenging test-cases by using the 2D and 3D Boussinesq equations. The results illustrate that closure models can be extended to multi-physics systems, by using multiple design parameters.

Higher Order 2D Virtual Elements for Elastic Materials at Finite Strains

Alex Kraus^{*}, Peter Wriggers^{**}

^{*}Leibniz Universität Hannover, Institute for Continuum Mechanics, ^{**}Leibniz Universität Hannover, Institute for Continuum Mechanics

ABSTRACT

The recently developed Virtual Element method shows promise as an alternative to finite element formulations and has gained a lot of attention in the last years due to its flexibility using meshes with convex and non-convex elements. However, for large strain applications this discretization technique has not been established as a standard engineering tool. This is mainly due to the need to stabilize this formulation. Based on the stabilization method proposed by Wriggers et al. 2017, a new method for the evaluation of the stabilizing term for a virtual element formulation was developed in this approach. Furthermore, a higher order formulation for finite deformations was developed.

A 3D Discontinuous Galerkin Cut Cell Immersed Boundary Method: Results and a View on Parallel Efficiency

Dennis Krause*, Florian Kummer**

*TU Darmstadt, **TU Darmstadt

ABSTRACT

In the past, we developed an immersed boundary solver in a cut cell context based on a cut cell (extended, unfitted) Discontinuous Galerkin (DG) discretization. To overcome the difficulty of quadrature on cut cells, we use the hierarchical moment fitting quadrature technique proposed by Müller et al. [1]. For coupled motion we use a simple Lie-Splitting approach for the moving domain. Furthermore, the boundary conditions at the interface are represented by Dirichlet values for velocity in the weak form of the discretization. In first two dimensional calculations we could proof very good agreement with other works in the field of immersed boundary methods for moving body flows. This can be shown for simple static boundary test cases as well as for typical fluid-structure interaction problems like an oscillating cylinder or coupled problems like a disk separating in a vertical channel due to gravity forces. Additionally, the crucial benefit is the save of total degrees of freedom comparing with particulate flow literature. However, also a dependence of the calculated forces on the penalty parameter chosen was discovered. All results mentioned have already been published [2]. For large 3D calculations, it became apparent, that two main topics had to be addressed, in order to reach the aforementioned goal: First, the direct solver MUMPS had been substituted by an iterative solver, i.e. GMRES with a suitable Preconditioning. Second, the total parallel efficiency of the solver had to be increased. Additionally, a dynamic load balancing approach had to be implemented in case of moving boundaries. The presentation will shortly introduce the method. After that, we will focus on suitable preconditioning for the linear equations systems and analyse the bottlenecks of performance arising from large 3D calculations. Acknowledgement: The work of D. Krause is supported by the Excellence Initiative of the German Federal and State Governments and the Graduate School of Computational Engineering at Technische Universität Darmstadt. The work of F. Kummer is supported by the German DFG through Collaborative Research Centre 1194/B06. [1] B. Müller, F. Kummer and M. Oberlack. "Highly Accurate Surface and Volume Integration on Implicit Domains by Means of Moment-Fitting.", Int. J. f. Num. Meth. in Engng., 96, no. 8 (2013): 512–528. [2] D. Krause and F. Kummer. "An Incompressible Immersed Boundary Solver with Applications to Moving Body Flows using a Cut Cell Discontinuous Galerkin Method.", Comput. Fluids 153 (2017): 118–29.

Parallel Multigrid Methods for Interface Problems

Rolf Krause^{*}, Patrick Zulian^{**}, Maria Nestola^{***}, Cyrill von Planta^{****}

^{*}Institute of Computational Science, USI, ^{**}Institute of Computational Science, USI, ^{***}Institute of Computational Science, USI, ^{****}Institute of Computational Science, USI

ABSTRACT

In this talk, we discuss the design of efficient parallel multigrid methods for contact and interface problems. Contact and interface problems pose particular challenges for the development of efficient parallel solution methods. On the one hand, the presence of the strongly local non-linearities, which are associated to the interface, requires a global convergence control strategy. On the other hand, in particular for the case of multi-body contact or embedded interfaces, the discretization of the interface itself and of the (non-penetration) constraints at the interface will give rise to additional communication between the different processors. Thus, standard parallelization strategies for standard linear multigrid methods can not be applied directly to contact and interface problems. In this talk, we discuss the difficulties related to global convergence control for the case of parallel multigrid methods. We present different convergence control strategies, which are based on successive energy minimization in parallel and exploit the fact that contact problems can be viewed as constrained minimization problems. Our strategies can be applied in the case of linear as well as non-linear material laws. We furthermore discuss how to build efficiently a parallel and inherently non-linear multilevel method for contact problems. Finally, we explain how to compute in parallel the inter-mesh dependencies at contacting or embedded interfaces. We will treat the case of non-overlapping (contact) as well as of overlapping (embedded interfaces) decompositions. Examples from geo-sciences and from fluid-structure interaction in cardiovascular applications will illustrate our findings.

Generation of Reliable Input Data for a Damage Model Taking Use of a Closed CAE-Chain Containing Material Interfaces

Constantin Krauss*, Siegfried Galkin**, Luise Kaerger***

*Karlsruhe Institute of Technology (KIT), Institute of Vehicle System Technology (FAST), Part Institute of Lightweight Technology, **Karlsruhe Institute of Technology (KIT), Institute of Vehicle System Technology (FAST), Part Institute of Lightweight Technology, ***Karlsruhe Institute of Technology (KIT), Institute of Vehicle System Technology (FAST), Part Institute of Lightweight Technology

ABSTRACT

Due to their high specific strength and stiffness, continuous fiber-reinforced polymers (CoFRP) are ideal lightweight materials for high performance structural components in the automotive sector. In addition, demands regarding economics, robustness and cycle times of the manufacturing processes are even higher in order to be able to compete with the commonly used metallic materials in large batch production. Such processes, for instance the Resin Transfer Molding, are further divided into a sequence of several sub processes containing draping, infiltration and curing steps. Developing and extending simulation models for these processes has been topic of numerous investigations in the past and present time and are quite well understood. Since in the field of composites, both the material and the actual part are results of the manufacturing, the material's history is crucial for the final structural performance. Occurring changes in fiber orientation, fiber volume content and additional effects such as fiber undulation or wrinkle formation and also remaining residual stresses need to be taken into account to avoid oversized or defective structures. Since material constitutive behavior, physics or reasonable mesh topology and size typically vary, different specialized software for each of the process steps is usually used. Therefore, the virtual interfaces between the individual simulation steps are going to play a key role in the future. Within these interfaces the exchange and transfer of relevant geometric and material data is managed. In the present moment, significant effort is required to develop and implement such interfaces, which are usually tailor-made for the current problem and not applicable to new cases. Within the EU research project ITEA-VMAP this issue is addressed by creating a new interface standard for virtual material modelling. The aim of this concept is to ease and accelerate the building of virtual process chains and thus of reducing the product's TTM. In this work, the virtual manufacturing route of an exemplary composite structure based of unidirectional non-crimp fabric reinforcement is presented. Hereby, the main focus is on the interface formulation and realization. It is demonstrated how the information flow within the CAE-chain is accomplished and how draping effects affect e.g. permeability, thermal expansion and strength. Eventually, a newly developed damage model is fed with the provided parameters resulting from the previous simulation steps. The main goal is to assess the impact on the load bearing capacity compared to computations neglecting the material's prehistory.

Adaptive Direct FEM Simulation

Ezhilmathi Krishnasamy*, Johan Jansson**, Massimiliano Leoni***, Niclas Jansson****, Johan Hoffman*****

*Computational Science and Technology, CSC, KTH, SE-10044 Stockholm, Sweden and BCAM - Basque Center for Applied Mathematics, Bilbao, Spain, **Computational Science and Technology, CSC, KTH, SE-10044 Stockholm, Sweden and BCAM - Basque Center for Applied Mathematics, Bilbao, Spain, ***Computational Science and Technology, CSC, KTH, SE-10044 Stockholm, Sweden and BCAM - Basque Center for Applied Mathematics, Bilbao, Spain, ****Computational Science and Technology, CSC, KTH, SE-10044 Stockholm, Sweden, *****Computational Science and Technology, CSC, KTH, SE-10044 Stockholm, Sweden

ABSTRACT

We present efficient way of solving incompressible Navier-Stokes Equations (NSE) for industrial applications involving turbulence modelling[1]. We named our methodology as Direct FEM Simulation (DFS)[2] which is based on the General Galerkin (G2); and it is defined by finite element method (FEM) with piecewise linear approximation in space and time, and with numerical stabilization in the form of a weighted least squares method based on the residual. The incompressible Navier-Stokes Equations (NSE) are discretized directly, without applying any filter. Thus, the method does not result in Large Eddy Simulation (LES) filtered solutions, but is instead an approximation of a weak solution satisfying the weak form of the NSE. This means no explicit turbulence model is used, and the effect of unresolved turbulent boundary layers is modeled by a simple parametrization of the wall shear stress in terms of a skin friction. Which leads to getting small skin friction on the boundary for the higher Reynolds number (in particular turbulence modelling) thus favors the slip boundary condition, and it requires not having solved costly (computationally expensive) boundary layer resolution. And another main advantage with our methodology is that adaptivity, which is achieved by doing posteriori error estimation using adjoint techniques[2], and it is defined as a goal functions, for example, lift and drag. This minimizes effort of computational domain manual mesh refinement. Our approach and methodology has been well tested against typical scientific and industrial benchmark models[2,3,4], in particular we have previously participated in HiLiftPW-2, HiLiftPW-3 and HiOCFD5 (tandem sphere test case). For example, even how one can get benefit (computational cost) using our methodology over higher order methods. And also we present parallel post processing based on the task parallelization using the VisIt[5] visualization tool. [1] FEniCS (2003), 'Fenics project', <http://www.fenicsproject.org>. [1] Hoffman, J. & Johnson, C. (2007), Computational Turbulent Incompressible Flow, Vol. 4 of Applied Mathematics: Body and Soul, Springer. [2] Hoffman, J. (2005), 'Computation of mean drag for bluff body problems using adaptive dns/les', SIAM J. Sci.Comput. 27(1), 184–207. [3] Hoffman, J. (2006), 'Adaptive simulation of the turbulent flow past a sphere', J.Fluid Mech. 568, 77–88. [4] Hoffman, J. (2009), 'Efficient computation of mean drag for the subcritical flow past a circular cylinder. [5] VisIt, <https://wci.llnl.gov/about-us>.

Modeling of Damage and Crack Growth in Semi-Crystalline Polymers

Martin Kroon^{*}, Eskil Andreasson^{**}

^{*}Linnaeus University, ^{**}Blekinge Technical University

ABSTRACT

Crack growth in semi-crystalline polymers, represented by polyethylene, is considered. The material considered comes in plates that had been created through an injection-molding process. Hence, the material was taken to be orthotropic. Material directions were identified as MD: molding direction, CD: transverse direction, TD: thickness direction. Uniaxial tensile testing was performed in order to establish the direction-specific elastic-plastic behaviour of the polymer. In addition, the fracture mechanics properties of the material was determined by performing fracture mechanics testing on plates with side cracks of different lengths. The fracture mechanics tests were filmed using a video camera. Based on this information, the force vs. load-line displacement could be established for the fracture mechanics tests, in which also the current length of the crack was indicated, since crack growth took place. The crack growth experiments were then simulated using Abaqus, where crack growth was enabled by use of a cohesive zone. The force-displacement-crack length data from the experiments could be well reproduced in the simulations, where different model parameters for the cohesive zone were explored. Furthermore, the direction-specific work of fracture had been established from the experiments and these energies could be compared to the values of the J-integral from the simulations for the different crack lengths.

Mesh Generation Techniques for Converting Triangular Meshes to Quadrilateral and Mixed-element Meshes with Applications to Shallow Water Flow

Ethan Kubatko^{*}, Dominik Mattioli^{**}, Dylan Wood^{***}

^{*}The Ohio State University, ^{**}The University of Iowa, ^{***}The Ohio State University

ABSTRACT

In this talk, we discuss the development and implementation of a new, simple indirect methodology for producing high-quality quadrilateral (quad) and quad-dominant meshes from any pre-existing, unstructured triangular mesh. One of the primary motivations for this work is to provide a tool for generating meshes that can be used within a discontinuous Galerkin (DG) finite element framework for modeling shallow water flow — a setting where meshes of mixed-element composition can be easily accommodated and where the computational advantages of using quad elements have been demonstrated [1]. Employed techniques include: A strategic merging sequence of neighboring triangular element pairs to form quads, several topological operators designed to improve the quality of the resulting quad elements and a direct (i.e., non-iterative) smoothing method to improve overall mesh quality. When paired with an existing triangular-element mesh generator, ADMESH+ [2], this new methodology results in a mesh generation tool capable of automatically producing high-quality triangular, quad and mixed-element meshes within one framework. Several example quad and quad-dominant meshes produced from the mesh generation tool will be presented, and numerical results of shallow water simulations obtained from the quad and quad-dominant meshes will be compared to the results obtained from their parent triangular meshes in terms of overall accuracy and efficiency. [1] Wirasaet, D., Kubatko, E.J., Michoski, C.E., Tanaka, S., Westerink, J.J., and Dawson C., Discontinuous Galerkin methods with nodal and hybrid nodal/nodal triangular, quadrilateral, and polygonal elements for nonlinear shallow water flow *Computer Methods in Applied Mechanics and Engineering*, 270, pp. 113–149, 2013. [2] Conroy, C., Kubatko, E.J., and West, D., ADMESH: An advanced, automatic unstructured mesh generator for shallow water models, *Ocean Dynamics*, 62 (10), pp. 1503–1517, 2012.

Meshless Remap for Earth System Models

Paul Kuberry^{*}, Pavel Bochev^{**}, Kara Peterson^{***}

^{*}Sandia National Laboratories, ^{**}Sandia National Laboratories, ^{***}Sandia National Laboratories

ABSTRACT

Global Earth System Models comprise multiple components, representing a diverse set of physical phenomena and employing different types of discretizations adapted to the particular scales and features of the underlying physical phenomena. As a result, the coupling of these components requires information exchanges (remap) between codes, which involve fields defined on different types of meshes and possibly having different representations, e.g., finite element vs. finite volume, or node-centered vs. cell-centered. Typically, the coupling takes place over a shared subdomain boundary, resulting in interface discretizations that are generally mismatched. For such couplings, a mesh-free approach to data transfer offers an attractive alternative to traditional, mesh-based remap. In this talk we present a flexible data transfer tool, employing Generalized moving least squares (GMLS), and which can handle a wide range of “native” field representations. GMLS is a meshless reconstruction technique for approximating a target functional from nearby neighbor information, which makes it particularly well-suited for our purposes. The GMLS data transfer tool is based on the recently developed Compadre meshless toolkit, which provides a wide range of utilities for mesh-free discretizations of PDEs. Compadre utilizes the Trilinos software stack to balance workloads over processors, execute k-d tree searches, reconstruct functionals using GMLS, and to provide many additional capabilities for meshfree PDE discretizations. The talk will highlight the ability of the toolkit to also support coupling codes such as components of Earth system models, by allowing for processor assignment of coordinates or sites where information is needed from the peer program. This information is constructed using neighbor information in the peer program and then transferred back. Transfer in this way allows for completely independent distributions of field data in each code being coupled. Numerical results will be presented demonstrating exact transfer of specific orders of polynomial solutions on the sphere, as well as the approximation error introduced when the solution being transferred is not within the span of the basis for the reconstruction.

BLADE TIP-TIMING SENSORS CALIBRATION AND ITS USAGE UNDER LOW LOAD CONDITION

Zdenek Kubin ^{*,†}, Tomas Misek [†], Jindrich Liska ^{*}

^{*} Faculty of Applied Sciences,
UWB in Pilsen, Univerzitní 22, Plzeň
306 14, Czech Republic
zdenek.kubin@doosan.com

[†] Doosan Skoda Power s.r.o.,
Tylova 1/57, Plzeň
301 28 Czech Republic

Key words: Blade Tip-Timing, Sensors, Calibration, Steam turbine, Vibration limits

Abstract. Blade Tip-Timing measurement becomes more and more valuable because power generation market is changing to the peak-load market. Today steam turbines have to full-fill high efficiency and reliability demand as well as increasing of number of cycles or operating under wide operational range which include windage or low load operation. The higher level of blade vibration is more common for windage and other non-nominal regimes. Blade Tip-Timing measurement offer solution for long term monitoring and safety operation.

The new last stage steam turbine blades have been developed with state of the art design features. The last stage moving blades are designed with integral shroud, mid-span tie-boss connection, and fir-tree dovetail. The blades are continuously coupled by blade untwist due to centrifugal force, and thus decreased vibrations and increased structural damping are provided. Unfortunately measurement of shrouded blades is much more complicated and the sensor to blade calibration has to be performed.

The Blade Tip-Timing measurement and sensor calibration is described in the paper. The calibration of magnetoresistive, optical sensors and eddy-current sensors was performed. The induction and optical reflection phenomena is described with their impact to shroud edge detection. The detection of shroud edges and its angle seems to be important in terms of calibration between tip deflections to high air foil stress identification. The comparison between the individual types of sensors is presented as well as the real results from 270MW steam turbine operation in wide operational range. The motivation to use multiple sensors and provide their calibration is reduced uncertainty of Blade Tip-Timing which is presented in many publications.

1 INTRODUCTION

In 2009, a new 48" steam turbine last stage blade (LSB) was developed by Doosan Skoda Power and in 2013 a new 42" LSB for 3000 RPM and high backpressure was developed with the application of new design features. Using modern computational instruments, airfoils with high flow efficiency were designed. Successful detuning of natural frequencies with respect to harmonics of rotational frequency has been achieved for both blades by using interconnecting elements near the mid-span and at the tip of the blades. Friction forces among the contact elements result from the constraint of blade untwist induced by centrifugal force. The mechanical properties of LSB were measured under rotation in a Campbell testing rig (vacuum chamber with rotating bladed disk and some source of blade excitation). Measurement proved that blades are out of synchronous resonances up to 7th harmonic frequency.

Synchronous excitation is the most common excitation in terms of the steam turbine blades. This excitation is closely related with circumferential asymmetry, blade passing and unbalance. On the other hand, resonances with non-synchronous excitation can occur as a result of aerodynamic excitation. Avoiding that is quite demanding task, because even very small aerodynamic excitation forces with wide frequency range can excite blades if the damping is insufficient. A big amplitudes of vibration during ventilation conditions was present several times as well as unstalled flutter observation during power output increase [5]. 3D unsteady CFD methodology under ventilation conditions was published by Megerle in 2012 [1]. Rotating aerodynamic excitation was measured and confirmed by CFD simulation, unfortunately there are still some unpredictable cell patterns. Previous study made by Shnee in 1974 [6] shows that there is a dynamic stress 2-3 times higher than the dynamic stresses at rated conditions in the range of 30 – 60 % of the nominal volume flow due to aerodynamic induced vibrations during ventilation.

From time to time customers want to operate the turbine in extraordinary conditions which can cause unpredictable blade excitations. These excitations have impact on dynamic stress of blades and reduced blade lifetime. Based on this, it was decided to measure blade vibration in a wide range of operation conditions in the power station and reduces mechanical stress of rotating blades thereby increasing their service life.

Damage of the blades causes changes in their frequency characteristics, which are measured using a contact or contactless method. The contact measurement by strain gauges provides direct information about the blade stresses during operation. However, this method is not suitable for long-term measurements, because the sensors service life is short in a corrosive environment. Furthermore, it is very difficult and expensive to monitor all blades of the bladed disc.

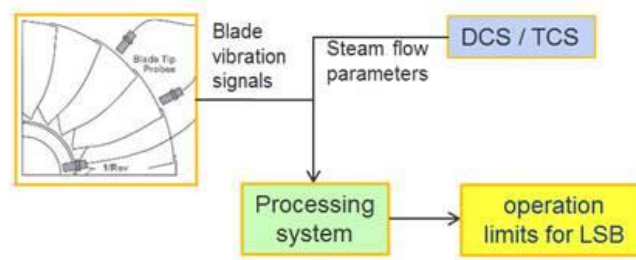


Figure 1 - Blade vibration monitoring system components

Noncontact measurement methods based on analysis of blade tip passing times are used for blade vibration measurement - blade tip-timing (BTT). The schematic description of BTT is shown on Figure 1. This method was used in 1970's for the first time. The manufacturers use abbreviations NSMS (Non- Intrusive Stress Measurement System), BSSM (Berührungslöse Schaufelschwingungsmessung) or usually Blade Tip Timing. BTT method is a cheaper alternative with a long-term instrumentation in comparison with strain gauges which offer a direct measurement of the blade stress but with a very short instrumentation lifetime. The BTT approach is based on sensors which are located circumferentially around bladed disk, radially mounted in the stator, watching tip of trailing edge [3, 4, 5]. This arrangement enables the measurement of blade tip passes. The system measures and analyses time differences of blades passing along the sensor position. The sensor itself is placed very close to the blade (order of ones-tens of millimetres depending on technology of the sensor), in order to guarantee fast response time and high sensitivity. The passing blade generates a trigger pulse which is captured by a high resolution time counter. All the data or timestamps are analysed and at the output of the system information on the blade vibration is provided.

It is important to monitor the blades frequency characteristics during turbine run-up, run-down and power changes. The measurement of vibrations provides information about blade deflection and blade residual lifetime. The long-term measurement of blade deflections is important for planning shutdowns and optimization of the maintenance cost and operation of the turbine.

Blade deflections are determined by differences between the real and expected passage times of the blades under the sensors. The deflection of the specific blade is sampled once per revolution. An antialiasing filter cannot be used in the measurement chain because the turbine rotation frequency is in fact the sampling frequency of the blade rotation movement and furthermore, the rotation speed changes. For these reasons, the vibrations of the specific blade are measured in a limited frequency range with lots of data mirrors at higher frequency and lower frequency resolution. Increasing the number of sensors does not often bring results adequate to expended resources.

Instead of single blade behaviour analysis, behaviour of the whole bladed disc could be analysed. The deflections are sampled by the passages of all blades. Then, the width of the frequency band is sufficient and aliasing doesn't manifest itself so much. The all-blade spec-

trum, which is the spectrum involving all blades of one disc, is calculated for each sensor from deflections measured for all blades passed under the sensor using short-time Fourier transform. Consequently, cross spectra are calculated from couples of the all-blade spectra from different sensors.

To obtain correct information about vibrations of shrouded blades, it was necessary to develop reliable measuring equipment for the shrouded blades. The key factor is to use adequate sensors [13, 14].

2 REQUIREMENTS FOR NON-CONTACT VIBRATION MEASUREMENTS ON SHROUDED BLADES

Observing the motion of rotating and vibrating blades in turbomachinery is a relatively demanding task. The sensors have to operate properly and precisely in a harsh environment characterized by temperatures up to 250°C and relative humidity of 100% (LP part of steam turbine). Concurrently, long-term stability, high accuracy and sensitivity of the sensors are required. Most present systems are therefore focused on the application of non-contact methods which can operate on a variety of principles. The limiting factor for non-contact measurement of blades vibration is the sampling frequency f_s . The sampling level has in BTT a significant influence on determining the vibration amplitude of the blades. Maximum resolution of the blade deflection is described by the following relation:

$$\Delta_a = \frac{2\pi \cdot r_{\text{senz}} \cdot f_{\text{rot}}}{f_s}, \quad (1)$$

where r_{senz} is the radius (measured from the center of the rotor) on which the sensor is placed. f_{rot} is the maximum rotational speed of the bladed disk in the measurements (typically 50 Hz). To illustrate the dependence between sampling rate and blade deflection amplitude resolution, the above relationship was used to provide the following table computed for rotation frequency of 50 Hz:

Table 1 - Resolution base on sampling frequency

f_s	blade 1220mm + 900mm rotor radius = 2120mm
100kHz (standard acquisition systems)	6660.2 μm
1MHz	666.0 μm
8MHz (oscilloscope standard)	83.2 μm
100MHz	6.6 μm
500MHz	1.3 μm

Table 1 shows the blade vibration resolution. It is clear that, for example, system resolution approaching units of microns should work with sampling frequencies of 500 MHz and

higher. Demand for a maximum resolution sensor should always be related to the largest bladed disk of the machine. For smaller diameters better resolution of measured deflection is always guaranteed, sampling frequency maintains.

The table above also shows that standard acquisition systems are not appropriate for BTT measurements (usually sampling frequency up to 100 kHz - 200 kHz). The biggest resolution of the measurement in such a case is in the order of millimetres, which is beyond the expected oscillatory behaviour of shrouded blades. For general diagnostic systems, which are able to monitor blades and evaluate their level of stress, it is necessary to use special hardware that allows the required sampling rate - hundreds of MHz. For the measurement of LSB, which is presented in this paper, the 200MHz system was used in combination with several types of sensors. This system seems to be sufficient to monitor LSB shrouded blades with vibration amplitudes 10 times under fatigue strength.

3 EDDY-CURRENT SENSOR CALIBRATION

The eddy-current sensors are most valuable in terms of robustness and cost. The principle is very simple see [13, 14]. There are magnet and coil in the sensor case. When the blade passes the sensor the eddy-current in the blade create magnetic field which induced the voltage in the sensor itself. The following equation describes the induced voltage in the sensor.

$$V = \frac{k \times \text{RPM} \times B(T) \times f(\text{RPM}, d_{\text{sensor}} \sqrt{[\mu\delta]_{\text{sensor}}(T)}) \times d_{\text{BLADE}} \sqrt{[\mu\delta]_{\text{BLADE}}(T)} \times T_{\text{sensor}}}{(\text{gap} + r)^6}, \quad (2)$$

where V is the blade pulse voltage, RPM is the rotor shaft speed, k is the calibration factor, $B(T)$ is the permanent magnetic field, which varies with temperature. The term $f(\cdot)$ describes the lowpass effect of the sensor signal due to eddy currents in the sensor itself, resisting the change in magnetic field. The frequency of the low pass effect is determined by the $\mu\sigma$ product of the material in the sensor, which varies with temperature. The term $d_{\text{BLADE}} \sqrt{[\mu\delta]_{\text{BLADE}}(T)}$ describes how the pulse amplitude increases with the $\mu\sigma$ product and the thickness of the blade. The $(\text{gap} + r)^6$ term relates how the pulse amplitude changes with changing gap. For the practical usage the equation 2 can be simplified as equation 3.

$$\text{gap} = K \left(\frac{\text{RPM}}{V - V_{\text{start}}} \right)^{1/6} - r, \quad (3)$$

To validate blade sensor model the computational model was created in ANSYS Maxwell – electromechanical FEM based simulation software. This model contained three blades (with cyclic symmetric condition), sensor and stator ring. The magnetic field around of the sensor is excited by a permanent magnet which is the part of the sensor. Magnetic flux lines are closing across the stator ring and blade shrouds. Changes in magnetic flux, caused by the shrouds rotation, are detected by the sensor coil.

By this model it was tried to cover the real conditions in a steam turbine. The blades rotate 50Hz that implies the tip speed 640m/s. This speed requires the simulation time and the simulation time step which had to be quite small.

For final evaluation the triggering algorithm was used. It was the same triggering algorithm which had been used for real BTT data. It is a very robust algorithm which contains high pass and low pass filtering, arm level which activates a trigger and finally the trigger which waits for a falling or rising edge going across the 0 level. (The algorithm was taken from HoodTech BTT acquire SW, because the authors have very good experience with it on-site).

This algorithm finally provides a time of arrival of individual blades which correspond to actual blade position. In next figure (Fig. 2) there are the times of arrival shown by cross markers (one cross for one axial position). It can be seen that these crosses correspond to outgoing edge of the shroud below the sensor coil.

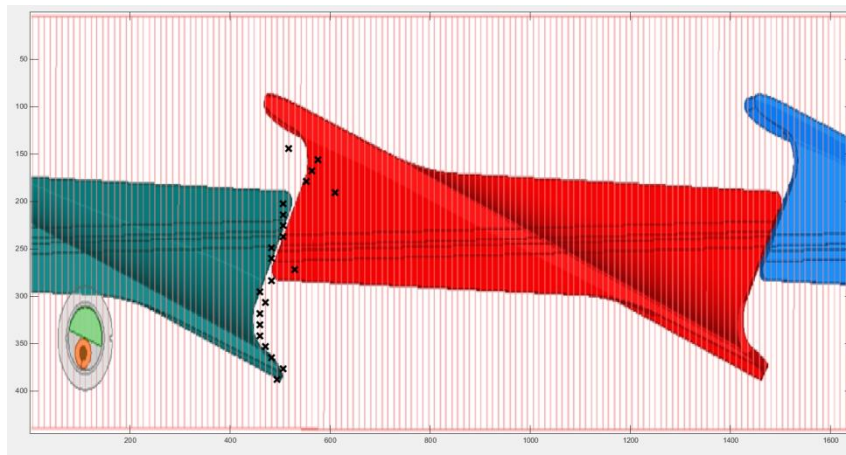


Figure 2 – Detection of the blade based on calculated signals and triggering algorithm

3.1 Experimental validation

The numerical calculation of the eddy-current sensor provides suitable solution. The next step was to verify the calculation by the measurement. The bladed disk was installed in to the Campbell machine. The Campbell machine is the vacuum chamber with rotor and one stage blade. The blades rotate in the vacuum with nominal speed and the vibration are excited by the electromagnets or oil jets.

The eddy-current sensors were installed into the vacuum chamber and used for measurement of time of arrival. The raw signals (before triggering algorithm usage) were recorded and then compared with calculation signals. The following figure 3 shows the comparison.

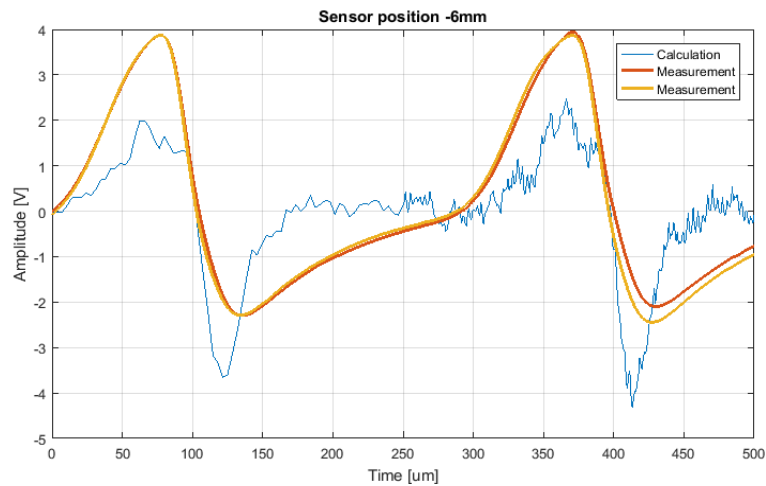


Figure 3 – Comparison of calculated signal (blue) and the measured signal from eddy-current sensor (red and yellow curves)

It is easy to see that calculated and real signals have same trends. The measured signals have lower noise than calculated one. The authors assume that the noise in the calculation is there because the 2 different meshes were used for the calculation – one for blades and second for electromagnetic surroundings. On the other hand the measured curve looks very smooth, it is happen because whole sensor system is behave like low pass filter.

4 MEASUREMENT IN POWER STATION UNDER REAL AND SPECIAL OPERATIONAL CONDITIONS

The crucial task for blade monitoring is to determine blade vibration limits (BVL) which are basically dependent on blade mode shapes. In case of integrally coupled blading the nodal diameter also affects vibration limits.

BVL are evaluated base on blade material fatigue limit (Goodman diagram) and safety factors. When the safety factors are applied then two critical blade locations are distinguish: airfoil and dovetail.

Maximal allowable cyclic stress is defined as

$$\text{Airfoil} \quad \sigma_{max} = \frac{\sigma_F}{S_b S_e}, \quad (4)$$

$$\text{Dovetail} \quad \sigma_{max} = \frac{\sigma_F}{S_b S_e S_f} \quad (5)$$

Where:

σ_F	Fatigue strength reflecting mean stress preload (Goodman diagram)
S_b	Basic safety factor
S_e	Safety factor for environment
S_f	Safety factor for fretting

Based on the FEM modal analysis the ratio R between dynamic cyclic stress at critical location and vibration amplitude of monitored tip location is determined for each mode shape and nodal diameter.

Maximal allowable vibration amplitude of the blade tip is determined as:

$$U_{max} = \frac{\sigma_{max}}{R}, \quad (6)$$

The BTT sensors monitor vibration only in circumferential direction therefore U_{max} has to be recalculated into proper direction in order to be used as BTT vibrational limits.

Figures 4 and 5 present typical U_{max} limits and BTT limits Y_C for the long LSB. Fatigue strength σ_F was determined based on the measured Wohler curve and Goodman diagram.

Figures 4 and 5 show that the most critical location from fatigue view is blade dovetail (root neck). This conclusion is also supported by the fact that the most cracks occur at the blade dovetails.

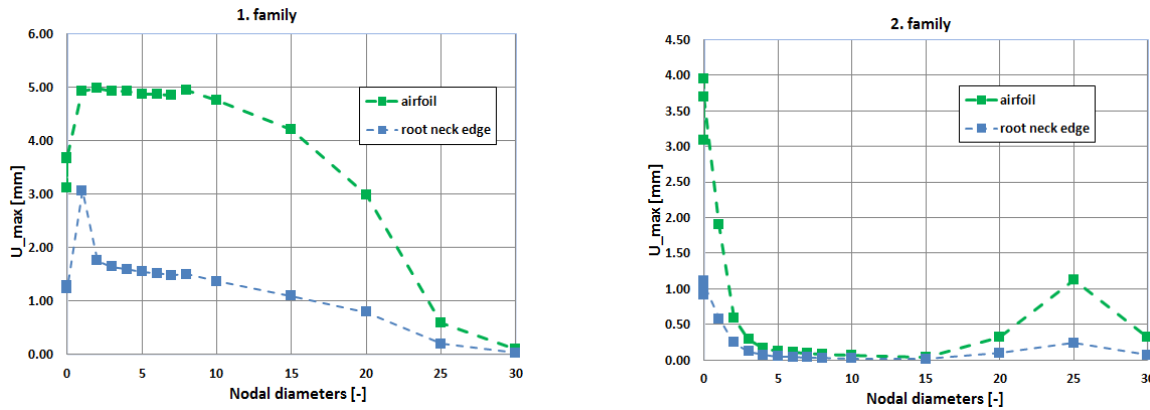


Figure 4 – Maximal allowable vibration amplitude at the blade tip for the first and second mode shape. Two critical locations are depicted

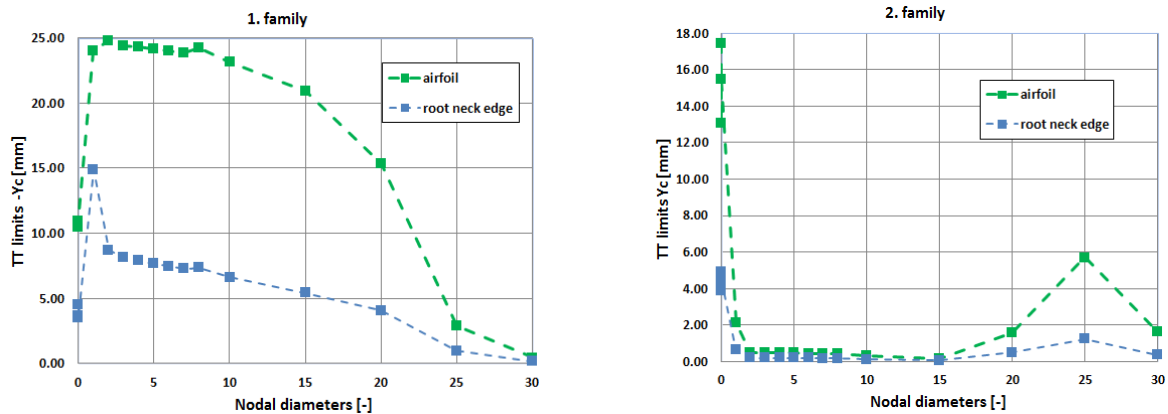


Figure 5 – BTT limits amplitude at leading edge for the first and second mode shape. Two critical locations are depicted

4.1 Field vibration monitoring setup

In early 2013 biaxial magnetoresistive, standard eddy-current and green laser optical sensors were installed into the 270 MW steam turbine. The sensors were located in LP part and watched LSB tip trailing edge. Totally 18 sensors were installed non-uniformly around the half of bladed disk. There were 5 eddy-current sensors, 7 biaxial magneto-resistive sensors (2 pairs of 3 involved sensors and individual dual sensor) and 6 optical sensors. Blade tip timing system from Hoodtech was used with 200MHz sampling frequency and it was able to measure up to 32 channels. The system allows setting up a different trigger for each sensor which was necessary because the physical principle of the sensors were different. The differences between signals from optical and electrical based sensors are shown in Figure 6.

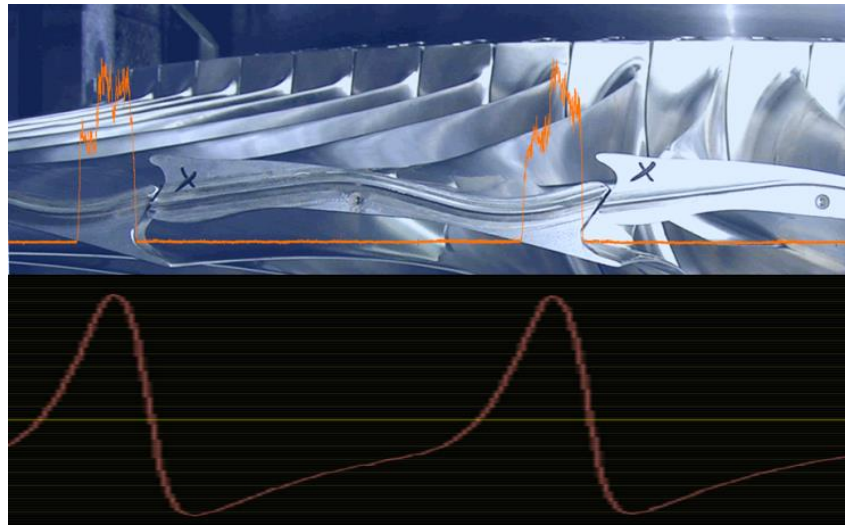


Figure 6 - different signal for triggering – upper picture represents optical signals and bottom picture is signal from eddy-current sensor

In 2016 on field blade monitoring was carried out at 135 MW steam turbine power plant. Seven different measuring runs were undertaken, see table 2. During the each run the back-pressure in condenser was gradually increasing from 10kPa to 42kPa. Both vacuum pumps were switched off one by one as required therefore vacuum drop control was limited however vacuum decay tendency (up to 2kPa/min) was still acceptable.

Table 2 - Measurement runs

1	1800rpm	Pre-heating of the turbine
2	3000rpm, 0MW	Large portion of steam was bypassed
3	20MW	Power control, certain portion of steam was bypassed
4	40MW	Power control, certain portion of steam was bypassed, LP re-generation switch on
5	65MW	Power control, LP regeneration switch on
6	90MW	Pressure control, not enough steam to maintain constant power
7	135MW	Pressure control, not enough steam to maintain constant power

Totally seven tests were done. Turbine reached seven different power outputs and then the back pressure was gradually changed (vacuum in condenser decrease from 0.05 up to 0.5 bar).

All measured data were evaluated by in-house code that was created for this purpose in MATLAB. It was found out that the blades vibrated under all operating regimes that were monitored:

- dominant vibration : 1st mode family, nodal diameters from 4 to 7 , ND5 – the most excited
- 2nd mode family was not observed

BTT vibration amplitudes were plotted in graphs with respect to nodal diameters see figures 7 to 8. Figures 9 show maximal BTT vibration amplitudes respectively.

Maximal vibrations in figure 9 are likely the most relevant amplitudes that should be focused on since they represent sum of all amplitudes but mostly those dominant related to ND4 to ND7. Even if the maximal vibration amplitudes are not presented continuously but only about 30% the total time a number of cycles related to these amplitudes are still sufficiently high in terms of high cycle fatigue (HCF).

The major output from the field monitoring of LSB is presented in the figures 7 to 9. It shows BTT amplitudes versus backpressure and volumetric flow. Red and black lines depict alarm and trip limits respectively. The colormap area in the above mentioned figures is limited by boiler capacity (mass flow) in other words the higher volumetric flow regimes for high backpressure than 42kPa are not reachable at this power plant.

After the evaluation of all data it became clear which type of sensor is the best. For operation with high steam parameters the laser sensor provides very accuracy signals without any electrical noise. On the other hand when the steam was wet and there were small water drops the signal was insufficient and it was not possible to measure blade vibration. Standard eddy-current sensors and newly developed magnetoresistive sensors [11] provided signals all the time. The differences between them could be shown only in all blade spectrums. The spectrum from biaxial magnetoresistive sensor is better in terms of signal to noise ratio. The 50 Hz and multiples of 50 Hz are very poor in spectrum of magnetoresistive sensor.

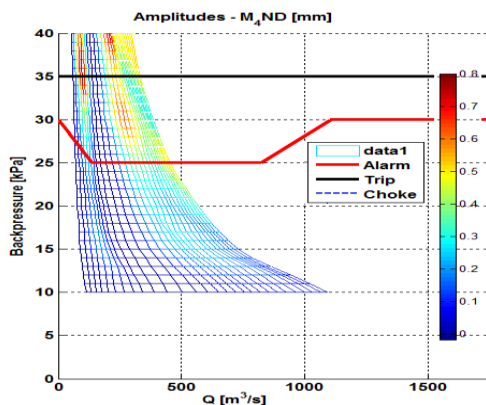


Figure 7 - TT vibration amplitudes (0-peak) for ND4

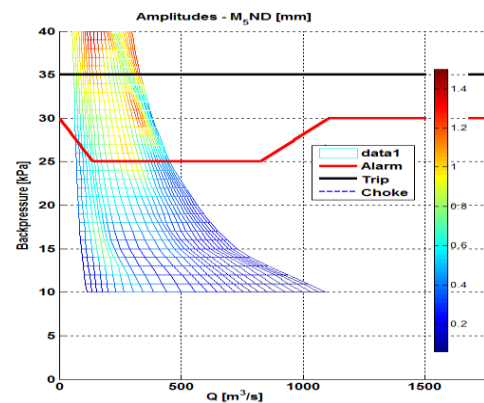


Figure 8 - TT vibration amplitudes (0-peak) for ND5

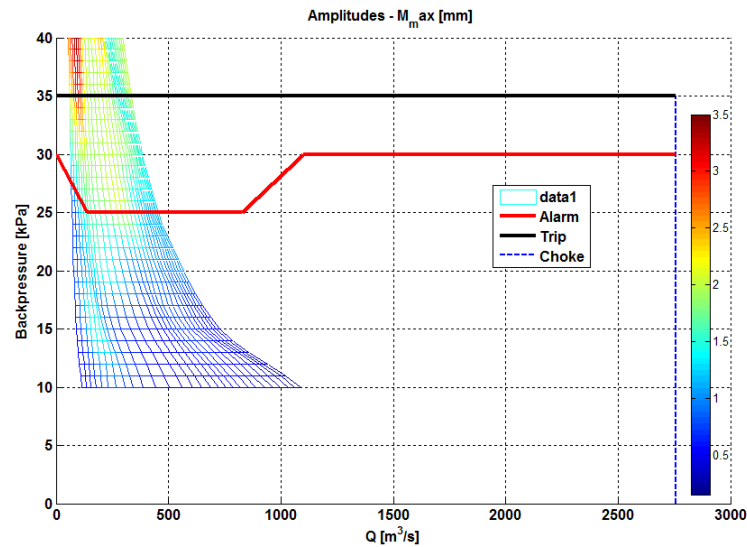


Figure 9 - BTT vibration amplitude - maximal from signal envelope (0-pk) versus backpressure and volumetric flow

5 CONCLUSION

The biaxial magnetoelectric and optical sensors have proven successful in all installations. The sensors are designed for operation under a long-term temperature of 200°C and a short-term temperature of 250°C. Using permanent magnets in MR sensors as the source of the magnetic field simplified the sensor construction and increased its reliability. The most favourable properties of the group of magnetoelectric sensors emphasized advantages of magnetoresistive sensors, which are characterized by high accuracy and sensitivity to displacement, wide frequency bandwidth (0 to 300 kHz) and a very important feature, which is the independence of the sensor output voltage magnitude on the speed of a blade passage. The advantage of this feature is that the sensors can be calibrated statically, for example using a positioning facility. The optical sensors with green laser source have been used in steam turbine with pretty good success. There are still some operational conditions in wet steam environment when the signal noise ratio is not good enough. Eddy-current sensors provide high quality signal as well and it was proven that it can be used for shrouded blades.

Several types of LSBs were measured under real and under special operational conditions. It was found out that the blades vibrated under all operating regimes that were monitored and the installed sensors were capable to identify the tip blade vibration.

It was proved that the blades can be operated in a wide range of operational conditions and they are resistant against high vibration.

The figures 7 - 9 proved Shnee hypothesis [7] that vibration in ventilation is 2-3 times higher. The windage condition are worst in terms of vibration which are 3 times higher than vibration at 100% volume even more the temperature increase dramatically.

References

- [1] Benjamin Megerle, "Numerical and experimental investigation of the aerodynamic excitation of a model low-pressure steam turbine stage operation under low volume flow. ", GT2012-68384, Proceedings of ASME Turbo Expo 2012, June 11-15, 2012, Copenhagen, Denmark
- [2] Naoki Shibukawa, Yoshifumi Iwasaki, "A correlation between vibration stresses and flow features of steam turbine long blades in low load condition", GT2011-46368, Proceedings of ASME Turbo Expo 2011, June 6-10, 2011, Vancouver, British Columbia, Canada
- [3] M. Zielinski and G. Ziller, Noncontact Blade Vibration Measurement System for Aero Engine Application. MTU Aero Engines GmbH Engine Control and Testing Division 80995 München, German.
- [4] P. Beauseroy, R. Lengellé, Nonintrusive turbomachine blade vibration measurement system. System Modelling and Dependability Group - FRE CNRS 2848, Charles Delaunay Institute, Université de Technologie de Troyes BP2060 10010 TROYES Cedex, France
- [5] Y. Kadoy, M. Mase, Y. Kaneko, S. Umemura, T. Oda, M. C. Johnson, "Noncontact Vibrational Measurement Technology of Steam Turbine Blade", JSME International Journal, Vol. 38, No. 3, 1995.
- [6] Zdenek Kubin, Vaclav Cerny, Pavel Panek, Tomas Misek, Jan Hlous, Lubos Prchlik. "Determination of crack initiation on L-1 LP steam turbine blades, Part 1: Measurements on rotor train, material specimens and blades", GT2011 – 46203, Proceedings of ASME Turbo Expo 2011, June 6-10, 2011 Vancouver Canada
- [7] Y. Shnee, et al., "Influence of the operational factors on dynamic stresses in moving blades of a turbine stage", Teploenergetika, vol. 21, pp. 49-52, 1974
- [8] MISEK, T., Kubin, Z., Duchek, K., 2009, "Static and Dynamic Analysis of 48" Steel Last Stage Blade for Steam Turbine", Proceedings of ASME Turboexpo: Power for Land Sea and Air, Orlando, USA
- [9] PRCHLIK, L., Kubin, Z., Duchek, K., 2009, "THE Measurement of dynamic vibration modes and frequencies of a large LP bladed disc", Proceedings of ASME Turboexpo 2009: Power for Land, Sea and Air, Orlando, USA
- [10] Misek, T., et al., 2014. "Development of the New 54" Titanium Last Stage Blade", Power-Gen Europe, Cologne, Germany.
- [11] P. Procházka, and F. Vaněk, , "New Methods of Non-Contact Sensing of Blade Vibrations and Deflections in Turbomachinery", IEEE Trans. Instrum. Meas., vol. 63, p. 1583-1592, June 2014.
- [12] Kubín, Z., Liška, J., Mišek, T., Procházka, Pavel, "Application of non-contact vibration measurements on a 48" blade under low load condition", DYMAMESI 2017. Cracow (PL), 28.02.2017-01.03.2017, s. 45-54. ISBN 978-80-87012-62-8.
- [13] Zdenek Kubin, Tomas Misek, Jan Hlous, Tereza Dadakova, Josef Kellner, Tibor Bachorec, „CALIBRATION OF BLADE TIP-TIMING SENSOR FOR SHROUDED 40" LSB“, Mechanical Systems and Signal Processing, Volume 108, August 2018, Pages 88-98
- [14] Nidhal Jamia, Michael I Friswell, Sami El-Borgi, Ralston Fernandes, Simulating eddy current senso outputs for blade tip timing, Advances in Mechanical Engineering, 2018, Vol. 10(1) 1–12, DOI: 10.1177/1687814017748020

A BASIC CELL MODELING METHOD FOR HOMOGENIZATION ANALYSIS OF PLAIN-WOVEN COMPOSITES WITH NESTING

G. KUBO*, T. MATSUDA[†], AND Y. SATO[†]

*Affiliation

Department of Engineering Mechanics and Energy
University of Tsukuba
Tsukuba, Ibaraki, Japan
Email address; s1730189@s.tsukuba.ac.jp

[†]Affiliation

Department of Engineering Mechanics and Energy
University of Tsukuba
Tsukuba, Ibaraki, Japan
Email address; matsuda@kz.tsukuba.ac.jp

Key words: Plain-woven composite, Nesting, basic cell, Homogenization, Viscoplasticity.

Abstract. A basic cell modeling method is newly developed for the homogenization analysis of plain-woven composites with nesting. For this, based on the periodicity and point-symmetry of internal structures of plain-woven composites with nesting, a hexagonal prism-shaped basic cell and its boundary conditions are proposed. The basic cell and boundary conditions are then introduced into the homogenization theory for nonlinear time-dependent composites developed by the authors. Using the present method, elastic-viscoplastic behavior of a plain-woven glass fiber-reinforced plastic (GFRP) composite with nesting subjected to on- and off-axis loading is analyzed. In the analysis, the present method is successful in significantly reducing the analysis domain, and in achieving the modeling of a high volume fraction of fiber bundles caused by nesting. This cannot be attained if conventional cuboid cells are employed as analysis domains. Moreover, it is shown from the analysis results that the present method accurately predicts experimentally observed macroscopic elastic-viscoplastic behavior of the plain-woven GFRP composite with nesting.

1 INTRODUCTION

Plain-woven composites have many positive features, for example, high specific strength, high specific stiffness and good formability. Therefore, they have been used as primary structural members in many industrial fields such as the aerospace, auto and energy-related industries. Plain-woven composites are generally produced by stacking plain fabrics and impregnating them with polymer materials (Fig. 1). During this forming process, fabric layers are not necessarily

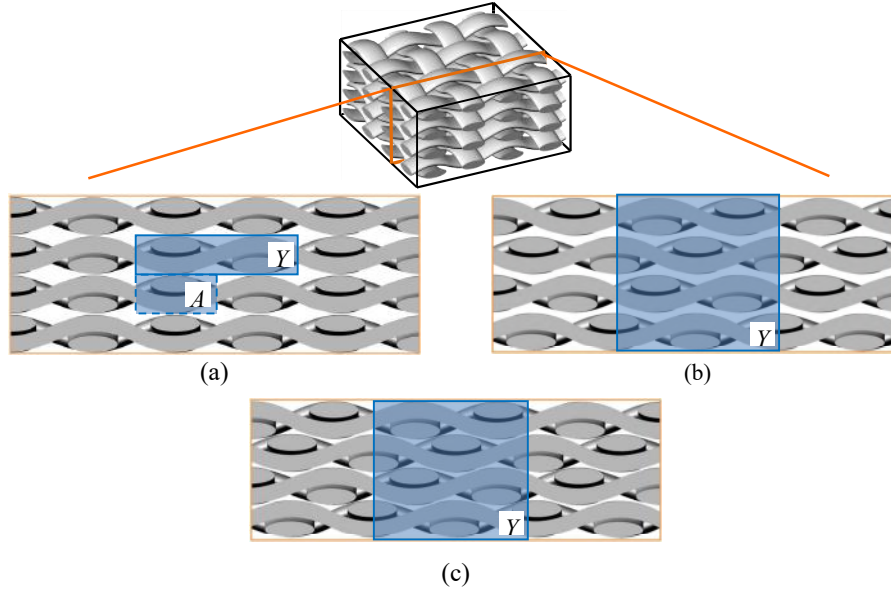


Fig. 1. Microstructures and unit cells of plain-woven laminates; (a) without misalignment, (b) with misalignment of $1/4$ unit cell length, (c) with nesting.

aligned (Fig. 1(a)), but can be shifted in the in-plane directions (Fig. 1(b)), which will be referred to as "laminate misalignment". Moreover, compression in the forming process causes the fabric layers to press into each other in the stacking direction. Consequently, complicated internal structures as illustrated in Fig. 1(c), which are generally called "nesting", can occur in plain-woven composites [1-5]. It is known that the nesting can affect the mechanical properties of plain-woven composites, which is not limited to elastic properties such as initial stiffness [5-8], but extends to inelastic properties such as damage behavior and strength [9]. Therefore, we should consider the effects of nesting when analyzing the mechanical properties of plain-woven composites.

For such mechanical analysis of plain-woven composites with nesting, numerical unit cell analysis based on the finite element method (FEM) or homogenization theory [10] is considered as one of the most promising methods. This is because it can explicitly take into account the nesting structures in plain-woven composites. Such analysis, however, encounters two main difficulties. One is how we can easily generate unit cell geometries and FE meshes for unit cells of plain-woven composites with nesting. In general, the aforementioned complicated internal structures of plain-woven composites with nesting make it difficult and cumbersome to generate their unit cells and FE meshes. The second difficulty is that enormous computational costs are required for the analysis because unit cells with nesting basically become much larger than that without nesting due to the restriction of the periodic boundary condition (see the unit cells Y in Fig. 1). This can be a critical issue, especially for nonlinear analysis accompanied by incremental computation. For these reasons, the nesting has been ignored in many unit cell analyses [11-13] including our previous studies [14-16].

To overcome the above-mentioned difficulties, some researchers developed the methods to generate geometries and FE meshes of unit cells of woven composites with nesting using micro-computed tomography (CT) or scanning electron microscope (SEM) digital images [17-20]. These methods provided easier generation of realistic geometries for unit cells, e.g. shapes of

fiber bundles and degree of nesting. However, the number of elements in the unit cells became considerably large to obtain appropriate solutions, resulting in application of the methods only to two-dimensional or elastic analyses. In addition, it is difficult for the image-based modeling methods to guarantee the periodic connectivity of unit cells.

In this study, a basic cell modeling method is newly developed for the homogenization analysis of plain-woven composites with nesting, and is applied to an elastic-viscoplastic analysis of plain-woven glass fiber-reinforced plastic (GFRP) composites with nesting. For this, focusing on the periodicity and symmetry of internal structures of plain-woven composites with nesting, a novel basic cell and its boundary conditions are proposed. The basic cell and boundary conditions are introduced into the homogenization theory for nonlinear time-dependent composites developed by the authors [21-23]. The proposed method is then applied to an elastic-viscoplastic analysis of plain-woven GFRP composites with nesting subjected to on- and off-axis loading. Comparing the analysis results with experimental data, we validate the present method.

2 BASIC CELL FOR PLAIN-WOVEN COMPOSITES WITH NESTING AND HOMOGENIZATION THEORY

2.1 Introduction of the basic cell and properties of internal distributions

We consider a plain-woven composite with nesting on the Cartesian coordinates y_i ($i = 1, 2, 3$) as illustrated in Fig. 2, in which each plain fabric is assumed to possess the same degree of nesting in the $y_3 - y_1$ plane. The composite is assumed to be subjected to a macroscopically uniform load, and to deform infinitesimally. Then, not a conventional cuboid cell [10-16] but a hexagonal prism cell shown in Fig. 2, which will hereafter be called "basic cell A ", is defined as an analysis domain. The boundary of A , Γ , is divided into Γ_α ($\alpha = 1, 2, \dots, 8$) as depicted in Fig. 3, where $\Gamma_1 - \Gamma_4$ are sequentially numbered in the counterclockwise direction from the upper right to the front boundary facets as indicated in Fig. 3(a), and $\Gamma_5 - \Gamma_8$ are also sequentially numbered in the counterclockwise direction from the lower left to the rear boundary facets as indicated in Fig. 3(b). It should be noted that A is much smaller than the unit cell Y [11, 13, 15] generally employed in the homogenization analysis on the basis of the so-called Y -periodic boundary condition.

Now, the microscopic velocity field $\dot{u}_i(\mathbf{y}, t)$ in A is expressed as [10]

$$\dot{u}_i(\mathbf{y}, t) = \dot{F}_{ij}(t)y_j + \dot{u}_i^\#(\mathbf{y}, t), \quad (1)$$

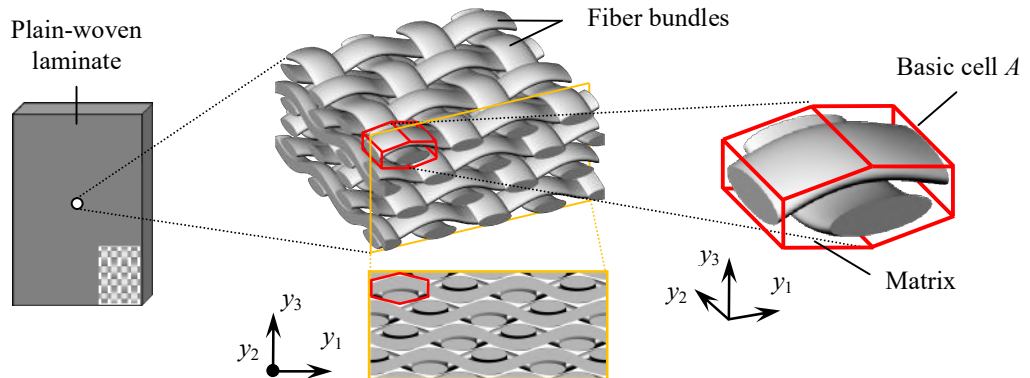
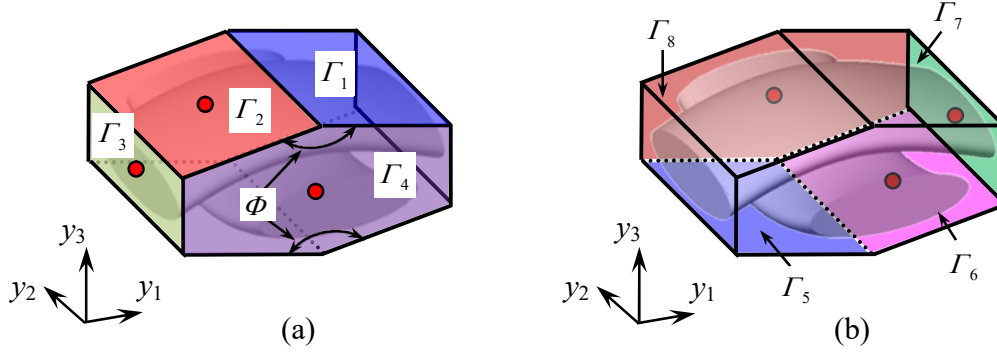


Fig. 2. Plain-woven composite with nesting in the $y_3 - y_1$ plane and basic cell A .

Fig. 3. Boundary facets of A ; (a) $\Gamma_1 - \Gamma_4$, (b) $\Gamma_5 - \Gamma_8$.

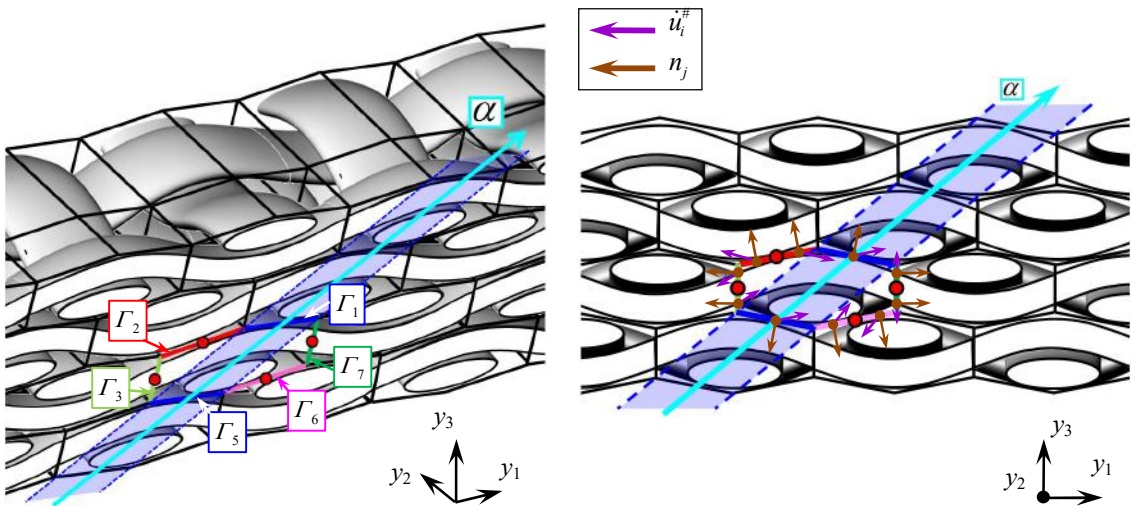
where (\cdot) indicates the differentiation with respect to t , $F_{ij}(t)$ is the macroscopic deformation gradient, and $\dot{u}_i^\#(y, t)$ is the perturbed velocity. In the present nesting case, it is found from the cross-sectional view as illustrated in Fig. 4 that the microstructure possesses the periodicity in the α -direction. Thus, $\dot{u}_i^\#$ must be periodically distributed on Γ_1 and Γ_5 . Further, one can find that the microstructure possesses the point-symmetries with respect to the centers of Γ_2 , Γ_3 , Γ_6 and Γ_7 . In addition, such point-symmetries are satisfied with respect to the centers of Γ_4 and Γ_8 . This suggests that $\dot{u}_i^\#$ on $\Gamma_2 - \Gamma_4$ and $\Gamma_6 - \Gamma_8$ should be point-symmetrically distributed with respect to these points (Fig. 4). It is clear that these periodicity and point-symmetries hold regarding the microscopic stress σ_{ij} and its rate $\dot{\sigma}_{ij}$.

2.2 Weak form of equilibrium of microscopic stress and its integral terms

The equilibrium of σ_{ij} in A can be expressed in a rate form as

$$\dot{\sigma}_{ij,j} = 0, \quad (2)$$

where $(\cdot)_{,j}$ denotes the differentiation with respect to y_j . The integration by parts and the divergence theorem allow Eq. (2) to be transformed to a weak form:

Fig. 4. Periodicity in the α -direction and point-symmetries with respect to the centers of Γ_2 , Γ_3 , Γ_6 and Γ_7 , and perturbed velocity field $\dot{u}_i^\#$ and unit normal vector n_i on each boundary facet.

$$\int_A \dot{\sigma}_{ij} v_{i,j} dA - \int_{\Gamma} \dot{\sigma}_{ij} n_j v_i d\Gamma = 0, \quad (3)$$

where $v(\mathbf{y}, t)$ is an arbitrary variation of $\dot{u}_i^\#$, and n_j is the unit vector outward normal to Γ . It is noted that the boundary integral term in Eq. (3) can be expressed as

$$\int_{\Gamma} \dot{\sigma}_{ij} n_j v_i d\Gamma = \sum_{\alpha=1}^8 \int_{\Gamma_\alpha} \dot{\sigma}_{ij} n_j v_i d\Gamma. \quad (4)$$

On Γ_1 and Γ_5 , the periodicity of v_i and $\dot{\sigma}_{ij}$ is satisfied as already described in the previous subsection, whereas n_j takes the opposite directions on these boundary facets (Fig. 4), leading to the following relationship:

$$\int_{\Gamma_1} \dot{\sigma}_{ij} n_j v_i d\Gamma + \int_{\Gamma_5} \dot{\sigma}_{ij} n_j v_i d\Gamma = 0. \quad (5)$$

On $\Gamma_2 - \Gamma_4$ and $\Gamma_6 - \Gamma_8$, in contrast, the point-symmetries of v_i and $\dot{\sigma}_{ij}$ with respect to the centers of these facets are satisfied, whereas n_j keeps the same direction on the facets (Fig. 4). Thus, the boundary integral terms with respect to these areas become zero, and we obtain

$$\int_{\Gamma_\alpha} \dot{\sigma}_{ij} n_j v_i d\Gamma = 0, \quad (\alpha=2-4, 6-8). \quad (6)$$

From Eqs. (4), (5) and (6), the second term on the left side of Eq. (3) vanishes, which enables Eq. (3) to be rewritten as

$$\int_A \dot{\sigma}_{ij} v_{i,j} dA = 0. \quad (7)$$

2.3 Homogenization

The constitutive equation of constituents in A is expressed in a rate form as

$$\dot{\sigma}_{ij} = c_{ijkl} (\dot{\epsilon}_{kl} - \beta_{kl}), \quad (8)$$

where c_{ijkl} and β_{kl} respectively denote the elastic stiffness and viscoplastic strain rate of the constituents, satisfying $c_{ijkl} = c_{jikl} = c_{ijlk} = c_{klij}$ and $\beta_{kl} = \beta_{lk}$, $\dot{\epsilon}_{kl}$ indicates the microscopic strain rate. As already stated in the previous subsection, Eq. (7) has the same form as that of the original homogenization theory [10, 21, 22]. Therefore, according to the earlier works [21, 22], we can derive the following evolution equation of microscopic stress, and the relation between macroscopic stress rate $\dot{\Sigma}_{ij}$ and macroscopic strain rate \dot{E}_{ij} :

$$\dot{\sigma}_{ij} = c_{ijpq} (\delta_{pk} \delta_{ql} + \chi_{p,q}^{kl}) \dot{E}_{kl} - c_{ijkl} (\beta_{kl} - \varphi_{k,l}), \quad (9)$$

$$\dot{\Sigma}_{ij} = \langle c_{ijpq} (\delta_{pk} \delta_{ql} + \chi_{p,q}^{kl}) \rangle \dot{E}_{kl} - \langle c_{ijkl} (\beta_{kl} - \varphi_{k,l}) \rangle, \quad (10)$$

where δ_{ij} indicates the Kronecker's delta, $\langle \# \rangle$ stands for the volume average in A , i.e. $\langle \# \rangle = |A|^{-1} \int_A \# dA$, where $|A|$ signifies the volume of A . Moreover, χ_p^{kl} and φ_k are the functions to be determined by solving the following boundary value problems for A :

$$\int_A c_{ijpq} \chi_{p,q}^{kl} v_{i,j} dA = - \int_A c_{ijkl} v_{i,j} dA, \quad (11)$$

$$\int_A c_{ijpq} \varphi_{p,q} v_{i,j} dA = \int_A c_{ijkl} \beta_{kl} v_{i,j} dA, \quad (12)$$

In general, the boundary value problems (11) and (12) are solved numerically to find χ_p^{kl} and φ_k using the FEM. In this analysis, we impose the combination of the periodicity and point-symmetries already described in the previous subsections on χ_p^{kl} and φ_k as the boundary conditions. It should be noted that the present modeling method, including the boundary conditions, enables us to substantially reduce the analysis domain for plain-woven composites with nesting compared with the previous methods mentioned in the introduction, which is eminently suitable for nonlinear analysis accompanied by incremental computation.

3 ELASTIC-VISCOPLASTIC ANALYSIS OF PLAIN-WOVEN GFRP COMPOSITES WITH NESTING

3.1 Basic cell

To determine the geometry of the basic cell A , we performed SEM observation of cross-sections of the plain-woven GFRP composite. It is noted that, in the composite, nesting predominantly existed in the plane parallel to the warp-direction, whereas there was less nesting in the plane parallel to the weft-direction. We then measured the wavelength, shape, size and volume fraction of the fiber bundles, the fiber volume fraction in fiber bundles, and calculated their averaged values. Based on these observation results and averaged values, A with nesting in the $y_3 - y_1$ plane with 69% volume fraction of fiber bundles was defined using the aforementioned hexagonal prism cell (Fig. 5), and was divided into eight-node isoparametric elements (1888 elements, 2329 nodes). It is noteworthy that the number of elements, 1888, is much smaller than in the preceding studies dealing with plain-woven composites with nesting [5, 17].

3.2 Material properties

Fiber bundles were regarded as E-glass/epoxy unidirectional composites, and as transversely isotropic elastic materials. Their material properties were calculated using the homogenization theory on the assumption that the fiber volume fraction in fiber bundles was 72% in the accordance with the microscope observation, and that the fiber bundles had a hexagonal fiber array. The elastic constants of the E-glass fibers and epoxy used in the calculation were set as

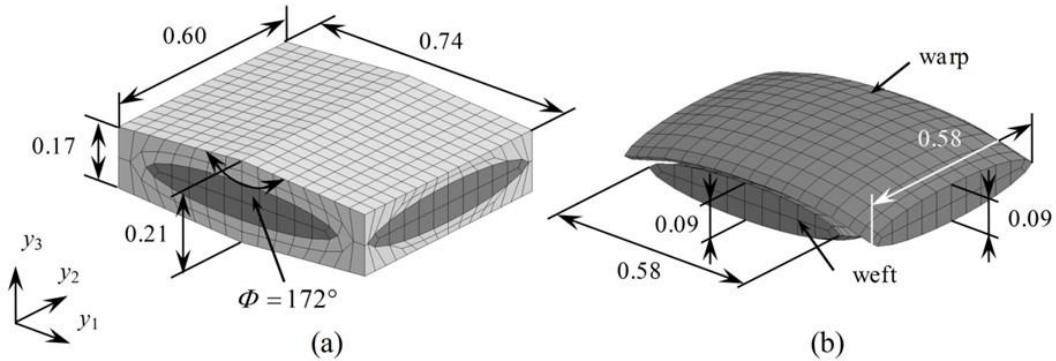


Fig. 5. Basic cell A of plain-woven GFRP laminates with nesting (1888 elements, 2329 nodes) with dimensions in mm; (a) full view, (b) fiber bundles (weft and warp) in A .

listed in Table 1. The epoxy matrix, on the other hand, was regarded as an isotropic elastic-viscoplastic material that obeyed the following constitutive equation [21-23]:

$$\dot{\epsilon}_{ij} = \frac{1+\nu_m}{E_m} \dot{\sigma}_{ij} - \frac{\nu_m}{E_m} \dot{\sigma}_{kk} \delta_{ij} + \frac{3}{2} \dot{\epsilon}_0^p \left[\frac{\sigma_{eq}}{g(\bar{\epsilon}^p)} \right]^n \frac{s_{ij}}{\sigma_{eq}}, \quad (13)$$

where E_m , ν_m and n represent material constants, $g(\bar{\epsilon}^p)$ stands for the exponential hardening function (Voce's hardening function) depending on the equivalent viscoplastic strain $\bar{\epsilon}^p$ [19,24], $\dot{\epsilon}_0^p$ signifies the reference strain rate, s_{ij} denotes the deviatoric part of σ_{ij} , and $\sigma_{eq} = [(3/2)s_{ij}s_{ij}]^{1/2}$. In this study, no failure of the fiber bundles and epoxy, and no delamination between the fiber bundles and epoxy were considered.

3.3 Loading condition

The plain-woven GFRP composites were subjected to a macroscopically uniaxial tensile load at a constant strain rate of 10^{-5} s^{-1} at room temperature. Five kinds of off-axis angles, i.e. $\theta = 0, 15, 30, 45$ and 90° , were considered.

3.4 Results of analysis

Figure 6 shows the macroscopic stress-strain relations obtained from the present analysis and the tensile tests of the plain-woven GFRP composite with nesting subjected to the uniaxial

Table 1 Material constants.

E-glass	$E_f = 80.0 \times 10^3$ $\nu_f = 0.22$		
Epoxy	$E_m = 3.5 \times 10^3$	$\nu_m = 0.35$	$\dot{\epsilon}_0^p = 1.0 \times 10^{-5}$
	$n = 30$	$g(\bar{\epsilon}^p) = 19 - 18 \times \exp(-190 \times \bar{\epsilon}^p)$	

MPa (stress), mm/mm (strain), s (time)

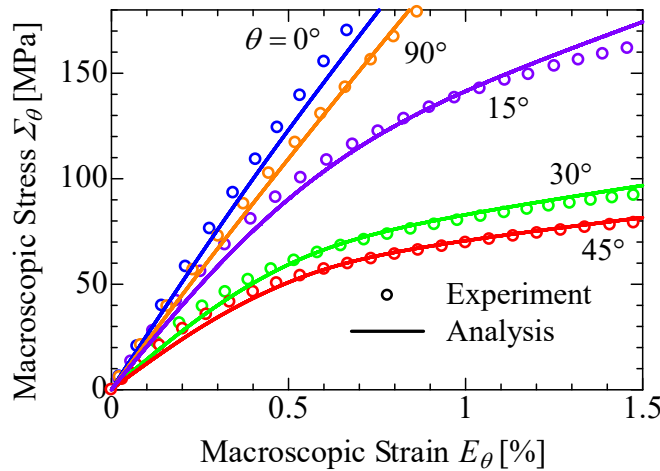


Fig. 6. Macroscopic stress-strain relations of plain-woven GFRP laminate with nesting at $\theta = 0, 15, 30, 45$ and 90° at $\dot{E}_\theta = 1.0 \times 10^{-5} \text{ s}^{-1}$.

tension with $\theta = 0, 15, 30, 45$ and 90° . In the figure, the analysis and the experimental results are respectively indicated by the solid lines and open circles. As seen from the experimental results in Fig. 6, the macroscopic stress-strain relations markedly depend on θ , indicating that the plain-woven GFRP composite possesses remarkable elastic-viscoplastic anisotropy [13-15]. Comparing such experimental data with the analysis results, it is found that the present modeling method is successful in predicting the macroscopic behavior of the plain-woven GFRP composite.

4 CONCLUSIONS

- The present method enabled us to substantially reduce the analysis domain for the homogenization analysis of plain-woven composites with nesting compared with the previous methods. This is eminently suitable for nonlinear analysis accompanied by incremental computation including the elastic-viscoplastic analysis performed in this study.
- High volume fraction of fiber bundles (69% in the present case) was achieved using the present modeling method. This could not be attained if conventional cuboid cells were employed. The present method therefore becomes significantly effective, especially in the case of the high volume fraction of fiber bundles caused by nesting as seen in the plain-woven GFRP composite dealt with in this study.
- Comparison between the analysis and the experimental results revealed that the present method was capable of accurately predicting the in-plane macroscopic elastic-viscoplastic behavior of the plain-woven GFRP composite with nesting.

ACKNOWLEDGMENTS

This presentation is based on results obtained from a project (P16010) commissioned by the New Energy and Industrial Technology Development Organization of Japan (NEDO). The presenter, G. Kubo, is grateful to the International Association for Computational Mechanics (IACM) for providing the IACM Scholarship covering his registration fee to participate in the 13th World Congress on Computational Mechanics (WCCM XIII) and the 2nd PanAmerican Congress on Computational Mechanics (PANACM II).

REFERENCES

- [1] Mesogitis, T.S., Skordos, A. and Long, A.C. Uncertainty in the manufacturing of fibrous thermosetting composites: A review. *Compos. Part A Appl. Sci. Manuf.* (2014) 57:67-75.
- [2] Yurgartis, S.W., Morey, K. and Jortner, J. Measurement of yarn shape and nesting in plain-weave composites. *Compos. Sci. Technol.* (1993) 46:39-50.
- [3] Saunders, R.A., Lekakou, C. and Bader, M.G. Compression and microstructure of fibre plain woven cloths in the processing of polymer composites. *Compos. Part A Appl. Sci. Manuf.* (1998) 29:443-454.

- [4] Hagiwara, K., Ishijima, S., Takano, N., Ohtani, A. and Nakai, A. Parameterization, statistical measurement and numerical modeling of fluctuated meso/micro-structure of plain woven fabric GFRP laminate for quantification of geometrical variability. *Mech. Eng. J.* (2017) 17-00053:1-12.
- [5] Lomov, S.V, Verpoest, I., Peeters, T., Roose, D. and Zako, M. Nesting in textile laminates: geometrical modeling of the laminate. *Compos. Sci. Technol.* (2003) 63:993-1007.
- [6] Naik, N.K. and Kuchibhotla, R. Analytical study of strength and failure behaviour of plain weave fabric composites made of twisted yarns. *Compos. Part A Appl. Sci. Manuf.* (2002) 33:697–708.
- [7] Ito, M. and Chou, T.W. An analytical and experimental study of strength and failure behaviour of plain weave composites. *J. Compos. Mater.* (1998) 32:2–30.
- [8] Olave, M., Vanaerschot, A., Lomov, S.V. and Vandepitte, D. Internal geometry variability of the stiffness. *Polym. Compos.* (2012) 33:1335-1350.
- [9] Olave, M., Vara, I., Husabiaga, H., Aretxabaleta, L., Lomov, S.V. and Vandepitte, D. Nesting effect on the mode I fracture toughness of woven laminates. *Compos. Part A Appl. Sci. Manuf.* (2015) 74:166-173.
- [10] Suquet, P.M. Elements of homogenization for inelastic solid mechanics. In: Sanchez-Palencia E., Zaoui, A., editors. *Homogenization techniques for composite media, lecture notes in physics*, 272. Berlin: Springer-Verlag; 1987.
- [11] Takano, N., Uetsuji, Y., Kashiwagi, Y. and Zako, M. Hierarchical modeling of textile composite materials and structures by the homogenization method. *Model. Simul. Mater. Sci. Eng.* (1999) 7:207-231.
- [12] Zako, M., Uetsuji. Y. and Kurashiki. T. Finite element analysis of damaged woven fabric composite materials. *Compos. Sci. Technol.* (2003) 63:507-516.
- [13] Carvelli, V., Poggi, C. A homogenization procedure for the numerical analysis of woven fabric composites. *Compos. Part A Appl. Sci. Manuf.* (2001) 32:1425-1432.
- [14] Matsuda, T., Nimiya, Y., Ohno, N. and Tokuda, M. Elastic-viscoplastic behavior of plain-woven GFRP laminates: Homogenization using reduced domain of analysis. *Compos. Struct.* (2007) 79:493-500.
- [15] Matsuda, T., Kanamaru, S., Yamamoto, N. and Fukuda, Y. A homogenization theory for elastic-viscoplastic materials with misaligned internal structures. *Int. J. Plast.* (2011) 27:2056-2067.

- [16] Matsuda, T., Kanamaru, S., Honda, N., Ohno, N. Macro/micro elastic-viscoplastic analysis of woven composite laminates with misaligned woven fabrics. *Adv. Struct. Mater.* (2013) 19:251-261.
- [17] Hivet, G. and Boisse, P. Consistent 3D geometrical model of fabric elementary cell. Application to a meshing preprocessor for 3D finite element analysis. *Finite. Elem. Anal. Des.* (2005) 42:25-49.
- [18] Faes, J.C., Rezaei, A., Paepegem, W. V. and Degrieck, J. Accuracy of 2D FE models for prediction of crack initiation in nested textile composites with inhomogeneous intra-yarn fiber volume fraction. *Compos. Struct.* (2016) 140:11-20.
- [19] Kim, J.H., Ryou, H., Lee, M., Chung, K., Youn, J.R. and Kang, T.J. Micromechanical modeling of fiber reinforced composites based on elastoplasticity and its application for 3D braided Glass/Kevlar composites. *Polym. Compos.* (2007) 28:722-732.
- [20] Potter, E., Pinho, S.T., Robinson, P., Lannucci, L. and McMillan, A.J. Mesh generation and geometrical modelling of 3D woven composites with variable tow cross-section. *Comp. Mater. Sci.* (2012) 51:103-111.
- [21] Ohno, N., Wu, X. and Matsuda, T. Homogenized properties of elastic-viscoplastic composites with periodic internal structures. *Int. J. Mech. Sci.*(2000) 42:1519-1536.
- [22] Ohno, N., Matsuda, T. and Wu, X. A homogenization theory for elastic-viscoplastic composites with point symmetry of internal distributions. *Int. J. Solids. Struct.*(2001) 38:2867-2878.
- [23] Matsuda, T., Ohno, N., Tanaka, H. and Shimizu, T. Effects of fiber distribution on elastic-viscoplastic behavior of long fiber-reinforced laminates. *Int. J. Mech. Sci.* (2003) 45:1583-1598.
- [24] Ilchev, A., Marcadon, V., Kruch, S. and Forest, S. Computational homogenisation of periodic cellular materials: Application to structural modeling. *Int J Mech. Sci.* (2015) 93:240-255.

A Control Volume Finite Element Approach for Modeling Molten Corium Spreading and Solidification

Alec Kucala^{*}, Rekha Rao^{**}, Lindsay Erickson^{***}, David Noble^{****}

^{*}Sandia National Laboratories, ^{**}Sandia National Laboratories, ^{***}Sandia National Laboratories, ^{****}Sandia National Laboratories

ABSTRACT

When the core is breached during a severe nuclear accident, a molten mixture of nuclear fuel, cladding, and structural supports is discharged from the reactor vessel, which is often referred to as “corium”. This scenario poses a difficult modeling problem due to the presence of large Peclet and Reynolds numbers, whereby the standard Galerkin based finite-element method (GFEM) technique is inadequate in suppressing the spurious oscillations in the mass, momentum, and energy equations. To address these oscillations, we implement a control volume finite element method (CVFEM) which allows for an upwinding treatment of the advection terms in the momentum and energy equations. Modeling the spreading of molten corium also requires a robust and accurate representation of the corium/air interface in two- and three-dimensions. To accomplish this, the conformal decomposition finite element method (CDFEM) is utilized to dynamically discretize the moving interface, allowing for the direct application of boundary conditions at the melt/air interface, such as surface tension and radiative energy transfer to the surrounding air. This CVFEM-CDFEM approach is used to model the spreading of molten corium in two- and three-dimensions, where the solidification of the melt is modeled using a temperature-dependent viscosity model. First, it is shown that the CVFEM technique is able to suppress spurious oscillations that GFEM cannot, where upwinding is introduced in the advection terms of the level set, momentum and energy equations. Our model is then compared directly with the FARO L26 corium spreading experiments and with previous numerical simulations in two- and three-dimensions. In these comparisons, good agreement is obtained with the evolution of the time-dependent corium spreading front.

Evaluation of Vehicle Aerodynamic Performance with Lane Change and Passing Using CFD and MBD

Toshifumi Kudo*

*Altair Engineering

ABSTRACT

Evaluation of aerodynamic performance using Wind Tunnels and CFD analysis conducted in each OEMs has great contribution to improve fuel consumption and performance of automobiles. The CFD has become more detail and has been able to solve a bigger scale problem in every year, a deviation between experimental and analysis results almost negligible and it is an effective tool for design and development process. However, is it enough to perform only Wind Tunnel experiments and CFD? Cross wind and air flow coming from various kind of other vehicles has a significant impact in actual driving. Furthermore, a vehicle posture changes due to the influence of air flow. That flow changes as the change of the vehicle attitude. Thus, in fact it is more complicated and fundamentally different from Wind Tunnel experiments. In principle, in order to better understand a physical phenomenon occurred, it is important to grasp a complex physical phenomenon rather than only solve a particular phenomenon. However, since governing equations vary in every physical phenomenon, it is important to couple each one. For this reason, this research aims to carry out analysis in a real condition and thus, the coupled analysis of mechanical and fluid is performed. As an example, we assume the following situation. Two cars are moving while receiving crosswinds, the latter vehicle changes its lanes and passing thru the front run vehicle. The vehicle has a steering and suspension system and the vehicle attitude changes as the change of the wind or lane. In order to carry out the simulation with taking all these conditions into consideration, the suspension and steering mechanism are included in Driver model of Multibody Dynamics analysis(MBD). It is then required to simulate the fluid flowing around the vehicle and to solve them simultaneously. In MBD we calculate displacement of the tire, steering, vehicle attitude, and store the displacement results to the CFD side. The CFD solver calculates the air flow using the calculated displacements obtained by MBD. At the end, force and moment are applied to the vehicle and we alternately performs this analysis through Multibody Dynamics analysis. Based on this simulation, it is now possible to estimate behavior of the vehicle which is not actually obtained by Wind Tunnel experiments including the influence of air flow from side wind, other vehicles. It is expected to be useful method in the product development process with higher accuracy and higher efficiency.

ON NON-UNIFORM TORSION IN FGM BEAM STRUCTURES AND THE EXTRACTION OF RELEVANT STIFFNESS QUANTITIES BASED ON SAFE

STEPHAN KUGLER*, PETER A. FOTIU* AND JUSTIN MURIN†

*University of Applied Sciences Wiener Neustadt,
Department of Applied and Numerical Mechanics, Austria
kugler@fhwn.ac.at; www.fhwn.ac.at

†Slovak University of Technology in Bratislava, FEI, Institute of Automotive Mechatronics,
Department of Applied Mechanics and Mechatronics, Slovak Republic
justin.murin@stuba.sk; www.stuba.sk

Key words: Non-uniform torsion; Vlasov's theory of torsion; Bescoter-related theory of torsion; Identification of stiffness parameters; SAFE

Abstract. All but axi-symmetric cross-sections warp during torsion, i.e. the cross-section deforms axially, and a warping or non-uniform theory of torsion has to be applied. Since the corresponding influence is severe in thin-walled open profiles much of the literature only covers thin-walled cross sections by Vlasov's theory of torsion. In this paper the classical Vlasov - theory is generalized to end up in a model similar to Bescoter's theory which is shown to be more accurate. A procedure to evaluate all arising stiffness quantities in arbitrarily shaped cross-sections accompanied with arbitrarily distributed constitutive parameters is proposed based on a reference beam problem in connection with semi-analytical finite elements. For the proposed theories of warping torsion effective finite beam elements are derived, and challenging benchmark-problems show the accuracy and the efficiency of the proposed formulations.

1 INTRODUCTION

Beam structures made of a Functionally Graded Materials (FGMs) show location dependent material parameters throughout their arbitrarily shaped cross-section. The load case of torsion introduces warping of the cross-section and a non-uniform theory of torsion has to be applied to achieve accurate solutions using one-dimensional finite elements. Starting with a suitable kinematic assumption where the cross-section rotates rigidly in its projection plane pivoting at the shear or drill center, the axial motion of a generic point is quantified based on an unknown warping function (depending

on the cross-section coordinates) multiplied with an axial field quantifying the amount of warping. The well-known and frequently applied Vlasov's theory of torsion [1] uses the first derivative of torsion angle φ'_x to quantify warping axially. This leads to two independent stiffness quantities (torsion stiffness and warping stiffness) which have to be identified in connection with one fourth order ordinary differential equation (ODE).

Alternatively, if the axial distribution of warping may be related to a yet unknown independent field rather than to the rate of twist, we end up with two coupled second order ODEs with four stiffness quantities. Such a calculation strategy is similar to the theory of Benscoter [3]. It can be shown by example that this theory leads to more accurate results compared to Vlasov's theory, especially for thick shafts. While the analytical evaluations regarding a set of two coupled ODEs are somewhat more involved very efficient finite beam elements can be derived based on linear shape functions. The evaluations of the related stiffness quantities can be carried out using a reference beam problem of arbitrary length in connection with three dimensional elasticity solutions where semi-analytical finite elements (SAFE) are applied. Due to SAFE and a specialized load case for the reference problem a true dimensional reduction is achieved and stress distributions, relevant cross-section parameters and stiffness quantities are accessible based on discretization of the cross-section only [2].

2 THEORY OF NON-UNIFORM TORSION

Under torsion any cross-section rotates about a specific location¹ with respect to the axial direction. The torsional angle $\varphi_x(x)$ is found from a differential equation which is derived from suitable kinematic hypotheses, the strain displacement relations and the constitutive equations. The derivation is based on the principle of virtual work which is well suited to generate two-noded finite elements. If a cross-section warps during torsional loading the points of the cross-section undergo axial displacements u_x . The displacement field $u_x(x, y, z)$ at a specific cross-section x is assumed in a multiplicative form,

$$u_x(x, y, z) = F(x)\omega(y, z), \quad (1)$$

where $\omega(y, z)$ is the warping function. Figure 1 depicts the kinematics of torsion problems: There, we model an arbitrary cross-section with arbitrary material distributions in the y_m - z_m , where the elastic center C (decoupling axial from bending deformations) and the shear center S (congruent with the drill center) is known (see [2]). The origin of the beam's coordinate system is located at C and the y - and z -axis is directed into the cross-sections principal directions. Any other orientation of the corresponding coordinate system might be possible without any further complexities for torsional loading, however, in light of shear force bending such an orientation is typically suggested. We then assume that the cross-section rotates rigidly about the shear (or drill) center S in terms of the torsional angle $\varphi_x(x)$ and a generic point of the cross-section undergoes axial deformations,

¹This specific location is called the drill center S and is congruent with the shear center of the cross-section which decouples torsion from shear force bending.

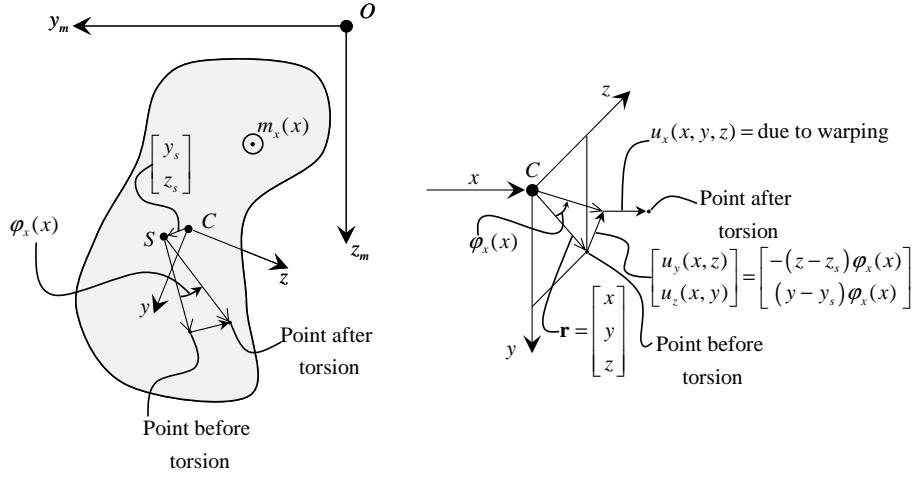


Figure 1: Kinematics of torsion

i.e. the cross-section is assumed to be rigid in its projection plane (any distortional deformations are neglected) but warps axially. According to the assumption (1) Vlasov assumes $F(x) = \varphi'_x(x)$ while the Bencoter theory leaves $F(x)$ to be determined. Hence, we have,

$$\text{Vlasov: } u_x(x, y, z) = \omega(y, z) \varphi'_x(x), \quad (2)$$

$$\text{Bencoter: } u_x(x, y, z) = \omega(y, z) F(x). \quad (3)$$

2.1 Vlasov's theory of torsion

According to Fig. 1 a generic point of the cross-section at x with the position vector $\mathbf{r} = [x \ y \ z]^T$ displaces in the cross-section according to

$$u_y(x, z) = -(z - z_s) \varphi_x(x), \quad (4)$$

$$u_z(x, y) = (y - y_s) \varphi_x(x), \quad (5)$$

where $\varphi_x(x)$ denotes the torsional angle and displaces out of that plane according to (2). Based on the above described kinematics we evaluate the strain fields according to the strain displacement relations,

$$\epsilon_{xx}(x, y, z) = \frac{\partial u_x(x, y, z)}{\partial x} = \omega(y, z) \varphi''_x(x), \quad (6)$$

$$\epsilon_{yy} = \frac{\partial u_y(x, z)}{\partial y} = 0, \quad \epsilon_{zz} = \frac{\partial u_z(x, y)}{\partial z} = 0, \quad (7)$$

$$\begin{aligned}\gamma_{xy}(x, y, z) &= \frac{\partial u_x(x, y, z)}{\partial y} + \frac{\partial u_y(x, z)}{\partial x} = \\ &= \left(\frac{\partial \omega(y, z)}{\partial y} - (z - z_s) \right) \varphi'_x(x) = (\omega_{,y} - (z - z_s)) \varphi'_x(x),\end{aligned}\quad (8)$$

$$\begin{aligned}\gamma_{xz}(x, y, z) &= \frac{\partial u_x(x, y, z)}{\partial z} + \frac{\partial u_z(x, y)}{\partial x} = \\ &= \left(\frac{\partial \omega(y, z)}{\partial z} + (y - y_s) \right) \varphi'_x(x) = (\omega_{,z} + (y - y_s)) \varphi'_x(x),\end{aligned}\quad (9)$$

$$\gamma_{yz} = \frac{\partial u_y(x, z)}{\partial z} + \frac{\partial u_z(x, y)}{\partial y} = -\varphi_x(x) + \varphi_x(x) = 0, \quad (10)$$

and the non-vanishing stress fields are found according to the constitutive relations,

$$\sigma_{xx}(x, y, z) = E(y, z)\epsilon_{xx}(x, y, z) = E(y, z)\omega(y, z)\varphi''_x(x), \quad (11)$$

$$\tau_{xy}(x, y, z) = G(y, z)\gamma_{xy}(x, y, z) = G(y, z)(\omega_{,y} - (z - z_s))\varphi'_x(x), \quad (12)$$

$$\tau_{xz}(x, y, z) = G(y, z)\gamma_{xz}(x, y, z) = G(y, z)(\omega_{,z} + (y - y_s))\varphi'_x(x), \quad (13)$$

where isotropy at each material point is understood (Young's modulus E and shear modulus G). Using the principle of virtual work $\delta W_a + \delta W_i = 0$ with prescribed kinematic boundary conditions at both beam ends ($\delta\varphi_x(0) = \delta\varphi_x(l) = \delta\varphi'_x(0) = \delta\varphi'_x(l) = 0$) we have an external load due to a line moment $m_x(x)$ [N],

$$\int_l m_x(x)\delta\varphi_x(x)dx - \int_V \sigma_{xx}\delta\epsilon_{xx}dV - \int_V \tau_{xy}\delta\gamma_{xy}dV - \int_V \tau_{xz}\delta\gamma_{xz}dV = 0, \quad (14)$$

and further,

$$\begin{aligned}& \int_l m_x(x)\delta\varphi_x(x)dx - \underbrace{\int_l \int_A E(y, z)\omega^2(y, z)dA \varphi''_x(x)\delta\varphi''_x(x)dx}_{=E_TC_\omega} - \\ & - \underbrace{\int_l \int_A G(y, z) [(\omega_{,y} - (z - z_s))^2 + (\omega_{,z} + (y - y_s))^2] dA \varphi'_x(x)\delta\varphi'_x(x)dx}_{=G_T I_T} = 0,\end{aligned}\quad (15)$$

where warping stiffness E_TC_ω [Nm⁴] and the torsional stiffness $G_T I_T$ [Nm²] are defined. Applying integration by parts,

$$\int_l m_x(x)\delta\varphi_x(x)dx - \int_l E_TC_\omega\varphi_x''''(x)\delta\varphi_x(x)dx + \int_l G_T I_T\varphi_x''(x)\delta\varphi_x(x)dx =$$

$$= \int_l \left(m_x(x) - E_T C_\omega \varphi_x''''(x) + G_T I_T \varphi_x''(x) \right) \delta \varphi_x(x) dx = 0, \quad (16)$$

delivers for arbitrary variations of the torsional angle the describing differential equation for warping torsion,

$$E_T C_\omega \varphi_x''''(x) - G_T I_T \varphi_x''(x) = m_x(x). \quad (17)$$

2.2 A Bencoter related theory of torsion

In Bencoter's theory [3] the kinematics are assumed according to (1)

$$u_x(x, y, z) = \omega(y, z) F(x), \quad (18)$$

and

$$u_y(x, z) = -(z - z_s) \varphi_x(x), \quad u_z(x, y) = (y - y_s) \varphi_x(x), \quad (19)$$

where axial warping deformations vary according to an unknown function $F(x)$ along the beam's axis. This approach is also discussed in [4]. The non-vanishing strain fields read,

$$\epsilon_{xx}(x, y, z) = \frac{\partial u_x(x, y, z)}{\partial x} = \omega(y, z) F'(x), \quad (20)$$

$$\gamma_{xy}(x, y, z) = \frac{\partial u_x(x, y, z)}{\partial y} + \frac{\partial u_y(x, z)}{\partial x} = \omega_{,y} F(x) - (z - z_s) \varphi_x'(x), \quad (21)$$

$$\gamma_{xz}(x, y, z) = \frac{\partial u_x(x, y, z)}{\partial z} + \frac{\partial u_z(x, y)}{\partial x} = \omega_{,z} F(x) + (y - y_s) \varphi_x'(x), \quad (22)$$

and the stress fields are

$$\sigma_{xx}(x, y, z) = E(y, z) \epsilon_{xx}(x, y, z) = E(y, z) \omega(y, z) F'(x), \quad (23)$$

$$\tau_{xy}(x, y, z) = G(y, z) \gamma_{xy}(x, y, z) = G(y, z) \left(\omega_{,y} F(x) - (z - z_s) \varphi_x'(x) \right), \quad (24)$$

$$\tau_{xz}(x, y, z) = G(y, z) \gamma_{xz}(x, y, z) = G(y, z) \left(\omega_{,z} F(x) + (y - y_s) \varphi_x'(x) \right). \quad (25)$$

The principle of virtual work with the kinematic variables φ_x and F gives for prescribed kinematic variables at both beam ends ($\delta \varphi_x(0) = \delta \varphi_x(l) = \delta F(0) = \delta F(l) = 0$),

$$\begin{aligned} & \int_l m_x(x) \delta \varphi_x(x) dx - \int_l \int_A E(y, z) \omega^2(y, z) dA F'(x) \delta F'(x) dx - \\ & - \int_l \int_A G(y, z) \omega_{,y}^2 dA F(x) \delta F(x) dx + \end{aligned}$$

$$\begin{aligned}
 & + \int_l \int_A G(y, z) \omega_{,y} (z - z_s) dA \left(F(x) \delta \varphi'_x(x) + \varphi'_x(x) \delta F(x) \right) dx - \\
 & - \int_l \int_A G(y, z) (z - z_s)^2 dA \varphi'_x(x) \delta \varphi'_x(x) dx - \int_l \int_A G(y, z) \omega_{,z}^2 dA F(x) \delta F(x) dx - \\
 & - \int_l \int_A G(y, z) \omega_{,z} (y - y_s) dA \left(F(x) \delta \varphi'_x(x) + \varphi'_x(x) \delta F(x) \right) dx - \\
 & - \int_l \int_A G(y, z) (y - y_s)^2 dA \varphi'_x(x) \delta \varphi'_x(x) dx = 0,
 \end{aligned} \tag{26}$$

which can be rewritten as,

$$\begin{aligned}
 & \int_l m_x(x) \delta \varphi_x(x) dx - \underbrace{\int_l \int_A E(y, z) \omega^2(y, z) dA F'(x) \delta F'(x) dx}_{=E_T C_\omega} - \\
 & - \underbrace{\int_l \int_A G(y, z) (\omega_{,y}^2 + \omega_{,z}^2) dA F(x) \delta F(x) dx}_{=K_1} - \\
 & - \underbrace{\int_l \int_A G(y, z) ((y - y_s) \omega_{,z} - (z - z_s) \omega_{,y}) dA \left(F(x) \delta \varphi'_x(x) + \varphi'_x(x) \delta F(x) \right) dx}_{=K_2} - \\
 & - \underbrace{\int_l \int_A G(y, z) ((y - y_s)^2 + (z - z_s)^2) dA \varphi'_x(x) \delta \varphi'_x(x) dx}_{=K_3} = 0,
 \end{aligned} \tag{27}$$

defining four stiffness quantities, $E_T C_\omega$ and K_i for $i = 1, 2, 3$. Note, that (27) coincides with (15) if $F(x) = \varphi'_x(x)$ is and

$$G_T I_T = K_1 + 2K_2 + K_3. \tag{28}$$

Integrating (27) by parts yields,

$$\begin{aligned}
 & \int_l m_x(x) \delta \varphi_x(x) dx + \int_l E_T C_\omega F''(x) \delta F(x) dx - \int_l K_1 F(x) \delta F(x) dx - \\
 & - \int_l K_2 \left(-F'(x) \delta \varphi_x(x) + \varphi'_x(x) \delta F(x) \right) dx + \int_l K_3 \varphi''_x(x) \delta \varphi_x(x) dx = 0,
 \end{aligned} \tag{29}$$

giving the Euler-Lagrange equations representing a system of coupled differential equations²,

$$m_x(x) + K_2 F'(x) + K_3 \varphi_x''(x) = 0, \quad (30)$$

$$E_T C_\omega F''(x) - K_1 F(x) - K_2 \varphi_x'(x) = 0. \quad (31)$$

Note that the strong form (30) (31) cannot be converted into the formulation (15) anymore and different results are expected.

3 EVALUATION OF STIFFNESS QUANTITIES AND STRESS DISTRIBUTIONS BASED ON SAFE

The identification of relevant stiffness quantities (warping stiffness $E_T C_\omega$ and torsional stiffness $G_T I_T$ (15) accompanied with K_i for $i = 1, 2, 3$ (27)) is performed on a reference beam problem (modeled in the y_m - z_m coordinate system) of arbitrary length l_{RB} which is analyzed by a three-dimensional elasticity formulation and the procedures discussed in [2]. The beam is assumed to rest on fork supports, i.e. $\varphi_x = \sigma_{xx} = 0$ at both beam ends. Transverse volume forces f_i for $i = y_m, z_m$ are applied (varying as a sine function with $\alpha = n\pi/l_{RB}$, $n = 1$)

$$f_{y_m} = f_{y_{m0}} \sin(\alpha x_m) = (b_{y0} + b_{yy} y_m + b_{yz} z_m) E(y_m, z_m) \sin(\alpha x_m), \quad (32)$$

$$f_{z_m} = f_{z_{m0}} \sin(\alpha x_m) = (b_{z0} + b_{zy} y_m + b_{zz} z_m) E(y_m, z_m) \sin(\alpha x_m), \quad (33)$$

which are scaled by the location dependent Young's modulus $E(y_m, z_m)$. The constant quantities $b_{uv} \neq b_{vu}$ with $u = y, z$ and $v = 0, y, z$ are unknowns at this stage, however, they can be identified by requiring that the reference beam problem has to react as shaft. Hence, we require

$$q_{y_{m0}} = \int_A f_{y_{m0}} dA = 0 \quad (34)$$

$$q_{z_{m0}} = \int_A f_{z_{m0}} dA = 0 \quad (35)$$

$$m_{x0} = \int_A (y_m f_{z_{m0}} - z_m f_{y_{m0}}) dA = 1 \quad (36)$$

We thus have three equations with six unknown parameters which can be solved by the Moore-Penrose pseudo-inverse. The mean torsional angle amplitude can be evaluated,

$$\bar{\varphi}_x = b_{y0} \bar{\varphi}_x^{b_{z0}} + b_{yy} \bar{\varphi}_x^{b_{zy}} + b_{yz} \bar{\varphi}_x^{b_{zz}} + b_{z0} \bar{\varphi}_x^{b_{z0}} + b_{zy} \bar{\varphi}_x^{b_{zy}} + b_{zz} \bar{\varphi}_x^{b_{zz}}, \quad (37)$$

²This formulation introduces four stiffness parameters, but it can be shown that $K_1 = -K_2$ if the same warping function ω is used for either Vlasov's theory or the Benscoter-related theory.

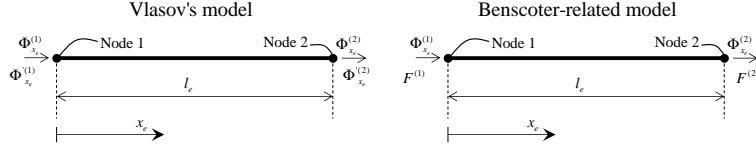


Figure 2: Two-noded beam finite element for Vlasov's and Benscoter's theory of torsion

where $\bar{\varphi}_x^{b_{uv}}$ denote the mean value of torsional angle with respect to the cross-section's area evaluated from the reference beam problem due to the application of b_{uv} only (see [2] for additional details). According to Vlasov's theory the out of plane motion,

$$u_x(x, y_m, z_m) = \omega(y_m, z_m) \varphi'_x(x), \quad (38)$$

is proportional to $\varphi'_x(x)$ and we find the nodal warping amplitudes ω as

$$\omega = \frac{\mathbf{U}_x}{\alpha \bar{\varphi}_x} = \frac{\sum_{u=y}^z \sum_{v=0}^z b_{uv} \mathbf{U}_x^{b_{uv}}}{\alpha \bar{\varphi}_x}. \quad (39)$$

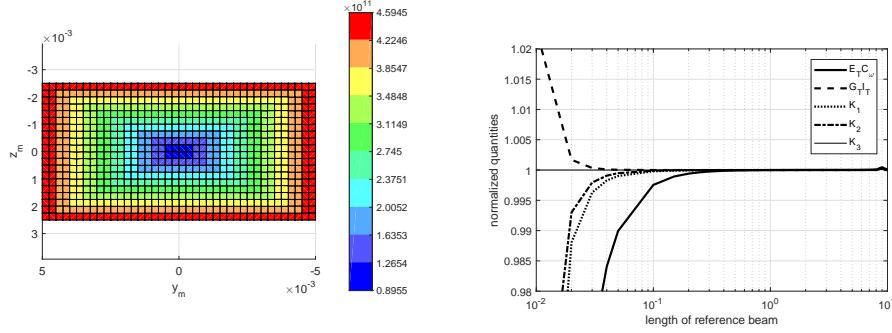
Once the warping distribution is at hand all stiffness properties can be evaluated. As a side product axial and shear stress distributions due to a unity torsional moment and unity bimoment $M_\omega = \int_A \omega \sigma_{xx} dA$ are found without any additional effort. The reference beam problem is analyzed by semi-analytical finite elements (SAFE) (see [2, 5]) where only the cross-section of the beam has to be discretized since axial variations are assumed to be analytical functions. The only remaining free parameter of the reference problem is the length of the reference beam l_{RB} , where it can be shown that accurate solutions can be achieved for $10r < l_{RB} < 500r$, where r denotes a characteristic geometrical dimension of the actual cross-section. For $l_{RB} < 10r$ beam theory is no longer accurate since cross-sectional distortions become important. For lengths $l_{RB} > 500r$ some numerical problems regarding SAFE start to emanate.

4 FINITE ELEMENT FORMULATIONS

In this section we present very briefly a two-noded beam finite element of length l_e for both theories (see Fig. 2). The nodal degrees of freedom are the torsional angle Φ_x and either Φ'_x or F . We use polynomial shape functions (cubic for Vlasov's theory and linear for Benscoter's model). This yields to the following equations

Vlasov:

$$\left\{ \frac{E_T C_\omega}{l_e^3} \begin{bmatrix} 12 & 6l_e & -12 & 6l_e \\ 6l_e & 4l_e^2 & -6l_e & 2l_e^2 \\ -12 & -6l_e & 12 & -6l_e \\ 6l_e & 2l_e^2 & -6l_e & 4l_e^2 \end{bmatrix} + \frac{G_T I_T}{30l_e} \begin{bmatrix} 36 & 3l_e & -36 & 3l_e \\ 3l_e & 4l_e^2 & -3l_e & -l_e^2 \\ -36 & -3l_e & 36 & -3l_e \\ 3l_e & -l_e^2 & -3l_e & 4l_e^2 \end{bmatrix} \right\} \begin{bmatrix} \Phi_{x_e}^{(1)} \\ \Phi_{x_e}^{'(1)} \\ \Phi_{x_e}^{(2)} \\ \Phi_{x_e}^{'(2)} \end{bmatrix} = \frac{m_{x0} l_e}{2} \begin{bmatrix} 1 \\ l_e/6 \\ 1 \\ -l_e/6 \end{bmatrix}. \quad (40)$$



(a) Distribution of Young's modulus in rectangular FGM cross-section (b) Convergence characteristic for either parameters with respect to large variations of RB-lengths

Figure 3: Rectangular FGM cross-section

Benscoter:

$$\begin{bmatrix} \frac{K_3}{l_e} & -\frac{K_2}{2} & -\frac{K_3}{l_e} & -\frac{K_2}{2} \\ -\frac{K_2}{2} & \frac{K_1 l_e}{\chi_1} + \frac{E_T C_\omega}{l_e} & \frac{K_2}{2} & \frac{K_1 l_e}{\chi_2} - \frac{E_T C_\omega}{l_e} \\ -\frac{K_3}{l_e} & \frac{K_2}{2} & \frac{K_3}{l_e} & \frac{K_2}{2} \\ -\frac{K_2}{2} & \frac{K_1 l_e}{\chi_2} - \frac{E_T C_\omega}{l_e} & \frac{K_2}{2} & \frac{K_1 l_e}{\chi_1} + \frac{E_T C_\omega}{l_e} \end{bmatrix} \begin{bmatrix} \Phi_{x_e}^{(1)} \\ F_{x_e}^{(1)} \\ \Phi_{x_e}^{(2)} \\ F_{x_e}^{(1)} \end{bmatrix} = \frac{m_{x0} l_e}{2} \begin{bmatrix} 1 \\ 0 \\ 1 \\ 0 \end{bmatrix} \quad (41)$$

The constants χ_1 and χ_2 in equation (40) depend on the order of integration,

$$\text{Full integration (2 Gauss-points) : } \chi_1 = 3, \chi_2 = 6, \quad (42)$$

$$\text{Reduced integration (1 Gauss-point) : } \chi_1 = \chi_2 = 4. \quad (43)$$

It can be shown by example that the selectively reduced formulation converges much faster since locking effects are resolved.

5 EXAMPLE, RESULTS AND DISCUSSION

For sake of space only one example can be described here where we consider a rectangular cross-section (height $h = 5 \cdot 10^{-3}$, width $w = 10 \cdot 10^{-3}$) which is made from pure aluminum (Al6061-TO, $E = 69\text{GPa}$, $\nu = 0.33$) in the core and pure titancarbid (TiC, $E = 480\text{GPa}$, $\nu = 0.33$) at the outer surfaces. Due to Murin et al. [8] the variation of the material properties is assumed to be linear in both transverse directions (see Fig. 3a where ten layers are used to approximate the continuous distribution). The mesh density defines the model of the continuous variation of Young's modulus, i.e. the continuous variation is approximated by layers of one element horizontally and two elements vertically. It is shown in [8] that the application of ten layers delivers good accuracy regarding the stiffness quantities which are evaluated using a completely different procedure compared to

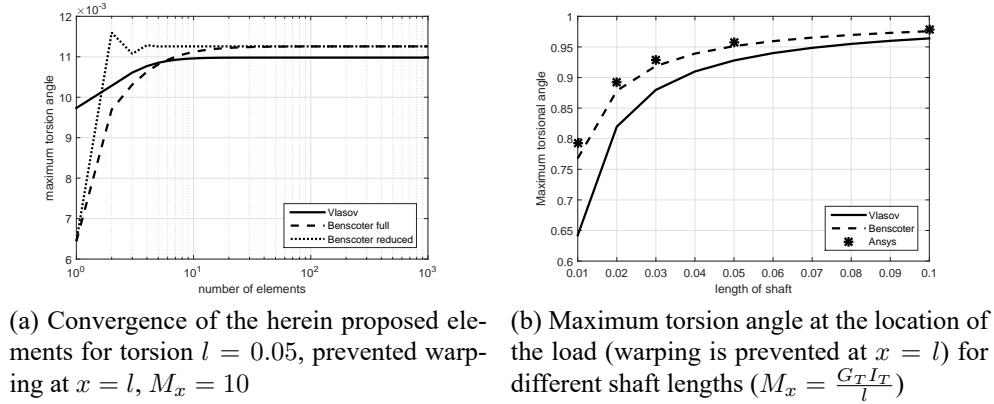


Figure 4: Results in a clamped shaft

the present one. The stiffness quantities are found using the proposed procedure and $l_{RB} = 1$ as the length of the reference beam ($E_T C_\omega = 1.3727e - 04$, $G_T I_T = 42.2540$, $K_1 = 35.3680$, $K_2 = -35.3681$ and $K_3 = 77.6221$). The convergence characteristic over a wide range of reference beam lengths is shown in Fig. 3b which indicates a relative error of less than two percent within an interval of $0.04 < l_{RB} < 5$ (all quantities are normalized to the corresponding ones using $l_{RB} = 1$).

Using these stiffness parameters we analyze the torsional behavior of a shaft of length l which is clamped at $x = 0$ ($\varphi_x = 0$ and $u_x = 0$) and loaded with a torsion moment M_x at $x = l$. Reference solutions are found using Ansys (regular mesh of linear brick elements with enhanced strain formulation, edge length: $0.25 \cdot 10^{-3}$) where the load is applied using a rigid contact with pilot (RBE2 element) and a concentrated torsional moment on the pilot node. The application of the load using an RBE2 element causes restrained warping at $x = l$. The corresponding outcome indicates good agreement of both theories of torsion compared to Ansys. Nevertheless, Vlasov's theory of torsion delivers a relative error of three percent while Benscoter's theory leads to 0.6 percent relative error for $l = 0.1$ and $l = 0.05$. This indicates that Benscoter's theory is slightly more predictive in that problem. The convergence characteristic of the proposed finite beam elements regarding a shaft length of $l = 0.05$ for Vlasov's cubic element, Benscoter's fully integrated linear element and Benscoter's reduced integrated linear element are shown in Fig. 4a, where accurate results are indicated for more than ten elements (Benscoter's fully integrated linear element shows the worst convergence characteristic indicating two percent error for ten elements). The maximum torsional angle at the location of the load due to $M_x = \frac{G_T I_T}{l}$ is shown in Fig. 4b for different shaft length and compared to Ansys. As expected all results converge to $\varphi_x^{max} = 1$ for rather long shafts where warping is not important anymore (St. Venant problem), however, the system becomes stiffer in case of short shafts due to non-negligible warping effects. It turns out that the results due to the Benscoter-related model are much more accurate compared to Vlasov's model in the problem of short shafts.

6 ACKNOWLEDGMENT

This work has been supported by Grant Agency VEGA(Grant No. 1/0102/18).

References

- [1] V. Vlasov, Thin walled elastic beams, National Science Foundation, Washington, 1961.
- [2] S. Kugler, P. Fotiu, J. Murin, The application of safe to extract relevant stiffness quantities for efficient modelling of fgm beam structures - axial deformations and shear force bending, 13th World Congress on Computational Mechanics (WCCM XIII) and 2nd Pan American Congress on Computational Mechanics (PANACM II), July 22-27, 2018, New York City, NY, USA.
- [3] S. Benscoter, A theory of torsion bending for multicell beams, Journal of Applied Mech (1954) 25–34.
- [4] K. Saade, Finite Element Modeling of Shear in Thin Walled Beams with a Single Warping Function, PhD Thesis University of Bruxelles, 2004.
- [5] O. C. Zienkiewicz, R. L. Taylor, Finite Element Method: Volume 2, Solid Mechanics (Finite Element Method), Butterworth-Heinemann, 2000.
- [6] E. Onate, Structural Analysis with the Finite Element Method - Linear Statics - Volume 1: Basis and Solids, Springer, 2009.
- [7] E. Dvorkin, D. Celentano, A. Cuitino, G. Gioia, A vlasov beam element, Computers & Structures 33 (1989) 187–196.
- [8] J. Murin, M. Aminbaghai, J. Hrabovsky, R. Gogola, S. Kugler, Beam finite element for modal analysis of FGM structures, Engineering Structures (2016) 1–18.

Phase Field Modeling of Cracks in Heterogeneous Materials

Charlotte Kuhn^{*}, Ralf Müller^{**}

^{*}University of Kaiserslautern, ^{**}University of Kaiserslautern

ABSTRACT

One of the reasons why the phase field approach has become very popular for modeling fracture processes is that therein the entire evolution of fracture follows from energetic principles without the need for different criteria for crack initiation, nucleation, kinking or branching. Furthermore, these models allow for a straightforward numerical implementation with standard finite elements, since displacement jumps and stress singularities are avoided in these models. Consequently, phase field fracture models are now also used to model and simulate fracture of heterogeneous materials such as composites, where cracks may be arrested, deflected or bifurcated at interfaces between the different components of the composite material, resulting in complicated crack patterns. The crack propagation is not only controlled by the elastic and fracture properties of the bulk phases of the material but also by the properties of the interfaces in between. Thus, it is crucial to take these interface properties into account, and there are conceptually different approaches on how to integrate them into phase field fracture models. In [1] interfaces are modeled as zones of finite width with appropriately adjusted fracture parameters. Contrary, a combination with a cohesive type of modeling interface fracture is proposed in [2]. Another approach, which makes use of a new energetic formulation mixing bulk and cohesive surface energies, is proposed in [3]. In this work, interfaces are equipped with a fracture energy corresponding to the phase field fracture energy of the bulk phases in order to model the interface fracture properties. In the finite element implementation, the interfaces are modeled by means of surface elements without introducing additional degrees of freedom. The convergence behavior of the proposed model with respect to the sharp interface limit of the phase field fracture model as well as energy release rates during crack propagation are analyzed in numerical studies in order to verify the model. [1] A.C. Hansen-Dörr, P. Hennig, M. Kästner, K. Weinberg: A numerical analysis of the fracture toughness in phase-field modelling of adhesive fracture. *Proc. Appl. Math. Mech.* (submitted), 2017. [2] C.V. Verhoosel, R. de Borst: A phase-field model for cohesive fracture. *Int. J. Numer. Meth. Engng* 2013, 96:43-62 [3] T.T. Nguyen, J. Yvonnet, Q.-Z. Zhu, M. Bornert, C. Chateau: A phase-eld method for computational modeling of interfacial damage interacting with crack propagation in realistic microstructures obtained by microtomography. *Comput. Methods Appl. Mech. Engrg.* 2015, 312: 567-595

Augmented Total-FETI Algorithm for Computationally Efficient Micromechanical Analysis of a Representative Volume Element

Nagesh Kulkarni*, BP Gautham**, Salil Kulkarni***

*TCS Research, Tata Consultancy Services Ltd. India, presently pursuing PhD at Mechanical Engineering Dept. IIT Bombay, India, **TCS Research, Tata Consultancy Services Ltd., India, ***Mechanical Engineering Dept., IIT Bombay, India

ABSTRACT

Representative Volume Element (RVE) is the smallest material volume that represents the material in terms of effective properties of interest. Analysis of a RVE is typically carried out to obtain response of material as a function of its underlying microstructure for a given load path. Periodic boundary conditions, which simulate the effect of embedding the RVE in a spatially infinite periodic structure, are commonly used in the analysis. They do not necessarily provide a good estimate of the effective properties if the size of the RVE is not very small as compared to the overall dimensions of the structure. The aim of this work is to develop an accurate and computationally efficient algorithm that effectively utilizes the principle of domain decomposition methods in a novel and natural way for estimating the effective properties of a periodic microstructure which is spatially finite in extent. The microstructure is assumed to be composed of a basic unit called cell which is spatially repeating. Instead of assuming the cell to be a RVE and applying periodic boundary conditions, the RVE is assumed to be composed of multiple identical cells glued together. It is then subjected to either uniform traction or uniform displacement boundary conditions as these are more representative of the actual boundary conditions in such case. A domain decomposition method called Total Finite Element Tearing and Interconnection (TFETI) method is used to perform the analysis. The proposed method of enlarging the size of the RVE using identical copies of the base cell and then using TFETI to computationally solve the problem is referred to as the Augmented TFETI method. Here subdomain level computations for the unit cell are directly used while performing calculations using the RVE. To demonstrate the applicability of the method, sample problem of finite size and having periodic microstructure is solved using the Augmented TFETI. It consists of a cell which has an eccentric hole embedded in an isotropic matrix. Uniform displacements are applied to the RVE's of increasing size. It is seen that the results obtained using RVE's of different sizes converge as the sizes of the RVEs increase. In addition the computational performance of the propose method is compared to that of using the standard finite element to solve problem with increased RVE size. It was also observed that the augmented TFETI is 50% computationally more efficient than the standard FEM applied to the RVE's with increased size.

EFFECT OF MICRON-SCALE CONSTITUTIVE AND DAMAGE MODELING ON MULTISCALE CRACK PREDICTION IN POLYMER-MATRIX COMPOSITE LAMINATES

Yuta Kumagai^a, Yoshiteru Aoyagi^b, and Tomonaga Okabe^a

^aDepartment of Aerospace Engineering, Tohoku University
6-6-01, Aramaki-Aza-Aoba, Aoba-ku, Sendai, Miyagi 980-8579, Japan
kumagai@plum.mech.tohoku.ac.jp

^bDepartment of Finemechanics, Tohoku University
6-6-01, Aramaki-Aza-Aoba, Aoba-ku, Sendai, Miyagi 980-8579, Japan

Key words: Multiscale Modeling, Polymer-Matrix Composites, Failure Prediction

Abstract. Damage accumulation on the fiber-diameter scale causes failure of carbon fiber-reinforced plastics (CFRPs). Therefore, microscopic damage prediction is important to evaluate structural safety of composite structures made from CFRPs. In this study, effect of matrix modeling on the fiber-diameter scale is investigated using a multiscale approach that consists of macroscopic and microscopic analyses. On the macroscopic analysis, laminate-scale finite-element analysis assuming each lamina to be a homogeneous body is conducted to obtain strain histories at failure-expected points. On the microscopic analysis, periodic unit-cell (PUC) analysis considering heterogeneity of materials is performed to predict initiation of crack in the matrix phase of CFRP, based on strain histories obtained from macroscopic analysis. Two constitutive models and four sets of failure criteria are applied to the matrix phase on the PUC analysis, and compared with each other to evaluate important factors in multiscale failure prediction of CFRP laminates.

1 INTRODUCTION

Carbon fiber reinforced plastics (CFRPs) have been widely applied to aircraft structures because of their excellent mechanical properties. In the structures made of CFRPs, the initial cracking strain has been utilized as one of the design criteria of structures. However, it is difficult to accurately predict the initial cracking strain due to structural features of CFRP laminate, such as stacking sequence, free surface, ply drop-off, and heterogeneous microscopic

structure. These structural features cause inhomogeneous stress fields in laminate, and affect fiber-diameter scale crack formation. Therefore, development of accurate multiscale analysis methods that can consider both macroscopic deformation behavior and microscopic material structure is desired.

Thermosetting or thermoplastic resin used for polymer-matrix composites exhibits nonlinear inelastic behavior with damage evolution^{1,2}. To predict such nonlinear deformation and damage evolution of polymers, various constitutive and damage models have been developed^{1,3-7}, and implemented into the fiber-diameter scale unit-cell analysis^{4,7-9}. These studies provide good understanding of micron-scale failure events in polymer-matrix composites. However, comprehensive evaluation of constitutive and damage models for the matrix phase of composites under practical loading conditions is still limited.

In this study, influence of constitutive models and failure criteria applied to matrix resin on crack prediction capability of multiscale analysis is investigated. Multiscale analysis, which consists of macroscopic finite-element (FE) analysis and microscopic periodic unit-cell (PUC) analysis, is developed. Two constitutive models and four sets of failure criteria are implemented to PUC analysis, and simulated results are compared with experiment in the previous studies to evaluate factors that need to consider for initial crack prediction in CFRP laminate.

2 SIMULATION METHOD

In this study, in order to evaluate important factors in failure criteria for the matrix phase of CFRP, constitutive models and failure criteria for microscopic crack prediction are examined through the comparison of simulated results with experiment data in the previous studies¹⁰. In this section, macroscopic FE analysis and microscopic PUC analysis are explained, and then two-scale simulation procedure is described.

2.1 Macroscopic FE analysis of unidirectional laminates

Unidirectional CFRP laminates under off-axis loading exhibit nonlinear stress-strain behavior because of plastic deformation of matrix resin. To reproduce this nonlinear behavior, macroscopic analysis is conducted based on an anisotropic elasto-plastic constitutive law proposed by Yokozeki et al.¹¹. Implementation of the constitutive law in multiscale analysis is described in the literature¹². The material properties used in the macroscopic analysis are listed in Table 1.

A schematic view of the computational model is presented in Fig. 1. The fiber angles of

Table 1 Elastic properties of unidirectional laminates used in macroscopic FE analysis.

Longitudinal Young's modulus E_1	151 GPa
Transverse Young's modulus E_2, E_3	9.16 GPa
Shear modulus G_{12}, G_{13}	4.62 GPa
Shear modulus G_{23}	2.55 GPa
Poisson's ratio ν_{12}, ν_{13}	0.302
Poisson's ratio ν_{23}	0.589

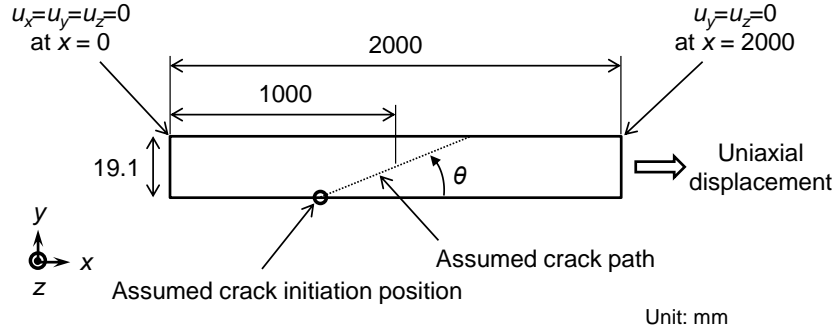


Fig.1 Schematic view of macroscopic FE analysis model.

unidirectional laminates are 10° , 20° , 25° , 30° , 35° , 40° , 45° , and 90° . The length of the computational model and the assumed initial cracking site are determined based on the literature^{12, 13, 14}. Incremental uniaxial displacement is applied to the edge of the analysis model with the displacement rate of 0.01 mm/s.

2.2 Microscopic periodic unit-cell analysis

To predict crack initiation under several loading conditions, a three-dimensional unit-cell model, which consists of five carbon fibers and matrix resin, is utilized. A FE model used for microscopic analysis is shown in Fig. 2. The carbon fiber is modeled as an orthotropic elastic body, and the matrix resin is modeled as an isotropic inelastic body explained later. The fiber diameter is 5 μm , and the fiber volume fraction is 56%. In this study, the interface between fiber and matrix resin is assumed to be perfectly bonding to focus on only matrix cracking. In addition, the periodic boundary condition is imposed on the unit-cell model. Material properties used in the PUC analysis are listed in Table 2.

To evaluate the effect of matrix constitutive modeling on two-scale FE analysis, two constitutive models were applied to matrix resin of PUC analysis. First one is an elasto-viscoplastic model³ proposed to reproduce mechanical responses of ductile polymers. This

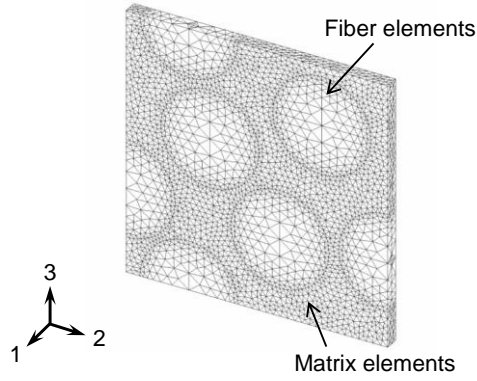


Fig.2 FE model for microscopic PUC analysis.

Table 2 Material properties of carbon fiber and epoxy resin used in the PUC analysis.

Fiber longitudinal Young's modulus E_L	294 GPa
Fiber transverse Young's modulus E_T	19.5 GPa
Fiber longitudinal Poisson's ratio ν_L	0.17
Fiber transverse Poisson's ratio ν_T	0.46
Fiber's coefficient of thermal expansion for the longitudinal direction α_L	$-1.1 \times 10^{-6} / K$
Fiber's coefficient of thermal expansion for the transverse direction α_T	$10 \times 10^{-6} / K$
Matrix Young's modulus E_m	3.2 GPa
Matrix Poisson's ratio ν_m	0.38
Matrix's coefficient of thermal expansion α_m	$60 \times 10^{-6} / K$

model includes a one-parameter damage variable based on the hypothesis of strain equivalence.

$$\dot{\boldsymbol{\sigma}} = (1 - \omega^*) \mathbf{C}_m^e : \dot{\boldsymbol{\varepsilon}} - (1 - \omega^*) \frac{3\mu \dot{\bar{\varepsilon}}^p}{\bar{\sigma}} \boldsymbol{\sigma}' - \frac{\dot{\omega}^*}{1 - \omega^*} \boldsymbol{\sigma} \quad (1)$$

Here, $\boldsymbol{\sigma}$ is the stress tensor, \mathbf{C}_m is the elastic stiffness tensor for the matrix resin, $\boldsymbol{\varepsilon}$ is the strain tensor, μ is the Lamé constant, $\bar{\varepsilon}^p$ is the equivalent plastic strain, $\bar{\sigma}$ is the von Mises stress, $\boldsymbol{\sigma}'$ is the deviatoric stress tensor, and ω^* is the scalar variable that gives the stiffness degradation rate. The equivalent plastic strain rate $\dot{\bar{\varepsilon}}^p$ is determined by the following equation used by Matsuda et al.¹⁵, including hydrostatic stress dependence⁹:

$$\dot{\bar{\varepsilon}}^p = \dot{\varepsilon}_r \left(\frac{\bar{\sigma} + \beta \sigma_m}{g(\bar{\varepsilon}^p)} \right)^{\frac{1}{m}}, \quad (2)$$

$$g(\bar{\varepsilon}^p) = g_1(\bar{\varepsilon}^p)^{g_2} + g_3. \quad (3)$$

Here, $\dot{\varepsilon}_r$ is the reference strain rate; σ_m is hydrostatic stress; m is an exponent regarding strain-rate sensitivity; β is hydrostatic stress sensitivity; and g_1 , g_2 and g_3 are material constants.

The second model is an inelastic constitutive model¹ that accounts for the effect of free volume variation in polymer on mechanical responses.

$$\dot{\sigma} = C_m^e : \dot{\varepsilon} - \frac{\sqrt{2}}{\tau} \dot{\gamma}^p \sigma', \quad (4)$$

where

$$\dot{\gamma}^p = \dot{\gamma}_0 \int_0^\infty \psi(\Delta F) \left[\exp \left\{ -\frac{\Delta F - \tau \Delta v_\tau^*}{kT} \right\} - \exp \left\{ -\frac{\Delta F + \tau \Delta v_\tau^*}{kT} \right\} \right] d\Delta F. \quad (5)$$

Here, $\dot{\gamma}_0$ is macroscopic inelastic strain rate, ΔF is an activation energy for transformation, ψ is a probability density function of activation energy, τ is equivalent shear stress, T is temperature, Δv_τ^* is shear activation volume, k is the Boltzmann constant, and σ' is local transformation strain energy. Detailed expressions of variable's evolution laws are described in the literature¹.

Material parameters used for each constitutive model were identified through the comparison of neat-resin FE analysis with neat-resin experiment of Fiedler et al.². We employed $\dot{\varepsilon}_r = 1.0 \times 10^{-5}$, $m = 1/35$, $\beta = 0.2$, $g_1 = 90$ MPa, $g_2 = 0.08$, and $g_3 = 20$ MPa for Eqs. (2) and (3); and $\dot{\gamma}_0 = 1.51 \times 10^7$ 1/s, $T = 297$ K, and $\Delta v_\tau^* = 1.24 \times 10^{-18}$ mm³ for Eq. (5).

To investigate important factors in failure criteria of composites, four sets of failure criteria are applied to matrix resin individually. Three criteria predict crack initiation based on the tensile and compressive strengths of matrix. Another criterion models crack initiation under elastic and plastic deformation, using two failure models.

The first criterion is von Mises criterion, expressed by the following equation.

$$\frac{1}{2} \left[(\sigma_{11} - \sigma_{22})^2 + (\sigma_{22} - \sigma_{33})^2 + (\sigma_{33} - \sigma_{11})^2 \right] + 3(\sigma_{12}^2 + \sigma_{23}^2 + \sigma_{31}^2) \leq \sigma_t^2 \quad (6)$$

Here, σ_i is the stress component with respect to material principal axis, and σ_t is tensile strength of matrix resin.

The second criterion is Drucker-Prager criterion¹⁶, which includes the hydrostatic stress

effect on yielding behavior.

$$\frac{3}{2} \left(\frac{1}{\sigma_m} - \frac{1}{\sigma_Y} \right) \sigma_m + \frac{1}{2} \left(\frac{1}{\sigma_m} + \frac{1}{\sigma_Y} \right) \bar{\sigma} \leq 1 \quad (7)$$

Here, σ_m is compressive strength of matrix resin.

The third criterion is Christensen's failure criterion⁵, which considers brittle failure under elastic deformation as well as ductile failure under plastic deformation.

$$3 \left(1 - \frac{\sigma_m}{\sigma_Y} \right) \hat{\sigma}_m + \hat{\sigma}^2 \leq - \quad (8)$$

Here, $\hat{\sigma}_m$ and $\hat{\sigma}$ are hydrostatic and equivalent stresses normalized by compressive strength σ_m , respectively. On the PUC analysis with Eq. (7), (8), or (9), σ_m^* in Eq. (1) is set at zero to independently evaluate each failure criterion, and a matrix crack is assumed to occur when the stress state in an element satisfies each equation.

The fourth criterion is the combined criterion¹² that consists of two failure models to predict brittle failure under elastic deformation and ductile failure under plastic deformation. The first model is the dilatational energy density criterion, proposed by Asp et al.⁶. The dilatational energy density of a linear elastic body, U_v , is given by

$$U_v = \frac{3(1-2\nu)}{2E} \sigma_m^2 \quad (9)$$

where ν is Poisson's ratio and E is Young's modulus. A matrix crack is assumed to occur when U_v reaches a critical value, U_v^{crit} , under elastic deformation. We employ $U_v^{\text{crit}} = 0.9$ MPa, referring to the literature¹². The second model is based on the damage parameter, D , calculated by the following evolutionary equation⁷, which is based on the Gurson-Tvergaard-Needleman model^{17, 18}.

$$\dot{D} = H(\bar{\sigma} - \sigma_Y) \left(1 - \frac{\sigma_Y}{\bar{\sigma}} \right) \left\langle \dot{\epsilon}_m^p \right\rangle + \left(\alpha_0 + \alpha_1 \right) \dot{\epsilon}^p. \quad (10)$$

Here,

$$\left\langle \dot{\epsilon}_m^p \right\rangle = \left[\left(\frac{\langle \sigma_m \rangle}{\hat{\sigma}} \right)^2 \right]^{\bullet} \quad (11)$$

The first term on the right-hand side in Eq. (10) represents void growth caused by mean plastic vertical strain, and the second term indicates damage evolution caused by shear deformation. Here, H is the Heaviside function, $\hat{\sigma}$ is the reference stress, σ_Y is the linearity limit of the matrix resin, and α_0 , α_1 and α_2 are non-dimensional constants. We employ $\hat{\sigma} = 73$

MPa, $\sigma_0 = 1.5$, $\sigma_0 = 0.6$, and $\sigma_1 = 0.6$, referring to the literature¹². σ^* is introduced to include the effect of the rapid evolution of damage due to the coalescence of micro voids¹⁸.

$$\sigma^* = \begin{cases} \sigma & (\sigma < \sigma_c) \\ \sigma_c + \frac{\sigma_{crit}^* - \sigma_c}{\sigma_{crit} - \sigma_c} (\sigma - \sigma_c) & (\sigma \geq \sigma_c) \end{cases} \quad (12)$$

Rapid damage evolution starts when σ reaches the threshold value σ_c . Here, σ_{crit}^* is the critical value of σ^* , and σ_{crit} is the critical value of σ . A matrix crack is assumed to occur when σ reaches the critical value, σ_{crit} , under plastic deformation. We utilize $\sigma_c = 0.08$, $\sigma_{crit}^* = 0.25$, and $\sigma_{crit} = 1/1.5$, referring to the literature¹⁹. Furthermore, to avoid the mesh dependence of matrix damage, the nonlocalization of the variables that relate to failure criteria is conducted according to the literature²⁰.

2.3 Computational procedure

To consider microscopic structure of composites and macroscopic deformation behavior of laminate simultaneously, multiscale analysis that consists of microscopic PUC analysis and macroscopic FE analysis is carried out. The computational procedure of the multiscale analysis is summarized as follows.

- 1) On the macroscopic scale, displacement-controlled tensile test analysis is performed to predict strain fields in laminate. The strain history is extracted at the assumed crack initiation point presented in Fig. 1.
- 2) On the PUC analysis, temperature decrease analysis is carried out to calculate thermal residual stress generated in the manufacturing process. Through the analysis, temperature is decreased by 150 K, which corresponds to the difference from curing temperature to room temperature. Macroscopic strain increment, which is uniformly applied to whole unit-cell, is controlled in order that volume-averaged stress of unit-cell will be zero, which reproduces the thermal shrinkage of laminate. Stress and strain fields obtained from this calculation are defined as initial states of laminate.
- 3) Macroscopic strain increment based on the strain history obtained from procedure 1) is applied to unit-cell to predict crack initiation in laminate subjected to tensile loading. Initial cracking strain is defined as the applied strain of the laminate when the failure criterion described in the section 2.2 is firstly satisfied in an element.

3 RESULTS AND DISCUSSION

Firstly, the effect of matrix constitutive modeling on laminate nonlinear response prediction was examined. Figure 3 shows the comparison of simulated results obtained from PUC analysis with experiment data of Yoshioka et al.¹⁰. The horizontal axis indicates applied strain, and the vertical axis represents volume-averaged stress over the unit cell. Multiscale predictions with both constitutive models reproduced inelastic stress-strain relationship of laminate. In the case of unidirectional laminate under off-axis loading, appropriate constitutive modeling, which is established based on experiment data, provides reasonable prediction of nonlinear stress-strain response.

Failure criteria were compared with each other, using the constitutive model of Eq. (1). Parameters and were identified through the comparison of simulated cracking strains with experiment results of unidirectional off-axis tensile tests conducted by Yoshioka et al.¹⁰. Figure 4 shows simulated failure strains obtained from multiscale analysis with each failure criteria, using identified parameters. Except for von Mises criterion, simulated results qualitatively agree with experiment data. The identified parameters and shown in Fig. 4 are feasible because these values are in the range of experimentally measured strength^{2, 21}.

For more detailed evaluation, initial cracking sites obtained from each failure criterion were compared. Figure 5 shows the initial cracking sites predicted by each failure criterion in the 30° off-axis test. The hydrostatic and equivalent stress distributions obtained from the PUC analysis with the combined criterion are also shown in Fig. 5. In this case, initial crack was initiated

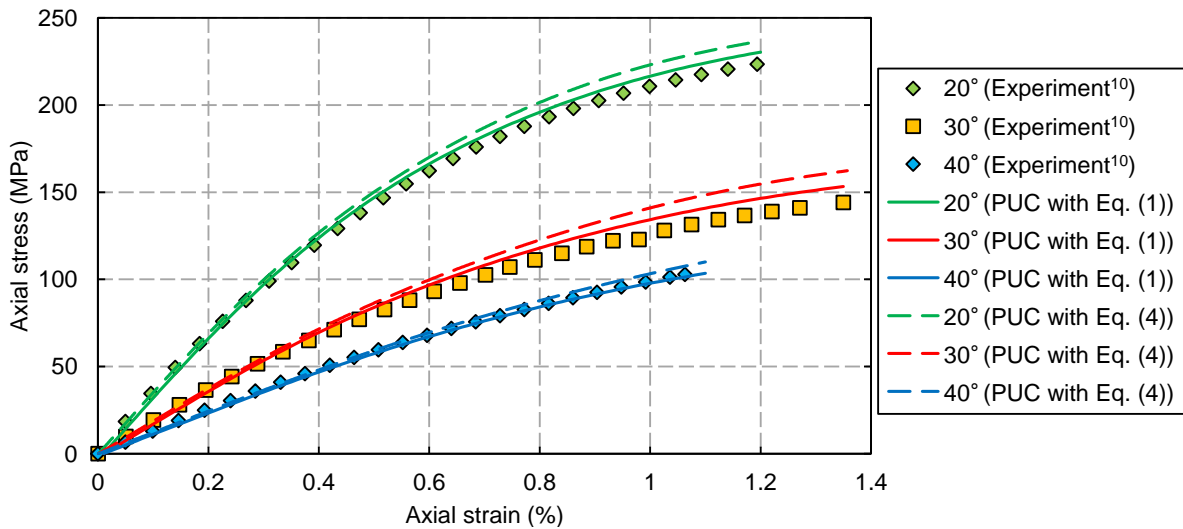


Fig. 3 Comparison of simulated off-axis tensile response of laminate with experiment data.

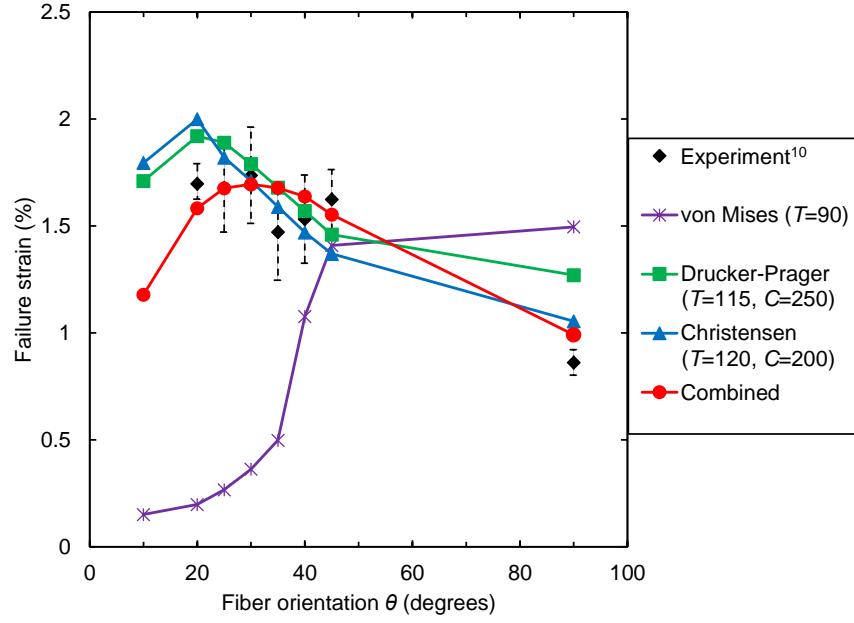


Fig. 4 Comparison of initial cracking strains obtained from multiscale analysis with experiment.

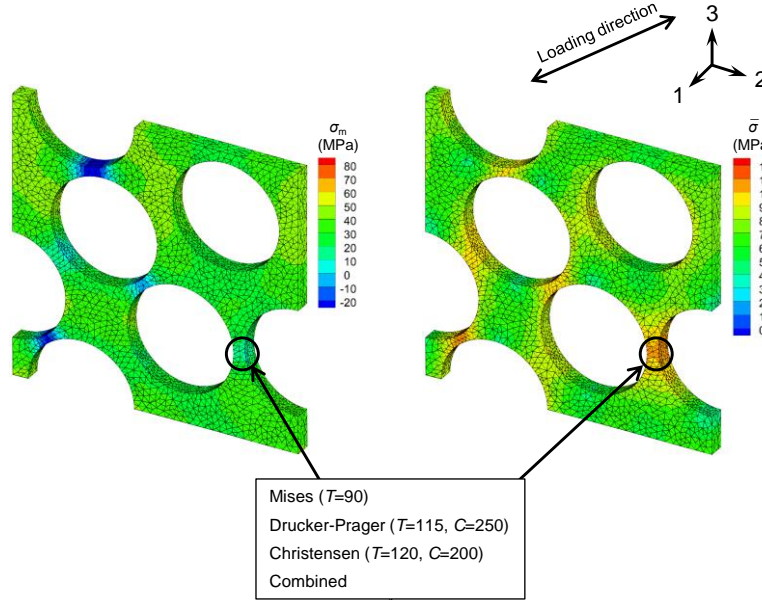


Fig. 5 Initial cracking sites predicted by each failure criterion and hydrostatic and equivalent stress distribution obtained from 30° off-axis analysis with combined criterion.

between fibers where large equivalent stress occurs. This large equivalent stress was caused by the shear deformation of laminate, and it led to crack formation under plastic deformation.

Figure 6 shows the initial cracking sites predicted by each failure criterion in the transverse

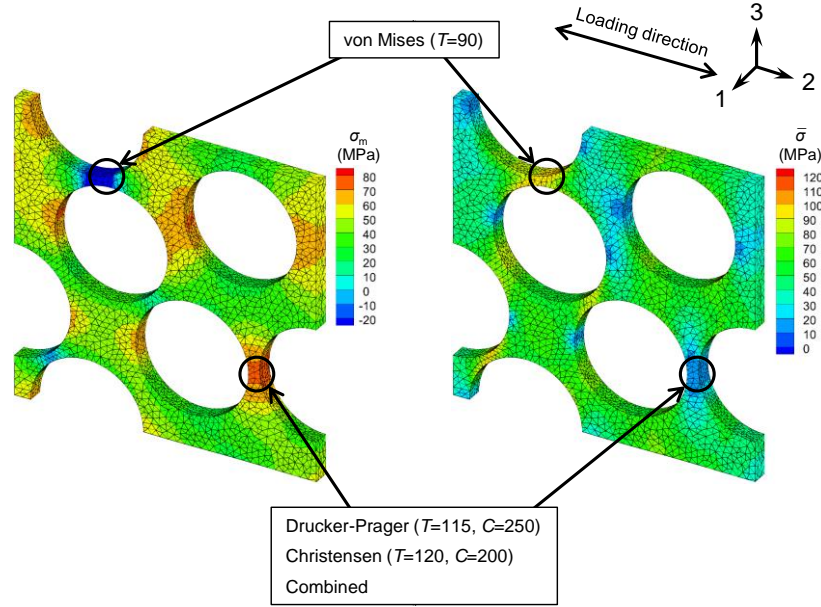


Fig. 6 Initial cracking sites predicted by each failure criterion and hydrostatic and equivalent stress distribution obtained from 90° off-axis analysis with combined criterion.

tension test. Figure 6 also shows the hydrostatic and equivalent stress distributions obtained from the PUC analysis with the combined criterion. In the case of the Drucker-Prager, Christensen and combined criteria, the initial crack occurred between fibers that are aligned parallel to the loading direction. These results agree well with previous experimental work²¹ and numerical results^{8,9}. On the other hand, in the case of von Mises criterion, the initial crack was initiated between fibers that are aligned perpendicular to the loading direction. The von Mises criterion cannot reproduce the initial cracking site under transverse loading because this criterion does not consider the hydrostatic stress effect that causes cavitation-induced brittle failure reported by Asp et al.^{6,8}. These results indicate that a failure criterion for matrix resin should include not only the distortional component that causes ductile failure but also the dilatational component that induces brittle failure to predict initial failure under practical loading conditions.

4 CONCLUSIONS

In this study, the effect of constitutive and failure modeling of matrix resin on crack prediction capability of multiscale analysis is investigated. Two constitutive models were applied to matrix resin of PUC analysis to examine their influence on nonlinear stress-strain

response prediction of CFRP laminate. For unidirectional laminate, inelastic constitutive models with experimentally identified parameters provided reasonable multiscale prediction of material nonlinearity. Four sets of failure criteria were implemented to microscopic PUC analysis to evaluate factors that need to predict crack initiation in composite laminate. Except for von Mises criterion, simulated results qualitatively agreed with experiment data. This is because von Mises criterion does not consider the hydrostatic stress effect on crack formation. These results imply that a failure criterion for matrix resin ought to take account for not only the distortional effect that leads to ductile failure but also the dilatational effect that induces brittle failure to predict crack formation. We will conduct multiscale matrix modeling evaluation with practical laminate to develop matrix modeling strategy for multiscale failure prediction, which is capable under more complex loading conditions.

REFERENCES

- [1] Hasan, O. A., and Boyce, M. C., A constitutive model for the nonlinear viscoelastic viscoplastic behavior of glassy polymers, *Poly. Eng. Sci.* (1992) 35:331-344.
- [2] Fiedler, B., Hojo, M., Ochiai, S., Schulte, K., and Ando, M., Failure behavior of an epoxy matrix under different kinds of static loading, *Compos. Sci. Technol.* (2001) 61:1615-1624.
- [3] Kobayashi, S., Tomii, D., and Shizawa, K., A modelling and simulation on failure prediction of ductile polymer based on craze evolution and annihilation, *Trans. Jpn Soc. Mech. Eng. Ser. A* (2004) 70:810-817. (in Japanese).
- [4] Bai, X., Bessa, M. A., Melro, A. R., Camanho, P. P., Guo, L., and Liu, W. K., High-fidelity micro-scale modeling of the thermo-visco-plastic behavior of carbon fiber polymer matrix composites, *Compos. Struct.* (2015) 134:132-141.
- [5] Christensen, R. M., *The Theory of Materials Failure*, Oxford University Press (2013).
- [6] Asp, L. E., Berglund, L. A., and Talreja, R., A criterion for crack initiation in glassy polymers subjected to a composite-like stress state, *Compos. Sci. Technol.* (1996) 56:1291-1301.
- [7] Nishikawa, M., *Multiscale modeling for the microscopic damage and fracture of fiber-reinforced plastic composites*, Dr. Eng. Thesis, The University of Tokyo (2008). (in Japanese).
- [8] Asp, L. E., Berglund, L. A., and Talreja, R., Prediction of matrix-initiated transverse failure in polymer composites, *Compos. Sci. Technol.* (1996) 56:1089-1097.
- [9] Okabe, T., Nishikawa, M., and Toyoshima, H., A periodic unit-cell simulation of fiber

- arrangement dependence on the transverse tensile failure in unidirectional carbon fiber reinforced composites, *Int. J. Solids Struct.* (2011) 48:2948-2959.
- [10] Yoshioka, K., Kumagai, Y., Higuchi, R., Lee, D., and Okabe, T., Multiscale Modeling of Failure Strain in Off-Axis Tensile Testing of UD-CFRP, *Mater. Sys.* (2016) 34:7-13. (in Japanese).
- [11] Yokozeki, T., Ogihara, S., Yoshida, S., and Ogasawara, T., Simple constitutive model for nonlinear response of fiber-reinforced composites with loading-directional dependence, *Compos. Sci. Technol.* (2007) 67:111-118.
- [12] Sato, Y., Okabe, T., Higuchi, R., and Yoshioka, K., Multiscale approach to predict crack initiation in unidirectional off-axis laminates, *Adv. Compos. Mater.* (2014) 23:461-475.
- [13] Pipes, R. B., and Gosse, J. H., An Onset Theory for Irreversible Deformation in Composite Materials, in: *17th International Conference on Composite Materials* (2009).
- [14] Tran, T. D., Kelly, D., Prusty, B. G., Gosse, J. H., and Christensen, S., Micromechanical modelling for onset of distortional matrix damage of fiber reinforced composite materials, *Compos. Struct.* (2012) 94:745-757.
- [15] Matsuda, T., Ohno, N., Tanaka, H., and Shimizu, T., Homogenized in-plane elastic-viscoplastic behavior of long fiber-reinforced laminates, *JSME Int. J. Ser. A* (2002) 45:538-544.
- [16] Drucker, D., and Prager, W., Soil Mechanics and Plastic Analysis or Limit Design, *Quart. Appl. Math.* (1952) 10:157-165.
- [17] Gurson, A. L., Continuum theory of ductile rupture by void nucleation and growth: Part I- Yield criteria and flow rules for porous ductile media, *J. Eng. Mater. Technol.* (1977) 99:2-15.
- [18] Tvergaard, V., and Needleman, A., Analysis of the cup-cone fracture in a round tensile bar, *Acta Metall.* (1984) 32:157-169.
- [19] Tvergaard, V., and Needleman, A., Effects of nonlocal damage in porous plastic solids, *Int. J. Solids Struct.* (1995) 32:1063-1077.
- [20] Bažant, Z. P., and Pijaudier-Cabot, G., Nonlocal continuum damage, localization instability and convergence, *J. Appl. Mech.* (1988) 55:287-293.
- [21] Hobbiebrunken, T., Hojo, M., Adachi, T., De Jong, C., and Fiedler, B., Evaluation of interfacial strength in CF/epoxies using FEM and in-situ experiments, *Compos. Part A* (2006) 37:2248-2256.

Hydrodynamics and Nutrient Transport Inside a Cell-Seeded Hollow Fibre Membrane Bioreactor

Prakash Kumar*, Raja Sekhar G. P.**

*Indian Institute of Technology Kharagpur, India 721302, **Indian Institute of Technology Kharagpur, India 721302

ABSTRACT

Introduction Biodegradable extracellular matrix (ECM), also termed as the scaffold, are manufactured using natural materials such as collagen, glycosaminoglycan, and chitosan. In addition to natural materials, artificially synthetic polymers like polyglycolic acid (PGA), polylactic acid (PLA), and polycaprolactone (PCL) have also been used; moreover, most of the products used are deformable in nature [1]. The objective of this study is to provide a mathematical model of HFMB bioreactor along with deformable scaffold so that a uniform distribution of nutrient concentration can be supplied to each part of the bioreactor. Methods In order to deal with deformation of the solid phase and movement of the fluid phase, we adopt biphasic mixture theory equations [2]. The flow inside the lumen is governed by Stokes equation. We close the model using the appropriate boundary conditions at the wall and the interphase of the bioreactor. The flow inside the bioreactor is assumed to be unidirectional and the advection-diffusion-reaction equation is used to get the momentum balance of the nutrient in scaffold and lumen region. We use asymptotic methods to reduce the system (lubrication approximation) to obtain leading order nutrient concentration. This leads to a coupled system of partial differential equations (PDEs) with time-dependent variables. Laplace transformation is used to deal with time-dependent terms and Durbin's algorithm was used to retrieve time dependency. Results The effect of fluid velocity and the solid displacement is analyzed with respect to varying pressure gradient, porosity, the permeability of the scaffold region. The convection in the nutrient balance equation is affected by the composite velocity inside the scaffold region. The reaction rate of different cells based on available experimental data is used to study the effect on nutrient concentration. The factors affecting the nutrient concentration are lumen radius, porosity, and permeability of the scaffold, Thiele modulus, pressure gradient etc. Total mass transfer rate is computed to analyze the movement of nutrient supply in each cross-section of the bioreactor. Nutrient concentration inside the bioreactor increases with increase in the thickness of the lumen whereas porosity and permeability have significant role in the uniformity of nutrient concentration. Nutrient concentration decreases with higher Thiele modulus and the mass transfer increases with the increase in the thickness of scaffold region. References 1. P. Chumtong, et al. Mechatronics and Automation (ICMA), 2014 IEEE International Conference on. IEEE, 2014. 2. K. R. Rajagopal, Mathematical Models and Methods in Applied Sciences 17.02 (2007): 215-252.

A C 0 Interior Penalty Discontinuous Galerkin Method for Fourth Order Total Variation Flow

Rahul Kumar^{*}, Chandi Bhandari^{**}, Ronald H.W Hoppe^{***}

^{*}Basque Center for Applied Mathematics (BCAM), Bilbao, Spain, ^{**}University of Houston, Houston, ^{***}University of Houston, Houston, USA

ABSTRACT

We consider the numerical solution of the regularized fourth order total variation flow problem based on an implicit discretization in time and a C 0 Interior Penalty Discontinuous Galerkin (C 0 IPDG) method in space. In particular, we prove coerciveness and boundedness of the associated C 0 IPDG form with respect to a mesh dependent C 0 IPDG-norm of the underlying function space. The main result is an a priori error estimate of the global discretization error in the mesh dependent C 0 IPDG-norm. The derivation of the error estimate requires an Aubin-Nitsche type argument by considering an appropriate boundary value problem for the adjoint of the linearized partial differential operator. Numerical results are also provided illustrating the performance of the C 0 IPDG method and confirming the theoretical findings. Finally documentation of applications to medical imaging will be produced.

Enhanced Local Maximum Entropy Approximation for Stable Meshfree Simulations

Siddhant Kumar^{*}, Dennis Kochmann^{**}, Kostas Danas^{***}

^{*}California Institute of Technology, ^{**}ETH Zürich, ^{***}École Polytechnique

ABSTRACT

We propose an improved meshfree approximation scheme which is based on the local maximum-entropy strategy as a compromise between shape function locality and entropy in an information-theoretical sense. The improved version is specifically designed for severe, finite deformation and offers significantly enhanced stability as opposed to the original formulation. This is achieved by (i) formulating the quasi-static mechanical boundary value problem in a suitable updated-Lagrangian setting, (ii) introducing anisotropy in the shape function support to accommodate directional variations in nodal spacing with increasing deformation, (iii) spatially bounded shape function support to restrict the domain of influence and increase efficiency, (iv) truncating shape functions at interfaces in order to stably represent multi-component systems like composites or polycrystals. The new scheme is applied to benchmark problems of severe elastic deformation that demonstrate its performance both in terms of accuracy (as compared to exact solutions and, where applicable, finite element simulations) and efficiency. Importantly, the presented formulation overcomes the classical tensile instability found in most meshfree interpolation schemes, as shown for stable simulations of, e.g., the inhomogeneous extension of a hyperelastic block up to 300% or the torsion of a hyperelastic cube by 270 degrees – both without the need for remeshing.

A Cluster-based Microstructural Topology Optimization

Tej Kumar^{*}, Krishnan Suresh^{**}

^{*}University of Wisconsin, Madison, ^{**}University of Wisconsin, Madison

ABSTRACT

The advent of 3D printing has enabled the possibility of custom designed microstructures for demanding applications. Microstructures were initially employed in structural optimization to create repeating structures using a single set of microstructural design variables. Later, macro-structural variables were included together with a local volume constraint to achieve a two-level optimization [1, 2]. The local volume constraint was found to be essential to avoid completely degenerate (entirely solid, or entirely void) microstructures. However, this additional constraint inhibited the design from achieving peak performance. Here, we propose to get rid of both the macro-structural variables, as well as the local volume constraint. Instead, we directly impose a volume constraint via the microstructural variables. This leads to spatially varying, and optimal, microstructures. To address the computational cost, we generalize the grid-based clustering strategy proposed in Sivapuram et al. [1]. In particular, we propose several alternate clustering strategies that lead to significant improvement in performance, without significantly affecting the computational cost. Clusters are allowed to remain fixed or can adapt, during optimization. The clustering strategies are developed based on the well-known k-clustering algorithm, using multiple metrics. The effectiveness of these strategies is demonstrated through several examples. Associated computational cost and performance are studied with varying number of clusters. [1] Sivapuram, R., Dunning, P. D., Kim, H. A. (2016). Simultaneous material and structural optimization by multiscale topology optimization. *Structural and Multidisciplinary Optimization*, 54(5), 1267–1281. <https://doi.org/10.1007/s00158-016-1519-x> [2] Chen, W., Tong, L., & Liu, S. (2017). Concurrent topology design of structure and material using a two-scale topology optimization. *Computers and Structures*, 178, 119–128. <https://doi.org/10.1016/j.compstruc.2016.10.013>

Numerical Modeling of Contact Friction Problems Using Phase-Field Model of Fracture

Vivek Kumar*, Maurizio Chiaramonte**

*Civil and Environmental Engineering Dept, Princeton, NJ, **Civil and Environmental Engineering Dept, Princeton, NJ

ABSTRACT

Correctly predicting the behavior of faults and fissures in rocks or concrete-to-concrete sliding in civil engineering structures is important to prevent structural failure. These essentially turn into solving contact problems between fractured surfaces. Earlier approaches to solve contact problems based on extended finite element method (X-FEM) suffer from numerical instability and the contact pressure so obtained between cracked surfaces show spurious oscillations. Moreover, these oscillations persist or become worse with mesh refinement. Hence, various stabilization techniques had to be employed to overcome the numerical instability. Some of the commonly employed stabilization techniques are Nitsche's stabilization, bubble stabilization, reduced Lagrange methods and polynomial pressure projection. In this article we discuss a new method for solving frictional contact problems which do not suffer from such issues. In this work, we develop a phase-field model of fracture for solving frictional contact problems. Phase field model is a diffusive model of fracture based on the introduction of an auxiliary field called phase field. The phase-field model used in this article is based on the work of Miehe et. al [Miehe C, Hofacker M, Welschinger F. A phase field model for rate-independent crack propagation: Robust algorithmic implementation based on operator splits. *Computer Methods in Applied Mechanics and Engineering*. 2010 Nov 15;199(45):2765-78.]. We detail the mathematical formulation for extending the use of phase-field for frictional contact problems and implement the scheme using FEniCS, an open source computing platform for solving partial differential equations. Benchmark problems involving both frictionless and frictional contact are solved to demonstrate the advantages of this new method. Finally, the above method is used to simulate the crack growth when surfaces with frictional contact move past each other, and the results are compared with those found in literature.

On the Combination of Extended Galerkin Methods with Mesh Adaptation

Florian Kummer*

*TU Darmstadt/Fluid Dynamics

ABSTRACT

Over the past years, we developed a high-order numerical method for multi-phase flow problems, such as droplets or bubbles, which employs a sharp interface representation by a level-set and an extended discontinuous Galerkin (XDG) discretization for the flow properties. The shape of the XDG basis functions is dynamically adapted to the position of the fluid interface, so that the spatial approximation space can represent jumps in pressure and kinks in velocity accurately. By this approach, the high-order convergence property of the discontinuous Galerkin (DG) method can be preserved for the low-regularity, discontinuous solutions, such as those appearing in multi-phase flows. However, in realistic droplet setups one observes length scales which may cover several magnitudes. While extended methods are well suited to embed arbitrary interfaces or surfaces on (e.g. Cartesian) background meshes they lack the capability to adapt to different length scales. Therefore, an extended method has to be combined with techniques like adaptive mesh refinement. This refinement can be feature-based, e.g. controlled by the local curvature of the fluid interface. Our presentation will focus on some of the critical building-blocks of the method and their integration in the full solver.

The Lie Symmetries of Forced Duffing Type Oscillators

Bidisha Kundu*, Ranjan Ganguli**

*Ph.D Student, **Professor

ABSTRACT

In the era of advanced computation techniques and tools, still, the researchers are interested in inventing new ways of calculation. Their interests lie in searching analytical solutions, exact or closed form of the solutions to save the computation time. The Lie symmetry method is the most famous and successful among them for applying on different types of differential equations. The Norwegian mathematician Sophus Lie (1842-1899) first introduced this technique and later it was developed more and employed in several problems [1]. This method is the mixture of two branches of mathematics- algebra and analysis. There are various kinds of motivations for studying the Lie method such as to find the symmetries of the system, an equivalent form of the equation by reducing the order of the equation or linearize the nonlinear equation, and the invariant solutions which are in exact or closed form in most of the cases. In this work, we mainly concentrate on the nonlinear damped spring-mass system with external force. Due to nonlinear restoring force (Duffing oscillator), or for the damping (van der Pol oscillator), the nonlinearities appear. In [2], the general Liénard type equations were studied but without forcing effect. We follow the Lie symmetry procedure to understand the symmetries and try to find the similarity transformation dependent on the damping coefficient, force etc. Duffing type oscillators with external force effect are studied here. So, time variable is explicitly present in the equation, and the equation is nonautonomous. In this case, the Lie method will help us to investigate this system to get the invariant solution, and it may also linearize the equation. In this presentation, at first, I will discuss the fundamental theories and background of the Lie method and the application procedure. The primary challenge is to solve the determining equations which provide the transformations. We have solved them analytically and found a relationship between the damping coefficient, stiffness nonlinearity and the force. We hope we can extract more information and extend our work to coupled Duffing type oscillators. References: [1] Olver P. J., Applications of Lie Groups to Differential Equations, vol. 107 (Springer Science & Business Media, New York, 2012). [2] Pandey, S.N., Bindu, P.S., Senthilvelan, M., Lakshmanan, M., J. Math. Phys. 50, 082702 (2009).

Particle Image Velocimetry-based Validation of a CFD Model for the Treatment of Intracranial Aneurysms Using a Shape Memory Polymer Embolization Device

Robert Kunkel^{*}, Devin Laurence^{**}, Donnie Robinson^{***}, Joshua Scherrer^{****}, Aichi Chien^{****},
Bradley Bohnstedt^{*****}, Yi Wu^{*****}, Yingtao Liu^{*****}, Ching-Hao Lee^{*****}

^{*}University of Oklahoma, ^{**}University of Oklahoma, ^{***}University of Oklahoma, ^{****}University of Oklahoma,
^{*****}University of California Los Angeles Medical School, ^{*****}The University of Oklahoma Health Sciences Center,
^{*****}University of Oklahoma, ^{*****}University of Oklahoma, ^{*****}University of Oklahoma

ABSTRACT

Intracranial aneurysms (ICAs) are localized dilations of blood vessels in the brain caused by weaknesses in the vessel walls. ICAs have a prevalence of 0.5% - 6% in adults. While the aneurysm itself is typically asymptotic, incidental rupture of an ICA produces subarachnoid hemorrhage (SAH), leading to 5% of all strokes and the death of roughly 10% of patients before receiving medical attention [1]. Computational fluid dynamic (CFD) modeling of the hemodynamics of ICAs can be used by physicians to inform the treatment process once an aneurysm has been diagnosed. The objective of this study is to develop a CFD model for simulating the velocity patterns within ICAs, and eventually for accommodating a novel endovascular treatment method utilizing an aliphatic urethane shape memory polymer. The CFD model will be developed from patient-specific brain computed tomography (CT) angiography in ANSYS Fluent. The model will be validated using in-house particle image velocimetry (PIV) analysis of patient-specific aneurysm phantoms under pulsatile flow conditions. The current clinical practice includes two main treatment methods for ICAs— a clipping device that is surgically attached around the outer neck of the aneurysm and an endovascular embolization method that uses an intravenous delivery device to coil flexible wire within aneurysm sac [2]. We are developing a novel treatment using patient-specific shape memory polymer (SMP) inserts for an endovascular embolization technique capable of achieving a higher volume fill rate and providing more permanent occlusion. CFD is used to evaluate which treatment method will result in the most favorable flow conditions once implemented. For our innovative therapeutics, we plan to use a stereolithographic 3D printer to cure SMP in geometries based on CT scan image data from individual patients. The SMP will then be deformed into a thin filament capable of being delivered intravenously, and will be thermally activated to revert to its original geometry once arriving at the aneurysm. To properly demonstrate the feasibility of this treatment, the developed CFD model will need to accurately predict the velocity patterns within the untreated aneurysm, and account for interactions between the blood flow and the boundary of the SMP device. The developed CFD-based aneurysm treatment simulation platform will provide a useful tool for predicting the effectiveness of SMP based occlusion in patient-specific scenarios. References: [1] S. Yu and J. Zhao, Medical Engineering & Physics 1999, 21(3): 133–141. [2] Y. Hoi, Journal of Biomechanical Engineering, 2006, 128(6): 844.

Micro-FE Modeling for Multiscale Coupled Analysis of Resistance Spot Welding

Hiroyuki Kuramae^{*}, Tomoya Niho^{**}, Tomoyoshi Horie^{***}

^{*}Osaka Institute of Technology, ^{**}Kyushu Institute of Technology, ^{***}Kyushu Institute of Technology

ABSTRACT

Since electrical contact resistance is an important property in the numerical simulations for resistance spot welding, a multiscale coupled finite element (FE) procedure for resistance spot welding is proposed to evaluate the high accuracy of the electrical contact resistance. This analysis consists of macroscopic coupled FE analysis for the resistance spot welding and microscopic the electrical contact resistance analysis using three-dimensional (3D) thermal elasto-plasticity contact FE simulation. The multiscale analysis is based on coupled FE procedure among structural deformation, electric current and temperature distributions to evaluate a nugget growth by Joule heating in the macro-scale analysis, and to calculate the electrical contact resistance in the micro-scale analysis. Temperature-dependent material properties such as yield stress, work hardening rate and resistivity are considered in both scale analyses. A rigid plate is contacted to the micro-FE model with contact pressure and temperature that are obtained by macro-analysis, to calculate electrical contact resistance by elast-plasticity contact FE analysis including large deformation theory combined with electric FE analysis based on the phi-method. The micro-scale analysis is a very computationally expensive process because of evaluation of electrical contact resistance distribution on the macro-contact surface every time step. A micro-FE model, which corresponds to statistically similar representative volume element (SS-RVE), was constructed based on a surface roughness measurement of a steel sheet using laser microscope apparatus with 0.139 micrometers interval. In this study, an optimum size of SS-RVE in-plane was determined based on correlational analyses between frequency distribution of the microscopic surface roughness between measured 284.7×213.5 square micrometers and various sampling size. The optimum size of SS-RVE was determined as 100×100 square micrometers in-plane. Resolution of 3D FE mesh in-plane is also examined by the micro-scale electrical contact resistance analyses. In addition, to analyze realistic electrical contact resistance of steel plate contact in the micro-scale analysis, an oxide film FeO on the surface is considered. The oxide film is 3nm thickness and is introduced into the surface of the micro-FE model. The electrical contact resistance with the oxide film was higher accuracy than without one.

Comparison of Fracture Behavior in Concrete between FEM and DIC

Mao Kurumatani^{*}, Yusuke Koakutsu^{**}, Kazuya Hashiguchi^{***}

^{*}Ibaraki University, ^{**}Ibaraki University, ^{***}Ibaraki University

ABSTRACT

We present a comparison of fracture behavior in reinforced concrete between simulation and experiment toward the V&V analysis which has recently been required in the field of computational mechanics. Particularly, the V&V for the fracture simulation in concrete seems to be difficult because many studies still have been made on the numerical methods for crack propagation for a long time. In this study, the FEM with a damage model is applied to simulate the fracture behavior with cracking in concrete. The damage model is based on fracture mechanics for concrete in consideration of cohesive zone in the fracture process, which is equivalent to a kind of energy balance approach in terms of fracture energy. The modified von-Mises criterion is introduced into the damage model to evaluate the cracking in concrete while the von-Mises plasticity is applied to model the plastic behavior of steel-reinforcements. To measure the crack propagation in concrete, we employ the digital image correlation (DIC) method which has been developed in our laboratory. A numerical simulation with the FEM and experimental measurement with the DIC are performed for 4-point bend test of RC beams with different shear reinforcements. The quantitative comparison of crack propagation between the numerical and experimental results offer valuable insight into the V&V for the fracture simulation of concrete and reinforced concrete.

Autonomous Materials Research Systems: Phase Mapping

A. Gilad Kusne^{*}, Brian DeCost^{**}, Jason Hattrick-Simpers^{***}, Ichiro Takeuchi^{****}

^{*}National Institute of Standards & Technology, ^{**}National Institute of Standards & Technology, ^{***}National Institute of Standards & Technology, ^{****}University of Maryland

ABSTRACT

The last few decades have seen significant advancements in materials research tools, allowing researchers to rapidly synthesis and characterize large numbers of samples - a major step toward high-throughput materials discovery. Machine learning has been tasked to aid in converting the collected materials property data into actionable knowledge, and more recently it has been used to assist in experiment design. In this talk we demonstrate the next step in machine learning for materials research - an autonomous materials measurement system. The software system controls X-ray diffraction measurement systems both in the lab and at the beamline to identify composition-temperature phase maps from composition spreads with a minimum number of measurements. The algorithm also capitalizes on prior knowledge in the form of physics theory and external databases, both theory-based and experiment-based, to more rapidly hone in on the optimal results. Materials of interest include Fe-Ga-Pd, TiO₂-SnO₂-ZnO, and Mn-Ni-Ge.

FINITE BEAM ELEMENT WITH PIEZOELECTRIC LAYERS AND FG MATERIAL OF CORE

VLADIMÍR KUTIŠ*, JUSTÍN MURÍN†, JURAJ PAULECH† AND
GABRIEL GÁLIK†

*†Department of Applied Mechanics and Mechatronics
Institute of Automotive Mechatronics
Faculty of Electrical Engineering and Information Technology
Slovak University of Technology
Ilkovičova 3, 812 19 Bratislava
Slovak Republic
vladimir.kutis@stuba.sk
justin.murin@stuba.sk
juraj.paulech@stuba.sk
gabriel.galik@stuba.sk

Key words: Beam Element, FEM, Piezoelectric Analysis, State Space Model.

Abstract. New smart materials have been developed in material science, that are suitable for broad mechatronic applications. Modern mechatronic systems are focusing on minimizing size, active control and low energy consumption. To improve performance of such systems, new materials and technologies are developed – one of them, which found broad application usage in mechatronics is Functionally graded material (FGM). Connection of FGM beam with piezoelectric layers can be considered as suitable smart material composition for mechatronics. In the contribution, finite element beam with thick FGM core and thin piezoelectric layers is presented. FGM finite element beam with piezolayers has 6 structural degree of freedom and 4 electric degree of freedom. Stiffness matrix and mass matrix of beam element is computed using transfer functions and transfer constants, where the homogenization process of FGM core and piezoelectric layers is applied.

1 INTRODUCTION

Smart structures are widely used in modern engineering applications. They can combine the progress in material science, control theory, electronics and informatics. The best way how to examine such structures before their production is to create their mathematical model. Finite element method is dominant mathematical tool to analyzed such structures and with combination with control can be able to create model of smart structure.

In the presented paper, beam element with core made of functionally graded material in

transversal and longitudinal direction and with piezoelectric layers is presented. The goal is to create dynamic representation of beam structures with active parts made from piezoelectric layers, which can be also used for model of control of the structure.

2 HOMOGENIZED MATERIAL PROPERTIES OF BEAM

Let us consider straight sandwich beam with core made from functionally graded material (FGM) and top and bottom layers made from piezoelectric material with constant material properties – Fig. 1. Cross-section of FGM core has height h_{FGM} and depth b , one piezoelectric layer has height h_p and depth b .

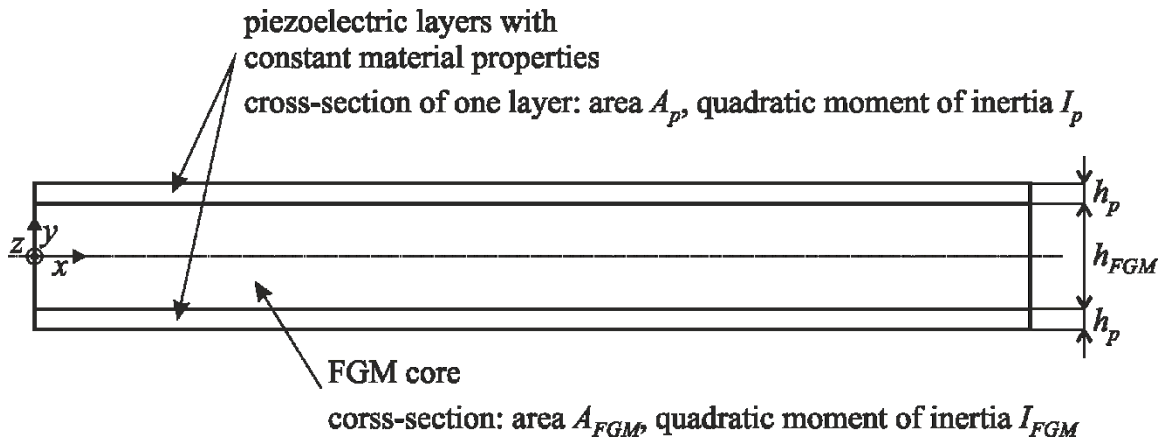


Fig. 1: Piezoelectric beam with core made from FGM material

The composite material of the FGM core arises by mixing two components (matrix and fibers) that are approximately of the same geometrical form and dimensions.

Both the fiber volume fraction $v_f(x, y)$ and matrix volume fraction $v_m(x, y)$ are chosen as a polynomial function of longitudinal position x , and with continuous and symmetrical variation through its height h with respect to the neutral plane of the FGM core. The volume fractions are assumed to be constant through the cross-section depth b . At each point of the FGM core it holds: $v_f(x, y) + v_m(x, y) = 1$.

Young modulus of the constituents (fibers - $E_f(x, y)$ and matrix - $E_m(x, y)$) can analogically vary as it is stated by the variation of volume fractions. For effective Young's modulus $E_{FGM}(x, y)$ of FGM core we can write [1,2]

$$E_{FGM}(x, y) = v_f(x, y)E_f(x, y) + v_m(x, y)E_m(x, y) \quad (1)$$

2.1 Homogenized properties of FGM core

Homogenized Young's modulus for axial loading $E_{FGM}^{HN}(x)$ and bending $E_{FGM}^{HM}(x)$ of FGM core with cross-section A_{FGM} (height h_{FGM} and depth b) and quadratic moment of inertia I_{FGM} can be expressed in form

$$E_{FGM}^{HN}(x) = \frac{\int_{-h_{FGM}/2}^{h_{FGM}/2} b E_{FGM}(x,y) dy}{A_{FGM}} \quad (2)$$

$$E_{FGM}^{HM}(x) = \frac{\int_{-h_{FGM}/2}^{h_{FGM}/2} b y^2 E_{FGM}(x,y) dy}{I_{FGM}} \quad (3)$$

Both homogenized Youngs' moduli of FGM core are dependent only on axial location x and not on transversal location y .

2.2 Homogenized properties of beam with FGM core and piezoelectric layers

Homogenized Young's modulus for axial loading $E^{HN}(x)$ and bending $E^{HM}(x)$ of beam with FGM core and piezoelectric layers can be expressed in form

$$E^{HN}(x) = \frac{A_{FGM}}{A} E_{FGM}^{HN}(x) + \frac{2A_p}{A} E_p \quad (4)$$

$$E^{HM}(x) = \frac{I_{FGM}}{I} E_{FGM}^{HN}(x) + \frac{2I_{pz}}{I} E_p \quad (5)$$

where A is total cross section ($A = A_{FGM} + 2A_p$), I is total quadratic moment of inertia and I_{pz} is quadratic moment of inertia of piezolayer to global axis z .

Both homogenized Youngs' moduli of beam with FGM core and piezoelectric layers are dependent only on axial location x .

3 PIEZOELECTRIC BEAM FINITE ELEMENT EQUATIONS

3.1 Piezoelectric constitutive equations

Piezoelectric constitutive equations describe the relation between mechanical and electrical quantities. The form of the constitutive equations depends on chosen mechanical and electrical quantities and can be expressed in two basic configurations. The first configuration is expressed by stress tensor components σ_{kl} and vector components of electric intensity E_k and has form

$$\begin{aligned} \varepsilon_{ij} &= d_{ijk} E_k + s_{ijkl}^E \sigma_{kl} \\ D_i &= \epsilon_{ik}^\sigma E_k + d_{ikl} \sigma_{kl} \end{aligned} \quad (6)$$

where ε_{ij} are strain tensor components, D_i are components of electric displacement vector, d_{ijk} are tensor components of piezoelectric constants, ϵ_{ik}^σ are components of permittivity tensor on conditions constant mechanical stress and s_{ijkl}^E are components of compliance tensor on conditions constant electric intensity [3].

The constitutive equations can be also expressed by strain tensor components ε_{kl} and vector components of electric intensity E_k and has form

$$\begin{aligned}\sigma_{ij} &= c_{ijkl}^E \varepsilon_{kl} - e_{ijk} E_k \\ D_i &= e_{ikl} \varepsilon_{kl} + \epsilon_{ik}^\varepsilon E_k\end{aligned}\quad (7)$$

where new quantities are components of stiffness tensor c_{ijkl}^E and components of piezoelectric modulus tensor e_{ikl} .

The other equations, which play important role, are relation between the components of strain tensor ε_{ij} and components of deformation u_i and relation between vector components of electric intensity E_i and electric potential φ . These relations can be expressed as

$$\begin{aligned}\varepsilon_{ij} &= 1/2 (u_{i,j} + u_{j,i}) \\ E_i &= -\varphi_{,i}\end{aligned}\quad (8)$$

Tensor equations (6) and (7) can be expressed in matrix forms, which is more suitable for finite element formulations, using symmetry of mechanical and electrical quantities as well as material properties. Matrix formulations of constitutive equations (7) can be expressed as

$$\begin{aligned}\boldsymbol{\sigma} &= \mathbf{c}^E \boldsymbol{\varepsilon} - \mathbf{e}^T \mathbf{E} \\ \mathbf{D} &= \mathbf{e} \boldsymbol{\varepsilon} + \boldsymbol{\epsilon}^\varepsilon \mathbf{E}\end{aligned}\quad (9)$$

where $\boldsymbol{\sigma}$ is vector (in mathematical meaning) of 6 stress tensor components, \mathbf{D} is vector of 3 electric displacement vector components, $\boldsymbol{\varepsilon}$ is vector of 6 strain tensor components, \mathbf{E} is vector of 3 electric intensity vector components, \mathbf{c}^E is 6x6 matrix of mechanical properties, $\boldsymbol{\epsilon}^\varepsilon$ is 3x3 matrix of electrical properties and \mathbf{e} is 3x6 matrix of piezoelectric properties.

3.2 Piezoelectric FEM equations

Piezoelectric governing equations for dynamic problems can be obtained by Hamilton's principle, which can be written in form

$$\int_{t_1}^{t_2} (\delta L + \delta W) dt = 0 \quad (10)$$

where L is Lagrangian, W is work of external mechanical and electrical forces and t_1 and t_2 defined considered time interval. Lagrangian of piezoelectric structure is given by

$$L = T - U + W_e \quad (11)$$

where T , U and W_e is kinetic energy, potential energy and electric energy of investigated structure, respectively. They can be expressed as

$$\begin{aligned} T &= \int_{(V)} \frac{1}{2} \rho \dot{\mathbf{u}}^T \dot{\mathbf{u}} dV \\ U &= \int_{(V)} \frac{1}{2} \boldsymbol{\varepsilon}^T \boldsymbol{\sigma} dV \\ W_e &= \int_{(V)} \frac{1}{2} \mathbf{E}^T \mathbf{D} dV \end{aligned} \quad (12)$$

where $\dot{\mathbf{u}}$ is velocity vector with 3 components. Virtual work of external mechanical and electrical forces can be expressed as

$$\delta W = \sum \delta \mathbf{u}^T \mathbf{F} - \sum \delta \phi Q \quad (13)$$

where \mathbf{u} is displacement vector with 3 components, \mathbf{F} is force vector with 3 components, ϕ is electric scalar potential and Q is electric charge.

Hamilton's principle (10) can be using equations (12), (13) and constitutive equation (9) expressed in following form

$$\int_{t_1}^{t_2} \left[- \int_{(V)} \rho \delta \mathbf{u}^T \dot{\mathbf{u}} dV - \int_{(V)} \delta \boldsymbol{\varepsilon}^T \mathbf{c}^E \boldsymbol{\varepsilon} dV + \int_{(V)} \delta \boldsymbol{\varepsilon}^T \mathbf{e}^T \mathbf{E} dV + \int_{(V)} \delta \mathbf{E}^T \mathbf{e} \boldsymbol{\varepsilon} dV + \int_{(V)} \delta \mathbf{E}^T \boldsymbol{\epsilon}^E \mathbf{E} dV + \sum \delta \mathbf{u}^T \mathbf{F} - \sum \delta \phi Q \right] dt = 0 \quad (14)$$

Relationship between displacement of point and nodal displacement of finite element and between scalar electric potential of point and nodal scalar electric potential of finite element can be expressed by shape functions of element

$$\begin{aligned} \mathbf{u} &= \mathbf{N}_u \mathbf{u}^e \\ \phi &= \mathbf{N}_\phi \phi^e \end{aligned} \quad (15)$$

\mathbf{N}_u and \mathbf{N}_ϕ are matrices with shape functions. Relationship between components of strain and components of nodal displacements and relationship between components of electric intensity and nodal electric scalar potential have forms

$$\begin{aligned}\boldsymbol{\varepsilon} &= \mathbf{B}_u \mathbf{u}^e \\ \mathbf{E} &= -\mathbf{B}_\phi \boldsymbol{\phi}^e\end{aligned}\tag{16}$$

\mathbf{B}_u and \mathbf{B}_ϕ are matrices with derivative of shape functions. Hamilton's principle (10) can be rewritten by equations (15) and (16) into form

$$\begin{aligned}& \int_{t_1}^{t_2} \delta(\mathbf{u}^e)^T \left[- \left(\int_{(V)} \mathbf{N}_u^T \rho \mathbf{N}_u dV \right) \ddot{\mathbf{u}}^e - \left(\int_{(V)} \mathbf{B}_u^T \mathbf{c}^E \mathbf{B}_u dV \right) \mathbf{u}^e - \left(\int_{(V)} \mathbf{B}_u^T \mathbf{e}^T \mathbf{B}_\phi dV \right) \boldsymbol{\phi}^e + \right. \\ & \left. + \sum \mathbf{N}_u^T \mathbf{F} \right] dt + \int_{t_1}^{t_2} \delta(\boldsymbol{\phi}^e)^T \left[- \left(\int_{(V)} \mathbf{B}_\phi^T \mathbf{e} \mathbf{B}_u dV \right) \mathbf{u}^e + \left(\int_{(V)} \mathbf{B}_\phi^T \boldsymbol{\epsilon}^E \mathbf{B}_\phi dV \right) \boldsymbol{\phi}^e - \right. \\ & \left. \sum \mathbf{N}_\phi^T Q \right] dt = 0\end{aligned}\tag{17}$$

FEM equations of individual element can be derived from (17) in form

$$\begin{bmatrix} \mathbf{M}_{uu}^e & \mathbf{0}^e \\ \mathbf{0}^e & \mathbf{0}^e \end{bmatrix} \begin{bmatrix} \ddot{\mathbf{u}}^e \\ \ddot{\boldsymbol{\phi}}^e \end{bmatrix} + \begin{bmatrix} \mathbf{K}_{uu}^e & \mathbf{K}_{u\phi}^e \\ \mathbf{K}_{\phi u}^e & \mathbf{K}_{\phi\phi}^e \end{bmatrix} \begin{bmatrix} \mathbf{u}^e \\ \boldsymbol{\phi}^e \end{bmatrix} = \begin{bmatrix} \mathbf{F}^e \\ \mathbf{Q}^e \end{bmatrix}\tag{18}$$

The equation (18) represents dynamic behavior of piezoelectric material without mechanical damping. If the damping is considered, then the equation (18) has form

$$\begin{bmatrix} \mathbf{M}_{uu}^e & \mathbf{0}^e \\ \mathbf{0}^e & \mathbf{0}^e \end{bmatrix} \begin{bmatrix} \ddot{\mathbf{u}}^e \\ \ddot{\boldsymbol{\phi}}^e \end{bmatrix} + \begin{bmatrix} \mathbf{C}_{uu}^e & \mathbf{0}^e \\ \mathbf{0}^e & \mathbf{0}^e \end{bmatrix} \begin{bmatrix} \dot{\mathbf{u}}^e \\ \dot{\boldsymbol{\phi}}^e \end{bmatrix} + \begin{bmatrix} \mathbf{K}_{uu}^e & \mathbf{K}_{u\phi}^e \\ \mathbf{K}_{\phi u}^e & \mathbf{K}_{\phi\phi}^e \end{bmatrix} \begin{bmatrix} \mathbf{u}^e \\ \boldsymbol{\phi}^e \end{bmatrix} = \begin{bmatrix} \mathbf{F}^e \\ \mathbf{Q}^e \end{bmatrix}\tag{19}$$

where individual submatrices are defined as follows:

$$\mathbf{M}_{uu}^e = \int_{(V)} \mathbf{N}_u^T \rho \mathbf{N}_u dV; \mathbf{K}_{uu}^e = \int_{(V)} \mathbf{B}_u^T \mathbf{c}^E \mathbf{B}_u dV; \mathbf{K}_{u\phi}^e = \int_{(V)} \mathbf{B}_u^T \mathbf{e}^T \mathbf{B}_\phi dV;$$

$$\mathbf{K}_{\phi u}^e = \int_{(V)} \mathbf{B}_\phi^T \mathbf{e} \mathbf{B}_u dV; \mathbf{K}_{\phi\phi}^e = \int_{(V)} \mathbf{B}_\phi^T \boldsymbol{\epsilon}^E \mathbf{B}_\phi dV; \mathbf{C}_{uu}^e = \alpha \mathbf{M}_{uu}^e + \beta \mathbf{K}_{uu}^e$$

\mathbf{F}^e and \mathbf{Q}^e represent nodal forces and nodal charges on considered element.

For whole structure we can formally write

$$\begin{bmatrix} \mathbf{M}_{uu} & \mathbf{0} \\ \mathbf{0} & \mathbf{0} \end{bmatrix} \begin{bmatrix} \ddot{\mathbf{u}} \\ \ddot{\boldsymbol{\phi}} \end{bmatrix} + \begin{bmatrix} \mathbf{C}_{uu} & \mathbf{0} \\ \mathbf{0} & \mathbf{0} \end{bmatrix} \begin{bmatrix} \dot{\mathbf{u}} \\ \dot{\boldsymbol{\phi}} \end{bmatrix} + \begin{bmatrix} \mathbf{K}_{uu} & \mathbf{K}_{u\phi} \\ \mathbf{K}_{\phi u} & \mathbf{K}_{\phi\phi} \end{bmatrix} \begin{bmatrix} \mathbf{u} \\ \boldsymbol{\phi} \end{bmatrix} = \begin{bmatrix} \mathbf{F} \\ \mathbf{Q} \end{bmatrix}\tag{20}$$

3.3 FEM equations of FGM beam with piezoelectric layers

2D beam element with piezoelectric layers and FGM core with degree of freedom is shown in Fig. 2.

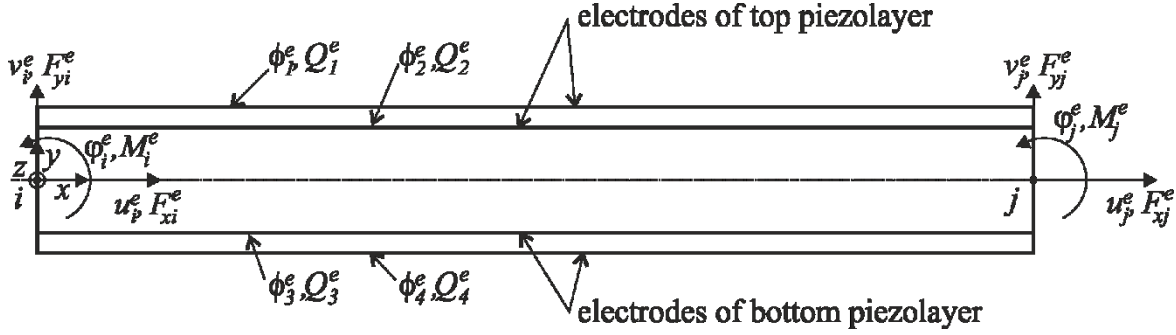


Fig. 2: 2D beam element with piezoelectric layers – degree of freedom and internal forces

Length of beam element is L^e , cross-section of FGM core is A_{FGM} and cross-section of piezolayer is A_p . Homogenized Youngs' moduli for axial loading and bending are computed according equations (4) and (5). Mechanical degree of freedom of element are displacements and rotations in both nodes $(u_i^e, v_i^e, \phi_i^e, u_j^e, v_j^e, \phi_j^e)$, electrical degree of freedom are electric potential on all 4 electrodes of both piezoelectric layers $(\phi_1^e, \phi_2^e, \phi_3^e, \phi_4^e)$. Internal element mechanical loads are forces and moments in both nodes $(F_{xi}^e, F_{yi}^e, M_i^e, F_{xj}^e, F_{yj}^e, M_j^e)$, internal element electric loads are electric charge on all 4 electrodes of both piezoelectric layers $(Q_1^e, Q_2^e, Q_3^e, Q_4^e)$ [4].

FEM equation of 2D piezoelectric beam with FGM core has formally the same equation as equation (20), but individual stiffness submatrices have different form, because they are using transfer constant and not classical shape functions. Mass submatrix \mathbf{M}_{uu}^e can be constructed by classical shape functions.

The structural submatrix for the beam element with piezoelectric layers can be expressed in a form

$$\mathbf{K}_{uu}^e = \begin{bmatrix} k'_u & 0 & 0 & -k'_u & 0 & 0 \\ 0 & k'_{v2} & k'_{v3} & 0 & -k'_{v2} & k_{v2} \\ 0 & k'_{v3} & k'_{v33} & 0 & -k'_{v3} & k_{v3} \\ -k'_u & 0 & 0 & k'_u & 0 & 0 \\ 0 & -k'_{v2} & -k'_{v3} & 0 & k'_{v2} & -k_{v2} \\ 0 & k_{v2} & k_{v3} & 0 & -k_{v2} & k_{v23} \end{bmatrix} \quad (21)$$

Computation of individual components of the structural submatrix contains the influence of FGM core and piezoelectric layers, where homogenized material properties of beam is considered. The computation is performed numerically using concept of transfer constants.

The electrical submatrix for the beam element with piezoelectric layers can be expressed in a form

$$\mathbf{K}_{\phi\phi}^e = \begin{bmatrix} -\frac{A_p L \epsilon^\varepsilon}{h_p^2} & \frac{A_p L \epsilon^\varepsilon}{h_p^2} & 0 & 0 \\ \frac{A_p L \epsilon^\varepsilon}{h_p^2} & -\frac{A_p L \epsilon^\varepsilon}{h_p^2} & 0 & 0 \\ 0 & 0 & -\frac{A_p L \epsilon^\varepsilon}{h_p^2} & \frac{A_p L \epsilon^\varepsilon}{h_p^2} \\ 0 & 0 & \frac{A_p L \epsilon^\varepsilon}{h_p^2} & -\frac{A_p L \epsilon^\varepsilon}{h_p^2} \end{bmatrix} \quad (22)$$

where ϵ^ε is permittivity of piezoelectric layer under constant strain.

Submatrices of piezoelectric coupling can be expressed in following forms

$$\mathbf{K}_{u\phi}^e = \begin{bmatrix} -\frac{A_p d_{21} E_p}{h_p} & \frac{A_p d_{21} E_p}{h_p} & -\frac{A_p d_{21} E_p}{h_p} & \frac{A_p d_{21} E_p}{h_p} \\ 0 & 0 & 0 & 0 \\ \frac{A_y d_{21} E_p}{h_p} & -\frac{A_y d_{21} E_p}{h_p} & \frac{A_y d_{21} E_p}{h_p} & -\frac{A_y d_{21} E_p}{h_p} \\ \frac{A_p d_{21} E_p}{h_p} & -\frac{A_p d_{21} E_p}{h_p} & \frac{A_p d_{21} E_p}{h_p} & -\frac{A_p d_{21} E_p}{h_p} \\ 0 & 0 & 0 & 0 \\ -\frac{A_y d_{21} E_p}{h_p} & \frac{A_y d_{21} E_p}{h_p} & -\frac{A_y d_{21} E_p}{h_p} & \frac{A_y d_{21} E_p}{h_p} \end{bmatrix} \quad (23)$$

$$\mathbf{K}_{\phi u}^e = \begin{bmatrix} -\frac{A_p e_{21}}{h_p} & 0 & \frac{A_y e_{21}}{h_p} & \frac{A_p e_{21}}{h_p} & 0 & -\frac{A_y e_{21}}{h_p} \\ \frac{A_p e_{21}}{h_p} & 0 & -\frac{A_y e_{21}}{h_p} & -\frac{A_p e_{21}}{h_p} & 0 & \frac{A_y e_{21}}{h_p} \\ -\frac{A_p e_{21}}{h_p} & 0 & \frac{A_y e_{21}}{h_p} & \frac{A_p e_{21}}{h_p} & 0 & -\frac{A_y e_{21}}{h_p} \\ \frac{A_p e_{21}}{h_p} & 0 & -\frac{A_y e_{21}}{h_p} & -\frac{A_p e_{21}}{h_p} & 0 & \frac{A_y e_{21}}{h_p} \end{bmatrix} \quad (24)$$

where $A_y = \frac{1}{2} A_p (h_{FGM} + h_p)$, d_{21} and e_{21} are piezoelectric constants.

4 STATE SPACE EQUATIONS OF PIEZOELECTRIC BEAM FINITE ELEMENT

Smart structures made from piezoelectric material, are usually connected to controller in order to have required behavior of structure. For this purpose, FEM equations are transformed to state space equations [5].

The voltage actuation and charge sensing are considered. Actuation is done by imposing a voltage on the actuators and sensing by imposing a zero voltage and measuring the electric

charges appearing on the sensors. Vector of nodal displacement of the structure \mathbf{u} can be expressed by truncated modal decomposition

$$\mathbf{u} = \mathbf{Z}\mathbf{x} \quad (25)$$

where \mathbf{Z} represents chosen n modal shapes of structure and \mathbf{x} represents modal amplitudes. Using equation (25) can be FEM equation of whole structure (20) rewritten to form

$$\mathbf{M}_{uu} \mathbf{Z}\ddot{\mathbf{x}} + \mathbf{C}_{uu} \mathbf{Z}\dot{\mathbf{x}} + \mathbf{K}_{uu} \mathbf{Z}\mathbf{x} + \mathbf{K}_{u\phi} \boldsymbol{\phi} = \mathbf{0} \quad (26)$$

$$\mathbf{K}_{\phi u} \mathbf{Z}\mathbf{x} + \mathbf{K}_{\phi\phi} \boldsymbol{\phi} = \mathbf{Q} \quad (27)$$

Using orthogonality property of mode shapes

$$\mathbf{Z}^T \mathbf{M}_{uu} \mathbf{Z} = \text{diag}(\mu_k) \quad (28)$$

$$\mathbf{Z}^T \mathbf{K}_{uu} \mathbf{Z} = \text{diag}(\mu_k \omega_k^2) \quad (29)$$

$$\mathbf{Z}^T \mathbf{C}_{uu} \mathbf{Z} = \text{diag}(2\xi_k \mu_k \omega_k) \quad (30)$$

equations (26) and (27) can be rewritten into form

$$\boldsymbol{\mu} \ddot{\mathbf{x}} + 2 \boldsymbol{\xi} \boldsymbol{\mu} \boldsymbol{\omega} \dot{\mathbf{x}} + \boldsymbol{\mu} \boldsymbol{\omega}^2 \mathbf{x} + \mathbf{Z}^T \mathbf{K}_{u\phi} \boldsymbol{\phi} = \mathbf{0} \quad (31)$$

$$\mathbf{K}_{\phi u} \mathbf{Z}\mathbf{x} + \mathbf{K}_{\phi\phi} \boldsymbol{\phi} = \mathbf{Q} \quad (32)$$

where matrices $\boldsymbol{\mu}$, $\boldsymbol{\omega}$ and $\boldsymbol{\xi}$ represent matrix of modal masses, modal frequencies and modal damping ratios of structure, respectively. After some manipulation, we can from equation (31) obtain

$$\ddot{\mathbf{x}} = -2 \boldsymbol{\xi} \boldsymbol{\omega} \dot{\mathbf{x}} - \boldsymbol{\omega}^2 \mathbf{x} - \boldsymbol{\mu}^{-1} \mathbf{Z}^T \mathbf{K}_{u\phi} \boldsymbol{\phi} \quad (33)$$

Equation (33) and (32) can be rewritten into form

$$\begin{bmatrix} \dot{\mathbf{x}} \\ \ddot{\mathbf{x}} \end{bmatrix} = \begin{bmatrix} \mathbf{0} & \mathbf{I} \\ -\boldsymbol{\omega}^2 & -2 \boldsymbol{\xi} \boldsymbol{\omega} \end{bmatrix} \begin{bmatrix} \mathbf{x} \\ \dot{\mathbf{x}} \end{bmatrix} + \begin{bmatrix} \mathbf{0} \\ -\boldsymbol{\mu}^{-1} \mathbf{Z}^T \mathbf{K}_{u\phi} \end{bmatrix} \boldsymbol{\phi} \quad (34)$$

$$\mathbf{Q} = [\mathbf{K}_{\phi u} \mathbf{Z} \quad \mathbf{0}] \begin{bmatrix} \mathbf{x} \\ \dot{\mathbf{x}} \end{bmatrix} + \mathbf{K}_{\phi\phi} \boldsymbol{\phi} \quad (35)$$

Equations (34) and (35) represents state space model of structure with piezoelectric sensors and actuators and can be used to analyzed structure from control viewpoint.

5 CONCLUSION

The paper presents beam finite element with piezoelectric layers, where core of the beam can be made of FGM materials. Such combination of materials is very attractive for mechatronic applications, because material composition of FGM core can be optimized for design stress state and deformation can be controlled by voltages on electrodes. FEM equations are rewritten to state space equations using truncated modal decomposition. Such model of beam structure can be easily incorporated into control model.

REFERENCES

- [1] Murín, J., Kutiš, V., Masný, M. Composite (FGMs) beam finite elements. In: Composites with Micro- and Nano-Structure. Edited by: V. Kompiš, Springer Science+Business Media B.V., (2008), ISBN 978-1-4020-6974-1, p. 209 – 239.
- [2] Kutiš, V., Murín, J., Belák, R., Paulech, J. Beam element with spatial variation of material properties for multiphysics analysis of functionally graded materials. Computers & Structures, (2011) 89:1192–1205.
- [3] Moheimani, S.O.R. and Fleming, A.J.. Piezoelectric Transducers for Vibration Control and Damping. Springer, (2006).
- [4] Bruant, I., Coffignal, G., Lene, F., Verge, M. Active control of beam structures with piezoelectric actuators and sensors: modeling and simulation. Smart Material Structures (2001), 10:404–408.
- [5] Piefort, V. Finite Element Modeling of Piezoelectric Structures, PhD Thesis, Université Libre de Bruxelles, (2001).

Performance Engineering for Advanced Lattice Boltzmann Methods in CFD

Konstantin Kutscher*, Manfred Krafczyk**, Martin Geier***, Martin Schönherr****

*TU Braunschweig, iRMB, **TU Braunschweig, iRMB, ***TU Braunschweig, iRMB, ****TU Braunschweig, iRMB

ABSTRACT

We report on techniques developed for and implemented in our research CFD code VirtualFluids which has been developed as a C++-library for massively parallel CFD simulation. Its modular structure includes the following functionality: hybrid block based tree type grid, generation based on geometric objects and/or CAD data, restart options for different parallel setups, D3Q27 Cumulant LBM kernel including a so-called Esoteric Twist approach to reduce memory requirements, second order accurate grid refinement, implicit turbulence model, a hybrid parallelization based on MPI and pthreads, restart/checkpointing based on MPI/IO as well as parallel In-situ visualization and output in Paraview parallel format. The code is developed using of object-oriented techniques and design patterns which foster support and functional extension. We will report on various massively parallel CFD benchmarks for real-world problems including examples running on GPGPUs and discuss future options for code extensions for usage of hybrid CPU/GPU clusters.

Limiting Techniques and hp Adaptivity for Continuous High-order Bernstein Finite Element Approximations

Dmitri Kuzmin^{*}, Christopher Kees^{**}, Manuel Quezada de Luna^{***}

^{*}TU Dortmund University, ^{**}US Army Engineer Research & Development Center, ^{***}US Army Engineer Research & Development Center

ABSTRACT

In this talk, we present three new approaches to blending a continuous high-order Bernstein finite element discretization with a monotone piecewise-linear approximation based on the same nodal points. The first approach is a predictor-corrector method which constrains the difference between the high and low-order solutions using a localized flux-corrected transport (FCT) algorithm. The second approach constrains the difference between the residuals of the underlying discretizations using nodal limiters to adjust monotonicity-preserving artificial diffusion coefficients. This correction leads to nonlinear algebraic systems which are solved iteratively. The third approach combines the high and low-order finite element bases using a continuous piecewise-linear limiter function. This low-level limiting strategy represents a new kind of hp adaptivity. The proposed method adjusts the local order of approximation in a continuous manner while keeping the number of degrees of freedom fixed. The pros and cons of each limiting technique for high-order finite elements will be discussed and results of numerical studies for 2D test problems will be presented.

Reduced Order Models for Divergence-Conforming Isogeometric Flow Simulations

Trond Kvamsdal^{*}, Eivind Fonn^{**}, Harald van Brummelen^{***}, Adil Rasheed^{****}

^{*}Norwegian University of Science and Technology, ^{**}SINTEF Digital, ^{***}Eindhoven University of Technology,
^{****}SINTEF Digital

ABSTRACT

Repetitive solutions of parametrized flow problems can be quite demanding, each solution involving a million or more degrees of freedom, that takes hours or days of computational time. A promising methodology to reduce the (on-line) computational effort is the use of Reduced Order Modelling (ROM). ROM offers the possibility to balance loss of accuracy with gain in efficiency. We have tied ROM with a divergence-conforming isogeometric high-fidelity method for incompressible flow simulations and achieved (significant) additional speedup compared to non-conforming methods. The additional speedup is related to less computations related to the so-called supremizers needed for avoiding that the ROM model get a rank-deficient velocity-pressure block. We will illustrate the performance of the development method by doing high fidelity simulations of stationary Navier-Stokes were performed of flow around a NACA0015 airfoil where we varies the inflow velocity and the angle of attack.

Performance Characteristics of a High-order Finite Element Application on a Modern High Performance Computing System – Blue Waters

JaeHyuk Kwack*, Gregory Bauer**

*National Center for Supercomputing Applications / University of Illinois at Urbana-Champaign, **National Center for Supercomputing Applications / University of Illinois at Urbana-Champaign

ABSTRACT

Performance indices of high performance computing (HPC) systems poorly represent the performance of science and engineering applications on the HPC systems. The most popular performance index of HPC systems, the TOP500, relies on a traditional LINPACK benchmark that is very limitedly used for modern HPC applications. The HPC community has recently made significant efforts to include more general numerical algorithms to represent the performance of modern HPC applications. This study is one of our continued efforts to find out the most optimal way to represent the performance of HPC systems and HPC applications [1,2,3]. We employed a high-order finite element application optimized for modern HPC systems to analyze performance characteristics depending on several configurations such as the order of shape functions, employed linear algebra solvers and structure for MPI and OpenMP hybrid computing. We profiled the application in scale with Cray Performance Measurement and Analysis Tools (CPMAT) on Blue Waters at National Center for Supercomputing Applications (NCSA). We present collected hardware counter data for flops, flop-rates, L1/L2/L3 data cache accesses and memory access for several important routines. In addition, we discuss potential rooflines of the system performance by analyzing the performance characteristics of the crucial routines for the considered configurations. With the above analysis, we provide our recommendations to help scientists and engineers optimize their algorithms for science and engineering applications on modern HPC systems. [1] J. Kwack, G. Bauer, S.Koric, "Performance Test of Parallel Linear Equation Solvers on Blue Waters - Cray XE6/XK7 system", Proceedings of the Cray Users Group Meeting (CUG2016), London, England, May 2016. [2] G. Bauer, V. Anisimov, G. Arnold, B. Bode, R. Brunner, T. Cortese, R. Haas, A. Kot, W. Kramer, J. Kwack, J. Li, C. Mendes, R. Mokos, C. Steffen, "Updating the SPP Benchmark Suite for Extreme-Scale Systems", Proceedings of the Cray Users Group Meeting (CUG2017), Redmond, WA, May 2017. [3] J. Kwack and G. Bauer, "HPCG and HPGMG benchmark tests on Multiple Program, Multiple Data (MPMD) mode on Blue Waters - a Cray XE6/XK7 hybrid system", Concurrency and Computation, Practice and Experience journal, 30(1), 10.1002/cpe.4298, 2017.

Numerical Simulation of Wave/Current-Induced Scour Below Pipelines Using RKPM Method

On Lei Annie Kwok*, Pai-Chen Guan**, Chien-Ting Sun***

*National Taiwan University, **National Taiwan Ocean University, ***National Taiwan Ocean University

ABSTRACT

Stability of marine pipelines and marine cables can be significantly affected by the presence of scour due to repeated wave and current action. In this study, RKPM (reproducing kernel particle method)-based numerical framework is used to simulate this fluid-structure-soil interaction process. Semi-Lagrangian reproducing kernel incompressible fluid method is employed to model the ocean wave and tidal flow while the pipeline is analyzed by RKPM Mindlin plate formulation. A non-cohesive seabed sediment is considered and modeled by a semi-Lagrangian reproducing kernel method. A contact algorithm is used to handle the interaction between fluid (waves), structure (pipelines) and solid (soil sediment). This investigation focuses on the effect of pipeline embedment, water depth to pipeline diameter ratios and soil properties on the stability of submarine pipelines/cables.

Method to Analyze Welding Deformation Based on a Visualization Model for Plant Construction

KiYoun Kwon*

*Kumoh National Institute of Technology

ABSTRACT

The ship and offshore plant are designed by dividing it into several blocks which constitute the hull, and each block is constructed separately and assembled. Blocks are usually made by assembling small parts fabricated by machining steel plates, and the plant is constructed through the assembly of large blocks from the small blocks. During these process, welding deformation causes many problems [1]. In order to prevent welding deformation, FEA (finite element analysis) is widely used. In this paper, we propose a mesh generation method to enable welding analysis based on a visualization model. The visualization model is widely used for visualizing and sharing large cad data in PLM (product lifecycle management) [2]. This model is mainly composed of triangular elements to minimize the file size and improve rendering performance. The method proposed in this paper is as follows. The visualization model has no information about the welding line. First, boundary curves are restored from the triangle elements of visualization model. After matching the connectivity of triangular elements, boundary element edges are extracted. Boundary curves are generated by connecting these boundary element edges. If the restored boundary curve lies on another part, it is classified as a welding line. Then, a polygon surface is created by using triangle elements constituting boundary curves for each plate, and a trim surface is created to include welding lines. The number of elements is given to the boundary curves and the welding lines, and a quadrilateral mesh is generated by using the domain decomposition method [3]. Finally, the welding line attribute information is added to the elements included in the welding line so that thermal deformation analysis is possible

References 1. Heo, H. and Chung, H, 2014, Stochastic assessment considering process variation for impact of welding shrinkage on cost of ship production, International Journal of Production Research, pp. 6076-6091 2. Ball, A., Ding, L. and Patel, M., 2007, Lightweight Formats for Product Model Data Exchange and Preservation, PV 2007 Conference, pp. 9-11. 3. Chae, S. W. and Kwon, K. Y., Quadrilateral Mesh Generation on Trimmed NURBS Surfaces, KSME International Journal, Vol. 15, pp. 592~601, 2001.

Hygroelastic Multiscale Modeling of Epoxy-based Nanocomposites

Sunyong Kwon*, Man Young Lee**, Seunghwa Yang***

*Chung-Ang University, **Agency for Defense Development, ***Chung-Ang University

ABSTRACT

Hygroscopic aging occurs inevitably by consistent exposure to moisture in service condition of epoxy-based nanocomposites. Slow and steady process of aging causes swelling, plasticization, and degradation of mechanical and interfacial properties of epoxy-based nanocomposite eventually leading to the fast fracture of nanocomposites. Since the aging is a long-time process, experimental approach of hygroscopic aging is burdensome because it needs accelerated aging environment accompanied by time-to-time preparation of epoxy coupons for evaluation of properties. Therefore, in order to access hygroelastic behavior with computational mechanics, molecular dynamics (MD) simulation is firstly applied. To determine the aged structure-to-hygroelastic property relationship of epoxy-based nanocomposite, varying cross-linking and water contents of diglycidyl ether of bisphenol F (EPON862®)/ triethylenetetramine (TETA) epoxy system is studied. A defect-free single layer graphene is added in the nanocomposite structure as reinforcement. The dynamic cross-linking method is used to set the crosslinking ratio of epoxy from 30 to 70%. For each cross linking ratio, moisture weight fraction of 0, 2, 4 wt% is considered in each nanocomposite unit cell. Through the classical ensemble simulation incorporated with ab-initio parameterized PCFF forcefield, coefficient of moisture expansion (CME), diffusion coefficient of water, and elastic modulus and cohesive zone law of epoxy/graphene nanocomposite models are predicted. To efficiently diagnose and predict hygroscopic aging in real life conditions, establishing ternary correlation of aging time-micro structure- macro property is necessary. However, as MD simulation can only describe couple microseconds of material status, continuum scale computational analysis with well-established time dependent property analysis is essential to overcome the limitations of MD simulation in describing hygroscopic aging behavior of epoxy-based nanocomposites. Furthermore, hygroelastic and interfacial properties of epoxy/graphene nanocomposite calculated by MD simulation are essential element for implementing multi-scale analysis. Therefore, MD simulation incorporated with micromechanics theory and finite element method (FEM) is presented in this study. Thus, based on the previous calculation of hygroelastic and interfacial properties by MD simulation, moisture expansion elastic constitutive equation model and stress-strain behavior of moisture absorbed nanocomposite constitutive equation model approximation can be developed. Also, mapping of elastoplastic properties by connecting time dependent moisture concentration profile and Young's moduli of epoxy-based nanocomposite will be analyzed.

Adaptive Isogeometric Analysis with Hierarchical B-Splines

Markus Kästner*, Paul Hennig**, Marreddy Ambati***, Laura De Lorenzis****

*Institute for Solid Mechanics, TU Dresden, **Institute for Solid Mechanics, TU Dresden, ***Institute for Applied Mechanics, TU Braunschweig, ****Institute for Applied Mechanics, TU Braunschweig

ABSTRACT

The finite element discretisation of a large class of boundary value problems requires highly refined meshes to appropriately resolve, e.g., singularities in contact problems, shear bands in elasto-plasticity or steep local gradients in the field variables of phase-field models. If these domains evolve during the simulation, adaptive local mesh refinement and coarsening are essential for efficient computations. As Isogeometric Analysis (IGA) introduced by Hughes et al. [1] overcomes the disjunction between geometry and computational models it is the ideal discretisation technique to be combined with adaptive mesh refinement because already the coarsest mesh provides an exact geometry representation which is preserved during refinement. Tedious interactions with an underlying geometry during re-meshing, which is required to increase the accuracy of the geometry representation in standard FEM, are avoided. We present projection methods and transfer operations required for adaptive mesh refinement/coarsening in problems with internal variables at integration point level. By extending the results of Hennig et al. [2], we propose three different local and semi-local least squares projection methods for field variables and compare them to the standard global version. We discuss the application of two different transfer operators for internal variables. An alternative new operator inspired by superconvergent patch recovery [3] is also proposed. The presented projection methods and transfer operations are tested in benchmark problems and applied to phase-field modelling of spinodal decomposition and brittle and ductile fracture. REFERENCES [1] T. Hughes, J. Cottrell, Y. Bazilevs, Isogeometric analysis: CAD, finite elements, NURBS, exact geometry and mesh refinement, *Comput. Methods Appl. Mech. Eng.* Vol. 194, pp. 4135–4195, 2005. [2] P. Hennig, S. Müller, M. Kästner, Bézier extraction and adaptive refinement of truncated hierarchical NURBS. *Comput. Methods Appl. Mech. Eng.* Vol. 305, pp. 316 – 339, 2016. [3] M. Kumar, T. Kvamsdal, K. A. Johannessen, Superconvergent patch recovery and a posteriori error estimation technique in adaptive isogeometric analysis, *Comput. Methods Appl. Mech. Eng.* Vol. 316, pp. 1086 – 1156, 2017

Coupled Electro-Physiology, Mechanical and Fluid Structure Interaction for Heart Simulation Using LS-DYNA

Pierre L'Epplattenier^{*}, Sarah Bateau-Meyer^{**}, David Benson^{***}, Inaki Caldichoury^{****},
Facundo Del Pin^{*****}, Attila Nagy^{*****}

^{*}Livermore Software Technology Corporation, Livermore, CA, USA, ^{**}Livermore Software Technology Corporation, CA, USA, ^{***}Livermore Software Technology Corporation, Livermore, CA, USA, ^{****}Livermore Software Technology Corporation, Livermore, CA, USA, ^{*****}Livermore Software Technology Corporation, Livermore, CA, USA, ^{*****}Livermore Software Technology Corporation

ABSTRACT

Heart diseases are the leading cause of death in the western World. A deeper understanding of the heart functioning can provide important insights for medical doctors and clinicians in treating cardiovascular diseases but its extraordinary complexity represents a challenge for scientists and clinicians studying it. In this respect, some recent efforts have been made to be able to model the functioning of the heart along the entire heartbeat using the finite element commercial software LS-DYNA [1]. The model starts with Electro-Physiology (EP) which simulates the propagation of the wave of cell transmembrane potential in the heart. Different models, called "mono-domain" or "bi-domain", couple the diffusion of the potential along the walls of the heart with ionic equations describing the exchanges between the inner and the outer parts of the cells. These models give in particular the local intracellular calcium ion which provides the activation part of the heart muscle myofilament models, hence the input for the mechanical tissue models. The mechanical deformations of the heart are coupled with the hemodynamics using the Fluid and Structure Interaction (FSI) model of LS-DYNA. Benchmarks of the different parts of the model will be presented, followed by coupled multiphysics simulations of parts of the heart as well as an example of a full heart beat. The model will also be used to show the difference between a healthy heart and different heart diseases such as cardiac arrhythmia, in term of EP behaviors, mechanical deformations and pumped blood. [1] Hallquist, J.O., LS-DYNA Theory Manual. ISBN 0-9778540-0-0, LSTC, Livermore, CA, USA, 2006.

SIMNANO: A Highly Efficient Molecular Systems Energy Minimizer

NIKOS LAGAROS*, STAVROS CHATZIELEFTHERIOU**

*Institute of Structural Analysis & Antiseismic Research, School of Civil Engineering, National Technical University of Athens, **Institute of Structural Analysis & Antiseismic Research, School of Civil Engineering, National Technical University of Athens

ABSTRACT

In this study a new energy computationally highly efficient minimizer is presented, achieving excellent convergence properties; therefore, becomes suitable for dealing with large-scale molecular systems. SimNano relies on the analytical calculation of the gradient vectors and hessian matrices of the molecular systems by applying a computational modeling framework, possessed by the authors (J. Chem. Inf. Model. 2016, 56 (10), 1963-1978), that was inspired from structural mechanics and the finite element method. In order to present the efficiency of the proposed energy minimizer several test cases are examined and the results are compared with those obtained by one of the most popular molecular simulations software (LAMMPS). The comparative results indicate that the proposed minimizer depict superior convergence properties to those of the algorithms that are generally employed in the field. SimNano energy minimizer can be downloaded for free from the site: <http://users.ntua.gr/nlagaros/simnano.html>.

Optimization of Stiffened Composite Plate Using Artificial Neural Network-based Differential Evolution Algorithm

THUAN LAM-PHAT*, Son Nguyen-Hoai**, Quan Nguyen-Anh***

*GACES, HCMC University of Technology and Education, Vietnam, **GACES, HCMC University of Technology and Education, Vietnam, ***GACES, HCMC University of Technology and Education, Vietnam

ABSTRACT

In this paper, a new algorithm called ABED (Artificial neural network Based Differential Evolution) is used to find the optimal design for the stiffened composite panel structure. This ABED algorithm is formed by the combination of an improved version of the Differential Evolution (DE) algorithm with the Artificial Neural Network technique and is adopted to look for suitable values of the fiber angle and the thickness of the stiffened composite plate. The ANN is used to compute the fitness of the object functions and evaluate the values related to the constraint conditions, meanwhile, the DE algorithm is used for optimization task. To verify the accuracy and the effectiveness of the algorithm, numerical solutions obtained from the proposed method are compared with those of other available approaches.

A Novel First-order Reliability Method Based on Performance Measure Approach for Highly Nonlinear Problems

Gang LI^{*}, Bin Li^{**}, Hao Hu^{***}

^{*}Dalian University of Technology, ^{**}Dalian University of Technology, ^{***}Yancheng Institute of Technology

ABSTRACT

The first-order reliability method (FORM) is widely used in structural reliability analysis for its simplicity and efficiency. When searching the MPP in traditional FORM, gradient-based algorithms may fail to converge due to oscillation or chaos if the performance function is highly nonlinear. Evolutionary algorithms could achieve convergence solutions even for highly nonlinear performance function, usually with expensive computational cost. To overcome their drawbacks, we propose a new reliability analysis method called PMA-IACC to search the most probable failure point (MPP). As the inverse reliability analysis and reliability analysis are reversible each other, the performance measure approach (PMA) of the inverse reliability analysis could be used for the reliability analysis based on the multi-objective optimization theory. With the iterative calculation of performance measure, the approximate MPP and reliability index would be gradually close to the true MPP and reliability index. Furthermore, the improved adaptive chaos control (IACC) method is also proposed to further improve the robustness and efficiency of inverse reliability analysis by updating and choosing suitable chaos control factors, without additional computational efforts at each iteration. And then, the IACC is integrated into the PMA reliability analysis strategy. The proposed PMA-IACC method has outstanding performance, which has been illustrated by five highly nonlinear examples with different dimensions, distributions and local optimal solution. Compared with some traditional reliability analysis methods, the proposed PMA-based reliability analysis methods (PMA-MCC, PMA-ACC, PMA-IACC) always show better accuracy and efficiency, among which the PMA-IACC is the best and is beneficial to the application in complex engineering problems. Furthermore, although it is hard to obtain the exact probability of failure currently by our proposed method in frame of FORM, our current work could be further used for higher-order reliability analysis based on the MPP-based DRM in the future study.

Multiscale Modeling of Soft Contact and Imulation of Cell Motility

SHAOFAN LI*

*University of California-Berkeley

ABSTRACT

Experimental observations have shown that the elasticity of the extracellular substrate has significant influence on cell motility and cell rotation. To explain such bio-physical or physiology phenomenon has been one of focuses of cell biology or cellular mechanobiology. In this work, we shall discuss multiscale modeling and simulations of soft matter contact and cell adhesion. In particular, our work is focused on modeling and simulation of contact and adhesion of cell on substrates with different rigidities and micro-structures. We have developed a soft matter cell model for actin filament aggregate, and a coarse-grained contact model that is based on a recently proposed multiscale adhesion model, which can take into account the long-range Van der Waals force, steric force, and colloidal interactions etc. By modeling the cell as an isotropic amphiphilic aggregate, it may be shown that under external stimulus the cell can change its microstructure, conformation, as well as configuration. We have used the soft matter cell model, the multiscale cell adhesive and contact model in conjunction with recently proposed Multiscale Moving Contact Line theory to successfully simulate cell motility in a virtual environment. In this presentation, we shall present our latest results on numerical simulations of cell contact, adhesion, spreading, and self-moving.

Multiscale Crystal Defect Dynamics (MCDD): Towards an Atomistically Determined Crystal Plasticity via Multiscale Dislocation Patter Dynamics

SHAOFAN LI*, Dandan Lyu**

*University of California-Berkeley, **University of California-Berkeley

ABSTRACT

In this work, we present the latest development of multiscale crystal defect dynamics (MCDD) for modeling of crystal plasticity by simulating crystal defect evolutions at small scales. The main novelties of the proposed MCDD are: (1) We use the dual-lattice tessellation to construct a process zone model that can represent dislocation patterns in single crystal; (2) We adopt a fourth-order (four scales) hierarchical strain gradient theory to model constitutive behaviors of various dislocation patterns, in which the atomistic-informed higher order Cauchy–Born rule is employed, and (3) We employ the Barycentric finite element technique to construct finite element shape functions for polygonal and polyhedral process zone elements. The proposed MCDD method provides an efficient and viable alternative to both molecular dynamics (MD) and dislocation dynamics (DD) in simulations of defect evolutions such as dislocation nucleation, and growth. In particular, MCDD offers a mesoscale description for dynamic lattice microstructure, defect microstructure, and their interactions. The method offers a possible solution for studying nanoscale and mesoscale crystalline plasticity. In this approach, coarse-grained models are adopted for both bulk media and material interphase or process zone. In bulk elements, the first order Cauchy-Born rule is adopted, so we can formulate an atomistic enriched continuum constitutive relation to describe the material behaviors. All the nonlinear deformation is assumed to be confined inside the process zone, and the process zone between the bulk elements is remodeled as a finite-width strip whose lattice constants and atomistic potential may be the same or different from those of the bulk medium. Inside the interphase zone, the higher order Cauchy-Born rules are adopted in process zones, and a higher order strain gradient-like coarse grain constitutive model is derived, which can capture the size-effect at the small scales. All interphase or process zones are constructed such that they are part (a subset) of slip planes in a lattice space. The multiscale crystal defect dynamics has been applied to simulate both dislocation motion and crack propagations in both single crystals and polycrystalline solids. Crack branching and void formation have been found possible for different element mesh stacking fault energies, which are dictated, by the effective lattice structure or microstructure in the process zone elements.

Modified Inherent Strain Theory for the Metal Additive Manufacturing Process with Experimental Validation Using Embedded Optical Fiber

XUAN LIANG^{*}, Albert To^{**}

^{*}University of Pittsburgh, ^{**}University of Pittsburgh

ABSTRACT

Additive manufacturing (AM) has been paid increasing attention over the past few years, since usually arbitrarily-shaped parts can be manufactured through a bottom-up approach with little geometric limitation. However, residual stress and distortion have been the most critical issue for metal AM process. It is important to give an accurate prediction of residual stress and distortion in order to guarantee the quality of the printed metal parts. Usually thermomechanical simulation is employed to calculate the residual stress and strain; however, it is too time-consuming to simulate the printing process of a metal part containing thousands of layers. The inherent strain theory was established for solving residual stress and distortion for simple welding problem. It has been proved that the original theory is not accurate for calculating the residual stress and strain of the metal AM process. Therefore, the modified inherent strain theory is proposed in this work, taking the detailed physical process of metal AM into consideration. The modified method considers two different states in the metal AM process. On the one hand, an intermediate state is concerned where rapid solidification occurs, and the plastic strain is extracted correspondingly as the first part of the inherent strains. On the other hand, the increment of the elastic strains of the intermediate and final state is considered to be the other source of the inherent strain. This source of the inherent strain indicates the influence of the changing mechanical boundaries due to the new depositions in the multi-layer printing process. Based on the two different contributions, the modified inherent strains can be obtained. To capture the two important states in the metal AM process, the embedded optical fiber is used to measure the strain distribution in real time. Based on the measurement, the modified inherent strains can be calculated. Uniform averaged inherent strains are applied to a layer in a macroscale geometrical model as equivalent coefficients of thermal expansion. Meanwhile, variation of the inherent strains as a function of the distance to the deposition substrate will be employed in the layer depositing direction. After all the inherent strains are loaded, unit temperature change is applied to the model. Through a one-time full-body static analysis, the residual stress and distortion can be predicted in short time. Compared with the experimental measurement, good accuracy of the modified inherent strain method has been validated, which shows great potential for application to the metal AM field.

INVESTIGATION ON VIBRATION CHARACTERISTICS OF THE HUMAN MIDDLE EAR AND APPLICATION FOR CLINICS IN TYMPANOPLASTY

Y. LIU*, T. HIGASHIMACHI *, AND R. TORIYA[†]

*Department of Mechanical Engineering, Sojo University
4-22-1 Ikeda, Nishi-ku, Kumamoto-shi, Kumamoto, JAPAN
Email address: liu@mec.sojo-u.ac.jp

[†]Toriya ENT Clinic
5-7-12 Kuhonji, Chuo-ku, Kumamoto-shi, Kumamoto, JAPAN

Key words: Human middle ear, Vibration characteristics, Auditory ossicles, Columella.

Abstract. In this paper, investigation on vibration characteristics of the human middle ear was carried out using the finite element harmonic vibration analysis. It was clarified that there is a relationship between hearing ability and stapes displacement including frequency characteristics. In tympanoplasty, the linkage of auditory ossicles may be reconstructed using the column article called the columella. It was also confirmed that stapes displacement changes according to the shape of columella or its mounting position to malleus. Then, a new method is proposed for estimating the hearing restoration effect prior to the tympanoplasty operation. That is, the hearing restoration effect can be estimated by a comparison of the differences in the stapes displacement between the reconstruction model and a healthy subject. In this study, as a part of the optimum design of the columella with the aim of better sound conduction efficiency, the correlation of columella junction area to the auditory ossicles and hearing restoration effect was clarified.

1 INTRODUCTION

In 2012, the World Health Organization (WHO) reported that there are 360 million persons in the world (5.3% of the world's population) with disabling hearing loss [1], which is one of the most severe problems in usual life activity of the human being. Conductive hearing loss is the most common case due to problems in the middle ear or the outer ear at times. A human middle ear which includes auditory ossicles (malleus, incus and stapes) and the tympanic membrane is a mechanical system. A key function of the mechanical system is to transmit sound energy from the air into the inner ear. The audition process begins in the tympanic membrane, which receives sound energy from outside and this causes the membrane to vibrate. Then the vibrations are amplified by the auditory ossicles while being transmitted through the malleus, incus and stapes. Finally, The stapes is responsible for transferring the vibrations into the cochlea fluid of the inner ear so that the hair cells in the inner ear can generate the neuronal signals. The conductive

hearing loss occurs when the middle ear is damaged by various ear diseases, and sounds hardly transfer through the ear canal to the eardrum and three ossicles. The chronic otitis media or middle ear cholesteatoma in which the ossicular chain in middle ear is damaged causes severe conductive hearing loss. The tympanoplasty operation is often carried out to reconstruct the damaged ossicular chain, and to improve the sound conduction efficiency. In the ossicular chain reconstruction, the columella is produced and used instead of incus which is generally broken. In this operation, the sound conduction efficiency changes by the variations in the shape, material and mounting position of the columella. Currently, the operation is carried out based on the workmanship and experience of the surgeon. Identification of the dynamic characteristics of the middle ear is very important in many areas including hearing aids, hearing loss evaluation, and design of middle ear prostheses. Many experimental measurements have been conducted in order to understand the dynamics of the middle ear. H. Wada et al. measured Young's modulus, thickness and damping ratio of the human eardrum by using measuring apparatus developed by themselves [2]. S. E. Voss et al. reported the measurements on human cadaver ears that describe sound transmission through the middle ear [3]. R. Aibara et al. measured the middle-ear pressure gain in 12 fresh human temporal bones for the 0.05 to 10 kHz frequency range [4]. However, experiments on live humans and cadavers are very limited. The dynamic characteristics of the middle ear exhibit a very complex behavior as well as individual variations. Several researchers on middle ear system use finite element analysis (FEA) in their study. The FEA is a powerful tool to analyze the vibration of a middle ear because the middle ear has a complicated shape. As for dynamics analysis on the middle ear system, a cat eardrum was firstly investigated by a finite element analysis on the curved conical eardrum by W. R. I. Funnell and C. A. Laszlo [5]. After that, H. Wada et al. made a three-dimensional FEM model of a human right middle ear, which included ossicles and the mechanical properties and boundary conditions of the middle ear were determined by a comparison between the numerical results obtained and the measurement results [6]. R. Z. Gan et al. performed a three-dimensional finite element analysis of the human ear that included the external ear canal, eardrum, ossicular bones, middle ear suspensory ligaments/muscles, and middle ear cavity [7] [8]. Q. Sun et al. proposed a practical and systematic method for reconstructing accurate computer and physical models of entire human middle ear [9]. T. Koike et al. performed the finite element analysis of the human middle ear and compared calculated results with measurement data [10]. Moreover, Liu et al. carried out a three-dimensional finite element analysis of human ear in order to analyze lesion of ossicular chain [11]. Computational modeling methodology of multi-body system was examined in order to simulate and study the middle ear mechanical response to acoustic stimulus by F. Bohnke et al. [12]. D. D. Greef et al. performed dynamics analysis on a new anatomically-accurate model composed of the tympanic membrane and malleus using the finite element method [13]. Lee, D. and Ahn, T. S. proposed statistical calibration framework effectively improves the middle ear FE model performance [14]. Nevertheless, there are few studies regarding clinical applications and aiming at improvement of the sound conduction efficiency in tympanoplasty. As mentioned upon, in the tympanoplasty operation, the shape, material and mounting position of the columella have been decided based on the workmanship and experience of the surgeon. In this paper, we introduce a new numerical approach using the finite element harmonic vibration analysis for estimating the hearing restoration effect prior to the tympanoplasty operation. This kind of approach makes it possible to propose a new medical treatment for the recovery of conductive or cochlear hearing loss. First of all, precise geometric models of the middle ear, including healthy type model and tympanoplasty type models, were

constructed on the basis of the computerized tomography (CT) scanning data. Then, frequency response characteristics of the stapes displacement in sound conduction were clarified using three-dimensional finite element harmonic vibration analysis. The vibration analysis was also carried out to investigate the effect on the frequency response characteristics caused by changes in the characteristics of the annular ligament and the division of the tympanic membrane. Based on the investigation results of vibration characteristics of the human middle ear, we proposed that the hearing restoration effect can be estimated by a comparison of the differences in the stapes displacement between the reconstruction model and the healthy subject. As an application for clinics in tympanoplasty, four kinds of models that change the mounting location of the columella were analyzed in order to investigate the difference of the displacement of the stapes basal plane. By comparing those analytical results with the result for a healthy model as a standard, the possibility of a clinical application of our method has been verified. Furthermore, as a part of the optimum design of the columella with the aim of better sound conduction efficiency, the correlation of columella junction area to the auditory ossicles and hearing restoration effect was clarified.

2 THE HUMAN MIDDLE EAR AND ITS FUNCTION

Figure 1 shows the structure of the ear. The middle ear is composed of the tympanic membrane, tympanic cavity, auditory ossicles and others. Auditory ossicles are behind the tympanic membrane in a small space (tympanic cavity), and they are composed of malleus, incus and stapes. The stapes basal plane connects with the inner ear through an oval window.

The tympanic cavity is a space filled with air. The inner wall of the tympanic cavity is covered with a mucous membrane. The air pressure of the tympanic cavity is controlled at the appropriate value by ventilation in order to keep the important function that is the sense of hearing. Furthermore, the tympanic cavity has a washing function that absorbs and removes bacterial waste by the secretion and reabsorption of the mucus. Each part of the auditory ossicles is connected with the joints. They are suspended by ligaments and muscles in the tympanic cavity. The vibration amount of the tympanic membrane is amplified about 17 times by the area ratio of the stapes basal plane and the tympanic membrane. In addition, the vibration amount of the tympanic membrane is amplified about 1.3 times by the lever motion of the auditory ossicles.

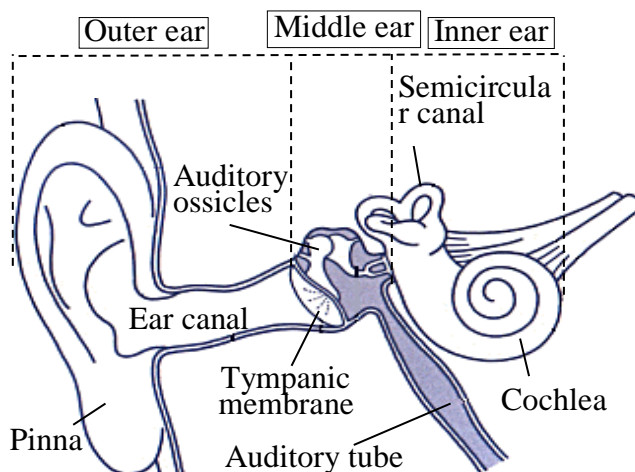


Fig. 1 Structure of the human ear

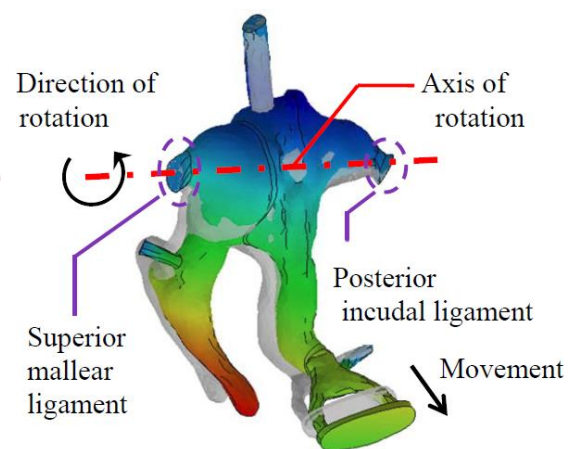


Fig. 2 Deformation of auditory ossicles

Figure 2 shows that the auditory ossicles turn about the axis connecting the superior ligament and the posterior incudal ligament [15]. By this rotary motion, the vibration of the tympanic membrane is efficiently converted into Z-direction (perpendicular to the stapes basal plane) movement of the stapes. The stapes vibration is transmitted to the labyrinthine fluid of the internal ear and converted to electrical signals, which are then recognized as sound in the brain. In this study, we consider that there is a certain relationship between hearing ability and the Z-direction displacement of the stapes.

3 GEOMETRIC MODELING OF THE MIDDLE EAR

The precise geometry of ossicles was obtained through CT scanning of the human head. As shown in Fig. 3, the two-dimensional slice images of the CT scanning data were transformed into three-dimensional solid geometries using a post-processing software and the region which contains the three ossicles was separated from the CT scanning data. Then, the 3D geometries were refined and converted to DICOM data, and further converted into STL data, which were imported into a general-purpose structure analysis software to create a FEM model. The geometric model for a healthy subject for finite element harmonic vibration analysis is shown in Fig. 4. This model is composed of the tympanic membrane, auditory ossicles, ligaments, joints, stapedial muscle and others.

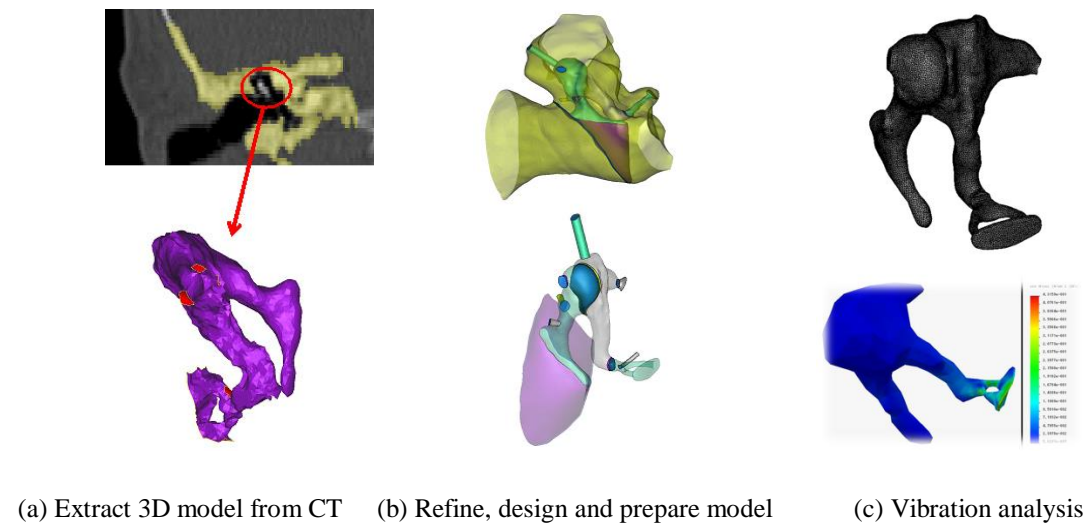
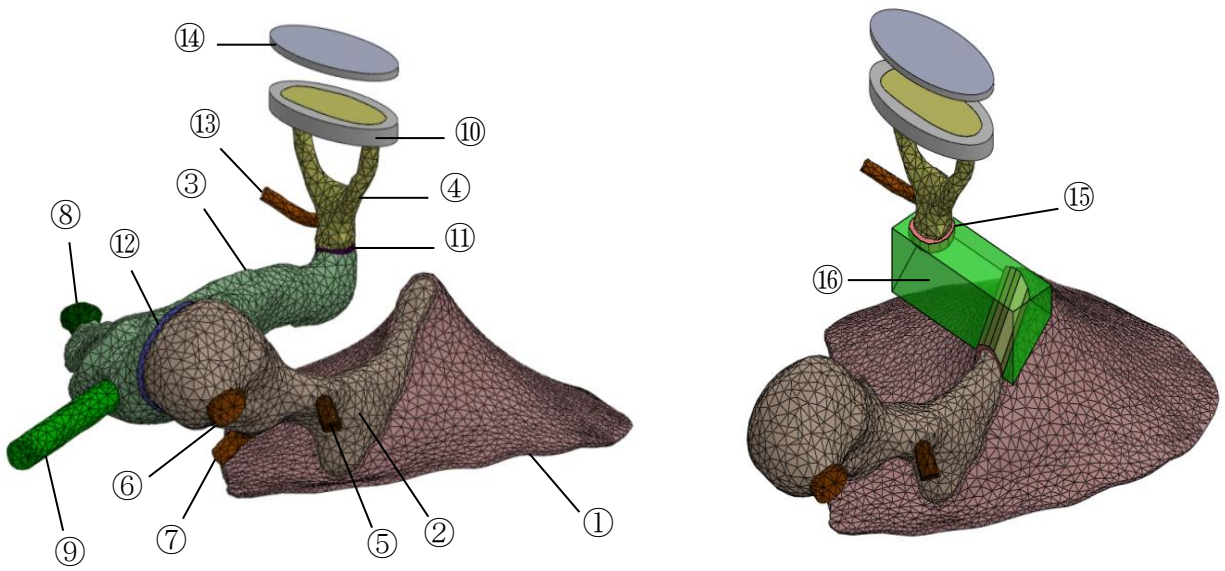


Fig. 3 Construction of a 3D model of human middle ear for vibration analysis

4 HARMONIC VIBRATION ANALYSES

4.1 Material data

Material data of the analysis model are shown in Table 1 [9] [10] [17]. The anatomical parts name number in the table corresponds to the number in Fig. 4. The base plate 14 is a virtual part for supporting the spring. Therefore, its Young's modulus can be assumed to be that of a rigid body.



(a) Healthy subject model of middle ear

(b) Operation model of middle ear

Fig. 4 Model of middle ear

Table 1 Material data

Anatomical name	Young's Modulus (MPa)	Density (kg/m ³)	Poisson's ratio
①Tympanic membrane	33.4	1,200	0.3
②Malleus	13,436	4,350	
③Incus			
④Stapes			
⑤Lateral mallear ligament	21	2,500	
⑥Superior mallear ligament			
⑦Anterior mallear ligament			
⑧Posterior incudal ligament	0.65		
⑨Superior incudal ligament			
⑩Stapedial annular ligament			
⑪Incudostapedial joint	6	1,200	
⑫Incudomallear joint			
⑬Stapedial muscle	0.52	2,500	
⑭Base plate	1×10 ¹⁰	-	
⑮Columella (joint)	6	1,200	
⑯Columella (Main body)	112,400	2,330	0.28

4.2 Boundary conditions

The tympanic membrane circumference, edges of ligament and muscle, and base plate were perfectly fixed in load conditions. A sound pressure of 90dB was converted into pressure using the equation (1) as load conditions.

$$L_p = 20 \log_{10}(P/P_0) \quad (1)$$

In Eq. (1), $L_p = 90\text{dB}$ is the setting sound pressure (a relative noisy level) and $P_0 = 20 \times 10^{-6}\text{Pa}$ a standard value (the lowest value of the sound intensity which is audible for humans). As a result, a pressure of $P = 0.632\text{Pa}$ was obtained. However, in this analysis, $P = 15.2\text{Pa}$ was given at the contact surface of the tympanic membrane and malleus. The ratio $15.2/0.632$ equals the ratio of the total area of the tympanic membrane to the contact surface area of the tympanic membrane and malleus. A spring of 40N/m spring constant was installed between the stapes and the base plate referring to the research of Gan et al [8]. Rayleigh damping was assumed and damping factors of $\alpha = 0\text{s}^{-1}$, $\beta = 7.5 \times 10^{-5}\text{s}$.

4.3 Finite element analysis results of the healthy model

In this research, harmonic vibration analysis was done as a dynamic analysis using the finite element method. Fig. 5 shows the harmonic vibration analysis results for a healthy subject. The longitudinal axis shows the displacement of the stapes bottom in a perpendicular direction to the basal plane, and the lateral axis represents the frequency. In cases of a healthy subject, it is said that there is a resonance region of the middle ear at $0.5 \sim 2\text{ kHz}$ in frequency, that is, conversation range. Average displacement of the stapes basal plane shows the peak of the resonance to be near 1.3 kHz in frequency in the analytical results for a healthy subject. This displacement decreases gradually with an increase in frequency over 2 kHz . It is possible to reproduce the resonance phenomena to some extent by our finite element model. Fig. 5 shows that the average displacement of the stapes base for the sound pressure of 90dB is $5.09 \times 10^{-6}\text{ mm}$, which was used as a standard value in this study. If the change in this displacement is compared, the hearing restoration effect can be estimated prior to the tympanoplasty operation, in the case where the medical device, called columella, is substituted for the deficient auditory ossicles, or in the case of stiffening of the ligament. This kind of approach makes it possible to propose a new medical treatment for the recovery of conductive or cochlear hearing loss.

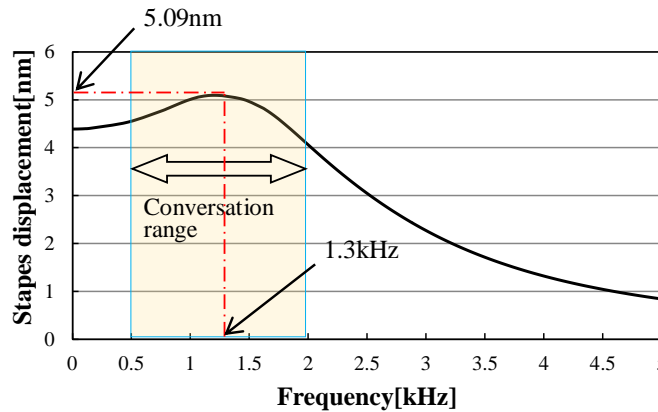
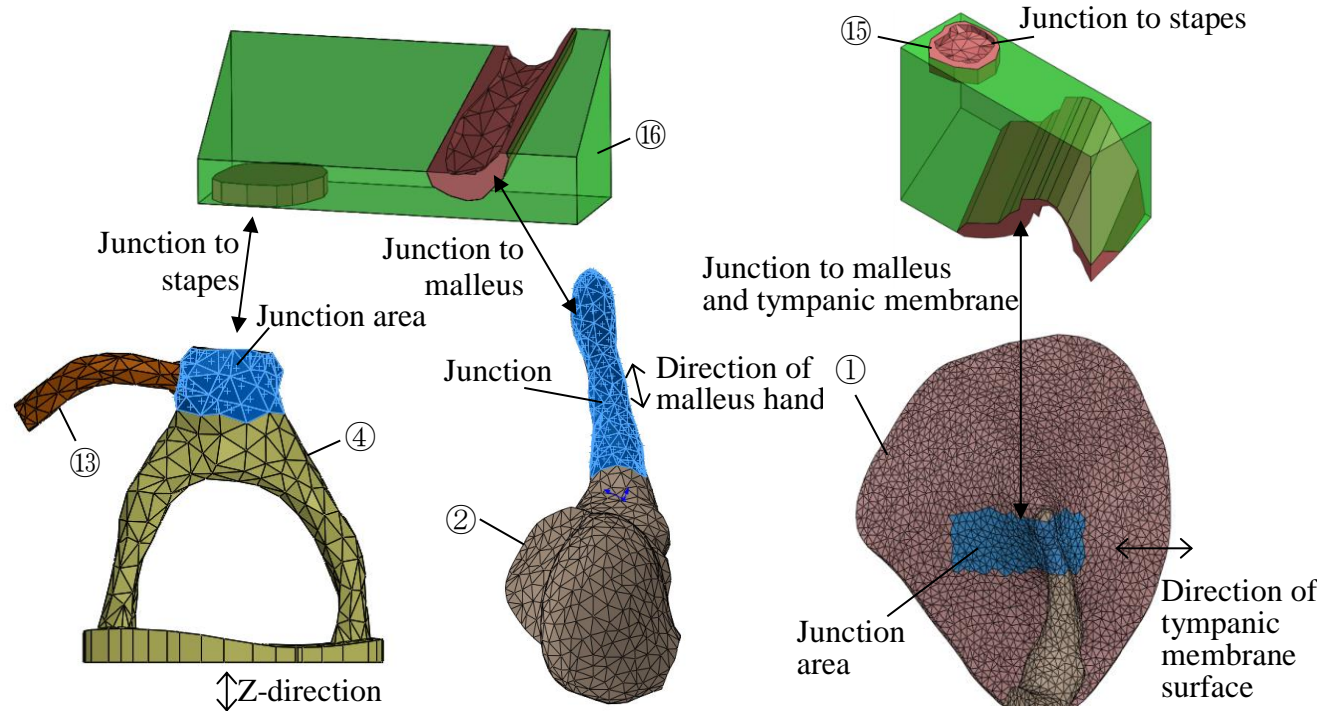


Fig. 5 Frequency response graph of healthy subject model

5 APPLICATION FOR CLINICS IN TYMPANOPLASTY

As mentioned in Section 1, the tympanoplasty operation is often carried out to reconstruct the damaged ossicular chain to improve the sound conduction efficiency when auditory ossicles were damaged for chronic otitis media, etc.. In the ossicular chain reconstruction, as shown in Fig. 4(b), the column article called columella is produced and used instead of incus which is generally broken. As a part of the optimum design of the columella with the aim of better sound conduction efficiency, the correlation of columella junction area to the auditory ossicles and hearing restoration effect was studied.



(a) Junction area for the stapes (b) Junction area for the malleus (c) Junction area for the tympanic membrane
Fig. 6 Definition of the junction area

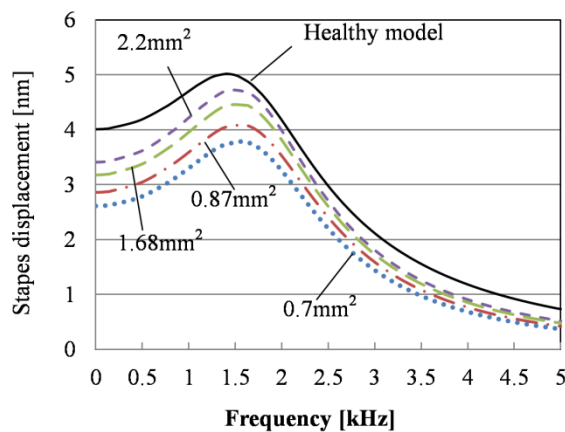


Fig. 7 Frequency response graph for the Fig. 6(a) model

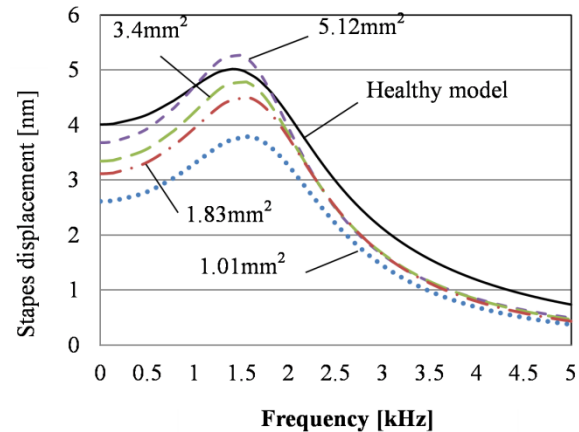


Fig. 8 Frequency response graph for the Fig. 6(b) model

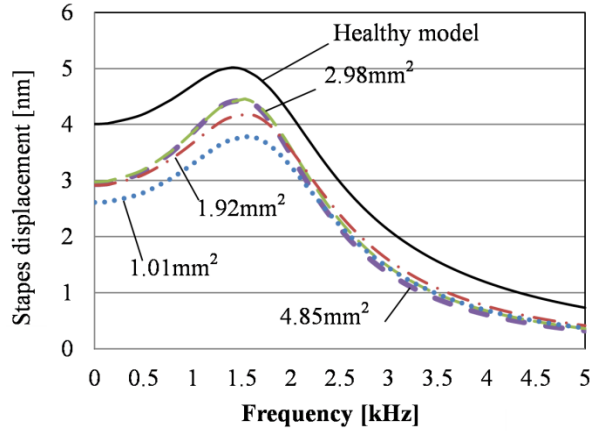


Fig. 9 Frequency response graph for the Fig. 6(c) model

The junction area is the contact area between a columella and malleus, stapes or tympanic membrane. The junction area is changed by the change of shape of the columella. A standard model of columella is shown in upside of Fig. 6. The junction area for the stapes side is shown in Fig. 6(a). In the case of stapes side, the shape of the columella is changed in the Z-direction, which is perpendicular to the basal plane of stapes. The junction area for the malleus side is shown in Fig. 6(b). In the case of malleus side, the shape of the columella is changed in the direction along the handle of malleus. The junction area for the tympanic membrane side is shown in Fig. 6(c). In the tympanic membrane side, the shape of the columella is changed in the direction along the tympanic membrane surface. The number of ①, ②, ④, ⑬, ⑮, ⑯ in Fig. 6 corresponds to the number in Fig. 4 and Table 1. The influence by the change of the junction area is examined, and the correlation of hearing restoration effect and junction area is clarified.

A frequency response graph obtained by the finite element analysis is shown in Fig. 7~9. These figures show the relation between the normal displacement of stapes bottom and frequency. Figure 7 shows the results in case the junction area for the stapes side changes. The solid line shows the result for a healthy subject, and the dotted line shows the result for the model where the junction area equals 0.7mm^2 . Moreover, the dashed and single-dotted line is the result for the model where the junction area is 0.87mm^2 . The long dashed line is the result for the model where the junction area is 1.68mm^2 . The short dashed line is the result for the model where the junction area is 2.2mm^2 .

Figure 8 shows the results in case the junction area for the malleus side changes. The solid line shows the result for a healthy subject. The dotted line shows the result for the model where the junction area equals 1.01mm^2 . The dashed and single-dotted line is the result for the model where the junction area is 1.83mm^2 . Long dashed line is the result for the model where the junction area is 3.4mm^2 . The short dashed line is the result for the model where the junction area is 5.12mm^2 .

Figure 9 shows the results in case the junction area for the tympanic membrane side changes. The solid line shows the result for a healthy subject. The dotted line shows the result for the model where the junction area equals 1.01mm^2 . The dashed and single-dotted line is the result

for the model where the junction area is 1.92mm^2 . The long dashed line is the result for the model where the junction area is 2.98mm^2 . The short dashed line is the result for the model where the junction area is 4.85mm^2 .

Figures 7 and 8 show that the stapes displacement increases with the increase of junction area between auditory ossicles (stapes or malleus) and the columella. By increasing the junction area, it is possible to more firmly connect the columella. Therefore, it seems to improve the transfer efficiency of sound. Fig. 9 shows that the stapes displacement increases with the increase of junction area between tympanic membrane and columella, but there is a limit in the increase. Tympanic membrane is not suitable to transmit the force, because the Young's modulus of the tympanic membrane is considerably lower than that of auditory ossicles as shown in Table 1. In previous research [16], we have obtained the same results in static analysis. The vibration of the tympanic membrane cannot sufficiently transmit to the stapes due to its low rigidity.

6 CONCLUSIONS

The vibration characteristics of the human middle ear were investigated in this paper and were applied to improve the sound conduction efficiency in tympanoplasty. We have proposed that the hearing restoration effect can be estimated by comparison of the displacement of stapes basal plane prior to the operation. The validity of our proposal was confirmed by analyzing various types of operation models using harmonic vibration analysis and compared with a healthy subject. Furthermore, as a part of the optimum design of the columella with the aim of better sound conduction efficiency, the correlation of hearing restoration effect and junction area of the auditory ossicles was clarified. It is possible and important to optimize the columella from the engineering viewpoint using the finite element method. This kind of approach makes it possible to propose a new medical treatment for the recovery of conductive or cochlear hearing loss.

ACKNOWLEDGEMENT

This work was supported by JSPS KAKENHI Grant Number JP17K14581.

REFERENCES

- [1] WHO global estimates on prevalence of hearing loss. WHO (2012).
- [2] Wada H, Kobayashi T, Nagamura H, Tashizaki H. Analysis of dynamic characteristics of eardrum : Young's modulus, thickness, and damping ratio of human eardrum. Transactions of the Japan Society of Mechanical Engineers Series C (1990) 56:1431–4.
- [3] Voss SE, Rosowski JJ, Merchant SN, Peake WT. Acoustic responses of the human middle ear. Hearing Research (2000)150:43 – 69.
- [4] Aibara R, Welsh JT, Puria S, Goode RL. Human middle-ear sound transfer function and cochlear input impedance. Hearing Research (2001)152:100 –9.

- [5] Funnell WRJ, Laszlo CA. Modelling of the cat eardrum as a thin shell using finite element method. *The Journal of the Acoustical Society of America* (1978) 63:1461–7.
- [6] Wada H, Metoki T, Kobayashi T. Analysis of dynamic behavior of human middle ear using a finite-element method. *The Journal of the Acoustical Society of America* (1993)92:3157–68.
- [7] Gan RZ, Dyer RK, Wood MW, Dormer KJ. Mass loading on the ossicles and middle ear function. *Annals of Otology, Rhinology & Laryngology* (2001)110:478–85.
- [8] Gan RZ, Feng B, Sun Q. Three-dimensional finite element modeling of human ear for sound transmission. *Annals of Biomedical Engineering* (2004) 32:847–59.
- [9] Sun Q, Gan RZ, Chang KH, Dormer KJ. Computer integrated finite element modeling of human middle ear. *Biomechanics and Modeling in Mechanobiology* (2002)1:109–22.
- [10] Koike T, Wada H. Modeling of the human middle ear using the finite element method. *The Journal of the Acoustical Society of America* (2002)111:1306–17.
- [11] Liu Y, Li S, Sun X. Numerical analysis of ossicular chain lesion of human ear. *Acta Mechanica Sinica* (2009) 25:241–7.
- [12] Frank Bohnke F, Bretan T, Lehner S, Strenger T. Simulations and measurements of human middle ear vibrations using multi-body systems and laser-doppler vibrometry with the floating mass transducer. *Materials* (2013) 6:4675–88.
- [13] Greef DD, Aernouts J, Aerts J, Cheng JT, Horwitz R, Rosowski JJ, et al. Viscoelastic properties of the human tympanic membrane studied with stroboscopic holography and finite element modeling. *Hearing Research* (2014) 312:69 – 80.
- [14] Lee D, Ahn TS. Statistical calibration of a finite element model for human middle ear. *Journal of Mechanical Science and Technology* (2015) 29:2803–15.
- [15] Higashimachi T, Shiratake Y, Maeda T, Toriya R. Three-dimensional finite element analysis of the human middle ear and an application for clinics for tympanoplasty. *Surface Effects and Contact Mechanics, XI, WIT Transactions on Engineering Sciences* (2013) 78:61–72.
- [16] Higashimachi T, Maeda T, Oshikata T, Toriya R. Finite element analysis of the human middle ear and an application for clinics for tympanoplasty (static and harmonic vibration analysis). In: *The 3rd International Conference on Design Engineering and Science, ICDES 2014* (2014).
- [17] Higashimachi T, Suga K, Sasahara H. Structural mechanical analysis and evaluation for extension of teeth lifetime. *Journal of Japanese Society of Precision Engineering* (2009)75:428–3.

Fracture Mechanism for Porous Single Crystals under Various Stress States

ZHIGANG LIU*

*IHPC

ABSTRACT

Void growth and coalescence are well known as the main mechanism of ductile fracture. While less effort has been devoted to investigating the process of void growth and coalescence in single crystal. This work examines the onset of void coalescence, the void behaviors that often precede eventual failure in ductile porous single crystal. The occurrences depends largely on the stress states in the solid, characterized by the stress triaxiality (T) and the Lode parameter (L). In employing a 3D unit cell simulation with crystal plasticity constitutive model, the strain at onsets of void coalescence behaviors can be operationally defined for different crystal orientation. Validated against known experimental and numerical works, we have demonstrated the stress state dependence of void coalescence. The crystal orientation and stress states on void coalescence are studied with five original single crystal orientations and two initial void volume fractions.

Stochastic Geometric Nonlinear Analysis of Functionally Graded Circular Shallow Arches

Zhanpeng LIU^{*}, Wei GAO^{**}, Di WU^{***}, Guoyin LI^{****}

^{*}Centre for Infrastructure Engineering and Safety (CIES), School of Civil and Environmental Engineering, The University of New South Wales, Sydney NSW 2052, Australia, ^{**}Centre for Infrastructure Engineering and Safety (CIES), School of Civil and Environmental Engineering, The University of New South Wales, Sydney NSW 2052, Australia, ^{***}Centre for Infrastructure Engineering and Safety (CIES), School of Civil and Environmental Engineering, The University of New South Wales, Sydney NSW 2052, Australia, ^{****}Department of Applied Mathematics, The University of New South Wales, Sydney NSW

ABSTRACT

In this study, a stochastic geometric nonlinear analysis of functionally graded (FG) shallow arch is investigated. The constitutive material composition of the FG arch varies along the radial direction of the cross section, so the mechanical performance of the arch can be well controlled for various engineering design purposes. Based on the Euler-Bernoulli hypothesis, both geometric linear and nonlinear analytical solutions of the structural responses (i.e., displacements, axial compressive force and bending moment) of the FG arch subjected to uniform distributed load are derived by using the virtual work method. The boundary condition of the investigated FG arch is identified as pin-ended support at both ends. By adopting the derived analytical solution, the relationship between the structural response and the various FG material properties can be analysed efficiently. Once the analytical solutions of the deterministic structural responses of the FG arch are established, the stochastic analysis of the FG arch structure is performed by direct Monte Carlo simulation method. Both uncertain material properties and loading conditions can be incorporated within the simulative analysis framework. One numerical example is presented to demonstrate the applicability and effectiveness of the proposed nondeterministic analysis framework for the geometric nonlinear analysis of FG arch structures.

Computational Investigation of Bio-inspired Composite Nano Rotor Blade

Zhen LIU*, Chen BU**, Shanyong ZHAO***

*State Key Laboratory for Strength and Vibration of Mechanical Structures, school of Aerospace, Xi'an Jiaotong University, **State Key Laboratory for Strength and Vibration of Mechanical Structures, school of Aerospace, Xi'an Jiaotong University, ***State Key Laboratory for Strength and Vibration of Mechanical Structures, school of Aerospace, Xi'an Jiaotong University

ABSTRACT

At ultra-low Reynolds number, the propulsive performance of nano rotor drops dramatically, which has a profound impact on the flight performance of NAV. The bio-inspired blade motion is introduced to improve the performance of nano rotor. However, the complex flow interacts with the flexible composite blade structure resulting in the variation of propulsion performance of nano rotor and the vibration of blade structure. In this paper, the nano-scale composite rotor with blade-pitching motion was studied computationally with a computational solvers based on a preconditioned compressible NS equations, Roe-scheme, LUSGS-?ts dual-time marching method coupling with a finite element solver. A non-contact modal experimental platform was established using sound excitation instrument and laser vibrometer. The structural characteristics of the composite nano rotor were measured. It was found that the natural frequencies are very close for the first two orders. The finite element model of composite rotor was created accordingly. The modal was studied computationally with FEM solver. It was found that the simulation results matched well with the experimental results which verified the correctness of the finite element model. The CFD model was established and the propulsive performance of nano rotor without bio-inspired motion was studied, respectively. The results showed that the computational results from Fluid-structure solver matched better than that for CFD solver. It is indicted that the fluid-structure method has a higher precision for nano rotor simulation. It is evident that it is necessary to consider the flexibility of the composite nano rotor when investigating the propulsion performance of bio-inspired nano rotor. Then the flow field of flexible nano rotor was also analyzed at different bio-inspired pitching frequency and the response of blade structure was also studied with the fluid-structure solver. Results showed that the propulsive performance for bio-inspired pitching rotor at different pitching frequency. It was found that the thrust and torque for the bio-inspired pitching rotor are higher than those for the rotor without bio-inspired motion. And it was also found that the propulsive performance for the nano rotor with bio-inspired pitching frequency of two times of that rotation frequency is higher than that with only one times pitching frequency. It is evident that the improvement enhanced with the increase of the pitching frequency. And the blade structure was also found vibrate with a small amplitude. In general, it was found that the bio-inspired pitching motion can improve the performance of nano rotor.

Multibody Dynamics to Build a Reduced Ordered Model of a Car Crash Simulation

Tanguy LOREAU*, Philippe SERRE**, Laurent NOYELLE***, Jean-Luc DION****

*QUARTZ EA 7393 - SUPMECA, **QUARTZ EA 7393 - SUPMECA, ***GROUPE RENAULT, ****QUARTZ EA 7393 - SUPMECA

ABSTRACT

Finite element models for vehicle crash studies are unsuited for upstream design: they have a large number of degrees of freedom and require precise information. Furthermore, their complexity implies high computational costs that make them unusable for short optimization loops. A way to overcome this complexity is to adapt results from another finite element simulation or crashtest of a vehicle close to the one to design. But this process uses only one part of the knowledge of the company, which restrains the new vehicle to be close to the previous one and requires a long time modeling and calculation making it a bad candidate for optimization. In this study, we aim to build a fast computing and robust model from all the knowledge of the company on crash simulation. A first approach is to apply a well suited and designed reduced ordered model method (POD, PGD, Deep Learning) on the simulation database. Yet these methods all have weaknesses that make them unusable for the crash reduction: either they need a quantity of data the company can't provide, or they are not adapted in contact detection, or the produced model needs parameters that are not available in upstream phases and, in all cases, these methods don't relate about physics so the model can't be so much extrapolated. A second approach, which is presented in this work, is to see a car during a crash as a rigid multibody system articulated with dissipative links (Carvalho & Ambrosio, 2011, Development of generic road vehicle multibody models for crash analysis using an optimization approach, International Journal of Crashworthiness). Indeed, an energetic analysis of a crash simulation shows that a very small quantity of parts explains most of the phenomenon. These parts can be modeled as sets of rigid bodies articulated with plastic links which localization and rheological parameters come from the finite element simulation. The method presented here proposes a way to read finite element simulations to soundly place sensors on finite element models and then, after a new simulation, to get rheological parameters and positions of links to build a multibody model from a finite element simulation. This new multibody model, after a well suited correlation and validation, will represent a car crash simulation.

The Magneto-electric Coupling in Multiferroic Composites: Magnetostrictive Preisach and Ferroelectric Switching Model

Matthias Labusch*, Jörg Schröder**

*University Duisburg-Essen, Germany, **University Duisburg-Essen, Germany

ABSTRACT

Multiferroic materials combine two or more ferroic properties and can exhibit an interaction between electric polarization and magnetization. This magneto-electric (ME) coupling can find applications in sensor technology or in magneto-electric data storage devices. Since most ME single-phase materials show such a coupling far below room temperature, the manufacturing of two-phase composites, consisting of a ferroelectric matrix with magnetostrictive inclusions, becomes important. Due to the interaction of both constituents the composites generate a strain-induced ME coupling at room temperature, where we distinguish between the direct and the converse ME effect. The direct effect characterizes magnetically induced polarization, where an applied magnetic field yields a deformation of the magnetostrictive phase, which is transferred to the ferroelectric phase. Due to the electro-mechanical properties of the matrix material the composite exhibit a change in polarization. On the other hand, the inverse ME effect characterizes electrically induced magnetization. The ME coupling significantly depends on the microscopic morphology and the ferroic properties of the individual constituents. In order to take both aspects into account, a finite element (FE²) homogenization approach is performed, which combines via a scale bridging the macro-and microscopic level [1]. Thereby, the microscopic morphology is characterized by representative volume elements and the ferroic properties of the phases are described by suitable material models. The typical ferroelectric hysteresis curves are modeled by considering the switching behavior of the spontaneous polarizations of barium titanate unit cells [2], whereas the magnetic hysteresis loops are described by a Preisach operator [3]. [1] J. Schröder, M. Labusch, and M.-A. Keip: Algorithmic two-scale transition for magneto-electro-mechanically coupled problems – FE²-scheme: Localization and homogenization. *Computer Methods in Applied Mechanics and Engineering* 302, 253 – 280 (2016). [2] S. Hwang, C. Lynch, and R. McMeeking: Ferroelectric/Ferroelastic interaction and a polarization switching model. *Acta metall. Mater.* 43, 2073-2084 (1995). [3] M. Kaltenbacher, B. Kaltenbacher, T. Hegewald, and R. Lerch: Finite Element Formulation for Ferroelectric Hysteresis of Piezoelectric Materials. *Journal of Intelligent Material Systems and Structures* (2010).

A Posteriori Estimation and Adaptivity for the Parabolic p-curl from Applied Superconductivity

Marc Laforest^{*}, Andy T. S. Wan^{**}, Yann-Meing Law^{***}, Frédéric Sirois^{****}

^{*}École Polytechnique de Montréal, ^{**}McGill University, ^{***}École Polytechnique de Montréal, ^{****}École Polytechnique de Montréal

ABSTRACT

The optimal design in 3D of new electrical components from commercially available high-temperature superconductors pushes the limits of current computational tools. Strong currents develop near the envelope of the superconductor and under AC, the nonlinear resistance induces sharp fronts in the currents and in the magnetic field density. These are challenges for finite element approximations but they also introduce subtle regularity issues recently identified by our group. In this presentation, we discuss the a posteriori error estimation of the critical-state model from applied superconductivity, both with and without linearization. We also review our work on the generation of diffusion, and energy loss, at the front and its approximation by both FE approximation and non-oscillatory approximations using a relaxation formulation of the problem. Regularity issues at the boundary are further related to error estimation and modeling.

Spectral Analysis of the Deflated Complex Shifted Helmholtz Operator

Domenico Lahaye^{*}, Kees Vuik^{**}

^{*}DIAM / TU Delft, ^{**}DIAM / TU Delft

ABSTRACT

The complex shifted Laplacian is widely recognized as a computationally very efficient preconditioner for the Helmholtz equation. It introduces a sequence of damped wave propagation problems. The linear systems that arise can efficiently be solved by for instance multigrid methods. This method can however be significantly accelerated by a procedure published in [1]. In this procedure, the preconditioner is multiplied with a deflation operator that employs multigrid vectors. The deflation operator thus accelerates the convergence of the preconditioner in a similar way that a coarse grid correction operator accelerates the convergence of a smoother in a multigrid method. The objective of this work is to analyze how damping influences the efficiency of the new hybrid method. We are especially interested in large amounts of damping that facilitates the approximate inversion of the preconditioner. Without the use of deflation operator, the converge of the outer Krylov method rapidly deteriorates with the amount of damping introduced. To study the influence of the deflation operator, we analyze the spectrum of the discrete Helmholtz operator preconditioned by a multiplicative combination of the first deflation operator and subsequently complex shifted Laplace preconditioner. We perform a Rigorous Fourier modal analysis of a one-dimensional model problem in which the Helmholtz equation with homogeneous Dirichlet boundary conditions discretized by a second order finite difference scheme on a uniform fine and coarse grid. With these choices, the discrete Helmholtz operator, the complex shifted Laplacian and the coarse grid operator share a set of eigenmodes. Our spectral analysis reveals that the inversion of the near-singular coarse grid operator causes the eigenvalues of the deflated operator spreads in tails along both sides of the real axis. The subsequent action of the preconditioner is to shrink, rotate and shift the set of eigenvalues. Unlike the case in which merely the preconditioner is employed, the smallest eigenvalue remains bounded away from zero for larger values of the damping parameter. Numerical results show that the eigenvalue distribution and the GMRES number of steps are well correlated. A much larger damping parameter than in algorithms without deflation can be used. This holds great promises for the future application of the new method. [1] A.H. Sheikh, D. Lahaye, L. Garcia Ramos, R. Nabben and C. Vuik, Accelerating the shifted Laplace preconditioner for the Helmholtz equation by multilevel deflation, Journal of Computational Physics, 322: 473--490, 2016.

Phase Field Modelling of Brittle Fracture in Thin Shells Accounting for Cracks Partly Through the Thickness

Wenyu Lai^{*}, Jian Gao^{**}, Yihuan Li^{***}, Marino Arroyo^{****}, Yongxing Shen^{*****}

^{*}University of Michigan-Shanghai Jiao Tong University Joint Institute, Shanghai Jiao Tong University, Shanghai, China, ^{**}University of Michigan-Shanghai Jiao Tong University Joint Institute, Shanghai Jiao Tong University, Shanghai, China, ^{***}University of Michigan-Shanghai Jiao Tong University Joint Institute, Shanghai Jiao Tong University, Shanghai, China, ^{****}Laboratori de Calcul Numeric, Universitat Politecnica de Catalunya, Barcelona, Spain, ^{*****}University of Michigan-Shanghai Jiao Tong University Joint Institute, Shanghai Jiao Tong University, Shanghai, China

ABSTRACT

In this work, we present a phase field fracture model for the brittle fracture of the Euler-Bernoulli beam theory and the Kirchhoff-Love shell theory under the principle of minimum potential energy. To account for transverse part-through cracks, we employ an ansatz for the phase field using two scalar fields within cross section, allowing variation of the phase field through the thickness. The problem then reduces to a one-dimensional nonlinear differential equation for the beam problem, or a two-dimensional nonlinear differential equation over the mid-surface for the shell problem, which can be solved with the finite element method. Combined with a phase field model discriminating tension and compression, this special treatment permits simulating fracture due to bending loads and to membrane loads. The continuous formulation then can be discretized using any standard numerical method allowing H^2 continuity of the basis functions. In the presentation, we will talk about efficient simulation schemes for the numerical algorithm.

Modelling and Numerical Algorithm for Contact Problems with Frictional Heat Generation and Wear in Peridynamics

Xin Lai^{*}, Lisheng Liu^{**}

^{*}Wuhan University of Technology, ^{**}Wuhan University of Technology

ABSTRACT

For multi-body contact problems, accurate modelling and numerical algorithm of the contact interaction between objects are very important to ensure the reliability of the numerical simulation. Especially, the frictional heat generated in the sliding and contacting progress, which is usually neglected, has great effect on the behavior of the material and the structure in material cutting, wearing, and impact problems. In such circumstances, the dramatic increasing of temperature caused by the frictional heat may change the physical properties, mechanical properties, or even the states of the material. Therefore, Frictional heat should be considered when dealing with high-speed contact problems. In this work, contact interactions including frictional heat has been modelling and numerically implemented in Peridynamic framework, which is recently widely used in impact damage problems. Numerical examples are carried out to validate the validity and accuracy of our algorithm. Comparisons have been made to show the influence of the material behavior affected by the frictional heat.

Dispersion, Spurious Reflections and Spurious Bifurcation of Flexural Waves

José Laier*

*Engineering School of São Carlos USP

ABSTRACT

Wave velocity dispersion, spurious bifurcation (numerical instability) and spurious reflections of the flexural wave model produced by numerical integration were investigated [1]. Classic cubic beam finite elements of two nodes with consistent mass matrix are taken into account [2]. The Newmark average acceleration integration method of single step is used for integration in time. The resultant system of difference equation is then analytically integrated in non-finite terms (numerical wave solution) using complex notation. Numerical results reveal that even for refined mesh the spurious reflections can be significant.

A Positive Asymptotic Preserving Scheme for Linear Kinetic Transport Equations

M. Paul Laiu^{*}, Martin Frank^{**}, Cory Hauck^{***}

^{*}Oak Ridge National Laboratory, ^{**}Karlsruhe Institute of Technology, ^{***}Oak Ridge National Laboratory

ABSTRACT

We present a new positive and asymptotic preserving numerical scheme for solving linear kinetic transport equations. The proposed scheme is developed based on the standard spectral angular discretization and the classical micro-macro decomposition. The three main ingredients of the proposed scheme are a semi-implicit time discretization, a dedicated finite difference space discretization, and positivity limiters. We show that the proposed scheme is asymptotic preserving in the sense that when the mean free path of the particles goes to zero, the scheme achieves a correct numerical scheme for the limiting diffusion equation, without restrictive time step constraints. We also prove that the proposed scheme preserves positivity of the spatial particle concentration in the solution, which fixes a common defect of spectral angular discretizations. The proposed scheme is tested on two benchmark problems on a two-dimensional spatial domain, one with a single material and one with two types of material embedded as a checkerboard.

An HPC Enhanced Agent Based System for Simulating Mass Evacuations

Maddeggedara Lalith*, Muneo Hori**, Wasuwat Petprakob***, Leonel Aguilar****

*Earthquake Research Institute, The University of Tokyo, **Earthquake Research Institute, The University of Tokyo,

Dept. of Civil Eng., The Univ. of Tokyo, *Dept. of Humanities, Social and Political Sciences, ETH

ABSTRACT

We present the details of implementation and applications of an HPC enhanced Agent Based Model (ABM) for simulating tsunami triggered evacuation of large coastal regions. In seeking various strategies to accelerate evacuation process, quantitative evaluation of their effectiveness, identifying unforeseen problems, etc., numerical simulations are invaluable to disaster mitigation authorities. Simple queue models with 1D networks are widely used for mass evacuations due to the ease of use, limited of computer resources, etc. These simplified models are inadequate for studying certain scenarios in congested urban regions which demand the use of accurate high resolution model of environment and complex models of individuals. Some of the scenarios requires best use of the available narrow spaces, debris, visibility in night time, pedestrian-vehicle interactions, etc. With the aim of simulating such demanding scenarios, we developed an ABM which includes a high resolution model of environment and sophisticated agents capable of perceiving the environment in high resolution [1, 2]. Environment is modeled as a hybrid of high resolution grid and a graph which contains the topological connectivity of accessible spaces in the grid. Each agent scans its surrounding in the grid in high resolution mimicking the eyes of an evacuee. This allows them to perceive dynamic changes in environment like progression of inundation and act accordingly. Agent store their experiences with reference to the topological graph and use those information in decision making. In order to meet the high computational demand of sophisticated agents in high resolution environment, we implemented MPI+OpenMP hybrid HPC extension. The heterogeneous nature of agents, the movements of agents from the domain of one CPU to other, etc. give rise to significant load imbalance among CPUs. To cope with this load imbalance, we implemented a dynamic load balancer using the measured execution time of each agent as a heuristic.

A Multiscale and Multiphase Model for the Description of Paracetamol-induced Hepatotoxicity Using the Example of the Human Liver

Lena Lambers*, Navina Waschinsky**, Tim Ricken***

*Institute of Mechanics, Structural Analysis, and Dynamics; University of Stuttgart, **Chair of Mechanics, Structural Analysis, and Dynamics; TU Dortmund University, ***Institute of Mechanics, Structural Analysis, and Dynamics; University of Stuttgart

ABSTRACT

The liver is the most important human organ responsible for metabolic homeostasis. A further central task of the human liver is the detoxification of the blood since toxic substances or excessive medication can cause damage in the liver structure which can lead to acute liver failure. One example for a medicine which can cause hepatotoxicity is the analgesic Paracetamol (Acetaminophen). The toxic metabolites of the Paracetamol are normally bound by the internal Glutathione. When the concentration of Glutathione is exhausted, the metabolites react with cellular proteins causing liver necrosis. The detoxification capability of the liver can be affected by several liver diseases, e.g. the non-alcoholic fatty liver disease (NAFLD). The developed model is an extension of a previous published work, where a multicomponent, poro-elastic multiphase and multiscale function-perfusion approach based on the Theory of Porous Media (TPM), see [1], [2] has been presented, cf. [3]. Additionally, the decomposition of toxic metabolites causing cell damage is supplemented using the example of Paracetamol. Since the liver has a complex structure and different sizes, a scale bridging approach is requested. The total organ consists of liver lobules, where the toxic metabolites, just like other nutrients and substances, are initiated into the liver with an anisotropic blood flow via the sinusoids. As the structure of the lobules is extremely complex, we use a multicomponent mixture theory based on the Theory of Porous Media (TPM) see [1], [2] to describe the lobule scale. The computational model consists of a tetra-phasic component body, composed of a porous solid structure, fat tissue with the ability of growth, a liquid phase representing the blood and a solid phase, which characterizes the necrotic cells. The phases consist of a carrier phase, also called solvent, and solutes, representing microscopic components, solved in the solvent and consisting of the nutrients responsible for the liver metabolism. The metabolism takes place in the liver cells, which are located along the sinusoids. To calculate the metabolism processes on the cell scale, an embedded set of coupled ordinary differential equations (ODE) is used. [1] De Boer, R. [2002], „Theory of porous media: highlights in historical development and current state'', Springer Science & Business Media. [2] Ehlers, W. [2002], „Foundations of multiphase and porous materials“, Springer-Verlag Berlin, Heidelberg, New York., S. 3–86. [3] Ricken, T., et al. [2010], „A biphasic model for sinusoidal liver perfusion remodeling after outflow obstruction.'', Biomech Model Mechanobiol, 9. Jg., Nr. 4, S. 435-450.

Deep Learning for Protein Structure Prediction and Protein Folding

Guillaume Lamoureux*

*Concordia University

ABSTRACT

I will be presenting our recent progresses on the development of deep neural networks for the prediction of the structure of a protein from its amino acid sequence. We are interested in neural network architectures that mimic the protein folding process and that learn not only the native structure of a protein but the shape of the folding funnel leading to it. In particular, we use neural networks designed to respect translational and rotational invariance, and to generate structures that obey the rules of molecular folding and assembly.

Coupled Thermal Mechanical Model of the LORELEI Experimental Device with Multiple Interactions and Heat Sources during Controlled Transients and Accident Scenarios

Eran Landau^{*}, Hadas Shanha^{**}, Moran Ezra^{***}, Niv Moran^{****}, Avner Sasson^{*****}

^{*}Rotem Industries LTD., ^{**}Nuclear Research Center Negev, ^{***}Rotem Industries LTD., ^{****}Nuclear Research Center Negev, ^{*****}Rotem Industries LTD.

ABSTRACT

A primary component within the LORELEI experimental device designed for single-rod Loss of Coolant Accident (LOCA) experiments in the French JHR research reactor, is a double-wall pressure flask with unique geometry and loading conditions containing the fuel rod and a peripheral heater. During the experiment sequence, the fuel power is controlled by moving the entire systems position relative to the reactor core. Heat transfer between the fuel, a surrounding heater (and instrumentation holder) and the double-wall flask result in significant axial and azimuthal temperature variations over the flask walls. The resulting temperatures are also influenced by the gamma heating of the structure materials, and the Zirconium cladding exothermal oxidation reaction and ballooning during the transient. In Addition, the system is also subjected to several notable external loads and constraints. Design-by-analysis initially relied on separate heat transfer and temperature-displacement analysis (uncoupled). This method however, produced relatively large displacements resulting in significant contact between the inner and outer flask walls, which in turn should have a strong effect over the resulting temperature field. For this reason, a fully coupled thermal and mechanical model of the LORELEI experiment device is developed, using a transient ABAQUS/Implicit solver with several tailored user-subroutines. The model employs a "simplified" approach for heat transfer over a gap (Radiation and Conduction/Convection) between cylindrical bodies using controlled (programmed) interactions, to accurately enable transient heat transfer between the deformable surfaces. Volumetric heat generation (nuclear, gamma, oxidation) is computed in user-subroutine HETVAL for each material model using several solution dependent variables (SDV's), Common block parameters and spatial functions, defined in user-subroutines USDFLD and UAMP. The device velocity, position, and the heater power are controlled by two independent PID controllers using temperature sensors on the cladding and heater hot-spots. The fully-coupled simulation displays notable differences in the temperature variation over the flask walls, and helps examine the influence of the existing pre-loads, cladding ballooning, added design features (such as centering pins) and the desired controller functions. LORELEI design calculations and safety analysis are based on qualified models. At this stage in development, the model is employed in evaluating safety margins and possible optimization that would result from future qualification of the model. In this presentation, special challenges in the development of the model and important findings will be discussed. [1] L.Ferry, D.Parrat, C.Gonnier, C.Blandin, Y.Weiss, A.Sasson. "The LORELEI Test Device for LOCA Experiments in the Jules Horowitz Reactor" WRFPM 2014

Reduced-Order Models with Space-Adapted Snapshots

Jens Lang^{*}, Sebastian Ullmann^{**}

^{*}Technische Universität Darmstadt, Germany, ^{**}Technische Universität Darmstadt, Germany

ABSTRACT

Space-adaptive numerical methods have recently found their way into reduced-order modeling of parametrized PDEs [1, 2, 3]. Standard techniques assume that all snapshots are computed with one and the same spatial mesh, which is often not appropriate for multi-scale problems. Instead, we consider unsteady adaptive finite elements, where the spatial discretization varies over time or stochastic sampling. Our focus is on reduced-order models obtained by a Galerkin projection onto a proper orthogonal decomposition (POD) of solution samples. In this context, adaptive snapshot computations allow a reduction of computational complexity in the offline-phase of the reduced-order model. The following points will be discussed in the talk: (i) How can the effort for creating reduced-order models with space-adapted snapshots be minimized? (ii) How can the union of all snapshot meshes be avoided? (iii) What is the main difference between static and adaptive snapshots in the error analysis of Galerkin reduced-order models? Numerical test cases illustrate the convergence properties with respect to the number of POD basis functions. References: [1] M. Ali, K. Steih, and K. Urban. Reduced basis methods with adaptive snapshot computations. *Adv. Comput. Math.*, 43:257-294, 2017. [2] S. Ullmann, M. Rotkvic, and J. Lang. POD-Galerkin reduced-order modeling with adaptive finite element snapshots. *J. Comput. Phys.*, 325:244–258, 2016. [3] M. Yano. A minimum-residual mixed reduced basis method: exact residual certification and simultaneous finite-element reduced-basis refinement. *ESAIM: M2AN*, 50:163–185, 2016.

A Condensed Approach to Investigate Electromechanical Induced Phase Transitions in Lead Zirconate Titanate (PZT)

Stephan Lange*, Philip Uckermann**, Andreas Ricoeur***

*University of Kassel, **University of Kassel, ***University of Kassel

ABSTRACT

Ferroelectric materials are used for a variety of technical applications, for example fuel injection or hearing devices. Despite containing lead, lead zirconate titanate (PZT) remains one of the most common actor materials because of its favorable electromechanical properties, particularly at the morphotropic phase boundary (MPB). PZT at the MPB consists of both tetragonal and rhombohedral unit cells. One of the most accepted theories for those properties is the existence of fourteen instead of six (tetragonal) or eight (rhombohedral) domain variants. The condensed method was developed to calculate e.g. hysteresis loops or residual stresses for polycrystalline materials without spatial discretization, resulting in low computational effort and large numerical stability [1]. It is suitable for efficient implementation of various constitutive behaviors, accounting for interactions of grains or different constituents of a material compound. Hitherto it has been applied to tetragonal ferroelectrics, ferromagnetics and multiferroic compounds [2] as well as to life time predictions in ferroelectrics [3]. In this research the approach is expanded towards transitions of tetragonal and rhombohedral phases. Therefore, the evolution law needs to be extended with respect these multiphase aspects. It contains energy barriers which can be reached by electrical or mechanical loads and distinguishes between phase transitions and domain wall motions. Some alternatives for modeling these barriers and the related consequences on material responses will be analyzed. Finally, the influences of the existence of two different types of unit cells and of phase transitions on properties of PZT at the MPB will be critically discussed. References [1] Lange, S. and Ricoeur, A., A condensed microelectromechanical approach for modeling tetragonal ferro- electrics, *International Journal of Solids and Structures* 54, 2015, pp. 100 – 110. [2] Ricoeur, A., Avakian, A. and Lange, S., Microstructured multiferroic materials: modelling approach towards efficiency and durability. In: Altenbach, H., Jablonski, F., Müller, W. H., Naumenko, K. and Schneider, P. (eds.), *Advances in Mechanics of Materials and Structural Analysis, Advanced Structural Materials*, 80, Springer 2017 (in press). [3] Lange, S. and Ricoeur, A., High cycle fatigue damage and life time prediction for tetragonal ferroelectrics under electromechanical loading, *International Journal of Solids and Structures* 80, 2016, pp. 181 – 192.

Numerical Transition Behavior Modeling of High-Strength Low-Alloy Steels (HSLA) Extending a Gurson Model with a Modified Orowan Criterion

Julius Langenberg*, Victoria Brinnel**, Sebastian Münstermann***

*RWTH Aachen University, **RWTH Aachen University, ***RWTH Aachen University

ABSTRACT

Traditional design rules are hindering the usage of High-Strength Low-Alloy steels (HSLA) in constructions. Numerical studies performed by (1) on a modified Gurson-Tvergaard-Needleman model (GTN), prove that HSLA steels offer huge ductile resources. Yet, ductile as well as brittle failure properties are important to characterize the mechanical behavior of HSLA steels. The pure GTN model however is unable to simulate cleavage fracture. The aim of the presented study was therefore to combine the GTN model with a suitable cleavage fracture model to provide a tool for modelling the full transition behavior. Combinations of Gurson and Beremin models are widely used to characterize cleavage fracture (2). The probabilistic Beremin model bases on a threshold stress integrated in a test volume. Therefore, it may only be applied as a postprocessor computation. A prediction of the inverse transition behavior of ductile failure and cleavage fracture is thus not possible. Additionally, most Beremin models are not taking any stress triaxialities and plastic strains into account. A possible solution for this is an extended Orowan cleavage fracture criterion as proposed by (3), which defines failure in dependence of critical stress- and strain states for a single element. Such a single element formulation enables a prediction of transition zone behavior using interactive online coupling for the cleavage fracture and ductile failure mechanism. So far, the extended Orowan criterion is not combined with any Gurson model. This study focuses on numerical modeling of the transition behavior of HSLA steels by extending a Gurson model with a modified Orowan criterion. The extended Orowan cleavage fracture model proposed by (3) will be summarized and an overview on its implementation into the GTN model is given. Moreover, an experimental calibration scheme as well as the influence of stress triaxialities and plastic strains on cleavage fracture are discussed. The developed formulation of the GTN model helps to characterize transition behavior of high-strength steels. Thus, this study supports the structural application of HSLA steels by considering their combined ductile failure and cleavage fracture properties in design.

References 1. Brinnel, Victoria. 2017. Improved Limit State Definitions for Pressure Vessels by a Scalebridging Application of Damage Mechanics. Aachen 2. Pineau, Andre. 2008. Modeling ductile to brittle fracture transition in steels -micromechanical and physical challenges. International Journal of Fracture. 150: 129-156 3. He, Jinshan; Lian, Junhe; Golisch, Georg; Jie, Xiaodong; Münstermann, Sebastian. 2017. A generalized Orowan model for cleavage fracture. Engineering Fracture Mechanics. 186: 105-118

Meshing Images with OOF3D

Stephen Langer^{*}, Andrew Reid^{**}

^{*}NIST, ^{**}NIST

ABSTRACT

The OOF project [1] at NIST develops software for analyzing materials with complex microstructures, starting with real or simulated micrographs. The OOF2 program reads and analyzes two dimensional micrographs, while OOF3D works in three dimensions. In both cases, the OOF user assigns continuum material properties to features in a micrograph, creates a finite element mesh, and performs virtual experiments on the mesh. An important step in the process is to match the finite element mesh to the microstructural geometry given by the micrograph. The crucial cpu-intensive part of matching the mesh is to compute the homogeneity of each element: the degree to which the 2D pixels or 3D voxels inside the element all have the same material properties. This requires the computation of the area or volume of the intersection of an element with a conglomeration of pixels or voxels (treating each pixel or voxel independently is too slow). In 2D this calculation is relatively straightforward, but in 3D it is complex and fraught with subtleties. If done incorrectly, microscopic round-off errors in the calculation of the position of an intersection can lead to macroscopically wrong answers. A new technique, based on Powell and Abel's "3d" graph clipping algorithm [2] is fast and robust. The boundary of a voxel set is represented by a planar graph, and the graph is clipped sequentially by each face plane of a finite element. The method depends only on the topology of the voxel set and round-off errors only lead to small changes in the final volume. I will discuss the algorithm, how to construct the graph efficiently, and modifications to the algorithm to handle concavities in the voxel set. [1] <http://www.ctcms.nist.gov/oof> [2] D. Powell and T. Abel, "An exact general remeshing scheme applied to physically conservative voxelization", Journal of Computational Physics 297 (2015) 340–356.

Some Statistical Properties of the Frequency Response Functions of Random Systems

Robin Langley*

*University of Cambridge UK

ABSTRACT

Professor Soize has made seminal contributions to the theory of random structures, and this paper considers some of the properties of the frequency response functions (FRFs) of such systems. Initially the properties of causal complex frequency response functions are discussed, and it is shown that under certain conditions these functions obey the Analytical Ergodicity (AE) condition, in that the average value of a function of the FRF is equal to the value of the function when evaluated using the average value of the FRF. This property can be used to derive simple expressions for power input to complex systems. Attention is then turned to the statistical properties of the energy FRFs of built-up systems. It is shown that by combining Statistical Energy Analysis (SEA) with random vibration theory, expressions can be obtained for the mean rate (as a function of frequency) at which an energy FRF crosses a critical level. Results are also derived for the probability that the FRF will cross a critical level at least once over a prescribed frequency range. The same analysis leads to results for the mean number of peaks in the FRF over a specified frequency range, and for the mean trough-to-peak height. The latter results are useful for auralisation (i.e. sound reconstruction) when using SEA: the averaging employed in SEA removed all detail from an FRF, and the present results provide metrics that should be met when reconstructing this detail.

Meshfree Partition of Unity Radial Basis Function Methods

Elisabeth Larsson^{*}, Victor Shcherbakov^{**}, Alfa Heryudono^{***}

^{*}Uppsala University, ^{**}Uppsala University, ^{***}University of Massachusetts Dartmouth

ABSTRACT

In this talk, we present how to build on radial basis function (RBF) approximation to obtain a numerical method for PDE solving that is high order accurate, numerically robust, and computationally efficient. Global RBF methods are too expensive for large scale problems, so the first step in achieving computational efficiency is to localize the approximations. We use a partition of unity approach, where local RBF approximations on overlapping patches are combined into a global approximation. Radial basis function methods are in general counted as meshfree methods, but there can still be sensitivity to the node layout. We avoid this by letting each patch have an identical optimized node layout. This introduces nodes outside of the computational domain, but we then use oversampling within the computational domain, and in the end perform a least squares fitting of the problem. This final ingredient also provides the numerical robustness for large scale problems.

A Two-scale Modeling Framework for Fracturing Solids Based on Smeared Macro-to-Micro Transitions of Discontinuities

Fredrik Larsson*, Erik Svenning**, Martin Fagerström***

*Chalmers University of Technology, **Chalmers University of Technology, ***Chalmers University of Technology

ABSTRACT

In computational homogenization of solids, the effective response can be obtained from underlying simulations on, e.g., Statistical Volume Elements (SVEs). Although standard nowadays, such an approach leads to poor results when strain localization and fracture occurs in the material. Remedies to this problem exists in the literature, however, the proposed approaches all tend to focus on particular choices of constitutive models on the microscale. In the present work, we aim to circumvent the need for explicit fine-scale discontinuity tracking by developing a two-scale scheme for fracturing solids, where the eXtended Finite Element Method (XFEM) is chosen for representation of the macroscale discontinuities, see [1]. The formulation, which is based on Variationally Consistent Homogenization (VCH), leads to a weak problem of finding the (possibly discontinuous) displacement field. The macroscale weak equilibrium equations contains, in addition to the standard bulk contribution, a term of cohesive zone type and a novel correction term. The macroscale discontinuities are imposed on the microscale SVEs using weakly periodic boundary conditions that are aligned to the macroscale localization direction. A key feature is that the smearing width employed in the discontinuity transitions is related to the SVE size used for the fine scale analysis at the effective discontinuity. By combining the smeared discontinuity transitions with the strict ellipticity condition, we obtain a modeling framework that can be employed without restrictive assumptions on the constitutive models employed on the microscale. Numerical investigations are presented in two spatial dimensions. In particular, it is noted that the method does not result in pathological dependence on macroscale mesh-size, nor on the size of the SVE. References [1] E Svenning, F Larsson and M Fagerström: Two-scale modeling of fracturing solids using a smeared macro-to-micro discontinuity transition. Computational Mechanics 2017: 627–641.

DEM-CFD Simulation of the Effect of Air on Powder Flow During Die Filling

Simon Larsson*, Gustaf Gustafsson**, Pär Jonsén***, Hans-Åke Häggblad****

*Luleå University of Technology, **Luleå University of Technology, ***Luleå University of Technology, ****Luleå University of Technology

ABSTRACT

In the field of powder metallurgy (PM), complex components with complicated shapes can be manufactured. One important step in the PM process is the powder pressing process, where powder is consolidated during a forming operation into a desired shape, normally by applying pressure. During powder pressing, the mechanical properties of powder materials change dramatically. PM manufacturers tend to produce components with shapes of increasing complexity, requiring improved pressing equipment and methods. The most crucial aspect is to control the powder flow during die filling and the final powder density distribution after the filling stage, which has been shown to affect the strength of the final component significantly [1]. To investigate the non-homogeneity of the density of PM components, experimental studies combined with numerical simulations of the die filling stage are exploited. This work covers the numerical modelling and simulation of die filling. The discrete element method (DEM) [2] was used to model the powder, and computational fluid dynamics (CFD) to model the air. To study the effect of air on powder flow, the DEM was coupled to the CFD using a two-way coupling approach. Experimental measurements with digital speckle photography (DSP) from a previous study [3] were used for comparison with the numerical simulations. The comparison of the DSP measurements and the numerical simulations showed similar macroscopic flow characteristics. Thus, the adequacy of the proposed DEM-CFD model has been demonstrated in a metal powder die filling operation. The DEM-CFD method has been shown to be an effective method for the numerical simulation of the interaction between powder and air. References [1] Zenger, D. & Cai, H. (1997). Handbook of the Common Cracks in Green P/M Compacts. Metal Powder Industries Federation, MPIF. Worcester, USA. [2] Cundall, P. A., & Strack, O. D. (1979). A discrete numerical model for granular assemblies. *geotechnique*, 29(1), 47-65. [3] Larsson, S., Gustafsson, G., Jonsén, P. & Häggblad, H.-Å. (2016). Study of Powder Filling Using Experimental and Numerical Methods. In: World PM2016 Congress & Exhibition, Hamburg, October 9-13, 2016.

Modelling of Red and White Thrombus Formation in Intracranial Aneurysms after Flow Diversion

Toni Lassila^{*}, Ali Sarrami-Foroushani^{**}, Mostafa Hejazi^{***}, Alejandro Frangi^{****}

^{*}University of Sheffield, ^{**}University of Sheffield, ^{***}University of Sheffield, ^{****}University of Sheffield

ABSTRACT

Treatment of intracranial aneurysms with flow-diverting stents is a highly successful minimally invasive technique. It typically results in the stable embolisation, endothelialisation, and complete elimination of the aneurysm. Computational fluid dynamics simulation of post-operative flow reduction inside the aneurysm has shown utility in predicting whether or not the procedure will be successful. However, in some cases the aneurysm fails to develop a stable clot or recurs even when sufficient levels of flow reduction are attained. It is not fully understood why some aneurysms fail to develop a stable clot. We believe that computational prediction of thrombus formation dynamics can help predict the post-operative response in these challenging cases. In this work, we propose a new model of thrombus formation inside intracranial aneurysms (Sarrami-Foroushani et al. 2018) that builds on previously proposed models of haemostatic thrombosis at the site of vascular injury (Wu et al., 2017). Our novel contributions are: 1) the initiation mechanism, where we modelled post-operative flow stasis as the thrombosis initiator, and 2) the combination of platelet activation and transport models with fibrin generation models that are key in characterising stable and unstable thrombus. The model is based on post-mortem observations of two types of thrombus inside aneurysms: red thrombus (erythrocyte- and fibrin-rich) can be found in unstable clots, while white thrombus (fibrin- and platelet-rich) can be found in stable clots. The thrombus generation model is coupled to 3-D CFD model developed in ANSYS CFX. The coupled flow and thrombus formation model is simulated until a steady state is reached, after which point the quality of the resulting thrombus is evaluated as a combination of platelet content and fibrin concentration within the aneurysm. Computational predictions of thrombus quality are validated against two idealised flow diversion scenarios. The first is an in vitro phantom study (Gester et al. 2016) of two flow-diverting stents with different sizings. We demonstrate that our model accurately predicts the lower thrombus stability that results in the oversized stent scenario. The second validation study explores the behaviour of the proposed thrombus quality indicator in a range of idealised sidewall aneurysms with variable aspect ratio and diameter. References Sarrami-Foroushani A, et al. A mathematical model of thrombus formation in intracranial aneurysms, Biomech. Model. Mechanobiol., submitted, 2018 Wu, WT, et al. Multi-constituent simulation of thrombus deposition. Sci.Rep. 7: 42720, 2017 Gester K, et al. In vitro evaluation of intra-aneurysmal, flow-diverter-induced thrombus formation: a feasibility study. Am. J. Neuroradiol. 37.3:490-496, 2016

Time-Independent Formulations for Growth and Remodeling of Soft Tissues

Marcos Latorre^{*}, Jay Humphrey^{**}

^{*}Yale University, ^{**}Yale University

ABSTRACT

Most biological soft tissues exhibit a remarkable ability to adapt to sustained changes in mechanical loads. These macroscale adaptations, including growth (changes in mass) and remodeling (changes in microstructure), are important determinants of physiological behaviors at a systems level and thus clinical outcomes. Necessarily, growth and remodeling (G&R) processes are time dependent due to the finite periods needed for material to be synthesized, deposited, degraded, and/or reorganized. Moreover, because soft tissues appear to have some material “memory” during G&R, hereditary integral formulations [1], as commonly used in viscoelasticity, have proven useful in describing and predicting evolving responses of soft tissues under diverse conditions. As frequently done in many areas of mathematical physics, however, these time-dependent models can be specialized to respective time-independent formulations that provide tremendous simplification and yet considerable insight. We present a new time-independent approach for modeling the evolution of soft tissue G&R [2] that arises from a general constrained mixture model. We discuss the mathematical conditions, in terms of ratios of characteristic times of tissue responses and external loading, that yield the particularized formulation. In these cases, integral-type evolution equations can be written in terms of an equivalent set of time-independent, algebraic nonlinear equations that can be solved efficiently. We show that the simplified theory captures well the predictions of a fully general constrained mixture theory at a fraction of the computational expense for problems defined by particular characteristic times. Additionally, with the present pre-integrated model at hand, we compute exactly the long-term outcomes of G&R processes in response to sustained external stimuli following a direct approach. The present formulation plays parallel roles as in Fung’s theory of pseudoelasticity to better understand complex G&R of soft tissues, in general, and of arteries, in particular. Indeed, simplified formulations of this type can serve as efficient tools for studies of parameter sensitivity, uncertainty quantification, and optimization, which tend to be even more demanding computationally. Acknowledgements US NIH: R01 HL105297, U01 HL116323, R01 HL128602, R01 HL134712. Spain: CAS17/00068, DPI2015-69801-R. UPM: “Ayudas al personal docente e investigador para estancias breves en el extranjero 2017”. References [1] JD Humphrey, KR Rajagopal (2002). A constrained mixture model for growth and remodeling of soft tissues. *Math Models Methods Appl Sci*, 12, 407-430. [2] M Latorre, JD Humphrey. Critical Roles of Time-Scales in Modeling Soft Tissue Growth and Remodeling. Invited. Under review.

Micropolar Crystal Plasticity Finite Element Models with Grain Shape Effects on Slip Resistance

Marat Latypov^{*}, Jason Mayeur^{**}, Irene Beyerlein^{***}

^{*}University of California Santa Barbara, ^{**}CFD Research Corporation, ^{***}University of California Santa Barbara

ABSTRACT

Emerging manufacturing routes for advanced materials (such as additive manufacturing) often result in complex microstructures at the mesoscopic length scale. These complex microstructures with features (e.g., grains) far from equiaxed shapes require advanced modeling approaches. In this contribution, we present size-dependent crystal plasticity finite element framework that explicitly accounts for grain shape effects. The intrinsic length scale and size dependence are captured at the single crystal constitutive level by the micropolar theory. This subclass of micromorphic higher-order continuum theory considers lattice rotations as generalized displacements and incorporates couple stresses that lead to kinematic hardening of slip systems originating from gradients of lattice rotations. The grain shape effect is accounted for at two levels: (i) at the slip system level where slip resistance for each grain is calculated according to the chord length along the slip direction and (ii) at the finite element model level where the actual grain shapes are constructed. Potential applications of the proposed framework include improved predictions of effective yield strength or high-cycle fatigue crack initiation of polycrystals.

Binding to Glutamate Receptors: Follow the Yellow Brick Road

Albert Lau^{*}, Alvin Yu^{**}, Hector Salazar^{***}, Andrew Plested^{****}

^{*} Johns Hopkins University School of Medicine, ^{**} Johns Hopkins University School of Medicine, ^{***} Humboldt University Berlin, ^{****} Humboldt University Berlin

ABSTRACT

Ionotropic glutamate receptors (iGluRs) mediate neurotransmission at the majority of excitatory synapses in the brain. Little is known, however, about how the neurotransmitter glutamate reaches the recessed binding pocket in iGluR ligand-binding domains (LBDs). Here we report the process of glutamate binding to a prototypical iGluR, GluA2, in atomistic detail using both enhanced sampling and unbiased molecular dynamics simulations. Charged residues on the LBD surface are found to form pathways that facilitate glutamate binding by effectively reducing a three-dimensional diffusion process to a spatially-constrained two-dimensional one. Free energy calculations identify residues that metastably interact with glutamate and help guide it into the binding pocket. These simulations also reveal that glutamate can bind in an inverted conformation and also reorient while in its pocket. Electrophysiological recordings demonstrate that eliminating these transient binding sites slows activation and deactivation, consistent with slower glutamate binding and unbinding. These results suggest that binding pathways have evolved to optimize rapid responses of GluA-type iGluRs at synapses.

An Atomistic Study of the Microstructure and Mechanical Properties in Bamboo under Uniaxial Tension

Devnid Lau^{*}, Huali Han^{**}

^{*}City University of Hong Kong, ^{**}City University of Hong Kong

ABSTRACT

There is an increasing requirement for lightweight materials that are able to be served in engineering such as transportation, buildings, and energy storage and conversion. The natural materials of hierarchical structures have low density and outstanding mechanical properties inspiring us to design and fabricate bio-materials with unprecedented combinations of stiffness, strength and toughness at low density by replicating their structures [1]. In this work, the bamboo is used as the example to study the structure-properties relationship for the bio-material design because bamboo has a greater stiffness-to-weight and strength-to-weight ratio than that of common wood, cast iron, aluminum alloy and structural steel. According to the experimental characterization of the bamboo, the bamboo fibers that are resource of the mechanical properties have lamellar structures where the cellulose microfibrils are embedded in the matrix of lignin and hemicellulose [2]. The dynamic evolution of the modeled constituents under uniaxial tension is observed with the help of the molecular dynamics simulations to disclose the role of the basic constituents in the mechanical behavior of bamboo fibers. It is found that the cellulose mainly provides the strength and the matrix is responsible for the load transformation. The interfacial interaction between the cellulose and the matrix of hemicellulose and lignin is also studied. The interaction of different constituents combining with the molecular conformation evolution of the individual constituents during the deformation enables us to figure out the relationship between the microstructure and mechanical performance of bamboo fibers and to understand the critical structural features for the outstanding mechanical properties in the bamboo. Our work provides a guideline for the design of synthetic materials by replicating the structural characteristics of their natural counterparts. Moreover, the computation methods used in our work can also be worked as an efficient way to synthesize novel compounds with improved performance. [1] U G.K. Wegst, H. Bai, E. Saiz, A.P. Tomsia and R.O. Ritchie. Bioinspired structural materials. *Nature Materials*, 14 (2015) 23-36. [2] M.K. Habibi, L-H. Tam, D. Lau, Y. Lu. Viscoelastic damping behavior of the structural bamboo material and its microstructural origins. *Mechanics of Materials*, 97 (2016)184-198.

Development of a Multiscale Computational Modeling Framework for the Tricuspid Valve – Linking Valvular Interstitial Cell Mechanobiology with Organ-Level Function

Devin Laurence*, Yi Wu**, Chung-Hao Lee***

*The University of Oklahoma, **The University of Oklahoma, ***The University of Oklahoma

ABSTRACT

The tricuspid valve (TV) is located in the right side of the heart and prevents the retrograde blood flow between the right ventricle and right atrium during systole. Functional tricuspid regurgitation (FTR) occurs when the TV's three leaflets are unable to fully close, causing an undesired backflow into the right atrium as the right ventricle contracts to move blood through the pulmonary vascular system. Approximately 1.6 million Americans are affected by FTR annually with only 8,000 undergoing surgical repair; furthermore, there exists a disappointing recurrence rate (~20%) of FTR 10 years after the initial repair.^{1,2} Recent investigations have demonstrated and quantified the multiscale behavior of the mitral valve (MV) under both physiological and pathophysiological conditions,³ but no such extensive investigation has been performed for the TV. In this work, we are developing a multiscale computational framework of the TV to provide insight into the underlying mechanisms behind TR initiation and progression, which contains three anatomical scales: the tissue-level, the downscale cellular microenvironment, and the organ-level. First, the tissue-level model is developed by considering the underlying constituents (extracellular matrix, collagen, and elastin), which is validated against previously acquired biaxial tension data to accurately capture tissue's anisotropic behaviors. Then, the tissue-level deformation is prescribed as boundary conditions to the downscale microenvironment model (containing the ECM and heterogeneously dispersed valvular interstitial cells (VICs)) to provide insight into the VIC mechanobiology. Finally, the information obtained from the tissue-level and microenvironment models is combined with realistic valve geometry and heterogeneous mapping of leaflet constituents (i.e., collagen, elastin, and VICs) in high-fidelity organ-level finite element simulations of the TV. Our preliminary investigations have demonstrated the VIC's interaction with the surrounding ECM, specifically the VIC cytoplasm's key function in transferring mechanical stimuli from the ECM to VIC nucleus. The ongoing development will facilitate patient-specific modeling of the TV in healthy, diseased, and repaired states. Moreover, the developed model can be extended to provide objective recommendations to surgeons for repair timing and individual-optimized therapy to significantly increase the repair longevity. Acknowledgments AHA SDG (16SDG27760143) for CHL; OU UROP (2018) and MRF (2017-2018) for DL. References [1] Sturge O, et al., JTSC (2006). [2] Ballazhi F., et al., TCS (2016). [3] Ayoub S., et al., JRSI (2017).

Gradient-Enhanced Parametric Optimization of Vibro-Acoustic Problem Using Xfem and a Dedicated Metamodel

Luc Laurent*, Antoine Legay**

*Laboratoire de Mécanique des Structures et des Systèmes Couplés, Conservatoire National des Arts et Métiers, case 2D6R10, 2 rue Conté, 75003 Paris, France, **Laboratoire de Mécanique des Structures et des Systèmes Couplés, Conservatoire National des Arts et Métiers, case 2D6R10, 2 rue Conté, 75003 Paris, France

ABSTRACT

Noise reduction is a design constraint which is more and more taken into account. For instance, this constraint occurs in aircraft cabin design on which the noise propagation is minimized by finding the optimal arrangement. Classical design processes require many expensive numerical computations. In order to reduce the computation time, a new strategy is proposed based on two specific tools integrated in a dedicated optimization strategy: (1) a finite element solver which provides responses and gradients of the objective function to (2) a gradient-enhanced metamodel which interpolates both kinds of information. Solving the mechanical problem remains to solve a coupled problem composed of structural and fluid domains. The acoustic fluid problem is governed by the Helmholtz's equation. A porous material present in the acoustic cavity is modeled by the Biot-Allard's constitutive law. The structural problem corresponds to thin walls placed in the fluid and governed by elasto-dynamics equation. The air-structure problem is solved using xfem in order to be able to consider an arbitrary structure placed in the acoustic cavity. In order to reduce the computation time, a reduced model is built from the full coupled problem using a Craig-Bampton's approach. In addition to the resolution of the coupled problem, the calculation of the gradients with respect to the design parameters is proposed by considering an intrusive approach. Due to the fact that design parameters govern only the position of the structure in the acoustic cavity, the calculation of the gradients requires only calculation of gradients of the xfem's operators which can be done analytically. The global optimization based on this mechanical problem requires a large number of calls of the mechanical solver. Therefore a gradient-enhanced surrogate-based optimization is used. The approach is based on the Efficient Global Optimization composed of two phases: (1) a gradient-enhanced cokriging metamodel is built using only a few sample points and associated responses and gradients and (2) an iterative scheme using the expected improvement allows us to find the global minimum by adding smartly new sample points to the initial surrogate model. The whole strategy has been applied on some 2D and 3D cavity on which the position of a wall is determined in order to minimize the mean quadratic pressure in a control volume. Some examples will be presented for illustrating the performance of the proposed approach.

Multilevel Monte Carlo for Inverse Problems

Kody Law*

*University of Manchester

ABSTRACT

Uncertainty is recently becoming a requisite consideration in complex applications which have been classically treated deterministically. This has led to an increasing interest in recent years in uncertainty quantification (UQ). Another recent trend is the explosion of available data. Bayesian inference provides a principled and well-defined approach to the integration of data into an a priori known distribution. The posterior distribution, however, is known only point-wise (possibly with an intractable likelihood) and up to a normalizing constant. Monte Carlo methods have been designed to sample such distributions, such as Markov chain Monte Carlo (MCMC) and sequential Monte Carlo (SMC) samplers. Recently, the multilevel Monte Carlo (MLMC) framework has been extended to some of these cases, so that approximation error can be optimally balanced with statistical sampling error, and ultimately the Bayesian inverse problem can be solved for the same asymptotic cost as solving the deterministic forward problem. This talk will concern the recent development of multilevel Monte Carlo methods for inverse problems and data assimilation in the context of complex engineering applications. This class of algorithms are expected to become prevalent in the age of increasingly parallel emerging architecture, where resilience and reduced data movement will be crucial algorithmic considerations.

ARCHITECTURAL LAYOUT DESIGN FOR RAILWAY STATION PLATFORMS TO MITIGATE PASSENGER HAZARD RISK DUE TO TERRORIST EXPLOSIONS

VIVIAN LAWRENCE*, SAKDIRAT KAEWUNRUEN[†], AND CHARALAMPOS
BANIOTOPOULOS[†]

* School of Engineering, The University of Birmingham
52 Pritchatts Road
Edgbaston B152TT United Kingdom
Email address; VJL693@student.bham.ac.uk;

[†] School of Engineering, The University of Birmingham
52 Pritchatts Road
Edgbaston B152TT United Kingdom
Email addresses: s.kaewunruen@bham.ac.uk (S. Kaewunruen); C.Baniotopoulos@bham.ac.uk
(C. Baniotopoulos)

Key words: Passenger safety, explosive blast, physical and cyber threats, hazard risk, railway systems, platform layout design; layout optimization.

Abstract. The first priority in operating transportation and transit systems is public safety. Generally, operators are expected highly to assure the reliable and safe day-to-day journeys of public transports. However, based on recent factual evidences, extreme physical and cyber threats are no longer uncommon and these unpreventable measures are even more dangerous to the public's daily lives. Such clear examples are the terrorist attacks in Saint Petersburg in 2017, in London in 2017, in Stockholm in 2017, in Brussels in 2016, in Nice in 2016, and so many more. These examples have one thing in common. The transportation and transit system hubs are the clear target: either on rail, bus, car or truck, etc. This research establishes a novel and innovative development and optimization of architectural layout design on the railway platform in order to improve safety, manage risks, and mitigate uncertainties where perspectives from the humanities and the operations are fully considered. Computational multi-physics simulations have been used to simulate blast effects from terrorist attacks at a railway platform. Birmingham Grand Central railway station has been selected for case study modelling using LS-Dyna. A platform layout design as structural wave barriers has been used to illustrate the hazard risk mitigation for train passengers due to explosive blast pressures. The reflected air blast from a simulated terrorist bomb has been calculated using LS-Dyna CFD in comparison with the US Army guideline. The new insight will guide a new platform layout design to minimize damage and hazard risks to rail passengers. This research aligns with United Nation's Sustainable Development by creating novel engineering solutions enabling a safer built environment.

1 INTRODUCTION

Since the 1970's, terrorist attacks in Western Europe have remained a constant threat [1]. The number of attacks and fatalities can be seen in Figure 1. Therefore, it is of paramount importance to consider blast attack resistance in all design processes of new built environments and the assessment of existing ones in order to mitigate risks and minimise hazards to the public. To put the physical and cyber threats into context, areas of high importance and potential targets include train stations, airports, shopping centres, sport stadiums, malls, concert halls and theatres. In other words, anywhere that could have a large number of casualties or have a detrimental effect on transport and infrastructure networks or the economy [2].

There are currently no official standards governing the testing or specification of blast-resistant structures in Eurocodes [3]. However, there are accepted technical manuals for blast-resistant design, including but not limited to:

- EN 1990: Eurocode - Basis of structural design
- GSA-TS01-2003: US General Services Administration Standard Test Method for Glazing and Window Systems Subject to Dynamic Overpressure Loadings
- ASTM F2912 – 11: Standard Specification for Glazing and Glazing Systems Subject to Air blast
- UFC 3-340-02: Structures to resist the effects of accidental explosions.

Railway assets are a critical infrastructure that requires active monitoring and protection against man-made hazards (such as terrorist attack, severe vandalism, derailments, and human errors). The loading actions and design criteria are complex in nature with strict considerations for systemic and sub-systemic compatibility [3-7]. With the active engagement in overseas military missions, Europe's critical infrastructures remain at high risk of terrorist attack, especially at crowded railway stations as shown in Figure 2. Based on a critical literature review, most studies into blast effects are focussed on the damage on built environments or on building structures. In fact, the impact on passengers or human responses, especially at railway platforms, has not been thoroughly investigated. In this study, we pioneer a novel and innovative development in re-designing and optimising the railway platform layout in order to minimise blast damage to railway passengers. This type of development is highly in significant demand in this modernised but conflicted world.

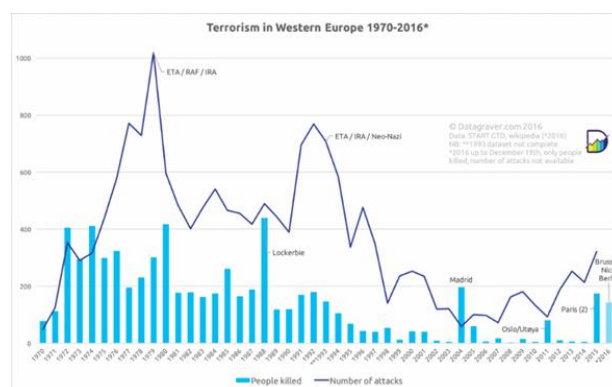


Fig.1: Terrorism in Western Europe [1]



Figure2: Birmingham Grand Central Station

It is important to note that only high explosives will be considered as a terrorist threat within this research project. The high explosives are often in solid form. TNT is used as a universal reference point for determining a scaled distance from the blast wave source, by converting the charge mass of an explosive into the equivalent mass of TNT. This is done by multiplying the charge mass by a conversion factor derived from the specific energy and charge mass of TNT [8].

An explosion is defined as a sudden release of energy, dissipated as shock waves, projecting missiles and thermal radiation [9]. The detonation of high explosives generates hot gases and high pressures, which rapidly expands, compressing a layer of air and forming a shock wave [10]. As shown in Figure 3, the shock wave instantaneously increases the surrounding pressure above ambient atmospheric pressure, P_o , to peak pressure, P_{so} . This deteriorates as the shockwaves expand outwards from the epicentre [11]. Once the wave front has passed, after a short period of time, the pressure may drop below the ambient air pressure, producing a partial vacuum. This, together with suction winds, can carry debris for long distances away from the centre of the explosion [11]. Pape et al. [10] also explains that the overpressure, which is any pressure above ambient atmospheric pressure, tapers off and goes below ambient pressure, later returning to equilibrium. It can also be seen in Figure 3 that the area of positive pressure is called the 'positive phase' and the area of negative pressure is called the 'negative phase'. Both the positive and negative phases can contribute to causing damage. The time-pressure curve seen in Figure 3 can usually be approximated using Friendlander's equation, seen in Eq.1:

$$p(t) = p_s \cdot \left(1 - \frac{t}{t_0}\right) \exp\left(-\frac{bt}{t_0}\right) \quad (1)$$

There are 3 types of explosion: unconfined explosions, confined explosions and explosions attached to the structure [12]. Unconfined explosions are categorised into two types; an air-burst and a surface-burst, which create shock waves that interact in different ways. Surface-bursts are often the most common type of burst when it comes to terrorist activities, as they usually occur in built-up areas, where devices are placed on or close to the ground surface [12]. Only a surface-burst will be considered for purposes of this study. A surface-burst is when detonation occurs on the near the ground surface, causing initial shockwaves to be immediately reflected and

amplified by the ground surface, forming a single wave front, from both the initial and reflected shockwaves [13-14].

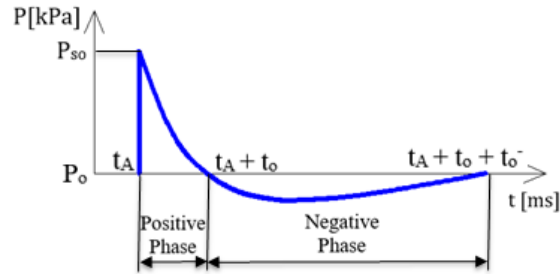


Fig.3: Shockwave pressure progression [6]

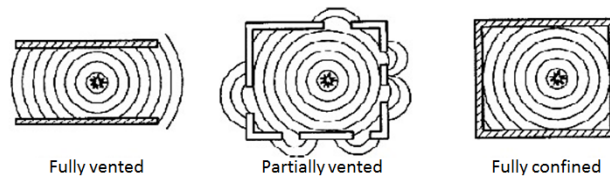


Fig.4: Degree of confinement [12]

The effects of an explosion inside a structure will need to be considered, which will depend on the degree of confinement, which in turn depends on the location of a blast. A confined explosion occurs where the initial peak pressures are very high, enhanced by refraction within the structure [13]. Examples of degrees of confinement can be seen below in Figure 4. Other factors that affect the amount of damage inflicted will include ventilation, temperatures, accumulation of gas pressure, blast characteristics, weight of the explosives and location of detonation [15].

2 RAILWAY STATION MODELLING

Birmingham Grand Central railway station has been re-developed and opened for multi-purpose uses in September 2015. As illustrated in Figure 5, Grand Central underwent a major overhaul as part of the New Street Station Gateway Plus redevelopment. The mall has been redesigned with a glass atrium roof as centrepiece, and is home to over 60 stores across 500,000 ft². Many of the shops, restaurants and cafés are creating very vibrant and extremely crowded malls that are fully integrated to one of the UK busiest rail hubs, with 12 train platforms.

In this study, the chosen platform is an island platform with a width of 16m. There are several structural columns situated 12m apart. The columns are 3m high and 1m wide. Fig .6 shows the finite element modelling of the platform. Two types of blast protective barriers have been installed in the simulation at a symmetrical distance in order to measure the comparable impact. The meshing optimization was used to suit the analysis purpose [16-20]. The platform and columns are to be modelled as reinforced concrete. The function `CONSTRAINED_LAGRANGE_IN_SOLID` is a validated solution to model the rebar within the concrete mesh. The concrete material uses the function `MAT_CSCM_CONCRETE`. Through which C32/40 concrete properties are imputed. The rebar and steel barriers are both defined to be

MAT_PLASTIC_KINEMATIC. Transverse rebar is 16 millimetres diameter; longitudinal rebar is 10 millimetres diameter. The steel properties of the barrier are shown in Table 1.



Figure 5: Birmingham Grand Central Station

Table 1: Steel Properties

Property	Value	Unit
Mass Density	7850	kg/m ³
Young's Modulus	2.1×10^5	MPa
Poisson's Ratio	0.3	
Yield Stress	400	MPa

3 EXPLOSIVE BLAST MODELLING

The platform, one scenario of terrorist attacks is simulated, both using 15kg of TNT.

- The bomb is placed in a bag and left on the floor of the platform (0m above G.L).

The barrier design and orientations from the previous study were used [21], as shown in Fig. 6. LS-DYNA software was used to simulate the air blast created from TNT. LS-DYNA has an empirical function LOAD_BLAST_ENHANCED which computes to a high degree of calibration, the pressure exerted on a Lagrangian structure from an air blast. LS-DYNA calculates pressure by measuring the distance from segment to charge, and the angle of incidence from the segments normal. To identify the blast load criticality, the document Unified Facilities Criteria (UFC), Structures to Resist the Effects of Accidental Explosions [5] has been reviewed.

$$Z = \frac{R}{\sqrt[3]{W}} \quad (2)$$

where R is the distance between the point of the detonation and the structure, W is the weight of the charge.

The scaled distance is computed. `LOAD_BLAST_ENHANCED` uses both of these variables at every cycle to calculate the pressure. The pressure can also be calculated by hand using this formula to validate the pressure computed by LS-DYNA. `LOAD_BLAST_ENHANCED` enables the blast to be located at any point throughout the model. The function can allow for four different types of blast shape. This research uses the hemispherical blast with reflected waves, as well as a free air blast with reflective waves. The model was created through LS-DYNA Prepost and is based on Birmingham New Street Station as shown in Figure 6. The floor slab and roof slab were made completely rigid to simulate a blast underground.

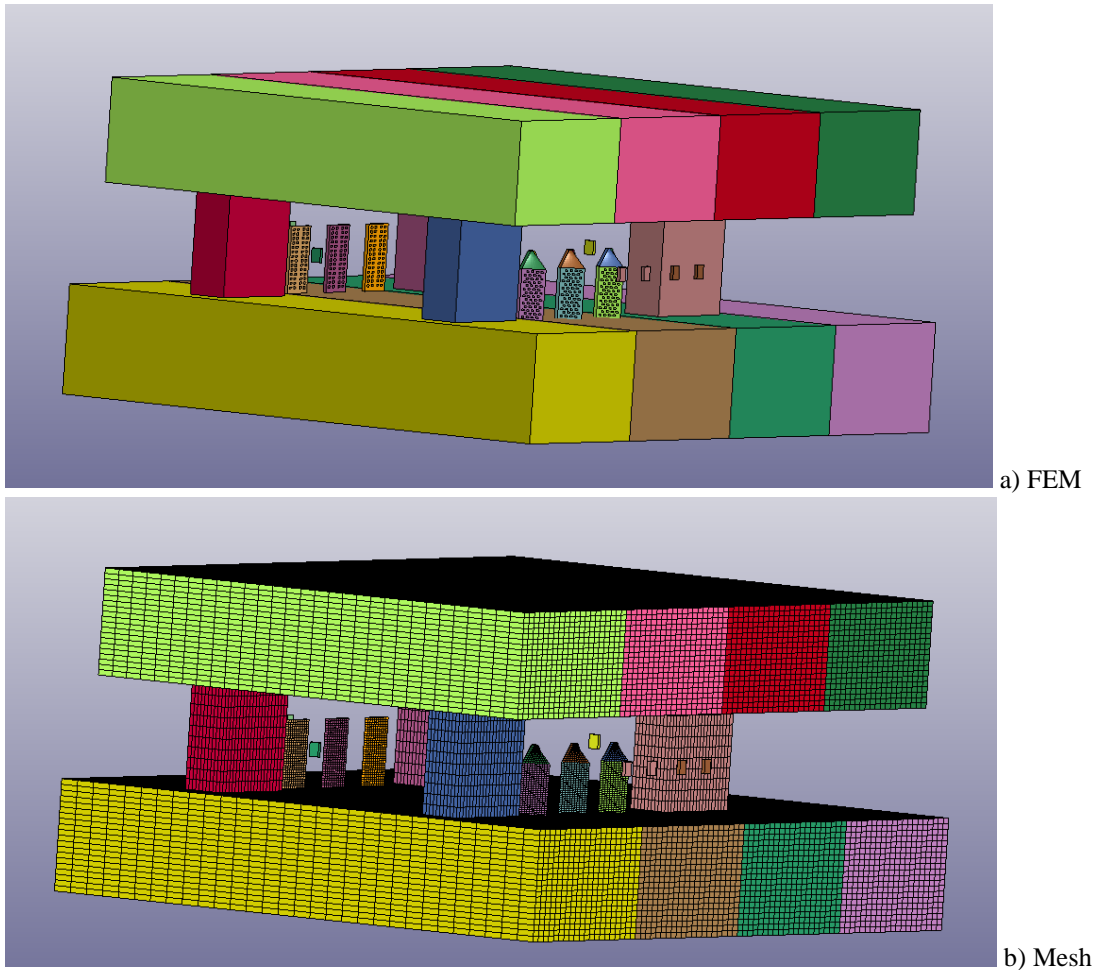


Fig.6: Platform modelling with blast protective barriers

The architectural barrier layout arrangements are presented in Figure 7. It can be seen that the different arrangements have been setup to evaluate the hazard risks to the rail passengers measured by sensors (at locations that affect human).

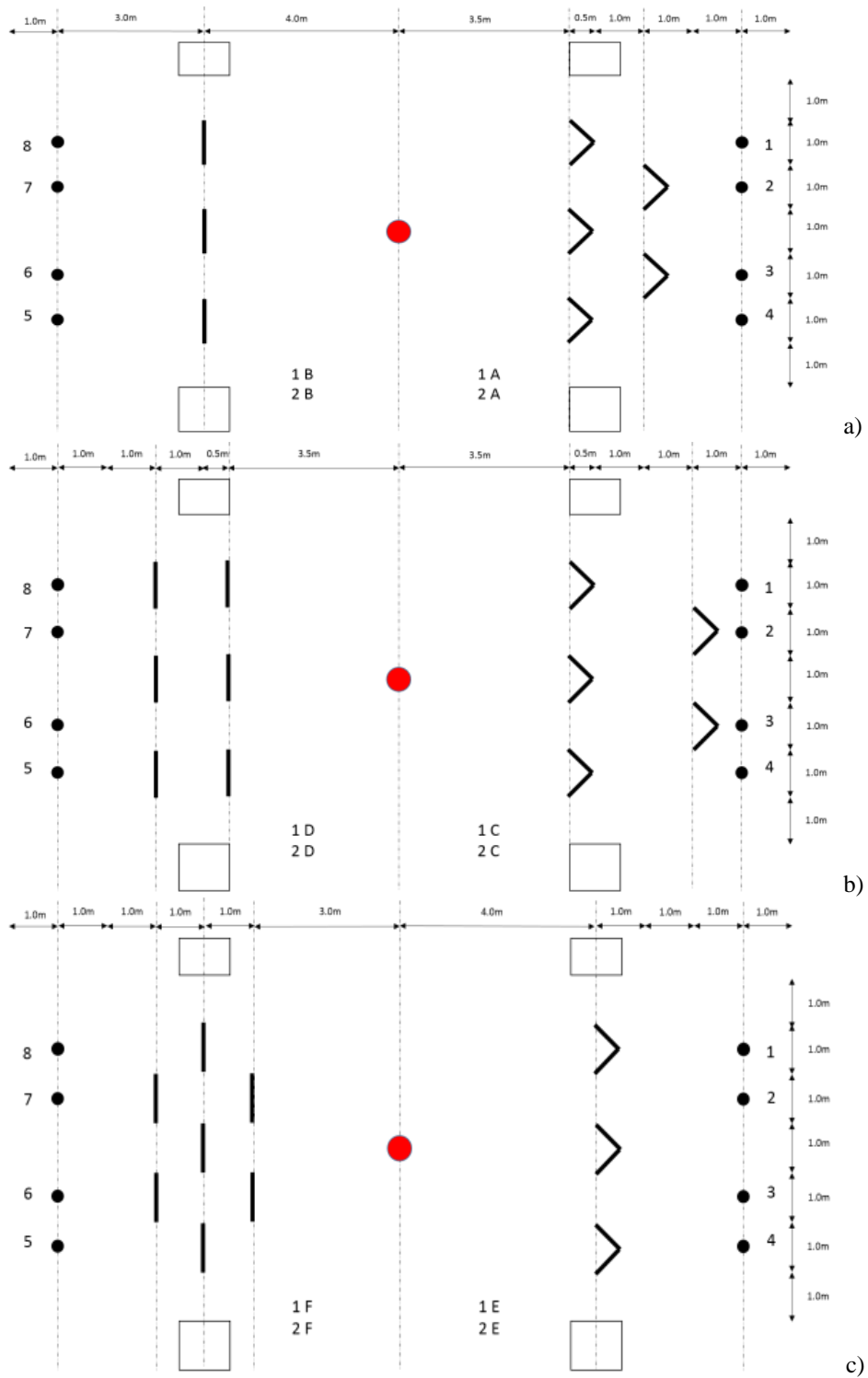


Figure 7: Layout optimization of architectural blast protective barriers

4 RESULTS AND DISCUSSION

Table 2 shows the pressure on the sensors due to near surface blast. When comparing the control sensor values with arrangements 1B and 1E the two central sensors have an increased pressure. The increased pressure is caused by the blast pressure reflecting and intensifying as it is transmitted through the barriers. It is noted that the flow of a shock wave expands directly after the barrier gap, resulting in the velocity of the wave intensifying [22]. The two external sensors of both arrangements were predicted to act the same due to the findings of recent study [21]. Concluding that the shape of the barriers placed in identical orientation has minimal effect on mitigating the blast wave. It is also concluded that a blast wave travels over a barrier, reforming a reduced pressure wave on the other side.

Table 2: Near surface blast pressure (kPa)

Sensor Number	1A	1B	1C	1D	1E	1F
1 & 8	254	289	238	248	289	211
2 & 7	279	339	276	315	339	237
3 & 6	279	339	276	315	339	237
4 & 5	266	305	250	261	305	221

Arrangement 1A and 1C were created to investigate this conclusion. Arrangement 1C is the same orientation as 1A but the barriers have a greater distance between them. From the results 1C reduced the overall pressure of the blast wave. The two external sensors of 1C both have a decreased pressure of 16 KPa than 1A. As found by [22], the reformed blast wave travels a longer distance until reaching the second row of barriers. Within this distance the wave is dissipating, thus reducing in force. However, the two central sensors show a very minimal decrease in pressure. The cause of both outcomes is as a result of the shape of the transmitted shock wave. As demonstrated in [22] the peak of a transmitted shock wave is created at the centre point between two barriers. The remaining transmitted wave travels in a ‘close to’ hemispherical shape, depending on the angular degree of barrier shape.

1C allows for the transmitted blast wave to dissipate and reduce more, before impacting the external sensors. The peak transmitted blast wave travels identically in both 1A and 1C resulting in minimal reduction at the central sensors. Arrangement 1F insured the two most vulnerable sensors (central) were protected from the peak transmitted blast wave. 1F increased the number and density of the barriers. Comparing the results with the other arrangements, 1F has significantly decreased the pressure over all sensors.

5 CONCLUSION

The safety in and within public transport is significantly paramount to every society globally. This study aligns with United Nation’s Sustainable Development by creating novel engineering solutions enabling a safer built environment. The project develops architectural layout design for protective blast barriers to mitigate primary and secondary dangers to train passengers and commuters at a railway platform. Considering recent factual evidences, extreme physical and cyber threats are no longer uncommon and these protective measures could be adopted to prevent damage and improve safety of the public’s daily lives.

Computational multi-physics simulations using LS-Dyna have been used to simulate blast effects from terrorist attacks at a railway platform. Birmingham Grand Central railway station has been selected for case study. A platform layout design as structural wave barriers has been used to illustrate the hazard risk mitigation for train passengers due to explosive blast pressures. The numerical three-dimensional simulations are in excellent agreement with empirical estimates developed by US Army. This study reveals that the layout of blast barriers does have an impact on the reduction of blast pressure. Increasing the amount of barriers between the explosion and target can increase the chance of survival. The results show that layouts 1F and 2F both had very successful effects compared with other layouts. In addition, this study is the first to demonstrate that the shape of the barrier provides minimal effect on the mitigation of blast pressure to rail passengers. The new insight will guide a new platform layout design to minimize damage and hazard risks to rail passengers.

ACKNOWLEDGEMENT

The second author wishes to thank the Australian Academy of Science and Japan Society for the Promotion of Sciences for his Invitation Research Fellowship (Long term), Grant No. JSPS-L15701 at the Railway Technical Research Institute and The University of Tokyo, Tokyo Japan. The authors wish to gratefully acknowledge the financial support from European Commission for H2020-MSCA-RISE Project No. 691135 “RISEN: Rail Infrastructure Systems Engineering Network,” which enables a global research network that tackles the grand challenges in railway infrastructure resilience and advanced sensing under extreme events (www.risen2rail.eu).

REFERENCES

- [1] DataGraver, People killed by terrorism per year in western europe 1970-2015. [online]. Available from: <http://www.datagraver.com/case/people-killed-by-terrorism-per-year-in-western-europe-1970-2015> [Accessed 5 December 2016] (2016)
- [2] Remennikov, A. and Carolan, D., “Building vulnerability design against terrorist attacks.” In Stewart, M. and Dockrill, B. (1st ed.) Proceedings of the Australian Structural Engineering Conference 2005. Australia: Tour Hosts Pty Ltd. pp. 1-10, (2005).
- [3] Larcher, M., Arrigoni, M., Bedon, C., Van Doormaal, J. C. A. M., Haberacker, C., Hüskén, G., Millon, O., Saarenheimo, A., Solomos, G., Thamie, L., Valsamos, G., Williams, A. and Stolz, A., Design of blast-loaded glazing windows and façades: a review of essential requirements towards standardization. *Advances in Civil Engineering*, 1-14, (2016).
- [4] Kaewunruen, S., Sussman, J. M., and Matsumoto, A. Grand challenges in transportation and transit systems. *Frontiers in Built Environments*, 2:4, (2016) doi:10.3389/fbuil.2016.00004
- [5] Unified Facilities Criteria (UFC), Structures to Resist the Effects of Accidental Explosions, U. S. Army Corps of Engineers, Naval Facilities Engineering Command, Air Force Civil Engineer Support Agency, UFC 3-340-02, 5 December (2008).
- [6] Kaewunruen, S., Pompeo, G., Bartoli, G., “Blast simulations and transient responses of long-span glass roof structures: A case of London's railway station”, Proceedings of the 25th UKACM Conference on Computational Mechanics, 12–13 April 2017, University of Birmingham, Birmingham, U.K., (2017).

- [7] United States DoD. "UFC 3-340-02: Structures to resist the effects of accidental explosions". Washington D.C.: US Department of Defense (USDOD), (2008).
- [8] Draganić, H. and Sigmund, V., Blast loading on structures. *Technical Gazette*, 19 (3): 643-652, (2012).
- [9] Kinney, G. and Graham, K., Explosive shocks in air. 2nd ed. New York: Springer, (1985).
- [10] Pape, R., Mniszewski, K. R. and Longinow, A. "Explosion phenomena and effects of explosions on structures i: phenomena and effects". *Practice Periodical on Structural Design and Construction*, 15 (2): 135-140., (2010).
- [11] Ngo, T., Mendis, P., Gupta, A. and Ramsay, J. Blast loading and blast effects on structures – an overview. *EJSE Special Issue: Loading on Structures*, 2007: 76-91, (2007).
- [12] Koccaz, Z., Sutcu, F. and Torunbalci, N., Architectural and structural design for blast resistant buildings. The 14th World Conference on Earthquake Engineering. [online]. Available from: http://www.iitk.ac.in/nicee/wcee/article/14_05-01-0536.PDF [Accessed 5 December 2016]
- [13] Mali, P., Lokare, S. and Chitra, V. Effect of blast loading on reinforced concrete structures. *International Journal of Scientific Engineering Research*, 5 (12): 14-16, (2014).
- [14] Remennikov, A.M., Kaewunruen, S., A review on loading conditions for railway track structures due to wheel and rail vertical interactions. *Structural Control and Health Monitoring*, 15(2): 207-234, (2008).
- [15] Lawrence, V., Ngamkhanong, C., Kaewunruen, S. "An investigation to optimize the layout of protective blast barriers using finite element modelling", *International Conference on Mechanical Engineering*, 19-21 October 2017, University of Birmingham, Birmingham, U.K., (2017).
- [16] Griffin, D.W.P., Mirza, O., Kwok, K., and Kaewunruen, S., "Finite element modelling of modular precast composites for railway track support structure: A battle to save Sydney Harbour Bridge", *Australian Journal of Structural Engineering* 16 (2), 150-168, (2014).
- [17] Remennikov, A.M., "A review of methods for predicting bomb blast effects on buildings", *Journal of Battlefield Technology* 6 (3), 5, (2003).
- [18] Remennikov, AM and Kaewunruen, S, Simulating shock loads in railway track environments: experimental studies, *Proceedings of 14th International Congress on Sound and Vibration*, Cairns, Australia, 9-12 July 2007. Copyright 2007 Australian Acoustics Society, Australia, (2007).
- [19] Kaewunruen, S and Remennikov, AM, "An Experimental Evaluation of the Attenuation Effect of Rail Pad on Flexural Behaviour of Railway Concrete Sleeper under Severe Impact Loads." In E. F. Gad & B. Wong (Eds.), *Proceedings of the 2008 Australasian Structural Engineering Conference (ASEC)* (p. [10]), Melbourne, Australia, June 26-27, (2008).
- [20] Kaewunruen, S and Remennikov, AM, "Experimental simulation of the railway ballast by resilient materials and its verification by modal testing", *Experimental Techniques* 32 (4), 29-35, (2008).
- [21] Hajek R and Foglar M *Structures Under Shock and Impact XIII* **141** 265-275, (2015).
- [22] Berger S, Ben-Dor G. and Sadot O. *Journal of Fluids Engineering* **137** 41203-1-41203-11, (2015).

Mesoscale Finite Element Modeling of Concrete Materials

William Lawrimore^{*}, Jameson.d.shannon@usace.army.mil Shannon^{**}, Mei Chandler^{***},
Stephen Akers^{****}, Charles Burchfield^{*****}, Zackery McClelland^{*****}, Robert Moser^{*****}

^{*}US. Army Engineer Research and Development Center, ^{**}US. Army Engineer Research and Development Center,
^{***}US. Army Engineer Research and Development Center, ^{****}US. Army Engineer Research and Development
Center, ^{*****}US. Army Engineer Research and Development Center, ^{*****}US. Army Engineer Research and
Development Center, ^{*****}US. Army Engineer Research and Development Center

ABSTRACT

The topological complexity of concrete materials has been a barrier against the development of a high fidelity computational modeling methodology with which to analyze them. Hierarchical multiscale modeling methods have shown remarkable capacity to enhance the computational analyses in other material genomes. As a part of the multiscale hierarchy, this work is focused on efforts to model concrete materials at the mesoscale in order to harvest crucial deformation mechanism information to be used at higher scales in the multiscale modeling hierarchy. Two approaches using idealized topological representations of concrete are demonstrated herein. The first approach simplifies aggregate inclusions to be spherical within a cementitious matrix where the size distribution of the aggregate is prescribed from experimental data and the virtual topologies are built using the Virtual Composite Structure Generator (VCSG) method. The second approach utilizes microstructure data generated from the Virtual Cement and Concrete Testing Lab (VCCTL) as a source from which a voxel mesh is built for mesoscale finite element analysis. Both approaches feature Interface Transition Zones (ITZ) between the aggregate and cement matrix. Results from each approach are compared and discussed.

Rate and Size Effects on Dynamic Tensile Strength of Quasibrittle Structures

Jia-Liang Le^{*}, Anna Gorgogianni^{**}, Josh Vievering^{***}, Jan Elias^{****}

^{*}University of Minnesota, ^{**}University of Minnesota, ^{***}University of Minnesota, ^{****}Brno University of Technology

ABSTRACT

In this study, we develop a rate-dependent finite weakest-link model of strength statistics of quasibrittle structures. The model involves a length scale influenced by the applied strain rate, which captures the transition from localized damage to diffused damage as the strain rate increases. The present model predicts that the probability distribution of the nominal tensile strength depends on both the specimen size and the strain rate. At low strain rates, the strength distribution varies from a predominantly Gaussian distribution to a Weibull distribution as the specimen size increases, whereas at high strain rates the strength distribution follows a Gaussian distribution and its variance decreases with an increasing specimen size. In parallel with analytical modeling, a set of stochastic simulations is performed to study the dynamic tensile fracture of aluminum nitride (AlN) specimens. The simulations use a stochastic discrete element model (DEM), which explicitly takes into account the randomness of both the microstructural geometry and the fracture properties of AlN. In the DEM, the fracture behavior of the grain boundary is described by a mixed-mode failure model, in which the tensile and shear strengths and mode-I and mode-II fracture energies are considered to follow some prescribed probability distributions. The dynamic equilibrium equations are solved by the implicit Newmark method. The model is applied to simulate the nominal tensile strengths of geometrically similar AlN square plates of different sizes subjected to a range of strain rates. The simulations indicate that, as the applied strain rate increases, the size dependence of the mean structural strength diminishes while the coefficient of variation (CoV) of the strength exhibits a strong size effect. This simulated rate dependence agrees well with the prediction by the rate-dependent finite weakest-link model. The rate and size effects on strength distribution have important implications for stochastic simulations of dynamic quasibrittle fracture.

A Force Treatment of Immersed Boundary Method for Light-weighted Structures Interacting with Fluids

Trung Le*

*Medical College of Wisconsin

ABSTRACT

Performing Fluid-Structure Interaction with immersed boundary method at high Reynolds numbers is challenging due to the spurious force oscillation (SFO) phenomenon on the fluid-solid interface. In this work, we present a new development of enforcing the incompressibility condition on the fluid-solid interface so that the SFO is limited. The application of the method is in the hydrokinetic turbine application. The hydrokinetic blade is simulated with a thin-walled beam model, which is derived for variable cross-section structures. The beam model does not require any priori definition of cross-sectional warping but compute it directly from the final solution. The deformation pattern is superimposed on the bending deformation described by Euler-Bernoulli beam theory. Due to the combination between the beam and finite element assumptions, all sectional properties are automatically incorporated in the analysis when the final system of equations is assembled. The resulted model is suitable to simulate the dynamics of wind/hydrokinetic turbine blade with low computational cost under the fluid-structure interaction (FSI) simulation. A number of test cases have been carried out to validate the structural model which shows good agreement between the computational results and analytical solutions. Finally, FSI simulation of a hydrokinetic blade under critical flow condition is carried out to exemplify the capability of the current FSI model in practice.

State Health Monitoring of High-speed Train Suspensions by Bayesian Calibration Based on Gaussian Surrogate Modeling

David Lebel^{*}, Christian Soize^{**}, Guillaume Perrin^{***}, Christine Fünfschilling^{****}

^{*}Université Paris-Est, ^{**}Université Paris-Est, ^{***}CEA, ^{****}SNCF

ABSTRACT

The work presented here deals with the development of a state health monitoring method for high-speed train suspensions using in-service measurements by embedded accelerometers. Mathematically, it consists in solving a statistical inverse problem. A rolling train is a dynamic system excited by the track geometric irregularities. They consist of small displacements of the rails relatively to the theoretical track design. The suspension elements play a key role for the ride safety and comfort. The train dynamic response being dependent on the suspensions mechanical characteristics, information about the suspensions state can be inferred from acceleration measurements in the train. This information would allow for providing a more efficient maintenance. Track geometry is subject to damage caused by railway traffic and to maintenance operations. Consequently, it evolves through time. Because of the high sensitivity of the train dynamic response to the track geometric irregularities, their evolution must be taken into account through the use of train dynamics simulation. Because the system input (the track geometric irregularities) and output (the train dynamic response) are stochastic quantities, the inverse problem is solved in the Bayesian framework. The monitoring method thus consists in performing a Bayesian calibration of a simulation-based model using joint measurements of the system input and output. Its objective is to identify the posterior distribution of the model parameters describing the suspensions mechanical characteristics. Classical Bayesian calibration implies the computation of a likelihood function using a stochastic model and experimental data. This likelihood function is then used to estimate the posterior distribution of the model parameters. This step can be performed by Markov Chain Monte Carlo (MCMC) algorithms, which require numerous calls to the likelihood function. If the latter is expensive to compute, it may result in unaffordable computational costs, which is the case here. To address this issue, we propose to rely on surrogate models. They are usually used to provide an algebraic approximation of the system output. However, in the present case, the output is functional, which makes a surrogate model difficult to build. Instead, we propose a calibration method based on a Gaussian surrogate model of the scalar likelihood function. We present how such a random surrogate model can be used to estimate the model parameters distribution, how the new uncertainty it introduces can be taken into account to correctly evaluate the calibration accuracy, and the results of the method applied to our railway monitoring case.

Numerical Modeling of the Propagation of Planar 3D Hydraulic Fracture in Material with Anisotropic Toughness

Brice Lecampion*, Haseeb Zia**

*EPFL, **EPFL

ABSTRACT

Sedimentary rocks often exhibit a transverse isotropy due to fine scale layering. We investigate numerically the effect of the anisotropy of fracture toughness on the propagation of a planar 3D hydraulic fracture perpendicular to the isotropy plane: a configuration commonly encountered in sedimentary basins. We extend a fully implicit level set scheme for the simulation of hydraulic fracture growth to the case of anisotropic fracture toughness. We derive an analytical solution for the propagation of an elliptical hydraulic fracture in the toughness dominated regime - a shape which results from a particular form of toughness anisotropy. The developed numerical solver closely matches this solution as well as classical benchmarks for hydraulic fracture growth with isotropic toughness. We then quantify numerically the transition between the viscosity dominated propagation regime at early time -where the fracture grows radially- to the toughness dominated regime at large time where the fracture reaches an elliptical shape in the case of an elliptical anisotropy. The time scale at which the fracture starts to deviate from the radial shape and gets more elongated in the direction of lower toughness is in accordance with the viscosity to toughness transition time-scale for a radial fracture defined with the largest value of fracture toughness. Similarly, the toughness dominated regime is fully reached along the whole fracture front when the time gets significantly larger than the same transition time-scale defined with the lowest value of toughness. Using different toughness anisotropy functions, we also illustrate how the details of the complete variation of fracture toughness with propagation direction governs the final hydraulic fracture shape at large time. Our results highlight toughness anisotropy as a possible hydraulic fracture height containment mechanism as well as the need for its careful characterization beyond measurements in the sole material axes (divider and arrester) directions.

Elucidating Metal Powder Rheology via Discrete Element Simulations and Mechanically Stirred Powder Rheometry

Jeremy Lechman^{*}, Dan Bolintineanu^{**}, Anne Grillet^{***}

^{*}Sandia National Laboratories, ^{**}Sandia National Laboratories, ^{***}Sanida National Laboratories

ABSTRACT

Bulk solids composed of many discrete particles, i.e., grains and powders, are present in numerous engineering applications from mining to materials processing to energy storage to consumer products to food. In addition, particles are often added to materials to enhance their properties and subsequent performance in some fashion. Although particulate materials are ubiquitous, there remains a general lack of predictive understanding of their behavior; leading to a deficiency in effective, efficient control of the processing of such materials. At the core of this poor understanding is a shaky fundamental explanation of how the dynamics of individual particles, in ensemble, lead to the complicated dilative, yield stress, pressure dependent rheological behaviors of the bulk material. This challenge is particularly acute at low confining stresses for small, mildly cohesive particles. In this paper, we will present work to simulate, via the Discrete Element Method (DEM), the dynamics of individual particles of metal powders in a mechanically stirred powder rheometer. Our aim is to elucidate the connection between particle dynamics and powder rheology. In addition, we will assess the use of powder rheometry as a means of validating DEM models. Sandia National Laboratories is a multimission laboratory managed and operated by National Technology and Engineering Solutions of Sandia LLC, a wholly owned subsidiary of Honeywell International Inc. for the U.S. Department of Energy's National Nuclear Security Administration under contract DE-NA0003525.

Primal Hybrid DG Finite Element Formulations for the Biot Consolidation Problem

Ismael Ledoino*, Abimael Loula**

*LNCC/MCTIC, **LNCC/MCTIC

ABSTRACT

As a model problem we consider the linear Biot's consolidation problem in two space dimensions whose existence and uniqueness of solution are proved in [1]. It is well known that Finite element approximations for the Biot's consolidation problem based on the Continuous Galerkin method may present spurious oscillations in the pressure due to the incompressibility constraint on the displacement field in the beginning of the consolidation process, as analyzed in [2,3]. Some combinations of finite element interpolations, including equal order for both fields, are unstable due to the incompressibility constraint on the displacement field in the initial state, as analyzed in [2,3]. To gain more flexibility in the choice of stable finite element spaces and to improve stability and accuracy we propose here stabilized hybrid Discontinuous Galerkin finite element methods with Lagrange multipliers associated with the traces of the displacement and pore pressure fields. Stability of low order approximations are recovered including equal order for all fields. [1] A. Zenisek, The existence and uniqueness theorem in Biot's consolidation theory. *Aplik. Matem.*, 29 (1984), pp. 194-210. [2] M. A. Murad, A. F. D. Loula, Improved accuracy in finite element analysis of Biot's consolidation problema. *Comput. Methods Appl. Mech. Engrg.*, 95 (1992), pp. 359-382. [3] M. A. Murad, V. Thomee, A. F. D. Loula, Asymptotic Behavior of Semidiscrete Finite Element Approximations of Biot's Consolidation Problem. *SIAM Journal on Numerical Analysis*, Vol. 33, No. 3 (1996), pp. 1065-1083.

Parallel Surface Mesh Adaptation for Manycore Architecture

Franck Ledoux^{*}, Hoby Rakotoarivelo^{**}, Franck Pommereau^{***}

^{*}CEA, DAM, ^{**}CEA, DAM, ^{***}IBISC, Université Paris-Saclay

ABSTRACT

In this work, we design a dedicated process to adapt triangular meshes for the purpose of simulation codes on 3D CAD models in the HPC context where manycore architectures are used. Our technical contribution is to provide a standalone library that can be called from any C++ simulation code to adapt a surface mesh M while both preserving some surface geometric properties and taking into account some relevant data given by the simulation code. More precisely, the simulation code must give the expected number of points in the final mesh and either provide a scalar function F defined on the mesh M or directly specify the desired size and direction of elements everywhere in the computational domain. When function F is given, sizes and directions are derived from it. Formally, sizes and directions are encoded using a metric field that we will call a computational metric field. Another metric field, called geometric metric field, is used to represent surface properties. By combining computational and geometric metric fields, we drive the mesh adaptation process, which consists in iteratively applying several meshing kernels (edge swapping, triangle splitting, smoothing,) until getting the expected size and direction for each triangle on the surface. Several meshing techniques are used to achieve it: computational and geometric metric fields are intersected to preserve both the computational requirements and the surface geometry; gradation is computed to handle strong anisotropy; sharp features induce specific cases in each meshing kernel, ... In order to obtain good performances on modern manycore architectures, we follow a 3-steps schema for every kernel: (1) we build a task graph of the local operations that have to be done; (2) we extract an ordering set of independent tasks from this graph; (3) Extracted independent tasks are finally performed in parallel. Note that every step is done in a lock-free manner and the overhead induced by steps (1) and (2) is very low. Our solution has been tested and validated on different target architecture with up to several hundred of threads, different CAD models and input computational field. In practice good weak and strong scalings are obtained thanks to the 3-steps schema we apply and with dedicated mesh data structures.

High-Dimensional Stochastic Sensitivity Analysis and Design Optimization for Dependent Random Variables

Dongjin Lee^{*}, Sharif Rahman^{**}

^{*}The University of Iowa, ^{**}The University of Iowa

ABSTRACT

Stochastic sensitivity analysis plays a central role in robust design optimization and reliability-based design optimization of complex systems. For calculating design sensitivities of a stochastic response of interest, the finite-difference method constitutes the most straightforward approach, but it mandates repeated stochastic analyses for different instances of design variables, rendering the method prohibitive for practical design optimization. The other prominent method, the score function method [1], has been used when the input random variables are independent with product-type probability measures, where both the stochastic response and its sensitivities are obtained from a single stochastic simulation. In reality, though, the random variables are often statistically dependent producing non-product-type probability measures, invalidating most available methods, including the existing score function method [1]. This paper presents a novel computational method for calculating design sensitivities of statistical moments and reliability of high-dimensional complex systems subject to dependent random variables with arbitrary, non-product-type probability measures. The method represents a novel integration of the referential dimensional decomposition (RDD) [2] of a multivariate stochastic response function and score functions adapted for dependent random variables. Applied to the statistical moments, the method provides mean-square convergent analytical expressions of design sensitivities of the first two moments of a stochastic response. For reliability analysis, the method exploits the combination of embedded Monte Carlo simulation of the RDD approximation and score functions. The statistical moments or failure probabilities and their design sensitivities are both determined concurrently from a single stochastic analysis or simulation. Numerical examples, including a 100-dimensional mathematical problem, indicate that the new method developed provides not only theoretically convergent, but also computationally efficient design sensitivities for dependent random variables. A practical example involving robust design optimization of a three-hole bracket illustrates the usefulness of the proposed method. [1] Rahman, S. and Ren, X., "Novel Computational Methods for High-Dimensional Stochastic Sensitivity Analysis," International Journal for Numerical Methods in Engineering, Vol. 98, 2014, pp. 881–916. [2] Rahman, S., "Approximation Errors in Truncated Dimensional Decompositions," Mathematics of Computation, Vol. 83, No. 290, 2014, pp. 2799-2819.

Investigation of Transient Temperature of Pharmaceutical Tablets during Compaction Utilizing Infrared Thermography and Computational Modeling

Hwahsiung Lee^{*}, Bereket Yohannes^{**}, Alberto Cuitino^{***}

^{*}Rutgers University, ^{**}Rutgers University, ^{***}Rutgers University

ABSTRACT

Compaction of pharmaceutical tablets from powders is always accompanied by the conversion of irreversible mechanical work of compaction into heat. The heat is generated due to friction between powder particles, particles and the die wall, plastic deformation of particles, bonding, and other irreversible processes. The resulting temperature increase could significant effect tablet's performance including mechanical properties, disintegration times, and drug release profiles. Temperature rise can also affects physiochemical properties of the medicinal substances, including chemical stability, crystallinity and polymorphous state. The temperature increase in the powder during compaction is detrimental to heat sensitive APIs with low heat conductivity, such as most organic materials used in pharmaceutical formulations. Therefore, it is important to understand the thermomechanical behavior of powders during compaction. Infrared thermography (IR) provides a useful tool to trace the temperature distribution evolution of the tablet surface after ejection from the tablet press in laboratory experiments but also during manufacturing, in particular as in-line process analytical technology (PAT) tool for quality control. In the present work, we show that utilizing infrared thermography as a nondestructive and noncontact PAT tool that allows accurate tablet surface temperature fields acquisition in real time to accuracy of ± 0.1 °C during tablet compaction. Heat transfer of particulate systems in pharmaceutical tablet manufacturing is important element to be considered, yet is not fully understood. In this study, we utilize computational tools based on particle-mechanics to describe the formation of networks during the consolidation process. These heterogeneous networks are subsequently used to simulate the heat transfer process after ejection. We demonstrate the computational modeling match well with experimental results from infrared measurement, which have not been previously reported.

Unconditionally Energy Stable and High-Order Time Accurate Schemes for the Multi-Component System

Hyun Geun Lee^{*}, Jaemin Shin^{**}, June-Yub Lee^{***}

^{*}Kwangwoon University, ^{**}Ewha Womans University, ^{***}Ewha Womans University

ABSTRACT

In contrast to the well-developed convex splitting schemes for gradient flows of two-component system, there were few efforts on applying the convex splitting idea to gradient flows of multi-component system, such as the vector-valued Cahn-Hilliard (vCH) equation. In the case of the vCH equation, one need consider not only the convex splitting idea but also a specific method to manage the partition of unity constraint (the sum of concentration fields must be unity) to design an unconditionally energy stable scheme. In this study, we propose a constrained convex splitting scheme for the vCH equation, which is based on a convex splitting of the energy functional for the vCH equation under the constraint. We show analytically that the scheme satisfies the constraint at the next time level for any time step thus is unconditionally energy stable. Note that the scheme is first-order accurate in time thus we extend it to high-order time accuracy by applying the recently developed scheme for gradient flows. We also show analytically that the high-order schemes are unconditionally energy stable. Numerical experiments are presented demonstrating the accuracy, energy stability, and efficiency of the proposed first-, second-, and third-order constrained convex splitting schemes.

Verification and Validation of Bioprosthetic Heart Valve FSI Simulations

Jae Lee^{*}, Boyce Griffith^{**}, Alex Rygg^{***}, Brent Craven^{****}, Robert Hunt^{*****}, Pierre-Yves Passaggia^{*****}

^{*}University of North Carolina at Chapel Hill, ^{**}University of North Carolina at Chapel Hill, ^{***}U.S. Food and Drug Administration, ^{****}U.S. Food and Drug Administration, ^{*****}University of North Carolina at Chapel Hill, ^{*****}University of North Carolina at Chapel Hill

ABSTRACT

Every year, 300,000 heart valve repair/replacement procedures are performed worldwide in order to treat stenosis or regurgitation. This number continues to increase as these procedures become less invasive by using more transcatheter aortic valve replacement (TAVR) or by expanding access to cardiac surgery and interventional cardiology. Heart valves can be replaced with prosthetic or manufactured heart valves, but there are still difficulties with current prosthetic heart valves. Mechanical heart valves (MHVs) are durable but yield non-physical flow patterns that induce platelet activation, possibly causing other complications such as stroke, pulmonary embolism, or myocardial infarction. As a result, patients with MHVs need blood thinners for lifetime, which increases a risk of bleeding. Bioprosthetic heart valves (BHVs), which are made out of either bovine or porcine pericardium, are becoming increasingly popular because they yield hemodynamics flow patterns that are similar to the native valve, allowing patients to avoid complications from using MHVs. However, currently available BHVs require replacement after 10-15 years due to degradation of the tissue. A fluid-structure interaction (FSI) approach is necessary in modeling heart valves, which are thin elastic structures that interact with the blood flow. This presentation will describe ongoing work to develop computational models of prosthetic heart valve dynamics using extensions of the immersed boundary (IB) method. This work starts by evaluating the accuracy of the approach using benchmark problems associated with such modeling. The accuracy of the computational model is assessed by comparing with experimental measurements acquired in a left heart pulse duplicator system. This will ultimately lead to developing high-fidelity predictive models to perform simulations that can help answer challenging questions about optimal device performance, device selection, regulation for future cardiovascular devices, and surgical planning.

An Efficient Structural Optimization Strategy Based on a Parametric Reduced-Order Model Using the Selection and Interpolation of Substructural Modes

Jaehun Lee^{*}, Maenghyo Cho^{**}

^{*}Kyungnam University, ^{**}Seoul National University

ABSTRACT

In this study, an efficient structural design optimization strategy is presented by combining the interpolation-based parametric reduced-order model (IB-PROM) with the component mode synthesis (CMS) in the finite element framework. In particular, to enhance the robustness of the IB-PROM combined with the CMS [1] for the structural design optimization, we employ a substructural mode selection method to the interpolation of the component mode. In general, for the ROMs that consist of off-line and on-line stages, the off-line sampling of a large-scale structure containing many parameters requires numerous computations to explore the parameter-dependency of a dynamical system. Therefore, we suggest to divide the structure into multiple subdomains to execute the sampling in the substructural level. Since one design variable does not usually change the whole mesh configuration of a structure, synchronizing design domains with substructures is possible, which should be done before the sampling. As a result, the computation time for sampling is greatly reduced compared with that using a full order model. For the CMS that is effective to solve the eigen-problem of a large-scale structure, we usually employ domain decomposition algorithms to divide the structure into nearly uniform substructures in size. Then we select a dominant substructural modes by the frequency cut-off method. However, the design variables of a large-scale system might not be uniformly distributed different from the subdomains divided automatically. Therefore, the substructural modes selected by the frequency cut-off might not be regarded as the optimum when we use the CMS to structural design problems. In addition, the selection of the important substructural mode can be changed depending on the value of the parameter. As a consequence, the ROM might lose its accuracy as the parameters vary over a wide range. Therefore, we employ the mode selection method to improve the accuracy of the ROM. Among the various mode selection methods, a moment matching-based method (CMS?, [2]) is applicable to the present method since it can be performed in near real-time. Numerical examples including the dynamic response optimization of large-scale system support the strength of the proposed method. [1] J. Lee and M. Cho, An interpolation-based parametric reduced order model combined with component mode synthesis, *Comput. Methods Appl. Mech. Engrg.*, Vol. 319, pp. 258-286, 2017. [2] B.-S. Liao, Z. Bai and W. Gao, The important modes of subsystems: A moment-matching approach, *Int. J. Numer. Meth. Engng.*, Vol. 70, pp. 1581-1597, 2007.

COMPUTATIONAL ANALYSIS FOR DRY-ICE MIXED CO₂ JET IMPINGEMENT FLOW AND SUBLIMATION EFFECT

SONGMI KWAK* and JAESEON LEE*

*Ulsan National Institute of Science Technologies (UNIST)
Ulsan, S. Korea (ROK)
JaeseonLee@unist.ac.kr

Key words: Jet impingement, carbon dioxide, sublimation, solid-gas multi-phase flow.

Abstract. The flow and heat transfer characteristics of a novel gas - solid two - phase impinging jet have been studied numerically. When the high pressure carbon dioxide (CO₂) flow passes through a nozzle or orifice, it experiences the sudden expansion and the rapid temperature drop occurred by Joule-Thomson effect. This temperature drop causes the lower bulk jet fluid temperature than the CO₂ sublimation line, so dry-ice becomes formed. By using CO₂ gas-solid mixture as a working fluid of jet impingement, it is expected the heat transfer enhancement can be achieved due to the low bulk temperature and the additional phase change sublimation heat. In this study, 2D computational model is created to predict the cooling effect of gas-solid CO₂ jet. The gas-solid CO₂ flow is considered by Eulerian approach of mixed phase and the additional heat transfer module is embedded to account for the sublimation phenomena of the solid state CO₂. The jet flow and heat transfer performance of gas-solid CO₂ jet is investigated by the variance of flow parameter like Reynolds number, solid phase concentration and jet geometries.

1 INTRODUCTION

An impinging jet is a flow in which a fluid accelerated through a nozzle or an orifice is projected onto a target surface. Such impinging jets can be used for a variety of engineering purposes, such as heating, cooling, drying or cleaning solid surfaces. This technique has been studied for decades in various heat transfer applications. Since high heat transfer rates can be obtained near the jet stagnation point, impinging jets are widely used in applications where tight area thermal management is required. Typical applications include processing glass or metal and cooling gas turbine or electronic components.

Numerous experimental and numerical studies of single-phase impinging jets have been performed and various methods to improve their heat transfer efficiency have been suggested. Caggese *et al.*¹ showed a change in the heat transfer enhancement of the confined jet with

varying nozzle spacing. The flow recirculation caused by a confined jet affects the wall jet flow streams over the target surface and the heat transfer performance. Behnia *et al.*² showed the differences in flow characteristics between confined and free jets.

Carbon dioxide has some advantages for impinging jet cooling process. First, carbon dioxide has a high Joule-Thomson coefficient. In the case of a gas jet, the source of the gas working fluid is generally in the form of a compressed gas in the vessel and the jet flow is generated by the pressure difference between this source and the environment. The pressurized gas expands over some steps and the state of gas is continuously changed during expansion. The final state of injected gas is affected by the condition of ambient, but it is obvious that the gas temperature should be changed during expansion. Especially the change of gas temperature in expansion process is related to Joule-Thomson coefficient. Due to the high Joule-Thomson coefficient of carbon dioxide, the temperature of injected carbon dioxide gas jet drops rapidly. Theoretically the temperature of carbon dioxide from highly pressurized source becomes lower than the sublimation temperature and solid carbon dioxide particle becomes to be formed. Thus, the created particle and cold carbon dioxide gas exits the nozzle and gas-solid mixture phase is made. If the gas-solid carbon dioxide mixture is used for impinging jet cooling and the jet is injected to ambient air, the temperature of ambient air and heat transfer from the target surface can cause the sublimation of solid carbon dioxide particles. Sublimation during jet cooling absorbs the heat energy and it may add the additional benefits of target surface of cooling. Recently, experimental studies have been reported to use these sublimation properties of carbon dioxide for cooling³⁻⁵.

In this study, jet impingement cooling with sublimation effect was investigated through computational analysis. There are two issues concerning numerical analysis of gas-solid multiphase flow including sublimation phenomena. One is a method for simulating a bulk gas-solid multiphase flow and the other is a method for simultaneously integrating a sublimation phenomenon to the bulk flow. To simulate the gas-solid mixture carbon dioxide jet, this study uses Euler-Euler method which considers solid particle flow as granular flow. This method assumes the solid particle phase as a kind of pseudo fluid. The method can simulate the bulk motion of solid particle flow but cannot show the state or condition of each individual particle in flow. Using Euler-Euler method, particle sublimation should be calculated by adjusting the phase fraction of particle flow in a cell. The rate of sublimation is assumed as the linear function of temperature. The Euler-Euler method is suitable for a relatively large number of solid particles in comparison to the volume of the gaseous phase. Considering the amount of dry ice that can be observed in high-pressure carbon dioxide jet experiments³, it seems to be the preferred approach

2 NUMERICAL STUDY

2.1 Eulerian multiphase slot jet model

Figure 1 shows the details of a 2-D single unconfined slot jet which is a computational domain of current study. Key boundary conditions are also shown in the figure. The nozzle width (w) is 1 mm and the nozzle inlet condition is a velocity inlet. The origin of the coordinates is located at the center of the target heater block surface, and the x direction is set parallel to the surface of the heater block and the surrounding insulating material. The nozzle inlet conditions were 216.36 and 510 a, which is the result of carbon dioxide in the 5.5 MPa container first being depressurized by the regulator valve³. This temperature condition has already caused the sublimation of carbon dioxide and the nozzle inlet is a mixture of solid and gas. The jet cooling surface is a heated copper surface and the insulating material (G10) insulates everything but the jet exposed surface of the copper block. The properties of copper are $\rho = 8978 \text{ kg/m}^3$, $c_p = 381 \text{ J/kg} \cdot \text{K}$, $k = 387.6 \text{ W/m} \cdot \text{K}$. The properties of G10 are $\rho =$

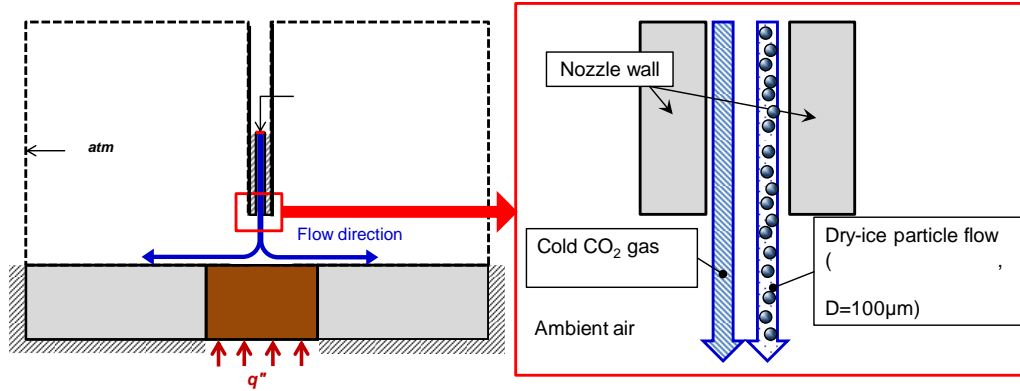


Figure 1 Details of boundary conditions and inlet flow for the linear sublimation model.

1818 kg/m^3 , $c_p = 800 \text{ W/kg} \cdot \text{K}$ and $k = 0.288 \text{ W/m} \cdot \text{K}$. A constant heat flux is exerted on the bottom of the copper block. All the insulation surfaces that are not contact with jet flow are assumed to be adiabatic with a constant temperature. A species model is used to depict the carbon dioxide jet. As the jet is injected into the ambient air, a mixed gas state of carbon dioxide and air must be considered. The properties of the air are constant: $\rho = 1.225 \text{ kg/m}^3$, $c_p = 1006.43 \text{ J/kg} \cdot \text{K}$ and $k = 0.0242 \text{ W/m} \cdot \text{K}$.

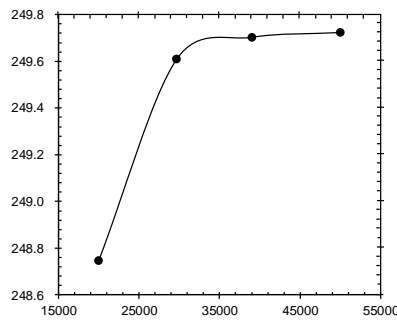
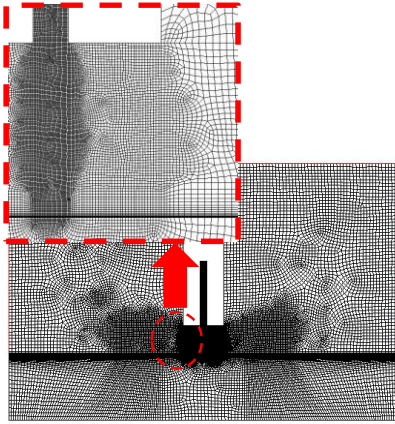


Figure 2 a Computational grid construction b Grid dependency test.

1562 kg/m^3 , $c_p = 54.55 \text{ J/kg} \cdot \text{K}$ and $k = 0.086 \text{ W/m} \cdot \text{K}$.

A pressure-based steady solver using a coupled scheme for pressure-velocity coupling was applied and a second-order upwind scheme was used for the momentum, pressure, and energy equations. The realizable k- ϵ model was chosen for each gas phase turbulent flow model. A multiphase Eulerian model was chosen to account for the multiphase flow of mixed solid phase of carbon dioxide. The schematic of inlet flow and computational domain is described in Figure 1. The primary phase is the gaseous phase, the mixture of air and gas state carbon dioxide. The secondary phase is solid carbon dioxide (dry ice), a solid particle phase. There are few previous studies to quantitatively measure dry ice production by pressure and temperature drop. For this reason, it was assumed that the flow conditions at the nozzle inlet consisted of 90% carbon dioxide gas and 10% solid particulate carbon dioxide. The diameter of the carbon dioxide solid particles was also assumed to be a constant of 100 microns. This diameter is the size that can be observed with ordinary human eyes, and is considered a reasonable assumption based on experimental experience³.

The governing equations of the multiphase Eulerian model are summarized as follows^{6,7}.

$$\frac{\partial}{\partial t}(\alpha\rho) + \nabla \cdot (\alpha\rho\vec{v}) = \frac{dm}{dt} \quad (2)$$

$$\frac{\partial}{\partial t}(\alpha\rho\vec{v}) + \nabla \cdot (\alpha\rho\vec{v}\vec{v}) = -\alpha\nabla p + \nabla \cdot \vec{\tau} + \alpha\rho\vec{g} + \vec{F} + \vec{R} \quad (3)$$

$$\frac{\partial}{\partial t}(\alpha_s\rho_s\vec{v}_s) + \nabla \cdot (\alpha_s\rho_s\vec{v}_s\vec{v}_s) = -\alpha_s\nabla p + \nabla p_s + \nabla \cdot \vec{\tau}_s + \alpha_s\rho_s\vec{g} + \vec{F}_s + \vec{R} \quad (4)$$

$$\vec{R} = K_s(\vec{v} - \vec{v}_s) \quad (5)$$

$$\frac{\partial}{\partial t}(\alpha\rho i) + \nabla \cdot (\alpha\rho\vec{v}i) = \alpha\frac{\partial p}{\partial t} + \vec{\tau} : \nabla\vec{v} - \nabla \cdot \vec{q} + \frac{dE}{dt} + Q \quad (6)$$

The continuity, momentum, and energy equations were solved for each phase. \vec{F} contains external body force, lift force, and wall lubrication force. \vec{R} is the phase interaction force that depends on the friction, pressure, cohesion, and other effects between phases. Equation (4) is the modified momentum equation for the solid phase and p_s is the solid pressure term. The phase interaction force term \vec{R} can be obtained by equation (5), where K_s is the interphase momentum exchange coefficient. The K_s value between the fluid and the solid phase is obtained by the Syamlal-O'Brien model¹⁸, which is already implemented in commercial CFD code FLUENT[®]. The Q and $\frac{dE}{dt}$ terms of the energy conservation equation (6) represent the heat transfer amount between phases and the sublimation heat amount through sublimation, respectively. For the latter term, a more detailed description is provided in the next section. The multiphase Eulerian model recognizes that it is impossible for any phase to have both fluid and solid particle trajectories at the same time. The computational domain was constructed mainly with quadrilateral elements, as shown in Figure 2 (a). In the nozzle, core jet, and jet stagnation zones where complex flows exist, a finer grid is created. A fine grid was also added near the surface of the heater and the insulation where the wall jet flow was formed. Grid sensitivity tests were performed by examining the surface temperature of the heater block as the number of mesh elements increased. The average temperature of the block becomes almost constant when the number of mesh elements is above 40,000. Therefore, the current studies were conducted using a 40,000 elements quadrilateral grid.

2.2 Solid to gas phase change modeling

In conventional commercial CFD solvers, there is no way to analyze the phenomenon of phase change between gas and solid which is the main subject of this study. In this study, the internal code for considering the carbon dioxide sublimation process in the jet flow was embedded to the existing CFD solver. FLUENT®, the CFD solver used in this study, provides a melting and solidification module. The present sublimation model was applied in such a way that the melting and solidification model was modified by considering the physical exchanges in mass and energy during sublimation process. Because it was calculated by modifying the existing commercial code module, it is possible to use the existing variable name as it is in the explanation below (Ex. *liquidus*, *solidus*, *etc.*). Among these parameters, the melting model parameters related to the liquid phase represent gas phase in the sense of the present study. The enthalpy of the material (i) is calculated as the sum of the sensible enthalpy (i_s) and the latent heat of sublimation material (I).

$$i = i_s + I \quad (7)$$

$$i_s = i_{ref} + \int_{T_{ref}}^T c_p dT \quad (8)$$

$$I = \beta L \quad (9)$$

β is the sublimation rate fraction and L is the latent heat. β is modeled to be varied by the material temperature in the mushy zone, which is the gas-solid two-phase region originated from the melting or solidification module⁶. β is defined as

$$\beta = 0 \quad \text{if } T < T_{solidus} \quad (10)$$

$$\beta = 1 \quad \text{if } T > T_{liquidus} \quad (11)$$

$$\beta = \frac{T - T_{solidus}}{T_{liquidus} - T_{solidus}} \quad \text{if } T_{solidus} \leq T \leq T_{liquidus}. \quad (12)$$

The sublimation rate is expected to vary depending on the difference between the dry ice particle and the ambient temperature. When the temperature increases, the sublimation rate also increases, but the rate will converge to a constant value. In this study, a simple carbon dioxide sublimation rate model is assumed. The assumption is that the sublimation rate is a linear function of temperature difference and all solid phase vanish when the environmental temperature becomes higher than the criterion temperature which is assumed as 10 °C higher than sublimation saturation temperature in this study. The setting of these 10 °C temperature differences in the current research phase is arbitrary. Since the sublimation heat is relatively small, it can be believed that the sublimation can be sufficiently completed within this setting value. However, it is a set value that needs to be supplemented through further future investigations.

$$\frac{dm}{dt} = -\frac{\rho \alpha_s}{\Delta} \frac{T - T_{sat}}{T_c - T_{sat}} \quad (13)$$

$$\frac{dE}{dt} = L_{CO2} \frac{dm}{dt} = -L_{CO2} \frac{\rho \alpha_s}{\Delta} \frac{T - T_{sat}}{T_c - T_{sat}} \quad (14)$$

Δt is time step size of flow time for each individual cell and T_c is the criterion temperature at which the sublimation is finally completed. L_{CO_2} is the latent heat of sublimation of carbon dioxide (545 J/g at 194.67 K; Giaque⁹). From equation (13), the mass exchange rate is calculated in each cell. When the temperature of a solid carbon dioxide particle exceeds the criterion temperature, all the solid carbon dioxide particles in the cell are vanished. The equation for the rate of change of the energy is the product of the sublimation latent heat and the mass change rate. This equation plays an important role in the temperature change by adding the role of sublimation in the jet flow energy exchange with environment.

3 RESULTS OF ANALYSIS

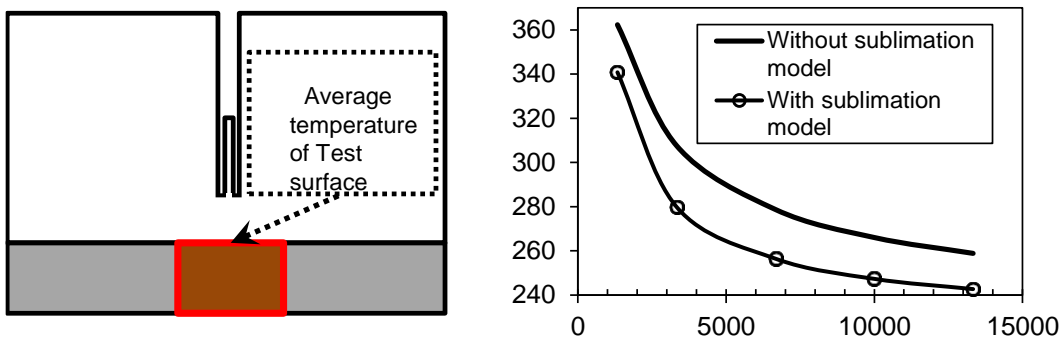


Figure 3 Average temperature of copper bloc test surface by the change of Re_w $q = 10 \text{ W}$.

The distribution of the solid phase fraction of the jet flow varies greatly depending on whether the sublimation model is applied or not, and accordingly, the heat transfer characteristic changes. Reynolds number is used for the variable which describes inlet velocity and nozzle width is selected as characteristic length. Reynolds number (Re_w) is defined as $Re_w = \rho v w / \mu$ and v is velocity of inlet flow. ρ is density of gas phase and μ is dynamic viscosity of gas phase. The different cases with Re_w variation from about 1,300 to 13,000 were analyzed and the results with and without applying the sublimation model were compared. Figure 3 shows the average change in temperature of the top surface of the heater block with variation in Re_w . A total heat of 10 W was applied to the heater. As in the case of the other jet flows, the surface temperature decreases as the Reynolds number increases. The analytical results with the sublimation model predict lower surface temperatures than those not included. The additional cooling effect by sublimation is effectively expressed in the results. It can be seen that the cooling effect for this sublimation is relatively weak at low Reynolds number flow. However, as the Reynolds number increases, a certain amount of sublimation cooling effect is maintained. Figure 4 shows the dry ice volume fraction and temperature distribution according to CFD analysis when the sublimation model is not applied. All the solid-phase carbon dioxide escapes from the computational domain of Fig. 4 without a large change in the volume fraction. The thickness of the solid phase volume fraction gradient becomes thinner as Re_w increases. Figure 4 (b) shows the temperature distribution with

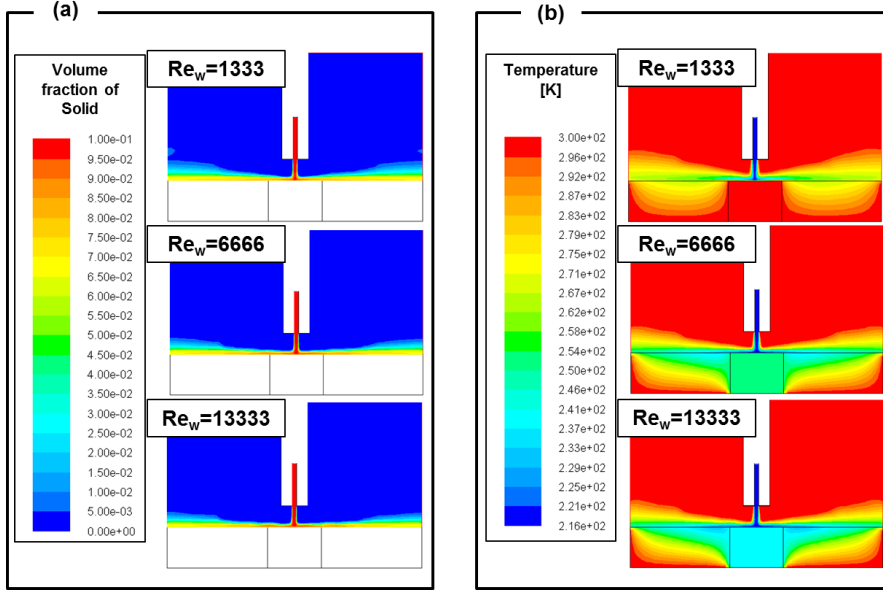


Figure 4 a Dry ice phase volume fraction contour variation and b Temperature distribution without the sublimation model.

variation in e_w . If the e_w is high due to the fast jet velocity, the jet flow will be kept cooler and the heater block will be maintained as colder temperature.

Figure 5 shows the results when the sublimation model is activated. The volume fraction of the solid carbon dioxide phase decreases when the solid carbon dioxide bulk temperature is

higher than the carbon dioxide saturation temperature in Figure 5 (a). Thus, application of the sublimation model changes the distribution of the solid phase volume fraction. In all cases, when the sublimation model is applied, the solid carbon dioxide phase disappears before reaching the domain outlet. As e_w increases, the point at which all the solid carbon dioxide phase disappears is delayed toward the downstream. The solid phase volume fraction contour

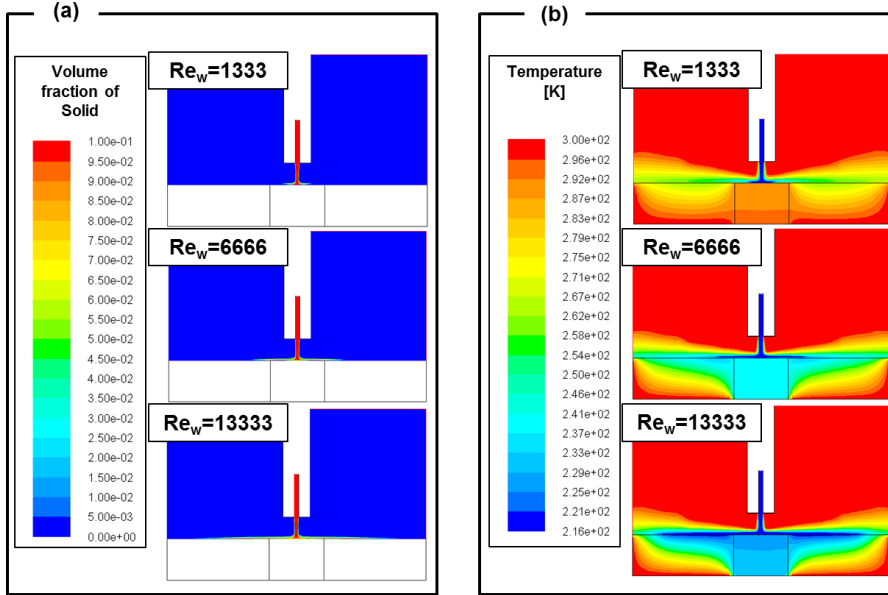


Figure 5 a Dry ice phase volume fraction contour variation and b Temperature distribution with the sublimation model.

almost coincides with the low temperature distribution of the temperature contour in Figure 5 (b).

The plots in figure 6 show the volume fraction of solid phase carbon dioxide along the x direction, which is the direction of the jet flow near the wall, and the y direction, which is the cross-sectional direction of the wall jet. The horizontal position of

the data is 0.5 mm above the test surface and figures 6 (a) and (b) show dry ice volume fraction variations when the sublimation model is not applied and when applied, respectively. The vertical location of the data is 2.5 mm from the center of the jet core and the vertical distribution results are represented in figure 6 (c). As all of the data are symmetrical with regard to the center of the jet core, the results represent only one side of the domain. The center of jet core represents the stagnation point of the impinging jet. When the sublimation model is not applied in the calculation, the volume fraction changes slightly along the x direction as shown in figure 6 (a). The reason that the volume fraction of solid carbon

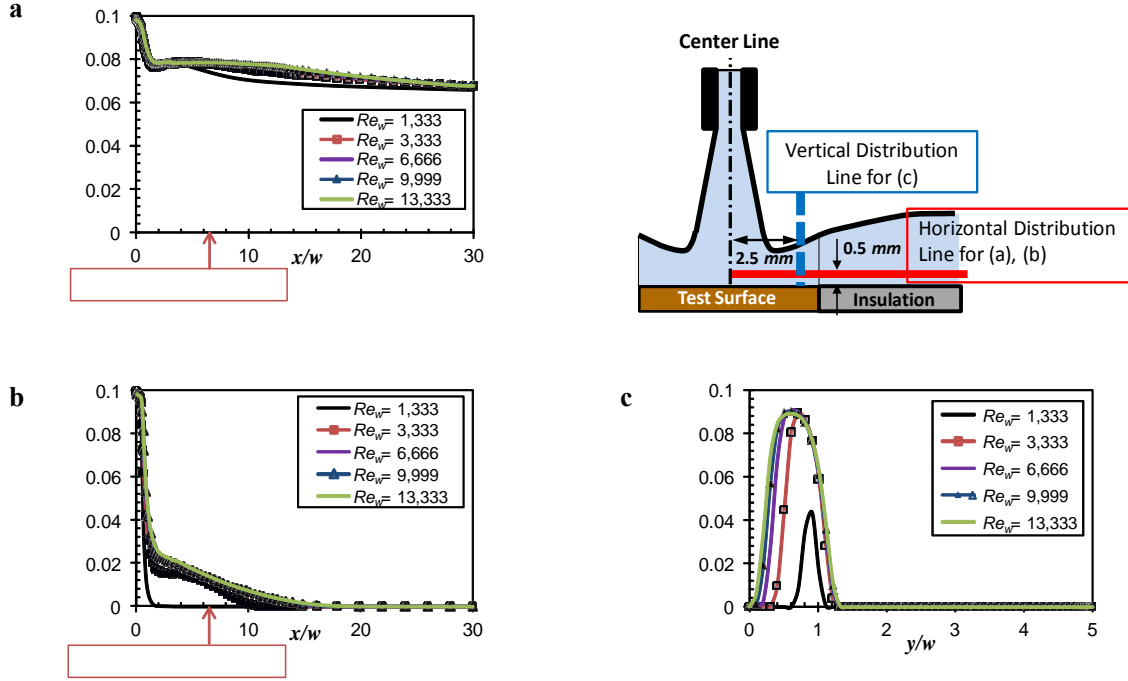


Figure Dry ice volume fraction distribution **a** without the sublimation model in horizontal direction **b** with the sublimation model in horizontal direction **c** with the sublimation model in vertical direction.

dioxide phase is reduced to a small amount is because the jet flow diffuses along the x direction even though sublimation is not considered. A greater change is observed when the sublimation model is applied, in figure 6 (b). All solid phase carbon dioxide disappears before the main jet flow escapes the domain outlet and the solid phase volume fraction lasts longer when the Reynolds number is higher as shown in figure 5 (a). Especially when $Re_w = 1,333$, all of the solid phase carbon dioxide sublimates before the jet flow passes the end of the heater block. The low-temperature distribution corresponding to the solid carbon dioxide phase distribution is related to heat transfer enhancement and will be discussed below. Figure 6 (c) shows the vertical distribution of solid carbon dioxide volume fraction at the fixed horizontal location of $x/w = 5$. Sublimation is actively induced by the thermal energy supplied near the wall surface, so that the volume fraction of the solid phase is lowered and the maximum volume fraction is obtained at a constant height position. As the jet flow increases, that is, as the Re_w number increases, the position of this maximum volume fraction approaches the wall

due to the momentum of the jet flow.

4 CONCLUSIONS

Due to the high Joule-Thompson coefficient, carbon dioxide can be easily lowered below the sublimation point by the throttle effect, and the formation of dry ice can easily occur. In this study, numerical analysis on the enhancement of jet impingement heat transfer caused by sublimation and simultaneous collision of dry ice on cooling surface was performed. The jet flow of the gas-solid mixture was simulated by the Eulerian multiphase flow analysis method and mass and energy transfer equations for analyzing the phase change between dry ice gas-solid phase were added. The key conclusions are listed below.

- The analysis of the impinging jet flow with solid dry ice particle was performed by adding a module for the analysis of gas-solid phase change which is lacking from the conventional CFD code.
- The latent heat of dry ice sublimation keeps the jet bulk flow at low temperature. As the flow rate, or e_w , increases, the temperature of the jet bulk flow is maintained at a lower level for a longer period of time.
- When e_w is low, all solid carbon dioxide is sublimated before the jet flow reaches the end of the heater surface. Also, the low temperature jet bulk flow is not maintained on the near heater wall surface, so the heat transfer enhancement effect is limited to the minimum area of heater surface.
- As the jet flow rate or e_w increases, the effect of sublimation of a larger amount of solid dry ice appears on near the surface of the heater. The temperature of the impinging surface is reduced and the effect of the heat transfer enhancement occurs in a larger area.
- It can be seen that the heat transfer coefficient of the dry ice jet flow is greatly increased due to the absorption of the additional heat energy by sublimation above a certain flow rate condition.
- The proposed dry ice sublimation model is integrated with the existing Eulerian multiphase flow analysis to show that it can effectively describe the characteristics of dry ice impinging jet flow.

Acknowledgement

This material is based upon work supported by the research funding from Basic Science Research Program through the National Research Foundation of Korea (NRF) funded by the Ministry of Education (Grant No. NRF-2017R1D1A1B03029858) and Ulsan National Institute of Science and Technology (Grant No. 1.180038.01).

REFERENCES

- [1] O. Caggese, G. Gnaegi, G. Hannema, A. Terzis and P. Ott, "Experimental and numerical investigation of a fully confined impingement round jet", *International journal of heat and mass transfer*, vol. 65, 873-882, 2013.

- [2] M. Behnia, S. Parneix, Y. Shabany and P. A. Durban, "Numerical study of turbulent heat transfer in confined and unconfined impinging jets", *International journal of heat and fluid flow*, vol. 20, 1-9, 1999.
- [3] D. Kim and J. Lee, "Experimental investigation of CO₂ dry-ice assisted jet impingement cooling", *Thermal Engineering*, vol. 107, 927-935, 2016.
- [4] M. R. O. Panão, J. J. Costa, M. R. F. Bernardo, "Thermal assessment of sublimation cooling with dry-ice sprays", *International journal of heat and mass transfer*, vol. 118, 518-526, 2018.
- [5] Robert. S, "Carbon Dioxide Snow Cleaning", *Particulate Science and Technology*, Vol. 25, 37-57, 2007.
- [6] *ANSYS Fluent 15.0 Theory Guide, Fluent user's Guide*, Fluent Inc, Canonsburg, PA, 2013.
- [7] *ANSYS Fluent 15.0 UDF Manual, Fluent user's Guide*, ANSYS Inc, Canonsburg, PA, 2013.
- [8] M. Syamlal and T. J. O'Brien. "Computer Simulation of Bubbles in a Fluidized Bed", *AIChE Symposium Series*, 85, 22-31, 1989.
- [9] W. F. Giauque and C. J. Egan, "Carbon dioxide. The heat capacity and vapor pressure of the solid. The heat of sublimation. Thermodynamic and spectroscopic values of the Entropy", *Journal of chemical physics*, vol. 5, 45-54, 1937.

Pattern Design of Permanent Magnet Segments using Topology Optimization

Jaewook Lee^{*}, Tsuyoshi Nomura^{**}, Ercan Dede^{***}

^{*}School of Mechanical Engineering, Gwangju Institute of Science and Technology (GIST), ^{**}Toyota Central R&D; Labs, ^{***}Toyota Research Institute of North America

ABSTRACT

In this work, the patterns of permanent magnet segments are designed using topology optimization. Specifically, the optimal border and magnetization directions of permanent magnet segments are designed using the topology optimization technique for the given design goal. For this, an orientation design variable in Cartesian coordinate system is assigned at each finite element. The orientation variable controls the magnetization direction of permanent magnets. Compared to the polar coordinate design variable, the variable in Cartesian coordinate is known to be beneficial to the optimization problem stability. To achieve the segmented permanent magnet arrays with discrete magnetization directions, a penalization scheme is applied. In this scheme, the strength of permanent magnet is controlled by the magnetization directions. The permanent magnet strength becomes weak where the magnetization direction is located between target discrete directions. Through this penalization, the design result composed of discrete target magnetization directions can be obtained. As a numerical example, a Halbach cylinder pattern is designed using topology optimization. The design result is compared with the analytical pattern design result derived by Halbach.

Multiscale Modeling of Surface Functionalized Graphene-Polymer Nanocomposite

Jeong-ha Lee^{*}, Seunghwa Yang^{**}, Inseok Jeon^{***}

^{*}Chung-Ang University, ^{**}Chung-Ang University, ^{***}Chung-Ang University

ABSTRACT

Graphene, a 2-dimensional single layered carbon nanostructure, is a promising material due to its excellent electrical, thermal and mechanical properties. Among the promising applications of the graphene, the reinforcement into a polymer nanocomposite (PNC) is one of the most well-known processes of strengthening polymer structure. However, restacking issue on dispersed graphene nanosheets [1] caused by the van der Waals forces decrease PNCs mechanical and thermal properties. Moreover, weak van der Waals interaction between polymer and graphene reduces their thermoelastic behavior and cohesive zone energy at the materials' interface. To improve the intrinsic weak interfacial strength between the graphene and polymer and to improve the dispersion state of the graphene in PNCs, several surface functionalization such as oxygen functionalization as well as covalent grafting have widely been applied to the nanocomposites. In this study, multiscale modeling approach for pristine and covalently functionalized graphene reinforced polypropylene (PP) nanocomposites is proposed. The representative molecular unit cells consisting of single layer graphene and PP matrix are modeled for molecular dynamics simulations with periodic boundary conditions. Direct covalent grafting between graphene and PP matrix are constructed via a dynamics cross linking method based on the cut-off methods. In molecular dynamics (MD) simulations, reactive forcefield is used for graphene including the grafted carbon-carbon covalent bond while classical potential model is used for the matrix phase. Through the statistical ensemble simulations, thermoelastic properties of PNCs are determined according to the grafting density at the interface. For equivalent continuum modeling to account for the effect of covalent grafting, the mean field micromechanics model [2] is incorporated to characterize the effect of covalent grafting on the interfacial and interphase properties of nanocomposites. Besides the interfacial point of view, contribution of the covalent grafting to the dispersion of graphene inside the polymer matrix is examined. [1] Dan Li, Marc B. Muller, Scott Gilje, Richard B. Kaner and Gordon G. Wallace, "Processable aqueous dispersions of graphene nanosheets", Nature Nanotechnology, Vol 3, pp. 101-105, 2008. [2] Seunghwa Yang, Maenghyo Cho, "Scale bridging method to characterize mechanical properties of nanoparticle/polymer nanocomposites", Appl. Phys. Lett., 93, 043111, 2008.

Root-Finding Absorbing Boundary Conditions for Wave Propagation Problems in Infinite Media

Jin Ho Lee*

*Pukyong National University

ABSTRACT

The theory of wave propagation is the basis of understanding various physical phenomena in fields such as civil engineering, mechanical engineering, offshore engineering, seismology, meteorology, and oceanography. Because many wave propagation phenomena occur in extensive, unbounded or infinite media, it is required that the dynamic behaviors of such media is simulated accurately and efficiently. Wave propagation phenomena in infinite media can be simulated using computational treatments such as those based on the finite element method and the finite difference method. However, since these treatments were developed originally for problems in finite domains, it is necessary to use a special numerical or mechanical model that can precisely consider the energy radiation into infinity. Therefore, various models such as consistent transmitting boundaries, boundary elements, infinite elements, high-order absorbing boundary conditions (ABCs), and perfectly matched layers (PMLs) have been developed and used for various wave propagation problems in infinite media. Various nonlinear behaviors, for example, material nonlinearities, may occur in wave propagation phenomena. These can be addressed most conveniently in the time domain. Therefore, with infinite media, it is best to consider energy radiation into infinity directly in the time domain. Accuracy and efficiency depend on how well we can account for energy radiation into infinity in the time domain. Among the models mentioned above that can consider the influence of the infinite domain, the higher-order ABCs and PMLs can guarantee both accuracy and efficiency in the time domain and have been applied widely to wave propagation problems. Both approaches for time-domain applications entail their own advantages and disadvantages. The high-order ABCs approximate the dispersion equation of waves in the infinite region by rational expressions or a series of simple differential operators while the PMLs introduce artificial damping through complex transformations of the spatial coordinate system. Recently, a new absorbing boundary condition for scalar-wave propagation problems has been developed [1] on the basis of solutions of the dispersion equation using a root-finding algorithm such as the Newton-Raphson method. This boundary condition is referred to as a Root-Finding Absorbing Boundary Condition (RFABC). In this study, the RFABC is extended to elastic waves. The accuracy of the newly developed boundary condition is demonstrated by application to time-domain analysis of an elastic-wave propagation problem. References 1. Lee JH, Tassoulas JL. Absorbing boundary condition for scalar-wave propagation problems in infinite media based on a root-finding algorithm, *Computer Methods in Applied Mechanics and Engineering* 2018; 330: 207-219.

Topology Optimization Considering Stress Constraint for Dynamic Load Using Response Filtering Method

Jongwook Lee*, Gilho Yoon**

*Hanyang university, Seoul, Korea, **Hanyang university, Seoul, Korea

ABSTRACT

When a sudden collision, explosion or earthquake occurs, the stress wave from that region propagates to the surroundings. Since the propagating stress wave can cause unexpected failure, it is possible to design a safer structure considering the stress wave in the design stage. In this study, we focused on structural optimization techniques considering these stress waves. To consider the stress wave, the propagating stress is calculated numerically. However, when numerically calculating the stress wave, numerical inaccuracies appear [1-2]. Especially, undershoot and overshoot are found in numerical solutions, which cause ambiguity in the design of structures considering stresses. Therefore, we have developed a new filtering technique called RFM (Response Filtering Method) to eliminate these numerical errors. Numerical errors of propagating stress waves can be reduced by this method. In addition, accuracy was improved when compared with the exact solution. In addition, it is confirmed that the frequency characteristic is also similar to the exact solution in this research. Acknowledgement This work was supported by the National Research Foundation of Korea (NRF) grant funded by the Korea government (MEST) (NRF-2015R1A2A2A11027580). References [1] Cook, Robert D., et al., Concepts and applications of finite element analysis. New York: Wiley. 1974. [2] Daryl L. Logan., A first course in the finite element method, fifth ed., Thomsom, 2011.

Development of a Three-Dimensional Parallel Volume Integral Equation Method

Jungki Lee*

*Hongik University, Sejong Campus

ABSTRACT

A three-dimensional parallel volume integral equation method (PVIEM) is applied for the analysis of elastostatic problems in an unbounded isotropic matrix containing multiple anisotropic inclusions. It is necessary to use standard parallel programming, such as MPI (message passing interface), to speed up computation in the volume integral equation method (VIEM). It should be noted that this numerical method does not require the use of the Green's function for the anisotropic inclusion - only the Green's function for the unbounded isotropic matrix is needed. A detailed analysis of stress field at the interface between the isotropic matrix and the central anisotropic inclusion is carried out for simple cubic packing arrangements of multiple spherical inclusions. The effects of multiple anisotropic spherical inclusions on the stress field at the interface between the matrix and the central inclusion are investigated. The accuracy of the parallel volume integral equation method for the interfacial stress field is compared by the finite element method (FEM). The PVIEM is shown to be very accurate and efficient for solving general three-dimensional elastostatic and elastodynamic problems involving multiple anisotropic inclusions whose shape and number are arbitrary.[1-3] References [1] A volume integral equation technique for multiple inclusion and crack interaction problems - Journal of Applied Mechanics, Volume 64, Issue 1, March 1997, pp. 23-31. Jungki Lee, Ajit Mal. [2] Calculation of interfacial stresses in composites containing elliptical inclusions of various types - European Journal of Mechanics, A/Solids, Volume 44, 2014, pp. 17-40. Jungki Lee, Sangmin Oh, Ajit Mal. [3] Multiple scattering using parallel volume integral equation method: Interaction of SH waves with multiple multilayered anisotropic elliptical inclusions - Mathematical Problems in Engineering, Volume 2015, 2015, Article ID 809320, 48 pages. Acknowledgements This research was supported by the International Science and Business Belt Program through the Ministry of Science and ICT (2017K000451) and Korea Institute of Science and Technology Information (KISTI) supercomputing center through the strategic support program for the supercomputing application research (KSC-2017-C1-0004).

Automated Framework for Efficient Surrogate Model Building with Machine Learning Techniques

Kyungeun Lee*, ikjin Lee**

*Ph.D candidate, Mechanical Engineering, KAIST, **Associate professor, Mechanical Engineering, KAIST

ABSTRACT

Variable selection is needed not only to improve computational efficiency but also accuracy of the analysis by eliminating unnecessary variables and focusing on the relevant ones. Especially, variable selection is essential for surrogate modeling with high-dimensional problems because the number of required sampling for the model building highly depends on the size of dimension. However, in practical, there is a limit on the number of training samples provided because most experiments or analysis are cost or time-consuming. Even the current computational performance is greatly improved, many FEM solving still take long time according to the nonlinearities or amount of elements. That kinds of model needs surrogate modeling. However, many computations are spent in variable selection itself prior to build a surrogate model which aims to replace time-consuming calculations. Moreover, after variable selection, new samples for the surrogate modeling are often required because the orthogonality of the initial sample with selected sub-dimension is broken. Therefore, in this study, we suggest to perform variable selection and surrogate model building at the same time with as few samples as possible. The key point of this study is that subset selection and model accuracy evaluation are performed simultaneously and iteratively in every loop. Gaussian process regression (GPR) is selected as the surrogate modeling methodology for its stochastic property. GPR can handle the perturbation caused by dimensionality reduction with covariance function. The overall process is as follows. At first, initial sample is drawn carefully to preserve the orthogonality and space-filling property with the sub-dimension as possible, using maximum projection design. Next, initial surrogate modeling is performed and the marginalized maximum likelihood (ML) derived after hyperparameter optimization of GPR is used as a subset selection fitness. K-means clustering is utilized to classify the ML values into converged and non-converged groups. The best subset is chosen as the minimum-sized subset in the converged group to prevent the overfitting and remove redundant variables. Model accuracy is evaluated with Leave-One-Out cross validation. If the model is proved to be inaccurate or converged/non-converged groups are not discriminating, next sequential sample is chosen focused on the most recently selected subset dimension. By this process, when the algorithm is finished which means both model accuracy is validated and subset selection is converged, variable selection and surrogate model building is completed at the same time. This research suggests efficient stochastic surrogate modeling framework.

Flooding Simulation Method of Railway Infrastructure by Using Open Data Schema-based 3D Information Model

Sang-Ho Lee^{*}, Young-Hoon Jang^{**}, Kyung-Wan Seo^{***}, Tae Ho Kwon^{****}

^{*}Yonsei University, ^{**}Yonsei University, ^{***}Yonsei University, ^{****}Yonsei University

ABSTRACT

The damage of railway infrastructure from flooding has been steadily increasing as a recent climate change. The predicting the particular damage situation can be one of the effective provisions for reducing the damage of structures. The flooding simulation totally depends on the structure's information, and the information of a railway infrastructure is the complex, tangled, and linked various application fields. It needs, therefore, multidisciplinary approach for the successful flooding simulation of the railway infrastructure. BIM is a new paradigm that can interoperably manage the lifecycle information on facility, it can effectively satisfy the requirements for flooding simulation of the railway infrastructure. Industry Foundation Classes (IFC) is the BIM standard open data schema developed by buildingSMART. The IFC, however, has limitations to represent the exact city information model including the railway infrastructure since it focuses on building structures. The CityGML is the open data schema to build a city model while IFC is developed for one specific facility. The IFC is a relatively detailed schema that can support the whole lifecycle of facility, whereas the CityGML is rough but can be considering the relationship between facilities. This study aimed to build an effective and detailed city information model focused on the railway infrastructure based on open data schema and to conduct flood damage assessment by 3D model-based simulation. For this procedure, the authors have been proposed the IFC-based extended data schema for the railway infrastructure and developed converting method from IFC-based model to CityGML-based model. The hydraulic analysis data were spread on terrain model and the flooding damage assessment was simulated through conflict check between 3D city object model and hydraulic analysis model. The damage assessment of flooding situation was categorized casualty, property damage estimation, and availability check of railway infrastructure. The simulating results of flood damages were stored in linked external database. By using this, it could be possible to capture semantic data by a query according to the condition of the flood occurrence. The authors have examined the proposed modeling and simulation method on the part of the real city and checked the feasibility of the methods.

<Acknowledgement> This research was supported by a grant (16RTRP-B104237-03) from Railroad Technology Research Program funded by Ministry of Land, Infrastructure and Transport (MOLIT) of Korean government.

A Kernel-based Learning Approach for Mechanical Characterization of Soft Tissue

Sangrock Lee^{*}, FNU Rahul^{**}, Uwe Kruger^{***}, Suvranu De^{****}

^{*}Rensselaer Polytechnic Institute, ^{**}Rensselaer Polytechnic Institute, ^{***}Rensselaer Polytechnic Institute,
^{****}Rensselaer Polytechnic Institute

ABSTRACT

In recent years, elastography has emerged as a viable technique for non-invasive assessment of mechanical properties of tissue. Elastography techniques rely on imaging modalities, such as ultrasound imaging, to quantitatively assess changes in the elasticity of soft tissue in various pathologies, which is useful for diagnostic purposes [1]. However, these techniques require solving an inverse problem to identify the mechanical properties of soft tissue while under external load, which is computationally expensive particularly for tissues that exhibit nonlinear mechanical characteristics under finite deformation [2]. We propose a kernel-based machine learning approach for rapid assessment of mechanical properties of soft tissue based on a training dataset for which the deformation map represents the cause and the corresponding spatial distribution of material parameter, or elasticity map, is the response to be predicted. A nonlinear kernel-based partial least square (KPLS) regression model is employed to learn the relationship between the deformation map and corresponding elasticity map. KPLS is a chemometric tool that is particularly useful in situations where the number of cause variables exceeds the number of observations [3], which is often the case with clinical patient specific dataset. Hence, KPLS is chosen to directly address this problem of small elastography datasets. A Gaussian kernel is used to construct the nonlinear mapping for the KPLS model. The parameters of KPLS model, i.e. the latent variable sets and Gaussian kernel parameter, are obtained by n-fold cross-validation to guarantee an independent assessment of the model. The prediction error of the KPLS regression model is estimated by n-fold cross validation on a synthetic dataset. References [1] Sigrist, R.M., Liao, J., El Kaffas, A., Chammas, M.C., Willmann, J.K., 2017. Ultrasound Elastography: Review of techniques and clinical applications. *Theranostics*, 7, 1303-1329. [2] Dargar, S., Akyildiz, A.C., De, S., 2017. In situ mechanical characterization of multilayer soft tissue using ultrasound imaging. *IEEE Transactions on Biomedical Engineering*, 64, 2595-2606. [3] Rosipal, R., Trejo, L.J., 2001. Kernel partial least squares regression in reproducing kernel Hilbert space. *Journal of Machine Learning Research*, 2, 97-123.

Micromechanics-based Homogenization Method Applicable to a Wide Range of Interfacial Damage for Reinforced Composites Having Anisotropic Matrix

Sangryun Lee*, Jinyeop Lee**, Seunghwa Ryu***

*Korea Advanced Institute of Science and Technology, **Korea Advanced Institute of Science and Technology,

***Korea Advanced Institute of Science and Technology

ABSTRACT

In this study, we study a micromechanics model to predict effective moduli of a reinforced composite having interfacial damage using linear spring model. We propose a modified Eshelby tensor of an anisotropic matrix which is applicable to the entire range of interfacial damage from perfect bonding to complete de-bonding. Then, we obtain a modified strain concentration tensor by decomposing the damaged interface problem of single inhomogeneity into three independent elasticity problems. Also, we derived exterior Eshelby tensor and exterior strain concentration tensor and validate our analytic model against finite element analysis (FEA) results. Combining the modified Eshelby tensor and strain concentration tensor in the Mori-Tanaka framework, we derive the effective moduli of a particle-reinforced composite having an anisotropic matrix and interfacial damage with correct upper bound (perfect bonding) and lower bound (porous medium). We study the effect of penetration at the interface because the micromechanics model can not account for contact behavior which is a highly nonlinear behavior. To study the effect of the penetration on the effective moduli of composite, we use FEA to compute the effective modulus of the composite having contact behavior at the interface and compare with the micromechanics model allowing penetration. Besides, we compute stress strain curve of the composite and stress state of each phase theoretically considering interfacial damage under uniaxial loading, which allows us to compute the ultimate strength of nanocomposites in a wide range of interfacial damage.

Blood Flow Simulation from Cellular Interaction to Microvascular-network

Tae-Rin Lee^{*}, Seokjin Park^{**}, Ji-Ah Hong^{***}

^{*}Advanced Institutes of Convergence Technology, Seoul National University, ^{**}Department of Mechanical Engineering, Ajou University, ^{***}Department of Mechanical Engineering, Ajou University

ABSTRACT

Blood flow in the microvasculature is a key component to understand various phenomena in the field of biomedical engineering, e.g. angiogenesis, tumor growth, metastatic cancer and etc. However, the nonlinear properties in hemodynamics make it difficult to precisely understand the blood flow. In this talk, we will introduce an immersed boundary method for simulating blood cells in microvessels and for quantifying hemodynamic properties at the microvascular-network level. Specifically, blood cells are modeled by material points with springs. The fluid-structure interaction (FSI) force is generated by using a direct-forcing technique. Based on the FSI method, we will estimate the plasma skimming effect in bifurcated microvessels for predicting the blood flow in the microvasculature. Here, the cellular level interaction for simulating blood flow in the microvasculature is limited in a few microvessels and thousands of cells. Therefore, it is required to develop an 1-D blood flow model for simplifying the complex blood flow in continuously bifurcating microvessels. We will computationally construct microvascular geometries and simulate the blood flow through them by using an extended 1-D blood flow model with plasma skimming effect. The suggested model will be compared with experimental data in rat mesentery and mouse cortex. Based on the simulation results, the linking between cellular model and network model is fully discussed.

Improving the Accuracy of Consumer Preference Estimation Using Economic Simulation Model

Ungki Lee*, Namwoo Kang**, Ikjin Lee***

*Korea Advanced Institute of Science and Technology, **Korea Advanced Institute of Science and Technology,

***Korea Advanced Institute of Science and Technology

ABSTRACT

The research field of the design for market systems (DMS) gives insights to decision makers to find profit-maximized product design [1]. After estimating the consumer preferences toward the product attributes, product design can be formulated as a mathematical optimization problem, and the optimum design that maximizes the expected value can be achieved. Therefore, it is important to predict a market share of a product using product attributes and consumer preferences when designing a product [2]. To obtain individual level consumer preference, choice-based conjoint (CBC) study is executed to extract actual responses results of consumers collected from surveys. Then a hierarchical Bayesian (HB) approach is used to estimate the part-worths on product attributes which indicate preferences of consumers [3]. However, the number of people who can conduct a survey is limited, and the number of questionnaires per person should not be large. This influences the predictive capability of HB in estimating consumer preferences on product attributes. This paper introduces an approach to improve the accuracy of consumer preference estimation using a simulation model despite the small number of actual survey data. Based on the demographic data of consumers surveyed, each consumer's discount rate which shows how future income or expenditure is valued at present can be obtained using optimization technique, and an economic simulation model that can replace each individual's choice on product can be established. Then the economic simulation model conducts virtual surveys which consist of a combination of various product attribute levels, and the achieved simulation data is calibrated with actual survey data to improve predictive capability. Some of the actual survey data is used to estimate consumer preferences, while some are used to validate the estimated consumer preferences. Validation calculates how much the marketing model which is generated through the calibration of actual survey data and economic simulation model data can match the actual survey results. [1] Lewis, K. E., Chen, W., Schmidt, L. C., and Press, A., 2006, Decision Making in Engineering Design, ASME Press, New York. [2] Kang, N., Ren, Y., Feinberg, F. M., and Papalambros, P. Y., 2016, "Public Investment and Electric Vehicle Design: A Model-based Market Analysis Framework with Application to a USA-China Comparison Study," Des. Sci., 2, p. e6. [3] Kang, N., Feinberg, F. M., and Papalambros, P. Y., 2017, "Autonomous Electric Vehicle Sharing System Design," ASME J. Mech. Des., 139(1), 011402.

Multiscale Analysis of the Domain Patterns in Ferroelectrics

Yi-Chien Lee*, Nien-Ti Tsou**

*Dept. of Materials Science and Engineering, National Chiao-Tung University, Hsinchu, Taiwan, **Dept. of Materials Science and Engineering, National Chiao-Tung University, Hsinchu, Taiwan

ABSTRACT

Ferroelectric materials have been widely used in many applications of sensors, actuators and memory devices in recent decades. These materials have strong electrical, thermal, or mechanical coupling, giving an opportunity for crystals to sense the change of external loading or boundary conditions. The microstructure is the most important factor to determining the crystal properties. However, there are some limitations of typical microstructural modeling. For example, certain patterns of microstructure are assumed for sharp interface models, and the small calculation regions for phase field methods. Thus, the aim of this study is to develop a multiscale analysis scheme combining the merits of sharp interface and phase field models. Firstly, the microstructure pattern can be obtained by sharp interface model based on compatibility equations. Wherein the pattern is determined with the assumption of flat interfaces. Then, the pattern is set as the initial state of the phase field model, for further energy minimization to eliminate the flat interface assumption. The phase field algorithm is implemented by a commercial software COMSOL Multiphysics. Microstructures of the tetragonal and rhombohedral ferroelectrics crystal are both examined in order to demonstrate the validity of the current work. Interesting laminate structures, such as herringbone patterns and stripe patterns, are generated. Also the effect of depolarization energy, applied load and applied electric field will be examined. The current multiscale model eliminates the assumption of flat interfaces, and at the same time, has better efficiency for engineering purposes. Keywords: phase-field method, ferroelectric, compatible pattern, interfacial energy

Topology Optimization of Synthesized, Stochastic Microstructures

Sylvain Lefebvre*

*INRIA

ABSTRACT

In this presentation I will discuss recent work made within our team regarding the optimization of objects filled with microstructures that are synthesized from stochastic processes. I will present two different approaches. The first, inspired by example-based texture synthesis techniques from Computer Graphics, allows designers to specify the local shape of porosities by providing an example. A global optimizer distributes material such as to obtain globally rigid shapes, while locally the material form porosities resembling the ones in the exemplar. The second approach relies on stochastic processes to generate microstructures resembling foams. By controlling the statistics of the generation process, we show that it is possible to control the final average elastic behavior. These techniques can be used in two-scale topology optimization problems, where a shape is globally optimized at a coarse scale, while the random process quickly generates a fine scale foam having the desired homogeneous behavior.

Qualitative and Quantitative Inverse Analysis of Layered Pavement Properties from Falling Weight Deflectometer Data Using Artificial Neural Networks

Marek Lefik^{*}, Marek Wojciechowski^{**}

^{*}Technical University of Lodz, Poland, ^{**}Technical University of Lodz, Poland

ABSTRACT

Falling Weight Deflectometer (FWD) is an instrument for “in situ” test, commonly used to evaluate mechanical parameters and to assess the quality of layered structures of road and airfield pavements. The deflection response of the pavement to an falling weight (measured in several points aligned on a rigid support) is used as an indicator of material properties, and structural performance of the pavement. Determination of the mechanical parameters of the layers is classically done by minimization of a distance between the measured and a theoretical deflection (function of parameters of the model). Slow convergence of this method is described in [2]. Using ANN, it is possible to approximate directly the inverse relation between the set of parameter of the FE model of the layered half space and the deflection of its upper surface, computed for this set of parameters. To do this, the input of the ANN is valued with the deflections and the output with the corresponding set of parameters of the model. FE model can be constructed for many qualitatively different hypotheses concerning the mechanics of the layers (see [1]). For example, the influence of a quality of interlayer junction is crucial for the behavior of asphaltic pavements. Novel algorithm of the stepwise identification that we propose starts with qualitative identification. It is possible to train the ANN with sets of deflections computed according to different qualitative models, such that the ANN computes at the output the integers labelling these models. Having the qualitative solution of the inverse problem, the ANN is retrained with samples computed in frame of the identified FE model and for a coarse sampling of the multidimensional space of parameters. If the error of the solution is not sufficiently small, in the next step a retraining of the ANN is performed again with some set of samples from a neighborhood of the parameters identified in the previous step. If the solution of the inverse problem exists and is ambiguous, this procedure converges. Our own FE code is used to generate solutions of the forward problem. [1] Maoyun Li, Hao Wang, Guangji Xu, Pengyu Xie. Finite element modeling and parametric analysis of viscoelastic and nonlinear pavement responses under dynamic FWD loading, *Construction and Building Materials*, 141 (2017) 23-35 [2] P. Ruta, B. Krawczyk, A. Szydło, Identification of pavement elastic moduli by means of impact test, *Engineering Structures*, 100 (2015) 201–211

A New FEM/DEM Multiscale Model to Solve Immersed Granular Flows Based on Suspension Drops Simulations

Vincent Legat^{*}, Matthieu Constant^{**}, Jonathan Lambrechts^{***}, Frédéric Dubois^{****}

^{*}Ecole Polytechnique de Louvain (UCL/EPL), ^{**}Ecole Polytechnique de Louvain (UCL/EPL), ^{***}Ecole Polytechnique de Louvain (UCL/EPL), ^{****}Université de Montpellier, France

ABSTRACT

This paper is devoted to the study of an hybrid multiscale model for flows mixing fluid and grains. The grains are solved at a fine scale using a Lagrangian approach with the Discrete Element Method. It provides the trajectories and the force applied on the grains with an accuracy that is needed to describe small scales phenomena happening in these flows. The dynamics of the fluid is deduced from a continuous representation of the mixture between grains and fluid at the coarse scale. We present an hybrid multiscale model for immersed granular flows using the Finite Element Method to solve the fluid phase and a non-smooth grains model to solve the contacts. This model will be validated on two-dimensional simulations of the suspension drops that refers to cluster of grains settling in a viscous fluid. The challenging point of this method stays in the coupling of the two different representation scales. Applying this model to the well-known problem of suspension drops provides validation and insight in this kind of methodology. All the features of a swarm of grains settling in a viscous fluid can be found to validate the model and its generality provides easily simulations at regimes where inertia is dominant compared to Stokeslet or Oseenlet simulations usually encountered in literature. Just after the drop begins to move, some grains escape from the closed envelop and form a tail that grows in time until it separates from the swarm. The tail contains grains from the rear of the swarm as well as grains from inside because of the recirculation that leads grains outside the closed envelop. The rate of grains leakage is linked to the falling velocity of the swarm, the radius of the swarm and the radius of the grains. At some time the centre of the swarm contains not enough grains and the tail breaks up. The fluid can go through the center of the swarm and it changes into an open torus that destabilises during expansion and contraction phases to form two (or more) secondary droplets.

Topology Optimization and Model Reduction of Elastomer Damping Devices

Antoine Legay^{*}, Sylvain Burri^{**}, Jean-François Deü^{***}

^{*}Structural Mechanics and Coupled Systems Laboratory, Conservatoire National des Arts et Métiers, 292 rue Saint-Martin, 75141 Paris Cedex 03, France, ^{**}Structural Mechanics and Coupled Systems Laboratory, Conservatoire National des Arts et Métiers, 292 rue Saint-Martin, 75141 Paris Cedex 03, France, ^{***}Structural Mechanics and Coupled Systems Laboratory, Conservatoire National des Arts et Métiers, 292 rue Saint-Martin, 75141 Paris Cedex 03, France

ABSTRACT

Due to their damping properties, elastomer materials are commonly used in the industry to achieve anti-vibration junctions between mechanical subsystems. These links are usually made of various materials (metallic, composites and elastomers). Their geometries may be optimized in order to fulfill the needs of the specific targeted application. Moreover, in order to predict the dynamic behavior of these junctions in their environment, efficient numerical dynamic models have to be developed. These models should take into account the viscoelastic behavior of the elastomer and the material and geometric nonlinearity. Thus, the objective of this work is thus to develop methods to optimize flexible damping devices made of elastomer as well as to build efficient models for the prediction of their dynamic behavior. Firstly, a three-dimensional finite element code using viscoelasticity constitutive relations is developed for the numerical modeling of the elastomer junctions. A Zener fractional derivative of the viscous behavior is implemented. Secondly, a topology optimization [1] of the damping device is achieved in order to find the best geometry shape. The objective function is based on the dynamic compliance of the whole system (the structure and its damping devices) in the frequency domain. A dual method using Lagrange function is used to find the optimum of the objective function, under a volume constraint. Thirdly, a reduced order model is developed. It is based on a component mode synthesis method adapted to highly damped structures by using a multi-model approach [2]. The final reduced element representing the junction is obtained by a dynamic condensation on the external rigid faces in contact with the sub-structures for a total of 12 dofs (6 dofs per face) [3]. The presented application is a junction used to damp the transmitted vibrations from a vibrating base such as a space launcher to a CubSat satellite during takeoff. [1] M.P. Bendsoe, O. Sigmund. Topology Optimization. Theory, Methods, and Applications. Springer, 2004. [2] L. Rouleau, J.-F. Deü, A. Legay. A comparison of model reduction techniques based on modal projection for structures with frequency-dependent damping. Mechanical Systems and Signal Processing, 90, 110–125, 2017. [3] A. Legay, J.-F. Deü, B. Morin. Reduced order models for dynamic behavior of prestressed elastomer damping devices. Proceedings of the VII European Congress on Computational Methods in Applied Sciences and Engineering, the ECCOMAS Congress 2016, Hersonissos, Crete, Greece, June 5-10, 2016.

A Phase Field Model for Three-phase System with Tunable Interfacial Energy and Its Application to Solid Oxide Fuel Cell

Yinkai Lei^{*}, Tianle Cheng^{**}, Youhai Wen^{***}

^{*}National Energy Technology Laboratory, Albany OR, ^{**}National Energy Technology Laboratory, Albany OR,

^{***}National Energy Technology Laboratory, Albany OR

ABSTRACT

An improved phase field model has been developed to simulate the microstructure evolution in three-phase system. Detailed analysis reveals that a cross term between the gradient of order parameters is essential to make the interfacial energy tunable. We demonstrate that the ratio between the energy of grain boundary and interphase boundary (or surface) can be easily tuned in our model. We use this model to simulate the microstructure evolution in both the anode and cathode of solid oxide fuel cell. The results show that our model is well applicable to two different three-phase systems, i.e. Ni-YSZ-pore for anode and LSM-YSZ-pore for cathode.

Stochastic Agent-based Modeling of Cell Death and Tissue Shrinkage

Emma Lejeune*, Christian Linder**

*Stanford University, **Stanford University

ABSTRACT

Cell death, a process which occurs both naturally and in response to external factors, is both a complex and diverse phenomenon. A better understanding of how cell death manifests on the population and tissue scales is relevant to both morphogenesis and tumor response to treatment. Under certain conditions, dying cells actively contract, which causes neighboring cells to rearrange and maintain tissue integrity. Under other conditions, dying cells leave behind gaps, which results in tissue separation. Here we establish a computational framework to study the effects of cell death on population scale shrinkage. In order to better quantify model uncertainty and parameter interactions, we implement a recently developed technique for conducting a variance-based sensitivity analysis on a stochastic model. In particular, we define appropriate technique for prescribing stochastic model components and constructing a meta-model to make sensitivity analysis with a computationally expensive simulation feasible. With this framework, we explore cell death implemented in a peridynamics based mechanical model [1]. Peridynamics, a theoretical and computational framework designed to unify the mechanics of continuous and discontinuous media, is a promising tool for coupling mechanical and algorithmic biological behavior. In our model, algorithmic rules applied on the cellular level interact with mechanical behavior and emerge on the population scale where their effects are quantified. We find that parameters such as cell shrinkage during death are as important as the fraction of dying cells for determining population scale shrinkage. Looking forward, we anticipate that the methods and results presented here are a starting point for significant future investigation toward modeling and understanding cell death in multiscale and multiphysics settings. [1] Lejeune, E. & Linder, C. Biomech Model Mechanobiol (2017) 16: 1141.

Modeling the Capillary Transport of Deformable Nanoconstructs and Cells via a Lattice Boltzmann Method

Pietro Lenarda^{*}, Alessandro Coclite^{**}, Marco Miali^{***}, Hilaria Mollica^{****}, Anna Lisa Palange^{*****}, Paolo Decuzzi^{*****}

^{*}Fondazione Istituto Italiano di Tecnologia, ^{**}Fondazione Istituto Italiano di Tecnologia, ^{***}Fondazione Istituto Italiano di Tecnologia, ^{****}Fondazione Istituto Italiano di Tecnologia, ^{*****}Fondazione Istituto Italiano di Tecnologia, ^{*****}Fondazione Istituto Italiano di Tecnologia

ABSTRACT

In the treatment and imaging of diseases, nanoconstructs and engineered cells are emerging as powerful tools for the tissue specific delivery of multiple agents. Generally, nanoconstructs and cells are injected systemically and could reach any site within the circulatory system as they are transported by the blood flow. In the case of nanoconstructs, the size, shape, surface properties and softness – 4S parameters – can be tailored during the synthesis process to enhance their specific accumulation within the diseased tissue. Similarly, stem cells, macrophages and other types of cell can be engineered ex-vivo to express specific surface receptors that would facilitate the recognition of the biological target. Given, the variety of independent parameters and the complexity of the biophysical problem, sophisticated computational tools to guide scientists in the rational selection of the most effective delivery strategy are urgently needed.[1] In this study, a computational framework based on coupling Lattice Boltzmann (LB) and Immersed Boundary (IB) methods is employed to predict the vascular transport and adhesion of nanoconstructs and cells in capillary flows. The fluid solver for the incompressible Navier-Stokes equations is based on the three dimensional D3Q19 Lattice-Boltzmann Method. The dynamics of deformable nanoconstructs and cells is simulated through a neo-Hookean membrane constitutive model coupled iteratively with the fluid. [2] Nanoconstructs and cells are decorated with ligand molecules interacting through probabilistic laws with receptors deposited along the blood vessel walls. The proposed numerical scheme is validated against known computational and experimental benchmarks. The vascular dynamics (margination) and adhesion of nanoconstructs and cells is predicted in terms of the 4S parameters – size, shape, surface and softness – and of vascular features – caliber, wall shear rate, receptor density and affinity. Numerical data are directly compared with experiments performed in microfluidic chips.[3] Implications on the rational design of nanoconstructs and efficiency of cell delivery are critically discussed. References 1. Decuzzi, P., Facilitating the Clinical Integration of Nanomedicines: The Roles of Theoretical and Computational Scientists. ACS Nano, 2016. 10(9): p. 8133-8. 2. Kruger, T., F. Varnik, and D. Raabe, Efficient and accurate simulations of deformable particles immersed in a fluid using a combined immersed boundary lattice Boltzmann finite element method. Computers & Mathematics with Applications, 2011. 61(12): p. 3485-3505. 3. Coclite, A., et al., Predicting different adhesive regimens of circulating particles at blood capillary walls. Microfluidics and Nanofluidics, 2017. 21(11): p. 168.

Optimal Gear Design to Minimize Vibrations Through the Path Gear-Shaft-Bearing-Gearhousing

Jesson Xavier Leon-Medina*, Henry Octavio Cortes-Ramos**

*Universidad Nacional de Colombia-Sede Bogotá, **Universidad Nacional de Colombia-Sede Bogotá

ABSTRACT

In this work, the dynamic behavior of a gearbox is optimized. We consider the interaction between the housing, the bearing, the shaft and the gears. We minimize the excitation sources generated by the meshing process, among which are included, the static transmission error-STE and the variation of the mesh stiffness. For the analysis of static transmission error, several methods have been generated, most of which are based on the finite element method for a set of successive positions of the driving wheel [1]. The STE is presented due to differences between ideal and real designs, such as deflections of teeth and manufacturing errors [2]. We seek to find the best gear profiles to reduce the vibrations present in a gearbox, taking into account the transmission effect involved in the interaction between gear, shaft, bearing and housing . This interaction can be modeled by two methods, the finite element method or the lumped mass method a hybrid method combining the advantages of the two methods can be employed to avoid some problems such as modeling error, time consuming and computing cost, etc. [3].
References [1] Rigaud, E., & Barday, D. (1999). Modelling and analysis of static transmission error. Effect of wheel body deformation and interactions between adjacent loaded teeth. In 4th World Congress on Gearing and Power Transmission (pp. 1961-1972). [2] Carbonelli, A., Perret-Liaudet, J., Rigaud, E., & Le Bot, A. (2011). Particle swarm optimization as an efficient computational method in order to minimize vibrations of multimesh gears transmission. Advances in Acoustics and Vibration, 2011. [3] Gao, W., & Wang, L. (2015). Research on dynamic transmission characteristics of box-like structures based on a hybrid model method. In Advanced Intelligent Mechatronics (AIM), 2015 IEEE International Conference on (pp. 1190-1194). IEEE.

Towards a Unified FSI and Multiphysics Heart Simulator for Clinical Applications

Massimiliano Leoni^{*}, Cem Degirmenci^{**}, Johan Jansson^{***}, Johan Hoffman^{****}

^{*}KTH Royal Institute of Technology and Basque Center of Applied Mathematics, ^{**}Basque Center of Applied Mathematics, ^{***}KTH Royal Institute of Technology and Basque Center of Applied Mathematics, ^{****}KTH Royal Institute of Technology and Basque Center of Applied Mathematics

ABSTRACT

We present our plan and latest developments on our unified framework for multiphysics simulation of a human heart. Our project is built on top of our Unified Continuum formulation for fluid-structure interaction, where we solve the conservation equations for the fluid and the solid parts in a unified computational framework based on a stabilized finite elements method [1]. The long-term idea is to be able to couple this model with various domain-specific model, ideally individually designed to simulate a specific clinical procedure or heart disease, in a modular and flexible way. As a first, intermediate milestone, we already developed a simulator, for radiofrequency ablation of cardiac tissue, that solves a coupled system consisting of fluid motion, heat conduction and electrical diffusion; we plan to couple this solver with our Unified Continuum model in order to get a more reliable simulator of radiofrequency ablation of a beating heart. As an additional option, we also plan to pair Unified Continuum's intrinsic adaptive formulation into our framework, allowing for adaptivity to increase the computational efficiency of the whole procedure. More than one option is possible in this direction: h-adaptivity, where refinement is performed at the end of a primal-dual solver run on the cells that most contribute to the error on the computation of some cost functional [2], or r-adaptivity, where the mesh is moved during the computation in order to follow characteristic features of the solution as it is being computed. Our software is implemented in the FEniCS-HPC software framework for automated finite elements simulations, which has proven records of parallel performance on modern supercomputers [3].

References [1] Hoffman, J., Jansson, J., Stöckli, M. (2011). Unified Continuum Modeling of Fluid-Structure Interaction. Mathematical Models and Methods in Applied Sciences. [2] Jansson, J., Degirmenci, N. C., Hoffman, J. (2016). Adaptive Unified Continuum FEM Modeling of a 3D FSI Benchmark Problem. International Journal for Numerical Methods in Biomedical Engineering. [3] Jansson, N., Hoffman, J., Jansson, J. (2012). Framework for Massively Parallel Adaptive Finite Element Computational Fluid Dynamics on Tetrahedral Meshes. SIAM Journal on Scientific Computing.

Nuclear Fuel Assembly Deformation, Reduced Mechanical Model Dedicated to FSI Simulation

Bertrand Leturcq*

*CEA, DEN, DANS, DM2S, SEMT, LM2S, F-91191 Gif sur Yvette, France

ABSTRACT

In the pressure vessel of a PWR the core is constituted of a number of fuel assemblies. Under operation, they all suffer from various phenomena, among them, initial trapped efforts, thermal expansion, irradiation growth, creeping, tightening relaxation and rod slipping. Each fuel assembly may develop contacts with its neighbors and strongly interacts with the fluid. It then undergoes vertical as well as lateral fluid forces, which are partly coupled with its instantaneous shape. As a consequence the fuel assembly tends to get distorted during and still after operation. The first concern is economic: at the end of a cycle, when changing the assembly position in the core, the contact interactions with its neighbors due to its distorted shape sometimes delay the handling. The second concern is that the shutdown rods have to slide into the deformed shape of the guide tube and might be slowed due to excessive friction forces. In order to precisely assess these situations it is necessary to simulate numerically a complete core, taking into account all of the previously mentioned phenomena. For that purpose, we propose a light but relevant reduced mechanical model of a fuel assembly, partially based on a POD analysis performed on a detailed fuel assembly model. We then show that a rather simple model, still based on classical finite elements can be used and simplifies the integration of the local nonlinear constitutive equations. We then compare both of the detailed and reduced model on typical situations and show excellent agreement. The CPU time ratio between them, for a full nonlinear simulation of a single fuel assembly under operation, is over 1000, which is competitive against separation of variables based reduced order methods such as POD, PGD and even APHR[1]. So, yet still with a simplified FSI approach, the drastic memory and CPU reductions obtained now enable us to complete a 3D core simulation representing at least 4 years under operation (4 cycles), with as much as 241 individual fuel assemblies, in a reasonable time of a few hours. [1] David Ryckelynck, Djamel Missoum-Benziane. Multi-level A Priori Hyper-Reduction of mechanical models involving internal variables. Computer Methods in Applied Mechanics and Engineering, Elsevier, 2010, 199, pp.1134-1142. <10.1016/j.cma.2009.12.003>. <hal-00461492>

Microscale Phase Field Modeling of Phase Transformation and Its Interaction with Discrete Dislocation Plasticity

Valery Levitas*, Ehsan Esfahani**

*Iowa State University and Ames Laboratory, **Iowa State University

ABSTRACT

A microscale phase field approach with strain softening is developed to model microstructure evolution during stress-induced multivariant martensitic phase transformations [1]. In contrast to traditional phase field models, the current model is applicable to scales larger than 100 nm and without an upper limit. Gradient energy terms is omitted, but rate-type of regularization is used. During phase transformation, strain softening and related strain localization lead to separated band-like multivariant martensitic regions. The volume fraction of the martensite is the order parameter; the volume fraction of each martensitic variant is just the internal variable, and interfaces between variants are not reproduced. The model is used to study the phase transformation of a single- and polycrystal cubic (B2) austenite to monoclinic (B19') multivariant martensite in nitinol shape memory alloy. All twelve martensitic variants are engaged during the simulation of NiTi, and anisotropic elasticity is assumed for both high and low-temperature phases. Finite element model was developed and implemented into code ABAQUS. Simulations based on the presented model are showing the formation of martensitic microstructures which are in qualitative agreement with experimental observations. The results are mesh-independent and are also weakly strain-rate dependent for small strain rates. The effect of crystal orientation, polycrystalline structure, number and location of nucleation sites, an athermal friction on the evolution of the morphology of the transformed regions and global stress-strain curves are investigated under cyclic loading. In addition, pressure and shear strain-induced phase transformations in a bicrystal of a model material at the evolving dislocations pile-up have been studied at the microscale, in contrast to our previous nanoscale studies [2]. Strong stress concentrator at the tip of the dislocation pile-up significantly increases the local thermodynamic driving force for the phase transformation, which drastically reduces transformation pressure in comparison with a hydrostatic loading. This allows us to explain reduction of the transformation pressure by an order of magnitude due to plastic shear in some experiments [2,3]. 1. Esfahani S.E., Ghamarian I., Levitas V.I., Collins P.C. Microscale Phase Field Modeling of the Martensitic Transformation During Cyclic Loading of NiTi Single Crystal. Submitted. 2. Javanbakht M. and Levitas V.I. (2016) Phase field simulations of plastic strain-induced phase transformations under high pressure and large shear. Physical Review B, 94, 214104. 3. Ji C., Levitas V. I., Zhu H., et al. (2012) Shear-Induced Phase Transition of Nanocrystalline Hexagonal Boron Nitride to Wurtzitic Structure at Room Temperature and Low Pressure. PNAS, 109, 19108-19112.

Effect of Fibre and Sheetlet Distribution on Physiological Models for Heart Contraction

Francesc Levrero-Florencio*, Ricardo Ruiz Baier**, Alfonso Bueno-Orovio***, Vicente Grau****, Blanca Rodriguez*****

*University of Oxford, **University of Oxford, ***University of Oxford, ****University of Oxford, *****University of Oxford

ABSTRACT

Cardiac disease is, according to the World Health Organization (2015), the first cause of death worldwide, making the study of its underlying mechanisms a priority. A current popular and non-invasive alternative to animal testing or clinical trials is multi-scale computational modelling, particularly that which takes into account the contraction mechanisms of the heart. The heart achieves its primary role of pumping blood through the circulatory system by means of active contraction of cardiomyocytes. Cardiomyocytes have a well-defined local fibre orientation. Moreover, during systole, myocytes slide over each other in compounds of sheetlets, leading to a wall thickening of $\geq 25\%$. In order to reproduce physiological ranges of thickening, cardiac electro-mechanical models require to incorporate such sliding mechanisms in addition to realistic fibre and sheetlet architectures. Furthermore, conditions which affect the fibre orientation distribution, such as hypertrophic cardiomyopathy (fibre disarray) might also lead to contraction abnormalities if these mechanisms are not considered. The developed models include the description of multi-physics and spatial/temporal multi-scale mechanisms and consider the coupling between electrical activation, excitation-contraction coupling, and solid mechanics. The passive mechanical behaviour is modelled with an anisotropic and incompressible hyperelastic constitutive law; the active strain orthotropic model with sliding filaments from Rossi et al. (2014) is used to represent the active contraction; electrical propagation throughout the myocardium is modelled with the bidomain equations. At the single cell level, biophysical processes underlying electrophysiology, contraction and relaxation of cardiomyocytes are represented in the model through the coupling of two systems of ODEs: the O'Hara-Rudy model for cell electrophysiology and the Land et al. (2017) excitation-contraction coupling model. The biophysical detail of this multi-scale model enables simulation of microscopic mechanisms, such as disease-induced remodelling or pharmacological blocks of specific ionic currents. The impact of the model choices on the deformation obtained for different normal or abnormal sheetlet distributions (see e.g. Potse et al., 2006) is studied. We also address an additional application considering local fibre disarray, in which the obtained deformation is compared to the normal case. This study contributes to assessing the effect of healthy and diseased sheetlet distributions on the mechanical deformation during contraction of the ventricles, and it will serve to increase the predictive capabilities of electro-mechanical cardiac models, particularly during diseased conditions. References: - Rossi et al., 2014. Eur J Mech A Solids. - Potse et al., 2006. IEEE Trans Biomed Eng. - Land et al., 2017. J Mol Cell Cardiol.

Probably Robust Directional Vertex Relaxation for Geometric Mesh Optimization

Adrian Lew^{*}, Ramsharan Rangarajan^{**}

^{*}Department of Mechanical Engineering, Stanford University, ^{**}Department of Mechanical Engineering, Indian Institute of Science Bangalore

ABSTRACT

We introduce an iterative algorithm called directional vertex relaxation that seeks to optimally perturb vertices in a mesh along prescribed directions without altering element connectivities. Each vertex update in the algorithm requires the solution of a max-min optimization problem that is nonlinear, nonconvex and nonsmooth. With relatively benign restrictions on element quality metrics and on the input mesh, we show that these optimization problems are well posed and that their resolution reduces to computing roots of scalar equations regardless of the type of the mesh or the spatial dimension. We adopt a novel notion of mesh quality and prove that the qualities of mesh iterates computed by the algorithm are nondecreasing. The algorithm is straightforward to incorporate within existing mesh smoothing codes. We include numerical experiments which are representative of applications in which directional vertex relaxation will be useful and which reveal the improvement in triangle and tetrahedral mesh qualities possible with it.

Numerical Implementation of an Invariant-Based Model for Foamed Elastomers with Strain Softening and Nonlinear Time Dependent Response

Matthew Lewis*

*Los Alamos National Laboratory

ABSTRACT

A hyperelastic strain energy function (Lewis, 2017) has been developed to describe the mechanical response of elastomeric foams. The model for compression as the relative density (ratio of foam density to parent material density) approaches and even exceeds unity is based on the compaction of a spherical cavity in a compressible elastomer with a Neo-Hookean response and a logarithmic pressure- volume relationship. The relative volume is multiplicatively decomposed into a part resulting from the compressibility of the solid elastomer and a part resulting from isochoric deformation of this solid. Because of this formulation, even very low porosities and large compressions can be modeled using this strain energy function. A simplified continuum damage model was introduced to capture the strain softening effect in many foamed elastomers. Additionally, a nonlinear, viscous, inelastic response after the manner of Bergstrom and Boyce (1998) has been incorporated to introduce hysteresis and rate and time dependence into the model. Details of the numerical implementation of these aspects of the model and verification are presented. Lewis, M. "A Robust, Compressible, Hyperelastic Continuum Model for the Mechanical Response of Foamed Rubber," *Technische Mechanik* 36, 1-2 (2016), 88- 101. Bergstrom, J.S. and Boyce, M.C., "Constitutive modeling of the large strain time- dependent behavior of elastomers," *JMPS* 46, 5, (1998), 931-954.

Simulation of Material Transport in Complex Geometry of Neurons Using Isogeometric Analysis

Angran Li^{*}, Xiaoqi Chai^{**}, Ge Yang^{***}, Yongjie Jessica Zhang^{****}

^{*}Carnegie Mellon University, ^{**}Carnegie Mellon University, ^{***}Carnegie Mellon University, ^{****}Carnegie Mellon University

ABSTRACT

Neurons exhibit strikingly complex and diverse geometry in their highly branched networks of neurites, i.e. axons and dendrites. The geometry is essential to function of individual neurons and formation of neural circuits. However, because material synthesis and degradation in neurons are carried out mainly in the cell body, neurons must constantly transport a wide variety of essential materials throughout the complex neurite network to survive and function. How material transport is carried out in the complex neuronal geometry remains a fundamental yet unanswered. Answering this question is critical to understanding the physiology and disease of neurons. To this end, we develop an isogeometric analysis (IGA) based solver to simulate the material transport in complex neurite networks of neurons. The material transport process is described by generalizing a one-dimensional motor-assisted transport model of intracellular particles to three dimensions. We start the modeling and simulation from a single neurite, a neurite bifurcation, to a simple neurite tree structure, which are the basic structural units of the complex neurite network in neurons. We use a skeleton sweeping method to construct hexahedral meshes for them. To solve the transport equations, we first develop a Navier-Stokes equation solver based on the variational multiscale method (VMS) to obtain the velocity field of material transport in neurons. Then, we develop the solver of the motor-assisted transport equations based on the streamline upwind/Petrov-Galerkin method (SU/PG). Finally, specific boundary conditions and initial conditions based on experiments are set to validate the simulations. Our simulation can reliably reproduce the spatiotemporal dynamics of material transport in neurons.

Investigation of Dynamic Load Effect on LiCoO₂ Cathode of Lithium- ion Battery with Nanomechanical Raman Spectroscopy Analysis

Bing Li*, Ryan Adams**, Jafr Kazmi***, Vikas Tomar****, Vilas Pol*****, Tom Adams*****,
William Kellerhals*****

*Purdue University, **Purdue University, ***United States Military Academy at West Point, ****Purdue University,
*****Purdue University, *****Naval Surface Warfare Center, Crane Division, *****Purdue University

ABSTRACT

For mechanical property and in service behavior analyze of material with complex composition and morphology, nano level mechanical tests including nano-impact have been proved successful for application on alloy and metallic powder[1]. For decades lithium- ion battery (LIB) has been accepted in energy storage industry as one of the most mature yet promising secondary batteries. However there are still safety flaws of LIB, one main hazard is dynamic impact generated defects in transportation, which could cause battery capacity drop. With most dynamic effect evaluation carried out at battery level, there exists need for evaluation of dynamic response of electrode excluding contribution of battery housing. Electrode material of LIB is typically in form of powder mixture consists of electroactive material, conductive agent and binder with particle diameter at level of micrometer. Considering composite composition and powder morphology nature, it is essential for battery design to obtain information of response and effect of dynamic load of electroactive material at nano level to reveal effect on electrode structure and influence on battery performance. Technique of nanomechanical Raman spectroscopy analysis developed by Interfacial Multiphysics group of Purdue University[2] was applied for investigation of dynamic response and corresponding structural change of LiCoO₂ cathode. Electrode was exposed to dynamic load for direct impact, with electrochemical structure evaluation carried out with analysis of impact history and nanomechanical Raman analysis, applied dynamic load was related with electrode structural response at nano level and battery electrochemical performance for first time. It was shown that direct dynamic impact is related with noticeable capacity drop of electrode which presented proportional relation with impact cycles. Change of electrochemical material structure was represented with positive Raman shift observed. [1]. Beake, B. D., et al. "Investigating the correlation between nano-impact fracture resistance and hardness/modulus ratio from nanoindentation at 25–500° C and the fracture resistance and lifetime of cutting tools with Ti1?xAlxN (x= 0.5 and 0.67) PVD coatings in milling operations." Surface and Coatings Technology 201.8 (2007): 4585-4593. [2]. Gan, Ming, and Vikas Tomar. "Surface stress variation as a function of applied compressive stress and temperature in microscale silicon." Journal of Applied Physics 116.7 (2014): 073502.

Concurrent Multiscale Modeling of Ductile Failure Mechanisms in Metals

Bo Li^{*}, Hao Jiang^{**}

^{*}Case Western Reserve University, ^{**}Case Western Reserve University

ABSTRACT

We propose a high-performance computing based multiscale computational tool for the high fidelity prediction of ductile failure mechanisms in metals undergoing arbitrary deformations. A three-dimensional finite element model of the polycrystalline structure of metals at the mesoscale is reconstructed by incorporating the probability distribution functions (PDF) of grain sizes, orientation and misorientation angles from the experimental EBSD data. In particular, grain boundaries are explicitly represented by a thin layer of elements with non-zero misorientation angles. The behavior of the material at each finite element is obtained from a concurrent analysis of a representative volume element (RVE). Accordingly, we refer to the RVE as the packed hollow sphere (PHS) model and solved by a Ritz–Galerkin method based on spherical harmonics, specialized quadrature rules, and exact boundary conditions at the microscale. A single crystal plasticity model with the strain hardening law related to the local misorientation angle is employed at each quadrature point to predict the deformation of the hollow sphere and void growth in the RVE. The finite element at the mesoscale fails as the void of the representative hollow sphere grows beyond some critical size. As a result, the model predicts the strong coupling between polycrystal plasticity and void deformation to simulate the ductile failure mechanism in polycrystalline structures. The proposed method is validated in an example of spallation fracture in aluminum alloys under high velocity impact conditions.

A Micro-Mechanical Model of Saturated Granular Soils Using Discrete-Elements and a Lattice Boltzmann Form of the Averaged Navier-Stokes Equations

Bo Li^{*}, Mourad Zeghal^{**}

^{*}Rensselaer Polytechnic Institute, ^{**}Rensselaer Polytechnic Institute

ABSTRACT

Saturated granular soils consists of grains forming a solid skeleton and water filling the pores. These soils exhibit a broad range of response patterns depending on the level of confining stresses and pore pressures, including granular flow, liquefaction, dilation and others. A number of studies were successfully conducted using a continuum-discrete approach to model the hydro-mechanical response of these soils. The solid phase is modeled using the Discrete Element method and the fluid phase is idealized using volume-averaged Navier Stokes (VANS) equations. The numerical solution of these equations is often tackled using the finite volume technique, which has limitation when used to solve complex-geometry problems. In this study, the lattice Boltzmann method (LBM) is modified and adapted to solve the VANS equations for incompressible pore fluid flow. This method employs fine lattice meshes and is highly effective in accommodated complex conditions. A new pressure correction term is introduced to resolve the solution inaccuracy and instability at the interface between zones of highly dissimilar permeabilities. A modified mass-source term is employed to ensure an accurate and stable solution to dynamic problems in which the porosity varies with time. A series of benchmark tests were preformed, and the proposed LBM scheme was found to agree well with analytical solutions.

Correlation Analysis of Statistical Descriptors for Heterogeneous Materials

Chenfeng Li^{*}, SQ Cui^{**}, JL Fu^{***}

^{*}Swansea University, ^{**}Swansea University, ^{***}Swansea University

ABSTRACT

Heterogeneous materials such as rock, concrete, composite often exhibit a random micro-structure, where two or more material phases distribute randomly through the medium. It is known that the mechanical, electrical, thermal properties of the heterogeneous material are closely related to the random morphology of micro-structure. For a specific heterogeneous material, a central requirement that is often raised is to predict the macro-scale properties from the morphological features of micro-structure. To achieve this goal, a number of statistical descriptors have been proposed in material science and computational mechanics to quantify the random morphology of heterogeneous materials. However, these statistical descriptors have very different mathematical formulation, and even worse some do not even have a closed form equation. As such, it is very difficult, if not impossible, to understand clearly the relationship between these statistical descriptors, which has long hampered the research progress of heterogeneous materials. This work address this challenge, by proposing a novel machine-learning base approach to quantitatively measure the correlation between various statistical descriptors. Furthermore, based on the correlation analysis, the statistical descriptors can be classified into different groups with similar descriptors grouped together. This classification not only helps to understand the characteristics of heterogeneous materials, but it also guide the researchers and engineers in material design and evaluation.

Thermomechanical Extended Layerwise Method of Laminated Composite Plates

Dinghe Li^{*}, Jacob Fish^{**}

^{*}Civil Aviation University of China/Columbia University, ^{**}Columbia University

ABSTRACT

With accelerating use of aeronautic and aerospace composite structures in the high-temperature operating conditions, numerous research works were published on heat transfer and thermal stress analysis of laminated composite plates and shells during the last three decades. In order to uncouple heat transfer and thermal stress analyses, the thermomechanical dissipation was neglected in most of the existing analytical and numerical models. In addition, considerable research works were carried out under the steady-state assumption by considering the thermal effect as an additional term in the constitutive relationship. However, when the dynamic disturbances resulting from the heat flow are considered, the thermomechanical dissipation is of primary interest. Existing works mainly focus on the thermomechanical fracture problem of delamination or transverse cracking, but only few studies have been conducted on multiple delaminations and problems in which the delamination and transverse cracks interact. In the present work, a Thermomechanical Extended Layerwise Method (TELM) is developed for the laminated composite plates with multiple delaminations and transverse cracks. The discontinuity of displacements and temperature induced by multiple delaminations is simulated by strong discontinuous function while the discontinuity of strain and temperature gradient between dissimilar layers is modeled by a weak discontinuous function. Transverse cracks are modeled using classical Extended Finite Element Method (XFEM). The coupled thermomechanical variational principle is employed to derive the Euler equations and the discrete forms. Since the displacement and temperature fields are solved simultaneously, a fully coupled time integration method is developed based on the Newmark integration algorithm and Crank-Nicolson scheme. The strain energy release rate for multiple delamination fronts and stress intensity factors for transverse cracks are calculated by the Virtual Crack Closure Technique and the Interaction Integral Method, respectively. The proposed method is applied to the steady-state thermomechanical problems, elastic and thermomechanical dynamic problems for isotropic and composite plates with transverse cracks and multiple delaminations.

Development of Efficient Algorithms in the Design of Phononic Crystals / Acoustic Metamaterials

Eric Li^{*}, ZC He^{**}

^{*}Teesside University, ^{**}Hunan University

ABSTRACT

The phononic crystals (PCs) / acoustic metamaterials (AMs) are periodic man-made composite materials. In this paper, a mass-redistributed finite element method (MR-FEM) is formulated to study the wave propagation within fluid PCs, solid/fluid PCs and fluid/solid PCs with fluid-structural interaction. With a perfect balance between stiffness and mass in the MR-FEM model, the dispersion error of longitudinal wave is minimized by redistribution of mass. In addition, the mathematical model to predict the upper and lower bounds of mechanical response of AMs with uncertainty parameters such as Young's modulus, Poisson's ratio and density, is established by the nonlinear interval perturbation hybrid node-based smoothed finite element method (NIPH-NS/FEM). One of the main features of NIPH-NS/FEM with a softened effect in the discretized model is capable to overcome the volumetric locking issue of incompressible rubber in the standard finite element method (FEM).

A Two-Scale Generalized FEM for the Evaluation of Stress Intensity Factors at Spot Welds in Large Structures

Haoyang Li^{*}, Carlos Duarte^{**}

^{*}University of Illinois at Urbana-Champaign, ^{**}University of Illinois at Urbana-Champaign

ABSTRACT

Spot welds are commonly used to join thin gauge metallic structural components of automotive and aerospace vehicles. The failure of spot welds in these components may lead to the catastrophic loss of the structure. One of the common failure modes of spot welds is fatigue crack propagation through the surrounding material of the spot weld edge. Hence, resolving the local stress fields and extracting Stress Intensity Factors (SIFs) with high fidelity is rather important. The goal of this research is to simulate a large number of spot welds in representative aircraft panels and to calculate SIF variations at each weld with high accuracy and efficiency. This class of problem poses three major challenges. First, the disparate scales involved in a large structure with hundreds of spot welds prevent the discretization of all spot welds in a single FEM model. Second, a proper finite element (FE) approximation is needed to capture the singularity along spot weld edges. Third, an accurate extraction method is required to compute SIFs based on the FE solutions. In this presentation we report on a novel two-scale Generalized Finite Element Method with global-local enrichment (GFEMgl) to solve the target problem. This GFEMgl is a scale-bridging method which uses the solution of a local problem defined for each spot weld as enrichment functions for the structural-scale (global) model. This methodology allows the discretization of each spot weld independently of each other using fine meshes at the local scale, while keeping the global mesh fairly coarse. While solving local problems, a GFEM with singular function enrichments is deployed to capture the stress field along the crevice of each spot weld. With the help of the global-local enrichment, the localized phenomena can be accurately recovered in the global model. Finally, the Displacement Correlation Method (DCM) is adopted to evaluate SIFs along spot weld edges. Numerical experiments show that the proposed GFEMgl framework combined with the DCM can address all the aforementioned challenges and achieve comparable accuracy to the direct finite element simulation with the fine-scale features discretized in the global mesh. Furthermore, the proposed two-scale framework offers greater parallel efficiency in the simulation of structures with a large number of spot welds since local problem solutions are inherently parallel.

Data Compression in Multiscale Analysis for Composite Materials

Hengyang Li^{*}, Jiaying Gao^{**}, Cheng Yu^{***}, Modesar Shakoor^{****}, Wing Kam Liu^{*****}

^{*}Northwestern University, ^{**}Northwestern University, ^{***}Northwestern University, ^{****}Northwestern University,
^{*****}Northwestern University

ABSTRACT

Composite materials, such as fiber reinforced plastic, filled rubber, and composite laminates, are widely used in the industry. Their complex microstructures can be modeled at the scale of structures using multiscale analysis but with a huge computational burden. The discovery of efficient and accurate multiscale modeling methods is a challenge for researchers. Concurrent homogenization can be coupled to reduced order modeling techniques to efficiently generate material laws directly from the solution of Representative Volume Element (RVE) problems and use them in a finite element model of the structure. This presentation will present recent developments in concurrent multiscale modeling using data science to generate material laws. In particular, the recently proposed Self-consistent Clustering Analysis method [1][2][3] is used to solve RVE problems based on the assumption that material points of the RVE that have similar mechanical response can be associated to the same degrees of freedom. This association is generated automatically using data clustering techniques such as k-means, Self-organizing Map. The large RVE can be homogenized into a group of clusters. This will largely reduce the calculation cost in the following analysis. However, the influence of different data compression algorithms still needs more study. This presentation focusses on the accuracy and efficiency of different data science algorithms on data compression in multiscale analysis. Suggestion will be given based on comparison between difference data science algorithms. [1] Liu, Zeliang, M. A. Bessa, and Wing Kam Liu. "Self-consistent clustering analysis: an efficient multi-scale scheme for inelastic heterogeneous materials." Computer Methods in Applied Mechanics and Engineering 306 (2016): 319-341. [2] Liu, Zeliang, Mark Fleming, and Wing Kam Liu. "Microstructural material database for self-consistent clustering analysis of elastoplastic strain softening materials." Computer Methods in Applied Mechanics and Engineering 330 (2018): 547-577. [3] Bessa, M. A., et al. "A framework for data-driven analysis of materials under uncertainty: Countering the curse of dimensionality." Computer Methods in Applied Mechanics and Engineering 320 (2017): 633-667.

A Multiphysics Model for Characterization of Responsive Performance of Urea-Sensitive Hydrogel

Hua Li^{*}, K. B. Goh^{**}, K. Y. Lam^{***}

^{*}Nanyang Technological University, Singapore, ^{**}Nanyang Technological University, Singapore, ^{***}Nanyang Technological University, Singapore

ABSTRACT

A remarkable feature of biomaterials is their ability to deform in response to certain external bio-stimuli. In this talk, a novel biochemo-electro-mechanical model is presented for the numerical characterization of the urea-sensitive hydrogel in response to the external stimulus of urea. Usually the urea sensitivity of the hydrogel is characterized by the states of ionization and denaturation of the immobilized urease, as such that the model includes the effect of the fixed charge groups and temperature coupled with pH on the activity of the urease. Therefore, a novel rate of reaction equation is proposed to characterize the hydrolysis of urea that accounts for both the ionization and denaturation states of the urease subject to the environmental conditions. After examination with the published experimental data, it is thus confirmed that the model can characterize well the responsive behaviour of the urea-sensitive hydrogel subject to the urea stimulus, including the distribution patterns of the electrical potential and pH of the hydrogel. The results point to an innovative means for generating electrical power via the enzyme-induced pH and electrical potential gradients, when the hydrogel comes in contact with the urea-rich solution, such as human urine.

Integrated Thermal-fluid-structural Analysis of Metallic Powder-substrate Interaction Using Phase Field Method

Ji-Qin Li*, Tai-Hsi Fan**

*Department of Mechanical Engineering, University of Connecticut, **Department of Mechanical Engineering,
University of Connecticut

ABSTRACT

Selective laser melting of metallic powders is broadly applied in additive manufacturing process for building geometrically complicated parts. Understanding the underlying transport phenomena that control the fusion dynamics of the metallic powders is important to enhance the surface quality of the additive manufacturing parts and reduce their residual stress during the thermal manufacturing processes. Theoretical analysis focusing on resolving the small scale dynamics at the powder level, especially on the laser-powder-substrate interactions, is therefore critical on improving the process technology and product quality. Phase field method provides an excellent platform to develop new theoretical model that can combine thermal fluids, interfacial evolution, and elastic structural response into an integrated framework to simulate the process dynamics of metallic powders on various substrates. Here we present phase field formulation and simulation of the dynamics of single powder-substrate interactions driven by a pulsed laser beam. The entropy-based approach is applied in deriving the integrated model to ensure thermodynamical consistency of the deformable interfaces. Without the complication of evaporation from the liquid metal, this simplified 2D model describes fully coupled phenomena including melting, partially deforming interfaces, thermal capillary flow, and thermal expansion and elastic structure response during the heating and cool off processes. Thermal physical properties including thermal conductivity, viscosity of the liquid metal, and surface tension are considered temperature-dependent. The process dynamics is computationally resolved and characterized by the temperature distribution, interfacial evolution, thermal capillary pattern, thermal stress induced in the bulk substrate, and the overall morphology change after the pulse heating. The conceptual theoretical framework is important for further development on predicting complicated morphology involving many or hybrid powders, and for the prediction of void formation due to incomplete melting or fusion of metallic powders.

Microstructural Analysis for the Nano-Indentation in Shape Memory Alloys by Using Molecular Dynamics Simulation

Ji-Ting Li^{*}, Nien-Ti Tosu^{**}

^{*}NCTU, ^{**}NCTU

ABSTRACT

Shape memory alloys (SMAs) have been widely used in medicine, aerospace and industry because of its superelasticity and shape memory effect. Many experimental measurements are used to study the origin of these two special properties, such as temperature-induced and stress-induced martensitic transformation. Nano-indentation is one of the stress-induced martensitic transformation way and particularly useful to characterize the properties of SMAs, such as hardness, elastic modulus, and the level of shape memory effect. However, only the macroscopic properties were considered and the discussion about the variants of microstructures due to the martensitic transformation is still limited. In recent years, Molecular Dynamics (MD) simulations opens an opportunity for SMA analysis. Most of these studies only focus on the crystal system after the martensitic transformation but mention the variants few. Typically, these methods identify limited sets of the crystal variants. The aim of this study is to develop a method to identify the variants in MD simulation, and then, apply to study the microstructures due to the martensitic transformation in NiTi SMAs. So far, this method had been successfully used in the temperature-induced martensitic transformation model. In this study, we focus on the microstructure evolutions of stress-induced martensitic transformation during the indentation process. The volume of each variant during the indentation process can be predicted. The interfaces between crystal variants are also examined by compatibility theory. Besides, the relationship between microstructure and mechanical properties are defined, such as hardness. Moreover, the curve features with the corresponding microstructures and the force-displacement distribution of the crystal are also discussed. It is expected to provide the design guidelines in current studies for the SMA applications. Keywords: Shape memory alloys, Molecular dynamics, Indentation, Crystal variants, Microstructure

The Shifted Interface Method for Embedded Interface Computations

Kangan Li^{*}, Alex Main^{**}, Guglielmo Scovazzi^{***}

^{*}Duke University, ^{**}Duke University, ^{***}Duke University

ABSTRACT

Based on the previous work on surrogate boundary method for embedded domain computations, we extend it to the embedded interface problems. The key idea of this approach is shifting the real interface to the surrogate interface. In order to preserve optimal convergence rate of the numerical solution, the shifted interface jump conditions are enforced weakly by using the minimum distance and Taylor expansions. From our view of point, this method is efficient and robust. We apply this concept here to the Poisson interface problems. In particular, we also present the numerical analysis and simulations for Poisson equations defined on complicated geometries.

Three-dimensional Finite Element Modeling of Dynamic BMP Gradient Formation in Zebrafish Embryonic Development

Linlin Li^{*}, Xu Wang^{**}, Adrian Buganza Tepole^{***}, Tzu-ching Wu^{****}, David Umulis^{*****}

^{*}Purdue University, ^{**}Purdue University, ^{***}Purdue University, ^{****}Purdue University, ^{*****}Purdue University

ABSTRACT

Bone Morphogenetic Proteins (BMPs) play a significant role in dorsal-ventral (DV) patterning of the early zebrafish embryo. BMP signaling is regulated by extracellular, intracellular, and cell membrane components. BMPs pattern the embryo during development at the same time that cells grow and divide to enclose the yolk during a process called epiboly. We developed a new three-dimensional growing finite element model to simulate the BMP patterning and epiboly process during the blastula stage. Quantitative whole mount RNA scope data of BMP2b and phosphorylated-SMAD data are collected and analyzed to precisely test the hypotheses of gradient formation in our model. We found that the growth model results in consistent spatially and temporally evolving BMP signaling dynamics within a range of biophysical parameters including a minimal rate of ligand diffusion.

Influence of Volume Fraction on the Effective Friction Law for Transient Granular Avalanche

Liuchi Li^{*}, José Andrade^{**}

^{*}Caltech, ^{**}Caltech

ABSTRACT

We experimentally measure the dynamics of transient granular avalanche with two different types of grain in a rotating drum and for the first time carry out 3D soft particle simulations that are able to produce quantitatively comparable results, from which we discover a non-one-to-one relation of the widely used μ_I law. We suggest that such phenomenon is caused by the relative dilation or contraction of granular material with respect to its steady state as transient flow develops and accordingly we propose a modification for μ_I that can capture our major simulation observations. This finding provides important physical insight into understanding transient flow in comparison to steady flow by revealing the significance of volume fraction variation and its close connection with the effective friction coefficient, both of which can be key ingredients in accurately modeling the dynamics of transient flow that the current incompressible visco-plastic granular flow model fails to produce quantitative agreement with experimental measurements such as density variation and velocity evolution.

Numerical Simulation of Sloshing Flows of Liquid Tanks in Waves

Qi Li^{*}, Decheng Wan^{**}

^{*}Shanghai Jiao Tong University, ^{**}Shanghai Jiao Tong University

ABSTRACT

The exploitation and the transportation of liquid natural gas energy is very challenging and dangerous in Ocean Engineering. In order to solve these problems, a new type of offshore unit FLNG (floating liquefied natural gas vessel) has been proposed. Among many problems that threatening the survival performance of FLNG, the liquid sloshing problem caused by partially filled LNG tanks has a significant coupling influence on FLNG motion. Different from the potential flow method in previous researches, computational fluid dynamics (CFD) method has its unique advantages, such as the consideration of fluid viscosity and the strong nonlinear phenomena. Using our in-house unsteady RANS solver, naoe-FOAM-SJTU, which is developed and based on the open source tool libraries of OpenFOAM, the sloshing coupled effect of a floating box which equipped with liquid tanks is simulated in numerical wave conditions in this paper. Firstly, the motions of the floating box with empty tanks in waves are simulated, the accuracy and effectiveness of the solver are validated by comparing its results with experiment results. Next, to clarify the sloshing influence on ship motion, several tank filling ratios (24.3%, 38.3%, 61.3%) are considered under the same incident wave frequency. The time histories of the corresponding motions are given and discussed, and the influence of the sloshing resonance frequency on sloshing phenomena is revealed and studied. Meanwhile, naoe-FOAM-SJTU solver can also calculate the moments on inside wall and outside wall of the liquid tank, so the coupling influence on the structure motion caused by sloshing and wave force can be studied individually. It is noticed that the amplitude of the rolling motion of the liquid tank has an obvious connection with the phase differences between sloshing moment and wave moment. All above results agree well with the experimental results, which shows that the naoe-FOAM-SJTU solver can effectively simulate the sloshing-motion coupling problem under the wave environment. Besides, on the basis of this study, further researches about other sloshing factors can be carried out in the future.

Atomic-scale Investigation of Tensile Mechanical Properties of Nano-twinned Cu-Ag Multilayers

Qian Li*, Yonggang Zheng**, Hongwu Zhang***, Hongfei Ye****

*Dalian University of Technology, P. R. China, **Dalian University of Technology, P. R. China, ***Dalian University of Technology, P. R. China, ****Dalian University of Technology, P. R. China

ABSTRACT

Understanding the mechanical properties and plastic deformation mechanisms of nano-twinned multilayered materials is essential to provide design parameter in the preparation of multilayer composites. Though extensive experiments and simulations conducted in recent years showed that the strength of nanoscale multilayered metallic materials is strongly dependent on the individual layer thickness, there is still a lack of a thorough understanding on the strengthening effect and underlying mechanism mediated by the hetero interface and twin boundary. In our recent work, we investigated the tensile mechanical properties and plastic deformation mechanisms of nano-twinned Cu//Ag multilayered materials based on molecular dynamics simulations. The simulation results show that, due to the different hetero interfacial configurations, the hetero-twin interfaces have a stronger resistance effect on the dislocation motion than that of the cube-on-cube hetero interfaces, the strength of hetero-twin multilayered materials is higher than that of the cube-on-cube samples. The strength increases with the increase of layer thickness of nano-twinned Cu//Ag multilayered materials with a constant twin spacing, while it decreases with the increase of layer thickness for twin-free ones, which is due to the stronger strengthening effect of the twin boundary than both the cube-on-cube and hetero-twin interfaces between Cu and Ag layers. The confined layer slip of dislocation is found to be the dominant plastic deformation mechanism for twin-free hetero-twin multilayered materials and the strengthening effect of twins follows the conventional Hall-Petch relationship in the nano-twinned multilayered composites. These results may provide guidelines to the fabrication of high strength nano-twinned multilayered metallic materials. References [1] Zheng, Y.; Li, Q.; Zhang, J.; Ye, H.; Zhang, H.; Shen, L. Hetero interface and twin boundary mediated strengthening in nano-twinned Cu//Ag multilayered materials. *Nanotechnology*. 2017, 28, 415705. [2] Zhang, J.; Zhang, H.; Ye, H.; Zheng, Y. Free-end adaptive nudged elastic band method for locating transition states in minimum energy path calculation. *J. Chem. Phys.* 2016, 145, 094104. [3] Zhang, J.; Zhang, H.; Ye, H.; Zheng, Y. Twin boundaries merely as intrinsically kinematic barriers for screw dislocation motion in FCC metals. *Sci. Rep.* 2016, 6, 22893.

Topology Optimization for Biomedical Engineering Applications

Qing Li^{*}, Zhongpu Zhang^{**}, Keke Zheng^{***}, Ali Entezari^{****}, Junning Chen^{*****}, Michael Swain^{*****}, Chaoy Rungsiyakull^{*****}

^{*}The University of Sydney, ^{**}The University of Sydney, ^{***}The University of Sydney, ^{****}The University of Sydney, ^{*****}Exeter University, ^{*****}The University of Sydney, ^{*****}Chiang Mai University

ABSTRACT

Biomedical engineering signifies a class of important problems facing to computational mechanics society. Advanced numerical techniques and computational optimization have been extensively used in biomechanics and biomedical engineering which enables to promote computer aided surgical design and plan for enhancing therapeutic outcomes. Nowadays, numerous prosthetic devices are employed to replace damaged/lost tissues in human body to restore proper functionality. Such artificial structures are required to withstand various mechanical loading over a desired service duration without failure. Further, implantable prostheses need to play a role in engaging the surrounding tissue for osseointegration and bone remodeling, thereby strengthening the entire system of prosthesis - tissues. While these issues have drawn significant attention over the past two decades, one critical problem that remains to be studied is design optimization for various biomedical engineering applications. As a well-established engineering method, topology optimization has been mature through development of rigorous algorithms for general engineering and physics problems. This paper aims to introduce its applications to biomedical problems by outlining the grand challenges and specific features, through a series of clinical case scenarios in dentistry [1,2], cardiology [3], orthopedics [4,5], tissue engineering [6] and biofabrication. References 1. J Chen, R Ahmad, H Suenaga, W Li, K Sasaki, MV Swain, Q Li (2015) Shape optimization for additive manufacturing of removable partial dentures - a new paradigm for prosthetic CAD/CAM. PLoS One 10 (7), e0132552. 2. J Chen, C Rungsiyakull, W Li, Y Chen, M Swain, Q Li (2013) Multiscale design of surface morphological gradient for osseointegration. Journal of the Mechanical Behavior of Biomedical Materials 20, 387-397 3. S Tammareddi, G Sun, Q Li (2016) Multiobjective robust optimization of coronary stents. Materials &&&&&&& Design 90, 682-692. 4. K Zheng, C Scholes, J Chen, D Parker, Q Li (2017) Multiobjective optimization of cartilage stress for non-invasive, patient-specific recommendations of high tibial osteotomy correction angle. Medical Engineering &&&&&&& Physics 42, 26-34. 5. B Miles, E Kolos, R Appleyard, W Theodore, K Zheng, Q Li, AJ Ruys (2016) Biomechanical optimization of subject specific implant positioning for femoral head resurfacing to reduce fracture risk. Journal of Engineering in Medicine 230 (7), 668-674. 6. Y Chen, SW Zhou, Q Li (2011) Microstructure design of biodegradable scaffold and its effect on tissue regeneration. Biomaterials 32:5003-5014.

Analytic Modelling of Reactive Diffusion for Transient Electronics

Rui Li^{*}, Yonggang Huang^{**}, John A. Rogers^{***}

^{*}State Key Laboratory of Structural Analysis for Industrial Equipment, Department of Engineering Mechanics, and International Research Center for Computational Mechanics, Dalian University of Technology, ^{**}Northwestern University, ^{***}Northwestern University

ABSTRACT

Transient electronics [1] is a class of technology that involves components which physically disappear, in whole or in part, at prescribed rates and at programmed times. Enabled devices include medical monitors that fully resorb when implanted into the human body (“bio-resorbable”) to avoid long-term adverse effects, or environmental monitors that dissolve when exposed to water (“eco-resorbable”) to eliminate the need for collection and recovery. Analytic models for dissolution of the constituent materials represent important design tools for transient electronic systems that are configured to disappear in water or biofluids [2, 3]. In this talk, solutions for reactive-diffusion are presented in both single- and double-layered structures, in which the remaining thicknesses and electrical resistances are obtained analytically. The dissolution time and rate are defined in terms of the reaction constants and diffusivities of the materials, the thicknesses of the layer, and other properties of materials and solution. These models are well validated by the experiments, and provide effective approaches to new designs of biofluid barriers for flexible electronic implants. Keywords: transient electronics, biofluid barrier, reactive diffusion, analytic model [1] S.-W. Hwang, H. Tao, D.-H. Kim, H. Cheng, J.-K. Song, E. Rill, M. A. Brenckle, B. Panilaitis, S. M. Won, Y.-S. Kim, Y. M. Song, K. J. Yu, A. Ameen, R. Li, Y. Su, M. Yang, D. L. Kaplan, M. R. Zakin, M. J. Slepian, Y. Huang, F. G. Omenetto, J. A. Rogers, *Science* 2012, 337, 1640. [2] R. Li, H. Cheng, Y. Su, S.-W. Hwang, L. Yin, H. Tao, M. A. Brenckle, D.-H. Kim, F. G. Omenetto, J. A. Rogers, Y. Huang, *Adv. Funct. Mater.* 2013, 23, 3106. [3] E. Song, Y. K. Lee, R. Li, J. Li, X. Jin, K. J. Yu, Z. Xie, H. Fang, Y. Zhong, H. Du, J. Zhang, G. Fang, Y. Kim, Y. Yoon, M. A. Alam, Y. Mei, Y. Huang, J. A. Rogers, *Adv. Funct. Mater.* 2017, 1702284.

A Novel Homogenisation-Aided Topology Optimisation Method for Fast Design of Graded Microstructures in Additive Manufacturing

Shaoshuai Li^{*}, Yichao Zhu^{**}, Weisheng Zhang^{***}, Xu Guo^{****}

^{*}Dalian University of Technology, ^{**}Dalian University of Technology, ^{***}Dalian University of Technology, ^{****}Dalian University of Technology

ABSTRACT

Devices equipped with graded microstructures (GMs) whose constituting cells gradually deform in space have seen their vast engineering potentials in various industrial sectors, especially after the introduction of the 3D printing techniques. Given the fact that microscopic search for the optimal design of GMs is in general computationally unaffordable, homogenisation-aided topology optimisation (termed as “HATO”) approaches provide numerous perspectives on fast design of additively manufacturable GMs. Up to now, however, a majority of existing HATO methods are dedicated for studying periodic lattice configurations. Here we present a novel homogenisation-aided topology optimisation approach (termed as “HATO plus”), where the originally multiscale optimisation problem gets asymptotically decomposed into two sub-problems concurrently taking place on different length scales. Compared to traditional HATO methods, HATO plus exhibits essential advantages which make it a suitable platform for the fast design of additively manufacturable GMs. Firstly, HATO plus stores GMs in a highly compressible manner. Under the HATO plus framework, a GM can be expressed with fewer design parameters. Secondly, existing common topology optimisation methods such as solid isotropic material with penalization (SIMP)/level-set approaches and moving morphological components (MMC)/voids (MMV) can be readily implemented within the HATO plus framework. Thirdly, HATO plus accommodates far more design freedom for GMs than traditional inverse-homogenisation-based schemes. Finally, the proposed HATO plus framework enjoys a diminishing FE-analytical scale compared to methods built on finer grid, while the abundance of its describable configurations is well maintained at the same time. Several simulation results will be presented to demonstrate the aforementioned advantage displayed by the HATO plus scheme.

Multi-scale and Multi-physics Simulations for Dusty Flows in Proto-Planetary Disks

Shengtai Li*

*Los Alamos National Laboratory

ABSTRACT

The recent observations from the ALMA telescope have revealed much detailed structures in many observed proto-planetary disks. The disks can be modeled as turbulent dusty gas motions around a central star with potential embedded planets. To simulate the formation of those disks and its interaction with embedded planets, we have developed a multi-scale and multi-physics numerical tool that can handle the interactions between gas and gas, gas and dust, dust and dust, disk and planets simultaneously. The dusty gas motion is solved as bi-fluid Navier-Stokes equations with the dust treated as the pressure-less flow. The stiff coupling between the dust and gas are solved by a semi-implicit method to improve the time step. The dust coagulation and fragmentation is treated using a partial equilibrium method. Numerical results are presented to demonstrate the effectiveness of our method.

Multiscale Continuous Discontinuous Element Model and the Progressive Failure Rate

Shihai Li^{*}, Qindong Lin^{**}, Dong Zhou^{***}, Chun Feng^{****}, Yongbo Fan^{*****}

^{*}Institute of Mechanics, Chinese Academy of Sciences, ^{**}Institute of Mechanics, Chinese Academy of Sciences,
^{***}Institute of Mechanics, Chinese Academy of Sciences, ^{****}Institute of Mechanics, Chinese Academy of Sciences,
^{*****}Institute of Mechanics, Chinese Academy of Sciences

ABSTRACT

The main features of the continuum discontinuum element method (CDEM), that is based on the generalized Lagrange equation, are introduced. The basic framework of this method is to express the variables in the continuous field and discontinuous field with the variables defined on discrete nodes, which are regarded as generalized variables of the generalized Lagrange equation. The unified expression for fluid, solids and discrete bodies can be obtained. A multi-scale calculation framework for the rock mass by CDEM is established. The physical meaning and the relationship of each scale are expressed, which including engineering scale for engineering problems, element scale for the numerical model, test scale for the continuous media model, micro particle scale for the continuous property and molecular scale for energy dissipation. The failure load on the microplanes within the representative volume element (RVE) is defined, that is the dot product of the stress intensity and the plane vector on microplane. On this basis, the concept of the progressive failure rate for heterogeneous media is proposed, which is defined as the ratio of the force on the microplane and the boundary force. The progressive failure rate represents the heterogeneity of the strength on the microplanes, which is equal to 1 when the strength of the microplanes are the same and will become higher when the loads on the microplanes are more inhomogeneous. The relationship between the force of the particle size and the Van Der Waals force between molecules is discussed. The progressive failure ratio can be also expressed as the ratio of the fracture force of the molecular bond and the load between particles. The results show that the progressive failure model on the molecular scale can describe the material properties of solids reasonably. When used as a constitutive model in the numerical computation, the influence of the mesh shape become much less, which could be an effective way to resolve the mesh dependence problem.

Wrinkling of a Vesicle in Viscous Fluid

Shuwang Li*

*Illinois Institute of Technology

ABSTRACT

We study the nonlinear, nonlocal dynamics of two-dimensional vesicles in a time-dependent, incompressible viscous flow at finite temperature. We focus on a transient wrinkling instability that can be observed when the surface tension becomes negative, e.g. the direction of applied flow is suddenly reversed. In the quasi-circular limit, we derive a Langevin type stochastic differential equation. Using a stochastic immersed boundary method with a biophysically motivated choice of thermal fluctuations, we find that thermal fluctuations actually have the ability to attenuate variability of the characteristic wavelength of wrinkling by exciting more wrinkling modes. Reference: Liu, Kai and Hamilton, Caleb and Allard, Jun and Lowengrub, John and Li, Shuwang, Wrinkling dynamics of fluctuating vesicles in time-dependent viscous flow, *Soft Matter*, 2016, 5663-5675.

Finite-element Analysis of Fracture Toughness of Bovine Cortical Bone: Effect of Osteonal Micro-morphology

Simin Li^{*}, Mayao Wang^{**}, Vadim Silberschmidt^{***}

^{*}Loughborough University, ^{**}Loughborough University, ^{***}Loughborough University

ABSTRACT

A crack-propagation process in cortical bone is difficult to comprehend using only in-situ experimental studies. A previous work [1] assessed quantitatively the fracture toughening mechanisms of cortical bone using a compact-tension experiment, characterising a linear rising fracture resistance curve, R-curve. Even though a final crack-propagation path could be observed with microscopy, the effect of osteonal morphology and their interaction with a surrounding matrix are still not documented properly. In this paper, a finite-element method employing a zero-thickness cohesive-element scheme was used to analyse the effect of micro-morphology of cortical bone on the crack-propagation process in a bone tissue. Microstructured models of cortical bone, incorporating statistical realisations of main features of the osteonal structure, consisting of osteons, cement lines and an interstitial matrix, were developed. They were based on osteonal morphometric parameters, acquired from experimental samples at posterior cortex of bovine cortical bone and used to simulate the process of crack propagation in the compact-tension experiment. The results of numerical simulations, validated experimentally, demonstrated that the suggested approach is an efficient method for investigation of the crack-growth process and fracture mechanics at micro-level. Observations from the experiments and simulation results indicated that the cement line acted as crack-inhibiting mechanism attracting surrounding cracks, while preserving the osteons. Crack-ligament bridging, another extrinsic toughening mechanism of cortical bone, happens for osteons with relatively large Haversian canals. Still, it is difficult to reduce the damage to osteons during a crack growth. Fracture mechanics, as shown in this paper, is influenced significantly by the micro-morphological parameters of osteons, and studying systematically such interplay between osteonal micro-morphology and crack propagation, one could gain an insight into individual fracture toughening mechanisms of cortical bone and their contribution towards tissue-level fracture resistance.

Design and Simulation of a Nanomaterial-based Reverse Osmosis Device with an Intrinsic Anti-fouling Mechanism

Tiange Li^{*}, Shaofan Li^{**}

^{*}University of California, Berkeley, ^{**}University of California, Berkeley

ABSTRACT

A concept of the porous graphene membrane centrifuge is proposed aiming at fabrication of large scale, fouling free desalination machine with nanomaterial-based reverse osmosis (RO) modules. The concept as well as operation strategy of such porous rotating graphene membrane device is validated through molecular dynamics (MD) modeling and simulation of a nano-fluidic device in order to make a quantitative evaluation. One of the challenges in the development of such a device is the tendency of the ions to block the pores on the membrane wall, which is called the fouling problem in RO desalination. The fouling problem can be quantified in terms of ion concentration polarization or ion density distribution. The ion density distribution may become higher close the membrane wall, while the water density distribution becomes low. In order to investigate the distribution of ions, the ion density distribution as a result of the conducted MD simulations is plotted in the radial direction. It is observed that the ion density concentration is almost zero at the membrane wall, which implies that concentration polarization does not exist for the proposed nano-porous membrane centrifuge. Accordingly, it is demonstrated that the proposed desalination device has an intrinsic anti-fouling mechanism, which can be attributed to the presence of the Coriolis force along the tangential direction. After overcoming this significant challenge, several other aspects, related to the design and operation of the developed device, are investigated. First, an analytical formulation is derived for the critical angular velocity, above which the centrifugal force is able to counter-balance osmosis pressure, so that the RO desalination process can proceed. Moreover, energy efficiency and flux rate analyses are conducted for the proposed desalination device, and relationships are developed between fresh water flux rate and energy efficiency and several design parameters, such as the angular velocity, pore size and length of the device. Overall, it is demonstrated that the proposed desalination device can significantly improve desalination efficiency with its important features of the anti-fouling mechanism and adaptable design to achieve maximum efficiency.

Hydraulic Fracture Modeling Based on Poromechanical Method

WANG Li^{*}, CAO yunxing^{**}

^{*}Henan Polytechnical University, ^{**}Henan Polytechnic University

ABSTRACT

Hydraulic fracturing(HF) is an important technique in enhancing the permeability of petroleum and gas reservoirs. The mechanisms of fracture propagation are well understood and involve the propagation of a fluid-driven fracture, inclusive of the effects of fluid transport and fluid lag at the tip. Where propagation is in fluid saturated porous media, the interaction of the fracturing fluid and the formation fluid are intimately coupled and may influence propagation. The complexity and nonlinearity of the principal physical interactions mean that numerical methods are the favored choice in representing response. And typically, domain methods such as finite element (FEM) and finite difference (FDM) methods are the preferred vehicles for solution as these enable nonlinear effects in the porous medium adjacent to the propagating fracture to be rigorously accommodated. The direct coupling is also referred to as strongly coupled or implicit, where the multiple physical field variables are taken as the unknown field variable vector and the final solution is recovered by solving the simultaneous equations. However, many engineering problems do not satisfy the conditions of strong coupling, especially for problems of damage-induced fracture - where it is difficult to ensure solution convergence. The load transfer method approaches a solution of the unknown field variables by successively solving the multi-physical field equations, in which one field variable is used as an input for the solution of another, and repeated through the sequence of couplings until a tolerance for an equilibrium solution is reached. We present a load transfer coupling finite element model (FEM) to represent hydraulic fracture propagation in porous media. The model represents: (1) poro-mechanical coupling of fluid and solid response for slightly compressible fluid; (2) damage localization, to calculate hydraulic fracture opening; (3) tensors of damage and permeability to denote the evolution of fracture-induced anisotropic properties; and (4) a loading scheme using full flow rate. The model is validated against a geometry of hydraulic fracture propagation in a three-layer reservoir. We demonstrate that the model returns the correct morphology of the evolving fracture zone and fluid pressure distribution and its variation with injection schedule. The simulation seamlessly follows four stages of fracture propagation (which are fracture nucleation, kinetic propagation, steady propagation and propagation termination) and represents the coupling between fracture tip and fluid front.

Moment Closure for Radiative Transfer Based on Beta Distribution

Weiming Li^{*}, Ruo Li^{**}

^{*}Beijing Computational Science Research Center and Hong Kong University of Science and Technology, ^{**}Peking University

ABSTRACT

We present an approximation of the M2 model for radiative transfer in three-dimensional space based on a combination of beta distributions. It is an extension of the second-order extended quadrature method of moments (EQMOM) to multiple dimensions. Like the M2 closure, the ansatz of the new model can capture both isotropic and strongly peaked solutions. Also, the new model has fluxes in closed-form, making it cost-effective for numerical simulations. The rotational invariance, realizability, and hyperbolicity of the model are studied. We will also present numerical experiments testing the effectiveness of the new model.

An New Algebraic Subgrid-scale Model for Flow within Vegetation Canopies

Weiyi Li^{*}, Marcelo Chamecki^{**}, Marc Parlange^{***}, Marco Giometto^{****}

^{*}Columbia University, ^{**}University of California-Los Angeles, ^{***}Monash University, ^{****}Columbia University

ABSTRACT

In flows over and within vegetation canopies, the presence of branches and leaves profoundly modifies the structure of turbulence, impacting transfer rates of energy, momentum and mass. In current Smagorinsky-type large-eddy simulations of such flow systems, the canopy-wake contributions to the subgrid-scale viscosity and diffusivity is not included. This flow feature is known to significantly affect scalar transfer rates deep within uniform dense canopies. In this contribution, an algebraic correction to the Smagorinsky model is proposed to encode the effect of the wake turbulence. The model is validated in neutrally-stratified pressure-driven atmospheric boundary-layer flow over and within uniform vegetation canopies. Vegetation is accounted for via a drag term in the momentum conservation equation which is a function of the canopy leaf-area density parameter. Predictions from the new proposed subgrid-scale model, classic Smagorinsky type models and one equation closure model are inter-compared against turbulent statistics from experimental measurements

Numerical study on Shale Mechanical Properties based on Mesoscale Stochastic Digital Models

Xiang Li^{*}, Dongyang Chu^{**}, Zhanli Liu^{***}, Shaoqing Cui^{****}

^{*}Tsinghua University, ^{**}Tsinghua University, ^{***}Tsinghua University, ^{****}Swansea University

ABSTRACT

With the advancement of hydraulic fracturing techniques, shale gas exploitation has been significantly developed over the past decades. In order to provide essential information for hydraulic fracturing engineering design, it is vital to understand the mechanical properties of shale. However, it has been observed that shale is a complex heterogeneous material that contains multiple types of mineral components. The mineral components percentage and distribution manner differ among different shale samples. For this reason, it is important to establish the precise mesoscale mechanical model of shale. However, to date, most mesoscale digital shale models are developed in order to study permeability characteristics of the fluid, and not much attention has been given to the relation between mineral components of shale and its overall mechanical properties. In this research, mesoscale mechanical models of shale are established based on scanning electron microscopy images. A statistical reconstruction algorithm is introduced to generate stochastic models. As is known, it is difficult to adopt traditional fracture mechanics to investigate crack evolution in complex materials such as shale. The phase field method, on the other hand, employs a diffusive phase field variable to represent the crack surface, avoiding the complexity of modeling and tracing discontinuous crack surfaces. Since no additional criterions are required in dealing with crack deflecting and branching, the method exhibits significant advantages in simulating complex crack evolution. Therefore, a phase field method is implemented to study the damage characteristics and complex crack evolution in the mesoscale shale models. The mechanical properties of shale obtained from simulation results are compared with lab experiments. A three-field-coupling phase field model is further developed based on Biot poroelasticity theory. Solid deformation, fluid seepage, and damage evolution are fully coupled in this numerical model. The model is utilized to study the damage characteristics of shale as fluid is present. [1] Bennett K C, Berla L A, Nix W D, Borja R I. Instrumented nanoindentation and 3D mechanistic modeling of a shale at multiple scales. *Acta Geotechnica* 2015; 10(1):1-14. [2] Walls J D, Diaz E, Cavanaugh T In Shale reservoir properties from digital rock physics, SPE/EAGE European Unconventional Resources Conference & Exhibition-From Potential to Production, 2012. [3] Miehe C, Mauthe S. Phase field modeling of fracture in multi-physics problems. Part III. Crack driving forces in hydro-poro-elasticity and hydraulic fracturing of fluid-saturated porous media. *Computer Methods in Applied Mechanics and Engineering* 2016; 304,619-655.

Absorbing Boundary Conditions for Atomistic and Electron Structure Calculations

Xiantao Li^{*}, Xiaojie Wu^{**}

^{*}Pennsylvania State University, ^{**}Pennsylvania State University

ABSTRACT

This talk will present a systematic approach to derive and approximate absorbing boundary conditions (ABC) for dynamics models involving atoms and electrons. The emphasis will be placed on the following issues: 1. Appropriate linearizations. ABCs can only be expressed explicitly for linear models. Ideally, one needs to retain the nonlinear interactions around lattice defects, and linearizes the interactions with the surrounding bath. This is a nontrivial task for multi-body interatomic interactions which extend beyond nearest neighbors. We present a partially-harmonic approximation that achieves this goal. Overall, this approximation is still consistent up to second order. 2. General expressions for the ABCs. We present a Dirichlet-to-Neumann map approach that yields an explicit representation of the boundary conditions, for domains of general geometry, including multiply connected domains. This is motivated by the observation that typical simulations involve multiple material defects. 3. Local approximations of the ABCs. We present a hierarchy of approximations that eliminate the nonlocality of the exact ABCs, which makes the implementation very efficient. 4. Stability. In practice, it is quite easy to end up with unstable boundary conditions. We will show how to determine the coefficients in the approximate ABCs to ensure nonlinear stability, using Lyapunov functionals.

Structural and Electromechanical Properties of III-nitride Nanoribbons Using First-principles Calculations

Xiaobao Li^{*}, Huanlin Zhou^{**}, Changwen Mi^{***}

^{*}Dr., ^{**}Dr., ^{***}Dr.

ABSTRACT

It has been found that III-nitride monolayers possess promising applications in high power electronic devices and optoelectronics. In this work, we have performed first-principles calculations on the mechanical and electro-mechanical properties of the pristine and chemically-passivated III-nitride nanoribbons. In particular, we investigate the edge stability in terms of the edge stress as well as the deformation for two typical types of edges, i. e. armchair and zigzag edges. It is found that the edges of all three pristine nitride nanoribbons are in compression and the deformation behavior due to the edge stresses along the edges are further confirmed by the molecular dynamics simulations. Moreover, since for such kind of compound nanoribbons, there are two distinct terminated zigzag edges which are also studied in detail in this work. The electromechanical properties are also presented for both pristine and chemically passivated nanoribbons. Our results highlight the importance of the edge properties in the application of 2D III-V monolayer crystalline.

Multiscale Modeling and Characterization of Coupled Damage-Healing-Plasticity for Granular Materials by Concurrent Computational Homogenization Method

Xikui Li^{*}, Zenghui Wang^{**}, Qinglin Duan^{***}

^{*}Dalian University of Technology, ^{**}Dalian University of Technology, ^{***}Dalian University of Technology

ABSTRACT

A multiscale modeling and characterization method for coupled damage-healing-plasticity occurring in granular material is proposed. The characterization is performed on the basis of multiscale modeling of granular material in the frame of concurrent second-order computational homogenization method, in which granular material is modelled as gradient-enhanced Cosserat continuum at the macroscale. The damage-healing-plasticity is characterized in terms of meso-structural evolution of discrete particle assembly within representative volume elements (RVEs) assigned to selected local material points in macroscopic continuum, with no need to specify macroscopic phenomenological constitutive models, failure criteria along with evolution laws, and associated macroscopic material parameters. The proposed modeling and characterization method for coupled damage-healing-plasticity in granular material is comprised of the following three constituents. The incremental non-linear constitutive relation for the discrete particle assembly of RVE is first established. Then the meso-mechanically informed incremental non-linear constitutive relation of macroscopic gradient-enhanced Cosserat continuum is derived. Finally meso-mechanically informed anisotropic damage and healing factors, anisotropic net damage factors combining both damage and healing effects, plastic strains are defined in the thermodynamic framework. Densities of thermodynamic net damage, plastic and total dissipative energies as scalar internal state variables are provided to compare the effects of damage, healing and plasticity on material failure and structural collapse. The numerical example of strain localization and softening problem is performed to demonstrate the performance and applicability of the proposed multiscale modeling and characterization method of coupled damage-healing-plasticity for granular materials.

Consistent Coupling of Nonlocal Diffusion

Xingjie Li^{*}, Qiang Du^{**}, Xiaochuan Tian^{***}, Jianfeng Lu^{****}

^{*}University of North Carolina at Charlotte, ^{**}Columbia University, ^{***}University of Texas at Austin, ^{****}Duke University

ABSTRACT

Nonlocal models have been developed and received lot of attention in recent years to model systems with important scientific and engineering applications. While it is established that the nonlocal formulations can often provide more accurate descriptions of the systems, the nonlocality also increases the computational cost compared to conventional models based on PDEs. The goal is to combine the accuracy of nonlocal models with the computational and modeling efficiency of local PDEs. In this talk, I will introduce a new self-adjoint, consistent, and stable coupling strategy for nonlocal diffusion models, inspired by the quasi-nonlocal atomistic-to-continuum method for crystalline solids. The proposed coupling model is coercive with respect to the energy norms induced by the nonlocal diffusion kernels as well as the L_2 norm, and it satisfies the maximum principle. A finite difference approximation is used to discretize the coupled system, which inherits the property from the continuous formulation. Furthermore, we design a numerical example which shows the discrepancy between the fully nonlocal and fully local diffusion, whereas the result of the coupled diffusion agrees with that of the fully nonlocal diffusion.

A Multiscale Framework to Quantify the Competing Failure Mechanisms in Metal Matrix Composites

Yan Li*

*California State University, Long Beach

ABSTRACT

The development of high performance MMCs requires careful microstructure design which can improve fracture toughness while maintaining high strength. Although a great deal of research has focused on the effect of microstructural properties on fracture toughness and strength of MMCs, the relations being established are mostly qualitative. In metal matrix composite materials, reinforcement cracking and interface debonding are two competing failure mechanisms observed during the crack-reinforcements interactions. For ductile MMCs, the fracture resistance depends on the sum of energy spent on both surface generation and the plastic deformation of the matrix material. Interface debonding usually leads to more tortuous crack paths and in turn enhances surface energy dissipation. However, it is not clear if this form of fracture can also lead to more pronounced plastic deformation in the metal matrix. While more significant plastic energy dissipation is beneficial to the toughening of a MMC, it has negative effect on its material strength. The objective of this study is to elucidate the two levels of competitions by considering the effect of microstructure and loading conditions: one being the competition between interface debonding and reinforcement cracking, and the other being the competition between crack formation and the deformation of matrix material. The systematic studies focus on Al/SiC metal matrix composites. The cohesive parameters employed in the computational models are calibrated through Digital Image Correlation analysis.

3D Frequency-Domain Elastic Wave Modeling Using the Spectral Element Method

Yang Li^{*}, Ludovic Métivier^{**}, Romain Brossier^{***}

^{*}ISTerre, Univ. Grenoble Alpes, ^{**}ISTerre, LJK, CNRS, Univ. Grenoble Alpes, ^{***}ISTerre, Univ. Grenoble Alpes

ABSTRACT

High resolution geophysical seismic imaging by full waveform inversion can be tackled either in time or frequency domains. While it has been proven that frequency-domain can be an approach of choice under the acoustic approximation of the wave equation, taking benefit of recent developments of the computational facilities and optimized finite differences schemes, most of the successful and large scales applications still rely on the time domain formulation. Application of 3D large scale frequency-domain wave modeling is currently limited by the high computational burden resulting from the resolution of huge sparse linear system, i.e., the discretized wave equation. Recent attempts are made either using the multifrontal direct solvers with hierarchically semi-separable (HSS) or block low-rank compression, or using massively parallel iterative solvers with preconditioners like shifted Laplacian or specifically designed method like CARP-CG. These attempts have all been conducted with the finite difference discretization of the wave equation, mainly for visco-acoustic media. However, application in complex area involving complex topographies and free surface boundary conditions lead to severe limitation for the finite difference method. Therefore, in this study, we rely on the finite spectral element method, which has proven to be successful and efficient for considering complex topographies and free surface boundary conditions in the time domain. As the free surface boundary condition is naturally satisfied when considering the weak form of the wave equation, no extra effort need to be made. Wave modeling could also benefit from the high-order accuracy of spectral element method. For instance, only 5 degree of freedom per minimum wavelength is known to be sufficient for P4 spectral element method. Moreover, higher order could also be used in the frequency-domain, as the restriction coming from the CFL condition of the time step does not exist anymore. The mesh could therefore be significantly coarsened at higher order, resulting in a decrease of the linear system size. We start from the most general case where all of the 21 elastic parameter are considered. An anisotropic perfectly matched layer technique and sponge absorbing boundary condition will be investigated to simulate the wave propagation in limited computational area. Several direct solvers and iterative solvers will be studied in solving the derived linear system.

Dimensionless Damage Factor Method: A New Computational Methodology for Evaluating the Residual Strength of Aluminum Plates

Yanping Li^{*}, Weiguo Guo^{**}, Kangbo Yuan^{***}, Jin Guo^{****}, Xueyao Hu^{*****}

^{*}School of Aeronautics, Northwestern Polytechnical University, ^{**}School of Aeronautics, Northwestern Polytechnical University, ^{***}School of Aeronautics, Northwestern Polytechnical University, ^{****}School of Aeronautics, Northwestern Polytechnical University, ^{*****}School of Aeronautics, Northwestern Polytechnical University

ABSTRACT

Abstract: By consulting the relevant literature on calculating the residual strength of cracked aluminium plates, it's found that there is a difference between the experimental results and the calculated values of the existing models. Thus, a more accurate method is expected to predict the residual strength for the aluminium plates. In this paper, we introduce the dimensionless damage factor which is used to quantify the initial damage degree of a plate, and then propose a new computational methodology for evaluating the residual strength of aluminium plates. The dimensionless damage factor can be used as a parameter to describe the material tolerance for damage; it is determined by the ratio between crack length and ultimate plastic zone diameter. (As the ultimate plastic zone diameter is related to apparent fracture toughness and the ultimate tensile strength, their accuracy will have great influence on the predictive value by this method.) For further calculating, establish the function of residual strength reduction coefficient through regression analysis of the data from reference and boundary conditions. The empirical curve of residual strength reduction coefficient decreases with the damage degree increasing. The plates ranged from intact to completely damaged would have the corresponding residual strength reduction coefficients according to their dimensionless damage factors. Illuminated by Jean Lemaitre's damage variable, combining the mechanical parameters and the damage degree, a new methodology presented in the framework of linear elastic fracture mechanics. Then, the comparisons with the other typical two models are carried out, respectively on middle crack tension specimens and multiple site damage specimens. The results show that the dimensionless damage factor method gives the most accurate predictive residual strength, and it is valid on the plates with no crack, a through-thickness crack and multiple site damage. Keywords: Residual strength, Dimensionless damage factor method, Fracture toughness, Residual strength reduction coefficient, Multiple site damage Reference [1] Uwe Zerbst, Markus Heinemann, Claudio Dalle Donne, Dirk Steglich. Fracture and damage mechanics modeling of thin-walled structures-An overview. Engineering Fracture Mechanics 2009; 76:5-43 [2] CHERRY C, MALL S Residual strength of unstiffened aluminum panels with multiple site damage [J] Engineering Fracture Mechanics 1997, 57(6):701-713 [3] Jean Lemaitre. A continuous damage mechanics model for ductile fracture. Journal of Engineering Materials & Technology, 1985, 107 (107) :83-89

Fluid-Rigid Body Interaction Simulation Based on ISPH Incorporated with Impulse-based Method

Yi Li*, Mitsuteru Asai**

*Kyushu University, **Kyushu University

ABSTRACT

Particle-based fluid-rigid body interaction simulation techniques have been proposed. In our research, ISPH method has been used for fluid simulation and rigid body representation, and the penalty method was utilized for the contact force calculation between rigid bodies. However, precision of the contact force calculated by penalty method is strongly affected by the time increment and the penalty parameter. Then, the impulse-based contact method, which is widely used for the multiple rigid body simulation in computer graphics area, is introduced to ISPH in the fluid-rigid body interaction simulation. The magnitude of contact force in the penalty method is calculated according to the overlap between rigid bodies which can reproduce the procedure of compression and restitution in contact problems. However, it needs a very small time increment. In the meantime, an appropriate time increment in the penalty method is always much smaller than the one in ISPH method. Choosing a smaller time increment will slower the efficiency of the entire simulation because the number of water particles is always hundred times larger than the number of rigid body particles. An impulse-based method is applied, where instead of contact force, impulse is calculated without any calibrations. The velocity change caused by the impulsive force during a very short instant can be easily decided by the coefficient of restitution. By comparing the penalty method with the impulse-based method, it is clear that the impulse-based method can reproduce reasonable and robust rigid body motion with a large time increment. In order to discuss the accuracy of ISPH incorporated with impulse-based method, a comparison between an experiment with several rigid bodies and a simulation result will be demonstrated.

Mechanical and Thermal Properties of 2D Polycrystalline Graphene Structures

Yinfeng Li*

*Shanghai Jiao Tong University

ABSTRACT

Research on two-dimensional (2D) atomic materials has been a leading topic in condensed matter physics and materials science for many years. A large number of 2D crystals are currently available and isolated atomic crystals can be further reassembled into planar and multilayer heterostructures for desirable electronic and optical properties. In this talk, we present our recent progresses on the mechanical and thermal properties of polycrystalline graphene structures using classical Molecular Dynamics method, density functional theory calculation and disclination theory. Grain boundaries (GBs) as typical defective graphene structure have significant influence on the overall properties of 2D graphene structures. The fracture strength of hydrogenated graphene with tilt GBs composed of pentagon–heptagon defects is systematically investigated and anomalous tunable mechanical and thermal characteristics are revealed for graphene with hydrogenation either on or near the GBs because of the interaction between polar stress fields of hydrogenated pentagon–heptagon defects. GB is also found a vulnerable spot for planar polycrystalline heterostructure of graphene and hexagonal boron nitride under uniaxial tension. The disclination theory is successfully adopted to predict the stress field caused by the lattice mismatch at GB. What's more, the thermal transfer efficiency of hybrid GB is also revealed to depend not only on the mismatch angle of grains but also the direction of thermal flux. Thermal transfer efficiency from graphene to h-BN is higher than that from h-BN to graphene. Detailed analyses for the phonon density of states of GB atoms are carried out for the mismatch angle-dependence of interfacial conductance. Extraordinary dependence of thermal conductivity of polycrystalline graphene on surface hydrogenation and inplane strains are revealed, and PG with different average grain sizes shows different sensitivities to tensile strain. Our results provide useful insights into the application of two dimensional polycrystalline heterostructures for next-generation electronic and flexible devices.

Understanding Receptor-Mediated Endocytosis of Elastic Nanoparticles Through Coarse Grained Molecular Dynamic Simulation

Ying Li^{*}, Zhiqiang Shen^{**}, Huilin Ye^{***}

^{*}University of Connecticut, ^{**}University of Connecticut, ^{***}University of Connecticut

ABSTRACT

For nanoparticle (NP)--based drug delivery platforms, the elasticity of NPs has significant influence on their blood circulation time and cellular uptake efficiency. However, due to the complexity of endocytosis process and inconsistency in the definition of elasticity for NPs in experiments, the understanding about the receptor-mediated endocytosis process of elastic NPs is still limited. In this work, we developed a coarse-grained molecular dynamics (CGMD) model for elastic NPs. The energy change of elastic NPs can be precisely controlled by the bond, area, volume and bending potentials of this CGMD model. To represent liposomes with different elasticities, we systematically varied the bending rigidity of elastic NPs in CGMD simulations. Additionally, we changed the radius of elastic NPs to explore the potential size effect. Through virtual nano-indentation tests, we found that the effective stiffness of elastic NPs was determined by their bending rigidity and size. Afterwards, we investigated the receptor-mediated endocytosis process of elastic NPs with different sizes and bending rigidities. We found that the membrane wrapping of soft NPs was faster than stiff ones at early stage, due to the NP deformation induced large contact area between the NP and membrane. However, because of the large energy penalties induced by the NP deformation, the membrane wrapping speed of soft NPs slows down during the late stage. Eventually, the soft NPs are less efficient than stiff ones during the membrane wrapping process. Through systematic CGMD simulations, we found a scaling law between the cellular uptake efficiency and phenomenal bending rigidity of elastic NPs, which agrees reasonably well with experimental observations. Furthermore, we observed that membrane wrapping efficiencies of soft and stiff NPs with large size were close to each other, due to the stronger ligand-receptor binding force and smaller difference in stiffness of elastic NPs. Our computational model provides an effective tool to investigate the receptor-mediated endocytosis of elastic NPs with well controlled mechanical properties. This study can also be applied to guide the design of NP-based drug carriers with high efficacy, by utilizing their elastic properties.

Dissipative Particle Dynamics Methods for Mesoscopic Problems

Zhen Li*, George Karniadakis**

*Division of Applied Mathematics, Brown University, **Division of Applied Mathematics, Brown University

ABSTRACT

The traditional dissipative particle dynamics (DPD) model was initially proposed as a minimal working version for mesoscopic simulation of fluids. Regardless of many successful applications of DPD to material science, rheology of complex fluids and computational biology, it only considers the momentum equation governing the evolution of flow field, which precludes the traditional DPD method from modeling many interesting problems involving coupling of flow field with other physical fields, e.g., thermal field, concentration field and electrostatic field. To this end, we have developed several extensions of the DPD method in recent years for tackling the challenges in diverse multiphysics applications involving multiple physical fields, which are beyond the capability of the traditional DPD model. In this talk, we will present three DPD extensions including energy-conserving DPD (eDPD)[1], transport DPD (tDPD)[2] and charged DPD (cDPD)[3]. In particular, the eDPD method solves the energy equations in the DPD framework and is able to consider the coupling of fluctuating hydrodynamics and heat flow, which has been applied to investigation of temperature-induced self-assemblies of thermoresponsive polymers; the tDPD method solves the advection-diffusion-reaction equations and momentum equations in the DPD framework and is able to model mesoscopic diffusive and reactive transport in many biological systems, such as the dynamic process of blood coagulation; the cDPD method solves the equation to consider the It describes the solvent explicitly in a coarse-graining sense as DPD particles, while the ion species are described semi-implicitly using a Lagrangian description of ionic concentration fields associated with each moving cDPD particle, which provides a natural coupling between fluctuating electrostatics and hydrodynamics. These DPD extensions consistently incorporate thermal fluctuations and are capable of describing certain mesoscopic features that deterministic macroscopic methods cannot model. References: [1] Z. Li, Y.-H. Tang, H. Lei, B. Caswell and G.E. Karniadakis. Energy-conserving dissipative particle dynamics with temperature-dependent properties. *Journal of Computational Physics*, 2014, 265: 113-127. [2] Z. Li, A. Yazdani, A. Tartakovsky and G. E. Karniadakis. Transport dissipative particle dynamics model for mesoscopic advection-diffusion-reaction problems. *The Journal of Chemical Physics*, 2015, 143: 014101. [3] M. Deng, Z. Li, O. Borodin and G.E. Karniadakis. cDPD: A new dissipative particle dynamics method for modeling electrokinetic phenomena at the mesoscale. *The Journal of Chemical Physics*, 2016, 145: 144109.

Failure Analysis of Composite Laminates with Big Cutouts

Zheng Li^{*}, Pengcheng Chu^{**}, Jianlin Chen^{***}

^{*}Peking University, ^{**}Peking University, ^{***}Peking University

ABSTRACT

According to the extensive application of composite laminates in practical engineering, there are many composite laminates with big cutouts to be designed and applied. However, the stress concentration and the complicated failure modes around the cutout are very difficult to be studied. The progressive failure process induced by the stress concentration needs to be thoroughly investigated because it is essential for predicting the performance of composite structures and designing reliable and safety structures. In the case of more complex structures and complicated stress states, most of the failure criteria are not suitable to predict the propagation of failure and the ultimate strength directly. Therefore, a simulation approach is developed in this paper by combining the finite element method and the progressive damage model to analyze the progressive failure process of composite structures. In this study, the composite laminates with different lay-up and different sizes of big cutouts are considered to figure out the failure behaviors of composite laminates. In the numerical analysis, the onset of failure is predicted by Hashin criteria and the evolution of failure is simulated using a continuum damage model, in which the failure evolution is based on the fracture energy dissipation and the stiffness reduction of matrix is controlled by a set of scalar damage variables. And two kinds of damage degradation model are used to simulation linear and exponential soften relation between stress and strain. The shear nonlinearity was also considered for composite laminates, and shear nonlinearity constitutive relations for the laminates were defined with the Ramberg-Osgood equation. The model has been implemented in the finite element software Abaqus using a UMAT subroutine. All simulation results are compared with experimental tests. The failure evolution in simulation results shows that the proposed model preforms well for predicting the failure behavior of composite laminates with big cutouts. We found that the exponential degeneration law performs better than linear degradation law for predicting the ultimate strength for the selected composite laminates. And the simulation using shear nonlinearity gives better results for predicting the nonlinear relation between displacement and force. Furthermore, the finite element based failure model of composite laminates can be used in composite structures with arbitrary configurations under complex stress states to make up for the shortage of analytical failure analysis.

Extension of Shape-free Low-order Unsymmetric Finite Elements for Geometric Nonlinear Analysis

Zhi Li*, Song Cen**, Cheng-Jin Wu***, Yan Shang****, Chen-Feng Li*****

*Tsinghua University, **Tsinghua University, ***Tsinghua University, ****Nanjing University of Aeronautics and Astronautics, *****Swansea University

ABSTRACT

ABSTRACT Two recent low-order element models, the unsymmetric 4-node, 8-DOF quadrilateral element US-ATFQ4 [1] and the unsymmetric 8-node, 24-DOF hexahedral element US-ATFH8 [2], which exhibit excellent precision and distortion-resistance for linear elastic problems, are successfully extended to geometric nonlinear analysis. Since the original linear elements contain the analytical solutions for pure bending and twisting, how to modify such formulae into incremental forms for nonlinear applications and design an appropriate updated algorithm become the key of the whole job. First, the analytical trial functions should be updated at each iterative step in the framework of updated Lagrangian (UL) formulation that takes the configuration at the beginning of an incremental step as the reference configuration during that step. Second, an appropriate stress update algorithm that the Cauchy stresses are updated by the Hughes-Winget method [3] is adopted to estimate current stress fields. The present geometric nonlinear formulations of element US-ATFQ4 and US-ATFH8 are compiled and implemented in commercial software SIMULA Abaqus via the user element subroutine (UEL). Numerical examples using traditional regular and new distorted mesh divisions are employed to assess the performance of the new formulations, including the slender elastic cantilever beam subjected to end shear force or end moment, the post-buckling nonlinear behavior of the Lee's frame buckling problem and so on. These numerical examples show that the new nonlinear formulations also possess amazing performance for geometric nonlinear analysis, no matter regular or distorted meshes are used. It again demonstrates the advantages of the unsymmetric finite element method with analytical trial functions, although these functions only come from linear elasticity.

ACKNOWLEDGEMENTS The authors would like to thank for the financial supports from the National Natural Science Foundation of China (11272181, 11702133), the Tsinghua University Initiative Scientific Research Program (2014z09099) and the Natural Science Foundation of Jiangsu Province (BK20170772). **REFERENCES** [1] Cen S, Zhou PL, Li CF, Wu CJ. An unsymmetric 4-node, 8-DOF plane membrane element perfectly breaking through MacNeal's theorem. *International Journal for Numerical Methods in Engineering* 2015;103(7):469-500. [2] Zhou PL, Cen S, Huang JB, Li CF, Zhang Q. An unsymmetric 8-node hexahedral element with high distortion tolerance. *International Journal for Numerical Methods in Engineering* 2017;109(8):1130-1158. [3] Hughes TJR, Winget J. Finite rotation effects in numerical integration of rate constitutive equations arising in large-deformation analysis. *International Journal for Numerical Methods in Engineering* 1980;15(12):1862-1867.

Numerical Simulation of Head Dynamic Process and Potential Mechanism of Brain Injury during Blast Loading

Zhijie Li^{*}, Xiaochuan You^{**}, Zhuo Zhuang^{***}, Zhanli Liu^{****}

^{*}Tsinghua University, ^{**}Tsinghua University, ^{***}Tsinghua University, ^{****}Tsinghua University

ABSTRACT

Blast-induced traumatic brain injury (b-TBI) is a signature injury of the current military conflicts. And the corresponding mechanism of brain injury and head protection strategy have been the hot research. In this paper, numerical simulation study is conducted to investigate the dynamic response of head and the brain injury mechanics during the blast loading. Based on the software of Hypermesh, a three-dimensional (3-D) finite element model of the human head with high fidelity is constructed, which is to be verified by simulating the impact experiment of cadaver head with ABAQUS software. The simulation and experiment results are in satisfactory agreement, showing the accuracy and validity of the numerical head model. At the same time, based on the coupled Eulerian-Lagrangian (CEL) theory the fluid-structure coupled model of explosive blast and head is developed, and then adopted to conduct the simulation of the head dynamic process under the blast loading with the peak pressure of 500 KPa. The potential mechanism for the brain injury is analyzed from four aspects, namely flow distribution, brain pressure, impulse and acceleration. These corresponding conclusions provide the theoretical basis for the treatment of brain injury and the development of protection equipments.

Multi-Scale Modeling of Damage and Failure in Heterogeneous Composite Subject to High Strain Rate Impact and Blast

Zhiye Li^{*}, Zhang Xiaofan^{**}, Somnath Ghosh^{***}

^{*}Department of Civil Engineering, Johns Hopkins University, ^{**}Department of Civil Engineering, Johns Hopkins University, ^{***}Department of Civil Engineering, Johns Hopkins University

ABSTRACT

This work aims to develop an efficient explicitly multiscale model incorporating material heterogeneities to study multi-physics damage and failure of fiber reinforced composites under extreme dynamic environments. First, micromechanical analysis of S-glass fiber reinforced epoxy composites is performed in conjunction with the phenomenon of stress wave propagation in the representative volume elements (RVEs) subjected to high strain rate deformation. The stress wave propagation process is correctly performed by novel space-time boundary conditions (STBCs) for extreme high strain rate impact or blast. Deformation and failure response of RVE model exhibiting fiber and matrix damage as well as interfacial cohesive crack. The rate-dependent nonlocal damage model is validated by DER 353 Epoxy donut impact experiment. In this calibration-validation study of high-speed impact experiment, adiabatic heating is observed in the specimens and implemented in the thermos-mechanical damage model. The dynamic rate-dependent cohesive models are validated by cruciform experiment and micro-droplet experiment. With model parameters calibrated from experiments, characterization of failure properties and microstructure criteria is studied in realistic microstructure models by using a Voronoi cell characteristic method, e.g. cracking nucleation, growth and spacing decrease. Then macroscopic constitutive damage law is obtained through the homogenized response of the micromechanical model. To connect the damage mechanism in micro-scale with macroscopic damage evolution, a fourth order tensor governing the initiation and evolution of the damage is introduced, and it is calibrated as a function of the macroscopic damage state in heterogeneous materials. After this fourth order tensor is calibrated for a specific composite system, the constitutive damage law can be obtained by this Parametrically Homogenized Continuum Damage model (PHCDM) model without performing a micro-mechanical analysis. Meanwhile, the microscopic damage and failure history at any specific location of a macroscopic model can be recovered from a top-down process of this hierarchical model. Finally, this PHCDM model is incorporated in ABAQUS user-subroutine to describe the material behavior for the composite system, making the analysis of macro-scale structures computationally feasible. This presentation shows theoretical math model and experimentally validated application examples of this multi-scale damage model. Results show that the bilateral combination of micromechanics model and PHCDM model for heterogeneous composite systems can be used for the material-by-design loop and meanwhile able to predict the damage behavior at both micro- and macro- scales.

A 9-Node Co-rotational Curved Quadrilateral Shell Element for Smooth, Folded and Multi-Shell Structures

Zhongxue Li^{*}, Tianzong Li^{**}, Loc Vu-Quoc^{***}, Bassam A. Izzuddin^{****}

^{*}Zhejiang University, ^{**}Zhejiang University, ^{***}University of Illinois at Urbana-Champaign, ^{****}Imperial College London

ABSTRACT

A 9-node co-rotational curved quadrilateral shell element for smooth, folded and multi-shell structures is presented. Its co-rotational framework is defined by the two bisectors of the diagonal vectors generated from the four corner nodes and their cross product. In this framework, the element rigid-body rotations are excluded in calculating the local nodal variables from the global nodal variables. The two smallest components of each nodal normal vector of mid-surface are defined as rotational variables for smooth shell, and three smaller components of two nodal orientation vectors at intersections of folded and multi-shell structures are employed as rotational variables, leading to the desired additive property for all nodal variables in a nonlinear incremental solution procedure. Different from other existing co-rotational finite-element formulations, the resulting element tangent stiffness matrix is symmetric owing to the commutativity of the local nodal variables in calculating the second derivative of strains energy with respect to these nodal variables. To alleviate membrane and shear locking phenomena, the membrane strains and the out-of-plane shear strains are replaced with assumed strains for obtaining the element tangent stiffness matrices and the internal force vector using the Mixed Interpolation of Tensorial Components (MITC) approach. Finally, a series of typical and challenging smooth, folded and multi-shell structures undergoing large displacements and large rotations are solved to demonstrate the reliability, computational accuracy of the proposed formulation.

A Cellular Automaton Finite Element Method to Predict Grain Evolution for Directed Laser Fabricated IN718 Alloy

Yanping Lian^{*}, Zhengtao Gan^{**}, Gregory Wagner^{***}, Wing Kam Liu^{****}

^{*}Northwestern University, ^{**}Northwestern University, ^{***}Northwestern University, ^{****}Northwestern University

ABSTRACT

The grain structure of build part by the additive manufacturing (AM) technology, e.g., Directed Laser Fabrication (DLF), has attracted widespread interest because it plays an essential role in deciding the mechanical property of the build part and can be tailored through the use of reasonable processing parameters in AM. Most of the existing simulation works have been focused on the 2D problem. However, for the accurate quantitative prediction of solidification and grain structure 3D modeling is necessary. In this work, a 3D cellular automaton finite element method is proposed to predict the microstructure of IN718 alloy in DLF, where the thermal field along with the molten pool flow is solved by the finite element method. An enriched grain heterogeneous nucleation scheme is implemented in the cellular automaton model to take into account of both epitaxial grain growth and grain growth from the re-nucleation, following the experimental observation. The simulated microstructure results are shown to be in good agreement with experimental complements, which demonstrates the ability of the proposed method. Moreover, additional simulations are conducted to disclose the influence of the laser scan speed and the laser power on the grain structure and texture, which sheds light on the relationship between the AM process parameters and the as-built grain structure.

An Improved Koiter-Newton Method for Tracing the Geometrically Nonlinear Response of Structures

Ke Liang^{*}, Qin Sun^{**}

^{*}School of Aeronautics, Northwestern Polytechnical University, ^{**}School of Aeronautics, Northwestern Polytechnical University

ABSTRACT

The original Koiter-Newton(KN) method has been approved to be a numerically accurate and computationally efficient algorithm to trace the nonlinear equilibrium path in a stepwise manner, especially in the presence of buckling. In each step, this method works by combining a nonlinear predictor and a few Newton iteration-based corrections. Although the predictor is obtained from the ROM, corrections to the exact equilibrium path relies exclusively on the full model. In this paper, we extend the method such that the reduced order model can be used also in the correction phase. In the proposed predictor-corrector strategy, the exact nonlinear model is used only to calculate force residuals. This significantly reduces the computational cost of the method. As a side product, the method has better error control and more robust step size adaptation strategies, benefiting from the corrections applied in each solution step of the ROM. We demonstrate the potential of the proposed method and the high quality of the analysis results with a set of benchmark and real engineering problems. Both reliability and accuracy of the approach are remarkable. The proposed method show great advantages in computational efficiency, compared to both the original method and the conventional Newton path-following method. Acknowledgement This work was supported by the National Natural Science Foundation of China (Grant No. 11602286, 51375386). References [1] Liang, M. Abdalla, Z. Gurdal, A Koiter-Newton approach for nonlinear structural analysis, International Journal for Numerical Methods in Engineering 96(12) (2013) 763–786. [2] Liang, M. Ruess, M. Abdalla, The Koiter-Newton approach using von Kármán kinematics for buckling analyses of imperfection sensitive structures, Computer Methods in Applied Mechanics and Engineering 279(1) (2014) 440–468.

Predicting Effective Properties of Peridynamic Composites Based on Boundary Element Method

Xue Liang^{*}, Linjuan Wang^{**}, Jianxiang Wang^{***}

^{*}Peking University, ^{**}Peking University, ^{***}Peking University

ABSTRACT

The effective properties of composite materials have been intensively and extensively studied within the framework of classical local theory. Today, some composite materials may have hierarchical microstructures such that non-locality may emerge and need to be considered in predicting their properties. Here, we predict the effective elastic properties of composites that are composed of a continuous matrix and discrete inhomogeneities, where both the matrix and inhomogeneities are peridynamic media. To this end, we calculate the displacement field in the composites with the peridynamic boundary element method (PD-BEM). Then, the effective properties are made to correspond to the elastic constants of classical orthotropic composites, and also to the micromodulus functions of the bond-based peridynamic theory. We also examine the effects of various parameters and the correlations with the classical theory.

Canonical Dual Theory of Discrete Variable Topology Optimization and its Numerical Algorithm

Yuan Liang*, Gengdong Cheng**

*Dalian University of Technology, **Dalian University of Technology

ABSTRACT

The mathematical essence of topology optimization is nonlinear integer programming. To overcome the huge computational burden for solution of large scale integer programming, the popular way is to relax the 0-1 variable constraint and transform the integer programming to continuous variable programming by introduction of the interpolation schemes for the material properties vs design variables as it allows to use gradient based mathematical programming methods. With this strategy, the well-know SIMP (Solid Isotropic Material with Penalty) method achieves great success and popularity. However, there is no doubt that tackling the discrete problems directly is very important. In order to overcome the combination complexity in integer programming, this paper resort to a kind of penalty-dual theory named by Canonical Dual Theory(CDT). This theory is developed by Dvaid Gao[1] in nonconvex mechanics and global optimization. In contrast to the classic Lagrange dual in integer programming, CDT can get any order smooth and differentiable dual function. The present paper develops a CDT formulation of structural topology optimization and applies an effective fixed point iterative algorithm to solve discrete variable topology optimization subproblems which is constructed by sensitivity information. Numerical experiments show that the fixed point iterative algorithm can get approximate solutions with good properties in excellent short time. And this paper shows that the dual gap of this method is negligible. Move limit strategies are supposed to be key role in discrete variables topology optimization. Therefore, this paper also combines some different move limits within the new method. The new method successfully solve the classic minimization of structural compliance, design dependent load problem, multiple constraints problem and heat conduction problems. The results of these problems exhibit that the new method can deal with much more design variables compared to the general branch and bound method. The new method can get black and white solutions and slightly lower compliance than SIMP. On the other hand, in comparison with the BESO method which is also widely used in structural topology optimization, the new method don't need any thresholds for sensitivities or heuristics. Finally, the new method also can solve multi-constraints optimization problems in a unified way and have more hopeful prospects in large-scale discrete topology optimization with local constraints. Reference [1]. Gao D., Gao, D.Y. and Ruan, N. (2010). Solutions to quadratic minimization problems with box and integer constraints. J. Glob. Optim. 47 463484

Time-extrapolation of Dynamic, Particulate Flows with Recurring Patterns

Thomas Lichtenegger*

*Department of Particulate Flow Modelling, Johannes Kepler University, Linz, Austria; Linz Institute of Technology,
Johannes Kepler University, Linz, Austria

ABSTRACT

Granular systems exhibit clearly separated, characteristic time-scales. Microscopically, particle collisions last only a few microseconds while the macroscopic motion takes place on the order of (fractions of) seconds. Slow processes like heat transfer or chemical conversion which might happen over minutes or hours eventually render conventional particle-based simulation approaches unfeasible. Inspired by the observation that many systems which evolve over very long durations either run into a steady state or repeat their motion in an approximate, completely irregular fashion, we have recently proposed a novel technique employing recurrence statistics [1] to describe the latter class [2]. This presentation deals with its application to heat transfer in a lab-scale, bubbling fluidized bed. Time-series analysis of the flow fields obtained from CFD-DEM shows that their dynamics starts to reproduce itself after a relatively short duration of a few seconds. After this period, hardly any new states appear, which allows us to extrapolate the bed's behavior using only the information contained within the initial phase. We demonstrate that these fields suffice to study a slow, almost passive process like heat transfer between gas and particles in (semi-)quantitative agreement with experiments over long durations at small fractions of the computational costs of CFD-DEM [3]. Finally, we discuss limitations and envisioned future developments of the method for extremely fast, accurate simulations of large-scale, industrial processes. [1] J.-P. Eckmann, S. O. Kamphorst and D. Ruelle. "Recurrence plots of dynamical systems." *Europhys. Lett.* 4.9 (1987): 973. [2] T. Lichtenegger and S. Pirker. "Recurrence CFD – A novel approach to simulate multiphase flows with strongly separated time scales." *Chem. Eng. Sci.* 153 (2016): 394-410. [3] T. Lichtenegger et al. "A recurrence CFD study of heat transfer in a fluidized bed." *Chem. Eng. Sci.* 172 (2017): 310-322.

Multi-scale Mechanics in Bioengineering

Kim Meow Liew*

*City University of Hong Kong

ABSTRACT

Due to the extremely small size of micro- and nano-structures, experimental studies are generally quite difficult. Although experimental studies can capture certain phenomena, it is impossible to understand their delicate properties well through experimental investigations alone. In addition to a large amount of experimental work, theoretical analysis and numerical modeling play an important role in capturing the delicate behavior of complex materials systems. Theoretical and numerical approaches can be generally classified into two categories: microscale method and macroscale method. Microscale method can capture the microscale mechanism of micro- and nano-structures and yield results that are in many cases explicit in nature. However, microscale methods consume a large amount of computational resources, and thus computation is limited to a very small size. This huge computational cost largely restricts their application. Macroscale continuum simulation can largely reduce the degrees of freedom in problems, and the theoretical and numerical analysis of large-size structures thus become possible. However, continuum simulations cannot reflect the microscale physical laws, and are not adequate. The limitations of microscale method as well as macroscale method have stimulated extensive research into multi-scale method that couples microscale method and continuum description. Multi-scale method can overcome the length and time scale limits in an efficient manner, and is emerging as a feasible and efficient approach for complex materials systems. This talk will present recent research work on multi-scale mechanics problems, focussing in bioengineering application.

Interface-conformal Hex Meshing Techniques and Mesh Sensitivities in Crystal Plasticity Finite Element Simulations

Hojun Lim^{*}, Steve Owen^{**}, Corbett Battaile^{***}, James Foulk^{****}

^{*}Sandia National Laboratories, ^{**}Sandia National Laboratories, ^{***}Sandia National Laboratories, ^{****}Sandia National Laboratories

ABSTRACT

Crystal plasticity-finite element (CP-FE) models explicitly capture individual grains within a polycrystalline domain and it is important to accurately reproduce their features using finite elements. In order to better incorporate microstructures in continuum scale models, we use a novel finite element (FE) meshing technique to generate three-dimensional polycrystalline aggregates from a phase field model of grain microstructures. The proposed meshing technique creates hexahedral FE meshes with conformal smooth interfaces between adjacent grains. Three-dimensional realizations of grain microstructures from the phase field model were used in crystal plasticity simulations of polycrystals. It is shown that the conformal meshes significantly reduce artificial stress localizations in voxelated meshes that exhibit the so-called wedding cake interfaces. In addition, mesh sensitivities in CP-FE simulations using polycrystalline and single crystal microstructures are investigated with various constitutive factors.

An Alternative Approach of Parallel Preconditioning for 2D Finite Element Problems

Leonardo Lima^{*}, Sérgio Bento^{**}, Riedson Baptista^{***}, Paulo Barbosa^{****}, Lucia Catabriga^{*****},
Isaac Santos^{*****}

^{*}UFES, ^{**}UFES, ^{***}UFES, ^{****}UFES, ^{*****}UFES, ^{*****}UFES

ABSTRACT

We propose an alternative approach of parallel preconditioning for finite element analysis. This technique consists in a proper domain decomposition with reordering that produces narrow-band linear systems from finite element discretization, allowing to consider traditional preconditioners as Incomplete LU Factorization (ILU) or even sophisticated parallel preconditioners as SPIKE [1] without significant efforts. We also employ preconditioners based in element-by-element [2] storage with minimal adjustments. Another feature of that approach is the facility to recalculate finite element matrices whether for nonlinear corrections or for time integration schemes. That means parallel finite element application is performed indeed in parallel, including matrices calculations, residue updating, and linear systems calculation. Moreover, our approach provides load balancing and improvement to MPI communications that can be evidenced through consistent studies using an analyzer tools as TAU (Tuning Analysis Utilities). We demonstrate the robustness and scalability of these parallel preconditioning strategies for a set of benchmark experiments, considering two-dimensional fluid flow problems modeled by transport, Euler, and Navier-Stokes equations to evaluate the ILU, SPIKE, and element-by-element preconditioners. We also provide a comparison between our implementation and standard implementations using the Portable, Extensible Toolkit for Scientific Computation (PETSc). [1] L. M. de Lima, B. A. Lugon, and L. Catabriga. An Alternative Approach of the SPIKE Preconditioner for Finite Element Analysis. High Performance Computing (HiPC), 2016 IEEE 23rd International Conference on. IEEE, 2016. [2] L. K. Muller, L. M. de Lima, and L. Catabriga. A Comparative Study of Local and Global Preconditioners for Finite Element Analysis. In: Ibero-Latin American Congress on Computational Methods in Engineering - CILAMCE, 2017, Florianópolis, Brazil. Proceeding of the XXXVIII Ibero-Latin American Congress on Computational Methods in Engineering. Florianópolis, Brazil: ABMEC, 2017. p. 1-19.

Evaluating High Order Discontinuous Galerkin Discretizations of the Boltzmann Collision Integral in $O(N^2)$ Operations Using the Discrete Fourier Transform

Jeffrey Limbacher*, Alexander Alekseenko**

*California State University Northridge, **California State University Northridge

ABSTRACT

Continuing progress in a number of important applications of slow flows and/or time dependent flows of non-continuum gases requires design of new efficient scalable deterministic methods for solution of the Boltzmann equation. The key difficulty in numerical solution of the Boltzmann equation is evaluation of the multifold collision integral that accounts for interactions of gas molecules. Development of numerical algorithms for efficient and accurate evaluation of the collision integral is at the forefront of recent advances in kinetic theory. We present a novel approach for evaluating the Boltzmann collision operator in $O(N^2)$ operations where N is the number of discrete velocity points. The method is formulated for high order nodal discontinuous Galerkin (DG) discretizations of the Boltzmann equation in the velocity variable. At the foundation of the new approach is the convolution form of the Galerkin projection of the collision integral. To achieve efficiency, the solution and the collision kernel are periodically extended and the direct convolution in R^3 is replaced by a circular convolution. The discrete Fourier transform is used to rewrite the collision operator as a weighted convolution in the frequency space. The approach is formulated, implemented, and tested for uniform meshes, however, generalizations to octree meshes are possible. Accuracy of the method was investigated by comparing it to the direct evaluation of convolution and an established DSMC solver. Different forms of the collision operator were investigated. It was found that the non-split form, in which the gain and loss terms are kept together, is the most suitable for fulfillment of the conservation laws. Also, the macro-micro decomposition, in which the solution is represented as a sum of the local Maxwellian and a correction term (not small) was found to help maintain the conservation laws. Evaluation of the collision operator using the discrete Fourier transform results in a two orders of magnitude increase in speed as compared to the direct evaluation.

A Versatile Hyperbolic Constitutive Framework for Soft Tissue Elasticity-Application to Skin Mechanics

Georges Limbert*

*University of Southampton

ABSTRACT

Over the last two decades, soft tissue mechanics has been a very active area of research resulting in a wide range of constitutive theories. Nowadays, scientists, engineers and clinicians jointly capitalise on these advances to make practical and quantitative predictions about biological systems and their interactions with engineered devices. This is typically done through the use of computational models developed in concert with dedicated physical experiments. Although constitutive models of soft tissues have reached a high level of sophistication in terms of their ability to capture anelastic and mechanobiological phenomena, as well as their integration of microstructural information, there is still the need for simple versatile phenomenological models featuring a minimum number of physically meaningful constitutive parameters. The objective of this research was to develop such a generic constitutive framework, capable of reproducing a wide range of responses (e.g. low stiffness at moderate strains, strain hardening and locking), whilst also capturing different types of material symmetry for various soft tissues. The constitutive model is based on hyperbolic functions and traditional isotropic and anisotropic tensor invariants but can also accommodate invariants arising from fully decoupled modes of deformation [1] which can capture matrix-to-fibre and fibre-to-fibre interactions. Properties of polyconvexity and stress-free configuration in the reference placement are enforced a priori. A parametric smooth version of the Heaviside step function was also devised to enable a no- or little-compression option when fibres are subjected to compression along their main axis. Constitutive parameters were identified from experimental data obtained from physical tests on skin and arteries samples. The constitutive model was shown to reproduce very well the experimental macroscopic multi-axial properties of these tissues. The constitutive formulation was implemented into a non-linear finite element code using a three-dimensional enhanced strain formulation [2]. Direct sensitivity routines were also developed to assess the influence of constitutive parameters, geometry and loads on the mechanical response of a multi-layer finite element model of the skin subjected to various loading scenarios. The conceptually simple formulation should prove useful for a wide range of biological soft tissues. References [1] Limbert, G. 2011. J Mech Behav Biomed Mater, 4 1637-1657. [2] Korelc, J. et al. 2010. Comput. Mech., 46 641-659.

Simulations of Turbulent Flow over Periodic Hills with Multiple-relaxation-time Lattice Boltzmann Method on Multi-GPU Cluster

Chao-An Lin^{*}, Chi-Wei Su^{**}, Xiao-Ying Huang^{***}

^{*}National Tsing Hua University, ^{**}National Tsing Hua University, ^{***}National Tsing Hua University

ABSTRACT

Laminar and turbulent channel flows over periodic hills were simulated with single-relaxation-time and multiple-relaxation-time lattice Boltzmann method. To speed up the simulation, the computation was conducted on multi-GPU cluster with two-dimensional decomposition by message passing interface(MPI). The laminar flow was simulated at Reynolds number $Re = 25, 50, 75, 100$ and compared with benchmark solutions for validation. For turbulent flow simulations, the Reynolds number was set to be $Re = 700$ and the results were in comparison with DNS results. Both results are compared and are in good agreement. In addition, the parallel performance was tested by the strong scaling test on the GPU cluster.

Consistent Strong Enforcement of Essential Boundary Conditions in Meshfree Methods

Kuan-Chung Lin*, Michael Hillman**

*The Pennsylvania State University, **The Pennsylvania State University

ABSTRACT

Essential boundary condition enforcement in meshfree methods requires special techniques since nodal coefficients of shape functions are not the actual field values. Strong enforcement of boundary conditions at nodes can be accomplished in several ways, such as the transformation method [1], use of a singular kernel [2], and so on. With these approaches, the standard weak form with kinematically admissible approximations is employed, yet between nodes, test functions are generally non-zero, while trial functions also may not satisfy the essential boundary conditions either. In this work, it is first shown that the consequence of employing the standard weak form with these methods is not negligible, as much lower rates of convergence are obtained than expected for meshfree basis functions higher than linear, and in some cases, for linear. Two weighted residual formulations are proposed that allow for test and trial functions which are not kinematically admissible, including a version which yields a symmetric stiffness matrix. When employed with the transformation method, optimal convergence rates are restored, and in general much lower error is obtained in the solution. [1] Chen, J. S., Pan, C., Wu, C. T., and Liu, W. K., 1996. Reproducing kernel particle methods for large deformation analysis of non-linear structures. *Computer Methods in Applied Mechanics and Engineering*, 139(1–4), pp.195–227. [2] Chen, J. S., and Wang, H. P., 2000. New boundary condition treatments in meshfree computation of contact problems. *Computer Methods in Applied Mechanics and Engineering*, 187(3–4), pp.441–468.

Computational Investigation of Hot-spots Generation by Micocracks in Carbon Nanotube Reinforced Composite under Dynamic Loading

Liqiang Lin^{*}, Justin Wilkerson^{**}, Xiaowei Zeng^{***}

^{*}University of Texas at San Antonio, ^{**}Texas A&M; University, ^{***}University of Texas at San Antonio

ABSTRACT

The sensitivity of polymer-bonded explosives (PBXs) can be tuned through adjusting binder material and volume fraction, crystal composition and morphology. To obtain a better understanding on correlation between grain-level failure and hot-spots generation in energetic composites as they undergo mechanical and thermal processes subsequent to impact, a recently developed interfacial zone finite element model (IZFEM) was used to study the dynamic response of polymer-bonded explosives. The IZFEM can capture the contributions of deformation and fracture of the binder phase as well as interfacial debonding and subsequent friction on hot-spots generation. In this study, a 2D computational model of carbon nanotube reinforced polycrystalline composite was developed. The proposed computational model has been applied to simulate hot-spots formation in polymer-bonded explosives with different carbon nanotube volume fraction under dynamic loading. Our simulation showed that the carbon nanotubes will provide additional dissipation pathways for impact energy as well as conduct heat away from energy localizations.

Performance of AMG-based Preconditioners for Fully-coupled Newton-Krylov Methods for Implicit Continuum Plasma Simulations

Paul Lin^{*}, Roger Pawlowski^{**}, John Shadid^{***}, Edward Phillips^{****}, Eric Cyr^{*****}

^{*}Sandia National Laboratories, ^{**}Sandia National Laboratories, ^{***}Sandia National Laboratories, ^{****}Sandia National Laboratories, ^{*****}Sandia National Laboratories

ABSTRACT

Abstract The computational simulation of continuum models of plasma physics systems can be extremely challenging. These difficulties arise from both the strong nonlinear coupling of fluid and electromagnetic phenomena, as well as the significant range of time-scales that the interactions of these physical mechanisms produce. From this point of view, fully-implicit formulations, coupled with effective robust nonlinear iterative solution methods, become attractive, as they have the potential to provide stable, higher-order time-integration of these complex multiphysics systems when long dynamical time-scales are of interest. For the solution of the discrete nonlinear system, the use of fully-coupled Newton-Krylov solution approaches can be advantageous because of their robustness. To enable scalable and efficient solution of the large-scale sparse linear systems generated by the fully-coupled Newton linearization, multilevel/multigrid preconditioners are developed. The multigrid preconditioners are based on two differing approaches. The first technique employs a graph-based aggregation method applied to the nonzero block structure of the Jacobian matrix [1-2]. The second approach utilizes approximate block decomposition methods and physics-based preconditioning approaches that reduce the coupled systems into a set of simplified systems to which multigrid methods are applied [3]. This talk considers the scaling and performance of these algebraic multigrid (AMG) based solution approaches for both MHD and multifluid plasma models with finite element type methods on unstructured meshes. The focus is on large-scale, transient plasma simulations. Studies are presented for scaling and performance on both CPU (IBM Blue Gene/Q and Intel Xeon) and Intel Xeon Phi Knights Landing platforms. References [1] J. Shadid, R. Pawlowski, E. Cyr, R. Tuminaro, P. Weber and L. Chacon, "Scalable Implicit Incompressible Resistive MHD with Stabilized FE and Fully-coupled Newton-Krylov-AMG," Computer Methods in Applied Mechanics and Engineering, 2016, Vol. 304, pp. 1-25 [2] P.T. Lin, J.N. Shadid, J.J. Hu, R.P. Pawlowski, E.C. Cyr, "Performance of Fully-coupled Algebraic Multigrid Preconditioners for Large-scale VMS Resistive MHD," Journal of Computational and Applied Mathematics, 2017, in press (<https://doi.org/10.1016/j.cam.2017.09.028>) [3] E. Phillips, J. N. Shadid, E. C. Cyr, and R. Pawlowski. Fast linear solvers for multifluid continuum plasma simulations. Extended abstract and presentation NECDC 2016.

The Research on Settlement and Damage Characteristics of Pavement Structure under Impulse Load by CDEM (Continuous-discontinuous Element Method)

Qindong Lin^{*}, Chun Feng^{**}, Shihai Li^{***}

^{*}Institute of Mechanics, Chinese Academy of Science, ^{**}Institute of Mechanics, Chinese Academy of Science,
^{***}Institute of Mechanics, Chinese Academy of Science

ABSTRACT

The load of Falling Hammer Crusher and Falling Weight Deflectometer can be reduced to instantaneous impulse load. Finite Element Method is usually used to study the impact of impulse load on pavement structure, but it can't accurately describe the damage characteristics. An explicit numerical calculation method CDEM that based on the coupling of FEM and DEM is used to simulate the gradual destruction of the material. With the method of CDEM, the influence of impulse load on the deformation and damage characteristics of pavement structure was discussed. Taking the linear elastic model coupled with Mohr-Coulomb criterion and the maximum tensile stress criterion as constitutive model of element of pavement structure and subgrade material in CDEM. The virtual interface and the real interface in CDEM are described by the brittle fracture Mohr-Coulomb model and the maximum tensile stress criterion. Impulse load is reduced to a trapezoidal load with a certain amplitude and pulse width. Through the comparison with the test results of falling weight deflectometer, the computational accuracy of the CDEM method for calculating the small impact load elasticity problem is proved. By comparing with commercial software Abaqus, the computational accuracy of CDEM simulating plastic rupture problem is proved. The calculation results show that: 1. CDEM can explicitly expresses the initiation and expansion process of cracks. 2. The crack shape of the pavement structure is related to the area, amplitude of the impulse load and pavement structure. Vertical cracks occur in the layers and horizontal cracks occur between the layers. 3. When the cracks occur in the layers, the settlement will increase, this is due to cracks that reduce the structural integrity of the pavement and its ability to dissipate the load. What's more, the increasing proportion of cement concrete pavement is greater than that of asphalt concrete pavement. 4. The settlement of the pavement is positively correlated with the amplitude, time and area of the impulse load. 5. When the layer can be broken, the curve of settlement in one direction will have obvious inflection point. These conclusions have important guiding significance for the research on the crushing of concrete pavement and the settlement of pavement structure under impulse load.

A Numerical Method for Simulation of Flow Past a Square Cylinder with Porous Wall

San Yih Lin^{*}, Ya Hsien Chin^{**}, Jeu Jiun Hu^{***}

^{*}National Cheng Kung University, ^{**}Overseas Chinese University, ^{***}Shu-Te University

ABSTRACT

The IB-Penalization pressure correction method is developed to simulate a flow past a square cylinder with porous wall. The numerical method can deal with fluid-porous-solid system by using a direct-forcing immersed boundary (IB) method to handle flow past a solid body and a penalization method to handle flow in porous wall. About the fluid field, the method uses a pressure correction method to solve the solutions of incompressible Navier-Stoke equations. The physical model creates intermediate porous media between the solid body and the fluid to modify the boundary layer behavior. First, we two numerical methods, direct-forcing IB and penalization, are used to simulate the flow past a solid square cylinder. Two numerical results will be compared each other. Then the IB-Penalization pressure correction method is developed to simulate the flow past a square cylinder with porous wall. A parametric study is performed to investigate the effect of the porosity and thickness on the porous layer.

A Nonlinear Gradient-based Reliability Assessment Method (GRAM) for Reliability-Based Design Optimization (RBDO)

Shu-Ping Lin*, Po Ting Lin**

*National Taiwan University of Science and Technology, **National Taiwan University of Science and Technology,
Taiwan

ABSTRACT

This paper presents a nonlinear Reliability-Based Design Optimization (RBDO) method, which estimates a new reliability assessment based on gradient evaluated at the Most Probable Failure Point (MPFP) and formulates a nonlinear probabilistic constraint at the Allowable Reliability Point (ARP). At first, the MPFP for each performance constraint is determined in terms of minimizing the distance between the design point and the constraint in the original design space (not in the standard normal space). The advantage of finding the MPFP in the original design space is that the new method does not require transformation to the standard normal space, which sometimes is difficult to determine. Next, an approximated constraint function is formulated based on expansion at the MPFP. The approximated constraint function is then shifted along the negative gradient direction, that is evaluated at the MPFP, toward the feasible space by the distance of a Gradient-based Reliability Assessment (GRA), which equals the distance between the design point and the Most Probable Target Point (MPTP). MPTP is located at the position where the failure probability of the shifted constraint function equals to the allowable probability. The second advantage of the proposed method is that it provides a better approximation of the nonlinear probabilistic constraint than traditional first-order reliability methods. Several numerical examples will be examined to show the numerical performances of the proposed Gradient-based Reliability Assessment Method (GRAM).

A Balanced-forced Level Set Method on Unstructured Meshes for Thermal Multiphase Flows

Stephen Lin^{*}, Jinhui Yan^{**}, Gregory Wagner^{***}

^{*}Northwestern University, ^{**}Northwestern University, ^{***}Northwestern University

ABSTRACT

The interaction between multiple phases (such as solid, liquid and gas) drive many industrial processes, such as additive manufacturing. Physical driving mechanisms driving the free-surface evolution involve surface tension and Marangoni forces at the gas and fluid interface; therefore an accurate computation of these forces is necessary to sufficiently resolve the free-surface evolution. In this work, we present a balanced-force level set formulation on unstructured meshes using a control volume finite element method (CVFEM) for large-scale parallel simulations of thermal multiphase flows that capture the evolution of the liquid, gas and solid phases. We demonstrate that our balanced-force algorithm is able to exactly balance the resulting pressure gradient and surface tension forces for a specified curvature; validation examples show that this balanced-force is necessary to achieve convergence for flows driven by surface force applications. These interfacial forces become significant in engineering applications that exhibit highly localized phenomena including melting and subsequent flow of molten metals in additive manufacturing processes.

Variational Inequalities for Saddle Point Functionals in Continuum Mechanics and Their Relevance to Error Estimates

Christian Linder^{*}, Andreas Krischok^{**}

^{*}Stanford University, ^{**}Stanford University

ABSTRACT

We present a variational approach towards identifying conditions for stability and uniqueness of Galerkin methods based on saddle point problems in continuum mechanics and continuum thermodynamics. The framework aims to generalize the inf-sup theory in the context of general problems in an arbitrary number of fields for both linear and nonlinear settings. In utilizing a linearized second derivative test for admissible variations, the proposed framework is purely based on uniqueness properties of a mixed Lagrangian around the solution, thus combining requirements that descend from variational calculus with error estimates for finite-dimensional Galerkin methods. In particular, due to its universal form and its straightforward connection to generalized numerical tests, the proposed framework is trusted to provide a helpful tool for the development of mixed methods that arise in many novel engineering problems due to the coupling of multiple physical phenomena.

Defect Estimation within the Limitations of Computational Welding Mechanics

Lars-Erik Lindgren Lindgren*, Joar Draxler**, Andreas Lundbäck***, Jonas Edberg****

*Luleå University of Technology, Sweden, **Luleå University of Technology, Sweden, ***Luleå University of Technology, Sweden, ****Luleå University of Technology, Sweden

ABSTRACT

The approaches developed from the 1970ies and onward regarding modelling of welding are also applicable to additive manufacturing when limiting the focus on the macroscopic scale excluding details of the process zone as well as addition of filler material or the existence of powders. The aim of Computational Welding Mechanics (CWM) is to model the overall mechanical performance of the welded component or structure. CWM models can be combined with models for microstructure evolution coupled with thermo-mechanical. The centrepiece in welding simulations is the heat generation process. Its description belongs to the domain of thermo-mechanics in the case of explosive welding, friction welding and friction stir welding. Resistance welding need the inclusion of the electrical field also. However, the process becomes much more complex for fusion welding processes. Weld process modelling (WPM) focuses on modelling the physics of the heat generation. The limiting region between these models is the liquid-solid boundary. They have different time and spatial scales and are not easily solved simultaneously. Therefore most CWM models start with a calibrated heat source model and exclude fluid flow. There are various approaches that have been used over the last decades to estimate the risk for cracking. The talk reviews these approaches and also describes developments for enable better descriptions in the near weld region for crack initiation estimates.

Modelling of Bulk Metallic Glass Formation in Powder Bed Fusion

Johan Lindwall*, Victor Pacheco**

*Luleå University of Technology, **Uppsala University

ABSTRACT

Additive manufacturing by the powder bed fusion process can provide cooling rates high enough to avoid crystallization, i.e. create bulk metallic glasses. The small melting pool connected to a relatively large volume of cooling material gives cooling rates many orders of magnitude larger than the critical cooling rate for the studied glass forming alloy AMZ4. However, subsequent reheating of built material may cause devitrification, i.e. crystallization of the amorphous phase. The present work aims to simulate the thermal cycles of the powder bed fusion process in order to evaluate and mitigate the risk of devitrification. This is done by combining finite elements simulations with a phase transformation model for the amorphous and crystal phases. The response of AMZ4, in the present case limited to heating of amorphous material from room temperature, was evaluated using DSC measurements with varying low heating rates. This limited set of information is used to construction the lower part of the crystallization diagram based on a JMAK-model. Previous work has developed simulation techniques for efficient simulations of glass formation in powder bed fusion. Temperatures can be computed with sufficient accuracy and considerable reduced computational time compared to a fully detailed model. The simplifications were based on temporal reduction by consolidating the heat source to strings or entire layers by assuming infinite scanning speed in one or two directions. The JMAK- model will now be used combined with these techniques. Further understanding of when and where crystals may be formed can be acquired by the presented work.

IMPROVEMENT AND APPLICATION OF THE LARGE SCALE 2D 3D HYBRID TSUNAMI NUMERICAL MODEL

**GUOMING LING* JUNICHI MATSUMOTO† ETHAN J. KUBATKO‡
AND KAZUO KASHIYAMA§**

*Research and Development Initiative, Chuo University

Kasuga 1-13-27, Bunkyo-ku

Tokyo, Japan

Email address: lingguoming@civil.chuo-u.ac.jp

†National Institute of Advanced Industrial Science and Technology (AIST)

Namiki 1-2-1, Tsukuba

Ibaraki, Japan

Email address: matsumoto-junichi@aist.go.jp

‡Department of Civil, Environment and Geodetic Engineering, Ohio State University

417D Hitchcock Hall, 2070 Neil Avenue

Columbus, OH 43210, U.S.A

Email address: kubatko.3@osu.edu

§Department of Civil and Environmental Engineering, Chuo University

Kasuga 1-13-27, Bunkyo-ku

Tokyo, Japan

Email address: kaz@civil.chuo-u.ac.jp

Key words: 2D-3D Hybrid Model, Tsunami Simulation, Overlapping Method, Arbitrary Grid.

Abstract. This paper presents some improvements and applications of a large-scale 2D-3D hybrid tsunami numerical model which we have developed. The overlapping method based on arbitrary grid is applied as a two-way coupling method to connect a 2D model and a 3D model. For the 2D model, the shallow water equations are applied as the governing equations. For the 3D model, the phase-field model (PFM) governed by the Allen-Cahn equation is applied for the free surface flow. The numerical accuracy of the present method is verified on several numerical

examples.

1 INTRODUCTION

Since the tsunami disaster occurred by the 2011 Great East Japan Earthquake, awareness has been improved that not only the prediction of the inundation area of the tsunami but also the damage prediction of structure is extremely important. In practice, the two dimensional (2D) shallow water equations have been widely used for simulating the inundation damage of tsunami. However, in order to compute the fluid force acting on the structure precisely, the three dimensional (3D) free surface flow simulation is needed. But it is still not realistic for simulating tsunami waves from the source area to urban area all by 3D considering the huge computation cost. Therefore, a hybrid model can be an efficient and a reasonable tool by simulating the wave propagation in ocean by a 2D model and in the target area with structures by a 3D model.

In recent years, several 2D-3D hybrid models have been proposed. Some of the 2D-3D hybrid models are based on structured Cartesian grids, e.g. Masamura *et al.* ^[1], Tomita *et al.* ^[2], Fukui *et al.* ^[3], Pringle *et al.* ^[4], Arikawa *et al.* ^[5]. These models have shown the 2D-3D hybrid models can significantly reduce the calculation load comparing to the fully 3D model, and they also can reproduce the characteristics of 3D flows which cannot be reproduced by the 2D model. However, since these methods use structured grids, meshing the structure or the terrain with a complex geometry exactly is difficult in numerical simulation. To this reason, Takase *et al.* ^[6] proposed a 2D-3D hybrid model based on the stabilized finite element method which can use arbitrary grid. In this model, the multiple point constraint (MPC) method is employed to connect the 2D and 3D models, for which a shared border boundary has to be set between the 2D and 3D domains. The applications were limited to some simple numerical examples. Recently, Mitsume *et al.* ^[7], Asai *et al.* ^[8] proposed the 2D-3D hybrid models using particle method, but they are one-way coupling models.

The objective of our study is to develop a 2D-3D hybrid model for large-scale tsunami simulation, which can treat with complicate geometry in a two-way coupling. In this paper, we aim to improve the accuracy and the robustness of the 2D and 3D models we used in the proposed 2D-3D hybrid model ^[9]. The shallow water equations are applied as the governing equations for the 2D model, the Navier-Stokes equations and the Allen-Cahn equation are applied as the governing equations for the 3D model. The stabilized finite element method ^[6, 10] is applied for the spatial discretization. The Crank-Nicolson method is applied for the temporal discretization. The Message Passing Interface (MPI) is employed as the parallel computing method. Several numerical examples are simulated to show the validity and efficiency of the present method.

2 GOVERNING EQUATIONS

The governing equations for the 2D and 3D models are described in this section.

2.1 Shallow water equations for the 2D model

The wave propagation from source area to offshore area is governed by the non-linear shallow water equations,

$$\frac{\partial(U_i H)}{\partial t} + \frac{\partial(U_j U_i H)}{\partial x_j} + \nu_e \frac{\partial^2(U_i H)}{\partial x_j^2} + \frac{g n^2 U_i \sqrt{U_j U_j}}{H^{\frac{1}{3}}} + g H \frac{\partial(H + z)}{\partial x_i} = 0 \quad (1)$$

$$\frac{\partial H}{\partial t} + \frac{\partial(U_i H)}{\partial x_i} = 0 \quad (2)$$

where U_i is the average velocity in x_i direction, H is the total water depth, g is the gravitational acceleration, ν_e is the eddy viscosity coefficient, n is the Manning's roughness coefficient and z is the height of bottom.

2.2 Navier Stokes equations and Allen Cahn equation for the 3D model

The 3D free surface flow model is governed by the Navier-Stokes equations, continuity equations and the Allen-Cahn equation ^[11],

$$\rho \left(\frac{\partial u_i}{\partial t} + u_j \frac{\partial u_i}{\partial x_j} - f_i \right) + \frac{\partial p}{\partial x_i} - \mu \frac{\partial}{\partial x_j} \left(\frac{\partial u_i}{\partial x_j} + \frac{\partial u_j}{\partial x_i} \right) = 0 \quad (3)$$

$$\frac{\partial u_i}{\partial x_i} = 0 \quad (4)$$

$$\frac{\partial \phi}{\partial t} + u_j \frac{\partial \phi}{\partial x_j} = -M_a \left[\xi(\phi) - \kappa_\phi \left(\frac{\partial^2 \phi}{\partial x_j^2} + \kappa \left| \frac{\partial \phi}{\partial x_k} \right| \right) \right] \quad (5)$$

where ρ, u_i, f, p, μ are the density, velocity, body force, pressure, viscosity coefficient, respectively. ϕ is the phase function, $\phi = 1$ denotes fluid, $\phi = 0$ denotes gas, $\phi = 0.5$ denotes free surface. M_a , $\xi(\phi)$, κ_ϕ , κ are defined as,

$$M_a = \frac{2b^2}{\delta^2} M\gamma, \quad b = 2\tanh^{-1}(1 - 2\lambda), \quad \delta = a_\delta h_\delta$$

$$\xi(\phi) = \frac{\partial f(\phi)}{\partial \phi}, \quad f(\phi) = \phi^2(1 - \phi)^2,$$

$$\kappa_\phi = \frac{\delta^2}{2b^2},$$

$$\kappa = \nabla \cdot \mathbf{n}, \quad \mathbf{n} = \frac{\nabla \phi}{|\nabla \phi|}$$

where $M, \gamma, \delta, h_\delta, \kappa, \mathbf{n}$ are the interface mobility, interface energy, continuously changing gas-liquid interface width, representative length of element, interface curvature, interface normal vector.

2.3 Discretization methods

For the spatial discretization, the stabilized finite element method based on the SUPG method^[10] is applied to Eqs. (1), (2), (5), the stabilized finite element method based on the SUPG/PSPG method^[6] is applied to Eqs. (3), (4). For the temporal discretization, the Crank-Nicolson method with second order accuracy is applied. And to solve the simulation linear equations, the element-by-element Bi-CGSTAB (Bi-Conjugate Gradient STABILized) method is applied.

4 2D 3D OVERLAPPING METHOD

In this study, the 2D-3D overlapping method shown in the **Figure 1** based on arbitrary grid is developed. In this method, the computational domain is separated into a 2D domain and a 3D domain. An overlap domain for the 2D and 3D domains is set. The domains and the grids of 2D and 3D can be arbitrary. Then the inner boundary of the 2D domain is defined as a 2D connection boundary, while the outer boundary of the 3D domain is defined as a 3D connection boundary. At the 2D connection boundary and the 3D connection boundary, the nodes of 2D and 3D can be located at different places. For the computation, the flow velocities and the water depth computed from the 3D domain are used as the boundary conditions of the 2D connection boundary. As the same, the flow velocities and the water depth computed from 2D domain are used as the boundary conditions of the 3D connection boundary. For the computation of real terrain tsunami simulation, the 3D domain can be chosen anywhere we want to compute precisely. Because of the place for the nodes of 2D and 3D is different, the boundary condition of 2D/3D connection boundary should be computed by making interpolation. The flowchart of

the 2D-3D overlapping method is shown in the **Figure 2**.

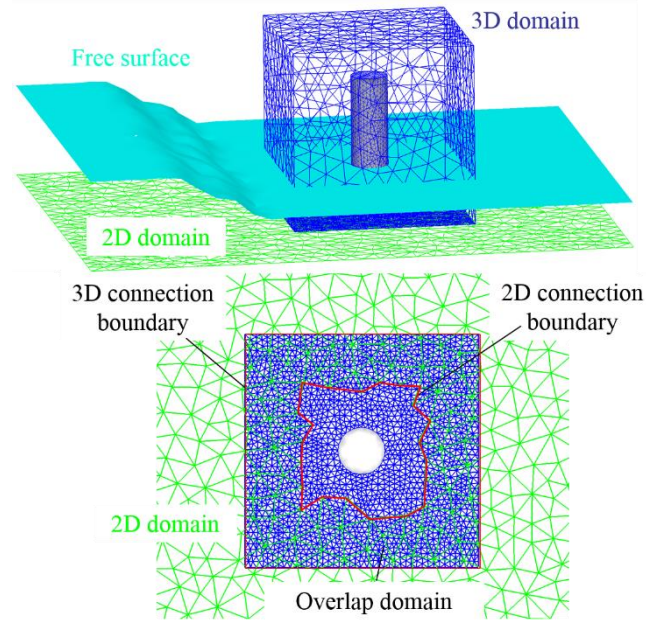


Figure 1 Overlapping method

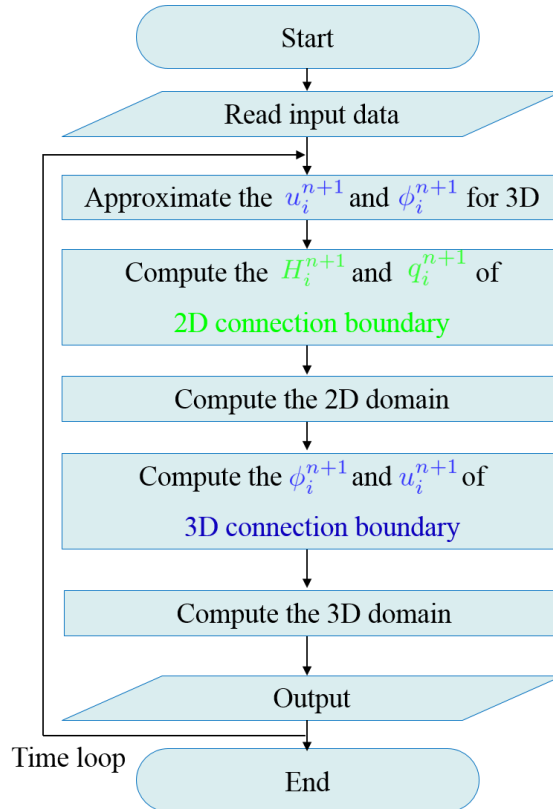


Figure 2 Flowchart for 2D 3D overlapping method

NUMERICAL EXPERIMENTS

3.1 Runup of solitary wave problem

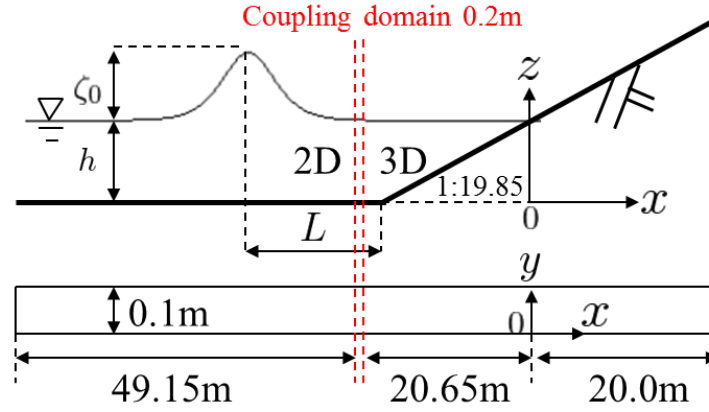


Figure 3 Computational model

The runup of a solitary wave problem shown in **Figure 3** is simulated to investigate the applicability of the 2D-3D hybrid model. The computational results are compared to the experimental results ^[12], the results of 2D model and 3D model. For the initial conditions, the initial wave height is set by the following equation,

$$\zeta(x, t = 0) = \frac{\zeta_0}{h} \operatorname{sech}^2 \left(\sqrt{\frac{3\zeta_0}{4h}} (x - x_0) \right) \quad (4)$$

the ratio of the wave height ζ_0 and the static depth h is set to be 0.3. x_0 is the location of wave crest. The initial flow velocity is set by the following equation,

$$u(x, t = 0) = \zeta(x, t = 0) \sqrt{\frac{g}{h}} \quad (5)$$

The wave crest is located at the half solitary wave length from the front end of the slope.

$$L = \sqrt{\frac{4h}{3\zeta_0}} \operatorname{arccosh} \left(\sqrt{\frac{1}{0.05}} \right) \quad (6)$$

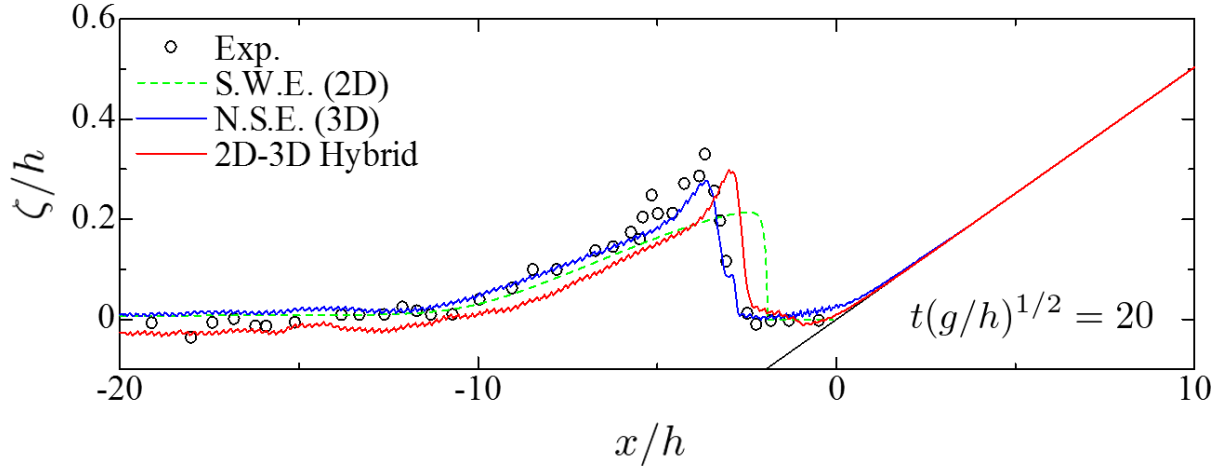


Figure 4 Surface elevation at $t'=20$

For the computational condition, the mesh size is 0.05m and the time increment is 0.001s.

The comparison of the surface profiles at $t' = t\sqrt{g/h} = 20$ is shown in the **Figure 4**. From this figure, we can see the result of the 3D model is in the best agreement with the experimental result. The result of the 2D-3D hybrid model show better agreement with the experimental results than the results of the 2D model.

.2 Tsunami simulation on real terrain

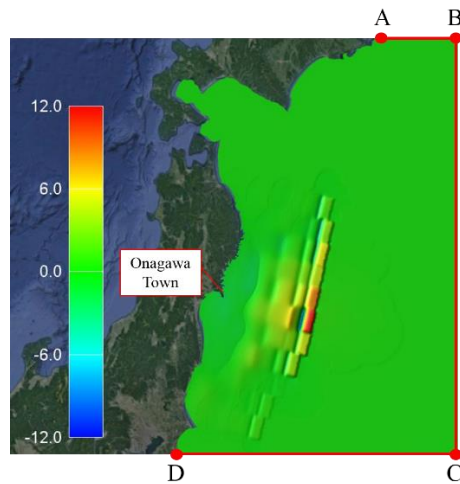


Figure Computational model initial condition

In order to test the applicability of the 2D-3D hybrid tsunami numerical model to the real terrain, the computational model shown in **Figure** is simulated. For this example, the area around the Onagawa town is simulated by 3D while the other area by 2D. For the initial

condition, the fault model of Ver. 8.0 by Satake *et al.* ^[13] is applied. For the boundary conditions, the shoreline is non-slip condition and the ABCD boundary is set open boundary condition. The mesh information of the 2D and 3D domains is shown in **Table 1**. The time increment is 0.1s.

Figure shows the computational result at 2000.0s, in the figure, the green denotes the results of 2D domain and the blue denotes the 3D domain. We can see the buildings are flooded by the tsunami waves. The applicability of the present method to the real terrain has been confirmed by this numerical example.

Table 1 Mesh information

	2D	3D
Number of nodes	557,252	23,232,416
Number of elements	1,103,938	134,768,640

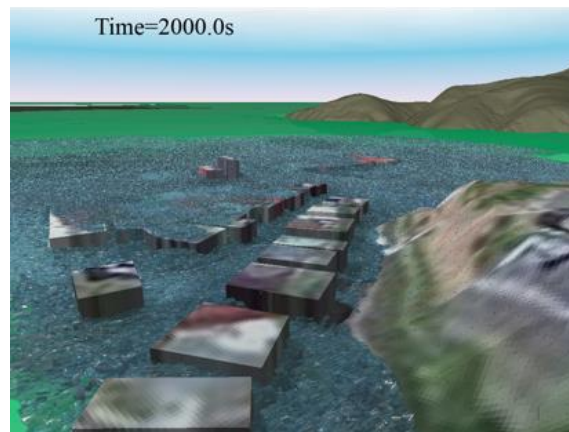


Figure Computational result at 2000.0s

CONCLUSIONS

In this paper, a 2D-3D hybrid tsunami numerical model using the overlapping method based on arbitrary grid was developed. By the numerical examples, the following conclusions can be drawn.

- From the runup of solitary wave problem, the numerical result of the present method is in good agreement with the experimental results.
- From the application to the tsunami caused by the Great East Japan Earthquake, the applicability of the present method has been confirmed.

For the future work, we are planning to apply the present 2D-3D hybrid model to solve the

fluid structural interaction (FSI) problems.

REFERENCES

- [1] Masamura, K., Fujima, K., Goto, C., Iida, K. and Shigemura, T. Numerical analysis of tsunami by using 2d/3d hybrid model. *Journal of JSCE*, (2001), pp. 49-61. (in Japanese)
- [2] Tomita, T. and Kakinuma, T. Storm surge and tsunami simulation in oceans and coastal areas (STOC). Report of the Port and Airport Research Institute, (2005), pp. 83-98.
- [3] Fukui, T., Koshimura, S. and Matsuyama, M. 2D-3D Hybrid Simulation of Tsunami Inundation Flow by Lattice Boltzmann Method. *Journal of Japan Society of Civil Engineers, Ser. B2 (Coastal Engineering)*, Vol. 66(1), (2010), pp. 61-65. (in Japanese)
- [4] Pringle, W., Yoneyama, N. and Mori, N. Two-way coupled long wave - RANS model: Solitary wave transformation and breaking on a plane beach. *Coastal Engineering*, Vol. 114, (2016), pp. 99-118.
- [5] Arikawa, T. and Tomita, T. Development of High Resolution Tsunami Runup Calculation Method Based on a Multi Scale Simulation. Report of the Port and Airport Research Institute, Vol. 53(2), (2014), pp. 3-18. (in Japanese)
- [6] Takase, S., Moriguchi, S., Terada, K., Kato, J., Kyoya, T., Kashiya, K. and Kotani, T. 2D-3D hybrid stabilized finite element method for tsunami runup simulations. *Comput. Mech.*, Vol. 58, (2016), pp. 411-422.
- [7] Mitsume, N., Donahue, A.S., Westerink, J.J. and Yoshimura, S. One-way coupling model based on Boussinesq-type and Navier-Stokes equations for multi-scale tsunami analysis. *Proceedings of the conference on computational engineering and science, CD-ROM, C-5-3*, (2016). (in Japanese)
- [8] Asai, M., Miyagawa, Y., Idris, N., Muhari, A. and Imamura, F. Coupled tsunami simulations based on a 2D shallow-water equation-based finite difference method and 3D incompressible smoothed particle hydrodynamics. *Journal of Earthquake and Tsunami*, Vol. 10(5), (2016). 1640019.
- [9] Ling, G., Matsumoto, J. and Kashiya, K. Large scale tsunami simulation by 2D-3D hybrid method based on arbitrary domain. *COMPSAFE, Chengdu, China*, (2017).
- [10] Takase, S., kashiya, K., Tanaka, S. and Tezduyar, T.E. Space-time SUPG formulation of the shallow-water equation, *International Journal for Numerical Methods in Fluids*, Vol. 64, (2010), pp. 1379-1394.
- [11] Beaucourt, J., Biben, T., Leyrat, A. and Verdier, C. Modeling breakup and relaxation of Newtonian droplets using the advected phase field approach. *Physical Review E*, Vol. 75, (2007), pp. 021405(1-8).
- [12] Synolakis, C.E. The runup of solitary wave. *Journal of Fluid Mechanics*, Vol. 185, (1987).

Guoming Ling, Junichi Matsumoto, Ethan J. Kubatko and Kazuo Kashiya

pp. 523-545.

[13] Satake, K., Fujii, Y., Harada, T. and Namegaya, Y. Time and Space Distribution of Coseismic Slip of the 2011 Tohoku Earthquake as Inferred from Tsunami Waveform Data. Bulletin of the Seismological Society of America, Vol. 103, (2013). pp. 1473-1492.

On the Role of Patient-specific Predictions by Functional MRI Informed Constitutive Modeling

Kevin Linka^{*}, Amelie Schäfer^{**}, Mikhail Itskov^{***}

^{*}Department of Continuum Mechanics, RWTH Aachen University, ^{**}Department of Continuum Mechanics, RWTH Aachen University, ^{***}Department of Continuum Mechanics, RWTH Aachen University

ABSTRACT

Osteoarthritis is strongly associated with a degeneration of cartilaginous tissue, which, in turn, is accompanied by tissue softening. One promising non-invasive approach towards its detection appears to be an assessment of multiparametric magnetic resonance (MR) imaging [1,2]. However, so far, there is no reliable correlation between the exact tissue properties and the multiparametric MR image mapping. In this contribution, we developed a constitutive framework in order to inform a cartilage model by sample-specific multiparametric MR maps (T1, T1rho, T2 and T2*) generated by a clinical 3.0-T MR imaging system. The model predictions of individual patients were fitted against their sample-specific stress responses by enforcing a global set of material parameters. Accordingly, we obtained suitable relations between the specific MR maps and the biomechanical properties. These relations serve as an input for the proposed constitutive law in order to predict the individual stress response of the tested cohort. References [1] Nebelung, S., Sondern, B., Oehrl, S., Tingart, M., Rath, B., Pufe, T., ... & Truhn, D. (2016). Functional MR imaging mapping of human articular cartilage response to loading. *Radiology*, 282(2), 464-474.. [2] K. Linka, M. Itskov, D. Truhn, S. Nebelung, J. Thüning, T2 MR imaging vs. computational modeling of human articular cartilage tissue functionality, *JMBBM*, 74(2017), 477-487.

Design through Fabrication Systems for Carpentry

Jeffrey Lipton^{*}, Daniela Rus^{**}

^{*}MIT CSAIL, ^{**}MIT CSAIL

ABSTRACT

Carpentered items are a critical part of modern lives. They make up the houses people live in along with the furniture and cabinetry inside them. With the Industry 4.0 movement and efforts towards mass customization, laymen are able to design and create a greater number of custom items. This explosion of ability is powered by 3D printing, CNC manufacturing and other robotic fabrication tools. Carpentry however, has few digital design tools that include fabrication. Wood cannot be 3D printed in a meaningful way, and CNC and robotic fabrication methods are expensive and time consuming to setup. Most carpentered items are made by hand with lathes, drill presses and saws. As a result, customization of these items currently requires expert skill, restricting customization to professional and hobbyist carpenters and those who can afford their labor. Recent developments in mobile robotics and digital design tools move us towards mass customization of carpentered items. These advances are predicated on understanding the constraints on the movement of standard carpentry tools and how humans use them. Fabrication and design systems can be made around a tool once its constraints are modeled. Fabrication systems use the model as the basis of path planning and manipulation. Design systems need to know the constraints to ensure parts are in a fabricate-able form. Currently two of the key tools have been modeled, the Jigsaw and the chop saw [1]. These are non-holonomic tools that are model as modified Reeds-Shepp cars. I used this model to make a generic path planning algorithm and combining that with a robotic movement system to turn a jigsaw into a scalable computer controlled cutting machine [1]. For the chop saw I developed fabrication algorithms that control the tolerance stack and allow mobile robots to cut pre-specified lengths of wood with a similar cut quality to a human, despite the robots' movements being imprecise. Through integration of professional CAD systems with user-friendly customization, verification, and robotic fabrication tools, these two tools became the basis of a template design system for co-design of carpentered items. I will discuss motivations and methods for developing constraint models on carpentry tools and discuss how such tools can become the basis of design through fabrication systems for more intricate carpentered items. References [1] J. I. Lipton, Z. Manchester and D. Rus, "Planning cuts for mobile robots with bladed tools," Internation Confrence on Robotics and Automation, pp. 572-579, 2017.

Optimized Local Bases and Efficient Implementation of Multiscale GFEM

Robert Lipton^{*}, Ivo Babuska^{**}, Paul Sinz^{***}, Michael Stuebner^{****}

^{*}Center for Computation and Technology and Mathematics Louisiana State University, ^{**}Institute for Computational and Engineering Sciences University of Texas, ^{***}Department of Computational Mathematics and Science and Engineering Mich. State Univ., ^{****}University of Dayton Research Institute

ABSTRACT

We present a computationally efficient method for implementing domain decomposition for multiscale problems. Our approach is to use nearly optimal local bases functions within the Generalized Finite Element Method. Here optimality is measured in terms of the Kolomoragov n -width. In this talk we describe the new approach and provide several computational examples. We demonstrate the how this method scales favorably with problem size.

Multiscale Solid Mechanics on Next-Generation Computing Hardware

David Littlewood*, Michael Tupek**, J. Antonio Perez***, Brian Lester****

*Sandia National Laboratories, **Sandia National Laboratories, ***University of New Mexico and Sandia National Laboratories, ****Sandia National Laboratories

ABSTRACT

Concurrent multiscale approaches for solid mechanics can resolve small-scale mechanisms within engineering-scale simulations. Their widespread use remains limited, however, due in large part to computational expense. This motivates the adaptation of simulation codes for optimal performance on next-generation computing platforms, which have the potential to enable multiscale and multiphysics models that have been considered intractable to date. In this presentation, we review an ongoing effort to adapt constitutive models within the Library of Advanced Materials for Engineering (LAME) [1] for improved performance on emerging computer architectures characterized by on-node hierarchical parallelism [2]. Increased parallelism is achieved primarily through the Kokkos software package [3], which provides an advanced parallel-for mechanism suitable for the evaluation of constitutive models. Here, memory management is a key issue due to differences in optimal access patterns across disparate architectures. An additional concern is the evolving nature of next-generation hardware, which is addressed by encapsulating hardware-specific source code so that it can be altered at a later date without the need for invasive changes to the material models themselves. The implementation strategy will be discussed, followed by performance analysis of constitutive models in the context of both single-scale and multiscale simulations. Simulations across multiple length scales utilize the well-known FE-squared approach, which associates sub-models that resolve the fine scale with material points in the macroscale model. It is shown that concurrent multiscale modeling is made increasingly viable for engineering-scale simulations by emerging, next-generation computing architectures. [1] W.M. Scherzinger and D.C. Hammerand. Constitutive models in LAME. Report SAND2007-5873, Sandia National Laboratories, Albuquerque, NM and Livermore, CA, 2007. [2] D.J. Littlewood and M.R. Tupek. Adapting material models for improved performance on next-generation hardware. Memorandum SAND2007-5873, Sandia National Laboratories, Albuquerque, NM and Livermore, CA, 2017. [3] H.C. Edwards, C.R. Trott, and D. Sunderland. Kokkos: Enabling manycore performance portability through polymorphic memory access patterns. Journal of Parallel and Distributed Computing, 74(12), 2014.

The Cracks Competition Propagation Simulations for the Composite Adhesively Bonded Joint or Repair Based on Cohesive Zone Model and Hashin Criteria

Bin Liu^{*}, Rui Yan^{**}

^{*}Northwestern Polytechnical University, ^{**}Xi'an Aeronautical University

ABSTRACT

Abstract Composites bonded technique are being used widely in the composite joints and repairs of the advanced air vehicle, such as Boeing 747 using bonding junction of 62% among the surface structures, Lockheed C-5A has 3250 m² bonding structures. A.B. Harman studied the impact, the compression after impact of composite scarf repair and found that mechanical performance of both the compressional and the tension after impact were affected obviously by the low velocity impact [1]. Generally, the fibers are discontinuous and the adhesive are the new material for the original matrix and fibers. The damage mechanics FEM model contains the intralaminar solid elements, the interlaminar cohesive zone elements[2,3], and the adhesive cohesive zone elements. In the intralaminar solid elements, fiber fracture, matrix crack and matrix plastic were considered based on the three dimensional Hashin Criteria[4]. The cohesive zone elements considered the composites delamination[5] and adhesive cracks. All the damage elements stiffness would be degraded once the material goes in failure state. The cracks competition propagation was simulated for different loadings. Under the in plane load, the ultimate failure mode is the adhesive shear fracture. The matrix cracks occur at the earliest. Under the out plane impact load, the earliest damage is the delamination and the matrix crack. The delamination dominates the earlier impact stage. When the impact energy increasing to a critical level, the higher-strength adhesive starts cracking. The adhesive cracking also leads to matrix damage. Keywords composite; adhesive; joints; repair; CZM; impact; fracture; delamination Reference [1] A.B. Harman, A.N. Rider. Impact damage tolerance of composite repairs to highly-loaded, high temperature composite structures. Composites Part A: 2011 (42): 1321-1334. [2] B. Liu, F. Xu, W. Feng, R. Yan, W. Xie. Experiment and design methods of composite scarf repair for primary-load bearing structures. Composites Part A: Applied Science and Manufacturing, 2016 (88): 27-38. [3] Panos Papanastasiou, Ernestos Sarris, Cohesive zone models. Woodhead Publishing, 2017:119-144 [4] Z. Hashin. Failure Criteria for Unidirectional Fiber Composites. Journal of Applied Mechanics, 1980 (47): 329-334. [5] Xueling Fan, M.N. Yuan, Q. Qin. Failure mechanisms of Ti-Al₃Ti metal-intermetallic laminate composites under high-speed impact. Rare Metal Materials and Engineering. 2017,46(3):403-408

An Efficient and Robust Numerical Integration Scheme for Embedded Interfaces: Application to Fluid-structure Interaction

Bin Liu^{*}, Rajeev Kumar Jaiman^{**}

^{*}Department of Mechanical Engineering, National University of Singapore, ^{**}Department of Mechanical Engineering, National University of Singapore

ABSTRACT

An efficient, accurate and robust numerical scheme is developed for immersed interface problems with application to fluid-structure interaction (FSI). The incompressible Navier-Stokes equations are solved by the Petrov-Galerkin Finite Element formulation on Cartesian Eulerian grids with finite cell method. In contrast to body-fitted methods, unfitted FEM techniques offer attractive properties for FSI modeling with large displacement and rotation with possible solid-to-solid contact. In a finite-cell unfitted FEM, geometric interfaces of immersed bodies are embedded within each element, termed as a cut cell and the Dirichlet boundary condition is imposed weakly along these interfaces via Nitsche's type method. These interfaces represent a discontinuity embedded in the cut cell, which imposes a difficulty to the conventional numerical integration algorithm. Existing techniques require a sub-division of cut cell into the integration cells and interpolation of scalar values and their gradients from the nodes of the cut cell. Of particular the approximation of the gradients depends on the shape of the cut cell, which leads the degradation of accuracy to resolve complex interface geometry. We introduce a robust and accurate numerical integration technique to deal with the cut cells with embedded discontinuity. Each cut cell is refined into the integration cells. We recognize that elemental matrices of cut cell can be reconstructed at matrix level from the summation of similar matrices from its integration cells. The numerical integration is undertaken in each integration cell with respect to the nodes of its own. Each integration cell takes as minimal supporting area/volume as possible along the discontinuity, thus the accurate and robust interpolation of the scalar values and their gradients are preserved in each integration cell. The proposed numerical integration has been tested on the stationary and rotating circular cylinder and cavity flow problems. Good convergence and stability have been achieved with unfitted grids. Finally, we extend the proposed formulation to fluid-structure interaction application with solid-wall contact effects. References [1] Zou, Zilong, Wilkins Aquino, and Isaac Harari. "Nitsche's method for Helmholtz problems with embedded interfaces." *International Journal for Numerical Methods in Engineering* 110.7 (2017): 618-636. [2] de Prenter, F., et al. "Condition number analysis and preconditioning of the finite cell method." *Computer Methods in Applied Mechanics and Engineering* 316 (2017): 297-327. [3] Natarajan, Sundararajan, D. Roy Mahapatra, and Stephane Bordas. "Integrating strong and weak discontinuities without integration subcells and example applications in an XFEM/GFEM framework." *International Journal for Numerical Methods in Engineering* 83.3 (2010): 269-294.

Generalized Isogeometric Analysis by a Differential Quadrature Hierarchical Finite Element Method

Bo Liu^{*}, Cuiyun Liu^{**}, Yufeng Xing^{***}

^{*}The Solid Mechanics Research Center, School of Aeronautic Science and Engineering, Beihang University, Beijing 100191, PR China, ^{**}The Solid Mechanics Research Center, School of Aeronautic Science and Engineering, Beihang University, Beijing 100191, PR China, ^{***}The Solid Mechanics Research Center, School of Aeronautic Science and Engineering, Beihang University, Beijing 100191, PR China

ABSTRACT

Generalized isogeometric analysis (IGA) by a differential quadrature hierarchical finite element method (DQHFEM) [1] is carried out through representing the geometry by the differential quadrature hierarchical (DQH) basis in the solution space of DQHFEM for dependent variables. The exact CAD geometry, similar to IGA, is matched by a coarse mesh of “DQH elements” using the hierarchical basis. Not only tensor product domains like quadrilateral and hexahedral DQH elements, triangular, tetrahedral and triangular prism DQH elements using Fekete points on the simplexes were also discussed. The DQH method in weak form is called DQHFEM. In DQHFEM, the number of nodes on different edges of an element can be different, and the number of nodes inside an element does not rely on the number of nodes on the edge of the element. So the geometry represented by DQH elements can be easily constructed to be water-tight and to be matched with the nodes of neighboring elements. The DQH method is of high accuracy, so the transformation of exact CAD geometry to be DQH elements will not lose accuracy in general. The DQH method uses high order or very high order basis. A whole NURBS element can be modeled by one DQH element, and any further mesh refinement or further communication with the CAD system is usually not necessary. The accuracy of DQH method can be improved by increasing the order of basis. As is well known that IGA [2] needs mesh refinement in order to keep isoparametric although it does not need to communicate with CAD system. In this work, the DQH elements in physical field is allowed to be sub-parametric or super-parametric, so it is a generalization of the IGA. Water-tight, mesh adaptive and high accuracy properties of the generalized IGA using DQH bases were demonstrated through application of the method to vibration of plate and shell structures. A discussion of obtaining a coarse mesh of “DQH elements” through trimmed NURBS surfaces is also presented. References [1] C.Y. Liu, B. Liu, L. Zhao, Y.F. Xing, C.L. Ma, H.X. Li. A differential quadrature hierarchical finite element method and its applications to vibration and bending of Mindlin plates with curvilinear domains. *Int. J. Numer. Meth. Engng* 109 (2016) 174–197. [2] T.J.R. Hughes, J.A. Cottrell, Y. Bazilevs. Isogeometric analysis: CAD, finite elements, NURBS, exact geometry and mesh refinement. *Comput. Methods Appl. Mech. Engrg.* 194 (2005) 4135–4195.

Concurrent Design of Additive Manufacturing-Oriented Shell-Infill Graded Lattice Structures Through Explicit Topology Optimization

Chang Liu^{*}, Weishang Zhang^{**}, Zongliang Du^{***}, Xu Guo^{****}

^{*}Dalian University of Technology, ^{**}Dalian University of Technology, ^{***}Dalian University of Technology, ^{****}Dalian University of Technology

ABSTRACT

Lattice structures with well-designed periodic microstructures have excellent mechanical, thermal, optical and acoustical properties. Structural topology optimization has successfully been used in optimum design of such periodic lattice/porous structures. Nowadays, with the rapid development of modern fabrication technology, it is no longer difficult to fabricate structures with more complicated microstructures. Actually, a structure constituted by graded microstructures can inherit many merits from the ones constitute by uniform periodic microstructures and usually has better performances. In addition, from an aesthetic point of view, using grade structures is also an effective means to make structures having a sense of beauty. Therefore, recent years witnessed a growing interest on developing methods to design graded structures. In the present work, a new approach for designing graded lattice structures is developed based on the Moving Morphable Components/Voids (MMC/MMV) topology optimization framework. For the convenience of additive manufacturing, the structures are designed to have two sub-structures, i.e., a solid shell forming the exterior and graded lattice structures filled in it, which can be optimized simultaneously. The essential idea is introducing a coordinate perturbation in the topology description functions (TDF) for describing the geometries of the components/voids in the design domain, in order to achieve graded structure design by optimizing the coefficients in the perturbation basis functions. Within the current design approach, both the complex solid shell and graded infills with explicitly geometrical parameters can be optimized simultaneously with a very small number of design variables under various loading conditions and coordinate systems. Numerical examples demonstrate the effectiveness and efficiency of the proposed approach.

Vorticity Tensor and Vorticity Vector Decomposition for Turbulence Study

Chaoqun Liu^{*}, Yisheng Gao^{**}

^{*}University of Texas at Arlington, ^{**}University of Texas at Arlington

ABSTRACT

Abstract For long time, there is a lack of mathematical definition for vortex, which is one of major obstacles causing many confusions in turbulence study. Classical theories usually decompose the velocity gradient tensor to a symmetric part which is corresponding to deformation and an anti-symmetric part which is corresponding to vorticity. Many people think vorticity represents fluid rotation, but it is not correct. In this paper the vorticity tensor is further decomposed to an anti-symmetric tensor which is corresponding to rigid rotation and another anti-symmetric tensor which is corresponding to non-rotational shear. The existence and uniqueness of the decomposition are proved. Based on the tensor decomposition, the vorticity vector is decomposed to a vortex vector which is called "Rortex" and a shear vector. This decomposition clearly shows that vorticity is a vector and vortex vector is another vector, but they are different vectors. $\text{Vorticity} = \mathbf{R} + \mathbf{S}$ is a very important formula to study turbulence and it clearly shows vorticity cannot be used to describe the vortex structure in turbulence since vorticity is not vortex vector and \mathbf{S} plays an important role in 3-D viscous flow. Vortex is also not necessary to be a region where vorticity is concentrated since vortex is a region with large \mathbf{R} but not large vorticity. Since Rortex only represents fluid rotation, unlike vorticity, it can be generated and ended inside flow field. As a new important physical quantity to represent vortex, through dynamics analysis Rortex can clearly show the vortical structure in turbulence and how turbulence is generated, developed, and sustained. The DNS for boundary layer transition is taken as an example to demonstrate the capability of Rortex to clearly and correctly show the vortex structure in flow transition.

Buckling Optimization of Variable-Stiffness Composite Panels Based on Flow Field Function

Chen Liu^{*}, Peng Hao^{**}, Xuanxiu Liu^{***}

^{*}Dalian University of Technology, ^{**}Dalian University of Technology, ^{***}Dalian University of Technology

ABSTRACT

Buckling is the main failure mode for composite thin-walled panels under axial load or combined load. Cutouts are widely existed in various branches of thin-walled structures to accommodate the need of easy access, inspection, electric lines, especially for launch vehicles, aircrafts, etc. When axial compression load is applied, buckling is usually the governing failure mechanism for these types of structures, and the buckling resistance would be reduced due to the presence of cutouts. Due to the non-uniform in-plane stress distribution, variable-stiffness panel with curvilinear fiber paths is a promising structural concept for cutout reinforcement of composite structures under axial compression, due to the more diverse tailorability opportunities than simply choosing the best straight stacking sequence. Traditional curvilinear fiber path functions lack the local variation capacity of fiber orientation angles to compensate the stiffness loss caused by cutouts. However, traditional representation methods of curvilinear fiber path are usually not flexible for cutout reinforcement. In this study, variable-stiffness panels based on flow field is employed to meet the requirement of cutout reinforcement, since the stress distribution is highly non-uniform for the panel with cutout, and stiffness tailoring is significant for improving the stress distribution and load-carrying efficiency. The cocurrent and equipotential lines are used to parameterize each pair of adjacent plies. The flow field function containing a uniform field and several vortex fields is utilized to represent the fiber path due to its inherent non-intersect and orthotropic features, and a bi-level optimization framework of variable-stiffness panels considering manufacturing constraints is then proposed. The flow field function is utilized to represent the global orientation and local variation of fiber path, which can enhance the design flexibility with only few variables. A typical rectangular panel with multiple cutouts is established to demonstrate the advantage of flow field function and proposed framework. The buckling modes and fiber paths of obtained optimum designs are examined in detail. Also, the effects of boundary condition and manufacturing constraint are investigated. By comparison with other fiber path functions, including linear variation function, cubic polynomial function, contour lines of cubic function. Flow fiber path only needs few variables to finely describe the fiber path, which can provide satisfying and manufacturable fiber paths by combination use of curvature constraint. Results indicate that variable-stiffness panel based on flow field function is a promising structural concept compared to common variable stiffness designs, especially for cutout reinforcement of composite structures under axial compression.

Modeling Strong and Weak Discontinuities without Element-partitioning in Reservoir Models

Chuanqi Liu^{*}, N. Sukumar^{**}, Jean H. Prevost^{***}

^{*}Princeton University, ^{**}University of California at Davis, ^{***}Princeton University

ABSTRACT

For reservoir, faults are either barriers to flow or fluid flow conduits. By using the extended finite element method, faults can be introduced into a three-dimensional reservoir mesh without meshing them explicitly and a structured mesh suffices since the faults can arbitrarily cut the elements. To capture the various properties of the faults, the enrichment functions in the model can be strongly (faults working as barriers) or weakly (faults working as fluid flow conduits) discontinuous. We implement a new integration scheme without element-partitioning to obtain the residual of the pressure equation. In the integration scheme, the integration of homogeneous monomials over each polyhedron is converted into the integration of the same monomials over the one-dimensional edges of the polyhedron by using Stokes's theorem and Euler's homogeneous function theorem. Several numerical examples are given to assess the performance of this new integration scheme in terms of computational time. It is found that the new integration scheme is over 50% more efficient than the integration scheme using element-partitioning procedure.

A Multi-scale Modeling Approach for Computational Design of Knitted Textiles

Dani Liu*, Seid Koric**, David Breen***, Antonios Kotsos****

*Theoretical & Applied Mechanics Group, Department of Mechanical Engineering & Mechanics, Drexel University, Philadelphia, PA, **National Center for Supercomputer Applications-NCSA, University of Illinois Urbana-Champaign, ***Department of Computer Science, Drexel University, Philadelphia, PA, ****Theoretical & Applied Mechanics Group, Department of Mechanical Engineering & Mechanics, Drexel University, Philadelphia, PA

ABSTRACT

Knitted textiles are viewed in this talk as hierarchically structured materials. Compared to the manufacturing methods for materials such as fiber-reinforced composites, modern knitting machines provide much finer control which is comparable to CAD-based advanced manufacturing methods and capable of creating a variety of structures using a range of input materials. The mechanical behavior of knitted textiles, however, is difficult to be predicted by traditional computational methods due to their complex architectures. This talk presents results from a developing computational framework for modeling and design of knitted textiles. Specifically, predictions of mechanical behavior of knitted textiles are first obtained by employing direct numeric simulation (DNS) using 3D Finite Element Analysis (FEA). Given the geometrical details of the entangled yarns included in the 3D models used, the DNS approach is capable of investigating the influence of various design parameters at the yarn level, including loop architecture, material properties, as well as interfacial interactions. However, since knitted textiles are treated as free standing structures both kinetic and kinematic effects become important resulting in significant increase of the computational degrees of freedom as a function of domain size analyzed. To address this issue DNS of the mechanical behavior of knitted textiles are for the first time conducted on High Performance Computing (HPC) using the explicit FEA method which was compared to implicit analysis. The results presented demonstrate satisfying accuracy and higher order efficiency with reduced memory requirements of the explicit method which allows for improved efficiency in simulations of larger computational domains, while also demonstrate that HPC could be a valuable resource for computational material design applied to advanced manufacturing. Furthermore, efforts to develop Reduced Order Models (ROM) for knitted textiles based on the available DNS results are also presented which are shown to provide an alternative approach to predict multiscale behavior in addition to consist a tool that could be leveraged in future microstructure optimization investigations. Moreover, to address the issue of size effects a first order, two-scale homogenization scheme was modified and applied by considering the yarn-level knitted textile models as a material point in the far field. The equivalent macro stress and consistent material stiffness were derived from the micro-level where specific 3D textile models were used. The macro field with unknown material properties was linked to the micro-level by a user subroutine which can convey the equivalent macro stress and stiffness in a looped form of the FE code.

Modeling Competing Hydraulic Fracture Propagation with the Extended Finite Element Method

Fushen Liu^{*}, Peter Gordon^{**}, Dakshina Valiveti^{***}

^{*}ExxonMobil Research and Engineering Company, ^{**}ExxonMobil Research and Engineering Company,

^{***}ExxonMobil Upstream Research Company

ABSTRACT

Hydraulic fracturing process is essential in enhancing productivity in low permeability reservoirs. In practice, it is common to create several perforation clusters to facilitate simultaneous growth of multiple hydraulic fractures per stage. However, the reported production log data suggests that only a small portion of perforation clusters in a stage may be effectively contributing to the overall production. The uneven fracture propagation results from the nonlinear coupling of wellbore friction, perforation friction, fracture propagation and stress interaction. We present a stabilized extended finite element framework to numerically study competing hydraulic fracture propagation in one stage. The framework is capable of modeling fully-coupled hydraulic fracturing processes including fracture propagation, elasto-plastic bulk deformation and fluid flow inside both fractures and the wellbore. Dynamic fluid allocation among fractures during propagation is solved, by considering both wellbore pressure loss and perforation pressure loss. With the numerical examples, we identify and verify the dimensionless parameters determining the transition from uniform fracture propagation to preferential fracture propagation.

Thermo-viscoplastic Analysis with Robust Solution Strategy for Extrusion

Guomai Liu^{*}, Xiaoliang Qin^{**}, Hongyan Yuan^{***}

^{*}Fujian University of Technology, ^{**}Fujian University of Technology, ^{***}University of Rhode Island

ABSTRACT

Extrusion is a plastic deformation process in which a billet is heated and pressed to flow through a die opening of a much smaller cross-sectional area than the original billet. In recent years, numerical simulation using finite element method has been increasingly used in extrusion die design. The challenges of extrusion simulation come from the large distortion of rate sensitive materials and the coupling of the material flow and heat transfer. It is hard to model extrusion process in a Lagrangian reference frame because the excessive element distortion will fail the analysis as the material pass through the die. Element remising and results mapping are usually required in a Lagrangian reference frame. However, the re-meshing method is computationally costive. The extrusion process can be effectively modeled by treating the problem as a steady flow of viscoplastic material in an Eulerian frame. In this work, a stabilized Eulerian formulation for fully coupled thermal-mechanical steady state viscoplastic flow is presented. Plastic heat generation and frictional heat are considered in this work. Streamline Upwind Petrov-Galerkin (SUPG) method is used to stabilize the incompressible equation and the convection term in heat transfer equation. A mixed P2-P1 tetrahedral element is developed to enhance the stability further. Anand's viscoplastic constitutive material model is used in this study. A two-step cut off strain rate reduction solution method is introduced to provide a robust and efficient convergence by solving the Anand's model in the Eulerian formulation using the Newton-Raphson method. The Eulerian formulation is implemented in an OpenMP finite element program called OnExtrude. Two numerical examples are studied to validate the accuracy and efficiency of the Eulerian formulation.

OPTIMIZATION OF RESIN PELLET SHAPE FOR IMPROVING FLOWABILITY

JIHONG LIU

DAIKIN INDUSTRIES, LTD.
1-1, Nishi-Hitotsuya
Settsu, Osaka 566-8585, Japan
jihong.liu@daikin.co.jp; <http://www.daikin.com/>

Key words: Optimal Pellet Shape, Hopper, Flowability, Dynamic Explicit FEM.

Summary: *In this paper, we proposed a simulation approach based on the dynamic explicit FEM (Finite Element Method) to evaluate the flowability of resin pellets in a hopper of an extruder. Using the simulation approach, we clarified that the shape of the resin pellets had a large influence on its flowability, and found the optimal pellet shapes that can improve the flowability of the resin pellets in the hopper.*

1 INTRODUCTION

The demand for LAN (Local Area Network) cables is greatly increasing with the rapid progress of information technology. LAN cables are made up of electrical wires which are coated with resins. The resins are usually manufactured into pellets of about several millimeters for easy processing.

It is sometimes seen that the coating layer on the electrical wires is not uniform. One of the reasons for this is presumed to be that the outflow rate of the resin pellets from a hopper of an extruder is not constant and the resin pellets are not stably supplied to the electrical wires during coating processes.

Although it is empirically known that the shape of resin pellets affects the outflow behavior of the resin pellets from a hopper, only a few theoretical researches and simulation studies on it have been conducted ^[1, 2]. There are two reasons for this. One is that the governing equations of resin pellets motion are not yet established theoretically due to the fact that resin pellets are discrete and the interactions between resin pellets are complicated. Another is that it is difficult to simulate actual flow phenomenon of resin pellets in a hopper because of the limitations on the scale of resin pellets simulation model and calculation time.

At present, the shape of resin pellet is mainly determined based on the experience and intuition of engineers. In order to improve the stability of the coating layer of electrical wires, it is desired to elucidate the influence of the shape of resin pellets on its flowability in a hopper of an extruder.

In this paper, we proposed a simulation approach based on the dynamic explicit FEM (Finite Element Method) to evaluate the flowability of resin pellets in a hopper of an extruder, which fill into the hopper by free-fall and then flow out from the hopper by gravity.

In particular, first, we verified simulation results in a small scale model by statistical method to ensure the randomness of the filled state of resin pellets in the hopper and established a simulation approach of resin pellet flow. Next, we confirmed that we can deduce simulation results in a large scale model from those in a small scale model. Then, using the simulation approach, we clarified that the shape of resin pellets has a large influence on its flowability and found an optimal pellet shape of oblate and prolate spheroid respectively that can improve the flowability of resin pellets in a hopper. Finally, we confirmed that the optimal resin pellet shape is in dependent of the amount of pellets, kind of material and angle of hopper. It is an interesting phenomenon that the optimal oblate and prolate spheroid have a reciprocal relationship between ratios of equatorial diameter to polar diameter respectively.

2 FLOW SIMULATIONS OF RESIN PELLETS IN A HOPPER

The above-mentioned simulation approach is described in detail below. In this paper, we model a resin pellet by using finite elements. A resin pellet cluster includes a plurality of the resin pellets, and we create its simulation model that can be calculated using a workstation.

2.1 Analysis model

In this paper, we assume that the shape of a resin pellet can be expressed approximately by a spheroid. Here, as shown in Figure 1, a resin pellet is modeled with solid elements, and a hopper is modeled with shell elements.

In the simulations, first, a resin pellet cluster placed in a higher position than the hopper free-falls to the hopper whose outlet is closed with a lid, and thereby creates a random filled state of resin pellets in the hopper. Next, the randomly filled resin pellets flow out from the hopper under the action of gravity by removing the hopper outlet lid, and the outflow time of the resin pellets from the hopper is calculated.

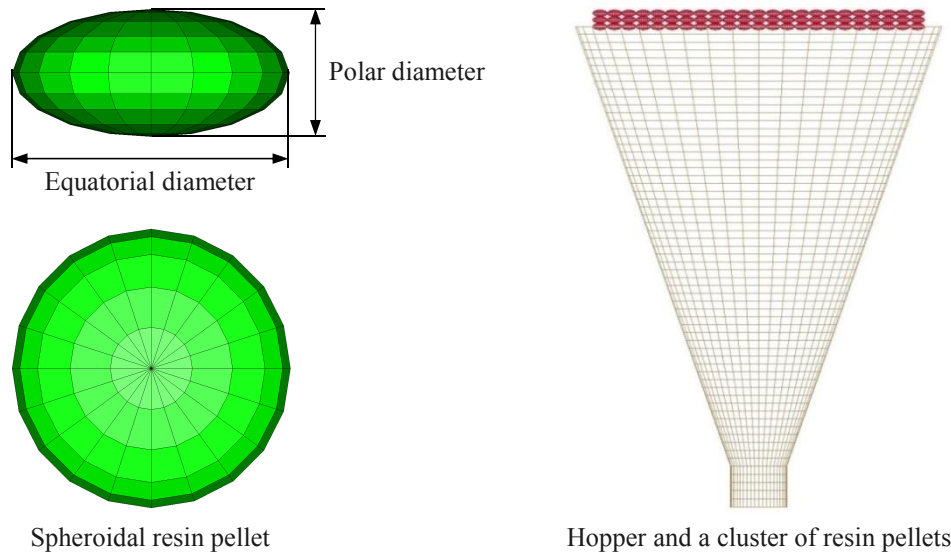


Figure 1. Finite element model of a spheroidal resin pellet, a hopper and a cluster of spheroidal resin pellets in a higher placement position than the hopper

2.2 Verification of simulation results

Simulations are performed on the filling of FEP (tetrafluoroethylene-hexafluoropropylene copolymer) pellet clusters with different initial placement state into a hopper and the outflow of filled FEP pellets from the hopper. Nonlinear dynamic explicit software LS-DYNA^[3, 4] is used in the simulations.

2.2.1 Creation of filled state of pellets and verification of its randomness

Figure 2 shows the FEP pellet clusters with mass of 10g and different initial placement state No.1 to No.7, and the filled state of pellets in the hopper owing to free fall. According to the results, it seems that there is no difference in randomness in the filled state of the pellets corresponding to the initial placement state No.1 to No.7. Figure 3 shows the distributions of the pellet center distances in each filled state of the pellets. It is seen that the each filled state of the pellets shows almost the same distribution, and it can be judged that they have equivalent randomness and that there is no difference between them.

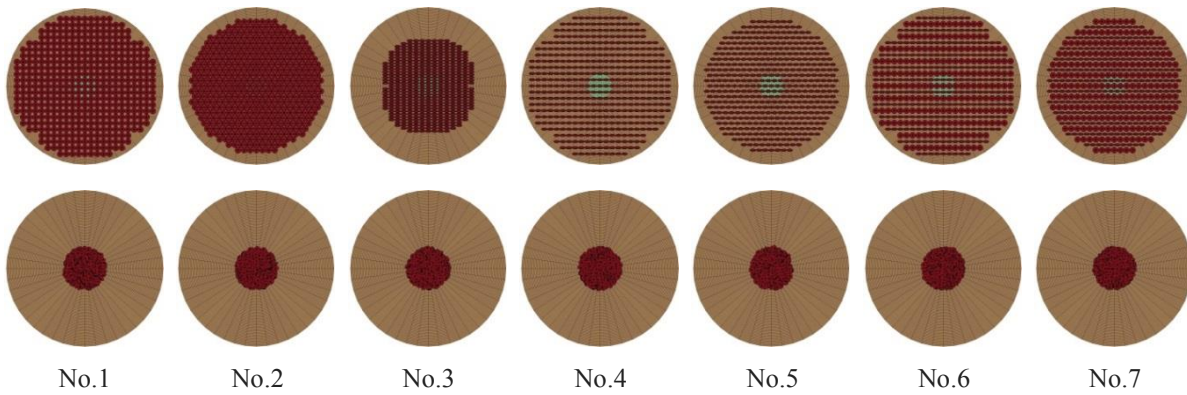


Figure 2. The FEP pellet clusters of 10g with different initial placement state (upper row) and the filled state of the pellets in the hopper due to the free-fall (lower row).

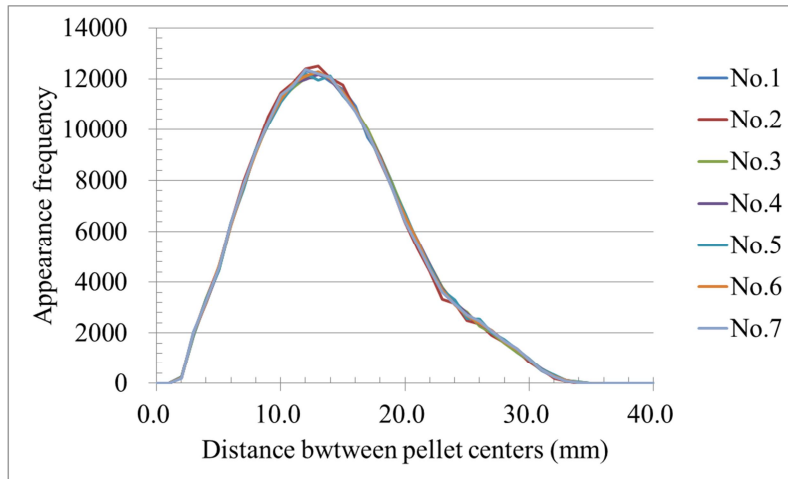


Figure 3. Appearance frequency distributions of the distance between pellet centers of 10g FEP pellet clusters

Figure 4 shows the filling process of the FEP pellets of 10g into a hopper and the outflow process of the filled FEP pellets from the hopper as an example.

2.2.2 Outflow time of pellets from a hopper

Figure 5 shows the simulation results of the outflow time of the FEP pellet clusters No.1 to No.7 with mass of 10g, 20g and 30g from the hoop, respectively. According to the results, it is found that there is a slight difference in the outflow time of the pellets due to the differences in initial placement state. The outflow time of the pellets is statistically processed and the relationship between the number of simulations and the variation coefficient of the outflow time is shown in Figure 6. It is found that the coefficient of variation of the outflow time of the pellets is as low as 2% or less in either case. It can be also seen from Figure 6 that the coefficient of variation of the outflow time decreases with an increase in the amount of the pellets. For example, when the pellet cluster is 10g, the variation coefficient of the outflow time is about 2%, but in the case of the pellet cluster of 30g, it is obvious that the variation coefficient of the outflow time decreases to 1% or less. It can be also seen from Figure 6 that when the amount of the pellets reaches 30g or more, the variation coefficient of the outflow time due to the differences in the number of simulations does not change.

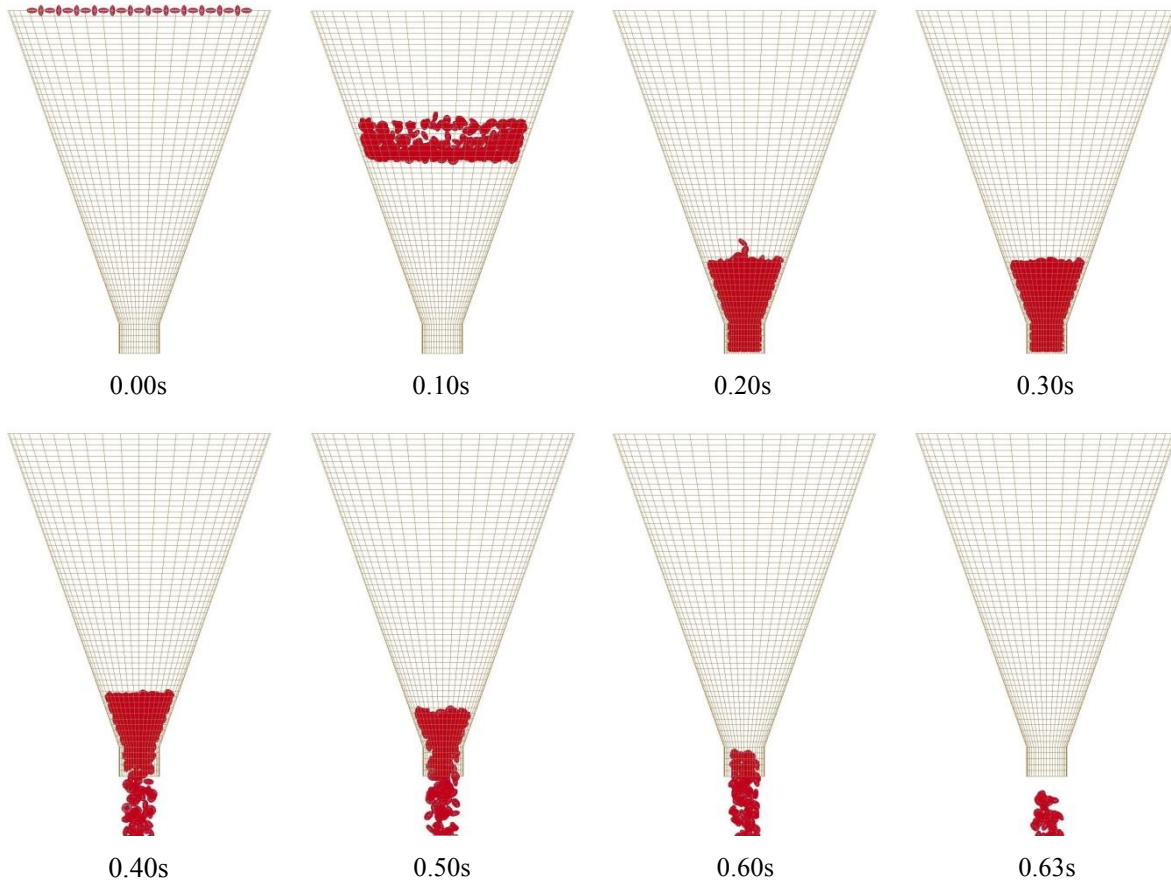


Figure 4. Filling of the FEP pellets of 10g into a hopper and the outflow of the FEP pellets from the hopper

To summarize the simulation results of the outflow time of the FEP pellets described above, it is expected that the statistical influences will not be given to the simulation results of the filled state of the pellets in the hopper and the outflow time of the pellets from the hopper if any pellet cluster of any initial placement state is used. This means that the simulation results of the filled state of pellets in a hopper and the outflow time of the pellets from the hopper obtained by using any pellet cluster of any initial placement state have statistically the same randomness.

2.2.3 Relationship between amount of resin pellets and outflow time

It is revealed that there is no statistical differences in the filled state of pellets in a hopper and the outflow time of the pellets from the hopper even if the initial placement state of the pellets is different. In this section, we simulate the filling of the FEP pellets into the hopper

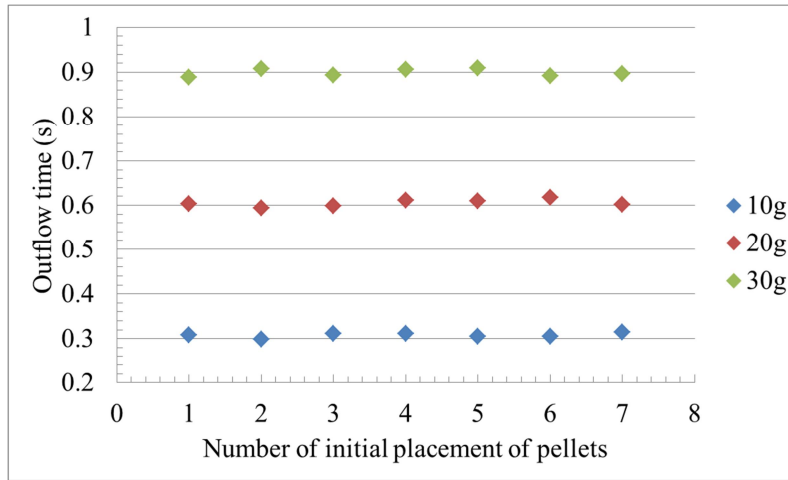


Figure 5. Changes in outflow time due to the differences in initial placement state of FEP pellets and in mass

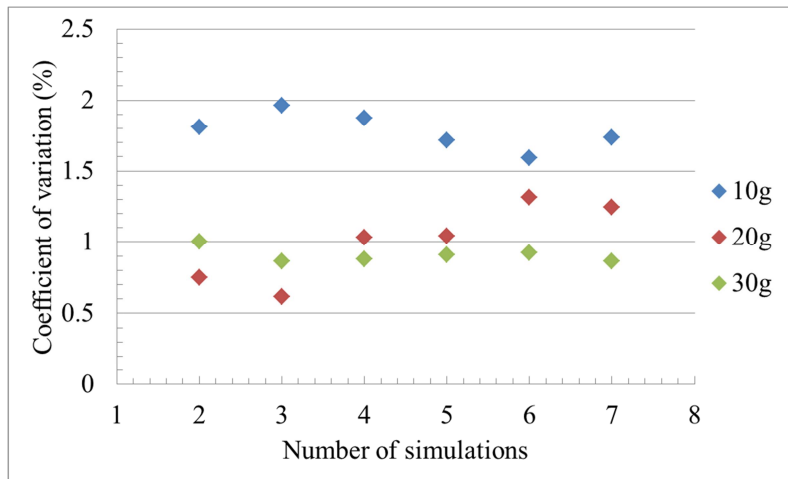


Figure 6. Number of simulations and coefficient of variation of outflow time of FEP pellets with different mass

and the outflow of the pellets from the hopper when the initial placement state No.7 is used to increase the mass of the pellets up to 80g at intervals of 10g.

The relationship between the mass of the FEP pellets and the outflow time of the pellets from the hopper is shown in Figure 7. At the same time, an approximate curve showing the relationship between the mass and the outflow time of the FEP pellets is also shown in the Figure 7. It can be seen that the relation between the mass and the outflow time of the FEP pellets from the hopper can be approximated by a linear function equation $y=0.0299x$. Here, x is the mass (g) of the FEP pellets, and y is the outflow time of the FEP pellets from the hopper. Using this formula, it is possible to easily predict the outflow time of the FEP pellets of arbitrary mass.

In this paper, the accuracy of the predicted outflow time of the FEP pellets by the formula is verified with the case of the FEP pellets of 300g as an example. Since the simulation model of the pellets of the same mass is large in scale and the calculation time is enormous and not realistic, we predict the outflow time of the pellets on a real scale using simulation results in a small scale model and indirectly verify the accuracy of the simulation.

Table 1 shows the comparisons between the test results and the predicted results of the outflow time of the FEP pellets with mass of 300g. Here, it is assumed that the variation coefficient of the simulation results due to the randomness of the filled state of the pellets is 1%. According to the results, it is revealed that the average error between the predicted results and the test results is 5.97%, which is sufficiently good from the viewpoint of engineering. We think that the simulation approach used in this paper is valid because the predicted results and the test results almost agree with each other. As one of the causes of the differences between the predicted results and the test results, uncertainty of the friction coefficient between the pellets, between the pellets and the hopper can be mentioned. In addition to this, the pellets of uniform shape and size are used in the simulations, but the pellets in the test are not completely uniform shape and size. This is also considered to be the cause of the differences between the predicted results and the test results.

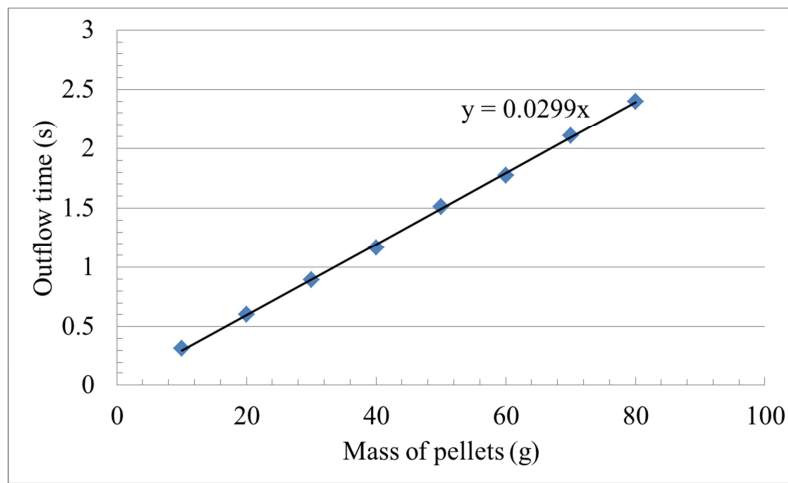


Figure 7. Relationship between the mass of the FEP pellets and the outflow time of the FEP pellets from the hopper, and an approximate formula to predict the outflow time of the FEP pellets of arbitrary mass

Table 1. Predicted and test outflow time of FEP pellets of 300g

Results		Error (%)		
Test	Prediction	Avg.	Max.	Min.
9.54±0.054	8.97±0.090	5.97	7.44	4.49

To summarize the above analysis results, it is found that filling of the pellets into the hopper and outflow of the pellets from the hopper can be predicted by the simulations using the dynamic explicit FEM. This makes it possible to grasp the flow behavior of the pellets having different shapes by the simulations.

3 SEARCHES FOR PELLET SHAPE FOR IMPROVING FLOWABILITY

Conventionally, the pellet shape is determined by trial and error based on the experience and intuition of engineers and therefore the theoretical and simulation studies on the pellet shape are insufficient. In this section, we elucidate the influence of the pellet shape on the flowability of the pellets using the above proposed simulation approach and reveal the optimal pellet shapes that can improve flowability of the pellets in a hopper.

3.1 Case of similar pellet shape

Figure 8 shows some examples of similar spheroidal pellet shape having the same ratio of equatorial diameter to polar diameter. Here, the unit of the diameter is millimeter and the ratio is denoted as α . Figure 9 shows the changes in the outflow time of the FEP pellets from the hopper due to the differences in mass and equatorial diameters of the pellets having the same α of 2.1875. It is revealed that when the mass is the same, the outflow time becomes linearly shorter as the equatorial diameter of the pellet becomes smaller. This means that, in the case of the pellets having a similar shape, smaller pellets can flow out more smoothly from the hopper and the flowability is better. It is to be noted that since the pellets tend to become more electrostatic as the pellets become smaller, it is necessary to determine the actual pellet size considering the balance between flowability and chargeability.

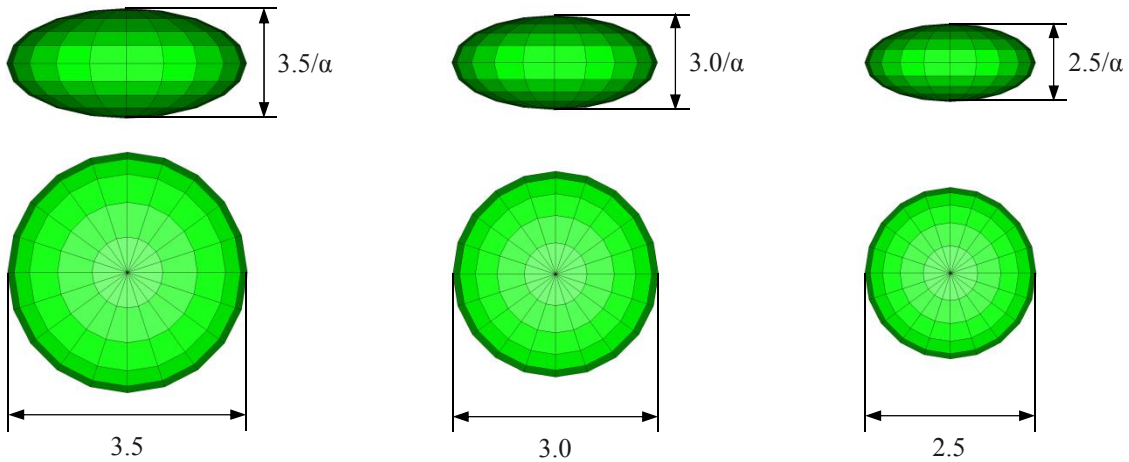


Figure 8. Some similar spheroidal pellets with the same ratio of equatorial diameter to polar diameter, α

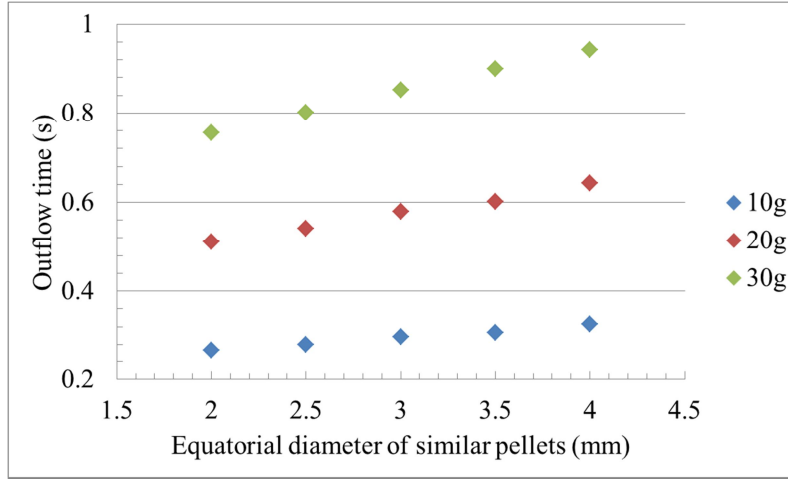


Figure 9. Equatorial diameter, mass and outflow time of FEP pellets with the same α of 2.1875

3.2 Case of isovolumetric pellets with a different shape

Figure 10 shows some examples of isovolumetric spheroidal pellets in which the ratio of equatorial diameter to polar diameter is varied. Figure 11 shows the changes in the outflow time of the isovolumetric spheroidal FEP pellets of 10g with the varying ratio of equatorial diameter to polar diameter. According to the results, it is revealed that an optimal oblate spheroid and a prolate spheroid with good flowability exist compared to the sphere which is perceived to have the best flowability. Specifically, for example, when the ratio of equatorial diameter to polar diameter is 2.19, it is found that the flowability of the pellets is the most excellent. On the other hand, in the optimal prolate spheroid, the ratio of equatorial diameter to polar diameter is 0.47. It is strangely found that the optimal oblate and prolate spheroid have a reciprocal relationship ($0.47 \times 2.19 = 1.00$) between ratios of equatorial diameter to polar diameter respectively.

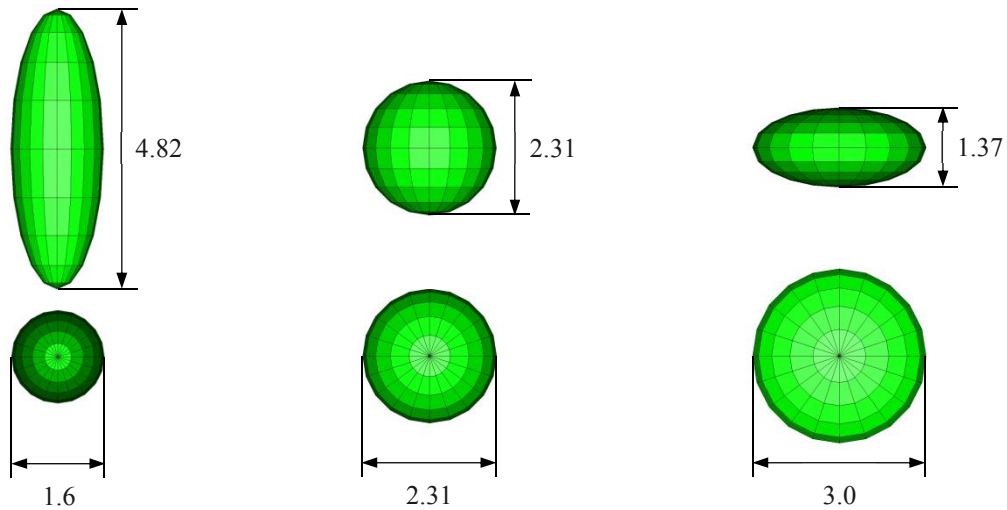


Figure 10. Some isovolumetric spheroidal pellets with varying ratio of equatorial diameter to polar diameter

Concerning the generality of the optimal pellet shapes, it is confirmed below by the simulations based on the above approach whether the optimal pellet shapes for improving flowability of the pellets are in dependent of the amount of pellets, kind of material and angle of hopper.

3.2.1 Influence of amount of pellets

Figure 12 shows the change in the outflow time due to the difference in the ratio of equatorial diameter to polar diameter and in the FEP pellets with mass of 10g and 20g. It is found that even when the amount of the pellets is changed, the optimal pellet shapes for improving flowability does not change. That is, the optimal pellet shapes do not depend on the amount of pellets.

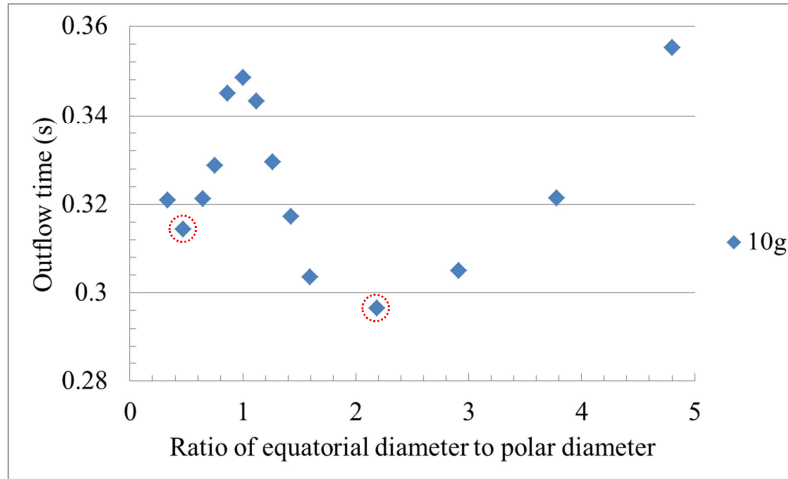


Figure 11. Relationship between the ratio of equatorial diameter to polar diameter and the outflow time of the FEP pellets of 10g

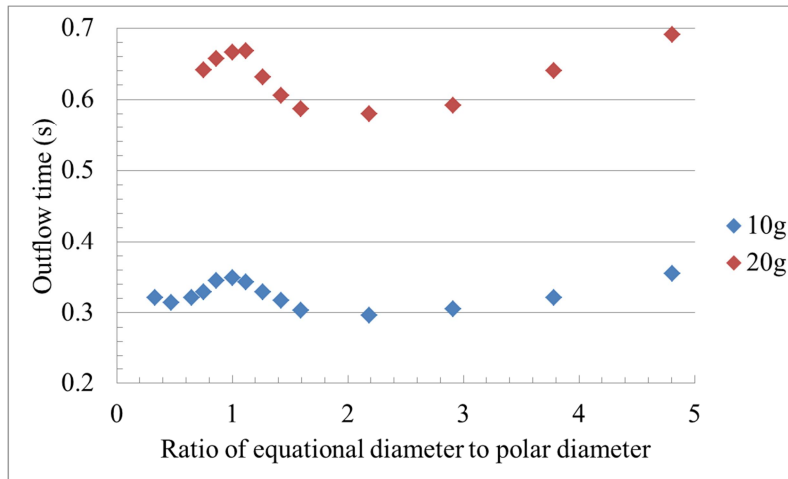


Figure 12. Change in the outflow time due to differences in the ratio of equatorial diameter to polar diameter and in the FEP pellet mass of 10g and 20g

3.2.2 Influence of material type of pellets

Figure 13 shows the change in outflow time due to the differences in the ratio of equatorial diameter to polar diameter and in the material type of the FEP and PE (polyethylene) pellets. It turned out that even if the material type of the pellets are changed from FEP to PE, the optimal pellet shapes for improving flowability does not change. That is, the optimal pellet shapes do not depend on the material type.

3.2.3 Influence of hopper angle

Figure 14 shows the outflow time of the FEP pellets of 10g due to the difference in the ratio of equatorial diameter to polar diameter when the hopper angle is changed. It is seen that the optimal shapes for improving flowability do not change even if the hopper angle is different. This means that the optimal pellet shapes are independent of the hopper angle.

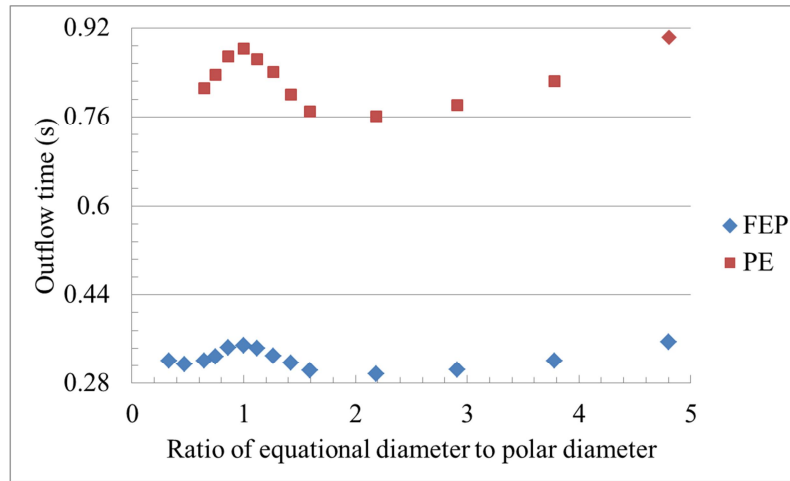


Figure 13. Outflow time of the FEP and PE pellets of 10g

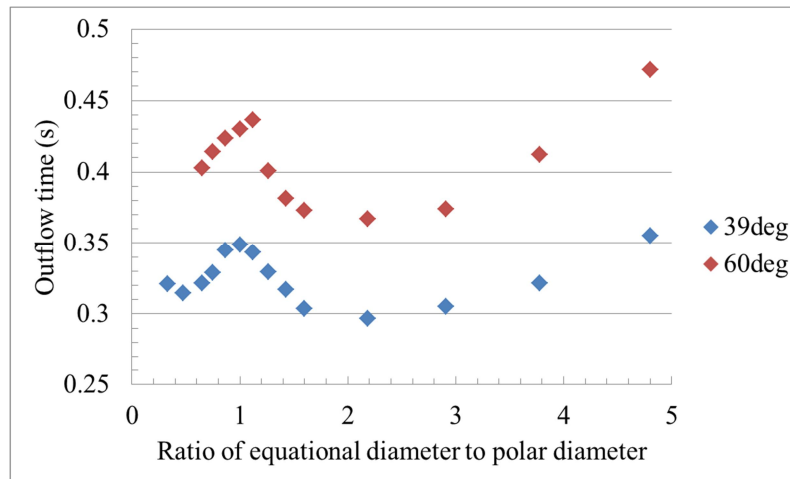


Figure 14. Outflow time of the FEP pellets of 10g with different hopper angles

4 CONCLUSIONS

In this paper, using the simulations based on the dynamic explicit FEM, we found the optimal pellet shapes with an oblate and a prolate spheroid respectively, which can improve the flowability of the pellets in a hopper. The ratios of equational diameter to polar diameter in the optimal oblate and prolate spheroid are 2.19 and 0.47, respectively.

It is confirmed by the simulations that the optimal spheroid shapes of the pellets are in dependent of the amount of pellets, the kind of material and the angle of a hopper.

It is also an interesting phenomenon that the optimal oblate and prolate spheroid have a reciprocal relationship between ratio of equatorial diameter and polar diameter respectively.

The optimal oblate spheroid shape is applied to our Neoflon FEP pellets and contributed to the improvement of the pellet flowability and its commercial value.

REFERENCES

- [1] Potente, H. and Pohl, T. C. Polymer pellet flow out of the hopper into the first section of a single screw, *International Polymer Processing* (2002) 17:11-21.
- [2] Rowe, R. C, York, P., Colbourn, E. A. and Roskilly, S. J. The influence of pellet shape, size and distribution on capsule filling—A preliminary evaluation of three-dimensional computer simulation using a Monte-Carlo technique, *International Journal of Pharmaceutics* (2005) 300:32-37.
- [3] LSTC, LS-DYNA KEYWORD USER'S MANUAL VOLUME I, II, Version971 R6.1.0 (2012).
- [4] JSOL Corporation, LS-DYNA Usage Guide, Second Edition (2012).

ALTO: A Super-Lightweight Topology Optimization Method and Its Application to Support Structure Design for Additive Manufacturing

Jikai Liu^{*}, Albert To^{**}

^{*}University of Pittsburgh, ^{**}University of Pittsburgh

ABSTRACT

This research introduces a new topology optimization method, named ALTO (Accelerated Lightweight Topology Optimization). The basic idea of ALTO is to arbitrarily place a number of plates inside the design domain and then perform simultaneous optimization of the shape and material distribution of each plate, as well as the layout of the plates. Unlike conventional topology optimization methods where a 3D background mesh is needed, only the 2D shell element mesh is used to discretize each plate in ALTO, while the shape of each plate is represented by a negative-signed distance function. To ensure smooth convergence and accuracy, finite element nodes will be placed on the joint connections between plates in each optimization iteration. These geometric representation and discretization strategies allow for a rigorous and robust topology optimization method to be formulated. As indicated by its name, this new method has two key advantages: (i) high computational efficiency since no 3D background mesh is required; and (ii) extremely small material volume fraction (such as below 0.02), since material volume is calculated by counting the plate elements, and thickness of the plates can approach a very small value. Effectiveness of the proposed method is proved by studying a few numerical examples. Other than the basic method description, the method will be used to address a tough problem: support structure design in additive manufacturing. Support structure is often encountered in additive manufacturing, which functions in supporting the printing of large overhangs. However, utilizing support structure consumes extra metallic powders, lengthens the printing process, and requires post-machining to remove it after printing. Therefore, overhang free topology optimization has attracted the attention but the overhang free design often severely deviates from the unconstrained optimal. In such a situation, lightweight support structure design through topology optimization is appealing but has been less focused, i.e. residual distortion/stress constrained topology optimization. This problem is challenging due to the involved transient thermo-mechanical analysis is computationally expensive, and to address this problem, we have proposed the inherent strain theory based fast method for residual distortion prediction which have demonstrated pretty good prediction result. Therefore, the inherent strain based ALTO algorithm for super lightweight support structure design will be explored in this research.

A Unified Continuum and Variational Multiscale Formulation for Fluids, Solids, and Fluid-structure Interaction

Ju Liu^{*}, Alison Marsden^{**}

^{*}Stanford University, ^{**}Stanford University

ABSTRACT

Traditionally, there has been a dichotomy in computational mechanics: the governing equations for fluids are typically written in terms of the velocity and pressure, while the governing equations for solids are often written in terms of the displacement. This difference is fundamentally due to different stress responses in the constitutive laws, and it leads to developments of different numerical strategies for fluids and solids. It is desirable to formulate a unified framework for fluids and solids to facilitate construction of a consistent and unified numerical framework. Furthermore, a unified framework will benefit the algorithm design for fluid-structure interaction problems. In this work, we first present a unified continuum modeling framework for viscous fluids and hyperelastic solids using the Gibbs free energy as the thermodynamic potential [2]. This framework naturally leads to a pressure primitive variable formulation for the continuum body, which is well-behaved in both compressible and incompressible regimes. Then we perform variational multiscale (VMS) analysis for this general continuum body. The resulting VMS formulation recovers the residual-based variational multiscale formulation for the Navier-Stokes equations. For hyperelastic materials, the VMS formulation provides a mechanism to circumvent the inf-sup condition for low-order tetrahedral elements [1, 3]. After that, we present a novel unified formulation for fluid-solid coupled problems. We show that the proposed numerical scheme enjoys several appealing numerical properties. Numerical examples will be presented to provide corroboration. Lastly, we will discuss possible extensions in biomedical and engineering applications. References [1] A.J. Gil, C.H. Lee, J. Bonet, M. Aguirre. A stabilised Petrov-Galerkin formulation for linear tetrahedral elements in compressible, nearly incompressible and truly incompressible fast dynamics. *Computer Methods in Applied Mechanics and Engineering*, 276:659–690, 2014. [2] J. Liu and A.L. Marsden. A unified continuum and variational multiscale formulation for fluids, solids, and fluid-structure interaction. [arXiv:1711.01322](https://arxiv.org/abs/1711.01322) [physics.comp-ph]. [3] G. Scovazzi, B. Carnes, X. Zeng, and S. Rossi. A simple, stable, and accurate linear tetrahedral finite element for transient, nearly, and fully incompressible solid dynamics: a dynamic variational multiscale approach. *International Journal for Numerical Methods in Engineering*, 106:799–839, 2016.

Mixed Precision Iterative Methods for Complex Symmetric Systems

Lijun Liu^{*}, Masao Ogino^{**}, Kazuaki Sekiya^{***}

^{*}JST ACT-I, ^{**}Information Technology Center, Nagoya University, ^{***}Graduate School of Information Science,
Nagoya University

ABSTRACT

Electricity devices play an important role in our daily life and in the development of human society. In the processes of designing electricity devices and controlling the quality, electromagnetic field simulations are required. In the electromagnetic field simulations, complex systems of linear equations are generated. In some cases, e.g. the finite element formulation of the E method for Maxwell equations including displacement current, the complex systems are symmetric. To solve complex symmetric systems, many numerical methods are proposed and widely used. When the coefficient matrix is dense and has no special properties to enable fast matrix-vector multiplication, full GMRES is usually the method of choice. If the coefficient matrix is sparse or if storage becomes a problem for full GMRES, COCG, COCR, QMR, MINRES-like_CS[1], CSYM[2], CS-MINRES-QLP[3] are used. Except for GMRES, the bases of the other methods are computed by recursion and not fully stored. Since all the computations are implemented in finite precision arithmetic, the algorithms are unstable, and the performance of the methods are not only affected by the methods themselves but also depending on the machine precision. To overcome the algorithm's instability and provide adequate accuracy, high precision arithmetic is useful. For the current machines, GCC Version 4.6 or later provides `__float128` type as a system software support, and the IBM POWER9 has hardware support of 128-bit quad-precision floating-point operations. And also, many arbitrary precision algorithms and libraries have been developed using the fixed precision arithmetic. However, computations with high precision are usually time-consuming. In this work, we develop mixed precision iterative methods for complex symmetric systems to achieve high accuracy and at the same time decrease runtime. Keywords: mixed precision arithmetic, complex symmetric, iterative methods

References [1] M. Ogino, A. Takei, S. Sugimoto, and S. Yoshimura, "A numerical study of iterative substructuring method for finite element analysis of high frequency electromagnetic fields", *Comput. Math. Appl.*, (2016). [2] A. Bunse-Gerstner, R. Stöver, "On a conjugate gradient-type method for solving complex symmetric linear systems", *Linear Algebra Appl.* 287 (1999) 105–123. [3] S., Choi, "Minimal Residual Methods for Complex Symmetric, Skew Symmetric, and Skew Hermitian Systems", Report ANL/MCS-P3028-0812, Computation Institute, University of Chicago, (2013).

DEM-SPH Coupling Simulation with Dilated Polyhedral Elements

Lu Liu^{*}, Shunying Ji^{**}

^{*}Dalian University of Technology, ^{**}Dalian University of Technology

ABSTRACT

The Minkowski sum theory is adopted to generate the dilated polyhedral element which is used for the discrete element method (DEM). The constrained minimization problem in the contact detection between dilated polyhedra employs an envelope function which replaces the true dilated polyhedron shape. The parameters of the envelope function are studied about the influence to the efficiency and accuracy of the contact detection. Meanwhile, a bond model is adopted in DEM to simulate the breaking process of continuum. The weakly compressible smooth particles hydrodynamics (SPH) is adopted to simulate the liquid in the coupling with DEM. The force between DEM particles and SPH particles uses the repulsive force model. The GPU-based parallel technology, CUDA is used to accelerate the simulation. Typical simulation examples are simulated by the DEM-SPH model to calibrate the parameters and validate the results. The ice-water coupling including the fracture of ice is simulated by the DEM-SPH coupling model. Real scaled physical model of ice-water coupling is implemented for engineering in cold regions. The results is analyzed and validated with standards to evaluate the accuracy of the simulation ultimately.

Meshfree Particle Simulation of Explosive/impact Welding

Moubin Liu*

*Peking University

ABSTRACT

Explosive welding (EXW) involves processes like the detonation of explosive, impact of metal structures and strong fluid-structure interaction, while the whole process of explosive welding has not been well modeled before. In this paper, a novel smoothed particle hydrodynamics (SPH) model is developed to simulate explosive welding. In the SPH model, a kernel gradient correction algorithm is used to achieve better computational accuracy. A density adapting technique which can effectively treat large density ratio is also proposed. Typical phenomena in EXW such as the wavy interface, jetting formation, temperature and pressure distribution at the interfaces and melting voids are investigated by the present SPH simulations, which are usually difficult for grid based methods. The mechanisms of wave formation are investigated, specially, two well-known mechanisms namely, the jet indentation mechanism and the vortex shedding mechanism are studied with the present simulations. Based on the well captured interfacial morphologies, the weldability windows for the impact welding (IMW) are given and are compared with the experimental and theoretical results. Furthermore, the weldability windows for EXW with respect to explosive quantity and initial welding angle are obtained. Meanwhile, welding limits and effective explosive quantity for EXW are discussed in detail.

RATIONAL BEZIER TRIANGLES FOR THE ANALYSIS OF ISOGEOMETRIC HIGHER ORDER GRADIENT DAMAGE MODELS

Ning Liu Ann E. Jeffers[†]

*Department of Civil and Environmental Engineering, University of Michigan
2350 Hayward Street
Ann Arbor, Michigan, 48109, USA
Email address: ningliu@umich.edu

[†] Department of Civil and Environmental Engineering, University of Michigan
2350 Hayward Street
Ann Arbor, Michigan, 48109, USA
Email address: jffrs@umich.edu; website: <https://sites.google.com/umich.edu/jeffers>

Key words: Isogeometric Analysis, Higher-Order Gradient Damage Model, Feature Preserving, Rational Bézier Triangles, Lagrange multipliers.

Abstract. The computational approach of modeling smeared damage with quadrilateral elements in isogeometric analysis (e.g., using NURBS or T-splines) has limitations in scenarios where complicated geometries are involved. In particular, the higher-order smoothness that emerges due to the inclusion of higher-order terms in the nonlocal formulation is not always easy to preserve with multiple NURBS patches or unstructured T-splines where reduced continuity is observed at extraordinary points. This drawback can be bypassed with the use of Bézier triangles for domain triangulation. The use of a triangular meshing scheme significantly increases the flexibility in the discretization of arbitrary spaces and facilitates the handling of singular points that result from sharp changes in curvature. Moreover, the process of mesh generation can be completely automated and does not require any user intervention. We also adopt in this research an implicit higher-order gradient damage model in order to fix the non-physical mesh dependency exhibited in continuum damage analysis. For the solution of the fourth- and sixth-order gradient damage models, Lagrange multipliers are adopted to elevate the global smoothness to a desired order in an explicit fashion. The solution algorithm initializes with the cylindrical arc-length method and switches to a dissipation-based arc-length control for better numerical stability as the damage evolves. A number of numerical examples with singularities demonstrated improvements in terms of efficiency and accuracy, as compared to the damage models represented by Powell-Sabin triangles.

1 INTRODUCTION

Continuum damage analysis has limitations in approximating diffusive fracture due to the lack of an internal length scale that propagates damage. We address this problem by the use of nonlocal higher-order gradient damage models [1], where nonlocality is introduced by a damage variable that is a function of the nonlocal quantity, which is evaluated as the Taylor expansion of the volume average of the local quantity. Higher-order terms in the Taylor approximation of the nonlocal integral are included due to the lack of accuracy of the second-order gradient damage model.

The formulations of fourth- and sixth-order gradient damage models require a global smoothness of C^1 and C^2 , respectively. The high-order continuity of basis functions can be automatically satisfied with the use of Non-Uniform Rational B-splines (NURBS) [2,3] and T-splines [4] in isogeometric analysis (IGA). However, it is not always easy to preserve the high-order smoothness when modeling complicated geometries, where reduced continuity is observed at multi-patch interfaces or extraordinary points in unstructured T-splines. In such cases, domain triangulation appears to be a powerful tool for parameterization as it is not topologically constrained to the four-sided meshgrid. The use of Powell-Sabin (PS) triangles in fourth-order gradient damage models was studied in [5] and showed promising results. However, due to the definition of PS triangles, which are required to contain all the associated PS points in order to obtain positive basis functions, the control points of PS triangles are positioned randomly. This may be inconvenient in cases where Dirichlet/Neumann boundary conditions have to be specified at a given point. Moreover, the definition of quintic PS triangles for C^2 -continuity is complicated, compared to enforcing higher-order continuities on Bézier triangles. Additionally, it is not clear how the PS triangle formulation could be extended to three dimensions for tetrahedral meshing.

As an alternative, we adopt rational Bézier triangles [6,7] for domain triangulations. The process of mesh generation starts from C^0 Bézier triangles, meaning that one can resort to a wide number of existing meshing tools and automate the meshing process. To raise the global continuity to a desired order, Lagrange multipliers are used to impose continuity constraints in an explicit fashion. Due to the use of the rational form of the Bézier triangles, exact boundary can be fully recovered. Moreover, in order to capture small geometric features and increase the flexibility in discretization, a Delaunay-based feature-preserving triangulation is adopted. This turns out to be beneficial in capturing the initiation and early-stage propagation of damage. Additionally, instead of uniformly refining the mesh, we adopt a local refinement approach called Rivara's method [8] that bisects marked triangles while keeping the final mesh conformal and well-conditioned. The method is used to locally refine the regions where damage initiates and propagates.

In this contribution, the implicit fourth- and sixth-order gradient damage models are considered, since the inclusion of higher-order terms has the potential to accurately approximate the nonlocal solution, with minimal computational effort. The solution initializes with the cylindrical arc-length control [9] and switches to a dissipation-based arc-length control [10] for better numerical stability with the evolution of damage. Numerical examples demonstrate the benefits of higher-order gradient damage models, as well as the accuracy and ease of generalization into arbitrary high-order global smoothness in the use of the feature-preserving rational Bézier triangles.

2 DELAUNAY BASED FEATURE PRESERVING TRIANGULATION

Our solution procedure initiates with a closed NURBS curve as input and makes use of a number of existing meshing technologies (e.g., TriGA [6,7]). The main idea is a Delaunay-based triangulation with a series of Laplacian smoothing operation. The algorithm attempts to construct a high-quality polygon approximation of the original NURBS curves (Fig. 1b and 1c), which is then followed by a quadtree decomposition (Fig. 1d) that matches the local geometry features to evaluate the element size distribution needed to resolve the geometry. The algorithm optimizes the control point placement and mesh topology through an iterative process (Fig. 1e and 1f). In particular, a constrained Delaunay triangulation is performed in each iteration with a series of Laplacian smoothing operation. After a high-quality triangulation is obtained, the polynomial degree is raised to cubic and the control points at the domain boundary are replaced by the control points of the original NURBS to exactly recover the boundary. The solution process is briefly discussed in the following and illustrated in Fig. 1.

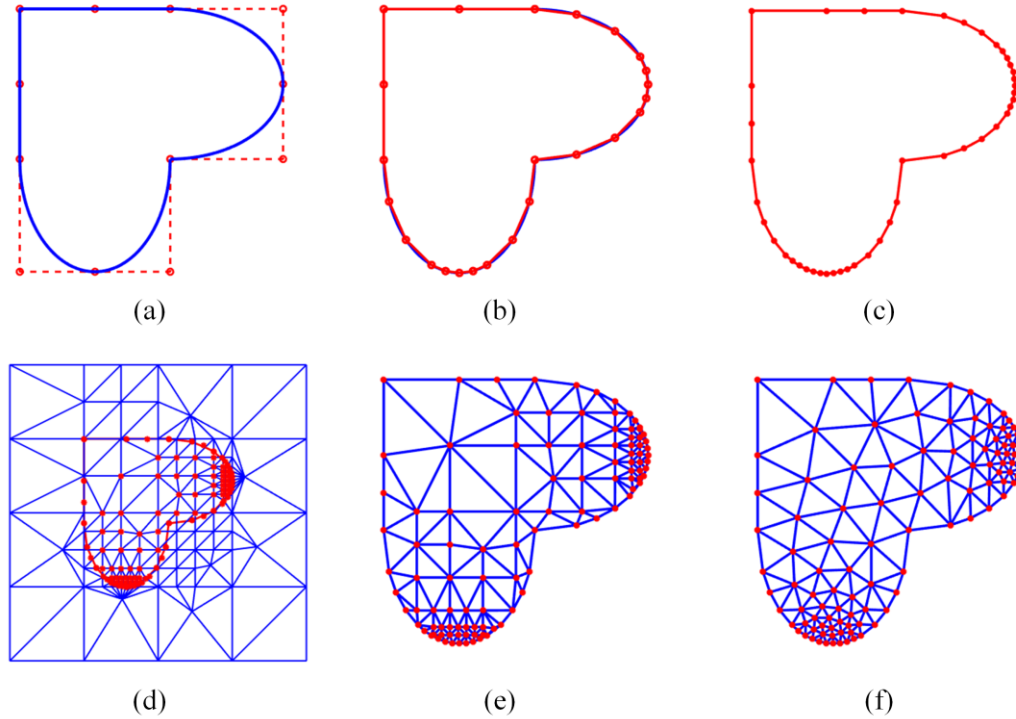


Fig. 1. Delaunay-based feature-preserving triangulation: (a) input NURBS curve; (b) initial polygon approximation after step 1; (c) final polygon approximation after step 2; (d) quadtree decomposition and control points considered for triangulation; (e) constrained Delaunay triangulation (CDT) at the first iteration; and (f) final CDT.

A . Initial polygon approximation. The step is controlled by the relative difference between the length of the curve for each knot span and the length of the corresponding polygon that approximates it. The algorithm iteratively subdivides the input NURBS curve until the relative differences for all the knot spans are below a given threshold.

B . quadtree decomposition. In this step, a quadtree background mesh is constructed and used to further refine the polygon. Specifically, the algorithm generates a bounding box, which is then recursively subdivided until the dimension of each box matches the local geometry feature size. A size function is also evaluated at the quadtree vertices based on the minimum neighboring box dimension. Next, the quadtree mesh is triangulated (Fig. 1d) so that the size function can be linearly interpolated at the polygon control points. Knot insertion is performed if the ratio of the edge length to the size function is above a given threshold.

C . Delaunay based triangulation with inner smoothing. The polygon approximation from Step () is triangulated using the quadtree decomposition. The initial control points of the mesh are taken as a combination of the fixed polygon nodes and the internal nodes from the quadtree mesh (Fig. 1e). The algorithm optimizes the node placement and mesh topology via an iterative process. In particular, a constrained Delaunay triangulation is constructed at every iteration. Nodes are then added or removed from the mesh to meet the required element size distribution. A Laplacian smoothing operation such as a spring-based smoothing is then performed. The process iterates until all the triangles meet the element size constraints.

D . Polynomial degree elevation and boundary recovery. In this step, we raise the polynomial degree to cubic via linear interpolation. Additionally, knot insertion is performed on the input NURBS curves until the knots corresponding to the polygon vertices have multiplicity 3. As a result, there exist four control points at each knot span corresponding to the edge control points of the boundary triangles. The control points at the boundary are then substituted by the control points of the input NURBS curves for exact boundary recovery.

3 LOCAL REFINEMENT

As is commonly acknowledged, it is unnecessary and computationally costly to uniformly refine the mesh. Therefore, we adopt a local refinement scheme (i.e., Rivara's method [8]) that is capable of generating high-quality mesh while keeping the final mesh conforming and well-conditioned. The algorithm firstly bisects marked triangles and then iteratively bisects non-conforming triangles until the mesh becomes conforming. A pseudo-code is provided in Fig. 2.

Algorithm 1 Rivara's method of bisecting triangles for local refinement

```

1: for all marked triangles  $\tau \in \Gamma$  do
2:   Bisect  $\tau$  by the midpoint  $P$  of the longest edge.
3: end do
4: Find the set of non-conforming triangles  $\tau_n \in \Gamma_n$ 
5: while cardinality of  $\Gamma_n \neq 0$  do
6:   Bisect  $\tau_n$  by the midpoint  $Q$  of its longest side
7:   if  $P \neq Q$  then
8:     Join  $P$  and  $Q$ 
9:   end if
10: Find the set of non-conforming triangles  $\Gamma_n$ 
11: end do

```

Fig. 2. A pseudo-code for Rivara's method of bisecting triangles for local refinement

4 HIGHER ORDER GRADIENT DAMAGE MODELS

4.1. Continuum formulation

The nonlocal damage analysis is a coupled analysis where a diffusion equation representing the damage propagation needs to be solved in addition to the equilibrium equation representing the structural deformation. On the one hand, the structural deformation can be expressed as

$$\frac{\partial \sigma_i}{\partial x_i} = 0 \quad (1)$$

and may be subjected to Dirichlet boundary conditions $u_i = \bar{u}_i$ on $\partial\Omega_u$ and Neumann boundary conditions $\sigma_i n_i = h_i$ on $\partial\Omega_h$.

On the other hand, the representation of damage propagation requires an additional scalar variable $\omega \in [0,1]$, with $\omega = 0$ the undamaged state and $\omega = 1$ the fully damaged state. As a result, the stress-strain relationship can be written as

$$\sigma_i = (1 - \omega) \epsilon_i \quad (2)$$

where ϵ_i is the elasticity tensor and ϵ is the infinitesimal strain tensor

$$\epsilon_i = \frac{1}{2} \left(\frac{\partial u_i}{\partial x} + \frac{\partial u}{\partial x_i} \right) \quad (3)$$

The damage variable ω is a function of a monotonically increasing history parameter κ , $\omega = \omega(\kappa)$. The evolution of κ is controlled by the Kuhn-Tucker conditions:

$$f \leq 0, \quad \dot{\kappa} \geq 0, \quad \dot{\kappa} f = 0 \quad (4)$$

with f the loading function, $f = \bar{\eta} - \kappa$, and $\bar{\eta}$ the nonlocal equivalent strain. The nonlocal equivalent strain $\bar{\eta}$ can be calculated using the average of the local equivalent strain η over a finite volume Ω

$$\bar{\eta}(x) = \frac{\int_{\hat{x} \in \Omega} g(x, \hat{x}) \eta(\hat{x}) d\hat{x}}{\int_{\hat{x} \in \Omega} g(x, \hat{x}) d\hat{x}} \quad (5)$$

with $g(x, \hat{x})$ the weighting function,

$$g(x, \hat{x}) = \exp \left(- \frac{\|x - \hat{x}\|}{2l_c^2} \right) \quad (6)$$

and l_c the internal length parameter.

In order to avoid a computationally expensive evaluation of the above volume integral, the Taylor expansion of the local equivalent strain η is often employed. In particular,

$$\eta(\hat{x}) = \eta|_{\hat{x}=x} + \frac{\partial \eta}{\partial \hat{x}_i} \bigg|_{\hat{x}=x} (\hat{x}_i - x_i) + \frac{1}{2} \frac{\partial^2 \eta}{\partial \hat{x}_i \partial \hat{x}_j} \bigg|_{\hat{x}=x} (\hat{x}_i - x_i)(\hat{x}_j - x_j) + O((\hat{x}_i - x_i)^3) \quad (7)$$

Substituting Eq. (7) into Eq. (5) and assuming that the integral ranges from negative infinity to infinity result in the explicit gradient formulation of the nonlocal equivalent strain

$$\bar{\eta}(x) = \eta(x) + \frac{1}{2} l_c^2 \frac{\partial^2 \eta(x)}{\partial x_i^2} + \frac{1}{8} l_c^4 \frac{\partial^4 \eta(x)}{\partial x_i^2 \partial x_j^2} + \frac{1}{48} l_c^6 \frac{\partial^6 \eta(x)}{\partial x_i^2 \partial x_j^2 \partial x_k^2} + \dots \quad (8)$$

In order to include the second- and fourth-order terms from Eq. (8), 1 - and 2 - continuous basis functions are required, respectively. As an alternative, the implicit gradient formulation can be obtained through differentiation and multiplication of Eq. (8)

$$\eta(x) = \bar{\eta}(x) - \frac{1}{2} l_c^2 \frac{\partial^2 \bar{\eta}(x)}{\partial x_i^2} + \frac{1}{8} l_c^4 \frac{\partial^4 \bar{\eta}(x)}{\partial x_i^2 \partial x_j^2} - \frac{1}{48} l_c^6 \frac{\partial^6 \bar{\eta}(x)}{\partial x_i^2 \partial x_j^2 \partial x_k^2} + \dots \quad (9)$$

The above implicit formulation only requires 0 -continuity for the second-order gradient model and is therefore suitable for standard FEA. However, the accuracy of the solution is often not satisfactory. In our approach, the fourth- and sixth-order gradient damage terms are also considered through the use of Lagrange multipliers [7] to raise global continuity.

Combining Eq. (1) and Eq. (9) leads to the govern equations for the higher-order gradient damage model. Through multiplication of a perturbation term δu and $\delta \bar{\eta}$ to Eq. (1) and Eq. (9), respectively, and integration by parts over the domain Ω , the weak form can be obtained

$$\begin{aligned} \int_{\Omega} \frac{\partial \delta u_i}{\partial x} \sigma_i d &= \int_{\partial \Omega_h} \delta u_i h_i d \\ \int_{\Omega} \delta \bar{\eta} \bar{\eta} + \frac{1}{2} l_c^2 \frac{\partial \delta \bar{\eta}}{\partial x_i} \frac{\partial \bar{\eta}}{\partial x_i} + \frac{1}{8} l_c^4 \frac{\partial^2 \delta \bar{\eta}}{\partial x_i \partial x_j} \frac{\partial^2 \bar{\eta}}{\partial x_i \partial x_j} + \frac{1}{48} l_c^6 \frac{\partial^3 \delta \bar{\eta}}{\partial x_i \partial x_j \partial x_k} \frac{\partial^3 \bar{\eta}}{\partial x_i \partial x_j \partial x_k} d &= \int_{\partial \Omega_h} \delta \bar{\eta} \eta d \end{aligned} \quad (10)$$

4.2. Discretization

The domain of interest is discretized into n elements by the feature-preserving triangulation in Section 2. We can rewrite the displacement u , the nonlocal equivalent strain $\bar{\eta}$ and their derivatives in terms of the Bézier basis functions and the deformation of the associated control points

$$u = \mathbf{R}_u \mathbf{u}, \varepsilon = \mathbf{B}_u \mathbf{u}, \bar{\eta} = \mathbf{R}_{\bar{\eta}} \bar{\eta}, \frac{\partial \bar{\eta}}{\partial x_i} = \mathbf{B}_{\bar{\eta}} \bar{\eta}, \frac{\partial^2 \bar{\eta}}{\partial x_i \partial x} = \mathbf{B}_{\bar{\eta}\bar{\eta}} \bar{\eta}, \frac{\partial^3 \bar{\eta}}{\partial x_i \partial x \partial x} = \mathbf{B}_{\bar{\eta}\bar{\eta}\bar{\eta}} \bar{\eta} \quad (11)$$

where

$$\begin{aligned} u &= \begin{bmatrix} u_x & u_y \end{bmatrix}, \varepsilon = \begin{bmatrix} \varepsilon_{xx} & \varepsilon_{yy} & 2\varepsilon_{xy} \end{bmatrix}, \frac{\partial \bar{\eta}}{\partial x_i} = \begin{bmatrix} \frac{\partial \bar{\eta}}{\partial x} & \frac{\partial \bar{\eta}}{\partial y} \end{bmatrix}, \\ \frac{\partial^2 \bar{\eta}}{\partial x_i \partial x} &= \begin{bmatrix} \frac{\partial^2 \bar{\eta}}{\partial x^2} & \frac{\partial^2 \bar{\eta}}{\partial y^2} & \sqrt{2} \frac{\partial^2 \bar{\eta}}{\partial x \partial y} \end{bmatrix}, \\ \frac{\partial^3 \bar{\eta}}{\partial x_i \partial x \partial x} &= \begin{bmatrix} \frac{\partial^3 \bar{\eta}}{\partial x^3} & \frac{\partial^3 \bar{\eta}}{\partial y^3} & \sqrt{3} \frac{\partial^3 \bar{\eta}}{\partial x^2 \partial y} & \sqrt{3} \frac{\partial^3 \bar{\eta}}{\partial x \partial y^2} \end{bmatrix}, \\ \mathbf{R}_u &= \begin{bmatrix} \mathbf{R} & \mathbf{R} \end{bmatrix}, \mathbf{B}_u = \begin{bmatrix} \frac{\partial \mathbf{R}}{\partial x} & \frac{\partial \mathbf{R}}{\partial y} \\ \frac{\partial \mathbf{R}}{\partial y} & \frac{\partial \mathbf{R}}{\partial x} \end{bmatrix}, \mathbf{R}_{\bar{\eta}} = \mathbf{R}, \mathbf{B}_{\bar{\eta}} = \begin{bmatrix} \frac{\partial \mathbf{R}}{\partial x} & \frac{\partial \mathbf{R}}{\partial y} \end{bmatrix}, \end{aligned} \quad (12)$$

$$\mathbf{B}_{\bar{\eta}\bar{\eta}} = \begin{bmatrix} \frac{\partial^2 \mathbf{R}}{\partial x^2} & \frac{\partial^2 \mathbf{R}}{\partial y^2} & \sqrt{2} \frac{\partial^2 \mathbf{R}}{\partial x \partial y} \end{bmatrix}, \mathbf{B}_{\bar{\eta}\bar{\eta}\bar{\eta}} = \begin{bmatrix} \frac{\partial^3 \mathbf{R}}{\partial x^3} & \frac{\partial^3 \mathbf{R}}{\partial y^3} & \sqrt{3} \frac{\partial^3 \mathbf{R}}{\partial x^2 \partial y} & \sqrt{3} \frac{\partial^3 \mathbf{R}}{\partial x \partial y^2} \end{bmatrix}$$

Substituting the discretized form into Eq. (10) leads to

$$\begin{aligned} \delta \mathbf{u} \left(\int_{\Omega} \mathbf{B}_u (1-\omega) \mathbf{C} \mathbf{B}_u d\mathbf{u} - \int_{\partial\Omega_h} \mathbf{R}_u \mathbf{h} d \right) &= 0 \\ \delta \bar{\eta} \left(\int_{\Omega} \mathbf{R}_{\bar{\eta}} \mathbf{R}_{\bar{\eta}} + \frac{l_c^2}{2} \mathbf{B}_{\bar{\eta}} \mathbf{B}_{\bar{\eta}} + \frac{l_c^4}{8} \mathbf{B}_{\bar{\eta}\bar{\eta}} \mathbf{B}_{\bar{\eta}\bar{\eta}} + \frac{l_c^6}{48} \mathbf{B}_{\bar{\eta}\bar{\eta}\bar{\eta}} \mathbf{B}_{\bar{\eta}\bar{\eta}\bar{\eta}} d\bar{\eta} - \int_{\Omega} \mathbf{R}_{\bar{\eta}} \eta d \right) &= 0 \end{aligned} \quad (13)$$

NUMERICAL EXAMPLES

In this section, we consider the classical L-shaped domain and its variant, which is an L-shaped domain with curved inside corner. For both problems, we employ a 28-point quadrature rule for integration over the triangle. We also use quintic elements in order to impose higher-order continuity.

1 L shaped domain

As the first numerical example, we consider the classical L-shaped domain problem. The setup of the problem is shown in Fig. 3(a). The thickness of the plate is $t=200$ mm. The material

is linear elastic, with the Young's modulus $E=10\text{GPa}$ and Poisson's ratio is $\nu=0.2$. A state of plane stress is assumed.

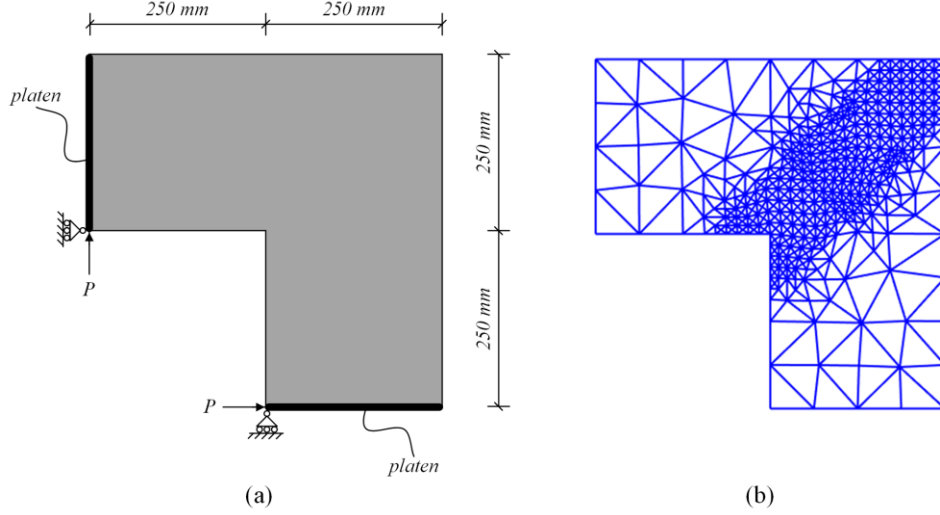


Fig. 3. The classical L-shaped domain: (a) the problem setup, and (b) the resulting mesh after applying Rivara's method five times (number of control points (NCP): 12631).

The two platens at the ends of the plate are realized by imposing linear constraints in the form of Lagrange multipliers. The modified von Mises local equivalent strain is used

$$\eta(\varepsilon) = \frac{-1}{2(1-2\nu)} I_1(\varepsilon) + \frac{1}{2} \sqrt{\left(\frac{-1}{1-2\nu} I_1(\varepsilon) \right)^2 + \frac{12}{(1+\nu)^2} J_2(\varepsilon)} \quad (14)$$

with $I_1(\varepsilon)$ the first invariant of the strain tensor, $J_2(\varepsilon)$ the second invariant of the deviatoric strain tensor, and β representing a parameter that accounts for the variation in strength between compression and tension, $\beta = 10$.

The damage law employed in this example is

$$\omega(\kappa) = \begin{cases} 0 & \kappa \leq \kappa_0 \\ 1 - \frac{\kappa_0}{\kappa} (1 - \alpha + \alpha \exp(\beta(\kappa_0 - \kappa))) & \kappa > \kappa_0 \end{cases} \quad (15)$$

with $\kappa_0 = 4 \times 10^{-4}$, $\alpha = 0.98$ and $\beta = 80$. The internal length parameter is $l_c = 5\sqrt{2}\text{mm}$.

Instead of uniformly refining the entire domain, we directly apply Rivara's method to locally refine the diagonal region, which is the region that damage will propagate. Fig. 3(b) shows the final mesh after applying Rivara's method five times to the region bounded by two lines $y \geq x - 75$ and $y \leq x + 75$, with the inside corner taken as the origin.

The force-displacement relationships are plotted in Fig. 4, where they are also compared to the solutions from literature using T-splines [1] and PS triangles [5]. The displacement is

measured at the location the point load is applied to. For this problem, we use the nonlocal solution using T-splines as our reference solution. By comparing the solutions of different order gradient formulations on the locally refined mesh (LRM), we observe an obvious improvement in accuracy with the inclusion of the fourth- and sixth-order terms. In comparison to the result of the fourth-order gradient damage formulation using PS-triangles, our solution appears to be more accurate. In terms of NCP, the solution using PS-triangles uses 26463 control points, whereas our LRM only employs 12631 control points, which demonstrates significant computational saving.

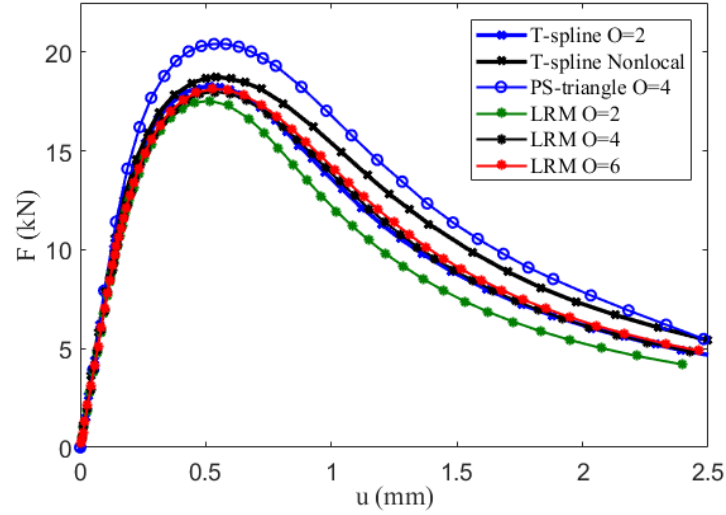


Fig. 4. The force-displacement relationships of the L-shaped domain

To better illustrate the accuracy of the proposed approach, the contour plots for the damage propagation and maximum principal stress distribution at $u = 1.95\text{mm}$ are also plotted in Fig. 5.

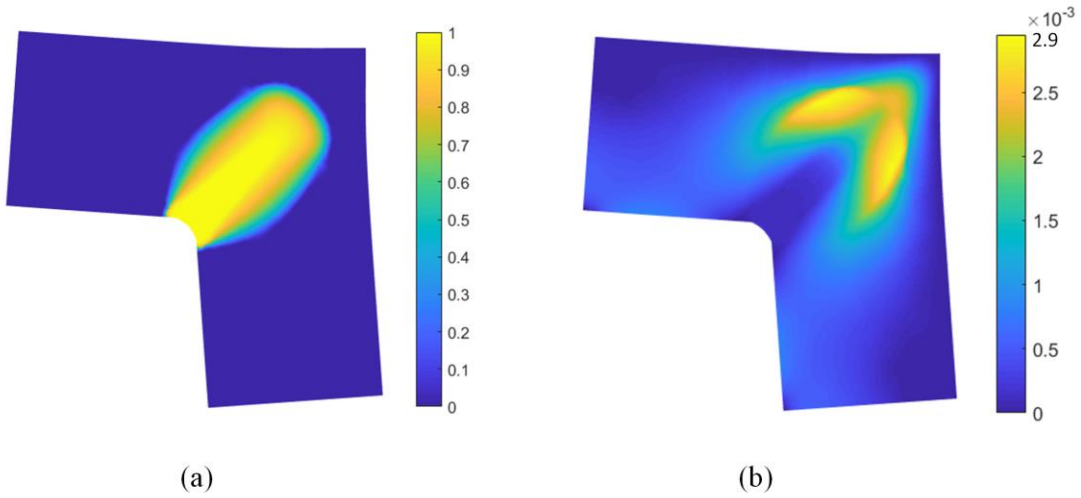


Fig. 5. Control plot for the L-shaped domain at $u = 1.95\text{mm}$ (the deformation is amplified by a factor of 20):
 (a) damage propagation and (b) maximum principal stress distribution.

.2 L shaped domain with curved inside corner

For the second example, only a slight change is made to the L-shaped domain, with the inside corner being curved instead of at a right angle (see Fig. 6(a)). Our aim is to investigate the performance of the feature-preserving algorithm on capturing the damage initiation and the early-stage damage diffusion. The sixth-order gradient damage formulation is adopted.

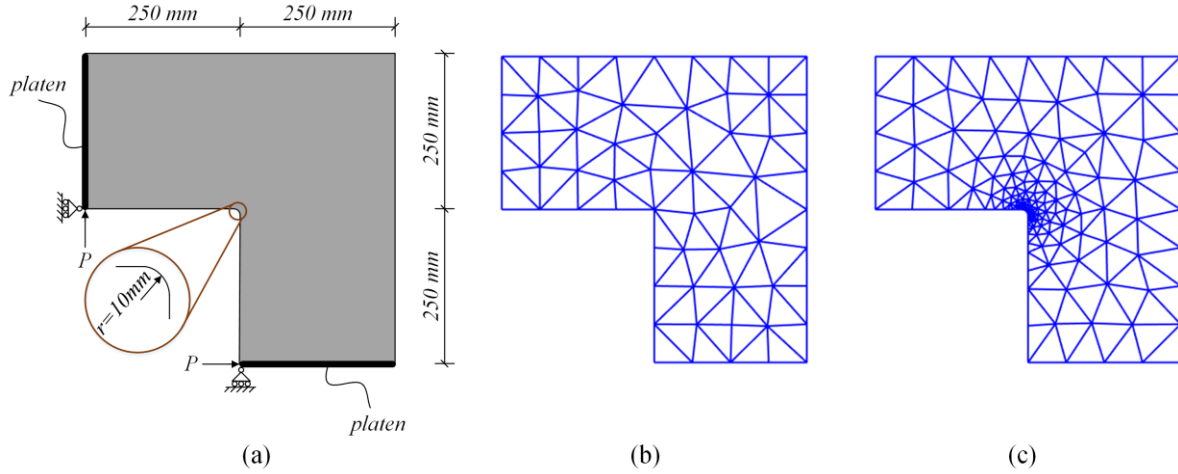


Fig. 6. The L-shaped domain with curved inside corner: (a) the problem setup, (b) the initial mesh, and (c) the feature-preserving triangulation

The final mesh from the feature-preserving meshing algorithm is plotted against the initial mesh of the classical L-shaped domain without before the local refinement technique is applied (see Fig. 6(b)). As we can see, the inside corner is resolved with high resolution (Fig. 6(c)).

The force-displacement relationships obtained using the above two meshes are plotted in Fig. 7. In comparison to the result obtained using the mesh in Fig. 6(b), we see a more accurate prediction of the entire deformation path using the mesh in Fig. 6(c), especially in the damage initiation phase that corresponds to the onset of yielding. The feature-preserving mesh is able to provide a fairly accurate solution up to $u \approx 0.4\text{mm}$, after which the damage propagates into the region of relatively large elements and locally refinement as demonstrated in the first numerical example is needed. In general, the feature-preserving triangulation can be employed to predict the early-stage damage propagation, and then a coupled adaptive meshing should be used to refine meshes in the direction of damage growth.

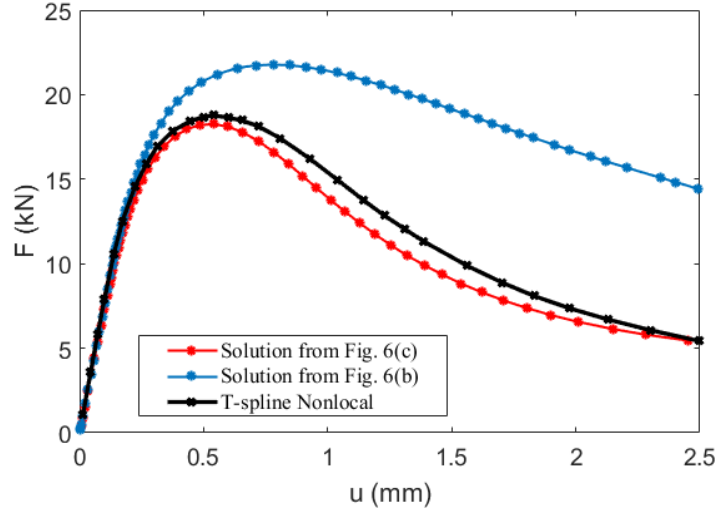


Fig. 7. The force-displacement curves obtained using the two mesh cases in Fig. 6

To better demonstrate the capability of the feature-preserving triangulation in capturing the early-stage damage propagation, the contour plots of damage growth at $u = 0.43mm$, $u = 0.90mm$ and $u = 1.25mm$ are provided in Fig. 8.

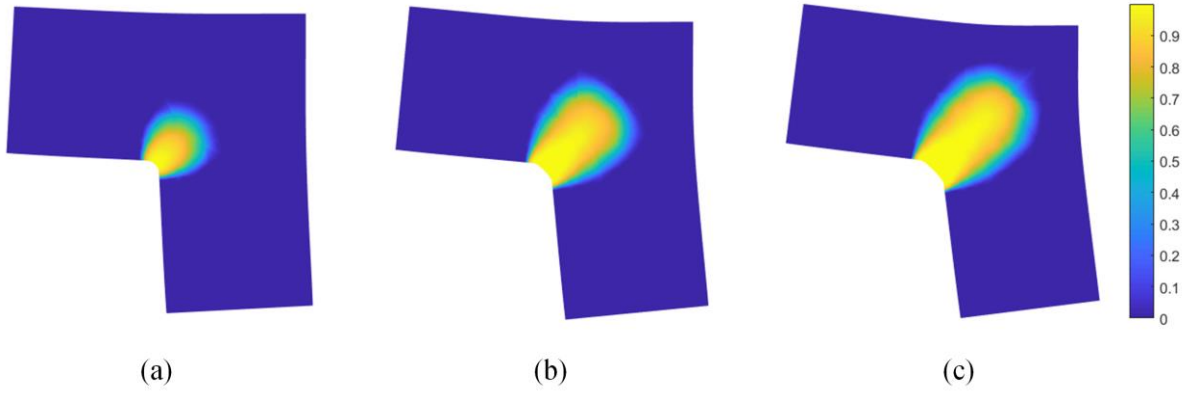


Fig. 8. The contour plots of damage growth in the L-shaped domain with curved inside corner (deformation is amplified by a factor of 50) at (a) $u = 0.43mm$, (b) $u = 0.90mm$ and (c) $u = 1.25mm$

. CONCLUSION

The Delaunay-based feature-preserving rational Bézier triangles are a powerful tool in modeling smeared damage, especially in cases where complicated geometries are involved. They not only bypass the reduced continuity issue in NURBS and T-splines, but they also increase the flexibility in discretization. As is indicated in the second example, a general modeling framework can be constructed where the feature-preserving meshing can be employed to predict the damage growth at an early stage. As the damage propagates, a suitable

local refinement technique such as the Rivara's method can be adopted to further refine the mesh in the direction of damage growth. Furthermore, the use of Lagrange multipliers makes it possible to impose higher-order continuity constraints to the resulting mesh. In terms of the formulation of the implicit gradient damage models, the inclusion of higher-order terms results in a more accurate prediction of the deformation path, while the additional computational effort is trivial. The accuracy and efficiency of the proposed modeling approach are verified by a number of numerical examples, where superiority is observed over other domain triangulation methods such as PS triangles.

Nevertheless, it must be mentioned that domain triangulation is not an undisputedly better approach over quadrilateral meshing techniques (e.g., T-splines). An obvious defect of domain triangulation methods is that typically high-order polynomials (e.g., quartic and quintic) have to be used in order to enforce higher-order global continuity. In contrast, C^2 continuity can be easily achieved with cubic NURBS/T-splines.

REFERENCES

- [1] C. V. Verhoosel, M.A. Scott, T.J.R. Hughes, R. de Borst, An isogeometric analysis approach to gradient damage models, *Int. J. Numer. Methods Eng.* 86 (2011) 115–134.
- [2] N. Liu, A.E. Jeffers, Adaptive isogeometric analysis in structural frames using a layer-based discretization to model spread of plasticity, *Comput. Struct.* 196 (2018) 1–11.
- [3] N. Liu, A.E. Jeffers, Isogeometric analysis of laminated composite and functionally graded sandwich plates based on a layerwise displacement theory, *Compos. Struct.* 176 (2017) 143–153.
- [4] Y. Bazilevs, V.M. Calo, J.A. Cottrell, J.A. Evans, T.J.R. Hughes, S. Lipton, M.A. Scott, T.W. Sederberg, Isogeometric analysis using T-splines, *Comput. Methods Appl. Mech. Eng.* 199 (2010) 229–263.
- [5] S. May, R. de Borst, J. Vignollet, Powell-Sabin B-splines for smeared and discrete approaches to fracture in quasi-brittle materials, *Comput. Methods Appl. Mech. Eng.* 307 (2016) 193–214.
- [6] L. Engvall, J.A. Evans, Isogeometric triangular Bernstein-Bézier discretizations: Automatic mesh generation and geometrically exact finite element analysis, *Comput. Methods Appl. Mech. Eng.* 304 (2016) 378–407.
- [7] N. Liu, A.E. Jeffers, A geometrically exact isogeometric Kirchhoff plate: Feature-preserving automatic meshing and C^1 rational triangular Bézier spline discretizations, *Int. J. Numer. Methods Eng.* (2018) 1–15.
- [8] M.C. Rivara, Algorithms for refining triangular grids suitable for adaptive and multigrid techniques, *Int. J. Numer. Methods Eng.* 20 (1984) 745–756.
- [9] N. Liu, P. Plucinsky, A.E. Jeffers, Combining Load-Controlled and Displacement-Controlled Algorithms to Model Thermal-Mechanical Snap-Through Instabilities in Structures, *J. Eng. Mech.* 143 (2017) 1–11.
- [10] C. V. Verhoose, J.J.C. Remmers, M.A. Gutiérrez, A dissipation-based arc-length method for robust simulation of brittle and ductile failure, *Int. J. Numer. Methods Eng.* 77 (2009) 1290–1321.

Understanding Evolution Mechanisms of Site-specific Grain Structures during Metal Additive Manufacturing

Pengwei Liu^{*}, Yanzhou Ji^{**}, Zhuo Wang^{***}, Chunlei Qiu^{****}, Alphons A. Antonysamy^{*****},
Long-Qing Chen^{*****}, Xiangyang Cui^{*****}, Lei Chen^{*****}

^{*}Hunan University, ^{**}Pennsylvania State University, ^{***}Mississippi State University, ^{****}Cardiff University, ^{*****}GKN Aerospace Filton, ^{*****}Pennsylvania State University, ^{*****}Hunan University, ^{*****}Mississippi State University

ABSTRACT

A multiscale model is developed to investigate the evolution mechanisms of site-specific grain structures during additive manufacturing (AM) of metallic alloys, using Ti-6Al-4V fabricated by selective electron beam melting (SEBM) as an example. These rapid processes are difficult to observe in experiments. Specifically, finite-element method is utilized to predict the thermal response at macroscale during SEBM, and the extracted thermal information is then input into a temperature-dependent phase-field model to simulate the grain growth at mesoscale. The thermal-gradient-dictating grain nucleation and anisotropic grain boundary energy are incorporated to account for the strongly anisotropic grain structures and textures. The development of large vertical columnar grains in the thick wall and inward growing slanted columnar grains in the thin wall can be attributed to the competition and collaboration between the thermal gradient and the crystallographically preferred grain orientations, as shown from the different growth stages in the simulations. The simulation results reveal that the thermal gradients control the grain nucleation angles during a layer-wise printing, and play a dominant role in grain structure development at the initial and intermediate stages. As the printing proceeds, the developed large columnar grains, either vertical or slanted, prohibit and swallow the nucleated grains in the newly deposited layer. The crystallographically preferred grain orientations gradually take over and contribute more to the grain texture development. The present study potentially offers valuable insights and guidance toward designing AM conditions to tailor the grain structures and textures. Keywords: Grain structures; Evolution mechanisms; Additive manufacturing; Titanium alloys; Phase-field method; Finite-element.

Concurrent Topology Optimization of Macrostructures and Microstructures of Viscoelastic Materials under Periodic Dynamic Loads

Qiming Liu^{*}, Xiaodong Huang^{**}

^{*}Swinburne University of Technology, Australia, ^{**}Swinburne University of Technology, Australia

ABSTRACT

The damping characteristics of the viscoelastic materials are often utilized in the applications of dynamic structures, whereas there is no report on concurrent topology optimization of dynamic structures and their viscoelastic materials. Based on the bi-direction evolutionary structural optimization (BESO) method, this paper proposes a two-scale topology optimization algorithm which minimizes the dynamic compliance of structures by employing viscoelastic materials with optimal damping characteristics. The macrostructure is constructed by viscoelastic composite, whose microstructure is represented by periodic unit cells (PUCs). The effective properties of the viscoelastic composite are extracted by the homogenization theory and further integrated into the analysis of macrostructures. The sensitivity analysis with regard to design variables at macro- and micro- scale levels is conducted for iteratively updating the topologies at both scale levels synchronously. Numerical results show the developed topology algorithm can obtain the optimal topologies of the structure at the macro-scale level and microstructure of its viscoelastic material at the micro-scale level simultaneously, so that the resulting structure possesses the minimum dynamic compliance and the maximum damping under the prescribed weight.

Liquid Evaporation-Driven Self-Assembly of 3-D Architected Structures: Atomistic Modeling and Simulations

Qingchang Liu^{*}, Baoxing Xu^{**}

^{*}University of Virginia Charlottesville, ^{**}University of Virginia Charlottesville

ABSTRACT

Low-dimensional deformable 2-D graphene have attracted tremendous attention for its many unique properties. However, a single piece of graphene is too delicate to be useful in most applications, for example, high-performance electrodes in energy storage, filters for waste water/gas treatments in environmental systems, and lightweight structures. Assembling these nanomaterials into three-dimensional (3-D) scaffolds to achieve superior overall performance with multiple functionalities has attracted growing interests, yet this is challenging in manufacturing. In particular, graphene tends to aggregate/restack due to strong van der Waals attraction such as restacking of 2-D flat graphene sheets, which not only results in a tremendous reduction of their accessible surface area and poor mass/ion transport, but also degrades with processing and/or application environments such as mechanical loadings, hence adversely affecting their properties and subsequent applications. A liquid evaporation-assisted manufacturing technique is considered to provide a facile route, where 2-D graphene will experience large deformation and severe instability under evaporation-induced compression to create spacings when assembled, which is highly desirable to minimize restacking and retain the large surface areas of graphene in the assembled 3-D architectural structures. In the present study, we develop an atomistic modeling and simulation technique to first probe the deformation and self-folding mechanism of individual 2-D graphene suspended in a liquid environment, and then extend it for understanding crumpling and assembling multiple 2-D graphene sheets by liquid evaporation. The proposed modeling and simulations results will help finding key controlling parameters including concentration, evaporation rate in experiments and provide a direct guidance for evaporation-assisted manufacturing technique.

A Coupled Finite Element Method/Peridynamic for 2D Dynamic Fracture Analysis

Shuo Liu^{*}, Bing Wang^{**}, Guodong Fang^{***}, Jun Liang^{****}

^{*}Harbin Institute of Technology, ^{**}Harbin Institute of Technology, ^{***}Harbin Institute of Technology, ^{****}Beijing Institute of Technology

ABSTRACT

Abstract: A new coupling scheme of peridynamic (PD) and finite element method (FEM) is proposed in this paper to analyze the 2D brittle material transient crack propagation problem. The coupling scheme makes full use of the advantages of PD to deal with discontinuous problems and the high efficiency of FEM. It is easy to perform, without setting the overlap region between PD and FEM. By using the adaptive partitioning of the solution domain, the PD model is used only in the vicinity of the crack to reduce the computational effort. In the coupling region, the stiffness of FEM and the interaction between PD particles are assembled into a global stiffness matrix. Ghosts test analysis verifies the reliability of the coupling method. The numerical example shows that the proposed coupling scheme has high accuracy and efficiency in the simulation of dynamic crack bifurcation problems. Key words: coupling, damage; crack propagation and bifurcation; FEM; peridynamic

Harmonic Balance Method for Unsteady One-Dimensional Periodic Flows

Wei Liu^{*}, Zhenxia Chai^{**}, Ming Zeng^{***}, Xiaoliang Yang^{****}

^{*}National University of Defense Technology, ^{**}National University of Defense Technology, ^{***}National University of Defense Technology, ^{****}National University of Defense Technology

ABSTRACT

In recent years, the harmonic balance method (HBM) has been developed as a novel nonlinear frequency domain method for modeling periodic unsteady flows. In this paper, two one-dimensional computational fluid dynamics (CFD) codes were developed to investigate the behavior of the harmonic balance method. The first work investigated harmonic balance solutions of one-dimensional inviscid wave equation subject to a variety of periodic boundary conditions. Next, harmonic balance solutions of the inviscid Burgers' equation were investigated. Accuracy will be determined through comparison with accurate results and conventional time domain method's results. The impact of number of harmonics, amplitude and frequency of the boundary conditions, and grid density on the harmonic balance solution were investigated. Computational results demonstrate that a flow that is smoothly unsteady without moving discontinuities will require fewer harmonics for HBM computation than a flow containing a moving shock to achieve the same accuracy with the time domain method. As amplitude increased, solutions for boundary conditions containing moving waves ranging from smooth disturbances to strong discontinuities. The larger of amplitude, the stronger of the discontinuities, and the more harmonics are required for HBM computation. In contrast, as the disturbance frequency increased, the number of harmonics required for HBM computation usually decreased. The results also show that the coarse grid can eliminate the non-physical oscillations resulted in beneficial smoothing, but the coarse grid damping effect caused considerable degradation in higher-frequency solution. The harmonic balance method was more sensitive to grid density than the time domain method.

A Simulation Toolkit for the Microstructure Modelling Guided Design of the Damage Tolerant High-strength Steel

Wenqi Liu^{*}, Sebastian Münstermann^{**}, Junhe Lian^{***}

^{*}RWTH Aachen University, ^{**}RWTH Aachen University, ^{***}RWTH Aachen University

ABSTRACT

A simulation toolkit is developed in this study for the damage tolerant microstructure design of the advanced high strength steel. Toolkit is an improved integrated computational materials engineering approach fostering sustainable component design option. It provides a method of tailoring steels for a specific industry application and improving material performance by new mechanism. In this study, crash box manufactured by a dual-phase steel sheet (DP1000) in the automotive industry is focused on. With the help of macro- and micro-mechanical models, the component performance, i.e. the crashworthiness of crash box, can be transferred to the required mechanical property profiles and the optimized microstructure features. Toolkit starts at the targeted component performance, crash box tests are performed on the drop tower to characterize the crashworthiness. An Extended Modified Bai Wierzbicki (eMBW) damage considering the effects of stress state, strain rate and temperature on the plasticity and damage/fracture behavior is developed for transfer the component performance to the required macromechanical property profiles. An extensive experimental program at lab scale is designed to calibrate the material parameters and validate the model, involving dog-bone specimens, notched tension specimens, central-hole specimens, and punch specimens to cover a wide range of stress states. These tests are performed at quasi-static and high speeds conditions to obtain the plasticity and fracture description of material response at various strain rates and temperatures. For the linking between the microstructure features and the mechanical properties, the representative microstructure model is employed allowing consideration of the microstructure parameters and at the same time bridging the equivalent quantities from microstructure to macroscopic level by incorporating a crystal plasticity material model. To balance the representativeness and computational capability of the 3D representative volume elements (RVEs), A criterion considering the effects of RVE size and mesh discretization is proposed to characterize the RVE representativeness. Nanoindentation tests are carried out on both ferrite and martensite to calibrate the crystal plasticity parameters. The micromechanical models are validated by uniaxial tensile test, with which the flow curve of the reference material is naturally captured. For microstructure optimization, the integrated microstructural features, such as phase fraction, grain size, grain shape, texture, and second phase morphology et.al., are taking into account for their effects on the macroscopic mechanics. Finally, the tailored damage tolerant microstructure is designed for the targeted component performance.

Data-Driven Process-Structure-Property Simulation Models for Additive Manufacturing

Wing Kam Liu*

*Northwestern University

ABSTRACT

This talk presents our latest work on the comprehensive materials modeling of process-structure-property relationships for additive manufacturing (AM) materials. The numerous influencing factors that emerge from the AM process motivate the need for novel rapid design and optimization approaches. For this, we propose data-mining as an effective solution. Such methods - used in the process-structure, structure-properties and the design phase that connects them - would allow for a design loop for AM processing and materials. As a specific application, the developed data-driven simulation models are employed to study, understand, and manipulate thermos-capillary flow in additive manufacturing. Thermo-capillary flow, driven by Marangoni stress and buoyant force, dramatically affect the heat and mass transfer, solidification behavior, and microstructure formation in the melt pool. It is still challenging to understand the thermo-capillary flow and to manipulate it so as to tailor microstructure and properties in AM of Superalloys. Surfactants, which are the elements or compounds remarkably affecting surface tension of liquid metal, are introduced. The effects of surfactants on thermo-capillary flow is demonstrated as well as the possibility of manipulating thermo-capillary flow by adding specific surfactant. The surfactant-affected thermo-capillary flow in AM will be discussed.

Welcome Remarks

Wing Kam Liu*, Jacob Fish**

*Northwestern, **Columbia University

ABSTRACT

Opening words of welcome.

An Efficient Strategy for Large Scale 3D Simulation of Heterogeneous Materials

Xiaodong Liu^{*}, Julien Réthoré^{**}, Antonius A. Lubrecht^{***}, Marie-Christine Baietto^{****}, Philippe Sainsot^{*****}

^{*}Ecole Centrale de Nantes, ^{**}Ecole Centrale de Nantes, ^{***}INSA-Lyon, ^{****}INSA-Lyon, ^{*****}INSA-Lyon

ABSTRACT

The development of imaging techniques based on X-ray tomography permits one to obtain the inner structure and the details of materials at a microscopic scale. To take into account such detailed information as an input for numerical simulations is becoming more and more common. The difficulties are the computational cost, mesh generation in the context of finite element simulation and the high discontinuities of material properties (Gu et al., 2016) which can lead to convergence problems. The subject of this presentation is the application of MultiGrid methods coupled with homogenization methods for coarse grid operators (Sviercoskiet al., 2015). The method allows us to solve large scale 3D thermal conduction problems in a material with highly heterogeneous properties. Hybrid MPI-OpenMP parallel computing has been used to save computational time. The material structure is obtained from a real X-ray tomography image. The influence of material heterogeneity is analyzed as well as the ratio of material properties for the thermal conduction. The efficiency of the strategy of using MultiGrid coupled with homogenization based coarse grid operators shows the possibility to carry out numerical simulations at microscopic scale with a low computational cost. References Gu, H., Réthoré, J., Baietto, M.-C., Sainsot, P., Lecomte-Grosbras, P., Venner, C. H., Lubrecht, A. A., 2016. An efficient multigrid solver for the 3d simulation of composite materials. Computational materials science 112, 230–237. Sviercoski, R. F., Popov, P., Margenov, S., 2015. An analytical coarse grid operator applied to a multiscale multigrid method. Journal of Computational and Applied Mathematics 287, 207–219.

NONLINEAR DYNAMIC LATERAL RESPONSES OF CURVED RAILWAY TRACK ASSOCIATED WITH HIGH-FREQUENCY SQUEAL NOISES

CHAYUT NGAMKHANONG^{1,2}, XIN LIU³, AND SAKDIRAT KAEWUNRUEN^{1,2}

¹Department of Civil Engineering, School of Engineering,
University of Birmingham, Birmingham B152TT, United Kingdom
Email address; cxn649@student.bham.ac.uk, s.kaewunruen@bham.ac.uk

²Birmingham Centre for Railway Research and Education, School of Engineering,
University of Birmingham, Birmingham B152TT, United Kingdom

³Department of Civil Engineering, Beijing Jiaotong University,
Haidian district, Beijing 100044, China
Email address; 15125863@bjtu.edu.cn

Key words: Dynamic Response, Railway Track, Lateral Responses, Curved Railway Track, Squeal Noise.

Abstract. In urban environment, curve squeal is a strongly tonal noise emitted from wheel/rail contact caused by the passage of the train in tight curve rail. Wheel/rail contact can cause a traveling source of sound and vibration, which constitutes high-pitch noise pollution inducing a considerable concern of rail asset owners, commuters and people living or working along the rail corridor. The sound and vibration can be expressed in various forms and spectra. The undesirable sound and vibration on curves are often called squeal noises. This type of noise is commonly emitted in tight curve rails and can be annoying to nearby residents due to its tonal nature and uncertain excitation mechanism. This paper studies the effect of curve radii on the possible occurrence of curve squeal, which is devoted to systems thinking the approach and dynamic assessment in resolving railway curve noise problems. Curve track models in three-dimensional space have been built using finite element package, STRAND7. The moving train loads are applied in order to simulate nonlinear dynamic responses of curve track associated with squeal noise. The simulations of railway tracks with different curve radii have been carried out to develop state-of-the-art understanding into lateral track dynamics. Parametric studies have been conducted to evaluate static and dynamic responses. The dynamic responses of the track are found to be sensitive to the change of curve radii. The resonance peak in the lateral direction is related to the agreement of corresponding natural frequency of rail and the vibration excitation frequency under an individual rolling velocity. The outcome of this study will help provide some key parametric insights into fundamental dynamics of track in the lateral direction and establish the development of the dynamic design of curve track.

1 INTRODUCTION

Railway vibration and noise are a serious concern as it makes an annoyance to people nearby and affects property in the surrounding area [¹⁻³]. Wheel/rail interaction is a traveling source of

excitation, sound radiation and vibration along the railway corridors. The sound and vibration can be in various forms and spectra. There are many types of noise occurred on railway track during train passage; ground-borne, impact, rolling, squeal and flange. However, one of the loudest and most annoying noise sources from railways is squeal noise ^[4] which is often occurred on curved track. The occurrence of squeal induces significant environmental impacts immensely annoying people living nearby due to its high frequencies characteristics ^[5]. Curve squealing occasionally arises when railway vehicles run through tight curves at low speed ^[4, 6]. Table 1 shows different types of railway noise associated with different frequencies. It can be seen that the frequency range concerned with squeal noise is between 1000 and 5000Hz.

Table 1 Frequency range for different types of railway noise ^[7-9].

Noise type	Frequency range (Hz)
Ground-borne vibration	4-80
Impact noise	50-250 (speed dependant)
Rolling noise	30-5000
Squeal noise	1000-5000
Flange noise	5000-10000

It should be noted that ^[10-13] unsteady lateral creepage at the wheel/rail contact is thought to be the prime reason of squeal noise, while other mechanisms such as longitudinal creepage and flange contact, do not necessarily eliminate squeal noise thereby are determined to be of secondary importance ^[14-16]. Previous work indicated that squeal only occur when the curve radius is smaller than 100b, where b is the bogie wheelbase ^[17]. The results of on-site measurements also presented that there is no significant reduction in wheel squeal associated with limiting operation speed. According to the data collected from fields, it is suggested that diverse range of curving behaviour are largely relevant to curve radii. Although there are many possible treatments ^[18-20] that can be taken for mitigating the effects of squeal such as improving curving behaviour, modifying rail profiles, adding lubrications or friction modifiers, increasing the damping of wheel or rail, it is still uncertain to what extent the track lateral response is affected by rail radii, cants etc. It is noted that lateral track dynamic characteristic has not been fully investigated. The various curve radii, cants and lateral loads are taken into account in this study.

This paper illustrates the dynamic influences of curve radii, cants, lateral loads on the lateral dynamic vibrations, which are the possible mechanism for development of curve squeal under mode-coupling theory. The study is devoted to systems thinking the approach and dynamic assessment in resolving railway curve noise problems. Finite element package, STRAND7 has been used to build the curve track models in three-dimensional space. The dynamic responses of curve track have been simulated by applying a moving train load. The simulations of railway tracks with different curve radii have been implemented to develop a comprehensive understanding of lateral track dynamics, containing dynamic behaviors of rail, cant, gauge and overall track responses.

2. TRACK MODEL

The track model comprises two-dimensional Timoshenko beam, which takes into account shear deformation and rotational bending effects. This beam has been proven to be the best options for modelling rail and concrete sleeper due to its bending characteristics in both vertical and lateral directions to reflect the behaviour of thick beam ^[21-22]. It is noted that Timoshenko beam is suitable for solving the problem of beam subjected to high-frequency excitation when the wavelength approaches the thickness of the beam. The 60kg rail cross section (Area: 17659.8mm²; Second moment of Area: 43.2x10⁶) are considered in this track model ^[23]. While, the trapezoidal cross-section is allocated to the sleeper elements with medium section (204mm top-wide, 250mm bottom-wide and 180mm deep). The non-linear tensionless beam support can be used to demonstrate ballast under the sleeper. It is noted that the tensionless support allow beam to lift over the support while the tensile support is omitted ^[24]. Thus, this option can correctly reflect the real ballast characteristics ^[25]. It is noted that the partial support condition is believed to vastly conform with real condition of standard gauge tracks. The rail pads at the rail seat are simulated by using series of spring dash-pot elements. The high-density polyethylene pads are assigned to these spring-dashpot elements both in vertical and lateral direction. It should be noted that the model has been developed and validated previously using experimental parameters, field data and previous laboratory results ^[26-28]. The finite element models in three-dimensional space for an in situ railway track with both curve and tangent are presented in Figure 1.

Table 2 Material properties.

Parameters	Characteristic value	Unit
Rail		
Length, l_r	10.8	m
Gauge, g	1.5	m
Modulus, E_r	2e5	MPa
Poisson's ratio, ν_r	0.25	-
Density, d_r	7850	Kg/m ³
Railpad		
Vertical stiffness, k_{pv}	17	MN/m
Lateral stiffness, k_{pl}	70	MN/m
Sleeper		
Length, l_s	2.5	m
Spacing, s	0.6	m
Modulus, E_s	3.75e4	MPa
Shear modulus, G_s	1.09e4	MPa
Density, d_r	2740	Kg/m ³
Ballast		
Stiffness, k_b	13	MN/m

The curve radius of railway track considered varies from 100m to 600m. Cant is also considered with the range from 100cm to 300cm. It is simplified to 2points loads (1 axle) with a speed of 10m/s and 100kN in magnitude, 2m apart (common passenger bogie centre), on each

side of the rail track. The impulse excitations of a period of 0.0001s starting at 0.005s are assigned. In order to cover high frequency squeal noise, the calculation time step is set to be 0.00005. While, the lateral loads are set to be the proportion of vertical loads (Lateral to Vertical, L/V). The schematic lateral load case used is shown in Figure 2.

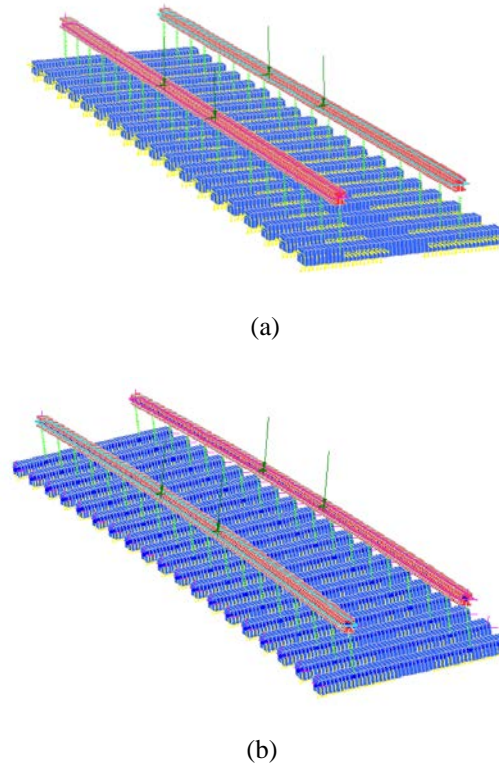


Figure 1 Dynamic track models: (a) The model of curve track (b) The model of tangent track.

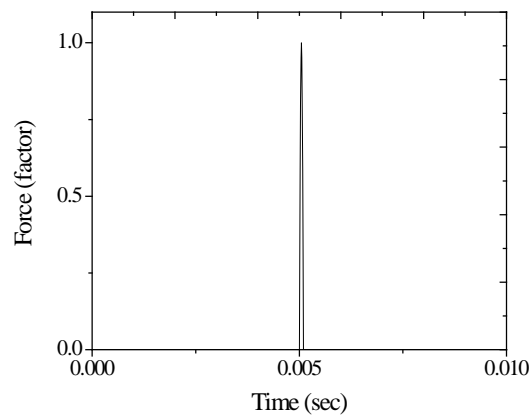


Figure 2 Schematic load case.

3 RESULTS AND DISCUSSIONS

The Nonlinear Transient Solver in STRAND7 is used to solve the dynamic responses of curved track. The eigenfrequencies and corresponding eigenmodes are calculated up to 10kHz in order to cover modes of squeal noises vastly. For curve track, the parameters concerned are curve radius, cants and lateral loads. The moving loads are applied with the velocity of 10m/s and thus the calculation time of 5s is considered for the whole process. In this study, lateral track displacement, lateral track velocity and lateral track mobility are presented.

3.1 Displacement responses

Dynamic lateral displacements of rail under different lateral load intensity are shown in Figure 3. The vertical loads are fixed to be 100kN as a benchmark for passenger train bogie, while the lateral loads varies from 5kN to 40kN. It can be seen that railway track with higher curve radius or tangent track have severe lateral displacement than that with tight curve. This is because the tight curve has higher lateral resistance and stiffness. It is interesting to note that the trends of rail lateral displacement with respect to curve radius are nonlinear as can be seen in Figure 3. In addition, as for track with 300cm cant, the lateral responses tend to be nonlinear as well as railway track without cant. However, it is noted that the increase of cant can significantly reduce lateral displacement by about 20-30%. As for from 100m to 200m curve radius, about 78% increase of lateral displacement of track without cant is observed. While, only 3.2% increasing rate is expected to occur from 500m to 600m radius. It can be concluded that, for large curve, lateral displacement has a slight change with the increase of radius and thus the radius plays a little role on dynamic response of large curved track but play a significant role on dynamic responses of tight curve. Therefore, the possibility of occurrence of curve squeal noise might be decreased on large curved track.

The obtained results demonstrate that the increase of track radius has a significant positive effect on the reduction of lateral responses which might decrease the possibility of curve squeal. This implies that lateral displacement responses are more sensitive corresponding to low radii, which gave evidence on the appearance of squeal during train negotiating tight curves. It can also be observed from the graph that the lateral track displacement of tangent track is similar to the value of track with a radius of 600m. For large curve radius, the lateral displacement of the track no longer change significantly with increasing radius therefore the increase of radius plays a little role on the dynamic amplitude of track. In reality, this phenomenon is evident from the less flange contact between wheel and rail while train traveling in large curve. The results above indicate that the increased track radius has positive effect on reducing curve squeal and squeal noise would disappear when the curve radius comes to a certain value.

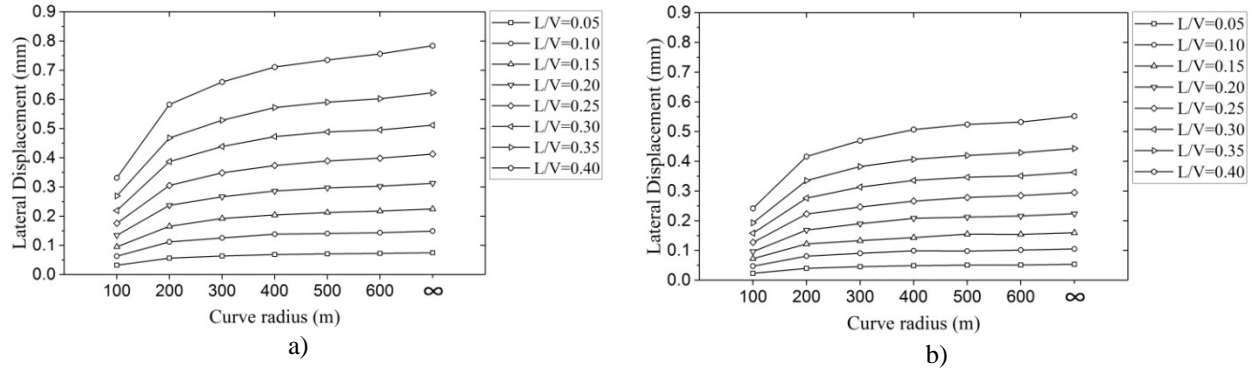


Figure 3 Dynamic lateral displacements of track at rail seat with different curve radius a) without cant
b) with 300mm cant.

3.2 Lateral velocity

The time histories of lateral rail velocity are presented in Figure 4. It is noted that the velocity of 10m/s and lateral loads of 20kN are taken into account in this part. Overall, it is shown that the velocity at mid-span is slightly higher than that at rail seat. It is also interesting to note that the peak of the lateral velocity at rail does not occur at the position where train load is applied. This is because there is a delay for the happening of maximum responses. The responses induced by the first sets of loads are smaller than that induced by following train load as a result of the superposition effects of moving loads.

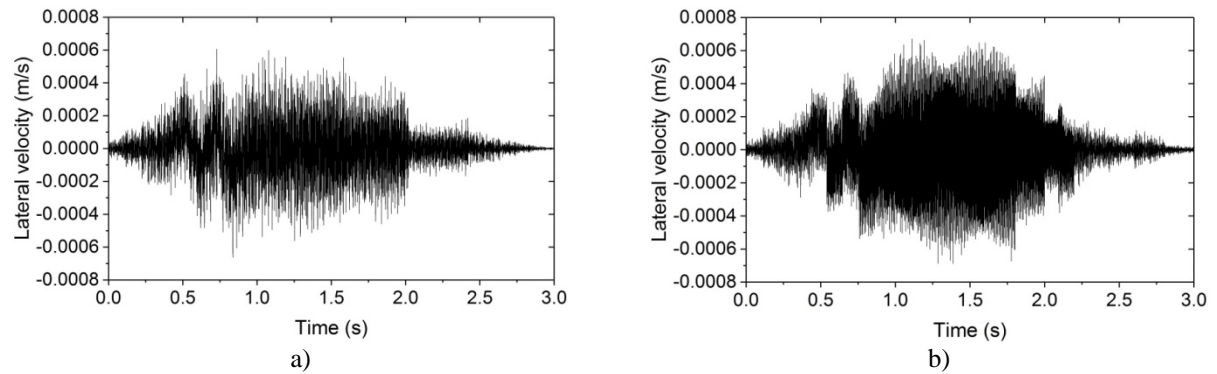


Figure 4 Rail lateral velocity of track with 100m radius under $L/V=0.2$ at a) rail seat b) mid-span.

The dynamic excitations are comprehensively displayed in terms of the lateral mobilities of the track. The lateral mobility spectrums obtained by a fast Fourier transform are shown in Figure 5 as a comparison of three types of track by virtue of logarithmic distribution in dB re. 10^{-9} m/s. Overall, it is clearly seen that the curve track with smaller radius has the higher lateral mobilities, in both positions as expected especially between 1000Hz and 5000Hz which is the range of squeal noise. Interestingly, the increasing of curve radius in both cases moves pinned-pinned resonance to higher frequencies and the depth of resonances are effectively reduced. For

example, the sharp peaks at 730Hz, which corresponding to pin-pin resonant frequencies, significantly drop by 20dB with the transition of track radius from 200m to 500m.

This is due to the fact that curve radius considerably affects track dynamics. However, in the low frequency range, the lateral mobilities are generally unaffected by the curve radius. As for the frequency range of 1000-5000Hz, the responses from the various cases incur apparently differences due to the influence of wheel/rail interaction during train passage on curve. By comparison with curve track, tangent track globally exhibits much lower noise levels in high frequency, which implies curve squeal is not likely to occur on tangent track.

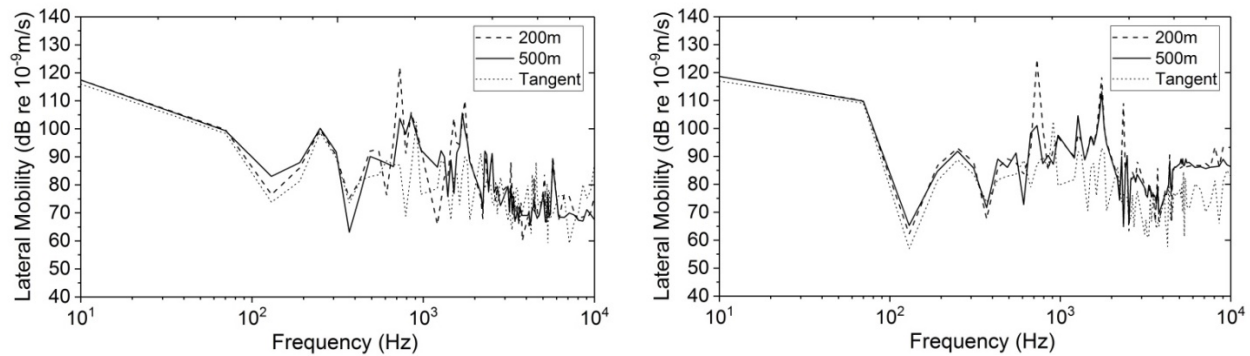


Figure 5 Spectra of the rail lateral mobility at (a) rail seat and (b) mid-span.

4 CONCLUSIONS

In this study, numerical simulation has been conducted to identify the lateral dynamic characteristics of both tangent and curved tracks with the consideration of track radii, cants and lateral loads. Track models have been established in three-dimensional space using a finite element package STRAND7. The results obtained are clearly shown that the increase of curve radius and cants have a positive effect on reducing lateral dynamic responses. The lateral displacement responses are more sensitive corresponding to low curve radii as clearly seen in the results between 100m and 200m radii. It has been noted from the literature that the frequency ranges of between 1000 and 5000Hz are corresponding to the squeal noise. In this region, it is observed that the vibration velocity of 200m radius curved track is lower than that of 500m radius and tangent tracks. Hence, increasing of track radius tends to vastly control the squeal noise at higher frequencies. This study put insight into the dominant influences of different track parameters to track lateral dynamic behaviors. Further studies and more experimental results are needed to investigate associated with these influencing parameters.

ACKNOWLEDGEMENTS

The authors are sincerely grateful to the European Commission for the financial sponsorship of the H2020-RISE Project No. 691135 “RISEN: Rail Infrastructure Systems Engineering Network”, which enables a global research network that tackles the grand challenge of railway infrastructure resilience and advanced sensing in extreme environments (www.risen2rail.eu) [²⁹].

REFERENCES

- [1] Connolly, D.P., Marecki, G.P., Kouroussis, G., Thalassinakis, I. and Woodward, P.K., 2016. The growth of railway ground vibration problems — a review. *Sci. Total Environ.* (2016) 568: 1276–1282.
- [2] Kouroussis, G., Van Parys, L., Conti, C. and Verlinden, O. Prediction of ground vibrations induced by urban railway traffic: an analysis of the coupling assumptions between vehicle, track, soil, and buildings. *Int. J. Acoust. Vib.* (2013) 18(4): 163–172.
- [3] Ngamkhanong, C., Kaewunruen, S. and Costa, B.J.A. State-of-the-Art Review of Railway Track Resilience Monitoring. *Infrastructures.* (2018) 3.
- [4] Thompson, D. Chapter 9 – Curve Squeal Noise. in: *Railw. Noise Vib.* (2009) :315–342. doi:10.1016/B978-0-08-045147-3.00009-8.
- [5] Wickens, A. *Fundamentals of Rail Vehicle Dynamics: Guidance and Stability.* (2003).
- [6] Liu, X., Ngamkhanong, C. and Kaewunruen, S. Nonlinear Dynamic of Curved Railway Tracks in Three-Dimensional Space. *IOP Conference Series: Materials Science and Engineering.* (2017) 280(1).
- [7] Ngamkhanong, C. and Kaewunruen, S. The effect of ground borne vibrations from high speed train on overhead line equipment (OHLE) structure considering soil-structure interaction. *Science of the Total Environment.* (2018) 627: 934-941.
- [8] Eadiea, D.T., Santoroa, M. and Kalousek, J. Railway noise and the effect of top of rail liquid friction modifiers: changes in sound and vibration spectral distributions in curves. *Wear.* (2005) 258: 1148–1155.
- [9] Liu, X. and Meehan, P.A. Investigation of the effect of relative humidity on lateral force in rolling contact and curve squeal. *Wear.* (2014) 310(1-2): 12-19. doi.org/10.1016/j.wear.2013.11.045.
- [10] Remington, P.J. Wheel/rail squeal and impact noise: What do we know? What don't we know? Where do we go from here? *J. Sound Vib.* (1987) 116: 339-353.
- [11] Fingberg, U. A model for wheel-rail squealing noise. *J. Sound Vib.* (1990) 143: 365-377.
- [12] Thompson, D.J. and Jones, C.J.C. A review of the modelling of wheel-rail noise generation. *J. Sound Vib.* (2000) 231: 519-536.
- [13] De Beer, F.G., Janssens, M.H.A. and Kooijman, P.P. Squeal noise of rail-bound vehicles influenced by lateral contact position. *J. Sound Vib.* (2003) 267: 497-507.
- [14] Koch, J.R., Vincent, N., Chollet, H. and Chiello, O. Curve squeal of urban rolling stock- Part 2: Parametric study on a 1/4 scale test rig. *J. Sound Vib.* (2006) 293: 701–709. doi:10.1016/j.jsv.2005.12.009.
- [15] Pieringer, A. A numerical investigation of curve squeal in the case of constant wheel/rail friction. *J. Sound Vib.* (2014) 333: 4295–4313. doi:10.1016/j.jsv.2014.04.024.
- [16] Vincent, N., Koch, J., Chollet, H. and Guerder, J. Curve squeal of urban rolling stock - Part 1: State of the art and field measurements. *J. Sound Vib.* (2006) 293: 691- 700.
- [17] Rudd, M.J. Wheel/rail noise – Part II: Wheel squeal. *Journal of Sound and Vibration.* (1976) 46: 381–394.
- [18] Nelson, J.T. *Wheel/rail noise control manual.* TCRP Report 23, 1997.
- [19] Kruger, F. *Schall- und Erschütterungsschutz im Schienenverkehr.* Expert Verlag, Renningen, (2001).
- [20] Muller, B., Jansen, E. and De Beer, F.G. Curve squeal WP3 tool box of existing measures. Union Internationale des Chemins de Fer, report prepared by SBB and TNO, (2003).
- [21] Grassie, S.L. Dynamic Modelling of Concrete Railway Sleepers. *J. Sound Vib.* (1995) 187:

- 799–813. doi:10.1006/jsvi.1995.0564.
- [22] Kaewunruen, S. and Remennikov, A.M. Experimental simulation of the railway ballast by resilient materials and its verification by modal testing. *Exp. Tech.* (2008) 32: 29–35. doi:10.1111/j.1747-1567.2007.00298.x.
 - [23] Standards Australia. AS1085.1 Rail. Australia: Sydney, (2001).
 - [24] Kaewunruen, S. and Remennikov, A.M. Effect of a large asymmetrical wheel burden on flexural response and failure of railway concrete sleepers in track systems. *Engineering Failure Analysis.* (2008) 15(8): 1065-1075.
 - [25] Ngamkhanong, C., Kaewunruen, S. and Baniotopoulos, C. A review on modelling and monitoring of railway ballast, *Structural Monitoring and Maintenance.* (2017) 4(3):195-220. doi: 10.12989/smm.2017.4.3.195.
 - [26] Kaewunruen, S., Lewandrowski, T. and Chamniprasart, K. Nonlinear modelling and analysis of moving train loads on interspersed railway tracks. 6th ECCOMAS Thematic Conference on Computational Methods in Structural Dynamics and Earthquake Engineering, Rhodes Island, Greece, 15–17 June 2017.
 - [27] Kaewunruen, S., Lewandrowski, T. and Chamniprasart, K. Dynamic responses of interspersed railway tracks to moving train loads. *International Journal of Structural Stability and Dynamics*, (2018) 18(1),1850011. doi: 10.1142/S0219455418500116
 - [28] Kaewunruen S, Freimanis A and Goto, K. Impact responses of railway concrete sleepers with surface abrasions. 25th International Congress on Sound and Vibration, 8-12 July 2018, Hiroshima, Japan.
 - [29] Kaewunruen, S., Sussman, J.M. and Matsumoto, A. Grand challenges in transportation and transit systems. *Frontiers in Built Environment.* (2016) 2(4). doi:10.3389/fbuil.2016.00004.

The Time Stepping Analysis by XFEM with a New Enrichment Scheme

Xuecong Liu^{*}, Qing Zhang^{**}, Xiaozhou Xia^{***}

^{*}Hohai University, ^{**}Hohai University, ^{***}Hohai University

ABSTRACT

Due to there is no need to re-mesh to adapt to the crack geometry in the simulation of failure, the extended finite element method (XFEM) has been widely used. In this talk, we want to present a new enrichment scheme of crack which is based on the framework of XFEM, and the stability of explicit time integration algorithm for dynamic problem is concerned. Based on the classical crack tip enrichment function, many new forms has been developed, such as using singular basis form [1] and Improved XFEM [2]. The new proposal enrichment scheme here is in the matrix form, the characteristics of the classical enriched functions are preserved completely by combining the classical function basis, and only two additional degrees of freedom related to tip are added at each node of the crack tip element. The governing equations are derived and evolved into the discretized form. The lumped mass and the explicit time algorithm are applied for dynamic problem. With different grid densities and different forms of Newmark scheme, the Dynamic Stress Intensity Factor (DSIF) is computed to reflect the dynamic response. DSIF is also as a parameter of judging the stability of numerical method. The applicability and availability of the proposed scheme has been sufficiently verified through the numerical examples, and the critical time stepping in different situations are listed and analyzed to illustrate the factors that affect the numerical stability. It is concluded that the grid density and the form of iterative method have obvious effects on stability. The critical time stepping varies with the grid density and the parameters of iterative method. In addition, a similar conclusions can be obtained by the standard FEM with the lumped mass, and the ratios of the two methods' critical time are relatively stable. Furthermore, the simulation results are found in good agreement with each other when they are stable and the computational efficiency will be involved during the presentation. Keywords: XFEM, DSIF, dynamic loading, time stepping References: [1] T.Menouillard, J.H. Song, Q. Duan, T. Belytschko: Time dependent crack tip enrichment for dynamic crack propagation. Int. J. Fract., 2010, 62 (1-2): 33-69. [2] R. Tian, L. Wen: Improved XFEM: An extra-dof free, well-conditioning, and interpolating XFEM. Comput. Methods Appl. Mech. Engrg., 2015, 285 (3): 639-658.

Numerical Investigation on the High-velocity Impact of Micron Particles in the Cold Spray

Yan Liu^{*}, Chenyang Xu^{**}, Xiong Zhang^{***}

^{*}Tsinghua University, ^{**}Tsinghua University, ^{***}Tsinghua University

ABSTRACT

The cold spray (CS) technique has been considered as a competitive additive manufacturing technique owing to its outstanding properties[1]. The key process of the CS technique is that the micron particles are accelerated to a high speed, and then the particles impact on and are bonded to the substrate. The working temperature is much lower than the melting point, so that the deposit layer has a low level of porosity, nice bonding strength and only compressive residual stress. The bonding mechanism of the CS technique, however, is still under investigation due to the strong nonlinearities aroused by the high-velocity impact. The traditional finite element method (FEM) may encounter mesh distortion and difficulties in modeling material failure when it is used to simulate the high-velocity impact process. In this presentation, the material point method (MPM) is successfully applied to investigate the high-velocity impact of micron particles in the cold spray process. The MPM[2], as one kind of meshfree particle methods, have many advantages over the traditional FEM when investigating the high-velocity impact process. No mesh distortion exists, and the fracture and fragmentation can be naturally simulated in the MPM framework. The high-velocity impacts of single micron copper particle or micron particle cluster onto the copper substrate are successfully simulated with the MPM. The configurations obtained by simulation agree well with the experimental results. The deformation of the sprayed particles and the substrate, the jetting at the rim of the particle, and the stress distribution are discussed in detail. Possible bonding mechanism between the sprayed particle and the substrate is also discussed based on the simulation results. [1] Sova A, Grigoriev S, Okunkova A, Smurov I. Potential of cold gas dynamic spray as additive manufacturing technology. *Int. J. Adv. Manuf. Technol.*, 69: 2269-2278, 2013. [2] Zhang X, Chen Z, Liu Y. *The material point method: A continuum-based particle method for extreme loading cases*. London: Academic Press, 2017

Structured Grid Based Method with Modified Boundary Basis Functions for Solid and Structure

Yanan Liu^{*}, Keqin Ding^{**}, Zhirong Yang^{***}

^{*}China Special Equipment Inspection and Research Institute, ^{**}China Special Equipment Inspection and Research Institute, ^{***}China Special Equipment Inspection and Research Institute

ABSTRACT

Structured Grid Based method with Modified Boundary Basis Functions for Solid and Structure Yanan Liu, Keqin Ding and Zhirong Yang China Special Equipment Inspection and Research Institute In this paper, the basis functions based on a structured grid are used for global approximation in solution domain. A boundary region is considered and the B-Spline basis functions are used to approximate the boundary curves (surfaces in 3D) and describe this boundary region. In this boundary region, boundary basis functions are constructed based on the same B-Spline basis functions used for representing the boundary region and corresponding weight functions are created for modification of the global basis functions and the boundary basis functions. The modified basis functions maintain high order continuity and can at least reconstruct linear polynomial. Based on the modified basis functions, the solution is created to satisfy the essential boundary conditions automatically. Meanwhile, the high accuracy of the solution near the essential boundaries can be guaranteed. Furthermore, the solutions also can be constructed to perform local refinement in the local region in which complex deformation exists. The present method has been used to solve some 2D and 3D elasticity problems. The numerical results are compared with analytical results and finite element analysis solutions to show that the new method is accurate, stable and effective. Keywords: Structured grid; Boundary region; Boundary basis functions; Local refinement

Numerical Study on Seismic Behavior of a Resilient Steel Bridge Pier

Yang Liu^{*}, Ying-ting Lv^{**}, Zi-xiong Guo^{***}, Qun-xian Huang^{****}

^{*}College of Civil Engineering, Huaqiao University, ^{**}College of Civil Engineering, Huaqiao University, ^{***}College of Civil Engineering, Huaqiao University, ^{****}College of Civil Engineering, Huaqiao University

ABSTRACT

An resilient steel bridge pier with replaceable steel slit dampers has been developed to meet the needs of rapid restoration of performance and functionality of bridge structures after earthquakes. This design concept is based on concentrating the damage in specially detailed components, which can be controlled and easily replaced once the damage occurs during the earthquake. Refined finite element model of the resilient steel bridge pier was established with ABAQUS and verified using existing experimental data. Numerical simulation on the seismic performance of the resilient steel bridge pier under constant axial load and cyclic horizontal load was then carried out. The main studied parameters are the axial compression ratio(n), effective slenderness ratio(?) and shear strength of the steel slit damper. It is indicated that with reasonable design principle, which is "strong column – weak damper", satisfactory seismic behavior, including high strength and stiffness, ample ductility, stable hysteretic behaviors, can be achieved for the resilient steel bridge pier. The plastic damage is concentrated on the steel slit dampers under large displacement reversals, while the main structure components remain nearly elastic.

Fast BEM for Modeling Cracks in 3D Using the Dual BIE Formulation

Yijun Liu^{*}, Yuxiang Li^{**}, Shuo Huang^{***}

^{*}University of Cincinnati, ^{**}University of Cincinnati, ^{***}University of Cincinnati

ABSTRACT

In this talk, we present some results in modeling crack problems in 3-D using the fast boundary element method (FastBEM). The BEM is based on the dual boundary integral equation (BIE) formulation, using a linear combination of the displacement and traction BIE. Fast multipole method is applied to solve the BEM equations and constant boundary elements are used in the discretization. The use of the constant elements is more efficient for solving large-scale BEM models of crack propagation problems. Numerical examples are presented to show the efficiency and accuracy of the developed approach. It is found that with enough numbers of boundary elements, the constant elements can be applied effectively to solve crack problems in 3-D solids, and it is more efficient compared with the FEM (ANSYS) in both the meshing and solution times. References: [1] Y. J. Liu, "On the displacement discontinuity method and the boundary element method for solving 3-D crack problems," *Engineering Fracture Mechanics*, 164, 35-45 (2016). [2] Y. J. Liu, Y. X. Li, and W. Xie, "Modeling of multiple crack propagation in 2-D elastic solids by the fast multipole boundary element method," *Engineering Fracture Mechanics*, 172, 1-16 (2017).

Locomotion Mechanism and Energy Efficiency of Soft Robots

Yilun Liu^{*}, Yingbo Yan^{**}, Langquan Shui^{***}

^{*}State Key Laboratory for Strength and Vibration of Mechanical Structures, School of Aerospace, Xi'an Jiaotong University, Xi'an 710049, China, ^{**}State Key Laboratory for Strength and Vibration of Mechanical Structures, School of Aerospace, Xi'an Jiaotong University, Xi'an 710049, China, ^{***}State Key Laboratory for Strength and Vibration of Mechanical Structures, School of Aerospace, Xi'an Jiaotong University, Xi'an 710049, China

ABSTRACT

In nature, a variety of limbless locomotion patterns flourish, from the small or basic life forms (*Escherichia coli*, amoebae, etc.) to the large or intelligent creatures (e.g., slugs, starfishes, earthworms, octopuses, jellyfishes, and snakes). Many bioinspired locomotion of soft robots have been developed in the past few decades. The locomotion/velocity efficiency and energy efficiency are two important characteristics to evaluate the performance of soft robot system. In this work, we first propose a broad set of innovative designs for soft mobile robots, based on the kinematics and dynamics of two representative locomotion modes (i.e., worm-like crawling and snake-like slithering). Inspired by and going beyond the existing biological systems, these designs include 1-D (dimensional), 2-D, and 3-D robotic locomotion patterns enabled by the simple actuation of continuous beams to achieve various locomotion functions, including crawling, rising, running, creeping, squirming, slithering, swimming, jumping, turning, turning over, helix rolling, wheeling, etc. The locomotion efficiency, functionality and adaptability for different locomotion modes are further analyzed. Then, a general framework is established to evaluate the energy efficiency of mobile soft robots by considering the efficiency of the energy source, actuator and locomotion, and some insights for improving the efficiency of soft robotic systems are presented. Four key factors related to the locomotion energy efficiency are identified, that is, the locomotion modes, material properties, geometric sizes, and actuation states. The results presented herein indicate a large space for improving the locomotion and energy efficiency of soft robots, which is of practical significance for the future development and application of soft robots.

A Phase Field Formulation for Cohesive Fracture with Application to Shock Wave Lithotripsy

Yingjie Liu^{*}, Rudy Geelen^{**}, John Dolbow^{***}, Pei Zhong^{****}

^{*}Duke University, ^{**}Duke University, ^{***}Duke University, ^{****}Duke University

ABSTRACT

This study concerns a novel phase field formulation for modeling cohesive-type fracture. Phase field formulations have become increasingly popular for simulating fracture due to their inherent strengths in representing complex fracture patterns, e.g., branching, kinking, merging, and etc. [1]. However, the applicability of many phase field formulations is limited by their basis on a Griffith model of fracture. An advanced phase field formulation is developed in this work that is distinguished by the fact that it converges to a cohesive model of fracture as the regularization length vanishes. In this work, we demonstrate how such an approach builds a foundation for the simulation of fracture in advanced materials with complex microstructure, bulk constitutive laws, and non-conventional fracture behavior. In the present study, in particular, it is applied to simulations of shock wave lithotripsy (SWL). SWL has proven to be a highly effective treatment for the removal of kidney stones [2]. The shock waves break up kidney stones through a dynamic fatigue process involving the contribution of various stress waves propagating inside the stones and cavitation produced in the surrounding liquid medium. In this work, we present a fully coupled acoustic-structural-fracture model for the simulation of SWL. Numerical experiments show ring-shaped cracks on the top surfaces of idealized stones, as well as radial cracks on the bottom surfaces. The details of the fracture patterns are shown to be sensitive to both the position and strength of the acoustic source driving the process. These findings are validated against experimental observations. Keywords: Phase Field; Cohesive Fracture; Anisotropic Solids; Shock Wave Lithotripsy References: [1] Miehe, C., Hofacker, M. and Welschinger, F., 2010. A phase field model for rate-independent crack propagation: Robust algorithmic implementation based on operator splits. *Computer Methods in Applied Mechanics and Engineering* 199, 45-48. [2] Weizer, A.Z., Zhong, P., and Preminger, G.M., 2007. New Concepts in Shock Wave Lithotripsy. *Urologic Clinics of North America* 34, 375-382.

Multiscale Microstructural Database for Concurrent Modeling of Nonlinear Softening Material with Damage and Failure

Zeliang Liu*, Wing Kam Liu**

*Livermore Software Technology Corp., **Northwestern University

ABSTRACT

Accurate and efficient computational methods for predicting fracture and damage of engineering materials are essential to design and failure analysis of materials with non-uniform or heterogeneous microstructural properties. Successful material models need to capture the non-trivial inter-dependence between material constituents at small scales that lead to dramatic performance effects in the macroscale response. Mechanistic understanding of this structure-property relation will also enable a collection of material microstructural database, which will accelerate material design and manufacturing. Traditional fracture mechanics and continuum damage mechanics are phenomenological macroscopic methods which are not sensitive to the material microstructures and require extensive testing and model calibration for new materials. In this work, we aim to solve the damage problem using a multiscale data-driven modeling framework, so that the macroscale material law is directly extracted from the homogenization of the microscale model. A new three-step homogenization scheme is presented, where the strain localization is distributed in the representative volume element (RVE) and the microscale equilibrium condition becomes well-posed even with the strain softening effect. The homogenization will continuously provide the effective behavior in the localization region, which is independent of the RVE size. The only material length parameter in the concurrent simulation is in the macroscale, and it can be measured or calibrated from numerical or physical experiment. The microscale RVE homogenization can capture the complex damage mechanism due to material heterogeneities, and explicitly provide a microstructure-sensitive material damage model for the macroscale without predefining the form. To increase the efficiency of the multiscale concurrent calculations, the self-consistent clustering analysis (SCA) with a new generalized formulation is proposed. By grouping material points with similar mechanical behavior into clusters, the number of degrees of freedom can be greatly reduced. With the microstructural database built in the offline stage, a reduced Lippmann-Schwinger equation is formulated and solved using a self-consistent scheme in the online stage. By comparing with direct numerical simulations (DNS) for plastic materials, the proposed method is shown to be accurate, with good convergence under refinement and computationally efficient. In the concurrent simulation, the predicted macroscale fracture patterns are observed to be sensitive to the combinations of microscale constituents, showing the capability of the SCA microstructural database.

Recent Development in Computational Mechanics of Soft Materials and Machines – an Overview

Zishun Liu*

*International Center for Applied Mechanics; State Key Laboratory for Strength and Vibration of Mechanical Structures, Xi'an Jiaotong University, China

ABSTRACT

Abstract: The elegance of nature's designs has inspired scientists to create soft machines. With development of soft machines, the mechanics of soft materials which are used by soft machines becomes an emerging field of applied mechanics. Therefore, the mechanical behaviors of soft materials are new and very current research topics, i.e. the large deformation studies of hydrogels, liquid crystal elastomers, dielectric elastomers and shape memory polymers (SMPs). In last decades, computational methods have become main approaches for studying mechanics of soft materials. Thus different numerical simulation methods are proposed to predict deformation behavior of soft materials, for example, FEM method, meshless method, molecular dynamics simulation etc. It is very imperative to reviewer and discuss the advances of different computational methods. In this presentation, we will review some of the recent works aligned with the direction of providing a better understanding of computational soft materials (gels, SMPs etc.). Then the transient deformation process of polymeric gels and numerical implementation for large deformation kinetics of polymeric gels are studied using the finite element method (FEM). The neutral and environmentally sensitive (such as temperature, pH-value, magnetics and light) hydrogels are investigated. For the SMPs study, we developed different constitutive models which can be used for different SMP materials and can be used for large strain large deformation analyses. To validate the model, simulated and predicted results are compared with experimental results. Finally, as many issues related to the mechanics of hydrogel and SMPs deformation behaviors remain open, we will list some outlines for plausible future directions in the research of computational mechanics of soft materials/machines. Furthermore, we will overview the recent development of computational mechanics in the study of soft materials and machines over the worldwide, especially; the advances of computational mechanics for soft materials in different research groups will be discussed and reviewed.

A Nonlocal Damage-Plasticity Model Based on a Smooth Elastic-Plastic Transition

Michal Livnani^{*}, Mahmood Jabareen^{**}

^{*}Technion – Israel Institute of Technology, ^{**}Technion – Israel Institute of Technology

ABSTRACT

Standard rate-independent elastic-plastic formulations use a yield function to separate elastic response and plastic response. Specifically, the consistency condition, which requires the yield function to vanish during loading, causes a sharp transition between elastic and plastic response with a break in the slope of the stress-strain curve. To eliminate this undesired response, a large deformation model, characterized by a smooth elastic-inelastic transition has been proposed (Hollenstein et al. 2013, Jabareen 2016). Also, their model unifies rate independent as well as rate dependent responses. Further, it is well-known that classical continuum damage models may not be able to capture the real mechanical behavior of materials due to localization associated with strain softening. In addition, if no adjustments are made, the region of localization will depend on the mesh size of the spatial discretization. The necessity to model damage, which is controlled by the microstructure, has driven the development of the nonlocal and gradient damage formulations. Nonlocal plasticity models incorporate a nonlocal variable defined as the spatial weighted average of a corresponding local field over the entire body. Often, the nonlocal quantity formulation includes an intrinsic length parameter that affects the weight amplitude in the vicinity of a material point. In the present study, an extension of a smooth inelasticity model to include softening and localization based on a strongly non local gradient-enhanced formulation is presented. A strongly objective integration scheme is developed based on the introduction of the relative deformation gradient – the deformation mapping between the last converged and current configuration. Also, a finite element formulation has been developed, which incorporates three variational fields for the equilibrium equations and an additional field for the Helmholtz type equation for the gradient-enhanced formulation. The numerical implementation of the proposed model will be presented, and the capabilities of the developed finite element will be demonstrated by few examples.

Rate-Dependent Phase-Field Fracture Model for Rubbers and its Experimental Validation

Pascal Loew^{*}, Bernhard Peters^{**}, Lars A. A. Beex^{***}

^{*}University of Luxembourg, SISTO Armaturen S.A., ^{**}University of Luxembourg, ^{***}University of Luxembourg

ABSTRACT

The failure of rubber-like materials depends amongst others on the strain-rate. In this presentation we discuss an isothermal phase-field fracture model for rate-dependent failure of rubber components. Miehe et al.[2] were the first to formulate a rate-independent phase-field damage model for rubbery polymers. Stumpf et al.[3] laid out the framework for thermodynamic consistent linear thermo-viscoelastic damage models. Extending these ideas, we formulate our new model. Introducing a crack phase field overcomes difficulties associating with the computational study of sharp discontinuities. This is particularly convenient when cracks branch and coalesce. The size of the crack phase field is determined by the length scale parameter l_0 . As a material parameter, depending on the microstructure, the length scale l_0 has a high influence on the local solution near the crack tip [1]. We demonstrate the performance of our model by conducting a series of tension tests for various geometries and clamp velocities. First, we compare the measured and numerical calculated global force-displacement curve and see a good agreement. Further, we measure the local strains near the crack tip by application of the Digital Image Correlation technology. Again, we can observe a good matching between experimental data and the numerical solution indicating a correct calibration of the length scale l_0 . Finally, we are showing a numerical example of several cracks coalescing to one. The resulting crack path agrees well with the experimentally determined. References [1] Geers, M. G. D., Borst, R., Brekelmans, W. A.M. and Peerlings, R. H. J. Validation and internal length scale determination for a gradient damage model: application to short glass-fibre-reinforced polypropylene International Journal of Solids and Structures (1999) 36, pp. 2557-2583. [2] Miehe, C. and Schaezel, L.-M Phase field modeling of fracture in rubbery polymers. Part I: Finite elasticity coupled with brittle failure Journal of the Mechanics and Physics of Solids (2014) 65, pp. 93-113. [3] Stumpf, H. and Hackl, K. Micromechanical concept for the analysis of damage evolution in thermo-viscoelastic and quasi-brittle materials. International Journal of Solids and Structures (2003) 40, pp. 1567-1584.

Textile Geometry Processors for Virtual Textiles and Textile Composites

Stepan Lomov*

*KU Leuven

ABSTRACT

Textiles, including textile reinforcements for composites, are fibrous materials, hence they are multi-scale and hierarchical. Modelling of textile fibrous structures is a necessary element of a simulation chain which streams the material description from fibre data and description of a textile manufacturing parameters via the fibrous assembly geometry model to the manufacturing and then performance of a final material or product, be it a textile reinforced composite, a textile element of an architectural structure or a nano-fibre based knited antenna. The paper presents a general philosophy of a virtual textile. It has as its key a Textile Geometry Processor, which accepts textile data (such as weave structure, yarns spacing, yarn dimensions etc.), parameters of the fibrous assembly (such as fibre volume fraction, layered geometry) and local (in relation to a scale of model) overall deformation of the textile (shear, compression etc.), and creates a geometrical model of the textile ready for use in the manufacturing and performance simulations of mechanical and physical phenomena (deformation response, damage initiation and development, flow through the material, electromagnetic properties, thermal conductivity etc). The paper describes general principles and a concrete realisation of a textile geometry processor, implemented in WiseTex and VoxTex software of the author. Two types of the textile data inputs are considered: models of the fibres geometry based on the interlacing topology description and micro-computed tomography data. The geometrical model of a unit cell (representative volume) of the textile is transformed into a “general purpose” meso-level finite element (FE) model of the unit cell, allowing further in-depth simulation of the textile or a textile composite properties and behaviour. The modelled textile structures can be seen as stochastic realisations with certain characteristics of their variability. The concept of the textile geometry processor allows implementation of the stochasticity and its advancement to Monte-Carlo variability modelling. The open data structure of the input allows multi-parametrical optimisation of the fibrous assembly.

Using the Material Point Method to Model Fracture and Multi-body Interactions Within a Single Velocity Field

Christopher Long*, Duan Zhang**, Yuri Bazilevs***, Georgios Moutsanidis****

*Los Alamos National Laboratory, **Los Alamos National Laboratory, ***University of California San Diego,
****University of California San Diego

ABSTRACT

A chief drawback of using the Material Point Method (MPM) for brittle failure is that a material cannot separate unless a crack has grown to at least one grid cell in thickness. This problem is exacerbated by the use of the Dual Domain Material Point Method (DDMP), which extends the numerical stencil of the particle-grid interactions. Thus, the resolution issues are inherent for brittle failure, as crack width is typically very small, creating artificially thick failure zones. We propose and will discuss a numerical methodology to construct a damage field on the particles which can be used to detect cracks that are sub-gridscale in thickness, and can then be used to separate materials which are otherwise still connected through the Eulerian mesh. This has been previously achieved by detecting a crack and partitioning the particles into multiple interacting velocity fields. [1] We achieve the same effect using a single velocity field through selective force and momentum transfers from particle to grid and vice-versa when a crack is present. The same methodology can be applied to model multi-body interactions and self-contact, by marking the surface particles of an object as a “crack”. Smooth Particle Hydrodynamics (SPH) and Reproducing Kernel Particle Method (RKPM) are introduced to MPM and are used to integrate the crack/damage field in lieu of traditional transfer methodologies. This allows us to model the gradient of the damage field more accurately, which allows us to compute the normal direction to the crack. We will present several numerical demonstrations of this capability, and compare to benchmarks in fracture mechanics. Additionally, we will compare to experimental results of quasi-statically loaded glass spheres (not a Brazil test). These experiments provide several benchmarks for comparison, including the average load at failure, average fractured particle size, and deflection to failure. The implementation of the single-velocity field fracture model will enable us to predict the correct average number of large fragments and ratio of large to small fragments using a much coarser resolution than has previously been required. [1] Homel, M. A., and Herbold, E. B. (2017) Field-gradient partitioning for fracture and frictional contact in the material point method. *Int. J. Numer. Meth. Engng*, 109: 1013–1044. doi: 10.1002/nme.5317.

DEM Modelling of Ice Load on Conical Structures under Influence of Cone Angle

Xue Long^{*}, Shunying Ji^{**}

^{*}Dalian University of Technology, ^{**}Dalian University of Technology

ABSTRACT

The conical structures are applied to effectively reduce the ice load and avoid serious damage to the structures caused by the sea ice. The reasonable parameters for the design of the anti-ice cone are important to show the anti-ice performance of cones. According to the failure characteristics of sea ice, the discrete element method (DEM) with a parallel-bond model is adopted to simulate the interaction between sea ice and conical structure. The accuracy of the DEM model is verified by comparing the calculated ice load and the failure process of sea ice with the test data of the Hamburg Ship Model Basin (HSVA). The simulation results show that the cone ice load increases with the increase of the cone angle, while the average broken length of sea ice decreases with the cone angle. It is found that the failure modes of sea ice are transformed from bending failure to crushing failure as the cone angle increases. Therefore, the anti-ice cone with 60° to 70° cone angle has a better performance to prevent the damage caused by the interaction with ice. The DEM simulations can provide a meaningful basis for the design of anti-ice structures.

A Plastic-damage Model of Concrete Subjected to Reversed Loading

Yuchuan Long^{*}, Yuming He^{**}, Chentao Yu^{***}

^{*}Chongqing University, China, ^{**}Sichuan College of Architectural Technology, China, ^{***}Chongqing University, China

ABSTRACT

A plastic-damage model was developed by using essential concepts of continuum damage mechanics and plastic flow theory, within the framework proposed by Lee and Fenves[1]. First, the mathematic expression of the model was given in this paper. It employed a non-associated plastic flow rule to model the evolution of irrecoverable deformation. The concept of energy-loss mechanism was utilized to develop the evolutionary rule of damage by defining the damage factor in terms of the fracture energy and accumulated dissipating energy. Then, the influence of mesh size on tensile damage factor was investigated using the crack band theory to alleviate the mesh sensitivity. The crack band theory, which modifying the stress-strain relation according to mesh size, was not sufficient to obtain objective responses under cyclic loading. To eliminate the effect of mesh size under unloading and reloading states, the equivalent relation of damage factor for different meshes was derived based on the assumption that the inelastic and plastic components of strain were concentrated in the damaged elements. According to the relation, the damage factor defined by the energy-loss mechanism was mesh-objective and equal to the equivalent damage factor corresponding to crack band width. Last, this model was implemented into ABAQUS and used to model concrete tests conducted by Kupfer[2] and Hordijk[3]. Numerical results such as stress-strain curves and load-deflection ones agreed well with those obtained from tests. The load-deflection responses obtained with different mesh were in close agreement when using the crack band theory and equivalent relation of damage factor, which indicates the equivalent relation of damage could eliminate the effect of mesh size. Moreover, the equivalent damage factors corresponding to crack band width in the cases of different mesh size were consistent to each other and therefore it could be used as a damage index to evaluate the damage degree of concrete structure. These numerical examples drew a conclusion that the plastic-damage model could model the nonlinear responses of concrete structures subjected to reversed loading. [1] Lee J, Fenves GL. Plastic-damage model for cyclic loading of concrete structures[J]. Journal of Engineering Mechanics, ASCE, 1998, 124(8): 892-900. [2] Kupfer H, Hilsdorf H K, Rusch H. Behavior of concrete under biaxial stresses[J]. Journal of ACI, 1969, 66(8): 656-666. [3] Hordijk D A. Local approach to fatigue of concrete[D]. Dissertation, Delft University of Technology, 1991.

Large Scale Approach of Dynamic Shear Localization-induced Failure of Viscoplastic Structures

Patrice Longère*, André Dragon**, Hannah Lois-Dorothy***

*Institut Clément Ader, **Pprime, ***Institut Clément Ader

ABSTRACT

Lightweight materials such as titanium alloys are widely employed in aircraft and other structures. The latter, while possessing high strength, are susceptible to a dynamic instability phenomenon called adiabatic shear banding which leads to a premature structural failure. Adiabatic shear bands (ASBs) are narrow shear localized regions resulting from thermomechanical instability and occur under high strain rate loading (involving quasi adiabatic conditions) as a consequence of the competition between hardening and softening mechanisms. The linear perturbation method is applied in the context of dynamic plasticity to determine the shear localization onset. Different softening mechanisms (e.g. thermal softening vs. dynamic recrystallization) triggering the adiabatic shear banding are studied (see [1]). A constitutive model is developed within a large scale postulate wherein the shear localization band is embedded within the representative volume element (RVE) and further finite element – and not the opposite as usually done. This facilitates numerical implementation of the model on large structures without the need for mesh refinement in the critical zones. The model describes the progressive anisotropic material deterioration induced by the ASB and further micro-voiding in the band wake as well as the kinematic consequences of the deterioration mechanisms at stake (ASB, micro-voiding) until the ultimate fracture (see [2], [3]). The model is implemented as user material subroutine in the engineering finite element computation code LS-DYNA and its performances are evaluated considering some initial boundary value problems such as dynamic shearing of hat shaped structure and ASB assisted chip serration in high speed machining. References [1] Longère, P., “Respective/combined roles of thermal softening and dynamic recrystallization in adiabatic shear banding initiation,” *Mech. Mater.*, vol. 117, pp. 81–90 (2018). [2] Longère, P. and Dragon, A., “Enlarged finite strain modelling incorporating adiabatic shear banding and post-localization microvoiding as shear failure mechanisms,” *Int. J. Damage Mech.*, vol. 25-8, pp. 1142-1169 (2016). [3] Dorothy, H.L., Longère, P. and Dragon, A., “Coupled ASB-and-microvoiding-assisted dynamic ductile failure,” *Procedia Eng.*, vol. 197, pp. 60–68 (2017).

A Numerical Framework to Analyze Fracture in Composite Materials: From Simulated Crack Resistance Curves to Homogenized Softening Laws

Cláudio S. Lopes*, Miguel Herráez**, Carlos González***

*IMDEA Materials Institute, Madrid, Spain, **IMDEA Materials Institute, Madrid, Spain, ***IMDEA Materials Institute, Madrid, Spain

ABSTRACT

A numerical framework to obtain the crack resistance curve (R-curve) and its corresponding softening law for fracture analysis in composite materials under small scale bridging is presented [1]. The use case addresses the intralaminar transverse tensile fracture of a unidirectional ply of carbon fiber-reinforced polymer AS4/8552. The R-curve is computed for this material using a micromechanical embedded model corresponding to the intralaminar transverse tensile fracture toughness characteristic. The model combines an embedded cell approach with the Linear Elastic Fracture Mechanics (LEFM) displacement field to analyze the local crack growth problem including fiber/matrix interface debonding and bridging of matrix ligaments as the main energy dissipation mechanisms. Due to the complexity of the problem, the methodology is illustrated to study the bidimensional propagation of a crack in a fiber reinforced unidirectional ply, including the fiber/matrix interface debonding and the ductile tearing of the matrix ligaments between fibers as energy dissipation mechanisms. This crack propagation problem is also known as the intralaminar crack propagation under transverse tension, characterized by the fracture toughness G_{2+} . The bidimensional formulation of the problem impedes the inclusion of higher length scale toughening mechanisms, as for instance, fiber bridging due to the lack of parallelism between fibers, so the material toughness and R-curve behavior obtained should be understood as lower bounds or initiation values rather than propagation over a finite crack length of some millimeters. Parametric analyses were carried out to assess the influence of the properties of the material constituents on the R-curve behavior and on the corresponding homogenized cohesive laws. Homogenized softening laws for the crack propagation problem in a unidirectional ply are presented for a wide range of micromechanical parameters including constituent properties as the fiber/matrix interface and matrix plastic/damage behavior. [1] M. Herráez, C. González, C.S. Lopes, A numerical framework to analyze fracture in composite materials: From R-curves to homogenized softening laws, International Journal of Solids and Structures (2017) 1–13, In Press.

Thermal Characterization of a Concrete Sample during Hydration Process by Solution of the Inverse Problem

Ruben Lopez^{*}, Antonio Aquino^{**}, Sebastian Farina^{***}, Fernando Diaz^{****}, Carlos Sauer^{*****},
Belen Martinez^{*****}

^{*}National University of Asuncion. Faculty of Engineering, ^{**}National University of Asuncion. Faculty of Engineering,
^{***}National University of Asuncion. Faculty of Engineering, ^{****}National University of Asuncion. Faculty of
Engineering, ^{*****}National University of Asuncion. Faculty of Engineering, ^{*****}National University of Asuncion.
Faculty of Engineering

ABSTRACT

During the curing process of concrete, chemical exothermic reactions with temperature increase and heat release take place. Studying the development of early thermal and mechanical properties of concrete becomes of primary importance, since the heat release throughout hydration process and the associated effects, such as temperature gradients, may lead to crack generation. To simulate this thermal behavior, it is necessary to obtain the thermal parameters. In this work, computational implicit algorithms using the Conjugate Gradient (CG) method were developed and applied aiming to obtain thermal conductivity k and specific heat c of concrete samples during the hydration process, solving the inverse problem. The algorithms were based on temperatures obtained by sensors placed on samples, having in count that the heat generation is minimum since the fourth day of the hydrating process, in order to reduce the ill-posed characteristic of the inverse problem. In addition, to reduce the computational cost of a pure implicit algorithm, the Douglas-Gunn alternate direction implicit (ADI) method was chosen, maintaining at the same time the unconditional stability of the implemented algorithm. Validation of the numerical method was done comparing the parameters obtained by the numerical model with experimental results. Samples manufactured with different cement kinds, and therefore having different strength, were studied. Comparison of temperature evolution curves and thermal parameters of interest was done. Results were, in general, coherent and satisfactory. The proposed model allows the solution of the heat transfer equation avoiding the chemical kinetics modelling, which is well-known for its complexity. Despite this, all the chemical phenomena related to heat generation are indirectly represented. For the studied samples, concretes with similar strength values produced similar Temperature-time plots, except for some pozzolanic samples. These pozzolanic samples produced a delayed temperature increase profile, and therefore delayed heat generation, and their peak temperatures were also noticeably lower than those corresponding to compound cement of similar strength. It could also be observed that the bigger the strength the bigger the temperature peak and thermal constants, except for some pozzolanic samples. In general, the results were satisfactory, which leads to conclude that the thermal characterization of concrete is achieved by means of these implicit numerical methods

Simulation of a Quadcopter Rotor in Hover at High Altitude

Omar D. Lopez Mejia^{*}, Luisa F. Prado Arellano^{**}, Santiago Mendoza Silva^{***}, Jaime A. Escobar^{****}

^{*}Universidad de los Andes, ^{**}Universidad de los Andes, ^{***}Universidad de los Andes, ^{****}ADVECTOR

ABSTRACT

Unmanned Aerial Vehicles (UAVs) have become an important technology for civil applications in last years. Among the different platforms available in UAVs, quadcopters are preferable due to its easier control in flight for drone operators and because of their rapid take-off capabilities. Typically, the research community has focused on the control system of these vehicles and simplifying the aerodynamic problem [1]. It is well known that the description and understanding of the wake of the rotor of a rotorcraft is a very complex fluid dynamic problem. The global efficiency of a quadcopter is highly dependant on the aerodynamic performance of the rotor and the interaction of the induced flow between the rotors and the fuselage [2]. In-flight testing of quadcopters is difficult due to space limitations and control of atmospheric conditions. Bench-testing of quadcopter rotors is commonly done, but limited in the information that can be obtained. In this context, Computational Fluid Dynamics (CFD) can play an important role in a clear understanding of the dynamics of such a complex flow. In the present work, CFD is used in order to quantify the influence of atmospheric conditions such as those found in Colombia (high altitude) in the aerodynamic performance of the rotor of the quadcopter ARAKNOS v2 developed by the Colombian company ADVECTOR. Numerical simulations are performed using the commercial software ANSYS-Fluent v17. The rotation is implemented with the Multiple Reference Frame (MRF) model and using the Spalart-Allmaras turbulence model with curvature correction. The influence of the four rotors is included by means of a double symmetry used in the implemented computational domain. Numerical results of torque and power were compared with experimental data measured in hover flight. It was also found that the temperature, atmospheric pressure and humidity have a great influence in the aerodynamic performance (Torque and power coefficients) of the rotor. A difference of approximately 20% was found between the experimental and computational results which can be attributed to the influence of the fuselage which is not included in the computational model. REFERENCES [1] Hoffmann, G. M., Huang, H., Waslander. S. L., and Tomlin C. J., "Quadrotor Helicopter Flight Dynamics and Control: Theory and Experiment" AIAA Guidance, Navigation and Control Conference and Exhibit: AIAA-2007-6461. American Institute of Aeronautics and Astronautics, 2007. [2] Potsdam, M., and Pulliam, T., "Turbulence Modelling Treatment for Rotorcraft Wakes," San Francisco CA : Specialist's Conference on Aeromechanics, 2008.

Nucleation and Propagation of Fracture and Healing in Elastomers: A Phase-Transition Theory & Numerical Implementation

Oscar Lopez-Pamies*, Aditya Kumar**, Gilles Francfort***

*University of Illinois at Urbana-Champaign, **University of Illinois at Urbana-Champaign, ***NYU

ABSTRACT

A macroscopic theory is proposed to describe, explain, and predict the nucleation and propagation of fracture and healing in elastomers undergoing arbitrarily large quasistatic deformations [1]. The theory, which can be viewed as a natural generalization of the phase-field approximation of the variational theory of brittle fracture of Francfort and Margio (1998) to account for physical attributes innate to elastomers that have been recently unveiled by experiments at high spatio-temporal resolution, rests on two central ideas. The first one is to view elastomers as solids capable to undergo finite elastic deformations and capable also to phase transition to another solid of vanishingly small stiffness: the forward phase transition serves to model the nucleation and propagation of fracture while the reverse phase transition models the possible healing. The second central idea is to take the phase transition to be driven by the competition between a combination of strain energy and hydrostatic stress concentration in the bulk and surface energy on the created/healed new surfaces in the elastomer. From an applications point of view, the proposed theory amounts to solving a system of two coupled and nonlinear PDEs for the deformation field and an order parameter, or phase field. A numerical scheme is presented to generate solutions for these PDEs in $N = 2$ and 3 space dimensions. This is based on an efficient non-conforming finite-element discretization, which remains stable for arbitrarily large deformations and elastomers of any compressibility, together with an implicit gradient flow solver, which is able to deal with the large changes in the deformation field that can ensue locally in space and time from the nucleation of fracture. We conclude by presenting sample simulations of the so-called poker-chip and Gent-Park experiments and confronting those with experimental results for various types of elastomers.

A Discontinuous Galerkin Immersed Boundary Method Using Unstructured Anisotropic Mesh Adaptation and Penalization Techniques

Marco Lorini^{*}, Cécile Dobrzynski^{**}, Vincent Perrier^{***}, Mario Ricchiuto^{****}

^{*}Inria Bordeaux Sud-Ouest, Team Cardamom, ^{**}Inria Bordeaux Sud-Ouest, Team Cardamom, ^{***}Inria Bordeaux Sud-Ouest, Team Cagire, ^{****}Inria Bordeaux Sud-Ouest, Team Cardamom

ABSTRACT

When dealing with meshing for Computational Fluid Dynamics (CFD) simulations, two possible methods can be employed. An attractive alternative to the well-known body-fitted approach is the use of embedded boundary methods, which are arousing interest mainly because they simplify the mesh generation process, particularly in the case of moving bodies. This kind of methods are characterized by the fact that the mesh covers the entire domain, so that a special treatment for the elements close to the body surface is needed. We propose an Immersed Boundary Method (IBM) in which the wall boundary conditions are taken into account through a penalization technique, i.e. through the addition of a penalty term to the Navier-Stokes equations. The localization of the solid bodies is done via a level set method, employing the signed distance function (SDF). With the combination of anisotropic mesh adaptation and unstructured simplicial meshes, the accuracy of the definition of the solid boundaries, not explicitly discretized, can be improved without increasing too much the computational cost of the simulation. The method was already proposed by some of the authors for a Finite Element (FE)/Finite Volume (FV) scheme [1] and Residual Distribution Schemes (RDS) [2] while it is now extended to the Discontinuous Galerkin (DG) context. DG methods are FE methods in which the solution of the variational form of the problem is approximated by piecewise polynomial functions with no global continuity requirement. Nowadays they are finding use in very diverse applications because of their robustness, accuracy and flexibility. These aspects combined with the compactness of the scheme have been advantageous for the parallel implementation of the proposed method. The presentation will first briefly cover the motivations and scope of the work. Details on the penalized Navier-Stokes equations and on the evaluation of the penalization operator will be also given before discussing the DG discretization of the equations employed in our solver as well as the mesh adaptation procedure. Results on two- and three-dimensional test cases will conclude the presentation. (1) Abgrall R., Beaugendre H. and Dobrzynski C., "An immersed boundary method using unstructured anisotropic mesh adaptation combined with level-sets and penalization techniques", *Journal of Computational Physics* 257 (2014) 83 - 101. (2) Nouveau, L., Beaugendre H., Dobrzynski C., Abgrall R. and Ricchiuto M., "An adaptive, residual based, splitting approach for the penalized Navier Stokes equations", *Comput. Methods Appl. Mech. Engrg.* 303 (2016) 208 – 230.

Fast Isogeometric Solvers for Implicit Dynamics Simulations of Heat Transfer and Elastic Wave Propagation Problems

Marcin Los^{*}, Maciej Paszynski^{**}, Victor Calo^{***}

^{*}AGH University, Krakow, Poland, ^{**}AGH University, Krakow, Poland, ^{***}Curtin University, Perth, Western Australia

ABSTRACT

The alternating directions method (ADS) was first introduced in 1960 [1] to deal with finite difference simulations for time-dependent problems. Nowadays, the method has been rediscovered as a tool to deal with simulations of difficult computational problems, such as time-dependent Maxwell equations, or incompressible flows [2]. The method introduces intermediate time steps to separate the differential operator and obtain a multi-diagonal structure of the matrices enabling for linear computational cost factorization. The alternating direction method has been recently rediscovered by [3] for fast solution of the isogeometric L2 projection problem in the context of isogeometric finite element method. In there, we do not have a time steps, but rather the projection problem discretized with tensor products B-spline basis functions. It has also been used for explicit dynamics isogeometric simulations [4]. In this talk, we show how to successfully apply the alternating direction method for isogeometric finite element method simulations of implicit dynamics. Namely, we focus on a parabolic problem and discretize it with B-spline basis functions in the spatial dimension, and we use implicit scheme for time discretization. We introduce intermediate time steps and separate our differential operator into a summation of the blocks, acting along particular axes in the intermediate time steps. We show that resulting stiffness matrix can be represented as multiplication of the two (in 2D) or three (in 3D) multiple diagonal matrices, each one with B-spline basis functions along with a particular axis of the spatial system of coordinates. As a result of our algebraic transformations, we get a system of linear equations that can be factorized in linear $O(N)$ computational cost in every time step of the implicit method. We verify our method by simulating heat transfer and linear elasticity problems. We also demonstrate that our implicit method is unconditionally stable for heat transfer problems (i.e., parabolic). We conclude our presentation with a discussion on the limitations of the method. The work has been supported by National Science Centre, Poland grant no. 2017/26/M/ST1/00281 [1] G. Birkhoff, R.S. Varga, D. Young, Alternating direction implicit methods, *Advanced Computing* 3 (1962) 189–273. [2] J. L. Guermond, P. Mineev, A new class of fractional step techniques for the incompressible Navier-Stokes equations using direction splitting, *Comptes Rendus Mathematique* 348(9-10) (2010) 581–585. [3] L. Gao, V.M. Calo, Fast Isogeometric Solvers for Explicit Dynamics, *Computer Methods in Applied Mechanics and Engineering*, 274 (1) (2014) 19-41

On Almost Pixel-exact Real-time Rendering of High-order Solution on Unstructured Meshes

Adrien Loseille^{*}, Rémi Feuillet^{**}

^{*}INRIA, ^{**}INRIA

ABSTRACT

OpenGL 4 with GLSL shading language have become a standard on many common architectures (Mac, Linux, Windows, , ...) from a couple of years. In the mean time, high-order methods (for flow solution and for meshing algorithm) are emerging. Many of them have proven their abilities to provide accurate results on complex (3D) geometries. However, the assessment of a particular meshing algorithm or of a high-order numerical scheme strongly relies on the capacity to validate and inspect visually the current mesh/solution at hand. However, having at the same time, an accurate and interactive visualization process for high-order mesh/solution is still a challenge as complex process are usually involved in the graphic pipeline: non linear root finding, ray tracing, GPU programming, ... In this presentation, we discuss the current status and issues of using the (raw) OpenGL 4 pipeline to render curved high-order entities, and almost pixel-exact solutions. We illustrate this process on meshes and solutions issued from high-order curved from CAD and with high-order interpolated solutions.

Numerical Flow Analysis and Optimal Management of a Fishway Model

Mohammed Louaked*

*Caen University, France

ABSTRACT

The need to preserve and enhance natural stocks of diadromous and resident fish have been recognized for, at least, the past century. Dams cut off the migratory route of fish. A fishway or fish-pass is an hydraulic structure that enable fish to overcome obstructions to their spawning and other river migration, and is built whenever it is required, based on ecological, economical, or legal considerations. The purpose of this work is to find the optimal form of fishway so that most many fish can go through rivers in the best conditions. The work involves modeling, mathematical analysis and numerical approximation of a coupled problem between a primal hyperbolic system and adjoint problem for the cost function of the optimal structure. We also obtain an expression for the gradient of the objective function via the adjoint system. Finally, we give numerical results obtained for the pools channel under study. References [1] A. Harten, (1983), High resolution schemes for hyperbolic conservation laws; J. Comp. Physics, 49, 357-393. [2] M. Louaked, (2008), TVD adaptive mesh redistribution scheme for the shallow-water equations; Int. J. Num. Meth. Fluids, 56, 1391-1397. [3] M. Louaked, A. Saidi, (2009), Pointwise control and hybrid scheme for water quality equation; Nonlinear Analysis, 71, 2337-2349. [4] M. Louaked, N. Seloula, S. Shuyu and S. Trabelsi, (2015), A pseudocompressibility method for the incompressible Brinkman-Forchheimer equations; Differential Integral Equations, 28, 3-4, 361-382. [5] Pk. Sweby, (1984), High-resolution schemes using flux limiters for hyperbolic conservation-laws ; Siam J. Numer. Analysis, 21, 995-1011, 361-382.

Asymmetric Breathing Motions of Nucleosomal DNA and the Role of Histone Tails

Sharon Loverde*, Kaushik Chakraborty**

*CUNY College of Staten Island, **CUNY College of Staten Island

ABSTRACT

The most important packing unit of DNA in the eukaryotic cell is the nucleosome [1]. It undergoes large-scale structural re-arrangements during different cell cycles [1,2]. For example, the disassembly of the nucleosome is one of the key steps for DNA replication, whereas reassembly occurs after replication. Thus, conformational dynamics of the nucleosome is crucial for different DNA metabolic processes. We perform three different sets of atomistic molecular dynamics (MD) simulations of the nucleosome core particle at varying degrees of salt conditions for a total of 0.7 microseconds simulation time. We find that the conformational dynamics of the nucleosomal DNA tails are oppositely correlated from each other during the initial breathing motions [3]. Furthermore, the strength of the interaction of the nucleosomal DNA tail with the neighboring H2A histone tail modulates the conformational state of the nucleosomal DNA tail. With increasing salt concentration, the degree of asymmetry in the conformation of the nucleosomal DNA tails decreases as both tails tend to unwrap. This direct correlation between the asymmetric breathing motions of the DNA tails and the H2A histone tails, and its decrease at higher salt concentrations, may play a significant role in the molecular pathway of unwrapping. Following, we perform even longer simulations (~ 5 microseconds) of the nucleosome core particle at high salt concentration (2 M NaCl). We find the formation of a bulge/loop of nucleosomal DNA that is initiated by the collapse of the H2B N-terminal tail. Using Umbrella Sampling, we next explore the initial stages of unwrapping at these high salt concentrations using the radius of gyration of the nucleosomal DNA tail as a reaction coordinate. [1] McGinty, R. K, Tan, S. Chemical Reviews 115, 2255 (2015). [2] Muller, M. M, Muir, T. W. Chemical Reviews 115, 2296 (2015). [3] Chakraborty, K., Loverde, S.M. Journal of Chemical Physics 147, 165101 (2017).

THE ENERGY FLUX INTEGRAL BASED FRACTURE CRITERION FOR ELASTIC PLASTIC CRACK GROWTH

Longkun Lu, Shengnan Wang

School of Aeronautics, Northwestern Polytechnical University
No. 127, Youyi Road (West), Beilin
Xi'an City, Shaanxi Province, China
1768614416@qq.com (L.K. Lu), wangshna@nwpu.edu.cn (S.N. Wang)

Key words: energy flux integral, elastic plastic crack growth, crack tip configurational force.

Summary: *The crack tip energy flux integral is derived from energy or power balance formula containing crack tip. This integral is found to be path independent and represents the power available for separating the crack surfaces during the crack propagation. On the foundation of this integral, a parameter is defined and this parameter is proved to be equal to the minus project of crack tip configurational force along crack growth direction. That is, this parameter is identical to the near tip J integral proposed by Simha et al (*J. Mech. Phys. Solids*. 2008;56: 2876-95), which is the thermodynamic crack driving force. Thus, a fracture criterion based on this parameter is proposed and its critical value is proved to be equal to the cohesive strength of cohesive model.*

1 INTRODUCTION

Plastic unloading is inevitable during crack propagation in elastic plastic materials. Thus, for elastic plastic growing cracks, deformation theory of plasticity ceases to be valid and increment theory of plasticity is required. Furthermore, increment theory of plasticity is not mature enough and intricate to apply. In other words, it is quite difficult to find

a parameter that can characterize the elastic plastic growing crack tip fields. However, the general crack tip integrals proposed by Moran and Shih^[1] have captured our attention. Moran and Shih have derived the general crack tip integrals based on momentum balance containing the crack tip. This work reminds us that energy balance is always satisfied and energy method may provide a novel view of elastic plastic growing cracks. And this paper attempts to shed some lights on this area.

Unlike the conventional way, the fracture process region (FPZ)^[2] is our focus. FPZ is a region near the crack tip where the microstructural fracture processes take place. From the standpoint of physical meaning, a parameter representing the states of FPZ can really reflect the fracture properties of materials. Usually, FPZ is small and it may be idealized as the crack tip in some cases^[2].

In this paper, the energy flux dissipated in FPZ is studied. And we found that this flux can be expressed as a path independent integral. In fact, this integral is also a kind of crack tip integral proposed by Moran and Shih^[1]. In Section 2, we have derived this energy flux integral through two methods, energy and power balance^[3]. And no restriction is imposed on the material response. Since this integral can be regarded as power available for separating the crack surfaces during crack growth, a force-like parameter F_T can be defined through power is equal to force multiplied by velocity. That is, F_T is the force conjugated to the crack tip velocity and it is the thermodynamic crack driving force. In Section 3, the relation between F_T and crack tip configurational force is established. And F_T is found to be equal to the minus project of crack tip configurational force along crack growth direction, which is identical to the near tip J integral proposed by Simha et al^[4]. In Section 4, a fracture criterion based on F_T is proposed. And the critical value of F_T is proved to be the cohesive energy of cohesive zone model. In Section 5, a puzzle arising in our minds is presented and some conjectures are also given. Conclusions are summarized in Section 6.

2 THE ENERGY FLUX AND CRACK DRIVING FORCE

The energy flux is first derived by energy balance containing crack tip. For a 2D elastic plastic continuum, A denotes its occupation and Γ denotes its boundary. And then according to equilibrium equation, we can obtain

$$\int_{\Gamma} \sigma_{ij} n_j u_i d\Gamma = \int_A \sigma_{ij} u_{i,j} dA \quad (1)$$

Body force is ignored and Cartesian coordinates are used in Eq. (1). n_j is the outer normal of the boundary Γ . The left side represents the external load work and the right side is the internal stress work.

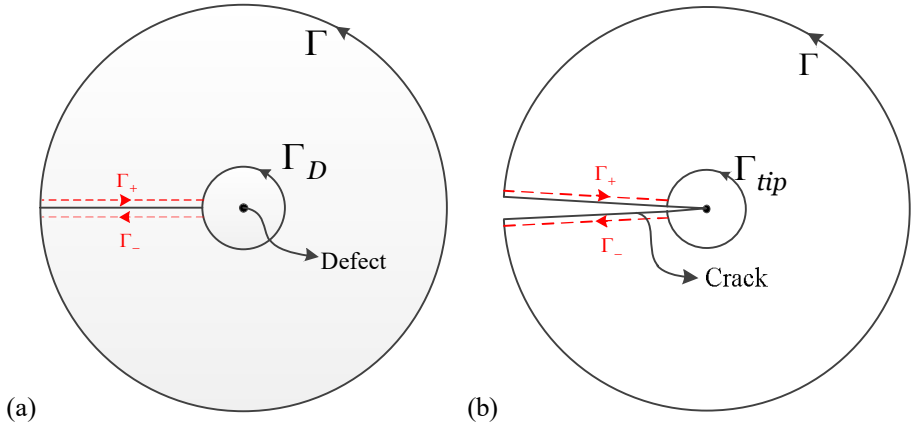


Fig. 1 The contour path when a defect is contained

As shown in Fig. 1 (a), if a defect exists in this body, the defect must be excluded to guarantee the validity of Green theorem. Consider Γ_D is an arbitrary curve surrounding the defect but included by Γ . A_D is the area surrounded by Γ_D . Because of the overlap between Γ_+ and Γ_- , Eq. (1) turns into

$$\int_{\Gamma-\Gamma_D} \sigma_{ij} n_j u_i d\Gamma = \int_{A-A_D} \sigma_{ij} u_{i,j} dA \quad (2)$$

Eq. (2) is also applicable to the crack case. As shown in Fig. 1 (b), the defect will become a crack when Γ_+ and Γ_- are separated. And Eq. (2) will keep invariable if the crack surface is traction free. Replace Γ_D with Γ_{tip} (A_{tip} is the area enclosed by Γ_{tip}), further result can be obtained,

$$\int_{\Gamma} \sigma_{ij} n_j u_i d\Gamma - \int_A \sigma_{ij} u_{i,j} dA = \int_{\Gamma_{tip}} \sigma_{ij} n_j u_i d\Gamma - \int_{A_{tip}} \sigma_{ij} u_{i,j} dA \quad (3)$$

If Γ_{tip} is chosen as the boundary of FPZ, Γ_{tip} is fixed and Γ can be chosen arbitrarily. Therefore, the left side of Eq. (3) is path independent. The line integral is the work applied to the region enclosed by Γ and the area integral is the strain energy stored in (or dissipated by) the materials. The physical meaning of the left side of Eq. (3) is the energy flowing into the crack tip. In addition, as shown by Broberg^[2], material separations take place in FPZ and continuum mechanics does not work. We assume that all of the external work is dissipated by micro damage and then the second term of the right hand will vanish. Thus,

$$\int_{\Gamma_{tip}} \sigma_{ij} n_j u_i d\Gamma = \int_{\Gamma} \sigma_{ij} n_j u_i d\Gamma - \int_A \sigma_{ij} u_{i,j} dA \quad (4)$$

Eq. (4) can also be explained by idealizing FPZ as the crack tip. In this case, $\Gamma_{tip} \rightarrow 0$. Since $\sigma_{ij} u_{i,j}$ has a singularity less than r^{-2} , the term $\int_{A_{tip}} \sigma_{ij} u_{i,j} dA$ vanishes. When crack grows in this body,

$$\frac{d}{da} \int_{\Gamma_{tip}} \sigma_{ij} n_j u_i d\Gamma = \frac{d}{da} \left[\int_{\Gamma} \sigma_{ij} n_j u_i d\Gamma - \int_A \sigma_{ij} u_{i,j} dA \right] \quad (5)$$

Where a is the crack length. FPZ will also move with respect to this crack tip and it is reasonable to assume FPZ is invariable in size^[5]. By fixing Γ in space, Eq. (5) will turn into

$$\Theta = \int_{\Gamma_{tip}} \sigma_{ij} n_j \dot{u}_i d\Gamma = \int_{\Gamma} \sigma_{ij} n_j \dot{u}_i d\Gamma - \int_A \sigma_{ij} \dot{u}_{i,j} dA \quad (6)$$

The superposed dot denotes the time derivative. Eq. (6) can also be obtained by power balance during crack propagation. Xiao S et al ^[3] have provided power available for separating the crack surfaces,

$$\text{Power} = \int_{\Gamma} \sigma_{ij} n_j \dot{u}_i d\Gamma - \int_A \sigma_{ij} \dot{u}_{i,j} dA \quad (7)$$

The first term of the right hand side is the power of the external force and the second term is the power of the internal force. From the angle of power balance, the total power of external load can be divided into two parts: One part is the power dissipated by the internal load, and the other is dissipated by FPZ. When the contour is the boundary of FPZ, the external power is totally dissipated by FPZ. And then Eq. (6) can be obtained.

Θ is the energy flux integral, which represents the energy flowing into FPZ. This integral has already been proved to be path independent during the derivation process. In addition, the energy flux integral can be considered as the power dissipated in FPZ (or the power available for separating the crack surfaces).

Since power is the product of load multiplied by velocity, a force like parameter can be defined as follows,

$$\Theta = F_T \cdot \dot{a} \quad (8)$$

Where \dot{a} is the crack growth velocity and F_T is the force conjugated to \dot{a} . F_T can thus be regarded as the thermodynamic crack driving force.

3 ENERGY FLUX AND CONFIGURATIONAL FORCE

Now we will recall Eq. (6) in initial undeformed configuration. Thus Cauchy stress tensor σ will become Piola-Kirchhoff stress tensor \mathcal{S} . The contour Γ_{tip} will turn into Γ_{tip}^{un} and the normal vector \mathbf{n} will become \mathbf{m} . Fig. 2 has shown this conversion. And then

$$\Theta = \int_{\Gamma_{tip}} (\boldsymbol{\sigma} \cdot \mathbf{n}) \dot{\mathbf{u}} d\Gamma = \int_{\Gamma_{tip}^{un}} (\mathbf{S} \cdot \mathbf{m}) \dot{\mathbf{u}} d\Gamma \quad (9)$$

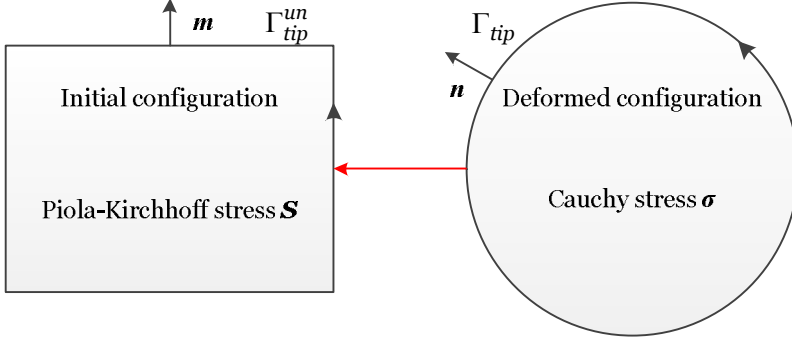


Fig. 2 Initial and deformed configuration

As provided by Moran and Shih^[1], the displacement fields satisfy

$$\dot{\mathbf{u}} \sim -\dot{a}_{un} \hat{\mathbf{e}} \cdot \frac{\partial \mathbf{u}}{\partial \mathbf{X}} \text{ as } \Gamma_{tip}^{un} \rightarrow 0 \quad (10)$$

In Eq. (10), \dot{a}_{un} is the crack growth velocity in initial configuration and $\hat{\mathbf{e}}$ is the direction of crack growth. \mathbf{X} is the Lagrange coordinate and \mathbf{x} is the corresponding spatial coordinate. Thus, Eq. (9) becomes

$$\Theta = \int_{\Gamma_{tip}^{un}} (\mathbf{S} \cdot \mathbf{m}) \dot{\mathbf{u}} d\Gamma = -\dot{a}_{un} \hat{\mathbf{e}} \cdot \int_{\Gamma_{tip}^{un}} (\mathbf{S} \cdot \mathbf{m}) \frac{\partial \mathbf{u}}{\partial \mathbf{X}} d\Gamma \quad (11)$$

Since $\mathbf{u} = \mathbf{x} - \mathbf{X}$ and substitute it into Eq. (11),

$$\Theta = -\dot{a}_{un} \hat{\mathbf{e}} \cdot \int_{\Gamma_{tip}^{un}} (\mathbf{S} \cdot \mathbf{m}) (\mathbf{F} - \mathbf{I}) d\Gamma = -\dot{a}_{un} \hat{\mathbf{e}} \cdot \int_{\Gamma_{tip}^{un}} (\mathbf{F}^T \cdot \mathbf{S}) \mathbf{m} d\Gamma \quad (12)$$

In Eq. (12), \mathbf{F} is the deformation gradient and the second equality has used $\int_{\Gamma_{tip}^{un}} (\mathbf{S} \cdot \mathbf{m}) d\Gamma = 0$, which is provided by Simha et al^[4].

Consider that Γ_{tip}^{un} is the boundary of FPZ in initial configuration and

the materials in FPZ always undertake microscope fracture. And then all of the external work is dissipated by microscope separations. That is no stored energy exists in FPZ (namely Γ_{tip}^{un}). If φ is the stored energy density, we can obtain

$$\int_{\Gamma_{tip}^{un}} (\varphi \mathbf{I}) \mathbf{m} d\Gamma = 0 \quad (13)$$

Eq. (13) can also be explained as follows: When FPZ is idealized as the crack tip, usual continuum mechanics is applicable near the crack tip and φ can be considered as stress work density. The elastic plastic growing crack tip field has a weaker singularity than static crack tip field [6]. Thus the singularity of φ is less than r^{-1} and Eq. (13) satisfies.

By adding Eq. (13) into Eq. (12),

$$\Theta = \dot{a}_{un} \hat{\mathbf{e}} \cdot \int_{\Gamma_{tip}^{un}} (\varphi \mathbf{I} - \mathbf{F}^T \cdot \mathbf{S}) \mathbf{m} d\Gamma \quad (14)$$

The crack tip driving force proposed by Simha et al [4] is

$$J_{tip} = \hat{\mathbf{e}} \cdot \int_{\Gamma_{tip}^{un}} (\varphi \mathbf{I} - \mathbf{F}^T \cdot \mathbf{S}) \mathbf{m} d\Gamma \quad (15)$$

And thus

$$\Theta = J_{tip} \cdot \dot{a}_{un} \quad (16)$$

It is noting that Eq. (16) is derived in initial configuration. Pull Eq. (16) forth to current configuration, Eq. (8) will be obtained. That is, the energy flux integral is indeed consistent with the thermodynamics crack driving force. And the parameter F_T proposed in Section 2 is equal to the minus project of crack tip configurational force along crack growth direction. In other words, F_T is identical to the Simha near tip J integral.

4 ENERGY FLUX BASED CRACK GROWTH CRITERION

Crack growth will happen only when micro-separations ahead of the

crack tip coalesce with the main crack. That is, the energy flowing into the crack tip must be large enough to support the above process in order to make crack propagate. Therefore, due to its physical meaning, the energy flux integral is a suitable fracture parameter. To keep the same dimension as J integral, we choose F_T here. And thus the crack growth criterion can be expressed as

$$F_T = F_T^c \quad (17)$$

F_T^c is the critical value of F_T , which is dependent on the fracture micro-mechanisms taking place in FPZ. According to Anderson^[7], the mechanisms depend on material properties and stress state (constraint level). And thus, for the same material and stress state, it is reasonable to assume that F_T^c is invariant during crack growth.

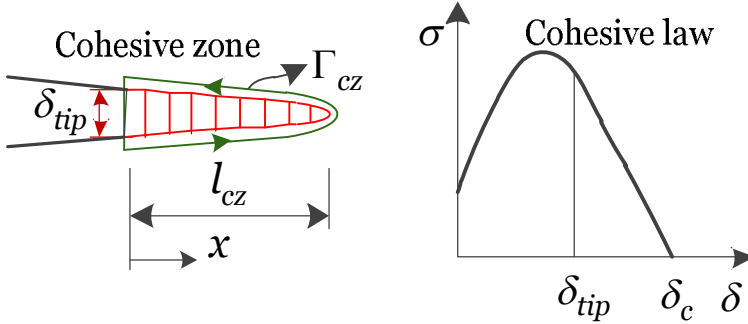


Fig. 3 Cohesive zone model

To determine F_T^c , FPZ can be idealized as the cohesive zone ahead of crack tip^[8-9]. The model is shown in Fig. 3, where l_{cz} is the length of the cohesive zone, δ_{tip} is the separation distance at the crack tip, δ_c is the critical separation when crack will grow and Γ_{cz} is the contour around the cohesive zone. The contour Γ_{cz} can be divided into two parts: the

upper and lower part. We have $n_1 = 1, n_2 = 0$ on the upper part; and for the lower part, we have $n_1 = -1, n_2 = 0$. Besides, all stress components except σ_{22} are zero. Thus, the power dissipated in cohesive zone is

$$F_T \cdot \dot{a} = 2 \int_0^{l_{cz}} \sigma_{22} \dot{u}_2 dx = \int_0^{l_{cz}} \sigma(\delta) \dot{\delta} dx \quad (18)$$

Where $\sigma_{22} = \sigma(\delta)$ and $\delta = 2u_2$. Since $\delta(0) = 0, \delta(l_{cz}) = \delta_c$ and $da = -dx$,

$$F_T = \int_0^{l_{cz}} \sigma(\delta) \frac{d\delta}{da} dx = \int_0^{\delta_c} \sigma(\delta) d\delta \quad (19)$$

Therefore, we can conclude that F_T^c is equal to the cohesive energy Γ_0 for cohesive zone model.

M (T) and C (T) specimens tested in reference ^[10] are used to verify Eq. (19). These specimens are 3 mm thick and made of AL 5083 H321 (L-T). The Young's modulus E is 68000 MPa and Poisson's ratio ν is 0.33. Scheider et al ^[10] have utilized cohesive zone model to predict crack extension of these specimens. The predicted results coincide with these tested results quite well when $\Gamma_0 = 10 \text{ N/mm}$. Table 1 has shows the specimen geometry and initial load. W is the total width, a_0 is the initial crack length and F_i is the applied load when crack initiates.

Table 1. Specimen geometry and initial load

Specimen type	$W(\text{mm})$	$a_0(\text{mm})$	$F_i(\text{KN})$
M (T)	100	15	39
M (T)	300	30	81
C (T)	50	25	2
C (T)	150	75	3.6

Since F_T^c is invariant during crack growth, the F_T value under F_i is equal to F_T^c . We assume that the crack tip fields are controlled by K factor when crack initiates. Combined Eq. (6) with (8),

$$F_T = - \int_{\Gamma} \sigma_{ij} n_j \frac{\partial u_i}{\partial x} d\Gamma + \int_A \sigma_{ij} \frac{\partial u_{i,j}}{\partial x} dA \quad (20)$$

By substituting linear elastic crack tip fields into Eq. (20),

$$F_T = \frac{3+\nu}{4} \frac{K^2}{E} \quad (21)$$

From F_i we can get the stress intensity factor when crack initiates, and then F_T^c can be obtained. Table 2 has summarized the validity results. All of these errors except 150 mm wide C (T) are less than 2%. The discrepancies of 150 mm wide C (T) may be due to the inappropriate application of linear elastic crack tip fields. Nonetheless, we can get from Table 2 that F_T^c is indeed consistent with the cohesive energy.

Table 2. Comparison between F_T^c and Γ_0

Specimen	M (T)-100	M (T)-300	C (T)-50	C (T)-150
F_T^c (N/mm)	9.87	9.83	10.15	10.97
Error	-1.3%	-1.7%	1.5%	9.7%

5 DISCUSSIONS

A puzzle exists here: For growing cracks, F_T is the thermodynamic crack driving force and thus F_T^c is indeed the fracture toughness. And we have shown that F_T^c is equal to Γ_0 of cohesive zone model. But Γ_0 alone is not enough to capture crack propagation in cohesive zone model. Any two parameters of Γ_0 , σ_{\max} and δ_c are required (σ_{\max} is the cohesive strength of cohesive law) in cohesive zone model.

There exist two conjectures about this puzzle:

The first conjecture is that $F_T = F_T^c$ must be satisfied to keep crack growing but this equality is not enough to represent the whole features of crack propagation. And another condition is required. Maybe there exists an energy ratio R_E for these structures. And R_E is defined as F_T^c

divided by the total dissipated work (F_T^c plus plastic dissipation). This ratio may be a truly geometry parameter, which is just dependent upon the geometry. Once the formula of R_E is obtained, the crack growth behavior can be totally decided by F_T^c .

The second conjecture is that $F_T = F_T^c$ is enough to represent the whole features of crack propagation. And there exist some conditions which are ignored by cohesive zone model. Usually, we choose cohesive law just on the basis of predicted results. That is, the cohesive parameters are first obtained from simple specimens and then are used to predict the crack growth behaviors of complex structures. And we guess that there may some standard procedure to get these parameters or some extra conditions that control these parameters. That is, once F_T^c is given, the corresponding cohesive law may be directly obtained. In this case, $F_T = F_T^c$ is enough to control the crack growth.

6 CONCLUSIONS

The crack tip energy flux integral is obtained from energy or power balance containing crack tip. This integral is also path independent. Besides, this integral can be considered as the power available for separating the crack surfaces or power dissipated in FPZ. Based on this physical meaning, a force-like parameter F_T conjugated to the crack tip velocity is defined. And F_T is found to equal to the minus project of crack tip configurational force along crack growth direction, which is identical to near tip J integral proposed by Simha et al ^[4]. Thus, a crack growth criterion based on F_T is proposed by us. Besides, we also prove that the critical value of F_T is equal to cohesive energy of cohesive zone model.

REFERENCE

[1] Moran B, Shih CF. Crack tip and associated domain integrals from

- momentum and energy balance. *Eng. Fract. Mech.* 1987;27: 615-42.
- [2] Broberg KB. *Cracks and fracture*. USA: Academic Press; 1999.
- [3] Xiao S, Wang HL, Liu B, Hwang KC. The surface-forming energy release rate based fracture criterion for elastic-plastic crack propagation. *J. Mech. Phys. Solids*. 2015;84:336-57.
- [4] Simha NK, Fischer FD, Shan GX, Chen CR, Kolednik O. J-integral and crack driving force in elastic-plastic materials. *J. Mech. Phys. Solids*. 2008;56:2876-95.
- [5] Tvergaard V, Hutchinson JW. The relation between crack growth resistance and fracture process parameters in elastic-plastic solids. *J. Mech. Phys. Solids*. 1992;40:1377-97.
- [6] Rice JR, Drugan WJ, Sham TL. Elastic-plastic analysis of growing cracks. *Fracture Mechanics: Twelfth Conference, ASTM STP 700*, American Society for Testing and Materials. 1980:189-21.
- [7] Anderson TL. *Fracture mechanics: fundamental and applications*. USA: CRC Press; 2017.
- [8] Barenblatt GI: The mathematical theory of equilibrium cracks in brittle fracture. *Adv Appl Mech*. 1962;7:55-129.
- [9] Dugdale DS: Yielding of steel sheets containing slits. *J Mech Phys Solids*. 1960;8:100-104.
- [10] Scheider I, Schodel M, Brocks W, Schonfeld W. Crack propagation analyses with CTOA and cohesive model: Comparison and experimental validation. *Eng. Fract. Mech*. 2006;73:252-63.

Phase Field Modeling of Hydraulic Fracture Propagation in Complex Formation Condition

Qianli Lu^{*}, Jianchun Guo^{**}, Lei Chen^{***}

^{*}Southwest Petroleum University, ^{**}Southwest Petroleum University, ^{***}Mississippi State University

ABSTRACT

Unconventional reservoir, especially shale reservoir, is featured with rock heterogeneity, in-situ stress anisotropy and abundant natural fractures. Due to these features, diverting, branching, offsetting and some other phenomena could occur while Hydraulic fracture propagate in the rock of unconventional reservoir. Commonly used sharp fracture topology models, such as the finite –element method (FEM), often suffer in complex fracture geometry due to computationally expensive remeshing and some other special handlings when fracture diverts or branches. In this paper, phase-field method (PFM) which is featured with diffusive fracture interface is proposed to quantitatively study the fracture propagation in complex formation condition with rock heterogeneity, stress anisotropy and natural fracture. The evolution of phase field is established by solving the energy balance between elastic energy, dissipation and external work by variational approach. The displacement field is solved by solid material wave equation with damping term. The advantage of this method is that no special handling or additional constitutive rule is needed to track the fracture interface and the fracture tip, and is free from pre-defining the propagation path, because the fracture diverting and branching is the solution of global optimal of the total energy of the system based on variational principal. The model is validated through fracture width, stress field and propagation against analytical model, ABAQUS and displacement discontinuity method. A hydraulic fracture interacts with an angled single natural fracture and a hydraulic fracture propagates in a shale main formation with a stiff heterogeneous strip across it are investigated. Study reveals that the approaching angle (θ) of natural fracture (NF) has great impact on hydraulic fracture propagation. For $\theta > 72^\circ$, hydraulic fracture directly penetrates natural fracture, and cannot initiate the natural fracture; for θ around 63° , hydraulic fracture penetrates and also initiates natural fracture, both fracture propagate simultaneously; for small $\theta < 45^\circ$, HF initiates NF, but cannot penetrate NF, fracture propagates along NF. In heterogeneous strip simulation, parametric study shows that fractures will branch as long as Young's modulus ratio ($ER = E_{strip}/E_{main}$) exceeds a critical value. The critical value increases accordingly as the principal in-situ stress difference (S_d) goes up. These results indicate that formation with around 63° approaching angle natural fractures, relatively low S_d and high ER has higher possibility to generate fracture network to increase production. The findings in this study could provide valuable insights in predicating and creating complex hydraulic fracture patterns.

Development of Commercial Finite Element Software Using Kratos Multiphysics Framework

Qiukai Lu^{*}, Erwan Beauchesne^{**}, Tadeusz Liszka^{***}, Mahender Reddy^{****}

^{*}Altair Engineering, Inc., ^{**}Altair Engineering, Inc., ^{***}Altair Engineering, Inc., ^{****}Altair Engineering, Inc.

ABSTRACT

Kratos Multiphysics platform developed as open source at CIMNE, Barcelona, [1], has been used to study thermo-mechanical analysis of material behavior during additive manufacturing (AM, called also 3-D printing) process. Kratos provides Finite Element solver basis, which relies on a set of open source components, including mesh and field variable data structures, matrix assembly, linear system solvers, and even parallelism for both shared and distributed memory systems. These, and other advanced features are under active development by the Kratos community, new ones are constantly being added to the code base, enable developers to quickly implement and test new solution algorithms. This development presents both opportunities to receive cutting edge functionality, and challenges to keep up with constantly changing, fluid environment. In this research, we developed proprietary features specific to AM simulation. These include customized meshing algorithms, moving heat source models, element activation strategies as well as material models. Some of the Altair development related to Kratos has been offered to Kratos community - this includes help in automated builds and testing, as well as interface layer to Altair pre- and post-processing products (Hyper Mesh(R), Hyper View(R), and H3D file format standard). In this talk we will present various aspects of the software development practices utilized by Altair to facilitate practical collaboration between open source and commercial software. We will also present a few results from the Altair AM solver. [1] Kratos Multiphysics (Version 5.2) [Computer software]. Retrieved January 12, 2018, from <https://github.com/KratosMultiphysics/Kratos>

An Improved FPM Method in the Discontinuous Interface Problems

Wang Lu^{*}, Xu Fei^{**}

^{*}Northwestern Polytechnical University, ^{**}Northwestern Polytechnical University

ABSTRACT

An Improved FPM Method in the Discontinuous Interface Problems Wang Lu¹?Yang Yang¹?Xu Fei¹ (1.School of Aeronautics, Northwestern Polytechnical University, Xi'an 710072, Shaanxi, P. R. China) Abstract: FPM (Finite Particle Method) is an important improvement of SPH (Smoothed Particle Hydrodynamics) method, which effectively improves the calculation accuracy of boundary particles. However, when the discontinuous physical field is solved by FPM, the accuracy in the vicinity of discontinuous interface is greatly reduced, and non-singularity of the matrix must be satisfied in FPM method, which requires an elaborate handling of the interface. Therefore, based on DSPH (Discontinuous SPH) method which is an improvement of traditional SPH for discontinuous problems, this paper proposed an improved FPM method — DSFPM(Discontinuous Special FPM) method, which considers discontinuous interface, aiming to improve the computational accuracy at interface and further improve the stability of FPM method and reduce the computational method. In this paper, the estimation accuracy of DSFPM method was analyzed firstly, and then the algorithm flow diagram of DSFPM method to deal with the different engineering problems is demonstrated. Next, DSFPM, DSPH and FPM methods are used to simulate the small deformation problem — elastic aluminum blocks impact, by comparing velocity and stress of the aluminum blocks, we verified the accuracy and computational efficiency of DSFPM method. Finally, the simulation of large deformation problem is realized by combination of DSFPM with DFPM (Discontinuous FPM) methods. Key words: FPM; interface; DSFPM; accuracy; computational cost References: [1] Liu MB, Liu G.R. Restoring particle consistency in smoothed particle hydrodynamics[J]. Applied Numerical Mathematics, 2006, 56(1):19-36. [2] Liu M B, Liu G R, Lam K Y. A one-dimensional meshfree particle formulation for simulating shock waves [J]. Shock Wave, 2003, 13: 201-211. [3] F. Xu?Y. Zhao? R. Yan? T. Furukawa. Multi-dimensional Discontinuous SPH method and its application to metal penetration analysis [J]. International Journal for Numerical Methods in Engineering. 2013,93:1125-1146.

Enhancing the Efficiency of Multiple Image Processing Tasks in Automatic Optical Inspection (AOI)

Wei-Hao Lu*, Po Ting Lin**

*National Taiwan University of Science and Technology, Taiwan, **National Taiwan University of Science and Technology, Taiwan

ABSTRACT

Automatic Optical Inspection (AOI) has been widely used in machinery and manufacturing industries. To complete each specific AOI mission, multiple image processing tasks, such as color balancing, contrast enhancement, filtering, transformation, pattern detection, etc., are used in a systematic arrangement with proper decisions of control parameters. As the complexity of the inspection mission increases, the required time to complete the entire image processing tasks increases dramatically. One way to speed up the image processing tasks is to use multithread computing in Graphics Processing Units (GPUs). However, the improvement by GPUs has a limit because the number of multiple image processing tasks remain the same. To further enhancing the efficiency, we investigated the effectiveness of each process (or each individual operation) and reduced the least effective processes in the entire multi-tasking processes. The balance between the process reduction and the image processing performance is optimized in terms of minimizing the computation time and maximizing the image processing accuracy simultaneously. Several numerical examples are examined to show the performance of the proposed method.

Computational Welding Vademecum for Parametric Studies: Identification of Nonlinear Material Properties

Ye Lu^{*}, Nawfal Blal^{**}, Anthony Gravouil^{***}

^{*}Univ Lyon, INSA-Lyon, CNRS UMR5259, LaMCoS, F-69621, France, ^{**}Univ Lyon, INSA-Lyon, CNRS UMR5259, LaMCoS, F-69621, France, ^{***}Univ Lyon, INSA-Lyon, CNRS UMR5259, LaMCoS, F-69621, France

ABSTRACT

In spite of the impressive progresses in computer science, traditional approaches remain prohibitive when dealing with nonlinear multiparametric problems, like inverse identification or optimization of welding, additive manufacturing or other complex processes. The use of model order reduction [1] can make available, at a cheaper cost, computational vademecum. Fast decisions can be then made by engineers. In this study, a novel non-intrusive reduced order strategy for construction of multiparametric welding computational vademecum is presented. This is based on an optimized database containing a limited number of standard finite element solutions selected in the underlying parameter space. These solutions can be obtained with any appropriate commercial code. An offline learning procedure based on Higher-Order Proper Generalized Decomposition method (HOPGD) [2, 3] is then carried out for searching a separated representation of the parametric solutions (space, time and controlled parameters). Once the separated parameter functions are constructed, new solutions for new parameter values (non-considered in precomputed set) are rapidly obtained by unidirectional interpolation methods at the online stage. The interpolation accuracy is controlled by an adaptive sparse grid sampling strategy in the parameter space. As an example, the multiparametric welding computational vademecum coupled with an online guidance algorithm is applied to inverse identification of non-linear constitutive model parameters. [1] A. Falcó, N. Montés, F. Chinesta, L. Hilario, M. C. Mora, On the Existence of a Progressive Variational Vademecum based on the Proper Generalized Decomposition for a Class of Elliptic Parameterized Problems. *Journal of Computational and Applied Mathematics* (2018). [2] D. Modesto, S. Zlotnik, A. Huerta, Proper generalized decomposition for parameterized helmholtz problems in heterogeneous and unbounded domains: Application to harbor agitation, *Computer Methods in Applied Mechanics and Engineering* (2015). [3] Y. Lu, N. Blal, A. Gravouil. "Multi-parametric space-time computational vademecum for parametric studies: Application to real time welding simulations." *Finite Elements in Analysis and Design* (2018).

Getting the Best of Damage Mechanics and Peridynamics: A Unified Approach for Objective Simulation of Material Degradation up to Complete Failure

Gilles Lubineau^{*}, Fei Han^{**}, Yan Azdoud^{***}, Yongwei Wang^{****}

^{*}KAUST, ^{**}KAUST, ^{***}KAUST, ^{****}KAUST

ABSTRACT

Despite many different approaches have been developed, the objective (mesh-independent) simulation of evolving discontinuities, such as cracks, remains a challenge. Current techniques are highly complex or involve intractable computational costs, making simulations up to complete failure difficult. We propose a framework as a new route toward solving this problem that adaptively couples local-continuum damage mechanics with peridynamics to objectively simulate all the steps that lead to material failure: damage nucleation, crack formation and propagation. Local-continuum damage mechanics successfully describes the degradation related to dispersed microdefects before the formation of a macrocrack. However, when damage localizes, it suffers spurious mesh dependency, making the simulation of macrocracks challenging. On the other hand, the peridynamic theory is promising for the simulation of fractures, as it naturally allows discontinuities in the displacement field. Here, we present a hybrid local-continuum damage/peridynamic model. Local-continuum damage mechanics is used to describe “volume&” damage before localization. Once localization is detected at a point, the remaining part of the energy is dissipated through an adaptive peridynamic model capable of the transition to a “surface&” degradation, typically a crack. We believe that this framework, which actually mimics the real physical process of crack formation, is the first bridge between continuum damage theories and peridynamics. This approach leverages at best both techniques as 1) damage mechanics helps in locating at low-cost where a peridynamics model should be introduced and 2) the peridynamics models helps in stabilizing the damage mechanics solution once the localization is achieved. Two-dimensional numerical examples are used to illustrate that an objective simulation of material failure can be achieved by this method.

Simulation of Micro-Scale Shear Bands Using Peridynamics with an Adaptive Dynamic Relaxation Method

Jiangyi Luo^{*}, Veera Sundararaghavan^{**}

^{*}University of Michigan, Ann Arbor, ^{**}University of Michigan, Ann Arbor

ABSTRACT

Size effects play an important role in material response. In classical elasticity, stress at a point is locally dependent on the strain at the same point which leads to prediction of singularities at crack tips and dislocation cores. It is therefore difficult for crystal plasticity finite element methods to properly predict strain localizations, in the form of fine shear bands, which have been observed by recent experiments. In contrast, the non-local method, peridynamics, is capable of handling damage and propagation of discontinuities. In peridynamics, strain at a point is calculated by tracking the motion of surrounding particles. An intrinsic length scale is introduced by the particle influence horizon to control the material responses. Recent results based on a crystal plasticity peridynamic model with an implicit Newton-Raphson solver have shown advantages of capturing finer shear bands in planar polycrystals. However, for crystal plasticity, the computation cost of calculating the tangent modulus matrix in implicit methods is high. In this presentation, we will present a peridynamic (PD) implementation of crystal plasticity with an adaptive dynamic relaxation method. Non-ordinary state-based peridynamics and the Newmark's dynamic method with artificial damping are employed to capture strain localizations in polycrystalline microstructures based on a rate-independent crystal plasticity model. The computational efficiency of the explicit PD model is demonstrated to be superior to the implicit PD model for modeling crystals. The stress field distribution, texture formation, and homogenized stress-strain response predicted by the finite element method and the new dynamic PD model are compared in numerical simulations. Finer strain localization bands are observed in the latter model. The effect of influence horizon size on localization bands are studied and instability is observed in PD results with larger horizon radius. Our future work will include: 1. More sophisticated controls of instability in peridynamics, such as introducing stress points; 2. 3D simulations to understand the effect of crystal structure on the activation and propagation of shear bands more accurately. Reference Luo, J., Ramazani, A. and Sundararaghavan, V., 2018. Simulation of micro-scale shear bands using peridynamics with an adaptive dynamic relaxation method. International Journal of Solids and Structures, 130, pp.36-48.

Coarse-grained Formulation of Point Defect Absorption at Interfaces and Its Application in Modelling Grain Boundary Migration Under Irradiation

Jing Luo^{*}, Yichao Zhu^{**}, Yang Xiang^{***}, Xu Guo^{****}

^{*}Dalian University of Technology, ^{**}Dalian University of Technology, ^{***}The Hong Kong University of Science Technology, ^{****}Dalian University of Technology

ABSTRACT

Interfaces are known to be ideal sink sites for point defects. Hence the introduction of high density interfaces provides an effective mean for developing materials with high irradiation tolerance. Nevertheless, limited works have been seen on modelling interface evolution induced by underlying point defect-interface interaction. In this talk, with use of matched asymptotic technique, we manage to upscale the (micro-scale) interaction between point defects and the constituting dislocation of low-angle grain boundaries (GBs), so as to derive a (macro-scale) Robin-type jump boundary condition. In comparison with the existing GB sink efficiency models, the derived condition takes into account (for the first time) the effect due to the point defects that penetrate GBs. Thus the study for GB sink efficiency in polycrystal is enabled. With use of the obtained jump Robin condition, we first derive a formula predicting sink efficiency of point defects for polycrystalline material as a function of its constituting grain sizes. Then in conjunction with the equation for point defect evolution in grain interiors, the GB migration behavior in the presence of irradiation is simulated. It is found that in contrast to the widely-used curvature-derived law, (which predicts symmetric evolution for cylindrical GBs), the GB deforms asymmetrically under irradiation. This work has laid a solid foundation for the investigation of interaction between interfaces and point defects, and useful insights for the dynamical behavior of interface are provided. This is essential for further investigations on nanocrystalline material behavior under irradiation.

Concrete Fragmentation Driven by Kinetic Energy of Forming Particles: Penetration of Projectiles of Various Impact Inclinations and Velocities

Wen Luo^{*}, Zdeněk Bažant^{**}

^{*}Northwestern University, ^{**}Northwestern University

ABSTRACT

The apparent increase of strength of concrete at very high strain rates experienced in projectile impact (10 s⁻¹ to 10⁶ s⁻¹), called 'dynamic overstress', has recently been explained by the theory of release of local kinetic energy of shear strain rate in finite size particles about to form. This theory gives the particle size and the additional kinetic energy density that must be dissipated in finite-element codes. In previous research, it was dissipated by additional viscosity, in a model partly analogous to turbulence theory. In the model presented here, it is dissipated by scaling up the material strength. Microplane model M7 is used and its stress-strain boundaries are scaled up by factors proportional to the -4/3rd power of the effective deviatoric strain rate and its time derivative. The scaled M7 model is seen to predict correctly the crater shapes and exit velocities of projectiles penetrating concrete walls of different thicknesses. Apart from orthogonal impacts, oblique impacts of projectiles into thin and thick concrete targets are also simulated. The choice of the finite strain threshold for element deletion criterion, which can have a big effect, is also studied. It is proposed to use the highest threshold above which a further increase has a negligible effect. References Bažant, Z.P., and Caner, F.C. (2013). "Comminution of solids caused by kinetic energy of high shear strain rate, with implications for impact, shock and shale fracturing." Proc., National Academy of Sciences 110 (48), 19291—19294 Bažant, Z.P., and Caner, F.C. (2014). "Impact comminution of solids due to local kinetic energy of high shear strain rate: I. Continuum theory and turbulence analogy." J. of the Mechanics and Physics of Solids 64, 223--235 (with Corrigendum, Vol. 67 (2014), p. 14). Bažant, Z.P., and Su, Yewang (2015). "Impact comminution of solids due to progressive crack growth driven by kinetic energy of high-rate shear." ASME J. of Applied Mechanics 82 (March), pp. 031007-1--031007-5. Su, Yewang, Bažant, Z.P., Zhao, Youxuan, Salvato. M., and Kirane. K. (2015). "Viscous energy dissipation of kinetic energy of particles comminuted by high-rate shearing in projectile penetration, with potential ramification to gas shale." Int. J. of Fracture 193 (1), 77-85.

A New Strong Formation Finite Element Method for Fracture Analysis of Functionally Graded Materials

Jun Lv^{*}, Xiao-Wei Gao^{**}

^{*}State Key Laboratory of Structural Analysis for Industrial Equipment, Dalian University of Technology, Dalian 116024, China, ^{**}State Key Laboratory of Structural Analysis for Industrial Equipment, Dalian University of Technology, Dalian 116024, China

ABSTRACT

In this paper, elastostatic crack analysis in continuously non-homogeneous, isotropic and linear elastic functionally graded materials and structures (FGMs) is presented. A new strong formation finite element method, Elemental Differential Method (EDM), is applied for this purpose, which establishes the system equations directly based on the equilibrium equations. The key aspect of this method is based on the direct differentiation of the shape functions of isoparametric elements used to characterize the geometry and physical variables of the solids. We develop a set of analytical expressions for computing first and second order partial derivative of the shape functions with respect to global coordinates. And then a new collocation approach is proposed to collocate the equilibrium equations collocated at the internal nodes inside elements, and collocate the traction equilibrium equations at the interface and outer surface nodes. Compared with standard FEM, the EDM does not require a variational principle to set up the computational system equation and no integrals are involved to form the coefficients of the system. Moreover, the stress results in EDM are calculated based on the constitutive relationship and can reflect the stress concentration phenomenon better than FEM. Special attention of the analysis is devoted to the computation of the most important crack-tip characterizing parameters of cracked FGMs, namely the stress intensity factors. Numerical examples for 2d and 3d crack problems in FGMs are presented and discussed to show the effects of the material gradation on the crack-opening-displacements and the stress intensity factors.

Symbolic-Numeric Methods for Solving Differential Equations in Scientific Computing

Dmitry Lyakhov*

*King Abdullah University of Science and Technology

ABSTRACT

Differential equations are the central objects in physical simulations. However, very rare cases admit exact analytical expressions as solutions. Typically, simulations of complex systems require to solve them numerically. This approach also suffers from drawbacks and limitations, like significant stiffness of the underlying physical systems. This usually requires tiny numerical step sizes to resolve accurately the behavior or to significant improvement of numerical method. Another problem is the lack of physical plausibility in long-term behavior, because it is hardly available to preserve physically important quantities like conservation laws at the discrete level. In this talk we describe modern methods of group analysis of differential equations and differential algebra in order to overcome these difficulties. First of all, we introduce the notion of symmetries and conservation laws, and how to construct symbolically methods to preserve them at the discrete level. Then, we present general algorithms from differential algebra in order to show how to extract all possible information from a differential system without solving it explicitly. Finally, theoretical approaches are illustrated by several relevant examples from scientific computing.

ProMesher: A Novel Code for Preprocessing of High-Order Finite Elements Applied to High-Speed Penetrations

Eric Lynd^{*}, Kent Danielson^{**}, Mark Adley^{***}

^{*}Geotechnical and Structures Laboratory, Engineering Research and Development Center, ^{**}Geotechnical and Structures Laboratory, Engineering Research and Development Center, ^{***}Geotechnical and Structures Laboratory, Engineering Research and Development Center

ABSTRACT

As part of modeling a deformable penetrator impacting a target, meshing of a pointed-nose projectile finite element model can be a non-trivial task requiring significant user interaction. For applications with nearly incompressible materials, such as typical metal plasticity models, the potential for significant locking issues generally precludes the use of “automatic” unstructured meshers using first-order tetrahedrons. In recent years, however, the authors have developed robust 2nd order finite elements for lumped-mass explicit methods that do not lock and thus can accurately model high-speed penetration events with unstructured meshes. Consequently, it is now possible to employ “automatic” meshers which utilize a variety of 2nd order mapping strategies for efficiently running analyses traditionally limited by select numerical phenomena. This presentation describes a code, developed by the authors, that easily creates high-quality hex-dominant finite element projectile meshes employing combinations of 2nd order element types TET15, WEG21, and HEX27. The code, penned ProMesher (Projectile Mesher), exploits inherent characteristics of the higher-order finite elements that can greatly simplify/automate the meshing and lead to significant reductions in required computation time. ProMesher can greatly improve productivity of analysts as well as provide the automation necessary for shape optimization and large tradespace analyses. Benefits of the computational approach for the case of high projectile penetration are demonstrated.

A Multiscale Control Volume Framework Using a Non-orthodox MPFA-D for the Simulation of Two-phase Flows on Truly Unstructured Grids

Paulo Lyra^{*}, Artur Souza^{**}, Lorena Barbosa^{***}, Darlan Carvalho^{****}

^{*}Federal University of Pernambuco (UFPE), ^{**}Federal University of Pernambuco (UFPE), ^{***}Federal University of Pernambuco (UFPE), ^{****}Federal University of Pernambuco (UFPE)

ABSTRACT

The advances in geostatistical modeling and characterization allow information from different scales to be integrated in order to generate geocellular models whose resolution typically range on the hundreds of millions cells, meanwhile the standard petroleum reservoir simulators handle only a fraction of this amount. In this way, multiple direct simulations on these high-resolution grids become infeasible. To overcome this limitation, scale-transferring methods have been devised. In essence, they allow high-resolution geostatistical data to be integrated onto the flow simulation grid. Among them, two branches of schemes stand out: the upscaling and the multiscale methods. Roughly speaking, the first generally employs a sort of homogenization of the field property, even when there is no formal separation between the scales. In these schemes a solution is found at the coarse-scale space leading to fast and robust results, but on the cost of losing information on the geological scale. To overcome this problem Multiscale Finite Volume Methods (MsFVM) devise conservative operators which are used to project the discrete system of equation onto the coarse-scale, solve the resulting coarse system and by using a set of operators, project back the solution onto the higher-resolution grid. Nonetheless, the MsFVM fail to deal with high-resolution geological properties on general grids as the multiscale operators are often calculated using a TPFA, which is only consistent for k-orthogonal grids. Furthermore, MsFVM lacks the framework capable of generating the geometric entities needed for simulation on unstructured coarse-scale meshes. The Multiscale Restricted Smoothed Basis (MsRSB) method creates this framework and expands the multiscale approach to unstructured coarse meshes. However, it fails to produce consistent solutions on fine-scale unstructured grids and for arbitrary permeability tensors as it also uses TPFA. In this article, we couple a MultiPoint Flux Approximation (MPFAD) with a Diamond stencil with the MsRSB to produce a consistent framework using unstructured grids on all scales. Additionally, we experiment with state of the art correction functions used to improve that quality of the multiscale flux in order to simulate some of the benchmark layers of the SPE. This framework showed prominent results producing accurate solutions for two-phase flow simulation in heterogeneous and mildly anisotropic medium with unstructured grids on coarse and fine scale.

Nonlinear Free Vibration Analysis of Defective FG Nanobeams Embedded in Elastic Medium

Zheng Lyu^{*}, Zhiping Qiu^{**}

^{*}Institute of Solid Mechanics, Beihang University (BUAA), Beijing 100191, China, ^{**}Institute of Solid Mechanics, Beihang University (BUAA), Beijing 100191, China

ABSTRACT

Defects in atomic structure can deteriorate the mechanical properties of nanomaterials. These defects can be used to tailor the local characteristics of nanostructures and to achieve new functionalities, which is crucial to the potential application in nano electromechanical systems. The existing model cannot fully reflect accurate mechanical behaviors of nanostructures with material defects. Apparently, developing a more realistic model accounting for the nanomaterial defects is an interesting research topic. The presentation focuses on the effect of the material defects on nonlinear vibration behavior of embedded functionally graded (FG) nanobeam. The concept of defect degree is freshly introduced to quantify the material defects. Then a defective FG nanobeam model for nonlinear vibration behavior is developed in the framework of nonlocal strain gradient theory. The proposed defective model is an extension of the perfect model, which not only exhibits good performance in revealing the effect of material defect on vibration behavior, but also could be degenerated into the perfect model by eliminating defect degree. Based on set theory, two methods, i.e., sensitivity based interval analysis method (SIAM) and iterative algorithm based interval analysis method (IAM), are presented to solve the defective model for predicting nonlinear vibration frequency. The comparison between SIAM and IAM is discussed in the presentation. Subsequently, the detailed parametric investigations are carried out to understand the combined effects of the material defects and size-dependent parameter, elastic medium as well as power-law index on the vibration frequency. Some significant conclusions are given, which will offer guidance in the reliability design of new nanodevices. Our preliminary investigations suggest that the defective model and two numerical methods can also be applied to other nanostructures with material defects in various engineering problems. At the end of the presentation, further work on this field is put forward.

EXPLORING THE LIMITS OF EFFICIENCY FOR BENDING-ACTIVE STRUCTURES

CARLOS LÁZARO*[†], JUAN BESSINI[†], AND SALVADOR MONLEÓN[†]

*[†]Departamento de Mecánica de los Medios Continuos y Teoría de Estructuras
Universitat Politècnica de València, Camino de Vera s/n, 46022 Valencia, Spain
carlafer@mes.upv.es

Key words: active bending, tied arch, scale effect, activation forces, buckling resistance.

Abstract. This paper discusses the relationship between structural shape, activation forces and activation stress levels in bending-active tied arches. The study focuses on planar arches composed of a bent rod, lower spanning cables and three equally spaced perpendicular deviators. A general relation between activation forces and structural shape has been established. Numerical experiments have provided activation stress levels with reference to rise-to-span ratios and rod slenderness. Serviceability limits for different proportions and lengths have been also analyzed. Results are given in terms of non-dimensional magnitudes and are applicable to variable scales and cross-section properties.

1 INTRODUCTION

Bending-active structures constitute a recent field of interest in research and practice¹. They consist of initially straight slender members that are elastically bent to reach a post-buckled curved configuration and then stabilized by means of constraints, cables or membranes in tension. Finding the initial equilibrium configuration is one of the main difficulties during the conceptual phase due to the high non-linearity of the structural response of active members². To address this issue, computational form-finding methods are being developed and comprise an active research field.

Nonetheless, the number of investigations focused on the assessment of the structural performance and efficiency of bending-active structures is limited. Lienhard¹ includes the study of several typical cases subject to simple loadings after they reach the initial active state and analyzes the proportion of the different contributions to the stiffness for different configurations by means of FEM software. Lázaro *et al.*³ analyze the response of circular and elastica-shaped active arches subject to a point load, and quantify the relation between geometric stiffness, tangent stiffness and the angle at arch ends for different values of the slenderness. Douthe⁴ considers strength and stiffness criteria to assess the applicability of different materials for active grid-shell members.

The design of a bending-active structure involves a tradeoff between member strength and magnitude of the pre-deformation: significant member curvatures are needed to reach a suitable shape; they require slender members to keep stresses low enough in the target configuration. However, very slender members may lead to insufficient stiffness of the structure. In the design of gridshell-like structures, the structural configuration is typically targeted to obtain certain shape definition and the effect of external loads may not be the most critical. However, in the case of footbridges they must bear heavier loads and it is crucial to achieve a certain stiffness.



Figure 1: Prototype of a lightweight footbridge based on the active bending principle

The broad objective of our research is to find patterns of relationship between form, activation forces, and limits of utilization of bending-active structures that may be used in the field of footbridges. At this stage we stick to simple planar structures composed of a continuous flexible rod that is activated by cables and deviators (Figure 2). We will use the term *bending-active tied arch* to refer to them. The structural concept is a hybrid between a tied arch and a cable beam and is suited to resist self-weight and service live loads. We consider structures with three deviators to limit the number of cases and the complexity of the study. More complex and stiff three-dimensional systems can be built combining a pair of planar bending-active tied arches. (figure 1).

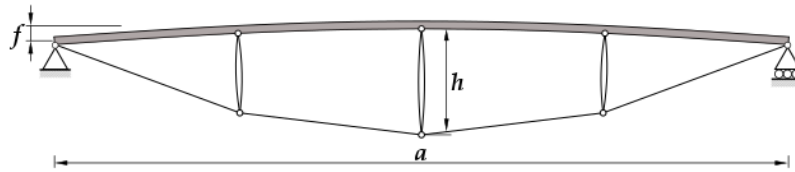


Figure 2: Three-deviator bending-active tied arch

In section 2, we start from fixed lengths and given cross-sections of rod and deviators. Introducing prestressing forces in cables, four different structural configurations that keep deviators perpendicular to the rod are form-found. From these results we establish a relation between the cable force ratio and the rise-to-span ratio of the activated structure, which is applicable for any scale. Through a series of numerical experiments, in section 3 we have obtained stress levels after the activation of the structure as functions of the rise-to-span ratio and the slenderness of the active member. Finally, further numerical analysis has led to establish relations between shape, length and slenderness associated to the serviceability limit state and ultimate limit state of the structure.

2 RELATIONSHIP BETWEEN SHAPE AND ACTIVATION FORCE

In a first step, we generate four different configurations for a bending-active tied arch with three equally spaced, perpendicular deviators. Simulations are carried out using Sofistik. The upper rod is a 4 m long continuous member with circular hollow cross-section with $EI = 23.72 \text{ kN m}^2$. The lengths of the deviators are $h = 0.4 \text{ m}$ (central) and 0.3 m (lateral). Cables are not continuous; therefore, cable forces will be different in each cable segment.

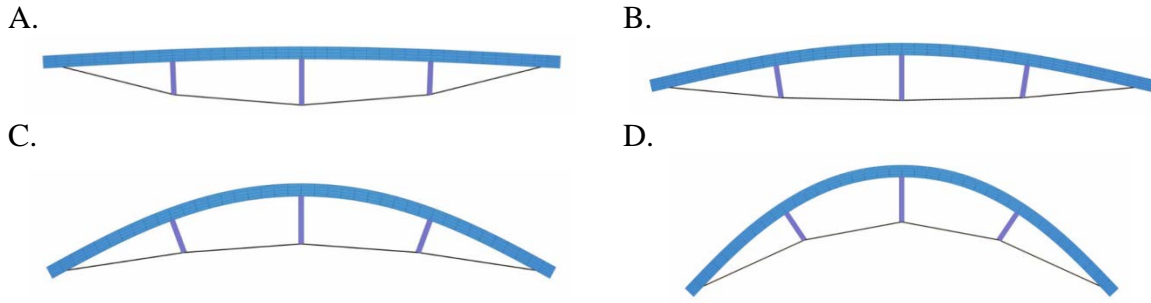


Figure 3: Four configurations for the hybrid structure with equal segment lengths and stiffness

For each self-stressed configuration, a force T^0 has been introduced in the outer cable segments; the force T^l in the inner cable segments has been chosen to achieve perpendicularity between rod and deviators at nodes. Table 1 lists characteristic data for each structure.

Table 1: Values of activation forces and resulting geometric ratios for each configuration

	A	B	C	D
T^0 (kN)	2.71	10.58	21.77	32.9
T^l (kN)	2.62	10.43	22.2	35.41
T^l / T^0	0.97	0.99	1.02	1.08
a (m)	3.996	3.947	3.753	3.366
f/a	0.0178	0.0727	0.1639	0.284

These results can be generalized for flexible members of any length and stiffness with equally spaced, perpendicular deviators whose proportions be: length of central deviator equal to 10% of the length of the rod; length of lateral deviators equal to 75% of the central deviator. Each segment of the rod behaves as a segment of inflexional elastica whose scale is determined by the critical length (Lázaro *et al.*⁵) $l_c = \pi\sqrt{EI/T}$. The ratio l_c^0/l_c^l between critical lengths of the outer and inner rod segments defines the shape of the whole structure. Consequently, the shapes and forces that have been obtained using specific sizes and dimensions of members can be scaled by increasing the critical lengths of each segment while keeping their ratio. Therefore, the relation between any non-dimensional size ratio and the activation force ratio in cables T^l / T^0 may be stated with generality for this structural type. Figure 4 represents the rise-to-span ratio and the depth-to-span ratio vs. the cable force ratio.

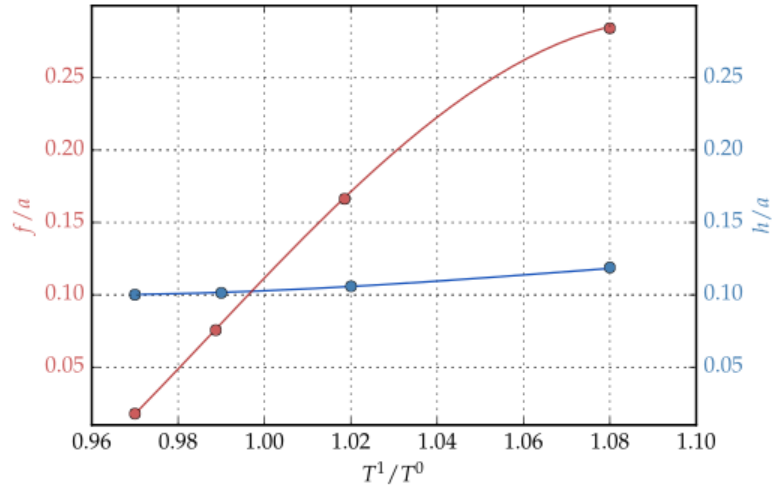


Figure 4: Relation between activation forces and proportions for tied arches with three deviators

Using figure 4 and the results in table 1, the configuration associated to a desired shape and size can be easily determined. For example, a 12 m span and 2.4 m rise arch ($f/a = 0.2$) has a force ratio $T^1/T^0 = 1.03$ (Figure 2). For this f/a ratio, in the original structure, $a = 3.68$ m and $T^0 = 25$ kN. The scaling factor for the desired structure will be $12/3.68 = 3.26$; therefore EI/T^0 should be $3.26^2 = 10.627$ times larger than in the original one. This can be done with a $3.26 \cdot 4$ m = 13.04 m long rod, using a stronger cross section, or decreasing the activation force, or a combination of both.

3 STRESS LEVELS AFTER ACTIVATION

The next step has been to establish limits to normal stresses in the bent rod after activation.

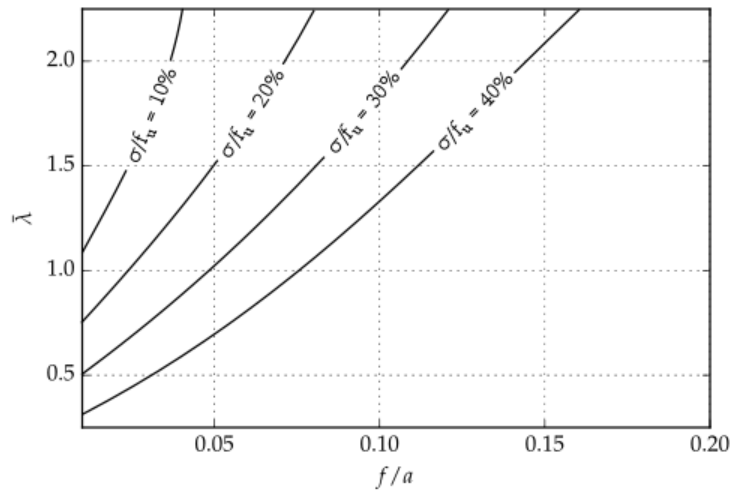


Figure 5: Stress ratio levels after activation in terms of rod slenderness and rise-to-span of the structure

For a single elastica, it can be shown that there is a direct relation between rise-to-span ratio and slenderness of the flexible rod for a given material, shape of cross section and level of normal stress due to bending. The following definition of slenderness has been selected: $\bar{\lambda} = \frac{s}{\pi} \sqrt{\frac{A}{I}} \sqrt{\frac{f_u}{E}}$,

where s is the length of the rod between deviators. As the bending-active tied arch is composed of a series of elastica sections, a similar relation between rise-to-span and slenderness is to be expected for a given structural topology. We have carried a series of numerical experiments with the same setup as in section 2. We have chosen GFRP for the rod (material properties of GFRP are $E = 30$ GPa, $f_u = 400$ MPa) and circular hollow cross-sections with thickness equal to 10% of the radius. Stresses in the rod have been evaluated for 12 values of $\bar{\lambda}$ and 40 values of the rise-to-span ratio. We have represented curves corresponding to several ratios of stress-to-ultimate-strength (Figure 5). As expected, higher rises lead to higher f/a ratios for the same slenderness. This diagram complements the results of section 2. Once the shape and size of the structure have been defined, it allows to select the minimum slenderness of the flexural member compatible with a prescribed stress level.

4 PERFORMANCE FOR SERVICE LOADS

To study the performance for service loads, it is necessary to define the cross-section of the activating cables and the magnitude of loading. The cable area has been selected so that its slenderness be 10 times the rod slenderness. The mechanical properties of the selected cables are: $E = 105$ GPa and $f_u = 1570$ MPa. Point loads corresponding to 40% of 5 kN/m^2 distributed on a variable wide which corresponds to the 10% of the rod length have been applied as frequent service load. Mid-span deflections have been evaluated for different lengths.

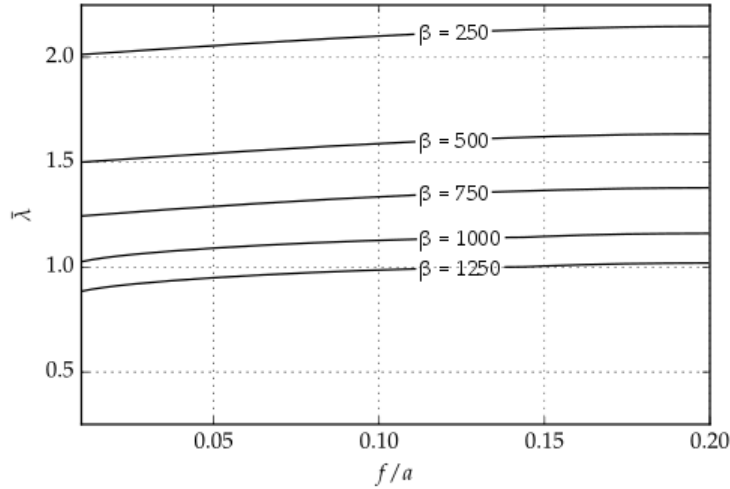


Figure 6: Deflections from $L/250$ to $L/1250$ for different lengths and a given load in terms of slenderness and shape

5 PERFORMANCE FOR ULTIMATE LOADS

A similar study has been carried out to assess the behavior at ultimate limit states. Structural proportions and cross-section dimensions are the same as the previous analysis. The design value for the point loads is obtained by the application of the partial factor for actions $\gamma_f = 1.35$. For several structures, we have checked normal forces and bending moments in the rod performing second order analysis of the structural model. Figure 7 shows the region of the slenderness-shape diagram where according to EN 1993-1-1 (Eurocode 3) the utilization ratio is less than 1, for different lengths and a given design load.

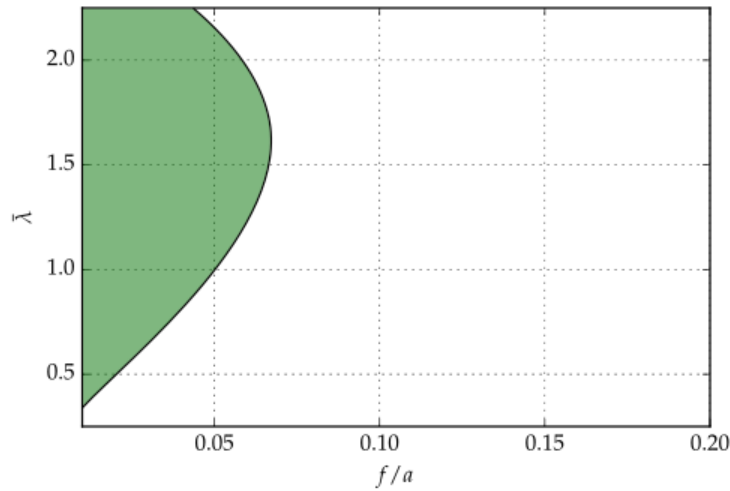


Figure 7: Safe region (green) against buckling for the model examples.

6 CONCLUSIONS

We have studied the activation process and the performance of bending-active tied arches with three perpendicular deviators. General non-dimensional relations between activation forces and structural shape, as well as stress levels in terms of shape and slenderness of the flexural member have been established. We have also studied the serviceability limit state and the ultimate limit state for prescribed loads and cable areas. Further research needs to be done to establish the limits of applicability of this type of active arch.

6 ACKNOWLEDGEMENTS

The authors gratefully acknowledge the financial support from the Spanish Ministry of Economy and Competitiveness through grant BIA2015-69330-P (MINECO) and the support from CALTER Ingeniería and SOFISTIK AG for providing a software license.

REFERENCES

- [1] Lienhard, J. *Bending-Active Structures: form-finding strategies using elastic deformation in static and kinetic systems and the structural potentials therein*. Universität Stuttgart, (2014).
- [2] Bessini, J., Lázaro, C. and Monleón, S. A Form-finding method based on the geometrically exact rod model for bending-active structures. *Engineering Structures*, (2017); 152:549–558. <https://doi.org/10.1016/j.engstruct.2017.09.045>.
- [3] Lázaro, C., Monleón, S. and Bessini, J. Tangent Stiffness in loaded elastica arches. *Proceedings of the IASS Symposium 2017. International Association for Shell and Spatial Structures*, (2017).
- [4] Douthe, C. *Etude de structures élancées précontraintes en matériaux composites, application à la conception des gridshells*. *Engineering Sciences [physics]*. Ecole des Ponts ParisTech, (2007).
- [5] Lázaro, C., Monleón, S. and Casanova, J. Can the force density method be extended for active bending structures? *Proceedings of the IASS Symposium 2015. International Association for Shell and Spatial Structures*, (2015).
- [6] Bessini, J., Piñol, R., Lázaro, C. and Monleón, S. Design of an experimental lightweight footbridge based on the active bending principle. *Proceedings of the IASS Symposium 2018. International Association for Shell and Spatial Structures*, (2018).

Pseudospin-spin Dynamics in AC-driven Single-layer Silicene

Alexander López^{*}, Antonio Di Teodoro^{**}, Francisco Mireles^{***}, John Schliemann^{****}, Benjamin Santos^{*****}

^{*}Escuela Politécnica del Litoral, ^{**}Universidad San Francisco de Quito, ^{***}Universidad Autónoma de México,
^{****}University of Regensburg, ^{*****}INRS-Energie et Materiaux Varennes

ABSTRACT

We study the pseudospin-spin fluctuation dynamical effects in single layer silicene due to the interplay of a periodically driven perpendicular electric field and the Rashba spin-orbit interaction. We find that spin non conserving processes of the real spin, induced by the rather weak Rashba coupling, manifest themselves as shifts of the resonances in the quasienergy spectrum in the low coupling regime to the driving field. Moreover, we find an interesting cooperative effect among the, in principle, competing spin-orbit contributions. This is explicitly illustrated by a perturbative analytical solution of the dynamical equations. In addition, we show that a finite Rashba spin-orbit interaction is necessary in order to get a non vanishing out of plane pseudospin polarization. We discuss the possible experimental detection schemes of our theoretical results and their relevance in new practical implementation of periodically driven interactions in silicene physics.

In recent years, synchrotron X-ray microtomography (SpCT) became an established method for the investigation of biological questions [1]. However, with the analysis and the ever-increasing amount of data, we are constantly facing new challenges. In particular, the segmentation of tomographic images is still the bottleneck in a fast evaluation of CT data sets, since in many cases the segmentation is done manually. We present the Biomedical Image Segmentation App (Biomedisa, <https://biomedisa.de>) which is a web application for the fast and accurate analysis of large tomographic data. It has already proven to be extremely effective in accelerating the tedious manual segmentation within the projects ASTOR and NOVA. Reducing the number of manually labeled slices, it can be seen as an interpolation between pre-segmented reference slices taking into account the image data. Its semi-automatic segmentation method is based on a highly scalable diffusion method, which is free of so-called hyperparameters making it easy to use [2]. The segmentation is performed using weighted random walks starting in the pre-segmented reference slices. Moreover, due to their independence, the random walks can be efficiently performed in parallel using GPUs. The image data and results can be visualized by means of a 2D slice viewer and 3D rendering software. By employing Biomedisa for segmentation of various extant and fossil insects from fast SpCT, we demonstrate the value of this tool for different research areas like functional morphology and paleontology. We scanned thousands of different specimens at the fast imaging stations of KIT's Institute for Photon Science and Synchrotron Radiation (IPS). When studying 30-million-year old mineralized fossils, we found that also insects from non-amber collections may contain detailed internal anatomical characters, thus allowing species description and phylogenetic analysis as done for extant specimens [3]. Biomedisa turned out to be much faster and more accurate than manual segmentation and proved to be invaluable when dealing with a huge amount of specimens. [1] T. van de Kamp, P. Vagovic, T. Baumbach, &&&&&&&& A. Riedel. A biological screw in a beetle's leg, *Science*, 333, 52, 2011. [2] P. Lösel &&&&&&&& V. Heuveline. Enhancing a diffusion algorithm for 4D image segmentation using local information, *Proc. SPIE 9784, Medical Imaging 2016: Image Processing*, 97842L, 2016. [3] A.H. Schwermann, T. dos Santos Rolo, M.S. Caterino, G. Bechly, H. Schmied, T. Baumbach &&&&&&&& T. van de Kamp. Preservation of three-dimensional anatomy in phosphatized fossil arthropods enriches evolutionary inference. *eLife* 5, e12129, 2016.

Computational Researches on Damage and Failure Mechanics of CFRP T-joints under Pulling Load

XUESHI MA*, YI WANG**, QINGDA YANG***, KE XIONG****

*State Key Laboratory of Mechanics and Control of Mechanical Structures, Nanjing University of Aeronautics and Astronautics, **State Key Laboratory of Mechanics and Control of Mechanical Structures, Nanjing University of Aeronautics and Astronautics, ***Department of Mechanical and Aerospace Engineering, University of Miami, ****State Key Laboratory of Mechanics and Control of Mechanical Structures, Nanjing University of Aeronautics and Astronautics

ABSTRACT

Abstract As a typical case of co-cured connection of composite structural components, T-joints represent potentially a vulnerable section affecting the overall integral structure reliability and efficiency. In this study, filler cracking and interface debonding of Carbon Fiber Reinforced Polymer (CFRP) T-joints (T700/QY8911) under pulling have been numerically investigated by Augmented Finite Element Method (AFEM) [1] – Cohesive Zone Model (CZM) as well as Extended Finite Element Method (XFEM) – Cohesive Zone Model (CZM), respectively. The two numerical and experimental results have been obtained and compared, describing the major failure modes (filler crack & interface debond) of the typical T-joints during pulling process. In addition, load-displacement responses of the T-joints have also been separately obtained from AFEM-CZM, XFEM-CZM and experimental pulling test. Comparing with the experiment data, there are good performances for AFEM-CZM and XFEM-CZM in predicting damage paths and failure status of the T-joints. From the results, it can be demonstrated that filler crack initiation occurs at early stage of pull-off and initiates at the top region which reveals that stress generally concentrates around top region under pulling load. Upon continuous pulling, tensile load subjected to the T-joint will increase until structural ultimate failure. During the whole tensile process, filler seems to make little contribution on load-bearing for the structure. However, debond starts to appear at stiffener-to-skin interface and filler-to-skin interface at the moment of onset failure, which means load-bearing capability of the T-joint mainly depends on debond durability of the interface related to skin. Furthermore, fiber-bridge could be considered to adopt for improving load-carrying of T-joints under pull-off based on the stress status predicted by numerical analyses. Key words: CFRP T-joint; AFEM-CZM; XFEM-CZM; Pulling References [1] W. Liu, Q. D. Yang*, et al. An efficient augmented finite element method for arbitrary cracking and crack interaction in solids. *Int. J. Numer. Meth. Engng* 2014;99:438-468. [2] Yi Sheng, Ke Xiong*, et al. Fracture behavior of carbon fiber T-joints under tensile load (with English abstract). *Acta Materialiae Composite Sinica* 30(6), (2013) 185-90. [3] X. Ma, K. Bian, K. Xiong*, et al. Experimental research on detection for interface debond of CFRP T-joints under tensile load. *Compos Struct* 2016;158:359-368.

Evaluation of FEM analysis model on solar module steel structure design

Yasuhiro MAEDA*, Yoshihito OZAWA⁺, and Naoto TAKEHANA[^],
Wataru TAKANO[^], Yuta ONODE[^]

* Graduate School of Fukushima University
Fukushima, Fukushima, Japan
s1671004@ipc.fukushima-u.ac.jp

⁺Fukushima University
Fukushima, Fukushima, Japan
ozawa@sss.fukushima-u.ac.jp

[^] Okuji Kensan Co., Ltd
Osaka, Osaka, Japan
n_takegahana@okuji.co.jp

Key word: FEM Analysis, Photovoltaic System, Support Structure Design, Buckling,

Abstract. In recent years, accidents have frequently occurred under the rapid spread of photovoltaic power generation system in Japan. The support structures of the system were deformed or destroyed due to strong wind or heavy snow when the support structure was designed improperly. The main cause is considered to be a mistake in the structural calculation model, especially the model for joint parts. In this study, we conducted a full-scale experiment simulating wind load and snow load on photovoltaic power generation system, furthermore, it was examined that the joint parts model proposed by the Authors is valid for safety design of the support structure. The buckling element was modeled with thin shell element and some reports on the deformation state until buckling were precisely shown from the results of elastoplastic analysis.

1 INTRODUCTION

In recent years, the use of renewable energy has been dramatically increased in each country. Especially "photovoltaic power generation system" (hereinafter called "PV system") has been attracting a wide attention around the world, and the scale of market is expanding continuously. In Japan, the introduction of PV system is beginning to be advanced, and then the number of large-scale PV system has rapidly increased because the Feed-in Tariff Law for Renewable Electric Energy (Fit Low) takes effect from July 1, 2012. In order to precede massive introduction of PV system in Japan, it is considered that there are found to be two problems as the current condition. The first is that the power generation cost is higher than that of the other major power supply. The second is that the structural accidents are frequently occurring along with the rapid spread of PV system. In order to solve these problems, it is an urgent issue to realize the safe and reasonable support structure. In addition, in the PV system, the support structures of the PV system were deformed or destroyed due to strong wind or heavy snow when the support structure

was designed improperly ^[1]. The main cause of inappropriate design is considered to be a mistake in the structural calculation model, especially the model for joint parts.

In this study, we compare the experimental results with the analysis results simulating wind load and snow load applied to the support structure of PV system which is composed of 1.6 mm in thickness thin steel plates as main structural elements ^[2]. Furthermore, we will examine that the joint parts model proposed by the Authors is valid for safely design of the support structure. The buckling element is modeled with thin shell elements and some reports on the process of buckling are precisely shown from the results of elastoplastic analysis.

2 LOADING TEST

2.1 Experimental Procedure

The support structure equipped with the solar cell module of four lines and two columns was treated as one unit ground installation of PV system. Then, two units to be simulated were arranged side by side as a specimen. The outline of the specimen is shown in Fig. 1. Table 1 shows the cross-sectional shape of the support structure elements used in the experiments, and Table 2 shows the conditions of wind load experiment ^[3, 4].

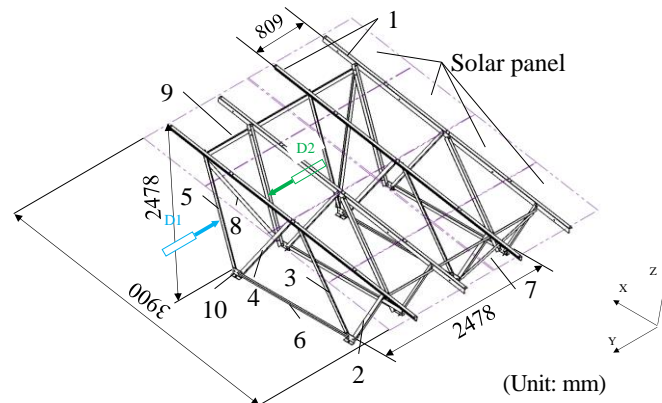


Fig. 1 Support structure of PV system

Table1 Cross-sectional shape of elements

	Cross-section shape [mm]
1	L-66.2×45×11.6×1.6
2	L-45×45×1.6
3	L-45×45×1.6
4	L-45×45×1.6
5	L-45×45×1.6
6	L-45×25×1.6
7	L-45×25×1.6
8	L-45×25×1.6
9	L-45×25×1.6
10	L-85×45×4.5

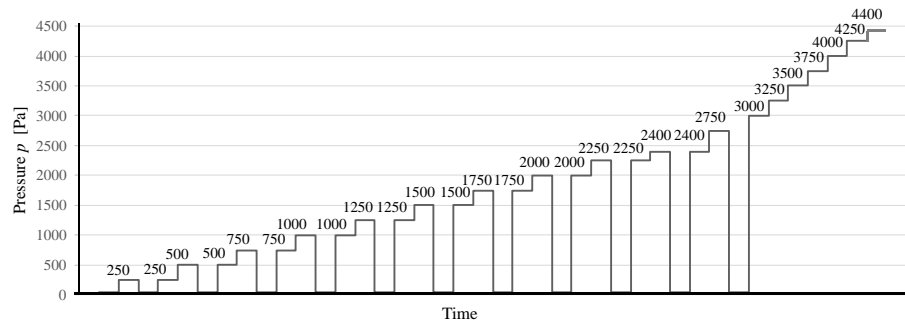


Fig. 2 Pressure step applied to the solar panels

Table 2 Condition of wind load experiment

Load	Design condition	Module surface inclination angle	Calculation method
Wind load	Design standard wind speed 38 m/s Ground roughness classification III	20 degrees	$W/A=C_f \times q=1.25 \times 1540=1925 \text{ Pa}$

In this experiment, we carried out an experiment procedure in order to simulate the positive pressure of the wind load (pressure to depress the PV system) by using a dynamic wind pressure chamber. The pressure step applied to the solar panels is shown in Fig. 2. Pressure p was applied until the specimen destroyed, and the evaluation of strength, deformation and fracture were conducted for the specimen. In the displacement measurement, since the displacement sensor would be damaged due to the breakage of the specimen, the measurement was continued until the final stage only for D1, but for D2 it was stopped at 2000 Pa.

2.3 Experimental result

Figure 3 shows the relationship between the pressure and the displacement at sensor position D1 and D2 shown in Fig. 1. The displacements of pillar element No. 5 from sensor positions D1 have minus value, opposite sign to data from D2 shown in Fig. 3. For pillar element No. 5, it was observed that the element deformed toward inside from visual observation. The relationship

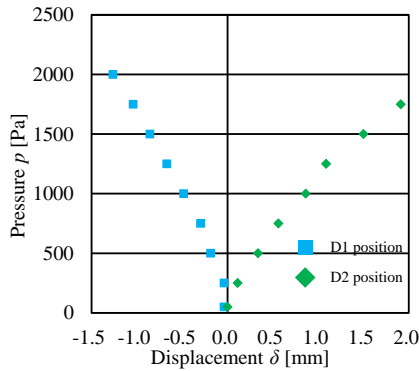


Fig. 3 Relationship between pressure and displacement

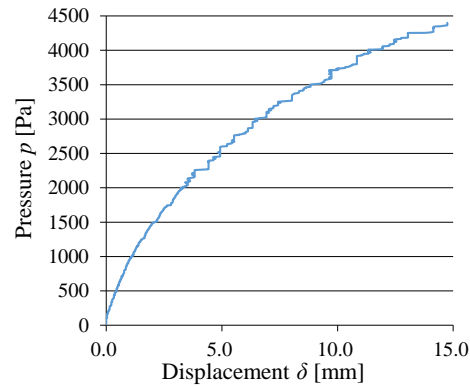


Fig. 4 Relationship between pressure and displacement in position of D3

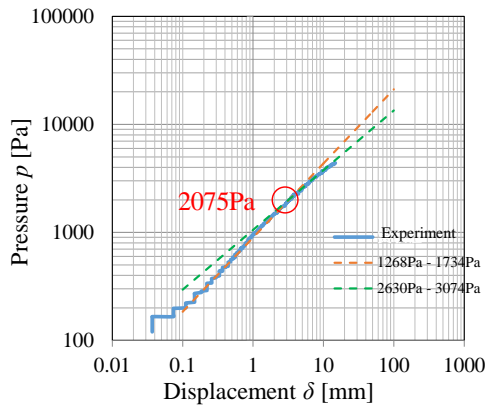


Fig. 5 Relationship between pressure and displacement with logarithm scale of both axis



Fig. 6 Destruction situation of specimen

between the pressure and the displacement up to the destroyed pressure at the position D1 is shown in Fig. 4. In order to evaluate the kink point of the deformation of support structure easily, Fig.5 shows for relationship between the pressure and displacement in logarithm scale of both axes. The point of intersection of the dotted lines indicated by the red circle in Fig. 5 was taken as the inflection point, and this stress level of 2075 Pa could be taken as the kink point of deformation of the pillar element No. 5. After continuing pressure, the specimen was suppressed from 4250 Pa to 4500 Pa, and then the pillar element No. 4 buckled and the specimen of PV system was destroyed as shown in Fig. 6.

In experiments for simulating snow load, experiments were conducted by using same specimens with different tilt angles of array surface. In the case of snow load, the pillar element No. 5 buckled and the breaking pressure was 5038 Pa.

3 FINITE ELEMENT METHOD

FEM analysis was carried out in order to examine the important effect of the joint parts model on the destruction accident, and the buckling process of the pillar elements in the experiment.

The mechanical properties used in the analysis are shown in Table 3. In the plastic range, the relationship between the stress and plastic strain is bilinear due to the relation to the yield stress and the tensile strength.

Table 3 Mechanical property of SS400

	Young's modulus [MPa]	Poisson's ratio	Yield stress [MPa]	Tensile strength [MPa]	Elongation
Analysis model	205000	0.3	235	400	33%

3.1.1 Three-dimensional elasticity analysis with beam element

At the joint parts of the support structure with the thin steel plate, the centroid axis of an element with L-shape deviates from that of an adjacent element. Accident occurred due to the lack of conscious on these mismatches. Especially it is important to simulate real joint parts model in FEM analysis by using beam elements. We proposed the joint parts model as follows and examined whether it is effective for the safety support structure design.

The analytical model used in analysis is a three-dimensional elastic beam element model. In order to simulate the joint parts of the actual structure, the joint nodes between two adjacent elements were not set at the along the same line, and the centroids of joint elements remain apart each other. Furthermore, we proposed a model with eccentricity that does not constrain the rotating motion only the bolt axis (Fig. 7 (a)) ^[5]. For the comparison, we also analyzed the non-eccentricity model (Fig. 7 (b)) simulated the joint parts node rigidity. For the initial conditions of the analysis, when simulating a wind load, a uniformly distributed load in the perpendicular direction acts on the element No. 1. And when simulating a snow load, an equally distributed load acts on the element No. 1 however in the vertical direction to the horizon.

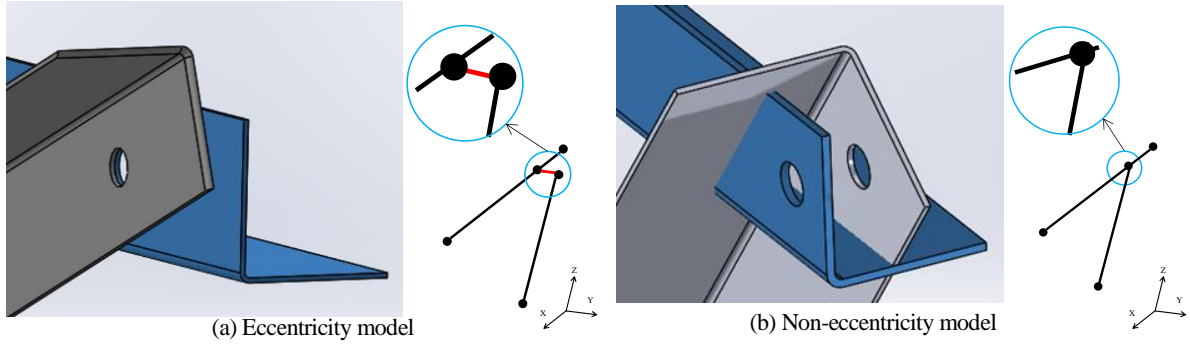


Fig. 7 Joint part model of elements

3.1.2 The results of analysis

Figure 8 shows the relationship between the pressure and the displacement at the same measurement position of the experiment shown in Fig.1. Figure 9 shows the deformation behavior by the use of the eccentricity model and the non-eccentricity model, when the wind load is applied. From Fig. 8, in the eccentricity model, the displacement of the pillar elements at D1 position become large as increasing the pressure, the displacement at D1 takes smaller value than that at D2, and with a opposite sign against that at D2. In the non-eccentricity model, the behavior at D1 is inverse relation to the eccentricity model and the displacement at D2 indicates nearly zero. In Fig. 9, the pillar elements No. 5 in the eccentricity model was deformed toward inside, and in the case of the non-eccentricity model, the deformation of the element tilts to one side. The same tendency was also observed for the experiments in the case of snow load.

For the element which experienced buckling in the experiment, the load level is coincided with

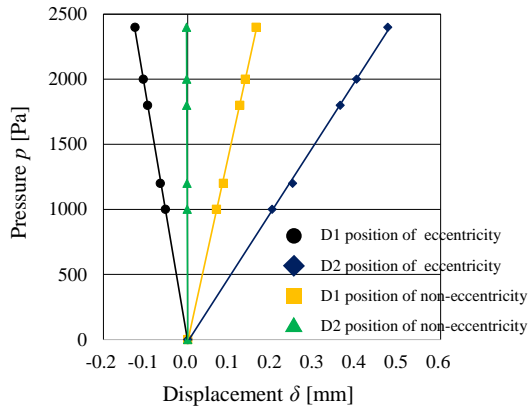


Fig. 8 Relationship between y direction pressure and displacement

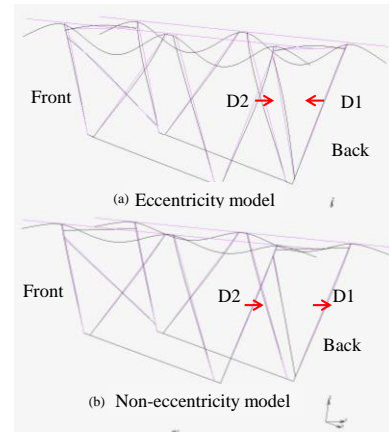


Fig. 9 Deformation diagram

Table 4 Analytical values of axial force and bending moment

		Axial force [N]	Bending moment [N·m]
Wind load	Eccentricity model	-1982.1	8173.6
	Non-eccentricity model	-1986.0	-867.4
Snow Load	Eccentricity model	-1471.8	-9769.6
	Non-eccentricity model	-1256.9	1035.1

the points where the axial force and the bending moment are maximized in the analysis results. Table 4 shows analytical values of axial force and bending moment for the buckled element in the eccentricity model and non-eccentricity mode. From Table 4, it can be seen that the bending moment takes on very large value in the eccentricity model. It can be seen from Figs. 8 and 9 that the bending deformation due to twisting of the joint part can be expressed in the eccentricity model.

3.2 Three-Dimensional Shell Element Elastoplastic Analysis

3.2.1 Shell Element Finite Element Model

In the experiment, the pillar elements buckled and the support structure was suddenly destroyed. Therefore, it is important to understand the buckling process of the structure and the behavior of a buckled element. In this Chapter, for the purpose to examine the deformation state until the pillar element is buckling, the elastoplastic analysis was conducted for a pillar element which buckled at onset of the support structure destruction.

Let us focus on the pillar element No. 4 buckled at first in the experiment for wind pressure. Figure 10 shows the applied load and the boundary conditions of the model. The model was analyzed with a bilinear thin-shell element. The displacement of lower end was completely constrained at all nodes of the bottom end, and that of upper end was set as a free end. The load was applied to the bolt circle center that is eccentric from the centroid. The axial force P obtained in the analytical result of Section 3.1.2 was applied at the free end as a load.

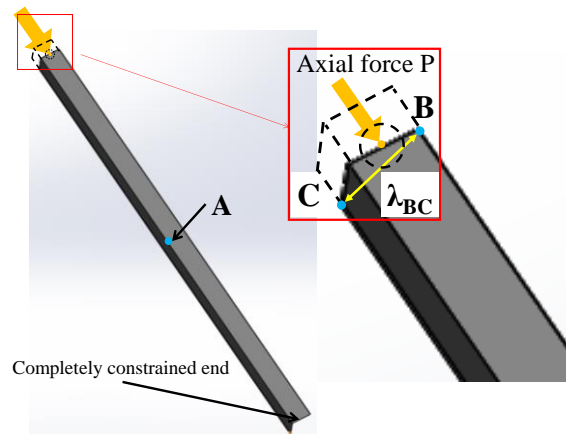


Fig. 10 Analysis model of pillar element No. 4

3.2.2 Analysis Results

Elastoplastic analysis was conducted with the pillar elements (No. 2 to 5). The pillar element No. 4 buckled at first in the analytical simulation as well as in the experiment. Therefore, the analytical result of the pillar element No. 4 will be precisely described below.

Figure 11 shows the relationship between the pressure and the displacement at the point A, which

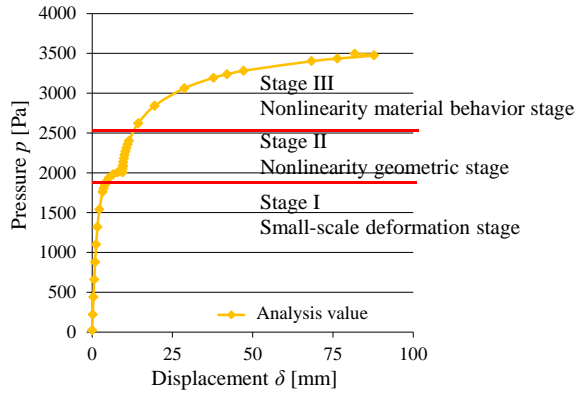


Fig. 11 Relationship between pressure and displacement (shell element model)

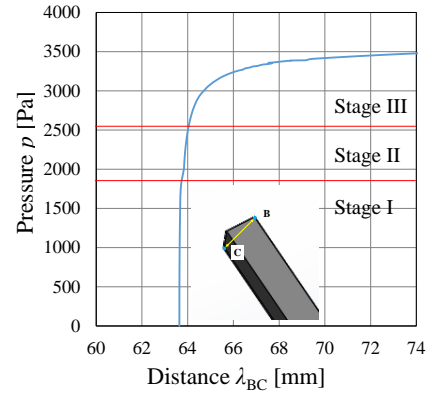


Fig. 12 Relationship between pressure and distance between B and C

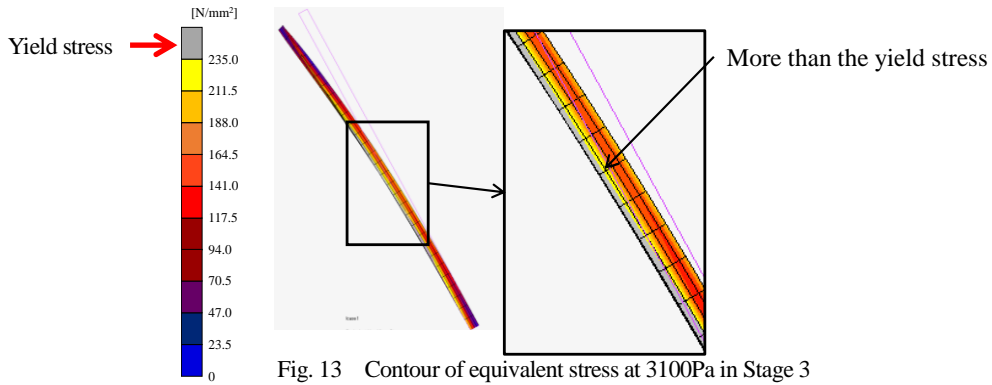


Fig. 13 Contour of equivalent stress at 3100Pa in Stage 3

is the center in the length direction of the element shown in Fig. 10. By examining the results for the kink point appeared in Fig. 11, the deformation state until the structure buckling was divided into three stages. In the Stage I, as a shown Fig. 11, it is a linear relationship between pressure and displacement is observed and in the elastic deformation. Therefore, it was defined as a small-scale deformation stage of the pillar element. The Stage II is a nonlinear deformation stage from in Fig. 11. It is seen that there is a kink point of deformation behavior near 2000Pa. From Fig. 12, the distance between two points B and C λ_{BC} starts to increase, so that the L-shaped of cross section is beginning to be deformed into flat shape in this stage. But the stress of the pillar element was found to be less than the yield stress. This is considered to be caused the reduction in the geometrical rigidity after the cross-sectional shape changes. Therefore, the Stage II was defined as a geometrical nonlinearity deformation stage. In the final Stage, the strong nonlinear behavior was observed as shown in Fig. 11. From the stress distribution of the element in Fig. 13, since the stress in the cross section of the pillar element is equal to be the yield stress or higher than it, the Stage III was defined as a nonlinear material behavior stage and buckling occur.

4 DISCUSSION

4.1 Evaluation of Joint Part Model of Beam Element Model

In the eccentricity model, the bending deformation of the pillar elements with the geometrical eccentricity at the joint part could be described with the sufficient accuracy correspond to the actual model. In order to evaluate the buckling load of the element No. 4, the procedure is shown in as follows;

The compressive stress of the element was calculated from the axial force and the bending moment of the analytical result by using the Eq. (1) ;

$$\sigma_T = P_y / A + M_y / Z \quad (1)$$

where σ_T is the vertical compressive stress [Pa], P_y is the axial force [N], A is sectional area of element [mm²], M_y is the bending moment [N·mm] and Z is section modulus [mm³]. The compressive load is calculated by multiplying the compressive stress σ_T by the cross-sectional area A , and then the relationship between the compressive load of pillar element $\sigma_T A$ and the experimental pressure p is shown in Figs. 14 (a) wind load and (b) snow load. The buckling load of the element No. 4 and No. 5 in Table 1 is calculated by using the Eq. (2) ;

$$P_{cr} = \pi^2 EI / l^2 \quad (2)$$

where P_{cr} is Euler buckling load [N], E is young's modulus [MPa], I is cross-sectional secondary moment [mm⁴] and l is the length of the beam [mm]. The buckling load of the element No. 4 and No. 5 is shown by the red line in Fig. 14 (a) and (b), respectively. It was seen that the buckling occurs at the intersection of the red line to the straight lines of the analytical results in the

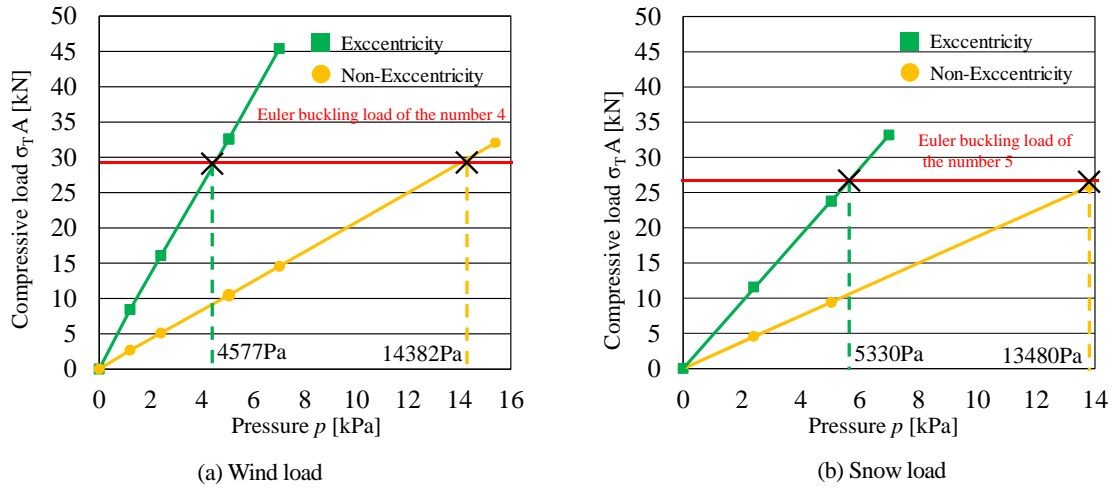


Fig. 14 Relationship between pressure and compressive load

Table 5 Comparison of the buckling stress between experimental results and analytical results

	Experiment	Eccentricity model	Non-Eccentricity model
Wind load [Pa]	4400	4577	14382
Snow load [Pa]	5038	5330	13480

eccentricity model and in the non-eccentricity model. Table 5 shows the comparison of the buckling loads in the experiment with the loads calculated from the simulation for two models. For the case of wind load and snow load, the buckling load with the eccentricity model shows good agreement with the experiments. The bending moment value in Table 4 is large in the eccentricity model and then, the bending deformations due to the twist of the joint part are well described in the analysis. Therefore, in the evaluation of buckling load, it was found that the simulation results that the eccentricity model shows better agreement with the experiments than the results with the non-eccentricity model.

4.2 Comparison between analysis results and experimental results deformation of a buckling element

Figure 15 shows comparison of the relationship between the pressure and the displacement in the dynamic wind pressure experiment and in the analysis where the buckling behavior of the pillar element is defined as three stages as in Fig. 11. From Fig. 15, the deformation behavior of the pillar element in the experiment is not in good agreement with in the analysis, however the kink point in the experiment shown in Fig. 11 is indicated about at the starting point of the geometrical nonlinear in the stage 2 of analysis. Although there is slight difference from the boundary conditions of the pillar element in the analysis, it means good suggestion for understanding a kink point observed in the deformation state. For better understanding these deformation behaviors, it is important to set exact boundary conditions of experiment in the further analysis.

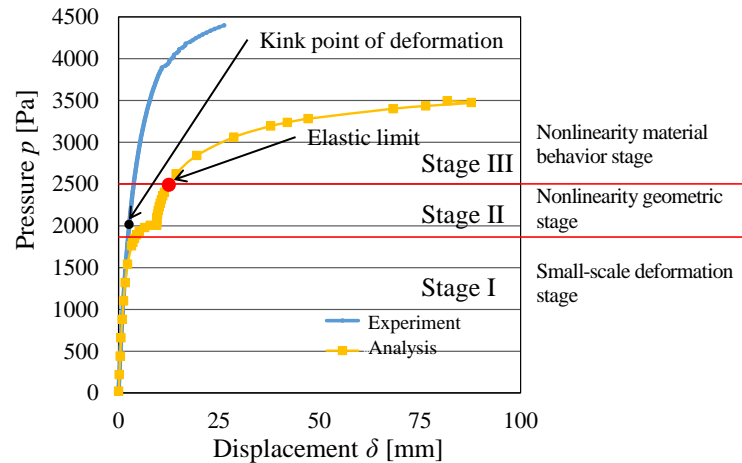


Fig. 15 Comparison of relationship between displacement and pressure in experiment and analysis

5 CONCLUSIONS

In order to design the strong and high rigidity support structure of PV system by the thin plate, we analyzed two joint part models in the FEM analysis with three dimensional elastic beam elements, and examined the structure deformation behavior and buckling load from the experiment result and the analytical result. In addition, in order to clarify the deformation behavior

until buckling of the pillar element, we conducted the elastoplastic analysis for the pillar element modeled with the thin shell element. The obtained results in this study are summarized as follows.

- i. From the deformation behavior and the evaluation of the buckling load, the FEM analysis with the eccentric model for the joint part in the actual structure successfully applied to be safety design of PV system.
- ii. The deformation behavior until buckling was clarified from the results of elastoplastic analysis of pillar element model with thin shell element. From this result, the kink point in the experiment was seen to be caused due to the effect of geometrical nonlinearity.
- iii. It was found that the kink point in the experiment is indicated about at the starting point of the geometrical nonlinear in the stage II of analysis. Although there is slight difference from the boundary conditions of the pillar element in the analysis, it means good suggestion for understanding a kink point observed in the deformation state.

In our future work, it might be required to consider not only the axial force but also the influence of the transvers force. In order to examine the stress distribution and deformation state of the entire support structure precisely, we will model the actual support structure by using three-dimensional shell elements and conduct elastoplastic analysis. By conducting a revised analysis, an analytical model which clarifies the buckling load and incorporate it into the whole model could be proposed for safe support structure of PV system.

ACKNOWLEDGMENTS

This paper is based on results obtained from a project commissioned by the New Energy and Industrial Technology Development Organization (NEDO).

REFERENCES

- [1] Takamori, K. Somekawa, D. Okuji, M. and Uematsu, Y. WIND RESISTANCE TEST OF A PHOTOVOLTAIC SYSTEM INSTALLED ON METAL ROOF. Proc. Symp. Wind Engng. 24th. (2016) 319-324 (in Japanese)
- [2] AIJ Design. Standard for Steel Structures Based on Allowable Stress Concept. (2017)
- [3] Somekawa, D. Koizumi, T. Taniguchi, T. and Taniike Y. WIND LOADS ACTING ON THE PHOTOVOLTAIC PANELS ARRAYED NEAR GROUND. Proc. Symp. Wind Engng. 22nd. (2012) 157-160 (in Japanese)
- [4] Somekawa, D. Koizumi, T. Taniguchi, T. and Taniike Y. WIND LOADS ACTING ON PV PANELS AND SUPPORT STRUCTURES WITH VARIOUS LAYOUTS. Proc. The Eighth Asia-Pac. Conf. Wind. Engng. (2013) 235-242
- [5] Mtsuura, M. Hatanaka, A. and Yamaguchi, T. Study on load carrying capacity of a small power transmission tower made of angle steel members. J. Struct. Engng. Vol. 58A., (2012) 50-61

Atomic Mixed-Mode Cohesive-Zone Laws of Hydrogen-Embrittled Grain Boundaries in Crystalline Metals via Nanoscale Field Projection Method

Nghia Trong MAI^{*}, Vinh Phu NGUYEN^{**}, Phuoc Quang PHI^{***}, Seung Tae CHOI^{****}

^{*}Chung-Ang University, ^{**}Chung-Ang University, ^{***}Chung-Ang University, ^{****}Chung-Ang University

ABSTRACT

Grain boundaries of polycrystalline materials can be one of the easiest paths for crack propagations, since atoms at grain boundaries experience less ordered interatomic interactions with neighboring atoms than those in homogeneous crystalline materials. Furthermore, thermodynamically, impurity atoms such as hydrogen, chrome, nickel, copper, and carbon atoms in polycrystalline iron, tend to segregate near grain boundaries, which may cause the degradation of mechanical properties and accelerate intergranular fracture. Recently, a field projection method (FPM) was established to extract the crack-tip cohesive zone law (CZL) from far field data using J- and M-based mutual integrals between the physical field and numerical auxiliary field. In this study, we extend the universality of the FPM for atomic mixed-mode CZL of a crack tip on an interface between two anisotropic solids by using an analytical auxiliary field, as well as the effective use of atomic-level J- and M-based mutual integrals. This augmented FPM has no convergence problems and does not need to find a numerical helper every time, depending on the given problem associated with finite elements solution. The atomic-level field projection is applied to characterize a cohesive crack-tip naturally arising from atomic deformation field, which can be obtained from molecular dynamic simulation of decohesion along the hydrogen-segregated grain boundaries in nickel. Our FPM results enable the development of a qualitative picture of the traction-separation relations and functional form and parameters for a cohesive surface constitutive model consisting of separate normal and shear traction-separation relations.

Automatic Isogeometric Models Generation from Standard B-REP Models – Application to Reduced Order Modeling

Tristan MAQUART*, Thomas Elguedj**, Anthony Gravouil***, Michel Rochette****

*Université de Lyon, CNRS, INSA-Lyon, LaMCoS UMR5259, France; ANSYS Research & Development, France,

Université de Lyon, CNRS, INSA-Lyon, LaMCoS UMR5259, France, *Université de Lyon, CNRS, INSA-Lyon, LaMCoS UMR5259, France, ****ANSYS Research & Development, France

ABSTRACT

Key Words: Isogeometric Analysis, NURBS, Global Parameterization, Cross Fields, Parametric geometry, Multiparametric, Singular value decomposition. We present an effective framework to automatically construct trivariate B-spline models of complicated geometry and arbitrary topology required for most mechanical applications and parametric studies. The input is a triangulation of the solid 3D model's boundary provided from B-Rep CAD models or scanned geometry. The boundary surface is decomposed into a set of cuboids [1], approximating the input boundary mesh. Due to its highly regular and trivariate structure, the polycube is suitable for serving as the canonical domain of the volume parameterization required for trivariate NURBS construction. The polycube's nodes and arcs decompose the input model globally into hexahedral domains. Using cross fields and aligned global parameterization [2], optimal compatible trivariate B-spline are reconstructed. For different parametric instances with the same topology (including sharp features) but different geometries, this method allows to have the same representation: i.e., meshes with the same topology (i.e., isotopological meshes : same mesh connectivity) where each point on a mesh have a homologue into another mesh (with possibly homologous sharp features). This method is used to build reduced order models (ROMs) [3]. Real time simulations remain intractable despite the impressive increasing computing power, we present an approach for building geometric multiparametric isogeometric models suitable for ROM construction. The efficiency and the robustness of the proposed approach are illustrated by solving mechanical equations given several geometric parameters.

REFERENCES [1] H. Al-Akhras, T. Elguedj, A. Gravouil, and M. Rochette, "3D Isogeometric Analysis Suitable Trivariate NURBS Models from Standard B-Rep CAD", *Computer Methods in Applied Mechanics and Engineering*, doi:10.1016/j.cma.2016.04.028, 2016. [2] Marcel Campen and Leif Kobbelt. "Quad layout embedding via aligned parameterization". In *Computer Graphics Forum*, volume 33, pages 69-81. Wiley Online Library, 2014. [3] Ye Lu, Nawfal Blal, Anthony Gravouil, Multi-parametric space-time computational vademecum for parametric studies: Application to real time welding simulations, In *Finite Elements in Analysis and Design*, Volume 139, 2018, Pages 62-72, ISSN 0168-874X,

Numerical Modeling of Pull-Out-Tests Using Finite Elements

YADIAN MENENDEZ ROSALES*, RAUL DURAND**

*UNIVERSITY OF BRASILIA, **UNIVERSITY OF BRASILIA

ABSTRACT

During the last decades, several researches have been studying the phenomenon of steel-concrete bond with the purpose of establishing parameters that express the evolution of the bond stress as a function of the rebar slip. This information is useful to develop constitutive models and to obtain material parameters needed for numerical predictions of reinforced concrete structures. In this regard, the pull-out test is one of the experimental tests widely used for these purposes. This work presents a contact model for the mechanical behavior of steel-concrete interface. This model is based on the one proposed by CEB-FIP MODEL CODE (2010) and the plasticity theory. The model was implemented in a finite element code and tested against a battery of experimental pull-out tests in cylindrical specimens of 100, 150 and 200 mm diameter and 200 mm height combined with different steel bars with diameters of 8, 10 and 12 mm and anchorage length of 100 mm. In the finite element model, the rebars were simulated using a novel semi-embedded approach which allows rod elements to cross solid (concrete) elements and, thanks to the contact model, predict rebar slip and contact failure. After the analyses, it was observed that the proposed contact model successfully reproduced the main characteristics of the pull-out-test. Numerical results, as for example load-displacement curves including softening, were in good agreement when compared with experimental results.

Nonlinear Analysis of Squeal and Whirl Mode Instabilities

Alexy MERCIER^{*}, Louis JEZEQUEL^{**}, Sébastien BESSET^{***}, Abdelbasset HAMDI^{****},
Jean-Frédéric DIEBOLD^{*****}

^{*}LTDS/Safran Landing Systems, ^{**}LTDS, ^{***}LTDS, ^{****}Safran Landing Systems, ^{*****}Safran Landing Systems

ABSTRACT

The "Whirl" and "Squeal" modes generate significant vibrations on an aircraft braking system. These vibrations strongly damage the brake structure and generate acoustic discomfort. Nowadays, several types of finite element (FE) models have been developed. In order to test and simply reproduce some important physics in these models (FE), analytical and phenomenological models have been developed. The ultimate goal is to have a tool to model as faithfully as possible braking dynamics. To accelerate computation time, model reductions such as synthesis or double modal synthesis are used. Finally, to ensure the convergence of vibration amplitudes, the major sources of nonlinearities have been identified and integrated into the model (FE). These nonlinearities are located at the different friction interfaces of the system and in the hydro-mechanical part.

High-Fidelity Seismic Response Analysis of a Nuclear Power Plant Using K computer

Tomoshi MIYAMURA*, Shinobu YOSHIMURA**, Tomonori YAMADA***

*Nihon University, **University of Tokyo, ***University of Tokyo

ABSTRACT

In the earthquake resistant design of a nuclear power plant, mass-spring models are usually used to simulate structural behavior. However, seismic responses of details of the plant cannot be simulated using such macro model. A high-fidelity 3D finite element model of integrated boiling water reactor and reactor building of the Unit 1 at the Fukushima Daiichi Nuclear Power Plants was constructed [1]. In the present study, the results of the seismic response analyses for the Tohoku Off-Pacific Coast Earthquake of 9.0 Mw using the analysis model are presented. The analyses are conducted using a parallel finite element structural analysis code, ADVENTURE_Solid 2.0 [2] implemented on the K computer that is one of the fastest supercomputers in the world. The finite element model is made of tetrahedral solid elements. Reactor building, pressure boundary including primary containment vessel, suppression chamber, bent pipes, and reactor pressure vessel are modeled precisely and integrated. Total DOFs of the mesh using linear elements (linear element model) is approximately two hundred million, and that of the mesh using quadratic elements (quadratic element model) is approximately fifteen hundred million. The linear element model is verified using the numerical results of the quadratic element model. The elastic seismic response analysis for 65 seconds is conducted using the linear element model. The numerical results including maximum acceleration and maximum stress at a number of points, and floor response spectra (acceleration response spectra) are compared with those of the conventional seismic response analysis using a lumped-mass model [3]. Computation performance of a parallel solution algorithm, that is, the hierarchical domain decomposition method with balancing domain decomposition preconditioner is evaluated on the K computer. Methods of data handling of huge output data such as an offline rendering technique and automatic generation of graphs are presented. A preliminary elastic-plastic seismic response analysis for 55 seconds is also conducted. Steel material of main pressure boundary components are supposed to be elastic-plastic using the von Mises yield criterion. The numerical results and computation performance are presented. References [1] S. Yoshimura, T. Yamada, H. Kawai, T. Miyamura, M. Ogino, and R. Shioya, Petascale coupled simulations of real world's complex structures, IACM Expression, No.37, pp. 9-13, 2015. [2] ADVENTURE project, <http://adventure.sys.t.u-tokyo.ac.jp/> [3]?TEPCO report on seismic response analysis results of building and important components and piping in Fukushima Daiichi Nuclear Power Stations utilizing observed data during Tohoku Off-Pacific Coast Earthquake in 2011, 2011 [in Japanese].

Similarities and Differences between the Thick Level Set and Cohesive Models for Quasi-brittle Failure

Nicolas MOES*

*Ecole Centrale de Nantes

ABSTRACT

Three topics will be summarized in the presentation. They correspond to the three papers listed below. The first topic deals with the equivalence of the cohesive zone model (CZM) and the Thick Level Set approach to fracture (TLS). The TLS is a continuum damage model in which the damage gradient is bounded. In the 1D setting (bar under tension), TLS and CZM parameters may be chosen so that they model the same global behavior. In the 2D setting, the TLS generalizes the CZM approach and offers more capabilities (no extra equations needed for crack growth direction, stress triaxiality taken into account and crack branching made possible). Based on the above equivalence, the TLS parameters have been identified to fit experimental data of size and shape effects. Even though it is continuum damage based, the TLS gives a great capability in fitting the experiments on a large spectrum of size and shapes. Finally, a second version of the TLS (TLS V2), unifies continuum damage and cohesive zone within a unique model. Damage is both surfacic and volumic. The TLS V2 allows to get high numerical performances even for long process zones. References. - Parrilla Gómez, A., Moës, N., & Stolz, C. (2015). Comparison between thick level set (TLS) and cohesive zone models. *Advanced Modeling and Simulation in Engineering Sciences*, 2(1), 18. <http://doi.org/10.1186/s40323-015-0041-9> - Parrilla Gómez, A., Stolz, C., Moës, N., Grégoire, D., & Pijaudier-Cabot, G. (2017). On the capability of the Thick Level Set (TLS) damage model to fit experimental data of size and shape effects. *Engineering Fracture Mechanics*, 184, 75–87. <http://doi.org/10.1016/j.engfracmech.2017.07.014> - B. Le, N. Moës & G. Legrain (2018), Coupling damage and cohesive zone models with the Thick Level Set approach to fracture *Journal: Engineering Fracture Mechanics*, *Engineering Fracture Mechanics*, to appear.

A Magnification-based Multi-asperity (MBMA) Model of Rough Contact Where the Greenwood-Williamson and Persson Theories Meet

Benben Ma^{*}, Xu Guo^{**}, Yichao Zhu^{***}

^{*}Dalian University of Technology, ^{**}Dalian University of Technology, ^{***}Dalian University of Technology

ABSTRACT

Contact analysis without adhesion is still a challenging problem, mainly owing to the multiscale and self-fractal characteristics of rough surfaces. Up to now, theories for analyzing contact behavior of rough surfaces in literature can be generally categorized into two groups: the asperity-based Hertz contact models initiated by Greenwood and Williamson (G-W model), which is shown more accurate under small indentation distance, and the magnification-based pressure diffusion theory initiated by Persson, which is shown to work well under full contact conditions. The aim of this paper is to propose a theoretical model that can effectively formulate the contact status of rough surfaces during the entire compression process. This is achieved by integrating the idea of magnification, or evolving resolution into an asperity representation of rough surfaces, and a magnification-based multi-asperity model is thus established. In the derived model, the originally complex contact problem is decomposed into a family of sub-problems each defined on a morphologically simpler contact islands. Benefiting from the explicit results given by Greenwood and Williamson, the proposed method is relatively easy for numerical implementation. Compared to other G-W type models, the proposed method has especially shown its strength in the computation of the contact area. Moreover, the G-W and Persson models are found well connected by the proposed approach. For its validation, the proposed model is well compared with existing theoretical, numerical and experimental results. In particular, the proposed model has shown its excellency through comparison with representative theoretical, numerical and experimental data compiled in the “contact challenge” test by Mueser et al.

Comparative Study on Seismic Design Method of Utility Tunnel

Hongmin Ma*, Jianxun Ma†

* Ph.D.Student

99 Yanxiang Road

Xi'an, Shaanxi, China

Email address: mahongmin@stu.xjtu.edu.cn

† Professor

99 Yanxiang Road

Xi'an, Shaanxi, China

Email address: matumu@163.com

Key words: Response Displacement Method, Response Acceleration Method, Time History Method, Single Deck Utility Tunnel, Double Deck Utility Tunnel.

Summary. *The response displacement method and the response acceleration method were studied and summarized from the principle. Two kinds of sectional utility tunnel models of single deck utility tunnel and double deck utility tunnel are established respectively. Then time history method, response displacement method and response acceleration method were used to carry out the seismic calculation of the two models. In the calculation, the universality of the calculation method was analyzed by changing the 3 types of factors, such as the seismic type and peak acceleration of seismic waves and the stiffness of the structure. The calculation results shows that the two pseudo-static methods all have high accuracy, but the response acceleration method is more accurate. By comparing the calculation results of two different cross-section forms of the utility tunnel, it can be found that the calculation results are the same as the whole, but the specific calculation results are different. Therefore, it should be carried out in accordance with the form of the structure and the factors considered in the seismic calculation of the utility tunnel. Detailed calculation and analysis is needed.*

1 INTRODUCTION

With the development of urbanization, people began to develop and utilize the underground space vigorously, and the underground structure engineering technology has also been greatly developed ^[1]. In 1995 Kobe earthquake ^[2] and the 1999 Chi Chi earthquake in Taiwan ^[3] have caused irreparable damage in a large number of subway stations, tunnels and utility tunnels, then raised the seismic research of underground structure in the world. At present, the commonly used pseudo static methods for seismic response analysis of underground structures include seismic

coefficient theory, free field deformation method, soil structure interaction coefficient method, response displacement method (RDM) [4-6], response acceleration method (RAM) [7,8], pushover method and integral response displacement method. Through the previous theoretical research, it is found that the response displacement method (RDM) and the response acceleration method (RAM) are more suitable for the seismic calculation of the utility tunnel. In this paper, the finite element software ABAQUS is used to establish a single deck utility tunnel and double deck utility tunnel model, which are calculated by RDM, RAM and time history method (THM) respectively. The error analysis of the two methods of RDM and RAM is carried out. Finally, based on the calculation results, the recommended method for seismic calculation of utility tunnel is given.

2 THE PRINCIPLE OF RDM AND RAM

2.1 A brief introduction to RDM

In 1970s, scholars from various countries research underground structural response characteristics under earthquake by field observation, experimental study and theoretical analysis. The results show that the underground structural vibration together with the surrounding soil under earthquake, structural displacement and acceleration are basically the same as the surrounding underground [4]. Then the Japanese scholars through seismic observation data to further understand the vibration characteristics of the underground structure, gradually realize the decisive effect on seismic response of underground structures is the deformation of surrounding soil not the inertial force of structure, then put forward RDM. The calculation model of the RDM is shown in Fig.1.

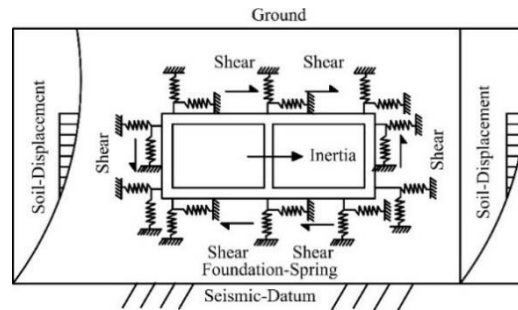


Figure 1. Model of RDM

2.2 A brief introduction to RAM

The response acceleration method is used to simulate the interaction between soil and structure by applying the inertial force by the analysis of seismic response of one dimensional soil layer in free field [9]. The calculation model is shown in Fig.2.

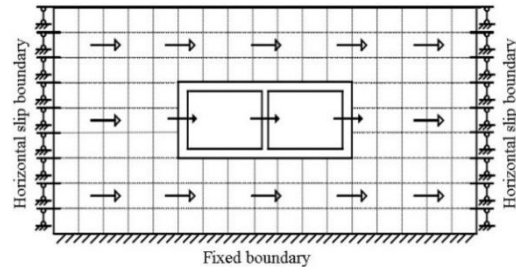


Figure 2. Model of RAM

3 CALCULATION MODEL AND CONDITION

3.1 Structure

In this calculation, two typical cross section utility tunnel of single deck utility tunnel (SDUT) and double deck utility tunnel (DDUT) are used. The total width of the single deck utility tunnel is 10m, the height is 4m, the thickness of the top panel, the bottom panel and the side wall are all 0.5m, and the thickness of the middle diaphragm is 0.4m. The total width of the double deck utility tunnel is 6m, the height is 6m, the thickness of the top panel, the bottom panel, the middle diaphragm and the side wall are all 0.3m. The size of the two structures is shown in Fig.3 and Fig.4 respectively.

The concrete material is C40, density $\rho=2500\text{Kg/m}^3$, elastic modulus $E=32.5\text{GPa}$, Poisson's ratio $\nu=0.2$.

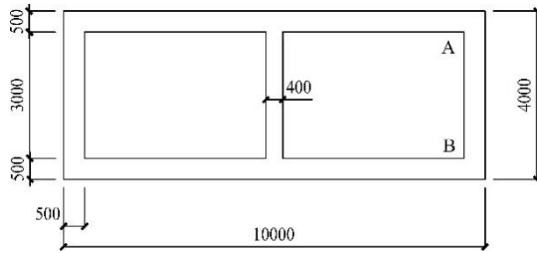


Figure 3. Cross section of SDUT (mm)

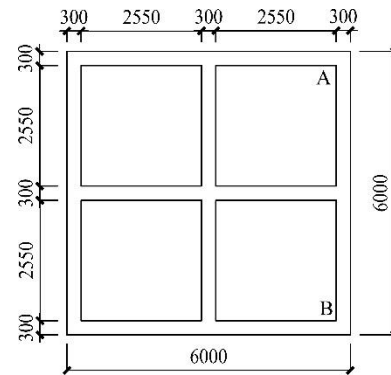


Figure 4. Cross section of DDUT (mm)

3.2 Soil

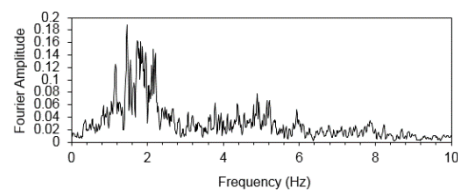
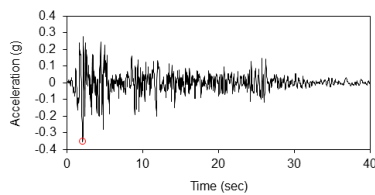
The layered soil is selected for calculation, and the specific soil information is shown in Table 1.

Table 1. Soil parameters

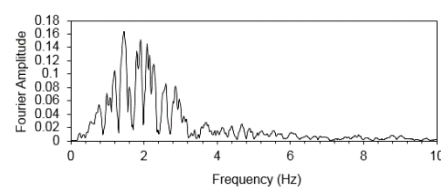
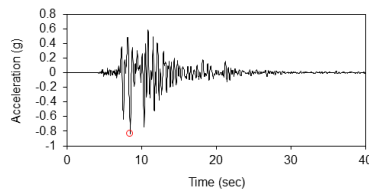
Serial Number	Type	Thickness (m)	γ (kN/m ³)	C (kPa)	Φ (°)	V_s (m/s)	G (MPa)	ν
1	Backfill	0.5	18.5	10	10	115	26	0.33
2	Fine Sand I	2.5	18.7	7	12	160	36	0.31
3	Fine Sand II	3	19	7	26	200	79.5	0.28
4	Silty Clay	34	20.1	13	20	251	120.3	0.30
5	Round Pebble		22			520		0.25

3.3 Seismic wave

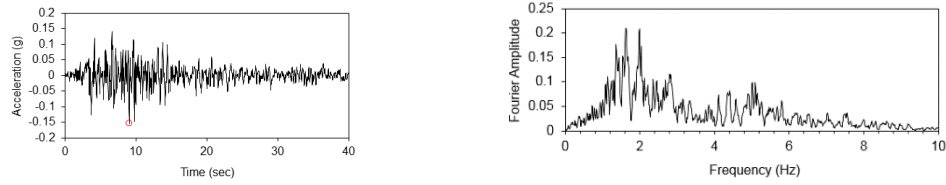
Because different seismic waves have different characteristics, 3 kinds of seismic waves commonly used in seismic calculation of subway stations are selected. The time history curves and fourier spectrum of 3 kinds waves are chosen such as El-Centro wave, Kobe wave and Taft wave and shown in Fig.5.



El-centro wave



Kobe wave



Taft wave

Figure 5. Acceleration time history curve and Fourier spectrum curve of input seismic wave

4 RESULTS AND ANALYSIS

When the calculation process to establish two-dimensional finite element model, the depth of utility tunnel is 3m, the width of soil is 7 times the width of the structure, the soil depth calculate to seismic datum (shear wave velocity $\geq 500\text{m/s}$). The calculation is simplified as follows: 1. There is no slip and separation between soil and structure during earthquake, and the structure is coupled with the soil layer. 2. It is assumed that both the soil and the underground structure are in the linear elastic state in the calculation process.

4.1 Different input seismic wave

The time history curves of 3 kinds of waves are chosen such as El-Centro wave, Kobe wave and Taft wave and shown in FIG.6. The PGA of these seismic waves is 0.2. The calculation results are shown in Table 4. It can be seen from Table 2 that the calculation error of RAM is smaller than that of RDM, no matter which kind of seismic wave is used in two structure. The maximum value of the relative error of the moment in RDM is 12.04% (Taft Wave), and the maximum relative error of the displacement is 11.50% (Kobe Wave) in SDUT. The maximum value of the relative error of the moment in RDM is 8.53% (Kobe Wave), and the maximum relative error of the displacement is 11.09% (El-Centro Wave) in SDUT. By comparing the relative error of the table, it is obvious that the error of RAM is smaller than that of RDM, no matter what kind of seismic wave.

4.2 Different peak ground acceleration

The Kobe wave is used to input the PGA to 0.05g, 0.2g, 0.5g and 0.8g respectively. The calculation results are shown in Fig. 5 and Fig. 6. The PGA of seismic wave is adjusted according to the following formula:

$$a'(t) = \frac{a'_{\max}}{a_{\max}} a(t) \quad (1)$$

Table 2. Calculation results under the different seismic waves

		The Results of RDM		The Results of RAM	
		Results	Relative Error	Results	Relative Error
The bending moment at B of SDUT (kN·m)	El-Centro wave	400.98	7.32%	412.98	4.55%
	Kobe wave	360.59	10.38%	410.23	2.03%
	Taft wave	351.01	12.04%	400.20	1.01%
The bending moment at B of DDUT (kN·m)	El-Centro wave	265.58	7.81%	279.32	3.39%
	Kobe wave	240.65	8.53%	253.21	3.80%
	Taft wave	212.96	5.19%	230.74	2.73%
The displacement of side wall of SDUT (mm)	El-Centro wave	4.91	1.03%	4.95	1.85%
	Kobe wave	4.56	11.50%	4.03	1.47%
	Taft wave	4.36	3.07%	4.38	3.55%
The displacement of side wall of DDUT (mm)	El-Centro wave	10.26	9.68%	12.62	11.09%
	Kobe wave	12.31	4.15%	11.95	1.10%
	Taft wave	8.26	8.42%	9.23	2.33%

The $a'(t)$ and a'_{\max} are the adjusted seismic acceleration curves and the PGA. $a(t)$ and a_{\max} are the seismic acceleration curves and the PGA of the original ground.

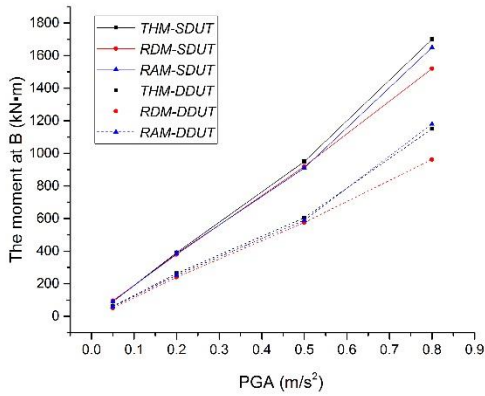


Figure 6. The bending moment at B (kN·m)

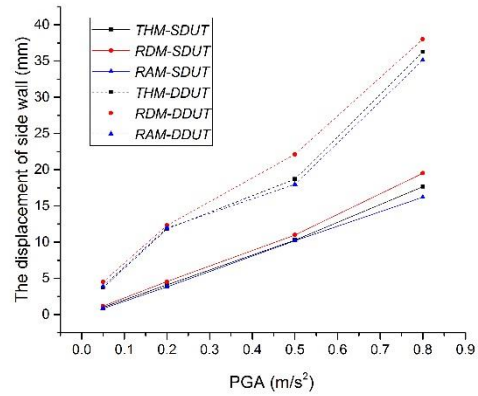


Figure 7. The displacement of side wall (mm)

By observing Fig.6 and Fig.7, we can see that with the increase of PGA, both the moment at B and the displacement of side wall all show an obvious upward trend. Because the thickness of the side plate of DDUT is smaller than that of SDUT, the bending moment of B is smaller than that of SDUT, while the side wall deformation is larger. In Fig.6 and Fig.7, it is found that SDUT and DDUT exhibit different regularity in bending moment and side panel deformation.

4.3 Different relative stiffness

Using the Kobe wave with PGA as 0.2g, the structural stiffness is calculated at 0.5 times, 1 times, 2 times and 5 times of the basic stiffness. The calculation results are shown in Fig.8 and Fig.9.

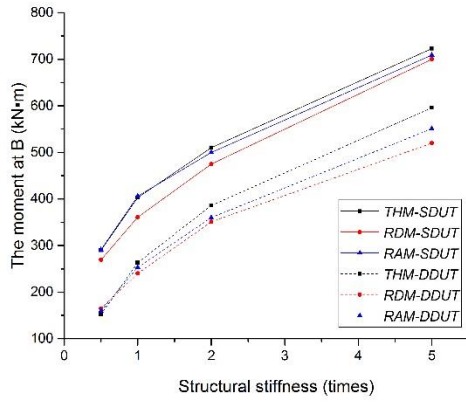


Figure 8. The bending moment at B (kN·m)

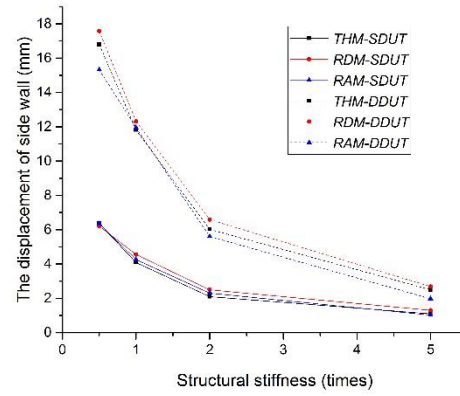


Figure 9. The displacement of side wall (mm)

From the above Fig.8 and Fig.9, it can be seen that the variation trend of the results of the three methods in SDUT and DDUT is the same when the structural stiffness is changed. The result curves of CAM are close to THM, it shows that RAM has higher computation accuracy while RDM has larger discrete type and lower computation accuracy.

5 CONCLUSIONS

In this paper, two kinds of sectional utility tunnel models of SDUT and DDUT are established respectively. Then THM, RDM and RAM methods are used to carry out the seismic calculation of the two models. In the calculation, the universality of the calculation method is analyzed by changing the 3 types of factors, such as the type and size of the input seismic waves and the stiffness of the structure. Through the calculation and analysis, the main conclusions are as follows:

- It is found that there are no abrupt changes in the calculation results of RDM and RAM, which show that these two methods are all can used in the seismic calculation of utility tunnel.

- Although the overall change trend of SDUT and DDUT is the same after changing the calculation parameters in the calculation, but the specific aspects are different, so the detailed analysis is needed in the calculation of the utility tunnel of different sections according to the form of the section and the factors considered.
- No matter what kind of calculation conditions, CAM has high accuracy, while CDM calculation results are discrete. Therefore, it is recommended that CAM be used for seismic response calculation of utility tunnel.

REFERENCES

- [1] Qian, Q.H. The fourth wave of geotechnology. *Underground Space*. (1999) 19: 267-272.
- [2] Zhao, Z.X. and Xv, J.R. In 1995 the Japanese earthquake in Kobe building collapse and the edge of the S wave and surface wave interference on the secondary Basin. *Chinese Science Bulletin*. (2003) 48:2566-2571.
- [3] Hao, M. Xie, L.L. and Xu, L.J. Some considerations on the physical measure of seismic intensity. *Acta Seismologica Sinica*. (2005) 27:245-250.
- [4] Newmark, M. Problems in wave propagation in soil and rock. *Proceedings of the International Symposium on Wave Propagation and Dynamic Properties of Earth Materials*. (1968).
- [5] Wang, N. Seismic design of tunnels: a simple state of the art design approach. New York: Parsons Brinckerhoff Quade and Douglas Inc. (1993).
- [6] Liu, J.B. Wang, W.H. and Zhao, D.D. Integral response deformation method for seismic analysis of underground structure. *Chinese Journal of Rock Mechanics and Engineering*. (2013) 32:1618-1624.
- [7] Kawashima, K. The seismic design of underground structures. Japan: Kashima Publishing. (1994).
- [8] Li, B. Theoretical analysis of seismic response of underground subway structures and its application. Beijing: Tsinghua University. (2005).
- [9] Liu, J.B. Liu, X.Q. and Li, B. A pushover method for seismic response analysis and design of underground structures. *China Civil Engineering Journal*. (2008) 41:73-80.

Uncertainty Quantification of Finite Element Analysis of Uni-axial Strength Test Holed Composite Laminates

Li Ma^{*}, Jeffrey Fong^{**}, Pedro Marcal^{***}, Robert Rainsberger^{****}, Alan Heckert^{*****}, James Filliben^{*****}

^{*}Theiss Research, ^{**}NIST, ^{***}MPACT Corp., ^{****}XYZ Scientific Applications, Inc., ^{*****}NIST, ^{*****}NIST

ABSTRACT

In the aerospace industry, open hole specimens of composite laminates have been used in standardized tests to generate design allowables. Using finite element method (FEM) based tool MicMac/FEA with ABAQUS code interface and statistical design of experiments, Shah, et al. in 2010 studied average-property-based failure envelope with uncertainty estimates of open hole specimen with quasi-isotropic carbon fiber-epoxy laminate. However, their FEM model is deterministic, without uncertainty analysis. In this paper, based on Shah's FEM model, we developed FEM model of uni-axial strength test of holed composite laminates using ABAQUS and ANSYS with a series of quadrilateral and triangle shell element designs. The mesh density ranges from the original 8 X 8 (very coarse) to 10x10 (coarse), 12x12 (normal), 14x14 (fine), and 16 X 16 (very fine). For each of the meshes, we compute the failure strength from Hashin failure criteria. Then we use a 4-parameter logistic function nonlinear least squares fit algorithm to obtain an estimate of the failure strength at infinite degrees of freedom (d.o.f) as well as its uncertainty at one-billion-d.o.f. and relative error convergence rates. Our results are then compared with Shah's with the additional advantage that our results have uncertainty quantification that can be compared with experimental data. The significance and limitation of our method on the uncertainty quantification of FEM model of uniaxial strength test of holed composite laminates are discussed.

An Adaptive Kirigami Metamaterial Plate for Broadband Anisotropic Elastic Wave Manipulation on a Subwavelength Scale

Qian Ma^{*}, Rui Zhu^{**}, Yangyang Chen^{***}, Guoliang Huang^{****}, Gengkai Hu^{*****}

^{*}Beijing Institute of Technology, ^{**}Beijing Institute of Technology, ^{***}University of Missouri, ^{****}University of Missouri, ^{*****}Beijing Institute of Technology

ABSTRACT

Although metamaterials possess peculiar negative material properties and subwavelength wave manipulation abilities, there are still unfilled gaps between current metamaterial design and engineering standards for practical applications. In fact, the subtractive microstructures and resonance-induced narrow bandgaps significantly prevent elastic metamaterials from successful engineering implementations. In this presentation, we propose an adaptive metamaterial plate with its microstructure consisting of built-on-top kirigami structures and shunted piezoelectric patches with feedback circuit control. First, an analytical model of the proposed metamaterial is developed to explain the mechanism of its adaptive bandgaps and switchable anisotropy for flexural wave propagation. Then, an additive unit cell design is conducted with lightweight kirigami microstructure and strategically positioned piezoelectric patches. Feedback control of the piezoelectric shunts is realized with the help of a semi-analytically determined transfer function, which provides tunable anisotropic mass density in a broad frequency range. Finally, full-wave simulations on the broadband directional flexural wave propagation as well as super-resolution hyperlens effect are conducted to demonstrate the robustness of proposed adaptive kirigami metamaterial in subwavelength-scale flexural wave control. This attachable and adaptive metamaterial opens a new avenue for practical elastic wave control and management in engineering structures.

High-order Two-scale Asymptotic Analysis and Computation of the Dynamic Piezoelectric Performance for Composite Structures with Axisymmetric Configuration

Qiang Ma^{*}, Junzhi Cui^{**}, Zhihui Li^{***}

^{*}College of Mathematics, Sichuan University, Chengdu, 610064, China, ^{**}LSEC, ICMSEC, The Academy of Mathematics and Systems Science, CAS, Beijing, 100190, China, ^{***}Hypervelocity Aerodynamics Institute, China Aerodynamics Research and Development Center, Mianyang, 621000, China

ABSTRACT

The high-order asymptotic expansion homogenization method is developed for the dynamic piezoelectric problem of the composite materials with axisymmetric configuration. The structure considered is periodically distributed in only radial and axial directions, while homogeneous in circumferential direction, and the constituent materials are assumed to be orthotropic. By reformulating the governing equations in the compact form, the multi-scale expansion of the displacement and electrical field is performed, the homogenized piezoelectric model is obtained and the second-order asymptotic approximations are also derived. Theoretical results are derived for some simplified problem in both 1-D and 2-D cases. The corresponding high-order finite element algorithm is proposed, and two numerical examples are carried out to demonstrate the effectiveness of our proposed model. It is also indicated that the second-order asymptotic approximations are more accurate to simulate the coupled piezoelectric performance of the composites.

FLUID-STRUCTURE INTERACTION NUMERTCAL SIMULATION OF DIFFERENTIAL PRESSERE PIPELINE INSPECTION GAUGE PASSING ABILITY

Rui MA^{*}, S Fan ZHU[†], D Yan SHI[†], H Xi REN[†]

^{*}College of Mechanical and Electrical Engineering, Harbin Engineering University
Harbin, Hei Longjiang, China
Email: marui1993@hrbeu.edu.cn

[†]College of Mechanical and Electrical Engineering, Harbin Engineering University
Harbin, Hei Longjiang, China
Email: zhushifan@hrbeu.edu.cn
Email: shidongyan@hrbeu.edu.cn

Key words: Pipeline Inspection Gauge; Fluid-Structure Interaction; CEL Method;
Mooney-Rivlin Model; Local Deformation

Summary: *Differential pressure Pipeline Inspection Gauge(PIG) can accurately scan and detect oil and gas pipelines. In order to achieve the scanning and detection of oil and gas pipelines, It must ensure that the pipeline detector through the oil and gas pipeline smoothly. Based on the method of coupled Euler-Lagrangian (CEL), a fluid-structure interaction model for the operation of the pipeline detector was established. The Mooney-Rivlin model was used to describe the superelastic and non-linear behavior of the polyurethane rubber. Analyzing the complex mechanical behavior of the local deformation of PIG when it passing through the pipeline. Based on the CEL simulation method, calculating the passability of PIG in the actual pipeline and analysising the factors which impact the passability. We have demonstrated in this paper that the amount interference of cup is a very important parameter. When the amount of interference is less than 15.0%, the detector can pass through the pipeline. When the pipe is in the deformation area, the height of the deformation part is less than 6.0 %. The detector can pass through the pipe smoothly. Through the research of this paper, we can provide theoretical basis and reference for the design and use of the detector in the pipeline.*

1 INTRODUCTION

At present, as one of the most economical and reliable ways of oil transmission, pipelines play a crucial role in modern industry. Due to the long-time of transmission, pipelines will be subject to corrosion by transmission medium. The detection method commonly used at home and abroad is placing detectors inside the pipeline to complete the scan inspection of the pipeline wall [1-2]. The use of differential pressure Pipeline Inspection Gauge (PIG) is one of the main techniques for pipeline inspection. PIG is exposed to pressure differences at both ends of the fluid medium, thus generating a driving force for the PIG [3-5].

The structure of PIG is a middle cabin with rubber cup at both ends. The number of rubber cup is generally 2 to 3 [6]. The rubber cup is an important part that directly contacts the pipe inner wall on the PIG. It is made from a non-linear solid material with characteristics of super-elasticity, volume incompressibility and large deformation. Its' material characteristics have important effect on the dynamic characteristic of PIG [7-9].

In order to further explore the mechanical behavior of PIG encountering pipeline local deformation. Zhang Hang [10-11] established a dynamic theoretical model for the transient migration of PIG passing girth welds in confined spaces of pipelines. The overall dynamics of PIG was analyzed. Liu Baoyu [12] established a geometrical theoretical model for the PIG bendability, and systematically analyzed the different structures of the cup. Durali M [13] established a one-dimensional equivalent spring and damping vibration model of PIG. He studied the vibration characteristics of the PIG passing solder joint deformation. The above research focuses on the one or two-dimensional theory and simplified simulation of the model. It lacks a complete PIG motion process with the inertia of the detector and the influence of friction. It even does not involve the coupling model construction of three-dimensional model and other important research work such as numerical simulation.

This paper is focused on the complex dynamics problem of PIG. Based on the CEL fluid-solid coupling method, study the key technology of fluid-solid coupling numerical simulation for non-linearity of PIG systematically.

2 FLUID-SOLID COUPLING MODELS

2.1 CEL method

The Coupled Euler-Lagrangian (CEL) method in ABAQUS combines the advantages of Euler method and Lagrangian method. It can handle large deformation, nonlinear, fluid-solid coupling and other issues correctly. In CEL method, the area to be analyzed is divided into an Euler area and a Lagrangian area according to the possibility of large deformation. In these two areas, the Euler finite element method and Lagrange are used respectively. The finite element method is used for calculation. Using CEL method for numerical analysis, the flow state of fluid material can be obtained by calculating the Euler Volume Fraction (EVF). Each Euler cell is assigned a percentage that represents the part of the Euler cell that is filled with material, if a Euler unit is completely filled with material, then $EVF=1$, if there is no material in the unit, $EVF=0$.

The CEL method in ABAQUS is a general contact based on a penalty function algorithm to solve the contact problem between Euler materials and Lagrangian materials. Creating boundary nodes on the edges and faces of Lagrangian cells, creating fixed reference point on the Euler material surface, and the penalty function contact method approaches the hard pressure-occlusal behavior. This method allows small Euler materials to penetrate into Lagrangian. area.

2.2 Geometric models and grids

The force condition of PIG is shown in Fig.1. Setting the length of the pipe to 6m, the diameter is 216mm, the length of the thin pipe section is 5m, and the inner diameter is 200mm. The PIG consists of three polyurethane-driven cups and a central cabin, the diameter of cups are 280mm.

The power received by the inner detector is the driving pressure generated by the fluid medium at the front and rear ends of the detector at different pressures. The pressures at both ends of PIG are P_1 and P_2 . The frictional resistance caused by the contact between cups and wall of pipe is the main resistance against the PIG.

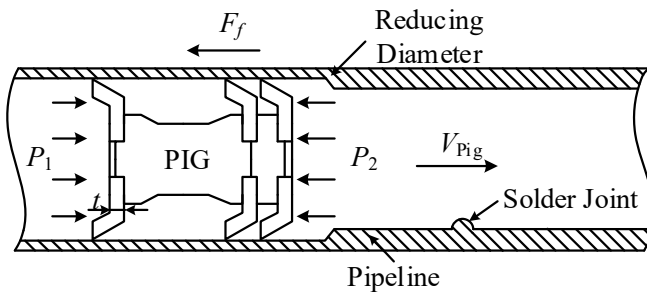


Fig.1 Force condition of Pipeline Inspection Gauge

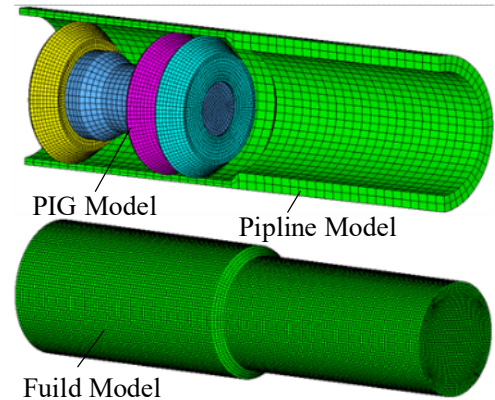


Fig.2 Fluid - Solid Coupling Finite Element Model for PIG

In order to analyze the complex dynamics characteristics of the PIG inside the pipe under the influence of fluid medium, a fluid-solid coupling finite element model is established by using CEL method, as shown in Fig. 2.

In order to ensure the accuracy of finite element analysis, a reasonable selection of cell types, shapes, and grid densities is required in order to maintain a good cell morphology during the analysis. In this paper, a linear reduction integration unit C3D8R is used to divide the PIG and set the grid density of the cup to be twice of the center cabin. The pipeline is set as a rigid body and is also divided by C3D8R units. The mesh density is approximately equal to the center cabin. The fluid is meshed with Euler cells. The cell type is an 8-node linear Euler solid cell EC3D8R. By default, the EC3D8R cell uses viscous hourglass control. In

order to make the simulation result more accurate, the solid grid density needs to be set to 3 to 5 times of the density of the fluid grid. In the numerical simulation process, the Euler material's initial material definition was controlled by the Volume Fraction Tool in ABAQUS which combined with the material's pre-defined field.

The smooth pipeline model and the local deformation pipeline model were established respectively, as shown in Figure 3. The smooth pipeline is used for the analysis of the mechanical motion of the PIG in straight pipeline, mainly to explore the effect of the interference of the cup on passing ability. The local deformation pipeline is used to analyze the mechanical motion of the PIG in irregular pipelines, mainly to explore the effect of the pipeline deformation on the passing ability. The local deformation shape of the pipeline is hemispherical which refer to the actual working conditions for internal processing in the pipeline.

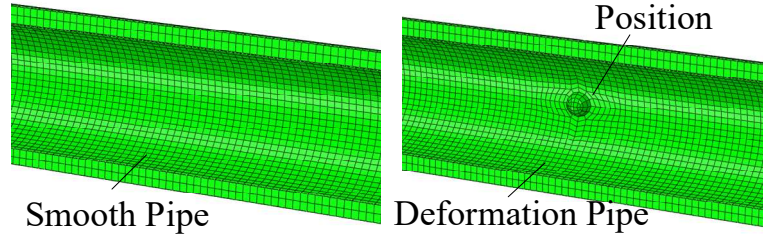


Fig.3 Finite Element Model of Smooth Pipeline and Deformation Pipe

2.3 Fluid material model

Based on ABAQUS's CEL method, the fluid material in the pipe is represented by the state equation (EOS) combined by Mie-Grüneisen and Hugoniot^[14-15], which defines the volumetric strength of the material and the ratio of pressure to density. The universal fluid Mie-Grüneisen's state equation is expressed as:

$$p = p_H \left(1 - \frac{\Gamma_0 \eta}{2} \right) + \Gamma_0 \rho_0 E_m \quad (1)$$

Where p_H and E_m are Hugoniot pressure and energy per unit mass respectively. They are functions of density ρ , ρ_0 is reference density, Γ_0 is material constant, and η is nominal volume compressive strain.

The pressure equation that usually satisfies the Hugoniot curve is expressed as:

$$p_H = \frac{\rho_0 c_0^2 \eta}{(1 - s\eta)^2} \quad (2)$$

Where c_0 is sound velocity in fluid, s is undetermined constant. The linear relationship between fluid impact velocity U_s and fluid particle velocity U_p , can be expressed as:

$$U_s = c_0 + sU_p \quad (3)$$

Substituting equation (2) into equation (1) can be expressed as:

$$p = \frac{\rho_0 c_0^2 \eta}{(1-s\eta)^2} \left(1 - \frac{\Gamma_0 \eta}{2} \right) + \Gamma_0 \rho_0 E_m \quad (4)$$

Based on the above equation, this paper set the density $\rho = 1000 \text{ kg/m}^3$, the viscosity $\mu = 0.001 \text{ kg/(m} \cdot \text{s)}$, the sound speed $C_0 = 1483 \text{ m/s}$ and $s = 0, \Gamma_0 = 0$.

2.4 Rubber cup constitutive model

The PIG's cups are made from urethane rubber. The Mooney-Rivlin material model is used to describe the properties of the rubber material. The general form of the strain energy density function for rubber materials can be expressed as:

$$U = C_{10}(\bar{I}_1 - 3) + C_{01}(\bar{I}_2 - 3) + \frac{1}{D_1}(J_{el} - 1)^2 \quad (5)$$

Where U is the strain energy per unit volume, C_{01} , C_{10} and D are material parameter which are related to temperature. \bar{I}_1 is the first and \bar{I}_2 is the second invariants of Cauchy-Green deformation tensors, expressed as:

$$\bar{I}_1 = \bar{\lambda}_1^2 + \bar{\lambda}_2^2 + \bar{\lambda}_3^2; \bar{I}_2 = \bar{\lambda}_1^{(-2)} + \bar{\lambda}_2^{(-2)} + \bar{\lambda}_3^{(-2)} \quad (6)$$

Where the offset $\bar{\lambda}_i = J^{-1/3} \lambda_i$, J is the total volume ratio, J_{el} is the elastic volume ratio, λ_i is the main extension, the initial shear modulus and bulk modulus are defined as:

$$G = 2(C_{10} + C_{01}) \quad K = \frac{2}{D_1} \quad (7)$$

In order to accurately express the stress-strain relationship of the rubber material, the data obtained through uniaxial tensile test, was fitted by Abaqus/Standard to obtain the hyper-elastic constitutive parameters of the rubber material. The mechanical properties curve of polyurethane materials as shown below:

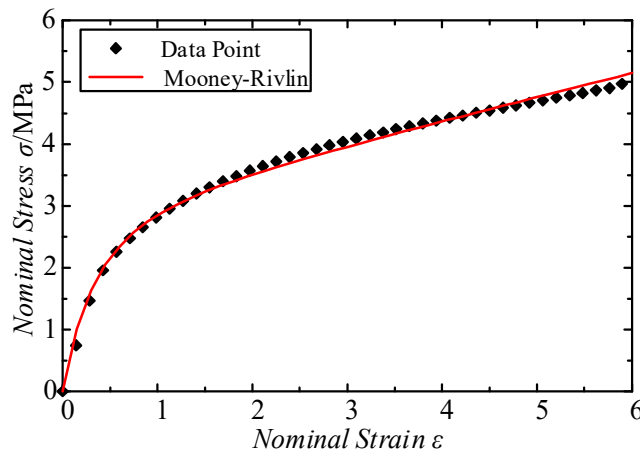


Fig.4 Stress-strain relationship of polyurethane rubber

In this paper, Mooney-Rivlin model is used to describe the mechanical behavior of rubber materials. The experimental results are used to fit the obtained polyurethane rubber cup constitutive model coefficients: $C_{10} = 1.93e6$, $C_{01} = 0.96e6$. The material is incompressible.

2.5 Boundary conditions and friction coefficients

The boundary conditions include the inlet and outlet boundaries of the pipeline, and the space constraints of the pipeline. In order to satisfy the hydrodynamic equation, the inlet boundary of the pipeline is set as the velocity boundary, and the outlet boundary of the pipeline is the natural flow. During the PIG runs in the pipeline, it is mainly affected by the force of the fluid and the force of the inner wall of the pipeline. The friction coefficient is an important parameter that affects the force. In this paper, the friction coefficient between the inner detector and the pipeline is set to 0.4.

3 SIMULATION RESULTS AND ANALYSIS

The PIG is mainly subjected to the action of the driving pressure and the friction force, that maintains a balance between the basic driving force and the friction force at a constant speed. In this paper, the fluid-structure coupled finite element model of the PIG movement in the pipeline is established by the nonlinear finite element software ABAQUS using the CEL method. Friction force and stress are taken as the research objects, and the influencing factors of the in-line detector are analyzed.

3.1 Analysis of straight pipe mechanics behavior

For the study of the relationship between the mechanical behavior and the interference of the cups in the operation of the straight pipe, three types of cups with 10mm, 14mm and 18mm thickness were used as the research object, and the pipe was 8-inch (internal diameter 200mm). limited the cups' interference range to 0 to 35mm with an interval of 5mm. Obtained numerical simulation data points, and after three times of polynomial fitting, to obtain the results of Figure 5~7.

Fig. 5 shows the relationship between the friction force and the interference magnitude of the cups. It can be seen that when the interference magnitude increases from 25mm to 35mm, the friction increment is larger and the curve is steeper. When the interference magnitude is from 10mm to 25mm, the increase in friction is smaller and more gradual. The data points from the 14mm and 18mm cup thickness deviate from the fitting curves, and the data points with the thickness of 10mm basically coincided with the fitting curve.

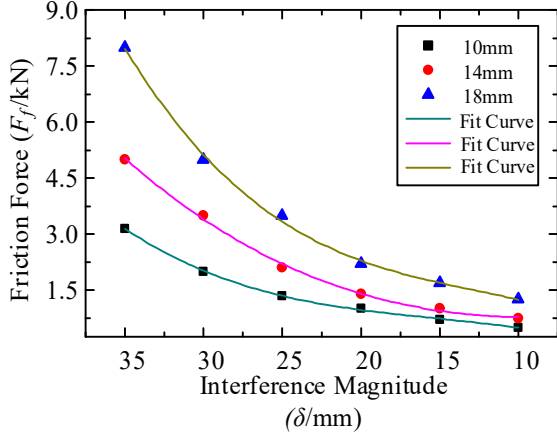


Fig.5 Relation between frictional force F and magnitude of interference δ

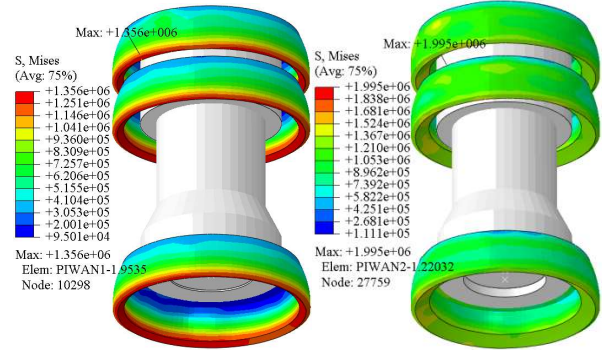


Fig.6 The Mises stress nephogram of PIG

The Mises stress on the detector is shown in Fig. 6. It can be seen that when the detector runs smoothly in a smooth pipe, the stress on the PIG is more uniform and appears at the interface between the cup and the inner wall of the pipe. Comparing the Mises stress cloud map with the thickness of 10mm and 18mm, it can be seen that with the same amount of interference magnitude, the stiffness of the cup increases significantly with the increase of the thickness of the cup.

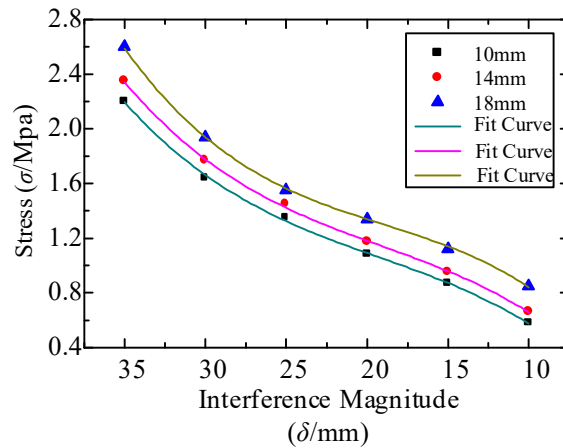


Fig.7 Relation between stress σ and magnitude of interference δ

Figure 7 shows the relationship between the stress of PIG and the change in the interference of the cup. It can be seen that when the interference increases from 10mm to 15mm, the stress on the detector increases more obviously. When the magnitude of interference is from 15mm to 30mm, the rising trend of the stress on the PIG is slowed down. When the interference magnitude is in the range of 30mm~35mm, the stress is greatly

increased. Exceeded the reasonable range of applications for the cups. As can be seen from the three fitting curves, the change trend of the curve is basically the same, and the coincidence degree between the simulated data point and the fitted curve is high, indicating that the thickness of the cups only has the effect of increasing the stiffness.

3.2 Analysis deformation mechanical behavior

To study the mechanical behavior of PIG at the local deformation of the pipe. When it running in the pipe, due to the super elastic and nonlinear characteristics of the sealed cups, when the shape of the pipe is abruptly changed, the complex dynamic behavior will occur great fluctuations. Setting the boundary velocity to 1m/s, 2m/s, and 3m/s respectively, the inner diameter of the pipe to 200mm, and the thickness of the cuvette to 14mm as the research object, to investigate the process of the pipe deformation (half-sphere) height increasing from 4mm to 20mm. The relationship between the friction force, the cup stress, and the deformation height is used to analyze the influence factors of the PIG passing ability.

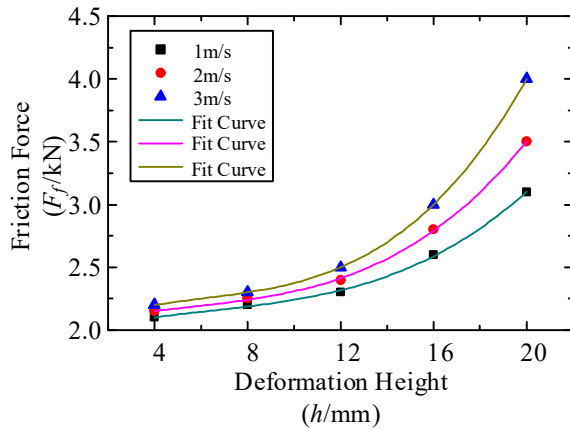


Fig.8 Relation between stress σ and deformation height h

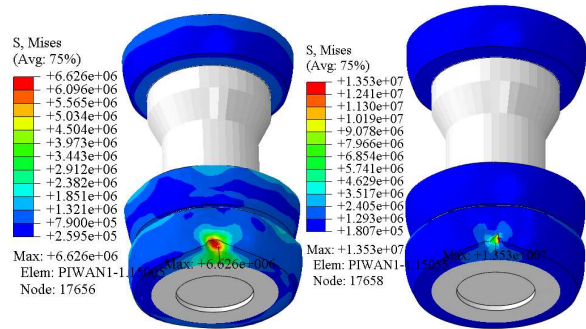


Fig.9 The Mises stress nephogram of PIG

Figure 8 shows the relationship between the friction force and the deformation height. Analysis of Figure 8 shows that when the deformation height changes in the interval of 4-12mm, the friction force of the detector changes more smoothly, and less than 2.5kN, the trend of the three fitting curves is similar; when the deformation height increases from 12mm to 20mm, at that time, friction increased significantly, and the increase of the three curves gradually increased. It shows that the speed will have a certain influence on the friction force that the PIG receives when it passes through the deformation zone of the pipeline, and the speed will lead the friction force to increase.

When PIG passes through the local deformation part of pipeline, the phenomenon of stress concentration will inevitably occur. As shown in Fig. 9, when passing through the local deformation zone of the pipeline, the stress exceeds the reasonable area of the cup, but after

through the deformation zone, due to the polyurethane. The material has a high degree of super-elastic, flying behavior, that will return to normal motion. However, through simulation, it can be seen that when the stress of the cup is very large, the damage to the cup is irreversible.

When the PIG passes through the deformation part of pipeline, due to the presence of the deformation part, the PIG will produce a significant stress concentration phenomenon. Figure 10 shows the relationship between the stress σ of PIG and the deformation height h . According to the fitting curve, the trend of the maximum stress change experienced by the cup is basically the same as that of the friction force. When the deformation height is less than 12mm, the stress changes less than 10 MPa, which is in line with the reasonable use range of the polyurethane rubber material; the stress change trend is also the same related to the passing speed, the working condition with a speed of 1m/s, the stress is obviously less, and less than 10MPa; the working condition with a speed of 3m/s, when the deformation height is 20mm, the maximum stress reaches 24.8MPa, showing the polyurethane material Strong superelastic, nonlinear behavior.

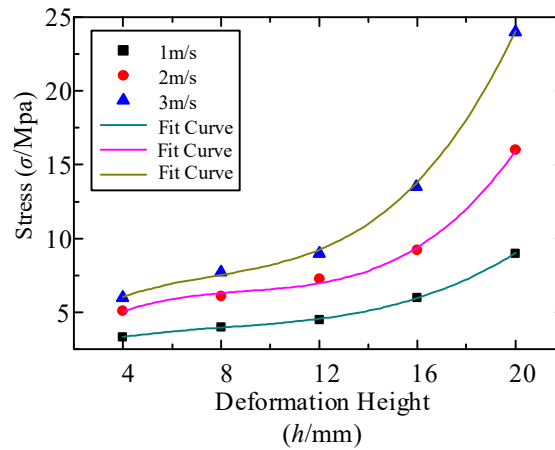


Fig.10 Relation between stress σ and deformation height h

When the PIG passes through the deformation part of pipeline, due to the presence of the deformation part, the PIG will produce a significant stress concentration phenomenon. Figure 10 shows the relationship between the stress σ of PIG and the deformation height h . According to the fitting curve, the trend of the maximum stress change experienced by the cup is basically the same as that of the friction force. When the deformation height is less than 12mm, the stress changes less than 10 MPa, which is in line with the reasonable use range of the polyurethane rubber material; the stress change trend is also the same related to the passing speed, the working condition with a speed of 1m/s, the stress is obviously less, and less than 10MPa; the working condition with a speed of 3m/s, when the deformation height is 20mm, the maximum stress reaches 24.8MPa, showing the polyurethane material Strong superelastic, nonlinear behavior.

3.3 Analysis of Passing Influence Factors

The above simulation method was used to numerically simulate the fluid-structure interaction of the PIG when passing through the smooth straight pipe section and local deformation of the pipe. The difference method [16] was used to do the surface fitting to the stress, and the fitting surface was shown in the Figure.11 and Figure 12.

As can be seen from Figure 11, when the pipe diameter does not change, the stress in the detector increases as the thickness of the cup increases, but the stress increases slowly when the amount of interference is constant. When the thickness of the cup increase from 10mm to 18mm, the stress increase value is less than 0.5MPa; when the cups' interference reaches 30mm, that is the 15.0% of pipe diameter, the stress change obviously increases obviously, indicating that the stress is beyond the range of reasonable use. It can achieve conclusion is in order to ensure that PIG can smoothly pass through the pipeline, the magnitude of interference should be less than 15.0% of the inner pipeline diameter.

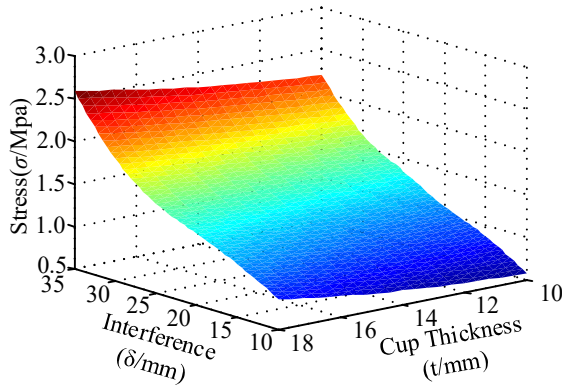


Fig.11 Relation of stress σ versus thickness t and magnitude of interference δ

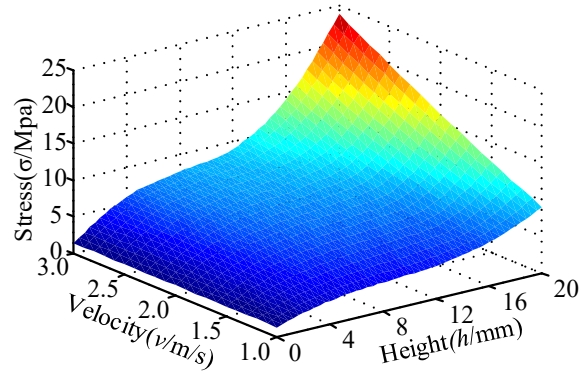


Fig.12 Relation of stress σ versus deformation height h and boundary velocity v

As can be seen from Fig. 12, when PIG's structure is unchanged, the deformation height is 0, the stress on the cups is basically at 2 MPa and remains unchanged, indicating that in the smooth straight pipeline, the change of velocity has little effect on the stress. But when the speed is less than 2m/s and the pipe deformation height is larger than 8.0% of the pipe inner diameter, the stress on the detector increases significantly, the speed is faster than 2m/s, and the pipe deformation height is bigger than 6.0% of the pipe inner diameter. The stress increases significantly, indicating that the faster the speed is, the larger stress on the cups. In order to ensure the high efficiency of PIG, when the deformation height is less than 12mm, as the 6.0% of the pipeline diameter. The device can pass through the pipeline smoothly.

4 Conclusion

In this paper, the CEL method is applied to the in-pipe detector simulation. The fluid-solid coupling model of the detector in the pipeline is established. The coupling effect of the

detector inside the pipeline and the fluid and the pipeline is considered. The dynamic model of the fluid material is established and the polyurethane rubber cup is established. Material experiments were performed using the Mooney-Rivlin hyperelastic constitutive model, and numerical simulations using the CEL method yielded the following conclusions:

1) When the detector is operated in the pipe, the maximum stress in the smooth pipe mainly occurs at the contact surface between the cup and the inner wall of the pipe, and the stress distribution is more uniform under steady state operation. In the local deformation of the pipeline, there is a large stress concentration.

2) The amount of interference of the inner detector tube sealer is a very important parameter for the passage of the inner detector in the pipeline. To ensure that the detector can smoothly pass through the pipeline, the amount of interference should be less than 15.0% of the inner diameter of the pipeline.

3) When the pipe is locally deformed, the height of the deformation determines the level of the passing performance of the detector. When the deformation height is less than 6.0% of the internal diameter of the pipe, the detector can smoothly pass through the pipe.

In addition, the CEL method is applied to the field of fluid-solid coupling dynamics of detectors in pipelines, and nonlinear dynamic analysis of detectors in pipelines is carried out to provide theoretical basis and technical basis for the design and manufacture of detectors in pipelines.

Acknowledgement

This paper is funded by the International Exchange Program of Harbin Engineering University for Innovation-oriented Talents Cultivation.

REFERENCES

- [1] Guan L, Osman A, Gao Y, et al. Analysis of Rolling Motion Effect on SINS Error Modeling in PIG[C]//Ieee/ion Plans. 2016.
- [2] DAI Bo, XU Guang. Analysis of motion state of detectors in pipelines based on effusion holes[J]. Journal of Computers and Applied Chemistry, 2013(8).
- [3] Kandroodi MR, Araabi BN, Bassiri MM, et al. Estimation of Depth and Length of Defects from Magnetic Flux Leakage Measurements: Verification with Simulations, Experiments, and Pigging data[J]. 2016, PP(99):1- 1.
- [4] Dai Bo, Yang Guang, Zhang Xiao, et al. Mathematical model for velocity control of detectors in differential pressure driven pipelines [J]. Journal of Computers and Applied Chemistry, 2016, 33(4).
- [5] Aksenov DV, Shcherbakov VI, Leshchenko V V. Selection of structural parameters of an inspection pig for arterial oil and gas pipelines from conditions of dynamics[J]. Chemical and Petroleum Engineering, 2013, 49(3):265-269.
- [6] Zhang H, Zhang S, Liu S, et al. Chatter vibration phenomenon of pipeline inspection gauges (PIGs) in natural gas pipeline[J]. Journal of Natural Gas Science & Engineering, 2015,

27:1129-1140.

- [7] Zhang Xing, Liu Shuhai, Li Qing, et al. Influence of the interference on the stiffness characteristics of sealed leather bowl of pig 1016mm pig[J]. Chemical Engineering Equipment and Tube, 2015, 52(6):82-86.
- [8] Gu Yaxiong, Zhou Qiongli, Yang Qiang. Design and Simulation of Detector Leakage Device in Gas Pipeline[J]. Instrumentation Users, 2013(3):81-82.
- [9] Zhang H, Zhang S, Liu S, et al. Collisional vibration of PIGs (pipeline inspection gauges) passing through girth welds in pipelines[J]. Journal of Natural Gas Science & Engineering, 2016, 37:15-28.
- [10] Zhang Xing, Zhang Shimin, Guo Shudun, et al. Dynamic simulation of the process of over-weld welding of straight-pipe pig cleaners[J]. Petroleum Mining and Related Machinery, 2015, 44(2):22-27.
- [11] Zhu X, Wang D, Yeung H, et al. Comparison of linear and nonlinear simulations of bidirectional pig contact forces in gas pipelines[J]. Journal of Natural Gas Science & Engineering, 2015, 27:151-157.
- [12] Liu Baoyu. Design and theoretical study of detectors in gas transmission pipelines [D]. China University of Petroleum, 2010.
- [13] Durali M, Fazeli A, Nabi A, et al. Investigation of Dynamics and Vibration of PIG in Oil and Gas Pipelines [C]// ASME 2007 International Mechanical Engineering Congress and Exposition. 2007:2015-2024.
- [14] Sillem A. Feasibility study of a tire hydroplaning simulation in a finite element code using a coupled Eulerian-Lagrangian method [J]. 2008.
- [15] Ahmadzadeh M, Saranjam B, Hoseini Fard A, et al. Numerical simulation of sphere water entry problem using Eulerian–Lagrangian method[J]. Applied Mathematical Modelling, 2014, 38(5–6):1673-1684.
- [16] Chen Shili, Gao Chunqian, Guo Shixu, et al. Research on the Penetration Simulation of Spherical Inner Detector in Submarine Riser[J]. Computer Engineering and Applications, 2015, 51(19): 265-270.

A Numerical Model for Calculating Atmospheric Corrosion Rate of Marine Steel Structures

Rujin Ma^{*}, Chuanjie Cui^{**}, Airong Chen^{***}

^{*}Tongji University, ^{**}Tongji University, ^{***}Tongji University

ABSTRACT

Atmospheric corrosion is particularly common but hazardous for marine steel structures in civil engineering. Nowadays, a great number of salt spray accelerated corrosion tests have been carry out to illuminate the corrosion rate and corroded structure performance. However the relationship between marine atmospheric corrosion and salt spray environment corrosion is still uncertain. In this research, the electrochemical principle of atmospheric corrosion is analysed and a numerical corrosion model in marine atmospheric environment is developed considering atmospheric humidity, chloride ion concentration and structure stress. The numerical simulation agrees well with the experimental results under same environment condition. At last, based on the numerical model, a parameter analysis of atmospheric humidity, chloride ion concentration and structure stress are studied. The results show that the corrosion rate increases with all of the three parameters. The growth rate increases with atmospheric humidity while decreases with chloride ion concentration and structure stress. This numerical model is certainly helpful for design and maintenance of marine steel structures such as cross-sea bridges, oil platforms and so on .

Topology Optimization of Cable Domes Based on Genetic Algorithm

Shuo Ma^{*}, Xing-Fei Yuan^{**}

^{*}Zhejiang University, ^{**}Zhejiang University

ABSTRACT

This study mainly focuses on topology optimization of cable domes based on genetic algorithm, in which the vertical stiffness is set as the objective of optimization. Modified stiffness matrix based form-finding method (mSMFF) is used for form-finding and structural analysis of self-stressed cable domes. An innovative encoding scheme which uses ground structures as well as 0-1 strings to generate connectivity matrix and rest lengths of members are adopted. The mSMFF method is then used to give the initial solution of topology, prestress and configuration. Constraint conditions including constant total mass, yielding and buckling constraints are processed by transforming initial solutions into feasible solutions, in which a nonlinear equation is solved for the coefficient of prestress. The objective function is set as the work done by vertically uniform load, which is a reflection of vertical stiffness. A simple genetic algorithm(SGA) is used for the topology optimization of cable domes. Numerical examples show that the proposed method is efficient in simultaneously searching new topology, prestress and configuration of cable domes with high vertical stiffness. Topology, configuration and prestress are the three main factors that affect the mechanical properties of a tensegrity structure, so the design and optimization of tensegrities can be classified into three categories respectively. There are large amounts of researches focuses on form-finding, force-finding as well as prestress and configuration optimization of tensegrity structures, while the study of topology optimization of tensegrity structures with certain mechanical properties is limited. To this end, the optimization of cable domes with high vertical stiffness is studied. This study proposes a novel encoding scheme to generate new cable domes and uses genetic algorithm to do topology optimization of cable domes with topology, configuration and prestress as variables simultaneously. The numerical results extend the existing forms of cable domes.

Phase Field Modeling of the Sintering Process

Weixin Ma^{*}, Yongxing Shen^{**}, Wentao Yan^{***}

^{*}University of Michigan-Shanghai Jiao Tong University Joint Institute, Shanghai Jiao Tong University, ^{**}University of Michigan-Shanghai Jiao Tong University Joint Institute, Shanghai Jiao Tong University, ^{***}Department of Mechanical Engineering, Northwestern University

ABSTRACT

Modeling of sintering process has been developed in different scales with different methods. Our work focuses on metals at the microscale, which is applicable to the preheat stage of 3D printing. We hope it could help to finding the proper temperature and time in preheating to improve the quality of 3D printing. We consider the sintering process between two metal powders. The governing equation is given by: Cahn-Hilliard Equation for the conserved density field c [1] $\frac{\partial c}{\partial t} = \nabla \cdot (M \nabla \mu)$ Allen-Cahn Equation for the un-conservative order parameter field ϕ [2] $\frac{\partial \phi}{\partial t} = -L \nabla^2 \phi$ where M is the concentration mobility tensor, F is the total free energy and L is the order parameter scalar mobility. x and t represent spatial position vector and time respectively. In our previous work [3], we model the sintering process of metal powder at the nanoscale. Only the grain boundaries at the grain surface are taken into account. However, for micro scale metal powders, each particle is consisted of several grains, which means grain boundaries are within each particles. The evolution of grain boundaries inside the particle and in between two particles now has been added. Representative examples will be included to showcase the method. References: [1] Cahn JW, Hilliard JE. J Chem Phys 1958;28:258. [2] Cahn JW. Acta Metall 1961;9:795. [3] Wentao Yan, Ya Qian, Weixin Ma, Bin Zhou, Yongxing Shen, Feng Lin, Modeling and Experimental Validation of the Electron Beam Selective Melting Process, Engineering, Volume 3, Issue 5, 2017, Pages 701-707.

Subdivision Stencils around Extraordinary Vertices with Quasi-G2 Continuity and with Applications in Isogeometric Analysis

Weiyin Ma^{*}, Yue Ma^{**}

^{*}City University of Hong Kong, ^{**}City University of Hong Kong

ABSTRACT

Abstract: This talk presents a novel method to construct subdivision/refinement stencils near extraordinary vertices with limit surfaces having quasi-G2 continuity at extraordinary positions. Most existing subdivision schemes result in unbounded curvature or highly oscillated curvature around an extraordinary vertex. Some researchers minimize the Gaussian curvature variation for a set of central surfaces through tuning the subdivision masks. Some other researchers explicitly optimize the local quadratic precision of eigenvectors corresponding to the subsubdominant eigenvalue utilizing the extra degrees of freedom obtained through tuning the subdivision stencils for triangle control meshes. In our work, we optimize the subdivision stencils to provide the best possible curvature behaviour near extraordinary vertices with respect to G2 requirements for stationary subdivision of quadrilateral meshes. The subdivision stencils include that for one-ring new face vertices, one-ring new edge vertices and updated vertex vertices near an extraordinary vertex similar to that of Catmull-Clark subdivision, but with maximum possible degrees of freedom for further optimizing the stencils. We first construct the subdivision stencils to ensure subdivision properties including G1 continuity with bounded curvature at extraordinary positions. The remaining degrees of freedom of the constructed subdivision stencils are further used to optimize the subdivision towards a scheme with G2 continuity through direct optimization of the eigenbasis functions corresponding to the subsubdominant eigenvalue of the subdivision and to achieve other desired limit surface properties. A systematic evaluation shows that the constructed subdivision stencils produce better limit surfaces in extraordinary regions than that of other similar existing subdivision schemes with respect to a necessary and sufficient criterion for C2 continuity (Peters and Reif 2008) and local curvature behaviour. The resulting subdivision stencils can be integrated with either subdivision schemes for quadrilateral meshes of arbitrary topology or unstructured T-splines (Scott et al. 2013). Applications of the resulting schemes using the proposed refinement stencils in isogeometric analysis (Hughes et al. 2005) are also discussed. References: [1] J. Peters and U. Reif, *Subdivision Surfaces*, Springer-Verlag Berlin Heidelberg, 2008. [2] M. A. Scott, R. N. Simpson, J. A. Evans, S. Lipton, S. P. A. Bordas, T. J. R. Hughes, T. W. Sederberg, Isogeometric boundary element analysis using unstructured T-splines. *Computer Methods in Applied Mechanics and Engineering* 254: 197-221, 2013. [3] T. J. R. Hughes, J. A. Cottrell and Y. Bazilevs, Isogeometric analysis: CAD, finite elements, NURBS, exact geometry and mesh refinement. *Computer Methods in Applied Mechanics and Engineering* 194(39-41):4135-4195, 2005.

A Semi-analytical Method for Critical Buckling Analysis of 2D Nano-materials

Yong Ma^{*}, Yuli Chen^{**}, Shengtao Wang^{***}, Yanguang Zhou^{****}

^{*}Institute of Solid Mechanics, Beihang University (BUAA), ^{**}Institute of Solid Mechanics, Beihang University (BUAA), ^{***}Institute of Solid Mechanics, Beihang University (BUAA), ^{****}Aachen Institute for Advanced Study in Computational Engineering Science (AICES), RWTH Aachen University

ABSTRACT

The performances of 2D nano-materials in micro- and nano-electronics and devices are significantly affected by their morphologies, which depend on the surface features of the supporting substrate. In practical applications, non-developable substrates are widely used, and thus it is of great importance to predict the final morphology of 2D nano-materials on non-developable substrates. To this end, energy-based theoretical models are developed for several substrates with different topographies and a mode-independent energy buckling analysis method (MIEM) is proposed to analyze the final morphology. By molecular dynamics simulations, three typical morphologies of 2D nano-materials, completely conforming, partial delamination and wrinkling, are observed. Based on simulation results, theoretical models are established for spherical, concave and convex substrate, respectively. Applying the principle of minimum energy, the strain in 2D nano-materials can be derived. And then we propose a half-analytical method to predict the critical buckling of structures, named mode-independent energy-based buckling analysis method (MIEM). In MIEM, the pre-knowledge of buckling mode is not required, and the modified Cauchy-Born rule is employed to obtain the equilibrium configuration of atom-structures, which can greatly reduce computation load. Meanwhile, it can take full advantage of the structure characteristics, such as periodicity and flatness, to further reduce the calculation amount so that the method is more suitable for large-scale nanostructures than the atomistic simulations. Besides, it is as accurate as atomic simulation because it is derived directly from the atomic potentials and no additional simplifications are made. With this method, whether the atom-structure buckles can be determined, and finally the critical conditions of different morphologies can be derived. These results can provide guidelines to design high quality graphene-based electronics and can be extended as the surface roughness standard for the supporting substrates. Reference [1] Zhou Y, Chen Y, Liu B, et al. Mechanics of nanoscale wrinkling of graphene on a non-developable surface[J]. Carbon, 2014, 84(1):263-271. [2] Chen Y, Ma Y, Wang S, et al. The morphology of graphene on a non-developable concave substrate[J]. Applied Physics Letters, 2016, 108(3):031905. [3] Wang S, Chen Y, Wu J, et al. A mode-independent energy-based buckling analysis method and its application on substrate-supported graphene[J]. International Journal of Solids and Structures, 2017, 124: 73-88. Acknowledgments National Natural Science Foundation of China (nos. 11622214, 11472027 and 11202012).

An Architecture of Flexible Host Platform for Multi-Physics Numerical Computation

Zhaosong Ma^{*}, Chun Feng^{**}

^{*}Institute of Mechanics, Chinese Academy of Sciences, ^{**}Institute of Mechanics, Chinese Academy of Sciences

ABSTRACT

A host platform has been designed for numerical computation, including FEM, FVM, DEM, as well as particle simulation. The platform supports any number of user-defined multi-physics variables, which are optionally shown via OpenGL. The solving flow can be driven by JavaScript, written by developer or end user. In addition, a result cache server has been developed to support high performance calculation and real-time post procession. The Platform is written in C++ language, with complete post-processing and limited pre-processing functionality, which can host user-written kernel solvers, user-written GUI modules. Users can define their own multi-physics problem description, problem associated parameters, DOFs, and any number of result variables. These variables can be of any data types. To define a variable, a C++ class should be filled to describe the variable's hierarchy, the variable's name and other information, with a self-defined sample variable to tell the host about the data type and data size. To improve post-processing performance, a cache mechanism has been designed by setting up an embedded result server to run in another worker thread. The server maintains a result queue with an adaptive size limit determined by system available memory. A kernel solver submits result asynchronously. When a solver module received a set of results, the server records the step number, the time stamp, and push the result data into the back of result queue, which is instantly rendered on the screen. If the queue size exceeds the limit, the front of the queue is popped up. Whatever the queue size exceeds the limit, the step result is written to disc. This process runs in background while the kernel solver is proceeding. A JavaScript host has also been implemented in the platform by means of windows script hosting technique which provides syntax checking, interpreting, and debugging functionality. The script engine supports ActiveX and COM Technology, which makes the platform able to call most third-party functionalities like CAD, CAE, GIS, word processing and database. The script can be from a source file or from a command input, either of them can take full control of the solving flow. Unlike Python and Java, JavaScript supports "Just in Time Operation" (JIT), which is very important to interactive computation. For example, users can change the solving flow whenever needed. The architecture of the platform is introduced and various results are shown.

Design of an Endovascular Chemofilter Device with CFD Modeling

Nazanin Maani^{*}, Daryl Yee^{**}, Julia Greer^{***}, Steven Hetts^{****}, Vitaliy Rayz^{*****}

^{*}Purdue, ^{**}Caltech, ^{***}Caltech, ^{****}UCSF, ^{*****}Purdue

ABSTRACT

Purpose: Intra-Arterial Chemotherapy (IAC) used for treating Hepatocellular Carcinoma by local injection of Doxorubicin (Dox) into the tumor, causes systemic toxicity due to 50-70% of the drug passing to the systemic circulation [1]. A catheter-based Chemofilter device can be deployed in the veins downstream of the tumor to filter the excessive Dox from blood during the IAC procedure. The optimal design of the Chemofilter will minimize pressure drop and flow disturbance, while providing sufficient binding sites for Dox chemical adsorption on the filter's surface. In this study, the effect of the Chemofilter's configuration, microstructure, and surface texture on hemodynamic performance of the device is investigated with CFD simulations. **Methods:** The chemofilter's membrane consists of 3D-printed micro-trusses that form an interconnected porous lattice of symmetric micro-units. The micro-units provide adequate porosity for the passage of blood cells, and large contact area for the Dox binding. To study the flow through the individual micro-units (100-200 μ m) as well as the whole device (about 10 mm), a multi-scale approach is used for CFD modeling of the Chemofilter. The general configuration of the membrane resembles an umbrella which is installed on a supporting structure, inspired by the RX AccUNET embolic protection device. The design parameters include 1) the leading angle, 2) the number of membrane sectors, 3) the thickness of membrane, and 4) the size of gap between the membrane and the vessel wall. The shark skin effect, i.e. surface texturing, is investigated to examine the shear stress reduction and platelet activation on the surface. The numerical results are obtained with the finite-volume solver Fluent (ANSYS). **Results:** The simulations of hemodynamic performance for different Chemofilter configurations indicate that the pressure drop across the membrane increases with the leading angle, the number of umbrella sectors, and the membrane thickness. However, an acute leading angle of the device can result in increased area of flow recirculation and stagnation. The fewer number of the sectors results in the larger gap near the wall, thus allowing a large fraction of the flow to bypass the filter. Therefore, the membrane sectors should be curved and extended to the wall in order to prevent escaping jets. The application of the shark-skin texture on the surface results in reduction of the shear stress, by shifting the regions of high velocity and vorticity away from the surface. **Reference:** M.S. Aboian et al., Biomed microdevices. 2016;18(6):98.

A Geometrically Exact Euler-Bernoulli Beam Formulation with an Interface to Arbitrary Nonlinear Material Laws

Sascha Maassen^{*}, Cátia da Costa e Silva^{**}, Paulo de Mattos Pimenta^{***}, Jörg Schröder^{****}

^{*}Universität Duisburg-Essen, ^{**}University of São Paulo, ^{***}University of São Paulo, ^{****}Universität Duisburg-Essen

ABSTRACT

In this work a geometrically exact Euler-Bernoulli beam finite element is presented, which is based on [1] and subject to [3]. The beam formulation is embedded into the three-dimensional space and obeys the Euler-Bernoulli hypothesis of remaining plain cross-sections and of shear rigidity when subjected to bending deformation. The rotational group is parametrized using Rodrigues formula with an efficient update scheme for the parameter set. In hand with out of plane warping, this allows for arbitrary large rotations and deformation within this model. For the implementation of arbitrary material laws, as shown in [2], the resulting deformation measure needs to result in stress states at each material point, that obeys the special stress condition of beams. This is enforced by a local iteration which allows application of arbitrary material laws. Throughout this presentation the restrictions of hyperelastic materials and rectangular cross-sections is made. On the element level a straight reference configuration is considered where the displacements are interpolated using C1 continuous Hermite polynomials which a priori leads to satisfaction of the shear rigidity constraint. In many engineering applications, non-straight connections of structural members with variable cross section geometries and/or materials have to be analyzed. We address this modelling challenge with a unique rotational continuity extension which allows for the modeling of material- and geometrical- discontinuities. The necessity of the continuous rotational group is enforced using Lagrange multipliers and a penalty method. The capabilities of the formulation will be displayed through numerical examples. 1.Pimenta P. M. and Yoo T., "Geometrically-exact analysis of spatial frames", Applied Mechanics Reviews, ASME, New York, v.46, 11, 118-128, 1993. 2.Klinkel, S. & Govindjee, S. "Using finite strain 3D-material models in beam and shell elements", Engineering Computations, v.19, 3,254-271, 2002. 3.Silva, C.C., Maassen, S., Pimenta, P.M. & Schröder, J. "Geometrically exact analysis of Bernoulli-Euler rods", in preparation for Computer Methods In Applied Mechanics and Engineering, 2017.

INVERSE METHOD FOR DETERMINATION OF HARDENING PARAMETERS OF DUCTILE MATERIALS BY A MULTI-IMAGE ANALYSIS OF INDENTATION PROFILES FROM HARDNESS TESTS: NUMERICAL AND EXPERIMENTAL ASPECTS

L.Q. MACHADO¹ AND L. MALCHER²

^{1,2} University of Brasília, Faculty of Technology, Department of Mechanical Engineering, Campus Darcy Ribeiro, Brasília – Distrito Federal – Brazil.

^{1.} lucasqmachado@gmail.com

^{2.} malcher@unb.br

Abstract: The plastic behavior of a material is resultant of non-linearities which leads to complex stress-strain fields, making it difficult to devise analytical relationships beyond the elastic domain. Traditionally, the material's stress-strain relationship has been acquired from uniaxial testing, which is widely used to describe its behavior under plastic deformation. However, the hardness test is more versatile, operative, cheaper and faster than the uniaxial test. Therefore, over the past years new techniques have been devised to obtain the stress-strain relationship of bulk metallic materials from the reaction curve of an indentation test with the formulation of an inverse method for parametrical identification, which is possible thanks to the development of numerical methods and instruments able to provide the load-displacement data by continuously measuring the depth of indentation. When it comes to traditional hardness tests, such as in the Brinell, Knoop, Rockwell and Vickers, they have been mostly used as a way to assess the capability a material has to resist plastic deformation by relating the applied load to the resultant area or depth of indentation. From the Brinell hardness test, due to its simplicity and versatility, a newer approach was devised to correlate this test to the material's full plastic characterization by finding its hardening parameters. The methodology consists of performing four Brinell hardness tests to have a representative material's response and from it do a multi-image comparison of the resultant indentation profiles obtained from a confocal laser microscope with the predicted output of repeated FEM modelling. The parametric identification is conducted by an optimization technique using the Trust-Region-Reflective Least Square Algorithm available in the MATLAB's Optimization Toolbox. In this process several trial stress-strain curves are provided to minimize the discrepancy between numerical and experimental data in an iterative FEM modeling of the indentation process until reaching the established tolerance and thus providing the hardening parameters that best fit the experimental data. The new method then numerically replicates the same indentation impression left in the specimen by the indenter in a real experiment. The methodology for characterizing the elastic-plastic properties from the indentation's reaction curve is also presented in parallel to the multi-image analysis to compare its performance, since both were developed seeking to replace the traditional uniaxial test. Finally, the hardening curves obtained from uniaxial and indentation tests are compared to corroborate the new methodology.

Keywords: parametric identification, indentation multi-image analysis, hardening curve, optimization process.

1 INTRODUCTION

Indentation hardness tests have been traditionally understood as a way to assess the capability a material has to resist plastic deformation by relating the applied load to the resultant area or depth of indentation, such as in Brinell, Knoop, Rockwell and Vickers hardness tests ¹. Over the past years, new techniques have been devised for probing the mechanical properties of materials by an indentation test. This is mainly due to the development of instruments able to provide the indentation load-displacement data by continuously measuring the depth of indentation while a normal load is being applied on the material and thanks to numerical methods, such as the Finite Element Method, that makes possible to analyze complex stress-strain fields in contact mechanics ²⁻⁵.

The plastic behavior of a material is resultant of non-linearities which leads to complex stress and strain fields, making it difficult to devise analytical relationships beyond the elastic domain. Traditionally, the material's stress-strain relationship acquired from uniaxial testing has been widely used to describe its behavior under plastic deformation. However, the hardness test is more versatile, operative, cheaper and faster than the uniaxial test. Therefore, efforts have been made in using the indentation hardness test to obtain the stress-strain relationship of a material under plastic deformation with the formulation of an inverse method for parametric identification aided by numerical methods.

While the uniaxial test is the forward method to obtain the plastic parameters of a material, the indentation test needs to be aided by numerical methods such as the FEM and other optimization methods in order to characterize the material's plastic behavior and then yielding the hardening parameters that describe the stress-strain relationship of it. The most popular way of evaluating the material response to an indentation load is by analyzing the material's indentation reaction curve^{3,4}. However, this work addresses the material response in a newer way by analyzing the resultant indentation impression profile. Basically, the process is the same, the difference is the data being analyzed. Since there are some other effects related to the indentation profile, such as pile-up and sink-in phenomena, this work seeks to provide a more precise assessment of the indentation process and thus a more accurate determination of the material's hardening parameters.

2 EXPERIMENTAL PROCEDURES

Both traditional tensile tests and indentation hardness tests are carried out for a marine grade steel. The tensile test is the direct way to determine the hardening parameters of the material, while the indentation hardness test is part of an inverse method of parametric identification aided by numerical methods. In this contribution, the hardening curve is approximated by an exponential function according to Ludwick (1909), and represented as:

$$\sigma_y(\bar{\epsilon}^p) = \sigma_{y0} + H\bar{\epsilon}^{pn}, \quad (1)$$

where σ_{y0} is the material's initial yield stress, H is the isotropic hardening modulus, $\bar{\epsilon}^p$ represents the accumulated plastic strain, and lastly, n is the so-called hardening exponent. Therefore, to have a way of comparison and to validate the new methodology, a uniaxial tensile test is performed. In the sequence, uniaxial and indentation hardness tests are addressed.

2.1 Uniaxial Tensile Test

The tensile test was conducted in an MTS machine (Figure 1) with a 100 kN load capacity, where the specimen was elongated until collapsing. The deformation was measured aided by a clip gauge of 25 mm of length gauge (+ 5 / -2.5 mm).

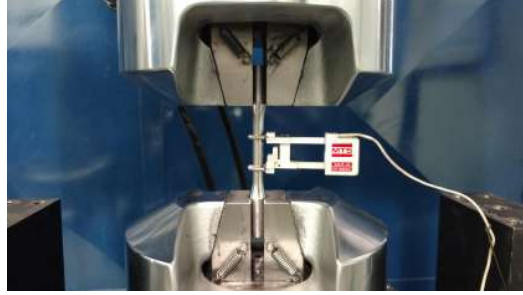


Figure 1: MTS with Clip Gauge Used for Tensile Test.

The hardening stress-plastic strain relationship is shown in Figure 2, which is later used to evaluate the proposed inverse method for parameter identification.

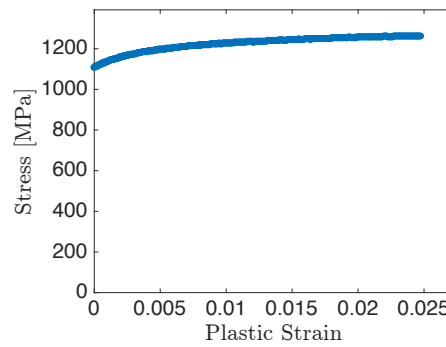


Figure 2. Stress-Strain Curve from Uniaxial Test and Nonlinear Regression.

2.2 Brinell Hardness Test

The Brinell indentation tests were realized in the Zwick/Roell ZHU250 universal hardness machine using a carbide tungsten indenter of 2.5 mm diameter, as shown in Figure 3.

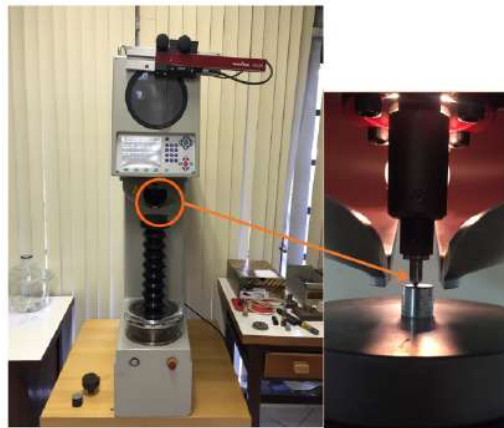


Figure 3. Zwick/Roell ZHU250 Universal Hardness Machine.

The specimen is then submitted to three different load configurations of the Brinell hardness test: HBW 31.25/2.5, HBW 62.5/2.5 and HBW 187.5/2.5. The indentation profiles (Figure 4) are assessed with a *LEXT OLS4100* laser confocal microscope

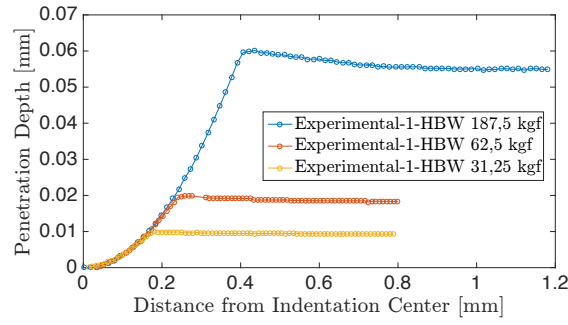


Figure 4. Indentation Profile

3 NUMERICAL APPROACH

The numerical analysis was carried out in a Finite Element Environment using Abaqus. This software is licensed by Dassault Systèmes, 2012 and is widely used by engineers to solve diverse problems encompassing a wide range of industrial applications. This section presents a discussion on contact formulation and mesh convergence to decide the most suitable model configuration. Therefore, comparisons are made in terms of contact pressure, penetration depth and simulation time for procedures comprising the elastic and the elastic-plastic formulations. For simulations purely elastic, the predicted output is compared to the analytical solution provided by Hertz's⁶ theory while the elastic-plastic numerical response is used for mesh convergence purposes. The elastic analyses are performed for a rigid indenter while the elastic-plastic assumes a deformable indenter with Elastic Modulus of 645 GPa and Poisson Ratio of 0.22. The specimen is a marine grade steel with Elastic Modulus of 200 GPa and Poisson Ratio of 0.3.

3.1 Part Module

The sphere-plane contact is modeled in a 2D axisymmetric configuration. Both bodies are defined as deformable shells, however, when necessary to grant a rigid characteristic to the sphere, its elastic modulus is assigned a value four orders greater than the specimen's elastic modulus.

In Figure 5, it can be seen that both, specimen and indenter, were partitioned into different regions. It was done to facilitate meshing, making it possible to have suitable refinement in the contact region and, at the same time, to avoid unnecessary elements in other regions less affected by the stress field due to the contact.

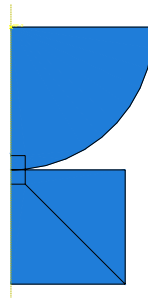


Figure 5. Contact Configuration

3.2 Property Module

Each defined part indenter and specimen is made of a different material, both isotropic. To define the indenter's material property is enough to consider it has only a linear elastic

behavior, which is done by informing its elastic modulus and Poisson ratio. The specimen may or may not behave elastically depending on the applied load it bears; therefore, it is necessary to perform an elastic-plastic analysis. The elastic-plastic analysis requires different fields depending on the plasticity model. For this case, besides the elastic definition, the classical metal plasticity model was adopted, which requires the knowledge of the stress-plastic strain data representing the material hardening behavior.

To every part must be assigned material property. Once the materials are defined, sections are created to attend the parts' specifications. Since each part is made of one material kind, one section is created to each part and the correct material property is associated to its respective section. Respecting the pre-established conditions, the section is defined as homogeneous solid with thickness of 1 *mm*.

3.3 Assembly Module

In the assembly, the part instances are created and positioned relatively to each other in a global coordinate system, as shown in Figure 5, in a way where the lowest point of the indenter is in contact with the leftmost upper point of the specimen.

3.4 Step Module

The simulation was carried out in three steps, defining in this manner the indentation test. In the initial step the contact interaction between indenter and specimen is defined, the boundary conditions establish that the specimen is fully restrained at its base and that there is a symmetry about a plane $X = \text{constant}$. A first step, called Penetration, defines that the indenter can only move vertically relatively to the specimen, deforming it. This vertical displacement is caused by a load applied to the indenter. Thereafter, the step two establishes that the indenter returns to its initial position, which allows the materials to spring back so that the impression's maximum depth is not the final depth. The conditions of each step are propagated to the following step, with exception of the load established on the Penetration step that is not propagated to the next step.

During Penetration, instabilities in the model may arise causing local velocities to increase due mainly to mesh size and material behavior. If that happen, part of the strain energy needs to be dissipated, which can be achieved by adding a viscous force to the global equilibrium equations. This viscous force is proportional to a damping factor that in turn is proportional to the nodal velocities. Therefore, an automatic stabilization method with a constant damping factor is considered. However, defining the appropriate damping factor is not an easy task and depends on results from previous runs. An optimal damping factor is found when converged solution is obtained and the dissipated stabilization energy is sufficiently small.

3.5 Interaction Module

The interaction module is used to define contact interactions, tie constraints and coupling constraints in the model. Addressing firstly the contact interactions, Abaqus makes it possible to define contact in three main ways: general contact, contact pairs and contact elements.

The model analyzed here counts with the contact of two bodies defined as deformable in a two-dimensional configuration. The physical proximity of these two bodies in the assembly does not indicate interaction, therefore it is necessary to specify what kind of interaction exists between their surfaces and its properties. The contact pair is the most suitable type of interaction for this case because there are only two surfaces that may interact with each other and having a pairwise specification of the contact results in a more robust analysis. Thus, in the Part Module the indenter and the specimen were divided in regions for contact definition

and efficiency purposes, so that the extension of its contact surfaces is appropriate for the contact.

Contact Formulation. Once the contact interaction type is determined, the contact formulation defined subsequently will have a considerable impact on how the surfaces interact. It is based on master and slave definitions, contact discretization and tracking approaching. Since the indenter is stiffer and may have coarser mesh, its contact surface is defined as master while the contact surface from the specimen acts as the slave surface. The contact discretization is defined as surface-to-surface and accounts for the way that conditional constraints are applied to interacting surfaces. For a given mesh refinement, the surface-to-surface discretization tends to provide more accurate stress and pressure results than the node-to-surface discretization. It happens because the surface-to-surface discretization resists penetrations in an average perspective over finite regions of the slave surface while the node-to-surface allows master nodes to penetrate the slave surface causing forces to concentrate at the slave nodes. This results in an uneven distribution of pressure over the surface. Figure 6 shows the contact pressure response for both contact discretization methods: surface-to-surface (a) and node-to-surface (b) for the same mesh refinement.

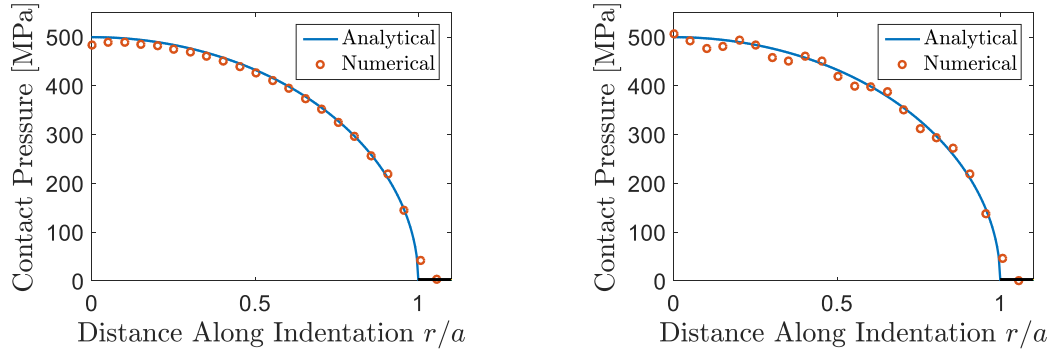


Figure 6. Contact Pressure Response from Surface-to-Surface (a) and Node-to-Surface (b) Contact Discretization Methods.

Along the numerical responses for contact pressure, the chart shows also the analytical result, as described by Hertz⁶. While the surface-to-surface method provides contact pressure values uniformly distributed along the analytical solution, the node-to-surface method provides values fluctuating up and down near the analytical values.

To have a better idea of which discretization method is more appropriate, a point to point scalar relative error is calculated comparing the exact and numerical results, which is shown in the Figure 7:

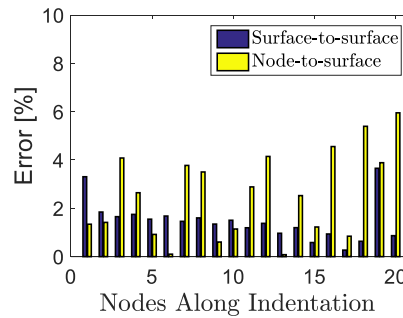


Figure 7. Contact Pressure Error for Each Node Along Indentation.

Figure 7 gives a clear understanding of the nodal pressure error distribution along indentation for the surface-to-surface and node-to-surface discretization methods. As it can be seen, the node-to-surface nodal errors oscillates from 0.08% to almost 6 % in the contact pressure prediction, while the surface-to-surface nodal errors does not oscillate as much. Thus, to decide which model is more appropriate, a second error calculation is performed measuring the Frobenius norm of the error and exact vectors, as shown in Equation 3:

$$Error = \frac{\|R_i^{FEM} - R_i^{Exact}\|_F}{\|R_i^{Exact}\|_F} \quad (2)$$

where R_i^{FEM} and R_i^{Exact} are the numerical and the analytical responses for each analysed node i . Equation 23 evaluates the numerical responses as a whole and yields a relative error of 1.69 % for the surface-to surface and 2.67 % for the node-to-surface contact discretization models. Since the computational time is not an issue for these analyses, the surface-to-surface contact discretization is the one that provides better results.

The tracking approach can be defined as finite-sliding or small sliding, being responsible for dictating the relative motion relationships between the interacting surfaces. For the case where the relative motion of the contact surfaces is small, the assumption of a contact pair defined from the undeformed body configuration is acceptable and the small-sliding tracking approach can be used. However, when facing significative relative motion, the finite-sliding is preferable since the contact pair is determined upon the relative tangential motion of the contact surfaces. Using the small-sliding tracking approach represents computational savings, but also means less accuracy. For the same model in analyses, the small sliding tracking approach yielded a pressure error of 1,58 % and 1:14 of computational time while the finite sliding tracking approach yielded 1.47 % pressure error and 1:17 of computational time.

For either cases, when using the node-to-surface discretization method or the small sliding tracking approach, it was necessary to apply a damping factor to force convergence, otherwise the simulation would fatally abort due to excessive node/element penetration. For all cases analyzed so far, the small sliding tracking approach was ignored. However, when the material being assessed is too soft and a high load is applied, convergence is more easily reached if a damping factor is considered and the node-to-surface contact discretization method is applied.

Contact Constraint Enforcement Methods. One of the issues that arises when dealing with computational contact mechanics has to do with defining a relationship that establishes a rule for surface's motion. The chosen contact constraint enforcement method establishes how contact constraints are resolved in the analysis. Two main approaches are the Penalty and the Lagrange Multiplier methods.

The penalty method in its formulation allows penetration whose amount depends on the stiffness that the penalty term grants to the system. Its kinematical constraint equation is fulfilled when the stiffness $\epsilon \rightarrow \infty$, yielding the same solution given by the Lagrange multiplier method⁷. For this reason, the Lagrange multiplier method usually add more degrees of freedom to the model and requires more iterations to achieve the solution, hence the computational costs increase.

For protection and efficiency against numerical errors related to ill-conditioning, that can occur if a high contact stiffness is in effect, the Augmented Lagrange Multiplier method is adopted, which uses the same kind of stiff approximation as the penalty method but with augmented iterations to improve the accuracy of the approximation.

Constraints Tie and coupling constraints are used in the model to define the relationships among part instances and references points. The tie constraint is used from the necessity to fuse two-part instances that belong to the same body but with dissimilar meshes, as can be seen in Figure 8 for the indenter (a) and the specimen (b):

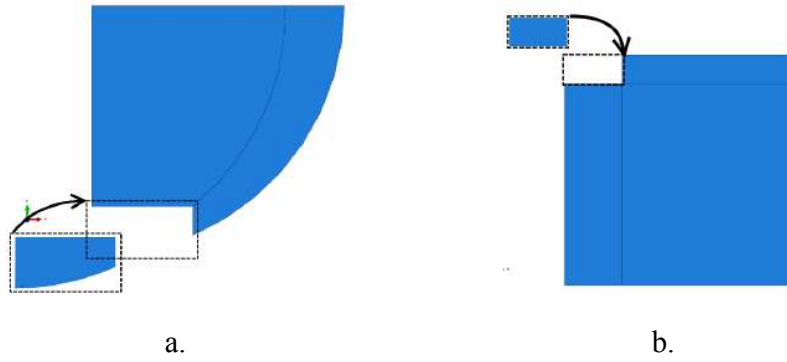


Figure 8. Tie Constraints Applied to the Indenter (a) and the Specimen (b)

There are two reference points whose motion constrains the motion of two surfaces, thus the necessity to use the coupling constraint to perform this task. The first reference point is used to transfer a concentrated force to the whole model by applying it to a reference point that has a coupling constrain relationship with the indenter's upper surface, as shown in Figure 9.a. Second, the bottom of the specimen is totally constrained with an encastre, However, for output readings purposes, this condition is applied to the reference point and a coupling constraint between this point and the specimen's bottom surface is applied, as shown in Figure 9.b.

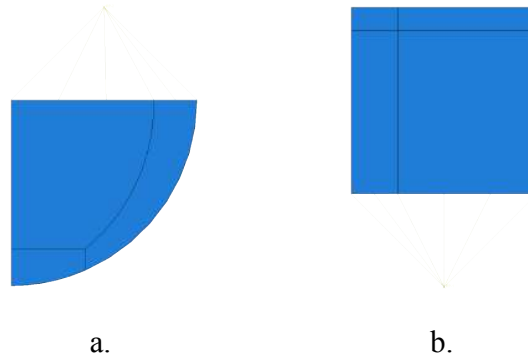


Figure 9. Coupling Constraints Applied to the Indenter (a) and to the Specimen (b).

3.6 Load Module

Load and boundary conditions are applied to the model, and since they are step-dependent objects it is necessary to specify in which steps they are active, as it has been described in the Step Module section. At the initial step, the encastre boundary condition is applied to a reference point that is coupled to the specimen's bottom surface (Figure 9.b). The axisymmetry boundary condition is applied to the specimen's and indenter's surfaces lying on the symmetry line. The indenter's initial position is defined by allowing its motion in the vertical direction only, by constraining the motion of the reference point that is coupled to the indenter's upper surface (Figure 9.a) in the horizontal direction and from rotating about the z-axis. In the subsequent step a concentrated force is applied to the reference point coupled to the indenter's upper surface so that the load is transmitted to the whole model. The last step consists in bringing the indenter back to its initial position allowing the specimen to spring back having an elastic recovery after unloading.

3.7 Mesh Module

The process of generating meshes requires a convergence study to guarantee the needs of the analysis. First, for efficiency purposes, a region of contact was defined in the indenter and in the specimen to make it possible to assign dissimilar meshes to the same body without the need of a zone of transition between them, as shown in Figure 10.

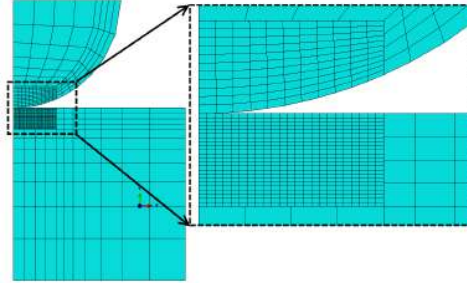


Figure 10. Meshing Assignment.

As it can be seen in Figure 10, the contact zone has a finer mesh than the other regions for efficiency purposes and the indenter's mesh is slightly coarser than the specimen's due to its greater stiffness and also to minimize the penetration of the master surface nodes in case of choosing the node-to-surface contact. The number of nodes and elements varies depending on the contact length, which in turn depends on the load applied, material definitions and if the analysis is purely elastic or elastic-plastic. In general, the contact length is estimated analytically, when dealing with elastic analysis, or experimentally, when for the elastic-plastic analysis. However, despite the length of contact, the coarser mesh is programmed in a way where the elements in the vicinity of the contact zone have five times the size of the finer mesh with a bias applied making it to increase in size until reaching an element size five times greater than the first one defined for the coarser mesh.

Using the surface-to-surface contact discretization method, a mesh converge assessment is carried out for two element types (Table 1) and five mesh refinement levels of the contact zone. The two element types are:

Table 1. Element Types Description.

Element Type	Description
CAX4R	A 4-node bilinear axisymmetric quadrilateral, reduced integration, hourglass control.
CAX4	A 4-node bilinear axisymmetric quadrilateral.

The refinement level takes into consideration the experimental contact length obtained from a Brinell Hardness test HBW 187.5/2.5 that yielded an indentation diameter of 1.03 mm. The number of nodes in the contact zone depends of two definitions: the length of the contact region and the mesh element size. For a better analysis, the length of the contact region is not defined as being of the same as the experimental one but assumes a size two times longer than the experimental indentation radius. Once the length of the contact region is defined, the number of nodes in the contact region depends only of the mesh element size. The equivalent plastic strain and the von Mises equivalent stress convergence are the assessed variables used to define the best refinement level. To capture its distribution along the contact, the mesh is initially built with an element size ten times smaller than the adopted contact length, then fifteen, twenty, twenty-five, and thirty.

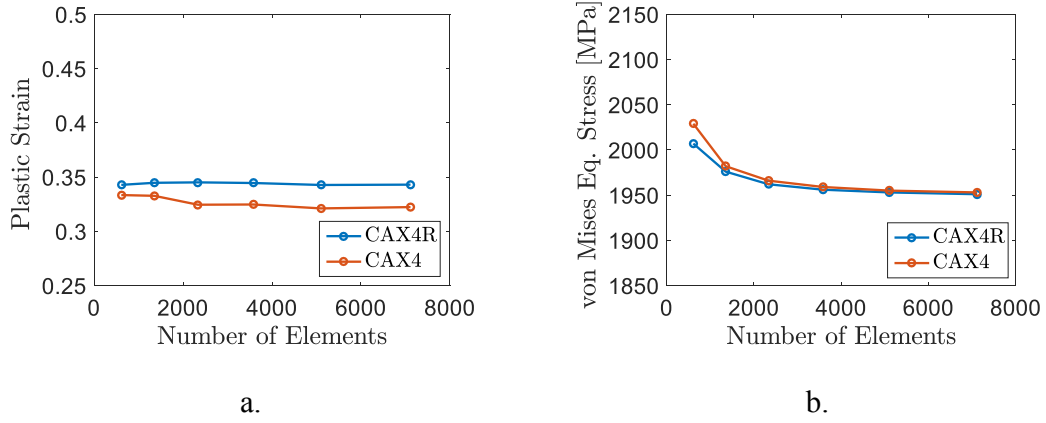


Figure 11. Mesh Convergence Analysis.

Figure 11 shows that, even though the full integration is more expensive than the reduced integration, both converge to the same amount of von Mises equivalent stress and keep approximates amount of equivalent plastic strain for different refinement levels. On the other hand, when going from reduced to full integration, the discrepancy between them is not significative enough to pay back the computational cost when using full integration. Therefore, the mesh configuration that yields the appropriate response in a suitable amount of time is composed of 2335 4-node bilinear axisymmetric quadrilateral elements with reduced integration.

4 RESULTS

The optimization procedure is a curve fitting process. New parameters are suggested until the numerical indentation impression (Figure 12.a) matches the experimental data (Figure 12.b).

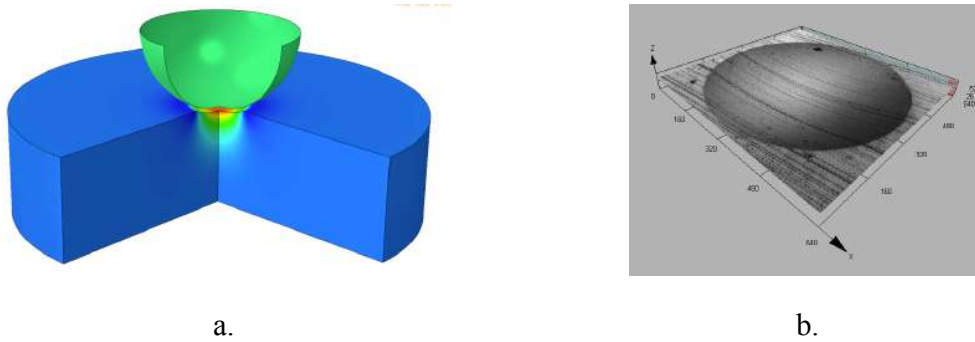


Figure 12. Simulation Configuration

The parametric identification is conducted by an optimization technique using the Trust-Region-Reflective Least Square Algorithm available in the MATLAB's Optimization Toolbox. After 27 global iterations, the objective function was satisfied, and the optimization process yielded the best fitting profile shown in Figure 13.

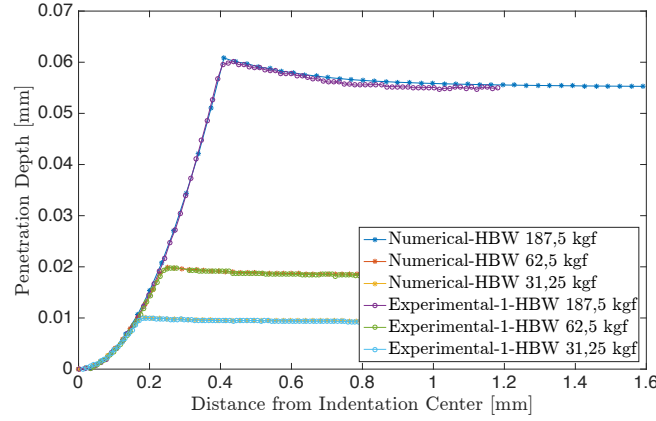


Figure 13. Profile Best Fitting.

The optimum hardening parameters that generated this best fitting are $\sigma_{y0} = 1081.3 \text{ MPa}$ for the initial the yield stress, $H = 769.9$ for the hardening modulus and $n = 0.43$ for the hardening exponent (Equation 1).

4.1 Comparative Analysis

The optimization routine generated the optimum parameters used to describe the hardening curve for the marine grade steel. The hardening curve obtained from the indentation test is presented in Figure 14 in comparison with that obtained from uniaxial test.

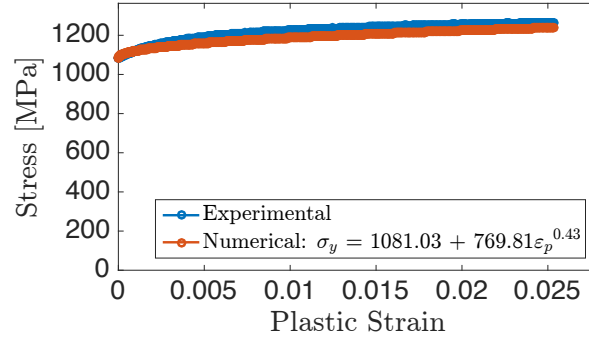


Figure 14. Comparison Between Hardening Curves Obtained by Tensile and Indentation Tests

From Figure 14, the error between numerical and experimental data is 2.5 %, calculated according to Equation (3).

$$Error = \frac{\|R_i^{FEM} - R_i^{Exact}\|_F}{\|R_i^{Exact}\|_F}, \quad (3)$$

where R_i^{FEM} and R_i^{Exact} are the numerical and the analytical responses for each analysed point i and $\|\cdot\|_F$ is the Frobenius norm.

Considering that the Brinell indentation test causes the material to plastic deform beyond the amount acquired from uniaxial test, Figure 15 shows the hardening curve used in the numerical simulation to generate the results shown in Figure 13. The Brinell hardness test in the configuration HBW 187.5/2.5 provides information for 25.2 % of plastic strain.

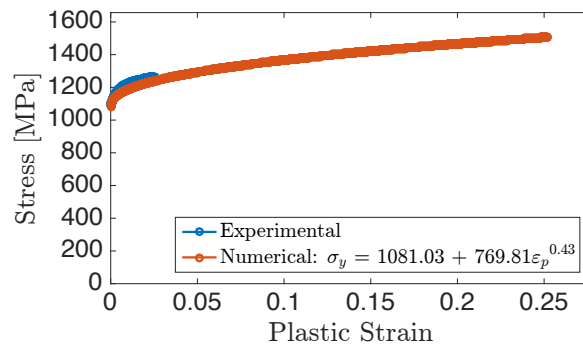


Figure 15. Hardening Curve Used for the Brinell Indentation Test Simulation Considering a Maximum Plastic Strain of 25.2 % in Comparison with the Experimental Hardening Curve Obtained from Tensile Test.

5 CONCLUSION

To determine the hardening parameters by an indentation test, a new approach was proposed considering the Brinell Hardness test to generate the experimental data set. This data set is then used to extract the mechanical properties of ductile materials through an inverse parametric identification method. Brinell hardness tests are performed and the indentation profile data, which is the indentation depth h and the impression diameter d , is extracted assisted by the *LEXT OLS4100* laser confocal microscope.

Since the goal is to provide hardening parameters that will describe the material's plastic behavior, the model was validated considering the case purely elastic whose solution is provided by Hertz⁶. The methodology consists of repeating FEM simulations of the indentation model and continuously comparing numerical and experimental data. In this way, the appropriate results are determined when the objective function reaches a minimum, yielding the parameters that leads to the best fitting.

Traditional and new approaches are compared by calculating the discrepancy in the stress-strain data yielded by the two methods. Taking the uniaxial test as a reference, the parameters resultant from the indentation multi-profile analysis present an error of 2.5 %.

REFERENCES

1. Chandler H. Introduction to Hardness Testing. *Hardness Test*. 1999;14. doi:10.1126/scisignal.2001965.
2. Oliver WC, Pharr GM. An improved technique for determining hardness and elastic modulus using load and displacement sensing indentation experiments. *J Mater Res*. 1992;7(06):1564-1583. doi:10.1557/JMR.1992.1564.
3. Dean J, Clyne TW. Extraction of plasticity parameters from a single test using a spherical indenter and FEM modelling. *Mech Mater*. 2017;105:112-122. doi:10.1016/j.mechmat.2016.11.014.
4. Kang J. Determination of elastic-plastic and visco-plastic material properties from instrumented indentation curves. 2013.
5. Guillonneau G, Kermouche G, Bec S, Loubet J-L. Determination of mechanical properties by nanoindentation independently of indentation depth measurement. *J Mater Res*. 2012;27(19):2551-2560. doi:10.1557/jmr.2012.261.
6. Johnson KL. Contact Mechanics. *J Am Chem Soc*. 1985;37(22):1-17. doi:10.1115/1.3261297.
7. Wriggers P. *Computational Contact Mechanics*.;2006. doi:10.1007/978-3-540-32609-0.

Multiscale Enrichment Method with Automatic Detection of Critical Regions for Modeling Composite Materials

Michael Macri^{*}, Andrew Littlefield^{**}

^{*}Benet Labs, ^{**}Benet Labs

ABSTRACT

This presentation reviews a methodology for solving an FEA simulation that uses the homogenization method [1] throughout the model and the multiscale enrichment method within critical regions. An algorithm has been developed that implements a partition of unity multiscale enrichment approach [2, 3] when an element exceeds a threshold criteria. The multiscale enrichment approach has been shown to capture the micro phenomena with improved accuracy compared to using the homogenization method [2, 3]. Thus, in critical regions of the model, the multiscale enrichment approach is implemented to accurately capture the material response, while the rest of the model is solved for using the more computationally efficient homogenization method. The elements surrounding the critical region are adapted to act as a transition from the multiscale region to the homogenization region. To avoid numerical errors, careful consideration was performed in the derivation of the enrichment functions for these transition or blended elements. Calculating the integrands in these elements and the material properties used is also discussed in this presentation. Within this discussion we present several examples, including the validation of the multiscale enrichment method with experimental data from testing. Additional results show that using the automatic detection algorithm can significantly reduce the computational cost. In the examples presented, the runtime of the simulation was reduced by up to 70% when compared to simulations performed using the multiscale enrichment method throughout the entire model. REFERENCES 1. Bakhvalov, N. & Panasenko, G. Homogenization: Averaging process in periodic media. Dordrecht: Kluwer Academic Publishers, 1989. 2. Fish, J. & Yuan, Z. "Multiscale enrichment based on partition of unity." International Journal for Numerical Methods in Engineering 24 (2005): 1341–1359. 3. Macri, M. & Littlefield A. "Enrichment Based Multi-scale Modeling of Composite Materials undergoing Thermo-Stress", International Journal for Numerical Methods in Engineering 93 (2013): 1147-1169.

Recent Applications in Multiobjective Optimization with Direct Search

Jose Madeira*

*IDMEC-IST and ADM-ISEL

ABSTRACT

In practical applications it is common to have to optimise problems with several conflicting objective functions in multi-objective optimization. Frequently, these functions are nondifferentiable or discontinuous, could be subject to numerical noise and, or be of black-box type, preventing the use of derivative-based techniques. An overview of some recent developments in derivative-free optimisation with direct search will be presented. The basic concepts and ideas commonly considered in multiobjective optimization will be given. Direct MultiSearch (DMS) [1] is a solver for multiobjective optimization problems, without the use of derivatives and does not aggregate any components of the objective function. It essentially generalizes all direct-search methods of directional type from single to multiobjective optimization. DMS maintains a list of feasible nondominated points. At each iteration, the new feasible evaluated points are added to this list and the dominated ones are removed. Successful iterations correspond then to an iterate list changes, meaning that a new feasible nondominated point was found. Otherwise, the iteration is declared as unsuccessful. MULTIGLODS [2] (global and local multiobjective optimization using direct search) is a well-established derivative-free optimization algorithm, based in directional direct search, which extends the concept of GLODS [3] to multiobjective optimization. In GLODS, for single-objective directional direct search, a strategy was proposed aiming at identifying several local minimizers. In MULTIGLODS we attempt to identify global and local Pareto fronts. Applications of these direct search algorithm to real problems will be presented. REFERENCES [1] A. L. Custódio, J. F. A. Madeira, A. I. F. Vaz, and L. N. Vicente. Direct multisearch for multiobjective optimization. SIAM J. Optim., 21:1109–1140, 2011. [2] A.L. Custodio, J. F. A. Madeira, MULTIGLODS: global and local multiobjective optimization using direct search. Submitted, 2017. [3] A.L. Custodio, J. F. A. Madeira, GLODS: Global and Local Optimization using Direct Search. Journal of Global Optimization, 62(1):1-28,2015.

Direct Coupling of Peridynamics with Finite Elements Without a Transition Zone

Erdogan Madenci*, Mehmet Dorduncu**, Atila Barut***, Nam Phan****

*University of Arizona, **University of Arizona, ***University of Arizona, ****Naval Air Systems Command (NAVAIR)

ABSTRACT

This study presents a variational approach to couple PeriDynamic (PD) and Finite Element (FE) analyses to take advantage of their salient features. The region of PD can be completely or partially surrounded by a region of traditional finite elements. There exists no transition region along the interface of these regions unlike the previous coupling techniques. Therefore, this approach does not require a morphing or a blending function that facilitates coupling over a transition zone. The PD region with an arbitrary geometry is interfaced with traditional local (conventional) elements while satisfying the displacement continuity through Lagrange multipliers. The resulting global system of equations includes the contributions arising from the PD points and the FE nodes. These equations are solved simultaneously without requiring an iterative procedure. Therefore, it is a direct coupling approach. This coupling approach is demonstrated by considering an isotropic plate under tensile loading. Part of the plate is modeled with PD points, and the remaining region with linear triangular elements. The PD region can share a boundary with FEM region or completely embedded in the FE region. The results from the coupled PD/FE approach agree well with those of PD and FE analyses.

Shared-Memory Parallel Implementation of High-Order Asynchronous Spacetime Discontinuous Galerkin Methods

Amit Madhukar^{*}, Robert Haber^{**}, Volodymyr Kindratenko^{***}, Reza Abedi^{****}

^{*}University of Illinois at Urbana-Champaign, ^{**}University of Illinois at Urbana-Champaign, ^{***}University of Illinois at Urbana-Champaign, ^{****}University of Tennessee Knoxville (UTK) / Space Institute (UTSI)

ABSTRACT

We present a new parallel-adaptive shared-memory implementation of high-order asynchronous spacetime discontinuous Galerkin methods for hyperbolic problems; see for example [1] for a serial implementation. We use the Tent Pitcher algorithm [2] to generate fully unstructured spacetime meshes that satisfy a causality constraint to enable locally implicit aSDG solutions. These involve local Galerkin projections on a sequence of spacetime patches (small clusters of spacetime finite elements) that inherit the stability of implicit solvers while the overall solution exhibits the linear computational complexity reminiscent of explicit methods. The duration of each patch is determined independently and is not restricted by the order of the local basis. The processes of constructing and solving patches are interleaved, asynchronous and share the same granularity, so most of the algorithm is embarrassingly parallel. Advancing a conforming space-like front mesh through the spacetime analysis domain subject to the causality constraint is the heart of the Tent Pitcher algorithm. This front mesh is the only global data structure. We copy fragments of the front mesh into private data structures called footprints that render the generation and solution of each new patch embarrassingly parallel. Gather and scatter operations between the front and footprint meshes are not embarrassingly parallel, but they represent a tiny fraction of the overall computational expense. In this presentation, we focus on the architectural details of our parallel implementation. These include coarse-grained, patch-level parallelization across multiple cores; strict separation of shared front-mesh and private patch-level data; task queues and use of hardware threads for asynchronous execution of major operations, such as footprint construction, patch generation, patch solution, and front updates; and NUMA-aware data storage. We present numerical performance results to demonstrate near perfect scaling for high-order models of varying order and the effects of various software optimizations. References: [1] R. Abedi, B. Petracovici, and R. B. Haber. "A spacetime discontinuous Galerkin method for linearized elastodynamics with element-wise momentum balance. *Comp. Methods Appl. Mech. Engrng.* 195(25-28), 3247–3273 (2006). [2] Shripad Thite. *Spacetime Meshing for Discontinuous Galerkin Methods*. Ph.D. thesis, Dept. Computer Science, Univ. Illinois Urbana-Champaign, August (2005).

A Diffuse Manifold Approach to the Exploration of Geometry of Damage in Composites

Anna Madra^{*}, Piotr Breitkopf^{**}

^{*}Massachusetts Institute of Technology, ^{**}UTC CNRS Roberval

ABSTRACT

The characterization of the geometry of damage in fiber-reinforced composites is a crucial element towards understanding failure mechanisms. Given that the geometry of damage varies from relatively simple to highly sophisticated, it is imperative to identify the main characteristics that would enable its characterization across different length scales. We propose a data-driven model of damage geometry based on 2D optical photos and 3D X-ray microtomographic scans of carbon fiber and epoxy laminates subject to different loading paths. High-dimensional snapshots of damage geometry are taken, and Singular Value Decomposition (SVD) of the centered observation matrix is performed providing basis vectors of affine feature space. Projection of the data points into the feature space allows to study the intrinsic dimensionality of the embedded low-dimensional manifold, providing consequently for a minimal parameterization of the damage geometry enabling thus to compare the efficiency of 2D and 3D characterization methods.

Explicit Computational Wave Propagation in Micro-Heterogeneous Media

Roland Maier^{*}, Daniel Peterseim^{**}

^{*}University of Augsburg, ^{**}University of Augsburg

ABSTRACT

Explicit time stepping schemes are popular for linear acoustic and elastic wave propagation due to their simple nature. However, explicit schemes are only stable if the time step size is bounded by the mesh size in space subject to the so-called CFL condition. In micro-heterogeneous media, this condition is typically prohibitively restrictive because spatial oscillations of the medium need to be resolved by the discretization in space. This talk presents a way to reduce the spatial complexity in such a setting and, hence, also enable a relaxation of the CFL condition. This is done using the Localized Orthogonal Decomposition method as a tool for numerical homogenization. References: [1] Daniel Peterseim and Mira Schedensack. Relaxing the CFL condition for the wave equation on adaptive meshes. *Journal of Scientific Computing*, 72(3):1196-1213, 2017. [2] Axel Målqvist and Daniel Peterseim. Localization of elliptic multiscale problems. *Mathematics of Computation*, 83(290):2583-2603, 2014.

On the Treatment of Body Forces in a Two-scale FE2 Scheme

Simon Maike^{*}, Jörg Schröder^{**}

^{*}Institute of Mechanics, University of Duisburg-Essen, ^{**}Institute of Mechanics, University of Duisburg-Essen

ABSTRACT

Many materials in engineering applications exhibit complex heterogeneous micro-structures. Even today, the simulation of such materials with respect to a full resolution of the microstructure is almost impossible due to tremendous computational costs. One possibility to tackle this problem is the incorporation of a homogenization procedure within a multiscale approach. Assuming a scale separation between the two appearing scales, the micro- and macroscale, and applying a FE2 scheme allows for the resolution of representative volume elements which are attached to each macroscopic point, see e.g. [1]. This method is well proven in various fields where the body forces in the balance of momentum or comparable quantities in other balance laws are neglected on the micro-scale. In contrast to that there are only a few works where these quantities are included as in [2]. Motivated by similar effects for the modeling of multiphase porous media, e.g. within the framework of the Theory of Porous Media (TPM) [3], in a multiscale approach, this contribution deals with the treatment of body forces within the FE2 method. The influence on the macro-homogeneity condition and therefore the boundary conditions on the micro-scale is investigated. The goal is to compute the stresses on the micro-scale as accurate as possible since these are crucial for the design of engineering structures, especially when irreversible material behavior is taken into account. Concluding, the results will be discussed with respect to the applicability within the TPM. References [1] J. Schröder: A numerical two-scale homogenization scheme: the FE 2-method, in J. Schröder, K. Hackl (editors) *Plasticity and Beyond*, CISM Vol. 550, Springer, 1–64, 2014. [2] E.A. de Souza Neto and P.J. Blanco and P.J. Sanchez and R.A. Feijoo, An RVE-based multiscale theory of solids with micro-scale inertia and body force effects. *MM*, 80, 136–144, 2015. [3] R. de Boer: *Theory of Porous Media*, Springer, 2000.

Integrating In Vivo Mechanics and Multi-scale Computational Models to Address Questions in Bone Cell and Tissue Mechanobiology

Russell Main^{*}, Kari Verner^{**}, Melanie Venderley^{***}, Eric Nauman^{****}

^{*}Purdue University, ^{**}Purdue University, ^{***}Purdue University, ^{****}Purdue University

ABSTRACT

The vertebrate skeleton is sensitive to externally applied mechanical stimuli and alters bone mass and shape in response to loading regimes different from those typically encountered during daily life. At the tissue level, there is evidence that new bone is formed in regions where the difference between habitual and increased applied tissue stresses and strains are greatest. However, the physical and biological mechanisms by which tissue-level stimuli are sensed and alter the biology of bone cells, such as osteoblasts and osteocytes, are still largely unknown. Through an ongoing series of complementary studies, we are using experimental biomechanics approaches to measure habitual loading environments in the limb bones of running animals. Using these in vivo characterizations, we are able to base the stimuli used in our in vivo applied loading studies relative to functional locomotor biomechanics. In order to isolate the in vivo skeletal response to load from age-, species-, or disease-related differences in systemic physiology, we have developed an ex vivo loading bone organ culture system. Here, we have characterized tissue deformation in relation to our in vivo loading model while maintaining living cells in a highly controlled environment to study interactions between chemical, physical, or thermal stimuli on bone cell and tissue mechanobiology. Ultimately, we believe that the bone cells, and very likely the matrix-embedded osteocytes, play a key role in governing the tissue response to organ-level mechanical stimuli. Therefore, assessing the mechanical environment at the cellular level becomes important for understanding how changes in tissue-level stimuli are perceived at the cell. To this end, we are developing lacunar-canalicular models of osteocytes using processed confocal microscopy images and application of mixture theory to characterize the effects of tissue-level deformation on fluid mechanics in the osteocyte peri-cellular space. Integration of these complementary approaches will ultimately allow us to base the results of both controlled in vivo and ex vivo adaptation studies relative to everyday mechanical stimuli and provide a cellular basis for the tissue-level bone adaptation.

ALTERNATIVE TO RETURN -MAPPING ALGORITHM FOR GEOMATERIALS WITH NON LINEAR INFLUENCE OF MEAN STRESS. APPLICATION TO CLAY MODELS REVISED BY THE SMP CRITERION

Siegfried Maiolino

Cerema/DTerCE/Department Laboratory of Lyon
25, avenue Mitterrand
69674 Bron cedex France
e-mail: siegfried.maiolino@cerema.fr

Keywords: Computing Methods, Elastoplasticity, Finite Element Methods, Numerical Methods, Geomechanics, Return Mapping

Abstract. *Computing plastic strain is a crucial issue in finite element methods. This problem is also known as closest point projection. The radial return used for circular models reduces the computations to literal expressions. But in geomechanics, the deviatoric shape of yield functions is generally non circular, so that return mapping algorithm becomes cumbersome and time consuming.*

Works that will be presented rather focus on a geometric based methods. It will be demonstrated that the numerical problem of closest point projection of the trial stress on the yield surface is equivalent to a geometrical bounded problem. Whereas this property is intuitive, the tools ensuring a straightforward equivalence between the two problems were to be developed.

We identify the geometric problem associated to the problem of the closest point projection in the deviatoric plane. The geometric problem is independent from the mechanical one, and can be solved with trigonometric and geometric laws. Those laws are integrated in a general algorithm to compute plastic strain, taking account of associated and non associated dilatancy for the computation of volumic plastic strains.

We adapted this method to models specific to clay : a Cam Clay model, modified to take into account the SMP

1 INTRODUCTION

The Mohr's envelope of many porous media - soils, rocks, bones, compacted powder, show their dependence to mean stress, and also differences in strength between triaxial extension and triaxial compression. Criteria like Coulomb or Hoek-Brown [3] take into account this dependence but present corners, whereas circular yield functions like Drucker-Prager don't. Experimental results using true triaxial tests prove that geomaterials present a triangular deviatoric shape with rounded corners [12]. Taking into account this particular shape in a smooth criterion involves using the third invariant. Various yield functions had been proposed, for soils [6, 10], concrete [15] or rocks [7].

The radial return [14] used for circular models reduces the computations to literal expressions [5]. The main drawback of non circular models is that return mapping algorithm becomes complex, expensive [13] and time consuming, even if the efficiency is increased with spectral decomposition techniques [1, 2]. Works that will be presented rather focus on a geometric based methods : in order to bypass the computational costs of return mapping algorithm, we will focus on simpler equivalent geometric problem.

2 POLAR DECOMPOSITION OF THE YIELD SURFACE

Traction stresses are positive, and the principal stresses ordered as follow : $\sigma_I \geq \sigma_{II} \geq \sigma_{III}$

2.1 Geometric parametrage

For a given mean stress ($\sigma_m = \text{Tr} \underline{\underline{\sigma}} / 3$), the yield surface can be reduced to its cross-sectional shape on the deviatoric plane, or π plane. A yield surface ($f(\underline{\underline{\sigma}}) = 0$) can be represented in a unique manner by the mean stress and the deviatoric invariants ($J_2 = \frac{1}{2} \text{Tr}(\underline{\underline{s}}^2)$, $J_3 = \frac{1}{3} \text{Tr}(\underline{\underline{s}}^3)$, with $\underline{\underline{s}} = \underline{\underline{\sigma}} - \sigma_m \underline{\underline{1}}$), but it is more practical to replace the third invariant by the Lode angle θ , to work in the π plane (deviatoric plane).

$$-\frac{\pi}{6} \leq \theta = \frac{1}{3} \arcsin \left(\frac{-3\sqrt{3}}{2} \frac{J_3}{\sqrt{J_2^3}} \right) \leq \frac{\pi}{6} \quad (1)$$

The set $(\sqrt{J_2}, \theta)$ define polar coordinates on one sixth of the deviatoric plane, which is sufficient for an isotropic criterion. Zienkiewicz and Pande [16], using the fact that a yield surface can be reduced to its polar expression, provided tools to study the regularity, the sensitivity to the extension and the convexity of a criterion starting from the shape function $g_p(\theta)$

$$\sqrt{J_2} = \sigma^+ g_p(\theta) \quad (2)$$

The deviatoric radius : $\sigma^+(\sigma_m) = \sqrt{J_2}_{\theta=\frac{\pi}{6}}$, gives the yield function in the meridional plane $(\sigma_m, \sqrt{J_2})$, for $\theta = \frac{\pi}{6}$. This value of the Lode angle corresponds to a classical triaxial test, or compression triaxial test ($\sigma_I = \sigma_{II} > \sigma_{III}$). The function $g_p(\theta)$ is the shape function of the yield surface in the deviatoric plane. It is normalized ($g_p(\frac{\pi}{6}) = 1$) and gives directly the value of the extension ratio $g_p(-\frac{\pi}{6}) = L_S$ which is more detailed in the following section.

2.2 Characteristic function of a material

The deviatoric radius σ^+ can be easily deduced from triaxial compression tests. Whether the shape is straight or parabolic, the deviatoric radius used can be the Coulomb or Hoek-Brown.

The extension ratio L_S has a physical meaning and can be determined from experiment. The condition $\theta = -\frac{\pi}{6}$ corresponds to extension triaxial tests ($\sigma_I > \sigma_{II} = \sigma_{III}$), which can be performed with the same triaxial cell as compression triaxial test.

$$L_S = \frac{\sqrt{J_2}(\theta = -\frac{\pi}{6})}{\sqrt{J_2}(\theta = \frac{\pi}{6})} = \frac{(\sigma_I - \sigma_{III})(extension)}{(\sigma_I - \sigma_{III})(compression)} \quad (3)$$

Physically, this means that for the same mean stress, the yield value of $\sqrt{J_2}$ would be lower in extension than in compression. The value of L_S is directly linked to the deviatoric shape of a yield surface. While this value can be independent from the mean stress (Coulomb), some rocks present a shape of their yield surface changing from triangular (low confinement) to circular (high confinement) [4], i.e, L_S increases from 0.5 to 1.

2.3 Introduction of the orthoradial tensor

We consider for stresses and strains (i.e. symetric second order tensors) the following scalar product. For two tensors, $\underline{\underline{T}}_1$ and $\underline{\underline{T}}_2$:

$$\underline{\underline{T}}_1 \cdot \underline{\underline{T}}_2 = \underline{\underline{T}}_1 : \underline{\underline{T}}_2 = \text{Tr} \underline{\underline{T}}_1 \underline{\underline{T}}_2 \quad (4)$$

Hence defining the following norm (Frobenius norm) for a symetric second order tensor $\underline{\underline{T}}$:

$$\| \underline{\underline{T}} \| = \sqrt{\underline{\underline{T}} : \underline{\underline{T}}} \quad (5)$$

We introduce the orthoradial tensor, $\underline{\underline{v}}$:

$$\underline{\underline{v}} = 3 \frac{\sqrt{3}}{2} \frac{1}{J_2} s^2 - \sqrt{3} \underline{\underline{1}} - \frac{9\sqrt{3}J_3}{4J_2^2} s \quad (6)$$

This tensor is orthoradial as $\underline{\underline{v}} \cdot \underline{\underline{1}} = \underline{\underline{v}} \cdot \underline{\underline{s}} = 0$, hence those three tensors, $\underline{\underline{1}}$, $\underline{\underline{s}}$, $\underline{\underline{v}}$ constitute an orthogonal basis of the space of symetric second order tensors, for the Frobenius scalar product.

We can then easily decompose the derivatives of the yield function along this orthogonal basis, as the expression of the gradient of invariants can easily be expressed. It is necessary to introduce the orthogonal tensor, as the gradient of the third invariant cannot be expressed using only the hydrostatic tensor or the deviatoric tensor. Expressions of the three gradients of invariants are the following :

$$\frac{\partial I_1}{\partial \underline{\underline{\sigma}}} = \underline{\underline{1}} \quad (7)$$

$$\frac{\partial J_2}{\partial \underline{\underline{\sigma}}} = \underline{\underline{s}} \quad (8)$$

$$\frac{\partial J_3}{\partial \underline{\underline{\sigma}}} = s^2 - \frac{2J_2}{3} \underline{\underline{1}} = \frac{3J_3}{2J_2} s + \frac{2J_2}{3\sqrt{3}} \underline{\underline{v}} \quad (9)$$

Hence the gradient of any yield surface can be orthogonally decomposed.

$$\frac{\partial f}{\partial \underline{\underline{\sigma}}} = f_u \underline{\underline{1}} + f_s \underline{\underline{s}} + f_v \underline{\underline{v}} \quad (10)$$

We can observe that the deviatoric part of the gradient, $\text{dev} \frac{\partial f}{\partial \underline{\underline{\sigma}}}$ can be split in two orthogonal component, a radial $f_s \underline{\underline{s}}$, and a orthoradial, $f_v \underline{\underline{v}}$. This later part is null for criteria independent from the third invariant.

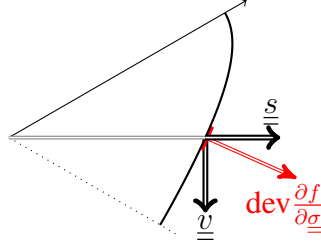


Figure 1: Orthogonal decomposition of the deviatoric part of the gradient

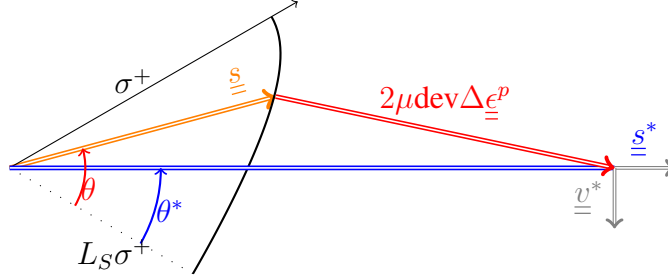


Figure 2: Physical problem in the deviatoric plane

2.4 Consequences for return mapping algorithm

Let us consider at an integration point, the increment from step n to $n + 1$. We want to calculate the plastic strain, if the trial stress $\underline{\underline{\sigma}}^*$ doesn't satisfy the yield condition. We want to implicitly solve the relation that gives the stress.

$$\underline{\underline{\sigma}}_{n+1} = \underline{\underline{\sigma}} = \underline{\underline{\sigma}}^* - \underline{\underline{L}} \Delta \underline{\underline{\epsilon}}^p \quad (11)$$

Where $\underline{\underline{L}}$ is the elasticity tensor. We can split this relation between two orthogonal components: an hydrostatic and a deviatoric.

$$\sigma_m - \sigma_m^* = -K \text{Tr} \Delta \underline{\underline{\epsilon}}^p \quad (12)$$

$$\underline{\underline{s}} - \underline{\underline{s}}^* = -2\mu \text{dev} \Delta \underline{\underline{\epsilon}}^p \quad (13)$$

Where K is the bulk modulus and μ the shear modulus.

We can notice that the hydrostatic part (12) is purely scalar and that the main difficulties come from the deviatoric part(13).

3 GEOMETRIC EQUIVALENCE OF CLOSEST POINT PROJECTION

We introduce the following quantity [8, 9]:

$$\rho = \frac{\sqrt{J_2^*}}{\sigma^+(\sigma_m^* + \Delta \sigma_m)} \quad (14)$$

The closest point projection of $\underline{\underline{s}}^*$ on the trace of yield surface (Figure 2) is equivalent to the following geometric problem(Figure 3): find the closest point projection (polar coordinates:

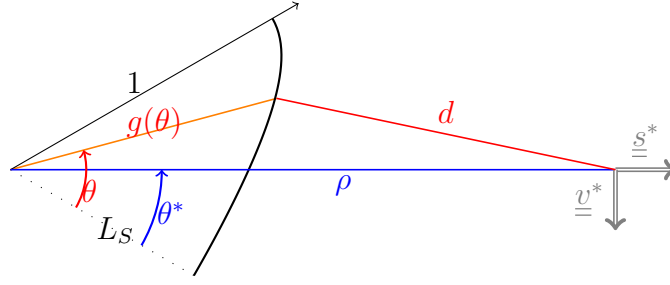
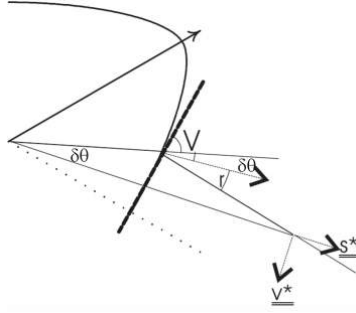


Figure 3: Geometric problem in polar coordinates

Figure 4: Angular relations: $V + r + \delta\theta = \frac{\pi}{2}$, $(\delta\theta = \theta - \theta^*)$

$(\theta, g_p(\theta))$ of the point (ρ, θ^*) on the curve defined by the shape function $g_p(\theta)$. The function $d(\theta)$ reaches its minimum at this point.

$$d(\theta)^2 = g_p^2(\theta) + \rho^2 - 2g_p(\theta)\rho\cos(\theta - \theta^*) \quad (15)$$

Expression of the norm of the deviatoric plastic strain is straightforward:

$$\|\text{dev}\Delta\epsilon^p\| = \frac{d(\theta)\sigma^+}{\sqrt{2}\mu} \quad (16)$$

Now, $\text{dev}\Delta\epsilon^p$ can be expressed in the local base associated to the trial stress

$$\text{dev}\Delta\epsilon^p = \|\text{dev}\Delta\epsilon^p\| \left(\frac{\cos r}{\sqrt{2}\sqrt{J_2^*}} \underline{s}^* + \frac{\sin r}{\|\underline{v}^*\|} \underline{v}^* \right) \quad (17)$$

The value of the r angle can be deduced from trigonometric considerations (figure 4), V being the angle between the tangent to a polar curve and the radial axis :

$$\tan V = \frac{g}{g'} \quad (18)$$

4 COMPUTATION OF DEVIATORIC AND HYDROSTATIC PLASTIC STRAIN

4.1 General algorithm

The geometric equivalence allows to get the plastic strain if $\Delta\sigma_m$ is known. This quantity is calculated using an iterative method. Initially, $\Delta\sigma_m^0 = 0$, and the stopping condition c is satisfied when the ratio between hydrostatic and deviatoric parts is equal to the dilatancy angle δ .

$$c(\Delta\sigma_m, \|\text{dev}\Delta\epsilon^p\|, \tan \delta) = \|\text{dev}\Delta\epsilon^p\| \sqrt{3}K \tan \delta + \Delta\sigma_m < \varepsilon \quad (19)$$

We use the following definition of the dilatancy angle :

$$\tan \delta = \frac{g_u \sqrt{3}}{\sqrt{g_s^2 \|\underline{s}\|^2 + g_v^2 \|\underline{v}\|^2}} \quad (20)$$

With g_u , g_s and g_v are the components of the normal to the plastic potential :

$$\frac{\partial g}{\partial \underline{\sigma}} = g_u \underline{1} + g_s \underline{s} + g_v \underline{v} \quad (21)$$

The dilatancy angle can be deduced from the expression of the yield function (associated potential) or from a non associated potential. Whereas it is not easy to identify the potential, without extensive true triaxial tests, the dilatancy angle can be easily identified using classical triaxial compression tests.

If $\delta > 0$ material is said to be dilatant. The alternative return mapping algorithm can be expressed as follow, at a given integration point, for a dilatant material

1. Compute $\underline{\sigma}^* = \underline{\sigma}^0 + \underline{L} \left(\underline{\epsilon}_{n+1} - \underline{\epsilon}_n^p \right)$
2. Check $f(\underline{\sigma}^*) > 0$? No set $\underline{\sigma}_{n+1} = \underline{\sigma}^*$ and exit.
3. Yes : set $i = 0$ and $\Delta \sigma_m^0 = 0$
4. Set $\rho^i = \frac{\sqrt{J_2^*}}{\sigma^+(\sigma_m^* + \Delta \sigma_m^i)}$ and if L_S depends of mean stress : $L_S^i = L_S(\sigma_m^* + \Delta \sigma_m^i)$
5. Compute θ^i , $d(\theta^i)$, $\sqrt{J_2^i}$ and $\|\text{dev} \Delta \underline{\epsilon}^p\|^i$
6. Evaluate $\tan \delta^i = \tan \delta(\sigma_m^* + \Delta \sigma_m^i, J_2^i, J_3^i)$
7. Evaluate stopping criterion $|c(\sigma_m^* + \Delta \sigma_m^i, \|\text{dev} \Delta \underline{\epsilon}^p\|^i, \tan \delta^i)| < \epsilon$. If Yes compute angle r and tensor $\Delta \underline{\epsilon}^p$. Update $\underline{\sigma}_{n+1} = \underline{\sigma}^* - \underline{L} \Delta \underline{\epsilon}^p$ and exit.
8. If No, set $i = i + 1$ and $\Delta \sigma_m^i = \Delta \sigma_m^{i-1} + \Delta^2 \sigma_m$, then loop to step 4.

The evaluation of $\Delta^2 \sigma_m$ depends of the nature of yield function f and δ

4.2 Evaluation of mean stress increment

One natural way to compute $\Delta^2 \sigma_m$ is to apply a Newton-Rhapson like iterative function to (19), but it can be not so straightforward and be costly, even for circular criteria, as the Cam Clay model, because of the presence derivative of the deviatoric radius. So

$$\Delta^2 \sigma_m = -c(\Delta \sigma_m^{i-1}) \frac{\Delta \sigma_m^{i-1} - \Delta \sigma_m^{i-2}}{c(\Delta \sigma_m^{i-1}) - c(\Delta \sigma_m^{i-2})} \quad (22)$$

Where c can be directly expressed :

$$c(\Delta \sigma_m) = \sqrt{\frac{2}{3}} \frac{K}{\mu} \tan \delta(\sigma_m^* + \Delta \sigma_m) \left(\sqrt{J_2^*} - g_p(\theta(\Delta \sigma_m)) \sigma^+(\sigma_m^* + \Delta \sigma_m) \right) + \Delta \sigma_m \quad (23)$$

With the following expression for the first increment :

$$\Delta \sigma_m^1 = -\sqrt{\frac{2}{3}} \frac{K}{\mu} \left(\sqrt{J_2^*} - g_p(\theta^0) \sigma^+(\sigma_m^*) \right) \tan \delta(\sigma_m^*) \quad (24)$$

5 Cam Clay model revised by the SMP criterion

Cam Clay models and modified Cam Clay models don't take into account the influence of the third invariant. This influence can be taken into account through a transformation of the stress tensor [11], so that the deviatoric shape is the one of Matsuoka-Nakai.

Another solution is to use the Maiolino general yield function [7] :

$$f(\underline{\sigma}) = \frac{3}{2}\sqrt{3}(1 - L_S)J_3 + (L_S^2 + 1 - L_S)\sigma^+J_2 - \sigma^{+3}L_S^2 \quad (25)$$

When fitted with Coulomb deviatoric radius and extension ratio, this criterion is equal to standard Matsuoka-Nakai.

We can also use the deviatoric radius of Cam Clay (with $p = -\sigma_m$ and $q = \sqrt{3}\sqrt{J_2}$), so that :

$$\sigma^+ = -\sigma_m M \sqrt{\frac{1}{\sqrt{3}} \left(1 + \frac{p_0}{\sigma_m}\right)} \quad (26)$$

To integrate the SMP, we have to determinate the extension ratio. We can adopt the following value :

$$L_S = \frac{3 - \sin \phi_i}{3 + \sin \phi_i} \quad (27)$$

With ϕ_i an instantaneous friction angle :

$$\sin \phi_i = \frac{3 \frac{\partial \sigma^+}{\partial \sigma_m}}{\frac{\partial \sigma^+}{\partial \sigma_m} + 2\sqrt{3}} \quad (28)$$

6 CONCLUSIONS

We have shown that for J_3 dependant yield function, the problem of closest point projection is equivalent to a pure geometric problem in polar coordinates. For different values of (ρ, θ^*) , solutions can be computed and values of $d(\theta) \sin 3\theta$ and $g_p(\theta)$ are saved, allowing to shortcut computational costs of return mapping in the deviatoric plane. For the hydrostatic part, we propose a general algorithm that allows to take account of the dilatancy in the computation of plastic strain.

This general algorithm can be applied to Cam Clay models revised by the SMP criterion. Further work will be done to take into account non associate deviatoric plastic flow, and adapt the framework to pressure dependent elasticity.

7 Acknowledgment

The work presented and this communication are part of the project Anticipation and mitigation of slow landslides in the Alps (MLA3) that benefits of the support of the European Union and Provence-Alpes-Côte d'Azur (PACA) Region through the European Regional Development Fund (ERDF) interregional operational program "Massif des Alpes" (POIA).

References

- [1] R. Borja, K. Sama, and P. Sanz. On the numerical integration of three invariant elasto-plastic constitutive models. *Comput. Methods Appl. Mech. Engrg*, 192(9-10):1227–1258, 2003.

- [2] C. Foster, R. Regueiro, A. Fossum, and R. Borja. Implicit numerical integration of a three-invariant, isotropic/kinematic hardening cap plasticity model for geomaterials. *Comput. Methods Appl. Mech. Engrg.*, 194(50-52):5109–5138, 2005.
- [3] E. Hoek and E. Brown. Empirical strength criterion for rock masses. *J. Geotech. Engng DIV., ASCE*, 106(GT9):1013–1035, 1980.
- [4] M. Kim and P. Lade. Modelling rock strength in three dimensions. *Int. Journ. Rock Mech. Min. Sci. Abstracts*, 21(1):21–33, 1984.
- [5] R. D. Krieg and S. M. Key. Implementation of a Time Dependant Plasticity Theory into Structural Computer Programs. *Constitutive Equations in Viscoplasticity : Computational and Engineering Aspects*, 20:125–137, 1976.
- [6] P. V. Lade. Elasto-plastic stress-strain theory for cohesionless soil with curved yield surfaces. *Int. Journ. Solids Structures*, 13:1019–1035, 1977.
- [7] S. Maïolino. Proposition of a general yield function in geomechanics. *Comptes Rendus Mécanique*, 333:279–284, 2005.
- [8] S. Maïolino. *Fonction de charge générale en géomécanique : application aux travaux souterrains*. PhD thesis, École Polytechnique, 2006. General yield function in geomechanics : application to tunneling (in French).
- [9] S. Maïolino. Numerical abacuses method based on the equivalence between the closest point projection and a bounded geometric problem. In *8th. World Congress on Computational Mechanics (WCCM8) , 5th European Congress on Computational Methods in Applied Sciences and Engineering (ECCOMAS 2008)*, Venice, July 2008.
- [10] H. Matsuoka and T. Nakai. Stress-deformation and strength characteristics of soil under three different principal stresses. In *Proc. JSCE*, volume 232, pages 59–70, 1974.
- [11] H. Matsuoka, Y. Yao, and D. Sun. The cam–clay models revised by the smp criterion. *SOILS AND FOUNDATIONS*, 39(1):81–95, 1999. doi: 10.3208/sandf.39.81.
- [12] P. Michelis. True triaxial yielding and hardening of rock. *J. Geotech. Engng DIV., ASCE*, 113(6):616–635, 1987.
- [13] J. Simo and T. Hughes. *Computational Inelasticity*. 1998.
- [14] J. L. Wilkins. Calculation of Elastic-plastic Flow. *Methods of Computational Physics*, 8, 1964.
- [15] K. William and E. Warnke. Constitutive models for the triaxial behavior of concrete. In *International Association of Bridge and Structural Engineering (IABSE) Seminar on "Concrete Structures Subjected to Triaxial Stresses"*, Bergamo, volume 19, pages 1–30, 1975.
- [16] O. C. Zienkiewicz and G. N. Pande. Some useful forms of isotropic yield surfaces for soil and rock mechanics. In *Numerical methods in soil and rock mechanics*, Karlsruhe, pages 3–16, september 1975.

Numerical Study on Nonlinear Electrophoresis of a Charged Dielectric Droplet

Partha Sarathi Majee*, Somanth Bhattacharyya**

*Indian Institute of Technology Kharagpur, **Indian Institute of Technology Kharagpur

ABSTRACT

The study of electrophoresis of a charged spherical droplet is important for its wide applications in atmospheric physics, inkjet printers, pharmaceutical, lab-on-a-chip, and electrospray applications. The dielectric polarization of the droplet under an external electric field creates a nonlinear dependence of the electrophoretic velocity on the applied electric field. The surface of the droplet is not stationary and a lower droplet viscosity increases the fluid convection in the Debye layer, which in turn enhances the double layer polarization and surface conduction. The polarization effect of double layer due to fluid convection is analyzed extensively in the present work. The electrophoresis of a charged spherical droplet of an immiscible dielectric liquid in an electrolyte in response to an applied electric field is studied. Fluid inside and outside the droplet is governed by the Navier-Stokes equations, ion transport in electrolyte is described by Nernst-Planck equation, the electric potential within and outside the droplet is governed by the Laplace and Poisson equations, respectively. Governing equations along with proper boundary conditions are solved numerically through a control volume approach over a staggered grid arrangement. Discretized equations are solved through the pressure correction based iterative SIMPLE (Semi-Implicit Method for Pressure-Linked Equations) algorithm. Electrophoretic velocity of the droplet is determined by balancing the electric and drag forces experienced by the droplet. The present numerical model successfully accounts the double layer polarization and relaxation effects. Solutions are obtained without invoking weak field condition or thin Debye layer assumption unlike the analytic solutions of Ohshima et al.(1984) or thin layer analysis of Schnitzer et al.(2013). The electrophoretic velocity is presented to analyze its dependency on droplet-to-electrolyte viscosity ratio, Debye length, droplet-to-electrolyte permittivity ratio. Electrophoretic velocity diminishes with the increase of droplet-to-electrolyte viscosity ratio and it also decreases with the rise of droplet-to-electrolyte permittivity ratio. The present solutions over-estimate the results of Ohshima et al.(1984) for thinner Debye layer. At a fixed surface potential the mobility shows a non-linear variation with the droplet size. The enhancement rate of mobility with the decrease of droplet-to-electrolyte viscosity ratio is higher for a thinner Debye length compares to a thick one. Surface conduction effect slows down the increment rate of mobility with droplet charge at thinner Debye layer. References [1] H. Ohshima, T. W. Healy, and L. R. White, J. Chem. Soc. Faraday Trans. 80(12), 1643–1667 (1984). [2] O. Schnitzer, I. Frankel, and E. Yariv, J. Fluid Mech. 722, 394–423 (2013).

Field-Controlled Soft-Matter Electronics with Ferromagnetic Elastomers and Liquid Metal

Carmel Majidi*

*Carnegie Mellon University

ABSTRACT

There has been extraordinary progress in recent decades in the development of electronics that are mechanically soft and stretchable. These range from conductive elastomer composites and fabrics to circuits with wavy metal electrodes or liquid metal (LM) traces. Most of this work has focused on wiring and electrical interconnects, although there has also been progress in soft electronics that have active properties for electrical switches, diodes, and tunable radio transmission. The ultimate goal is to produce “field-controlled” soft electronics that, like conventional semiconductor-based field effect transistors (FETs) or electromagnetic relays, change their state in response to an applied electrical or magnetic field. Such elements would help broaden the electronic functionality of soft materials within emerging applications like wearable computing, soft robotics, inflatable structures, and shape-programmable matter. In this talk, I will present recent efforts by my research group (CMU Soft Machines Lab) to introduce field-controlled soft electronics using soft elastomers (silicone rubber), ferromagnetic microparticles (Fe, Ag-coated Ni), and Ga-based LM alloy (eutectic gallium indium; EGaIn). I will primarily focus on elastomers embedded with LM droplets[1] or LM-coated ferromagnetic microparticles[2]. These composites can be engineered to exhibit a broad range of electrical and thermal properties, from electrical conductors that maintain fixed electrical conductivity when stretched or damaged (e.g. tearing, puncture) to high-k dielectric insulators with metal-like thermal conductivity. They can also be integrated into an electrical switches that reversibly open and close in response to an electrical or magnetic field. In addition to experimental implementations, I will present analytic models that combine theories of elasticity and Maxwell’s equations to predict electromagnetic responses that are in strong agreement with measurements. I will close the talk by discussing potential applications of LM-elastomer and LM-ferroelastomer composites to the emerging field of soft robotics. If time permits, I will also present recent efforts with an electrochemical LM switch that responds to low voltage activation.[3] This switch exhibits some features of a traditional FET – e.g. source/drain/gate layout, ~1V response, high on/off switching ratio – and can be extended to other active functionalities. References: [1] M. D. Bartlett, N. Kazem, M. J. Powell-Palm, X. Huang, W. Sun, J. A. Malen, and C. Majidi, “High thermal conductivity in soft elastomers with elongated liquid metal inclusions,” *Proceedings of the National Academy of Sciences* 114 2143–2148 (2017). [2] V. Ramachandran, M. D. Bartlett, J. Wissman, C. Majidi, “Elastic instabilities of a ferroelastomer beam for soft reconfigurable electronics,” *Extreme Mechanics Letters* 9 282-290 (2016). [3] J. Wissman, M. D. Dickey, C. Majidi, “Field-Controlled Electrical Switch with Liquid Metal,” *Advanced Science* 4 1700169 (2017).

Towards the Tensegrity Beam Structural Element

Manoranjan Majji^{*}, Edwin Peraza Hernandez^{**}, Robert Skelton^{***}

^{*}Dept. of Aerospace Engineering, Texas A&M; University, ^{**}Dept. of Aerospace Engineering, Texas A&M; University, ^{***}Dept. of Aerospace Engineering, Texas A&M; University

ABSTRACT

A novel paradigm that is the basis for an innovating multibody dynamics approach to model flexible structures is presented in this work. We particularly focus on modeling flexible beams. As opposed to the traditional approximations based on the superposition principle, the new approach decomposes the continuum into discrete tensegrity structures (denoted as tensegrity elements). A matrix approach for modeling tensegrity systems is employed to model the individual elements and the Newton-Euler and Lagrangian approaches for multibody dynamics are used to assemble the individual tensegrity elements to realize the beam structure. The goal of this multibody tensegrity discretization process is to match the dynamic characteristics of the flexible structure. To this end, we perform topology optimization studies pertaining to the natural frequency and mode shape matching as a function of the number and topology of the tensegrity elements involved in the discretization process. To baseline our proposed approach, we use finite element approximations using cubic spline elements and the assumed modes methods employing eigenfunctions for Euler-Bernoulli beams subjected to a variety of loading and boundary conditions. Since nonlinear tensegrity elements are used to furnish constituent approximations, new tools are developed to solve the resulting nonlinear eigenvalue problems for the mode shapes of the structure and the calculation of the natural frequencies. Theoretic concepts of dynamic response of the nonlinear structure will be employed to identify natural frequencies.

Modeling of Work Hardening and Strain-rate Sensitivity of Precipitation Strengthened Ultrafine-grained and Nanostructured Materials

Janusz Majta*, Remigiusz Bloniarz**, Krzysztof Muszka***

*AGH University of Science and Technology, Krakow, Poland, **AGH University of Science and Technology, Krakow, Poland, ***AGH University of Science and Technology, Krakow, Poland

ABSTRACT

This study aims at understanding the work hardening ability of precipitation strengthened ultrafine-grained (UFG) and nanostructured (NS) materials at different strain rates. The investigations were performed for two materials: high strength Nb microalloyed ferrite (b.c.c.) and austenite (f.c.c.). A range of different grain sizes was developed using multiaxial compression tests (MaxStrain). As a result different nanostructures were observed in the investigated alloys characterized by different grain size and dislocation density. From a microscopic viewpoint, plastic deformation and work-hardening of a crystal are caused by dislocation motions and dislocation accumulations. In order to model mechanical behavior of UFG and NS precipitation strengthened materials, there is a need, first of all, to understand the deformation and strengthening mechanisms governing the plastic deformation of such material. To capture these phenomena in a sufficient way, multiscale modelling approach was applied in the present study, since the conventional material models are not amendable to bridge the gap arising from different scales at which those phenomena are taking place. Multiscale modeling was based on the combination of discrete techniques such as continuous finite element (FE) models as well as on the combination of traditional differential equations describing material behavior in the micro scale with FE models. Stochastic processes, such as new grains nucleation on the grain boundaries, development of the shear bands and its influence on the nucleation process, as well as influence of defects or inclusions on nucleation process, have been taken into account. Analysis was performed in the nano- and micro- scale with respect to the dislocation structures evolution during processing. The data needed for a successful and complete interpretation of all mechanical tests, performed to define the correlation between microstructure and mechanical properties was possible due to the results of the transmission electron microscopy (TEM) and scanning electron microscopy (SEM) with EBSD analysis. The Taylor test and Split Hopkinson Pressure Bar (SHPB) tests were applied in the analysis of the mechanical response of the UFG and NS materials under dynamic loading conditions. Based on the study of the precipitation and substructure strengthening a modification of the Khan-Huang-Liang flow stress model was proposed, so it relates the strain hardening with strain, strain rate and precipitates as well as dislocation cell sizes. Our approach was tailored to the unique aspects of UFG and NS microalloyed steels, with the thrust being and understanding of the key physical mechanisms that govern plastic deformation behavior under dynamic loading.

Strain Hardening and Crack Growth in '2.5D' Discrete Dislocation Dynamics

Eleanor Mak^{*}, William Curtin^{**}

^{*}École Polytechnique Fédérale de Lausanne, ^{**}École Polytechnique Fédérale de Lausanne

ABSTRACT

Discrete dislocation dynamics (DD) methods have been widely used to investigate plasticity-related phenomena at the sub-continuum scale. Although 3D models can capture the realistic generation, motion, and interaction of dislocation loops, they are often prohibitively expensive in computational cost for the non-homogeneous loading, complex boundaries, and explicit interfaces in crack growth problems. Thus, 2D models are commonly used as a computationally tractable framework to provide insight to plastic flow and fracture. Strain hardening from forest dislocations, which emerges due to the entanglement of loops on intersecting slip planes, is inherently a 3D effect which cannot be captured by conventional 2D models. A new '2.5D' DD framework addresses this major shortcoming by projecting 3D effects onto a 2D problem [1]. The '2.5D' parameters are physically motivated and are obtained from 3D DD, and hardening behavior then emerges naturally. Here, a cohesive zone (CZ) model with realistic cohesive parameters is combined with the '2.5D' DD framework using the O'Day and Curtin [2] superposition method. Crack growth, near-crack dislocation structuring and hardening, and Mode I fracture toughness are then studied as a function of material yield strength, strain hardening, and internal material length scales. [1] Keralavarma, S. M., & Curtin, W. A. (2016). Strain hardening in 2D discrete dislocation dynamics simulations: A new '2.5 D' algorithm. *Journal of the Mechanics and Physics of Solids*, 95, 132-146. [2] O'Day, M. P., & Curtin, W. A. (2004). A superposition framework for discrete dislocation plasticity. *Transactions of the ASME-E-Journal of Applied Mechanics*, 71(6), 805-815.

Effect of the Stress Triaxiality on the Mechanical Behavior of Ductile Materials

Lucival Malcher^{*}, LEONEL LEONARDO DELGADO MORALES^{**}, André Trajano^{***}

^{*}Group of Fatigue, Fracture and Materials - GFFM University of Brasília, ^{**}Group of Fatigue, Fracture and Materials - GFFM University of Brasília, ^{***}Group of Fatigue, Fracture and Materials - GFFM University of Brasília

ABSTRACT

The correct determination of the mechanical behavior of materials is one of the main challenges faced by researchers and an important step for the design of mechanical components. Stress triaxiality is one of the elastoplastic parameters with the greatest influence on the behavior of ductile materials and is determined as a function of the ratio between the hydrostatic stress and the equivalent stress. In this context, this contribution contemplates the study of this parameter on the mechanical behavior of the SAE 4340 alloy, annealed and normalized. In order to achieve the desired objective, experimental tests are carried out for smooth and notched cylindrical specimens, as well as, specimens subjected to pure shear. Furthermore, it is also proposed the implementation of Gao's elastoplastic model, with nonlinear isotropic hardening, in an academic finite element framework, through an implicit integration strategy. The experimental and numerical reaction curves for the specimens are analyzed and fracture curve, showing the influence of the stress triaxiality on the behavior of the material. At the end, it is proposed a correction in the reaction curve, assuming the calibration of the Gao's model, and an equation that characterizes the fracture curve for the material 4340 alloy, regarding wide range of stress triaxiality.

A Hybridized Discontinuous Galerkin Framework for High-Order Conservative Particle-Mesh Methods

Jakob Maljaars^{*}, Robert Jan Labeur^{**}, Nathaniel Trask^{***}, Deborah Sulsky^{****}, Matthias Möller^{*****}

^{*}Delft University of Technology, ^{**}Delft University of Technology, ^{***}Sandia National Laboratories, ^{****}The University of New Mexico, ^{*****}Delft University of Technology

ABSTRACT

Despite successful applications, since its introduction in the late 1950s [1], the particle-in-cell (PIC) method still faces some unresolved issues. In particular, PIC-methods have difficulty unifying accuracy and exact, local conservation. More specific to incompressible flows, maintaining local volume conservation remains a daunting task for PIC-based methods. These are not exclusively issues with PIC, but of particle methods in general (eg. [2]). Whereas various grid-based methods, hybridized Discontinuous Galerkin (HDG) (eg. [3]) among them, can achieve high accuracy with exact conservation, there are still difficulties associated with discretization of nonlinear advection terms and choices of numerical fluxes. This contribution presents a novel particle-mesh operator-splitting framework, utilizing particles and HDG, to resolve these challenges. More precisely, the particle-mesh interactions are interpreted in terms of a PDE-constrained minimization problem in order to reconcile accuracy and exact conservation. The key idea in formulating the constraint equations is that from a mesh-perspective the particle motion must satisfy an advection operator. Derivation of the corresponding optimality conditions reveals that the HDG-method is indispensable in providing the required optimality control. Consistency and rigorous conservation of the resulting scheme are derived. By means of various numerical examples for the linear advection-diffusion equation and the non-linear Navier-Stokes equations the accuracy of the method is further unveiled. High Reynolds-number tests give further evidence for the robustness of the scheme. Given its crucial importance, specific attention is paid to the uniformity of the particle distribution when simulating transient, incompressible fluid flows. Apart from using an accurate particle advection scheme, it will be demonstrated that another important criterion for maintaining a correct particle distribution is to transport the particles in velocity fields being H(div)-conforming. We will show how this criterion can be met in the scope of the HDG-framework [3]. Practical impediments of not satisfying the H(div)-criterion are extensively discussed by comparing the particle distributions obtained for a numerical test using Taylor-Hood elements, and using a HDG-based method both with and without H(div)-conforming velocity fields. [1] M. Evans, F. Harlow, E. Bromberg. The particle-in-cell method for hydrodynamic calculations. Technical report, Los Alamos Scientific Laboratory, 1957. [2] G. Dils, A. Haque, J. Wallin. Tuned local regression estimators for the numerical solution of differential equations, volume 26 of Lecture Notes in Computational Science and Engineering, pages 87–104. Springer-Verlag, Berlin, 2003. [3] S. Rhebergen, G.N. Wells. A hybridizable discontinuous Galerkin method for the Navier–Stokes equations with pointwise divergence-free velocity field. 2017.

In-silico Assisted Evaluation of the Airflow Resistance in Canine Upper Airways Comparing Different Dog Breeds

Mauro Malvè*, Rocío Fernández-Parra**, Pascaline Pey***, Luca Zilberstein****

*Public University of Navarra, **Western College of Veterinary Medicine, University of Saskatchewan, ***Antech Imaging Services, ****École Nationale Vétérinaire d'Alfort

ABSTRACT

Brachycephalic breeds are prone to breathing difficulties due to their upper airways anatomy that includes stenotic nares, intranasal turbinates swelling, reduced tracheal lumen and elongated soft palate [1]. Several surgical techniques exist to correct these anatomical pathologies that focus on widening the nasal apertures and/or reducing tissue of the soft palate. Since many problems still remains after surgery, further knowledge is necessary for improving clinical outcomes. In this study we have developed high-performance computational fluid dynamics models of different canine breeds with aim of comparing pressure-based airflow resistances. Larger grids were required in order to capture in details the canine nasal airways structure that has been reconstructed from computerized tomography. The numerical simulations modeled the respiratory flow as turbulent and performed steady inspiration imposing breed-specific physiological airflow rates. The mesh independent study performed to one selected dog skull anatomy pushed the grid refinements up to 50x106 cells. While the results suggest that the computed pressure drop is moderately grid independent as found by other authors [2,3], the rigorous finite volume-based computational study performed to nine non-pathological healthy dogs allowed a comprehensive fluid dynamics comparison between different canine morphologies. The latter revealed higher resistance regions in healthy brachycephalic dogs with respect to meso- and dolichocephalic breeds. Additionally, different brachycephalic dogs presented different airways resistances at different locations. The proposed methodology represents a novel non-invasive approach for quantifying the upper airways flow structure, pressure and resistance that can be used as a surgical planning in veterinary medicine as widely proposed for humans in biomechanics and in the biomedical engineering. [1] Hostnik et al. 2017, Quantification of nasal airflow resistance in English bulldogs using computed tomography and computational fluid dynamics, *Veterinary Radiology Ultrasound*, American College of Veterinary Radiology, 58:542-551. [2] Craven et al., 2009, Development and Verification of a High-Fidelity Computational Fluid Dynamics Model of Canine Nasal Airflow, *Journal of Biomechanical Engineering*, 131:091002-1/11. [3] Craven et al., 2009, The fluid dynamics of canine olfaction: unique nasal airflow patterns as an explanation of macrosmia, *Journal of Royal Society Interface*, doi:10.1098/rsif.2009.0490.

TENSOR-VALUED RANDOM FIELDS DESCRIBING THE PIEZOELECTRIC EFFECT

ANATOLIY MALYARENKO* AND MARTIN OSTOJA-STARZEWSKI†

*Professor, Mälardalen University
Västerås, Sweden

anatoliy.malyarenko@mdh.se, <http://www.mdh.se/ukk/personal/maa/amo01>

†Professor, University of Illinois at Urbana-Champaign
Urbana, IL, USA

martinos@illinois.edu, <http://martinos.mechanical.illinois.edu>

Key words: Piezoelectricity, Symmetry Class, Representation, Random Field.

Abstract. The 18-dimensional space of piezoelectric tensors carries a natural action of the group $O(3)$ of the orthogonal matrices. By the result of Geymonat and Weller (C. R. Math. Acad. Sci. **335** (10), 847–852, 2002), this action has 16 symmetry classes. For each class, consider the corresponding fixed point set V . It carries an orthogonal representation ρ of a symmetry group G . Our task is to describe the one- and two-points correlation tensors of a V -valued homogeneous and isotropic random field as well as the spectral expansion of the field in the form of stochastic integrals with respect to scattered orthogonal random measures.

We give an affirmative answer for the typical cases: a) the representation ρ is trivial; b) the group G is a subgroup of the group $SO(3)$ and ρ is nontrivial; c) the group G is of type III and ρ is nontrivial; d) the most complicated case when $G = O(3)$ and $\rho = 2\rho_1 \oplus \rho_2 \oplus \rho_3$. We describe and use a general method of obtaining such spectral expansions.

1 INTRODUCTION

Let B be a subset of the three-dimensional affine Euclidean space E^3 occupied by a body. Let $\mathbf{D}(\mathbf{x}): B \rightarrow \mathbb{R}^3$ (resp. $\mathbf{E}(\mathbf{x}): B \rightarrow \mathbb{R}^3$, resp. $\varepsilon(\mathbf{x}): B \rightarrow \mathbb{S}^2(\mathbb{R}^3)$, resp. $\mathbf{e}(\mathbf{x}): B \rightarrow \mathbb{S}^2(\mathbb{R}^3) \otimes \mathbb{R}^3$) be the induction vector field (resp. the electric vector field, resp. the dielectric permeability tensor field, resp. the piezoelectric tensor field). The symbol $\mathbb{S}^2(\mathbb{R}^3)$ denotes the set of rank 2 *symmetric* tensors over \mathbb{R}^3 . The above fields are connected by the constitutive equation

$$D_i = e_{ijk}\varepsilon_{jk} + \varepsilon_{ik}E_k,$$

that describes the piezoelectric effect. Here, the Einstein summation convention is in use.

In the presence of spatially random material microstructure, we have to consider the body B as a *random medium*. Then, the piezoelectric tensor field $\mathbf{e}(\mathbf{x})$ becomes random. That is, there is a probability space $(\Omega, \mathfrak{F}, \mathbf{P})$ and a function of two variables $\mathbf{e}(\mathbf{x}, \omega): B \times \Omega \rightarrow \mathbf{S}^2(\mathbb{R}^3) \otimes \mathbb{R}^3$ such that for any point $\mathbf{x}_0 \in B$ the map $\omega \mapsto \mathbf{e}(\mathbf{x}_0, \omega)$ is a $\mathbf{S}^2(\mathbb{R}^3) \otimes \mathbb{R}^3$ -valued random tensor.

Assume that the random field $\mathbf{e}(\mathbf{x})$ is *second-order*, that is, $E[\|\mathbf{e}(\mathbf{x})\|^2] < \infty$ for all $\mathbf{x} \in B$, and *mean-square continuous*, that is,

$$\lim_{\|\mathbf{x} - \mathbf{x}_0\| \rightarrow 0} E[\|\mathbf{e}(\mathbf{x}) - \mathbf{e}(\mathbf{x}_0)\|^2] = 0, \quad \mathbf{x}_0 \in B.$$

Assume that the random field $\mathbf{e}(\mathbf{x})$ is a restriction to B of a random field defined on all of E^3 . Introduce a Cartesian coordinate system in E^3 and identify the resulting space with the *space domain* \mathbb{R}^3 . When one shifts the origin of the introduced system, the random field $\mathbf{e}(\mathbf{x})$ is not changing. In particular, the *one-point correlation tensor* $\langle \mathbf{e}(\mathbf{x}) \rangle = E[\mathbf{e}(\mathbf{x})]$ does not depend on $\mathbf{x} \in \mathbb{R}^3$, while its *two-point correlation tensor* $\langle \mathbf{e}(\mathbf{x}), \mathbf{e}(\mathbf{y}) \rangle = E[(\mathbf{e}(\mathbf{x}) - \langle \mathbf{e}(\mathbf{x}) \rangle) \otimes (\mathbf{e}(\mathbf{y}) - \langle \mathbf{e}(\mathbf{y}) \rangle)]$ depends only on the difference $\mathbf{z} = \mathbf{y} - \mathbf{x}$. Such a field is called *wide-sense homogeneous*. In what follows we omit the words “wide-sense”.

The *orthogonal group* $O(3)$ of 3×3 orthogonal matrices naturally acts in the space $\mathbf{S}^2(\mathbb{R}^3) \otimes \mathbb{R}^3$. For any point $\mathbf{x} \in \mathbf{S}^2(\mathbb{R}^3) \otimes \mathbb{R}^3$, let $G_{\mathbf{x}} = \{g \in O(3): g \cdot \mathbf{x} = \mathbf{x}\}$ be the *stationary subgroup* of the point \mathbf{x} . Call two stationary subgroups $G_{\mathbf{x}}$ and $G_{\mathbf{y}}$ *conjugate*, if there is $h \in O(3)$ such that $G_{\mathbf{y}} = \{hgh^{-1}: g \in G_{\mathbf{x}}\}$. The equivalence classes of this relation are called *piezoelectricity classes*.

Geymonat and Weller [1] proved that there are 16 piezoelectricity classes. For a representative G_0 of a fixed piezoelectricity class, let V be the linear subspace of the space $\mathbf{S}^2(\mathbb{R}^3) \otimes \mathbb{R}^3$ defined as is the maximal linear subspace where the group G_0 acts *trivially*:

$$V = \{\mathbf{x} \in \mathbf{S}^2(\mathbb{R}^3) \otimes \mathbb{R}^3: g \cdot \mathbf{x} = \mathbf{x} \text{ for all } g \in G_0\}.$$

The space V is the space of all piezoelectric tensors of a fixed symmetry defined by the group G_0 . There may exist a group G such that G_0 is a proper closed subgroup of G but the space V is *invariant* under the action of G , that is, $g \cdot \mathbf{x} \in V$ for all $\mathbf{x} \in V$ and for all $g \in G$. It turns out that a group G has the above property if and only if it is a closed subgroup of the *normaliser* $N(G_0) = \{h \in O(3): hG_0h^{-1} = G_0\}$. The group G acts in V by an *orthogonal representation* ρ , that is, the functions $\rho(g): V \rightarrow V$ acting by $\rho(g)\mathbf{x} = g \cdot \mathbf{x}$ is an orthogonal linear operator in V satisfying $\rho(g_1g_2) = \rho(g_1)\rho(g_2)$.

Assume that the random field $\mathbf{e}(\mathbf{x})$ takes values in V . What happens when one rotates or reflects the Cartesian coordinate system by means of a matrix $g \in G$? After the transformation g the point \mathbf{x} becomes the point $g\mathbf{x}$. Evidently, the tensor $\mathbf{e}(\mathbf{x})$ is transformed into $\rho(g)\mathbf{e}(\mathbf{x})$. It is easy to see that the one- and two-point correlation tensors of the initial and transformed fields are equal if and only if

$$\begin{aligned} \langle \mathbf{e}(g\mathbf{x}) \rangle &= \rho(g)\langle \mathbf{e}(\mathbf{x}) \rangle, \\ \langle \mathbf{e}(g\mathbf{x}), \mathbf{e}(g\mathbf{y}) \rangle &= (\rho \otimes \rho)(g)\langle \mathbf{e}(\mathbf{x}), \mathbf{e}(\mathbf{y}) \rangle. \end{aligned} \tag{1}$$

The fields satisfying (1) are called *wide-sense isotropic*. As before, we will omit the words “wide-sense” in what follows.

We would like to find the general form of one- and two-point correlation tensors of a homogeneous and isotropic random field describing the piezoelectric effect and the spectral expansion of the field with respect to orthogonal random scattered measures.

The rest of the extended abstract is organised as follows. In Section 2, we describe the idea of solution and find the spectral expansion of the two-point correlation tensor of a homogeneous and isotropic random field taking its values in a fixed piezoelectricity class. In Section 3, we show how the methods of Section 2 work in practice by giving examples of spectral expansions of random fields for several typical cases.

2 AN IDEA OF SOLUTION

First, note that the answer to our question depends on the choice of a coordinate system in V . We try to write as many formulae as possible in the coordinate-free form and choose an appropriate coordinate system as late as possible.

Second, the solution can be naturally divided into two stage. At the first stage, we describe all homogeneous random fields. Then, we choose those fields that are isotropic.

Unfortunately, there exist no complete description of homogeneous random fields taking values in a finite-dimensional *real* linear space. Such a description exists for the case of a *complex* linear space and has been found by Cramér [2]. Equation

$$\langle \mathbf{e}(\mathbf{x}), \mathbf{e}(\mathbf{y}) \rangle = \int_{\hat{\mathbb{R}}^3} e^{i(\mathbf{p}, \mathbf{y} - \mathbf{x})} dF(\mathbf{p}), \quad (2)$$

where $\hat{\mathbb{R}}^3$ is the *wavenumber domain*, establishes a one-to-one correspondence between the set of two-point correlation tensors of second-order mean-square continuous W -valued homogeneous random fields and the set of measures defined on the Borel σ -field $\mathfrak{B}(\hat{\mathbb{R}}^3)$ and taking its values in the set of Hermitian nonnegative-definite linear operators on a finite-dimensional *complex* linear space W .

Recall that a *real structure* on W is an operator $J: W \rightarrow W$ satisfying the following conditions:

$$J(\alpha \mathbf{x} + \beta \mathbf{y}) = \bar{\alpha} J(\mathbf{x}) + \bar{\beta} J(\mathbf{y}), \quad J^2 = I$$

for all $\alpha, \beta \in \mathbb{C}$, $\mathbf{x}, \mathbf{y} \in W$, where I is the identity operator in W . The set of all eigenvectors of J corresponding to the eigenvalue 1 is a *real* linear space, call it V . Let (\cdot, \cdot) be an inner product in W . We adopt the *physical* convention: an inner product is linear in its second argument and anti-linear in the first one. For a linear operator L in W , let L^\top be the linear operator defined by

$$(LJ\mathbf{x}, \mathbf{y}) = (J\mathbf{x}, L^\top \mathbf{y}), \quad \mathbf{x}, \mathbf{y} \in W$$

(it's just the coordinate-free definition of the transposed matrix).

We do not know *necessary and sufficient conditions* under which the W -valued random field $\mathbf{e}(\mathbf{x})$ takes values in V . However, we know a *necessary condition*: if $\mathbf{e}(\mathbf{x})$ takes values in V , then

$$F(-A) = F(A)^\top, \quad A \in \mathfrak{B}(\hat{\mathbb{R}}^3), \quad (3)$$

where $-A = \{-\mathbf{p}: \mathbf{p} \in A\}$.

Let $\mathbf{e}_0 \in V$ be the one-point correlation tensor of the homogeneous random field $\mathbf{e}(\mathbf{x})$. The first line in Equation (1) means that $\mathbf{e}_0 \in V_0$, where

$$V_0 = \{x \in V: \rho(g)x = x \text{ for all } g \in G\}.$$

In the language of representation theory, V_0 is the maximal subspace of V where the multiple of the trivial representation acts.

Similarly, the second line in Equation (1) means that

$$F(gA) = (\rho \otimes \rho)(g)F(A), \quad g \in G, \quad A \in \mathfrak{B}(\hat{\mathbb{R}}^3), \quad (4)$$

where we used Equation (2). The next idea is as follows: we would like to replace Equations (3) and (4) by *one* equation. To do this, we need more notation.

The conjugacy classes of closed subgroups of the group $O(3)$ fall into three types.

Type I The subgroups of the group $SO(3)$.

Type II The subgroups containing $-I$.

Type III The remaining subgroups.

Let Z_2^c be the subgroup of the group $O(3)$ defined by $Z_2^c = \{I, -I\}$. This group has two irreducible orthogonal representations: $A_g(h) = 1$ and $A_u(h) = \det h$, $h \in Z_2^c$. Let $\pi: O(3) \rightarrow SO(3)$ be the projection of the Cartesian product $O(3) = SO(3) \times Z_2^c$ to the first term. The space $S^2(V)$ is an invariant subspace of the representation $\rho \otimes \rho$. Denote by $S^2(\rho)$ the restriction of the representation $\rho \otimes \rho$ to the above subspace. Similarly, the space $\Lambda^2(V)$ of rank 2 skew-symmetric tensors over V is an invariant subspace, and the restriction of the representation $\rho \otimes \rho$ to this subspace is denoted by $\Lambda^2(\rho)$. Finally, let ρ be a representation of a group G of type III, let ρ^π be the representation of the group $\pi(G)$ defined by $\rho^\pi(g) = \rho(\pi^{-1}(g))$, and let $\widehat{\Lambda^2(\rho^\pi)}$ be the representation of $\pi(G)$ given by

$$\widehat{\Lambda^2(\rho^\pi)} = \begin{cases} \Lambda^2(\rho^\pi), & \text{if } g \in G \cap \pi(G), \\ -\Lambda^2(\rho^\pi), & \text{otherwise.} \end{cases}$$

Lemma 1. *There exists a group \tilde{G} and its orthogonal representation $\tilde{\rho}$ in a real finite-dimensional space \tilde{V} such that the measure F takes values in \tilde{V} and Equations (3) and (4) are equivalent to the equation*

$$F(\tilde{g}A) = \tilde{\rho}(\tilde{g})F(A), \quad \tilde{g} \in \tilde{G}, \quad A \in \mathfrak{B}(\hat{\mathbb{R}}^3). \quad (5)$$

Moreover:

- If G is of type I, then $\tilde{G} = G \times Z_2^c$, $\tilde{V} = V \otimes V$, and

$$\tilde{\rho} = S^2(\rho) \hat{\otimes} \dim S^2(\rho) A_g \oplus \widehat{\Lambda^2(\rho^\pi)} \hat{\otimes} \dim \widehat{\Lambda^2(\rho^\pi)} A_u.$$

- If G is of type II, then $\tilde{G} = G$, $\tilde{V} = S^2(V)$, and $\tilde{\rho} = S^2(\rho)$.
- If G is of type III, then $\tilde{G} = \pi(G) \times Z_2^c$, $\tilde{V} = V \otimes V$, and

$$\tilde{\rho} = S^2(\rho^\pi) \hat{\otimes} \dim S^2(\rho^\pi) A_g \oplus \widehat{\Lambda^2(\rho^\pi)} \hat{\otimes} \dim \widehat{\Lambda^2(\rho^\pi)} A_u.$$

Remark 1. Malyarenko and Ostoj-Starzewski [3] considered the case of *elasticity classes*. In this case, all groups G are of type II, and the second part of Lemma 1 have been formulated and proved there. The complete proof may be found in the forthcoming book by Malyarenko and Ostoj-Starzewski [4].

Consider the measure μ defined by $\mu(A) = \text{tr } F(A)$, the trace of the operator $F(A)$. It is well-known that the measure F is absolutely continuous with respect to μ , and the Radon–Nykodym derivative $f(\mathbf{p})$ is a measurable function taking values in the set of nonnegative-definite operators with unit trace. Equation (2) takes the form

$$\langle \mathbf{e}(\mathbf{x}), \mathbf{e}(\mathbf{y}) \rangle = \int_{\mathbb{R}^3} e^{i(\mathbf{p}, \mathbf{y} - \mathbf{x})} f(\mathbf{p}) d\mu(\mathbf{p}),$$

while condition (5) becomes

$$f(\tilde{g}\mathbf{p}) = \tilde{\rho}(\tilde{g}) f(\mathbf{p}), \quad \mu(\tilde{g}A) = \mu(A), \quad \tilde{g} \in \tilde{G}, \quad A \in \mathfrak{B}(\mathbb{R}^3). \quad (6)$$

The description of all measures μ satisfying the second condition is well-known, see Bourbaki [5]. Consider the action of the group \tilde{G} on \mathbb{R}^3 by matrix-vector multiplication. This action is an orthogonal representation of a compact group \tilde{G} and has finitely many symmetry classes, see Duistermaat and Kolk [6]. Introduce a partial ordering on the set of symmetry classes: $[G_1] \leq [G_2]$ if and only if any representative of the class $[G_1]$ is conjugate to a subgroup of G_2 . The maximal element of the introduced partial ordering is $[G_0] = [G]$. Enumerate the remaining elements in such an order that $[G_i] \leq [G_j]$ if $i \leq j$. There is also the minimal element $[G_{M-1}]$, where M is the number of symmetry classes. Any chain of this ordering has at most $1 + \dim \mathbb{R}^3 / \tilde{G}$ many elements, where \mathbb{R}^3 / \tilde{G} is the orbit space of the action. Denote by $(\mathbb{R}^3 / \tilde{G})_m$ the set of all orbits whose stationary subgroups are representatives of the class $[G_m]$, $0 \leq m \leq M-1$. The sets $(\mathbb{R}^3 / \tilde{G})_m$ are manifolds. We have $[G_i] \leq [G_j]$ if and only if $(\mathbb{R}^3 / \tilde{G})_j$ is a subset of the closure of $(\mathbb{R}^3 / \tilde{G})_i$. In particular, the set $(\mathbb{R}^3 / \tilde{G})_{M-1}$ is open and dense in \mathbb{R}^3 / \tilde{G} , it is called the *principal orbit type*, while $(\mathbb{R}^3 / \tilde{G})_0 = \{\mathbf{0}\}$.

Denote by ν_m the probabilistic G_m -invariant measure on the orbit \tilde{G}/G_m . The measure μ has the form

$$\mu = \sum_{m=0}^{M-1} \int_{(\mathbb{R}^3 / \tilde{G})_m} \nu_m d\mu_m,$$

where μ_m are arbitrary finite measures on the Borel σ -fields $\mathfrak{B}((\hat{\mathbb{R}}^3/\tilde{G})_m)$. For simplicity, assume that there exists a chart $\boldsymbol{\varphi}^m$ of the manifold \tilde{G}/G_m and a chart $\boldsymbol{\lambda}^m$ of the manifold $(\hat{\mathbb{R}}^3/\tilde{G})_m$ with dense domains. The two-point correlation tensor of the random field $\mathbf{e}(\mathbf{x})$ takes the form

$$\langle \mathbf{e}(\mathbf{x}), \mathbf{e}(\mathbf{y}) \rangle = \sum_{m=0}^{M-1} \int_{(\hat{\mathbb{R}}^3/\tilde{G})_m} \int_{\tilde{G}/G_m} e^{i((\boldsymbol{\lambda}^m, \boldsymbol{\varphi}^m), \mathbf{y}-\mathbf{x})} f(\boldsymbol{\lambda}^m, \boldsymbol{\varphi}^m) dv_m(\boldsymbol{\varphi}^m) d\mu_m(\boldsymbol{\lambda}^m).$$

It remains to analyse the first condition in Equation (6). Denote

$$V_m = \{ \mathbf{x} \in \tilde{V} : \tilde{\rho}(\tilde{g})\mathbf{x} = \mathbf{x} \text{ for all } \tilde{g} \in G_m \}.$$

The subspace V_m has positive dimension, because the representation $\tilde{\rho}$ contains at least one trivial irreducible component. The intersection of V_m with the convex compact set of Hermitian nonnegative-definite linear operators with unit trace is a convex compact set, call it C_m . Let $\boldsymbol{\varphi}_0^m$ be the coordinate of the point of \tilde{G}/G_m with stationary subgroup G_m . The function $f(\boldsymbol{\lambda}^m, \boldsymbol{\varphi}_0^m)$ is an arbitrary measurable function on $(\hat{\mathbb{R}}^3/\tilde{G})_m$ taking values in C_m . By the first condition in Equation (6), the function $f(\boldsymbol{\lambda}_m, \boldsymbol{\varphi}_m)$ becomes

$$f(\boldsymbol{\lambda}^m, \boldsymbol{\varphi}^m) = \tilde{\rho}(\boldsymbol{\varphi}^m) f(\boldsymbol{\lambda}^m, \boldsymbol{\varphi}_0^m),$$

and the two-point correlation tensor of the random field $\mathbf{e}(\mathbf{x})$ takes the form

$$\langle \mathbf{e}(\mathbf{x}), \mathbf{e}(\mathbf{y}) \rangle = \sum_{m=0}^{M-1} \int_{(\hat{\mathbb{R}}^3/\tilde{G})_m} \int_{\tilde{G}/G_m} e^{i((\boldsymbol{\lambda}^m, \boldsymbol{\varphi}^m), \mathbf{y}-\mathbf{x})} \tilde{\rho}(\boldsymbol{\varphi}^m) f(\boldsymbol{\lambda}^m, \boldsymbol{\varphi}_0^m) dv_m(\boldsymbol{\varphi}^m) d\mu_m(\boldsymbol{\lambda}^m).$$

To calculate the inner integral, choose a basis $\mathbf{e}^1, \dots, \mathbf{e}^{\dim V}$ in the space V . The tensor square $V \otimes V$ has several different bases. The *coupled basis* is the set of tensor products $\mathbf{e}^i \otimes \mathbf{e}^j$, $1 \leq i, j \leq \dim V$. The *m th uncoupled basis* is constructed as follows. The space $\tilde{V} \subseteq V \otimes V$ falls into the direct sum of several subspaces, where the irreducible components of the representation $\tilde{\rho}$ act. Let $H^{m11}, \dots, H^{m1k_1}, \dots, H^{mL_m1}, \dots, H^{mL_mk_{L_m}}$ be the set of all subspaces that satisfy the following conditions.

- The irreducible component ρ^l acts in the spaces $H^{m11}, \dots, H^{m1k_l}, 0 \leq m \leq M, 1 \leq l \leq L_m$.
- $H^{mlk} \cap V_m \neq \{0\}, 0 \leq m \leq M, 1 \leq l \leq L_m, 1 \leq k \leq k_l$.

Choose a basis $\{\mathbf{e}^{mlkn} : 1 \leq n \leq \dim H^{mlk} \cap V_m\}$ in the intersection $H^{mlk} \cap V_m$ and complement the chosen basis to a basis of the space $V \otimes V$ arbitrarily. The tensors of the coupled basis are linear combinations of the tensors of the m th uncoupled basis:

$$\mathbf{e}^i \otimes \mathbf{e}^j = \sum_{l=1}^{L_m} \sum_{k=1}^{k_l} \sum_{n=1}^{\dim H^{mlk} \cap V_m} c_{ijmlkn} \mathbf{e}^{mlkn} + \dots,$$

where the dots denote non-essential terms. One needs to choose bases in such a way that the *Clebsch–Gordan coefficients* c_{ijmlkn} are calculating as easy as possible. Let $f^{mlkn}(\boldsymbol{\lambda}^m, \boldsymbol{\varphi}_0^m)$ be the components of the tensor $f(\boldsymbol{\lambda}^m, \boldsymbol{\varphi}_0^m)$ in the m th uncoupled basis. Then we have

$$\begin{aligned} \langle \mathbf{e}(\mathbf{x}), \mathbf{e}(\mathbf{y}) \rangle_{ij} &= \sum_{m=0}^{M-1} \sum_{l=1}^{L_m} \sum_{k=1}^{k_l} \sum_{q=1}^{\dim \rho^l} \sum_{n=1}^{\dim H^{mlk}} \int_{(\hat{\mathbb{R}}^3/\tilde{G})_m} \int_{\tilde{G}/G_m} e^{i((\boldsymbol{\lambda}^m, \boldsymbol{\varphi}^m), \mathbf{y}-\mathbf{x})} \\ &\times \rho_{qn}^l(\boldsymbol{\varphi}^m) f^{mlkn}(\boldsymbol{\lambda}^m, \boldsymbol{\varphi}_0^m) d\nu_m(\boldsymbol{\varphi}^m) d\mu_m(\boldsymbol{\lambda}^m). \end{aligned}$$

By the Fine Structure Theorem [7], there is a subset N_{ml} of the set $\{1, 2, \dots, \dim H^{mlk}\}$ such that the functions $\sqrt{\dim \rho^l} \rho_{qn}^l(\boldsymbol{\varphi}^m)$, $1 \leq q \leq \dim \rho^l$, $n \in N_{ml}$, form an orthonormal basis in the space of square-integrable functions on the orbit \tilde{G}/G_m with respect to the measure μ_m . Denote

$$j_{qn}^{ml}(\boldsymbol{\lambda}^m, \mathbf{y} - \mathbf{x}) = \int_{\tilde{G}/G_m} e^{i((\boldsymbol{\lambda}^m, \boldsymbol{\varphi}^m), \mathbf{y}-\mathbf{x})} \rho_{qn}^l(\boldsymbol{\varphi}^m) d\mu_m(\boldsymbol{\lambda}^m).$$

Then we obtain the spectral expansion of the two-point correlation tensor of the field:

$$\langle \mathbf{e}(\mathbf{x}), \mathbf{e}(\mathbf{y}) \rangle_{ij} = \sum_{m=0}^{M-1} \sum_{l=1}^{L_m} \sum_{k=1}^{k_l} \sum_{q=1}^{\dim \rho^l} \sum_{n \in N_{ml}} \int_{(\hat{\mathbb{R}}^3/\tilde{G})_m} j_{qn}^{ml}(\boldsymbol{\lambda}^m, \mathbf{y} - \mathbf{x}) f^{mlkn}(\boldsymbol{\lambda}^m, \boldsymbol{\varphi}_0^m) d\mu_m(\boldsymbol{\lambda}^m).$$

To obtain the spectral expansion of the field $\mathbf{e}(\mathbf{x})$, write down the complex exponent as

$$e^{i((\boldsymbol{\lambda}^m, \boldsymbol{\varphi}^m), \mathbf{y}-\mathbf{x})} = e^{i((\boldsymbol{\lambda}^m, \boldsymbol{\varphi}^m), \mathbf{y})} \overline{e^{i((\boldsymbol{\lambda}^m, \boldsymbol{\varphi}^m), \mathbf{x})}},$$

and apply the Fine Structure Theorem to each term *separately*. Then, apply Karhunen’s Theorem [8]. We perform this in the following examples in each case separately.

3 EXAMPLES

Example 1. The *dihedral group* D_2 generated by the rotation about the z -axis with angle π and the rotation about the x -axis with the same angle, is a piezoelectric class. Its symmetry class V has dimension 3, and the group D_2 acts in V trivially. The basis of V is

$$T^1 = \frac{1}{\sqrt{2}} \begin{pmatrix} 0 & 1 & 0 \\ 1 & 0 & 0 \\ 0 & 0 & 0 \end{pmatrix} \otimes \begin{pmatrix} 0 \\ 0 \\ 1 \end{pmatrix}, T^2 = \frac{1}{\sqrt{2}} \begin{pmatrix} 0 & 0 & 1 \\ 0 & 0 & 0 \\ 1 & 0 & 0 \end{pmatrix} \otimes \begin{pmatrix} 0 \\ 1 \\ 0 \end{pmatrix}, T^3 = \frac{1}{\sqrt{2}} \begin{pmatrix} 0 & 0 & 0 \\ 0 & 0 & 1 \\ 0 & 1 & 0 \end{pmatrix} \otimes \begin{pmatrix} 1 \\ 0 \\ 0 \end{pmatrix}.$$

The group \tilde{G} is $\tilde{G} = D_2 \times Z_2^c$. The orbit type stratification is

$$\begin{aligned} (\hat{\mathbb{R}}^3/D_2 \times Z_2^c)_1 &= \{ (0, 0, p_3): p_3 > 0 \}, \\ (\hat{\mathbb{R}}^3/D_2 \times Z_2^c)_2 &= \{ (0, p_2, 0): p_2 > 0 \}, \\ (\hat{\mathbb{R}}^3/D_2 \times Z_2^c)_3 &= \{ (p_1, 0, 0): p_1 > 0 \}, \\ (\hat{\mathbb{R}}^3/D_2 \times Z_2^c)_4 &= \{ (p_1, p_2, 0): p_1 > 0, p_2 > 0 \}, \\ (\hat{\mathbb{R}}^3/D_2 \times Z_2^c)_5 &= \{ (p_1, 0, p_3): p_1 > 0, p_3 > 0 \}, \\ (\hat{\mathbb{R}}^3/D_2 \times Z_2^c)_6 &= \{ (0, p_2, p_3): p_2 > 0, p_3 > 0 \}, \\ (\hat{\mathbb{R}}^3/D_2 \times Z_2^c)_7 &= \{ (p_1, p_2, p_3): p_1 > 0, p_2 > 0, p_3 > 0 \}. \end{aligned}$$

Let Φ be a finite measure on $\hat{\mathbb{R}}^3/D_2 \times Z_2^c$, and let $f(\mathbf{p})$ be a Φ -equivalence class of measurable functions acting from $\hat{\mathbb{R}}^3/D_2 \times Z_2^c$ to the set of nonnegative-definite Hermitian linear operators on $V_{\mathbb{C}}$ with unit trace. Let $u_n(\mathbf{p}, \mathbf{x})$ be 8 different products of cosines and sines of $p_i x_i$:

$$\begin{aligned} u_1(\mathbf{p}, \mathbf{x}) &= \sin(p_1 x_1) \sin(p_2 x_2) \sin(p_3 x_3), & u_2(\mathbf{p}, \mathbf{x}) &= \cos(p_1 x_1) \cos(p_2 x_2) \sin(p_3 x_3), \\ u_3(\mathbf{p}, \mathbf{x}) &= \cos(p_1 x_1) \sin(p_2 x_2) \cos(p_3 x_3), & u_4(\mathbf{p}, \mathbf{x}) &= \sin(p_1 x_1) \cos(p_2 x_2) \cos(p_3 x_3), \\ u_5(\mathbf{p}, \mathbf{x}) &= \cos(p_1 x_1) \cos(p_2 x_2) \cos(p_3 x_3), & u_6(\mathbf{p}, \mathbf{x}) &= \sin(p_1 x_1) \sin(p_2 x_2) \cos(p_3 x_3), \\ u_7(\mathbf{p}, \mathbf{x}) &= \sin(p_1 x_1) \cos(p_2 x_2) \sin(p_3 x_3), & u_8(\mathbf{p}, \mathbf{x}) &= \cos(p_1 x_1) \sin(p_2 x_2) \sin(p_3 x_3). \end{aligned}$$

The one-point correlation tensor of a homogeneous and $(D_2, 3A)$ -isotropic random field $\mathbf{e}(\mathbf{x})$ is

$$\langle \mathbf{e}(\mathbf{x}) \rangle_{ijk} = \sum_{m=1}^3 C_m \mathsf{T}_{ijk}^m,$$

where $C_m \in \mathbb{R}$. Its two-point correlation tensor has the form

$$\begin{aligned} \langle \mathbf{e}(\mathbf{x}), \mathbf{e}(\mathbf{y}) \rangle &= \int_{\hat{\mathbb{R}}^3/D_2 \times Z_2^c} \cos(p_1 z_1) \cos(p_2 z_2) \cos(p_3 z_3) f_S(\mathbf{p}) \, d\Phi(\mathbf{p}) \\ &\quad + \int_{(\hat{\mathbb{R}}^3/Z_2 \times Z_2^c)_7} \sin(p_1 z_1) \sin(p_2 z_2) \sin(p_3 z_3) f_A(\mathbf{p}) \, d\Phi(\mathbf{p}), \end{aligned}$$

The field has the form

$$\begin{aligned} \mathbf{e}_{ijk}(\mathbf{x}) &= \sum_{m=1}^3 C_m \mathsf{D}_2^2 \mathsf{T}_{ijk}^m + \sum_{m=1}^3 \sum_{n=1}^4 \int_{\hat{\mathbb{R}}^3/D_2 \times Z_2^c} u_n(\mathbf{p}, \mathbf{x}) \, dZ_{mn}^1(\mathbf{p}) \mathsf{T}_{ijk}^m \\ &\quad + \sum_{m=1}^3 \sum_{n=5}^8 \int_{(\hat{\mathbb{R}}^3/Z_2 \times Z_2^c)_7} u_n(\mathbf{p}, \mathbf{x}) \, dZ_{mn}^2(\mathbf{p}) \mathsf{T}_{ijk}^m, \end{aligned}$$

where $\mathbf{Z}^{1n}(\mathbf{p}) = (Z_{1n}^1(\mathbf{p}), \dots, Z_{3n}^1(\mathbf{p}))^\top$ (resp. $\mathbf{Z}^{2n}(\mathbf{p}) = (Z_{1n}^2(\mathbf{p}), \dots, Z_{3n}^2(\mathbf{p}))^\top$) are centred \mathbf{V} -valued random measures on $\hat{\mathbb{R}}^3/D_2 \times Z_2^c$ (resp. on $(\hat{\mathbb{R}}^3/D_2 \times Z_2^c)_7$) with control measure $f_S(\mathbf{p})$ and cross-correlation

$$\mathbb{E}[\mathbf{Z}_n^S(A) \otimes \mathbf{Z}_{n+4}^A(B)] = -\mathbb{E}[\mathbf{Z}_n^A(A) \otimes \mathbf{Z}_{n+4}^S(B)] = \int_{A \cap B} f_A(\mathbf{p}) \, d\Phi(\mathbf{p}).$$

Example 2. The dihedral group D_4 acts in the space \mathbf{V} of Example 1 by the nontrivial representation $\rho = A_1 \oplus 2B_1$ (for the notation used, see [9]). The basis of \mathbf{V} is

$$\mathbf{T}^{1,3} = \frac{1}{\sqrt{2}} \left[\begin{pmatrix} 0 & 1 & 0 \\ 1 & 0 & 0 \\ 0 & 0 & 0 \end{pmatrix} \otimes \begin{pmatrix} 1 \\ 0 \\ 0 \end{pmatrix} \pm \begin{pmatrix} 0 & 0 & 0 \\ 0 & 0 & 1 \\ 0 & 1 & 0 \end{pmatrix} \otimes \begin{pmatrix} 0 \\ 0 \\ 1 \end{pmatrix} \right]$$

and the same \mathbf{T}^2 as the one in Example 1.

The group \tilde{G} is $\tilde{G} = D_4 \times Z_2^c$. The orbit type stratification is

$$\begin{aligned} (\hat{\mathbb{R}}^3/D_4 \times Z_2^c)_1 &= \{ (0, 0, p_3) : p_3 > 0 \}, \\ (\hat{\mathbb{R}}^3/D_4 \times Z_2^c)_2 &= \{ (p_1, p_2, 0) : p_1 = p_2 > 0 \}, \\ (\hat{\mathbb{R}}^3/D_4 \times Z_2^c)_3 &= \{ (p_1, 0, 0) : p_1 > 0 \}, \\ (\hat{\mathbb{R}}^3/D_4 \times Z_2^c)_4 &= \{ (p_1, p_2, 0) : 0 < p_2 < p_1 \}, \\ (\hat{\mathbb{R}}^3/D_4 \times Z_2^c)_5 &= \{ (p_1, p_2, p_3) : p_1 = p_2 > 0, p_3 > 0 \}, \\ (\hat{\mathbb{R}}^3/D_4 \times Z_2^c)_6 &= \{ (p_1, 0, p_3) : p_1 > 0, p_3 > 0 \}, \\ (\hat{\mathbb{R}}^3/D_2 \times Z_2^c)_7 &= \{ (p_1, p_2, p_3) : 0 < p_2 < p_1, p_3 > 0 \}. \end{aligned}$$

Let Φ be a finite measure on $\hat{\mathbb{R}}^3/D_4 \times Z_2^c$, and let $f^{3,7}(\mathbf{p})$ be a Φ -equivalence class of measurable functions acting from $\hat{\mathbb{R}}^3/D_4 \times Z_2^c$ to the set of nonnegative-definite Hermitian operators on \mathbf{V} with unit trace. Let an equivalence class $f^{0,1}(\mathbf{p})$ acts to the set of diagonal matrices, $f^2(\mathbf{p})$ acts to the set of matrices satisfying $f_{12}^2(\mathbf{p}) = f_{13}^2(\mathbf{p}) = 0$, and $f^{4,6}(\mathbf{p})$ acts to the set of matrices with real-valued entries. Finally, define σf as follows:

$$(\sigma f)_{12} = f_{21}, \quad (\sigma f)_{13} = f_{31},$$

and $(\sigma f)_{ij} = f_{ij}$ otherwise. Denote

$$\begin{aligned} u_1(\mathbf{p}, \mathbf{x}) &= \cos(p_1 x_1) \cos(p_2 x_2) \cos(p_3 x_3), \\ u_2(\mathbf{p}, \mathbf{x}) &= \sin(p_1 x_1) \sin(p_2 x_2) \sin(p_3 x_3), \\ u_3(\mathbf{p}, \mathbf{x}) &= \cos(p_1 x_2) \cos(p_2 x_1) \cos(p_3 x_3), \\ u_4(\mathbf{p}, \mathbf{x}) &= \sin(p_1 x_2) \sin(p_2 x_1) \sin(p_3 x_3). \end{aligned}$$

The one-point correlation tensor of a homogeneous and $(D_4, A_1 \oplus 2B_1)$ -isotropic random field $\mathbf{e}(\mathbf{x})$ is

$$\langle \mathbf{e}(\mathbf{x}) \rangle_{ijk} = C \mathbb{T}_{ijk}^1,$$

where $C \in \mathbb{R}$. Its two-point correlation tensor has the form

$$\begin{aligned} \mathbf{e}_{ijk}(\mathbf{x}) = & \int_{(\hat{\mathbb{R}}^3/D_4 \times Z_2^c)_{0,1}} [u_1(\mathbf{p}, \mathbf{x}) f_S^{0,1}(\mathbf{p}) + u_2(\mathbf{p}, \mathbf{x}) f_A^{0,1}(\mathbf{p}) \\ & + u_3(\mathbf{p}, \mathbf{x}) (\sigma f)_S^{0,1}(\mathbf{p}) + u_4(\mathbf{p}, \mathbf{x}) (\sigma f)_A^{0,1}(\mathbf{p})] d\Phi(\mathbf{p}) \\ & + \int_{(\hat{\mathbb{R}}^3/D_4 \times Z_2^c)_2} [u_1(\mathbf{p}, \mathbf{x}) f_S^2(\mathbf{p}) + u_2(\mathbf{p}, \mathbf{x}) f_A^2(\mathbf{p}) \\ & + u_3(\mathbf{p}, \mathbf{x}) (\sigma f)_S^2(\mathbf{p}) + u_4(\mathbf{p}, \mathbf{x}) (\sigma f)_A^2(\mathbf{p})] d\Phi(\mathbf{p}) \\ & + \int_{(\hat{\mathbb{R}}^3/D_4 \times Z_2^c)_{3,7}} [u_1(\mathbf{p}, \mathbf{x}) f_S^{3,7}(\mathbf{p}) + u_2(\mathbf{p}, \mathbf{x}) f_A^{3,7}(\mathbf{p}) \\ & + u_3(\mathbf{p}, \mathbf{x}) (\sigma f)_S^{3,7}(\mathbf{p}) + u_4(\mathbf{p}, \mathbf{x}) (\sigma f)_A^{3,7}(\mathbf{p})] d\Phi(\mathbf{p}) \\ & + \int_{(\hat{\mathbb{R}}^3/D_4 \times Z_2^c)_{4,6}} [u_1(\mathbf{p}, \mathbf{x}) f_S^{4,6}(\mathbf{p}) + u_2(\mathbf{p}, \mathbf{x}) f_A^{4,6}(\mathbf{p}) \\ & + u_3(\mathbf{p}, \mathbf{x}) (\sigma f)_S^{4,6}(\mathbf{p}) + u_4(\mathbf{p}, \mathbf{x}) (\sigma f)_A^{4,6}(\mathbf{p})] d\Phi(\mathbf{p}). \end{aligned}$$

Example 3. The *prismatic group* D_4^h of order 8 is generated by the product of the rotation about the z -axis with angle $\pi/2$ and the reflection through the plane normal to the same axis, and the rotation about the x -axis with angle π . It acts in the space V of Example 1 by the nontrivial representation $\rho = 2A_1 \oplus B_1$. The basis of V and the group \tilde{G} are the same as in Example 2.

Let Φ be a finite measure on $\hat{\mathbb{R}}^3/D_4 \times Z_2^c$, and let $f(\mathbf{p})$ be a Φ -equivalence class of measurable functions acting from $\hat{\mathbb{R}}^3/D_4 \times Z_2^c$ to the set of nonnegative-definite Hermitian linear operators on V with unit trace. Let $f^S(\mathbf{p})$ be its symmetric part, and let $if^A(\mathbf{p})$ be its skew-symmetric part. Let $f^{S,B}(\mathbf{p})$ be the same class with $f_{13}^{S,B}(\mathbf{p}) = f_{23}^{S,B}(\mathbf{p}) = 0$. Let $f^{A,B}(\mathbf{p})$ be the same class with $f_{12}^{A,B}(\mathbf{p}) = 0$, and let $f^{A,A}(\mathbf{p})$ be the same class with $f_{13}^{A,A}(\mathbf{p}) = f_{23}^{A,A}(\mathbf{p}) = 0$.

The one-point correlation tensor of a homogeneous and $(D_4^h, 2A_1 \oplus B_1)$ -isotropic random field $\mathbf{e}(\mathbf{x})$ is

$$\langle \mathbf{e}(\mathbf{x}) \rangle = C_1 \mathbb{T}_{ijk}^1 + C_2 \mathbb{T}_{ijk}^3.$$

Its two-point correlation tensor is

$$\begin{aligned}
 \langle \mathbf{e}(\mathbf{x}), \mathbf{e}(\mathbf{y}) \rangle &= \frac{1}{2} \int_{(\hat{\mathbb{R}}^3/D_4 \times Z_2^c)_{3,4,6,7}} \cos(p_1 z_1) \cos(p_2 z_2) \cos(p_3 z_3) f^S(\mathbf{p}) d\Phi(\mathbf{p}) \\
 &+ \frac{1}{2} \int_{(\hat{\mathbb{R}}^3/D_4 \times Z_2^c)_{0,1,2,5}} \cos(p_1 z_1) \cos(p_2 z_2) \cos(p_3 z_3) f^{S,B}(\mathbf{p}) d\Phi(\mathbf{p}) \\
 &+ \frac{1}{2} \int_{(\hat{\mathbb{R}}^3/D_4 \times Z_2^c)_{3,7}} \cos(p_1 z_1) \sin(p_2 z_2) \cos(p_3 z_3) f^A(\mathbf{p}) d\Phi(\mathbf{p}) \\
 &+ \frac{1}{2} \int_{(\hat{\mathbb{R}}^3/D_4 \times Z_2^c)_2} \cos(p_1 z_1) \sin(p_2 z_2) \cos(p_3 z_3) f^{A,B}(\mathbf{p}) d\Phi(\mathbf{p}) \\
 &+ \frac{1}{2} \int_{(\hat{\mathbb{R}}^3/D_4 \times Z_2^c)_5} \cos(p_1 z_1) \sin(p_2 z_2) \cos(p_3 z_3) f^{A,A}(\mathbf{p}) d\Phi(\mathbf{p}).
 \end{aligned}$$

The field has the form

$$\begin{aligned}
 \mathbf{e}_{ijk}(\mathbf{x}) &= C_1 \mathbb{T}_{ijk}^1 + C_2 \mathbb{T}_{ijk}^3 + \frac{1}{\sqrt{2}} \sum_{m=1}^3 \sum_{n=1}^8 \int_{(\hat{\mathbb{R}}^3/D_4 \times Z_2^c)_{3,4,6,7}} g_n(\mathbf{p}, \mathbf{x}) dZ_{mn}^S(\mathbf{p}) \mathbb{T}_{ijk}^m \\
 &+ \frac{1}{\sqrt{2}} \sum_{m=1}^3 \sum_{n=1}^8 \int_{(\hat{\mathbb{R}}^3/D_4 \times Z_2^c)_{0,1,2,5}} g_n(\mathbf{p}, \mathbf{x}) dZ_{mn}^{S,B}(\mathbf{p}) \mathbb{T}_{ijk}^m \\
 &+ \frac{1}{\sqrt{2}} \sum_{m=1}^3 \sum_{n=1}^8 \int_{(\hat{\mathbb{R}}^3/D_4 \times Z_2^c)_{3,7}} g_n(\mathbf{p}, \mathbf{x}) dZ_{mn}^A(\mathbf{p}) \mathbb{T}_{ijk}^m \\
 &+ \frac{1}{\sqrt{2}} \sum_{m=1}^3 \sum_{n=1}^8 \int_{(\hat{\mathbb{R}}^3/D_4 \times Z_2^c)_5} g_n(\mathbf{p}, \mathbf{x}) dZ_{mn}^{A,B}(\mathbf{p}) \mathbb{T}_{ijk}^m \\
 &+ \frac{1}{\sqrt{2}} \sum_{m=1}^3 \sum_{n=1}^8 \int_{(\hat{\mathbb{R}}^3/D_4 \times Z_2^c)_2} g_n(\mathbf{p}, \mathbf{x}) dZ_{mn}^{A,A}(\mathbf{p}) \mathbb{T}_{ijk}^m,
 \end{aligned}$$

where $\mathbf{Z}_n^S(\mathbf{p}) = (Z_{1n}^S(\mathbf{p}), \dots, Z_{3n}^S(\mathbf{p}))^\top$ (resp. $\mathbf{Z}_n^{S,B}(\mathbf{p})$, resp. $\mathbf{Z}_n^A(\mathbf{p})$, resp. $\mathbf{Z}_n^{A,B}(\mathbf{p})$, resp. $\mathbf{Z}_n^{A,A}(\mathbf{p})$) are uncorrelated centred $\mathbb{V}^{D_4^h}$ -valued random measures on $\hat{\mathbb{R}}^3/D_4 \times Z_2^c$ with control measure $f^S(\mathbf{p})$ (resp. $f^{S,B}(\mathbf{p})$, resp. $f^A(\mathbf{p})$, resp. $f^{A,B}(\mathbf{p})$, resp. $f^{A,A}(\mathbf{p})$) and cross-correlations

$$\begin{aligned}
 \mathbb{E}[\mathbf{Z}_1^S(A) \otimes \mathbf{Z}_3^A(B)] &= \mathbb{E}[\mathbf{Z}_2^S(A) \otimes \mathbf{Z}_4^A(B)] = \int_{A \cap B} f_A(\mathbf{p}) d\Phi(\mathbf{p}), \\
 \mathbb{E}[\mathbf{Z}_1^A(A) \otimes \mathbf{Z}_3^S(B)] &= \mathbb{E}[\mathbf{Z}_2^A(A) \otimes \mathbf{Z}_4^S(B)] = - \int_{A \cap B} f_A(\mathbf{p}) d\Phi(\mathbf{p}),
 \end{aligned}$$

and where $g_n(\mathbf{p}, \mathbf{x})$ are 8 different products of cosines and sines of $p_i x_i$.

Example 4. Let $G = O(3)$ and let ρ be the natural orthogonal representation of G in the space $V = S^2(\mathbb{R}^3) \otimes \mathbb{R}^3$.

The one-point correlation tensor of a homogeneous and $(O(3), \rho)$ -isotropic random field $C(\mathbf{x})$ is equal to 0. Its two-point correlation tensor has the spectral expansion

$$\langle \mathbf{e}(\mathbf{x}), \mathbf{e}(\mathbf{y}) \rangle_{ijk i' j' k'} = \sum_{n=1}^3 \int_0^\infty \sum_{q=1}^{21} N_{nq}(\lambda, \rho) L_{i i k i' j' k'}^q(\mathbf{y} - \mathbf{x}) d\Phi_n(\lambda),$$

The measures $\Phi_n(\lambda)$ satisfy the condition

$$\Phi_1(\{0\}) = 2\Phi_2(\{0\}).$$

The spectral expansion of the field has the form

$$\begin{aligned} \mathbf{e}_{ijk}(\rho, \theta, \varphi) = & 2\sqrt{\pi} \sum_{n=1}^3 \sum_{\ell=0}^\infty \sum_{m=-\ell}^\ell \int_0^\infty j_\ell(\lambda \rho) \sum_{(\ell', m', i', j', k') \leq (\ell, m, i, j, k)} L_{\ell m i j k, n}^{\ell' m' i' j' k'}(\lambda) \\ & \times dZ_{ijk \ell m}^n(\lambda) S_\ell^m(\theta, \varphi), \end{aligned}$$

where $S_\ell^m(\theta, \varphi)$ are real-valued spherical harmonics, $j_\ell(\lambda \rho)$ are the spherical Bessel functions, and where $Z_{ijk \ell m}^n$ are centred uncorrelated real-valued random measures on $[0, \infty)$ with control measures Φ_n . The functions $N_{nq}(\lambda, \rho)$ and $L_{i i k i' j' k'}^q(\lambda)$ are given in [4].

REFERENCES

- [1] Geymonat, G. and Weller, T. Classes de symétrie des solides piézoélectriques. C. R. Math. Acad. Sci. Paris (2002) 335:847–852.
- [2] Cramér, H. On the theory of stationary random processes. Ann. of Math. (1940) 41:215–230.
- [3] Malyarenko, A. and Ostoja-Starzewski, M. A random field formulation of Hooke’s law in all elasticity classes. J. Elasticity (2017) 127:269–302.
- [4] Malyarenko, A. and Ostoja-Starzewski, M. Tensor-valued random fields for continuum physics. Cambridge University Press (2019), Cambridge.
- [5] Bourbaki, N. Integration. II. Chapters 7–9. Springer (2004), Berlin.
- [6] Duistermaat, J.J., and Kolk, J.A.C. Lie groups. Springer (2000), Berlin.
- [7] Hofmann, K.H., and Morris, S.A. The structure of compact groups. De Gruyter (2013), Berlin.
- [8] Karhunen, K. Über lineare Methoden in der Wahrscheinlichkeitsrechnung. Ann. Acad. Sci. Fennicae. Ser. A. I. Math.-Phys. (1947) 37:1–79.
- [9] Altmann, S.L., and Herzog, P. Point-group theory tables. Clarendon Press (1994), Oxford.

Detection and Selection System of Healthily Growth Seedlings for a Plant Factory

Yasuhiko Manabe^{*}, Hitohide Usami^{**}, Taiyo Maeda^{***}, Shigeo Kawata^{****}

^{*}National Institute of Technology, Numazu College, ^{**}Tamagawa University, ^{***}Saitama Institute of Technology,
^{****}Utsunomiya University

ABSTRACT

We study about an automatic detection and selection of healthily growing seedlings and an automatic robot planting in a plant factory. The plant factory has various problems that should be solved. For example, the healthily growing seedlings are almost selected manually by experienced staffs of the plant factory. The detection speed has a limit. The employment cost of the staffs cannot also be ignored. If this process is automated, the production efficiency of the plant factory would be improved. Our PSE (Problem Solving Environment) system for the automatic detection, selection and planting in plant factory aims to automate these processes. This automation will contribute to reduce the total cost of the plant factory. In addition, the production efficiency will be improved at the plant factory. At first we describe about the automatic detection of the healthily growth seedlings. The PSE system takes pictures of the seedlings on a tray. Each seedling is labeled with markers. The system determines that where the seedlings exist on the tray by using markers. The pictures are analyzed by the image processing: the pictures are divided into each seedling area. Then the area of leaves of each seedling is calculated by the divided seedling pictures. Before the analysis, the pictures must be converted into grayscale color spaces. Because the pictures taken is in the RGB color spaces. However, if the pictures of RGB color spaces are converted into the grayscale, the color information of the pictures has been lost. Therefore, it becomes difficult to obtain the form of the leaves from the grayscale pictures. We use the HSV color spaces instead of RGB. The HSV color space has an advantage of the extracting particular colors. Thus, the HSV color spaces is suitable to obtain the shapes of the leaves. We obtain the clear shapes of the leaves by using the HSV color spaces. We can also obtain the area of the leaves by counting the white pixels of the pictures. The system determines healthily good seedlings from the area of the leaves. In addition, when the robot grips the healthy seedlings, the roots of the seedling hang by the gravity. The system also measures the length of the roots. The requirement of the healthy seedling includes the length. The robot transfers the really healthy seedlings to the next tray, which is transferred into the inside of the plant factory.

Atomic-scale Simulations of High Velocity Impact of Nanocrystalline Nanoparticles: Effect of Surface Roughness

Poshit Nag Mandali^{*}, Moneesh Upmanyu^{**}, Alireza Shahabi^{***}, Sinan Muftu^{****}

^{*}Northeastern University, ^{**}Northeastern University, ^{***}Northeastern University, ^{****}Northeastern University

ABSTRACT

High velocity impact of nanoparticles onto growing substrates has the potential for a range of next-generation additive manufacturing techniques. Nanoparticle synthesis techniques such as gas atomization usually result in rough surfaces, and the effect of the roughness on the impact dynamics remains poorly understood. In this talk, we focus aspects related to surface roughness of both the impacting nanoparticle, as well as the substrate. Molecular dynamics simulations of high velocity (500-2000 m/s) impact of Al nanocrystalline particles on single and polycrystalline substrates show that the dissipation of the kinetic energy is dramatically altered by the roughness. In addition to deformation of the substrate, the amorphization and flow of the roughness related asperities becomes an important aspect that determines the nature and extent of particle impingement. We present a simple theoretical model that captures the modified dissipation mechanism. The implications on additive techniques such as cold spray and laser-shock processing are discussed.

Scalable, Multi-Scale Methods for Coastal Modeling

Kyle Mandli^{*}, Jiao Li^{**}

^{*}Columbia University, ^{**}Columbia University

ABSTRACT

Coastal flooding due to severe storms is one of the most wide-spread and damaging hazards faced around the world. The threat of these events has grown not only due to increased population and economic reliance on coastal regions but also due to climate change impacts such as sea-level rise. Computational predictive capabilities are critical to addressing this threat but require the ability to handle multiple, disparate scales, handle the physics relevant at each of these scales, and remain tractable under the necessity of large ensembles to handle uncertainty in the input. In this context we present a novel Riemann solver based method developed to handle coastal barriers that are not required to align with a computational grid while not needing to be restricted by arbitrary CFL time-step restrictions made problematic by such approaches. Importantly the properties of the original Riemann solver, such as conservation and correct wet-dry interfaces, are maintained while allowing for the application of adaptive mesh refinement.

Dimensional Reduction of FEM-based Eigenvector Functions

Herbert A. Mang*

*Vienna University of Technology & College of Civil Engineering, Tongji University

ABSTRACT

Historically, stability limits on nonlinear prebuckling paths were often determined by means of so-called accompanying linear eigenvalue analysis in the framework of the Finite Element Method (FEM). One of the two coefficient matrices of the underlying linear eigenvalue problems was the tangent stiffness matrix, whereas the other one was an arbitrary real symmetric matrix. The aim of the present work is to support the hypotheses that (a) the absolute value of the initial vector velocity and (b) the ratio of the absolute value of the vector acceleration to its initial value are invariants with respect to the second coefficient matrix. By “vector velocity” and “vector acceleration” the first and the second derivative of the “fundamental eigenvector” of the linear eigenvalue problem concerned, with respect to a pseudo time, is meant. It must be equal to the arc length of the load-displacement path. At the stability limit, the “fundamental eigenvector” corresponds to the null eigenvalue. The mechanical background of the aforementioned hypotheses is the assumption that the product of the two asserted invariants is equal to one half of the non-membrane percentage of the strain energy. The nucleus of this work is computation of curves on the unit sphere, described by the vertex of the non-uniformly moving “fundamental eigenvector” of the linear eigenvalue problem concerned. To determine these curves, the N-dimensional “fundamental eigenvector” must be “reduced” to a vector, the vertex of which is defined by the two spherical coordinates. This “dimensional reduction” is based on the split of a relation for the rate of change of the radius of curvature of the surface curves to be determined. It allows for computation of the rate of change of the zenith angle, which is a prerequisite for determination of the azimuth angle. The practical added value of this work is the possibility to choose a particularly simple form of the underlying linear eigenvalue problem, with the unit matrix as one of the two coefficient matrices, to compute the non-membrane percentage of the strain energy. This quantity provides insight into the load-carrying mechanism of structures, subjected to proportional loading [1]. References: [1] H.A. Mang, Evolution and verification of a kinematic hypothesis for splitting of the strain energy. *Comput. Methods Appl. Engrg.*, Vol. 324, pp. 74-109, 2017.

Mechanical Positioning of Multiple Myonuclei in Muscle Cells

Angelika Manhart*, Alex Mogilner**

*Courant Institute, New York University, **Courant Institute, New York University

ABSTRACT

Many types of large cells have multiple nuclei. In long muscle cells, the nuclei are distributed almost uniformly along their length. This nuclear positioning is crucial for cell function. Mechanisms of the nuclear positioning remain unclear. We examine computationally the hypothesis that a force balance generated by microtubules positions the nuclei. Rather than assuming what the forces are, we allow various types of forces between the pairs of nuclei and between the nuclei and cell boundary to position the nuclei according to the laws of mechanics. Mathematically, this means that we start with a great number of potential models. We use the reverse engineering approach by screening the models and requiring their predictions to fit imaging data on nuclei positions and shapes from hundreds of muscle cells of *Drosophila* larva. Computational screens result in a small number of feasible models, the most adequate of which suggests that the nuclei repel from each other and cell boundary with forces that decrease with distance. This suggests a hypothesis that microtubules growing from nuclear envelopes push on neighbouring nuclei and cell boundary, which is sufficient for the nearly-uniform nuclear spreading. We support this hypothesis with simulations of an agent-based mechanical model. The model makes nontrivial predictions about the increased nuclear density near the cell poles, zigzag patterns of the nuclei positions in wider cells, and about correlations between the cell width and elongated nuclear shapes, which we confirm by image analysis of the experimental data.

Simulation and Learning for Process Modeling and Control of Powder-Bed Metal Additive Manufacturing

Antoinette Maniatty^{*}, Souvik Roy^{**}, James Dolan^{***}, Sandipan Mishra^{****}, Alexander Shkoruta^{*****}

^{*}Rensselaer Polytechnic Institute, ^{**}Rensselaer Polytechnic Institute, ^{***}Rensselaer Polytechnic Institute, ^{****}Rensselaer Polytechnic Institute, ^{*****}Rensselaer Polytechnic Institute

ABSTRACT

A finite element simulation tool for modeling metal powder-bed additive manufacturing is developed and used to study the effect of processing parameters on metrics associated with part quality. An efficient finite element formulation is derived that predicts temperature, phase (melt/solid), and porosity for given processing parameters – power, beam diameter, and path history. In the formulation, we introduce two state variables into the first law of thermodynamics, a phase parameter to characterize the transition between solid and melt, and a consolidation parameter to characterize the degree of consolidation from powder to dense material, which naturally predict local porosity. The model is fully implicit, and is expressed in a total Lagrangian framework that accounts for the changing geometry as the powder consolidates. The formulation is implemented in a parallel simulation framework allowing for scalable computations on high performance computing platforms. From the temperature and phase history, the evolution of the grain structure at key locations in the part are predicted using a novel Monte Carlo algorithm for predicting grain growth in the presence of time varying temperature gradients. Input and output data from the simulations is analyzed to develop control-oriented low order models. Such control-oriented models can be used for designing and certifying feedback and feedforward control algorithms that can regulate, for example, melt pool geometry or temperature fields inside the melt pool itself. As an example, an iterative learning control algorithm is designed based on this lower order model to update processing parameters for improved part performance. The algorithm is then validated on the simulation tool to certify its performance. Test cases for a single layer process and for a multi-layer partial part build are used to demonstrate the simulation capabilities and quality improvement through process control applied to the simulation tool.

On Modeling Cyclic Mobility of Sand

Majid Manzari*

*The George Washington University

ABSTRACT

Cyclic mobility of medium dense saturated sands subjected to cyclic shearing is the cause of significant deformations in civil infrastructure systems that are subjected to severe ground shaking. While several existing elastoplastic constitutive models are shown to capture the observed responses of sands in monotonic shearing, these models are rarely able to produce realistic simulations of sand behavior in cyclic shearing, particularly when cyclic mobility is involved. In this work, the capabilities of a critical state two-surface plasticity model of sand (Manzari and Dafalias, 1997; Dafalias and Manzari, 2004, Manzari and Yonten, 2010) are evaluated against a range of stress and strain paths that are caused by earthquakes. In particular, the model performance is evaluated in simulation of cyclic direct simple shear tests on medium dense soils that exhibit cyclic mobility. The key similarities and differences between the numerical simulations and the experimentally observed responses are noted and analyzed. Specific enhancements are then proposed to improve the capabilities of the model in simulation of cyclic mobility. The proposed enhancements are implemented in a fully-coupled stress-flow finite element platform for analysis of seismic response of saturated soil structures. Two boundary value problems that involve cyclic mobility of medium dense sands are then simulated and the role of model enhancement in the improvement of the simulation results are identified. It will be shown that a more accurate simulation of plastic shear strains in the calibration phase of the constitutive model will lead to noticeable improvement of the ability of the model and the numerical simulation platform to simulate permanent deformations of saturated sand deposits that are subjected to significant shaking levels. 1. Manzari, M.T. and Dafalias, Y. F. (1997). A critical state two-surface plasticity model for sands. *Geotechnique*, Volume 47 Issue 2, April 1997, pp. 255-272. <https://doi.org/10.1680/geot.1997.47.2.255> 2. Dafalias, Y.F. and Manzari, M.T. (2004). Simple Plasticity Sand Model Accounting for Fabric Change Effects. *Journal of Engineering Mechanics*, Vol. 130, Issue 6, [https://doi.org/10.1061/\(ASCE\)0733-9399\(2004\)130:6\(622\)](https://doi.org/10.1061/(ASCE)0733-9399(2004)130:6(622)). 3. Manzari, M. T. and Yonten, K. (2011). Analysis of post-failure response of sands using a critical state micropolar plasticity model, *Interaction and Multiscale Mechanics*, Vol. 4, No. 3, <http://dx.doi.org/10.12989/imm.2011.4.3.187>.

Adaptive Stopping Criterion for Iterative Linear Solvers in an Anisotropic Stabilized AFEM Framework, with Applications to Convection-dominated Problems

Gabriel Manzinali^{*}, Youssef Mesri^{**}, Elie Hachem^{***}

^{*}MINES ParisTech, PSL - Research University, CEMEF - Centre for material forming, ^{**}MINES ParisTech, PSL - Research University, CEMEF - Centre for material forming, ^{***}MINES ParisTech, PSL - Research University, CEMEF - Centre for material forming

ABSTRACT

Adaptive finite elements methods (AFEM) are nowadays well known to be a reliable approach to achieve better accuracy in the solution of PDEs, at a reduced computational cost. A typical adaptation procedure starts from a solution on an initial discretization of the computational domain, computes the estimated error distribution on that mesh, and using this information defines the topology of the new spatial discretization. The solving step implies the solution of the linear system that stems from the discretization of the continuous problem. Usually the solution of this system is assumed to be exact. In real-world application however, this kind of system can be solved efficiently only with an iterative procedure, which provides an approximation to the exact solution. The accuracy of this approximation is controlled by the stopping criteria used to drive the convergence of the iterative procedure. As remarked by Becker, Johnson, and Rennacher in their seminal work [1], ad hoc stopping criteria are commonly used. These criteria are straightforward to implement, but have no direct link to the actual error in the approximate solution. This could possibly affect efficiency and accuracy. On one hand, a highly accurate approximation is inefficient and most likely unnecessary, on the other hand, a poor approximation affects the accuracy of the solution and the convergence of the adaptation procedure. In this work we propose an adaptive stopping criterion that follows the approach proposed in [2], integrated with the anisotropic mesh adaptation procedure. Using information from this procedure we provide an adaptive control for the linear solver that proves to be effective to considerably reduce the number of iteration needed by the solver, without spoiling the accuracy of the solution. We apply this framework to convection-diffusion problems in 2D and 3D, relying on a stabilized finite element method. References: [1] Roland Becker, Claes Johnson, and Rolf Rannacher. Adaptive error control for multigrid finite element. *Computing*, 55(4):271–288, 1995. [2] Marco Picasso. A stopping criterion for the conjugate gradient algorithm in the framework of anisotropic adaptive finite elements. *International Journal for Numerical Methods in Biomedical Engineering*, 25(4):339–355, 2009.

Three-dimensional multiscale modeling of concrete based on the use of finite element with high aspect ratio and coupling finite elements

Osvaldo L. Manzoli*, Eduardo A. Rodrigues**, Luís A. G. Bitencourt Jr.***, Pedro R. Cleto****, Heber A. A. Fabbri*****

*Sao Paulo State University (UNESP), **Sao Paulo State University (UNESP), ***Polytechnic School at the University of Sao Paulo, ****Sao Paulo State University (UNESP), *****Sao Paulo State University (UNESP)

ABSTRACT

The mechanical properties and arrangement of the constituents of concrete in mesoscale determine its mechanical behavior and failure process. Modeling a representative distribution of the coarse aggregates into the mortar matrix constitutes a typical situation that requires a three-dimensional arrangement representation. This work proposes a three-dimensional concurrent multiscale model for plain concrete, consisting of two well-separated macro and mesoscale. In the macroscale the concrete is treated as an elastic material with homogenized elastic parameters. To construct the concrete in mesoscale, coarse aggregates with regular and irregular shaped are generated from a grading curve and placed into the mortar matrix randomly, using the 'take-and-place' method. To represent the interfacial transition zone (ITZ) and simulate the crack propagation process the mesh fragmentation procedure is used [1]. This technique is based on the use of standard finite elements with high aspect ratio, which are inserted in between all regular finite elements of the mortar matrix and in between the mortar matrix and aggregate elements, representing the ITZ [2]. A tension damage constitutive relation between stresses and strains consistent with the Continuum Strong Discontinuity Approach (CSDA) is used to describe crack formation and propagation. The use of coupling finite elements (CFEs) [3] is proposed to enforce the continuity of displacements between the non-matching meshes corresponding to the two different finer and coarser scales. These CFEs can ensure the correct connection between these scales without increasing the total number of degrees of freedom of the problem. Numerical examples are performed to show the ability of the proposed method to predict the behavior of cracks initiation and propagation in the tensile region of the material. The numerical results are compared with the experimental ones. Keywords: 3D numerical analysis, multiscale analysis, finite element, damage model, interface finite element, coupling finite element, plain concrete, cracks propagation. References: [1] Manzoli OL, Maedo MA, Bitencourt Jr. LAG, Rodrigues EA. On the use of finite elements with a high aspect ratio for modeling cracks in quasi-brittle materials. *Engineering Fracture Mechanics*, 153: 151-170, 2016 [2] Rodrigues EA, Manzoli OL, Bitencourt Jr LAG, Bittencourt TN. 2D mesoscale model for concrete based on the use of interface element with a high aspect ratio. *International Journal of Solids and Structures*, 94–95: 112–124, 2016. [3] Bitencourt Jr. LAG, Manzoli OL, Prazeres PGC, Rodrigues EA, Bittencourt TN. A coupling technique for non-matching finite element meshes. *Comput. Methods Appl. Mech. Engrg.*, 290: 19–44, 2015.

Data-driven Computing with Deep Neural Networks for Inverse Modeling of Two-phase Flows

Xiaoyu Mao^{*}, Vaibhav Joshi^{**}, Tharindu Pradeeptha Miyanawala^{***}, Rajeev Kumar Jaiman^{****}

^{*}National University of Singapore, ^{**}National University of Singapore, ^{***}National University of Singapore,
^{****}Natioanl University of Singapore

ABSTRACT

Efficient prediction of fluctuating wave force on a floating or a submerged body is of great significance in many offshore and marine engineering applications. While a tremendous amount of wave-body interaction data is generated in offshore engineering via both CFD simulations and experiments, the results are generally underutilized. Design space exploration and motion control of such practical scenarios are still time-consuming using high-fidelity physical data. In this talk, we present a Convolutional Neural Network (CNN) based data-driven computing to predict the unsteady wave forces on submerged bodies due to the free-surface wave motion. The wave forces are investigated by the stabilized finite element method solver based on the Navier-Stokes equations and the Allen-Cahn phase-field approach. For the interface capturing, the Allen-Cahn equation is solved in the mass-conservative form by imposing a Lagrange multiplier technique [1]. An alternative to semi-analytical modeling, CNN is a class of deep neural network for solving inverse problems which are efficient in parametric data-driven computation and can use the domain knowledge [2]. In this study, CNN-based data-driven computing is utilized to predict the wave forces on bluff bodies with different geometries and distances to free surface. The predictions are made after the CNN is trained by a constructed input function based on input parameters and the target data generated by the full-order model. The proposed CNN-based model reduction procedure has a profound impact on the parametric design of bluff bodies experiencing wave loads. Following this, we next propose a deep neural network procedure, which combines Convolutional Neural Network (CNN) and Recurrent Neural Network (RNN) to construct the reduced-order model for two-phase modeling. While the CNN is responsible for processing the spatial information in the flow field, the RNN performs the predictions for the temporal evolution based on the training flow field data from the full-order model. After training for several initial time steps, the neural network is utilized for the fast prediction with a reduced computational cost in the following time steps. We demonstrate the accuracy and validation of the proposed data-driven technique for increasing complexity of problems. References [1] Joshi, V., and Jaiman, R. K., 2017. "A positivity preserving and conservative variational scheme for phase-field modeling of two-phase flows". Journal of Computational Physics, <http://arxiv.org/abs/1710.09831> [2] Miyanawala, T. P., and Jaiman, R. K., 2017. "An efficient deep learning technique for the Navier-Stokes equations: Application to unsteady wake flow dynamics". arXiv preprint arXiv:1710.09099

Fracture of Elastomeric Materials by Crosslink Failure

Yunwei Mao^{*}, Lallit Anand^{**}

^{*}Department of Mechanical Engineering, MIT, ^{**}Department of Mechanical Engineering, MIT

ABSTRACT

If an elastomeric material is subjected to sufficiently large deformations it eventually fractures. There are two typical micromechanisms of failure in such materials: chain scission and crosslink failure. The chain scission failure mode is mainly observed in polymers with strong covalent crosslinks, while the crosslink failure mode is observed in polymers with weak crosslinks. In two recent papers we have proposed a theory for progressive damage and rupture of polymers with strong covalent crosslinks. In this talk we extend our previous framework and formulate a phase field damage theory for modeling failure of elastomeric materials with weak crosslinks. We first introduce a model for the deformation of a single chain with weak crosslinks at each of its two ends using statistical mechanics arguments, and then upscale the model from a single chain to the continuum-level for a polymer network. Finally, we introduce a damage variable to describe the progressive damage and failure of polymer networks. A central feature of our theory is the recognition that the free energy of elastomers is not entirely entropic in nature, there is also an energetic contribution from the deformation of the backbone bonds in a chain and/or the crosslinks. For polymers with weak crosslinks this energetic contribution is mainly from the deformation of the crosslinks. It is this energetic part of the free energy which is the driving force for progressive damage and fracture of elastomeric materials. We have numerically implemented this theory in an open-source finite element code MOOSE by writing our own application. Using this simulation capability we have presented results from simulations of: (i) fracture of single-edge-notched specimens; (ii) fracture of an asymmetric double-edge-notched specimen; and (iii) fracture of a sheet specimen with multiple circular and elliptical holes, under our plane stress conditions. These examples show the powerful capability of our gradient damage theory and its numerical implementation to simulate the complicated fracture process of nucleation, propagation, branching and merging of cracks in elastomeric materials in arbitrary geometries undergoing large deformations. We expect that our theory and numerical simulation capability will be useful in studying various interesting phenomena such as crazing and cavitation in soft materials.

Dynamic Elasto-Plasticity in Metals Computed by a Discrete Element Method

Frédéric Marazzato^{*}, Alexandre Ern^{**}, Christian Mariotti^{***}, Karam Sab^{****}

^{*}Université Paris-Est, Cermics (ENPC), F-77455 Marne-la-Vallée cedex 2 and Inria Paris, EPC SERENA, F-75589 Paris, France and CEA, DAM, DIF, F-91297 Arpajon, France, ^{**}Université Paris-Est, Cermics (ENPC), F-77455 Marne-la-Vallée cedex 2 and Inria Paris, EPC SERENA, F-75589 Paris, France, ^{***}CEA, DAM, DIF, F-91297 Arpajon, France, ^{****}Université Paris-Est, Laboratoire Navier (UMR 8205), CNV, ENPC, IFSTTAR, F-77455 Marne-la-Vallée, France

ABSTRACT

Since their first use by Hoover et al (1974) in models for crystalline materials and Cundall & Strack (1979) in geotechnical problems, Discrete Elements methods (DEM) have found a large field of application in granular materials, soil and rock mechanics. The handling of a set of particles interacting by means of forces and torques allows a variety of models for the expression of these bonds and for the material's behavior. L. Monasse and C. Mariotti (2012), have been able to simulate the deformation and fragmentation of a three-dimensional linear elastic brittle material. The discretisation is achieved through rigid convex polyhedral particles. The forces and torques are computed directly through macroscopic quantities like the distance and relative rotation between two particles. The aim of this presentation is to introduce an extension of this formalism with the goal to compute anisothermal dynamic plasticity with strain rate dependence in metals. The behaviors considered are for instance the Johnson-Cook model (1983). Elements of proof for the well-posedness and convergence of the discretisation will also be given. A special attention has been given to the correct approximation of the elastic inequality constraint. In addition, since energy dissipation is crucial for cracking phenomena, a special energy-conserving time-integration scheme has been developed in (F. Marazzato et al, 2017) to compute the solid dynamics.

Note on Initiation of Turbulence, a Systemic View

Pedro Marcal*

*Mpact Corp.

ABSTRACT

Turbulence is a much studied subject in Fluid Flow. Though we are able to predict some of its behavior numerically, other features remain somewhat obscure. In particular, at what point does a laminar flow transition into turbulence? Launder and Spalding used a two equation transport model [1] for turbulence. This model requires an initial seeding of turbulence. In this note we will make some assumptions as to the nature of the phenomenon and then using a Least Squares Finite Element Method (LSFEM, Jiang [2]) implemented in the MPACT code, we carry out a simulation to gain some further insight. Here we follow methods similar to those used in linear fracture mechanics [3], where we use a balance of energy for pre and post fracture conditions. Because of the nature of the viscous flow, we consider a balance of the rate of work prior to turbulence and post turbulence. This balance gives the initiation conditions which include the transition of one or more elements (volume) to turbulent flow. The transition elements are assumed to transform into elements with a large number of frequencies and as such contribute nearly nothing to the laminar flow. The balance of rate of work is established by numerical analysis of the flow system. When we increase the velocity of flow, the equivalent stress increases to a point where the fluid system can no longer support any further increase in stress so that the laminar flow morphs into a turbulent flow. We assume it turns into local eddies of random and high frequencies that are subsequently dissipated. We assume that turbulence initiation takes place in the elements in the regions of max equiv_stress. One for each region to maintain symmetry of flow. The chosen elements are assumed to have reduced flow with no memory of the applied stress caused by the flow. Its assumed to have a reduced shear rate modulus that is a tenth or less of its original value, in order to keep up the mean flow. References [1] B.E. Launder; D.B. Spalding, D.B., The numerical computation of turbulent flows,. Computer Methods in Applied Mechanics and Engineering. 3 (2): 269–289, 1974 [2] Bo-Nan Jiang, Louis A. Povinelli, Least-squares Finite Element Method for Fluid Dynamics, NASA Technical Memorandum 102352, ICOMP-89-23, 1989 [3] J.R. Rice, A path independent integral and the approximate analysis of strain concentrations by notches and cracks, J. Appl. Mechanics, 35, 379-386, 1968

Influence of Meso-Structure on the Mechanical Response of FDM 3D Printed Material

Sonia Marfia^{*}, Gianluca Alaimo^{**}, Ferdinando Auricchio^{***}, Elio Sacco^{****}

^{*}Department of Civil and Mechanical Engineering, University of Cassino and Southern Lazio, Italy, ^{**}Department of Civil Engineering and Architecture, University of Pavia, Italy, ^{***}Department of Civil Engineering and Architecture, University of Pavia, Italy, ^{****}Department of Structures for Engineering and Architecture, University of Naples Federico II, Italy

ABSTRACT

Lately, Additive Manufacturing (AM) processes via 3D printers have made several progress with the aim of becoming rapid manufacturing methods to produce finished components. A crucial point in the use of AM solutions for direct production is the satisfactory evaluation of the mechanical properties of the printed components, so that they can be correctly accounted for in the design phase [1]. The present study focuses on the determination of the mechanical properties of Fused Deposition Modeling (FDM) 3D-printed objects. In FDM processes a thermoplastic filament is heated and extruded: the material is deposited layer by layer on a printing surface. Each printed layer is made of filaments, called fibers and deposited in a plane parallel to the printing surface, and of voids, since the deposited material is not able to full the space due to geometrical and process constraints. Thus, the obtained material can be considered as a composite with two phases, i.e. fibers and voids. Process parameters, such as fiber thickness, width and orientation and fiber-to-fiber overlap significantly influences the printed material overall mechanical response. Some studies have been proposed in literature to investigate the response of FDM 3D-printed materials [2]. Accordingly, the aim of the present study is to develop a meso-macro analysis for studying the mechanical response of FDM 3D-printed material. To this end a representative volume element (RVE) of the heterogeneous material made by the filament and the voids is analyzed. Initially, a micromechanical approach based on nonlinear finite element analyses is developed. Finite elements characterized by 3D displacement fields that do not vary along the fiber axis are proposed. Then, a homogenization technique, based on Transformation Field Analysis [3], is implemented. The homogenization approach is able to model the nonlinear phenomena occurring at the mesoscale level, introducing an approximation for the inelastic strain field. Thus, a proper constitutive model for the filament, able to describe all the non-linear phenomena occurring in the material, is proposed. The RVE is divided in subsets, and in each subset the inelastic strain is considered uniform. A numerical procedure is developed to study the evolution of the subset inelastic strains that represent the internal variables of the problem. Several types of RVEs characterized by different distribution of filaments and by the presence of voids of different shapes are studied. In order to assess the efficiency of the proposed micromechanical approach and homogenization technique comparisons with experimental data are performed.

Computational Strategies for Chemo-Mechano-Biological Response to Arterial Injury

Michele Marino^{*}, Meike Gierig^{**}, Malte Rolf-Pissarczyk^{***}, Peter Wriggers^{****}

^{*}Institute of Continuum Mechanics, Leibniz Universität Hannover, ^{**}Institute of Continuum Mechanics, Leibniz Universität Hannover, ^{***}Institute of Continuum Mechanics, Leibniz Universität Hannover, ^{****}Institute of Continuum Mechanics, Leibniz Universität Hannover

ABSTRACT

A common approach for modeling stress-induced growth and remodeling on a continuum level is the introduction of a multiplicative split of the deformation gradient into an elastic and inelastic part. The evolution of the inelastic part is described by physically motivated growth and remodeling laws governed by a target function based on a homeostatic stress value. These laws allow to govern the effects related to changes in the stress-free configuration induced by mass variations of tissue constituents that are optimal for the maintenance of a physiological stress [1]. On the other hand, in living systems, the injury of a tissue activates a cascade of cell-cell interactions, involving biologically active molecular species (e.g., growth factors, proteinases and cytokines) that induce changes in the composition and the histology of extracellular matrix, as well as growth of specific cell species [2]. Although these mechanisms can be implicitly incorporated in classical approaches for growth and remodeling, a mechanistic insight on these chemo-mechano-biological mechanisms provide a special insight on non-functional responses to tissue injury, such as the ones occurring during in-stent restenosis. Accordingly, this work presents computational strategies for incorporating the explicit description of chemo-mechano-biological effects in the context of tissue growth and remodeling following arterial tissue injury. From the theoretical and computational point of view, the aim of present work inherits significant challenges: the deformation gradient is decomposed into an elastic and an inelastic part to consider elastoplastic effects [3]; an ad hoc invariant-based Helmholtz free energy is formulated in order to include the anisotropic tissue mechanical response [2,3]; a transport problem modeling cell-cell signaling pathways is defined and regulated by the internal variable associated with plastic mechanisms [3]; growth and remodeling laws are defined on the basis of the resulting molecular concentrations. The computational models are firstly implemented in a staggered way. Then, by exploiting the separation of the characteristic time scales, strategies for coupling these multiphysics simulations are traced. Parametric simulations will be conducted, considering both idealised and patient-specific geometries, as well as variations in the diffusivity properties of a tissue, in loading conditions associated with different physio-pathological conditions, or in mechanobiological relationships between transport and growth and remodeling. [1] Cyron, C.J., Aydin, R.C., Humphrey, J.D. Biomechanics and Modeling in Mechanobiology, 15(6):1389-1403 (2016). [2] Marino, M., Pontrelli, G., Vairo, G., Wriggers, P. Journal of the Royal Society Interface 14:20170615 (2017). [3] Gasser, T.C., Holzapfel, G.A. Computational Mechanics 40:47-60 (2007).

A Meshless Method for Quasi-static Crack Propagation in 3D Heterogeneous Elastic Media

Anatoly Markov^{*}, Sergei Kanaun^{**}

^{*}Tecnologico de Monterrey, ^{**}Tecnologico de Monterrey

ABSTRACT

An efficient mesh-free numerical method for the solution of the problem of slow crack growth in an infinite 3D-homogeneous medium containing inhomogeneities (cracks and inclusions) is developed. A finite region of the medium containing the inhomogeneities is subjected to arbitrary external forces. The problem is reduced to a system of surface integral equations for crack opening vectors and volume integral equations for stress tensors inside the inclusions. Stress fields inside inclusions and crack opening vectors are approximated by Gaussian functions centered at a system of nodes. The elements of this matrix are calculated in closed analytical forms (for inclusions) or expressed in terms of five standard 1D-integrals (for cracks). For regular node grids, the matrix of the discretized system has Toeplitz's structure, and Fast Fourier Transform technique can be used for calculation of matrix-vector products with such matrices. An iterative process is proposed for the construction of the crack shape in the process of crack growth. At every iteration of this process, calculation of so-called equilibrium crack is required. For such a crack, the stress intensity factors (SIFs) on the crack edge are equal to the corresponding material fracture toughness. Examples of crack evolution for various properties of medium and types of loading are presented.

Thrust Membrane Analysis of Masonry Vaults

Francesco Marmo^{*}, Luciano Rosati^{**}

^{*}Università di Napoli Federico II, ^{**}Università di Napoli Federico II

ABSTRACT

Based on Heyman's principles of limit analysis of no tension structures, the Thrust Network Analysis (TNA) was firstly contributed by O'Dwyer [Funicular analysis of masonry vaults. Computers and Structures, 73:187-197, (1999)] who proposed a technique for modelling the principal stresses in a masonry vault as a discrete network of forces in equilibrium with the applied loads. Using projective geometry and linear optimization algorithms, Block [Thrust Network Analysis. PhD thesis, Massachusetts Institute of Technology, (2009)] provided a graphical and intuitive interpretation of O'Dwyer's method. O'Dwyer's and Block's versions of the method have been recently reformulated by Marmo and Rosati [Reformulation and extension of the thrust network analysis. Computers and Structures, 182:104-118, (2017)] where the methodology is extended to include the effects of horizontal forces and the presence of holes or free edges. The generality and efficiency of this recent improved approach has been witnessed by his application to masonry stairs of very complicated geometry. All versions of the TNA model membrane stresses as concentrated thrust forces lying along the branches of the network. Hence, although the method is very general and applicable to the limit analysis as well as to the form finding of structures having a very complicated geometry, the evaluation of the membrane stresses starting from the value of branch thrust is still an issue. Here we present the preliminary results of the application of an alternative strategy in which the membrane thrusts within the structure are modeled by triangular stress elements. These elements substitute the classical network branches so that the correspondence between thrust stresses and the equilibrium condition of the membrane nodes is straightforward. The method is applied to the limit analysis of a cross vault in which membrane elements, representing the membrane stresses within the vault, and branch elements, representing thrust forces within the groins, are both used within the same model.

EULER-EULER MODELLING OF THE INTERACTION OF A GAS-PARTICLE MIXTURE WITH A DETACHED SHOCK

G. MAROIS^{*†}, P. VILLEDIEU^{#†}, J. MATHIAUD^{*}

gentien.marois@cea.fr
philippe.villedieu@onera.fr
julien.mathiaud@cea.fr

^{*}CEA CESTA, 14 Avenue des Sablières, Le Barp, France

[†]INSA-TOULOUSE, 135 Avenue de Rangueil, Toulouse, France

[#]ONERA/DMPE, Université de Toulouse, F-31055 Toulouse (France)

Key words: Multiphase flows, Gas-particle mixtures, Shock Disturbance.

Abstract. This work deals with the interaction of a mist of solid particles and a stationary detached shock wave. Experiments over a 3 inches sphere were done in the 70's at the Boeing Hypersonic Wind Tunnel^[1]. A very strong modification of the detached shock was observed. The aim of the present work was to check the capability of numerical simulations based on an Euler-Euler approach to reproduce this behavior. Comparisons with Hulin and Znaty^[2] simulations (performed with an Eulerian-Lagrangian approach) have been carried out and the results are discussed.

1 INTRODUCTION

Studies of gas-particle two-phase flows (both subsonic and supersonic) are fairly recent and complex since they involve a lot of additional physical phenomena compared to single-phase flows. The work presented here deals with the interaction of a stationary detached shock wave with a mist of spherical particles (that are solid particles in the scope of the present study). Such interactions are encountered in a large range of scientific and engineering applications, from planetary explorations to motors design.

During last decades, several studies have been devoted to this problem. Analytical works were done for example by Carrier^[3] or Marble^[4]. Experimental investigations were performed, for example in Boeing laboratories^[1,5] and were completed by numerical simulations (Papadopoulos^[6], Palmer^[7]). These numerical studies were all based on the so-called Eulerian-Lagrangian method which consists in an Eulerian treatment of the gas phase and a Lagrangian treatment of the particulate phase. This approach is very popular since it can be quickly implemented and allows to easily take into account complex physical phenomena like particle breakup, complex wall-particle interactions, etc. However, when one is interested in the rate of particle impact on a surface or the density of particles in the vicinity of an obstacle, this approach requires the use of a very large number of numerical particles to get accurate results. In addition, due to load balancing issues, this approach is very difficult to implement efficiently on a massively parallel computer.

To overcome this limitation, in the present work, the Eulerian-Eulerian approach has been preferred even if it is more complex both from a numerical and a physical point of view. A finite volume method has been used to solve the equations of both phases. The particulate phase being very diluted in all targeted applications, its volume fraction (but not its mass density) is assumed to be negligible and its influence on the gas flow is taken into account via source terms in the right-hand side of the gas equations.

The paper is divided into four parts. First, the model is presented. We then detail the numerical method used as well as some results of validation tests carried out to ensure that the method has been correctly implemented and gives the expected results in simple but representative cases of application. The last part is devoted to attempts to replicate the Boeing experiment of the 70's concerning the interaction of a shock wave with a mist of particles.

2 PROBLEM FORMULATION

2.1 Eulerian model for the gas

The gas phase is modeled by the Navier-Stokes equations adapted for reacting gases (including vibrational energy effects, chemical reactions of dissociation, etc.). More details can be found in ^[8]. These equations can be schematically written as:

$$\partial_t \mathbf{U}_g + \partial_x \mathbf{G}(\mathbf{U}_g, \nabla \mathbf{U}_g) = \mathbf{S}_{\text{ext}} + \mathbf{S}_{\text{ch}} + \mathbf{S}_p \quad (1)$$

where \mathbf{U}_g denotes the vector of the gas phase conservative variables, \mathbf{G} corresponds to the flux terms, \mathbf{S}_{ch} corresponds to the chemical reaction source terms, \mathbf{S}_p denotes the source terms that takes into account the influence of the particles on the gas flow, and \mathbf{S}_{ext} is a source term that takes into account other effects like external forces, etc.

2.2 Eulerian model for the particles

In this paper, we limit ourselves to the case where the dispersed phase is composed of solid spherical particles whose only interactions with the gas phase are the exchange of momentum (via the drag force) and heat (by forced convection). However, the model presented below as well as its numerical treatment can be adapted to deal with more general cases (in particular the case of liquid particles), for which other phenomena must be taken into account like particle evaporation, sublimation, break-up, etc.^[18]

There are several variants of the Eulerian approach for the treatment of the particulate phase (see for example ^[6, 7]). Here, we have chosen the sampling method ^[9] which has the advantage of being the simplest to implement. It consists of dividing the particulate phase into N classes, each characterized by its number density field $n_i(t, \mathbf{x})$, its mass density field $m_i(t, \mathbf{x})$, its velocity field $\mathbf{v}_i(t, \mathbf{x})$ and its temperature field $T_i(t, \mathbf{x})$. Assuming that all the particles belonging to the same class and located at the same point have the same velocity, same diameter and same temperature, the following set of conservation equation can be easily derived:

$$\begin{cases} \partial_t n_i + \nabla_x(n_i \mathbf{v}_i) = 0 \\ \partial_t m_i + \nabla_x(m_i \mathbf{v}_i) = 0 \\ \partial_t m_i \mathbf{v}_i + \nabla_x(m_i \mathbf{v}_i \otimes \mathbf{v}_i) = n_i \mathbf{F}_i \\ \partial_t m_i h_i + \nabla_x(m_i \mathbf{v}_i h_i) = n_i H_i \end{cases} \quad (2)$$

where $h_i = h_p(T_i)$ denotes the specific enthalpy of the particles of class i (supposed to be very close to their specific internal energy $e_p(T_i)$), \mathbf{F}_i denotes the drag force acting on the particles of class i and H_i correspond the convective heat flux for the particles of class i . The drag force is given by:

$$\mathbf{F}_i = -\frac{\pi}{8} d_i^2 \rho_f C_D \|\mathbf{v}_i - \mathbf{u}_g\| (\mathbf{v}_i - \mathbf{u}_g) \quad (3)$$

where C_D is the drag coefficient. The particle mass density m_i , the particle number density n_i , the particle diameter d_i and the particle temperature T_i are linked by the following relationship:

$$m_i = \frac{\pi}{6} n_i \rho_p(T_i) d_i^3 \quad (4)$$

where ρ_p denotes the particulate phase bulk density (supposed to depend only on the temperature). The drag coefficient C_D depends on the particle Reynolds number Re_i and particle Mach number M_i . It can be calculated by combining Swain^[10] with Clift and Gauvin^[11] empirical formula:

$$\begin{cases} C_D^1(M_i, Re_i) & \text{for } M_i < 0.6 \\ C_D^2(M_i, Re_i) & \text{for } M_i > 1.3 \\ C_D^1(0.6, Re_i) + \frac{M_i - 0.6}{0.7} (C_D^2(1.3, Re_\infty) - C_D^1(0.6, Re_i)) & \text{elsewhere} \end{cases}$$

with: (5)

$$\begin{aligned} C_D^1(M_i, Re_i) &= \frac{24}{Re_i} (1 + 0.15 Re_i^{0.687}) + \frac{0.42}{1 + 42500 Re_i^{-1.16}} \\ C_D^2(M_i, Re_i) &= 1 + 4.66 Re_i^{-0.5} \end{aligned} \quad (6)$$

Introducing the Nusselt number, Nu_i , the heat flux H_i can be defined as:

$$H_i = \lambda_g \pi Nu_i d_i (T_g - T_i) \quad (7)$$

with the Nusselt number being calculated thanks to Fox formula^[12] which is an extension of classical subsonic fits^[13] to supersonic flows:

$$Nu_i = \frac{2 \exp(-M_i)}{1 + 17 M_i / Re_i} + 0.459 Pr^{0.33} Re_i^{0.55} \frac{1 + 0.5 \exp(-17 M_i / Re_i)}{1.5} \quad (8)$$

The particulate source term in the r.h.s. on the gas phase balance equations can be easily deduced from the conservation of momentum and energy. It writes:

$$S_p = - \begin{pmatrix} 0 \\ \sum_{i=1}^N n_i \mathbf{F}_i \\ \sum_{i=1}^N n_i \mathbf{F}_i \cdot \mathbf{v}_i + n_i H_i \end{pmatrix} \quad (9)$$

where $n_i \mathbf{F}_i \cdot \mathbf{v}_i$ corresponds to the power of the drag force. This term does not appear in the particles' equations (2) because the last equation involves the particle specific enthalpy (or G. internal energy) instead of the particle total energy. It is worth mentioning that this formulation is adapted even in the case of supersonic flows because the fields associated with the particulate phase is not discontinuous through shocks (due to the finite relaxation time scales of the particles). If the gas equations are coupled with a turbulence model, it is also necessary, at least from a theoretical point of view and for consistency reasons, to take into account the influence of the particulate phase on turbulence production and dissipation by adding source terms in the turbulence model equations. We will come back to this question in section 5.3.

In most applications, particle interactions with solid walls play a fundamental role. In the Eulerian approach, since all the particles of a given class and located at the same point are supposed to have the same velocity (no pressure term in the momentum equation contrary to the gas phase), it is mandatory to introduce additional classes to deal with the secondary particles created during the impact of particles onto a wall (due to rebound, fragmentation and erosion). The number of additional classes will depend on the complexity of the impact model. In the present work, for the sake of simplicity, we have only considered the simplest model which consists of allocating only one secondary class to each primary class.

Let's denote by i_r the index of the class of secondary particles corresponding to the class i_p of primary particles. At the beginning of the calculation, there is no particle in class i_r (which means that $m_{i_r} = 0$ in all mesh cells). When particles of class i_p impinge the wall, new particles are created in the corresponding class i_r . In the present work, the following model was used to compute the mass flux of the reemitted particles, their velocity, their diameter and their temperature:

$$\begin{cases} \mathbf{v}_{i_r} \cdot \mathbf{n} = \epsilon_n \mathbf{v}_{i_p} \cdot \mathbf{n} \\ \mathbf{v}_{i_r} \cdot \mathbf{t} = \epsilon_t \mathbf{v}_{i_p} \cdot \mathbf{n} \\ \epsilon_n m_{i_r} = G m_{i_p} \\ \epsilon_n n_{i_r} = F n_{i_p} \\ T_{i_r} = H T_{i_p} \end{cases} \quad (10)$$

G is a mass gain parameter which allows to take into account the creation of new particles by erosion effects ($G = 1$ corresponds to mass conservation during impact). F is a parameter which accounts for the combined effect of erosion and fragmentation (which both lead to the creation of new particles and thus to $F > 1$). The parameter H allows to take into account the energy transfer during the particle impact. ϵ_n and ϵ_t correspond to the normal and tangential restitution coefficients. Naturally a model has to be prescribed for G , F , H , ϵ_n and ϵ_t .

3 NUMERICAL TREATMENT OF THE PARTICLE PHASE EQUATIONS

The generalized Navier-Stokes equations for the gas phase are solved using a classical finite volume scheme on structured meshes that will not be described here. Details can be found for example in ^[14,15,16].

Regarding the spatial discretization of (2), the following finite volume method has been used. For each class, let's first introduce the vector \mathbf{V}_i of specific variables defined as follows:

$$\mathbf{V}_i = (n_i/m_i, 1, \mathbf{v}_i, h_i)^t \quad (11)$$

Using this notation, system (2) can be rewritten under the following generic form:

$$\partial_t m_i \mathbf{V}_i + \nabla_x (m_i \mathbf{v}_i \mathbf{V}_i) = \mathbf{S}_i \quad (12)$$

which is more suited for the numerical discretization. Introducing $|K|$ the volume (or area) of a given control volume K and $|e|$ the area (or length) of the cell edge e , and integrating (12) on K leads to the semi-discretized equation:

$$|K| d_t (m_i \mathbf{V}_i) + \sum_{e \in \partial K} \Phi_{ie,K} |e| = |K| \mathbf{S}_i \quad (13)$$

where $\Phi_{ie,K}$ denotes the flux through the edge e . Let's define the edge mean particle velocity (for the class of particles i) by:

$$\mathbf{v}_{ie} = \frac{m_{i,K} \mathbf{v}_{i,K} + m_{i,Ke} \mathbf{v}_{i,Ke}}{m_{i,K} + m_{i,Ke}} \quad (14)$$

Applying an upwind scheme based on the sign of $\mathbf{v}_{ie} \cdot \mathbf{n}_{e,K}$ the expression of the flux $\Phi_{ie,K}$ reads:

$$\Phi_{ie,K} = v_{ie,K}^+ \mathbf{V}_{i,K} + v_{ie,K}^- \mathbf{V}_{i,Ke} \quad (15)$$

where $v_{ie,K}^+$ and $v_{ie,K}^-$ denote the positive (respectively negative) part of $\mathbf{v}_{ie} \cdot \mathbf{n}_{e,K}$. In addition, this space discretization scheme can be combined with the MUSCL approach ^[15,17] to get a second order accurate scheme.

As far as the time discretization is concerned, a first order semi-implicit scheme has been used which consists of using an explicit scheme for the flux terms and a partially implicit scheme for the treatment of the source terms. An advantage of this method is that, under a CFL-like condition, it can be shown to insure the positivity of the number density and to satisfy a maximum principle on the components of \mathbf{V}_i (which are directly related to the particle velocity, temperature and diameter).

Regarding the treatment of the particle source term in the gas phase equations, \mathbf{S}_p , a relaxation method has been implemented to enforce the stability of the coupling in dense zones.

4 BASIC VALIDATION TESTS

Several tests case were carried out in order to check the correct implementation of the above described numerical model and to assess its capability to accurately reproduce basic interactions between a gas flow and a cloud of particles. Here, for the sake of concision, we only present a one-dimensional test case (but performed using a 2D mesh).

The test consists of injecting gas and particles in a tube in non-equilibrium conditions. The gas flow at the inlet being supersonic, the whole gas and particle states are prescribed at the inlet. No boundary condition is imposed at the outlet. The gas is supposed to be perfect and inviscid and heat conduction effects are neglected. The objective of the test case it to assess the capability of the code to calculate the relaxation towards the equilibrium between the two phases along the tube.

In the first variant of the test, we only focus on the solution at the outlet of the tube which is assumed to be long enough for the particles and the gas to be at equilibrium at the output. By using the conservation of particle mass, particle number, gas mass, global momentum and global energy, it is possible to compute analytically the expression of the equilibrium velocity, pressure and temperature at the tube outlet for any inlet conditions. This calculation was done and numerical tests were performed for several inlet conditions. For all cases, the numerical results were in perfect agreement with the theoretical solution, showing that the global conservation properties are correctly ensured by the code. Due to the lack of room, the results of these tests will not be shown here.

The second variant of the test consists in computing the steady state solution according to the abscissa x along the tube. Solving analytically the full non-linear system is not possible. However, it is possible to compute the analytical solution of the linearized system around an equilibrium state. Each quantity q can be written as the sum of its equilibrium value \bar{q} and a small perturbation \hat{q} . In the simplest case when it is possible to neglect the heat transfer between the gas and the particles, the solution of the linearized system reads:

$$\begin{cases} \hat{\rho}_g = -\frac{\bar{m}_p}{\bar{u}} \frac{M^2}{M^2 - 1 + \epsilon M^2} [\hat{u}_p(0) - \hat{u}_g(0)] \left\{ 1 - \exp \left[\frac{-x}{\tau_{\mathcal{F}} \bar{u}} \left(1 + \epsilon \frac{M^2}{M^2 - 1} \right) \right] \right\} \\ \hat{m}_p = \frac{\bar{m}_p}{\bar{u}} \frac{M^2 - 1}{M^2 - 1 + \epsilon M^2} [\hat{u}_p(0) - \hat{u}_g(0)] \left\{ 1 - \exp \left[\frac{-x}{\tau_{\mathcal{F}} \bar{u}} \left(1 + \epsilon \frac{M^2}{M^2 - 1} \right) \right] \right\} \\ \hat{u}_g = \hat{u}_g(0) + \frac{\epsilon M^2}{M^2 - 1 + \epsilon M^2} [\hat{u}_p(0) - \hat{u}_g(0)] \left\{ 1 - \exp \left[\frac{-x}{\tau_{\mathcal{F}} \bar{u}} \left(1 + \epsilon \frac{M^2}{M^2 - 1} \right) \right] \right\} \\ \hat{u}_p = \hat{u}_p(0) - \frac{M^2 - 1}{M^2 - 1 + \epsilon M^2} [\hat{u}_p(0) - \hat{u}_g(0)] \left\{ 1 - \exp \left[\frac{-x}{\tau_{\mathcal{F}} \bar{u}} \left(1 + \epsilon \frac{M^2}{M^2 - 1} \right) \right] \right\} \\ \hat{p}_g = -\frac{\gamma \bar{p}_g \epsilon}{\bar{u}} \frac{M^2}{M^2 - 1 + \epsilon M^2} \left\{ 1 - \exp \left[\frac{-x}{\tau_{\mathcal{F}} \bar{u}} \left(1 + \epsilon \frac{M^2}{M^2 - 1} \right) \right] \right\} \end{cases} \quad (16)$$

where \bar{m}_p is the equilibrium particle mass density, \bar{p}_g is the equilibrium pressure, \bar{u} is the equilibrium velocity of both phases, $M = \frac{\bar{u}}{\sqrt{\frac{\gamma \bar{p}_g}{\bar{\rho}_g}}}$ is the corresponding Mach number, γ is the classical heat capacity

ratio, $\epsilon = \frac{\bar{m}_p}{\bar{\rho}_g}$ is the equilibrium mass loading ratio and $\tau_{\mathcal{F}} = \frac{\bar{\rho}_p d^2}{18 \mu_g}$ is the dynamic relaxation time of the particles (Stokes regime) and μ_g is the viscosity.

Figures 1 show the density and velocity profiles for the two phases. The dashed line corresponds to the asymptotic solution given by the global conservation equations. It can be seen that the numerical results (full line) agree very well with the two analytical profiles.

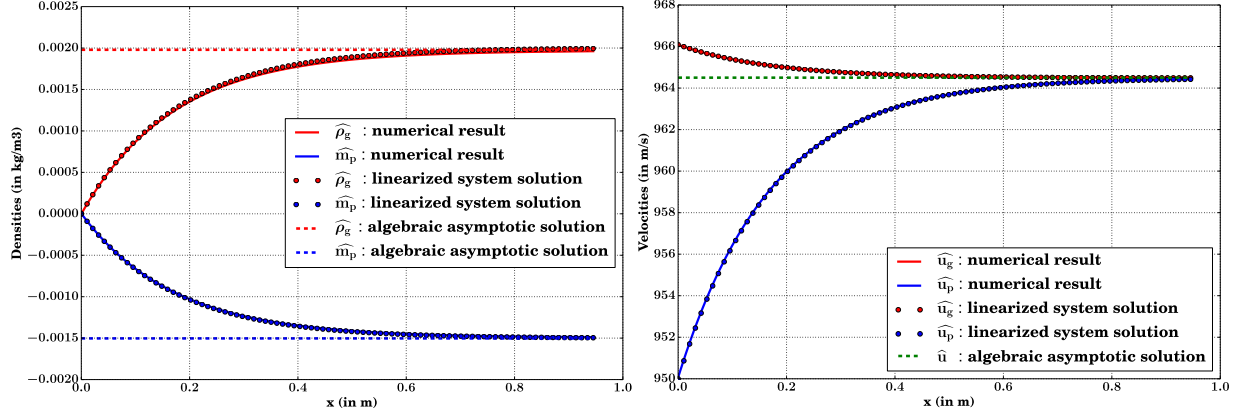


Figure 1: Left: evolution of the gas density and particle mass density along the tube at the steady state. Right: evolution of the gas and particle velocity along the tube at the steady state. Solid lines: numerical results - Dotted lines: theoretical solution - Green dashed line: equilibrium theoretical solution.

5 SIMULATION OF BOEING HYPERSONIC WIND TUNNEL EXPERIMENT

5.1 Experimental conditions

In the 70's experiments were carried out at the Boeing Hypersonic Wind Tunnel (BHWT) ^[1]. In these experiments, a solid metallic sphere was plunged into a Mach 6.1 free stream flow containing silica particles. In table 1, the flow stagnation conditions (at the input of the tunnel) and the infinity flow conditions (inlet of our computational domain) of the considered test run are summarized:

	Stagnation flow conditions	Infinity flow conditions
Pressure	44.8 10^5 Pa	2564 Pa
Temperature	633.1 K	75 K
Density	24.6 kg.m^{-3}	0.12 kg.m^{-3}
Sound speed	504.4 m.s^{-1}	173.6 m.s^{-1}

Table 1: Stagnations and infinity flow conditions

The silica particles injected in the flow were of 100 μm diameter. In the following, c_∞ will denote the ratio between the particles mass flow rate and the gas mass flow rate. Its value was:

$$c_\infty = \frac{\dot{m}_{part}}{\dot{m}_{gas}} = 7.3 \cdot 10^{-4} \quad (17)$$

A strong shock disturbance was observed due to the presence of the particles, especially in the vicinity of the symmetry axis. The objective of the numerical simulations presented hereafter was to check the ability

of model (1)-(2)-(10) to capture this phenomenon and, as far as possible, to use the results to better understand its physical origin.

5.2 Modeling choices of HULIN and ZNATY^[2]

Numerical simulations of BHWT experiments have already been successfully performed by Hulin and Znaty^[2] but using a Lagrangian approach for the particulate phase. These researchers performed two types of simulation. In the first case, each numerical particle was associated with a real particle so as to account for the discrete nature of the solid phase and the fact that in the experiment the average distance between two neighboring particles is in the order of a few mm which is far from being negligible in the considered application. In the second case, the number of numerical particles that they used was much larger than the number of real particles. Each numerical particle was therefore assigned a weight that could be associated with a probability of presence. This second method, for which the concentration field of the particulate phase is quasi-continuous is therefore very close to an Eulerian approach. As Hulin and Znaty say in their paper that they get the same results in both cases, we expected to obtain comparable results with the Eulerian approach.

Hulin and Znaty have proposed a set of hypotheses to take into account the influence of fragmentation and erosion phenomena due to particle impacts. According to their model, after an impact,

- each incident particle is supposed to fragment into 5 smaller particles ;
- erosion leads to the creation of new particles with the same characteristics as the particles created by fragmentation of the incident particles ; the total mass of the eroded particles is supposed to be four times the mass of the incident particles ;
- the total kinetic energy of the reemitted particles (initial particle fragments + eroded particles) is supposed to represent 30% of the incident kinetic energy ;
- the restitution parameters, ϵ_n and ϵ_t are supposed to have the same value.

These assumptions lead to the following values for the impact model parameters (see equation (10)): $G = 5$, $F = 25$, $\epsilon_n = \epsilon_t = 0.24$. Since no assumption was mentioned in [2] regarding thermal effects, we simply assumed that $H=1$ for the sake of simplicity, even if it is not realistic from a physical point of view.

5.3 Results

The classical $k-\omega$ model[20] was used to account for the effect of turbulence on the gas flow mean properties. We performed two different numerical simulations with the particles. In the first simulation, we did not take into account any influence of the particles on the turbulence production and dissipation. In the second simulation, the turbulence source term model proposed by Hulin and Znaty^[2] was used. As far as the turbulent kinetic energy source term is concerned, their model reads:

$$S_p^k = \sum_{i=1}^N n_i \mathbf{F}_i \cdot (\mathbf{v}_g - \mathbf{v}_i) \quad (18)$$

It is worth noticing that this model is not correct as it involves the mean slip velocity between the gas and the particles instead of the gas fluctuating velocity as it should be the case from a theoretical point of view. The correct expression should be:

$$S_p^k = \sum_{i=1}^N n_i \overline{\mathbf{F}_i' \cdot \mathbf{v}_g'} \quad (19)$$

Since the mean slip velocity is very high behind the shock, model (18) necessarily leads to a very high production rate of turbulent kinetic energy. It is thus not surprising that the presence of particles has a strong influence on the turbulence level, as noticed by Hulin and Znaty.

We point out that the calculations made in this paper do not reach a steady state. Indeed, the particles indefinitely accumulate along the shock. This phenomenon will be discussed later. This accumulation makes difficult the establishment of a steady state. This is why the results presented below are snapshots taken during the calculation.

Figures 2 show a comparison of the obtained numerical results for the gas phase density field without particles (left), with particles but without any turbulence production by the particle (middle), with particles and turbulence production by the particles using model (18) (right). Figures 3 and figures 4 show a similar comparison but for the gas Mach number field and for the turbulent kinetic energy field respectively.

We can see that without any influence of the particles on the turbulence production rate, no shock disturbance is observed whereas a clear modification of the shock appears if model (18) is applied. According to these results, the shock disturbances that have been observed in BHWT experiments seem to result from the strong production of turbulence by the particles in the vicinity of the shock. We recover similar conclusions as in ^[2] even if our numerical results do not exactly coincide with theirs. However, as already mentioned above, model (18) is not correct and is expected to strongly overestimate the turbulence production due to the presence of particles. We can therefore question the truth of this conclusion. To investigate this question, this will need at least to replace model (18) by a more correct one derived from (19) using closure assumptions. This will be the subject of future work.

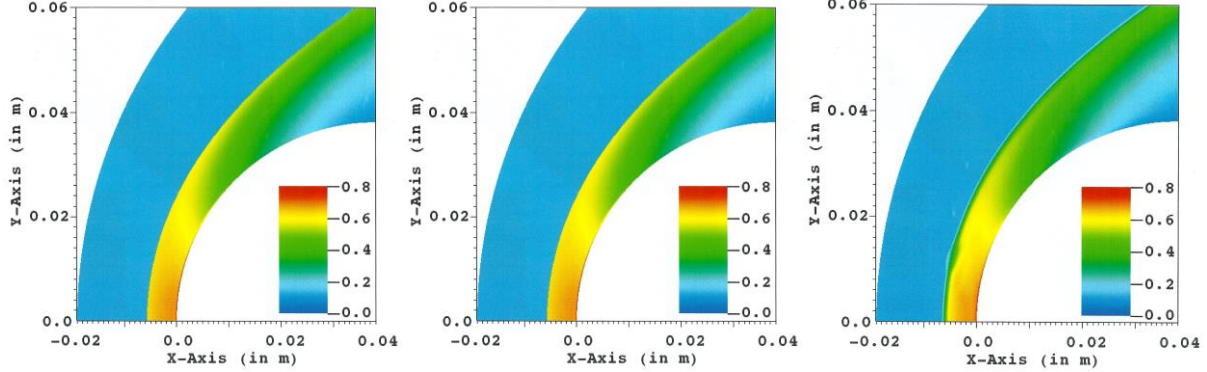


Figure 2: Gas phase density field (in kg.m^{-3}). Without particles (left) – With particles but without turbulence production by the particles (middle) – With particles and model (18) for turbulence production by the particles (right)

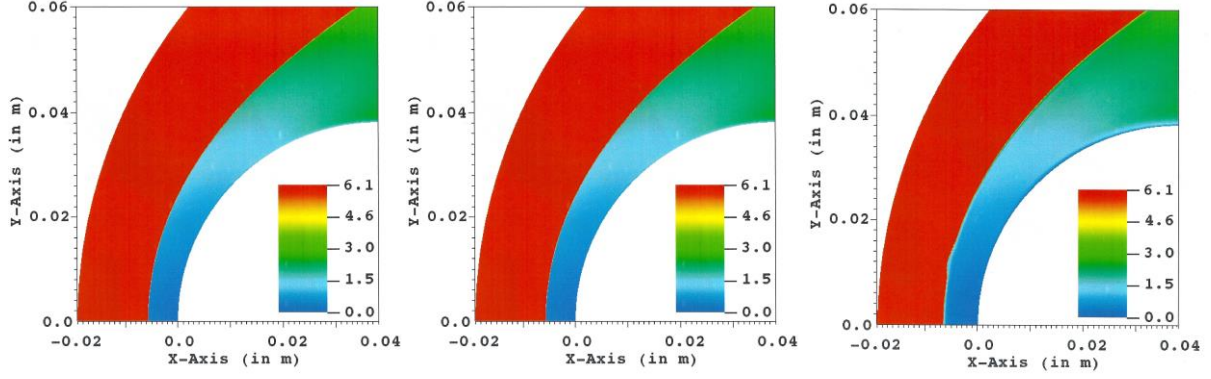
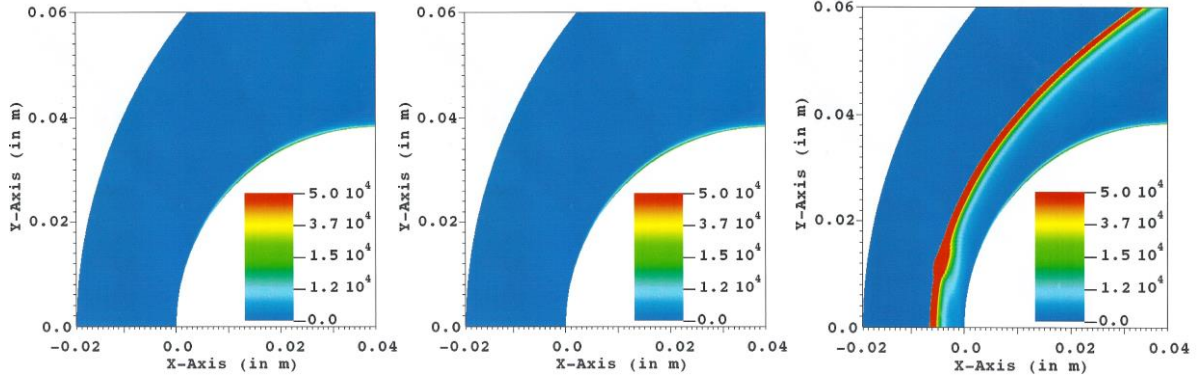


Figure 3: Gas Mach number field. Same legend as for Figure 2.

Figure 4: Turbulent kinetic energy field (in $\text{kg.m}^2.\text{s}^{-2}$). Same legend as for Figure 2.

Another interesting consequence of the interaction of the particles with the detached shock can be observed in Figures 5 on the particle mass density fields. The secondary particles that are reemitted from the wall due to fragmentation and erosion phenomena are strongly decelerated by the gas flow and tend to accumulate in the vicinity of the shock, leading to very high density of particles compared to the far field. Even if this phenomenon is certainly overestimated by the Eulerian treatment of the particle phase (well-known effect of single-velocity Eulerian model ^[19]), it is physically plausible and could also play a role in the shock disturbance mechanism.

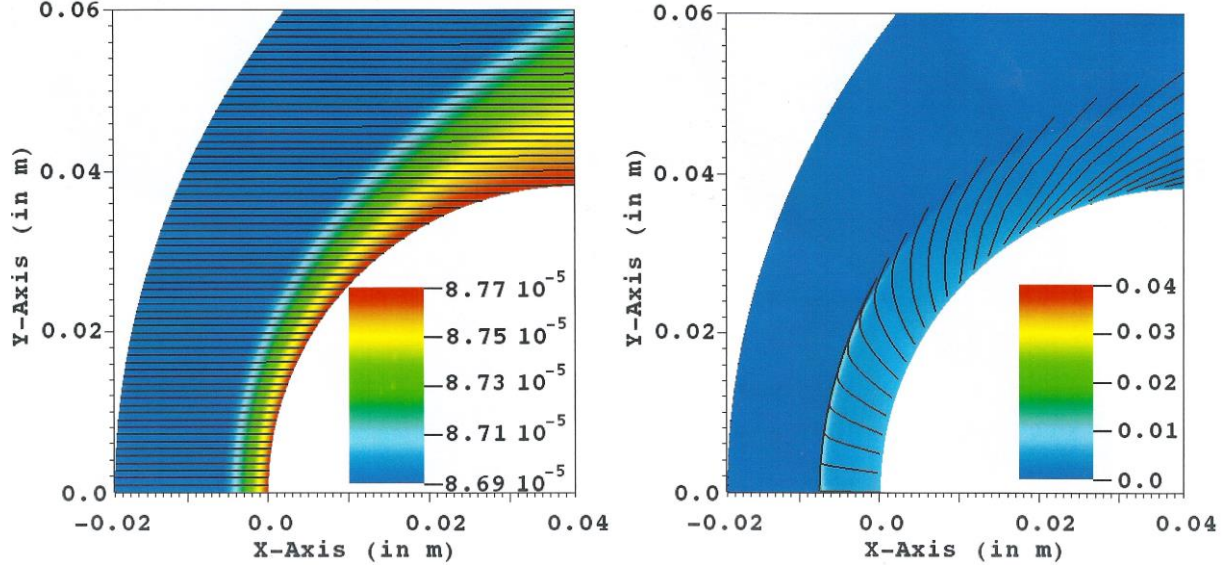


Figure 5: Particle mass density field (in kg.m⁻³) and particle velocity streamlines. – Left : primary particle class – Right : secondary particle class

CONCLUSION

In this work, an Eulerian-Eulerian approach has been proposed to simulate particle laden hypersonic flows. It has been applied to the simulation of the BHWT experiment with the aim to reproduce the particle induced shock disturbances that were experimentally observed. We have obtained similar results as Hulin and Znaty^[2] who already performed the same simulations in the past but using an Euler-Lagrange approach. In the numerical simulations, the influence of the particles on the turbulent kinetic energy production rate in the vicinity of the shock seems to play a determinant role for shock disturbances to appear. However the model used by Hulin and Znaty^[2] (and that was used as well in the present study for the sake of comparison) is not correct from a theoretical point of view and tends to strongly overestimate the turbulence generation by the particles. The validity of the simulation results obtained with this model are thus strongly questionable. Further investigations are necessary to better understand the physical phenomena at the origin of the shock displacement and to ensure that Euler-Euler, and as well Euler-Lagrange models, are able to reproduce the experimental results.

REFERENCES

- [1] W.FLEENER and R.WATSON. Convective heating in dust-laden hypersonic flows. In 8th Thermophysics Conference, page 761, 1973.
- [2] A.HULIN and E.ZNATY. Aerodynamic modelling of hypersonic erosive reentry flows. In *Aerothermodynamics for space vehicles*, volume 367, page 391, 1995
- [3] G.F.CARRIER. Shock waves in a dusty gas. *Journal of Fluid Mechanics*, 4(4):376–382, 1958.
- [4] F.E.MARBLE. Dynamics of dusty gases. *Annual Review of Fluid Mechanics*, 2(1):397–446, 1970.
- [5] L.DUNBAR, J.COURTNEY, and L.MCMILLEN. Heating augmentation in particle erosion environments. In 8th Aerodynamic Testing Conference, page 607, 1974.
- [6] P.PAPADOPOULOS, M.E.TAUBER, and I.D.CHANG. Heatshield erosion in a dusty martian atmosphere. *Journal of Spacecraft and Rockets*, 1993.
- [7] G.PALMER, Y.K.CHEN, P.PAPADOPOULOS, and M.TAUBER. Reassessment of effect of dust erosion on heatshield of mars entry vehicle. *Journal of Spacecraft and Rockets*, 37(6):747–752, 2000.
- [8] J.D.ANDERSON Jr. *Hypersonic and High Temperature Gas Dynamics*. AIAA Publications, AIAA, Reston, VA, 2000.
- [9] F.LAURENT and M.MASSOT. Multi-fluid modelling of laminar polydisperse spray flames: origin, assumptions and comparison of sectional and sampling methods, 2001.
- [10] C.E.SWAIN. The effect of particle/shock layer interaction on reentry vehicle performance. 1975.
- [11] R.CLIFT, J.R.GRACE, and M.WEBER. *Bubbles, drops and particles*. Academic, New York, 1978.
- [12] TW FOX, CW RACKETT, and JA NICHOLLS. Shock wave ignition of magnesium powders. 1978.
- [13] R.M.DRAKE. Discussion: “Forced Convection Heat Transfer From an Isothermal Sphere to Water” (Vliet, GC, and Leppert, G., 1961, *ASME J. Heat Transfer*, 83, pp. 163–170). *Journal of Heat Transfer*, 83(2), 170–172, 1961
- [14] W.K.ANDERSON, J.L.THOMAS, and B.VAN LEER. Comparison of finite volume flux vector splittings for the Euler equations. *AIAA journal*, 24(9):1453–1460, 1986.
- [15] E. F.TORO. *Riemann solvers and numerical methods for fluid dynamics: a practical introduction*. Springer Science & Business Media, 2013.
- [16] B.VAN LEER, J.L.THOMAS, P.L.ROE, and R.W.NEWSOME. A comparison of numerical flux formulas for the Euler and Navier-Stokes equations. 1987.
- [17] B.VAN LEER. Towards the ultimate conservative difference scheme V: a second-order sequel to godunov’s method. *Journal of computational Physics*, 32(1):101–136, 1979.
- [18] G.MAROIS, PhD Thesis, Toulouse University, in preparation, 2018
- [19] O.Desjardin, R.Fox, Ph.Villedieu. A quadrature-based moment method for dilute fluid-particle flows. *Journal of Computational Physics*, 227(4), 2514–2539, 2008
- [20] D.C. WILCOX, *Turbulence models for CFD*. DCW Industries, La Cañada, CA, EUA, 1998

An Accurate and Robust Immersed Method for Flow Problems

Alexandre Marques^{*}, Jean-Christophe Nave^{**}, Rodolfo Rosales^{***}

^{*}Massachusetts Institute of Technology, ^{**}McGill University, ^{***}Massachusetts Institute of Technology

ABSTRACT

We present an immersed method that solves flow problems to high order of accuracy using compact discretization stencils. High order of accuracy is especially important for computing derivatives of flow variables adjacent to the immersed boundaries. For instance, derivatives of the velocity are needed to compute stresses acting on the boundaries, which is required in fluid-structure interaction applications. This method, named the Correction Function Method (CFM), is based on three main concepts: (i) defining smooth extensions of the flow variables across the immersed boundaries as solutions to a Cauchy problem, (ii) solving the Cauchy problem locally for each discretization stencil that crosses the immersed boundaries, and (iii) solving the Cauchy problem via a least squares minimization. The result is a general framework to compute smooth extensions of the flow variables across immersed boundaries to high order of accuracy, and that are independent of the underlying computational grid. These smooth extensions can then be applied with standard discretizations that may straddle the boundaries, maintaining their original order of accuracy and compactness. Furthermore, because the CFM is independent of the underlying computational grid, it is very robust with respect to the arbitrary shape the boundaries can assume under deformation. Similarly, the CFM seamlessly solves problems where multiple interfaces are arbitrarily close. The CFM also facilitates the implementation of complex boundary conditions that arise in the context of high-order methods to solve the incompressible Navier-Stokes equations, such as boundary conditions that involve the divergence or the curl of the velocity. In this talk we will present results of a fourth order implementation of the CFM.

Computational Modeling of the Cardiovascular System: Origins, Recent Advances, and Contributions of TJR Hughes

Alison Marsden*

*Stanford University

ABSTRACT

In this talk, I will aim to highlight the early contributions of Thomas JR Hughes to the development of cardiovascular modeling, starting with his early work on 1D blood flow solvers and progressing to his pioneering work on development of patient-specific modeling and finite element blood flow simulations. I'll then highlight how these contributions are continuing to impact current work in the field of cardiovascular simulation and treatment planning. In particular, I will discuss recent advances in computational methodology for cardiovascular modeling, including large-deformation fluid structure interaction simulations, physiologic coupled boundary conditions, uncertainty quantification, optimization, and high-throughput image segmentation. I will then highlight recent applications to clinical problems in pediatric and adult cardiovascular disease, including single ventricle physiology, coronary artery bypass graft surgery, and cardiac development.

Improvements in the Accuracy of the Theta Method for the Calculation of the Stress Intensity Factors in 3D

Alexandre Martin^{*}, Matthieu Le Cren^{**}, Claude Stolz^{***}, Patrick Massin^{****}, Nicolas Moes^{*****}

^{*}IMSIA, UMR EDF-CNRS-CEA-ENSTA ParisTech 9219, ^{**}IMSIA, UMR EDF-CNRS-CEA-ENSTA ParisTech 9219,

^{***}IMSIA, UMR EDF-CNRS-CEA-ENSTA ParisTech 9219, ^{****}IMSIA, UMR EDF-CNRS-CEA-ENSTA ParisTech 9219, ^{*****}Ecole Centrale de Nantes, UMR CNRS 6183

ABSTRACT

The theta method was proposed by Destuynder et al. [1] to compute the energy release rate and stress intensity factors. This method is based on domain integrals and Lagrangian derivation of the potential energy with respect to a virtual crack extension velocity field. Currently, the method allows obtaining very good results in 2D but has several drawbacks for three-dimensional cracks that will be addressed. To better understand the problems encountered, we propose to study two 3D cases: -- a 3D case that is an extrusion of a 2D case so that the solution is the same for the 2D case and the 3D case along the extrusion direction. -- a Penny-shaped crack which has also an analytical solution [2]. In each case, the results of the calculation for the energy release rate and stress intensity factors will be obtained with the extended finite element method [3] and the finite element method in order to compare both. First, we propose an improvement of the theta field discretization and secondly, an extension of the asymptotic fields for the computation of the stress intensity factors in order to obtain more accurate results with the curved cracks. [1] P. Destuynder, M. Djaoua, S. Lescure. Some remarks on elastic fracture mechanics J. Méca. Théo. Appl. Vol. 2, N° 1, 113-135, 1983. [2] H. Tada, P. Paris, G. Irwin, The stress analysis of cracks handbook, 3ème éd., 2000 [3] N. Moes, J. Dolbow et T. Belytschko, «A finite element method for crack growth without remeshing», International Journal for Numerical Methods in Engineering, pp. 135-150, 1999.

Risk Average Optimal Control Problem for Elliptic PDEs with Uncertain Coefficients

Matthieu Martin^{*}, Fabio Nobile^{**}, Sebastian Krumscheid^{***}

^{*}CSQI, Institute of Mathematics, Ecole Polytechnique Federale de Lausanne, 1015 Lausanne, Switzerland, ^{**}CSQI, Institute of Mathematics, Ecole Polytechnique Federale de Lausanne, 1015 Lausanne, Switzerland, ^{***}CSQI, Institute of Mathematics, Ecole Polytechnique Federale de Lausanne, 1015 Lausanne, Switzerland

ABSTRACT

We consider a risk averse optimal control problem for an elliptic PDE with uncertain coefficients. The control is a deterministic distributed forcing term and is determined by minimizing the expected L^2 -distance between the state (solution of the PDE) and a target deterministic function. An L^2 -regularization term is added to the cost functional. We consider a finite element discretization of the underlying PDE and derive an error estimate on the optimal control. Concerning the approximation of the expectation in the cost functional and the practical computation of the optimal control, we analyze and compare two strategies. In the first one, the expectation is approximated by either a Monte Carlo estimator, and a steepest descent algorithm is used to find the discrete optimal control. The second strategy, named Stochastic Gradient is again based on a steepest-descent type algorithm. However the expectation in the computation of the steepest descent is approximated with independent Monte Carlo estimators at each iteration using possibly a very small sample size. The sample size and possibly the mesh size in the finite element approximation could vary during the iterations. We present error estimates and complexity analysis for both strategies and compare them on few numerical test cases.

Finite Element Analysis of Steel-Concrete Composite Floor Systems under Traveling Fire Exposures

Jason Martinez*, Ann Jeffers**

*University of Michigan - Ann Arbor, **University of Michigan - Ann Arbor

ABSTRACT

Preliminary research has shown that the structural response of a building can be significantly influenced by the size and spread rate of a traveling fire. However, prior works have only focused on 2D structural frames, without taking into account the floor system. To address this limitation, this presentation highlights a computational investigation that was undertaken to better understand the global behavior of a 3D steel-concrete composite (SCC) floor system under a traveling fire exposure. Using the Traveling Fires Methodology, a range of spatially and time-varying fire exposures were applied to a 3D finite element model of a SCC floor system. The sequentially coupled thermal-mechanical simulations were carried out using ABAQUS, where the modeling approach was verified against existing test data on full-scale fire test. Essential factors influencing the fire resistance of SCC floor systems, namely the passive fire protection scheme, and the burning size of the fire, were varied to investigate the global structural response. Simulation results indicate that structural response during a traveling fire is not only dominated by material stiffness and strength reduction during heating, but also by large axial forces in the beam-to-column connections during the heating and cooling phase of the fire, structurally-significant displacements of the floor slab, and load redistribution between columns occurring as the fire progresses across the floor plan. Additionally, useful trends were observed, in particular the dependency of the slab displacement rate and the maximum displacement to both the distance from the fire origin and fire burning size.

Numerical Modelling of the Combined Effect of Mechanical Deployment and Drug Delivery in Endovascular Devices

Miguel A. Martinez*, Javier Escuer**, Martina Cebollero***, Estefania Peña****

*Aragón Institute of Engineering Research, University of Zaragoza, Spain. Centro de Investigación Biomédica en Red en Bioingeniería, Biomateriales y Nanomedicina (CIBER-BBN), Spain, **Aragón Institute of Engineering Research, University of Zaragoza, Spain, ***Aragón Institute of Engineering Research, University of Zaragoza, Spain, ****Aragón Institute of Engineering Research, University of Zaragoza, Spain. Centro de Investigación Biomédica en Red en Bioingeniería, Biomateriales y Nanomedicina (CIBER-BBN), Spain

ABSTRACT

Cardiovascular diseases are the first cause of death and disability in developed countries. Specifically, atherosclerotic disease results in millions of sudden deaths annually. Endovascular devices such as stents and balloons have become very successful devices to treat advanced atherosclerotic lesions. However, one of the main issues with these interventions is the development of restenosis that is related with the migration of SMCs from the media to the intima causing intima hyperplasia and possible lumen obstruction. An important advance in the treatment of this postsurgical effect is the development drug eluting devices. The controlled delivery of anti-proliferative drugs limits this restenosis phenomenon avoiding the migration and proliferation of SMC, however an excessive drug concentration can have a toxic consequence delaying re-endothelialization of the intima. Many mathematical models describing the drug elution from the device and transport in arteries have been developed. However, most of them do not consider how the mechanical expansion of the endovascular device compresses the porous arterial wall and the transport properties are modified by the mechanical deformation. Therefore the main objective of this work is to study the influence of the mechanical expansion of the device in the diffusion properties of the vessel and on the spatial concentration of the drug. To simulate the mechanical expansion, a fibre-reinforced hyperelastic constitutive model is used to describe arterial wall behaviour and a linear elastic model for the device. Blood flow is modeled by Navier-Stokes equations in the arterial lumen domain. Concerning to drug diffusions properties, the arterial wall is modelled as a multilayer anisotropic porous structure distinguishing intima, media and adventitia. Darcy's law is used to calculate filtration velocity through porous layers and convection-diffusion equations are used to model drug transport through blood, intima, media and adventitia, incorporating a reaction term for the media layer. Endothelium, internal and external elastic laminae are treated as semipermeable membranes and the flux across them is described by Kedem-Katchalsky equations¹. A non-linear saturable reversible binding model describes binding of drug to specific and non-specific sites. The transport properties of the arterial wall are modified by the local deformation caused by the device deployment. The inclusion of the mechanical expansion of the device modifies the peak concentration on points of the media layer with maximum compressive deformation. The long-time drug average concentration is unaffected by the consideration of device expansion. [1] Bozsak, F., Chomaz, J.M., Barakat, A.I. (2014). Biomech. Model. Mechanobiol. 13(2), 327–347.

3D Reconstruction of Histological Sections with Constituent and Morphological Analyses

Pedro Martins*, Carolina Rocha**, Rita Rynkevic***, Marco Parente****, António Fernandes*****

*INEGI, University of Porto, Faculty of Engineering, **University of Porto, Faculty of Engineering, ***INEGI, University of Porto, Faculty of Engineering, ****INEGI, University of Porto, Faculty of Engineering, *****INEGI, University of Porto, Faculty of Engineering

ABSTRACT

The microstructure of soft biological tissues has a significant influence on the mechanical properties at a macroscopic level. Using the ovine animal model, a good agreement between tissue contents (collagen, elastin, smooth muscle and myofibroblasts) and biomechanical properties [1] has been established. Despite the importance of constituents' quantity on the overall mechanical behavior of a given biological soft tissue, their three-dimensional arrangement will ultimately dictate the macroscopic mechanical response. In this work, tissue from ovine ewes was collected, and consecutive histology samples were prepared. A 3D reconstruction of the multiple sections of the vagina (full-thickness) was carried out using Mimics software. From this analysis it was possible to study the 3D arrangement of tissue constituents through the tissue thickness. The volumetric estimation of tissue constituents was also a direct result of the current work. References: [1] R. Rynkevic, P. Martins, L. Hympanova, H. Almeida, A. A. Fernandes, and J. Deprest, "Biomechanical and morphological properties of the multiparous ovine vagina and effect of subsequent pregnancy," *Journal of Biomechanics*, vol. 57, pp. 94–102, 2017.

Design and Numerical Analysis of a Gasket Based on Auxetic Structures

Arturo A. Martínez*, Fernando Velázquez**

*Universidad Nacional Autónoma de México, **Universidad Nacional Autónoma de México

ABSTRACT

In the present article the design and analysis of a bell and spigot joint gasket based on an auxetic materials is proposed to solve leaks produced by severe misalignment. With current gaskets, misalignments in the joints can produce separations between his elements, which can represent a major environmental, health or economic problem. The auxetic structure design is analyzed and evaluated by finite element (FE) analysis to simulate the auxetic behavior of the proposed structure. The auxetic structure used is based on a simple geometry in periodical arrangements. The proposed gasket modifies its volume, maintaining contact with the surfaces to be sealed even with large joint deflection.

A Machine Learning Tool for the Mechanical Characterization of Cardiovascular Tissues

Javier Martínez*, Myriam Cilla**, Ignacio Pérez-Rey***, Miguel Ángel Martínez****, Estefanía Peña*****

*4.-Department of Natural Resources and Environmental Engineering, University of Vigo, Vigo, Spain. 5.-Centro Universitario de la Defensa (CUD), Marín, Spain, **1.-Centro Universitario de la Defensa (CUD), Zaragoza, Spain. 2.-Aragon Institute of Engineering Research (I3A), University of Zaragoza, Zaragoza, Spain. 3.-3CIBER's Bioengineering, Biomaterials and Nanomedicine (CIBER-BBN), Spain, ***4.-Department of Natural Resources and Environmental Engineering, University of Vigo, Vigo, Spain, ****2.-Aragon Institute of Engineering Research (I3A), University of Zaragoza, Zaragoza, Spain. 3.-3CIBER's Bioengineering, Biomaterials and Nanomedicine (CIBER-BBN), Spain, *****2.-Aragon Institute of Engineering Research (I3A), University of Zaragoza, Zaragoza, Spain. 3.-3CIBER's Bioengineering, Biomaterials and Nanomedicine (CIBER-BBN), Spain

ABSTRACT

Introduction The research of the mechanical response of biological tissues is the basis for the creation of computational models which can accurately reproduce their mechanical behaviour. The experimental data are used to estimate the material model parameters through a Strain Energy Function (SEF) within the framework of the continuum theory of large deformation hyperelasticity. Traditionally, material parameters associated with the material model have been fitted by means of a Levenberg-Marquardt type minimization algorithm and/or inverse models combined with finite element models. However, motivated by the well-known problem of these numerical methods based on gradients, that is, their limitation to find local optimization, and therefore, their instability and dependence of the selected initial seed, a new approach is explored in the presented study. The use of Artificial Neural Networks (ANNs) is proposed to solve the parameter identification of constitutive laws for soft biological tissues. **Methods** Data is collected from circumferential and longitudinal uniaxial tests carried out on cardiovascular tissues. 1080 analytical curves, which cover a range of response from highly anisotropic to quasi-isotropic, were used. From uniaxial tests, it is possible to recover stress-strain pairs for each longitudinal and circumferential cases. The input of the ANN was defined by extracting three customized parameters (initial slope, middle point and final slope) from test results. The ANN was trained with these inputs providing the parameters which define the behavior of the tissue by means of the SEF defined by Gasser et al. [1]. The tool was trained repetitively until convergence and it was carried out by considering a different number of neurons in the hidden layers. A validation with new observations of analytical curves (previously unseen observations by the ANN) and with eight kinds of cardiovascular experimental data was performed. **Results** The train and test errors show a great efficiency during the training process to find correlations between inputs and outputs; besides the correlation coefficients were very close to 1. In addition, the results show an excellent agreement between the prediction of the material parameters of the SEF and the analytical curves. **Discussion** We found that the method was able to consistently identify model parameters, and we believe that the use of this numerical tools could imply an improvement in the characterization of cardiovascular tissues. **References** [1] C.T. Gasser, R.W. Ogden and G.A. Holzapfel. Hyperelastic modelling of arterial layers with distributed collagen fibre orientations. *Journal of The Royal Society of Interface*- 3:15:35. 2006.

ADVANCES IN THE TREATMENT OF TRIMMED CAD MODELS DUE TO ISOGEOMETRIC ANALYSIS

BENJAMIN MARUSSIG^{*,†}

^{*}Graz University of Technology
Graz Center of Computational Engineering (GCCE)
Krenngasse 37/I, 8010 Graz, Austria
marussig@tugraz.at; www.gcce.tugraz.at

[†]Graz University of Technology
Institute of Mechanics
Kopernikusgasse 24/IV, 8010 Graz, Austria

Key words: Isogeometric Analysis, Trimming, SSI operation, CAGD

Abstract. Trimming is a core technique in geometric modeling. Unfortunately, the resulting objects do not take the requirements of numerical simulations into account and yield various problems. This paper outlines principal issues of trimmed models and highlights different analysis-suitable strategies to address them. It is discussed that these concepts not only provide important computational tools for isogeometric analysis, but can also improve the treatment of trimmed models in a design context.

1 INTRODUCTION

Isogeometric analysis (IGA) aims to bridge the gap between computer aided geometric design (CAGD) and analysis by using CAGD technologies for numerical simulations. Since the introduction of IGA in 2005, it has been demonstrated that the synthesis of these disciplines allows not only an improved interaction, but yields many computational advantages¹⁻³. Nowadays, IGA is widely recognized as a powerful alternative to the conventional analysis methodology. In the following, the attention is drawn to a somewhat different aspect, namely (potential) benefits for CAGD due to developments made in IGA. It is focused on challenges concerning robustness and interoperability. In particular, the treatment of trimmed models is addressed, because these representations play a central role in engineering design and the integration of design and analysis⁴. First, the evolution of trimmed CAD models is presented in order to outline the related problems. Based on that, corresponding advances of IGA are discussed.

2 A BRIEF HISTORY OF TRIMMED SOLID MODELS

The problem of computing surface-to-surface intersections (SSI) is closely related to trimming and thus, it is discussed at the beginning of this section. Then, the formulation of solid models defined by trimmed surfaces is presented and finally related robustness issues and the role of trimmed models with respect to the exchange of CAD data are discussed.

2.1 SSI operations

Computing intersections of surfaces is a crucial task in various types of modeling processes. First of all, it is the core ingredient for Boolean operations which are the most important functions in creating CAD objects⁵. In general, the intersection of two parametric surfaces

$$\mathbf{S}_1(u, v) = (x_1(u, v), y_1(u, v), z_1(u, v)) \quad (1)$$

$$\mathbf{S}_2(s, t) = (x_2(s, t), y_2(s, t), z_2(s, t)) \quad (2)$$

leads to a system of three nonlinear equations⁶. These equations represent the three coordinate differences of the surfaces, \mathbf{S}_1 and \mathbf{S}_2 , with the four unknown surface parameters u, v, s, t . In most cases, the solution describes a curve, but intersection points, subsurfaces, or empty sets may occur as well.

Efficiently providing *all* features of these solutions is the purpose of SSI operations⁷. The development of a good SSI procedure is a very challenging task due to the fact that the operation has to be *accurate*, *efficient*, and *robust*. These attributes are indeed quite contradictory and the definition of an adequate balance between them depends strongly on the application context. Early solid modeling systems employed analytic methods to compute exact parametric descriptions of intersections between linear and quadratic surfaces⁸. Unfortunately, the algebraic complexity of an intersection increases rapidly with the degree of \mathbf{S}_1 and \mathbf{S}_2 , which has been thoroughly discussed by Sederberg and co-workers^{9–11} in the 1980s. This makes analytic approaches impractical; a fact often illustrated by the algebraic degree of an intersection of two general bicubic surfaces which is 324.

Hence, alternative SSI schemes are needed. These concepts can be broadly classified as lattice evaluation schemes^{12,13}, subdivision methods¹⁴, and marching methods^{15,16}. The former reduces the dimensionality of the problem by computing intersections of a number of isocurves of \mathbf{S}_1 with \mathbf{S}_2 and vice versa. The second strategy uses approximations of the actual surfaces, often defined by a set of piecewise linear elements, and computes the related intersections with respect to the simplified objects. Finally, marching methods define an intersection curve by stepping piecewise along the curve. This requires detection of appropriate starting points, determination of point sequences along the intersection that emit from the starting points, and proper sorting and merging of these individual sequences. Marching methods are by far the most widely used schemes due to their generality and ease of implementation¹⁷. However, each intersection strategy has its advantages and drawbacks, hence SSI algorithms usually use hybrid concepts that combine different features of these approaches^{17–19}.

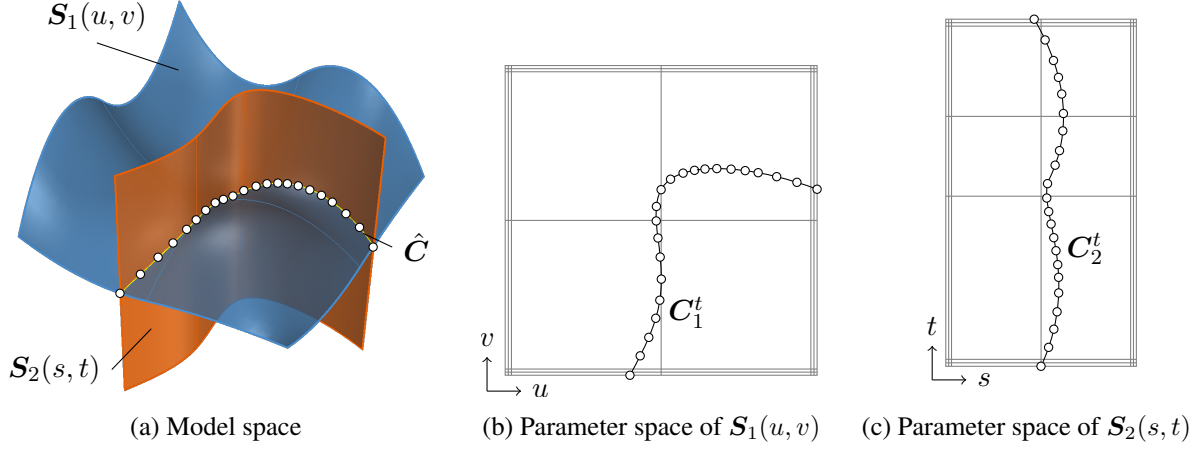


Figure 1: Independent curve interpolation of an ordered point set to obtain approximations of the intersection of two patches $S_1(u, v)$ and $S_2(s, t)$. The set of sampling points depends on the SSI algorithm applied. The subsequent interpolation of these points is performed in (a) the model space and the parameter space of (b) $S_1(u, v)$ and (c) $S_2(s, t)$ leading to independent curves \hat{C} , C_1^t , and C_2^t .

Irrespective of the scheme applied, the initial result of a SSI operation is usually a set of sampling points that represent the intersection²⁰. An *approximate* intersection curve in model space \hat{C} is subsequently obtained by some curve-fitting technique such as point interpolation or least-squares approximation. Thus, \hat{C} does not lie on either of the intersecting surfaces in general. Furthermore, the sampling points are mapped into the parameter spaces of S_1 and S_2 , where they are again used as input for a curve-fitting procedure. This yields the main result of the SSI process, namely *trimming curves* C^t in the two-dimensional parametric domains. These C^t are usually represented by spline curves. They are essential because they allow the definition of arbitrarily shaped partitions within a tensor product surface, which enables proper visualization of intersecting surfaces and the application of Boolean operations. Every C^t can be mapped into model space, but the resulting image \tilde{C}^t will not coincide with \hat{C} . In short, SSI operations yield various independent approximations of the actual intersection (see Figure 1), rather than an unambiguous solution. It is emphasized that there is no direct mapping between these different approximations and that the sampling point data for their construction is usually discarded once the curves are computed.

2.2 Trimmed solid models

There are various approaches for representing geometric objects^{20–22}. The most popular one in engineering design is the boundary representation (B-Rep) and the benefits of storing an object's shape by means of its boundary were already elaborated in the seminal work of Braid²³. B-Rep solid modeling utilizes SSI schemes to create arbitrarily defined free-form geometric entities. The corresponding algorithms, however, require more than the computation

of intersection curves. Essential attributes of geometric modeling operators are²⁴:

- the determination of the geometric surface descriptions,
- the determination of the topological descriptions, and
- the guarantee that the geometry corresponds unambiguously to the topology.

Topological data is not metrical, but addresses connectivity and dimensional continuity of a model²⁰. Its determination requires the classification of the neighborhood of various entities (faces, edges, and vertices) involved in the intersections²¹. In CAGD, the term *solid* model emphasizes that a representation contains the descriptions of an object's shape, i.e., the geometry, as well as its structure, i.e., the topology; it does not refer to the dimension of the object defined.

The idea of a trimmed model appeared already in 1974 and was proposed by Pierre Bézier²⁵. However, the approach was presented with little theoretical support and it took some time to develop a rigorous way to represent trimmed free-form solid models. The first formulation supporting Boolean operations and free-form geometry was presented by Farouki²⁶ as well as Casale and Bobrow^{27,28} in the late 1980s. In general, the connectivity between intersecting surfaces is established by assigning the approximate intersection curves (which do not coincide) to a single topological entity. Further, Boolean operations define the relation of the faces, edges, and vertices of a model. Various data structures for B-Reps have been proposed to find a compromise between storage requirements and response to topological questions. The crucial discrepancy, which still exists, is that solid modeling is concerned with the use of *unambiguous* representations, but SSI schemes introduce approximations and do not provide a unique representation of an intersection. In other words, all these modeling approaches have to deal with imprecise data and thus, fail to guaranty exact topological consistency²⁹. Thus, the robustness of a trimmed B-Rep becomes a crucial factor.

2.3 Robustness issues of trimmed models

Several robustness issues arise in case of imprecise geometric operations. As a matter of fact, numerical output from simple geometric operations can already be quite inaccurate - even for linear elements²¹. For SSI schemes, ill-conditioned intersection problems are particularly troublesome. Such cases occur when intersections are tangential or surfaces overlap, for instance. Since geometrical decisions are based on *approximate* data and arithmetic operations of *limited* precision, there is an interval of uncertainty in which the numerical data cannot yield further information³⁰ and the fact that SSI operations do not provide a unique intersection curve makes the situation even more delicate.

The most common strategy to address robustness issues is the use of tolerances¹⁴. They shall assess the quality of geometrical operations and may be adaptively defined^{31,32} or dynamically updated³³. Alternative approaches employ interval arithmetic³⁴ or exact arithmetic³⁵, but

these concepts have certain drawbacks (especially with respect to efficiency) and hence, tolerance based approaches are usually preferred. Unfortunately, tolerances cannot guarantee robust algorithms since they do not deal with the inherent problem of limited-precision arithmetic.

Overall, the formulation of *robust* solid models with trimmed patches is still an open issue. This is particularly true when a model shall be transferred from a CAD system to another software tool. Since there is no canonical representation of trimmed solid models, different systems may employ different data structures and robustness checks. Consequently, data exchange involves a translation process which can lead to misinterpretation. This makes the treatment of trimmed solid models a key aspect for the interoperability of design and analysis.

3 DEVELOPMENTS IN ISOGEOMETRIC ANALYSIS

Since the introduction of IGA, more and more scientists in the field of computational mechanics have become aware of the advantages and deficiencies of design models and various analysis-suitable approaches dealing with CAD-related challenges have been proposed. Here, we highlight advances made in the context of local refinement of multivariate splines, which are important to derive watertight models, and the treatment of trimmed geometries.

3.1 Local refinement

The lack of local refinement of conventional tensor product splines was one of the first issues tackled by the IGA community. The topic emerged to an active area of research and several techniques have been developed, such as T-splines^{36,37}, LR-B-splines^{38,39}, hierarchical B-splines^{40–42}, and truncated hierarchical B-splines⁴³. Some of these concepts were first presented in the context of CAGD (e.g., T-splines and hierarchical B-splines). However, their application in an analysis setting has provided a huge impetus to their further enhancement. In fact, these concepts have become so technically mature that the question is no longer if local refinement of multivariate spline is feasible, but what technique do you prefer.

Besides the apparent computational benefits, these advances in local refinement techniques also offer new possibilities for the design community. Admittedly, these local refinement concepts are usually not incorporated in current CAD systems (yet), but a strong indicator for the impact of IGA is a novel capability of the next version of the Standard for the Exchange of Product Model Data (STEP) – the most involved neutral exchange standard. That is, it will include entities that facilitate a canonical representation of locally refined tensor product splines⁴⁴. To be precise, this feature affects the part “geometric and topological representations,” which focuses on the definition of geometric models and represents a core component of STEP. Regarding trimmed models, the ability of local refinement can be a powerful tool as well. For instance, effects of trimming may be localized⁴⁵ or trimmed surfaces may even be joined as it is done during the conversion of trimmed B-Reps to watertight T-spline models⁴⁶.

3.2 Dealing with non-watertight representations

The term "non-watertight" is commonly used to stress that trimmed models have small gaps and overlaps between their intersecting surfaces. They occur due to the inevitable approximations introduced by SSI operations as discussed in Section 2.1. Watertight representations, on the other hand, possess unambiguously-defined edges and a direct link between adjacent elements. This link is missing in case of trimmed models and has to be established (or at least taken into account) in order to make them analysis-suitable. Current attempts for the integration of trimmed geometries into IGA can be divided into global and local approaches⁴. The former aims to convert trimmed solid models to watertight ones in a pre-processing step (or even already during the design stage), whereas the latter intends to enhance the simulation tool so that it is able to cope with the models' flaws.

3.2.1 Local approaches

The basic idea of local approaches is that trimmed parameter spaces are used as background parameterization for the simulation. Hence, there is a close relation to fictitious domain methods and the corresponding challenges are indeed similar: First, the elements needed for the analysis have to be detected^{47–49}. Second, special integration techniques for elements cut by a trimming curve^{47–54} have to be employed. Third, weak enforcement of boundary conditions or weak coupling of adjacent surfaces has to be addressed^{50,53,55,56}. Finally, stability issues of cut elements with small support should be taken into account^{45,57}. The main difference to fictitious domain methods is that an additional effort is required to associate the degrees of freedom of adjacent patches, keeping in mind that their intersections have non-matching parameterizations, gaps, and overlaps. Usually, point inversion algorithms^{58,59} are utilized to establish a link between adjacent surfaces. Alternatively, simulation methods that allow discontinuities between elements^{57,60} can be applied.

The majority of the publications on IGA with trimmed geometries employs such local concepts. A possible reason could be that these approaches focus on analysis aspects and thus, may seem more feasible for researchers in the field of computational mechanics. On the other hand, this also means that the number of subjects that may affect CAGD is relatively small. The essential common ground is the problem of finding robust procedures and the use of tolerances to achieve a proper model treatment. However, this does not mean that the task is trivial. As outlined in Section 2.3, the robust treatment of trimmed models is a really challenging issue in CAGD. Regarding IGA, an additional obstacle complicates the situation, that is, analysis software has to deal with extracted data. In other words, the input data provides only a reduced portion of the information that would be available in the initial CAD tool. Furthermore, this portion may be altered due to the translation process that might be required for the exchange. This aspect could be improved when the exchange procedure is tailored to a specific CAD system using its native data format. Yet, this would require vendor interaction and the restriction to a single software. Most importantly, this option is not very sustainable since a native format

of a CAD system may become obsolete after a new software version is released.

3.2.2 Global approaches

Global approaches decompose trimmed model components into a set of regular surfaces or replace them by other spline representations such as subdivision surfaces or T-splines. Similar to the developments regarding local refinement, some strategies may originate from CAGD. For instance, isogeometric analysis with subdivision surfaces^{61,62} and T-splines^{36,63} can be included into the class of global techniques. Reconstruction concepts proposed in the context of analysis usually aim to replace trimmed surfaces by a set of regular ones. This is done by means of ruled surfaces⁶⁴, Coons patches⁶⁵, triangular Bézier patches⁶⁶, or a reconstruction based on isocurves⁶⁷.

Global approaches seek to resolve the core problem of trimmed solid models and hence, they are more related to CAGD than their local counterpart. Consequently, advances in this research area are more likely to have an impact in the design community. T-splines are a prime example in this regard. The introduction of T-splines in IGA has led to various enhancements such as analysis-suitable T-spline spaces that guarantee linear independent basis functions and it would be no exaggeration to say that IGA has been a driving force for the development T-splines in the past years. Approaches emerging from an analysis perspective can also be very useful for design applications. For instance, the reconstruction scheme introduced by Urlick⁶⁷ could be utilized to create watertight Boolean operations. This possibility is currently under investigation and a preliminary example is illustrated in Figure 2. Note that Figure 2(c) shows a single surface with a matching parameterization across the computed intersection.

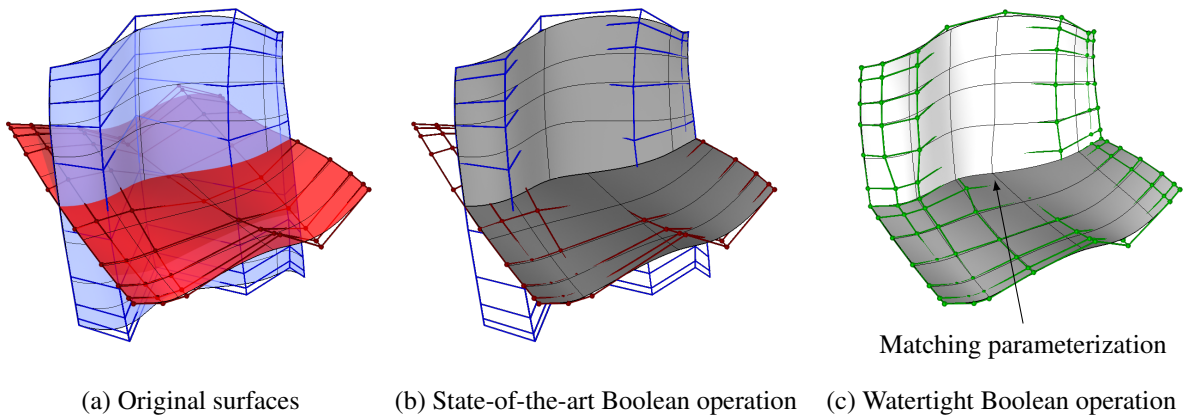


Figure 2: Comparison of conventional and watertight Boolean operations: (a) initial surfaces and their control grids colored in blue and red, respectively, (b) the outcome based on a conventional Boolean operation, and (c) the result of the watertight counterpart. The control grids in (a) and (b) are identical, whereas in (c) the control points are updated to reflect the intersection which is defined as an isocurve of the watertight surface.

In contrast to local approaches, it is hard to identify general ingredients associated to global reconstruction procedures. Each global strategy requires a self-contained concept which becomes more and more sophisticated with its capabilities. This is indeed a potential drawback, especially when new features are added later on. Once a global scheme can be successfully applied, that is, it leads to a watertight model, two fundamental questions have to be addressed: (i) the representation of unstructured meshes and (ii) the treatment of extraordinary points (EPs). These topics are indeed of great interest for CAGD. Current model data is usually based on a structured mesh setting, where all control points of a surface are arranged in a regular grid. When local refinement of tensor product surfaces is considered as well, a structured mesh admits only interior points of valence 4 and T-junctions. But in case of smooth watertight models points with any valence (e.g., 3, 4, 5, ...) can occur and the arising non-regular points are referred to as EPs. These EPs also affect analysis properties and hence, their proper treatment is important for IGA⁶⁸. It is worth noting that IGA researchers are also included in recent attempts seeking to include the capability of representing unstructured meshes in STEP.

Looking at the overall scope of global schemes, it is fair to say that they do address core issues of trimmed models. A compelling analysis-suitable approach could eventually resolve the robustness and interoperability of trimmed models not only for analysis, but all downstream applications. On the other hand, they are more complex and their success will also depend on their acceptance in CAGD.

4 CONCLUSION AND OUTLOOK

A brief overview of the development of surface-to-surface intersection operations and the formulation of trimmed solid models is provided to indicate the potential problems related to these popular computer aided geometric design (CAGD) representations. Strategies for isogeometric analysis (IGA) with trimmed geometries are listed and divided into two categories: (i) local approaches aim to enhance the analysis process and (ii) global approaches try to convert trimmed objects to regular models before the simulation. It is argued that these advances also bring new insights for CAGD, indicating the mutual benefits due to the interaction of the design and analysis communities. That IGA solutions lead to improvements for analysis as well as design has already been demonstrated by the evolution of local refinement concepts for multivariate splines and the recent developments regarding the treatment of trimmed models are indeed on a similar trajectory.

REFERENCES

- [1] J. A. Cottrell, A. Reali, Y. Bazilevs, T. J. R. Hughes, Isogeometric analysis of structural vibrations. *Computer Methods in Applied Mechanics and Engineering*, 195(41–43), 5257–5296, 2006.
- [2] J. Cottrell, T. Hughes, A. Reali, Studies of refinement and continuity in isogeometric

- structural analysis. *Computer Methods in Applied Mechanics and Engineering*, 196(41–44), 4160–4183, 2007.
- [3] S. Lipton, J. A. Evans, Y. Bazilevs, T. Elguedj, T. J. R. Hughes, Robustness of isogeometric structural discretizations under severe mesh distortion. *Computer Methods in Applied Mechanics and Engineering*, 199(5–8), 357–373, 2010.
 - [4] B. Marussig, T. J. R. Hughes, A review of trimming in isogeometric analysis: Challenges, data exchange and simulation aspects. *Archives of Computational Methods in Engineering*, 1–69, 2017.
 - [5] J. Corney, T. Lim, *3D modeling with ACIS*. Saxe-Coburg, 2001.
 - [6] E. Cohen, R. F. Riesenfeld, G. Elber, *Geometric modeling with splines: An introduction*. A K Peters, 2001.
 - [7] N. M. Patrikalakis, T. Maekawa, *Shape interrogation for computer aided design and manufacturing*. Springer Science & Business Media, 2009.
 - [8] C. M. Brown, PADL-2: A technical summary. *IEEE Computer Graphics and Applications*, 2(2), 69–84, 1982.
 - [9] T. W. Sederberg. *Implicit and parametric curves and surfaces for computer aided geometric design*. PhD thesis, Purdue University, 1983.
 - [10] T. W. Sederberg, D. C. Anderson, R. N. Goldman, Implicit representation of parametric curves and surfaces. *Computer Vision, Graphics, and Image Processing*, 28(1), 72–84, 1984.
 - [11] S. Katz, T. W. Sederberg, Genus of the intersection curve of two rational surface patches. *Computer Aided Geometric Design*, 5(3), 253–258, 1988.
 - [12] A. Limaiem, F. Trochu, Geometric algorithms for the intersection of curves and surfaces. *Computers & Graphics*, 19(3), 391–403, 1995.
 - [13] J. R. Rossignac, A. A. G. Requicha, Piecewise-circular curves for geometric modeling. *IBM Journal of Research and Development*, 31(3), 296–313, 1987.
 - [14] J. Hoschek, D. Lasser, *Grundlagen der geometrischen Datenverarbeitung*. Vieweg+Teubner, 1992.
 - [15] C. L. Bajaj, C. M. Hoffmann, R. E. Lynch, J. E. H. Hopcroft, Tracing surface intersections. *Computer Aided Geometric Design*, 5(4), 285–307, 1988.
 - [16] R. T. Farouki, The characterization of parametric surface sections. *Computer Vision, Graphics, and Image Processing*, 33(2), 209–236, 1986.
 - [17] S. Krishnan, D. Manocha, An efficient surface intersection algorithm based on lower-dimensional formulation. *ACM Transactions on Graphics*, 16(1), 74–106, 1997.
 - [18] E. G. Houghton, R. F. Emnett, J. D. Factor, C. L. Sabharwal, Implementation of a divide-and-conquer method for intersection of parametric surfaces. *Computer Aided Geometric Design*, 2(1), 173–183, 1985.
 - [19] R. E. Barnhill, S. Kersey, A marching method for parametric surface/surface intersection. *Computer Aided Geometric Design*, 7(1–4), 257–280, 1990.

- [20] M. E. Mortenson, *Geometric modeling*. Wiley, 2nd edition, 1997.
- [21] C. M. Hoffmann, *Geometric and solid modeling*. Morgan Kaufmann, 1989.
- [22] M. Mäntylä, *An introduction to solid modeling*. Computer Science Press, 1988.
- [23] I. C. Braid, *Designing with volumes*. Cantab Press, Cambridge University, England, 2 edition, 1974.
- [24] K. J. Weiler. *Topological structures for geometric modeling*. PhD thesis, Rensselaer Polytechnic Institute, 1986.
- [25] P. Bézier, Mathematical and practical possibilities of UNISURF. In R. E. Barnhill, R. F. Riesenfeld, editors, *Computer Aided Geometric Design*, 127–152. Academic Press, 1974.
- [26] R. T. Farouki, Trimmed-surface algorithms for the evaluation and interrogation of solid boundary representations. *IBM Journal of Research and Development*, 31(3), 314–334, 1987.
- [27] M. S. Casale, Free-form solid modeling with trimmed surface patches. *IEEE Computer Graphics and Applications*, 7(1), 33–43, 1987.
- [28] M. S. Casale, J. E. Bobrow, A set operation algorithm for sculptured solids modeled with trimmed patches. *Computer Aided Geometric Design*, 6(3), 235–247, 1989.
- [29] R. T. Farouki, C. Y. Han, J. Hass, T. W. Sederberg, Topologically consistent trimmed surface approximations based on triangular patches. *Computer Aided Geometric Design*, 21(5), 459–478, 2004.
- [30] C. M. Hoffmann, J. E. Hopcroft, M. S. Karasick. Towards implementing robust geometric computations. In *Proceedings of the Symposium on Computational Geometry*, 106–117. ACM, 1988.
- [31] D. J. Jackson. Boundary representation modelling with local tolerances. In *Proceedings of the Symposium on Solid Modeling and Applications*, 247–254. ACM, 1995.
- [32] M. Segal, Using tolerances to guarantee valid polyhedral modeling results. *SIGGRAPH Computer Graphics*, 1990.
- [33] S. F. Fang, B. Bruderlin, X. H. Zhu, Robustness in solid modeling: A tolerance-based intuitionistic approach. *Computer-Aided Design*, 1993.
- [34] C.-Y. Hu, N. M. Patrikalakis, X. Ye, Robust interval solid modelling part I: representations. *Computer-Aided Design*, 28(10), 807–817, 1996.
- [35] S. Krishnan, D. Manocha, M. Gopi, T. Culver, J. Keyser, BOOLE: A boundary evaluation system for boolean combinations of sculptured solids. *International Journal of Computational Geometry & Applications*, 11(1), 105–144, 2001.
- [36] Y. Bazilevs, V. M. Calo, J. A. Cottrell, J. A. Evans, T. J. R. Hughes, S. Lipton, M. A. Scott, T. W. Sederberg, Isogeometric analysis using T-splines. *Computer Methods in Applied Mechanics and Engineering*, 199(5–8), 229–263, 2010.
- [37] T. W. Sederberg, J. Zheng, A. Bakenov, A. Nasri, T-splines and T-NURCCs. *ACM Trans. Graph.*, 2003.
- [38] T. Dokken, T. Lyche, K. F. Pettersen, Polynomial splines over locally refined box-

- partitions. *Computer Aided Geometric Design*, 30(3), 331–356, 2013.
- [39] K. A. Johannessen, T. Kvamsdal, T. Dokken, Isogeometric analysis using LR B-splines. *Computer Methods in Applied Mechanics and Engineering*, 269, 471–514, 2014.
 - [40] P. B. Bornemann, F. Cirak, A subdivision-based implementation of the hierarchical b-spline finite element method. *Computer Methods in Applied Mechanics and Engineering*, 253, 584–598, 2013.
 - [41] R. Kraft, *Adaptive and linearly independent multilevel B-splines*. SFB 404, 1997.
 - [42] A. V. Vuong, C. Giannelli, B. Jüttler, B. Simeon, A hierarchical approach to adaptive local refinement in isogeometric analysis. *Computer Methods in Applied Mechanics and Engineering*, 2011.
 - [43] C. Giannelli, B. Jüttler, H. Speleers, THB-splines: The truncated basis for hierarchical splines. *Computer Aided Geometric Design*, 2012.
 - [44] V. Skytt, J. Haenisch. Extension of ISO 10303 with isogeometric model capabilities. ISO TC 184/SC 4/WG 12, *ISO*, 2013.
 - [45] B. Marussig, R. Hiemstra, T. J. R. Hughes, Improved conditioning of isogeometric analysis matrices for trimmed geometries. *Computer Methods in Applied Mechanics and Engineering*, 334, 79–110, 2018.
 - [46] T. W. Sederberg, X. Li, H. W. Lin, H. Ipson, G. T. Finnigan, Watertight trimmed NURBS. *ACM Transactions on Graphics*, 2008.
 - [47] R. Schmidt, R. Wüchner, K.-U. Bletzinger, Isogeometric analysis of trimmed NURBS geometries. *Computer Methods in Applied Mechanics and Engineering*, 241–244, 93–111, 2012.
 - [48] H.-J. Kim, Y.-D. Seo, S.-K. Youn, Isogeometric analysis for trimmed CAD surfaces. *Computer Methods in Applied Mechanics and Engineering*, 198(37–40), 2982–2995, 2009.
 - [49] H.-J. Kim, Y.-D. Seo, S.-K. Youn, Isogeometric analysis with trimming technique for problems of arbitrary complex topology. *Computer Methods in Applied Mechanics and Engineering*, 199(45–48), 2796–2812, 2010.
 - [50] M. Ruess, D. Schillinger, A. I. Özcan, E. Rank, Weak coupling for isogeometric analysis of non-matching and trimmed multi-patch geometries. *Computer Methods in Applied Mechanics and Engineering*, 269, 46–71, 2014.
 - [51] B. Marussig. *Seamless integration of design and analysis through boundary integral equations*. PhD thesis, Graz University of Technology, 2015.
 - [52] Y.-W. Wang, Z.-D. Huang, Y. Zheng, S.-G. Zhang, Isogeometric analysis for compound B-spline surfaces. *Computer Methods in Applied Mechanics and Engineering*, 261–262, 1–15, 2013.
 - [53] M. Breitenberger, A. Apostolatos, B. Philipp, R. Wüchner, K.-U. Bletzinger, Analysis in computer aided design: Nonlinear isogeometric B-Rep analysis of shell structures. *Computer Methods in Applied Mechanics and Engineering*, 284, 401–457, 2015.
 - [54] B. Philipp, M. Breitenberger, I. D’Auria, R. Wüchner, K.-U. Bletzinger, Integrated design

- and analysis of structural membranes using the isogeometric B-Rep analysis. *Computer Methods in Applied Mechanics and Engineering*, 303, 312–340, 2016.
- [55] M. Breitenberger. *CAD-integrated design and analysis of shell structures*. PhD thesis, Technische Universität München, 2016.
 - [56] Y. Guo, J. Heller, T. J. R. Hughes, M. Ruess, D. Schillinger, Variationally consistent isogeometric analysis of trimmed thin shells at finite deformations, based on the STEP exchange format. *Computer Methods in Applied Mechanics and Engineering*, 336, 39–79, 2018.
 - [57] B. Marussig, J. Zechner, G. Beer, T.-P. Fries, Stable isogeometric analysis of trimmed geometries. *Computer Methods in Applied Mechanics and Engineering*, 316, 497–521, 2016.
 - [58] Y. L. Ma, W. T. Hewitt, Point inversion and projection for NURBS curve and surface: Control polygon approach. *Computer Aided Geometric Design*, 2003.
 - [59] L. A. Piegl, W. Tiller, *The NURBS book*. Springer, 2nd edition, 1997.
 - [60] J. Zechner, B. Marussig, G. Beer, T.-P. Fries, The isogeometric Nyström method. *Computer Methods in Applied Mechanics and Engineering*, 306, 212–237, 2015.
 - [61] F. Cirak, Q. Long, Subdivision shells with exact boundary control and non-manifold geometry. *International Journal for Numerical Methods in Engineering*, 88(9), 897–923, 2011.
 - [62] A. Riffnaller-Schiefer, U. H. Augsdörfer, D. W. Fellner, Isogeometric shell analysis with NURBS compatible subdivision surfaces. *Applied Mathematics and Computation*, 272, Part 1, 139–147, 2016.
 - [63] M. A. Scott. *T-splines as a design-through-analysis technology*. PhD thesis, 2011.
 - [64] G. Beer, B. Marussig, J. Zechner, A simple approach to the numerical simulation with trimmed CAD surfaces. *Computer Methods in Applied Mechanics and Engineering*, 285, 776–790, 2015.
 - [65] H. Harbrecht, M. Randrianarivony, From Computer Aided Design to wavelet BEM. *Computing and Visualization in Science*, 13(2), 69–82, 2010.
 - [66] S. Xia, X. Qian, Isogeometric analysis with Bézier tetrahedra. *Computer Methods in Applied Mechanics and Engineering*, 316, 782–816, 2016.
 - [67] B. Urick. *Reconstruction of tensor product spline surfaces to integrate surface-surface intersection geometry and topology while maintaining inter-surface continuity*. PhD thesis, The University of Texas at Austin, 2016.
 - [68] D. Toshniwal, H. Speleers, T. J. R. Hughes, Smooth cubic spline spaces on unstructured quadrilateral meshes with particular emphasis on extraordinary points: Geometric design and isogeometric analysis considerations. *Computer Methods in Applied Mechanics and Engineering*, 327, 411–458, 2017.

Computational Design of Lattice Models of Next-generation Structural Materials under Testing

Ida Mascolo^{*}, Mariano Modano^{**}, Francesco Fabbrocino^{***}, Francesco Colangelo^{****}, Ilenia Farina^{*****}

^{*}University of Salerno, Italy, ^{**}University of Naples Federico II, Italy, ^{***}Pegaso Telematic University, Italy,
^{****}University of Naples Parthenope, Italy, ^{*****}University of Naples Parthenope, Italy

ABSTRACT

Keywords: Tensegrity, prestress, frequency bandgaps. Recent studies have explored the use of additively manufactured reinforcing elements of innovative construction materials, which consist of fibers with structural hierarchy manufactured from computer-aided design (CAD) data, employing additive manufacturing techniques based either on photopolymers (SLA) and the electron beam melting (EBM) of a metallic powder [1][2]. The present study employs strut-and-tie lattice models [3][4] to capture the experimental response of such materials under short-beam shear tests, which are aimed at determining the first-crack strength and toughness of the material. A comparative theory vs. experiment study shows that the employed lattice models accurately describe the actual response of prismatic elements in correspondence with the cracked regime. Their use to predict the mechanical properties of nextgeneration composite materials, such as, e.g., the overall strength and fracture toughness of totally or partially additively manufactured composites, awaits attention.

Automated Conformal Discretization Of Complex Heterogeneous Microstructures

Thierry J. Massart*, Karim Ehab Moustafa Kamel**, Bernard Sonon***

*Université libre de Bruxelles (ULB), **Université libre de Bruxelles (ULB), ***Université libre de Bruxelles (ULB)

ABSTRACT

The response of heterogeneous materials is highly dependent on their micro-morphology. Fine scale constitutive models are therefore developed to establish a link between experimental observations and the physical underlying mechanisms, coupled to information on the morphology of microstructures of interest. Such ingredients are nowadays routinely upscaled using computational homogenization techniques. However, this requires the availability of some Representative Volume Elements (RVEs) of the microstructure, which can be obtained either experimentally (e.g. CT scans) or numerically by using algorithms aiming to reproduce the main micro-morphological features [1]. The complexity of discretizing complex geometries motivated the development of XFEM approaches based on the concept of partition of unity over the last decade. The use of available conventional finite packages is however still of interest for multi-scale analyses as it allows using existing formulations and constitutive models, especially when large strains and/or coupled processes are considered. This motivated the development of a hierarchical Delaunay mesh generator based on an extended Persson-Strang truss analogy optimization [2], and using an input level set function in order to produce conformal tetrahedral meshes. A local control of element sizes is enforced using an analogy with the equilibrium of a truss system made of the element edges. Desired bar lengths evaluated from a constructed element size function are used in combination with distances from material interfaces to compute nodal forces acting on the truss nodes to converge to an equilibrated truss situation when the targeted element size is reached. A mesh of material interfaces is first obtained starting from an initial Delaunay surface mesh. An optimized shape of these surface elements is reached by controlling their size with a tension/compression force field in the bars to reach the targeted lengths. This is achieved while preventing nodal displacements away from interfaces based on a level set (distance) function. A 3D mesh is subsequently obtained based on same optimization principles, using a constrained Delaunay generation based on the material interfaces discretization. The versatility of the approach will be illustrated based on computationally generated RVEs for 3D woven composites and porous materials; as well as for experimentally obtained images of metallic materials. [1] B. Sonon, B. François, T.J. Massart (2012). A unified level set based methodology for fast generation of complex microstructural multi-phase RVEs. *Comp. Meth. Appl. Mech. Engng.*, 223–224, 103-122. [2] P.O. Persson and G. Strang (2004). A simple mesh generator in MATLAB, *SIAM Review*, 46(2), 329-345.

Cut Discontinuous Galerkin Methods for Surface and Multi-dimensional Coupled Problems

Andre Massing*, Ceren Gürkan**

*Umeå University, **Umeå University

ABSTRACT

In this talk, we present novel stabilized cut discontinuous Galerkin methods (cutDGM) for the numerical treatment of surface and multi-dimensional problems coupling partial differential equations on domain of different topological dimensionality. The domains of interest such the surface or the bulk domain can be embedded arbitrarily into a background mesh and are generally not fitted to it. To remedy the numerical challenges caused by small cut cells, we combine stabilization techniques from the cut finite element method [1] with the interior penalty discontinuous Galerkin methods (DG) for elliptic [2] and hyperbolic problems [3]. Using only a few abstract assumptions on the employed cutDG stabilization, we can establish geometrically robust optimal a priori error and condition number estimates irrespective of how the embedded geometry cuts the background mesh. Motivated by flow and transport problems in fractured porous media, the theoretical properties are corroborated by a number of numerical experiments for surface problems, interface problems on surfaces and coupled surface/interface-bulk problems. REFERENCES [1] E. Burman, S. Claus, P. Hansbo, M. G. Larson, and A. Massing. CutFEM: discretizing geometry and partial differential equations. *Internat. J. Numer. Meth. Engrg.*, 104(7):472- 501, November 2015. [2] D.N. Arnold. An interior penalty finite element method with discontinuous elements. *SIAM J. Num. Anal.*, 19(4):742-760, 1982. [3] F. Brezzi, L. D. Marini, and E. Süli, *Math. Models Methods Appl. Sci.* 14(12):1893-1903, 2004.

A Discontinuous Galerkin Method for Thermoelasticity at Finite Strains

Arif Masud*, Pinlei Chen**

*University of Illinois at Urbana-Champaign, **University of Illinois at Urbana-Champaign

ABSTRACT

This talk presents a stabilized Discontinuous Galerkin (DG) method at finite strains for thermomechanical problems that have embedded weak and strong discontinuities in the mechanical and thermal fields. The new method is designed to address technical issues that present themselves in the emerging field of additive manufacturing. Starting from a thermomechanically coupled formulation, a Lagrange multiplier method is developed that couples fields across the embedded interfaces. Employing ideas from VMS based stabilization that are applied to internal interfaces arising across discontinuities, an interfacial fine scale problem is derived. The interfacial fine scales are expanded via edge bubbles and are resolved locally to extract analytical models for Lagrange multipliers in terms of the jumps in the fields and their fluxes. Since the derived expressions are a function of the mechanical and thermal fields, the resulting stabilized formulation contains numerical flux and stability tensors that provide an avenue to variationally embed interfacial kinetic and kinematic models for a robust representation of interfacial physics. A significant contribution of the method is that it is free of any ad hoc or user defined parameters. Several benchmark problems are presented to show stability and variational consistency of the method. References: [1] A. Masud and T. Truster, A Framework for Residual-Based Stabilization of Incompressible Finite Elasticity: Stabilized Formulations and F-bar Methods for Linear Triangles and Tetrahedra. *Computer Methods in Applied Mechanics and Engineering*, vol. 267, 359-399, 2013. [2] P. Chen, T.J. Truster, and A. Masud, Interfacial Stabilization at Finite Strains for Weak and Strong Discontinuities in Multi-Constituent Materials. *Computer Methods in Applied Mechanics and Engineering*. 328, 717–751, 2018.

Prediction of Numerical Analysis Results using Machine Learning

Masato Masuda*, Yasushi Nakabayashi[†], AND Yoshiaki Tamura^{††}

*Center for Computational Mechanics Research, Toyo University
1-1-1, Yayoi, Bunkyo, Tokyo, Japan
masuda.masato@mail.u-tokyo.ac.jp

[†]Toyo University
2100, Kujirai, Kawagoe, Saitama, Japan
nakabayashi@toyo.jp

^{††}Toyo University
2100, Kujirai, Kawagoe, Saitama, Japan
tamura@toyo.jp

Key words: CFD, Convolutional Neural Network(CNN), Long Short-Term Memory(LSTM), Convolutional LSTM

Abstract. This study is to predict the solution of the nonlinear problem of computational fluid dynamics (CFD) using machine learning. We predict the results of CFD analysis using Convolutional LSTM(Long Short-Term Memory) which expanded to handle time series data based on Convolutional Neural Network. In this paper, we did not use physical quantities of CFD results. For simplicity, we used visualized images of CFD results. A visualized image of a vorticity field (1-channel) was used for learning. The training image and the untrained image were input using the model after learning and the learning accuracy was verified by Mean Squared Error and Structural Similarity Index Measure. In addition, assuming that physical quantities are to be input, learning is performed by increasing the number of channels of the image to 2-channels. It was confirmed that learning accuracy was the same as in the case of 1-channel.

1 Introduction

In recent years, an artificial intelligence boom is coming back by the image recognition competition^[1] and Google's cat^[2]. In this artificial intelligence boom, research and development using deep learning is mainstream. In image recognition, it is known that CNN (Convolutional Neural Network) can obtain better results than conventional feature extraction techniques^[1], and is widely used not only in images but also in many fields such as speech recognition^[3]. In deep learning, LSTM (Long Short-Term Memory) which extends Recurrent Neural Network (RNN) is used to realize learning that adds temporal state information^[4].

On the other hand, in the field of numerical analysis, highly accurate analysis using computer power is very active ^[5] ^[6], such as ultra-large-scale analysis, coupled analysis, multiscale analysis, complex shape analysis, etc. However, it takes a lot of time for ultra-large-scale analysis or complicated analysis, and calculation may take time from several days to several weeks in one case. Therefore, if we could know the approximate analysis result in advance, we can obtain clues for detailed analysis. Therefore, it is thought that reduction of the number of trials of analysis leads to shortening of total analysis time. Besides, convergence of the calculation could be improved by predicting the initial value in the internal iterations of an implicit solution.

The final goal of this research is prediction of numerical analysis results using deep learning. We construct a network that predicts the state at the next time from the state of arbitrary analysis time. Since the analysis results of numerical analysis have physical quantities on nodes, the spatial information is very important. CNN is capable of feature extraction maintaining spatial information. However, although CNN can hold spatial information, it is not good to hold time information. On the other hand, LSTM is good at handling time information, but it cannot handle spatial information. So, we use Convolutional LSTM (ConvLSTM)^[7] which combines the advantages of the two methods. It combines features that can keep spatial information holding of CNN and handling time series of LSTM. Originally, ConvLSTM is a network developed to predict future images from moving images. By giving the physical quantity of the node as the input channel of the convolution layer, it is possible to predict the numerical analysis result by treating the node information as spatial information. In this paper, we propose to use ConvLSTM for prediction of numerical analysis result. In this paper, in order to investigate whether it is possible to predict the analysis result, learning was performed using images visualizing the vorticity of the analysis result. By using the visualized image, it is possible to represent part of the physical quantity of the analysis result, simplifying the coding and speeding up the learning. We use the trained ConvLSTM to predict the analysis result and compare it with the correct image. And we demonstrate the usefulness of the proposed method. MSE and SSIM are used as quantitative evaluation. In addition, we added images of pressure field to the network input. This is 2-channels learning. This is an experiment to increase the number of channels for the physical quantities as input in future. It confirms that there is no problem in prediction accuracy even when the number of channels increases.

2 Convolutional LSTM^[7]

LSTM is one type of method for estimating the future state based on temporal state information. LSTM conventionally calls 1-dimensional feature quantity information recursively. When predicted, input vector of the current step and feature quantity vector of the previous step are merged and treated as input information for learning. Convolutional LSTM (ConvLSTM) can extend the 1-dimensional feature information to 2-dimensional Convolutional layer and store past input information. Therefore, it is possible to track spatial information temporally. Equation 1 shows each gate and activation function of ConvLSTM.

$$\begin{aligned}
 i_t &= \sigma(W_{xi} * X_t + W_{hi} * \mathcal{H}_{t-1} + W_{ci} \circ C_{t-1} + b_i) \\
 f_t &= \sigma(W_{xf} * X_t + W_{hf} * \mathcal{H}_{t-1} + W_{cf} \circ C_{t-1} + b_f) \\
 C_t &= f_t \circ C_{t-1} + i_t \circ \tanh(W_{xc} * X_t + W_{hc} * \mathcal{H}_{t-1} + b_c) \\
 o_t &= \sigma(W_{xo} * X_t + W_{ho} * \mathcal{H}_{t-1} + W_{co} \circ C_t + b_o) \\
 \mathcal{H}_t &= o_t \circ \tanh(C_t)
 \end{aligned} \tag{1}$$

Here, X represents the input group, \mathcal{H} is the state of the hidden layer, and C is the output of the cell. i, f, o represent the gates of input, forget, and output, respectively.

These variables have a 3rd-order tensor, which time t and 2-dimensional spatial information (row, column). The calculation symbol "*" is the convolution product, and "o" is the Hadamard product.

3 Analysis data for learning

Deep learning and neural networks require a lot of training data. Training data must be correct combination data of input vector and output vector. ConvLSTM generally uses image data for both input and output. The input and output vector used in this research are visualized images of analysis results. By replacing this image data with the physical quantity of the numerical analysis result, it is possible to predict the physical quantity of the numerical analysis result. For simplicity, this time visualized image data is assumed.

The analysis model is an incompressible flow around a two-dimensional cylinder, and the computational domain was discretized with 1250×800 equidistant Cartesian grid. The pseudo compressibility method was used for analysis method, and the third order upwind difference was used for the convective terms. The analysis conditions are shown in Table 1.

Table 1 Analysis conditions

Cylinder Diameter	40
Reynolds number	1,000
Courant number	0.25

The training data is image data visualizing the vorticity distribution of the numerical analysis result. One image is generated every 100 steps and 300 images are collected. The image size is 512×476 pixels, and by expressing it in gray scale of 256 gradations, the channel of the Convolutional layer is taken as 1-channel of vorticity distribution. The image was trimmed with a size of 200×100 , that the flow field of the cylinder and the cylinder wake was captured. In this paper, we created the learning data to predict the input of the past 4 frames and an image of the future vorticity fields 1 frame later. Also, training data was created from the pressure field likewise. The training data of the pressure field is learned together with the vorticity field at the time of learning of two channels.

4 Construction of learning device

The input to the network is the image size (200, 100), the input image is a visualized grayscale image of the vorticity distribution, and the number of channels is (1). When the pressure field is also used, the number of channels is (2). Therefore, the input vector is (200, 100, 1 or 2). In this network, 4-layers of ConvLSTM are laminated from the input layer, and in the uppermost layer, 3-dimensional Convolutional layer is arranged. We built a total of 6-layers of networks. Figure 1 shows the network structure for 1-channel. The kernel size of ConvLSTM was set to (3×3) for all layers. The inputs of the three dimensional Convolutional layer(the uppermost layer) are (20, 4, 200, 100) and the kernel size is $(3 \times 3 \times 3)$. The stride was (1, 1) and (1, 1, 1) in all layers. The loss function cross entropy was adopted for the loss function, optimization used Adadelta, weights were modified by back propagation method.

5 Results of Learning

The data of 250 images (frame number $t = 0$ to 249) were used as the input data for training. The number of epochs is 10,000. First, using the learned model, the image used for learning was given to the input, and the predicted image was generated. The predicted image is shown in Fig.2. In Fig.2, "Actual" is a visualized image of numerical analysis result. "Predicted" is an image predicted by input data of 4 visualized images of the numerical analysis results from 4 frames before. For example, images of time $t-3$, $t-2$, $t-1$, t are given to input data, and an image of time $t+1$ is predicted. Although the prediction results of training data are shown in this paper, similar results were obtained for untrained input data. The prediction result in the case of 2-channels is shown in Fig.3. And the output images were evaluated by MES (Mean Square Error) and SSIM (Structural Similarity Index Measure) (Table 2). Each calculation formula is shown below. MES is an indicator of how much difference is between the images. When the value is small, the error of the image is small. SSIM is an image similarity index. Similarity is high if the value is close to 1.

$$MES = \frac{1}{row \cdot col} \sum_{i=0}^{row-1} \sum_{j=0}^{col-1} (Actual - Predicted) \quad (2)$$

$$SSIM(x, y) = \frac{(2\mu_x\mu_y + C_1)(2\sigma_{xy} + C_2)}{(\mu_x^2 + \mu_y^2 + C_1)(\sigma_x^2 + \sigma_y^2 + C_2)} \quad (3)$$

Here, row and col represent image sizes, and Actual and Predicted are correct images and predicted images. Taking the square root of MES gives the difference in gradation of the pixel. It is the average of pixel differences across the images. SSIM is calculated for each small area (window) in the image, and the average value of the entire an image is calculated. Equation 3 indicates a process on window. x, y are index having each pixel in the window as an element. μ is the average value of pixels in each window. σ_x, σ_y are standard deviations of pixel values within the window. σ_{xy} is the covariance of x and y . C is a constant, here $C_1 = (0.01 \times 255)^2$, $C_2 = (0.03 \times 255)^2$ were used.

From Fig.2, we can see that predictive images similar to "Actual" are obtained by learning. The vortices in the wake are slightly blurry, but it seems to be maintaining a qualitatively correct structure. In addition, the SSIM of the quantitative evaluation result of Table 2 shows prediction accuracy about 70%. From the results, it was confirmed that structurally similar images were output. Since MES also shows a relatively low value, it was confirmed that ConvLSTM can be predicted to some extent. Even when the number of input channels is increased, the results are the same as for single channel.

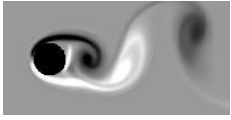
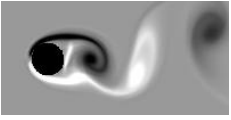
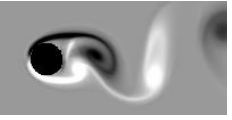
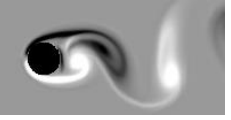
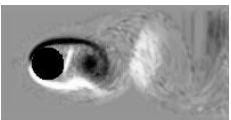
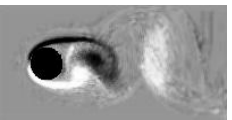
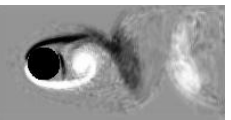
	t-1	t	t+1	t+2
Actual (Vorticity)				
Predicted (Vorticity)				

Fig.2 Prediction of analysis results using Convolutional LSTM (t is frame of figure, t=31.)

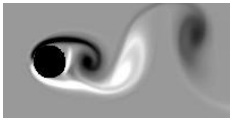
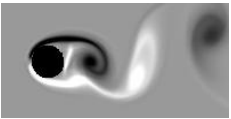
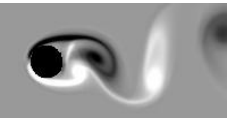
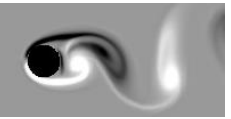
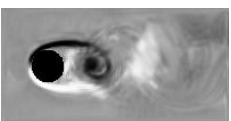
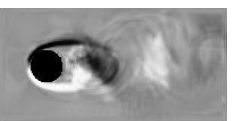

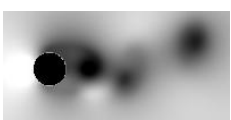



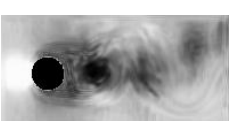
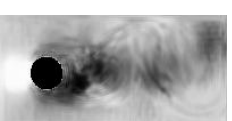

	t-1	t	t+1	t+2
Actual (Vorticity)				
Predicted (Vorticity)				
Actual (Pressure)				
Predicted (Pressure)				

Fig.3 Prediction of analysis results by 2-channels (t is frame of figure, t=31.)

Table 2 Result of MES & SSIM
(1ch is only vorticity field, 2ch is both fields of vorticity and pressure)

		t	t+1	t+2
1ch	MES (Vorticity)	248.862	257.929	127.669
	SSIM (Vorticity)	0.7196	0.750	0.759
2ch	MES (Vorticity)	357.922	361.254	322.959
	MES (Pressure)	501.031	381.589	327.583
	SSIM (Vorticity)	0.728	0.722	0.723
	SSIM (Pressure)	0.702	0.719	0.724

6 Conclusions

In this research, we proposed to use ConvLSTM for prediction of numerical analysis results. Numerical analysis results of 1 or 2 channels were predicted using training data. The obtained results are as follows.

- (i) We succeeded in generating the visualized image of the next frame by giving the visualized image of the analysis result of the past 4 frames to the input.
- (ii) It was confirmed that prediction images can be generated even when 2 images of vorticity and pressure are given to the input, and increasing the number of channels does not affect the prediction accuracy.
- (iii) We evaluated output images by MES and SSIM. The SSIM results showed about 70% similarity. Moreover, it was found that the error per pixel in the MES result is relatively small.

It was confirmed that ConvLSTM is useful for predicting numerical analysis results. In the future, we implement the following two things. First, we will change the input vector from image to physical quantity. Next, we will implement algorithms to learn the whole calculation area.

Acknowledgements

This research was partly supported by grants from the Project of the NARO Bio-oriented Technology Research Advancement Institution(R&D matching funds on the field for Knowledge Integration and innovation).

REFERENCES

- [1] Alex Krizhevsky, Ilya Sutskever, Geoffrey E. Hinton, ImageNet Classification with Deep Convolutional Neural Networks, NIPS2012, 2012.
- [2] Quoc V. Le, Marc’Aurelio Ranzato, Rajat Monga, Matthieu Devin, Kai Chen, Greg S. Corrado, Jeff Dean, Andrew Y. Ng, Building High-level Features Using Large Scale Unsupervised Learning, International Conference on Machine Learning, 2012.

- [3] Alex Graves, Abdel-rahman Mohamed, Geoffrey Hinton, Speech recognition with deep recurrent neural networks, IEEE International Conference on Acoustics, Speech and Signal Processing, pp.6645-6649, 2013.
- [4] Klaus Greff, Rupesh Kumar Srivastava, Jan Koutník, Bas R. Steunebrink, Jürgen Schmidhuber, LSTM: A Space Odyssey, arXiv:1503.04069, 2015.
- [5] Masao OGINO, Kaworu YODO, Ryuji SHIOYA, Hiroshi KAWAI, Two-level extension of the hierarchical domain decomposition method, Mechanical Engineering Letters, vol.4(No.18-00088) 1-8, 2018.
- [6] Yuri Bazilevs, Kenji Takizawa, Tayfun E. Tezduyar, Computational Fluid-Structure Interaction: Methods and Applications, Wiley, 2013.
- [7] Xingjian Shi, Zhourong Chen, Hao Wang, Dit-Yan Yeung, Wai-kin Wong, Wang-chun Woo, Convolutional LSTM Network: A Machine Learning Approach for Precipitation Nowcasting, arXiv:1506.04214v2, 2015.

Integrated Computational Materials Engineering

Karel Matous*

*University of Notre Dame

ABSTRACT

With concentrated efforts from the material science community to develop new multifunctional materials using unique processing conditions, the need for modeling tools that accurately describe the physical phenomena at each length scale has only further been emphasized. For example, additive manufacturing and shock synthesis lead to unique material morphologies that need to be understood for reliable engineering analysis and product safety assessments. Considering these material complexities, Direct Numerical Modeling (DNM) is accessible only for moderate system sizes. Thus, a multiscale strategy must recognize that just a relatively small part of the material will typically be instantaneously exposed to rapid material transformations. Macroscopic constitutive models obtained from homogenization, of the complex but slowly varying microstructure, may adequately describe the rest of the material. Nonlinear model reduction, pattern recognition and data-mining are a key to future on-the-fly modeling and rapid decision making. To address these challenges, we present an image-based (data-driven) multiscale framework for modeling the chemo-thermo-mechanical behavior of heterogeneous materials while capturing the large range of spatial and temporal scales. This integrated computational approach for predicting the behavior of complex heterogeneous systems combines macro- and micro-continuum representations with statistical techniques, nonlinear model reduction and high-performance computing. Our approach exploits the instantaneous localization knowledge to decide where more advanced computations are required. Simulations involving this wide range of scales, $O(10^6)$ from nm to mm, and billions of computational cells are inherently expensive, requiring use of high-performance computing. Therefore, we have developed a hierarchically parallel high-performance computational framework that executes on hundreds of thousands of processing cores with exceptional scaling performance. Any serious attempt to model a heterogeneous system must also include a strategy for constructing a complex computational domain. This work follows the concept of data-driven (image-based) modeling. We will delineate a procedure based on topology optimization and machine learning to construct a Representative Unit Cell (RUC) with the same statistics (n-point probability functions) to that of the original material. Our imaging sources come from micro-computed-tomography (micro-CT), focused ion beam (FIB) sectioning, and advanced photon source nano-tomography at the Argonne National Laboratory. We show that high-performance DNM of these statistically meaningful RUCs coupled on-the-fly to a macroscopic domain is possible. Therefore, well-resolved microstructure-statistics-property (MSP) relationships can be obtained. Finally, the integrated V&V/UQ program with co-designed simulations and experiments provides a platform for computational model verification, validation and propagation of uncertainties.

Space-time Characterization of Macroscopic Thermo-Mechanical Behavior Reflecting Microscopic Unsteady Heat Conduction

Seishiro Matsubara^{*}, Kenjiro Terada^{**}

^{*}Tohoku University, ^{**}Tohoku University

ABSTRACT

The present study proposes a method of space-time characterization of the macroscopic thermo-mechanically coupled behavior in consideration of the microscopic unsteady heat conduction. An emphasis is placed on how the unsteadiness of microscopic temperature distribution affects the macroscopic thermo-mechanical behavior. The incremental variational formulation (IVF) [1] is employed to define the global and local saddle point problems for thermo-mechanically coupled phenomena within a certain time interval. The unsteadiness of heat conduction arises from the time rate of entropy change, which is determined by not only the thermal expansion and specific heat in the case of thermo-elastic solids, but also the inelastic part of free energies in general dissipative solids. In fact, the heat sources due to self-generated heat are formulated as the gradients of the inelastic dual dissipation potential with respect to the rates of both the deformation and state variables, and in turn affect the unsteadiness of heat conduction involving for general dissipative solids. To this end, the relationship between time rates of micro- and macroscopic entropies must be determined through appropriate numerical material testing within the standard computational homogenization framework that enables us to characterize the macroscopic heat conduction under the assumption that both the geometry of microstructures of composites under consideration and the time evolution are periodic. Nonetheless, since the temporal scale need not be periodic in the present problem setting, the standard space-time homogenization scheme cannot be applied. Instead, we introduce the concept of time-homogenization that defines the macroscopic time increment by the time spent to attain the microscopic steady state. We begin with formulating two-scale problem under the assumption of periodicities of state variables in space and time along the line of the two-scale spatial discretization approach [2] and then the integration factor in the IVF is utilized to define the micro- and macroscopic time scales. Several numerical examples are presented to demonstrate the idea and concept of our new space-time homogenization for thermo-mechanical coupled problems. A series of numerical material testing are performed to illustrate the capability in characterizing the macroscopic thermo-mechanical behavior reflecting the microscopic unsteady heat conduction. [1] Q. Yang and L. Stainier and M. Ortiz: A variational formulation of the coupled thermomechanical boundary-value problem for general dissipative solids, *J. Mech. Phys. Solids*, Vol.54 (2006), No.2, pp.401-424. [2] I. Temizer and P. Wriggers: Homogenization in finite thermoelasticity, *J. Mech. Phys. Solids*, Vol.59 (2011), No.2, pp.344-372.

Development of Homeschooling Support Framework Using Desktop Robotic Arm with Computer Vision

Masami Matsumoto*

*National Institute of Technology, Yonago College

ABSTRACT

In this research, we propose a Problem Solving Environment (PSE) for education that supports homeschooling using robotic arm with computer vision. A useful system is necessary for science, technology, engineering, mathematics (STEM) education. The purpose of this research is to develop self-study support system using information communication (ICT) environment. The developed system consists of four hardware elements: a system control unit, a robotic arm, a smart pad, and a camera. The framework developed for operating the system interactively controls the robotic arm by using the image analysis result photographed by the two cameras. This system is built by Linux system on a small single board computer developed to promote the basic computer science lecture. The robotic arm is controlled by the G-code sent from the control unit via the serial line. G-code is used for head control of numerical control (NC) machines and 3D printers, and porting to other systems is also easy. Users can interactively use the basic actions registered in the library. Images from two cameras attached to the overhead view camera and robotic arm are analyzed by the computer. By exchanging data with the GPU server on the Internet via wireless LAN, various processing becomes possible. Since, this system can be expected to increase the visual effect by using the robot arm with motion as the user interface. This system provides scoring, searching, and task management functions. Problems imposed on users are semi-automatically generated from Web pages provided in Wikipedia format. The answers solved on a paper basis can also be scored by the robotic arm. Users create their own drill type problems and learn by scoring interactively. Simultaneously, handwritten characters are recognized by Artificial Intelligence (AI) system, and information is digitized and stored. In addition, a problem management system using the Web is provided. The management system provides guidance that makes task deadlines important. Give the user a badge to accomplish the task within the deadline and admire it. It is also expected to expand the voice operation function by introducing the smart speaker. Practice of science and technology education is an important issue in modern society. The user extends the framework provided in this research and pushes forward homeschooling.

Boundary Integral Based Method for Treatment of Solid Wall in a Particle Method

Takuya Matsunaga^{*}, Kazuya Shibata^{**}, Seiichi Koshizuka^{***}

^{*}Department of Systems Innovation, The University of Tokyo, ^{**}Department of Systems Innovation, The University of Tokyo, ^{***}Department of Systems Innovation, The University of Tokyo

ABSTRACT

Many important applications in engineering involve an incompressible fluid flow with moving boundaries. For such background, particle methods in computational fluid dynamics have been becoming more important. One representative particle method for incompressible fluid dynamics is the moving particle semi-implicit (MPS) method. When it first emerged, a solid wall was represented by a set of spatially-fixed particles called wall particles [1]. While the representation by wall particles has high numerical stability and thus reliable, difficulties are encountered when it is used for complicated geometry, especially in three dimensions. On the other hand, the polygon wall boundary model proposed by Harada et al. (2008) [2] is known suited for such cases. It represents solid wall by surface mesh (a set of polygons). Thus, even in three dimensions it can be handled easily using CAD tools. Today, this technique has been used widely in engineering applications. However, it is known that unphysical behaviors of particles are often observed, and improvement of accuracy is desired. In these circumstances, this study has been done to propose a novel numerical treatment for solid wall boundary. In our approach, wall geometry is represented by a surface mesh and thus suited for problems with three-dimensional complicated boundaries. The wall contribution is derived using the integration over boundary surface. Since present method considers boundary shape more precisely, computational accuracy is expected to be improved compared to the polygon wall boundary model. Main differences between other boundary integral based approaches such as by Feldman and Bonet (2007) [3] and ours are related to derivation of the wall contribution term in discrete equation. In the present scheme, not only the particle number density but also the spatial derivatives are evaluated considering the volume integration over truncated domain. The volume integrations are mathematically transformed into the surface integral form using the divergence theorem. The proposed method was applied to several test problems. As a result, it was clarified that the present boundary integral based scheme has an accuracy comparable with the wall particle method and much better than the polygon wall boundary model. [1] S. Koshizuka et al., Int. J. Numer. Methods Fluids 26, 751-769 (1998). [2] T. Harada et al., Transactions of JSCES, 20080006 (2008). (in Japanese) [3] J. Feldman and J. Bonet, Int. J. Numer. Meth. Engng. 72, 295-324 (2007).

Uncertainty Quantification in Drug-induced Arrhythmias

Kristen Matsuno^{*}, Franciso Sahli^{**}, Paris Perdikaris^{***}, Jiang Yao^{****}, Ellen Kuhl^{*****}

^{*}Stanford University, ^{**}Stanford University, ^{***}Massachusetts Institute of Technology, ^{****}Dassault Systemes,
^{*****}Stanford University

ABSTRACT

The QT interval of an electrocardiogram signal, which begins with the activation of the ventricles and ends with their recovery, is a function of both heart rate and ventricular repolarization time. A prolonged QT interval is typically indicative of a patient's vulnerability to Torsade de Pointes, a potentially fatal arrhythmia characterized by rapid depolarization and repolarization of the ventricles. Various drugs have undesired side effects associated with a prolongation of the QT interval and an increased pro-arrhythmic risk. Two landmark parameters that quantify the effect of drug are the drug concentration IC₅₀ at 50% blockage of an ion channel, and the slope, h of the dose-response curve at this point. Here we present a novel high resolution, multi-scale, multi-fidelity computational model to predict the QT interval for a wide ranges of IC₅₀ and h values [0]. The experimental variability of these two parameters is the origin of uncertainty in the model. Using previously developed hierarchical Bayesian inference methods [2], we sample a set of 500 IC₅₀ and h parameter pairs from the experimental dose-response data for 30 common drugs [1]. For each pair of parameters and a chosen drug concentration, we calculate the conductance block of a specific ion channel. Using these ion channel blocks, we adopt a multi-fidelity model to predict a set of QT intervals via Gaussian process regression. We use Gaussian kernel density estimations to produce the probability density function of the QT interval at each concentration. Our uncertainty quantification reveals that, for a compound with three dose-response experiments, the QT interval has up to 76% variability at the maximum concentration compared to a baseline case of zero concentration and zero ion channel blockage. Our results contribute to predict the pro-arrhythmic risk of common drugs and assess their effect on cardiovascular performance. [0] F. Sahli, J. Yao, E. Kuhl. Predicting drug-induced arrhythmias by multiscale modeling. 2017; submitted. [1] Johnstone RH, Bardenet R, Gavaghan DJ and Mirams GR. "Hierarchical Bayesian inference for ion channel screening dose-response data" [version 2; referees: 2 approved] Wellcome Open Research 2017, 1:6 (doi: 10.12688/wellcomeopenres.9945.2) Copyright: © 2017 Johnstone RH et al. [2] Crumb, William J., et al. "An evaluation of 30 clinical drugs against the comprehensive in vitro proarrhythmia assay (CiPA) proposed ion channel panel." Journal of pharmacological and toxicological methods 81 (2016): 251-262.

A Padé-localized Absorbing Boundary Condition for 2D Time-harmonic Elastodynamic Scattering Problems

Vanessa Mattesi^{*}, Marion Darbas^{**}, Christophe Geuzaine^{***}

^{*}University of Liège, Belgium, ^{**}University of Picardie Jules Verne, Amiens, France, ^{***}University of Liège, Belgium

ABSTRACT

We focus on the construction of an absorbing boundary condition (ABC) for 2D isotropic elastic waves in high frequency regime. Problem statement We consider a spherical obstacle of radius r_{int} , the propagation domain is its complementary into the plane. Considering a time-harmonic incident wave, the scattering problem is formulated as follows: find the displacement in domain solution to the Navier equation with a Dirichlet boundary condition on the boundary of the obstacle and satisfying the Kupradze radiation conditions at infinity. The stress tensor is isotropic. In view of a finite element discretization, the infinite media is truncated by an artificial boundary, which delimits the bounded domain under study. On the fictitious boundary, we put an ABC involving an absorbing operator. Comparisons of two ABCs Multiple choices are possible for the absorbing operator \mathcal{B} , the optimal operator being the exact exterior Dirichlet-to-Neumann map. We investigate two approximations: *The Lysmer and Kuhlemeyer condition: We point out the limitations of this low-order condition in high-frequency regime and/or with incident S-waves. It motivates the investigation of a high-order condition. *A Padé-localized condition: it involves the tangential Günter derivative [1] and two operators using Padé local representations of the inverse of the square-root operator with rotating branch-cut [2]. We detail the choice of the different parameters and the construction of this high-order condition which is an adaptation of Chaillat et al. [1] to the 2D case. Numerical simulations in low and high frequency regime attest the efficiency of this ABC. [1] S. Chaillat, M. Darbas and F. Le Louër, Approximate local Dirichlet-to-Neumann map for three-dimensional time-harmonic elastic waves, in Computer Methods in Applied Mechanics and Engineering, 297 (2015), pp. 62-83. [2] S. Chaillat, M. Darbas and F. Le Louër, Fast iterative boundary element methods for high-frequency scattering problems in 3D elastodynamics, in J. Comput. Phys. 341 (2017), pp. 429-446.

Bayesian Inverse Problems and Low-Rank Approximations

Hermann Matthies*

*Technische Universitaet Braunschweig, Institute of Scientific Computing

ABSTRACT

We look at Bayesian updating in the frame work of updating a random variable (RV) whose distribution is the prior distribution. It is assumed that this RV is a function of many more elementary random variables. Furthermore it is assumed that computationally the RV is represented in either a sampling format or in a functional or spectral representation like the the polynomila chaos expansion. The samples resp. the coefficients may be viewed as a high degree tensor, and hence it is natural to assume a low-rank approximation for this. Conditioning, the central element of Bayesian updating, is theoretically based on the notion of conditional expectation. Here we use this construct also as the computational basis, namely the ability to compute conditional expectations. With this in hand, we formulate an updating process, which produces a new RV through successively finer approximations, whose law resp. distribution is the sought posterior distribution. This is in effect a kind of filter. It will be shown that it the filter can be computed using low-rank tensor approximations, and that it directly operates on the low-rank representation of the RV representing the prior, to produce a low-rank represenatation of the posterior RV.

Calibration and Propagation of Model Discrepancy Across Experiments

Kathryn Maupin*, Laura Swiler**

*Sandia National Laboratories, **Sandia National Laboratories

ABSTRACT

Model inadequacy due to model form error remains a concern in all areas of mathematical modeling, despite continuing advances in statistical inversion and the availability of cost-effective high-performance computing infrastructure. The Bayesian paradigm naturally integrates uncertainties from both experimental data and model formulation, including initial or boundary conditions, model form and parameters, and numerical approximation. However, model error is unavoidable in many situations due to incomplete understanding of the underlying physics, likely in addition to large and possibly poorly characterized uncertainties in calibration and validation data. Put simply, infinite amounts of data may still result in inadequate models. Model correction techniques have the potential to increase the range of applicability and enhance the predictive power of models that suffer from model-form error. It has been argued that some approaches preserve the physical meaning and improve the transferability of parameters of physics-based models. Calibrating a discrepancy model requires careful consideration regarding problem-specific formulation, parameter estimation, and uncertainty quantification. In the presence of large data sets, it may be necessary to select only those points which are the most informative of the discrepancy model. Furthermore, the validity of the original physical model, the inadequacy model, and the combined model for the prediction of quantities of interest remains in question. A generalized approach and implementation of model discrepancy detection, construction, and propagation into a predictive setting is presented in the context of Bayesian model calibration.

The Variational Phase-field Models of Brittle Fracture with Anisotropic Surface Energy

Corrado Maurini*, Bin LI**

*Sorbonne Universit'es, **Sorbonne Universit'es

ABSTRACT

Combining Griffith's theory and a suitable crack path selection criterion, one can successfully predict the crack path for the fracture of brittle materials with isotropic surface energy and quasi-static conditions. However, many materials have anisotropic surface energy because of their inherent microstructure or the manufacturing process, which can strongly influence the crack path. The understanding of the crack path selection criterion is under question for this case [2,3]. Experimental results [3,4] show that even a relatively small anisotropy in the surface energy always present in common materials, can cause the real crack paths to significantly deviate from those predicted with the assumption of an isotropic surface energy. The great success of the variational approach to fracture suggests that the variational model for fracture could provide a unifying and general framework capable of addressing fracture with anisotropic surface energy. A recent work [1] within the framework of variational approach to fracture had reproduced the key features of strongly anisotropic fracture and strikingly well recent experimental observations [2]. However, there are still a lot of fundamental questions that are open and need to be addressed, e.g. it is not clear that the energetic penalty for crack bending is intrinsic or extrinsic in real materials with strongly anisotropic surface energy, and what is the physical meaning of such energetic penalty; what crack path criterion in three dimensional and anisotropic surface energy setting. In this contribution, we formulate a phase-field model depending on the Hessian of phase-field, which can capture both weakly and strongly anisotropic surface energy with orthorhombic and cubic symmetry. The variational nature of the model suggests that the underlying crack-path selection principle is related to the maximum energy release rate (MERR) criterion. We verify this point by comparing the crack propagation directions observed from simulations under various loading and strength of anisotropy with MERR criterion predictions. We also analyze the energetic penalty for crack bending implicit in the model and highlight the difference of quenched crack behaviors between isotropic and anisotropic fracture surface energy. [1] B. Li, C. Peco, D. Millán, I. Arias, M. Arroyo, 2015. INT J NUMER METH ENG 102 (3-4), 711-727. [2] A. Takei, B. Roman, J. Bico, E. Hamm, F. Melo, 2013. Phys. Rev. Lett 110 (14), 144301. [3] A. Ibarra, B. Roman, F. Melo, 2016. Soft Matter 12, 5979-5985. [4] P. Judt, A. Ricoeur, G. Linek, 2015. ENG FRACT MECH 138, 33-48.

Meshless Solution of Thermomechanical Slice Model of Continuous Casting of Steel

Boštjan Mavri?*, Tadej Dobravec**, Robert Vertnik***, Božidar Šarler****

*Institute of Metals and Technology, Ljubljana, and University of Ljubljana, **Institute of Metals and Technology, Ljubljana, ***Store Steel and Institute of Metals and Technology, Ljubljana, ****University of Ljubljana and Institute of Metals and Technology, Ljubljana

ABSTRACT

The continuous casting of steel is well established process for producing steel billets, blooms and slabs used as semi-products for further downstream processing. The demand of the various steel consumers for ever higher quality products influences the steel producers to continuously improve the casting process. To achieve this, the producers increasingly rely on computer models. The traveling slice model [1] is particularly useful to model continuous casting. The model assumes that diffusion and deformation processes occur only perpendicular to the casting process and that the advection is the principal process in the direction of the casting. These assumptions, valid for most of the involved fields, allow the slice model to be computationally very effective. It can thus serve as a standard off-line tool for multiobjective optimization of the process parameters with respect to the quality and productivity as well as in on-line mode for regulation. In this work we develop a solid mechanics model to complement the existing traveling slice model of heat transport, solidification and grain growth [2]. The solid mechanics model is stated in plane stress formulation and a two-phase model is used to determine stress equilibrium of the inhomogeneous material. The governing equations are discretized by a local RBF collocation method augmented by first order monomials [3]. The shape parameter is determined automatically by adjusting the condition number of the interpolation matrix. The implicit Euler method is used to perform the time stepping to facilitate the coupling of the solid shell to the liquid through the mushy zone. The results from the mechanical model are integrated into a hot-tearing criterion and used to predict the occurrence of cracks in the material. We compare the results for the shape of the billet and the prediction of crack nucleation points with the experience from the industry. [1] A. Z. Lorbiecka et al., "Numerical modeling of grain structure in continuous casting of steel," *Comput. Mater. Contin.*, vol. 8, no. 3, pp. 195–208, 2009. [2] T. Dobravec, B. Mavri?, R. Vertnik, and B. Šarler, "Meshless modelling of microstructure evolution in the continuous casting of steel," in *Coupled problems VII?: proceedings of the VII International Conference on Coupled Problems in Science and Engineering*, Rhodes Island, 2017, pp. 156–166. [3] B. Mavri? and B. Šarler, "Local radial basis function collocation method for linear thermoelasticity in two dimensions," *Int. J. Numer. Methods Heat Fluid Flow*, vol. 25, no. 6, pp. 1488–1510, 2015.

Continuous and Discrete Energy Based Methods for Accurate Force Computations on Shells in the Immersed Boundary Method

Ondrej Maxian^{*}, Andrew Kassen^{**}, Wanda Strychalski^{***}

^{*}Case Western Reserve University, ^{**}University of Utah, ^{***}Case Western Reserve University

ABSTRACT

The immersed boundary method is a mathematical formulation and numerical method for solving fluid-structure interaction problems. For many biological problems, such as models that include the cell membrane, the immersed structure is a two-dimensional infinitely thin elastic shell immersed in an incompressible viscous fluid. When the shell is modeled as a hyperelastic material, forces can be computed by taking the variational derivative of an energy density functional. A new method for computing a continuous force functional on the entire surface of a hyperelastic elastic shell is presented. The method extends work from [1], where forces on a hyperelastic solid were computed without using stress tensors. The new method is compared to a previous formulation from [2] where the surface and energy functional are discretized before forces are computed. For the case of Stokes flow, a method for computing quadrature weights is provided to ensure the integral of the elastic spread force density remains zero throughout a dynamic simulation. Tests on the method are conducted when the shell is represented using spherical harmonics. Results show that it yields more accurate force computations than previous formulations as well as more accurate geometric information including mean curvature. The method is then applied to a new 3D model of cellular blebbing. [1] D. Devendran, C. S. Peskin, An immersed boundary energy-based method for incompressible viscoelasticity, J. Comput. Phys. 231 (14) (2012) 4613–4642. [2] T. G. Fai, B. E. Griffith, Y. Mori, C. S. Peskin, Immersed boundary method for variable viscosity and variable density problems using fast constant-coefficient linear solvers I: Numerical method and results, SIAM J. Sci. Comput. 35 (5) (2013) B1132–B1161.

A Multiscale Approach to Determine Permeability Tensor for Simulation of Composites Manufacturing Using RTM

Ravisankar Mayavaram*, Wentao Xu**, Mohit Tyagi***, Jacob Fish****

*Altair Engineering, Inc., **Columbia University, ***Altair Engineering India Pvt. Ltd., ****Columbia University

ABSTRACT

Composite materials are of great importance to aerospace and auto industry owing to the high strength to weight ratio exhibited by these materials. Resin Transfer Molding (RTM) and its variants such as VARTM are used to manufacture composite parts. Fundamentally, these processes involve infusing a preform with a thermosetting resin. In the numerical simulation of an RTM process, one of the major challenges is to have an accurate characterization of the material preform data. This is an expensive procedure and not offered as part material characterization services by most laboratories. We aim to address this challenge by numerically determining the permeability tensor of the preform using multiscale modeling. This numerical determination is performed using Altair's commercial CFD solver AcuSolve® and the subsequent RTM simulation is done using HyperXtrude®-RTM solver. We first determine the permeability tensor by taking into account the periodic microstructures in the preform and the Darcy's law. Using the microscale permeability, we then perform the mesoscale modeling. Finally, we upscale mesoscale permeability to perform macroscale RTM simulation at an optimal cost and increased accuracy. We demonstrate this approach by performing RTM simulation of a cylindrical pressure vessel with hemispherical ends. This simulation involves the use of multiple local coordinate systems. Results demonstrate an innovative approach to perform a complete simulation of the RTM process starting with material characterization.

Parameter Estimation and Uncertainty Quantification in Hurricane Storm Surge Modeling

Talea Mayo*

*University of Central Florida

ABSTRACT

Storm surges pose a significant threat to coastal regions. They are the primary cause of life and property loss during a hurricane. Real-time forecasting as well as long-term risk analysis are both critical to protecting coastal environments and their inhabitants. Due to the sparsity of hurricanes and storm surge events, hydrodynamic storm surge models have become increasingly important to the preservation of life and property, particularly as the climate and storm climatology change, and coastal populations increase. The effectiveness of both real-time forecasting and long-term risk analysis is largely dependent on the accuracy of the storm surge models employed. In recent decades, storm surge models have become increasingly accurate due to improvements in numerical methods and advancements in high performance computing. However, these models remain dependent on parameters which are often uncertain or unknown. For example, uncertainties in storm surge models largely result from uncertainties in the winds that are used to drive them, and specifically from uncertainties in how the winds are represented. Uncertainties in other model parameters such as bottom friction are also common sources of error. Parameter estimation methods can be implemented to reduce these types of model uncertainties using observed data. However, traditional inverse modeling techniques are often computationally intensive and can generally only be implemented offline, i.e. they are not feasible for the timely prediction of hurricane storm surges. Alternatively, statistical data assimilation techniques are non-intrusive methods that have been developed to estimate model parameters in real-time. In addition to parameter estimates, they provide estimates of associated uncertainties. In this talk, such approaches to parameter estimation and uncertainty quantification are discussed.

Automated Composite Material Model Development with Multiscale Designer

Colin McAuliffe^{*}, Robert Crouch^{**}, Jeff Wollschlager^{***}, Jacob Fish^{****}, Venkat Aitharaju^{*****},
Roger Ghanem^{*****}

^{*}Altair Engineering Inc, ^{**}Altair Engineering Inv, ^{***}Altair Engineering Inc, ^{****}Columbia University, ^{*****}General Motors, ^{*****}University of Southern California

ABSTRACT

Development of accurate computational models for composite materials presents a challenge for industry practitioners. The input parameters to a multiscale model of a composite are the properties of the constituent materials, e.g. carbon fiber and epoxy. It is often not possible to fully characterize a complex constituent material like carbon fiber from performing experiments on them individually. Even if it were, manufacturing processes may result in different in situ properties. Model development therefore must be accomplished through inverse identification, where experimental observations on the composite are used with a model to infer the constituent properties. This presents its own set of challenges, since inverse problems are notoriously difficult to solve correctly. Additionally, the success of the inverse solution requires that each of the constitutive properties be constrained by at least one experimental observation. Due to the expense associated with testing of composites, there is strong motivation to minimize the number of tests. Multiscale Designer employs both deterministic and stochastic approaches to the model development problem for linear and nonlinear property identification. These approaches are automated and highly accessible to practicing engineers. The stochastic approaches provide crucial insight into the reliability of the inverse solution, and can inform the analyst when the lack of a particular experimental observation negatively impacts this solution. In this case, a purely deterministic approach may give the false impression of a good solution. In this presentation, the technical details of these approaches are presented, and their ability to successfully identify composite properties is demonstrated.

A Low-Mach Number Preconditioner for the 10-Moment Closure with Application to Non-Equilibrium Gas Flows

James McDonald*, Fabien Giroux**

*University of Ottawa, **University of Ottawa

ABSTRACT

The ten-moment, Gaussian closure of gas dynamics is an accurate mesoscopic model for low-Mach-number laminar gas flows in which heat transfer does not play a significant role. This is true in the traditional continuum regime, as well as for higher-Knudsen-number transition-regime flows. Unfortunately, for exactly these low-speed applications, the partial differential equations governing the model can be numerically difficult to solve. This is due to the fact that there is a large discrepancy between the magnitude of the wave speeds present in the system. In such ill-conditioned hyperbolic systems, computational time-steps are limited by fast-moving acoustic-like waves, while processes of interest are related to slower-moving waves. The result is long run times and excessive numerical dissipation. There are several preconditioners available for traditional continuum models that alleviate this issue for classical low-speed flows. These local preconditioners alter the eigenstructure of the system such that all wave speeds are of the same order, even at low Mach numbers. The subject of this talk is the derivation and application of a similar low-Mach-number preconditioner for the Gaussian closure with the BGK collision operator. Preconditioning of the Gaussian closure brings an added difficulty as compared to traditional models. This is because of the interplay between the hyperbolic wave nature of the model and the effects of the collision operator. The apparent waves display a dispersive nature with wave speeds that depend on the timescale of gas-particle collisions. The preconditioner must, therefore, be constructed to effectively control the condition number across all possible flow regimes, from continuum to free molecular. The current preconditioner is inspired by the traditional Weiss-Smith preconditioner for the Euler equations, but extended for the ten equations of the Gaussian model and adapted to work effectively from the continuum to the free-molecular regime. This presentation demonstrates the construction of the preconditioner as well as a dispersion analysis that demonstrates its effectiveness across all levels of rarefaction. A numerical implementation is briefly reviewed and the ability of the preconditioner to effectively control run times and numerical dissipation for canonical low-speed transition-regime flows is demonstrated.

Free Energy Analysis of Cell Spreading on Collagen Coated Elastic Substrates

Eoin McEvoy*, Patrick McGarry**

*National University of Ireland Galway, **National University of Ireland Galway

ABSTRACT

Cell behaviour has been shown to depend on substrate stiffness and surface collagen density. In this study we provide new insights into the processes underlying cell mechano-sensitivity by developing a novel modelling framework. Beginning with a thermodynamic description of sub-cellular actin-myosin interactions, we demonstrate that spreading of cells is driven by a competition between passive and active cytoskeletal free energy. The cell explores its physical environment as it attempts to achieve a homeostatic free energy. This dynamic process is simulated on substrates of differing stiffness and surface collagen density using a Markov chain Monte-Carlo(MCMC) scheme. This entails the simulation of 2.5 million spread states and the associated distributions of stress fibres and focal adhesions. Our MCMC simulations predict an ensemble of cell spread states on compliant and rigid substrates. For cells on a rigid substrate, both the mean and standard deviation of the spread area are predicted to increase as the collagen density increases. As substrate stiffness decreases, lower spread areas are computed. These predictions are extremely similar to experimentally observed cell behaviour.

Modelling Transient Active Force Generation in Cell Stress Fibres

Patrick McGarry*, Eoin McEvoy**

*National University of Ireland Galway, **National University of Ireland Galway

ABSTRACT

Mechanical priming strategies have been developed in an ongoing drive to engineer tissues with increased functional viability. As cells actively respond to loading in the 3D microenvironment, the development of a fundamental mechanistic understanding of the effects of mechanical conditioning on cell biomechanics is critical. In this study we develop a novel framework for active cell contractility when subjected to uniaxial and biaxial dynamic loading conditions. Uniaxial and biaxial experiments are simulated using an active thermodynamically motivated model for cell contractility. The modelling framework includes a novel cross-bridge cycling formulation for transient force generation and an anisotropic constitutive law for collagen realignment and compaction. The active model predicts that highly aligned high concentration sarcomeres are formed when the stress state is uniaxial, whereas a biaxial stress state leads to the computation of unaligned low concentration sarcomeres. The model also accurately predicts measured tissue forces. Model results confirm that the small experimentally measured difference (36%) in uniaxial and biaxial force for contractile tissue (compared to the large difference (100%) for a passive hydrogel) is due to stronger sarcomere formation and alignment induced by a uniaxial stress state.

Shape Morphing of Non-periodic Metamaterial Sheets

Connor McMahan^{*}, Paolo Celli^{**}, Chiara Daraio^{***}, Brian Ramirez^{****}, Basile Audoly^{*****}

^{*}California Institute of Technology, ^{**}California Institute of Technology, ^{***}California Institute of Technology,
^{****}California Institute of Technology, ^{*****}LMS, École Polytechnique, CNRS, Université Paris-Saclay

ABSTRACT

The dominant approach in the design of mechanical metamaterials revolves around ordered arrangements of mesoscale constituents. In this work, we demonstrate that the shape morphing abilities of two-dimensional architected sheets can be enhanced by resorting to non-periodic (graded, or fully aperiodic) geometries. Through theoretical considerations, numerical simulations and desktop-scale experiments, we demonstrate that rectangular sheets can morph shape, in-plane and out-of-plane, when subjected to carefully-engineered load patterns. Leveraging modes of inextensional deformation, the systems are designed to display large deformations for small input energies.

An Evaluation of Mesh-free Hydrodynamic Methods for Blast Wave Modeling and Blast-Structure Interaction

Casey Meakin^{*}, Dominic Wilmes^{**}, Fabien Teulieres^{***}

^{*}Karagozian & Case, Inc., ^{**}Karagozian & Case, Inc., ^{***}Karagozian & Case, Inc.

ABSTRACT

The advantages provided by mesh-free numerical methods for modeling solids and fluids are becoming more attractive as simulation models become more complex. The ability to rapidly develop models by side-stepping the often time consuming process of mesh generation is of particular interest. Mesh-free algorithms can also provide elegant solutions to several notable limitations associated with grid based methods including large deformation in solids and contact tracking at fluid interfaces. Despite growing interest in mesh-free methods for fluids dynamics, however, their performance for treating shock waves and shock-structure interactions remain poorly characterized. In order to address this issue, the effectiveness of using a recently developed class of fully conservative, consistent, mesh-free hydrodynamic methods for these types of problems is investigated. Key performance metrics considered include computational efficiency, accuracy, and ease of model development compared to more traditional grid-based hydrodynamic solvers.

Fully Explicit Three-Dimensional Lagrangian Simulation of Fluid-Structure-Interaction Problems

Simone Meduri^{*}, Umberto Perego^{**}, Massimiliano Cremonesi^{***}

^{*}Politecnico di Milano (Italy), ^{**}Politecnico di Milano (Italy), ^{***}Politecnico di Milano (Italy)

ABSTRACT

A partitioned fully Lagrangian and fully explicit approach for the simulation of FSI problems is presented. Partitioned approaches are particularly interesting for the application to real engineering problems because of the possibility to make use of existing software. Moreover, explicit methods can be advantageous in many large scale applications characterized by fast dynamics and/or a high degree of nonlinearity. In this work, we propose an explicit version of the Particle Finite Element Method (PFEM) [1] for the weakly compressible fluid domain, coupled with the commercial software Abaqus/Explicit for the structural one. The Gravouil and Combescure approach [2] has been chosen to enforce a strong coupling together with a global system of fully decoupled (explicit) equations [3]. Nonconforming meshes and time increments in the fluid and solid subdomains can be used to optimize the discretization for the overall efficiency of the coupled solver. The use of a commercial software as structural solver allows including in the model its advanced functionalities, such as the libraries of material constitutive models and finite elements and other advanced features. Furthermore, the fully Lagrangian framework of the coupled PFEM-FEM approach makes this method particularly suitable for applications with free-surface fluid flows and large displacements of the solid partition. In 3D problems, a frequent remeshing of the fluid domain is required by the PFEM. The resulting new mesh is often of a bad quality, with many slivers (tetrahedra with almost zero volume), leading to a vanishing critical time step size. A novel efficient mesh smoothing technique has been developed to produce a regular mesh, with a reasonably large stable time increment for the explicit solver. This smoothing algorithm is fully explicit and parallelizable, because it exploits the same architecture of the fluid solver thanks to an elastic analogy. Several three-dimensional examples have been considered to validate the approach against available analytical, experimental and numerical solutions, confirming the robustness and effectiveness of the proposed method. [1] E. Onate, S. Idelsohn, "The particle finite element method: an overview." *Int J Comput Meth*, 2004;2:267-307. [2] A. Gravouil, A. Combescure, "Multi-time-step explicit-implicit method for non-linear structural dynamics." *Int J Numer Meth Engng*. 2001;50:199-225. [3] S. Meduri et al. "A partitioned fully explicit Lagrangian finite element method for highly nonlinear fluid-structure interaction problems." *Int J Numer Meth Engng*. 2018;113:43-64.

EVALUATION OF THE PERFORMANCE OF BUND WALL SYSTEMS UNDER THE EFFECT OF CATASTROPHIC FAILURE OF STORAGE TANKS VIA NUMERICAL MODELLING

ISLEM MEGDICHE WILLIAM ATHERTON CLARE HARRIS GLYNN
ROTHWELL⁴ AND DAVID ALLANSON

¹ Department of Civil Engineering, Liverpool John Moores University
15-21 Webster St, Liverpool L3 2ET
I.Megdiche@2015.ljmu.ac.uk

² Department of Civil Engineering, Liverpool John Moores University
Peter Jost Enterprise Centre, 3 Byrom St, Liverpool L3 3AF
W.Atherton@ljmu.ac.uk, <https://www.ljmu.ac.uk/about-us/staff-profiles/faculty-of-engineering-and-technology/departement-of-civil-engineering/bill-atherton>

³ Department of Civil Engineering, Liverpool John Moores University
Peter Jost Enterprise Centre, 3 Byrom St, Liverpool L3 3AF
C.B.Harris@ljmu.ac.uk, <https://www.ljmu.ac.uk/about-us/staff-profiles/faculty-of-engineering-and-technology/departement-of-civil-engineering/clare-harris>

⁴ Department of Maritime and Mechanical Engineering, Liverpool John Moores University
James Parsons Building, 3 Byrom St, Liverpool L3 3AF
G.Rothwell@ljmu.ac.uk, <https://www.ljmu.ac.uk/about-us/staff-profiles/faculty-of-engineering-and-technology/departement-of-maritime-and-mechanical-engineering/glynn-rothwell>

⁵ Department of Maritime and Mechanical Engineering, Liverpool John Moores University
James Parsons Building, 3 Byrom St, Liverpool L3 3AF
D.R.Allanson@ljmu.ac.uk, <https://www.ljmu.ac.uk/about-us/staff-profiles/faculty-of-engineering-and-technology/departement-of-maritime-and-mechanical-engineering/david-allanson>

Key words: bund wall, Fluid Structure Interaction, storage tank, impact load.

Abstract. The failure of storage tanks is a very serious problem that has occurred in many countries around the world due to natural disasters and accidental releases. The consequences of such failures recorded in the literature have impacts on the environment, the immediate community and the economy. The United States (US) is one of the countries that has suffered most from this kind of problem and lately many above-ground storage tanks have ruptured in the Houston area due to Hurricane Harvey. Usually, refineries, chemical plants and oil depots are required to provide safety measures to mitigate the effects of the rupture of storage tanks where the collapse is unavoidable due to extreme natural disasters or because of the use of decades-old technology already in place. These safety measures imply the use of a secondary containment surrounding the storage tanks where the intention is to contain any spilled materials. The secondary containment is referred to as a bund wall. In the UK, bund walls are designed according to BS EN 1992-3:2006, where only static pressure is accounted for due to

slow leaks. However, in the wake of the catastrophic failure of storage tanks, the bund wall is subjected to the impact of the rapidly escaping fluid. Such scenarios require accounting for the dynamic pressure in addition to the traditional approach, especially since previous failures proved that bund walls designed for static pressure only, were ineffective and collapsed under the impact of surging fluids. In this study, it is proposed to investigate the performance of a bund wall system under the effect of fluid impact via the use of numerical modelling. The analysis involves the interaction between the structure and the fluid domains. The fluid problem is modelled as a multiphase flow and solved using OpenFoam software, while the structural problem is solved with the dynamic explicit solver of Abaqus. The coupling between the two computational fluid dynamics (CFD) and finite element modelling (FEM) packages was carried out using MpCCI software. Numerous load configurations and bund shapes have been analysed. The numerical analysis indicates that the bund walls constructed from plain concrete (block) are not able to withstand the impact of the fluid and ruptured providing no secondary containment.

1 INTRODUCTION

Throughout many years, numerous incidents related to the storage of hazardous substances have occurred in many countries^[1]. The most affected country is the United States of America (USA) as it is subjected to many natural disasters apart from the accidental releases that pose further risk for the sudden failure of the primary storage (tank) facility. Recently, an explosion took place at the Husky Energy oil refinery on April 2018 in Superior, Wisconsin. It was reported that a tank of asphalt exploded at 10 a.m. on 26th April. Later on, on the following day, at 3.15 p.m. another tank caught the fire^[2]. The root cause of the explosion is still unclear, however the blast occurred while the workers were preparing to shut down the facility, which is considered one the most sensitive times, where the risk of failure increases. It was also reported that at the time of the explosion, staff were carrying out construction work, which might have contributed to the failure^[3]. The consequences were deemed very disastrous, resulting in the shaking of buildings up to one mile away from the scene. The ignition of a huge fire and the spread of thick smoke across a wide area around the refinery was evident. This resulted in the evacuation of the residents living in a three miles radius around the plant, together with the evacuation of schools and a hospital in the affected region. A state of emergency was also declared in Douglas County. The smoke was very harmful as it contained mixes of hydrocarbons and other chemical mixtures and was extremely dense, as people living 30 miles away for the incident could see the smoke spreading. In terms of casualties, the number of injured persons is not exact, but at least 11 persons were injured with one person being seriously affected^[4].

Natural disasters are considered potential factors that trigger the failure of storage tanks. Texas is an area subjected to hurricanes, and during Hurricane Harvey, that swept Houston on August 2017, many failures were subsequently reported. Houston is a hub of oil refineries, chemical plants and storage facilities. The capacity of the crude storage of the region has increased from 21 million barrels to 56 million in the last six years. Many companies use floating roof storage tanks, about 400 out of more than 1000 storage tanks in Houston itself.

The design proved to be inadequate, as many companies reported failures of these tanks due to the huge weight of accumulated water on the roofs that reached 50 inches, while the roofs are only designed to hold up to 10 inches of rain. The storm caused the roofs to flip, releasing toxic materials into the atmosphere. The technology of floating roofs was deemed responsible for spills as well. It was reported that 500,000 gallons of gasoline escaped from two storage tanks located in the Galena Park storage complex, which belongs to Magellan Midstream Partners [5]. Additionally, many large companies reported leaks and spillages at their facilities, such as BASF, which is the second largest producer of chemical products in North America. Tanks overflowed leaving chemicals to spill in a diked area which itself then overflowed to the surrounding area [6]. At Exxon Mobil's Beaumont Oil Refinery, storage tanks leaked, resulting in the oil escaping to the nearby county road. The spills were considered small enough compared to those recorded in the aftermath of Hurricane Katrina, where millions of gallons were released into the residual areas [7].

Safety measures are essential to reduce the extent of any failure. In many parts of the world such as the UK and the USA, companies that perform any activity associated with hazardous materials are required to provide secondary containment in the form of a wall that surrounds a single or multiple storage tanks to contain spillage caused by the rupture of the tanks. The secondary containment is known as bund wall and can be constructed from concrete, bricks or earth [1]. In the UK, it is designed according to BS EN 1992-3:2006, where it is only required to withstand the static pressure of the released material. During catastrophic failures and major events, a number of facilities failed to withstand the torrential waves of the escaping materials, which is a subsequent mode of failure [8].

In this study, it is proposed to investigate the performance of the bund walls under the effect of the catastrophic failure of storage tanks that gives rise to a surge of fluid. Three different shapes of bund walls were investigated namely, circular, square and rectangular bund walls with a centered and off-centered storage vessel. Results indicated that a better performance is obtained when using a circular wall, while the square and rectangular bund walls behaved almost the same manner, with a slightly better performance for the square bund wall.

2 METHODOLOGY

At the moment of complete failure of storage tank, a column of fluid falls under the effect of gravity until it hits the bund wall. Then, depending on the shape and the height of the wall, part of the fluid will be diverted back in the banded area and the rest of the fluid overtops and escapes to the surrounding area. The bund wall might exhibit damage, depending on the severity of the surging wave. A numerical modelling approach involving fluid/structure interaction was used to model this problem. The fluid part was solved following a multiphase flow modelling approach using OpenFoam software. For the structural part, the bund wall was modelled using Abaqus software and the coupling between the fluid and the structural codes was performed using the MpCCI coupling environment.

For the OpenFoam side, InterDyFoam was used to solve the Navier Stokes equation (1) and a specie transport equation (2) derived from the conservation of mass equation, based on the Volume of Fluid (VoF) method, with α being the phase fraction. The Navier Stokes equation

contains an additional term to model the surface tension between the considered fluids which are oil and air ^[9].

$$\frac{\partial \rho U}{\partial t} + \nabla \cdot (\rho U U) = -\nabla p + [\nabla \cdot \mu \nabla U + \nabla U \cdot \nabla \mu] + \rho g + \int_{S(t)} \sigma k' n' \delta(x - x') dS \quad (1)$$

$$\frac{\partial \alpha}{\partial t} + \nabla \cdot (U \alpha) = 0 \quad (2)$$

The turbulence was modelled using the low Reynolds version of the shear stress Transport (SST) - $k-\omega$ model, as it can accurately model the behaviour of fluid flow exhibiting droplet formation and separation that occurs at the moment of the impact.

InterDyMFoam solves the multiphase flow using a dynamic mesh. Although, InterFoam was able to predict the flow behaviour and yields accurate results for certain configurations of tank and bund wall arrangements, the dynamic solver was used because MpCCI requires the dynamic solver to move the interface between the structural and fluid domains.

The InterDyMFoam solver uses the Multidimensional Universal Limiter for Explicit Solution (MULES) method that allows maintenance of the boundedness of the phase fraction ^[9]. The discretization schemes are not therefore restricted to those, which are bounded. The discretization schemes used are: The Euler scheme for the temporal term, which is first order, implicit and bounded allowing the determination of a stable solution, the Gauss linear upwind scheme for the convective term, utilized to obtain improved accuracy, the Gauss linear scheme for the gradient term and the Gauss VanLeer scheme for the compression flux in the specie transport equations ensuring boundedness.

The total time for the simulation is 2s which is believed (on the basis of experimental and numerical results) to be a sufficient time for the wave to settle. The time step is equal to 0.001s and the maximum Courant number was allowed to reach unity because of the use of the semi-implicit version of the MULES algorithm. Regarding the convergence control, tolerances were specified for each physical quantity. They are 10^{-7} for pressure, 10^{-5} for all of velocity, kinetic energy and specific dissipation rate and 10^{-8} for phase fraction, α .

In regards to boundary conditions, it is assumed that the fluid is not able to penetrate through the surrounding walls of the computational domain and the ground, walls are not slippery and, that the domain is free to atmosphere (a reasonable assumption given the ratio of the mass densities involved and the open domain). The boundary conditions that permit modelling in OpenFoam are: fixed flux pressure equal to zero for pressure and fixed value equal to zero for velocity, zero fixed flux pressure and zero velocity (no-slip) is applied to all surrounding walls and the ground. Total pressure, pressure inlet outlet velocity and inlet outlet boundary conditions for the pressure, velocity and phase fraction respectively to model the free surface.

For Abaqus, an explicit approach was adopted using the explicit solver, which is the appropriate solver for problems involving impacts. The geometric model was discretized using hexahedral, first order and reduced integration elements with an aspect ratio equal to unity. These types of elements are efficient in modelling contact impact or large distortions problems ^[10]. For the material modelling, the Concrete Damage Plasticity (CDP) was used for its suitability for problems involving dynamic loading ^[11]. The model requires the density of the concrete, the Poisson Ratio and Young's Modulus parameters, to model the elastic behaviour of the concrete. For the plastic behaviour modelling, the stress- strain and stress-displacement

relationships for the compressive and tensile curves need to be defined. In order to account for the damage of the concrete, additional tabular data representing the damage-displacement has to be provided. The tensile damage is modelled because of the weakness of concrete under tensile loading. The material parameters were taken from ^[11] and summarized in Table 1.

Table 1: Material properties for the CDP model for plain concrete finite element modelling

Density		2643	
<u>Concrete Elasticity</u>			
Elastic modulus (GPa)		31	
Poisson’s ratio		0.15	
<u>The parameters for CDP model</u>			
Dilation angle (degrees)		36.31	
Eccentricity		0.1	
f _{b0} / f _{c0}		1.16	
K _c		0.667	
μ		0	
<u>Compressive behaviour of the concrete</u>			
Yield stress (Pa)		Inelastic strain	
13000000		0	
24000000		0.001	
<u>Concrete tension stiffening</u>			
Yield stress (Pa)	Displacement (m)	Damage variable	Displacement (m)
2900000	0	0	0
1943930	6.6185E-05	0.381217	6.6185E-05
1303050	0.00012286	0.617107	0.00012286
873463	0.000173427	0.763072	0.000173427
585500	0.00022019	0.853393	0.00022019
392472	0.000264718	0.909282	0.000264718
263082	0.000308088	0.943865	0.000308088
176349	0.00035105	0.965265	0.00035105
118210	0.000394138	0.978506	0.000394138
79238.8	0.000437744	0.9867	0.000437744
53115.4	0.000482165	0.99177	0.000482165

For MpCCI, the coupling procedure consists of 5 steps: Models step, Coupling step, Monitors step, Edit step and the Go step ^[12]. The Models, coupling and Monitors steps are mandatory to couple OpenFoam and Abaqus. The Models step consists of defining the coupled software and the input files for OpenFoam and Abaqus models. The Coupling step consists of defining the global variables, creating and configuring the coupling regions. For this problem, the global variable represents the time step that is sent from OpenFoam to Abaqus, and the coupling region represents the surface of the bund wall as represented in Fig.1. During the computation, OpenFoam solves the governing equations of the fluid domain and sends the

pressure to Abaqus denoted in MpCCI by RelWallForce. Abaqus uses those values to solve the governing equations of the structure and then sends the deformations back to OpenFoam. The final step in the coupling process is the Go step in which the coupling scheme, the initial quantities transfer and other parameters need to be defined. Here, the explicit-transient coupling scheme was used, which is the only possible coupling scheme to solve for the transient problem when using the Abaqus explicit solver. The initial quantities transfer determines whether the coupling is serial or parallel. For this problem, the initial quantities transfer are receive and exchange modes for Abaqus and OpenFoam respectively which yields a serial coupling.

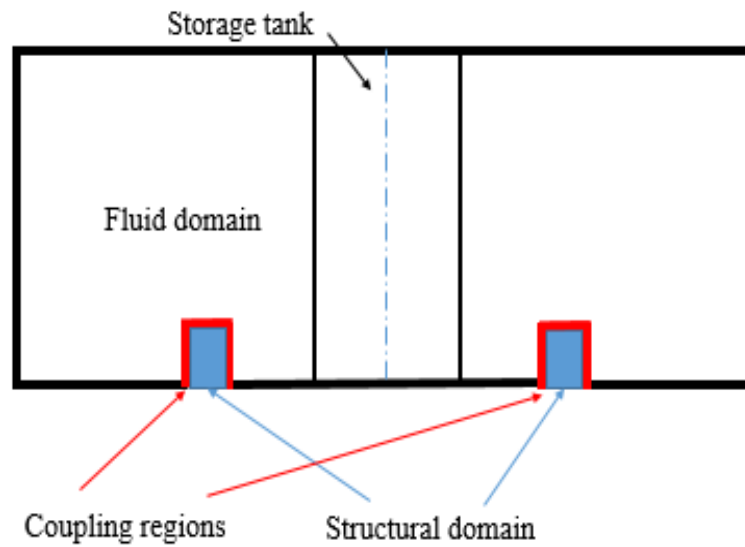


Fig.1: Fluid-Structure domain

The dimensions of the bund walls were calculated based on a scale factor of 30. Three shapes of bund walls were tested which were the circular, square and rectangular. The bund walls have the same volume for the banded region, the height of the circular bund wall is 0.24m while the height of the square and rectangular bund walls are 0.12m. The thickness of all walls is 0.007m. The bund walls were subjected to the impact of a column of oil with an initial height of 6m, which was determined by increasing the height of the fluid until damage appeared in the concrete when using a circular wall. The effect of the asymmetric load modelled by an off-centred tank has been investigated by moving the column of fluid by 0.05m from the central position along x or y-axes. Such a situation is considered in case the fluid escapes the tank in a non-symmetric fashion. In total, seven simulations were run, three simulations when the load is centred with the three different bund shapes, and four simulations when the load is off-centred. For the rectangular bund wall, the load is off-centred in the x and y directions with the same magnitude. Fig. 2 represents a nomenclature of the three different bund walls.

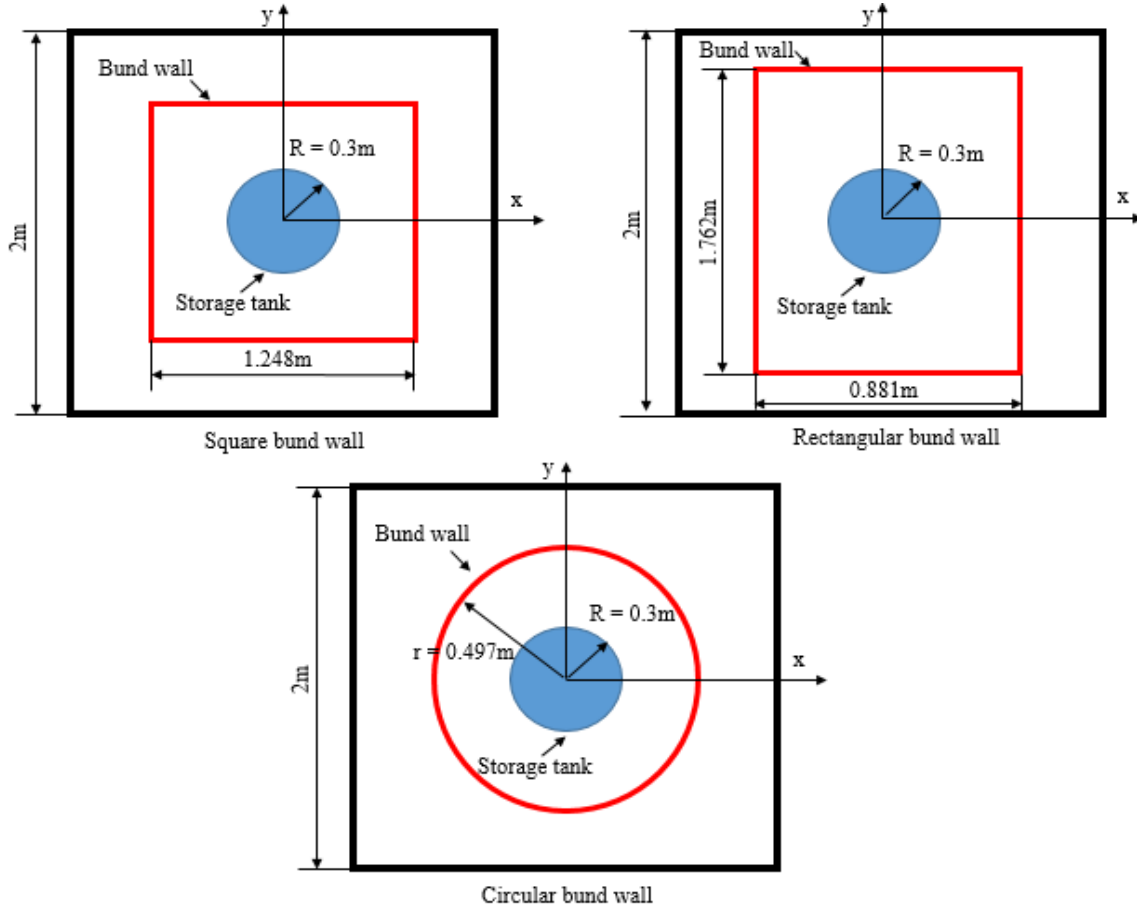


Fig. 2: Nomenclature for bund walls

3 RESULTS AND DISCUSSIONS

Figs.3, 4 and 5 show the flow structure and the bund wall behaviour in terms of tensile damage corresponding to the circular, square and rectangular bund walls with centred releases. Due to the page limit of this paper, figures of the behaviour of the structures under an off-centred release are not included, but results of dynamic pressure, VonMises stress and tensile damage denoted damageT are presented in Tables 2, 3, 4 and 5 as a function of time until the failure occurs. A comparison between the three shape configurations shows that a circular bund outweighs square and rectangular bund walls in terms of the maximum pressure that it can take and the magnitude of damage incurred. A circular bund wall withstands 40kPa with only minor damage of the order of 0.3%. In contrast, square and a rectangular bund walls are structurally weaker. The performance of the square bund wall is slightly better than a rectangular bund wall, i.e. a square bund wall fails slightly after the rectangular bund wall (0.653s for the square wall versus 0.6074s for the rectangular wall). A temporal comparison between the magnitude of the damage indicates that the square bund wall exhibits less damage compared to a rectangular bund; for example at $t = 0.5s$, the tensile damage of a square bund wall is 40.48% versus 69.71%

for a rectangular bund wall.

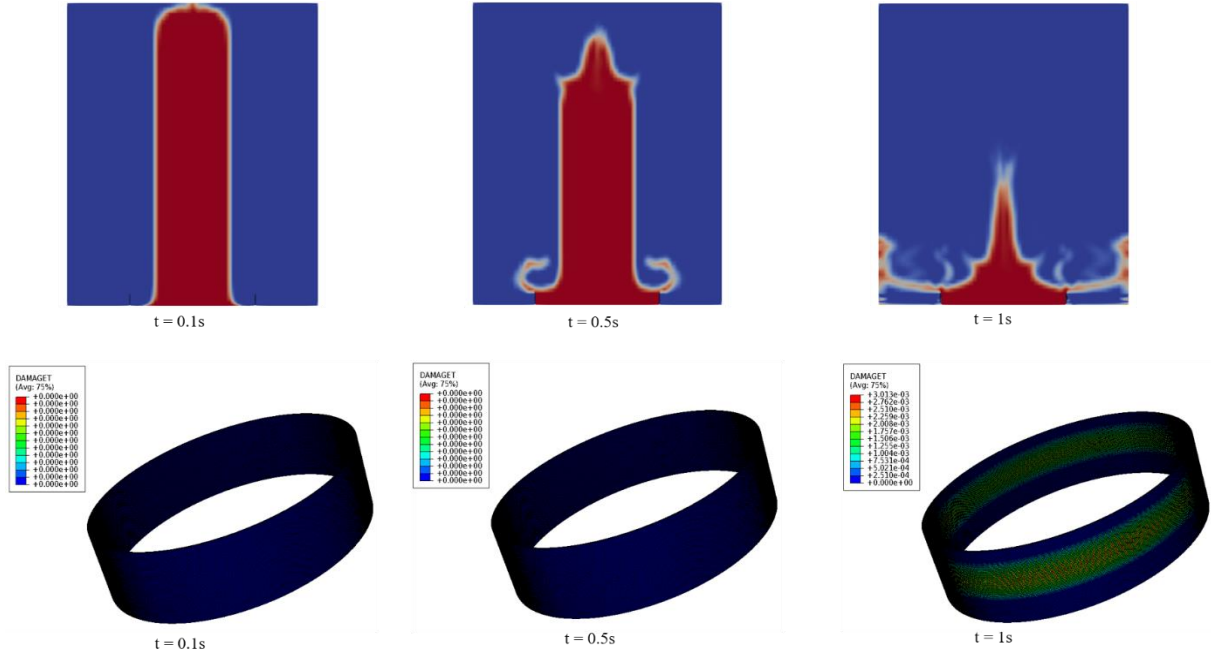


Fig.3: Flow and structural behaviour for a circular bund wall

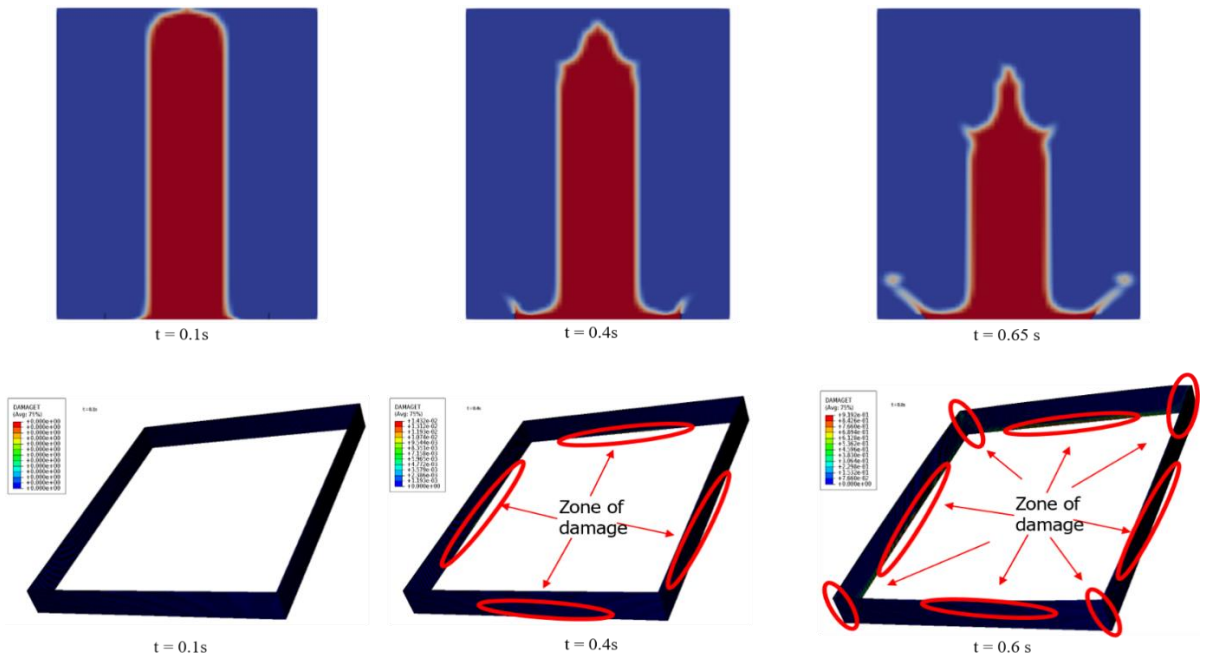


Fig.4: Flow and structural behaviour for a square bund wall

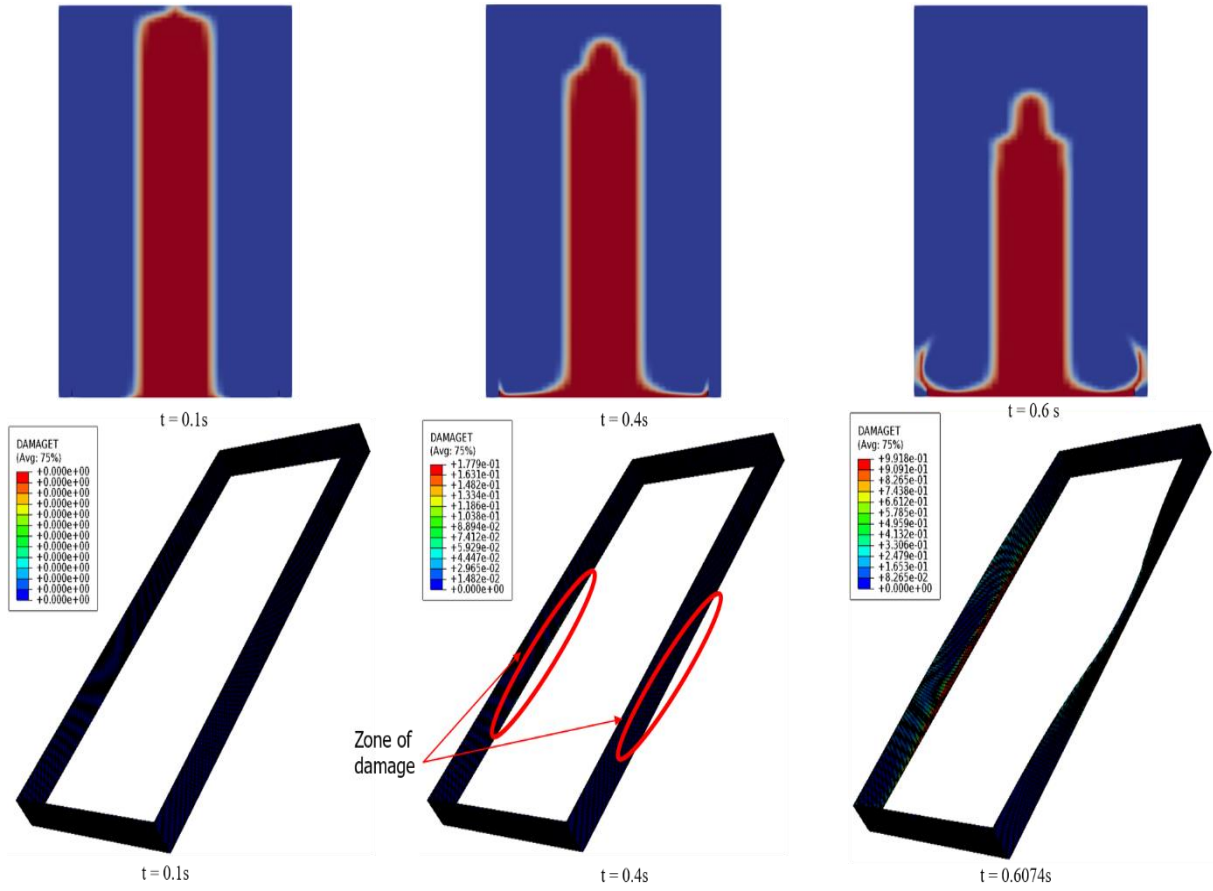


Fig.5: Flow and structural behaviour for a rectangular bund wall

The assumption of a centred release is ideal, as during the failure, the fluid flow moves in a different fashion with respect to the direction. This asymmetry of the load is due to the fluid flow as it hits an obstacle in the bundled region. To take this into consideration, the fluid column was shifted by 0.05m from the centre along x or y-axes. From Tables 2, 3, 4 and 5 a comparison between the performance of the bundled configurations of the same shape, under a centred and an off-centred load shows that generally, the bund wall exhibits a higher magnitude of damage with an off-centred load. As an example, the damage to a circular bund wall is 0.34% with an off-centred load compared to 0.30% with a centred load at $t = 1.1s$. This increase in damage is minor for the circular bund wall, while for a square bund wall the increase in the tensile damage is more significant. For example at $t = 0.5s$, the damage increases from 40.48% with a centred load to 47.01% with off-centred load. This behaviour is due that the fluid flow hits one side of the bund before hitting the other sides, which triggers an earlier damage and higher magnitude of damage, as only one side will be initially subjected to the load. The only exception of this behaviour is with a rectangular bund wall, when the load is moved along the y axis which is in the direction of the longest side of the rectangular bund wall.

A comparison between the shape of bund walls under an off-centred load leads to the same conclusion as when using a centred load. The circular bund wall withstands a higher level of dynamic pressure without significant damage, while the performance of square and rectangular bund walls is almost the same.

Table 2: Results of dynamic pressure, tensile damage and stress for a circular bund wall

Time (s)	centred load			Time (s)	off centred load		
	Dynamic pressure near the bund wall (Pa)	damage (%)	Maximum VonMises stress (MPa)		Dynamic pressure near the bund wall (Pa)	damageT	Maximum VonMises stress (MPa)
0	2500	0	0	0	2500	0	0
0.1	2800	0	0.18	0.1	2800	0	0.18
0.2	4200	0	0.25	0.2	5400	0	0.36
0.3	8300	0	0.55	0.3	8900	0	0.63
0.4	13000	0	0.90	0.4	13000	0	0.91
0.5	14000	0	1.01	0.5	15000	0	1.05
0.6	19000	0	1.41	0.6	20000	0	1.45
0.7	26000	0	1.92	0.7	24000	0	1.79
0.8	32000	0	2.29	0.8	32000	0	2.39
0.9	39000	0	2.79	0.9	38000	0	2.74
1	42000	0.3	2.75	1	43000	0.33	3.13
1.1	17000	0.3	1.17	1.1	18000	0.34	1.85
1.2	16000	0.3	0.62	1.2	36000	0.34	1.15
1.3	17000	0.3	0.53	1.3	9900	0.34	1.13
1.4	18000	0.3	0.51	1.4	5700	0.34	0.78
1.5	18000	0.3	0.55	1.5	4500	0.34	0.55
1.6	23000	0.3	0.48	1.6	5400	0.34	0.56
1.7	16000	0.3	0.49	1.7	5600	0.34	0.53
1.8	13000	0.3	0.6	1.8	9300	0.34	0.69
1.9	12000	0.3	0.73	1.9	13000	0.34	0.95
2	19000	0.3	0.81	2	14000	0.34	0.91

Table 3: Results of dynamic pressure, tensile damage and stress for a square bund wall

Time (s)	centred load			Time (s)	off centred load		
	Dynamic pressure near the bund wall (Pa)	damageT	Maximum VonMises stress (MPa)		Dynamic pressure near the bund wall (Pa)	damageT	Maximum VonMises stress (MPa)
0	1900	0	0	0	1900	0	0
0.1	2300	0	0.46	0.1	2300	0	0.46
0.2	3800	0	0.46	0.2	3800	0	0.46
0.3	6000	0	1.07	0.3	6000	0	1.64
0.4	9000	1.43	2.91	0.4	9000	4.12	3.02
0.5	13000	40.48	4.38	0.5	13000	47.01	4.56
0.6	17000	91.92	6.02	0.6	17000	98.88	6.6
0.65	20000	-		0.6393	-	99.18	-
0.6536	-	99.18	-	-	-	-	-

Table 4: Results of dynamic pressure, tensile damage and stress for a rectangular bund wall

Time (s)	Centred load			Time (s)	Off centred load		
	Dynamic pressure near the bund wall (Pa)	damageT	Maximum VonMises stress (MPa)		Dynamic pressure near the bund wall (Pa)	damageT	Maximum VonMises stress (MPa)
0	1900	0	0	0	1900	0	0
0.1	2300	0	0.29	0.1	2300	0	0.295
0.2	4600	0	1.11	0.2	4700	0	1.81
0.3	6300	0	2.58	0.3	6500	0.14	2.61
0.4	9200	17.79	2.97	0.4	9200	20	3.03
0.5	13000	69.71	5.28	0.5	13000	77.12	5.88
0.6	17000	99.18	8.96	0.55	15000	99.18	-
0.6074	-	99.18	-	0.5946	-	-	-

Table : Results of dynamic pressure, tensile damage and stress for a rectangular bund wall with off-centred load

Time (s)	Off centred load y		
	Dynamic pressure near the bund wall (Pa)	damageT	Maximum VonMises stress (MPa)
0	1900	0	0
0.1	2300	0	0.29
0.2	4500	0	1.08
0.3	6200	0	2.58
0.4	9200	17.06	2.97
0.5	13000	69.17	5.31
0.6	17000	99.18	6.72
0.619	-	99.18	-

4 CONCLUSIONS

In this paper, the performance of bund walls, which are structures that surround storage tanks to retain any spillage of hazardous materials in the event of failure were investigated. A numerical approach was followed, which involved the fluid/structure interaction using OpenFoam, Abaqus and MpCCI packages. In total, three configurations of bund walls were analysed, which were circular, square and rectangular bund walls under a centred and off-centred load. The simulations showed that a circular bund wall is superior in terms of structural performance. The square and rectangular bund walls behave almost in the same manner. When the load is off-centred, the bund wall exhibits more extensive damage. For future work, the performance of the square and rectangular bund walls need to be enhanced, as they are used most commonly within the industry.

Ac knowledgements

The first author would like to thank Liverpool John Moores University for the financial support provided for this project.

REFERENCES

- [1] Atherton, W. *n Empirical investigation of catastrophic and partial failures of bul storage vessels and subse uent bund wall overtopping and dynamic pressure*. PhD thesis, Liverpool John Moores University, 2008.
- [2] Forliti, A. and Baenen, J. Police: Evacuation order lifted following Wisconsin refinery blast injured 11 [Internet]. Chicago Tribune. 2018 [cited 10 May 2018]. Available from: <http://www.chicagotribune.com/news/nationworld/midwest/ct-wisconsin-refinery->

- [explosion-20180426-story.html](#)
- [3] Millar, J. Wisconsin explosion: Dozens hurt after ‘Sonic Boom’ in US city – Evacuation underway [Internet]. Express UK. 2018 [cited 10 May 2018]. Available from: <https://www.express.co.uk/news/world/951698/wisconsin-explosion-Husky-oil-refinery-injuries-police>
 - [4] Dellinger, A.D. City Evacuated, State of emergency declared in Wisconsin country following oil refinery explosion [Internet]. Gizmodo UK. 2018 [cited 10 May 2018]. Available from: <https://gizmodo.com/city-evacuated-state-of-emergency-declared-in-wisconsin-1825583765>
 - [5] Blum, J. Failures of floating-roof oil tanks during Harvey raise concerns [Internet]. Houston Chronicle. 2017 [cited 10 May 2018]. Available from: <https://www.houstonchronicle.com/business/energy/article/Failures-of-floating-roof-tanks-during-Harvey-12269513.php#photo-14326482z>
 - [6] Mufson, S. Chemical companies have already released 1 million pounds of extra air pollutants, thanks to Harvey [Internet]. The Washington post. 2017 [cited 10 May 2018]. Available from: https://washingtonpost.com/news/energy-environment/wp/2017/09/04/chemical-companies-have-already-released-1-million-pounds-of-extra-air-pollutants-thanks-to-harvey/?noredirect=on&utm_term=.0770b2c3c6df
 - [7] Associated Press. Tank failures in Harvey reveal vulnerabilities in storm [internet]. Wtop. 2017 [cited 10 May 2018]. Available from: <https://wtop.com/business-finance/2017/09/tank-failures-in-harvey-reveal-vulnerabilities-in-storm/>
 - [8] BS EN 1992-3:2006, *Design of concrete structures. Part 3: Design of retaining and containing structures*. BSI, ISBN:0 580 48267 7, 2006.
 - [9] Greenshields, C.J. (2017). OpenFOAM: User guide. Retrieved from <http://foam.sourceforge.net/docs/Guides-a4/OpenFOAMUserGuide-A4.pdf>
 - [10] Othman, H. A. B. *Performance of ultra high performance fibre reinforced concrete plates under impact loads*. . PhD thesis, Ryerson University, 2016.
 - [11] ABAQUS (2016), ABAQUS Documentation, Dassault Systèmes Simulia Corp, Providence, RI, USA.
 - [12] MpCCI 4. 5.2 (2018), MpCCI coupling environment, Fraunhofer Institute for Algorithms and Scientific Computing SCAI, Germany.

Integrated Stochastic Prediction for Composites

Loujaine Mehrez^{*}, Roger Ghanem^{**}, Ziad Ghauch^{***}, Venkat Aitharaju^{****}, William Rodgers^{*****}, Arnaud Dereims^{*****}, Praveen Pasupuleti^{*****}

^{*}University of Southern California, ^{**}University of Southern California, ^{***}University of Southern California,
^{****}General Motors Research Center, ^{*****}General Motors Research Center, ^{*****}ESI Group, ^{*****}ESI Group

ABSTRACT

Mechanical properties of NCF composites are the byproduct of a manufacturing process that involves a sequence of steps where multiple physical processes, operating at distinct time and spatial scales. Mathematical and computational models of these processes are necessarily incomplete, resulting in both modeling and parametric uncertainties. Predicted performance of these composites, in the elastic and inelastic regimes, as well as near instabilities, is thus dependent on the details of their manufacturing process, and inherit uncertainties accumulated throughout the modeling of that process. Further, as the details of the manufacturing process predict the morphology of the composite on a fine scale and its constituents properties, methods for upscaling to large-scale performance must be relied upon. The challenge in predicting device-scale performance is further exacerbated by the need to account for uncertainties in the manufacturing process in addition to uncertainties in the upscaling process. A key challenge is computational, requiring multi-physics/multiscale simulations in a high-dimensional parameter space. A second challenge is conceptual (as well as numerical, and deals with modeling errors. We present an integrated procedure for tackling both of these challenges. Our procedure relies on adapted and doubly stochastic polynomial chaos expansions that permit highly-accurate approximations in high-dimensional stochastic spaces. By treating the coefficients of the polynomial chaos expansions as random, modeling errors becomes an integral part of the modeling and computational process. The methodology is demonstrated on the validation of a stochastic model for a composite component.

Efficient Stochastic Analysis and Prediction for Infrastructure Networks Using Compressive Sampling

Hadi Meidani*, Negin Alemazkoor**

*University of Illinois at Urbana-Champaign, **University of Illinois at Urbana-Champaign

ABSTRACT

In order to efficiently quantify the uncertainties in the behaviors of high dimensional infrastructure networks, fast analytical surrogates can be used to replace full-scale simulation models. Polynomial chaos expansion (PCE) is one of the widely adopted surrogates. To build PCEs, non-intrusive stochastic techniques such as regression can be used. These techniques in spite of their increasing use still suffer from the curse of dimensionality. This is because the number of required samples for accurate surrogate estimation rapidly increases with the number of random inputs. This is while the PCE surrogates for infrastructure networks are typically sparsely represented in terms of input uncertainties. Therefore, compressive sampling can be used to build these PCE with a significantly small number of sampled simulations. In this work, we apply novel compressive sampling approaches on the analysis of transportation and power systems. Specifically, we consider uncertain travel demands in the transportation network, and random power consumptions and generations in a power system with renewable energy sources are uncertain. Reliable short-term control of these systems require fast stochastic computation of system's response, e.g. travel time in transportation system and voltage levels in power system. To bypass the need to run a prohibitively large number of expensive simulations and facilitate fast, and almost real time analysis and prediction, we use polynomial surrogates using compressive sampling. In particular, we employ an incremental algorithm to identify the influential parameters, e.g. origin-and-destination pairs that their demand significantly impacts a given link's travel time and network nodes at which power consumption/generation substantially affect the voltage at another given node. Identifying important random inputs and removing uninfluential ones not only results in more accurate analysis, but also since our algorithm ranks random inputs based on their influence, it can be readily used for control purposes. We show the applicability and efficiency of our algorithm using benchmark problems in transportation and power systems, namely the Sioux Falls road network and the IEEE 33 bus test system.

Metal Additive Manufacturing by Selective Laser Melting: Modeling and Simulation Approaches Across Length Scales

Christoph Meier*, A. John Hart**, Wolfgang A. Wall***

*Mechanosynthesis Group, Massachusetts Institute of Technology, 77 Massachusetts Ave, Cambridge, MA 02139, USA / Institute for Computational Mechanics, Technical University of Munich, Boltzmannstraße 15, D-85748 Garching, Germany, **Mechanosynthesis Group, Massachusetts Institute of Technology, 77 Massachusetts Ave, Cambridge, MA 02139, USA, ***Institute for Computational Mechanics, Technical University of Munich, Boltzmannstraße 15, D-85748 Garching, Germany

ABSTRACT

Among the manifold of existing additive manufacturing (AM) processes, selective laser melting (SLM) of metals has attracted much scientific attention because it offers near-net-shape production of near-limitless geometries, and eventual potential for pointwise control of microstructure and mechanical properties. However, the overall SLM process is complex and governed by a variety of (competing) physical mechanism, motivating the development of elaborate modeling and simulation approaches in order to gain further understanding. The existing modeling approaches in the context of SLM processes can typically be classified in three categories: macroscopic, mesoscopic and microscopic models [1]. Macroscopic models typically treat the powder phase as a homogenized continuum resulting in efficient numerical tools capable of simulating entire SLM-manufactured parts. These models commonly aim to determine spatial distributions of temperature, residual stresses as well as dimensional warping within SLM parts, without explicitly resolving the fluid dynamics within the melt pool. On the contrary, mesoscopic models resolve individual powder grains and account for the melt pool thermo-hydrodynamics in an explicit manner. Mesoscopic models commonly predict resulting melt pool and part properties such as melt track stability, surface quality and layer-to-layer adhesion as well as creation mechanism of defects such as pores and inclusions. Last, microscopic models consider the evolution of the metallurgical microstructure involving the resulting grain sizes, shapes and orientations as well as the development of thermodynamically stable or unstable phases. The presentation will review existing modeling and simulation approaches on different length scales. In this context, also the first steps of the authors' ongoing research work in developing a mesoscopic simulation model for the SLM processes will be presented. Our approach especially focuses on the particle-to-particle interaction between individual powder grains, both, during the actual selective laser melting process but also in the initial powder coating process. The latter, which has rarely been studied so far, is crucially governed by adhesive forces prevalent at this length scale and essentially determines powder bed properties such as packing density, surface roughness or particle coordination number and, thus, also the properties of the final metal part after the rapid melting and solidification process in SLM. References: [1] C. Meier, R. Penny, Y. Zou, J.S. Gibbs, A.J. Hart. Thermophysical phenomena in metal additive manufacturing by selective laser melting: Fundamentals, modeling, simulation and experimentation. Annual Review of Heat Transfer, accepted for publication.

Photosynthesis and Its Biomedical Applications: NMR Properties of FMO Light-harvesting Complexes

Roderick Melnik*, Shyam Badu**

*MS2Discovery Institute, Wilfrid Laurier University, **MS2Discovery Institute, Wilfrid Laurier University

ABSTRACT

The bacteriochlorophyll is one of the most important molecular systems found in the light-harvesting complex in which the photosynthesis event occurs. Most recently, bacteriochlorophylls, found in the light-harvesting complexes, have been used for the photodynamic therapy for treatment of some forms of cancer. In order to understand the application of these photosynthetic materials in biomedicine, as well as in the plant cycle and other life science applications, it is very important to understand the structure of these molecules. Therefore, in this contribution, we study the structural properties of the bacteriochlorophyll taken from the Fenna-Matthew-Olsen light-harvesting complex found in the green sulfur bacteria. Specifically, in our current study, we present the nuclear magnetic resonance (NMR) spectrum of the bacteriochlorophyll that is directly taken from the FMO complex, as well as the spectrum for this system for its optimized geometry. We use density functional theory to calculate the optimized geometry and the NMR spectra of the bacteriochlorophyll. From our calculations, we found that the chemical shift values are slightly lower for the optimized geometry of the bacteriochlorophyll than the values obtained for the unoptimized bacteriochlorophyll. The differences observed between these two spectra are due to the fact that the unoptimized structure of the bacteriochlorophyll possesses the influence of the protein environment of FMO complex.

Investigation on Generation Method of Meso-scale Simulation Model for W-Cu Shaped Charge Liner and its Dynamic Response under Explosive Loading

Jianbing Men^{*}, Fang Wang^{**}, Jianwei Jiang^{***}, Shuyou Wang^{****}, Mei Li^{*****}

^{*}Beijing Institute of Technology, ^{**}Beijing Institute of Technology, ^{***}Beijing Institute of Technology, ^{****}Beijing Institute of Technology, ^{*****}Beijing Institute of Technology

ABSTRACT

Tungsten-copper(W-Cu) is a kind of composites constituted of two immiscible phases which are mechanically mixed without interfacial reaction. It is always regarded as homogeneous material in conventional simulations. However, the dynamic response of W-Cu under explosive loading is still unclear especially in the meso-scale scope due to the significant difference between the chemical and physical properties of tungsten and copper. In order to investigate the mesoscopic mechanism of W-Cu shaped charge jet formation, the generation program of W-Cu meso-discrete model was developed based on the random particles principle. The discrete models of W-Cu liner with different ratios of two phases and various diameters of tungsten particles were successfully established by the program. The multi-scale finite element numerical simulations were carried out on the particle-matrix materials and the referenced equivalent homogeneous material by using Autodyn-2D Euler solver. The results show that the average velocity of Cu phase is much higher than W phase, leading to a phase segregation and composition gradient in W-Cu jet during its forming process. The content of Cu is higher in the jet tip compared with the liner material while the W particles mainly concentrate in the slug. A novel recovery experiment was designed to verify the microstructural change of W-Cu composite during the jet formation process. The W-Cu jet residue recovered from the target surface was observed by scanning electron microscopy. The experiment results also indicate that composition gradient exists in the W-Cu jet, which was in good agreement with the simulation results. Reference: [1]D. Eakins, N.N. Thadhani. Discrete Particle Simulation of Shock Wave Propagation in a Binary Ni+Al Powder Mixture [J]. Journal of Applied Physics, 2007, 101, 043508 [2]Liu Jintao, Cai Hongnian, Wang Fuchi etc. Multiscale Numerical Simulation of the Shaped Charge Jet Generated from Tungsten-copper Powder Liner [J]. Journal of Physics: Conference Series, 2013, 419: 1-8 [3]Seong Lee, Moon-hee Hong, Joon-wong Noh etc. Microstructural Evolution of a Shaped-charge Liner and Target Materials during Ballistic Tests [J]. Metallurgical and Materials Transactions A, 2002, 33A: 1069-1074

Analysing the Relationship between the Hopper Angle and the Mass Flow Rate in Conical Hoppers

David Mendez^{*}, Raul Cruz Hidalgo^{**}, Diego Maza^{***}

^{*}University of Navarra, ^{**}University of Navarra, ^{***}University of Navarra

ABSTRACT

The accurate prediction of the mass flow rate in silos and bins is obviously important in many industries. In past decades, accurate correlations predicting the mass flow rate in granular hoppers were introduced [1,2]. However, there is a lack of a generalized formulation connecting the mass flow rate with the grains properties, the hopper geometry, and the macroscopic stress field. On the other hand, examining industrial silos by R&D factories and technical offices, continuous models are the most commonly used numerical tools. Those algorithms are usually very sophisticated and have many tuning parameters, so they require an extensive experimental calibration. In this work, we use a continuous description [3] to analyze the relationship between the hopper angle and the mass flow rate in conical hoppers. Adjusting the parameters of the simulation and feedbacking the code with experimental results, we develop an accurate calibration procedure, which can be employed in both simplified lab conditions and industrially relevant systems. Furthermore, executing a systematic study, changing the hopper angle and the size of the aperture, we find that the used numerical implementation captures the main features of the granular flux through the orifice, such as the velocity and density profiles. Moreover, the results suggest that the hopper angle controls the system's dynamics near the exit, determining the discharge rate at the outlet. [1] W. A. Beverloo, H. A. Leniger, and J. J. Van de Velde, Chem. Eng. Sci. 15, 260 (1961) [2] C. Mankoc, A. Janda, R. Arévalo, M. Pastor, I. Zuriguel, A. Garcimartin, and D. Maza, Granular Matter 9, 407 (2007) [3] A. Janda, I. Zuriguel, and D. Maza, Phys. Rev. Lett. 108, 248001 (2012) [4] ANSYS Fluent <http://www.ansys.com/Products/Fluids/ANSYS-Fluent>

Study on Pull-out Failure of Headed Inserts in Concrete Based on Peridynamic Theories

Xianhong Meng^{*}, Jianan Bi^{**}, bo Jiang^{***}, Xiaofeng Wang^{****}

^{*}Shenyang Jianzhu University?Shenyang?China?110168, ^{**}Shenyang Jianzhu University?Shenyang?China?110168, ^{***}China Academy of Building Research?Beijing?China?100013, ^{****}China Academy of Building Research?Beijing?China?100013

ABSTRACT

The metal inserts are widely used in lifting and handling of concrete components. The concrete cone capacity of headed inserts subjected to axial tension load was studied by many researchers, However, the research on the numerical simulation method is still insufficient. The finite element simulation results are far from the actual situation, and the reason is that the continuum mechanics is difficult to describe the discontinuous problem of concrete cracking. The peridynamic(PD) method is more advantageous in solving the problem about the concrete crack expansion and material damage, etc. A peridynamic(PD) model based on PMB was established, two kinds of critical stretch of the bond in concrete and the lifting inserts were applied to distinguish the different tensile strength, and the bond of linkage between the concrete and the lifting inserts took the mean value of the above two kinds of critical stretch. Through this model and the continuous medium finite element model, the failure process of the embedded headed inserts was simulated. The comparison between the simulation results and the experimental results indicated that the PD model was closer to the actual situation than the finite element method in solving the crack propagation of the concrete cone failure. It was proved that PD method can be used to analyze the pull-out damage of the lifting inserts in the concrete, provided a theoretical basis for the engineering application of the lifting inserts. [1]Karin Lundgren,Kent Gylltoft.A model for the bond between concrete and reinforcement[J].Magazine of Concrete Research,2000,52(1):53-63 [2]HUANG Dan,ZHANG Qing,QIAO Pi-zhong,et al.A review on peridynamics method and its applications[J].Advances in Mechanics,2010,40(4):448-459. [3]SHI Hongshun?QIAN Songrong?XU Ting?YUAN Qunsheng?ZHANG Guo-hao.Study on reinforced concrete structure failure based on peridynamic theories[J].Guizhou Science,2016,34(06):64-68.

SCRAMJET Design Optimization Using SNOWPAC in Dakota

Friedrich Menhorn^{*}, Youssef Marzouk^{**}, Florian Augustin^{***}, Michael Eldred^{****}, Gianluca Geraci^{*****}

^{*}Technical University of Munich, ^{**}Massachusetts Institute of Technology, ^{***}MathWorks/ Massachusetts Institute of Technology, ^{****}Sandia National Laboratories, ^{*****}Sandia National Laboratories

ABSTRACT

SNOWPAC (Stochastic Nonlinear Optimization With Path-Augmented Constraints) [Augustin & Marzouk 17] is a method for stochastic derivative-free optimization, developed to treat nonlinear constrained optimization problems with uncertain parameters. These uncertain parameters represent, for example, a lack of knowledge about the system under consideration, or other errors in the models entering the objective and constraints. Optimization in these settings employs measures of robustness and risk in order to describe a suitable solution—for instance, to identify solutions that are relatively insensitive to parameter uncertainties. SNOWPAC extends the path-augmented constraint framework introduced by NOWPAC [Augustin & Marzouk 14], via a noise-adapted trust region approach and Gaussian process approximations. It solves optimization problems where Monte Carlo sampling is used to estimate robustness or risk measures comprising the objective function and/or constraints. We consider problems where expensive black box model evaluations are needed to construct these estimates, and thus we focus on a small sample size regime. This regime involves significant noise in the estimators, which slows the optimization process. To mitigate the impact of noise, SNOWPAC employs Gaussian process regression to smooth models of the objective and constraints in the trust region. In a recent development, SNOWPAC has been integrated with the Dakota framework, which offers a highly flexible interface to couple the optimizer with different sampling strategies and surrogate models. In this presentation, we showcase the combined SNOWPAC-Dakota capability by performing design optimization under uncertainty in two challenging problems: a bump in a 2D supersonic duct and supersonic turbulent spray combustion in a SCRAMJET engine. The SCRAMJET follows the HIFiRE design and is modeled by an LES simulation code developed by Sandia National Laboratories. We compare deterministic optimization results with results obtained by introducing uncertainty in the inflow parameters. As a sampling strategy, we contrast simple Monte Carlo sampling with more sophisticated multilevel Monte Carlo approaches. Here, Dakota serves as the driver of the optimization process, employing SNOWPAC as optimization method on the black box problem. We show that all approaches provide reasonable optimization over the design while seeking/maintaining feasibility in the final minimized objective. Furthermore, we see significant improvements in the computational cost when employing multilevel approaches that combine solutions from different grid resolutions.

Impact Modelling of Bioinspired Pseudo-ductile Composite Laminates with Hierarchical Energy Absorption Mechanism

Michele Meo^{*}, F. Rizzo^{**}, F. Pinto^{***}

^{*}University of Bath, ^{**}University of Bath, ^{***}University of Bath

ABSTRACT

The intrinsic layered nature of carbon fiber and their weak resistance to out-of-plane loads leads to oversized composite structural parts, preventing the full exploitation of their unique characteristics and limiting their use in harsh environments. Therefore, composite laminates able to respond with a pseudo-ductile behaviour when subjected to an out-of-plane load is of crucial importance as it would eliminate the need of oversized parts and extend the range of applications available to composite structures. This paper presents the design, manufacturing and characterisation of a bioinspired CFRP laminate in which the pseudo-ductility arises from an ordered pattern of discontinuities which are created over the surface of the different layers before the curing reaction, called platelets. The presence of this carved pattern creates a hierarchical interplay of high-strength carbon fibre segments and elastic soft matrix-rich areas which resembles the interaction between the β -sheets crystalline domains and amorphous helical and β -spiral structures typical of spider silk and other biological structures (e.g. cellulose, hair) which enables a combination of high mechanical strength and elasticity. The effect of different geometrical parameters of the carved pattern such as critical length, shape and dimensions, on the mechanical properties of the laminate were modelled via Finite Element Analyses in order to identify the optimal configuration of the discontinuities, finding the best trade-off between in-plane and out-of-plane mechanical properties. Samples with different carved patterns were then manufactured and their properties were assessed by subjecting them to Low Velocity Impacts (LVIs). An optimisation process was carried out to optimise critical fiber length of the platelets. The predicted internal distribution of damaged areas was compared to experimentally measured damage using different Non Destructive Techniques. The energy absorption improvement was assessed by comparing it to the behaviour of traditional CFRP. Results showed that the presence of the artificial discontinuities is able to induce pseudo-ductile behaviour into the CFRP, improving the energy absorption mechanism during out-of-plane solicitations without severely affecting the in-plane properties. 1. Pinto, F., A. White, and M. Meo, Characterisation of ductile preregs. *Applied Composite Materials*, 2013. 20(2): p. 195-211. 2. Keten, S., et al., Nanoconfinement controls stiffness, strength and mechanical toughness of β -sheet crystals in silk. *Nature materials*, 2010. 9(4): p. 359. 3. Mirkhalaf, M. and F. Barthelat, Nacre-like materials using a simple doctor blading technique: Fabrication, testing and modeling. *Journal of the mechanical behavior of biomedical materials*, 2016. 56: p. 23-33.

Variational Model for Solid and Hydraulic Fracturing Problems Using Interface Elements

Günther Meschke*, Ildar Khisamitov**

*Ruhr University Bochum, **Ruhr University Bochum

ABSTRACT

In this presentation, we propose a variational formulation for fracture in brittle materials, which is inspired by the class of phase-field models [1, 2] but which is incorporated into a zero-thickness interface modeling framework instead of a continuum damage framework [3]. The fractured structure is variationally formulated as the sum of bulk elastic and fracture surface energies. With the help of a damage variable used as an additional degree of freedom, the fracture propagates according to a minimization principle of the total potential energy. As a criterion for the crack propagation, an energy criterion, checking, if the elastic energy within the interface surface exceeds the critical energy release rate is used. Equilibrium of the discretized structural boundary value problem is found using a staggered scheme, solving first the mechanical problem and then searching for the solution for the updated damage variable. The model is first presented in the context of crack propagation simulations in structures made of quasi-brittle materials. In a second step, the computational model is formulated in a coupled poromechanics framework to enable the numerical simulation of hydraulic fracturing problems. This type of analysis finds applications in hydraulic stimulation of deep geothermal reservoirs, which is characterized by the creation of hydraulically driven fractures, which eventually interact with pre-existing fractures and natural faults. Besides selected benchmark tests, also various laboratory tests fluid induced fracture propagation are analyzed numerically and compared with experimentally obtained fracture paths. [1] Bourdin, B., Francfort, G.A. and Marigo, J.J., The variational approach to fracture , *Journal of elasticity*, 91, 5–148 (2008). [2] Miehe, C., Welschinger, F. and Hofacker, M., Thermodynamically consistent phase-field models of fracture: Variational principles and multi-field FE implementations , *International Journal for Numerical Methods in Engineering*, 83, 1273–1311 (2010). [3] Khisamitov, I. and Meschke, G., Variational approach to interface element modeling fracture propagation, *Computer Methods in Applied Mechanics and Engineering*, 328, 452-476 (2018).

Phase-field Modeling of Anisotropic Phase-change and Fracture in Silicon Anodes in Li-ion Batteries

Ataollah Mesgarnejad*, Alain Karma**

*Northeastern University, **Northeastern University

ABSTRACT

The chemo-mechanical modes of failure in Li-ion battery remain poorly understood. In this talk, motivated by new experimental observations, we will present the results of our simulations of complex finite elasto-plastic model for Si/Ge-anode structures. Due to their high theoretical capacity, Silicon and Germanium as anode material for Li-ion batteries has attracted wide interest in the research community. However, the intercalation of Li ions in crystalline Si (or Ge) results in phase change and amorphization of Si to Li_xSi accompanied by ~ 300% volume expansion. Amorphization, in turn, results in an inelastic deformation flow and fracture. Furthermore, the intercalation occurs as a reaction-controlled invasion of Li where the sharp amorphous-crystalline interface between Li-rich amorphous phase and crystalline phase moves anisotropically due to the crystallographic directions. Over the past two decades, the phase-field models have emerged as exceptional computational tools for modeling a spectrum of physical phenomena from phase change to fracture. The variational nature of these models allows for coupling between a range of physical phenomena. To model intercalation of Si structures, we combine formulations of finite neo-Hookean elasticity and finite J-2 plasticity with a modified Allen-Cahn model of the amorphous-crystalline phase change and a phase-field fracture. We show how our numerical simulations reproduce the experimentally observation where the crystalline directions significantly modify the onset of fracture and its propagation direction.

Anisotropic Mesh Adaptation on Emerging Architectures

Youssef Mesri^{*}, Philippe Meliga^{**}, Franck Pigeonneau^{***}, Rudy Valette^{****}, Elie Hachem^{*****}

^{*}Mines Paristech, ^{**}CNRS, ^{***}Mines Paristech, ^{****}Mines Paristech, ^{*****}Mines Paristech

ABSTRACT

This work is motivated by the success of the anisotropic adaptive finite element methods in accurately simulating complex physical systems in science and engineering. The parallel implementation of anisotropic adaptive finite element methods is a challenging task for which efficiency continues to be a significant issue due to its dynamic data structure modification along the simulation. We have developed and optimized in the last years, mesh adaptation tools and algorithms to manage efficiently the dynamic load balancing in the context of SPMD based parallelism [1, 4]. However, the performance of these algorithms is deteriorated with the advent of new architectures such as Intel Xeon Phi Knights Landing processors or GPUs. Indeed, the heterogeneity of the hardware resources and the memory hierarchy require the adaptation of the existing algorithms according to these characteristics. The effort should then goes back to focus only on the efficiency of a single computing node. The leading question that arises from this analysis is then as follows: Which effort is the most rewarding: code optimization, algorithmic adaptation or both? In this paper, we present the recent improvements brought to the anisotropic mesh adaptation tools to meet the efficiency challenges imposed by the heterogeneity of the emerging architectures. Indeed, we developed algorithms and techniques to efficiently use CPU and memory. The main data arrays are vectorized with Intel AVX-512 intrinsics, the data locality is improved by considering a suitable renumbering algorithm for unstructured meshes, and the mesh is efficiently mapped into the threads. We conduct performance analysis over different CFD benchmarks to highlight effectiveness of the proposed approach.

REFERENCES [1] Y. Mesri, H. Dignonnet, T. Coupez. Advanced parallel computing in material forming with CIMLib. E. J. of Computational Mechanics, 18(7-8):669-694, 2009. [2] Mesri Y., Dignonnet H., Guillard H. Mesh Partitioning for Parallel Computational Fluid Dynamics Applications On a Grid. Finite Volumes for complex applications IV. Hermes Science Publisher, pp. 631—642, 2005 [3] Y. Mesri, H. Dignonnet, T. Coupez, Hierarchical adaptive multi-mesh partitioning algorithm on heterogeneous systems. Parallel Computational Fluid Dynamics 2008, 299-306 [4] Mesri Y., Gratien J.-M., Ricois O., Gayno R. Parallel Adaptive Mesh Refinement for Capturing Front Displacements: Application to Thermal EOR Processes. SPE paper, 2013

Optimization of Periodic Structures with Convolutional Neural Network Surrogate Models

Mark Messner*

*Argonne National Laboratory

ABSTRACT

The development of additive manufacturing methods has spurred interest in the optimization of periodic, mesoscale structural unit cells. These unit cells can be printed to fill a component shape, forming an effective material on the macroscale with optimized material properties. This presentation describes a method for optimizing the effective, homogenized material properties of such periodic mesostructures using neural network surrogate models. Convolutional neural networks are a machine learning tool that has been successfully applied to a variety of image recognition problems. The convolutional network structure is also ideally suited for solid mechanics homogenization: the homogenization of a particular periodic mesostructure can be viewed as an image recognition problem. This presentation describes the development and training of a convolutional neural network surrogate model that can accurately predict the effective elastic and inelastic properties of 2D periodic mesostructure. A forward evaluation of the model is six orders of magnitude faster than a corresponding finite element simulation. Such fast surrogate models can be used to find globally optimal material mesostructures through genetic algorithm optimization. This presentation details the results of several example optimization problems. For the simplest, elastic optimization problems the surrogate model approach finds similar structures to those found through conventional, gradient based topology optimization methods. The surrogate modeling approach can also optimize for inelastic effective material properties like energy dissipation. These kinds of optimization problems are harder to solve with conventional methods and are relevant to finding optimally dissipative structures for armor and ballistic protection applications.

Variability Response Function of Axial Characteristic

Mladen Mestrovic*

*University of Zagreb

ABSTRACT

The axial characteristic of beam used in second order theory of beam bending is taken for stochastic analysis. The flexural rigidity of the beam is assumed to be random variable with given expectation, variance and coefficient of variation. That assumption leads to variability of axial characteristic. Variability response function of axial characteristic is defined to determinate its expectation, variance and coefficient of variation. The coefficient of variation of axial characteristic is expressed as function of coefficient of variation of flexural rigidity. The variation of axial characteristic is needed for further investigation of variability of the beam stiffness matrix defined according the second order theory of elasticity.

Modeling Strategies for Magnetosensitive Elastomers on Different Scales: A Link between Microscopic and Macroscopic Models

Philipp Metsch*, Karl Alexander Kalina**, Jörg Brummund***, Markus Kästner****

*Institute of Solid Mechanics, TU Dresden, **Institute of Solid Mechanics, TU Dresden, ***Institute of Solid Mechanics, TU Dresden, ****Institute of Solid Mechanics, TU Dresden

ABSTRACT

Magnetosensitive elastomers (MSEs) represent a class of active materials which typically consist of micron-sized magnetizable particles embedded in a cross-linked elastomer matrix. Due to mutual interactions of the particles, MSEs are able to alter their effective material behavior reversibly if subjected to an external magnetic field. Moreover, they show a large magnetostrictive response: compared to pure ferromagnetic materials, their field-induced deformation is increased by orders of magnitude. This strong coupling of magnetic and mechanical fields facilitates a variety of applications in the fields of actuators and sensors. Within this contribution, a modeling strategy for MSEs is presented: starting from the properties of the magnetizable particles and the elastomer matrix, a continuum formulation of the problem is applied on the microscale in order to determine the macroscopic material behavior by means of a computational homogenization [1]. The governing equations are solved using the finite element method. For these calculations, an efficient monolithic solution scheme is developed in order to account for the strong nonlinear coupling of magnetic and mechanical fields [2]. Initially, the modeling approach is applied to investigate the influence of microstructural geometric as well as constitutive properties of MSEs on their behaviour. A comparison between our simulations and experiments is used to identify deformation mechanisms which can be observed in both simplified and complex MSE samples [3]. Moreover, the discrepancy between widely used two-dimensional approaches and a full three-dimensional solution of the problem is investigated qualitatively and quantitatively. Based on these findings, the macroscopic behavior of MSEs is predicted by performing a statistical evaluation of different random microstructures. The results of our approach are used to identify parameters of available macroscopic models from the literature - an optimization procedure for the parameter identification allows for the link between microscopic and macroscopic models. This strategy allows for an efficient prediction of the effective behavior of realistic MSE samples. References: [1] Metsch, P., Kalina, K. A., Spieler, C., Kästner, M., A numerical study on magnetostrictive phenomena in magnetorheological elastomers, *Computational Materials Science*, 124, pp. 364-374 (2016) [2] Kalina, K. A., Metsch, P., Kästner, M., Microscale modeling and simulation of magnetorheological elastomers at finite strains: A study on the influence of mechanical preloads, *International Journal of Solids and Structures*, 102-103, pp. 286-296 (2016) [3] Puljiz, M., Huang, S., Auernhammer, G. K., Menzel, A. M., Forces on Rigid Inclusions in Elastic Media and Resulting Matrix-Mediated Interactions, *Physical Review Letters*, 117, pp. 238003 (2017)

Surface Mechanics Improved Solutions to an Elastic Half-space Subjected to Nanoscale Surface Traction

Changwen Mi^{*}, Xiaobao Li^{**}

^{*}Southeast University, China, ^{**}Hefei University of Technology, China

ABSTRACT

To better understand the impact of surface stress effects on fundamental solutions of elasticity, a three-dimensional stress analysis is performed for an elastic half-space subjected to surface tractions applied within a nanoscale circular portion of its plane boundary. The method of Boussinesq displacement functions is used to address the problem, where local elastic field including displacements and stresses in the vicinity of the loading area is semi-analytically determined by solving a set of improper integral equations. Numerical results are presented to examine effects and the stress disturbances caused by the coupling of surface loads and surface mechanics. The results show that a metallic layer with properly designed mechanical behavior coated on the free surface of a half-space substrate of even the same material can function as a stiffener and stress reliever. The results suggest a means of optimizing the local displacements, strains and stresses by controlling the material properties of the half-space boundary. Keywords: Surface mechanics; Half-space; Surface loads; Stress disturbance

CFD and FFD Method for Lines Optimization Design of Twin-skeg Ship

Aiqin Miao^{*}, Decheng Wan^{**}

^{*}Shanghai Jiao Tong University, ^{**}Shanghai Jiao Tong University

ABSTRACT

The optimization design method for a twin-skeg ship's stern shape is presented here. The stern shape of a twin-skeg ship greatly affects its resistance, propulsion and maneuverability. Therefore, to improve hydrodynamic performance, the local hull lines of a twin-skeg ship's stern can be optimized in the preliminary design stage according to some scientific transformation method. This paper intends to optimize the stern of a twin-skeg ship based on OPTShip-SJTU, a solver for ship optimization design developed independently by Computational Marine Hydrodynamics Laboratory (CMHL). Free-form Deformation (FFD) method is introduced and developed to transform twin skegs locally. The total resistance and the wake fraction in the stern are considered as two objective functions, calculated by our in-house CFD solver, naoe-FOAM-SJTU based on the viscous flow theory. Finally, NSGA-II algorithm is called for the multi-objective optimization solution to obtain optimal hulls with the best resistance and propulsion performance in the design space. Notably, in order to reduce the numerical computational cost, the relationship between ship transformation parameters (design variables) and hydrodynamic performance (objective functions) is expressed as two surrogate models by design of experiment and Kriging method. These two models are directly applied to evaluate the objective functions of any new individual in the optimization process, instead of direct numerical simulations. The selected optimal ship is compared with the parent ship in terms of the wave elevation, pressure distribution, vorticity field and wake field. It turns out that the research provides an effective guide to the stern shape design of the twin-skeg ship and the solver OPTShip-SJTU is practical for ship optimization design.

The Importance of Geometry and Mesh Association in Adaptive Meshing

Todd Michal*

*Boeing Research and Technology

ABSTRACT

The last decade has seen an increased use of adaptive meshing in computational analysis. Adaptive meshes are continuously changing throughout the analysis requiring a close association between the mesh and geometry model. In this talk the importance of associating the geometry and mesh and tracking that association throughout the analysis will be explored. Examples from the context of anisotropic adaptive meshing on complex aerospace applications will be presented.

Multi-Scale simulation for Part-Level Metal AM

Pan Michaleris^{*}, Jeff Irwin^{**}, Erik Denlinger^{***}, Michael Gouge^{****}, Serge Sidorov^{*****}

^{*}Autodesk, ^{**}Autodesk, ^{***}Autodesk, ^{****}Autodesk, ^{*****}Autodesk

ABSTRACT

A primary challenge for Laser Powder Bed Fusion (LPBF) to become a reliable and economically feasible method of component production is the warping of parts during production. This distortion adds expense of the process, can take weeks or months of experimentation to minimize, and may prematurely end the businesses case for implementing AM into production. Autodesk offers a software, Netfabb Simulation, which can predict and mitigate build failure prior to manufacture, by using a multi-scale modeling approach. This study shows through simulation-experimental comparisons that this software can be used to make timely and useful predictions of distortion for common AM metals. It will also document the successful modeling of the secondary failure mechanisms of support structure delamination and recoater blade interference. Simulation based distortion mitigation will be demonstrated by simulating a part and compensating the build geometry to reduce deformation. Finally, the concept of multi-scale modeling will be extended to the prediction of hot-spots and lack of fusion related defects on Part-Level AM builds.

Modeling of Masonry Walls under Blast Loads

Georgios Michaloudis*, Norbert Gebbeken**

*University of the Bundeswehr Munich, **University of the Bundeswehr Munich

ABSTRACT

Masonry walls represent one of the most common applied constructions in civil engineering and architecture. The inhomogeneous nature of masonry imposes a challenge in the development of robust modeling techniques especially under high dynamic loads. Under extreme loading conditions the numerical model must take into account failure mechanisms which do not occur under static loads. In this contribution some modeling strategies are discussed which are suitable for the simulation of unreinforced masonry walls under detonation loads. The damage formation in the wall under loads resulting from far-field as well as contact detonations is investigated. Firstly the issue of an appropriate material model for bricks under high strain rates is discussed. Through a proper adaptation of a material model initially developed for concrete under blast loads we derive all the necessary parameters for the bricks. In this way we develop a suitable strength model as well as an equation of state for the simulation of the material behavior under high strain rates. We apply the simplified micro-model as the general strategy for the modeling of the walls. The numerical results resulting from the simulation of the walls under far-field detonation loads are validated with experiments. Subsequently we refine these models in order to be able to capture the local damage formation and the resulting debris due to a contact detonation. Small parts of the wall in the proximity of the explosion separate from the main body of the wall and travel at high velocities. They can establish an additional danger for persons and infrastructure which theoretically lie in a secure distance from the target of the explosion. This failure mechanism is dominant in contact detonation but negligible in far-field blast scenarios. We propose a numerical algorithm in order to alter the numerical model in the regions where formation of debris is expected due to a contact detonation. The algorithm is based in Lagrangian finite elements so that the general formulation of the model (Lagrangian) does not need to be changed. The numerical results also of the contact detonation scenarios are validated with appropriate experiments.

State-of-the-art of Analysis Techniques for Masonry Arches and Shells Subjected to Seismic Loading and Their Applicability to Conceptual Design

Tim Michiels*, Sigrid Adriaenssens**

*Princeton University, **Princeton University

ABSTRACT

The design of new masonry shells is attracting renewed attention because the embodied energy of masonry structures is exceptionally low, making them environmentally friendly construction solutions [1]. Extensive research has led to a wide array of analysis methods for masonry arches and shells, but only few of these methods have been translated into tools for their conceptual design. While most of these conceptual design tools focus on gravitational loading, earthquakes can be the design-guiding stressors for masonry shells. And while also for seismic loads, analysis methods for masonry are well established, tools for shape-finding in seismic areas are nearly non-existent. Therefore, this presentation provides an overview of the available analysis techniques to evaluate the seismic response of masonry arches and shells and evaluates the usefulness of each technique to perform conceptual design for shells in earthquake areas. The considered methods include upper-and lower-bound equilibrium approaches – such as thrust line and network analysis, kinematic limit state analysis and membrane analysis and explain while these are the most promising tools for form-finding. Furthermore, while analytic solution methods have been developed for arches, the application of these analytic solutions to 3D-geometries has not yet been accomplished. Instead, researchers typically resort to macro-modelling, such as non-linear finite element modeling (FEM) techniques assuming homogeneous material behavior. It is shown how these methods are more suitable for validation, than to perform conceptual design due to their high computational demand. Similarly, it is shown that distinct element methods can be an excellent analysis technique for shells or arches which can be discretized into realistic discrete blocks. Additionally, a set of recently published, lesser-known methods, such as the reformulated thrust-network analysis and the relaxed-funicularity method are discussed because of their potential for form-finding [2]. Finally, examples are provided that show how simplified equilibrium methods can be used to find new shapes for masonry shells in seismic areas, while their seismic capacity is validated using non-linear FEM [3].

1. De Wolf, C., M. Ramage, and J. Ochsendorf, Low Carbon Vaulted Masonry Structures. Journal of the International Association for Shell and Spatial Structures, 2016 (Vol. 57 (2016) No. 4 December n. 190): p. 275-284.
2. Gabriele, S., V. Varano, G. Tomasello, and D. Alfonsi, R-Funicularity of form found shell structures. Engineering Structures, 2018. 157: p. 157-169.
3. Michiels, T. and S. Adriaenssens, Form-finding algorithm for masonry arches subjected to in-plane earthquake loading. Computers & Structures, 2018. 195: p. 85-98.

Multiscale and Multiphysics Integrated Computational Materials Engineering Framework for Linking Additive Manufacturing Process Parameters with Part Performance

John Michopoulos^{*}, Athanasios Iliopoulos^{**}, John Steuben^{***}, Andrew Birnbaum^{****}

^{*}US Naval Research Laboratory, ^{**}US Naval Research Laboratory, ^{***}US Naval Research Laboratory, ^{****}US Naval Research Laboratory

ABSTRACT

Additive manufacturing (AM) has become an important technology for the fabrication of a wide variety of components and structures. Interest in AM has been primarily driven by the potential for object fabrication relatively free of geometric constraints as well as the introduction of features across multiple length scales. Despite these advantages, currently implemented AM processes continue to be highly non-uniform in terms of undesirable, process-induced features both from material and geometry perspectives. Experimental studies have shown that these non-uniformities lead to AM-induced micro/meso structures and morphologies that differ drastically from those produced by conventional methods. Consequently, additively manufactured products suffer from issues including geometric errors, residual stresses and strains that may be very large, layer delamination, as well as porosity and poor or indeterminate material properties. These issues lead to further uncertainty in functional performance that often preclude the use of AM technology in performance-critical applications. To address these issues our team has embarked on the development of a Multiscale and Multiphysics Integrated Computational Materials Engineering (MMICME) framework for AM. Our description will be the topic of this talk. This framework incorporates multiscale multiphysics modeling and experimentation in order to fully encapsulate the important roles that micro- and meso-structures play in tailoring material properties and responses in engineering applications. The immediate goals of this effort is to enable on-demand control of AM processes for tailoring meso- and micro-structures to endow desirable properties and eliminate undesirable ones. This talk describes an overview of the multiscale and multiphysics modeling and simulation elements, which have been developed in order to implement our MMICME framework for AM.

APPLICATION OF THE MESHLESS METHOD TO THE FILTRATION EQUATION

MAGDALENA MIERZWICZAK*

*Poznan University of Technology, Institute of Applied Mechanics
Jana Pawła II 24,
60-965 Poznan, POLAND
magdalena.mierzwiczak@wp.pl

Key words: Beavers-Joseph boundary condition, permeability, slip constant, fibrous porous media, meshless methods.

Abstract. In this paper the permeability and the slip constant on the boundary of the considered fibrous porous region are determined by numerical simulation of the imaginary physical experiment. The porous medium is modeled by a parallel bundle of straight fibers arranged in a regular triangular, square, or hexagonal array. In order to determine the permeability, the flow driven by the pressure gradient in an unbounded porous medium is considered. To determine the slip constant, the shear flow between a flat immovable wall containing both the porous and free flow layers is considered. In both numerical simulations, the meshless procedure is applied. The influence of the volume fraction of the fibres on the value of the permeability and the slip constant is investigated. In all considered cases the value of the slip constant is lower than one. The slip constant decreases with increasing the volume fraction of fibers for a high porosity. For a square and hexagonal array the value of slip constant starts increasing for small porosity. For the same volume fraction of the fibers, both the permeability and the slip constant for the triangular array is smaller than for the square and the hexagonal array. Proposed algorithm is easy to implementation, accurate and is mesh free.

1 INTRODUCTION

The viscous fluid flow in a channel coupled with the flow through an adjacent porous region is often found in several engineering applications. In order to solve this type of problem numerically, a set of proper governing equations for the flow through two distinct, neighboring and interconnected domains has to be established. The incompressible flow in the fluid region is well represented by Navier-Stokes equations, while Darcy equation is used to describe the flow in the adjoining porous medium. For these governing equations problem is with the boundary condition. Beavers and Joseph [1] proposed that the interfacial velocity of the freely flowing fluid and the fluid velocity in the porous matrix could be related by

$$\frac{du}{dx} = \frac{\alpha}{\sqrt{k}}(u - q) \quad (1)$$

where u is a velocity of the fluid flow calculated at boundary (slip velocity), k is a permeability of porous medium, and q is a seepage velocity measured at small distance outside the interface, suggesting the existence of a thin layer just inside the porous medium over which the velocity transition occurs. The dimensionless slip coefficient α is an independent of the fluid viscosity and apart from permeability depends on the structural parameters of the porous medium and is specific to the geometric features of the interface.

For determination the slip coefficient, Beavers and Joseph described experiments performed in a parallel-plate channel, one of the bounding walls was made of the porous material while the other one was impermeable. Identical axial pressure gradients were imposed on the channel and the porous medium, thereby giving rise to parallel axial flows.

This paper presents a numerical simulation of the Beavers-Joseph's experiment for the fibrous porous media. The longitudinal laminar flow in a parallel-plate conduit is considered. The first half of the considered region is a porous medium and the second one is a free fluid region. The porous medium is modelled as a bundle of parallel fibres. The purpose of the present consideration is determination of the slip constant in the Beavers-Joseph boundary condition for Newtonian fluid. But for do this the permeability of the porous medium is required. For to determine the last one the flow with the pressure gradient in unbounded porous medium was considered. Numerical simulations are conducted using the Trefftz method [2]. Essential novelty of this paper is numerical simulation of the Beavers-Joseph experiment for the Newtonian fluid. The influence of the volume fraction of the fibres on the value of the slip constant is investigated.

2 DETERMINATION OF THE SLIP CONSTANT

It is convenient in numerical simulations to use directly the Beavers-Joseph boundary condition to determined the slip coefficient. Let us consider a plane infinite channel adjoining with a plane infinite porous region in which flow is governed by the Darcy law in the following form

$$\frac{du}{dx} = \frac{\alpha}{\sqrt{k}} \left(u - \frac{k}{\mu} \frac{dp}{dz} \right). \quad (2)$$

Let us introduce the following dimensionless variables

$$U = \frac{\mu \cdot u}{-b^2 \cdot \frac{dp}{dz}}, \quad X = \frac{x}{b}, \quad \sigma = \frac{b}{\sqrt{k}}, \quad (3)$$

where b is the characteristic dimension.

Substituting Eq. (3) into Eq. (2) the following dimensionless condition is obtained

$$\frac{dU}{dX} = \frac{\alpha}{\sigma} (\sigma^2 U - 1). \quad (4)$$

Assuming that values of the dimensionless slip velocity, the derivative of the dimensionless slip velocity on the boundaries dU/dX and the dimensionless parameter of the permeability are known, the slip coefficient can be determined from the following formula

$$\alpha = \frac{\sigma \frac{dU}{dX}}{\sigma^2 U - 1} \quad (5)$$

In such approach in which the slip constant is determined by means of the numerical simulation the permeability of the porous medium is calculated independently. Thus two independent numerical experiments are needed. In both numerical experiments the porous medium is modeled by a bundle of a regular fibers. The radius of the fibers is equal to a , and the distance between the fibers is equal to $2b$. In the first experiment the considered bundle of fibers is infinite in all directions (Fig. 1). Because of the symmetry that fluid flow can be considered in the repeating part of the region (Fig. 2) and the permeability of the porous medium can be determined. In the second experiment a regular bundle of fibers is located between two parallel walls (Fig. 4). However the porous medium is located only in one half of this channel. Fluid flow is considered only in the repeating element of the considered channel (Fig. 6). The slip velocity U and the derivative dU/dX on the boundary can be calculated. Then the slip constant is determined from Eq. (5).

3 THE MICRO STRUCTURAL BOUNDARY VALUE PROBLEMS FOR DETERMINATION OF THE PERMEABILITY

In this section a porous medium modeled by a regular array of parallel fibers is considered. Square, triangular and hexagonal arrays of fibers (see Fig. 1) are analyzed.

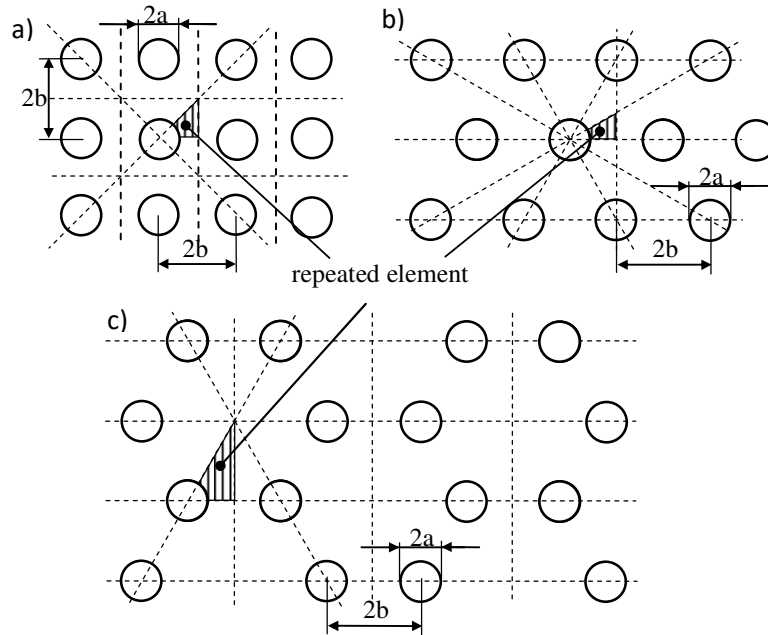


Fig. 1. Unbounded porous medium: (a) square array, (b) triangular array, (c) hexagonal array.

One of the basic method for determination of the permeability of the porous medium is an experiment in which the flow rate is measured. In the present paper the solution is obtained using the special purpose Trefftz functions [3, 4]. This method is semi-analytical. That means, that

application of the method gives analytical form of the dimensionless permeability of the porous medium.

Let us consider steady, fully developed, laminar, isothermal flow of an incompressible viscous fluid driven by a constant pressure in a system of regular parallel fibers. The flow is longitudinal with respect to fibers. In such case the equation of motion is reduced to a single partial differential equation in the polar coordinate system by

$$\frac{\partial^2 w}{\partial r^2} + \frac{1}{r} \frac{\partial w}{\partial r} + \frac{1}{r^2} \frac{\partial^2 w}{\partial \theta^2} = \frac{1}{\mu} \frac{dp}{dz}, \text{ in } \Omega_F \quad (6)$$

where w is the velocity component in the z -axis direction [m/s], dp/dz is the constant pressure gradient [Pa/m], μ is the viscosity of the fluid [Pa·s], and Ω_F is the fluid domain.

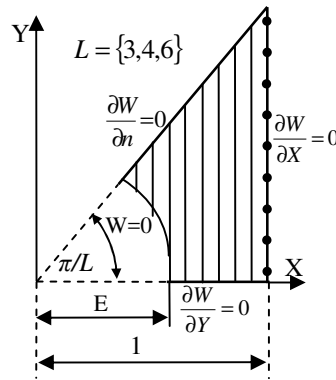


Fig. 2. Repeated element Ω_F of unbounded porous medium.

It is convenient to introduce the dimensionless variables

$$W = -\frac{w}{b^2 \frac{dp}{dz}}, \quad R = \frac{r}{b}, \quad E = \frac{a}{b}. \quad (7)$$

Now, the governing Eq. (6) has the form

$$\frac{\partial^2 W}{\partial R^2} + \frac{1}{R} \frac{\partial W}{\partial R} + \frac{1}{R^2} \frac{\partial^2 W}{\partial \theta^2} = -1, \quad (8)$$

and is solved with the boundary conditions

$$W = 0 \text{ for } R = E, \quad (9a)$$

$$\frac{\partial W}{\partial \theta} = 0 \text{ for } \theta = \begin{cases} 0, \\ \pi/L, \end{cases} \quad (9b)$$

$$\frac{\partial W}{\partial X} = 0 \text{ for } X = 1, \quad (9c)$$

The fiber volume fraction is given by

$$\varphi = \frac{\Omega_P}{\Omega_T} = \frac{\pi \cdot E^2}{L \cdot \tan\left(\frac{\pi}{L}\right)}. \quad (10)$$

where $\Omega_T = 0.5 \tan(\pi/L)$ is the total area of the repeated element (the fluid and the fiber areas together) and $\Omega_P = 0.5 E^2 \cdot \pi/L$ is the area of the fiber in the repeated element (Fig.2).

The exact solution of Eq. (8) can be expressed using the special purpose Trefftz functions

$$W(R, \theta) = -\frac{1}{4}(R^2 - E^2) + \sum_{k=1}^{N-1} B_k \left(R^{Lk} - \frac{E^{2Lk}}{R^{Lk}} \right) \cos(Lk\theta) + B_N \ln\left(\frac{R}{E}\right), \quad (11)$$

The solution (11) satisfies exactly the boundary conditions (9a)–(9b). The unknown coefficients B_k ($k = 1, \dots, N$) are determined by solving the system of linear equations resulting from satisfying of the boundary condition (9c) using the boundary collocation technique [5, 6]. Using the definition of the non-dimensional velocity (7) and introducing the fiber volume fraction (10) the longitudinal component of the filtration velocity can be expressed as

$$q_z = -\frac{b^2}{\mu} F(\varphi) \frac{dp}{dz}, \quad (12)$$

where

$$F(\varphi) = \frac{k}{\beta \cdot b^2} = \frac{\iint_{\Omega_F} W(X, Y) dXdY}{\beta \cdot \Omega_T} = \frac{2}{L \tan\left(\frac{\pi}{L}\right)^2} \int_0^{\frac{\pi}{L} \sec(\theta)} \int_E W \cdot R dR d\theta \quad (13)$$

is the non-dimensional component of the permeability tensor in the direction parallel to the fibers, $\Omega_F = \Omega_T - \Omega_P$ is the region occupied by the fluid in the repeated element (Fig. 2). A dimensionless parameter of the porous medium is calculated as $\beta = L \tan(\pi/L)$.

After analytical integration in Eq. (13) the dimensionless permeability is a function of the number of collocation points N and can be calculated from

$$F = \left(\frac{E^2}{4} - \frac{1}{12} - \frac{1}{24 \cos\left(\frac{\pi}{L}\right)^2} \right) - \frac{\pi E^4}{8L \tan\left(\frac{\pi}{L}\right)} + \frac{2}{\tan\left(\frac{\pi}{L}\right)} \sum_{k=1}^{N-1} B_k \left[\frac{H_k E^{2Lk}}{Lk - 2} + \frac{G_k}{Lk + 2} \right] + B_N \left[\ln\left(\frac{1}{E \cos\left(\frac{\pi}{L}\right)} \right) - \frac{3}{2} \right] \quad (14)$$

where

$$H_k = \frac{\sin\left[(1 - Lk)\frac{\pi}{L}\right]}{(1 - Lk) \left[\cos\left(\frac{\pi}{L}\right) \right]^{1-Lk}}, \quad G_k = \frac{\sin\left[(1 + Lk)\frac{\pi}{L}\right]}{(1 + Lk) \left[\cos\left(\frac{\pi}{L}\right) \right]^{1+Lk}}. \quad (15)$$

The value of the dimensionless permeability as a function of the fibers volume fraction is presented in Fig. 3. Permeability $F(\varphi)$ for all types of fiber arrays is similar and substantially different for $\varphi > 0.3$. The problem was solved for $N = 7$ collocation points on the boundary. The

numerical results (marks) are compared with the analytical presented by Drummond and Tahir [7] (line). Compatibility between the results is great.

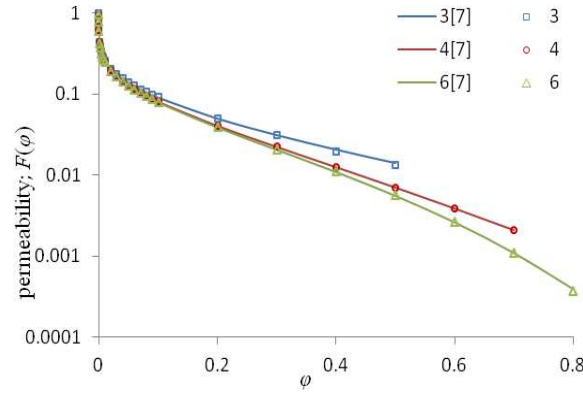


Fig. 3. The non-dimensional component of the permeability tensor in the direction parallel to the fibers. The numerical results (marks) compared with the analytical solution (line).

4. THE MICRO STRUCTURAL BOUNDARY VALUE PROBLEMS FOR DETERMINATION OF THE SLIP CONSTANT

After determination of the permeability, the microstructural flow in the layer of porous medium can be considered (Fig. 4).

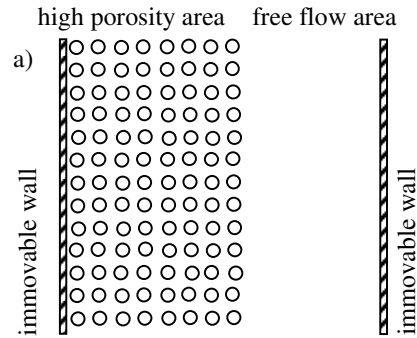


Fig. 4. Porous medium with very high porosity in the presence of free fluid region between two impermeable walls.

Let us consider a layer of the porous medium located between two fixed plates (Fig. 4). The problem is governed by the dimensionless Poisson equation

$$\frac{\partial^2 W}{\partial R^2} + \frac{1}{R} \frac{\partial W}{\partial R} + \frac{1}{R^2} \frac{\partial^2 W}{\partial \theta^2} = -1 \quad (16)$$

with the no-slip boundary conditions: $W = 0$ on the immovable wall.

Since the array of fibers is streaked and periodic in one direction it is sufficient to consider the problem only in one repeated strip which is depicted in Fig. 5. In all cases the repeated strip is divided into smaller elements associated with each of the fibers which are called large finite elements.

The boundary between the porous and fluid regions is located for $X = H$. The value of slip velocity U and the derivative dU/dX at this boundary can be calculated by numerical integration.

The slip constant can be determined from Eq. (5) where $\sigma = \frac{1}{\sqrt{\beta \cdot F}}$ is the permeability

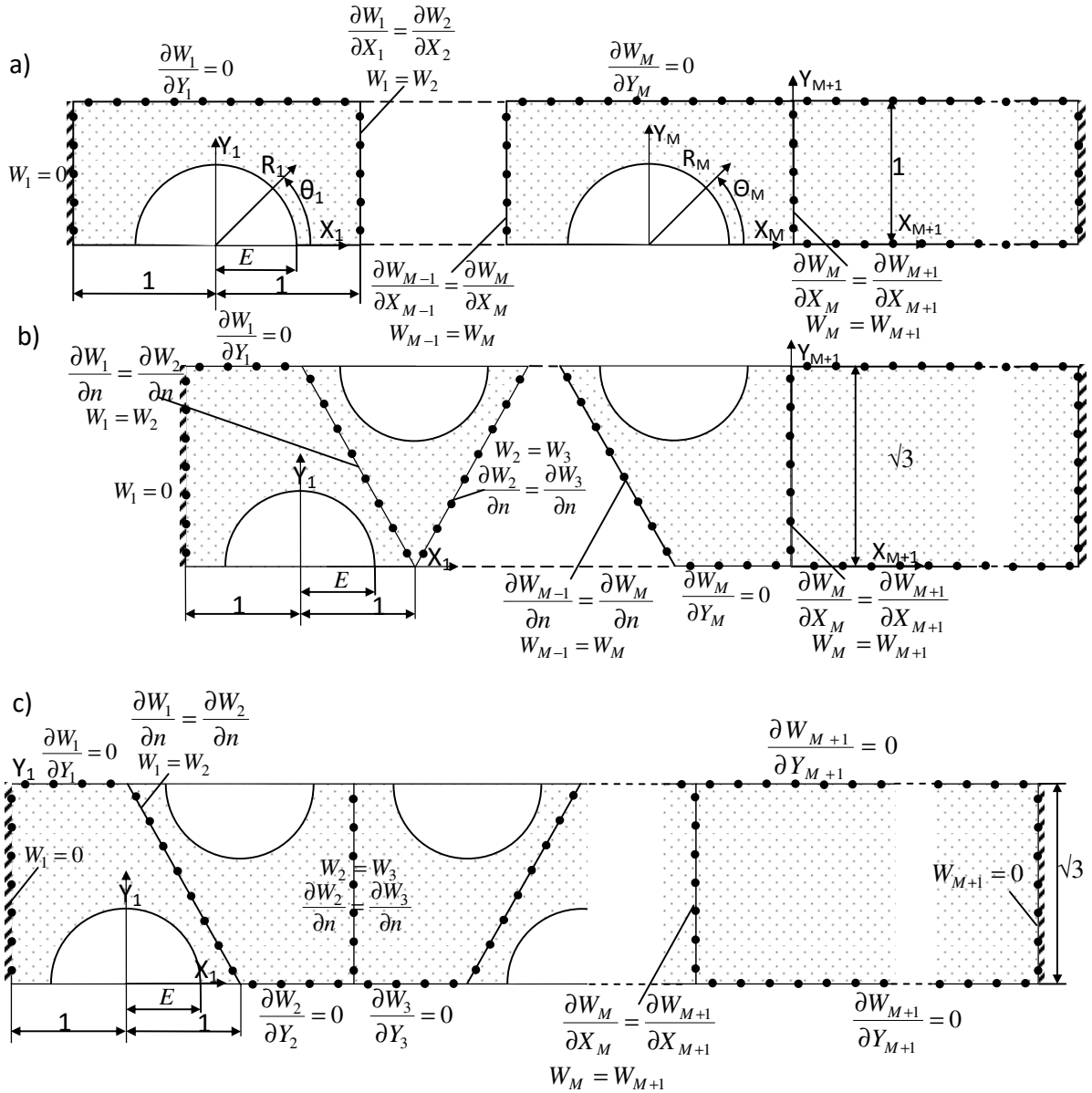


Fig. 6. The repeating part of the considered region with the boundary and contact conditions for square (a), triangular (b) and hexagonal array (c)

5. NUMERICAL RESULTS AND DISCUSSION

In the first part of the numerical experiment the value of the dimensionless effective permeability as a function of the fibers volume fraction is calculated. The results are presented in Fig. 3. In that case 7 collocation points and the same number of trial function are used.

In the next part the slip constant on the boundary is determined for 10 rows. The width of the porous and free flow area were the same and equals to $H = 2 \cdot LR$ for square, $H = 3 \cdot LR$ for hexagonal and $H = 1 + LR$ for triangular array, where LR is the number of rows of fibers. For each single edge of the repeated element we chosen $Mc = 4$ collocation points. For the upper and lower edge of free flow area the number of collocation points are calculated by the formula $H \cdot Mc / 4$. The total number of collocation points for the free flow area was equals $Nc = 2 \cdot (H \cdot Mc / 4 + 2)$. The total number of collocation points for the porous area was equals $Nc = 2 \cdot LR \cdot Mc$ for square, $Nc = 2 \cdot Mc(LR + 1)$ for triangular and $Nc = 6 \cdot Mc \cdot LR$ for hexagonal array.

Figure 7 shows the slip constant, α as a function of the volume fraction of fibers, ϕ . The value of the slip constant is lower than 1.0 and decreases with increasing the volume fraction of fibers for the high porosity. For the hexagonal and square array of the fibers, α increases for a large share of fibers ϕ . For the triangular array the α decreases also for a low porosity.

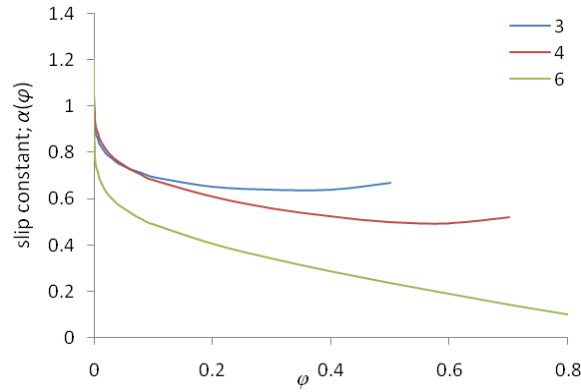


Fig. 7. The slip constant α as a function of the fiber volume fraction ϕ for square (4), triangular (6) and hexagonal (3) array of fibers for $LR = 10$, $Mc = 4$

The effect of the number of rows of the fibers LR on the value of the effective permeability for the triangular, square and hexagonal array was examined. Figure 8 shows the obtained numerical results. The influence of the number of the fibers rows is significant and its effect disappears for LR equal to 12. The influence of the number of the fibers rows is more significant for the porous medium with high porosity (small ϕ). For small value of the volume fraction of fibers, ϕ just four rows of the fibers are sufficient for determining the slip constant, α .

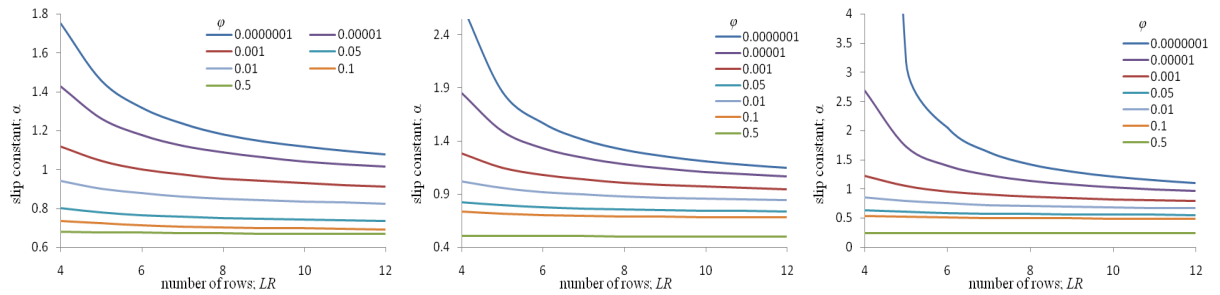


Fig. 8. Influence of the number of rows at a slip constant for a hexagonal, square and triangular array of fibers

6. CONCLUSIONS

In this paper the permeability and the slip constant on the boundary of the considered region were determined by numerical simulation of the imaginary physical experiment. The porous medium was modeled by a parallel bundle of straight fibers arranged in a regular triangular or square array. In order to determine the permeability, the flow driven by the pressure gradient in an unbounded porous medium was considered. To determine the slip constant, the shear flow between a flat immovable wall containing both the porous and free flow layers was considered. In both numerical simulations, the Trefftz method with the special purpose Trefftz functions and trial functions was applied. In all considered cases the value of the slip constant is lower than one. The slip constant decreases with increasing the volume fraction of fibers for a high porosity. For a square and hexagonal array the value of slip constant starts increasing for small porosity. For the same volume fraction of the fibers, both the permeability and the slip constant for the triangular array is smaller than for the square and the hexagonal array. The number of collocation points has inconsiderable effect on the simulation results. To determine the permeability a few collocation points are enough to get an accurate result ($Mc = 4$). More visible influence has the number of rows, especially for high porosity. For all the cases 10 rows of fibers is sufficient to determine the slip constant. Proposed algorithm is easy to implementation, accurate and is mesh free.

ACKNOWLEDGMENTS

This work was supported by the grant 2015/19/D/ST8/02753 from the National Science Center, Poland.

REFERENCES

- [1] G. S. Beavers and D. D. Joseph, Boundary conditions at a naturally permeable wall, *J. Fluid Mech.*, 30 (1967) 197-207.
- [2] Trefftz E.: Ein Gegenstück zum Ritzschen Verfahren, *Proceedings of the 2nd International Congress of Applied Mechanics (Zurich)*, Orell Fussli Verlag (1926): 131-137.
- [3] J.A. Kolodziej and W. Dudziak, The determination of the stationary incompressible laminar viscous flow past a hexagonal lattice parallel cylindrical bars by means of boundary collocation (in Polish), *Archiwum Budowy Maszyn* (1979) 26:101-114.
- [4] J.A. Kolodziej, Influence of the porosity of a porous medium on the effective viscosity in Brinkman's filtration equation, *Acta Mech.* (1988) 75:241-254.
- [5] G. Fairweather and A. Karageorghis, The method of fundamental solutions for elliptic boundary value problems, *Adv. Comput. Math.* (1998) 9:69-95.
- [6] J.A. Kolodziej and A.P. Zieliński, *Boundary Collocation Techniques and their Application in Engineering*, WIT Press, Southampton (2009).
- [7] J.E. Drummond and M.I. Tahir, Laminar viscous flow through arrays of parallel solid cylinders. *Int. J. Multiphase Flow* (1984) 10:515-540.

Maximum Entropy-based Uncertainty Modeling at the Finite Element Level

Marc Mignolet^{*}, Pengchao Song^{**}

^{*}Faculties of Mechanical and Aerospace Engineering, Arizona State University, ^{**}Faculties of Mechanical and Aerospace Engineering, Arizona State University

ABSTRACT

A novel approach is proposed for the modeling of uncertainties in finite element models of linear structural or thermal problems. This uncertainty is introduced at the level of each finite element by randomizing the corresponding elemental matrices (e.g., mass, stiffness, conductance) using maximum entropy concepts. In performing this randomization, it is first recognized that elemental matrices corresponding to different elements cannot be simulated independently of each other. Doing so would induce very high spatial frequency variations which are unphysical. Rather, it is proposed here to adopt the matrix field modeling proposed in [1] which views each randomness generating matrix as the transformation of a zero mean, unit variance Gaussian field with a specified, parametrized stationary autocorrelation function. The second requirement is that the correlation between random elemental matrices of neighboring finite elements implied by the above algorithm must be reflected on every component of the assembled matrix. That is, if a strong correlation is expected between two different finite elements, then there must exist a similarly strong correlation between the components of their elemental matrices as they are added together in the construction of the global matrix. Since the elemental matrix is built from independent fields, this condition can be satisfied if: (1) the elemental matrices of the mean and uncertain models are expressed in the same (i.e., global) frame of reference, and (2) each simulated sample of the random global matrix is independent of the ordering of the nodes in each element. The proposed approach is characterized by a limited set of parameters, one expressing the overall level of uncertainty with the rest characterizing the correlation structure underlying the random elemental matrices. It is exemplified on a structural example and the effects of the overall uncertainty level and correlation length of the random elemental matrices are analyzed. [1] C. Soize, Non-Gaussian positive-definite matrix-valued random fields for elliptic stochastic partial differential operators. Computational Methods in Applied Mechanics and Engineering, 195, pp. 26-64, 2006.

Analysis of Elliptical and Semi-Elliptical Fatigue Crack Propagation

Yozo Mikata*

*Bechtel

ABSTRACT

The fatigue crack propagation of a 3D crack is investigated under a uniform loading. As for crack geometry, an elliptical crack and a semi-elliptical crack are considered. The focus of this paper is to solve a pair of coupled differential equations derived from Paris law. Stress intensity factors are approximate except for an elliptical crack in an infinite body, for which an exact result is available. The approximate stress intensity factors used for semi-elliptical cracks are based on an empirical equation given in Newman and Raju.

Mechanically-evoked ATP Release is Regulated by Facilitated Membrane Resealing in Murine Osteoblasts

Nicholas Mikolajewicz*, Elizabeth Zimmerman**, Bettina Willie***, Svetlana Komarova****

*McGill University, **Shriners Hospital for Children, Canada, ***McGill University, ****McGill University

ABSTRACT

Mechanical environment is an important determinant of bone health. ATP release is one of the first events induced by mechanical stimulation of bone-forming osteoblasts and bone-resident osteocytes; however, the dominant pathways of ATP release remain disputed. We examined the mechanism of ATP release from mechanically-stimulated compact bone or bone marrow-derived osteoblasts. We demonstrated that 70 ± 24 amol ATP/cell were released in response to single cell membrane deformation and 21 ± 11 to 422 ± 97 amol ATP/cell in response to turbulent fluid shear stress. Mechanical stimulation induced exocytosis of quinacrine-positive ATP-containing vesicles. Pharmacological activation of protein kinase C (PKC) potentiated vesicular exocytosis, while PKC inhibition reduced exocytosis. Unexpectedly, increase in vesicular release coincided with a significant decrease in released ATP, and vice versa. To examine the contribution of injury to ATP release, we evaluated membrane integrity during and after mechanical stimulation using membrane impermeable markers. We demonstrated that in vitro or in vivo mechanical stimuli induced magnitude-dependent repairable cell membrane injury. Ca^{2+} /PLC/PKC-dependent vesicular release was critical for successful repair of membrane damage, suggesting that rather than delivering ATP to extracellular space, vesicular exocytosis limits the much larger efflux of intracellular ATP through damaged membranes. Prior activation of PKD/vesicular signaling improved membrane integrity and limited ATP release induced by subsequent mechanical stimulation. Our study suggests a new model of biological adaptation to mechanical forces that combines graded perception of mechanical environment through membrane injury and an ability to effectively counteract the destructive potential of mechanical forces through membrane repair.

Computational Investigation of a Blast Loaded Surrogate Head Model with Application Towards Traumatic Brain Injury

Scott Miller^{*}, Candice Cooper^{**}, Paul Tayloer^{***}, Adam Willis^{****}, Ricardo Mejia-Alvarez^{*****}

^{*}Sandia National Laboratories, ^{**}Sandia National Laboratories, ^{***}Sandia National Laboratories, ^{****}San Antonio Military Medical Center, ^{*****}Michigan State University

ABSTRACT

Blast-induced Traumatic Brain Injury (bTBI) is a signature wound of modern warfare and can leave victims at risk for persistent neurologic/behavioral symptomatology, including headaches, sleep disorder, cognitive impairment and mood disturbance. Clinical experience and neuropathologic analysis has identified some unique features of this injury: injury to the blood vessels at both large and small length scales manifesting with brain swelling, subarachnoid hemorrhage or pseudoaneurysm, vasospasm, and astroglial scarring at multiple intracranial interfaces. The mechanisms and thresholds of these injuries are not yet understood mechanically. In this talk, we discuss an on-going project whose goal is to build a model which reproduces the human intracranial injury after blast exposure in order to isolate the mechanism(s) of injury. A surrogate head model was developed and tested experimentally. Computational simulations were performed that coupled an Eulerian shock-physics model of the incident blast to a Lagrangian finite element model of the test object. We will present the coupling methodology and our current results. Particular emphasis is placed on cavitation modeling and resolution near fluid-structure interfaces.

Computational Framework for Assessment of Injection-based Drug Delivery

David Milner*, Prateek Dixit**, John Mould***, Mahesh Kailasam****

*Thornton Tomasetti, **Thornton Tomasetti, ***Thornton Tomasetti, ****Thornton Tomasetti

ABSTRACT

Delivery of drugs via injection is a widely and long-used method to administer continuous and low dose drug treatments. With the advent of new types of drugs such as biologics, the increased usage of self-administered injections, and other developments, there is increasing need for a more systematic evaluation of delivery mechanisms. Such evaluations can facilitate more precise specification of drug delivery location and rate, selection of the most appropriate needle type, and reduction of pain. These issues have traditionally been investigated via laboratory experiments, analytical assessments, and clinical trials. Advances in computational modeling, however, now facilitate virtual testing which is rapid, cost-effective, and provides more insights than are available through traditional physical testing. With these benefits, computational modeling is becoming increasingly attractive, especially when used in combination with advances in imaging technologies. In this study, a systematic computational framework is developed to understand various mechanisms involved in drug injection. Using the finite element method, coupled pore pressures and tissue stresses are computed to predict bolus growth, including advancement of the wetting fronts and the corresponding tissue strains, as the drug perfuses through tissue. The computational methodology is first validated by comparing computed bolus growth to experimental data obtained by x-ray/CT imagery of porcine tissue injected with fluids such as saline (Kim, 2017) or insulin; multiple injection rates, needle types, and tissue types are considered. Once validated, various parameters are modified, including the volume, viscosity, and injection rate of the perfusate, and the permeability, porosity, and mechanical properties of the tissue. The effects of these parameters on bolus size, shape, and growth are assessed. Tissue stresses and strains are also computed and compared as a measure of relative pain. (Finocchietti, 2012) Insights provided by this framework will allow both the development and selection of more effective delivery methodologies depending on patient characteristics and other care requirements. References Kim, Hyejeong; Park, Hanwook; Lee, Sang Joon. Effective method for drug injection into subcutaneous tissue. Scientific Reports 7: 9613, 2017 Finocchietti, Sara; Takahashi, Ken; Okada, Kaoru; Watanabe, Yasuharu; Graven-Nielsen, Thomas; Mizumura, Kazue. Deformation and pressure propagation in deep tissue during mechanical painful pressure stimulation. Medical &&& Biological Engineering &&& Computing, Volume 51 (2), 2012

Stress-constrained Multi-Material Topology Optimization Considering Thermal Expansion

Seungjae Min^{*}, Youngsuk Jung^{**}

^{*}Department of Automotive Engineering, Hanyang University, Seoul, Korea, ^{**}Department of Automotive Engineering, Hanyang University, Seoul, Korea

ABSTRACT

This paper presents a stress-based topology optimization method of the multi-material structure by considering thermal expansion. As the use of multiple materials increases with the demand for lightweight structure design, the design with mixed-materials using welding and adhesion is increasing. However, the different thermal expansion between dissimilar materials make the unexpected stress increments in the interface area, and it could lead to the product failure and to decrease performance. Deaton [1] suggest the single material thermal structures with a stress constraint using topology optimization, and Tong [2] suggest the multi-material thermal structure design for the compliance minimization problem. However, the multi-material design and the stress constraints were not considered simultaneously, and only single temperature condition was allowed for each optimum design. In this paper, we perform a multi-material topology optimization with the stress constraints for various temperature conditions. We formulate the optimization problem that minimizes the weight with the stiffness performance and the stress constraints of each material. For the validation of the proposed method, the design example of an automotive component with the operating temperature range -40° to +85° was considered. For the stable optimization of the design-dependent loads, the RAMP (Rational Approximation of Material Properties) model is adopted to interpolate of material properties such as elastic modulus and thermal expansion coefficient. From the design example results, we can find that the optimum result has different layouts depending on the set of temperature conditions, and we can get a robust design against the temperature change by taking into account the multiple temperature conditions. [1] J. D. Deaton and R. V. Grandhi, "Stress-based design of thermal structures via topology optimization", Struct. Multidisc. Optim., 2015 [2] G. Tong et al., "Topology optimization of thermo-elastic structures with multiple materials under mass constraint", Struct. Multidisc. Optim., 2016

DEM Simulations for the Investigations of the Mechanochemical Activation of Copper Ores

Masaya Minagawa^{*}, Shosei Hisatomi^{**}, Tatsuya Kato^{***}, Giuseppe Granata^{****}, Chiharu Tokoro^{*****}

^{*}Graduate School of Creative Science and Engineering, Waseda University, ^{**}Graduate School of Creative Science and Engineering, Waseda University, ^{***}Graduate School of Creative Science and Engineering, Waseda University, ^{****}Faculty of Science and Engineering, Waseda University, ^{*****}Faculty of Science and Engineering, Waseda University

ABSTRACT

The high demand of copper has been pushing the copper industry to process low-grade ores. For this reason, the developments of new technologies able to promote the dissolution of copper from refractory ores are highly anticipated. The mechanochemical activation is a phenomenon resulting in the enhancement of leachability of metal minerals due to the transfer of large amounts of energy through high-intensity grinding operations. The enhancement can be result of a decrease of the particle size and/or the consequence of induced transformation of the crystal structure. Although the occurrence and the effectiveness of this phenomenon towards the enhancement of leaching have been proved, its quantitative relation to provided mechanical energy is not fully elucidated. In this study, we elucidated the mechanism of mechanochemical activation of covellite with two types of dry grinding technologies: vertical stirred ball milling and planetary ball milling. We performed grinding experiments under different operating conditions and then DEM simulations to assess the collision energy involved in the grinding process. Following this step, we carried out leaching experiments by sulfuric acid to determine the leaching rate constant to be related to the collision energy of grinding. DEM simulations were performed with considering both collisions of grinding media and grinded particles. XRD and XAFS results after grinding revealed the partial amorphization of covellite by intensifying the grinding conditions. As a consequence, the leaching of samples grinded under more intense conditions resulted into higher leaching rate constants. In order to understand whether the increase was due to a simple increase of surface area or due to an induced-transformation of the crystal structure of covellite, we performed a correlation between collision energy and leaching rate-constants. The rate constants had a unique correlation to the collision energy calculated by DEM for the two different mills. The correlation between leaching rate constant and collision energy exhibited a sudden increase of the rate constant beyond 0.25 J/mol?sec. This increase can be considered as a consequence of the occurred mechanochemical reaction previously confirmed by XRD results.

3D-Printable Soft-Actuator Composites

Aslan Miriyev*, Hod Lipson**

*Columbia University in the City of New York, **Columbia University in the City of New York

ABSTRACT

One of the main gaps in conventional robotics is the lack of compliance, resulting in poor human-robot interface, thus preventing the ability of humans to work side by side with robots. Soft-material robotics is an emerging domain aiming to provide compliant robots, allowing soft-bodied locomotion and soft touch. The main challenge in soft robotics is development of multi-functional materials, combining actuation and sensing with computerized control. I will demonstrate a new-developed compact approach, allowing to replace conventional motors and existing massive soft-actuation devices by self-contained 3D-printable composite materials. Specifically, I will present a silicone/ethanol composite material, capable of exhibiting actuation stress and strain exceeding those of natural muscles. The working mechanism, properties and performance of the soft-actuator composites, as well as their fabrication by 3D-printing, will be discussed.

Reduced Order Modeling of Coronary Blood Flow

Mehran Mirramezani*, Shawn Shadden**

*UC Berkeley, **UC Berkeley

ABSTRACT

Reduced-order modeling (ROM) of blood flow offers the possibility to study hemodynamics of large cardiovascular networks with negligible computational cost. A basic approach is to use lumped-parameter (LP) models, which describe regional pressure-flow relationships in vascular beds. The accuracy of such models may become questionable for resolving hemodynamics at individual-artery-scale especially when complex flow features are present. The goal of this study is to compare and develop ROM to capture pressure and flow dynamics in the coronary arteries. To model coronary hemodynamics, we developed 3D time-dependent (3D+t) fluid structure interaction (FSI) simulations and 3D+t rigid wall (CFD) simulations as gold standards. Minimal difference was observed between 3D-FSI and 3D-CFD. We then considered ROM starting from 2D “multiring” method and then classical 1D formulations. As an alternative to these PDE models, we developed a novel distributed LP approach, that assigns a net effective resistance to each vascular segment by considering various sources of energy dissipation. We sought two main objectives. The first was a fully LP-type model that could resolve vessel-level hemodynamics throughout the coronaries with minimal computational cost. The second was the specific ability compute transstenotic pressure drop and fractional flow reserve (FFR) in diseased coronaries, since such information is highly relevant to clinical diagnosis of coronary artery disease (CAD) and a major driver of coronary modeling. We considered a series of image-based models that included major coronary arteries. We considered patient-specific models with CAD, without CAD, and synthetically generated lesions to enable systematic exploration. We first considered the ability of ROM to accurately predict FFR by considering ROM of only the stenotic artery, and then we then considered ROM of the entire aortic-coronary complex. For computation of transstenotic pressure drop and FFR, major differences were observed between 3D and 2D and 1D models. Major differences were also observed between algebraic models; however, a particular algebraic model was found to have strong agreement with 3D simulations, including for patient-specific stenoses. We next considered the ability of a fully LP-type framework to accurately predict pressure and flow throughout the coronary tree. We developed a quasi-LP approach that demonstrated strong agreement with fully 3D+t simulations. Average errors in pressure at coronary outlets were $\leq 3\%$, including arteries with significant stenosis. The developed framework as made fully automated and requires ≤ 10 sec runtime on a desktop computer. These results support the notion that an appropriately-derived LP framework may provide high diagnostic value for coronary modeling.

Reinforcing and Scattering Reduction for Flexural Vibrations in a Rectangular Lattice

Diego Misseroni^{*}, Davide Bigoni^{**}, Alexander B. Movchan^{***}

^{*}DICAM, Univeristy of Trento, Italy, ^{**}DICAM, University of Trento, Italy, ^{***}University of Liverpool, UK

ABSTRACT

A novel concept has been introduced and tested for reduction of the scattering by faults in a flexural lattice. The majority of the relevant published works are based on the so-called “cloaking transformation”. This approach originally came from electromagnetism and optics, and is linked to the Maxwell system of equations or, in special cases, to the Helmholtz equation. In the present work, we address an elastic system and apply a different principle, concerning a reinforcement of the boundary and a redistribution of mass. We demonstrate that this approach, which is simple in nature, enables one to significantly reduce the coefficients in the multipole expansion of the scattered field. Accurate numerical simulations and a quantitative analysis of the scattered fields for ‘cloaked’ and uncloaked faults are provided. A constructive simple algorithm has been proposed and verified through numerical simulations in a wide range of frequencies. The results are accurate and supplied with evaluation of the Fourier coefficients on two circular contours enclosing the square hole in the lattice, which shows a significant reduction of the scattered field for the case of a hole, with the appropriately reinforced boundary and redistributed mass. This method can also be considered an ‘approximate cloaking’, and being simple in nature it is appealing in a range of practical applications involving flexural waves in plates with defects.

A Statistical Learning Based Characterization of Lithium-Ion Battery Electrodes

Aashutosh Mistry^{*}, Chance Norris^{**}, Partha Mukherjee^{***}

^{*}Purdue University, ^{**}Purdue University, ^{***}Purdue University

ABSTRACT

With recent advances in X-ray tomography based imaging, lithium-ion battery electrode microstructures can be probed with sufficient resolution. Such porous electrode structures, obtained from 3D X-ray imaging, exhibit spatial heterogeneity, which requires appropriate representative volume element (RVE) delineation for analyzing the influence of interface and transport properties, which in turn affect the electrochemical performance. For example, a typical electrode volume imaging based on X-ray tomography, may contain several RVEs, which can be analyzed to build a correlation among structural features and effective properties. This statistical learning map can be used to further analyze microstructural variations. In this work, statistical learning based characterization is presented for tomographed datasets of Li-ion battery electrodes, including a discussion on the microstructural variabilities emanating from processing conditions.

SAND2017-13837 A: Upscaling Microstructural Effects by Combining Local/Nonlocal Models

John Mitchell*

*Sandia National Laboratory

ABSTRACT

Shock wave propagation in solids has a long history [1], yet modeling microstructure effects for weak shocks remains elusive. Aggregate effects of grain size and shape, residual stresses, and grain orientations cause shock fronts to spread; non-uniform states of shear stress occur at grain size length scales due to differing grain orientations and residual stresses of adjacent grains. These nonlocal effects inhibit formation of sharp elastic-plastic wave fronts. In this talk, a nonlocal peridynamic inspired yield function [2] is used to incorporate and upscale microstructure features; this function is used in conjunction with a more traditional local plasticity model. In this way, existing local computational frameworks for shock propagation are leveraged while at the same time important microstructural and nonlocal effects are incorporated. This approach is applied to microstructures arising from additive manufacturing and welding [3] where grain sizes approach macroscale (1 mm) and morphologies are non-equiaxed. Mathematical constructs for the model will be introduced and simple demonstration calculations will be presented. Time permitting, key computational aspects will be discussed. [1] Asay, James R. and Chhabildas, Lalit C. and Lawrence, Jeffery R., and Sweeney, Mary Ann. "Impactful Times," Springer, 2017. [2] Mitchell, J.A., "A non-local, ordinary-state-based plasticity model for peridynamics," Sandia National Laboratories Report SAND2011-8064, 2011. [3] Rodgers, Theron M., Mitchell, John A., and Tikare, Veena, "A Monte Carlo model for 3D grain evolution during welding", Modeling and Simulation in Materials Science and Engineering, Volume 25, Number 6, September 2017.

Parallel Simulation of Thermal Conduction in Coal Gasification Vessel Coupled with Cooling Pipe Model

Naoto Mitsume^{*}, Byungsoo Song^{**}, Tomonori Yamada^{***}, Shinobu Yoshimura^{****}

^{*}The University of Tokyo, ^{**}The University of Tokyo, ^{***}The University of Tokyo, ^{****}The University of Tokyo

ABSTRACT

Research and development with regard to advanced coal-fired power plants to reduce CO₂ emission have been conducted. Coal gasification is one of the key technologies. In reactor for the coal gasification, coal is crushed into fine particulate matter and then partially burned into gas in a high-pressure environment in the reactor. Our research group has carried out a project to tackle a coupled problem of thermo-fluid-structure interaction for quantification of its efficiency, environmental load, and structural integrity. As one of key components of the project, we present a large-scale parallel simulation of three-dimensional (3D) thermal conduction in a gasification vessel. As a parallel solver for thermal conduction, we adopt ADVENTURE_Thermal [1], which is based on the hierarchical domain decomposition method and the balancing domain decomposition preconditioner. To simulate effect of cooling pipes in the vessel, we model heat transfer in the pipe as a one-dimensional (1D) convection-diffusion equation, and develop a discontinuous Galerkin-based solver [2]. These 3D and 1D solvers are coupled by a staggered coupling scheme with a subcycling technique [3] to deal with different time increments in the 1D and 3D analyses. We perform a validation test for our proposed system for the coupled analysis and discuss parallel efficiency. [1] Mukaddes, A. M. M., Ogino, M., Kanayama, H., Shioya, R.: A scalable balancing domain decomposition based preconditioner for large scale heat transfer problems. JSME International Journal Series B Fluids and Thermal Engineering 49(2), 533-540 (2006) [2] Cockburn, B., Shu, C. W.: The local discontinuous Galerkin method for time-dependent convection-diffusion systems. SIAM Journal on Numerical Analysis 35 (6), 2440–2463 (1998) [3] Farhat, C., Lesoinne, M.: Two efficient staggered algorithms for the serial and parallel solution of three-dimensional nonlinear transient aeroelastic problems. Computer Methods in Applied Mechanics and Engineering 182(3), 499–515 (2000)

Polycrystalline Grain Growth Simulations Using the Molecular-Dynamics and Multi-Phase-Field Methods

Eisuke Miyoshi^{*}, Tomohiro Takaki^{**}, Yasushi Shibuta^{***}, Munekazu Ohno^{****}

^{*}Kyoto Institute of Technology, ^{**}Kyoto Institute of Technology, ^{***}The University of Tokyo, ^{****}Hokkaido University

ABSTRACT

During the heat treatment of a polycrystalline material, grain growth occurs after completion of solidification, allotropic transformation, or recrystallization. The ability to predict and control the microstructural evolution through grain growth is crucial for developing materials with superior mechanical properties. Therefore, in order to predict the microstructural evolution systematically, numerical simulations of grain growth have been frequently performed in recent years. Grain growth simulations are classified into two categories according to their methodologies: one is the atomic level calculations including the molecular dynamics (MD) method or phase-field crystal method. The other is the continuum model-based simulations using the phase-field method, Monte-Carlo method, vertex method, and so forth. The former can express spontaneous nucleation process, enabling successive simulation of grain growth and its preceding phenomena such as solidification. However, owing to the large computational cost, it is difficult to simulate grain growth until the late stage. On the other hand, the continuum-based methods allow for relatively efficient computations. In particular, the multi-phase-field (MPF) method [I. Steinbach and F. Pezzolla, *Physica D*, 134 (1999) 385], which is an extension of the phase-field method to multi-phase and polycrystalline systems, is widely employed as the most powerful tool capable of simulating grain growth with accuracy and efficiency; however, the MPF method requires some assumption to reproduce nucleation process, and the simulated results are strongly dependent upon the used assumption. The purpose of this study is to enable comprehensive prediction of the microstructural evolutions from nucleation to late-stage grain growth by using the MD and MPF methods successively; in this framework, nucleation process is simulated by the MD method, and the obtained microstructure is used as the initial structure for MPF grain growth simulation. To this effect, we propose a novel method to convert MD-generated atomic configurations into phase-field profiles. In addition, MPF and MD grain growth simulations are directly compared using the proposed method, through which the accuracy of the MPF simulation is examined.

CONSTRUCTION OF DAMAGE OBSERVATION SYSTEM FOR BOTH STRUCTURAL AND NON-STRUCTURAL MEMBERS WITH OVERLAYING

YASUNORI MIZUSHIMA*, YOICHI MUKAI^{†1}, YASUYUKI NAGANO^{†2}

* Takenaka Corporation

1-5-1, Ohtsuka, Inzai-shi, Chiba, 270-1395, Japan

E-mail: mizushima.yasunori@takenaka.co.jp

^{†1}Kobe University

1-1, Rokkodai-cho, Nada-ku, Kobe, 657-8501, Japan

E-mail: ymukai@port.kobe-u.ac.jp

^{†2} Graduate School of Simulation Studies, University of Hyogo

7-1-28, Minatojima-Minamimachi, Chuo-ku, Kobe 650-0047, Japan

E-mail: nagano@sim.u-hyogo.ac.jp

Key words: Structural Analysis, Large-Scale Model, FEM Analysis.

Abstract. This study presents the first step in the development of a visualization system that would predict simultaneously the expected entire seismic damage of both structural and non-structural members, such as non-structural walls and ceilings, in building, by superposing seismic analytical results of non-structural members on those of structural members. A large-scale FE structural analysis of a building was conducted to evaluate structural damages and to extract local responses that will be used to evaluate non-structural damages on the building.

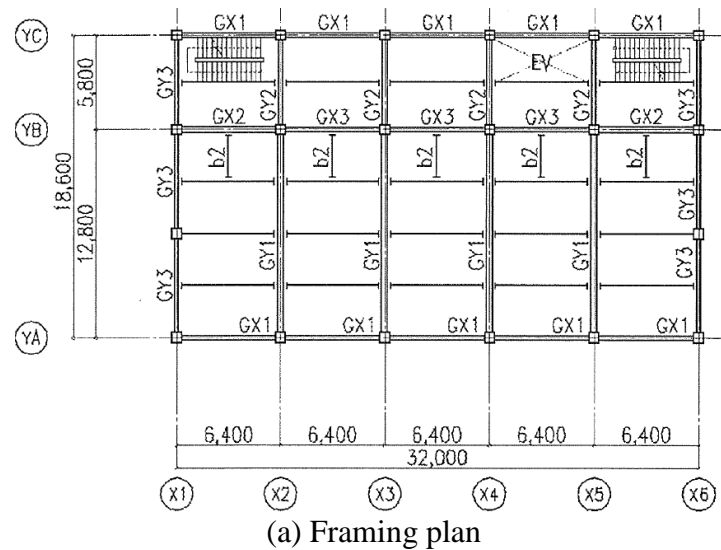
1 INTRODUCTION

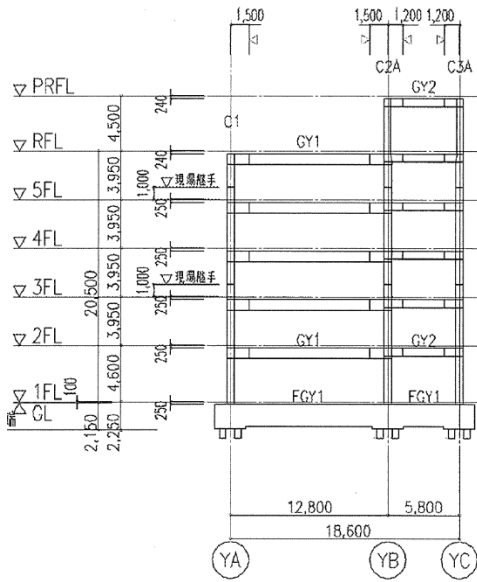
This study aims to develop a system that can show the seismic damage undergone by structural and non-structural members at the same time. Past seismic damage examples showed that harms on humans had been caused by not only structural damages but also by damages of non-structural members. Whereas safety of structural members is constantly confirmed in the structural design process of buildings, there is no detailed process for safety of non-structural members as they are made by specification design without any consideration to their locations. In order to reduce damage to non-structural members that may harm humans, non-structural members should be designed considering local seismic responses. To accurately evaluate local seismic responses of non-structural members, it is necessary to accurately evaluate seismic responses of structural members on which non-structural members are attached.

In this study, the structural damage in a building was evaluated accurately by using detailed finite element (FE) model of all structural members of the building. The authors showed, in a previous study, that a detailed and entire FE model of the building structure simulated accurately the actual seismic behavior of the building^[1]. By the detailed FE model, local seismic responses of the structural parts on which non-structural members were connected could be extracted because the original shapes of all the structural members were reproduced as precisely as possible in the model. The local responses could be used to evaluate the seismic damage to the non-structural members.

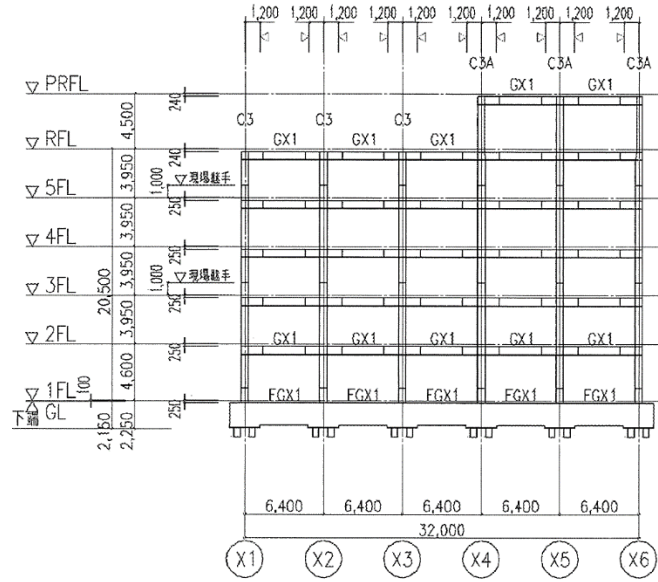
2 ANALYTICAL TARGET BUILDING^[2]

An analytical target is shown in Fig. 1. The building was a 7-story (include Pent house), 5-bay in X-direction and 3-bay in Y-direction. The columns were made of square tube(BCR295) and beams were made of H-shaped steel. The properties of columns are listed in Table 1, and those of beams are listed in Table 2.





(b) Framing elevation 1



(c) Framing elevation 2

Fig.1 Structural drawings of analytical target building

Table 1 Section list of columns

	C1	C2, C2A	C3, C3A	C4
RF		B-460×16	B-460×16	-
5F	B-500×22	B-500×22	B-500×22	B-500×22
4F				
3F				
2F				
1F				

Table 2 Section list of beams

	GX1		GX2		GX3	
	edge	center	edge	center	edge	center
PRF	H-600×250×12×19		H-600×250×12×22		H-600×200 ×12×22	
RF						
5F			H-600×200 ×12×25	H-600×200 ×12×22		
4F						
3F	H-600×250 ×12×22	H-600×250 ×12×19	H-600×200 ×12×22	H-600×200 ×12×19	H-600×250 ×12×22	H-600×250 ×12×19
2F						

	GY1		GY2		GY3	
	edge	center	edge	center	edge	center
PRF	-		H-600×200×12×19		-	
RF	H-800×350×16×25				H-600×200 ×12×22	
5F					H-600×200 ×12×25	H-600×200 ×12×22
4F						
3F			H-600×200 ×12×22	H-600×200 ×12×19	H-600×250 ×12×22	H-600×250 ×12×19

3 ANALYTICAL MODEL

An outline of the analytical model is shown in Fig. 2. In this study all steel members were modeled with 1st order planer elements that have 4-node at a unit length of 40mm. The planer elements had 4 integration points in the thickness direction and 1 integration point in the plane. As the concrete parts, 8-node solid elements were used. In the model, beam elements were used as the reinforcement bar and headed stud. The concrete mesh and reinforcement mesh were generated separately, so that their nodes were not shared in the model. The solid elements which was used for slabs and the beam elements which was used for reinforcement were coupled by constraint methods. The number of elements and nodes was 6,526,889 and 7,381,537, respectively.

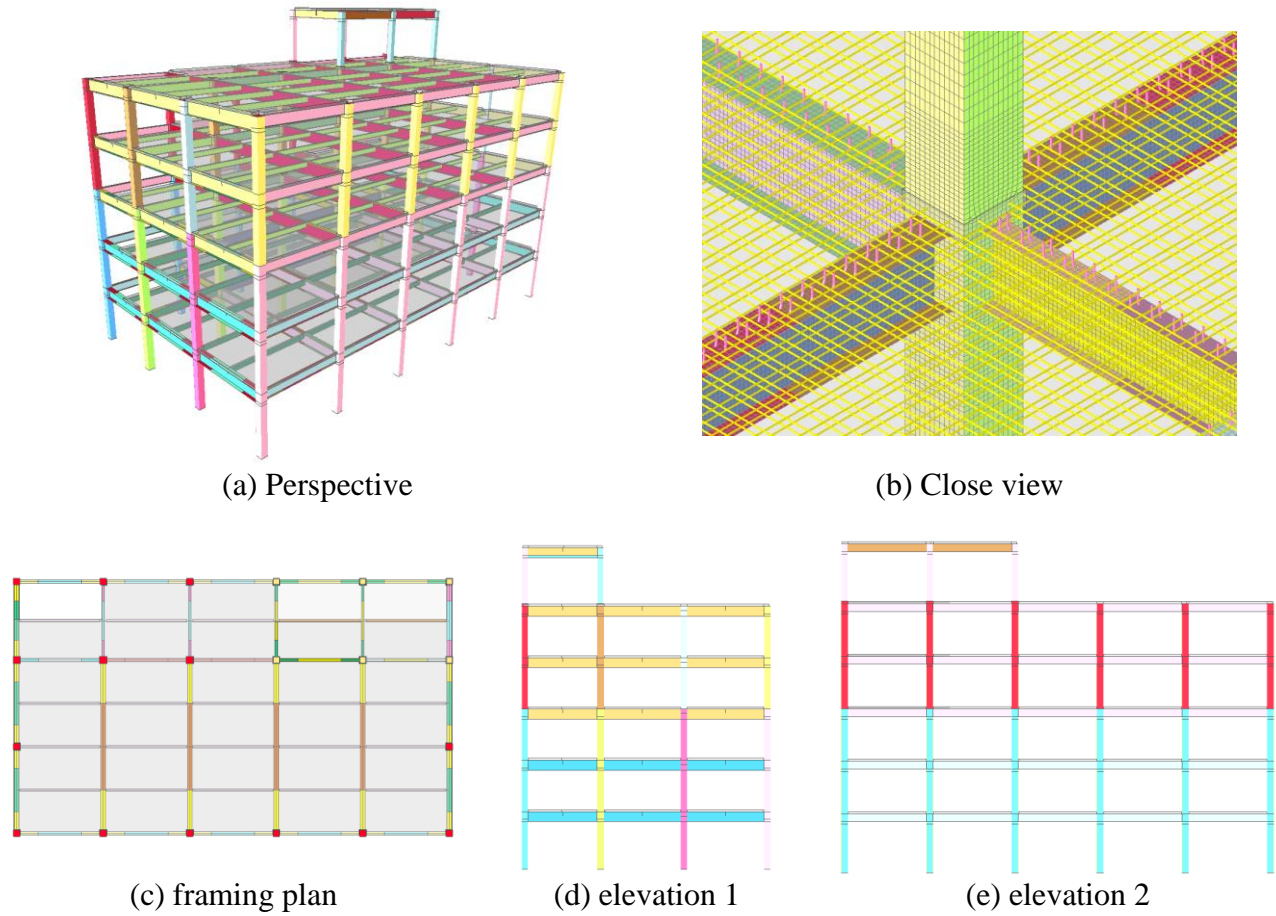


Fig.2 Analytical model

Input motion used in this study was 3-directional JR-Takatori wave, which was recorded at a railway station in Hyogo-ken Nambu earthquake(1995). Time histories of acceleration of the input motion are shown in Fig.3. Input motions that were recorded in north-south, east-west and up-down direction were inputted, respectively, X, Y and Z directions that was defined in the analytical model.

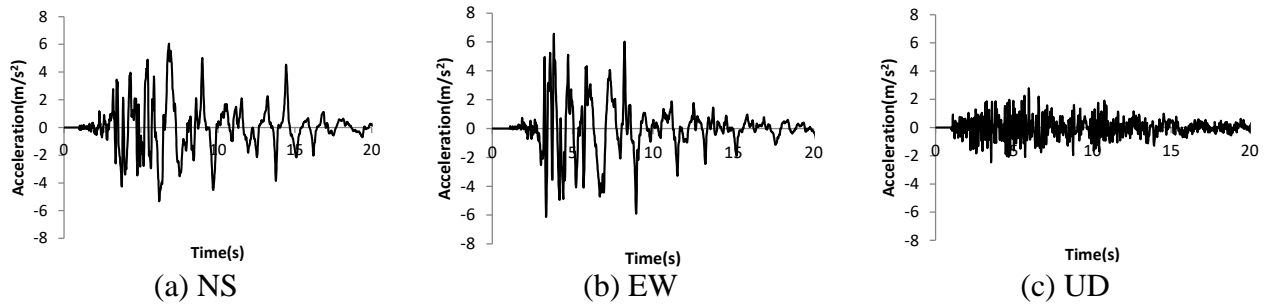


Fig.3 Input motion

3 ANALYTICAL RESULT AND CONECTION TO ANALYSIS FOR NON-STRUCTURAL MEMBERS

Time histories of story drift are shown in Fig.4. Maximum story drift reached 191mm and 90mm in X and Y direction, respectively. Deformation and stress distributions obtained from the analysis are shown in Fig.5. These results were observed at a time when the maximum story drift in X direction occurred. It can be seen that local buckling of bottom of columns occurred at 1st story. Torsional motion was observed because times when the maximum story drift was different between X and Y directions. Local response that will be used to evaluate non-structural damages is shown in Fig.6 The local response is relative displacement between input motion and points that will be connected to suspension rod for ceilings.

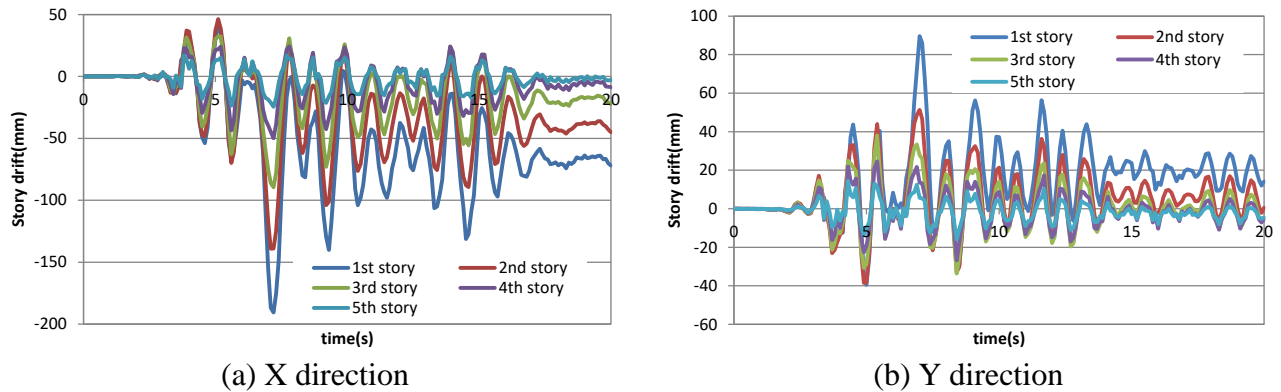
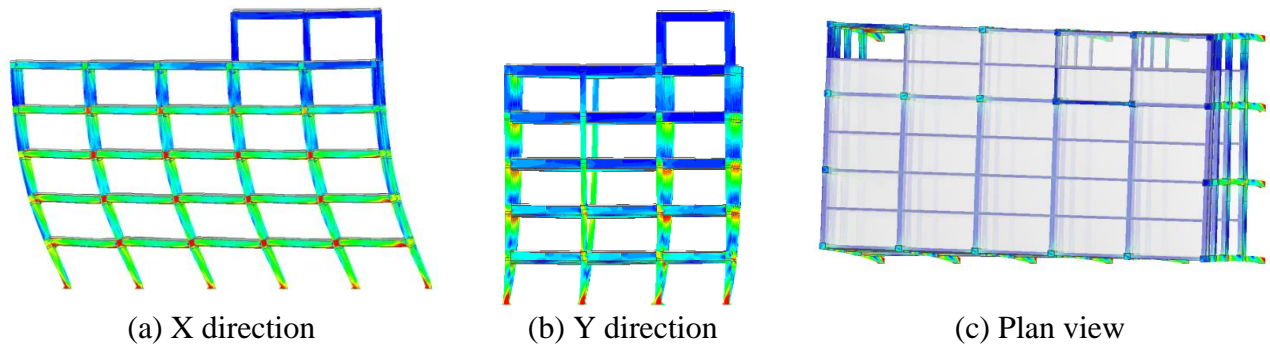


Fig.4 Story drift



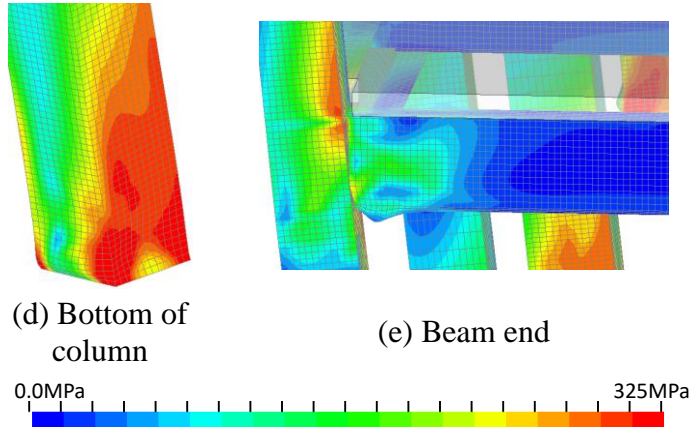


Fig. 5 Deformations and von Mises stress distribution

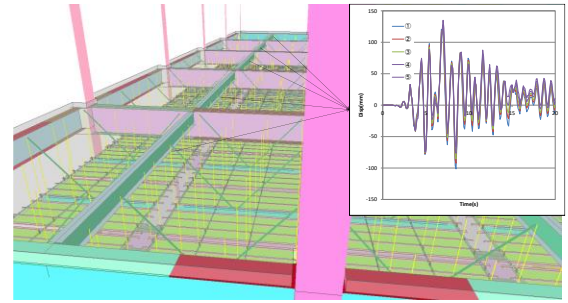


Fig.6 Local response

6 CONCLUSIONS

- Structural analysis of the entire building was carried out. Steel structural members in the model were modeled by shell element in order to replicate their original shapes.
- Local responses of the model can be extracted and the result will be used to evaluate non-structural damages on the building.

ACKNOWLEDGMENTS

This work was supported by JSPS KAKENHI Grant Number JP16H03124.

REFERENCES

[1] Yasunori Mizushima, Yoichi Mukai, Hisashi Namba, Kenzo Taga and Tomoharu Saruwatari : Super-detailed FEM simulations for full-scale steel structure with fatal rupture at joints between members -Shaking-table test of full-scale steel frame structure to estimate influence of cumulative damage by multiple strong motion: Part 1, *Japan Architectural Review*, AIJ, Vol.1, Issue 1, pp.96-108, Jan., (2018)
DOI : <https://doi.org/10.1002/2475-8876.10016>

[2] The Japan Building Disaster Prevention Association: Case Examples of Structural Design of Buildings and Their Members, (2007) (in Japanese)

An Unbiased Nitsche's Formulation of Frictional Contact and Self-contact

Rabii Mlika^{*}, Yves Renard^{**}, Franz Chouly^{***}

^{*}INSA-Lyon, France., ^{**}INSA-Lyon, France., ^{***}Université Bourgogne Franche-Comté, France

ABSTRACT

In this work, we present a new formulation of frictional contact between two elastic bodies based on Nitsche's method. Nitsche's method was adapted to unilateral contact in [1]. It aims to treat the interface conditions in a weak sense, thanks to a consistent term stabilized with a Nitsche parameter. At first, we introduce the study carried out in the small strain framework for an unbiased version of the method. The non-distinction between a master surface and a slave one will allow the method to be more generic and directly applicable to the self-contact problem. As in [1], we describe a class of methods through a generalization parameter θ . Particular variants have different properties from a numerical point of view, in terms of accuracy and robustness. The restrictive framework of small strain and Tresca friction allowed us to obtain theoretical results on the consistency and convergence of the method (see [2]). The Nitsche's method is then extended to the large strain case more relevant for industrial applications and situations of self-contact. The method is formulated for an hyper-elastic material and declines in the two versions: biased and unbiased. To prove the accuracy of the method for large deformations, we provide several validation tests (Taylor patch test, elastic half ring, cross tubes ...). The description of the method and all the results are detailed in [3]. We provide, finally, a study of the influence of numerical quadrature on the accuracy and convergence of the method. This study covers a comparison of several integration rules (element-based, segment-based, non-symmetric integration) proposed in the literature for other integral methods. References [1] F. Chouly, P. Hild, and Y. Renard. Symmetric and non-symmetric variants of Nitsche's method for contact problems in elasticity: theory and numerical experiments. *Mathematics of Computation*, 84:1089–1112, 2015. [2] F. Chouly, R. Mlika, and Y. Renard. An unbiased Nitsche's approximation of the frictional contact between two elastic structures. To appear in *Numerische Mathematik*, Available on HAL as hal-01240068, 2016. [3] R. Mlika, Y. Renard, and F. Chouly. An unbiased Nitsche's formulation of large deformation frictional contact and self-contact. *Computer Methods in Applied Mechanics and Engineering*, 325(Supplement C):265 – 288, 2017.

An Efficient DDM with Cross-points for the Parallel Finite Element Solution of Helmholtz Problems

Axel Modave^{*}, Xavier Antoine^{**}, Christophe Geuzaine^{***}

^{*}CNRS, POEMS, University of Paris-Saclay, France, ^{**}Institut Élie Cartan de Lorraine, Université de Lorraine, France, ^{***}University of Liège, Belgium

ABSTRACT

Solving high-frequency time-harmonic scattering problems using finite element techniques is challenging, as such problems lead to very large, complex and possibly indefinite linear systems. Optimized Schwarz domain decomposition methods (DDMs) are currently a very promising approach, where subproblems of smaller sizes are solved using sparse direct solvers, and are combined with iterative Krylov subspace techniques. It is well-known that the convergence rate of these methods strongly depends on the transmission condition enforced on the interfaces between the subdomains. Local transmission conditions based on high-order approximations of the free-space Dirichlet-to-Neumann (DtN) operator have proved well suited. They represent a good compromise between basic impedance conditions (which lead to suboptimal convergence) and the exact DtN map related to the complementary of the subdomain (which is very expensive to compute). However, a direct application of this approach for domain decomposition configurations with cross-points, where more than two subdomains meet, leads to disappointing convergence results. In this talk, we will present novel strategies to efficiently address configurations with cross-points. These strategies are based on corner treatments developed for high-order absorbing boundary conditions. Computational results obtained with the GetDP and GetDDM environments will be presented.

Sampling Full Extreme Event Statistics for Nonlinear Dynamical Systems through Sequential Surrogate Models

Mustafa Mohamad*, Themistoklis Sapsis**

*Courant Institute of Mathematical Sciences, **Massachusetts Institute of Technology

ABSTRACT

We develop a method for the evaluation of extreme event statistics associated with nonlinear dynamical systems, using a small number of samples. Extreme events in this context are related to intermittent behavior that occur on short-time scales and have large magnitude responses. From an initial dataset of design points, we formulate a sequential strategy that provides the 'next-best' data point (set of parameters) that when evaluated results in improved estimates of the probability density function (pdf) for a scalar quantity of interest. The approach utilizes Gaussian process regression to perform Bayesian inference on the parameter-to-observation map describing the quantity of interest. We then approximate the desired pdf along with uncertainty bounds utilizing the posterior distribution of the inferred map. The 'next-best' design point is sequentially determined through an optimization procedure that selects the point in parameter space that maximally reduces uncertainty between the estimated bounds of the pdf prediction. Since the optimization process utilizes only information from the inferred map it has minimal computational cost. Moreover, the special form of the criterion emphasizes the tails of the pdf. This strategy is unlike traditional failure probability methods in that we determine the full pdf not just the probability of a desired failure level. The method is applied to estimate the extreme event statistics to several examples including a high-dimensional system with millions degrees of freedom: an offshore platform subjected to three-dimensional irregular waves. It is demonstrated that the developed approach can accurately determine the extreme event statistics using orders from a small of samples.

Intergranular and Transgranular Fracture Modes in H.C.P. Alloys

I. Mohamed*, S. Ziaei**, M. Zikry***

*North Carolina State University, **North Carolina State University, ***North Carolina State University

ABSTRACT

A dislocation-density based multiple slip crystalline plasticity formulation and a new computational fracture approach have been used to investigate and predict intergranular and transgranular fracture in hexagonal cubic packed (h.c.p.) materials with a focus on h.c.p. alloys subjected to large changes in strains, strain-rates, and temperatures. This validated predictive framework has been used to understand and predict the interrelated effects of dislocation-density interactions, generation, and recovery on the competition between intergranular and transgranular crack nucleation and propagation. The predictions indicate that iodine pits that have diffused into the GB dominate intergranular fracture and that transgranular fracture is dominated by interrelated dislocation-density interactions and threshold fracture stresses along transgranular cleavage planes.

Wind Reliability Assessment of Power Transmission Lines Using an Error Rate-Based Adaptive Kriging Method

Yousef Mohammadi Darestani^{*}, Kyunghwa Cha^{**}, Zeyu Wang^{***}, Abdollah Shafieezadeh^{****}

^{*}Ohio State University, ^{**}Ohio State University, ^{***}Ohio State University, ^{****}Ohio State University

ABSTRACT

Estimation of wind reliability of transmission line systems is critical for risk assessment and management of power grids. This is a complex task considering various uncertainties involved in structural properties and wind load parameters. Conventional Monte Carlo simulation techniques can be utilized to analyze the reliability of these structures. However, considering the large number of random variables involved, these methods would require a significantly large number of realizations of uncertain parameters to accurately estimate failure probabilities. On the other hand, the mechanistic behavior of transmission line systems under extreme wind loadings is considerably complex. Given that these structures are composed of a large number of components such as lattice members and connections and considering large uncertainties involved, there exist numerous potential modes of failure. Analysis of numerical models capable of capturing these complex behaviors is considerably time-consuming. In order to efficiently estimate the probability of failure of transmission line systems, the current study adopts an advanced error rate-based adaptive Kriging method proposed by the authors. In this regard, a small set of realizations of uncertain variables are generated using Latin Hypercube sampling method and the limit state function for each realization is estimated subsequently using a high-fidelity nonlinear model of the tower in OpenSEES Finite Element platform. Nonlinear static pushover analyses are employed with failure defined as the event of exceeding the capacity of the system determined via pushover analyses. A Kriging model is constructed to evaluate the established limit state function. The initial surrogate model is refined continually by strategically selecting additional random realizations of uncertain variables from a novel effective sampling region (ESR). The region refers to a set of realizations that have a joint probability density larger than a threshold. The additional training points are chosen from those within ESR based on an Expected Learning Function that prioritizes points that are near the limit state function and/or have high variance. The model is improved adaptively until the maximum error rate associated with the Kriging prediction of probability of failure is less than a desired threshold. The error rate here is estimated using an extension of central limit theorem based on Lindeberg condition. Results indicate that error rate-based adaptive Kriging method can significantly reduce the number of Finite Element simulations in order to accurately estimate the probability of failure of transmission line systems.

Computational Modeling of Large People Traffic in Building Environments with Fuzzy Logic

Gray Moita*, Henrique Braga**, Paulo Eduardo Almeida***

*Centro Federal de Educação Tecnológica de Minas Gerais (CEFET-MG), Brazil, **Centro Federal de Educação Tecnológica de Minas Gerais (CEFET-MG), Brazil, ***Centro Federal de Educação Tecnológica de Minas Gerais (CEFET-MG), Brazil

ABSTRACT

The traffic of people in building environments is an important issue whose knowledge and implications directly influences the quality of life of everyone, including our own safety. Tragedies, as occurred in Brazil in 2013 [1], where 242 peoples lost their life and hundreds were injured, can be avoided, or at least minimized, if the human flow was correctly considered, both in normal situations and in case of an emergency. Due to the high number of people who can occupy a building at the same time, and therefore are subject to various risks, it can be said that this is a matter of great public and social interest. Thus, there are several prescriptive legal criteria that establish parameters of design and occupation of these highly diverse environments in search of more controllable human movement. Still, these codes are often nonspecific, not being able to promote certain improvements, and even to avoid dangerous situations. In this way, the existence of computational tools that can help in the verification of the conditions of quality, fluidity and safety of an environment becomes very relevant. However, different from the usual granular mechanical modeling, human movement must also consider several qualitative and quantitative aspects related to human behavior, including mental and cognitive features. This is lacking in many of the available models. In this work, a brand new model is introduced. It is called Fuga, Version 2.0, in which the dynamics of people flow is simulated by the association of artificial intelligence techniques and fuzzy logic, to emulate the human decision making process, taking into account several of the ergonomics aspects. The main focus here is to detail the step-by-step of the entire system, with specific examples, and its relation with the ergonomic human aspects. In the sequence, it is shown how this fuzzy system is transformed into a fuzzy table, and how this knowledge is introduced into the modeling program. This is a necessary step in order to improve the model performance in large scale situations, fundamental when it involves hundreds (sometimes thousands) of people moving at the same time. Examples of effective simulations of human movement using the system are presented and discussed, showing the relevance of the model to contribute in the design and maintenance of safer building. [1] H.C. Braga, G.F. Moita. On the Boate Kiss Fire and the Brazilian Safety Legislation - what we can learn. Collective Dynamics, v. 2, 2017.

A Combined NFEM - Conservative Level-Set Method for Interface Propagation

Jorge Molina-Moya^{*}, Pablo Ortiz^{**}, Alejandro Martínez-Castro^{***}

^{*}University of Granada, ^{**}University of Granada, ^{***}University of Granada

ABSTRACT

The conservative Level-Set (CLS) [1] is one of the most successful interface-capturing methods [2]. Frequently, the CLS is composed of very high order schemes for the transport, and of fast marching methods (FMM) to reconstruct the signed distance function. Although this kind of procedures gives proper results for interfaces propagation problems, they are computationally expensive, even for structured meshes. We propose a methodology consisting of a second order non-oscillatory finite element method (NFEM) [3] applied to the phase function transport step and of a reinitialization step formulated as a non-linear diffusion equation. Reinitialization is completed by the use of the NFEM sign-preserving correction to obtain the final solution. Calculation of interface normals in the CLS leads recurrently to oscillations in the phase function. In this work we propose a simplified local computation of normals with substantial savings on computational cost. Concerning hydrodynamics solution, we employ an improved NFEM for incompressible flows. Numerical model is tested for typical stringent experiments as the Zalesak disk, and dam-break problem. Numerical experiments are also focused on the propagation of air cavities in ducts during pressurized stages. Results are satisfactory both in terms of error norms and in terms of enclosed volume conservation, and are competitive with those obtained from very high order schemes. Acknowledgements: This research is supported by MICIIN Grant #BIA-2015-64994-P (MINECO/FEDER). REFERENCES [1] Olsson, Elin and Kreiss, Gunilla, A conservative level set method for two phase flow. J. Comput. Phys., Vol. 210, pp. 225–246, 2005. [2] Cruchaga, Marcela et al., Numerical Modeling and Experimental Validation of Free Surface Flow Problems. Arch. Computat. Methods Eng., Vol. 23, pp. 139–169, 2016. [3] Ortiz, Pablo, Non-oscillatory continuous FEM for transport and shallow water flows. Comput. Methods Appl. Mech. Engrg., Vol. 223, pp. 55–69, 2012.

Three-dimensional Fluid Structure Interaction between a Compressible Fluid and a Fragmenting Structure with a Conservative Immersed Boundary Method

Laurent Monasse*

*Inria Sophia Antipolis

ABSTRACT

In this work, we present a conservative method for three-dimensional inviscid fluid-structure interaction problems. On the fluid side, we consider an inviscid Euler fluid in conservative form, discretized with a Finite Volume method on a Cartesian grid. On the solid side, we consider an elastic deformable solid with possible fragmentation. We use a Discrete Element method (particles connected with springs) for the discretization of the solid. Body-fitted methods are not well-suited for large displacements or fragmentation of the structure, since they involve possibly costly remeshing of the fluid domain. We use instead an immersed boundary technique through the modification of the finite volume fluxes in the vicinity of the solid, in the spirit of cut-cell methods. The method is tailored to yield the exact conservation of mass, momentum and energy of the system and exhibits consistency properties [1, 2]. In the event of fragmentation, void can appear due to the velocity of crack opening. Since the numerical flux used is not stable in the presence of void, we resort locally to the Lax-Friedrichs flux near cracks [3]. Since both fluid and solid methods are explicit, the coupling scheme is designed to be explicit too. The computational cost of the fluid and solid methods lies mainly in the evaluation of fluxes on the fluid side and of forces and torques on the solid side. It should be noted that the coupling algorithm evaluates these only once every time step, ensuring the computational efficiency of the coupling. We will present numerical results showing the robustness of the method in the case of a fragmenting solid coupled with a compressible fluid flow. [1] M. A. Puscas, L. Monasse, A three-dimensional conservative coupling method between an inviscid compressible flow and a moving rigid solid body, SIAM Journal on Scientific Computing 37, pp. 884-909, 2015 [2] M. A. Puscas, L. Monasse, A. Ern, C. Tenaud, C. Mariotti, V. Daru, A time semi-implicit scheme for the energy-balanced coupling of a shocked fluid flow with a deformable structure, Journal of Computational Physics 296, pp. 241-262, 2015 [3] M. A. Puscas, L. Monasse, A. Ern, C. Tenaud, C. Mariotti, A conservative embedded boundary method for an inviscid compressible flow coupled with a fragmenting structure, International Journal for Numerical methods in Engineering 103(13), pp. 970-995, 2015

Modeling Fracture in BCC-Fe Using Cohesive Zone Model Coupled with Crack-tip Plasticity in Multiphysics Object Oriented Simulation Environment (MOOSE)

Geeta Monpara*, Ray Fertig**, Wen Jiang***

*University of Wyoming, **University of Wyoming, ***Idaho National Laboratory

ABSTRACT

Ferritic steels with 9-12%Cr are a candidate material for Gen-IV nuclear fission reactors due to their improved creep resistance with respect to current generation of steels. Fission process releases high energy particles, which interact with the structural components surrounding the nuclear fuel rods, such as cladding, pressure vessel etc. Such interactions lead to large displacement of atoms in the bulk of a material, resulting in many microstructural defects. Such defects could cause radiation-induced segregation and embrittlement of the grain boundaries. This leads to a change in cohesive energy of a grain boundary, which can affect fracture of the material. The Multiphysics Object-Oriented Simulation Environment (MOOSE) is used to model fracture in our study. MOOSE is a finite-element, multiphysics framework primarily developed by Idaho National Laboratory. In this study, we use cohesive zone model for grain boundary fracture in pure body-centered cubic (BCC) Fe. The cohesive law is implemented in MOOSE framework using Extended Finite Element Method module. All commercial finite element packages use viscous regularization to improve convergence issues. A study by Kuhn and Fertig show that use of energy conserving trilinear cohesive law obsoletes viscous regularization, resulting load-displacement curve matches well with the experimental data [1]. Such trilinear cohesive law is implemented for mode-I fracture in MOOSE. We simulate a micro-cantilever beam to model fracture along a grain boundary. Fracture is set to initiate at a notch on the grain boundary. The cantilever beam is loaded to propagate the crack from notch according to a cohesive law. The tip of the crack sees significant plastic deformation. The plastic zone ahead of the crack tip is modeled with a crystal plasticity model. Here, Crystal plasticity model is based on modified Schmid's law. This is derived from atomistic studies to incorporate nonplanar nature of a screw dislocation core in BCC materials [2]. Results of load-displacement curves are compared with the experimental data from our collaborators. References: 1. Kuhn, K. and R. Fertig III. A Physics-Based Fatigue Life Prediction for Composite Delamination Subject to Mode I Loading. in Proceedings of the American Society for Composites: Thirty-First Technical Conference. 2016. 2. Koester, A., A. Ma, and A. Hartmaier, Atomistically informed crystal plasticity model for body-centered cubic iron. Acta Materialia, 2012. 60(9): p. 3894-3901.

Spline Parameterization of 2D and 3D Geometries for its Application in Isogeometric Analysis

Rafael Montenegro*, Marina Brovka**, José Iván López***, José María Escobar****

*University Institute for Intelligent Systems and Numerical Applications in Engineering (SIANI), University of Las Palmas de Gran Canaria, Spain, **University Institute for Intelligent Systems and Numerical Applications in Engineering (SIANI), University of Las Palmas de Gran Canaria, Spain, ***University Institute for Intelligent Systems and Numerical Applications in Engineering (SIANI), University of Las Palmas de Gran Canaria, Spain, ****University Institute for Intelligent Systems and Numerical Applications in Engineering (SIANI), University of Las Palmas de Gran Canaria, Spain

ABSTRACT

We present an optimization based method for parameterization of 2D and 3D geometries for its application in isogeometric analysis. This method is a continuation of our previous works [1, 2, 3]. The proposed technique allows to obtain a good quality global spline parameterization from the boundary representation of the domain. The key of strategy lies in the simultaneous untangling and smoothing procedure used for the relocation of the interior control points in order to obtain optimal quality spline parametric mapping. Optimization is based on the mean ratio shape quality measure which attains its maximum when the mapping is conformal. Another important feature of the technique is the use of the regularized distortion measure which allows to perform unconstrained smooth optimization pursuing two goals at the same time: a valid parametric mapping (positive Jacobian) and a mapping as conformal as possible. We give a detailed description of the proposed method and show some examples. Also, we present some examples of the application of isogeometric analysis in geometries parameterized with our method. REFERENCES [1] Brovka M., López J.I., Escobar J.M., Cascón J.M., Montenegro R. (2014) A new method for T-spline parameterization of complex 2D geometries. *Engineering with Computers* 30: 457-473. [2] López J.I., Brovka M., Escobar J.M., Montenegro R., Socorro G.V. (2016) Strategies for optimization of hexahedral meshes and their comparative study. *Engineering with Computers* 33: 33-43. [3] López J.I., Brovka M., Escobar J.M., Montenegro R., Socorro G.V. (2017) Spline parameterization method for 2D and 3D geometries based on T-mesh optimization. *Computer Methods in Applied Mechanics and Engineering* 322: 460-482.

A Complex Variable Finite Element-Based Approach for Rapid Estimates of Residual Stress Variance

Arturo Montoya^{*}, Harry Millwater^{**}, Randal Fielder^{***}, Patrick Golden^{****}

^{*}University of Texas at San Antonio, ^{**}University of Texas at San Antonio, ^{***}University of Texas at San Antonio,
^{****}Air Force Research Laboratory

ABSTRACT

Residual stresses can be introduced intentionally to structural components as a means to improve their fatigue performance. Methods for introducing beneficial residual stresses include autofrettage, cold working, low plasticity burnishing and laser shot peening. However, there is frequently significant uncertainty regarding the magnitude of the induced residual stresses due to variation in material properties, loading, geometry, variables of the thermo/mechanical processes, and measurement uncertainty. The residual stress variation must be quantified in order to have confidence that the behavior of a structure, during its entire operation time, will be within safety limits. The traditional approach to estimate this variance is the Monte Carlo simulation (MCS). However, MCS requires a large number of simulations to accurately predict the variance, and becomes prohibitively time consuming for large-scale models and nonlinear analyses. This paper presents a unique, efficient approach to quantifying the uncertainty associated with residual stresses induced during manufacturing processes. The variance in the residual stresses is approximated using a few nonlinear complex-variable finite element analyses. The key ingredient for this method is to compute the sensitivities of the residual stress field with respect to each random variable using the complex variable finite element method, ZFEM. This sensitivity information are fed to a first order Taylor series approximation in order to provide a first-order estimate of the residual stress variance. The method was verified using the autofrettage process of a sphere subject to random stress-strain properties, internal pressure, and geometry. Four ZFEM nonlinear analyses were conducted to obtain the sensitivities of the residual stress field with respect to the four random variables of interest. The CPU time required for the four ZFEM analyses was about 2% of the total CPU time required to generate the MCS results from 1000 realizations. In addition, the approximate method provided a sensitivity analysis that allowed the most critical random variables to be identified quickly. Although demonstrated using the autofrettage process, the ZFEM-based methodology is general and can be applied to other residual stress inducing processes.

Multiscale Analysis of Photomechanics of Liquid Crystalline Polymer via Coarse-grained Molecular Dynamics Simulation

Junghwan Moon^{*}, Byungjo Kim^{**}, Joonmyung Choi^{***}, Maenghyo Cho^{****}

^{*}Seoul National University, ^{**}Seoul National University, ^{***}Samsung Electronics Co., ^{****}Seoul National University

ABSTRACT

Crosslinked liquid crystalline polymer (LCP) containing azo-based photochromic mesogens is a kind of photo-responsive polymers (PRPs), which can realize reversible mechanical deformation under irradiation of ultraviolet (UV) and visible lights. The difficulty in precise prediction of the photo-actuated deformation originates from the multiscale and multiphysics nature of the phenomenon. Even though some finite element method (FEM)-based computational models have been established [1,2], those cannot reflect the dependence of the molecular architecture on the macroscopic deformation. Also, full-atomistic molecular dynamics (MD) simulations have limitations of massive computational costs for describing diverse liquid crystalline phases. Therefore, we developed a multiscale computational framework, which combines the information at different scales to establish a relation between microscopic photochemical reaction and corresponding mechanical actuation. First, a photo-switching potential, which can be derived by a density functional theory (DFT) calculation, was utilized to describe the trans -to cis- isomerization of the azobenzene moieties in the MD simulation [3]. Then, light-induced liquid crystalline structural changes are reflected to the mesoscale simulation by deriving the coarse-grained (CG) potentials. Especially, we used a structure-based iterative Boltzmann inversion (IBI) method to derive the non-bonded energy of the CG MD simulation. As a result, our multiscale computational model efficiently described thermal and light response of the azo-LCP. The smectic-nematic-isotropic phase transition temperature and photo-strain had a good accordance with those of the experimental findings. Furthermore, a relationship between microscopic LC order parameters and shape parameter of the polymer networks was characterized with various molecular architectures, which is useful to precisely predict the macroscopic photo-mechanical deformation in continuum scale analysis. We expect our multiscale simulation scheme can broaden the applicability of the computational mechanics in research fields of the photo-responsive soft actuators. Acknowledgements This work was supported by a grant from the National Research Foundation of Korea (NRF) funded by the Korea government (MSIP) (Grant No. 2012R1A3A20488 41). References [1] Y. Lin, L. Jin, Y. Huo, Int. J. Solids. Struct. 2012, 49, 2668-2680. [2] H. Chung, J. Park, M. Cho, Phys. Rev. E 2016, 94, 042707. [3] J. Choi, H. Chung, J.-H. Yun, Appl. Phys. Lett. 2014, 105, 221906.

Recent Developments in Polygonal and Polyhedral Discontinuous Petrov-Galerkin Methods (PolyDPG)

Jaime Mora^{*}, Federico Fuentes^{**}, Leszek Demkowicz^{***}, Ali Vaziri Astaneh^{****}

^{*}University of Texas at Austin, ^{**}University of Texas at Austin, ^{***}University of Texas at Austin, ^{****}MSC Software Corporation

ABSTRACT

After the birth of PolyDPG methods, that is, the introduction of the discontinuous Petrov-Galerkin methodology (DPG) into the flourishing family of polytopal discretization techniques, these have kept maturing as a suitable set of finite element methods for general polytopes. This ongoing development of PolyDPG methods has involved both their mathematical foundations and their applications, and new extensions that may be of great interest to this community are currently in progress. In [1], the initial stage of 2D PolyDPG was consolidated, therein delivering: (1) a clear procedure for the discretization using the broken ultraweak formulation in meshes of arbitrary polygonal elements; (2) a complete proof of convergence as a conforming method for the mentioned variational formulation; and (3) a few practical examples where PolyDPG successfully satisfied the expectations arisen from the theory. Now, a new set of results of PolyDPG for two-dimensional problems is provided, where our methodology shows how competitive it is with respect to other polygonal technologies. Additionally, PolyDPG has been extended to the three-dimensional realm. Given the limitations of some of the ideas that work in 2D when extrapolated to polyhedra, three possibilities for the 3D problem can be explored: (i) considering polyhedral elements of triangular and quadrilateral faces only; (ii) using alternative shape functions for the polygonal faces (which require some degree of continuity across edges); or (iii) implementing a non-conforming DPG methodology. To conclude, the first sample of results of PolyDPG in 3D is presented and discussed. [1] A. Vaziri Astaneh, F. Fuentes, J. Mora, L. Demkowicz, High-order polygonal discontinuous Petrov–Galerkin (PolyDPG) methods using ultraweak formulations, *Comput. Methods Appl. Mech. Engrg.* (2017), <https://doi.org/10.1016/j.cma.2017.12.011>

Constrained Relative Entropy for Coarse-Grained Force Field Development of Room Temperature Ionic Liquids

Alireza Moradzadeh^{*}, Hossein Motevaselian^{**}, Sikandar Mashayak^{***}, Narayana Aluru^{****}

^{*}Department of Mechanical Science and Engineering Beckman Institute for Advanced Science and Technology University of Illinois at Urbana-Champaign, ^{**}Department of Mechanical Science and Engineering Beckman Institute for Advanced Science and Technology University of Illinois at Urbana-Champaign, ^{***}Department of Mechanical Science and Engineering Beckman Institute for Advanced Science and Technology University of Illinois at Urbana-Champaign, ^{****}Department of Mechanical Science and Engineering Beckman Institute for Advanced Science and Technology University of Illinois at Urbana-Champaign

ABSTRACT

Room temperature ionic liquids (RTILs) are an emerging class of solvents with many potential applications in energy-storage, biochemistry, etc. Molecular dynamics (MD) simulation is a powerful tool to study RTILs behavior in order to connect their microscopic behavior with their macroscopic properties. However, the high computational cost hinders the all-atom MD (AAMD) simulations of RTILs for large time- (~ μ s) and length-scales (~ μ m). During the past decade, coarse-grained (CG) simulations have become popular to study systems on larger time- and length-scales. In this study, we extend the relative entropy method with the addition of a constraint to reproduce the thermodynamics properties such as pressure in addition to the structure. In this study, the constrained relative entropy (CRE) method is applied for (CG) force field development of imidazolium-based ionic liquids. In addition to Lagrange multiplier for CRE minimization, we treat Coulombic interaction in a more systematic manner, which is of significant importance in RTILs behavior. To do so, we consider a global charge scalar for CG force field and obtain its optimal value within the CRE framework. Finally, we demonstrate that our CG force-field can accurately predict the structural, thermodynamic, and dynamical properties of imidazolium-based ionic liquids. The coarse-graining method presented in this study is also applicable for other classes of RTILs, such as Pyridinium-based and di-cationic ILs.

Finite Element Simulations of Two-phase Flow and Floating Bodies Using FEniCS-HPC

Margarida Moragues Ginard*, Daniel Castañón Quiroz**, Niyazi Cem Degirmenci***, Johan Jansson****, Vincenzo Nava*****, Ezhilmathi Krishnasamy*****, Johan Hoffman*****

*Basque Center for Applied Mathematics (BCAM), **University of Montpellier, ***Basque Center for Applied Mathematics (BCAM), ****KTH Computational Technology Laboratory and Basque Center for Applied Mathematics (BCAM), *****Tecnalia R&I; and Basque Center for Applied Mathematics (BCAM), *****Basque Center for Applied Mathematics (BCAM), *****KTH Computational Technology Laboratory

ABSTRACT

We present a variational multiscale stabilized finite element method to solve the variable density incompressible Navier-Stokes equations for the simulation of two-phase flow. We introduce a level-set method based on the compression technique similar to [1]. For the simulation of floating devices we make use of a simplified rigid body motion scheme and a deforming mesh approach [2]. The mesh deforms elastically following the movement of the body. An implicit turbulence model is used where turbulence is modelled by the numerical stabilization. The described methods are implemented in the open source software framework FEniCS-HPC [3] provided with an automated methodology for discretization and error control. We are working in a project for marine energy generation together with Tecnalia R&I. In this context we simulate floating platforms that will be used for marine energy generation or device experimentation in the ocean. The aim is to study the dynamics of this kind of off-shore devices. Our simulation results are compared against the experimental data obtained by Tecnalia R&I company in the experimental tank of CEHIPAR in Spain. We also participate in the IEA-OES Task 10 project where different simulations of floating bodies are carried out. The results are compared against other groups simulations that use different methodologies. [1] E. Olsson, G. Kreiss, A conservative level set method for two phase flow, *Journal of Computational Physics* 210 (1) (2005) 225-246. [2] A.A. Johnson and T.E. Tezduyar, Mesh update strategies in parallel finite element computations of flow problems with moving boundaries and interfaces, *Computer Methods in Applied Mechanics and Engineering* 119 (1) (1994) 73-94 [3] Hoffman J., Jansson J., Jansson N., FEniCS-HPC: Automated Predictive High-Performance Finite Element Computing with Applications in Aerodynamics, PPAM 2015. *Lecture Notes in Computer Science*, vol 9573 (2016). Springer, Cham

Three-Dimensional Model for Smooth Muscle Contraction: Urinary Bladder Wall Application

Enrique Morales Orcajo^{*}, Robert Seydewitz^{**}, Tobias Siebert^{***}, Markus Böl^{****}

^{*}Institute of Solid Mechanics, Braunschweig, Germany, ^{**}Institute of Solid Mechanics, Braunschweig, Germany,

^{***}Institute of Sport and Motion Science, Stuttgart, Germany, ^{****}Institute of Solid Mechanics, Braunschweig, Germany

ABSTRACT

The urinary bladder wall is a soft tissue that constitute the bladder organ and control all its functions. Such a functionality is achieved due to a specific hierarchical layered structure which featured non-linear hyperelastic mechanical response with hysteresis and softening effects as well as regional variability across the organ. Therefore, a detailed constitutive model of urinary bladder wall that account for its singularities will provide a useful tool for medicine and biomedical engineering applications. To work in that direction, a recently developed model for smooth muscle contraction of the urinary bladder [Seydewitz et al. 2017] is improved with new region-specific mechanical and histological data. The model features the urinary bladder wall in two layers: One layer with passive mechanical properties, the tunica mucosa, and another layer with passive and active response, the tunica muscularis. For the passive response, location-specific biaxial tests of the intact bladder wall as well as the mucosa and muscularis layers independently were use to identify the parameters. At the same positions, the smooth muscle orientation was histologically measured catching the in-plane and transmural fibre distribution. For the active response, layer-specific orientation-dependent uniaxial test were use. As a result, the temporal progression of four variables namely, electrical potential, calcium concentration, degree of activation and von Mises stress are simulated in a three-dimensional urinary bladder model. References R. Seydewitz, R. Menzel, T. Siebert, M. Böl, Three-dimensional mechano-electrochemical model for smooth muscle contraction of the urinary bladder, Journal of the Mechanical Behavior of Biomedical Materials, 75, 128-146, 2017.

A New Shell Formulation for Composite Delamination Modelling under Transient Dynamic Loading

Lionel Morancay^{*}, Said Mamouri^{**}, Jean-Baptiste Mouillet^{***}, Juan Pedro Berro Ramirez^{****}

^{*}ALTAIR Engineering, ^{**}ALTAIR Engineering, ^{***}ALTAIR Engineering, ^{****}ALTAIR Engineering

ABSTRACT

When composite structures are subject to highly dynamic loading such as crash or impact, it may be necessary to take into account delamination, especially if it is necessary to estimate energy absorption and failure modes. A first approach consists in either a full solid elements (in which all layers are modelled with solid element) or modelling each layer with one element connected by cohesive elements to take into account the delamination properties. With the ever increasing size of models in term of element size and number of plies, those approach are becoming very expensive in terms of computation time especially for “full vehicle models”. In addition, solid CAD are sometimes difficult to handle within the industrial processes for modelling full components, the shell approach being often preferred for instance in automotive industry. To reduce computational time and model design time, a new shell element was developed and implemented in the RADIOSS transient non-linear explicit code. Based on the MICT4 shell [1], the model is enriched by introducing additional degrees of freedom for representing the relative motion of the plies wrt actual positions of the - through the thickness - integration points. These additional degrees of freedom are calculated according to the interlayer properties, which are based on the transverse material properties of the laminate. A delamination criterion such as Ladevèze [2] can be associated. Full element delamination in mode I or II is modelled by relaxation of the corresponding interlayer stiffness. This approach results in a shell modelling approach, giving CPU times comparable to shell models and significantly faster than “full3D models”, while the transverse behaviour is significantly better represented and it allows to identify delamination phenomenon in crash or impact situation on thin structures. The so-called PLY-XFEM shell formulation will be first presented. To assess the capacities of modelling delamination, the PLY-XFEM formulation is next compared to solid elements on an ENF test. Another application of a bird strike onto a Kevlar plate at 45 degrees incidence is presented. References [1] E. Dvorkin and K. J. Bathe, “A Continuum Mechanics Based Four-Node Shell Element for General Nonlinear Analysis”, Engineering Computations, 1, 77-88, 1984. [2] O. Allix and P. Ladevèze, “Interlaminar interface modeling for the prediction of delamination”, Composite Structures, 22, 235-242, 1992.

Mesh Refinement for T-Splines in Any Dimension

Philipp Morgenstern*

*Leibniz University Hannover, Germany

ABSTRACT

T-splines are a generalization of tensor-product B-splines to non-uniform meshes. They have been introduced as a free-form geometric technology in the Computer-Aided Design community and have therefore caught much attention in Isogeometric Analysis, particularly with regard to constructing a mesh-adaptive Galerkin Method that uses the data structures from CAD applications. We present a generalized adaptive refinement procedure for n-dimensional axis-parallel box meshes with user-defined grading, i.e., the user chooses the number of children in a single elements' refinement. We prove linear independence of the T-spline functions that correspond to the generated meshes, nestedness of the generated T-spline spaces and linear computational complexity of the refinement procedure in terms of the number of marked and generated mesh elements. REFERENCES [1] P. Morgenstern, Globally structured three-dimensional analysis-suitable T-splines: Definition, linear independence and m-graded local refinement, SIAM Journal on Numerical Analysis 54 (2016), no. 4, 2163–2186. [2] P. Morgenstern, Mesh refinement strategies for the adaptive isogeometric method, Ph.D. thesis, Institut für Numerische Simulation, Universität Bonn, 2017.

DEM-based Optimal Design of Rockfall Protection Walls

Shuji Moriguchi^{*}, Hasuka Kanno^{**}, Kenjiro Terada^{***}

^{*}International Research Institute of Disaster Science, Tohoku University, ^{**}Department of Civil and Environmental Engineering, Tohoku University, ^{***}International Research Institute of Disaster Science, Tohoku University

ABSTRACT

Strong variability is generally involved in rockfalls. Although the variability comes from both the epistemic and aleatory uncertainties, the latter uncertainty that originates in complex movements of rockfalls is focused in this study. When we predict the behavior of rockfalls, there should be different rockfall paths to be considered. Because this variability is an irreducible uncertainty, it must be one of the important aleatory uncertainties in the prediction of rockfall movement. This study presents an optimal design of rockfall protection retaining walls in consideration of the variability of rockfall paths and kinetic energies. Although a retaining wall is generally designed to resist the energies of rockfalls, the determination of optimal position and width of retaining walls is also demanded in practice. In particular, it is difficult to evaluate an effect of the horizontal distance between toe of slopes and retaining walls, while this parameter is quite important for designing retaining walls. The proposed framework enables us to determine optimal horizontal distance and width of retaining walls based on results of DEM [1] simulations. A cost function is selected as an objective function with these design parameters along with a safety indicator as a constraint condition. A number of DEM simulations are conducted to obtain appropriate sets of rockfall paths and kinetic energies so that a response surface of the objective function can be formed. The response surface is approximately constructed by a polynomial function with the help of multiple linear regression analyses. Then, the optimization becomes possible to determine the optimal parameters under the employed constraint condition. Selecting a virtual site with a simple slope condition, a numerical example is presented to demonstrate the capability of the suggested optimal design approach. During the course of the demonstration, the appropriateness of each element of the suggested method is also examined; the selection of design parameters, the definition of a cost function and constraint conditions and the accuracy of a response surface as a surrogate model of the cost must be subjects of study.

Improvements on Highly Viscous Fluid Simulation Using a Particle Method and Its Application to Landslide Problems

Daniel Morikawa^{*}, Mitsuteru Asai^{**}

^{*}Kyushu University, ^{**}Kyushu University

ABSTRACT

The objective of this work is to show some improvements on highly viscous fluid simulation using the Smoothed Particle Hydrodynamics (SPH). SPH is one of the Lagrangian particle methods, and it is used on fluid dynamics problems [1]. It is already well recognized for dealing with problems of low viscosity fluids (eg., water). However, SPH needs some modifications in order to accurately simulate for highly viscous fluids, which need to model the landslide problems as a macroscopic continuum model. The main improvement is related to the free-surface treatment. In the original SPH method, there is no transition between inner particles and the void space outside the fluid domain which causes some instability on the free-surface particles. Here, we propose the concept of Space Potential Particles (SPP) in order to overcome this problem. Although the original SPP formulation introduced by Tsuruta et al [2] was used to avoid gaps inside the fluid domain, the present work promotes its usage to create fictitious mass around the free-surface. This implementation increases the free-surface stability. In addition, most of highly viscous simulations with the SPH method do not account for an accurate pressure distribution of the fluid particles. To overcome this problem, we applied a relaxation of the density invariance condition together with a semi-implicit time integration scheme proposed by Asai et al [1]. Validation of these improvements includes the hydrostatic problem for pressure distribution calculation and free-surface verification. Combining these improvements, we are able to calculate accurately both the particle movement and the pressure distribution throughout the fluid domain. To demonstrate it, we will present the viscous fluid coiling effect validation problem, which requires highly accurate modelling in the viscous term. Results of this problem agree with some of the experiments on Ribe et al. [3]. At last, we will show some examples of landslide simulations using the proposed solution with the aim of improving disaster prevention measures. References [1] Asai, M., Aly, A. M., Sonoda, Y., Sakai, Y. (2012). A Stabilized Incompressible SPH Method by Relaxing the Density Invariance Condition. International Journal for Applied Mathematics No. 20130011. [2] Tsuruta, N., Khayyer, A., Gotoh, H. (2015). Space Potential Particles to Enhance the Stability of Projection-based Particle Methods. International Journal of Computation Fluid Dynamics. DOI: 10.1080/10618562.2015.1006130. [3] Ribe, N. M., Habibi, M., Bonn, D. (2012). Liquid Rope Coiling. The Annual Review of Fluid Mechanics. DOI: 10.1146/annurev-fluid-120710-101244.

Rail Pad Super-Elements for Track Decay Rate Computation

Benjamin Morin^{*}, Bart Van Damme^{**}, Gwenael Hannema^{***}, Armin Zemp^{****}

^{*}Empa, ^{**}Empa, ^{***}Empa, ^{****}Empa

ABSTRACT

The state of art mechanical model for the superstructure of railway tracks, rail pads, sleepers and ballast is to represent the whole assembly as a parallel array of mass and springs [1]. This kind of model is used to compute the Track Decay Rate (TDR) which is considered to be a key parameter in limiting the radiated rail noise. As a result of the spring representation, only the stiffness of the rail pads has an influence on the TDR. Neither the frequency-(pre)load-temperature dependent properties of material nor the pads geometry are described. Ageing, which is of primary importance for maintenance purpose is also missing. The proposed approach is to use the finite element method to obtain a more complete representation of the rail pads. As a first step, the present work focuses on adding visco-thermo-elasticity [2] to the pads model and also on high preloads affects the pads behaviour. The resulting model is able to (i) access the behavior of pads under finite strain preloads, (ii) exhibit stiffness/damping related to frequency and temperature, (iii) represent the possibly complex geometry of the pads. To achieve practical computation time, a Craig-Bampton type reduction method is used to obtain a super-element of pads based on the finite element model. Following [3], the frequency dependence of pads is implemented in the super-element and similar features can be achieved for thermo-elasticity and preload. Thanks to the reduction method, interfaces between the pads and the rails or sleepers can still be modeled and for instance introduce contact/friction in the model. To validate the proposed approach, TDR computed by using super-elements will be compared to in-situ measured TDR. The material parameters of the pads are characterized experimentally. This work is part of the “Novel Rail Pads for Improved Noise Reduction and Reduced Track Maintenance” project, funded by the Swiss Federal Office for the Environment. [1] D. Thompson. (2008). *Railway Noise and Vibration: Mechanisms, Modelling and Means of Control.*, Elsevier Science. ISBN: 978-0-08-045147-3 [2] Lion, A. (1997). A physically based method to represent the thermo-mechanical behaviour of elastomers. *Acta Mechanica*, 123(1–4), 1–25. DOI: 10.1007/BF01178397 [3] B. Morin et al. (2016). Reduced Order Models for Dynamic Behavior of Elastomer Damping Devices. *J. Phys. Conf. Ser.* DOI: 10.1088/1742-6596/744/1/012134

Implementation of Higher-order Vertical Finite Elements in ISSM for Improved Ice Sheet Flow Modeling over Paleoclimate Timescales

Mathieu Morlighem^{*}, Joshua Cuzzone^{**}

^{*}University of California Irvine, ^{**}University of California Irvine

ABSTRACT

Ice sheet models are being used in conjunction with paleoclimate proxies to determine how the Greenland ice sheet responded to past changes, particularly during the last deglaciation. Although these comparisons have been a critical component in our understanding of the Greenland ice sheet's sensitivity to past warming, they rely on modeling experiments that favor minimizing computational expense over increased model physics. Over Paleoclimate timescales, simulating the thermal field within an ice sheet has large implications on the modeled ice viscosity, which can feedback onto the basal sliding and ice flow. To accurately capture the thermal field, models often require a high number of vertical layers. This is not the case for the stress balance computation, however, where a high vertical resolution is not necessary. Accordingly, since both computations are generally performed on the same model mesh, more time is spent on the stress balance computation than is otherwise necessary. For these reasons, running a higher-order ice sheet model (e.g. Blatter-Pattyn) over timescales equivalent to the paleoclimate record has not been possible without incurring a large computational expense. To mitigate this issue, we propose a method that can be implemented within ice sheet models, whereby the vertical interpolation along the z-axis relies on higher-order polynomials, rather than the traditional linear interpolation. This method is tested within the Ice Sheet System Model (ISSM) using quadratic and cubic finite elements for the vertical interpolation on an idealized case and a realistic Greenland configuration. A transient experiment for the ice thickness evolution of a single dome ice sheet demonstrates improved accuracy using the higher-order vertical interpolation compared to models using the linear vertical interpolation, despite having fewer degrees of freedom. This method is also shown to improve a model's ability to capture sharp thermal gradients in an ice sheet particularly close to the bed, when compared to those models using a linear vertical interpolation. This is corroborated in a thermal steady-state simulation of the Greenland ice sheet using a higher-order model. In general, we find that using a higher-order vertical interpolation decreases the need for a high number of vertical layers in a model, while dramatically decreasing model runtime for transient simulations. The findings suggest that this method will allow higher-order models to be used in studies investigating ice sheet behavior over paleoclimate timescales at a fraction of the computational cost than would otherwise be needed for a model using a linear vertical interpolation.

Linking High-Throughput Binary Calculations to Phase Evolution in Multicomponent Alloys

James R. Morris^{*}, Louis Santodonato^{**}, M. Claudia Troparevsky^{***}, Raymond R. Unocic^{****},
Peter K. Liaw^{*****}

^{*}Oak Ridge National Lab, ^{**}Oak Ridge National Lab, ^{***}Oak Ridge National Lab, ^{****}Oak Ridge National Lab,
^{*****}University of Tennessee

ABSTRACT

The development of high-throughput calculations provides significant data available for materials discovery. In this work, we demonstrate how the large amount of data associated with high-throughput first-principles calculations may be directly utilized for studying high entropy and related alloys, which have many components in near equal composition. These alloys are quite far from the binaries, and from traditional alloys that are based on one- or two-component systems, with minor alloying additions. We have demonstrated [Troparevsky 2015] that these calculations may be used to predict high entropy alloys with single-phase compositions. We have also examined the Al(x)CrFeCoNi materials as a function of Al content, utilizing a Monte Carlo model derived from high-throughput calculations, and demonstrate that the predicted phase evolution is remarkably close to results from neutron scattering and in situ microscopy experiments. This work demonstrates that the development of materials databases may be utilized for discovery and elucidation of materials. [Troparevsky 2015] M. C. Troparevsky, J. R. Morris, P. R. C. Kent, A. R. Lupini, and G. M. Stocks, Criteria for predicting the formation of single-phase high-entropy alloys, Phys. Rev. X 5, 011041 (2015); M. C. Troparevsky, J. R. Morris, M. Daene, Y. Wang, A. R. Lupini, and G. Malcolm Stocks, Beyond atomic sizes and Hume-Rothery Rules: Understanding and predicting high entropy alloys, JOM 67, 2350 (2015). This work has been supported by the USDOE BES MSED program, by the High Flux Isotope Reactor and Spallation Neutron Source, and through a user proposal at the Center for Nanophase Materials Sciences, a USDOE Office of Science User Facility. PKL acknowledges support from the USDOE Office of Fossil Energy.

Representing Model Inadequacy in Interacting Systems, Using Physics-Constrained Data-Driven Stochastic Operators

Rebecca Morrison*, Youssef Marzouk**

*Massachusetts Institute of Technology, **Massachusetts Institute of Technology

ABSTRACT

An emerging area in computational modeling is the effective combination of physics-based and data-driven models. This combination is well-suited to address problems of model error and, in particular, model inadequacy for desired prediction goals. Often we cannot improve a model purely through physics-based approaches, either because we do not have better descriptions of the physics or because doing so would be computationally infeasible. An alternative is to develop a data-driven representation of the model inadequacy. Yet there is often rich physical information that can and should be used to constrain such a representation. This work explores how to represent model inadequacy via physics-constrained stochastic operators in the context of interacting systems, exemplified here by the generalized Lotka-Volterra (LV) equations. These equations are a generalization of predator-prey models to an arbitrary number of species S , and consist of a set of S ordinary differential equations (ODEs). The dynamics of this system are governed by a random intrinsic growth rate vector and a random interaction matrix. Given: (i) a reduced model representing the dynamics of S species, where $S < S$; (ii) limited observations of the original S -species system; and (iii) information about the species growth rates and interactions, we construct a stochastic operator to capture the error in the reduced model. Rather than simply correcting the model output to the data, this operator is embedded within the reduced set of ODEs. The latter approach---capturing the model error where it occurs---is critical when using the augmented model to make predictions beyond the regime of available observations.

Computed Binding of Peptides to Proteins with Information-Accelerated Molecular Dynamics Simulation

Joseph Morrone*

*IBM T.J. Watson Research Center

ABSTRACT

The in silico prediction of binding modes and affinities for peptide-protein complexes is a challenging problem, particularly as peptides may undergo large conformational changes upon binding. Significant strides have been made by developing a method that combines molecular dynamics simulation with sparse, ambiguous external information that restricts sampling to regions of interest. This technique, known as MELD (Modeling Employing Limited Data), was developed for protein structure prediction and fully accounts for peptide flexibility. Only weak information about the binding motif is employed and not knowledge of the detailed binding mode that is typically required by other free-energy-based methods. MELD is implemented on large-scale, parallel GPU clusters and is illustrated by studying the association of peptide inhibitors with the P53-regulator-proteins MDM2 and MDMX. It is found that binding induces the peptide into the correct helical conformation, resulting in binding modes that are in excellent agreement with experiment. In addition, relative binding affinities may also be estimated. Reference: (1) Morrone, J. A.; Pérez, A.; MacCallum, J.; Dill, K. A. Computed Binding of Peptides to Proteins with MELD-Accelerated Molecular Dynamics. *J. Chem. Theory Comput.* 2017, 13 (2), 870–876. (2) Morrone, J. A.; Pérez, A.; Deng, Q.; Ha, S. N.; Holloway, M. K.; Sawyer, T. K.; Sherborne, B. S.; Brown, F. K.; Dill, K. A. Molecular Simulations Identify Binding Poses and Approximate Affinities of Stapled α -Helical Peptides to MDM2 and MDMX. *J. Chem. Theory Comput.* 2017, 13 (2), 863–869.

Simulation of Fracture and Fragmentation of Glass Lites under Blast Loading Using the Applied Element Method with Comparison to the Finite Element Method

Jonathan Moss^{*}, Adam Howe^{**}, Matthew Whelan^{***}, David Weggel^{****}

^{*}The University of North Carolina at Charlotte, ^{**}The University of North Carolina at Charlotte, ^{***}The University of North Carolina at Charlotte, ^{****}The University of North Carolina at Charlotte

ABSTRACT

The Applied Element Method (Meguro and Tagel-Din, 2000), which has been developed into an effective alternative to the Finite Element Method, features distinct advantages compared to other methods of analysis when applied to blast simulation problems featuring fracture and fragmentation. The advantages of the Applied Element Method render the method especially well-suited for predictive simulations involving element separation, which is an important aspect in the simulation of blast events that could potentially result in material fracturing or debris field formation. In this study, the Applied Element Method is explored as a tool for post-blast forensics investigation through comparison of predicted fracture, fragmentation, and debris field formation under blast loading against field observations and measurements. An overview of the Applied Element Method will be presented with specific details on the development of a model for simulating fracture and fragmentation of a glass fenestration system under blast loading. Experimental data from a set of six open arena blast tests performed on a façade structure consisting of six glass lites supported by aluminum mullions on a steel reaction frame will be used for assessment of the predictive fidelity of the simulations. Measurement of incident and reflected blast pressures, high-speed videography, 3D scanning and scene reconstruction, and a vertical witness panel to capture hazardous glass fragments were employed across each test to provide an experimental reference. Results obtained using the Applied Element Method will be compared to results obtained from similar analytical models developed using commercial Finite Element Method software. Specifically, the comparisons will focus on the predicted dynamic response of the lites under blast loading, fracture patterns, and fragmentation. Meguro, K. and Tagel-Din, H. (2000) "Applied Element Method for Structural Analysis: Theory and Applications for Linear Material," Structural Engineering/Earthquake Engineering JSCE, 17(1). 21-35.

The Schwarz Alternating Method for Quasistatic Multiscale Coupling in Solid Mechanics

Alejandro Mota^{*}, Coleman Alleman^{**}, Irina Tezaur^{***}

^{*}Sandia National Laboratories, ^{**}Sandia National Laboratories, ^{***}Sandia National Laboratories

ABSTRACT

We advance the Schwarz alternating method as a means for concurrent multiscale coupling in finite deformation solid mechanics. We prove that the Schwarz alternating method converges to the solution of the problem on the entire domain and that the convergence rate is geometric provided that each of the subdomain problems is well-posed, i.e. their corresponding energy density functions are quasi-convex. It is shown that the use of a Newton-type method for the solution of the resultant nonlinear system leads to two kinds of block linearized systems, depending on the treatment of the Dirichlet boundary conditions. The first kind is a symmetric block-diagonal linear system in which each diagonal block is the tangent stiffness of each subdomain, i.e. the off-diagonal blocks are all zero and the coupling terms appear only on the right-hand side. The second kind is a nonsymmetric block system with off-diagonal coupling terms. Several variants of the Schwarz alternating method are proposed for the first kind of linear system, including one in which the Schwarz alternating iterations and the Newton iterations are combined into a single scheme. This version of the method is particularly attractive, as it lends itself to a minimally intrusive implementation into existing finite element codes. Finally, we demonstrate the performance of the proposed variants of the Schwarz alternating method on several one-dimensional and three-dimensional examples. Support for this work was received through the U.S. Department of Energy's (DOE) Advanced Simulation and Computing (ASC) Program at Sandia National Laboratories. Sandia National Laboratories is a multimission laboratory managed and operated by National Technology and Engineering Solutions of Sandia, LLC., a wholly owned subsidiary of Honeywell International, Inc., for the U.S. Department of Energy's National Nuclear Security Administration under contract DE-NA-0003525.

Generation of Training Data for Scene Labeling Using Neural Network

Yuichiro Motegi^{*}, Takahiro Suzuki^{**}, Yuta Matsuda^{***}, Makoto Murakami^{****}

^{*}Toyo University, ^{**}Toyo University, ^{***}Toyo University, ^{****}Toyo University

ABSTRACT

Some researchers have proposed neural networks for scene labeling which assigns class label to each pixel of an image. The class accuracy for objects included enough in a training set such as sky or road is high, but the accuracy for objects included less in the training set tends to be low. To improve the average per-class accuracy, we need to increase variations of training images in each class, and reduce the difference in the number of training images/pixels in each class. But it takes time to annotate a lot of images at the pixel level manually to make training set. There are some researches to generate many pixel-level annotated images using computer graphics. We propose the method to generate large training set for scene labeling. In our system users register 3D models and the corresponding class labels. And the users input some constraints of the object positions such as "tables must be on the floor" or "cups must be on tables or desks". And the users input some hyper parameters for training neural network, such as the structure of the network, loss function, etc. The system put some objects in the virtual space based on the constraints, and generates a large set of images labeled at each pixel, to increase the variations of images in each class and to flatten the number of pixels in each class. The neural network is trained using the large set of generated labeled images. And the system repeats training and evaluating while increasing the variations of training images, and output the network parameters which minimize the generalization error measured with the average per-class accuracy. We captured some real images of indoor environment, and labeled each pixel of them using the neural network trained with our system. To evaluate our system we changed some settings of the system and compared the obtained results.

A Point Dipole CG Model and Quasi-Continuum Treatment of Confined Water

Mohammad Motevaselian*, Sikandar Mashayak**, Narayana Aluru***

*University of Illinois, **University of Illinois, ***University of Illinois

ABSTRACT

In this study, we have developed a systematic, point dipole-based coarse-grained (CG) model using the relative entropy method to reproduce the radial distribution function (RDF) and bulk dielectric permittivity of water in an all-atom (AA) molecular dynamics description of water. The bulk CG potentials may not adequately describe the structure and dielectric permittivity variation of water inside confined slit graphene channels. To overcome this, we introduce a modified/corrected wall-fluid potential to accurately predict the structural variations close to the interface. Next, we employ the CG water potential and the water-fluid potential in the empirical potential-based quasi-continuum theory to predict the water density profiles inside the graphene slit-like channels of various widths, and the results are in good agreement with both AA and CG representations. Furthermore, we have also simulated water close to positively and negatively charged walls. We show that although the dipole-dipole correlations are treated using the mean field approximation (MFA) in the EQT framework, EQT can accurately predict the density and polarization variations of the point dipole CG model close to the charged walls. Our results also reveal that, in addition to the dipolar interactions, the secondary effects such as hydrogen bonding, can also play an important role in determining the water structure and polarization at these interfaces. Hence, to quantitatively reproduce water interfacial properties these effects should be included in the CG models.

Simulation of Blast Load Effects Using the Duke Human Population XCAT Phantom Data Set

John Mould*, Kerim Genc**, Patrick Tompsett***, Andrew Nicholson****, Mahesh Kailasam,*****

*Thornton Tomasetti, Inc., **Synopsys Inc., ***Synopsys Inc., ****Thornton Tomasetti, Inc., *****Thornton Tomasetti, Inc.

ABSTRACT

Computational modeling and simulations have proven effective in predicting the effects of blast loads of different intensities and types. This includes effects of airblast due to various reasons, such as terrorist attack, vapor-cloud explosions or other mishaps, on structures and facilities and even underwater explosions on ships and submarines[a]. Simultaneously, computational modeling and simulations of the human body have made significant advances to the point where the behavior of organs, such as the heart or brain, under impact loads can be assessed fairly accurately[b]. In this study, we use the Duke Human Population XCAT Phantom Data Set to develop a framework for efficient assessment of blast effects on reference human bodies at different distances and orientations relative to the blast source. The XCAT models were created[c] using clinical CT images as the source data for the human body along with sophisticated morphing methods to create 150+ highly detailed phantoms of varying body-mass indices (BMIs). These methods reduce manual segmentation and model generation time for a virtual population and capture interior variability from person-to-person resulting in a population representation. We demonstrate the XCAT models, with initially reduced levels of interior details for rapid, assessment of blast effects on a gathering. This can then be followed by more thorough assessments by restoring the details of the human body as needed. The ability to scale the detail level of the models provides an efficient mechanism to tailor the simulations based on the level of accuracy desired. Furthermore, the XCAT models allow the ability to model different sized bodies thereby more accurately representing groups of people, which could prove useful in threat reduction assessments. References a Vaughan, D.; Mould, J.; Levine, H.; Tennant, D. Simulating Explosive Detonations Within Multiroom Buildings. ASME Pressure Vessels and Piping Conference, 2013 b Cotton, R.; Pearce, C.; Young P.; Kota, N.; Leung, A.; Bagchi, A.; Qidwai, S. Development of a geometrically accurate and adaptable finite element head model for impact simulation: The Naval Research Laboratory–Simpleware Head Model. Comput Methods Biomech Biomed Engin. 19(1), 2016; c Genc, K.; Segars, P.; Cockram, S.; Thompson, D.; Horner, M.; Cotton R.; Young, P. Workflow For Creating a Simulation Ready Virtual Population For Finite Element Modeling. J. Med. Devices 7(4), 2013

Three-dimensional Simulation of Obstacle-mediated Chemotaxis

Adrian Moure^{*}, Hector Gomez^{**}

^{*}Purdue University, ^{**}Purdue University

ABSTRACT

Amoeboid cells exhibit a highly dynamic motion based on the extension and retraction of actin-rich protrusions called "pseudopods". Amoeboid cell motility can be directed by external chemical signals, through the process of chemotaxis. Here, we extend the model of amoeboid motion presented in [1,2], which focus on the spontaneous migration of Dictyostelium Discoideum, and propose a three-dimensional model for chemotactic motion of amoeboid cells. By using the diffuse domain (or phase-field) method, we account for the interactions between the extracellular substances, the membrane-bound proteins, and the cytosolic components involved in the signaling pathway that originates cell motility. The motion of the cell is driven by the actin filament network, which is assumed to be a Newtonian fluid subject to the forces caused by the cell motion machinery (membrane surface tension, cell-substrate adhesion, actin-driven protrusion, myosin contraction, and a repulsive force accounting for the interaction with obstacles or fibers). The use of the diffuse domain method permits to solve equations posed on deformable domains (i.e., the cytosol, the membrane, and the extracellular medium) by using a fixed mesh only. We show two- and three-dimensional simulations of cell migration on planar substrates, flat surfaces with obstacles, and fibrous networks. The results show that our model reproduces the main features of chemotactic amoeboid motion. Our simulations unveil a complicated interplay between the geometry of the cell's environment and the chemoattractant dynamics that tightly regulates cell motion. [1] Moure, A. and Gomez, H. 2016. Computational model for amoeboid motion: Coupling membrane and cytosol dynamics. Physical Review E, 94(4), 042423. [2] Moure, A. and Gomez, H. 2017. Phase-field model of cellular migration: Three-dimensional simulations in fibrous networks. Comp. Methods in App. Mech. Eng., 320, 162-197.

Time-variant Reliability Based Risk Optimization Using Surrogate Modeling

Maliki Moustapha^{*}, Henrique Kroetz^{**}, André Téofilo Beck^{***}, Bruno Sudret^{****}

^{*}ETH Zurich, Chair of Risk, Safety and Uncertainty Quantification, ^{**}São Carlos School of Engineering, University of São Paulo, ^{***}São Carlos School of Engineering, University of São Paulo, ^{****}ETH Zurich, Chair of Risk, Safety and Uncertainty Quantification

ABSTRACT

Structural design optimization is an important part of designing structures that allows one to select among alternate concepts or configurations the one with the best compromise between the conflicting goals of economy, performance and safety. Deterministic design optimization may only partially achieve this as uncertainties, which are ubiquitous to all engineering applications, need to be taken into account. Reliability-based design optimization has been widely used in the literature in an attempt to trade the cost with the probability of failure. However, it is often argued that the solution of the latter is largely dependent on the target failure probability set as constraints of the problem (Beck and Gomes, 2012). Risk optimization addresses this issue by introducing a more global framework where the failure is directly integrated by quantifying and minimizing its associated cost. This framework may also include the cost of construction, operation and/or maintenance. This contribution focuses on a basic formulation of the risk optimization problem where the cost of failure is computed throughout the expected lifetime of the structure using time-variant reliability. For the latter, approaches based on the so-called out-crossing rate are considered. Such approaches may rely on either approximation (FORM) or crude Monte-Carlo simulation. In any case, the computational cost of this procedure is extremely high because of the integration along the time dimension. This is even more so when accounting for the repeated computations associated to different design configurations. To address this issue and allow for efficient solution when expensive computational models are considered, adaptive surrogate modeling is considered. The efficiency and validity of the approach is demonstrated on two application examples. REFERENCES Beck, A. T. and W. J. S. Gomes (2012). A comparison of deterministic, reliability-based and risk-based structural optimization under uncertainty. Prob. Eng. Mech. 28, 18–29.

A New Immersed IGA-RKPM Phase Field Framework for Brittle Fracture under Blast Loading

Georgios Moutsanidis*, David Kamensky**, Yuri Bazilevs***

*University of California, San Diego, **University of California, San Diego, ***University of California, San Diego

ABSTRACT

We present a newly developed hyperbolic phase field model for brittle fracture coupled with an immersed formulation for air-blast-structure interaction [1]. A fixed background discretization provides the basis functions used to approximate the unknowns of the coupled fluid-structure interaction problem, while foreground lagrangian particles are used to track the position of the solid, store the history dependent variables, and perform numerical quadrature on the solid terms. In addition, the foreground particles provide the basis functions to approximate the governing equation of the damage field. Isogeometric basis functions are used for the background discretization, while reproducing kernel shape functions are assigned to the particles and approximate the damage field. The presented air-blast-structure interaction problems show the methodology's ability to handle brittle fracture under blast loading. References: [1] Bazilevs, Y., Moutsanidis, G., Bueno, J., Kamran, K., Kamensky, D., Hillman, M.C., Gomez, H. and Chen, J.S., 2017. A new formulation for air-blast fluid-structure interaction using an immersed approach: part II—coupling of IGA and meshfree discretizations. Computational Mechanics, pp.1-16.

Practical Multiscale Approach for Analysis of Reinforced and Prestressed Concrete Structures

Arturo Moyeda^{*}, Jacob Fish^{**}

^{*}Columbia University, ^{**}Columbia University

ABSTRACT

We present a multiscale approach for analysis of reinforced and prestressed concrete structures , that overcomes two major hurdles in utilization of multiscale technologies in practice: (1) coupling between material and structural scales due to consideration of large representative volume elements, and (2) computational complexity of solving complex nonlinear multiscale problems. The former is accomplished using a variant of computational continua framework that accounts for sizeable reinforced concrete RVEs by adjusting the location of the quadrature points. The latter is accomplished by means of reduced order homogenization customized for structural elements.

Optimal Design of a Smart Wind Turbine Based on Neural Network, Evolutionary Optimization Technique and CFD

Javier Luis Mroginski*, Juan Manuel Podesta**, Hugo Guillermo Castro***

*Applied Mechanical Dept., Universidad Nacional del Nordeste, Argentina, **Universidad Nacional del Nordeste, Argentina, ***CONICET and Applied Mechanical Dept., Universidad Nacional del Nordeste, Argentina

ABSTRACT

It is well known that one of the global priorities is to implement new technologies that allow us to use in a more efficient manner alternative and renewable energy sources, in order to reduce the consumption of conventional energy sources. Wind is one of the most promising renewable energy and, for a number of years, several different types of wind turbines were used, mainly classified as horizontal axis wind turbines (HAWT's) and vertical axis wind turbines (VAWT's). Nevertheless, there are still many issues to explore or improve in this subject. Regarding its type, some researches support the fact that VAWT's perform better in urban environments than HAWT's [1]. In this work a new model of VAWT is proposed, designed as a combination of the Savonius and Darrieus VAWT's, where the simplest model is the so-called "H" turbine. The optimization of the proposed model is made by coupling computational fluid dynamics (CFD) and neural networks, leading to a "smart" wind turbine with the capability to switch between Savonius and Darrieus types according to the velocity and direction of the incident wind. Furthermore, it is shown how changing length and angle of attack of the blades modify its performance for different wind speeds. The prototype consists of three blades of NACA 0018 profile, initially vertical, with 2 meters high (H) and radius (R) of 1 meter. By means of an opening mechanical device, the operational principle can be interchanged, allowing to start the turbine at relatively low wind speeds. For the CFD simulation, the open-source toolbox OpenFOAM is used with sliding mesh on the rotational domain and SST k- ω turbulence model [2]. Considering the wind incidence angle together with the angle of attack of the blades and the average radius of the turbine as optimization variables, the optimal performance of the wind turbine is obtained associated to the maximum energy production and equipment regularity. [1] Li, Q; Maeda, T.; Kamada, Y.; Hiromori, Y.; Nakai, A.; Kasuya, T.; "Study on stall behavior of a straight-bladed vertical axis wind turbine with numerical and experimental investigations" Journal of Wind Engineering and Industrial Aerodynamics, 164 pp.1-12, 2017. [2] H.G. Castro, R.R. Paz, J.L. Mroginski, M.A. Storti "Evaluation of the proper coherence representation in random flow generation based methods" Journal of Wind Engineering and Industrial Aerodynamics, 168, pp 211–227 (2017)

Evolutionary Topology Optimization of Lightweight Structures with Fatigue Constraints

Mirosław Mrzygłod*

*Opole University of Technology

ABSTRACT

The necessity to carry out research in the field of fatigue design of lightweight structure is mainly related to the needs of the industry - the getting lighter structures, which maintain a high level of fatigue durability is very important for aviation and automotive. Answers to these needs can only be found in the combination of the implementation of the latest research in the field of material fatigue with modern design optimization algorithms. Available commercial tools have great limitations, both in terms of obtaining solutions for light structures as well as the application of modern fatigue constraints. The paper presents a proposal of a new methodology of topological optimization with the use of evolutionary methods dedicated for use in the optimization of lightweight structures with fatigue constraints. The research includes the use of modern hypotheses of multi-axis fatigue of materials and methods of damage accumulation for complex load regime. It can be mentioned criteria based on the critical plane approach, criteria based on stress invariants and criteria based on stress averages in elementary volume [1]. As a part of the research, selected fatigue hypotheses and the procedure of cumulative damage summation were numerically implemented. In addition, new methods have been developed to improve the efficiency of searching for low-mass solutions for the evolutionary algorithm of topological optimization. The Constant Criterion Surface Algorithm (CCSA) was used for research in this area, which was enriched with new procedures [2]. To illustrate the proposed design methodology, several examples of optimization of benchmark structural problems have been presented [3]. In addition to obtaining optimal numerical solutions, they were verified using virtual prototyping methods. The effect of the conducted research is new numerical procedures for rapid estimation of fatigue damages of several multiaxial fatigue criteria and the effective evolutionary topology optimization algorithm dedicated to the design of lightweight structure with fatigue constraints. References [1] Papadopoulos I.V., Davoli P., Gorla C., Filippini M., Bernasconi A., A comparative study of multiaxial high-cycle fatigue criteria for metals, *International Journal of Fatigue*, 19, 1997, 219-235. [2] Mrzygłod M., Multi-constrained topology optimization using constant criterion surface algorithm, *Bulletin of the Polish Academy of Sciences – Technical Sciences*, 60(2), 2012, 229-236. [3] Rozvany G.I.N., Exact analytical solutions for some popular benchmark problems in topology optimization, *Structural Optimization*, 15, 1998, 42-48.

QUANTITATIVE OBSERVATION AND COMPUTER SIMULATION OF WINDOW GLASS FRAGMENT INTO PIECES AND THEIR SCATTERING DUE TO COLLISION OF FLYING OBJECT

YOICHI MUKAI*, HIROTO KOHARA*, YASUFUMI KANNO[†],
MASAKI MATSUMOTO[†], YOSHIRO HORI[†], AND FUMIHIKO CHIBA[†]

*Kobe University
1-1 Rokkodai-cho, Nada-ku, Kobe, Hyogo 657-8501, Japan
ymukai@port.kobe-u.ac.jp

[†]YKK AP Inc.
3-22-1 Kamezawa, Sumida-ku, Tokyo 130-8521, Japan
mas_matsumoto@ykkap.co.jp

Key words: Collision Action, Window Glass Fragment, Non-structural Member, Flying Object, Impact load, FEM Analysis.

Abstract. In this study, destruction moment of glass window due to flying object is observed with high-speed cameras at the impact-loading experiments, and the behavior of scattering broken glass pieces is estimated through the motion-capturing and the position-data-extracting process. Various types of the projectile objects were shot on the front surface of the plate glass window. Different weight and impacting speed of the flying objects, and thickness of the plate glasses are tested. Each test specimen and test situation is also simulated in the FEM analysis. Numerical results are compared with the actual motions recorded by the high-speed camera. This study clarifies that numerical simulations can adequately reproduce window glass behavior broken into pieces and their scattering motion as observing in the experimental tests. The variation of the material parameters of the projectile object or the plate glass are evaluated to make assure these parameters sensitivity on the numerical simulation results. Through these case studies, the validity of the FEM modeling and the FEM analyses to reproduce the scattering behaviors of broken glass pieces is also discussed.

1 INTRODUCTION

A window glass destruction due to impact objects must cause serious human injury, thus, consideration of window glass property placed on a building facade is important for shock-resistant building design against impact actions [^{1,2}]. However, there are few studies to observe and to analyze quantitatively the behavior of scattering pieces of broken glass caused by the impact action of flying or colliding objects.

This study focuses on the destruction moment of plate glass windows due to flying objects and the scattering behavior of broken glass pieces [3]. For this aim, impact-loading experiments are carried out and colliding actions caused by the projectile object are observed using high-speed cameras. The behavior of scattering glass pieces is estimated through the motion-capturing and the position-data-extracting procedures by using recorded video photography in the tests. A launching apparatus with compressive air was used for the experimental tests and various types of the projectile objects were shot on the front surface of the plate glass window. Different weight and impact speed of the projectile object, and thickness of the plate glass are tested. Through the experimental tests, the relationship between the impact action of the projectile object and the scattering motions of the broken glass pieces are quantified and investigated.

Test specimen and test situation are also simulated in the FEM analyses. Numerical results are compared with the actual motion recorded by the high-speed camera. Reproducibility of the actual fracture behavior of plate glass in the numerical simulation is considered in this study. The variation of the material parameters of the projectile object and the impacted plate glass are investigated parametrically to make assure the sensitivity of these parameters on the numerical simulation results. Adequate model condition and parameters are considered for the validity of the FEM analyses to reproduce the scattering behaviors of broken glass pieces.

2 EXPERIMENTAL TESTS

To observe the fracture behavior of float plate glass for building windows, the impact tests using the projectile object shot by launching apparatus were carried out. This experimental test focuses on quantifying the scattering motion of broken glass pieces, thus the high-speed cameras were used to record the behavior the impact action of the projectile object and the fracture behavior of the plate glass specimen.



(a) Launching apparatus and test specimen



(b) High-speed camera setting

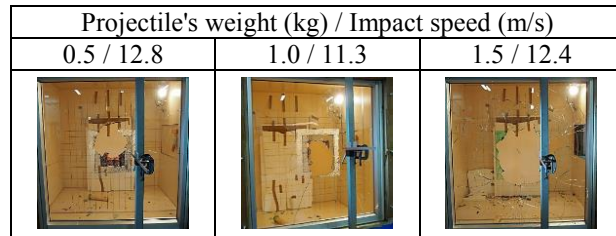
Figure 1 View of experimental test configuration

2.1 Outline of experimental test equipment and specimens

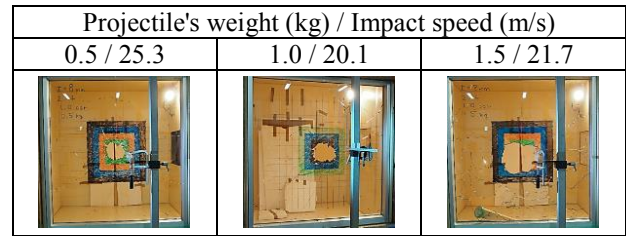
The experimental test configurations are displayed in Figure 1. The launching apparatus is set in front of the test specimen of window plate glass where is placed at 2 m of the front from the muzzle of the gun barrel of the launching apparatus. The plate glass specimen is equipped to the aluminum

sash frame, which is 1120 mm width and 1160 mm height, with 8 mm margins to suspend its whole periphery glass edge by placing rubber cushioning. Two kinds of specimens of plate glass which are 6 mm and 8 mm thickness are provided for this test. Both wooden and stainless projectiles are used as the impact objects and these are shot from the launching apparatus for the center of the plate glass window specimen. Wooden projectiles are the two kinds which have circular (94.2 mm diameter) and elliptic (78 mm x 37 mm in major/minor axis) sections. A stainless projectile is a hollow cylinder (95 mm diameter) whose ends are capped stainless plate. Weights of the wooden projectiles are adjusted by their length and three kinds of weights, 0.5 kg, 1.0 kg, and 1.5 kg, are tested. Weights of the stainless projectile are adjusted by the inserting weight into the cylinder and two kinds of weights, 0.5 kg and 1.0 kg, are tested. Impact speed of the projectile object is controlled by the compression air pressures, and the impact tests are operated under three kinds impact speeds, about 15 m/s, 25 m/s and 35 m/s.

Fracture behavior of window plate glass is photographed by using high-speed video cameras, and then, the recorded motions of scattering broken glass pieces are analyzed to extract their trajectory on the photo screen. Two high-speed video cameras are used; one is placed over the test specimen (as seen in Figure 1(b)) to pick up an image from above of the window plate glass to downward, and the other is placed in the front-side of the test specimen to image from the just beside of the projectile object toward the window surface and to measure its impact speed.

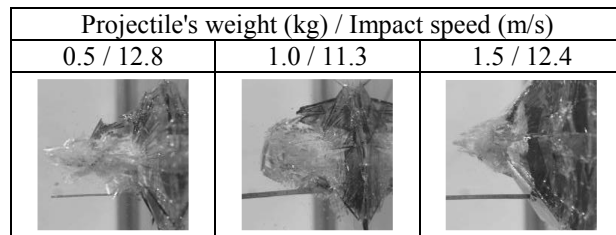


(a) Launching pressure : 0.6 bar

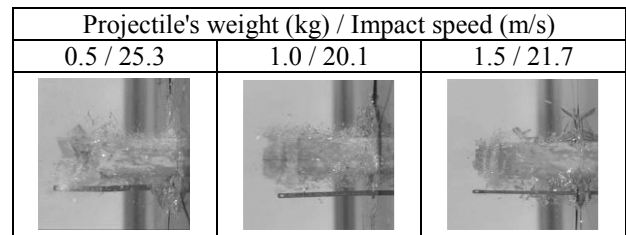


(b) Launching pressure : 1.0 bar

Figure 2 Damage state after penetration of ellipse-section wooden projectile (Glass thickness : 8 mm)



(a) Launching pressure : 0.6 bar



(b) Launching pressure : 1.0 bar

Figure 3 Scattering fragments by collision of ellipse-section wooden projectile (Glass thickness : 8 mm)

2.2 Observation of window glass fracture behavior

The front view photographs of the broken plate glass window which remains in the aluminum sash frame are displayed in Figure 2. These are at the case that the ellipse-section wooden projectile is used for shooting to the plate glass of 8 mm. Figure 3 displays scattering glass pieces and penetrating

projectile which are captured by the high-speed camera. As seen in Figures 2 and 3, different fracture modes can be observed depending on the impact speed of the projectile object. When the impact speed is fast (in this study, it is around 20 m/s or more), the projectile object goes through a narrow part and loss of area in broken plate glass is limited to small part. On the other hand, when the impact speed is slow (in this study, it is around 10 m/s), the projectile object breaks a wide part of the plate glass and the plate glass surface are broken with out-of-plane deformation.

2.3 Motion capture analysis of scattering glass pieces

Scattering motion of the broken glass pieces caused by collision of the projectile object is extracted using the two-dimensional motion analysis software (DIIP-Motion V/2D, DITECT Co.) for the video movies photographed by the high-speed camera. Displacements of some flying pieces of broken glass on the screen are evaluated by tracking the positions of "markers", which are the designated image areas included on the glass pieces, by every image frame. These markers are chosen from the leading fragments pushed in front of the projectile object, and the scattering speed of the window glass pieces are estimated as the average speed of these designated pieces. Every markers are designated on the photographed video frame after the tests through the software and displacing pixel number of each markers between frames is measured, and then time series of these pixels are decoded to the glass pieces motions. To convert pixels to length for this motion data extraction, a ruler of 150 mm which is equipped by protruding from the glass window is used as the referential length. Photographing frame resolution is 1280×800 pixels and frame rate is 1000 fps.

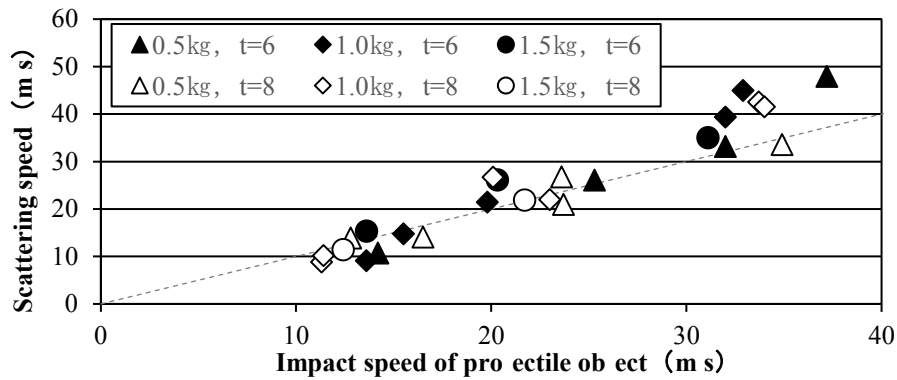


Figure 4 Scattering glass pieces speed vs. collision speed of projectile object (Experimental results)

Relations between scattering glass piece speed and collision object speed for the tests under different projectile objects, impact speeds and plate glass specimens are depicted in Figure 4. Collision speed of projectile object is determined as the just before moment to collide for the plate glass and it is evaluated by using the high-speed camera placed in the front-side of the test specimen. Under this test condition, is assured that the scattering glass piece speed is proportionally increased depending on the collision object speed and that the scattering glass piece speed has similar value of the collision object speed. However, when the collision object speed becomes large (in this study, it is around 30 m/s or more), the scattering glass piece speeds seem to increase and the variance of these are observed enlarging. While the obvious dependence to the collision object speed is observed

for the scattering glass piece speeds, it is assured that the difference of material or weight of the projectile object influence less to the scattering glass piece speeds within the test condition operating in this study.

3 FEM SIMULATIONS

To reproduce the actual behavior of scattering glass pieces caused by collision of projectile objects in the numerical simulations, FEM analyses are carried out. The finite element models are composed by considering the test specimen's features and configurations using in the impact experimental tests. LS-DYNA is used for calculating fracture of plate glass model caused by the projectile object collision. Reproducibility of the analyses is investigated through the comparison with the experimental results.

3.1 Numerical modelling and its parameters

For the FEM analyses, both the projectile object and the plate glass window are composed by the solid element model. As depicted in Figure 5, the center area of the plate glass window, where seem to be broken by the impact of the projectile object, has dense mesh division, and the single element size is 14 mm width x 14 mm height x 2 mm depth, while the single element at the surrounding area is 56 mm width x 56 mm height x 2 mm depth. Three or four layers are given in the thickness direction for the plate glasses of 6 mm or 8 mm. The number of the entire elements and the entire nodes are 3026 elements and 19996 nodes for the plate glass of 6 mm thickness and 4218 elements and 26236 nodes for the plate glass of 8 mm thickness, respectively.

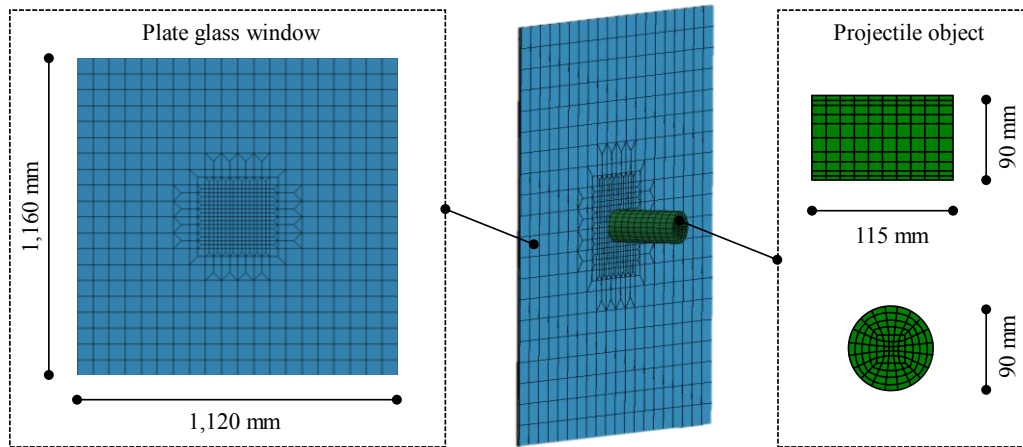


Figure 5 FEM analysis model

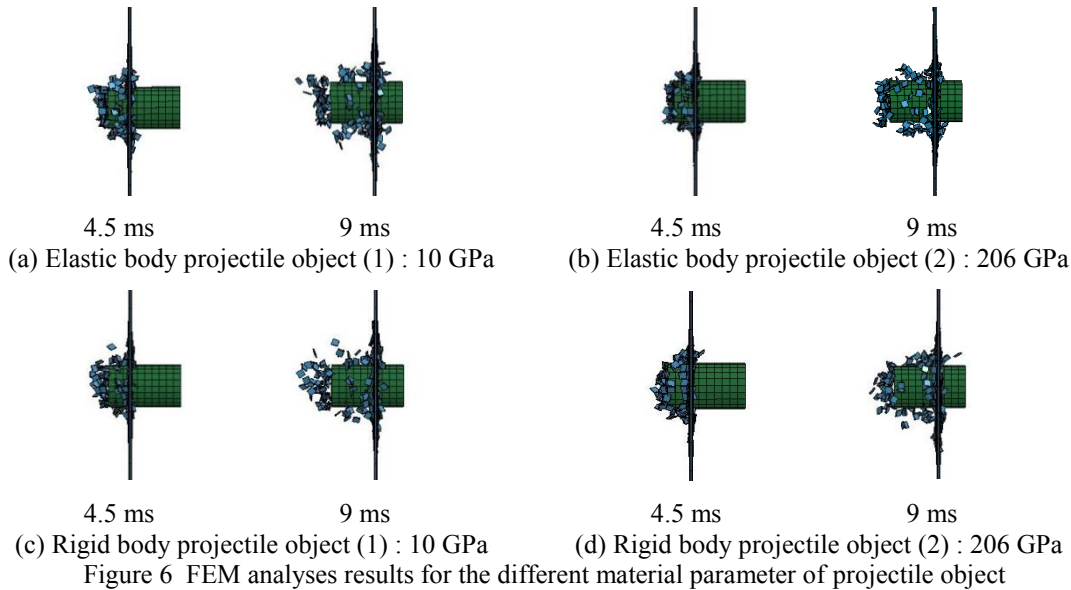
In this numerical study, all surrounding glass edge are assumed to be fixed rigidly. The projectile object part is applied to be contacted automatically to the plate glass part. Numerical calculations are started from the initial situation that the projectile object is placed at the initial position just coming into contact to the plate glass surface, and the impact action is simulated by applying the initial impact speed to the projectile object. To reproduce the scattering behavior of the broken glass

pieces in the simulations, all elements of the plate glass part are provided the condition that any element is restricted to all adjacent ones at its all nodes until reaching their rupture limitation, thus elements of the plate glass are separated at the nodes beyond the rupture limitation, and then the fracture behavior is simulated. In this study, the rupture limitation is considered at the situations when exceeding 0.24% for the equivalent plastic strain or exceeding 60 MPa for the tensile strength, and the node restriction is released [4].

Material model parameters of window plate glass and impact object are listed in Table 1. Material model for the plate glass is applied to the JOHNSON-HOLMQUIST-CERAMICS (MAT110) [5] which is adequate to represent the behavior of the brittle material and the real constants for the material parameter for this model are employed from the values indicated in Hidallana-Gamage's literature [4]. Material model for the projectile object is applied to the normal elastic material model (MAT001) [5], and the normal rigid body material model (MAT20) [4] is also used for comparative investigations with the elastic material model.

Table 1 Material model constants of plate glass and projectile object

Material	Mass density (kg/m ³)	Young's modulus (GPa)	Poisson's ratio
Plate glass	2530	72	0.22
Projectile object (1)	507	10	0.3
Projectile object (2)	507	206	0.3



3.2 Sensitivity analysis for material parameters : Projectile object

At first, parameter sensitivity in FEM analyses is evaluated for the material constants about the projectile object model. In this study, two kinds of the material constant about Young's modulus of the projectile object material as seen in Table 1 are considered for the two kinds of material model types which are the elastic body and the rigid body. Figure 6 displays the fracture behaviors of the

plate glass of 6 mm thickness while colliding 0.5 kg projectile object which has 14.2 m/s of the impact speed. Each case displays the fracture situation images at 4.5 ms and 9 ms after the impact moment. Figure 6 (a) and (b) are corresponding to the cases using the elastic material model for the projectile object with Young's modulus of 10 GPa and 206 GPa, respectively. Figure 6 (c) and (d) are corresponding to the cases using the rigid body material model for the projectile object with Young's modulus of 10 GPa and 206 GPa, respectively. By comparing Figure 6 (a) and (b), or by comparing Figure 6 (c) and (d), it is assured that the difference of the speed and displacement of scattering broken glass pieces are quite small even if the different Young's modulus is considered but the same material model type is applied. This result is consistent to the experimental observation that the scattering speeds of broken glass pieces had less dependence to the difference of projectile object material. By comparing Figure 6 (a) and (c), or by comparing Figure 6 (b) and (d), the speed and displacement of scattering broken glass pieces are reduced in the case using the elastic material model, because of consideration of the local deformation of the projectile object in calculations.

3.3 Sensitivity analysis for material parameters : Plate glass

Parameter sensitivity in FEM analyses for the material fracture parameters about the plate glass model are also evaluated. In this study, the equivalent plastic strain and the tensile strength are considered as the fracture index of the plate glass. As the referential case, the rupture limitation of plate glass material is considered 0.24% for the equivalent plastic strain and 60 MPa for the tensile strength. By using the elastic material model with Young's modulus of 10 GPa for the projectile object, the case study about the fracture behavior of the plate glass of 6 mm thickness while colliding the projectile object of 0.5 kg under the impact speed of 14.2 m/s.

Three different parameters of the plate glass fracture limitation for the equivalent plastic strain, which are 0.12%, 0.24% and 0.48%, are investigated under the same fracture limitation of 60 MPa for the tensile strength. And then, three different parameters of the plate glass fracture limitation for the tensile strength, which are 30 MPa, 60 MPa and 120 MPa, are investigated under the same fracture limitation of 0.24% for the equivalent plastic strain.

Figure 7 displays the numerical results of the fracture situation images at 4.5 ms and 9 ms after the impact moment for five cases. Figure 7 (a), (b) and (c) are corresponding to the cases using the plate glass fracture limitation of the equivalent plastic strain of 0.12%, 0.48% and 0.24%, respectively. The same limitation of the tensile strength of 30 MPa are assumed in these 3 cases. By comparing these figures, it is assured that the fracture parameter dependence on the equivalent plastic strain of the plate glass is comparatively small, thus the remarkable difference of the scattering speed of broken glass pieces and the penetration length of the projectile objects are not observed.

Figure 7 (c), (d) and (e) are corresponding to the cases using the plate glass fracture limitation of the tensile strength of 60 MPa, 30 MPa and 120 MPa, respectively. The same limitation of the equivalent plastic strain of 0.24% are assumed in these 3 cases. By comparing these figures, it is assured that the fracture parameter dependence on the tensile strength of plate glass is comparatively small for the the scattering speed of broken glass pieces and the penetration length of the projectile objects. On the other hand, it is observed that loss of area in broken plate glass becomes narrow in the case of the weak strength (30 MPa), and that loss of area in broken plate glass becomes wide in the case of the strong strength (120 MPa).

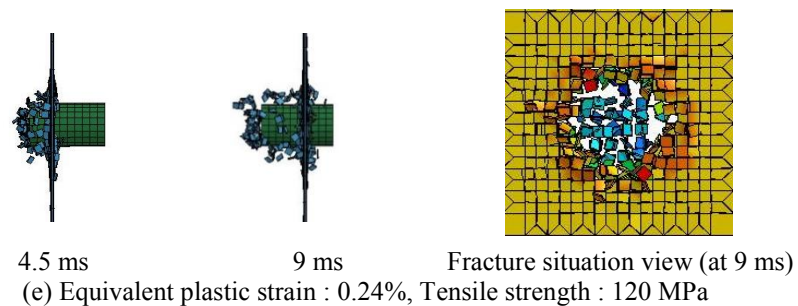
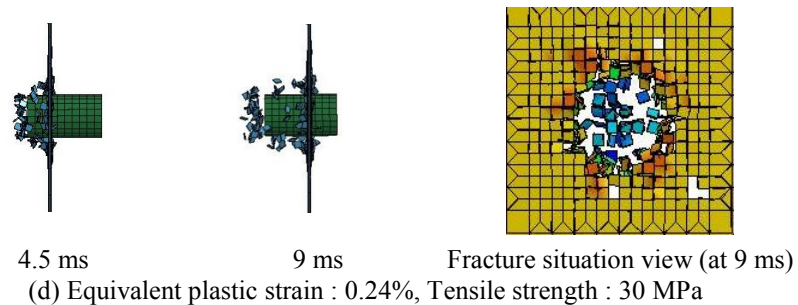
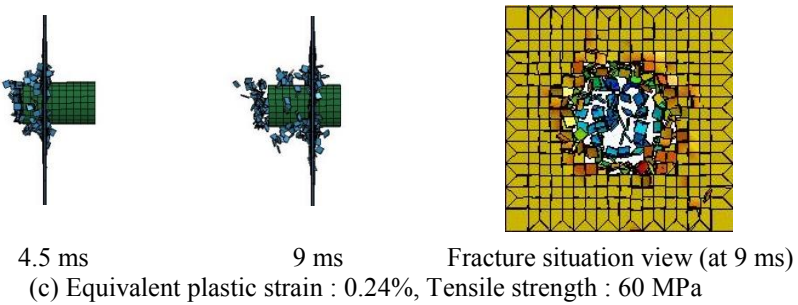
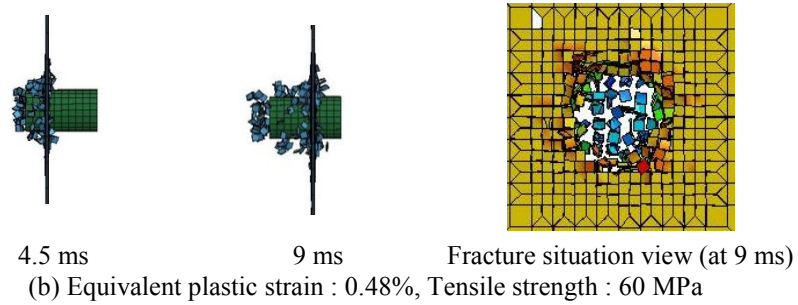
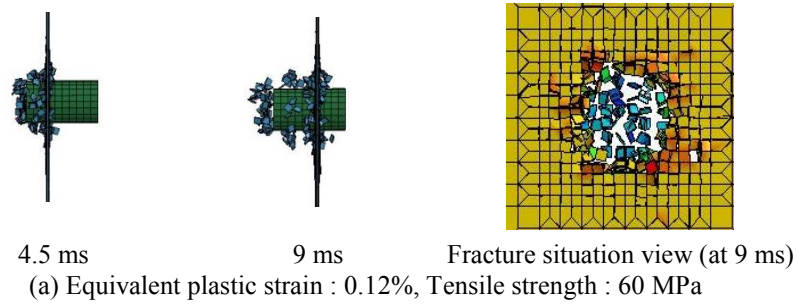


Figure 7 FEM analyses results for the different material parameters of plate glass fracture

3.4 Comparative study between FEM analyses and experimental tests

FEM analyses corresponding to every cases of the different test parameters carried out in the experimental tests are executed. The collision speeds of the projectile objects in the simulations are adjusted to each speed observed in the experiment. In this simulation study, FEM model of the projectile object is applied as the elastic material with Young's modulus of 206 GPa, and the rupture limitations of the plate glass are considered to 0.24% for the equivalent plastic strain and 60 MPa for the tensile strength. Relations between scattering glass pieces speed and collision object speed for the different projectiles weight, impact speed and plate glass thickness are depicted in Figure 8.

Under the FEM analyses, it is assured that the scattering glass pieces speed is proportionally increased depending on the collision object speed, and that the scattering glass pieces speed has similar value of the collision object speed. By comparing this numerical result with the experimental result as seen in Figure 4, it is confirmed that the fracture behavior of plate glass can be reproduced capably. When the collision object speed becomes large (around 30 m/s or more), the scattering glass pieces speeds become to increase and the variance of these are observed enlarging in FEM analyses likewise. The dependence on the collision object speed is also observed for the scattering glass pieces speeds, and the weight of the projectile object has also less influence to the scattering glass pieces speeds in the simulation results.

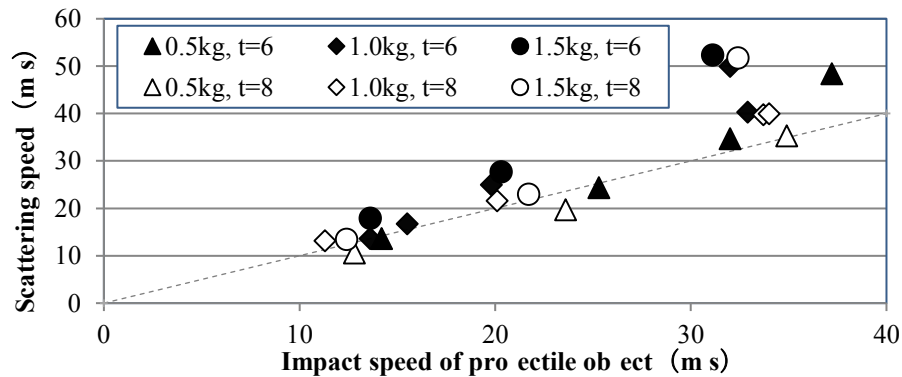
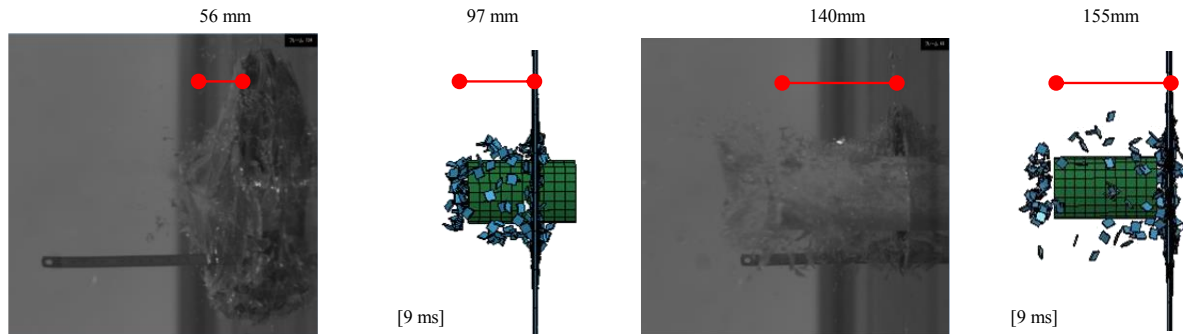


Figure 8 Scattering glass pieces speed vs. collision speed of projectile object (Numerical results)



(a) Collision speed : 14.2 m/s (b) Collision speed : 25.3 m/s
Figure 9 Comparison between FEM analyses and experimental tests results about penetrating length

Figure 9 displays comparison between the experiment and the FEM analysis results about penetrating length of the projectile object after collision on the plate glass. Figure 9 (a) and (b) are corresponding to the low speed collision (14.2 m/s) and the high speed collision (25.3 m/s), respectively. Both of these cases are the collision of the ellipse-section wooden projectile of 0.5 kg to 6 mm thickness plate glass and both images are corresponding to the instance at 9 ms after impact. FEM analyses are operated using the elastic material model with Young's modulus of 206 GPa, and the rupture limitation of plate glass material is considered 0.24% for the equivalent plastic strain and 60 MPa for the tensile strength.

By comparing the experimental and the numerical results about penetrating length of the projectile object, larger length in the FEM analyses are observed than the experimental results. More difference between the simulation and the test appears in the low speed collision case (as seen in Figure 9 (a)), while difference between them is not much in the high speed collision case. As a reason for this, it is considered that less energy loss of the projectile object is evaluated at the FEM analyses than an actually obtained experimental result. This seems to be the issue to have further consideration about the rupture limitations parameters of the plate glass in the FEM analyses, or the estimation about element mesh size of the plate glass part is also thought about as a new issue.

4 CONCLUSIONS

This study executed the experimental test to observe and photograph the fracture behavior caused by collision of the projectile object. High-speed cameras are used to record the scattering motion of broken glass pieces and the quantitative evaluation of the fracture behavior of plate glass are performed through 2D motion analyses procedures. FEM analyses to reproduce the actual fracture situation of the plate glass are also carried out and the sensitivity of the material model parameters for the FEM models are investigated. By comparing the FEM simulation results with the experimental results, adequateness of the FEM analyses to evaluate the fracture behavior of the plate glass is also discussed. The findings through this study are summarized in the followings.

- Different fracture modes were observed depending on the impact speed of the projectile object. When the impact speed is fast (around 20 m/s or more), the projectile object goes through a narrow part and loss of area in broken plate glass is limited small part. When the impact speed is slow (around 10 m/s), the projectile object breaks a wide part of the plate glass and its surface are broken with out-of-plane deformation.
- Relations between scattering glass pieces speeds and collision object speed for the tests under different projectile objects, impact speeds and the plate glass thicknesses are investigated. It was observed that the scattering glass pieces speed is proportionally increased depending on the collision object speed and it has similar value of the collision object speed, while the difference of material or weight of the projectile object influence less to the scattering glass pieces speeds.
- Numerical simulations can adequately reproduce window glass behavior broken into pieces and their scattering as observing in the experimental tests. While the tendency that influences the results, which are related by the difference of weight or impact speed of the projectile object, or the thickness of the plate glass, could be reappeared in FEM

analyses.

- The penetrating length of the projectile object is observed larger in the FEM analyses than the experimental results. More difference between the simulation and the test appears in the low speed collision case, while difference between them is not much in the high speed collision case. This seems to be depending on evaluation of less energy loss of the projectile object in the FEM analyses than an actually obtained experimental tests.
- The difference of the speed and displacement of scattering broken pieces are quite small even if the different Young's modulus are considered but the same material model type is applied. The speed and displacement of scattering broken glass pieces are reduced in the case using the elastic material model, because of consideration of the local deformation of the projectile object in calculations.
- The fracture parameter dependence on the equivalent plastic strain of plate glass is comparatively small, thus the remarkable difference of the scattering speed of broken glass and the penetration length of the projectile object are not observed in the simulations with the different rupture limitation of the equivalent plastic strain.
- The fracture parameter dependence on the tensile strength of plate glass is comparatively small for the the scattering speed of broken glass and the penetration length of the projectile object. On the other hand, it is observed that loss of area in broken plate glass becomes narrow in the case of the weak strength, and that loss of area in broken plate glass becomes wide in the case of the strong strength.

ACKNOWLEDGMENTS

The part of this work were supported by JSPS grant No.R2904 in the program for Advancing Strategic International Networks to Accelerate the Circulation of Talented Researchers and JSPS KAKENHI Grant Number 26420552, 16H03124 and 17K18924. Authors also acknowledge Mr. Tsubasa Hattori who graduated the master course of Kobe University for his contribution to the experimental tests and the numerical simulations in this study.

REFERENCES

- [1] Architectural Institute of Japan. Recommendations for Loads on Buildings, AIJ Design Guideline. AIJ, (2015). (in Japanese)
- [2] Architectural Institute of Japan. Introduction to Shock-Resistant Design of Buildings, AIJ Design Concept. AIJ, (2015). (in Japanese)
- [3] Matsumoto, M. Study on Destructive Behavior of Window Glass by Collision due to Flying Object. Summaries of technical papers of Annual Meeting, Architectural Institute of Japan. Structures I. (2017) 285-288. (in Japanese)
- [4] Hidallana-Gamage, H.D. et al. Numerical modelling and analysis of the blast

Yoichi Mukai, Hiroto Kohara, Yasufumi Kanno, Masaki Matsumoto, Yoshiro Hori and Fumihiko Chiba

performance of laminated glass panels and the influence of material parameters. *Engrg. Failure Analysis*. (2014) 45: 65-84.

[5] JSOL. LS-DYNA Version 971, User's Manual Volume II. (2016) 461-463.

Hybrid Particle-continuum Computational Models for Thrombus Biomechanics

Debanjan Mukherjee*, Shawn C. Shadden**

*University of California, Berkeley, **University of California, Berkeley

ABSTRACT

Thrombosis and embolisms comprise the primary cause of major cardiovascular diseases like heart attack and stroke, which amount to significant morbidity and mortality worldwide. Additionally, thrombotic and embolic events during surgical procedures or medical device deployment can cause serious complications. Computational tools have rapidly advanced to become a valuable non-invasive technique for investigating cardiovascular phenomena, complementing experimental and clinical investigations. However, developing computational models for thrombus biomechanics within large artery hemodynamics remains a key challenge. Resolving the interaction of a realistic thrombus, comprising arbitrary shape and heterogeneous microstructure, with pulsatile viscous flow is critical. Additionally, robust modeling of the deformation and embolization of these heterogeneous thrombi often requires specialized techniques. Here, we present our recent advancements towards addressing these challenges by devising a mesoscale particle-continuum framework. A thrombus is reconstructed as a heterogeneous aggregate of discrete particles based on medical or experimental image-data. Arterial hemodynamics around this aggregate is resolved by coupling the particle reconstruction to blood flow using a fictitious domain finite element method. Thrombus deformation mechanics is modeled based on the particle reconstruction using a discrete element approach, wherein individual particles interact via effective forces and potentials, and via a network of force-chains interspersing the particles (mimicking the intrinsic fibrin network of thrombi). Each element of the force chain comprises a combination of springs, dashpots, and sliders. The collective dynamics emerging from the particle interactions effectively describe thrombus deformation. Rupture and embolization is recovered by removing particles from the aggregate based on particle-network connectivity and inter-particle forces. We present numerical experiments using model thrombus geometries reconstructed from experimental data reported in the literature. We demonstrate that our methods can resolve not only the complex unsteady flow around large-arterial thrombi, but also estimate the intra-thrombus perfusion flow. Simulations performed on mechanically deforming thrombus aggregates embedded in plasma demonstrated the efficacy of our methods in capturing aggregate thrombus deformation biomechanics. Additionally, we establish that our approach can capture the initiation of thrombus rupture and rupture propagation until complete embolization. Micro-mechanical properties like microstructural order parameters can also be directly computed and compared with experiments. These results, thus, demonstrate the utility of our hybrid particle-continuum treatment in addressing current challenges in thrombus biomechanics modeling. [Acknowledgements: AHA Award: 16POST27500023, NSF Award: 1354541, BWF-CRTG Award: 1016360]

Stochastic Time Domain Spectral Element Analysis of Timoshenko Beam with Non-Gaussian Properties

Shuvajit Mukherjee*, Ranjan Ganguli**, S. Gopalakrishnan***

*Department of Aerospace Engineering, Indian Institute of Science, Bangalore-560012, India., **Department of Aerospace Engineering, Indian Institute of Science, Bangalore-560012, India., ***Department of Aerospace Engineering, Indian Institute of Science, Bangalore-560012, India.

ABSTRACT

Material uncertainty effects are studied for static, free vibration and dynamic analysis of Timoshenko beam. Uncertainty is inevitable in engineering structures. So, for reliable design of engineering structures, it should be incorporated into the modeling. In this work, random field based modeling is used to account the spatial variability of the material properties. A stochastic time domain spectral element method (STSEM) is proposed for Timoshenko beam. The material properties are considered as 1-D non-Gaussian random fields and optimal linear estimation (OLE) [1] is used for the discretization of the random fields. The OLE-based discretization of a random field allows simulating the random fields digitally followed by the simulation of realizations of stiffness, mass matrix, and dynamic stiffness matrix. Recently, Sasikumar et al. [2] proposed a framework which suggests different independent meshing for random field and finite element discretization resulting in the saving of CPU time. In this current work, computationally efficient time domain spectral element method (TSEM) [3] is used instead of finite element method (FEM) to develop the STSEM formulation. The STSEM reduces the CPU time significantly as the number of degrees of freedom (DOF) is very less than that of FEM. TSEM also provides a consistent diagonal mass matrix and Gauss–Lobatto–Legendre (GLL) quadrature requires less computational cost than the Gauss–Legendre quadrature which lessens the CPU time. Unlike Monte Carlo, the computation time follows almost linear relationship with the number of simulations. In this work, STSEM of Timoshenko beam is proposed and as well as the effect of correlation length on the response statistics is also studied. The deflection statistics of the beam for both static and dynamic cases are investigated considering various boundary conditions. The computational efficiency of the proposed method and effect of material variability on response statistics are discussed. This STSEM formulation can also be applied for complex structural and computationally demanding wave propagation problems. 1. C.-C. Li, A. Der Kiureghian, Optimal discretization of random fields, *Journal of Engineering Mechanics* 119 (6) (1993) 1136–1154. 2. P. Sasikumar, R. Suresh, S. Gupta, Stochastic finite element analysis of layered composite beams with spatially varying non-gaussian inhomogeneities, *Acta Mechanica* 225 (6) (2014) 1503–1522. 3. A. T. Patera, A spectral element method for fluid dynamics: laminar flow in a channel expansion, *Journal of Computational Physics* 54 (3) (1984) 468–488.

A CLOSED-FORM FUNCTIONAL DIFFERENTIAL QUADRATURE METHOD (f-DQM) WITH APPLICATIONS IN COMPUTATIONAL MECHANICS

FAISAL M. MUKHTAR*

* Department of Civil & Environmental Engineering,
King Fahd University of Petroleum & Minerals,
31261, Dhahran, Saudi Arabia.

Email; faisalmu@kfupm.edu.sa

Key words: Differential Quadrature Method, Closed-form Solution, Symbolic Computation, Radial Basis Functions.

Abstract. As a popular numerical technique, the differential quadrature method (DQM) expresses each derivative and/or integral, in the differential or integro-differential equations, as a weighted sum of the solution values at some selected nodes. This allows discrete values of the primary solution variable(s) to be obtained with only few grid points. The method has gained wide acceptance in the area of computational mechanics. Despite its advantages, DQM requires extra efforts for additional quadrature formulations each time any other secondary variable is needed. Moreover, result at few discrete points hinders sufficient visual representation of the overall solution pattern, and results of the non-sampled points may not be obvious in some cases. Also, some terms in nonlinear problems necessitates inconvenient use of intermixed summation indices. In order to increase the flexibility of the method while maintaining its accuracy, this paper proposes the functional differential quadrature method (f-DQM) that yields a symbolic/functional form of the solution valid throughout the domain under consideration. Some of the advantages of the proposed method include (1) ease in post-processing, as any other secondary variable of interest can be obtained by directly operating on the closed-form solution, (2) means for better visual pattern/description of the solution while utilizing quadrature-based formulation to achieve high accuracy with only few nodes, and (3) possibility for direct analytical computation of differentials and/or integrals during the solution process for terms that require inconvenient use of nested quadrature formulations. The convenience and power of symbolic software programs can be harnessed both during the pre and post-processing stages. Problems of bending of a thin plate and linear and nonlinear elastoplastic torsion of a bar are analyzed to illustrate the features of the proposed method.

1 INTRODUCTION

Interest in the use of differential quadrature method (DQM) and/or its variants results, largely, due to their efficiency. Origin of the method can be traced back to Bellman and Casti [1] with full

details later given by Bellman et al. [2]. DQM requires relatively few grid points to achieve accurate results. It has been popularly applied to many works in computational mechanics as well as developing its variances aiming at addressing some of its associated short comings and challenges.

The basis of the method stems from the derivative approximation, rather than the solution approximation. Any n^{th} derivative of a function with respect to a space variable (say, x or y) is written as a linear combination of some weighting coefficients multiplied by the discrete values of the function itself at selected sampling points. The weighted sum requires the use of some suitably selected shape functions whose choice, in addition to the number and distribution of points, dictates the accuracy of the final solution. Since the invention of the method, the impetus of research on the subject mainly focuses on the selection of the shape functions and algorithm for the method's implementations. Example of commonly used shape functions includes the polynomial basis function proposed by Shu and Richards [3], the Fourier expansion by Shu and Chew [4], the radial basis function by Wu and Shu [5], etc. With slight modification, a local DQM can be used to tackle problems with irregular boundaries (for example, see [6]).

Suitable selection of the shape functions apriori allows the solution of the weighting coefficients, first, which are then used to obtain the solution for the problem at hand. A tasking exercise in DQM is the need for having to always cast the expression for any secondary variable (such as the stresses) using the quadrature rules, thereby requiring extra efforts in post-processing. In addition, the discrete nature of the solution implies that results for those locations that have not been initially selected as sampling points will be missing. If such results need to be captured, it becomes necessary to use many sampling points before the solution behavior becomes representative of the whole domain. However, the use of unnecessarily more points than is required for accuracy neutralizes the major advantage of the method: few grid points that provides good accuracy. Last, but not the least, is the fact that the formulation of some highly nonlinear derivative terms becomes more involved due to the need for many nested quadrature formulations. This could be inconvenient with a more likelihood of human error resulting from many intermixed summation indices.

This paper proposes and develops a new version of DQM, the functional differential quadrature method (f-DQM), which addresses the aforementioned concerns. The method warrants a chance to increase the flexibility of traditional DQM by (i) presenting its results in symbolic/functional form of the solution valid throughout the domain under consideration which results in the ease in post-processing so that any other secondary variable of interest can be obtained by directly operating on the closed-form function for the solution, (ii) preserving the main advantage of DQM in using fewer points while providing a means for better visual pattern/description of the solution, and (iii) making it possible for direct analytical computation of differentials and/or integrals during the solution process for terms that require inconvenient use of nested quadrature formulations. In addition to the number and distribution of points and shape functions in the conventional DQM, there exists a possibility of choosing different candidate solutions that provide the means to refine the accuracy to different extents in f-DQM. Another secondary advantage of the proposed method is the convenience in utilizing symbolic computational tools capabilities. Overall, the proposed f-DQM provides a means to harness advantages similar to those of the closed-form analytical counterparts and, yet, maintaining high accuracy associated with the conventional DQM.

2 TRADITIONAL DQM FORMULATION

The most basic form of DQM is explained here, where for a two-dimensional domain consisting of the spatial variables x and y , the derivatives of any given function are, first, sought. For example, consider the rectangular domain of dimensions L_x by L_y where the derivative approximation at a typical point (x_i, y_j) , shown with the symbol \bullet in Fig. 1(a) will be determined. The m^{th} derivative with respect to x requires the weighted sum of the linear combination of the function values at the grid points represented with the symbol \circ in the same figure. This derivative is given by Eq. (1). Similarly, the n^{th} derivative with respect to y , given by Eq. (2), requires the weighted sum of linear combination of the function values at the grid points represented with the symbol \oplus in Fig. 1(a). It can be shown that mixed derivative can be written in the form given by Eq. (3).

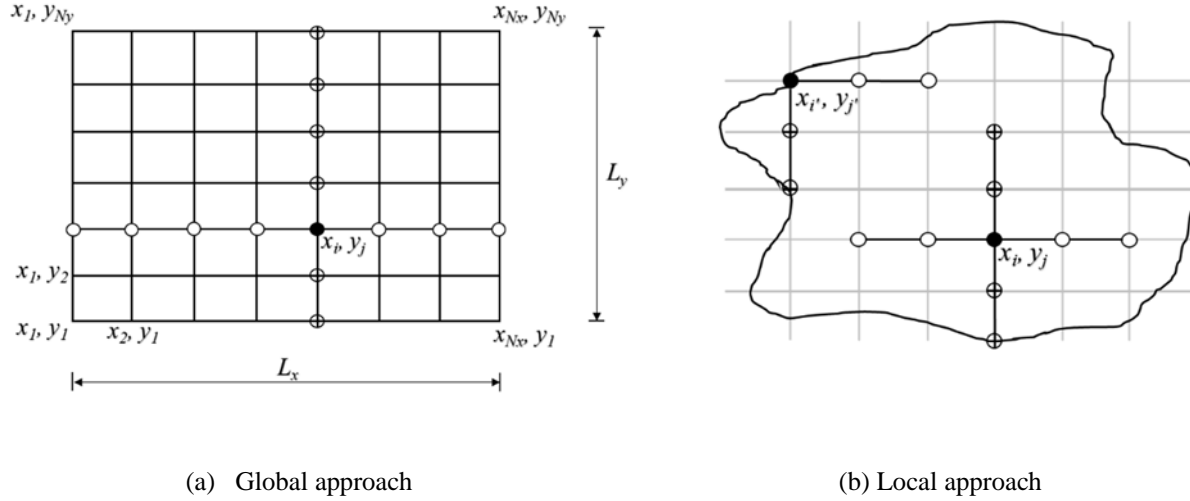


Figure 1: Idea of problem discretization in DQM

$$\frac{\partial^m \psi(x_i, y_j)}{\partial x^m} = \sum_{k=1}^{N_x} \alpha_{ik}^{(m)} \psi(x_k, y_j), \quad i = 1, 2, \dots, N_x \quad \text{at any point } y = y_j \quad (1)$$

$$\frac{\partial^n \psi(x_i, y_j)}{\partial y^n} = \sum_{l=1}^{N_y} \beta_{jl}^{(n)} \psi(x_i, y_l), \quad j = 1, 2, \dots, N_y \quad \text{at any point } x = x_i \quad (2)$$

$$\frac{\partial^{(m+n)} \psi(x_i, y_j)}{\partial x^m \partial y^n} = \sum_{k=1}^{N_x} \alpha_{ik}^{(m)} \sum_{l=1}^{N_y} \beta_{jl}^{(n)} \psi(x_k, y_l), \quad i = 1, 2, \dots, N_x \text{ and } j = 1, 2, \dots, N_y \quad (3)$$

The unknown coefficients α and β are determined by selecting appropriate test function $\psi(x, y)$ and forcing it to satisfy Eq. (1) at N_x sampling points and Eq. (2) at N_y sampling points, respectively. An alternative discretization to the global approach is the use of local DQM discretization, as typically depicted in Fig. 1(b). This becomes particularly useful in cases of irregular geometries where both the internal and boundary points such as (x_i, y_j) and (x_i', y_j') can be treated comfortably.

After determining α and β as described above, any problem of interest such as that described by the general linear (**L**) or nonlinear (**NL**) governing differential equation subject to some boundary condition (**BC**) given by Eq. (4) can be solved. Where, f and g are some constants or

functions of the spatial variables. However, while solving Eq. (4), the same domain and its discretization as that used for obtaining α and β needs to be maintained. This is achieved by substituting Eqs. (1) to (3) into Eq. (4) by using $u(x_i, y_j)$ instead of $\psi(x_i, y_j)$ to enable the primary solution variable $u(x_i, y_j)$ to be obtained at the discrete points (x_i, y_j) over the domain.

$$\mathbf{NL}(u, \partial_x u, \partial_y u, \dots, \partial_x^m \partial_y^n u) = f \quad \text{in } \Omega \subset \mathbb{R}^d \quad (4a)$$

$$\mathbf{BC}(u, \partial_x u, \partial_y u, \dots) = g \quad \text{in } \partial\Omega \quad (4b)$$

$$\text{Where, } \partial_x^m(\dots) = \frac{\partial^m(\dots)}{\partial x^m}, \quad \partial_y^n(\dots) = \frac{\partial^n(\dots)}{\partial y^n}, \quad \text{and} \quad \partial_x^m \partial_y^n(\dots) = \frac{\partial^{(m+n)}(\dots)}{\partial x^m \partial y^n}$$

3 CLOSED-FORM FUNCTIONAL DIFFERENTIAL QUADRATURE METHOD (f-DQM)

It is obvious that the formulation of the basic DQM presented in the previous section consists of the derivative approximation using quadrature rules and the subsequent solution of the problem of interest at discrete values. As mentioned earlier, in order to obtain other secondary variables, additional quadrature rules must be used for the derivatives. Yet, both the primary and secondary solution variables can only provide results at discrete points. This and the other earlier identified challenges, including the non-representativeness of non-sampled points as well as the issue of nonlinear derivative or integral terms, in DQM can be addressed by the formulations in this section. Instead of only the derivative approximation in traditional DQM, the present work proposes the use of both derivative and the solution approximations as follows.

The solution to Eq. (4) or for a corresponding one dimensional case can be approximated using the linear combination of some function $\phi(x, y)$ or $\phi(x)$, respectively, given by Eq. (5). The coefficients λ_{ij} or λ_i are unknowns that needs to be determined.

$$u(x, y) = \sum_{i=1}^{N_x} \sum_{j=1}^{N_y} \lambda_{ij} \phi_{ij}; \quad u(x) = \sum_{i=1}^{N_x} \lambda_i \phi_i; \quad (5)$$

Depending on their performance, polynomials, radial basis functions (RBFs) or other suitable approximating functions, can be selected as ϕ in Eq. (5). For instance, if a Taylor series expansion around a point c is selected in a 1D problem, then $u(x) = \sum_{i=1}^{\infty} \frac{y^i(c)}{i!} (x - c)^i \approx \sum_{i=1}^{N_x} \lambda_i \phi_i$. Similarly, if a suitably chosen RBF centered at x^{ij} is used for a 2D case, then $\phi_{ij} = \phi(\bar{x}, x^{ij})$. Where, $\bar{x} = (x, y)$ and $x^{ij} = (x_i, y_j)$.

Writing the quadrature analogue of Eq. (4) results in Eq. (6), which is a system of $N_x \times N_y$ equations that can be solved for the $N_x \times N_y$ discrete unknowns u at the sampling points.

$$\mathbf{NL}\left(u(x_i, y_j), \sum_{k=1}^{N_x} \alpha_{ik}^{(m)} u(x_k, y_j), \sum_{l=1}^{N_y} \beta_{jl}^{(n)} u(x_i, y_l), \dots, \sum_{k=1}^{N_x} \alpha_{ik}^{(m)} \sum_{l=1}^{N_y} \beta_{jl}^{(n)} u(x_k, y_l)\right) = f \quad (6a)$$

$$\mathbf{BC}\left(u(x_i, y_j), \sum_{k=1}^{N_x} \alpha_{ik}^{(m)} u(x_k, y_j), \sum_{l=1}^{N_y} \beta_{jl}^{(n)} u(x_i, y_l), \dots\right) = g \quad (6b)$$

However, instead of the direct solution of discrete u values, the assumed symbolic solution $u(x, y)$ given by Eq. (5) is substituted in Eq. (6) to obtain Eq. (7), where $\phi_{pq}^{mn} = \phi(\bar{x}^{pq}, x^{mn})$ and $\bar{x}^{pq} = (x_p, y_q)$. Solving Eq. (7) yields the $N_x \times N_y$ unknowns λ_{ij} which are then substituted back into

Eq. (5) to obtain the final approximate solution in a closed/functional form from which any other secondary variables can be obtained by directly operating on the solution u rather than having to spend extra effort in using additional quadrature formulations to achieve the same.

$$NL \left[\sum_{m=1}^{N_x} \sum_{n=1}^{N_y} \lambda_{mn} \phi_{ij}^{mn}, \sum_{k=1}^{N_x} \alpha_{ik}^{(m)} \left(\sum_{m=1}^{N_x} \sum_{n=1}^{N_y} \lambda_{mn} \phi_{kj}^{mn} \right), \sum_{l=1}^{N_y} \beta_{jl}^{(n)} \left(\sum_{m=1}^{N_x} \sum_{n=1}^{N_y} \lambda_{mn} \phi_{il}^{mn} \right), \dots, \sum_{k=1}^{N_x} \alpha_{ik}^{(m)} \sum_{l=1}^{N_y} \beta_{jl}^{(n)} \left(\sum_{m=1}^{N_x} \sum_{n=1}^{N_y} \lambda_{mn} \phi_{kl}^{mn} \right) \right] = f \quad (7a)$$

$$BC \left[\sum_{m=1}^{N_x} \sum_{n=1}^{N_y} \lambda_{mn} \phi_{ij}^{mn}, \sum_{k=1}^{N_x} \alpha_{ik}^{(m)} \left(\sum_{m=1}^{N_x} \sum_{n=1}^{N_y} \lambda_{mn} \phi_{kj}^{mn} \right), \sum_{l=1}^{N_y} \beta_{jl}^{(n)} \left(\sum_{m=1}^{N_x} \sum_{n=1}^{N_y} \lambda_{mn} \phi_{il}^{mn} \right), \dots \right] = g \quad (7b)$$

It is important to mention that the selection of RBF as the function ϕ in Eq. (5) does not make the f-DQM and Kansa method [7] the same. While Kansa method works by directly operating on the approximated solution in its formulation, the f-DQM utilizes quadrature-based differentials and/or integrals. In fact, the use of ϕ as RBF is just one possibility out of the many choices one may deem fit. The second example in Section 4 illustrates that even if RBF is selected for the function ϕ , there exists a difference in performance between the proposed f-DQM and the Kansa method.

4 NUMERICAL IMPLEMENTATION

To illustrate the performance of the proposed f-DQM, two examples are presented. The first, brief, example on bending of thin plates is used to provide a quick overview of the method's application. A more in-depth discussion about the method's many interesting features is provided in the second example; linear elastic and nonlinear elastoplastic torsion of bars. In both the two examples, multiquadric RBF is chosen as the function $\phi_{pq}^{mn} = \sqrt{\|\bar{x}^{pq} - x^{mn}\|^2 + c^2}$. Where \bar{x}^{pq} and x^{mn} are as earlier defined in Section 3, $\|\bar{x}^{pq} - x^{ij}\|$ denotes a radial distance between the point \bar{x}^{pq} and the center x^{mn} of the RBF. c is a constant called the shape parameter whose choice is one of the factors that dictate the accuracy of the f-DQM.

4.1 Bending of thin plates

Consider a rectangular simply supported thin plate of planar dimensions L_x by L_y , thickness h and loaded with a uniform load q per unit area. The governing equation and boundary conditions describing the flexural behavior of such plates in terms of the displacement w can be written as in Eq. (8).

$$D \nabla^2 \nabla^2 w = -q \quad \text{in } \Omega \subset R^2 \quad (8a)$$

$$w = 0; \quad (\partial_{xx} w)n_1 + (\partial_{yy} w)n_2 = 0 \quad \text{on } \partial\Omega \quad (8b)$$

The flexural rigidity is $D = Eh^3/12(1 - \nu^2)$. ν and E are, respectively, the Poisson ratio and modulus of elasticity. n_1 and n_2 are the outward unit normal vectors of the boundaries.

The proposed f-DQM is used by, first, approximating the displacement function $w(x, y) = \sum_{m=1}^{N_x} \sum_{n=1}^{N_y} \lambda_{ij} \phi_{ij}^{mn}$. The quadrature analogue of Eq. (8a) is then written as Eq. (9a) considering

the definition of the biharmonic operator on the function w as $\nabla^2 \nabla^2 w = \frac{d^4 w}{dx^4} + 2 \frac{d^4 w}{dx^2 dy^2} + \frac{d^4 w}{dy^4}$. Similarly, Eqs. (9b) to (9d) are the quadrature forms of the original boundary conditions (Eq. (8b)).

$$D \left[\sum_{k=1}^{N_x} \alpha_{ik}^{(4)} \left(\sum_{m=1}^{N_x} \sum_{n=1}^{N_y} \lambda_{mn} \phi_{kj}^{mn} \right) + 2 \sum_{k=1}^{N_x} \alpha_{ik}^{(2)} \sum_{l=1}^{N_y} \beta_{jl}^{(2)} \left(\sum_{m=1}^{N_x} \sum_{n=1}^{N_y} \lambda_{mn} \phi_{kl}^{mn} \right) + \sum_{l=1}^{N_y} \beta_{jl}^{(4)} \left(\sum_{m=1}^{N_x} \sum_{n=1}^{N_y} \lambda_{mn} \phi_{il}^{mn} \right) \right] = -q \quad (9a)$$

$$\sum_{m=1}^{N_x} \sum_{n=1}^{N_y} \lambda_{mn} \phi_{ij}^{mn} = 0 \quad \text{for (I) } i = 1, N_x; \quad j = 1, 2, \dots, N_y, \quad \& \quad \text{(II) } i = 2, 3, \dots, N_x - 1; \quad j = 1, N_y \quad (9b)$$

$$\sum_{k=1}^{N_x} \alpha_{ik}^{(1)} \left(\sum_{m=1}^{N_x} \sum_{n=1}^{N_y} \lambda_{mn} \phi_{kj}^{mn} \right) = 0 \quad \text{for } i = 1, N_x; \quad j = 2, 3, \dots, N_y - 1 \quad (9c)$$

$$\sum_{l=1}^{N_y} \beta_{jl}^{(1)} \left(\sum_{m=1}^{N_x} \sum_{n=1}^{N_y} \lambda_{mn} \phi_{il}^{mn} \right) = 0 \quad \text{for } i = 2, 3, \dots, N_x - 1; \quad j = 1, N_y \quad (9d)$$

Uniform grid spacing is used in the discretization as shown in Fig. 2, and Eq. (9a) is applied on $i = 3, 4, \dots, N_x - 2$ and $j = 3, 4, \dots, N_y - 2$. Plot of the solution predicted by traditional DQM and the proposed f-DQM (with the parameter $c = 1$) are given in the same figure for a unit square plate with $q = 1 \text{ kN/m}^2$, $h = 5 \text{ cm}$, $\nu = 0.3$ and $E = 87,360 \text{ kN/m}^2$. The solution proves that the continuous nature of the f-DQM provides a better visualization. In addition, there is the ease of directly operating on the functional form of the solution rather than using extra quadrature-based formulations to post-process other desirable secondary variables (such as moment, shear, e.t.c.). Many other important advantages of the method are discussed in the next example.

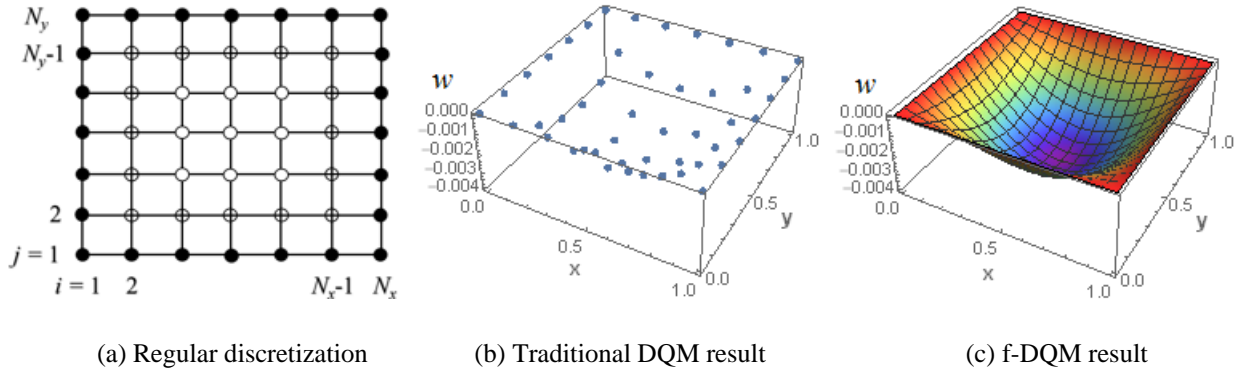


Figure 2: Discretized plate and solution for the displacement w

4.2 Linear elastic and nonlinear elastoplastic torsion of bars

For more detailed discussion about the features of the proposed f-DQM, both linear elastic and nonlinear elastoplastic torsion of a bar are analyzed. The governing equation and the boundary condition of the problem, in terms of a non-dimensionalized stress function Ψ , are given by Eq. (10). Details about the non-dimensionalization of the variables can be found in [8, 9] where similar problem was solved using MFS and pure Kansa approaches, respectively.

$$\nabla^2 \Psi = -\beta - g(x, y) \quad \text{in } \Omega \subset R^2 \quad (10a)$$

$$\Psi = 0 \quad \text{on } \partial\Omega \quad (10b)$$

Where $\nabla^2(\dots) = \frac{\partial^2(\dots)}{\partial x^2} + \frac{\partial^2(\dots)}{\partial y^2}$ is the Laplacian operator. The effect of the angle of twist θ per unit length and the modulus of rigidity G are contained in the parameter $\beta = 2G\theta$. The two stress components can be computed from the solution Ψ using Eq. (11), and the nonlinear function $g(x, y)$ that describes the plastic behavior of the section under twisting action is given by Eq. (12).

$$\tau_{xz} = \frac{\partial \Psi}{\partial y}, \quad \tau_{yz} = -\frac{\partial \Psi}{\partial x} \quad (11)$$

$$g(x, y) = 2G \left(\frac{\partial \gamma_{xz}^p}{\partial y} - \frac{\partial \gamma_{yz}^p}{\partial x} \right) \quad (12)$$

γ_{xz}^p and γ_{yz}^p are the total plastic strains that need to be added to the elastic strains to obtain the total strains, γ_{xz} and γ_{yz} , using Eq. (13).

$$\gamma_{xz} = \frac{\tau_{xz}}{G} + \gamma_{xz}^p; \quad \gamma_{yz} = \frac{\tau_{yz}}{G} + \gamma_{yz}^p \quad (13)$$

The equivalent total and plastic strains, ε_t and ε_p , are given by Eq. (14). ν is the Poisson ratio and m is the strain-hardening parameter defined as the ratio between the slope of linear strain-hardening curve to the slope of the elastic curve. Based on deformation theory of plasticity and the Von Mises yield criterion, the plastic strains can be calculated using Eq. (15).

$$\varepsilon_t = \sqrt{(\gamma_{xz}^2 + \gamma_{yz}^2)/3}; \quad \varepsilon_p = \frac{\varepsilon_t - (2/3)(1+\nu)}{1 + (2/3)(1+\nu)(m/(1-m))} \quad (14)$$

$$\gamma_{xz}^p = \frac{\varepsilon_p}{\varepsilon_t} \gamma_{xz}; \quad \gamma_{yz}^p = \frac{\varepsilon_p}{\varepsilon_t} \gamma_{yz} \quad \text{for } \varepsilon_p > 0 \quad (15a)$$

$$\gamma_{xz}^p = \gamma_{yz}^p = 0 \quad \text{for } \varepsilon_p \leq 0 \quad (15b)$$

For the case of elastic torsion, $g(x, y) = 0$ and the problem simplifies to a linear one that can be analyzed in a single step. For the elastoplastic torsion, however, the function $g(x, y)$ is nonlinear and as can be seen from Eqs. (11) to (15), proper solution can only be obtained using an iterative scheme.

For both the linear elastic and nonlinear elastoplastic torsion problems, the torsional capacity of the section can be computed from the solution Ψ using Eq. (16).

$$M = 2 \iint_{\Omega} \Psi \, dx dy \quad (16)$$

A traditional DQM formulation of the governing equation and boundary condition (Eq. (10)) is given by Eq. (17), where it is seen that several quadrature derivative formulations are necessary. For example, Eq. (17a) requires the derivatives of both the solution variable Ψ and the plastic strains on the right hand side to be written in quadrature form. However, the plastic strains themselves contain other nested nonlinear quadrature formulations inside them. This complicates

the iterative solution formulation. Despite such inconvenience, this effort only yields discrete solution results which require a large number of points before the solution behavior becomes obvious. In addition, it will be reiterated that any post-processing using the discrete results to obtain other secondary variables require different quadrature formulations. Sometimes even integral quadrature formulations become necessary for some secondary variables such as the moment in Eq. (16).

$$\sum_{k=1}^{N_x} \alpha_{ik}^{(2)} \Psi(x_k, y_j) + \sum_{l=1}^{N_y} \beta_{jl}^{(2)} \Psi(x_i, y_l) = -\beta - 2G \left(\sum_{l=1}^{N_y} \beta_{jl}^{(1)} \gamma_{xz}^p(x_i, y_l) - \sum_{k=1}^{N_x} \alpha_{ik}^{(1)} \gamma_{yz}^p(x_k, y_j) \right) \quad (17a)$$

$$\Psi(x_1, y_j) = \Psi(x_{N_x}, y_j) = \Psi(x_i, y_1) = \Psi(x_i, y_{N_y}) = 0 \quad \text{for } i = 1, 2, \dots, N_x; j = 1, 2, \dots, N_y \quad (17b)$$

The proposed f-DQM is implemented to analyze the elastic torsion problem described by Eq. (10) on a unit square section $(x, y) \in (0, 1) \times (0, 1)$. The power of the method is illustrated by solving and analyzing both the elastic and elastoplastic behavior more conveniently. Firstly, the stress function Ψ is approximated by Eq. (18) and the quadrature analogues of the original governing equations with the boundary conditions given by Eq. (10) are written as Eq. (19). For convenience, the nonlinear function $g(x, y)$ is evaluated analytically; thanks to the symbolic form of the proposed f-DQM. This justifies the use of direct analytical computation of differentials and/or integrals during the processing stage in f-DQM for terms that will, otherwise, require inconvenient use of nested quadrature formulations.

$$\Psi(x, y) = \sum_{i=1}^{N_x} \sum_{j=1}^{N_y} \lambda_{ij} \phi_{ij}^{mn} \quad (18)$$

$$\sum_{k=1}^{N_x} \alpha_{ik}^{(2)} \left(\sum_{m=1}^{N_x} \sum_{n=1}^{N_y} \lambda_{mn} \phi_{kj}^{mn} \right) + \sum_{l=1}^{N_y} \beta_{jl}^{(2)} \left(\sum_{m=1}^{N_x} \sum_{n=1}^{N_y} \lambda_{mn} \phi_{il}^{mn} \right) = -\beta - g(x_i, y_j) \quad (19a)$$

$$\sum_{m=1}^{N_x} \sum_{n=1}^{N_y} \lambda_{mn} \phi_{ij}^{mn} = 0 \quad \text{for (I) } i = 1, N_x; j = 1, 2, \dots, N_y, \quad \& \quad \text{(II) } i = 2, 3, \dots, N_x - 1; j = 1, N_y \quad (19b)$$

Elastic behavior for the problem is obtained by solving Eq. (19) while setting $g(x_i, y_j) = 0$. The nonlinear elastoplastic solution, however, is obtained in an iterative manner by, first, using the elastic solution for Ψ as its first iteration. The second iteration starts by using the elastic solution to compute the two stress components in Eq. (11). Next, the total strain components are computed from Eq. (13) while setting the plastic strain components to zero. The equivalent total and plastic strains are then obtained from Eq. (14) after which a check is run for possible onset of plastic zones (i.e. $\varepsilon_p > 0$). The new plastic strain components are obtained using Eq. (15). This completes the second iteration. The procedure is repeated in the subsequent iterations, where the updated values of the variables from previous iterations are used, until convergence.

The parameter $\beta = 3$ is used in the simulation. Exact solution for the elastic problem exists elsewhere [10], and it is used to calculate the function Ψ plotted in Fig. 3(a). The elastic solution using the traditional DQM based on Eq. (17) is shown in Fig. 3(b and c). It is obvious that while

the said approach has the power of achieving accurate results with only few grid points, but its inability to provide representative behavior with such a few number of nodes is a setback. It will, thus, be a wasted effort of having to use more nodes in traditional DQM as shown in Fig. 4(c) before the solution depicts the actual behavior similar to that of Fig. 3(a). Interestingly, use of the proposed f-DQM based on Eq. (19) provides a true representative solution with only few nodes as shown in Fig. 4 (a and b). The use of only one domain node in Fig. 4 (a) implies a relatively coarse discretization (3×3 grid) in which neither the DQM nor the f-DQM predicts the solution in exact sense. Yet, it is obvious that despite this relatively coarse discretization, the proposed f-DQM has captured the solution behavior more closely compared to the traditional DQM: An advantage credited to having an interpolated form of the solution (Eq. (18)). More interestingly, however, is the fact that while a grid of 5×5 for the traditional DQM (Fig. 3(c)) hardly provides an idea about the solution pattern in the remaining parts (non-sampled points) of the domain, the f-DQM (Fig. 4(b)) is able to achieve that. It should be noticed that the DQM and f-DQM agree with each other at the sampling points. Hence, there is a similar accuracy between the two methods at such points. Therefore, it only remains desirable to illustrate how the f-DQM and the Kansa RBF collocation method compare to each other. This fact is highlighted in following paragraph.

Eq. (16) is used to compute the torsional moment for different discretization density using the proposed f-DQM formulation and the result is shown in Table 1. For performance comparison, the RBF collocation method is formulated and used to solve the same problem. The remarkable performance of f-DQM is obvious in the table.

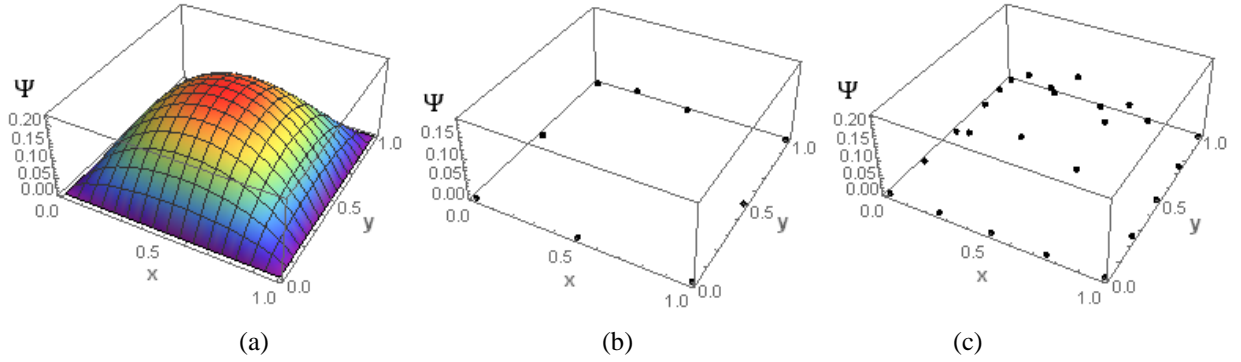


Fig. 3: Elastic solution for the stress function Ψ (a) Exact [9] (b) Traditional DQM with 3×3 grid (c) Traditional DQM with 5×5 grid

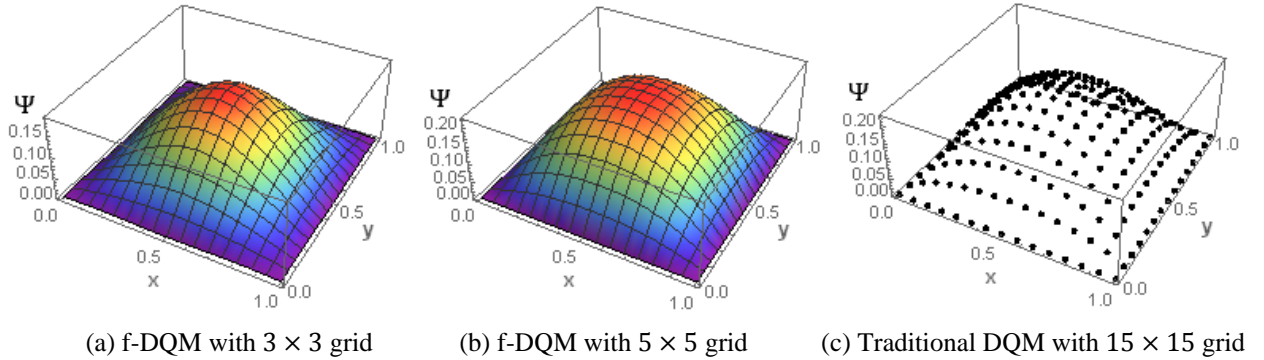


Fig. 4: Ability of the proposed closed-form f-DQM to predict the true elastic solution behavior with fewer nodes compared with traditional DQM

Table 1: Torsional moment (Eq. (16)) for the elastic solution

Discretization	f-DQM ($c = 0.74$)	Error (%)	RBF ($c = 0.84$)	Error (%)
3×3	0.1392	34.0	0.0938	55.5
4×4	0.1748	17.1	0.1512	28.3
5×5	0.2038	3.4	0.1838	12.9
6×6	0.2067	1.9	0.1942	7.9
7×7	0.2097	0.6	0.2034	3.6
8×8	0.2101	0.4	0.2059	2.4
9×9	0.2106	0.1	0.2086	1.1
10×10	0.2108	0.0	0.2094	0.7

The elastoplastic solution using the f-DQM (Eq. (19)) is also obtained based on the iterative approach described earlier due to the nonlinearity of the problem. The check in Eq. (15) using ε_p determines whether or not a given location in the computational domain undergoes plasticity. The computer code written to solve the problem is programmed in such a way to capture and plot any point at which the behavior becomes plastic. Using a discretization grid of size 10×10 and the parameter $\beta = 3$, the f-DQM predicts that the whole cross-section remains elastic as seen in Fig. 5. The two stress components, τ_{xz} and τ_{yz} , corresponding to the mentioned loading parameter are shown in the same figure. Increase in the value of β above 3 results in gradual propagation of the plastic region captured by the f-DQM as shown in Fig. 6.

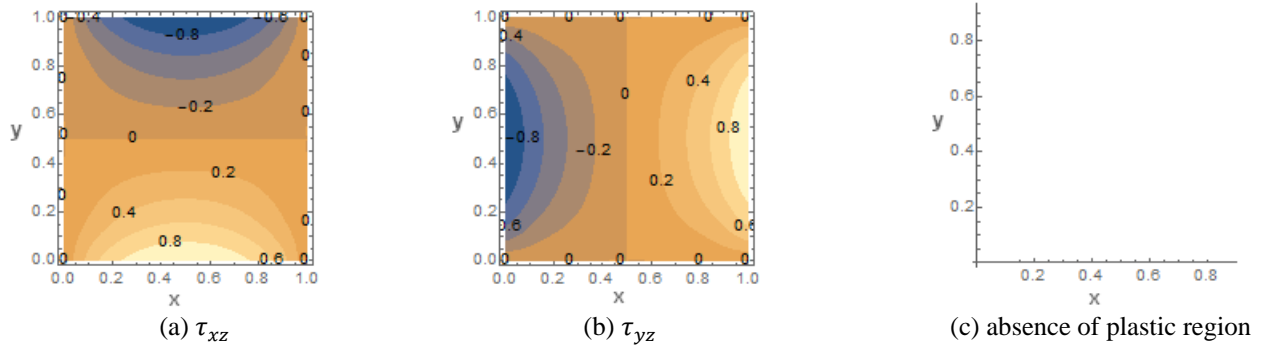


Fig. 5: Computed stresses using f-DQM and a prove of pure elastic behavior at low value of the displacement-controlled loading parameter $\beta = 3$

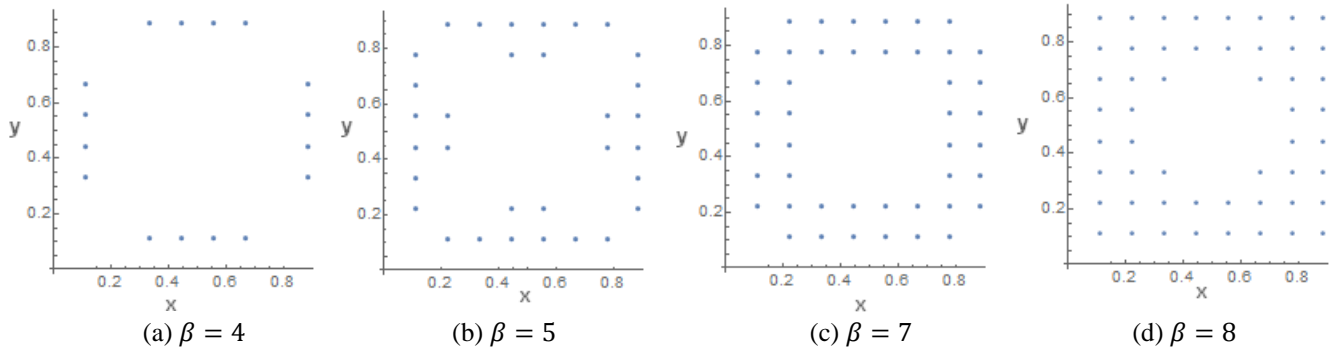


Fig. 6: Plastic region propagation (predicted using f-DQM) as the elastic region diminishes with increase in the displacement-controlled loading parameter β

Table 2 summarizes the post-processing formulations in f-DQM compared with those required in the conventional DQM. It is clear that all the secondary variables in the former are obtained using direct analytical differentiation or integration of the symbolic solution for Ψ against the need for additional differential or integral quadrature formulations required in the latter.

Table 2: Comparison of post-processing formulations between DQM and f-DQM

Secondary variable	DQM	f-DQM
$\tau_{xz} = \frac{\partial \Psi}{\partial y}$	$\sum_{l=1}^{N_y} \beta_{jl}^{(1)} \Psi(x_i, y_l)$	$\frac{\partial \Psi(x, y)}{\partial y}$
$\tau_{yz} = -\frac{\partial \Psi}{\partial x}$	$-\sum_{k=1}^{N_x} \alpha_{ik}^{(1)} \Psi(x_k, y_j)$	$-\frac{\partial \Psi(x, y)}{\partial x}$
$M = 2 \iint_{\Omega} \Psi \, dx dy$	$2 \sum_{k=1}^{N_x} \zeta_k \sum_{l=1}^{N_y} \eta_l \Psi(x_k, y_l)$	$2 \iint_{\Omega} \Psi(x, y) \, dx dy$

* ζ_k and η_l are the weighting coefficients for integral quadrature

5 CONCLUSIONS

A closed-form functional differential quadrature method (f-DQM) is proposed and applied to analyze two problems, namely, bending behavior of a thin plate as well as an elastic and elastoplastic torsion of a bar. Based on the method's performance, the following conclusions are be derived.

1. The proposed f-DQM outperforms the traditional DQM in flexibility and convenience.
2. The symbolic nature of the method makes it possible to harness its advantages similar to those of the analytical counterparts in terms of ease in post-processing.
3. The proposed approach harnesses the convenience and power of a symbolic software package both during preprocessing and post-processing, especially for problems involving terms that require inconvenient use of nested quadrature formulations.
4. The method can be used to yield a truly RBF-DQ approach with a preferable name of RBF-DQ-RBF in cases when the shape functions used in evaluating the weighting coefficients are RBF.
5. Despite some of its common features with RBF collocation (Kansa method) when RBF is chosen as the approximating function, the f-DQM and RBF collocation are not the same; accuracy of the proposed f-DQM is more pronounced, at least, in the torsion problem analyzed in this work.

ACKNOWLEDGMENT

The author would like to acknowledge the support of King Fahd University of Petroleum & Minerals (KFUPM).

REFERENCES

- [1] Bellman, R.E. and Casti, J. Differential quadrature and long-term integration. *J. Math. Anal. Appl.* (1971) 34: 235 – 238.
- [2] Bellman, R.E., Kashef, B.G. and Casti, J. Differential quadrature: a technique for the rapid solution of nonlinear partial differential equations. *J. Comput. Phys.* (1972) 10: 40 – 52.
- [3] Shu, C. and Richards. B.E. Application of generalized differential quadrature to solve two-dimension incompressible Navier-Stokes equations. *Int. J. Numer. Methods Fluids.* (1992) 15: 791–798.
- [4] Shu, C. and Chew, Y.T. Fourier expansion-based differential quadrature and its application to Helmholtz eigenvalue problems. *Comm. Numer. Meth. Eng.* (1997) 13: 643–653.
- [5] Wu, Y.L. and Shu, C. Development of RBF-DQ method for derivative approximation and its application to simulate natural convection in concentric annuli, *Comput. Mech.* (2002) 29: 477 – 485.
- [6] Shu, C., Ding, H. and Yeo, K.S. Local radial basis function-based differential quadrature method and its application to solve two-dimensional incompressible Navier-Stokes equations, *Comput. Methods Appl. Mech. Eng.* (2003) 192: 941 – 954.
- [7] Kansa, E.J. Multiquadrics – A scattered data approximation scheme with applications to computational fluid-dynamics—I surface approximations and partial derivative estimates, *Comput. Math. Appl.* (1990) 19: 127 – 145.
- [8] Kolodziej, J.A. and Gorzelanczyk, P. Application of method of fundamental solutions for elasto-plastic torsion of prismatic rods, *Eng. Anal. Boundary Elem.* (2012) 36: 81 – 86.
- [9] Mukhtar, F.M. and Al-Gahtani, H.J. Application of radial basis functions to the problem of elasto-plastic torsion of prismatic bars, *Appl. Math. Model.* (2015) 40: 436 – 450.
- [10] Timoshenko, S. and Goodier, J.N. *Theory of Elasticity.* McGraw Hill Book Company Inc., (1951).

Chemo-mechanical Regulation of Embryo Development with Time-delay Differential Equations

Jose J Munoz^{*}, Enrique Martín-Blanco^{**}, Katerina Karkali^{***}, Manuel Wenzel^{****}

^{*}Universitat Politècnica de Catalunya, Barcelona, Spain, ^{**}Insitut de Biologia Molecular de Barcelona, Spain,
^{***}Alexander Fleming Biomedical Sciences Research Center, ^{****}Karlsruhe University, Germany

ABSTRACT

Time oscillations are ubiquitous during embryo development. Strikingly, these systems have a negligible mass and thus cannot be described through hyperbolic equations. One possible source of these oscillations is the chemo-mechanical coupling between the biological signaling and the active response of the tissue [1]. We here study such interaction for the Central Nervous System during embryo development of *Drosophila* fly. We analyse the strain field and deduce plausible stresses that may generate the observed deformations [2] by solving an inverse problem on the three-dimensional images and assumed field of dipoles at the CNS. We reproduce those results by using a direct problem that is mathematically expressed as differential equation with a delay parameter, i.e. a Delay Differential Equation (DDE). The delay represents the retarded mechanical response of the cells due to a signaling stimulus. The DDE stem from an active rest length change and a linear stress-strain constitutive law. The resulting system of equations can be solved analytically [3] and also numerically. From our results we deduce a critical time delay, below which no oscillations are present. Such critical delay depends on the ability of the cell to adapt the rest length change (remodeling rate) and the tissue stiffness. We are also able to simulate the segmented distribution on space of the oscillations, which can be obtained by using segmented values of the material properties. References [1] Solon J, Kaya-Çopur, Colombelli, Brunne D. Pulsed Forces Timed by a Ratchet-like Mechanism Drive Directed Tissue Movement during Dorsal Closure, *Cell* 137:1331-1342, 2009. [2] JJ Muñoz, D Amat, V Conte. Computation of forces from deformed visco-elastic biological tissues. *Inverse Problems*, Accepted. [3] Kolmanovskii V., Myshkis A. General theory. In: *Applied Theory of Functional Differential Equations. Mathematics and Its Applications (Soviet Series)*, vol 85. Springer, 1992.

Investigating Blend Morphology of P3HT: PCBM Organic Solar Cells by Coarse-grained Molecular Simulations

Joydeep Munshi^{*}, Ganesh Balasubramanian^{**}, Teyu Chien^{***}, Wei Chen^{****}

^{*}Lehigh University, Bethlehem, PA, ^{**}Lehigh University, Bethlehem, PA, ^{***}University of Wyoming, Laramie, Wyoming, ^{****}Northwestern University, Evanston, IL

ABSTRACT

Organic photovoltaic bulk heterojunctions (BHJ) typically contain interpenetrating phases of semiconducting polymer acceptors along with fullerene donor materials. Morphology and dynamics of the BHJ active layers significantly affect the power conversion efficiency of solar cells. Mixtures of poly-(3-hexyl-thiophene) (P3HT) and phenyl-C61-butyric acid methyl ester (PCBM) have been widely employed over the past decade as acceptor-donor materials, respectively, for the active layer of the BHJ. The material selection has been driven by the simple and inexpensive synthesis of the flexible semiconducting polymer P3HT, and the high thermal and mechanical stability of both acceptor and donor materials in the BHJ morphology. Atomistic simulations are able to provide insights into the dynamics of blend morphology of organic materials and overcome the experimental challenges in extracting microstructural characterization due to poor contrast in electron microscopy. In addition, coarse-grained molecular dynamics (CGMD) modeling is able to simulate structures approaching the experimental length scales and processing conditions. We present results from CGMD simulations describing the morphological evolution of P3HT:PCBM active layer while solution processing in chlorobenzene. A decrease in the P3HT-PCBM contact areas with increasing solvent temperature reveals an enhanced phase separation of the two materials, and hence an improved crystal growth of the P3HT phase at a solvent temperature of 373K. Thermal annealing of the solvent-free morphology increases the ordering of the P3HT phase, and the predicted microstructures are compared against the as-cast morphologies to determine the changes in the molecular arrangements. We discuss the advantages of thermal annealing for BHJ active layer fabrication in the context of complementary experimental findings.

Phase-field Simulation and Neural Network Analysis of the Relationship between Material Parameters and Martensite Microstructure in Low-carbon Steels

Yoshihiro Murai^{*}, Yuhki Tsukada^{**}, Toshiyuki Koyama^{***}

^{*}Nagoya University, ^{**}Nagoya University, ^{***}Nagoya University

ABSTRACT

The lath martensite appears in most heat-treatable commercial steels. The size and morphology of martensite phase and dislocation density influence the mechanical properties of steels. The martensite microstructure varies depending on the alloy composition and heat treatment condition. On the other hand, various material parameters such as lattice constants and elastic constants are composition- and temperature-dependent. The relationship between the martensite microstructure and material parameters has not yet been clarified. In this study, phase-field simulation and neural network analysis are used for elucidating the influence of material parameters on the martensite microstructure. Most recently, a phase-field model was developed which considered the fcc-to-bct lattice deformation and slip deformation during the martensitic transformation (MT) in low-carbon steels [1]. Using the developed phase-field model, we performed three-dimensional simulations of the MTs near the martensite finish temperatures in Fe-0.1~0.4mass%C alloys. The composition and temperature dependences of material parameters were considered in the simulations. The simulation results show that the MT progresses with forming the cluster composed of three tetragonal variants of the martensite phase. By analyzing total of 4200 microstructure data obtained by the simulations, fifteen characteristics of the martensite microstructure were measured. For example, the total number of isolated variant domains on {100} cross-sections of the parent phase was counted and used as a measure of the variant domain size. The dislocation density was estimated from the simulated slip deformation field. A feed-forward neural network was trained in order to express the relationship between twelve material parameters and the fifteen characteristics of the martensite microstructure. The prediction error of the trained neural network was confirmed to be sufficiently small. Using the weight parameters and bias parameters of the trained neural network, sensitivity of material parameters to characteristics of martensite microstructure was calculated. It has been found that the yield stress, cubical dilatation of fcc-to-bct lattice deformation, and lattice parameter of the parent phase have significant influences on the martensite microstructure. Reference: [1] Y. Tsukada et al., Proc. of the 5th International Symposium on Steel Science (ISSS 2017), in press.

High-Order Hybridized Discontinuous Galerkin (HDG) Method and a Multigrid Solver for MHD Applications

Sriramkrishnan Muralikrishnan^{*}, Tim Wildey^{**}, Tan Bui-Thanh^{***}, John Shadid^{****}

^{*}The University of Texas at Austin, ^{**}Sandia National Labs, ^{***}The University of Texas at Austin, ^{****}Sandia National Labs

ABSTRACT

In this talk we will present a high-order hybridized discontinuous Galerkin (HDG) method and an efficient solver for MHD systems. The advantages of high-order HDG methods over DG methods is that they have much less globally coupled degrees of freedom when combined with implicit time integration schemes. The coupled unknowns are only the hybrid variables introduced on the skeleton of the mesh, which for high-order is much less compared to the total volume unknowns. Here we will present a multi-grid approach defined entirely on the skeletal system (hence least number of unknowns) and demonstrate its scalability. Multigrid solvers on the skeletal system represent difficulty because of the non-nested nature of the grids i.e. new edges/faces appear on refinement which does not have parents from the previous level. With examples from incompressible and compressible MHD systems we will show the effectiveness and scalability of the multigrid solver.

A Multiscale Analysis of Formation of Ferroelastic Phase in Metallic Oxide

Mayu Muramatsu^{*}, Tatsuya Kawada^{**}, Kenjiro Terada^{***}

^{*}Department of Mechanical Engineering, Keio University, ^{**}Graduate School of Environmental Studies, Tohoku University, ^{***}International Research Institute of Disaster Science, Tohoku University

ABSTRACT

In this study, we discuss the changes of the macroscopic material properties of a metallic oxide $\text{La}_{0.6}\text{Sr}_{0.4}\text{Co}_{0.2}\text{Fe}_{0.8}\text{O}_{3-\delta}$ (LSCF) in relation to its ferroelastic microstructure formation. LSCF is a material which is often used as a cathode electrode of Solid Oxide Fuel Cell (SOFC), and its crystal structure becomes rhombohedral below 700-1100K and cubic above that temperature level. When the cubic structure of LSCF changes to a rhombohedral one with temperature decrease after a cell is sintered, the single crystal grain in a polycrystalline aggregate accommodates some stable phases due to the lattice misfit between crystal structures. The stable rhombohedral phase, which is called ferroelastic phase, is known to exhibit stress relaxation due to the crystal re-orientation when stress is applied. In this study, emphasizes are placed on the mechanism of ferroelastic phase transformation caused by the change of lattice structure during temperature decrease. In order to incorporate the mechanical behavior of ferroelastic phase [1] into the stress analysis of SOFC in consideration of elastic, creep, thermal and reduction strains [2], we propose a mathematical model to predict the formation of ferroelastic phases in crystal grains of a metallic oxide LSCF [3]. The phase-field model equipped with the elastic energy is introduced to realize the morphology formation of ferroelastic phases in a crystal grain. We conduct a series of three-dimensional numerical simulations to reproduce the deformation-induced nucleation and growth of ferroelastic phases of LSCF. The crystal orientations of matrices are also considered in the simulation so that the ferroelastic phase transformation in the polycrystalline aggregates can be reproduced. Then, the changes of the macroscopic material properties are discussed in relation to the ferroelastic microstructure formation. References [1] M. Muramatsu, K. Terada, T. Kawada, K. Yashiro, K. Takahashi and S. Takase, Characterization of time-varying macroscopic electro-chemo-mechanical behavior of SOFC subjected to Ni-sintering in cermet microstructures, Computational Mechanics, Vol. 56, pp. 653-676, 2015. [2] Y. Kimura, J. Tolchard, M.-A. Einarsrud, T. Grande, K. Amezawa, S. Hashimoto and T. Kawada, The Effect of Ferroelasticity of $\text{La}_{1-x}\text{Sr}_x\text{Co}_{1-y}\text{Fe}_y\text{O}_{3-\delta}$ on the Mechanical Stability of Solid Oxide Fuel Cells, ECS Transactions, Vol. 57, pp. 635-642, 2013. [3] M. Muramatsu, K. Yashiro, T. Kawada and K. Terada, Simulation of Ferroelastic Phase Formation Using Phase-field Model, International Journal of Mechanical Sciences, (Accepted).

A Novel Non-Parametric Optimization Method for Free-Orientation of a Laminated Composite Shell Structure for Tailoring Thermal Deformation

Yoshiaki Muramatsu*, Masatoshi Shimoda**

*Graduate School of Advanced Science and Technology, Toyota Technological Institute, **Department of Advanced Science and Technology, Toyota Technological Institute

ABSTRACT

Abstract: Shell structures with composite materials such as carbon fiber reinforced plastics (CFRP) have been widely utilizing in various structural design of cars, aircrafts and so on. They have higher specific mechanical performances, and especially anisotropic materials can be used for tailoring the elastic tensor of a shell structure. From the practical point of view, most of the industrial products are exposed to a thermal load and needs for controlling the thermal deformation to maintain the mechanical performance. On the other hand, there are other industrial products which use the thermal deformation proactivity such as bimaterial thermal actuators. In this study, we propose a material orientation optimization method for optimum design of laminated composite shell structures consisting of anisotropic materials. We aim at controlling thermal displacements to target values without varying shape or thickness. The square displacement error norm is minimized by varying the material orientation of each layer as the design variable. The optimum design problem is formulated as a distributed-parameter optimization problem, and the sensitivity function with respect to the material orientation variation is theoretically derived based on the variational method. The optimal material orientation variations are determined by using the H1 gradient method [1][2], where the sensitivity functions aforementioned are applied as the Robin condition to vary and optimize the material orientation. In detail, after deriving the sensitivity function, we transfer it to the internal heat generation and determine the material orientation variation by using the Poisson's equation for fictitious-heat transfer analysis to ensure the continuously distribution of the material orientation. The optimum design examples show that the proposed optimization method can effectively obtain the optimum material orientation with the smooth curvilinear distribution and can tailor the thermal deformation, simultaneously. Reference: [1] Shimoda M, Liu Y. A non-parametric free-form optimization method for shell structures. *Structural Multidisciplinary Optimization* 2014;50:409–423. [2] Muramatsu Y, Shimoda M. Optimization approach for designing free-orientation of orthotropic materials of a shell structure. *Transactions of the Japan Society of Mechanical Engineers*. 2017;83(851):1-15 (in Japanese).

Interfacial Mixing in High-energy-density Matter with Multiphysics Kinetic and Molecular Dynamics Models

Michael S. Murillo^{*}, Liam Stanton^{**}, Jeff Haack^{***}

^{*}Michigan State University, ^{**}Lawrence Livermore National Laboratory, ^{***}Los Alamos National Laboratory

ABSTRACT

At the National Ignition Facility, high-powered laser beams are used to compress a small target to generate fusion reactions. A critical issue in achieving this is the understanding of mix at the ablator/fuel interface. Mixing occurs at various length scales, ranging from atomic inter-species diffusion to hydrodynamic instabilities. Because the interface is preheated by energy from the incoming shock, it is important to understand the dynamics before the shock arrives. The interface is in the warm dense matter phase with a deuterium/tritium fuel mixture on one side and a plastic mixture on the other. We would like to understand various aspects of the evolution, including the state of the interface when the main shock arrives, the role of electric field generation at the interface, the 'kinetic-ness' of the system, and the character and time scales for diffusion. We present a multiscale approach to model these processes, which combines molecular dynamics to simulate the ionic degrees of freedom with orbital-free density functional theory to calculate the electronic structure. Simulation results are presented and compared with a newly developed multispecies BGK model, and connections to hydrodynamic models are discussed.

THE FGM BEAM FINITE ELEMENT INCLUDING WARPING TORSION

J. MURIN*, M. AMINBAGHAI**, V. KUTIS*, J. HRABOVSKY*, J. PAULECH*,
S. KUGLER[†]

* Department of Applied Mechanics and Mechatronics of IAMT, Faculty of Electrical Engineering and Information Technology, Slovak University of Technology in Bratislava, Ilkovičova 3, 812 19 Bratislava, Slovakia
justin.murin@stuba.sk

** Institute of Mechanics of Materials and Structures, Vienna University of Technology, Karlsplatz 13, A-1040 Vienna, Austria
mehdi.aminbaghai@ac.at

[†] Department of Applied and Numerical Mechanics, University of Applied Sciences Wiener Neustadt, Johannes Gutenberg-Straße 3, A-2700 Wiener Neustadt, Austria
kugler@fhwn.ac.at www.fhwn.ac.at

Key words: 3D-FGM beam finite element, Warping torsion, Elastostatic and modal analyses.

1 INTRODUCTION

Structures with spatially inhomogeneous material properties are of great practical importance in modern product and system design. Functionally Graded Materials (FGMs) are formed by a continuous gradation of two or more constituents over the physical volume, while composites show a discontinuous variation of constitutive properties. The specific variations can be tailored properly in order to achieve optimized characteristics of the component. The numerical assessment of the mechanical or multiphysical behaviour is a critical issue in the product development process and new and enhanced strategies have to be developed. Accurate and efficient structural finite elements like beams, plates and shells require suitable homogenization procedures to arrive effective stiffness quantities for the membrane, bending, transverse and torsional shear properties accompanied with a suitable warping stiffness regarding non-uniform torsion [^{1,2,3}]. In the literature, a huge amount of papers can be found, which deal with modelling and simulation of static and dynamic problems of FGM beams. In [^{4, 5}], a review of the principal developments in FGM structures is processed. A common feature of the cited articles is that constant material properties of the beams in the longitudinal direction are assumed. According to our knowledge, especially for torsion of the FGM beams with longitudinally varying material properties, the warping effect has not yet been considered.

This contribution is an extension of our previous work dealing with derivation of the FGM beam finite elements (with 12x12 stiffness and mass matrix) with longitudinally varying effective material properties that is suitable for analysis of beam structures made of spatially varying FGM. Effects of axial and shear forces are included as well as the Winkler elastic foundation and the Saint Venant torsion is considered in our previous papers. Homogenization of the spatially varying material properties in the real FGM beam and the calculation of effective parameters are done by extended mixture rules and by the multilayer method (MLM) and the direct integration methods (DIM), e.g. [6]. If only symmetric transversal and lateral variations of material properties are considered in the real FGM beam, longitudinally constant effective material properties arises from the homogenization. For spatially varying material properties, where the transversal and lateral variation is symmetric, a longitudinally variation of effective material properties has been obtained, [6, 7, 8, 9]. This method can also be used in the homogenization of multilayer beams with discontinuous variation of material properties in transversal and lateral direction.

In the contribution, the 3D FGMs Timoshenko beam finite element with 14x14 stiffness and mass matrices for doubly symmetric open and closed cross-section is presented including warping torsion effect (non-uniform torsion). A longitudinal continuous variation of effective material properties is considered by the finite element equations derivation, which is obtained by homogenization of the spatially varying material properties in real FGM beam. Results of numerical elastostatic analysis of the cantilever beam with rectangular hollow cross-section are presented and the accuracy and effectiveness of the new FGM beam finite element is discussed and evaluated.

2 THE FGM BEAM FINITE ELEMENT EQUATIONS

Let us consider a straight Timoshenko beam finite element of doubly symmetric cross-section –

Figure 1. The Saint Venant torsion is assumed in the first step of this study. The degrees of freedom at node i according to transfer matrix method (TMM) notation are: the displacements u_i, v_i, w_i in the local directions x, y, z , and the cross-sectional area rotations about the x, y, z directions - $\varphi_{x,i}, \varphi_{y,i}, \varphi_{z,i}$. The degrees of freedom at the node j are denoted in a similar manner. The internal forces at node i according to transfer matrix method (TMM) notation are: the axial force N_i , the transversal forces $R_{y,i}$ and $R_{z,i}$, the bending moments $M_{y,i}$ and, the torsion moment $M_{x,i}$. Furthermore, $n_x = n_x(x)$ denotes the axial force distribution, $q_z = q_z(x)$ and $q_y = q_y(x)$ are the transversal and lateral force distributions, $m_x = m_x(x)$, $m_y = m_y(x)$ and $m_z = m_z(x)$ are the distributed moments, $\mu_x = \rho A = \mu_y = \mu_z = \mu$ denote the mass distribution, $\bar{\mu}_y = \rho I_y$, $\bar{\mu}_z = \rho I_z$ and $\bar{\mu}_{xT} = \rho I_p$ refer to the distributions of mass moments of inertia, $\rho = \rho_L^H(x) \equiv \rho_L^H$ is the homogenized effective mass density distribution, A is the cross-sectional area, I_y and I_z are the second moments of area, $I_p = I_y + I_z$ denotes the polar moment of area, $k_x = k_x(x)$, $k_y = k_y(x)$, $k_z = k_z(x)$, $\bar{k}_y = \bar{k}_y(x)$, $\bar{k}_z = \bar{k}_z(x)$ are the elastic foundation modules (the torsional elastic foundation is not considered), and ω is the circular frequency. The effective homogenized and longitudinally varying stiffness reads as follows: $EA = E_L^{NH}(x)A$ is the axial stiffness ($E_L^{NH}(x) \equiv E_L^{NH}$ is the effective elastic modulus for axial loading), $EI_y = E_L^{MyH}(x)I_y$ is the flexural stiffness about the y -axis ($E_L^{MyH}(x) \equiv E_L^{MyH}$ is the

effective elastic modulus for bending about axis y), $EI_z = E_L^{M_z H}(x)I_z$ is the flexural stiffness in axis z , ($E_L^{M_z H}(x) \equiv E_L^{M_z H}$ is the effective elastic modulus for bending about axis z), $G\bar{A}_y = G_{Ly}^H(x)k_y^{sm}A$ is the reduced shear stiffness in y -direction ($G_{Ly}^H(x) \equiv G_{Ly}^H$ is the effective shear modulus and k_y^{sm} is the average shear correction factor in y -direction), $G\bar{A}_z = G_{Lz}^H(x)k_z^{sm}A$ is the reduced shear stiffness in z - direction ($G_{Lz}^H(x) \equiv G_{Lz}^H$ is the effective shear modulus and k_z^{sm} is the average shear correction factor in z - direction), $G_L^{M_x H}(x)I_T$ is the effective torsional stiffness, $G_L^{M_x H}(x) = G_L^{M_x H}$ is the torsional elastic modulus and I_T is the torsion constant – $I_p = I_T$ for the circular and ring cross-section). The homogenization of spatially varying material properties is described in more detail in [6,7,8,9].

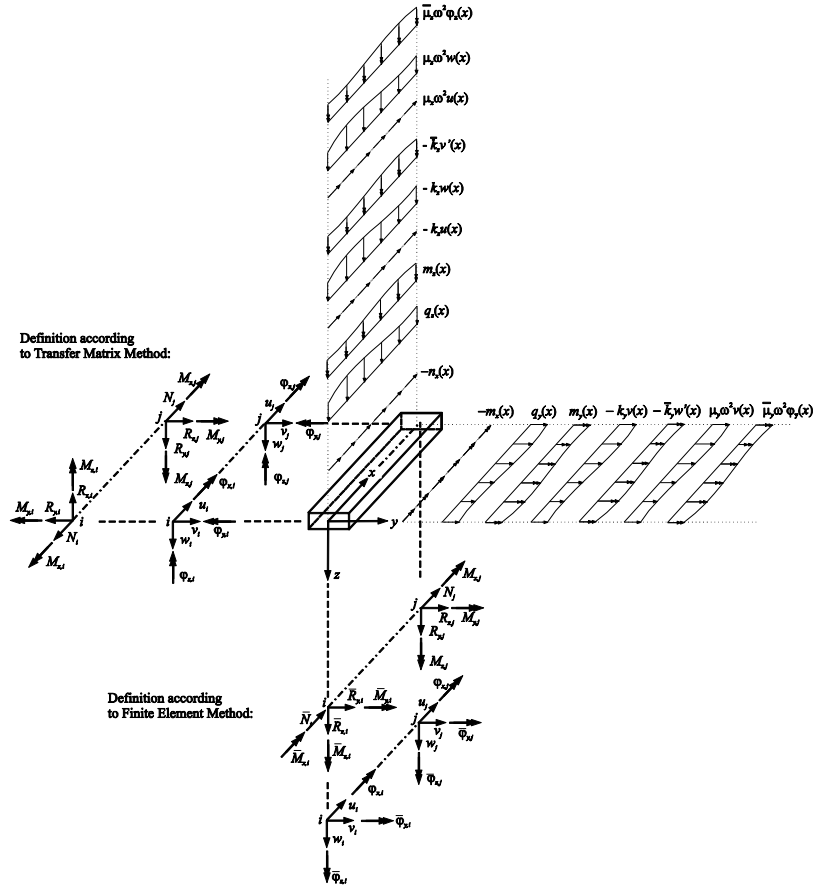


Figure 1: The local internal variables and loads for 12x12 Timoshenko FGM beam finite element.

The derivatives with respect to x of the relevant variable is denoted with an apostrophe “ ’ ” throughout the article. For establishing the FGM warping torsion beam finite element equations with 14x14 element matrix we use the matrices for axial, transversal lateral loading (according the Figure 1) that were derived and described in our previous papers [6,7,8,9]. The warping torsion equations are described in more detail in the next subchapter.

2.1 Non-uniform torsion of the FGM beams with STMDE

Fig. refers to determination of the eigenvibrations due to non-uniform torsion. It shows the torsional moment $M_T(x)$, representing the sum of the primary torsional moment $M_{Tp}(x)$ and

the secondary torsional moment $M_{Ts}(x)$, and the bimoment $M_\omega(x)$ according to the formulation in the framework of the transfer matrix method (TMM).

Fig. 2 also shows the angle of twist $\psi(x)$, corresponding to $M_{Tp}(x)$. It represents the sum of the angle of twist, resulting from the primary deformation, $\psi'_M(x)$ and from the secondary deformation, $\psi'_S(x)$.

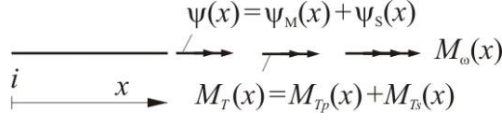


Fig. 2: Non-uniform torsion: torsional moments, bimoment, and angles of twist.

Fig. 3 illustrates the beam element for non-uniform torsion. It is loaded by the equivalent inertial torsional line moment $\omega^2 I_p \rho(x) \psi(x)$, the equivalent inertial line bimoment

$\omega^2 I_\omega \rho(x) \psi'_M(x)$, where I_ω stands for the warping constant, and the torsional line moment $m_T(x)$, which is equal to zero for modal analysis. These line moments represent the static equivalent of the respective dynamic action. In the following, the equilibrium equations for TMM will be formulated. They are obtained as

$$M'_T(x) = -m_T(x) - \omega^2 I_p \rho(x) \psi(x), \quad (1)$$

where $m_T(x) = \sum_{k=0}^{\max k} \eta_{m_T,k} x^k$ is the polynomial representation of the torsion moment with the parameters $\eta_{m_T,k}$, and

$$\begin{aligned} M'_\omega(x) &= M_T(x) - M_{Tp}(x) + m_\omega(x) + \omega^2 I_\omega \rho(x) \psi'_M(x) = \\ &= M_{Ts}(x) + m_\omega(x) + \omega^2 I_\omega \rho(x) \psi'_M(x), \end{aligned} \quad (2)$$

where $m_\omega(x) = \sum_{k=0}^{\max k} \eta_{m_\omega,k} x^k$ is the polynomial representation of the warping moment with the parameters $\eta_{m_\omega,k}$, and

$$M_T(x) = M_{Tp}(x) + M_{Ts}(x). \quad (3)$$

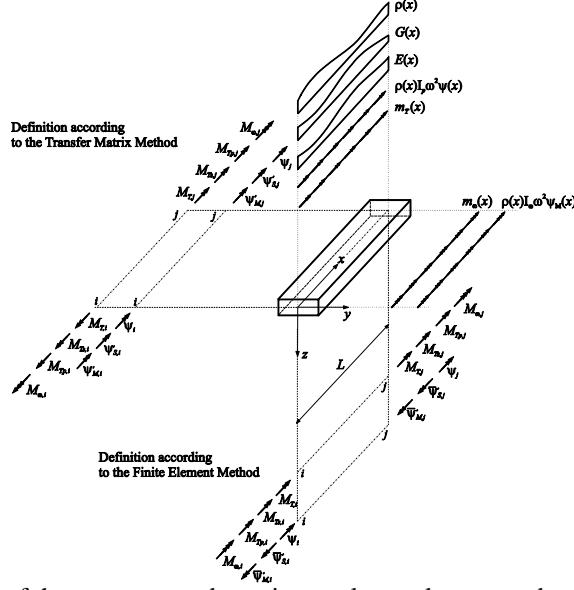


Fig. 3: Positive orientation of the moments and rotation angles at element nodes for the TMM and the FEM.

According to [10,11],

$$\psi''_M(x) = -\frac{M_{\omega}(x)}{E(x)I_{\omega}}, \quad (4)$$

and

$$\psi'(x) = \psi'_M(x) + \psi'_S(x), \quad (5)$$

with

$$\psi'(x) = \frac{M_{Tp}(x)}{G(x)I_T}, \quad (6)$$

and

$$\psi'_S(x) = \frac{M_{Ts}(x)}{G(x)I_{Ts}}, \quad (7)$$

where I_{Ts} denotes the secondary torsion constant and $E(x)$ and $G(x)$ stand for the longitudinally varying effective elasticity modulus and shear modulus, respectively. The new polynomial $G(x)I_{Ts}$ is obtained by multiplication of the secondary torsion constant I_{Ts} with the polynomial for the effective shear modulus, $G(x)$.

The polynomial $E(x)I_{\omega}$ is obtained by multiplication of the warping constant I_{ω} with the polynomial representation of Young's modulus, $E(x)$. After mathematical manipulation, [10,11], the following differential equation of fourth order, with the load polynomial $\eta_L(x)$, is obtained:

$$\eta_4(x)\psi''''(x) + \eta_3(x)\psi'''(x) + \eta_2(x)\psi''(x) + \eta_1(x)\psi'(x) + \eta_0(x)\psi(x) = \eta_L(x). \quad (8)$$

The variable polynomial coefficients and establishing of the local finite element are given in [10]. The local finite element equations for non-uniform torsion (in particular for free torsional vibrations) read as follows (considering the definitions of positive quantities in the framework of the FEM, resulting in $\bar{M}_{T,i} = -M_{T,i}$, $\bar{M}_{\omega,i} = -M_{\omega,i}$, $\bar{\psi}'_{M,i} = -\psi'_{M,i}$, and $\bar{\psi}'_{M,j} = -\psi'_{M,j}$):

$$\begin{bmatrix} \bar{M}_{T,i} \\ \bar{M}_{\omega,i} \\ M_{T,j} \\ M_{\omega,j} \end{bmatrix} = \begin{bmatrix} B_{4,4} & B_{4,7} & B_{4,11} & B_{11,14} \\ B_{7,4} & B_{7,7} & B_{7,11} & B_{7,14} \\ B_{11,4} & B_{11,7} & B_{11,11} & B_{11,14} \\ B_{14,4} & B_{14,7} & B_{14,11} & B_{14,14} \end{bmatrix} \cdot \begin{bmatrix} \psi_i \\ \bar{\psi}'_{M,i} \\ \psi_j \\ \bar{\psi}'_{M,j} \end{bmatrix} + \begin{bmatrix} F_4 \\ F_7 \\ F_{11} \\ F_{14} \end{bmatrix}. \quad (9)$$

In order to include warping, an additional degree of freedom is added to the classical nodal variables at each element nodal point. As mentioned previously, the warping part of the first derivative of the twist angle, \mathcal{G}'_M , is considered as this degree of freedom [7]. This is advantageous for the formulation of boundary conditions. If the effect of the secondary torsional moment on the deformations is not considered, $\mathcal{G}'_M(x) \equiv \mathcal{G}'(x)$. Here, $\mathcal{G}'(x)$ is the first derivative of the angle of twist (bicurvature) that is very often used as a 7th degree of freedom in the usual non-uniform torsion formulations [12,13,14]. A detailed description of the matrix coefficients in (9) is presented in [10] and [11]. The local finite element matrix B in (18) is symmetric.

3 THE FINITE ELEMENT EQUATIONS OF THE 3D TIMOSHENKO BEAM WITH WARPING

By combination of the equations for axial and bending loads ([6,7,8,9]) and the non-uniform torsion, following system of finite element equations is obtained

$$\begin{bmatrix} F_{int}^e \end{bmatrix} = \begin{bmatrix} B^{le} \end{bmatrix} \begin{bmatrix} u^e \end{bmatrix} + \begin{bmatrix} F^e \end{bmatrix} \quad (10)$$

where $\begin{bmatrix} u^e \end{bmatrix}^T = \{u_i \ v_i \ w_i \ \psi_i \ \varphi_{y,i} \ \varphi_{z,i} \ \psi'_{M,i} \ u_j \ v_j \ w_j \ \psi_j \ \varphi_{y,j} \ \varphi_{z,j} \ \psi'_{M,j}\}$

is the displacement vector, and

$$\begin{bmatrix} F_{int}^e \end{bmatrix}^T = \{N_i \ R_{y,i} \ R_{z,i} \ M_{x,i} \ M_{y,i} \ M_{z,i} \ M_{\omega,i} \ N_k \ R_{y,j} \ R_{z,j} \ M_{x,j} \ M_{y,j} \ M_{z,j} \ M_{\omega,j}\}$$

is the internal load vector and $\begin{bmatrix} F^e \end{bmatrix}$ is the external load vector. The local finite element matrix reads

$$\begin{bmatrix} B^{le} \end{bmatrix} = \begin{bmatrix} B_{1,1} & 0 & 0 & 0 & 0 & 0 & 0 & B_{1,8} & 0 & 0 & 0 & 0 & 0 & 0 \\ & B_{2,2} & 0 & 0 & 0 & B_{2,6} & 0 & 0 & B_{2,9} & 0 & 0 & 0 & B_{2,13} & 0 \\ & & B_{3,3} & 0 & B_{3,5} & 0 & 0 & 0 & 0 & B_{3,10} & 0 & B_{3,12} & 0 & 0 \\ & & & B_{4,4} & 0 & 0 & B_{4,7} & 0 & 0 & 0 & B_{4,11} & 0 & 0 & B_{4,14} \\ & & & & B_{5,5} & 0 & 0 & 0 & 0 & B_{5,10} & 0 & B_{5,12} & 0 & 0 \\ & S & & & & B_{6,6} & 0 & 0 & B_{6,9} & 0 & 0 & 0 & B_{6,13} & 0 \\ & & Y & & & & B_{7,7} & 0 & 0 & 0 & B_{7,11} & 0 & 0 & B_{7,14} \\ & & & M & & & & B_{8,8} & 0 & 0 & 0 & 0 & 0 & 0 \\ & & & & M & & & & B_{9,9} & 0 & 0 & 0 & B_{9,13} & 0 \\ & & & & & E & & & & B_{10,10} & 0 & B_{10,12} & 0 & 0 \\ & & & & & & T & & & & B_{11,11} & 0 & 0 & B_{11,14} \\ & & & & & & & R & & & & B_{12,12} & 0 & 0 \\ & & & & & & & & I & & & & B_{13,13} & 0 \\ & & & & & & & & & C & & & & B_{14,14} \end{bmatrix}. \quad (11)$$

The local finite element matrix B^{le} in (11) consists formally of the linear stiffness matrix K_L and the linearized geometric stiffness matrix K_N (containing the terms with second order axial force N^{II} that has to be known or has to be evaluated by a linear elastic-static calculation)

and the consistent mass matrix M :

$$[B^{le}] = [K_L + K_N - \omega^2 M]. \quad (12)$$

Solution algorithm for calculation of the matrix B^{le} and the loads vector F^e is implemented into the software MATHEMATICA [15]. In the modal analysis, the eigenvalue problem is solved. For given axial forces N^H and the geometrical parameters and the homogenized material properties and the global boundary conditions, the circular frequency ω is increased until the determinant of the global beam structure matrix tends to zero. This circular frequency is the natural circular frequency from which the natural frequency (eigenfrequency) can be calculated. Further, the mode shapes can be calculated by the transfer relations [8]. In elastostatic analysis, the circular frequency is set to zero, and the load vector has to be established.

4 NUMERICAL EXPERIMENTS

Results of numerical experiments on several combined loadings of FGM beams including Saint Venant torsion are presented in articles [8,9,10,11,12]. Issues of modal and elastostatic analyses of thin walled FGM beams with warping consideration is prepared for publication in more detail in papers [10,11]. Due to the limited scope of this paper, only the particular results of numerical experiments on the non-uniform torsion of thin-walled beam with rectangular hollow cross-section will be presented in this contribution. The cantilever FGM beam with a hollow rectangular cross-section of length $L = 0.1\text{m}$ is considered as shown in Fig. 5. The beam is loaded by the torsional moment $M_T = 1\text{Nm}$ at point k . The moment was applied as a distributed load on the whole hollow cross-section. The FGM consists of a mixture of aluminium (denoted with the index m) and tungsten (denoted with the index f). The material properties are shown in Table1.

Material properties:		
Young's modulus	$E_f = 4.8 \cdot 10^{11}, E_m = 0.69 \cdot 10^{11}$	Pa
Poisson's ratio	$\nu_f = 0.2, \nu_m = 0.33$	-
Shear modulus	$G_f = 2.0 \cdot 10^{11}, G_m = 0.26 \cdot 10^{11}$	Pa

Table1: Material properties of the FGM constituents.

The longitudinal polynomial variation of the effective Young's modulus and the effective Poisson's ratio (13) is assumed as:

$$E(x) = E_f + (E_m - E_f) \left(\frac{x}{L} \right)^n, \quad \nu(x) = \nu_f + (\nu_m - \nu_f) \left(\frac{x}{L} \right)^n \quad (13)$$

In (13), n is the order of the polynomial. The effective shear modulus reads as:

$$G(x) = \frac{E(x)}{2(1 + \nu(x))}. \quad (14)$$

The longitudinal beam axis x begins at the clamped end of the cantilever beam

($x = 0$). The axial variations of the material properties are shown in Fig. 4 for $n \in \langle 1, 5 \rangle$.

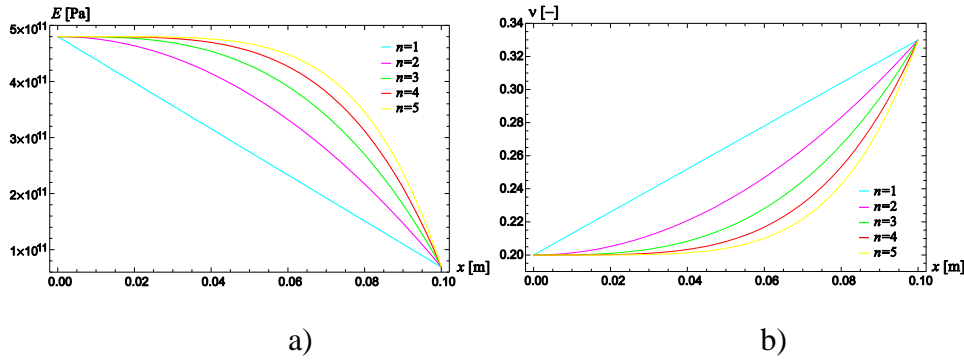


Fig. 4: Variation of the effective Young's modulus and a) and Poisson's ratio b).

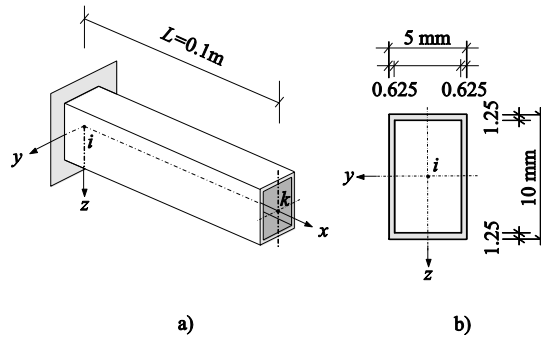


Fig. 5: Cantilever beam with a rectangular hollow cross-section: a) system, b) cross-section.

The cross-sectional parameters of the beam (Figure 5b)) are calculated by ANSYS [16] and by Thin Tube Theory - TTT). They are listed in

Table 2.

Cross-sectional parameters		
Cross-sectional area	$A = 0.21875 \cdot 10^{-4}$	m^2
Second moment of area about the y-axis	$I_z = 0.71208 \cdot 10^{-10}$	m^4
Second moment of area about the z-axis	$I_y = 0.28483 \cdot 10^{-9}$	m^4
Polar moment of area	$I_p = I_y + I_z = 0.31209 \cdot 10^{-9}$	m^4
Torsion constant	$I_T = 0.16748 \cdot 10^{-9}$	m^4
Secondary torsion constant	$I_{Ts} = 0.717773 \cdot 10^{-10}$	m^4
Warping constant	$I_\omega = 0.240426 \cdot 10^{-15}$	m^6

Table 2: Cross-sectional parameters of the hollow cross-section.

The elastostatic torsional analyses were calculated by:

a) only one warping torsion beam finite element (FGM-WT with STMDE); b) a very fine mesh (number of 500) of our WT BEAM ^[17] finite elements. Constant material properties of relevant finite element is obtained as an average value, calculated from their values in the element nodes, according the variation in Fig. 4; c) a very fine mesh of 3D SOLID186 finite elements (number of 577000 FE) of the software ANSYS ^[16].

The results of the analyses, considering the angle of twist and internal moments at the nodes i and k for $n = 1$, are shown in Table 3.

Variables	FGM-WT with STMDE	WT BEAM ^[17]
ψ_k [rad]	0.0071	0.0072
$\psi'_{M,k}$ [rad/m]	0.1916	0.1916
$M_{\omega,i}$ [kNm ²]	-1.0352×10^{-6}	-1.0351×10^{-6}
$M_{Tp,i}$ [kNm]	7.0×10^{-4}	7.0×10^{-4}
$M_{Tp,k}$ [kNm]	9.497×10^{-4}	4.487×10^{-4}
$M_{Ts,i}$ [kNm]	3.0×10^{-4}	3.0×10^{-4}
$M_{Ts,k}$ [kNm]	5.027×10^{-5}	5.512×10^{-4}

Table 3: Twist angl and internal moments for $n = 1$.

The longitudinal distribution of the angle of twist and bimoment, due to non-uniform torsion for the cantilever beam of the hollow-cross-section calculated by the FGM-WT with STMDE is shown in Figure 6. Longitudinal distribution of the angle of twist and the bimoment obtained by the WT BEAM is very close to the ones shown in Fig. 6, and therefore is not depicted separately here.

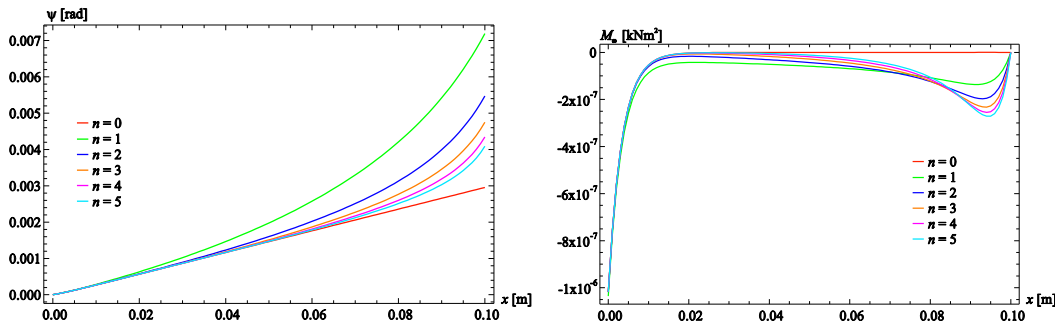


Fig. 6: Angle of the twist, ψ [rad] and bimoment, M_{ω} [kNm²].

As presented in Fig. 6, a significant impact of the material properties variation on the twist angle can be observed. On the other hand, the maximal value of the bimoment in the clamped cross-section is not affected significantly by the considered variation of material properties. Some bimoment changes occur at the site of a rapid change in material properties in the beam field. In following, the bimoment normal and torsional shear stress at clamped beam end is calculated (the position of the corners is assumed at the intersection of the center lines of the cross section walls (Fig 7.)). The cross-section is loaded by the bimoment

$M_{\omega,i} = -1.0352 \times 10^{-6} \text{ kNm}^2 = -0.0010352 \text{ Nm}^2$ and primary torsional moment $M_{Tp,i} = 7.0 \times 10^{-4} \text{ kNm} = 0.7 \text{ Nm}$ and secondary torsional moment $M_{Ts,i} = 3.0 \times 10^{-4} \text{ kNm} = 0.3 \text{ Nm}$. The bimoment normal stress at the clamped cross-section corners is: $\sigma_{\omega,i} = \pm \frac{M_{\omega,i}}{I_{\omega}} \omega_R = \pm 24.72 \text{ MPa}$, where $|\omega_R| = \frac{hb}{4} \frac{ht - bs}{ht + bs} = 5.74 \text{ mm}^2$ is the warping ordinate at the corners, (Fig. 7a)). The shear stress resulting from the secondary torsional moment is given as:

$$\tau_{s,1} = \frac{M_{Ts}}{t I_{\omega}} S_0 = 3.13 \text{ MPa}, \quad \tau_{s,2} = \frac{M_{Ts}}{s I_{\omega}} S_0 = 6.27 \text{ MPa}, \quad \tau_{s,3} = \frac{M_{Ts}}{t I_{\omega}} S_1 = 10.9 \text{ MPa},$$

$$\tau_{s,4} = \frac{M_{Ts}}{s I_{\omega}} S_2 = -9.40 \text{ MPa}, \quad \text{where } S_0 = \frac{h^2 - b^2}{6\gamma} \omega_R = 3.140258790 \times 10^{(-12)} \text{ m}^4,$$

$$S_1 = S_0 + A_G \frac{\omega_R}{4} = 1.099090576 \times 10^{(-11)} \text{ m}^4, \quad S_2 = S_0 - A_S \frac{\omega_R}{4} = -4.710388182 \times 10^{(-12)} \text{ m}^4,$$

are the auxiliary constants with the web and flange areas

$$A_S = sh = 0.00000546875 \text{ m}^2 \quad \text{and} \quad A_G = tb = 0.00000546875 \text{ m}^2.$$

The shear stress resulting from the primary torsional moment is obtained as:

$$\tau_{p,1} = \frac{M_{Tp} sbh}{I_T (ht + bs)} = 7.31 \text{ MPa}, \quad \tau_{p,2} = \frac{M_{Tp} t bh}{I_T (ht + bs)} = 14.63 \text{ MPa}.$$

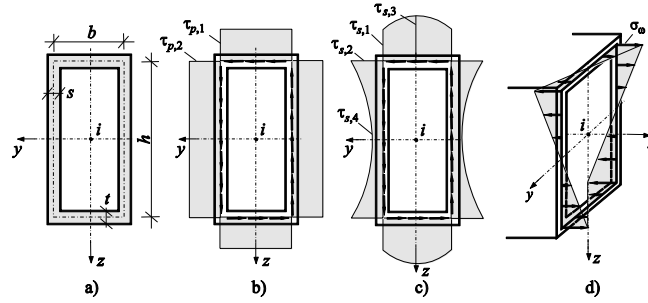


Fig. 7: a) Cross-section, b) primary shear stress, c) secondary shear stress, d) axial stress due to warping.

According to Fig. 7, the total shear stresses are obtained as follow:

$$\tau_1^{total} = \tau_{s,1} + \tau_{p,1} = 10.45 \text{ MPa}, \quad \tau_3^{total} = \tau_{s,3} + \tau_{p,1} = 18.28 \text{ MPa},$$

$$\tau_2^{total} = \tau_{s,2} + \tau_{p,2} = 20.89 \text{ MPa}, \quad \tau_4^{total} = \tau_{s,4} + \tau_{p,2} = 5.22 \text{ MPa}.$$

As can be observed from the above calculations, the magnitude of the normal warping stress in the clamped beam end is comparable to the torsional shear stress magnitude. Distribution of the bimoment normal stress along the beam edges is proportional to the bimoment distribution shown in Fig. 6. To verify the results achieved, numerical analysis of the same beam is done using a very fine mesh of the SOLID186 [16] finite elements. For variation $n = 1$, results obtained are shown in Table 4 and Fig. 8. From their comparison, a good match of the achieved results can be found for the angle of twist. By the solid FEM model, the twist angle at the beam free end is calculated from the displacements of the points lying on the hollow cross-section symmetry stress. Some discrepancies occur in both the values and the positions of the maximum normal stress. The SOLID186 solution exhibits maximum normal stresses at points that are offset from the corners of the clamped cross section. This local effect may be caused by an uneven cross sectional wall thickness of the profile and by different base of the beam and solid finite elements modelling. From the detailed stress distribution in Fig. 8 also follows that normal stress in the middle point of the wall thickness at the corners agree well with the results obtained by our FGM-WT beam finite element.

Variables for:	FGM-WT with STMDE	WT BEAM	SOLID186
ψ_k [rad]	0.0072	0.0072	0.0077
$\sigma_{\omega,i}$ [MPa]	24.72	24.71	17.2/20.0

Tab. 4: Results comparison for $n = 1$.

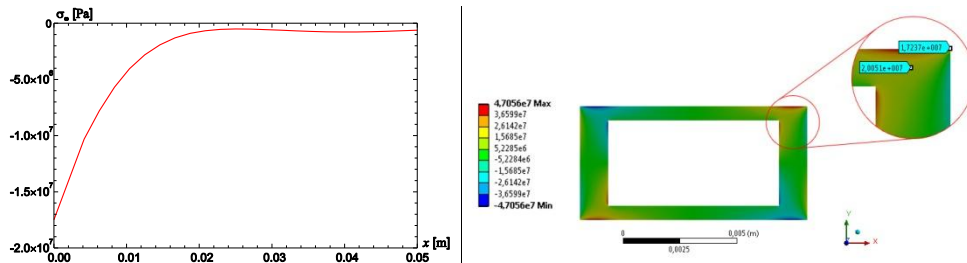


Fig. 8: Distribution of the normal stress along the top edge of the beam and on the clamped cross-sectional area.

5 CONCLUSIONS

In the contribution, the 3D FGMs Timoshenko beam finite element with 14×14 stiffness and mass matrices for doubly symmetric open and closed cross-section is presented including warping torsion effect (non-uniform torsion) and the STMDE. A longitudinal continuous variation of effective material properties is considered. This element can be used for modal and elastostatic analysis of FGM beams. The results of the analyzes confirm an acceptable accuracy and very high effectiveness of the new finite element comparing to results obtained by solid FE. FGM beam with continuous spatial variation of material properties can be modelled with only one new FGM-WT beam finite element. This FE is implemented into the 14×14 matrix of the 3D FGM beam finite element that can be used for analysis of the beam structures built of beams with spatially varying material properties.

Acknowledgement: The authors gratefully acknowledge financial support by the Slovak Grant Agencies: VEGA No. 1/0102/18 and No. and 1/0081/18.

REFERENCES

- [1] Murin, J. and Aminbaghai, M. and Hrabovsky, J. and Gogola, R. and Kugler, S. Beam finite element for modal analysis of FGM structures. *Eng. Struct.* (2016) 121: 1 – 18.
- [2] Tsipisis, I.N. and Sapountzakis, and E.J. Generalized warping and distortional analysis of curved beams with isogeometric methods. *Comp. Struct.* (2017) 191: 33 – 50.
- [3] Yoon, K. and Lee, P.S. and Kim, D.N. Geometrically nonlinear finite element analysis of functionally graded 3D beams considering warping effects. *Comp. Struct.* (2015) 132: 1231 – 1247.
- [4] Abrate, S. and Sciuva M. D. Equivalent single theories for composite and sandwich structures: A review. *Comp. Struct.* (2017) 179:482–494.
- [5] Attenshamudin, S.S. and Yuvaraj, M.G. Modeling and analysis of functionally graded sandwich beams: A review. *Mech. of Ad. Mat. and Struct.* (2018) DOI 10.1080/15376494.2018.1447178.
- [6] Murin, J. and Goga, V. and Aminbaghai, M. and Hrabovsky, J. and Sedlar, T. and Mang, H.A. Measurement and modelling of torsional warping free vibrations of beams with rectangular hollow cross-sections. *Eng. Struct.* (2017) 136: 68 – 76.
- [7] Kutis, V. and Murin, J. and Belak, R. and Paulech, J. Beam element with spatial variation of material properties for multiphysics analysis of functionally graded materials. *Comp. and Struct.* (2011) 89: 1192 – 1205.
- [8] Aminbaghai, M and Murin, J. and Balduzzi, G. and Hrabovsky, J. and Hochreiner, G. and Mang, H.A. Second-order torsional warping theory considering the secondary torsion-moment deformation-effect. *Eng. Struct.* (2017) 147: 724 – 739.
- [9] Murin, J. and Goga, V. and Aminbaghai, M. and Hrabovsky, J. and Sedlar, T. and Mang, H.A. Measurement and modelling of torsional warping free vibrations of beams with rectangular hollow cross-sections. *Eng. Struct.* (2017) 136: 68 – 76.
- [10] Murin, J. et al. Torsional warping eigenmodes of FGM beams with longitudinally varying material properties. (2018). Sent for publication.
- [11] Aminbaghai, M. et al. Torsional warping elastostatic analysis of FGM beams with longitudinally varying material properties. (2018). In preparation.
- [12] Aminbaghai M, Murin J, Hrabovsky J, Mang H.A. Torsional warping eigenmodes including the effect of the secondary torsion moment on the deformations. *Eng. Struct.* (2016) 106: 299 – 316.
- [13] ABAQUS/CAE, Version 6.10-1, Dassault Systems Simulia Corp. Providence, RI, USA.
- [14] Przemieniecki, J.S. Theory of matrix structural analysis. McGraw-Hill, NY, 1968.
- [15] Wolfram Mathematica 9.0.1.0, Wolfram Research 2013.
- [16] ANSYS Swanson Analysis System, Inc., 201 Johnson Road, Houston, PA 15342/1300, USA.
- [17] Murin, J. and Aminbaghai, M. and Kutis, V. and Kralovic, V. and Sedlar, T. and Goga, V. and Mang, H.A. A new 3D Timoshenko finite beam element including non-uniform torsion of open and closed cross sections. *Eng. Struct.* (2014) 59: 153 – 160.

In Vitro Biaxial Contraction Tests Identify Changes in Arterial Mechanical Properties Not Observed in Isometric Uniaxial Contractions

Sae-I Murtada^{*}, Jay Humphrey^{**}, Gerhard Holzapfel^{***}

^{*}Yale University, ^{**}Yale University, ^{***}Graz University of Technology

ABSTRACT

Multiscale modeling that includes a description of relevant structural components and their interrelations is facilitated to better understand the underlying mechanisms of vascular smooth muscle contractility in intact arteries. Much focus has been given to study the uniaxial length-tension relationship described through changes in the actin and myosin filament overlap for studying characteristics of smooth muscle contractility even though this experimental arrangement does not mimic the in vivo vascular geometry or loading. In contrast, biaxial contraction of an inflated and axially extended vessel provides considerable information, both passive and active, under realistic conditions. Filament lattice spacing has also been reported to have a significant effect in muscle contractility (1), but a clear explanation of its influence has not yet been given. Few investigations have compared these two in vitro approaches directly, namely how their results overlap, how they differ, and if they provide unique complementary information. We present a multiscale mathematical model of arterial contractility accounting for structural and functional constituents at molecular, cellular, and tissue levels. The artery is assumed to be a thick-walled incompressible cylinder described by an anisotropic model of the extracellular matrix and novel model of smooth muscle contractility. The latter includes a three-dimensional structural sensitivity to deformation, including muscle filament overlap and filament lattice spacing. The overall model was able to capture both uniaxial (2) and biaxial (3) experimental contraction data, which was not possible when accounting for filament overlap alone. The model was also used to conduct a parameter sensitivity study that reveals that uniaxial contraction tests are not as efficient as biaxial tests for identifying changes in vascular smooth muscle contractility. References 1. C.D. Williams, M.K. Salcedo, T.C. Irving, M. Regnier, T.L. Daniel, The length-tension curve in muscle depends on lattice spacing, 2013, *Proc Biol Sci.* 280:20130697. 2. S.-I. Murtada, S. Lewin, A. Arner, J.D. Humphrey. Adaptation of active tone in the mouse descending thoracic aorta under acute changes in loading, 2016, *Biomech Model Mechanobiol* 15:579–592. 3. S.-I. Murtada, J Ferruzzi, H. Yanagisawa, J.D. Humphrey. Reduced biaxial contractility in the descending thoracic aorta of fibulin-5 deficient mice, 2016, *J Biomech Eng* 138:051008

Modeling Texture Inhomogeneity during Accumulative Angular Drawing Process of Ti-6Al-4V

Krzysztof Muszka^{*}, Lukasz Madej^{**}, Janusz Majta^{***}, Jakub Kawalko^{****}, Irene Beyerlein^{*****},
Sven Vogel^{*****}

^{*}AGH University of Science and Technology, ^{**}AGH University of Science and Technology, ^{***}AGH University of Science and Technology, ^{****}AGH University of Science and Technology, ^{*****}University of California Santa Barbara, ^{*****}Los Alamos National Laboratory

ABSTRACT

In the present work, initial results regarding self-consistent computer model for prediction of texture evolution during Accumulative Angular Drawing process of Ti-6Al-4V will be presented. AAD process is recently developed method of Severe Plastic Deformation that allows for production of drawn wires with controlled inhomogeneity of microstructure. It introduces controlled strain path changes that activate additional deformation mechanisms – compared to conventional wire drawing processes. Apart from reduction of the area, bending, torsion and burnishing mechanisms act on the drawn wire. This way, it is possible to accumulate high deformation energy and deform materials that are characterized by low number of possible slip planes and hence limited ductility. Due to a number of process parameters that are characteristic for AAD process, computer modeling offers a robust way to optimize the microstructure and properties of the deformed wires. In the current work, model assumptions and initial results will be presented and compared with microstructural data.

Error Representation and Space-Time Goal-Oriented Adaptivity for the Advection-Diffusion Equation Employing Explicit Runge-Kutta Methods

Judit Muñoz-Matute^{*}, Victor M. Calo^{**}, David Pardo^{***}, Elisabete Alberdi^{****}

^{*}University of the Basque Country (UPV/EHU), Leioa, Spain, ^{**}Applied Geology, Curtin University, Perth, Australia,

^{***}University of the Basque Country (UPV/EHU), Leioa, Spain, ^{****}University of the Basque Country (UPV/EHU),
Leioa, Spain

ABSTRACT

In goal-oriented adaptivity for space-time problems, it is crucial to represent the error in the quantity of interest as an integral over the whole space-time domain. In that way, we can express the error in the quantity of interest as a sum of local element contributions, and perform the adaptive process. A full space-time variational formulation allows such integral representation [2]. Many authors employ implicit methods in time to perform goal-oriented adaptivity [1], like Backward Euler or Crank-Nicholson, as it is well known that these methods present variational structure [3]. However, the variational formulation of explicit methods in time for partial differential equations remains elusive. In this work, we build a Petrov-Galerkin formulation for the advection-diffusion equation that is equivalent to the Forward Euler method in time. Then, we derive an error representation and an explicit goal-oriented adaptive algorithm, enabling dynamic meshes in space. Some numerical results are provided in 1D to illustrate the proposed explicit algorithm. Finally, we provide an overview of how to construct higher order Runge-Kutta methods using a variational formulation and describe a similar goal-oriented procedure. References: [1] W. Bangerth, M. Geiger, and R. Rannacher. Adaptive Galerkin finite element methods for the wave equation. *Computational Methods in Applied Mathematics*, 10(1):3–48, 2010. [2] P. Díez and G. Calderón. Goal-oriented error estimation for transient parabolic problems. *Computational Mechanics*, 39(5):631–646, 2007. [3] D. Estep and A. Stuart. The dynamical behavior of the discontinuous Galerkin method and related difference schemes. *Mathematics of Computation*, 71(239):1075–1103, 2002.

Patient-specific Finite Element Models of Normal Pregnancy Derived from Time-course Maternal Ultrasound Scans

Kristin Myers^{*}, Andrea Westervelt^{**}, Lindsey Carlson^{***}, Chia-Ling Nhan-Chang^{****}, Joy Vink^{*****}, Timothy Hall^{*****}, Helen Feltovich^{*****}

^{*}Columbia University, ^{**}Columbia University, ^{***}University of Wisconsin, ^{****}Columbia University Medical Center, ^{*****}Columbia University Medical Center, ^{*****}University of Wisconsin, ^{*****}University of Wisconsin

ABSTRACT

Preterm birth (PTB) is a global health dilemma. It is the leading cause of childhood death worldwide, affecting 1 in 10 babies. In 2016, the PTB rate in the U.S. rose for the second consecutive year. A likely reason for this is misdirected investigation due to combining the multiple phenotypes of PTB into a single diagnosis. Ultrasound measurement of cervical length (CL) is the current standard-of-care for PTB prediction, presumably because it provides information about cervical structural integrity. While this has a strong negative predictive value (0.97), its positive predictive value is weak (0.23) [1]. We hypothesize this is partially because CL provides a 1-dimensional metric for a complex 3-dimensional structure. The overall objective of our research is to develop etiology- and patient-specific models that describe the biomechanical interrelationships of the uterus, cervix, and fetal membranes during pregnancy. In this study, we investigate the patient-specific mechanical environment of a cohort of women at low-risk for PTB to establish normal maternal mechanics. Specifically, we measure maternal anatomy longitudinally throughout pregnancy using multiple ultrasound measurements and characterize tissue stress and stretch using Finite Element Analysis (FEA). For this ongoing study, we recruited 21 multiparous and 9 nulliparous patients. Each has received transabdominal and transvaginal ultrasound exams at four pregnancy timepoints (8-12 weeks, 14-18 weeks, 22-24 weeks, and 32-34 weeks). At each visit, ultrasound images of the uterus and cervix are acquired (Siemens S3000) from both supine and standing orientations. From these, maternal anatomical parameters (uterine diameters, uterine wall thickness, cervical length and diameter, angle between the cervical canal and the anterior lower uterine segment, and the posterior location of the cervix) are measured. 3D computer models of the first timepoint of each patient's anatomy are built and meshed in Trelis 16.1 (csimsoft) using a custom parameterized script. Anatomical boundary conditions and material properties [2] are prescribed and gestation-matched intrauterine pressure [3] applied to the inner fetal membrane surface using FEBio 2.6.4 (febio.org). Material parameters are remodeled so FEA predictions of anatomy shape of later pregnancy timepoints match the experimental data. The uterine, fetal membranes, and cervical tissue stress and stretch is characterized and compared between patients at gestation-matched time points to reveal the common load-bearing and tissue remodeling features of maternal anatomy throughout normal pregnancy. References [1] van Baaren GJ, et al. *ObGyn.* 2014;123:1185–1192. [2] Westervelt AR, et al. *ASME. J Biomech Eng.* 2017;139(5). [3] Fisk, et al. (1992). *BJOG*, 99: 18–22.

PHASE FIELD BASED MULTIMATERIAL TOPOLOGY OPTIMIZATION

ANDRZEJ M. MYSLINSKI^{1,2}

¹ Systems Research Institute,
ul. Newelska 6, 01-447 Warsaw, Poland,
e-mail: andrzej.myslinski@ibspan.waw.pl

² Warsaw University of Technology,
Faculty of Manufacturing Engineering, ul. Narbutta 85
02-524 Warsaw, Poland
e-mail: a.myslinski@wip.pw.edu.pl

Key words: topology optimization, unilateral contact, Tresca friction, phase field regularization, operator splitting method.

Abstract. *The paper is concerned with the robust numerical method to solve numerically the multimaterial topology optimization problems for bodies in unilateral contact. This contact phenomenon with Tresca friction is governed by the elliptic boundary value problem with inequality boundary conditions. The body is assumed to consist from more than two distinct isotropic elastic materials. The materials distribution function is chosen as the design variable. The structural optimization problem consists in finding such topology of the domain occupied by the body that the normal contact stress along the boundary of the body is minimized. The original cost functional is regularized using the multiphase volume constrained Ginzburg-Landau energy functional rather than the perimeter functional. The first order necessary optimality condition is recalled and used to formulate the generalized gradient flow equations of Allen-Cahn type. The optimal topology is obtained as the steady state of the phase transition governed by the generalized Allen-Cahn equation. The optimization problem is solved numerically using the operator splitting approach combined with the alternating gradient projection method. Numerical examples are reported to validate the applicability of the proposed approach.*

1 INTRODUCTION

The goal of the multimaterial structural topology optimization is to find the optimal distribution of several elastic materials in a given design domain to minimize a functional describing the mechanical or the thermal properties of the structure or its cost [1,2]. The loaded structure is assumed to satisfy the volume or mass constraints imposed on it. In recent years multiple phases topology optimization problems have become subject of the growing interest [3,4,5,6,7]. The use of multiple number of phases during the design of engineering structures opens a new opportunities in the design of smart and advanced structures in material science and/or industry. In contrast to single material design the use of multiple number of materials extends the design space and may lead to better design solutions. Different aspects of the multimaterial structural optimization, including both analytical and numerical, are subject of intensive research (see references in [3,4,5,6,7]). Many methods including the homogenization method [1], the Solid Isotropic Material Penalization (SIMP) method [2], topological derivative method [8] or different methods based on the level set approach [9,10] or phase field approach [11,12,13] successful in single material optimization, have been extended to deal with the multimaterial optimization. The extension of these methods faces several challenges. A crucial issue in the solution of the multimaterial optimization problems is the lack of physically based parametrization of the phases mixture [3,7]. Although in the literature are proposed different material interpolation schemes, in general, they may influence the optimization path in terms of the computational efficiency and the final design. The level set methods can eliminate the need of the material interpolation schemes provided that interfaces are actually tracked explicitly [3]. Among others, in [3] a multimaterial topology optimization problem for the plane elasticity system has been solved using the level set method. The elasticity tensor has been smeared out using the signed distance function. In [7] similar optimization problem has been solved numerically using a generalized Allen–Cahn equation.

The paper is concerned with the structural topology optimization of unilateral contact problems with Tresca friction between the surfaces of the elastic bodies [14] and extends the results from [6]. The optimization problem consists in finding such topology of the domain occupied by the body that the normal contact stress along the boundary of the body is minimized. In literature [10,12] this problem usually is considered as two-phase material optimization problem with voids treated as one of the materials. In the paper the domain occupied by the body is assumed to consist from several elastic materials rather than two materials. Material fraction function is a variable subject to optimization. The regularization of the objective functional by the multiphase volume constrained Ginzburg-Landau energy functional is used. The derivative formula of the cost functional with respect to the material fraction function is calculated and is employed to formulate a necessary optimality condition for the topology optimization problem. The cost functional derivative is also used to formulate a gradient flow equation for this func-

nal in the form of the generalized Allen–Cahn equation governing the evolution of the material phases. The optimal topology is obtained as a steady state solution to this equation. Two step operator splitting approach [7] is used to solve this gradient flow equation. Finite difference and finite element methods are used as the approximation methods. Numerical examples are reported and discussed.

2 PROBLEM FORMULATION

Consider deformations of an elastic body occupying two–dimensional bounded domain Ω with the smooth boundary Γ (see Fig. 1). The body is subject to body forces $f(x) = (f_1(x), f_2(x))$, $x \in \Omega$. Moreover, the surface tractions $p(x) = (p_1(x), p_2(x))$, $x \in \Gamma$, are applied to a portion Γ_1 of the boundary Γ . The body is clamped along the portion Γ_0 of the boundary Γ and the contact conditions are prescribed on the portion Γ_2 . Parts $\Gamma_0, \Gamma_1, \Gamma_2$ of the boundary Γ satisfy: $\Gamma_i \cap \Gamma_j = \emptyset$, $i \neq j$, $i, j = 0, 1, 2$, $\Gamma = \bar{\Gamma}_0 \cup \bar{\Gamma}_1 \cup \bar{\Gamma}_2$.

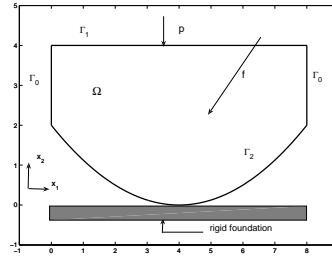


Figure 1: Elastic body occupying domain Ω in unilateral contact with the foundation.

The domain Ω is assumed to be occupied by $s \geq 2$ distinct isotropic elastic materials. Each material is characterized by Young modulus. The voids are considered as one of the phases, i.e., as a weak material characterized by low value of Young modulus [1]. The materials distribution is described by a phase field vector $\rho = \{\rho_m\}_{m=1}^s$ where the local fraction field $\rho_m = \rho_m(x) : \Omega \rightarrow R$, $m = 1, \dots, s$, corresponds to the contributing phase. The phase field approach allows for a certain mixing between different materials. This mixing is restricted only to a small interfacial region. In order to ensure that the phase field vector describes the fractions the following pointwise bound constraints called in material science the Gibbs simplex [4,7,8] are imposed on every ρ_m

$$\alpha_m \leq \rho_m \leq \beta_m, \text{ for } m = 1, \dots, s, \text{ and } \sum_{m=1}^s \rho_m = 1, \quad (1)$$

where the constants $0 \leq \alpha_m \leq \beta_m \leq 1$ are given and the summation operator is understood componentwise. The second condition in (1) ensures that no overlap and gap of fractions are

allowed in the expected optimal domain. Moreover the total spatial amount of material fractions satisfies

$$\int_{\Omega} \rho_m(x) dx = w_m |\Omega|, \quad 0 \leq w_m \leq 1, \text{ for } m = 1, \dots, s, \text{ and } \sum_{m=1}^s w_m = 1. \quad (2)$$

The parameters w_m are user defined and $|\Omega|$ denotes the volume of the domain Ω . From the equality (1) it results that $\rho_s = 1 - \sum_{m=1}^{s-1} \rho_m$ and the fraction ρ_s may be removed from the set of the design functions. Therefore from now on the unknown phase field vector ρ is redefined as $\rho = \{\rho_m\}_{m=1}^{s-1}$. Due to the simplicity and robustness the SIMP material interpolation model [3,7] is used. Following this model the elastic tensor $\mathcal{A}(\rho) = \{a_{ijkl}(\rho)\}_{i,j,k,l=1}^2$ of the material body is assumed to be a function depending on the fraction function ρ :

$$\mathcal{A}(\rho) = \sum_{m=1}^s g(\rho_m) \mathcal{A}_m = \sum_{m=1}^{s-1} g(\rho_m) \mathcal{A}_m + g(1 - \sum_{m=1}^{s-1} \rho_m) \mathcal{A}_s, \quad (3)$$

with $g(\rho_m) = \rho_m^3$. The constant stiffness tensor $\mathcal{A}_m = \{\tilde{a}_{ijkl}^m\}_{i,j,k,l=1}^2$ characterizes the m -th elastic material of the body. For detailed discussion of the interpolation of the material elasticity tensor see [3,7,16]. It is assumed, that elements a_{ijkl} and $\tilde{a}_{ijkl}^m(x)$, $i, j, k, l = 1, 2$, $m = 1, \dots, s$, of the elasticity tensors \mathcal{A} and \mathcal{A}_m , respectively, satisfy [14,15] usual symmetry, boundedness and ellipticity conditions. Denote by $u = (u_1, u_2)$, $u = u(x)$, $x \in \Omega$, the displacement of the body and by $\sigma(x) = \{\sigma_{ij}(u(x))\}$, $i, j = 1, 2$, the stress field in the body. Consider elastic bodies obeying Hooke's law, i.e., for $x \in \Omega$ and $i, j, k, l = 1, 2$,

$$\sigma_{ij}(u(x)) = a_{ijkl}(\rho) e_{kl}(u(x)), \quad e_{kl}(u(x)) \stackrel{\text{def}}{=} \frac{1}{2}(u_{k,l}(x) + u_{l,k}(x)), \quad (4)$$

where $u_{k,l}(x) = \frac{\partial u_k(x)}{\partial x_l}$. We use here and throughout the paper the summation convention over repeated indices [14]. The stress field σ satisfies the system of equations in the domain Ω [14]

$$-\sigma_{ij}(x)_{,j} = f_i(x) \quad \sigma_{ij}(x)_{,j} = \frac{\partial \sigma_{ij}(x)}{\partial x_j}, \quad x \in \Omega, \quad i, j = 1, 2. \quad (5)$$

The following boundary conditions are imposed on the boundary $\partial\Omega$

$$u_i(x) = 0 \quad \text{on } \Gamma_0, \quad \sigma_{ij}(x)n_j = p_i \quad \text{on } \Gamma_1, \quad i, j = 1, 2, \quad (6)$$

$$(u_N + v) \leq 0, \quad \sigma_N \leq 0, \quad (u_N + v)\sigma_N = 0 \quad \text{on } \Gamma_2, \quad (7)$$

$$|\sigma_T| \leq 1, \quad u_T \sigma_T + |u_T| = 0 \quad \text{on } \Gamma_2, \quad (8)$$

where $n = (n_1, n_2)$ is the unit outward versor to the boundary Γ . Here $u_N = u_i n_i$ and $\sigma_N = \sigma_{ij} n_i n_j$, $i, j = 1, 2$, represent [14] the normal components of displacement u and stress σ , respectively. The tangential components of displacement u and stress σ are given [14] by $(u_T)_i = u_i - u_N n_i$ and $(\sigma_T)_i = \sigma_{ij} n_j - \sigma_N n_i$, $i, j = 1, 2$, respectively. $|u_T|$ denotes the Euclidean norm in R^2 of the tangent vector u_T . A gap between the bodies is described by a given function v .

2.1 Phase Field Based Topology Optimization Problem

Before formulating a structural optimization problem for the system (5)-(8) let us introduce a set U_{ad}^p of the admissible suitable regular fraction functions:

$$U_{ad}^p = \{\rho : 1 - \beta_s \leq \sum_{m=1}^{s-1} \rho_m \leq 1 - \alpha_s, \\ \alpha_m \leq \rho_m \leq \beta_m, \int_{\Omega} \rho_m dx = w_m \mid \Omega \mid \text{ for } m = 1, \dots, s-1\}. \quad (9)$$

The set $U_{ad}^p \subset H^1(\Omega; R^{s-1})$ is assumed to be nonempty. The aim of the structural optimization problem for the bodies in unilateral contact is to reduce the normal contact stress responsible for wear, vibrations, fatigue of the contacting surfaces as well as for a generated noise. The structural optimization problem with normal contact stress functional is difficult to analyze it and to solve it numerically. Therefore following [10] we shall use the cost functional $J_\eta : H^1(\Omega) \rightarrow R$ approximating the normal contact stress on the contact boundary Γ_2

$$J_\eta(u(\rho)) = \int_{\Gamma_2} \sigma_N(u(\rho)) \eta_N(x) ds, \quad (10)$$

depending on a given auxiliary bounded function $\eta(x) \in M^{st}$. The set M^{st} is given by

$$M^{st} = \{\eta = (\eta_1, \eta_2) \in H^1(\Omega; R^2) : \eta_i \leq 0 \text{ on } \Omega, i = 1, 2, \|\eta\|_{H^1(\Omega; R^2)} \leq 1\},$$

where functions σ_N and η_N are the normal components of the stress field σ corresponding to a solution $u(\rho)$ satisfying the system (5)-(8) and the function η , respectively. The optimization problem consisting in finding such $\rho \in U_{ad}^p$ to minimize the functional $J_\eta(u(\rho))$ in general has no solutions [1,4,7,14,16]. In order to ensure the existence of optimal solutions let us regularize the cost functional (10) by adding to it a regularizing term $E(\rho) : U_{ad}^p \rightarrow R$ rather than the standard perimeter term [1,16]

$$J(\rho, u(\rho)) = J_\eta(u(\rho)) + E(\rho). \quad (11)$$

The Ginzburg-Landau free energy functional $E(\rho)$ is expressed as [7,16]

$$E(\rho) = \sum_{m=1}^{s-1} \int_{\Omega} \psi(\rho_m) d\Omega, \quad \psi(\rho_m) = \frac{\gamma \varepsilon}{2} |\nabla \rho_m|^2 + \frac{\gamma}{\varepsilon} \psi_B(\rho_m), \quad (12)$$

where $\varepsilon > 0$ is a real constant governing the width of the interfaces, $\gamma > 0$ is a real parameter

related to the interfacial energy density. Moreover $\nabla \rho_m \cdot n = 0$ on Γ for each m . The function $\psi_B(\rho_m) = \rho_m^2(1 - \rho_m)^2$ is a double-well potential [22] which characterizes the concentration of the material phases [7]. The structural optimization problem for the system (5)-(8) takes the form: *find* $\rho^* \in U_{ad}^\rho$ *such that*

$$J(\rho^*, u^*) = \min_{\rho \in U_{ad}^\rho} J(\rho, u(\rho)), \quad (13)$$

where $u^* = u(\rho^*)$ denotes a solution to the state system (5)-(8) depending on ρ^* and the set U_{ad}^ρ is given by (9). The existence of an optimal solution $\rho^* \in U_{ad}^\rho$ to the problem (13) follows by classical arguments (see [5]). Remark due to (12) the problem (13) is dependent on the interface width parameter ε .

3 NECESSARY OPTIMALITY CONDITION

The Lagrangian approach combined with adjoint state approach has been applied to compute the derivative of the cost functional (11) with respect to the function ρ . This derivative is determined for all $\zeta \in H^1(\Omega; R^{s-1})$ and $i, j, k, l = 1, 2$ as

$$\begin{aligned} \int_{\Omega} \frac{\partial J}{\partial \rho}(\rho, u) \zeta dx &= \int_{\Omega} \frac{\partial L}{\partial \rho}(\rho, u, \lambda, p^a, q^a) \zeta dx = \sum_{m=1}^{s-1} \int_{\Omega} [\gamma \varepsilon \nabla \rho_m \cdot \nabla \zeta_m + \\ &\quad \frac{\gamma}{\varepsilon} \psi'_B(\rho_m) \zeta_m] dx + \int_{\Omega} [a'_{ijkl}(\rho_m) e_{ij}(u) e_{kl}(p^a + \eta) - f_i(p_i^a + \eta_i)] \zeta_m dx. \end{aligned} \quad (14)$$

where (p^a, q^a) denotes the adjoint state. For details see [12]. From (1), (3) and (12) it results the derivatives of the tensor element $a_{ijkl}(\rho_m)$ and the function $\psi_B(\rho_m)$ with respect to ρ_m are equal to $a'_{ijkl}(\rho) = 3\rho_m^2 \tilde{a}_{ijkl}^m - 3\rho_s^2 \tilde{a}_{ijkl}^s$ and $\psi'_B(\rho_m) = 4\rho_m^3 - 6\rho_m^2 + 2\rho_m$, respectively. Using (14) the necessary optimality condition to the optimization problem (13) takes the form [1, 15]:

Let U_{ad}^ρ be a nonempty closed convex subset of $H^1(\Omega; R^{s-1})$ and $\rho^* \in U_{ad}^\rho$ be an optimal solution to the structural optimization problem (13). Then

$$\int_{\Omega} \frac{\partial J}{\partial \rho}(\rho^*, u^*)(\rho - \rho^*) dx \geq 0 \quad \forall \rho \in U_{ad}^\rho. \quad (15)$$

The functions (u^*, λ^*) and (p^{a*}, q^{a*}) in the derivative formula (14) denote the solutions to the state system (5)-(8) and the adjoint systems for $\rho = \rho^*$, respectively. Using the orthogonal projection operator $P_{U_{ad}^\rho} : L^2(\Omega; R^{s-1}) \rightarrow U_{ad}^\rho$ from $L^2(\Omega; R^{s-1})$ on the set U_{ad}^ρ condition (15) can be written [7] in the form:

if $\rho^* \in U_{ad}^\rho$ is an optimal solution to the structural optimization problem (13), then for $\mu \in R$ and $\mu > 0$

$$P_{U_{ad}^\rho}[\rho^* - \mu \frac{\partial J(\rho^*, u^*)}{\partial \rho}] - \rho^* = 0. \quad (16)$$

The parameter ε governing the width of the interface zone between the phases in the model (11)-(13) and the optimality systems (15)-(16) is assumed to be fixed. In a case when this parameter tends to zero, i.e., $\varepsilon \rightarrow 0$ from (11)-(13) it follows this parameter may be also controlled by the parameter γ . As the interfaces between the material phases subdomains shrink to the subdomain boundaries the phase field model evolves [7] into sharp interface model characterized by boundaries dividing a design domain into subdomains. The sharp interface model corresponds to the level set approach [4,5,6,13]. The transition from phase field model to the sharp interface model is equivalent to the investigation of the convergence of the solutions to the phase field model as the interface width parameter tends to zero. This convergence for the contact problems has been investigated in [5]. Using the theory of bounded variations spaces and the notion of Γ convergence, for the interface width parameter tending to zero the Γ -convergence in the space L^1 of the sequence of phase field regularized functionals to the sharp interface functional regularized using the perimeter term has been shown in [5].

3.1 Generalized Allen–Cahn Gradient Flow Equation

Recall [16] the structural optimization problem (13) can be considered as a phase transition setting problem consisting in such evolution of the phases to minimize the cost functional (11) with respect to the initial configuration. In order to describe the evolution of phases in time let us assume that the phase field vector ρ depends not only on $x \in \Omega$ but also on time variable $t \in [0, T]$, $T > 0$ is a given constant, i.e., $\rho = \rho(x, t) = \{\rho_m(x, t)\}_{m=1}^{s-1}$. The variable t may be interpreted as an artificial time or iteration number in the computational algorithm [7,16]. Using the right hand side of (16) let us formulate the constrained gradient flow equation of Allen–Cahn type [4,7,8,14,22,23] for the cost functional (11): *find function $\rho \in U_{ad}^\rho$ satisfying the initial boundary value problem:*

$$\frac{\partial \rho}{\partial t} = -P_{U_{ad}^\rho}[\rho - \mu \frac{\partial J(\rho, u)}{\partial \rho}] + \rho \quad \text{in } \Omega, \forall t \in [0, T], \quad (17)$$

$$\nabla \rho \cdot n = 0 \quad \text{on } \partial \Omega, \forall t \in [0, T], \quad (18)$$

$$\rho(0, x) = \rho_0(x) \quad \text{in } \Omega, t = 0, \quad (19)$$

with $\rho_0(x) = \{\rho_{0m}(x)\}_{m=1}^{s-1}$ denoting a given $H^1(\Omega; R^{s-1})$ regular function. For such ρ_0 the system (17)-(19) possesses a solution ρ (see [4,8]). The stationary solutions of (17)-(19) fulfill the first order necessary optimality conditions (15) or (16) for the problem (13) [4,8]. For $\frac{\partial \rho}{\partial t} = 0$ the right hand side of the equation (17) vanishes and $\rho(x, t) = \rho^*(x, t)$ is an optimal solution to the problem (13).

For the sake of numerical calculations we reformulate the initial boundary value problem (17)-(19) using the operator splitting approach [7]. Remark, the cost functional (11) may be represented as a sum of two functionals, i.e.,

$$J(\rho, u) = J_1(\rho, u) + J_2(\rho) \quad (20)$$

given by

$$J_1(\rho, u) = J_\eta(u(\rho)) + \sum_{m=1}^{s-1} \int_{\Omega} \frac{\gamma}{\varepsilon} \psi_B(\rho_m) d\Omega, J_2(\rho) = \sum_{m=1}^{s-1} \int_{\Omega} \frac{\gamma \varepsilon}{2} |\nabla \rho_m|^2 d\Omega.$$

The derivatives of these functionals result from formula (14). Assume the time interval $[0, T]$ is divided into N subintervals with stepsize $\Delta t = t_{k+1} - t_k$, $k = 1, \dots, N$ and $\rho_k = \rho(t_k)$ is known. The design variable ρ_{k+1} at the next time step t_{k+1} is calculated in two substeps. First the trial value $\tilde{\rho}$ is calculated from the gradient flow equation (17) for the functional J_1 only. Next this solution is updated to ensure its $H^1(\Omega)$ regularity [4] by solving the gradient flow equation (17) for the functional J_2 only with the boundary condition (18), i.e.,

$$\frac{\partial \tilde{\rho}}{\partial t} = -P_{U_{ad}^\rho} \left[\tilde{\rho} - \frac{\partial J_1(\tilde{\rho}, u)}{\partial \rho} \right] + \tilde{\rho}, \quad \tilde{\rho}(t_k) = \rho_k, \quad t_k < t \leq t_{k+1}. \quad (21)$$

$$\frac{\partial \rho}{\partial t} = -\frac{\partial J_2(\rho)}{\partial \rho}, \quad \rho(t_k) = \tilde{\rho}_{k+1}, \quad t_k < t \leq t_{k+1}. \quad (22)$$

4 NUMERICAL RESULTS

The topology optimization problem (13) has been discretized and solved numerically. Time derivatives are approximated by the forward finite difference. Piecewise constant and piecewise linear finite element method is used as discretization method in space variables. The derivative of the double well potential is linearized with respect to ρ_m . Primal-dual active set method [4,7,12] has been used to solve the state system (5)-(8) and the adjoint system. The initial boundary value problem (17)-(19) has been solved in two steps according to scheme (21)-(22). The algorithms are programmed in Matlab environment. As an example a body occupying 2D domain

$$\Omega = \{(x_1, x_2) \in \mathbb{R}^2 : 0 \leq x_1 \leq 8 \wedge 0 < v(x_1) \leq x_2 \leq 4\}, \quad (23)$$

is considered. The boundary Γ of the domain Ω is divided into three disjoint pieces

$\Gamma_0 = \{(x_1, x_2) \in R^2 : x_1 = 0, 8 \wedge 0 < v(x_1) \leq x_2 \leq 4\}$, $\Gamma_1 = \{(x_1, x_2) \in R^2 : 0 \leq x_1 \leq 8 \wedge x_2 = 4\}$, $\Gamma_2 = \{(x_1, x_2) \in R^2 : 0 \leq x_1 \leq 8 \wedge v(x_1) = x_2\}$. The domain Ω and the boundary Γ_2 depend on the function $v(x_1) = 0.125 \cdot (x_1 - 4)^2$. Domain Ω is filled with $s = 3$ elastic materials. The Poisson's ratio of each material is $\nu = .3$. The Young's moduli of materials are: $E_1 = 6 \cdot E_0$, $E_2 = 3 \cdot E_0$ and $E_3 = E_0$, $E_0 = 2.1 \cdot 10^{11}$ Pa. The parameters w_1, w_2, w_3 are equal to .25, .5 and .25 respectively. As an initial design ρ_0 a feasible design with the uniform material distribution has been taken. The body is loaded by the boundary traction $p_1 = 0$, $p_2 = -5.6 \cdot 10^6$ N along the boundary Γ_1 , the body forces $f_i = 0, i = 1, 2$. The auxiliary function η is selected as a piecewise linear on Ω and is approximated by a piecewise linear function. The domain Ω is divided into 80×40 grid. The parameters ε and γ are equal to the mesh size and to 0.5, respectively. The total number of iterations k_{max} in the optimization algorithm has been set to 90. It is approximately equivalent to final time $T = 125$ s. Fig. 2 presents the optimal topology domain obtained by solving structural optimization problem (13) using the necessary optimality condition (17)-(19). The areas with the weak phases appear in the central part of the body and near the fixed edges. The areas with the strong phases appear close to the contact zone and along the edges.

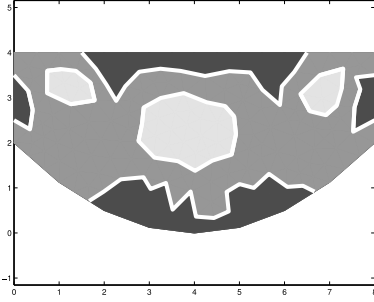


Figure 2: Optimal material distribution in domain Ω^* .

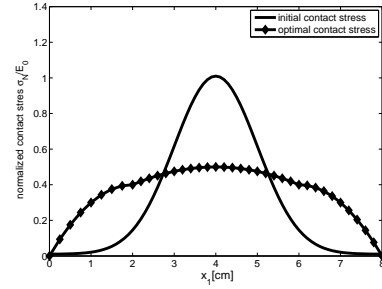


Figure 3: Initial and optimal normal contact stress.

The rest of the domain is covered with the intermediate phase. The obtained normal contact stress for the optimal topology is almost constant along the contact boundary and has been significantly reduced comparing to the initial one (see Fig. 3). The cost functional value decreases almost monotonically when the number of iterations increases. At the beginning this decrease is significant and finally the cost functional value is almost steady. Similarly, after a few initial iterations the gradient of the cost functional also almost monotonically decreases to reach the steady state.

5 CONCLUSIONS

- The obtained numerical results indicate that the optimal topologies are qualitatively comparable to the results reported in other phase-field topology optimization methods.
- Since the optimization problem is non-convex it has possibly many local solutions dependent on initial estimate.
- Gradient flow method employed in H^1 space is more regular and efficient than standard Allen-Cahn approach. The obtained solution depends on the interface width parameter. As this parameter tends to zero the optimal solutions to this optimization problem are expected to converge to optimal solution of the perimeter regularized problem.

REFERENCES

- [1] Allaire, G. Shape optimization by the homogenization method, Springer, New York, (2001).
- [2] Bendsoe, M.P., Sigmund, O. Topology Optimization: Theory, Methods, and Applications, Springer, Berlin, (2004).
- [3] Allaire, G., Dapogny, C., Delgado, G., Michailidis, G. Multi-phase structural optimization via a level set method, ESAIM - Control Optimisation and Calculus of Variations, (2014)20:576–611.
- [4] Blank, L., Garcke, H., Hecht, C., Rupprecht, Ch. Sharp interface limit for a phase field model in structural optimization, SIAM J. Control Optim., (2016)54:1558–1584.
- [5] Myśliński, A. Multimaterial Topology Optimization of Variational Inequalities, in System Modeling and Optimization, eds. L. Bociu, J.P. Desideri, A. Habbal, IFIP AICT 494, 27 th IFIP TC 7 CSMO, Sophia Antipolis, France, June 29 July 3, 2015, Revised Selected Papers, Springer International Publishing, (2016):380 – 389.
- [6] Myśliński, A. Multimaterial Topology Optimization of Contact Problems Using Allen-Cahn Approach, in Advances in Structural and Multidisciplinary Optimization, Eds: A. Schumacher, T. Vietor, S. Fiebig, K.U. Bletzinger, K. Maute, Springer International Publishing, ISBN 978-3-319-67987-7, (2018):1069 - 1082.

- [7] Tavakoli, R. Multimaterial Topology Optimization by Volume Constrained Allen–Cahn System and Regularized Projected Steepest Descent Method, *Comput. Meth. Appl. Mech. Eng.* (2014)276:534–565.
- [8] Kovtunen, V.A., Leugering, G. A Shape-Topological Control Problem for Nonlinear Crack-Defect Interaction: The Antiplane Variational Model, *SIAM Journal on Control and Optimization* (2016)54(3):1329–1351.
- [9] van Dijk, N.P., Maute, K., Langlaar, M., van Keulen, F. Level-set methods for structural topology optimization: a review, *Structural and Multidisciplinary Optimization* (2013) 48:437–472.
- [10] Myśliński, A. Piecewise Constant Level Set Method for Topology Optimization of Unilateral Contact Problems, *Advances in Engineering Software* (2015)80:25–32.
- [11] Burger, M., Stainko, R. Phase-field relaxation of topology optimization with local stress constraints, *SIAM J. Control. Optim.*, (2006)45:1447–1466.
- [12] Myśliński, A., Wróblewski, M. Structural optimization of contact problems using Cahn-Hilliard model, *Computers & Structures*, (2017)180:52–59.
- [13] Penzler, P., Rumpf, M. and Wirth, B. A phase-field model for compliance shape optimization in nonlinear elasticity, *ESAIM: COCV*, (2012)18(1):229–258.
- [14] Haslinger, J., Mäkinen, R. Introduction to Shape Optimization. Theory, Approximation, and Computation, SIAM Publications, Philadelphia, (2003).
- [15] Tröltzsch, F. Optimal control of partial differential equations: Theory, methods and applications, American Mathematical Society, Graduate Studies in Mathematics 112, Providence, Rhode Island, (2010).
- [16] Dede, L., Boroden, M.J., Hughes, T.J.R. Isogeometric analysis for topology optimization with a phase field model, *Archives of Computational Methods in Engineering*, (2012)19(3):427–465.

Making Use of Symmetries in the Elastic Inverse Homogenization Problem

Carlos Méndez^{*}, Juan Manuel Podestá^{**}, Sebastián Toro^{***}, Alfredo Huespe^{****}, Javier Oliver^{*****}

^{*}CIMEC – Universidad Nacional del Litoral, Santa Fe, Argentina., ^{**}CIMEC – Universidad Nacional del Litoral, Santa Fe, Argentina., ^{***}CIMEC – Universidad Nacional del Litoral, Santa Fe, Argentina., ^{****}CIMEC – Universidad Nacional del Litoral, Santa Fe, Argentina., ^{*****}CIMNE - Universitat Politècnica de Catalunya, Barcelona, Spain.

ABSTRACT

It is a known fact that even the highest symmetry (isotropic) of the elastic tensor can be achieved through topology design using a unit cell with arbitrary shape whose material distribution does not present any symmetry (think about a polycrystal or an amorphous material). However, it is also well known that an adequate choice of the unit cell and the symmetries imposed in the design process can significantly facilitate the finding of certain classes of composites (like Vigdergauz microstructures or new ones proposed by Sigmund [1]). In this work, we make a comprehensive analysis of the connection between the symmetry of the material distribution in the microstructure and the properties of the resulting elastic tensor. Considering periodic structures, we analyze all the possible Bravais lattices and all the plane (wallpaper) groups in order to study the way in which the symmetries of these patterns are reflected in the homogenized elastic tensor. For the unit cell we adopt Wigner-Seitz cells, which are primitive cells that preserve all the symmetries of the subjacent Bravais lattice and simplify the implementation of plane groups. Given an arbitrary elastic tensor, we propose a procedure for the inverse homogenization that allow us to choose the most convenient shape for the unit cell and to select the symmetries to be imposed that guarantee (during the whole optimization process) that the homogenized elastic tensor will have the same symmetry of the tensor to be designed. Concerning the design, several well established tools were used, such as algorithms for the rotation of the tensor to their material axes [2] and topology optimization methods based on SIMP [1] and topological derivative [3]. Some examples regarding the search of new classes of extreme materials are shown, where it can be seen how different composites classes emerge depending on the enforced symmetries. [1] O. Sigmund (2000). A new Class of Extremal Composites. *Journal of the Mechanics and Physics of Solids*, 48(2), 397-428. [2] N. Auffray and P. Ropars (2016). Invariant-based reconstruction of bidimensional elasticity tensors. *International Journal of Solids and Structures*, 87, 183-193. [3] S. Amstutz et al. (2010). Topological derivative for multi-scale linear elasticity models applied to the synthesis of microstructures. *International Journal for Numerical Methods in Engineering*, 84(6), 733-756.

Theory and Application of Reactive Inelasticity Framework for Modeling Tendon Viscoelasticity, Plastic Deformation, and Damage

Babak N. Safa^{*}, Michael Santare^{**}, Dawn Elliott^{***}

^{*}University of Delaware, ^{**}University of Delaware, ^{***}University of Delaware

ABSTRACT

The major inelastic behaviors in tendon are viscoelastic, plastic deformation, and damage. Of these, plastic deformation and damage are particularly significant, because of their potential relation to tissue dysfunction and repair. However, these behaviors have overlapping effects, which hinders their experimental measurement. As a result, a theoretical framework is needed to formulate and characterize them. We have formulated a structurally inspired inelasticity framework for modeling tissue inelasticity, Reactive Inelasticity (RIE), based on the kinetics of molecular bonds [1], and further applied it to experimental data on rat tail tendon fascicles, to determine the role of the inelastic behaviors in the mechanical response of tendon tissue. The RIE framework is based on the kinetics of molecular bonds and assumes different molecular bond types that break and reform when subjected to loading, to model the inelastic behaviors. Three types of bonds are defined: (1) Formative (for viscoelasticity), (2) Permanent (for hyperelasticity), and (3) Sliding (for plastic deformation). The same sets of constitutive equations are used to formulate each of these bonds, with the major difference being the kinetics rate of breakage and reformation of bonds. Further, damage is added to the model by reducing the number of each bond type. To determine the role of each one of the inelastic behaviors in tendon, based on the RIE framework we built two independent models, each specific to plastic deformation or damage, and applied them to a set of experimental stress data on rat tail tendon fascicles [2]. Further, the models were validated against another set of experiments [3]. Overall, both of the models had a similar success in fitting and predicting the mechanical response. Further experimental studies, specifically designed to differentiate between plastic deformation and damage are needed. This study is significant in addressing inelastic behaviors of tendon based on its molecular structure, which can be used to identify structural relationships between its mechanical behavior and external loading. References: [1] B.N. Safa, et al., Summer Biomechanics, Bioengineering, Biotransport Conf., 2017, 434. [2] A.H. Lee, et al., Acta Biomaterialia, 2017, 57, 363. [3] S.E. Szczesny, et al., PloS one, 2014, 9, e99588.

Macroscopic Models for Crack Propagation in Heterogeneous Lattices based on Phase Field Method

Nhu NGUYEN*, Julien RETHORE**, Julien YVONNET***

*Université Paris-Est Laboratoire MSME UMR CNRS 8208 5 Bd Descartes 77454 Marne-la-Vallée Cedex 2, France., **Institute de Recherche en Génie Civil et Mécanique-GeM UMR CNRS 6183, École Centrale de Nantes 1 rue de la Noë 44321, Nantes, France, ***Université Paris-Est Laboratoire MSME UMR CNRS 8208 5 Bd Descartes 77454 Marne-la-Vallée Cedex 2, France.

ABSTRACT

In heterogeneous quasi-brittle materials like civil engineering materials micro-cracks can propagate and merge to create macro-cracks. Modelling precisely the micro-cracks as well as the heterogeneities in materials and tracking the propagation of micro-cracks is cumbersome and computationally intractable. The phase field approach to fracture has brought appealing advantages in modelling cracks process including the possibility to handle nucleation, propagation, branching and merging of cracks branching and merging of cracks with no predefined path. In heterogeneous materials, propagation of cracks is a multiscale process. Unfortunately, homogenization of damage behavior is associated with many difficulties, including: (i) the intrinsic nonlinearity of the problem; (ii) the difficulty to define an RVE due to localization; (iii) the numerical lack of convergence and of stability at the macroscale; (iv) the definition of the characteristic length scale at both scales. Among many approaches to fracture in a multiscale framework, in the present work, we follow [1] by identifying the different parameters of a damage model at the macroscale but in a direct manner, by fitting the effective parameters of a mechanical test response under crack initiation and propagation in a structure where all heterogeneities are explicitly described. The macroscopic parameters are identified and can then be used without concurrent computations for the macroscale calculations using the phase field method. Specifically, depending on the regularized length, which is considered as a material parameter, the isotropic phase field model [2] is employed to study cracks in the equivalent homogeneous medium or its extensions to anisotropic crack propagation [3] will be used to handle the effects of preferential crack propagation in regular lattices. Within this framework, the scale separation is not required and allows avoiding concurrent (FE2-like) costly computations. Keywords: Phase field method, multiscale modelling, damage, homogenization, crack propagation, quasi-brittle materials. References [1] Hossain M, Hsueh CJ, Bourdin B, Bhattacharya K (2014) Effective toughness of heterogeneous media. *Journal of the Mechanics and Physics of Solids* 71:15–32 [2] Nguyen T, Yvonnet J, Zhu QZ, Bornert M, Chateau C (2015) A phase field method to simulate crack nucleation and propagation in strongly heterogeneous materials from direct imaging of their microstructure. *Engineering Fracture Mechanics* 139:18–39 [3] Nguyen T, Rethore J, Yvonnet J, Baietto M (2017) Multi-phase-field modeling of anisotropic crack propagation for polycrystalline materials. *Comput Mech* 60(2):289–314

Tribological Behaviors of Grafted-Nanoparticles on Polymer-Brushed Walls: A Dissipative Particle Dynamics Study

Vinh Phu NGUYEN*, Phuoc Quang PHI**, Nghia Trong MAI***, Seung Tae CHOI****

*Chung-Ang University, **Chung-Ang University, ***Chung-Ang University, ****Chung-Ang University

ABSTRACT

Synthetic polymer brushes on tribological surfaces have wide potential industrial and medical applications as lubricants, since they are close to biological systems and do not produce any pollute waste like oil lubricants. Understanding the tribological behavior of the polymer brush-coated surfaces under high normal loading can be considered as the first step to enhance their tribological properties and to realize their practical applications. In this study, grafted nanoparticles are proposed as nano bearings on polymer brush-coated surfaces to alleviate the harsh working conditions of polymer brushes and to improve their mechanical stability. As a mesoscale simulation technique, dissipative particle dynamics (DPD) is adapted for the first time to investigate the tribological interaction between grafted nanoparticles and parallel walls with non-charged polymer brushes. DPD simulations are performed to investigate the influences of seven parameters (solvent quality, brush miscibility, grafting density and chain length of nanoparticle brushes, shear rate and hollowness of nanoparticles, and separation distance of parallel walls) on the tribological behavior of the system. Density profile, number of inter-brush interactions and kinetic friction coefficient are analyzed from DPD simulation results to find out the tendencies of structural and tribological responses caused by the variations of the seven parameters. The grafted nanoparticles do obviously act as nano-bearings that partially replace the sliding contact between two walls' brushes with the rolling contact between the grafted nanoparticle itself and two walls' brushes. The solvent quality has a strong effect on kinetic friction coefficient as already known in the literature. The grafting density and chain length of the grafted nanoparticle, which are important to prevent the agglomeration of nanoparticles, also influence the kinetic friction coefficient. However, their effects are relatively weaker than the solvent quality. For some cases, the number of interbrush interactions in the middle of the simulation box is better correlated to the friction coefficient than the total number of interbrush interactions. The DPD simulation results and analysis performed in this study would be beneficial in designing the polymer-brushed surfaces and grafted nanoparticles, predicting their tribological performance, and thus, developing new lubricants, especially water-based lubricants for green technology, both experimentally and computationally.

A Multi-phase-field/Polycrystal Plasticity for the Brittle-ductile Transitions of Crystalline Rock with Precipitating Fluid

SeonHong Na^{*}, WaiChing Sun^{**}

^{*}Columbia University, ^{**}Columbia University

ABSTRACT

A safe and permanent repository for nuclear waste disposal using rock salt has drawn attention due to increasing demand of a sustainable and clean energy. The usage of rock salt for the geological repository is highly related to its desired characteristics, such as high thermal conductivity, low permeability and self-healing mechanism. These complicated physical and chemical mechanisms are closely related to the microscopic properties of rock salt. Previous efforts for investigating rock salt have focused on capturing the phenomenological behaviors. Nevertheless, the induced anisotropy and the rate-dependent behaviors of polycrystalline salt are often originated from the microstructures. In this work, we present an alternative approach in which the crystalline nature and the migration of brine as inclusions and precipitated fluid along the grain boundaries are explicitly modelled. We formulate a phase field framework for rock salt that explicitly model the interactions among crystal grain, grain boundaries and brine inclusions. A multi-phase-field method to capture brine migration due to dissolution and precipitation mechanism of halite under temperature gradient. Meanwhile, the crystal plasticity theory is adopted for modeling each grain to account for the crystallographic properties of rock salt. The texture of the multi-grains of salt is assumed to be random by assigning different sets of orientations to each grain. Numerical examples demonstrate that the proposed model is able to capture the brine migrations, interactions of the brine inclusion inside the halite grain and the fluid precipitating in grain boundaries.

A Kriging-PGD Algorithm to Couple Enriched Multifidelity Metamodels and Reduced-order Model to Handle Multiparametric Problem

Stéphane Nachar^{*}, Pierre-Alain Boucard^{**}, David Néron^{***}

^{*}LMT (ENS-Cachan/CNRS/Université Paris-Saclay), ^{**}LMT (ENS-Cachan/CNRS/Université Paris-Saclay), ^{***}LMT (ENS-Cachan/CNRS/Université Paris-Saclay)

ABSTRACT

The advent of Virtual Testing and industry's willingness for hyper fine structural optimization impose technical constraints for computational mechanics community. Optimize mechanical criterion for a turbine blade with classical techniques costs around months of CPU computation. To handle this issue, many cost-killer methods have been developed and two major families can be distinguished: surrogate models for an optimal approximation of mechanical criteria in the whole design space or around global optimum; and reduced-order models to approximate mechanical fields and allows evaluation of criteria in real-time. Our contribution is to unify these strategies around an nonlinear solver, well-designed for multiparametric problem: the LATIN-PGD method [Ladevèze, 1999]. It has two key features: each LATIN iteration gives an MOR-approximation of mechanical fields at each time step, known as time-space PGD modes; and it can be (re)started with fields from another solution. With these features, we can consider low-fidelity data from a non-converged LATIN solution, and harness the possibility to create a spatial modes basis for (re)start computation with other parameters set from design space, which drastically cut time computation. Our algorithm relies on building a initial surrogate model of the mechanical criterion with multi-fidelity data observations from a non-converged LATIN solution [Forrester, 2007]. This surrogate model will be enriched with well-choosed points from MSE or EI criterion and spatial modes arising from previous computations will be used to accelerate LATIN convergence. Attention will be focused towards the number of initial points on design space, and the way to choose low-fidelity data. This new algorithm will be presented on an elasto-visco-plastic case, using parallel computing. [Forrester, 2007] Forrester, Alexander I.J., András Sóbester, and Andy J. Keane. "Multi-Fidelity Optimization via Surrogate Modelling." Proceedings of the Royal Society A: Mathematical, Physical and Engineering Sciences 463, no. 2088 (December 8, 2007): 3251–69. [Ladevèze, 1999] Ladeveze, Pierre. Nonlinear Computational Structural Mechanics: New Approaches and Non-Incremental Methods of Calculation. Springer Science & amp; Business Media.

Image-base Material Homogenization Using Neural Networks under the cgFEM Framework

Enrique Nadal*, Borja Ferrandiz**, Manuel Tur***, Juan José Ródenas****, F. Javier Fuenmayor*****

*Universitat Politècnica de València. Centro de Investigación en Ingeniería Mecánica, **Universitat Politècnica de València. Centro de Investigación en Ingeniería Mecánica, ***Universitat Politècnica de València. Centro de Investigación en Ingeniería Mecánica, ****Universitat Politècnica de València. Centro de Investigación en Ingeniería Mecánica, *****Universitat Politècnica de València. Centro de Investigación en Ingeniería Mecánica

ABSTRACT

Metal foams, such as aluminium foam, is taking interest due to its acoustic properties, impact energy absorption, etc. However, the structural analysis using the Finite Element Method (FEM) of such structures is complex since the geometry is not available in a CAD file. In fact, the geometry of a metal foam is obtained from a CT-scan. In order to avoid the unneeded step of generating an artificial CAD model from the CT-scan, some new FEM formulations have emerged. Some of them associate one element per pixel, whose elastic properties are related to the pixel color [1], leading to a model with an unaffordable number of elements. In order to avoid this problem, CellFEM [1] and cgFEM [2] methods allow several pixels to be associated with one single element. The latter one uses a special integration quadrature with one integration point per pixel. This methodology is precise, although the high number of integration points used makes it inefficient. In order to speed up the cgFEM, the authors propose in this work to carry out an off-line machine learning (ML) process, based on neural networks, for the homogenization process at each element. The ML process relates the low frequency terms of the Discrete Cosines Transform of the group of pixels falling into one element, which can be extracted from the JPEG compression, with its homogenized material properties. Therefore, a standard quadrature is used speeding up the Finite Element analysis. Results show that the use of 3 DCT coefficients is accurate enough in terms of deformation energy and displacements with respect to the reference solution. References: [1] A. Düster, J. Parvizian, Z. Yang, E. Rank. The finite cell method for three-dimensional problems of solid mechanics. *Computer Methods for Applied Mechanical Engineering*. 198: 3768-3782, 2008 [2] L. Giovannelli, J.J.Rodenas, J. M. Navarro, M. Tur. Direct medical image-based finite element modelling for patient-specific simulation of future implants. *Finite Elements in Analysis and Design*. 136:37-57, 2017. [3] E. Nadal. Cartesian grid FEM (cgFEM): High performance h-adaptive FE analysis with efficient error control: application to structural shape optimization. Ph.D. Thesis, Universitat Politècnica de València, 2014. Acknowledgements The financial support to this work of Generalitat Valenciana (PROMETEO/2016/007) and the Spanish Ministerio de Economía, Industria y Competitividad (DPI2017-89816-R) is greatly acknowledged.

Computational Micromechanics of Defects' Influence and Fiber Kinking on the Response of Fiber-Reinforced Composites

Mehdi Naderi^{*}, Nagaraja Iyyer^{**}, Nicole Apetre^{***}, Kishan Goel^{****}, Nam Phan^{*****}

^{*}Technical Data Analysis, Inc., ^{**}Technical Data Analysis, Inc., ^{***}Technical Data Analysis, Inc., ^{****}US Naval Air Systems Command, ^{*****}US Naval Air Systems Command

ABSTRACT

The influence of defects and fiber waviness on the tensile/compressive response of fiber-reinforced composite is studied in this paper via micromechanical approach. Augmented finite element method (AFEM) is used to provide high-fidelity data on damage initiation and propagation along with micromechanical analysis. A python program is written to generate the micromechanical model as the input file for Abaqus model. We also discuss the three dimensional AFEM, developed as Abaqus User Element (UEL). Zero-thickness cohesive elements are inserted on fiber/matrix interface for modelling fiber/matrix interface delamination. Both automatic damage initiation and propagation algorithm is implemented in AFEM to capture discontinuities. Within micromechanical analysis, the effects of fiber volume fractions, fiber shapes are also considered to capture the stochastic behavior of the composite under tensile loading. In order to investigate the effects of voids and defects on ultimate strength of composite, we carry out simulations with random voids and defects. These results strongly show the importance of including defects and voids in the finite element analysis. To study composite response with fiber misalignment under compressive loading, random degree of waviness are considered in different sets of representative volume elements (RVEs). The results show how detrimental is the fiber misalignment to the structural integrity of composite components under compressive loading. It is also seen that the damage initiation and propagation locations are controlled by the degree and location of waviness. [1] M. Naderi, J. Jung, Q. D. Yang, A three dimensional augmented finite element for modeling arbitrary cracking in solids, *International Journal of Fracture*, 2016, 197: 147-168. [2] M Naderi, N Apetre, and N Iyyer. Effect of interface properties on transverse tensile response of fiber-reinforced composites: Three-dimensional micromechanical modeling. *Journal of Composite Materials*, 2017,51: 2963-2977. [3] M Naderi and N Iyyer. 3D modeling of arbitrary cracking in solids using augmented finite element method. *Composite Structures*, 2017, 160: 220–231.

6D Response Statistics by Path Integration of a Nonlinear Rotating Shaft Subjected to Colored Noise

Arvid Naess*, Oleg Gaidai**, Michael Dimentberg***

*NTNU, Norway, **JUST, China, ***WPI, USA

ABSTRACT

The paper studies extreme response statistics of random vibrations for a Jeffcott-type rotor with non-linear restoring force, under uniaxial colored noise excitation. The latter type of dynamic system is of wide use in stability studies of rotating machinery. System response statistics are studied by applying the path integration (PI) method. The Jeffcott rotor response statistics are then obtained by solving the Fokker–Planck-Kolmogorov (FPK) equation for a 6D dynamic system. The resulting response probability distributions can serve as an engineering input for a wide range of design issues, e.g. estimates of characteristic values, extreme value statistics and system reliability. Assessment of transverse random vibrations of shafts in rotating machinery may be of practical importance for applications with substantial environmental dynamic loads on supports, particularly in transport/vehicle engineering. Colored noise is a step forward compared to white noise excitation forces, but it raises the mechanical system dimension from 4D to 6D. The major advantage of path integration, relative to direct Monte Carlo simulation, is that path integration yields high accuracy in the probability distribution tail. Improved implementation of the PI algorithm was applied, specifically, the fast Fourier transform (FFT) was used to simulate the additive noise of the dynamic system. PI was accelerated by using a Monte Carlo based estimate of the joint PDF as an initial input. Finally, the key feature of this work is the advance to 6D problems, where very little PI research has been done. The obvious reason is of course the formidable computation load arising from decent 6D mesh. This paper, however, gives a practical solution to the latter challenge, enabling 6D PI calculation on an ordinary desktop within a reasonable amount of time. Using modern computational hardware with a decent GPU (Graphic Processing Unit) will significantly facilitate 6D calculation, making it an easy engineering task.

Atomistic-Continuum Coupling for Random Alloys

Shankha Nag*, William Curtin**

*École polytechnique fédérale de Lausanne, **École polytechnique fédérale de Lausanne

ABSTRACT

Random alloys are multicomponent systems where occupancy of any lattice site by an atom type is independent of its surrounding. Such systems have statistical fluctuations in local atomic configurations and properties, which prevents accurate application of standard atomistic/continuum coupling methods [1]. Here, two methods for atomistic/continuum coupling that mitigate errors are proposed, studied, and validated. In one method, a fully-relaxed atomistic sample, with atoms displaced from the perfect lattice sites, is carved out of a larger random sample. The outer atoms of the atomistic sample then (i) define nodal positions from which an outer continuum model is constructed and (ii) serve as so-called pad atoms that move with the continuum nodes and transmit forces onto the atoms in the inner atomistic domain. This method ensures no spurious stresses at zero loading, and only small spurious stresses arise under loading. But it requires creation of a much larger initial sample and is specific to that particular atomic distribution. A second method considers an atomistic domain with two outer layers of atoms and then the additional pad region represented as by “average” atoms interatomic potentials [2] that, in principle, match the average bulk lattice and elastic constants of the random alloy. This method separates the random/homogeneous boundary from the atomistic/continuum boundary, avoiding the serious errors that arise when the two boundaries are at the same position. This method creates small spurious stresses under zero load, due to small mismatches in the actual properties of the “average” atoms as compared to the real atoms, and small additional spurious stresses under applied load. The two methods are examined for three different solid solution alloys (dilute Al-5%Mg, Ni-15%Al, and medium entropy FeNiCr, all described by EAM interatomic potentials). Spurious errors for both methods and across all three materials are small (~ 10 MPa) up to applied strains of 10^{-3} . These methods enable the accurate study of mechanics boundary value problems in random alloys, such as High Entropy Alloys, for problems where it is essential to capture atomistic phenomena in some localized region of the sample. [1] Modelling Simul. Mater. Sci. Eng. 11 (2003) R33–R68 [2] Phys. Rev. B 93, 104201

KEY ELEMENT BUILDINGS DESIGN METHOD WITH BIDIRECTIONAL EVALUATION BETWEEN STRUCTURAL ANALYSIS AND EVACUATION ANALYSIS

YASUYUKI NAGANO*, YOICHI MUKAI^{†1}, KENSUKE YASUFUKU^{†2},
YASUNORI MIZUSHIMA^{†3} AND TOMOHARU SARUWATARI^{†4}

* Graduate School of Simulation Studies, University of Hyogo
7-1-28, Minatojima-Minamimachi, Chuo-ku, Kobe 650-0047, Japan
E-mail: nagano@sim.u-hyogo.ac.jp

^{†1}Kobe University
1-1, Rokkodai-cho, Nada-ku, Kobe, 657-8501, Japan
E-mail: ymukai@port.kobe-u.ac.jp

^{†2} Osaka University
2-1, Yamadaoka, Suita, Osaka, 565-0871, Japan
E-mail: yasufuku@cmc.osaka-u.ac.jp

^{†3} Takenaka Corporation
1-5-1, Ohtsuka, Inzai-shi, Chiba, 270-1395, Japan
E-mail: mizushima.yasunori@takenaka.co.jp

^{†4} JSOL Corporation
Tosabori Daibiru Bldg. 2-2-4, Tosabori, Nishi-ku, Osaka, 550-0001, Japan
E-mail: saruwatari.tom@jsol.co.jp

Key words: Key Element Design, Structural Analysis, Evacuation, FEM Analysis.

Abstract. In this study, we aim to construct a ‘Damage Simulator’ which can quantitatively evaluate the damage of nonstructural materials in the building. To avoid human casualties in a large building at the time of big earthquakes, we predict the damage caused by falling furniture inside the building, interior and exterior etc. by using computer simulation. First, we will develop a ‘Damage Assessment Observer’ function that accurately calculates the response of each part of the building using a structural simulator and visualizes and evaluates the degree of damage of nonstructural material. At the same time, the evacuation simulator will develop a ‘Damage Control Operator’ function that creates critical damage sites that cause significant evacuation difficulties, and performs key design elements of nonstructural materials from the importance of

Yasuyuki Nagano, Yoichi Mukai, Kensuke Yasufuku, Harunori Mizushima and Tomoharu Saruwatari

evaluation of nonstructural materials. Subsequently, by integrating the structural simulator and the evacuation simulator, we construct a damage simulator that can comprehensively design necessary specifications and evaluate the performance of nonstructural materials. We propose key elements in the design of a building or a structure by utilizing the damage simulator.

Nonstructural material of buildings is determined by designers in the overall cost plan of the building unlike the structural material. In ordinary building design, quantitative verification of damage created by nonstructural material is not taken into account. On the other hand, if the detailed model structure analysis based on the assumed ground motion during an earthquake is carried out, since the local behavior of the building can be comprehended, it is also possible to determine the damage degree of each nonstructural material. If the degree of damage can be evaluated for each nonstructural material, by assessing the damage resistance of each nonstructural material based on the evacuation simulation results, it is possible to design the nonstructural material to reduce casualties. We propose this new method of evaluating both the structural analysis result of where the building is likely to sustain damage due to an earthquake and the evacuation analysis result by considering the damage caused to the nonstructural material.

1 INTRODUCTION

In this study, by combining the incidental functions of the structural simulator and the evacuation simulator, the result of the evacuation simulation is vital to determine the furniture layout of buildings and the specifications of interior and exterior finishing materials. Considering both damage evaluation and damage control, we build a damage simulator. Fig. 1 shows a conceptual diagram of integrated simulation.

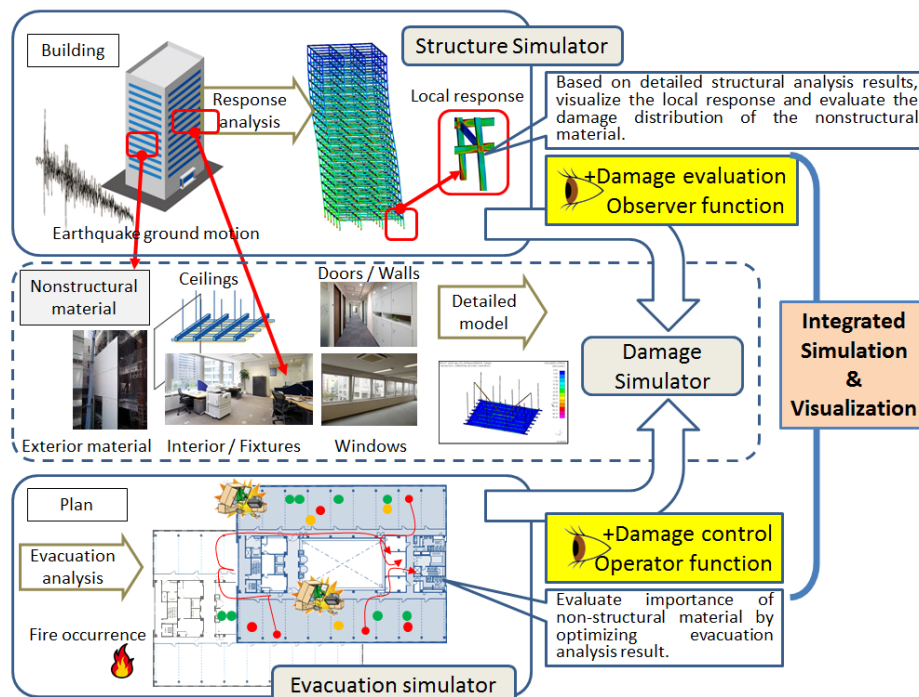


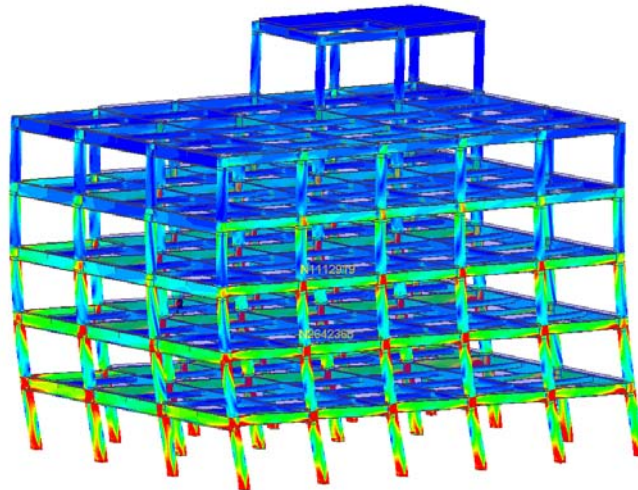
Fig. 1 Conceptual diagram of integrated simulation

2 DETAILED STRUCTURAL ANALYSIS WITH FINITE ELEMENT METHOD ^[1]

This study presents the first step in the development of a visualization system that would predict simultaneously the expected seismic damage of both structural and nonstructural members, such as walls and ceilings, by superposing seismic analytical results of nonstructural members on those of structural members.

Past seismic damage examples showed that human casualties had been caused by not only structural damages but also by damages of nonstructural members. Whereas the safety of structural members is constantly confirmed in the structural design process of buildings, there is no detailed process regarding the safety of nonstructural materials as they are made by specification design without any consideration to their locations. In order to reduce damage to nonstructural members that may cause harm to humans, nonstructural members should be designed considering local seismic responses. To accurately evaluate local seismic responses of nonstructural members, it is necessary to accurately evaluate seismic responses of structural members to which nonstructural members are attached. Therefore, it is important to have an overview of the overall responses of structural and nonstructural members.

This study aims to develop a system that can indicate the seismic damage undergone by structural and nonstructural members at the same time. The structural damage in a building was evaluated accurately by using the detailed finite element (FE) model of all structural members of the building (Fig. 2). The authors showed, in a previous study, that a detailed and complete FE model of the building structure simulated accurately the actual seismic behavior of the building. Through the detailed FE model, local seismic responses of the structural parts to which nonstructural members were connected could be extracted because the original shapes of all the structural members were reproduced as precisely as possible in the model. The local responses could be used to evaluate the seismic damage to the nonstructural members. Furthermore, superposing these analytical results enabled the comprehension of the relationship between the damaged members. This may lead to a structural design method that can reduce seismic damage to nonstructural members.



An Example of Stress Distribution

Fig. 2 Detailed finite element model of whole structural members of a building

3 ANALYZING THE SEISMIC BEHAVIOR OF NON-STRUCTURAL MEMBERS OF BUILDINGS BY USING THE LARGE-SCALE PARALLEL CALCULATION METHOD [2]

After large-scale earthquake, it is often reported that serious damage was caused to the nonstructural members, for example ceilings and claddings, of buildings with large open spaces such as gymnasiums and assembly halls.

The technical standard for preventive measures against collapsing ceilings is available for buildings, but its application is limited to preventing the damage caused by a middle-scale earthquake for which the behavior of the ceiling can be predicted to some extent. In order to expand this technical standard to the prevention of damage caused by an extremely rare earthquake (large-scale earthquake), it is necessary to have first clarified the behavior of the ceilings that are suspended from the building structure, and then to make the complete structure analysis model. To realize this, the specific analysis methods to evaluate the response of nonstructural members as precisely as possible according to the accurately predicted response of the structural frame of the building against the earthquake.

This study, suspending the ceilings in long-span structures as an example, prepares the detailed structural analysis models made by means of modeling the shape of the structural members so as to reflect the real one as truthfully as possible, and tries to obtain the extremely accurate earthquake response of the structural frame by a large-scale parallel calculation method (Fig. 3).

In the future, the aim will be to evaluate the behavior of a whole building through piling the results of the earthquake response of the ceilings by means of making as the boundary conditions the responses obtained by extremely accurate analysis of the structural frame from which the ceilings are suspended.

1: Max 66200748 : 1.523913E+02, Min 57857 : 1.631545E-13

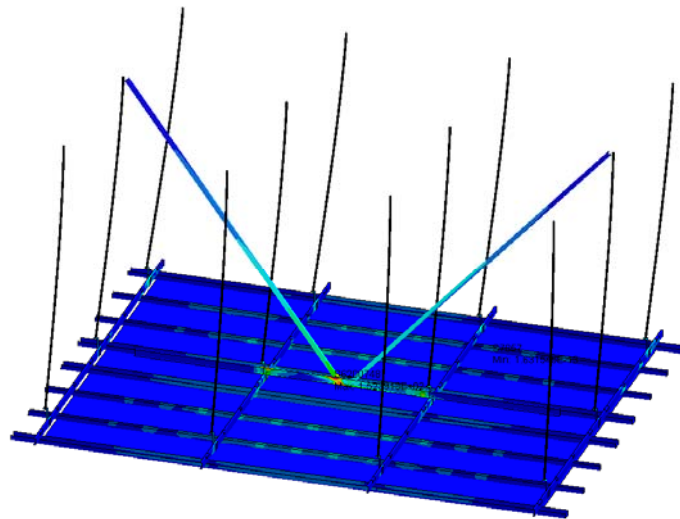


Fig. 3 Suspended ceilings FEM model installed in long-span structures

4 EVACUATION ANALYSIS CONSIDERING MULTIPLE PATH FAILURES WITH MULTI AGENT SYSTEM [3]

When verifying whether all the residents of a building can evacuate safely in the event of a major earthquake, it is necessary to consider various path failures due to earthquakes. For example, evacuation routes may be blocked due to debris such as damaged window panes, walls, ceilings and other exterior and interior (nonstructural) materials, movement of furniture fixtures, falling parts, and the like, which may affect evacuation safety. On the other hand, in recent years, the number of cases where a simulation method based on a multi-agent system that takes individual movements of evacuees into consideration for the evaluation of evacuation safety of buildings is increasing, and it is possible to promptly predict detailed evacuation properties under various conditions.

In this chapter, we propose a method to conduct evacuation analysis by using a multi-agent system, considering multiple path obstacles caused by damage of nonstructural material etc., in order to verify the evacuation safety of the building at the time of a large earthquake occurrence.

4.1 Multi-agent system and route fault setting

The evacuation analysis in this paper is based on the Multi-agent System^[4]. As an evacuation behavior model, the Social Force model is used. Our model has a feature that the shape of the agent is represented by an ellipse so that it can deal with higher density of crowd flow. In addition, when planning routes of agents and avoiding collisions with obstacles, the plan of the building is divided by a square mesh of 20 cm on each side, and a data structure is held for evacuation route information and obstacle information in each mesh. The evacuation route uses a mesh as a network structure to calculate the shortest route, and the agent refers to the information and selects the shortest route in the real space.

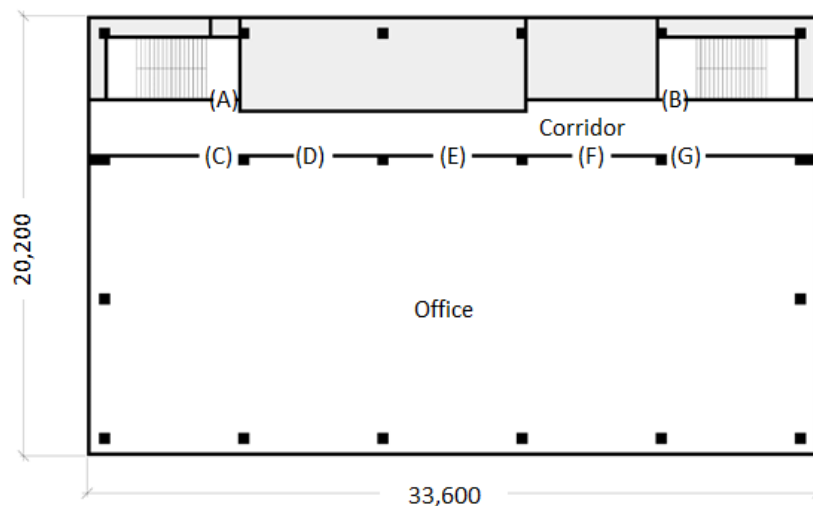


Fig. 4 Case study plan of the reference floor

Table 1 Setting of impassable route

	A	B	C	D	E	F	G
Case 1	✓	✓	✓	✓	✓	✓	✓
Case 2	✓	×	✓	✓	✓	✓	✓
Case 3	✓	×	×	×	✓	✓	✓
Case 4	✓	×	✓	✓	✓	×	×

✓: Passable ×: Impassable

Fig. 4 shows the standard floor plan of a general office building as a case study. The number of residents is randomly arranged as 57 people (0.125 people/m^2) and evacuation starts at once. As a route fault setting of the office building, situations where either one of the emergency stairs (A, B) cannot be used, or where one or more of the living room exits (C, D, E, F, G) cannot be used. The case of this route failure is summarized in Table 1. Evacuation routes for each case shall be set as the shortest route avoiding the route fault with the emergency staircase as the destination.

4.1 Results and discussion

Fig. 5 shows the transition of the number of evacuees completed in each case. Case 1 is a setting with no route fault, evacuate to the nearest one of the two emergency stairs A and B. The floor evacuation time is the shortest (41.1 seconds). The changes in the number of evacuees completed slowed to around 30 seconds. It indicates that one emergency staircase is not being used, and there are variations in the number of evacuees. There is a possibility that the evacuation time can be further shortened by appropriate evacuation guidance.

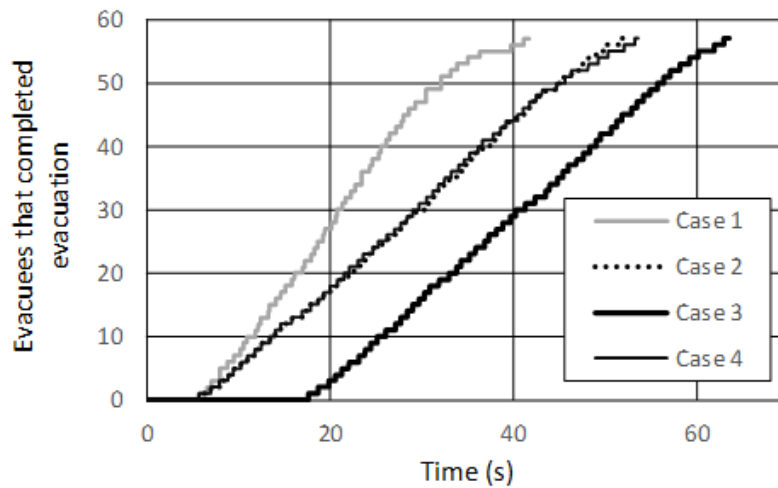


Fig. 5 Changes of number of evacuees that completed evacuation

In Cases 2 to 4, evacuation can take place only from emergency staircase A. Emergency staircase B is set to be unable to be used. Apart from that, the office room exits that can be used are different. Floor evacuation time is 51.8 seconds in Case 2, 63.0 seconds in Case 3, and 53.2 seconds in Case 4. The evacuation time and the evacuation completed number of cases in Case 2 and Case 4 are almost the same. In Case 2, all office room exits can be used, but Case 4 is set to be impassible at two exits F and G. However, since F and G are located far from the emergency staircase that can be used in Case 4, there was almost no influence on the floor evacuation time. On the other hand, in Case 3, it is impossible for two exits of the office room exits C and D close to the emergency staircase A (passable) to pass. It is necessary for the evacuees to take a detour and evacuate, and the floor evacuation time takes longer. However, the flow coefficients from Cases 2 to 4 to the staircase room are almost equal.

Next, the changes in the number of visitors in office rooms and corridors are shown in Fig. 6 and 7. In cases of evacuation of the office room, examples cases 1 and 2, there is no obstacle at the office room exit, so the room evacuation time is as short as 13 seconds. In cases 3 and 4, since 2 of 5 room exits are impossible to pass, it takes 22.5 seconds in Case 3 and 21 seconds in case 4 evacuation time. The reason for this is that there are evacuees whose walking distance in the living room is longer, and evacuees are concentrated in the room exit E. The reason why the evacuation time differs between Cases 3 and 4 is that because Case 3 is unable to pass through exits C and D on the left side and emergency stairs B on the right side, walking on the corridor becomes longer, this is caused by the occurrence of confluence of crowds in the room E and the corridors. From the simulation screen 17 seconds after the start of the simulation in Case 3 shown in Fig. 8, it is also understood that the crowd density is high near the corridor center. Even if there are no changes in the number and width of room exits that can be passed through, it is simulated that the crowd properties and the evacuation time differ due to the confluence of evacuees by the positional relationships and routes with the emergency staircases.

Focusing on the number of people in the corridor, the density of residents in Case 3 is the highest, and that of Case 4 is the lowest. Particularly in Case 4, there are two impassable room exits as compared with Case 2, which takes a long time to evacuate the office room and the number of people staying in the corridor simultaneously decreases. Also, since the distance between the passable room exits and the emergency stairs that can pass through is short, the evacuation time required in the corridor is shortened, and the difference between the final floor evacuation time and Case 2 has disappeared. Fig. 9 shows a simulation screen 10 seconds after the start of simulation in Case 4. As the room exit F and G are unable to pass, more than half of the residents are evacuated from the room exit E. However, because the exit width is suitable, the congestion is small in the office room, you can see that the evacuation is relatively smooth up to the corridor.

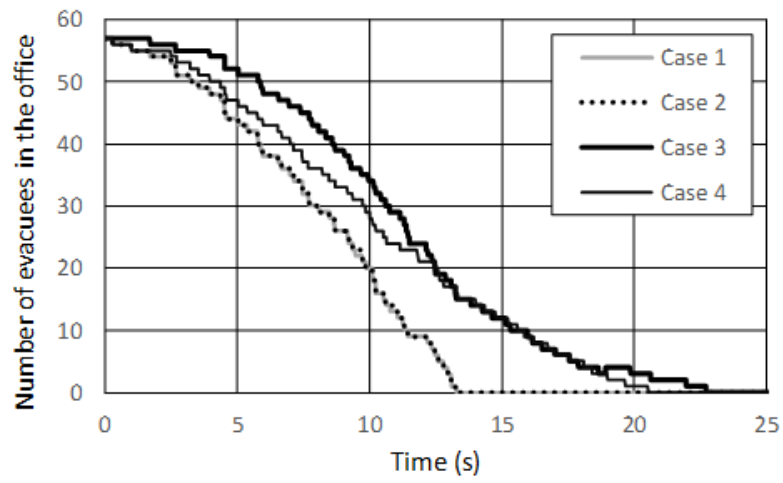


Fig. 6 Changes of number of evacuees in the office

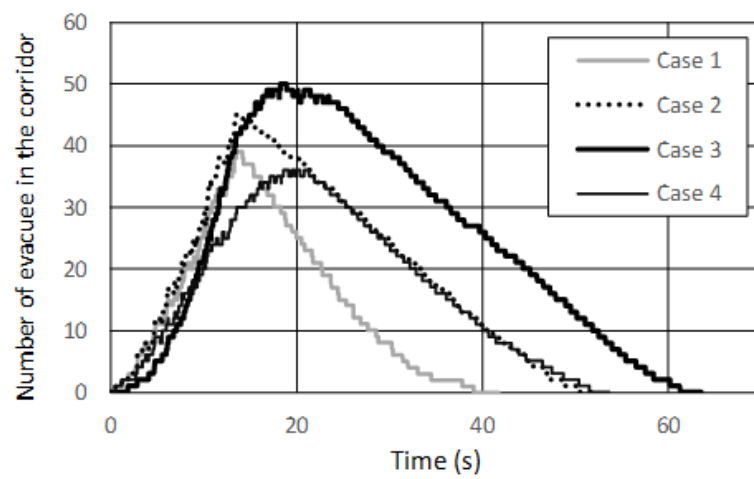


Fig. 7 Changes of number of evacuees in the corridor

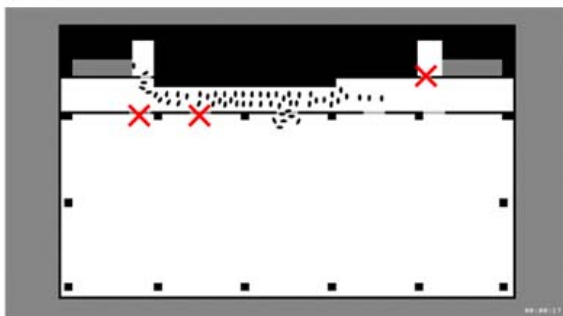


Fig. 8 Evacuation Simulation of Case 3

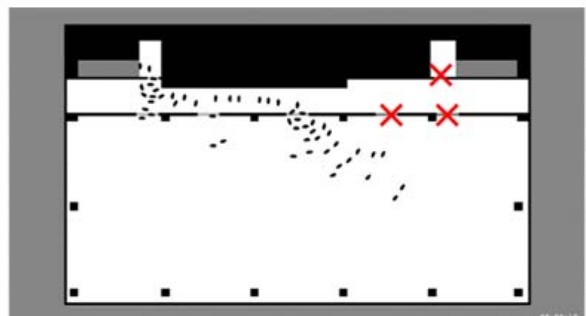


Fig. 9 Evacuation Simulation of Case 4

5 INTEGRATED VISUALIZATION

For the mutual link between the structure simulator, the damage simulator, and the evacuation simulator, we have constructed a visualization system that can test each analysis result from an engineering point of view. Fig. 10 shows the overall view, and Fig. 11 shows the detail view.



Fig. 10 Overall view of integrated visualization

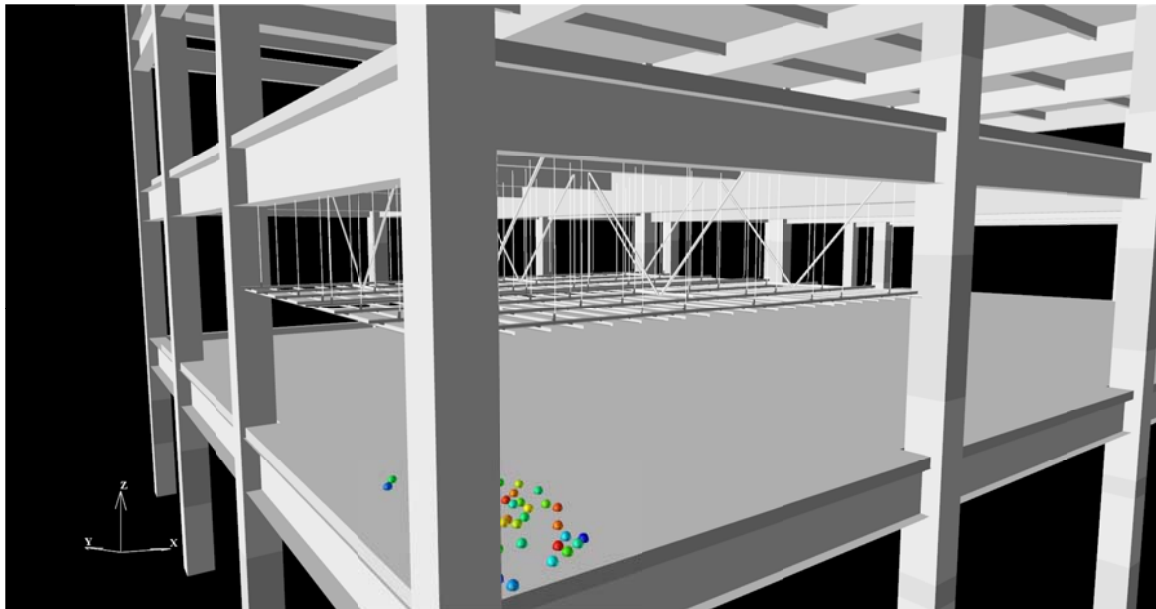


Fig. 11 Detail view of integrated visualization

6 CONCLUSIONS

- Structural analysis of the entire building, ceiling material of nonstructural members and evacuation analysis were carried out respectively, and the all results were integrated visualized.
- By looking at the result of the integrated visualization, we developed a function that allows us to judge what the key elements regarding building design are and where in the building they should be implemented.

ACKNOWLEDGMENTS

This work was supported by JSPS KAKENHI Grant Number JP16H03124.

REFERENCES

- [1] Yasunori Mizushima, Yasuyuki Nagano and Yoichi Mukai : Construction of damage observation system for both structural and nonstructural members with overlaying, #2019117, *proc. 13th WCCM* (2018).
- [2] Tomoharu Saruwatari, Yasuyoshi Umezu, Yoshitaka Ushio, Lyu Zhilun and Yasuyuki Nagano : Earthquake response analysis of nonstructural members of buildings by using the large-scale parallel calculation method, #2020310, *proc. 13th WCEE* (2018).
- [3] Kensuke YASUFUKU and Yasuyuki NAGANO : Evacuation Analysis of Several Impassable Routes by Using Multi-agent System, 387-388, *AIJ*, (2017). (in Japanese)
- [4] Kensuke YASUFUKU : REPRODUCTION OF PEDESTRIAN MOVEMENT IN QUEUE BY USING MULTI-AGENT SYSTEM AND ANALYSIS OF CROWD FLOW AFFECTED BY FOLLOWING BEHAVIOR, *J. Archit. Plann.*, *AIJ*, Vol.81 No.722, 821-829, Apr., (2016). (in Japanese)
DOI : <https://doi.org/10.3130/aija.81.821>

Aircraft Traffic Model Using Step Back Cellular Automaton

Shinsuke Nagaoka^{*}, Tomoaki Tatsukawa^{**}, Kozo Fujii^{***}, Eri Ito^{****}

^{*}Tokyo University of Science, ^{**}Tokyo University of Science, ^{***}Tokyo University of Science, ^{****}Electronic Navigation Research Institute

ABSTRACT

In recent years, the number of flights is drastically increasing, and arrival delays are occurring every day worldwide, especially in the Asia-Pacific area. Originally, all of airplanes should fly along the planned routes based on flight plans. However, some airplanes are not able to go through the planned route due to various factors during flight. The most common factor is the over-capacity of the arrival airport. When the arrival airport is already over the capacity, some flights are controlled by "Holding", "Vectoring", "Late departure" or "Flight deck interval management" etc. Airplane delay contributes to various socio-economic problems. Of course, Japanese airport is also no exception. Especially, a great many delay is occurring every day in Tokyo international airport that is the world 5th largest airport. About 70% domestic flights concentrate to the Tokyo International Airport. Moreover, 1.5 times more international and cross over flights are expected in 2015. In addition, number of aircraft for Tokyo international airport is expected to exceed the limit of air traffic capacity of air traffic controllers around 2025. In this kind of situation, there are concerns that is safety aspect too. Based on this situation, we think that more automation support is needed. The objective of this study for socio-economic problems is to develop a computer program for agent model simulation. Specifically, we construct the two-dimension Step Back Cellular Automaton method (SBCA) which is based on Cellular Automaton method. The method is including Base of Aircraft Data (BADA) to calculate behavior of airplane. BADA is preferred by Eurocontrol which has many parameter data, for example velocity, altitude, mass, fuel consumption and so on. Moreover, the method considers multiple routes which is based on actual way point from all airports in Japan to Tokyo international airport as same as actual flight route. By using this method, we compare analysis result with actual flight time table to investigate the effectiveness of the air traffic management model around Tokyo international airport by our proposed method. As a future work, we unravel air traffic congestion around the Tokyo international airport.

A Virtual Testing Framework for the Analysis of Damage in Composite Structures

Manish Hassan Nagaraj^{*}, Erasmo Carrera^{**}, Ibrahim Kaleel^{***}, Marco Petrolo^{****}

^{*}Department of Mechanical and Aerospace Engineering, Politecnico di Torino, Italy, ^{**}Department of Mechanical and Aerospace Engineering, Politecnico di Torino, Italy, ^{***}Department of Mechanical and Aerospace Engineering, Politecnico di Torino, Italy, ^{****}Department of Mechanical and Aerospace Engineering, Politecnico di Torino, Italy

ABSTRACT

The present work involves the progressive damage analysis of composite structures using refined beam elements based on advanced structural theories, developed within the framework of the Carrera Unified Formulation (CUF) [1]. The main concept of CUF is the use of expansion functions across the cross-section (for 1D beam elements) and thickness (for 2D shell/plate elements) to enrich the kinematics of the element. Such an approach removes the restrictive assumptions associated with classical 1D and 2D finite elements, resulting in a 3D-like accuracy of the solution at a highly reduced computational cost with respect to standard 3D FEA. It is, therefore, an ideal framework for the virtual testing of failure mechanisms in composite structures, since such a non-linear analysis is extremely computationally expensive. Various computational tools available in CUF are used to predict the progression of damage within the structure. A multi-scale analysis is performed by considering a representative volume element (RVE) at the micro-scale, where the fiber and matrix are independently modeled using Component-Wise (CW) analysis [2]. The CW approach is based on Lagrange-type polynomials leading to a physically based description of the RVE, which results in a high-fidelity model and correspondingly accurate stress fields. Matrix and fiber failure can thus be detected at the microscopic level, where matrix non-linearities are taken into account using an elasto-plastic constitutive model. Interface modeling capabilities are present, via which delamination and debonding effects can be considered. Delamination is modeled using cohesive elements governed by a traction-separation law. Interface modeling can be extended to the domain of contact mechanics by introducing contact elements, thus gaining the ability to solve a new class of structural problems. A combination of the above tools is used to obtain an accurate material response of the structure in the non-linear regime, from the structural level, i.e., macro-scale to the constituent material level, i.e. the micro-scale, in a computationally efficient manner, providing a suitable virtual testing environment for the progressive damage analysis of composite structures. References [1] Carrera E, Cinefra M, Petrolo M, Zappino E. "Finite element analysis of structures through unified formulation", John Wiley & Sons (2014). [2] Kaleel I., Petrolo M., Waas A.M., Carrera E., "Micromechanical Progressive Failure Analysis of Fiber-Reinforced Composite Using Refined Beam Models", Journal of Applied Mechanics (2018), 85.

A New Non-Iterative Mesh Generation Algorithm for Modeling Problems with Complex Geometries

Anand Nagarajan^{*}, Soheil Soghrati^{**}

^{*}The Ohio State University, ^{**}The Ohio State University

ABSTRACT

We present an integrated computational framework relying on a new non-iterative mesh generation technique, named Conforming to Interface Structured Adaptive Mesh Refinement (CISAMR), for creating high fidelity FE models of composite materials. A NURBS-based reconstruction algorithm is implemented to synthesize the material microstructure by packing arbitrary shaped particles, morphologies of which are extracted from digital data such as micro-computed tomography images. A genetic algorithm (GA) based optimization framework is also employed to simulate the target statistical microstructural descriptors such as the size distribution, volume fraction, and spatial arrangement of particles. CISAMR is then employed to create a FE model of the material by transforming a structured mesh into a high quality conforming mesh with low element aspect ratios and a negligible discretization error. This non-iterative transformation is carried out by combining customized versions of four algorithms: h-adaptivity, r-adaptivity, face-swap, and sub-tetrahedralization. Compared to enriched methods such as extended FEM, CISAMR obviates the additional computational burden associated with evaluating enrichment functions and provides a higher accuracy for recovering the gradient field. Further, unlike conventional mesh generation algorithms such as the Delaunay triangulation, CISAMR can easily handle problems with highly complex geometries without the use of iterative smoothing or relaxation algorithms to improve the elements quality. In this work, we show the application of this integrated reconstruction-meshing framework for simulating the failure response a variety of heterogeneous materials, including particulate and fiber-reinforced composites, as well as non-woven entangled materials such as fiberglass insulation packs. Multiple sources of material and geometrical nonlinearity, including the damage, contact, and cohesive debonding are considered in each simulation.

Development of Stress Analysis System Using XFEM to Evaluate Strength of Composite Structures

Toshio Nagashima*

*Sophia University

ABSTRACT

Finite Element Analyses (FEAs) are utilized to perform stress analyses for evaluation of structural integrity of CFRP (Carbon Fiber Reinforced Plastics) composite structures. In order to perform such analysis effectively, the extended finite element method (XFEM) in conjunction with the level set method is employed in this study. Two kinds of method based on XFEM have been developed. One is an XFEM code using three-node triangular shell elements enriched with a step function, which can perform stress analyses of thin-walled structures with an open hole. Another is an XFEM code using 6-node pentahedral elements enriched with Heaviside function [1][2], which can perform damage propagation analyses considering both matrix cracks and delamination. In the presentation, both stress analyses of a CFRP stiffened panel with a maintenance hole and damage propagation analyses of an OHT (Open Hole Tension) specimen are demonstrated and validated through comparisons with experimental results. [1] Nagashima, T., Sawada, M. : Development of a damage propagation analysis system based on level set XFEM using the cohesive zone model, Computers and Structures. 174(2016) 42-53. [2] R. Higuchi, T. Okabe, T. Nagashima, Numerical simulation of progressive damage and failure in composite laminates using XFEM/CZM coupled approach, Composites Part A, 95(2017) 197-207.

Investigation of Relationship between Copper Liberation and Inner Force of High Pressure Grinding Roll by Applying DEM Simulation

Yu Nagata*, Yukihiro Sawamura**, Masaya Minagawa***, Yuki Tsunazawa****, Giuseppe Granata*****, Ryo Kawarabuki*****, Kohei Mitsunashi*****, Kouji Tsukada*****, Takashi Misumi*****, Chiharu Tokoro*****

*Graduate School of Creative Science and Engineering, Waseda University, **Graduate School of Creative Science and Engineering, Waseda University, ***Graduate School of Creative Science and Engineering, Waseda University, ****National Institute of Advanced Industrial Science and Technology, *****Faculty of Science and Engineering, Waseda University, *****Research & Development Department, Nittetsu Mining Co., Ltd., *****Research & Development Department, Nittetsu Mining Co., Ltd., *****Design Department Industrial Machinery Section, Furukawa Industrial Machinery Systems Co. Ltd., *****Technology Division, Furukawa Co., Ltd., *****Faculty of Science and Engineering, Waseda University

ABSTRACT

Although in the recent years the demand of copper products has been rapidly increasing, the decrease of copper grade in copper ores and the increase of arsenic impurities have become major issues for the copper industry. In this scenario, the development of a new process to efficiently separate and concentrate copper minerals is highly anticipated. Among the available comminution techniques, the high pressure grinding roll (HPGR) was found able to determine an efficient comminution and a high mineral liberation with a relatively low energy consumption. However, a significant barrier to the further develop of this method is determined by the requirement of large amounts of ore samples for pilot-scale tests. In this research, we performed discrete element method (DEM) simulations based on the T10 breakage model to determine the optimum conditions for HPGR pilot-scale tests on copper ore including chalcopyrite and bornite. First, we conducted piston press tests to produce pressing phenomena similar to HPGR. From these tests we determined the model parameters for the ore under investigation. Following this step, we performed DEM simulations by changing four operating variables: pressing force per mm², roll rotational speed, initial roll gap and height of the feed. In order to evaluate the effect of different operating conditions, the liberation of copper was determined by mineral liberation analysis (MLA). Upon determination of the T10 parameters, the DEM simulations could reproduce throughput, roll gap, the energy consumption for all tested conditions. Moreover, the simulation could describe the results of pilot-scale tests, thus confirming the reliability of the method. According to the obtained results, the liberation of copper minerals improved by increasing the roll pressing force from 3 to 7 N/mm² and by lowering the initial gap between the rolls from 6 to 3 mm. Under these conditions, the normal direction component of the contact force increased. On the other hand, under the conditions which did not improve the mineral liberation, the normal contact force did not change, thus suggesting that the normal component of the contact force greatly contributes to the liberation of copper minerals.

Nanomechanics of Metal Matrix Nanocomposites Embedded with 1D and 2D Materials

Arun Nair*

*University of Arkansas

ABSTRACT

Graphene is a 2-D material with superior mechanical properties. It also possesses an exceptionally high aspect ratio, which makes it highly desirable for use as a fiber in nanocomposites. Previous studies have predicted that the presence of graphene will have a significant impact on the failure mechanisms of metal-graphene nanocomposites. In this talk, we use molecular dynamics to predict how different loading directions and crack orientations will impact the failure mechanisms of metal-graphene nanocomposites. We study both pristine and polycrystalline graphene as part of our nanocomposite model. Different failure mechanisms depending on loading direction, crack orientation, graphene structure (pristine or polycrystalline graphene sheets) will be discussed. Carbyne is a 1-D carbon chain that could be considered the strongest material. Recent experiments have shown that stable chains with lengths of thousands of atoms can be developed. As carbyne manufacture advances, it is important to determine possible applications for use in nanocomposites. We use both using density functional theory and molecular dynamics methods to predict the mechanical properties of metal-carbyne nanocomposites composed of multiple carbyne chains sandwiched within a metal matrix. These studies show that the mechanical properties of metal matrix can be improved with the addition of these 1D and 2D materials and also provide an insight into better design of metal nanocomposites.

A Tale of Two Velocities

John Nairn^{*}, Chad Hammerquist^{**}

^{*}Oregon State University, ^{**}FracGeo

ABSTRACT

The material point method has two velocity fields - the velocities stored on the particles and the velocities of those particles represented on the grid. Each time step involves extrapolation of velocities from the particles to the grid and then back to update both particle velocity and position. The availability of two velocities opens up interesting options for modifications in MPM but new options are prone to errors if not done consistently. For example, two ways to implement damping are to reduce acceleration by velocity on the particle or by velocity on the grid. By implementing both these damping options one can unify standard MPM update methods (called FLIP) with alternative update methods (called PIC or hybrid FLIP/PIC) into a single scheme. The new view reveals that PIC is specific damped form of FLIP and the damping characteristics can be quantified. By re-examining velocity extrapolation back to the particles, we have derived a third MPM update method called XPIC(m). XPIC(1) is identical to PIC, which is a highly damped form of FLIP. As m increases, XPIC(m) optimizing damping performance such that it selectively damps null-space noise resulting a new form of MPM with reduced noise and enhanced stability. The null space arises because typical simulations have more particles than nodes and thus more degrees of freedom on the particles than on the grid. XPIC(m) selectively damps modes on the particles that are invisible to the grid. A potential for error in new MPM options is to focus solely on velocity extrapolations and ignore the role the method has when updating particle positions. Each new MPM update scheme for velocity (FLIP, PIC, or XPIC(m)) also requires modification to the particle position update. The new position methods are non-intuitive but essential for accurate results. This talk will present MPM extrapolations and particle updates in an abstract form and then show how each potential MPM method fits within the abstract scheme. Examples will be given for properties of XPIC(m) and the importance of proper particle position update. For example, MPM modeling with explicit cracks needs to track position of the particle surfaces. By implementing new position update methods for crack surfaces, the surface tracking is significantly improved.

Design of Nonlinear Materials Using a Multi-scale NURBS-based Shape Optimization Scheme

Ahmad Najafi^{*}, Masoud Safdari^{**}, Daniel Tortorelli^{***}, Philippe Geubelle^{****}

^{*}Department of Mechanical Engineering and Mechanics, Drexel University, ^{**}Department of Aerospace Engineering, University of Illinois at Urbana-Champaign, ^{***}Department of Mechanical Science and Engineering, University of Illinois at Urbana-Champaign, ^{****}Department of Aerospace Engineering, University of Illinois at Urbana-Champaign

ABSTRACT

Due to recent advances in manufacturing techniques over the past decades, the tailoring of materials with specific macroscopic properties has been the focus of active research in mechanical engineering and materials science over the past decade. The key challenge in this line of work is how to optimize the material microstructure at the mesoscale to achieve a desired macroscopic constitutive response. In this work, we present a method to design the structure of particulate composites at the mesoscale using a shape optimization scheme to minimize or maximize a nonlinear objective function at the macroscale while satisfying a set of constraints (associated, for example, with the volume fraction of inclusions or with the manufacturing technique). Three key elements of the presented technique are i) multiscale nonlinear modeling, ii) sensitivity analysis, and iii) optimization. The multiscale modeling is based on a nonlinear finite element scheme, which combines a classical homogenization scheme with a NURBS-based Interface-enriched Generalized Finite Element Method (NIGFEM) used for accurate and efficient capturing of the displacement field in a heterogeneous material with a finite element discretization that does not conform to the material interfaces. Damage evolution is captured using a three-parameter isotropic damage model, which is applicable to a wide range of failure responses. To perform sensitivity analysis, we formulate a NIGFEM-based analytic nonlinear sensitivity scheme, which is simplified by the fact that only the enrichment control points on material interfaces move, appear or disappear during the shape optimization process. The selected scheme avoids the technical difficulties encountered in the finite difference schemes when the boundary intersects an element very close to a node in a non-conforming mesh. In these situations, the boundary may move to another element during the design perturbation step, resulting in changes of the mesh topology, making the differentiation of the stiffness matrix and load vector problematic. The last part is a gradient-based shape optimization scheme that relies on the stationary nature of the non-conforming meshes used to discretize the periodic unit cell, thereby avoiding mesh distortion issues that plague conventional finite-element-based shape optimization studies. In the current approach, the finite element approximation space used in the NIGFEM is augmented with NURBS to allow for the accurate capture of the weak discontinuity present along complex, curvilinear material interfaces. To demonstrate the performance of the method, we present a set of microstructural shape optimization problems with applications in linear and nonlinear design of heterogeneous particulate composites.

Application Development Framework for Manycore Architectures -from Exascale to Post Moore Era-

Kengo Nakajima*

*The University of Tokyo

ABSTRACT

"ppOpen-HPC" is an open source infrastructure for development and execution of optimized and reliable simulation code on post-peta-scale (pp) parallel computers based on many-core architectures, and it consists of various types of libraries, which cover general procedures for scientific computation. Source code developed on a PC with a single processor is linked with these libraries, and the parallel code generated is optimized for post-peta-scale systems with manycore architectures, such as the Oakforest-PACS system of Joint Center for Advanced High Performance Computing (JCAHPC). "ppOpen-HPC" is part of a five-year project (FY.2011-2015) spawned by the "Development of System Software Technologies for Post-Peta Scale High Performance Computing" funded by JST-CREST. The framework covers various types of procedures for scientific computations, such as parallel I/O of data-sets, matrix-assembly, linear-solvers with practical and scalable preconditioners, visualization, adaptive mesh refinement and dynamic load-balancing, in various types of computational models, such as FEM, FDM, FVM, BEM and DEM. Automatic tuning (AT) technology enables automatic generation of optimized libraries and applications under various types of environments. We release the most updated version of ppOpen-HPC as open source software every year in November (2012-2015), which is available at <http://ppopenhpc.cc.u-tokyo.ac.jp/ppopenhpc/>. In 2016, the team of ppOpen-HPC joined ESSEX-II (Equipping Sparse Solvers for Exascale) project (Leading P.I. Professor Gerhard Wellein (University of Erlangen-Nuremberg)), which is funded by JST-CREST and the German DFG priority programme 1648 "Software for Exascale Computing" (SPPEXA) under Japan (JST)-Germany (DFG) collaboration until FY.2018. In ESSEX-II, we develop pK-Open-HPC (extended version of ppOpen-HPC, framework for exa-feasible applications), preconditioned iterative solvers for quantum sciences, and a framework for automatic tuning (AT) with performance model. In the presentation, various types of achievements of ppOpen-HPC, ESSEX-II, and pK-OpenHPC project, such as applications using parallel preconditioned iterative solvers will be shown. Finally, future perspectives towards the Post Moore Era will be discussed.

Response Analysis of Soil-Foundation-Structure Interaction System of RC Building Using Nonlinear 3-dimensional FEM against Strong Earthquake

Naohiro Nakamura*, Takuya Suzuki**

*Hiroshima University, **Takenaka Corporation

ABSTRACT

It is important to consider the behavior of buildings against earthquakes beyond the current design level because no one can deny the possibility that buildings are attacked by such earthquakes. In this paper, the behavior of middle-rise RC buildings which are not designed by dynamic analysis are studied against the earthquake up to 2 times for the design level using detailed 3-dimensional nonlinear FEM considering soil-foundation-structure interaction. 3 type of soil models (Type1, Type2 and Type3) and 6story building models are used for the analysis. These models are considered with the nonlinear effect of both soil and buildings and the soil structure interaction effect, and analyzed by large scale FEM. The input earthquake level is from 1.0 to 2.0 times of Japanese Level 2 design earthquake. Based on these study, following results are obtained. 1) In the model of the hard soil, as the input increased, the plasticity of the building advanced, but the plasticity of the pile did not proceed. In the soft soil model, as the input increases, the plasticity of the pile progresses but the progress of the plasticity of the building was small. Also, in the model of the second type of general ground, as the input increased, both the plasticity of the building and the pile advanced. These qualitative properties are almost the same as the previous studies. On the other hand, quantitative evaluation is necessary to apply it to real problems. Regarding Level 2 and higher input levels, it is not clear how much accuracy the existing model has. Therefore, it is necessary to compare the accuracy of these models and study to make more suitable model. 2) We compared the models A and B which changed the behaviors of the piles after the ultimate stress. As a result, model A, which loses stiffness after ultimate stress, does not necessarily have the larger response than model B. In the case where the response of model B is large, the subsequent seismic motion is inputted, and the maximum response value is generated there. It is considered that the difference of the vibration characteristics of the coupled system in that state is the cause of the difference of the maximum response value.

Application of XFEM Magnetic Field Analysis Using Conformal Mapping to Kinked and Curved Crack Problem

Shogo Nakasumi*

*National Institute of Advanced Industrial Science and Technology (AIST)

ABSTRACT

Extended Finite Element Method (XFEM) is a method that makes the solution more accurate than the conventional FEM due to the effect of the enrichment function. We are researching on XFEM analysis which utilizes conformal mapping and potential flow theory by restricting the problem to two-dimensions. Non-destructive inspection technology is our engineering application field. So far, we have proposed XFEM magnetic field analysis for two-dimensional internal defects [1]. In that method, we could obtain accurate solution by using the Joukowski mapping even with coarse mesh division. In this presentation, we will present a two-dimensional XFEM analysis that maps the enrichment function of straight-line cracks to kinked cracks and/or curved cracks. In these mappings, we use the power function of the complex numbers and use the linear-transformation (or Moebius-transformation). The feature of this presentation is to create enrichment functions by utilizing conformal mapping, limiting the problem to two dimensions. Since the nature of the enrichment function does not change after mapping, high accuracy can be expected. Also, the two-dimensional X and Y coordinates correspond to the real part and the imaginary part of the complex number respectively, and the operation of the complex number is performed in this research. We could obtain almost reasonable solutions in the numerical examples for verification. [1] S. Nakasumi and M. A. Schweitzer, Magnetostatic XFEM Analysis for Internal Multiple Cracks based on Joukowski Mapping, Proceedings of 12th World Congress on Computational Mechanics (WCCM12), 2016.

Nonlinear parallel FEM analysis on thermal warpage of multilayered high-density wiring interposer

Shinji Nakazawa^{*}, Kazuya Goto^{**}, Gaku Hashimoto^{***}, Hiroshi Okuda^{****}, Naoki Iwasaki^{*****}

^{*}Shinko electric industries co., ltd., ^{**}PEXProCS, LLC., ^{***}The university of Tokyo, ^{****}The university of Tokyo, ^{*****}Shinko electric industries co., ltd.

ABSTRACT

It is one of the most important issues to reduce the warpage of semiconductor package substrate (interposer), which is caused by the thermal loadings in IC mounting processes, from the viewpoints of connection reliability or product yield. To predict such the behavior of thermal warpage, the finite element analysis has been widely used at the stage of interposer designing and development. However, since a typical interposer for microprocessor has very fine wiring structure with dimensions of the order of several microns in the substrate of several tens of millimeters square, the number of finite element meshes required for the FEM analysis can reach up to several hundreds of million. Therefore, some approximation techniques such as the material homogenization method have been applied to reduce the number of finite element mesh. In our previous work [1], we showed large-scale finite element analyses of interposer warpage, where the finite element meshes were generated as high resolution as possible to recognize the wiring patterns; the maximum number of finite element was 210 million. However, all of our analyses in the above were done in the frame of the linear theory (infinitesimal deformation theory). Moreover, the temperature-dependency or the viscoelasticity, which are thought to be essential to understand the warpage behaviors especially when the temperature is higher than glass-transition temperature (around 200 deg.C), did not be taken into account. In this study, we have performed the large-scale nonlinear analysis of interposer warpage by using FrontISTR, which is an open-source, finite element analysis software that enables massively parallel computations. New point in this work is that viscoelasticity and geometric nonlinearity, which were ignored in our previous work[1], are included. Furthermore, our analysis will be compared with the measurement by means of the digital image correlation (DIC) method. [Reference] 1] Shinji Nakazawa, Naoki Iwasaki, Tatsuro Yoshida, Ryuichi Matsuki, Kazuya Goto, Gaku Hashimoto and Hiroshi Okuda, A Large-Scale Finite Element Analysis for Predicting Thermal Warpage of a Semiconductor Package Substrate, WCCM &&&& APCOM 2016, pp. 2492-2492, 2016.

Numerical Analysis of Flows in Coating Processes

Jaewook Nam^{*}, J. Alex Lee^{**}, Matteo Pasquali^{***}, Heechan Jung^{****}

^{*}Seoul National University, ^{**}Saint-Gobain Northboro, ^{***}Rice University, ^{****}Sungkyunkwan University

ABSTRACT

Various parts of modern electronic devices, e.g., battery electrodes, solar cell panels, and mobile displays, contains multi-functional films. Continuous liquid coating processes can produce these films in fast and efficient manner. Coating liquids include various type, shape, and size of organic and inorganic particles. Due to these particles, the rheological characteristics of the coating liquids become complex. Therefore, one has to consider such rheological aspects into the design of coating apparatuses or devices. In this respect, computational fluid mechanics plays a vital role in the process design. In this presentation, we will cover two types of flows: a liquid-bridge break-up flow of polymeric solutions with free surfaces and highly loaded suspension flows inside channels, called coating die manifold. We proposed an efficient method for the time-stepping algorithm, trapezoidal rule based on finite difference interrupt for viscoelastic non-Newtonian flows of a liquid-bridge breakup phenomena. For highly-loaded suspension flows, we considered the shear-induced particle migration. This migration can affect the distribution of non-Brownian particles inside the flows that may lead to problematic situations including particle flocculation or coagulation that can cause coating defects. For the prediction of the particle distribution, we implemented the particle transport model by Phillips et al. (1992) in three-dimensional die manifold flows. Navier-Stokes equations and the particle transport equation are discretized by a space-time finite element method with Galerkin-least squares stabilization for large-scale computations. Using this computational approach, we will explain the diffusive particle fluxes under the non-homogeneous shear rate flows that typically encountered in the coating flows.

A Forward Incremental Prestressing Method for Biological Membranes

Nitesh Nama^{*}, Miquel Aguirre^{**}, C Alberto Figueroa^{***}

^{*}University of Michigan, USA, ^{**}Tecnalia Research & Innovation, Spain, ^{***}University of Michigan, USA

ABSTRACT

Computational techniques to simulate cardiovascular flows in three-dimensional models of arteries have attracted significant interest owing to their applications in disease research, medical device design, and surgical planning. To model the blood flow in compliant arteries, various fluid-structure interaction (FSI) methods such as Arbitrary Lagrangian-Eulerian methods, immersed methods, and Coupled Momentum Method have been employed. To reduce the computational costs while simulating large 3D FSI models of vasculature, a membrane formulation can be employed to model the deformation of the arteries. The membrane assumption for the arteries is reasonable in view of the long wavelength of the cardiac pulse compared to the diameters of arteries.¹ The patient-specific vessel geometry is typically obtained through in-vivo medical imaging techniques. These geometries are known to represent a deformed configuration under in vivo loading conditions, thereby necessitating knowledge of the current state of stress to perform computational study predicting accurate stress values. Inverse methods that rely on the computation of a stress-free configuration are unsuitable for membrane formulations owing to the instabilities and non-uniqueness in case of buckling during the calculation of stress-free configuration. An alternative to inverse methods is the forward incremental approach presented by Grytz and Downs² for 3D solids, where the state of stress is calculated in an accurate and unique manner. In this work, we adapt this methodology to biological membranes to determine the state of prestress in a medically-obtained vessel anatomy. We provide a description of the different configurations in curvilinear coordinates, the tangent vectors, and of the evaluation of a constitutive model from an unknown unloaded configuration. As in 3D solid formulation², this methodology results in an equivalent Lagrangian description formulated onto the in-vivo reference configuration, thereby requiring minor modifications to a standard total Lagrangian forward membrane algorithm. We present results for a variety of constitutive models including the isotropic Neo-Hookean model as well as a four fiber-family constitutive model. Several benchmark problems are presented to verify the accuracy of the method. Furthermore, patient-specific geometries are used to assess the adequacy of the method for cardiovascular FSI computations. [1] Figueroa, C. A. et al., Computer methods in applied mechanics and engineering, 195(41), 5685-5706, 2006. [2] Grytz, R. and Downs, J.C., Computer methods in biomechanics and biomedical engineering, 16(7), pp.768-780, 2013.

Simulations of Shock Front Evolution in a Submicron Thick Nanocrystalline Aluminum: A Study of the Role of Grain Size in the Formation of Atomistic Defects

Raju Namburu^{*}, Ramakrishna Valisetty^{**}, Arunachalam Rajendran^{***}, Avinash Dongare^{****},
Ianni James^{*****}

^{*}US ARL, ^{**}US ARL, ^{***}University of Mississippi, ^{****}University of Connecticut, ^{*****}Leidos

ABSTRACT

The role of the grain size in designing nanocrystalline aluminum (nc-Al) for superior shock strength was investigated via the study of the Hugoniot elastic limit (HEL, or the shock precursor) decay under one dimensional strain condition using large scale molecular dynamics (MD) simulations†. For this purpose, shock fronts' evolution and shock fronts' progression were simulated at impact velocities in the range of 0.7 km/s to 1.5 km/s in a range of atom systems that span a length scale from the nano- to the sub-micron scale range. Spanning the nano-scale range were considered five 920 Å thick 20 million nc-al atom systems each with grains with an average size in the range of 60 Å to 180 Å. Spanning the sub-micron scale range were considered three 5000 Å thick 2 billion nc-al atom systems each with grains with an average size in the range of 180 Å to 1000 Å. The evolving shock front profiles were studied in detail via the averaged shock stress distributions in the shock fronts' travel direction and the HEL decay curves were generated by the shock stress rise behavior post-HEL. To further identify the compression process in the nano-grains, the atomistic defects evolving upstream under the rising shock fronts were identified and quantified using a crystal analysis algorithm and a twin dislocation identification method. The results showed that certain dislocation partials are strongly influenced by the elastic-plastic transition response past the HEL. The atomistic defects generated were very much dependent on the grain size with the lower grain size leading to more defects and more plasticity.

Numerical Simulation of Crack Propagation Using CT Specimen under Low Cycle Fatigue

Yoshiki Namita^{*}, Yoshitaka Wada^{**}, Rekisei Ozawa^{***}

^{*}Kindai University, ^{**}Kindai University, ^{***}Kindai University

ABSTRACT

Crack growth under the elastic-plastic fracture is an important issue of the structural integrity, because seismic wave causes low cycle fatigue in the engineering structure. Many researchers have worked for many experiments and numerical analyses, however obvious and general criterion cannot be found until now. In order to develop a three-dimensional fracture criterion, the fully automated and state-of-the-art FE crack growth simulation should be realized. In the numerical simulation system, there are three important processes which are generation of the model with crack, stable and accurate FE analysis and post-processing for fracture evaluation. Crack growth simulation requires each process to be stable and connected each other in the one system. On the other hand, experiment should be conducted to determine material properties such as cyclic stress strain curve, crack tip opening displacement, J integral and so on. In particular, determination of parameters for appropriate cyclic stress strain curve is very important to actual evaluation of seismic loading. In order to reproduce the fundamental experiment result of a CT specimen under low cycle fatigue, we have developed the mesh generation scheme with thumbnail crack shape for a CT specimen. The present work shows the result of contact analysis of a CT specimen at the low cycles, because contact behavior of crack surfaces occurs under the applied cyclic loading with stress ratio $R = ?1$. To show the effectiveness of the criterion using stress triaxiality and equivalent plastic strain along a crack front in the CT specimen, the conventional generation phase and application phase analyses are conducted. The work shows comparisons between experimental result and numerical simulation results. We discuss the effectiveness of the criterion using stress triaxiality and equivalent plastic strain for crack growth criterion under the low cycle fatigue.

Fully-Resolved Simulation of Multiphase Fluid-Structure Interaction Problems Using a Constraint-Based Immersed Boundary Method on Adaptive Meshes

Nishant Nangia^{*}, Amneet Pal Singh Bhalla^{**}, Neelesh A. Patankar^{***}

^{*}Northwestern University, ^{**}Lawrence Berkeley National Laboratory, ^{***}Northwestern University

ABSTRACT

Many industrial fluid flow problems involve the interaction between heavy, rigid objects and one or more fluid phases. Fictitious domain and immersed boundary methods for simulating fluid-structure interaction (FSI) have been gaining popularity in the past few decades because of their robustness in handling arbitrarily moving bodies on regular Cartesian meshes. One such technique is the constraint-based immersed boundary method (cIB), which involves an additional projection step to enforce a rigidity constraint within the solid body domain [1]. However, in cases where the density ratio between the solid and fluid is large and the inertia of the rigid object must be adequately simulated, the cIB method can suffer from numerical instabilities. In this work, we outline the formulation and development of a parallel, variable-coefficient, constraint-based immersed boundary method using adaptive mesh refinement. The variable density and viscosity of the flow field are handled implicitly using an unsplit, incompressible Navier-Stokes solver that uses a projection method based preconditioner [2]. This enables efficient and stable simulations of large density and viscosity ratio FSI problems. The numerical technique is validated using past experimental studies of multiphase particulate flows. Novel applications of this method include simulation of sports ballistics problems and self-propelled vehicle aerodynamics, in which the density ratio between the fluid and solid regions are more than three orders of magnitude. [1] Bhalla, A. P. S., Bale, R., Griffith, B. E., & Patankar, N. A. (2013). A unified mathematical framework and an adaptive numerical method for fluid-structure interaction with rigid, deforming, and elastic bodies. *Journal of Computational Physics*, 250, 446-476. [2] Cai, M., Nonaka, A., Bell, J. B., Griffith, B. E., & Donev, A. (2014). Efficient variable-coefficient finite-volume Stokes solvers. *Communications in Computational Physics*, 16(5), 1263-1297.

A Bayesian Interpretation of Kernel-Based Methods for Multifidelity Approximation

Akil Narayan*

*University of Utah

ABSTRACT

A recently developed technique for forward uncertainty quantification (UQ) uses the induced reproducing kernel Hilbert space from a low-fidelity parametric model as a tool to understand the parametric variability of a more expensive high-fidelity model. This has been the cornerstone of a multifidelity simulation technique that seeks to attain accuracy comparable to an expensive high-fidelity model with the cost of an inexpensive low-fidelity model. We show that this methodology, explicitly developed for forward UQ problems, has an interesting Bayesian interpretation by introducing suitable notions of prior and posterior distributions.

Fluctuating Hydrodynamics Simulations of Hydrodynamic Instabilities at Meso- and Macro-scales

Kiran Narayanan*, Ravi Samtaney**

*King Abdullah University of Science and Technology, **King Abdullah University of Science and Technology

ABSTRACT

Traditional deterministic hydrodynamic equations such as the compressible Navier-Stokes equations (CNS) describe macroscopic systems where the probabilistic effects of thermal fluctuations are negligible. However, there are systems in which thermal fluctuations can drive the macroscopic physical phenomenon; one such example is hydrodynamic instability at fluid-fluid interfaces where they affect the flow both quantitatively and qualitatively [1]. Here, we obtain numerical solutions of the two-fluid fluctuating compressible Navier-Stokes equations (FCNS) in order to study the effect of such fluctuations on the mixing behavior in the Richtmyer-Meshkov instability (RMI) and Kelvin-Helmholtz instability (KHI). FCNS are a system of stochastic partial differential equations that are a coarse-grained representation of microscopic dynamics, constitute a meso-level model of the system and provide a compromise between computational cost and the ability to capture thermal fluctuations. Their validity for non-equilibrium systems was derived by Espanol [2]. The numerical solver was developed in-house and verified using the equilibrium spectrum of fluctuations of hydrodynamic quantities. For RMI, we present results from simulations of three systems having length scales with decreasing order of magnitude ($O(10^{-5})$, $O(10^{-6})$, $O(10^{-7})$ meters) that span from macroscopic to mesoscopic, with a corresponding increase of thermal fluctuations. Simulations show that for all systems, deterministic mixing behavior emerges as the ensemble-averaged behavior of several fluctuating instances, with the FCNS solution providing bounds on the growth rate of the amplitude of the mixing layer. Traditionally, a stochastic flux $Z(x,t)$ is discretized using a regularization factor that scales as the inverse square root of (h^*dt) for spatial interval h , time interval dt , with h greater than h_0 where h_0 produces the right equilibrium spectrum. For the mesoscale RMI systems simulated, it was desirable to use a cell size smaller than this limit in order to resolve the viscous shock. This was achieved by using a modified regularization factor that scaled as the inverse square root of $(\max(h,h_0)*dt)$ with h_0 being an integer multiple of h when $h \leq h_0$. For KHI, ensemble-averaged mixing behavior for similar length-scale systems will be presented. References [1] K. Kadau, C. Rosenblatt, J. L. Barber, T. C. Germann, Z. Huang, P. Carles, B. L. Holian, and B. J. Alder, "The Importance of Fluctuations in Fluid Mixing," Proc. Nat. Acad. Sci. U.S.A., vol. 104, pp. 7741–7746, 2007 [2] P. Español, "Stochastic differential equations for non-linear hydrodynamics," Physica A: Statistical Mechanics and its Applications, Vol. 248, No. 1-2, pp. 77–96, Jan 1998.

DNS of Near-Wall Flame Propagation

Kosuke Narukawa^{*}, Yuki Minamoto^{**}, Masayasu Shimura^{***}, Mamoru Tanahashi^{****}

^{*}Tokyo Institute of Technology, ^{**}Tokyo Institute of Technology, ^{***}Tokyo Institute of Technology, ^{****}Tokyo Institute of Technology

ABSTRACT

Laminar flame speed is an important quantity for combustion analysis and turbulent combustion modeling. In a previous study [1], time-resolved CH chemiluminescence of methane-air flames impinging a wall were measured, and the flame displacement speed was estimated as a function of wall distance. They concluded that the flame displacement speed just before flame quenching corresponds to the laminar flame speed of a corresponding thermochemical condition. In this study, to explore the applicability of the above feature to experimental measurements of laminar flame speed, relationship between laminar flame speed and near-wall flame behavior is investigated under various conditions based on direct numerical simulations (DNS). Two-dimensional DNS of ignition combustion between two parallel walls are performed for methane, hydrogen, and n-heptane/air premixed flames under several mixture temperatures, wall temperatures and ignition positions. The mixture temperature is set to 300 K or 700 K, and the wall temperature is set to 300 K, 500 K or 700 K. An initial high-temperature region set in the center of the computational domain is given by a Gaussian function. The dependence of the results on the distance from ignition position to the wall is investigated by changing the computational domain. The distance from ignition position to the wall is 1.5 mm, 2.0 mm, 2.5 mm or 3.0 mm. In all cases, equivalence ratio and pressure are set to 1.0, 0.1 MPa respectively. Using the results of DNS, the flame front position nearest to the wall and defined by the point where the gradient of OH mass fraction takes maximum value, and the flame displacement speed defined by the temporal variation of this position are calculated. By estimating the flame speed under various conditions as a function of the distance from the wall, it is clarified that the near-wall flame propagation has unique characteristics and following results are obtained. (i) Under the conditions where the wall temperature equals unburnt gas temperature, the flame speed has a local minimum or inflection point near the wall, and this value corresponds to the laminar flame speed of the mixture. (ii) Similar trends are observed in near-wall flame speed variation regardless of mixture temperature, ignition position or fuels. Furthermore, the effect of the wall on the flame is investigated, and the mechanism for these characteristics is also discussed. References [1] Tsuzuki et al. , Proceedings of Thermal Engineering Conference, 2009, pp. 7-8.

Feasibility of Myocardial Material Parameter Estimation from 2D Images

Anastasia Nasopoulou*, David Nordsletten**, Steven Niederer***, Pablo Lamata****

*Department of Biomedical Engineering, King's College London, **Department of Biomedical Engineering, King's College London, ***Department of Biomedical Engineering, King's College London, ****Department of Biomedical Engineering, King's College London

ABSTRACT

Myocardial material parameter estimation is an essential step towards both the personalization of cardiac biomechanical models and the in vivo estimation of myocardial stiffness, a proposed clinical index of diagnostic and prognostic value. Currently the process requires the use of 3D cardiac imaging data, which -unlike the ubiquitous 2D ultrasound images- are costly and not widely available in clinical practice. Aiming to translate recent advances in cardiac modelling into the clinic, we develop in this study a method for myocardial material parameter estimation from 2D images, such as provided by 2D or 3D speckle tracking echocardiography. The proposed methodology relies on previous work [1], where an energy based cost function (CF) was introduced to address the inability of displacement/strain based CFs to uniquely confine the parameter space. In this study, a modified version of the CF is used based on the 'virtual works' principle (VWP) for more flexibility to adapt to the limited data, while the myocardial material behavior is described by a popular transversely isotropic model [2]. Using a combination of the modified CF and the VWP expressed at end diastole, our pipeline focuses on recovering two of the most inter-correlated parameters by keeping the remaining two exponential parameters fixed. To test the accuracy and robustness of the pipeline against model assumptions and data noise, two synthetic data sets were created from the passive inflation of a truncated ellipsoid, mimicking the availability of pressure recordings and 'long axis images' with either 3D or 2D displacement and deformation information. Using the proposed pipeline, the parameter estimation in the synthetic dataset recovered the ground truth values. A sensitivity analysis showed that the method was robust to offsets of the imaging plane from the axis of symmetry, when 3D deformation data is available. The most critical factor identified was the image quality, while model assumptions concerning the tissue microstructure (including the fixed exponential parameter values) had the least impact on results. Our study has demonstrated that accurate predictions of myocardial material parameters can be performed from 2D imaging data. In future work, the pipeline is applied to clinical data from heart failure patients. [1] Nasopoulou et al. Improved identifiability of myocardial material parameters by an energy-based cost function. BMMB (2017). [2] Guccione et al. Passive material properties of intact ventricular myocardium determined from a cylindrical model. J Biomech Eng (1991).

Functionality of the Pelvic Floor after Vaginal Delivery with Episiotomy

Renato Natal*, Dulce Oliveira**, Marco Parente***, Teresa Mascarenhas****

*INEGI, **INEGI, ***INEGI, ****Hospital São João

ABSTRACT

Introduction To increase the birth canal and prevent extensive vaginal tears, incisions in the perineal region were made. Currently, a policy of restrictive episiotomy is favored for spontaneous deliveries [1]. To identify the influence of episiotomy in the functionality of the pelvic floor, numerical simulations of vaginal deliveries in different fetal positions were performed based on the Finite Element Method. **Methods** In general terms, the childbirth model includes the most requested muscles of the pelvic floor region and the fetus. Two fetal positions were simulated, occipitoanterior (OA) and occipitoposterior (OP). Hyperelastic material models were used to describe the material behavior of the several structures of the model. **Results** As expected, the forces opposing the descent of the fetus are higher for deliveries with the fetus in OP position. Without episiotomy, the maximum value of force observed is around 20% higher in OP position. For deliveries with episiotomy, the forces reduction may be as high as 60% in OP position and greater than 50% in OA position. A lag between the moment of the peak force in the two positions is observed, which coincides with the moment when the pelvic diameters for the OP and OA positions are maximums. Regarding the widening of the incision, the highest values observed were for the episiotomies performed at 30°, which corresponds to the incisions that caused greater reductions in the values of the forces opposing the descent of the fetus. Analyzing the maximum principal stress along the lower portion of the muscles, it is verified that the insertion points in the symphysis pubis are the ones presenting the higher values, followed by the middle portion. The episiotomy at 30° is the closest to this middle region, which makes sense to be the one with the best results. Considering the medial portion, the stress values are higher in the rightmost portion. These results predict that, in this model, episiotomies performed on the right side would lead to better outcomes. **Conclusions** Fetal malposition (OP) induces greater extension of the muscles compared to normal position (OA), leading to increases of stretch. Also, the higher value of force required to achieve delivery might justify the increased need of surgical interventions. In mechanistic terms, episiotomy has proven to be a protective factor during delivery, reducing the risk of other pelvic floor injuries, and urogynecological complaints. **References** 1. Carroli G, Mignini L, (2009) In: Cochrane Database of Systematic Reviews, pp1-53.

A Novel Error Indicator and an Adaptive Refinement Technique Using the Scaled Boundary Finite Element Method

Sundararajan Natarajan^{*}, Ean Tat Ooi^{**}, Pramod ALN^{***}, Song Chongmin^{****}

^{*}Department of Mechanical Engineering, Indian Institute of Technology-Madras, ^{**}School of Engineering and Information Technology, Federation University Australia, VIC 3350, Australia., ^{***}Department of Mechanical Engineering, Indian Institute of Technology-Madras, ^{****}School of Civil and Environmental Engineering, University of New South Wales, Sydney, Australia.

ABSTRACT

In this talk, an adaptive displacement based formulation based on the scaled boundary finite element method on quadtree meshes for linear elasticity problems is discussed. Within this framework, the elements with hanging nodes are treated as polygonal elements and thus does not require special treatment. The adaptive refinement is supplemented with a novel error indicator. The local error is estimated directly from the solution of the scaled boundary governing equations. The salient feature is that it does not require any stress recovery techniques. The efficacy and the robustness of the proposed approach is demonstrated with a few numerical examples from linear elasticity.

A Numerical Model for Quantifying the Reduction in the Structural Service Life of Flexible Pavements due to Dynamic Axle Loads

Fermín Navarrina*, Luis Ramírez**, José París***, Xesús Nogueira****, Ignasi Colominas*****,
Manuel Casteleiro*****, Manuel Ruiz*****, José R. Fernández-de-Mesa*****

*University of La Coruna, **University of La Coruna, ***University of La Coruna, ****University of La Coruna,
*****University of La Coruna, *****University of La Coruna, *****University of La Coruna, *****University of La
Coruna

ABSTRACT

A numerical model for the fatigue analysis of flexible pavements considering the effects of dynamic axle loads is presented in this paper. The main objective of this work is to quantify the reduction in the structural service life of the pavement due to the rise of the dynamic axle loads exerted by the traffic, as the progressive deterioration of the road profile occurs. First, the procedure for the fatigue analysis of flexible pavements, as defined in the Spanish Standard 6.1-IC [1], is explained in detail. The implementation herein presented is specific for this Standard, but the underlying concepts are not restrictive, and the model can be easily adapted to fit the distinctive features of other regulations. Second, the concepts of accumulated damage and structural service life are formalized in mathematical terms. Next, dynamic axle loads are introduced, which leads to the definition of a suitable accumulated fatigue damage indicator that takes into account these effects. Dynamic axle loads are introduced in this formulation by means of a so-called effective dynamic load amplification factor. For the quantification of this factor, the Quarter-Car model is extended to allow for computing the time evolution of the dynamic axle load exerted by a heavy vehicle on the pavement [2]. The model is completed by adding a simple procedure for simulating how the road profile deteriorates over time. Finally, an application example is presented. [1] DGC / Dirección General de Carreteras, Secretaría de Estado de Infraestructuras. Norma 6.1-IC "Secciones de Firme" de la Instrucción de Carreteras. Orden FOM/3460/2003 de 28 de noviembre (BOE de 12 de diciembre de 2003). Centro de Publicaciones del Ministerio de Fomento, Gobierno de España, 2003. [2] F. Navarrina, L. Ramírez, J. París, X. Nogueira, I. Colominas, M. Casteleiro y J.R. Fernández-de-Mesa. Comprehensive Model for Fatigue Analysis of Flexible Pavements Considering Effects of Dynamic Axle Loads. Transportation Research Record: Journal of the Transportation Research Board, DOI: 10.3141/2524-11, No. 2524, pp. 110-118, Washington (2015).

Recovery of the Contact Stress Field in the Cartesian Grid Finite Element Method (cgFEM)

José Manuel Navarro-Jiménez*, Héctor Navarro-García**, Enrique Nadal***, Manuel Tur****, Juan José Ródenas*****

*Universitat Politècnica de València, **Universitat Politècnica de València, ***Universitat Politècnica de València, ****Universitat Politècnica de València, *****Universitat Politècnica de València

ABSTRACT

This paper proposes an adaptation of the SPR-C technique[1] (Superconvergent Patch Recovery[2] with constraints) for the evaluation of a recovered stress field at the contact area of mechanical components. In the context of the finite element method for the resolution of 2D linear elasticity problems, ref. [1] presented a procedure, based on the use of Lagrange multipliers, by means of which the polynomials used to describe the locally recovered stress field were enforced to satisfy the equilibrium and compatibility equations. In this work, we have extended the technique described in [1] to improve the stress field around the contact. To do this, and for the patches of elements involved in the contact, we simultaneously evaluate two stress fields (one for each of the contacting bodies) satisfying not only the previously mentioned equilibrium and compatibility equations but also the contact equilibrium equations. This is obtained by imposing the continuity of the normal and tangential stresses of the two stress fields along the contact surface. One of the most relevant characteristics of this work is that it has been developed within a Cartesian grid framework (cgFEM [3]) where the FE mesh is independent of the geometry. The numerical results show a considerable accuracy enhancement of the stress field at the contact area that improves the behaviour of the contact algorithm and its accuracy. Acknowledgements: The financial support to this work of Generalitat Valenciana (PROMETEO/2016/007) and the Spanish Ministerio de Economía, Industria y Competitividad (DPI2017-89816-R) is greatly acknowledged. REFERENCES [1] JJ Ródenas, M Tur, FJ Fuenmayor, A Vercher "Improvement of the superconvergent patch recovery technique by the use of constraint equations: The SPR-C technique". International Journal for Numerical Methods in Engineering 70, 705–727 (2007). [2] OC Zienkiewicz, JZ Zhu. "The superconvergent patch recovery and a posteriori error estimates. Part I: The recovery technique". International Journal for Numerical Methods in Engineering, 33, 1331-1364 (1992). [3] E Nadal, JJ Ródenas, J Albelda, M Tur, JE Tarancón, FJ Fuenmayor. Efficient Finite Element Methodology Based on Cartesian Grids: Application to Structural Shape Optimization. Abstract and Applied Analysis 2013, Article ID 953786, 19 pages (2013).

Fracture Prediction in Patients with Skeletal Metastasis with CT-Based Rigidity Analysis

Ara Nazarian*, Vahid Entezari**, David Zurakowski***, Nathan Calderon****, John Hipp****,
Timothy Damron*****, Brian Snyder*****

*BIDMC and HMS, **BIDMC and HMS, ***CHB and HMS, ****BIDMC and HMS, *****Orthomet, *****SUNY
Upstate, *****BIDMC and HMS

ABSTRACT

Cancer patients are living longer due to new and aggressive treatments, yet at sites of skeletal metastasis patients experience significant complications. The dilemma for the physicians is to decide whether the metastatic tumor has weakened the bone such that pathological fracture is imminent. A multi-center, prospective, in-vivo study was conducted to identify significant predictors of physicians' treatment plan for skeletal metastasis based on clinical fracture risk assessments (Mirels score) and the proposed CT-based Rigidity Analysis (CTRA). One hundred and twenty four patients with 149 appendicular skeletal metastatic lesions were enrolled. Orthopaedic-oncologists were asked to select a treatment plan based on their initial risk assessment using Mirels method and follow up on patients over a 4-month period. Then, CTRA was performed on CT scans of the involved bones, and the results were provided to the enrolling physicians, who were asked to reassess their treatment plan. The pre- and post-CTRA treatment plans were compared to identify cases where treatment plan could be changed resultant from the CTRA report. Patient follow up resulted in 7 fracture cases, where the CTRA method was 100% sensitive and 90% specific, whereas Mirels method was 71% sensitive and 50% specific. Pain, lesion type and lesion size were significant predictors of the pre-CTRA plan. After providing the CTRA results, physicians changed their plan for 36 patients. CTRA results, pain and primary source of metastasis were significant predictors of post-CTRA plan. Lesion type and size along with pain level were relevant clinical information that influenced physician's plan for management of metastatic appendicular lesions. Physician's treatment plan and fracture risk prediction were significantly influenced by introduction of the CTRA results.

Roughness, Toughness and the Possibility of Crack Path Engineering

Alan Needleman^{*}, Ankit Srivastava^{**}, Shmuel Osovski^{***}

^{*}Department of Materials Science & Engineering, Texas A&M; University, College Station, TX, ^{**}Department of Materials Science & Engineering, Texas A&M; University, College Station, TX, ^{***}Faculty of Mechanical Engineering, Technion - Israel Institute of Technology, Haifa, Israel

ABSTRACT

Fracture surfaces of structural metals are rough and the statistics of that roughness are largely set by the material microstructure together with the nature of the imposed loading. A material's resistance to crack growth is also set by the same factors. Hence a basic question is: what is the relation, if any, between measures of the statistics of fracture surface roughness and measures of the material's crack growth resistance? Simulations of ductile fracture will be discussed that address this issue. The calculations are carried out within a continuum mechanics framework with a model of void nucleation, growth and coalescence incorporated into the constitutive relation. Simulations will be discussed that suggest the possibility that a material's crack ductile growth resistance can be significantly increased by suitably designing the microstructure to control the crack path. The results also suggest the possibility that suitably adding defects to a material can alter the crack path in a way that increases its ductile fracture resistance.

A Comparison of Hertzian and Differential-variational Inequality Contact Models

Dan Negrut^{*}, Arman Pazouki^{**}, Michał Kwaśny^{***}, Kyle Williams^{****}, William Likos^{*****}, Radu Serban^{*****}

^{*}University of Wisconsin-Madison, ^{**}California State University, ^{***}University of Wisconsin-Madison, ^{****}University of Wisconsin-Madison, ^{*****}University of Wisconsin-Madison, ^{*****}University of Wisconsin-Madison

ABSTRACT

We present and numerically compare two manifestly different contact models using a set of granular dynamics experiments. The first contact model, referred to herein as DEM-P from “discrete element method via penalty”¹, is a force-displacement model that is commonly used in the soft matter physics and geomechanics communities. The second approach, called DEM-C from “complementarity”², considers the grains perfectly rigid and enforces non-penetration via complementarity conditions; it is commonly used in robotics and computer graphics applications. Herein, we use a cone-complementarity formulation that formulates DEM-C as a global quadratic optimization problem subjected to conic constraints. DEM-P and DEM-C are manifestly unlike each other since they use different (1) approaches to model the frictional contact problem; (2) sets of model parameters to capture the physics of interest; and (3) classes of numerical methods to solve the differential equations that govern the dynamics of the granular material. Herein, we report numerical results for five experiments: shock wave propagation, cone penetration, direct shear, triaxial loading, and hopper flow, which we used to compare the DEM-P and DEM-C solutions. This experiments helped us reach two conclusions. First, both DEM-P and DEM-C are predictive; i.e., they predict well the macro-scale emergent behavior by capturing the dynamics at the micro-scale. Second, there is no clear winner insofar as handling granular dynamics is concerned. DEM-P runs into difficulties when handling complex geometries owing to its (1) ad-hoc approach to producing the friction and contact forces under these circumstances; and, (2) sensitivity to contact information; i.e., the geometrical or collision detection component, when small variations in contact information lead to sizable changes in forces. To a point, we found DEM-P insensitive to shearing rates, which could be increased, and to contact stiffness, which could be decreased, both by orders of magnitude. This lack of sensitivity can be traded for larger simulation step-sizes that led in some experiments to significant speedups over DEM-C. The DEM-P vs. DEM-C comparison was carried out using a public-domain, open-source software package called Chrono.

Development of the CAVEMAN Human Body Model: Lower Extremity Injury Assessment in Underbody Blast Accelerative Loading Conditions

Ryan Neice^{*}, Matthew Panzer^{**}, Kevin Lister^{***}, Kent Butz^{****}, Chad Spurlock^{*****}, Rajarshi Roy^{*****}

^{*}University of Virginia, ^{**}University of Virginia, ^{***}Corvid Technologies, ^{****}Corvid Technologies, ^{*****}Corvid Technologies, ^{*****}Corvid Technologies

ABSTRACT

The use of improvised explosive devices (IED) against U.S. military vehicles in recent conflicts has led to an increased need for accurately predicting mounted warfighter injuries. The lower extremities are the most often injured region of the body in underbody blast (UBB) events. Computational injury assessment in conjunction with the use of experimental anthropomorphic test devices (ATD) in loading conditions similar to UBB events provides more comprehensive occupant safety analyses for military vehicles. A major benefit of computational injury assessment is its ability to describe soft tissue failures that are otherwise difficult to capture in experimental ATD testing. The Computational Virtual Experiment Man (CAVEMAN) is a detailed human body model focused on expanding injury prediction capabilities for skeletal and soft tissues. The CAVEMAN finite element model is based on a 50th percentile human male developed for use in high performance computing. Comparisons to PMHS experimental data have been performed with the CAVEMAN lower extremity model in order to validate its sub-injurious response (Butz, et al. 2017). Current efforts are focused on injury prediction capabilities with the CAVEMAN model as compared to an injurious PMHS experimental data set (Bailey 2016). In addition, a sensitivity study concerning biological variabilities such as positioning, material properties, and anatomical geometry was performed to understand how such parameters affect injury localization and severity in an underbody blast loading event. References: Butz, K., Spurlock, C., Roy, R., Bell, C., Barrett, P., Ward, A., Xiao, X., Shirley, A., Welch, C., and Lister, K. (2017). Development of the CAVEMAN Human Body Model: Validation of Lower Extremity Sub-Injurious Response to Vertical Accelerative Loading. Stapp Car Crash Journal, Vol. 61 Bailey, A. (2016). Injury Assessment for the Human Leg Exposed to Axial Impact Loading. University of Virginia, Department of Mechanical and Aerospace Engineering, PHD.

An Immersed Boundary Method for the Fluid-structure Interaction Simulations Based on the Variational Transfer

Maria G.C. Nestola^{*}, Barna Becsek^{**}, Hadi Zolfaghari^{***}, Dominik Obrist^{****}, Patrick Zulian^{*****}, Rolf Krause^{*****}

^{*}Institute of Computational Science, Università della Svizzera italiana, Lugano, ^{**}University of Bern ARTORG Center for Biomedical Engineering Research, Bern, ^{***}University of Bern ARTORG Center for Biomedical Engineering Research, Bern, ^{****}University of Bern ARTORG Center for Biomedical Engineering Research, Bern, ^{*****}Institute of Computational Science, Università della Svizzera italiana, Lugano, ^{*****}Institute of Computational Science, Università della Svizzera italiana, Lugano

ABSTRACT

In the last years, the Fluid-Structure Interaction (FSI) analysis of the cardiovascular system has become an active area of research for assessing the hemodynamic risk in physiological and pathological conditions. To this aim, several approaches have been developed to reproduce the interaction between blood and a solid structure, which can be classified in the boundary-fitted and not boundary-fitted method. In this work, we present a novel and completely parallel approach for Fluid-Structure Interaction simulations. Our approach is inspired by the Immersed Boundary technique introduced by Peskin [1] and it makes use of the finite-element method for discretizing the equations of the solid structure and the finite-difference method for simulating the fluid flow. A segregated scheme is adopted to solve the fully coupled FSI problem [2]. More specifically, we first transfer the fluid velocity from the structured Cartesian fluid grid to the unstructured solid mesh. The fluid velocity field is used as a boundary condition for the elastodynamic problem, thus obtaining the reaction forces. These are then transferred to the fluid solver to compute the new velocity field. In addition, a fixed point (Picard) iteration scheme is used to solve the arising coupled non-linear discrete FSI system. The main characteristics of our FSI framework are the description of the solid body motion obtained by solving the elastodynamics equations and the use of a variational transfer to couple the solid and the fluid sub-problems. To this aim, we attach Lagrangian basis functions to the Finite Difference discretization and define the corresponding finite element space [3]. The proposed approach provides great flexibility and enables the modeling of deformable and rigid bodies with non-homogeneous and anisotropic properties embedded in different flow regimes. To demonstrate the robustness and flexibility of the computational framework we illustrate numerical results for 2D and 3D benchmark configurations. Finally, applications to the FSI simulations of a bioprosthetic aortic valve are also presented. 1) Peskin, Charles S. "The immersed boundary method." Acta Numerica 11 (2002): 479-517 2) Maria GC Nestola, Barna Becsek, Hadi Zolfaghari, Patrick Zulian, Dominik Obrist and Rolf Krause. An immersed boundary method based on the variational L2-projection approach. DD24 conference proceedings (under review) 3) Fackeldey, K., Krause, D., Krause, R., & Lenzen, C. (2011). Coupling molecular dynamics and continua with weak constraints. Multiscale Modeling & Simulation, 9(4), 1459-1494.

Software-in-the-Loop based Optimization of Actuator/Sensor Placement for Active Vibration Control

Tamara Nestorovic*, Atta Oveisi**, Afshin Sattarifar***

*Ruhr-Universität Bochum, Mechanics of Adaptive Systems, **Ruhr-Universität Bochum, Mechanics of Adaptive Systems, ***Ruhr-Universität Bochum, Mechanics of Adaptive Systems

ABSTRACT

Modern engineering concepts and interdisciplinary development often require coupling of different techniques, methods and tools towards finding optimal solutions. Optimization is a crucial step in smart engineering structures development and design. One of the often addressed problems in smart structures is active vibration/noise control (AVC/ANC), which requires both the controller design expertise and structural dynamics modeling and characterization knowledge. While the control community on one hand often deals with mainly mathematically based development of novel controllers (state or output feedback based ones), state reconstruction and disturbance estimation, anti-windup compensators, and input/output filters, with implementation often restricted to abstract numerical examples or reduced order problems without real-world applications, the engineering community on the other hand requires implementation of such methods to different problems (among others AVC and ANC) ranging from civil structures to aerospace ones. This contribution aims at closing this gap by proposing a new Software-in-the-Loop (SiL) scheme which enables a control engineer to design AVC based on optimization of actuator/sensor placement on an approximation of a real-world application without requiring a very deep knowledge of the structural dynamics phenomena. The proposed SiL scheme is based on coupling structural dynamics modeling and controller design tools, i.e. the finite element (FE) package ABAQUS and MATLAB. The focal contribution of this coupling scheme is in adopting FORTRAN as a messenger between ABAQUS kernel and MATLAB engine. In contrast to the methods in the literature, this interconnection enables the user to call and execute functions within MATLAB in an online setting. Further coupling involves a Python script which defines the structural properties such as geometry, material and assembly of the CAE model, whereas the FORTRAN UAMP subroutine controls the MATLAB function execution. Sensor elements on a predefined set of nodes are specified in ABAQUS output variables, while the actuation is realized through the user-defined load amplitudes. UAMP subroutine determines the value of the user-defined amplitude (control signal) in feedback from the sensor variables. The novelty in establishing the feedback is defined at this stage, by forwarding the sensor values from UAMP subroutine to MATLAB engine. This procedure enables the use of functions in MATLAB and implementation of arbitrary control laws, which in turn define the optimization criteria with respect to actuator/sensor placement. In this contribution we show the implementation of the method on a benchmark AVC problem. Accordingly, all the benchmark problems in AVC can be efficiently investigated in this framework.

Multiscale Elastography Using Multimodal Image Data Combined with Inverse Modeling

Corey Neu^{*}, Luyao Cai^{**}, Soham Ghosh^{***}

^{*}University of Colorado Boulder, ^{**}Purdue University, ^{***}University of Colorado Boulder

ABSTRACT

Quantification of high resolution spatiotemporal motion, structural, and spatial changes in biological tissues are required to understand the mechanobiological regulations in physiological or pathological altered mechanical environments. Visualization of internal tissue and cellular displacements and strains require specialized, multiscale imaging techniques including displacements MRI or microscopy. However, displacement and strain information does not directly correlate with spatial distributions of stiffness, which are critical to the understanding pathology and deviations from normal. To overcome these limitations, we describe a general approach to quantitatively assess spatiotemporal strain and material properties in biological systems using an imaging and inverse modeling-based technique. We acquired displacement-sensitive image data for hydrogels, in situ ovine tibiofemoral joint cartilage, and single cells. We prepared complex, heterogeneous tissues or mimics, including layered agarose constructs of 2% and 4% w/v, and skeletally-mature ovine stifle (knee) cartilage. Deformation was computed in samples that were cyclically loaded within an MRI system. Additionally, we visualized deformation in nuclei of cardiomyocytes isolated from mouse embryos. We utilized finite element-based hyperelastic (e.g. neo-Hookean) constitutive formulations to account for complex 3D joint geometry, and topology optimization. The design variable was the relative density of each finite element, which was varied to minimize the absolute difference of the displacements at N discrete points between the simulation and the imaging data. The optimization formulation was solved using an iterative design process, where elemental relative densities were updated with the iteration until a stop criterion was satisfied, and scaled to the modulus at each location using known loading/boundary conditions. Distributions of the absolute stiffness in samples were derived from MRI/microscopy displacement data and topology optimization. The stiffness maps showed distinct differences between materials, with the averaged value for 2% and 4% agarose respectively as 5.4 kPa and 15.7 kPa. Heterogeneous stiffness distributions were also observed in ovine cartilage and cardiomyocyte nuclei, and related to structural characteristics. Combined imaging data with topology optimization allows for measurement of quasi-static elastography in biological tissues and cells over multiple length scales. Our results show stiffness maps that are robust to noise, but that also require careful attention to boundary condition settings, to ensure stability during the optimization process. This method may allow for the noninvasive measurement of tissue/cell stiffness following damage, as a promising functional imaging biomarker.

Fatigue Life Prediction by Extended Gurson Model for SAE 1045 and S460N Steels

Raniere Neves^{*}, Lucival Malcher^{**}, Guilherme Ferreira^{***}

^{*}University of Brasília, ^{**}University of Brasília, ^{***}University of Brasília

ABSTRACT

Several machines components and structures are subjected to cyclic loading and the phenomenon of progressive rupture, known as fatigue, can be analyzed. The study of fatigue is very important during the design of component because it is necessary to avoid sudden failures that may result in accidents and also avoid oversizing components so that it does not lose competitiveness. This contribution suggests fatigue life prediction for two different materials (SAE 1045 and S460N steels) by means of an iterative approach based on the evolution of the void volume fraction accounted for an extended Gurson model after each cycle of loading. Due to its characteristics, the traditional Gurson damage model (1977) can not be used to fatigue life prediction. The first limitation that model shows an unreal healing behavior for cases of cyclic axial loads, where all void growth generated during the tension step is cured during the compression step, therefore there is no evolution of damage variable cycle to cycle. The second limitation is the fact that the Gurson model does not account the void distortion during predominantly shear loads, so does not occur the evolution of the damage variable in this cases. In order to overcome both limitations, this paper proposes an extended Gurson model where an unrecovered parameter is added to the void growth law with the role of identifying by means of stress triaxiality whether the material is being tensioned or compressed and thus change the response of the material to avoid the total recovery of the damage generated during tension step and the paper also proposes the coupling of void shearing mechanism of damage proposed by Nahshon and Hutchinson (2008) to the Gurson model in order to account for damage in predominantly shear loads too. This contribution presents the validation of the proposed approach by means of the simulation of axial, torsional and axial torsional cyclic loads taken from the literature for SAE 1045 and S460N steels.

Multi-Physics, Multi-scale Performance Assessment of Geological CO₂

Pania Newell^{*}, Mario Martinez^{**}

^{*}University of Utah, ^{**}Sandia National Laboratories

ABSTRACT

Deep geological formations are considered as a potential tool for permanent storage of large amounts of carbon dioxide over long periods of time (10^3 - 10^4 years). Their overall performance is highly affected by various trapping mechanisms such as structural, capillary, solubility, and mineral mechanisms. The presence of faults, joints, pre- or newly-formed fractures and other mechanical discontinuities that range in scale from micro-cracks (micrometers) to fractures (10s-100s of meters) to faults (100s meters to km) affect the state of stress and influencing the structural trapping mechanisms. Opening/closure or generation of new fractures can alter the flow paths for injection or withdrawal of fluids. The magnitude of the pore pressure also depends on hydrological and geomechanical properties of rock formation, wellbore orientation, injection rate and injection schedule. In this presentation, we will address (i) geomechanical testing at core scale for material model calibration, (ii) impact of formation thickness, wellbore orientation, injection rate, presence of fault and pre-existing fractures within the caprock to highlight the importance of the spatial and temporal scales and coupled processes within geological formations. Moreover, our results indicates that the integration between experimental and numerical modeling is critical to understand the long-term behavior of geological carbon storage. Sandia National Laboratories is a multimission laboratory managed and operated by National Technology and Engineering Solutions of Sandia, LLC., a wholly owned subsidiary of Honeywell International, Inc., for the U.S. Department of Energy's National Nuclear Security Administration under contract DE-NA-0003525.

DISCRETE ELEMENT MODELLING OF SLEEPER-BALLAST INTERACTION UNDER IMPACT LOADING

CHAYUT NGAMKHANONG^{1,2} AND SAKDIRAT KAEWUNRUEN^{1,2}

¹Department of Civil Engineering, School of Engineering,
University of Birmingham, Birmingham B152TT, United Kingdom
Email address; cxn649@student.bham.ac.uk, s.kaewunruen@bham.ac.uk

²Birmingham Centre for Railway Research and Education, School of Engineering,
University of Birmingham, Birmingham B152TT, United Kingdom

Key words: Impact Loading, Discrete Element Modelling, Sleeper, Ballast, Railway Track.

Abstracts. Generally, track structure experience impact load (also called “shock load”) due to the irregularities of either wheel or rail. The impact load, that may greatly exceed the static wheel load, are mainly caused by wheel/rail abnormalities such as poor weld geometry, rail corrugation, and rail defects like spalling, wheel burns and squats. Impact load is transient by nature which occurs over a short period with a high magnitude. This corresponds to the frequency range from 0 to 2000 Hz. In fact, ballast is a nonhomogeneous and discontinuities by nature. Based on literature, the conventional method, continuum modelling, cannot provide insight into the interaction of ballast particles. Hence, continuum modelling should be replaced by discrete element modelling (DEM) which has a finite number of ballast particles. The discrete element modelling is an approach to present the discontinuity of material. The ballast particles with various radii are modelled in LS-DYNA. The spherical shapes are modelled instead of polyhedral due to the lower cost of computational time and memory consumption. Even though the spherical model has limitation on the contact interlocking, this can be compensated by adopting the contact model. One bay ballasted track modelling has been conducted. The impact load associated with actual train load is applied on the rail. The interaction between sleeper and ballast are highlighted. Moreover, sleeper and ballast particle movement are presented. This study will provide greater insight into the ballast particle and the sleeper motion induced by impact load associated with actual train load.

1 INTRODUCTION

Railway ballast track, which has been widely used throughout the world, typically comprises rails, sleepers, fastening system, ballast, sub-ballast and subgrade. This type can be divided into two main components: superstructure and substructure. Superstructure, which is a multilayered construction supported by substructure, consists of rails, sleepers, fastening system and ballast. While, substructure includes sub-ballast and subgrade [¹⁻²]. It is known that ballast is placed between superstructure and substructure. The duties of ballast are to transfer the load from superstructure to underlying structure, to provide stability of the track, to support sleepers

uniformly, to absorb noise and vibration, to provide drainage system etc [³⁻⁶]. It is noted that ballast is one of the prone area to experience deteriorations which lead to track deterioration.

Previously, it was believed that the continuum method was capable to solve all the engineering problems [⁷]. However, it has been proven that this method cannot be used to solve some problems as this is only useful for solving homogeneous material [⁸⁻¹⁰]. By nature, the interactions among ballast aggregate particles are mostly discontinuous. Ballast shapes are sharp, angular, complex, and irregular. Since railway ballast normally consists of large particles of typical size approximately 40-60 mm, it is difficult to treat such a material as a continuum. It can be seen in many literatures that this approach could not perform the particle behaviour and difficult to highlight any significant phenomena such as particles interaction, ballast fouling, ballast breakage etc. Thus, discrete element modelling (DEM) is an alternative method, which was firstly introduced for rock and soil materials [¹¹]. This approach is a numerical method for computing the motion and effect of a large number of small particles with its interactions in a granular assembly. The discontinuous behaviour can also be included. DEM can provide insight into the micro-mechanical behaviour of railway ballast.

Railway track is usually subjected to dynamic impact load. Such load is a large magnitude applied over a short period. This may induce damage in railway track. It is noted that the typical impact load varies between 100kN to 750kN. Based on field works and many literatures [¹²⁻²⁰], it can be seen that the dynamic impact loads are caused by the irregularities of wheel or rail as well as the resonance effect produced among the track components [¹]. It should be also noted that the impact capacity of sleepers can be reduced due to the modification of their cross section [²¹⁻²⁴] and time-dependent behaviour [²⁵⁻²⁷].

A three dimensional finite element model was firstly conducted using ANSYS [²⁸⁻³⁰]. This model was validated by full-scale experiment based on the European standard [³¹]. The three-dimensional finite element software LS-DYNA was then used to analyze the dynamic responses of single bay ballasted track. The model has been validated against experimental drop impact tests [³²⁻³⁴]. This study presents the dynamic responses and sleeper-ballast interaction under impact loading. The outcome of this study can help improve the understanding of ballast movement of each particle under impact loading.

2 MODELLING

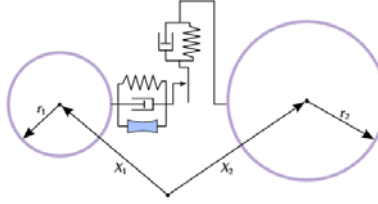
In this study, finite element package LS-Dyna is used to analyze the dynamic response of single span ballasted track. The sleeper and rails are modelled by solid element with eight nodes with three degree of freedom (translation). Truss element is used to model the prestressing wires by assuming perfect bond between prestressing wires and concrete. It should be noted that truss element cannot resist bending moment and shear force. The modulus of elasticity of concrete (E_c) was estimated based on AS3600 [³⁵]. The material properties of each element are shown in Table 1.

Table 1 Material properties of ballasted track.

Parameters	Characteristic value	Unit
Rail		
Modulus of elasticity	200000	MPa
Density	7870	Kg/m ³
Possion's ratio	0.25	
Sleeper		
Concrete		
Modulus of elasticity	98000	MPa
Density	2400	Kg/m ³
Possion's ratio	0.2	
Prestressing wire		
Modulus of elasticity	200000	MPa
Density	7850	Kg/m ³
Possion's ratio	0.25	
Rail pad		
Modulus of elasticity	1250	MPa
Density	960	Kg/m ³
Possion's ratio	0.42	
Ballast		
Layer thickness	30	cm
Modulus of elasticity	1000	MPa
Density	2600	Kg/m ³
Possion's ratio	0.3	
Diameter	20-50	mm
Spring constant (Tangential)	1	
Spring constant (Normal)	0.3	
Damping constant (Tangential)	0.7	
Damping constant (Normal)	0.4	
Friction coefficient	1	
Rolling friction coefficient	0.3	

The extended finite element model was calibrated using vibration data [^{30, 36}]. The updated finite element model was then transferred to LS-Dyna [^{33, 34}], as shown in Figure 3. The simulation results were achieved by assigning the initial velocity to the drop mass to generate an impact event, similarly to the actual drop tests.

The ballast particles were firstly generated and packed into the cubic element. The contacts between each particle were assigned in terms of spring and damper by keyword *CONTROL_DISCRETE_ELEMENT. The friction coefficient can be also applied. The contacts between each component were assigned using keywords *CONTACT_AUTOMATIC_SURFACE _ TO_SURFACE and *CONTACT_AUTOMATIC_NODES_TO_SURFACE. The friction coefficient between rails and sleepers, sleeper and ballast, were 0.3 and 0.3, respectively. The contact interactions were defined using keywords *CONTROL_DISCRETE_ELEMENT. The contact parameters are shown in Table 1. The schematic contact between each particle is shown in Figure 1. It should be noted that the friction and rolling coefficient were applied into the contact between the ballast in order to compensate the disadvantage of spherical element.

Figure 1 Schematic contact between each ballast particle [³⁷].

It is noted that particle size varied between 20-50 mm were packed randomly into the concrete box, as shown in Figure 2. The gravity acceleration (9.81m/s^2) was applied to the ballast, sleeper and rails before applying the velocity to the impactor. It should be noted that ballast, sleeper and rails fell down freely without constraint in any directions. The velocity of impactor was 1.94 m/s which equivalent to the drop height 0.2 m the test rig [³²⁻³⁴]. The modeling has been validated against experiment. It was found that the finite element model was fairly sufficient for use in predicting impact responses. The trends of peak acceleration responses are quite close to the experiment obtained [³²⁻³⁴], although there is certain phase and pulse duration differences.

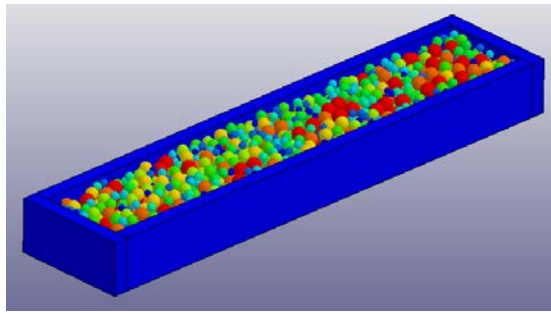


Figure 2 Various size of ballast packed into concrete box.

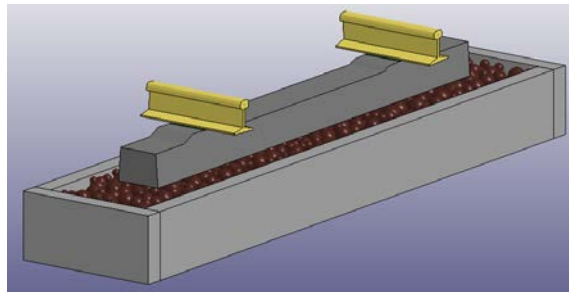


Figure 3 Finite element modelling of railway ballast track.

3 RESULTS AND DISCUSSIONS

The contact force between sleeper and ballast is shown in figure 4a. It is observed that about 340 kN is the contact force between sleeper and ballast due to the applied velocities of drop mass of 1.94 m/s . It is also noted the pulse durations is about 2.6ms . While, the maximum sleeper/ballast contact force is about 150 kN , as seen in figure 4b.

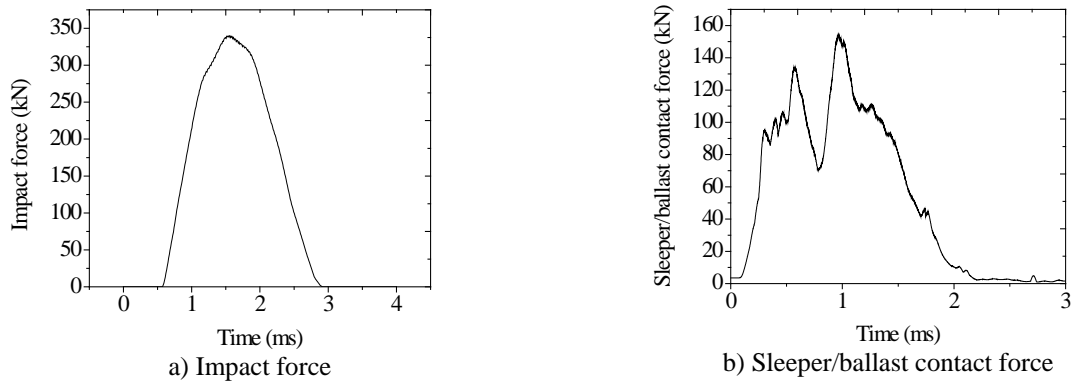


Figure 4 Contact force between sleeper and ballast.

Figure 5 presents the displacement contour at time of 0.64s and the displacement time history of sleeper at rail seat and mid-span. It should be noted that all components are in equilibrium within 0.5s after applying gravity acceleration. The result shows that the positive displacement is observed so that there is a slight uplift of sleeper at rail seat during unloading. The permanent displacement is also observed after all components are in equilibrium at about 0.9s due to the settlement and packing of ballast. The displacement of sleeper at rail seat (loaded side) is larger than that at mid span and another rail seat.

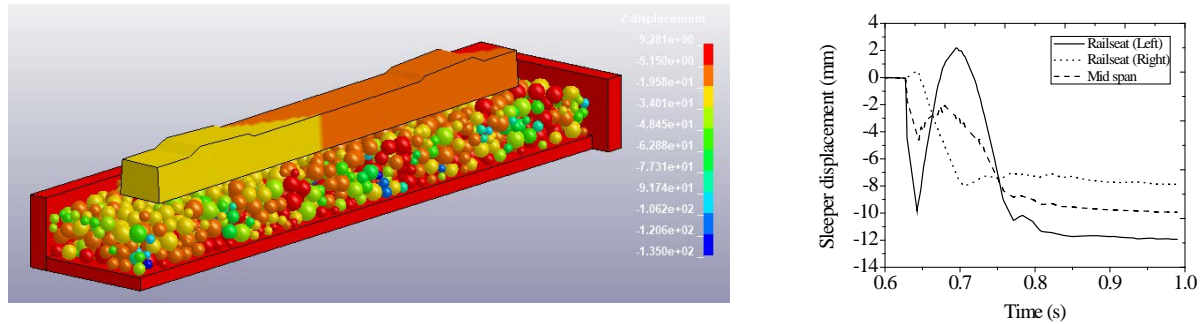
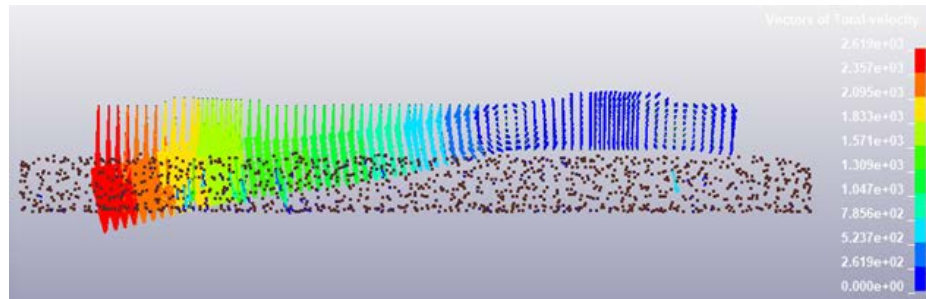
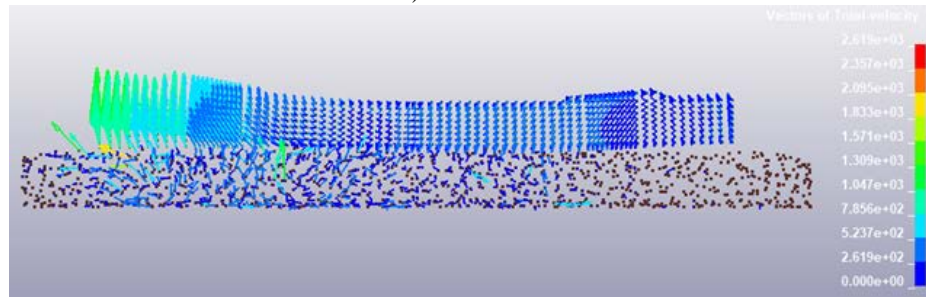


Figure 5 Vertical displacement contour and sleeper displacement time history.

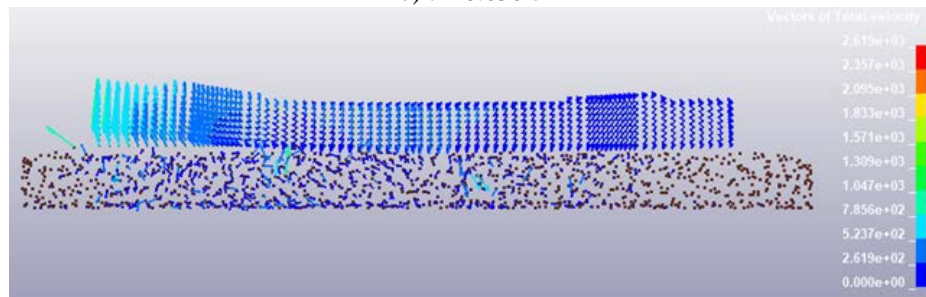
The movements of ballast particles and sleeper at each node are presented in terms of displacement vectors as shown in figure 6. Figure 6a displays the ballast and sleeper responses at the initial stage under gravity. Figure 6b-d shows the responses of ballast and sleeper under impact loading at each time step. It should be noted that the displacements contour and vector are cumulatively presented from the starting of applied gravity acceleration so that the displacements displayed are not due to only impact loading but also gravity at the first stage. Hence, figure 6 illustrate the node vector velocities of ballast and sleeper instead of displacement as it can show the behaviour at particular time. It is clearly seen that sleeper and ballast on loaded side moves down significantly and tends to lift up when unloading as previously describe. It is finally seen that ballast has a permanent settlement which lead to the permanent settlement of sleeper. These can be compared to the time history response obtained in figure 5.



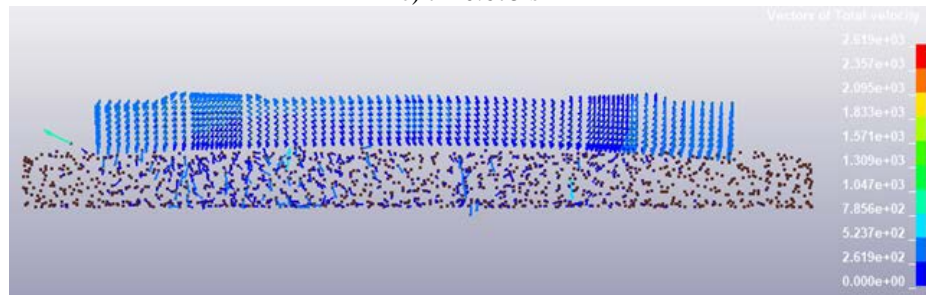
a) $t = 0.625$ s



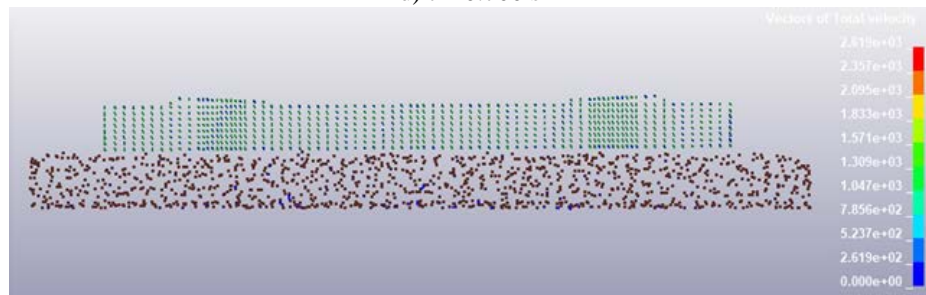
b) $t = 0.650$ s



c) $t = 0.675$ s



d) $t = 0.700$ s



e) $t = 0.100$ s

Figure 6 Velocity vectors of ballast and sleeper at each time.

It should be noted again that this study did not consider the lateral resistance of sleeper as we only consider the vertical movement. However, due to the random placement of various size of ballast, sleeper was not completely flatly placed on ballast bed. Also, in fact, longitudinal rail and fastening system can considerably constrain the movement of sleeper in longitudinal and transverse directions and they may also help reduce uplift effect.

4 CONCLUSIONS

Discrete element modelling (DEM) is an alternative method to take into account the nature of granular and heterogeneous materials. This method has been firstly used for granular material and then adapted to railway ballast. This method is very useful and powerful as it provides the multi scale mechanic behaviour and the movement of each ballast particle. A commercial finite element package, LS-Dyna, has been employed to extend the model for impact analysis and it has been validated against experimental drop impact tests. The spherical particle was employed since it can provide a better computational time and memory consumption than polyhedral. Although the simple spherical cannot provide insight into the real shape and particle contact, this can be fitted by adapting the proper contact coefficient between each particle. In fact, railway track normally experiences impact load, which is a shock load applied in short duration, due to the irregularities of either wheel or rail. It should be noted that the magnitude is much higher than static load. Thus, the vertical velocity of drop mass of 1.94 m/s associated with actual train loads was applied to the rail. It should be noted that this equivalent to about 340 kN. The results show that the maximum displacement occurred at rail seat under impact load while the displacement on another side of rail seat is lower than that at mid-span. The permanent deformation of sleeper is also observed. This is because ballast particles are packed and settled and then sleeper is pressed down into the ballast bed. Moreover, it is noted that uplift of the sleeper is observed during unloading. It should be noted that the relative uplifts of the sleepers tend to cause deteriorations of railway tracks over time, such as ballast breakage, excessive dilation and densification, which can cause further track differential settlements. In fact, ballast can be broken and crushed due to the impact load which leads to severe track degradation. However, this study did not consider ballast breakage. Hence, it is recommended to take into account the spherical cluster particle and ballast breakage under impact loading for further study.

ACKNOWLEDGEMENTS

The authors are sincerely grateful to the European Commission for the financial sponsorship of the H2020-RISE Project No. 691135 “RISEN: Rail Infrastructure Systems Engineering Network”, which enables a global research network that tackles the grand challenge of railway infrastructure resilience and advanced sensing in extreme environments (www.risen2rail.eu) [³⁸].

REFERENCES

- [1] Remennikov, A.M. and Kaewunruen, S. A review of loading conditions for railway track structures due to train and track vertical interaction. *Struct. Control. Health Monit.*

- (2008) 15(2):207-234.
- [2] Ngamkhanong, C., Kaewunruen, S. and Baniotopoulos, C. A review on modelling and monitoring of railway ballast, *Structural Monitoring and Maintenance*. (2017) 4(3):195-220. doi: 10.12989/smm.2017.4.3.195.
 - [3] Selig, E.T. and Waters, J.M. *Track Geotechnology and Substructure Management*, Thomas Telford Publishing, UK, (1994).
 - [4] Indraratna, B., Salim, W. and Rujikiatkamjorn, C., *Advanced Rail Geotechnology-Ballasted Track*, Taylor & Francis Group, London, UK, (2011).
 - [5] Remennikov, A.M. and Kaewunruen, S. Experimental load rating of aged railway concrete sleepers. *Eng. Struct.* (2014) 76(10):147-162.
 - [6] Kaewunruen, S. and Remennikov, A.M. Dynamic properties of railway track and its components: Recent findings and future research direction. *Insight: Non-Destructive Testing and Condition Monitoring*. (2010) 52(1):20-22.
 - [7] Nguyen, V., Duhamel, D. and Nedjar, B. A continuum model for granular materials taking into account the no-tension effect. *Mech. Mater.* (2003) 35:955-967.
 - [8] Alva-Hurtado, J.E. and Selig, E.T. Permanent strain behavior of railroad ballast. *Proceeding of the International Conference on Soil Mechanics and Foundation Engineering*. (1981) 1:543-546.
 - [9] Shenton, M. Ballast deformation and track deterioration. *Track technology*. (1985):253-265.
 - [10] Sato, Y. Japanese studies on deterioration of ballasted track. *Vehicle Syst. Dynam.* (1995) 24(1):197-208.
 - [11] Cundall, P.A. A Computer Model for Simulating Progressive, Large Scale Movements in Blocky Rock Systems. *International Symposium on Rock Fracture*, I.S.R.M. Nancy, France, (1971).
 - [12] Remennikov, A.M., Murray, M.H. and Kaewunruen, S. Reliability based conversion of a structural design code for prestressed concrete sleepers. *Proceedings of the Institution of Mechanical Engineers: Part F Journal of Rail and Rapid Transit*. (2012) 226(2):155-73.
 - [13] Wakui, H. and Okuda, H. A study on limit-state design for prestressed concrete sleepers. *Concrete Library of JSCE*. (1999) 33:1-25.
 - [14] Wang, N. Resistance of concrete railroad ties to impact loading. PhD Thesis, University of British Columbia, Canada, (1996).
 - [15] Gustavson, R. Structural behaviour of concrete railway sleepers. PhD Thesis, Department of Structural Engineering, Chalmers University of Technology, Sweden, (2002).
 - [16] Stevens, N.J. and Dux, P.F. A method of designing a concrete railway sleeper. *International Patent No WO 2004/019772 A1*, World Intellectual Property Organisation, International Bureau, (2004).
 - [17] Lilja, J., Preliminaries for probabilistic railway sleeper design. Licentiate Thesis, Chalmers Applied Mechanics, Chalmers University of Technology, Gothenburg, (2006).
 - [18] Leong, J. Development of a limit state design methodology for railway track. Master of Engineering Thesis, Queensland University of Technology, QLD, Australia, (2007).
 - [19] Kaewunruen, S., Remennikov, A.M. and Murray, M.H. Limit states design of railway concrete sleepers. *Proc. of ICE Transport Journal*. (2012) 164(TR1). doi: 10.1680/tran.9.00050
 - [20] Ngamkhanong, C., Kaewunruen, S. and Costa, B.J.A. State-of-the-Art Review of Railway Track Resilience Monitoring. *Infrastructures*. (2018) 3.

- [21] Ngamkhanong, C., Li, D. and Kaewunruen, S. Impact capacity reduction in railway prestressed concrete sleepers with vertical holes. IOP Conference Series: Materials Science and Engineering. (2017) 236(1).
- [22] Ngamkhanong, C., Kaewunruen, S. and Remennikov, A.M. Static and dynamic behaviours of railway prestressed concrete sleepers with longitudinal through hole. IOP Conference Series: Materials Science and Engineering. (2017) 251(1).
- [23] Ngamkhanong, C., Li, D. and Kaewunruen, S. Impact capacity reduction in railway prestressed concrete sleepers with surface abrasions. IOP Conference Series: Materials Science and Engineering. (2017) 245(3).
- [24] Ngamkhanong, C., Li, D., Kaewunruen, S. and Remennikov, A.M. Capacity Reduction in Railway Prestressed Concrete Sleepers due to Dynamic Abrasions. International Journal of Structural Stability and Dynamics. (2018). (Accepted)
- [25] Li, D., Ngamkhanong, C. and Kaewunruen, S. Influence of vertical holes on creep and shrinkage of railway prestressed concrete sleepers. IOP Conference Series: Materials Science and Engineering, (2017) 236(1).
- [26] Li, D., Ngamkhanong, C. and Kaewunruen, S. Time-dependent topology of railway prestressed concrete sleepers. IOP Conference Series: Materials Science and Engineering. (2017) 245(3).
- [27] Li, D., Ngamkhanong, C. and Kaewunruen, S. Influence of Surface Abrasion on Creep and Shrinkage of Railway Prestressed Concrete Sleepers. IOP Conference Series: Materials Science and Engineering. (2017) 245(3).
- [28] Kaewunruen, S. and Remennikov, A.M. Effect of a large asymmetrical wheel burden on flexural response and failure of railway concrete sleepers in track systems. Engineering Failure Analysis. (2008) 15(8): 1065-1075.
- [29] Kaewunruen, S. and Remennikov, A.M. Experimental simulation of the railway ballast by resilient materials and its verification by modal testing. Experimental Techniques. (2008) 32(4):29-35.
- [30] Kaewunruen, S. and Remennikov, A.M. Nonlinear finite element modeling of railway prestressed concrete sleeper. Proceedings of the 10th East Asia-Pacific Conference on Structural Engineering and Construction. (2006) 4:323-328.
- [31] British Standards Institute (BSI) European Standard BS EN13230 Railway applications. Track. Concrete sleepers and bearers. London, UK, (2016).
- [32] Kaewunruen, S. and Remennikov, A.M. Low-velocity impact analysis of prestressed concrete sleepers. Proceedings of the 23rd Biennial Conference of the Concrete Institute of Australia: Design, Materials, and Construction. Adelaide, Australia, (2007):659-668.
- [33] Kaewunruen, S. and Remennikov, A.M. Impact responses of prestressing tendons in railway concrete sleepers in high speed rail environments. Proceedings of the 5th Computational Methods in Structural Dynamics and Earthquake Engineering. May 25-27, Crete Island, Greece, (2015).
- [34] Kaewunruen, S., Remennikov, A.M. and Minoura, S. Dynamic responses of railway ultra-highstrength concrete sleepers under extreme impact loading. Proceedings of the 6th Computational Methods in Structural Dynamics and Earthquake Engineering. June 15-17, Rhodes Island, Greece, (2017).
- [35] Standards Australia. Design of concrete structures. Australian Standard: AS3600-2001. (2001).
- [36] Gamage, E.K., Kaewunruen, S., Remennikov, A.M. and Ishida, T. Toughness of Railroad

- Concrete Crossties with Holes and Web Openings. *Infrastructures*. (2017) 2(3). doi:10.3390/infrastructures2010003.
- [37] Livermore Software Technology Corporation (LSTC). *LS-DYNA KEYWORD USER'S MANUAL VOLUME I*. (2013).
- [38] Kaewunruen, S., Sussman, J.M. and Matsumoto, A. Grand challenges in transportation and transit systems. *Frontiers in Built Environment*. (2016) 2(4). doi:10.3389/fbuil.2016.00004.

Performance of the Polygonal Finite Element Method in Modelling Complex Natural Structures

Tuan Ngo^{*}, Abdallah Ghazlan^{**}, Tuan Nguyen^{***}, Hung Nguyen-Xuan^{****}

^{*}University of Melbourne, ^{**}University of Melbourne, ^{***}University of Melbourne, ^{****}Ho Chi Minh City University of Technology (Hutech)

ABSTRACT

Well-organised polygonal structures have been observed in nature in many instances, such as polygonal brick and mortar found in nacreous seashells, functionally graded polygonal foams in porcupine quills and trabecular bone, arbitrary cellular structures in bamboo, beetle wing striations, and so on. These structures show unique structural configurations, which are effective under large deformations, and also in deflecting cracks and distributing damage. They can be approximated by voronoi diagrams, which is a powerful tool in computational geometry capable of generating complex and well-organised polygonal and polyhedral patterns by simply controlling a set of points. However, the loss in performance and accuracy in modelling complex natural structures is evident by the significant increase in elements introduced in the meshing process. In this study, the efficacy of the polygonal finite element method, which uses one element per voronoi polygon, is investigated in modelling the polygonal microstructure found nacre from mollusc shells, which can consist of millions of platelets. The voronoi diagram is generated using the well-known sweep line algorithm, which traverses a set of points and constructs the polygonal cells efficiently. The polygonal finite element method is benchmarked against the finite element method in ABAQUS and shown to significantly improve performance by reducing the computation time.

Free Vibration of Cracked FG Plates Based on Strain-Gradient Theory

Hoang Nguyen^{*}, Elena Atroshchenko^{**}, Hung Nguyen-Xuan^{***}, Thuc Vo^{****}

^{*}Northumbria University, ^{**}University of Chile, ^{***}HCMC University of Technology, ^{****}Northumbria University

ABSTRACT

This study aims to investigate the free vibration responses of functionally graded (FG) cracked small-scale plates using the strain-gradient theory and the extended isogeometric analysis (XIGA). While the strain-gradient elasticity is employed to account for the size-dependent effects, the displacement fields of plate structures are described based on the refined plate theory (RPT). The simple strain-gradient theory with one additional length scale parameter, apart from Lamé's constants, is capable of effectively capturing the small-scale effects in nano/micro structures [1]. The RPT with four unknowns not only is able to improve the accuracy of the results for both thin and thick plates but also helps to describe the nonlinear distribution of the shear stress through the plate's thickness without using shear correction factor. The combination of SGE and RPT ends up requiring C2 elements, which causes difficulty if traditional finite element is involved to solve for approximate solutions. The isogeometric analysis (IGA) [2] is employed as a prominent numerical method to solve the problems that require higher-order elements. This recently developed method utilises the non-uniform rational B-splines (NURBS) functions to establish approximation functions and describe geometry domains simultaneously. In order to model the discontinuity at the cracks within the plates, the extended IGA with enrichment functions for crack path and crack tip is involved. The primary results for the free vibration of functionally graded plates show that the proposed approach is able to predict both the fracture behaviours and size-dependent effects well. It yields appropriate and reliable results in which the stiffness of the structures, consequently the fundamental frequency, is increased as the length scale ratio becomes larger. It also demonstrates that strain-gradient theory plays a significant role in the prediction of size-dependent effects of nano/micro structures which classical continuum theory could fail to capture. REFERENCES [1] R.D.Mindlin, Micro-structure in linear elasticity, Archive for Rational Mechanics and Analysis, 16, 51–78, 1964. [2] T.J.R. Hughes, J.A. Cottrell, Y. Bazilevs, Isogeometric analysis: CAD, finite elements, NURBS, exact geometry and mesh refinement, Computer Methods in Applied Mechanics and Engineering, 194, 4135-4195, 2005.

An Iterative Local Corrector Scheme for the Multiscale Finite Element Method

Lam Nguyen^{*}, Dominik Schillinger^{**}

^{*}University of Minnesota, ^{**}University of Minnesota

ABSTRACT

Fine-scale features such as scale separation and periodicity are usually used to simplify simulations of heterogeneous materials and reduce the computational cost. Without these features, we need to fully resolve all microstructures to obtain accurate results, involving tremendous computational memory and time. The multiscale finite element method is one of the multiscale techniques that can be applied to this problem. Constraints on multiscale basis functions at element interfaces, however, prevent convergence to the fine-scale solution. In this work, we overcome this challenge by introducing an iterative corrector scheme which enables communication between fine-scale solutions across coarse element interfaces. In our approach, a first solution is found by using initial multiscale basis functions. The corrector scheme is then applied to improve the multiscale basis functions at element interfaces by solving local boundary problems in separate patches of coarse elements. The new multiscale basis is used to find a new multiscale solution. We repeat the procedure until reaching the desired accuracy. With this technique, we can solve large problems with significantly fewer degrees of freedom while retaining the same accuracy as the fully resolved discretization of the fine scale. In this talk, we briefly describe our method, discuss implementation aspects, and illustrate it with numerical examples.

Adaptive Isogeometric Collocation Method Based On Reproducing Kernel Meshfree Formulation For Large Deformation Frictional Contact Problems

Nhon Nguyen*, Kun Zhou**

*School of Mechanical and Aerospace Engineering, Nanyang Technological University, 50 Nanyang Avenue, Singapore 639798, Singapore, **School of Mechanical and Aerospace Engineering, Nanyang Technological University, 50 Nanyang Avenue, Singapore 639798, Singapore

ABSTRACT

Collocation has recently shown as a powerful alternative to Galerkin's method in the context of isogeometric analysis (IGA). In this method, the strong form of the governing differential equations of the problem is enforced at a set of discrete collocation points, equal in number to the control points. Isogeometric collocation (IGA-C) exhibits a strongly reduced computational cost when compared with Galerkin approaches while maintaining higher-order convergence rates. However, IGA has certain shortcomings in terms of numerical analysis. Because of the tensor-product form of non-uniform rational basis spline, the control points must belong to a structured grid, which causes an excessive overhead of control points with increasing refinement. In this work, adaptive IGA-C method based on reproducing kernel meshfree formulation for large deformation frictional contact problems are presented. The proposed reproducing kernel meshfree representation of IGA-C basis functions provides a reliable meshfree strategy which is flexible adaptive refinement. The shape functions in the refined regions can be naturally constructed in a straightforward meshfree manner. The consistency and independence of the shape functions required by the subsequent computational analysis are ensured by the consistency conditions of reproducing kernel meshfree formulation. Moreover, a large deformation contact formulation is subsequently developed and tested in the frictional setting, where collocation confirms the excellent performance already obtained for the frictionless case.

A Deterministic-stochastic Method for Computing the Boltzmann Collision Integral in $O(MN)$ Operations

Truong Nguyen^{*}, Alexander Alekseenko^{**}, Aihua Wood^{***}

^{*}Wright State University, ^{**}California State University, Northridge, ^{***}Air Force Institute of Technology

ABSTRACT

Abstract: We developed and implemented a numerical algorithm for evaluating the Boltzmann collision operator with $O(MN)$ operations, where N is the number of the discrete velocity points and $M \ll N$. At the base of the algorithm is nodal-discontinuous Galerkin discretizations of the collision operator on uniform grids and a bilinear convolution form of the Galerkin projection of the collision operator. Efficiency of the algorithms is achieved by applying singular value decomposition compression of the discrete collision kernel and by approximating the kinetic solution by a sum of Maxwellian streams using a stochastic likelihood maximization algorithm. Accuracy of the method is established on solutions to the problem of spatially homogeneous relaxation. The method achieves more than ten fold speedup in comparison to the fully deterministic evaluation of the collision integral presented in [1,2].
References: [1] A. Alekseenko and E. Josyula, Deterministic solution of the Boltzmann equation using a discontinuous Galerkin velocity discretization, in 28th International Symposium on Rarefied Gas Dynamics, 9-13 July 2012, Zaragoza, Spain, AIP Conference Proceedings, American Institute of Physics, 2012, 8. [2] A. Alekseenko and E. Josyula, Deterministic solution of the spatially homogeneous Boltzmann equation using discontinuous Galerkin discretizations in the velocity space, Journal of Computational Physics, 272 (2014), 170-188.

Multiscale Modeling of Wave Propagation in Periodic Fluid-saturated Poroelastic Media

Vu-Hieu Nguyen*, Eduard Rohan**, Salah Naili***

*bLaboratoire Modélisation et Simulation Multi Echelle, MSME UMR 8208 CNRS, Université Paris-Est, France,

aEuropean Centre of Excellence, NTIS – New Technologies for Information Society Faculty of Applied Sciences, University of West Bohemia, Czech Republic, *Laboratoire Modélisation et Simulation Multi Echelle, MSME UMR 8208 CNRS, Université Paris-Est, France

ABSTRACT

This work is motivated by the need for characterizing porous materials with heterogeneity at different scales, e.g natural and artificial porous materials such as biological tissues, soils, rocks and foams. We aim to study the propagation of acoustic waves in periodic mixture of two fluid saturated poroelastic materials which exhibit the presence of heterogeneity at scales much larger than microstructure scales but much smaller than the wavelengths [1,2,3]. For describing the acoustic wave propagation in such materials, both porous materials at the mesoscale are modeled by using Biot's theory. Then, a two-scale homogenization scheme has been carried out for deriving the effective dynamic equations at the macroscale. Depending on the contrast between the permeability and the poroelastic coefficients of two phases, two different models have been derived. Finite element formulations were developed for computing the effective acoustic properties of the material at macroscopic scale from given mesoscale structural geometries. We also present a down-scale post-processing procedure for estimating the local dynamic responses at the mesoscale from solutions of homogenized medium at the macroscale. The proposed method is validated by considering a plane wave propagation problem in a half-space under harmonic excitations. The solutions obtained by using homogenized models are compared with the ones obtained by using a model which take into account all geometrical details at the mesoscale. The numerical validations showed that the high-contrast model can capture some phenomena which are not described by the standard homogenization treatment of a low contrast model. The domain of validity for high contrast model may also be determined. REFERENCES [1] Nguyen, V.-H., Rohan, E., & Naili, S. (2016). Multiscale simulation of acoustic waves in homogenized strongly heterogeneous porous media. *International Journal of Engineering Science*, 101, 92–109. [2] Rohan, E., Naili, S., & Nguyen, V.-H. (2016). Wave propagation in a strongly heterogeneous elastic porous medium: Homogenization of Biot medium with double porosities. *Comptes Rendus Mécanique*, 344(8), 569–581 [3] Rohan, E., Nguyen, V. H., & Naili, S. (2017). Numerical modelling of waves in double-porosity Biot medium. *Computers and Structures* (in press, DOI: 10.1016/j.compstruc.2017.09.003)

Heat and Moisture Conduction and Hydrothermal Analysis in Laminated Plates Using Higher Order Zig-zag Theory

Ngoc Nguyen-Sy^{*}, Jaehun Lee^{**}, Maenghyo Cho^{***}

^{*}Seoul National University, ^{**}Kyungnam University, ^{***}Seoul National University

ABSTRACT

This work developed higher order zig-zag theory to predict accurately the coupling hygroscopic-thermal-mechanical behaviors for viscoelastic composite laminated plates. All in-plane displacement, temperature, and moisture fields through the thickness are constructed by combining the locally linear zig-zag term and globally cubic polynomial distribution. The Laplace transform is employed to avoid such integration of the viscoelastic constitutive equation as well as improve accuracy and efficiency. All formulations are simplified in Laplace domain. The hydrothermal variation principle is employed to determine the temperature and moisture distributions through the thickness. Then, viscoelastic relaxation modulus with various hydrothermal shift factors in each layer are calculated in the general form of Prony series. The final numerical results of stresses and deformations are obtained by using inverse Laplace techniques. To demonstrate the efficiency and accuracy of the present theory, some numerical examples for long-term creep and relaxation processes are performed. The present theory is suitable for the predictions of coupled hygroscopic-thermal-mechanical behaviors for thick viscoelastic composite laminated plates.

An Adaptive Strategy Based on Conforming Quadtree Meshes for Kinematic Limit Analysis

Hung Nguyen-Xuan*

*Hutech University, Ho Chi Minh City, Vietnam

ABSTRACT

We propose a simple and efficient scheme based on adaptive finite elements over conforming quadtree meshes for collapse plastic analysis of structures. Our main interest in kinematic limit analysis is concerned with both purely cohesive-frictional and cohesive materials. It is shown that the most computational efficiency for collapse plastic problems is to employ an adaptive mesh strategy on quadtree meshes. However, a major difficulty in finite element formulations is the appearance of hanging nodes during adaptive process. This can be resolved by a definition of conforming quadtree meshes in the context of polygonal elements. Piecewise-linear shape functions in barycentric coordinates are used to approximate the velocity field. Numerical results prove the reliability and benefit of the present approach.

NUMERICAL SIMULATION OF ICE LOADS IN THE PROCESS OF SHIP ICE COLLISION BASED ON NONLINEAR ELEMENT METHOD

Li Z.P.¹ Ni B. Y.¹ Yang D.² Han D. F.¹

1. College of Shipbuilding Engineering, Harbin Engineering University, Harbin, China, 150001;
Email address: nibaoyu@hrbeu.edu.cn
2. Wuhan Second Ship Design and Research Institute, Wuhan, China, 430205

Key words: ship, ice loads, collision, finite element method, nonlinearity.

Abstract. More and more ships are operating and will navigate in cold regions, particularly in the arctic route. The maneuverability of ship in level ice is complex no matter the ship is in straight motion or rotational motion. To study this complex, strong and nonlinear collision between ice and ship, nonlinear finite element method is adopted with appropriate ice material and failure modes. Numerical results are compared with that from empirical formula. On this basis, combined movement of an icebreaker including straight motion and rotational motion is studied and the characteristics of ice loads are discussed. The influences of forward and angular velocities are also analyzed.

1 INTRODUCTION

Along with global warming, the arctic route and resource exploration in Arctic areas are becoming more practical. As a result, more and more ships are operating and will navigate in cold regions. When a ship navigates in the Arctic area, its structural response and motion state are influenced by various external loads, including ice, winds, waves, and currents, etc. Among these external loads, the most important one may be the ice loads, which may induce severe dynamic structural response on the ship during the process of ship-ice collisions. When a ship is maneuvering in the level ice, the ship-ice interaction can be very complex. In the condition of straight-forward motion, due to the rake of the stem, the main force exerted on the ice sheet by the ship is the vertically downward force. As a result, the breaking mode of the ice sheet is bending failure mainly. However, when a ship turns in the level ice, the ice is extruded by the midship whose face is perpendicular to the ice sheet. Thus, the breaking mode of the ice sheet is compression failure mainly. The strong nonlinear impact between the ship and ice generates challenges on simulating the motion of the ship in the ice, especially in a rotational motion.

In numerical simulations, there has been researches on ship-ice collisions. Valanto (2007) [1] simulated the straight-forward resistance of a ship moving in level ice by establishing a three-dimensional finite element model of the ship. Numerical results were compared with the actual measured data and good agreement was achieved, which denotes their model can predict ice resistance well. Wang et al. (2008) [2] adopted commercial software MSC.DYTRAN to simulate the collision between LNG ships and crushable ice based on nonlinear finite element analysis. The results indicated that the ship structure under ice loads presented two major failure modes: the large plastic deformation and the local buckling. Su (2011) [3] developed a kind of ‘point-face’ contact algorithm to predict the ice loads on the ship surfaces. On this basis, the resistance and maneuverability of the ship were simulated by self-programming. Liu (2012) [4] developed a type of ice material and inserted it into commercial software LS-DYNA to analyze the collision between a ship and an iceberg. The iceberg was defined as a plastic material and the corrosion of the unit was used to simulate the growth of the cracks. Kim et al. (2013) [5] simulated the resistance performance of a cargo ship under the conditions of broken ice. The numerical simulated results were compared with the results of the non-frozen model ice test in a water tank in South Korea and the cut ice test in an ice tank in Canada, and good agreements were both achieved. Kajaste-Rudnitski & Kujala (2014) [6] adopted commercial software ABAQUS to simulate the three-degree-of-freedom motion of the ship in the level ice. The results showed that the ice breaking is a stochastic process and time history of ice loads present a series of high peaks with very short duration.

It can be seen that most researches concerned the collision process between ice and ship when the ship is in a straight-forward movement. Seldom work studied ice-ship collision when the ship in a rotational motion. However, in the actual voyage, ship usually needs to turn or move in a curvilinear motion. At that time, the side of hull squeezes the ice strongly, so the transverse loads increase a lot. To study this problem, based on the nonlinear finite element method, this paper sets up a three-dimensional finite element model of the ship and the ice to simulate the process of ice-ship collision when the ship in a rotational motion. The longitudinal and transverse load curves of the hull are obtained, and the effects of various parameters are analyzed, including tangential velocity and angular velocity of the ship.

2 MODELLING PRINCIPLES

When a ship moves in the level ice, its bow breaks ice before the hull slides in the broken ice. The velocity of the ship is affected by the ice loads and may vary. However, in this paper, to simplify the simulation, we firstly assume that the ship is in a forced motion with a constant speed, whether the ship is in a straight motion or a rotational motion. Secondly, the effect of the water is assumed to be neglectable, considering the water load is small compared with the strong ice load. Under these assumptions, we consider a combined motion of the ship in the level ice. The ship moves straight forwards in a constant speed before turns in a constant angular velocity, so the velocity

in the global coordinates can be expressed as follows:

$$\begin{cases} x = \\ y = 0 \end{cases} \quad (t \leq t_0, \text{ or in the straight motion}) \quad (1)$$

$$\begin{cases} x = \cos[\omega(t - t_0)] \\ y = \sin[\omega(t - t_0)] \end{cases} \quad (t > t_0, \text{ or in the rotational motion}) \quad (2)$$

where v is the given constant speed, ω is the given angular velocity, t is the total time and t_0 is the end moment of the straight motion. Only 3 degrees of freedom of the ship movement are allowed—surge(x), sway(y) and yaw (φ). The origin of the local coordinates along with the body is fixed at the center of gravity of the ship, as shown in Fig.1, whose x axis points forwards, y axis points towards port and z axis points upwards. At the initial moment, the local coordinates coincide with the global coordinates.

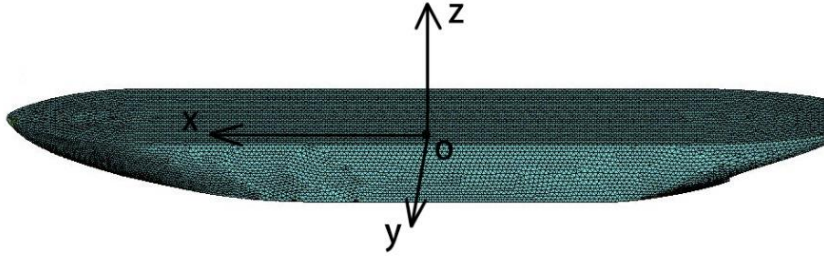


Figure1. Sketch of coordinates and finite element model of the ship

The length between perpendiculars of the ship is 147m, the beam of ship is 22.6m and the displacement is 18000DWT. The surface of the ship is meshed by triangular element, which is also shown in Fig. 1. The ship hull is presented as a rigid body. On the other hand, the main dimension of the level ice is 600m*350m*1m, and the boundary conditions of the ice is non-reflecting boundary. The material property of ice is simplified as Isotropic Elastic-Plastic with Failure model. When the stress or the strain of the element exceeds the set value in the finite element model, the element is invalid and will be deleted from the model. Ralston [7] first studied the yield conditions and plastic deformation of the failure of the ice, which proved the feasibility of ice materials by using the plastic theory. For ice, the principle of isotropic hardening is usually adopted to regulate the change rule of the yield function in the stress space after the material enters the plastic deformation. The von Mises yield criterion is used as the failure criterion of sea ice. The maximum plastic strain mode is used as the failure mode of materials, and the constant minimum pressure mode is used as the separation mode of materials [8].

In this paper, the model parameters of the ice are taken as those in Table 1:

Table.1 Ice model characteristics

RO Kg/m ³	G Gpa	$SIGY$ Mpa	$ETAN$ Gpa	$BULK$ Gpa	EPF	PRF Mpa	REM	$TREM$
900	2.2	2.12	4.26	5.26	0.35	-4	0	0

where RO is the mass density, G is the shear modulus, $SIGY$ is the yield stress, $ETAN$ is the plastic hardening modulus, $BULK$ is the bulk modulus, EPF is the plastic failure strain, PRF is the failure pressure, REM is the element erosion option, and $TREM$ is the time interval for the element removal.

3 SOLUTION METHOD

The nonlinear finite element method is adopted to simulate the ice-ship collision process. The solution method is introduced briefly. The motion equation of the ship can be expressed as:

$$Ma_n = F_n^{ext} + \quad_n - F_n^{int} - \quad v_n \quad (3)$$

where M is the mass matrix; \quad is the damping matrix; a_n and v_n are the acceleration vector and velocity vector at time t_n , respectively; F_n^{ext} is the external force vector; \quad_n is the hourglass resistance; F_n^{int} is the internal force vector, which is the sum of unit internal force and contact force. Eq. (3) can be rewritten as:

$$a_n = M^{-1}(F_n^{ext} + \quad_n - F_n^{int} - \quad v_n) \quad (4)$$

The center difference method is used to update the velocity vector v_{n+1} and displacement vector d_{n+1} of the ship in the time domain as:

$$v_{n+\frac{1}{2}} = v_{n-\frac{1}{2}} + \Delta t a_n \quad (5)$$

$$d_{n+1} = d_n + v_{n+\frac{1}{2}} \Delta t_{n+\frac{1}{2}} \quad (6)$$

where it is assumed that the acceleration is constant throughout the time step. Thus, if the node position d_n and acceleration a_n of the time step n and the node speed $v_{n-\frac{1}{2}}$ of time step $(n-1/2)$ have been obtained, the node speed $v_{n+\frac{1}{2}}$ of time step

$(n+1/2)$ and the displacement d_{n+1} of time step $(n+1)$ can be solved by using Eqs. (5) and (6).

As we know, the central difference method is conditionally stable and the time step must be smaller than a critical value Δt^{crif} to keep it stable. In this paper, it is found that this critical time step can be taken as:

$$\Delta t^{crif} = \frac{l}{c} \quad (7)$$

based on the numerical experience, where l is the minimum height of the unit, c is the sound velocity of material. In this paper, Δt is taken as 0.9 times of Δt^{crif} .

4 RESULTS AND DISCUSSIONS

4.1 Validation of numerical model

In order to validate the numerical model, we assume the ship in a straight motion and compare the ice resistance obtained by the numerical simulation with the empirical formula proposed by Lindqvist (1989) [9]. The moving velocity of the ship is taken as $=5\text{m/s}$.

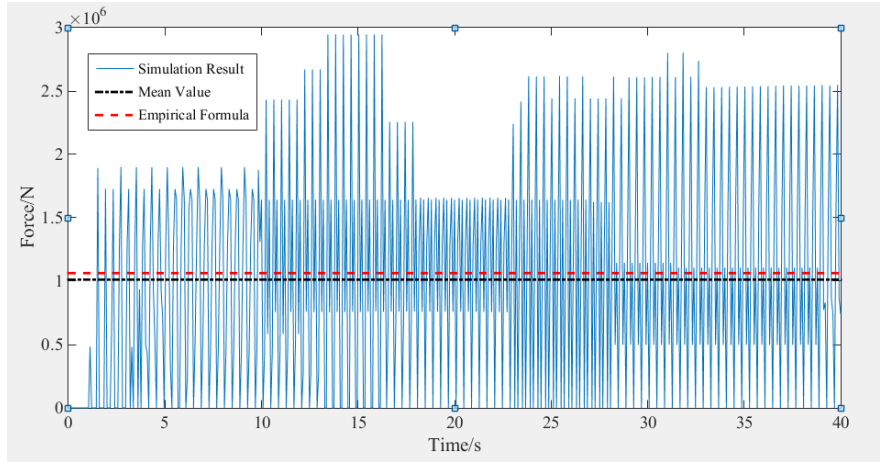


Figure 2. Comparison between results of numerical simulation and empirical formula

The comparison between results of numerical simulation and empirical formula is shown in Figure 2, where the fluctuate curve is calculated result with black dot-dash line as the mean value and the red broken line is the empirical-formula result. It can be seen that the average value of numerical simulation is very close to the value calculated by empirical formula. The result of empirical formula is 1.06MN and the average value of numerical simulation is 1.01MN, with a relative error 4.7%. Therefore, it can be considered that the numerical model is validated to some extent.

4.2 Analysis on ice loads

On the basis of the validation of numerical model, we consider the combined motion

of the ship in the level ice as mentioned in section 2. When the ship is in the rotational motion, the ice loads in local coordinates and those in global coordinates have the relationships as below:

$$F_{long} = F_x \cos(\omega(t-t_0)) + F_y \sin(\omega(t-t_0)) \quad (8)$$

$$F_{trans} = -F_x \sin(\omega(t-t_0)) + F_y \cos(\omega(t-t_0)) \quad (9)$$

where F_{long} and F_{trans} are the longitudinal and transverse ice forces in the local coordinate system, respectively; F_x and F_y are the x-directional and y-directional ice forces in the global coordinate system, respectively.

In this section, we take $v = 5\text{m/s}$, $\omega = 1^\circ/\text{s}$ and $t_0 = 40\text{s}$ as the example to discuss ice loads on the ship. Other parameters are taken same as section 2.

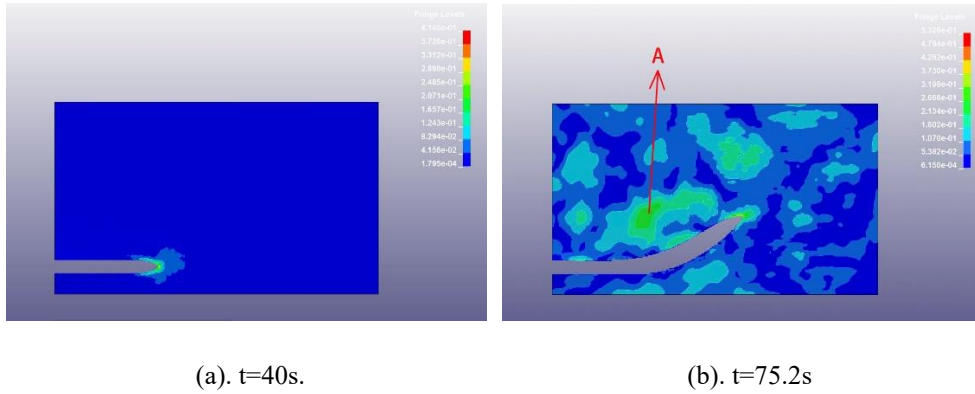
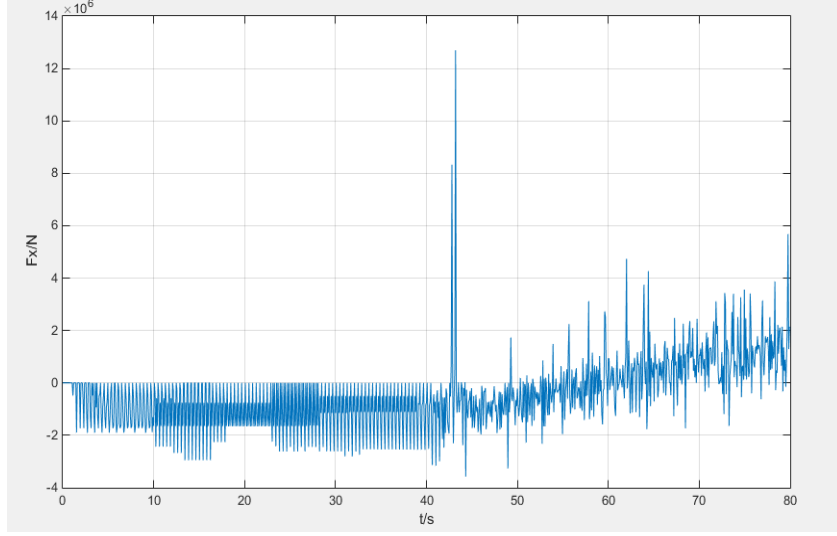


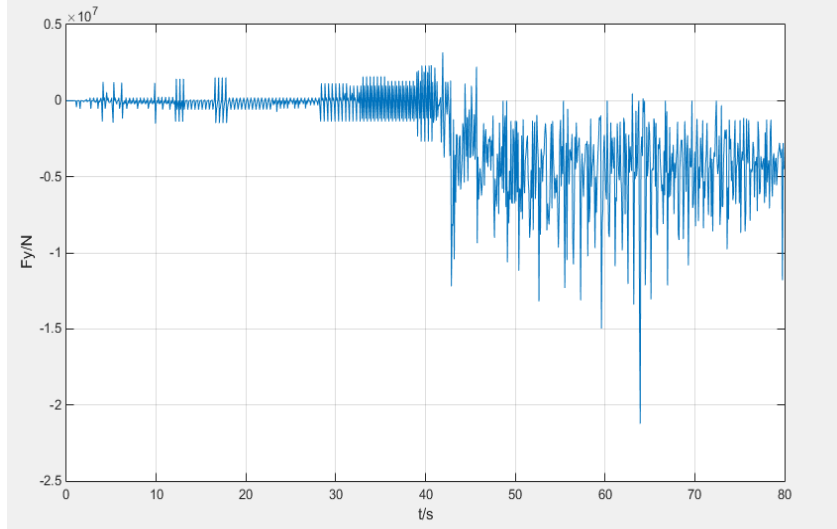
Figure 3. Von Mises stress contour on the level ice during ice-ship collision

Fig. 3 shows the trajectory of the ship and stress distribution on the level ice during ice-ship collision. Fig. 3 (a) and (b) correspond to straight forward and rotational stages, respectively. It can be seen in Fig.3 (a) that during the straight motion, the high-stress is mainly concentrated on the area near the bow. This is because the ice is extruded by the bow mainly and an ice channel whose width is a little wider than the ship beam is generated as a result. The rear part of the hull hardly contacts with the ice, so there is no stress almost. On the contrast, during the rotational motion, the stress presents a different distribution. There are two significant high-stress areas: one is in the area near the bow of the ship and the other is the area near the port of the ship. For the former, it can be understandable because the ship needs to open the channel like that in the straight motion stage. While for the latter, it is because the port of the ship contacts with and extrudes the ice in the inner side of the channel during its left constant-speed rotation. One may also notice there are also high-stress areas near the center of the turning circle. This phenomenon may be due to the ice material and failure mode adopted in this paper,

which will not be discussed here.



(a). F_x



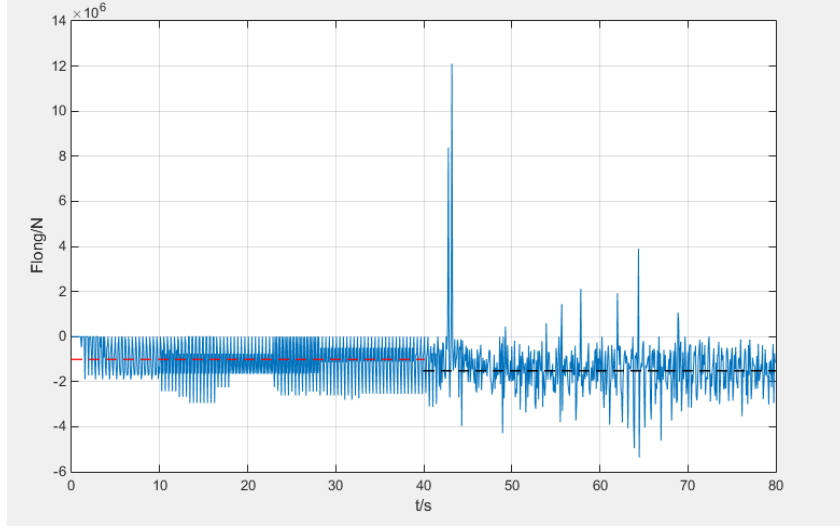
(b). F_y

Figure 4 Time histories of the ice loads in the global coordinates

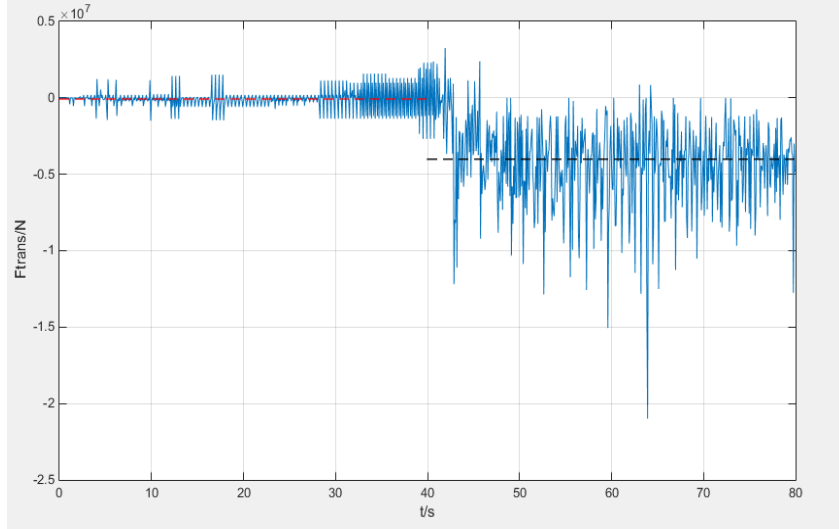
Time histories of ice loads F_x and F_y in the global coordinates are shown in the Fig. 4, where the first 40s corresponds to straight-forward motion. It can be seen from Fig. 4 that the time histories of ice loads present a series of high peaks with very short duration, which are the results of the transient and strong nonlinear ice-ship collision.

When the ship moves straight forward, F_x is always negative, which denotes the hull

is subjected to the resistance of ice, while F_y fluctuates around zero with an average value near zero. When the ship begins to rotate around the Z axis, the global reaction F_x and F_y in the global coordinates become complex and it will be easier to analyze in the local coordinates fixed on the ship, as shown in Fig.5.



(a). F_{long}



(b). F_{trans}

Figure 5. Time histories of the ice loads in the local coordinates

Time histories of the ice loads F_{long} and F_{trans} in the local coordinates are shown

in the Fig. 5. The relationships between Figs.4 and 5 are Eqs. (8) and (9). The ice loads in the straight-forward motion stage in Fig.4 and Fig.5 are the same, so we just discuss the ice loads in the rotational motion stage. From Fig. 5 (a), it can be seen that the oscillation of F_{long} gets larger under the effects of the turning movement. However, the average resistance of ice in the rotational motion stage is just a little larger than that in the straight-forward motion stage, because of the same forward velocity. On the other hand, F_{trans} becomes much larger negative when the ship starts to turn as shown in Fig. 5 (b). This great force to the starboard is due to the extrusion of the ice between the hull and the inner channel when the ship is turning left, or inwards herein, which can also be seen in the stress contour shown in Fig.3 (b). In other words, the ice will prevent the ship from moving inwards when the ship turns.

4.3 Influence of different parameters

The ice loads in the case study have been analyzed as shown in Sec.4.2. On this basis, the influences of forward velocity and angular velocity will be discussed in this section. As mentioned above, many scholars have studied the collision process at straight-forward movement. Therefore, this section only analyzes the effect of parameters on the ice loads during the rotation stage.

4.3.1 The effect of forward velocity

To study the effect of forward velocity, we keep angular velocity $\omega = 1^\circ/\text{s}$ constant and change forward velocity from $V = 2.5\text{m/s}$, to $V = 5\text{m/s}$ and then to $V = 7\text{m/s}$. The average longitudinal and the transverse ice loads of the ship in local coordinates at different forward velocities are shown in Fig. 6, where the minus denotes the force is opposite to the coordinate axis as discussed in Sec.4.2.

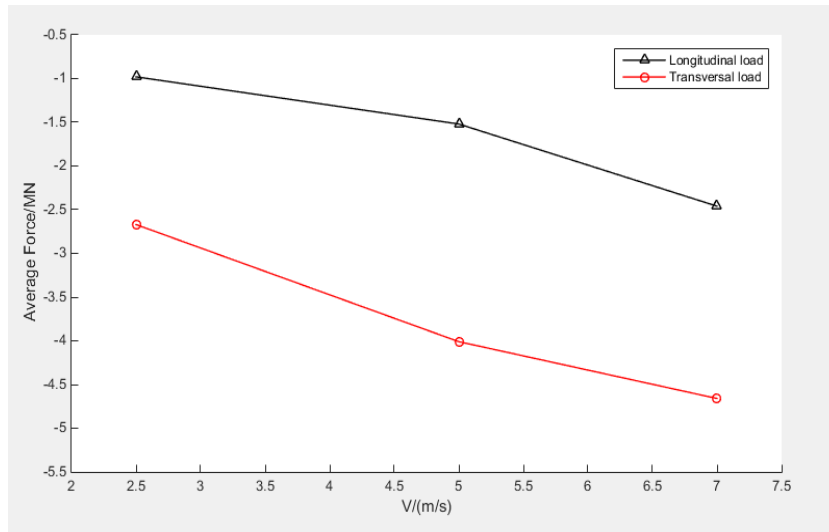


Figure 6. The change of ice loads with forward velocity ($\omega = 1^\circ/\text{s}$)

As can be seen from Fig. 6, both longitudinal and transverse ice loads increase significantly with forward velocity. In addition, the increase rate of the longitudinal force becomes larger than that of transverse force as the forward velocity rises. This can be predictable because the greater the forward velocity is, the severer the collision between the ice and ship is, particularly in longitudinal direction.

4.3.2 The effect of angular velocity

To study the effect of angular velocity, we keep forward velocity $V = 5\text{m/s}$ constant and change angular velocity from $\omega = 0.4^\circ/\text{s}$, to $\omega = 1^\circ/\text{s}$ and then to $\omega = 1.5^\circ/\text{s}$. The average ice loads of the ship at different angular velocities are presented in Fig. 7.

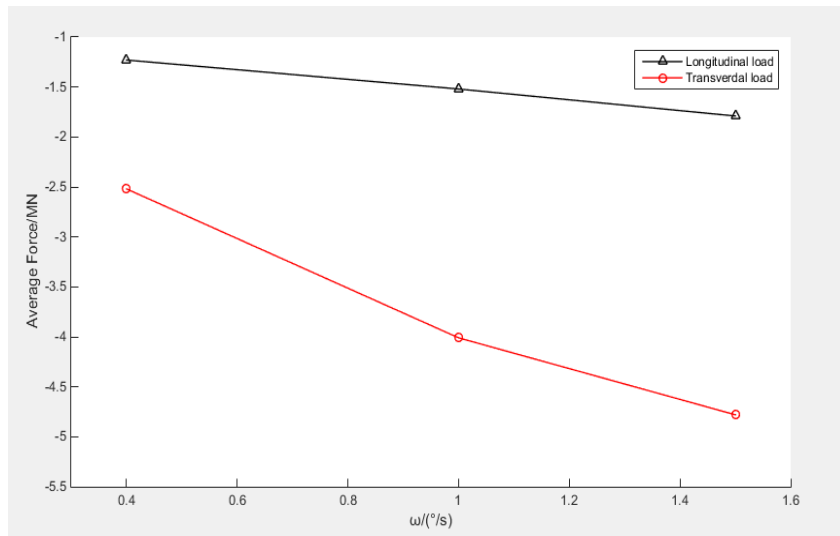


Figure 7. The change of ice loads with angular velocity ($V = 5\text{m/s}$)

It can be seen from Fig. 7 that both the longitudinal and transverse loads increase with the angular velocity, but it is obvious that the transverse load rises more rapidly. As one may know, $V = \omega R$, where R is the constant turning radius of the ship. When V remains and ω rises, one can easily obtain R reduces. A smaller turning radius will, of course, cause a severer contact, extrusion and collision for a given length of the ship during rotation, particularly in transverse direction.

CONCLUSIONS

In order to study the ice loads when the ship is moving in the level ice, the finite element method is adopted to simulate the motion of an ice-breaker under different movements. Main conclusions can be drawn from the numerical simulations:

- -Nonlinear finite element method is effective to study the transient and strong collision between ship and ice with appropriate ice material and failure modes. The ice loads present sawtooth configuration with large amplitudes and very high frequencies.

Its average loads in the straight motion is close to that obtained by the empirical formula.

- -Different from that only longitudinal ice resistance can be observed in the straight motion, both longitudinal and transverse loads can be obtained in the rotation motion. Transverse loads, which are caused by the extrusion between level ice and the side of the ship, prevent the ship from turning inwards.
- - Both absolute values of average longitudinal and transverse loads rise along with the increase of forward velocity or angular velocity. It is found that longitudinal ice loads rise more rapidly than transverse ones with forward velocity, while transverse ice loads rise more rapidly than longitudinal ones with angular velocity on the contrast.

ACKNOWLEDGEMENTS

This work is supported by the National Key R&D Program of China (No. 2017YFE0111400), National Natural Science Foundation of China (Nos. 51639004, 51579054 and 11472088), the Fundamental Research Funds for the Central Universities (No. HEUCFG201811), the 111 Project in HEU, and Lloyd's Register Foundation through the joint centre involving University College London, Shanghai Jiaotong University and Harbin Engineering University, to which the authors are most grateful. Lloyd's Register Foundation helps to protect life and property by supporting engineering-related education, public engagement and the application of research.

REFERENCES

- [1]. Valanto, P. Spatial distribution of numerically predicted ice loads on ship hulls in level ice. Report for Deliverable D6-3 of SAFEICE Project. (2007).
- [2]. Wang B, Yu H C, Basu R. Ship and Ice Collision Modeling and Strength Evaluation of LNG Ship Structure[C]// ASME 2008, International Conference on Offshore Mechanics and Arctic Engineering. 2008:121-6.
- [3]. Su B. Numerical Predictions of Global and Local Ice Loads on Ships[J]. Department of Marine Technology, 2011.
- [4]. Liu Z. Analytical and numerical analysis of iceberg collisions with ship structures[J]. Marin Teknologi, 2012.
- [5]. Kim M C, Lee S K, Lee W J, et al. Numerical and experimental investigation of the resistance performance of an icebreaking cargo vessel in pack ice conditions[J]. International Journal of Naval Architecture and Ocean Engineering, 2013, 5(1): 116-131.
- [6]. Kajaste-Rudnitski J., Kujala P. Ship propagation through ice field[J]. Rakenteiden Mekaniikka. (Journal of Structural Mechanics). 2014, 47(2):34-49.
- [7]. Ralston T D. Yield and plastic deformation in ice crushing failure: Preprint), ICSI/AIDJEX Symposium on Sea Ice--Processes and Models, Seattle, Washington, 1977.
- [8]. Hallquist J O. LS-DYNA Theory Manual[R]. California: Livermore Software Technology Corporation, 2006.

Li Z.P. Ni B. Y. Yang D. Han D. F.

[9]. Lindqvist G. A straightforward method for calculation of ice resistance of ships[J]. Performance, 1989.

A Hamiltonian-based Approach for Thermal Buckling of a Functionally Graded Magneto-electric Orthotropic Cylindrical Shell

Yiwen Ni^{*}, Zhenzhen Tong^{**}, Shengbo Zhu^{***}, Xinsheng Xu^{****}

^{*}Dalian University of Technology; City University of Hong Kong Shenzhen Research Institute, ^{**}Dalian University of Technology, ^{***}Dalian University of Technology, ^{****}Dalian University of Technology; City University of Hong Kong Shenzhen Research Institute

ABSTRACT

The magneto-electro-elastic (MEE) shells with coupling effects are widely used in a variety of intelligent systems such as sensors and actuators. In practice, the MEE shell usually has a non-uniform distribution of stresses. The bonding agent may crack or peel off at low temperature or may creep at high-temperature which could lead to reliability and lifetime limitations. To avoid this, functionally graded (FG) MEE shells without any bonding agent have attracted much attention in recent years. Therefore, the study on dynamic behaviors of such shells is of serious consequence for their strength and safety designs. This paper aims to present a new analytical symplectic solution for thermal buckling of FG MEE orthotropic cylindrical shells. Though adopting the Reissner's shell theory and the symplectic mathematics, the governing equations of MEE medium involving mechanical, electrical and magnetic fields in the classical Lagrangian system is rebuilt in the Hamiltonian system. The high-order governing differential equation is reduced to a set of ordinary differential equations which can be analytically solved by the method of separation of variables. The thermal buckling problem is converted into solving of the symplectic eigenvalues and eigenfunctions. Critical thermal buckling loads are computed and presented in the numerical examples. Comparisons are presented to show the accuracy of the analytical solution procedure. A detailed parametric study is carried out to investigate the influences of the FGM magneto-electric properties and boundary conditions. Some new results are given also. The present study demonstrates that the general solutions of displacement, electric potential and magnetic potential highly depend on the computation parameters. The pre-determined general solution (e.g., trigonometric functions) used in the classical analytical method may lead to inappropriate results in some cases. In addition, the present accurate cylindrical shell model will provide more reasonable guidance to the design.

Concurrently Coupled Peridynamics/Finite Element Simulation Based on Nonlocal Matching Boundary Condition

Clint Nicely^{*}, Dong Qian^{**}

^{*}Raytheon Space and Airborne Systems, ^{**}The University of Texas at Dallas

ABSTRACT

Peridynamics (PD) is a reformulation of the continuum theory based on an integro-differential formulation. With its unique capability in incorporating material length scale, there is a continuing interest in establishing multiscale computational methods that integrate PD with continuum scale simulation methods. In this presentation, a concurrent multiscale approach has been established to couple a stabilized non-ordinary peridynamics (SNOPD) with finite element method (FEM). In order to minimize the artificial wave reflection that is present within coupling methods a Non-Local Matching Boundary Condition (NMBC) is developed for treating the numerical peridynamic interface. The NMBC is cast in the form of a parameterized expression that involves the displacements and their higher-order time derivatives of peridynamic (PD) nodes at the numerical interface. Non-reflective and wave transmitting conditions are realized by zeroing the associated residual and its higher order derivatives that are functions of the dispersion relation at the particular wave length of interest. Both 1D and 2D versions of NMBCs have been established and it is shown that the 1st order NMBC for 2D SNOPD is applicable for both unidirectional and multidirectional waves. A bridging scale decomposition employing a projection approach is introduced in the concurrent multiscale discretization to realize a seamless information passage between the PD and FEM simulation. Multiple examples are given to demonstrate the effectiveness of the coupling method comparing a direct coupling, a coupling with only projection of the PD result, and finally a method using the projection and NMBC combined. These examples demonstrate the high effectiveness of the NMBC coupling approach.

A Stable Formulation of Resonant Maxwell's Equations in Cold Plasma

Anouk Nicolopoulos*, Bruno Després**, Martin Campos Pinto***

*LJLL, **LJLL/IUF, ***LJLL/CNRS

ABSTRACT

A hybrid resonance phenomena is considered here for the heating of magnetic confinement fusion plasma. It is obtained sending high frequency electromagnetic waves into the plasma. Mathematically, it corresponds to a singular solution of the harmonic in time Maxwell's equations. Under some uniformity assumptions of the plasma, we work on the equations in 1D. The problem is that the equations are ill posed, meaning that there is no uniqueness of the solution. But the equations can be regularized introducing a small viscosity parameter to modelize the friction between ions and electrons. We then select the physical solution to our limit problem making that viscosity go to zero. From a numerical point of view, taking a small viscosity parameter is not satisfying as this small parameter should be linked to the discretization in space step. This is why we chose to characterize the limit solution. Constructing a family of manufactured functions based on the expected singularity of one over x of our electric field, energy relations on the scaled difference between the real electromagnetic fields and the manufactured ones have then been derived to construct a variational formulation for the limit problem. The formulation we obtained fits in the frame of classical mixed variational formulations, and its structure allows us to ensure its well-posedness, in the sense that there is a solution, which is unique. Furthermore, this formulation is stable in the sense that it is the limit of a mixed variational formulation for the viscosity problem. This feature is interesting for numerical simulations as the viscosity is of various orders of magnitude in a tokamak, and it also gives us additional information on the solution of our resonant equations. This work will be illustrated by numerical results using the finite element method to discretize these formulations. First in the X-mode case, meaning the heating wave sent into the plasma is of normal incidence, and which allows us to decouple the equations into two systems. Then in the mode-coupling case of oblique incidence.

ULTRA-FAST, HIGH-FIDELITY COMPUTATIONAL FLUID DYNAMICS ON GPU FOR AUTOMOTIVE AERODYNAMICS

CHRISTOPH A. NIEDERMEIER*, CARLO DEL BENE*,
CHRISTIAN F. JANSSEN[†], BASTIAN SCHNEPF[†],
MARC RATZEL[†] AND THOMAS INDINGER*

*FluidDyna GmbH
Edisonstr. 3
85716 Unterschleißheim, Germany
{christoph.niedermeier,carlo.del.bene,thomas.indinger}@fluidyna.de

[†]Altair Engineering GmbH
Calwer Str. 7
71034 Böblingen, Germany
christian.janssen@altair.com, schnepf@altair.de, ratzel@altair.com

Key words: LBM, GPU, Automotive Aerodynamics.

Summary. In this work, we present the innovative commercial GPU-based Computational Fluid Dynamics (CFD) solver ultraFluidX. The software is based on the Lattice Boltzmann Method (LBM), which is explicit in time, hence inherently transient and which only requires nearest-neighbor information for each point of the computational grid. Therefore, LBM is a perfect match for the massively parallel architecture of GPUs and highly benefits from their tremendous computational power. Additionally, ultraFluidX can make use of multiple GPUs through an efficient implementation based on CUDA-aware MPI. The software thereby achieves unprecedented turnaround times of just a few hours for transient flow simulations of fully detailed production-level passenger and heavy-duty vehicles. This work features simulations of the DrivAer model, a generic, publicly available vehicle geometry that was developed by the Chair of Aerodynamics and Fluid Mechanics at the Technical University of Munich and which is widely used for testing and validation purposes nowadays.

1 INTRODUCTION

The optimization of aerodynamic properties of a vehicle plays a crucial role in the automotive design process. In the case of interurban travel, the biggest portion of the driving resistance is induced by aerodynamic drag. Moreover, there are other secondary goals, such as driving stability and ride comfort, that are influenced by the vehicle's aerodynamics. For such a sophisticated level of aerodynamic optimization, it is very important to have as much knowledge as possible about the flow field around the vehicle under consideration. This can only be achieved through a CFD simulation, where the full three-dimensional information can be easily extracted from the

numerical results in contrast to, e.g., wind tunnel testing. The flow field in such a case is very complex and highly unsteady, and the corresponding CFD simulations must be fully transient and highly resolved to capture all relevant physical effects. This was posing a big challenge for automotive OEMs so far, because such simulations based on pure CPU systems are typically constraint by available computational resources and in general also very expensive. The situation now changes drastically with GPU-based CFD, where well-suited methods like LBM can achieve turnaround times of just a few hours for the aforementioned use cases.

2 ULTRAFLUIDX

The current contribution is based on the commercial GPU-based CFD solver ultraFluidX. ultraFluidX is developed by FluidDyna GmbH, a wholly-owned subsidiary of Altair Engineering. The main motivation for the development of the code is to introduce higher fidelity models, fully transient analyses, small turnaround times and low total cost to automotive OEMs around the world. ultraFluidX is based on the Lattice Boltzmann Method, which is explicit in time, hence inherently transient and which only requires nearest-neighbor information for each point of the computational grid. Therefore, ultraFluidX highly benefits from the tremendous computational power of the massively parallel architecture of GPUs and can additionally make use of multiple GPUs through an efficient implementation based on CUDA-aware MPI. The solver thereby achieves unprecedented turnaround times of just a few hours for transient flow simulations of fully detailed production-level passenger and heavy-duty vehicles.

ultraFluidX uses a recent, highly accurate LBM collision operator based on Cumulants [1-3], which is accompanied by an LBM-consistent Smagorinsky LES model [4] and a wall modeling technique based on the work of Malaspinas & Sagaut [5] and Wang & Moin [6]. The Cartesian LBM base mesh is combined with an octree-based grid refinement. Starting from a relatively coarse Cartesian background grid, the mesh is consecutively refined towards the obstacle surface. Between each refinement level, the mesh spacing is reduced by a factor of 2. The first refinement levels are typically defined via axis-aligned bounding boxes, higher refinement levels closer to the geometry are either based on custom user-defined volumes or defined via geometry offsets. Kinks and thin parts are fully resolved in the volumetric preprocessing. Moreover, the appropriate physical modeling is selected automatically inside tight gaps and cavities. Representative production-level volume meshes are generated within the order of one hour.

In addition, the code contains several enhanced features for automotive applications. These features typically come with additional computational overhead, which has to be considered in the performance evaluation and in comparison to other available software packages. ultraFluidX nevertheless achieves a parallel strong scaling efficiency of more than 80% for a realistic production-level case even when using these enhanced features [7], which include, but are not limited to, porous media zones, support for moving floors (single- and five-belt systems), static floors with boundary layer suction, rotating wheel models (straightforward wall-velocity boundary conditions or more advanced MRF and overset grid approaches) and automatic convergence detection. The code also features advanced post-processing capabilities, such as window averaging, spatial drag/lift contributions, probe output and section cut output.

3 DRIVAER MODEL WITH ENGINE BAY FLOW

The DrivAer model [8] was introduced by Heft et al. [9] to address the need for a generic geometry for investigations of automotive aerodynamics that is somewhere in between rather simple, academic models like the Ahmed body and very complex, production-level vehicle geometries of automobile manufacturers. The original DrivAer model already featured different rear end and underbody designs, however, it was only available in mock-up configuration and hence missing the possibility to include flow through the engine bay. Therefore, Wittmeier & Kuthada [10] lately presented an update with additional underhood flow to make the model even more realistic. This model was then used by Collin et al. [11] in their recent work, where they performed both wind tunnel tests and numerical simulations of the 40% scale open cooling geometry using perforated aluminum sheets with different opening ratios to mimic different radiator properties. Below, we will compare some of the results from these wind tunnel tests with numerical results obtained with ultraFluidX.

3.1 Case setup

The simulations are performed with the 40% scale DrivAer open cooling notchback model with open wheelhouses and closed rims using a rectangular computational domain with a constant-velocity inlet, slip walls at the sides as well as at the top and a non-reflecting outlet. Additionally, Figure 1 shows the mixed boundary conditions that are used at the ground of this numerical wind tunnel to account for the moving belt system and the passive boundary layer scoop that were used for the experiments by Collin et al. [11] at the Technical University of Munich.

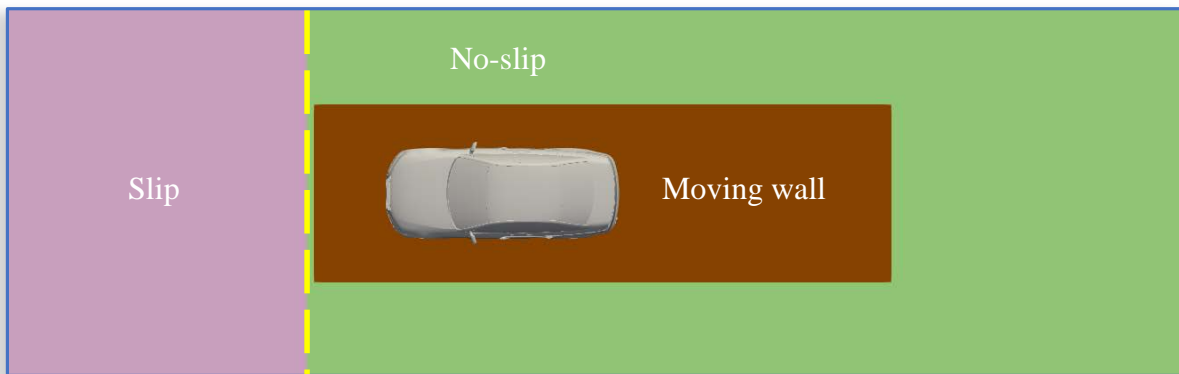


Figure 1: Boundary conditions at the wind tunnel ground.

The inlet velocity is 44 m/s and the density, temperature and kinematic viscosity of the air are assumed to be 1.135 kg/m³, 27.6 °C and 0.0000163 m²/s, respectively. Three different cases with opening ratios (A_o/A_c) of 12.3%, 19.7% and 28.3% for the perforated aluminum sheets are simulated. For doing so, each of the respective pressure drop curves provided by Collin et al. [11] is converted into viscous and inertial resistances that have to be provided as input parameters to the porous media zones in ultraFluidX.

A mixture of axis-aligned bounding boxes, user-defined volumes and geometry offsets is used to refine the computational grid in relevant areas like the wake, the engine bay and sensitive regions along the surface. The minimum grid size at refinement level 7 is 0.6 mm and the grid overall consists of 156.6 million voxels with 57.5 million so-called fine equivalents, Figure 2 shows the computational grid in the y-normal symmetry plane of the wind tunnel.

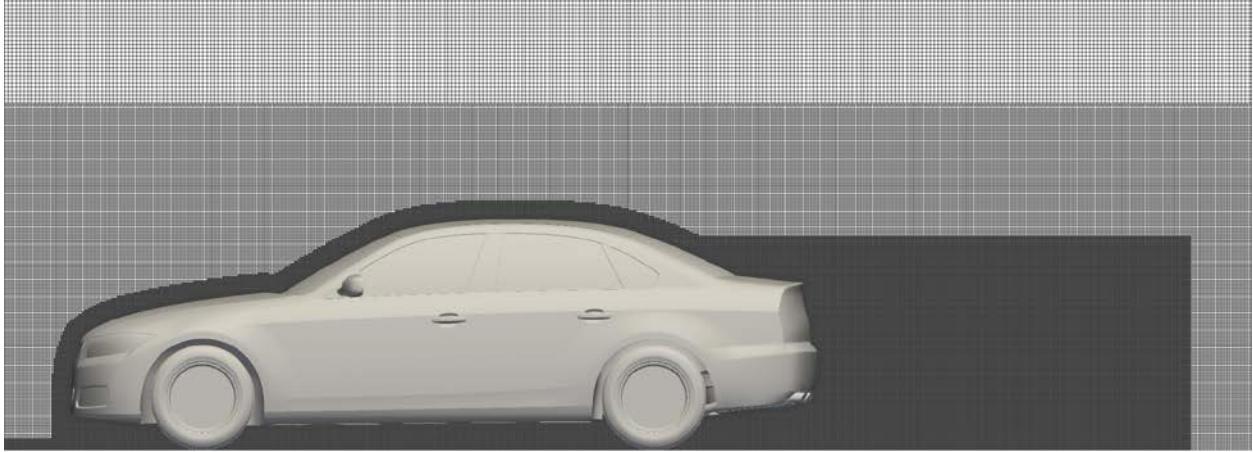


Figure 2: Computational grid in the y-normal symmetry plane of the wind tunnel.

The physical simulation time is 1.276 s, which corresponds to 30 flow passes over the vehicle. Additionally, the simulations are run at twice the original Mach number, which is a common technique for LBM to reduce the necessary number of iterations if only the aerodynamic properties are of interest.

3.2 Numerical results and performance

The simulations are performed on an NVIDIA DGX-1 with eight NVIDIA Tesla V100 GPUs, where they exhibit an overall performance of 2,208 million node updates per second (MNUPS), so 276 MNUPS per GPU. This results in a computation time of only 4.7 h with the case setup as mentioned above. If we also take into account the meshing time of 0.8 h, the total turnaround time is just 5.5 h.

A short time-to-solution is of course only beneficial if the solution is also accurate. Figure 3 shows the instantaneous velocity magnitude in the y-normal symmetry plane of the wind tunnel. Even small turbulent structures, e.g., in the wake region, are clearly visible, meaning that both the spatial as well as the temporal resolution of the simulation are sufficient to capture such effects. However, the most interesting quantities for an aerodynamic analysis are usually still the deltas between the drag and lift coefficients due to certain changes of the vehicle geometry or the simulation parameters. These deltas are then usually used to assess if a design change or an attachment part like, e.g., a spoiler has the desired aerodynamic effect.

In this work, we use the deltas between different opening ratios to analyze if ultraFluidX can predict the same trends for the drag, front lift and rear lift coefficients that were measured in the wind tunnel by Collin et al. [11]. For doing so, we use the opening ratio of 12.3% as a baseline

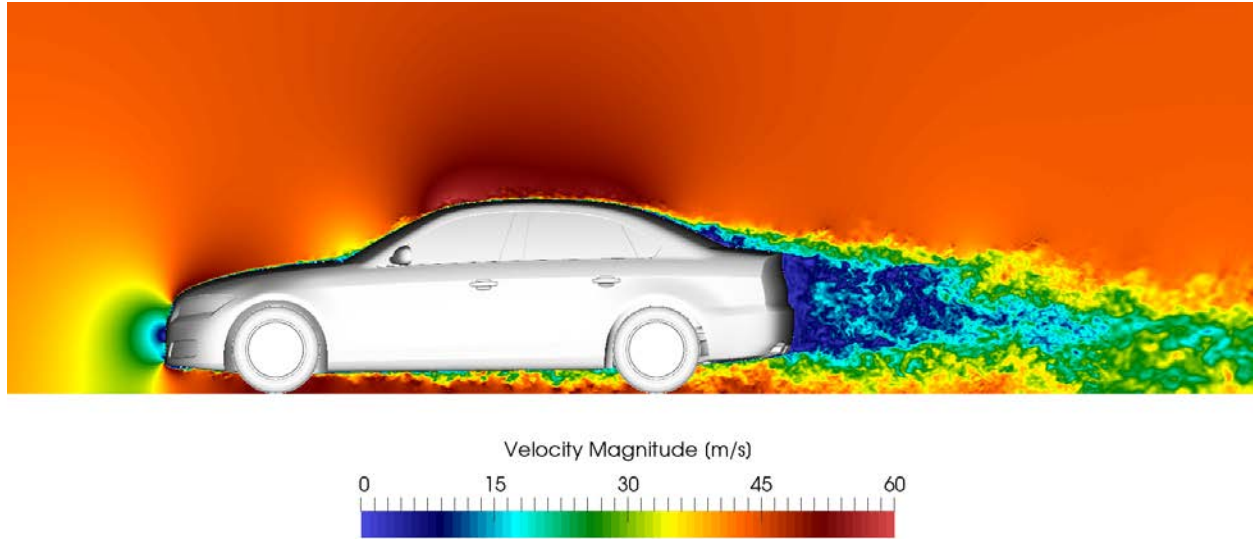


Figure 3: Instantaneous velocity magnitude in the y-normal symmetry plane of the wind tunnel.

and compare the deltas that we get for 19.7% and 28.3%. Figure 4 shows the deltas of the drag coefficient and the ultraFluidX results exhibit an excellent agreement to the deltas measured by Collin et al. [11] within less than 1 count, which means that the difference is less than 0.001. A similar observation can be made in Figure 5 for the deltas of the front lift coefficient, which almost exactly match for the opening ratio of 19.7% and still only differ by approx. 2 counts for 28.3%. Figure 6 finally shows the deltas of the rear lift coefficient, the agreement for 19.7% with a deviation of approx. one count is also excellent, just the difference for 28.3% is higher and reaches a maximum value of 6 counts. However, this is still within a reasonable range and the especially the trend from 12.3% to 19.7% and 28.3% is correctly captured for all coefficients, which is very important for a consistent evaluation of parameter changes.

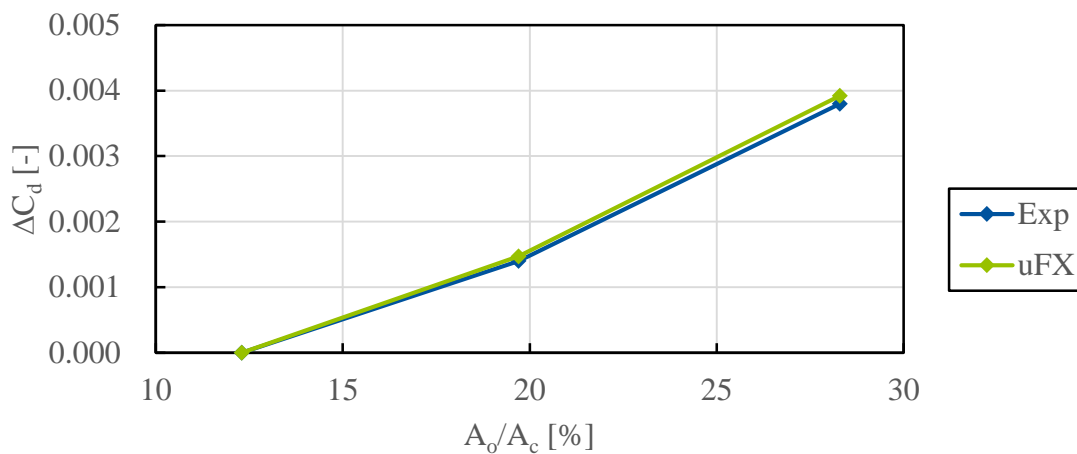


Figure 4: Deltas of the drag coefficient w.r.t. an opening ratio of 12.3% obtained with ultraFluidX (uFX) and compared with reference data by Collin et al. [11] (Exp).

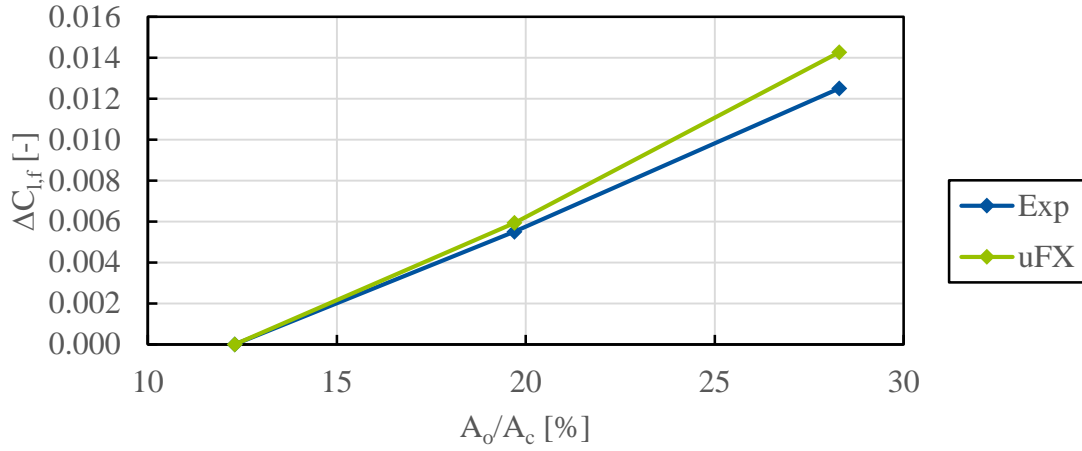


Figure 5: Deltas of the front lift coefficient w.r.t. an opening ratio of 12.3% obtained with ultraFluidX (uFX) and compared with reference data by Collin et al. [11] (Exp).

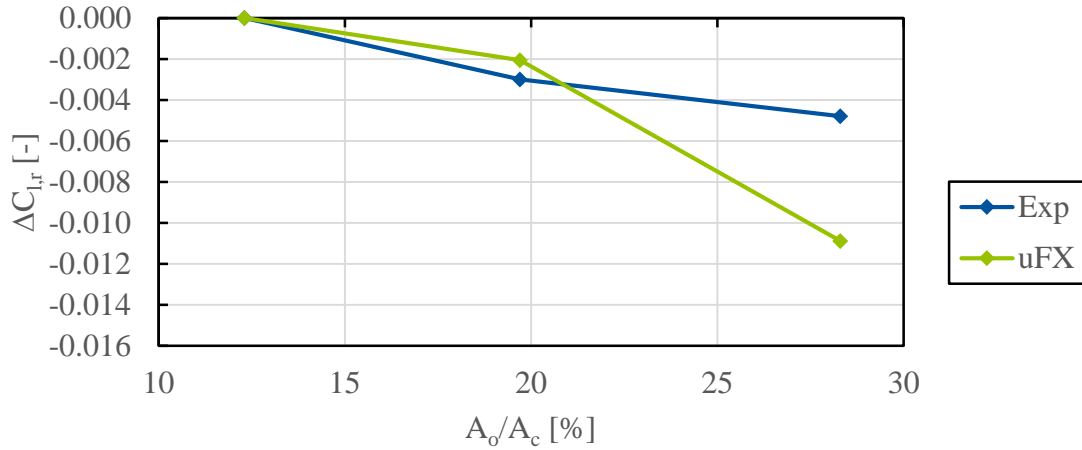


Figure 6: Deltas of the rear lift coefficient w.r.t. an opening ratio of 12.3% obtained with ultraFluidX (uFX) and compared with reference data by Collin et al. [11] (Exp).

4 SUMMARY AND CONCLUSION

In this work, we presented the innovative commercial GPU-based CFD solver ultraFluidX and used it to perform simulations of the recently updated 40% scale DrivAer notchback model with engine bay flow. Drag and lift trends compared to experimental reference data can be reproduced very well within just 5.5 h of total wall time per simulation, while the maximum resolution of the grid is as high as 0.6 mm and the total size of the case is more than 150 million voxels. Therefore, by using an advanced LBM collision operator and by leveraging the massively parallel architecture

of GPUs, ultraFluidX can deliver accurate, fully transient results within unprecedented turnaround times of just a few hours on a single compute node. This creates completely new possibilities for automotive OEMs to use even highly resolved, high-fidelity simulations for simulation-driven design processes on a daily basis.

REFERENCES

- [1] Geier, M., Schönherr, M., Pasquali, A., & Krafczyk, M. (2015). The cumulant lattice Boltzmann equation in three dimensions: Theory and validation. *Computers & Mathematics with Applications*, 70(4), 507-547.
- [2] Geier, M., Pasquali, A., & Schönherr, M. (2017). Parametrization of the cumulant lattice Boltzmann method for fourth order accurate diffusion part I: Derivation and validation. *Journal of Computational Physics*, 348, 862-888.
- [3] Geier, M., Pasquali, A., & Schönherr, M. (2017). Parametrization of the cumulant lattice Boltzmann method for fourth order accurate diffusion Part II: Application to flow around a sphere at drag crisis. *Journal of Computational Physics*, 348, 889-898.
- [4] Malaspinas, O., & Sagaut, P. (2012). Consistent subgrid scale modelling for lattice Boltzmann methods. *Journal of Fluid Mechanics*, 700, 514-542.
- [5] Malaspinas, O., & Sagaut, P. (2014). Wall model for large-eddy simulation based on the lattice Boltzmann method. *Journal of Computational Physics*, 275, 25-40.
- [6] Wang, M., & Moin, P. (2002). Dynamic wall modeling for large-eddy simulation of complex turbulent flows. *Physics of Fluids*, 14(7), 2043-2051.
- [7] Niedermeier, C. A., Janßen, C. F., & Indinger, T. (2018, June). Massively-parallel Multi-GPU Simulations for Fast and Accurate Automotive Aerodynamics. In *7th European Conference on Computational Fluid Dynamics*.
- [8] Technical University of Munich. DrivAer Model. Retrieved from <http://www.drivaer.com>
- [9] Heft, A. I., Indinger, T., & Adams, N. A. (2012). *Introduction of a new realistic generic car model for aerodynamic investigations* (No. 2012-01-0168). SAE Technical Paper.
- [10] Wittmeier, F., & Kuthada, T. (2015). Open grille DrivAer model-first results. *SAE International Journal of Passenger Cars-Mechanical Systems*, 8(2015-01-1553), 252-260.
- [11] Collin, C., Müller, J., Islam, M., & Indinger, T. (2017, September). On the Influence of Underhood Flow on External Aerodynamics of the DrivAer Model. In *FKFS Conference* (pp. 201-215). Springer, Cham.

Extreme-Scale Unstructured-Grid CFD Algorithms for a Many-Core Landscape

Eric Nielsen^{*}, Justin Luitjens^{**}, Aaron Walden^{***}, Mohammad Zubair^{****}

^{*}NASA Langley Research Center, ^{**}NVIDIA Corp, ^{***}NASA Langley Research Center, ^{****}Old Dominion University

ABSTRACT

We explore the transition of an unstructured-grid CFD code from a flat MPI model to a shared-memory model suitable for a many-core landscape. Included are node-level studies of computationally intensive CFD kernels on the Intel Xeon Phi Knights Landing, NVIDIA Pascal P100, and NVIDIA Volta V100 architectures. Performance comparisons are shown, and scaling studies on several modern supercomputing systems including the new IBM Power9/NVIDIA V100 system located at Oak Ridge National Laboratory known as Summit are also included. Meshes with billions of elements are used to demonstrate GPU performance equivalent to over one million Xeon cores.

Coupled Finite Element Analysis Model of Structural and Electrical Coupled Analysis for Electrical Contact Resistance

Tomoya Niho^{*}, Hiroyuki Kuramae^{**}, Daisuke Ishihara^{***}, Tomoyoshi Horie^{****}

^{*}Kyushu Institute of Technology, ^{**}Osaka Institute of Technology, ^{***}Kyushu Institute of Technology, ^{****}Kyushu Institute of Technology

ABSTRACT

Electrical contact resistance plays important role in melting and bonding of interface between steel sheets for resistance spot welding. Although many researchers have proposed theoretical models of electrical contact resistance[1], microscale structural and electrical coupled finite element analysis is required to evaluate electrical contact resistance because its characteristics depend on the real contact surface, elasto-plastic large deformation contact, electric current and temperature. In this study, we discuss a microscale structural and electrical coupled finite element analysis for the electrical contact resistance[2]. In this analysis, the structural analysis with elasto-plastic, large deformation and contact effect is performed using measured surface based finite element analysis model and temperature dependent material properties. Deformed shape obtained by the structural analysis is used for the electrical analysis considering temperature dependent electrical resistivity. In the microscale electrical contact resistance analysis, statistically similar representative volume element (SS-RVE) size and mesh resolution are important to obtain the accurate results. On the other hand, the large computational cost is required for 3D coupled analysis. The electrical contact resistance analyses are performed to discuss the SS-RVE size, mesh resolution and computational cost. The electrical contact resistance analyses are performed for 270 MPa grade, 440 MPa grade and 980 MPa grade tensile strength steel sheets to confirm the validity of the proposed analysis method. The dependency of the electrical contact resistance on the contact pressure and the temperature are compared with that of Babu's model[3] and experimental results from the viewpoint of these path dependencies. [1] M. Hamed and M. Atashparva. A Review of Electrical Contact Resistance Modeling in Resistance Spot Welding. *Welding in the World*, Vol. 61, No. 2, pp. 269 - 290, 2017. [2] T. Niho, K. Kubota, H. Aramaki, H. Kuramae, D. Ishihara and T. Horie, Microscale Electrical Contact Resistance Analysis for Resistance Spot Welding, *Proceedings of VII International Conference on Computational Methods for Coupled Problems in Science and Engineering 2017*, pp. 1152-1158, 2017. [3] S.S. Babu, M.L. Santella, Z. Feng, B.W. Riemer, and J.W. Cohron, Empirical Model of Effects of Pressure and Temperature on Electrical Contact Resistance of Metals, *Science and Technology of Welding and Joining*, Vol. 6, No. 3, pp. 126-132, 2001.

Geometry Optimization of Nitinol Stent Design: Comparing Old and New Design Using Finite Element Method

Dalibor Nikolic*, Igor Saveljic**, Nenad Filipovic***

*BioIRC - Research and Development Center for Bioengineering, **BioIRC - Research and Development Center for Bioengineering, ***Faculty of Engineering University of Kragujevac

ABSTRACT

OBJECTIVE In-stent restenosis struct shape and thickness have significant impact, especially if stent was implanted in the small arteries. In this paper author suggest novel approach for better geometry stent modeling – topology optimization process on existing stent design. For evaluation of the topology optimization and mechanical performance of nitinol stents and comparing differences between old design (non-optimized) and new optimized design the finite element method was used. The Z-shaped closed-cell self-expanding stent type for testing was used. This type of stent is most common in clinical practice. For better understanding of the mechanical process inside of the stent device for researcher is very important to simulate them and compare the results. **METHOD** Geometrically of stent model was used from Palmaz-Schatz first stent model. Finite element method (FEM) was performed assuming that the stents device used for this research were made by laser cutting, from tube form, by application of expanding and crushing force. The behavior of two different stent models was analyzed: old Palmaz-Schatz design and optimized design obtained based on the results from topology optimization of the Palmaz-Schatz design. Palmaz-Schatz stent geometry is a very simple geometry with enormous potential for modification this is the main reason why this geometry was used in this research. **RESULTS** By compering of simulation result between old Palmaz-Schatz and new modern and optimized design, it can be noticed that maximal stress and strain are much lower on the modern design model than on the old design model. Also, from distribution of stress and strain conclusion could be made that the old design has a lot of problematic positions with stress and strain concentration. **CONCLUSION** Performed simulation on stent models show that the new modern design has better clinical behavior due to lower contacting surface, higher radial resistive strength and much better superplastic behavior. Optimization process based on two optimization rules: minimization of the model volume and retention (or increase) of the maximal strain of the basic model.

Dynamic Analysis of B-train Articulated Vehicle

Barbieri Nilson*, Rubem Melo**, Key Lima***

*PUCPR, **PUCPR, ***PUCPR

ABSTRACT

The new Brazilian Regulations 210 and 211/2006 of the CONTRAN, had authorized the circulation of new Cargo Vehicles Combinations. Because their major load capacity, the numbers of these new models grew quickly, mainly b-trains, road-trains and semi-trailers with spaced axles. Certainly representative of a cargo vehicles evolution because the increase of productivity that provide and for the reduction of the costs and pollution with the road cargo transport, these new models must be observed about their characteristics of handling and security. Because the number of articulations, these combinations have specific phenomenon that affect their handling. Among them, the most important is the "rearward amplification". In consequence of this rear amplification, the last unit is exposed to highest lateral acceleration, and can rollover, taking with it other vehicles of combination. The semi-trailers with spaced axles have higher resistance to maneuvering that can bring tires wear and need higher friction demand in the tractor-vehicle during the maneuvers. A revision about the characteristics is necessary for the evolution of the vehicles project, roads design and traffic signs. There is also the necessity to include specific instructions for the drivers. In this work, the dynamic behavior of a b-train vehicle with liquid cargo is analyzed. The vehicle is subjected to evasive maneuvers and the vibration data is obtained through four accelerometers positioned along the vehicle. The liquid cargo is varied from 100, 80, 60 and 40% of the total capacity. The results evidential the phenomenon slosh through the variation in the loads of the wheels. Mathematical models use high order nonlinear polynomials to adjust system parameters. The results show great agreement between the numerical and experimental values of the lateral accelerations.

A Boundary Integral Equation (BIE) Method for Modeling Flow Through Non-deformable Porous Medium Using Brinkman Equation in Terms of Non-primitive Variables

Chandra Shekhar Nishad*, Anirban Chandra**, Timir Karmakar***, Raja Sekhar G.P.****

*Indian Institute of Technology Kharagpur, India, **Indian Institute of Technology Kharagpur, India, ***Indian Institute of Technology Kharagpur, India, ****Indian Institute of Technology Kharagpur, India

ABSTRACT

In this work, we propose a new boundary element technique for steady two-dimensional viscous incompressible Newtonian flow through non-deformable porous medium. We assume that the porous medium is isotropic and homogeneous, and utilize Brinkman equation to model the fluid flow. There are mainly two approaches to solve Brinkman equation using boundary integral methods, one in terms of primitive variables, namely velocity and traction (also known as Brinkmanlet formulation) and another in terms of non-primitive variables, namely stream function-vorticity variables (in case of two-dimensional or three-dimensional axisymmetric flows). Boundary integral formulation for Brinkman flows in terms of primitive variables is well known and available in the literature ([1], [2]). As per the knowledge of the authors, there does not exist any boundary integral formulation so far for two-dimensional Brinkman flows in terms of non-primitive variables, namely stream function-vorticity variables. Moreover, it is always advantageous to have an alternative approach which is efficient and easy to implement. In this context, first we present boundary integral equation (BIE) method for 2D Brinkman equation in terms of the non-primitive variables namely, stream-function and vorticity variables. Subsequently, a test problem namely, the lid-driven porous cavity over a unit square domain is presented to assert the accuracy of our BEM code. We observe that the rate of convergence increases with increasing Darcy number. Finally, we discuss an application of our proposed method to flows through porous wavy channel, which is a problem of significant interest in the microfluidics, biological domains and groundwater flows. For low Darcy number the streamlines follow the curvature of the wavy channel and no circulation occurs irrespective of the wave-amplitude, while for high Darcy number the flow circulation occurs near the crest of the wavy channel (when the wave-amplitude is large enough), which in many cases promotes the convective mixing and may prevent the leakage of carbon dioxide and support storage safety ([3]). References: [1]. Feng, J., Ganatos, P., Weinbaum, S.: Motion of a sphere near planar confining boundaries in a Brinkman medium. *Journal of Fluid Mechanics* 375, 265–296 (1998) [2]. Pozrikidis, C.: A study of linearized oscillatory flow past particles by the boundary-integral method. *Journal of Fluid Mechanics* 202, 17–41 (1989) [3]. Karmakar, T., Raja Sekhar, G.P.: A note on flow reversal in a wavy channel filled with anisotropic porous material. In: *Proc. R. Soc. A*, vol. 473, p. 20170193. The Royal Society (2017)

Implicit Particle-in-cell Formulation for Fluid-Structure Interaction Simulations with Hard Solid

Koji Nishiguchi^{*}, Rahul Bale^{**}, Shigenobu Okazawa^{***}, Makoto Tsubokura^{****}

^{*}RIKEN Advanced Institute for Computational Science, ^{**}RIKEN Advanced Institute for Computational Science,
^{***}University of Yamanashi, ^{****}RIKEN Advanced Institute for Computational Science, Kobe University

ABSTRACT

An implicit particle-in-cell method using a fixed Eulerian mesh and a set of Lagrangian particles is proposed to simulate fluid-structure interaction (FSI) problems. The authors have been developing a full Eulerian scheme for solid dynamics [1]. A full Eulerian method, however, cannot avoid the numerical dissipation of material interfaces and history-dependent variables of structures due to the advection. Even if a high-order advection scheme is adopted, material interfaces become diffusive gradually with time. To retain the sharp interface, K. Sugiyama et al. [2] proposed the particle-in-cell method for FSI simulations of flexible neo-Hookean tube flows in axisymmetric cylindrical coordinates. In this study, we propose a novel implicit particle-in-cell formulation using a fixed Cartesian mesh in order to relax limitation of small time increment in FSI simulations with hard solid such as metal materials. In the present method, the unified equation of motion for fluid and structure [3] is computed on the fixed Cartesian mesh. To avoid numerical dissipation of material interfaces and history-dependent variables of solid, Lagrangian particles represent the solid region and carry history-dependent variables such as solid deformation tensor. For an implicit time-integration for relaxing the time restriction stemming from an elastic wave, we assume the linear approximation using a fourth-order Jacobian tensor of hyperelastic stress tensor [4]. To verify the present approach, several numerical examples of FSI problem with hard solid will be demonstrated in the presentation. [1] K. Nishiguchi, S. Okazawa, M. Tsubokura: Multi-material Eulerian finite element formulation for pressure-sensitive adhesives, International Journal for Numerical Methods in Engineering, accepted, 2017. [2] K. Sugiyama, N. Nagano, S. Takeuchi, S. Ii, S. Takagi, Y. Matsumoto: Particle-in-cell method for fluid-structure interaction simulations of neo-Hookean tube flows, Theoretical and Applied Mechanics Japan, 59, 245-256, 2011. [3] K. Sugiyama, S. Ii, S. Takeuchi, S. Takagi, Y. Matsumoto: A full Eulerian finite difference approach for solving fluid-structure coupling problems, Journal of Computational Physics, 230(3), 596-627, 2011. [4] S. Ii, K. Sugiyama, S. Takeuchi, S. Takagi, Y. Matsumoto: An implicit full Eulerian method for the fluid-structure interaction problem, International Journal for Numerical Methods in Fluids, 65(1-3), 150-165, 2011.

Preliminary Investigation for Robust Topological Design Considering Nonlinear Structural Behavior

Takayuki Nishino^{*}, Takashi Kyoya^{**}, Junji Kato^{***}

^{*}TOHOKU university, ^{**}TOHOKU university, ^{***}TOHOKU university

ABSTRACT

Most studies on topology optimization find the optimum solution deterministically under a prescribed and unchanged boundary condition. However, in reality, uncertainty such as disturbances or errors in boundary conditions often occurs: this may degrade the structural performance or cause a serious structural problem if the optimized structure is sensitive with respect to the uncertainty. For this reason, the development of robust topology optimization considering an uncertainty is demanded. Many of the previous studies, however, deal with the conventional stiffness maximization problem assuming a linear elastic body, which is not related to a serious structural problem such as buckling. With this background, the present study addresses preliminary investigation for robust topology optimization to avoid a serious structural problem. One of the important uncertainties may be deviation from a prescribed loading condition, such as errors in loading angle, location and magnitude. These uncertainties and their influences onto the nonlinear structural response will be discussed in this study.

A Stochastic Analysis of Tensile Ductile Fracture for Polypropylene Solids

Koh-hei Nitta^{*}, Chun-yao Li^{**}

^{*}Institute of Science and Engineering, Kanazawa University, ^{**}Graduate School of Natural Science and Technology, Kanazawa University

ABSTRACT

Tensile fracture data from over 100 tensile tests of a polypropylene showed Gaussian distribution functions of fracture time and strength. With increasing tensile speed, the mean and deviation of fracture time decreased whereas those of toughness were independent of the tensile speed. We found a stochastic differential equation for predicting the fracture time under tension and the strength distribution can be determined uniquely from the stochastic equation.

Atomistic Simulation Study on Ultrasound-driven Aggregation Mechanism of Ceramic Nanoparticles

Xinrui Niu^{*}, Zijian Yao^{**}, Hao Zhang^{***}

^{*}City University of Hong Kong, ^{**}City University of Hong Kong, ^{***}University of Alberta

ABSTRACT

Nanoparticles (NPs) and their assemblies have been widely for many applications such as nanocomposites, nano medicines, microfluidic devices et al. Methods to assemble NPs have attracted considerable amount of research interests. Ultrasonication is a widely adopted method to treat NPs. The original goal was to break down NP agglomerations but later the method was demonstrated able to assemble NPs. Although ultrasound-driven NP assemblies have been observed experimentally, its formation mechanism is still unclear. This talk reports a recent effort to investigate mechanism of ultrasound driven NP aggregation. The work suggested that the NPs can be aggregated by partial melting of the NPs induced by the ultrasound driven collision. Critical aggregation velocity of NP under ultrasonication was estimated by molecular dynamics (MD) simulation. This work not only explained the phenomena observed in experiments but also indicates a possible novel method to assemble ceramic NPs through which ceramic NPs are aggregated through ultrasonication in standard ambient environment without any additional heat source or chemical treatment. Meanwhile, by predicting formation velocities of three different types of interparticle bondings, this work provided guidance to control and/or optimize the dispersion and/or aggregation of NPs, which could benefit the development of NP assembling technique.

Models and Finite Element Simulations of Nonlinear Electro-Thermo-Mechanical Problems with Application to the Shape Memory Polymer Medical Devices

Innocent Niyonzima^{*}, Jacob Fish^{**}

^{*}Columbia University, ^{**}Columbia University

ABSTRACT

Biomaterial implants, especially intelligent biomaterials have gained considerable attention in the biomedical community thanks to their ability to change physical properties (morphing, structural rigidity, etc.) when subjected to external stimuli such as temperature, pH, humidity, electromagnetic fields, etc. These materials are increasingly used for a large number of biomedical applications such as prevention and cure of coronary heart disease and stroke, ophthalmological applications, biosensors and drug delivery systems (S. K. Bhatia. "Biomaterials for clinical applications". Springer Science & Business Media, 2010). Among intelligent materials, shape memory polymers have a very promising future because they can be chosen biocompatible and biodegradable. For applications inside the human body, contactless control can be achieved by the addition of electric and/or magnetic particles that can react to electromagnetic fields, thus leading to a composite biomaterial. The difficulty of developing accurate numerical models for intelligent materials results from their multiscale nature and from the coupling of physical phenomena. This coupling involves electromagnetic, thermal and mechanical problems (C. Miehe et al., "Homogenization and multiscale stability analysis in finite magneto-electro-elasticity. Application to soft matter EE, ME and MEE composites". Comput. Methods Appl. Mech. Eng., 300 : 294–346, 2016). This research work will contribute to the multi-physical modelling of a shape memory polymer material used as a medical stent. The stent is excited by electromagnetic fields produced by a coil which can be wrapped around a failing organ. In this paper we develop Lagrangian formulations for the coupled electro-thermo-mechanical problem using the electric potential to solve the electric problem. The formulations are then discretized and solved using the finite element method. In the extended paper, the theoretical multi-physical model will be thoroughly detailed and the results will be validated by comparison with the experimental results present in the literature.

An Accurate and Well-Conditioned Conformal Decomposition Finite Element Method for Many Materials

David Noble*

*Sandia National Laboratories

ABSTRACT

Enriched finite element methods such as the Generalized Finite Element Method (GFEM), the eXtended Finite Element Method (XFEM), and the Conformal Decomposition Finite Element Methods (CDFEM) are powerful tools for multi-material problems. To capture the discontinuities across material interfaces, these methods introduce enrichment in the elements that contain multiple materials. Additional unknowns are assigned to the mesh entities (elements, nodes, sides, or edges) that are associated with these interfacial elements, and additional equations are formulated. However, as an interface comes arbitrarily close to background mesh nodes, the resulting equations may become linearly dependent. This problem is exacerbated when many materials intersect an element. To circumvent this issue, practitioners have omitted the enrichment in elements that intersect only a small fraction of material. In this way, the interface is snapped to the nodes of the background mesh. This approach incurs an error in the geometry to gain better conditioning. CDFEM is an enriched finite element method that can be used to describe discontinuous physics across material interfaces. Level sets are used to describe the domain of each material. Nodes are added at the intersection of each level set surface with the edges of the input mesh, and a conforming mesh is generated automatically. This allows the physics code to describe either weak or strong discontinuities across material interfaces using standard finite element methods. CDFEM can also produce poorly conditioned systems of equations when the interfaces come close to the background mesh nodes. This can be addressed by snapping the interface to the nearest node. However, this snapping introduces an error in the location of the interface. In the current work, an alternate approach is taken that removes the poor conditioning without introducing an error in the interface location. When an edge is crossed near one of its ends, the nearest node of the edge is moved to the crossing, instead of moving the crossing to the node. For simulations with many materials, the material interfaces may meet producing material intersection points, curves, and surfaces. In that case, the background mesh nodes are preferentially snapped to material interfaces that consist of a point, then curves, then surfaces. This approach improves the quality of the resulting decomposed meshes and produces systems of equations with dramatically better conditioning. The resulting system of equations is readily solved using traditional linear solvers. The method is described further and the improvement in the matrix conditioning is quantified.

*Sandia National Laboratories is a multimission laboratory managed and operated by National Technology and Engineering Solutions of Sandia, LLC, a wholly owned subsidiary of Honeywell International, Inc., for the U.S. Department of Energy's National Nuclear Security Administration under contract DE-NA0003525.

A Damage to Crack Transition Framework for Ductile Materials Accounting for Stress Triaxiality

Ludovic Noels^{*}, Julien Leclerc^{**}, Ling Wu^{***}, Van Dung Nguyen^{****}

^{*}University of Liege, ^{**}University of Liege, ^{***}University of Liege, ^{****}University of Liege

ABSTRACT

Predicting the entire ductile failure process is still a challenge task since it involves different processes: damage first diffuses before localizing, eventually leading to a micro-crack initiation and propagation. On the one hand, discontinuous approaches can describe localised processes such as crack propagation but fail in capturing diffuse damage evolution. On the other hand, continuous approaches such as continuum damage models are suited for diffuse damage modelling, but cannot represent properly physical discontinuities. In this work both approaches are combined in a hybrid implicit non-local damage model combined with an extrinsic cohesive law in a discontinuous Galerkin finite element framework [1]. The implicit non-local damage model reproduces the initial diffuse damage stage without mesh-dependency. Upon transition at void coalescence or intensive plastic localisation, a crack is introduced using a cohesive band model. Contrarily to cohesive elements, cohesive band models capture in-plane stretch effects, and thus account for stress triaxiality [2]. Indeed, by considering a band of small but finite thickness ahead of the crack surface, the strain field inside this band is evaluated from the neighbouring strains and from the cohesive jump [2]. Then, an appropriate damage model is used to compute the stress-state inside the band and the cohesive traction forces on the crack lips. The approach is first applied in the case of elastic damage for which the band thickness is evaluated to ensure the energetic consistency of the damage to crack transition with respect to purely non-local continuum damage mechanics [1]. Then, the scheme is formulated to the case of a non-local porous-plastic damage Gurson model. In particular, the law governing void growth accounts for shear effects, while the void coalescence mechanism, hence the damage to crack transition criterion, is predicted using the Thomason model [3]. [1] Leclerc J., Wu L., Nguyen V.D., Noels L. Cohesive band model: a cohesive model with triaxiality for crack transition in a coupled non-local implicit discontinuous Galerkin/extrinsic cohesive law framework. *Int. J. for Num. Methods in Eng.* (2017): In press. [2] Remmers J. J. C., de Borst R., Verhoosel C. V., Needleman A. The cohesive band model: a cohesive surface formulation with stress triaxiality. *Int. J. Fract.* 181 (2013). [3] Benzerga A.A., Leblond J.-B., Needleman A., Tvergaard V. Ductile failure modelling. *Int J Fract* 201 (2016).

Topology Optimization Applied to Pumps with Turbulent Flows

Luís Fernando Nogueira de Sá*, Emílio C. N. Silva**

*Polytechnic School of University of São Paulo, **Polytechnic School of University of São Paulo

ABSTRACT

The design of pumps by using topology optimization method is a powerful approach to improve these devices. When considering flow machines that operate at high rotations there are regions where the flow detaches from the blade and turbulence characteristics are present. The flow in the rotor of these machines have a considerably influence of their topology (Romero, 2014) and can be optimized to attend different design requirements. In this work we explore the topology optimization applied to rotors under turbulent flows by using the density method. The rotor is modeled in a rotary frame and the RANS equations coupled with the Spalart-Allmaras turbulence model are used. We use different material models between the constitutive equations, in a similar way as the work of Yoon (2016). The objective function used is the viscous energy dissipation (Borrvall and Peterson, 2003). The problem is implemented in the FEniCS environment with dolfin-adjoint and the Ipopt optimizer. At the present the flow is solved with arbitrary properties. Finally, blade topologies are presented and compared computationally with a traditional straight blade. Borrvall T, Petersson J (2003). Topology optimization of fluids in Stokes flow. *Int J Numer. Methods Eng* 41(1):77–107 Romero JS, Silva ECN (2014). A topology optimization approach applied to laminar flow machine rotor design. *Comput Methods Biomech Biomed Engin* 279:268–300 Yoon, Gil Ho (2016). Topology optimization for turbulent flow with Spalart–Allmaras model. *Computer Methods in Applied Mechanics and Engineering*, 303:288-311

Numerical and Analytical Investigation of a Phase Field Model for Ductile Fracture

Timo Noll^{*}, Charlotte Kuhn^{**}, Ralf Müller^{***}

^{*}University of Kaiserslautern, ^{**}University of Kaiserslautern, ^{***}University of Kaiserslautern

ABSTRACT

In phase field models for fracture a scalar valued order parameter describes the state of the material in terms of fracture on a fixed finite element mesh. Thus, in contrast to conventional fracture models, where cracks are described by sharp surfaces, computationally expensive remeshing and/or techniques are not necessary. In this contribution a phase field model for ductile fracture with linear isotropic hardening is presented. An energy functional consisting of an elastic energy, a plastic dissipation potential and a Griffith type fracture energy constitutes the model. The application of an unaltered radial return algorithm [1] on element level is possible due to the choice of an appropriate coupling between the nodal degrees of freedom, namely the displacement fields and the crack fields. The degradation function accomplishes the mentioned coupling by reducing the stiffness of the material and the plastic contribution of the energy density in broken material. Furthermore, to solve the global system of differential equations comprising the balance of linear momentum and the quasi-static Ginzburg-Landau type evolution equation, the application of a monolithic iterative solution scheme becomes feasible. Analytic considerations are presented demonstrating, that if the conventional, quadratic degradation function is used, the nominal plastic material parameters do not coincide with the effective parameters of the model and a reinterpretation of the parameters is necessary in order to relate simulation results to experimental data [2]. On the other hand, if certain cubic degradation functions [3], are used such a distinction between effective and nominal parameters is not necessary. Furthermore, the meaning of the fracture resistance, a model parameter stemming from the underlying brittle fracture model [4] is considered in context of ductile fracture and regarding its influence on e.g. the fracture strain compared to a plastic threshold function. In numerical examples, it is studied in how far the findings of the 1D considerations can be applied to the 3D cases. REFERENCES [1] J.C. Simó and T.J.R. Hughes, Computational Inelasticity, Interdisciplinary Applied Mechanics (Springer Berlin, New York, Heidelberg), 1998. [2] C. Kuhn, T. Noll, R. Müller, "On phase field modeling of ductile fracture", GAMM-Mitt., 39, 35-54 (2016). [3] C. Kuhn, A. Schlüter, R. Müller, "On degradation functions in phase field fracture models ", Comp. Mater. Sci., 108, 374-384 (2015). [4] C. Kuhn and R. Müller, "A continuum phase field model for fracture", J. Eng. Fract. Mech., 77, 3625-3634 (2010).

Multiscale Estimation of Effects of Coastal Vegetation in Consideration of Breakage and Washout During Tsunami

Reika Nomura^{*}, Shuji Moriguchi^{**}, Shinsuke Takase^{***}, Kenjiro Terada^{****}

^{*}Tohoku University, ^{**}Tohoku University, ^{***}Hachinohe Institute of Technology, ^{****}Tohoku University

ABSTRACT

This study presents a multiscale analysis method to estimate the positive and negative effects of coastal forests in consideration of the breakage and the washout of constituent trees by an incoming tsunami. More specifically, the proposed method is designed to characterize both the disaster mitigation effect and the washout risk of a coastal forest by performing numerical analyses under various conditions. To this end, we separate the coastal forest into two spatial scales; micro- and macro-scales. That is, the domain containing several trees is defined as a micro-structure, whereas the overall forest is a macrostructure. Numerical analyses are conducted for the micro-structure to characterize the macroscopic effects on the tsunami force/energy. A porosity model is employed to transmit the micro-scale information to the macro-scale in the scale-up evaluation process. That is, by regarding the coastal forest as a porous medium at the macro-scale, we expect that the overall flow resistance can be characterized by the mechanical behavior at the micro-scale. Thus, the proposed method can be recognized as a sort of homogenization methods. Based on the results of the micro-scale analyses, the flow resistance of the porous medium is defined as a function of not only the fluid velocity and the flow depth, but also the damage variable, which represents the degree of damage of trees during a tsunami. Since the damage variable develops according to the amount of trees breakage, the washout trees are described as a source of equivalent mass density advected to the overall flow. In numerical analyses, the stabilized Finite Element Method [1] is employed to solve the Navier-Stokes equation containing a porosity-related drag term, which is an alternative to the classical roughness coefficients modeling in the shallow water equation [2]. Several case studies are conducted and the numerical results are compared to the laboratory experiments for the validation. It is thus demonstrated that both assessments of mitigation effect of coastal forests and risk caused by the washout trees can be made for a whole coastal region with relatively low computational cost. [1] Tezduyar, T.E.: Stabilized finite element formulations for incompressible flow computations: Adv. Appl. Mech. 28, 1-44(1991) [2] Harada, K., Imamura, F.: Effects of coastal forest on tsunami hazard mitigation—a preliminary investigation, Tsunamis, Springer Netherlands, 279-292(2005)

Anisotropic Multi-Component Topology Optimization Method for Composite Shell Structures

Tsuyoshi Nomura^{*}, Kazuhiro Saitou^{**}, Yuqing Zhou^{***}

^{*}Toyota Research Institute of North America, ^{**}University of Michigan, ^{***}University of Michigan

ABSTRACT

This paper discusses about multi-component topology optimization for structures made of anisotropic materials, typically, fiber reinforced composite materials. The proposed method is capable of designing a variety of types of structures which are comprised by multiple components made of anisotropic materials. The topology of both the entire structure and each component is optimized by the conventional density design variables. The component is optimally divided under given constraints. In addition to that, the orientation distribution of the anisotropic material in each component is also optimized by means of anisotropic topology optimization. One major application field of this method is design of composite shell structures. Conventionally, this type of problem is formulated as a multi-material topology optimization problem, that is, a problem to find the optimal material distribution in an extended design domain. The most successful method for this problem is the discrete material optimization (DMO). As similar to isotropic topology optimization, the materials to be used in the design are given, a priori. For a composite shell structure design problem, they are given as a discrete set of options, such as, 0, 45, 90, 135 degrees. However, the selection of the discrete set severely affects the performance of the structure, and it is difficult to select the optimal angle option set beforehand. Another type of method for the composite shell structure design problem is based on continuous fiber angle optimization or anisotropic topology optimization. These types of methods handle topology optimization as a continuous angle field or a vector field distribution optimization problem; therefore, the orientation angle is optimized without any restriction. In addition to that, it is also capable of deriving designs with a discrete set of options by penalizing intermediate angles, but still, prescribed discrete options must be provided beforehand. The proposed method can solve this problem without a prescribed option set. The method is based on multi-component topology optimization and anisotropic topology optimization. The method optimizes the orientation distribution without any restriction, thanks to the nature of anisotropic topology optimization. To obtain a discrete angle design, it constraints the maximum allowed curvature in each component. The component partitioning occurs by this constraint up to the maximum allowed number of components. Therefore, it can provide discrete angle designs with the optimal angle for each component without a prescribed discrete set of options. Several numerical examples are provided in the presentation to show the usefulness of the proposed method.

3-dimensional Topology Optimization with Supershapes

Julián Norato*

*Assistant Professor, University of Connecticut

ABSTRACT

We present a method for the topology optimization of 3-dimensional structures made by the union of geometric primitives represented via supershapes. In two dimensions, supershapes are a generalization of hyperellipses that allow for different symmetries and thus can render not only circles and ellipses, but (approximately) any polygon. In three dimensions, the spherical product can produce sweeps of 2-dimensional supershapes in order to generate extruded and revolved solids. A distinct advantage of this parameterization is that it allows individual shapes to morph into several primitives via a single mathematical representation (the superformula). Being able to render a design made of primitives combined via Boolean operations is advantageous because that is exactly how most CAD programs build a solid model. The low-dimensional design representation thus constructed facilitates several aspects of the production process, such as providing convenient datum features for fabrication and assembly, specifying production tolerances and performing inspection of dimensional quality. To perform the analysis and optimization, we wish to retain one of the major advantages of classical topology optimization methods, namely the use of a fixed grid. To this end, we employ the geometry projection method to smoothly map the supershapes onto a density field discretely defined on the fixed grid. As customary, this field is used to define an ersatz material to perform the primal and sensitivity analyses. Unlike previous work by our group, where only a union of solid shapes is performed, in this work shapes can also be subtracted via a generalization of the geometry projection. We demonstrate the effectiveness of our method with several compliance minimization problems.

Stabilized and Multiscale Methods for Free Surface Flow Problems

Leo Nouveau^{*}, Guglielmo Scovazzi^{**}, Alex Main^{***}

^{*}Duke University, ^{**}Duke University, ^{***}Duke University

ABSTRACT

Embedded boundary methods obviate the need for continual re-meshing in many applications involving rapid prototyping and design. Unfortunately, many finite element embedded boundary methods for incompressible flow are also difficult to implement due to the need to perform complex cell cutting operations at boundaries, and the consequences that these operations may have on the overall conditioning of the ensuing algebraic problems. We present a new, stable, and simple embedded boundary method, which we call “shifted boundary method” (SBM), that eliminates the need to perform cell cutting. Boundary conditions are imposed on a surrogate discrete boundary, lying on the interior of the true boundary interface. We then construct appropriate field extension operators, with the purpose of preserving accuracy when imposing the boundary conditions. We demonstrate the SBM applied to several free surface flow problems.

The Biomimetic Method for Shape Optimization in 3D Elasticity

Michał Nowak*, Antoni Zochowski**, Jan Sokolowski***

*Chair of Virtual Engineering, Poznań University of Technology, Poland, **Systems Research Institute of the Polish Academy of Sciences, Poland, ***Institut Elie Cartan, Laboratoire de Mathématiques Université Henri Poincaré, France

ABSTRACT

This paper presents a new biomimetic approach to the structural design. The trabecular bone adapts its form to mechanical loads and is able to form lightweight but very stiff structures. In this sense, it is a problem (for the Nature) similar to the structural optimization. The remodeling phenomenon with strain energy density equalization on the trabecular bone surface assumption could be described from the stiffness point of view [1]. In the paper the structural optimization with shapes parameterization by the assumed energy density on the structural surface will be discussed. The structural optimization system based on shape modification using shape derivative [2] will be presented. The stiffest design is obtained by adding or removal material on the structural surface in the virtual space. The assumed value of the strain energy density on the part of the boundary subjected to modification could be related to the material properties. Change in the assumed value of the strain energy density results in change of the structural form – topology and volume. In general the problem of stiffest design (compliance minimization) has no solution. If the volume of the object is increasing, the compliance is decreasing. Thus, in the standard approach to the energy based topology optimization the additional constraint has to be added. Usually the volume of the material is limited. In the presented approach instead of imposing volume constraint the shapes are parameterized by the assumed energy density, which may be predicted from the yield criteria. The domain independence, functional configurations during the process of optimization and possibility to solve multiple load problems are the unique features of the biomimetic method, useful in mechanical design. To illustrate the algorithm functionality, the problem of determining the optimal internal wing structure will be discussed. For the purpose of aircraft wing design the numerical environment combining simultaneous structural size, shape, and topology optimization based on aeroelastic analysis was developed [3]. The optimal internal wing structure resulting from aeroelastic computation with different angles of attack will be presented. [1] Nowak M., Sokolowski J. Zochowski A., Justification of a certain algorithm for shape optimization in 3D elasticity, Struct Multidiscipl Optim, doi 10.1007/s00158-017-1780-7, 2017 [2] Sokolowski J., Zolesio J., Introduction to shape optimization. Shape Sensitivity Analysis. Springer, 1992 [3] Gawel D., Nowak M., Hausa H. et al., New biomimetic approach to the aircraft wing structural design based on aeroelastic analysis, Bull. Pol. Ac.: Tech. 65(5), pp. 741-750, 2017

Computational Modelling of Thermoplastic Behaviour of Inconel 718 in Application to Laser-Assisted Bending of Thin-Walled Alloy Tubes

Zdzisław Nowak*, Marcin Nowak**, Ryszard Pecherski***, Krzysztof Wisniewski****, Jacek Widłaszewski*****, Piotr Kurp*****

*Institute of Fundamental Technological Research, Polish Academy of Sciences, **Institute of Fundamental Technological Research, Polish Academy of Sciences, ***Institute of Fundamental Technological Research, Polish Academy of Sciences, ****Institute of Fundamental Technological Research, Polish Academy of Sciences, *****Institute of Fundamental Technological Research, Polish Academy of Sciences, *****Kielce University of Technology

ABSTRACT

At present, nickel based alloys are broadly used in the aerospace industry due to their excellent corrosion resistance and high mechanical properties. Laser-assisted tube bending process is a promising manufacturing process because of its ability to produce forms and shapes that cannot be achieved by mechanical bending. Laser bending is particularly suitable for the high hardness and brittle materials, such as nickel alloys, ceramics and cast iron. An experimental investigation of the Inconel 718 alloy is used in validation of the constitutive model. The multi-axial constitutive model accounts for the strength-differential behaviour under uniaxial tension/compression [1-3]. It encompasses softening phenomena as well as the coupling between temperature and strains, both of them observed in experiments. Bending of thin-walled tubes in a specially designed device is studied. Mechanical loading and simultaneous heating of the material by a moving laser beam are introduced in a controlled manner to obtain the required deformation. The current paper is focused on numerical simulations to provide more insight into the laser bending process of the Inconel 718 tubes. A 3D thermomechanical analysis model is developed in the FE code ABAQUS. The temperature, stress and deformation fields during thermo-mechanical loading of tubes are determined in a sequentially coupled thermo-mechanical analysis. Laser beam is modelled as a surface heat flux using the dedicated DFLUX procedure. The temperature field is then used as a thermal load in the static general step, together with an external mechanical load. The tube is discretized using the C3D8R. For the steel rollers with horizontal and vertical axes, the R3D4 element is used. The process of tube bending is controlled by the displacement of the piston rod, while the thrust force is the resulting value. References 1. Iyer S. K., Lissenden C. J., Multi-axial constitutive model accounting for the strength-differential in Inconel 718, Int. J. Plasticity, 19, 2055–2081, 2003. 2. Vadillo G., Fernandez-Saez J., Pecherski R. B., Some applications of Burzynski yield condition in metal plasticity, Materials and Design, 32, pp.628-635, 2011. 3. Pecherski R. B., Szeptynski P., Nowak M., An extension of Burzynski hypothesis of material effort accounting for the third invariant of stress tensor, Archives of Metallurgy and Materials, 56 (2), pp. 503-508, 2011.

Modeling Brain Tissue Degradation through Continuum Damage Mechanics

Lise Noël*, Ellen Kuhl**

*Stanford University, **Stanford University

ABSTRACT

Human brain is extremely sensitive to environmental changes and can exhibit different behaviors depending on the nature of the received stimuli. Undergoing large deformation over short time scale, the brain is unable to adapt to its environment. It is subject to damage and presents an inelastic material behavior. Modeling brain tissue degradation could lead to a better understanding of the mechanisms involved in neurodamage and neurodegeneration associated with various pathologies ranging from traumatic brain injuries to Alzheimer's disease. The basics of continuum damage mechanics (Kachanov 1958) can be adapted to describe damage in soft biological tissues. These ones are generally modeled as hyperelastic rubberlike materials, for which the stress-strain relation is established through a stored strain energy function. Material degradation can be accounted for by defining the damaged stored strain energy as a damage weighted function of the elastic stored strain energy. Directly impacting the material behavior, damage is represented by a scalar variable (if isotropic) that evolves from 0 for a virgin material to 1 for a complete failure. The material stress-strain curve is dependent on the loading history and damage is characterized resorting to a damage loading function. Assuming that damage is strain driven, its growth can be described by an evolution law including history dependency through an internal variable recording the largest strain state reached during the loading process. This work focuses on the role of mechanics in neurodamage. To model brain tissue damage, the mechanical model assumes finite strains and an hyperelastic constitutive material behavior based on an Ogden energy type. Degradation is introduced following continuum damage mechanics and the damage evolution law is calibrated with experimental results found in the literature (Franceschini et al. 2006, Goriely et al. 2015). The developed method is applied to two dimensional structures discretized resorting to the finite element method and the damage process is solved using Newton's method. Regular and arbitrary 2D structures, obtained from human brain medical imaging techniques, are considered. Kachanov, L. M., On creep rupture time. *Izvestiya Akademii Nauk SSSR. Otdelenie Tekhnicheskikh Nauk*, 8:26-31, 1958. Franceschini G., Bigoni D., Regitnig P. and Holzapfel G.A., Brain tissue deforms similarly to filled elastomers and follows consolidation theory. *Journal of the Mechanics and Physics of Solids*, 54:2592-2620, 2006. Goriely A., Budday S. and Kuhl E., Neuromechanics: From Neurons to Brain. In *Advances in Applied Mechanics*, 48:79-139, 2015.

A Time-multiscale Model Reduction Technique for Nonlinear Problems Involving High Number of Cycles

David Néron^{*}, Pierre Ladevèze^{**}, Shadi Alameddine^{***}, Mainak Bhattacharyya^{****}, Amélie Fau^{*****}, Udo Nackenhorst^{*****}

^{*}ENS Paris-Saclay, ^{**}ENS Paris-Saclay, ^{***}Leibniz Universität Hannover, ^{****}Leibniz Universität Hannover, ^{*****}Leibniz Universität Hannover, ^{*****}Leibniz Universität Hannover

ABSTRACT

The simulation of the mechanical response of structures subjected to cyclic loadings for a large number of cycles remains a challenge. The goal of this work is to develop a dedicated computational scheme for fatigue computations in problems involving nonlinear material behaviors described by internal variables. The focus is on the Large Time Increment (LATIN) method coupled with the PGD model reduction technique. This method has already been introduced in the 90s in this context but a new version, more robust, is proposed herein taking in particular into account the progress done recently. More, unilateral damage is considered here for the first time. In that scheme, a two-time-multiscale approach is proposed, that consists in computing the quantities of interest only at particular predefined cycles called the “nodal cycles” and using a suitable interpolation to estimate their evolution at the intermediate cycles. The proposed framework is exemplified for a structure subjected to cyclic loading, where, combined to visco-plasticity, damage is considered to be isotropic and micro-defect closure effects are taken into account. The combination of these techniques reduce the numerical cost drastically and allows to create virtual S-N curves for large number of cycles.

A Complete Model of Metal Additive Manufacturing: Requirements and Progress

Patrick O’Toole*, Vu Nguyen**, Paul Cleary***, Peter Cook****, Sharen Cummins*****,
Gary Delaney*****, Dayalan Gunasegaram*****, Anthony Murphy*****, Matthew
Sinnott*****, Mark Styles*****

*CSIRO, **CSIRO, ***CSIRO, ****CSIRO, *****CSIRO, *****CSIRO, *****CSIRO, *****CSIRO, *****CSIRO,
*****CSIRO

ABSTRACT

Metal additive manufacturing based on powder-bed fusion processes is becoming increasingly important production method. The technology has several advantages over conventional methods, for example in the manufacture of components having complex geometries and of custom-designed parts. The physical phenomena that occur in these processes are highly transient and difficult to monitor. Very challenging experiments requiring expensive sensing equipment are usually needed to obtain the data required for process understanding and improvement. Computational modeling of powder-bed fusion processes is therefore important from several points of view. These include obtaining an improved understanding of the phenomena occurring in the process, optimization of process parameters and component designs, and prediction of component properties. In the long term, it is foreseen that modeling will play an important role in qualification of components and in assisting process control. Several physical processes have to be considered to develop a complete model. These include the raking of the powder bed surface, the transfer of energy from the laser or electron beam to the metal, the melting and solidification of the powder, the flow of liquid metal in the melt pool, the heat transfer from the melt pool to the surrounding powder and solid metal, the evolution of the microstructure of the component, and the residual stress and deformation of the component. A further complication is that many of the processes are interdependent. The physical processes occur on very different length and time scales, and their treatment requires the use of different computational techniques. We are modeling powder bed raking using the discrete element method, and have obtained results for different particle shapes and sizes. We are applying two techniques, computational fluid dynamics and smoothed particle hydrodynamics, to treat the melt pool phenomena. A semi-empirical approach has been used to predict microstructure evolution, and we are now implementing the phase field method to obtain more detailed insights. The residual stress and deformation caused by the non-uniform heat fluxes is being modeled with the finite element method; the results obtained depend critically on the constitutive model that is used to describe the metal's thermomechanical properties. This paper discusses the rationale for developing a complete model, progress in developing the sub-models of the different physical processes at the disparate scales, and the framework that is envisaged to handle the interdependencies of the sub-models to allow the development of a predictive model of the full additive manufacturing process.

Explicit Dynamics IGA : LR B-Spline Implementation in the Radioss Solver

Matthieu OCCELLI*, Salim BOUABDALLAH**, Lionel MORANCAY***, Thomas ELGUEDJ****

*LaMCoS / Altair Engineering France, **Altair Engineering France, ***Altair Engineering France, ****LaMCoS

ABSTRACT

Isogeometric analysis has shown to be a very promising tool for an integrated design and analysis process [1]. A challenging task is still to move IGA from a proof of concept to a convenient design tool for industry and this work contributes to this endeavor. This communication deals with the implementation of IGA concept into Radioss explicit code in order to address crash and stamping simulation applications. To this end, the necessary ingredients to a smooth integration of IGA in a traditional finite element code have been identified and adapted to the existing code architecture. First, a solid NURBS element has been developed in Radioss and then, an existing contact interface has been extended in order to work seamlessly with both NURBS and Lagrange finite elements, using a node to surface formulation. Some academic and simple industrial cases will be presented to show the obtained results and the relevance of the retained solution. Mesh refinement is the third ingredient added to this integration, as local refinement is needed for solution approximation and for patch connection. After comparing it with several existing refinement methods such as Hierarchical B-Splines (HBS) and Truncated Hierarchical B-Splines (THBS) in term of additional data requirements and implementation aspects, we implemented the approach of locally refined B-Splines (LRBS) [3]. This approach is validated on industrial benchmarks, for validation cases conventionally used for industrial codes like stamping and drop test. REFERENCES [1] J.A. Cottrell, T.J.R. Hughes and Y. Bazilevs, Isogeometric Analysis: Toward integration of CAD and FEA, John Wiley & sons, 2009. [2] L. Piegl and W. Tyler, The NURBS book, 2nd ed., Springer, 1997. [3] K.A. Johannessen, T. Kvamsdal and T. Dokken, Isogeometric analysis using LR B-splines, Comput. Methods Appl. Mech. Engrg, 269, 471-514, 2014.

Modal Synthesis for Sloshing Modeling. Reduced Order Model and Summation Rule

Roger OHAYON*, Jean-Sebastien SCHOTTE**

*Conservatoire National des Arts et Metiers (CNAM), Paris, France, **ONERA, The French Aerospace Lab., France

ABSTRACT

The application of modal synthesis methods to the modeling of the coupling between a deformable structure and a quiescent fluid was the subject of many works [Morand & Ohayon (1995)]. Although this approach is limited to the study of the low amplitude vibrations of a coupled fluid-structure system, it has the advantage of allowing the efficient construction of reduced models, useful for an intuitive frequency analysis of the coupling between both sub-systems. In particular, it permits to generalize the representation method of a sloshing fluid by equivalent mechanical systems (mass-spring or pendulum) to cases of deformable tanks with complicated geometrical shapes [Schotté & Ohayon (2009)]. Starting from a pressure formulation for the fluid and a decomposition of its response on the modal basis of its sloshing modes, completed by some particular quasi-static solutions, the reduced coupled equations of the fluid-structure system are established and a summation rule concerning the various fluid mass operators is exposed. The interest of this approach is illustrated by comparison with the classical mass-spring or pendulum approach. Finally, an extension of this model, to take the capillarity effects into account, is tackled with the aim to adapt this approach to the case of fluid-structure systems in micro-gravity (for satellite applications) [El-Kamali, Schotté & Ohayon (2011), Ohayon & Soize (2016)].

References Morand & Ohayon (1995): Fluid-Structure Interaction: Applied Numerical Methods, Wiley Schotté & Ohayon (2009): Various modelling levels to represent internal liquid behavior in the vibratory analysis of complex structures, CMAME, 198: 1913-1925 El-Kamali, Schotté & Ohayon (2011): Three-dimensional modal analysis of sloshing under surface tension, IJNMF, 65: 87-105 Ohayon & Soize (2016): Nonlinear model reduction for computational vibration analysis of structures with weak geometrical nonlinearity coupled with linear acoustic liquids in the presence of linear sloshing and capillarity, Computers & Fluids, 141: 82-89

A Generic Metallurgical Phase Transformation Framework Applied to Additive Manufacturing Processes

Victor Oancea*, Qi Zhang**, Jiawen Xie***, Tyler London****

*Dassault Systemes SIMULIA Corp., Johnston, RI, USA, **Brown University/Dassault Systemes SIMULIA Corp.,
Dassault Systemes SIMULIA Corp., *TWI Ltd, Cambridge, UK

ABSTRACT

While significant progress has been made in the last few years, the reliability of AM manufactured parts is often questionable as they suffer from manufacturing defects and hence subpar strength/fatigue life. Like in many other fields before, numerical methods are sought to provide insight into the process and help accelerate progress in raising the quality of AM parts, including predicting thermal evolutions, part distortions and residual stresses. In metal applications, assessing the amount of unfused powder, melt pool volumes, grain growth, and metallurgical phase transformations are often of interest. Ultimately, process-controlled microstructures can lead to superior designs and desirable mechanical properties. In previous work, a highly customizable general simulation framework was demonstrated and validated for a wide spectrum of additive manufacturing processes (laser and electron beam powder bed fabrication, direct energy deposition, arc welding, polymer extrusion, ink jetting) as implemented on the Dassault Systemes 3DX Platform based on new FE technology implemented in Abaqus. The framework allows for: 1) arbitrary meshes of CAD representations; 2) exact specification in time and space of processing conditions (e.g., powder addition, laser trajectories, dwell times, etc.); 3) precise tracking of the progressive raw material addition to each element in the mesh via complex geometric computations; 4) precise integration of the moving energy sources (e.g., laser, electron beams, arc welds, high temperature polymer extrusion) and; 5) automatic computation of the continuously evolving convection and radiation surfaces. In the current work, in conjunction with the general simulation framework above, we are introducing a generic metallurgical phase transformation framework applicable to arbitrary metal alloys. The framework accounts for phase transformations (physical state changes) from stock feed (e.g., powder) via melting/vaporization/solidification followed by metallurgical solid state phase transformations induced by either rapid heating/cooling events associated with typical 3D printing sequences but also with slower rate temperature evolutions as associated with heat treatment applications. The user defines in a systematic fashion all possible transformations that can take place via a parent-children paradigm (e.g., austenite to martensite); the temperature conditions when transformations can occur with associated TTT/CCT diagrams; and whether the transformations are reversible, diffusional/non-diffusional. The framework predicts temperature evolutions, calibrates JMA/KM models, and predicts phase transformations during print and heat treatment. Grain growth and aspect ratio assessment models are also included. A few verification/validation exercises for two different alloys are presented

New Application Domains for the Variational Multiscale Method

Assad Oberai*

*University of Southern California

ABSTRACT

One of Prof. Hughes's lasting contribution to the field of computational mechanics is the Variational Multiscale Method (VMS). The variational multiscale method was developed as a tool to derive numerical methods for solving partial differential equations. In this context, it has been applied to a large class of problems that include incompressible and compressible fluid flow, MHD and turbulence modeling. However, more recently, its applications in other areas have emerged. These include PDEs with stochastic parameters, discrete reduced order models, goal-oriented error estimates, and phase change problems. In this talk, I will begin with a brief description of the variational multiscale method, and then discuss its application in these new areas.

An Accelerated Molecular Dynamics Study of Yield Stress of Ultrafine-grained Metals

Shigenobu Ogata*

*Osaka University

ABSTRACT

Plastic deformation and yielding of nanocrystalline metals is mostly governed by a dislocation nucleation from grain boundaries. A newly developed accelerated molecular dynamics simulation method computes temperature and strain-rate dependent yield stress, which is corresponding to a stress of onset of dislocation nucleation from grain boundaries. Since the accelerated molecular dynamics allows to analysis very rare events, the yield stress is computed over very wide ranged strain rate, 10^{-4} to 10^{10} 1/s, which never be covered by conventional molecular dynamics simulation methods. In addition, the accelerated molecular dynamics reveals a mechanism transition and strong stress, temperature and strain-rate dependencies of the dislocation nucleation events. At stress levels up to 90% of the ideal dislocation nucleation stress, atomic shuffling at the E structural unit in a grain boundary acts as a precursor to dislocation nucleation, and eventually a single dislocation is nucleated. At very high stress levels near the ideal dislocation-nucleation stress, a multiple dislocation is collectively nucleated. In these processes, the activation free energy and activation volume depend strongly on temperature. The strain-rate dependence of the critical nucleation stress shows that the mechanism transition from the shuffling-assisted dislocation-nucleation mechanism to the collective dislocation-nucleation mechanism occurs during the strain rate increasing.

HYBRID MORI-TANAKA/FINITE ELEMENT METHOD: AN EFFICIENT HOMOGENIZATION OF COMPOSITE MATERIALS WITH VARIOUS REINFORCEMENT SHAPE AND ORIENTATION

WITOLD OGIERMAN*

*Institute of Computational Mechanics and Engineering,
Faculty of Mechanical Engineering, Silesian University of Technology
ul. Konarskiego 18A, Gliwice, Poland
witold.ogierman@polsl.pl; <http://www.icme.polsl.pl/>

Key words: Homogenization, Mori-Tanaka method, Composite materials, Micromechanics

Abstract. The main goal of this study is to use the hybrid Mori-Tanaka/Finite element homogenization method for determination of effective properties of composite materials reinforced with particles of arbitrary shape. Mori-Tanaka homogenization method, that is based on Eshelby's fundamental solution, provides very efficient solution. On the other hand, it has got several limitations, for example it allows to consider only ellipsoidal shape of the reinforcement. A hybrid Mori-Tanaka/Finite element method can overcome the limitations of standard Mori-Tanaka approach. In this case mean field relations between per phase stresses and strains are combined with numerical solution of the equivalent inclusion problem by the finite element method. The numerical model of equivalent inclusion problem requires very simple geometry containing single inclusion and embedding matrix. An influence of size of the embedding matrix on the strain concentration tensor has been investigated by considering different volume fractions of the single inclusion and comparing the obtained results with analytical solution. The accuracy of hybrid M-T/FE method has been verified by performing direct FE homogenization based on the representative volume element containing substantial number of inclusions.

1 INTRODUCTION

Effective properties of composite materials corresponding to the material behavior at the macroscale can be determined by using homogenization procedures. Methods of homogenization allow to take into account an influence of microstructural features on the effective material properties. One way of using homogenization is to solve a boundary value problem (BVP) by using numerical methods like finite element method (FEM) [1, 2, 3] or boundary element method (BEM) [4, 5, 6]. In this case the macroscopic quantities are computed as volume averages of the microscopic quantities over the representative volume element (RVE). The RVE can be defined as a volume of heterogeneous material that is sufficiently large to be statistically representative of the composite [7]. Therefore, the RVE must include a sufficient number of the composite inhomogeneities like fibers, particles etc. On the other hand, the RVE should be small enough to provide reasonable computational cost. The RVEs corresponding to composites containing inclusions of complex shape and orientation distribution typically require taking into account large number of

inhomogeneities that makes the computational homogenization time consuming. Another group of homogenization methods is based on the Eshelby's fundamental solution [8]. In this case several different approaches can be distinguished like for example self-consistent schemes [9] and Mori-Tanaka method [10]. In particular, the Mori-Tanaka (M-T) method found wide popularity in analysis of composite materials due to good predictive capabilities and low computational cost [11]. Tucker and Liang [12] studied different mean field methods and recommend the M-T method as the best choice for estimating the stiffness of aligned short-fiber composites. M-T method can be also used in modeling of composites with misaligned inclusions by using the orientation averaging procedure [13]. On the other hand, Eshelby's solution is limited to the case of the ellipsoidal shape of inclusions only. However, the numerical solution of equivalent inclusion problem, instead of using the Eshelby's tensor, allowing the M-T method to be extended so as to involve the arbitrary shapes of the inhomogeneities. Therefore, usage of hybrid Mori-Tanaka/Finite element (M-T/FE) method can overcome the limitations of standard M-T approach. In this case mean field relations between per phase stresses and strains are combined with numerical solution of the equivalent inclusion problem by the finite element method (in standard M-T method Eshelby's tensor is used in this case). This approach is generally more computationally effective than direct analysis of RVE by the FEM, as it requires very simple geometrical model containing single inclusion and embedding matrix. The feasibility and effectiveness of the hybrid approach has been presented by Bradshaw et al. [14] who investigated the influence of nanotube waviness on effective properties of nanotube reinforced composite. Klusemann et al. [15] analyzed different shapes of reinforcing particles however authors restricted their calculations to the plane strain conditions. Three dimensional models corresponding to the fiber reinforced composites have been developed by Srinivasulu et al. [16], authors reported good agreement between results obtained by hybrid method and pure numerical solution. Brassart et al. [17] developed hybrid approach that accounts for elastic-plastic material behavior. In the present work, hybrid M-T/FE method is applied in modeling of effective elastic properties of composites reinforced with particles of arbitrary shape, as an example composite reinforced with cubic particles is presented. An influence of size of the embedding matrix on the accuracy of the obtained results has been investigated. The accuracy of hybrid M-T/FE method has been verified by performing direct FE homogenization based on the RVE containing substantial number of inclusions.

2 HYBRID HOMOGENIZATION METHOD

The Mori-Tanaka approach provides the effective stiffness tensor C^{EFF} by the following expression:

$$C^{EFF} = C_m + f_i(C_i - C_m)A[(1 - f_i)I + f_iA]^{-1}, \quad (1)$$

where C_m and C_i are isotropic stiffness tensors of matrix and inclusion respectively, f_i is volume fraction of inclusions, A is strain concentration tensor, I is identity tensor [10]. The strain concentration tensor relates the average strain in the inclusion ε_i to the far field strain (macro strain) ε :

$$\begin{bmatrix} \varepsilon_{11}^i \\ \varepsilon_{22}^i \\ \varepsilon_{33}^i \\ \varepsilon_{23}^i \\ \varepsilon_{13}^i \\ \varepsilon_{12}^i \end{bmatrix} = \begin{bmatrix} A_{11} & A_{12} & A_{13} & A_{14} & A_{15} & A_{16} \\ A_{21} & A_{22} & A_{23} & A_{24} & A_{25} & A_{26} \\ A_{31} & A_{32} & A_{33} & A_{34} & A_{35} & A_{36} \\ A_{41} & A_{42} & A_{43} & A_{44} & A_{45} & A_{46} \\ A_{51} & A_{52} & A_{53} & A_{54} & A_{55} & A_{56} \\ A_{61} & A_{62} & A_{63} & A_{64} & A_{65} & A_{66} \end{bmatrix} \begin{bmatrix} \varepsilon_{11} \\ \varepsilon_{22} \\ \varepsilon_{33} \\ \varepsilon_{23} \\ \varepsilon_{13} \\ \varepsilon_{12} \end{bmatrix}. \quad (2)$$

The strain concentration tensor for the M-T method depends on the Eshelby's tensor S as follows:

$$A = [S(C_m^{-1}C_I - I) + I]^{-1}. \quad (3)$$

The principle of the hybrid method is replacement of strain concentration tensor expressed by the equation 3 by strain concentration tensor determined numerically. Therefore, the numerical solution of equivalent inclusions problem is required. The equivalent inclusion problem is connected with analysis of single inclusion embedded in an infinite matrix. Numerical model approximates the infinite medium by rectangular prism whose finite dimensions are large enough in comparison with the size of the inclusion. In order to obtain the strain concentration tensor by using numerical method six FE simulations have to be performed by prescribing displacement boundary conditions that enforce the unit strains as follows (superscript denotes the analysis number):

$$\varepsilon^{(1)} = \begin{bmatrix} 1 \\ 0 \\ 0 \\ 0 \\ 0 \\ 0 \end{bmatrix} \quad \varepsilon^{(2)} = \begin{bmatrix} 0 \\ 1 \\ 0 \\ 0 \\ 0 \\ 0 \end{bmatrix} \quad \varepsilon^{(3)} = \begin{bmatrix} 0 \\ 0 \\ 1 \\ 0 \\ 0 \\ 0 \end{bmatrix} \quad \varepsilon^{(4)} = \begin{bmatrix} 0 \\ 0 \\ 0 \\ 1 \\ 0 \\ 0 \end{bmatrix} \quad \varepsilon^{(5)} = \begin{bmatrix} 0 \\ 0 \\ 0 \\ 0 \\ 1 \\ 0 \end{bmatrix} \quad \varepsilon^{(6)} = \begin{bmatrix} 0 \\ 0 \\ 0 \\ 0 \\ 0 \\ 1 \end{bmatrix}. \quad (4)$$

At the post processing stage of the finite element computations the strains inside the inclusion ε_i are averaged in the following way:

$$\langle \varepsilon^i \rangle = \frac{1}{V^i} \int_{V^i} \varepsilon^i dV^i \quad (5)$$

where V^i is volume of the inclusion. The volume averaging is performed for each strain component, due to assumption of the unit macro strains (equation 4) the components of strain concentration tensor A are directly regarded as $\langle \varepsilon^i \rangle$. An influence of the rectangular prism size (embedding matrix) on the strain concentration tensor has been investigated by considering different volume fractions of single spherical inclusion. The numerical solution has been compared with analytical result for spherical inclusion which is achieved by substituting the Eshelby's tensor whose nonzero components are given by [18]:

$$\begin{aligned}
 S_{11} = S_{22} = S_{33} &= \frac{7-5\nu}{15(1-\nu)}, \\
 S_{12} = S_{23} = S_{31} = S_{13} = S_{21} = S_{32} &= \frac{5\nu-1}{15(1-\nu)}, \\
 S_{44} = S_{55} = S_{66} &= \frac{4-5\nu}{15(1-\nu)},
 \end{aligned} \tag{6}$$

to the equation 3. In case of numerical model fine finite element mesh consisting of hexahedral elements have been applied. View on one-eighth of model containing inclusion whose volume fraction is 0.001 is presented in Fig.1a and corresponding finite element mesh is presented in Fig. 2b. During the analysis the following elastic constants related to the matrix and inclusion have been taken into account: $E_m=70$ GPa, $\nu_m=0.30$, $E_i=415$ GPa, $\nu_i=0.16$ which are typical for aluminum alloy and silicon carbide.

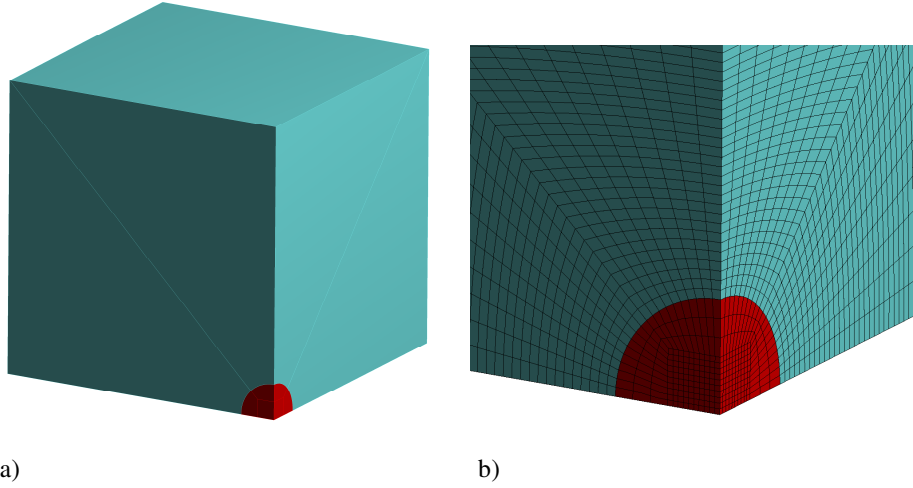


Figure 1. Model of equivalent inclusion problem involving spherical inclusion: a) view on the one-eighth of the model, b) detailed view on the finite element mesh

The error of numerical solution of equivalent inclusion problem has been quantified by comparing the components of strain concentration tensor determined analytically and numerically:

$$\chi_{ij} = \frac{|A_{ij}^{ANA} - A_{ij}^{NUM}|}{A_{ij}^{ANA}} 100\% \tag{7}$$

The dependence of the volume fraction of the single inclusion on the error χ_{ij} is presented in Fig. 2 (due to isotropic behavior only A_{11} and A_{12} components are compared).

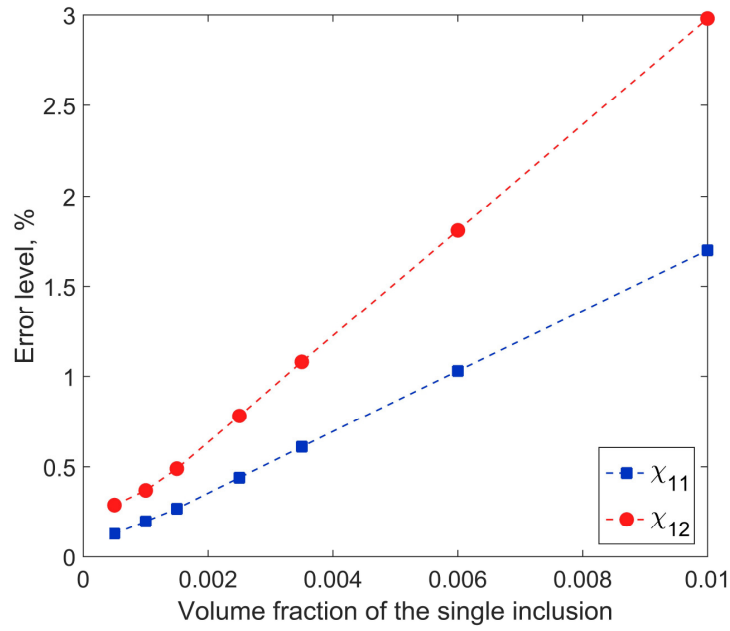


Figure 2. Dependence of the volume fraction of the single inclusion on the error of numerical solution of equivalent inclusion problem

Analysis of the Fig. 2 lead to conclusion that 0.001 volume fraction of the single inclusion provides good approximation of the equivalent inclusion problem. Strain concentration tensors computed analytically and numerically involving 0.001 volume fraction of single inclusion have the following form respectively:

$$A^{ANA} = \begin{bmatrix} 0.31203 & 0.04085 & 0.04085 & 0.00000 & 0.00000 & 0.00000 \\ 0.04085 & 0.31203 & 0.04085 & 0.00000 & 0.00000 & 0.00000 \\ 0.04085 & 0.04085 & 0.31203 & 0.00000 & 0.00000 & 0.00000 \\ 0.00000 & 0.00000 & 0.00000 & 0.27117 & 0.00000 & 0.00000 \\ 0.00000 & 0.00000 & 0.00000 & 0.00000 & 0.27117 & 0.00000 \\ 0.00000 & 0.00000 & 0.00000 & 0.00000 & 0.00000 & 0.27117 \end{bmatrix}, \quad (8)$$

$$A^{NUM} = \begin{bmatrix} 0.31264 & 0.04070 & 0.04070 & 0.00000 & 0.00000 & 0.00000 \\ 0.04070 & 0.31264 & 0.04070 & 0.00000 & 0.00000 & 0.00000 \\ 0.04070 & 0.04070 & 0.31264 & 0.00000 & 0.00000 & 0.00000 \\ 0.00000 & 0.00000 & 0.00000 & 0.27170 & 0.00000 & 0.00000 \\ 0.00000 & 0.00000 & 0.00000 & 0.00000 & 0.27170 & 0.00000 \\ 0.00000 & 0.00000 & 0.00000 & 0.00000 & 0.00000 & 0.27170 \end{bmatrix}. \quad (9)$$

3 ANALYSIS OF REINFORCEMENT OF ARBITRARY SHAPE

One of the main goals of this study is to use the hybrid homogenization method for determination of effective properties of composite materials reinforced with particles of arbitrary shape. This section presents the results obtained for cubic particles. The results obtained by using hybrid homogenization method are compared with pure numerical solution based on the direct finite element (FE) analysis of representative volume element (RVE) containing substantial number of inclusions. The numerical model of equivalent inclusion problem has been formulated in a way described in section 2 by considering single cubic inclusion of volume fraction 0.001 (Fig. 3) and the same elastic constants as previously.

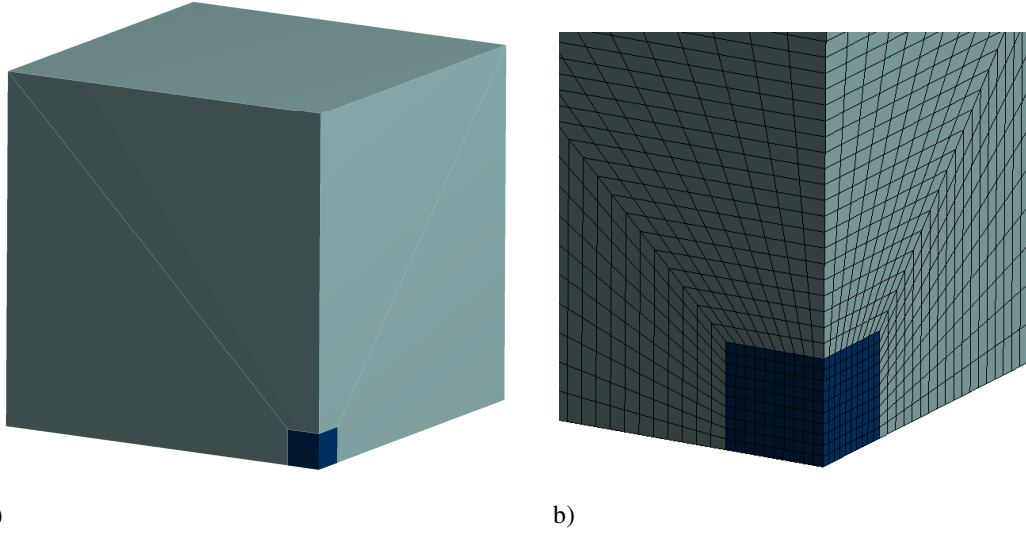


Figure 3. Model of equivalent inclusion problem involving cubic inclusion: a) view on the one-eighth of the model, b) detailed view on the finite element mesh

Strain concentration tensor obtained for cubic inclusion is given by:

$$A^{NUM_CUBE} = \begin{bmatrix} 0.34391 & 0.03273 & 0.03273 & 0.00000 & 0.00000 & 0.00000 \\ 0.03273 & 0.34391 & 0.03273 & 0.00000 & 0.00000 & 0.00000 \\ 0.03273 & 0.03273 & 0.34391 & 0.00000 & 0.00000 & 0.00000 \\ 0.00000 & 0.00000 & 0.00000 & 0.28037 & 0.00000 & 0.00000 \\ 0.00000 & 0.00000 & 0.00000 & 0.00000 & 0.28037 & 0.00000 \\ 0.00000 & 0.00000 & 0.00000 & 0.00000 & 0.00000 & 0.28037 \end{bmatrix}. \quad (10)$$

The effective stiffness tensor determined in terms of tensor A^{NUM_CUBE} exhibit cubic symmetry. For example, effective stiffness tensor obtained for 0.2 volume fraction of particles has the following form:

$$C = \begin{bmatrix} 122.326 & 46.544 & 46.544 & 0.000 & 0.000 & 0.000 \\ 46.544 & 122.326 & 46.544 & 0.000 & 0.000 & 0.000 \\ 46.544 & 46.544 & 122.326 & 0.000 & 0.000 & 0.000 \\ 0.000 & 0.000 & 0.000 & 36.876 & 0.000 & 0.000 \\ 0.000 & 0.000 & 0.000 & 0.000 & 36.876 & 0.000 \\ 0.000 & 0.000 & 0.000 & 0.000 & 0.000 & 36.876 \end{bmatrix}. \quad (11)$$

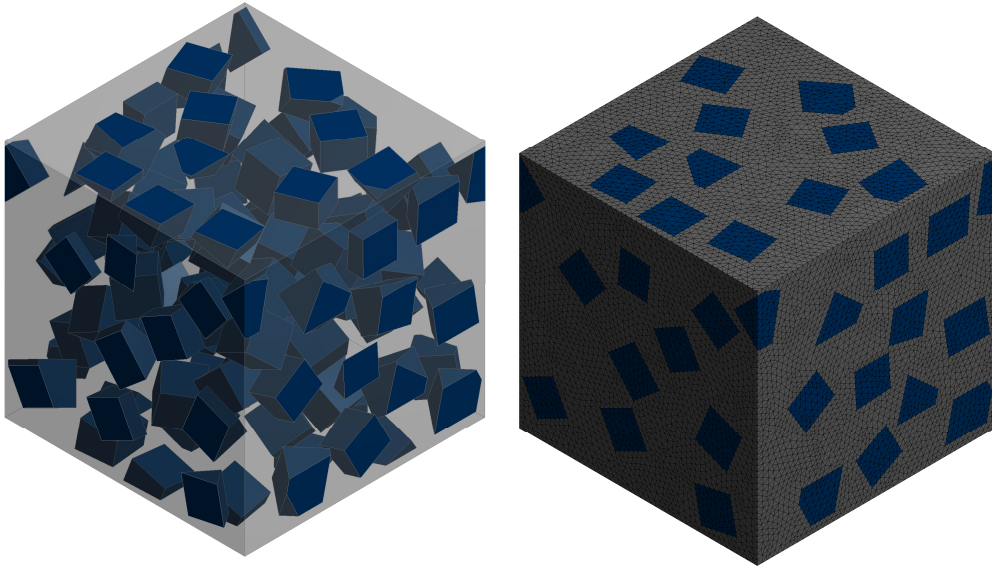
However, in many cases, particle reinforced composites contain the inclusions which are distributed randomly hence the material is characterized by isotropic symmetry. Therefore, the orientation averaging procedure has been employed to model the random orientation of cubic particles. The effective stiffness tensor of the material with random orientation of the inclusions can be determined by integration over the unit sphere:

$$C^{RANDOM} = \int_{\theta=0}^{\pi} \int_{\varphi=0}^{2\pi} C(\theta, \varphi) \psi(\theta, \varphi) \sin \theta d\theta d\varphi, \quad (12)$$

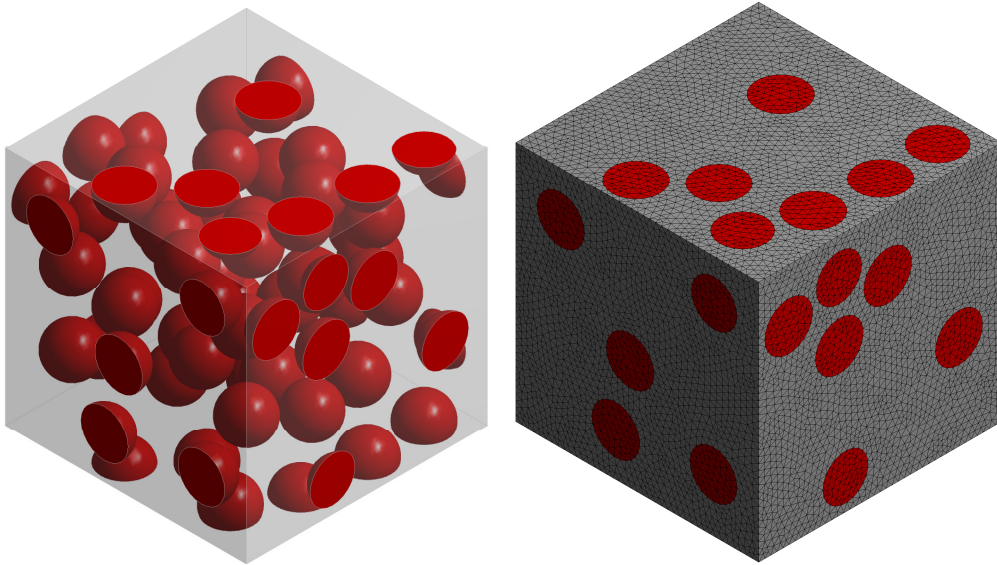
where θ and φ are spherical angles, $C(\theta, \varphi)$ is transformed stiffness tensor determined in terms of tensor A^{NUM_CUBE} , $\psi(\theta, \varphi)$ is orientation distribution function [19, 20]. The stiffness tensor obtained after orientation averaging which represents the material with randomly oriented cubic particles of volume fraction 0.2 is given by:

$$C^{RANDOM} = \begin{bmatrix} 121.514 & 46.950 & 46.950 & 0.000 & 0.000 & 0.000 \\ 46.950 & 121.514 & 46.950 & 0.000 & 0.000 & 0.000 \\ 46.950 & 46.950 & 121.514 & 0.000 & 0.000 & 0.000 \\ 0.000 & 0.000 & 0.000 & 37.282 & 0.000 & 0.000 \\ 0.000 & 0.000 & 0.000 & 0.000 & 37.282 & 0.000 \\ 0.000 & 0.000 & 0.000 & 0.000 & 0.000 & 37.282 \end{bmatrix}. \quad (13)$$

Afterwards the direct FE homogenization has been performed on the basis of the representative volume elements (RVE) whose exemplary models are presented in Fig. 4-5. During the direct FE homogenization periodic boundary conditions [1] have been applied in order to enforce the unit strains in the similar way to the equation 4. In this case tetrahedral finite elements with quadratic shape functions have been used where the nodes on opposite faces of the RVE model are consistent that makes application of periodic boundary conditions convenient. Cubic and spherical shapes of the reinforcement have been studied involving four different volume fractions: 0.1, 0.15, 0.20, 0.25 hence eight different cases have been studied.



a) b)
Figure 4. RVE containing cubic inclusions used in direct FE homogenization: a) geometrical model, b) finite element mesh



a) b)
Figure 5. RVE containing spherical inclusions used in direct FE homogenization: a) geometrical model, b) finite element mesh

For example, effective stiffness tensors obtained after direct FE homogenization corresponding to the materials reinforced with cubic and spherical particles of volume fraction 0.2 have the following form:

$$C^{FE_CUB} = \begin{bmatrix} 122.751 & 46.975 & 46.466 & -0.328 & 0.103 & -0.017 \\ 46.975 & 122.482 & 46.435 & -0.104 & -0.065 & -0.125 \\ 46.466 & 46.435 & 123.008 & 0.135 & 0.039 & 0.198 \\ -0.328 & -0.104 & 0.135 & 38.170 & -0.004 & -0.042 \\ 0.103 & -0.065 & 0.039 & -0.004 & 37.718 & 0.036 \\ -0.017 & -0.125 & 0.198 & -0.042 & 0.036 & 37.615 \end{bmatrix}, \quad (14)$$

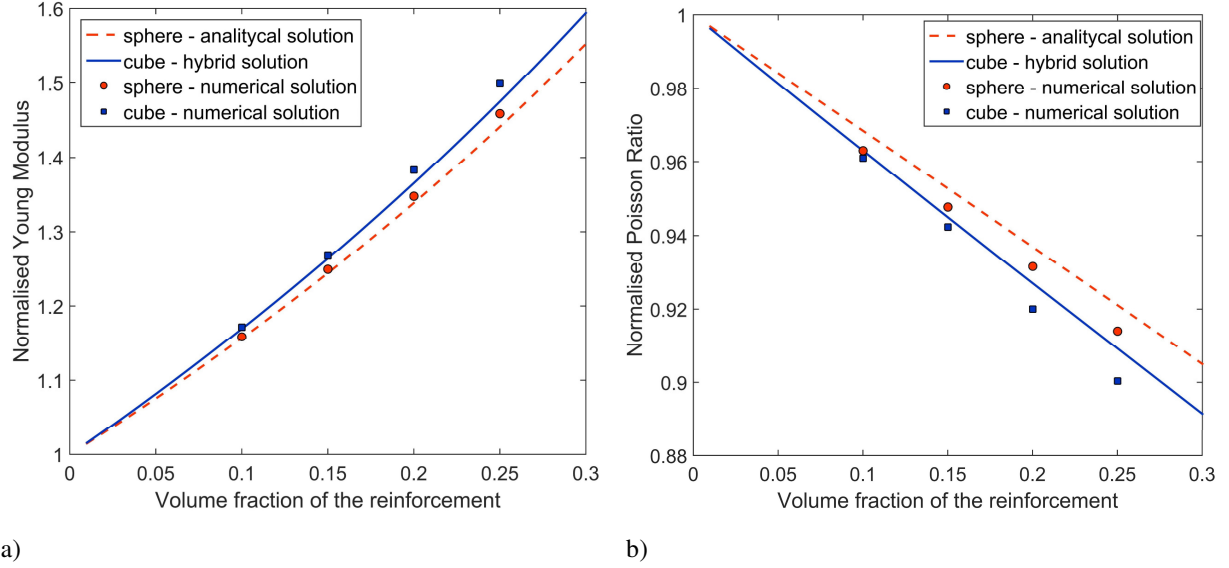
$$C^{FE_SPH} = \begin{bmatrix} 120.653 & 46.666 & 46.702 & 0.055 & -0.104 & 0.134 \\ 46.666 & 120.430 & 46.801 & 0.090 & 0.019 & 0.098 \\ 46.701 & 46.800 & 120.289 & -0.054 & 0.010 & 0.159 \\ 0.055 & 0.090 & -0.054 & 36.826 & 0.215 & -0.012 \\ -0.104 & 0.019 & 0.010 & 0.215 & 36.822 & -0.028 \\ 0.134 & 0.098 & 0.160 & -0.012 & -0.028 & 36.947 \end{bmatrix}. \quad (15)$$

The obtained stiffness tensors do not exhibit the isotropic symmetry exactly therefore in order to extract the effective Young modulus and Poisson ratio the procedure of the best isotropic approximation of elastic anisotropies discussed by Cavallini ^[21] has been applied. The result of approximation is given by the following stiffness tensors:

$$C^{FE_CUB_ISO} = \begin{bmatrix} 122.566 & 46.716 & 46.716 & 0.000 & 0.000 & 0.000 \\ 46.716 & 122.566 & 46.716 & 0.000 & 0.000 & 0.000 \\ 46.716 & 46.716 & 122.566 & 0.000 & 0.000 & 0.000 \\ 0.000 & 0.000 & 0.000 & 37.925 & 0.000 & 0.000 \\ 0.000 & 0.000 & 0.000 & 0.000 & 37.925 & 0.000 \\ 0.000 & 0.000 & 0.000 & 0.000 & 0.000 & 37.925 \end{bmatrix}, \quad (16)$$

$$C^{FE_SPH_ISO} = \begin{bmatrix} 120.456 & 46.724 & 46.724 & 0.000 & 0.000 & 0.000 \\ 46.724 & 120.456 & 46.724 & 0.000 & 0.000 & 0.000 \\ 46.724 & 46.724 & 120.456 & 0.000 & 0.000 & 0.000 \\ 0.000 & 0.000 & 0.000 & 36.866 & 0.000 & 0.000 \\ 0.000 & 0.000 & 0.000 & 0.000 & 36.866 & 0.000 \\ 0.000 & 0.000 & 0.000 & 0.000 & 0.000 & 36.866 \end{bmatrix}. \quad (17)$$

Normalized effective Young moduli and Poisson ratios have been determined on the basis of effective stiffness tensors, Fig. 6 presents results obtained by using: analytical solution for spherical inclusion, hybrid solution for cubic inclusion and pure numerical (FE) solution for both analyzed shapes of the inclusions. The effective properties are expressed in terms of volume fraction of the reinforcement.



a) b)
Figure 6. Effective material constants in terms of the reinforcement volume fraction: a) normalized Young modulus, b) normalized Poisson ratio

4 CONCLUSIONS AND FURTHER WORK

The work presents the hybrid Mori-Tanaka/Finite element (M-T/FE) homogenization method which allowed to determine the effective properties of composite materials reinforced with particles of arbitrary shape. The method is efficient, as it requires the numerical solution of equivalent inclusion problem involving very simple geometry. An influence of size of the embedding matrix on the strain concentration tensor has been investigated by considering different volume fractions of the single inclusion and comparing the obtained results with analytical solution. Carried out computations showed that single inclusion of volume fraction 0.001 allows to approximate the equivalent inclusion problem properly. The effective stiffness tensor determined for cubic inclusion exhibit the cubic symmetry and therefore the orientation averaging procedure has been applied to obtain the effective stiffness tensor corresponding to material reinforced with randomly oriented cubic particles. The accuracy of obtained results has been verified by performing direct FE homogenization based on the RVE containing substantial number of inclusions. The error of hybrid solution related to the direct FE results is increasing with increasing volume fraction of the inclusions. The hybrid solution underestimates the effective Young moduli and overestimates the effective Poisson ratios. A similar situation is present in case of analytical solution for spherical inclusion. Further work will focus on different shapes of inclusions and orientation distributions. In order to reduce the error of M-T/FE method in case of intermediate volume fractions of the reinforcement a double inclusion approach [22, 23] will be applied. While this paper focuses on linear-elastic material behavior only, the future work will be devoted to extension of M-T/FE method for nonlinear composites.

ACKNOWLEDGEMENT

The research for this paper was financially supported by the National Science Centre, Poland (Grant No. UMO-2016/21/N/ST8/01119)

REFERENCES

- [1] Segurado, J. and Llorca, J. A numerical approximation to the elastic properties of sphere-reinforced composites. *J. Mech. Phys. Solids*. (2002) 50:2107–2121.
- [2] Kouznetsova, V., Brekelmans, W.A.M. and Baaijens, F.P.T. Approach to micro-macro modeling of heterogeneous materials. *Comput. Mech.* (2001) 27:37–48.
- [3] Burczyński, T., Kuś, W. and Brodacka, A. Multiscale modeling of osseous tissues. *J. Theor. Appl. Mech.* (2010) 48:855–870.
- [4] Kamiński, M. Boundary element method homogenization of the periodic linear elastic fiber composites. *Eng. Anal. Bound. Elem.* (1999) 23:815–823.
- [5] Fedeliński, P., Górski, G., Czyż, T., Dziatkiewicz, G. and Ptaszny, J. Analysis of effective properties of materials by using the boundary element method. *Arch. Mech.* (2014) 66: 19–35.
- [6] Ptaszny, J. Accuracy of the fast multipole boundary element method with quadratic elements in the analysis of 3D porous structures. *Comput. Mech.* (2015) 56:477–490.
- [7] Kanit, T., Forest, S., Galliet, I., Mounoury, V. and Jeulin, D. Determination of the size of the representative volume element for random composites: Statistical and numerical approach. *Int. J. Solids Struct.* (2003) 40:3647–3679.
- [8] Eshelby, J.D. The determination of the elastic field of an ellipsoidal inclusion, and related problems. *Proc. R. Soc. Lond. A. Math. Phys. Sci.* (1957) 241:376–396.
- [9] Benveniste, Y. Revisiting the generalized self-consistent scheme in composites: Clarification of some aspects and a new formulation. *J. Mech. Phys. Solids*. (2008) 56: 2984–3002.
- [10] Benveniste, Y. A new approach to the application of Mori-Tanaka's theory in composite materials. *Mech. Mater.* (1987) 6:147–157
- [11] Sadowski, P., Kowalczyk-Gajewska, K. and Stupkiewicz, S. Consistent treatment and automation of the incremental Mori–Tanaka scheme for elasto-plastic composites. *Comput. Mech.* (2017) 60:1–19.
- [12] Tucker, I.C. and Liang, E. Stiffness predictions for unidirectional short-fibre composites: review and evaluation. *Compos. Sci. Technol.* (1999) 59:655–671.
- [13] Ogierman, W. and Kokot, G. A study on fiber orientation influence on the mechanical response of a short fiber composite structure. *Acta Mech.* (2016) 227:173–183.
- [14] Bradshaw, R.D., Fisher, F.T. and Brinson, L.C. Fiber waviness in nanotube-reinforced polymer composites-II: Modeling via numerical approximation of the dilute strain concentration tensor. *Compos. Sci. Technol.* (2003) 63:1705–1722.
- [15] Klusemann, B., Böhm, H.J. and Svendsen, B. Homogenization methods for multi-phase elastic composites with non-elliptical reinforcements: Comparisons and benchmarks. *Eur. J. Mech. A/Solids*. (2012) 34:21–37.
- [16] Srinivasulu, G., Velmurugan, R. and Jayasankar, S. A hybrid method for computing the effective properties of composites containing arbitrarily shaped inclusions. *Comput. Struct.* (2015) 150:63–70.
- [17] Brassart, L., Doghri, I. and Delannay, L. Homogenization of elasto-plastic composites coupled with a nonlinear finite element analysis of the equivalent inclusion problem. *Int. J. Solids Struct.* (2010) 47:716–729.
- [18] Mura, T. *Micromechanics of defects in solids*, Martinus Nijhoff Publishers, Dordrecht (1987)

- [19] Doghri, I. and Tinel, L. Micromechanics of inelastic composites with misaligned inclusions: Numerical treatment of orientation. *Comput. Methods Appl. Mech. Eng.* (2006) 195, 1387–1406.
- [20] Ogierman, W. and Kokot, G. Homogenization of inelastic composites with misaligned inclusions by using the optimal pseudo-grain discretization. *Int. J. Solids Struct.* (2017) 113–114:230–240.
- [21] Cavallini, F. The best isotropic approximation of an anisotropic Hooke's law. *Bollettino di Geofisica Teorica ed Applicata* (1999) 40: 1-18.
- [22] Lielens, G. Micro–Macro Modeling of Structured Materials. PhD thesis (1999) Universite' Catholique de Louvain, Belgium.
- [23] Friebel, C., Doghri, I. and Legat V. General mean-field homogenization schemes for viscoelastic composites containing multiple phases of coated inclusions. *Int. J. Solids Struct.* (2006) 43:2513–2541.

An Efficient Many-core Implementation of Non-overlapping Domain Decomposition Methods

Masao Ogino*

*Nagoya University

ABSTRACT

To solve complex problems in science and industrial applications, the finite element analysis with large-scale unstructured mesh has been widely used on parallel computers. Moreover, the iterative methods such as Krylov subspace method has been usually adopted for solving the large-scale system of the linear equation. However, solving large-scale linear systems from actual problems suffer from slow convergence rate. Therefore, numerical methods having both robust convergence and scalable parallel efficiency are in great demand. The domain decomposition method (DDM) is well known as the iterative substructuring method, and is an efficient approach for parallel finite element methods. As an implementation of the DDM, the hierarchical domain decomposition method (HDDM) [1] has high scalability on distributed-memory parallel computers. As a preconditioner for the non-overlapping DDM, the balancing domain decomposition (BDD) method [2] have robust convergence for the number of subdomains and is expected to be high convergence rate compared to conventional preconditioners. This study focuses on an implementation of the non-overlapping DDM and the BDD method. Especially, parallel scalability of many-core CPUs and multi-GPUs is investigated by using the BDD method based on the HDDM. Moreover, an efficient linear solver of subdomain-interior problems is investigated. To indicate that our system has both robust convergence and high parallel efficiency, some numerical results are demonstrated on the Fujitsu PRIMEHPC FX100 consisting of 32-core CPU and a supercomputer consisting of multi-CPU and multi-GPU. [1] Yagawa, G. and Shioya, R. (1994) Parallel finite elements on a massively parallel computer with domain decomposition, *Computing Systems in Engineering*, 4, 495-503. [2] Mandel, J. (1993) Balancing domain decomposition, *Communications on Numerical Methods in Engineering*, 9, 233-241.

Numerical Investigations on Pattern Formation in Surface Earthquake Faults

Kenji Oguni*, Sayako Hirobe**

*Keio University, **Keio University

ABSTRACT

Surface earthquake faults due to underground strike slip often show a typical echelon fault pattern on the top surface of the embedded soil. This typical echelon fault pattern is called Riedel shear. Based on the observations from model experiments for Riedel shear using a box of sand, the twist of the fault surface growing from the strike-slip at the bottom could be suspected as the fundamental source of the periodical pattern of the Riedel shear. On the other hand, experiments using transparent gelatin specimen show that Riedel shear is the consequence of the consecutive choice of the bifurcated solution. These experimental observations with contradicting appearances prevent us from the complete explanation of the mechanism behind Riedel shear. The purposes of this study are to simulate Riedel shear caused by strike-slip faults and to identify the governing mechanism of the Riedel shear. The periodical pattern formation observed in Riedel shear implies the importance of bifurcation in the governing mechanism of this phenomenon. Therefore, numerical analysis method with the capacity of the fracture-induced bifurcation analysis is required. For this purpose, PDS-FEM (particle discretization scheme finite element method) has been employed and elasto-dynamic analysis of a plate of homogeneous elasticity subject to strike-slip at the bottom surface has been carried out as the simplest model of the Riedel shear. The periodical echelon fault pattern generated by numerical simulation shows reasonable agreement with the Riedel shear observed in sandbox experiment in its size, orientation, and pitch. The detail investigation of the internal structure of the numerically generated faults has revealed the formation process of the Riedel shear. The Riedel shear starts from the segmentation of the straight strike-slip line into short echelon faults with small twist, then, as the cracks evolve upwards, these short segments undergo consecutive bifurcation with alternative choice of the growing segments. As this process proceeds, the cracks reach to the top surface, the twist angle of the cracks increases, and the number of the cracks decreases as the consequence of the consecutive bifurcation.

Mitigation of Boundary Effect in Nonordinary State-based Peridynamics by Addition of Mirroring Nodes

Seong Eun Oh^{*}, Jung-Wuk Hong^{**}

^{*}Korea Advanced Institute of Science and Technology, ^{**}Korea Advanced Institute of Science and Technology

ABSTRACT

In this research, the boundary effect of the nonordinary state-based peridynamics (PD) in the displacement controlled simulation is investigated and mitigated by adding mirroring nodes along the boundary. The peridynamic variables at each node are collectively calculated using the configurations and variables at neighboring nodes within its horizon [1]. If there exists an intersection between a certain horizon and the boundary, the domain within the horizon is not completely spherical, yielding inaccurate estimation of tensors and state variables. In order to mitigate this boundary effect, virtual nodes are deployed by mirroring the interior nodes residing within the body with respect to the boundary. In specific, the shape tensors of the peridynamic nodes that have incomplete spherical horizons are calculated by considering both the interior peridynamic nodes and the mirrored virtual nodes. For the calculation of the force states, the displacements of the peridynamic nodes in the body are extrapolated to the virtual nodes anti-symmetrically, and the interacting forces between the interior nodes and the virtual nodes are added to the nodal forces. In order to validate the proposed methodology, displacement-controlled simulations are carried out by exerting axial elongation and shear deformation on the left and right sides of a solid cube. For different horizons ($1\delta x$, $2\delta x$ and $3\delta x$), the numerical results from the proposed mirroring method are compared with the results from the original nonordinary state-based peridynamics, and the differences are investigated. The proposed methodology yields more accurate results than the original methodology, especially around the boundary. [1] Silling, S.A., Epton, M., Weckner, O., Xu, J., Askari, E., 2007. Peridynamic states and constitutive modeling. Journal of Elasticity 88, 151-184.

Extension of Quantitative Phase-field Simulations to Prediction of Macroseggregation Based on Machine Learning

Munekazu Ohno*

*Hokkaido University

ABSTRACT

Segregation arises during alloy solidification. It is generally classified into microsegregation on a dendritic scale and macrosegregation on an ingot scale. Prediction of macrosegregation requires precise description of microsegregation during dendritic growth. Several analytical models were developed for prediction of microsegregation and they have played an important role in making progress in understanding the microsegregation behavior. Effects of microstructural change and multicomponent diffusion are the important factors to be taken into account for better description and prediction of microsegregation behavior. The phase-field model is a powerful tool to describe microstructural evolution processes in alloy solidification. Importantly, quantitative phase-field model (Q-PFM), which is formulated based on the thin-interface limit, enables us to carry out quantitative description and prediction of microstructural evolution processes. However, the early developed Q-PFMs are applicable to alloy systems without diffusion in the solid phase(s) and therefore these models cannot be utilized for the analysis of microsegregation. In order to describe the microsegregation behavior, Q-PFM was extended by our group to deal with alloy systems with diffusion in the solid in multicomponent alloys. In this talk, we show that Q-PFM enables highly accurate prediction of microsegregation behavior in Fe-Mn and Al-Cu alloy systems. Several simulation models have been proposed for prediction of macrosegregation. The improvement of accuracy of the early developed models requires the improvement of microsegregation calculation in these models in which the details of microstructural change are not taken into account. In this study, we propose the macrosegregation model in which the microsegregation behavior predicted by Q-PFM is introduced by means of machine learning.

Edge Wrinkle or Crease in Very Thin Rectangular Plates under Gravity

Akira Ohta^{*}, Hideo Koguchi^{**}

^{*}Niigata Institute of Technology, ^{**}Niigata Institute of Technology

ABSTRACT

A precise position control of glass substrates is required in a process of manufacturing an organic electroluminescence display. The precise position of glass is the most important process, which determines the definition of the display. Recently, glass substrates tend to be larger every year to increase a productive efficiency. The thickness of the glass substrate reduces every year since a market demands thinner end products. Furthermore, material of the substrate is required to be replaced except glass. In the manufacture process, multiple deformation modes in the glass substrate are frequently observed. In a deformation mode, when the glass substrate is pushed up by a finger from the bottom and release the finger, the deformation mode of the substrate varies stably. When a different place in the substrate is pushed up with a finger in the same manner, the plate becomes stable at the different shape. We can simulate this phenomenon in a computer and real manufacture process. We will present a mechanism of occurrence for multiple deformation modes and the relationship of thickness, elasticity, the size and the density of the substrate. When a thin plate is supported only at side edges, the center area of the plate deflects due to gravity, the side edge is dragged along the side and compressed. When compressive stress exceeds a critical value, buckling occurs at the side edges. The local buckling occurs in a part of the thin plate, that is, buckling does occur in the whole plate. This local buckling is the cause of multiple unstable deformation. In a production site, it is required that multiple unstable deformation never occurs. A method for calculating a occurrence limit of phenomenon is needed. We would like to present a method for calculation. Furthermore, it is investigated that the buckling occurs under what kind of condition using this method. Here, the ratio of the thickness and the area of the plate is referred to as the degree of thin plate. The ratio of the stiffness and the density of the plate is referred to as a specific stiffness. The occurrence limit of the unstable deformation will be shown using these ratios.

UMMDp and UMMDr: Unified User Subroutine Libraries for Nonlinear Material Models in Advanced Finite Element Applications

Kai Oide^{*}, Hideo Takizawa^{**}, Takashi Terajima^{***}, Junji Yoshida^{****}, Toshihiko Kuwabara^{*****}

^{*}Mechanical Design & Analysis Corporation, ^{**}Nippon Institute of Technology, ^{***}Meiji Rubber & Chemical CO., LTD, ^{****}University of Yamanashi, ^{*****}Tokyo University of Agriculture and Technology

ABSTRACT

With the spread of commercial finite element software, numerical simulation has become widely used throughout many fields, not only in advanced industrial applications, as a method for solving practical problems. Appropriate solutions for daily routine design work can easily be identified using the extensive analytical functions of these software programs. For example, large displacement problems, large strain problems, and contact problems are becoming common tasks for general design engineers. However, in nonlinear material application fields, if more advanced problems are attempted, material models that are not prepared in default analysis options are needed. Analysts have to customize the available options in finite element programs, and prepare material constants through appropriate material testing. These kinds of technical processes require professional knowledge and skills, and are therefore not yet widely available. The Japan Association for Nonlinear Computer Aided Engineering (JANCAE), a non-profit organization, has held lectures twice a year for four days each since 2001 to provide training on theories and technology related to nonlinear simulation; more than 3000 people have participated so far. Over the last decade, it has held working groups during which participants have developed and verified two user-subroutine libraries: the Unified Material Model Driver for Plasticity (UMMDp) for anisotropic yield functions, and the Unified Material Model Driver for Rubber (UMMDr) for modeling rubber materials. These working groups were established to provide a multidisciplinary forum for steel researchers, rubber researchers, design engineers, and software engineers to collaborate through the medium of advanced finite element codes. The UMMDp contains a subroutine library that includes practically recognized anisotropic yield functions (e.g. Yoshida's 6th-order polynomial, Barlat's Yld2000-2d and Yld2004, Banabic's BBC2008). In UMMDr, a subroutine library combines the isochoric components of hyperelastic models (e.g. a stretch-based model such as Ogden, Shariff, and an invariants-based model such as Mooney Rivlin.), damage models (e.g. Simo, Miehe, Ogden-Roxburgh), visco-elastic models (e.g. Simo, Holzapfel, Reese-Govindjee), and the volumetric components of the hyperelastic models. Both subroutine libraries provide multi-port capabilities that can be used with commercial finite element software, such as Abaqus, ADINA, ANSYS, LS-DYNA and MSC.Marc. Moreover, new material models can be added to both subroutine libraries. Each subroutine is verified with basic tests, and both libraries are verified with one elements test and multiple practical tests. This paper introduces the development of the UMMDp and UMMDr, and discusses some verification methods and example simulations.

A FUNDAMENTAL STUDY ON DAMAGE DETECTION BASED ON DEEP LEARNING USING DATA OBTAINED FROM SHAKE TABLE TESTS OF A STEEL FRAME

**KAZUYA OKA*, KENTA WATANABE*, MASAYUKI KOHIYAMA*,
TAKUZO YAMASHITA†, KAZUTOSHI MATSUZAKI‡, AND YUJI MORI‡**

*Graduate School of Science and Technology, Keio University
3-14-1 Hiyoshi, Kohoku-ku, Yokohama 223-8522, Japan
kazuyaoka@a8.keio.jp

†National Research Institute for Earth Science and Disaster Resilience
3-1 Tennodai, Tsukuba-shi, Ibaraki, 305-0006, Japan

‡Mizuho Information & Research Institute, Inc.
2-3 Kanda-Nishikicho, Chiyoda-ku, Tokyo 101-8443, Japan

Key words: Damage Identification, Deep Learning, Structural Health Monitoring, Brace, Steel Frame, Shaking Table Test

Abstract. To employ neural networks in structural health monitoring, a large volume of training data is required. The data can be obtained by a generative learning method based on high-precision simulation of seismic responses. We investigate appropriate machine learning parameters such as the numbers of layer nodes in a deep neural network and the number of epochs for training. Response records measured in shaking table tests of a steel frame structure are used as training, validation, and test data. Our results show that response data of only the translational component can achieve high accuracy of damage pattern classification. Regarding the length of response data, clear difference is not observed in two durations of 1 s and 2 s. We propose a method to detect unlearned damage pattern data using the Mahalanobis distance.

1 INTRODUCTION

Structural health monitoring (SHM) systems have not been extensively applied to existing buildings, and it is expected to improve damage estimation accuracy of these systems. Some SHM systems employ a neural network (NN); many studies have been conducted on damage detection using NN. For example, with respect to the NN input data, Ferregut et al.^[1] used resonance frequency and Choi and Kwon^[2] used responses measured by strain gauges and acceleration sensors for the truss bridge under traffic vibrations. Chang et al.^[3] used modal parameters such as natural periods and mode shapes, and Lee et al.^[4] used mode vectors of a

linear model. However, these studies performed damage detection based on linear responses rather than nonlinear responses, which are often observed under strong ground motion.

To consider nonlinear responses, Lautour and Omenzetter^[5] predicted damage indices by numerical simulations using a nonlinear finite element method, and Derkevorkian et al.^[6] also took a nonlinear response into account and proposed a time-marching framework to predict damage from the change. Rafiei and Adeli^[7, 8] proposed a global and local SHM system that can detect damage using only ambient vibrations of high-rise building structures before damage occurs. However, these methods cannot detect damage of individual members, such as columns, beams, and braces.

Recently, Abdeljaber et al.^[9] developed a method to detect damage of individual members through deep learning of distribution from raw acceleration responses of random vibrations for damage patterns. In addition, Zhang et al.^[10] presented a machine learning framework using peak plastic hinge rotation obtained from a nonlinear response analysis of a four-story and three-span reinforced-concrete building under simulated ground motion. These studies use the acceleration of all joints; therefore, it is necessary to develop systems that can be applied to models installed with less sensors.

To overcome problems in the field of SHM described above, we use the shaking table test data of a steel structure and nonlinear responses at a limited number of joints to train deep NN. We analyze the identification accuracy of damage patterns. Additionally, we propose and verify a detection method of unlearned damage pattern data.

2 OUTLINE OF THE SHAKING TABLE TEST

In this research, response records measured in the shaking table tests of a steel frame structure are used as training, validating, and test data instead of response data simulated by E-Simulator, a high-precision finite element analysis software. The test specimen (Fig. 1) is a small-scale model of a four-story steel frame structure with a longitudinal direction width of 12 m, a transverse direction width of 6 m, and a height of 14 m. The test specimen has a height of 1.157 m and a first natural period of 0.21 s. We install four braces in the second story of the specimen and assume eight different damage patterns of the braces, as shown in Fig. 2, which are simulated by relaxing the turn buckle of the braces before shaking. We prepare simulated ground motions for horizontal uniaxial shaking; an example of input waves is shown in Fig. 3. The simulated ground motions are synthesized based on a modified method for design ground motion prescribed by the Notification of Building Standard Law of Japan, which uses time-domain envelope functions, design acceleration response spectrum, and random phases. Approximately 100 different simulated ground motions with small to large amplitudes and short to long durations are input to the specimen with each state of damage. We install inertial measurement units, M-G550-PC made by Seiko Epson Corporation, throughout the specimen and measure three translational acceleration components and three angular velocity components with a sampling frequency of 500 Hz.

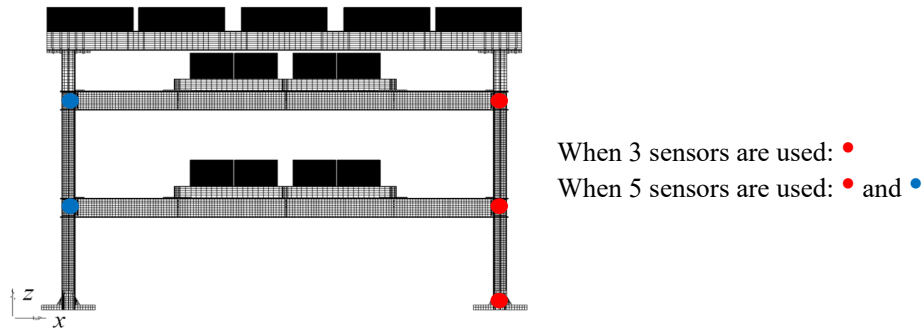


Figure 1. The test specimen and sensor location used in the study

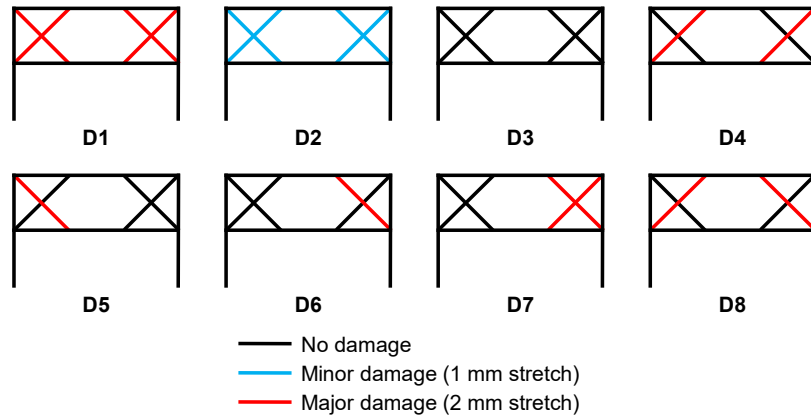


Figure 2. Damage patterns of braces

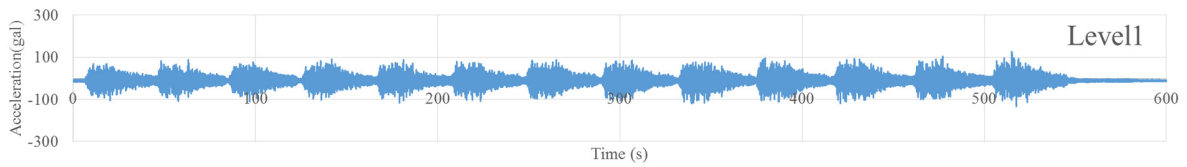


Figure 3. An example of simulated ground motion input in a shaking table test

3 ANALYSIS ON ACCURACY OF DAMAGE PATTERN IDENTIFICATION

We identify damage patterns of the specimen using the damage pattern identification system based on a multi-layer NN, which was developed by the National Research Institute for Earth Science and Disaster Resilience and Mizuho Information & Research Institute. For data input of NNs, a sample is a raw measurement record divided and extracted with a time length of 1 s or 2 s (two cases), which is 5 or 10 times that of the first natural period, 0.21 s, of a specimen without braces. The input dataset is randomly divided into two groups, one for training and the other for validation, and cross validation is performed.

To clarify hyper-parameters that improve the accuracy of damage pattern identification, accuracies are compared among different combinations of the components of the measurement records, the number of middle layers nodes, the sample length, and the number of training epochs. The number of sensors used is three or five (two cases), as shown in Fig. 1. We fixed the number of middle layers of NNs to three, and three cases of the numbers of middle layers nodes are compared: (100, 50, 25), (500, 250, 125), and (1000, 500, 250), values are ordered from the middle layer closest to the input layer. Two cases of the sample length, 1 s and 2 s, are compared.

Figure 4 shows the learning curves representing the relationship between the number of training epochs and the accuracy rate, i.e., a fraction of the number of samples with a damage pattern correctly identified over the total number of samples, for the case of the highest accuracy. A blue curve shows the average accuracy rate of the training data and a red curve is that of the cross-validation data. To reduce computation time, the average accuracy rate of the cross-validation data is calculated sparsely. When comparing two curves, the red curve decreases at the epoch size of 100 due to overfitting. Among the compared hyper-parameter combinations, the highest accuracy is achieved when there are three sensors, three components (only the translational acceleration component in the x-axis direction), the middle layer nodes (500, 250, 125), the sample length is 1 s, and the number of learning epochs is ninety. The cross-validation results at the hyper-parameter combination are shown in Table 1. The average accuracy rate is 88%.

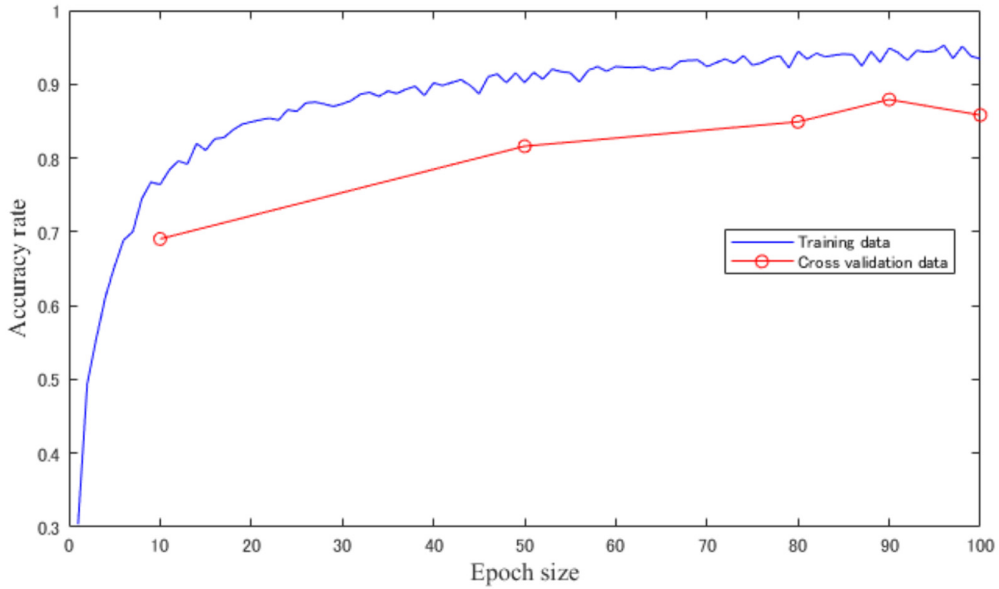


Figure 4. Relation between training epoch size and accuracy rates

Table 1. Cross-validation results with three sensors, one component, middle layers nodes (500, 250, 125), a sample length of 1 s, and 90 learning epochs.

		Damage pattern in experiment (true value)								Total
		D1	D2	D3	D4	D5	D6	D7	D8	
Cross validation result	D1	5099	1595	23	13	0	0	5	9	6744
	D2	1476	4987	6	27	0	0	3	7	6506
	D3	4	2	6532	7	18	6	0	0	6569
	D4	6	11	1	5919	36	15	257	133	6378
	D5	0	0	32	43	6195	448	10	1	6729
	D6	0	0	5	14	341	5969	87	20	6436
	D7	2	1	1	347	10	150	5795	502	6808
	D8	13	4	0	230	0	12	443	5928	6630
Total		6600	6600	6600	6600	6600	6600	6600	6600	52800
Accuracy rate		0.773	0.756	0.990	0.897	0.939	0.904	0.878	0.898	0.879

4 METHOD TO DETECT SAMPLE DATA OF UNLEARNED DAMAGE PATTERNS

We consider the input space of the output layer node, and detect unlearned damage pattern data at Mahalanobis distance, as shown in Figure 5. Therefore, the detection criterion of the unlearned pattern is given as

$$\sqrt{(\mathbf{x}_n - \boldsymbol{\mu}^k)^T (\mathbf{X}^k)^{-1} (\mathbf{x}_n - \boldsymbol{\mu}^k)} > \theta_\alpha^k \text{ for all } k \text{ and } n (k = 1, 2, \dots, K; n = 1, 2, \dots, N) \quad (1)$$

where $\mathbf{x}_n = (x_{n,1}, x_{n,2}, \dots, x_{n,K})^T$ is the input of the node in the output layer of sample n ; K is the number of learned damage patterns, and N is the number of test samples. Let $\mathbf{x}_m^k = (x_{m,1}^k, x_{m,2}^k, \dots, x_{m,K}^k)^T$ ($k = 1, 2, \dots, K; m = 1, 2, \dots, M_k$) be the input of the node in the output layer of the training sample m whose damage pattern is k (where M_k is the number of training samples of damage pattern k), the component of the average value $\boldsymbol{\mu}^k = (\mu_1^k, \mu_2^k, \dots, \mu_K^k)^T$ ($k = 1, 2, \dots, K$) of \mathbf{x}_m^k is $\mu_i^k = (1/M_k) \sum_{m=1}^{M_k} x_{m,i}^k$, and the covariance matrix $\mathbf{X}^k = (X_{ij}^k | i, j = 1, 2, \dots, K)$ has $X_{ij}^k = (1/M_k) \sum_{m=1}^{M_k} (x_{m,i}^k - \mu_i^k)(x_{m,j}^k - \mu_j^k)$. By setting the significance level α of detection, and for each damage pattern, searching a sample of the α -quantile point counted from a point where the Mahalanobis distance is far from the training data distribution, the threshold θ_α^k is defined by the distance.

5 VERIFICATION OF DETECTION METHOD

We conducted a verification test of the proposed method to detect sample data of unlearned damage patterns. First, we used damage patterns D1 to D8 as training data, and new data were obtained by inverting the sensor location and sign of the measurement records as data of an unlearned damage pattern. As a result, all the 660 samples were detected as “unlearned” at the significance level $\alpha = 5\%$.

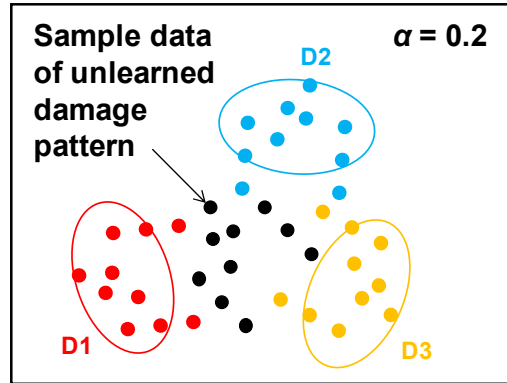


Figure 5. A method to detect sample data of unlearned damage patterns

A different dataset was also investigated; we used D1, D3, D4, D5, D6, and D8 as training data, and D7 as an unlearned damage pattern. It was observed that the samples detected as unlearned at $\alpha = 5\%$ was 0 out of 660. Eleven of 660 were detected as unlearned at $\alpha = 25\%$. In the proposed method, classification accuracy will decrease when training data of learned damage patterns do not follow a normal distribution in the space of the input values of the output layer nodes. Therefore, it is necessary to improve the method.

6 CONCLUSIONS

The accuracy of damage pattern classification based on a deep NN was analyzed using response records of a shaking table experiment as training and test data. It was confirmed that the average accuracy rate was approximately 88% under the condition that the sample length was 1 s, which is about five times the natural period of the target structure, and the number of installed sensors was one per layer. We constructed a method of detecting unlearned damage pattern data using the Mahalanobis distance. The classification accuracy significantly varied depending on the learned damage pattern; therefore, improvement of the method is needed in the future.

REFERENCES

- [1] Ferregut, C.M., Osegueda, R.A., and Ortiz, J. Artificial neural networks for structural damage detection and classification. *Proc. SPIE*. (1995) 2446:68–80.
- [2] Choi, M-Y. and Kwon, I-B. Damage detection system of a real steel truss bridge by neural networks. *Proc. SPIE*. (2000) 3988:295–306.
- [3] Chang, C.C., Chang, T.Y.P., and Xu, Y.G. Structural damage detection using an iterative neural network. *J. Intell. Mater. Syst. Struct.* (2000) 11:32–42.

- [4] Lee, J.J., Lee, J.W., Yi, J.H., Yun, C.B., and Jung, H.Y. Neural networks-based damage detection for bridges considering errors in baseline finite element models. *J. Sound Vib.* (2005) 280:555–578.
- [5] De Lautour, O.R. and Omenzetter, P. Prediction of seismic-induced structural damage using artificial neural networks. *Eng. Struct.* (2009) 31:600–606.
- [6] Derkevorkian, A., Hernandez-Garcia, M., Yun, H.-B., Masri, S.F., and Li, P. Nonlinear data-driven computational models for response prediction and change detection. *Struct. Control Health Monit.* (2015) 22:273–288.
- [7] Rafiei, M. H. and Adeli, H. A novel machine learning-based algorithm to detect damage in high-rise building structures. *Struct. Des. Tall Special Buildings* (2017) 26:1400. <https://doi.org/10.1002/tal.1400>.
- [8] Rafiei, M.H. and Adeli, H. A novel unsupervised deep learning model for global and local health condition assessment of structures. *Eng. Struct.* (2018) 156:598–607.
- [9] Abdeljaber, O., Avci, O., Kiranyaz, S., Gabbouj, M., and Inman, D.J. Real-time vibration-based structural damage detection using one-dimensional convolutional neural networks. *J Sound Vib.* (2017) 388:154–170.
- [10] Zhang, Y., Burton, H.V., Sun, H., and Shokrabadi, M. A machine learning framework for assessing post-earthquake structural safety. *Struct. Saf.* (2018) 72: 1–16.

Parameter Estimation during Solidification of Metals based on Data Assimilation

Yukimi Oka^{*}, Munekazu Ohno^{**}, Tomohiro Takaki^{***}, Yasushi Shibuta^{****}, Kiyotaka Matsuura^{*****}

^{*}Hokkaido University, ^{**}Hokkaido University, ^{***}Kyoto Institute of Technology, ^{****}The University of Tokyo, ^{*****}Hokkaido University

ABSTRACT

It is essential for production of casts with high quality to control the solidification microstructures. However, it is difficult to clarify the formation process of solidification microstructure in detail, because the solidification process is a multi-physics problem involving thermo-solutal diffusion and fluid dynamics. Moreover, it is generally not possible to directly observe the dynamics of solidification by experimental approaches. Therefore, computational studies have contributed to understanding of such a complicated solidification process and predicting of solidification microstructure. A phase-field method is a method of choice in simulating the dendrite structure, which is typical growth morphology in solidification of metals. In order to predict solidification microstructure precisely by the means of phase-field simulation, physical parameters must be determined accurately. Especially, solid-liquid interfacial energy and its anisotropy largely affect the morphology of the dendrite structure. Hence, it is indispensable to use accurate values of these interfacial properties. However, it is difficult and/or cumbersome to determine interfacial properties by means of experimental methods. Although calculation methods for interfacial properties based on molecular dynamics (MD) simulations have been developed, the application of these methods is limited to the equilibrium state. Also, it is not easy to calculate accurate values of interfacial energy and its anisotropy even by MD simulations. Therefore, it is very important to develop a reliable method for estimation of interfacial properties in both equilibrium and non-equilibrium states. In this study, data assimilation is utilized for the estimation of interfacial properties at the solid/liquid interface during solidification of metals. The data assimilation is a method based on Bayesian inference developed in the field of data science. In this study, the data assimilation is employed for estimation of interfacial properties of the phase-field simulation. The applicability of the data assimilation to the estimation of interfacial properties at the solid/liquid interface during solidification of metal is systematically investigated on the basis of the twin experiment.

CAE Simulation in OMRON Co. And My Idea about CAE Using “Big Data” and AI

Hiroshi Okada*

*OMRON

ABSTRACT

Omron Corp. has worked extensively to improve product development process utilizing CAE. However, the market requests are more demanding for higher quality, improved functionality, smaller dimension and appropriate delivery time. Moreover, the market is requesting Omron Corp. to develop the product which can be used safely with severe environmental impact. At first, I explain how Omron Corp. uses CAE for the many different field problems such as structural and thermal problems in the development process of our industrial products. Next, I will explain how Omron Corp. will extend CAE to make use of AI and Big Data Analytics. The extended CAE includes AI technology, especially Deep Learning with Neural Network, which can be used for the regression of complex design space (Big Data) generated by extensive parametric simulations. Last, I will explain how Omron Corp. will utilize the extended CAE for the future in order to satisfy the market requests.

Computations of Fracture Mechanics Parameters for 3D Arbitrary Shaped Crack in Welded Joint and Functionally Graded Material

Hiroshi Okada^{*}, Tatsuro Ishizaka^{**}, Masahiro Ono^{***}, Yasunori Yusa^{****}

^{*}Tokyo University of Science, ^{**}Tokyo University of Science, ^{***}Tokyo University of Science, ^{****}Tokyo University of Science

ABSTRACT

In this presentation, the formulations and the computations of fracture parameters, such as the stress intensity factors and the energy release rates for 3D arbitrary shaped crack in welded joint and functionally graded material are discussed. Welded joints and functionally graded materials have common features such that the mechanical properties have continuous and discontinuous spatial variations. Furthermore, residual stresses generally develop in welded joints. Classical ways to compute the fracture parameters often assume the material to be homogeneous. The weld residual stresses are not assumed. In the present investigation, a series of related developments to perform realistic 3D fracture mechanics analyses have been carried out. First, the use of general finite element program with the quadratic tetrahedral element along with an automatic mesh generation technique based on the constrained Delaunay tessellation technique was proposed (Okada et al. [1]). Then, methodologies to compute the J and the interaction integrals (Daimon and Okada [2]) were presented. They are presently extended to the problems of welded joints (Nose et al. [3]). We assume that residual stresses are present but the prior strain histories are not known. Furthermore, mechanical properties have spatial variations. The key issues are in the treatments on additional terms arising due to the spatial changes of mechanical properties and the existence of residual stress. To make all the methodologies tractable for application engineers, only a general purpose finite element program with the automatic meshing technique is used. The J- and the interaction integral evaluations are carried out as their post processes by separate software. In the presentation, the discussions on the additional terms, their numerical treatments and their numerical results are presented. Acknowledgements: A part of present research was supported by JSPS (Japan Society for the Promotion of Science) Grant-in-Aid for Scientific Research (C) No.16K05988. The support is acknowledged. References: [1] H. Okada, H. Kawai, T. Tokuda, Y. Fukui, Fully automated mixed mode crack propagation analyses based on tetrahedral finite element and VCCM (virtual crack closure-integral method), International Journal of Fatigue, Vol. 50, pp. 33-39, 2013. [2] R. Daimon, H. Okada, Mixed-mode stress intensity factor evaluation by interaction integral method for quadratic tetrahedral finite element with correction terms, Engineering Fracture Mechanics, Vol. 115, pp. 22-42, 2014. [3] M. Nose, H. Amano, H. Okada, Y. Yusa, A. Maekawa, M. Kamaya, H. Kawai, Computational crack propagation analysis with consideration of weld residual stresses, Engineering Fracture Mechanics, Vol. 182, pp. 708-731, 2017.

DES of Pulsatile Turbulent Flow Through a Double 90° Bend Pipe for Flow Analysis of an Automotive Exhaust System

Junichi Oki^{*}, Haruna Yanagida^{**}, Yukika Kuga^{***}, Ryo Yamamoto^{****}, Kazuhiro Nakamura^{*****},
Hideaki Yokohata^{*****}, Keiya Nishida^{*****}, Yoichi Ogata^{*****}

^{*}Hiroshima University, ^{**}Mazda Motor Corporation, ^{***}Hiroshima University, ^{****}Mazda Motor Corporation,
^{*****}Mazda Motor Corporation, ^{*****}Mazda Motor Corporation, ^{*****}Hiroshima University, ^{*****}Hiroshima
University

ABSTRACT

The present study focuses on pulsatile turbulent flow that is encountered in an exhaust system of an internal combustion engine. Whereas most of numerical studies related to exhaust flows have used Reynolds-averaged Navier-Stokes modeling even though such a flow is highly unsteady [1,2], our numerical simulation is performed using detached-eddy simulation (DES) [3] capable of calculating with a coarser spatial resolution close to the wall compared with large-eddy simulation approach. The flow configuration and condition are determined from our pulsatile flow rig with a square-sectioned S-shaped test section comprising a double 90° bend. The inlet boundary condition for the velocity and the outlet boundary condition for the pressure are respectively set based on the measured data with a hot-wire anemometer and a piezoelectric pressure sensor, resulting in a Reynolds number of 36,400 and a Womersley number of 59.9. The numerical result is validated against the experimental data obtained from the phase-locked stereo PIV conducted in the pipe cross sections located downstream of the bends. The comparisons show good agreement between the numerical and experimental results in terms of the phase-averaged secondary and axial velocities. The DES can capture the Dean-type secondary vortices downstream of the first bend and the Lyne-type vortices developing through the double bend. This implies that our numerical simulation is capable of accurately predicting the development process of the turbulent flow through the straight pipe as well as the bend under the pulsatile condition, because the inflow velocity distribution to the bend plays a significant role in the secondary flow formation. This study improves the understanding of pulsatile turbulent flow structures in bends through the computation, and confirms the capability of the DES approach for industrial application. [1] Jeong S.-J. (2014) A full transient three-dimensional study on the effect of pulsating exhaust flow under real running condition on the thermal and chemical behaviour of closed-coupled catalyst. Chemical Engineering Science, Vol. 117, pp. 18-30. [2] Rao H.K.S., S. Raviteja, Kumar G.N. (2017) Computational Analysis of Unsteady Flow in Turbine Part of Turbocharger. In: Saha A., Das D., Srivastava R., Panigrahi P., Muralidhar K. (eds) Fluid Mechanics and Fluid Power – Contemporary Research. Lecture Notes in Mechanical Engineering. Springer, New Delhi. [3] Spalart P.R., Jou W.-H., Strelets M., Allmaras S.R. (1997) Comments on the feasibility of LES for wings, and on a hybrid RANS/LES approach. First AFOSR International Conference on DNS/LES.

3D Vertex Modeling and Computational Simulations of Multicellular Dynamics

Satoru Okuda*

*PRESTO, Japan Science and Technology Agency

ABSTRACT

Multicellular dynamics have a key role in determining the macroscopic behaviors of living tissues in development, homeostasis, and disease. Such multicellular dynamics emerge from the integration of mechanical cell behaviors in three-dimensional (3D) space, such as cell deformation, movement, division, and apoptosis. Typical examples of 3D multicellular dynamics are epithelial deformations in morphogenesis and collective cell migration in cancer metastasis. However, while such 3D multicellular dynamics is fundamental to general soft tissue dynamics, little is about how individual cell behaviors are spatiotemporally coordinated in the macroscopic level. To simulate such 3D multicellular dynamics, we have developed a versatile 3D vertex model framework. Here, we show the mathematical framework of the model and its applications to morphogenesis.

Mechanism of Strain Softening Predicted by an Extended Flory-Rehner Model for Swollen Elastomers

Dai Okumura^{*}, Shoji Shimizu^{**}, Takafumi Mano^{***}

^{*}Osaka University, ^{**}Nagoya University, ^{***}Nagoya University

ABSTRACT

In this study, we investigate the ability of two scaling exponents to describe swelling-induced strain softening of elastomers. Two scaling exponents are included in the extended version of the Flory-Rehner (F-R) model [1], and are introduced into elastic strain energy functions that are separated into deviatoric and volumetric components [2]. The two scaling exponents are used to adjust the swelling effects on the Young's modulus and osmotic pressure of swollen elastomers, resulting in the ability to describe swelling-induced strain softening under uniaxial and biaxial deformations [2]. Swelling-induced strain softening can be related with strain localization followed by swelling-induced rupture. In Gee's experiments [3], natural rubbers exhibited swelling-induced rupture when a small extension was applied in good solvents. This tendency was successfully predicted when the two scaling exponents were determined based on experiments [2]. To investigate the detailed mechanism, mechanical properties such as the Young's modulus and Poisson's ratio are explicitly derived from linear perturbation analysis of the extended F-R model. This derivation is performed by considering an arbitrary deformation state. The onset point of swelling-induced strain softening are analysed using the combination of the explicit expressions of the mechanical properties. It is found that swelling-induced strain softening can be caused with negative Poisson's ratio, which appears under deformation states at equilibrium swelling and that it depends on the combination of the two scaling exponents. References [1] Flory, P.J., Rehner, J., "Statistical mechanics of cross-linked polymer networks II. swelling", The Journal of Chemical Physics, Vol.11, page 521-526 (1943). [2] Okumura, D., Kondo, A., Ohno, N., "Using two scaling exponents to describe the mechanical properties of swollen elastomers", Journal of the Mechanics and Physics of Solids, Vol.90, page 61-76 (2016). [3] Gee, G., "The interaction between rubber and liquid. X. some new experimental tests of a statistical thermodynamic theory of rubber liquid systems", Transactions of Faraday Society, Vol.42, page B033-B044 (1946).

A Marginalized Unscented Kalman Filter for Efficient Parameter Estimation with Applications to Finite Element Models

Audrey Oliver^{*}, Andrew Smyth^{**}

^{*}Columbia University, ^{**}Columbia University

ABSTRACT

This paper focuses on the problem of combined state/parameter estimation in dynamical systems with many degrees of freedom, for instance finite element models, using measured data from the system and nonlinear Bayesian filtering techniques for the estimation. An efficient nonlinear Kalman filtering technique is developed (marginalized UKF), based on a combination of extended Kalman filtering for state estimation and unscented filtering for parameter learning. While extended filtering requires computations of Jacobians, which might become cumbersome in large dimensional cases, unscented filtering is a gradient-free method that requires only function evaluations of the forward problem and could thus be combined with an external FE software. However, the number of required function evaluations grows linearly with the number of states, rendering this approach computationally cumbersome when considering FE models with many degrees-of-freedom. Instead, the algorithm presented herein implements the principle of marginalization to the unscented transform to conveniently combine extended and unscented filtering. The algorithm can then take advantage of the fact that Jacobians of the system equations with respect to the dynamic states, required in extended Kalman filtering, can be easily related to outputs of the finite element analysis such as the tangent stiffness matrix of the finite element model, thus greatly facilitating the use of extended filtering with respect to the dynamic states. In this talk we will first review basics of Bayesian filtering for combined state/parameter estimation, then we will present the specifics of the marginalized UKF and how it can be used to solve for inverse problems in finite element analysis. We will then demonstrate the applicability of this algorithm to perform efficient parameter estimation using simulated data from different types of finite element models. Systems which exhibit linear or nonlinear behaviors with respect to both the states and/or the parameters will be considered.

BDDC Methods for the Simulation of High Temperature Superconductors

Marc Olm^{*}, Santiago Badia^{**}, Alberto Martín^{***}

^{*}Technical University of Catalonia, CIMNE, ^{**}Technical University of Catalonia, CIMNE, ^{***}Technical University of Catalonia, CIMNE

ABSTRACT

In this work, we present numerical results using BDDC methods for preconditioning the systems arising from finite element discretizations of the time-domain quasi-static approximation of Maxwell's equations with Nédélec (or edge) elements of arbitrary order. First, we show the scalability of the proposed schemes on a set of academical linear problems with a highly scalable implementation based on overlapped multilevel task implementation in FEMPAR. Next, in order to model the behaviour of High Temperature Superconductors (HTS), resistivity is assigned a stiff power law depending on the magnetic field itself, introducing a strong nonlinearity. On the other hand, a constant resistivity value is kept in a large dielectric region, which completely surrounds the superconducting device. A h-adaptive meshing technique customized for Nédélec elements leads to a smart mesh coarsening in the dielectric region, where no results of interest are found but nevertheless it allows us to impose realistic external conditions far away from the HTS sample. Then the problem is linearized with a Newton-Raphson scheme, and nonlinear convergence is boosted with a line search technique. Finally, our BDDC preconditioners are composed with Krylov-subspace iterative methods to solve the linearized problems arising at every nonlinear iteration. References [1] S. Badia, A. Martín and J. Principe. A Highly Scalable Parallel Implementation of Balancing Domain Decomposition by Constraints. SIAM Journal on Scientific Computing, 36(2):C190–C218, 2014. doi:10.1137/130931989 [2] M. Olm, S. Badia, and A. Martín. Simulation of high temperature superconductors and experimental validation. arXiv:1707.09783 [physics], 2017.

A Blended Force-based Atomistic-to-continuum Coupling Method for Multilattice Materials

Derek Olson^{*}, Xingjie Li^{**}

^{*}Rensselaer Polytechnic Institute, ^{**}University of North Carolina--Charlotte

ABSTRACT

Atomistic-to-continuum coupling methods are a general class of methods which combine nonlocal atomistic models of materials with a local continuum mechanics description. Recently, the blended-force based quasicontinuum method, which operates by smoothly blending atomistic and continuum forces over a blending (or transition region), has been proposed and analyzed for general multilattice crystals. In this talk, we survey recent developments in applying the force-based quasicontinuum method to 2D materials for which out-of-plane behavior including bending is incorporated into the model. This results in changes to both the formulation of the method and the analysis.

On the Three-dimensional Simulation of Endocytosis

Yannick A. D. Omar*, Amaresh Sahu**, Kranthi K. Mandadapu***, Roger A. Sauer****

*RWTH Aachen University, **University of California, Berkeley, ***University of California, Berkeley, ****RWTH Aachen University

ABSTRACT

During endocytosis, an important mode of intercellular trafficking, cells form invaginations by internalizing parts of the plasma membrane to transport cargo into the cell. Endocytic events are mediated through a protein coat, which attaches to the outer membrane of the cell. The protein's structure induces curvature into the cell membrane, which thus forms an invagination and subsequently a bud which carries the material to be transported. When the neck of the bud is sufficiently constricted, scission occurs at the bud's neck and a vesicle is formed. Lipid bilayers are usually modeled as liquid shells which do not have any shear resistance in their in-plane directions (Sahu et al., 2017). There are few non-axisymmetric continuum studies on lipid bilayers available and axisymmetry has also commonly been assumed for continuum simulations of endocytosis. In contrast, we will review a recently developed, three-dimensional, C1-continuous Finite Element formulation (Sauer et al., 2017) with which non-axisymmetric simulations of endocytosis have been conducted. Further, we will discuss potential numerical pitfalls of lipid bilayer simulations. For endocytosis, we find that axisymmetric solutions in the high tension regime can only be regarded as metastable states. We show that small perturbations, either of numerical or physically-motivated type, are sufficient to trigger nonaxisymmetric shapes. Furthermore, we identify several parameters that determine the stability of axisymmetric solutions such as the surrounding tension, viscous dissipation, and shape of the protein coat. In the low surface tension regime, we find, similar as in the axisymmetric setup, closed buds with a constricted neck. However, the newly obtained shapes show a bud that is twisted relative to the flat lipid bilayer. Additionally, we present a newly observed transition from constricted buds to elongated tubes at relatively low surface tensions. These newly obtained shapes will be put in perspective using experimental data. Based on that comparison, the physical and physiological implications of nonaxisymmetry in lipid bilayers, such as the existence of a spontaneous Gaussian curvature, will be presented. Finally, we will critically evaluate the material formulation, in particular with respect to the protein coat model, and will discuss alternative modeling approaches. Sauer, R. A., Duong, T. X., Mandadapu, K. K., & Steigmann, D. J. (2017). A stabilized finite element formulation for liquid shells and its application to lipid bilayers. *Journal of Computational Physics*, 330, 436-466. Sahu, A., Sauer, R. A. & Mandadapu, K. K. (2017). Irreversible thermodynamics of curved lipid membranes. *Physical Review E* 96, 042409.

Computing Stochastic Stress Intensity Factors as a Result of Uncertain Material Properties by Generalized Polynomial Chaos

Netta Omer*, Zohar Yosibash**

*Afeka College of Engineering, Tel-Aviv, Israel, **Tel Aviv University, Ramat Aviv, Israel

ABSTRACT

Realistic material properties, as the Young modulus E and Poisson ratio ν (isotropic materials), are measured by experimental observations and are inherently stochastic. Having their stochastic representation $E(?)$ or $\nu(?)$ where $?$ is a random variable, we investigate the elastic solution of the stochastic elasticity system in the vicinity of a crack tip. An efficient method is presented to compute the stress intensity factors (SIF) and eigenfunctions by generalized polynomial chaos (GPC) [1], at a fraction of the computational cost compared to Monte Carlo simulations. We show that the stochastic asymptotic displacements are compound of a series of stochastic eigenpairs (with deterministic eigenvalues and stochastic eigenfunctions) multiplied by a stochastic polynomial representation of the Edge Stress Intensity Functions (ESIFs). The stochastic eigenpairs are computed explicitly and the stochastic ESIFs are computed numerically using the Quasi Dual Function Method (QDFM). The stresses, on the other hand, are represented in an asymptotic series so that the stochastic behavior is only manifested in the SIF. The GPC is used to compute the stochastic SIF from deterministic finite element solutions. As an example we consider either the stochastic Young modulus or the Poisson ratio to be given as random variable with a normal distribution. We present numerical examples of the computation of the stochastic eigenpairs, ESIFs and the SIF. These functions are obtained using deterministic finite element analyses [2] as a series of Hermite polynomials in the stochastic space. Monte Carlo simulations are used to demonstrate the efficiency of the proposed methods. References [1] Dongbin Xiu, Numerical methods for stochastic computations: A spectral method approach, Princeton University Press, 2010. [2] Neta Omer and Zohar Yosibash, On the path independency of the point-wise J-integral in three-dimensions, Int J Fracture, 136, pp. 1 - 36, 2005

An Imaged-based Fluid Structure Coupling Investigation on the Hemodynamic Origin of Intraluminal Thrombus Formation

ChiWei Ong^{*}, ChoonHwai Yap^{**}, Foad Kabinejadian^{***}, Fei Xiong^{****}, Fangsen Cui^{*****}, Pei Ho^{*****}, HwaLiang Leo^{*****}

^{*}Biofluid Mechanics Research Laboratory, Department of Biomedical Engineering, National University of Singapore, Singapore, ^{**}Cardiovascular Biomechanics and Ultrasound Laboratory, Department of Biomedical Engineering, National University of Singapore, Singapore, ^{***}Department of Biomedical Engineering, Tulane University, New Orleans, USA, ^{****}Biofluid Mechanics Research Laboratory, Department of Biomedical Engineering, National University of Singapore, Singapore, ^{*****}Institute of High Performance Computing, A*STAR, Singapore, Singapore, ^{*****}Department of Cardiac, Thoracic & Vascular Surgery, National University Health System, Singapore, ^{*****}Biofluid Mechanics Research Laboratory, Department of Biomedical Engineering, National University of Singapore, Singapore

ABSTRACT

Intraluminal thrombus (ILT) has been shown to be associated with the growth of aneurysm. However, the underlying factors that generate ILT are still unclear. We hypothesize that formation of ILT under the influence of unusual and unfavorable hemodynamic patterns is subjected to the patient-specific geometry. Three cases of thoracic aortic aneurysms (TAA) were reconstructed using retrospective CT images in the present study. Only one case developed ILT, and for this case, simulation was conducted with the removal of ILT to understand the hemodynamics origin of the ILT formation. It was observed in ILT case that an unusual and interesting stationary vortex near the aortic isthmus at the proximal end of the aneurysm, not observed for the other cases. This vortex exerted elevated stresses on blood particles and trapped them in recirculation, before dispersing them into the ILT locality during early diastole. The exposure of the aortic wall to blood elements under fluid-induced stress may be one factor that contribute to the formation of the ILT. Further simulations were performed to understand the factors leading up to the formation of this stationary vortex. It was found that the sharp curvature at the aortic isthmus was the primary factor causing this stationary vortex while reduction of vascular curvature prevented its formation. Reduction of the size of the aneurysm delayed the vortex formation, and shortened the duration of the vortex's existence. On the other hand, our study showed that shifting the location of aneurysm distally did not significantly alter the recirculation and particle dispersion dynamics, although it relocated the vortex to the proximal end of aneurysm.

Development of a Fully Parallelized Code for Phase Field Simulation of Microstructure Evolution in Solid Oxide Fuel Cell Electrodes

Junya Onishi^{*}, Zhenjun Jiao^{**}, Naoki Shikazono^{***}

^{*}Institute of Industrial Science, The University of Tokyo, ^{**}Institute of Industrial Science, The University of Tokyo,

^{***}Institute of Industrial Science, The University of Tokyo

ABSTRACT

Solid oxide fuel cell (SOFC) has gathered much attention as a next-generation power generation system because of its high conversion efficiency, low emissions, fuel flexibility, and so on. SOFCs consist of a porous cathode and anode electrodes, and a solid oxide electrolyte, which is used as a conductor of oxygen ions. The use of the solid oxide electrolyte requires very high operating temperature, typically between 500 and 1000 degree Celsius. As a result, capillary-driven microstructure evolution, such as grain growth and coarsening of material particles, is observed at both electrodes. It is of critical importance to predict this microstructure evolution because it highly influences the performance of SOFCs, through the density of triple phase boundary and the tortuosity of each phase. To predict the long-time behavior of microstructure evolution observed in a typical SOFC anode, which is composed of nickel phase and yttria-stabilized zirconia, some of the authors have developed a numerical model based on the phase field approach and have successfully simulated the morphological change of the nickel phase [Z. Jiao and N. Shikazono, Journal of The Electrochemical Society, 161 F577-F582 (2014)]. However, the total period achieved in their simulation is not sufficiently long for the purpose of assessing the performance degradation in practical applications. Furthermore, it is not clear if the computational grid is fine enough to resolve all relevant structures of grains and particles. These limitations are mainly due to the programming model and the numerical algorithm used in their code. In this research, we develop a highly scalable code for simulating the large-scale and long-time behavior of microstructure evolution with sufficient grid resolution. To do this, firstly, we employ a finite difference method to discretize the governing equations, instead of a spectral method adopted in the previous study. This employment of the finite difference method is intended to avoid communication overhead in large-scale parallel computation. Next, we introduce a hybrid programming model (MPI and OpenMP) for parallelization. In the parallelization, the computational domain is decomposed into sub-domains, and each sub-domain is assigned to one MPI process. To reduce the communication overhead, we implement a communication hiding algorithm for exchanging halo data and evaluate its impact on the parallel performance. Additionally, in the thread parallelization, we investigate the effects of decomposition strategy, including block decomposition and cyclic decomposition. Currently, it is confirmed that the developed code achieves 95% weak scaling parallel efficiency on 32,768 K-computer nodes.

Element-wise Selective Smoothed Finite Element Method for 10-node Tetrahedral Elements in Large Deformation Problems

Yuki Onishi^{*}, Ryoya Iida^{**}, Kenji Amaya^{***}

^{*}Tokyo Institute of Technology, ^{**}Tokyo Institute of Technology, ^{***}Tokyo Institute of Technology

ABSTRACT

A novel 10-node tetrahedral (T10) FE formulation that overcomes the shear/volumetric locking, spurious zero-energy modes, pressure checkerboarding, and reaction force oscillation issues is proposed. The proposed method utilizes the selective reduced integration technique and the smoothed finite element method (S-FEM)[1] with T10 element subdivision[2]. In contrast to the conventional Selective S-FEMs[3], this method applies the strain smoothing technique only within each element and thus never across the elements. Each T10 element is divided into 12 subelements of 4-node tetrahedra (T4) with 1 dummy node at the element center framed by 30 edges. The deformation gradient of each subelement is then given in the manner of the standard T4 element. The hydrostatic stress on each element is derived with the weighted mean of all the 12 subelements. On the other hand, the deviatoric stress on each subelement is derived with the edge-based S-FEM from subelements to edges followed by the cell-based S-FEM from edges to subelements. The stress integration is then performed in the manner of the selective reduced integration to obtain the nodal internal force. This formulation is regarded as an element-wise S-FEM; therefore, it is capable to be introduced as a user-defined add-on element of the general-purpose FE codes such as ABAQUS in contrast to the conventional S-FEMs. Moreover, this formulation is a purely displacement-based formulation, which means it can be directly applied to not only static implicit analyses but also dynamic implicit/explicit analyses. Several example analyses including complex shapes, large deformation, nearly incompressible materials and contact problems reveal that our method has superior accuracy and stability in comparison to the conventional T10 formulations. [1] G.R. Liu et al., "Smoothed Finite Element Methods", CRC Press. [2] J.T. Ostien et al., "A 10-node composite tetrahedral finite element for solid mechanics", IJNME, 2016. [3] Y. Onishi et al., "A locking-free selective smoothed finite element method using tetrahedral and triangular elements with adaptive mesh rezoning for large deformation problems", IJNME, 2014.

Scientific Workflow Tailored for Capacity Computing of Product Design

Kenji Ono^{*}, Tomohiro Kawanabe^{**}

^{*}Research Institute for Information Technology, Kyushu-University, ^{**}Advanced Institute for Computational Science,
RIKEN

ABSTRACT

Design paradigm of industrial products has been changing along with the progress of computer power and computational methodologies. The capacity computing is one of the effective approach to exploit vast amount of distributed parallel computational resources, which drastically changes the design paradigm of industrial products, however, demanding the mechanism of the efficient management and execution for many simulation cases to be performed. For specific purpose of design, e.g., the robust design or the optimization, engineers explore the solution space formed from the obtained simulation results and try to find suitable parameters. Scientific workflow system is the promising and essential infrastructure to proceed the capacity computing and is providing the function such as the description of flow of tasks on web user interface, automation of task flow, reuse of the workflow, management of tasks, control of task on a remote machine, resilience from errors, tracking of task, and provenance. This paper introduces the novel workflow system developed with the modern information technology widely used and its application examples.

Membrane Rotors: from Euler Vorticity Dynamics to Quasi-geostrophic Flows

Naomi Oppenheimer^{*}, Michael Shelley^{**}

^{*}Flatiron Institute at the Simons Foundation, ^{**}Flatiron Institute at the Simons Foundation

ABSTRACT

We show that the dynamics of rotors embedded in a quasi 2D membrane exhibit a power law transition in their interactions, from Euler fluid at small distances ($1/r$), to quasi-geostrophic at large distances ($1/r^2$). We derive a Hamiltonian for a discrete system of rotors and describe the conserved quantities. We develop a coarse-grained description for a density field of rotors. Theory and simulations for both the discrete and the continuous cases are presented. Although the membrane rotors are both driven and embedded in a viscous system, they show strong resemblance to vorticity in an ideal fluid. We discuss the analogies and the differences. references: P. Lenz, J.-F. Joanny, F. Ju ?licher, and J. Prost, 2004. Eur. Phys. J. E 13, 379–390 D. Cordoba, M A. Fontelos, A. M. Mancho, and J. L. Rodrigo, 2005. PNAS 102, 5949-5952

This study deals with the wave dispersion analysis in 1-D nonlinear elastic metamaterials made of tensegrity units. According to a novel model for tensegrity prisms formulated in recent years [1], a newly discovered extremely soft mode is considered in addition to the extremely stiff behaviour already studied for prisms with rigid bases [2]. In the present study the nonlinearity is related to large elastic strains within the prisms. Consequently, the wave motion is amplitude-dependent and may influence the band-structure characteristics of the system [3, 4]. A parametric analysis is hence performed varying the main mechanical and geometric variables. The scope is to detect the existence, the location and the size of the band gaps especially in the low frequency region, in consideration of their great interest for advanced engineering applications within the field of vibration protection and acoustic insulation. References [1] Fraternali, F. et al., "On the mechanical modeling of the extreme softening/stiffening response of axially loaded tensegrity prisms", *JMechanPhysSolids*, 74, 136–157, (2015) [2] Oppenheim, I., Williams, W., "Geometric effects in an elastic tensegrity structure", *JElas* 59, 51-65 (2000). [3] Khajehtourian, R., Hussein, M. I., "Dispersion characteristics of a nonlinear elastic metamaterial", *AIP ADVANCES* 4, 124308, (2014) [4] Herbold, E. B., Kim, J., Nesterenko, V. F., Wang, S. Y., Daraio, C., & "Pulse propagation in a linear and nonlinear diatomic periodic chain: effects of acoustic frequency band-gap", *Acta Mech*, 205, 85–103, (2009)

Development of hp-Adaptive $H(\text{curl})$ -conforming Approximation Spaces for Photonic Waveguide Analysis

Francisco Orlandini^{*}, Philippe Devloo^{**}, Hugo Figueroa^{***}

^{*}FEEC - State University of Campinas, ^{**}FEC - State University of Campinas, ^{***}FEEC - State University of Campinas

ABSTRACT

A hierarchical strategy for creating $H(\text{curl})$ -conforming elements is introduced in the context of a Finite Element Method (FEM) scheme for modal analysis of photonic waveguides. The hierarchical $H(\text{curl})$ -conforming elements are used for the transversal component of the electric field, coupled with scalar $H(1)$ elements for its longitudinal component. The Nédélec elements of the first kind were chosen for this work, and the easy integration with p-adaptivity schemes motivated the hierarchical construction of the FE basis. The application of hp-adaptivity schemes leads to a reduction of the computational effort, still obtaining high accuracy in the dispersion parameters with a significant decrease in the resultant generalized eigenvalue problem size. Curved geometries are dealt with using the Piola mapping, allowing the analysis of complex intricate geometries without increase of the computational effort, since both the basis functions and their curl are calculated directly in the reference element. Since the Nédélec elements naturally allow the analysis of inhomogeneous waveguides and the precise imposition of tangential boundary conditions, the present scheme is able to deal with the complex geometries and the interfaces between materials with contrasting properties present in the field of photonic waveguides. Different numerical examples in increasing complexity are used to demonstrate the features of the strategy, and finally an example with a Photonic Crystal Fiber illustrates the accuracy and the generalized eigenvalue problem size when dealing with a scenario requiring hp-adaptivity for high precision on the dispersion parameters.

Conservative Corrected FEM for Free Surface Frictional Flows

Pablo Ortiz^{*}, Jorge Molina^{**}

^{*}University of Granada, Spain, ^{**}University of Granada, Spain

ABSTRACT

Abstract Simulation of natural flows requires a proper numerical approach for the dynamics on the dry–wet interface, avoiding spurious residuals during front propagation and computing proper celerity of the wavefront. Errors due to mass and momentum imbalances during interface propagation are associated with the method employed in partially wet cells, with the criteria to specify wet or dry computational cells, and with the treatment of terms coming from correction procedures. In recent years we introduced a finite element model to simulate shallow flows with dry fronts (e.g.[1]), extending the formulation to flows coupled with erodible–non erodible sediment interfaces [2]. The method is developed by integrating a high order continuous finite element procedure with a conservative sign-preserving correction. Corrected continuous model has an inherent solution for the motion of interfaces, and does not need extensive modifications to compute flooding and evolutionary beds. The incorporation of relevant sources could produce high order conservation errors in the solution by standard flux correction procedure. In this work we present an extended conservative finite element method based on flux limiters with improved conservation properties after correction. We introduce applications of the procedure to severe frictional flows, such as experiments of dam–break flow type problems over erodible and non–erodible beds, and scrutinize propagation and conservation properties of the improved corrected method. Acknowledgements This work was supported by the MICIIN Grant #BIA-2015-64994-P (MINECO/FEDER) References [1] P.Ortiz, “Non oscillatory continuous FEM for transport and shallow water flows”, Comput. Methods Appl. Mech. Engrg., 223-224, 55–69 (2012). [2] P. Ortiz, J. Anguita, M. Riveiro, “Free surface flows over partially erodible beds by a continuous finite element method”, Environ. Earth Sci., 74, 7357–7330 (2015).

The Virtual Element Decomposition: A New Paradigm for Developing Convergent and Stable Meshfree Galerkin Methods

Alejandro Ortiz-Bernardin*

*Universidad de Chile

ABSTRACT

In the numerical solution of partial differential equations, meshfree Galerkin methods are numerical methods that use a cloud of nodes for domain discretization. Smooth nonpolynomial basis functions are constructed using this nodal discretization. Even though these methods do not need an underlying mesh for construction of the nodal basis functions, they require a mesh to perform the numerical integration of the Galerkin weak form integrals. Due to the nonpolynomial character of the meshfree nodal basis functions, there exist inaccuracies in the numerical integration that affect the consistency and stability of the method. This work presents a new paradigm for developing consistent and stable meshfree Galerkin methods: via the virtual element decomposition, the numerical integration issue is tackled in such a way that consistency and stability of the numerical solution are ensured by construction. Linear and quadratic consistency will be discussed along with new possibilities for developing consistent and stable nodal integration techniques. Some numerical examples are presented to demonstrate the performance of the method.

Universal Fragment Descriptors for Predicting Properties of Inorganic Crystals

Corey Oses^{*}, Olexandr Isayev^{**}, Cormac Toher^{***}, Eric Gossett^{****}, Alexander Tropsha^{*****},
Stefano Curtarolo^{*****}

^{*}Duke University, ^{**}University of North Carolina at Chapel Hill, ^{***}Duke University, ^{****}Duke University,
^{*****}University of North Carolina at Chapel Hill, ^{*****}Duke University

ABSTRACT

Although materials discovery has historically been driven by a laborious trial-and-error process, knowledge-driven materials design can now be enabled by the rational combination of Machine Learning methods with materials databases. Here, data from the AFLOW repository for ab initio calculations [1] is combined with Quantitative Materials Structure-Property Relationship models to predict important properties: metal/insulator classification, band gap energy, bulk/shear moduli, Debye temperature, and heat capacities. The accuracy of the predictions compares well with the quality of the training data for virtually any stoichiometric inorganic crystalline material, as well as with the available thermo-mechanical experimental data. The universality of the approach is attributed to the construction of the descriptors: Property-Labeled Materials Fragments [2]. While the models are trained on the full suite of properties available in the AFLOW repository, the predictions require only minimal structural input, allowing straightforward implementations of simple heuristic design rules. Access to these models and their predictions is streamlined through the development of an open RESTful API, available online at aflow.org/aflow-ml [3], facilitating easy integration into any application workflow. [1] C. Toher, C. Oses, et al., The AFLOW Fleet for Materials Discovery, submitted arXiv:1712.00422 (2017). [2] O. Isayev, C. Oses, C. Toher, E. Gossett, S. Curtarolo, and A. Tropsha, Universal fragment descriptors for predicting properties of inorganic crystals, Nature Communications 8, 15679 (2017). [3] E. Gossett, C. Toher, C. Oses, O. Isayev, F. Legrain, F. Rose, E. Zurek, J. Carrete, N. Mingo, A. Tropsha, and S. Curtarolo, AFLOW-ML: A RESTful API for machine-learning predictions of materials properties, submitted arXiv:1711.10744 (2017).

Spatial-Temporal Nonlocal Homogenization Model for Transient Wave Propagation in Periodic Viscoelastic Composites

Caglar Oskay*, Ruize Hu**

*Vanderbilt University, **Vanderbilt University

ABSTRACT

Wave propagation in manufactured composite materials has received increasing research interest over the past decade due to the opportunities for achieving favorable dynamic properties within targeted frequency ranges (e.g., acoustic band gaps). Phononic crystals and acoustic metamaterial demonstrate significant potential in many novel engineering applications, such as cloaking, acoustic diode and blast mitigation. These materials exhibit unique wave propagation and attenuation patterns possible through the design of the microstructure and constituent material properties. It has been recently recognized that employing viscoelastic materials could significantly expand the possibilities for these materials by leveraging the interactions between material damping and heterogeneity induced dispersion, such as shifting the stop band to lower frequencies and enhancing wave attenuation. We present a spatial-temporal nonlocal homogenization model for transient wave propagation in composites accounting for wave dispersion and attenuation due to material heterogeneity and damping. The proposed model is formulated through asymptotic homogenization with higher order corrections incorporated to extend the applicability of the homogenization theory to shorter wavelength regime. A homogenization model that is nonlocal in both space and time is consistently derived with all model parameters directly computed from the microstructure equilibrium. A reduced order model is then proposed for efficient transient wave propagation analysis. The reduced model retains the dispersive character of the original nonlocal model through the effective stiffness tensor. A Hybrid Laplace Transform/Isogeometric Analysis (HLT/IGA) is developed to solve the macroscale momentum balance equation, which provides high convergence rate for high frequency wave propagation simulation. Transient wave propagation in two-dimensional domain with periodic elastic and viscoelastic microstructures is investigated and the proposed models were verified against direct numerical simulations. The key contributions of our work are: (1) the proposed model captures the wave dispersion in the first pass band and stop band; (2) all the model parameters are computed directly from the microscale equilibrium as an off-line process.

Strain-Rate and Temperature Effects in Ductile Damage and Element Removal Threshold and Its Influence in FEM Orthogonal Cutting Simulations

Juan Camilo Osorio Pinzon*, Juan Pablo Casas Rodriguez**, Sepideh Abolghasem***, Edgar Alejandro Marañon Leon****, Niyireth Alicia Porras Holguin*****

*Universidad de los Andes, **Universidad de los Andes, ***Universidad de los Andes, ****Universidad de los Andes, *****Universidad de los Andes

ABSTRACT

Orthogonal cutting processes for ductile materials imposes severe plastic deformation, which involves ductile material failure at high strain-rates and the accompanying temperature rise. Plastic constitutive model parameters, ductile damage initiation parameters, damage evolution and damage threshold are directly affected by the complicate interactions among the thermomechanical conditions during the cutting process. During FEM simulation element removal threshold and damage threshold are needed to perform an accurate cutting simulation taking into account plastic, thermodynamic and damage effects in the workpiece, since reasonable parameters estimation can potentially lead to reliable solutions for cutting force, thrust force, temperature rise and residual stress among others. This study presents the experimental results for damage threshold and critical damage values for various strain - rate and temperature conditions using two different test devices: a conventional quasi-static test apparatus and a drop weight impact test (DWIT) adapted for tensile tests, covering strain rate values from 0.01/s to 10/s. Relationship between material damage threshold and critical damage value with strain – rate and temperature rise are presented, as well as, its effects during orthogonal cutting FEM simulation and accurate chip thickness prediction. Simulations with different damage parameters are presented and compared with previous works to verify convergence as well as, experimental results to show the importance of accurate damage parameter determination in cutting force prediction using numerical simulations.

How to Choose a Length Scale?

Shmuel Osovski*

*Technion - Israel Institute of Technology

ABSTRACT

The continuing efforts in improving the mechanical properties of structural alloys have led to a variety of materials with multiple characteristic length scales resulting from the underlying microstructure. A successful attempt at modeling the process of ductile fracture in such materials requires the implementation of the relevant microstructural length scale into the numerical models. As length scales in a given material system can vary drastically, it is impossible to explicitly represent all of them. As such, it is necessary to choose the relevant microstructural feature, which in turn can be identified based on experimental data. Recently it was suggested that the microstructural length scale, which has dictated the fracture process, could be extracted from fractured samples through a statistical analysis of the fracture surface. Here, we will present a detailed analysis on the statistical features of fracture surface roughness parameters obtained from 3D FE simulations with several microstructural features. The material is modeled using an elastic visco-plastic constitutive relation for a progressively cavitating solid, and each microstructural feature is allowed to accumulate damage through a different set of parameters. The propensity of each microstructural feature to fail is varied systematically with respect to the others and the resulting fracture surfaces are compared. The applicability of such an analysis in identifying the dominant microstructural feature, dictating the crack growth process, will be discussed with relation the experimental capabilities.

Mathematical Model Connecting Biological Processes and Physical Chemistry of Hydroxyapatite Formation in Bone Tissue

Borys Ostapienko*, Svetlana V. Komarova**

*McGill University, Department of Biomedical Engineering, **Department of Biomedical Engineering, Faculty of Medicine and Faculty of Dentistry, McGill University, Shriners Hospital for Children-Canada

ABSTRACT

Mathematical Model connecting Biological processes and Physical chemistry of Hydroxyapatite formation in Bone tissue Borys Ostapienko, Svetlana V. Komarova Department of Biomedical Engineering, Faculty of Medicine and Faculty of Dentistry, McGill University, Montreal, Quebec; Shriners Hospital for Children-Canada, Montreal, Quebec Abnormal mineralization of bone matrix results in severe clinical problems including bone deformities and fractures, such as observed in osteogenesis imperfecta and vitamin D deficiency. To better understand the physicochemical processes occurring during bone mineralization, we have developed a mathematical model that examines hydroxyapatite mineral formation on collagen matrices. The model describes biological components of bone mineralization in the form of kinetics of collagen matrix maturation, turnover of mineralization inhibitors and formation of nucleators. Chemical reactions occurring between Ca^{2+} , PO_4^{3-} and OH^- ions in the aqueous phase as well as hydroxyapatite precipitation as single solid phase mineral are accounted for in kinetic reactions, mass balance and electro-neutrality requirements. We examined the roles of biological processes in generating normal and abnormal mineralization patterns characterized using two outcome measures: mineralization lag time and degree of mineralization. Model parameters describing inhibitor homeostasis most effectively changed the mineralization lag time, while a parameter describing the rate of matrix maturation was found to increase both the mineralization lag time and the degree of mineralization. When the effect of physicochemical factors, including ion concentrations, pH and temperature, was examined, we found a more prominent effect of varying $[\text{PO}_4^{3-}]$ compared to $[\text{Ca}^{2+}]$ on mineralization kinetics, as well as a significant effect of changing pH in the physiological range. This model can be applied for qualitative predictions of genotype/phenotype relationship for bone mineralization, and adapted to study physiological and pathological calcification of other tissues, including formation of kidney stones and vascular calcification.

Exponential Integrators

Alexander Ostermann*

*University of Innsbruck, Austria

ABSTRACT

In recent years there has been a considerable progress in the construction, analysis and implementation of new types of time discretization schemes for evolution equations. In this talk we will concentrate on exponential methods, a class of integrators which dates back to the late 1950ies. We start with a historical account on these methods and emphasize their relation to linearly implicit time integration, an alternative approach which was developed concurrently. The larger part of the talk, however, is devoted to recent developments. In particular, we will touch upon applications of exponential integrators in computational mechanics. Exponential integrators rely on an appropriate linearization of the vector field and employ the exponential and related functions of the Jacobian of this linearization. The efficient evaluation of the action of such matrix functions on vectors is of paramount importance for getting competitive schemes. This topic will also be addressed in the talk.

Implementation of Modular Plasticity Models for Hyperelastic Material Response Including Coupled Damage

Jakob Ostien^{*}, William Scherzinger^{**}, Brian Lester^{***}, Brandon Talamini^{****}

^{*}Sandia National Laboratories, ^{**}Sandia National Laboratories, ^{***}Sandia National Laboratories, ^{****}Sandia National Laboratories

ABSTRACT

As a foundational technology in the engineering practice of modeling the large deformation of ductile metals up to and including failure, accurate models for constitutive response and efficient implementation into finite element codes remains a challenge. The purpose of this talk is to discuss implementation details for a class of hyperelastic plasticity models applicable for a family of yield surfaces and rate dependent models. The choice of finite deformation strain tensor facilitates direct comparison to the more broadly established hypoelastic versions of the models. Emphasis is placed on formulation, numerical integration, and verification of the algorithms. Efficacy of the models will be demonstrated on engineering applications and coupled damage formulations will be highlighted against two Sandia Fracture Challenge scenarios. Sandia National Laboratories is a multi-mission laboratory managed and operated by National Technology & Engineering Solutions of Sandia, LLC., a wholly owned subsidiary of Honeywell International, Inc., for the U.S. Department of Energy's National Nuclear Security Administration under contract DE-NA0003525.

Tensor-Valued Random Fields for Continuum Physics

Martin Ostoja-Starzewski*, Anatoliy Malyarenko**

*University of Illinois at Urbana-Champaign, **Mälardalen University

ABSTRACT

Continuum mechanics/physics typically involves fields of dependent quantities (temperature, displacement, stress...) and those of constitutive response (conductivity, stiffness...). In each case, there is a random field taking values in a linear space of tensors of a fixed rank: hence, a tensor-valued random field (TRF). First, we discuss most general and explicit representations of correlation functions of 2nd, 3rd, and 4th rank TRFs, which are wide-sense stationary and statistically isotropic having anisotropic realizations [MEMOCS 2(2), 209-231, 2014; ZAMP 67(3), 20, 2016; J. Elast. 127(2), 269-302, 2016]. Next, we examine the consequences for TRFs in 2d and 3d problems of classical continuum mechanics: velocity field in incompressible fluids, heat flux in steady-state heat conduction, or stress in quasi-static continuum mechanics. By extension, this leads to a study of consequences in stochastic micropolar theories [Math. Mech. Solids 20(4), 418-432, 2015]. Finally, we report what TRFs may arise if they are to represent most general constitutive responses in 2d or 3d heat conduction, (visco-thermo)elasticity, piezoelectricity, damage mechanics, or wave propagation [Adv. Appl. Mech. 49, 111-211, 2016]. By micro-physics and micro-mechanics arguments, such TRFs should be employed as input into stochastic partial differential equations or stochastic finite elements, instead of the commonly assumed locally isotropic (i.e. scalar) random fields.

Automated Feature Recognition of 3D CAD Models for Pre-and Post-Processing of CAE

Koji Otani*, Kazuyuki Mikami**

*Integral Technology Co., Ltd., **Integral Technology Co., Ltd.

ABSTRACT

It is time consuming to create FEM models for simulation and to analyze the simulation results especially when dealing with large assembly models. To create FEM mesh for input CAD models ensuring a certain quality of simulation result, it is important to follow specific mesh rules as simulation results may vary depending on the input FEM mesh. As large-scale modeling in FEM analysis increases, the importance of being able to create adequate FEM mesh for the input CAD models automatically is growing. This paper describes a method to recognize various features of 3D CAD models to create mesh according to mesh rules and to make post-processing efficient. In pre-processing step, recognizing features of input CAD models and generating mesh satisfying the detailed mesh rules automatically help to reduce manual mesh modifying work dramatically. In post-processing step, the recognized feature data makes it easier to analyze the simulation result by showing the result for each feature that is recognized. The feature recognition data can be post processed by linking recognized feature data and created FEM mesh data. To recognize specific features of input CAD models, we used characteristics of each face of the input CAD models, face type data that is calculated from the characteristics, combination of faces, and cross sectional shapes of the faces. This algorithm is capable of recognizing features of both mid-surface models such as sheet metal parts and solid models such as cast or resin parts. The features that we recognize with this algorithm include 2D/3D simple holes, stepped holes, steps on plane, embosses, beads, flanges, fillet flows, chamfers, corner fillets, ribs, grooves, gear teeth, and screws. After recognizing these features, FEM mesh for each feature can be generated with the information on the feature data and the mesh rules that are embedded and controlled by external control files. With this feature recognition algorithm, we achieved to recognize and create mesh meeting mesh rules in pre-processing step. In post-processing step, we proposed to link the recognized feature data and mesh data to analyze simulation results more efficiently.

Automated Simulation Model Preparation with Machine Learning

Steven Owen^{*}, Timothy Shead^{**}, Shawn Martin^{***}

^{*}Sand, ^{**}Sandia National Laboratories, ^{***}Sandia National Laboratories

ABSTRACT

We propose using machine learning to reduce the bottleneck in the engineering analyst workload. We discuss a potential rich new area of research where current machine learning methods can be applied to model preparation tasks such as defeating, resolution of dirty geometry and decomposition for hex meshing while maintaining high confidence in results. Because of the engineering judgment involved in these tasks, there can be wide ranges of good and bad solutions for any given problem, with bad solutions leading to inaccurate or misleading results and suboptimal engineering decisions. In order to effectively move the state-of-the-art towards full automation, analysts must have high confidence that the models created using automatic solutions are at least as good as the models they would otherwise build on their own. We believe that machine learning can prove useful in accomplishing this goal, providing algorithms that can reproduce the choices made by expert analysts. To accomplish this, the tasks now currently performed by analysts can be identified and used to train machine learning models, by capturing and labelling operations performed by experts using existing software tools as part of the model preparation process. We introduce an initial proof-of-concept environment, extending Sandia's Cubit geometry and meshing toolkit to utilize machine learning methods. In this software, geometric operations that are most likely to be effective for handling particular geometric characteristics of a CAD model are presented to the user. The ability to easily preview, execute, undo or even ignore the suggested operations are made available through an interactive user interface. Since the suggested solutions are based on previous training data, they draw upon the expertise of past users in similar simulations, while respecting the engineering judgment of the current user. While machine learning is widely used in text, image, audio, and video analysis, there has been little research on the application of machine learning to model preparation for simulation. Many important questions on how to use machine learning in this domain remain unexplored. In this talk we also introduce several open questions that need to be explored in order for machine learning techniques to be effectively applied in model preparation tasks. ^{*}Sandia National Laboratories is a multi-program laboratory managed and operated by Sandia Corporation, a wholly owned subsidiary of Lockheed Martin Corporation, for the U.S. Department of Energy's National Nuclear Security Administration under contract DE-AC04-94AL85000

A Game Theoretic Approach to Numerical Approximation and Algorithm Design

Houman Owhadi*

*Caltech

ABSTRACT

This talk will cover interplays between Game Theory, Numerical Approximation and Gaussian Process Regression. We will illustrate this interface between statistical inference and numerical analysis through problems in multiscale analysis, the design of fast solvers, the identification of operator adapted wavelets, and computation with dense kernel matrices. This talk will cover joint work with F. Schäfer, C. Scovel, T. Sullivan and L. Zhang.

Design Optimization Under Uncertainty Using Polynomial Chaos Expansions and Conditional Value-At-Risk

Geoffrey Oxberry*

*Lawrence Livermore National Laboratory

ABSTRACT

Recent advances in additive manufacturing have enabled the manufacture of parts of almost any shape. Although topology optimization searches this large design space systematically, deterministic problem formulations assume that boundary conditions (e.g., loads for structural physics), material properties, and the correspondence between designed part and manufactured part (e.g., geometric variability) are known. In practice, these assumptions are violated, and deviations from assumptions can affect substantially design performance. To compensate for uncertainties in topology optimization problem formulations, we present a stochastic programming approach to topology optimization that incorporates the effects of known uncertainties, and represent these uncertainties using polynomial chaos expansions. We compare traditional mean-standard-deviation approaches with the $x\%$ conditional value-at-risk, which is the average over the $x\%$ of worst cases (average-worst-case), arguing that the latter better compensates for worst-case events when uncertainties are skewed. We also compare the polynomial chaos expansion approach to computing the mean, standard deviation, and conditional value-at-risk directly via deterministic quadrature, and to computing these quantities using Monte Carlo sampling.

A Second-order in Time Approximation of Fluid-structure Interaction Problem

Oyekola Oyekole*, Catalin Trenchea**, Martina Bukac***

*University of Notre Dame, **University of Pittsburgh, ***University of Notre Dame

ABSTRACT

Fluid-structure interaction (FSI) problems arise in many applications, such as aerodynamics, geo-mechanics and biomedical engineering. They are characterized by highly non-linear coupling between two different physical phenomena. As a result, the development of robust numerical algorithms is a subject of intensive research. Since coupled FSI problems give rise to large and ill-conditioned systems of algebraic equations, partitioned methods have often been used to split the coupled problem into smaller and better-conditioned sub-problems. However, in applications where the density of the structure is comparable to the density of the fluid (such as the interaction between blood and arterial walls), classical partitioned schemes suffer from instabilities known as the added mass effect. In this case, the development of stable, non-iterative numerical schemes for FSI problems is challenging – even for first-order accurate solution techniques. We propose and analyze a novel, second-order accurate in time, partitioned method for the interaction between an incompressible, viscous fluid and a thin, elastic structure. The proposed numerical method is based on the Crank-Nicolson discretization scheme, which is used to decouple the system into a fluid sub-problem and a structure sub-problem. The scheme is loosely coupled, and therefore at every time step, each sub-problem is solved only once. Energy and a priori error estimates for a fully discretized scheme using finite element spatial discretization are derived. We prove that the scheme is stable under a CFL condition, second-order convergent in time and optimally convergent in space. We also present two numerical examples that support the theoretically obtained results. Using realistic parameter values for blood flow in a human common carotid artery, our simulation results demonstrate that the proposed scheme is stable and accurate when applied to problems related to blood flow modeling.

Turbulence-resolving Two-Phase Flow Simulations of Current Supported Turbidity Flows over Erodible and Non-erodible Beds

Celalettin Ozdemir*, Sahar Haddadian**

*Louisiana State University, **Louisiana State University

ABSTRACT

Although their existence was discovered more than two decades ago, wave- and current-supported turbidity currents (WCSTC) are now considered to be a major carrying agent that shapes the submarine geomorphology and deliver sediment from its source to its sink in the deep ocean with growing evidence. These flows are usually very thin at the seafloor and their occurrence is episodic which make their observation in the field very hard with the available sensor technology. To that end, turbulence-resolving two-phase flow simulations of WCSTC can be considered as virtual experiments to understand the full range of mechanisms that are responsible for and/or affect these currents. In this study, we present the culmination of two-phase, turbulence-resolving simulations, i.e. Direct Numerical Simulations (DNS), of alongshore current-supported fine sediment turbidity currents across mild bathymetric slopes. This type of flows exhibits rich hydrodynamic features because the flow is forced by both a non-uniform density difference due to suspended sediment concentration and a constant pressure gradient. Here, we analyze the alongshore current supported turbidity currents under two boundary conditions. First, suspended sediments are considered to be wash load. Second, we allow sediment mass exchange at the bottom boundary by using Krone-Partheniades type of erosion formula. Our results show a competition between sediment-induced density stratification and the horizontal flow created by the sediment-induced density difference to dampen and generate turbulence, respectively. Our numerical simulations also provide significant insights on how to model these turbidities in regional-scale models which will then be used to estimate the location of mud depocenters and the dynamics of submarine geomorphology such as in the clinoform development at the continental margin.

Time Integration Schemes for Transient Problems with Enhanced Stability and Accuracy via Finite Increment Calculus (FIC)

Eugenio Oñate*

*International center for Numerical Methods in Engng (CIMNE), Barcelona, Spain

ABSTRACT

The Finite Increment Calculus (FIC) (sometimes termed “finite calculus”) was proposed by Oñate [1] as a conceptual framework for deriving stabilized numerical methods for solving problems in mechanics for situations where numerical methods typically fail (i.e. high Peclet/Reynolds numbers and incompressible situations). The essence of the FIC approach lays in solving the modified form of the governing differential equations in mechanics obtained by writing the equations for balance of heat, momentum and mass in a space-time domain of finite size, and not in a domain of infinitesimal size, as it is usually done. The FIC governing equations involve the balance domain dimensions. The merit of the FIC equations is that they are a natural starting point for deriving stabilized numerical schemes [1-5]. In the presentation it is shown that the FIC equations in time are the starting point for deriving new explicit and implicit time integration schemes with increased stability and accuracy. Examples of the promising features of the FIC-Time approach for solving more efficiently and accurately a number of transient problems in mechanics are given. References [1] Oñate, E. Derivation of stabilized equations for numerical solution of advective-diffusive transport and fluid flow problems. *Comp. Meth. Appl. Mech. Eng* 151(1-2), 233–265 (1998). [2] Felippa C. A. and Oñate E., Nodally exact Ritz discretizations of 1D diffusion-absorption and Helmholtz equations by variational FIC and modified equation methods, *Computational Mechanics*, Vol. 39, pp. 91 - 111, 2007 [3] Oñate E., Miquel J. and Nadukandi P., An accurate FIC-FEM formulation for the 1D advection-diffusion-reaction equation, *Computer Methods in Applied Mechanics and Engineering*, Vol. 298, pp. 373-406, 2016 [4] Oñate E., Miquel J. and Nadukandi P., Accurate FIC-FEM formulation for the multidimensional steady-state advection–diffusion–absorption equation, *Comput. Meth. Appl. Mech. Eng.*, Vol 327, 352-368, 2017 [5] Felippa, C.A., Oñate, E., Idelsohn, S.R. , Variational Framework for FIC Formulations in Continuum Mechanics: High Order Tensor-Derivative Transformations and Invariants, *Archives of Comput. Meths.in Engng*, 10.1007/s11831-017-9245-0, 45 pp, 2018.

Experimental Characterisation and Constitutive Modelling of the PC/ABS Polymeric Blend

Fernando P. B. Macedo*, Shenghua Wu**, Daniel de Bortoli***, Francisco M. A. Pires****

*INEGI - Instituto de Ciência e Inovação em Engenharia Mecânica e Engenharia Industrial; FEUP - Faculdade de Engenharia da Universidade do Porto, **INEGI - Instituto de Ciência e Inovação em Engenharia Mecânica e Engenharia Industrial, ***INEGI - Instituto de Ciência e Inovação em Engenharia Mecânica e Engenharia Industrial, ****FEUP - Faculdade de Engenharia da Universidade do Porto

ABSTRACT

Keywords: Mechanics of Solid Polymers; Amorphous Polymers; Polymer Blends; Constitutive Modelling. **Abstract.** Polymeric blends are widely used in industrial applications in order to improve the mechanical performance and physical specifications of the individual constituents [1]. A case of interest is the ternary amorphous Polycarbonate/ABS blends – although neat PC has high ductility, thermal stability and durability, it lacks in high notch-sensitivity and fracture toughness, properties that are highly improved by the addition of ABS, a rubber-toughened polymer [2]. It is known that the fracture behaviour of rubber toughened polymers is governed by matrix shear yielding and crazing, interconnected with cavitation of the rubber particles. In this work, several experimental tests are performed to study the deformation behaviour of PC/ABS with different volume fractions of the blend constituents under different stress states, strain rates and temperatures. After that, a constitutive formulation framework was proposed, based on Gearing and Anand model [3], to describe the mechanical behaviour of PC/ABS blends. The proposed constitutive model accounts for the plastic deformation mechanisms described above (shear yielding, crazing, and cavitation) and is implemented within an implicit integration scheme. A representative set of numerical examples is analysed covering a wide range of parameters of the model. The predictions of the model are appraised against an experimental set of results obtained by our group. **REFERENCES:** [1] Helbig, M.; van der Giessen, E.; Clausen, A.H.; Seelig, T. (2016). Continuum-micromechanical modeling of distributed crazing in rubber-toughened polymers. *European Journal of Mechanics and Solids*, 57, 108-120. [2] Greco, R.; Astarita, M.F.; Dong, L.; Sorrentino, A. (1994). Polycarbonate/ABS blends: Processability, thermal properties, and mechanical and impact behavior. *Advances in Polymer Technology*, 13 (4), 259-274. [3] Gearing, B.P.; Anand, L. (2004). Notch-sensitive fracture of polycarbonate. *International Journal of Solids and Structures*, 41, 827-845.

Circumventing the Solution of Inverse Problems in Mechanics through Deep Learning

Dhruv PAtel^{*}, Assad Oberai^{**}, Adriana Vega^{***}, Raghav Tibrewala^{****}, Li Dong^{*****}

^{*}Rensselaer Polytechnic Institute, ^{**}University of Southern California, ^{***}City University of New York, ^{****}Indian Institute Technology, Chennai, ^{*****}University of Texas, Austin

ABSTRACT

Recent studies have demonstrated that images of mechanical heterogeneity of a tumor, and its nonlinear elastic response can be used to distinguish benign tumors from their malignant counterparts. These images of the linear and nonlinear parameters of tissue are typically obtained by using a measured displacement field and solving a complicated inverse elasticity problem. In this talk we circumvent the step of solving the inverse problem by using the displacement measurements as direct input to a deep convolutional neural net, and training it to directly classify tumors based on their heterogeneity and nonlinear elastic response. We explore the use of transfer learning in this context as a means to work with a reduced training data set, and also examine the characteristics of the trained model to understand the process through which the CNN extracts features from the raw displacement images.

Vornoi Tessellation with ShaPo

Joachim POUDEROUX^{*}, Florian CHEVASSU^{**}, Marc CHAREST^{***}, Mack KENAMOND^{****},
Mikhail SHASHKOV^{*****}

^{*}Kitware SAS, ^{**}Kitware SAS, ^{***}LANL, ^{****}LANL, ^{*****}LANL

ABSTRACT

Voronoi meshes are polygonal or polyhedral meshes that have properties that are appreciated in many scientific fields like computational fluid dynamics or geo-physics. In the particular context of the implementation of Reconnection-Based ALE family of methods at LANL, we are developing a cross platform C++ software library called ShaPo. This tool produces Voronoi meshes from a domain defined by a set of complex boundaries (convex or non-convex, simply or multi-connected) and user defined set of seeds. ShaPo integrates different algorithms to generate, in serial or in parallel, 2D and 3D Voronoi meshes with different properties, and it provides a complete API to retrieve the full connectivity of the generated meshes. In this talk we will present the core algorithms of ShaPo and expose the common pitfalls of the development of a Voronoi tessellation algorithm which can seem straightforward in theory but appears to be very complex to implement in practice, especially if you consider reliability, robustness and speed. We will also explain our algorithm to compute the tessellation in a MPI parallel context and how we establish the global mesh connectivity. Finally we will detail an important feature of ShaPo which is its capability to remesh a subregion of an existing unstructured mesh with a Voronoi tessellation and reconstruct the full mesh connectivity.

A Mid-frequency Method to Model Coupled Vibro-acoustic Response of a Railway Track

Guillaume PUEL^{*}, Raphaël CETTOUR-JANET^{**}, Pierre-Etienne GAUTIER^{***}, Andrea Barbarulo^{****}

^{*}CentraleSupélec, ^{**}CentraleSupélec, ^{***}SYSTRA, ^{****}CentraleSupélec

ABSTRACT

With metropolis and transport grid densification, the result of vibro-acoustic impact assessment has a pivotal role in rail network expansion. Indeed, for railway neighbors, the pass-by train noise is a key issue. One of the main source is the rolling noise: Roughness on the wheel and rail surface produce an imposed displacement on the both last. This last one generates vibrational response of wheels and the railway track and their acoustic radiation. The frequency range is 50-5000 Hz. In this work, a vibro-acoustic model of the ballasted railway track is presented. For vibrational response, analytical models (beam, mass, springs, ...) and finite elements do not allow to simulate correctly the behavior of the track. In this work, a generic element is simulated. It is constituted of a piece of rail and a half sleeper at the both ends. Semi-analytical finite element method (SAFEM) is used to simulate this element. This method uses a FEM mesh in the cross section and analytical formulation in the third dimension. Consequently, it allows to reduce computation time while taking account the 3 dimensions of the model. Infinite part and periodicity between supports are simulated using Floquet theorem and injecting the force produced by the support at the ends of the generic element. However, this technique suffers from numerical problems which imposed an adaptive algorithm. The second-order Arnoldi method (SOAR) is used before solving the SAFEM equation. This reduction allows to eliminate critical values that induce numerical problems. Moreover, the orthogonal basis created by this method allows improving the robustness of the algorithm. This method is validated thanks to a comparison with experimental results. For acoustic radiation, high frequency simulation prevents using conventional techniques (FEM, BEM, ...) . This imposes to use mid frequency techniques. Railway track geometry can be decomposed into big cavities. Consequently, the Variational theory of complex ray is particularly well adapted to this case. The principal features of VTCR approach are the use of a weak formulation of the acoustic problem, which allows to consider automatically boundary conditions between sub-domains. Then, the use of an integral repartition of plane waves in all the direction allows to simulate the acoustic field. The unknowns of the problem are their amplitudes. This method well assessed for closed domain has been extended to open domain and coupled to vibrational response. Comparison with FEM simulation at low frequency allows to validate the method.

Temperature Induced Structural Instabilities in Two-dimensional Buckled Honeycomb Systems

Alejandro Pacheco-Sanjuán*, Salvador Barraza-Lopez**

*Universidad Técnica Federico Santa María, **University of Arkansas

ABSTRACT

Non-linear deformations and phase changes in 2D buckled honeycomb crystals are analyzed by First-principles molecular dynamics simulations and discrete differential geometry. Unlike graphene, Silicene (Si) and Germanene (Ge) are not absolutely planar, but have buckled heights of 0.44 Å and 3.97 Å respectively. The low buckled (LB) configurations for these two structures exhibit positive frequencies for the phonon dispersion and therefore it is considered to be stable. At high temperatures, these systems are excited so they can cross the energy barrier and locally shift the positions of atoms from the LB to the high buckled (HB) state, generating a pattern of linear defects. Abrupt changes in the local geometry of Si and Ge are detected at a critical temperature T_c well below the melting point T_m . Distributions of the invariants for the local curvature and metric tensors are computed and compared for temperatures below and above T_c for both structures. Dynamical changes at T_c are also detected by the frequency shifting of non-linear modes in the power spectra. The geometrical analysis shows that this local disorder arises when nearest neighboring atoms are reassigned when the system is thermally excited at temperatures greater than T_c .

Numerical Simulation of Fuel Rod Vibrations Induced by Turbulence in the Vicinity of the Fuel Assembly Inlet Zone

Julien Pacull^{*}, Yasmail Akariouh^{**}, Valérie Biscay^{***}, Serge Delafontaine^{****}, Pierre Badel^{*****}

^{*}Framatome, ^{**}Framatome, ^{***}CEA, ^{****}CEA, ^{*****}EDF

ABSTRACT

This work pertains to the safety and performance analysis of fuel assembly components (i.e. fuel rods) of pressurized water reactor nuclear plants. Inside the reactor core of pressurized water reactors, fuel assemblies experience significant thermal, hydraulic, and irradiation loads during operation. These loads may induce large scale fuel rod oscillations that might result in fuel rod cladding fretting wear or fuel assembly motions that may contribute to significant assembly fretting. To address the flow induced vibrations of fuel rods subjected to the most generic form of excitation from turbulence-induced fields, a new nonlinear structural model is proposed. The model is constructed by beams with six degrees of freedom simulating the response of a single fuel rod subjected to a turbulent flow field. Mechanical non-linearities originate from the relative motion of the fuel rod cladding with respect to its supports, which becomes prominent especially for irradiated fuel for which the grid spring relaxation leads to degraded supporting conditions. Impacts and sliding motion can be derived from the simulations to support subsequent fretting wear risk assessment. The excitation field is generated by high fidelity unsteady CFD simulations, which are performed on a geometry representative of the fuel assembly components. As a post-treatment of the flow simulation, the Power Spectral Density of the fluctuating pressure is computed, to serve directly as excitation input for the nonlinear fuel rod model with no further empirical adjustment needed. This numerical tool is used to simulate the turbulent-induced vibrations of fuel rods in the vicinity of the bottom nozzle. In that zone, the flow complex topology is driven primarily by the axial flow jet coming through the holes in the lower core plate, combined with the hydraulic redistribution stemming from the bottom nozzle. The rod vibration amplitude and frequencies are compared with experimental data obtained from a full-scale fuel assembly testing in order to validate the prediction capability of the analytical tool.

Sensitivity Analysis and Optimization of Transient Responses

Narayanan Pagaldipti*, Shaobin Liu**

*Altair Engineering, Inc., **Altair Engineering, Inc.

ABSTRACT

Sensitivity Analysis and Optimization of Transient Responses Narayanan Pagaldipti and Shaobin Liu Altair Engineering, Inc. 2030 Main Street, Suite 100, Irvine, California 92614, USA E-mail: pagaldip@altair.com Dynamic analyses of engineering systems are conducted in the frequency domain (frequency response analysis) and the time domain (transient response analysis). Altair OptiStruct¹, a leading commercial Computational Mechanics and Design Optimization software, supports these analyses extensively and offers accurate, efficient and innovative solutions not only for Noise, Vibration and Harshness (NVH) applications but also in the broad CAE space and Multidisciplinary Design Optimization (MDO). OptiStruct is the established leader in topology, sizing and shape optimization for many applications. For dynamic applications, design optimization is supported for natural frequencies, frequency response displacements, stresses, Equivalent Radiated Power (ERP) and also for transient analysis using the Equivalent Static Load method (ESL Method). This paper will present recent developments for supporting transient responses directly in design optimization. The motivation is to rigorously capture the stiffness, inertial and damping effects in the sensitivity calculations along with the time integration of the transient analysis. Unlike the ESL Method, this rigorous approach is better equipped to offer robust designs, albeit at an increased computational price. Both direct and adjoint sensitivity methods will be covered with the latter being a necessity for supporting topology optimization. Peak transient responses will be automatically considered in the optimization formulation without requiring the design engineer to specify any specific time instants or geometric locations for the response evaluations. Several design studies based on this implementation will be presented to validate its robustness, efficiency and practical use. Comparative studies against the more efficient ESL Method will also be conducted to establish the robustness of the new, more rigorous method. References: 1. Altair OptiStruct 2017: Users Guide. Altair Engineering, Inc., Troy, Michigan.

Reduced Order Modeling for Uncertainty Quantification of the Cardiac Function

Stefano Pagani^{*}, Andrea Manzoni^{**}, Alfio Quarteroni^{***}

^{*}École polytechnique fédérale de Lausanne, ^{**}Politecnico di Milano, ^{***}Politecnico di Milano

ABSTRACT

A growing number of biomedical applications are bringing new challenges dealing with the integration of high-dimensional and complex data (possibly affected by uncertainty) within mathematical models built on partial differential equations (PDEs). The mathematical and numerical modeling of the cardiovascular system requires a huge amount of data when trying to reproduce both physiological and pathological behaviors. Often partially missing, these data show a considerable intra- and extra-subject variability and are inevitably hampered by uncertainty, e.g., in (i) the computational domain, (ii) physical parameters and (iii) boundary conditions, among others. These are the main reasons behind the very rapid growth of applications of uncertainty quantification (UQ) methods to cardiovascular problems in the past decade, in view of both model calibration and personalization -- that is, the adaptation of model inputs to subject-specific conditions. Forward UQ problems are strictly related to the task of parametric studies, multi-scenario and sensitivity analyses, whereas backward UQ problems involve parameter (and state) estimation and data assimilation. In particular, Bayesian methods provide a rigorous framework for the solution of backward UQ problems. Sampling algorithms, such as the Markov chain Monte Carlo (MCMC) or the (ensemble) Kalman filter, enable to estimate the distribution of quantities of interest (model parameters, state of a system) from noisy (non)-invasive clinical measurements. Numerical strategies for UQ problems in this context involve the approximation of PDEs for several (usually, order of thousands) input parameter values, thus making high-fidelity, or full-order, techniques (e.g. the finite element method) ill-suited, despite the constant growth of computer resources available. Reduced-order models (ROMs) such as the reduced basis (RB) method, are emerging methodologies in the UQ framework since they are aimed at reducing the computational complexity entailed by the repeated solution of PDEs. In this talk we show how to take advantage of ROM techniques to treat forward and backward propagation of uncertainty in relevant problems dealing with cardiac electrophysiology and electromechanics.

Identification of Nonlinear Parameters of a Nuclear Fuel Rod

Brian Painter^{*}, Marco Amabili^{**}, Stanislas Le Guisquet^{***}, Prabakaran Balasubramanian^{****},
Kostas Karazis^{*****}

^{*}AREVA NP Inc, ^{**}McGill University, ^{***}McGill University, ^{****}McGill University, ^{*****}AREVA NP Inc.

ABSTRACT

In Pressurized Water Reactors (PWRs), fuel assemblies are made up of fuel rods, long slender tubes filled with uranium pellets, bundled together using spacer grids. These structures are subjected to fluid-structure interaction, due to the flowing coolant surrounding the fuel assemblies inside the core, coupled with large-amplitude vibrations in the case of external seismic excitation. Therefore, understanding the nonlinear response of the structure, and, particularly, its dissipation, is of paramount importance for the choice of safety margins, in the design of fuel assemblies, to ensure their functionality and safety in the worst external condition scenarios. To model the nonlinear dynamic response of fuel rods, the identification of the nonlinear stiffness and damping parameters is required. A tool based on the harmonic balance method was developed to identify these parameters from the experimentally obtained force-response curves, considering one-to-one resonance phenomenon present in axisymmetric structures such as cylindrical tubes and shells. To validate the tool, it was applied to the reference case of a circular cylindrical shell filled with water, which revealed an increase of damping with the excitation amplitude. More recently, the more realistic case of a single fuel rod with clamped-clamped boundary conditions was investigated by applying harmonic excitation at various force levels in the presence of a surrounding fluid. The nonlinear parameters including damping were extracted from experimental results by means of the adapted tool. An increase in damping with excitation amplitude has been shown according to earlier studies.

An Elasto-plastic Dynamic Response Analysis of E-Defense Large-scale Experiment on Soil-underground Structure Interaction

Mahendra Kumar Pal*, Takuzo Yamashita**, Shintaro Ohno***, Atsushi Iizuka****

*National Institute for Earth Science and Disaster Resilience (NIED), Japan, **National Institute for Earth Science and Disaster Resilience (NIED), Japan, ***Kajima Corporation, Japan, ****Kobe University, Japan

ABSTRACT

In this study, an elasto-plastic dynamic response analysis of Soil-Structure Interaction (SSI) specimen, with an aim to validate the numerical results of E-Simulator, is presented. A large-scale soil-underground structure specimen was tested against multiple seismic waves [1], to assimilate a comprehensive understanding of SSI. Specimen is comprised of two inclined layers of soil-strata, two vertical shafts, two horizontal shield tunnels and one cut-and-cover tunnel interconnecting the shafts. All structural component and soil-layers of specimen are discretized using solid 3-Dimensional linear tetrahedral elements to generate a high fidelity finite element model of test specimen. Interface between soil and structures is modeled using conforming mesh. To achieve conforming mesh, soil mesh around the structures is adaptively refined with an aim to generate mesh, which is compatible with high-resolution meshes of structures. Soil laminar container is modeled using rigid-body elements with linear interpolatory constraints. Modified Cam-Clay model [3] has been employed to simulate nonlinear behaviour of soil, in which cyclic plasticity, development of anisotropy and collapsibility of soil-structure are modelled using extended sub-loading surface, rotational hardening and super-loading surface, respectively. Dynamic response analysis of the detailed FE model of the specimen is analysed using E-Simulator. E-simulator [3] is in-house high performance parallel finite element (FE) package developed at-and-by E-Defense to reproduce the damage mechanism of buildings and civil structures against seismic loading. Acceleration and displacement time history responses of numerical simulation at various critical locations of specimen are compared with those of experiment. A comparative study of profiles of curvature, rotation and displacement along depth of specimen is also demonstrated. The obtained numerical results are in reasonable agreement with the E-Defense large-scale experiment. A torsional deformation of cut-and-cover tunnel is also reported. Keywords: Soil-Structure-Structure Interaction, Large-scale Shake Table Test, Underground Structures, Modified Cam-Clay Model, E-Simulator, E-Defense. References: 1) Yohsuke Kawamata, Manabu Nakayama, Ikuo Towhata, Susumu Yasuda, "Dynamic behaviour of underground structure in E-Defense shaking experiment", Soil dynamics and earthquake engineering, 82, pp. 24-39, 2016. 2) Shintaro Ohno, "Elasto-plastic constitutive models derived from non-linear description of soil contractancy", Doctoral thesis submitted to Tokyo Institute of Technology Japan, 2006. 3) Takuzo Yamashita, Muneo Hori, Koichi Kajiwar. "Petascale Computation for Earthquake Engineering", Computing in Science and Engineering, 13(4), pp.44-49, 2011

Tunable Dynamic Response in Tensegrity Based Lattices

Raj Kumar Pal^{*}, Massimo Ruzzene^{**}, Julian Rimoli^{***}

^{*}Georgia Institute of Technology, ^{**}Georgia Institute of Technology, ^{***}Georgia Institute of Technology

ABSTRACT

Tensegrity-based lattices exhibit mechanical properties very distinct from their constituent materials due to their geometry, topology and nonlinear interaction between the members. They also have potential to exhibit significant tunability in their dynamic properties by varying the cable prestrain. As the prestrain increases, the bars buckle leading to a change in the effective stiffness. We investigate the linear wave properties of such tunable tensegrity-based beams, plates and solids, where the basic building block is a truncated octahedron. We show the presence of three distinct stages of dynamic behavior as the cable prestrain is varied, with sharp transitions in wave speeds between them. These transitions are analogous to phase transitions in condensed matter systems, and lead to qualitative change in wave response. For example, we show that, in a range of cable prestrains, tensegrity solids exhibit dilational response, where the shear waves travel faster than pressure waves. Our dispersion analyses are verified by detailed numerical simulations. This work provides a robust and simple framework for developing tunable tensegrity-based periodic media in three dimensions.

Nonlinear Static Analysis of a Celestial Icosahedron Vacuum Lighter Than Air Vehicle

Anthony Palazotto*, Kyle Moore**

*Air Force institute of technology, **Air Force Institute of technology

ABSTRACT

The idea of a lighter than air vehicle (LTAV) which uses an internal vacuum to achieve buoyancy has been around since the 17th century, but advancements in engineering and manufacturing processes are just now allowing for this concept to be feasible. Research on vacuum LTAVs has been conducted at AFIT since 2013. A new design for such a vehicle, called the Celestial Icosahedron design, was proposed by Brian Cranston in 2016 as part of his PhD dissertation but has not yet been analyzed as thoroughly as previous designs. The design itself is composed of 9 intersecting, circular hoops made of a carbon nanotube (CNT) composite, spaced out and revolved at 45 degree increments. The frame is covered by a thin membrane-like, Graphene skin. The research for this particular design followed that of previous AFIT designs. The research includes a boundary condition study of the frame in order to ensure symmetry, as well as a comparison of different sized designs (variation of diameter) with the goal of achieving the smallest possible structure (diameter less than 3 feet). The structure's nonlinear static response to a loading condition that is representative of sea-level pressure was analyzed using the Finite Element Analysis (FEA) program, Abaqus including adoptive stabilization. Spherical stresses and displacements show the level of material and structural nonlinearity based on the various boundary conditions. Matlab is used in order to optimize both the size and the weight to buoyancy ratio of the structure. The frame of the structure has been built using additive manufacturing. A small, feasible design is to be implemented in the intelligence, surveillance, and reconnaissance (ISR) field with an emphasis on cramped urban environments. Future research will include a comparison of different structural materials, further optimization and dynamic response including instability.

Flow Diverter Treatment Outcome of Intracranial Aneurysms is Associated with Blood Flow Modifications: In Silico Computational Analysis of Clinical Cases

Nikhil Paliwal^{*}, Robert Damiano^{**}, Jason Davies^{***}, Adnan Siddiqui^{****}, Hui Meng^{*****}

^{*}Mechanical and Aerospace Engineering, Toshiba Stroke and Vascular Research Center, University at Buffalo,

^{**}Mechanical and Aerospace Engineering, Toshiba Stroke and Vascular Research Center, University at Buffalo,

^{***}Neurosurgery, Toshiba Stroke and Vascular Research Center, University at Buffalo, ^{****}Neurosurgery, Toshiba Stroke and Vascular Research Center, University at Buffalo, ^{*****}Mechanical and Aerospace Engineering,

Neurosurgery, Toshiba Stroke and Vascular Research Center, University at Buffalo

ABSTRACT

Introduction Flow diverters (FDs) are the preferred treatment modality for endovascular treatment of intracranial aneurysms (IAs). Densely woven stent-meshes structure of FDs disrupt blood flow within the aneurysm to induce pro-thrombotic conditions, and serves as a scaffold for endothelial ingrowth and arterial remodeling. Despite good clinical success of FDs, complications like incomplete occlusion and post-treatment rupture have been reported.[1] In silico analysis of FD-treated IA patients can shed light on the contrasting hemodynamics in different clinical outcomes. To that end, this study aims to investigate differences in hemodynamics in patients with completely and partially occluded IAs after FD-treatment. **Methods** Patients with following criteria were included in this study: (1) sidewall aneurysm at the ICA treated using one FD, (2) pre-treatment images and 6-month follow-up available. Patients were divided into "occluded" and "residual" groups based on their 6-month clinical outcome. Images were segmented to obtain patient-specific IA models. Virtual stenting workflow[2] was used to recapitulate the clinical FD deployment in each IA. CFD was performed on the untreated and virtually-treated IA geometries using STAR-CCM+ (CD-adapco, Melville, NY) under physiological flow conditions, with blood modeled as Newtonian (density: 1056 kg/m³, viscosity: 0.0035 Pa-s). Time-averaged reductions in shear rate (SR), aneurysmal average velocity (AAV), wall shear stress (WSS) and inflow rate (IR) were calculated for each case. A two-tailed Student's t-test was performed for statistically significant differences in hemodynamic parameters between the groups. **Results** Thirty-eight IAs in 35 patients fulfilled the inclusion criteria and were included in the study. At 6-month clinical follow-up, 27 aneurysms were occluded and 11 aneurysms were patent (residual). IAs in the occluded group had higher hemodynamic reductions than the residual group. IR was significantly different between the two groups with a p-value of 0.04. SR, AAV and WSS showed no significant difference between the groups. **Discussion** Our results shows higher flow reduction in successfully occluded IAs at 6-month follow-up. This is in accordance with previous findings that larger hemodynamic reductions are associated with successful occlusion of FD-treated IAs.[3] Statistically significant differences in IR between the groups implies that higher flow reductions at the aneurysmal neck may be required for complete occlusion of FD-treated sidewall IAs. Large prospective studies are required to confirm our findings, and develop statistical models for a priori prediction of the occlusion outcome of FD-treated IAs. **References** 1. Siddiqui et al., Neurosurgery, 2012 2. Paliwal et al., CMBME, 2016 3. Ouared et al., JNIS, 2016

Schwarz Alternating Implicit Enrichment Methods for Analysis of Kirchhoff-Love Plate Model with Angular Corners

Birce Palta*

*The University of North Carolina at Charlotte

ABSTRACT

We develop numerical methods for analysis of Kirchhoff-Love plate model with angular corners. Even though this thin plate model has no boundary layer problems, we have to handle fourth order partial differential equations whose finite element approach requires smoother basis functions. It is known that Isogeometric Analysis (IGA) can effectively handle this type of problems whenever plate is a simple convex domain. However, IGA with single patch encounters difficulties in dealing with irregular shaped polygonal plates. In literatures, for analysis of thin plates with angular corners, multi-patches approaches, discontinuous Galerkin method (DGA), penalty methods, domain decomposition methods (DDM), and so on, are suggested. In this paper, in order to handle thin plate model with singularities, we introduce implicitly enriched Galerkin method combined with smooth flat-top partition of unity functions. Unlike XFEM, this approach does not have singular integral problems. For the cases where multi-patches are necessary, we combine DDM and implicitly enriched Galerkin method. Numerical examples show effectiveness of the proposed methods in dealing with cracked and L-shaped plates.

On the Numerical Study of Ballistic Performance of Multi-ply Woven Fabrics

Emre Palta^{*}, Howie Fang^{**}

^{*}The University of North Carolina at Charlotte, ^{**}The University of North Carolina at Charlotte

ABSTRACT

Studies on ballistic performance of woven fabrics possess considerable importance because woven fabrics are one of the most commonly used materials for soft body armor equipment. The ballistic impact performance of single-ply woven fabrics has been widely evaluated both experimentally and numerically in literature. Although a soft body armor equipment is always made of multi-ply woven fabrics, there are few experimental and numerical studies dealing with multi-ply woven fabrics. In this study, a multi-scale numerical modeling technique was developed to evaluate in detail the ballistic performance of multi-ply woven fabrics. The multi-scale modeling technique was validated against experimental data and was found to reduce computational expense while maintaining adequate solution accuracy. The multi-scale models of four multi-ply woven fabric targets with three, five, seven, and ten plies, respectively, were created and used in the evaluation of the ballistic performance of multi-ply woven fabrics in terms of ballistic limits, transverse displacements, and perforation mechanism.

OPTIMIZED STRATEGIC TASK ALLOCATION FOR THE MITIGATION OF OFF NOMINAL EVENTS IN THE FUTURE AIR TRAFFIC MANAGEMENT SYSTEM

Roberto Palumbo and Edoardo Filippone

*CIRA, Italian Aerospace Research Center
Via Maiorise
Capua (CE), 81043 Italy
r.palumbo@cira.it; www.cira.it

Key words: ATM performance; resilience engineering; optimal path search; task allocation.

1 INTRODUCTION

The growing density of air transportation operations and airspace users, has increased the complexity of the Air Traffic Management (ATM) system. For this reason, in recent years international programs, such as SESAR in Europe and NextGEN in the US, are developing new operational concepts to redesign and reorganize the ATM system in a more efficient way improving capacity, efficiency and safety, thus avoiding the increase of costs, delays and emissions as well as the increase of workload of air traffic controllers. More specifically the goal is to fulfil the performance expectations expressed in the 11 Key Performance Areas defined by ICAO plus Human Performance [1]. To this end, the new and future air traffic management paradigms will focus on:

- increasing the level of automation of the system (to reduce workload)
- moving toward a network centric approach to information sharing (to improve situational awareness)
- moving toward time-based operations (to increase sector capacity).

In the context of this future highly automated system, disruptive events will call for an efficient re-allocation of tasks and authority sharing between humans and automated systems in order to mitigate the degradation of performance caused by the off-nominal condition. Recently, the ATM research community is giving more and more attention to the concept of resilience as a possible way to analyze the capabilities of the ATM system to recover an acceptable level of performance when non-nominal conditions occur. In fact the original definition of resilience comes from the material science domain where it is considered a property of a system that describes its ability to return to its original state (at some later time), after the removal of a [deforming] stress. In 2009, EUROCONTROL has given a specific interpretation of resilience in the context of air traffic management. In fact according to Ref. 2,

resilience is “the intrinsic ability of a system to adjust its functioning prior to, during, or following changes and disturbances, so that it can sustain required operations under both expected and unexpected conditions”. This definition, while explaining well the desired behavior of a resilient ATM system, it does not, however, provide a quantitative framework to evaluate the resilience of the ATM system. Recently, the SESAR JU E2.21 SAFECORAM (Sharing of Authority in Failure/Emergency Condition for Resilience of Air traffic Management) project, introduced a quantitative methodology to measure the level of resilience of the ATM system based on the concept of tasks re-allocation and authority sharing between humans and systems within the future ATM system (year 2050) [3, 4]. The following sections will describe the methodological approach developed in the SAFECORAM project, together with some applications from different operational perspectives.

2 SAFECORAM METHODOLOGY

The SAFECORAM definition of resilience is based on a quantitative measure of the global performance of the ATM system. To quantify resilience, it is therefore necessary to define the meaning of global performance. The global performance of the ATM system can be thought as the fulfilment of the aforementioned performance expectations in the 11 Key Performance Areas (KPAs) defined by ICAO plus Human Performance. With reference to Figure 1a, if we are able to assign a performance level to each KPA, then we could interpret the yellow area, as the global performance of the ATM system at a given state. When an off-nominal condition occurs, the ATM system can no longer perform in its nominal conditions and its global performance will inevitably change. Of course the ATM system reacts to the disturbance applying a set of mitigation tasks and actions that are aimed at restoring the nominal level of performance (i.e. the original yellow area) as much as possible. This residual level of global performance is what SAFECORAM defines as the resilience of the system. Therefore an ATM system is more resilient the more it is able to reorganize itself towards the most similar state with respect to the reference (nominal) one.

It is important to remark that not all mitigation strategies are alike. Different mitigation strategies may recover different levels of global performance (Figure 1b). This means that among all the possible sets of mitigation actions suitable to face the disruptive event, some of them are better at minimizing performance loss. In other words, it is possible to define an optimization problem aimed at maximizing the resilience of the system (i.e. minimize performance loss). This optimization is based on the optimal re-allocation of tasks between different ATM actors, in order to preserve the highest possible level of residual performance of the system when an off-nominal condition occurs.

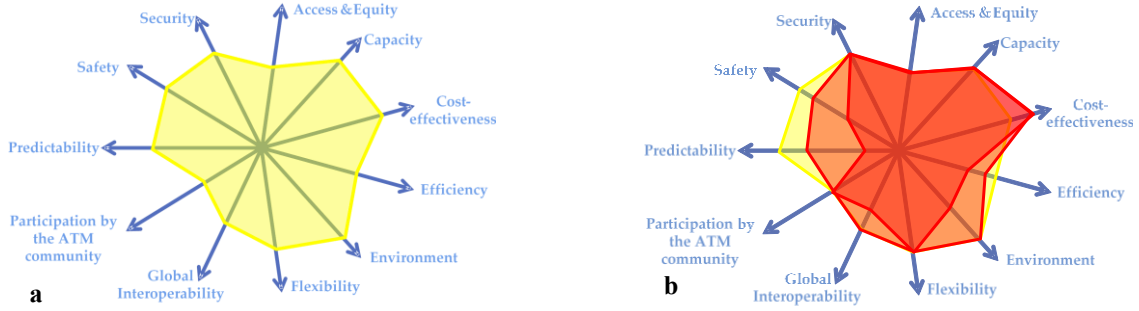


Figure 1. Global Performance of the system (a). Residual global performance in off-nominal conditions (b).

Therefore, to quantify the global performance of the ATM system in nominal and off-nominal conditions it is necessary to provide:

- a methodology to quantify the performance levels of the KPAs and how they are degraded once the off-nominal condition occurs;
- a methodology to establish the best re-allocation of tasks.

2.1 Scenario Based Approach

The SAFECORAM methodology was derived following a scenario based approach. This means that the methodology was developed starting from the definition and analysis of several ATM scenarios. Basically, a scenario represents a description of a set of nominal and non-nominal situations affecting the ATM system. In SAFECORAM, the objective of a scenario is to explore alternative behaviors of the system when an off-nominal condition is triggered.

In Section 3, we will describe an explanatory case study scenario (developed with the help of ATM operational experts) which is very useful to understand the application of the SAFECORAM approach.

In general, the approach consists of several steps (see Figure 2): first of all, the ATM scenario is described in nominal conditions, then a disturbance is considered leading to off-nominal conditions and possible different task reallocation strategies are analyzed. These strategies are then evaluated and optimized in terms of global performance yielding the best mitigation strategy which finally defines the resilience of the system.

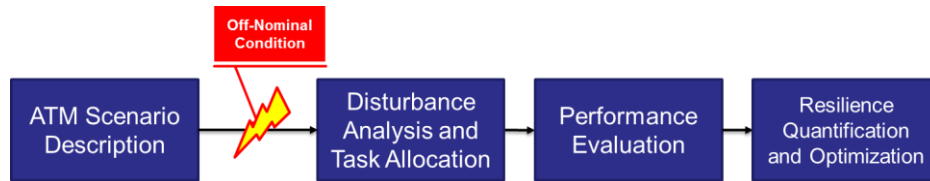


Figure 2. The SAFECORAM methodology steps.

3 CASE STUDY SCENARIO

Before describing the details of the case study scenario it is important to state some basic assumptions:

- the framework is the future ATM system (year 2050): this means that the SESAR ConOps are fully deployed, the ATM system is highly automated and Remotely Piloted Aerial Systems (RPAS) and Personal Air Transportation Systems (PATs) (with their related infrastructure) are fully integrated as airspace users;
- the stochastic nature of the events that can affect the scenarios is not taken into account.

3.1 Scenario Description

The scenario consists of four en-route airplanes that according to their flight plan have to cross a specific air sector and 4 airplanes that depart from an airport inside that same air sector. Nominally the four en-route airplanes fly their assigned 4D trajectory contract crossing the specific air sector, and the departing four airplanes depart from the airport inside the air sector. The unexpected event that triggers the application of a mitigation strategy is the fact that the airspace sector is affected by a temporary GNSS unavailability that impairs the navigation systems of the vehicles.

3.2 Disturbance Analysis and Task Allocation

In general, the scenario description may be broken down into a flow of tasks and actions performed by the actors of the scenario. The nominal flow is the set of tasks and actions that describes the nominal execution of the scenario and guarantees the nominal global performance.

When the off-nominal condition occurs, there are several task reallocation alternatives and different flows of actions that may be performed to mitigate the effect of the disturbance. Each of these alternatives determine different paths characterized by a different, yet degraded level of global performance. Comparing the degraded global performances of each alternative flow with the nominal global performance, it is possible to identify the mitigation strategy which minimizes performance loss.

Figure 3 shows the task breakdown identified for this case study scenario. Basically the ACC Manager must decide how to deal with the off-nominal condition inside the specific air sector, either closing the sector (deviating the en-route airplanes and grounding the departing ones) or allowing only a limited number of airplanes through the airspace sector (either departing or crossing the area).

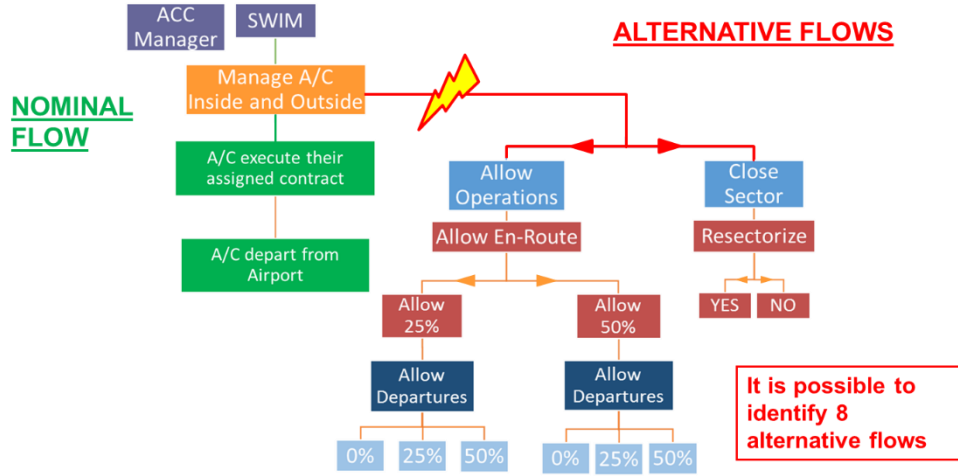


Figure 3. Nominal flow and alternative mitigation strategies for the Case Study.

3.3 Global Performance Evaluation and Optimization

As it can be seen, eight possible alternative flows can be identified. Now, in order to evaluate the global performance of the system for each of these alternative flows, we consider a quantitative evaluation of the performance in certain KPAs through the use of specific Key Performance Indicators (KPIs). Specifically:

- K1 - efficiency (fuel burn);
- K2 - efficiency (delay);
- K3 - environment (emissions);
- K4 - capacity (throughput).

In general, once the nominal flow and the off-nominal flows are completely described, it is possible to analyze and optimize the performance through the use of graph theory results. As a matter of fact both the nominal flow and the alternative flows may be represented in the form of weighted directed acyclic graphs (DAGs), in which vertices are tasks whose contribution to performance degradation is weighted along the connecting edges [4].

A computer program written in Java maps the graph and finds the task reallocation strategies (which are all of the possible paths of the graph) with their associated level of global performance. Given a path distance function $d(\cdot)$ between the nominal task flow and the alternative ones, it is possible to quantify resilience as the shortest path which is basically the one that minimizes performance loss. Specifically – in line with Figure 1b – we have chosen as distance function the difference between the areas that are generated by the performance levels expressed by the KPIs for all of the possible mitigation strategies [3, 4].

3.4 Results

In this specific case study we have obtained the graph shown in Figure 4 and the results shown in Figure 5. As it can be seen, the more the global performance area of the off-nominal strategies is close to the nominal one, the more the system is resilient.

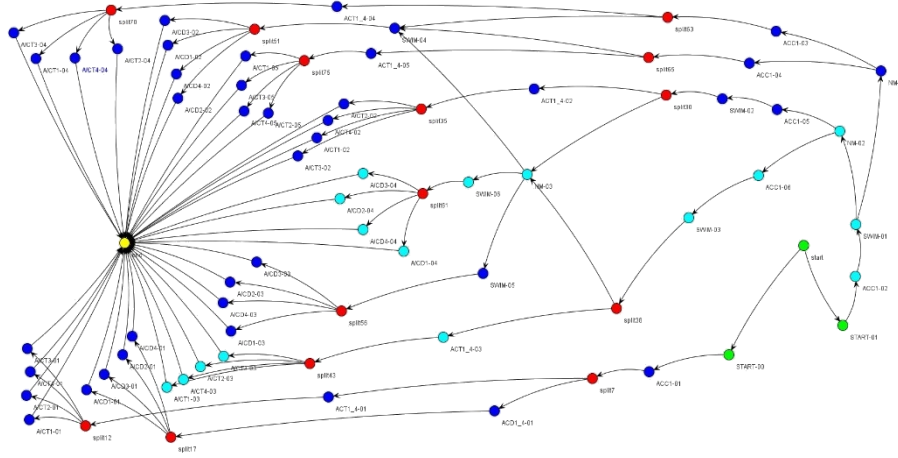


Figure 4. Generated DAG graph for the Case Study.

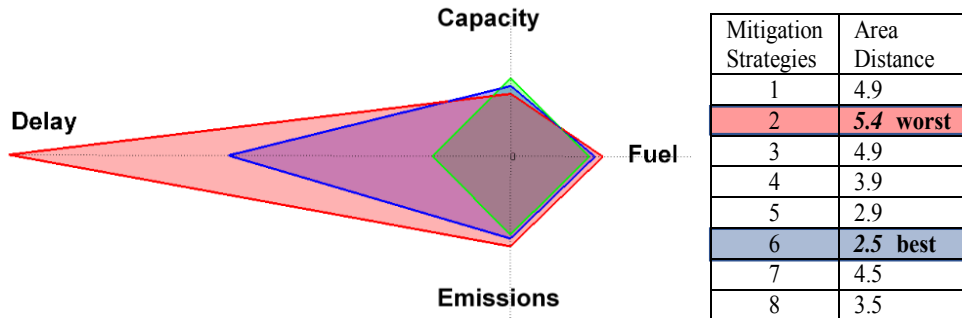


Figure 5. Results of the resilience optimization for the Case Study.

As seen, the analysis of this Case Study is quite straightforward and – in principle – it does not need a computational approach. However, the analysis of different scenarios throughout the development of the SAFECORAM project has demonstrated that the system can become extremely complex and impossible to treat without a computational approach and graph theory results.

4 SAFECORAM METHODOLOGY AS A DECISION SUPPORT TOOL

While the methodology defined in the SAFECORAM project is mainly oriented at defining an operational way to quantify the resilience of the future ATM system, it can also be employed as a decision-support tool in performance optimization analyses related to ATM contexts.

In this section, we use the SAFECORAM approach as a cost-benefit analysis tool for airlines dealing with potential flight cancellations or replanning due to a volcanic ash cloud. This idea – which is still currently work in progress – stems from the well-known volcanic ash aviation crisis of 2010, one of the most common actual events referred in ATM resilience studies.

4.1 The 2010 Volcanic Ash Aviation Crisis

Between April and May 2010, the European airspace was massively disrupted by the eruption of the Icelandic volcano Eyjafjallajökull which caused the presence of a large cloud of fine ash drifting south east. In fact many national aviation authorities, following the “zero ash tolerance” regulation advised by ICAO (because of the threat posed by ash to aircraft engines) and relying on the ash cloud forecast carried out by the Volcanic Ash Advisory Centre in London, decided to shut-down many air sectors for days, grounding thousands of flights and millions of passengers, causing huge economic losses to airlines and airports. As a matter of fact, during the ash crisis, several airlines conducted a number of independent flight tests and safety assessments demonstrating the limitations of the precautionary “zero ash tolerance” criterion in areas where the ash concentration was lower than 2 mg/m^3 [5]. As a consequence, after some pressure from the airlines and in agreement with jet engine experts, ICAO decided to raise the threshold for dangerous ash concentration and a new safety code was roughed out. Specifically, any ash concentration:

- higher than 2 mg/m^3 , is a no-fly zone;
- between 2 mg/m^3 and 0.2 mg/m^3 , requires airlines to take extra precautions
- below 0.2 mg/m^3 is considered no threat at all.

This new regulation allowed most of the airspace to be reopened. In fact in the aftermath of the crisis, EUROCONTROL ultimately decided that, “while each individual state remains responsible for deciding whether or not to impose restrictions on flights in its airspace, [...] decisions to perform flights in airborne contamination (such as ash or sand), should be made by airlines, based on the conclusions of their safety risk assessment” [6].

4.2 Simulated Ash Cloud Scenario Description

The objective of this section is to describe and analyze an ash cloud crisis scenario similar to the one of 2010. This study will show how the SAFECORAM approach can be used as a cost-benefit analysis tool that may help to find the best mitigation strategy in terms of economic damage caused by ash cloud flight disruptions.

As study reference scenario, we consider a one-day flight schedule of a generic low-cost airline operating a B737-800 fleet from London, UK, to several European cities.

In the nominal strategy, 14 daily flights are carried out nominally (see Figure 6) and the airline expenses for each flight are the nominal reference costs.

We then consider two consecutive days of ash cloud crisis. We assume the following:

- the post 2010 ash crisis regulation holds, therefore the ash cloud is divided into three areas with high, medium and low levels of ash concentration. Areas with concentration levels higher than 2 mg/m^3 are considered no fly zones, while areas with levels below 0.2 mg/m^3 are totally safe;
- areas with medium concentration levels are assumed to have a homogeneous value of 1.1 mg/m^3 and are all safe to cross, however the airline is faced with additional maintenance costs [7];
- the vertical distribution of the ash cloud is uniform between FL200 and FL350 while its horizontal distributions (in the 2 days) slightly resemble those observed on April 18-19, 2010 [5];
- the ash cloud topology for each day is not a function of time, i.e. the cloud is constant across the day of operation.

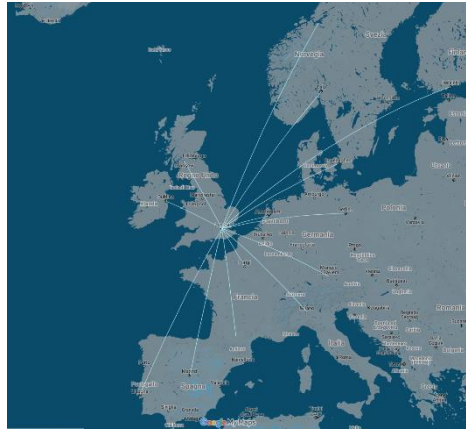


Figure 6. Route structure of the generic low-cost airline considered in the Scenario.

4.3 Disturbance Analysis and Task Allocation

As far as the mitigation strategies are concerned, we assume that for each flight of the day the airline can decide:

- to cancel the flight, or
- to fly directly to the destination (modifying as little as possible the trajectories that should intersect no-fly zones), or

- to deviate the flight in order to reduce as much as possible the flight time within the medium concentration ash cloud.

These options have all different impacts on the overall flight costs.

4.4 Global Performance Evaluation and Optimization

In fact the KPI used in this analysis is the overall cost that the airline has to face in order to tackle the flight operations in each day of the crisis. The overall cost is then normalized with respect to the nominal case (i.e. flights carried out nominally without any contingency measure due to the ash cloud).

Degradation of the KPI is brought about by costs due to additional flight time when rerouting the airplane to avoid the ash cloud, and to additional maintenance when crossing the medium concentration ash cloud.

The determination of flight costs has been carried out collecting data from different literature sources [^{8,9}] relative to the B737 type of aircraft. Delay costs and cancellation costs were taken from [^{9,10}]. All costs were expressed in terms of dollars per block hour. No literature references were found on the cost of maintenance due to flights within ash clouds of medium concentration. However, according to Ref. 7, the maximum tolerable exposure dose to volcanic ash of a turbine engine before mandatory engine inspection is around $15\text{g}\cdot\text{s}/\text{m}^3$. From this piece of information, assuming that the cloud has a constant concentration of $1.1\text{ mg}/\text{m}^3$, we were able to draw some conclusions on the additional costs of maintenance per flight hour within the cloud, as this process reduces the time interval between routinary engine inspections.

Using these data and assuming (realistically) constant average speed for each flight, we were able to determine the cost of each flight per day for the three different aforementioned alternative airline choices.

4. Results

Analyzing the resulting decision tree it is possible to determine the most convenient flight management for both days of operations.

Figure 7 shows the route structure assuming that all flights during Day 1 (above) or Day 2 (bottom) are either direct (left) or deviated (right). On Day 1 some routes are not disrupted by the ash cloud, while some routes marked as DIRECT are slightly deviated to avoid the high density ash cloud. In both ash cloud situations there are some flights that must be cancelled since their destination is not reachable without crossing the no-fly zone.

Table 1 and Table 2 summarize the resulting flight management schedule in the best case (lowest economic damage) and worst case (highest economic damage). The tables report the Cost KPI for each flight (normalized with respect to the nominal cost of that flight) and also a Best and Worst Total Cost Index which is the total cost of the day of operations normalized to the overall nominal cost of the same day. It can be seen that on both days, although the total

cost to the airline will obviously grow, there are mitigation strategies that generate a total cost lower than 1.5 times the nominal cost, while other (worse) strategies could cost up to more than twice the nominal cost.

DAY 1	Best Management			Worst Management	
Route	Flight Status	Cost KPI		Flight Status	Cost KPI
LHR-CDG	DIRECT	3.21	Not Affected	DEVIATED	6.82
LHR-AMS	DEVIATED	1.23		CANCELED	3.61
LHR-DUB	DIRECT	1.00		DIRECT	1.00
LHR-GLA	DIRECT	1.00		DIRECT	1.00
LHR-MAD	DIRECT	1.30	Not Affected	DEVIATED	2.40
LHR-SXF	DEVIATED	1.02		CANCELED	2.13
LHR-CPH	DIRECT	1.00		DIRECT	1.00
LHR-OSL	CANCELED	1.95		CANCELED	1.95
LHR-LIN	DIRECT	1.63	Unreachable	CANCELED	2.13
LHR-LIS	DIRECT	1.21		DEVIATED	1.63
LHR-HEL	CANCELED	1.38		CANCELED	1.38
LHR-MUC	DIRECT	1.46		CANCELED	2.23
LHR-TLS	DIRECT	1.78	Unreachable	DEVIATED	3.16
LHR-TRD	CANCELED	1.56		CANCELED	1.56
Best Total Cost Inde				1.43	
Worst Total Cost Inde				2.	

Table 1. Day 1: Most convenient and least convenient flight planning (in terms of economic damage).

DAY 2	Best Management			Worst Management		
Route	Flight Status	Cost KPI		Flight Status	Cost KPI	
LHR-CDG	DIRECT	1.62	Unreachable	CANCELED	4.70	
LHR-AMS	DEVIATED	1.10		CANCELED	3.61	
LHR-DUB	DIRECT	1.39		CANCELED	3.33	
LHR-GLA	CANCELED	2.93		CANCELED	2.93	
LHR-MAD	DIRECT	1.17		DEVIATED	1.79	
LHR-SXF	DEVIATED	1.07		CANCELED	2.13	
LHR-CPH	DIRECT	1.46		CANCELED	2.13	
LHR-OSL	DIRECT	1.25		DEVIATED	2.51	
LHR-LIN	DIRECT	1.55		DEVIATED	5.21	
LHR-LIS	DIRECT	1.17		CANCELED	1.38	
LHR-HEL	DIRECT	1.29		DEVIATED	1.53	
LHR-MUC	DIRECT	1.48		DEVIATED	2.87	
LHR-TLS	DIRECT	1.36		DEVIATED	3.61	
LHR-TRD	DIRECT	1.22		DEVIATED	2.33	
Best Total Cost Inde				1.3		
Worst Total Cost Inde				2. 1		

Table 2. Day 2: Most convenient and least convenient flight planning (in terms of economic damage).

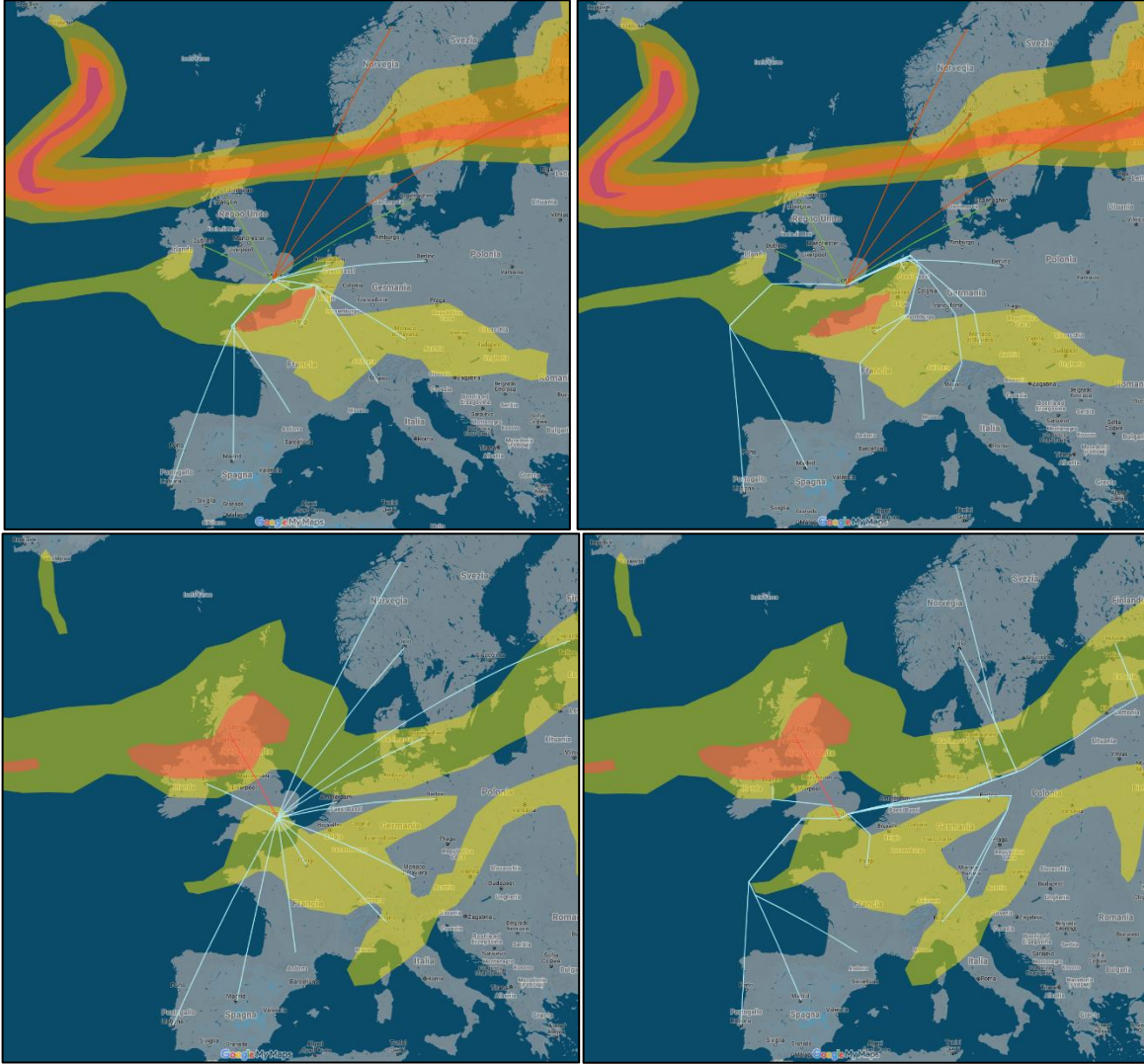


Figure 7. Direct and deviated routes considered in the Scenario.

CONCLUSIONS

This work describes the SAFECORAM approach, a methodology to quantify and optimize the ATM system resilience. The application of this approach to realistic case studies demonstrated the consistency of the methodology. In fact in non-nominal conditions that could disrupt, locally or extensively, the ATM system operability, the proposed approach allows to

select the proper task allocations that optimize the recovery of the global performance of the ATM system. We have also employed the SAFECORAM methodology as a support-decision tool in a cost-benefit analysis for a generic airline, evaluating a volcanic ash crisis kind of scenario, using a cost index as Key Performance Indicator.

Future work will expand this approach to consider the full ATM performance framework, merging several KPIs related to different key performance areas.

REFERENCES

- [1] Graham, R., Pilon, N., Tabernier, L., Koelman, H. and Ravenhill, P., Performance framework and influence model in ATM, Digital Avionics Systems Conference, IEEE/AIAA (2009).
- [2] EUROCONTROL, A white paper on resilience engineering for ATM, Report of the Project Resilience Engineering for ATM (2009).
- [3] Palumbo, R., Filippone, E., A Quantitative Approach to Resilience Engineering for the Future ATM System: Case Studies Results, 12th USA/Europe Air Traffic Management Research and Development Seminar (2017).
- [4] Filippone, E., Gargiulo, F., Errico, A., di Vito, V. and Pascarella, D., Resilience management problem in ATM systems as a shortest path problem, *J. Air. Tra. Man.* (2016) 56:57-65.
- [5] Folch, A., Costa, A., Basart, S., Validation of the FALL3D ash dispersion model using observations of the 2010 Eyjafjallajökull volcanic ash clouds, *Atmos. Environ.* (2012) 48:165-183.
- [6] EUROCONTROL, What has changed for aviation in dealing with volcanic ash since 2010?, retrieved from <http://www.eurocontrol.int/articles/what-has-changed-aviation-dealing-volcanic-ash-2010>
- [7] Clarkson, R., Simpson, H., Maximising Airspace Use During Volcanic Eruptions: Matching Engine Durability against Ash Cloud Occurrence, STO-MP-AVT-272 (2017).
- [8] Aviation Week, July 30, 2012.
- [9] EUROCONTROL, Standard Inputs for EUROCONTROL Cost-Benefit Analyses (2015).
- [10] Cook, A., Tanner, G., Jovanović, R., Lawes, A., The Cost of Delay to Air Transport in Europe – Quantification and Management, 13th Air Transport Research Society World Conference (2009).

Data-driven Discovery of Closure Models

Shaowu Pan^{*}, Karthik Duraisamy^{**}

^{*}University of Michigan, Ann Arbor, ^{**}University of Michigan, Ann Arbor

ABSTRACT

In this work, we discover closures for reduced-dimensional dynamical systems using data from high-dimensional dynamical systems. In contrast to parameter estimation or function reconstruction, the entire evolution operator of the closure term is extracted from data. Inspirations for the closure are derived from the Mori-Zwanzig formalism of statistical mechanics, which is a formal procedure to address coarse-graining of multi-scale problems. A key characteristic feature of this approach is that the closed lower-dimensional system is capable of emulating the non-Markovian character of the true reduced-dimensional dynamics. For Machine learning, we pursue global features (via non-linear regression) and local approaches (via neural networks), and the limitations of both approaches are discussed. Applications will be demonstrated in reduced order models of transport PDEs.

A Consistent Adaptive-resolution Meshless Method

Wenxiao Pan^{*}, Wei Hu^{**}, Guannan Guo^{***}, Xiaozhe Hu^{****}

^{*}University of Wisconsin-Madison, ^{**}University of Wisconsin-Madison, ^{***}University of Wisconsin-Madison, ^{****}Tufts University

ABSTRACT

We seek to accelerate and increase the size of simulations for fluid-structure interactions (FSI) by using adaptive resolutions in the spatial discretization of the equations governing the time evolution of systems displaying two-way fluid-solid coupling. To this end, we propose an adaptive-resolution smoothed particle hydrodynamics (SPH) approach, in which spatial resolutions adaptively vary according to a recovery-based error estimator of velocity gradient as flow evolves. The second-order consistent discretization of spatial differential operators is employed to ensure the accuracy of the proposed method. The convergence, accuracy, and efficiency attributes of the new method are assessed by simulating different flows. In this process, the numerical results are compared to the analytical and finite element solutions. We anticipate that the proposed adaptive-resolution method will enlarge the class of SPH-tractable FSI applications.

Lattice Type Model in Fracture Analysis of Cementitious Materials: A Brief Review on Achievements and Developments During the Past 30 Years

Zichao Pan^{*}, Rujin Ma^{**}, Airong Chen^{***}, Dalei Wang^{****}

^{*}Department of Bridge Engineering, Tongji University, ^{**}Department of Bridge Engineering, Tongji University,
^{***}Department of Bridge Engineering, Tongji University, ^{****}Department of Bridge Engineering, Tongji University

ABSTRACT

The lattice model is a discrete model that is typically used to simulate the fracture process of brittle materials such as mortar and concrete. This review briefly summarizes the most important achievements of the lattice model in fracture mechanics during the past 30 years. The lattice type models can be generally divided into (1) lattice spring model (LSM), and (2) lattice beam model (LBM), where the classical LSM can only simulate a fixed Poisson's ratio. This problem can be solved by using (1) extra nodal DOFs, (2) extra shear springs, (3) extra nonlocal energy parameters, and (4) higher dimensional normal springs. The lattice model has already been successively applied in simulations of fracture processes of different materials including mortar and concrete, and under different loads. The innovative areas of future research in reference to the use of the lattice model in engineering practice include constitutive relations, failure criteria, anisotropic material modeling and efficient computing techniques to expand its use and range of applications.

A Probabilistic Model for Aircraft Freeplay Dynamics

J. Panchal^{*}, H. Benaroya^{**}, S. Mottaghi^{***}

^{*}Rutgers University, ^{**}Rutgers University, ^{***}William J. Hughes Technical Center, FAA

ABSTRACT

A probabilistic approach is developed to model the potentially unstable dynamics, known as flutter, of airfoils due to nonlinearities in the behavior of the coupled fluid-structural system. One source of nonlinearity is freeplay, which is a regime where stiffness is zero or almost zero. There is a break in the stiffness force around zero displacement or rotation. The literature on this is substantial. It is generally agreed that this freeplay nonlinearity lowers the flutter onset velocity, and typically introduces a limit cycle oscillation mode of flutter. While not necessarily divergent, this behavior can significantly accelerate the accumulation of structural fatigue damage and degrade controllability. Experimental, as well as computational and analytical studies have explored this behavior. Regimes of instability have been mapped. Damping-driven hysteretic behavior has been identified, as well as snap-through behavior. Reduced-order models have been derived based on classical aerodynamic theory, for sub- and transonic regimes. These reduced-order models generally allow one or two structural degrees of freedom, depending on the allowable motion of the airfoils. Cubic spring hardening nonlinearity is common. In many instances the aerodynamic force and moment are assumed to be linear. Damping is rarely included in the analytical models. Most analyses are deterministic, with a few including aerodynamic turbulence in the model, in which cases random responses are examined, where it appears that there is a coupling between the nonlinearity and the random external excitation. Current regulatory guidance is based on relatively old data on structural models that no longer closely resemble today's aircraft. There is much interest in deriving a better understanding of this phenomenon due to the seriousness of its impact on safety, reliability and maintenance. Our work is based on the development of stochastic dynamic models for the above phenomena. Based on experimental evidence, there appear to be substantial variabilities in the parameters that define the freeplay, as well as the regimes of structural response, in particular, the onset of instabilities. We believe that the freeplay characterization is not only nonlinear, but also stochastic in loading as well as in system properties. The freeplay region likely changes with age. System parameters, including damping, in principle, need to reflect random changes in parameter values with time. We present our modeling efforts.

An Irving-Kirkwood Based Homogenization Procedure for Thermomechanical Continua

Sushrut Pande^{*}, Panayiotis Papadopoulos^{**}, Robert Taylor^{***}

^{*}University of California, Berkeley, ^{**}University of California, Berkeley, ^{***}University of California, Berkeley

ABSTRACT

This talk presents a homogenization procedure to model material behaviour for thermomechanical continua. The procedure[1] is derived using an approach inspired by Irving and Kirkwood [2] which only homogenizes extensive quantities namely mass, linear momentum and energy. In conjunction with continuum balance laws, expressions are derived for the macroscopic stress and heat flux in terms of microscopic quantities. The procedure is compared with the classical energy-conserving Hill-Mandel condition. The talk will also describe the implementation of this procedure using a continuum-to-continuum FE2 solution - whereby every material point is associated with an RVE (representative volume element) which represents the underlying microstructure. An RVE boundary-value problem is solved at the microscale and the results are homogenized to obtain macroscopic quantities. The two scales are linked by means of Lagrange multiplier constraints, which indirectly impose various kinds of boundary conditions on the RVE at the microscale which will be discussed. Some numerical examples which illustrate the application of this procedure to practical problems will also be presented. References: [1] Mandadapu, K.K., Sengupta, A., Papadopoulos, P. A homogenization method for thermomechanical continua using extensive physical quantities. Proc. R. Soc. A., 486, pp 1696--1757, 2012. [2] Irving, J.H., Kirkwood, J.G. The statistical mechanical theory of transport processes. IV. The equations of hydrodynamics. J. Chem. Phys., 18, pp. 817--829, 1950.

A Numerical Algorithm for the Solution of the Fluid-Structure Interaction Problem in the Corneal Air Puff Test

Anna Pandolfi^{*}, Andrea Montanino^{**}, Maurizio Angelillo^{***}

^{*}Politecnico di Milano, ^{**}Politecnico di Milano, Italy, ^{***}Universita' di Salerno, Italy

ABSTRACT

The air puff test is a clinical exam commonly used in ophthalmology to determine the intraocular pressure (IOP), the pressure exerted on the cornea by the fluid filling the anterior chamber of the eye. The test consists in applying a rapid and localized air jet pulse on the anterior surface of the cornea, provoking a transient local change of sign of the mean curvature: the level of external pressure exerted by the air jet when the cornea is locally flattened is correlated to IOP. More recently, the air puff test has been regarded as a possible tool to retrieve patient-specific material parameters of the corneal structure. In this respect, the numerical modelling of the air puff test has assumed interest, in view of conducting inverse analyses correlating medical images and numerical simulations, that can provide information about the material parameters of the corneal material and finally, a more accurate patient specific model of the eye, a goal of great interest in refractive surgery. From the mechanical side point of view, the air puff test is a Fluid-Structure Interaction (FSI) problem, due to the mutual interaction between the corneal deformation and changes in the pressure load due to fluid movement. In this work we present an algorithm for the simulation of the FSI problem of the air puff test. For the numerical simulation we use a staggered approach, consisting in the use of two different solvers for the two subdomains, allowing to preserve the advantages of each solver. In particular, we use a finite element code for the solid elastic problem of the cornea, already used in [1], and a meshless method for the fluid domain [2], using a Lagrangian formulation, particularly suitable for fluid-dynamic problems with moving boundaries. The coupling between subdomains is made through an iterative Dirichlet-Neumann algorithm, following the formulation already used in [3] for the axis-symmetric case. The results we present confirm the computational efficiency of the numerical approach in dealing with the corneal-humor aqueous interaction, and provide useful information for the determination of the mechanical properties of the corneal tissue. [1] Pandolfi, A. and Manganiello, F. "A model for the human cornea: constitutive formulation and numerical analysis." BMMB 5.4(2006):237-246. [2] Asprone, D., et al. "A Modified Finite Particle Method: Multi-dimensional elasto-statics and dynamics." IJNME 99.1(2014):1-25. [3] Montanino, A., et al., "Modelling with a meshfree approach the cornea-aqueous humor interaction during the air puff test." JMBS 77(2018):205-216.

Minimal Worst-Case Stress Microstructure Design

Julian Panetta^{*}, Denis Zorin^{**}

^{*}École Polytechnique Fédérale de Lausanne (EPFL), ^{**}New York University

ABSTRACT

The power of modern additive fabrication technologies to rapidly and inexpensively manufacture special-purpose customized objects has spurred the development of computational tools for designing objects to meet specific performance goals. However, many such design goals--for instance, achieving particular deformations under applied forces--require precise control of the fabrication material's elastic properties beyond the capabilities of even advanced multi-material 3D printers. Furthermore, many behaviors are impossible to achieve with ordinary fabrication materials (e.g., negative Poisson's ratios). Several recent works address this limitation by using periodic microstructures to emulate a large space of elastic materials. This approach to tailoring material properties is a perfect fit for additive fabrication, which can produce parts of arbitrary complexity at a cost proportional to only the material consumed. Unfortunately, one significant problem blocks practical applications: the structures tend to feature thin joints that concentrate stress, leading to plastic deformation or fracture. My talk addresses this problem; I describe how to design microstructures that minimize stress, thereby improving the resulting metamaterials' robustness in practice. First, I introduce an efficient, exact solution to the worst-case stress analysis problem for periodic microstructures. Because microstructures behave like general-purpose materials, it is most natural and computationally efficient to build a single complete metamaterial library up-front instead of re-solving the microstructure design problem in the inner loop of each macroscopic design optimization. Consequently, the specific loads a microstructure will experience are unknown during its design. To ensure that every microstructure in the library is robust in generic use, we must design each to withstand its worst-case load: the load most likely to induce failure at any given point. I show that, for several different stress-based failure criteria (e.g., maximum principal stress or von Mises stress), determining a periodic structure's worst-case loads can be formulated as solving an inexpensive tensor eigenvalue problem for each point in the structure. Next, I introduce a method to design microstructures that experience minimal worst-case stresses while producing a wide range of elastic material properties. The design problem is formulated as a parametric shape optimization and incorporates constraints to ensure manufacturability on 3D printers without support structure. Finally, I demonstrate how the worst-case stress reductions achieved by the method (typically a reduction factor of roughly 5x) translate into practical robustness improvements visible in lab tests on 3D printed samples. [1] Panetta, J., Rahimian, A., Zorin, D. 2017. Worst-case Stress Relief for Microstructures. ACM Trans. Graph. 36, 4 (July), 122:1--122:16.

Strength Distributions of Brittle Heterogenous Materials and Its Scale Effects on Stochastic Simulations of Fracture

Sze Dai Pang*

*National University of Singapore

ABSTRACT

It has been well accepted that the probability distribution function of structural strength follows the Gaussian distribution for ductile materials by virtue of the central limit theorem of the theory of probability while it follows the Weibull distribution for brittle materials by virtue of the weakest-link theory of probability. Recently, it has been shown that the probability distribution function of structural strength for brittle heterogenous materials lies somewhere between Gaussian and Weibull distributions and depends on type of loading, structure size and geometry (Bažant and Pang, 2006; Le et al. 2011). In fact, it has been argued theoretically and matched experimentally that the probability distribution function of these quasibrittle materials comprises of a Gaussian distribution with a transition to Weibull distribution at the tail probabilities. The point of transition is largely dependent on the size of the representative volume element (RVE) and the number of equivalent RVEs in the structure. The coefficients of variation for the Weibull and Gaussian distribution segments are found to be dependent on the stress distribution and redistribution within the RVE and size of the RVE. A proper treatment will necessitate a probability distribution function that can reproduce the Gaussian distribution at small size limit and Weibull distribution at large size limit. Such is the probability distribution function proposed by Bažant and Pang (2006) which is size dependent and also relies on the knowledge of the size and statistical property of each RVE. When the FE mesh coincides with the size of the RVE, the material strength can be treated as brittle with its random field being sampled from the proposed probability distribution function which would have accounted for the stress redistribution with the RVE. In most cases, the size of the FE mesh does not correspond to the size of the RVE and this inevitably leads to a scale effect on the probability distribution of strength which is further complicated by the stress redistribution (having the effect of sharing the loads analogous to extending the Gaussian core). The scaling of the probability distribution ought to lead to mesh objectivity in FE simulations which is investigated in this study. REFERENCES Bažant, Z.P., and Pang, S.-D. (2006). Proc. of the National Academy of Sciences 103(25), 9434-9439. Le, J.-L., Bažant, Z.P., and Bažant, M.P. (2011). Journal of the Mechanics and Physics of Solids 59, 1291-1321.

Robust Hex-Dominant Mesh Generation Using Field-Guided Polyhedral Agglomeration

Daniele Panozzo*

*New York University

ABSTRACT

While hexahedral meshes are generally preferred for solving nonlinear partial differential equations, automatic techniques capable of producing them robustly are still out of reach despite three decades of extensive research dedicated to this topic. Hexahedral-dominant meshes strike a good balance: they are easier to generate, since they can contain a small number of irregular elements, while offering good numerical properties. Building upon the 2D instant meshing (IM) approach, we introduce a novel algorithm to efficiently, robustly, and automatically create field-aligned hex-dominant meshes. The first part of the talk will cover a quaternionic representation for a volumetric cross-field, which will guide the edge alignment of the hex-dominant mesh. When paired with a hierarchical accelerations structure, this representation enables us to interpolate user-defined constraints, while naturally aligning to shape features. The volumetric cross-field is used to define a position field encoding the position of the nodes of the hex-dominant mesh. The second part of the talk will complete the pipeline, providing a robust extraction algorithm guaranteed to extract a compatible manifold mesh from any field-aligned parameterization — it is designed to work with local parameterizations that are characteristic of the output produced by the IM technique, but it can also be applied to any global parameterization generated by other means. The algorithm uses a sequence of local topological operations to collapse and split edges, faces, and polyhedra of the input mesh, eventually converting the input tetrahedral mesh into a hex-dominant output mesh. Topological invariants are checked before each operation, and only those preserving the invariants are executed, which ensures that both genus and manifoldness of the input are preserved throughout this process. While the two contributions are independently useful in existing meshing pipelines, they have been designed together to extend the IM pipeline to the volumetric cases. Combined, they lead to a simple, robust, automatic, and scalable pipeline that automatically remesh a benchmark composed of 106 meshes, with no user-interaction and no parameter tweaking.

Introduction to Geometry Processing and Field-Aligned Mesh Generation

Daniele Panozzo^{*}, Denis Zorin^{**}, Leif Kobbelt^{***}

^{*}NYU, ^{**}NYU, ^{***}NYU

ABSTRACT

Introductory comments on MS 812 topic.

Flaw Tolerance of Architected Metamaterials

Panos Pantidis^{*}, Andrew Gross^{**}, Katia Bertoldi^{***}, Simos Gerasimidis^{****}

^{*}PhD Candidate, University of Massachusetts, Amherst, ^{**}Post-Doctoral, Harvard University, Boston, USA,
^{***}Professor, Harvard University, Boston, USA, ^{****}Assistant Professor, University of Massachusetts, Amherst

ABSTRACT

Recent advancements in the area of bio-inspired lattice-truss metamaterials have allowed the design and fabrication of new lightweight materials with unique and tunable properties. High fabrication rates may though result in a higher probability of producing defects, whereas the term 'defect' is utilized to describe the presence or absence of a member-strut in the lattice-truss topology. This work constitutes a systematic approach to examine and identify the mechanical properties of defected architected meta-materials. Using advanced nonlinear finite element techniques, a variety of bending- and stretching-dominated topologies are investigated under quasi-static compression and their characteristic mechanical properties such as the effective elastic modulus, the yield stress and the damage propagation path of the failure mode are assessed. The randomness of the defect spatial distribution for a given defect percent is accounted for through exhaustive sampling using Monte Carlo simulations, and the evolution of the mechanical properties is monitored as the total defect percent increases in magnitude. Additional idealizations of cluster defect scenarios are conducted, providing insight on the behavior of the different topologies when voids exist within their domain. The impact of fixed boundary conditions in finite defected tessellation sizes versus infinite defected periodic geometries is also investigated. The experimental part of this work is conducted using the two-photon lithography approach, an advanced additive manufacturing technique capable of printing polymer struts with sub-micron cross-sectional dimensions. Representative specimens of intact and defected metamaterials topologies are fabricated and they are compared to the numerical results, providing a detailed picture of the actual behavior of defected lattice-truss materials at different connectivity levels.

Defect Generation and Nanostructure Deformation during Focused Ion Beam Processes of Nanomaterials

Chun-Wei Pao*, Cheng-Lun Wu**

*Research Center for Applied Sciences, Academia Sinica, Taiwan, **Research Center for Applied Sciences,
Academia Sinica, Taiwan

ABSTRACT

Focused ion beam (FIB) is a versatile tool with applications across disciplines ranging from optoelectronic devices, metamaterials, bioimaging, and even to archaeology. Nevertheless, the nanoscale machining precision of FIB is often accompanied by damages to the nanostructures due to energetic ion beam bombardment. In this talk, we will present our recent works on studying the nanostructure deformation as well as defect generation mechanisms during FIB processes using a series of large-scale molecular dynamics (MD) simulations. We will focus on two subjects: 1) the mechanisms leading to FIB-induced self-fold behavior of nanostructures, and 2) defect generation and suppression during FIB patterning of 2D materials. We will reveal that mass transport from ion beam irradiation is responsible for the nanostructure self-folding, and the constrained scattering of atoms from 2D materials is the primary source of damage to 2D materials during FIB patterning. Hence, by understanding the mechanisms behind nanostructure deformation and defect generation during FIB processes, it is possible to fabricate nanostructures with complicated geometries, as well as patterning 2D materials with nanoscale precision using FIBs.

Consistent Bayesian Updating for Multiscale Analysis Using Subset Simulation

Vissarion Papadopoulos*, Marios Impraïmakis**, Dimitris Giovanis***, Ioannis Kalogeris****

*National Technical University of Athens, **National Technical University of Athens, ***Johns Hopkins University,
****National Technical University of Athens

ABSTRACT

Bayesian updating is a powerful method to learn and calibrate models with data and observations, facts that is of utmost importance in multiscale problems with uncertain microscale status like very random and hard predicted nanocomposite behavior. In this work BUS (Bayesian Updating with Structural reliability methods) with SuS (Subset Simulation) in a multiscale environment is employed to compute the posterior distribution of microscale random parameter in a framework that microscale with mesoscale and microscale with macroscale pair models converge into each experimental data simultaneously. More specific, every sample cluster of every subset within SuS in this parallel double problem forced to agree with the other one. In the end, the samples in the final subset (posterior samples in Bayesian terms) have the best agreement with experimental data. This methodology is very promising for nanomaterial reinforced composites which have big uncertainty range with quite unexpected measurements and really large number of parameter. It is a gainful direction for engineering practice and non-costly experimental investigations, being concurrently quite appropriate for every multiscale modeling applications.

Enhanced Computational Techniques for Improving the Performance of Isogeometric Analysis

Manolis Papadrakakis*, George Stavroulakis**, Dimitrios Tsapetis***, Manos Trypakis****, Christos Gritzalis*****, Alex Karatarakis*****

*Institute of Structural Analysis and Antiseismic Research, National Technical University of Athens, Greece,

**Institute of Structural Analysis and Antiseismic Research, National Technical University of Athens, Greece,

***Institute of Structural Analysis and Antiseismic Research, National Technical University of Athens, Greece,

****Institute of Structural Analysis and Antiseismic Research, National Technical University of Athens, Greece,

*****Institute of Structural Analysis and Antiseismic Research, National Technical University of Athens, Greece,
*****Microsoft Corporation, Seattle, USA

ABSTRACT

Due to high regularity across mesh elements, isogeometric analysis (IGA) achieves higher accuracy per degree of freedom and improved spectrum properties, among others, compared with finite element analysis. However, this inherent feature of isogeometric analysis increases the density of the stiffness matrix and requires more elaborate numerical integration schemes for its computation. Furthermore, the augmented continuity of the shape functions in IGA results in greater bandwidth and overlapping of the resulting matrices, raising the computational cost of solving the corresponding linear systems of equations. For these reasons, both the assembly of the stiffness matrix and the solution of the resulting algebraic equations in isogeometric analysis is a computationally demanding task, which needs special attention in order to be affordable for real-world applications. In this paper we address the computational demanding task of assembling the stiffness matrix using the standard element-wise Gaussian quadrature. A novel approach is proposed for the formulation of the stiffness matrix which exhibits several computational merits, among them, its amenability to parallelization and the efficient utilization of the graphics processing units (GPU) to drastically accelerate computations. In addition, an efficient, scalable and load balanced solution algorithm is proposed that combines the advantages of the preconditioned conjugate gradient (PCG) algorithm and domain decomposition methods (DDM) by introducing a preconditioner based on the isogeometric tearing and interconnecting (IETI) solution method. The proposed preconditioner circumvents the dependency between domain subdivisions and patches that IETI imposes, decoupling load balancing and scalability properties from the model geometry. Numerical examples demonstrate the efficiency of the proposed handling of matrix assembling and solution algorithm, when compared to other matrix assembling schemes and previously presented domain decomposition methods. As a result, the proposed methodologies enables minimization of the computational cost for solving demanding problems with IGA and thus widens its applications in large-scale real life applications. [1] A. Karatarakis, P. Karakitsios, M. Papadrakakis, GPU Accelerated Computation of Isogeometric Analysis Stiffness Matrix, *Comput. Methods Appl. Mech. Engrg*, 269, 334-355, 2014. [2] M. Papadrakakis, G. Stavroulakis, A. Karatarakis, A New Era in Scientific Computing: Domain Decomposition Methods in Hybrid CPU-GPU Architectures, *Comput. Methods Appl. Mech. Engrg*, 200, 1490-1508, 2011. [3] S. Kleiss, C. Pechstein, B. Juttler, S. Tomar, IETI – Isogeometric Tearing and Interconnecting, *Comput. Methods Appl. Mech. Engrg*, 247-248, 201-215, 2012.

Identifying Far From Equilibrium Microstructures in Crystal Plasticity and Other Crackling Noise Phenomena

Stefanos Papanikolaou*

*West Virginia University

ABSTRACT

When far from equilibrium, many-body systems display behavior that strongly depends on the initial conditions. A characteristic such example is the phenomenon of plasticity of crystalline and amorphous materials that strongly depends on the material history. In plasticity modeling, the history is captured by a quenched, local and disordered flow stress distribution. While it is this disorder that causes avalanches that are commonly observed during nanoscale plastic deformation, the functional form and scaling properties have remained elusive. In this presentation, a generic formalism is developed for deriving local disorder distributions from field-response (eg stress/strain) timeseries in models of crackling noise. We demonstrate the efficiency of the method in the hysteretic random-field Ising model and also, models of elastic interface depinning that have been used to model crystalline and amorphous plasticity. We show that the capacity to resolve the quenched disorder distribution improves with the temporal resolution and number of samples. Moreover, we demonstrate how this method may apply to nanoindentation of FCC crystals.

A Unified Framework for Multiscale Modeling Using the Mori-Zwanzig Formalism and the Variational Multiscale Method

Eric Parish^{*}, Karthik Duraisamy^{**}

^{*}University of Michigan, Ann Arbor, ^{**}University of Michigan, Ann Arbor

ABSTRACT

We describe a paradigm for multiscale modeling that combines the Mori-Zwanzig (MZ) formalism of Statistical Mechanics with the Variational Multiscale (VMS) method of Hughes. The MZ-VMS approach leverages both VMS scale-separation projectors as well as phase-space projectors to provide a systematic modeling framework that is applicable to non-linear partial differential equations. Spectral as well as continuous and discontinuous finite element methods are considered. The framework leads to a formally closed equation in which the effect of the unresolved scales on the resolved scales is non-local in time and appears as a convolution or memory integral. The resulting non-Markovian system is used as a starting point for model development. We discover that unresolved scales lead to memory effects that are driven by an orthogonal projection of the coarse-scale residual and inter-element jumps. It is further shown that an MZ-based finite memory model is a variant of the well-known adjoint-stabilization method. For hyperbolic equations, this stabilization is shown to have the form of an artificial viscosity term. We further establish connections between the memory kernel and approximate Riemann solvers.

Computational Design of Quantum Spin Hall-Based Phononic Topological Insulators

Harold Park^{*}, S.S. Nanthakumar^{**}, Xiaoying Zhuang^{***}, Timon Rabczuk^{****}

^{*}Boston University, ^{**}Leibniz University Hannover, ^{***}Leibniz University Hannover, ^{****}Bauhaus-University Weimar

ABSTRACT

We present a new topology optimization framework to design phononic topological insulators based on electronic quantum spin hall-based principles. We discuss the methodology, and show numerical examples demonstrating the resulting phononic topological insulators.

Prediction of Quasi-static Yield of Amorphous Epoxy Polymers Using Temperature Accelerated Molecular Dynamics

Hyungbum Park^{*}, Byungjo Kim^{**}, Maenghyo Cho^{***}, Joonmyung Choi^{****}

^{*}Seoul National University, ^{**}Seoul National University, ^{***}Seoul National University, ^{****}Samsung electronics Co.

ABSTRACT

It has been challenging to derive the quasi-static dynamic responses of amorphous polymer systems in the molecular dynamics (MD) simulations, since it demands tremendous computational costs owing to the inherent short timestep of MD simulations. In an efforts to derive the quasi-static mechanical response of amorphous polymer, we propose a temperature accelerated approach using the physical equivalence of time and temperature involving the yield behaviors of polymer system. Herein, quasi-static yield behaviors of amorphous epoxy polymers are predicted using the stress-strain relationship of various elevated temperatures. To predict the yield stress at low strain rate which cannot be explored with classical MD environment, a method to construct Eyring's plot is proposed by quantifying the correlation between increasing temperature and decreasing strain rate. In this study, the obtained results reveal that the strain rate sensitivity of reduced yield stress is getting lower with increasing temperature. This observation opens an avenue for constructing the Eyring's plot toward the low rate condition by sequential shifting of yields at elevated temperature. The predicted quasi-static yield stress of epoxy polymers is validated with the experimental literature, showing good agreement each other. The proposed acceleration approach provides a good way to design of amorphous polymer based materials enabling the estimation of quantitatively comparable constitutive equation to the experimental tests.

Use of Perimeter Control for Geometrically Complex Structures in Topology Optimization

Jaejong Park^{*}, Alok Sutradhar^{**}, Jami J Shah^{***}, Glaucio H Paulino^{****}

^{*}The Ohio State University, ^{**}The Ohio State University, ^{***}The Ohio State University, ^{****}Georgia Institute of Technology

ABSTRACT

Perimeter control emerged into topology optimization to alleviate the common numerical instabilities. For instance, solution space employing checkerboard can be discarded during the optimization process by introducing the upper bound on the perimeter. Earlier research efforts in filters and basic projection functions in topology optimization also attempts to reduce the topological complexity that leads to a reduction of the perimeter. However, some design problems demand a high level of geometric complexity with large perimeter value. Simulating designs found in nature requires a solution to have complex internal structures with lots of holes. For instance, stress shielding phenomenon between bone and the implant is of immense importance in the implant design industry. The inherent property mismatch between the bone and implant material can be reduced by designing them with fine members interconnected in a complex manner. Conventional topology optimization formulated as density distribution problem cannot achieve this goal without additional restrictions. In this work, this is attained by confining a lower bound on the perimeter. By restricting the design space by means of the perimeter, intricate design features can be obtained. Three different bone regions with well-known physical loadings are selected to illustrate the efficacy of the method, i.e., femur, calcaneum, and midface. Additionally, we observed the perimeter value and the pattern of the initial distributions play a vital role in obtaining natural looking structural members with various curvatures. We also witnessed the initial material distribution is required to have a sufficient perimeter value to avoid excessive islanding. The desired structural complexity can also be obtained by manipulating the target perimeter. The approach demonstrates great potential in engineering problems that requires geometric complexity to cope with uncertainties in the design domain and to promote reliable structure options with high porosity. Issues with aforementioned stress shielding and inadequate mass transfer in medical implant industry could be tackled with the technique described in this work.

A Study on Selective Bivariate Dimension Reduction Method for Efficient Reliability Analysis

Jeongwoo Park*, Ikjin Lee**

*KAIST, **KAIST

ABSTRACT

As reliability of engineering systems under uncertainty becomes more important in various industries due to global competitive market situation, a safer and more reliable product design to satisfy consumers' needs is required. To satisfy these requirements, there have been various attempts to accurately and efficiently compute the product reliability, which is obtained from reliability analysis and used as a probabilistic constraint of reliability-based design optimization. Among various reliability analysis methods, analytical reliability analysis methods such as the first-order reliability method (FORM), the second-order reliability method (SORM), and the most probable point based dimension reduction method (MPP-based DRM) are available. Reliability analysis using MPP-based DRM, the most recently proposed method, has advantages of the FORM and SORM in terms of efficiency and accuracy. However, the reliability analysis using the MPP-based univariate DRM does not obtain high accuracy because it does not consider the cross-term of the performance function. To increase the accuracy, the MPP-based bivariate DRM can consider the cross-term, but the efficiency decreases as the number of integration points required increases as the dimension of the performance function increases. The main objective of this paper is to develop an efficient methodology for the MPP-based bivariate DRM by using the subspaces considering cross-term. In the proposed method, a partial F-test is introduced to evaluate cross-term and the axial sensitivity. The MPP search points are used in this process, no additional function evaluation is required. In the partial F-tests, F-values and p-values are suggested as criteria to assess sensitivity, the variables selected in the cross-term direction are applied to the bivariate DRM, and the variables selected in the axial direction are increased in the number of integration points of the Gaussian quadrature integration method. Since the partial F-test suggests the application direction of the DRM and the number of integration points, the proposed method can present selection criteria of FORM, univariate DRM, and bivariate DRM for each variable. Several numerical examples demonstrate the improvement of the accuracy and the efficiency of the probability of failure estimation and the feasibility of partial F-tests. Reference [1] Lee, I., Choi, K.K., Du, L. and Gorsich, D., Inverse analysis method using MPP-based dimension reduction for reliability based design optimization of nonlinear and multi-dimensional systems, *Computer Methods in Applied Mechanics and Engineering*, 198(1), p.14–27, 2008. [2] Geladi, P., and Kowalski, B.R., Partial least-squares regression: a tutorial, *Analytica chimica acta*, 185, p.1-17, 1986.

Partitioned Symmetric Formulation and Solution Algorithms of Thermoelastic Interaction Problems

K. C. Park^{*}, Carlos Felippa^{**}, Charbel Farhat^{***}

^{*}University of Colorado, ^{**}University of Colorado, ^{***}Stanford University

ABSTRACT

A partitioned formulation of transient coupled thermoelastic problems is presented, which yields a four-field symmetric set of partitioned governing equations. The present formulation can be reduced to conventional two-field non-symmetric coupled thermoelastic equations as a special case, thus validating the present partitioned formulation. A key feature of the present formulation is the addition of the constraint enforcement of energy exchanges between the elastic body and the thermal conduction body, each of which occupying the same volume space. The variational formulation of the elastic body and the thermal conduction part is independently constructed as if they are uncoupled. Various solution algorithms are suggested including explicit-implicit, implicit-implicit time integration strategies.

Multiscale Modelling Framework for Predicting Mechanical Properties of Concrete

S.M. Park^{*}, Bezawit Haile^{**}, D.W. Jin^{***}, B.J. Yang^{****}, H.K. Lee^{*****}

^{*}Korea Advanced Institute of Science and Technology, ^{**}Korea Advanced Institute of Science and Technology,
^{***}Korea Advanced Institute of Science and Technology, ^{****}Korea Institute of Science and Technology, ^{*****}Korea
Advanced Institute of Science and Technology

ABSTRACT

Cement concrete is the most widely employed construction material, while its heterogeneous nature, i.e., presence of multiple phases such as unreacted clinkers, hydrates, aggregates and pores at various length scales, makes modelling approaches extremely difficult. The present study summarizes a portion of a work conducted by Haile et al. [1], which proposes a multiscale modelling framework for predicting mechanical properties and durability of cementitious materials. The elastic properties of various phases present in a cement paste (e.g., silicate and aluminate hydrates) are calculated by considering molecular dynamics, while the phase assemblage is predicted by coupling Parrot and Killoh's hydration kinetic model [1] and a thermodynamic modelling approach. This information is carried forward to a micromechanics model, in which the different phases present are considered as inhomogeneous inclusions, in order to predict the mechanical properties of concrete at macroscale. The modelling strategy, its perspectives, and validation with experimental results reported in the literature will be discussed in detail. Acknowledgement This study was supported by the National Research Foundation (NRF) of the Korean government (Ministry of Science&amp; ICT) [Grant No. 2017R1A5A1014883] through Smart Submerged Floating Tunnel System Research Center. References [1] Haile, B.F, Jin, D.W., Yang, B.J., Park, S.M. and Lee, H.K. (2018). Multiscale modelling framework for predicting mechanical properties of cementitious composites, in preparation. [2] Parrot L.J. and Killoh D.C. (1984). Prediction of cement hydration, Proc. Br. Ceram. Soc. No. 35, pp. 41.

Design Optimization for Loading Arm of LNG Bunkering System Considering Dynamic Behavior

Sanghyun Park^{*}, Jaewon Oh^{**}, Dongho Jung^{***}, Hong-Gun Sung^{****}, Cheonhong Min^{*****}, Tae Hee Lee^{*****}, Su-gil Cho^{*****}

^{*}Korea Research Institute of Ships & Ocean Engineering, ^{**}Korea Research Institute of Ships & Ocean Engineering, ^{***}Korea Research Institute of Ships & Ocean Engineering, ^{****}Korea Research Institute of Ships & Ocean Engineering, ^{*****}Korea Research Institute of Ships & Ocean Engineering, ^{*****}Hanyang University, ^{*****}Korea Research Institute of Ships & Ocean Engineering

ABSTRACT

The LNG bunkering system means a technique for supplying Liquefied Natural Gas (LNG) fuel to a ship in a stably and efficiently. Since liquefied cargoes, such as crude oil and natural gas, have inherent risk of accident such as fire or explosion, it is very important to transfer it safely to ship. In offshore, the loading arm, which is composed of pipe, is mechanically controlled and used for LNG transport because of its high stability. In this study, therefore, the design optimization of the loading arm is carried out for the safe transfer to the ship supplied from the LNG carrier. First of all, the loading arm should keep the center of gravity stable from the stationary mode to the operation mode in the 5K condition (meaning the distance between ship and ship) and minimize the reaction force acting on each joint part structurally. Secondly, the most important operating condition is when injecting fuel of the loading arm. The hydraulically actuated loading arm should not be damaged at the connection of the Quick Connect/Disconnect Couplers (QC/DC) with the moored ship. Since the behavior of ship cannot be precisely controlled, the reaction force acting on the fastening part of the QC/DC must be minimized. In this regard, the loading arm is a multi-objective optimization problem and to find the optimal weight of dual-type counterweight. Finally, we perform design verification of the loading arm based on optimized result. The loading arm should be satisfied with the required requirements in EN 1474 for the design. EN 1474 considers various loading conditions and environmental loading conditions, such as dead load, earthquake load, fluid load, thermal load, wind load.

Subsurface Applications for Peridynamics

Michael Parks*

*Sandia National Laboratories

ABSTRACT

Peridynamics is a nonlocal reformulation of continuum mechanics that is suitable for representing fracture and failure, see [1, 2] and the references therein. Better understanding and control of the subsurface is important to the energy industry for improving productivity from reservoirs. We motivate and explore two relevant subsurface applications for peridynamics. The first involves solving inverse problems in heterogeneous and fractured media, which may be useful in characterizing subsurface stress-state conditions [3]. The second involves the study of fracture initiation and growth from propellant-based stimulation of a wellbore [4]. Simple models and proof-of-concept numerical studies are presented. [1] S. A. Silling, Reformulation of elasticity theory for discontinuities and long-range forces, J. Mech. Phys. Solids 48, (2000), 175-209. [2] S. Silling, M. Epton, O. Weckner, J. Xu, and E. Askari, Peridynamic states and constitutive modeling, J. Elasticity 88, (2007), 151-184. [3] D. Turner, B. van Bloemen Waanders and M.L. Parks, Inverse problems in heterogeneous and fractured media using peridynamics, Journal of Mechanics of Materials and Structures, 10(5), pp. 573-590, 2015. [4] R. Panchadhara, P.A. Gordon, and M.L. Parks, Modeling propellant-based stimulation of a borehole with peridynamics, International Journal of Rock Mechanics and Mining Sciences, 93, pp. 330-343, 2017.

Reproducing Kernel Enhanced Peridynamics

Marco Pasetto^{*}, J. S. Chen^{**}

^{*}University of California, San Diego, ^{**}University of California, San Diego

ABSTRACT

Peridynamics is a nonlocal reformulation of continuum mechanics in which balance laws are computed through integration rather than differentiation [1]. For this reason, the peridynamic theory does not require any assumptions on the spatial differentiability of the displacement fields and remains valid in the presence of displacement discontinuities. Peridynamics is thus directly applicable to problems involving material failure and damage. The two most common discretization methods for peridynamic models used in engineering problems are the Finite Element method, based on a weak formulation and a meshfree method, based on nodal integration of the strong form. The former is computationally expensive and limited by the need of adapting the mesh to track evolving cracks. The latter approach discretizes peridynamic domains by a set of nodes, each associated with a nodal cell with a characteristic volume, leading to a particle based description of continuum systems. The behavior of each particle is then considered representative of its cell, limiting the convergence rate to first-order [2]. This work proposes the use of a meshfree Reproducing Kernel (RK) approximation [3] to the field variables in the peridynamic equations in order to increase the order of convergence of peridynamic numerical solutions. In this work, the peridynamic framework and the RK approximations are reviewed, the proposed approach is presented and the improved convergence rates in static peridynamic problems obtained using the proposed method is shown through numerical examples. REFERENCES [1] Silling, S.A., "Reformulation of elasticity theory for discontinuities and long-range forces", Journal of the Mechanics and Physics of Solids, 48, 175-209, 2000. [2] Seleson, P., Littlewood, D.J., "Convergence studies in Meshfree Peridynamics", Computers and Mathematics with Applications, 71, 2432-2448, 2016. [3] Chen, J. S., Pan, C., Wu, C. T., and Liu, W. K., "Reproducing Kernel Particle Methods for Large Deformation Analysis of Nonlinear Structures", Computer Methods in Applied Mechanics and Engineering, 139, 195-227, 1996.

Isogeometric Residual Minimization (iGRM)

Maciej Paszynski^{*}, Marcin Los^{**}, Victor Calo^{***}, Ignacio Muga^{****}

^{*}AGH University, Krakow, Poland, ^{**}AGH University, Krakow, Poland, ^{***}Curtin University, Perth, Western Australia, ^{****}University of Valparaiso, Chile

ABSTRACT

The residual minimization methods allow finding the best possible approximation in the trial space while increasing the test space. The residual minimization method allows stabilizing the numerical simulations of challenging computational problems. The isogeometric analysis (IGA) is a modern rapidly growing numerical method integrating Computer Aided Design (CAD) with Computer Aided Engineering (CAE) [1]. The IGA allows to perform the computations directly on B-splines and NURBS, and the computations can be integrated with CAD tools, such as AutoCAD. The alternating directions method (ADS) introduced in 1960 [2] deals with finite difference simulations for time-dependent problems. Due to its linear computational cost, it is used nowadays to deal with difficult computational problems on parallel machines. The ADS has been recently used [3] for fast solution of the isogeometric L2 projection problem in the context of IGA. The method has also been applied for explicit dynamics simulations of different physical phenomena expressed as a sequence of isogeometric L2 projections [4]. In this talk we present a new computational method for a stable, accurate solution of stationary and time-dependent problems, which we call Isogeometric Residual Minimization (iGRM) method, with the following unique features: 1) Linear computational cost $O(N)$ of the direct solver solution; 2) Unconditional stability of the implicit time integration scheme; 3) Unconditional stability in the spatial domain. This method mixes benefits of the Discontinuous Petrov-Galerkin method (DPG), the Isogeometric Finite Element Method (IGA-FEM), and Alternating Direction solvers (ADS). We verify our method on some computational problems, including the advection skew to the mesh, Ericsson problem, two- and three-dimensional propagation of pollutant from a chimney. For all these problems we present a superior convergence of the iGRM stabilization. We also emphasize that our method is not problem specific, and thus switching from one problem to another is straightforward. [1] J. A. Cottrell, T. J. R. Hughes, Y. Bazilevs, *Isogeometric Analysis: Toward Unification of CAD and FEA*, John Wiley and Sons, (2009) [2] G. Birkhoff, R.S. Varga, D. Young, Alternating direction implicit methods, *Advanced Computing* 3 (1962) 189–273. [3] L. Gao, V.M. Calo, Fast Isogeometric Solvers for Explicit Dynamics, *Computer Methods in Applied Mechanics and Engineering*, 274 (1) (2014) 19–41. [4] M. Los, M. Wozniak, M. Paszynski, A. Lenharth, M. A. Hassan, K. Pingali, IGA-ADS: Isogeometric analysis FEM using ADS solver, *Computer & Physics Communications* 217 (2017) 99–116. The work has been supported by National Science Centre, Poland grant no. 2017/26/M/ST1/00281

A Study of Approximation Error in Eulerian Hydrocodes

Parth Patel^{*}, David Littlefield^{**}

^{*}The University of Alabama at Birmingham, ^{**}The University of Alabama at Birmingham

ABSTRACT

In this study we examine a number of approximations in the formulation of hydrocodes. These approximations were borne out of an original requirement for the code to run as fast as possible – i.e. with accuracy being secondary to speed. Many of these approximations originated from the 1970's when computers were slow and memory was at a premium. Although speed and memory are not as much of an issue today, these approximations are still used to formulate the hydrocodes. In this study, the effect of these approximations is examined systematically. The lumped mass approximation is a simplification to the consistent mass formulation and is routinely used in hydrocodes. While this approximation is computationally efficient, the consistent mass formulation is the most accurate (and computationally expensive) option. There are other levels of approximation between these two extremes that trade off computational efficiency for accuracy. As is shown in this work, some of these result in tridiagonal systems which are very computationally efficient to solve. Linear finite elements are also used pervasively in hydrocodes. Like the lumped mass approximation, the use of linear elements was borne out of the requirement for computational efficiency and not accuracy. Surprisingly, linear elements are still used routinely today, despite their numerous accuracy issues such as realistic representation of geometry and the need for hourglass stabilization. In this work higher order finite elements, including quadratic and cubic elements, are examined. Special attention is placed on quadrature order used in integration and its effect on overall accuracy. The 2D version of ALEAS (Arbitrary Lagrangian-Eulerian Adaptive Solver), an in-house ALE research code, is used in this work. The Taylor impact test is used as the benchmark problem to assess and quantify the effect of higher order approximations in Eulerian hydrocodes.

3-D Conditional Hyperbolic Quadrature Method of Moments for Dilute Gas-particle Flows

Ravi Patel^{*}, Olivier Desjardins^{**}, Rodney Fox^{***}

^{*}Cornell University, ^{**}Cornell University, ^{***}Iowa State University

ABSTRACT

Although dilute gas-particle flows are common in many industrial processes, efficient and faithful simulation of such flows remains a challenge. When the particle phase is in a regime with finite Stokes and Knudsen numbers, the dynamics may stray far from equilibrium and require a more complete kinetic description to capture than is assumed with commonly used hydrodynamic techniques. To reduce the computational cost of integrating the full kinetic equation, moment methods transform the kinetic equation to evolution equations for a set of moments of the number density function (NDF). Quadrature based moment methods (QBMM) solve the resulting closure problem by constructing a NDF comprised of weighted Dirac deltas from a given set of moments. It has been shown that QBMM in conjunction with kinetic based finite volume schemes maintain realizable sets of moments during transport [1]. However previous QBMM either fail to maintain the strict hyperbolicity of the kinetic equations or use alternatives to Dirac delta functions that restrict the sets of moments that can be reconstructed. The conditional hyperbolic quadrature method of moments (CHyQMOM) has recently been introduced as a QBMM that maintains both the strict hyperbolicity of the kinetic equation and the Dirac delta representation of the NDF [2]. In this talk, we present the 3-D extension to CHyQMOM and results from simulations of particle-laden flows using CHyQMOM. Comparing with benchmark Lagrangian simulations, we demonstrate that CHyQMOM is capable of capturing the complex dynamics resulting from non-equilibrium effects in gas-particle flows. [1] V. Vikas, Z. J. Wang, A. Passalacqua, and R. O. Fox. Realizable high-order finite-volume schemes for quadrature-based moment methods. *J. Comput. Phys.*, 230(13):5328–5352, 2011. [2] R. O. Fox, F. Laurent, and A. Vie. Conditional Hyperbolic Quadrature Method of Moments for Kinetic Equations. hal-01632813, 2017.

Data-driven Homogenization Technique for Mechanical Property Prediction in Composite Materials

Mehtab Pathan^{*}, Sathiskumar Anusuya Ponnusami^{**}, Borja Erice^{***}, Nik Petrinic^{****}

^{*}University of Oxford, ^{**}University of Oxford, ^{***}University of Oxford, ^{****}University of Oxford

ABSTRACT

This research aims to explore the potential of data science and machine learning techniques following Bessa et al. [1], in developing a model to predict the mechanical properties of composite materials using their geometric (microstructural) and constituent properties. Numerical homogenisation techniques are utilised to extract effective properties of a composite material. Subsequently, a training database is created by analyses of large set of Representative Volume Elements (RVE) with varying parameters involving size and spatial distribution of the reinforcing phases as well as the constituent material properties. Elastoplastic constitutive models involving damage are used for the material behaviour of the matrix phase while the reinforcement phase is assumed to be linear elastic. Periodic boundary condition is enforced on the analysed RVEs and a case of transverse tensile loading is considered. Each analysed RVE and its calculated effective properties are correlated with a 'microstructural fingerprint' i.e. a combination of its geometric and constituent material parameters. The geometric parameters of the microstructures are quantified using a variety of spatial descriptive metrics (see [2]) such as the pair-correlation function, Ripley's K-function etc. as well as the reinforcement volume fraction. Thus a complete mapping of microstructural features to the computed effective property is established. Subsequently, supervised machine learning techniques are then applied to this dataset with an aim to develop a model to predict effective properties of an arbitrary, user-defined microstructure. Exploratory data analysis is used to highlight the underlying relationships between independent predictors i.e. microstructural features and the computed effective properties. The effectiveness of the developed machine learning model is then validated using high-fidelity finite element simulations. Finally, an inverse problem is solved using optimization techniques in order to find an optimal microstructure for a given set of material parameters and for a user defined property (stiffness, yield stress, ultimate stress). Keywords: Composites, Machine learning, Optimization, Microstructure, Data Science References 1. Bessa, M.A., Bostanabad, R., Liu, Z., Hu, A., Apley, D.W., Brinson, C., Chen, W., Liu, W.K., 2017. A framework for data-driven analysis of materials under uncertainty: Countering the curse of dimensionality. *Computer Methods in Applied Mechanics and Engineering* 320, 633–667. 2. Niezgoda, S. R., Yabansu, Y. C. & Kalidindi, S. R., 2011. Understanding and visualizing microstructure and microstructure variance as a stochastic process. *Acta Materialia* 59, 6387–6400.

Hybrid Finite Element Strategy for Simulation of Coupled Electro/Magneto-Thermoelastic Interactions in Microsystems

Kunal Patil*, Chandrashekhar Jog**

*Indian Institute of Science (IISc), Bangalore, India, **Indian Institute of Science (IISc), Bangalore, India

ABSTRACT

An efficient numerical solution strategy for problems involving multiple energy domains is of importance not only for predicting the underlying coupled behaviour, but also for subsequent optimization. Many applications in Micro-Electro-Mechanical Systems (MEMS) or dielectric elastomers etc. involve chunky structural geometries in combination with thinner elements such as beams, plates or shells etc., and subjected to strongly or weakly interacting fluid, thermal, electric or magnetic forces. Computational modelling of such multi-physical systems using Finite Elements (FE) have to deal with the challenges posed by the 'locking' phenomenon associated with the use of standard displacement based finite elements, while modelling small aspect ratio geometries and incompressible materials, and the problem of spurious stress oscillations while modelling thermoelastic coupling. The problems of locking and spurious thermal stress oscillations were circumvented using the Hybrid FE strategy in the context of coupled electro-elasticity [1], and coupled thermoelasticity [2]. In this work, we discuss the non-trivial extension of the Mixed/Hybrid FE strategy for modelling monolithically the non-linear coupled electro/magneto-thermoelastic behaviour for microsystems. The efficacy of the developed computational strategy is demonstrated using several numerical examples, with an emphasis on predicting accurately the onset of static and dynamic pull-in instabilities associated with microsystems. References [1] Jog C, Patil KD. A hybrid finite element strategy for the simulation of mems structures. International Journal for Numerical Methods in Engineering 2016; 106(7):527–555. [2] Jog C, Gautam G. A monolithic hybrid finite element strategy for nonlinear thermoelasticity. International Journal for Numerical Methods in Engineering 2017; 112(1):26–57.

An Immersed Interface Finite Element Method for the Analysis and Design of Multi-Material Systems

Mayuresh Patil*

*Virginia Tech

ABSTRACT

Design of multi-material systems involve the optimal placement of multiple materials within a base material. The optimal design takes the form of a shape or interface design problem. Large number of interface design variables require the use of gradient based optimization which need interface sensitivities, i.e., the effect of change in interface on the performance of the material. There are two computational issues with interface design using current discrete or continuum shape sensitivity analyses: remeshing at each design iterations and the need for either mesh Jacobian sensitivities (domain velocity form) or solution gradients (boundary velocity form). An alternate way to design multi-materials systems is the use of immersed interface method for analysis. The present effort is focused on developing and presenting an immersed interface method based on the splitting of material constitutive law along the interface and normal to it. This leads to a solution that converges to the exact multi-material solution as the number of finite elements are increased. To verify the results of the multi-material immersed interface finite element method a multi-material patch test is developed. It is shown that the proposed approach satisfies the multi-material patch test which guarantees convergence of the analysis. Finally, the method is used to calculate the sensitivities of the analysis solution to interface change. Future work will focus on using the analysis and sensitivity computation based on the present method for optimal design of multi-material systems.

Integrating the Use of Multiple Models Based on Complex Mass Flows

Abani Patra*

*University at Buffalo, SUNY

ABSTRACT

In this talk, we will outline recent work on integrating the use of multiple models based on different rheological assumptions to improve predictive power when modeling complex flows where the ideal rheology is hard to determine a priori or changing in the course of the flow as a result of entrainment or deposition. We begin by a careful statistical analysis of major extant models to establish the most significant factors arising from different rheological assumptions. These can then be put together in a problem specific manner to produce predictive simulations that exploit all the models.

Wave Motion in an Elastically Connected Double Beam Using Super-convergent Finite Element Formulation

Shweta Paunikar*, Srinivasan Gopalakrishnan**

*Indian Institute of Science, **Indian Institute of Science

ABSTRACT

Adhesively bonded metallic and composite joints are an inseparable part of today's aerospace industry. Wave propagation across such joints is an effective way of monitoring their health for delamination and aging. In this work, a new semi-analytical double beam element is developed to model wave propagation characteristics of a bonded joint. A double beam element is constituted of two parallel Timoshenko beam-rod elements connected to each other by continuously distributed vertical elastic springs. Different values of spring stiffness are used to simulate different levels of adhesion, which is required for monitoring the health of adhesive bond between the two beams. First order shear deformation theory is used for assessing the displacement field, namely, axial, transverse, and shear components each for top and bottom beams. Six coupled equations governing dynamic interactions between two parallel beams are obtained. While using conventional finite elements, discrete springs modelling the elastic layer must have stiffness values depending on the node spacing, sometimes even having negative stiffness values. Therefore, a new set of stiffness values needs to be found for each frequency and mesh refinement. This tedious nature of finite element modelling is the motivation for developing a novel, simpler and more accurate formulation for elastically coupled beams. In this formulation, the exact solutions to the static part of the axial-flexure-shear coupled governing equations are obtained. The exact interpolating functions ensure the exactness of stiffness matrix, thus largely reducing the error in approximation in comparison with finite element method. The order of interpolating function of transverse displacement, thus obtained, is one order higher than that of the beam slope. As a result, the beam element has super-convergent properties and is free from shear locking. Hence, obtaining the wave propagation behaviour in elastically coupled metallic and symmetric or asymmetric composite beams accurately and within a short time is possible with this double beam element. This approach also makes it feasible to model various level of bonding in beams by varying stiffness values of the spring. Consequently, more accurate models for health monitoring of adhesively bonded metallic or composite joints can be developed with this element.

Joint Image Segmentation and Registration Based on a Dynamic Level Set Approach Using Hierarchical B-splines

Aishwarya Pawar^{*}, Yongjie Zhang^{**}, Cosmin Anitescu^{***}, Timon Rabczuk^{****}

^{*}Carnegie Mellon University, ^{**}Carnegie Mellon University, ^{***}University of Weimar, ^{****}University of Weimar

ABSTRACT

We present an efficient approach for joint image segmentation and nonrigid registration based on a level set formulation. Joint image segmentation and registration is an efficient tool as it incorporates automatic structural analysis into the image processing framework. This method has shown an improved performance as compared to carrying out the segmentation and registration methods separately [1,2]. Unlike previous approaches, the implicit level set function defining the segmentation contour and the spatial transformation that maps the deformation for the image registration are both defined using C2 continuous hierarchical B-splines. This joint level set framework uses a variational form of an atlas-based segmentation together with a nonrigid registration method which can compute large deformations with cubic splines. The minimization of the variational form is accomplished by dynamic evaluations on a set of successively refined adaptive grids at multiple image resolutions. The improvement in the description of the segmentation result using higher order splines leads to a better accuracy of both the image segmentation and registration process. The performance of the proposed method is demonstrated on 2D synthetic and medical images to show the advantages of the proposed method as compared to other joint segmentation and registration methods. Keywords: joint image registration and segmentation, adaptive refinement, level set framework, partial differential equation models, hierarchical B-splines, dynamic scheme REFERENCES: [1] A. Pawar, Y. J. Zhang, C. Anitescu, Y. Jia, T. Rabczuk. DTHB3D_Reg: Dynamic Truncated Hierarchical B-Spline Based 3D Nonrigid Image Registration. Communications in Computational Physics, 23(3):877-898, 2018. [2] A. Pawar, Y. Zhang, Y. Jia, X. Wei, T. Rabczuk, C. L. Chan, C. Anitescu. Adaptive FEM-based Nonrigid Image Registration Using Truncated Hierarchical B-splines. A Special Issue of FEF 2015 in Computers and Mathematics with Applications, 72:2028-2040, 2016.

Application of the Concept of Virtual Material for the Design of Additive Manufacturing Processes of Open Cell Foams

Piotr Pawlowski*, Ryszard Pecherski**, Marcin Nowak***, Zdzislaw Nowak****, Marek Sklodowski*****

*Institute of Fundamental Technological Research Polish Academy of Sciences, **Institute of Fundamental Technological Research Polish Academy of Sciences, ***Institute of Fundamental Technological Research Polish Academy of Sciences, ****Institute of Fundamental Technological Research Polish Academy of Sciences, *****Institute of Fundamental Technological Research Polish Academy of Sciences

ABSTRACT

The subject of the presented paper is the model based on a digital microstructure called also virtual material, in particular open cell foams characterised with the skeleton formed of convex or re-entrant cells. The study is based on the following hypothesis: Computed Tomography analysis of polyurethane foam with convex or re-entrant cells provides an adequate basis for the computational reconstruction of a “virtual cellular material.” It enables one to simulate numerically the thermomechanical processes for assumed properties of the skeleton material. The hypothesis is based on visible similarity in the structure of convex or re-entrant cells of the observed polyurethane and metallic cellular materials that are reported in many papers discussed in [1]. The virtual foam structure is derived from the real polyurethane foam specimens produced and studied in [2] with use of computed tomography images implementing the procedures described in [1]. The additive manufacturing (AM) methods used for metallic materials mostly require numerical models composed of large sets of 2-D slices of the 3-D structural model. The necessary steps of computational design and pre-processing of additive manufacturing of open cell foams are discussed, including voxel-based and smoothed geometry generation algorithms, positioning and supporting in the working volume of the AM system, slicing, and post-processing. To demonstrate the feasibility of the study, the open-cell multifunctional structures were manufactured, which can be used as e.g., crush-resistant heat exchangers, heat capacitors, etc. The structures were produced using selective laser melting process in the powder bed fusion technology using aluminium and maraging steel powders. References 1. R.B. Pecherski, M. Nowak, Z. Nowak, Virtual metallic foams. Application for dynamic crushing analysis, International Journal for Multiscale Computational Engineering, 15, 431-442, 2017. 2. A. Streck, Production and study of polyether auxetic foam, Mech. Control, 29,78–87, 2010.

Towards a Hybrid Multi-fluid/PIC Plasma Capability

Roger Pawlowski^{*}, John Shadid^{**}, Edward Phillips^{***}, Sidafa Conde^{****}, Stephen Bond^{*****},
Eric Cyr^{*****}, Sean Miller^{*****}, Matthew Bettencourt^{*****}

^{*}Sandia National Laboratories, ^{**}Sandia National Laboratories, ^{***}Sandia National Laboratories, ^{****}Sandia National Laboratories, ^{*****}Sandia National Laboratories, ^{*****}Sandia National Laboratories, ^{*****}Sandia National Laboratories, ^{*****}Sandia National Laboratories, ^{*****}Sandia National Laboratories

ABSTRACT

Plasma physics systems are often simulated by either a continuum approach (e.g. magnetohydrodynamics or multi-fluid plasma models) or a charged particle description (e.g. Boltzmann equation). Particle-in-cell (PIC) methods are typically applied to solve the Boltzmann equation that is the fundamental equation for the distribution function describing particle motion in the presence of electromagnetic fields. As the plasma density and collisional interaction increases, PIC becomes intractable to simulate directly due to the large number of particles required. In this case, fluid PDE models such as the single fluid magnetohydrodynamics (MHD) and multi-species fluid models are often utilized. In transition regions certain problems may require a hybrid model that combines the fluid and PIC descriptions for tractability. This presentation describes an initial effort to couple a finite element (FE) multi-species fluid model to a PIC description. The multi-fluid model consists of continuity, momentum and energy equations for each species coupled to Maxwell's equations for the electromagnetic field. The equations are discretized using the continuous Galerkin FE method with a compatible basis to enforce the electric field (edge basis) and magnetic field (face basis) involutions from Maxwell's equations. The resulting set of fluid equations contains a wide range of multiple time and length-scale physical mechanisms, producing a stiff system. To evolve the coupled kinetic-PIC / fluid system for the time scales of interest, we explore the use and development of IMplicit-EXplicit (IMEX) Runge-Kutta time integration methods and pursue initial comparisons with operator split methods. For robustness, efficiency, and scalability the implicit nonlinear fluid physics are solved using a Newton-Krylov method with a GMRES linear solve and an approximate block factorization preconditioner. Algebraic multigrid is applied within the blocks. Code verification problems will be presented to assess accuracy and efficiency of the algorithm.

Multilevel Hierarchy of Shear Banding in Viscoplastic Flow and Failure

Ryszard Pecherski*

*Institute of Fundamental Technological Research, Polish Academy of Sciences, Warsaw, Poland

ABSTRACT

Experimental observations show that inelastic deformation of metals is often produced as an effect of competing mechanisms of crystallographic glide, twinning and micro-shear banding. The micro-shear bands are observed as concentrated shear zones in the form of transcrystalline layers of the thickness of the order 0.1 μm . It has been observed that the change of the mechanism of inelastic deformation has strong influence on ductile failure processes in different length scales. Therefore, the identification and elucidation of physical mechanisms that are responsible for initiation, growth and evolution of micro-shear bands is of fundamental importance for understanding the macroscopic behaviour of metallic materials, [1]. A new physical model of multilevel hierarchy and evolution of shear bands is proposed with use of the analysis of recent state of the art of the investigations carried on different levels of observations: uni-axial and bi-axial mechanical tests enhanced with digital image correlation method and in-situ tests with use of electron microscopy as well as atom probe tomography in relation with ab initio and molecular dynamics computational simulations. The difficulties with application of a direct multiscale integration scheme are discussed and an original idea of an extension of the representative volume element concept with use of the known theory of the propagation of the singular surfaces of microscopic velocity field is proposed, [2]. A new formulation of the description of rate of shear strain generated by multilevel hierarchy of shear bands is formulated in the workflow integration approach, in which information from molecular simulation at different levels flows into the decision process, [3]. [1] R.B. Pecherski, Macroscopic effects of micro-shear banding in plasticity of metals, *Acta Mechanica*, 131, pp 203–224, (1988). [2] R.B. Pecherski, Finite deformation plasticity with strain induced anisotropy and shear banding, *Journal of Materials Processing Technology*, 60, pp. 35-44, (1996). [3] G. Goldbeck, Foreword, in: *Industrial Applications of Molecular Simulations*, M. Meunier (ed.), CRC Press, Taylor & Francis Group, Boca Raton, (2012).

Efficient Reduced Coupling of PDEs Based on Weak Transmission Conditions

Luca Pegolotti^{*}, Simone Deparis^{**}

^{*}École polytechnique fédérale de Lausanne, ^{**}École polytechnique fédérale de Lausanne

ABSTRACT

We present a non-conforming domain decomposition method based on weakly imposed transmission conditions. The continuity of the global solution is enforced by Lagrange multipliers defined over the interfaces of adjacent subdomains. The method falls into the class of primal hybrid methods [1], which include also the well-known mortar method [2]. In contrast with the mortar method, we discretize the space of basis functions at each interface independently of the discretization of the two adjacent domains. The advantages of this choice are twofold. Firstly, the accuracy of the coupling can be tuned accordingly to the specific application, because the continuity of the global solution and its normal derivatives at the interface depends on the richness – i.e. the number of basis functions – of the space of Lagrange multipliers. Secondly, the global solution is independent of any partition of the subdomains into master and slave domains, which, in the mortar method, must be done a priori. Being a non-conforming method, applications of our approach include e.g. the solution of problems with finite element spaces built on non-conforming meshes or with different polynomial degrees, or the coupling of solutions obtained using otherwise incompatible methods such as the finite element method, the spectral element method and isogeometric analysis. The method can be also used to couple solutions obtained on reduced basis spaces. We explore some of these possibilities with numerical experiments. [1] D. Boffi, F. Brezzi, M. Fortin. Mixed finite element methods and applications, Springer (2013) [2] C. Bernardi. A new nonconforming approach to domain decomposition: the mortar element method, Nonlinear partial equations and their applications (1989)

Multifidelity Monte Carlo Estimation with Adaptive Low-Fidelity Models

Benjamin Peherstorfer*

*University of Wisconsin-Madison

ABSTRACT

Multifidelity Monte Carlo (MFMC) estimation combines low- and high-fidelity models to speedup the estimation of statistics of the high-fidelity model outputs. MFMC optimally samples the low- and high-fidelity models such that the MFMC estimator has minimal mean-squared error for a given computational budget. In the setup of MFMC, the low-fidelity models are static, i.e., they are given and fixed and cannot be changed and adapted. We introduce the adaptive MFMC (AMFMC) method that splits the computational budget between adapting the low-fidelity models to improve their approximation quality and sampling the low- and high-fidelity models to reduce the mean-squared error of the estimator. Our AMFMC approach derives the quasi-optimal balance between adaptation and sampling in the sense that our approach minimizes an upper bound of the mean-squared error, instead of the error directly. We show that the quasi-optimal number of adaptations of the low-fidelity models is bounded even in the limit case that an infinite budget is available. This shows that adapting low-fidelity models in MFMC beyond a certain approximation accuracy is unnecessary and can even be wasteful. Our AMFMC approach trades-off adaptation and sampling and so avoids over-adaptation of the low-fidelity models. Besides the costs of adapting low-fidelity models, our AMFMC approach can also take into account the costs of the initial construction of the low-fidelity models ("offline costs"), which is critical if low-fidelity models are computationally expensive to build such as reduced models and data-fit surrogate models. Numerical results demonstrate that our adaptive approach can achieve orders of magnitude speedups compared to MFMC estimators with static low-fidelity models and compared to Monte Carlo estimators that use the high-fidelity model alone.

A Mesoscale-based Homogenization Study of Sand

Gerald Pekmezi*, David Littlefield**

*The University of Alabama at Birmingham, **The University of Alabama at Birmingham

ABSTRACT

In recent years, renewed research effort has been directed toward characterizing soils in transient applications. The main approach favored towards that end, has been to use one of many “cap” models derived from Mohr-Coulomb failure theory. In addition to a friction-based yielding stress like Mohr-Coulomb, typically such models incorporate a pressure cap. More advanced three-phase models also take into account the great difference in soil response with degree of saturation through “effective” stress. Effective stress isolates the stress in the solid skeleton of the material, from the bulk behavior. One such model, the Hybrid Elastic Plastic (HEP) model has been used extensively to model soils subjected to energetic, highly-transient phenomena using hydrocodes, a class of explicit computational packages geared toward such phenomena. Geomaterials such as soils, differ from other common engineering materials like metals, polymers, and many composites, in that the fundamental evolution of the underlying structure may reasonably be considered to occur at a higher scale, i.e. at the mesoscale rather than the microscale. This offers a somewhat unique opportunity to be able to characterize the underlying structural evolution of the material, and use that characterization to inform a general constitutive framework to model the behavior of a wide spectrum of soils under a range of pressures and distortional transient loading conditions. In the current work, experimental and laboratory data of a poorly graded sand previously modeled using the HEP model, is used to explore the internal evolution of the sand by carrying out particle-based simulations of the behavior at the mesoscale. These simulations are used to conduct a homogenization study of the granular subdomain. This is done in order to 1) identify the threshold at which the transition from discrete mesoscale to the Representative Volume Element (RVE) occurs, and 2) to quantify the uncertainty associated with discretization below that threshold. Additionally, the mesoscale results are used to formulate an effective stress model that matches the behavior observed in the particle-based simulations. This new effective stress model is then compared with the predictions of the sand behavior from the HEP model.

Combining Tetrahedra into Valid Finite-Element Hexahedral Cells

Jeanne Pellerin^{*}, Amaury Johnen^{**}, Jean-François Remacle^{***}

^{*}Université catholique de Louvain, ^{**}Université catholique de Louvain, ^{***}Université catholique de Louvain

ABSTRACT

To generate automatically hex-dominant meshes for general domains, indirect methods take advantage of the existence of tetrahedral mesh generation algorithms and combine tetrahedra in hexahedra, prisms and pyramids. Existing indirect methods rely on a small set of predefined patterns of subdivision of the hexahedron into tetrahedra. However these patterns do not account for the whole range of valid finite-element hexahedron geometries since the patterns are limited to hexahedra with planar faces. Valid cells, i.e. which have a strictly positive Jacobian, have bilinear faces by definition, may be quite distorted and/or non-convex. We describe an algorithm that overcomes this limitation and identifies all combinations of tetrahedra into valid finite element hexahedral cells. All combinations of eight vertices of a tetrahedral mesh which are candidates to define a valid hexahedron are generated in a first step. The tetrahedra are computed in a second step. The core of the algorithm is a combination generator which efficiency is drastically improved by tests discarding invalid hexahedra as early as possible. We reach 300,000 potential hexahedra computed per second on a laptop. Our algorithm does not depend on any pattern and is actually able to discover new patterns that are compared using an edge-colored graph formalism. We have discovered more than a hundred patterns that do correspond to valid hexahedral cell geometries. Our unexpected result includes the ten previously used patterns. It shows how the complexity of tetrahedral meshes propagates to indirect meshing methods. We exhibit subdivisions of hexahedral cells valid for finite-element computation into up to fourteen tetrahedra without additional vertices. We further study the discovered patterns in terms of occurrence, maximum quality and show how these values are linked to the point set quality for hexahedral meshing and on the tetrahedral mesh chosen.

Multiscale Modeling of a Red Blood Cell Passing through the Human Spleen

Zhangli Peng^{*}, Huijie Lu^{**}

^{*}University of Notre Dame, ^{**}University of Notre Dame

ABSTRACT

We developed a boundary integral formulation to study a red blood cell (RBC) squeezing through a submicron slit under prescribed inlet and outlet pressures. The motivation of this study is to investigate splenic filtrations of RBCs and corresponding in vitro mimicking microfluidic devices, during which RBCs regularly pass through inter-endothelial slits with a width less than 1 micrometer. We first derived the boundary integral equations of a RBC immersed in a confined domain with both Neumann and Dirichlet boundary conditions, and gave the explicit matrix forms of equations and numerical procedures to solve these equations. In addition, we also developed accurate treatments of nearly singular integrals and corner singularities, which are especially important in this fluid-structure interaction study with strong lubrication. After validations against analytical and experimental results, we explored the membrane tension, shear deformation, and bilayer-cytoskeletal interactions under various conditions. We systematically studied the effects of pressure drop, volume-to-surface-area ratio, internal viscosity, and membrane stiffness on RBC deformation and internal stress. The numerical methods developed will not only be important for understanding RBCs physiology and diseases related to splenic filtration, but also be useful for studying elastic capsules, vesicles, and other cells squeezing small slits in drug delivery and extravasation.

Preconditioning the Virtual Element Method

Micol Pennacchio^{*}, Silvia Bertoluzza^{**}, Daniele Prada^{***}

^{*}CNR-IMATI, Pavia, Italy, ^{**}CNR-IMATI, Pavia, Italy, ^{***}CNR-IMATI, Pavia, Italy

ABSTRACT

The Virtual Element Method [1] is a quite recent discretization framework which can be viewed as an extension of the Finite Element Method. The Virtual Element Method allows to easily handle meshes consisting of very general shaped polygonal or polyhedral elements, while keeping simplicity in implementation as far as accuracy and stability of the resulting numerical schemes. However, in order to make the method more competitive, it is also necessary to deal with the efficient solution of the associated linear system of equations, and, in particular, to provide good preconditioners. Here we deal with a Domain Decomposition approach [2] and we focus on a non overlapping domain decomposition method: the Dual-Primal Finite Element Tearing and Interconnecting (FETI-DP) method. We prove polylogarithmic condition number bounds in two [3] and three dimensions, independent of the number of subdomains, the mesh size, and jumps in the diffusion coefficients. Numerical results validate the theory. [1] L. Beirao da Veiga, F. Brezzi, L.D. Marini, A. Russo: The hitchhiker guide to the Virtual Element Method, Math. Models Methods Appl. Sci., Vol. 24, 1541-1573, (2014). [2] A. Toselli, O. Widlund: Domain Decomposition Methods - Algorithms and Theory. Springer Series in Computational Mathematics volume 34, 2005. [3] S. Bertoluzza, M. Pennacchio, D. Prada: BDDC and FETI-DP for the Virtual Element Method. Calcolo, 54(4), 1565-1593, (2017),

TWO-DIMENSIONAL CHAPEAU FUNCTION RECURSION RELATIONS

SOGOL PIRBASTAMI*, DARRELL W. PEPPER*

*University of Nevada, Las Vegas
4505 S Maryland Pkwy,
NV, Las Vegas, USA
Sogol.pirbastami@unlv.edu

*University of Nevada, Las Vegas
4505 S Maryland Pkwy,
NV, Las Vegas, USA
Darrell.pepper@unlv.edu

Key words: Finite Element, Chapeau Function, Strongly Implicit Procedure

Abstract. In this study, a simple Galerkin-based finite element approach is used to solve the advection-diffusion equations in two-dimensional. The finite element method (FEM) is a powerful technique that is commonly used for solving complex engineering problems. However, the implementation of the FEM in two or Three-dimensional problems can be computationally expensive. A simple finite element algorithm based on the bilinear triangular, bilinear quadrilateral and Quadratic Lagrangian approximation is employed to discretize the 2D convection-diffusion equations. This algorithm is an extension of the 1D Chapeau (linear element) technique which employed a tridiagonal recursion expression common to the classical central finite-difference approach. In this case, the global matrix now becomes penta-diagonal (for 2D). Hypermetrics and the natural coordinate system are used to transform the integral expressions. Then, integrating and assembling the set of relations over the i th node within the patch of four bilinear elements (similar to assembling the one-dimensional linear chapeau function), a recursion relation is established for the 2D equations. The transient term is finally approximated in a forward-in-time difference, and the assembly becomes complete. The FEM algorithm is validated by applying the method to a simple problem in a two-dimensional square and Strongly Implicit Procedure (SIP) method used as a solver.

INTRODUCTION

The most commonly used numerical techniques used in Computational Fluid Dynamics (CFD) simulations are the finite difference (FDM), finite volume (FVM), and finite element (FEM) methods. Due to the mathematical robustness and flexibility of the finite element method, the FEM is popular for solving the general class of transport equations. However, the implementation of the FEM in 2 or 3-dimensions can be computationally expensive.

In this study a simple Galerkin-finite element recursion-based algorithm for the 2-D general transport equation is examined. The algorithm is based on integrating and assembling eight bilinear triangular elements, 4 bilinear quadrilateral elements, or one Lagrangian quadratic quadrilateral element over the i^{th} node within the patch of 9 nodes. A recursion relation is established which can be solved using the strongly implicit method (SIP) instead of a more direct Gaussian elimination matrix solver, i.e., the global matrix. The purpose of this method is to speed up the computational time while eliminating the issue of minimizing global bandwidth associated with global matrix assembly[4].

Pepper and Baker [1] used linear basis functions for each element in a simple finite element algorithm (chapeau function) to derive the 1-D advection-diffusion transport equation. Hypermatrices and natural coordinates were employed to evaluate the integral forms of the algorithm and then assembly was conducted over two adjacent elements, creating a tridiagonal recursion relation which resembles a central FDM. Multidimensional problems were solved using time splitting for the 2D/3D equations, i.e., treating the discretized equations as a series of 1D algorithms. Long and Hicks [8] used the 1D chapeau function to model atmospheric boundary layer flow, and found that the method produced fourth order accuracy and stable solutions. For transient problems in 2D and 3D, Marchuk's time splitting method was employed.

Pepper et al [5] studied quasi-Lagrangian cubic-spline and chapeau-function (Galerkin) methods for general dispersion models. Both methods showed more accurate results and stability compared to finite difference methods. Both methods used low storage and were simple to code. In simple advection with uniform discretization, the chapeau function showed 4th order accuracy but in unequal mesh spacing, the cubic spline had slightly lower dispersion errors. The chapeau function method is based on the use of linear basis functions, or hat-shaped (chapeau) expressions in 1-D.

FINITE ELEMENT ALGORITHM OF 2D CHAPEAU FUNCTION

In a conventional Galerkin approach, the weighting functions are set equal to the basis functions, converting a PDE into a series of algebraic equations. The general 2D transport equation can be discretized using either 2D triangular elements or quadrilateral elements and then assembled over eight triangular elements, four quadrilateral elements, or one quadratic Lagrangian quadrilateral element, consecutively, to establish a set of recursion relations.

eneral transport e uation

$$\frac{\partial c}{\partial t} + \nabla(Vc) - \nabla \cdot (D(\nabla c)) = S \quad (1)$$

For simplicity, we consider the source term, S , to be zero and define c as a scalar transport, e.g. temperature.

The 1D chapeau function is described in Pepper and Baker [1]. The linear shape function and weighted residual method are used for two consecutive elements. After assembly (creating a 3x3 global matrix), the recursion relation for the i^{th} node can be established:

inear shape function

$$N_{i-1} = \frac{x_i - x}{\Delta x} \quad (2)$$

$$N_i = \frac{x - x_{i-1}}{\Delta x} \quad (3)$$

The approximation for linear function can be expressed as:

$$c = N_{i-1} * c_{i-1} + N_i * c_i \quad (4)$$

Weighted residual method for 1D:

$$\int W. \left(\frac{dc}{dt} + u * \frac{dc}{dx} - D * \left(\frac{d^2c}{dx^2} \right) \right) \quad (5)$$

when $W=N$. Thus, the integral relation for the 1D element spanning nodes $i-1$ to i can be written as

$$\int N_i * N_{i-1} dx. \left\{ \frac{c'_i - 1}{c'_i} \right\} + U * N_i \int N_i. \frac{dN_{i-1}}{dx} dx. \left\{ \frac{ci - 1}{ci} \right\} D * \int \frac{dN_i}{dx} \frac{dN_{i-1}}{dx}. \left\{ \frac{ci - 1}{ci} \right\} = 0 \quad ()$$

The integral terms are similarly evaluated for elements spanning i to $i+1$. Thus, for the two adjacent linear elements,

For $\Delta x_- = x_i - x_{i-1}$

$$\frac{\Delta x_-}{6} \begin{bmatrix} 2 & 1 \\ 1 & 2 \end{bmatrix} * \left\{ \frac{ci - 1}{ci} \right\} + \frac{-1}{2} \begin{bmatrix} -1 & 1 \\ -1 & 1 \end{bmatrix} * \left\{ \frac{ci - 1}{ci} \right\} + \frac{-1}{\Delta x_-} \begin{bmatrix} 1 & -1 \\ -1 & 1 \end{bmatrix} * \left\{ \frac{ci - 1}{ci} \right\} = 0 \quad (7)$$

For $\Delta x_+ = x_{i+1} - x_i$

$$\frac{\Delta x_+}{6} \begin{bmatrix} 2 & 1 \\ 1 & 2 \end{bmatrix} * \left\{ \frac{ci - 1}{ci} \right\} + \frac{-1}{2} \begin{bmatrix} -1 & 1 \\ -1 & 1 \end{bmatrix} * \left\{ \frac{ci - 1}{ci} \right\} + \frac{-1}{\Delta x_+} \begin{bmatrix} 1 & -1 \\ -1 & 1 \end{bmatrix} * \left\{ \frac{ci - 1}{ci} \right\} = 0 \quad (8)$$

Assembling the two adjacent elements in a global matrix,

$$\frac{1}{6} \begin{bmatrix} 2\Delta x_- & \Delta x_- & 0 \\ \Delta x_- & 2\Delta x_- + 2\Delta x_+ & \Delta x_+ \\ 0 & \Delta x_+ & 2\Delta x_+ \end{bmatrix} * \left\{ \begin{matrix} c'_i + 1 \\ c'_i \\ c'_i - 1 \end{matrix} \right\} + \frac{1}{2} \begin{bmatrix} -1 & 1 & 0 \\ -1 & 0 & 1 \\ 0 & -1 & 1 \end{bmatrix} * \left\{ \begin{matrix} ci + 1 \\ ci \\ ci - 1 \end{matrix} \right\} + \frac{1}{6} \begin{bmatrix} \frac{1}{\Delta x_-} & \frac{-1}{\Delta x_-} & 0 \\ \frac{-1}{\Delta x_-} & \frac{1}{\Delta x_-} + \frac{1}{\Delta x_+} & \frac{-1}{\Delta x_+} \\ 0 & \frac{-1}{\Delta x_+} & \frac{1}{\Delta x_+} \end{bmatrix} * \left\{ \begin{matrix} ci + 1 \\ ci \\ ci - 1 \end{matrix} \right\} = 0 \quad (9)$$

The recursion relation in 1D is obtained by stripping out the central expression within the global matrix, i.e.,

$$\frac{1}{6} * (C'_{i-1} + 4C'_i - C'_{i+1}) + \frac{U}{2 * \Delta x} (C_{i+1} - C_{i-1}) - \frac{K}{\Delta x^2} (C_{i+1} - 2C_i + -2C_{i-1}) = 0 \quad (10)$$

For 2D, the shape functions bilinear triangular and quadratic elements are used. Employing isoparametric transformations and applying Galerkin's weighted residual method, the 2D recursion relation for bilinear elements and triangular elements are shown:

$$\int_{-a}^a \int_{-b}^b F(x, y) dx dy = \int_{-1}^1 \int_{-1}^1 f(\xi, \eta) |J| d\xi d\eta \quad (11)$$

$$[M]\dot{c} + [F]c - [K]c = s \quad (12)$$

$$[M] \text{ Mass matrix} \quad (13)$$

$$[F], [K] \text{ Stiffness matrix} \quad (14)$$

$$[M]\dot{c} = \int_{-1}^1 \int_{-1}^1 \frac{\partial c}{\partial t} \cdot Ni dx dy = \int_{-1}^1 \int_{-1}^1 [Ni \cdot Nj |J| d\xi d\eta] \left[\frac{\partial ci}{\partial t} \right] \quad (15)$$

$$[F]c = \int_{-1}^1 \int_{-1}^1 \left[(u \cdot Ni \cdot Ni \frac{\partial Nj}{\partial x} + v \cdot Ni \cdot Ni \frac{\partial Nj}{\partial y}) |J| d\xi d\eta \right] [ci] \quad (16)$$

$$[K]c = \int_{-1}^1 \int_{-1}^1 \left[D * \left(\frac{\partial Nj}{\partial x} \frac{\partial Nj}{\partial x} + \frac{\partial Nj}{\partial y} \frac{\partial Nj}{\partial y} \right) |J| d\xi d\eta \right] [ci] \quad (17)$$

After establishing the global matrices for a patch consisting of 8 bilinear triangular elements, 4 bilinear quadrilateral elements, and one Lagrangian quadratic quadrilateral element, a set of recursion relations for the T_{ij} node can be established.

The set of finite element expressions, defined over a rectangular subspace and formulated using chapeau basis functions, can be interpreted as integrated averaged finite difference approximations. After applying Galerkin's method, integrating by parts, and using isoparametric transformations, we obtain the equations as follows:

2D bilinear triangular elements:

$$\begin{aligned} & \frac{1}{36} * [(3C'_{i+1j+1} + 3C'_{i-1j-1} + 3C'_{i+1j} + 3C'_{i-1j} + 3C'_{ij+1} + 3C'_{ij-1}) + 54 C'_{ij}] + \frac{U}{6 * \Delta x} * [(C_{i+1j+1} - C_{i-1j} + \\ & 2C_{i+1j} - 2C_{i-1j} + C_{i+1j} - C_{i-1j-1})] + \frac{V}{6 * \Delta y} [(C_{i-1j} - C_{i-1j-1} + 2C_{ij+1} - 2C_{ij-1} + C_{i+1j+1} - C_{i+1j})] + \\ & \frac{K}{\Delta x^2} [(-C_{i-1j-1} + 2C_{ij} - C_{i+1j+1})] + \frac{K}{\Delta y^2} [(-C_{ij+1} + 2C_{ij} - C_{ij-1})] = 0 \end{aligned} \quad (19)$$

2D bilinear quadrilateral elements:

$$\begin{aligned} & \frac{1}{9} * [(C'_{i-1j+1} + C'_{i+1j+1} + C'_{i-1j-1} + C'_{i+1j-1}) + 4(C'_{i+1j+1} + C'_{i-1j} + C'_{i+1j} + C'_{ij-1}) + 52 C'_{ij}] + \frac{U}{6 * \Delta x} * \\ & [(2C_{i+1j+1} - 2C_{i-1j+1} + 8C_{i+1j} - 8C_{i-1j} + 2C_{i+1j-1} - 2C_{i-1j-1})] + \frac{V}{6 * \Delta y} [(2C_{i-1j+1} - 2C_{i-1j-1} + 8C_{ij+1} - \\ & 8C_{ij-1} + 2C_{i+1j+1} - 2C_{i+1j-1})] + \frac{K}{6 * \Delta x^2} [(-4C_{i-1j} + 8C_{ij+1} - 4C_{i+1j} - C_{i-1j} + 2C_{ij} - C_{i+1j} - C_{i-1j-1} + 2C_{ij-1} - \\ & C_{i+1j-1})] + \frac{K}{6 * \Delta y^2} [(-C_{i-1j+1} + 2C_{i-1j} - C_{i-1j-1} - 4C_{ij+1} + 8C_{ij} - 4C_{ij-1} - C_{i+1j+1} + 2C_{i+1j} - C_{i+1j-1})] = 0 \end{aligned} \quad (20)$$

2D Quadratic Lagrangian quadrilateral element:

$$\begin{aligned} & \frac{1}{225} * [(C'_{i-1j+1} + C'_{i+1j+1} + C'_{i-1j-1} + C'_{i+1j-1}) + 8(C'_{i+1j+1} + C'_{i-1j} + C'_{i+1j} + C'_{ij-1}) + 16 C'_{ij}] + \frac{U}{45 * \Delta x} * \\ & [(16C_{i+1j+1} - 16C_{i-1j+1} + 128C_{i+1j} - 128C_{i-1j} + 16C_{i+1j-1} - 16C_{i-1j-1})] + \frac{V}{45 * \Delta y} [(16C_{i-1j+1} - 16C_{i-1j-1} + \\ & 128C_{ij+1} - 128C_{ij-1} + 16C_{i+1j+1} - 16C_{i+1j-1})] + \frac{K}{45 * \Delta x^2} [(-8C_{i-1j} + 16C_{ij+1} - 8C_{i+1j} - 64C_{i-1j} + 128C_{ij} - \\ & 64C_{i+1j} - 8C_{i-1j-1} + 16C_{ij-1} - 8C_{i+1j-1})] + \frac{K}{45 * \Delta y^2} [(-8C_{i-1j+1} + 16C_{i-1j} - 8C_{i-1j-1} - 64C_{ij+1} + 128C_{ij} - \\ & 64C_{ij-1} - 8C_{i+1j+1} + 16C_{i+1j} - 8C_{i+1j-1})] = 0 \end{aligned} \quad (21)$$

Basis Functions

The general 2D bilinear element configuration are shown in Fig. 1. Notice that the triangular element array permits either a 9-node configuration or a 5-node configuration.

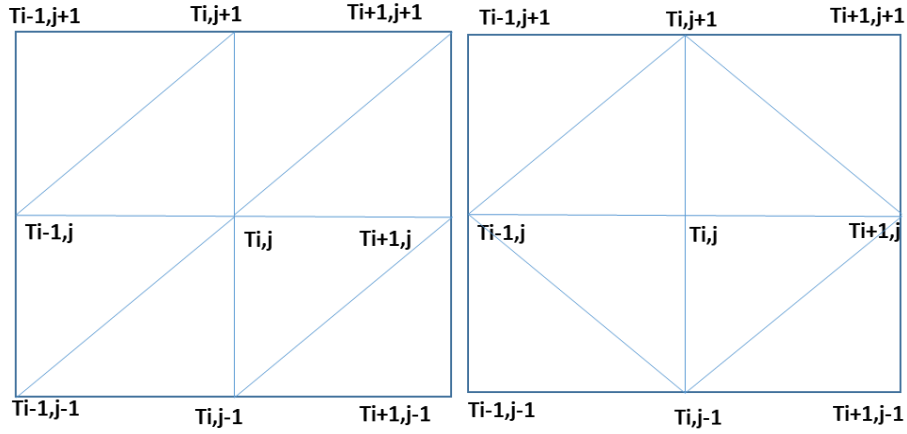


Figure1. Basis Function-Triangular element

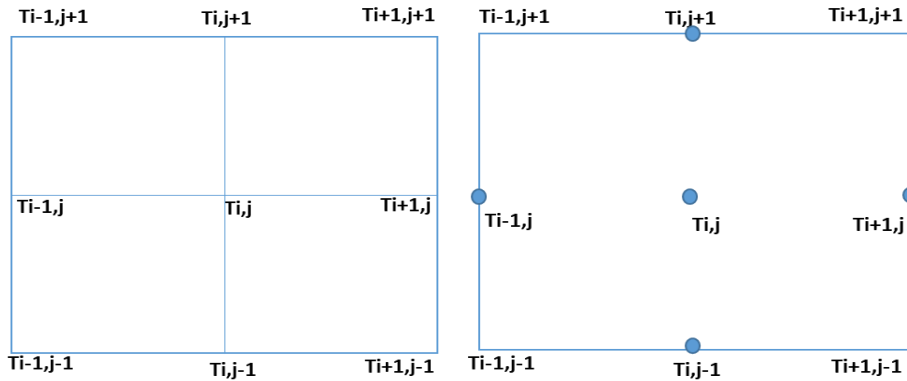


Figure2. Basis Function-Quadrilateral element

STRONGLY IMPLICIT PROCEDURE

For large algebraic systems, conventional solvers and direct solvers are computationally expensive. In the one-dimensional chapeau function study by Pepper and Baker [1], the ADI method was used to solve a set of tridiagonal matrices. In this study, SIP (Strongly Implicit Procedure) is considered for the penta-diagonal matrices but modified since we have 9 diagonal stripes in the overall matrix structure. While SIP was developed to solve 2-D transport equations, the overall SIP solution modifies the 5-stripe matrix into a 9-stripe matrix, hence involving the 9 nodes obtained from the triangular or quadrilateral patch. SIP has been shown to produce fewer iterations and lower computational cost compared to ADI conventional methods [Stone, 1968]. The SIP method decomposed the original matrix into upper and lower triangular matrices, i.e.

$$[A]x = B \quad (22)$$

$$[A + M]x = [A + M]x - ([A]x - B) \quad (23)$$

$$[A + M] = [L][U] \quad (24)$$

$$[L][U] * \{\delta\}^{n+1} = \{R\}^n \quad (25)$$

$$[V]^{n+1} = [U] * \{\delta\}^{n+1} \quad (26)$$

$$[L][V]^{n+1} = \{R\}^n \quad (27)$$

$$[U] * \{\delta\}^{n+1} = \{V\}^{n+1} \quad (28)$$

$[A+M]$ is a modified matrix that can be decomposed to L and U matrices. This method can be applied to 5-stripe penta-diagonal matrices (produced in a 2D central FDM discretization). In this study, we employ the modified SIP (MSIP) used by Schneider and Zedan [4] to resolve the 9-diagonal matrix[2,6,7].

APPLICATION AND RESULTS

In this simulation, a simple 2D domain (1 x 1) was used with a source established near the lower left corner. A simple diffusion test was first run, followed by an advection test, and then the combination of the two. The time dependent transport equation was solved for a 5 x 5 rectangular domain which was discretized into 32 triangular elements, 25 rectangular bilinear elements and 4 Lagrangian elements. Here we assume velocity $U=V=1$ and diffusion coefficient $\alpha_x = \alpha_y = 1$ and also $\Delta y = \Delta x$ (constant) with fluxes set to zero at the outer boundaries.

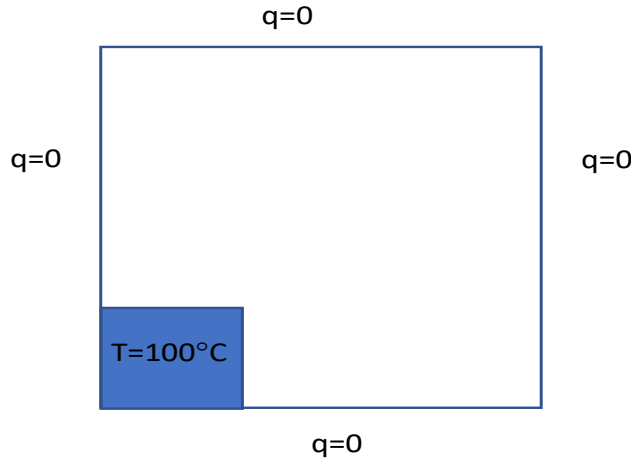


Figure3. Application Domain

Both a conventional FEM assembly (global matrix method) and SIP were used to solve the 2-D general transport equation. For a square patch of 5 by 5 rectangular elements, results from both conventional method and MSIP are shown in Fig. 4,5 for the triangular elements and in Fig. 6,7 for the bilinear quadrilateral and Lagrangian quadratic elements. While a little dispersive noise is observed in the simulations, the errors associated with the numerical methods are very low in the diffusion simulations, but become more noticeable as the advection terms become more dominant. Table 1 lists the CPU times (running on a 64-bit, 12GB Ram PC) for the various simulations. All programming was conducted using MATLAB. After almost 400 iteration for various simulation the residual become less than residual was less than $1e^{-4}$ for time step of 0.1(s).

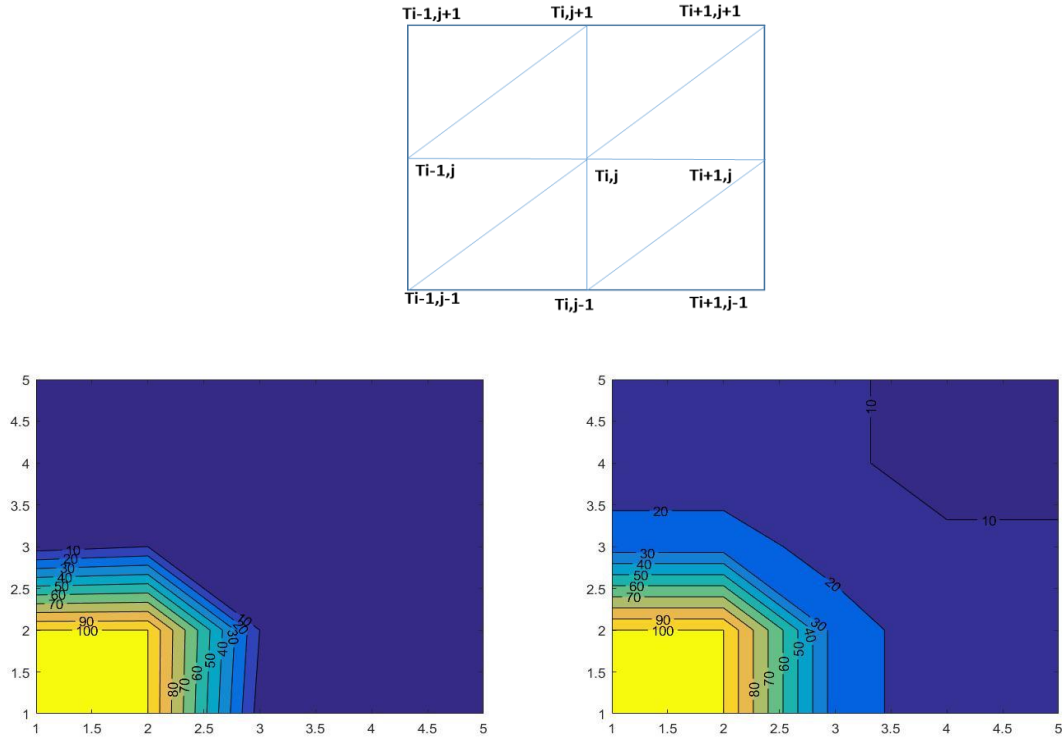
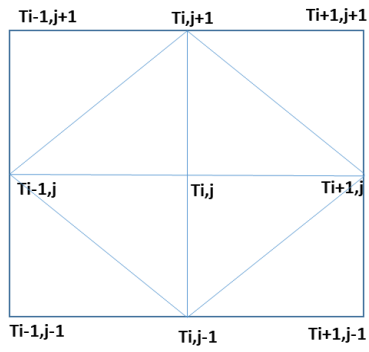


Figure4.

Left, Triangular-32 elements-conventional. Right, Triangular-32 elements-MSIP



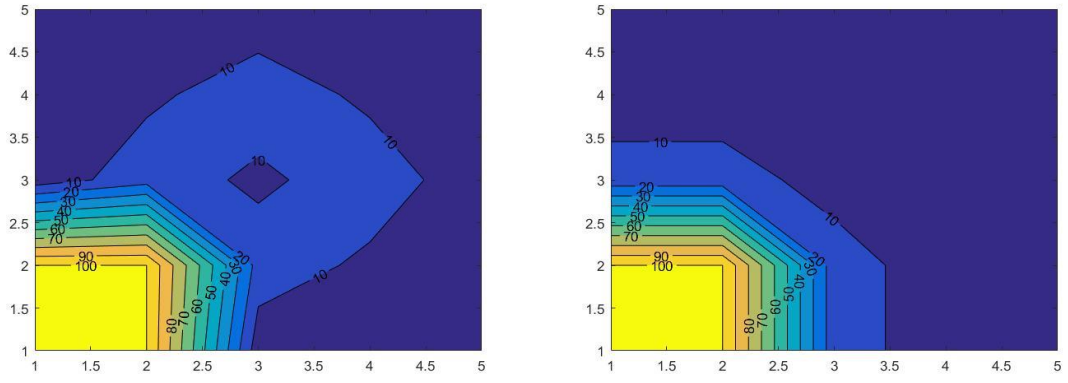


Figure5. Left, Triangular-32 elements-conventional method. Right, Triangular-32 elements-MSIP

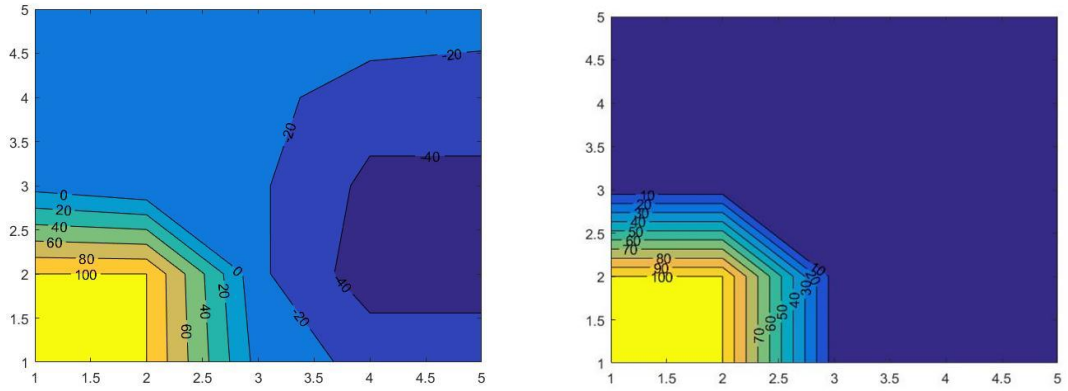
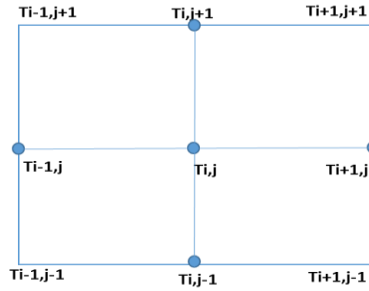


Figure6. Left, Bilinear-25 elements-conventional. Right, Bilinear-25 elements-MSIP

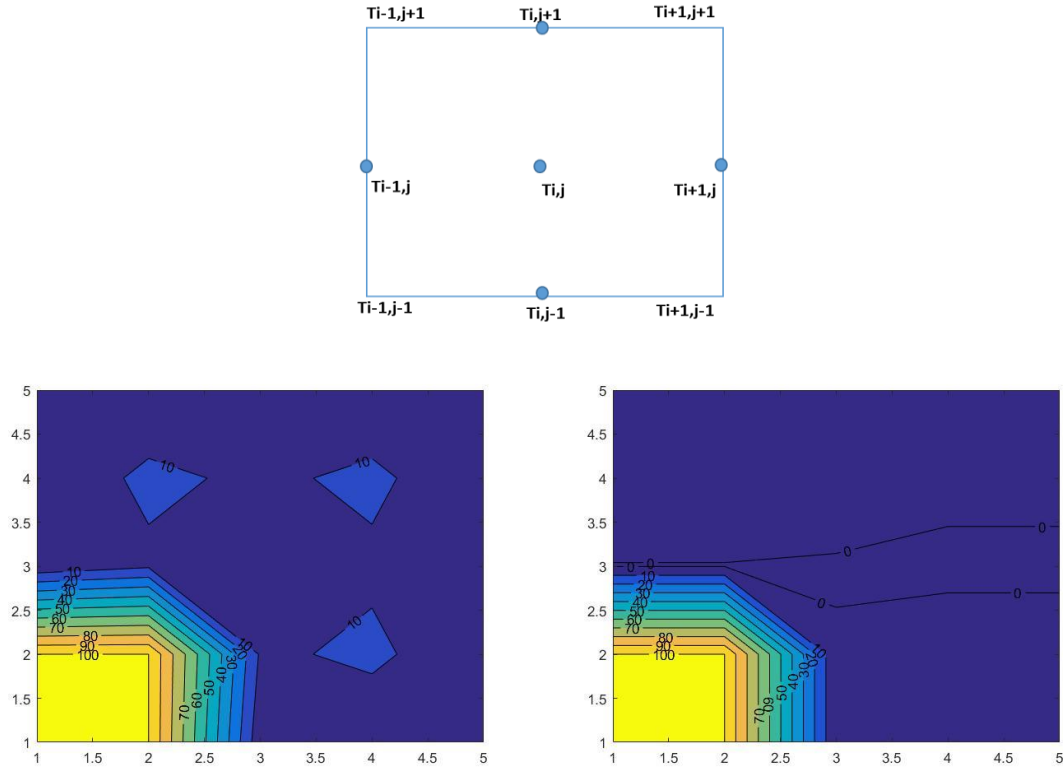


Figure7.Left,Lagrangian-25elements- Conventional. Right, Lagrangian-25elements- MSIP

Table 1. Comparison of CPU times

Shape function	Conventional (time, s)	MSIP (time, s)
Triangular(1)	5.5 (S)	1.4 (S)
Triangular(2)	5.4 (S)	1(S)
Bilinear	0.5 (s)	0.1(s)
Lagrangian	1.2(s)	0.2(s)

Conclusions

The MSIP method is significantly faster than the conventional solution approach and provides a means for solving an implicit equation involving 5 (or 9) unknown nodal values. By establishing a recursion expression for a series of element patches, a conventional finite element method employing either triangular or quadrilateral elements can be converted into a pseudo finite difference approximation. This eliminates the need for renumbering global node numbers in order to minimize global bandwidth. While values using the Chapeau function approach provide values close to conventional FEM results, there is a slight loss in numerical accuracy. However, the use of 2D Chapeau functions provides a very convenient and easy methodology to resolve problem domains more routinely solved using conventional finite element techniques.

References

- [1] Pepper, D.W. and Baker, A.J. A SIMPLE ONE-DIMENSIONAL FINITE-ELEMENT ALGORITHM WITH MULTIDIMENSIONAL CAPABILITIES, Numerical Heat Transfer, vol 2, 1979, pp 81-95.
- [2] Halada L., Lucká M. A Parallel Strongly Implicit Algorithm for Solving of Diffusion Equations. In: Zinterhof P., Vajteršic M., Uhl A. (eds) Parallel Computation. ACPC 1999. Lecture Notes in Computer Science, vol 1557, Springer, Berlin, Heidelberg, 1999.
- [3] P. E. Long and D. W. Pepper , A Comparison of Six Numerical Advection Schemes for Calculating the Advection of Atmospheric Pollution , Proc. AMS 3d Symp. Atmospheric Turbulence Diffusion and Air Quality, Raleigh, N.C., Oct. 19–22 , 1976 , pp. 181 – 187 .
- [4] Diersch, H. and Heidelberg, S. FEFLOW - Finite Element Modeling of Flow, Mass and Heat Transport in Porous and Fractured Media, Springer, (2018).
- [5] Pepper, D., Kern, C. and Long, P. Modeling the dispersion of atmospheric pollution using cubic splines and chapeau functions. Atmospheric Environment, 1979.
- [6] Azevedo, J.L.T., Durst, F., Pereira, J.C.F., Comparison of strongly implicit procedures for the solution of the fluid flow equations in finite difference form, Applied Mathematical Modelling, 1988
- [7] Schneider, G. E., Zedan, M., A MODIFIED STRONGLY IMPLICIT PROCEDURE FOR THE NUMERICAL SOLUTION OF FIELD PROBLEMS, Numerical Heat Transfer, 1981
- [8] Long P. E., Shaffer W. A., Kemper J. E. and Hicks F. J. The state of the Techniques Development Laboratory's boundary layer model, 1977.

Modeling Abrasive Wear by the Discrete Elements Method

Franco Perazzo*, Rainald Löhner**

*Universidad Técnica Federico Santa María, **George Mason University

ABSTRACT

The discrete elements method (DEM) is a computational method used to describe the movement of a large number of particles of different sizes and shapes, which interact through a contact model. Among other applications, the DEM is used as an effective way of addressing engineering problems to model the behavior of granular materials, mechanics of dust and rocks. In the field of mining, the DEM has been used mainly to predict the trajectory of the material inside SAG mills and in chutes of mineral transfer [1]. Within the applications of interest in this area, there is also the modeling of wear. There are many processes where wear limits the life of equipment, affecting its productivity and operating costs. However, no calculations that predict the wear of the enclosing walls have been performed to date. After an extensive review of the literature, a methodology to predict wear via DEM and phenomenological wear models has been developed. The decision was taken to use Archard's model [2], one of the simplest yet most accurate models proposed to date in the context of DEMs. The Archard model was used to predict the rate and the wear pattern on a structural steel plate A37-24 ES under different granulometry conditions of copper ore. One of the key stages is the correct characterization of the granular medium in order to be able to calibrate the numerical model. The numerical results obtained to date show a correct behavior with respect to the experimental values, which allows to establish that the model can to predict the phenomenon of abrasive wear and to compute realistic wear patterns. [1] P. Cleary, Modelling comminution devices using DEM; Int. J. Numer. Anal. Methods Geomech. 25, 83–105, 2001. [2] J.F. Archard, Contact and Rubbing of Flat Surfaces; J. Appl. Phys. 24, 981-988, 1953.

Effects of Microstructural and Production Inhomogeneities on the Macroscopic Behavior of Dual Phase Steels

Semih Perdahcioglu*, Erkan Asik**, Ali Torkabadi***, Ton Van den Boogaard****

*University of Twente, **University of Twente, ***University of Twente, ****University of Twente

ABSTRACT

It is well established that microstructural inhomogeneities such as crystal orientations, grain boundaries and second phase particles play a direct role on the macroscopic mechanical behavior of materials. The statistical distribution of these inhomogeneities however is equally important as it results in a microscopic distribution of mechanical quantities such as strain and stress fields. Using a lower order gradient enhanced crystal plasticity approach and realistic but computer generated microstructures representing a class of multiphase steels the effect of material as well as production induced inhomogeneity distributions is studied. The adopted crystal plasticity framework is rate-independent elastoplastic with gradient enhancement enforced at the finite element mesh using a staggered approach that makes it applicable directly to many commercial software packages efficiently. The production route is simulated by generating solid state phase transformations with volumetric mismatch which results in local stress fields as well as GNDs. Further steps in production such as discrete rolling operations are applied as simplified boundary conditions on the same RVE. It is shown that many relevant macroscopic phenomena such anelasticity and Bauschinger effect can be observed when a sufficiently accurate mechanical history of the material is taken into account in terms of stress and GND distributions. Furthermore a Mean-Field homogenization approach is adopted to incorporate these distributions in a statistical manner in order to reproduce the aforementioned phenomena directly using simple phenomenological constitutive models for material fractions. To this end, a multiphase self-consistent elastoplastic framework is utilized. The results show that the distributions that occur as a result of production deformations as well as microstructural inhomogeneities play a significant role in dictating the macroscopic behavior of this class of materials.

Physics Informed Neural Networks

Paris Perdikaris*, Maziar Raissi**

*University of Pennsylvania, **Brown University

ABSTRACT

We introduce physics informed neural networks – neural networks that are trained to solve supervised learning tasks while respecting any given law of physics described by general nonlinear partial differential equations. In this two part treatise, we present our developments in the context of solving two main classes of problems: data-driven solution and data-driven discovery of partial differential equations. Depending on the nature and arrangement of the available data, we devise two distinct classes of algorithms, namely continuous time and discrete time models. The first form a new class of data-efficient spatio-temporal function approximators, while the latter allow the use of arbitrarily accurate Runge-Kutta time stepping schemes with up to 500 stages. Their effectiveness is demonstrated through a collection of classical problems in fluids, quantum mechanics, and reaction-diffusion systems.

Advances in the Approximation Theory for Functional Reconstructions Using GMLS and Applications to Meshless Discretization of Differential Equations

Mauro Perego^{*}, Paul Kuberry^{**}, Pavel Bochev^{***}, Peter Bosler^{****}, Nathaniel Trask^{*****}, Kara
Peterson^{*****}

^{*}Sandia National Laboratories, ^{**}Sandia National Laboratories, ^{***}Sandia National Laboratories, ^{****}Sandia
National Laboratories, ^{*****}Sandia National Laboratories, ^{*****}Sandia National Laboratories

ABSTRACT

In this talk we present existence and approximation results for the reconstruction of a few classes of linear functionals, including differential and integral functionals, using the Generalized Moving Least Square (GMLS) method. These results extend or specialize classical GMLS theoretical results, and they rely both on the classic approximation theory for finite elements and on existence/approximation results for scattered data. In particular, we will consider the reconstruction of vector fields in Sobolev spaces and, more in general, the reconstruction of differential k-forms. We show how these results can be applied, in a rather straightforward way, to a variety of meshless schemes such as staggered stable discretizations for local/nonlocal diffusion and elasticity problems.

A Mixed-Mode Delamination Model Accounting for Large Openings and Fiber-Bridging

Umberto Perego*, Federica Confalonieri**

*Politecnico di Milano, **Politecnico di Milano

ABSTRACT

When large openings or extensive fiber-bridging phenomena are involved, classical cohesive models formulated under the assumption of small relative displacements often fail to predict the delamination growth. In the presence of large openings, the rotational equilibrium of the cohesive element is not satisfied [1], while the development of large scale fiber-bridging sensibly enhances fracture energy [2]. This effect, mainly governed by the normal opening, has been experimentally observed in several DCB tests performed on fiber-reinforced composites and is described in terms of R-curves, expressing the progressive growth of the toughness up to a steady-state value. In this work the isotropic damage cohesive model formulated in [3] under the assumption of small openings is extended to properly model both the cases of small and large openings and the presence of large-scale bridging or interfacial fibrillation. The considered cohesive model is specifically conceived for the case of mixed-mode delamination with variable mode ratios. Since the fiber bridging is mainly induced by mode I loading conditions, two distinct traction-separations laws are introduced for Mode I and II. A classical bilinear traction-separation law is adopted in pure Mode II, while the traction separation law in pure Mode I is, instead, characterized by a trilinear softening branch, consisting of an initial linear branch, followed by a plateau and by a second linear branch up to complete decohesion. Assuming that the fiber bridging occurs when the plateau is reached allows formulating a simple activation criterion that can be generalized also to mixed-mode conditions. To account for the transition from small to large openings, the classical interface element is substituted with a fibril element, whose constitutive behaviour is defined such that no discontinuity in the dissipated energy or in the transmitted cohesive tractions is introduced. As shown in [2], this kind of elements is able to account for large openings in a consistent way, since the interface tractions and openings are colinear. [1] Vossen, Schreurs, van der Sluis, Geers, On the lack of rotational equilibrium in cohesive zone elements, *Computer Methods in Applied Mechanics and Engineering*, 254, 146-153 (2013) [2] Dávila, Rose, Camanho, A procedure for superposing linear cohesive laws to represent multiple damage mechanisms in the fracture of composites, *International Journal of Fracture*, 158, 211-223 (2009) [3] Confalonieri, Perego, A mixed-mode cohesive model for delamination with isotropic damage and internal friction, *Proceedings of the sixth ECCOMAS Thematic Conference on the Mechanical Response of Composites* (2017)

Buckling of Viscoplastic Bingham Fluid Filaments under Compression Stresses

Anselmo Pereira^{*}, Mehdi Khalloufi^{**}, Elie Hachem^{***}, Romain Castellani^{****}, Rudy Valette^{*****}

^{*}Université Paris Sciences et Lettres (PSL), MINES ParisTech, Centre de Mise en Forme de Matériaux (CEMEF), 1 Rue Claude Daunesse, 06904 Sophia Antipolis, France, ^{**}Université Paris Sciences et Lettres (PSL), MINES ParisTech, Centre de Mise en Forme de Matériaux (CEMEF), 1 Rue Claude Daunesse, 06904 Sophia Antipolis, France, ^{***}Université Paris Sciences et Lettres (PSL), MINES ParisTech, Centre de Mise en Forme de Matériaux (CEMEF), 1 Rue Claude Daunesse, 06904 Sophia Antipolis, France, ^{****}Université Paris Sciences et Lettres (PSL), MINES ParisTech, Centre de Mise en Forme de Matériaux (CEMEF), ^{*****}Université Paris Sciences et Lettres (PSL), MINES ParisTech, Centre de Mise en Forme de Matériaux (CEMEF), 1 Rue Claude Daunesse, 06904 Sophia Antipolis, France

ABSTRACT

Fluid buckling instabilities represent a major source of irregularities for several industrial and natural processes such as container filling, glass plate fabrication and folding of geological structures. Despite some recent and significant works regarding such instabilities in Newtonian fluids, the buckling of non-Newtonian materials remains scarcely explored in the literature. In the present work, we analyse through scaling laws and direct numerical simulations the buckling of filaments of a viscoplastic Bingham fluid compressed at constant velocity by two parallel plates. Under low gravity conditions (the Laplace pressure exceeds the hydrostatic pressure), three regimes are observed for slender filaments: a first one driven by the capillary force and during which there is no deflection and a folding regime that is dominated by the compressive viscous force and for which the inertia is negligible, as found by Le Merrer, Quéré and Clanet [PRL 109, 064502 (2012)]; and a twist/coil regime appearing at larger Reynolds number. Introducing a yield stress induces localization that restricts the buckled flow dimensions. Our main results are summarized in a four-dimensional phase diagram whose axes are a slenderness parameter, capillary number, Reynolds number and Bingham number.

An Asynchronous Task-Based Parallelization Strategy for Multiscale Solid Mechanics

J. Antonio Perez^{*}, Jeremiah Wilke^{**}, David Littlewood^{***}, Janine Bennett^{****}, David Hollman^{*****}, Jonathan Lifflander^{*****}

^{*}University of New Mexico and Sandia National Laboratories, ^{**}Sandia National Laboratories, ^{***}Sandia National Laboratories, ^{****}Sandia National Laboratories, ^{*****}Sandia National Laboratories, ^{*****}Sandia National Laboratories

ABSTRACT

Concurrent multiscale approaches for solid mechanics combine the use of a low-cost macroscale model, applied over the bulk of the domain, with a high-cost, high-fidelity model operating at a lower length scale. This combination of modeling approaches with vastly different computational expenses and memory requirements greatly complicates the management of tasks within a parallel simulation code. Recent work in Asynchronous Many-Task (AMT) scheduling provides a framework for multiscale mechanics that addresses this complexity through a task-based programming model and a flexible, highly-scalable runtime environment. In this presentation, we explore the use of the DARMA AMT programming model within a FE-squared multiscale mechanics code [1]. The FE-squared approach, which associates independent mesoscale finite-element problems with material points in the macroscale model, is naturally compatible with AMT scheduling on next-generation, heterogeneous computing platforms. We first review the implementation of a traditional parallelization strategy based on direct application of the MPI programming model, which illustrates the challenges of parallelization and provides a performance baseline. We then present an alternative parallelization approach based on AMT. In this approach, the software design follows a paradigm that compartmentalizes work in a set of tasks with explicitly-defined interdependencies. Applied in combination with an overdecomposition strategy, the task-based model enables the AMT runtime to execute work asynchronously and to migrate work among hardware resources to accommodate load-balancing requirements that may evolve over time. We present example simulations for single-scale and multiscale solid mechanics that span a range of computational expense and load-balancing requirements. Results obtained using AMT scheduling are compared against those obtained using traditional parallelization to illustrate both the advantages and the challenges associated with AMT scheduling for computational mechanics. [1] J. Bennett, M. Bettencourt, R. Clay, H. Edwards, M. Glass, D. Hollman, H. Kolla, J. Lifflander, D. Littlewood, A. Markosyan, S. Moore, S. Olivier, J. Perez, E. Phipps, F. Rizzi, N. Slattengren, D. Sunderland, and J. Wilke. ASC ATDM level 2 milestone #6015: Asynchronous many-task software stack demonstration. Report SAND2017-9980, Sandia National Laboratories, Albuquerque, NM and Livermore, CA, 2017.

Stochastic Partial Linearization Approach for Nonlinear Reduced Order Models of Thin Panels

Ricardo Perez^{*}, Benjamin Smarslok^{**}, Marc Mignolet^{***}

^{*}Universal Technology Corporation, ^{**}U.S. Air Force Research Laboratory, ^{***}Arizona State University

ABSTRACT

Finite element analysis (FEA) of the dynamic response of aircraft panels in extreme aeroacoustic environments requires substantial computational resources, which has led to numerous research efforts on the development of nonlinear reduced order models (ROMs). ROMs reduce the finite element model to a low-order system of nonlinear modal-like equations which can be integrated in the time domain [1]. Although much more computationally efficient than FEA, it may still be expensive to build and solve the ROM equations of motion for large structures (i.e., built-up panels) owing to the large number of nonlinear terms involved [2]. The proposed approach seeks to further reduce the computational cost by building a sparse ROM that only includes the nonlinearity in the dominant modes of the basis. The methodologies stem from previous observations that only a subset of the modes in the basis are dominant [2], while the rest of them respond significantly less to the loading or are parametrically excited by nonlinear coupling with the most important modes. Yet, the contributions of the non-dominant modes cannot simply be ignored without unduly affecting the accuracy of the predictions. Their small level of response has however suggested that the nonlinear terms involving them may be neglected, a process referred to here as partial linearization. The selection of the number of dominant modes can be made as aggressively or conservatively as desired (i.e., as many or as few) leading to a varying tradeoff between degree of accuracy of the solution and computational cost. The solution approximation error introduced by this process is recognized as an epistemic uncertainty, which is modeled by randomizing the linear stiffness terms of the non-dominant modes. The nonparametric stochastic approach [3] is adopted for this modeling and its uncertainty level is estimated using maximum likelihood estimation. The approach is verified on the ROM of a 96,000 degrees-of-freedom, 9-bay panel, where significant computational gains are observed for dynamic simulations. [1] Mignolet, M.P., Przekop, A., Rizzi, S.A., and Spottswood, S.M., "A Review of Indirect/Non-Intrusive Reduced Order Modeling of Nonlinear Geometric Structures," *Journal of Sound and Vibration*, Vol. 332, 2013. [2] Perez, R., Wang, X.Q., and Mignolet, M.P., "Non-Intrusive Structural Dynamic Reduced Order Modeling for Large Deformations: Enhancements for Complex Structures," *Journal of Computational and Nonlinear Dynamics*, Vol. 9, 2014. [3] Soize, C., "Stochastic linearization method with random parameters for SDOF nonlinear dynamical systems: prediction and identification procedures," *Probabilistic Engineering Mechanics*, Vol. 10, 1995.

Bayesian Identification of the Random Elasticity Field of a Heterogeneous Microstructure

Guillaume Perrin*, Christian Soize**

*cea, **Université Paris-Est

ABSTRACT

This paper presents a statistical inverse method for identifying the mechanical properties of a heterogeneous microstructure, which is modeled by a random elastic media. To this end, several experimental tests are performed on a series of specimens made of the same material. For each experiment, the applied force field is supposed to be imposed, and the induced displacement field is measured on the contours of the specimens only. In parallel, for given properties of the random media, it is possible to simulate independent realizations of the elasticity random field, and to approximate (using the Finite Element Method) the displacements that are induced by the experimental force field. Based on the comparison of the statistical properties of the displacement fields on the contours of the specimens in the experimental and the simulated cases, a method is thus proposed to identify the most likely properties of the random media characterizing the heterogeneous microstructure (such as the mean elasticity field, the dispersion and the correlation lengths). It should be noted that the elasticity field is not a real-valued random field, but a tensor-valued random field, and that the different components of this random field cannot be identified separately due to algebraic constraints. Additionally, the quantity of interest on which the identification procedure is based is not a scalar, but a high-dimension vector. This requires the introduction of dedicated reduction techniques. Last but not least, the number of code evaluations that is generally required for the identification procedure can quickly become burdensome. To circumvent this problem, statistical extrapolation techniques and iterative procedures will be presented to maximize the precision of the identification at a reduced computational cost. Validations of the procedure are eventually presented using simulated data in two and three dimensions.

Modeling of Laser Powder Bed Fusion Additive Manufacturing Using The eXtended Discrete Element Method (XDEM)

Bernhard Peters*, Mehdi Baniasadi**, Maryam Baniasadi***

*Université du Luxembourg, **Université du Luxembourg, ***Université du Luxembourg

ABSTRACT

The production of parts via laser powder bed fusion additive manufacturing (LPBF-AM) of metallic powders is growing exponentially. LPBF-AM involves complex physical processes such as the laser interaction with the bed, powder bed melting, solidification, the melt formation, and Marangoni effect. The bed structure can significantly affect the local heat transfer, fluid formation, and the porosity distribution. The shape and surface of the transient fluid flow along with its internal porosity distribution will form the final product. Therefore, the final product quality is a strong function of all the above-mentioned parameters. In order to be able to model the bed structure along with the melt formation, the combined continuous-discrete methods are of interest. The eXtended Discrete Element Method known as XDEM [1,2] an advanced numerical tool based on discrete-continuous concept able to address the thermophysical phenomena involved during laser powder bed fusion is presented. Within this platform, the continuous phases such as gas and liquid phases are coupled to the discrete entities such as powders through mass, momentum and energy exchange. It can predict the position, temperature distribution and phase change for each particle in conjunction with each fluid phases' temperature, velocity, and volume fraction. In this contribution, the XDEM is used as an alternative approach for laser powder bed fusion additive manufacturing of metallic powders. To this aim, a bed of powders is constructed and a moving heat source representing the laser will melt the exposed powders and the melt phase will form. In this concept, the melting and shrinking of the powders, as well as the formation of the melt pool and heat transfer, are well studied. References [1] Mehdi Baniasadi, Maryam Baniasadi, Bernhard Peters, Coupled CFD-DEM with Heat and Mass transfer to Investigate the Melting of a Granular Packed Bed, doi:10.1016/j.ces.2017.12.044. [2] Bernhard Peters, Gabriele Pozzetti, Flow characteristics of metallic powder grains for additive manufacturing, The European Physical Journal Conferences, 2017, doi:10.1051/epjconf/201714013001.

A Divergence-Conforming Hybridized Discontinuous Galerkin Method for the Incompressible Reynolds Averaged Navier-Stokes Equations

Eric Peters*, John Evans**

*University of Colorado Boulder, **University of Colorado Boulder

ABSTRACT

We introduce a hybridizable discontinuous Galerkin method for the incompressible Reynolds Averaged Navier-Stokes equations coupled with the Spalart-Allmaras one equation turbulence model for the scalar eddy viscosity. With a special choice of velocity and pressure spaces for both element and trace degrees of freedom, we arrive at a method which returns point-wise divergence-free velocity fields and properly balances momentum and energy at an element-level. We further demonstrate how to directly enforce a non-negativity constraint on the eddy viscosity field without loss of accuracy through the intelligent utilization of constrained optimization. Finally, we examine the use of different polynomial degrees and meshes for the flow and turbulence variables to most efficiently represent the flow field (which is typically smooth) and the eddy viscosity (which is typically rough). As is standard with hybridized discontinuous Galerkin methods, static condensation can be employed to remove the element degrees of freedom and thus dramatically reduce the global number of degrees of freedom. Numerical results illustrate the effectiveness of the proposed methodology both in the case of no turbulence model as well as in the case of the Spalart-Allmaras turbulence model.

Explicit Partitioned Methods for Multiphysics Coupling

Kara Peterson^{*}, Pavel Bochev^{**}, Paul Kuberry^{***}

^{*}Sandia National Laboratories, ^{**}Sandia National Laboratories, ^{***}Sandia National Laboratories

ABSTRACT

Complex multiphysics applications often require the efficient and stable coupling of individual codes or separately meshed regions through non-matching interfaces. A characteristic example of this type of coupling occurs between atmospheric and ocean codes in global Earth system models where conservation of fluxes as they are passed between the different code discretizations is crucial. In this talk we describe an explicit Lagrange multiplier-based interface coupling method and its application to advection-diffusion equations and to a simplified ocean/atmosphere system. To obtain a Lagrange multiplier formulation that is fully compatible with explicit time integration we consider a coupling condition which enforces the continuity of the time derivatives of the states across the interface. Assuming that the initial data are continuous across the interface, this alternative coupling condition implies continuity of the state while enabling a fully explicit treatment. For the explicit partitioned method we compute the Lagrange multiplier directly and use it for boundary data in partitioned solves on each domain. Numerical results for advection-diffusion equations demonstrate the stability of the formulation and second-order convergence in both the advection and diffusion dominated regimes.

DPG Multigrid Solvers for High Frequency Time-harmonic Wave Propagation Problems

Socratis Petrides*, Leszek Demkowicz**

*Institute for Computational Engineering and Sciences, UT Austin, **Institute for Computational Engineering and Sciences, UT Austin

ABSTRACT

We present a novel adaptive DPG multigrid (MG) solver for the solution of high-frequency wave propagation problems in both two and three space dimensions. In stark contrast to traditional MG methods, this solver operates only on the trace variables defined on the mesh skeleton. Since trace variables supported on new faces created upon h-refinements have no predecessors, coarse grid basis functions have no fine grid representatives. Thus, an auxiliary mesh is constructed by statically condensing these trace variables. Therefore, communication between meshes involves both an inclusion and a Schur complement extension operator. True to the DPG spirit, this solver is applicable to a general class of second order problems, cast in any DPG formulation. However, in this talk we focus on high-frequency wave propagation problems with localized solutions (e.g. simulation of Gaussian beams). For very large wavenumbers, h^p -adaptivity is crucial in order to keep the computational cost and the memory requirements under control. The DPG unconditional mesh-independent discrete stability and its built-in error indicator provide efficient and reliable adaptive mesh refinements starting from very coarse meshes. The need for iterative solvers, comes from the fact that the problem has to be solved several times throughout the adaptive procedure. Employing a direct solver, at every adaptive step is far from optimal and unnecessary. We use the aforementioned multigrid technology as a preconditioner for the Conjugate Gradient method. The resulting iterative solution scheme is employed in order to produce partially converged solutions, accurate enough to drive the adaptive refinements. Our results show convergence in terms of iterations at a rate independent of the mesh and the wavenumber. The efficacy of the above construction (in the two-grid case) has already been demonstrated for high-frequency acoustics problems in 2D in [1]. [1] Petrides, S. and Demkowicz, L. (2017). An Adaptive DPG Method for High Frequency Time-harmonic Wave Propagation Problems. Comput. Math. Appl.

An Experimental and Numerical Study of Deformation and Decohesion Mechanisms During Peel Testing of a Laminate Packaging Material

Simon Pettersson^{*}, Stephen Hall^{**}, Jonas Engqvist^{***}, Håkan Hallberg^{****}, Nils Toft^{*****}

^{*}Lund University, ^{**}Lund University, ^{***}Lund University, ^{****}Lund University, ^{*****}Tetra Pak Packaging Solutions AB

ABSTRACT

The material used in packages for the food and dairy industries comprise multiple laminate layers, each serving different purposes in preserving and protecting the package content and by providing the appropriate package rigidity during handling. Already during package manufacturing and filling, the package material is subject to large deformations and a range of thermal and chemical processes that sometimes cause delamination between the laminate layers. This, in turn, can lead to a reduced product shelf lifetime and unsatisfactory package performance. In addition, controlled delamination can also be a required material property, for example in the case of package folding or opening mechanisms. Aspects like these emphasize a great need for increased understanding of adhesion and for the ability to predict adhesion properties of different packaging materials and under different handling conditions. In order to quantify the delamination strength, more or less standardized peel tests are often employed. In such tests, a laminate layer is partly separated to provide the peel arm which is pulled off from the substrate layer(s) at a constant angle. The required peel force is measured along with the peel arm deformation and provides a measure of the delamination strength of the laminate package material. However, the measured force is not only the force component required to separate the layers, but it is also due to deformation of the peel arm and possibly also additional deformation mechanisms in the substrate layer(s). Therefore, not only the cohesive bond between individual laminate layers, but also the properties of the individual laminate layers themselves must be properly characterized. In the present work, peel test experiments have been conducted and the peel force and displacement as well as the peel arm geometry have been monitored. The same peel test has also been studied by numerical simulations using a cohesive zone modeling framework. The influence of the cohesive model formulation and the choice of constitutive model for the peel arm material are investigated in relation to the experimental observations and different delamination mechanisms are observed.

Computational Modelling of Carotid Atherosclerotic Plaque Formation and Development on Patient-specific Geometries

Estefania Peña*, Patricia Hernández**, Myriam Cilla***, Miguel A. Martínez****

*Aragón Institute of Engineering Research (I3A), University of Zaragoza, Zaragoza, Spain; CIBER de Bioingeniería, Biomateriales y Nanomedicina (CIBER-BBN), Zaragoza, Spain, **Mechanical Engineering Department, University of Zaragoza, Zaragoza, Spain, ***1. Centro Universitario de la Defensa. Academia General Militar, Spain; Aragón Institute of Engineering Research (I3A). University of Zaragoza, Spain; Centro de Investigación Biomédica en Red de Bioingeniería Biomateriales y Nanomedicina (CIBER-BBN), Spain, ****Aragón Institute of Engineering Research (I3A), University of Zaragoza, Zaragoza, Spain; CIBER de Bioingeniería, Biomateriales y Nanomedicina (CIBER-BBN), Zaragoza, Spain

ABSTRACT

Atherosclerosis is the process in which atheroma plaques are built up in the walls of the arteries causing narrowing, hardening of the arteries and loss of elasticity. Cyclic stretch, laminar and oscillatory shear stress, effects of vessel compliance, curvature, pulsatile blood flow or cardiac motion are considered the main triggers of atherosclerosis initiation. The location of atherosclerosis is associated with flow separation and turbulence. Therefore, many studies have identified haemodynamic shear stresses as an important determinant of endothelial function and phenotype in atherosclerosis disease. We propose a mathematical model of atheroma plaque initiation and early development in carotid arteries. Our current approach is on the process on plaque initiation and intimal thickening rather than in severe plaque progression and rupture phenomena. This model uses the Navier–Stokes equations and Darcy's law for fluid dynamics, convection–diffusion–reaction equations for modelling the mass balance in the lumen and intima, and the Kedem–Katchalsky equations for the interfacial coupling at membranes, i.e. endothelium. The volume flux and the solute flux across the interface between the fluid and the porous domains are governed by a three-pore model. The main species and substances which play a role in early atherosclerosis development have been considered in the model, i.e. LDL, oxidized LDL, monocytes, macrophages, foam cells, smooth muscle cells, cytokines and collagen. This model has been applied to model the plaque formation patient-specific geometries of carotid artery where the atherosclerotic plaque has been removed in order to validate the mathematical framework. Our results for plaque localization correspond to low shear stress zone and the plaque location is compared with the patient-specific geometries with atheroma. References M. Cilla, E. Peña, and M. A. Martínez. Mathematical modelling of atheroma plaque formation and development in coronary arteries. *J. R. Soc. Interface* 11:201308661–2013086616, 2014. U. Olgac, V. Kurtcuoglu, and D. Poulikakos. Computational modeling of coupled blood-wall mass transport of LDL: effects of local wall shear stress. *Am. J. Physiol. Heart Circ. Physiol.* 294(2):909–919, 2008. Acknowledgements Support from the Spanish Ministry of Economy and Competitiveness through the research projects DPI2016-76630-C2-1-R.

Layer-specific Failure Mechanics of Thoracic and Abdominal Aorta and Related Constitutive Modeling

Juan A. Peña*, Miguel A. Martínez**, Estefanía Peña***

*Department of Management and Manufacturing Engineering, Faculty of Engineering and Architecture University of Zaragoza, Spain, **Aragón Institute of Engineering Research (I3A), Mechanical Engineering Department University of Zaragoza, Spain, ***Aragón Institute of Engineering Research (I3A), Mechanical Engineering Department University of Zaragoza, Spain

ABSTRACT

Mechanical force at the tissue level leads to local stress concentrations within the tissue, and, if high enough, starts damaging it at specific spots. In healthy tissues at physiological stress levels, healing continuously repairs such defects to maintain the tissue's structural integrity. Despite increasing experimental and analytical efforts to investigate failure-related irreversible effects of soft biological tissue, the underlying mechanisms are still poorly understood. The goal of this study was characterize the failure properties of the intact wall and each separated layer (intima, media and adventitia) of the descending thoracic and infrarenal abdominal aorta and to test the hypothesis that the failure properties of layer-separated thoracic arteries differ depending on arterial location in the aorta (Peña et al. 2015). To test this hypothesis, we performed uniaxial tests to study the mechanical behavior of both intact and layer-separated porcine aortic tissue samples taken from descending thoracic and infrarenal abdominal aorta until complete failure. The damage behavior required a continuum damage theory commonly used to describe the softening of soft tissues under large deformations. The structural model here presented was built within the framework of nonlinear continuum mechanics (Calvo et al. 2007). Tissue damage was simulated considering different damage behaviors for the matrix and the fibers. We reported values of constitutive parameters using the damage model that can be used by biomedical engineers for investigating better therapies and developing artery-specific devices. References Calvo, B., Peña, E., Martínez, M.A., Doblaré, M., 2007. An uncoupled directional damage model for fibered biological soft tissues. Formulation and computational aspects. *Int. J. Numer. Meth. Eng.* 69, 2036–2057. Peña, J.A., Martínez, M.A., Peña, E., 2015. Layer-specific residual deformations and uniaxial and biaxial mechanical properties of thoracic porcine aorta. *J. Mech. Behav. Biomed.* 50, 55–69. Acknowledgements Support from the Spanish Ministry of Economy and Competitiveness through the research projects DPI2016-76630-C2-1-R and the Instituto de Salud Carlos III (ISCIII) through the CIBER initiative.

Incremental POD and Custom Integration Schemes for Hyper-reduced Automotive Crash Analysis

Pierre Phalippou^{*}, Piotr Breitkopf^{**}, salim bouabdallah^{***}, pierre villon^{****}

^{*}Altair/UTC, ^{**}UTC, ^{***}Altair, ^{****}UTC

ABSTRACT

Industrial usage of numerical math-based tools such as the finite element method may in some applications become prohibitive due to the computational cost. This is particularly true in the automotive sector when optimizing the shape of a vehicle in crash situations. Model Order Reduction addresses this issue. Most model order reduction methods rely on the construction of a reduced basis to project the model on. The Proper Orthogonal Decomposition (POD) builds a modal basis from solution observations called snapshots. Data are in a first stage taken from full order model runs and then processed in a so-called 'off-line phase' to give the reduced basis which is then used to build the reduced model. Some difficulties arise in the POD. In industrial applications, the data generated in the observation phase may become huge and hard to manipulate. Moreover, the computational cost for post-processing this data may as well explode. Another issue concerns the numerical integration schemes, i.e. the position of numerical integration points and the integration weights. The incremental Singular Value Decomposition originates from streamed visual content. This method is based on rank one modifications of a given matrix decomposition. In the POD framework it allows post-processing observations as soon as they are available. This method leads to memory savings and possible computational savings during the 'off-line phase', as data are not kept in memory and redundant or nonrelevant observations are automatically rejected by the method. Another benefit of this method is the ease to manipulate the POD basis by adding new observations or removing others. For the integration of internal forces, we propose a reduced integration scheme, with integration sites and weights obtained as the solution of a Linear Programming problem. This allows us to add to the training set additional constraints such as an exact integration of monomials or of other explicit base functions. The proposed approach has been implemented in ALTAIR's solver RADIOSS® and applied to a structural impact problem. Results regarding computation time, developed features such as estimation of the Reduced Basis error of approximation as well as visual representations illustrate this work. The presentation will focus on the integration of such approach in the whole reduction process, highlighting the attractiveness of the method as well as the required developments to make the whole reduction process incremental.

The Web Force-Field (WebFF) Project: Ontology Based Force-field Repository for Soft Materials at Multiple Levels of Granularity

Frederick Phelan Jr.*, Huai Sun**

*NIST, **Shanghai Jiao Tong University

ABSTRACT

In this talk, we will describe WebFF, an open and extensible force-field repository, designed to support the Materials Genome Initiative (MGI) for organic and related soft materials. The repository is built using the NIST Materials Data Curation System (MDCS). The MDCS has a web-based interface built on top of the RESTful API and a NoSQL database system to support ontology based database descriptions using XML schema. Users interact with the repository through two main portals. The Data Curation Portal supports upload of published force-field data with appropriate metadata descriptors to support provenance based data sharing. New datasets may be curated interactively or using a python based toolset to upload large datasets en masse. The User Portal supports search for curated force-field data based on the metadata descriptors and download in a number of common formats. The initial release of the repository will feature a number of integrated XML schemas. The first schema supports Class I organic force-fields in such as OPLS, Amber and CHARMM style representations. The second supports Class II style force-fields such as CFF, PCFF, COMPASS and TEAMFF. We have also developed a schema for representing a wide range of coarse-grained force-field data ranging from united-atom style models to tabulated potentials. The methods, requirements and goals of force-field data sharing, and the plan for extending the initial repository to include other classes of force-field data will also be described.

Modeling the Nonlinear Response of Complex Periodic Truss Lattices Using a Modified Quasicontinuum Method

Greg Phlipot^{*}, Dennis Kochmann^{**}

^{*}California Institute of Technology, ^{**}ETH Zurich

ABSTRACT

Recently, there has been significant interest in periodic truss lattices down to the micro- and nanoscales, but the computational modeling of these metamaterials remains a challenge due to the fine scale of the truss architecture and the resulting large numbers of truss members to be modeled. In this talk, we model periodic truss lattices using an extension of the quasicontinuum (QC) method [1]: a multiscale tool originally designed to significantly reduce the computational cost of atomic lattice simulations, which has recently been extended to model simple (Bravais) truss lattices and fiber networks with inelasticity and failure [2]. The QC method is a set of interpolation and energy approximation rules that allows for full resolution of the microstructure to be obtained in areas of interest, while drastically reducing the number of degrees of freedom by coarse-graining in areas requiring less resolution. We present results from a new, fully-nonlocal formulation of the QC method capable of modeling the nonlinear response of more general three-dimensional periodic truss (multi)lattices that uses an optimal summation rule [3] to approximate the total energy of the system. Corotational beam elements are used to capture the geometric nonlinearities on the microscale, while the degrees of freedom of the beams are linearly interpolated in coarse-grained regions. Adaptive mesh refinement is also used, which allows us to expand the fully-resolved region as necessary to accurately capture local nonlinear phenomena. Importantly, this approach does not rely upon a separation of scales and is thus a powerful tool to bridge across scales in a concurrent manner. References: [1] E.B. Tadmor, R. Phillips, M. Ortiz, "Mixed atomistics and continuum models of deformation in solids", *Langmuir*, v. 12, p. 4529-4534, 1996. [2] L.A.A. Beex, R.H.J. Peerlings, M.G.D. Geers, "A multiscale quasicontinuum method for dissipative lattice models and discrete networks", *Journal of the Mechanics and Physics of Solids*, v. 64, p. 154-169, 2014. [3] J. S. Amelang, G. N. Venturini, and D. M. Kochmann, "Summation rules for a fully nonlocal energy-based quasicontinuum method," *J. Mech. Phys. Solids*, 2015.

An Adaptive Method to Verify the Lack of Collision Between Solid Bodies in a 2D Incompressible Viscous Flow

Marco Picasso^{*}, Samuel Dubuis^{**}, Peter Wittwer^{***}

^{*}Institute of Mathematics, EPFL, Switzerland, ^{**}Institute of Mathematics, EPFL, Switzerland, ^{***}Department of Theoretical Physics, University of Geneva, Switzerland

ABSTRACT

Our goal is to check numerically a Theorem of Hillairet (Communications in Partial Differential Equations 32(9) 2007) which states that a solid body falling in a constant-density incompressible viscous fluid cannot reach the bottom of the cavity in finite time. A penalty method is used to formulate the fluid flow problem in the whole cavity, thus avoiding the solid-liquid interface to be tracked explicitly. However, an adaptive method in space and time is advocated, the error indicators in space and time being derived on simplified problems. Space adaptivity requires the use of anisotropic finite elements. Numerical experiments indeed show that the solid body does not reach the bottom of the cavity in finite time.

Strain Control via Level Set Topology Optimization: An Energy Harvesting Application

Renato Picelli^{*}, Carol Featherston^{**}, H. Alicia Kim^{***}, John McCrory^{****}, Scott Townsend^{*****},
Stephen Grigg^{*****}

^{*}Cardiff University, ^{**}Cardiff University, ^{***}Cardiff University / University of California, San Diego, ^{****}Cardiff University, ^{*****}Cardiff University, ^{*****}Cardiff University

ABSTRACT

Topology optimization has been previously applied to manipulation of displacements (compliant mechanisms) and failure (stress isolation), but not to strain control. This work formulates a level set topology optimization method to strain integral functions, thus facilitating the manipulation of strain in a specified region of a structure (sub-structure). A general shape sensitivity analysis is developed herein, with the sub-structure considered fixed and the external structure variable. Such a scenario finds use in the design of structural supports for strain-based sensors without a need to optimize the sensor material itself, e.g., piezoelectric skins. Numerical results demonstrate effective strain minimization/maximization for a range of directions. An application of the method to the design of a cantilever beam for use in vibrational energy harvesting is presented. The piezoelectric device is located in the sub-structure, with the surrounding beam shape designed to maximize the strain caused by ambient vibrations in a predefined frequency range. Experimental results show excellent agreement regarding location of natural frequencies and relative magnitude of harvested power.

A Practical Finite Element Method to Include Osmotically Induced Prestretch\Prestress in Image-Driven Simulations of Cartilage

David M. Pierce^{*}, Xiaogang Wang^{**}, Thomas S.E. Eriksson^{***}, Tim Ricken^{****}

^{*}University of Connecticut, ^{**}University of Connecticut, ^{***}FOI – Swedish Defense Research Agency, ^{****}Stuttgart University

ABSTRACT

Medical imaging, e.g. MRI, is generally performed in vivo, hence finite element (FE) models constructed from medical images of cartilage represent geometries under Donnan osmotic loading even when the articulating joint is physically unloaded. Thus, an osmotically induced stretch/stress exists prior to constructing the geometry of the FE model, and we refer to it as prestretched/prestressed. When applying classical modeling approaches to patient-specific simulations of cartilage a theoretical inconsistency arises: the in-vivo imaged geometry (used to construct the model) is not an unloaded, stress-free reference configuration. Furthermore, cartilage specimens removed from the joint and placed into a physiological bathing solution, are commonly in this equilibrium state, and thus mechanical testing commonly occurs on prestretched/prestressed specimens. If one assumes that the resulting experimental data begin from a stress-free reference configuration when fitting nonlinear constitutive models that include osmotic swelling (to obtain material parameters) the fitted stress-strain relationship (parameters) obtained will actually describe a different behavior. The objectives of this study are two-fold: (1) to establish practical computational method to include osmotically induced prestretch in image-driven simulations of cartilage; and (2) to investigate (by apply the new methods) the influence of considering the prestretched/prestressed state when fitting fiber-reinforced, biphasic (swelling) constitutive models of cartilage. Towards objective (1) we extend our recent constitutive model for cartilage (Pierce et al., 2016, JMBBE 15:229-244) to include the mechanical effects of osmotic pressure, and determine the prestretched/prestressed state within the solid matrix induced by osmotic loading in the (imaged) initial configuration of the FE model using the backward displacement method (Bols et al., 2013, JCAM 246:10-17) prior to solving boundary value problems of interest. We compare results from simulations with/without including osmotic contributions. Towards objective (2) we fit our new constitutive model for cartilage with/without considering osmotic contributions and considering different initial configurations, and compare the resulting stress-stretch responses and parameters. Our results highlight the importance of determining the prestretched/prstressed state within the solid matrix induced by osmotic loading in the imaged configuration prior to solving boundary value problems of interest. With our new constitutive model and modeling methods, we hope to improve the fidelity of FE-based, patient-specific biomechanical simulations of joints and cartilage. Improved simulations can provide medical researchers with new information often unavailable in a clinical setting, information that may contribute to better insight into the pathophysiology of cartilage diseases. With our new fitting approach, we can also better fit available experimental data.

The Comparison of Parametric and Non-Parametric Estimation of an Uncertainty for Parameters of a Modified Surface Layer

Jacek Pietraszek^{*}, Norber Radek^{**}, Renata Dwornicka^{***}

^{*}Cracow University of Technology, ^{**}Kielce University of Technology, ^{***}Cracow University of Technology

ABSTRACT

The quantitative estimation of an uncertainty is one of the most important issues in the industrial statistics, especially in the design of experiment (DoE) being a source of specific experimental schemes for a quick and effective knowledge acquisition. The classic parametric approach based on the normal distribution is usually applied however it is only very rough approximation of data obtained from the real tests. Since Efron's papers [1, 2], the bootstrap approach is well recognized method for non-parametric estimation of distributions and their statistics including confidence intervals, especially for relatively small datasets where reliable selection of the particular family of distributions is not possible. Decade later, Owen proposed [3] another non-parametric approach based on Wilks's theorem, subsequently extended to the non-parametric maximum likelihood estimation method (NPMLE). The authors conducted the real experiment on a surface layer coated by a wear-resistant material (WC-Cu) and next modified by a laser beam impulse. The modified material is very important for a mechanical engineering and machining due to a longer life-time of parts, especially for friction pairs. The analyzed dataset contained many mechanical and geometrical properties of a such layer, hardness and friction among them. The comparison a classic parametric model and non-parametric approach was performed. The obtained non-parametric results were generally consistent with parametric however some significant differences were observed. The main advantage was the rejection of the arbitrary assumption on a distribution shape. The paper presents obtained results, their discussion, conclusions and guidelines for future works. References: 1. B. Efron: Bootstrap Methods: Another Look at the Jackknife. The Annals of Statistics 7, 1979, pp. 1–26. 2. B. Efron: Bootstrap confidence intervals for a class of parametric problems. Biometrika 72, 1985, pp. 45-58. 3. A.B. Owen: Nonparametric Likelihood Confidence Bands for a Distribution Function. Journal of the American Statistical Association 90, 1995, pp. 516-521.

Prediction of Distribution of Microstructural Parameters in Steels Described by Differential Equations with Recrystallization Term: Two Possible Approaches.

Maciej Pietrzyk^{*}, Paweł Morkisz^{**}, Piotr Oprocha^{***}, Paweł Przybyłowicz^{****}, Danuta Szeliga^{*****}, Jan Kusiak^{*****}

^{*}AGH University of Science and Technology, ^{**}AGH University of Science and Technology, ^{***}AGH University of Science and Technology, ^{****}AGH University of Science and Technology, ^{*****}AGH University of Science and Technology, ^{*****}AGH University of Science and Technology

ABSTRACT

The high strength and elongation of DP (Dual Phase) steels are due to combination of soft ferrite with hard martensite. These steels, however, are characterised by large gradients of properties, which cause poor local formability. Contrary, steels with a more heterogeneous microstructure have superior formability. This leads to a question: is it possible to achieve more balanced properties of multiphase steels by tailoring microstructure gradients? More detailed models of the microstructure are required to answer this question. A hypothesis was made that application of the distribution functions of various internal variables will allow to predict gradients of final product properties. The objective of the paper was to investigate the possibility of multiscale modelling of microstructure evolution based on distribution functions. Thermomechanical FE code was used to describe the macro scale during hot forming. A differential equation describing evolution of dislocation populations was considered as the first approach in the micro scale. This equation is based on K-M model [1] with the dynamic recrystallization introduced in [2]. Numerical solutions of this equation assuming average dislocation density is frequent in the literature. The present work aims at description of evolution of dislocation populations by distribution function and choice of parameters which assure consistency with real process. From mathematical point of view, we look for accurate description of associated Frobenius-Perron operator, representing evolution of densities when considered system evolves in time (see [3]) following the macro scale results. Due to the recrystallization, the underlying differential equation has discontinuous righthand side. Two approaches were considered to deal with this problem. First is to regularize the vector field via sigmoid function and then to apply suitable numerical method for stiff equations. The second is to use Filippov's framework (e.g. see [4]) for discontinuous differential equations together with appropriate numerical scheme based on time stepping or event detection. These two strategies and their utility from material science point of view were compared. Prediction of distribution of microstructural parameters is the main output of the paper.

1. Mecking H., Kocks U.F., Acta Metallurgica, 29, 1981, 1865-1875.
2. Sandstrom R., Lagneborg R., Acta Metallurgica, 23, 1975, 387-398.
3. Lasota A., Mackey M. C., Chaos, fractals, and noise. Stochastic aspects of dynamics. Applied Mathematical Sciences, 97. Springer-Verlag, New York, 1994.
4. Filippov, A. F. Differential equations with discontinuous righthand sides. Mathematics and its Applications (Soviet Series), 18. Kluwer Academic Publishers Group, Dordrecht, 1988.

Stabilized Monolithic FEM for Cahn-Hilliard/Navier-Stokes Equations on Anisotropic Unstructured Meshes

Franck Pigeonneau^{*}, Youssef Mesri^{**}, Rudy Valette^{***}, Elie Hachem^{****}

^{*}Mines-Paristech, CEMEF, ^{**}Mines-Paristech, CEMEF, ^{***}Mines-Paristech, CEMEF, ^{****}Mines-Paristech, CEMEF

ABSTRACT

Two-phase flows are involved in a large range of industrial processes for which the interfacial dynamics plays an important role on the overall behavior. It is particularly true in boiling devices for which the wetting properties on wall are crucial to determine the occurrence of the nucleation process. To investigate this kind of problems, phase-field or diffusive interface approach is chosen to describe the dynamics of two immiscible fluids. Four fields are involved: two for the phase-field (order parameter and chemical potential) and two for the fluid dynamics (pressure and velocity). To solve the Cahn-Hilliard equation which is a bi-harmonic non-linear equation, a coupled method is used to solve two second-order equations stabilized when advection is dominant. When the order parameter and the chemical potential are known, the Navier-Stokes equations are solved using a mixed-formulation stabilized with variational multiscale method. An anisotropic mesh adaptation is also implemented to capture accurately the interface dynamics. The numerical solver is applied to study the capillary rising in a tube, or the drop spreading on a substrate. A comparison with numerical results or with experimental data previously published is provided.

Multiscale Modeling of Notched Composites under Compression with Improved Shear Toughening Through Nano-reinforcement

Evan Pineda^{*}, Gregory Odegard^{**}, Hashim Al Mahmud^{***}, Matthew S. Radue^{****}, Sorayot Chinkanjanarot^{*****}, William Pisani^{*****}

^{*}NASA Glenn Research Center, ^{**}Michigan Technological University, ^{***}Michigan Technological University, ^{****}Michigan Technological University, ^{*****}Michigan Technological University, ^{*****}Michigan Technological University

ABSTRACT

Nano-reinforcement can be utilized to improve the properties of traditional carbon fiber reinforced polymers (CFRPs). One critical design parameter for CFRP structures is the open hole compression (OHC) strength. As the specimen is compressed, initially misaligned fibers rotate, inducing shear stress in the matrix. The shear stress acts to degrade the stiffness of the matrix through micro-cracking which permits further rotation. The interaction between matrix damage and fiber rotation leads to an instability wherein the fibers buckle and a kink band is formed. Thus, OHC failure is a result of micro buckling of the fibers which is primarily governed by the shear toughness of the polymer matrix. As such, nano-particles can be utilized to improve the shear toughness of the matrix, and hence increase the OHC strength of the material system. In this work, graphene nano-platelets (GNPs) are mixed into the resin system to produce nano-reinforced composite panels. The CFRP/GNP materials exhibited an improved shear toughness as compared to the baseline CFRP system. Neat resin, CFRP, and CFRP/GNP experiments are used to characterize the multiscale progressive damage analysis (MPDA) models. The MPDA model includes five disparate length scales ranging from the nano-scale up to the laminate scale. Numerous analytical, semi-analytical and numerical are integrated into the MPDA framework to provide predictions of the OHC strength of CFRP and CFRP/GNP. Molecular dynamics (MD) is used predict the elastic properties of a representative volume element (RVE) of a GNP with epoxy at the nano-scale. The generalized method of cells (GMC) is used to bridge the nano and continuum scales by modeling a repeating unit cell of epoxy with the appropriate volume fraction of GNP. The nonlinear behavior of the matrix is modeled using the multi-axial mixed-mode continuum damage mechanics (MMCDM) model, and the MD simulations are used to provide the properties of the homogenized GNP-epoxy subcell. An analytical technique is used to average the non-linear response of the GNP-epoxy RUC over all possible physical orientations of GNP within the matrix. MMCDM is then used to capture the non-linear response of the homogenized GNP-epoxy matrix in an additional GMC model containing a carbon fiber and GNP-epoxy matrix. Finally, Schapery theory (ST) is used to predict shear micro-cracking in the matrix of OHC specimens. The MPDA predictions indicate that the addition of a very small percentage of GNP may lead to a substantial increase in the OHC strength of the composite.

Computational Homogenization of Heterogeneous Materials in the Presence of Contact Interactions

Rodrigo Pinto Carvalho*, Thiago Doca**, Igor Rodrigues Lopes***, Francisco Andrade Pires****

*Institute of Science and Innovation in Mechanical and Industrial Engineering, **Department of Mechanical Engineering, Faculty of Technology, University of Brasilia, ***Institute of Science and Innovation in Mechanical and Industrial Engineering, ****Institute of Science and Innovation in Mechanical and Industrial Engineering

ABSTRACT

In past decades, the need to accurately predict the constitutive behavior of complex materials by explicitly taking into account their properties at finer physical scales has gained considerable attention and, with the increasing advent of computing capacity, nowadays the field of Multi-Scale computational modeling has become a well-established discipline among the field of computational mechanics. In particular, the analysis of a microscopic Representative Volume Elements (RVE) to investigate the impact of microstructure properties on the homogenized macroscopic response has been extensively exploited within many different applications. The main purpose of the present contribution is to further extend the numerical modeling capacity at the micro-scale by incorporating contact mechanics within a finite deformation computational homogenization framework. Specifically, contact interactions are modeled by using the well-known dual Mortar method combined with a semi-smooth Newton method [1,2]. In order to evaluate the algorithm, the constitutive behavior of a two-phase composite with debonded inclusions is analyzed and the numerical results compared with existing analytical solutions [3]. References: [1] Hübner, S., Stadler, G., & Wohlmuth, B. I. (2008). A primal-dual active set algorithm for three-dimensional contact problems with Coulomb friction. *SIAM Journal on Scientific Computing*, 30(2), 572-596. [2] Gitterle, M., Popp, A., Gee, M. W., & Wall, W. A. (2010). Finite deformation frictional mortar contact using a semi-smooth Newton method with consistent linearization. *International Journal for Numerical Methods in Engineering*, 84(5), 543-571. [3] Zhao, Y. H., & Weng, G. J. (1996). Plasticity of a two-phase composite with partially debonded inclusions. *International Journal of Plasticity*, 12(6), 781-804.

Dynamics of Porous FG Curved Beams with Uncertain Parameters

Marcelo Piovan^{*}, Lucas Digiorgio^{**}

^{*}Universidad Tecnológica Nacional, FRBB, ^{**}Universidad Tecnológica Nacional, FRBB

ABSTRACT

This article deals with the stochastic dynamics of curved beams constructed with ceramic and metallic materials that vary in a given functional form. The construction process of this type of structures conducts to the presence of porosity in its domain. The porosity and a non-constant curvature radius may be source of uncertainties in the dynamic behavior. The beam model is deduced in the context of common variational principles, incorporating shear flexibility, variable curvature. It serves as a mean deterministic approach to the studies on stochastic dynamics and uncertainty quantification, which are the main objective of the present article. The uncertainty quantification procedure considers the employment of random variables to characterize the uncertainty in material or geometric properties such as elasticity moduli and/or density of the material constituents, curvature radius of the beam, porosity parameters, among others. The probability density functions of the random variables are derived appealing to the Maximum Entropy Principle. Then the probabilistic model is constructed with the basis of the deterministic model and both discretized with finite element approaches. Once the probabilistic model constructed, the Monte Carlo Method is employed to perform statistical realizations. Numerical studies are carried out to show the main advantages of the modeling schemes employed, as well as to quantify the propagation of the uncertainty in the dynamics of curved FG beams.

Comparison of Structural Properties of Bare-metal Stents versus Bioresorbable Stents

Sogol Pirbastami*, Darrell Pepper**

*University of Nevada, Las Vegas, **NCACM, University of Nevada Las Vegas

ABSTRACT

Stents are wire loop shaped devices placed in coronary artery to provide short term support to open the narrowed or obstructed coronary artery and repair the blood passage for flow. Over the last decade, numerous types of stents have been developed. The first generation of stents was bare-metal, which are still in use today. However, the main drawback is that they remain permanently inside the body and increase the risk of restenosis and in-stent thrombosis. Also, this type of stent cannot be used for pediatric patients due to the limitations associated with vessel growth. The next generation of stents was coated with drug-eluting material to decrease the thrombosis, but the stent would still remain in the vessel as a bare metal stent. The new generation of stents is bioresorbable, where the blood flow is restored and the arterial wall is remodeled, and gradually degrades and becomes reabsorbed by the body. Since the new generation of stents is in the early stage of development, additional studies are still required to provide information about their mechanical properties, material composition, design, and performance. In this study, a computational model is developed for both bare-metal and bioresorbable stents, and their mechanical properties examined with regards to shear stresses and deformations in straight and curved vessels. Inserting a stent in a tortuous coronary artery can produce high shear stresses at both ends of the stent, impacting the shape of the artery. Deformation in metal stents is less than in bioresorbable stents. Over the long term, the bioresorbable stent conforms to the shape of the curved artery and applies less stress to surrounding tissues. The metal stent can create a tear in the arterial wall, resulting in restenosis. In this study, the COMSOL Multiphysics finite element code is used to investigate the wall shear stresses and the deformations to the tissues and artery walls. Results indicate that the bioresorbable stent is more flexible and conforms more readily to the shape of an arterial wall, producing lower stress levels than bare-metal stents.

Simulation of a Proposed FSI Validation Case

Jonathan Pitt*

*The Pennsylvania State University

ABSTRACT

A new validation test case for low-frequency, large amplitude deformation Fluid-Structure Interaction (FSI) codes is proposed, and simulations of the experiment are presented. This validation case extends previous benchmarks in the literature, by providing high Reynolds number, turbulent, three-dimensional experimental and computational data for FSI algorithms and solution methods comparison. The proposed case consists of a flexible flag attached to a vertically mounted square rod immersed in fully developed pipe flow. This flow is created in the test section of Penn State's twelve-inch water tunnel loop facility. As the flow passes over the square rod, vortices are generated which subsequently excite the flag and cause it to oscillate. The deformation of the flag is the key metric used for experiment-simulation comparison, similar to the two-dimensional laminar computational benchmark of Turek and Hron [1]. A high-resolution simulation of the proposed experiment is performed using an FSI solver previously developed at Penn State [2]. This solver implements a partitioned, overset grid enabled ALE-based method for the solution of tightly coupled FSI problems. In particular, overset meshes are attached to the immersed deformable structure, and permitted to move independently of the static background mesh. The overset grid capability is the enabling technology to allow large deformation of body fitted meshes, required to capture the turbulent boundary phenomena, without the need to re-mesh or distort the grid beyond usability. This approach also allows for simplified meshing of complex geometries, and a reduced domain size for mesh motion calculations, providing for significant reductions in computational cost. Comparison of computational results to experimental measurements are presented. [1] S. Turek and J. Hron. "Proposal of Numerical Benchmarking of Fluid-Structure Interaction Between and Elastic Object and Laminar Incompressible Flow", Fluid-Structure Interaction, Vol. 53, pp. 371–385, 2006. [2] S. T. Miller, R. L. Campbell, C. W. Elsworth, J. S. Pitt, and D. A. Boger. "An Overset Grid Method for Fluid-Structure Interaction", World Journal of Mechanics, Vol. 4, No. 7, pp. 217–237, 2014.

Yield Surfaces for Heterogeneous Materials Using a Multi-Scale Approach

José Julio de Cerqueira Pituba*, Wanderson Ferreira Santos**

*Federal University of Goiás, **Federal University of Goiás

ABSTRACT

This work deals with numerical simulation of the mechanical behavior of materials composed of heterogeneous ductile microstructures using a multi-scale approach considering plasticity processes and phase debonding. Due to few studies about yield surfaces of metal matrix composites (MMC) with weak interfaces presented in the literature, the major goal of this work is to propose yield surfaces for metal matrix composites reinforced by rigid inclusions. All simulations in this section have been performed by employing the computational homogenization under the plane stress assumption in small strain regime. The average stress is obtained by imposing the macro-strain over the RVE and subsequently solving the microscopic initial boundary value problem for the defined boundary condition assumed [1]. The yield surfaces are obtained for Representative Volume Elements (RVEs) of materials presenting perfectly bonded inclusions and phase debonding in the interface zone. The matrix is considered an ideally plastic material governed by von Mises model, whereas the interface zone is modeled by means contact and fracture constitutive models incorporated in a proposed finite element [2]. Also, RVEs containing different distributions and volume ratios of voids are analyzed. Considering the phase debonding, for compressive loadings the RVE behaves like RVE with perfectly bonded inclusions whereas for tension loadings the RVE presents a behavior quite similar to the one with voids. On the other hand, the concentration of voids in the RVE decreases its mechanical strength. [1] Fernandes, G.R., Pituba J.J.C., Souza Neto, E.A. (2015b). FEM/BEM formulation for multi-scale analysis of stretched plate, *Engineering Analysis with Boundary Elements* 54: 47-59. [2] Pituba, J.J.C., Fernandes, G.R., Souza Neto, E.A. (2016). Modelling of cohesive fracture and plasticity processes in composite microstructures. *Journal of Engineering Mechanics* 142: 04016069.1-04016069.15.

Dissipative Particle Dynamics for Soft Matter Simulations

Igor Pivkin*

*Institute of Computational Science, USI Lugano, Switzerland

ABSTRACT

Particle-based methods have been extensively used to study many biophysical systems in recent years. Dissipative Particle Dynamics (DPD) is a Lagrangian method that was originally proposed as a coarse-grained version of Molecular Dynamics. The popularity of this method is due to several essential properties. First, DPD provides an accurate hydrodynamics due to mass and momentum conservation. It also allows to model complex interactions between particles representing fluid, solid walls and soft matter in a unified way by defining proper DPD interaction parameters. Finally, DPD is a scale-free method meaning that it can be used for modeling processes on different length scales, from nanometers to microns and above. In this talk, we will present DPD models for soft matter applications, including modeling of cells in complex flow domains.

Multiscale Method with Patches for the Solution of Linear Parabolic Equations with Localized Uncertainties

Florent Pled^{*}, Anthony Nouy^{**}, Mathilde Chevreuil^{***}

^{*}Université Paris-Est, Laboratoire Modélisation et Simulation Multi Echelle, MSME UMR 8208 CNRS, ^{**}Université de Nantes, Laboratoire de Mathématiques Jean Leray, UMR 6629 CNRS, ^{***}Université de Nantes, Ecole Centrale Nantes, Institut de Recherche en Génie Civil et Mécanique, GeM UMR 6183 CNRS

ABSTRACT

Uncertainty quantification in computational engineering is nowadays an essential step to perform the robust design of mechanical systems. Analyzing the propagation of localized uncertainties in computational models allows for robust predictions of the model response with respect to the input uncertainties. Such uncertainties may represent either natural variabilities in the material properties or epistemic variabilities due to a lack of knowledge in the geometry, the boundary or initial conditions. Traditional monoscale approaches based on local refinement or enrichment techniques can be relatively difficult to implement in the existing commercial softwares and computationally demanding for solving high-dimensional stochastic problems. Consequently, concurrent multiscale approaches based on substructuring, domain decomposition or multigrid methods have been proposed to tackle large-scale engineering applications and perform stochastic computations of multiscale problems. A multiscale method has been recently introduced in [1] for solving linear elliptic equations with localized uncertainties and extended to a wider class of semi-linear elliptic equations with localized uncertainties and non-linearities in [2]. It relies on a decomposition of the domain into several subdomains of interest (called patches) containing the sources of uncertainties and possible non-linearities, and a complementary subdomain. A global-local iterative algorithm is then introduced to compute the multiscale solution and calls for the solution of a sequence of linear global problems (with deterministic operators and uncertain right-hand sides) over a deterministic domain, and (non-)linear local problems (with uncertain operators and right-hand sides) over the patches. In this work, the method is extended to linear parabolic equations with localized uncertainties. The convergence of the iterative algorithm is analyzed. The proposed multiscale approach allows for considering independent computational models, adapted discretization spaces and solvers for both types of problems. The stochastic local problems are solved using sampling-based approaches along with adaptive sparse approximation methods [3] to efficiently compute sparse representations of high-dimensional stochastic local solutions with arbitrarily-high accuracy. The performances of the multiscale method are illustrated on a transient linear advection-diffusion-reaction stochastic problem with localized random material heterogeneities. [1] M. Chevreuil, A. Nouy, and E. Safatly. A multiscale method with patch for the solution of stochastic partial differential equations with localized uncertainties. *CNAME*, 255:255–274, 2013. [2] A. Nouy and F. Pled. A multiscale method for semi-linear elliptic equations with localized uncertainties and non-linearities. *ESAIM: M2AN*, submitted, 2017. [3] A. Chkifa, A. Cohen, R. DeVore, and C. Schwab. Sparse adaptive Taylor approximation algorithms for parametric and stochastic elliptic PDEs. *ESAIM: M2AN*, 47(1):253– 280, 2013.

Electronic Structure Calculations with Bezier-extraction-based Isogeometric Analysis

Jiri Plešek^{*}, Robert Cimrman^{**}, Matyáš Novák^{***}, Jiri Vackar^{****}, Miroslav Tuma^{*****}, Radek Kolman^{*****}

^{*}Institute of Thermomechanics, The Czech Academy of Sciences, ^{**}New Technologies Research Centre, University of West Bohemia, ^{***}New Technologies Research Centre, University of West Bohemia, ^{****}Institute of Physics, The Czech Academy of Sciences, ^{*****}Institute of Computer Science, The Czech Academy of Sciences, ^{*****}Institute of Thermomechanics, The Czech Academy of Sciences

ABSTRACT

We present an application of isogeometric analysis based on Bézier extraction in electronic structure calculations [1]. A computational strategy [2] for non-periodic electronic structures based on the density functional theory, environment-reflecting pseudopotentials and the isogeometric analysis with Bézier extraction has been developed and tested. The approach is especially suitable for calculating the total energy and its derivatives, particularly for evaluation of atomic forces based on the Hellmann-Feynman theorem. In the contribution, we present of convergence properties of this numerical method in electronic structure calculations [3]. The results are compared with results obtained by the finite element method based on the Lagrangian shape functions. Acknowledgements to projects: CSF 17-12925S. MEYS CZ.02.1.01/0.0/0.0/15_003/0000493 (Plešek, Kolman) under AV0Z20760514 and MEYS CZ.02.1.01/0.0/0.0/15_0 03/0000358. REFERENCES [1] R.M. Martin, Electronic Structure: Basic Theory and Practical Methods, Cambridge University Press, (2005). [2] R. Cimrman, M. Novák, R. Kolman, M. Tuma and J. Vacká?, Isogeometric analysis in electronic structure calculations, Math. Comput. Simul., vol. 145, p. 125-135, 2018. doi: 10.340 1016/j.matcom.2016.05.011 [3] R. Cimrman, M. Novák, R. Kolman, M. Tuma, J. Plešek and J. Vacká?, Convergence study of isogeometric analysis based on Bézier extraction in electronic structure calculations, Applied Mathematics and Computation, vol. 319, p. 138-152, 2018. <http://dx.doi.org/10.1016/j.amc.2017.02.023>

Progress on an MPI+X Scalable, Multiscale GFEM for Large-scale Simulations

Julia Plews*, Matthew Mosby**

*Sandia National Laboratories, **Sandia National Laboratories

ABSTRACT

This presentation will demonstrate recent progress toward a data-parallel generalized finite element method with global–local enrichment functions (GFEMgl) for large-scale, multiscale computational mechanics problems. The GFEMgl simultaneously resolves fine-scale (e.g., crack- or material-scale) and coarse-scale (e.g., component- or structural-scale) physics in interdependent local and global boundary value problems. Local solutions are inserted into the global basis as enrichment functions to achieve strong coupling of fine- and coarse-scale response without sacrificing fine-scale fidelity. The embarrassing parallelism of GFEMgl local problems has led to promising scalability on shared memory computers while maintaining good accuracy relative to direct simulation [1,3]. However, scalable algorithms for the next generation of manycore high-performance computing platforms must exploit a combination of distributed parallel communication and on-node thread, or MPI+X, parallelism. This talk will focus on a new MPI-parallel version of the GFEMgl with particular emphasis on strategies for task-parallelism similar to [2] and minimizing communication of fine-scale data across compute nodes. REFERENCES [1] D.-J. Kim, C. Duarte, and N. Sobh. Parallel simulations of three-dimensional cracks using the generalized finite element method. *Computational Mechanics*, 47(3):265–282, 2011. [2] M. Mosby and K. Matous?. *Computational homogenization at extreme scales. Extreme Mechanics Letters*, 6:68–74, 2016. [3] J. Plews and C. Duarte. Bridging multiple structural scales with a generalized finite element method. *International Journal for Numerical Methods in Engineering*, 102(3–4):180–201, 2015.

Preston-Tonks-Wallace (PTW) Model Parameterization of Gamma (FCC) - Cerium

JeeYeon Plohr*

*Los Alamos National Laboratory

ABSTRACT

Cerium (Ce) is an scientifically interesting material for which there are seven allotropies; it goes through phase transformation between alpha and gamma phases via localization/delocalization of f electron with a large volume collapse; the liquid phase has a larger volume than solid phase in low pressure regime (less than 3GPa), and it has a critical point at low pressure/temperature. As part of an effort to have a better material model parameters for Ce, we have fitted the Preston-Tonks-Wallace (PTW) viscoplasticity model [1]. In doing so, we have used a newly generalized thermoelasticity model that provides the analytic expressions of shear modulus and melt curve [2]. The experimental data needed were provided by Russian Federal Nuclear Center (RFNC) where the split Hopkins bar tests were performed for seven sets of strain rate and temperature regimes from which stress-strain data were extracted, and we have used them to find the best fitting PTW model parameters. However, due to the lack of large strain data, there remains a big uncertainty in selecting the parameters. [1] D. L. Preston, D. L. Tonks, and D. C. Wallace, Model of Plastic Deformation for Extreme Loading Conditions, J. Appl. Phys. 93 (2003), 211-220 [2] L. Burakovsky, J. N. Plohr, S. K. Sjøe, and D. J. Luscher, Thermoelasticity Model for Cerium, in preparation.

A Micromorphic Computational Homogenization Framework for Heterogeneous Materials

Leong Hien Poh*

*National University of Singapore

ABSTRACT

The first-order computational homogenization approach is restricted to problems where the macro characteristic length scale is much larger than the underlying RVE. In this contribution, focusing on matrix-inclusion composites, a novel computational homogenization framework is proposed such that standard continuum models at the micro-scale translate onto the macro-scale to recover a micromorphic continuum. Departing from the conventional FE2 framework where a macroscopic strain tensor characterizes the average deformation within the RVE, our formulation introduces an additional macro kinematic field to characterize the average strain in the inclusions. The two macro kinematic fields, each characterizing a particular aspect of deformation within the RVE, thus provide critical information on the underlying rapid fluctuations. The net effect of these fluctuations, as well as the interactions between RVEs, are next incorporated naturally into the macroscopic virtual power statement through the Hill-Mandel condition to recover a micromorphic continuum at the macro-scale. The length scale parameter associated with the higher-order term characterizes the nonlocal interaction between neighbouring micro-mechanisms, which in turn provides a regularization effect and enables an accurate prediction of the size-effect. The excellent performance of the proposed homogenization approach is illustrated by benchmarking its predictions against reference DNS solutions. Considering a shear wave loading problem, it is shown that the homogenized micromorphic model adequately captures the material responses, even in the absence of a clear separation between the loading wavelength and the RVE size. Specific choices for the decomposition of kinematic fields, as well as the boundary conditions adopted, will also be elaborated.

Coupling MD with Phase Field Models: Atomistically Informed Free Energy Representation for Applications in Organic Electronics

Balaji S Sarath Pokuri^{*}, Shi Li^{**}, Sean Ryno^{***}, Chad Risko^{****}, Baskar Ganapathysubramanian^{*****}

^{*}Iowa State University, ^{**}University of Kentucky, ^{***}University of Kentucky, ^{****}University of Kentucky, ^{*****}Iowa State University

ABSTRACT

Phase field based simulation strategies have been shown to be quite useful in exploring process-structure relationships for solvent based fabrication of organic electronics. The free energy functional predominantly contains the specifications of the material system. Standard free energy functional representations are simplistic. However, with the increasing complexity of the molecular structure (conjugated, diverse side groups, anisotropic) of the materials that are currently being developed and utilized, standard Flory-Huggins type parametrization may be insufficient. This is further exacerbated by the need to accurately model multi component systems (consisting of donor, acceptor, solvent, solvent additives). In this work, we tackle this problem through an atomistically-driven construction of the free energy of representative material systems. The free energy construction is formally represented as a regression problem using a finite number of MD simulations. MD calculations of free energy are performed using the 2PT method with all-atom MD simulations. In order to minimize the number of MD simulations, we use a Bayesian optimization approach to intelligently sample the configuration space to spawn MD simulations. Under assumptions of smoothness of the free energy, we can provide rigorous bounds on the number of MD simulations required to construct the free energy functional (given a error threshold). We illustrate the framework through a few examples of increasing complexity.

Search for the Optimum Simple Computational Model of the Turbine Bladed Disk

Pavel Polach*

*Research and Testing Institute Plzen

ABSTRACT

Motivation for introducing this paper is the topical application of the method using the rotational periodicity of the structure at calculating natural vibration characteristics of the steam turbine bladed disk with continuous binding, in this case in the form of an integral shrouding and in the middle of the blade with the tie-boss connection. Part of the shroud and part of the tie-boss are the integral parts of the blade. Blades are free at non-rotating bladed disk. Blades of the advanced design are continuously coupled in the zone of the shroud and in the tie-boss zone by the blades untwist caused by the centrifugal forces acting at the turbine rotation. The method used for the calculation of natural frequencies and mode shapes rotational periodicity of the structure supposes that the finite periodic system (in this case of the bladed disk with the continuous binding) is composed of the definite number of identical parts – subsystems. The subsystem discretization (in this case using the finite element method) will be performed in such a way that it may be coupled to their left-side and right-side adjacent subsystems in identical number of points in identical degrees of freedom. Mathematically, this approach to the problem formulation leads to assembling and solving the matrix difference equations. This method does not enable to model real contact properties. The contact must be modeled by the flexible connection. Stiffness of the connection in the zones of adjoining blades contact was tuned at turbine operational speed (i.e. at 3000 rpm) in such a way that the values of calculated natural frequencies might come as near as possible to the values of the measured natural frequencies. Calculated value of the first natural frequency associated to mode shape with zero nodal diameter appears to be problematic. It differs from the measured natural frequency associated to mode shape with zero nodal diameter by 30 per cent. The paper deals with searching for the approach to the creation of the model of the steam turbine bladed disk with continuous binding that would improve the compliance of this natural frequency with the measured natural frequency.

Branched Covering Surfaces – New Shapes, New Materials and New Processes

Konrad Polthier*

*FU Berlin

ABSTRACT

The classic geometric view on smooth surfaces hardly fits to the complex and often multiscale physical surface shapes in nature and, nowadays, in industrial applications. In this talk we will introduce a new class of surface shapes derived from classic complex analysis. Multivalued functions and differential forms naturally lead to the concept of branched covering surfaces and more generally of branched covering manifolds in the spirit of Hermann Weyl's book "The Idea of a Riemann Surface " from 1913. We will illustrate and discretize basic concepts of branched (simplicial) covering surfaces starting from complex analysis and surface theory up to their recent appearance in geometry processing algorithms and artistic mathematical designs. Applications will touch discrete and differential based surface modeling, image and geometry retargeting, optimal surfaces, and novel weaved geometry representations with serious industrial applications.

Acceleration in Molecular Dynamics Simulations Using Phase Space Sampling

Mauricio Ponga*

*University of British Columbia

ABSTRACT

Molecular Dynamics (MD) simulations have proven to be a useful tool to understand many phenomena at the nanoscale. Although the capabilities of MD simulations for predicting properties of systems with great accuracy, many limitations still hamper widespread usage of this technique. One such limitation is the time scale that can be simulated. Since MD needs to resolve the phonon vibrations of atoms and molecules, the critical time for conditional stability -the maximum time step that can be taken in order to maintain stability in the system- in the simulations is a fraction of this frequency. This, in turn, gives a critical time step of the order of $1 \text{ fs} = 10^{-15} \text{ sec}$. The restriction in the timescale places several limitations in the total time that can be modeled with MD and, therefore, the loads and deformation are usually applied at exceedingly large rates that do not represent most of the everyday working condition of systems and components. In this work, we propose a new technique for sampling the free-energy and time acceleration of atomic systems. The new technique is based on the concept of macroscopic evolution of systems at finite temperature and acceleration of rare events by phase space sampling at accelerated rates. We show how the free energy of the system and the average atomic forces for a given temperature can be computed by making a separation of slow-fast variables of motion and subsequent phase average. Thus, the evolution of the free-energy at the desired temperature computed in terms of the macroscopic variables of the system can be sampled at a much higher rate with the aid of an artificial large temperature leading to an accelerated sampling technique. We use this idea to accelerate the dynamics of the system and the transition rate of rare events. Several validation cases are studied to show the acceleration of MD simulations in relevant problems of interest such as dislocation climb, vacancy diffusion, and vacancy cluster collapse in dislocation cores.

A Mortar Finite Element Approach for Modeling Point, Line and Surface Contact

Alexander Popp*, Philipp Farah**, Wolfgang A. Wall***

*Bundeswehr University Munich, **Technical University of Munich, ***Technical University of Munich

ABSTRACT

In this contribution, a new approach for investigating finite deformation frictional contact problems with a special emphasis on non-smooth geometries such as sharp corners and edges is presented [1]. The contact conditions are separately enforced for point contact, line contact and surface contact by employing three different sets of Lagrange multipliers and, as far as possible, a variationally consistent discretization approach based on mortar finite element methods. The discrete Lagrange multiplier unknowns are eliminated from the system of equations by employing so-called dual or biorthogonal shape functions. For the combined algorithm, no transition parameters are required and the decision between point contact, line contact and surface contact is implicitly made by the variationally consistent framework, which has not been possible until now with any other mortar-based approach from the literature [2]. One core ingredient of the proposed formulation for non-smooth contact geometries is a suitable modification of the discrete Lagrange multiplier spaces for line contact and surface contact in the vicinity of non-smooth geometric entities such as vertices and edges, respectively. If, for example, a line contact element in 2D is connected to a vertex, the vertex node would carry both a discrete line Lagrange multiplier and a discrete point Lagrange multiplier. Thus, partition of unity would not be guaranteed anymore. In order to recover consistency, the line Lagrange multiplier shape functions have to be modified in the vicinity of the vertex node. It should be pointed out that such modifications are quite well-established in mortar finite element methods in the context of so-called crosspoints, which arise when multiple subdomains meet at one point [3]. Similar modifications of the Lagrange multiplier shape functions have also been devised for 3D surface contact. In addition, a novel static condensation procedure for dual (biorthogonal) mortar methods is presented that allows for removing all discrete Lagrange multiplier degrees of freedom from the global system of equations at negligible computational costs. [1] P. Farah, W. A. Wall, and A. Popp. A mortar finite element approach for point, line and surface contact. *International Journal for Numerical Methods in Engineering*, accepted for publication, 2017. [2] A. Popp, A. Seitz, M. W. Gee, and W. A. Wall. Improved robustness and consistency of 3D contact algorithms based on a dual mortar approach. *Computer Methods in Applied Mechanics and Engineering*, 264:67-80, 2013. [3] B. I. Wohlmuth. Variationally consistent discretization schemes and numerical algorithms for contact problems. *Acta Numerica*, 20:569-734, 2011.

Orthogonality Constrained Gradient Reconstruction for the Super-convergent Computation of Stress Intensity Factors

Roberto Porcù^{*}, Maurizio M. Chiaramonte^{**}

^{*}Princeton University, ^{**}Princeton University

ABSTRACT

The accurate prediction of crack propagation requires the careful computation of the Stress Intensity Factors (SIFs) to determine whether the crack propagates, as well as its direction of propagation. The Stress Intensity Factors are a measure of the stress divergence near the crack tip and can be computed through the evaluation of linear and continuous functionals, termed Interaction Integrals functionals [1]. The argument of the latter is the gradient of the displacement field of the deforming elastic solid, a quantity that is often approximated using finite element methods. As the error in the computation of the SIF is bound by the error in the approximation of the displacement gradient, we propose a novel gradient reconstruction technique to enhance the accuracy of the computed SIFs. The salient feature of the proposed approach is that, by recognizing that the convergence properties of linear and continuous functionals are strongly tied to a Galerkin-orthogonality-like condition of its argument, we perform an orthogonality constrained gradient reconstruction. We will showcase that the proposed approach for gradient recovery preserves the super-convergent property of the reconstructed gradient and further, unlike previous methods, it enhances the convergence of linear functionals of the reconstructed gradient. We will combine this novel technique with Mapped Finite Element Methods [2], a finite element method for the optimal approximation of problems on cracked domains, to compute super-convergent SIFs. We will showcase that, by combining the aforementioned technologies, the SIFs can be computed to arbitrary orders of accuracy without any considerable computational overburden. References [1] M. M. Chiaramonte, Y. Shen, L. M. Keer, and A. J. Lew. Computing stress intensity factors for curvilinear cracks. *Int. Journal For Numerical Methods in Engineering*, Submitted, 2015. [2] Maurizio M. Chiaramonte, Yongxing Shen, and Adrian J. Lew. Mapped finite element methods: High-order approximations of problems on domains with cracks and corners. *International Journal for Numerical Methods in Engineering*, 2017.

IDENTIFICATION OF POROUS STRUCTURE PARAMETERS USING AN ARTIFICIAL IMMUNE SYSTEM

ARKADIUSZ POTERALSKI^{*}, AND JACEK PTASZNY[†]

Institute of Computational Mechanics and Engineering

Silesian University of Technology

Konarskiego 18A, 44-100 Gliwice, Poland

^{*}arkadiusz.poteralski@polsl.pl, [†]jacek.ptaszny@polsl.pl

www.icme.polsl.pl

Key words: Porous Structure, Identification, Artificial Immune System, Computational Homogenization, Linear Elasticity.

1 INTRODUCTION

Optimization and identification by using artificial immune systems (AIS) are interesting and give good results methods in comparison to other global optimization algorithms. Intensive research on the development of such algorithms in application to optimization and identification problems has been carried out in recent years [1]. The paper presents an application of the fast multipole boundary element method (FMBEM) coupled with artificial immune system (AIS) to the identification of a porous structure. Shape and orientation of ellipsoidal voids in a porous material are identified. 3D representative volume elements (RVE) of linear elastic porous materials are modelled by the FMBEM, that requires only the discretization of the boundary. The RVE contains uniformly distributed identical cavities. For this RVE effective elastic constants are calculated. This paper is organized as follows. In Section 2, the AIS is briefly reviewed. In Section 3, the numerical example of identification of a porous structure is presented. Finally, concluding remarks are given in Section 4.

2 ARTIFICIAL IMMUNE SYSTEM

The artificial immune systems (AIS) are developed on the basis of a mechanism discovered in biological immune systems. An immune system is a complex system which contains distributed groups of specialized cells and organs. The main purpose of the immune system is to recognize and destroy pathogens - fungi, viruses, bacteria and improperly functioning cells. The lymphocytes cells which play a very important role in the immune system are divided into several groups of cells (two main groups are: B and T cells). The B cells contain antibodies, which could neutralize pathogens and are also used to recognize pathogens. The B cells are produced in the bone marrow in long bones. The B cells undergo a mutation process to achieve big diversity of antibodies. The T cells mature in thymus and only T cells

recognizing non self cells are released to the lymphatic and the blood systems. There are also other cells like macrophages with presenting properties, the pathogens are processed by a cell and presented by using MHC (Major Histocompatibility Complex) proteins.

The recognition of a pathogen is performed in a few steps. In the first stage, the B cells or macrophages present the pathogen to a T cell using MHC the T cell decides if the presented antigen is a pathogen. The T cell gives a chemical signal to B cells to release antibodies (figure 1).

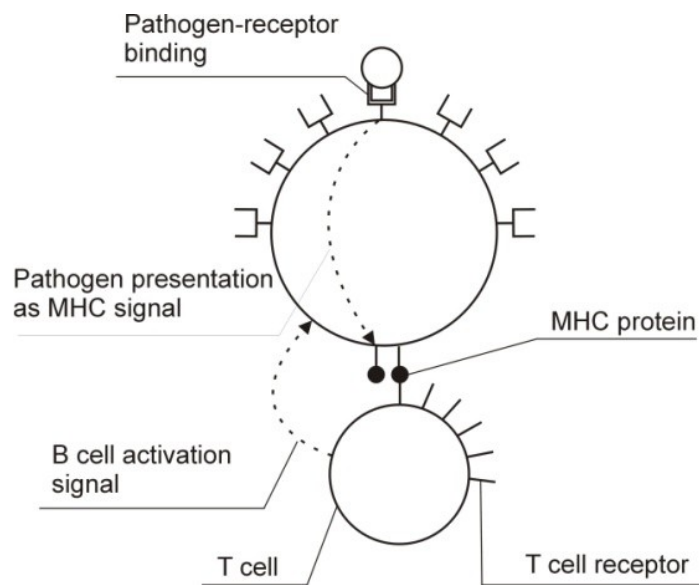


Figure 1. The recognition of a pathogen

A part of stimulated B cells goes to a lymph node and proliferate (clone). A part of the B cells changes into memory cells, the rest of them secrete antibodies into blood (figure 2a). The secondary response of the immunology system in the presence of known pathogens is faster because of memory cells. The memory cells created during primary response, proliferate and the antibodies are secreted to blood (figure 2b). The antibodies bind to pathogens and neutralize them. Other cells like macrophages destroy pathogens. The number of lymphocytes in the organism changes, while the presence of pathogens increases, but after attacks a part of the lymphocytes is removed from the organism.

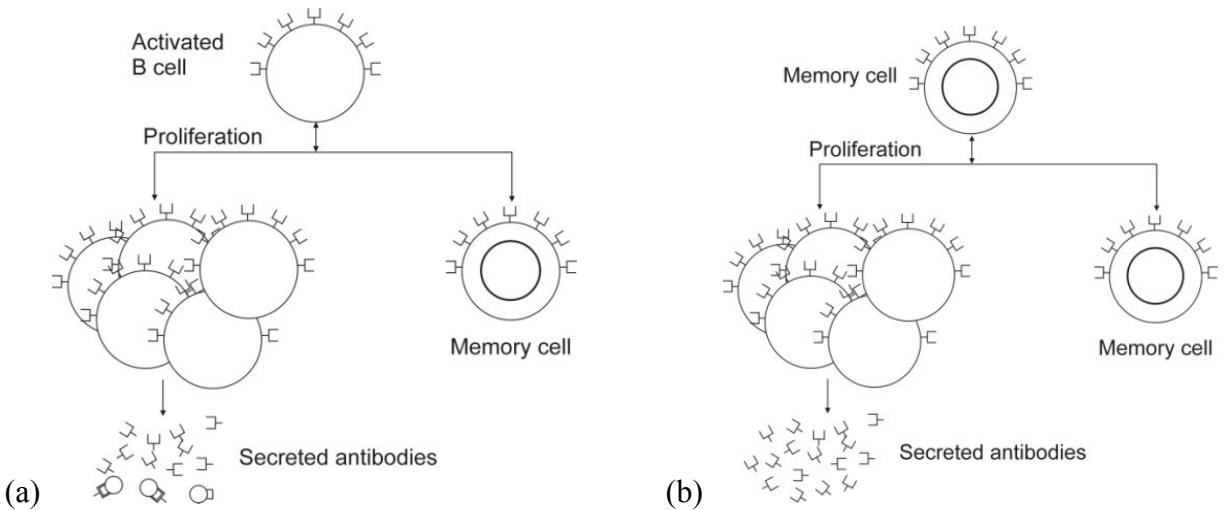


Figure 2. The proliferation of the a) B cells and b) memory cells

The artificial immune systems [2,3] take only a few elements from the biological immune systems. The most frequently used are the mutation of the B cells, proliferation, memory cells, and recognition by using the B and T cells. The artificial immune systems have been used to many optimization or identification problems [4] where the unknown global optimum is the searched pathogen. The memory cells contain design variables and proliferate during the optimization process. The B cells undergo mutation are created from memory cells. The B cells evaluate and better ones exchange memory cells. In this version of artificial immune system the crowding mechanism is used. Using this operator the diverse between memory cells is forced. A new memory cell is randomly created and substitutes the old one, if two memory cells have similar design variables. The crowding mechanism allows finding not only the global optimum but also other local ones.

The figure 3 presents the flowchart of an artificial immune system. In the first stage of AIS the memory cells are created randomly. In the next stage the memory cell are proliferated and mutated creating new B cells. The number of clones created by each memory cell is determined by the memory cells objective function value (the objective function for each B cell is evaluated). The selection process exchanges some memory cells for better B cells. The selection is performed on the basis of the geometrical distance between each memory cell and B cells (measured by using design variables). The crowding mechanism removes similar memory cells. The similarity is also determined as the geometrical distance between memory cells. The process is iteratively repeated until the stop condition is fulfilled. The stop condition can be expressed as the maximum number of iterations.

The optimization process using artificial immune system is controlled by several parameters [5,6]:

- the number of memory cells,
- the number of clones,
- the probability of occurrence of a crowding mechanism (crowding factor) ,
- the probability of Gaussian mutation

The settings of individual parameters of the artificial immune system affect the efficiency of the optimization process. Therefore, it is important to properly select the parameters of AIS. In general, the settings of these parameters is dependent from the scientist's experience. For each new problem we have to search the new and the best parameters of AIS.

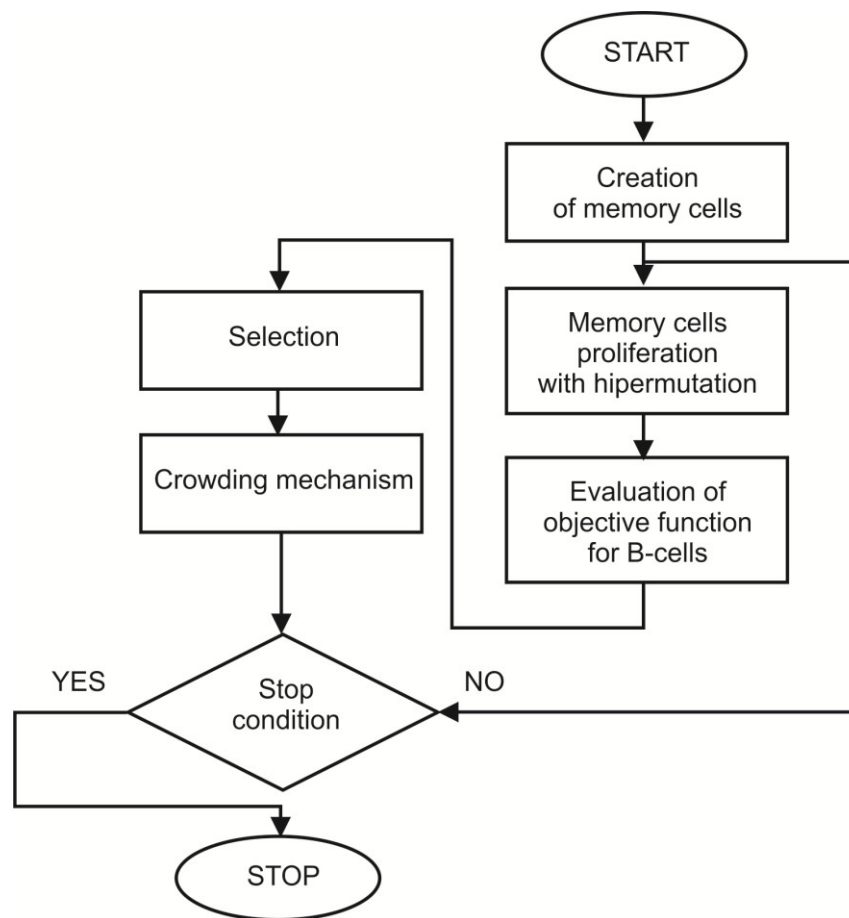


Figure 3. An artificial immune system

3 NUMERICAL EXAMPLE

Shape and orientation of ellipsoidal voids in a porous material are identified. A representative volume element (RVE) is modeled and effective elastic constants are calculated. The RVE contains uniformly distributed identical cavities. The shape and orientation of single cavity is defined by five parameters that are identified, namely a , b , α , β and γ . First two parameters describe the shape of single cavity and refer to ellipsoid radii in x_1 and x_2 directions. The parameters are defined as:

$$a = \frac{2a'}{A} \cdot 100\%, \quad b = \frac{2b'}{A} \cdot 100\%, \quad (1)$$

where a' and b' are absolute values of the ellipsoid radii, and A is the dimension of a cubic region containing single cavity. The third radius, c' , that is shown in Figure 4a, is dependent on a' and b' , and is calculated to preserve constant porosity value of 10%. The three other parameters indicate the Euler angles that define the orientation of a single cavity in the x_3 - x_1 - x_2 convention. In this convention, the void is rotated by the angles α , β and γ respectively. As a result of the rotation, the ellipsoid symmetry axes, that are initially the x_i axes (figure 4a), become x'''_i ($i = 1, 2, 3$) as shown in figure 4b. The description of identified parameters with bounds for box constraints is summarized in table 1.

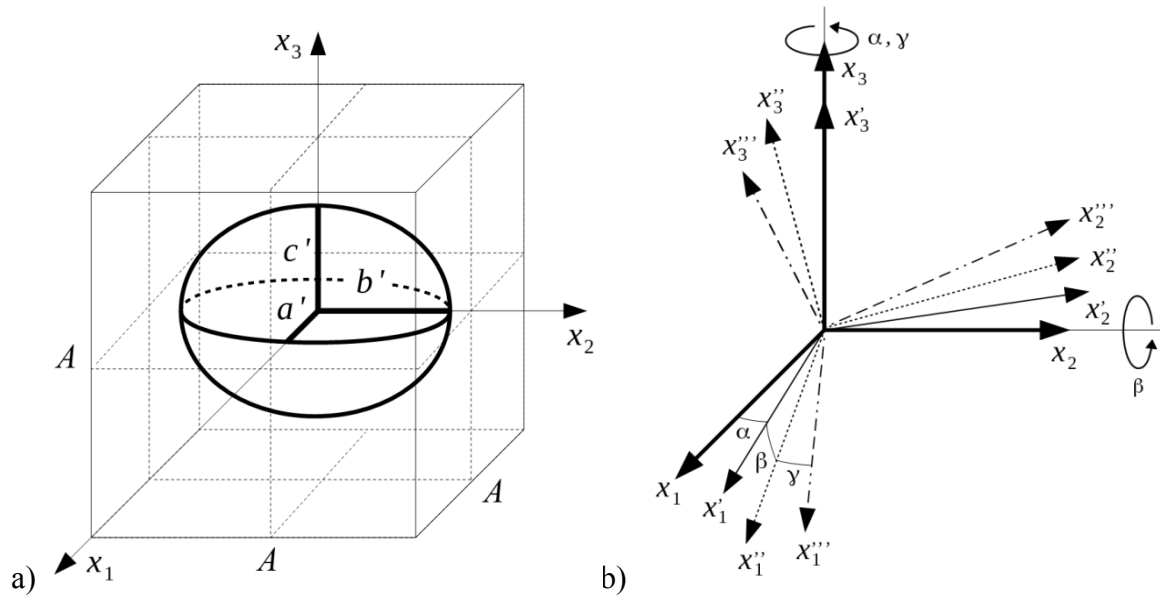


Figure 4. Parameters of single spheroidal cavity: a) initial orientation of the symmetry axes x_i , b) orientation of the rotated cavity symmetry axes x'''_i

Table 1. Description of the void parameters

Parameter	Meaning	Unit	Lower bound	Upper bound
g_1	a	%	45	90
g_2	b	%	45	90
g_3	α	deg	0	90
g_4	β	deg	0	45
g_5	γ	deg	0	90

The analysed RVE contains 4x4x4 (64) cavities. On the external boundary, displacement boundary conditions are applied to evaluate the matrix of effective elastic constants of the porous material \mathbf{C} [7]. The external boundary is a cube with side length equal of $4 \times A = 1$ mm. The properties of the solid linear elastic material are Young's modulus $E = 200$ GPa and Poisson's ratio $\nu = 0.3$. The RVE is modelled by the fast multipole boundary element method with 8-node Serendipity boundary elements [8, 9]. In this method, only the boundaries are discretized. For the generation of cavities, a boundary element mesh for single cavity is scaled, rotated, translated and duplicated. The number of degrees of freedom (DOF) of the model is 69 510. Probably, the number of DOF for corresponding finite element model would be by order of magnitude higher [10].

In the identification problem, the following cost function is minimized:

$$f(\mathbf{g}) = \frac{\|\log \mathbf{C}(\mathbf{g}) - \log \mathbf{C}^{\text{tet}}(\mathbf{g}^0)\|}{\|\log \mathbf{C}(\mathbf{g}^0) - \log \mathbf{C}^{\text{tet}}(\mathbf{g}^0)\|}, \quad (2)$$

where $\mathbf{C}(\mathbf{g})$ is the matrix of the material with pores described by the vector $\mathbf{g} = [g_1, g_2, g_3, g_4, g_5]^T$. \mathbf{g}^0 is a reference vector that describes the identified pore geometry. It is equal to $\mathbf{g}^0 = [46, 46, 0, 0, 0]^T$. Because $\mathbf{C}(\mathbf{g}^0)$ is a numerical solution of a boundary value problem in the micro scale, it is not ideally symmetric. By taking into account the pore shape and orientation, it is assumed that the elastic matrix exhibits the tetragonal symmetry. Thus, the matrix $\mathbf{C}^{\text{tet}}(\mathbf{g}^0)$ is introduced that is the Euclidean projection of the matrix $\mathbf{C}(\mathbf{g}^0)$ onto this type of symmetry. The cost function (2) involves the log-Euclidean norm that possesses the property that it is invariant under inversion. The norm was applied in [11] to the problem of finding the closest elasticity tensor to a tensor obtained from experiments. The form of function (2) allows one to evaluate the relative distance between the current elastic matrix of \mathbf{g} and the idealized (symmetrized) matrix of \mathbf{g}^0 , with respect to the distance between the matrix of \mathbf{g}^0 and its symmetric projection. The function takes its minimal value $\min[f(\mathbf{g})] = 1$ for $\mathbf{g} = \mathbf{g}^0$. Typical structures with corresponding cost function values are shown in figures 5a and 5b. The reference structure is shown in figure 6a.

The identification problem is solved by using the AIS described in Section 2. Parameters of the method are given in table 2. The stop criterion was set as 10 iterations. 10 test were performed and their results are listed in table 3. The identified structure is shown in figure 6b. It is shown, that the identified parameters are close to the reference structure, although the found values of α and γ are not equal to zero. It is caused by the fact, that for the considered structure, any change of these angles does not influence the void shape if $\beta = 0$. For the best identified solution \mathbf{g}^* , denoted by $\mathbf{5}^*$ in table 3, $g_4(\beta)$ is less than one degree.

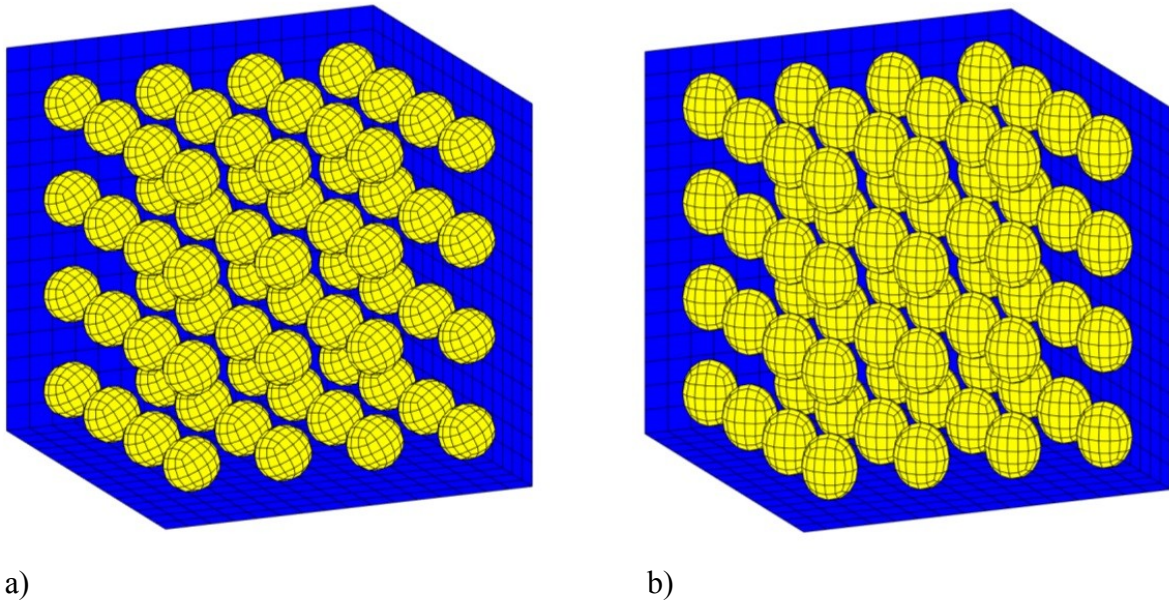


Figure 5. Typical RVEs with 64 voids corresponding to:

a) $\mathbf{g}=[59.8, 56.7, 27.1, 26.9, 77.3]^T, f(\mathbf{g}) = 150.4$

b) $\mathbf{g}=[57.8, 47.1, 15.8, 0.1, 36.7]^T, f(\mathbf{g}) = 91.3$

Table 2. AIS parameters

No. of design variables	No. of memory cells	No. of clones	Crowding factor	Gaussian mutation
5	8	5	0.5	0.5

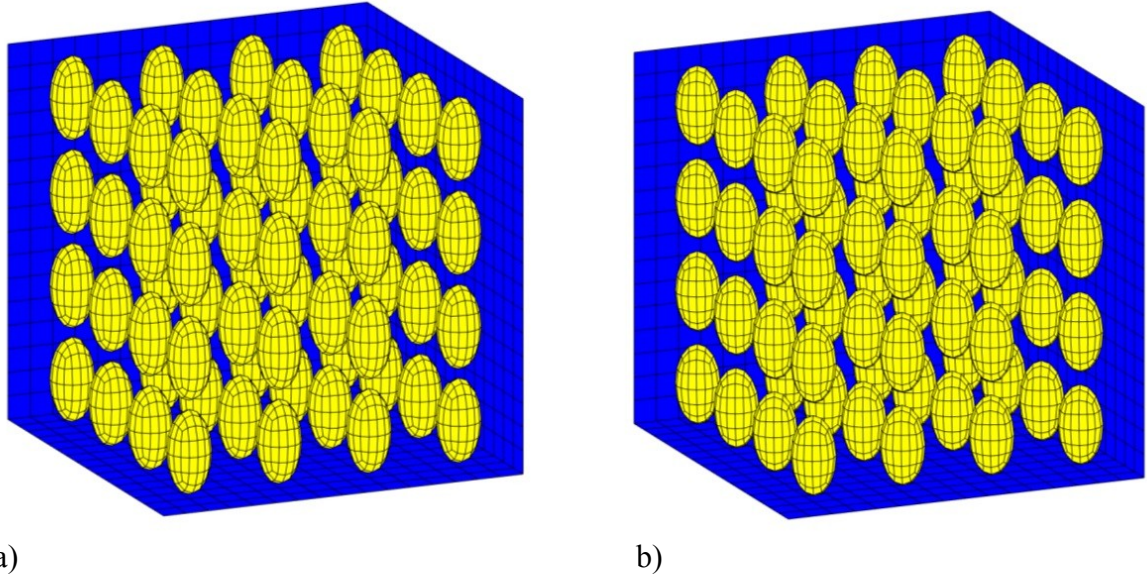


Figure 6. RVEs corresponding to: a) reference $\mathbf{g}^0 = [46, 46, 0, 0, 0]^T$, $f(\mathbf{g}^0) = 1$,
 b) identified $\mathbf{g}^* = [46.7, 47.4, 26.8, 0.7, 36.7]^T$, $f(\mathbf{g}^*) = 14.6$

Table 3. Identification results

Test no.	g_1	g_2	g_3	g_4	g_5	$f(\mathbf{g})$
1	53.7	49.7	78.7	1.4	47.0	73.1
2	51.0	50.7	45.0	7.6	48.0	72.6
3	50.4	51.7	61.9	15.1	55.6	84.3
4	47.2	49.4	77.4	2.7	89.0	33.6
5*	46.7	47.4	26.8	0.7	36.7	14.6
6	48.2	48.3	90	4.8	22.8	33.0
7	50.2	49.8	62.0	14.4	22.9	69.3
8	47.2	46.9	85.0	5.7	68.8	24.9
9	56.3	52.4	63.5	11.5	29.8	108.6
10	57.3	48.5	30.8	3.8	74.3	92.8

4 CONCLUSIONS

- An AIS was applied to the identification of ellipsoid pore geometry (shape and orientation) in a porous material with periodic microstructure, on the basis of its overall elastic matrix. The cost function involved the log-Euclidean metric for the measurement of the distance between the current solution and the referenced (searched) structure. To the computational homogenization, the FMBEM was applied.
- The FMBEM allowed us to only discretize the boundary and made the model preparation easy in comparison to the usually applied FEM [4]. The log-Euclidean norm involved in the cost function allowed for identification of both dimensions and orientation of the ellipsoidal cavities.
- The preliminary results show that the proposed approach can be applied to the optimization of material microstructure of other porous materials, composites, etc. This can be achieved by the minimization of the elastic distance between an optimized structure and a desired tensor of effective elastic constants. The desired tensor can be characterized e.g. by maximized moduli, specific ratio of moduli, etc.
- Efficiency of the proposed method can be improved by distributing computations or using hybrid global optimization algorithm, like hybrid artificial immune system [12].

ACKNOWLEDGEMENTS

The scientific research was funded by National Science Centre, Poland, grant no. 2015/19/B/ST8/02629.

REFERENCES

- [1] de Castro L.N. and Von Zuben F.J.: Learning and optimization using the clonal selection principle, IEEE Transactions on Evolutionary Computation, Special Issue on Artificial Immune Systems (2002) 6,3:239-251.
- [2] Wierzchoń S.T. Sztuczne systemy immunologiczne. Teoria i zastosowania (Artificial Immune Systems. Theory and Applications). EXIT, Warszawa (2001) (in polish).
- [3] Ptak M. and Ptak W. Basics of Immunology. Jagiellonian University Press, Cracow, (2000).

- [4] Poteralski A., Szczepanik M., Beluch W. and Burczyński T. Optimization of composite structures using bio-inspired methods. *Artificial intelligence and soft computing*. ICAISC (2014) 8468:385-395.
- [5] Poteralski A. Optimization of mechanical structures using artificial immune algorithm. *Beyond Databases, Architectures, and Structures*. *Communications in Computer and Information Science* (2014) 424:280-289.
- [6] Poteralski A. Data processing in immune optimization of the structure. *Beyond Databases, Architectures, and Structures (BDAS)*. *Communications in Computer and Information Science* (2015) 521:309-319.
- [7] Zohdi, T.I. and Wriggers, P. *An Introduction to Computational Micromechanics*. Springer (2008).
- [8] Ptaszny, J. Accuracy of the fast multipole boundary element method with quadratic elements in the analysis of 3D porous structures. *Comput. Mech.* (2015) 56: 477–490.
- [9] Ptaszny, J. Parallel fast multipole boundary element method applied to computational homogenization. *AIP Conference Proceedings* (2018) 1922: 140003. DOI 10.1063/1.5019145.
- [10] Ptaszny, J., and Hatlas, M. Evaluation of the FMBEM efficiency in the analysis of porous structures, *Eng. Computation*. (2018) 35: 843-866.
- [11] Moakher, M. and Norris, A.N. The closest elastic tensor of arbitrary symmetry to an elasticity tensor of lower symmetry, *J. Elasticity* (2006) 85: 215–263.
- [12] Poteralski A. Hybrid artificial immune strategy in identification and optimization of mechanical systems. *Journal of Computational Science* (2017) 23:216–225.

Property Prediction and Damage Modeling in Ultra High Temperature Ceramics Using the Material Point Method

Stefan Povolny^{*}, Gary Seidel^{**}, Carolina Tallon Galdeano^{***}

^{*}Virginia Tech, ^{**}Virginia Tech, ^{***}Virginia Tech

ABSTRACT

Ultra high temperature ceramics (UHTCs) show promise for use in material systems operating in extreme environments, such as leading edges on hypersonic aerospace vehicles. Enabling the design of such systems necessitates developing an understanding of UHTC properties and behavior. Experimental characterization is an option, but can be difficult and expensive when emulating hypersonic operating conditions where temperatures regularly exceed 2000 °C. This motivates a need for computational UHTC characterization, which is the main subject of this manuscript. The specific material system being characterized was produced with a manufacturing technique intended to introduce multiscale porosity. It is desired to predict effective material properties (such as elastic modulus and thermal conductivity) along with material behavior (such as damage initiation and propagation) as a function of porous microstructure variations, and to correlate computational results with experimental ones. Various physical phenomena are anticipated to be relevant in this problem. Examples include damage initiation and propagation during compressive loading, large deformations and rotations due to buckling of slender microstructure features, and extensive self-contact. In lieu of the finite element method (FEM), which is the typical choice for property prediction of solids, the material point method (MPM) is proposed as an appropriate tool to capture the aforementioned phenomena and thus adequately model the behavior of the highly porous material. The MPM discretizes a body using particles and incrementally updates their states by interpolating to a background grid to solve relevant equations of motion. The resulting hybrid Eulerian-Lagrangian nature of the method is often touted as its primary advantage, as it allows it to capture large deformation behavior without needing to worry about mesh degradation. Furthermore, the single-valued nature of the particles' velocity/displacement fields in the original MPM allows for automatic treatment of non-slip contact. Although the non-slip aspect is non-physical, having some contact treatment provides a starting point to explore UHTC behavior under high compressive loads. In this work, an MPM and continuum damage approach will be applied towards the modelling of large scale compression and fracture of porous ceramic microstructures in order to obtain effective mechanical properties. In addition, MPM will be used to capture changes in the effective thermal properties at various levels of damage. Future work will take advantage of more sophisticated kernel-based and multi-field treatments for contact and fracture that already exist in the literature.

XFEM/AMR Coupling for Efficient Crack Patterns Analyzes

Benoit Prabel^{*}, Clémentine Jacquemoud^{**}

^{*}Den-SERVICE d'études mécaniques et thermiques (SEMT), CEA, Université Paris-Saclay, F-91191, Gif-sur-Yvette, France, ^{**}Den-SERVICE d'études mécaniques et thermiques (SEMT), CEA, Université Paris-Saclay, F-91191, Gif-sur-Yvette, France

ABSTRACT

In some situations, multiple cracks may exist and interact in structures. Taking them into account in a “traditional” finite element analysis may be cumbersome as a fine and conforming mesh representing the crack pattern is needed. When the crack pattern is a parameter of the simulation (in term of number of cracks, size and location), the engineer has to build complex procedures that are generally not generic to the whole range of possible situations. Hence, it is proposed in this paper to develop a methodology combining XFEM (eXtended Finite Element Method) and AMR (Adaptative Mesh Refinement) for the study of stationary interacting cracks in 2 or 3 dimensions, in both linear and nonlinear fracture mechanics context. The declination of this approach implemented in Cast3M to the implicit/explicit crack description and to the enrichment strategy is deeply explained. Also integration technique compatible with crack propagation in history-dependent material is adopted. In the present paper only two main examples are considered to point out the benefit of the method. First the 2D case of a periodic crack pattern with a parametric description of its size and tilt angle is presented. The numerical results obtained feed a cohesive model for combined mode I+III crack propagation [1]. The proposed procedure is demonstrated to be more efficient than standard finite element analysis : time spent by engineer for the numerical model definition is far lower and the computation is possible for a wider range of parameter. Refining the mesh locally enables to maintain the computational time reasonable for a very good accuracy. Then the 3D case of multiple cracks in a nonlinear material will be discussed. This example is representative of the mechanical analysis undertaken to assess potential interaction between quasi-laminar or tilted cracks. In particular XFEM/AMR coupling is shown to be directly applicable to 3D non-linear case for complex crack geometry, saving time and effort of discretization, and thus allowing the modelling of numerous cracks configurations. Numerical results are directly validated by associated experiments. Extension to crack propagation is an undergoing work discussed in [2]. [1] Leblond, J. B., Lazarus, V., & Karma, A. (2015). Multiscale cohesive zone model for propagation of segmented crack fronts in mode I+ III fracture. *International Journal of Fracture*, 191(1-2), 167-189. [2] Gibert, G., Prabel, B., & Jacquemoud, C. (2018). XFEM/AMR coupling for crack propagation in inelastic media. 13th World Congress on Computational Mechanics (WCCM).

Virtual Element Modeling of the Perfusion of the Lamina Cribrosa

Daniele Prada^{*}, Silvia Bertoluzza^{**}

^{*}Istituto di Matematica Applicata e Tecnologie Informatiche "Enrico Magenes", ^{**}Istituto di Matematica Applicata e Tecnologie Informatiche "Enrico Magenes"

ABSTRACT

In this study, we theoretically investigate blood perfusion of the lamina cribrosa, a collagen structure located in the optic nerve head that plays a critical role in ocular pathologies, especially glaucomatous optic neuropathy [1]. The lamina is modeled as a porous material where capillaries are viewed as isotropically distributed pores in a solid matrix comprising collagen, elastin, extracellular matrix and neural tissue. The permeability tensor of the lamina is isotropic and homogeneous with a scalar value that is estimated according to the volume averaging method. We test this method on a morphologically-based micro structural model of the lamina using the Virtual Element Method (VEM) for the solution of the averaging closure problems. After estimating the permeability, blood pressure and perfusion velocities are approximated by a mixed virtual element space [2]. In view of coupling this three dimensional model with a zero dimensional model accounting for systemic factors that influence the local perfusion, a boundary condition of integral type is used [3]. Simulated distributions of blood pressure and perfusion velocity within the lamina are quantitatively close to realistic data. These results, together with the high flexibility that VEM allows in the treatment of complex geometries, suggest that VEM is a promising candidate for modeling the perfusion of the lamina cribrosa. [1] D. Prada, A. Harris, G. Guidoboni, B. Siesky, A. M. Huang, J. Arciero, Autoregulation and neurovascular coupling in the optic nerve head. *Surv Ophthalmol*, Vol. 61:2, pp. 164-186, 2016. [2] L. Beirao da Veiga, F. Brezzi, L. D. Marini, A. Russo, $H(\text{div})$ and $H(\text{curl})$ conforming virtual element methods. *Numer Math*, Vol. 133, 303-332, 2016. [3] S. Bertoluzza, G. Guidoboni, R. Hild, D. Prada, C. Prud'homme, R. Sacco, L. Sala, M. Szopos, An implementation of HDG methods with Feel++ and application to problems with integral boundary conditions. Manuscript in preparation, 2017.

Interface Thickness Effect on Impact Induced Failure in Energetic Material using Cohesive Finite Element Method

Chandra Prakash*, Emre Gunduz**, Vikas Tomar***

*Purdue University, **Purdue University, ***Purdue University

ABSTRACT

Energetic materials are susceptible to unwanted detonation due to the hot-spot formation, which may be triggered by defects occurred due to impact or shock. One of the main factors that can contribute to this type of defect is the failure initiated at the interfaces. Examples include failure at interfaces such as those between Hydroxyl-terminated polybutadiene (HTPB)-Ammonium Perchlorate (AP) in an example energetic material. In order to analyze the hot-spot behavior of energetic materials, a better understanding the impact behavior of interfaces is important. It has been shown that by coating the binder-particle interface with a low-density polymer can considerably lower the shock sensitivity of energetic materials. Interface size and composition also depend on the type of matrix, particle, binding agent, mixing time, etc. One way to change the interface composition is to add a binding agent to the matrix-particle mixture. In this work, we study the effect of interface thickness on the impact behavior of a single particle HTPB-AP material. A power law viscoplastic constitutive model is used in the simulation which is obtained from a dynamic impact experiment. Stress-strain-strain rate data was fitted in order to obtain constitutive behavior of interfaces, particle, and matrix. The experiments were conducted with indenter of radius $1\mu\text{m}$ on the interfaces with varying amount of binding agent Tepanol. Results show that interfacial properties are affected by the rate of loading and are also dependent upon the binding agent. Stress maps are obtained near the interface using In-situ Mechanical Raman Spectroscopy to analyze the changes in the stress distribution around interfaces for different loads till failure. The stress required for the delamination of the interface is called the interface strength. A bilinear cohesive zone model parameters were obtained from the consideration of local stress during failure and the cohesive energy required for delamination of AP from HTPB matrix. Effect of binding agent on the interface strength is found to be quite significant. The cohesive zone parameters and the viscoplastic model obtained from the experiment were then used in the cohesive finite element method to simulate the delamination between the matrix and the particle due to high-speed impact.

Peridynamics Applied to Deformation and Damage Sensing in Polymer Bonded Explosive Materials

Naveen Prakash*, Gary Seidel**

*Los Alamos National Laboratory, **Virginia Tech

ABSTRACT

Peridynamics, a recently developed non-local theory of continuum mechanics is gaining momentum as a novel method to model complex phenomena in solids such as the crack initiation, branching and propagation. The non-local nature of peridynamic equations allows one to overcome issues such as mesh dependent results and ill conditioned matrices. Peridynamic equations have also been extended to model multiphysics problems such as heat diffusion, coupled thermomechanics, fluid flow, corrosion among others. Polymer bonded explosives are complex materials susceptible to damage in low velocity impact events during transportation and handling, which can weaken the material in addition to the possibility of accidental ignition. Therefore to maintain reliability and efficacy, it is important to monitor in real time, the structural health of the material for safe transportation and handling [1]. It is proposed that dispersing carbon nanotubes within the binder phase will allow for in-situ structural health monitoring owing to the unique piezoresistive properties of nanocomposites [2]. In this work, a computational electromechanical framework based on peridynamics is used to investigate the strain and damage sensing properties of nanocomposite bonded explosive materials (NCBX) [3]. The peridynamics computational framework allows in capturing key deformation mechanisms like interface debonding and granular fracture which are important in assessing the piezoresistive response in the damage regime. The computational results presented in this work indicate that there is promise for in - situ monitoring of granular energetic materials based on the piezoresistive properties of nanocomposites which may prove to be advantageous over current methods. Some ongoing work with respect to including temperature effects, generating PBX/PBS microstructures and calibrating peridynamic model parameters will also be presented. Refs: 1. Han D K, Pecht M G, Anand D K and Kavetsky R 2007 Energetic material/systems prognostics Reliability and Maintainability Symposium, 2007. RAMS'07. Annual 59–64 (IEEE). 2. Sengezer, Engin C., and Gary D. Seidel. "Structural health monitoring of nanocomposite bonded energetic materials through piezoresistive response." *AIAA Journal* (2017): 1-14. 3. Prakash, Naveen, and Gary Don Seidel. "Effects of microscale damage evolution on piezoresistive sensing in nanocomposite bonded explosives under dynamic loading via electromechanical peridynamics." *Modelling and Simulation in Materials Science and Engineering* (2017).

A Configurational Energy Criterion Using Discrete Dislocation Plasticity for the Prediction of Fatigue Crack Nucleation Sites in Ni Superalloys

Nikoletta Prastiti^{*}, Zebang Zheng^{**}, Fionn Dunne^{***}, Daniel Balint^{****}

^{*}Imperial College, ^{**}Imperial College, ^{***}Imperial College, ^{****}Imperial College

ABSTRACT

High-performance nickel-based superalloys commonly find application as safety critical rotatory components in the automotive, power and aerospace industries due to their exceptional mechanical properties. This kind of application involves cyclic loading and therefore, the dominating failure mechanism is fatigue. The stage of crack nucleation during fatigue may consume a considerable fraction of the life of an engineering component compared to that for crack propagation. In addition, the former is not as well understood, in the sense of obtaining useful quantitative predictions of safe component lifetimes and therefore leading to highly conservative and expensive safe-life component design. The key for accurate quantitative predictions lies in the mechanistic understanding of crack nucleation. A new stored energy criterion [1] that has been established and used within a crystal plasticity framework to predict the location of fatigue crack nucleation sites, has been reproduced in a more fundamental way using a discrete dislocation methodology [2] that explicitly represents the dislocations and dislocation pile ups in regions that could potentially act as fatigue crack nucleation sites. Integrated experimental, characterisation and computational crystal plasticity studies in Ni single and oligo crystals [3] were used for the critical appraisal of the new discrete dislocation approach which showed satisfactory qualitative agreement. References [1] Wan, V. V. C., D. W. MacLachlan, and F. P. E. Dunne. "A stored energy criterion for fatigue crack nucleation in polycrystals." International Journal of Fatigue 68 (2014): 90-102. [2] Van der Giessen, Erik, and Alan Needleman. "Discrete dislocation plasticity: a simple planar model." Modelling and Simulation in Materials Science and Engineering 3.5 (1995): 689. [3] Chen, Bo, Jun Jiang, and Fionn PE Dunne. "Microstructurally-sensitive fatigue crack nucleation in Ni-based single and oligo crystals." Journal of the Mechanics and Physics of Solids 106 (2017): 15-33.

The Mechanical Response and Failure of Al-TiB₂ Composites Produced by Spark Plasma Sintering: A Multi-Scale Computational Study

Elad Priel^{*}, Brigit Mittelman^{**}, Nir Trabelsi^{***}, Nissim Navi^{****}, Noa Bitton^{*****}, Or Rahamim^{*****}, Shlomo Haroush^{*****}, Shmuel Hayun^{*****}, Nachum Frage^{*****}

^{*}Shamoon College of Engineering, ^{**}Shamoon College of Engineering & NRCN, ^{***}Shamoon College of Engineering, ^{****}Shamoon College of Engineering & NRCN, ^{*****}NRCN, ^{*****}Ben-Gurion University of the Negev, ^{*****}NRCN, ^{*****}Ben-Gurion University of the Negev, ^{*****}Ben-Gurion University of the Negev

ABSTRACT

Aluminum matrix composites (AMC) are highly attractive structural materials due to their high strength to weight ratio. Mechanical properties of AMC can be tailor made to suite a specific application, by controlling the particle volume fraction, size and distribution. A good control of these parameters can be achieved by using a powder metallurgy approach. In the present study, AMC specimens were fabricated by Spark Plasma Sintering (SPS) of a mixture of Al and TiB₂ powders with 0-15% volume fraction of TiB₂. Uniaxial compression of cylindrical specimens and Small Punch Test (SPT) experiments were conducted to examine the mechanical response and failure modes of the composite in both compression and bi-axial tension loading modes. A multi-scale finite element framework was used to investigate the relation between the micro-structure and mechanical properties of the composites. First, macro-scale models were used in conjunction with the compression and SPT experiments to determine the effective constitutive response. Next, micro-scale models of representative volume elements (RVE&amp;amp;amp;apos;s) were constructed from Scanning Electron Microscopy (SEM) images of the sintered material. Computational homogenization methods were used to determine the effective properties derived from the micro-structure as well as to investigate failure modes within the micro-scale. Finally, the effective mechanical properties derived from the RVE computations were compared to the effective properties derived from the macro-scale analysis. This comparison provides insight on the role of particle-matrix interactions in the resulting effective mechanical properties and failure modes.

Determining Critical Scenarios of Porosity in the Fatigue Behavior of Additively Manufactured IN 718 via Crystal Plasticity

Veerappan Prithivirajan*, Michael Sangid**

*Purdue University, **Purdue University

ABSTRACT

Selective laser melting (SLM) can be used to fabricate components for aerospace applications, in order to realize several advantages that are well documented. However, prior to their use in safety critical components, the failure mechanisms have to be well understood, especially for the unique defects within SLM materials. The focus of our work is on the influence of porosity towards fatigue behavior of a Ni-based super alloy, IN 718, produced by SLM. A fatigue crack in a SLM IN718 microstructure may either initiate at a crystallographic feature (grain boundary, triple points, etc.) or at a pore, and this depends on multiple factors like grain attributes, grain neighbor interactions, pore size and pore interactions. In our work, a crystal plasticity based framework is developed to identify the critical porosity, which quantifies the scenarios of the crack initiating at the pore rather than the crystallographic features. 3D virtual microstructures are developed based on the characterization of SLM IN718 and are used as input to crystal plasticity finite element (CP-FE) simulations. Damage indicator parameters (DIPs) such as the plastic strain accumulation, elastic stress anisotropy, resolved shear stress and triaxiality, obtained from the CP-FE simulations are used to identify the most probable locations of crack initiation. Pores are added to the microstructure instantiations in a systematic manner by varying the size, location, and proximity between pores. The critical pore size is defined as the size beyond which the crack nucleation transitions from crystallographic features to the pore vicinity, which is determined to be 20 microns with respect to an average grain size of 48 microns . This work is beneficial in qualifying SLM materials given the natural porosity inherent to the manufacturing process, by reducing the number of fatigue experiments. Additionally, this study informs the choice of non-destructive evaluation methods and subsequent post-processing steps.

Improving the Efficiency of a Surge Model via Adaptive Mesh Resolution

Jennifer Proft*

*The University of Texas at Austin

ABSTRACT

Storm-induced waves and flooding can be predicted using the computational model ADCIRC+SWAN modeling system for storm surge applications such as mapping of floodplain flood risk and forecasting of storm surge and inundation. This modeling system has been shown to be efficient in parallel computing environments. It is implemented on static meshes and with a static parallelization, and thus it does not evolve as a storm approaches and inundates a coastal region. This implementation can be inefficient when large portions of the mesh remain dry during the simulation. We improve the parallel implementation of ADCIRC by using large-scale adaptivity, in which a mesh is refined by incorporating entire portions of another, higher-resolution mesh. Instead of subdividing an individual element, we will increase resolution by adding elements from a pre-existing mesh that has been well-validated. This technology will decrease the computational cost and better utilize the available resources. We show developed technologies to improve the efficiency of ADCIRC+SWAN simulations, thus allowing for more model runs in ensemble-based design applications, and for faster simulations in time-sensitive applications such as operational forecasting.

A Multi Level Moving Particles Method for Uncertainty Quantification and Reliability Analysis

Carsten Proppe*

*Dept. of Engineering Mechanics, Karlsruhe Institute of Technology

ABSTRACT

Markov Chain Monte Carlo simulation methods allow estimating small failure probabilities efficiently, even for problems that involve a high-dimensional vector of input random variables. Subset simulation can be considered as the most prominent method in this class. In subset simulation, the failure probability is computed as the telescoping product of larger probabilities that require sampling from conditional distributions. Recently, a generalization of subset simulation in the sense of particle methods has been proposed [1], where a threshold is associated to each sample, samples are moved to new positions in the design space and the number of moves for the initial samples to reach the failure region are counted and yield an estimator for the failure probability, which is of comparable accuracy and efficiency as the subset simulation estimator. The algorithm allows for an easy parallel implementation. Just as for subset simulation, sampling from conditional distributions is required when moving a particle. In most practical applications, the limit state function is approximated numerically to a certain level h . In order to obtain an efficient simulation algorithm, it is necessary to balance the statistical error and the numerical error. In this presentation, we propose a multi level moving particles simulation method that balances both errors by computing a telescoping sum of estimates for the number of moves. For each term in the telescoping sum, it is necessary to compute as corrector the difference of the number of moves for each initial sample with two consecutive accuracy levels using the same random numbers in the Markov Chain Monte Carlo simulation. For the multi level moving particles method, the sample variance decreases with decreasing numerical error. Thus, the number of samples that has to be evaluated with high accuracy is reduced compared to a single level computation. Therefore, the proposed algorithm is very efficient for problems where highly accurate evaluations of the limit state function are necessary and require a tremendous computational effort. References: [1] C. Walter: "Moving particles: A parallel optimal Multilevel Splitting method with application in quantiles estimation and meta-model based algorithms". In: Structural Safety 55 (2015), pp. 10–25.

Goal-oriented Formulation of Boundary-value Problems for Accurate Estimation of Quantities of Interest

Serge Prudhomme^{*}, Kenan Kergrene^{**}, Marc Laforest^{***}, Ludovic Chamoin^{****}

^{*}École Polytechnique Montréal, ^{**}École Polytechnique Montréal, ^{***}École Polytechnique Montréal, ^{****}École Normale Supérieure de Paris-Saclay

ABSTRACT

We will present in this talk a mathematical formulation of boundary-value problems aiming at constructing finite element or model reduction approximations for accurate estimation of quantities of interest. The main idea is to reformulate a boundary-value problem as a minimization problem that involves inequality constraints on the error in the goal functional so that the resulting model is capable of delivering quantities of interest within some prescribed tolerance. Chaudhry et al. [1] have proposed a similar method in which constraints are imposed via a penalization approach. However, an issue with that approach is concerned with the selection of suitable penalization parameters. Our goal in this work aims at circumventing this difficulty by enforcing the inequality constraints through Lagrange multipliers [2]. We will also show how to design an adaptive strategy to construct adapted meshes based on a posteriori error estimates. Such a paradigm represents a departure from classical goal-oriented approaches in which one computes first the finite element solution and then adapts the mesh by controlling the error with respect to quantities of interest using dual-based error estimates. The proposed formulation will be extended to the construction of reduced models using the so-called proper generalized decomposition (or low-rank approximation) method. Numerical examples will be presented in order to demonstrate the efficiency of the approach. References: [1] J.H. Chaudhry, E.C. Cyr, K. Liu, T.A. Manteuffel, L.N. Olson, L. Tang, Enhancing least-squares finite element methods through a quantity-of-interest, SIAM J. Numer. Anal. 52 (6), 3085–3105 (2014). [2] K. Kergrene, S. Prudhomme, L. Chamoin, M. Laforest, A new goal-oriented formulation of the finite element method, Comput. Methods Appl. Mech. Engrg. 327, 256–276 (2017).

Soil-structure Interaction in Masonry Arch Bridges: A Hybrid Approach

Bora Pulatsu^{*}, Ece Erdogmus^{**}, Paulo B. Lourenço^{***}

^{*}PhD Candidate, ^{**}Professor, ^{***}Professor

ABSTRACT

Masonry structures constitute a large portion of the architectural heritage, transportation system and residential buildings all around the world. Therefore, understanding their structural behavior has a crucial role in avoiding excessive amount of interventions and preserving the historical characteristics of those structures. However, it has been a challenge for engineers to analyze masonry structures, due to its composite and highly non-linear nature. This problem becomes even more complicated in masonry arch bridges when soil-masonry interaction is considered to capture structural behavior. In present research, up-to-date numerical modeling strategies are combined, so called discrete and finite element methods in the framework of discrete element modeling (DEM), in which equations of motions are solved by an explicit finite-difference method. To achieve that, masonry units are modeled as distinct blocks, which interact along their boundaries, whereas backfill material is considered as a continuous medium consisting of tetrahedral finite elements. There is no mortar assumed to replicate dry-joint masonry which has zero cohesion and tensile strength at the joints. The contact forces are calculated depending on the stiffness and amount of inter-penetration between blocks. The goal of this study is to demonstrate the interaction between backfill and masonry under static loads in three-dimensions, including development of damage and crack propagation. In this context, a published experimental study is utilized to validate proposed methodology. Further, the influence of the constitutive properties of contact parameters such as normal stiffness, shear stiffness, cohesion and friction angle, are investigated by sensitivity analysis. The results of the analysis indicated that presented approach captures soil-structure interaction and provides insight into the masonry arch bridge behavior by taking the advantage of both computational methods.

Trimming Methods in Isogeometric Analysis

Riccardo Puppi^{*}, Annalisa Buffa^{**}, Rafael Vazquez Hernandez^{***}

^{*}EPFL, ^{**}EPFL, ^{***}EPFL

ABSTRACT

Trimming is one of the most fundamental tools in Computer Aided Design (CAD) that allows the construction of complex geometries. At the same time it constitutes a source of difficulty in the interplay between CAD and the numerical analysis of PDEs. When the superfluous surface areas are cut away, the visualization of the resulting surface changes, but its mathematical description remains unchanged. It turns out that we have to deal with elements unfitted with the boundary, making the research for efficient quadrature rules and the imposition of boundary conditions a challenge. Moreover there are basis functions, whose support has been cut, affecting the conditioning of the related linear system. In this regard, ideas from the Cut-FEM literature come to help. For the sake of simplicity and in order to be able to provide rigorous mathematical proofs, we confine our attention to the Laplace equation. In particular we study methods based on a modification of the weak form, e.g. Nitsche's method, enriched with suitable stabilizations. We present a stabilized method which delivers optimal accuracy and is parameter free. This stabilization needs to be coupled with ad-hoc preconditioners to restore good condition numbers of the underlying systems. Finally, numerical tests in the Matlab code GeoPDEs (<http://rafavzqz.github.io/geopdes/>) are provided to confirm our theoretical results. [1] Erik Burman. Ghost penalty. *Comptes Rendus Mathématique*, 348 (21), pp. 1217-1220, 2010. [2] Jaroslav Haslinger and Yves Renard A New Fictitious Domain Approach Inspired by the Extended Finite Element Method. *SIAM Journal on Numerical Analysis*, 47 (2), pp. 1474-1499, 2009.

Investigation in Stable Symmetric or Two-pass Contact Algorithms

Michael Puso^{*}, Jerome Solberg^{**}

^{*}Lawrence Livermore National Laboratory, ^{**}Lawrence Livermore National Laboratory

ABSTRACT

It's become common practice to apply the mortar contact approach in production applications due to its robustness and its recent appearance in most of the major commercial code applications. It is typically the clear choice when a single-pass (slave-master) contact algorithm is tractable. Of course, there are many situations where it becomes less attractive, particular when self-contact can occur. For most commercial codes, the only consistent schemes available would be the penalized two-pass mortar scheme or deprecated Lagrange multiplier constraint scheme. Potential approaches for stable symmetric algorithms are few. One method approaches the self-contact problem using the single-pass contact approach augmented with a binary tree that attempts to choose unique (nodal) contact pairs to avoid redundancy [1]. Lately, the Nitsche approach as in [e.g. 2] has been given more attention although it is not clear how this would perform in an explicit finite element setting. Here we present a stabilized two-pass mortar scheme and evaluate its performance against the canonical single-pass method. Comparison to other symmetric approaches along with potential techniques to alleviate computational cost will also be discussed. [1] B Yang, TA Laursen, "A large deformation mortar formulation of self-contact with finite sliding", Computer Methods in Applied Mechanics and Engineering, 198 (47), 3656-3669, (2009) [2] R Mlika, Y Renard, F Chouly, "An unbiased Nitsche's formulation of large deformation frictional contact and self-contact". ", Computer Methods in Applied Mechanics and Engineering, 325 (1), 265-288, (2017).

Multiphysics Problems for Viscoelastic Contact Mechanics

Carmine Putignano*, Giuseppe Carbone**

*Politecnico di Bari, **Politecnico di Bari

ABSTRACT

Lubrication between soft viscoelastic solids has crucial peculiarities that only very recently have started to be investigated by the lubrication science community. Indeed, in the last decades, massive research efforts have been dedicated to understand the role of non-Newtonian lubricants, but very little has been done to get what occurs when the lubricated solids are not linearly elastic, but exhibit a different rheology. However, such a topic is acquiring an increasingly marked prominence: all the biological cases, where the so-called soft lubrication occurs, are only examples of situations where the solids into contact cannot be considered linearly elastic. This work contains an innovative numerical methodology to assess the lubrication regime occurring between a rigid sphere and a linear viscoelastic layer. In detail, an explicit finite difference scheme is coupled to a Boundary Element solver in order to study the viscoelastic lubrication without any limitation in terms of material properties, geometry and viscosity. The results and, specifically, the film thickness, the contact pressure and, ultimately, the friction force show marked differences in comparison with classic lubrication theory. Indeed, we observe that the film thickness minimum moves from the flow outlet to the inlet, where consistently we found a maximum for the fluid pressure. This can be explained only accounting for the actual viscoelastic rheology of the contacting bodies. Finally, we notice that such results have been validated by means of experiments specifically developed to deal with soft matter.

Algebraic Decomposition as a Variance Reduction and Multiscale Coupling Technique

Jean-Philippe Péraud*, Nicolas Hadjiconstantinou**

*Corning Incorporated, **Massachusetts Institute of Technology

ABSTRACT

Stochastic particle methods, such as direct Monte Carlo simulations, are very well suited to the solution of kinetic equations because they lend themselves to intuitive simulation methods that handle the advection process elegantly and require no grid-based discretization. For problems characterized by small deviations from equilibrium, which are very common, if not prevalent, at the nanoscale (e.g. small Mach number flow), computational savings of several orders of magnitude (4 to 8 depending on the problem [1]) can be achieved by simulating only the deviation from the nearby equilibrium state [1, 2]. This algebraic decomposition of the distribution function into an equilibrium and a non-equilibrium part can be viewed as a control-variate variance-reduction technique, in which the (large) uncertainty associated with the evaluation of the equilibrium part of the distribution function is removed with no approximation. The remaining uncertainty, associated with the (small) non-equilibrium part of the distribution, scales with the signal, leading to a constant signal to noise ratio and a method that can capture arbitrarily small deviations from equilibrium at constant cost. [1] In other words, deviational Monte Carlo methods use significantly fewer computational particles for the same resolution, or alternatively, provide significantly improved resolution, compared to traditional Monte Carlo methods for the same computational cost. In fact, by limiting the use of computational resources to regions where deviations from a known state occur, these methods function as hybrid multiscale methods which employ different descriptions in different regions of the computational domain in order to reduce the computational cost associated with multiscale problems [1,2]. Deviational methods will be presented and discussed using examples from both nanoscale gas flow and solid-state heat transfer. For the case of phonon transport, we show that additional computational savings can be obtained by using a kinetic-type of Monte Carlo simulation with no time discretization [3]. We will also discuss adjoint methods for further accelerating problems which require fine resolution in small regions of phase space [3]. References: [1] Péraud, J-P. M. and N.G. Hadjiconstantinou, "Efficient Simulation of Multidimensional Phonon Transport Using Energy-based Variance-reduced Formulations," *Physical Review B*, 84, 205331, 2011. [2] Radtke, G.A., J-P. M. Péraud and N.G. Hadjiconstantinou, "On Efficient Simulations of Multiscale Kinetic Transport," *Philosophical Transactions of the Royal Society A*, 371, 20120182, 2013. [3] Péraud, J-P.M., C.D. Landon, and N.G. Hadjiconstantinou, "Monte Carlo Methods for Solving the Boltzmann Transport Equation," *Annual Reviews of Heat Transfer*, 17, 205-265, 2014.

Phase-field Modeling for Crack Propagation in Bio-inspired Composites

heeyeong jeong*

*Korea Advanced Institute of Science and Technology

ABSTRACT

In nature highly stiff and highly tough materials are found in living organism's body due to evolution in harsh environment. Such materials have less stress concentration near crack tips even when cracks exist in the material. Also their crack paths are lengthened by deflection, which increases the toughness of material. Here, crack phase-field modeling was utilized to investigate behavior of cracks in bio-material. crack phase-field simulation can model crack propagation in bio-material more properly than previous crack propagation simulation. Through crack phase-field modeling, we found that high toughness of bio-material can be achieved by difference between young's modulus within material. we investigated staggered plates structure in nacre and structure of haversian system in bone. toughness increase was observed in both structures.

Study of Vibration Analysis of Automotive Seating Seat

heeyong jung*

*Hyundai-dymos

ABSTRACT

The purpose of this study is to develop of vibration analysis of automotive seating seat. In the paper, test results show that variation of natural frequency according to the conditions of frame, seat assembly and seating. Using the test results and FE dummy, it made a finite element model similar test results. Also the equivalent FE model was developed for the FE dummy to reduce the analysis time. Topics of interest include, but are not limited to: - Vibration analysis of automotive seating seat - Equivalent model - Reduced analysis time

A Parallel Shared-Memory Implementation of an Overlay Grid Method

nicolas le goff^{*}, franck ledoux^{**}, jean-christophe janodet^{***}

^{*}Commissariat à l'énergie atomique et aux énergies alternatives, ^{**}Commissariat à l'énergie atomique et aux énergies alternatives, ^{***}Université d'Évry-Val-d'Essonne

ABSTRACT

Some overlay grid methods [OW08] take a cartesian grid or an adaptively refined grid carrying materials volume fraction data as an input and produce an unstructured mesh with pure cells as an output. This can be used in particular when the geometry is not explicitly known, or in an intercode context where two simulation codes are executed one after the other, the first one providing the data needed to build the input of the second one. We have implemented an overlay grid method that relies on the Bulk-Synchronous Parallelism (BSP) model and a thread-safe mesh data structure. By adopting a BSP, parallel regions are gathered in steps where data consistency must then be ensured at the beginning and the end of each step. In our mesh data structure, a basic set of operations such as mesh entity creation and destruction is designed with thread-safe properties, while data races still have to be managed by the developer. We extended our data structure GMDS [FL08], a C++ Generic Mesh Data Structure that allows the developer to select the mesh entities and connectivities his algorithm requires on-the-fly, using the Kokkos [Ko] programming model and its containers in order to provide the needed thread-safe functionalities. The performance and scalability of our implementation were measured on the Haswell processor as well as the Xeon Phi manycore architecture for several examples. [OW08] S. Owen, M. Staten and M. Sorensen. Parallel Hex Meshing from Volume Fractions. 17th International Meshing Roundtable (2008) [FL08] F. Ledoux, J.-C. Weill and Y. Bertrand. GMDS: a Generic Mesh Data Structure. 17th International Meshing Roundtable (2008) [Ko] <https://github.com/kokkos>

Minimising Stress Concentration around the Voids by Location Optimisation

dedao liu^{*}, Louis N. S. Chiu^{**}, Chris Davies^{***}, wenyi yan^{****}

^{*}Monash University, ^{**}Monash University, ^{***}Monash University, ^{****}Monash University

ABSTRACT

Structural optimisation has experienced fast development during the past decades. It plays a vital role in component designs. Three major aspects, size optimisation, shape optimisation and topology optimisation are included in structural optimisation. The three aspects correspond to the size, shape, and topology of design features. However, it should be noted that in between shape and topology, the location information of design feature has not been clearly stated. For a design feature with given shape and size, its location can be defined as the location of its characteristic point, such as its centroid. The location of design feature also has a significant effect on the stress distribution in the component. And such "location optimisation" is believed to be useful especially in additive manufacturing. In traditional manufacturing, a component's complexity is usually constrained by the accessibility of tools in processes including cutting, drilling etc. In additive manufacturing, however, this kind of constraints can be removed and it's much easier to build complex features such as internal voids to reduce the component weight. The locations of these internal voids need to be optimised to minimise stress concentration. A random search method with hill-climbing algorithm has been used to solve this "location optimisation" problem in this paper. Case studies have achieved stress minimization via such "location optimisation".

Effect of the Clamping Force on Stress Redistribution for a CFRP Interference-fit Bolted Joint

ping liu^{*}, kaifu zhang^{**}, yuanxin duan^{***}

^{*}NWPU IN CHINA, ^{**}NWPU IN CHINA, ^{***}NWPU IN CHINA

ABSTRACT

Carbon fiber reinforced polymer (CFRP) composites as a typical kind of multilayers material have widely been applied on the primary structure of airplanes due to the relentless pursuit of the lighter weight and higher performance. The joint is often the weakest area in a composite structure and the bolted joint. Compressive residual stresses induced by interference-fit installation can reduce the effective hoop stress in the vicinity of the fastener hole and cause significant improvement in fatigue life of the composite joints. The clamping force along the axial direction produced by the nut and bolt head screw in assembly process, which has a significant influence on the strength of the composite structure. In the interference-fit installation process, the effect of the clamping force combining with the interference compressive force, the stress will redistribution for the composite bolted joints after the nut fastening stage. In this paper, the theoretical model of the stress distribution in the vicinity of the hole was established based on the consideration of the interference-fit amount and the clamping force. The influence of the change of the interference amount and the clamping force on the stress redistribution was studied by combining the results of the finite element simulation. Through these analyses, the following conclusions can be drawn. ? Quadratic function distribution model of the axial compressive stress in the clamping region was constructed by the hydrodynamic semi-inverse method. The compressive stress has a maximum value at the boundary of the whole wall, and then the value decreases gently to zero at the boundary of the clamping area. The amplitude and range were related to clamping force, taper angle, effective extrusion ratio coefficient and so on. ? The equivalent transformation equation of the axial compressive deformation for the perimeter of the hole was deduced based on the equivalent anisotropy of the composite material. And the radial stress distribution equation around the hole was established taking the amount of interference-fit and clamping force into account. ? Comparing the results of finite element simulation with theoretical calculation, the validity of the analytical model was verified. The influence of the interference-fit amount and clamping force on the stress distribution were analyzed. It is found that when the small interference-fit amount and big pre-tightening force occurs, stress distribution appears "peak shift", that is, the wave crests/troughs deviates from coordinate axis and move closer to the middle.

First Principle Based Multi-scale Modeling to Predict Bondline Strength of Co-cured Composite-metal Joints

xianfeng ma^{*}, Bozhi Heng^{**}, Stephanie TerMaath^{***}

^{*}The University of Tennessee,Knoxville, ^{**}The University of Tennessee,Knoxville, ^{***}The University of Tennessee,Knoxville

ABSTRACT

Compared to traditional composite-metal joints such as bolts or rivets that usually cause unacceptable damage in hybrid structure design, the emerging co-cured composite-metal joints are attractive as they avoid damage to load bearing fibers, reduce stress concentrations in substrates, and thus are less prone to fatigue and do not suffer from the manufacturing pitfalls associated with fabrication of bolted joints. [1] However, evaluating the damage propagation and potential joint failure of co-cured composite-metal joints has been challenging since the bondline failure is non-visible and difficult to detect. [2,3] Therefore, improved understanding of the bondline physics is critical to resulting desired structural performance and reliable inspection schedules for bondline damage. In this work, we present our effort to integrate quantum-mechanical based calculation and microscale simulation to develop a first principle based multi-scale modeling framework for understanding the bondline behavior of co-cured composite-metal joints. Electronic and atomic structure calculations within the formulation of density functional theory (DFT) are performed to determine the equilibrium structure and properties (lattice constants, bulk/shear moduli, and elastic constants) of each component in the joint systems. [4] Based on the obtained material constants, the microscale level study on the bondline strength is carried out through peridynamics theory, [5] a theory of mechanics that extends classical continuum solid mechanic to include discrete particles and growing cracks. We demonstrated the capability of our approach through the Aluminum substrates co-cured to E-glass/Epoxy composite joints system, where we established the correlation between the composite layer structures and the corresponding bondline behavior for the joints under service loading like bending, uniaxial tension, and low velocity impact. The approach enables us to discover the optimal design parameters of the composite-metal co-cured joints with maximum performance. References: [1] S. A. Ucsnik and G. Kirov, Mater. Sci. Forum 690, 465 (2011). [2] B. Heng and S. C. TerMaath, AIAA SciTech Forum, 2018. [3] T. J. Truster and A. Masud, Comput. Mech. 52, 499 (2013). [4] X. Ma and H. Xin, Phys. Rev. Lett. 118, 36101 (2017). [5] S. A. Silling and R. B. Lehoucq, Adv. Appl. Mech. 44, 73 (2010).

Macro-zone Size Effect in Polycrital Alloys Compute with FFT-based Crystal Elastic-Visco-Platic Simulations of Structured Polycrystal

Azdine nait-ali^{*}, Samuel Hémery^{**}

^{*}Institut Pprime, ^{**}Institut Pprime

ABSTRACT

In this study, we want to define the effects of the "crystal microstructure" of the deformation and plasticity mechanisms of Titanium alloys. Numerical modeling of the elastic stress field in a real Ti-6Al-4V microstructure was performed using the FFT technique. We have observed a strong influence of the microstructure gradient on the mechanical fields and therefore on the critical stress of the solved shear stress (CRSS). In a first study, we simulate a virtual aggregate while maintaining the morphology of the grains of the initial material and especially of the same structure . Conservation of the grains morphology in order to separate the effects of the morphology of the effects of the crystallographic orientations. The 3D calculations based on FFT allowed us to estimate an influence distance of the macrozone. We highlight the influence of the texture of local crystals, as well as the effect of the "real" macrozone present in the study material. A second study, we try to highlight the influence of the morphology of the macrozone on the mechanical fields and on the CRSS. We modify the size (volume) by creating a spherical macrozone, and varying the orientation of the ellipsoid. This information aims to highlight an effect of macrozone too often overlooked in the literature, is based on a house code of the elastic-visco-plate model based on FFT.

Multilevel Optimisation of Laminated Composite Thin-walled Structures Using Isogeometric Analysis

SHUANG QU*

*SHANDONG JIANZHU UNIVERSITY

ABSTRACT

Due to the heterogeneity of CAD and CAE system, the general finite element analysis method cannot calculate the local mechanical response of the structure with high precision during the process of optimizing complex structures. The Isogeometric Analysis will be applied to the optimisation of complex structures, and the problem will be simplified by using multilevel approach. Based on the Isogeometric Analysis, the research will involve three major contents: the design model construction and mesh subdivision research, research of structure analysis method and development of the corresponding software, research of multilevel optimisation method and development of the corresponding software. The aim of this research is to apply the Isogeometric Analysis to the multilevel optimisation design, and to set up a multilevel optimisation design system for the laminated composite thin-walled structures. The achievements of the research will open up a new direction for the application of the Isogeometric Analysis in the field of structural optimisation, and at the same time, it will provide a new design method with high efficiency and high safety for the industrial design of thin-walled structures.

Low-Dimensional Reduced-Order Models for Statistical Response and Uncertainty Quantification in Turbulent Systems

Di Qi^{*}, Andrew Majda^{**}

^{*}Courant Institute, New York University, ^{**}Courant Institute, New York University

ABSTRACT

A low-dimensional reduced-order statistical closure model is developed for quantifying the uncertainty in statistical sensitivity and intermittency in principal model directions with largest variability in high-dimensional turbulent system. Imperfect model sensitivity is improved through a recent mathematical strategy for calibrating model errors in a training phase, where information theory and linear statistical response theory are combined in a systematic fashion to achieve the optimal model performance. The idea in the reduced-order method is from a self-consistent mathematical framework for general systems with quadratic nonlinearity, where crucial high-order statistics are approximated by a systematic model calibration procedure. Model efficiency is improved through additional damping and noise corrections to replace the expensive energy-conserving nonlinear interactions. Model errors due to the imperfect nonlinear approximation are corrected by tuning the model parameters using linear response theory with an information metric in a training phase before prediction. A statistical energy principle is adopted to introduce a global scaling factor in characterizing the higher-order moments in a consistent way to improve model sensitivity. Stringent models of barotropic and baroclinic turbulence are used to display the feasibility of the reduced-order methods. It is demonstrated that crucial principal statistical quantities in mean and variance in the most important large scales can be captured with accuracy and efficiency using the reduced-order model in various dynamical regimes of the flow field with distinct statistical structures.

A Computational Study on Colloidal Gold-Nanoparticle Interaction with Ultra-short Pulse Laser

Dong Qian^{*}, Mohammad Rezaul Karim^{**}, Xiuying Li^{***}, Jaona Randrianalisoa^{****}, Zhenpeng Qin^{*****}

^{*}University of Texas at Dallas, ^{**}University of Texas at Dallas, ^{***}University of Texas at Dallas, ^{****}University of Reims Champagne-Ardenne, ^{*****}University of Texas at Dallas

ABSTRACT

With the recent advances in laser-based manufacturing, there is a continuing interest in exploring the fundamental mechanisms of laser-material interaction to improve the performance of diverse engineering applications. The unique spatial and temporal profiles of lasers provide a wide range of capabilities for material processing and device fabrication. In this talk, we present a computational study on the responses of colloidal plasmonic vesicles subjected to ultra-short pulse laser. The plasmonic vesicle consists of multiple nanocrystals on a liposome surface or within a polymer coating and provides an important class of template for biomedical applications such as drug delivery, ultrasensitive bio-sensing and imaging. To capture the key mechanisms, a multiphysics computational framework that couples the electric field with molecular dynamics simulation has been established. The simulation demonstrates that the responses of the nanoparticles depend strongly on the laser intensity, the inter-particle distance and water-particle interaction. This study identifies key factors responsible for the observed nanoparticle transformation and the significant role of water in the inter-particle interactions. The presentation concludes with validation against the experiment and perspectives on applications.

Topology Optimization of Self-supporting Support Structures for Additive Manufacturing

Xiaoping Qian^{*}, Francesco Mezzadri^{**}, Vladimir Bouriakov^{***}

^{*}UW-Madison, ^{**}UW-Madison, ^{***}UW-Madison

ABSTRACT

In this research, we formulate the generation of support structures for additive manufacturing as a topology optimization problem. We have formulated the problem as a compliance minimization that presents analogies with compliance minimization of bridges and of roof supports, with, however, a difference in the setting of zero-displacement boundary conditions. This difference fosters a comparison with transmissible loads which, together with other mechanical considerations, helps explaining why the computed structures are generally self-supporting. Compared with usual geometric considerations based support structure design, this formulation affords mechanistic meaning to the computed support structures. We show the generality of the procedure by computing supports for a variety of parts in both two and three dimensions, including a complex model of the mascot of the University of Wisconsin-Madison. The resulting support structures have also been 3D printed, demonstrating that the computed designs can successfully be used as supports. Moreover, a comparison with supports generated by existing software shows that the computed structures indeed employ less material than other approaches currently used.

Study of Numerical Model for Stress Corrosion of Bioabsorbable Zinc Alloy Stent

Aike Qiao^{*}, Zihao Li^{**}, Xinyang Cui^{***}, Kun Peng^{****}

^{*}Beijing University of Technology, ^{**}Beijing University of Technology, ^{***}Beijing University of Technology,
^{****}Beijing University of Technology

ABSTRACT

Background The use of biodegradable stents for interventional treatment of coronary heart disease has become a hot research. Iron and magnesium and their alloys were considered as bioabsorbable stent materials during the last decade. However, zinc alloy exhibits a suitable degradation performance and become the hot research in bioabsorbable stent. The numerical model for stress corrosion of the zinc alloy is not clear at present. The present work aims to establish a elementary numerical model for stress corrosion of a new zinc alloy Zn-5Al-1Mg. **Method** First?finite element method (FEM) was used to simulate the stent expansion in an idealized coronary stenosis model, and to obtain the max Mises stress. According to the formula: $\dot{D} = (1-D)^n$, $D = 0$, when the material is undamaged and $D = 1$ when it is completely damaged and loses its ability to sustain loads. Once D reaches a critical value D_{cr} , the element “fails”, and then it is deleted. A uniaxial stress stretching of the model is a simple and convenient model for stress corrosion simulation of different biodegradable materials. Thus, a simple stress damage model of Zn-5Al-1Mg alloy is established according to the stress corrosion equation in the literature. The uniaxial stress stretching of the model is performed, and the stress of stretching is the max Mises stress of the FEM. A subroutine was developed in ABAQUS to mimic the stress corrosion process. **Results** Stress corrosion started when the equivalent stress reaches 50% of the yield stress. After the beginning of stress corrosion, it is obvious that the damage factor shows an increasing trend. The time unit of the model was 220. The increasing trend is becoming steeper and steeper. After reaching the set damage factor and the time unit was 247, it will not change and the element was deleted in the model. **Conclusion** This study presents a numerical modeling approach to describe the stress corrosion of Zn-5Al-1Mg through a phenomenological model. In the future work, the pulsation force will be added to the model according to the pulsation of the blood vessel, and the stress corrosion of the model can be observed. Then, the stress corrosion model can be applied to the stent expansion idealized stenosis vessel model to calculate the stress corrosion of the material of the stent in complex geometry and complex contact. **Acknowledgement:** Science and Technology of Beijing Municipal Education Commission and Beijing Natural Science Foundation (KZ201710005007).

Characterizing Elastic Turbulence in Channel Flows at Low Reynolds Number

Boyang Qin^{*}, Paulo Arratia^{**}

^{*}University of Pennsylvania, ^{**}University of Pennsylvania

ABSTRACT

In this talk, the flow of a viscoelastic fluid is experimentally investigated using particle velocimetry methods in a microfluidic device. The device is a long and straight microchannel that is 100- μm wide and deep; the channel has a short 3-mm region that contains a linear array of cylinders (perturbation region) followed by a 3-cm long and straight region (parallel shear region). We find that, both in the wake of the cylinders and far downstream in the parallel shear region, the flow is excited over a broad range of frequencies and wavelengths. Dye injection experiments and pressure tap measurements show enhanced mixing and increased flow resistance in the parallel shear region. These key flow features are consistent with those characterizing elastic turbulence at low Re . In the wake of the cylinder, we find that the decay in velocity temporal and spatial spectra is approximately -2.7 and -3.0, respectively. However, the decay of the initial elastic turbulence around the cylinders is followed by a growth downstream in the straight region. The emergence of distinct flow characteristics both in time and space suggests a new type of elastic turbulence, markedly different from that near the curved cylinders.

Predicting Residual Stress and Deflection in an Eulerian Frame by Extended Finite Element Method

Xiaoliang Qin*

*Onfea Computing LLC

ABSTRACT

The moving laser heat in the metal additive manufacturing results in residual stresses and distortion, which can cause the crack, warpage, and delamination of the 3d printed part. Residual stress and distortion have been predicted using the Lagrangian formulation. A fully coupled thermal-mechanical transient simulation for an additive manufacturing process using a Lagrangian frame is computational costive. The moving heat problem can be treated as a quasi-steady state process in an Eulerian reference frame for some cases. In a quasi-steady state Eulerian analysis, the process can be solved within one time increment. Thus the computational cost and time spent on large time increment in a Lagrangian transient analysis can be saved. This paper is a continuation and extension of earlier work of Dr. Qin and Dr. Michaleris [1] [2]. In our previous work, the elasto-viscoplastic Eulerian formulation with four unknown fields (velocity, stress, deformation gradient and internal variable) is developed to predict residual stress and strain from the Eulerian frame. The formulation is shown to be able to accurately predict residual stress for Friction Stir Welding. However, this method cannot predict the deflection of the material, it is because the velocity is used as the primary unknown in the Eulerian reference frame. In this work, an additional unknown field is introduced to denote the signed distance from the free surface of the deformed material. Level set evolution equation is used to track the material surface deformation. Extended Finite Element Method (XFEM) is implemented to integrate the elements which are split by the signed distance function in the Eulerian frame. The Newton-Raphson method is used to solve this five fields formulation implicitly. The formulation is implemented in an in-house code. Two numerical examples are implemented to verify the accuracy of the direct equilibrium Eulerian formulation. Reference [1] Xiaoliang Qin and P. Michaleris. Thermo-Elasto-Visco-Plastic Modeling of Friction Stir Welding. Science and Technology in Welding, 14(7): 640-649, 2009. [2] Xiaoliang Qin and P. Michaleris. Eulerian Elasto-Visco-Plastic Formulations for Residual Stress Prediction. International Journal for Numerical Methods in Engineering, 77(5): 634-663, 2009.

Computation on Effective Elastic Properties of Flexible Chiral Honeycomb Cores

Kepeng Qiu^{*}, Zhi Wang^{**}

^{*}Northwestern Polytechnical University, ^{**}Northwestern Polytechnical University

ABSTRACT

Cellular materials are widely applied in various fields due to their high stiffness-to-weight ratio and designable features [1], particularly for lightweight aircraft structures. And cellular materials are known to have properties: structures and mechanisms [2]. Therefore, one may design structures with cellular materials while controlling stiffness and flexibility [3]. The application of flexible honeycomb materials to morphing aircraft, the development of which has become a subject of great interest in recent years, is of particular relevance, due to their low density and low in-plane and high out-of-plane stiffness. Flexible chiral honeycomb cores generally exhibit nonlinear elastic properties due to the large geometric deformation. To rapidly and efficiently analyze the mechanical properties of chiral honeycomb sandwich structures, it is standard to replace the actual core structure in analyses with a homogenized core material presenting reasonably equivalent elastic properties. As such, a convenient and efficient method is required to evaluate the equivalent elastic properties of flexible chiral honeycomb cores. Here we develop analytical expressions based on a deformable cantilever beam under the large deformation. Firstly, the Euler-Bernoulli beam theory and micropolar theory are used to calculate the effective elastic modulus under the small deformation. The aim is to analyze the deflection characteristic of chiral honeycombs during the effective calculation. On that basis, the equivalence expressions are improved by including the stretching deformations of the chiral honeycomb structure on an infinitesimal section of a unit cell. Finite element analysis is subsequently performed for two examples of flexible chiral honeycomb cores. Equivalent results indicate that the analytical expressions under consideration of the geometric nonlinearity are more suitable to flexible chiral honeycomb cores under conditions of high strain and low elastic modulus. ACKNOWLEDGMENTS This work is supported by the National Natural Science Foundation of China (11772258). REFERENCES [1] L.J. Gibson, M.F. Ashby, Cellular Solids: Structure and Properties, 2nd ed., Cambridge University Press, Cambridge, 1997. [2] H. Heo, J. Ju, D.M. Kim. Compliant cellular structures: Application to a passive morphing airfoil. Composite Structures, 2013, 106: 560-569. [3] I. K. Kuder, A.F. Arrieta, W.E. Raither, P. Ermanni. Variable stiffness material and structural concepts for morphing applications. Progress in Aerospace Sciences, 2013 63: 33-55.

Modeling Rolling Contact Problems in Mining Industry

Xiangjun Qiu*

*Metso Minerals

ABSTRACT

Rolling contact is a phenomenon, which exists in industries in various form, such as tire to road contact rolling, idler to conveyor indentation rolling, metal sheet to mill plastic rolling, ore to ore or ore to steel ball comminution rolling in various mills and etc.. Accurate modeling of the rolling contact problems, such as rolling resistance, contact stresses, standing waves and comminution, in industrial applications is of significant scientific and economic value. This presentation focus on the modeling of rolling mechanisms in two types of industrial contact rolling problems: viscoelastic contact rolling and comminution contact rolling. The viscoelastic rolling contact problem is characterized as a thin layer of rubber material involved in contact rolling process, in which rolling resistance and standing wave are of primary concerns. The comminution rolling contact problem is characterized as geomaterial (ore) breakage in a rolling contact cycle, in which particle breakage efficiency is of primary concern. It is demonstrated that both types of rolling contact problems can be accurately modeled, the rolling processes can be numerically simulated, and the modeling tools have been successfully integrated into engineering design and/or optimization process. In the presentation, several examples are given to show the modeling based design and optimization process in mining industry.

Puncture Mechanics of Soft Membranes with Large Deformation

Shaoxing Qu^{*}, Junjie Liu^{**}

^{*}Zhejiang University, China, ^{**}Zhejiang University, China

ABSTRACT

Soft elastic membrane structures are widely used in biological and engineering application, owing to their ability of spanning relatively large areas despite low weight. Usually, large local deformation can be induced by indentation of rigid solids on the soft elastic membranes. The indentation of the soft elastic membrane structure is followed by puncture when continuously indented by a rigid solid, which is one of the primary failure modes for membrane structures. However, the puncture of soft elastic membrane is not so well understood compared with the indentation of elastic membranes such as metallic thin films. The main challenges in puncture are the difficulties to obtain the large local deformation around the rigid indenter and to set up the failure criteria for puncture. We study the puncture of silicone rubber membrane by rigid cylindrical indenters both experimentally and theoretically, focusing on the effects of indenter size, prestretch of the membrane, and contact friction between the soft elastic membrane and the rigid indenter. In the experiment, cylindrical steel indenters with various radius are adopted to puncture the prestretched silicone rubber membranes. Puncturing force-displacement relationship, as well as the deformation configurations, of the silicone rubber membrane are obtained. It is also observed that the membrane is punctured along the corner of the cylindrical indenter and a circular hole is left at the center of the membrane. The analytical model based on continuum mechanics is developed to predict the puncture behavior of the membrane observed in experiment. Gent model is used to describe the elasticity and the stiffening effect of the silicone rubber material. The deformed membrane of three distinct regions is considered as an out-of-plane axisymmetric configuration. There is no contact between membrane and the indenter in region I, while the membrane contacts with the indenter along its side surface in region II. In region III, the membrane contacts with the indenter along its fact tip surface. We adopt the Coulomb friction law to descript the contact friction behavior between the membrane and the indenter. The governing equations and boundary conditions for each region are developed for the membrane. Analytical results show that the punctured membrane fails accompanied with large deformation near the indenter tip. The first invariant of the right Cauchy-Green deformation tensor is adopted to characterize the rupture of the membrane. Once it reaches a critical value, the membrane is punctured. In this study, the analytical results agree well with the experimental observations.

IFMM-Preconditioning for 2D Stokes Flow in Porous Media

Bryan Quaife^{*}, Pieter Coulier^{**}, Eric Darve^{***}

^{*}Florida State University, ^{**}Velo3D, ^{***}Stanford University

ABSTRACT

We consider a boundary integral equation (BIE) formulation of the two-dimensional Stokes equations in a porous geometry. While BIEs are well-suited for resolving the complex geometry, they lead to a dense linear system of equations that is computationally expensive to solve. A fast multipole accelerated iterative method is possible, but for complex geometries, many iterations are required. Therefore, we apply the inverse fast multipole method (IFMM), which is based on the framework of H^2 matrices, to precondition the linear system. We examine the effect of the preconditioners tolerance and compare its efficacy with a block-diagonal preconditioner on several geometries.

A Partitioned and a Monolithic Approach to Fluid-Composite Structure Interaction

Annalisa Quaini^{*}, Davide Forti^{**}, Martina Bukac^{***}, Suncica Canic^{****}, Simone Deparis^{*****}

^{*}University of Houston, ^{**}Ecole Polytechnique Federale de Lausanne, ^{***}University of Notre Dame, ^{****}University of Houston, ^{*****}Ecole Polytechnique Federale de Lausanne

ABSTRACT

We study a nonlinear fluid-structure interaction (FSI) problem between an incompressible, viscous fluid and a composite elastic structure consisting of two layers: a thin layer (membrane) in direct contact with the fluid, and a thick layer (linearly elastic structure) sitting on top of the thin layer. The coupling between the fluid and structure, and the coupling between the two structures is achieved via the kinematic and dynamic coupling conditions modeling no-slip and balance of forces, respectively. The coupling is evaluated at the moving fluid-structure interface with mass, i.e., the thin structure. To solve this nonlinear moving-boundary problem in 2D a partitioned approach based on Lie–operator splitting was developed, while a monolithic method was used for 3D problems. Both methods are combined with an Arbitrary Lagrangian-Eulerian (ALE) approach to deal with the motion of the fluid domain. This class of problems and its generalizations are important in e.g., modeling FSI between blood flow and arterial walls, which are known to be composed of several different layers, each with different mechanical characteristics and thickness. By using this model we show how multi-layered structure of arterial walls influences the pressure wave propagation in arterial walls, and how the presence of atheroma and the presence of a vascular device called a stent, influence intramural strain distribution throughout different layers of the arterial wall.

A PGD-based Numerical Microscope for Evaluating Processing-induced Defects on Composites Structural Performances: Towards a Macroscopic Data-based Hybrid Modeling

Giacomo Quaranta*, Emmanuelle Abisset-Chavanne**, Anaïs Barasinski***, Jean Louis Duval****, Francisco Chinesta*****

*ESI Group Chair at Ecole Centrale de Nantes, **ESI Group Chair at Ecole Centrale de Nantes, ***Ecole Centrale de Nantes, ****ESI Group, *****ESI Group Chair at ENSAM ParisTech

ABSTRACT

Composites structures exhibit deviations from nominal conditions considered for determining structural performances. These deviations come from both, the intermediate material (e.g. pre-impregnated tapes or plies) and the final part processing. Thus, pre-impregnated plies sometimes exhibit fluctuations in the reinforcement distribution, irregularities at the surface level, where a non-negligible roughness on the fiber and matrix distribution is observed, as well as impregnation defects that results in micro-cavities with different shapes and sizes located inside the ply. When processing these pre-impregnated plies or tapes, the process exacerbates some of the existing defects, creating inter-ply polymer layers (where the concentration of fibers is almost negligible) with its own roughness, micro-cavities at the ply interfaces, or gaps between contiguous tapes originated during their placement or even discontinuities originated when during the placement tapes break and process re-starts. High fidelity calculations can be performed at the ply and defect level thanks to the use of the space separated representation characteristic of PGD-based solvers, constituting a sort of numerical microscope that zooms defect effects, in order to evaluate the parametric effect of each defect in both static and dynamic loadings, and their associated mechanical performances. Finally, if macroscopic models coming from nominal designs exhibit too large deviations with respect to the ones incorporating defects and deviations existing in real parts, and because creating enriched models that include details at the fine scale is too difficult, data-based models assimilating static and dynamical mechanical responses could be included and added to the nominal model to better describe the real part and consequently guarantee model predictability, without renouncing to a fully-macroscopic description. References 1) B. Bognet, A. Leygue, F. Chinesta, A. Poitou, F. Bordeu. "Advanced simulation of models defined in plate geometries: 3D solutions with 2D computational complexity". Computer Methods in Applied Mechanics and Engineering, 201, 1-12, 2012. 2) F. Chinesta, A. Leygue, F. Bordeu, J.V. Aguado, E. Cueto, D. Gonzalez, I. Alfaro, A. Ammar, A. Huerta. "Parametric PGD based computational vademecum for efficient design, optimization and control". Archives of Computational Methods in Engineering, 20/1, 31-59, 2013.

Application of a Strain-based Formulation of PDS-FEM for the Simulation of Dynamic Crack Propagation

Lionel Quaranta^{*}, Lalith Wijerathne^{**}, Tomoo Okinaka^{***}, Muneo Hori^{****}

^{*}University of Tokyo, ^{**}Earthquake Research Institute, Tokyo, ^{***}Kindai University, ^{****}Earthquake Research Institute, Tokyo

ABSTRACT

We present an application of a strain-momentum based Hamiltonian to dynamic crack propagation, using PDS-FEM [1] as the numerical method. While Lagrangian based formulations are widely used in continuum mechanics, the existing applications of Hamiltonian in continuum mechanics are based on the displacement and momentum variables. In this work, we consider a strain-momentum based Hamiltonian. Our objective is to compare the traditional displacement-momentum form with the strain-momentum form regarding numerical accuracy and computational cost. By developing a strain-based formulation of the dynamic Hamiltonian system in the PDS-FEM frame, and using adapted symplectic time integration, we derive a numerical method which reproduces accurately the dynamic crack propagation with a relatively low computational effort. Symplectic time integrators have the advantage of ensuring the symplectic character of the flow of local variables, and variational integrators ensure in particular the conservation of total momentum throughout the computation, and the average conservation of the total energy. This participates to an improved accuracy and stability for long-time integration. PDS-FEM is used as the numerical technique due to its simple and numerically efficient crack treatment. The PDS-FEM implementation is verified by comparing with analytical solutions, and validated by comparing with dynamic mode-I crack propagation and resulting photoelastic fringe patterns captured with a 1Mfps camera. Our preliminary results show that this method is successful in reproducing the crack patterns observed experimentally for standard 2D and 3D problems, especially for mode I cracks, as well as the variation of the stress distribution around the crack tip during the propagation. A further objective will be to extend this approach to simulate the generation of crack under high strain rates, in particular shockwave induced rupture, and use it to design an accurate damage prediction method for full-scale civil infrastructures after extreme events such as hypothetical near field super-shear earthquakes. Keywords: dynamic crack propagation, Hamiltonian, symplectic algorithms, PDS-FEM, photoelasticity [1] Hori, M., Oguni, K., Sakaguchi, H., (2005) Proposal of FEM implemented with particle discretization scheme for analysis of failure phenomena, J. of Mech. and Phys. of Solids, 53 681–703.

Numerical Experiments on the Convergence Properties of State-based Peridynamic Laws and Influence Functions in Two-Dimensional Problems

Alejandro Queiruga*, George Moridis**

*Lawrence Berkeley National Lab, **Lawrence Berkeley National Lab

ABSTRACT

Peridynamics is widely used as the theoretical basis for numerical studies of fracture evolution, propagation, and behavior. While the theory has been shown to converge to continuum mechanics in the theoretical limit, its behavior as a discrete numerical approximation with respect to classic problems has been largely neglected in the literature. We present the results published in Queiruga and Moridis, 2017 in which standard analytical solutions were used to thoroughly test the numerical accuracy and rate of convergence of the spatial discretization obtained by peridynamics. We analyze the accuracy and rate of convergence of three different peridynamic constitutive responses: of these, two involve a state-based dilation, and the third is based on the estimation of the deformation gradient. The peridynamic influence function is also varied in each of the constitutive responses. The methods are tested using classical results from mechanics for uniaxial compression, isotropic compression, and simple shear, as well as Westergaard's solution for a pressurized thin crack. The two dilation-based peridynamic constitutive responses are found to only converge to one of the constant-strain solutions, while the deformation gradient-based law converges in all cases with certain influence functions. We show that a cubic influence function is the best choice of those considered in all methods. Only the deformation gradient-based model converges to the classic solutions for all three linear deformation problems, but is less accurate than the dilation-based models for the thin crack problem because of instabilities.

Phase Conservative, Monolithic Level-Set Method for Multiphase Flow

Manuel Quezada de Luna*, Dmitri Kuzmin**, Christopher Kees***

*Us Army ERDC-CHL, **TU Dortmund, ***US Army ERDC-CHL

ABSTRACT

In fluid mechanics the interaction of fluids with distinguishable material properties (e.g. water and air) is referred as multiphase flow. This problem is important due to its wide range of applications. In this work we consider two-phase incompressible flow and concentrate on the representation and time evolution of the interface. There is an extensive list of methods to treat material interfaces. Popular choices include the volume of fluid and level set techniques. We propose a novel level-set like methodology for multiphase flow that preserves the initial mass of each phase. The model combines ideas from the volume of fluid and level set methods by solving a non-linear conservation law for a regularized Heaviside of the (distance function) level-set. This guarantees conservation of the volume enclosed by the zero level-set. The equation is regularized by a consistent term that assures a non-singular Jacobian. In addition, the regularization term penalizes deviations from the distance function. The result is a nonlinear monolithic model for a phase conservative level-set where the level-set is given by the distance function. The continuous model is monolithic; meaning that only one equation is needed, doesn't require any post-processing like: numerical stabilization, re-distancing, artificial compression, flux limiting and others, all of which are commonly used in either level-set or volume of fluid methods. In addition, we have only one parameter that controls the strength of regularization/penalization in the model. We start the presentation reviewing the main ingredients of this model: 1) a conservative level-set method by [1], which combines a distanced, non-conservative level-set method with the volume of fluid method via a non-linear correction and 2) elliptic re-distancing by [2]. Afterwards, we manipulate the conservative level-set method by [1] to motivate our formulation. We present a first model which we then modify to resolve some difficulties. Finally, we present a full discretization given by continuous Galerkin Finite Elements in space and a high-order Implicit-Explicit time integration. We demonstrate the behavior of this model by solving different benchmark problems in the literature of level-set methods. Then, we present results of this model coupled with a Navier-Stokes solver to simulate water-air interaction problems in two and three dimensions. [1] C.E. Kees, I. Akkerman, M.W. Farthing, and Y. Bazilevs. A conservative level set method suitable for variable-order approximations and unstructured meshes. *Journal of Computational Physics*. [2] C. Basting and D. Kuzmin. A minimization-based finite element formulation for interface-preserving level set reinitialization. *Computing*.

Approximation of the Weakly Symmetric Elasticity Problem on Quadrilaterals

Thiago Quinelato^{*}, Abimael Loula^{**}, Maicon Correa^{***}, Todd Arbogast^{****}

^{*}LabMeC - University of Campinas, ^{**}National Laboratory for Scientific Computing, ^{***}University of Campinas,
^{****}The University of Texas at Austin

ABSTRACT

A family of stable finite element spaces for the mixed $H(\text{div})$ -conforming formulation for elasticity is introduced. These spaces are shown to be suitable for quadrilateral meshes and are based on the satisfaction in the variational sense of the symmetry condition on the stress tensor. The main contribution is that the convergence order for the stress field in the $H(\text{div})$ -norm is the same as the one for displacements in the L_2 -norm, even on non-affine quadrilateral elements. The approximation strategy is based on the combination of ABF spaces (Arnold, Boffi, and Falk, 2005) with polynomials on quadrilateral meshes, resulting in a formulation that is locking-free under both compressible and incompressible regimes. Numerical experiments are used to confirm the analysis and to illustrate the stability of the approximation. References: D. N. Arnold, D. Boffi, and R. S. Falk. Quadrilateral $H(\text{div})$ finite elements. SIAM J. Numer. Anal., 42(6):2429-2451, 2005.

Automatic Constructions of Patient-specific Finite Element Models, Study of the Load Bypass Induced by TKR Implant Placement

Jean-Baptiste RENAULT*, Sébastien PARRATTE**, Patrick CHABRAND***

*1. Aix-Marseille University, France; 2. APHM, Institute for Locomotion, France, **1. Aix-Marseille University, France; 2. APHM, Institute for Locomotion, France, ***1. Aix-Marseille University, France; 2. APHM, Institute for Locomotion, France

ABSTRACT

Introduction Historically, total knee replacement (TKR) has been performed by placing the implants in a 90° position relative to the “mechanical” axis but this concept has been recently challenged [1]. TKR failure has several non-exclusive modalities, aseptic loosening could be initiated by stress shielding. Tibial implants generally have a stem, but they might cause load bypass [2]. In this study, we investigate if the stem position relative to the tibial cortical shell could explain the load bypass better than the implant frontal orientation. **Materials and Methods** 15 Varus-aligned tibias were segmented from QCT (MIMICS®). An in-house MATLAB® algorithm automatically selected and placed the implants in 7 different angular configurations. The 105 automatically created finite elements models comprised of the tibia, the implant and a 1.5mm thick cement layer, materials were assumed linear elastic isotropic. Bone elasticity modulus was mapped from QCT and parts meshed with quadratic tetrahedron. The distal tibia was fully constrained and several load cases, representative of daily activities, were applied on the implant. Surface interactions between parts were modeled as cohesive. The centrality of the stem was defined as the ratio of the minimal over average distance between the stem tip and tibia surfaces, and the load bypass by the percentage of axial force transiting by the stem tip. **Results** Centrality explains most of the load bypass variance ($R^2 = 0.54$, $p < 0.001$), while the linear relation between the Valgus angle and the load bypass was low ($R^2 = 0.002$, NS). The load transiting through the stem tip ranged from 10 to 27% of the total axial load applied to the implant. General and intra-subject linear regressions agreed: increasing centrality resulting in lower load bypass in both case. **Discussion** Those results can be explained by an increase in rigidity caused by a structural effect, the closer to the cortical shell the stiffer, and a trabecular bone heterogeneity effect, its stiffness increases as getting closer to the cortical shell. **Conclusion** Our preliminary results suggest that stem centrality is a good predictor of stem tip loading. Those results could partly explain the discrepancies between post-op alignment and functional outcome, and give a potential cause for the pain associated with malrotation of the tibial implant [3]. **References** [1] Parratte et al., JBJS Am. 92:2143-9, 2010. [2] Au et al., J Biomech. 40:1410-6, 2007 [3] Nicoll et al., JBJS Br. 92-B:1238-44, 2010.

A Gaussian Surrogate Model for Complex Manufacturing Processes

Jean-Christophe ROUX*, Rémi LACROIX**, Vincent ROBIN***, Eric FEULVARCH****

*Univ Lyon, ENISE, LTDS, UMR 5513 CNRS, **ESI Group, ***Electricité de France R&D, ****Univ Lyon, ENISE, LTDS, UMR 5513 CNRS

ABSTRACT

A surrogate model is developed for the mechanical analysis of complex manufacturing processes, involving non-linear, strongly coupled and time-consuming models. The objective is to build a simple and fast model for calculating mechanical quantities (e.g. residual stresses) as a function of the dimensions, material properties, process parameters and so on. This model is based on numerical experiments which are made of costly multi-physical finite element simulations and it is built by means of a full factorial design of experiments technique. The main interest of this model is that: - it is entirely numerical, - it has the ability to calculate results for the mechanical analysis in a multi-physical context, - it is based on Gaussian processes [1] used as a regression technique in non-linear structural mechanics. This Gaussian surrogate model is first applied to the computation of residual stresses induced by orbital multi-pass TIG welding of metal pipes [2]. The analysis of variance (ANOVA) is used to attest the great influence of the input parameters and the classical polynomial approach and the Gaussian process are compared for calculating the residual hoop stresses. Experience shows that the Gaussian process can be very successful for non-linear multiphysical welding applications. Then Gaussian processes are used as a surrogate model in fractures mechanics to predict the structure behavior according to the inputs parameters. Since Gaussian processes and their results quality are fully specified by the use of parametrized covariance functions, a discussion is held on the choice and construction of such functions, as well as on the values of their hyperparameters and approaches for these parameters estimations. References [1] C.E. Rasmussen, C.K.I. Williams. Gaussian processes for machine learning. MIT Press, 2006. [2] L. Portelet, J.-C. Roux, V. Robin, E. Feulvarch, A Gaussian surrogate model for residual stresses induced by orbital multi-pass TIG welding, Computers & Structures, Vol. 183, 27-37, 2017 <https://doi.org/10.1016/j.compstruc.2017.01.009>.

Micromechanical Modeling of the Fracture of Nacre-like Alumina Using a Discrete Approach

Kaoutar Radi^{*}, David Jauffres^{**}, Christophe L Martin^{***}

^{*}Univ. Grenoble Alpes, CNRS, Institute of Engineering Univ. Grenoble Alpes, SIMaP, F-38000 Grenoble, France,

^{**}Univ. Grenoble Alpes, CNRS, Institute of Engineering Univ. Grenoble Alpes, SIMaP, F-38000 Grenoble, France,

^{***}Univ. Grenoble Alpes, CNRS, Institute of Engineering Univ. Grenoble Alpes, SIMaP, F-38000 Grenoble, France

ABSTRACT

Ceramics exhibit an unmatched combination of high stiffness and strength, which makes them a suitable choice for high stress and/or high temperature applications. However, their brittleness limits their use for a wide range of applications. Interestingly, several damage-resistant materials that include ceramics are used for structural purposes in nature. Nacre is the perfect example of nature's design of damage-resistant materials. Due to its complex hierarchical "brick and mortar" structure, nacre can achieve high strength and toughness simultaneously. In this context, a new bio-inspired material, nacre-like alumina, was designed from brittle constituents arranged as brick and mortar (Bouville 2014). The intrinsic and extrinsic toughening mechanisms in this material are still poorly understood. A better insight on the reinforcement mechanisms and on the microstructure/properties relationships together with microstructural optimization are paramount for this new class of materials. Using Discrete Element Modeling (DEM) which is a very suitable method to model cracks and topological modifications in materials made from brittle components (Jauffres 2012), we have developed a pseudo-3D numerical model to study the influence of the microstructural key parameters (the aspect ratio of bricks, the thickness of the mortar and their relative strength and stiffness) on fracture and crack propagation of nacre-like alumina. We account for both intrinsic and extrinsic reinforcement mechanisms, which improves on previous models (elastic/elasto-plastic) that only consider intrinsic reinforcement. Compared to previous numerical models, the increase of fracture resistance as the crack propagates due to crack bridging is studied. The model is calibrated on both elasticity and fracture for the bricks and the mortar, which are modeled by a packing of spherical discrete particles. The model is validated against the analytical model of Barthelat (Barthelat 2014) on a 2D periodic unit cell of an idealized brick and mortar geometry. Depending on the overlap region, the bricks volume fraction and the strength of the mortar, we are able to retrieve two failure modes, mortar failure and bricks failure. We determine the parameters that prevent bricks failure and control the failure mode. Building on this validated model, an example of a realistic microstructure encompassing a few hundred platelets is created to investigate crack propagation, extrinsic reinforcement mechanisms such as crack bridging and to show the rising R-curve. Bouville, & al, (2014), Nature Materials. Barthelat, (2014), Journal of the Mechanics and Physics of Solids. Jauffres & al, (2012), Acta Materialia.

Advances in the Application of Discontinuous Galerkin Methods to Material and Structural Failure

Raul Radovitzky^{*}, Brandon Talamini^{**}, Bianca Giovanardi^{***}, Anwar Koshakji^{****}

^{*}MIT, ^{**}MIT, ^{***}MIT, ^{****}MIT

ABSTRACT

In this talk, I will discuss progress in the application of discontinuous Galerkin methods to material and structural failure. Topics will include: large-scale simulation of shell structures, challenges and approaches in describing quasi-static crack propagation, and the development of a scalable algorithm to describe hydraulic fracture in three dimensions.

Multiscale Modeling of Carbon Fiber/Carbon Nanotube/Epoxy Hybrid Composites: Comparison of Epoxy Matrices

Matthew Radue^{*}, Gregory Odegard^{**}

^{*}Michigan Technological University, Houghton, MI 49931, USA, ^{**}Michigan Technological University, Houghton, MI 49931, USA

ABSTRACT

The growing usage of carbon fiber (CF) composites attests to the demand of stiff-yet-lightweight materials. However, these composites presently demonstrate some weaknesses that limit their applicability: low compressive strength, susceptibility to delamination upon impact, and low thermal conductivity. It is conjectured that the inclusion of nanoparticles in the matrix may address these issues collectively. The noteworthy mechanical and thermal properties of carbon nanotubes (CNTs) make these nanoparticles attractive candidates for enhancing the deficiencies of traditional CF composites. Some studies have sought to understand what matrix characteristics promote good CNT-matrix interaction, showing that CNTs have a greater reinforcing effect on more ductile epoxies compared to stiff epoxies. Despite the important knowledge that has been gained, it is still unclear how the functionality of the epoxy (i.e., di-functional, tri-functional, tetra-functional) influences the CNT-matrix interaction and the overall elastic properties of CF/CNT/epoxy hybrid composites. The objective of this study is to employ Molecular Dynamics (MD) to compare the interfacial and mechanical response of three different crosslinked epoxy systems on the molecular level. A micromechanics approach is then utilized to predict the effective properties of realistic CNT/epoxy nanocomposites and CF/CNT/epoxy hybrid composites. At each step, the dissimilarities due to the three matrices are identified. The MD results demonstrate that the strength of the CNT-epoxy interaction correlates with the epoxy's ability to conform to the CNT and closely pack around it. Analysis of the interface and interphase region revealed that the tetra-functional epoxy did not adhere well to CNT (as compared to the other epoxies), which was detrimental to the stiffness of the MD model. However, the tri-functional resin paired with CNT outperforms the other models with respect to stiffness. The multiscale model was used to determine whether the excellent properties of the CNT/tri-functional resin MD model ultimately translate into a superior nanocomposite at the bulk level. The results indicate the tri-functional epoxy does indeed deliver the highest modulus nanocomposite and CF/CNT/epoxy hybrid composites for high CNT loadings. However, for CNT concentrations up to 5 wt%, the tri- and tetra-functional epoxies are expected to result in composites with comparable stiffness. For CNT composites with even higher concentrations, the tri-functional epoxy is more promising because of the combination of good bulk stiffness and strong interaction with CNT.

Analysis of Reliability of Levees against Slope Instability Using FLAC3D and an Adaptive Kriging-Based Monte Carlo Simulation Method

Mehrzad Rahimi^{*}, Zeyu Wang^{**}, Abdollah Shafieezadeh^{***}, Dylan Wood^{****}, Ethan J. Kubatko^{*****}

^{*}The Ohio State University, ^{**}The Ohio State University, ^{***}The Ohio State University, ^{****}The Ohio State University, ^{*****}The Ohio State University

ABSTRACT

Over 100,000 miles of levees in the United States protect communities from storm surge. Analysis of reliability of these systems against surge hazard is critical to determine the likelihood of failures and develop cost-effective risk mitigation solutions. Instability along with external erosion, internal erosion, and hydraulic failure are considered as primary failure processes of levees. Levee instability, in particular, occurs when the sum of destabilizing forces exceeds the resistance to failure on a failure surface. This type of failure can manifest in the form of shallow or deep sliding along the shear surface within the embankment in the waterside or landside of levees. Many former investigations used factor of safety evaluated through strength reduction method as the limit state function to evaluate the reliability of levees. In this approach, material strengths of levees are continually reduced by strength reduction factors until failure is reached. A primary shortcoming of this approach is that the same strength reduction factor is applied to all soil properties that affect the shear strength of soil in order to bring the slope to the state of instability [1]. Moreover, the factor of safety determined using this approach does not necessarily correspond to a shear surface that can lead to collapse of the slope and hence levee breach. To address these limitations in this study, limiting equilibrium states of the model are identified as an assembly of grid points in critical zones of levee embankments with rate of displacement increase higher than a critical threshold. Numerical analyses of levees to determine the rate of increase in displacement of various points in embankments are conducted in finite difference platform of FLAC3D. A new reliability analysis technique called REAK is used here to analyze the probability of failure of levees with respect to embankment instability. REAK employs Kriging surrogate modeling for adaptive and strategic sampling of random variables to generate most effective training points for model refinement. This feature significantly reduces the high computational demand for failure probability analyses of systems with complex numerical models. Results indicate the high efficiency of the proposed procedure for reliability analysis of levees and potentially for other geotechnical structures. 1. Li, D. Q., Xiao, T., Cao, Z. J., Phoon, K. K., & Zhou, C. B. (2016). Efficient and consistent reliability analysis of soil slope stability using both limit equilibrium analysis and finite element analysis. Applied Mathematical Modelling, 40(9), 5216-5229.

Parallel, Contact-aware Simulations of Concentrated Stokesian Suspensions in 3D

Abtin Rahimian^{*}, Libin Lu^{**}, Denis Zorin^{***}

^{*}University of Colorado Boulder, ^{**}New York University, ^{***}New York University

ABSTRACT

We present an efficient, accurate, robust, and parallel-scalable method for simulation of dense suspensions of deformable and rigid particles immersed in Stokesian fluid in three dimensions. We use a well-established boundary integral formulation for the problem as the foundation of our approach. This type of formulation, with a high-order spatial discretization and an implicit and adaptive time discretization, have been shown to be able to handle complex interactions between particles with high accuracy. Yet, for suspensions with high volume fractions, very small time-steps or expensive implicit solves as well as a large number of discretization points are required to avoid non-physical contact and intersections between particles, leading to infinite forces and numerical instability. Our method maintains the accuracy of previous methods at a significantly lower cost for dense suspensions. The key idea is to ensure interference-free configuration by introducing explicit contact constraints into the system. While such constraints are unnecessary in the formulation, in the discrete form of the problem, they make it possible to eliminate catastrophic loss of accuracy by preventing contact explicitly. Introducing contact constraints results in a significant increase in stable time-step size for explicit time-stepping, and a reduction in the number of points adequate for stability.

AllQuad, a New Automatic High Quality 3D Quadrilateral Mesher

Robert Rainsberger*, John Rogers**

*XYZ Scientific Applications, Inc., **XYZ Scientific Applications, Inc.

ABSTRACT

A new automatic 3D multi-block structured all quadrilateral mesh generation algorithm for arbitrary composite surfaces with non-self intersecting boundaries is described in this paper. It can be used to form shell element meshes or to form the boundary mesh for an automatic 3D multi-block structured all hexahedral mesh generator under development. The surfaces can have any number of holes. First, the surfaces are sewn together to form one polygonal surface approximating the composite surface. Nodes are selected along the boundaries. Nearly geodesic 3D curves connect critical points on the boundary, dividing the polygonal surface into nearly convex patches. One of sixty templates is chosen to mesh each patch. Finally, the composite mesh is smoothed on the actual surfaces. This method is designed to maintain element quality while minimizing the number of irregular nodes. Examples are given.

Hidden Physics Models: Machine Learning of Nonlinear Partial Differential Equations

Maziar Raissi^{*}, Paris Perdikaris^{**}, George Karniadakis^{***}

^{*}Brown University, ^{**}University of Pennsylvania, ^{***}Brown University

ABSTRACT

A grand challenge with great opportunities is to develop a coherent framework that enables blending conservation laws, physical principles, and/or phenomenological behaviours expressed by differential equations with the vast data sets available in many fields of engineering, science, and technology. At the intersection of probabilistic machine learning, deep learning, and scientific computations, this work is pursuing the overall vision to establish promising new directions for harnessing the long-standing developments of classical methods in applied mathematics and mathematical physics to design learning machines with the ability to operate in complex domains without requiring large quantities of data. To materialize this vision, this work is exploring two complimentary directions: (1) designing data-efficient learning machines capable of leveraging the underlying laws of physics, expressed by time dependent and non-linear differential equations, to extract patterns from high-dimensional data generated from experiments, and (2) designing novel numerical algorithms that can seamlessly blend equations and noisy multi-fidelity data, infer latent quantities of interest (e.g., the solution to a differential equation), and naturally quantify uncertainty in computations. The latter is aligned in spirit with the emerging field of probabilistic numerics.

A Monolithic Constraint-Based Approach for Handling Fluid-Solid Interaction Problems via Smoothed Particle Hydrodynamics

Milad Rakhsha^{*}, Arman Pazouki^{**}, Radu Serban^{***}, Dan Negrut^{****}

^{*}University of Wisconsin-Madison, ^{**}California State University, ^{***}University of Wisconsin-Madison, ^{****}University of Wisconsin-Madison

ABSTRACT

We present a meshless discretization of Navier-Stokes equations that draws on a differential-algebraic equation (DAE) formulation and results in a monolithic coupling between the fluid and solid phases. The methodology is particularly attractive when dealing with Fluid-Solid Interaction (FSI) problems containing a large number of bodies whose dynamics are governed by kinematic constraints, friction, and contact. In this approach, the dynamics of the fluid phase is resolved by Smoothed Particle Hydrodynamics (SPH) and is formulated as a set of DAEs. Particularly, the mass conservation is satisfied by enforcing bilateral constraints on the density of SPH markers at the velocity level, which consequently ensures a divergence-free velocity field. Moreover, our formulation for DEAs prevents drift from incompressibility condition at the position level. Therefore, both the constant-density and the divergence-free velocity conditions are naturally satisfied with the current methodology; this is particularly an advantage of the current methodology compared to the conventional projection-based methods where special care is required to satisfy both conditions simultaneously (Hu and Adams, Journal of Computational Physics, 2007, Mitsuteru Asai et al., Journal of Applied Mathematics, 2012). Overall, the solution to the fluid-solid interaction problem is cast as a Cone Complementarity Problem (CCP), which is posed as the first-order optimality condition of a convex quadratic optimization problem with conic constraints. We use a Nesterov-type method, Accelerated Projected Gradient Descent (APGD), to efficiently solve the optimization problem at every time-step. We present numerical results demonstrating the scalability and accuracy of the current approach for three test studies (dam break, incompressibility, sloshing). Furthermore, we demonstrate the capability of the current method when dealing with real world problems such as tracked-vehicle fording simulation. In conclusion, the resulting FSI solution is both fast and scalable. It is fast owing to the semi-implicit and monolithic nature of the approach that results in two-orders of magnitude larger time steps compared to an explicit SPH approach. It is scalable owing to its reliance on a matrix-free iterative solver for the solution of the underlying optimization problem. [1] X. Y. Hu and N. A. Adams. An incompressible multi-phase SPH method. Journal of Computational Physics, 227(1):264-278, Nov 10, 2007. [2] Mitsuteru Asai, Abdelraheem M Aly, Yoshimi Sonoda, and Yuzuru Sakai. A stabilized incompressible sph method by relaxing the density invariance condition. Journal of Applied Mathematics, 2012.

A Finite Temperature Quasicontinuum analysis of Recrystallization of Amorphous Silicon

Amuthan Arunkumar Ramabathiran*

*Indian Institute of Technology Bombay

ABSTRACT

The recrystallization of amorphous silicon plays an important role in many technological applications, most notably in microelectronics in the context of device miniaturization. A variety of computational and experimental studies of recrystallization have been carried out in the past by investigating the amorphous/crystalline (a/c) interface and measuring the rate of recrystallization. In this work, a new strategy to extend the quasicontinuum method for non-crystalline solids is proposed, and subsequently utilized to study the recrystallization process in pure Si. In particular, the temperature dependence of the a/c interface velocity and the atomistic mechanisms operative during recrystallization are investigated. The recrystallization of amorphous silicon is also numerically interesting from the point of view of the quasicontinuum method since the fraction of silicon atoms in amorphous form is significant in comparison with that in crystalline form. As a first step, a study of the recrystallization process using a previously developed finite temperature extension of the quasicontinuum method, in conjunction with an adaptive coarse-graining strategy that tracks all the atoms in the amorphous region and only those atoms in the crystalline region that are near the a/c phase boundary, is presented and validated using molecular dynamics simulations. The validated quasicontinuum model subsequently serves as a useful benchmark to test new ideas related to the extension of the quasicontinuum method for non-crystalline solids. One possible extension of the quasicontinuum method for amorphous materials is proposed in this work via a statistical algorithm based on the local atomic neighborhood. In the context of the recrystallization study, the statistical nature of the method results in a probability distribution for the a/c interface growth rate. Convergence studies of the recrystallization rate distribution according to the proposed algorithm and detailed comparisons with both numerical and experimental data are presented to highlight the usefulness of the proposed coarse-graining technique for studying non-crystalline solids. Limitations of the current approach and promising ideas that refine and extend this framework will also be discussed.

High-order Chimera Method Based on Moving Least Squares for Fluid-Structure Interaction

Luis Ramirez*, Xesús Nogueira**, Pablo Ouro***, Fermín Navarrina****

*Grupo de Métodos Numéricos en Ingeniería (GMNI), E.T.S.I. Caminos, Canales y Puertos Universidade da Coruña, Campus Elviña, 15171, A Coruña, Spain, **Grupo de Métodos Numéricos en Ingeniería (GMNI), E.T.S.I. Caminos, Canales y Puertos Universidade da Coruña, Campus Elviña, 15171, A Coruña, Spain,

***Hydro-Environmental Research Centre, School of Engineering, Cardiff University, The Parade, Cardiff, UK,

****Grupo de Métodos Numéricos en Ingeniería (GMNI), E.T.S.I. Caminos, Canales y Puertos Universidade da Coruña, Campus Elviña, 15171, A Coruña, Spain

ABSTRACT

The Chimera/overset approach is widely used in the numerical simulation of flows involving moving bodies. In this approach, first used by Steger et al. in 1983 [1], the domain is subdivided into a set of overlapping grids, which provide flexible grid adaptation, the ability to handle complex geometries and the relative motion of bodies in dynamic simulations. In this work a higher-order (> 2) accurate finite volume method [2,3] for the resolution of the Euler/Navier-Stokes equations on Chimera grids is presented. The formulation is based on the use of Moving Least Squares (MLS) approximations [4] for transmission of information between the overlapped grids [5]. The accuracy and performance of the proposed method is demonstrated by solving different benchmark problems. An example of fluid structure interaction using this method is shown with the application of the proposed scheme to the computation of a Vertical Axis Turbine. REFERENCES [1] Steger, J., Dougherty, F., Benek, J., "A Chimera Grid Scheme", ASME, Mini-Symposium on Advances in Grid Generation, Houston, June 1982. [2] Cueto-Felgueroso, L., Colominas, I., Nogueira, X., Navarrina, F., Casteleiro, M., "Finite volume solvers and Moving Least-Squares approximations for the compressible Navier-Stokes equations on unstructured grids", Computer Methods in Applied Mechanics and Engineering, 196 :4712-4736, 2007. [3] X. Nogueira, L. Ramirez, S. Khelladi, J.C. Chassaing, I. Colominas, "A high-order density-based finite volume method for the computation of all-speed flows", Computer Methods in Applied Mechanics and Engineering, 298, 229–251, 2016. [4] Lancaster, P., Salkauskas, K., "Surfaces generated by moving least squares methods", Mathematics of Computation 37, 155: 141-158, 1981. [5] L. Ramirez, C. Foulquié, X. Nogueira, S. Khelladi, J.C. Chassaing, I. Colominas, New high-resolution preserving sliding mesh techniques for higher-order finite volume schemes. Computers & Fluids, vol 118, 114–130, 2015.

A Multicomplex Finite Element Approach for Curvilinear Progressive Fracture

Daniel Ramirez Tamayo^{*}, Harry Millwater^{**}, Arturo Montoya^{***}

^{*}The University of Texas at San Antonio, ^{**}The University of Texas at San Antonio, ^{***}The University of Texas at San Antonio

ABSTRACT

A unique, curvilinear fracture algorithm for simulating crack growth has been developed based on the complex variable finite element method, ZFEM. ZFEM has the capability of computing arbitrary-order derivatives of a structure's response variable under a single finite element run. In previous publications [1-2], ZFEM analyses of first order have been used to conduct fracture mechanics analyses undergoing different loading conditions such as thermal, mechanical and mixed mode. The energy release rate, a critical fracture parameter, has been computed as the first order derivative of the strain energy with respect to the crack size. In this study, higher order derivatives of the strain energy with respect to the crack size are obtained by expanding ZFEM to multicomplex algebras. The proposed crack progression methodology consists of constructing an arbitrary order Taylor series approximation of the strain energy as a function of crack propagation. This Taylor series is formed by the high order derivatives that are obtained from the multicomplex finite element analyses. Using this local energy response function, a curvilinear crack path is predicted along the maximum energy release rate direction. The approach was tested by comparing the crack path measured by Miranda et al. [3] on a homogeneous steel specimen with a hole to the results provided by the proposed approach. The crack path predictions were performed for response functions constructed with different derivative orders, 1 to 4. The numerical results were in excellent agreement with the experimental paths. Nonetheless, fewer crack path increments were required when higher order derivatives were considered. This method offers significant advantages over traditional methods models that predict a curved crack path using several small linear crack increments. ZFEM curvilinear capabilities yield to higher accuracies and require less simulation steps. References [1] Millwater, H., Wagner, D., Baines, A., Montoya, A., 2016. A virtual crack extension method to compute energy release rates using a complex-valued finite element method. *Engineering Fracture Mechanics* 162, 95–111. [2] Daniel Ramirez Tamayo, Arturo Montoya, Harry Millwater, A Virtual Crack Extension Method for Thermoelastic Fracture using a Complex-variable Finite Element Method, *Engineering Fracture Mechanics*, 2017. [3] A.C.O. Miranda, M.A. Meggiolaro, J.T.P. Castro, L.F. Martha, and T.N. Bittencourt. Fatigue life and crack path predictions in generic 2d structural components. *Engineering Fracture Mechanics*, 70(10):1259 – 1279, 2003.

Hierarchic Isogeometric Shell Formulations Intrinsically Avoiding Locking

Ekkehard Ramm*, Bastian Oesterle**, Renate Sachse***, Manfred Bischoff****

*University of Stuttgart, Germany, **University of Stuttgart, Germany, ***University of Stuttgart, Germany,
****University of Stuttgart, Germany

ABSTRACT

The contribution addresses novel concepts emerging on the basis of Isogeometric Analyses (IGA) offering smooth function spaces (as NURBS) with higher inter-element continuity. They allow avoiding locking phenomena a priori on the theory level before discretization. IGA easily satisfies C1-continuity Kirchhoff-Love (KL) finite elements with low order trial functions. These results are taken as basic building block for a Reissner-Mindlin (RM) model. Instead of introducing total rotations as primal variables modified parametrizations in a sense of hierarchic formulations are chosen superimposing the transverse shear parts in an incremental way. Since the function spaces of these extra parts are separated from the KL basis the formulation is completely free from shear locking independent of the kind of discretization. Two different parametrizations are described. In the first concept [1] both transverse shear components are introduced as hierarchic (incremental) rotations superimposed on the KL-rotations, which in turn depend per definition on the mid-plane displacements. Since it turned out that the shear stress resultants still show a tendency to oscillate due to an unbalance in spaces, a second concept [2] is proposed, in which the two displacement fractions responsible for the transverse shear are superimposed as hierarchic displacement parameters to the total displacements. This leads to a shear deformable, rotation-free isogeometric shell formulation intrinsically free of shear locking showing excellent performance for shear stress resultants. Both formulations have been extended into the geometrically non-linear regime [3]. In the majority of practically relevant cases the transverse shear rotations can be assumed to be small. Thus, this linearized part can be added hierarchically to the fully non-linear KL shell model following the same additive procedure as in the case of small rotations, avoiding the cumbersome treatment of large rotations, for instance using Rodrigues parameters. A corresponding primal formulation to avoid membrane locking is still a challenge. Therefore, this defect has been remedied by applying either mixed formulations, or we resort directly to the Discrete Strain Gap (DSG) method. [1] R. Echter, B. Oesterle, M. Bischoff, A hierarchic family of isogeometric shell finite elements, *Comput. Methods Appl. Mech. Engrg.* 254 (2013) 170-180. [2] B. Oesterle, E. Ramm, M. Bischoff, A shear deformable, rotation-free isogeometric shell formulation, *Comput. Methods Appl. Mech. Engrg.* 307 (2016) 235-255. [3] B. Oesterle, R. Sachse, E. Ramm, M. Bischoff. Hierarchic isogeometric large rotation shell elements including linearized transverse shear, *Comput. Methods Appl. Mech. Engrg.* 321 (2017) 383-405.

Evolution of Shell Formulations - from Love to IGA

Ekkehard Ramm*, Manfred Bischoff**

*University of Stuttgart, Germany, **University of Stuttgart, Germany

ABSTRACT

The contribution gives a brief outline how shell formulations evolved in the last 130 years. It starts with the seminal paper of A.E.H. Love published in 1888 [1]. The subsequent period was concentrating on finding analytical solutions known at that time from mathematical physics like Euler or Bessel ODEs or applying corresponding energy expressions. Thus, Love's general equations were specialized to specific rotational or translational shells or to subclasses like deep and shallow shells; in addition minor terms were neglected simplifying the analysis. This period until the mid of the 20th century was of utmost importance for understanding the physical behavior of these delicate structures. In addition, first steps into the non-linear regime were made, in particular investigating buckling phenomena (von Karman, Koiter et al.). Beginning of the second half of the 20th century shell theories were extended and refined in many ways. Further mechanical effects were added to the basic formulation such as transverse shear deformations, higher order kinematics, heterogeneous layout across the thickness as well as geometrical and material nonlinearities, again mostly for simplified models. The potential for concrete analyses dramatically changed after the advent of modern computers and the rapid developments of numerical solution schemes, above all the finite element method. In the first decade, the C1-continuity requirement for the (Kirchhoff-) Love (KL) model was a major challenge, so that around 1970 versions with C0-continuity applying the so-called Reissner-Mindlin (RM) kinematics including transverse shear deformations were favored. Due to locking problems, innumerable un-locking schemes were proposed. In this period, shell problems in the entire spectrum of the computational environment have been investigated in the non-linear, multi-scale, multi-physics regime including multilayer and solid shell models. When in 2005 Hughes and co-workers introduced the Isogeometric Analysis it was soon recognized that low order NURBS (or subdivision) discretizations allow satisfying the continuity requirement for KL shells. Starting from this model recently hierarchic shell formulations were developed which intrinsically avoid geometrical locking problems on the theory level [2]; these formulations utilize hierarchic rotations or displacements in the sense of a re-parametrization of primary variables. [1] A.E.H. Love, The Small Free Vibrations and Deformation of a Thin Elastic Shell, Phil. Trans. R. Soc., 1888, 179A , 491-546. [2] B. Oesterle, E. Ramm, M. Bischoff, A shear deformable, rotation-free isogeometric shell formulation, Comput. Methods Appl. Mech. Engrg. 307 (2016) 235-255.

Using Micro-computed Tomography for Image-based Material Testing of Particulate Composites to Quantify Microscale Damage

Katherine Ramos*, Karel Matouš**

*University of Notre Dame, **University of Notre Dame

ABSTRACT

Understanding the mechanical behavior that arises from the heterogeneity at different length scales of natural and synthetic heterogeneous materials is essential. X-ray micro-computed tomography (micro-CT) has become a popular method in the materials science community for nondestructive analysis of the internal microstructure in these complex materials. In particular, this technology allows in situ analysis of materials under mechanical loading. The power of this experimental technique is enhanced through detailed statistical analysis of the evolution of various structural features through robust image processing strategies at various stages of loading. In this work, we develop an image-based material testing approach using micro-CT to understand the influence of microstructure and local damage phenomenon on the effective mechanical response of rubber-glass bead composites. Furthermore, a nondestructive, three-dimensional image-based analysis protocol which provides high fidelity of sample testing and data assessment has been established. An investigation was performed on various microstructure compositions of silicone rubber reinforced with silica particles. In situ compression experiments were used to study how the microscale damage (void creation from debonding) develops and evolves in the context of four primary studies: i) effect of particle volume fraction ii) effect of particle diameter iii) local damage phenomena and its evolution (incremental loading/unloading) and iv) effect of surface treatments on bonding characteristics. We use image analysis tools to quantify damage in the composites through calculations of void volume fractions and void size distributions. Additionally, we exploit the ability to directly examine the material's microstructure before and after loading to determine multiscale linking and evolution of fields when assessing the damage. The rich data analysis collected from the various experimental studies offers an understanding of the complex phenomena attributing to the material's response to loading including the mechanical and morphological response of non-linear viscoelastic materials subjected to uniaxial compression. In addition to the fundamental understanding, these experiments serve as validation data sets for multi-scale modeling approaches. In particular, the analysis will serve as a foundation in the development of better constitutive theories for Finite Element Analysis (FEA) of these heterogeneous microstructures. Focus is placed on the development of non-linear viscoelastic constitutive models with damage/debonding for these complex heterogeneous systems. This analysis and framework yields new insight of these composite materials required for the optimal material design. Additionally, the thorough and reliable experimental and image processing framework established supplements existing image-based modeling techniques substantially.

Topology Optimized Functionally Graded Structures for Impact Applications

Francisco Ramírez-Gil*, Esteban Foronda-Obando**, Wilfredo Montealegre-Rubio***

*Universidad Nacional de Colombia, **Universidad Nacional de Colombia, ***Universidad Nacional de Colombia

ABSTRACT

Functionally graded materials (FGM) are a kind of composites in which the microstructure, composition, porosity or other characteristics is changed continuously through one or more directions allowing a smooth variation of properties over the volume [Miyamoto et al., 1999]. In particular, the concept of FGM can be used for impact applications where the material is designed at macroscopic level with varying stiffness from the surface to the core looking for the best relation of parameters to enhance the energy absorption [Ramírez-Gil et al., 2016]. Although there are several options to design impact-resistant FGMs, in this research the density of the material of a rectangular plate is changed by controlling its porosity throughout its thickness. This approach is commonly used by nature in structures subjected to impact such as bones, teeth, horns, bird beaks and wood [McKittrick et al., 2010]. The topology optimization method (TOM) is used herein for optimal generation of the holes (size, shape, location, and the number of pores) by discretizing the plate in several layers, allowing each of them to have a different thickness and volume fraction constraint in order to achieve a functionally graded structure. Commercial software, LS-TaSC in conjunction with LS-DYNA, is used to get the topologies. The impact is assessed with the explicit finite element software and the model considers an elastoplastic material behavior at sub-ordnance velocity. Several patterns of holes are obtained and compared to a solid plate in terms of weight and energy absorption capability. The results show that it is possible to design the pattern of holes reducing the weight of the plate without having a substantial detriment on its structural response, which can be useful in applications where the weight is a priority. Finally, further research should be developed so that this design technique can be applied to components subjected to more complex impact phenomena produced by medium- and high-velocity impacts. References • Miyamoto et al., Functionally Graded Materials. Design, Processing and Applications. Springer, 1999. • Ramírez-Gil et al., "Optimization of functionally graded materials considering dynamical analysis," in Advanced Structured Materials, Springer, 205–237, 2016. • McKittrick et al., Energy absorbent natural materials and bioinspired design strategies: A review. Materials Science and Engineering C, 30(3), 331-342, 2010.

Concurrent Optimization of Topology and Distributed Transverse Isotropy for 3D Structures

Narindra Ranaivomiarana^{*}, Dimitri Bettebghor^{**}, François-Xavier Irisarri^{***}, Boris Desmorat^{****}

^{*}Onera, Chatillon, France, ^{**}Onera, Chatillon, France, ^{***}Onera, Chatillon, France, ^{****}Sorbonne Universite, Centre Nationale de la Recherche Scientifique, UMR7190, Institut Jean le Rond d'Alembert, Paris, France

ABSTRACT

This research project is funded by STELIA Aerospace. Reducing weight and costs of structures is crucial for aeronautic industry. Thus, great effort is placed in the development of new methodologies for mass minimization. Topology optimization is a relevant method on the rise. It consists of determining the best shape of structural components or the best layout of structures for a given bulk and predefined loadings. Most of the works in the field deals with isotropic materials, especially metallic ones. However, composites are increasingly used to lighten structures. These materials give new degrees of freedom for the optimization as it is possible to tailor the material anisotropy through the fiber orientations. Composite structures design and optimization is classically performed with fixed predefined shapes, most of the time derived from the preexisting metallic parts. Nevertheless, such a practice is questionable since the material anisotropy influences the optimal shape. The aim of the present project is to bridge the gap between topology optimization and composite optimization by developing an innovative method for simultaneous topology and anisotropy optimization of three dimensional structures. In the present paper, transversely isotropic materials are used. This work generalizes previous work by the authors about compliance minimization with a maximal volume constraint in two dimensions. The problem is solved numerically with an optimality criteria algorithm. The algorithm iterates between local minimizations in each element with fixed stress and re-actualization of the stress field with fixed design variables using finite element analysis. The material distribution is parameterized by a continuous density variable, penalized with the SIMP method (Solid Isotropic Method Penalization). The distributed anisotropy is parameterized using elasticity tensor invariants by change of frame. In two dimensions, the polar invariants are used. In three dimensions, significant work has been done to identify the adequate invariants and to solve the local minimizations. The results show that the optimal orientation of the transversely isotropic material is in the same direction as the highest absolute eigenvalue of the stress tensor's deviator. The optimal values of anisotropic invariants are found with explicit expressions. The developed method is applied on academic and industrial test cases. Compared with sequential optimization results where the shape is first optimized with a fixed isotropic material and then the material distribution is optimized with the obtained shape, the simultaneous optimization leads to a stiffer optimal design with a different shape.

A Comparison of Viscoelastic Level Set Formulations: Property Averaging versus Equation Averaging

Rekha Rao*, Weston Ortiz**

*Sandia National Laboratories, **University of New Mexico

ABSTRACT

In this work, we extend a finite element, Newtonian, level set implementation to viscoelastic flow, where a separate stress tensor must be solved in addition to the velocity and pressure. We investigate formulations where one fluid is viscoelastic and the other is Newtonian. We look at two viscoelastic level set (VE-LS) approaches; one based on the traditional property averaging common in level set implementations and the other using an equation averaging approach for the polymeric extra stress tensor. The viscoelastic equations are discretized using DEVSS-G method with LBB elements for the velocity and pressure spaces and bilinear interpolation for the stress and velocity gradient space. A Phan-Thien-Tanner (PTT) exponential constitutive equation is used to describe the viscoelastic response. Surface tension forces play a key role in many two-phase and immiscible fluid problems, especially in microfluidic flows where capillary forces can become dominant. For level set implementations, surface tension implementations can be plagued by parasitic currents. We investigate and compare multiple methods for reducing parasitic currents. The approaches are benchmarked against an arbitrary-Lagrangian-Eulerian (ALE) implementation for viscoelastic die swell into a Newtonian gas phase and a Newtonian droplet in a viscoelastic fluid traveling through a microfluidic constriction. In general, we have found that the results are better using equation averaging, though this is a costlier algorithm. *Sandia National Laboratories is a multi mission laboratory managed and operated by National Technology and Engineering Solutions of Sandia, LLC., a wholly owned subsidiary of Honeywell International, Inc., for the U.S. Department of Energy's National Nuclear Security Administration under contract DE-NA0003525.

Temporal Decomposition Strategies for Long-horizon Dynamic Optimization

Vishwas Rao*, Mihai Anitescu**

*Argonne National Laboratory, **Argonne National Laboratory

ABSTRACT

In this work, we investigate a temporal decomposition approach to long-horizon dynamic optimization problems. The problems are discrete-time, time-dependent and with box constraints on the control variables. These problems typically arise as optimal planning problems in electrical power industry for transmission or generation expansion. Planning analysis for these problems involves a production cost model (PCM). A PCM simulates the operation of generation and transmission systems by solving a nonlinear constrained optimal control problem for each time-interval in order to arrive at a least-cost solution to meet the energy demands. Many studies require simulating a PCM on an hourly scale for 1-20 years under different scenarios and this would mean that the number of time-intervals exceed 100,000. Additionally, each time interval involves tens of thousands of state and control variables, making the solution to a PCM a computationally expensive proposition. In this study, we propose an approximate temporal decomposition using overlapping time-intervals for approximate temporal decomposition of long-horizon dynamic optimization problem. The proposed approach opens up avenues to expose temporal-parallelism and hence creates an opportunity for faster computation. We demonstrate the effectiveness of this approach for Alternative Current Optimal Power Flow (ACOPF) and Security Constrained ACOPF (SCACOPF).

On the Formulation of Dissipative Path-Following Constraints in the Embedded Finite Element Method

Giuseppe Rastiello*, Francesco Riccardi**, Benjamin Richard***

*DEN - Service d'études mécaniques et thermiques (SEMT), CEA, Université Paris-Saclay, France, **LMT, ENS Cachan, CNRS, Université Paris-Saclay, France, ***DEN - Service d'études mécaniques et thermiques (SEMT), CEA, Université Paris-Saclay, France

ABSTRACT

The present contribution aims to investigate the formulation of dissipative path-following constraints [1] within the Embedded Finite Element Method (E-FEM) [2,3] framework. According to this approach, cracking is described by distinguishing between a global problem (where the displacement field is regular) and a finite set of local problems driving the response of element-wise defined strong discontinuities. At the embedded discontinuity level, a discrete traction-separation law describes the interaction between the crack surfaces. Furthermore, traction-continuity conditions ensure that each finite element crossed by the discontinuity line/surface satisfies the momentum balance equation. The localization and propagation of cracks often lead, however, to unstable structural responses characterized by snap-backs. Path-following procedures allow overcoming these instabilities. Accordingly, the equilibrium problem is augmented by an additional global unknown (the loading factor) which should comply with a dedicated equation: the path-following constraint equation. Thanks to the enhanced kinematic description provided by the E-FEM, this contribution shows that it is possible to formulate constraint equations where the controlled quantities are directly related to the dissipation process occurring at the strong discontinuity level. Several dissipative path-following constraints and their numerical implementation (based on an operator-splitting method) are illustrated. Simple two-dimensional quasi-static simulations, involving unstable structural responses characterized by multiple snap-backs, are presented. A comparison with some well-known path-following constraints used in non-linear finite element simulations is also established. This allows illustrating the main features of the proposed methods, as well as their effectiveness in controlling embedded discontinuity finite element simulations of failure in solids. [1] De Borst, R., Crisfield, M.A., Remmers, J.J.C, Verhoosel, C.V., Nonlinear finite element analysis of solids and structures. John Wiley & Sons (2012). [2] Oliver, J., Modeling strong discontinuities in solid mechanics via strain softening constitutive equations. Part-2: Numerical Simulation, International Journal for Numerical Methods in Engineering, 39, 3601-3623 (1996). [3] Linder, C., Armero, F., Finite elements with embedded strong discontinuities for the modeling of failure in solids, International Journal for Numerical Methods in Engineering, 72, 1391-1433 (2007).

Multiscale Model of Cooling after Cold Forging Based on the Solution of Diffusion Equation in the Micro Scale

Lukasz Rauch^{*}, Krzysztof Bzowski^{**}, Marek Wilkus^{***}

^{*}AGH University of Science and Technology, ^{**}AGH University of Science and Technology, ^{***}AGH University of Science and Technology

ABSTRACT

The structure and final properties of forgings after the thermo-mechanical treatment are a result of all operations, including the heating of the charge material itself, forging and controlled cooling. Performing the heat treatment of the forging during cooling, using the heat of the forging, is the main challenge today. Therefore, for the design of the process with the heat treatment directly after hot forging it is necessary to possess precise information on the whole process, which is possible to be acquired by applying modern numerical modelling methods. Development of the multiscale model of this process was the main objective of the paper. The common approach is to connect finite element (FE) model in the macro scale with mean field model (e.g. JMAK) in the micro scale. However, information supplied by this approach is constrained to the phase composition in the final product. On the other hand, the properties of the product depend on some additional parameters such as morphology of phases and distribution of carbon and alloying elements in each phase. Therefore, a new approach was proposed in which FE code in macro scale is connected with the FE solution of the diffusion equation in the micro scale. The latter is described in Authors earlier publications [1]. In this solution level set method was used to control motion of the interphase. New position of the interface in each time step was determined by the mass balance, interphase mobility and interphase curvature. Connection of the micro model with the FE model of the forging process is computationally costly. Therefore, searching for a balance between predictive capabilities of the model and computing costs was the next objective of the work. Possibilities of decreasing the computing costs while the accuracy of the model remains on a reasonable level were considered [2]. Distributed computing was applied. Results of simulation including distribution of microstructural features in the volume of the forging is the main output of the paper. Acknowledgement: The work is financed in TECHMATSTRATEG1/348491/10/NCBR/2017 project by NCBiR. References 1. Pernach M., Bzowski K., Pietrzyk M., Numerical modelling of phase transformation in DP steel after hot rolling and laminar cooling, International Journal for Multiscale Computational Engineering, 12, 2014, 397–410.. 2. Rauch L., Kuziak R., Pietrzyk M., From high accuracy to high efficiency in simulations of processing of Dual-Phase steels, Metallurgical and Materials Transactions B, 45B, 2014, 497-506.

Patient-specific Models of Tricuspid Valves Based on Healthy Human Heart Explants

Manuel Rausch*, William Meador**, Chen Shen***, Marcin Malinowski****, Tomasz Jazwiec*****, Tomasz Timek*****

*University of Texas at Austin, **University of Texas at Austin, ***University of Texas at Austin, ****Spectrum Health, *****Spectrum Health, *****Spectrum Health

ABSTRACT

Functional tricuspid regurgitation (FTR), i.e., a leaking tricuspid valve (TV) due to valve extrinsic causes, is a significant source of morbidity and mortality [1]. Our treatment options are currently suboptimal with a large number of patients exhibiting signs of recurrence within few years after surgery. Little is known about the mechanics of the TV, in health or disease, which may be impairing our ability to devise better treatment strategies for FTR and improve our current clinical standard. Toward a deeper understanding of the mechanics of the TV, we are setting out to develop detailed computational models of healthy human valves. We inform these models with in-situ experiments of healthy human hearts that were rejected from transplantation and with in-vitro experiments of the matched tissue samples. Specifically, we use sonomicrometry to determine the in-situ shape of the TV annulus in a beating human heart temporarily maintained in an organ preservation system. Upon termination of the experiments, we perform histo-mechanical analyses of the valve leaflets and chordae tendineae of the same valves to extract the mechanical properties of these tissues, their microstructural composition, and their geometry. Subsequently, we merge the matched sonomicrometry data with the mechanical, histological, and geometric data to build the first, patient-specific, finite element models of healthy human hearts. Additionally, we include chordae tendineae in our models whose origin and insertion sites are identified based on tissue samples. Using the non-linear, implicit finite method, we simulate the opening and closing behavior of the TV during one full cardiac cycle. To this end, we impose Dirichlet boundary conditions, which we derive from our in-vivo sonomicrometry data, to the annular geometry of our patient-specific models of the TV. In addition, we impose the in-situ measured transvalvular pressure to the ventricularis surface of the valve's three-leaflets. The TV shows a complex closing behavior, with a Y-shaped coaptation line that originates from its three distinct leaflets. Naturally, the leaflet stresses are largest during peak systole and smallest during diastole with the belly regions showing maximal stresses. Moving forward, we will employ these models to virtually test and optimize different treatment strategies for FTR. Our main focus will be on the shape of annuloplasty devices, the current gold-standard treatment of FTR. In conclusion, we developed a first patient-specific model of the TV and tested the feasibility of our combined in-situ/in-vitro experimental/computational framework. References [1] Rausch et al. Ann Biomed Eng, 2017

Patient-Specific Drug Elution Simulations in Stented Coronary Arteries Using a Combined Experimental-Numerical Scheme

Atefeh Razavi^{*}, John LaDisa^{**}, Harkamaljot Kandail^{***}

^{*}Marquette University, ^{**}Marquette University/Medical College of Wisconsin, ^{***}Eindhoven University of Technology

ABSTRACT

Cardiovascular disease (CVD) is a major cause of death worldwide. For example, about 92M Americans (28%) have CVD, a heart attack happens every 34 seconds, and someone dies from a coronary artery event every ~1 minute(1). Drug eluting stents (DES) have revolutionized CVD treatment, but restenosis forces >200,000 repeat coronary interventions in the US annually(2). Remodeling occurs after stenting, which causes changes in local coronary artery geometry and adverse hemodynamics on the wall. For bare metal stents it is known that adverse wall shear stress (WSS) is associated with restenosis, and can be improved through stent design. For DES, however, the details of how WSS-related parameters may impact restenosis are not known since many studies lack realistic representations for arterial geometry and hemodynamics due to limitations of the imaging or modeling methods, material properties of the coronary plaque, drug characteristics and/or biological reaction terms. The objective of the current study is to develop a combined experimental-numerical scheme leading to the most realistic study of hemodynamics after coronary artery DES implantation to date. Limited literature on drug and plaque properties prevents the implementation of realistic conditions in coronary artery DES simulations. To address this issue, stress-strain curves, diffusion coefficients, and reaction terms are determined using human coronary arteries with atherosclerotic plaques classified using the modified American Heart Association (AHA) criteria after patient-specific geometry is reconstructed from optical coherence and computed tomography(3). Experimentally derived nominal stress-strain curves are used to calibrate ABAQUS' isotropic hyperelastic material models. Diffusion coefficients are obtained by measuring drug concentration at various coronary artery locations. Binding capacity and equilibrium dissociation values are extracted from these measurements and bulk drug solution to identify biological reaction terms. Empirical values are then applied to the deformed artery geometry in FlowVision (Capvidia, Belgium) to conduct patient-specific simulations of drug-elution patterns for ultimate use in identifying patients at greater risk of restenosis. This approach also addresses challenges from minuscule faces that present in complex patient-specific DES models through the use of an improved cut-cell method within FlowVision, thereby extending the scheme to a cohort of DES patient models with malposition between the stent and artery. This work is expected to result in the most detailed characterization of plaque properties to date for use in more realistic patient-specific simulations of coronary artery DES. 1. Go et al. Circulation. 2013;127:e6-e245 2. Garg et al. JACC. 2010;56:S1-42 3. Ellwein et al. Cardiovasc Eng Tech. 2011;2(3): 212-7

Isogeometric Simulation of Structures: Recent Advances with a Focus on Composites

Alessandro Reali*

*University of Pavia

ABSTRACT

Tom Hughes is surely one of the most talented and influential researchers in the history of Computational Mechanics, given the incredible quality and quantity of fundamental contributions he was able to give to all aspects of this field. The latest of them, Isogeometric Analysis, has established itself as one of the hottest topics in Computational Mechanics despite its relatively young age, attracting a huge interest from many researchers around the world, testified by the exponentially growing number of related papers, talks, and citations. In this presentation, after a brief introduction on Isogeometric Analysis, I will review some of the new possibilities that this family of methods has allowed to develop in the context of structural simulation techniques. I will finally focus on a novel approach for composite structures, which takes advantage of the accuracy and high-regularity properties of Isogeometric Analysis to build a cost-effective stress recovery procedure based on equilibrium in strong form.

Analytical and Numerical Investigations of Locking in Transversely Isotropic Elasticity

Daya Reddy*, Faraniaina Rasolofoson**, Beverley Grieshaber***

*University of Cape Town, **University of Cape Town, ***University of Cape Town

ABSTRACT

For isotropic materials the concept of volumetric locking in the context of low-order finite element approximations is well understood, and a variety of effective remedies exist: for example, the use of mixed methods, discontinuous Galerkin (DG) methods, or selective underintegration. Corresponding studies have been carried out, to a limited extent, to determine conditions under which locking related to inextensibility occurs, in small- and large-deformation contexts [1,2]. The models treated in these works are of an isotropic material, with inextensibility imposed as a constraint. The present work is concerned with transversely isotropic linear elastic materials, which are characterized by 5 material parameters [3]. The behaviour under limiting conditions of near-incompressibility and near-inextensibility are investigated. It is shown both through numerical examples and an analysis of finite element approximations that locking behaviour for low-order elements depends critically on the degree of anisotropy of the material, that is, on the ratio of Young's moduli and Poisson ratios for the directions parallel and transverse to the direction characterizing transverse isotropy. In addition to conforming finite element approximations, the use of DG approximations is also pursued: for these, it is shown that behaviour is locking-free. References 1. Auricchio F., Scalet G. and Wriggers P. Fibre-reinforced materials: finite elements for the treatment of the inextensibility constraint. *Compute. Mech.* (2017) 60:905:922. 2. Wriggers P., Schröder J. and Auricchio F. Finite element formulations for large strain anisotropic material with inextensible fibers. *Adv Model Simul Eng Sci* (2016) 3(1):25. 3. Spencer, A.J.M. The formulation of constitutive equations for anisotropic solids. In *Mechanical Behavior of Anisotropic Solids* (J. P. Boehler, ed.) Martinus Nijhoff Publishers, The Hague (1982) 2–26.

Mathematical Modelling of Drug Delivery to the Targeted Organs through Bio-Absorbable Nanoparticles

J V Ramana Reddy*, Dasari Srikanth**, Sint Sundar***

*Indian Institute of Technology Madras, **Defence Institute of Advanced Technology, ***Indian Institute of Technology

ABSTRACT

It is proposed to control the thermal and concentration dispersion from drug-coated nanoparticles in the blood flow. It is assumed that the temperature sensitive drug is coated on the surface of the bio-absorbable nanoparticles. The mixture of blood together with the nanoparticle is modelled as nano-polar fluid. The formulation is useful to understand the impact of the deformation of the blood components on hemodynamics. The physiological pressure gradient caused due to the cardiac cycle, and the flexible arterial wall is also incorporated in the model. To make the model more realistic, the hematocrit has been considered along with the variable viscosity in the blood flow model. The resultant highly non-linear coupled modelled governing equations of flow are simulated by the Marker and Cell along with the suitable choice of the boundary and initial conditions. The numerical stability is also checked with the desired accuracy. The rate and the amount of drug release are controlled by the temperature provided by the catheter in the targeted region. The influence of various parameters which are arising out of the fluid and geometry considered on the physiological blood flow characteristics are computed numerically. The mathematical understanding of the drug release and blood flow through stenosed tapered arteries with flexible walls is having direct applications in lessening the adverse effects caused due to the medication, helps in designing the pharmaceutical drug, deemed to be a great help in the treatment of vascular diseases, and also the biomedical engineers.

Microscale Multiphysical Modeling of Tool Steels and Cast Irons

Konstantin Redkin^{*}, Christopher Hrizo^{**}, Isaac Garcia^{***}

^{*}WHEMCO Inc, ^{**}WHEMCO Inc, ^{***}University of Pittsburgh

ABSTRACT

Applied image-based 2D finite element modeling approach was developed to simulate microscale multiphysical behavior of highly alloyed steels and cast irons, which are used as the rolls' materials for cold and hot rolling mill applications. Combined image processing, advanced materials characterization techniques, thermodynamic-kinetics modeling and finite element analysis enabled one to simulate microscale deformation and heat transfer phenomena of considered microstructures. A fundamental understanding of composite-like materials' behavior will be shown and discussed, leading to more comprehensive materials engineering for industrial scale applications.

Data Mining for Electromechanical and Phase Change Properties of Over 1000 2D Materials

Evan Reed*

*Stanford University

ABSTRACT

We have utilized data mining approaches to elucidate over 1000 2D materials and several hundred 3D materials consisting of van der Waals bonded 1D subcomponents, or molecular wires. We find that hundreds of these 2D materials have the potential to exhibit observable piezoelectric effects, representing a new class of piezoelectrics. Another subset of these materials has the potential to exhibit structural changes under a variety of external stimuli including electrostatic gating. I will discuss calculations of phase diagrams, recent experimental results demonstrating the predicted electrostatic gating phase change effect, and potential phase change applications for these materials. We find that the nature of mechanical constraint has a significant impact on the phase diagram.

Uncertainty Quantification of the Performance of Seismic Waveguides through Reduced Order Model Interpolation

Heather Reed^{*}, Alex Kelly^{**}, Jeffrey Cipolla^{***}, Andrew Shakalis^{****}

^{*}Thornton Tomasetti – Weidlinger Applied Science, ^{**}Thornton Tomasetti – Weidlinger Applied Science,
^{***}Thornton Tomasetti – Weidlinger Applied Science, ^{****}Thornton Tomasetti – Weidlinger Applied Science

ABSTRACT

In seismic applications, incident waves are redirected, causing them to avoid a structure in their path of normal incidence. Seismic cloaking enables 'hiding' a structure through the selection or construction of a material that has specific waveguide properties. The material and mechanical properties required to achieve the cloaking effects are not found in nature, and therefore heterogeneous materials (metamaterials) are fabricated by gradually layering manufactured unit cell microstructures, resulting in a (usually smooth) variation of properties. Advances in additive manufacturing (i.e. 3D printing) have enabled these complex metamaterials to be fabricated relatively quickly, compared to conventional manufacturing methods. Metamaterials, however, present challenges in optimization for any desired waveguide effect. Homogenization methods, which assume Cartesian symmetry, are a staple in metamaterial design, but these only approximate a feasible optimum. Moreover, total reliance on homogenized continuum models provides no information about the actual cloak performance, and presents problems in functionally graded applications. To overcome this, a full field, explicit time domain finite element simulation of the wave propagation is required in the cloaking design process, resulting in a computationally expensive cloak optimization problem. Another challenge in the design of such waveguides stems from the uncertainty in the manufacturing process. Additive manufacturing is notorious for generating highly variable component properties. As the design process heavily depends on these metamaterial base properties, the uncertainty surrounding those properties must be quantified and accounted for in the simulation. A Monte Carlo analysis enables determination of the cloak performance uncertainty by integrating over the base material parameter space. However, because each evaluation of the integral entails evaluating the costly finite element model, a projection-based reduced order model (ROM) is leveraged to drastically decrease the deterministic model computational time. A ROM adaptation procedure is implemented, where projection-based ROMs are seen as points on a Riemannian manifold and are tracked and interpolated during the sampling process from a database of precomputed ROMs [1]. This approach ensures that an appropriate ROM is used for the model evaluation in every region of the parameter space, thus leading to computational savings while conserving sufficient accuracy. [1] Amsallem, David; Cortial, Julien; Carlberg, Kevin; Farhat, Charbel. A method for interpolating on manifolds structural dynamics reduced-order models. International Journal for Numerical Methods in Engineering Vol. 80, Iss. 9, (Nov 26, 2009): 1241-58.

Proper Orthogonal Decomposition (POD) Combined with Hierarchical Tensor Approximation (HTA) in the Context of Uncertain Parameters

Stefanie Reese^{*}, Steffen Kastian^{**}, Dieter Moser^{***}, Lars Grasedyck^{****}

^{*}RWTH Aachen, Germany, ^{**}RWTH Aachen, Germany, ^{***}RWTH Aachen, Germany, ^{****}RWTH Aachen, Germany

ABSTRACT

The evaluation of robustness and reliability of realistic structures in the presence of polymorphic uncertainty involves numerical simulations with a very high number of degrees-of-freedom, as well as a high number of parameters. Some of these parameters are certain in the way that they are a priori known. However, most of the parameters are uncertain, since they are based on incomplete information or imprecise measurements. To account for this uncertainty it is necessary to observe the high dimensional parameterspace. Therefore, a huge amount of simulation is required. In this context a method of model order reduction is used to reduce the cost of each simulation. In the present contribution, the POD [1] is chosen for this purpose. In order to get accurate results by means of the POD method it is essential to find proper projection matrices. The goal of the present contribution is to significantly improve the accuracy and efficiency of the existing POD method by developing adaptive projection matrices during the simulation. A moderate number of quantities of interest can be found in most technical problems. This could be for example the maximum displacement or the maximum stress in a deformed object. For several uncertain parameters the number of possible combinations of different parameters can be very high. The HTA [2] is a very good candidate to overcome this issue. The HTA needs several precalculations which can be speeded up by combining it with the POD method. In the next step the HTA can be used for uncertainty quantifications. This includes the calculation of the average, maximum and minimum value of the quantity of interest. [1] A. Radermacher, S. Reese, 2016. POD-based model reduction with empirical interpolation applied to nonlinear elasticity, International Journal for Numerical Methods in Engineering, 107 (6), 477--495 [2] L. Grasedyck, R. Kriemann, C.Löbbert, A. Nägel, G. Wittum, K. Xylouris, 2015. Parallel tensor sampling in the hierarchical Tucker format, Computing and Visualization in Science, 17 (2), 67--78.

Three-Dimensional Large Deformation Micromorphic Elastostatics with Microstructural Linkage and Comparison to Micropolar Elastostatics

Richard Requeiro*, Farhad Shahabi**, Volkan Isbuga***

*University of Colorado Boulder, **University of Colorado Boulder, ***Hasan Kalyoncu University

ABSTRACT

A three-dimensional (3D), large deformation, finite element analysis (FEA) framework accounting for material micro-structure is presented for micromorphic continuum mechanics. A fundamental assumption of the theory is that material micro-structure satisfies the governing equations of classical continuum mechanics within a "micro-element." The micro-element deformation with respect to a mass-centered macroscopic continuum point (called a "macro-element") is governed by an independent micro-deformation tensor. Assuming that proper constitutive models may be formulated, and material parameters calibrated, the theory may fill the gap between microstructural and macroscopic continuum length scales. The aim of the paper is to provide insight into micromorphic continuum mechanics, including the linkage between micro- and macro-element deformation, through numerical examples comparing static micromorphic and micropolar elasticity, while investigating the effects of boundary conditions which will influence the "length-scale effect." A 3D large deformation FEA framework for materially-linear isotropic micromorphic elastic materials is developed and applied to illustrate the effects of independent microstructural deformation on the macroscopic micromorphic and micropolar continuum-scale responses.

A Materials Scientists View of Crystal Plasticity -- The OOF Project

Andrew Reid^{*}, Shahriyar Keshavarz^{**}, Stephen Langer^{***}

^{*}NIST, ^{**}NIST / Theiss Research, ^{***}NIST

ABSTRACT

The OOF software tool, developed at the National Institute of Standards and Technology, is designed to allow users with a materials science background to quickly and flexibly assess the behavior of possibly complex microstructures, using as inputs an image of the microstructure, and the constitutive properties of the phases making up the system. Users do not have to be experts in the relevant physics, nor in the underlying Finite Element mathematics, in order to undertake useful explorations of structure-property relationships. As initially constructed, the software was principally focussed on solving problems that are easily posed as partial differential equations, including nonlinear and time-dependent PDEs. This covers a large fraction of materials problems, but is ultimately not sufficient to solve interesting problems in solid mechanics. A current development focus for this tool is the incorporation of crystal plasticity into the tool. Efforts so far have proven to be a useful exercise in testing the extensibility of the code, as well as in abstracting the large space of crystal plastic constitutive rules and techniques into categories of use and interest to our materials. This talk will focus on the progress to date in incorporating crystal plasticity into the OOF code, as well as related projects which have arisen from a materials-focused approach to crystal plasticity, including some potentially useful statistical approaches.

Expressing the Differences in Code Optimizations between Intel Knights Landing and NEC SX-ACE Processors

Thorsten Reimann^{*}, Hiroyuki Takizawa^{**}, Kazuhiko Komatsu^{***}, Takashi Soga^{****}, Ryusuke Egawa^{*****}, Akihiro Musa^{*****}, Hiroaki Kobayashi^{*****}

^{*}Technische Universität Darmstadt, ^{**}Tohoku University, ^{***}Tohoku University, ^{****}Tohoku University, ^{*****}Tohoku University, ^{*****}Tohoku University, ^{*****}Tohoku University

ABSTRACT

The latest processor of the Intel Xeon Phi architecture, called Knights Landing (KNL), has AVX-512 instructions for efficiently executing “vectorizable” loops, and one might hence consider that it is a kind of vector processors. However, code optimizations for KNL could be different from those for orthodox vector processors. This work thus discusses the differences in code optimizations between orthodox vector computing systems and KNL. In this case study, an incompressible flow solver, FASTEST, is optimized for a vector computing system, NEC SX-ACE. In addition to restructuring its kernel loops to help compiler’s vectorization, we employ the wavefront reordering for increasing the vector length of the most time-consuming kernel, called the SIPSOL kernel. That is, the FASTEST code is optimized so that it can achieve a higher performance on the SX-ACE system. Then, the KNL performance for the optimized FASTEST code is evaluated to discuss the similarities and differences in code optimizations between KNL and SX-ACE. The performance evaluation results show that code optimizations for KNL have certainly some similarities with those for vector computing systems such as SX-ACE, which mainly focus on increasing the lengths of innermost loops. However, some optimization techniques for SX-ACE obviously have negative impacts on the KNL performance. The wavefront reordering can increase the innermost loop length, and hence significantly improve the performance on the SX-ACE system. On the other hand, it also causes irregular memory access patterns and results in a higher cache miss ratio, leading to the KNL performance degradation. Accordingly, different processor architectures often require different code optimization techniques. Finally, we use the Xevolver code transformation framework to express system-specific code optimizations as user-defined code transformations. By using some custom code transformation rules, we can transform the original FASTEST code in different ways, depending on the target system, i.e., KNL or SX-ACE. As a result, we can achieve not only high performance but also high performance portability across different systems without maintaining multiple versions of a kernel for each system. In the case where a kernel already has multiple versions, each of which is optimized for a different system, Xevolver allows users to even simplify the kernel by preserving only one version and removing the others. The removed versions can be generated by transforming the remaining one if a rule for the code transformation is properly defined. Maintaining only a single version of each kernel is beneficial to keep the whole code tractable.

The Local Cohesive Zone Method for Efficient Modelling of Delamination in Large Composite Structures Under Low Velocity Impact

Johannes Reiner^{*}, Reza Vaziri^{**}

^{*}The University of British Columbia, ^{**}The University of British Columbia

ABSTRACT

Damage tolerance is an advantageous characteristic of composite materials. Computational models for structural design solutions need to consider interlaminar delamination in composite laminates in order to represent their behavior more realistically and utilize their full potential and weight saving benefits. Within Finite Element Analysis (FEA), the Cohesive Zone Method (CZM) is a common tool to simulate initiation and growth of interlaminar cracks. Detailed modelling of pre-inserted interconnecting cohesive elements between different plies is required to accurately capture the mechanics of separation of plies. This leads to high modelling complexity and computational cost. Hence, such models are not feasible to use in large-scale industrial applications. The Local Cohesive Zone Method (LCZ) [1] is a novel computational concept to adaptively insert cohesive elements only within local regions where interlaminar delamination has the potential to initiate. Computational cost is significantly reduced which makes the method applicable to large-scale composite structures. LCZ is verified and validated against composite structures in Mode I, Mode II and Mixed-Mode fracture tests [1] as well as under axial crushing and transverse impact loading [2]. We are presenting the latest modifications and applications of LCZ with regards to low velocity impact simulations of automotive carbon fiber reinforced composite structures. Implemented in the commercial FE solver LS-DYNA, interlaminar damage in LCZ is combined with intralaminar continuum damage models to account for matrix and fiber damage. Results are compared with conventional interlaminar modelling techniques using pre-inserted cohesive elements. References: [1] Shor, O., & Vaziri, R. (2015). Adaptive insertion of cohesive elements for simulation of delamination in laminated composite materials. *Engineering Fracture Mechanics*, 146, 121-138. doi:<http://dx.doi.org/10.1016/j.engfracmech.2015.07.044> [2] Shor, O., & Vaziri, R. (2017). Application of the Local Cohesive Zone Method to Numerical Simulation of Composite Structures under Impact Loading. *Engineering Fracture Mechanics*, 104, 127-149. doi: <https://doi.org/10.1016/j.ijimpeng.2017.01.022>

Damage Analysis of Shells Using a Consistent Anisotropic Puck-based Damage Model for Laminated Fiber-reinforced Composites

José Reinoso^{*}, Giuseppe Catalanotti^{**}, Ana Vallecillos-Portillo^{***}, Antonio Blázquez^{****},
Federico París^{*****}, Pedro P. Camanho^{*****}

^{*}Universidad de Sevilla, ^{**}Queen's University Belfast, ^{***}Universidad de Sevilla, ^{****}Universidad de Sevilla,
^{*****}Universidad de Sevilla, ^{*****}Universidade do Porto

ABSTRACT

The engineering use of carbon and glass fiber-reinforced polymer (CFRP and GFRP, respectively) composites has significantly increased in the last three decades. This tendency is especially relevant in aerospace and aeronautical components, whereby their superior material properties in terms of their specific stiffness and strength ratios play a central role. The exploitation of the load bearing capacities of such materials requires a comprehensive understanding of the different damage mechanisms that characterize their mechanical performance. On the basis of composite laminates, damage events can be arranged into two principal categories: (i) interlaminar failure (delamination), and (ii) intralaminar failure. From the computational point of view, FEM has been the most popular method to develop computational models that allows triggering this inelastic response upon failure. In this contribution, a novel anisotropic damage criterion for intralaminar damage in laminated fiber-reinforced composites using the 3D-version of the Puck failure criterion is presented [1]. This failure theory distinguishes between inter-fibre fracture (IFF) and fibre fracture (FF) which are accounted for through the definition of the corresponding set of damage variables. The current model specifically complies with the thermodynamic consistency by means of exploiting the additive decomposition of the Helmholtz free-energy function [2]. Additionally, the model endows: (i) an energetic-based evolution for the corresponding damage variables and (ii) the derivation of the consistent tangent operator to be integrated into a nonlinear FE solution scheme. Derived from its 3D character, the proposed model is integrated into a solid shell element to model intralaminar damaged in thin-walled structures. The solid shell formulation herein used relies in the mixed-enhanced formulation. Finally, the proposed model is assessed by means of several examples, exhibiting an excellent accuracy with respect to experimental data. References [1] Puck, A., Schürmann, H. Failure analysis of frp laminates by means of physically based phenomenological models. Compos Sci Technol, 62:1633–1662, 2002. [2] Reinoso, J, Catalanotti, G., Blázquez, A., Areias, P, París, F., Camanho, P.P. A consistent anisotropic damage model for laminated fiber-reinforced composites using the 3D-version of the Puck failure criterion. Int. J. Solids and Structures, 126-127:37-53, 2017.

Adaptive Curvilinear Meshing

Jean-François Remacle^{*}, Amaury Johnen^{**}, ruili zhang^{***}

^{*}Université catholique de Louvain, ^{**}Université catholique de Louvain, ^{***}Université catholique de Louvain

ABSTRACT

Assume a unit square $(x,y) \in [0,1] \times [0,1]$ and a smooth function $f(x,y)$ defined on the square. The question we want to address is the following: is it possible to compute the P^2 mesh with N triangles that minimizes the approximation error? Note of course that the elements of our optimized mesh have the freedom to be curved. In this talk, we present a way to generate such a mesh.

Ductile Rupture under Cyclic Loadings conditions

Al Mahdi Remmal^{*}, Jean-Baptiste Leblond^{**}, Stephane Marie^{***}

^{*}Framatome - Sorbonne Université, Faculté des Sciences et Ingénierie (formerly Université Pierre et Marie Curie), CNRS, UMR 7190, Institut Jean Le Rond d'Alembert, ^{**}Sorbonne Université, Faculté des Sciences et Ingénierie (formerly Université Pierre et Marie Curie), CNRS, UMR 7190, Institut Jean Le Rond d'Alembert, ^{***}Framatome

ABSTRACT

It is known that for ductile porous materials, cyclic loadings lead to lower fracture strains than monotone ones. This reduction of ductility probably arises from an effect called “ratcheting of the porosity” [1] that consists of a continued increase of the mean porosity during each cycle with the number of cycles. Finite element based micromechanical simulations [2] confirmed this interpretation. Recently [3], the authors proposed a Gurson-type “layer model” better fit that Gurson’s original one, which does not predict the ratcheting of the porosity, for the description of the ductile behavior under cyclic loading conditions. A very good agreement was obtained between the results of the micromechanical simulations and the model predictions for a rigid-hardenable material. Yet, the ratcheting of the porosity is a consequence of both hardening and elasticity; and the theory of sequential limit analysis used [3] in order to get the “layer model” is strictly applicable in the absence of elasticity. Based on an expression of the porosity rate accounting for elasticity, a proposal is made to improve the new model with regard to elasticity. This proposal is assessed through comparison of its predictions with the results of micromechanical simulations and with the results of tests on notched tensile and Compact Tensions specimens subjected to cyclic loadings. [1] P. Gilles, B. Jullien and G. Mottet. Analysis of cyclic effects on ductile tearing strength by a local approach of fracture, *Advances in Fracture/Damage Models for the Analysis of Engineering Problems*, ASME Publication AMD - Vol. 137, pp. 269-284, 1992. [2] J. Devaux, M. Gologanu, J.B. Leblond and G. Perrin. On continued void growth in ductile metals subjected to cyclic loadings, *Proceedings of IUTAM Symposium on Nonlinear Analysis of Fracture*, Cambridge, GB, J. Willis, ed., Kluwer, pp. 299-310, 1997. [3] L. Morin, J.C. Michel, and J.B. Leblond. “A Gurson-type layer model for ductile porous solids with isotropic and kinematic hardening.” *International Journal of Solids and Structures* 118 (2017): 167-178.

Study on Hydraulic Concrete Cracking Criterion in Smeared Crack Numerical Model

Qingwen Ren^{*}, Yajuan Yin^{**}

^{*}Hohai University, ^{**}Hohai University

ABSTRACT

The representative volume element (RVE) is defined as the smallest volume element, but sufficiently large to represent the effective properties of a composite at a large scale. It plays an important role in the study of concrete properties. Meanwhile, the RVE size determination itself is an issue that needs further study. Primarily, the RVE itself can be the measured object in laboratory testing of the macroscopic properties of material. Another advantage of RVE is related to the mechanistic modelling of concrete mixtures. Recently, the calculation meso-mechanical model has drawn more and more attention from the community of concrete mechanics, in an effort to establish the relationship between meso-structure and macro-mechanical properties when studying the failure of heterogeneous materials, which involves the two dimensions of meso and macro scales. For the first time, the problem of determining RVE size based on several factors is regarded as a multi-objective decision-making problem. A new method of entropy weight–grey correlation model is proposed, by comprehensively considering the influence of coarse aggregate content, aggregate average particle size and aggregate fineness modulus. A two-dimensional concrete aggregate specimen, randomly generated by numerical simulation with aggregate size of 5–20 mm, is taken as a case study, and the RVE size is determined as 6–7 times the maximum aggregate size. Then the finite-element method is used to verify its mechanical properties. This new method has an advantage of less dependency on variable data over the traditional method, indicating a wider range of applicability. Additionally, the model is applied to determine the RVE size of three-dimensional concrete, which is similar to two-dimensional concrete. It provides a new comprehensive insight for the study of concrete RVE size, which could also be extended to apply to the RVE determination of other composite materials. Acknowledgements: The financial supports provided by the National Natural Science Foundation of China (51739006)

Modeling and Simulation of Moving Contact Lines in Multi-phase Fluids

Weiqing Ren*

*National University of Singapore and IHPC

ABSTRACT

Contact line forms when a fluid interface intersects with a solid wall. The moving contact line problem is a classical problem in fluid mechanics. The difficulty stems from the fact that the classical Navier-Stokes equation with no-slip boundary condition predicts a non-physical singularity at the contact line with infinite rate of energy dissipation. Many modified continuum models have been proposed to overcome this difficulty. Though they all succeed in removing the singularity, it is not clear whether they describe the real physics near the contact line region. In this talk, we will discuss how the continuum theory, molecular dynamics and the more recently developed multiscale techniques can be combined to give us a better understanding of the fundamental physics of the moving contact line and formulate simple and effective models. We also illustrate how this model can be used to analyze the behavior of the apparent contact angle, hysteresis and other important physical problems for the moving contact line. [1] W. Ren, P. H. Trinh and W. E, On the distinguished limits of the Navier slip model of the moving contact line problem, J. Fluid Mech. vol 772, 107-126 (2015) [2] W. Ren, D. Hu and W. E, Continuum models for the contact line problem, Phys. Fluids, vol 22, 102103 (2010) [3] W. Ren and W. E, Boundary conditions for the moving contact line problem, Phys. Fluids, vol 19, 022101 (2007)

High-Fidelity T-Spline Based Isogeometric Analysis for 3D Complex Structures

Xiang Ren^{*}, Yongjie Jessica Zhang^{**}, Jim Lua^{***}, Xiaodong Wei^{****}

^{*}Global Engineering & Materials, Inc., ^{**}Carnegie Mellon University, ^{***}Global Engineering & Materials, Inc.,
^{****}Carnegie Mellon University

ABSTRACT

Isogeometric analysis (IGA) has shown its attractive feature recently for integrating a Finite Element Analysis (FEA) and Computer Aided Design (CAD) into a single unified process. For stress analysts, it is common practice to convert a spline/NURBS based CAD model to polynomial based finite element mesh for analysis. However, for complex geometries such as optimized 3D printing objects, it is known that smooth curvature cannot be exactly reserved by the discretized finite element mesh. As a consequence the simulation results can either be imprecise due to the geometric misrepresentation or a great larger number of degrees of freedom is needed to achieve a convergent solution. As such, T-spline based 3D IGA is developed by us to fill the gap. A 3D CAD geometry is first automatically converted to a T-spline control mesh, and then converted to analysis suitable T-spline elements for a high fidelity analysis. With unified and higher order T-spline basis functions selected for the geometry representation, FEA is directly conducted on the smooth CAD geometry without loss of any key design details. By taking advantage of the Bézier transformation, FEA is conducted by implementing IGA via customization of Abaqus' user-defined elements (UELs). To further enhance the IGA analysis capability without strong reliance on the generation of an analysis suitable T-spline for the entire geometry, a hybrid "T-spline and finite element" modeling approach is developed to preserve the smooth surface geometry of a complex 3D object. To accurately prescribe boundary conditions for an IGA solution domain, special algorithms are implemented for mapping both Cauchy and Dirichlet type boundary conditions from a physical boundary to the control points. A suite of numerical examples are selected to demonstrate the accuracy and rate of convergence for the stress response prediction of complex 3D components.

Phantom Paired Elements Approach for Matrix Cracking and Segmented Cohesive Interface for Failure Prediction of Composite Laminates

Xiang Ren^{*}, Xiaodong Cui^{**}, Jim Lua^{***}

^{*}Global Engineering and Materials, Inc., ^{**}Global Engineering and Materials, Inc., ^{***}Global Engineering and Materials, Inc.

ABSTRACT

Modeling and characterization of discrete damage and interaction of matrix cracks and interface delamination have received growing interests for the failure analysis of composite structures due to its ability to capture mechanisms of energy dissipation associated with crack and delamination failure progression. Fracture mechanics based approaches coupled with a kinematic description of discrete cracks have been extensively developed based on XFEM, RFXFEM, AFEM, floating node, or phantom paired elements approaches. A key problem that has not been well addressed is an accurate characterization of the interaction of matrix cracks and interface delamination when matrix cracks of different orientations from the top or bottom ply intersect a ply interface, namely the 'segmented cohesive interface'. The bridging forces (Mode I & Mode II) applied by a segmented cohesive interface on the surfaces of matrix cracks located on the top or bottom side of the interface are essential not only in capturing the stiffness but also the dissipated energy of the cracked layer system (cracked ply bonded by segmented cohesive interface). In the literature, a superimposed approach based on a cohesive interface cut by matrix cracks from its top and bottom was used and the combined bridging effects were characterized via an average approach assuming an equal contribution from the cracked interface from its top and bottom side. In order to better characterize the bridging effect of the segmented cohesive interface, an energy based phantom paired elements approach is developed for the cracked layer system to describe kinematic admissible displacement discontinuities without introducing a conforming mesh. A subdomain energy superposition is used to determine the overall response of the segmented cohesive interface influenced by its top and bottom side. A verification study is performed to examine its validity and effects of segmented cohesive interface using an Abaqus model of a conforming mesh for a given cracked configuration. Application examples are used next to demonstrate the proposed method for the discrete damage characterization and failure prediction driven by the evolution of matrix cracking, interface delamination, and their synergistic effect.

An Unbiased Nitsche's Formulation for Frictional Contact and Self-contact : Numerical Integration Aspects

Yves Renard^{*}, Franz Chouly^{**}, Rabii Mlika^{***}

^{*}INSA-Lyon, ^{**}Université de Franche Comté, ^{***}INSA-Lyon

ABSTRACT

In this work, we present a formulation of frictional contact between two elastic bodies based on Nitsche's method. Nitsche's method was adapted for unilateral contact in [1]. It aims to treat the interface conditions in a weak sense, thanks to a stabilized consistent term. At first, we introduce the study carried out in the small strain framework for an unbiased version of the method. The non-distinction between a master surface and a slave one will allow the method to be more generic and directly applicable to the self-contact problem. The restrictive framework of small strain and Tresca friction allowed us to obtain theoretical results on the consistency and convergence of the method (see [2]). Our Nitsche's method is then extended to the large strain case more relevant for industrial applications and situations of self-contact. The method is formulated for an hyper-elastic material and declines in the two versions: biased and unbiased. As in [1], we describe a class of methods through a generalization parameter γ . Particular variants have different properties from a numerical point of view, in terms of accuracy and robustness. To prove the accuracy of the method for large deformations, we provide several validation tests (Taylor patch test, elastic half ring, cross tubes ...). The description of the method and all the results are detailed in [3]. The presentation will focus on the influence of numerical quadrature on the accuracy and convergence of the method. This study covers a comparison of several integration rules (element-based, segment-based, non-symmetric integration) proposed in the literature for other integral methods. References [1] F. Chouly, P. Hild, and Y. Renard. Symmetric and non-symmetric variants of Nitsche's method for contact problems in elasticity: theory and numerical experiments. *Mathematics of Computation*, 84:1089–1112, 2015. [2] F. Chouly, R. Mlika, and Y. Renard. An unbiased Nitsche's approximation of the frictional contact between two elastic structures. To appear in *Numerische Mathematik*, Available on HAL as hal-01240068, 2016. [3] R. Mlika, Y. Renard, and F. Chouly. An unbiased Nitsche's formulation of large deformation frictional contact and self-contact. *Computer Methods in Applied Mechanics and Engineering*, 325(Supplement C):265 – 288, 2017.

Discontinuous Galerkin Material Point Method for Hyperbolic Problems in Solid Mechanics

Adrien Renaud^{*}, Laurent Stainier^{**}, Thomas Heuzé^{***}

^{*}Ecole Centrale of Nantes, ^{**}Ecole Centrale of Nantes, ^{***}Ecole Centrale of Nantes

ABSTRACT

A wide variety of physical problems in solid mechanics, such as impact on structures or high-speed forming techniques, involve waves propagating in solids submitted to large strains. The Material Point Method is now well established as an effective tool for dealing with finite deformations due to the use of particles that can move in an arbitrary Eulerian grid. However, the MPM can be viewed as an extension of classical Finite Element Method with moving quadrature points and therefore inherits the high frequency noise introduced in the vicinity of discontinuities by classical time integrators. Oscillations are troublesome for tracking the paths of waves in order to accurately assess residual stresses and strains. On the other hand, Discontinuous Galerkin methods are based on discontinuous shape functions across element boundaries and allow the use of efficient tools to accurately track waves fronts. First, the DG approximation permits to introduce the characteristic structure of the solution of hyperbolic problems within a Finite Element scheme through the computation of interface fluxes. Second, numerical strategies developed for Finite Volume methods can be employed so as to build Total Variation Bounded or Total Variation Diminishing in the Means finite element schemes. The purpose of this work is to extend the MPM to the DG framework in order to accurately capture both continuous and discontinuous waves. The resulting Discontinuous Galerkin Material Point Method uses the same space discretization than that of the MPM with an arbitrary computational grid supporting the DG approximation. Interface fluxes arising in the weak form of a system of conservation laws, written element-by-element on the reference configuration, are computed by means of an approximate Riemann solver. As for MPM, projection steps are required since particles carry all the fields of the problem while discrete equations are solved at nodes. A von Neumann stability analysis shows that the DGMPM can be used with a less restrictive Courant condition compared to that of the MPM and the DGFEM. In particular, a special space discretization yields the optimal CFL condition. This method is illustrated and compared to the original MPM and a developed analytical solution on one-dimensional problems, and to the classical FEM for two-dimensional ones. D. Sulsky, Z. Chen, H. L. Schreyer, A particle method for history-dependent materials, Computer methods in applied mechanics and engineering 118 (1-2) (1994) 179–196. B. Cockburn, Discontinuous galerkin methods for convection-dominated problems, High-order methods for computational physics, Springer, 1999, pp. 69–224.

Multiscale Strategy for Modelling the Mechanical Performance of Hook and Loop Fasteners Based On a Detachment Process Zone Model: Mode I

Vanessa Restrepo*, Pablo Zavattieri**, Chris Gallant***

*Purdue University, **Purdue University, ***Velcro USA Inc

ABSTRACT

Inspired by the natural mechanism of burdock burr seed, George de Mestral created a provisional and reversible closure system based on hooks and loops fasteners. The mechanics and physics involved in the detachment process of the hook and loop fastener are complex but present an excellent opportunity for the development of novel modelling strategies. A multiscale mechanical model that can capture the right mechanics of the hook and loop mating was developed through a bottom-up approach. The main dissipative mechanisms, the deformation and failure modes, and relevant length scales were explicitly incorporated into a high-fidelity micromechanical model of a Representative Hook and Loop Element (RHLE). An algorithm generates the fibrous surface taking into account the random variation on the geometric parameters of the material. The mechanical behaviour of polypropylene microfibers was characterized by a tensile set of experimental data and ESEM imaging. Subsequently, a macroscopic model was developed, where the length scale at which the entire specimen in the peel test is modelled explicitly. The information obtained from the RHLE model is bridged with the macroscopic model through a User-defined cohesive model (Park et al., 2009) inside the Detachment Process Zone (DPZ). Experimental and numerical peel tests were created to validate the accuracy of the multiscale model. The model accurately captures the mechanical performance of the fastening joint given a geometrical description and material information of the hooks and loops. Therefore, the computational model facilitates the design process and predictions allowing for quick changes and tests in the design parameters and virtually testing the performance of the new fasteners. Keywords: multiscale model, computational model, detachment process zone, hook and loop fasteners. Park, K., Paulino, G.H., Roesler, J.R., 2009. A unified potential-based cohesive model of mixed-mode fracture. J. Mech. Phys. Solids 57, 891–908. <https://doi.org/10.1016/j.jmps.2008.10.003>

Cementitious Composites Based on Bismuth Oxide Nanoparticles for X-ray Shielding

Luciana Restuccia^{*}, A. Favero^{**}, Giuseppe Ferro^{***}, Pravin Jagdale^{****}

^{*}Politecnico di Torino, ^{**}Politecnico di Torino, ^{***}Politecnico di Torino, ^{****}Politecnico di Torino

ABSTRACT

In this research work, a new kind of composite produced with the addition of Bismuth oxide nanoparticles has been investigated, to enhance the x-ray shielding properties of cement-based materials. Bismuth - a cheap, non-toxic and biocompatible element, characterized by having a high atomic number Z ($Z=83$) - has been used as additive by considering different percentages of addition (1%, 5% and 10% with respect the weight of cement for each composition). The experimental activity was focused on the preparation of cement-paste samples with and without addition of bismuth oxide nanoparticles. Water deionized and Portland-Limestone Cement (CEM II/B-LL 32,5 R) were used with a w/c ratio equal to 0.50. X-ray shielding effectiveness has been investigated by using a CT-Scanner for medical tomography: samples have been exposed to the ionising radiations afterwards the 28 days curing time for the complete cement hydration. Through the processing of the data acquired by the CT scanner it has been possible to appreciate the good reactivity of the new cement composites. The radio-opacity of the samples is directly related to the content of bismuth oxide nanoparticles: the higher the percentage, the opaquer they are. Furthermore, by analysing the averages of measurable ROI data for single slice (distance per slice: 4/10 mm), it has been possible evaluate the good homogeneous distribution of bismuth oxide nanoparticles added for each batch. The shielding properties shown by the experimental samples during the tests allow to state that bismuth can be used as a "smart" nanomaterial in cement-based composites, thanks to its chemical-physical properties and above all its non-hazardousness and its low cost.

Preconditioning for HDG and EDG: Stokes Problem

Sander Rhebergen^{*}, Garth Wells^{**}

^{*}University of Waterloo, ^{**}University of Cambridge

ABSTRACT

In this talk we introduce optimal preconditioners for linear systems that arise from discretizing the Stokes problem by hybridizable and embedded discontinuous Galerkin finite element methods. This talk presents an initial step towards preconditioning space-time hybrid finite element methods for the Navier-Stokes equations. Recently we introduced hybrid finite element methods for the Stokes problem which were constructed such that the approximate velocity field is pointwise divergence free and $H(\text{div})$ -conforming [1]. The interesting aspect of these hybrid methods is that the discretization is pressure-robust, compatible with discontinuous Galerkin discretizations of transport equations and, in the case of the Navier-Stokes problem, our method is locally conservative and energy stable [2]. These properties are achieved by introducing a Lagrange multiplier to enforce normal continuity of the velocity field across facets and a Lagrange multiplier to penalize the fact that the approximate velocity field is not in H^1 . Typical of hybrid methods is that it is possible to eliminate element degrees of freedom from the linear system so that the Lagrange multipliers are the only globally coupled degrees of freedom. This static condensation significantly reduces the size of the discrete problem. This talk focusses on optimal preconditioners of these statically condensed linear systems. [1] S. Rhebergen and G.N. Wells, Analysis of a hybridized/interface stabilized finite element method for the Stokes equations. SIAM J. Numer. Anal., Vol. 55/4, pp. 1982-2003, 2017. <https://doi.org/10.1137/16M1083839> [2] S. Rhebergen and G.N. Wells, A hybridizable discontinuous Galerkin method for the Navier-Stokes equations with pointwise divergence-free velocity field, 2017. Submitted. <http://arxiv.org/abs/1704.07569>

A Multi-Fidelity Approach for Aircraft Aero-Structural Optimization

Sergio Ricci^{*}, Alessandro De Gaspari^{**}

^{*}Politecnico di Milano, ^{**}Politecnico di Milano

ABSTRACT

The need for more efficient aircraft, coupled with a request for a significant reduction of the environmental impact, is driving the design of new. Despite the development of new numerical procedures and methods, as well the availability of more powerful computational tools, the development of a fully integrated Aero-structural optimization still represents a challenging goal. Martins in [1] presents a comprehensive overview of the current multidisciplinary design-optimization. The paper presents a multi-fidelity aero-structural design and optimization framework for the optimal design of aircraft wings taking into account the combination of aerodynamic and structural goals. The framework is mainly based on in-house developed tools that are combined in a weak but efficient way. In our case we adopted a typical conceptual design tool, named NeCASS, for the global analysis and aeroelastic optimization of the free flying full flexible aircraft. The structural model adopted is based on a stick representation of the structural components while the aerodynamic model is based on the classical VLM and DLM approaches. While this level of fidelity is usually enough at conceptual design level, this is not true in case of more detailed aero-structural indices have to be included into the optimization loop. For this reason, two different fidelity enhancements are included. The first one concerns the structural model, i.e. for each configuration analyzed a detailed wingbox is generated and optimized externally using the Nastran SOL200. The second fidelity enhancement includes a 2.5D module able to estimate the total Drag starting from the inviscid calculation. The aero-structural coupling is weakly defined by imposing the deformed shape resulting from the aeroelastic trimmed configuration on the aerodynamic mesh used for the Drag estimation. The obtained procedure is driven by a DOE engine to sample the design space that includes also geometrical design variables such as the aspect ratio and the swept angle. The results of the DOE analysis are used for a multi objectives optimization able to offer to the designer a Pareto front on which pick up the most promising configuration. The results concerning an application example will be included in the final paper. [1] Joaquim R. R. A. Martins and Andrew B. Lambe. "Multidisciplinary Design Optimization: A Survey of Architectures", AIAA Journal, Vol. 51, No. 9 (2013), pp. 2049-2075.

Fluid Forces Acting on a Confined Oscillating Cylinder

Guillaume Ricciardi*

*CEA Cadaracge

ABSTRACT

Earthquakes can irreversibly damage nuclear power plants especially in the core, where the nuclear fuel assemblies containing enriched uranium dioxide have to be particularly resistant. Before building a nuclear power plant, it is necessary to make sure that the core will resist the worst possible earthquake conditions liable to occur at the reactor site. Therefore, safety measures are required to insure the drop of control rods and that the core is cooled when the fuel assembly spacer grids strike each other during seismic excitation of a Pressurized Water Reactors. A way to insure these two criteria is to prevent the spacer grids from buckling. Engineers need special tools for designing and maintaining reactor cores. The reactor core made of fuel assemblies is subjected to an axial water flow to cool the reactor. The flow strongly modifies the dynamical behaviour of the fuel assemblies which is made of cylinders; therefore the identification of the fluid forces is important to provide a relevant modelling of the fuel assemblies' behaviour. It is proposed in this paper to perform turbulent CFD of a cylinder in a confined flow accounting for moving boundaries. An ALE method is used for the moving boundaries and a k epsilon model is applied for the turbulence. The Reynolds number is about 50 000. Dynamic simulations are compared the steady simulation with an inclination of the cylinder. Simulations are made for various flow velocities and inclinations. Results are compared to literature and experimental results.

A Continuum Mechanical Bi-scale PDE-ODE Multiphase Model for Alloy Solidification Processes Including Columnar to Equiaxed Transition (CET)

Tim Ricken*, Lukas Moj**, Carla Henning***

*University of Stuttgart, **University of Stuttgart, ***University of Stuttgart

ABSTRACT

ABSTRACT: Numerical hot working process simulations have gained significant importance for steel making industries in order to improve manufacturing. Hence, a thermal driven, bi-phasic, two-scale model consisting of a macro and a micro scale for describing thermo-mechanical loading as well as the physics of solidification is presented. A special focus will be given on the description of the columnar to equiaxed transition (CET). **Macro-Scale:** At macro level, the solid and liquid phases represent the steel physical states based on the theory of porous media (TPM) , cf. DE BOER [2000]. Following the concept of volume fraction, a local, discrete, spatial resolving of the phases is not required. The steel mechanical properties are strongly temperature dependent. Therefore, finite plasticity superimposed by a secondary power creep law as well as finite viscoelasticity are utilized for the solid and the liquid phase, respectively. One temporal and place dependent temperature field for both phases without any interface energy exchange is assumed. This macro-level description leads to a coupled partial differential equation (PDE) system. **Micro-Scale:** On micro-scale, the solidification behavior is described by a coupled ordinary differential equation (ODE) system based on a diffusion-driven dendrite growth model cf. WANG & BECKERMANN [1993]. This process description enables tracking of the transition between columnar and equiaxed dendritic growth (CET), and the influence of solute diffusion on the solidification progression. The strong coupling between volume fractions and concentrations of the alloying element considers the ejection of atoms from the crystal lattice and the associated change in solidification temperature range. **Example:** This two scale PDE-ODE approach has been already successfully applied from our group. This process description enables tracking of the transition between columnar and equiaxed dendritic growth (CET), and the influence of solute diffusion on the solidification progression. The strong coupling between volume fractions and concentrations of the alloying element considers the ejection of atoms from the crystal lattice and the associated change in solidification temperature range. By means of significant examples, the model approaches and the scale coupling will be presented, as well as pro and cons will be discussed. **REFERENCES:** de Boer, R. 2000, "Theory of Porous Media", Springer, New York. Wang, C.Y., and Beckermann, C. (1993), "A Multiphase Solute Diffusion Model for Dendritic Alloy Solidification," Metall. Trans. A, Vol. 24A, pp. 2787-2802.

Data Analytics Using Canonical Correlation Analysis and Monte Carlo Simulation

Jeffrey Rickman*

*Lehigh University

ABSTRACT

We describe the use of correlation analyses, coupled with Monte Carlo simulation, to solve data-intensive problems in materials science and engineering. With this approach, one can identify important, possibly non-linear, relationships among materials processing variables and properties, thereby reducing the dimensionality of large data spaces. We demonstrate the utility of our approach by considering two applications, namely 1.) determining the interdependence of processing and microstructural variables associated with doped polycrystalline aluminas, and 2.) relating microstructural descriptors to the electrical and optoelectronic properties of thin-film solar cells. Finally, we describe how this approach facilitates experimental planning and process control.

Small Changes with Large Impact: Developing Multiscale Models to Understand How Chemical Structure Impacts the Performance of Organic Semiconductors

Chad Risko*

*University of Kentucky

ABSTRACT

Semiconducting materials derived from organic, π -conjugated molecules or polymers have drawn the attention of materials chemists for decades because of the potential to modulate material (opto)electronic properties through well-established synthetic chemistry methods. Unfortunately, materials design remains highly Edisonian, due to limited knowledge of the intimate relationships that connect chemical composition and molecular architecture, materials processing, and the solid-state packing arrangements that determine material performance. We seek to address these connections through the development and application of multiscale, theoretical materials chemistry approaches that build upon principles from organic and physical chemistry, condensed matter physics, and materials science. In this presentation, we will focus on how these models can reveal the striking influence of seemingly modest changes in chemical structure on the processing and solid-state packing of organic semiconducting active layers and resulting materials characteristics. The chemical insight developed through these investigations is beginning to refine and offer novel design paradigms essential to the development of next generation organic semiconducting active layers, and is opening new pathways for in silico materials development.

Stochastic Modelling of Hysteretic Bit-Rock Interaction for Torsional Vibrations of a Drill-String

Thiago Ritto*, Fabio Real**, Anas Batou***, Christophe Desceliers****

*UFRJ, **INMETRO, ***University of Liverpool, ****Université Paris-Est

ABSTRACT

This paper aims at constructing a stochastic model for the hysteretic behaviour of the nonlinear bit-rock interaction of a drillstring under torsional vibrations, based on field data. The proposed model takes into account the fluctuations of the stick-slip oscillations and the hysteretic effect observed during the drilling process. Two nonstationary random processes are taken into account in this work, reproducing the high-frequency (added to the mean torque curve) and the low-frequency (multiplied to the mean torque curve) fluctuations, in order to represent the variation of the fluctuations with the bit speed, and the variations of independent stick-slip cycles respectively. The parameters of the proposed model for nominal hysteretic nonlinear torque are identified cycle by cycle with the least square method, in order to calculate the average parameters for the global nominal model. The coefficient of variation and the correlation length of high-frequency fluctuations are obtained for the stick-slip cycles as a part of the added stochastic fluctuations. Then, correlation length and one parameter that depends on the standard-deviation are identified to construct the low-frequency fluctuations over the independent stick-slip cycles. A nonlinear function of the bit speed is proposed, completing the model for the added fluctuations. Finally, independent trajectories of the proposed stochastic model are generated and used to simulate the stochastic response of the drillstring torsional dynamics in presence of random bit-rock interaction. The numerical results are compared with field data obtained from a 5km drillstring. Ritto, T. G., Soize, C., Sampaio, R., 2009, Nonlinear dynamics of a drill-string with uncertain model of the bit-rock interaction. *International Journal of NonLinear Mechanics*, vol. 44, no. 8, pp. 865-876. Ritto, T. G.; Aguiar, R.R. ; Hbaieb, S. . Validation of a drill string dynamical model and torsional stability. *Meccanica*, v. 52, p. 2959-2967, 2017.

Leveraging GPUs and the Multiple-Program Multiple-Data (MPMD) Computing Model to Enable Material-Aware Topology Optimization

Joshua Robbins^{*}, Miguel Aguilo^{**}, Thomas Voth^{***}, Brett Clark^{****}

^{*}Sandia National Laboratories, ^{**}Sandia National Laboratories, ^{***}Sandia National Laboratories, ^{****}Sandia National Laboratories

ABSTRACT

Additive Manufacturing (AM) expands the engineering design space by enabling creation of freeform geometries that can be driven by performance requirements rather than manufacturing constraints. Widespread adoption of this technology has been slow due to limitations in printed material quality and accompanying difficulties in part qualification. The most common approach in overcoming this qualification challenge is to pursue improvements in AM processes and resulting material quality. Alternatively, material imperfections can be incorporated into the design optimization problem so that designs are robust to deviations from the ideal material, thereby enabling the use of AM technology “as-is”. This presentation will cover the development of optimization based design tools that facilitate component qualification by accounting for AM material quality in the optimization process. By composing objectives that reflect details of the as-printed material, designs can be computed that i) use existing, well characterized AM processes, and ii) meet essential performance requirements. These tools use the multiple-program multiple-data (MPMD) computing model to distribute the evaluation of solutions, objectives, and gradients to available computing resources – including GPUs. Details of the formulation and implementation will be presented along with example applications that demonstrate our approach.

OceanMesh2D: A MATLAB Toolbox for 2-D Finite Element Mesh Development for Coastal Circulation Problems

Keith Roberts^{*}, Joannes Westerink^{**}, William Pringle^{***}

^{*}University of Notre Dame, ^{**}University of Notre Dame, ^{***}University of Notre Dame

ABSTRACT

Often, the most laborious process of geophysical finite-element type numerical simulations involve designing a “good” mesh that captures the features of interest adequately. Many times, the mesh is developed tediously through trial-and-error within a graphical user interface. This is undesirable because 1) it is not reproducible, 2) the development process is not objective, and 3) it frequently requires topological adjustments to ensure numerical stability and to correct flow conveyance. We present a toolbox written with an object oriented programming style in MATLAB to eliminate 1) and 2) and significantly reduce 3), the frequency of post-development adjustments to the mesh. The toolbox can construct large (> 5 million vertices), high quality and objectively built meshes in short computational times (< 1 hours) on an ordinary desktop machine. The mesh resolution is based on objective edge length functions that are derived from digital elevation models (DEMs). The mesh generation algorithm is based on the work of DistMesh2D (Persson and Strang, 2004) but with many improvements for quality solutions in large domains with irregular coastlines. Edge length functions determine how much resolution certain topographic length scales receive based on the following considerations: nodes per wavelength of the dominant tidal species nodes per topographic slope nodes to resolve geometrically complex nearshore features high resolution in deep-draft channels which funnel fluid flow. The edge length function is checked and adjusted to prevent CFL violations and for steep-transitions in mesh resolution. Additionally, the ability to design floodplain meshes where logic based wetting and drying severely limits numerical stability is considered. We illustrate the capabilities of the OceanMesh2D with some mesh sensitivity experiments using the Advanced CIRCulation (Luettich and Westerink 1991) model. The results motivate the selection of parameters used for the edge length function, which improve the objectivity in the mesh development process. In general, we show that meshes created with OceanMesh2D have fewer vertices than meshes developed by hand but have a comparably higher resolution nearshore. Luettich, Rick, Westerink, Joannes, Scheffner, N.W.: (1991). ADCIRC: an advanced three-dimensional circulation model for shelves, coasts and estuaries. Coast. Eng. Res. Ct., US Army Engs. Wtrways. Experiment Station, Vicksburg, MS Report 1: Theory and Methodology of ADCIRC-2DDI and ADCIRC-3DL. Persson, Per Olof, Strang Gilbert (2004): A Simple Mesh Generator in MATLAB. SIAM Review, vol. 46 (2), pp. 329-345.

Camellia for DPG and Other Finite Element Methods: New(er) Capabilities and Plans

Nathan V. Roberts^{*}, Brendan Keith^{**}

^{*}Sandia National Laboratories, ^{**}University of Texas at Austin

ABSTRACT

Camellia is a finite element library intended to facilitate rapid development of computationally efficient, hp-adaptive finite element solvers, starting with support for DPG. In the last couple of years, Camellia has gained several capabilities relevant to DPG and other high-order finite element methods. Among these, Camellia now supports discretizations involving C^0 continuous field variables, DPG* methods, and a platform for customized adaptive mesh refinement strategies, including goal-oriented strategies. In this talk, we will discuss these capabilities, including a new suite of tools for a posteriori error estimation with DPG* methods and some nascent work relating to running on next-generation platforms using Kokkos. [1] B. Keith and A. Vaziri Astaneh and L. Demkowicz. "Goal-oriented adaptive mesh refinement for non-symmetric functional settings." arXiv:1711.01996 [math.NA], 2017. [2] N. V. Roberts. "Camellia v1.0 Manual: Part I." Technical Report ANL/ALCF-16/3, Argonne National Laboratories, 2016.

Combination of Discrete and Finite Element Methods for Coupled Electrochemical-Mechanical Simulations of Lithium-Ion Battery Electrodes

Scott Roberts^{*}, Ishan Srivastava^{**}, Bradley Trembacki^{***}, Mark Ferraro^{****}, Jeremy Lechman^{*****}, David Noble^{*****}

^{*}Sandia National Laboratories, ^{**}Sandia National Laboratories, ^{***}Sandia National Laboratories, ^{****}Sandia National Laboratories, ^{*****}Sandia National Laboratories, ^{*****}Sandia National Laboratories

ABSTRACT

Discrete Element Methods (DEM) are a useful tool for capturing rheological behaviors of granular materials, such as those that arise during lithium-ion battery manufacturing processes, including coating and calendaring. We have extended the LAMMPS DEM simulator to realistically simulate the manufacturing of battery electrodes using experimentally-measured particle size distributions, physical particle interaction models of contact and cohesion, and realistic mechanical stresses introduced during manufacturing. This simulator has been used to create large mesostructures of NMC cathode particles at a wide variety of calendaring stresses. We will discuss these mesostructures and validate them against experimental data where available. The DEM-generated mesostructures are then fed into Finite Element Method (FEM) simulations of electrode performance, utilizing the Conformal Decomposition Finite Element Method (CDFEM) to efficiently create computable meshes of a large number of particles. We analyze the impact of manufacturing processes on relevant electrode-scale effective properties, such as electrical, ionic, and thermal conductivities. Sandia National Laboratories is a multi-mission laboratory managed and operated by National Technology and Engineering Solutions of Sandia, LLC., a wholly owned subsidiary of Honeywell International, Inc., for the U.S. Department of Energy's National Nuclear Security Administration under contract DE-NA0003525. Unclassified Unlimited Release: SAND2018-0016A.

The Role of Inter-constituent Mechanical Interaction in Left Ventricular Mechanics

Sara Roccabianca^{*}, Marissa Grobbel^{**}, Shavik Sheikh Mohammad^{***}, Stephanie Watts^{****}, Lik Chuan Lee^{*****}

^{*}Michigan State University, ^{**}Michigan State University, ^{***}Michigan State University, ^{****}Michigan State University, ^{*****}Michigan State University

ABSTRACT

Intro: Mechanical behavior of myocardial tissue is influenced primarily by two key constituents: myocytes and collagen fibers. These two constituents are often assumed to not be interacting mechanically in the tissue. However, an interaction between collagen fibers and myocytes may greatly influence the overall mechanical behavior of the myocardium. To better understand this interaction, opening angle tests were performed on intact left ventricular (LV) tissue and its isolated constituents. A constrained mixture with inter-constituent mechanical interaction (CMMI) modeling framework was then used to interpret experimental results. **Methods:** Ring-shaped tissues samples were extracted from LVs of healthy adult male rats. These samples were separated equally into three test groups: intact tissue, isolated myocytes, and isolated collagen fibers. Myocytes and collagen fibers were isolated through treatment with collagenase, and decellularization, respectively. We performed classical opening angle experiments [1] to quantify the contribution of the two constituents to overall LV residual stress. The CMMI modeling framework used was based on weighted strain energy function. Inter-constituent mechanical interaction in this framework was described by two parameters γ_m and γ_c that are, respectively, associated with the myocytes and collagen fibers stretch/compression when interacting mechanically. If the interaction is negligible, the CMMI framework should be able to predict the experimental opening angle without any interaction (i.e. $\gamma_m = \gamma_c = 1$). **Results:** Opening angles measured from the isolated collagen fibers ($106.45 \pm 23.02^\circ$) and isolated myocytes ($21.00 \pm 4.37^\circ$) were significantly higher and lower than the intact tissue ($57.88 \pm 12.29^\circ$), respectively. The traditional constrained mixture framework (i.e. no inter-constituent interaction) greatly overestimated the experimental opening angle. However, the experimental results were reproducible using the CMMI framework and introducing interaction described by the range of values from $\gamma_m = 0.1$ and $\gamma_c \leq 1.42$ to $\gamma_m = 0.9$ and $\gamma_c = 0.94$. **Discussion:** Results of the opening angle experiments allude to the idea that the collagen fibers are the key contributor to residual stress in the LV. Additionally, the traditional constrained mixture modeling framework was unable to reproduce the experimental results of this study without introducing some form of mechanical interaction between the collagen fibers and myocytes (CMMI). This interaction between constituents in intact cardiac tissue may greatly influence LV mechanics. **References** [1] Omens and Fung, Circ. Res., vol. 66, pp. 37-45, 1990.

SEPARATION OF MULTIPLE NATURAL FREQUENCIES IN TOPOLOGY OPTIMIZATION

Gustavo C. Rodrigues*, Ederval S. Lisboa*, João B. D. Moreira*, Fernanda B. Link* and
Walter J. P. Casas*

*Department of Mechanical Engineering, Federal University of Rio Grande do Sul
Rua Sarmiento Leite 425, 90050-170
Porto Alegre, Rio Grande do Sul, Brazil
www.ufrgs.br

Key Words: Frequency gaps, Natural frequencies, Topology optimization, Multiobjective Optimization.

Abstract. *In order to avoid mechanical resonance in vibrating structures, it is necessary to design said structures so that their natural frequencies do not coincide with their operational frequencies. Therefore, a machine with multiple modes of operation would need to avoid all of its resonant frequencies in each mode. As such, optimization algorithms can be used to search for a structural layout that maximizes the intervals between the different separated frequencies. This paper aims to accomplish the simultaneous separation of multiple distinct natural frequencies for various structures through the Bi-directional Evolutionary Structural Optimization (BESO) method of topology optimization. Introducing a set of variables representing the equipment's operational frequencies, the BESO algorithm is used to maximize the gap between the superior and inferior frequencies of said variables. As the separation of one pair of eigenfrequencies often affects the remaining eigenfrequencies of a structure, it is necessary to adopt a multi-objective formulation for the optimization problem. Therefore, to scalarize said problem the weighed sum method, where additional frequency intervals are added to the objective function, is utilized. The proposed method was implemented in the MATLAB programming environment and applied in examples of biclamped, unilaterally clamped and simply supported beams found in the literature. It is expected that different weighing coefficients within the optimization process result in varying frequency gaps in the final topologies. The resulting layouts and associated frequency gaps for each system are then presented. The results obtained by the proposed method demonstrate its applicability and efficiency for each case, and it is also shown that general Pareto frontiers for each analyzed system's frequency gaps can be inferred utilizing the resulting topologies.*

1. INTRODUCTION

Topology optimization techniques have become frequently used tools to aid designers and engineers when developing new products. Certain specifications, however, may come to impose limits on a product's natural frequencies, with the goal of avoiding structural mechanical resonance and failure modes. For instance, if a structure will be subjected to two

different known frequencies, the structure's natural frequencies would have to be as distant as possible from these entry frequencies. As such, it is of interest to study topological optimization procedures to develop band-gap structures.

The ESO method (*evolutionary structural optimization*) was first presented in 1993^[1], where in a given project domain, discretized by a fine grid, elements which contribute the least to the overall stiffness of a load-bearing structure are gradually removed, until a desired optimum is reached for the topology. The method was later rewritten^[2] utilizing the elemental deformation energy criteria, in an attempt to maximize structural stiffness. The method was further refined into bidirectional ESO (BESO)^[3], where materials can be added in regions with high stress, and removed in regions with low stress, typically implemented through the addition and removal of elements from the finite element method (FEM), meaning that elements that were removed in some previous iteration of the process can return in later iterations.

The method became very popular among structural optimization researchers, as can be seen in the literature^{[4] [5] [6]}. This method is well established and has evolved to more complex versions^[7], such as bidirectional ESO (BESO)^[4]; the multi-objective version based on fixed elements (MESO)^[8], the genetic ESO method (GESO)^[9]; the version for analysis of fluid-structure systems (BEFSO)^[10]; smoothing ESO (SESO)^[11], which applies a smoothing technique during the removal of inefficient elements from the grid, and the Evolutionary Topology Optimization method (ETO)^[12], capable of generating a smooth and clear boundary shape, in contrast with BESO's zigzagging outline, are just some of the various works found in the literature based on the general principles of the ESO method.

Optimization processes can be classified according to the number of objective functions as mono- or multi-objective problems. Although mono-objective type optimization problems are more widely researched, multi-objective type problems are closer to real problems faced in an engineering context. Unlike a typical mono-objective optimization problem, multi-objective problems do not necessarily have a solution that simultaneously minimizes or maximizes all the desired objective functions. Rather, different objectives can often conflict with each other, and the optimal parameters of one objective do not achieve the optimum of other objectives^[13].

According to the literature^{[14] [15]}, the solution to the multi-criteria problem is known as a Pareto optimum (or a non-inferior solution). For these multi-objective problems, the Pareto frontier of the entire design space is the most valuable tool a designer can have to select the most appropriate designs. Originally, the Pareto frontier is defined as the set of all solutions for which no other solution is better in all objectives^[16].

The ESO method was expanded for multi-criteria analysis on the design of structures with the objective of maximizing the fundamental frequency and minimizing flexibility, simultaneously^[17]. Furthermore, a multi-objective criterion for the optimization of a three-dimensional structure of a thermal protection system (TPS) was developed, in order to concurrently maximize the natural frequency, and minimize thermal stresses^[18].

Refining the BESO method through the implementation of a technique for adaptive removal of alternate and singular elements, propose the multi-objective optimization of frequency-stiffness was proposed ^[19], obtaining structures free from the checkerboard pattern problem.

Many solution algorithms attempt to combine all of the multi-objective functions in a single scalar objective using a weighted sum. The weighted sum is a simple, straightforward approximation to the solutions of the multi-objective optimization problem, employing a linear combination of different objectives, conflicting or not, aided by weights relative to the importance of an objective in relation to another.

This work aims to develop a multi-objective evolutionary structural optimization algorithm for structures with multiple band-gaps. First, section 2 introduces a theoretical foundation of the frequency optimization problem focused on frequency separation. Section 3 presents the proposed algorithm and its implementation concerning different natural frequency intervals. Section 4 presents the numerical procedures and tests realized utilizing the developed code in MATLAB, alongside the resulting Pareto sets from different weights. Finally, section 5 presents the results and conclusions regarding the implemented method.

2. THEORETICAL FOUNDATION

There are different mathematical techniques to define the multi-objective function and choose the optimal vector of variables which satisfies said objectives. Some of the most traditional techniques among them are weighted sum methods and compromise programming. We chose the weighted sum method due to its simplicity and ease of implementation.

The weighted sum method is an approximation for the multi-objective function that implements a linear combination of the different conflicting objectives, aided by artificial weights which measure the relative importance of one objective to another. As read in the literature ^[20], the aggregated objective function to be minimized is a combination of different performance indices, where the conflicting objectives are aggregated on a single function. For a given function \mathcal{A} , which represents the separation between any two consecutive adjacent frequencies, we can define the optimization problem as:

$$\text{Maximize : } A\lambda_{inf} + B\lambda_{sup} \quad (1.1)$$

$$\text{Such that: } (\mathbf{K} - \omega_k^2 \mathbf{M}) \mathbf{u}_k = \mathbf{0} \quad (1.2)$$

$$V_f - \sum_{i=1}^{N_{elements}} x_i V_i = 0 \quad (1.3)$$

$$x_i = 1 \text{ or } x_{min} \quad (1.4)$$

$$A + B = 1 \quad (1.5)$$

where \mathcal{A} can be obtained by equation (2), following from the equations previously presented in early papers^[21] as

$$\Lambda = \sum_{j=n}^m \frac{1}{(\omega_{n_j}^2 - \omega_0^2)} + \sum_{j=1}^{n-1} \frac{1}{(\omega_0^2 - \omega_{n_j}^2)} \quad (2)$$

where ω_0 represents an intermediary frequency between the n th natural frequency and its consecutive. The derivative of equation (2) in relation to a project variable x_i , may be expressed by Equation (3), which represents the function's sensitivity α .

$$\begin{aligned} \alpha = & \left[\sum_{j=n}^{n_{freq}} \frac{1}{(\omega_{n_j}^2 - \omega_0^2)} \right]^{-2} \sum_{j=n}^{n_{freq}} \frac{1}{(\omega_{n_j}^2 - \omega_0^2)} \mathbf{u}_j^T \left(\frac{1 - x_{min}}{1 - x_{min}^p} x_i^{p-1} [K^0] - \frac{\omega_{n_j}^2}{p} [M^0] \right) \mathbf{u}_j \\ & + \left[\sum_{j=1}^{n-1} \frac{1}{(\omega_0^2 - \omega_{n_j}^2)} \right]^{-2} \sum_{j=1}^{n-1} \frac{1}{(\omega_0^2 - \omega_{n_j}^2)} \mathbf{u}_j^T \left(\frac{1 - x_{min}}{1 - x_{min}^p} x_i^{p-1} [K^0] - \frac{\omega_{n_j}^2}{p} [M^0] \right) \mathbf{u}_j \end{aligned} \quad (3)$$

where x_{min} is a chosen minimum non-zero value for the design variable, p is the penalization factor, K^0 is the elemental stiffness matrix, M^0 is the elemental mass matrix, \mathbf{u}_j is the j -th eigenmode and n_{freq} is the chosen number of natural frequencies added to the function.

3. ALGORITHM AND METHODOLOGY

The BESO algorithm is a method of topology optimization based on iteratively removing or adding selected material according to a chosen criterion, according to the objective function. Originally developed for structural stiffness optimization, it was further adapted for multiple material, periodicity constraints and frequency optimization objectives^[5], proving to be a versatile and adaptive algorithm. This work implements a variation of the BESO algorithm, which is detailed in flowchart form in Figure 1.

In traditional frequency separation procedures, two frequencies are statically chosen at the beginning of the procedure, with an intermediary frequency between them, to be separated. It is expected that said frequencies do not fall when the volume fraction reaches lower than a certain threshold. However, this can be disruptive to the overall process as it is common that during an optimization run the chosen frequencies may be significantly altered from their initial values, potentially rising or falling below or above the intermediary frequency. This causes their separation to cease being an adequate distance metric for the entry frequency, and therefore we propose to consider the current upper and lower natural frequencies in any iteration, thus shifting the focus to the chosen intermediary frequency.

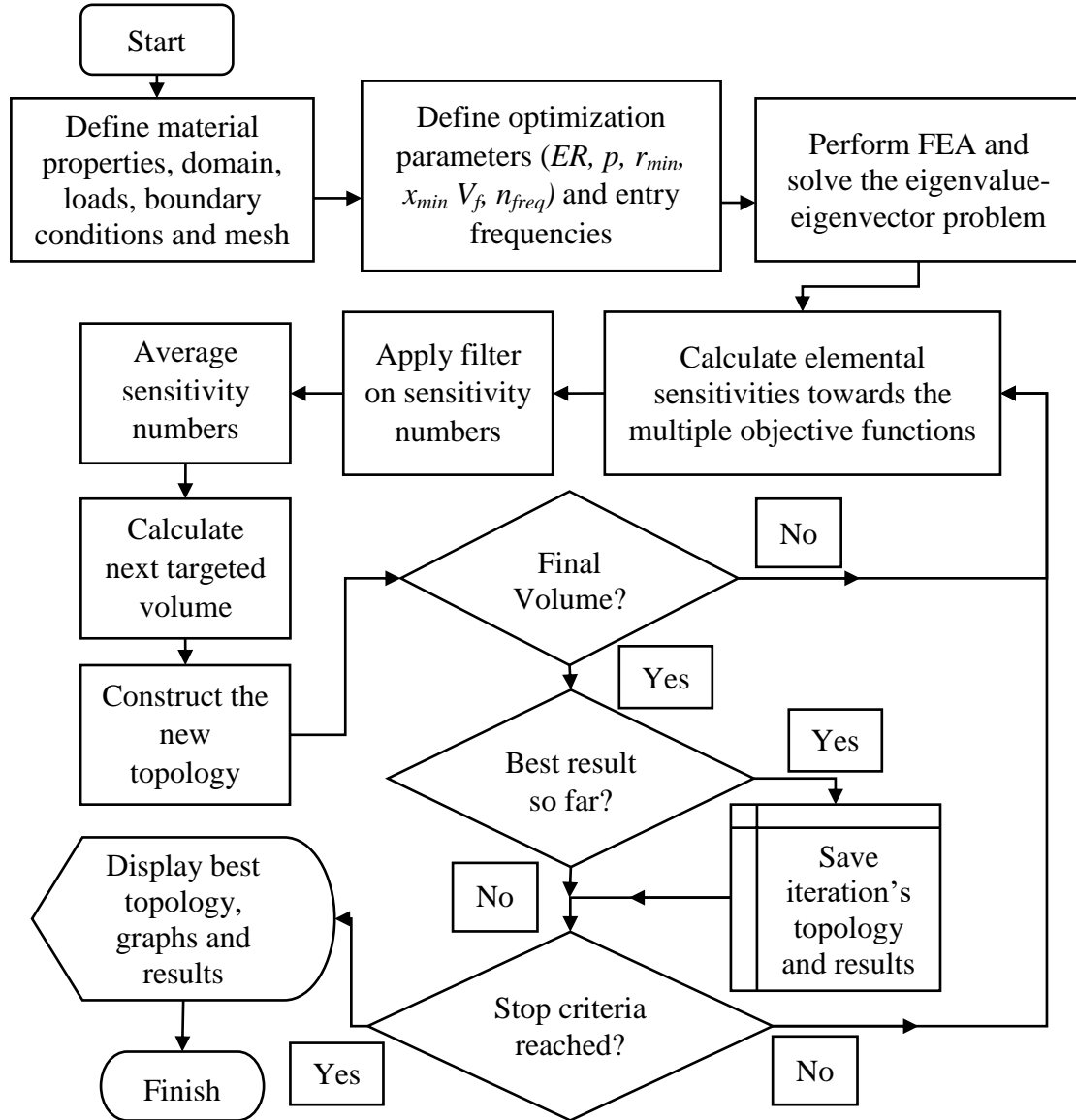


Figure 1. Flowchart of the proposed algorithm used in this work.

The algorithm used in this work adopted two further changes to the traditional BESO method: first, the adoption of a connectivity check between key structural elements (such as mass or support boundary conditions) and second, the selection of “best overall result” as the final structure. The first change is because in the examples chosen, we verified experimentally that if, during the optimization process, a structure loses integrity (for instance, a bi-clamped beam is separated in two) during any iteration, further iterations often do not remedy this

flaw, and the final iteration still presents this error. As such, in some cases we found it useful to stop the algorithm in the first iteration in which structural integrity is lost, and consider only the past iterations in the final procedure. The second change is due to instabilities in the final process. Due to the chosen objective function, the structure's natural frequencies can change wildly and sometimes unpredictably during a run, often to the detriment of the chosen objective. Therefore, it can be more interesting to consider only the best result, here defined as the topology with the highest obtained value S given by the weighted sum of the direct gaps related to the two entry frequencies, as given in equation (4)

$$S = A(\omega_{upper}^{inf} - \omega_{lower}^{inf}) + B(\omega_{upper}^{sup} - \omega_{lower}^{sup}) \quad (4)$$

in which $\omega_{upper}^{inf} - \omega_{lower}^{inf}$ refers to the separation between the closest higher and lower natural frequencies to the lower entry frequency, $\omega_{upper}^{sup} - \omega_{lower}^{sup}$ is the corresponding separation to the higher entry frequency, and A and B are the weights in Eq. (1.1) and (1.5).

4. NUMERICAL EXAMPLES

To analyze and test the proposed method, three key structure examples were chosen. For each case, we obtain the general Pareto frontier for the chosen parameters varying the weights from 0 to 1, as well as an example resulting topology and its natural frequencies along the iterations.

4.1 Simply supported beam

Following ^[22], a simply supported beam at both ends with dimensions of 10 m \times 1 m \times 1 m, as illustrated in Fig. 2, is studied. The material's Young's modulus is assumed to be $E = 10$ MPa, the density $\rho = 1$ kg/m³, and Poisson's ratio of $\nu = 0.3$.

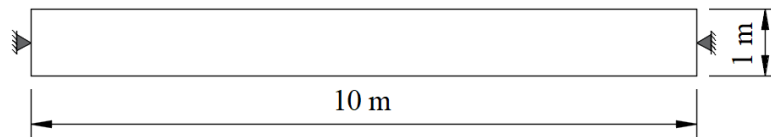


Figure 2 – Representation of the simply supported beam studied.

In this example, there are two entry frequencies, equal to 80 Hz and 390 Hz, respectively. The first entry frequency's sensitivity is calculated taking into account all the frequencies below it, and the first two immediately superior frequencies, while the second entry frequency's sensitivity is calculated taking into account all the natural frequencies below it, and all the natural frequencies above it, up to n_{freq} , here equal to 30. For a final volume V_f of

80%, the BESO process was carried out with $ER=4\%$, $p=6$, $r_{min}=4$ elements, $x_{min}=10^{-3}$ and $\tau=0.1\%$ with linearly varying weights. Figure 3a presents the topology with highest objective function value, while Figure 3b is its graph evolution in the optimization run and figure 3c presents the optimal solutions for different weights.

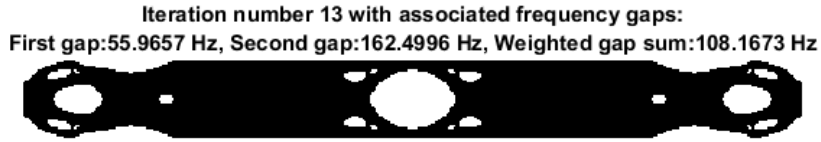


Figure 3a – Topology with the best weighted gap sum obtained in the optimization with weights $A=0.49$, and $B=0.51$.

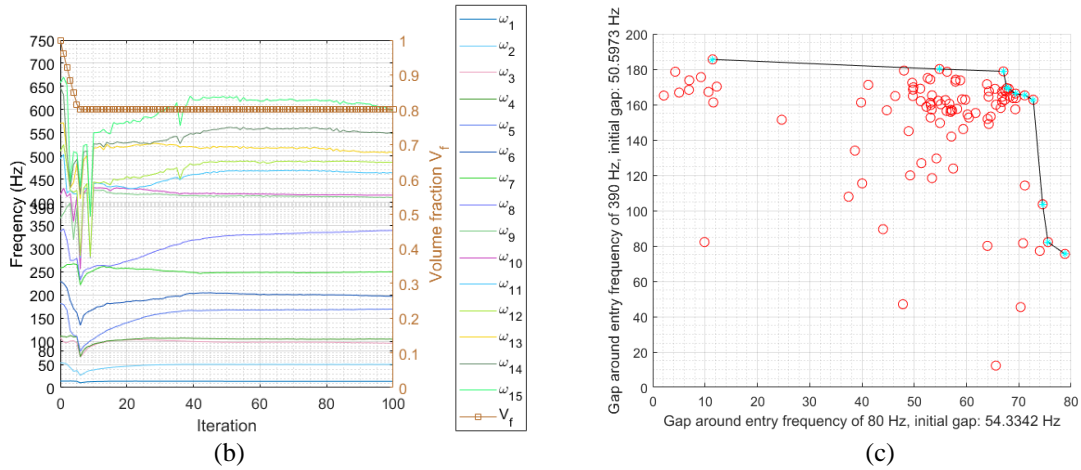


Figure 3b - Evolution of the natural frequencies for weights $A=0.49$ and $B=0.51$, and Figure 3c – Resulting data set obtained by varying the objective function's weights with points in the Pareto frontier.

4.2 Cantilever beam

For this case, a clamped $8 \text{ m} \times 4 \text{ m}$ beam with 1 m thickness, taken from [23] and seen in Fig. 4, is used. The material properties are elastic modulus $E = 10 \text{ GPa}$, density $\rho = 1000 \text{ kg/m}^3$ and Poisson's ratio $\nu = 0.3$, with a concentrated mass M of 16000 kg . The two entry frequencies are 100 and 300 Hz considering the same frequencies as the previous case, and the final volume was set as 60% . The parameters used are $ER=5\%$, $p=5$, $r_{min}=2.5$ elements, $x_{min}=10^{-3}$ and $\tau=0.1\%$.

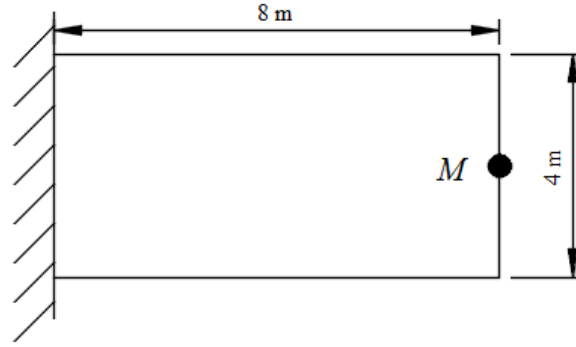


Figure 4 – Representation of the cantilever beam used.

Figure 5a contains the optimized topology for weights $A=0.3$ and $B=0.7$, with its evolution detailed in figure 5b. The resulting Pareto set for these parameters is shown in figure 5c.

Iteration number 34 with associated frequency gaps:
First gap: 77.1414 Hz, Second gap: 93.3807 Hz, Weighted gap sum: 88.5089 Hz

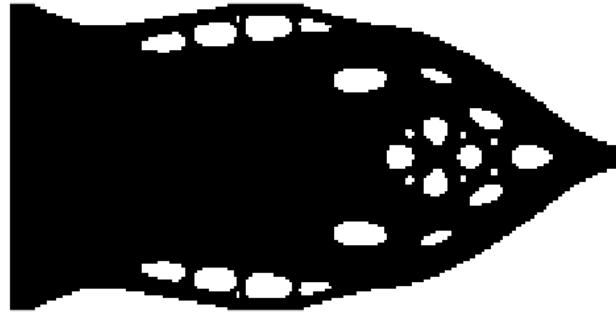
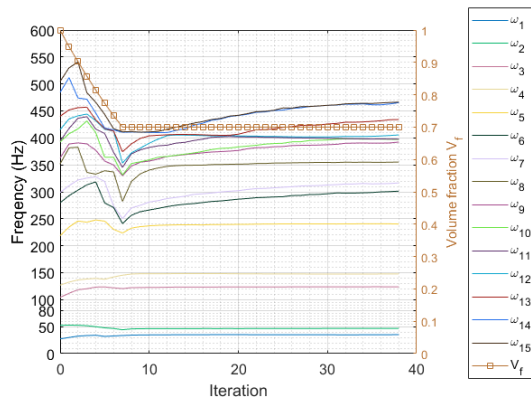
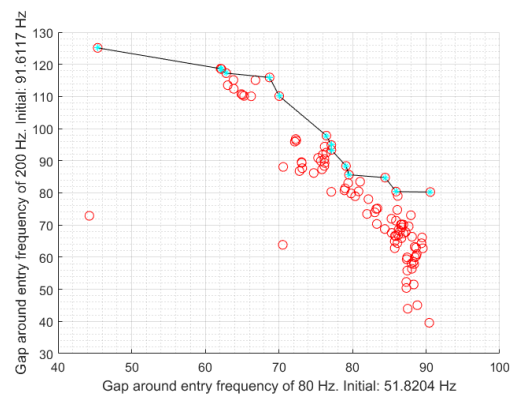


Figure 5a – Topology with the best weighted gap sum obtained in the optimization with weights $A=0.3$, and $B=0.7$.



(b)



(c)

Figure 5b - Evolution of the natural frequencies for weights $A=0.3$ and $B=0.7$, and Figure 5c – Resulting data set obtained by varying the objective function's weights with points in the Pareto frontier.

4.3 Biclamped beam

Finally, a biclamped beam with dimensions $8 \text{ m} \times 1 \text{ m}$ and thickness 0.001 m , based on ^[24] is tested, as in Figure 6. The material properties are elastic modulus $E = 10 \text{ MPa}$, density $\rho = 1 \text{ kg/m}^3$ and Poisson's ratio $\nu = 0.3$, with a concentrated mass M of 4 kg . The two entry frequencies are 100 and 300 Hz taking into account the same frequencies as the other two cases, and the final volume was set as 60% . The parameters used are $ER=4\%$, $p=6$, $r_{min}=4$ elements, $x_{min}=10^{-3}$ and $\tau=0.1\%$

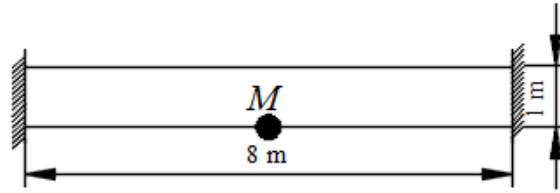


Figure 6 – Representation of the cantilever beam used.

Figure 7a contains the optimized topology for weights $A=0.26$ and $B=0.74$, with its evolution detailed in Figure 7b. The resulting Pareto set for these parameters is shown in Figure 7c.

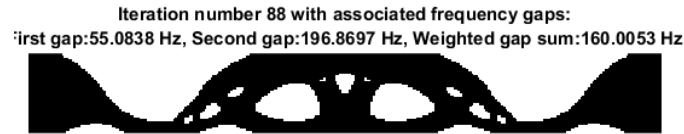
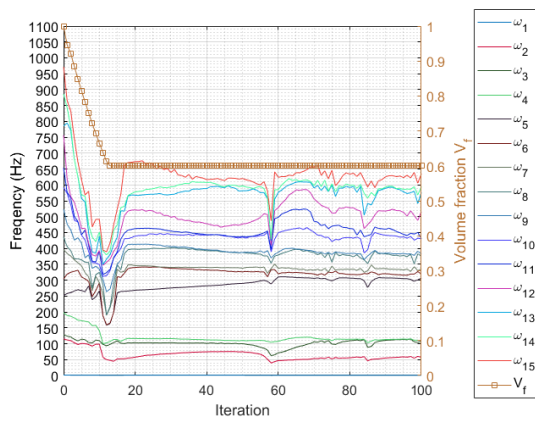
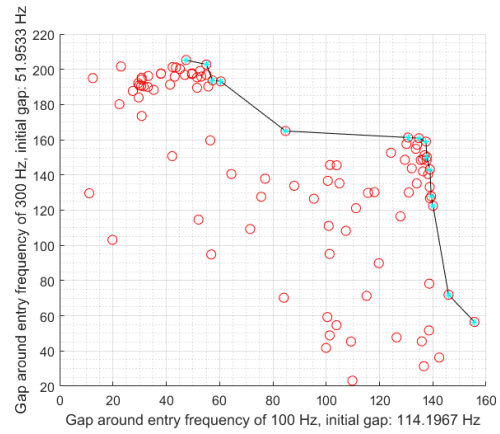


Figure 7a – Topology with the best weighted gap sum obtained in the optimization with weights $A=0.26$, and $B=0.74$.



(b)



(c)

Figure 7b - Evolution of the natural frequencies for weights $A=0.26$ and $B=0.74$, and Figure 7c – Resulting data set obtained by varying the objective function's weights with points in the Pareto frontier.

5. CONCLUSIONS

In this work, the BESO algorithm was applied to the concurrent separation of multiple natural frequencies within a structure given two entry frequencies. The objective function is the maximization of two frequency gaps, utilizing a multi-objective separation function which prioritizes the closest natural frequencies. For each iteration, the closest natural frequencies are re-evaluated and taken into account for the objective function and its sensitivity, thus shifting the focus towards the entry intermediary frequencies. Some numerical examples of topology optimization of 2D structures are carried out, obtaining the algorithm's optimal results in each case.

From the results obtained it is clear that, although extra cautions were taken into obtaining the best possible results from the implemented algorithm, it is still very unstable and may not actually converge to the desired optimum, even if it is capable of optimizing the natural frequency gaps in a structure. It is theorized that this is due to gap optimization objectives not being strictly conflicting, and because the chosen objective function is non-linear, thus being influenced unevenly by higher and lower frequencies. Furthermore, the scalarized weighing method proved to a poor choice to obtain the Pareto set, as it gives unevenly spaced points on its frontier.

6. REFERENCES

- [1] Xie, Y. M.; Steven, G. P. A simple evolutionary procedure for structural optimization. *Comp. & Struct.* (1993) 49: 885–896.
- [2] Chu, D. N.; Xie, Y. M.; Hira, A. and Steven, G. P. Evolutionary structural optimization for problems with stiffness constraints. *Finite Element Analysis*, (1996) 21:239–251.
- [3] Querin, O. M.; Steven, G. P.; Xie Y. M. Evolutionary structural optimisation (ESO) using a bidirectional algorithm. *Eng. Comp.* (1998) 15:1031–1048.
- [4] Huang, X. and Xie, Y. M. Convergent and mesh-independent solutions for the bidirectional evolutionary structural optimization method, *Finite Elements in Analysis and Design*, (2007) 43:1039–1049.
- [5] Huang, X. and Xie, Y. M. *Evolutionary Topology Optimization of Continuum Structures: Methods and Applications*. John Wiley & Sons Ltd. (2010a).
- [6] Huang, X. and Xie, Y. M. A further review of ESO type methods for topology optimization. *Struct. Multidiscip. Opt.* (2010b) 41:671–683.
- [7] Picelli, R. *Otimização Estrutural Evolucionária usando malhas hexagonais*, Masters Dissertation in Mechanical Engineering. Universidade Estadual de Campinas, (2011).

- [8] Tanskanen, P. A multiobjective and fixed elements based modification of the evolutionary structural optimization method. *Comp. Meth. App. Mech. and Engng.* (2006) 196:76–90.
- [9] Liu, X.; Yi, W.; Li, Q. S. and Shen, P. Genetic evolutionary structural optimization. *J. Const. Steel Research*, (2008) 64:305–311.
- [10] Vicente, W. M. *Otimização Topológica Evolucionária Aplicada a Sistemas Elasto-Acústicos*, Thesis (Doctorate in Mechanical Engineering). Universidade Estadual de Campinas, (2013).
- [11] Almeida, V. S.; Simonetti, H. L. and de Assis das Neves, F. Optimal topology selection for 2D structures with stress constraints via Smooth Evolutionary Structural Optimization, *Rev. Int. Mét. Num. Cál. Dsño. Ing.* (2014) 30:69–76.
- [12] Da, D.; Xia, L. and Li, G. Evolutionary topology optimization of continuum structures with smooth boundary representation. *Struct. Multidiscip. Opt.* (2018) 57:2143-2159.
- [13] Yang, X. H. *Engineering Optimization - An Introduction with Metaheuristic Applications*. John Wiley & Sons, (2010).
- [14] Carmichael, D. G. Computation of Pareto Optima in Structural Design, *Int. J. Num. Meth. Engng.* (1980) 15:925–952,
- [15] Koski, J. Multicriterion Structural Optimization. *Opt. Large Struct. Systems.* (1994) 231:793-804.
- [16] Pareto, V. *Cour deconomie politique*. Librairie Droz-Geneve (1964).
- [17] Proos, K. A.; Steven, G. P.; Querin, O. M. and Xie, Y. M. Stiffness and inertia multicriteria evolutionary structural optimisation. *Eng. Comp.* (2001) 18:1031-1054.
- [18] Kim, W. Y. and Grandhi, R. V. Multiobjective evolutionary structural optimization using combined static/ dynamic control parameters. *AIAA Journal.* (2006) 44:794-802.
- [19] Zuo, Z. X.; Xie, Y. M.; Huang, X. An improved bi-directional evolutionary topology optimization method for frequencies. *Int. J. Struct. Stab. & Dynm.* (2010) 10:55 – 75.
- [20] Messac, A. and Mullur, A. A. *Optimization of Structural & Mechanical Systems*. World Scientific (2007).
- [21] Ma, Z.-D., Cheng, H.-C. and Kikuchi, N. Structural design for obtaining desired eigenfrequencies by using the topology and shape optimization method. *Comp. Systems Engng.* (1994) 5:77-89.

- [22] Lopes, H. N., Pavanello, R. and Mahfoud, J. Topology Optimization for the Maximization of Frequency Separation Margin. VI Int. Symposium on Solid Mech – MecSol 2017 (Conference paper).
- [23] Zheng, J., Long, S. and Li, G. Topology optimization of free vibrating continuum structures based on the element free Galerkin method. *Struct. Multidisc. Optim.* (2012) 45:119-127.
- [24] Du, J. and Olhoff, N. Topological design of freely vibrating continuum structures for maximum values of simple and multiple eigenfrequencies and frequency gaps. *Struct. Multidisc. Optim.* (2007) 34:91-110.

Multi-Scale Analysis of Second-Order Effects at Finite Strains

Igor Rodrigues Lopes*, Francisco Andrade Pires**

*DeMec, Faculdade de Engenharia da Universidade do Porto, **DeMec, Faculdade de Engenharia da
Universidade do Porto

ABSTRACT

Multi-scale analyses are of utmost importance in order to understand the micro-scale mechanisms that influence the macroscopic material behaviour. Materials which are heterogeneous at a certain spatial scale may be modelled by a Representative Volume Element (RVE), where phenomena arising at the micro-scale due to a macro-scale loading may be analysed in detail, accounting for the effect of material heterogeneities. Computational analysis of RVEs behaviour are usually performed considering only the linear part of the macroscopic loading, e.g. by means of the insertion of a deformation gradient. However, in some applications, it may be interesting to include second-order effects through the macroscopic second-order displacement gradient [1,2]. In the present contribution, details on the implementation of a computational framework to analyse RVEs under second-order loadings are presented. Numerical simulations are performed in order to analyse the effects of including the second-order component of the macro-scale loading on RVEs representing materials with heterogeneous microstructures. Keywords: Multi-Scale, Heterogeneous materials, Second-order effects, Finite strain, Finite element method. References: [1] V.G. Kouznetsova, M.G.D. Geers and W.A.M. Brekelmans, Multi-scale constitutive modelling of heterogeneous materials with a gradient-enhanced computational homogenization scheme. *Int. J. Numer. Meth. Eng.*, Vol. 54, pp. 1235-1260, 2002. [2] D.J. Luscher, D.L. McDowell and C.A. Bronkhorst, A second gradient theoretical framework for hierarchical multiscale modeling of materials. *Int. J. Plast.*, Vol. 26, pp. 1248-1275, 2010.

Simulations of Rayleigh Bubble Collapse Near a Soft Object

Mauro Rodriguez*, Eric Johnsen**

*University of Michigan, Ann Arbor, **University of Michigan, Ann Arbor

ABSTRACT

Understanding the mechanics of bubble dynamics and shock wave propagation in viscoelastic media is important for various biomedical applications, particularly in the context of cavitation-induced damage. The application of interest is histotripsy, a therapeutic ultrasound treatment that uses high-amplitude (100 MPa peak positive pressure, -25 MPa peak negative pressure) and high-frequency (MHz) ultrasound waves to destroy tissue. The local/transient pressure changes lead to the formation of cavitation bubbles that grow and violently collapse, thus producing shock waves that propagate in the surroundings. Although not fully understood, the damage mechanism induced on the nearby object combines the effect of the incoming pulses and cavitation (bubble oscillation and collapse) produced by the high tension. In such problems, the constitutive models describing the soft material are non-trivial and include effects such as (nonlinear) elasticity, history (relaxation effects) and viscosity. Thus, the influence of the shock on the material and the response of the material to the shock are poorly understood. Understanding these mechanisms will provide invaluable insights to the further the development of histotripsy as a therapy tool for treating malignant tissues. To simulate this phenomenon, an in-house, solution-adaptive, high-order accurate shock- and interface-capturing method is used to solve the 3D equations for conservation of mass, momentum, energy in a Eulerian framework [1]. This method incorporates evolution equations for the elastic stresses and stress relaxation variables to solve multi-component flows including Zener-like viscoelastic media [2]. In this approach, the evolution equations are evaluated by taking the Lie objective time derivative of the constitutive relation that models the material of interest using strain rates. In the principal contributions to the field, a 3D canonical problem is considered which involves the Rayleigh collapse of a vapor bubble in a liquid next to a viscoelastic or elastic medium of a certain thickness. Using these simulations, scaling relations for the maximum pressures and temperatures produced during this process will be presented for different initial stand-off distances and shear moduli of the soft object. This research was supported in part by NSF grant CBET 1253157 and the Ford Foundation Dissertation Fellowship. [1] S. Alahyari Beig and E. Johnsen, Maintaining interface equilibrium conditions in compressible multiphase flows using interface capturing, J. Comput. Phys. 302 (2015) 548-566. [2] M. Rodriguez, E. Johnsen, A high-order accurate, finite-difference approach for numerical simulations of shocks interacting with interfaces between fluids and linear viscoelastic materials. In preparation. (2018)

Estimation of Material Coefficients for an Idealized Model of the Human Abdominal Aorta

Miguel Rodriguez*, Shawn Shadden**

*University of California, Berkeley, **University of California, Berkeley

ABSTRACT

The finite element method (FEM) has been used extensively to study the mechanics of arterial and cardiac tissue [1]. Magnetic resonance and computed tomography imaging techniques enable the extraction of a patient's cardiovascular geometry, which is then used to carry out patient-specific simulations. In most studies, the material coefficients required by constitutive equations are obtained through ex vivo patient-averaged material testing. For clinical applications however — and due to substantial patient variation in material properties — there exists a need for a patient-specific in vivo method to obtain these coefficients. We present a variational data assimilation (4DVar) technique applied to an idealized model of arterial walls. Before applying 4DVar techniques to patient data, we validate our framework using a thick-walled cylinder modeled as a neo-Hookean material. First, to produce a synthetic observation data set, a forward simulation of the time-dependent loading of the inner wall of the cylinder is carried out with known material coefficients, and the results are recorded. To test the robustness of this technique, white noise is added to the observation data. Then, material coefficient values different from those used to generate the observation data are fed to the 4DVar framework as the initial guess for the coefficients that are to be recovered. The forward problem is solved with this initial guess, and the gradient of the objective function quantifying the misfit between the simulation and observations with respect to the material coefficients is used to iteratively update the coefficient values. Preliminary results using the 4DVar framework show that the material coefficient simulation values are recovered within a 20% error of those used to produce the artificial observation data set with a signal-to-noise ratio as low as 2.25. Future work will focus on using different constitutive equations, as well as study the effect of adding regularization terms to the objective function. Developing and validating this framework will provide an automated technique for tuning simulations to specific patients, and in turn bring cardiovascular biomechanics closer to the clinical setting. 1. Holzapfel, Gerhard A. et al., Proc. R. Soc., 2010.

Dynamic Recrystallization and Adiabatic Shear Localization

José Rodríguez-Martínez*, Guadalupe Vadillo**, Daniel Rittel***, Ramón Zaera****, José Fernández-Sáez*****

*University Carlos III of Madrid, **University Carlos III of Madrid, ***Technion, ****University Carlos III of Madrid, *****University Carlos III of Madrid

ABSTRACT

It has recently been reported that, in alloys exhibiting early dynamic recrystallization (DRX), the onset of adiabatic shear bands (ASB) is primarily related to microstructural transformations, instead of the commonly assumed thermal softening mechanism, as shown by Rittel et al. (2008) and Osovski et al. (2012). Further, the dominant role of microstructural softening in the necking process of dynamically stretching rods showing DRX has been verified using linear stability analysis and finite element simulations by Rodríguez-Martínez et al. (2015). With the aim of extending this coupled methodology to shear conditions, this paper presents an analytical solution to the related problem of ASB in a material that undergoes both twinning and dynamic recrystallization. A special prescription of the initial and loading conditions precludes wave propagation in the specimen which retains nevertheless its inertia, allowing for a clear separation of material versus structural effects on the localization process. A parametric study, performed on the constants of the constitutive model, permits the identification of their relative role in the onset of the dynamic instability. The main outcome of the analysis confirms the strong destabilizing effect played by the development of DRX, consistently with the former statement regarding ASB, and contributes to rationalize the observations of other authors. We have also shown that the amount of DRX influences the width of the shear band, and the separation between shear bands in multiple shear band problems. Rittel, D., Landau, P., Venkert, A., 2008. Dynamic recrystallization as a potential cause for adiabatic shear failure. Phys. Rev. Lett. 101, 165501. Osovski, S., Rittel, D., Landau, P., Venkert, A., 2012b. Microstructural effects on adiabatic shear band formation. Scr. Mater. 66, 9–12. Rodríguez-Martínez, J.A., Vadillo, G., Zaera, R., Fernández-Sáez, J., Rittel, D., 2014. An analysis of microstructural and thermal softening effects in dynamic necking. Mech. Mater. 80B, 298-310.

TWO-SCALE MODELLING OF LARGE-DEFORMING FLUID-SATURATED POROUS MEDIA: RATE FORMULATION AND HOMOGENIZATION CONCEPT

EDUARD ROHAN*, VLADIMÍR LUKEŠ†

* Department of Mechanics, Faculty of Applied Sciences,
University of West Bohemia, Univerzitní 8, Pilsen, Czech Republic
rohan@kme.zcu.cz

† New Technologies for the Information Society, Faculty of Applied Sciences,
University of West Bohemia, Univerzitní 8, Pilsen, Czech Republic
lukes@kme.zcu.cz

Keywords: Porous media, Homogenization, Biot model, Updated Lagrangian formulation

Abstract: The paper deals with the homogenization of the locally periodic Biot medium subject to large deformation. As the main outcome, a consistent two-scale incremental scheme is derived, leading to a variant of the FE-square computational approach. A particular three compartment topology of the representative volume featured by large contrasts in the permeability is considered.

1 INTRODUCTION

Behaviour of the fluid-saturated porous media (FSPM) at finite strains has been studied within the mixture theories and also using the macroscopic phenomenological approach [1, 4]. The fluid retention in unsaturated media is so far not well understood in the context of deterministic models, a number of publications involve this phenomenon in computational models [5]. In any case, in this paper we consider only porous media with one phase fluids saturating the pores. In the context of homogenization, the FSPM has been treated *e.g.* in [12] At the pore level, the mechanical model describes interactions of an elastic, or hyperelastic skeleton and a compressible viscous fluid, see [8, 6] where the updated Lagrangian formulations has been employed. As an alternative, the ALE formulation provides some advantages [2]. Macroscopic treatment of the FSPM using the incremental updated Lagrangian formulations was reported in [13], the dynamic behaviour is confined to an approximation of the inertia effects associated with the relative fluid-solid motion so that the model is convenient for describing quasistatic loading of large-deforming porous structures.

In the present paper, we consider quasistatic loading of a FSPM medium with periodic heterogeneities related to the poroelastic and permeability coefficients of the Biot-Darcy model. More-

over, the double porosity structures are considered as an extension of the models developed by the homogenization to treat small deforming media, see [10]. At the macro-level, the computational algorithm is consistent with linearization of the residual formulation in the Eulerian framework, such that the incremental scheme (for a given time step) uses the updated Lagrangian approach. The equilibrium equation and the mass conservation expressed in the spatial configuration are differentiated using the material derivative with respect to a convection velocity field.

This yields linearized equations to which the homogenization can be applied, assuming locally periodic structures graded continuously at the macroscopic scale, cf. [8]. This allows us to establish the effective medium properties involved in the incremental formulation using the homogenization based on asymptotic analysis w.r.t the microstructure scale. In this way, modified poroelastic coefficients can be computed for given updated configurations, as in the linear case, cf. [9]. The proposed two-scale incremental formulation provides a basis for enrichment of the model by multiphysics effects, such as transport of electrolytes. The model is implemented in the SfePy code. A numerical example is presented.

2 PROBLEM FORMULATION AT THE MESOSCOPIC SCALE

In this section we introduce the residual formulation of the problem for a large deforming poroelastic medium with large contrast in the permeability coefficients. The initial configuration is associated with material coordinates X_i , $i = 1, 2, 3$ and with domain Ω_0 . The spatial (current) configuration at time t is associated with spatial coordinates x_i and with domain $\Omega(t)$. The deformation gradient $F_{ij} = \delta_{ij} + \partial u_i / \partial X_j$ is introduced using the displacement fields.

2.1 Weak formulations

The boundary conditions are prescribed on the boundary consisting of disjoint parts; two decompositions are considered: $\partial\Omega = \partial_u\Omega \cup \partial_\sigma\Omega$, where $\partial_u\Omega \cap \partial_\sigma\Omega = \emptyset$, and $\partial\Omega = \partial_p\Omega \cup \partial_w\Omega$, where $\partial_p\Omega \cap \partial_w\Omega = \emptyset$. This decompositions is reflected by the admissibility sets and corresponding linear spaces employed in the weak formulation,

$$\begin{aligned} V(t) &= \{\mathbf{v} \mid \mathbf{v} = \mathbf{u}^\partial \text{ on } \partial_u\Omega(t) \subset \partial\Omega(t)\} , \\ Q(t) &= \{q \mid q = p^\partial \text{ on } \partial_p\Omega(t) \subset \partial\Omega(t)\} , \\ V_0(t) &= \{\mathbf{v} \mid \mathbf{v} = 0 \text{ on } \partial_u\Omega(t) \subset \partial\Omega(t)\} , \\ Q_0(t) &= \{q \mid q = 0 \text{ on } \partial_p\Omega(t) \subset \partial\Omega(t)\} . \end{aligned} \tag{1}$$

The true (Cauchy) stress for the incompressible poroelastic medium $\boldsymbol{\sigma} = \boldsymbol{\sigma}^{\text{eff}} - p\mathbf{I}$ consists of the effective strain-dependent part $\boldsymbol{\sigma}^{\text{eff}}$, and the pore fluid pressure part $-p\mathbf{I}$. The state of the poroelastic medium is obtained as a solution of the nonlinear residual equation,

$$\Phi_t((\mathbf{u}, p); (\mathbf{v}, q)) = 0 \quad \forall (\mathbf{v}, q) \in V_0(t) \times Q_0(t), \tag{2}$$

consisting of the equilibrium equation and the Darcy flow driven balance of the fluid content,

$$\begin{aligned}\Phi_t((\mathbf{u}, p); (\mathbf{v}, 0)) &= \int_{\Omega(t)} \boldsymbol{\sigma} : \nabla \mathbf{v} - \int_{\Omega(t)} \rho \mathbf{b} \cdot \mathbf{v} \quad \forall V_0(t) , \\ \Phi_t((\mathbf{u}, p); (0, q)) &= \int_{\Omega(t)} (\nabla \cdot \dot{\mathbf{u}} q + \mathbf{K} \nabla p \cdot \nabla q) - \mathcal{J}_t(q) \quad \forall q \in Q_0(t) ,\end{aligned}\tag{3}$$

where $\dot{\mathbf{u}}$ is the skeleton (local) velocity, $\mathbf{K} = (K_{ij})$ is the permeability, \mathcal{J}_t is the fluid mass source/sink, ρ is the solid density and \mathbf{b} represents volume forces per mass. The linearization (2) involves the state increments $(\delta \mathbf{u}, \delta p)$; the following problem is subject to the homogenization, as described below: Given $(\bar{\mathbf{u}}, \bar{p})$ at time $t > 0$, compute a new state (\mathbf{u}, p) at time $t + \delta t$ such that

$$\Phi_{t+\delta t}((\mathbf{u}, p); (\mathbf{v}, q)) \approx \Phi_t((\bar{\mathbf{u}}, \bar{p}); (\mathbf{v}, q)) + \delta \Phi_t((\bar{\mathbf{u}}, \bar{p}); (\mathbf{v}, q)) \circ (\delta \mathbf{u}, \delta p, \delta t \mathcal{V}) ,\tag{4}$$

where $\delta \Phi_t((\bar{\mathbf{u}}, \bar{p}); (\mathbf{v}, q)) \circ (\delta \mathbf{u}, \delta p, \delta t \mathcal{V})$ is the increment due to the material derivative associated with convected field \mathcal{V} ,

$$\begin{aligned}\mathbf{u} &= \bar{\mathbf{u}} + \delta \mathbf{u} , p = \bar{p} + \delta p , \\ \text{where } \delta \mathbf{u} &= \dot{\mathbf{u}} \delta t , \quad \delta p = \dot{p} \delta t , \\ \Omega(t + \delta t) &= \Omega(t) + \delta t \{\mathcal{V}\}_{\Omega(t)}\end{aligned}\tag{5}$$

By differentiating $\boldsymbol{\sigma} = J^{-1} \mathbf{F} \mathbf{S} \mathbf{F}^T$ where \mathbf{S} is the 2nd Piola-Kirchhoff stress, $J = \det \mathbf{F}$ and \mathbf{F} is the deformation gradient, $F_{ij} = \delta_{ij} + \partial u_i / \partial X_j$, the Lie derivative of $\boldsymbol{\sigma}$ is obtained.

2.2 Time discretization

The time derivatives are approximated by backward differences $\delta \mathbf{u}^k = \mathbf{u}^k - \mathbf{u}^{k-1}$,

$$\begin{aligned}\dot{\mathbf{u}}(t_k) &\approx (\mathbf{u}^k - \mathbf{u}^{k-1}) / \delta t = \delta \mathbf{u}^k / \delta t , \\ \ddot{\mathbf{u}}(t_k) &\approx (\delta \mathbf{u}^k - \delta \mathbf{u}^{k-1}) / (\delta t)^2 = (\mathbf{u}^k - 2\mathbf{u}^{k-1} + \mathbf{u}^{k-2}) / (\delta t)^2 .\end{aligned}\tag{6}$$

The convection velocity field can be approximated by the backward, or forward difference of the displacements. We shall employ the following notation:

$$\begin{aligned}\delta \mathbf{u}^{k+1} &\mapsto \mathbf{u} , \quad \delta p^{k+1} \mapsto p , \\ \delta \mathbf{u}^k &\mapsto \bar{\mathbf{u}} , \quad \delta p^k \mapsto \bar{p} , \\ p^k &= \hat{p} .\end{aligned}\tag{7}$$

The incremental subproblem is imposed in the actual spatial configuration represented by domain $\Omega_k = \Omega$. Further abbreviated $\mathbb{D}^{\text{eff}}(t_k) = \mathbb{D}^{\text{eff}}$, $\boldsymbol{\sigma}^{\text{eff}}(t_k) = \boldsymbol{\sigma}^{\text{eff}}$, $\delta \mathbf{b}^{k+1} = \delta \mathbf{b}$.

To simplify notation, we shall introduce some further notation:

$$\begin{aligned}
\mathbf{I} &= (\delta_{ij}) , \quad (\mathbf{I})_{ij} = \delta_{ij} , \\
\mathbb{I} &= (\delta_{jl}\delta_{ik}) , \quad (\mathbb{I})_{ijkl} = \delta_{jl}\delta_{ik} , \\
\mathbf{B}^T(\mathbf{v}) &= (\mathbf{I} \otimes \mathbf{I} - \mathbb{I})\nabla \mathbf{v} , \\
\mathbf{H}(\mathbf{v}) &= (\nabla \cdot \mathbf{v})\mathbf{K} - \mathbf{K}(\nabla \mathbf{v})^T - (\nabla \mathbf{v})\mathbf{K}^T .
\end{aligned} \tag{8}$$

Note that $\mathbf{H}(\mathbf{v})$ is symmetric for any symmetric \mathbf{K} , whereas $\mathbf{B}^T(\mathbf{v})$ is non-symmetric in general; using the latter tensor we can simply write

$$\begin{aligned}
(\nabla \cdot \mathbf{v})(\nabla \cdot \bar{\mathbf{u}}) - \nabla \mathbf{v} \nabla \bar{\mathbf{u}} : \mathbf{I} &= (\nabla \bar{\mathbf{u}})^T : (\mathbf{I} \otimes \mathbf{I} - \mathbb{I})\nabla \mathbf{v} = (\nabla \mathbf{v})^T : (\mathbf{I} \otimes \mathbf{I} - \mathbb{I})\nabla \bar{\mathbf{u}} \\
&= \mathbf{B}(\mathbf{v}) : \nabla \bar{\mathbf{u}} = \mathbf{B}^T(\bar{\mathbf{u}}) : (\nabla \mathbf{v})^T = \mathbf{B}(\bar{\mathbf{u}}) : \nabla \mathbf{v} .
\end{aligned} \tag{9}$$

Using notation (8), the general incremental formulation (4) yields the linear subproblem: Find $(\mathbf{u}, p) \in \delta V(t_{k+1}) \times \delta Q(t_{k+1})$ which satisfy

$$\begin{aligned}
&\int_{\Omega} \mathbb{D}^{\text{eff}} e(\mathbf{u}) : e(\mathbf{v}) + \int_{\Omega} \boldsymbol{\sigma}^{\text{eff}} : \nabla \mathbf{v} (\nabla \mathbf{u})^T - \int_{\Omega} \hat{p} \mathbf{B}(\mathbf{u}) : \nabla \mathbf{v} - \int_{\Omega} p \mathbf{B}(\bar{\mathbf{u}}) : \nabla \mathbf{v} - \int_{\Omega} p \nabla \cdot \mathbf{v} \\
&= - \int_{\Omega} (\boldsymbol{\sigma}^k : \nabla \mathbf{v} - \rho \mathbf{b}^{k+1} \cdot \mathbf{v})
\end{aligned} \tag{10}$$

for all $\mathbf{v} \in V_0(t_k)$ and

$$\begin{aligned}
&\int_{\Omega} q \mathbf{B}(\bar{\mathbf{u}}) : \nabla \mathbf{u} + \int_{\Omega} q \nabla \cdot \mathbf{u} + \delta t \int_{\Omega} (\mathbf{K} + \mathbf{H}(\bar{\mathbf{u}})) \nabla p \cdot \nabla q \\
&= \delta t \mathcal{J}^{k+1}(q) - \delta t \int_{\Omega} (\mathbf{K} + \mathbf{H}(\bar{\mathbf{u}}) + \delta \mathbf{K}) \nabla \hat{p} \cdot \nabla q ,
\end{aligned} \tag{11}$$

for all $q \in Q_0(t_k)$.

3 HOMOGENIZATION

We consider a reference configuration generated as a periodic lattice by repeating the representative cell \hat{Y} . By virtue of the unfolding operation, the coordinates can be split into the macroscopic parts denoted by x and the local (microscopic) parts, denoted by y . As the consequence of the finite deformation and the incremental formulation, an updated configuration is established in terms of the locally representative periodic deformed cell.

3.1 Locally periodic microstructures

Using a diffeomorphic mapping $\mathcal{F}^\varepsilon \in C^1(\hat{\Omega}; \mathbb{R}^3)$ we may introduce “locally periodic microstructure”. For the location $x \in \Omega(t)$, there exists $\hat{x}^0 \in \Omega(0)$

$$x - \hat{x} = \mathcal{F}^\varepsilon(y^0, \hat{x}^0) , \quad \text{and} \quad Y^\varepsilon(\hat{x}) = \mathcal{F}^\varepsilon(\hat{Y}, \hat{x}^0) , \tag{12}$$

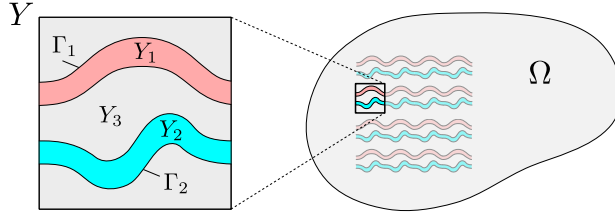


Figure 1: The representative cell with three porous compartments.

where \hat{x} is the spatial position of the cell central position $\hat{x}^0 \in \Omega(0)$ in the initial configuration. By $Y(\hat{x}) = \varepsilon^{-1}Y^\varepsilon(\hat{x})$ we denote the rescaled (but not necessarily unit) local reference cell representing the locally periodic microstructure, see Fig. 2. We recall that ε determines the ratio between the macro- and microscopic scales, the latter represented by the cell $Y(\hat{x})$; for $y, y' \in Y(\hat{x})$ the corresponding point $x, x' \in Y^\varepsilon(\hat{x})$ is given by $x - x' = \varepsilon(y - y')$. Evidently with ε getting smaller the number of cells Y^ε which cover any fixed subdomain of Ω increases. In this process any two adjacent cells, or those which are close enough, become almost identical. Thereby, in the limit case $\varepsilon \rightarrow 0$, each “macroscopic” point x is associated with the microstructure formed by periodic array of cells, which are defined as the Y -periodic translation of the representative cell $Y(\hat{x})$.

By Y we now abbreviate the local spatial reference cell $\varepsilon^{-1}Y^\varepsilon$ defined above in (12), without writing explicitly the macroscopic location. Since our interests are in porous media with large contrasts in the permeability coefficients, we shall introduce the following decomposition of Y into the sectors of primary and dual porosities.

Let Y_α , for $\alpha = 1, 2$ be mutually disconnected subdomains of Y with Lipschitz boundary, then Y_3 forms the complement (see Fig. 1)

$$Y_3 \equiv Y \setminus \bigcup_{\alpha=1,2} \overline{Y_\alpha}, \quad (13)$$

$$\text{interface } 3-\alpha: \quad \Gamma_\alpha = \partial_3 Y_\alpha = \partial_\alpha Y_3 \equiv \overline{Y_\alpha} \cap \overline{Y_3}.$$

Furthermore, we require that $\partial Y \cap \partial Y_k \neq \emptyset$, so that the all domains Ω_k^ε , $k = 1, 2, 3$ generated by repeating the cells εY_k are connected.

The parts of the periodic boundary will be denoted (interface $k-k$) by

$$\partial_k Y = \partial_k Y_k \equiv \overline{Y_k} \cap \partial Y, \quad k = 1, 2, 3.$$

The material parameters in deformed configuration depend on the deformation gradient $F_{ij}^\varepsilon(x)$. To define them in the local reference cell, we use the unfolding operation, [3], For the sake of brevity, we shall consider couples (y, x) implicitly matching, such that $y - \hat{y} = \varepsilon^{-1}(x - \hat{x})$. In the spatial configuration we introduce the permeability parameters, as follows:

$$K_{ij}^\varepsilon(x) = \begin{cases} \tilde{K}_{ij}^\alpha(x, y) & y \in Y_\alpha, \alpha = 1, 2, \\ \varepsilon^2 \tilde{K}_{ij}^3(x, y) & y \in Y_3. \end{cases} \quad (14)$$

We emphasize, that the scaling by ε^2 the permeability coefficients in the “matrix” compartment leads to the *double porosity* effect. Obviously, tensors \tilde{K}_{ij} are depend on the material deformation and should be modified from one time level to the next one using \tilde{F} .

3.2 Asymptotic expansions and decomposition of two-scale functions

This paper only summarizes those results which enable to construct a computational algorithm. In particular, the characteristic responses are introduced which allow for splitting the dependence of the two-scale responses describing the heterogeneous medium on the macroscopic fields (strain and pressures) and on the local microscopic configuration. With reference to the simplified notation (7), in the context of the incremental formulation we introduce truncated expansions of the time step increments,

$$\begin{aligned} \mathbf{u}^\varepsilon(x) &= \mathbf{u}^0(x) + \varepsilon \mathbf{u}^1(x, y) + O(\varepsilon^2) , \\ p^\varepsilon(x) &= \sum_{\alpha=1,2} \chi_\alpha(y) (p_\alpha^0(x) + \varepsilon p_\alpha^1(x, y) + O(\varepsilon^2)) + \chi_3(y) (\tilde{p}_3(x, y) + O(\varepsilon)) . \end{aligned} \quad (15)$$

Upon substituting (15) into (10)-(11) and passing to the limit $\varepsilon \rightarrow 0$, the limit two-scale equations of the weak formulation are obtained. Due to the linearity of these equations, we may introduce the following splits,

$$\begin{aligned} \mathbf{u}^1 &= \omega^{ij} \partial_j^x u_i^0 + \sum_{\alpha=1,2} \omega^\alpha p_\alpha^0 + \mathbf{u}^P \\ p_3 &= \pi^{ij} \partial_j^x u_i^0 + \sum_{\alpha=1,2} \pi^\alpha p_\alpha^0 + p_3^P , \\ p_\alpha^1 &= \eta_\alpha^k \partial_k^x p_\alpha^0 + p_\alpha^P , \end{aligned} \quad (16)$$

where ω , π and η are characteristic responses. Although these responses are governed by equations reflecting the local current configuration, so-called particular responses \mathbf{u}^P and p_k^P , $k = 1, 2, 3$ must be computed in addition, depending on the local actual stresses and pressures.

3.3 Microscopic local problems

These problems are established in terms of bilinear and linear forms (depending on a vector field parameter $\bar{\mathbf{u}}$) which involve the tangent elastic operator,

$$\mathbb{A} = \mathbb{D}^{\text{eff}} + \boldsymbol{\sigma}^{\text{eff}} \otimes \mathbf{I} - \hat{p}(\mathbf{I} \otimes \mathbf{I} - \mathbb{I}) , \quad A_{ijkl} = D_{ijkl}^{\text{eff}} + \sigma_{ik}^{\text{eff}} \delta_{jl} - \hat{p}(\delta_{ij} \delta_{kl} - \delta_{ik} \delta_{jl}) , \quad (17)$$

and further tensors depending on a two-scale vector fields $\bar{\mathbf{v}} = (\bar{\mathbf{v}}^0, \bar{\mathbf{v}}^1)$,

$$\begin{aligned} \tilde{\mathbf{B}}^T(\bar{\mathbf{v}}) &= (\mathbf{I} \otimes \mathbf{I} - \mathbb{I})(\nabla_x \bar{\mathbf{v}}^0 + \nabla_y \bar{\mathbf{v}}^1) , \\ \tilde{\mathbf{H}}^k(\bar{\mathbf{v}}) &= (\nabla_x \cdot \bar{\mathbf{v}}^0 + \nabla_y \cdot \bar{\mathbf{v}}^1) \tilde{\mathbf{K}}^k - \tilde{\mathbf{K}}^k (\nabla_x \bar{\mathbf{v}}^0 + \nabla_y \bar{\mathbf{v}}^1)^T - (\nabla_x \bar{\mathbf{v}}^0 + \nabla_y \bar{\mathbf{v}}^1) (\tilde{\mathbf{K}}^k)^T , \end{aligned} \quad (18)$$

defined for $k = 1, 2, 3$, the subdomain index.

The following bilinear and linear forms (depending on a vector field parameter $\bar{\mathbf{u}}$) will be employed:

$$\begin{aligned}
b_{Y_k}(\bar{\mathbf{u}}; q, \mathbf{u}) &= \int_{Y_k} q [\tilde{\mathbf{B}}(\bar{\mathbf{u}}) + \mathbf{I}] : \nabla_y \mathbf{u} , \quad k = 1, 2, 3 , \\
c_{Y_k}(\bar{\mathbf{u}}; p, q) &= \int_{Y_k} [\tilde{\mathbf{K}}^k + \tilde{\mathbf{H}}^k(\bar{\mathbf{u}})] : \nabla_y p \cdot \nabla_y q , \quad k = 1, 2, 3 , \\
a_Y(\mathbf{u}, \mathbf{v}) &= \int_Y \mathbb{A} \nabla_y \mathbf{u} : \nabla_y \mathbf{v} , \\
d_{Y_\beta}(p, q) &= \int_{Y_\beta} \delta \tilde{\mathbf{K}}^\beta \nabla_y p \cdot \nabla_y q , \quad \beta = 1, 2, 3 , \\
g_3^\alpha(\bar{\mathbf{u}}; p) &= \int_{\Gamma_\alpha} (\tilde{\mathbf{K}}^3 + \tilde{\mathbf{H}}(\bar{\mathbf{u}})) \nabla_y p \cdot \mathbf{n}^3 \, dS_y .
\end{aligned} \tag{19}$$

It should be noted, that all integrals over Y , or its sub-parts are defined in the reference deformed configuration $\varepsilon^{-1}Y^\varepsilon(\hat{x})$, see (12).

As announced above, the two-scale split (16) employed in the limit problem arising from (10)-(11) enables to extract autonomous local problems for the characteristic responses ω, π and η . The following problems associated with the poroelasticity in the whole cell Y and perfusion in the dual porosity Y_3 must be resolved for a given time step increment Δt .

1. Find $(\omega^{ij}, \pi^{ij}) \in \mathbf{H}_\#^1(Y) \times H_{\#0}^1(Y_3)$ such that

$$\begin{aligned}
a_Y(\omega^{ij} + \mathbf{\Pi}^{ij}, \mathbf{v}) - b_{Y_3}(\bar{\mathbf{u}}; \pi^{ij}, \mathbf{v}) &= 0 , \quad \forall \mathbf{v} \in \mathbf{H}_\#^1(Y) , \\
b_{Y_3}(\bar{\mathbf{u}}; q, \omega^{ij} + \mathbf{\Pi}^{ij}) + \Delta t c_{Y_3}(\bar{\mathbf{u}}; \pi^{ij}, q) &= 0 , \quad \forall q \in H_{\#0}^1(Y_3) .
\end{aligned} \tag{20}$$

2. Find $(\omega^\alpha, \pi^\alpha) \in \mathbf{H}_\#^1(Y) \times H_{\#0}^1(Y_3)$ such that

$$\begin{aligned}
a_Y(\omega^\alpha, \mathbf{v}) - b_{Y_3}(\bar{\mathbf{u}}; \pi^\alpha, \mathbf{v}) &= b_{Y_\alpha}(\bar{\mathbf{u}}; 1, \mathbf{v}) , \quad \forall \mathbf{v} \in \mathbf{H}_\#^1(Y) , \\
b_{Y_3}(\bar{\mathbf{u}}; q, \omega^\alpha) + \Delta t c_{Y_3}(\bar{\mathbf{u}}; \pi^\alpha, q) &= 0 , \quad \forall q \in H_{\#0}^1(Y_3) ,
\end{aligned} \tag{21}$$

where (in the sense of traces) $\pi^\alpha = \delta_{\alpha\beta}$ on $\partial_\beta Y_3 = \Gamma_\beta$.

3. Find $(\mathbf{u}^P, p_3^P) \in \mathbf{H}_\#^1(Y) \times H_{\#0}^1(Y_3)$, the particular response to the current reference state, such that

$$\begin{aligned}
a_Y(\mathbf{u}^P, \mathbf{v}) - b_{Y_3}(\bar{\mathbf{u}}; p_3^P, \mathbf{v}) &= -\langle \hat{\boldsymbol{\sigma}}^{\text{tot}}, \nabla_y \mathbf{v} \rangle_Y , \quad \forall \mathbf{v} \in \mathbf{H}_\#^1(Y) , \\
b_{Y_3}(\bar{\mathbf{u}}; q, \mathbf{u}^P) + \Delta t c_{Y_3}(\bar{\mathbf{u}}; p_3^P, q) &= -\Delta t (c_{Y_3}(\bar{\mathbf{u}}; \hat{p}_3, q) + d_{Y_3}(\hat{p}_3, q)) , \quad \forall q \in H_{\#0}^1(Y_3) ,
\end{aligned} \tag{22}$$

The two channels ($\alpha = 1, 2$) are related to the following microscopic problems:

1. The channel flow correctors: Find $\eta_\alpha^k \in H_\#^1(Y_\alpha)$ such that

$$c_{Y_\alpha}(\bar{\mathbf{u}}; \eta_\alpha^k + y_k, q) = 0, \quad \forall q \in H_\#^1(Y_\alpha). \quad (23)$$

2. The particular response for the current load response: Find $p_\alpha^P \in H_\#^1(Y_\alpha)$, $\alpha = 1, 2$, such that

$$c_{Y_\alpha}(\bar{\mathbf{u}}; p_\alpha^P, q) = d_{Y_\alpha}(\hat{P}_\alpha, q) - c_{Y_\alpha}(\bar{\mathbf{u}}; \hat{P}_\alpha, q), \quad \forall q \in H_\#^1(Y_\alpha), \quad (24)$$

where $\hat{P}_\alpha = \mathbf{y} \cdot \nabla_x \hat{p}_\alpha^0 + \hat{p}_\alpha^1$.

3.4 Homogenized coefficients and the macroscopic model

Let us consider the limit two-scale equations of the weak formulation tested by macroscopic fields, namely by the displacements \mathbf{v}^0 and the two pressures q_β^0 , $\beta = 1, 2$ associated with the channel pressure increments p_α^0 . In these equations involving the two-scale functions integrated over local reference cells $Y(x)$, due to the decomposed forms (16), we can identify the following homogenized coefficients.

- The viscoelastic incremental tensor, $\mathcal{D} = (\mathcal{D}_{ijkl})$,

$$\mathcal{D}_{ijkl} = |Y|^{-1} [a_Y(\boldsymbol{\omega}^{kl} + \boldsymbol{\Pi}^{kl}, \boldsymbol{\omega}^{ij} + \boldsymbol{\Pi}^{ij}) + \Delta t c_{Y_3}(\bar{\mathbf{u}}; \pi^{kl}, \pi^{ij})] . \quad (25)$$

- The Biot poroelasticity tensor, $\mathcal{B} = (\mathcal{B}_{ij})$,

$$\mathcal{B}_{ij}^\alpha = |Y|^{-1} [b_{Y_3}(\bar{\mathbf{u}}; \pi^\alpha, \boldsymbol{\Pi}^{ij}) + b_{Y_\alpha}(\bar{\mathbf{u}}; 1, \boldsymbol{\Pi}^{ij}) - a_Y(\boldsymbol{\omega}^\alpha, \boldsymbol{\Pi}^{ij})] . \quad (26)$$

- The averaged stress, $\mathcal{S}^{\text{tot}} = (S_{ij}^{\text{tot}})$,

$$S_{ij}^{\text{tot}} = |Y|^{-1} \int_Y \hat{\boldsymbol{\sigma}}^{\text{tot}} . \quad (27)$$

- The retardation stress, $\mathcal{Q} = (Q_{ij})$,

$$Q_{ij} = |Y|^{-1} [b_{Y_3}(\bar{\mathbf{u}}; p_3^P, \boldsymbol{\Pi}^{ij}) - a_Y(\mathbf{u}^P, \boldsymbol{\Pi}^{ij})] . \quad (28)$$

- The effective channel permeability, $\mathcal{C} = (\mathcal{C}_{ij})$,

$$\mathcal{C}_{ij}^\beta = |Y|^{-1} c_{Y_\beta}(\bar{\mathbf{u}}; \eta^i + y_i, \eta^j + y_j) . \quad (29)$$

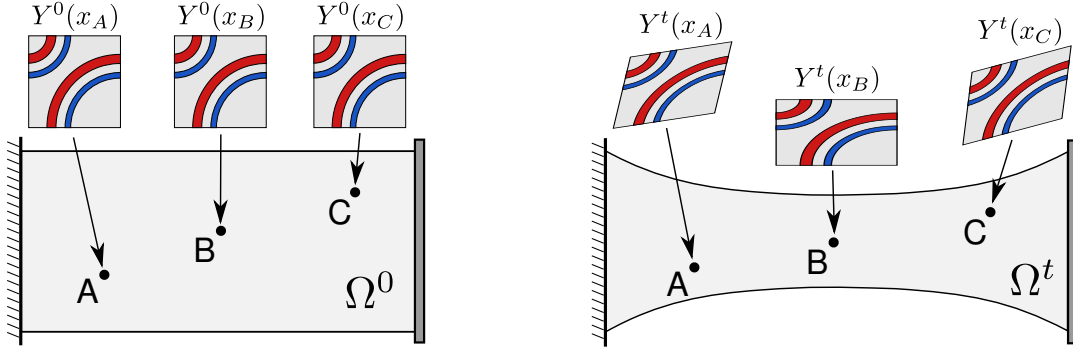


Figure 2: Schematic view of the deformed macroscopic specimen and of the local microstructures.

- The adjoint Biot poroelasticity tensor, $\mathcal{R} = (\mathcal{R}_{ij})$,

$$\mathcal{R}_{ij}^\alpha = |Y|^{-1} [b_{Y_\alpha}(\bar{\mathbf{u}}; 1, \boldsymbol{\omega}^{ij} + \boldsymbol{\Pi}^{ij}) + \Delta t g_3^\alpha(\bar{\mathbf{u}}, \pi^{ij})] . \quad (30)$$

- The perfusion coefficient,

$$\mathcal{G}_\beta^\alpha = |Y|^{-1} [g_3^\alpha(\bar{\mathbf{u}}, \pi^\beta) + (\Delta t)^{-1} b_{Y_\alpha}(\bar{\mathbf{u}}; 1, \boldsymbol{\omega}^\beta)] . \quad (31)$$

- The effective discharge due to deformation of the reference state; there are two coefficients:

$$\begin{aligned} \zeta_\alpha^{\text{eff}} &= (\Delta t |Y|)^{-1} b_{Y_\alpha}(\bar{\mathbf{u}}; 1, \mathbf{u}^P) + |Y|^{-1} g_3^\alpha(\bar{\mathbf{u}}, p_3^P + \hat{p}_3) + \oint_{Y_\alpha} \delta \tilde{\mathbf{K}}^3 \nabla_y \hat{p}_3 \cdot \mathbf{n}^3 \, dS_y , \\ \gamma_\alpha^{k, \text{eff}} &= |Y|^{-1} [c_{Y_\alpha}(\bar{\mathbf{u}}; \mathbf{y} \cdot \nabla_x \hat{p}_\alpha^0 + \hat{p}_\alpha^1, y_k) + d_{Y_\alpha}(\mathbf{y} \cdot \nabla_x \hat{p}_\alpha^0 + \hat{p}_\alpha^1, y_k) + c_{Y_\alpha}(\bar{\mathbf{u}}; p_\alpha^P, y_k)] . \end{aligned} \quad (32)$$

In the above expressions, the boundary integrals on the interface Γ_β^3 , $\beta = 1, 2$, can be computed using the residual form expression, which yields

$$\begin{aligned} g_3^\beta(\bar{\mathbf{u}}, \pi^\alpha) &= (\Delta t)^{-1} b_{Y_3}(\bar{\mathbf{u}}; \pi^\beta, \boldsymbol{\omega}^\alpha) + c_{Y_3}(\bar{\mathbf{u}}; \pi^\alpha, \pi^\beta) , \\ g_3^\beta(\bar{\mathbf{u}}, p_3^P + \hat{p}_3) &= (\Delta t)^{-1} b_{Y_3}(\bar{\mathbf{u}}; \pi^\beta, \mathbf{u}^P) + c_{Y_3}(\bar{\mathbf{u}}; p_3^P + \hat{p}_3, \pi^\beta) + d_{Y_3}(\hat{p}_3, \pi^\beta) . \end{aligned} \quad (33)$$

Moreover, the symmetry expression $\mathcal{B}^\alpha = \mathcal{R}^\alpha$ can be proved, $\alpha = 1, 2$.

Macroscopic equations On substituting the corresponding expressions of the homogenized coefficients in the limit problem arising from (10)-(11) by the homogenized coefficients, equations

of the macroscopic incremental problem are obtained which involve the increments \mathbf{u}, p_α ,

$$\begin{aligned} \int_{\Omega} \left(\mathcal{D} \nabla_x \mathbf{u} - \sum_{\alpha} p_{\alpha} \mathcal{B}^{\alpha} \right) : \nabla_x \mathbf{v} &= L^{\text{new}}(\mathbf{v}) + \int_{\Omega} (\mathcal{Q} - \mathbf{S}^{\text{tot}}) : \nabla_x \mathbf{v} , \\ \int_{\Omega} q_{\beta} \left(\mathcal{B}^{\beta} : \nabla_x \mathbf{u} + \Delta t \sum_{\alpha} \mathcal{G}_{\alpha}^{\beta} p_{\alpha} \right) &+ \Delta t \int_{\Omega} \mathcal{C}^{\beta} \nabla_x p_{\beta} \cdot \nabla_x q_{\beta} = -\Delta t \int_{\Omega} (\zeta_{\beta}^{\text{eff}} q_{\beta} + \gamma_{\beta}^{\text{eff}} \cdot \nabla_x q_{\beta}) . \end{aligned} \quad (34)$$

where $\beta = 1, 2$ and $L^{\text{new}}(\mathbf{v})$ is the functional defined by the volume and surface traction forces at time $t + \Delta t$. Boundary conditions for the two pressure increments can be introduced for a generalized decomposition of $\partial\Omega$. In particular, p_{α} can be prescribed on $\partial_{p,\alpha}\Omega \subset \partial\Omega$, whereas there is no relationship between $\partial_{p,1}\Omega$ and $\partial_{p,2}\Omega$; they can be disjoint or can overlap. This requires to establish two admissibility sets Q^{α} , $\alpha = 1, 2$ and, correspondingly, two spaces Q_0^{α} .

Incremental algorithm At each time level t , the reference two-scale configuration is established for a given FE discretization, so that at selected points $\hat{x}^k \in \Omega(t)$, $k = 1, 2, \dots$ (associated with the Gaussian quadrature points) the local problems (20)-(24) are solved. Consequently, the effective coefficients (25)-(32) are evaluated to constitute the macroscopic subproblem: Given the reference state, domain Ω and the microscopic configuration at time t , for the new load (associated with time $t + \Delta t$) find $(\mathbf{u}, p_1, p_2) \in V(\Omega) \times Q^1(\Omega) \times Q^2(\Omega)$ such that (34) holds for all test fields $(\mathbf{v}, q_1, q_2) \in V_0(\Omega) \times Q_0^1(\Omega) \times Q_0^2(\Omega)$. With the time increment computed from (34), the local configurations are updated in analogy with the procedure described in [8], cf. [7].

4 NUMERICAL ILLUSTRATION AND CONCLUSIONS

The two-scale model of the double porosity large deforming poroelastic medium has been implemented in the in-house developed SfePy code which is well suited for this kind of modelling. To illustrate capabilities of the homogenized model, we consider a 2D example with topology of the channels depicted in Fig. 1. It is not possible to provide periodic lattices with domains Ω_k^{ε} being simply connected for each $k = 1, 2, 3$. As the consequence, the homogenized permeabilities \mathcal{C}^{β} are rank-one, so that they must be regularized by adding a very small isotropic tensor. The macroscopic domain Ω is rectangular. On two opposite edges of $\partial\Omega$ the Dirichlet boundary conditions are prescribed which mimic that the structure is being stretched in the x_1 direction; the ramp-and-hold test is applied. The whole boundary $\partial\Omega$ is impermeable. Therefore, the fluid is being redistributed in the structure as the mere consequence of the deformation. The viscous effects captured by the retardation stress $\mathcal{Q}^{\varepsilon}$ are associated with the flow between the double porosity.

The proposed model describes behaviour of the Biot medium featured by the double porosity. The topology of the microstructure with two conductive channels leads to the two macroscopic pressure fields. For the linear case of small deformation, in [9], an analogous model of the periodic Biot medium with large contrast permeability was considered to describe tissue perfusion.

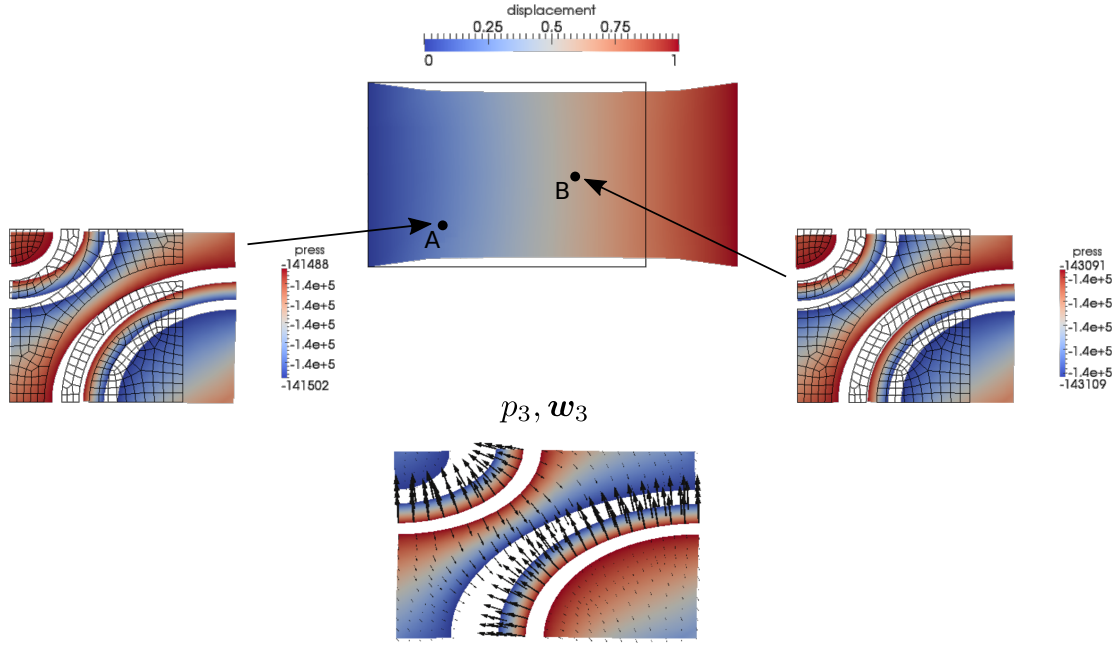


Figure 3: Macroscopic response of the deformation and displayed local reconstructions of the flow and pressure in the double porosity compartments Y_3 .

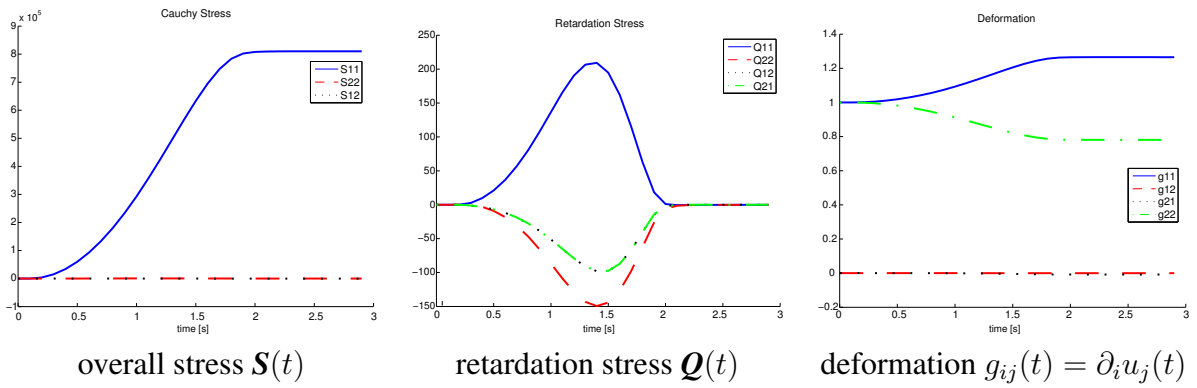


Figure 4: Macroscopic response computed at point B (see Fig. 3) in the time interval of the test

ACKNOWLEDGMENTS

The research and the participation in the conference was supported in part by the grant project GACR 16-03823S and by the the project LO 1506 of the Czech Ministry of Education, Youth and Sports.

REFERENCES

- [1] Biot, M. A. Variational Lagrangian-thermodynamics of non isothermal finite strain. mechanics of porous solid and thermomolecular diffusion. *Int J Solids Struct*, (1977) 13: 579–597.
- [2] Brown, D.L., Popov, P. and Efendiev, F. Effective equations for fluid-structure interaction with applications to poroelasticity. *Applicable Analysis*. (2014) 93: 771-790
- [3] Cioranescu, D., Damlamian, A., and Griso, G. The periodic unfolding method in homogenization, *SIAM Journal on Mathematical Analysis* (2008) 40: 1585–1620.
- [4] Coussy, O. *Poromechanics*. John Wiley & Sons, 2004.
- [5] Meroi, E. A. Schrefler, B. A. and Zienkiewicz, O. C. Large strain static and dynamic semisaturated soil behaviour. *Int J Numer Anal Met*, (1995) 19: 81–106.
- [6] Rohan, E. Sensitivity strategies in modelling heterogeneous media undergoing finite deformation. *Math Comput Simulat*, (2003)61): 261–270..
- [7] Rohan E. Modeling large-deformation-induced microflow in soft biological tissues. *Theoretical and Computational Fluid Dynamics* (2006) 20:251-276
- [8] Rohan, E., Cimirman, R., and Lukeš, V. Numerical modelling and homogenized constitutive law of large deforming fluid saturated heterogeneous solids *Computers and Structures* (2006)84:1095–1114
- [9] Rohan, E. and Cimirman, R. Two-scale modelling of tissue perfusion problem using homogenization of dual porous media. *Int. J. Multiscale Comput. Eng.*, (2010)8: 81–102.
- [10] Rohan, E., Naili, S., Cimirman, R. and Lemaire, T. Multiscale modeling of a fluid saturated medium with double porosity: Relevance to the compact bone. *J. Mech. Phys. Solids*, (2012) 60: 857–881.
- [11] Rohan, E. and Lukeš, V. On modelling nonlinear phenomena in deforming heterogeneous media using homogenization and sensitivity analysis concepts. *Appl Math Comput*, (2015)267:583–595.
- [12] Rohan, E., Naili, S., and Lemaire, T. Double porosity in fluid-saturated elastic media: deriving effective parameters by hierarchical homogenization of static problem. *Continuum Mech Thermodyn*, (2015)28: 1263–1293.
- [13] Rohan, E. and Lukeš, V. Modelling large-deforming fluid-saturated porous media using an Eulerian incremental formulation. *Advances in Engineering Software* (2017)113: 84–95.

On Size Effects Emerging in Pattern-Transforming Elastomeric Metamaterials

Ondrej Rokos*, Maqsood Ameen**, Ron H. J. Peerlings***, Marc G. D. Geers****

*Eindhoven University of Technology, **Eindhoven University of Technology, ***Eindhoven University of Technology, ****Eindhoven University of Technology

ABSTRACT

Cellular and foam-like materials have been successfully used in many engineering applications over decades due to their attractive overall properties such as light weight, high specific stiffness, or good ability to absorb impact. These properties result mainly from a particular arrangement of the base material in the underlying microstructural morphology, which nowadays can be controlled by means of additive manufacturing. Properties of such designed materials can range from a significant dependence of stiffness on overall deformation to more exotic ones, such as negative Poisson's ratio. In general, the entire class of materials with designed microstructures is usually referred to as mechanically tunable metamaterials, because their apparent properties cannot be observed in nature. It is of high engineering interest to design materials with specific effective properties, and to manufacture microstructures that are optimal with respect to their target application. To this end, an efficient homogenization procedure capable of accurate predictions of the mechanical response of mechanically tunable metamaterials needs to be provided. In the present study, we examine systematically and quantitatively size effects occurring in elastomeric voided metamaterial over a wide range of scale ratios, providing thus a solid basis for the development of advanced homogenization schemes. The elastomer under consideration follows the Mooney-Rivlin type of constitutive law, and its microstructural morphology consists of a periodic arrangement of circular holes. The resulting material exhibits an auxetic effect due to microstructural instabilities, followed by a rotational transformation of rigid islands positioned between individual holes. The effective behavior is obtained by considering an entire family of microstructures shifted randomly relative to specimen's geometry, making subsequently use of ensemble averaging. The ensemble averaged, homogenized response is shown to exhibit strong size effects, emerging either from boundary layers or steep strain gradients, which in certain parts of the specimen restrict the underlying kinematic microstructural mechanism that otherwise establishes long-range arrangements in the microstructure. Such long-range arrangements, and mainly their spatial variations, are one of the great challenges of homogenization theory. Based on the numerical solutions provided, first steps in enriching FE2 computational homogenization scheme capable of capturing these (size) effects will be discussed. Acknowledgement: The research leading to these results has received funding from the European Research Council under the European Union's Seventh Framework Programme (FP7/2007-2013) / ERC grant agreement no. [339392].

A New Workflow for an Experimental Testing and Simulation of Osteosynthesis Systems for Tibial Fractures

Michael Roland*, Thorsten Tjardes**, Bertil Bouillon***, Stefan Diebels****

*Saarland University, **Cologne Merheim Medical Center, ***Cologne Merheim Medical Center, ****Saarland University

ABSTRACT

A personalized approach to fracture therapy necessitates the integration of knowledge and techniques from mechanics, orthopedic trauma surgery and computer science. Merging the relevant knowledge of these disciplines can lead to the development of less invasive, individually tailored treatment approaches comprising the surgical technique and the implant used. Focusing on the case of distal tibia fractures, a new setup for a more realistic experimental testing of osteosynthesis systems is presented. Therefore, the experimental workflow is organized as follows: (1) starting point is a testing device to produce predefined tibia fractures, (2) the fractured lower extremities will be treated by an orthopedic trauma surgeon and (3) tested in a second testing device simulating the forces acting during a normal step forward. The experiments are realized with artificial bones from Sawbone as well as with fresh frozen human cadaveric specimen. During the first step of the workflow, the main goal is the repeatability of the fractures with respect to the applied forces and moments. Before the procedure starts, computed tomography scans of the bones are performed and are used as basis for the simulations. After the fracture is produced, an orthopedic trauma surgeon treats the lower extremity with an osteosynthesis locking plate and a second computed tomography scan is executed to enhance the computational model. Thereafter, in the last step of the testing workflow, the treated tibia is clamped in the second testing device and a mechanical loading scenario is applied on the bone-implant-system. The loading scenario is based on the OrthoLoad database and is calibrated by the subject-specific data of the human cadaveric specimen. During the test, stresses and strains are gained via a high-speed camera system combined with digital image correlation and several pressure and force measurements. This workflow allows a more realistic testing of tibia implants and gives information about the mechanical behavior of the fracture gap, like the interfragmentary move. The whole procedure is also simulated based on the performed tomograms. Therefore, the image stacks are segmented, the material parameters are assigned and passed to a meshing procedure. After that, finite element simulations are executed with respect to the testing parameters and protocols in order to validate and to verify the simulation process. Here, the investigation of the simulations is focused on the best possible match of the experiments and the achieved results.

Highly Scalable End-to-end Parallel Framework for Coupled Multi-scale and Multi-physics Fluid Dynamics

Sabine Roller^{*}, Harald Klimach^{**}, Daniel F. Harlacher^{***}

^{*}University of Siegen, Simulation Techniques and Scientific Computing, ^{**}University of Siegen, Simulation Techniques and Scientific Computing, ^{***}University of Siegen, Center for Information and Media Technology

ABSTRACT

This contribution is concerned with software engineering for HPC applications in engineering with a focus on multi-physics simulations such as fluid-acoustics, fluid-structure or fluid-electromagnetics applications. Our goals are easy usability, high maintainability, easy portability and of course high performance with high scalability, even when changing the characteristics of the application and/or the system. Usability is a key property to any application as it sets the bounds on the efficiency the user can work with it. But for developing new applications, also code maintainability is an important issue. In the context of multi-physics simulations, this introduces a conflict of objectives, considering modularity and encapsulation on the one hand, and integration and interaction on the other. With the focus on these objectives, we develop the APES simulation framework, consisting of a common core to handle meshes, modularized solvers, and additional helper tools for preprocessing, post-processing, steering and evaluation. The implementation of all parts ensures high scalability and good load balancing, allowing for workflows that are parallel from the very beginning to the final step. We call this the end-to-end-parallelization. Software engineering for the entire framework development guarantees for maintainability as well as feature development with the focus on efficiency, as any chain is only as strong as its weakest element. In this contribution, we will present an overview of the APES framework, show some software engineering principles like regular regression checks, and automatic code documentation, but also applications of different complexity together with the impacts on performance and load balancing. References: Roller S. et al. (2011): An Adaptable Simulation Framework Based on a Linearized Octree. In: Resch M., Wang X., Bez W., Focht E., Kobayashi H., Roller S. (eds) High Performance Computing on Vector Systems 2011. Springer, Berlin, Heidelberg Harlacher D.F., Klimach H., Roller S. (2015): Experiences in Developing HPC Software with Portable Efficiency. In: Resch M., Bez W., Focht E., Kobayashi H., Patel N. (eds) Sustained Simulation Performance 2014. Springer, Cham

Additive Manufacturing Inspired Computation

Anthony Rollett^{*}, Christopher Kantzos^{**}, Joseph Pauza^{***}, Tugce Ozturk^{****}, Ross
Cunningham^{*****}

^{*}Carnegie Mellon Univ., ^{**}Carnegie Mellon Univ., ^{***}Carnegie Mellon Univ., ^{****}Carnegie Mellon Univ.,
^{*****}Carnegie Mellon Univ.

ABSTRACT

Representative 3D synthetic microstructures were generated in Dream.3D, based on the characteristics of additively manufactured (AM) Ti-6Al-4V, and the input structures were modified for features of interest. The sensitivity to microstructure was quantified by performing full field simulations using a spectral elasto-viscoplastic code that uses parallelized fast Fourier Transforms (FFTs) and Hierarchical Data Format (HDF) for input/output. The strongest effect was related to volume fraction of the alpha phase. Texture in the original deposit produced anisotropy although this is mitigated by the multiplicity of variants that occurs in the beta to alpha transformation. To investigate the effect of surface roughness, computed tomography scans from AM samples made from two different size powders were used in the same elasto-plastic FFT code with isotropic properties. Near-surface voids and low points in the surface dominated the hot spots in stress. Subtle differences in hot spot character between von Mises stress and triaxiality were noted. These results were consistent with experimentally determined variations in fatigue life as a function of near-surface porosity in AM parts. The grain-scale microstructure of AM parts is well known to be sensitive to variations in processing conditions such as power, scan speed and hatch spacing. These variations are explored with the Monte Carlo ssparks code. Preliminary efforts are described to add the capability to simulate the preferred <100> growth direction in solidification of cubic materials.

Simulation of Dilute and Dense Non-Spherical Particle Laden Flows: Movement and Orientation Behaviour

Miguel A. Romero-Valle*, Hermann Nirschl**, Christoph Goniva***

*BASF SE, **Karlsruhe Institute of Technology, ***DCS Computing GmbH

ABSTRACT

The fast advancement of existing and new functional material systems, where particulate morphology differs from traditional systems (e.g. fibres, flakes, ...), demands technical know-how on the processing of non-spherical particles in liquid media. There are few to no technical relevant tools available for the prediction of such particulate systems, specifically when particle-particle interactions and particle orientation are relevant, making development of such processes time consuming and expensive. Therefore, a tool is needed to support process design and further understand non-spherical systems. On this work, a novel approach for the calculation of drag forces and drag induced torques for non-spherical particles in the context of CFD-DEM coupling (Kloss, Goniva, Hager, Amberger, & Pirker, 2012) is presented. The approach is inspired by Stokesian Dynamics for the computation of drag forces and torques (Joung, 2006) when using the multi-sphere method for the representation of non-spherical particles (Kruggel-Emden, Rickelt, Wirtz, & Scherer, 2008). In each multi-sphere particle, individual spheres of the multi-sphere clump have a hydrodynamic contribution to the multi-sphere drag force depending on the flow conditions that the sphere experiences, which in turn induces a torque on the multi-sphere representation. To consider the hydrodynamic proximity of the spheres within the multi-sphere clump, one computes the individual sphere contributions using Stokes's drag law and an Oseen type tensor, both which in a Stokesian Dynamics context are used to compute the mobility matrix of a particle suspension system. The method is validated for single rigid fibre particles in shear flow using an analytical solution given by an adaptation of Jeffery's orbits. Preliminary results show promise for dilute and semi-dilute rigid fibre suspensions, where a tapered channel is simulated and compared to experimental data. Potential relevant applications are discussed and evaluated. Joung, C. G. (2006). Dynamic simulation of arbitrarily shaped particles in shear flow. *Rheologica Acta*, 46(1), 143–152. <https://doi.org/10.1007/s00397-006-0110-6> Kloss, C., Goniva, C., Hager, A., Amberger, S., & Pirker, S. (2012). Models , algorithms and validation for opensource DEM and CFD-DEM. *Pcfd*, 12, 140–152. <https://doi.org/10.1504/PCFD.2012.047457> Kruggel-Emden, H., Rickelt, S., Wirtz, S., & Scherer, V. (2008). A study on the validity of the multi-sphere Discrete Element Method. *Powder Technology*, 188(2), 153–165. <https://doi.org/10.1016/j.powtec.2008.04.037>

Estimation of Modeling Errors in Local Quantities of Interest in the Elastostatic Analysis of Heterogeneous Solids

Albert Romkes*, Justin King**

*South Dakota School of Mines & Technology, **South Dakota School of Mines & Technology

ABSTRACT

We consider the analysis of the mechanics of multiphase composite materials, exhibiting complex microstructure with highly oscillatory material properties. It is generally prohibitive to numerically resolve all the features in the microstructure. Classical approaches have therefore focused on methods of homogenization, generally based on the assumption that the microstructure of the media is periodic, or on techniques for determining effective properties of representative volume elements. These averaged material models cannot account for local micromechanical effects that are critical factors in the initiation and evolution of failure mechanisms. To resolve this issue, Oden et al. [1] developed the Goal-Oriented Adaptive Modeling (GOAM) method. It represents an adaptive multi-scale modeling method based on control of modeling errors in a local quantity of interest of the material response, specified by the analyst. The GOAM method starts the analysis with an initial model of homogenized properties that are obtained via the classical averaging techniques. The homogeneous surrogate model is then enhanced in an iterative process of including the material microstructure in a local area surrounding the quantity of interest that increases in size with every iteration step. A critical element in the GOAM method is the ability to accurately estimate the modeling error. Currently, this is established by providing a residual-based a posteriori error estimator. It involves solving for a global influence function, related to the quantity of interest, and subsequently computing global integrals of governing residual functionals. Unfortunately, in the case of multiphase composite materials, this estimation process can be computationally prohibitive, again due to the complexity of the microstructure. We therefore propose a technique for local, goal-oriented estimation of the modeling error that resolves this computational issue. It is a continued effort by the authors in recent years and based on a local variational approach. It requires computing influence functions and residual integrals which are strictly local and can be computed at low computational cost and at high numerical accuracy. We introduce this approach for the linear elastostatic analysis of multiphase composites and the investigation of linear local quantities of interest. References: [1] J. T. Oden, S. Prudhomme, A. Romkes, P. Bauman. Multi-scale modeling of physical phenomena: Adaptive control of models. SIAM J. Sc. Comp., Vol. 28 (6), 2359-2389, 2006. [2] A. Romkes, T. C. Moody. Local Goal-Oriented Estimation of Modeling Error for Multi-Scale Modeling of Heterogeneous Elastic Materials. Int. J. Comp. Meth. Eng. Sc. Mech., Vol. 8 (4), 201--209, 2007.

Hamiltonian-based Buckling Analysis of Double-layered Orthotropic Nanoplate Systems Subjected to In-plane Magnetic Field

Dalun Rong^{*}, Zengbo Lian^{**}, Junhai Fan^{***}, Xinsheng Xu^{****}

^{*}State Key Laboratory of Structure Analysis of Industrial Equipment, International Research Center for Computational Mechanics, Dalian University of Technology, ^{**}State Key Laboratory of Structure Analysis of Industrial Equipment, International Research Center for Computational Mechanics, Dalian University of Technology, ^{***}State Key Laboratory of Structure Analysis of Industrial Equipment, International Research Center for Computational Mechanics, Dalian University of Technology, ^{****}State Key Laboratory of Structure Analysis of Industrial Equipment, International Research Center for Computational Mechanics, Dalian University of Technology

ABSTRACT

Due to the exceptional thermal, electrical, mechanical and magnetic properties, nanoscale structures have wide applications in nanoelectro-mechanical systems (NEMS). The double-layered orthotropic nanoplate system (DLNS) with magnetic effects is one of the fundamental components in the manufacture of high frequency and high sensitivity NEMS resonant magnetic field sensors. Therefore, a thorough understanding of the DLNS is of considerable importance for the design and fabrication of such sensors. However, the existing theoretical studies were concentrated on the DLNS with Levy-type boundaries. Exact solutions for dynamic behaviors of the DLNS with non Levy-type boundaries were rarely mentioned. Therefore, this paper aims to present an analytical symplectic method to find the exact solutions of buckling of the DLNS with two opposite edges clamped subjected to in-plane magnetic field based on Eringen's nonlocal theory. In the symplectic space, a new total unknown vector is introduced to establish the Hamiltonian system, so that the governing equations of biaxial buckling in the Lagrangian system are converted into its Hamiltonian dual form by a rigorous way. The governing equation of Hamiltonian system is reduced to a set of one-order ordinary differential equations instead of a high-order differential governing equation. Therefore, the method of separation of variables and the expansion of eigenfunctions are available to solve the governing equation and to derive the exact solution. For the Levy-type edges, the analytical critical buckling load equations are derived, and buckling mode shapes are expressed in terms of the total unknown vectors. Based on the obtained exact solution, DLNS with two opposite edges clamped are investigated by symplectic superposition technique. Closed-form solutions of the original problems are achieved by superposition of the exact solution from the fundamental subproblems. Comparisons validate the efficiency and accuracy of the proposed method. The comprehensive numerical examples demonstrate the effects of nonlocal parameters, boundary conditions, stiffness parameters, and magnetic field on the buckling behaviors of the nanoplate systems. This paper presents an analytical solution to nanoplate systems with two opposite edges clamped which can serve the design and fabrication of NEMS.

Topology Optimization Design of Broadband Elastic Hyperbolic Metamaterial

Junjie Rong^{*}, Wenjing Ye^{**}

^{*}The Hong Kong University of Science and Technology, ^{**}The Hong Kong University of Science and Technology

ABSTRACT

Metamaterials with delicately engineered architectures have been attracting considerable attention because of their unique properties and/or capabilities for wave manipulation. One such an example is metamaterials with hyperbolic dispersion, which have many promising applications such as negative refraction, partial focusing and super-resolution imaging [1]. However, compared with their acoustic and electromagnetic counterparts, the design of elastic hyperbolic metamaterials is more challenging due to the presence of both longitudinal and transverse waves [2]. In this talk, we present a computational approach for designing elastic hyperbolic metamaterial with a broad operation frequency band. A design formulation based on topology optimization is constructed and solved by a gradient-based optimizer. The material is designed to achieve the desired dispersion with a complete band gap in one direction and a single propagating state in the other direction. Proper constraints are imposed to avoid multiple mode interactions in the designed frequency band. Because the structural worthiness could be hampered by the perforation introduced in the design, the static effective modulus is incorporated into the optimization algorithm as a constraint in order to maintain a certain level of stiffness. Using the proposed optimization formulation, our designed metamaterial exhibits hyperbolic dispersion over a broad relative frequency range of 77%. Partial focusing and imaging with a super-resolution up to 0.25 times wavelength are also demonstrated. The developed approach could be extended to the design of other metamaterials with any desired dispersion. References: [1] Alexander Poddubny, Ivan Iorsh, Pavel Belov, Yuri Kivshar. Hyperbolic metamaterials. *Nature Photonics*, 7: 948-957, 2013. [2] Joo Hwan Oh, Hong Min Seung, Yoon Young Kim. A truly hyperbolic elastic metamaterial lens. *Applied Physics Letters*, 104: 073503, 2014.

The Effect of Shear Properties of Anterior Cruciate Ligament and of Patellar Tendon Grafts on Whole-Knee Biomechanics

Ryan Rosario*, Ellen Arruda**, Rhima Coleman***

*University of Michigan, **University of Michigan, ***University of Michigan

ABSTRACT

Finite element (FE) models of the knee are used to study how joint injury and repair affect joint kinematics and tissue mechanics. Ligaments are transversely isotropic, non-linear poro-viscoelastic materials. Typically, ligament material models are fit to uniaxial tension data along the predominant fiber direction (axial) and, less commonly, uniaxial tension data orthogonal to the fiber direction (transverse). Transversely isotropic material models can have excellent fit to axial and transverse data yet predict very different shear responses. These differences in shear behavior result in differences in tissue deformation and joint kinematics in whole joint models. In this study, the transversely isotropic freely-jointed eight-chain and the Holzapfel-Gasser-Ogden models were used to describe ACL behavior in a previously validated whole-knee FE model [1]. Material properties of the ACL were fitted to axial and transverse data with applied constraints to result in 3 shear response levels. Axial compression of the joint and anterior tibial shear were simulated. The same procedure was repeated for the patellar tendon. Under 800 N of axial compression, simulations showed that low shear stiffness resulted in the least overall joint motion in terms of knee flexion, external tibial rotation, and anterior tibial displacement, and mid shear stiffness resulted in the most. The high shear stiffness ACL model resulted in lowest maximum compression in the femoral articular cartilage. The mid shear stiffness model resulted in the highest maximum compression (12.1%). Differing shear properties can cause a 3.0° difference in external tibial rotation and a 1.0 mm difference in anterior tibial displacement under 800 N of axial compression. Small differences in joint kinematics can shift the location of maximum deformation in cartilage, potentially leading to the initiation and progression of osteoarthritis in cartilage [2]. Thus, to most accurately model the behavior of the knee in response to physical loads, material models of ligaments should also be well-fit to shear behavior. References: [1] Marchi B.C., et al., (2016). Biomech Model Mechanobiol. [2] Andriacchi T.P., et al., (2009). J Bone Joint Surg.

On the Application of Embedded Solution Techniques for the Solution of Computational Wind Engineering Problems

Riccardo Rossi^{*}, Ruben Zorrilla^{**}, Pooyan Dadvand^{***}, Roland Wuechner^{****}, Antonia Larese^{*****}, Jordi Cotela^{*****}

^{*}UPC, CIMNE, ^{**}UPC, CIMNE, ^{***}CIMNE, ^{****}TUM, ^{*****}CIMNE, ^{*****}TUM

ABSTRACT

Computational Wind Engineering (CWE) focuses on the assessment of the wind flow around structures. The simulation of city-scale problems is challenging due to the sheer size of the problem as well as due to the geometrical complexity of the problem. Current work combines a body fitted discretization of the surface with an embedded approach, employed in the simulation of the city buildings.

Locally-Implicit DG-FEM for Moment-Closure Approximations of Plasma

James Rossmanith*

*Iowa State University

ABSTRACT

In many applications broadly of interest to modern science, the dynamics of gas and plasma can be simulated using either kinetic or fluid models. Kinetic models are valid over most of the spatial and temporal scales that are of physical relevance in many application problems; however, they are computationally expensive due to the high-dimensionality of phase space. Fluid models typically have a more limited range of validity, but are generally computationally more tractable than kinetic models. One critical aspect of fluid models is the question of what assumptions to make in order to close the fluid model (i.e., what assumptions can we make about the microscale physics that will allow us to not explicitly resolve these scales). In principle, if the moment-closures are sufficiently information-dense, they allow fluid models to accurately capture important non-equilibrium dynamics. Determining such closures that also produce systems of well-posed partial differential equations is an ongoing area of research. In this work, we develop a class of high-order discontinuous Galerkin finite element methods (DG-FEM) for solving fluid models with various moment-closure approximations. The proposed methods are in the class of locally-implicit DG-FEM, which are built using a predictor-corrector approach. In particular, the predictor is a locally implicit spacetime method (i.e., the predictor is something like a block-Jacobi update for a fully implicit spacetime DG method). The corrector is an explicit method that uses the spacetime reconstructed solution from the predictor step. We develop limiters that guarantee that at each quadrature point the solution remains realizable. The schemes developed in this work are applied to a variety of moment-closures, including quadrature-based moment closures (QMOM) and ϕ -divergence moment closures. The resulting numerical methods are applied to several standard numerical tests in one dimension for both gas and plasma dynamics problems. These tests are used as benchmarks to verify and assess the accuracy and robustness of the method.

Application of Residual Strength Study to Improve Concrete Constitutive Models

Michael Roth^{*}, George Vankirk^{**}, Andreas Frank^{***}

^{*}US Army Engineer Research and Development Center, ^{**}US Army Engineer Research and Development Center,
^{***}US Army Engineer Research and Development Center

ABSTRACT

Impact and blast effects in geomaterials like concrete and soil is an area of important research interest for the U.S. Department of Defense. Events of specific interest include projectile penetration, shaped-charge penetration, and close-in explosive detonation, which involve a spectrum of challenging material behaviors and failure modes. Due to the events' high-rate impulsive nature, large deformations and material failure must be accurately represented; accurate representation of material behavior in the near and far-field regions from the event is especially critical to achieve reliable modeling results. The constitutive model must capture the high-rate, high-pressure mechanics occurring near a penetrator nose or explosive detonation that dominate the initial penetration and cavity formation. The model must also accurately represent shock-induced far-field effects such as brittle tensile failure and material heave, which dominate overall failure at the structural scale. Over the past decade technologies have evolved for this class of problems, with emphasis in areas like phenomenologically advanced material models to accurately predict material damage, failure, and residual strength. The proposed presentation will detail the results of a study on residual strength of a high-performance concrete. In this study, the residual unconfined compressive strength of a high-performance concrete ($f'_c \sim 130$ MPa) was investigated by using samples that were pre-loaded to specific states of triaxial confinement. The samples were first subjected to specified stress-strain paths corresponding to pure hydrostatic compression and uniaxial strain in compression. Both the hydrostatic compression and uniaxial strain tests were performed at low- and high-pressure levels under controlled conditions to prevent reaching the material failure limit. Once the samples were tested through either hydrostatic compression or uniaxial strain, they were recovered and subjected to unconfined compression until failure. Data from these samples were compared to the unconfined compressive strength of pristine samples from the same concrete batch. Residual strength was determined through a comparison of these values and as a means to quantify damage induced (both with and without shear) by the specified stress-strain paths. Applications of these data are discussed for future improvements to concrete constitutive models commonly used at the U.S. Army Engineer Research and Development Center to simulate dynamic events. Permission to publish was granted by Director, Geotechnical and Structures Laboratory.

Molecular Mobility in Driven Monomeric and Polymeric Glasses

Joerg Rottler*

*University of British Columbia

ABSTRACT

Glasses form when their structural relaxation time exceeds the experimentally accessible observation timescales, and the material falls out of equilibrium. However, relaxation speeds up greatly as soon as the glass is being deformed. The relaxation time is an important internal state variable in many theories of amorphous plastic flow, and can be measured with dynamic light scattering or fluorescence spectroscopy techniques. In this talk, we show with molecular simulations that in monomeric supercooled liquids and glasses that are plastically flowing at a constant shear stress while being deformed with fixed strain rate, the microscopic structural relaxation time equals a macroscopic "Maxwell time" that is proportional to the ratio of shear stress and strain rate. The equality holds for all rheological regimes from temperatures above the glass transition all the way to the athermal limit, and arises from the competing effects of elastic loading and viscous dissipation. In macromolecular (polymeric) glasses, however, the stress decouples from the Maxwell time and the relaxation time is in fact further reduced even through the stress rises during glassy strain hardening. Comprehensive expressions are developed that predict the accelerated dynamics during active deformation in terms of all relevant deformation variables.

Nanoindentation in Studying Mechanical Properties of Organic-rich Shale

Mo Rouainia^{*}, Majid Goodarzi^{**}, Andy Aplin^{***}

^{*}Newcastle University, ^{**}Newcastle University, ^{***}Durham University

ABSTRACT

Shale, or mudstone, is the most common sedimentary rock. It is a heterogeneous, multi-mineralic natural composite consisting of clay mineral aggregates, organic matter, and variable quantities of minerals such as quartz, calcite, and feldspar. Determination of the mechanical response of shales through experimental procedures is a challenge due to their heterogeneity and the practical difficulties of retrieving good-quality core samples. Therefore, in recent years extensive research has been directed at developing alternative approaches for the mechanical characterisation of shale rocks [1,2,3,4,5]. In this paper, several well-characterised shale samples have been subjected to indentation tests using different indenters in order to generate various stress-strain paths under controlled load conditions set at 500mN. Numerical modelling has been undertaken to back-calculate the plastic response of the shale samples using load-displacement curves obtained from indentation tests. Inverse analysis of the indentation tests was conducted by assuming only two material parameters, angle of friction and cohesion. The reduced modulus was derived from unloading curves and the value of Poisson's ratio dilation and contact friction were assumed. Issues related to indentation testing such as loading and unloading rate, tip shape and creep behaviour were studied. The capabilities and limitations of this test applied to shale rock were further clarified. References [1] Bennett K.C., Berla L.A., Nix W.D., Borja R.I. 2015. Instrumented nanoindentation and 3D mechanistic modeling of a shale at multiple scales. *Acta Geotechnica*, 10, 1-14. [2] Bobko C., Ulm F.J. 2008. The nano-mechanical morphology of shale. *Mechanics of Material*, 40, 318-337. [3] Goodarzi M., Rouainia M., Aplin A.C. 2016. Numerical evaluation of mean-field homogenisation methods for predicting shale elastic response. *Computational Geosciences*, Volume 20(5), 1109–1122 [4] Goodarzi M., Rouainia M., Aplin A.C. Cubillas P., de Block M. 2017. Predicting the elastic response of organic-rich shale using nanoscale measurements and homogenisation methods. *Geophysical Prospecting*, 65, 1597–1614. [5] Ortega J.A., Ulm F.J., Abousleiman Y. 2010. The effect of particle shape and grain-scale properties of shale: A micromechanics approach. *International Journal of Numerical and Analytical Method in Geomechanics* 34, 1124-1156.

Multi-scale Simulation of Seismic Wave Propagation

Varvara Roubtsova*, Mohamed Chekired**

*Hydro-Quebec (IREQ), **Hydro-Quebec (IREQ)

ABSTRACT

A numerical simulation of seismic wave propagation through the soils is an important part for the prediction of earthquake damage. The soils are a complex granular media with pore channels filled with water. The parameters of soils such as granulometry, density, shape of particles, etc. determine a capability to transmit and dissipate the seismic waves. On the other hand, the reflected wave at boundaries conditions between two soils must take into account. Furthermore, the soils characteristics vary under periodic loads up to critical state namely liquefaction. Liquefaction is a phenomenon whereby saturated soils lose strength. Finally a complex state is takes place in the soils because of interaction of p-waves (pressure primary waves) and s-waves (shear secondary waves) during earthquake. Simulations of the seismic wave propagation were carried out with Virtual Laboratory SiGran developed in Research Institute of Hydro-Quebec (IREQ). These codes are a bulk-parallel and can be run on GPU-devices. Smoothed Particle Hydrodynamics (SPH) method was used to model seismic waves at a macro level. At this level, the problem is described by the multiphysics continuum mechanics equations with the special rheological soil laws. The particles movement and their interactions with an increasing pore pressure and a water motion into pore channels under seismic loads determine a soil behavior during earthquake. The soils micro characteristics were modeled by coupling Discrete Element Method (DEM) with Marker And Cell (MAC) method. This coupling simulates the wet granular media as a matrix of particles with a free space (pore channels) filled with water. The information will be transferred from the micro level to a macro level by establishing of the rheological law. These codes were tested for many theoretical and physical problems. The possibilities of Virtual Laboratory will be presented.

Fluid Driven Discrete Cracks via 2D FDEM

Esteban Rougier*, Zhou Lei**, Antonio Munjiza***, Earl Knight****

*Los Alamos National Laboratory, **Los Alamos National Laboratory, ***University of Split, ****Los Alamos National Laboratory

ABSTRACT

In recent years the coupling of rock mechanics to fluid flow has become a critical topic for understanding the performance of energy systems including the production of unconventional oil and gas (e.g. hydraulic fracturing) where fluids are used to create fractures to increase the permeability of formations. On the rock mechanics modelling side the combined finite-discrete element method (FDEM) has become a tool of choice for simulations of complex fracture problems. In this work we combine our FDEM implementation with a novel fluid solver using an Integrated Solid Fluid (ISF) solver approach in order to simulate the key mechanisms that control fluid driven cracks. The main innovative aspects of the ISF solver are: the use of the same spatial discretization to describe the behavior of the solid (i.e., rock medium) and the fluid, the use of the same time step for both phases (solid and fluid); and the independence of the size of the critical time step with the fracture opening. This last point is extremely important because it means that the ISF simulations can use very fine meshes around areas of interest, such as a borehole, without penalizing the computational cost as fractures propagate (i.e., open) and the fluid flows through them. This paper presents a series of benchmark cases. The results shown in this work clearly demonstrate that the ISF approach is able to reproduce analytical results for fluid flow through a single crack. In addition, this approach is also able to reproduce analytical results for the problem of a fluid flow driven single crack propagation. The results shown also demonstrate that the same approach is robust enough to deal with complex fracture patterns and complex geometries; the obtained fluid driven fracture patterns in the vicinity of a borehole presented in this paper certainly stands to the scrutiny of human visual perception.

Size Dependent Crystal Plasticity Model Incorporating Strain-rate Effect and Temperature Dependence

Anish Roy^{*}, Qiang Liu^{**}, Vadim Silberschmidt^{***}, Ka Ho Pang^{****}

^{*}Loughborough University, ^{**}Loughborough University, ^{***}Loughborough University, ^{****}Loughborough University

ABSTRACT

Size-dependent crystal plasticity of metal single crystals is investigated using the finite-element method based on a phenomenological crystal-plasticity model, incorporating both first-order and second-order effects. The first-order effect is independent of the nature of the loading state and described by three phenomenological relationships based on experimental results. The second-order effect is considered in terms of storage of geometrically necessary dislocations, affected significantly by the loading state. The modelling approach is shown to capture the influence of loading conditions on the sample size effect observed in compression and bending experiments. The model accounts dislocation slip and twinning on different crystallographic systems. Special attention is paid to a strain-rate effect and temperature dependence in the constitutive description employed in the model. The model is extended for use in polycrystalline materials. Several case studies are performed to demonstrate the effect of strain-rates – as an example – micro scratching experiments are performed which are then used to first calibrate and then predict the effect of machining speeds on the structural integrity of the component.

Optimized Schwarz Methods for Time-Harmonic Elastodynamic Problems

Anthony Royer^{*}, Christophe Geuzaine^{**}, Vanessa Mattesi^{***}, Steven Roman^{****}

^{*}Université de Liège, ^{**}Université de Liège, ^{***}Université de Liège, ^{****}Université de Liège

ABSTRACT

Solving wave propagation problems in heterogeneous media is computationally challenging, especially in the high-frequency regime where discretizing the domain at the scale of the (small) wavelength leads to the solution of very large systems of equations. In the time-harmonic case (i.e. in Fourier space), recent progress has been made for acoustic and electro-magnetic wave problems, where quasi-optimal Schwarz domain decomposition methods have been proposed [1, 2, 3]. In this contribution we extend these results to the case of elastic waves, where we compare transmission conditions based either on Padé-localized approximations of the exact freespace Dirichlet-to-Neumann map, or on the use of perfectly matched layers. References [1] Y. Boubendir, X. Antoine, and C. Geuzaine. A quasi-optimal non-overlapping domain decomposition algorithm for the helmholtz equation. *Journal of Computational Physics*, 231(2):262–280, 2012. [2] M. El Bouajaji, B. Thierry, X. Antoine, and C. Geuzaine. A quasi-optimal domain decomposition algorithm for the time-harmonic maxwell's equations. *Journal of Computational Physics*, 294:38–57, 2015. [3] B. Thierry, A. Vion, S. Tournier, M. El Bouajaji, D. Colignon, N. Marsic, X. Antoine, and C. Geuzaine. Getddm: an open framework for testing optimized schwarz methods for time-harmonic wave problems. *Computer Physics Communications*, 203:309–330, June 2016.

Galerkin-RB-POD Reduced Order Methods: State of the Art and Perspectives with Focus on Parametric Computational Fluid Dynamics

Gianluigi Rozza*

*SISSA, International School for Advanced Studies, Trieste, Italy, Mathematics Area, mathLab

ABSTRACT

We provide the state of the art of Reduced Order Methods (ROM) for parametric Partial Differential Equations (PDEs), and we focus on some perspectives in their current trends and developments, with a special interest in parametric problems arising in Computational Fluid Dynamics (CFD). Systems modelled by PDEs are depending by several complex parameters in need of being reduced, even before the computational phase in a pre-processing step, in order to reduce parameter space. Efficient parametrizations (random inputs, geometry, physics) are very important to be able to properly address an offline-online decoupling of the computational procedures and to allow competitive computational performances. Current ROM developments in CFD include: a better use of stable high fidelity methods, considering also spectral element method, to enhance the quality of the reduced model too; more efficient sampling techniques to reduce the number of the basis functions, retained as snapshots, as well as the dimension of online systems; the improvements of the certification of accuracy based on residual based error bounds and of the stability factors, as well as the the guarantee of the stability of the approximation with proper space enrichments. For nonlinear systems, also the investigation on bifurcations of parametric solutions are crucial and they may be obtained thanks to a reduced eigenvalue analysis of the linearised operator. All the previous aspects are very important in CFD problems to be able to focus in real time on complex parametric industrial and biomedical flow problems, or even in a control flow setting, and to couple viscous flows -velocity, pressure, as well as thermal field - with a structural field or a porous medium, thus requiring also an efficient reduced parametric treatment of interfaces between different physics. Model flow problems will focus on few benchmark cases in a time-dependent framework, as well as on simple fluid-structure interaction problems. Further examples of applications will be delivered concerning shape optimisation applied to industrial problems. This work has been developed in collaboration with my research team in the framework of ERC AROMA-CFD, FARE-X-AROMA, HEaD, SOPHYA and PRELICA projects.

Local Yield Stress Analysis of Simulated Cu₆₄Zr₃₆ Bulk Metallic Glass

Dihui Ruan^{*}, Chris Rycroft^{**}, Sylvain Patinet^{***}, Michael Shields^{****}, Michael Falk^{*****}

^{*}Johns Hopkins University, ^{**}Harvard University, ^{***}Laboratoire PMMH, ESPCI, ^{****}Johns Hopkins University,
^{*****}Johns Hopkins University

ABSTRACT

The 'Local Yield Stress' (LYS) method is applied to an atomistic model of an as-quenched Cu₆₄Zr₃₆ metallic glass by shearing local regions of the glass along various orientations. By probing the structure in local shear modes, the LYS method measures the local yield stress as the minimum incremental stress required to trigger the onset of a plastic instability. This analysis is then utilized to identify the population of 'Shear Transformation Zones' (STZs), defined as local atomic clusters that rearrange cooperatively when the material is subjected to shear. These STZs are present in the as-quenched material structure. The population of STZs is correlated with the plastic events observed during a molecular dynamics simulation in which the glass is subjected to shear at the boundaries in order to assess the predictive capability and persistence of the derived STZ population while the material undergoes deformation.

A SIMPLE TECHNIQUE TO AVOID ACCURACY LOSS IN HIGHER ORDER FINITE-ELEMENT SIMULATIONS IN CURVED DOMAINS

VITORIANO RUAS*

* ∂ 'Alembert, Sorbonne Université - Campus de Jussieu
Couloir 55-65, 4^{ème} étage. 4 place Jussieu. 75005 Paris, France
and CNPq research grant holder, PUC-Rio, Brazil
ruas.vitoriano@gmail.com

Key words: Curved domain, Finite element, Hermite, Higher order, Simplex, Straight-edged.

Abstract. The isoparametric version of the finite element method for meshes consisting of curved triangles or tetrahedrons is widely employed to solve second order partial differential equations posed in curved domains. It allows to recover optimal approximation properties that hold for elements of order greater than one in the energy norm for polytopic domains. However so far it has mostly been applied to Lagrange interpolations. Even in this case it requires the manipulation of rational functions and the systematic use of numerical integration. Moreover natural isoparametric versions of other types of finite elements are still incipient, if not unavailable. We consider a simple alternative to deal with Dirichlet boundary conditions that bypasses these drawbacks, without eroding qualitative approximation properties. Applications involving prescribed values of an unknown field but also normal-component or normal-derivative degrees of freedom, illustrate the wide scope and the potential of the new technique.

1 INTRODUCTION

Among a few known techniques the isoparametric version of the finite element method (cf. [1]) for meshes consisting of curved triangles or tetrahedrons is the one most widely employed to solve partial differential equations with essential conditions prescribed on curved boundaries. It allows recovering optimal approximation properties that hold for elements of order greater than one in the energy norm for polytopic domains. However, besides a greater geometric complexity, this method requires the manipulation of rational functions and the use of numerical integration. We consider a simple alternative to deal with essential - that is, Dirichlet boundary

conditions that bypasses these drawbacks, without eroding qualitative approximation properties. Moreover, in contrast to other methods such as the isoparametric version of the finite element method, our technique is universal, for it applies to different types of degrees of freedom, such as normal components of vector or tensor fields. Actually the idea behind it was first disclosed during the talk given by the author on a Hermite method with normal-derivative degrees of freedom at ICNAAM - the International Conference of Numerical Analysis and Applied Mathematics -, which was held in Rhodes, Greece, in September 2016. Later on this work was published in the form of article [2]. In the present work we first recall the main principle the new technique is based upon, by taking as a model the solution of the Poisson equation with quadratic Lagrange finite elements. A detailed description thereof in both the two- and the three-dimensional case can be found in the open access article [3] and references therein. Then we show that the new method extends very naturally to both classical elasticity systems and viscous incompressible flow equations. This forms a basis for technique's application to the finite-element modeling of both fluid flow and solid-body deformation. In the particular case of the Stokes system, for instance, we show that the new method can be combined with any velocity-pressure pairing of global order greater than one. As an illustration we consider the classical Taylor-Hood (cf. [4]) and the Crouzeix-Raviart method, for which examples are given in two-dimension space. Some simulations of deformations of solid bodies of curved shape using our technique in connection with quadratic Lagrange finite elements are also supplied (see also [5]).

2 METHOD'S SHORT DESCRIPTION

First of all it is important to recall that the technique under consideration is aimed at interpolating Dirichlet conditions prescribed on curvilinear boundaries of bi- or tridimensional computational domains. It can provide a significant cost reduction of finite-element simulations in pure CFD or in Structural Calculus, as long as the method in use is of order greater than one. In this respect we can take as an example the popular Taylor-Hood method to solve the incompressible Navier-Stokes equations in a region delimited by two deformable excentric cylinders, both rotating with given angular velocities. The precision of this second order method to simulate the flow of an incompressible viscous fluid in such a domain will be considerably eroded, in case it is simply approximated by the polygon formed by the union of the straight-edged triangles, when a standard mesh is used. A classical solution to overcome such an accuracy loss is to employ the isoparametric version of the finite element method to represent the velocity of the fluid, which requires the use of elements with parabolic edges to approximate boundary portions. However, besides obvious geometric complications, this technique transforms the original local polynomial shape-functions into rational functions. Handling such functions can become a delicate issue. This is because the use of numerical integration is inevitable to compute the matrices inherent to the simulation, and the right choice of a quadrature rule is not always very clear. For all those reasons our method provides an efficient

efficient alternative, since it avoids the use of curved elements and handles only polynomial shape- and test-functions, thereby allowing for exact integration without any qualitative loss, as compared to the isoparametric technique.

Our method's guiding principle can be well understood in the framework of the finite-element solution of the following model-problem. Let us consider the Laplace equation $\Delta u = 0$ in a smooth curved plane domain Ω , with Dirichlet conditions $u=g$ on its boundary Γ , where g is assumed to be sufficiently smooth as well. Suppose that classical Lagrange finite elements are used to solve this problem, based on a straight-edged triangular mesh, in association with continuous functions which are a polynomial of degree less than or equal to k in each triangle.

Suppose again that Ω is approximated by the polygon Ω_h with boundary Γ_h , formed by the union of the triangles of a mesh with maximum edge-length equal to h . If the values of g at the nodes on Γ_h different from vertexes are taken from points on Γ close to them, it is well-known that, whatever $k > 1$, the error of the approximation of u in the energy norm will be an $O(h^{1.5})$ (see e.g. [6]), instead of the $O(h^k)$ one could hope for with this kind of interpolation. With the new technique it suffices to substitute the Lagrangian nodes in the interior of the edges contained in Γ_h , by nodes on Γ located nearby. The choice of the latter nodes is very wide, since anyway integration remains restricted to the triangles that form the polygon Ω_h . We further observe that the test-functions are not defined in this manner, but rather in the usual way for Lagrange finite elements. This is one of the main advantages of our method. In short this procedure allows generating approximations of optimal order k in the energy norm. A rigorous analysis of this property in both 2D and 3D can be found in two *arXiv* papers cited in [3].

A possible construction of the nodes located on Γ pertaining to the new method, generically denoted by P , is illustrated in Figure 1 for $k=3$.

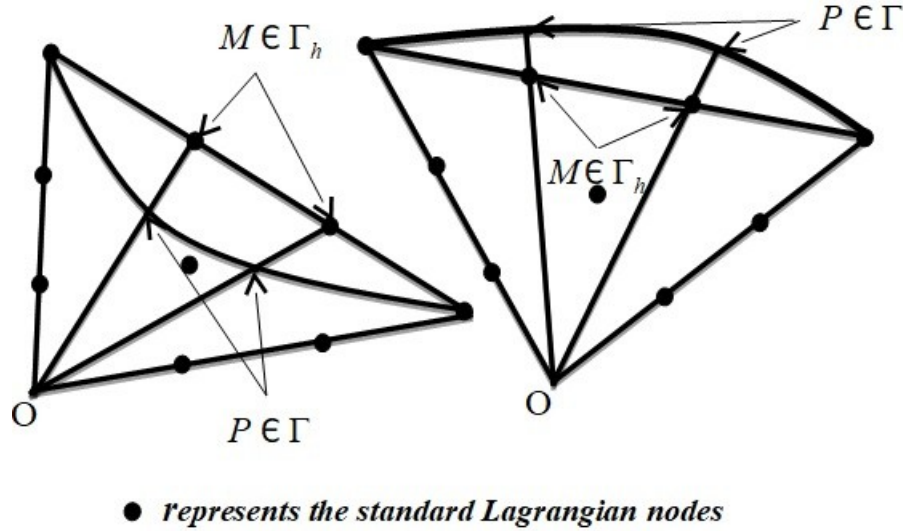


Figure 1- Lagrangian nodes $M \in \Gamma_h$ for $k=3$ and corresponding nodes $P \in \Gamma$ for typical boundary triangles

3 AN EXAMPLE WITH DEGREES OF FREEDOM OF THE NORMAL TYPE

In this section we apply the principles described in Section 2 to a finite element method based on Hermite interpolation incorporating degrees of freedom of the normal-derivative type. The aim is to show that, in contrast to classical methods to handle Dirichlet conditions for second order boundary-value problems posed in curved domains, the technique studied in this work is as universal as can be. For this purpose we solve a model-problem using a variant of the classical Raviart-Thomas mixed finite element of the lowest order [7], commonly known as RT_0 . This variant studied in author's work [8] among other papers of his, is to be employed in the framework of variational formulations mimicking corresponding mixed formulations. A Hermite interpolation with discontinuous piecewise quadratic functions allows for better accuracy of an approximate unknown field in the mean-square sense, as compared to the RT_0 finite element, though at equivalent cost. Solution's gradients in turn, are identically represented.

Suppose that we wish to determine the deflection u of an elastic membrane occupying a smooth plane domain Ω with edge Γ , under the action of a force density f perpendicular to its plane. It is well-known that this problem is governed by the Poisson equation $-c \Delta u = f$ in Ω , supplemented with appropriate boundary conditions, where c is a constant accounting for the mechanical properties of the material the membrane is made of. We consider that a portion Γ_0 of membrane's edge is kept fixed, that is, the essential boundary condition $u = 0$ holds on Γ_0 . On the other hand we assume zero traction on the complementary portion Γ_1 of Γ , which corresponds to the natural boundary condition $\partial u / \partial n = 0$ on Γ_1 , where $\partial u(\cdot) / \partial n$ denotes the outer normal derivative along Γ .

In order to solve this problem with our method, we first recast it in mixed form, by introducing the auxiliary field $\mathbf{p} = \text{grad } u$, which satisfies $\text{div } \mathbf{p} = -c^{-1}f$. The underlying mixed variational form writes: Find (\mathbf{p}, u) in $\mathbf{Q} \times W$ such that

$$\int_{\Omega} (v \text{div } \mathbf{p} + \mathbf{p} \cdot \mathbf{q} + u \text{div } \mathbf{q}) d\mathbf{x} = -c^{-1} \int_{\Omega} f v d\mathbf{x} \text{ for all } (\mathbf{q}, v) \text{ in } \mathbf{Q} \times W, \quad (1)$$

where W is the space of integrable functions in Ω (i.e. $W = L^2(\Omega)$), and \mathbf{Q} is a subspace of the space of vector fields which are square integrable in Ω , and whose divergence is also square-integrable in Ω , that is, the space $\mathbf{H}(\text{div}, \Omega)$ (cf. [7]). More precisely \mathbf{Q} is the subspace of $\mathbf{H}(\text{div}, \Omega)$ consisting of fields \mathbf{q} whose component $\mathbf{q} \cdot \mathbf{n}$ vanishes on Γ_1 , where \mathbf{n} is the outer normal vector to Γ .

It is important to recall that in the framework of formulation (1) the condition $\mathbf{p} \cdot \mathbf{n} = 0$ on Γ_1 is to be treated as an essential (Dirichlet) boundary condition, while the prescribed deflection $u = 0$ on Γ_0 is regarded as a natural (Neumann) boundary condition.

We actually solved a toy-problem with an empty Γ_0 . This requires taking an f satisfying the condition $\int_{\Omega} f d\mathbf{x} = 0$, and in this case u is defined up to an additive constant.

Now let \mathbf{T}_h be a mesh consisting of triangles with maximum edge length equal to h , satisfying the usual compatibility conditions (cf. [1]). Here again we denote by Ω_h the union of the triangles in \mathbf{T}_h and by Γ_h the boundary of this polygon. We define two subspaces \mathbf{Q}_h and W_h associated with \mathbf{T}_h , which are discrete counterparts of \mathbf{Q} and W . We recall that the Raviart-Thomas mixed method RT_0 consists of choosing W_h to be the space of functions which are constant in each triangle of the mesh. \mathbf{Q}_h in turn is the subspace of \mathbf{Q} consisting of fields of the form $a\mathbf{x} + \mathbf{b}$ in each triangle, where a is a real coefficient and \mathbf{b} is a vector of \mathbf{R}^2 , whose normal component is continuous on the edges of the elements in \mathbf{T}_h .

As for the Hermite variant of RT_0 , an approximation u_h of u is searched for in a space V_h defined as follows: In each triangle T of \mathbf{T}_h a function v in V_h is of the form $a\mathbf{x}^2/2 + \mathbf{b} \cdot \mathbf{x} + e$ where a and e are real coefficients and \mathbf{b} is a vector of \mathbf{R}^2 . Then, like the flux variable \mathbf{p} in the RT_0 method, the gradient of v is of the form $a\mathbf{x} + \mathbf{b}$ and its normal component along an edge is constant according to [7]. We require that this normal component of every v in V_h along a mesh edge be single valued if the edge is common to two triangles in the mesh, or to vanish if the edge is contained in Γ , in order to prescribe the zero traction condition on the edge of the membrane. Then following [8], we recast the finite-element counterpart of the mixed formulation (1) in the following variational form: Find u_h in V_h such that,

$$\sum_{T \in \mathbf{T}_h} \left[\int_T (v \Delta u_h + \text{grad } u_h \cdot \text{grad } v + u_h \Delta v) d\mathbf{x} \right] = -c^{-1} \int_{\Omega_h} f v d\mathbf{x} \quad \text{for all } v \text{ in } V_h. \quad (2)$$

Owing to these continuity requirements the local construction of functions in V_h must rely upon Hermite interpolation. Actually the degrees of freedom of V_h are precisely the (constant) normal derivatives along the edges, besides the function mean values in the elements of the mesh (cf. [8]). Since this method represents the gradient of the unknown field in the same way as the RT_0 mixed method, both methods differ only in the (discontinuous) representation of the deflection itself. Indeed in each triangle it is a linear function enriched with a quadratic term in the case of the Hermite method, whereas it is just constant for the mixed method. As long as Ω is a polygon, the Hermite variant of RT_0 described above is a second order method in the mean-square sense (cf. [8]), in contrast to the mixed method, which is just of the first order in the same sense.

Here we endeavor to show that, unless u_h is searched for in a suitable space U_h different from V_h such a property no longer holds, and moreover a substantial accuracy loss occurs in case Ω is a curved domain

Our choice of U_h is a space defined in the same way as V_h , except for elements in the subset of \mathbf{S}_h of \mathbf{T}_h consisting of triangles having an edge in Γ_h upon which a zero normal derivative condition must be enforced. However instead of enforcing this condition along such an edge, we require that the first order derivative of a function in U_h in the direction normal to it vanish along the tangent to the boundary at the intersection with it of the line joining the mid-point of this edge to the opposite vertex. This means that for each triangle in \mathbf{S}_h we pick up

the normal derivative where it is prescribed, that is, on the neighboring portion of the true boundary. This is precisely the counterpart of the Hermite finite element under study, for the technique designed to treat Dirichlet boundary conditions with Lagrange finite elements described in Section 2.

We next proceed to the numerical solution of our model-problem, taking $c = 1$ and Ω to be the ellipse with semi-axes equal to 0.5 and 1.0. We consider a manufactured exact solution given by $u(x,y) = (x^2/8+y^2/32-x^4/4-y^4/64-x^2y^2/8)$, f being defined accordingly. For symmetry reasons the computational domain is a quarter ellipse. We assess the convergence rates to the exact solution for three different approaches, namely, the classical RT_0 method, its Hermite variant taking $U_h=V_h$ and the latter combined with our method to approximate Dirichlet boundary conditions on curved boundaries. The meshes employed in these computations, indexed by an integer M with $h=1/M$, are the transformation of a uniform mesh of the unit square into the mesh of the quarter ellipse, by letting polar coordinates play the role of cartesian coordinates.

From the error evolution measured in the mean-square norm, it turned out that the power of h in the corresponding **OACR** is roughly 1, 1.8 and 2, respectively, where the acronym **OACR** stands for observed asymptotic convergence rate. We refer to Table 1 for such data. Moreover we checked the evolution as the mesh is refined of numerical solution's maximum absolute value at the centroids of the elements in the mesh. The **OACR** in this sense is roughly an $O(h^2)$ for the three methods. Nevertheless it is noteworthy that the accuracy of the boundary-modified Hermite variant of RT_0 in this respect is considerably improved, even for the coarser meshes, taking into account that the maximum absolute value of the exact solution is 1.56250, up to the fifth decimal. This comparison is illustrated in Figure 2.

All these results indicate that the modification in order to enforce on the true boundary the normal derivative boundary condition, with the Hermite variant of RT_0 , is indeed necessary whenever Ω is a curved domain. Indeed in doing so one takes the same advantage thereof in terms of accuracy enhancement, as in the case of polygonal domains (cf. [8]).

$M \rightarrow$	8	16	32	64	128	OACR
$h \rightarrow$	0.01250000	0.00625000	0.00312500	0.00156250	0.00078125	\downarrow
Raviart-Thomas mixed method RT_0	0.53435×10^{-3}	0.20712×10^{-3}	0.90368×10^{-4}	0.42781×10^{-4}	0.21005×10^{-4}	$O(h^{-1.0})$
Hermite variant of RT_0 ($U_h=V_h$)	0.32559×10^{-3}	0.99666×10^{-4}	0.29191×10^{-4}	0.83411×10^{-5}	0.24152×10^{-5}	$O(h^{-1.8})$
Modified Hermite variant of RT_0	0.18500×10^{-3}	0.48191×10^{-4}	0.12493×10^{-4}	0.32565×10^{-5}	0.82059×10^{-6}	$O(h^{-2.0})$

Table 1 - Absolute errors of the solution to a toy-problem in an ellipse in the mean-square norm

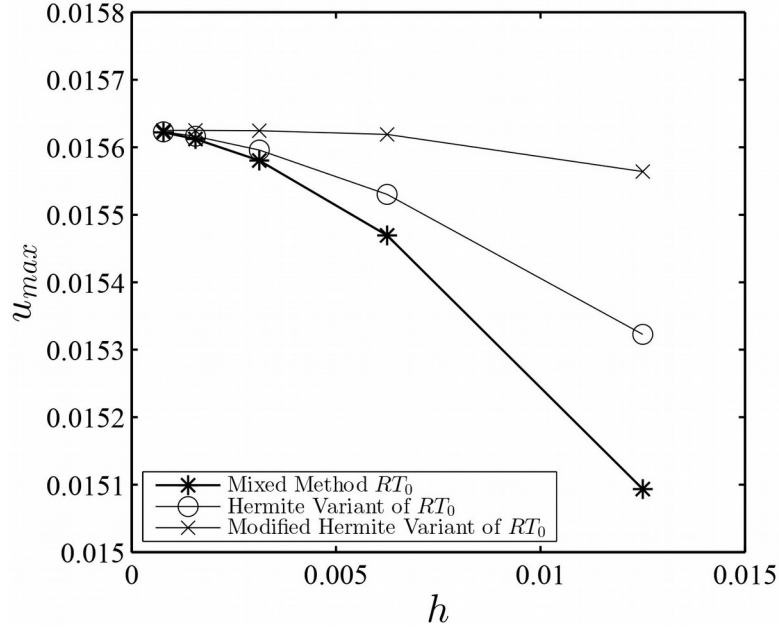


Figure 2 - Approximate solution's maximum absolute value u_{max} at the centroids of the elements

CONCLUSION

From the numerous experiments carried out so far with the new method to take into account Dirichlet boundary conditions prescribed on smooth curved boundaries, it is possible to assert that it is a simple, reliable and accurate tool to allow for higher order finite-element modeling. Moreover, as shown in this work, it is a universal technique, for it applies to different types of interpolations and degrees of freedom, and not only to those based only on function values, such as Lagrange finite elements.

To summarize we highlight the main features of the new method :

- Only polynomial local test- and shape-functions are employed;
- Curved domains are approximated by polytopes consisting of straight-edged N -simplexes;
- The method is universal, as far as degrees of freedom and interpolation types are concerned;
- Akin to classical techniques, optimal arbitrary order is attained;
- No numerical integration is necessary to compute element matrices;
- Implementation is simple and straightforward;
- The method is well-suited to adaptivity and the p -version of the finite element method;
- The multigrid or the h -version of the finite element method is not difficult to implement.

ACKNOWLEDGEMENT

The author gratefully acknowledges the financial support provided by CNPq through grant number 307996/2008-5. He is also thankful to his colleague Marco Antonio Silva Ramos for the diligent support in the preparation of this extended abstract.

REFERENCES

- [1] Zienkiewicz, O.C. and Taylor, R.L. The Finite Element Method. McGraw Hill, Vol. I., (1989), Vol. II., (1991).
- [2] Ruas, V. and Silva Ramos, M.A. A Hermite finite element method for Maxwell's equations. *Applied Mathematics and Information Sciences*, (2018) 12-2 : 271–283.
- [3] Ruas, V. Variational formulations yielding high-order finite-element solutions in smooth domains without curved elements. *Journal of Applied Mathematics and Physics*, (2017) 5-11: DOI:10.4236/jamp.2017.511174.
- [4] -, -. Accuracy enhancement for non-isoparametric finite-element simulations in curved domains; application to fluid flow. *Computer and Mathematics with Applications*, to appear.
- [5] -, -. Optimal Calculation of Solid-Body Deformations with Prescribed Degrees of Freedom over Smooth Boundaries. In: *Advanced Structured Materials*, H. Altenbach et al. Eds., Magdeburg, Springer International Publishing, Vol.1 (2018), 695–704.
- [6] Ciarlet, P.G., *The Finite Element Method for Elliptic Problems*, North-Holland, 1978.
- [7] Raviart, P.A. and Thomas, J.M. *Mixed Finite Element Methods for Second Order Elliptic Problems*, *Lecture Notes in Mathematics*, Springer Verlag, (1977) 292-315.
- [8] Ruas, V. Hermite finite elements for second order boundary value problems with sharp gradient discontinuities, *Journal of Computational and Applied Mathematics*, (2013) 246 : 234-242.

A Diffuse Interface Framework for Modelling the Evolution of Multi-cell Aggregates as a Soft Packing Problem

Shiva Rudraraju^{*}, Krishna Garikipati^{**}, Jiahao Jiang^{***}, Debabrata Auddya^{****}, Tugba Topal^{*****}, Luis Villa Diaz^{*****}

^{*}University of Wisconsin Madison, ^{**}University of Michigan Ann Arbor, ^{***}University of Michigan Ann Arbor,
^{****}University of Michigan Ann Arbor, ^{*****}University of Michigan Ann Arbor, ^{*****}Oakland University

ABSTRACT

We present a model for cell growth, division and packing under soft constraints that arise from the deformability of the cells as well as of a membrane that encloses them. Our treatment falls within the framework of diffuse interface methods, under which each cell is represented by a scalar phase field and the zero level set of the phase field represents the cell membrane. One crucial element in the treatment is the definition of a free energy density function that models cell-cell contact and adhesion. In order to properly represent cell packing and the associated free energy, we include a simplified representation of the anisotropic mechanical response of the underlying cytoskeleton and cell membrane through appropriate penalization of the cell shape change. Numerical examples are presented to demonstrate the evolution of multi-cell clusters, and the total free energy of the clusters as a consequence of growth, division and packing.

Instabilities in Magnetorheological Elastomers with Periodically Distributed Magnetizable Particles

Stephan Rudykh*, Artemii Godhkoderia**

*Technion, **Technion

ABSTRACT

We investigate the magneto-mechanical behavior of magnetorheological elastomers (MRE) undergoing large deformations subjected to magnetic fields. These magnetoactive materials can change their mechanical properties and develop large deformations when subjected to a magnetic field. We focus on the role of microstructures in the overall performance and stability of the deformable magnetoactive composites. We examine the coupled behavior of the active composites with (i) periodically and (ii) randomly distributed magnetizable particles embedded in soft matrix [3], and (iii) periodic laminates and anisotropic structured composites with chain like structures [2]. We identify the key parameters governing the magneto-mechanical couplings. We find that even very similar microstructures, such as periodic composites with hexagonal and rectangular representative volume elements (RVE), exhibit very different behavior in terms of actuation, and effective properties [3]. Next, we investigate the magnetomechanical instabilities [1] that may develop at different length-scales. Here, we focus on the so called macroscopic or long-wave magnetomechanical instabilities to obtain estimates of the onset of magnetomechanical instabilities. We explore the role of external magnetic fields, microstructure parameters, and phase properties on the onset of magneto-mechanical instabilities. To this end, we develop a finite element based code, which allows us to obtain the primary solution for various RVEs subjected to finite deformation and magnetic field ; moreover, the critical condition for the onset of macroscopic instability. By making use of the numerical tool, we identify the unstable domains for MRE composites with periodically distributed circular and elliptical inclusions embedded in a soft matrix. We use the isotropic Langevin model for magnetic behavior, to account for the initial (linear) susceptibility and saturation magnetization of the magnetoactive inclusions. We analyze the influence of the applied magnetic field and finite strains, as well as particle shape and material properties, on the stability of the MRE composites. We find that the stable and unstable domains can be significantly tuned by the applied magnetic field, depending on deformation, microstructure and magnetic properties of the inclusions such as initial susceptibility and saturation magnetization. REFERENCES: [1] Stability of magnetoactive composites with periodic microstructures undergoing finite strains in the presence of a magnetic field. Composites B 128:19-29 (2017) [2] Stability of Anisotropic Magnetorheological Elastomers in Finite Deformations : A Micromechanical Approach. J. Mech. Phys. Solids 61:949-967 (2013) [3] Magnetoactive elastomers with periodic and random microstructures. Int. J. Solids Struct. 51:3012-3024 (2014)

Mechanical Loading Maintains Bone Mass in vivo in Osteolytic Multiple Myeloma

Maximilian Rummler^{*}, Fani Ziouti^{**}, Anne Seliger^{***}, Maureen Lynch^{****}, Bettina Willie^{*****}, Franziska Jundt^{*****}

^{*}Research Centre, Shriners Hospital for Children-Canada, Department of Pediatric Surgery, McGill University, Montreal, Canada, ^{**}Medizinische Klinik und Poliklinik II-Hämatologie/Onkologie, Universitätsklinikum Würzburg, Germany, ^{***}Julius Wolff Institut, Charite- Universitätsmedizin Berlin, Germany, ^{****}University of Massachusetts, Amherst, USA, ^{*****}Research Centre, Shriners Hospital for Children-Canada, Department of Pediatric Surgery, McGill University, Montreal, Canada, ^{*****}Medizinische Klinik und Poliklinik II-Hämatologie/Onkologie, Universitätsklinikum Würzburg, Germany

ABSTRACT

Multiple myeloma (MM) is an incurable plasma cell derived neoplasia, leading to pathological osteoclast activity resulting in increased bone resorption. Treating MM bone disease is a major goal in MM therapy. We hypothesized, that loading would maintain bone mass in a mouse model of MM. The left tibiae of 40, 10wk old female BALB/c mice were either a) PBS injected, b) MOPC315.BM cell injected (2), or c) not injected. 14 days after injection, 25 mice (n = 7-10/treatment) underwent 3 wks of in vivo tibial loading (3) (left limb, right limb nonloaded), with the remaining 15 mice (n = 6 PBS, n = 9 tumor) serving as nonloaded controls. In vivo microCT was performed at day 0, 5, 10, 15 and 20 of loading, at proximal metaphysis and midshaft. Cortical and trabecular parameters were measured. An ANOVA assessed the effects of treatment, loading, and limb. After 20 days of loading, metaphyseal cortical bone formation (CtTh, CtAr, TAr, CtAr/TtAr, CtvTMD) was significantly greater and cortical porosity (CtPo) was lower compared to nonloaded right limbs and nonloaded groups. All right limbs had similar increases in cortical parameters over 20 days, indicating no systemic effects present. Left limbs of tumor-injected loaded group had + 41% cortical thickness, while left limbs of tumor-injected nonloaded group increased by 1%. In conclusion, these data indicate mechanical loading can maintain bone mass in this model of MM. 1) Lynch et al. JBMR 2013, 2) Hofgaard et al. PLoS One 2012, 3) Willie et al. Bone 2013

Computational Design and Fabrication of Foams for Actuators and Dampers in Robots

Daniela Rus^{*}, Jeffrey Lipton^{**}, Robert MacCurdy^{***}

^{*}MIT CSAIL, ^{**}MIT CSAIL, ^{***}UC Boulder

ABSTRACT

Computationally designing and 3D printing foam will be an important tool for the on-demand design and fabrication of robots. Impact protection and vibration isolation are important factors in robot design. In the past researchers and engineers have used foams as padding, vibration isolators, actuators, and as structural elements in robotic systems. With the explosion of soft robotics as a field, foams are increasingly becoming an integral element of robot design. Traditionally foams and other damping materials are available only in bulk or molded form. 3D Printing foams allows roboticists to produce custom shapes and distributions of material properties, enabling the rapid design and fabrication of robots. Methods of 3D printing foams work at three layers of the design and fabrication process: explicit geometry, print process control, and material blending. Explicit geometry methods rely on 3D representations of each cell and pore to be printed. Print process methods change the fabrication process to induce a porous foamed structure. For example, inducing viscous thread instability in direct write 3D printing generates open celled foams with controllable stiffness and pore size (1). Blending methods rely on two or more materials that are brought together before or during printing process (2). Researchers have used these foam-printing methods to make high force actuators, low force actuators and viscoelastic dampers. The foam actuators combined elastomers with phase change material. The high force actuators are made of printed wax-silicone blends and are capable of producing over 4.5 kN of blocked force (3). The lower force actuators combine silicone with ethanol. The viscoelastic dampers were closed cell foams of un-curing liquid encapsulated in a UV-curing acrylate elastomer. Varying the relative concentration of the un-curing liquid can adjust the elastic and damping modulus of the material over one order of magnitude. Engineers can programmatically control the shape and material properties produced using the empirical models of material properties. In this talk, we will discuss how these methods work and how they can be integrated into computation design systems for robots to produce actuators, dampers, and materials that change stiffness. References 1. 3D printing variable stiffness foams using viscous thread instability. Lipton, Jeffrey and Lipson, Hod. 2016, Scientific Reports, Vol. 6. 2. Printable programmable viscoelastic materials for robots. Lipton, Jeffrey I, et al. 2016, Intelligent Robotics and Systems, pp. 2628-2635. 3. Electrically Actuated Hydraulic Solids. Lipton, Jeffrey I, et al. 10, s.l. : Advanced Engineering Materials, 2016, Vol. 18. 10.1002/adem.201600271.

Pore-scale Computation of the Effective Diffusion and Hydrodynamic Dispersion in Inhomogeneous Porous Media

Héctor Rusinque*, Gunther Brenner**

*PhD Candidate, **Dr. Professor

ABSTRACT

In this study, a method for the quantification of effective diffusive and convective mass transport in porous media is presented. Engineering approaches to describe mass transport are based on averaged quantities such as effective diffusion coefficients to consider the diffusion inhibition due to the structure of the porous medium or the hydrodynamic dispersion coefficient in the transport is additionally determined by overlapping convection and diffusion. Here, the combined use of the Lattice-Boltzmann method and the lagrangian random-walk particle tracking method offers the possibility to accurately describe the transport phenomena at a pore scale. From the data obtained, effective parameters can be determined as needed in engineering models. This simulation approach requires a pore-scale reconstruction of the porous medium, resulting in the necessity of exceptional computational resources, such as those provided by supercomputers to perform pore-scale simulations. In the presentation, the method will be described and verified by means of known solutions, e.g. for the Taylor Aris dispersion. Based on this, the effective diffusion and hydrodynamic dispersion in beds of spherical and irregular particles are analyzed and effective parameters for the description of the mass transport are discussed. The focus is on packing in confined spaces with an inhomogeneous porosity distribution near the wall and porous media with designed transport pores.

The Virtual Element Method for Curved Domains

Alessandro Russo^{*}, Lourenco Beirao da Veiga^{**}, Giuseppe Vacca^{***}

^{*}University of Milano-Bicocca, ^{**}University of Milano-Bicocca, ^{***}University of Milano-Bicocca

ABSTRACT

In this talk I will present the first results about the investigation of the Virtual Element Method in the presence of curved elements. We consider the case of a fixed curved boundary in two dimensions, as it happens in the approximation of problems posed on a curved domain or with a curved interface. We show that the proposed Curved Virtual Elements lead to an optimal rate of convergence, independently of the shape of the curved edges.

Contribution to Multiscale Modelling of Additive Manufacturing: Selective Laser Melting

Romain Ruysen^{*}, Andrea Barbarulo^{**}, Hachmi Ben Dhia^{***}

^{*}CentraleSupélec, Université Paris Saclay, ^{**}CentraleSupélec, Université Paris Saclay, ^{***}CentraleSupélec, Université Paris Saclay

ABSTRACT

Additive Manufacturing refers to all processes creating parts by adding material from a numerical model. Those methods present several important advantages by making possible the creation of parts with complex shapes impossible to obtain with classical processes. However, although their utilization is expanding fastly for twenty years, their application remains marginal because of the lack of scientific and technical control of the process. Produced parts may not respect the specifications and the numerical simulations are a preferential way to determine key parameters for dimensioning. Several processes exist and we chose to focus on the Selective Laser Melting (SLM) process, wich is difficult to master due to the complexity of physical phenomena taking place during parts fabrication . The aim of this paper is to model the SLM by taking into account these several physical scales, and to this end, the multiscale Arlequin framework is especially suited for this problematic thanks to its great flexibility [1][2]. Indeed, this technique allowed to decompose our analysis by considering different scale levels. Firstly, a micro scale in the area under the laser have been used, to modelize precisely its heat inflow. A second zone has been modelled at mesoscopic scale for considering the phase changing phenomena thanks to the Latent Heat Source Method. The movement of this two domains, allows to modelize the microscopic material addition. Then, other scales (coarser at macroscale) are progressively and incrementally introduced during the process evolution as the laser and the high thermal gradients move far away from the previous layers. Moreover, we present a particular Model Order Reduction method infered by our simulations that leads to drastic reduction of computational costs. [1] Ben Dhia.H, Comptes Rendus de l'Académie des Sciences Series IIB Mechanics Physics Astronomy, 1998, Multiscale mechanical problems: the Arlequin Method. [2] Ben Dhia.H, International Journal for Multiscale Computational Engineering, 2008, Further Insights by Theoretical Investigations of the Multiscale Arlequin Method.

Topological and Localized Modes in Quasiperiodic Structures

Massimo Ruzzene*

*Georgia Institute of Technology

ABSTRACT

Phononic crystals and acoustic metamaterials are periodic structures that have drawn much attention to the engineering and physics communities due to their numerous applications in passive vibration and noise control. Topology concepts originally developed in electronics have recently inspired a number of applications in photonics and phononics. Many of these concepts rely on the existence of topological properties that lead to edge modes or interface wave modes. In this context, this paper explores quasiperiodicity, which has been the subject of extensive research in the fields of crystallography and photonics, as related to continuous quasiperiodic elastic structures. The objective is to find topological modes, such as localized modes in one-dimensional and two-dimensional quasiperiodic systems. These can be as interesting if not more useful than the interface modes that are found in periodic structures, as the quasiperiodicity framework provides a consistent methodology that leads to interfaces, which may be topologically protected. The concept is first illustrated for simple 1D quasiperiodic spring-mass chain that exhibits localized modes, introducing the mechanical analogues to the Harper models previously found in photonics. Next, the study investigates arrays of coupled rods, as analogues of a recent experiment conducted with a quasiperiodic photonic lattice designed to robustly transfer energy from one boundary to another. Finally, the investigation of plate structures with quasiperiodic arrangements of lumped masses and resonators are presented as structural components which support a variety of localized modes and that are suitable for the experimental characterization of the waveguiding behavior of these configurations.

Modeling Plasticity of FCC/BCC Micro-pillars Using Dislocation Dynamics

Ill Ryu*

*UT-Dallas

ABSTRACT

From the recent micro-pillar experiments, it is now known that the flow stress of metallic micro-pillars increases with decreasing sample size with and without the strain gradient by geometrically necessary dislocations. To understand size dependent plasticity, several models have been proposed, but the role of the dislocation sources in submicron sample is still under debate. In the present study, we make a three-dimensional, dislocation dynamics model to study collective dislocation behavior under tension/torsion in FCC/BCC micro-pillars. We follow both the evolution of the dislocation structure and the corresponding stress-strain relation. Our simulation results show the evident size effect and the effect of cross slip and clear Bauschinger effect, which appear to be good agreement with experimental results.

On the Fracture Strength Measurement of Polycrystalline Graphene Using Nanoindentation

Seunghwa Ryu^{*}, Sangryun Lee^{**}, Dongwoo Sohn^{***}, Jihoon Han^{****}

^{*}Korea Advanced Institute of Science and Technology, ^{**}Korea Advanced Institute of Science and Technology,

^{***}Korea Maritime and Ocean University, ^{****}Korea Advanced Institute of Science and Technology

ABSTRACT

The strength of pristine graphene and its grain boundaries (GBs) are mainly measured by nano-indentation with a spherical tip due to the difficulty of conducting uniaxial tensile tests. However, we recently showed that the fracture forces from the spherical indenter cannot be directly mapped onto the uniaxial strength. In this paper, employing a series of molecular dynamics simulations combined with a fracture mechanics analysis, we demonstrate that the fracture force from cylindrical indenters can be directly mapped onto the strength of graphene under uniaxial tension. Under indentation with cylindrical tips or uniaxial tension, the rupture of graphene sheets that have GBs with a low-tilt angle occurs simultaneously with the onset of crack nucleation at the GBs. On the contrary, when indented by a spherical indenter tip, the graphene sheets sustain the indentation loads until the crack size becomes comparable to the tip radius. Furthermore, the results show that estimating the strength with a cylindrical indenter is not very sensitive to the indentation site as well as angular misalignments that can be caused by human error or the limitations of the apparatus. We provide a detailed theoretical analysis on the crack growth based on the fracture mechanics. Our work presents the feasibility of obtaining the tensile strength from nanoindentation experiments, which may suggest a new standard to measure the tensile strength of graphene and related two-dimensional materials.

Gradient-based Optimization with the Cartesian Grid Finite Element Method (cgFEM)

Juan José Ródenas^{*}, Onofre Marco^{**}, Enrique Nadal^{***}, Francisco Javier Fuenmayor^{****},
Manuel Tur^{*****}

^{*}Research Centre in Mechanical Engineering (CIIM). Universitat Politècnica de València, ^{**}Laboratori de Càlcul Numèric (LaCàN). Universitat Politècnica de Catalunya, ^{***}Research Centre in Mechanical Engineering (CIIM). Universitat Politècnica de València, ^{****}Research Centre in Mechanical Engineering (CIIM). Universitat Politècnica de València, ^{*****}Research Centre in Mechanical Engineering (CIIM). Universitat Politècnica de València

ABSTRACT

This paper presents how an immersed boundary method, namely, the Cartesian grid Finite Element Method (cgFEM) described for the 2D case in [1], can be used to enhance the performance of gradient-based 3D shape optimization processes. To do this, we first developed a technique to perform the shape sensitivity analysis (SSA), used to evaluate the gradients required by the optimization algorithm, within the cgFEM framework [2]. This included a tailored evaluation of the design velocity field required by the SSA and the consideration of Dirichlet boundary conditions in non-fitted meshes. We then used the hierarchical Cartesian structure to improve the efficiency of the analysis of each geometry, as this structure allows for trivial data sharing between similar entities (including the exchange of information between different geometries) or for an optimal system matrix reordering, among other benefits. Finally, we developed a projection technique[3] based on [4] to directly create the h-adapted meshes required by each geometry to obtain the prescribed accuracy, thus eliminating the need to perform a full h-adaptive iteration for each geometry, consequently, improving the performance of the optimization algorithm. The numerical results obtained show the accuracy of the shape sensitivity analysis, its adequate behaviour in the cgFEM context, and a considerable improvement in the efficiency of the shape optimization algorithm.

REFERENCES [1] E Nadal, JJ Ródenas, J Albelda, M Tur, JE Tarancón, FJ Fuenmayor. Efficient Finite Element Methodology Based on Cartesian Grids: Application to Structural Shape Optimization. Abstract and Applied Analysis 2013, Article ID 953786, 19 pages (2013). [2] O Marco, JJ Ródenas, FJ Fuenmayor, M Tur. An extension of shape sensitivity analysis to an immersed boundary method based on Cartesian grids Computational Mechanics. <https://doi.org/10.1007/s00466-017-1522-0> (2017) [3] O Marco, JJ Ródenas, J Albelda, E Nadal, M Tur. Structural shape optimization using Cartesian grids and automatic h-adaptive mesh projection. Structural and Multidisciplinary Optimization. <https://doi.org/10.1007/s00158-017-1875-1> (2017) [4] G Buggedá, JJ Ródenas, E Oñate. An integration of a low-cost adaptive remeshing strategy in the solution of structural shape optimization problems using evolutionary algorithms. Computers & Structures (86)1563 – 1578 (2008). Acknowledgements: The financial support to this work of Generalitat Valenciana (PROMETEO/2016/007) and the Spanish Ministerio de Economía, Industria y Competitividad (DPI2017-89816-R) is greatly acknowledged.

Modelling the Musculoskeletal System - A Two-muscle Upper Arm Model

Oliver Röhrle^{*}, Michael Sprenger^{**}, Julian Valentin^{***}, Dirk Pflüger^{****}

^{*}University of Stuttgart, ^{**}University of Stuttgart, ^{***}University of Stuttgart, ^{****}University of Stuttgart

ABSTRACT

Investigating the interplay between muscular activity and motion is the basis to improve our understanding of healthy or diseased musculoskeletal systems. To be able to analyze the musculoskeletal systems, computational models are employed. Albeit some severe modeling assumptions, almost all existing musculoskeletal system simulations appeal to multi-body simulation frameworks. Although continuum-mechanical musculoskeletal system models can compensate for some of these limitations, they are essentially not considered due to their computational complexity and cost. Based on the two-muscle upper arm musculoskeletal framework proposed in [1] an efficient and for multi-muscle musculoskeletal system feasible modelling framework, in which the exerted skeletal muscle forces are computed using three-dimensional, continuum-mechanical skeletal muscle models and in which muscle activations are determined based on a constraint optimization problem, is proposed. In [1], the framework was limited to determine the state of activation of one of the two muscle or the positions of the bones based on the level of activation of both muscles. Now, a fully activation-driven musculoskeletal system model is feasible. Numerical feasibility is achieved by computing sparse grid surrogates with hierarchical B-splines. Adaptive sparse grid refinement further reduces the computational effort. The choice of B-splines allows the use of all existing gradient-based optimization techniques without further numerical approximation. To demonstrate this, we show several different test scenarios in which the upper limb model consisting of the elbow joint, the biceps and triceps brachii and an external load is subjected to different optimization criteria. In addition to the numerical framework, appropriate constitutive laws for the active behavior of the skeletal muscle tissue are needed. The presentation will conclude with an outlook on how one can extend this method to musculoskeletal systems with three or more muscles. [1] Röhrle O., Sprenger M., and Schmitt S. A two-muscle, continuum-mechanical forward simulation of the upper limb. *Biomechanics and Modeling in Mechanobiology*. 2017, 16(3), p. 743-762.

High-Order Time Stepping in Partitioned Fluid-Structure Interaction with Black-Box Solvers

Benjamin R  th^{*}, Benjamin Uekermann^{**}, Miriam Mehl^{***}, Hans-Joachim Bungartz^{****}

^{*}Technical University of Munich, ^{**}Technical University of Munich, ^{***}University of Stuttgart, ^{****}Technical University of Munich

ABSTRACT

Fluid-structure interaction problems are solved by applying either the monolithic or the partitioned approach [1]. While the monolithic approach usually provides more stable solutions, the partitioned approach has many advantages from a software engineering perspective as, for example, the reuse of well-tested existing solvers (participants) in a black-box fashion. However, this typically results in a degradation of time stepping to first order if applied in the standard way [2] - even if the used solvers are of higher order. In this talk, the convergence order of time-stepping for a simple 1D model problem is investigated. In our partitioned approach, the solvers are considered as black-boxes: Only nodal data at the wet interface between the fluid and the structure region is exchanged between the solvers. The aforementioned effect of order degradation is reproduced for state-of-the-art explicit (weak) and implicit (strong) coupling. Finally, an order conserving coupling scheme is introduced. This scheme allows to couple participants using arbitrary time stepping schemes and differing temporal meshes. Here, dense output is used to construct high-order local interpolants between the timesteps at low cost. Waveform relaxation iteratively improves the approximative, time-continuous solution at the boundary and windowing techniques are used to allow non-matching temporal discretization. In the future, we plan to implement this mechanism in the open source coupling library preCICE [3] to be able to solve complex multi-scale-multi-physics scenarios, such as turbulent fluid-structure interaction or fluid-structure-acoustics interaction. Currently, very small time steps are needed in this area due to degradation of convergence order and stability properties of the time-stepping scheme if a partitioned approach is in use. References [1] C Michler et al. "A Monolithic Approach to Fluid-Structure Interaction". In: Comput. Fluids (2004) [2] C. Farhat and M. Lesoinne. "Two efficient staggered algorithms for the serial and parallel solution of three-dimensional nonlinear transient aeroelastic problems". In: Comput. Methods Appl. Mech. Eng. (2000) [3] Hans-Joachim Bungartz et al. "preCICE - A fully parallel library for multi-physics surface coupling". In: Comput. Fluids (2016)

Analysis of Anisotropic Elastic Wave Field Using Boundary Element Method with Far- Field Approximation

Takahiro SAITOH*, Takashi ONODERA**, Akira FURUKAWA***, Sohichi HIROSE****

*Gunma University, **Gunma University, ***Tokyo Institute of Technology, ****Tokyo Institute of Technology

ABSTRACT

A new boundary element method (BEM) with far field approximation is presented for the elastodynamic problems of general anisotropy. The BEM has been developed as an effective and accurate numerical approach for wave propagation problems. However, the BEM for general anisotropic elastic solids still remains to be improved [1]. The fundamental solution for general anisotropic elastodynamics was developed by Wang and Achenbach [2]. The fundamental solution used in the BEM for anisotropic elastodynamic problems can be expressed by the sum of the static and dynamic part. The static part can be obtained by the closed form. However, the dynamic part of the fundamental solution cannot be obtained by the closed form and involves the numerical integration over a unit circle for 2-D and a unit sphere for 3-D problems. The evaluation of the numerical integration for them is very time consuming. Therefore, the most important key of the BEM analysis for general anisotropic elastodynamic problems is how to save the computational cost for the numerical integrations. Therefore, in this research, a far field approximation of the fundamental solution for general anisotropic elastodynamic problems is developed. The far-field approximation can be derived by using the stationary phase method. The far-field approximated fundamental solution has no integration over a unit circle for 2-D and a unit sphere for 3-D problems. Therefore, the development of the far-field approximated fundamental solution for BEM for general anisotropic elastodynamics can contribute to the reduction of the computational cost. In addition, parallel computing techniques, such as OpenMP, and MPI (Message Passing Interface) are utilized with the help of the supercomputer of Kyoto University for more reduction of the computational time. The numerical evaluation for the proposed far-field fundamental solution has been implemented and tested with numerical examples. The problems of elastic wave scattering by a cavity in general anisotropic elastodynamics are solved to validate the BEM with the proposed far-field approximation.

Low Impact Cratering on Granular Beds Under Low Gravity

Lucas SARDO*, Florian Thuillet**, Patrick Michel***, Elie Hachem****, Rudy Valette*****

*Center for Material Forming (CEMEF), MINES ParisTech, PSL Research University, France, **Lagrange Laboratory, University of Nice Sophia Antipolis, CNRS, Observatoire de la Côte d'Azur, France, ***Lagrange Laboratory, University of Nice Sophia Antipolis, CNRS, Observatoire de la Côte d'Azur, France, ****Center for Material Forming (CEMEF), MINES ParisTech, PSL Research University, France, *****Center for Material Forming (CEMEF), MINES ParisTech, PSL Research University, France

ABSTRACT

In the context of asteroid material sampling, landers are sent on the asteroid surface, which is made of regolith, that can be considered at first approximation as a granular bed. An important question is to understand the physics that governs the penetration of the lander in the granular bed, for a given impact velocity. For slow impact-induced flows on frictional non-cohesive granular beds on Earth, the soil behaves like a yield-stress fluid, where the yield-stress increases linearly with (depth induced) static pressure, and this rheology governs the penetration flow. However, for vanishing gravity, as encountered on asteroids, one expects dynamic (impact) pressure to dominate the penetration flow dynamics. In this paper, we model regolith as a $\mu(i)$ granular continuum fluid and propose both dimensional analysis and numerical simulations to identify asymptotic and coupled regimes for penetration of an impacting sphere from Earth to vanishing gravities. We find a penetration that scales quasi linearly with impact velocity for Earth gravity, that switch to sublinear for low enough gravities. The role of bed layer thickness and elasticity will be discussed and compared to discrete simulations.

New Unsymmetric Finite Elements Based on Analytical Trial Solutions Insensitive to Severe Mesh-Distortion

Yan SHANG*

*State Key Laboratory of Mechanics and Control of Mechanical Structures, College of Aerospace Engineering,
Nanjing University of Aeronautics and Astronautics, Nanjing 210016, China

ABSTRACT

The unsymmetric FEM is a very promising technique to produce finite elements with good numerical accuracies and high tolerances to mesh distortions. In this work, new high-performance unsymmetric quadrilateral element models are developed for analysis of the plane problems and Mindlin-Reissner plate problems within the framework of the so-called improved unsymmetric formulae, which is characterized by directly adopting a reasonable self-equilibrium stress field to be the element's trial functions. This stress field is obtained based on the analytical trial solutions of related problems and the quasi-conforming technique, thus can a priori satisfy the governing equations. Extensive numerical tests reveal that these new elements exhibit excellent capabilities for predicting results of both displacement and stress. In particular, they can still work very well in severely distorted meshes even when the element shapes deteriorate into concave quadrangle or degenerated triangle.

Simulation Analysis of the Optimal Position of Elastic Fixation for the Lumbar Spine

HONGFANG SONG*, QI LI**, ZHICHENG LIU***

*Capital Medical University, Beijing 100069, China, **Capital Medical University, Beijing 100069, China, ***Capital Medical University, Beijing 100069, China

ABSTRACT

The elastic dynamic fixation device COFLEX is approved to be an effective approach for the treatment of lumbar spine. What is the influence of different implantation depths on the motion of adjacent segments? This is still an open problem. The objective of the present work is to investigate the optimal position of elastic fixation COFLEX, and to provide the basis for clinical operation. The lumbar L1-L5 vertebral model was reconstructed based on CT images of volunteers. The intervertebral disc and nucleus pulposus model were established according to the upper and lower vertebral body by using CAD tools. The main ligaments of the control lumbar movement were added according to the anatomical structure, including the anterior longitudinal ligament, the posterior longitudinal ligament, the yellow ligament, the ligaments of the spine, the ligament of the transverse process, and the articulationes zygapophysiales ligament. The segments L3 - L4 were selected as the surgical segments. The complete group and the damage group models were constructed respectively. The 3d geometric structure of COFLEX was established by using laser scanning technique. Then 3 groups of models were built according to the depth from the U top of COFLEX to endorachis, and the different depths are 10 mm, 5 mm and 0 mm respectively. ABAQUS software was used to numerically analyze the movement of models under the flexion, left-right side bending and left-right rotation. The similarities to the complete group of motion variation range in the six motion states are in the descending order as 0 mm group, 5 mm group, 10 mm group and damaged instable group. In other words, the closer is the distance between the U top of COFLEX and endorachis, the closer is the variation range of lumbar vertebrae and adjacent segment to the complete group, while the difference in the instable group is the largest. Whether for the surgical segments or the overall lumbar spine, the closer is the U top of COFLEX to endorachis, the closer is the motion to the complete group. This indicates that COFLEX implanting close to the spine demonstrates good postoperative performance this good motion effect close to the complete spine. This phenomena is consistent with the experimental results. The elastic fixation device can be implanted as close to the dura as possible without injuring the nerve. Key words: lumbar spine; Elastic fixation; COFLEX; Finite element analysis; References 1?Divya V. Ambati, MS et al. Bilateral pedicle screw fixation provides superior biomechanical stability in transforaminal lumbar interbody fusion: a finite element study. The spine journal, available online 28 June 2014. 2?ZU Dan, HAI Yong, YUN Cai, et al.Adjacent segment range of motion after different insertion depth of lumbar interspinous dynamic stabilization device(Coflex): a biomechanical study. Chinese Journal of Spine and Spinal Cord, 2014, 24(10): 933-937. Acknowledgement: Project of Science and Technology of Beijing Municipal Education Commission (KM201410025012), Beijing Natural Science Foundation (7112056) Email?songhf@ccmu.edu.cn *corresponding, zcliu@ccmu.edu.cn

Roles of Length and Time Scales in Phase Transition Paradigm Shift

Qingping SUN*

*Hong Kong Univ. of Sci. & Tech.

ABSTRACT

Roles of Length and Time Scales in Phase Transition Paradigm Shift Qingping SUN¹, Mingpeng LI² ¹ Hong Kong University of Science and Technology, Hong Kong, China ² Wuhan University, China We report recent advances in the experimental and theoretical study of effects of material internal length scales (grain size, grain boundary and phase boundary) and time scales (loading time and heat conduction time) on the phase transition responses of NiTi polycrystalline shape memory alloy (SMA). For length scale effect [1-3], it is shown that, with grain size reduction, the energy of the elastic non-transformable grain boundary will gradually become dominant in the phase transition process and eventually bring fundamental changes of the deformation behaviors: breakdown of two-phase coexistence and vanishing of superelastic hysteresis dissipation. Such effects of length scale reduction originates from the large increase in the area-to-volume ratios of the interfaces (grain boundary and phase boundary) in the polycrystal, which provides a theoretical base to improve and control the performance of the existing NiTi SMA by grain size engineering. For the effects of time scales, it is shown that competition of physical processes (phase transition and heat transfer) with different time scales brings the emergence of a new length scale in the experimental observed domain patterns. Nucleation and growth of new phase, two-phase coexistence and the hysteresis dissipation are the key signatures of the first-order phase transition in materials and are widely used as the basic paradigms. It is shown that with the grain size reduction and/or loading time reduction, many unusual phenomena and properties will emerge, which not only open up new possibilities in the application but also lead to new paradigm building and shift in modelling and understanding. References [1] Li, M. P. and Q. P. Sun, "Nanoscale phase transition behavior of shape memory alloys — Closed form solution of 1D effective modelling", J. Mech. Phys. Solids, 110 (2018) 21–37. [2] Sun Q. P., A. Ahadi, Li M. P. and Chen M. X, "Effects of Grain Size on Phase Transition Behavior of Nanocrystalline Shape Memory Alloys", Science China Technological Sciences, 2014, 57: 671–679. [3] Aslan, A and Q. P. Sun, "Stress hysteresis and temperature dependence of phase transition stress in nanostructured NiTi—Effects of grain size", Applied Physics Letters 103, 021902 (2013).

Fluid/Solid Coupling for the Simulation of SLM Process

Yassine Saadlaoui^{*}, Jean-Michel Bergheau^{**}, Alexandre Delache^{***}, Eric Feulvarch^{****},
Jean-Baptiste Leblond^{*****}

^{*}Univ. Lyon, ENISE, ^{**}Univ. Lyon, ENISE, ^{***}LMFA UMR, ^{****}Univ. Lyon, ENISE, ^{*****}UPMC, Université Paris-6

ABSTRACT

Selective Laser Melting is among the additive manufacturing processes most used. It is one of the Powder Bed Fusion AM processes that consists in producing fully functional metal parts presenting high mechanical properties. The large use of SLM process and the need to improve and better control this process ability have led to the development of several numerical simulation approaches, which may provide valuable assistance to study the process's effects on the final parts. During SLM, the material undergoes thermal cycles which lead to state changes and fluid flows in molten pool. These fluid flows are related to the strong thermal gradient and caused by the effects of surface tension "Marangoni and curvature effects". This dynamic in molten pool can affect the temperature field distribution, the morphology of the molten zone and the generated stress field. Therefore, in order to reproduce as possible the physical phenomena occurring during the SLM process, it is very important to take into account the fluid flows during numerical simulation. Additionally, the type of coupling between fluid and solid computations is very important during the numerical simulation. Generally, a weak coupling is used to relate these computations. In this context, the aim of this work is to propose a new method to simulate the interaction between fluid flows and solid deformations. In first step, a new approach was developed, it consists to take into account the dynamic in molten pool through the two effects of surface tension (including both the "curvature effect" and the "Marangoni effect") and floatability. Additionally, the free surface was considered using an ALE method. To validate these methods, two numerical tests were used. Thereafter, two simulations of SLM were carried out, the first is a thermal computation without fluid flows and the second is a thermal-fluid computation with dynamic in molten pool. Finally, the authors have studied the effect of fluid flows on temperature evolution and weld pool morphology. The comparison of results between these two simulations shows a great influence of fluid flows on temperature and molten pool morphology. In second step, a new coupling strategy is developed to simulate the thermo-fluid flows and the solid-state stress field at each computing time step. The aim is to estimate residual stresses and distortions, in order to obtain final properties of SLM parts.

ICME Design of High Performance Ni-based and High-Entropy Turbine Alloys

James Saal^{*}, Jiadong Gong^{**}, Ricardo Komai^{***}, Greg Olson^{****}

^{*}QuesTek Innovations LLC, ^{**}QuesTek Innovations LLC, ^{***}QuesTek Innovations LLC, ^{****}QuesTek Innovations LLC / Northwestern University

ABSTRACT

Integrated Computational Materials Engineering (ICME) tools are being developed at QuesTek Innovations for the design of high-performance alloys for turbine blades, specifically (1) a highly castable yet creep-resistant low-Re Ni-based superalloy and (2) high entropy alloys (HEAs) for extreme environments. The integration of various CALPHAD calculations such as phase-equilibria, solidification pathways, diffusion fields, and precipitation behavior form an important foundation for designing high-performance alloys. Using internally developed processing-structure-property models and a parametric design platform integrated with both commercial and proprietary thermodynamic/mobility databases, QuesTek designed a novel low-Re castable SX Ni-based superalloy for blade applications. Select design criteria includes nominally 60% volume fraction of γ' , slight negative misfit between γ and γ' at 1000-1100°C, minimized propensity for TCP formation, and ability to be solution treatable without incipient melting, in addition to the processing and property objectives previously mentioned. The resulting design, termed QTSX, possesses an optimized combination of the processing constraints and property criteria specific for the blade application. HEAs, particularly those containing refractory elements, have the potential to surpass Ni-based superalloy performance in blade applications by enabling higher operating temperature. In addition to commercial CALPHAD databases, QuesTek is utilizing an internally developed database based on experimental data as well as exhaustive high-throughput density functional theory (DFT) calculations. Novel HEA compositions have been identified and experimentally verified by lab-scale alloy synthesis and characterization. A processing-structure-property framework has been created, and ongoing work focuses on the design of HEAs for high-temperature stability, strength, oxidation resistance, ductility, and creep resistance.

Virtual Element Method Approach for 2D Fracture Mechanics Problems

Elio Sacco^{*}, Edoardo Artioli^{**}, Sonia Marfia^{***}

^{*}, University of Naples Federico II, Naples, Italy, ^{**}University of Rome Tor Vergata, Rome, Italy, ^{***}University of Cassino and Southern Lazio, Cassino, Italy

ABSTRACT

The object of the present work is the development of an innovative methodology for 2D fracture mechanics problems based on the Virtual Element Method (VEM). The VEM is a new technology for the approximation of partial differential equations, which can be interpreted as an evolution of modern mimetic finite difference schemes, and which shares the same variational background of the finite element method. The main feature of the VEM is the possibility to construct an accurate Galerkin scheme with the flexibility to deal with highly general polygonal/polyhedral meshes, including “hanging vertices” and non-convex shapes, retaining the conformity of the method, i.e. the property to build an approximated solution which shares the same regularity features as the analytical solution of the problem under consideration [1,2]. In many interesting cases, this means that the discrete solution is continuous across adjacent elements. Owing to the powerful features of the VEM in relation with mesh generation and enhanced topological tools, the analysis will point to assessing accuracy and efficiency in the aforementioned computational fracture mechanics problem presenting a comparison with more established techniques [3]. In particular, the analysis will point out some interesting issues made possible using the innovative method, which are more cumbersome when resorting to standard FEM, namely the easiness of fracturing and segmenting existing elements whenever a fracturing path crosses them. Based on a wide variety of material models and fracture domain setups, an extensive numerical campaign will show the efficiency and accuracy of the proposed methodology which can then be seen as a powerful alternative classical methods. References [1] L. Beirão da Veiga, F. Brezzi, A. Cangiani, G. Manzini, L. D. Marini, and A. Russo, Basic principles of virtual element methods, *Math. Models Methods Appl. Sci.* 23 (2013), no. 1, 199–214. [2] E. Artioli, L. Beirão da Veiga, C. Lovadina, and E. Sacco, Arbitrary order 2D virtual elements for polygonal meshes: Part I, elastic problem, *Computational Mechanics* (2017), doi:10.1007/s00466–017–1404–5. [3] Moës, Nicolas; Dolbow, John; Belytschko, Ted (1999). “A finite element method for crack growth without remeshing". *International Journal for Numerical Methods in Engineering*. 46 (1): 131–150.

Investigating the Role of Interventricular Interdependence in Development of Right Heart Failure during LVAD Support: A Finite-element Methods-based Approach

Kevin L. Sack*, Thomas Franz**, Daniel Burkhoff***, Julius Guccione****

*University of California, San Francisco, USA, **University of Cape Town, South Africa, ***Columbia University, USA, ****University of California, San Francisco, USA

ABSTRACT

Patients with end-stage heart failure have limited treatment options and an extremely poor prognosis. The use of left ventricular assistance devices (LVADs) as a therapy offers much needed mechanical assistance to the left ventricle (LV) of these patients. However right heart failure, a substantial related adverse effect, occurs in 10-40% of LVAD patients, shortening their long-term morbidity and mortality [1]. Although the potential implications of ventricular interactions on right ventricle (RV) function during LVAD support are well appreciated, due to the mechanical complexity involved, no study has yet proven, in any setting, that LV unloading and septal shift can actually lead to RV failure. Computational modeling is well suited to investigate and elucidate the individual contributions of these primary hemodynamic factors. To investigate this LV-RV interdependence, we extend on our previous work [2] by introducing a patient-specific finite-element model of dilated chronic heart failure. This model consists of coupled subsystems describing ventricular wall mechanics and lumped circulatory fluid flow. The material parameters were calibrated using patient-specific clinical data, producing a realistic mechanical surrogate of the failing in vivo heart that predicts its dynamic strain and stress throughout the cardiac cycle. The coupled model of lumped circulatory flow was modified to include additional fluid exchanges between the LV and the systemic circuit, which simulate ventricular assistance. These incorporate experimentally recorded flow data for the HeartMate II LVAD a commonly used LVAD operating between 8k– 12k RPM. Our findings show that LVAD operation reduces myofiber stress in the LV (14.6 ± 8.0 vs. 5.26 ± 5.86 kPa) (no intervention vs. 12k RPM LVAD) and, to a lesser extent, RV free wall, while increasing leftward septal-shift with increased operating-speeds. These improvements were achieved with secondary, potentially negative effects on the interventricular septum which showed that LVAD support introduces unnatural bending of the septum and with it, increased localized stress regions. LVAD operation unloads the LV significantly and shifts the RV pressure-volume-loop toward larger volumes and pressures (19.5 vs. 24.1 mmHg) (no intervention vs. 12k RPM LVAD); a consequence of RV-LV interactions and increased flow to the systemic circuit. References 1. Hayek, S., et al., Assessment of right ventricular function in left ventricular assist device candidates. *Circulation: Cardiovascular Imaging*, 2014. 7(2): p. 379-389. 2. Sack, K.L., et al., Partial LVAD restores ventricular outputs and normalizes LV but not RV stress distributions in the acutely failing heart in silico. *Int J Artif Organs*, 2016. 39(8): p. 421-430.

On the 3D Mechanical Properties of Passive Myocardium Using a Novel Numerical-experimental Inverse Modeling Approach

Michael Sacks*, David Li**, Reza Avaz***

*University of Texas at Austin, **University of Texas at Austin, ***University of Texas at Austin

ABSTRACT

Recent studies have demonstrated the utility of the injection of biomaterials into the heart infarct region as bulking agents. Despite promising initial success, optimization of the mechanical characteristics and injection patterns of these polymers is limited by a lack of biomechanical knowledge of the remodeling events that occur as a result of MI and physical support by the injectate. We employed a novel 3D integrated numerical/experimental approach to apply 3D deformations to single soft tissue specimens, for characterizing the stress-strain response of non-contracting, healthy, drained LV myocardium. We developed an optimal set of displacement paths based on the full 3D deformation gradient tensor. We also performed studies on specimens injected with dual-crosslinked hyaluronic acid (HA)-based hydrogels. Diffusion tensor MRI was used to determine the local 3D orientation of myofibers. We then utilized an inverse finite element (FE) simulation of the experimental configuration embedded in a parameter optimization scheme for estimation of the SEDF parameters. Notable features of this approach include: (i) enhanced determinability and predictive capability of the estimated parameters following an optimal design of experiments, (ii) accurate simulation of the experimental setup and transmural variation of local fiber directions in the FE environment, and (iii) application of all displacement paths to a single specimen. Our results indicated that, in contrast to the common approach of conducting pre-selected tests and choosing an SEDF a posteriori, the optimal design of experiments integrated with a chosen SEDF and full 3D kinematics, leads to a more robust characterization of the mechanical behavior of myocardium. Resulting responses showed clearly nonlinear, fairly anisotropic, and slightly hysteretic behavior of the viable myocardium. We also confirmed detectable stiffening in mechanical behavior for samples injected with the HA hydrogel, which was also noted to stiffen the tissue anisotropically. To our knowledge, this work is the first of its kind on the robust fully 3D modeling of the tissue-level mechanical properties of viable myocardium. We found that the inclusion of optimal design of experiments was critical in our inverse model to minimize the dependence of the estimated values of the SEDF constants on the applied boundary conditions, and therefore to improve the predictive capability of the SEDF to capture the behavior of the myocardium under general in-vivo loading conditions. The results from this study will guide the development of a robust, clinically relevant organ-level model of injection therapies for the optimization of minimally invasive treatment of the post-MI heart.

A Macro-micro Modeling Approach to Determine In-situ Heart Valve Interstitial Cell Contractile Behaviors in Native and Synthetic Environments

Michael Sacks*

*University of Texas at Austin

ABSTRACT

Mechanical forces are known to regulate valve interstitial cell (VIC) functional state by modulating their biosynthetic activity, translating to differences in tissue composition and structure, and potentially leading to valve dysfunction. VICs can change phenotype dynamically; in diseased valves VICs switch to a myofibroblast-like phenotype and become contractile. Activated VICs display prominent SMA stress fibers and an increase in ECM remodeling. Yet, while advances have been made toward the understanding of VIC behavior ex-situ, the VIC biomechanical state in its native extracellular matrix (ECM) remains largely unknown. We hypothesize that improved descriptions of VIC biomechanical state in-situ, obtained using a macro-micro modeling approach, will provide deeper insight into VIC interactions with the surrounding ECM, revealing important changes resulting from pathological state, and possibly informing pharmaceutical therapies. To achieve this, a novel integrated numerical-experimental framework to estimate VIC mechanobiological state in-situ was developed. Flexural deformation of intact valve leaflets was used to quantify the effects of VIC stiffness and contraction at the tissue level. In addition to being a relevant deformation mode of the cardiac cycle, flexure is highly sensitive to layer-specific changes in VIC biomechanics. As a first step, a tissue-level bilayer model that accurately captures the bidirectional flexural response of AV intact layers was developed. Next, tissue micromorphology was incorporated in a macro-micro scale framework to simulate layer-specific VIC-ECM interactions. The macro-micro AV model enabled the estimation of changes in effective VIC stiffness and contraction in-situ that are otherwise grossly inaccessible through experimental approaches alone. While the use of native tissues provided much insight, we also utilized 3-D hydrogel encapsulation, which is an increasingly popular technique for studying VICs. Specifically, we employed poly(ethylene glycol) (PEG) gels to encapsulate VICs and study their mechanical response to the surrounding hydrogel stiffness and to varying levels of adhesion availability. Cell contraction was elicited through chemical treatments and the resulting mechanical properties of the constructs were measured through end-loading flexural deformation testing. We applied the downscale model, which was improved by 3D stress fiber visualization. The resulting cell force levels were comparable to native in-situ results. Overall, the developed numerical-experimental methodology can be used to obtain VIC properties in-situ. Most importantly, this approach can lead to further understanding of VIC-ECM mechanical coupling under various pathophysiological conditions and the investigation of possible treatment strategies targeting the myofibroblast phenotype characteristic of early signs of valvular disease.

Coupling Crystal-Plasticity Phase Field and Extended Finite Element Methods for Efficient Modeling of Fatigue Crack Initiation and Propagation

Alireza Sadeghirad^{*}, Kasma Momeni^{**}, Yanzhou Ji^{***}, Xiang Ren^{****}, Long-Qing Chen^{*****}, Jim Lua^{*****}

^{*}Global Engineering and Materials, Inc., ^{**}The Pennsylvania State University; Louisiana Tech University, ^{***}The Pennsylvania State University, ^{****}Global Engineering and Materials, Inc., ^{*****}The Pennsylvania State University, ^{*****}Global Engineering and Materials, Inc.

ABSTRACT

To model fatigue crack initiation and short crack within a grain or across grains, understanding behavior of the crack at microstructural level, considering the effects of crack size, shape, grain boundaries, and other microstructural features, is required. For this purpose, we integrated the phase field (PF) approach and the crystal plasticity (CP) theory following our recent coupling technique in the framework of the fast Fourier transform (FFT). Advantages of this coupled method include: (1) the PF and CP models are seamlessly coupled since both models use the FFT algorithm and (2) the spectral FFT formulation greatly reduce the computation cost at acceptable accuracy levels. We employed the coupled method to characterize realistic microstructures based on the electron backscatter diffraction (EBSD) data, and predict the fatigue micro-crack initiation using a microstructure-based failure model. The remaining issue is that the computational cost, associated with micro-mechanics simulation of crack initiation and propagation, is prohibitively large for length scales greater than a few millimeters. Noting that the effects of microstructural features are profound mainly for fatigue crack initiation and short-crack growth in metals justifies application of much more efficient linear elastic fracture mechanics (LEFM) modeling techniques for simulation of long-crack growth, e.g. the extended finite element method (XFEM). We developed a multiscale technique for unified fatigue crack initiation and propagation modeling in metallic alloys by combining two simulation techniques: (1) the coupled FFT-PF/CP method at micro-scale to simulate fatigue crack initiation taking into account the important microstructural features, and (2) the XFEM method at macro-scale to simulate fatigue long-crack growth. The motivation for this coupled modeling technique is to take advantage of the strengths of each method to physics-based predictions. A sequential coupling has been accomplished where the hot spots at each cyclic loading increment are determined using the XFEM model. The associated stress/strain values are then passed to the unit-cell PF model for accurate physics-based microstructure modeling and prediction of plasticity induced crack initiation. The accurate micromechanics model predicts the number of cycles for the crack initiation and the analytical crack growth models will be employed to propagate the initiated crack by the appropriate length to be inserted in the FE mesh. Finally, the XFEM method will be employed for the final stage of long crack growth prediction. Some numerical examples demonstrate the effectiveness of the proposed multiscale method.

Computational Modeling of the Intracellular Retrograde Flow During Cell Migration

Pablo Saez^{*}, Saskia Loosveldt^{**}, Kiran Sagar^{***}, Paris Mulye^{****}

^{*}Universitat Politecnica de Catalunya, ^{**}Universitat Politecnica de Catalunya, ^{***}École centrale de Nantes,
^{****}École centrale de Nantes

ABSTRACT

Actin dynamic is a key player in cell motility and migration [1]. Understanding the actin turnover at different spatial and temporal scales is of profound relevance in biology because it is involved in fundamental biological processes, e.g. in embryogenesis or wound healing. The retrograde flow protrudes the leading edge; one of the main exploratory mechanisms in the cell migration. The continuous flow of cellular components moves backward from the leading edge to the rear of the cell. This retrograde flow is conditioned by the actin polymerization against the plasma membrane and pushing forces exerted by myosin motors. Actin monomers polymerize rapidly after a period of slow nucleation. The resulting actin filaments undergo a complex reaction while forming and disassembling, providing a pool of new actin monomer [1]. Experimental cell biology has made the greatest progresses in understanding the actin turnover cycle and in the dynamic of the retrograde flow. Mathematical theories and computational models are highly reliable, low-cost and reliable tools to foster new insights and answer open questions in cellular motility. Complete mathematical models have also been proposed however the computational modeling of the cell migration has not been still extensively developed in literature. Pollard and co-workers [2] established the mathematical foundations of actin polymerization and depolymerization. Mogilner and coworkers, among many others, moved the field further with complete mathematical models [3]. Today, many question remain open in field of cell motility and migration. In this work, we have adopted a model of the main mechanisms involved in the dynamic of the retrograde flow and developed a fully coupled finite element model. We have focused on fast motile cells where the protrusion and the retrograde flow are steady during migration. We have reproduced some experimental results in literature. Furthermore, we modeled a number of flow responses under the effect of the manipulation of different assembly and disassembly rates. Using standard numerical techniques to solve complex models of actin turnover and cell motility opens tremendous opportunities in the understanding of cell migration. [1] T. D. Pollard and J. A Cooper. Actin, a central player in cell shape and movement. *Science*, 326(5957):1208–12, 2009. [2] T. D. Pollard. Rate constants for the reactions of ATP-and ADP-actin with the ends of actin filaments. *J. Cell Biol.*, 103(6):2747, 1986. [3] A. Mogilner and L. Edelstein-Keshet. Regulation of actin dynamics in rapidly moving cells: a quantitative analysis. *Biophys. J.*, 83(3):1237–1258, 2002.

MultiscaleHub: A Web-enabled Platform for Multiscale Modeling and Analysis of Materials

Masoud Safdari^{*}, Jacob Fish^{**}

^{*}Illinois Rocstar LLC, ^{**}Columbia University

ABSTRACT

In the current work, we present design, formulation, and prototyping of MultiscaleHub, a web-enabled platform for multiscale modeling and analysis of materials and chemistry. MultiscaleHub's design was performed based on previously published similar works. An established framework for multiscale discrete-to-continuum coupling was adopted in the formulation of MultiscaleHub. To simplify future development, a modular, extensible, and object-oriented structure was designed and implemented for MultiscaleHub. In the current form, the package provides general-purpose methods, data structure, tools and algorithms for encapsulating uniscale solvers, multiscale coupling, and analysis. A pair of open source atomistic and continuum computational physics solvers were selected and coupled together with MultiscaleHub. The preliminary capabilities of the package in solving multiscale structural and thermal problems were demonstrated using a series of illustrative examples and case studies. A web module and interface were designed and implemented for MultiscaleHub to providing Internet access to the package. The feasibility of delivering MultiscaleHub tools and capabilities on the web was demonstrated using a battery of preliminary example problems.

Machine Learning Materials Physics: Homogenization of Computed Martensitic Microstructures by Deep Neural Networks

Koki Sagiyama^{*}, Krishna Garikipati^{**}

^{*}University of Michigan, ^{**}University of Michigan

ABSTRACT

In this work, we study deep neural networks as a paradigm for abstracting the complexity of martensitic microstructures. This investigation is part of a larger exploration of the roles of machine learning in materials physics. The martensitic microstructures in our study are obtained by direct numerical simulations in three dimensions, based on non-convex elastic free energy functions. This model is regularized by Toupin's theory of gradient elasticity at finite strains. The computations use Isogeometric Analysis for the high-order continuity of spline basis functions, and fully resolve the laminae of martensitic variants [1,2]. The effective elastic response of the martensitic microstructures is explored to generate training data for standard deep neural network (DNN) representations of the constitutive relations. With the Lagrange strain components as features, we train DNNs for both: the nonlinear stress-strain response and the elastic free energy density function. Questions of symmetry representations and constitutive theory are addressed in the context of the DNNs. Finally, in order to accommodate arbitrary martensitic microstructures, we consider extensions of the feature vector to include microstructural variables. [1] Sagiyama, K., Garikipati, K., Unconditionally stable, second-order schemes for gradient-regularized, non-convex, finite-strain elasticity modeling martensitic phase transformations. (in review). [2] Sagiyama, K., Rudraraju, S., Garikipati, K., A numerical study of branching and stability of solutions to three-dimensional martensitic phase transformations using gradient-regularized, non-convex, finite strain elasticity. arXiv:1701.04564 (2017).

Euler-Lagrange Prediction of Aerosol Particle Transport and Deposition in Terminal Airways

Suvash Saha*, Mohammad Islam**

*School of Mechanical and Mechatronic Engineering, Faculty of Engineering and Information Technology, University of Technology Sydney, Ultimo NSW 2007, Australia, **School of Mechanical and Mechatronic Engineering, Faculty of Engineering and Information Technology, University of Technology Sydney, Ultimo NSW 2007, Australia

ABSTRACT

The knowledge of the complex aerosol transport procedure through the human respiratory system is important for dosimetry and respiratory health effects analysis. The studies over the last few decades have improved the understanding of the aerosol particle transport in the extra-thoracic and upper airways. However, almost all of the studies have predicted the particle transport and deposition for non-realistic anatomical model. A detail and complete prediction of the pharmaceutical aerosol transport and deposition in the terminal bronchioles of a large-scale whole lung model is still unknown. This study considered a large-scale realistic anatomical model to predict the deposition pattern in the terminal airways. High-resolution CT-DiCom images are used to construct the realistic anatomical model. Finite volume based ANSYS Fluent (18) solver is used to simulate the particle transport and deposition in the terminal airways. The micro-particle deposition pattern shows a new deposition hot spot for the realistic model, which could help the targeted drug delivery in the respiratory airways. The nanoparticle transport and deposition are also investigated for the large-scale model. The numerical study showed different deposition hot spot for different lobes. The deposition efficiency in the different lobes is different for different flow rates, which could help with the health risk assessment of respiratory diseases and eventually could help the targeted drug delivery system

A High Resolution Multiscale Model to Study Drug-induced Arrhythmias

Francisco Sahli Costabal*, Jiang Yao**, Ellen Kuhl***

*Stanford University, **Dassault Systemes Simulia Corp, ***Stanford University

ABSTRACT

Drugs often have undesired side effects. In the heart, they can induce lethal arrhythmias such as torsades de pointes. The risk evaluation of a new compound is costly and can take a long time, which often hinders the development of new drugs. Here we establish a high resolution, multiscale computational model to quickly assess the cardiac toxicity of new and existing drugs. The input of the model is the drug-specific current block from single cell electrophysiology; the output is the spatio-temporal activation profile and the associated electrocardiogram. We demonstrate the potential of our model for a low risk drug, ranolazine, and a high risk drug, quinidine: For ranolazine, our model predicts a prolonged QT interval of 19.4% compared to baseline and a regular sinus rhythm at 60.15 beats per minute. For quinidine, our model predicts a prolonged QT interval of 78.4% and a spontaneous development of torsades de pointes both in the activation profile and in the electrocardiogram. Our model reveals the mechanisms by which electrophysiological abnormalities propagate across the spatio-temporal scales, from specific channel blockage, via altered single cell action potentials and prolonged QT intervals, to the spontaneous emergence of ventricular tachycardia in the form of torsades de pointes. Our model could have important implications for researchers, regulatory agencies, and pharmaceutical companies on rationalizing safe drug development and reducing the time-to-market of new drugs.

Adaptive Construction of Locally Anisotropic Spectral Discretization for Stochastic PDEs

Onkar Sahni^{*}, Joseph Lapierre^{**}, Vignesh Srinivasaragavan^{***}, Jason Li^{****}

^{*}Rensselaer Polytechnic Institute, ^{**}Rensselaer Polytechnic Institute, ^{***}Rensselaer Polytechnic Institute,
^{****}Rensselaer Polytechnic Institute

ABSTRACT

Many multi-physics stochastic problems of interest exhibit anisotropic behavior in that some stochastic directions are more prominent than others. Furthermore, this behavior changes in a local fashion in the physical space. For example, in a local physical region, only a few stochastic directions have significant influence on the solution while the remaining majority of stochastic directions have zero to marginal influence. However, in a different physical region, other stochastic directions show significance. Such problems can be efficiently resolved by employing anisotropic adaptivity as not all stochastic directions require the same level of resolution to control the discretization error. In this presentation we will focus on the formulation and application of an anisotropic adaptive approach for stochastic PDEs with uncertain input data. In this approach, we employ finite element basis in the physical domain and spectral basis (based on generalized polynomial chaos) in the stochastic domain. Our approach is based on the variational multiscale (VMS) method for this basis setting. In the VMS method, the effect of missing/fine scales on resolved/coarse scales is modeled as an algebraic approximation within each element using the strong-form residual and a stochastic stabilization parameter. In addition, a model term of a similar form is derived to estimate the error in the numerical solution in a local/element-wise fashion. Variance-based sensitivity analysis is applied on the element-wise error to devise an anisotropic indicator. This anisotropic indicator is used in conjunction with the estimated measure of the local error to adaptively control the order of the spectral basis in each dimension of the stochastic space independently, resulting in anisotropic stochastic adaptivity. In summary, our approach is designed for the adaptive construction of locally anisotropic spectral discretizations for stochastic PDEs. We demonstrate the effectiveness of our approach on multiple example cases including transport problems where locally in the physical space the stochastic behavior is anisotropic.

Smart Constrained Layer Damping Analysis of Laminated Plates by Meshfree Method

Soumya Sahoo*

*Indian Institute of Technology, Kharagpur-721302, India

ABSTRACT

In this article, the performance of advanced piezoelectric composite (PZC) based smart constrained layer damping (SCLD) treatment is analysed in controlling vibration of laminated composite plates. The overall structure is comprised of a substrate laminated plate integrated with a viscoelastic layer and a piezoelectric composite layer attached partially or fully at the top surface of the plate. A mesh free (FE) model is formulated based on the element free Galerkin method to study the dynamic behaviour of the laminated composite plates with regular and irregular shaped SCLD treatments within the framework of a first order layer wise displacement field theory. Both symmetric cross-ply and antisymmetric angle-ply laminated plates are considered for the numerical analysis. It is observed that SCLD treatment significantly improves the active damping properties of the substrate plate. The numerical results also reveal that the performance of irregular shaped SCLD patches are more effective in controlling vibration of the laminated composite plates than the regular rectangular ones. Keywords: SCLD, vibration analysis, element free galerkin method, composite structure, laminated plate, layerwise plate theory

An Arbitrary Lagrangian--Eulerian Finite Element Formulation for Lipid Membranes

Amaresh Sahu^{*}, Yannick Omar^{**}, Roger Sauer^{***}, Kranthi Mandadapu^{****}

^{*}UC Berkeley, ^{**}RWTH Aachen University, ^{***}RWTH Aachen University, ^{****}UC Berkeley

ABSTRACT

Biological membranes comprised of lipids and proteins make up the boundary of the cell, as well as the boundaries of internal organelles such as the nucleus, endoplasmic reticulum, and Golgi complex. Lipid membranes, however, pose significant modeling challenges because they bend elastically out-of-plane yet flow in-plane as a two-dimensional fluid. In this work, we present the continuum mechanical equations of motion of an arbitrarily curved and deforming lipid bilayer. We then provide the theory underlying a novel arbitrary Lagrangian--Eulerian description of evolving two-dimensional surfaces, in which the in-plane and out-of-plane behavior can be treated differently. Finally, we demonstrate the utility of this description within an isogeometric finite element framework with C1-continuous basis functions. We apply the framework to study membrane shapes during endocytosis, and discuss how our framework can model large in-plane flows and their coupling to out-of-plane deformations.

Thermo-Mechanical Modelling of HTP Process: Prediction of Martensite Formation in Pearlitic Rail Steel

Loïc Saint-Aimé*, Aurélien Saulot**, Frédéric Lebon***, Grégory Antoni****

*IRT Railenium / INSA-Lyon / LaMCoS, **INSA-Lyon / LaMCoS, ***Université de Provence / LMA, ****Université de Provence / LMA

ABSTRACT

For about twenty years, some rails of railway network have been affected by a phenomenon called Tribological Surface Transformation (TST). These TSTs correspond to a permanent, quasi-surfacic solid-solid phase transformation, e.g. pearlitic-martensitic transformations. They are characterized by the formation of a thin white layer progressively appearing, in proportion to the number of loading cycles, on the near-surface of the rail. In the worst cases, and for a number of cycles depending on both the material and the loading, TSTs can eventually lead to the emergence of a crack, due to strong strain incompatibilities between the quasi-surfacic, "white phase" (e.g. martensite) and the volumetric, "bulk" phase (e.g. pearlite). Initially attributed to flash temperatures generated by frictional heating at the contact zone, followed by subsequent quenching, several studies have shown that the temperature increase is often too low to explain these phase transformations. Thus it is not unrealistic to assume that TSTs could result from a thermo-mechanical coupling; this is actually the main assumption underlying our study. In order to describe these TSTs, we propose a thermo-mechanical model based on previous work [Leblond et al. (1989)] for TRansformation Induced Plasticity (TRIP), which, however, are here extended for a thermo-mechanical coupling, relevant for TSTs, to be taken into account. Under rolling contact loading, rails are subjected to significant hydrostatic pressure simultaneously with shearing stress that could induce material transformations. With the aim to reproduce similar loading conditions High Pressure Torsion (HPT) experiments were conducted on the standard rail grade R260. Our purpose was to quantitatively assess load parameters (i.e., high pressure, shear and/or temperature) that could lead to WEL development. Therefore, these experimental data were used to calibrate the phenomenological thermo-mechanical model. Simulation of the HPT process has been the subject of a few studies with focus on the material behaviour and plastic flow as well as stress state and contact conditions between the sample and the anvils. However, the focus was on prediction of volume changes during phase transformation and the associated strain hardening. Hence the HPT process was simulated with the commercial FE software ABAQUS using an axi-symmetric model of the sample whose the material behaviour has been implemented as user material subroutines (UMAT). Good agreement between simulations and experimentally obtained stress-strain curves was achieved. Otherwise, the model was able to predict the emergence and progress of TSTs near the contact areas where the thermo-mechanical loading is applied.

Plastic Deformation Behavior in Nano-sized Metallic Wires Subjected to Drawing Process: Molecular Dynamics Simulation

Ken-ichi Saitoh^{*}, Kosuke Oda^{**}, Koki Yoshida^{***}, Tomohiro Sato^{****}, Masanori Takuma^{*****},
Yoshimasa Takahashi^{*****}

^{*}Kansai University, Faculty of Engineering Science, ^{**}Kansai University, Graduate School of Engineering(Student),

^{***}Kansai University, Graduate School of Engineering(Student), ^{****}Kansai University, Faculty of Engineering Science, ^{*****}Kansai University, Faculty of Engineering Science, ^{*****}Kansai University, Faculty of Engineering Science

ABSTRACT

The process of nano-sized wiredrawing is investigated by using molecular dynamics (MD) simulation in this study. Recently, in industrial wiredrawing process, a diameter of wire is going smaller and smaller such down to just several micrometers. It is supposed that this leads to a future demand of thin wire and an adequate mechanical process to produce it. The authors have constructed novel computation models of wiredrawing, in which a single wire has axisymmetric shape and is just a several nanometers in dimension (i.e. nano-sized wire). In those material models, a perfectly rigid or flexible die is attached to the wire so that the wire is smoothly drawn through it and is deformed to be thinner one. In MD simulations, all equations of motion for each atoms are solved numerically by using an interatomic potential which reproduces the needed properties for the simulated material. A many-body (EAM or MEAM method) and pairwise potential, both for pure iron (alpha-Fe) and iron-carbon binary (for pearlitic steel) systems, are adopted in this study. From MD results of the wiredrawing, we capture the dislocation mechanism inherent to nano-sized wire. According to crystalline orientations of drawing, the behavior of nucleated dislocations is quite different. We clarify that not only von Mises equivalent stress but also regional hydrostatic stress takes large effect on nucleation and subsequent motion of dislocations. We will also discuss an idea of aging status of each atom which is actually the history of atomistic and plastic stress or strain. By pearlite steel wire model, it is realized that the ferrite-cementite interface effectively offers high-speed paths for carbon atoms to diffuse from cementite to ferrite (it is called cementite decomposition in real system). It is observed that, when carbons diffuse, both ferrite and cementite crystals undergoes effectively microscopic plastic deformation, i.e. emission, movement, interaction and annihilation of many dislocations, as well as phase transition.

Technology of AI Aided Development for Electronic Devices

Akira Sakai^{*}, Tomo Kaniwa^{**}, Nobuyoshi Yamaoka^{***}, Serban Georgescu^{****}, Makoto Sakairi^{*****}

^{*}Fujitsu Advanced Technologies, ^{**}Fujitsu Advanced Technologies, ^{***}Fujitsu Advanced Technologies, ^{****}Fujitsu Laboratories of Europe, ^{*****}Fujitsu Advanced Technologies

ABSTRACT

Artificial Intelligence (AI) in the form of deep learning has made rapid progress during this decade and it started to influence a broad spectrum of technologies. We consider that “extended CAE technology” includes not only conventional CAD &&&& simulation technology but also AI. This presentation introduces three concrete examples of our contributions to extended CAE technology. (1) Predicting the number of substrate layers. Due to the recent progress in miniaturization and high performance of electronic devices, the number of necessary substrate layers has been increasing. However, predicting the number of necessary substrate layers largely relies on the skill of engineers. To make this task simple for everyone, we have developed a technology to predict the number of layers of the substrate by using Support Vector Machine (SVM), a machine learning technique. Furthermore, we confirmed that the required number of layers of the substrate can be correctly predicted with the probability of 96% by using this technology. (2) Component recognition of a 3D-object in a CAD system. 3D-CAD is frequently used in designing of electronic devices. However, there are cases where the labels for identifying the components are not attached making it necessary to manually check the components with defects. We have developed a technique to classify the 3D-components by recognizing them with 2D images to identify unlabeled components. By using this technology, we have achieved a probability of 96% in finding screw components. (3) Optimization technique combining AI and a genetic algorithm. The application of optimization technology to electronic device design has been actively discussed. However, optimization algorithms, including genetic ones, require hundreds of simulations, making it difficult to apply them in practice. One example of such problems is the optimization of the hole positions on the server. This belongs to the class of combinatorial optimization problems, which are regarded as the most difficult in the field. To solve this problem, we have developed method to accelerate the convergence of genetic algorithms by giving prerequisite knowledge using AI which leads to a reduction of the number of simulations. Finally, we are going to introduce the future prospects gained from our experiences.

Discrete Element Simulation for Industrial Applications

Mikio Sakai*

*The University of Tokyo

ABSTRACT

Abstract The discrete element method (DEM) is widely used in the simulations of industrial granular and multi-phase flows. Very recently, an innovative approach was developed by my group, where the DEM, computational fluid dynamics (CFD), signed distance functions [1], immersed boundary method [2] and coarse grain model [3] were employed. This approach makes it possible to simulate several complex and large-scale systems easily, e.g., a fluidized bed [3], die-filling for fine particles [4] and a wet ball milling [5]. This is because scaling law model can simulate an enormous number of particles with low calculation cost and because the arbitrary shape wall can be created by a simple algorithm. Adequacy of this approach was shown through the validation tests. References [1] Y. Shigeto, M. Sakai, "Arbitrary-shaped wall boundary modeling based on signed distance functions for granular flow simulations," Chem. Eng. J., 231, 464-476 (2013) [2] X. Sun, M. Sakai, "Immersed boundary method with artificial density in pressure equation for modelling flows confined by wall boundaries," J. Chem. Eng. Jpn., 50, 161-169 (2017) [3] M. Sakai, M. Abe, Y. Shigeto, S. Mizutani, H. Takahashi, A. Vire, J.R. Percival, J. Xiang, C.C. Pain, "Verification and validation of a coarse grain model of the DEM in a bubbling fluidized bed," Chem. Eng. J., 244, 33-43 (2014) [4] H. Yao, Y. Mori, K. Takabatake, X. Sun, M. Sakai, "Numerical investigation on the influence of air flow in a die filling process," J. Taiwan Inst. Chem. Eng. (accepted) [5] M. Sakai, "How should the discrete element method be applied in industrial systems?: A review," KONA Powder and Particle Journal, 33, 169-178 (2016)

Three-dimensional Phase-field Simulations during Directional Solidification of a Binary Alloy Considering Thermal-solutal Convection

Shinji Sakane^{*}, Tomohiro Takaki^{**}, Munekazu Ohno^{***}, Yasushi Shibuta^{****}, Takayuki Aoki^{*****}

^{*}Kyoto Institute of Technology, ^{**}Kyoto Institute of Technology, ^{***}Hokkaido University, ^{****}The University of Tokyo,
^{*****}Tokyo Institute of Technology

ABSTRACT

In terrestrial solidification of an alloy, a thermal-solutal convection inevitably occurs due to a liquid density difference caused by the special distribution of temperature and solute concentration in liquid. However, the thermal-solutal convection is usually not considered in simulations for predicting a solidification microstructure, because it needs large computational cost. Depending on the solidification conditions, the thermal-solutal convection greatly influences on the interdendritic microsegregation, dendrite fragmentation, and dendrite morphology. Therefore, for numerically evaluating the effects of thermal-solutal convection on the solidification microstructures, it is essential to enable a simulation taking into account all fields which occur during solidification, such as solute concentration, thermal field, and flow field. In this study, we develop a parallel computing code using multiple graphic processing units (GPU) to accelerate the phase-field simulations for dendrite growth of a binary alloy taking solute, thermal, and fluid fields into account. Then, the parallel efficiency and computational cost are evaluated for conditions with and without thermal and fluid fields. Moreover, we investigate the effects of thermal and fluid fields on the dendrite morphology and microsegregation during directional solidification of a binary alloy. Because these simulations become large-scale, the simulations are performed using the GPU supercomputer TSUBAME3.0 at Tokyo Institute of Technology.

Multiscale Stochastic Stress Analysis of FRP with a Successive Sensitivity Analysis Considering Randomness in Multi Fibers Location

Sei-Ichiro Sakata*, Takuro Sakamoto**

*Kindai University, **Graduate School of Kindai University

ABSTRACT

In this presentation, a multiscale stochastic stress analysis of composites considering microscopic geometrical randomness (location variation of inclusions) is discussed for estimation of the probabilistic properties of the maximum microscopic stresses. One of the reasons on uncertainty in an apparent strength of a composite material is randomness in microstructure. In particular, random variation of location of inclusions will have a large influence on its microscopic stress distribution, even if the influence on the homogenized elastic property is not so large [1]. For this problem, the Monte-Carlo simulation (MC) is one of standard approached, but because of some reasons, for instance computational costs, bias, or unclearness between the random variables and the responses, an effective computational method is needed. In particular, for the purpose of V&V or reliability-based optimization, non-MC method should be developed. For this purpose, from theoretical simplicity, the first, second or successive perturbation based approach is one of the attractive approaches. In previous reports, however, only one or two fibers variation were considered, and applicability of the perturbation-based approach to the problems was discussed [1]. These methods will be expensive and difficult to be applicable to a problem considering geometrical random variation when the number of random variables is large. From this background, a successive sensitivity analysis based approach is developed in this study. In this paper, random location variations of 3x3 fibers in a unit cell of a unidirectional fiber reinforced composite are considered as a first example, and the CV of the microscopic maximum stress is analyzed. For this problem, applicability of the proposed approach is discussed. In addition, the proposed approach is applied to a problem considering a unit cell including more fibers for a general case. As a numerical example, the proposed method is applied to the multiscale stochastic stress analysis of a unidirectional fiber reinforced composite plate under a tensile uniform load along transverse direction, and validity and effectiveness of the proposed method are discussed with comparison of the results of MC. [1] S. Sakata and I. Torigoe, "Multiscale Stochastic Stress Analysis for Randomness of Fiber Arrangement in Fiber Reinforced Composite Material", the proceedings of WCCM XI, 2014

Meso-mechanical Embedded Discontinuity Finite Element Modelling of Concrete Fracture Processes under Dynamic Loading

Timo Saksala*

*Tampere University of Technology, Tampere, Finland

ABSTRACT

This paper deals with numerical modelling of concrete fracture under dynamic loading. For this end, a 2D meso-mechanical model based on embedded discontinuity finite elements was developed. The aggregates are represented by polygons obtained by shrinking of Voronoi cells. The matrix, i.e. the mortar, and its failure are described by CST elements with three pre-embedded (before the analysis) discontinuities oriented parallel to the element edges. This approach is similar to the cohesive zone elements with the advantage of no need to double the nodes in the mesh since the embedded discontinuities are element-internal. The aggregates, also meshed with the CST elements, may fracture in mode-I and, consequently, a single discontinuity is embedded parallel to the first principal direction in the failing element inside an aggregate. The effect of the interfacial transition zone between the aggregates and the mortar matrix can be accounted for, to some extent, by lowering the strength of the elements in a narrow strip around the aggregates. The rate sensitivity is accommodated by adding a linear viscosity term to the static strength of an element. The finite element formulation of discontinuity kinematics is based on the enhanced assumed strains concept where the enhanced modes (variations of the crack opening displacement) are constructed in the strain space, orthogonal to the stress field. This formulation, with the CST element, results in a simple implementation where no crack length nor its exact location inside the element appears. Moreover, the multiple discontinuity approach alleviates, to some extent, the crack locking and spreading problems typical to low-order elements with embedded discontinuities. This kind of approach has two sources of heterogeneity. The first is the polygonal aggregates generated by shrinking of random seed Voronoi cells. The second source is the underlying non-structural CST mesh with (more or less) quasi-random triangle side orientations. As the finite elements representing the mortar have pre-embedded discontinuities parallel to the element sides, the strengths of the elements are quasi-random as well with respect to loading, say uniaxial compression for example. In the numerical examples, the performance of the model is demonstrated in uniaxial tension and compressive test simulations. The influence of the main parameters on the model behavior is tested. Finally, the dynamic Brazilian disc test is simulated. These simulations demonstrate that this kind of modelling approach is capable of capturing the salient features concrete under the various loading conditions.

Ocular Mathematical Virtual Simulator: A Hemodynamical and Biomechanical Study towards Clinical Applications

Lorenzo Sala^{*}, Christophe Prud'Homme^{**}, Giovanna Guidoboni^{***}, Marcela Szopos^{****}

^{*}IRMA UMR 7501, Université de Strasbourg, Strasbourg, France, ^{**}IRMA UMR 7501, Université de Strasbourg, Strasbourg, France, ^{***}Mizzou, University of Missouri, Columbia (MO), USA, ^{****}IRMA UMR 7501, Université de Strasbourg, Strasbourg, France

ABSTRACT

We present the development of a mathematical virtual simulator to model the interplay of biomechanics and hemodynamics in the human eye. This model provides a multiscale view of ocular physiology, in particular it simulates (i) the blood circulation in the retinal vasculature and the central retinal vessels via a circuit-based model, (ii) the blood perfusion within the lamina cribrosa via a porous-media model, and (iii) the biomechanical behavior of cornea, sclera, choroid, retina and lamina cribrosa via an isotropic linear elasticity system. Parts (ii) and (iii) within the lamina cribrosa are mathematically described by poro-elastic equations[1], whereas the coupling between the three-dimensional(3D) systems and the lumped-parameter circuit is achieved by employing an energy-preserving method in the spirit of [2]. To numerically solve the overall system, we implemented step (i) in OpenModelica and steps (ii) and (iii) in the multiphysics open-source platform Feel++ [3]. The 3D problem is solved by adopting a Hybridizable Discontinuous Galerkin (HDG) method, taking advantage of static condensation within the high performance computing environment developed in Feel++. In the present work, we aim to contribute to a better understanding of ocular neurodegenerative disease - in particular glaucoma, which is the second main condition that leads to blindness - in the context of biomedical research. Starting from clinically-measurable inputs of blood pressure, intraocular pressure and cerebrospinal fluid, the proposed virtual simulator is able to predict the main hemodynamical and biomechanical aspects of significant ocular components. In particular the model illustrates the spatial distribution of blood within the ocular tissues and the local displacement of the lamina cribrosa, which plays a crucial role in the pathogenesis of glaucoma. In addition, novel clinically relevant patient-specific insights can be obtained with respect to the central retinal vessels and other tissues of the eye included in the model. We envision this virtual simulator as a promising non-invasive clinical investigation tool in the biomedical context, after completion of thorough validation against experimental and clinical data. References: [1] Causin P et al. A poroelastic model for the perfusion of the lamina cribrosa in the optic nerve head. Mathematical biosciences. 2014. [2] Carichino L et al. Energy-based operator splitting approach for the time discretization of coupled systems of partial and ordinary differential equations for fluid flows: the Stokes case. Journal of Computational Physics. Submitted. [3] Sala L et al. An implementation of HDG methods with Feel++. Application to problems with integral boundary condition. In preparation.

Prestress Induced Phase Transitions In Tensegrity-Based Metamaterials

Hossein Salahshoor^{*}, Raj Kumar Pal^{**}, Julian Rimoli^{***}

^{*}Georgia Institute of Technology, ^{**}Georgia Institute of Technology, ^{***}Georgia Institute of Technology

ABSTRACT

Pre-stressing the cables of tensegrity structures is a widespread practice for enhancing their stability and mechanical properties. We chose a three dimensional tensegrity lattice [1] and have studied material symmetry phase transitions induced by varying the cable prestress. We studied several combinations of prestress cases and a vast regime of prestress values for each case. In each prestress scenario, we compute the effective elasticity tensor through a homogenization scheme. By examining the eigenspaces of the homogenized elasticity tensor, we study the material symmetries of the tensegrity lattice and characterize the effects of cable prestressing on it. We demonstrate symmetry breaking and phase transitions, occurring solely due to prestressing the members of our lattice. We observed several phase transitions including cubic to tetragonal and tetragonal to orthotropic and vice-verses. We also show that under a certain prestress condition, where the finite lattice exhibits orthotropic symmetry, we obtain tetragonal symmetry for the infinite lattice. This discrepancy in symmetries of the finite and infinite lattice is due to surface effects in finite size and the nonsymmorphic nature of the tensegrity lattice. Consequently, unlike the crystalline materials where surface effects increases the symmetries [2], we found a class of metamaterials where surface effects leads to symmetry reduction. [1] J. J. Rimoli, R. K. Pal, Mechanical response of 3-dimensional tensegrity lattices, Composites Part B: Engineering 115 (2017) 30{42. [2] P. Ayyub, V. Palkar, S. Chattopadhyay, M. Multani, Effect of crystal size reduction on lattice symmetry and cooperative properties, Physical Review B 51 (9) (1995) 6135.

Modeling of Crystal Plasticity by Using a Non-convex Energy Based on $GL(2, \mathbb{Z})$ Invariance

Oguz Umut Salman^{*}, Giovanni Zanzotto^{**}, Lev Truskinovsky^{***}, Roberta Baggio^{****}

^{*}CNRS/Paris 13, ^{**}Padova University, ^{***}CNRS/ESPCI, ^{****}ESPCI/Paris 13

ABSTRACT

For micro- and nano-sized samples, dislocation-mediated crystal plasticity is radically different from that described by classical engineering theories. At the microscale, plasticity evolves in a disordered manner through a sequence of intermittent events involving collective motion of dislocations and their interaction with each other and with existing lattice defects. Detailed mathematical modeling of these processes remains a major challenge in materials science. We present a mesoscopic post-DDD approach which involves constructing a coarse-grained non-convex energy invariant under the full symmetry group of lattices - such as $GL(2, \mathbb{Z})$ in the 2-d case. The model is thus informed by the inherent structure of the material, and is largely free of arbitrariness when dealing with the fast topological changes in dislocation configurations such as nucleation, annihilation, interaction with obstacles/other phases and with various other entanglements. We will also present an efficient numerical solver for the resulting equations.

A Phase Field Approach for Solid-state Dewetting

Marco Salvalaglio^{*}, Axdl Voigt^{**}, Rainer Backofen^{***}

^{*}TU Dresden, ^{**}TU Dresden, ^{***}TU Dresden

ABSTRACT

We consider a practical numerical scheme for a phase field approximation for surface diffusion to simulate solid-state dewetting phenomena. The scheme is based on a combined convexity splitting approach and a Rosenbrock method and uses a model with improved accuracy. We discuss modeling approaches to incorporate contact angles and show large scale simulations in comparison with experiments.

Optimization of Carbon Black Polymer Composite Microstructure for Rupture Resistance

Bingbing San^{*}, Haim Waisman^{**}

^{*}Hohai University, ^{**}Columbia University

ABSTRACT

In this manuscript, we study the optimal location of Carbon Black (CB) particle inclusions in a natural rubber (NR) matrix with the objective to maximize the rupture resistance of such polymer composites. Hyperelasticity is used to model the rubber matrix and stiff inclusions and the phase field method is used to model the fracture accounting for large deformation kinematics. A genetic algorithm is employed to solve the inverse problem in which three parameters are proposed as optimization objective, including maximum peak force, maximum deformation at failure-point and maximum fracture energy at failure-point. Two kinds of optimization variables, continuous and discrete variables, are adopted to describe the location of particles and several numerical examples are carried out to provide insight into the optimal locations for different objectives. The main conclusions from our studies are as follows: (i) location of particles has only a slight influence on the hardening part, but significantly affects the softening part after the peak force is reached; (ii) with the increase of particle numbers, the optimal position closet to notch is not changed, while other optimal position varies due to the inter-particle interactions; (iii) the location of particles does not change the overall crack propagation path; (iv) the fracture energy at failure-point is the most appropriate quantity to evaluate the effect of particle locations and yields most significant optimization results.

Influence of Microstructural Evolutions on Macroscopic Mechanical Behaviour of Cementitious Materials

Julien Sanahuja^{*}, Shun Huang^{**}, Luc Dormieux^{***}, Benoit Bary^{****}, Eric Lemarchand^{*****}

^{*}Edf lab Les Renardières, ^{**}Edf lab Les Renardières, ^{***}Ecole des Ponts ParisTech, ^{****}Den-Secr, CEA, Université Paris-Saclay, ^{*****}Ecole des Ponts ParisTech

ABSTRACT

Civil engineering facilities are, as any concrete structure, subject to ageing phenomena in association with environmental conditions, operating conditions and potential internal pathologies. Structure analysis and computations require relevant material constitutive models. The latter must integrate the influence of degradation, damage and ageing mechanisms. Such mechanisms often occur in pore space, or more generally at a much lower scale than the structure scale. This contribution examines the mechanisms associated to chemical processes. Through dissolution and precipitation, the latter induce progressive evolutions of microstructure. In turn, this microstructural evolution yields variations of the mechanical behaviour. Microstructure changes are thus the key linking the chemical processes occurring at lower scales to the mechanical behavior at the structure scale. To bridge the scales, micromechanics represents an appealing tool. Cementitious materials are the focus of this contribution, investigating both precipitation (due to hydration) and dissolution (due to leaching or hydration) mechanisms, and also elastic and creep behaviours. As far as upscaling is concerned, mean-field homogenization is used to benefit from its efficient computations. More precisely, when the considered behaviour does not involve time, such as elasticity, homogenization techniques can be readily used, on a time by time basis, to estimate the evolution of effective properties. But when the behaviour is intrinsically time-dependent, such as creep, modelling is much more involved as two processes coexist: microstructure evolution and the time-dependent individual behaviour of phases. The last part of this contribution proposes to take advantage of recent developments in micromechanics to investigate the influence of time-dependent microstructure changes, due to hydration, on the effective ageing viscoelastic behaviour of concrete. Model predictions are compared to experimental basic creep responses on VeRCoRs concrete loaded at various ages, and with a creep recovery experiment.

PDE-Constrained Optimization Framework and Inverse Design of Mechanical Metamaterials for Vibration Control

Clay Sanders^{*}, Timothy Walsh^{**}, Wilkins Aquino^{***}

^{*}Duke University, ^{**}Sandia National Laboratories, ^{***}Duke University

ABSTRACT

Harsh shock and vibration environments are commonly encountered in engineering applications involving dynamic loading. Acoustic/elastic metamaterials are showing significant potential as candidates for controlling wave propagation and isolating sensitive structural components. However, these materials have complex microstructures that must be properly designed to achieve their desired properties. In this talk we will present PDE-constrained, time and frequency-domain strategies for inverse design of elastic/acoustic metamaterials. A frequency-domain approach is typically the desirable strategy when designing band-gap or notch filter materials, whereas a time-domain strategy may be advantageous in a transient shock environment. For the frequency-domain optimization, a Modified Error in Constitutive Equation (MECE) objective function will be compared with the least squares counterpart in terms of effectiveness for designing a band-gap material. For the time-domain, a transient optimization formulation will be presented and demonstrated on a vibration isolation problem. Numerical examples will be presented on a variety of structural and acoustic cloaking scenarios. Sandia National Laboratories is a multimission laboratory managed and operated by National Technology and Engineering Solutions of Sandia, LLC., a wholly owned subsidiary of Honeywell International, Inc., for the U.S. Department of Energy's National Nuclear Security Administration. With main facilities in Albuquerque, N.M., and Livermore, C.A., Sandia has major R&D responsibilities in national security, energy and environmental technologies, and economic competitiveness.

Influence of Stress Triaxiality on Fracture Ductility for Stereolithography

Anjali Sandip*, Ravi Kiran Yellavajjala**

*University of North Dakota, **North Dakota State University

ABSTRACT

Stress triaxiality is one of the most important factors that controls fracture ductility [1]. The objective of this study was to investigate the influence of stress triaxiality on fracture ductility for specimens' printed using stereolithography. Dog bone shape specimens were printed using Formlabs® Form 2 Desktop SLA 3D printer. The specimens were built layer by layer with the help of this 3D printer. Each layer of liquid photopolymer is solidified through a computer-controlled ultraviolet (UV) light source with a laser spot size of 140 μm [1, 2]. A photopolymer resin supplied by the manufacturer which comprised of a proprietary mix of Methacrylated oligomers, Methacrylated monomer, photo initiators and trace amount of pigments and additives was used for printing the specimens. The length of the specimens was 92.06 mm and the width of the specimens in the gage length portion was 6 mm. Uniaxial tensile tests were conducted on 3D printed specimens. Numerical simulations of the uniaxial tensile tests were performed using the commercial finite element code, ABAQUS. Material properties of 3D printed specimens were calibrated using Abaqus/Isight. The stress triaxiality distribution in the critical cross section at a displacement corresponding to fracture displacement was evaluated. The maximum and average stress triaxialities at the critical cross section was recorded. Triaxiality versus equivalent strain to fracture was plotted for the tested specimens. The results indicate a strong dependence of fracture ductility on stress triaxiality for the 3D printed specimens investigated in this study. References: [1]. Bao, Y., & Wierzbicki, T. (2004). On fracture locus in the equivalent strain and stress triaxiality space. *International Journal of Mechanical Sciences*, 46(1), 81-98. [2]. Melchels, F. P., Feijen, J., & Grijpma, D. W. (2010). A review on stereolithography and its applications in biomedical engineering. *Biomaterials*, 31(24), 6121-6130. [3]. Crivello, J. V., & Reichmanis, E. (2013). Photopolymer materials and processes for advanced technologies. *Chemistry of Materials*, 26(1), 533-548.

Isogeometric Analysis and the k-refinement

Giancarlo Sangalli*

*Università di Pavia

ABSTRACT

k-refinement is one of the many great innovations proposed and promoted by Prof. Thomas J.R. Hughes. It has been described as one of the key features of isogeometric analysis, "a new, more efficient, higher-order concept", in the seminal work [1]. The idea of using high-degree and continuity splines (or NURBS, etc.) as a basis for a new high-order method appeared very promising from the beginning, and received confirmations from the next developments. k-refinement leads to several advantages: higher accuracy per degree-of-freedom, improved spectral accuracy, the possibility of structure-preserving smooth discretizations are the most interesting features that have been studied actively in the community. At the same time, the k-refinement brings significant challenges at the computational level: using standard finite element routines, its computational cost grows with respect to the degree, making degree raising computationally expensive. However, it has been understood recently that k-refinement is in fact superior from the point of view of computational efficiency, with respect to low-degree isogeometric discretizations, thanks to a proper code design that goes beyond standard finite element technology. I report the results obtained in collaboration with Mattia Tani, in [2]. In the proposed framework the k-refinement significantly improves not only the accuracy, but also the accuracy-to-computation-time ratio. The novelty is a matrix-free strategy, which is first used in this context but is well-known for other high-order methods. Matrix-free implementation speeds up matrix operations, and, perhaps even more important, greatly reduces memory consumption. Our strategy also employs the recently proposed weighted quadrature, which is an ad-hoc strategy to compute the integrals of the Galerkin system. The other key ingredient is a preconditioner based on the Fast Diagonalization method, an old idea to solve Sylvester-like equations. Numerical tests show that the new implementation is faster than the standard one (where the main cost is the matrix formation by standard Gaussian quadrature) even for low degree. But the main point is that, with the new approach, k-refinement leads to orders of magnitude faster execution, given a target accuracy. This is applicable to realistic differential problems, but its effectiveness will depend on the preconditioner stage, which is as always problem-dependent. [1] T.J.R.Hughes, J.A.Cottrell, Y.Bazilevs, Isogeometric analysis: CAD, finite elements, NURBS, exact geometry and mesh refinement, CMAME Volume 194, Issues 39–41, 1 October 2005, Pages 4135-4195 [2] G. Sangalli, M. Tani, Matrix-free isogeometric analysis: the computationally efficient k-method, arXiv:1712.08565

Utilizing Machine Learning and a Data-Driven Approach to Identify the Fatigue Crack Driving Force in Polycrystalline Materials

Michael Sangid^{*}, Andrea Rovinelli^{**}, Henry Proudhon^{***}, Ricardo Lebensohn^{****}, Wolfgang Ludwig^{*****}

^{*}Purdue University, ^{**}Purdue University, ^{***}Mines ParisTech, ^{****}Los Alamos National Lab, ^{*****}University of Lyon

ABSTRACT

Identifying the short crack driving force of polycrystalline engineering alloys is critical to correlate the inherent microstructure variability and the uncertainty in the short crack growth behavior observed during stage I fatigue crack growth. Due to recent experimental advancements, data of a short crack propagating at the relevant length scale is available via phase and diffraction contrast tomography. To compute the micromechanical fields not available from the experiment, crystal plasticity simulations are performed. Results of the experiment and simulations are combined in a single dataset and sampled utilizing non-local mining technique. Sampled data is analyzed using a machine learning Bayesian Network framework to identify statically relevant correlations between state variables, microstructure features, location of the crack front, and experimentally observed growth rate, in order to postulate a data-driven, non-parametric short crack driving force.

The Mechanics of Random Origami

Christian Santangelo*

*UMass Amherst

ABSTRACT

Origami is a new framework for the design of complex three-dimensional structures from an initially flat sheet or film, but has also been proposed as a way to fabricate mechanical metamaterials, which have effective mechanical response that is controlled by the material's architecture. In an origami structure, a fixed network of hinges along which the structure can be bent span a series of vertices. In this talk, I will discuss the interaction between origami geometry and the mechanical response of the folded structure. As I will discuss, the configuration space of an origami structure is characterized by an exponential number of distinct branches meeting at a bifurcation. Away from this, the dimension of the configuration space scales with the perimeter of the structure, allowing the rational design of mechanical response in these structures.

Effect of Topography on the Power Production and Wake Recovery of a Wind Turbine

Christian Santoni^{*}, Umberto Ciri^{**}, Stefano Leonardi^{***}

^{*}The University of Texas at Dallas, ^{**}The University of Texas at Dallas, ^{***}The University of Texas at Dallas

ABSTRACT

The performance of on-shore wind farms is largely affected the local topography of the region. Orographic features can induce velocity fluctuations that can be detrimental for the power production and increase fatigue loads. To address how the topography affects wind turbine power production and wake, Large Eddy simulations of a wind turbine located in a ridged terrain are performed. The hills are described by a sinusoidal wave. Two different amplitudes are considered, $0.10D$ and $0.05D$, where D is the rotor diameter. The wavelength is kept constant to $3D$. We investigate the effect of the position of the turbine within the domain by placing the turbine in the cavity and the crest of the hills and in a flat terrain downstream from the topography. Precursor simulations of a ridged topography are performed to obtain a fully developed flow to provide as an inflow condition. The numerical code is based on a finite difference scheme with a fractional step and a Runge-Kutta, providing a second order accuracy in space and time. It combines the immersed boundary method to model the tower, nacelle, and the topography with the actuator line method to represent the aerodynamic loads of the blades. It has been validated for surface roughness [1, 2] and turbine simulations [3]. Preliminary results show that fluctuations in the power production is not dependent on the location of the turbine with respect to the wavy wall but rather on the height of the ridges. Additionally, topography generated turbulence increases the entrainment of high momentum flow into the wake of the turbine increasing the recovery. This may be positive aspects considering wind farm configurations, because could mitigate wake interactions. References [1] Leonardi S, Orlandi P, Smalley RJ, Djenidi L and Antonia RA. Direct numerical simulations of turbulent channel flow with transverse square bars on one wall. *Journal of Fluid Mechanics* 2003; 491: 229-238. [2] Burattini P, Leonardi S, Orlandi P and Antonia RA. Comparison between experiments and direct numerical simulations in a channel flow with roughness on one wall. *Journal of Fluid Mechanics* 2008; 600: 403-426. [3] Santoni C, Carrasquillo K, Arenas-Navarro I and Leonardi S. Effect of tower and nacelle on the flow past a wind turbine. *Wind Energy*. 2017;20:1927–1939.

A Nonlinear Multiscale Method for Solving Incompressible Flow Problems

Isaac Santos^{*}, Riedson Baptista^{**}, Sérgio Bento^{***}, Leonardo Lima^{****}, Paulo Barbosa^{*****},
Lucia Catabriga^{*****}

^{*}Federal University of Espírito Santo, ^{**}Federal University of Espírito Santo, ^{***}Federal University of Espírito Santo,
^{****}Federal Institute of Espírito Santo, ^{*****}Federal University of Espírito Santo, ^{*****}Federal University of Espírito Santo

ABSTRACT

In this work we present a nonlinear variational multiscale method for solving incompressible flow problems with equal-order elements (P1/P1). The method is based on a two-level decomposition of the approximation space and consists of adding a residual-based nonlinear operator to the enriched Galerkin formulation, following a similar strategy of the methods presented in [1] for scalar advection-diffusion equation and in [2], [3] for compressible flow. The artificial viscosity acts adaptively in all scales of the discretization as a numerical stabilization and as a shock capturing scheme. In order to reduce the computational cost typical of two-scale methods, the subgrid scale space is defined using bubble functions whose degrees of freedom are locally eliminated in favor of the degrees of freedom that live on the resolved scales. Performance and accuracy comparisons with the streamline-upwind/Petrov-Galerkin (SUPG) formulation combined with the pressure stabilizing/Petrov-Galerkin (PSPG) method and shock capturing operators are conducted based on 2D benchmark problems.

Three-dimensional Fracture Analysis Using Scaled Boundary Polyhedral Elements

Albert Artha Saputra*, Ean Tat Ooi**, Chongmin Song***

*University of New South Wales, **Federation University Australia, ***University of New South Wales

ABSTRACT

A novel formulation based on scaled boundary finite element method is employed to construct a polyhedral element that can have an arbitrary number of planar faces. Each polygonal face can also be made up of an arbitrary number of vertices. Within each polyhedron, a volumetric scaling centre is chosen where the whole boundary is visible. Likewise, a surface scaling centre on each polygonal face is also selected such that it is able to see the whole perimeter of the polygon. Scaling in two scaled boundary coordinates is performed based on the two types of scaling centres. The displacements on each polygonal face are interpolated using the scaled boundary surface shape functions that are derived based on the boundary lines of the polygonal face [1]. These surface displacements are then scaled towards the volumetric scaling centre. Essentially, the dimension of the problem reduces by two, hence leaving the polyhedron to only be described by line elements (one-dimensional elements). Along the two scaling direction, analytical integration could be performed. This new formulation also enables the polyhedron to be constructed with arbitrary element order for each line. In the fracture analysis performed, the scaling centres of the polyhedron elements can be placed along the crack lines that allow the stress singularity of arbitrary order to be captured analytically [2]. The stress intensity factors can be simply extracted from the singular stress solution without a priori knowledge of the singularity order. Octree meshes [3] are also utilised such that smaller elements are placed around the crack that can transition quickly to larger elements for the other regions of the model. Keywords: three-dimensional, stress intensity factor, polyhedral element, scaled boundary finite element method, octree mesh References [1] Chiong, I., Ooi, E. T., Song, C., & Tin-Loi, F. (2014). Scaled boundary polygons with application to fracture analysis of functionally graded materials. *International Journal for Numerical Methods in Engineering*, 98(8), 562-589. [2] Saputra, A. A., Birk, C., & Song, C. (2015). Computation of three-dimensional fracture parameters at interface cracks and notches by the scaled boundary finite element method. *Engineering Fracture Mechanics*, 148, 213-242. [3] Saputra, A., Talebi, H., Tran, D., Birk, C., & Song, C. (2017). Automatic image-based stress analysis by the scaled boundary finite element method. *International Journal for Numerical Methods in Engineering*, 109(5), 697-738.

Mechanics of Pressure Ulcer: Application of Particle Based Methods

Sohan Sarangi*, Tetsu Uesaka**

*Department of Chemical Engineering, Mid Sweden University, **Department of Chemical Engineering, Mid Sweden University

ABSTRACT

Pressure ulcer is a silent epidemic in many of the developed countries. Elderly patients with limited mobility are particularly vulnerable to pressure ulcers (PUs). Although pressure is undoubtedly involved in PUs, there have not been good understandings of what mechanical environments induce complex bio-chemical reactions that leads to PUs. Factors related to the mechanical environment include the type of stresses, stress histories, damage evolutions, human body geometries and boundary conditions (e.g., bed mattress, clothes, diapers), for example. In order to model the specific features of PU problems, we have used particle-based methods. The human body model is based on the 3D reconstruction of a real human model from Visual Human Project. First, bones are modeled as a system of rigid bodies using Discrete Element Method (DEM). Bone joints can undergo rotations with the use of "ghost joint". Muscles, fat and skin are modeled as Smoothed Particle Hydrodynamics (SPH) particles, that follow a Mooney-Rivlin type hyperelastic constitutive equation with different material constants. We modified an open-source SPH code, "PySPH", in order to allow hyperelasticity, contact interactions, and DEM coupling. Validations have been made for cases of uniaxial tensile tests, multi-phase coupling, and stress concentrations around a hole. As the first step, we have performed the stress analysis of the whole human body which is lying in the bed. Unlike previous works using finite element method (FEM) with immobile bones, we have allowed complex joint movements with a multilayer discretization of human body. For interactions between bones and muscles, and also between skin and bed mattress (or diaper), the newly implemented contact model has been used. The results predicted the most vulnerable locations to the occurrence of pressure ulcer in the body, which are consistent to the clinical observations. We have also investigated the effect of friction coefficient (COF) between skin and underlying layer (e.g., diaper). The COF was varied from 0.3 to 1.3, the latter of which corresponds to wet skin case. The maximum shear and maximum compressive stresses were obtained on skin, fat and muscle layers. Increasing COF increased both maximum shear and principal compressive stresses, very much in the same way. Stresses on the fat region tended to flatten out for higher friction coefficient, but stresses on the muscle layer continued to increase with increasing friction. The implication of these results to damage evolution needs to be further investigated.

A Hybrid FE-FV Framework for Modeling Crack Propagation in Saturated Porous Media

Juan Michael Sargado^{*}, Eirik Keilegavlen^{**}, Inga Berre^{***}, Jan Martin Nordbotten^{****}

^{*}University of Bergen, ^{**}University of Bergen, ^{***}University of Bergen, ^{****}University of Bergen

ABSTRACT

Fluid driven fracture propagation in porous media has gained considerable attention in recent years due to its relevance to several important modern day applications. These include hydraulic fracturing of gas shales and the stimulation of enhanced geothermal systems, in which pressurized fluid is injected into the crack network to create or open up existing fractures, thereby improving the overall flow property of the reservoir. In this study, we develop a hybrid approach for solving the Biot poroelasticity equations coupled to a phase-field model for brittle fracture propagation. We begin by monolithically coupling a finite element approximation of stress equilibrium to a control volume form of the fluid mass balance. This subsystem is further coupled iteratively to a finite volume description of the phase-field evolution equation using an alternate minimization scheme. In particular, we leverage recent results dealing on alternative degradation functions that minimize spurious loss of stiffness in the mechanical response prior to fracture. Flow within open fractures is assumed to be of Poiseuille type, and it can be shown that accurately accounting for this additional flow can lead to mesh size constraints that are much more stringent than those coming from the phase-field equation. Performance of the proposed model is investigated by solving various numerical examples ranging from classical benchmarks to more sophisticated configurations.

Embedded Model Error Representation in Computational Models

Khachik Sargsyan^{*}, Xun Huan^{**}, Habib Najm^{***}

^{*}Sandia National Laboratories, ^{**}Sandia National Laboratories, ^{***}Sandia National Laboratories

ABSTRACT

Parameter calibration often assumes the computational model can replicate the true physical mechanism behind data generation. In practice, however, computational models rely on parameterizations, assumptions, and constitutive relations that entail significant model structural error. Ignoring such model errors can lead to overconfident calibrations and poor predictive capability, even when high-quality data are used for calibration. It is thus crucial to quantify and propagate uncertainty due to model error, and to differentiate it from parametric uncertainty and data noise. Traditional approaches accommodate model error through discrepancy terms that are only available for model output quantities used for calibration, and generally do not preserve physical constraints in subsequent predictions. The ability to extrapolate to other predictive quantities and to retain certain physical properties (e.g. conservation principles, positivity constraints) is often required in physical science and engineering applications. We develop a stochastically embedded model correction approach that enables these qualities, and illustrate computational methods for Bayesian inference of the correction terms together with model parameters [3]. Representing the correction terms using polynomial chaos expansions, the new formulation becomes a density estimation problem [1], and allows efficient quantification, propagation, and decomposition of uncertainty that includes contributions from data noise, parameter posterior uncertainty, and model error. The framework provides principled tools for the analyst, e.g. to examine the utility of corrections to specific suspect model components, and to identify the model components where model improvements are relevant for agreement with the data. We demonstrate the key strengths of this method on realistic engineering applications, including climate models, chemical kinetics [1, 3], and reacting flow simulations from a supersonic jet engine design [2].

Evaluation of Maximum Entropy Moment Closures for Predicting Radiative Heat Transfer Phenomena

Joaquim Sarr^{*}, Clinton Groth^{**}

^{*}University of Toronto, ^{**}University of Toronto

ABSTRACT

This study considers an evaluation of moment closures based on the principle of maximization of entropy for providing approximate solutions to the radiative heat transfer equation (RTE). Several representative tests cases in both one- and two-dimensions are considered whereby the predictions of the maximum-entropy closures are compared to those of the discrete ordinates method (DOM) as well as the more commonly used spherical harmonics solutions in terms of both accuracy and computational cost. More specifically, the present analysis is concerned with the lower-order approximations of the hierarchy of the maximum-entropy closures, namely the M1 and M2 closures and, for comparison purposes, the P1 and P3 spherical-harmonic closures are also considered. The discrete governing equations resulting from the application of a Godunov-type finite-volume method with anisotropic mesh refinement (AMR) to the system of moment equations in each case are solved using an inexact Newton method in which a generalized minimal residual (GMRES) technique is used to solve the linear system at each step of the Newton method. The proposed finite-volume method uses limited piecewise-linear solution reconstruction and Riemann solvers to evaluate the fluxes of the moments. The potential of the M1 and M2 closures is explored and discussed for a range of problems involving radiative heat transfer in gray media.

EARTHQUAKE RESPONSE ANALYSIS OF NON-STRUCTURAL MEMBERS OF BUILDING BY USING THE LARGE-SCALE PARALLEL CALCULATION METHOD

TOMOHARU SARUWATARI*, YASUYOSHI UMEZU^{†1}, YOSHITAKA USHIO^{†2},
LYU ZHILUN^{†3}, YASUYUKI NAGANO^{†4}

* JSOL Corporation

Tosabori Daibiru Bldg. 2-2-4 Tosabori, Nishi-ku, Osaka 550-0001, JAPAN

E-mail: saruwatari.tom@jsol.co.jp

^{†1} JSOL Corporation

Tosabori Daibiru Bldg. 2-2-4 Tosabori, Nishi-ku, Osaka 550-0001, JAPAN

E-mail: umezu.yasu@jsol.co.jp

^{†2} University of Hyogo

7-1-28, Minatojima-Minamimachi, Chuo-ku, Kobe 650-0047, Japan

E-mail: sb16q001@sim.u-hyogo.ac.jp

^{†3} University of Hyogo

7-1-28, Minatojima-Minamimachi, Chuo-ku, Kobe 650-0047, Japan

E-mail: sb15v003@sim.u-hyogo.ac.jp

^{†4} University of Hyogo

7-1-28, Minatojima-Minamimachi, Chuo-ku, Kobe 650-0047, Japan

E-mail: nagano@sim.u-hyogo.ac.jp

Key words: earthquake, non-structural members, Large-scale FEM, LS-DYNA.

Abstract. In large-scale earthquake disasters, it is reported that there were many serious damages of the non-structural members, such as ceilings and claddings, of the facilities with large space such as gymnasiums and assembly halls.

The technical standard for preventive measures against falling off is provided for the ceiling of the building, but it is applied only to prevent the damages caused by rare earthquake (middle-scale) at which the behavior of the ceiling can be predicted to some extent. In order to this problem, it is necessary to study the structure system after having clarified the behavior of the ceiling suspended from the building structure at the time of the extremely rare earthquake (large-scale earthquake).

To realize this, they need the analyzing methods to evaluate precisely the response of non-structural members according to the precisely predicted response data of the building structure against earthquake.

This study, making the suspended ceilings applied to large span structures as an example, prepares the detailed structural analysis models created by modeling the shape of the structural members through as faithfully following to the real one as possible, and tries to obtain the extremely precise earthquake response of the structures by means of large-scale parallel calculation.

In the future, it is aimed to evaluate the behavior of a whole building through piling of the results of the earthquake response of the ceilings by making as the boundary conditions the responses obtained by extremely precise analysis of the structure to which the ceilings are connected.

1 INTRODUCTION

In Japan, many cases of ceiling collapse and falling-down caused by earthquake was reported. For extremely rare earthquakes, it is necessary to study the real phenomenon in detail from the viewpoint of securing safety and evacuation plan at the time of earthquake^[7]. In this research, in order to solve these problems, we tried to analyze nonlinear dynamic transient response by a large scale parallel computer for a general suspended ceiling system used in Japan and to reproduce the behavior in detail.

2 NUMERICAL SIMULATION METHOD

Based on the use of large scale parallel computing environment, explicit non-linear dynamic response analysis was adopted. For software, LS-DYNA R 9.0.2 (double precision version) developed by Livermore Software Technology Corporation was used. We used the supercomputer system of the University of Hyogo for the calculator and parallel calculation by 160 to 320 parallel was carried out.

2.1 Finite element modeling

Modeling with BEAM elements and spring elements is often applied in FEM analysis because standard shape of channel sections are used for the parts that compose the suspended ceilings^[1]. These modeling methods have good accuracy with respect to elastic deformation, easy expression of rupture, and low calculation cost. However, it is difficult to express precision and complex destruction mode for nonlinear behavior at large deformation. On the other hand, if the shape of a member is precisely expressed by FE-MESH using the SHELL element or SOLID element, it is possible to express the nonlinear behavior due to buckling and yield, and to reproduce the failure mode accurately.

2.2 Finite element method

Explicit non-linear dynamic response analysis method is used for numerical calculation, and the software is DYNA R9.0.2 double precision version made by Livermore Software Technology

Corporation. This software, as its characteristics, has many non-linear material models, can precisely analyze non-linear large deformation and so on. Also, using the contact algorithm installed, it is possible to accurately analyze the change of the stress transmission mechanism due to contact and separation between parts at large deformation, and it is possible to express the phenomenon of collapse and damage with higher precision.

3 UNIT MODEL SIMULATION

In order to investigate the characteristics of the ceiling unit, static characteristic analysis and dynamic seismic response analysis were carried out. As for the suspended ceiling system, type 25, which is specified in the Japanese Industrial Standard JIS, was used ^[2, 3, 4].

3.1 Model Overview

Fig.1 shows a schematic diagram of a suspended ceiling model. In order to accurately express the shape of each part, all metal parts except the suspension rod were modeled with shell elements. The mesh pitch was based on 10 mm. The gypsum board and the rock wool board on the ceiling surface were modeled as one and the physical properties were determined so that the mass was equivalent. The mesh pitch was 100 mm.

The information specified in JIS for material property, and the elastic-plastic material model (*MAT_PIECEWISE_LINEAR_PLASTICITY) ^[9, 10] installed in the software for material model were used. Table.1 shows a list of material properties of the model.

Like the actual ceiling system, the suspension mechanism was expressed only by the contact between the parts. Only the contact condition is set between the hanger and the main channel and between the main channel and the clip, and no other fixed conditions are set. The total number of nodes was 26,806, the number of BEAM elements was 828, and the number of SHELL elements was 21,999 elements.

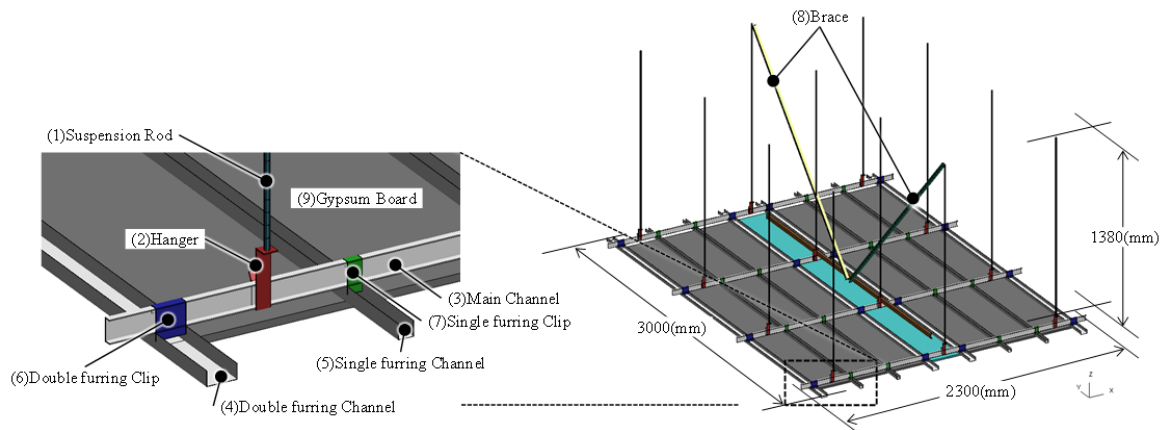


Fig.1 Suspended ceiling system

Table.1 material

	CODE	Material(JIS)	size	Density (ton/mm ³)	Young's modulus (MPa)	Poisson ratio	Yield Stress (MPa)
Suspension Rod	-	JIS G 3505	φ9	7.89E-09	206,000	0.3	215
Hanger	-	JIS G 3302	23x98x2.0				
Main Channel	CC-25	JIS G 3302	38x12x1.6				
Double Furring Channel	CW-25	JIS G 3302	50x25x0.5				
Single Furring Channel	CS-25	JIS G 3302	25x25x0.5				
Double Furring Clip	W-25	JIS G 3302	47.5x48.5x0.8				
Single Furring Clip	S-25	JIS G 3302	25x48.5x0.8				
Brace	AS-25	JIS G 3302	25x19x5x1.0	1.00E-09	28,900	0.2	-
Gypsum board + Rock wool sound absorbing plate	GB-R	JIS A 6901 JIS A 6301	t=9.0mm				

3.2 Push over analysis (Static characteristic)

A forced displacement of 50 mm was applied to the end of the model, and displacement-load relationship was obtained. Fig.2 shows the deformation of the system in the final stage. The calculation time was 1 h 24 m (160 parallel).

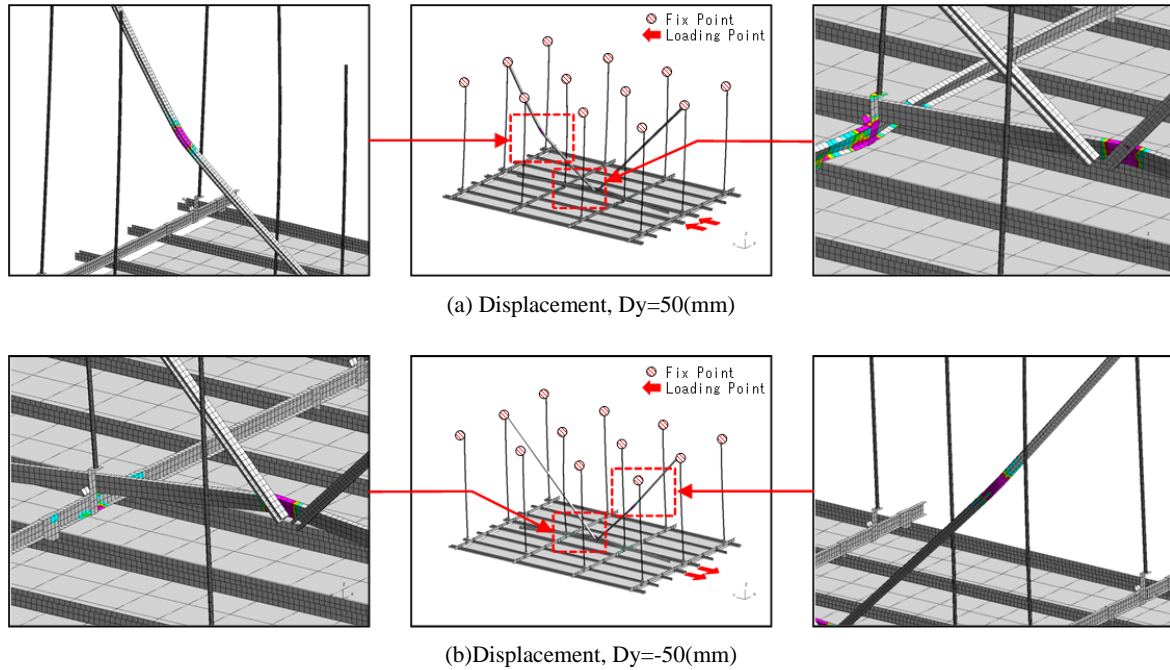


Fig.2 Plastic strain distribution

Forced displacement was loaded in the [+ y] and [- y] directions, and the load-displacement relationship were evaluated. The obtained load-displacement relationships of two loadings are shown in Fig.3

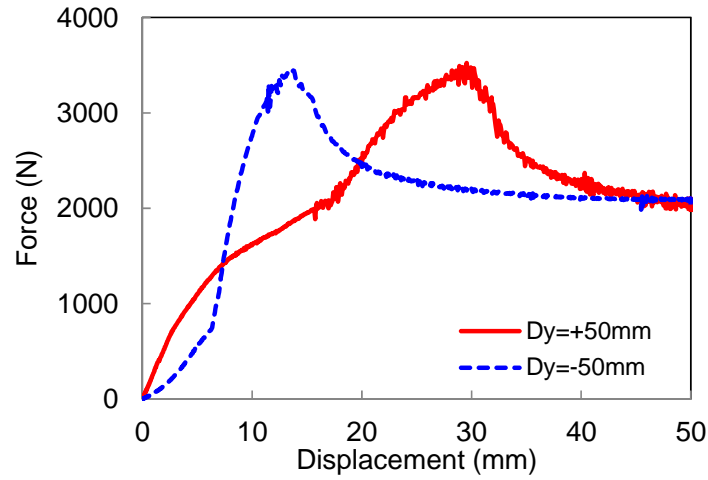


Fig.3 Force Displacement

3.3 Seismic response analysis (Dynamic characteristic)

By earthquake response acceleration wave was loaded to the upper end of the suspension rod, and earthquake response analysis was performed. As the seismic waves, "Takatori wave" observed JR Takatori station in Kobe in 1985 was used. The time history of the input seismic wave is shown in Fig.4.

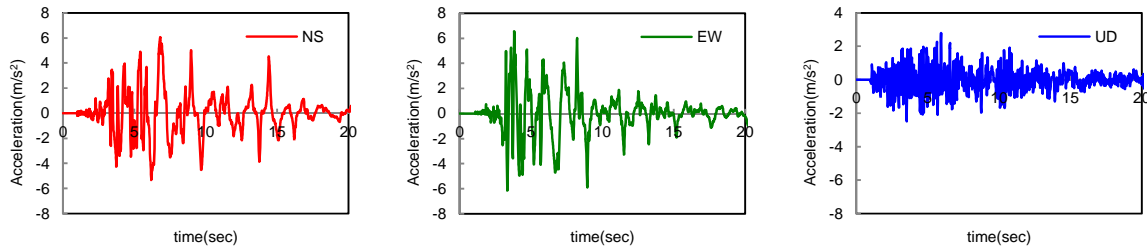


Fig.4 Input seismic acceleration

The calculation time is 5h36m (160 parallel). Fig.5 shows the response behavior.

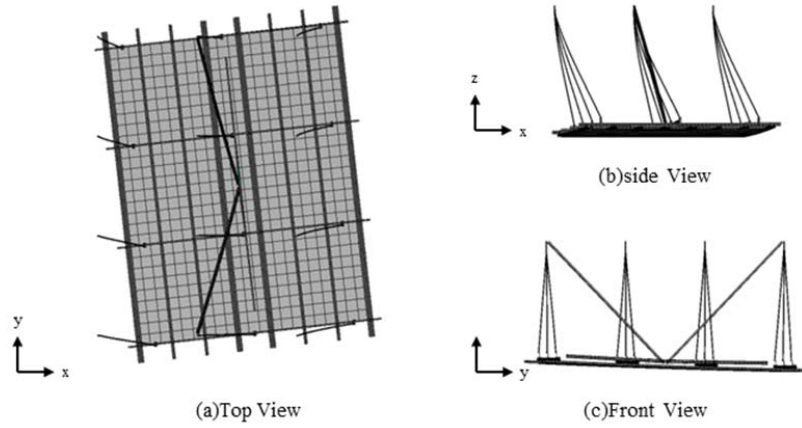


Fig.5 Displacement (t=8.0s)

Fig.6 shows the response displacement and the motion locus at the input (loading) points and the ceiling surface measurement points on the ceiling surface. From this, the ceiling surface responds greatly (swaying) in the X direction, but in the Y direction the brace for steady rest is effective and the response is small.

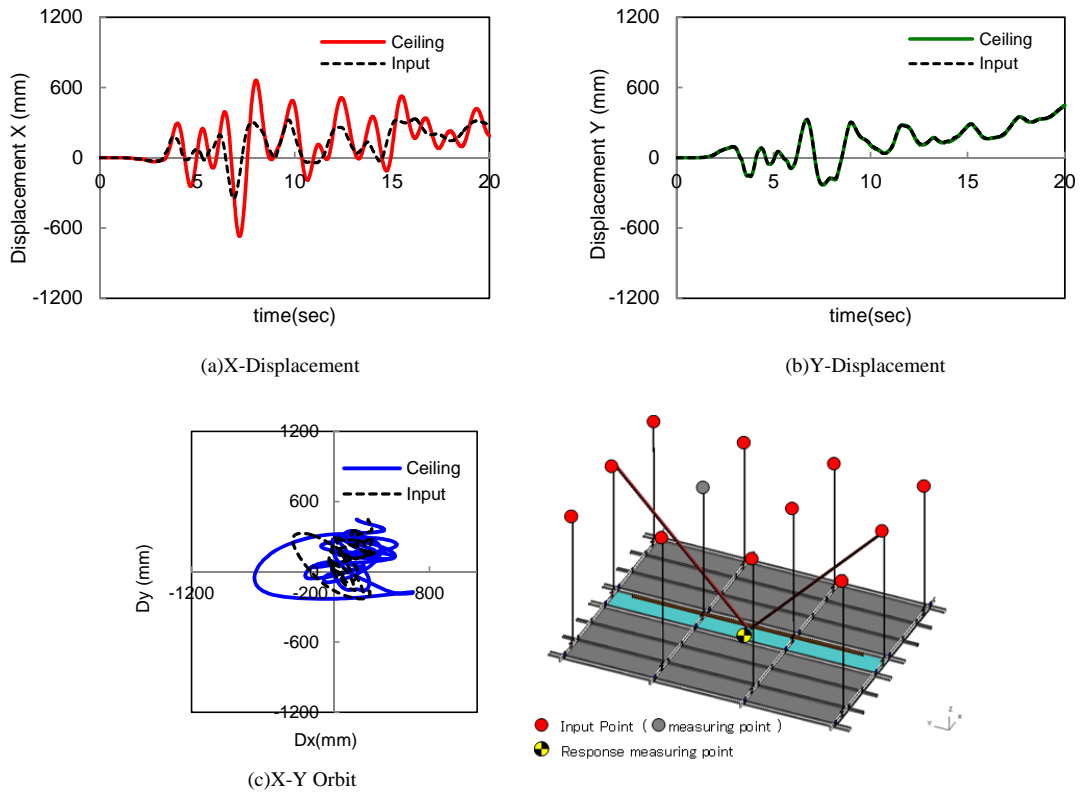


Fig.6 Time history of response displacement

4 BUILDING STRUCTURE MODELING

Since the input earthquake acceleration to the suspended ceiling is the earthquake response acceleration of the upper floor of the building, it is necessary to model the building, perform the earthquake response analysis, and input the result to the suspended ceiling. Detailed responses of the building should be obtained in general by detailed FEM analysis^[5,6], but, in this research, we tried to model the building into a simple frame model and incorporate the suspended ceiling model to the building frame model in order to reproduce the behavior of the suspended ceiling at the earthquake.

4.1 Model Overview

The plans and elevations of the building is shown in Fig. 7^[8], and the details of the structural members are shown in Table.2 and Table.3. The building is a 7-story steel frame structure including the penthouse, which has 5 spans in the X direction and 3 spans in the Y direction. The columns of the building were modeled into shell elements from the necessity of expressing the behavior of local buckling, and the beam was modeled into the BEAM element. The floor slab was modeled into a shell element. Both columns and beams were modeled as elastoplastic and all material models were installed in the software so that column models are in (*MAT_KINEMATIC_HARDENING_TRANSVERSELY_ANISOTROPIC) and beam model is in (*MAT_RESULTANT_PLASTICITY). For the floor slab, a reinforced concrete model is in (*MAT_CONCRETE_EC2). The total number of nodes was 242,812, the number of BEAM elements was 11,252, and the number of SHELL elements was 226,703.

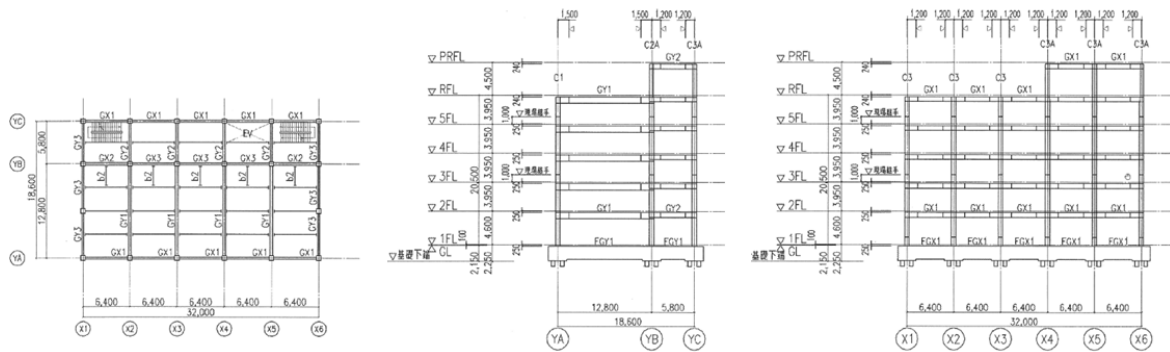


Fig.7 Framing plan

Table.2 Section list of columns

	C1	C2,C2A	C3,C3A	C4
RF	-	B-460x16	B-460x16	-
5F	B-500x22	B-500x22	B-500x22	B-500x22
4F				
3F				
2F				
1F				

Table.3 Section list of beams

	GX1		GX2		GX3	
	edge	center	edge	center	edge	center
PRF	H-600x250x12x19		H-600x250x12x22		H-600x200x12x22	
RF			H-600x200 x12x25 H-600x200 x12x22			
5F						
4F						
3F	H-600x250 x12x22	H-600x250 x12x19	H-600x200 x12x22	H-600x200 x12x19	H-600x250 x12x22	H-600x250 x12x19
2F						

	GY1		GY2		GY3	
	edge	center	edge	center	edge	center
PRF	-		H-600x200x12x19		-	
RF	H-800x350x16x25				H-600x200x12x22	
5F					H-600x200 x12x25	H-600x200 x12x22
4F						
3F					H-600x200 x12x22	H-600x200 x12x19

In order to evaluate the behavior of the ceiling of the 2nd floor of the building, a suspended ceiling model was placed under the 3rd floor. In the ceiling, three unit models explained in Chapter 3 of this paper were connected in the X direction and placed, and the upper end of the suspension rod was attached beneath the 3rd floor of the building. A schematic diagram of the analysis model is shown in Fig.8.

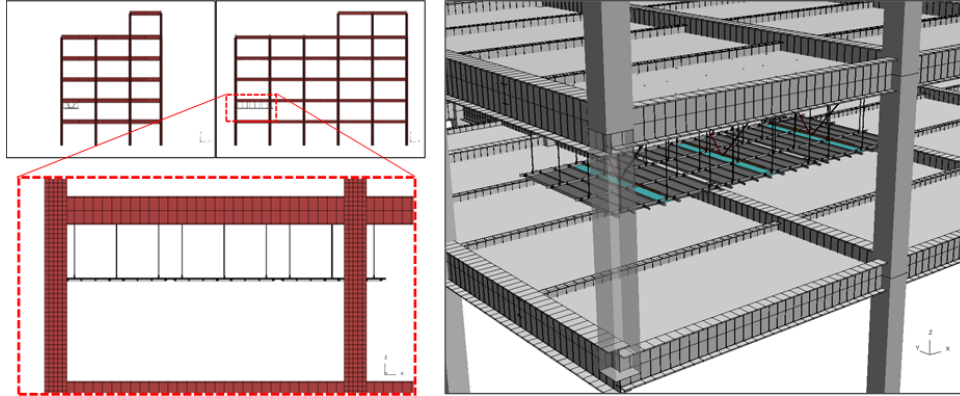


Fig.8 Building with ceiling system

4.2 Seismic response analysis

Earthquake response analysis was carried out by inputting the seismic wave (Takatori wave) shown in Fig. 4 to the column bases of the first floor of the building. The calculation time was 15 h 18 m (320 parallel). Fig. 9 shows the time history of displacement at the response measurement position of the column (X1 - YA) on the 3F, 6F floor and the ceiling surface.

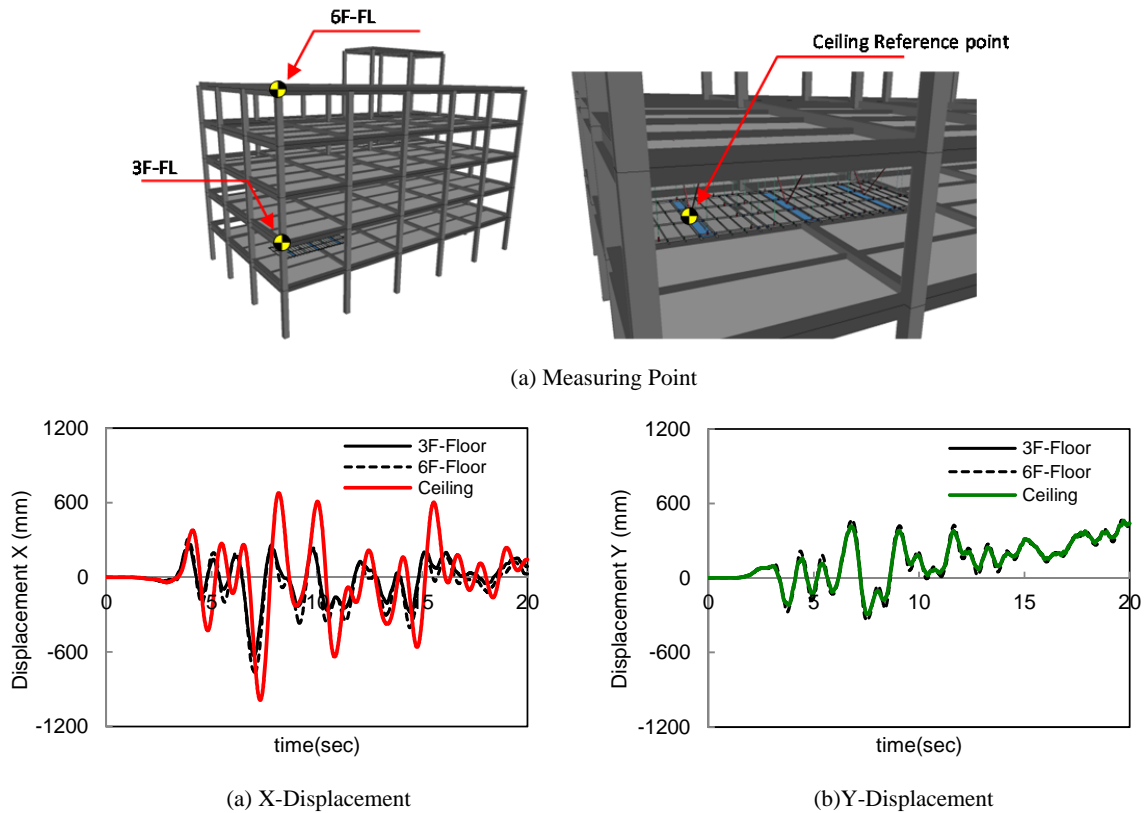


Fig.9 Time history of response displacement

It is understood that the response of the building in the X direction is large and the response displacement of the ceiling is larger than the building 3F - FL. In the Y direction the response of the building is small and the response to the ceiling is hardly seen due to the effect of the braces for steady rest.

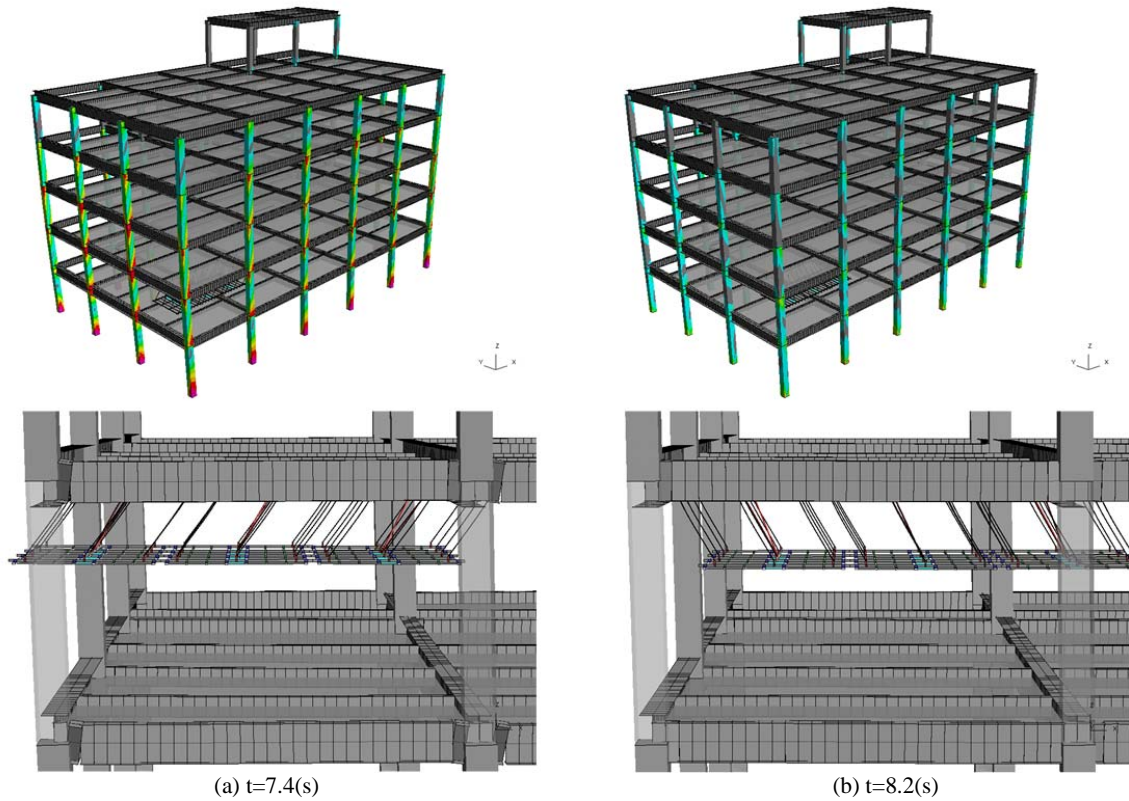


Fig.10 Building and ceiling behavior

The behavior during the earthquake response is shown in Fig10. The ceiling surface was greatly displaced, and the maximum displacement in the X direction was $+x = 678.9 \text{ mm}$ and $-x = 986.9 \text{ mm}$. The behavior of the ceiling in the response is shown in Fig.11. The dynamic behavior of the ceiling surface causes the clip to deform and slip, and it can be seen that the load is divergent from the stress distribution state.

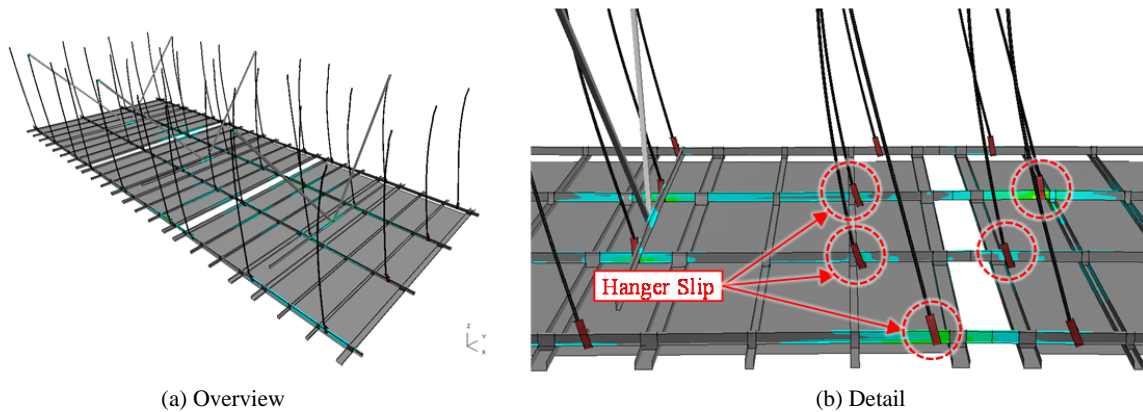


Fig.11 Detail around hanger (Von-Mises Stress)

5 CONCLUSIONS

- - By detailed modeling of suspended ceilings, the structural characteristics of the suspended ceiling system could be accurately reproduced.
- - Coupled analysis with buildings allowed us to explain in detail the dynamic behavior of the ceiling in the building at the time of the earthquake.
- - We were able to accurately grasp the changes in load transmission mechanism due to deformation and movement of parts.
- - It was suggested that the accurate grasp of the behavior of nonstructural members at the earthquake can contribute to improvement of safety of building and improvement of accuracy of evacuation plan.

ACKNOWLEDGMENTS

This work was supported by JSPS KAKENHI Grant Number JP16H03124.

REFERENCES

- [1] YAMAMOTO Takuya, TAGAWA Hiroyuki, YAMASHITA Takuzo and ISOBE Daigoro, Numerical Study on the Ceiling Collapse in Large-Space Building during Earthquakes –Part1 Basic Study, Summaries of technical papers of annual meeting Architectural Institute of Japan, 2014.9, 1107-1108. (in Japanese)
- [2] Shojiro MOTOYUI and Yasuaki SATO, EVALUATION METHOD FOR HORIZONTAL STIFFNESS OF CEILING WITH STEEL FURRING IN DIRECTION OF ‘NOBUCHI’, J. Struct. Constr. Eng., AIJ, Vol. 79 No. 703, 1395-1403, Sep., 2014 (in Japanese)
- [3] ARAI Tomokazu, Yuri Takayuki, and KOBAYASHI Toshio, Study on Aseismic

Tomoharu Saruwatari, Yasuyoshi Umezu, Yoshitaka Ushio, Lyu Zhilun, Yasuyuki Nagano

Ceiling Part 3 Lateral Loading Test of Ceiling with Steel Furrings, Summaries of technical papers of annual meeting Architectural Institute of Japan, 2006.9, 841-842. (in Japanese)

[4] Toshio KOBAYASHI, Takayuki YURI and Tomokazu ARAI, STUDY ON ASEISMIC SUSPENSION CEILING WITH STEEL FURRINGS, J. Struct. Constr. Eng., AIJ, Vol. 73 No. 630, 1295-1302, Aug., 2008 (in Japanese)

[5] Yasunori Mizushima, Yoichi Mukai, Hisashi Namba, Kenzo Taga and Tomoharu Saruwatari : Super-detailed FEM simulations for full-scale steel structure with fatal rupture at joints between members -Shaking-table test of full-scale steel frame structure to estimate influence of cumulative damage by multiple strong motion: Part 1, Japan Architectural Review, AIJ, Vol.1, Issue 1, pp.96-108, DOI : <https://doi.org/10.1002/2475-8876.10016>

[6] Yasunori Mizushima, Yasuyuki Nagano and Yoichi Mukai : Construction of damage observation system for both structural and non-structural members with overlaying, #2019117, proc. 13th WCCM(2018).

[7] Yasuyuki Nagano, Yoichi Mukai, Kensuke Yaufuku, Harunori Mizushima and Tomoharu Saruwatari : KEY ELEMENT BUILDINGS DESIGN METHOD WITH BIDIRECTIONAL EVALUATION BETWEEN STRUCTURAL ANALYSIS AND EVACUATION ANALYSIS, #2020193, proc. 13th WCCM(2018).

[8] The Japan building Disaster Prevention Association: Case Examples of Structural Design of Buildings and Their Members, (2007) (in Japanese)

[9] LS-DYNA KEYWORD USER'S MANUAL VOLUME (I) LS-DYNA R9.0 08/29/16 (r:7883), LIVERMORE SOFTWARE TECHNOLOGY CORPORATION (LSTC), 2016.

[10] LS-DYNA KEYWORD USER'S MANUAL VOLUME (II) LS-DYNA R9.0 08/29/16 (r:7883), LIVERMORE SOFTWARE TECHNOLOGY CORPORATION (LSTC), 2016.

Force-Driven Recruitment of Receptors into Cell Adhesion Sites

Alireza Sarvestani*

*Ohio University, Department of Mechanical Engineering, Athens OH 45701

ABSTRACT

The hallmarks of cell mechanotransduction shared by "focal adhesions" and intercellular "adherens junctions" include the enlargement and strengthening of these adhesion sites in response to actomyosin tension. We developed a thermodynamically admissible model for the mature adhesion sites subjected to time-dependent pulling tractions. The adhesion zone is presented by a bounded surface in which the ligands and receptors can interact and form physical bonds. Free receptors and/or ligands are mobile and can diffuse on cell membrane and cross the boundary of the adhesion site. Implementing the three fundamental laws, namely the conservation of receptors/ligands and first and second laws of thermodynamics along with the Hadamard jump condition at the boundary of the adhesion site, we found the fundamental equations that control the growth kinetics of the adhesion sites in response to an applied tension that changes with time. The coupled equations can be solved numerically, assuming a simple geometry for the adhesion site. We show that the pulling traction tilts the free energy landscape and mediates the flux of receptors into the adhesion zone and leads to its spontaneous growth, independent from any other sensory function.

Level Set-Based Topology Optimization of Fluid Flows Using the Moving Particle Semi-implicit Method

Yusuke Sasaki^{*}, Takayuki Yamada^{**}, Kazuhiro Izui^{***}, Shinji Nishiwaki^{****}

^{*}Kyoto University, ^{**}Kyoto University, ^{***}Kyoto University, ^{****}Kyoto University

ABSTRACT

Structural optimization has been successfully used in many industries. In particular, topology optimization [2] which has the most potential for exploring optimized structures, can be applied to a wide range of structural optimization problems such as stiffness maximization problems, thermal problems and fluid dynamics problems [3]. However, most existing topology optimization methods for fluid flows problems are based on the finite element method or finite volume method and have difficulty in handling problems which include free surface and two-phase flows, where the shape of the interface continuously changes depending on time. Moving particle semi-implicit (MPS) method is one of the particle methods, which can be used to analyze incompressible free surface flow without surface tracking. The motion of each particle is calculated through interactions with neighboring particles covered with the kernel function. This mesh-less numerical approach as a Lagrangian gridless particle method, proposed by Koshizuka, et al [1] has been proven to be useful in a wide range of engineering applications, such as numerical analysis of turbines and mixers. In this study, we propose a topology optimization method using the level set method and the MPS method for fluid dynamics problems, including free surface and two-phase flows. First, we explain briefly about topology optimization and the MPS method. Next, optimization problems are formulated based on the level set method and the MPS method. The design sensitivity analysis, performed using the adjoint variable method, is then explained. Finally, numerical examples are provided to confirm the validity and utility of the proposed method. [1] Koshizuka, Seiichi, and Yoshiaki Oka. "Moving-particle semi-implicit method for fragmentation of incompressible fluid." Nuclear Science and Engineering 123.3 (1996): 421-434. [2] Yamada, Takayuki, et al. "A topology optimization method based on the level set method incorporating a fictitious interface energy." Computer Methods in Applied Mechanics and Engineering 199.45 (2010): 2876-2891. [3] Deng, Yongbo, et al. "Optimization of unsteady incompressible Navier–Stokes flows using variational level set method." International Journal for Numerical Methods in Fluids 71.12 (2013): 1475-1493.

A Model Enhancement Approach for the Free Surface Simulations by the MRT-LBM Toward Three-dimensional Tsunami Analysis

Kenta Sato^{*}, Shunich Koshimura^{**}

^{*}Graduate School of Engineering, Tohoku University, ^{**}International Research Institute of Disaster Science,
Tohoku University

ABSTRACT

Free surface flow problems occur in numerous in disaster simulations such as tsunami in urban area. This application requires three-dimensional, highly resolved and efficient simulations. Consequently, the demand for powerful simulation models is larger than ever before. It is, however, difficult to carry out three-dimensional large-scale tsunami simulations because of the pressure Poisson equation in the incompressible Navier-Stokes fluid modeling. In recent years, the lattice Boltzmann method (LBM) has attracted attention as an efficient computational fluid dynamics tool. By contrast with traditional flow solvers, which calculate the macroscopic Navier-Stokes equations, LBM solves such problems on a microscopic scale and represents the fluid as the virtual particles. The key features of LBM are as follows: (i) fully explicit method in time integration, which means LBM does not have to solve the pressure Poisson equation, (ii) easy implementation with high-performance computing using multiple core processors or GPU because of the algorithmic operations and data locality. In this regards, LBM is considered to have an advantage to execute a high-performance three-dimensional tsunami simulation as an alternative tool of the other simulation methods. In current study, we have developed a three-dimensional free surface fluid model by LBM with the piecewise Linear Interface Reconstruction, Volume of Fluid (PLIC-VOF) approach. This type of VOF methods determines the interface location and hence the flux terms more accurately and avoids non-physical oscillations near the interface. The free surface is represented as a linear function segment, which can be determined by the interface normal and distance from Cartesian origin. It is well known that the lattice BGK model, which is the simple collision term of LBM, becomes numerical instability in high Reynolds number flow easily. In our model, the more advanced Multiple-Relaxation-Time (MRT) model is used to enhance the model robustness and accuracy. Three-dimensional breaking wave in a rectangular tank was simulated to verify our model. Lubin et al.[1] has calculated the benchmark by the three-dimensional PLIC-VOF with the incompressible Navier-Stokes equations. We used their solutions to compare our results. From the benchmark problem, we found that our model calculates the breaking waves well and is robustness in such complex flow field. We can conclude that our model is extremely useful as a way to simulate tsunami in three-dimensional flow field. [1] Lubin P., Vincent S., Abadie S., Caltagirone. J., Three-dimensional Large Eddy Simulation of air entrainment under plunging breaking waves, Coast. Eng., 53, pp.631-655. 2006.

Substitution Approach for De-coupled Two-scale Analysis of Composite Plates

Masami Sato^{*}, Mayu Muramatsu^{**}, Kenjiro Terada^{***}, Tatsuya Kawada^{****}

^{*}Tohoku University, ^{**}Tohoku University, ^{***}Tohoku University, ^{****}Tohoku University

ABSTRACT

We propose a new substitution approach to perform de-coupled nonlinear two-scale analysis for composite plates with an in-periodic meso-structure, which is referred to as in-plane unit structure (IPUS). In the suggested approach, the heterogeneity in the meso-structure is substituted or replaced by an equivalent laminated structure, which might not be unique, but must be proper in the sense that the macroscopic mechanical responses are uniquely determined. The macroscopic nonlinear mechanical characteristics of the plate are determined from the numerical plate testing for the IPUS that provides a set of relationships between macroscopic resultant stresses and generalized strains [1]. Since the obtained plate sectional properties cannot be represented by an equivalent homogeneous plate stiffness of a single material, we assume that an equivalent laminated structure (ELS) that exhibits the same macroscopic response can be substituted for the original composite plate. Then, the material parameters of each layer of an IPUS of this ELS, which is regarded as a mesoscopic substitution model (meso-SM), are identified by an optimization method so as to be equivalent to the original IPUS. After the parameter identification, the corresponding macroscopic substitution model (macro-SM) can be utilized with laminated plate elements to analyze the overall responses. We first validate the appropriateness of the proposed approach by comparing representative numerical examples with the results obtained by the original composite plate. Then, we apply the proposed approach to characterize the thermo-mechanical behavior of a plate-shaped device typified by solid oxide fuel cells (SOFC). Since the solid-shell type finite element modeling of the macro-SM is possible in the proposed method, we demonstrate the capability of analyzing a structure with stratified plate-shaped devices like a cell stack of SOFC. [1] K. Terada, N. Hirayama, K. Yamamoto, M. Muramatsu, S. Matsubara &&& S. Nishi Numerical plate testing for linear two-scale analyses of composite plates with in-plane periodicity, IJNME, 105, pp. 111–137, 2016.

Multiple-phase-field Simulation of Multiple Dendritic Growth with Motion

Ryotaro Sato*, Tomohiro Takaki**

*Kyoto Institute of Technology, **Kyoto Institute of Technology

ABSTRACT

Equiaxed structure formed during a solidification process of metals and alloys determines the mechanical property of those materials. Therefore, it is crucial to accurately predict and control the formation process of the equiaxed structure. Phase-field method has been widely used to predict the solidification microstructures as a powerful and accurate numerical model. Meanwhile, since the formation process of the equiaxed structure is very complex phenomenon including growth, motion and collision of multiple dendrites and subsequent grain growth after formation of grain boundary, there are no phase-field models expressing all physics in the formation process of equiaxed structure. In this study, we construct a new model which can express the growth, motion and collision of multiple dendrites and subsequent grain growth. In this model, the growth and motion of multiple dendrites are expressed by a multi-phase-field method and equations of motion, respectively, and the liquid flow is computed by lattice Boltzmann method. The collision and coalescence of multiple grains are also modeled in this model. The validity of the model is confirmed by performing simulations of a collision of two circular objects and a grain growth in three grains system. After that, the formation simulations of the equiaxed structure is demonstrated by employing the developed model.

Topology Optimization Incorporating Reliability Design under Geometrical Uncertainties

Yuki Sato^{*}, Kazuhiro Izui^{**}, Takayuki Yamada^{***}, Shinji Nishiwaki^{****}, Makoto Ito^{*****}, Nozomu Kogiso^{*****}

^{*}Kyoto University, ^{**}Kyoto University, ^{***}Kyoto University, ^{****}Kyoto University, ^{*****}Osaka Prefecture University,
^{*****}Osaka Prefecture University

ABSTRACT

Geometrical uncertainties caused by manufacturing errors and operational wear can affect the physical performance of various devices. In microfabrication processes, the effect of geometrical uncertainties can be particularly detrimental, due to the small dimensions at these scales. However, since the physical performance of a device usually depends on the details of its shape in implicit and radically non-linear ways, it is difficult for design engineers to predict the effects of geometrical variations and modify their designs accordingly. Therefore, consideration of geometrical uncertainties in the early design stage is of primary importance. For structural conceptual designs, topology optimization is a useful tool that can yield effective optimal configurations based on mathematical and physical principles. Since the pioneering study by Bendsøe and Kikuchi, topology optimization has successfully been applied to various physics problems, as widely reported in the literature. Some researchers have proposed robust topology optimization methods under geometrical uncertainties based on stochastic threshold Heaviside projection [1,2] or stochastic shifting of finite element nodes [3] under the assumption of sufficiently small perturbation. In the present study, we propose a reliability-based topology optimization under geometrical uncertainty. First, topology optimization is briefly discussed. Geometrical uncertainty is then modeled using an advection equation in which the advection velocity is treated as a stochastic field representing the magnitude and direction of variations, and the inverse reliability method is briefly discussed. Next, optimization problems are formulated based on the proposed geometrical uncertainty modeling, and the design sensitivity analysis, performed using the adjoint variable method, is explained. A two-level optimization algorithm is then constructed, where reliability analysis is conducted in the first level of the iterated procedure and the second level is used for updating design variables. Finally, the proposed method is applied in two numerical examples to demonstrate its validity and utility. References [1] M. Schevenels, B. S. Lazarov, O. Sigmund, Robust topology optimization accounting for spatially varying manufacturing errors, *Computer Methods in Applied Mechanics and Engineering*, Vol 200(49) 2011 pp. 3613–3627. [2] B. S. Lazarov, M. Schevenels, O. Sigmund, Topology optimization with geometric uncertainties by perturbation techniques, *International Journal for Numerical Methods in Engineering*, Vol 90(11) 2012, pp. 1321–1336. [3] M. Jansen, G. Lombaert, M. Schevenels, Robust topology optimization of structures with imperfect geometry based on geometric nonlinear analysis, *Computer Methods in Applied Mechanics and Engineering*, Vol 285 2015, pp. 452–467.

On the Isogeometric Modeling of Phase Transitions on Deforming Surfaces

Roger A. Sauer^{*}, Christopher Zimmermann^{**}, Deepesh Toshniwal^{***}, Chad M. Landis^{****},
Thomas J.R. Hughes^{*****}, Kranthi K. Mandadapu^{*****}

^{*}RWTH Aachen University, ^{**}RWTH Aachen University, ^{***}UT Austin, ^{****}UT Austin, ^{*****}UT Austin, ^{*****}UC
Berkeley

ABSTRACT

Many physical applications are governed by phase transitions. An example from biophysics are lipid membranes. They can separate into two distinct phases when quenched from high to low temperatures. Due to the coupling between in-plane phase transitions and out-of-plane bending, this can lead to severe shape changes of the membrane. This work presents a general theory and isogeometric finite element implementation for studying mass conserving phase transitions on deforming surfaces [1]. The mathematical problem is governed by two coupled fourth-order partial differential equations (PDEs) that live on an evolving two-dimensional manifold. For the phase transitions, the PDE is the Cahn-Hilliard equation for curved surfaces, which can be derived from surface mass balance in the framework of linear irreversible thermodynamics [2]. For the surface deformation, the PDE is the (vector-valued) Kirchhoff-Love thin shell equation. Both PDEs can be efficiently discretized using C1-continuous interpolations without derivative degrees-of-freedom (dofs). Structured NURBS and unstructured spline spaces with pointwise C1-continuity are utilized for this. The resulting finite element formulation is discretized in time by the generalized-alpha scheme with adaptive time-stepping, and it is fully linearized within a monolithic Newton-Raphson approach. A curvilinear surface parameterization is used throughout the formulation to admit general surface shapes and deformations [3]. The behavior of the coupled system is illustrated by several numerical examples exhibiting phase transitions on deforming spheres, tori and double-tori. [1] C. Zimmermann, D. Toshniwal, C.M. Landis, T.J.R. Hughes, K.K. Mandadapu and R.A. Sauer (2017), "An isogeometric finite element formulation for phase fields on deforming surfaces", arXiv:1710.02547 [2] A. Sahu, R.A. Sauer and K.K. Mandadapu (2017), "The irreversible thermodynamics of curved lipid membranes", Phys. Rev. E, 96:042409 [3] T.X. Duong, F. Roohbakhshan and R.A. Sauer (2017), "A new rotation-free isogeometric thin shell formulation and a corresponding continuity constraint for patch boundaries", Comput. Methods Appl. Mech. Engrg., 316:43-83

The Influence of Grain Size and Shape on the Mechanical Properties of AM Parts

Robert Saunders^{*}, Ajit Achuthan^{**}, Amit Bagchi^{***}

^{*}U.S. Naval Research Lab, ^{**}Clarkson University, ^{***}U.S. Naval Research Lab

ABSTRACT

Metal powder-based additive manufacturing (PAM) processes involve localized melting and solidification of a small amount of metallic powder, with large temperature gradients and cooling rates that influence the evolution of the local microstructure. Typically, the resulting microstructure has a texture and consists of columnar grains of different grain sizes, which affect the mechanical properties of the material. In a previous study, a microstructure-informed constitutive model was developed to describe the mechanical behavior of solidified material produced by PAM. This model was based on crystal plasticity and took into account the grain size and aspect ratio of the microstructure by considering a core and mantle configuration for the grain volume, with the mantle representing the grain boundary influence region. A representative volume element (RVE) using the developed constitutive model was used to validate the method and the overall mechanical properties were obtained. The results of the previous work showed that grain size and shape have a significant influence on individual grain strength and hardening modulus. In particular, smaller grains with larger aspect ratios exhibit the most dramatic effect. However, the influence of these size and shape effects on the overall mechanical behavior of the RVE is not known. In this work, a design of experiments (DoE) study is performed where the average grain aspect ratio, load direction, and grain size and shape influences of the RVE are varied. Preliminary results indicate that, as expected, the RVEs with their average aspect ratio larger have a higher predicted strength but little change in the hardening modulus. However, when the grains in the RVE are closer to equiaxial (i.e., microstructure of a conventionally cast metal part), the hardening modulus is greatly increased along with a lowered yield strength. This initial result indicates that there may be potential to tailor mechanical properties of a part by controlling the process parameters that determine the microstructure. The complete results of this DoE will help to determine the extent to which this tailoring can be done as well as shed light on the effect of grain size and shape on mechanical behavior of PAM parts.

Novel Kinetic Model and Kinetic Consistent Algorithm of Magneto Hydro Dynamics

Valeri Saveliev*, Boris Chetverushkin**, Andrey Saveliev***

*Institute of Applied Mathematics, Russian Academy of Sciences, **Institute of Applied Mathematics, Russian Academy of Sciences, ***Immanuel Kant Baltic Federal University

ABSTRACT

New kinetic model of dynamic of charged particles on base implementation of electromagnetic interactions inside Boltzmann like statistical distribution function and development of effective parallel algorithms for high performance computing systems will be presented. We propose a new approach to define of unified complex Boltzmann like distribution function, which includes the electromagnetic terms for the solution of the Boltzmann equation for charged particles in electromagnetic field. It was shown that electromagnetic fields do not destroy the validity of the Boltzmann equation which opened the way for the implementation of the electromagnetic term in the Boltzmann-like distribution function. Due to the vector nature of the electromagnetic interaction the distribution function should take into account the vector behavior and provide correct formulation for the evolution of the magnetic field, i. e. the magnetic field should be generally defined as a moment of the Boltzmann-like distribution function. In order to provide the validity of the proposed statistical complex distribution function, we show that the equilibrium state of Boltzmann equation for charged particles reproduced correctly the ideal magneto gas dynamics system of equations, including the evolution of the magnetic field. The computational algorithms are based on the kinetic consistent approach of the solution of the Boltzmann equation i.e. evolution of Boltzmann like statistical distribution function at discrete time and integration with the summational coefficients to getting the magneto gas dynamic system of equations. The numerical method is based on the explicit schemes. Due to logical simplicity and high efficiency, the algorithm is easily adopted to modern high performance parallel computing systems, including hybrid computing system with graphic processors. The weakness of explicit schemes is a strictly limited time step that ensures computational stability. This restriction becomes critical with the growing number of nodes and the reduction in the step of a spatial mesh. The advanced explicit kinetic finite difference schemes hyperbolic type have a soft stability condition giving the opportunity to enhance the stability and to use very fine meshes. The results of numerical calculations of test benches physical task of MHD in 3D space will be presented. It also can be mentioned the using of the proposed approach for the biomedical study in particular blood flow under strong magnetic field conditions.

Polytopal Stokes Weights Transport

Yann Savoye*

*Robert Gordon University

ABSTRACT

Deformation mechanism of non-rigid surfaces in motion is a long-standing problem in Computational Mechanics with numerous of applications in Engineering Sciences and Computer Graphics. In this work, we focus on estimating generalized coordinates on polyhedral meshes required for cage-based deformation. In particular; our approach relies on Computational Fluid Mechanism as a computational model of deformation mechanisms. Recent years have seen an increasing attention for physics-inspired rigging methods to enable visually-pleasant elastic shape animations. Cage-based deformation is a well-studied technique in Geometry Processing. Deformable Cages are purely shape-aware geometric subspaces, allowing non-isometric stretching strains. Also, shape coordinates are the key ingredients to rig an input coarse cage deformer to the enclosed surface, and then deform a shape with meaningful properties. Inspired by the mass-preserving vorticity in incompressible fluid transport, we reformulate the cage-based rigging as an incompressible Stokes problem to estimate weight functions suitable for cage-based deformation. Hence, we derive cage-based coordinates from Stokes equation by devising a vorticity-stream function formulation as the computational model for cage-based weighting functions. Our central contribution is a novel derivation of streamline-vorticity and its polyhedral discretization using finite difference method to obtain our compact-stenciled Stokes Coordinates. Our solver takes benefit from a linearization and biharmonization formulation. First, a linear formulation is derived from the Navier-Stokes equation. Then, starting from the linearized Stokes equations, we solve the Newtonian Stokes flow using the vorticity-velocity stream function. To speed up the computation, we approximate our Stokes-wise biharmonic operator using a compact second-order approximation with center-differencing. Finally, our cage-based Stokes Coordinates are the solution of the vorticity-stream equation for the Stokes flow at the steady state. We demonstrate the effectiveness of our Stokes Coordinates with several geometric applications such as shapes encoding, interactive cage-based shape editing as well as cartoon-style deformation of performance capture meshes. Overall, our technique does not modify the traditional cage-based metaphor for deforming objects such as point clouds, triangles soup, manifold or non-manifold surfaces. [1] - Stokes Coordinates, Yann Savoye, Proceedings of the 30th Spring Conference on Computer Graphics, 2017. [2] - Cage-based Performance Capture, Yann Savoye, SIGGRAPH ASIA 2016 Courses, 2016. [3] - Compact Stokes Coordinates for Cage-based Shapes, Yann Savoye, Proceedings of the 20th ACM SIGGRAPH Symposium on Interactive 3D Graphics and Games, 2016.

Application of the Harmony Search Algorithm to the Optimization of Laminated Composite Plates and Shells

Felipe Schaedler de Almeida*

*Federal University of Rio Grande do Sul

ABSTRACT

This work presents the application of an extended implementation of the harmony search algorithm (HSA) to the optimization of the stacking sequence of laminated composite plates and shells in order to maximize the buckling load of these structures. Due to usual manufacturing restraints, only few angles are allowed for the fiber direction of the plies, which are represented by discrete design variables in the optimization. Practical aspects such limitation to symmetric laminates and restraint on the number of plies with the same fiber orientation are also considered. The HSA used in this work extends the algorithm presented in de Almeida (2016) by the incorporation of additional strategies to dynamically change the parameters that control the generation of new design points. The modifications are introduced in order to adjust the exploration and exploitation efforts of the algorithm at different stages of the search. The first problem studied in this work deals with the optimization of a simply supported rectangular plate subjected to a biaxial uniform in-plane compressive load. The buckling load factor is given by an analytic expression, which make this a computationally inexpensive objective function. Many optimizations are performed for this problem in order to evaluate the reliability and efficiency of the method. The comparison of results obtained in this study to the result reported in other works shows that the modification proposed for the HSA can improve the performance of the algorithm. The last part of the paper shows the application of HSA to a more advanced structural optimization problem. The stacking sequence of a composite shallow shell is optimized to maximize the stiffness of the structure with respect to a pressure load. The objective function is formulated taking into account the critical load and the maximum displacement of the shell. These quantities are evaluated in a geometrically nonlinear analysis performed using a finite element solver presented by Almeida and Awruch (2009). The results obtained using HSA are compared to the optimizations performed by Almeida and Awruch (2009) using Genetic Algorithms. It is shown that the methodology used in this work reveals effective for the solution of optimization problems involving laminated composite structures with nonlinear behavior. de Almeida, F.S. Stacking sequence optimization for maximum buckling load of composite plates using harmony search algorithm. (2016) Composite Structures, 143. Almeida, F.S., Awruch, A.M. Design optimization of composite laminated structures using genetic algorithms and finite element analysis (2009) Composite Structures, 88 (3).

Runge-Kutta Based Generalised Convolution Quadrature Within an Elastodynamic BEM

Martin Schanz*

*Graz University of Technology

ABSTRACT

Boundary element formulations in time domain are well established in the engineering and the mathematical literature. In principle three types of formulations can be found: • Direct in time domain with analytical integration of the time convolution • Calculation in Laplace or Fourier domain with a subsequent numerical inverse transformation • Formulations based on the Convolution Quadrature Method (CQM) Common to all these approaches is the restriction to a constant time step size. The generalisation of the CQM to a non-uniform time mesh has been done by Lopez-Fernandez and Sauter [1], where the initial works use the implicit Euler as underlying time stepping method. To obtain higher order methods Runge-Kutta methods has been utilised within the generalised CQ [2]. These formulations have been presented for the single layer potential in acoustics or for acoustics with absorbing boundary conditions [3]. Here, the generalised CQ is applied to elastodynamics, where the single and double layer approach as well as a direct formulation for mixed boundary value problems will be presented. Essentially, the performance of the Runge-Kutta based generalized CQ is studied with respect to its convergence behaviour. As usual, the convergence order of the formulation is restricted by either the order of the Runge-Kutta method or by the spatial convergence order. In the presentation only a low order spatial discretisation is used. Numerical examples show the expected behavior. Further, first approaches to utilise fast methods within the generalised CQ will be presented. References [1] M. Lopez-Fernandez and S. Sauter, Generalized Convolution Quadrature with Variable Time Stepping. IMA Journal of Numerical Analysis 33 (2013), pp. 1156–1175. [2] M. Lopez-Fernandez and S. Sauter, Generalized Convolution Quadrature based on Runge-Kutta Methods. Numerische Mathematik 133 (2016), pp. 743–779. [3] M. Schanz and S. Sauter, Convolution Quadrature for the Wave Equation with Impedance Boundary Conditions. Journal of Computational Physics 334 (2017), pp. 442–459.

Effect of Occupant Size on Load and Displacement Response of the GHBM Detailed Occupant Models in a Frontal Sled Environment

Jeremy Schap*, Bharath Koya**, F. Scott Gayzik***

*Wake Forest School of Medicine, Virginia Tech-Wake Forest Center for Injury Biomechanics, **Wake Forest School of Medicine, Virginia Tech-Wake Forest Center for Injury Biomechanics, ***Wake Forest School of Medicine, Virginia Tech-Wake Forest Center for Injury Biomechanics

ABSTRACT

Computational human body models (HBMs) are playing a more prominent role in the development of safety systems across a variety of vehicle platforms. To use these tools to mitigate injuries, it is vital to take into account the full spectrum of potential occupant sizes. Therefore, the Global Human Body Model Consortium (GHBM) detailed occupant 5th percentile female (F05-O), 50th percentile male (M50-O) and 95th percentile male (M95-O) models were simulated in a frontal sled validation case. Comparisons were made between the three models to better understand effect of occupant size on load and displacement response. The previously published experimental sled decelerated from an initial velocity of 40 km/h with approximately 50th percentile male PMHS [1]. The sled minimized lower extremity movement via a rigid knee bolster and foot pan, each in contact with the PMHS throughout the event. No airbag or retractor was present. Three-dimensional kinematic response data were collected from the pelvis through head. Kinetic data were collected at each rigid part and seatbelt. By simulation, each HBM was first appropriately positioned and then gravity settled onto a published finite element sled model [2]. Then each HBM was belted in a three-point shoulder and lap belt. The experimental deceleration pulse was then applied to the rigid sled in the final simulation. Simulations ran with LS-Dyna R7.1.2 on a high-performance cluster. HBM biofidelity was first objectively verified by running CORA on M50-O load and displacement responses with respect to experimental corridors, created from five of the PMHS. The M50-O attained CORA scores of 0.84, 0.64, 0.77, 0.59, and 0.64 for seatbelt loads, reaction loads, head deflection, chest deflection, and spine deflection, respectively. The average score is 0.70, demonstrating reliable biofidelity. M95-O was morphed from M50-O. Additionally, CORA results for a morphed version of F05-O were previously published and were in line with the M50-O results. Higher load and displacement was generally observed as the size of the occupant increased. Compared with M50-O, peak forward head excursion is 11% greater and peak upper shoulder belt load is 7% greater in M95-O. M95-O experienced just over 60% higher chest compression on the left side of the chest where the shoulder belt passed compared to the M50-O. [1] Shaw et al., "Impact response of restrained PMHS in frontal sled", Stapp, 2009 [2] Poulard et al., "Contribution of pre-impact posture on restrained occupant", TIP, 2015

Interactions of Matrix and Interface Crack Growth in Composites

Johannes Scheel^{*}, Andreas Ricoeur^{**}

^{*}University of Kassel, ^{**}University of Kassel

ABSTRACT

Imperfect interfaces, e.g. occurring in composites, are having a crucial impact on propagating matrix cracks due to defect interaction [1]. The delamination, in return, is controlled not only by external loads but also by the matrix crack growth. In this numerical study, the interactions between the defects are investigated by examining the crack tip loadings, resulting crack paths and interface debonding, being crucial aspects of structural strength. The matrix crack tip loading is calculated by the J-integral. In order to incorporate the influence of imperfect interfaces, the J-integral needs to be reformulated. This influence depends on the appropriate modeling particularly of imperfect interfaces, where cohesive zones are an often used approach. The thermodynamical consistency of the implemented models is thus investigated. Above that, a consistent fracture mechanical frame work, involving both singular and cohesive cracks is presented, based on a thermodynamical approach. The matrix crack growth simulations require a continuous modification of the geometry due to incremental crack extensions. An intelligent re-meshing procedure is applied, where the loading history cannot be neglected due to the presence of dissipative processes at imperfect interfaces [2,3]. The distance between matrix crack tip and interface is essential for their interaction, going to extremes in the case of penetration, leaving several possibilities depending on the boundary value problem. The crack growth can stop, continue across the interface, in general with a kinking, or continue along the interface. In this regard, a criterion based on the J-integral is presented and applied to several test cases. [1] J. Scheel, A. Ricoeur; *Procedia Structural Integrity* 2017; 5: 255-262. [2] P. Judt, A. Ricoeur; *International Journal of Fracture* 2013; 182: 53-66. [3] P. Judt, A. Ricoeur, G. Linek; *Engineering Fracture Mechanics* 2015; 138: 33-48.

Nonlocal Modeling of Deformation and Damage Behavior of an Inhomogeneous Interphase in Nano-Particle Supercrystals

Ingo Scheider^{*}, Songyun Ma^{**}, Swantje Bargmann^{***}

^{*}Helmholtz-Zentrum Geesthacht, Institute of Materials Research, ^{**}RWTH Aachen, Institute of General Mechanics,

^{***}University of Wuppertal, Chair of Solid Mechanics

ABSTRACT

A novel nano-particle composite synthesized by bio-inspired design has been fabricated [1], which shows extraordinary mechanical characteristics due to the well-organized arrangement of soft and hard constituents in the microstructure. For this material, the inhomogeneous interphases surrounding the nano-particles play an important role in the mechanical performance of nano-composite. In order to describe this material on the nano-scale, particularly the interphase region, a nonlocal material model based on micropolar theory is proposed [2]. The new model is able to account for the scale of microstructure and describe the inelastic behavior, namely damage and plasticity, of interphases with gradient material properties. Micromechanical simulations are performed to investigate the relationship between nanostructures and mechanical properties of nanocomposites. The proposed damage model is validated by 3D micromechanical simulations for the nanoparticle super-crystals fabricated at different temperatures. The simulation results are in good agreement with the experimental data from micro-cantilever beams in terms of the stiffness, tensile strength and fracture energy absorption of the nanocomposites. [1] A. Dreyer, A. Feld, A. Kornowski, E. D. Yilmaz, H. Noei, A. Meyer, T. Krekeler, C. Jiao, A. Stierle, V. Abetz, H. Weller, G.A. Schneider, Organically linked iron oxide nanoparticle supercrystals with exceptional isotropic mechanical properties, *Nature Materials* 15(2016) 522{ 528. [2] S. Ma, I. Scheider, S. Bargmann; Ultrastrong nanocomposites with interphases: nonlocal deformation and damage behavior, submitted.

Robust Numerical Integration of Plasticity Models

William Scherzinger*, Brian Lester**

*Sandia National Laboratories, **Sandia National Laboratories

ABSTRACT

Recent work on the integration of plasticity models has enabled many high-fidelity models to be reliably implemented in production computing codes. A key aspect of this work is the adoption of line search methods for the return mapping algorithms. A Newton algorithm augmented with a line search method provides a very reliable technique for integrating plasticity models using a closest point projection algorithm. While the method is robust, little work has been done investigating the method to improve the convergence. Line search methods written for general minimization problems have a few parameters that govern the behavior of the method. Usually these parameters are set to some default value found in the optimization literature. However, for return mapping algorithms, improved convergence can be found by modifying these parameters. Furthermore, scaling, or conditioning, the residual can also improve the closest point projection algorithm. This work presents an overview of line search methods applied to closest point projection algorithms used with plasticity models, and looks to improve performance of the algorithms for complex plasticity models by choosing better line search parameters. The effect of scaling the residual is also examined with the goal of finding optimal scaling parameters for a given plasticity model. The anisotropic plasticity models of Barlat and co-workers are used to investigate the line search methods and scaling strategies. Results are presented that show significant improvement in the convergence of the return mapping algorithms.

In-Plane/Out-of-Plane Separated Representations of Navier-Stokes Solutions in Thin Geometries

Adrien Scheuer^{*}, Rubén Ibañez^{**}, Emmanuelle Abisset-Chavanne^{***}, Francisco Chinesta^{****},
Roland Keunings^{*****}

^{*}Université catholique de Louvain, Louvain-la-Neuve, Belgium; Ecole Centrale de Nantes, Nantes, France, ^{**}Ecole Centrale de Nantes, Nantes, France, ^{***}Ecole Centrale de Nantes, Nantes, France, ^{****}ENSAM ParisTech, Paris, France, ^{*****}Université catholique de Louvain, Louvain-la-Neuve, Belgium

ABSTRACT

Fluid flows in degenerated geometries, in which the characteristic length in one direction is much smaller than in the others, are a challenging task for standard mesh-based simulation techniques, that often require a tremendous number of discretization points or elements to provide accurate resolutions. Classically, ad-hoc simplifications or approximations (e.g. lubrication theory) are rather called for in order to conduct tractable simulations. In this work, we consider, within the Proper Generalized Decomposition (PGD) framework, an in-plane / out-of-plane separated representation of the solutions of the Navier-Stokes equations in thin geometries. The use of such separated representation let us decouple the meshes in the plane (coarse) and thickness (fine) directions, allowing a high-resolution representation of the solution evolution along the thickness coordinate while keeping the computational complexity characteristic of 2D simulations. This technique is particularly well suited to obtain efficiently fine and accurate solutions in boundary layers or in narrow geometries when approximations based on lubrication theory are not suitable.

A Small Strain Crystal Plasticity Formulation Based on the Primal Dual Interior Point Method

Lisa Scheunemann*, Paulo Salvador Britto Nigro**, Jörg Schröder***, Paulo Pimenta****

*Institute of Mechanics, University Duisburg-Essen, Germany, **Institute of Mechanics, University Duisburg-Essen, Germany, ***Institute of Mechanics, University Duisburg-Essen, Germany, ****Structural and Geotechnical Engineering, Polytechnic School at University of Sao Paulo Brazil Sao Paulo, Sao Paulo

ABSTRACT

Single crystal plasticity plays a major role in the analysis of material anisotropy. The polycrystalline material response is obtained upon considering a structure consisting of various individual, single grains, often also considering interface effects at the grain boundaries. On the individual grain level, single crystal plasticity can be treated in the mathematical framework of multisurface plasticity, leading to a constrained optimization problem wherein multiple constraints are defined as yield criteria on the different slip systems. Different approaches have been established in this field, see, e.g., [2], [3]. In rate-independent models, the set of active slip systems in the grain is possibly nonunique and is identified in, e.g., an active set search. Rate dependent approaches are based on power-type creep laws which do not differentiate into active or inactive slip systems. However, the constitutive equations of these formulations are often very stiff and require a small time increment. Here, a new algorithm for the solution of the constrained optimization problem based on the primal dual interior point method (PDIPM), [1], involving slack variables is presented for the framework of small strain single crystal plasticity. The use of slack variables therein stabilizes the conventional method and allows for a temporary violation of the constraint during the optimization. The optimization is solved using a Lagrange functional, wherein the nonlinear system of equations resulting from the derivation of the Lagrange functional is linearized using Taylor expansion and solved by a Newton Raphson scheme. All slip systems are considered simultaneously, omitting an iterative active set search. PDIPM has been found to lead to very efficient algorithms and better convergence rates than barrier or penalty methods. The stability of the algorithm would be especially beneficial in complex material models, such as a multiscale description of polycrystalline materials. Several numerical examples are presented, showing the performance of the developed algorithm based on academic slip system setups as well as face-centered-cubic crystals. References [1] El Bakry, A.S., Tapia, R.A., Tsuchiya, T. and Zhan, Y.: On the formulation and Theory of the Newton Interior Point Method for Nonlinear Programming. *Journal of Optimization Theory and Applications*, 89 (1996), 507-541. [2] Cuitino, A.M. and Ortiz, M.: Computational modelling of single crystals. *Modelling and Simulation in Materials Science and Engineering*, 1 (1992), 225-263. [3] Peirce, D., Asaro, R.J. and Needleman, A.: An analysis of nonlinear and localized deformation in ductile single crystals. *Acta Metallurgica*, 30 (1982), 1087-1119.

GENERIC-based numerical methods for the thermodynamically consistent simulation of coupled thermomechanical solids

Mark Schiebl^{*}, Peter Betsch^{**}

^{*}Institute of Mechanics, Karlsruhe Institute of Technology (KIT), Germany, ^{**}Institute of Mechanics, Karlsruhe Institute of Technology (KIT), Germany

ABSTRACT

This work deals with the Energy-Momentum-Entropy (EME) consistent time integration of open thermoelastic systems. While energy-momentum preserving integrators are well-known for conservative mechanical systems, Romero introduced in (I. Romero, Thermodynamically consistent time-stepping algorithms for nonlinear thermomechanical systems, *IJNME*, 79(6): 706-732, 2009) the class of thermodynamically consistent integrators for coupled thermomechanical systems, which further respect symmetries of the underlying coupled system and are therefore capable of conserving associated momentum maps. As mathematical framework for the geometric structure of the non-equilibrium thermodynamics the GENERIC (General Equation for Non-Equilibrium Reversible-Irreversible Coupling) framework is used. The GENERIC framework, originally proposed by Grmela and Öttinger for complex fluids (M. Grmela and H.C. Öttinger, Dynamics and thermodynamics of complex fluids. i. development of a general formalism. *Physical Review E*, 56(6):6620, 1997), expresses the evolution equation as the sum of reversible and irreversible contribution via a Poisson and a dissipative bracket. Since the GENERIC framework does not depend of a specific choice of the thermodynamical state variables (A. Mielke. Formulation of thermoelastic dissipative material behavior using generic. *Continuum Mechanics and Thermodynamics*, 23(3):233–256, 2011), we explore the structure of GENERIC framework using the entropy density, see e.g. (M. Krüger, M. Groß and P. Betsch. An energy-entropy-consistent time stepping scheme for nonlinear thermo-viscoelastic continua. *ZAMM-Journal*, 96(2):141–178, 2016), the absolute temperature, see e.g. (M. Hütter and B. Svendsen. Thermodynamic model formulation for viscoplastic solids as general equations for non-equilibrium reversible–irreversible coupling. *Continuum Mechanics and Thermodynamics*, 24(3):211–227, 2012), and further the internal energy density as thermodynamical state variable from which the weak form of the initial boundary value problem can be gained. Applying the notion of a discrete gradient in the sense of Gonzalez (O. Gonzalez. Design and analysis of conserving integrators for nonlinear Hamiltonian systems with symmetry. PhD thesis, Stanford University, 1996) leads to an EME integrator. As boundary conditions rely on the specific choice of the thermodynamical state variable we extend the GENERIC framework to be suitable for open systems following the procedure in (H. C. Öttinger. Nonequilibrium thermodynamics for open systems. *Physical Review E*, 73(3):036126, 2006). The presentation will indicate key differences and similarities between the alternative choices of thermodynamical state variables and will include several simulations with different boundary conditions using an energy-based termination criterion.

Superelements in a Screw Theory based Floating Frame of Reference Formulation

Jurnan Schilder^{*}, Marcel Ellenbroek^{**}

^{*}University of Twente, ^{**}University of Twente

ABSTRACT

The floating frame of reference formulation is a commonly applied method for the simulation of flexible multibody system dynamics in which the elastic behavior of each body is small relative to the body's local floating frame. Hence, the local elastic behavior of a body can be described by its linear finite element model. For this reason, the formulation naturally allows for use of substructuring methods, since modal order reduction techniques can be applied to describe the local elastic behavior with a limited number of generalized coordinates. The use of substructuring methods has led to the development of superelements for flexible multibody dynamics. In this, the absolute position and orientation of coordinate systems attached to a body's interface points are used as generalized coordinates. In terms of these coordinates, kinematic constraints between bodies can be enforced directly and do not require the use of Lagrange multipliers. In order to develop these superelements, a coordinate transformation is required that expresses the absolute floating frame coordinates and the local elastic displacement field in terms of the absolute interface coordinates. In literature, several methods for creating superelements have been proposed. In recent work [1], the authors presented a new method that enables a coordinate transformation to absolute interface coordinates in a way that the floating frame can be attached to a material point, not being an interface point. Here, Craig-Bampton interface modes are used as a reduction basis for the local mass and stiffness matrices. It is shown that by demanding zero elastic deformation at the location of the floating frame, the floating frame coordinates can be eliminated from the degrees of freedom. The method as described in [1] is formulated in terms of engineering coordinates, i.e. in terms of position vectors, rotation matrices, linear and angular velocities et cetera. In this work, this method is reformulated based on screw theory. In particular, a full and complete derivation of the inertia forces will be presented in terms of the twists of the interface points. In this way, the authors intend to make the method convenient to use for a broad range of fields and applications, independent of scientists and engineers use engineering coordinates or screw theory in that particular field. [1] Ellenbroek, M. & Schilder, J., "On the use of absolute interface coordinates in the floating frame of reference formulation for flexible multibody dynamics", J. Multibody Syst Dyn (2017). <https://doi.org/10.1007/s11044-017-9606-3>

Multiscale and Variational Modeling of Amorphous Silica Glass

William Schill^{*}, Michael Ortiz^{**}

^{*}California Institute of Technology, ^{**}California Institute of Technology

ABSTRACT

We develop a critical-state model of fused silica plasticity on the basis of data mined from molecular dynamics (MD) calculations. The MD data is suggestive of an irreversible densification transition in volumetric compression resulting in permanent, or plastic, densification upon unloading. The MD data also reveals an evolution towards a critical state of constant volume under pressure-shear deformation. The trend towards constant volume is from above, when the glass is overconsolidated, or from below, when it is underconsolidated. We show that these characteristic behaviors are well-captured by a critical state model of plasticity, where the densification law for glass takes the place of the classical consolidation law of granular media and the locus of constant volume states denotes the critical-state line. A salient feature of the critical-state line of fused silica, as identified from the MD data, that renders its yield behavior anomalous is that it is strongly non-convex, owing to the existence of two well-differentiated phases at low and high pressures. We argue that this strong non-convexity of yield explains the patterning that is observed in molecular dynamics calculations of amorphous solids deforming in shear. We employ an explicit and exact rank-2 envelope construction to upscale the microscopic critical-state model to the macroscale. Remarkably, owing to the equilibrium constraint the resulting effective macroscopic behavior is still characterized by a non-convex critical-state line. Despite this lack of convexity, the effective macroscopic model is stable against microstructure formation and defines well-posed boundary-value problems [1]. We study continuum mechanics examples of silica glass involving ballistic impact. We then study connections between this anomalous shear yield behavior and strain rate effects in loading of the glass employing time scale bridging techniques with specific interest in the behavior of amorphous solids. 1. W. Schill, S. Heyden, S. Conti, M. Ortiz, The Anomalous Yield Behavior of Fused Silica Glass, submitted to the Journal of Mechanics and Physics of Solids, 2017

Discontinuous Galerkin Methods through the Lens of Variational Multiscale Analysis

Dominik Schillinger^{*}, Stein K.F. Stoter^{**}, Bernardo Cockburn^{***}

^{*}Department of Civil, Environmental, and Geo- Engineering, University of Minnesota, Twin Cities, USA,

^{**}Department of Civil, Environmental, and Geo- Engineering, University of Minnesota, Twin Cities, USA, ^{***}School of Mathematics, University of Minnesota, Twin Cities, USA

ABSTRACT

The variational multiscale method was introduced by Tom Hughes and his students in the mid-1990s and has been primarily used as a unifying framework for stabilized finite element methods and to design effective subgrid-scale models in computational fluid dynamics. In this talk, we employ the variational multiscale method to open up an alternative perspective on discontinuous Galerkin methods. We first establish a multiscale variational formulation, based on the decomposition of the true solution into a discontinuous coarse-scale solution and a discontinuous fine-scale solution in each element domain. We tie discontinuous elements together by fine-scale interface conditions that naturally arise from the strong-form transmission conditions. We argue that the resulting multiscale variational form represents a general unifying framework for discontinuous Galerkin methods. In support of this claim, we show that standard discontinuous Galerkin methods can be recovered from this multiscale framework by choosing appropriate fine-scale closure models that relate coarse- and fine-scale solutions. We explain specific closure models for the examples of the interior penalty (IP) method and the local discontinuous Galerkin (LDG) method. We then show that these closure models offer new insights into the inner workings of the IP and LDG methods, in particular with respect to the numerical behavior at element interfaces. We close our talk with a few personal recollections of the speaker (D. Schillinger) on his advisor, mentor and friend Tom Hughes.

A Computational Modeling Approach to Model Patterned Strain Localizations in Magnesium Alloys

Sara Schlenker^{*}, Konstantinos Baxevanakis^{**}, Brian Wisner^{***}, Antonios Kotsos^{****}

^{*}Drexel University, ^{**}Drexel University, Loughborough University, ^{***}Drexel University, ^{****}Drexel University

ABSTRACT

A number of non-local constitutive theories have been developed to account for the phenomena of size dependence in material behavior. In the case of metals, several of these theories incorporate the gradient of plastic strain, or of plastic slip, as an independent state variable in the free energy equation. This introduces a dimensionally required length scale into the constitutive law and allows a connection between microstructural information and macrostructural behavior. Implementation of this class of theory into a finite element code additionally has been shown to induce patterning or localization of strains that could inform understanding of the mechanics and causes of the instabilities related to the transition from homogenous to locally-dominated behavior. This could additionally lead to more reliable predictions of plastic deformation in metal alloys such as in the case of Magnesium which is characterized by pronounced plastic anisotropy as well as the appearance of strain localization bands that have been associated with spatially inhomogeneous deformation twinning. Several computational methods used to predict strain localizations in the form e.g. of shear bands rely on geometrical changes such as reduction of thickness or a priori imposed defects to initiate such localized effects. In others, the material properties of a region are modified to induce localizations. In this talk, a computational model is presented which is capable to induce strain localizations as a result of the defined constitutive law. To achieve this goal, the approach explores the effect of gradient-based constitutive laws on inducing strain localizations in models free of triggering flaws. To demonstrate this approach, Finite Element models incorporating custom higher gradient constitutive laws are employed. The obtained simulation results are compared against available multiscale experimental strain measurements obtained using advanced optical metrology methods. Furthermore, an approach to include this computational formulation in a crystal plasticity framework is presented.

Imperfect Interfaces in Magnetoelectric Composites and Their Impact on Coupling Coefficients

Alexander Schlosser*, Andreas Ricoeur**

*University of Kassel, **University of Kassel

ABSTRACT

The efficiency in converting magnetic into electric energy and vice versa makes magnetoelectric (ME) composites promising candidates for many technical applications. The ferroelectric matrix as well as the magnetostrictive inclusions of particle composites and the layers of laminates are mostly ceramics or other brittle materials, thus being prone to cracking. Independent from the kind of composite the transmission of stresses via the interfaces between the constituents plays the key role in the functionality of ME composites. Therefore, the investigation of delamination processes is of great interest for the prediction of durability and coupling factors. In order to investigate delamination processes in ME composites, cohesive elements are being developed and applied in combination with nonlinear ME finite elements described in [1] and [2]. The mechanical behavior of the cohesive zone is classically prescribed by a bilinear traction-separation-law. Magnetic and electric fluxes emanate from evolution laws of magnetic and electric permeabilities, respectively, accounting for micro crack damage in the process zone and electrostatic stresses at the interfaces. Electric and magnetic properties change during damaging processes, being controlled by damage variables, which in turn are determined by the separation between the boundaries. Based on these cohesive elements, possible influence factors on delamination like the geometry of the composites or the ME poling processes are investigated, finally with regard to coupling coefficients. References: [1] Avakian, A., Gellmann, R., and Ricoeur, A. (2015). Nonlinear modeling and finite element simulation of magnetoelectric coupling and residual stress in multiferroic composites. *Acta Mechanica*, 226(8), 2789-2806. [2] Avakian, A., and Ricoeur, A. (2016). Constitutive modeling of nonlinear reversible and irreversible ferromagnetic behaviors and application to multiferroic composites. *Journal of Intelligent Material Systems and Structures*, 27(18), 2536-2554.

Relating the Horizontally Averaged Wind Profile to the Geometry of Idealized Urban Surfaces

Manuel F. Schmid^{*}, Marco G. Giometto^{**}, Marc B. Parlange^{***}

^{*}University of British Columbia, Vancouver, Canada, ^{**}Columbia University, New York, USA, ^{***}Monash University, Melbourne, Australia

ABSTRACT

The near-wall behavior of flow over rough surfaces depends on the geometry of the roughness. In urban areas, atmospheric models either have to resolve individual buildings or include a model for their effect on the flow. Large-scale models often employ one-dimensional urban canopy parameterizations to account for the unresolved surface elements. In this study, we attempt to model the wall-normal velocity profile in terms of statistical properties of the surface roughness. The Navier-Stokes equations are horizontally averaged to obtain an expression for the one-dimensional profile. The relationship between each term and the surface properties is assessed based on a series of large-eddy simulations of flow over idealized urban surfaces where roughness elements are resolved.

Stress and Driving Force Calculation within Multiphase-field Models: Applications to Martensitic Phase Transformation in Dual-phase Microstructures

Daniel Schneider^{*}, Ephraim Schoof^{**}, Felix Schwab^{***}, Christoph Herrmann^{****}, Michael Selzer^{*****}, Britta Nestler^{*****}

^{*}Institute of Applied Materials -- Computational Materials Science (IAM-CMS), Karlsruhe Institute of Technology (KIT) and Institute of Digital Materials Science (IDM), Karlsruhe University of Applied Sciences, ^{**}Institute of Applied Materials -- Computational Materials Science (IAM-CMS), Karlsruhe Institute of Technology (KIT), ^{***}Institute of Applied Materials -- Computational Materials Science (IAM-CMS), Karlsruhe Institute of Technology (KIT), ^{****}Institute of Digital Materials Science (IDM), Karlsruhe University of Applied Sciences, ^{*****}Institute of Applied Materials -- Computational Materials Science (IAM-CMS), Karlsruhe Institute of Technology (KIT) and Institute of Digital Materials Science (IDM), Karlsruhe University of Applied Sciences, ^{*****}Institute of Applied Materials -- Computational Materials Science (IAM-CMS), Karlsruhe Institute of Technology (KIT) and Institute of Digital Materials Science (IDM), Karlsruhe University of Applied Sciences

ABSTRACT

Numerical simulations based on phase-field methods are indispensable in order to investigate certain interesting and important phenomena in the evolution of microstructures. Microscopic solid state phase transitions are highly affected by mechanical driving forces and therefore the accurate calculation of the stresses in the transition region is essential. We present methods for stress calculations within the phase-field framework for finite deformations, which satisfy the mechanical jump conditions corresponding to sharp interfaces, although the sharp interface is represented as a volumetric region. The model allows to calculate phase inherent stresses and deformations even in regions where many phases coexist. Since the phase-inherent variables are known, appropriate methods can be used for the calculation of the internal variables in the bulk as well as in transition regions. We demonstrate that the models reflect the mechanical configurational forces for phase transitions and present applications to the martensitic phase transformation process in dual-phase microstructures. [1] D. Schneider, O. Tschukin, M. Selzer, T. Böhlke, B. Nestler, Phase-field elasticity model based on mechanical jump conditions. *Comp. Mech.* (2015) 5:887--901 [2] D. Schneider, F. Schwab, E. Schoof, A. Reiter, C. Herrmann, M. Selzer, T. Böhlke, B. Nestler, On the stress calculation within phase-field approaches: A model for finite deformations. *Comp. Mech.* (2017) 60:203--217 [3] D. Schneider, E. Schoof, O. Tschukin, A. Reiter, C. Herrmann, F. Schwab, M. Selzer, B. Nestler Small strain multiphase-field model accounting for configurational forces and mechanical jump conditions. *Comp. Mech.* (2017) in print [4] E. Schoof, D. Schneider, N. Streichhan, T. Mitnacht, M. Selzer, B. Nestler, Multiphase-field modeling of martensitic phase transformation in a dual-phase microstructure. *International Journal of Solids and Structures*. (2017) in print

GRAPH AND HEURISTIC BASED TOPOLOGY OPTIMIZATION OF CRASHWORTHINESS COMPOSITE PROFILE STRUCTURES MANUFACTURED BY VACUUM INFUSION AND GLUING

DOMINIK SCHNEIDER¹ SIMON LINK¹ ALEX SCHUMACHER¹ AND CHRISTOPHER ORTMANN²

¹ University of Wuppertal, Chair for Optimization of Mechanical Structures
Gaussstraße 20, 42119 Wuppertal, Germany
e-mail: dschneider@uni-wuppertal.de; simon.link@uni-wuppertal.de;
schumacher@uni-wuppertal.de website: <https://www.oms.uni-wuppertal.de/>

² Volkswagen Aktiengesellschaft
Letterbox 1777, 38436 Wolfsburg, Germany
e-mail: christopher.ortmann@volkswagen.de website: <http://www.volkswagen-ag.de/>

Key words: topology optimization, crashworthiness, heuristic, graph theory, composite profile, gluing.

Abstract. Composite structures enable lightweight solutions, which are required by the transportation industry to fulfil their weight targets. Many of those structures have high requirements regarding passive safety and manufacturing. Finding suitable designs for crashworthiness applications proves to be difficult because of material nonlinearities, contact, large displacements and in case of composite materials anisotropy, brittle failure and crushing. The graph and heuristic based topology optimization (GHTO) has already been utilized for the optimization of metal extrusion profiles under lateral crash loads. In order to enable the use of composite materials, the graph syntax, which is used to represent the geometry, is modified, so that it can carry information regarding fiber orientations and thicknesses of the layers. During the optimization, heuristics based on expert knowledge regarding crash applications evaluate the simulation data and propose new competing layouts with modified topologies. These designs are then evaluated with a single or multiple crash simulations in inner optimization loops. During the whole optimization process various manufacturing constraints prevent the occurrence of non-manufacturable designs.

This paper illustrates, how the GHTO can be extended for the optimization of crashworthiness composite profile structures under lateral loads. An extension of the graph syntax allows splitted structures which are glued together at flanges. New heuristics detect element failure and try to sustain the structural integrity. An optimization of a test specimen laterally impacted by a drop weight is carried out where the maximum contact force is minimized while restricting the maximum intrusion. Two improved designs and the initial design are manufactured and tested in a drop tower. The test results are presented and compared with the simulations.

1 INTRODUCTION

Composite materials enable lightweight structures because of their low density and high specific strength. In addition they show very good energy absorption capabilities if failing through stable crushing. They offer a great variety of design freedoms, like the type of matrix and fiber, the orientation and volume fraction of the fibers or the manufacturing process.

The large number of design freedoms and manufacturing constraints complicate the component development for crash applications. Popular commercially available topology optimization methods for linear static problems^[2,3] cannot be utilized in the process because of material nonlinearities, contact, large displacements and the explicit finite element method. Other methods^[4] try to overcome these issues. The Graph and Heuristic Based Topology Optimization (GHT)^[1] can be utilized to optimize the topology of structures with a constant cross section like extrusion profiles or rib layouts^[5]. The cross-section is described by a mathematical graph which enables algorithmic manipulations of the geometry while allowing to check manufacturing constraints. Heuristics that are based on expert knowledge regarding crash applications are used in an outer optimization loop to suggest new designs. They insert or remove walls from designs of the previous iteration after analysing their simulation results like nodal displacements, velocities, energy densities and element deletion. Inner optimization loops evaluate all new topologies by calling the commercial optimizer LS-OPT that changes e.g. the thicknesses to reach the given optimization objective while meeting the constraints. If desired a shape and sizing optimization of the best design can be carried out at the end of the optimization to try to reach further improvements.

To extend the field of application towards composite structures with constant cross-section, some adjustments are necessary, that are described in this paper. An optimization of a test specimen is carried out to demonstrate the procedure. The structure is built up by several parts with flanges that are glued together. Two improved designs as well as the initial design are manufactured by vacuum infusion and gluing to test the structures in physical experiments. Splitting the structure in several parts avoids the need to use pultrusion as the manufacturing process, which would have led to expensive tool costs for these small quantities.

2 ADAPTIONS FOR COMPOSITE STRUCTURES WITH FLANGES

Before using composite structures in an optimization, some adaptations in the GHT process are necessary. At first new information regarding the composite layup and the flanges have to be saved in the graph and taken into account while creating the input decks for the finite element simulations. In addition the material failure has to be considered. Besides new heuristics that are needed to address the material failure, the existing heuristics have to be modified to stop analyzing the finite element results after failure occurs in the observed area, since torn apart pieces flying through the space would lead to false interpretations of the deformation behavior. Furthermore the existing manufacturing constraints like limiting the minimum distance between two walls are extended by a new constraint that forbids to attach a new wall to a location with an already existing flange.

2.1 Graph syntax

The graph contains all the relevant information to describe the geometry of a structure with a constant cross section. As shown in Figure 1 each wall consists of different vertices connected by edges. The LINK-Vertices define the location of the walls with Cartesian coordinates. The BEAMG-Vertices save the thickness of each wall as well as its curvature and, in case of prescribed flange connections on outer walls, additional parameters like the overlapping length and the flange position. The BEAM1- and BEAM2-Vertices define the layer angles and layer fractions of a symmetrical composite layup or stay empty in case of applications with metal. Finally the PARAM-Vertex stores global parameters that describe the whole structure like the extrusion length and the density of the material, to allow internal mass calculations. In case of other applications like finding rib layouts^[5] the vertices can contain additional information like rib heights.

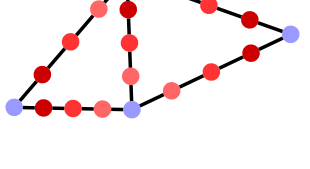
Graph Element	Contained information	
● BEAMG-Vertex	thickness, curvature, flange information	
● BEAM1-Vertex	composite layer angles	
● BEAM2-Vertex	composite layer fractions	
● LINK-Vertex	coordinates	
— EDGE	connected vertices	
○ PARAM-Vertex	e.g. extrusion length and density	

Figure 1: List of graph elements with their contained information, right: an exemplary graph

2.2 Flanges

There are two types of flanges currently implemented in the procedure. A custom flange connection can be defined on an outer wall by specifying the needed information in the BEAMG-Vertex. As displayed in Figure 2 the flange length, the flange position and the flange side can be stated. The overlapping length and the position are entered as a value between 0 and 1 with regard to the wall length. A position of 0 indicates that the flanges are located at the start of the wall and 1 respectively at the end, factoring in the edge direction. The side parameter controls on which side in edge direction the flange connection is established.

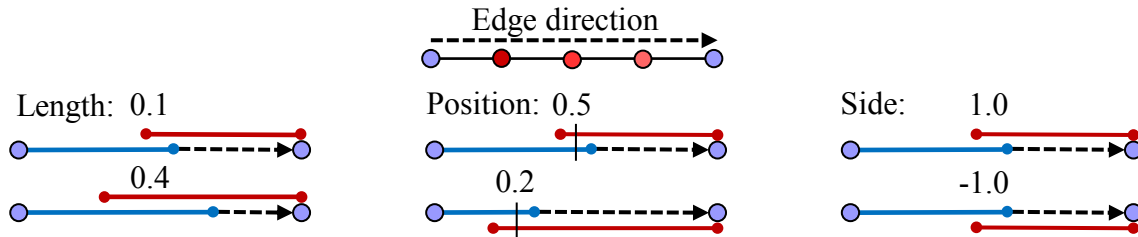


Figure 2: flange parameters, left: flange length, middle: flange position, right: side of the flange

Inner walls can automatically connect to the rest of the structure as new parts with flanges on both sides, so that each wall can be manufactured separately without undercuts. When inner walls share the same LINK-Vertex they connect to the other walls by creating a flange parallel to the next wall in clockwise direction, as displayed in Figure 3a. In case that two inner walls are connected nearly straight they are realised as a single part (Figure 3b).

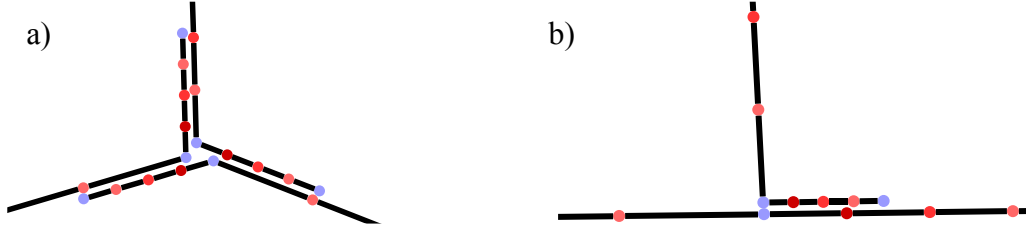


Figure 3: a) clockwise orientation of flanges of inner walls, b) no flanges created between straight connected inner walls

During the automatic creation of a finite element model, tied contacts are created between the flanges and the corresponding walls with a material defined by the user to represent the adhesive. Figure 4a shows an exemplary graph that is internally split into a converted graph (Figure 4b) with the presented rules to outline the flange connections. It is then extruded and meshed (Figure 4c) by GRAMB (Graph based Mechanics Builder), that was developed to create the input decks. As displayed, the composite layups are currently modeled with single layer elements, that contain the ply information in the material card (ESI VPS) or in the *PART_COMPOSITE definition (LS-DYNA), depending on the solver to be used. This approach saves computation time but is not capable of capturing delamination.

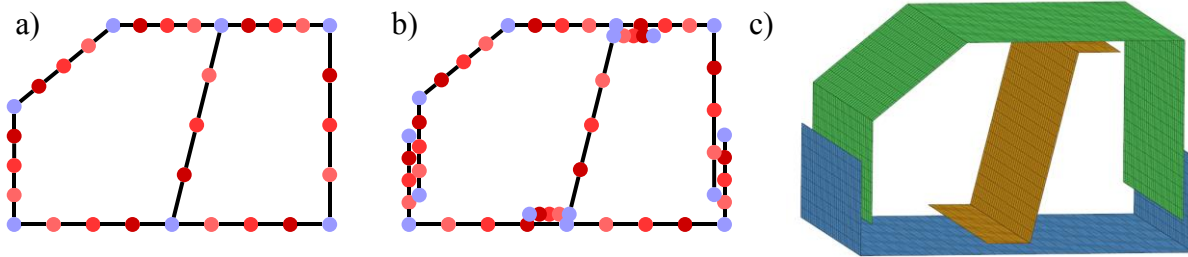


Figure 4: a) original graph, b) converted graph with flanges, c) extruded mesh

2.3 Heuristic Support Collapsin Walls

In addition to the existing heuristics^[1], the heuristic Support Collapsing Walls (SCW) is introduced to address a possible loss of the structural integrity through material failure. If detecting sudden and extensive failure, the wall with the highest failure index f is supported perpendicularly at the position of the most severe damage as displayed in Figure 5, where a cylinder impacts a structure that experiences material failure in the impact area. The failure index is calculated for each wall in each load case by formula (1).

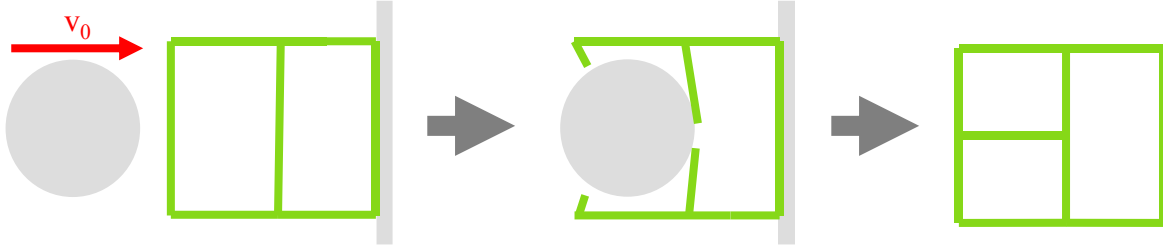


Figure 1: Principle of the heuristic Support Collapsing Walls

$$f = \max_{t_1, t_2} \left[\frac{n(t_1, t_2)}{0.9 \cdot \frac{(t_2 - t_1)}{\Delta t_{ref}} + 0.1} \right] \quad (1)$$

Here the number of elements deleted between the time t_1 and t_2 is divided by the fraction of this duration in relation to the period Δt_{ref} between the first and last occurrence of element deletion of the whole structure during the simulation. This allows to put more emphasis on strong failure in a short amount of time in contrast to less failure occurring during a longer period. To find the interval that delivers the highest failure index, t_1 and t_2 are varied in a heuristic approach to identify the maximum failure index for each wall. The heuristic then tries to support the wall with the highest failure index of all load cases perpendicular at the middle point of the deleted elements of the corresponding wall. If this fails the heuristic continues to support the wall with the next highest failure index.

2.4 Optimization variables

To evaluate the heuristic proposal, inner optimization loops can be carried out where the thicknesses of the structure are modified to improve the optimization goal. If working with composites an option is added to vary the global laminate direction that turns the complete layup of the composite. When running the final size and shape optimization, not only the thickness, the curvature and the shape can be optimized, but also the layer directions and/or the layer fractions of the layup of the whole structure. Changing the layer angles and fractions of each individual wall is not intended since it would lead to a large number of design variables that would increase the optimization time enormous and could not be handled efficiently by the optimization algorithms.

3 OPTIMIZATION OF A TEST SPECIMEN

With the new adaptations to the GHT, an optimization is carried out, that deals with a composite profile being laterally impacted by a semi-cylindrical weight in a drop tower. Since three different designs of the optimization will be manufactured and tested, the optimization problem and the simulation model are chosen to represent the test setup.

3.1 Simulation model and test setup

The simulation model is displayed on the left side of Figure 6. The rigid steel drop weight with a mass of 50 kg is guided along the Z-axis and moves with an initial velocity of 3 m/s against the Z-direction. The lower part of the drop weight has a semi-cylindrical shape with a diameter of 80 mm. The profile rests on a rigid steel plate, whose contact force with the profile is tracked during the simulation. For all contacts a friction of 0.2 is defined. The simulation is terminated by a sensor short after the drop weight starts to move back after the maximum intrusion. The model represents the test setup, visible on the right side of Figure 6. It only differs by the buffer elements on the sides that start to stop the drop weight roughly 27 mm before hitting the ground to avoid damaging the force sensor and the underlying structure in case the profile cannot stop the drop weight. Bidirectional $\pm 45^\circ$ -layers with 300 or 400 g/m² made of TENAX STS40 24K carbon fibers are used to create one of the following symmetric stacking sequences with the corresponding thicknesses assuming a fiber volume content of 48%:

- $[90^\circ, 0^\circ, 90^\circ, 0^\circ, 45^\circ, -45^\circ, 45^\circ, -45^\circ]_s \rightarrow 2.8 \text{ mm}$ with 300g/m²
- $[90^\circ, 0^\circ, 45^\circ, -45^\circ]_s \rightarrow 1.87 \text{ mm}$ with 400g/m²
- $[90^\circ, 0^\circ, 45^\circ, -45^\circ]_s \rightarrow 1.4 \text{ mm}$ with 300g/m²

The material cards for the tight contact and the composite are chosen from a set of existing cards of similar materials since no testing can be conducted to fit new material cards. Hence differences between the simulation model and the experiments are to be expected. The simulations are carried out with the commercial solver Pam-Crash.

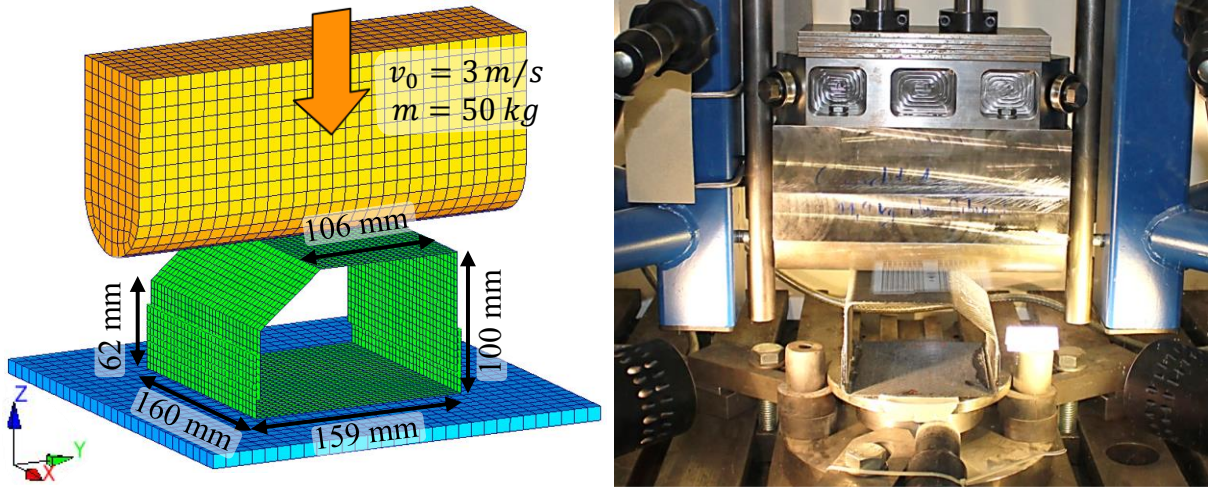


Figure 6: Simulation model (left) and corresponding test setup (right)

3.2 Optimization problem

As displayed in Table 1 the objective of the optimization is to minimize the maximum occurring force between the ground and the profile, filtered with a SAE-1000Hz-filter. The intrusion of the drop weight is restricted to 60 mm, to leave some deformation room in case the

drop weight is stopped later than predicted during the tests. During the heuristic evaluation the uniform thickness of the walls can be modified. In addition to that the shape can be varied in the final size and shape optimization. It should be mentioned that the restriction to forbid inner walls from ending at flanges of outer walls had not been implemented at the time of the optimization. All other manufacturing constraints are active and are listed in Table 1. The constraints are chosen quite restrictive to guarantee easy to manufacture structures, especially increasing the number of chambers would cause a much higher number of parts to be manufactured and glued together. During the inner optimization loops sequential domain reduction is applied combined with a genetic algorithm that is used for the optimization on the metamodel.

Table 1: Optimization problem

Objective	Minimize the maximum filtered contact force with the ground F_{max}
Constraints	Intrusion of drop weight (Z-direction) $d_z \leq 60$ mm
Design variables	Uniform thickness of the walls t Shape variables (only in final size and shape optimization)
Manufacturing constraints	Connection angle between two walls $> 60^\circ$ Wall distance > 20 mm Wall thickness > 1.4 mm and < 2.8 mm Size ratio between the largest and smallest chamber < 20 Number of chambers ≤ 3

3.3 Optimization results

The optimization starts with an empty profile without inner structures. During the Optimization in 3 Iterations 26 further designs are created and evaluated, causing about 1000 crash simulations for the heuristic evaluation and additional 1000 crash simulations for the final size and shape optimization of the so far best result. Three designs from that optimization, the initial design and the two best designs of the optimization, are chosen to be manufactured and tested. The graph and the results are displayed in Figure 7 and Table 2.

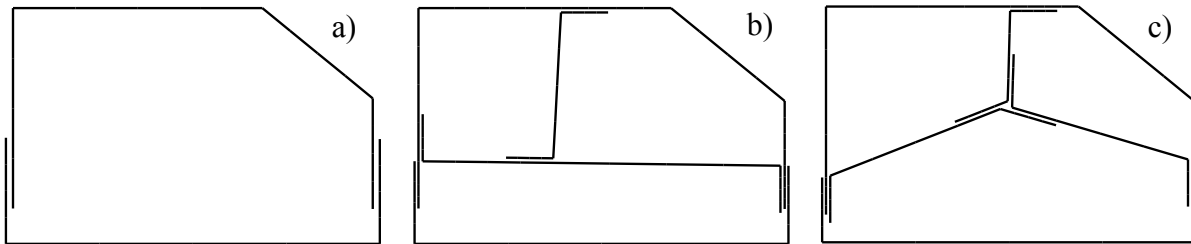


Figure 7: graphs (without vertices) of a) start design, b) option 1 and c) option 2

Table 2: Results of the selected designs from the optimization

Original Design	F_{max} [kN]	d_z [mm]	mass [kg]	t [mm]	Layup
Start	11.0	48.3	0.336	2.52	[90°,0°,90°,0°,45°,-45°,45°,-45°]s
Option 1	6.52	55.5	0.297	1.49	[90°,0°,90°,0°,45°,-45°,45°,-45°]s
Option 2	7.44	57.9	0.332	1.61	[90°,0°,90°,0°,45°,-45°,45°,-45°]s

The initial design only uses 80% of the allowed intrusion since a further reduction of the thickness would lead to a complete failure of the structure without stopping the mass. The new topologies meet the requirements to only consist of 3 chambers and are able to reduce the maximum force by 41% respectively 32%.

Since the optimization with continuous thicknesses delivers designs, that cannot be manufactured, the layups of the 3 designs are matched with the best fitting available stacking sequence for the inner and outer walls and new simulations are carried out (results in Table 3).

Table 3: Results of the adjusted designs

Adjusted Design	F_{max} [kN]	d_z [mm]	mass [kg]	t_{inner} [mm]	t_{outer} [mm]	Layup
Start S	15.3	26.0	0.372	-	2.8	[90°,0°,90°,0°,45°,-45°,45°,-45°]s
Option1 O1	7.72	55.3	0.313	1.87	1.4	[90°,0°,45°,-45°]s
Option2 O2	8.14	57.9	0.326	1.87	1.4	[90°,0°,45°,-45°]s

4 COMPARISON OF SIMULATION AND EXPERIMENT

For each adjusted design five test examples are manufactured by vacuum infusion and later glued together to create the structures displayed in Figure 8. Three of each structure are then tested in a drop tower and the results are compared with the simulations. The tests should deliver more knowledge about crash applications with composite profiles and point out necessary adjustments of the flange creation and new proposals for heuristics. Since not all structures are able to stop the drop weight before it hits the puffer elements, one of each structure is tested with a lower velocity of 2.45 m/s.

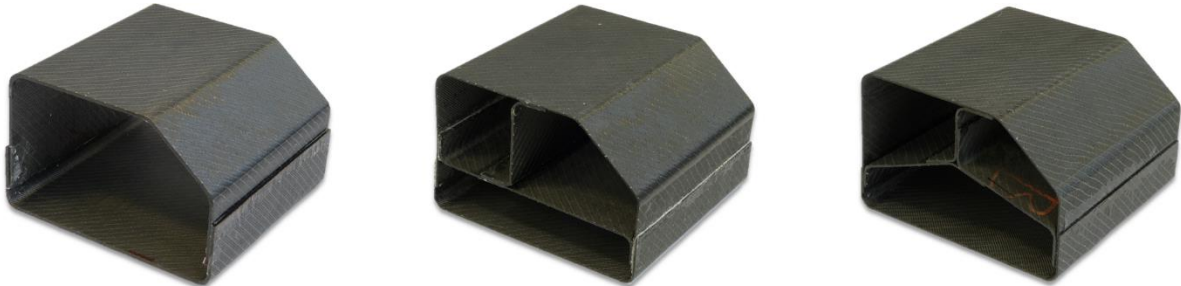


Figure 8: The manufactured profiles

4.1 Startin desin S

As displayed in Figure 9 and Figure 10 all tests of the start design S as well as the simulation are able to stop the drop weight although the maximum intrusion varies between 20 mm for experiment S-3 with the lower velocity and 40 mm for S-1. The simulation S-Sim delivers the highest peak force of 15.3 kN whereas the tests show more smooth force curves that reach between 9.6 and 12.8 kN. The general deformation behavior from the tests matches the simulation quite well, although the simulation develops a crack in the upper left corner. All flange connections remain undamaged during the tests and the simulation.

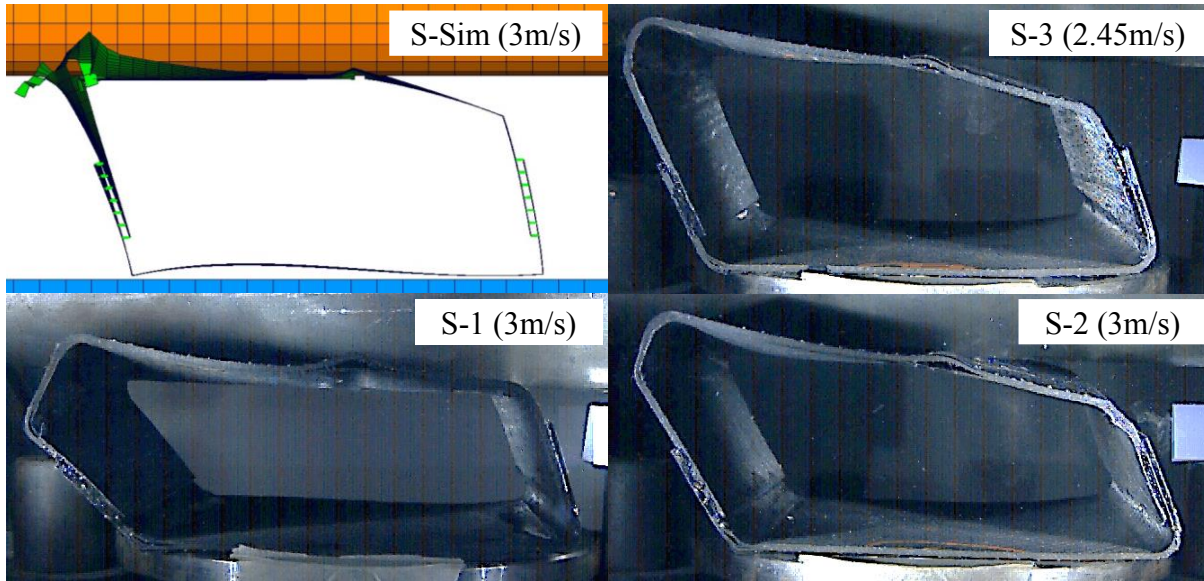


Figure 9: Deformations of the start designs S

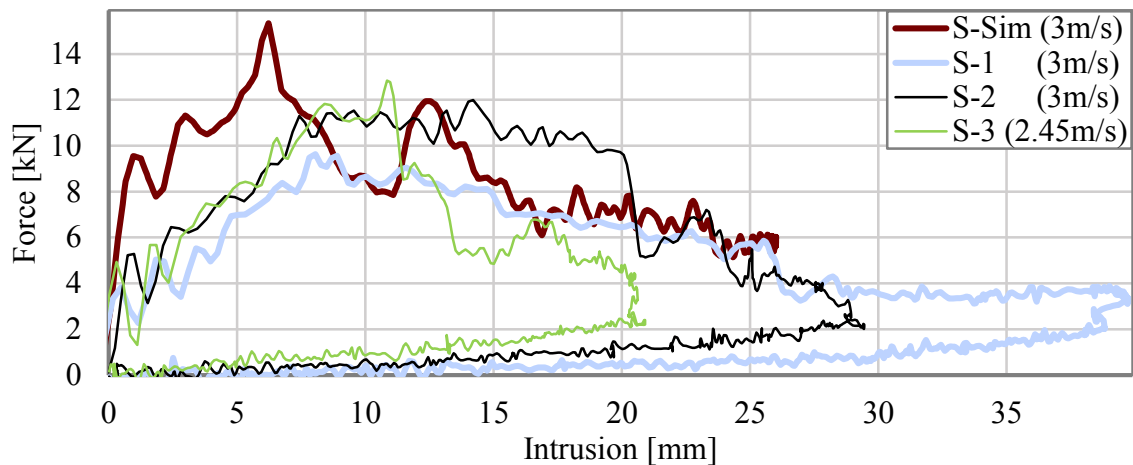


Figure 10: Force curves of the start designs S

4.2 Optimisation result O1

Figure 11 reveals more differences between the deformation behavior of the simulation and the tests. While the upper wall is torn apart in the simulation and some more areas experience damage, the tests reveal failing flange connections that in case of O1-2 even lead to the drop weight crushing the structure and only getting stopped by the puffer elements. During the deformation of O1-1 and O1-3 the flange on the left side fails but the perpendicular middle wall gets in contact with the ground and stays stable so that it increases the resistance against the drop weight and stops it. The force curves in Figure 12 also reveal the differing deformation behaviors. The maximum forces range between 5.3 kN for O1-3 and 10.4 kN for O1-1, although O1-2 could have also experienced a peak at the end if the energy of the drop weight had not been absorbed by the puffers, that were placed next to the force measuring plate. The intrusions vary between 52.1 mm (O1-3) and more than 81.8 mm (O1-2).

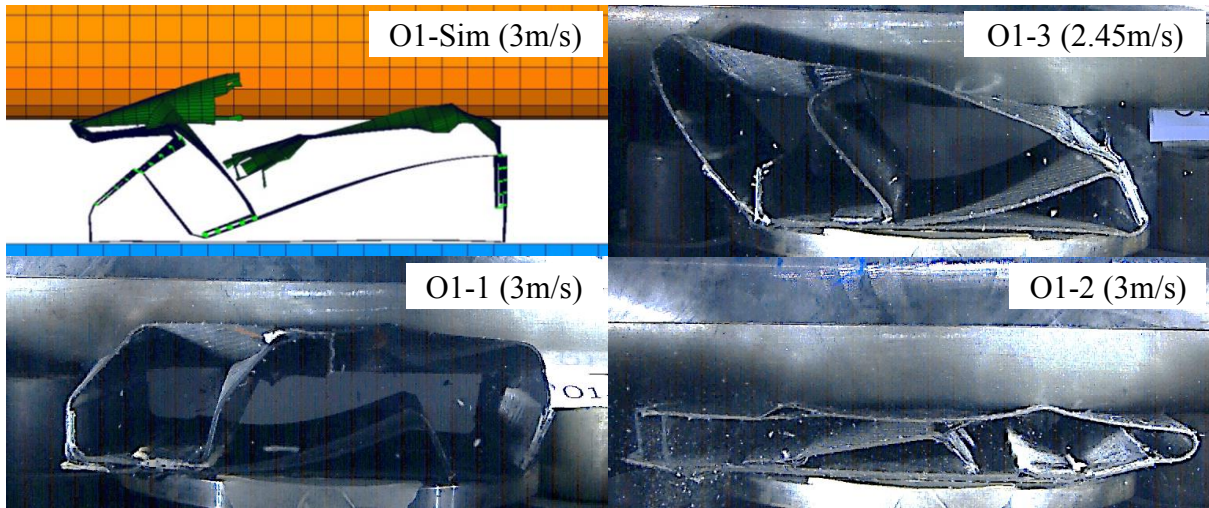


Figure 11: Deformations of the options 1 (O1)

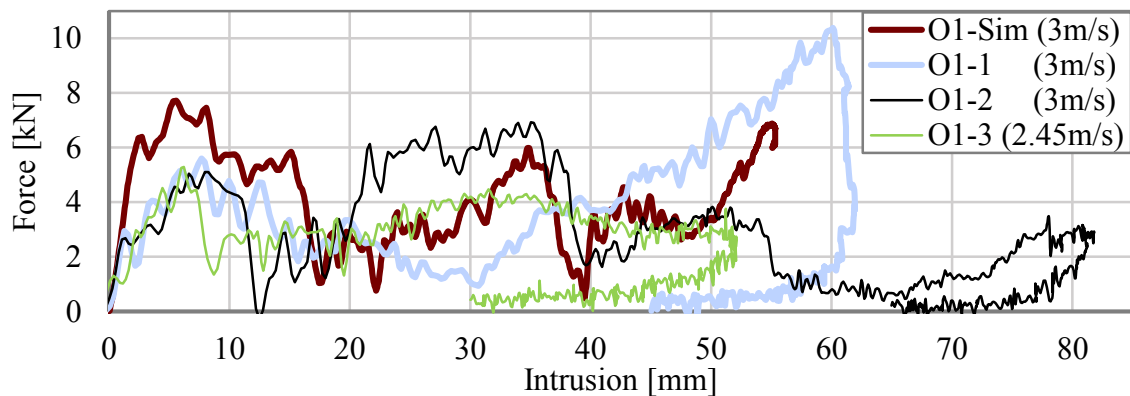


Figure 12: Force curves of the options 1 (O1)

4.3 Optimisation result O2

The results for O2 are shown in Figure 13. The results of O2-1 do not exist since the recording failed. Nevertheless in comparison to O1 the same difference of tearing and failing walls in the simulation versus detached flanges in the tests occurs. During the tests the perpendicular walls get in contact with the ground and resist against the drop weight and cause a higher force level towards the end of the simulation (Figure 14). The forces vary between 5.9 kN for O2-3 and 8.1 kN for O2-Sim and the intrusions between 57.9 mm for O2-Sim and 75.4 mm for O2-2, which comes slightly in contact with the puffer elements. Both tests exceed the allowed intrusion of 60 mm.

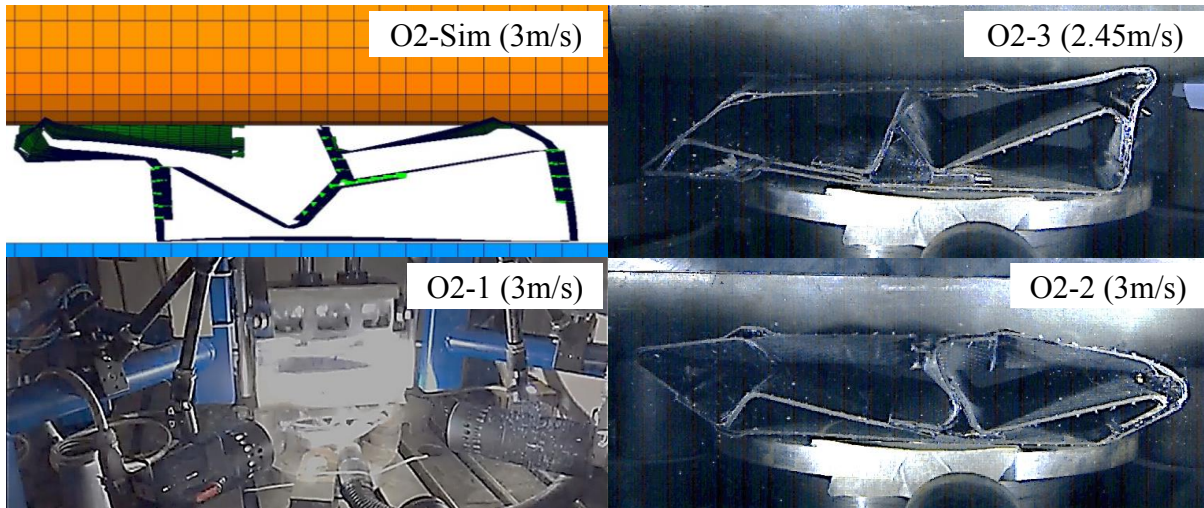


Figure 13: Deformations of the options 2 (O2)

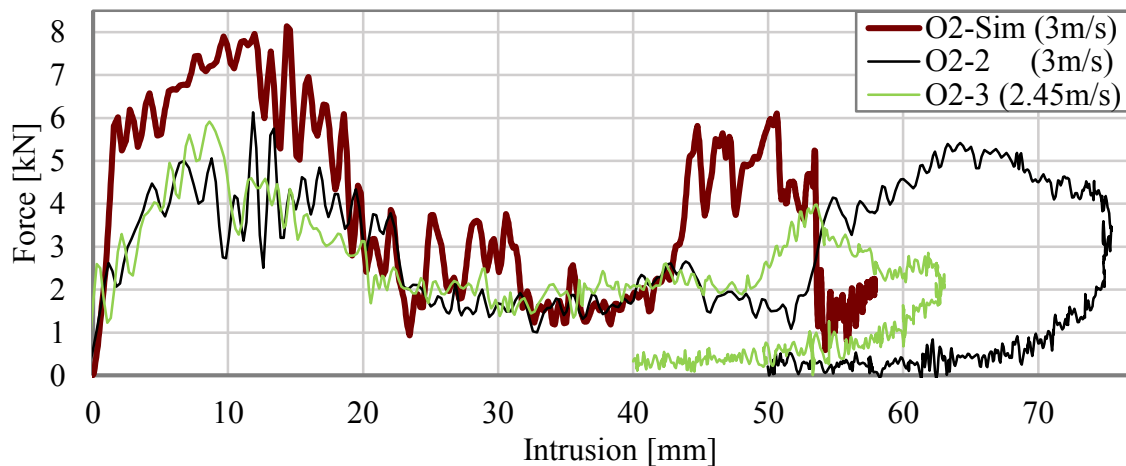


Figure 14: Force curves of the options 2 (O2)

CONCLUSIONS

This paper presents the adaptations that are necessary to consider composites during the optimization with the Graph and Heuristic Based Topology Optimization in a crashworthiness application. First, flange connections were introduced that allow to split the structure in several parts and enable to manufacture the structures by vacuum infusion without undercuts. Then a new heuristic was presented, that detects areas with sudden element failure and supports these locations with perpendicular walls. Also new options for composite specific design variables were presented. To demonstrate the process, the method was applied for a composite profile that is laterally impacted by a drop weight. During an optimization the maximum occurring force was minimized by up to 41% while not exceeding the maximum allowed intrusion. Since an optimization with discrete specified composite layups is not implemented yet, the layups of three chosen optimization designs were adjusted to fit the available composite stacks. The comparison between the drop tests and the simulations shows great deviations in the mechanical behavior. Especially the modeling of the adhesive does not depict the real behavior and underlines the importance of material testing. In addition the manufacturing by hand certainly favoured differing results. The start designs deformed more stable, but were not able to utilize the full potential of the allowed deformation space. In contrast the tests of the optimized designs exceed the intrusion restriction and show an undesired deformation behavior with risk of losing the structural integrity, which is caused by the more complex structures and the failing flanges. None of the structures experienced crushing during the tests, which is an important mechanism to increase the specific energy absorption of the composite. New heuristics could try to favour this mode of failure, although walls in lateral impacts rather tend to bending and breaking.

The method will be enhanced in further projects to fully capture the optimization of composite structures. Working with heuristics that analyze simulation data and suggest producible designs is a great opportunity for the optimization of crashworthiness applications in the future, where currently most structures are designed by empirical knowledge or trial and error without maxing out the potential of the structures.

REFERENCES

- [1] C. Ortmann and A. Schumacher, Graph and heuristic based topology optimization of crash loaded structures, *Structural and Multidisciplinary Optimization*, 47 (6), 839-854, 2013.
- [2] M. P. Bendsøe and O. Sigmund, Topology Optimization, Springer-Verlag, Berlin Heidelberg, 2004.
- [3] A. Schumacher, Optimierung mechanischer Strukturen, Springer-Verlag, Berlin Heidelberg, 2013.
- [4] J. Fang, G. Sun, N. Qiu et al., On design optimization for structural crashworthiness and its state of the art, *Structural and Multidisciplinary Optimization*, 55 (3), 1091-1119, 2017.
- [5] D. Schneider, A. Schumacher, Finding best layouts for ribs on surfaces for crash loads using the Graph and Heuristic Based Topology Optimization, *Advances in Structural and Multidisciplinary Optimization, Proceedings of the 11th World Congress of Structural and Multidisciplinary Optimization (M)*, Springer Nature, 1615-1628, 2018

A Leray Regularized Ensemble-Proper Orthogonal Decomposition Method for Parameterized Convection-Dominated Flows

Michael Schneier^{*}, Traian Iliescu^{**}, Max Gunzburger^{***}

^{*}Florida State University, ^{**}Virginia Tech, ^{***}Florida State University

ABSTRACT

Partial differential equations (PDE) are often dependent on input quantities which are inherently uncertain. To quantify this uncertainty these PDEs must be solved over a large ensemble of parameters. Even for a single realization this can be a computationally intensive process. In the case of flows governed by the Navier-Stokes equation, a method has been devised for computing an ensemble of solutions. Recently a reduced order model derived from a proper orthogonal decomposition (POD) was incorporated into a newly developed ensemble algorithm. Although the ensemble-POD method was successful in the numerical simulation of laminar flows, it yields numerical inaccuracies for convection-dominated flows. In this work we put forth a regularized model, the Leray ensemble-POD model, for the numerical simulation of convection-dominated flows. The Leray ensemble-POD model employs spatial filtering to smooth (regularize) the convection term in the Navier-Stokes. For the new Leray ensemble-POD algorithm, we also propose a numerical discretization with better stability properties than those of the numerical scheme for the standard ensemble-POD method. For this new numerical discretization, we prove its stability and convergence. Furthermore, we show that the Leray ensemble-POD method is more accurate than the standard ensemble-POD method in the numerical simulation of a two-dimensional flow between two offset circles.

Mapped Tent Pitching Schemes for Hyperbolic Systems

Joachim Schoeberl^{*}, Jay Gopalakrishnan^{**}, Christoph Wintersteiger^{***}

^{*}TU Wien, ^{**}Portland State University, ^{***}TU Wien

ABSTRACT

A spacetime domain can be progressively meshed by tent shaped objects. Numerical methods for solving hyperbolic systems using such tent meshes to advance in time have been proposed previously. Such schemes have the ability to advance in time by different amounts at different spatial locations. This paper explores a technique by which standard discretizations, including explicit time stepping, can be used within tent-shaped spacetime domains. The technique transforms the equations within a spacetime tent to a domain where space and time are separable. After detailing techniques based on this mapping, several examples including the acoustic wave equation and the Euler system are considered. J. Gopalakrishnan, J. Schoeberl and C. Wintersteiger, "Mapped tent pitching schemes for hyperbolic systems", SIAM J. Sci. Comput. 39-6 (2017), pp. B1043-B1063

On the Fly Coarse-Graining in Molecular Dynamics Simulations: Adaptive Identification of the Dimensionality

Markus Schoeberl^{*}, Nicholas Zabaras^{**}, Phaedon-Stelios Koutsourelakis^{***}

^{*}Center for Informatics and Computational Science, University of Notre Dame, USA, ^{**}Center for Informatics and Computational Science, University of Notre Dame, USA, ^{***}Technical University of Munich, Germany

ABSTRACT

The efficient exploration of the configurational space of non-trivial molecular compounds retains a challenging problem and is subject to current and future research. We present a general framework for enhancing sampling of highly complex distributions e.g. occurring in peptide simulations having several local free-energy minima by biasing the dynamics and learning a probabilistic coarse-grained (CG) model simultaneously. Its main component represents a Bayesian CG model which is trained on the fly during the simulation of the target distribution. We in turn use insights, gathered from that CG model, to bias the fine-grained potential in order to enhance the exploration of the configurational space and overcome high energy barriers. Next to biasing dynamics, the CG model serves as probabilistic predictor while we quantify the epistemic uncertainty arising due to information loss. An important component of the presented methodology builds the coarse-to-fine mapping which implicitly extracts lower dimensional collective variables, the CG variables. Those potentially reveal physical insight from the data. We propose a mixture model serving as coarse-to-fine mapping while we sequentially add mixture components and increase the mapping's flexibility. Moreover, the complexity of the employed components is consecutively increased by adding features based on an information theoretic metric. A second critical question pertains to the dimensionality of the CG variables. The advocated information theoretic metric is crucial for the adaptive identification of the dimensionality of collective variables. We demonstrate the capabilities of the proposed methodology in the context of peptide simulations.

Utilizing Topology Optimization for the Design of Mechanical Test Fixtures to Optimize Dynamic Response

Tyler Schoenherr^{*}, Peter Coffin^{**}

^{*}Sandia National Laboratories, ^{**}Sandia National Laboratories

ABSTRACT

Topology optimization is being used for many applications around the industrial world with objectives defined to reduce weight, minimize stress, and reduce costs through various means. Less common objective functions seek to match the dynamics (i.e. frequency response, mode shapes etc.) of a target model. One reason for optimizing on dynamic objectives would be to create shock and vibration test fixtures for laboratory tests. The goal of test fixture design is to replicate field hardware in a test laboratory. The dynamics of the test fixture affect how successful that effort is. This presentation will examine test fixture design utilizing topology optimization with dynamic objective functions to improve their performance.

Advances of a General Model for Tumor Growth and Drug Delivery

Bernhard A. Schrefler*, Raffaella Santagiuliana**, Johannes Krehheller***, Pietro Mascheroni****, Lena Yoshihara*****, Wolfgang A. Wall*****, Paolo Decuzzi*****

*Ias-Technical University of Munich, **Italian Institute of Technology, Genova, ***Technical University of Munich, ****University of Padua, *****Technical University of Munich, *****Italian Institute of Technology, Genova

ABSTRACT

We have developed a tumor growth model at macroscopic scale (tissue scale) based on first principles according to the concepts of transport onco-physics which state that physical properties of biological barriers control cell, particle, and molecule transport across tissues and this transport and its deregulation play an overarching role in cancer physics. The model allows not only for growth, hypoxia, necrosis and lysis of the tumor cells but also for invasion into the healthy tissue, transport of therapeutic agents and signalling molecules, mass exchange between the interstitial fluid and the cell populations, and angiogenesis. Further it includes deposition and remodelling of the extracellular matrix; the possibility of migration of the tumor cells through an existing ECM as is needed in case of ex-vivo experiments on decellularized extracellular matrix; the possibility of accounting for different interfacial tensions between the tumor cell, healthy cells, ECM, and interstitial fluid; mass exchange between the newly created and co-opted blood vessels and the interstitial fluid. All these features have been obtained with a growth model where the cell populations are treated as fluid phases, moving in a deformable ECM. Up to now the model was a four phases model consisting of tumor cells, healthy cells, interstitial fluid and extracellular matrix. Newly created vessels were modelled as a species of the IF. The model has now been extended to comprise the newly created vessels as a proper fifth phase which impacts the pores space. Further a diffusion advection equation has been added for the transport of therapeutic agents to the tumor. This model now allows to evaluate the efficacy of treatments which may either be based on chemotherapy or nanoparticle mediated drug delivery. Michor, F., J. Liphardt, M. Ferrari, and J. Widom, What does physics have to do with cancer? Nat Rev Cancer, (2011), 11(9): pp. 657-670. Santagiuliana, R., M. Ferrari, and B.A. Schrefler, Simulation of angiogenesis in a multiphase tumor growth model. Computer Methods in Applied Mechanics and Engineering, (2016), 304: pp. 197-216. Mascheroni, P., et al., Predicting the growth of glioblastoma multiforme spheroids using a multiphase porous media model. Biomechanics and Modeling in Mechanobiology, (2016), 15(5): pp. 1215-1228.

On Mixed Least-squares Finite Element Formulations for Finite J2 Plasticity

Jörg Schröder*, Maximilian Igelbüscher**, Alexander Schwarz***

*University of Duisburg-Essen, **University of Duisburg-Essen, ***University of Duisburg-Essen

ABSTRACT

The accurate approximation of the stress field is one important aspect in the field of elasto-plasticity, since the stresses are mainly responsible for the evolution of plastic deformations. Therefore, we discuss in this contribution an element formulation based on the least-squares finite element method (LSFEM) for finite J2 plasticity, see [3], where the stresses besides the displacements are used as an unknown field. A drawback within the consideration of elasto-plasticity using the LSFEM is that the variational approach given e.g. in [1], could lead to a discontinuity within the first variation of the functional initiated by the additional plastic constraint in the constitutive equation, see e.g. [2]. Thus, to avoid this drawback a modification of the method is performed to obtain a continuous first variation. Furthermore, an extended formulation is constructed by adding an additional redundant third residuum in order to enforce stress symmetry condition. For simplicity we restrict ourselves to a Neo-Hookean material model with a von Mises yield criterion regarding linear isotropic hardening. The numerical analysis is performed using a RTmPk finite element type, where m denotes the polynomial order of the stress approximation using vector-valued Raviart-Thomas functions and k is the interpolation order of the displacements considering standard Lagrange functions. Acknowledgment The authors acknowledge support by the Deutsche Forschungsgemeinschaft in the Priority Program 1748 “First-order system least squares finite elements for finite elasto-plasticity” (SCHR 570/24-1 and SCHW 1355/2-1). References [1] Z. Cai and G. Starke, Least-squares methods for linear elasticity. SIAM Journal on Numerical Analysis, 42, 826–842, 2004. [2] A. Schwarz and J. Schröder and G. Starke, Least-squares mixed finite elements for small strain elasto-viscoplasticity. IJNME, 77, 1351–1370, 2009. [3] J.C. Simo, Numerical analysis and simulation of plasticity. In P.G. Ciarlet and J.L. Lions, editors, Handbook of numerical analysis, No. 6. Elsevier Science, 1998.

The Logarithmic Finite Element Method: Approximation on a Manifold in the Configuration Space

Christian Schröppel*, Jens Wackerfuß**

*University of Kassel, **University of Kassel

ABSTRACT

The Logarithmic finite element method extends the Ritz-Galerkin method to approximations on a non-linear finite-dimensional manifold in the infinite-dimensional solution space. Formulating the interpolant on the logarithmic space allows for a novel treatment of the rotational component of the deformation, making this approach especially suitable for geometrically exact formulations involving large rotations. Using homogeneous coordinates, the logarithms of transformation matrices representing rotations and translations are given as elements of a linear subspace of the set of affine transformations, generating a Lie algebra. The degrees of freedom present in a finite element based on the LogFE method are associated with vector-valued shape functions which constitute the basis vectors of that subspace. Given an appropriate formulation of the finite elements, local degrees of freedom related to rotations and translations can be linked to global degrees of freedom and boundary conditions, and the interpolant is given by an immersion of the space of degrees of freedom into the configuration space. Thus, the LogFE method satisfies the general criteria for finite element models as given by Ciarlet [1]. A co-rotational formulation enables the model to exactly represent pure rigid body motions. This co-rotational formulation must also ensure that spurious high-order deformation components vanish with mesh refinement, in order to satisfy the interpolation theorem for finite elements [2]. Expanding on the work in [3], the authors will present co-rotational, geometrically exact formulations for both planar and spatial beam elements endowed with Bernoulli and Timoshenko kinematics. [1] Ciarlet, P.G. (1979) The Finite Element Method for Elliptic Problems. North-Holland, Amsterdam. [2] Oden, J.T. and Reddy, J.N. (2011) An Introduction to the Mathematical Theory of Finite Elements. Dover, Mineola. [3] Schröppel, C. and Wackerfuß, J. (2016) Introducing the Logarithmic finite element method: a geometrically exact planar Bernoulli beam element. Advanced Modeling and Simulation in Engineering Sciences, 3 (1).

A High-Order Method for Weakly Compressible Flows

Jochen Schuetz^{*}, Klaus Kaiser^{**}

^{*}Universiteit Hasselt, ^{**}RWTH Aachen University

ABSTRACT

It is well-known that the Euler equations at low Mach number constitute a singularly perturbed system of equations as the speed of sound approaches infinity. ‘Classical’ methods known from aerodynamics tend to fail because of the stiffness in the system. In particular, approaches based on purely explicit time integration suffer from a severe CFL restriction. On the other hand, purely implicit schemes introduce an excessive amount of numerical diffusion and, because the equations are nonlinear, are algebraically more difficult to solve. A remedy suggested in recent years is the use of mixed implicit/explicit (IMEX) time integration. IMEX schemes require a suitable identification of ‘stiff’ (to be treated implicitly) and ‘non-stiff’ (to be treated explicitly) terms. This is a highly nontrivial endeavor, because the splitting dictates such important features as stability, accuracy and efficiency. In this talk, we present a recently developed splitting [1-3] based on the incompressible limit solution of the Euler equations. Properties of the splitting are first discussed in a simplified, yet very instructive, ODE setting. The idea is then extended to the treatment of low Mach flows. We show that the combination of a discontinuous Galerkin scheme and IMEX time integration is asymptotically consistent, meaning that the discrete limit can be seen as an approximation to the incompressible limit. Numerical results demonstrate the behavior of the scheme. [1] Schütz, Kaiser, A new stable splitting for singularly perturbed ODEs, Applied Numerical Mathematics, Vol. 107, pp. 18-33, 2016 [2] Kaiser, Schütz, Schöbel, Noelle, A new stable splitting for the isentropic Euler equations, Journal of Scientific Computing, Vol. 70, pp. 1390-1407, 2017 [3] Kaiser, Schütz, A high-order method for weakly compressible flows, Communications in Computational Physics, Vol. 22, pp. 1150-1174, 2017

ON THE CURRENT NEED OF EXPERT RULES FOR THE TOPOLOGY OPTIMIZATION OF STRUCTURES WITH NON-LINEAR BEHAVIORS

AXEL SCHUMACHER

University of Wuppertal, Chair for Optimization of Mechanical Structures
Gaußstraße 20, 42119 Wuppertal, Germany
e-mail: schumacher@uni-wuppertal.de; website: <https://www.oms.uni-wuppertal.de/>

Key words: topology optimization, crash structures, non-linear material behavior, expert rules, heuristic.

Abstract. *In order to optimize the topology of structures with non-linear structural behavior like crash structures, pure mathematical optimization methods do not exist. This contribution shows the possibilities of the involving of expert rules and derived heuristics in the optimization process. It is a very interesting possibility to avoid time-consuming sensitivity calculations. Two methods are evaluated more precisely: The Hybrid Cellular Automaton (HCA), which works with one special rule and the Graph and Heuristic based Topology Optimization (GHT). The opportunities to find powerful design rules generated by experts or by analysis and clustering of many simulation data (big data) are shown. Supported by benchmarks examples, this contribution shows the limitation of optimization methods without expert rules and offers an overview of the possibilities to apply expert rules as an important part in an automatic topology optimization process.*

1 PROBLEM DESCRIPTION

Topology optimization for the layout finding of structures is commonly used for linear static mechanical problems within the industry. The most often used approach is the subdividing of the topology domain in small parts (pixel or voxel) and to distinguish whether there is material or not ^[1]. E.g. the well-known homogenization method minimizes the mean compliance considering a mass constraint. These methods work very fast, because they use existing analytical sensitivities of the most relevant objectives like mean compliance, stresses or mass.

Regarding to crash-loaded structures with highly non-linear behavior, there are a lot of more complex objectives and constraints:

- Consideration of special acceleration values like the head injury criterion (HIC-value)
- Energy absorption,

- Special force levels,
- Smooth force-displacement curve,
- Smooth acceleration-time curve,
- Special force paths for special loadcases.
- High stiffness of special parts, e.g. parts in a main force paths in the passenger area
- Low stiffness of special parts, e.g. at positions of the head contact of a pedestrian,
- Special safety criteria, e.g. no leakage of the petrol system.

In addition to these optimization functions, the behavior of the crash-loaded structures is strongly non-linear, normally calculated by the explicit finite element approach:

- Material plasticity and material failure models
- Geometric nonlinearities
- Contact phenomena
- Numerical and physical bifurcation points
- Non-smooth structural responses
- Mesh dependent results
- No analytical determination of the sensitivities (explicit time integration)
- Huge number of local optima in the design space

There are two possibilities for the definition of the design variables. The first possibility is the density of the material in the already mentioned small parts. Therefore there are millions of design variables. The second possibility is the CAD description of the structural elements e.g. by support of graph theory.

There is an urgent need of topology optimization methods for crash-loaded structures. Especially the automotive industry needs support from the optimization society, e.g. for fulfilled legal requirements. There, it is necessary to find new ideas for efficient methods. The considering of mean compliance and stress constraints is not enough. It is necessary to involve all relevant objectives and constraint functions.

2 POSSIBILITY: TOPOLOGY DERIVATIVES FOR NON-LINEAR PROBLEMS

It is very costly and often not beneficial to generate sensitivities by using explicit finite element calculations. Research activities to find efficient methods of necessary Topological Derivatives (TD) exist ^[2,3]. The idea is to find analytical or semi-analytical descriptions of the Topological Derivatives for an arbitrary state of displacements and stresses. For a functional $J(\Omega)$, the Topological Derivative is described by

$$TJ(x) = \lim_{\rho \downarrow 0} \frac{J(\Omega \setminus \overline{B_\rho(x)}) - J(\Omega)}{|B_\rho(x)|}. \quad (1)$$

Here, $B_\rho(x)$ denotes a ball (in a 3D structure) or a hole (in a 2D structure) with the radius. As an example, Figure 1 shows the scheme for the calculation of the Topology Derivatives depending on the principal stresses.

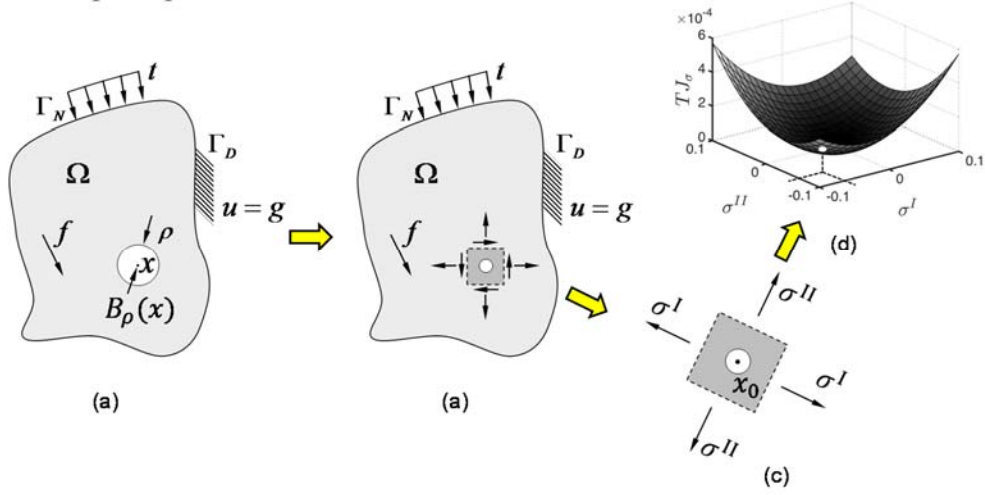


Figure 1: Calculation of Topological Derivatives depending on the principal stresses: a) mechanical Problem, b) Identification of the state in the area of the hole, c) Submodel for the numerical calculation of the Topology Derivatives, d) Meta-model of the Topological Derivatives depending on the principal stresses ^[2]

For creating the sample points for calculating the meta-model of the Topological Derivatives, the finite element model with a non-linear material behavior shown in Figure 2 is used as basic for the approximation in figure 3.

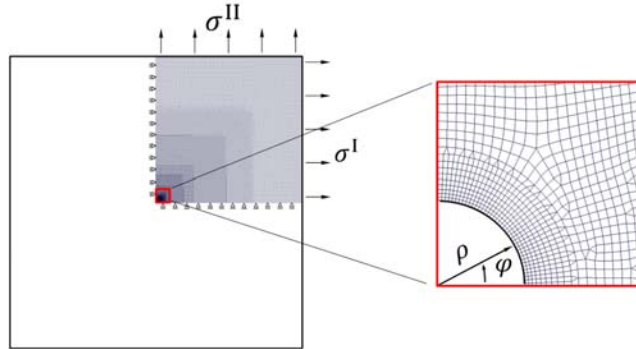


Figure 2: Finite element model with a non-linear material behavior ^[2]

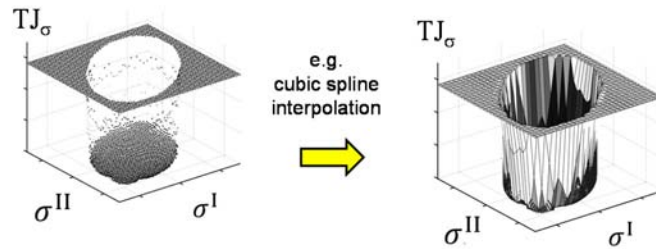


Figure 3: Approximation of the Topological Derivative depending on arbitrary principal stresses ^[2]

The research of finding Topology Derivatives is still at the beginning and it needs additional years to find a solution for structures with a highly non-linear behavior.

3 EXPERT RULES IN THE OPTIMIZATION PROCESS

Expert rules are a powerful possibility to avoid the need for the calculation of sensitivities. The idea is the addition of these automatic expert rules in the optimization process (Figure 4).

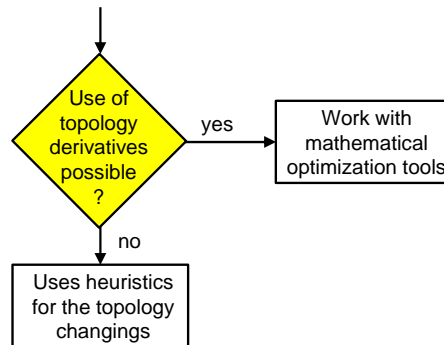


Figure 4: Practical approach for the topology optimization of structures with non-linear behavior

3.1 One-rule approaches - example: Hybrid Cellular Automaton (HCA)

The Hybrid Cellular Automaton (HCA) ^[4] is one example of an expert rule. The modification of the structure is carry out by finding a homogeneous distribution of the inner energy density. Neighboring elements in the Cellular Automaton lattice are considered. There is a direct connection of Cellular Automaton lattice and finite element mesh. The HCA is a density approach dealing with relative densities. A rule homogenizes the energy density in a way that no sensitivity calculation are necessary.

3.2 Competing rules approach - example: Graph and Heuristic based Topology Optimization (GHT)

For complex optimization tasks as mentioned in chapter 1, there is a need to consider different competing heuristics. The Graph and Heuristic based Topology Optimization (GHT) ^[5] combines topology, shape and sizing optimizations in one optimization process. It uses widely used finite element shell models for executing crash simulations. The optimization task is divided into an outer optimization loop, which performs the topology optimization with heuristics (derived from expert rules) and an inner optimization loop, which performs the mathematical shape optimization and sizing to evaluate the design. The heuristics use result data of finite element simulations like strains, stresses, displacement, velocities and accelerations. Based on this information the heuristics make proposals for modifications of the structure. Figure 5 shows the basic scheme of the GHT. For the flexible geometry description, mathematical graphs are used. The heuristics are used to perform structural modifications. The optimization problem is devised into two optimization loops, the outer loop for the structural modifications performed by heuristics (mainly topology changes) and the inner loop with a common shape and/or sizing optimization for a design layout, which is coming from the outer loop. The GHT has different strategies of the combination of the topology changing by heuristics and the shape optimization. E.g. the tracking of E competing designs in parallel (with $E \geq 1$) comes to a branching strategy to avoid local optima. A higher E leads to a higher probability to skip local optima, but leads to higher computer time.

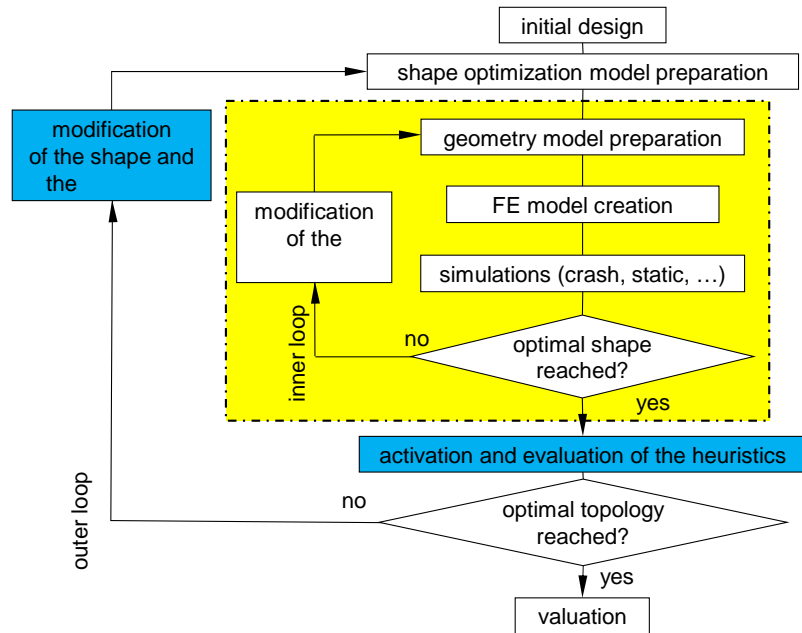


Figure 5: Basic scheme of the Graph and heuristic based topology optimization (GHT)

4 GENERATION OF RULES FROM EXPERT KNOWLEDGE

There are two possibilities for generating rules, first the organization of brainstorming meetings with experts and secondly the clustering of many simulation data (big data) ^[7]. This chapter has the focus on brainstorming meetings with crash development groups of several car producers ^[8]. Some results are sorted in the following list:

Increasing the stiffness in crash:

- Support components with buckling tendency
- Increasing of corner stiffness
- Inserting of Y-junctions
- Split high-loaded structures.
- No arch shaped components
- Use the full design domain:
- Filling of large cutouts
- If the torsion is to large, insert circular structures
- ...

Reducing the stiffness in crash:

- Including of crash elements
- Arching of straight components
- Inserting of triangle cutouts
- ...

Simplification:

- Delete unloaded components
- Use a small number of chambers
- ...

Balancing the energy density:

- Homogenize the buckling length
- Moderate changing of the wall thickness
- ...

Manufacturing constraints:

- Boundaries of the wall thicknesses,
- Boundary of the angle between two walls,
- Boundary of the distance between two walls
- ...

Based on the results of the brainstorming meetings the heuristics are implemented in the GHT software. Figure 6 shows the basic heuristics.

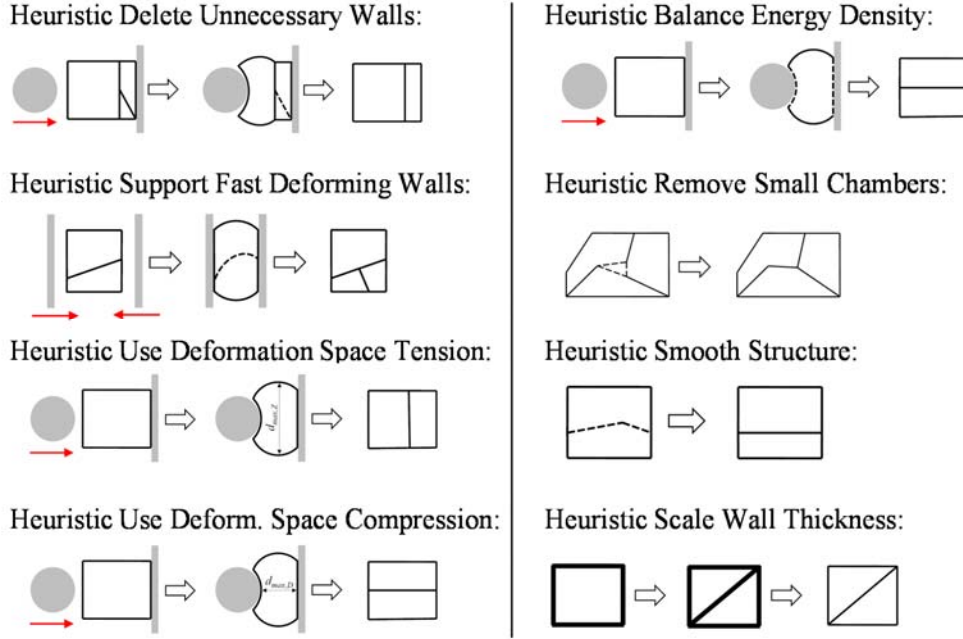


Figure 6: Examples of the implemented heuristics

5 BENCHMARK OPTIMIZATION RESULTS

Supported by benchmarks examples, this contribution shows the limitation of optimization methods without expert rules and offers an overview of the possibilities of using expert rules as an important part in an automatic topology optimization process.

5.1 Cantilever frame structure

The considered cantilever frame structure is shown in Figure 7. The optimizer has to find an optimal layout of walls in the structure. The optimization tasks are the following:

- Application 1: minimize maximum intrusion so that the frame mass ≤ 0.027 kg
- Application 2: minimize maximum acceleration so that the intrusion ≤ 49 m

The manufacturing constraints for both applications are:

- $0.5 \text{ mm} \leq \text{wall thickness} \leq 10 \text{ mm}$
- $\text{wall distance} \leq 10 \text{ mm}$
- $\text{wall connection angle} \leq 15^\circ$

The HCA can only optimize application 1 without the given manufacturing constraints. The results are shown in figure 7.

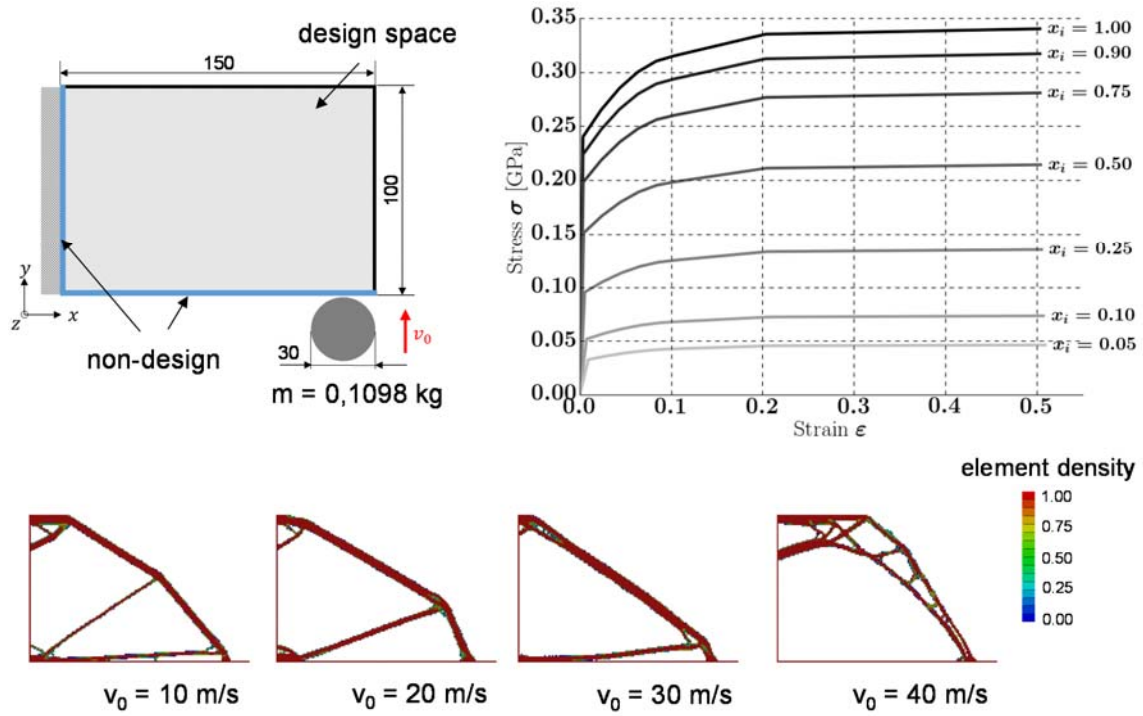


Figure 7: Maximum stiffness design with HCA for different initial velocities the mass m with the element density x_i [9]

Figure 8 shows the optimization results of the GHT.

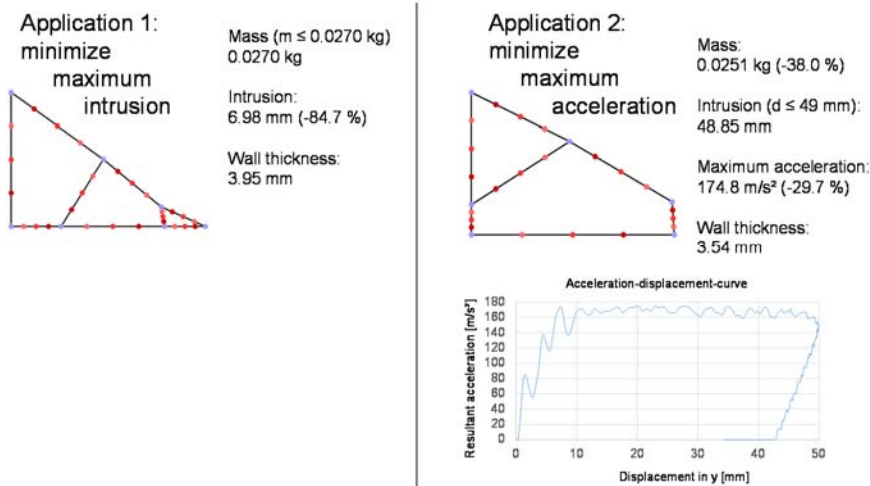


Figure 8: Maximum stiffness design with HCA for different initial velocities the mass m with the element density $v_0 = 25 \text{ m/s}$ x_i [5]

5.2 Rocker of a vehicle body-in-white structure

The optimization task is to find the optimal topology and shape of the cross section of the rocker profile shown in figure 9.

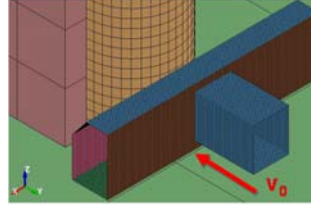


Figure 9: Mechanical problem of the rocker ^[6]

The objective is to minimize the maximal force at a moved rigid wall (velocity v_0), so that functional constraints

- mass ≤ 2.801 kg
- intrusion (pole crash) ≤ 70 mm
- stiffness(bending and torsion) ≥ 50 % stiffness initial design

and the manufacturing constraints

- $1.6 \text{ mm} \leq \text{wall thickness} \leq 3.5 \text{ mm}$
- distance of walls $\geq 10 \text{ mm}$
- connection angle of walls $\geq 15^\circ$
- maximum chamber size ration 1 : 20

are fulfilled. HCA is not able to optimize this problem, so figure 10 and 11 show only the GHT results.

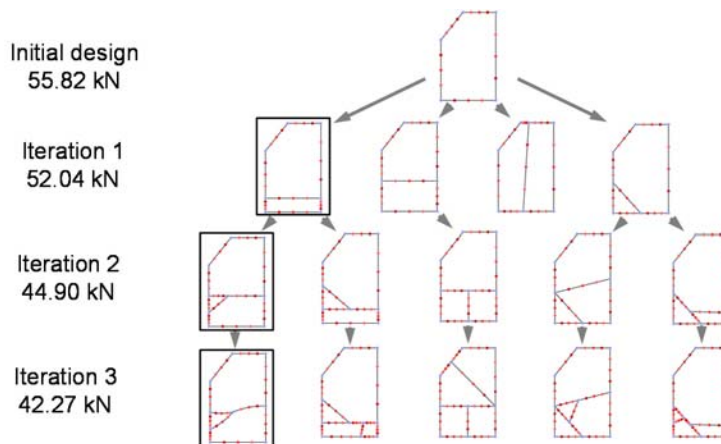


Figure 10: Optimization history (branching - competing designs) of the optimization of the rocker ^[6]

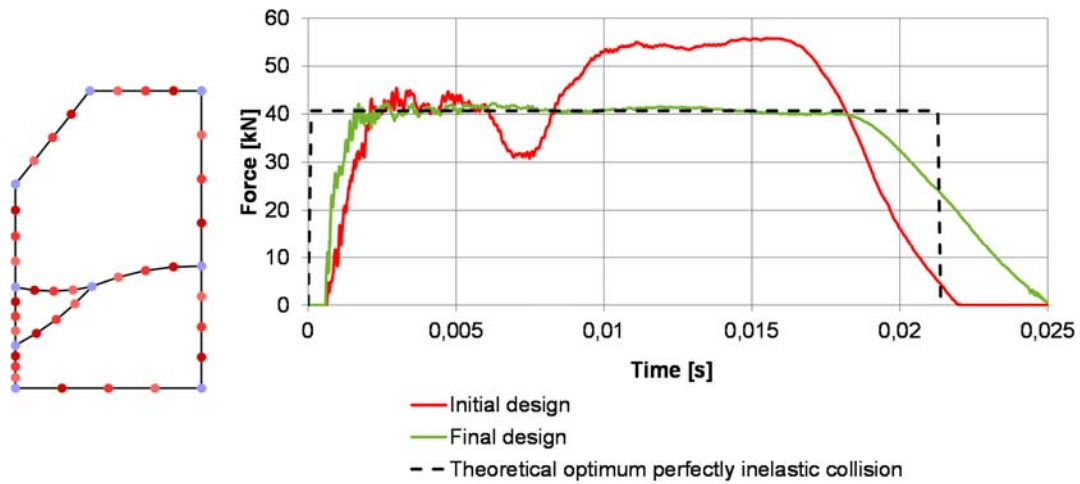


Figure 11: Optimization history (branching - competing designs) of the optimization of the rocker ^[6]

6 CONCLUSIONS

GHT and HCA as representatives of rule-based optimization methods provide interesting results, which cannot be achieved with purely mathematical methods. The expert knowledge based generation of powerful heuristics is time consuming. In the future, attention must be paid to a suitable interplay of mathematical methods and heuristics.

ACKNOWLEDGEMENT

The author thanks Katrin Weider for her contribution in the research project "Topological derivatives for layout generation of crash-loaded structures" founded by the German Research Foundation (DFG-No. Schu915/4-1, project number 350645830). He also thanks Christian Olschinka, Christopher Ortmann and Dominik Schneider for their works in the GHT method. He is also pleased about the numerous hints of the crash engineers of the German automotive industry in the scope of the research project "Methodological and technical realization of the topology optimization of crash loaded vehicle structures" founded by the German Federal Ministry for Education and Research within the scope of the research project ".

REFERENCES

- [1] M. P. Bendsøe and O. Sigmund, Topology Optimization, Springer-Verlag, Berlin Heidelberg, 2004.

- [2] K. Weider and A. Schumacher, A., On the calculation of Topological Derivatives considering an exemplary nonlinear material model, *Proc. Appl. Math. Mech.* 16, 717-718, 2016.
- [3] K. Weider and A. Schumacher, A topology optimization scheme for crash loaded structures using Topological Derivatives, *Advances in Structural and Multidisciplinary Optimization, Proceedings of the 12th World Congress of Structural and Multidisciplinary Optimization (WCSMO12)* Springer Nature, 1601-1614, 2018
- [4] N.M. Patel, B.S. Kang, J.E. Renaud and A. Tovar, Crashworthiness design using topology optimization. *J Mech Des* 131:061013.1–061013.12, 2009
- [5] C. Ortmann and A. Schumacher, Graph and heuristic based topology optimization of crash loaded structures, *Structural and Multidisciplinary Optimization*, 47 (6), 839-854, 2013.
- [6] C. Ortmann, Development of a graph and heuristic based method for the topology optimization of crashworthiness profile structures, *PhD thesis, University of Wuppertal*, 2014.
- [7] C. Diez, P. Kunze, D. Toewe, C. Wieser, L. Harzheim and A. Schumacher, A., Big-Data based rule-finding for analysis of crash simulations, *Advances in Structural and Multidisciplinary Optimization, Proceedings of the 12th World Congress of Structural and Multidisciplinary Optimization (WCSMO12)* Springer Nature, 396-410, 2018
- [8] A. Schumacher and C. Ortmann, Rule generation for optimal topology changes of crash-loaded structures, *Proceedings of the 10th World Congress on Structural and Multidisciplinary Optimization*, May 19 -24, 2013.
- [9] K. Weider, A. Marschner and A. Schumacher, A Systematic Study on Topology Optimization of Crash Loaded Structures using LS-TaSC, *Proc. of the 11th European LS-DYNA Conference 2017*, 9. - 11. Mai 2017, Salzburg, Austria, 2017

Characterization and Modeling of Spot Welds for Double-Lap Joints

Lilia Schuster^{*}, Silke Sommer^{**}, Vitali Schilow^{***}

^{*}Fraunhofer Institute for Mechanics of Materials IWM, ^{**}Fraunhofer Institute for Mechanics of Materials IWM,

^{***}Fraunhofer Institute for Mechanics of Materials IWM

ABSTRACT

Resistance spot welding is still the most commonly used process in the production of the body-in-white. Extensive research conducted on spot-welded single-lap joints has provided a good understanding of this type of spot weld joints. However, in order to adequately address material efficiency and construction limit aspects, automobile engineers are increasingly incorporating joints, which connect three layers of metal sheets with one single spot weld. These joints introduce an increasing complexity for possible combinations in sheet thickness, materials and load application points. Due to this large number of possible configurations it is not feasible to encompass the entirety of combinations by experimental testing. Therefore, the use of finite element simulations is necessary to investigate additional configurations to describe the load bearing capacity, fracture behavior and energy absorption in a comprehensive manner. Loading types such as tension, shear, torsion and bending lead to complex local stress states which require sophisticated damage and failure models. The GTN model is used to model the ductile failure under tensile loading and loadings with higher triaxialities and produces accurate predictions for various applications, but it is not capable to describe shear failure. Therefore the Gologanu damage model with additional fracture criteria was used by Sommer [1] and by Burget [2] to overcome this issue and simulate failure behavior of spot-welded single-lap joints under shear loading. It was able to provide reliable failure predictions for maximum load as well as fracture locations for single-lap joints of similar and dissimilar steel sheet metal joints. In this paper the arising challenges and modeling approaches in characterization of double-lap spot weld joints are outlined. Different loading cases like shear, tension and bending are investigated with variation of load points and their influences on load bearing capacities and fracture behavior are investigated. Also the sheet thicknesses, strength of sheet metals and layer positions in the spot-welded joints are varied. Experimental data will be presented for validation of the simulation results. [1] Silke Sommer, Modeling the fracture behavior of spot welds using advanced micro-mechanical damage models, IOP Conf. Ser.: Mater. Sci. Eng. 10 012057, 2010. [2] Sebastian Burget, Silke Sommer, Modeling of deformation and failure behavior of dissimilar resistance spot welded joints under shear, axial and combined loading conditions, 13th International Conference on Fracture, ICF 2013 pp.1589-1600.

Structural Metrics for the Collaboration of Design and Simulation Departments in Complex Product Development

Sebastian Schweigert*, Markus Zimmermann**

*Technical University of Munich, **Technical University of Munich

ABSTRACT

When managing product development including different sub-disciplines, communication at interfaces is crucial. Together with the increasing number and complexity of mechanical simulations, communication and collaboration of design and simulation departments becomes a system demanding for complexity management to handle it. Otherwise, wasted resources and demotivation especially in simulation departments occur. For instance, information generated by numerical simulations is not used, as redundant tests are performed even though numerical simulations were already conducted or design changes proposed by simulation experts never make it into the real product. Often this results from lacking trust between the two departments as emphasized by the following quote: "No one trusts in [numerical] simulation results, except those, who conducted the simulation. Everyone trusts in testing results, except those, who conducted the test." (Head of simulation, household appliances company) This contribution investigates barriers between design and simulation departments and recommendations to overcome them. Complexity management and network analysis are applied on collaboration graphs consisting of persons, artefacts, tasks, and tools. A toolset is proposed using structural metrics for engineering design processes of Kreimeyer and Lindemann (2011). Each metric is connected to barriers identified in an online survey and subsequent interview study. They include for instance lacking information transmission from design to simulation – especially in early design phases. Structural metrics like the number of unconnected nodes can identify those barriers from system graphs to find critical areas. Consequently, improvement measures like regular change notifications can be implemented. In an exemplary company with design and simulation departments consisting of dozens of experts the issue of lacking trust described above is met by integrating simulation experts earlier into product development processes. Using e-mails exchanged within and between departments and calendars of meetings, as well as product and simulation data management systems that track artifacts like CAD models or numerical simulation reports, system graphs of the collaboration and communication are generated. Within the graphs, nodes represent persons, tasks, artifacts, and tools, while edges represent communication channels, responsibilities, and links between datasets. Identifying people poorly integrated in the information flow by deleting edges of communication channels below a certain frequency and extracting the resulting unconnected nodes gives the possibility of systematically improving collaboration and communication and integrating these persons. The contribution of the approach lies in the systematic identification of barriers and suitable measures to improve the communication and collaboration of design and simulation departments in order to reduce avoidable epistemic uncertainty.

U-splines

Michael Scott^{*}, Derek Thomas^{**}, Kevin Tew^{***}, Stephen Schmidt^{****}

^{*}Brigham Young University, ^{**}Coreform, ^{***}Coreform, ^{****}Coreform

ABSTRACT

U-splines are a new spline technology which allows for local changes in mesh size, polynomial degree, and smoothness. There are no restrictions on proximity of T-junctions and it works for all degrees and smoothnesses. The resulting basis is positive, forms a partition of unity, and is complete. In this talk, U-splines will be described and applied as a basis for isogeometric analysis.

The Shifted Boundary Method: An Embedded Framework for Computational Mechanics

Guglielmo Scovazzi^{*}, Alex Main^{**}, Nabil Atallah^{***}, Ting Song^{****}

^{*}Duke University, ^{**}Duke University & ANSYS, ^{***}Duke University, ^{****}Duke University

ABSTRACT

Embedded boundary methods obviate the need for continual re-meshing in many applications involving rapid prototyping and design. Unfortunately, many finite element embedded boundary methods for incompressible flow are also difficult to implement due to the need to perform complex cell cutting operations at boundaries, and the consequences that these operations may have on the overall conditioning of the ensuing algebraic problems. We present a new, stable, and simple embedded boundary method, which we call “shifted boundary method” (SBM), that eliminates the need to perform cell cutting. Boundary conditions are imposed on a surrogate discrete boundary, lying on the interior of the true boundary interface. We then construct appropriate field extension operators, with the purpose of preserving accuracy when imposing the boundary conditions. We demonstrate the SBM on large-scale incompressible flow problems, multiphase flow problems, solid mechanics problems, and shallow water flow problems.

Stress Correlations in Discontinuously Thickening Suspensions

Omer Sedes^{*}, Abhinendra Singh^{**}, Jeffrey F Morris^{***}

^{*}CUNY City College of New York, Levich Institute, ^{**}CUNY City College of New York, Levich Institute, ^{***}CUNY City College of New York, Levich Institute

ABSTRACT

Very concentrated suspensions can shear thickening abruptly, and this is called discontinuous shear thickening. In the present work, the underlying statistical physical basis for this change in properties, which has the appearance of a nonequilibrium phase transition, are developed in terms of the spatial correlations of various measures of the contact network. We base our understanding on numerical simulations by a method which captures lubrication hydrodynamics, contact forces including friction, and stabilizing repulsive force or Brownian motion. At low stress, lubrication between particles maintains low viscosity, while at large stress, the stabilizing force is overwhelmed and a contact network develops. The stress correlations in these states will be described, as will be various measures of the contact network, to elucidate the role of the exchange of lubricated interactions for true contact in the abrupt change in properties. The behavior of similar measures in microrheology simulation, where a body is pulled through the suspension, will be briefly considered.

Towards a Scientific Understanding of Non-Schmid Behavior and Latent Hardening

Huseyin Sehitoglu*, Sertan Alkan**

*University of Illinois, **University of Illinois

ABSTRACT

In this presentation, we address two topics in crystal plasticity that need a better scientific understanding. The first topic is the modeling of CRSS (critical resolved shear stress) and the second topic is modeling of latent hardening. Firstly, we overview the dislocation-mediated slip in several alloys and then introduce a theory that addresses the strong non-Schmid behavior. By strong non-Schmid response, we refer to the strong orientation dependence and tension-compression asymmetry of the critical resolved shear stress for slip deformation. Unlike conventional fcc alloys, the critical resolved shear stress cannot be treated as a constant material parameter for BCC and B2 alloys. We show examples from transforming alloys such as shape memory alloys that exhibit strong tension-compression asymmetry and crystal orientation dependence. This deviation from the Schmid behavior has been overlooked in previous formulations and needs to be considered, and we illustrate its importance in this presentation. In the second part of the talk, we address the modeling of latent hardening and experiments to study the latent hardening phenomenon in metals. An empirical equation has been proposed in previous works in the literature and repeatedly used by the community. However, there are shortcomings with this empirical approach. The latent hardening behavior is rather complex especially in alloys that undergo simultaneous twinning and dislocation slip. It has been commonly accepted that latent hardening exceeds the hardening on the primary system which is a problematic assumption. We outline a new framework for determination of the latent hardening constants and show agreement with experimental trends in high entropy alloys.

Multiscale Modeling of Piezoresistivity and Damage Induced Sensing Of Nanocomposite Bonded Explosive Materials Under Dynamic Loading Using Electromechanical Peridynamics

Gary Seidel*, Naveen Prakash**, Krishna Talamadupula***, Engin Sengezer****

*Virginia Tech, **Virginia Tech, ***Virginia Tech, ****Virginia Tech

ABSTRACT

Polymer bonded explosives (PBXs) are composed of explosive grains at high volume fractions, for example RDX, HMX etc. surrounded by a polymer medium at low volume fractions such as epoxy, estane etc. They are susceptible to microstructural level damage due to impact events. This may degrade their operational reliability or even cause unwanted initiation leading to the detonation of the explosive. The prognostication of the life of PBX materials is therefore of significant interest. A nanocomposite piezoresistivity based sensing scheme is discussed as a solution to this problem. Carbon nanotube (CNT) based nanocomposite binders are used as the binder material in these explosive composites to give Nanocomposite Bonded Explosives (NCBXs). This leverages the ability of the CNTs to impart piezoresistive properties to the polymer and hence provide in situ sensing of strained and damaged states of NCBX materials. The effective piezoresistivity is derived from key multiscale aspects of the nanocomposite binder due to the presence of the CNTs such as electron hopping at the nanoscale, CNT bundle network formation and disruption at the microscale etc. The degree of piezoresistivity is informed in a hierarchical fashion from the lower scales to the microscale RVE being analyzed through a microscale gauge factor. A multifunctional coupled electromechanical peridynamics code is used to provide numerical analysis including the piezoresistive response of these composites under dynamic loading conditions. Peridynamics is a non-local theory of continuum mechanics that assumes material particles interact over a finite region. The strength of the peridynamic bonds are calibrated to their fracture energies in order to accurately reflect the energy dissipation during the fracture process. The model captures damage initiation and propagation mechanisms due to the progress of stress waves. In order to analyze the coupled piezoresistive and mechanical dynamic response, simulations are conducted on Charpy test specimens. This response is found to depend on many factors such as carbon nanotube content, electrical conductivity of the grain, impact velocity and fracture properties. The analysis of Charpy specimens enables comparisons with experimentally obtained preliminary piezoresistive and mechanical dynamic Charpy test data. This work aims to find qualitative agreement with the experimental data on the dynamic piezoresistive response of these nanocomposites to validate the sensing mechanism for explosive materials proposed here. It is expected that this study will improve the prognosis of life of NCBX materials.

Coupling Methods in Peridynamics for Effective Failure and Damage Simulation

Pablo Seleson*

*Oak Ridge National Laboratory

ABSTRACT

Predictive failure and damage simulation has been a topic of fundamental interest in materials science and engineering. A recently developed nonlocal theory called peridynamics has been a subject of increased interest in the computational mechanics community, due to its ability to naturally represent material discontinuities and handle complex dynamically evolving cracks. However, peridynamic simulations are significantly computationally more expensive than their classical (local) continuum mechanics analogues. Consequently, it is of interest to develop effective coupling methods with the capability to seamlessly combine nonlocal and local models. In this presentation, we will discuss methods to couple peridynamics and classical elasticity, and we will demonstrate the effectiveness of those methods through numerical simulations. References: [1] Seleson, Beneddine, Prudhomme, A force-based coupling scheme for peridynamics and classical elasticity, *Computational Materials Science* 66 (2013): 34–49. [2] Seleson, Ha, Beneddine, Concurrent coupling of bond-based peridynamics and the Navier equation of classical elasticity by blending, *International Journal for Multiscale Computational Engineering* 13(2) (2015): 91–113. [3] Silling, Littlewood, Seleson, Variable horizon in a peridynamic medium, *Journal of Mechanics of Materials and Structures* 10(5) (2015): 591–612.

Matrix Modulus and Ligand Density Effects on Cell Morphogenesis in Two-Dimensional and Three-Dimensional Cell Cultures

Dror Seliktar^{*}, Andrei Yosef^{**}, Olga Kossover^{***}, Iris Mironi-Harpaz^{****}, Arianna Mauretti^{*****},
Sonia Melino^{*****}, Joseph Mizrahi^{*****}

^{*}Technion, ^{**}Technion, ^{***}Technion, ^{****}Technion, ^{*****}University of Rome Tor Vergata, ^{*****}University of Rome Tor Vergata, ^{*****}Technion

ABSTRACT

There is a need to further explore the convergence of mechanobiology and dimensionality with systematic investigations of cellular response to matrix mechanics in 2D and 3D cultures. Here, we applied a semi-synthetic hydrogel capable of supporting both 2D and 3D cell culture to investigate cell response to matrix modulus and ligand density. The culture materials were fabricated from adducts of polyethylene glycol (PEG) or Pluronic®F127 and fibrinogen fragments, formed into hydrogels by free-radical polymerization, and characterized by shear rheology. Control over the modulus of the materials was accomplished by changing the concentration of synthetic PEG-diacrylate cross-linker, and by altering the molecular length of the PEG. Control over ligand density was accomplished by changing the fibrinogen concentration. Results indicate the modulus-dependent and ligand-dependent response from the cells in 2D culture was contradictory to the same measured responses in 3D culture. These differences arise from dimensionality constraints, most notably the encapsulation of cells in a non-porous hydrogel matrix. These insights underscore the importance of mechanical properties in regulating cell morphogenesis in a 3D culture milieu. The versatility of the hydrogel culture environment further highlights the significance of a modular approach when developing materials that aim to optimize the cell culture environment through static mechanical stimulation.

Modelling Ripple Morphodynamics Driven by Colloidal Deposition

Mathieu Sellier^{*}, James Hewett^{**}

^{*}University of Canterbury, ^{**}University of Canterbury

ABSTRACT

Fluid dynamics between a particle-laden flow and an evolving boundary are found in various contexts. We numerically simulated the morphodynamics of silica particle deposition from flowing water within geothermal heat exchangers using the arbitrary Lagrangian-Eulerian method. The silica particles were of colloidal size, with submicron diameters, which were primarily transported through the water via Brownian motion. First, we validated the Euler-Euler approach for modelling the transport and deposition of these colloidal particles within a fluid by comparing our simulation results with existing experiments of colloidal polystyrene deposition. Then we combined this multiphase model with a dynamic mesh model to track the gradually accumulated silica along the pipe walls of a heat exchanger. Surface roughness was modelled by prescribing sinusoidally-shaped protrusions on the wall boundary. The silica bed height grew quickest at the peaks of the ripples and the spacing between the protrusions remained relatively constant. The rough surface experienced a 20 % reduction in silica deposition when compared to a smooth surface. We also discuss the challenges of mesh deforming simulations with an emphasis on the mesh quality as the geometry changes over time.

Modeling and Quantification of Anisotropy and Heterogeneity in Geomaterials

Shabnam Semnani^{*}, Ronaldo Borja^{**}

^{*}Stanford University, ^{**}Stanford University

ABSTRACT

Geomaterials are often anisotropic and heterogeneous, and consist of various phases that form complex structures persisting at multiple scales. Microstructural morphology of these materials has a great impact on their overall behavior such as deformation, failure and transport properties, and needs to be incorporated into the computational modeling efforts. In this work, we present recent advances in addressing two aspects of structural morphology of geomaterials, namely, anisotropy and heterogeneity. In the first part, we describe a recently developed anisotropic thermo-plasticity framework for modeling the thermo-mechanical response of transversely isotropic geomaterials, which is then used to predict the inception of shear band and strength of rocks. In the second part, we focus on quantification of heterogeneity of geomaterials across scales using high-resolution imaging techniques. A stochastic framework is presented which uses high-resolution images to enhance low-resolution images obtained over larger fields of view by incorporating features below the resolution limit. The application of this method is demonstrated using images of shale samples with two different resolutions and fields of view obtained using X-ray micro-tomography. The proposed multi-scale imaging approach has vast applications to computational modeling such as computational homogenization, mesh sensitivity studies and multi-scale modeling methods.

Optimal Actuator Layout for Adaptive Structures under Quasi-Static Loading

Gennaro Senatore*

*Swiss Federal Institute of Technology (EPFL), School of Architecture, Civil and Environmental Engineering (ENAC), Applied Computing and Mechanics Laboratory (IMAC), Station 18, CH-1015 Lausanne

ABSTRACT

Adaptive structures are capable of counteracting the effect of external loads via controlled shape changes and redirection of the internal load path. These structures are integrated with sensors (e.g. strain, vision), control intelligence and actuators. Instead of using more material to cope with the effect of loads, controlled shape changes are employed to homogenise the stresses and to keep deflections within limits. Using a previously developed design methodology [1] it was shown that optimal material distribution in combination with strategic integration of the actuation system lead to significant whole-life energy savings when the design is governed by strong but rare loading events. The whole-life energy of the structure is made of an embodied part in the material and an operational part for structural adaptation. Experimental tests on a large scale physical prototype designed using this methodology [2], validated key assumptions confirming that for slender configurations adaptive structures can achieve up to 70% energy savings compared to passive structures. This presentation focuses on methods to derive optimal actuator layouts in reticular structures under quasi-static loading. A deformation vector akin to a lack of fit or eigenstrain is defined to assign the actuator length changes. A computationally efficient routine based on eigenstrain assignment via the Integrated Force Method is formulated to solve the actuator placement problem. The application of this method to planar and complex spatial structures is discussed to benchmark adaptive structures against optimised passive ones in terms of energy and monetary costs [3, 4]. References [1] G. Senatore, P. Duffour, S. Hanna, F. Labbe and P. Winslow, "Adaptive Structures for Whole Life Energy Savings," International Association for Shell and Spatial Structures (IASS), vol. 52, no. 4, pp. 233-240, 2011. [2] G. Senatore, P. Duffour, P. Winslow and C. Wise, "Shape Control and Whole-Life Energy Assessment of an "Infinitely Stiff" Prototype Adaptive Structure," Smart Materials and Structures, vol. 27, no. 1, p. 015022, 2018. [3] G. Senatore, P. Duffour and P. Winslow, "Exploring the Application Domain of Adaptive Structures," Engineering Structures, vol. 167, pp. 608-628, 2018. [4] G. Senatore, P. Duffour and P. Winslow, "Energy and Cost Analysis of Adaptive Structures - Case Studies," Journal of Structural Engineering (ASCE), 2018.

Uncertainty Quantification Methodologies and Linear Solvers in Cardiovascular Simulations in High-performance Computing

Jongmin Seo^{*}, Daniele Schiavazzi^{**}, Alison Marsden^{***}

^{*}Stanford University, ^{**}University of Notre Dame, ^{***}Stanford University

ABSTRACT

Cardiovascular simulations are widely used to aid in surgical planning and disease diagnostics. Cardiovascular blood flow simulations typically solve the incompressible Navier Stokes equations with physiologic boundary conditions in an anatomic model geometry constructed from image data. To account for variability of simulation predictions due to uncertainties in clinical data, material properties and the modeling process, we implement an uncertainty quantification (UQ) framework and report confidence intervals and output statistics on simulation prediction. We use non-intrusive UQ propagation strategies that requires multiple function evaluations. However, UQ propagation becomes numerically challenging when multiple function evaluations are required, each consisting of a solution of the Navier-Stokes equations in a complex 3-D patient specific geometry with deformable vessel walls. In this talk we compare a variety of numerical techniques aiming to accelerate forward uncertainty propagation for cardiovascular simulations. First, we assess the performance of several UQ propagation methodologies on an idealized coronary artery model coupled with a 0-D lumped parameter network (LPN) which consists of circuit elements to model the heart and coronary physiology. To obtain parameters for LPN network, we use parameter estimation methods to match clinical data for each patient. Performance of UQ methodologies including Markov-Chain Monte-Carlo, stochastic collocation, and a generalized multi-resolution expansion will be compared. The second part of this talk discusses the performance of iterative linear solver and preconditioning techniques in our flow solver on high performance clusters. We will show matrix characteristics from the linear system for example eigenvalues, bandwidth and condition number. Effect of boundary conditions and fluid-structure interaction on matrix characteristics and solver performance will be discussed. * Support from National Institute of Health (R01 EB018302) is greatly appreciated.

Towards Scalable Implicit FE Simulations of Continuum Plasma Physics Models

John Shadid*, Sibu Mabuza**, Roger Pawlowski***, Sidafa Conde****, Eric Cyr*****, Edward Phillips*****, Sean Miller*****, Paul Lin*****

*Sandia National Laboratories, **Sandia National Laboratories, ***Sandia National Laboratories, ****Sandia National Laboratories, *****Sandia National Laboratories, *****Sandia National Laboratories, *****Sandia National Laboratories, *****Sandia National Laboratories

ABSTRACT

The mathematical basis for the continuum modeling of plasma physics systems is the solution of the governing partial differential equations (PDEs) describing conservation of mass, momentum, and energy, along with various forms of approximations to Maxwell's equations. The resulting systems are characterized by strong nonlinear and nonsymmetric coupling of fluid and electromagnetic phenomena, as well as the significant range of time- and length-scales that the interactions of these physical mechanisms produce. To enable accurate and stable approximation of these systems a range of spatial and temporal discretization methods are commonly employed. In the context of finite element spatial discretization methods these include mixed integration, stabilized and variational multiscale (VMS) methods [1], and structure-preserving (physics compatible) approaches [2]. For effective long-time-scale integration of these systems the implicit representation of at least a subset of the operators is required [1,2]. Two well-structured approaches, of recent interest, are fully-implicit and implicit-explicit (IMEX) type time-integration methods employing Newton-Krylov type nonlinear/linear iterative solvers. To enable robust, scalable and efficient solution of the large-scale sparse linear systems generated by a Newton linearization, fully-coupled multilevel preconditioners are developed. The multilevel preconditioners are based on two differing approaches. The first technique employs a graph-based aggregation method applied to the nonzero block structure of the Jacobian matrix [1,3]. The second approach utilizes approximate block factorization (ABF) methods and physics-based preconditioning approaches that reduce the coupled systems into a set of simplified systems to which multilevel methods are applied [2]. To demonstrate the flexibility of implicit/IMEX FE discretizations and the fully-coupled Newton-Krylov-AMG solution approaches various forms of resistive magnetohydrodynamic (MHD) and multifluid electromagnetic plasma models are considered. In this context we first briefly discuss the development of the VMS formulation for subset of these systems and then present results for representative plasma physics problems of current scientific interest. Additionally, the discussion considers the robustness, efficiency, and the parallel and algorithmic scaling of the preconditioning methods. Weak scaling results include studies on up to 1M cores. References [1] J. Shadid, R. Pawlowski, E. Cyr, R. Tuminaro, P. Weber and L. Chacon, "Scalable Implicit Incompressible Resistive MHD with Stabilized FE and Fully-coupled Newton-Krylov-AMG," Computer Methods in Applied Mechanics and Engineering, 2016, Vol. 304, pp. 1-25 [2] E. Phillips, J. N. Shadid, E. C. Cyr, and R. Pawlowski. Fast linear solvers for multifluid continuum plasma simulations. Extended abstract and presentation NECDC 2017 [3] P.T. Lin, J.N. Shadid, J.J. Hu, R.P. Pawlowski, E.C. Cyr, "Performance of Fully-coupled Algebraic Multigrid Preconditioners for Large-scale VMS Resistive MHD," Journal of Computational and Applied Mathematics, 2017, in press (<https://doi.org/10.1016/j.cam.2017.09.028>)

Probabilistic Calibration of Soil Parameters in Total Stress Models of Levees Using Bayes' Theorem

Abdollah Shafieezadeh*, Mehrzad Rahimi**, Dylan Wood***, Ethan J. Kubatko****

*The Ohio State University, **The Ohio State University, ***The Ohio State University, ****The Ohio State University

ABSTRACT

Back analysis of parameters of geotechnical structures is an important yet challenging topic in geotechnical engineering. Deterministic approaches are the most commonly used techniques for back calculation of soil properties and model calibration. However, this group of techniques lack the ability to effectively utilize prior information on probabilistic properties of soil parameters and therefore may not yield realizations that have the highest likelihood. This paper proposes using post event investigations of the performance of levees to identify significant parameters, and Bayes' theorem to determine the posterior probability density function of identified significant parameters based on measured reliable responses of the system. The method is carried out on the total stress, plane strain numerical model of London Avenue South Canal in New Orleans, which is developed in FLAC3D finite difference platform. The horizontal displacement at the top of the floodwall is monitored under different water levels and compared with the measured response during a full-scale load test conducted on the same levee configuration. The calibration process involves evaluation of displacements of the levee model for a set of strategically selected training points. A response surface model is then fitted to these points in order to approximate the deviation of measured and simulated responses. Finally, posterior probability density functions of the significant variables are estimated according to Bayes' theorem [1] using Markov Chain Monte Carlo (MCMC) simulation strategy. Results of this study can help in proper and systematic calibration of soil properties of levee systems in a way that available information are effectively utilized and produced realizations of model parameters have the highest likelihood of occurrence. Produced calibrated models are essential for reliability analysis of levees and floodwalls, in particular, against extreme storm surge events. References: 1. Zhang, L. L., Zhang, J., Zhang, L. M., & Tang, W. H. (2010). Back analysis of slope failure with Markov chain Monte Carlo simulation. Computers and Geotechnics, 37(7), 905-912.

A Coupled Crystal Plasticity-Phase Field Framework for Modeling Ductile Failure in Polycrystals With Anisotropic Material Behavior

Ahmad Shahba^{*}, Jiahao Cheng^{**}, Xiaohui Tu^{***}, Somnath Ghosh^{****}

^{*}The Johns Hopkins University, ^{**}The Johns Hopkins University, ^{***}The Johns Hopkins University, ^{****}The Johns Hopkins University

ABSTRACT

Polycrystalline alloys with anisotropic material response, such as Al and Ti alloys, are widely used in the manufacturing of components for the aerospace and military applications. Failure of these components under service loads starts with the formation and propagation of short cracks at the microstructural level. Microstructural features, such as grain topology and crystallographic orientation, and dislocation-driven plasticity are known to affect the formation of microscale cracks. In this work, failure of polycrystalline alloys is modeled within a stabilized large-deformation crystal plasticity finite element framework coupled with a crack phase field model. The traditional phase field models require the elastic free energy density to be decoupled into dilatational and deviatoric parts; however, this decoupling is not generally achievable for anisotropic materials. Therefore, in this work a new model of crack phase field is proposed. Multiplicatively decomposing the elastic deformation gradient into fracture-sensitive and fracture-insensitive components and expressing the elastic free energy density in terms of the fracture-insensitive elastic deformation gradient, it is shown that one can simulate the fracture process in any anisotropic material. Furthermore, this methodology enables one to seamlessly accommodate the tension-compression asymmetry in the mechanical response of damaged materials. This feature is of paramount importance in modeling fatigue failure under partially (or fully) reversed cyclic loading conditions. Finite element modeling of degrading materials is numerically challenging since the traditional solvers fail to converge if instabilities, such as snap-back and snap-through, occur during the deformation. In this work, a simple remedy is proposed to overcome the numerical convergence issues in the event of instabilities as cracks propagate. To obtain plausible fracture patterns using crack phase field framework, fine discretization along the crack path is required in the computational domain. This requirement is crucial and can render the fracture simulations computationally intractable in problems where the crack path is not known a priori, such as failure in polycrystalline materials. An adaptive wavelet transformation-based projection technique is developed and mounted on a hierarchical finite element framework to model failure in polycrystalline materials. The hierarchical form allows one to increase the resolution on the fly in the critical region, i.e. the crack path, whereas the adaptive projection technique determines the necessary hierarchical degrees of freedom to keep and thus optimizes the computational cost. It is shown that this method can accurately predict the fracture patterns in polycrystals with nearly 25 times less number of nodes, compared to traditional finite element method.

A Multiscale Computational Homogenization Theory with Data-Driven Model Reduction for the Prediction of Ductile Damage

Modesar Shakoor*, Cheng Yu**, Orion L. Kafka***, Wing Kam Liu****

*Northwestern University, **Northwestern University, ***Northwestern University, ****Northwestern University

ABSTRACT

Metal forming processes such as extrusion or wire drawing induce large deformation and the nucleation, growth and coalescence of microscopic voids with complex distribution and morphology. The presence of these voids nucleated by either inclusion debonding or break-up can have disastrous effects and lead to ductile fracture both during processing and product life. There is hence an interest in modeling approaches that can relate microstructure to failure mechanisms in ductile materials. This presentation will introduce a multiscale computational homogenization theory with data-driven model reduction that can be applied at different stages of the life of metallic products. This theory is based on a FE-FFT method where the macroscale (product scale) problem is solved using a finite element approximation with a microscale problem solved at each integration point using a reduced version of the FFT-based numerical method [1]. The macroscale problem assumes a homogeneous material, while the microstructure's heterogeneity is modeled in microscale problems using model reduction. This model reduction is obtained by means of data clustering methods following the recently proposed Self-consistent Clustering Analysis (SCA) theory [2], herein extended to account for finite deformation and ductile damage. As opposed to its small strain version [2], the finite strain version of SCA requires a training data set for clustering that accounts for material nonlinearity, and micromechanical modeling of void nucleation, growth and coalescence. The latter is addressed in microscale problems using reduced versions of high-fidelity inclusion debonding and break-up models [3]. The potential of the new multiscale computational homogenization theory with reduced order modeling will be demonstrated through examples where heterogeneous deformation and stress states at the macroscale lead to heterogeneous microstructural evolution. For instance, the influence of macroscopic shear bands on the nucleation of voids and the evolution of their morphology will be investigated. [1] Moulinec, H., & Suquet, P. (1998). A numerical method for computing the overall response of nonlinear composites with complex microstructure. *Computer Methods in Applied Mechanics and Engineering*, 157(1–2), 69–94. [2] Liu, Z., Bessa, M. A., & Liu, W. K. (2016). Self-consistent clustering analysis: An efficient multi-scale scheme for inelastic heterogeneous materials. *Computer Methods in Applied Mechanics and Engineering*, 306, 319–341. [3] Shakoor, M., Bernacki, M., & Bouchard, P.-O. (2017). Ductile fracture of a metal matrix composite studied using 3D numerical modeling of void nucleation and coalescence. *Engineering Fracture Mechanics*. Article in Press.

Phase-field Modelling of Dislocation Interaction with Ordered Precipitates

Pratheek Shanthraj^{*}, Jaber Rezaei Mianroodi^{**}, Bob Svendsen^{***}

^{*}Max-Planck-Institut für Eisenforschung, ^{**}RWTH Aachen University, ^{***}RWTH Aachen University

ABSTRACT

Dislocation interaction with ordered precipitates is modeled here with the help of an extended atomistic phase-field micro-elasticity method taking into account elastic anisotropy and precipitate eigenstrain. In particular, the generalised stacking fault energy of the matrix and precipitate phases are incorporated into the free energy to capture dislocation dissociation and formation of planar faults. Ni-Al and Fe-Mn-Al-C alloys are considered as model systems and possible dislocation reactions and core structures in these alloys resulting in the formation of anti-phase boundaries and complex stacking faults inside the ordered precipitate are studied. Dislocations with different characteristics are placed in the matrix and driven toward the precipitate under external loading. The phase-field results thus obtained are also compared directly with the molecular dynamics simulation of the same system in order to validate the results.

Object Shape Feature Extraction from Motion Parallax Using Convolutional Neural Network

ChengJun Shao^{*}, Makoto Murakami^{**}

^{*}Toyo University, ^{**}Toyo University

ABSTRACT

We propose a neural network which can recognize objects from a sequence of RGB images captured with a single camera through two different convolutional neural networks. The learning process is divided into two steps: learning of CNN for spatial feature extraction and learning of CNN for spatiotemporal feature extraction. The spatial feature extraction CNN extracts spatial feature vectors with position invariance. And they are input to the following spatiotemporal feature extraction CNN, which convolutes them temporally to achieve depth information based on motion parallax. In the spatial feature extraction CNN, each frame of image sequence is convoluted with some spatial filters, the convoluted values are passed through an activation function, and some spatial features are extracted in the convolutional layer. The features are input to the local contrast normalization layer, and the following pooling layer for downsampling. With these three layers as a set, three sets of layers are concatenated to extract low, medium, and high level spatial features. Then, the high level features are converted to a one-dimensional vector, and weighted sums of elements of it are passed through an activation function in the fully connected layer. We may use dropout to reduce the degree of freedom of the network, and to prevent overfitting. In the spatiotemporal feature extraction CNN, a sequence of the low and medium spatial features extracted in the spatial feature extraction CNN with a frame length T is input to the convolutional layer. The sequence of the same spatial features is convoluted with some temporal filters, the convoluted values are passed through an activation function, and some temporal features including depth information from motion parallax can be extracted. The features are input to the local contrast normalization layer, the pooling layer, and the fully connected layer. And the high level spatial features extracted in the spatial feature extraction CNN are also input to the fully connected layer. And these different kinds of features are integrated in the output layer. To evaluate our proposed method we conducted an experiment using some objects with simple shapes, and extracted the shape information from motion parallax.

Global Sensitivity Analysis of Arlequin Method in Multiscale Models: Effect of Coupling Factors

Qian Shao^{*}, Qun Huang^{**}, Jian Liu^{***}, Shaobo Zhu^{****}, Heng Hu^{*****}

^{*}Wuhan University, ^{**}Wuhan University, ^{***}Wuhan University, ^{****}Wuhan University, ^{*****}Wuhan University

ABSTRACT

Being a kind of bridging techniques, the Arlequin method [1][3] uses Lagrange multipliers to couple mechanical or numerical models of different scales. Although this technique has been widely studied, the following key factors are still questionable: the definition of the weight functions, the choice of the characteristic length, the length of the coupling zone. The aim of this work is to investigate quantitatively and qualitatively the influences of these factors through the Global Sensitivity Analyses (GSA) [2]. The GSA uses Sparse Polynomial Chaos Expansion (SPCE) methodology that is based on the theory of Bayesian model averaging. In particular, Sobol' indices are calculated by variance decomposition to analyze the influence of each parameter on the accuracy of numerical model. Interaction effects among different parameters can also be captured. In this work, different multi-scale models (particle-continuum models and 2D-1D FE models) are analyzed by the proposed technique, and quantitative conclusions on the selection of the coupling factors are drawn. Keywords: Arlequin method; Global sensitivity analysis; Sparse polynomial chaos expansion; Bayesian model averaging; Multiscale models; References [1] H. Hu, N. Damil, M. Potier-Ferry. A bridging technique to analyze the influence of boundary conditions on instability patterns [J]. Journal of Computational Physics, 2011, 10: 3753–3764. [2] Q. Shao, A. Younes, M. Fahs, T. A. Mara. Bayesian sparse polynomial chaos expansion for global sensitivity analysis [J]. Computer Methods in Applied Mechanics &&&& Engineering, 2017, 318: 474-496. [3] H. B. Dhia, G. Rateau. The Arlequin method as a flexible engineering design tool [J]. International Journal for Numerical Methods in Engineering, 2005, 62(11): 1442-1462.

Immersed Boundary Methods for Rigid and Deformable Particles in Viscoelastic Flows

Eric Shaqfeh^{*}, Will Murch^{**}, Chris Guido^{***}, mengfei yang^{****}

^{*}Stanford University, ^{**}Stanford University, ^{***}Stanford University, ^{****}Stanford University

ABSTRACT

The immersed boundary method will be used with a finite volume fluid solver to develop a unique tool to examine the properties of a viscoelastic suspension of particles. The tool will employ unstructured grids and is massively parallel, thus allowing very complex geometries to be simulated. Since the internal stress of the particles is handled using a finite element solver, nearly arbitrary stress-strain relationships for the particles can be handled and their shape can deform continuously. A number of interesting physical problems will be examined with the code including 1) Sedimentation of particles in orthogonal shear, 2) the rheology of particulate suspensions in a viscoelastic uid under shear and 3) the swimming of C. Elegans in an elastic fluid.

Hermite Polynomial Based Variational and Galerkin Integrators for Forced Lagrangian Systems

Harsh Sharma^{*}, Mayuresh Patil^{**}, Craig Woolsey^{***}

^{*}Virginia Polytechnic Institute and State University, ^{**}Virginia Polytechnic Institute and State University, ^{***}Virginia Polytechnic Institute and State University

ABSTRACT

Conventionally, symplectic methods have been applied to conservative dynamical systems which require accurate long-time simulation. Unlike the traditional numerical integrators with numerical dissipation, these symplectic methods exhibit long-time stable energy behavior. Variational integrators, a subclass of symplectic methods, are momentum-preserving in presence of symmetries and have been shown to have bounded energy error for conservative dynamical systems. Their numerical performance in presence of external forcing though still remains unsettled. Motivated by Hermite interpolation polynomials approach to discretization this work presents two novel approaches to derive structure-preserving numerical integrators for Lagrangian systems. The first one, a variational approach, obtains the discrete Lagrangian by adopting the Hermite interpolation polynomial approach which gives the discrete analogue of the action integral in terms of discrete configuration states and velocities. We set the discrete action stationary with respect to both discrete configuration states and velocities to derive novel variational integrators. We also extend this proposed method to systems with external forcing by considering the discrete analogue of the Lagrange-d'Alembert principle. The second one, a Galerkin approach, discretizes the trajectories using the Hermite interpolation polynomials and the numerical integrators are then obtained by setting the weighted average of the residual of the equations of motion over a time step to zero. Both of the resulting methods are compliant to control analysis since they naturally yield configuration states and velocities as the output, without the need to interpolate like in variational integrators. This paper presents a detailed comparison of the two proposed methods and existing variational integrators. The goal is to establish numerical results pertaining to the computational cost and energy accuracy. The superior energy performance of the proposed methods compared to existing variational integrators is demonstrated by means of two numerical examples which are representative model problems of nonlinear solid-mechanics and multi-body dynamics. This paper also investigates to which extent the advantages of symplectic structure preservation for long-time simulation of conservative dynamical systems carry over to Lagrangian systems with external forcing.

A Comparative Study of Nonlocal Interphase Models for Interface Failure

Luv Sharma^{*}, Ron Peerlings^{**}, Pratheek Shanthraj^{***}, Franz Roters^{****}, Marc Geers^{*****}

^{*}Department of Mechanical Engineering, Eindhoven University of Technology, PO Box 513, 5600 MB, Eindhoven, The Netherlands, ^{**}Department of Mechanical Engineering, Eindhoven University of Technology, PO Box 513, 5600 MB, Eindhoven, The Netherlands, ^{***}Microstructure Physics and Alloy Design, Max-Planck-Institut für Eisenforschung, Max-Planck-Str. 1, 40237 Düsseldorf, Germany, ^{****}Microstructure Physics and Alloy Design, Max-Planck-Institut für Eisenforschung, Max-Planck-Str. 1, 40237 Düsseldorf, Germany, ^{*****}Department of Mechanical Engineering, Eindhoven University of Technology, PO Box 513, 5600 MB, Eindhoven, The Netherlands

ABSTRACT

In this work, we discuss FFT based modelling of interface decohesion. The method is developed keeping in mind the application to multiphase polycrystalline materials. FFT methods are based on a regular and uniform (voxelised) grid of material points. Therefore, interface models, which collapse the multi-scale physical behaviour of the interfaces to a sub-dimensional space cannot be implemented in a straightforward fashion. This limitation is remedied by using the idea of an interfacial band—an interphase band is introduced along the physically sharp interfaces. This interphase band contains material points in the neighbourhood of the interface. The material points inherit the elastic-plastic properties of the grains they originally belong to. The volumetric region of this interphase band dissipates the fracture energy and also models the kinematics associated with the decohesion. To model the anisotropic kinematics of the cracking process, a damage eigen strain is introduced [1]. The eigen strain is decomposed into normal and tangential opening modes, the driving forces for which are the respective resolved tractions. The evolution equations for the openings have a softening character, which induces localisation. In order to avoid the localisation associated with softening, two nonlocal strategies—gradient based nonlocal damage [2] and integral based averaging [3]—are considered. These regularisation strategies smear the damage content outside the interphase domains where the interfacial damage has no physical meaning. To confine the damage content within the interphase band, the boundary conditions at the two edges of the band become important. This is also important from the point of view of possible interaction with the intragranular damage model. We discuss the implementation of such regularisation in integral averaging and gradient based approaches. Their effectiveness in giving proper scaling for the fracture energy is first discussed for a 1D case and then for a propagating crack. Both nonlocal approaches will also be compared from ease of implementation considerations. Finally, an application to cluster of grains is presented. References [1] P. Shanthraj, B. Svendsen, L. Sharma, F. Roters, and D. Raabe. Elasto-viscoplastic phase field modelling of anisotropic cleavage fracture. *Journal of the Mechanics and Physics of Solids*, 99:19–34, 2017. [2] R.H.J. Peerlings, R. de Borst, W.A.M. Brekelmans, and J.H.P. de Vree. Gradient enhanced damage for quasi-brittle materials. *International Journal for Numerical Methods in Engineering*, 39(19):3391–3403, 1996. [3] Z.P. Bažant and G. Pijaudier-Cabot. Nonlocal Continuum Damage, Localization Instability and Convergence. *Journal of Applied Mechanics*, 55(2):287, 1988.

Atomistic and Molecular Modeling of Amorphous Germanium as Negative Electrode for Sodium Ion Battery

Vidushi Sharma^{*}, Kamalika Ghatak^{**}, Siva Nadimpalli^{***}, Dibakar Datta^{****}

^{*}New Jersey Institute of Technology, Newark, ^{**}New Jersey Institute of Technology, Newark, ^{***}New Jersey Institute of Technology, Newark, ^{****}New Jersey Institute of Technology, Newark

ABSTRACT

In recent years, there have been significant concerns that available lithium (Li) resources buried in the earth would not be sufficient to meet the ever-increasing demands for the ubiquitous Lithium Ion Batteries (LIBs). The abundance and low-cost of sodium (Na) in the earth and low reduction potential provide a lucrative inexpensive, safe, and environmentally benign alternative to LIBs. The major challenges in advancing Sodium Ion Battery (NIB) technologies lies in finding the better electrode materials. Experimental investigations showed the potency of Germanium (Ge) as suitable electrode materials for NIBs. However, a systematic multiscale computational investigation is necessary to understand the fundamental of capacity-voltage correlation, microstructural changes of Ge, as well as diffusion characteristics. We, therefore, performed the atomistic simulation (Density Functional Theory (DFT) and Ab Initio Molecular Dynamics (AIMD)) and atomistic-informed molecular simulation (Molecular Dynamics (MD) and Monte Carlo (MD)) to investigate the sodiation-desodiation kinetics in Germanium-Sodium system (Na₆₄Ge₆₄). We find the Ge electrode yields high theoretical capacity of 369 mAhg⁻¹. We analyzed the intercalation potential and capacity correlation for intermediate equilibrium structures and our computational results are in excellent agreement with the existing experimental data. We further investigated the diffusivity of sodium in amorphous Ge (a-Ge), volume expansion, and possible microstructural changes taking place during charging and discharging. We find the energy barrier for diffusion of Na in a-Ge is much lower as compared to crystalline Ge (c-Ge). We computed the volume expansion of Na-Ge alloy electrode to be approximately 149.51% in the fully sodiated state (Na₆₄Ge₆₄). We further investigated Radial Distribution Function (RDF) to examine the possible phase changes from amorphous to crystalline for intermediate structures of sodiated Ge. Furthermore, with input from DFT, we performed MD and MC computation to model the charge-rate of sodiated Ge. Moreover, we analyzed microstructural changes for a sodiated-Ge system with larger time and length scale. Our computational results provide a fundamental insight at the atomic and molecular level and help experimentalists design the Ge based NIBs for real-life applications.

Extracting Atomic Energy Barriers from Dynamics at Grain Boundaries

Tristan Sharp^{*}, Spencer Thomas^{**}, David Srolovitz^{***}, Andrea Liu^{****}

^{*}University of Pennsylvania, ^{**}University of Pennsylvania, ^{***}University of Pennsylvania, ^{****}University of Pennsylvania

ABSTRACT

The tendency for atoms at grain boundaries to rearrange leads to enhanced diffusion and permits phenomena such as lattice defect absorption and emission and grain boundary migration. Most grain boundaries have complex atomic structure which encumbers efforts to connect the local region with its likelihood to rearrange under thermal fluctuations. Here we investigate the connection between structure and atomic dynamics with a technique that uses machine learning (a support vector machine) to analyze simulations of poly-crystalline metals. Having trained on a portion of the simulation, the method applied to the full system readily distinguishes grain boundary atoms that tend to rearrange from those that will not. A quantity calculated from the support vector machine for each atom, “softness,” allows identification of structures that follow an approximately Arrhenius likelihood to rearrange, similar to previous findings in glasses. This indicates an energy barrier and generalized attempt frequency for rearrangements which may be determined for each atom. Correlations between softness and other microscopic quantities (e.g. local potential energy) led us to use a similar method with those quantities and find that consistent information could be extracted. Such considerations of the thermal atomic dynamics are a useful step towards machine-learning predictions of deformation of poly-crystalline materials.

Adaptive Reconnection-based Arbitrary Lagrangian Eulerian Method - A-ReALE

Mikhail Shashkov*

*XCP-4, Los Alamos National Laboratory

ABSTRACT

We present a new adaptive reconnection-based Arbitrary Lagrangian Eulerian method - A-ReALE. The main elements of an A-ReALE method are: An explicit Lagrangian phase on arbitrary polygonal mesh in which the solution and positions of grid nodes are updated; a rezoning phase in which a new grid is defined - both number of cells and their locations as well as connectivity (based on using Voronoi tessellation) of the mesh are allowed to change; and a remapping phase in which the Lagrangian solution is transferred onto the new grid. The design principles of A-ReALE method can be summarized as follows. First, it is using monitor (error indicator) function based on gradient or Hessian of some flow parameter(s), which is measure of interpolation error. Second, using equidistribution principle for monitor function for creating of adaptive mesh. Third, using weighted centroidal Voronoi tessellation as a tool for creating adaptive mesh. Fourth, we modify raw monitor function - we scale it to avoid very small and very big cells and smooth it to create smooth mesh and allow to use theoretical results related to weighted centroidal Voronoi tessellation. We present all details required for implementation of new adaptive ReALE methods and demonstrate their performance in comparison with standard ReALE method. on series of numerical examples.

Modeling Multi-Stage Hydraulic Fracturing from a Borehole within a GFEM Framework

Nathan Shauer^{*}, Carlos Armando Duarte^{**}, Alfredo Sanchez Rivadeneira^{***}, Piyush Gupta^{****}

^{*}University of Illinois at Urbana-Champaign, ^{**}University of Illinois at Urbana-Champaign, ^{***}University of Illinois at Urbana-Champaign, ^{****}University of Illinois at Urbana-Champaign

ABSTRACT

Hydraulic Fracturing is the process in which a fracture propagates through the injection of a pressurized fluid in its cavity. This process is widely used in the oil and gas industry to increase reservoir permeability which leads to high rates of both injection and production. Hydraulic fractures are normally created in a multi-stage process which leads to complex fracture geometries due to interactions and coalescence of fractures, and fracture realignment with preferential propagation direction. The fracture shape, and consequently pressure drop, varies significantly between fracture clusters. As a result, the majority of the gas and oil production, comes from only 20 to 30% of the clusters. Computational methods able to predict the near wellbore tortuosity and pressure drop can play a key role in improving the performance of multistage fracturing. This presentation reports on recent advances of an adaptive Generalized Finite Element Method (GFEM) for the simulation of multiple 3-D non-planar hydraulic fracture propagation near a wellbore. This method is particularly appealing for the discretization of the fractures since it does not require the fracture faces to fit finite element faces. Additionally, analytical asymptotic solutions are used to enrich the fracture fronts, which increases the accuracy of the approximation. Stress intensity factors (SIF) with fluid pressure on fracture faces are extracted using the displacement correlation method. The methodology is verified with analytical solutions and compared with experimental results from the literature. Various configurations and fracture geometries are investigated to demonstrate the non-intuitive propagation behavior in these near wellbore conditions and the robustness of the proposed GFEM methodology. P. Gupta and C.A. Duarte. Simulation of non-planar three-dimensional hydraulic fracture propagation. *International Journal for Numerical and Analytical Methods in Geomechanics*, 38:1397–1430, 2014. doi: 10.1002/nag.2305. P. Gupta and C.A. Duarte. Coupled formulation and algorithms for the simulation of non-planar three-dimensional hydraulic fractures using the generalized finite element method. *International Journal for Numerical and Analytical Methods in Geomechanics*, 40(10):1402–1437, June 2016. ISSN 1096-9853. doi: 10.1002/nag.2485. W. El Rabaa. 1987. 'Hydraulic Fracture Propagation in the Presence of Stress Variation';, in 62nd Annual Technical Conference and Exhibition of the Society of Petroleum Engineer, SPE, Dallas, TX, September 27-30.

On the Mechanical Response of Single Crystal Iron under Extreme Loading Conditions

Mu'asem Shehadeh*, Pascale El Ters**

*American University of Beirut, **American University of Beirut

ABSTRACT

Multiscale Discrete dislocation Dynamic Plasticity (MDDP) simulations are carried out to investigate the mechanical response and microstructure evolution of single crystal alpha-Fe subjected to high strain rate compression over wide range of temperature. The simulations are conducted at temperature ranging between 300K to 900K and strain rate ranging between 10^2 to 10^7 s⁻¹. Atomistically informed generalized mobility law was incorporated in MDDP to account for the effects of temperature and strain rate on dislocation mobility, Peierls stress and Elastic constants. MDDP based constitutive equation interrelating the temperature and strain rate with the flow stress at high strain rate monotonic and impact conditions are proposed. The simulation results of the yield strength, hardening rate and microstructure evolution are in good agreement with reported experimental results. Detailed investigations of the dislocation microstructure evolution show the formation of extended screw dislocation lines at temperatures below 340 K due large value of Peierls stress of the pure screw segments. Moreover, small sessile loops of radius in the order of few nanometers are formed; these sessile loops are facilitated by the easiness of multiple cross slip on available slip planes.

Statistical Reconstruction of Bone Microstructures to Study Osteoporosis

Azadeh Sheidaei*, Fayyaz Nosouhi**, Majid Baniassadi***, Daniel George****, Christine Chappard*****

*Iowa state university, **University of Tehran, ***University of Tehran, ****University of Strasbourg, *****University Paris Diderot

ABSTRACT

Osteoporosis is a major health problem for elderly people leading to weak bone stiffness and high risks of bone fracture under fall. The study and prediction of osteoporosis evolution is a difficult task. It involves both the development of multiphysics and multiscale models integrating bone physics and physiology through sophisticated theoretical numerical models (1-4) and it also requires to solve technical challenges about the integration of large scale numerical models to account for all the local physics through adequately homogenized theories (5). To address this problem, a 3D reconstruction of bone microstructures was extracted from high spatial resolution MR images. The real representation of the bone was converted into a finite element model based on small tetrahedral elements. To study potential microstructures distributions being patient dependent, an equivalent statistical representative volume element (RVE) has been created using a recently developed technique (6). Both real RVE and statistical RVE were studied and compare using FEM. The results showed good correlation between the two distributions. Several statistical RVEs were generated using the data obtained from MR images to study the effect of different parameters such as the influence of the geometrical distribution of the bone microstructure on its mechanical response. Study of the bone remodeling is currently our ongoing research project where the above bone microstructures are used to study and model the osteoporosis evolution. References 1. A. Madeo, D. George, T. Lekszycki, et al., A second gradient continuum model accounting for some effects of microstructure on reconstructed bone remodeling, *Compte Rendus Mécanique*, 2012, vol. 340 (8), pp. 575-589. 2. I. Scala, C. Spingarn, Y. Remond, et al., Mechanically-driven bone remodeling simulation : application to LIPUS treated rat calvarial defects, *Mathematics and Mechanics of Solids*, 2016, 22(10), 1976-1988. 3. D. George, C. Spingarn, C. Dissaux, et al., Examples of multiscale and multiphysics numerical modeling of biological tissues, *Bio-Medical Materials and Engineering*, 2017, 28(S1), S15-S27. 4. D. George, R. Allena, Y. Rémond, Mechanobiological stimuli for bone remodeling: mechanical energy, cell nutrients and mobility, *Computer Methods in Biomechanics and Biomedical Engineering*, 2017, 20(sup1), 91-92. 5. Y. Rémond, S. Ahzi, M. Baniassadi, et al., *Applied RVE Reconstruction and Homogenization of Heterogeneous Materials*, Ed. Wiley-ISTE, 2016; ISBN: 978-1-84821-901-4. 6. M. Tafazoli, M. Shakeri, M. Baniassadi, et al., Investigation of the geometric property hull for infiltrated solid oxide fuel cell electrodes, *International Journal of Energy Research*, 2017, 41(14), 2318-2331.

An Improved Formulation for Hybridizable Discontinuous Galerkin Fluid-Structure Interaction Modeling

Jason Sheldon^{*}, Jonathan Pitt^{**}, Scott Miller^{***}

^{*}Institute for Defense Analyses, ^{**}Applied Research Laboratory, The Pennsylvania State University, ^{***}Sandia National Laboratories

ABSTRACT

This work presents a novel application of the hybridizable discontinuous Galerkin (HDG) finite element method to the multi-physics simulation of coupled fluid–structure interaction (FSI) problems, along with formulation improvements that reduce the computational expense of the method. The FSI model utilizes monolithically coupled HDG formulations of nonlinear elastodynamics and incompressible arbitrary Lagrangian–Eulerian Navier–Stokes, with linear elastostatics for the motion of the fluid’s mesh. The elasticity formulations are written in a Lagrangian reference frame, with the nonlinear formulation restricted to hyperelastic materials. Two improvements over the HDG FSI formulation by Sheldon et al. [1] are presented: the elimination of a solid’s global displacement and the restriction of the mesh’s function spaces to only linear polynomials. These improvements significantly reduce the number of global degrees of freedom and reduce the method’s computational expense. The HDG FSI model formulations are compared to each other as well as to the FSI benchmark problem proposed by Turek and Hron [2]. [1] J. Sheldon, S. Miller, J. Pitt, A hybridizable discontinuous Galerkin method for modeling fluid–structure interaction, in: *Journal of Computational Physics*, 2016, pp. 91–114. [2] S. Turek, J. Hron, Proposal for numerical benchmarking of fluid–structure interaction between an elastic object and laminar incompressible flow, in: *Fluid–Structure Interaction*, 2006, pp. 371–385.

Damage and Failure Modeling of Heterogeneous Concrete Using Peridynamics

Feng Shen^{*}, Qing Zhang^{**}, Xiaozhou Xia^{***}, Dan Huang^{****}

^{*}School of Civil Engineering, Suzhou University of Science and Technology, Suzhou, China, ^{**}Department of Engineering Mechanics, Hohai University, Nanjing, China, ^{***}Department of Engineering Mechanics, Hohai University, Nanjing, China, ^{****}Department of Engineering Mechanics, Hohai University, Nanjing, China

ABSTRACT

The failure process and its mechanism of concrete structure is one of major concerns in the academic and engineering field for a long time. In the study of damage accumulation and progressive failure in concrete structures, nearly all traditional methods based on the classical theory of continuum mechanics attempt to solve the partial differential equations, but these methods are proved unsuitable since the limitations such as remeshing and mapping cannot be removed completely. To potentially solve this problem, a novel and promising non-local peridynamic theory is utilized in this paper. In contrast to these classical theories, the peridynamic equation of motion introduced by Silling is free of any spatial derivatives of displacement. After mathematical demonstration of the theory, peridynamics has been used in membranes, fibers, and so on. However, peridynamic theory has not been applied to model concrete very often. In this paper, a new constitutive model has been proposed, which was suitable for concrete based on the “bond-based” peridynamics, and some of its parameters have been discussed. Considering concrete as a heterogeneous material which is composed of aggregates, cement matrix and interfaces between them at the mesoscale, a mesoscale PD model was presented, which characterizing the microstructures of concrete, in order to reveal the failure mechanism of concrete and its whole process of damage. We have studied its deformation and characteristics under loading, and modeled the process of failure. Based on the result of peridynamics calculation, the whole process of microdefects growing, damage accumulation, crack initiation and propagation in concrete materials and structures were reappeared. The result of the example clarifies the unique advantage of modeling damage accumulation and progressive failure of concrete based on peridynamic theory. This study provides a new promising alternative for analyzing complicated discontinuity problems.

Acknowledgements This research is supported by the National Natural Science Foundation of China (Grants nos. 51709194, 11672101, 51679077). **References** [1] Silling S. A. Reformulation of elasticity theory for discontinuities and long-range forces[J]. Journal of the Mechanics and Physics of Solids, 2000, 48(1): 175-209. [2] Silling S.A., Bobaru F. Peridynamic modeling of membranes and fibers. International Journal of Non-linear Mechanics, 2005, 40(2): 395-409. [3] Shen Feng, Zhang Qing, Huang Dan. Damage and Failure Process of Concrete Structure under Uni-axial Compression Based on Peridynamics Modeling [J]. Mathematical Problems in Engineering, 2013.

Discrete Modeling of Concrete Thermal Spalling

Lei Shen^{*}, Gianluca Cusatis^{**}, Qingwen Ren^{***}, Giovanni Di Luzio^{****}, Weixin Li^{*****}, Xinwei Zhou^{*****}, Jun Feng^{*****}

^{*}Hohai University, ^{**}Northwestern University, ^{***}Hohai University, ^{****}Politecnico di Milano, ^{*****}Northwestern University, ^{*****}ES3 Company, ^{*****}Northwestern University

ABSTRACT

When concrete is exposed to fire, the high temperature leads to the development of thermal stresses and elevated pore vapor pressure, which, in turn, cause spalling of a surface concrete layer (mostly the concrete cover). Such spalling exposes the steel reinforcement to high temperature resulting in a drastic reduction of the carrying capacity of the affected structural elements. Despite the catastrophic effect of thermal spalling, a clear explanation of the underlying mechanisms remains elusive. To gain a better understanding of the overall phenomenon, a discrete hydro-thermo-chemical model for the simulation of temperature and pore pressure evolutions in concrete at high temperature is proposed. Such model is then coupled with the so-called lattice discrete particle model (LDPM) that simulates cracking and damage in concrete. The multi-physical coupled model features the effect of pore vapor pressure and temperature on the mechanical response and the effect of cracking on mass and heat transport. The model is validated by comparison with experimental data. Results show that damage localization and fracture significantly reduce local pore pressure built-up due to the increase of pore volume. Hence the pore pressure increase causes crack initiation but it is not enough to explain spalling. Also, results demonstrate that thermal stresses alone cause only minor damage. However, thermal spalling is very well reproduced if both effects are included: pore pressure causes cracks to develop parallel to surface and, subsequently, thermal stresses induce the buckling of the concrete layer generated by the cracks.

A Phase Field Model for Viscoelastic Fracture Accelerated by Viscous Energy Dissipation

Rilin Shen^{*}, Haim Waisman^{**}, Licheng Guo^{***}

^{*}Harbin Institute of Technology; Columbia University, ^{**}Columbia University, ^{***}Harbin Institute of Technology

ABSTRACT

Fracture of viscoelastic materials plays an important role in many applications in science and engineering but is not well understood. In addition to the time and rate-dependent response of viscoelastic materials, fracture of these materials may be accelerated by a viscous energy dissipation mechanism. Moreover, environmental factors further accelerate damage growth but are not easily accounted for by traditional fracture or damage models. To this end, we propose a modified phase field method for modeling the fracture of such viscoelastic materials. Unlike most phase field methods that are driven by pure elastic energy effects, herein we introduce viscous energy dissipation as an additional mechanism that drives fracture. Hence, with a single additional parameter, complex environmental factors could be introduced in order to obtain accelerated damage growth. Viscoelastic material behavior is obtained through Prony-Series expansion and the phase-field viscoelastic formulation is shown to be thermodynamically consistent. We study the effect of fracture driven by viscous dissipation on three 3D benchmark problems. First, the behavior of a bar under creep, relaxation and strain rate loading cases is examined. Then, crack propagation in mode I and mixed mode conditions are studied on a typical 3-point asphalt bending problem and validated against available experiments. In all cases, it is shown that viscous dissipation accelerates the fracture growth rate but essentially in principle do not affect crack path.

A Numerical Method for Crack Problems of Nonhomogeneous Materials Based on Cohesive Damage Model

Rinlin Shen^{*}, Yanyan Zhang^{**}, Jianchao Pang^{***}, Mengxiao Zhang^{****}, LiCheng Guo^{*****}

^{*}School of Astronautics, Harbin Institute of Technology, Harbin 150001, China, ^{**}Institute of Metal Research, Chinese Academy of Sciences, Shenyang 110016, China, ^{***}Institute of Metal Research, Chinese Academy of Sciences, Shenyang 110016, China, ^{****}Institute of Metal Research, Chinese Academy of Sciences, Shenyang 110016, China, ^{*****}School of Astronautics, Harbin Institute of Technology, Harbin 150001, China

ABSTRACT

Abstract: Fractures phenomena can often be found in nonhomogeneous materials (NM). This paper aims to develop a set of a micro-scale damage cohesive finite element model (CFEM) method, combining the digital image-based technique (DIT) for analyzing the crack initiation and growth problems of NM. The agreement of stress-strain curve and fracture mechanism between in-situ tensile experimental test and simulation results shows that the developed method works effectively. Keywords: Nonhomogeneous materials; Cohesive finite element method; Crack initiation.

A Homogenization-based Phase Field Approach to Fracture

Yongxing Shen*, Cheng Cheng**

*University of Michigan-Shanghai Jiao Tong University Joint Institute, Shanghai Jiao Tong University, **University of Michigan-Shanghai Jiao Tong University Joint Institute, Shanghai Jiao Tong University

ABSTRACT

The regularized variational theory of fracture, or so called phase field approach to fracture, has gained popularity due to its ability to predict crack nucleation, propagation, and branching without extra criteria. This approach works by minimizing a total energy functional with the displacement field and phase field (0=intact material, 1=crack) as arguments, and eliminates the cumbersome geometric tracking compared with traditional discrete crack methods such as the extended finite element method. Since 2009, a few variants of this approach have been proposed to account for the unilateral constraint. In this presentation, I will detail our formulation for the unilateral constraint based on homogenization theory and micromechanics, followed by a comparison with major existing models.

Nonlinear Dynamic Performance of a Viscoelastic Dielectric Elastomer Actuator

Junjie Sheng*, Bo Li**, Hualing Chen***, Yuqing Zhang****, Junshi Zhang*****

*China Academy of Engineering Physics, **Xi'an Jiaotong University, ***Xi'an Jiaotong University, ****China Academy of Engineering Physics, *****Xi'an Jiaotong University

ABSTRACT

Dielectric elastomer (DE) is a new type soft smart material. Subjected to a voltage, a DE reduces its thickness and generates large expansion in its area of a maximum area strain of 1600% [1] and can be used in high performance applications as DE actuator (DEA). Because of its viscoelasticity of the elastomeric polymer matrix, DEA is able to produce a time dependent electromechanical deformation [2]. The time-dependency of a DEA can cause dissipation in the system and significantly affect its dynamic performance and coupling efficiency [3]. In the current study, by using the a thermodynamic free energy model, an analytical model is developed to characterize the dynamic performance of a homogeneously deformed viscoelastic DEA by taking into account of the inertial force and damping force, and also taking into account of the temperature dependent dielectric constant and shear moduli. The nonlinear dynamic behaviors of viscoelastic DEA subjected to combined loads of the electric field and mechanical press undergoing periodic electric loading were analyzed. The numerical results, such as displacement response, phase diagrams and amplitude-frequency response were analyzed. Poincaré maps were presented to show the influence of temperature, viscoelasticity, pre-stresses and frequencies on the nonlinear dynamic stability of viscoelastic DEA. Numerical results indicated that temperature, viscoelasticity, pre-stresses, frequencies and applied voltages could tune the natural frequency and modify the dynamic behavior of DEA. The results may guide the design of high-performance DEA and the control of its dynamic deformation. References: [1]C. Keplinger, T. Li, R. Baumgartner, Z. Suo, and S. Bauer, Harnessing snap-through instability in soft dielectrics to achieve giant voltage-triggered deformation, *Soft Matter*, 8 (2), 285-288 (2012). [2] Lei Liu, Wenjie Sun, Junjie Sheng, Longfei Chang, Dichen Li and Hualing Chen, Effect of temperature on the electromechanical actuation of viscoelastic dielectric elastomers, *EPL*, 112, 27006 (2015). [3] Junshi Zhang, Hualing Chen, Bo Li, David McCoul and Qibing Pei, Coupled nonlinear oscillation and stability evolution of viscoelastic dielectric elastomers, 11, 7483 (2015).

HULLFORM DESIGN DRIVEN BY GLOBAL FLOW OPTIMIZATION FOR A SWATH

SHENGZHONG LI, FENG ZHAO, QIJUN NI, AND PENG LIN

China Ship Scientific Research Center
Wuxi, China
shengzhonglee@126.com

Key words: Hullform Design Optimization, SWATH, SBD Techniques; MOPSO Algorithm; CFD; Total resistance.

Abstract. Hull geometry modification and reconstruction, optimization algorithms and CFD technique are combined together into what is known as Simulation-based Design (SBD) techniques, and its essence is the hydrodynamic configurations design driven by global flow optimization. The purpose of this paper is to show how the improvement of the hydrodynamics performance of a Small Water-Plane-Area Twin Hull (SWATH) can be obtained by solving a shape optimization design problem at different speeds using the SBD technique. In this paper, an example of the technique application for the SWATH hullform optimization at different speeds is demonstrated. In the procedure, the Free-form Deformation method is chosen to automatically modify the geometry of submerged pontoon, and the Multi-Objective Particle Swarm Optimization (MOPSO) algorithm is adopted for exploring the design space. The two objectives functions, the total resistance at two different speeds (11kn and 15kn), are assessed by RANS solvers. The optimization results show that the decrease of total resistance is significant for the optimization case at two different speeds (11kn and 15kn), with a reduction of about 5.1% and 6.3% respectively. Meanwhile, the displacement increases 3.7% and the transverse section of submerged pontoon becomes "flower vase" type from ellipse. Finally, dedicated experimental campaigns for optimized model have been carried out to validate the computations and establish the effects of the optimization processes. It shows that the computations of optimization scheme mainly fit the results of model test. The given, practical examples demonstrate the practicability and superiority of the proposed SBD technique for the SWATH multiple speeds integrated optimization problem

1 INTRODUCTION

Energy conservation has attracted more and more attention in ship industry, and hullform optimization which is one of the most significant approach to meet the requirements of energy conservation for shipbuilding industry, has been studied for years. Traditional optimization which is conducted usually aiming at one specific speed. However, cruise speed and design speed which are regardful design points to the respectable ships. It is hard to make the ship performance obtain significant optimization effects in different design aspects by optimizing

hullform of ship. In this paper, the SWATH (Small Water-Plane-Area Twin Hull) which has outstanding seakeeping performance, roomy deck and the appropriate platform for scientific investigate, acoustics research and other oceangoing missions, was selected as the subject of study. However, the excellent performance of high performance ship is not inherent, meaning that elaborate design is need to bring the advantages of hullform into play.

Compared with traditional ship, total resistance of SWATH is quite sensitive to the variation of speed. Along with the increase of speed, resistance may change greatly. The hullform optimization design aiming at only one design factor is hard to guarantee that the benefit of SWATH resistance meet the requirements at other speeds as well, which will make an adverse impact on the holistic economy of ship. Furthermore, the uniqueness of SWATH hullform and the sensibility to variation of weight and center of gravity, bringing about new difficulties to hullform optimization design. Therefore, the hullform optimization design of SWATH at different speeds is necessary to be conducted to guarantee its better resistance performance at all speeds.

With the development of CFD (Computational Fluid Dynamics), CAD and Optimization theory, a new ship design method/mode also known as SBD (Simulation Based Design) technique opens a new way for hull-form optimization design and configuration innovation^[1]. In this process, the objective functions (the hydrodynamic performance of a ship) will be evaluated with CFD codes, and the solutions space of the design problem will be explored with optimization theory, then the optimized hullform under the given constraints will be attained at last. In summary, SBD techniques can solve the complex multi-objective hullform design optimization problem, and its essence is the hydrodynamic configurations design driven by global flow optimization.

2 GENERAL SPECIFICATIONS REVIEW OF SBD TECHNIQUE AND SWATH

For years, numerous researches around SBD technique have been conducted at home and abroad. Among them, it gives first place to the research related to monohull. Han, etc.^[2] conducts the optimization design of container ship and LPG (liquefied petroleum gas) ship. Different hullforms are obtained by varying the curve of transverse section area and the hullform geometry reconstruction is conducted based on Lackenby hullform transformation idea. Kim^[3] amends three shape parameters, including curve of transverse section area, waterline and bulbous bow, to achieve hull geometry reconstruction and conduct the multi-objective overall optimization of KVLCC2 ship model. Kim, Yang, etc.^[4] adopts ship overall geometry reconstruction method based on Lackenby transformation, hull part geometry reconstruction method based on radial basis function interpolation and the combination of these two methods to conduct optimization design on series 60 hullform. LI Shengzhong, etc.^[5] regards the total resistance and flow field of propeller disk as object function, adopts multi-objective particle swarm optimization (MOPSO) and FFD geometry construction method to conduct automatic optimization design on stern hullform of 6600DWT bulk cargo ship, and the results are satisfactory. Among them, one of the optimization schemes improves the wake flow field quality and decreases 10% of the residuary resistance.

The hullform and hydrodynamic performance characteristic of SWATH are different from monohull. On the aspect of appearance, SWATH is similar to catamaran and they both have two slices. SWATH is special on the following aspects: the waterplane area in design waterline is small; most of the volume locates in the underwater far away from waterplane, forming the pontoon shape which is called submerged body and connected with upper platform by strut. The special appearance of SWATH causes a decrease in wave turbulence and motion in waves, owning excellent seakeeping performance, which is the reason why this kind of hullform is high-profile. The developed countries, mainly including America, Japan and German, have built a great amount of SWATH with different purposes.

America is typical in this respect. The "Victorious" (3384T) and "Impeccable" (5380T) are all high seakeeping performance underwater acoustic surveillance ship, which are built by American navy at the end of 20th century and the beginning of 21th century^[6]. Two "Sea Slice" high speeds SWATH passenger ships used for oil field traffic and one 1000t SWATH harbor ferry with ice breaking function are built in this century. Japan has conducted related research in earlier period and built the first civil SWATH passenger ferry "Seagull" in 1979 and 12 SWATH ships with different purposes in total. German imports the relevant techniques from America from 1990s. Until 2012 September, 25 SWATH ships have been built, including 6 series and 11 types according to length and function which covers harbor diversion, test research, customs anti-smuggling, oceanographic survey and so on^[7]. In addition, other countries like Finland, Russia, Norway, Canada etc. also built SWATH with different purposes in succession.

SBD technique has been adapted to the design of multihull ship like catamaran and SWATH in recent years. Peri, Tahara, Campana etc.^[8, 9, 10] adopts MOGA, PSO and DRAGO mix algorithm to conduct single object optimization design of high speed catamaran at given speed, single object optimization design and multiple object optimization design at multi speed. Model test result of one of the optimization schemes indicates that the total resistance of optimal design scheme decrease 9.3% compared with original scheme. Stefano Brizzolara etc.^[11] conducted the concept design and hydrodynamic performance optimization of SWATH USV, adopting a set of automatic process which based on geometry parameters definition, latest CFD solver and unique differential evolution global minimum algorithm to conduct a systematic optimization.

It shows that SBD technique has attracted more and more attention in ship hydrodynamic design domain. In this paper, SBD is adopted to conduct double speeds optimization of SWATH. The main contents of this paper include the following three respects. Firstly, the concept and the key modules of SBD are introduced. Secondly, a double speeds (cruise speed and design speed) hullform optimization design is conducted on SWATH. During the optimization process, FFD free-form deformation is adopted to modify hull geometry shapes automatically, MOPSO is used to explore solution space and RANS solver is adopted to evaluate the resistance of ship at different speeds. Finally, resistance towing test is conducted on optimization scheme model to verify the accuracy of numerical calculation and reliability of optimization method.

3 SBD TECHNIQUE ELEMENTS AND FEATURES

SBD hullform optimization design technique includes three main modules: 1) Optimizer. This technique can be used to search overall optimal solution in hullform design space accurately and fast under the given constraint conditions; 2) hull geometry and mesh manipulation. It is used to provide the connection between optimization algorithm (design parameter) and evaluation of ship performance (object function); 3) CFD solver. It is not only the foundation of establishment of numerical model of hullform optimization problem, but also the bond between hull geometric shape and optimization platform. The relationship between each main module is shown in Fig. 1.

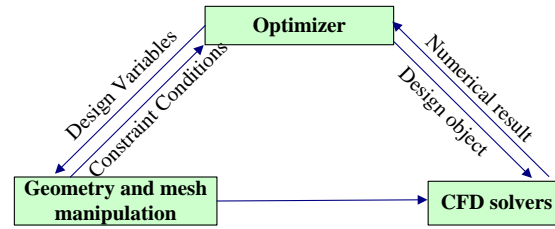


Figure 1 SBD-based hullform optimization design environment

3.1 Optimization method

Optimization is used to explore solution space and obtain the optimal solution of optimization problem. Therefore, to seek the optimal solution in design space quickly and accurately, the selection of optimization algorithm becomes one of the research emphasis in hullform optimization design. Random search algorithm does not rely on specific domain of problems and has high robustness and can find the overall solution easily. Among them, particle swarm optimization (PSO) has the following advantages compared with other random search algorithms. 1) It is simple and easy to implement; 2) It does not need a great amount of adjustments of parameters; 3) It has a stronger overall search ability in some particular areas; for instance, nonlinear problems. Therefore, overall optimization algorithm is recommended for solving practical engineer optimization problem. In this paper, MOPSO is adopted to solve the SWATH double speed design problems. The basic principle and its development are shown in Li [1].

3.2 Hullform geometry reconstruction

Hullform geometry reconstruction technique is the key link of SBD optimization technique and different reconstruction methods will make different influence on the degrees of freedom of optimization algorithm searching design space. Hullform geometry reconstruction should obey the following rules:

- 1) Taking a few control parameters to decrease the scale of problem;
- 2) Different hull shapes should be produced as more as possible to expand the scale of feasible solution;

3) When reconstructing part of hull, the reconstructed part hullform should connect the original hull smoothly;

4) The feasible scheme should be reserved, and the various constraint of geometric shape should be easy to realize in optimization process.

The free-form deformation (FFD) approach is proposed by Sederberg and Parry in 1986, which is a very flexible 3d geometry deformation approach, used for entire and part deformation. Nowadays, FFD approach is brought in the appearance optimization design domain such as ship, aviation and so on, used for the geometry reconstruction of design object. FFD approach is used for modifying hull geometry in this paper. The original approach and its development of FFD approach are shown in Sederberg [12] and Campana [13].

3.3 CFD solver

The CFD solver is adopted as the tools of analysis and forecast, the accuracy of which has a direct influence on the quality of optimization design. Generally, before the optimization design starts, the validity of CFD solver needs to be verified firstly. In addition, the improvement obtained by optimization design should exceed the numerical noise of CFD solver.

In order to redesign the existed appearance, accurate analysis tools are needed to be applied to lead the optimization platform to seek the optimal solution. To guarantee the success of optimization design, RANS method with high accuracy is adopted in this paper for numerical prediction of ship resistance. RANS method is the most widely applied numerical simulation method in practical engineer at present and it has low requirements for computer and high accuracy of prediction, and it is also capable of identifying the influence produced by the detailed variation of hullform geometry on ship performance in the optimization process and adaptable for hullform optimization design.

4 MULTIPLE SPEEDS INTEGRATED OPTIMIZATION OF A SWATH HULLFORM

The effect of ship shape on resistance performance is closely related to ship speed. It is not suitable for all ships to evaluate the resistance performance if only at the design speed. There are two main reasons. On the one hand, the optimal hull form obtained for a given speed may not have a consistent resistance reduction in the entire speed range. It may have a large resistance increase at other off-design speeds. On the other hand, for mid-high speed ship, the influence of hullform change on the resistance is closely linked with speed. In different speed range, the influence of the same hullform change is different, and even has very big difference. It is particularly obvious to the mid-high speed ships that utilize favorable wave interference by the bulb produced to reduce wave resistance. Thus, the present study is focused on the hydrodynamic optimization for a given speed range only, i.e., to develop optimal hull forms with minimum total resistance at the given design speeds.

In this paper, a SWATH is selected as the research object. Its main parameters are shown in table 1. The pontoon configuration is ellipsoid. The view is shown in Fig.2.

Table1 Principal Dimensions and Constraint Conditions

Principal dimensions and coefficients(λ =25)			Constraint conditions		
<i>Parameter</i>	<i>Ship</i>	<i>Model</i>	<i>Type</i>		<i>Definition</i>
<i>Lpp(m)</i>	86.7	3.468	<i>Main dimensions</i>	<i>Lpp</i>	<i>fixed</i>
<i>T (m)</i>	7.8	0.312		<i>T</i>	<i>fixed</i>
<i>B (m)</i>	32	1.280		<i>B</i>	<i>fixed</i>
∇ (t)	5850	0.374	<i>Displacement</i>		<i>Maximum variation: 2%~5%</i>
<i>S(m</i> ² <i>)</i>	1756	2.810	<i>Wetted surface area</i>		<i>Maximum variation: 1%~4%</i>
<i>L_{CB}(m)</i>	44.3	1.772	<i>Buoyancy position</i>		<i>Maximum variation: ±2.5%</i>

4.1 Definition of problems

1) Objective functions and its evaluation

In order to get obvious benefit in different speeds, the total resistance of ship at 11kn($F_n=0.186$) and 14kn ($F_n=0.254$) is regarded as object function as follows:

$$\begin{cases} F_1 = R_{t1}^1 / R_{t0}^1 & \text{at } F_n = 0.186 \\ F_2 = R_{t2}^2 / R_{t0}^2 & \text{at } F_n = 0.254 \end{cases} \quad (1)$$

Where R_{t0}^1 and R_{t0}^2 denote the total resistance evaluated for the original hull form and intermediate hull form obtained during the optimization process, respectively.

RANS flow solver is used to evaluate the value of object function. Cell-center finite volume method is applied to discretize the control equation of RANS. The convection item in RANS equation is discretized by second-order upwind scheme, and the viscous flow item is discretized by two-order center scheme. PISO algorithm is used for solving pressure-velocity coupling equation. Wall function is used to confirm the average speed and the wall boundary condition of vorticity transport equation. SST k- ω equation is selected as turbulence model. Level-set method is selected to numerically simulate the moving free surface. H-O multi-block structured grid is adopted as the mesh type (the background grid is Cartesian grid and the body-fitted grid is double-O grid). Hull mesh distributes more intensively near bow, stern, hull surface and free surface. The diagram of mesh generation is shown in Fig. 3.

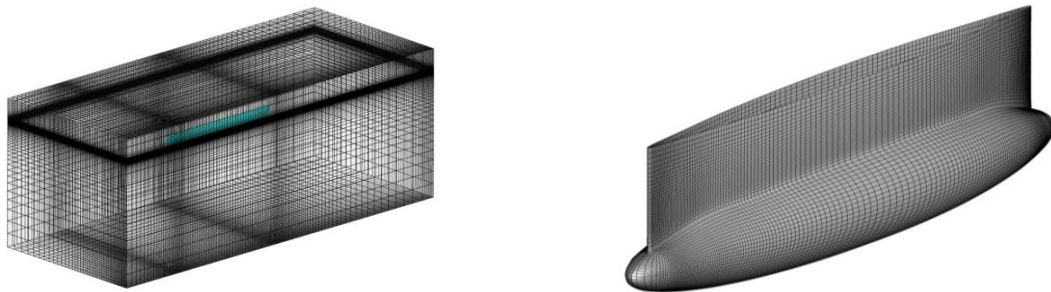


Figure 3 Computation region and hull surface mesh

In this paper, mesh amount and topology structure for the different hulls obtained in optimization process need to be coincident and the first level mesh of hull surface remain constant. Thus the numerical noise produced by the difference of mesh type is avoided.

2) Hull geometry reconstruction and constraint conditions

FFD approach is used for hull geometry reconstruction in the process of multi-objective optimization design for two different speeds. The whole hull area is normalized, and then it is put in a cube with 343 control points (see Fig.4). Twenty-four groups control points are chosen as Twenty-four design variables. Through the change of these design variables, the geometrical surface of the ship-hull at X, Y, Z directions can be reconstructed and deformed. The hull geometry FFD reconstruction diagram is shown in Figure 3. To introduce a realistic design problem, geometrical constraints about the submerged body length, buoyancy center, displacement and principal dimensions of the SWATH are imposed on the design variables. Complete definition of the problem, objective function and constraints, are given below in Tabell.

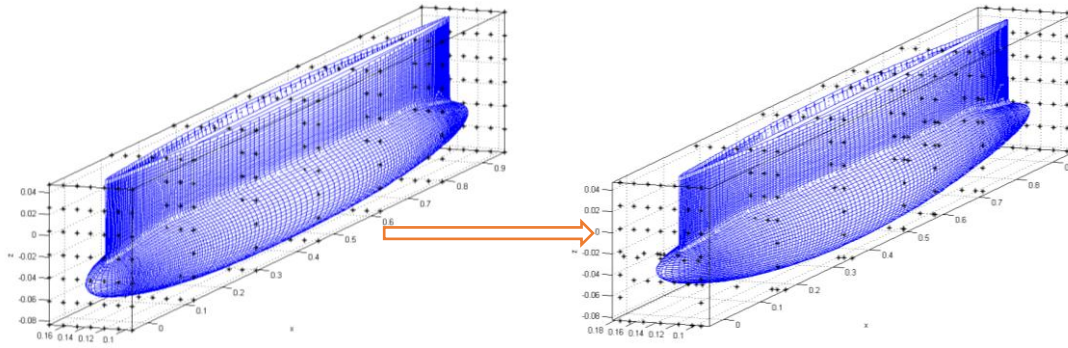


Figure 4 Hullform reconstruction using FFD approach

3) Multi-objective optimization algorithm

It is necessary to employ the multi-objective optimization algorithms to search for the hull forms that have possible resistance reduction at two design speeds. In this study, MOPSO algorithm has been extended to provide a set of optimal solutions using the Pareto front technique.

4.2 Design Optimization Results

In the SWATH optimization process, the particle population number is 36, generation number is 12. Only six points of the complete Pareto optimal sets of solutions are chosen to compare their resistance performances to the original ones. As shown in Table 2, the second and third columns report two objective functions, which are non-dimensionalized compared to its original value. The last three columns report the variation in wetted surface area, displacement and buoyancy position.

Table 2 The part optimal solution sets and constraint condition

Optimal Solutions	F_1	F_2	$(S'-S)/S$	$(\Delta'-\Delta)/\Delta$	$(L'_{CB} - L_{CB})/L$
<i>Opt1</i>	0.931	0.995	1.3%	1.7%	1.7%
<i>Opt2</i>	0.940	0.972	1.8%	2.3%	2.1%
<i>Opt3</i>	0.949	0.937	2.5%	3.7%	1.1%
<i>Opt4</i>	0.973	0.911	2.2%	3.2%	2.1%
<i>Opt5</i>	0.982	0.873	2.1%	2.6%	2.2%
<i>Opt6</i>	0.993	0.854	2.2%	3.4%	2.4%

According to the overall design requirement and resistance reduction effect, the optimized (Opt3) is more satisfactory in six optimized. Its model total resistance at $F_n=0.186$ and $F_n=0.254$ is reduced by 5.1% and 6.3%, respectively. In this paper, the resistances of the optimized at different speed are numerically simulated by RANS, and the results are shown in Table 3 and Fig.5. At the possible speed range, the total resistance coefficients is reduced by 4.5% ~ 19.5%, and the higher the speed, the greater the resistance reduction.

The comparison of hull shape between optimized (Opt3) and original case is shown in Fig. 6. It shows that the variation about transverse section hullform of the optimized has three main points compared with original. Firstly, the bottom of the transverse sections of pontoons becomes wider. Secondly, the vertical radius of transverse pontoon section decreases slightly except of the section near midship, while the transverse radius is nearly invariant. Thirdly, the strut breadth of different transverse sections increases. In general, the shape of section varies from ellipsoid to "vase shape".

Table 3 Comparison of resistance between the original and the optimized

F_n	R_{tm} (N)			C_{tm} (10^{-3})		
	<i>Design</i>	<i>Optimized</i>	<i>Reduction</i>	<i>Design</i>	<i>Optimized</i>	<i>Reduction</i>
0.169	12.2	11.9	-2.6%	4.101	3.915	-4.5%
0.186	15.1	14.3	-5.1%	4.190	3.898	-7.0%
0.203	17.7	16.9	-4.6%	4.141	3.873	-6.5%
0.220	22.5	20.4	-9.2%	4.468	3.975	-11.0%
0.237	25.1	23.0	-8.1%	4.301	3.872	-10.0%
0.254	30.5	28.6	-6.3%	4.565	4.191	-8.2%
0.271	44.3	37.8	-14.7%	5.816	4.861	-16.4%
0.300	52.3	43.0	-17.8%	6.087	4.901	-19.5%
0.318	49.4	44.9	-9.0%	5.124	4.568	-10.8%

The free surface wave profiles and the wave contours of the original model and the optimized models at two speeds are reported in Fig.7. The decrease of the bow wave amplitudes of the optimized is significant when compared to the original at $F_n=0.186$. When $F_n=0.254$, the wave amplitude of optimization is close to original nearbow and outboard of slice, while it increases slightly near the inboard of slice. However, the wave amplitude decreases obviously near the stern.

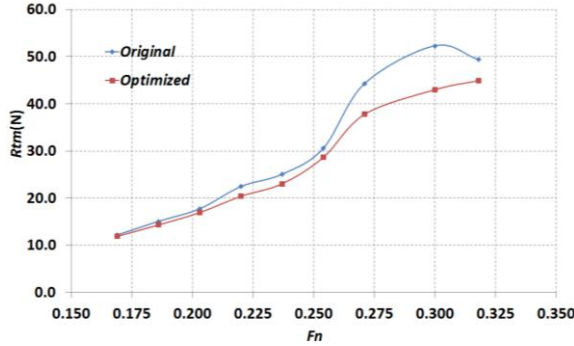


Figure 5 Comparison of the total resistance between the original and the optimized at different speeds

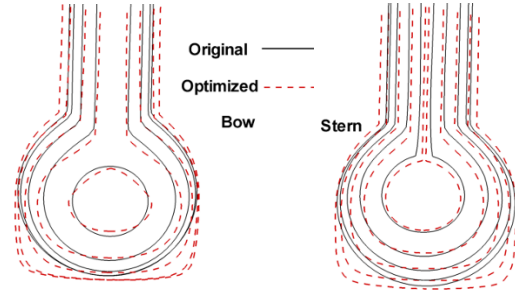


Figure 6 Comparison of transverse section between the original and the optimized

According to the design results mentioned above, through SBD technique, the design optimization problem in multiple speeds will be completed efficiently. The design results obtained decreases the resistance of SWATH in multiple speeds practically. It is hard to achieve only by traditional design method and experience of designer. At the same time, the optimized design results of the paper show the innovation capability of SBD technique, and the shape of the "vase" is obtained from the elliptic submarine line. Its essence is the hydrodynamic configurations design driven by global flow optimization.

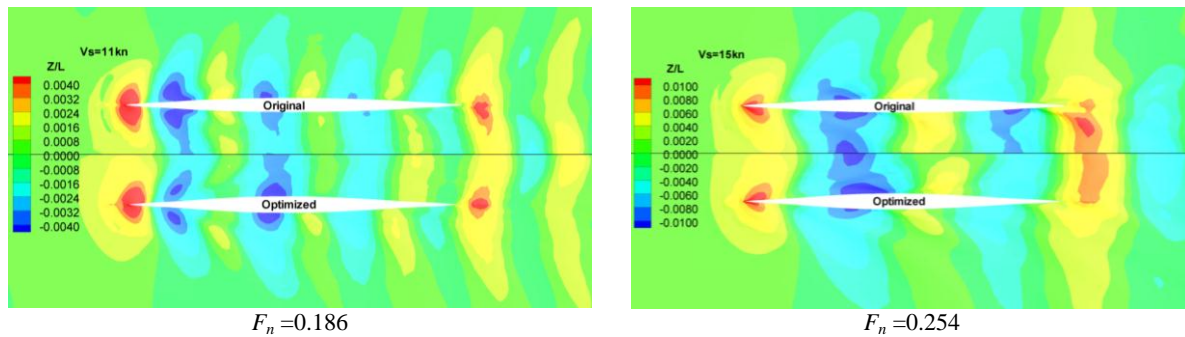


Figure 7 Comparison of wave contours between the original and the optimized

5 EXPERIMENTAL VALIDATION

In order to validate the reliability of optimization design results, the towing test of the optimized model is conducted in CSSRC towing tank. The photos are shown in Fig. 8 (Testing

condition: naked hull with rudders). The CFD (with rudders) and experiment results are shown in Table 4 and Fig.9 ~ Fig.11.

Table 4 The resistance results of experimental and CFD for the optimized with rudders

F_n	R_m (N)		C_{tm} (10^{-3})			θ (°)		δ_m (mm)	
	<i>Exp.</i>	<i>CFD</i>	<i>Exp.</i>	<i>CFD</i>	<i>Reduction</i>	<i>Exp.</i>	<i>CFD</i>	<i>Exp.</i>	<i>CFD</i>
0.169	11.908	12.338	3.865	4.005	3.6%	-0.08	-0.12	-69.1	-65.7
0.186	14.32	14.792	3.842	3.968	3.3%	-0.09	-0.15	-74.7	-78.0
0.203	17.174	17.645	3.871	3.978	2.8%	-0.12	-0.19	-93.7	-94.4
0.220	20.631	21.337	3.963	4.098	3.4%	-0.17	-0.25	-117.4	-114.3
0.237	23.325	23.964	3.863	3.969	2.7%	-0.21	-0.29	-143.6	-139.0
0.254	29.125	29.602	4.202	4.271	1.6%	-0.32	-0.44	-189.9	-160.9
0.271	40.284	39.333	5.108	4.987	-2.4%	-0.46	-0.55	-249.7	-203.1
0.300	44.501	44.594	4.998	5.009	0.2%	-0.49	-0.58	-279.2	-260.5

Through comparing the model experiment and CFD results, it is shown that the errors of total resistance, total resistance coefficient and heave value are relatively small. Although the pitch angle results contains some errors, the trend that pitch angle varies along with speed is similar. On the whole, the numerical calculation on the resistance of SWATH has relatively high accuracy and reliable result of prediction. Thus, according to the calculated results before, it is considered that the calculation of resistance benefit from optimization design is relatively credible. It also means the optimized has effect on resistance reduction to some extent at different speeds. When $F_n=0.186$ the total resistance decreases 5.1%, while when $F_n=0.254$ the total resistance decreases 6.3% accordingly.

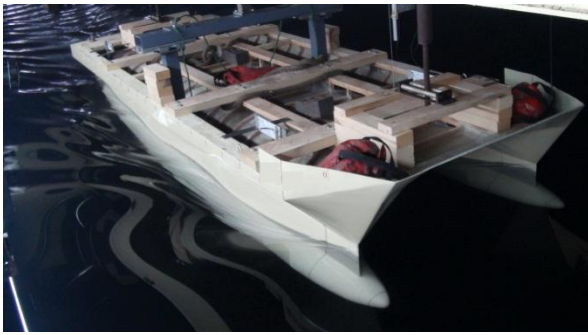


Figure 8 Experimental models of the optimized

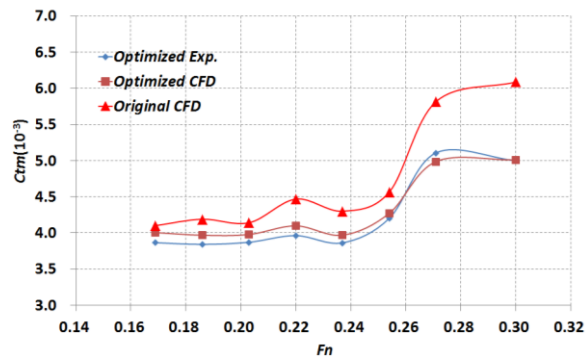


Figure 9 Comparison of the CFD and EFD results of the optimized total resistance coefficient

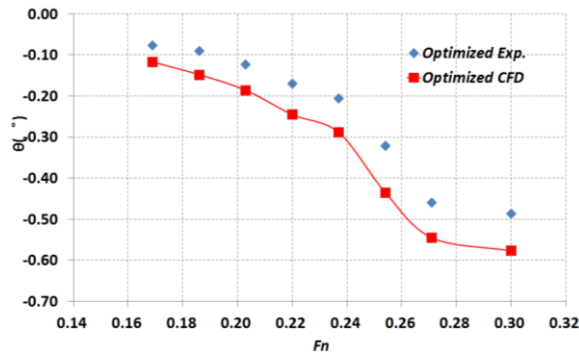


Figure 10 Comparison of CFD and EFD results of the optimized pitch angle

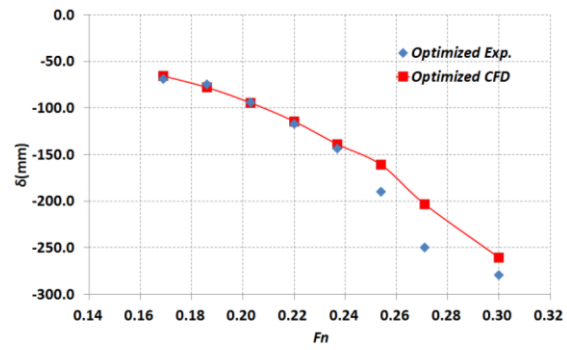


Figure 11 Comparison of CFD and EFD results of the optimized heave value

6 CONCLUSIONS

In this paper, SWATH is regarded as design object, of which the double speed integrated hullform optimization is performed by SBD technique. FFD approach is used to modify the hull geometry and MOPSO algorithm is applied to explore design space. The target response, i.e. total resistance is numerically calculated by high-precision solver based on RANS. Finally, dedicated experimental campaigns for the optimized model have been carried out to validate the accurate of the computations and the success of the optimization processes.

The optimization results show that the decrease of total resistance is significant for the optimization case at two different speeds (11kn and 15kn), with a reduction of about 5.1% and 6.3% respectively. The success of the optimization processes is nicely confirmed by the experimental measurements. The "vase" pontoon configuration is obtained from the ellipsoid, which fully demonstrates the innovation ability of SBD technique. In summary, the result of SWATH double speeds optimization given in this paper demonstrates that SBD technique is not only applicable for special appearance ship such as SWATH, but also quite practical and obviously effective. Its essence is the hydrodynamic configurations design driven by global flow optimization.

REFERENCES

- [1] Li Sheng-Zhong. Research on Hull Form Design Optimization Based on SBD Technique. Ph. D. Dissertation, China Ship Scientific Research Center, 2012.
- [2] Han S, Lee Y S, Choi Y B. Hydrodynamic hull form optimization using parametric models [J]. Journal Mar SciTechnol, 2012.
- [3] Kim H J, Chun H H. Optimizing using Parametric Modification Functions and Global Optimization Methods[C]//27th Symposium on Naval Hydrodynamics. Seoul, Korea, 2008.
- [4] Kim H, Yang C, Chun H H. A Combined Local and Global Hull Form Modification Approach for

Hydrodynamic Optimization. 28th Symposium on Naval Hydrodynamics, 2010[C].

- [5] LI Shengzhong, NI Qijun, ZHAO Feng, LIU Hui. Multi-Objective Design Optimization of Stern Lines for Full-Formed Ship[J]. Shipbuilding of China Vol. 54 No.3, 2013: 1-10
- [6] SHI Wen-qiang, YU Xian-zhao. The development and future trend of foreign SWATH ships [J]. Ship Science and technology Vol.34, Supplement 2, 2012: 4-19
- [7] ZHONG Kai, ZHANG Pei-yuan, ZHENG Ming. SWATH vessels development and future in Germany [J]. Ship Science and technology Vol.34, Supplement 2, 2012: 20-34, 51.
- [8] Peri D, Campana E F. Simulation Based Design of Fast Multihull Ship[C]. 26th Symposium on NavalHydrodynamics. Rome, Italy, 2006.
- [9] Campana E F, Peri D. Shape optimization in ship hydrodynamics using computational fluid dynamics[J]. Computer Methods in Applied. Mechanics and Engineering. 2006. 196: 634–651.
- [10] Tahara Y, Peri D, Campana E F, Stern F. Single and Multiobjective Design Optimization of a FastMultihull Ship: numerical and experimental results[C]. 27th Symposium on Naval Hydrodynamics.2008.
- [11] Stefano Brizzolara, Tom Curtin, Marco Bovio, Giuliano Vernengo. Concept design and hydrodynamic optimizationof an innovative SWATH USV by CFD methods [J]. Ocean Dynamics, 2012, 62:227–237
- [12] Sederberg T W, Parry S R. Free-Form Deformation of Solid Geometric Models [J]. Proc.SIGGRAPH'86, Computer Graphics, 20(4):151-159.
- [13] Campana E F, Peri D, Tahara Y, Kandasamy M, and Stern F. Numerical Optimization Methods for Ship Hydrodynamic Design[C], SNAME Annual Meeting 2009.

Geometry and Meshing for Automated High-Order Simulations

Mark Shephard^{*}, Mark Beall^{**}

^{*}Rensselaer Polytechnic Institute, ^{**}Simmetrix, Inc.

ABSTRACT

The development of isogeometric finite element methods represent a major advance in effective high-order discretization methods both in terms how high-order discretizations can be constructed and controlled, as well as in increased understanding of the properties and advantages of these methods. The application of high-order finite element methods place additional requirements on the mesh generation processes, and their interaction with the geometric domain definition, due to the need for elements on curved domain boundaries to be properly curved to those boundaries and the desire to often generate coarse meshes such that only a small number of finite elements are used to represent entire geometric model features. This presentation will summarize a set of technologies that have been, and continue to be, developed to support the automatic generation and adaptation of curved high-order meshes with an emphasis on being able to interact with the geometric domain definitions ranging for those housed in CAD systems [1], to domains defined by image data [2], to evolving domains as defined by the simulation of physical processes of interest. Key capabilities to be discussed and demonstrated are tools supporting the construction of proper geometric domain topological models from the original geometry, procedures to automatically generate and anisotropically adapt meshes for those geometries that maintain the required levels of geometric approximation while allowing the mesh configurations to be defined by the needs to most effectively represent the physical behavior being simulated. [1] Beall, M.W., Walsh, J. and Shephard, M.S., 2004. A comparison of techniques for geometry access related to mesh generation. *Engineering with Computers*, 20(3), pp.210-221. [2] Klaas, O., Beall, M.W. and Shephard, M.S., 2013. Construction of models and meshes of heterogeneous material microstructures from image data. In *Image-Based Geometric Modeling and Mesh Generation* (pp. 171-193). Springer Netherlands.

Modeling of Ultra-High Performance Concrete Flyer Plate Experiments

Jesse Sherburn*, William Heard**

*U.S. Army Engineer Research and Development Center, **U.S. Army Engineer Research and Development Center

ABSTRACT

Ultra-high performance concrete (UHPC) has emerged as a viable material in protective structures of interest to the defense community. A significant amount of research has been completed on characterizing UHPC under quasi-static loading conditions [1] and more recently under dynamic loading conditions [2] such as Koslky bar experiments. One area that has little study is under extreme loading conditions such as high velocity flyer plate impacts that induce shock wave propagation. Recent research efforts by Neel et al. [3] produced a number of carefully controlled flyer plate impact experiments for a UHPC. This data provides an excellent testbed to evaluate some current computational solid mechanics codes and their respective constitutive models ability to model this extreme loading condition. The data from Neel et al. [3] can be used to calibrate and validate various computational methods subjected to this type of loading condition. This study investigates modeling the flyer plate experiments of Neel et al. [3] using a number of different methods such the Eulerian shock wave code CTH, and the meshfree method known as the reproducing kernel particle method (RKPM). Multiple constitutive models in CTH and RKPM will be evaluated in order to match the flyer plate experiments. A discussion of the different current strengths and weaknesses of the respective models will be discussed as well as some future recommended research areas. [1] Williams, E.M., Graham, S.S., Reed, P.A., and Rushing, T.S. 2009. Laboratory Characterization of Cor-Tuf Concrete With and Without Steel Fibers. ERDC/GSL TR-09-22, U.S. Army Engineer Research and Development Center, Vicksburg, MS. [2] Martin, B.E., Heard, W.F., Loeffler, C.M., and Nie, X. 2017. Specimen Size and Strain Rate Effects on the Compressive Behavior of Concrete. *Experimental Mechanics*, <https://doi.org/10.1007/s11340-017-0355-2>. [3] Neel, C., Martin, B.E., and Chhabildas, L. 2017. Shock and Spall of the Ultra-High Performance Concrete Mortar "Cortuf" without Steel Fibers. AFRL-RW-EG-TR-2017-082, Air Force Research Laboratory, Eglin Air Force Base, FL. * Permission to publish was granted by Director, Geotechnical and Structures Laboratory.

FREE VIBRATION ANALYSIS OF BEAMS AND PLATES WITH ELASTIC BOUNDARY CONDITIONS BY DIFFERENTIAL QUADRATURE FINITE ELEMENT METHOD

Dongyan Shi*, Xianlei Guan[†], Gai Liu[‡]

*College of Mechanical and Electrical Engineering, Harbin Engineering University
Harbin, China
Email: shidongyan@hrbeu.edu.cn

[†]College of Mechanical and Electrical Engineering, Central South University
Changsha, China
Email: guanxianlei@hrbeu.edu.cn

[‡]College of Mechanical and Electrical Engineering, Harbin Engineering University
Harbin, China
Email: liugai@hrbeu.edu.cn

Keywords: Free vibration; DQFEM; Elastic boundary conditions; virtual springs

Summary: *A virtual or artificial spring technique is used in the weak form differential quadrature finite element method (DQFEM) in order to simulate the effects of elastic restraints in the analysis of free vibrations of beams and plates. By introducing the virtual spring technique, the applicability of the DQFEM is expanded to deal with free vibration problems with general elastic boundary conditions. The elastic boundary conditions can be easily achieved by setting the stiffness of corresponding springs to be desired values. Firstly, the expressions of the potential and kinetic energy of a beam or plate element are given based on the Timoshenko beam theory and Mindlin's plate theory, respectively, and the differential operators in which are discretized by the differential quadrature (DQ) rules. Secondly, the stiffness and mass matrices of beam element and plate element are derived in form of weighting coefficient matrices. Next, the translational springs and rotational springs are used to restraint the translational and rotational degree of freedoms of a node, respectively. Therefore, the potential energy of the springs is taken into account as part of the stiffness matrix of the elements. Finally, global stiffness and mass matrices of the whole system is*

assembled according to the traditional finite element method (FEM). Several numerical examples are presented. The accuracy of the present method is validated by comparing the results with those from references and FEM.

1 INTRODUCTION

The finite element method (FEM) and finite difference method (FDM) have been widely used in many engineering problems. Another alternative algorithm also called as the differential quadrature method (DQM) is proposed by Bellman et al. [1,2]. The greatest advantage of this algorithm is merely using a little of grid points to achieve high accuracy. However, there are some drawbacks in determining the weighting coefficients [3] in the original DQM. Many researchers have concerned the application of the multiple boundary conditions in DQM [4-5]. Recently, a differential quadrature finite element method (DQFEM) has been proposed by Yufeng Xing [6]. The discretization is operated on the partial derivative in the strain energy and kinetic energy, which is different from the operation in most of the literatures, where the discretization is operated directly on the differential equations [7-9]. Also, in DQFEM the boundary conditions are imposed similarly as that in FEM while in other literatures the discretized expressions of classical boundary conditions are imposed to modify the coefficient weighting matrix, which makes it complicated to apply the multiple boundary conditions to the structures.

The DQFEM has been used to solve many vibration problems with irregular geometries [10]. However, few works on the vibration characteristic of structures with elastic restraints can be found. The elastic restraints are simulated by employing translational and rotational springs linking the structure and the ground [11]. By setting different spring stiffness to achieve desired boundary conditions including several ideal classical boundary conditions. Many works have been done on the influence of spring stiffness on the vibration characteristic of the structure [11-15]. The main purpose of the authors is to introduce the concept of elastic restraints into the DQFEM to expand the application of the method to the analysis of vibration problems with elastic restraints as well as irregular domains.

The main contents of this paper are shown as follows: Firstly, introduce the basic rules of DQ and elaborate the specific principles of DQFEM. Then, a beam structure with elastic restraints is given to illustrate how the virtual translational and rotational springs are applied into equations of motion. Next, an example of a rectangular plate with elastic restraints is given to illustrate the procedures of applying the elastic restraints to a two-dimensional problem. Finally, the vibration of a plate with curved side is presented. Some numerical results are presented and compared with the literatures available, which proves the accuracy of the present work.

2 THEORY AND FORMULATIONS

2.1 The DQ rules

The basic idea of the DQM is to express the differential operator by the summation of a set of weighting coefficients multiplied by the function values corresponding to specified nodes. For instance, the s th-order derivative of function $f(x)$ can be written as:

$$\left. \frac{d^s f(x)}{dx^s} \right|_i = \sum_{j=1}^N A_{ij}^{(s)} f_j \quad (1)$$

where $A_{ij}^{(s)}$ is the first-order weighting coefficient. The partial derivatives of two-dimensional function $f(x,y)$ at grid point (x_i, y_j) can be written as

$$\left. \frac{\partial^r f}{\partial x^r} \right|_{ij} = \sum_{m=1}^M A_{im}^{(r)} f_{mj}, \quad \left. \frac{\partial^s f}{\partial y^s} \right|_{ij} = \sum_{n=1}^N B_{jn}^{(s)} f_{in}, \quad \left. \frac{\partial^{r+s} f}{\partial x^r \partial y^s} \right|_{ij} = \sum_{m=1}^M A_{im}^{(r)} \sum_{n=1}^N B_{jn}^{(s)} f_{mn} \quad (2)$$

where, $A_{im}^{(r)}$ and $B_{jn}^{(s)}$ are the weighting coefficients along x and y directions, respectively. Refer to references [16] for detailed expressions of the weighting coefficient matrix.

2.2 Equations of motion of the beam element

An elastically restrained beam is shown in Fig. 1. The stiffness of the translational springs and the rotational springs on the grid point x_1 and x_M are denoted by k_{t1} , k_{tM} and k_{r1} , k_{rM} , respectively. Base on the Timoshenko beam theory and take the axial effect of the beam into account, the displacements of a point in the beam can be given as:

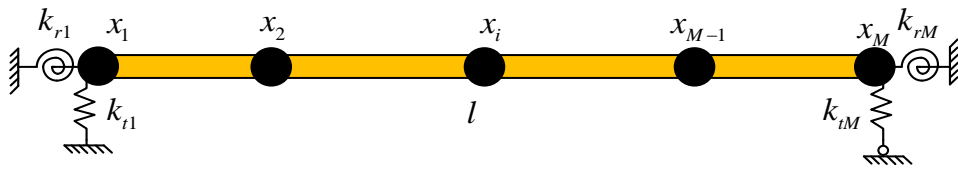


Fig. 1 The beam with elastic restraints on both ends.

$$u^e(x, z, t) = u_x^e(x, t) - z\varphi^e(x, t), \quad w^e(x, t) = w^e(x, t) \quad (3)$$

$$\{u_x^e(x), \varphi^e(x), w^e(x)\} = \sum_{i=1}^N l_i(x) \{u_{xi}^e, \varphi_i^e, w_i^e\}$$

where $l_i(x)$ is the i th Lagrange polynomial, $u_{xi}^e = u_x^e(x_i)$, $\varphi_i^e = \varphi^e(x_i)$ and $w_i^e = w^e(x_i)$ are the displacements at i th Gauss-Lobatto-Legendre (GLL) quadrature points [16]. According to the

elastic theory of Timoshenko beam, the normal and shear strain are

$$\boldsymbol{\varepsilon} = [\varepsilon_t \quad \varepsilon_b \quad \gamma_{xz}]^T = \left[\frac{\partial u_x}{\partial x} \quad -z \frac{\partial \varphi}{\partial x} \quad \frac{\partial w}{\partial x} - \varphi \right]^T \quad (4)$$

where the normal strain contains the compression and extension strain ε_t and bending strain ε_b . By applying the DQ rules, the derivatives in Eq. (4) can be written in the matrix form as

$$\boldsymbol{\varepsilon}^e = \begin{bmatrix} \mathbf{A}^{(1)} & \mathbf{0} & \mathbf{0} \\ \mathbf{0} & \mathbf{0} & -z\mathbf{A}^{(1)} \\ \mathbf{0} & \mathbf{A}^{(1)} & -\mathbf{E} \end{bmatrix} \begin{bmatrix} \mathbf{u}^e \\ \mathbf{w}^e \\ \boldsymbol{\varphi}^e \end{bmatrix} = \mathbf{B}\boldsymbol{\delta}^e \quad (5)$$

where

$$\mathbf{u}_x^e = [u_x^e(x_1) \quad u_x^e(x_2) \quad \cdots \quad u_x^e(x_N)]^T, \mathbf{w}^e = [w^e(x_1) \quad w^e(x_2) \quad \cdots \quad w^e(x_N)]^T \quad (6)$$

$$\boldsymbol{\varphi}^e = [\varphi^e(x_1) \quad \varphi^e(x_2) \quad \cdots \quad \varphi^e(x_N)]^T$$

The superscript e denotes that the corresponding displacement vectors is for element e , $\mathbf{A}^{(1)}$ is the first-order $N \times N$ weighting coefficient matrix for one-dimensional problem, \mathbf{E} is $N \times N$ unit diagonal matrix. Assuming the Young's modulus and the shear modulus are denoted by E and G , the normal and shear stresses of the beam can be obtained as

$$\boldsymbol{\sigma}^e = \begin{bmatrix} \mathbf{E}^* & \mathbf{0} & \mathbf{0} \\ \mathbf{0} & \mathbf{E}^* & \mathbf{0} \\ \mathbf{0} & \mathbf{0} & \kappa \mathbf{G} \end{bmatrix} \boldsymbol{\varepsilon}^e = \mathbf{D}\boldsymbol{\varepsilon}^e \quad (7)$$

where \mathbf{E}^* and \mathbf{G} are $N \times N$ diagonal matrices where the diagonal elements are Young's modulus and shear modulus, respectively. κ the shear correction factor of the beam.

The strain potential energy V is given as

$$V^e = \frac{1}{2} \iiint \boldsymbol{\sigma}^T \boldsymbol{\varepsilon} dx dy dz = \frac{1}{2} \iiint (\boldsymbol{\delta}^e)^T \mathbf{B}^T \mathbf{D} \mathbf{B} \boldsymbol{\delta}^e dx dy dz \quad (8)$$

The potential energy V_t stored in the translational springs and the potential energy V_r of the rotational springs are given as

$$V_t = \frac{1}{2} k_{t1} (w_1^e)^2 + \frac{1}{2} k_{tM} (w_M^e)^2, \quad V_r = \frac{1}{2} k_{r1} (\varphi_1^e)^2 + \frac{1}{2} k_{rM} (\varphi_M^e)^2 \quad (9)$$

The kinetic energy T of the beam is given as

$$T^e = \frac{1}{2} \iiint \rho \left[(\dot{u}_x^e)^2 + (-z\dot{\phi}^e)^2 + (\dot{w}^e)^2 \right] dx dy dz = \frac{1}{2} \int_0^l \rho (S\dot{u}^2 + S\dot{w}^2 + I\dot{\phi}^2) dx \quad (10)$$

The Lagrange function (L) of the beam can be expressed in terms of the total strain energy U and kinetic energy T as

$$L = T - U, \quad U = U_b + V_t + V_r \quad (11)$$

By applying the Hamilton's principle and extracting the time dependent function, one can get the stiffness matrix, mass matrix and the eigenvalue equations easily.

2.3. Equations of motion of the rectangular plate element

Next consider a plate meshed into M grid points along the x direction and N grid points along the y direction with translational and rotational springs supported at the grid points. In the two-dimensional problem, two types of rotational springs are introduced which are denoted by k_{rxi} and k_{ryi} . k_{rxi} restrains the rotation of the plate in x direction while k_{ryi} restrains the rotation in y direction. The displacement of point in the plate can be given as

$$u^e(x, y) = u_x^e(x, y) - z\phi_x^e(x, y), \quad v^e(x, y) = v_y^e(x, y) - z\phi_y^e(x, y); \quad w^e(x, y) = w^e(x, y) \\ \left\{ \begin{array}{c} u_x^e(x, y), v_y^e(x, y), \\ \phi_x^e(x, y), \phi_y^e(x, y), w^e(x, y) \end{array} \right\} = \sum_{i=1}^M l_i(x) \sum_{j=1}^N l_j(y) \left\{ \begin{array}{c} u_{xij}^e, v_{yij}^e, \\ \phi_{xij}^e, \phi_{yij}^e, w_{ij}^e \end{array} \right\} \quad (12)$$

where $l_j(x)$ is j th Lagrange polynomial in x direction, $u_{xij}^e = u_x^e(x_i, y_j)$, $v_{yij}^e = v_y^e(x_i, y_j)$, $\phi_{xij}^e = \phi_x^e(x_i, y_j)$, $\phi_{yij}^e = \phi_y^e(x_i, y_j)$ and $w_{ij}^e = w^e(x_i, y_j)$ are the displacements at the GLL quadrature points (x_i, y_j) . According to the Mindlin's plate theory, the shear deformation effect is taken into account. The normal and shear strain of a moderately thick plate are

$$\varepsilon_{xx}^e = \frac{\partial u^e(x, y)}{\partial x}, \quad \varepsilon_{yy}^e = \frac{\partial v^e(x, y)}{\partial y}, \quad \gamma_{xy}^e = \frac{\partial v^e(x, y)}{\partial x} + \frac{\partial u^e(x, y)}{\partial y} \\ \gamma_{xz}^e = \frac{\partial w^e(x)}{\partial x} + \frac{\partial u^e(x)}{\partial z}, \quad \gamma_{yz}^e = \frac{\partial w^e(x)}{\partial x} + \frac{\partial v^e(x)}{\partial z} \quad (13)$$

By applying the DQ rules, the derivatives in Eq. (13) can be written in the matrix form as the Eq. (14), in which $\mathbf{0}$ is $N \times N$ zero matrix, \mathbf{E} is $N \times N$ unit diagonal matrix, \mathbf{L}_t and \mathbf{L}_b are weighting coefficient matrix of tension or compression differential operators and bending differential operators, respectively.

Dongyan Shi, Xianlei Guan, Gai Liu

$$\boldsymbol{\varepsilon}_t^e = \begin{bmatrix} \varepsilon_{xxt}^e \\ \varepsilon_{yyt}^e \\ \gamma_{xyt}^e \end{bmatrix} = \begin{bmatrix} \mathbf{A}_{02}^{(1)} & \mathbf{0} \\ \mathbf{0} & \mathbf{B}_{02}^{(1)} \\ \mathbf{B}_{02}^{(1)} & \mathbf{A}_{02}^{(1)} \end{bmatrix} \begin{bmatrix} \mathbf{u}_x^e \\ \mathbf{v}_y^e \end{bmatrix} = \mathbf{L}_t \boldsymbol{\delta}_1^e; \quad \boldsymbol{\varepsilon}_b^e = \begin{bmatrix} \varepsilon_{xxb}^e \\ \varepsilon_{yyb}^e \\ \gamma_{xyb}^e \\ \gamma_{xz}^e \\ \gamma_{yz}^e \end{bmatrix} = \begin{bmatrix} -z\mathbf{A}_{02}^{(1)} & \mathbf{0} & \mathbf{0} \\ \mathbf{0} & -z\mathbf{B}_{02}^{(1)} & \mathbf{0} \\ -z\mathbf{B}_{02}^{(1)} & -z\mathbf{A}_{02}^{(1)} & \mathbf{0} \\ -\mathbf{E} & \mathbf{0} & \mathbf{A}_{02}^{(1)} \\ \mathbf{0} & -\mathbf{E} & \mathbf{B}_{02}^{(1)} \end{bmatrix} \begin{bmatrix} \boldsymbol{\phi}_x^e \\ \boldsymbol{\phi}_y^e \\ \mathbf{w}^e \end{bmatrix} = \mathbf{L}_b \boldsymbol{\delta}_2^e \quad (14)$$

Then, the normal and shear stresses are

$$\boldsymbol{\sigma}_t^e = \mathbf{D}_1 \boldsymbol{\varepsilon}_t^e, \quad \boldsymbol{\sigma}_b^e = \mathbf{D}_2 \boldsymbol{\varepsilon}_b^e$$

$$\mathbf{D}_1 = \frac{E}{1-\mu^2} \begin{bmatrix} \mathbf{E}^* & \mu\mathbf{E}^* & 0 \\ \mu\mathbf{E}^* & \mathbf{E}^* & 0 \\ 0 & 0 & \frac{1-\mu}{2}\mathbf{E}^* \end{bmatrix}; \quad \mathbf{D}_2 = \frac{E}{1-\mu^2} \begin{bmatrix} \mathbf{E}^* & \mu\mathbf{E}^* & \mathbf{0} & \mathbf{0} & \mathbf{0} \\ \mu\mathbf{E}^* & \mathbf{E}^* & \mathbf{0} & \mathbf{0} & \mathbf{0} \\ \mathbf{0} & \mathbf{0} & \frac{1-\mu}{2}\mathbf{E}^* & \mathbf{0} & \mathbf{0} \\ \mathbf{0} & \mathbf{0} & \mathbf{0} & \frac{1-\mu}{2}\kappa\mathbf{E}^* & \mathbf{0} \\ \mathbf{0} & \mathbf{0} & \mathbf{0} & \mathbf{0} & \frac{1-\mu}{2}\kappa\mathbf{E}^* \end{bmatrix} \quad (15)$$

where \mathbf{E}^* is $N \times N$ diagonal matrices where the diagonal elements are Young's modulus, κ is shear factor, usually $\kappa = \pi^2/12$.

The strain energy U_p and kinetic energy T for the plate are given as

$$V_p^e = \frac{1}{2} \iiint (\boldsymbol{\sigma}_t^{eT} \boldsymbol{\varepsilon}_t^e + \boldsymbol{\sigma}_b^{eT} \boldsymbol{\varepsilon}_b^e) dx dy dz$$

$$T^e = \frac{1}{2} \iiint \rho \left[(\dot{u}_x^e)^2 + (\dot{v}_y^e)^2 + (-z\dot{\phi}_x^e)^2 + (-z\dot{\phi}_y^e)^2 + (\dot{w}^e)^2 \right] dx dy dz \quad (16)$$

The potential energy V_{tx} , V_{ty} and V_{tw} stored in the three types of translational springs and the potential energy V_{rx} and V_{ry} of the two types of rotational springs are given as

$$V_{tx} = \frac{1}{2} \sum_{i=1}^2 \int_0^{l_i} k_{txi} (u_{xi}^e)^2 dl_i, \quad V_{ty} = \frac{1}{2} \sum_{i=1}^2 \int_0^{l_i} k_{tyi} (v_{yi}^e)^2 dl_i, \quad V_{tw} = \frac{1}{2} \sum_{i=1}^4 \int_0^{l_i} k_{twi} (w_i^e)^2 dl_i$$

$$V_{r1} = \frac{1}{2} \sum_{i=1}^2 \int_0^{l_i} k_{rxi} (\phi_x^e)^2 dl_i, \quad V_{r2} = \frac{1}{2} \sum_{i=1}^2 \int_0^{l_i} k_{ryi} (\phi_y^e)^2 dl_i \quad (17)$$

The Lagrange function (L) of the plate can be expressed in terms of the total strain energy U and kinetic energy T as

$$L = T - U, \quad U = U_p + V_{tx} + V_{ty} + V_{tw} + V_{rx} + V_{ry} \quad (18)$$

Similarly, by applying the Hamilton's principle and extracting the time dependent function, the stiffness matrix, mass matrix and the eigenvalue equations can be obtained.

2.4. Curvilinear quadrilateral plate element

The mass and stiffness matrices derived in the section 2.3 are limited to rectangular plates. It is necessary to extend the plate element to be applicable for irregular plate structures. Curvilinear quadrilateral plate defined in the Cartesian coordinate system can be mapped into a square parent domain defined in $-1 \leq \xi \leq 1$, $-1 \leq \eta \leq 1$, namely the natural coordinate system as shown in Fig. 3, through a mapping technique with serendipity element [16]:

$$x = \sum_{k=1}^{N_s} S_k(\xi, \eta) x_k, \quad y = \sum_{k=1}^{N_s} S_k(\xi, \eta) y_k \quad (19)$$

where x_k, y_k are the coordinates of nodes in the Cartesian coordinate system, S_k is the shape function with respect to node (x_k, y_k) . There are no limitations on the locations and the total numbers of the nodes except that the nodes are arranged anti-clockwise. Assuming the nodes distributions on the edges of a curvilinear quadrilateral plate are given as

$$\begin{aligned} \text{On side 1: } & (\alpha_1, -1), (\alpha_2, -1), \dots, (\alpha_{m-1}, -1), (\alpha_m, -1); \quad \text{On side 2: } (1, \beta_1), (1, \beta_2), \dots, (1, \beta_{n-1}), (1, \beta_n) \\ \text{On side 3: } & (\gamma_1, 1), (\gamma_2, 1), \dots, (\gamma_{p-1}, 1), (\gamma_p, 1); \quad \text{On side 4: } (-1, \lambda_1), (-1, \lambda_2), \dots, (-1, \lambda_{q-1}), (-1, \lambda_q) \end{aligned} \quad (20)$$

The general expressions of shape functions with respect to the i th node on each side except the corner nodes are given as

$$\begin{aligned} S_{1,i} &= \frac{1}{2}(1-\eta)(1-\xi^2) \frac{1}{1-\alpha_i^2} \prod_{\substack{j=2 \\ j \neq i}}^{m-1} \frac{\xi - \alpha_j}{\alpha_i - \alpha_j}, \quad S_{2,i} = \frac{1}{2}(1+\xi)(1-\eta^2) \frac{1}{1-\beta_i^2} \prod_{\substack{j=2 \\ j \neq i}}^{n-1} \frac{\eta - \beta_j}{\beta_i - \beta_j} \\ S_{3,i} &= \frac{1}{2}(1+\eta)(1-\xi^2) \frac{1}{1-\gamma_i^2} \prod_{\substack{j=2 \\ j \neq i}}^{p-1} \frac{\xi - \gamma_j}{\gamma_i - \gamma_j}, \quad S_{4,i} = \frac{1}{2}(1-\xi)(1-\eta^2) \frac{1}{1-\lambda_i^2} \prod_{\substack{j=2 \\ j \neq i}}^{q-1} \frac{\eta - \lambda_j}{\lambda_i - \lambda_j} \end{aligned} \quad (21)$$

The shape functions corresponding to the four corner nodes are given as

$$\begin{aligned} S_{p1} &= \frac{1}{4}(1-\eta)(1-\xi) \left[\prod_{j=2}^{m-1} \frac{\xi - \alpha_j}{-1 - \alpha_j} + \prod_{j=2}^{q-1} \frac{\eta - \lambda_j}{-1 - \lambda_j} - 1 \right]; \quad S_{p2} = \frac{1}{4}(1-\eta)(1+\xi) \left[\prod_{j=2}^{m-1} \frac{\xi - \alpha_j}{1 - \alpha_j} + \prod_{j=2}^{n-1} \frac{\eta - \beta_j}{-1 - \beta_j} - 1 \right] \\ S_{p3} &= \frac{1}{4}(1+\eta)(1+\xi) \left[\prod_{j=2}^{p-1} \frac{\xi - \gamma_j}{1 - \gamma_j} + \prod_{j=2}^{n-1} \frac{\eta - \beta_j}{1 - \beta_j} - 1 \right]; \quad S_{p4} = \frac{1}{4}(1+\eta)(1-\xi) \left[\prod_{j=2}^{p-1} \frac{\xi - \gamma_j}{-1 - \gamma_j} + \prod_{j=2}^{q-1} \frac{\eta - \lambda_j}{1 - \lambda_j} - 1 \right] \end{aligned} \quad (22)$$

The function $f(x, y)$ defined in the Cartesian coordinate system now can be expressed in terms of ξ and η in the natural coordinate system as $f=f[x(\xi, \eta), y(\xi, \eta)]$. Using the rule of differentiation, one can obtain the derivatives with respect to the ξ and η , namely the

expressions of $\partial f/\partial \xi$ and $\partial f/\partial \eta$ [16]. Then the modified weighting coefficient matrices derived for irregular plate can be obtained. By substituting the modified weighting coefficient matrices into the strain and stress expressions to replace the original matrices, the mass matrix and stiffness matrix for curvilinear quadrilateral plate can be obtained.

3 NUMERICAL EXAMPLES

In this section, several numerical examples will be presented to validate the accuracy of the present method. The discussions on the influence of the allocation of the nodes in the mapping procedures on the accuracy of the vibration results of curvilinear quadrilateral plate are also presented.

The convergence results of the first six frequency parameters $\lambda=l/\pi(\omega(\rho h/D)^{1/2})^{1/2}$ of a free beam are presented in Fig. 2(a), which shows that the results converge quickly to the accurate results as the number of nodes increases. Next example is a two-dimensional problem of a rectangular plate with length a and width b . The results of rectangular plate converge even faster than those of the beam from Fig. 2(b).

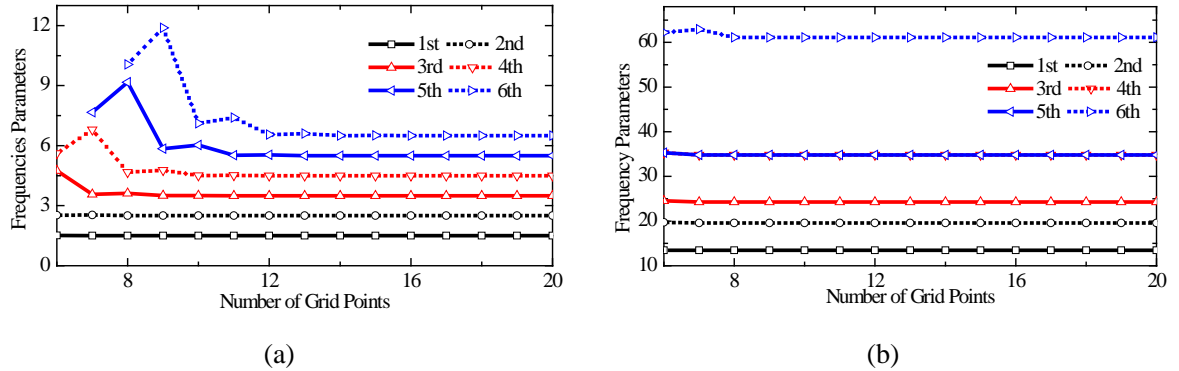


Fig. 2 Convergence studies of the first six frequency parameters of (a) free beam and (b) square plate.

Next, the virtual springs are introduced to simulate the practical boundary conditions and the effect on the natural frequencies and mode shapes are presented. Fig. 3 and Fig. 4 shows the variations of the frequency parameters with different stiffness of springs.

From Fig. 3, one can conclude that the frequency parameters increase as the stiffness of the translational springs increases firstly and then remain almost constant when the stiffness exceeds a certain value (for example $k_t/D=1e6$). For comparison, the results with classical boundary conditions: simply supported (SS) and clamped-clamped (CC) are also presented in Fig. 3(a) and Fig. 3(b), respectively. The same rules which can be observed as those for the beam from Fig. 4 are that the frequency parameters vary obviously in a certain interval of stiffness and remain almost constant when the stiffness is relatively small or large. Therefore, the simply supported boundary conditions can be achieved when the stiffness translational

springs is rather larger than the bending rigidity of the beam. The clamped boundary conditions can also be obtained by setting the stiffness of both the translational and rotational springs to be very large.

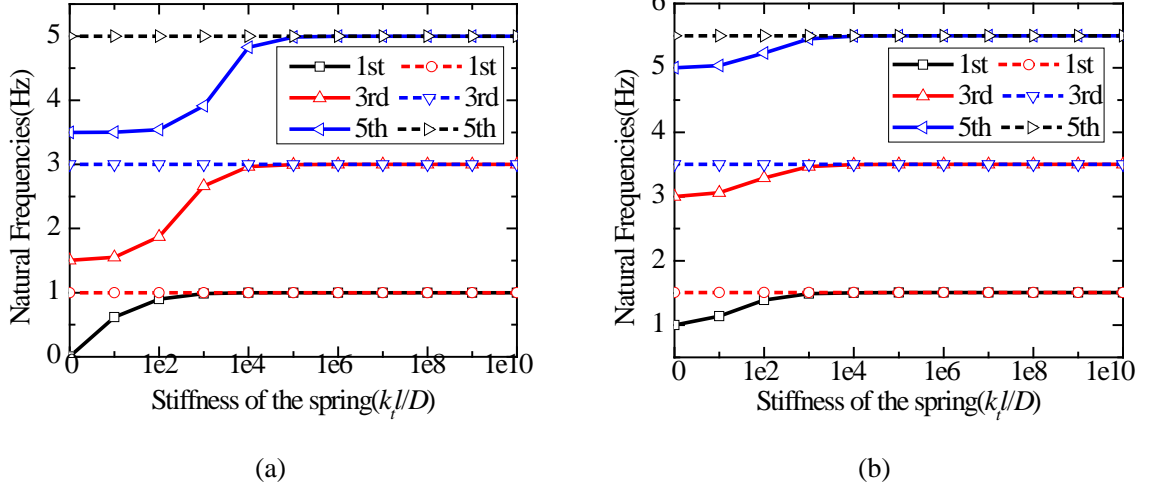


Fig. 3 Variations of the frequency parameters of a beam versus different stiffness of (a) translational springs and (b) rotational springs, —, elastic restraints, ---, classical boundary conditions.

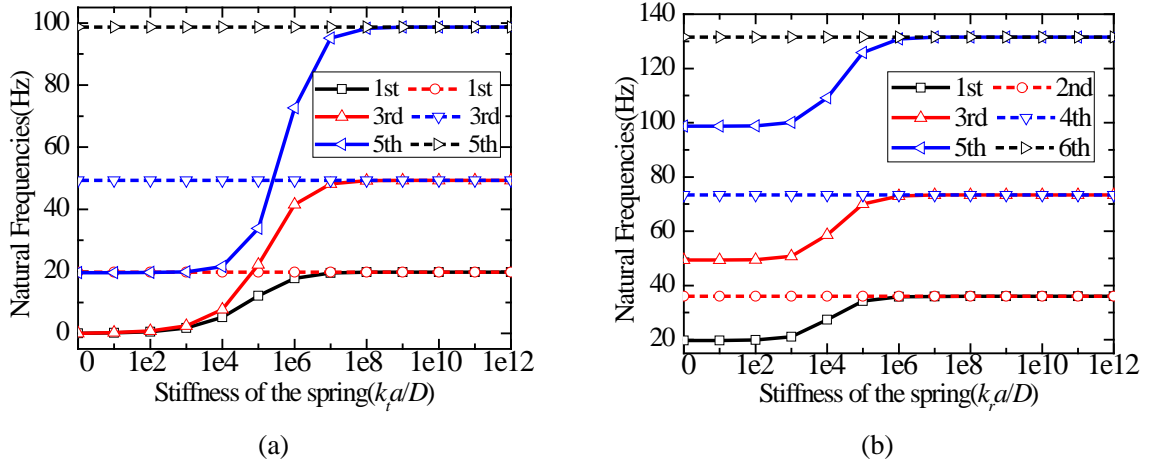


Fig. 4 Variations of the first six frequency parameters versus different stiffness of (a) translational springs and (b) rotational springs for $a/b=1$, —, elastic restraints, ---, classical boundary conditions.

The virtual springs introduced simplify the imposing procedures of boundary conditions. A certain boundary conditions can be easily achieved by setting the desired stiffness with respect to each spring. Table 1 lists some results obtained with different stiffness, which match well with the results in literature. The good agreement between the results

demonstrates the accuracy of the present method. The ^aresults come from the Ref[11].

Table 1 The first four frequency parameters $\lambda = l/\pi(\omega(\rho h/D)^{1/2})^{1/2}$ for various stiffness of the rotational springs.

$k_{rN}l$	Mode number			
	1	2	3	4
1	1.28657	2.27077	3.26479	4.26145
	1.28656 ^a	2.27081	3.26491	4.26175
10	1.41020	2.37137	3.34920	4.33353
	1.41020 ^a	2.37138	3.34927	4.33370
100	1.49137	2.47681	3.46883	4.46107
	1.49137 ^a	2.47681	3.46884	4.46108
10^{10}	1.50561	2.49975	3.50001	4.50000
	1.50562 ^a	2.49975	3.50001	4.50000

Table 2 The frequency parameters $\lambda = \omega a^2(\rho h/D)^{1/2}$ obtained with the 3rd type of nodes collocation methods of a free curvilinear quadrilateral plate under classical boundary conditions.

BC	Mode number					
	1	2	3	4	5	6
CCCC	96.01167	144.50359	190.18585	220.10220	258.74942	312.49447
	96.01943 ^a	144.28894	190.11589	220.48642	258.88697	311.99135
SSSS	49.85197	86.89633	132.00638	147.02897	197.77649	225.75121
	49.95280 ^a	87.00176	132.04367	147.41741	197.90891	225.37268
FFFF	20.96940	26.32154	55.37219	58.81766	74.03596	99.88516
	20.97836 ^a	26.31016	55.43785	58.77528	74.09149	99.83140
CCFC	29.00088	65.78078	95.81549	120.13331	158.34002	188.40518
	29.02093 ^a	65.78392	95.85332	120.11561	158.19744	188.25917
CFFF	12.51200	23.16806	39.38176	64.63335	83.98056	110.89167
	12.52553 ^a	23.13964	39.39007	64.69837	83.93515	110.76724

^aResults from FEM.

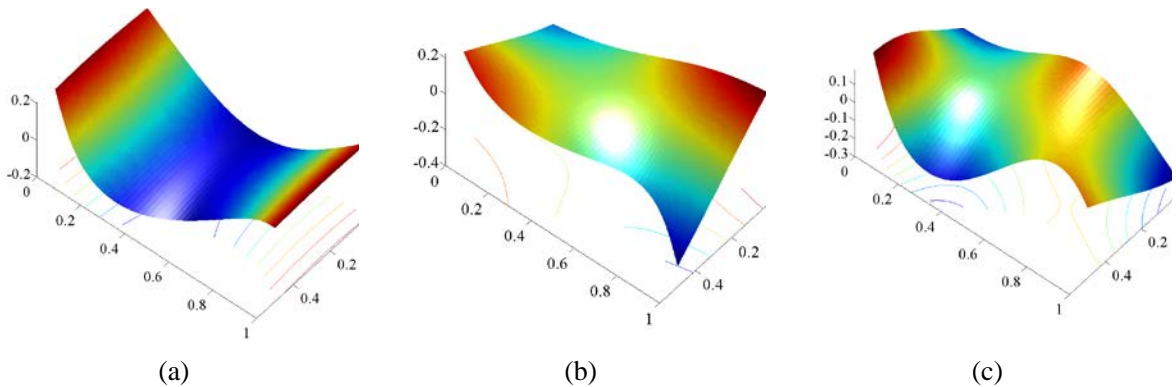


Fig. 5 The mode shapes except the rigid modes of the FFFF plate. (a) the 1st, (b) the 2nd, (c) the 3rd.

4 CONCLUSION

In this paper, the virtual springs are introduced into DQFEM to simulate the practical elastic restraints. The translational springs and rotational springs respectively restrain the translational movement and rotation of the point on the sides of the structures. Owing to the springs introduced, the imposing procedures of the boundary conditions are simplified so that a certain kind of boundary conditions can be achieved just by setting different stiffness of the springs. The frequency parameters and the mode shapes of the structures vary as the stiffness changes. The variations are obvious in a certain interval of stiffness of springs, beyond which the frequency parameters remain almost the same. Consequently, classical boundary conditions can be regarded as typical situations when stiffness is relatively small or large.

ACKNOWLEDGMENTS

This paper is funded by the International Exchange Program of Harbin Engineering University for Innovation-oriented Talents Cultivation. The works also supported by the National Natural Science Foundation of China (No. 51679056), and Natural Science Foundation of Heilongjiang Province of China (E2016024).

REFERENCES

- [1] Bellman, R., & Casti, J. Differential quadrature and long-term integration. *Journal of Mathematical Analysis and Applications*. (1971) 34:235-238.
- [2] Bellman, R., Kashef, B. G., & Casti, J. Differential quadrature: a technique for the rapid solution of nonlinear partial differential equations. *Journal of computational physics*. (1972) 10:40-52.
- [3] Du, H., Lim, M. K., & Lin, R. Application of generalized differential quadrature method to structural problems. *International Journal for Numerical Methods in Engineering*. (1994) 37:1881-1896.
- [4] Karami, G., & Malekzadeh, P. A new differential quadrature methodology for beam analysis and the associated differential quadrature element method. *Computer Methods in Applied Mechanics and Engineering*. (2002) 191:3509-3526.
- [5] Fung, T. C. Imposition of boundary conditions by modifying the weighting coefficient matrices in the differential quadrature method. *International Journal for Numerical Methods in Engineering*. (2003) 56:405-432.
- [6] Xing, Y., Liu, B., & Liu, G. A differential quadrature finite element method. *International Journal of Applied Mechanics*. (2010) 2:207-227.
- [7] Wang, X., & Wang, Y. Free vibration analyses of thin sector plates by the new version of

differential quadrature method. *Computer Methods in Applied Mechanics and Engineering*. (2004) 193:3957-3971.

[8] Wu, L., & Liu, J. Free vibration analysis of arbitrary shaped thick plates by differential cubature method. *International journal of mechanical sciences*. (2005) 47:63-81.

[9] Viola, E., Tornabene, F., & Fantuzzi, N. Generalized differential quadrature finite element method for cracked composite structures of arbitrary shape. *Composite Structures*. (2013) 106:815-834.

[10] Bert, C. W., & Malik, M. The differential quadrature method for irregular domains and application to plate vibration. *International Journal of Mechanical Sciences*. (1996) 38:589-606.

[11] Li, W. L. (2000). Free vibrations of beams with general boundary conditions. *Journal of Sound and Vibration*, 237(4), 709-725.

[12] Wang, Q., Shi, D., Liang, Q., & Shi, X. A unified solution for vibration analysis of functionally graded circular, annular and sector plates with general boundary conditions. *Composites Part B: Engineering*. (2016) 88:264-294.

[13] Wang, Q., Qin, B., Shi, D., & Liang, Q. A semi-analytical method for vibration analysis of functionally graded carbon nanotube reinforced composite doubly-curved panels and shells of revolution. *Composite Structures*. (2017) 174:87-109.

[14] Wang, Q., Shi, D., Liang, Q., & Pang, F. Free vibrations of composite laminated doubly-curved shells and panels of revolution with general elastic restraints. *Applied Mathematical Modelling*. (2017) 46:227-262.

[15] Wang, Q., Shao, D., & Qin, B. A simple first-order shear deformation shell theory for vibration analysis of composite laminated open cylindrical shells with general boundary conditions. *Composite Structures*. (2018) 184:211-232.

[16] Guan, X., Tang, J., & Wang, Q. Application of the differential quadrature finite element method to free vibration of elastically restrained plate with irregular geometries. *Engineering Analysis with Boundary Elements*. (2018) 90:1-16.

Effect of Rehabilitation Exercise Durations on the Dynamic Bone-repair Process by Coupling Polymer Scaffold Degradation and Bone Formation

Quan Shi^{*}, Qiang Chen^{**}, Zhiyong Li^{***}

^{*}School of Biological Science & Medical Engineering, Southeast University, 210096 Nanjing, PR China, ^{**}School of Biological Science & Medical Engineering, Southeast University, 210096 Nanjing, PR China, ^{***}School of Biological Science & Medical Engineering, Southeast University, 210096 Nanjing, PR China

ABSTRACT

Bone disorders are common, and the implantation of biodegradable scaffold is considered as a promising method to treat the disorders, but the knowledge of the dynamic mechanical process of the scaffold-bone system is extremely limited. In this study, based on the representative volume cell (RVC) of a periodic scaffold, the influence of rehabilitation exercise duration per day on the bone repair was investigated by a computational framework. The framework coupled the polymer scaffold degradation and the bone remodeling. The scaffold degradation was described by a function of stochastic hydrolysis independent of the mechanical stimulation, and the bone formation was remodeled by a function of the mechanical stimulation, i.e., strain energy density (SED). Then, numerical simulations were performed to study the dynamic bone repair process. The results showed that the scaffold degradation and bone formation in the process were competitive. The greater exercise duration per day could not improve the bone stiffness, and 0.3 is the optimal case. All exercise durations promoted the bone maturation with a final Young's modulus around 1.9 ± 0.3 GPa. The present study is helpful to understand and monitor the bone repair process, and useful for the bone scaffold design in bone tissue engineering.

Simulating Shrinkage Cracking in ECC Overlay Using an Efficient Discrete Model

Tiansheng Shi^{*}, Christopher K. Y. Leung^{**}

^{*}Hong Kong University of Science and Technology, ^{**}Hong Kong University of Science and Technology

ABSTRACT

Concrete structures always experience deterioration during their service time and a common practice of repairing is to replace the damaged part with an overlay system (usually made of mortar). However, the early age failures of the repair system are usually observed due to differential shrinkage between the old concrete substrate and the new overlay. With high ductility and good control of crack width, ECC is found to show an excellent performance in repairing the deteriorated concrete structure, and many numerical and experimental studies are carried out in this area to understand its behavior. Here a novel discrete model, which can efficiently simulate the realistic multiple cracking process in ECC, is adopted to assess the performance of ECC overlay system subjected to shrinkage. The proposed discrete model is first used to simulate a tensile test (for the purpose of model verification), and then the ECC overlay subjected to shrinkage. It is found that the failure modes of the overlay system, i.e., interface delamination and ECC multiple cracking, can be captured by the proposed model. The important parameters in the process are further discussed, which would provide insight in optimizing the overlay system.

A Numerical Simulation Model of Cleavage Crack Propagation in Steel Based on the Extended Finite Element Method

Kazuki Shibamura^{*}, Yuta Suzuki^{**}, Kazuya Kiriya^{***}, Takuhiro Hemmi^{****}, Hiroyuki Shirahata^{*****}, Shuji Aihara^{*****}, Katsuyuki Suzuki^{*****}

^{*}The University of Tokyo, ^{**}The University of Tokyo, ^{***}The University of Tokyo, ^{****}The University of Tokyo, ^{*****}Nippon Steel & Sumitomo Metal Corporation, ^{*****}The University of Tokyo, ^{*****}The University of Tokyo

ABSTRACT

Preventing crack propagation is extremely important in ensuring the integrity of steel structures such as hulls and cryogenic tanks. However, any theories and models to evaluate quantitative and universal relationship between microstructure and crack arrest toughness based on physical model of cleavage crack propagation has not been established. In the present study, we propose a model for cleavage crack propagation in steel based on the extended finite element method (XFEM) [1]. Although the cleavage crack propagation is a phenomenon without large plastic deformation, it is a geometrically complicated phenomenon, where the fracture surface is composed of cleavage plane facets formed in the respective grains. These features indicate that the linear fracture mechanics modeling using XFEM is suitable to simulate the cleavage crack propagation in steel. In the proposed model, geometries and spatial distribution of grains are defined independently from finite element mesh, as well as the crack. For simplification, only one cleavage facet is assumed to be formed in each grain. A criterion proposed by Aihara and Tanaka [2] is employed as fracture condition of crack propagation across a grain boundary. In the criterion, one of the three $\{1\ 0\ 0\}$ cleavage planes in a grain located in front of a crack front is selected so that normal stress acting on the plane is maximum and the grain is cleaved if the maximum normal stress exceeds the cleavage fracture stress. The normal stress on each $\{1\ 0\ 0\}$ plane is calculated from mixed mode local stress intensity factors which are evaluated by the fast interaction integral method. As validation of the proposed model, the numerical simulation results of fracture surface morphology are compared with experimental result obtained by the crack arrest test using double cantilever beam (DCB) specimen of low-alloy steel. The result shows that the proposed model can successfully simulate complicated cleavage crack propagation behaviors, such as micro-branching and wraparound of cracks on the fracture surface. In addition, the numerical and experimental results of distribution of the nominal directions of cleavage facets showed good agreement with each other. References [1] 2002 N. Moës, A. Gravouil, T. Belytschko, Non-planar 3D crack growth by the extended finite element and level sets - Part I Mechanical model, Int. J. Numer. Meth. Engng. 53 (2002) 2549-2568. [2] S. Aihara, Y. Tanaka, A simulation model for cleavage crack propagation in bcc polycrystalline solids, Acta Materialia 59 (2011) 4641-4652.

Multi-resolution Simulation by the Overlapping Particle Technique and the Ellipsoidal Particle Model for Particle Methods

Kazuya Shibata^{*}, Daisuke Yamada^{**}, Seiichi Koshizuka^{***}, Issei Masaie^{****}, Takuya Matsunaga^{*****}

^{*}Department of Systems Innovation, School of Engineering, The University of Tokyo, ^{**}Department of Systems Innovation, School of Engineering, The University of Tokyo, ^{***}Department of Systems Innovation, School of Engineering, The University of Tokyo, ^{****}Prometech Software Inc., ^{*****}Department of Systems Innovation, School of Engineering, The University of Tokyo

ABSTRACT

This presentation explains the overlapping particle technique [1] and the ellipsoidal particle model [2], which are multi-resolution techniques developed for fluid simulation of particle methods. The overlapping particle technique divides a whole simulation domain into sub-domains. Each sub-domain has an individual constant spatial resolution. The sub-domains partially overlap to give boundary condition about pressure and velocity. The ellipsoidal particle model allows us to use non-spherical particles. An extended Laplacian model for ellipsoidal particles was used to discretize the viscous term and the pressure Poisson equation. Compared to the traditional spherical particles, the ellipsoidal particles can reduce the required number of particles and the computation time. We applied the developed technique and model to the MPS method and SPH. Dam breaking and water waves were simulated by the multi-resolution techniques. The improved pressure calculation method [3] was applied to the MPS simulations. As a result, it was confirmed that the developed multi-resolution techniques can reduce the required number of particles and shorten the computation time of particle simulations. [1] K. Shibata, S. Koshizuka, T. Matsunaga, I. Masaie, The overlapping particle technique for multi-resolution simulation of particle methods, Computer Methods in Applied Mechanics and Engineering, Vol. 325, pp.434-462 (2017) [2] K. Shibata, S. Koshizuka, I. Masaie, Cost reduction of particle simulations by an ellipsoidal particle model. Computer Methods in Applied Mechanics and Engineering, Vol.307, pp.411-450 (2016) [3]K. Shibata, I. Masaie, M. Kondo, K. Murotani, S. Koshizuka, Improved pressure calculation for the moving particle semi-implicit method, Computational Particle Mechanics, Vol. 2, Issue 1, pp. 91-108 (2015)

Modeling Non-Gaussianity in Non-linear Stochastic Dynamic Systems

Michael Shields^{*}, Lohit Vandanapu^{**}, Hwanpyo Kim^{***}

^{*}Johns Hopkins University, ^{**}Johns Hopkins University, ^{***}Johns Hopkins University

ABSTRACT

It is well-known that nonlinear stochastic systems often exhibit non-Gaussian features. Examples of such phenomena are abundant in nature from fluid-structure interactions in turbulent flow to shoaling ocean waves. When modeling these non-Gaussian phenomena, it is common to develop an expansion for the stochastic process using methods such as the Karhunen-Loeve (K-L) expansion or spectral representation method (SRM). Under classical assumptions, the K-L expansion and SRM are used to model Gaussian processes and some non-linear transformation is then applied to induce the desired non-Gaussianity using e.g. translation process theory or orthogonal polynomials. However, in the more general case, the non-Gaussianity can be modeled by understanding the dependence structure of the random variables in the stochastic expansion. In this work, we derive analytical relationships relating phase difference distributions to higher-order spectra (bispectrum, trispectrum, etc.) in the spectral representation method that enable direct modeling of non-Gaussian stochastic processes derived from nonlinear dynamical systems. A brief comparison of the resulting models with classical non-linear transformation based approaches is provided along with some discussion of the advantages and disadvantages of each approach.

The Prediction of Bone-Remodeling Morphology and Peri-implant Osseointegration for Dental Implants

Chien Shih-Shun*, Nien Ti-Tsou**, Li Ming-Jun***

*National Chiao Tung University, **National Chiao Tung University, ***Industrial Technology Research Institute

ABSTRACT

In recent years, a number of algorithms have been proposed to predict the adaptive bone-remodeling, primary stability, and osseointegration around the dental implants under load, such as Strain energy density (SED) and cell differentiation based theory. The SED model can provide a balanced nonhomogeneous distribution state of the bone density/elastic modulus; the cell differentiation model can predict the osseointegration level between the considered implants and bones after surgical treatment. However, bone density and elastic modulus are typically assumed as constant in the most of the models. Thus, in order to improve the accuracy of the model, the current study firstly adopts SED model to determine the distribution of anisotropic bone density/elastic modulus around the natural teeth and set that distribution as the initial condition for the cell differentiation model. The SED and cell differentiation algorithms are incorporated by using finite element package ANSYS. The model consists with a 3-D segment of the mandible in premolar region, and the effect of the periodontal ligament is also considered. The current model is verified by the animal experiment. The results show that the current model has a more accurate prediction of osseointegration performance, compared with the model without considering the nature bone density and elastic distribution.

Multiscale Parametric Analysis of Strain Amplification in Cartilage under Different Loading and Tissue Conditions

Vickie Shim^{*}, Sophia Leung^{**}, David Musson^{***}, Sue McGlashan^{****}, Iain Anderson^{*****}, Jill Cornish^{*****}

^{*}University of Auckland, ^{**}University of Auckland, ^{***}University of Auckland, ^{****}University of Auckland, ^{*****}University of Auckland, ^{*****}University of Auckland

ABSTRACT

Articular cartilage lines the surfaces of diarthroidal joints and supports the joint motion by providing a load bearing and low friction material. Due to its large deformation under normal daily activities, the cells in the cartilage (chondrocytes) are exposed to a complex mechanical environment. The cartilage tissue also exhibits complex material properties that are both location and rate dependent. Yet, the avascular nature of the tissue means that any damage to the tissue is irreversible and as a result, osteoarthritis is one of the most widespread causes of morbidity and impaired quality of life in the western world. However, the pathogenesis of cartilage degeneration is largely unknown and the disease is untreatable. We have developed a unique system that combines multiscale computational models with a cell mechanical device. Our multiscale knee joint model is composed of three levels – joint, tissue and cell levels for predicting strains at multiple spatial scales [1]. Our cell device is a novel mechanical device that is capable of applying tension, compression and shear strains to cell seeded 3D cultures [2]. We have performed mechanical experiment that measured cell deformation patterns under these three mechanical loading conditions with confocal microscope imaging. Our results showed that chondrocytes experience significant strain amplification (up to 50 %) under mechanical loading and shear strains caused the highest strain amplifications. This result was then used in our multiscale computational model to predict how different loading conditions and tissue mechanical properties affect the degree of strain amplification. A parametric study was performed to quantitatively analyse the role of tissue stiffness and different loading conditions on cellular strains. Our results indicate that a change in tissue stiffness due to degeneration is one of the leading causes of abnormal strain amplification in chondrocytes. This result will be used in designing functional tissue engineering constructs for replacing damaged cartilage.

1. SHIM, V; MITHRARATNE, K., LLOYD, D., BESIER, T., FERNANDEZ, J. 'The influence and biomechanical role of cartilage split-line pattern on tibiofemoral cartilage stress distribution during the stance phase of gait' *Biomechanics and Modeling in Mechanobiology* 2016 15 (1), 195-204

2. LEUNG, S.; MCGLASHAN, S., MUSSON, D., ANDERSON, I.A.; CORNISH, J.; MCGLASHAN, S., SHIM, V; Investigation of strain fields in 3D hydrogels under dynamic confined loading, *Journal of Medical and Biological Engineering* (Accepted for publication)

Petascale Computing to Accelerate High-Temperature Alloy Design

Dongwon Shin^{*}, Patrick Shower^{**}, James Morris^{***}, Amit Shyam^{****}, James Haynes^{*****}

^{*}Oak Ridge National Laboratory, ^{**}The University of Tennessee, ^{***}Oak Ridge National Laboratory, ^{****}Oak Ridge National Laboratory, ^{*****}Oak Ridge National Laboratory

ABSTRACT

Recent progress in high-performance computing and data informatics has opened up numerous opportunities to aid and accelerate the design of advanced materials. Herein, we demonstrate a computational workflow that includes rapid population of high-fidelity materials datasets via petascale computing, utilization of those datasets for multi-scale modeling, and subsequent analyses with modern data science techniques. We use a first-principles approach based on density functional theory to derive the segregation energies of 34 microalloying elements at the coherent and semi-coherent interfaces between the aluminum matrix and the θ -Al₂Cu precipitate, which requires several hundred supercell calculations. We also perform extensive correlation analyses to identify materials descriptors that affect the segregation behavior of solutes at the interfaces. These atomic-scale data are integrated into a micro-scale model using phase field theory to investigate the effect of solute segregation on the high-temperature microstructural stability, and the temperature-dependent effects of both thermodynamic driving forces and kinetics. Finally, we show an example of leveraging machine learning techniques to predict segregation energies without performing computationally expensive physics-based simulations. The approach demonstrated in the present work can be applied to any high-temperature alloy systems for which key materials data can be obtained using high-performance computing. The research was sponsored by the Laboratory Directed Research and Development Program of Oak Ridge National Laboratory, managed by UT-Battelle, LLC, for the U. S. Department of Energy.

Convex Splitting Runge-Kutta Methods to Solve the Phase Field Equations

Jaemin Shin^{*}, Hyun Geun Lee^{**}, June-Yub Lee^{***}

^{*}Ewha Womans University, ^{**}Kwangwoon University, ^{***}Ewha Womans University

ABSTRACT

We introduce Convex Splitting Runge-Kutta (CSRK) methods to solve the gradient flow considering the energy stability, which provide a simple unified framework. The gradient systems have been fundamental in the development of many important concepts in dynamical systems. In particular, it is important in many phenomenological models of phase transition like as the phase field model. The core idea of CSRK method is the combination of convex splitting methods and multi-stage implicit-explicit Runge-Kutta methods. The proposed methods are high-order accurate in time. In addition, the energy stability is completely proved when we consider the special design of implicit-explicit Runge-Kutta tables, called a resemble condition. We present numerical experiments with the phase field equations to show the numerical accuracy and stability of the proposed methods. [1] Eyre, D. J., "An unconditionally stable one-step scheme for gradient systems", Unpublished article, 1998. [2] Shin, J., Lee, H. G. and Lee, J.-Y., "Convex Splitting Runge-Kutta methods for phase-field models", Computers & Mathematics with Applications, Vol. 73, 2017, pp. 2388-2403. [3] Shin, J., Lee, H. G. and Lee, J.-Y., "Unconditionally stable methods for gradient flow using Convex Splitting Runge-Kutta scheme", Journal of Computational Physics, Vol. 347, 2017, pp. 367-381.

CYBER-INFRASTRUCTURAL COMPUTE/DATA FRAMEWORK FOR THE AERODYNAMIC RESEARCH OF INDUSTRIAL AIRFOILS

JUNGHUN SHIN*, JEONGHWAN SA[†], JIN MA[†],
SIK LEE[†], AND KUMWON CHO[†]

*Supercomputing Division, Korea Institute of Science and Technology Information (KISTI)
245 Daehak-ro, Yuseong-gu
Daejeon, Republic of Korea
shandy77@kisti.re.kr

[†]Supercomputing Division, Korea Institute of Science and Technology Information (KISTI)
245 Daehak-ro, Yuseong-gu
Daejeon, Republic of Korea
sa_c@kisti.re.kr, majin@kisti.re.kr, siklee@kisti.re.kr, ckw@kisti.re.kr

Key words: Instructions, Multiphysics Problems, Applications, Computing Methods Abstract.

Abstract. This document provides information and instructions for preparing an extended abstract to be made available for downloading from the WCCM2018 website.

1 INTRODUCTION

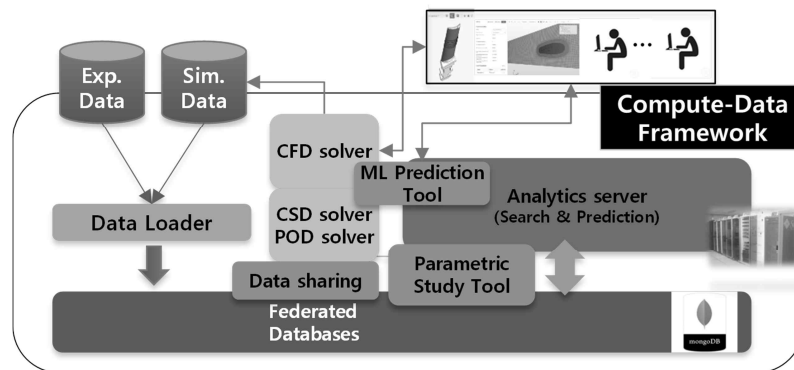
Computation has traditionally played a powerful role in a wide range of research and development areas, from the beginning of the computer to scientific research, product development, and knowledge services¹. The engineering analysis for industrial wings or blades has been performed in various disciplines such as aerodynamics analysis. This study was motivated by a blade manufacturer who was interested in the shape error effects in the earlier stage of the manufacturing.

From the manufacturers' viewpoint, the airfoil aerodynamics is a fundamental that must go through. In this study, a cyber-infrastructure framework which could conduct both compute and data techniques was developed to research airfoil aerodynamic performances, targeted for quickly predicting the aerodynamic performances and discussing them to make decision soon. Although the aerodynamic parameters differ from industries, in this study, the aerodynamic coefficients were employed following the wing airfoil ways².

In addition to the studies on the theoretical models and computer simulation techniques that have been actively carried out in industry and academia, there are not many ones about the environments in which this simulation studies can be performed. Currently, it became common for commercial software companies and many hardware system companies to construct the environment for running computer simulations, but it is difficult to maintain it costly unless it is

a large organization. In this situation, it would be helpful especially for small and medium companies to have high accessibility to large computing resources, to be able to perform analysis easily, to share information such as simulation results, and to produce additional information using some data analytics tools. Now it is believed that this kind of a compute-data framework for communicational or educational purposes can help apply the digital technology appropriately to the advanced manufacturing process³. Recently, new service types that can perform computation in the emerging cloud environment of internet technology have appeared, and there have been various kinds of technology prototypes in which the computation and the network are merged⁴. For example, an emerging software team company originated from the ‘Solidworks’ which is a representative CAD tool provided a cloud service called Onshape⁵ to perform CAD work and access to the data on web browsers or mobile devices without installing additional software. ANSYS, a software manufacturer of engineering analysis software, and many engineering consulting service companies, are developing a cloud-based analysis environment, which unlike the CAD cloud displays only the screen on the user's desktop or terminal. It is based on the Virtual Desktop Infrastructure (VDI), which is a method performed at the backend. Engineering consulting service companies in Europe, such as Simscale⁶ and CONSELF⁷, are administering novel cloud computing simulation environments which are different from VDI method to provide engineering consulting and community services. In the case of professional cloud computing companies such as Rescale⁸, there is a tendency to acquire a large number of users by providing cloud services including both of them. Besides there have been similar developments to the current cloud services based on high-performance computers^{9, 10}.

This paper aims to efficiently utilize gas turbine blade aerodynamics computer simulation and data-driven analysis with cyber-infrastructure resource at the product development site. Fig. 1 shows the concept of the framework. As for the data-driven analysis, recently accepted techniques of machine learning were tried for airfoil aerodynamics and the feasibility was evaluated preliminarily. Therefore, it introduces and develops contents and features of computerized research environment (user-specific authority and resource allocation, CAD and grid processing, analysis execution, sharing various information) using web browser based cloud computing system service model similarly to Onshape and Simscale described above. Finally the use scenario using the analytical system was presented. The development of airfoil aerodynamics solvers was briefly described, and the details will be discussed in separate documents.



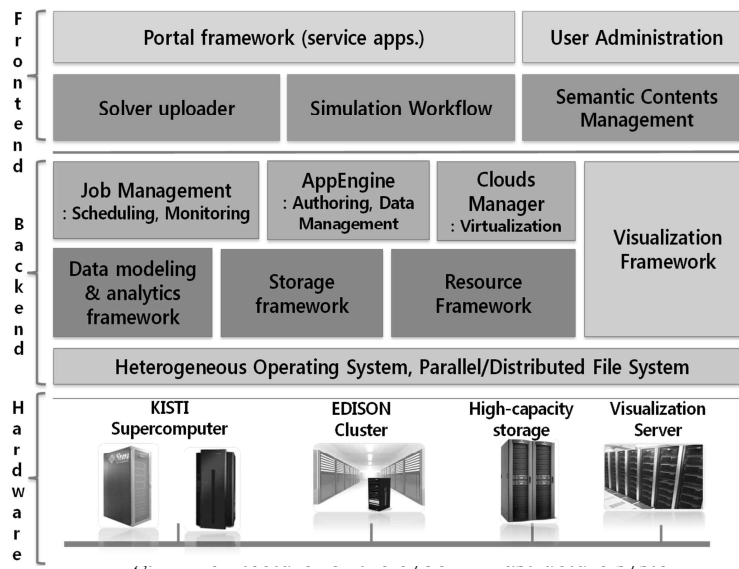
2 REQUIRMENT AND FUNCTION DESIGN

In manufacturing sites, engineers always conduct quality assessment by measuring shape error and etc. The aerodynamic performance is considered to be most affected by the shape deviation, which is the main concern of this paper. For example, it is known in the field that there is a case where a free vibration characteristic is changed due to some manufacturing error and is discarded. Two-dimensional airfoil analysis provides information that they can understand aerodynamic performance variations most intuitively.

The aerodynamic solver can hold two-dimensional airfoil and three-dimensional blade RANS analysis. It could not be only a single airfoil or blade, but also multi-staged. In addition, flows experienced by gas turbine blades are very complex, but especially in large gas turbines, complex turbulent flows occur in the full speed range of subsonic, transonic, and supersonic speeds. Therefore, the aerodynamic solver must be able to simulate the full speed range and also simulate moving rotor, vane stator interface treatment, centrifugal flow, and etc. They are originated from the fact that the blades in gas turbine show multi-staged arrangement. Finally, a flow model for turbulent transitions should be included since there is a transitional heat transfer in which the heat transfer characteristics vary greatly at the surface due to the shape of the blade with a large curvature. The aerodynamic solver using structured grid system has already been verified for the simulation efficiency and accuracy of various wings¹¹, so appropriate tuning of the base flow solver was performed to suit the turbine blade analysis, reflecting the above requirements.

Considering data-driven techniques using the dataset generated from the above full-order model (FOM) analysis could improve the efficiency of computation by applying a reduced-order modeling (ROM) such as proportional orthogonality decomposition (POD) method¹² and recently emerging machine-learning (ML) techniques. In this study, we handle with ML based simulation results reusing techniques.

The detailed description of the above solvers will be provided in other papers.



3 SYSTEM ARCHITECTURE AND COMPUTATIONAL MODULES

Fig. 2 shows the base architecture of the engineering system. This architecture was developed by modifying an existing system of so-called EDISON compute platform⁹ into compute-data platform which data modeling and analytics modules were added. The computational science and engineering platform host various compute software like flow solvers and share the input/output data. The computational procedures can be performed via the web-portal.

3.1 Computational modules

Fig. 3(a) depicts primary user interface of the web-portal. The web-based pages are quite friendly so that community could be build-up using project-sharing module, social network service module and etc. Fig. 3(b) shows the flow solver running tool which can throw

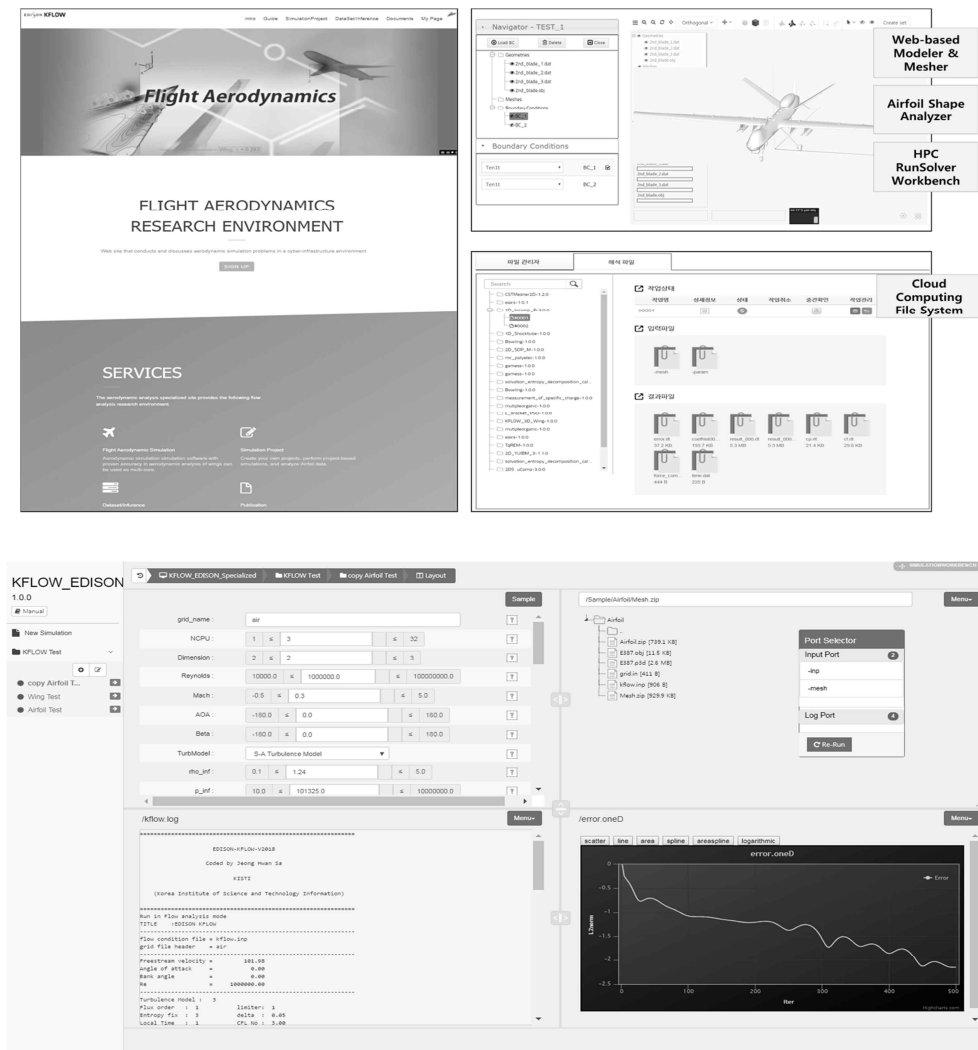


Fig. 3 Web-portal for cloud computing and data

parallelized jobs into the backend high performance computing system

The simulation data were arranged in accordance with shape parameter schema since the shape parameters are used to distinguish the airfoil shape. The airfoil might abruptly changes aerodynamic characteristics even if the shape is slightly different, so it is necessary to use numerically expressed parameters so that it can be accurately classified. It should be able to accurately express the airfoil shape using as few parameters as possible. As the number of parameters increases, the process of classifying shapes becomes complicated. In this study, the airfoil shape was defined using the Bezier-Parsec parameter¹³. The Bezier-Parsec parameter used the thickness profile and camber profile to represent the airfoil shape. Thickness and Camber curves were obtained by combining two cubic Bezier curves, respectively. One cubic Bezier curve requires eight control points in total using four control points in the horizontal and vertical directions respectively. Because there are the leading edge and trailing edge coordinates and overlapping control points, the thickness curve uses 8 control points and the camber curves uses 9 control points respectively. In order to extract the 17 control points constituting the Bezier-Parsec parameter from the airfoil shape, the Newton Raphson method was used until the error between the shape realized by the parameter and the airfoil shape became 10^{-4} or less. Because the number of control points and the number of coordinates to compare shapes are not same, the Least Squares Method has been used. The generated 17 parameters are used to define and compare the shape, and the parameters of the shape used are databased and updated continuously to the data-driven system. Fig. 4(b) shows the meshing tool which can automatically handle the small deviations of airfoils.

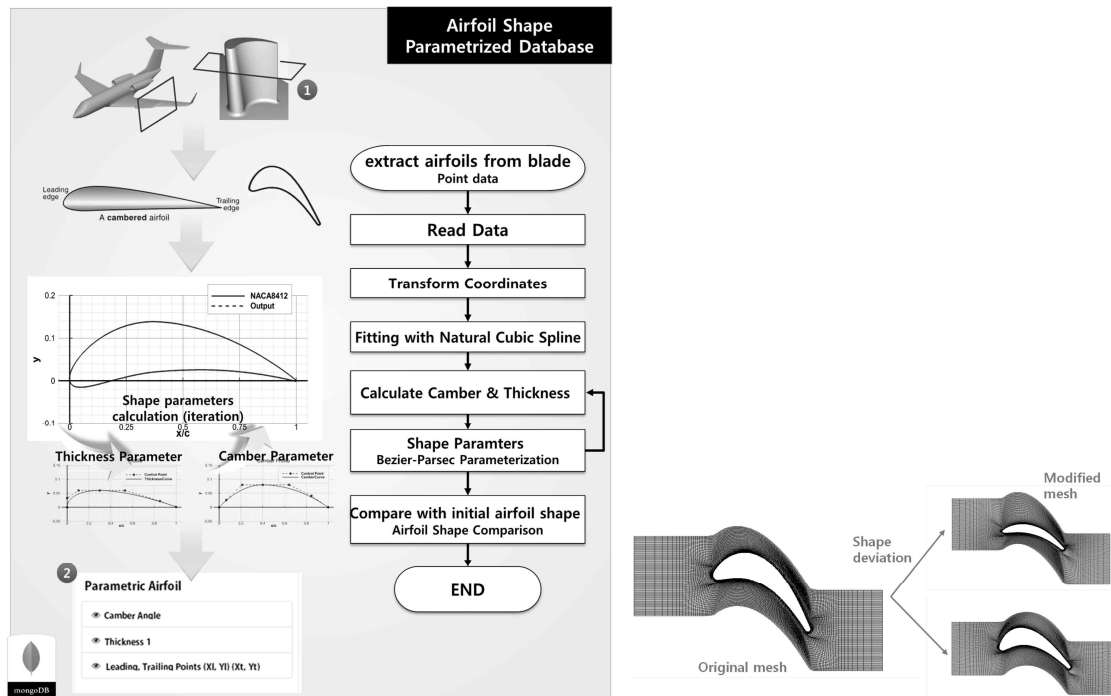


Fig. 4 Airfoil shape parametrization and meshing process

3.2 Data-driven inference module

The Navier-Stokes equations, which are mainly used in modern computational fluid dynamics, cannot be obtained exact Solutions, so approximate numerical solutions must be obtained through discretization of space and time and numerical analytical techniques. To do this, it is necessary to obtain the converged solution while reducing the error of the numerical solution through iterative calculation. Even if the computation time is reduced by the development of hardware or numerical algorithms, there is a limit in reducing the time required for such iterative calculations. In this study, data-driven technology was used to increase the efficiency of flow analysis.

The main function of currently developed data-driven system for the airfoil is three.

- a. Loading simulation results
- b. Re-using simulation results
- c. Predicting simulation results

Fig. 5 shows the overall system of operation process. When the user submits the airfoil shape and flow conditions, shape parameters are extracted through the data system. Then, multidimensional data mining using R is performed, and when the same or similar shape is found in the analysis database stored in Mongo DB, the result is transmitted to the user. However, if there is no identical shape, the prediction is performed through machine learning, the result is displayed to the user, and the information is stored in the analysis database.

Machine Learning analytics framework used Mongo DB to store simulation results and metadata in JSON documents. We used R to develop the prediction function, and we used JAVA as the development language to call the commands of the R script.

We used Node.js to retrieve the results of the simulation requested by the user through the web interface.

The main functions provided by machine learning analytics framework¹⁴ are as follows:

- A. Simulation Result Load
 - a. Loading the execution result of simulation program into Mongo DB as JSON document.
 - b. Bulk loading function.
 - c. Implemented language: Java
- B. Simulation Query Interface
 - a. Retrieves the execution result of the simulation requested by the user through the web interface and returns the result.
 - i. If the result is in the database, return it immediately without re-executing.
 - ii. If the result is not in the database, give the user a prediction option.
 - b. Implemented language: Node.js
- C. Simulation Result Reuse
 - a. If the simulation results you have requested are already in the database, return results directly without performing a simulation
- D. Simulation Result Predict
 - a. If the simulation result requested by the user is not in the database, analyze and predict results
 - b. Implemented language: JAVA (internally calls R script execution command)

- c. Then, use of several statistical machine learning techniques
- i. Multiple Linear Regression (MLR)
 - ii. General Addictive Model (GAM)
 - iii. Support Vector Machine (SVM)
 - iv. Classification and Regression Trees (CART)
 - v. Random Forests (RF)
 - vi. Generalized Boosted Models (GBM)
 - vii. Multivariate adaptive regression splines (MARS)
 - viii. Local Regression (LR)
 - ix. K-Nearest Neighbor Regression (KNN)
 - x. Multi-Layer Neural Network (MLNN)

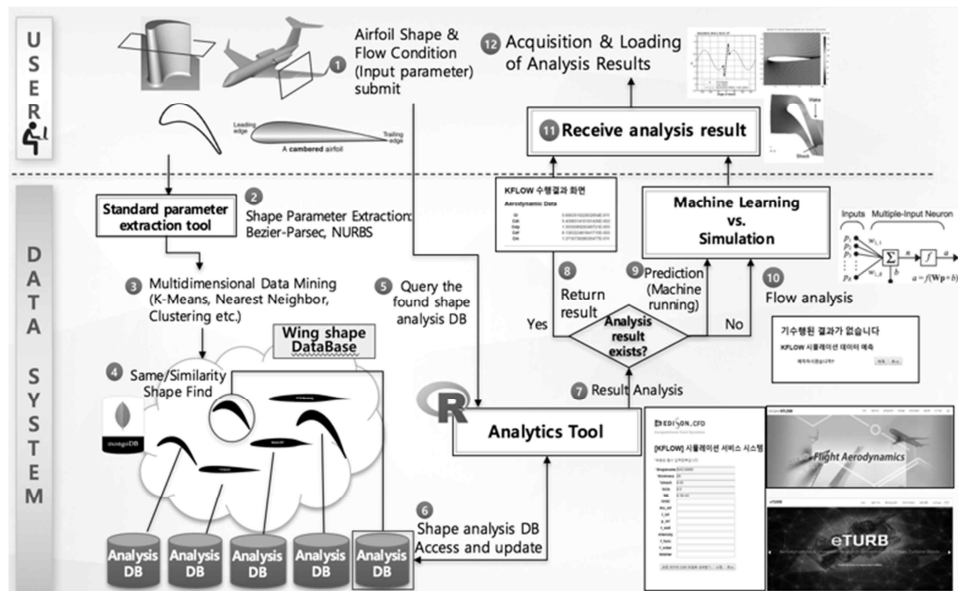
3.3 Verification study using the compute-data framework

Table 1 describes how the dataset was generated from FOM-calculated result data. The four input parameters were selected as the data indexes. Therefore high-fidelity flow solver was run with these indexes, and resulted in a dataset with the number of 7,679 simulation data.

Table 1. Configuration of airfoil aerodynamics dataset

Airfoil thickness	NACA 0009, 0010, 0011, 0012
Mach number	0.05, 0.10, 0.15, ..., 0.6
Angle of attack	0, 1, 2, ..., 10
Reynolds number	1x10 ⁵ , 2x10 ⁵ , ..., 10 ⁶

Now learning with various ML methods were conducted in 70% of the simulation data, then prediction tools was developed. We could test the results of 30% of the simulation data, which



means the comparisons of the ML-inferred and FOM-simulated values. Table 2 shows the comparison errors between ML-inferred and FOM-simulated values which include five features of the aerodynamic coefficients: lift, total/pressure/friction drag, and moment coefficients.

Table 2. Inference errors in accordance with ML techniques

	CL	CDt	CDp	CDf	CM	Avg.	Rank.
MLR	12.6	46.3	153	10.9	59.3	56.4	10
GAM	10.6	41.1	130	8.70	65.1	51.1	9
SVM	3.70	6.90	19.6	2.50	21.4	10.8	6
CART	5.80	7.20	15.2	3.50	17.4	9.82	5
RF	0.9	1.60	2.60	1.20	7.50	2.76	1
GBM	23.7	3.40	7.80	2.20	18.3	11.1	7
MARS	3.90	9.30	20.7	3.70	30.9	13.7	8
LR	1.30	1.70	2.70	1.10	7.40	2.84	2
KNN	3.00	3.70	6.50	2.00	10.3	5.10	3
MLNN	2.10	2.80	13.8	3.00	10.6	6.46	4

The comparison results indicate that Local Regression and famous decision-tree based method called Random Forest showed better accuracy performance.

It was worth being noted that the computation time of the ML-inference was immediate while the FOM simulation time was about 50 min.

4 CONCLUSIONS

A new web-based compute/data engineering system for the aerodynamics analysis of industrial airfoils has been explained in this paper. Some conclusions can be summarized as follows:

- Cyber-infrastructural engineering system can run a high-fidelity aerodynamic simulation and also machine learning based inference tool using the pre-run simulation results. The web-based running environment is expected to work particularly for quick airfoil aerodynamics prediction and compute-data correlation researches.
- Machine learning based framework of inferring aerodynamic coefficients was developed. The full-order flow simulation results in a platform-like computation system are consistently loaded into a database. The framework learned and tested the pre-run dataset using ten primary machine learning methods. The results showed that Local Regression and Random Forest Regression ranked the highest.

More indexes like more detailed airfoil shape and more features like other output parameters will be considered in the future

ACKNOWLEDGEMENTS

This research was supported by the EDISON Program through the National Research Foundation of Korea (NRF) funded by the Ministry of Science & ICT (No. NRF-2011-0020576). This research was supported by Korea Institute of Science and Technology Information (KISTI- 2018)

REFERENCES

- [1] Glotzer, S. C. et al, 2009, International Assessment of Research and Development in Simulation-Based Engineering and Science, WTEC Report, Maryland.
- [2] Petrilli, Justin, Paul, Ryan, and Gopalarathnam, Ashok, 2014, A CFD Database for Airfoils and Wings at Post-Stall Angles of Attack, *31st AIAA Applied Aerodynamics Conference* (AIAA 2013-2916).
- [3] Andreadis, G., Fourtounis, G., Bouzakis, K. D., 2015, Collaborative design in the era of cloud computing, *Advances in Engineering*, 81, pp. 66-72.
- [4] Sakellari, G., Loukas, G., 2013, A survey of mathematical models, simulation approaches and testbeds used for research in cloud computing, *Simulation Modelling Practice and Theory*, 39, pp. 92-103.
- [5] Onshape, <https://www.onshape.com/>.
- [6] SIMSCALE GmbH, <https://www.simscale.com/>.
- [7] CONSELF Url, <https://consself.com/>.
- [8] Rescale Url, <https://www.rescale.com/>.
- [9] Yu, J. L., Ryu, H., Byun, H. J., Lee, J. R., K. W. Cho, and Jin, D. S., 2013, EDISON Platform: A Software Infrastructure for Application-Domain Neutral Computational Science Simulations, *Lecture Note in Electrical Engineering*, 235, pp. 283~291.
- [10] Seo, D. W., Lee, J. Y., Lee, S. M., Kim, J. S., and Park, H. W., 2013, Multi-View Supporting VR/AR Visualization System for Supercomputing-based Engineering Analysis Services, *Korean Journal of Computational Design and Engineering*, 18(6), pp. 428-438.
- [11] Sa, J.H., Park, S.H., Kim, C.J., and Park, J.K., 2015, Low-Reynolds number flow computation for Eppler 387 wing using hybrid DES/transition model, *Journal of Mechanical Science and Technology*, 29(5), pp.1837-1847.
- [12] Taira, K. et al, 2017, Modal Analysis of Fluid Flows: An Overview, *AIAA Journal*, 55(12), pp. 4013-4041.
- [13] Derksen, R.W. and Rogalsky, T., 2010, Bezier-PARSEC: An optimized aerofoil parameterization for design, *Advances in Engineering Software*, 41, pp. 923-930
- [14] Lee, K. Y., Suh, Y. K., and Cho, K. W., 2017, Development of a simulation result management and prediction system using machine learning techniques, *Int. J. Data Mining and Bioinformatics*, 19(1), pp.75-96.

A method for seamless transition from degradation of material stiffness to formation of strong discontinuity

Yuichi Shintaku^{*}, Seiichiro Tsutsumi^{**}, Kenjiro Terada^{***}

^{*}University of Tsukuba, ^{**}Osaka University, ^{***}Tohoku University

ABSTRACT

The objective of this contribution is to develop a method for seamless transition from degradation of material stiffness to formation of a strong discontinuity of displacement with theoretical consistency of cohesive zone models (CZMs) for fracture. In existing CZMs, a fracture process is divided into two stages to realize the crack nucleation and propagation. At the first stage of the fracture process, the material stiffness reduces at a macro-scale due to the evolution of defects at a micro-scale, which is supposed to form a crack tip of the cohesive fracture. At the final stage, which corresponds to the crack propagation process after the stress reaches the maximum value in the material response, the displacement field develops an explicit crack opening due to the coalescence of the microscopic defects. In this study, the macroscopic stiffness reduction at the first stage is represented by the cohesive-traction embedded constitutive law, which is a damage-like constitutive law capable of embedding an appropriate CZM. Then, the proposed method bridges a transition from continuous to discontinuous displacements by the combination of the same CZM, employed to represent the first stage of the fracture process, and the finite cover method (FCM)[1]. In other words, a finite element in which the cohesive traction attains the maximum value is adaptively divided into two domains to represent the strong discontinuity by the FCM endowed with the CZM at their interface. Moreover, these two stages of the cohesive fracture process are seamlessly connected thanks to the unique feature of the cohesive-traction embedded damage-like constitutive law, in which deformation under tensile loading is consistent with the conventional CZMs. Several numerical examples are presented to verify the equivalence between the fracture processes represented by the cohesive-traction embedded damage-like constitutive law and the FCM combined with the CZM. After validating the performance of the proposed constitutive law, we demonstrate the capability of the proposed method of crack propagation equipped with the suggested seamless transition algorithm from the degradation of the material stiffness to the formation of an actual crack propagating within finite elements. . [1] T. Ishii, K. Terada and T. Kyoya, Int. J. Num. Meth. Engng, 67, 960-988 (2006).

Space - Time Trefftz-DG Approach for Elasto-Acoustic Wave Propagation Problem

Elvira Shishenina^{*}, H  l  ne Barucq^{**}, Henri Calandra^{***}, Julien Diaz^{****}

^{*}Team-project Magique-3D, Inria, LMAP-CNRS, France; Total S.A., USA, ^{**}Team-project Magique-3D, Inria, LMAP-CNRS, France, ^{***}Total S.A., USA, ^{****}Team-project Magique-3D, Inria, LMAP-CNRS, France

ABSTRACT

Discontinuous Finite Element Methods (DG FEM) have proven their numerical accuracy and flexibility. However, numerically speaking, the high number of degrees of freedom required for computation makes them more expensive, compared to the standard techniques with continuous approximation. Among the different variational approaches to solve boundary value problems there exists a distinct family of methods, based on the use of trial functions in the form of exact solutions of the governing equations. The idea was first proposed by Trefftz in 1926 [1], and since then it has been largely developed and generalized. By its definition, Trefftz-DG methods reduce numerical cost, since the variational formulation contains the surface integrals only. Thus, it makes it possible exploration of the meshes with different geometry, in order to create more realistic application. Trefftz-type approaches have been widely used for time-harmonic problems, while their implementation is still limited in time domain. The particularity of Trefftz-DG methods applied to the time-dependent formulations is in the use of space-time meshes. Even though it creates another computational difficulty, due to a dense form of the matrix, which represents the global linear system, the inversion of the full "space-time" matrix can be reduced to the inversion of one block-diagonal matrix, which corresponds to the interactions in time. In the present work, we develop a theory for solving the coupled elasto-acoustic wave propagation system. We study well-posedness of the problem, based on the error estimates in mesh-dependent norms. We consider a space-time polynomial basis for numerical discretization. The obtained numerical results are validated with analytical solutions [2]. Regarding the advantages of the method, the following properties have been proven by the numerical tests: high flexibility in the choice of basis functions, better order of convergence, low dispersion. References [1] E. Trefftz. Ein Gegenstuck zum Ritzschen Verfahren. Proc 2nd Int Cong Appl Mech Zurich (1926), 131–137. [2] H. Barucq, H. Calandra, J. Diaz, and E. Shishenina. Space-Time Trefftz - Discontinuous Galerkin Approximation for Elasto-Acoustics. Research Report, Inria RR-9104 (hal-01614126), (2017).

A Heterogeneous Multiscale Method Connecting Kinetic Theory and Molecular Dynamics

Gil Shohet^{*}, Jake Price^{**}, Jeff Haack^{***}, Mathieu Marciante^{****}, Michael S. Murillo^{*****}

^{*}Stanford U, ^{**}University of Washington, ^{***}Los Alamos National Laboratory, ^{****}Los Alamos National Laboratory,
^{*****}Michigan State University

ABSTRACT

Multimethod multiscale modeling, in which two or more separate models are used simultaneously to describe disparate scales in the same problem, provides an avenue for increasing the accuracy of macroscale models used in isolation. We have developed a concurrent multiscale using the traditional heterogeneous multiscale method (HMM) framework where molecular dynamics (MD) provides the missing microscale closure information for a macroscale kinetic model. The kinetic model is constructed such that only collision times are needed from the MD, greatly decreasing the memory and computation times needed. Computational cost is further reduced by a simple machine learning model that predicts future collision time information based on previous MD data. We illustrate the new model for the simple problems of temperature and momentum relaxation in a plasma composed of both weakly and strongly coupled species; we chose these zero dimensional problems to allow for a complete molecular dynamics solution, which allows us to examine choices made in the coupling between the two methods. HMM variants of this kind should be very useful for modeling a wide range of high energy-density environments.

High-precision Control Method for Large Space Structure Subject to Thermal Deformation

Kaori Shoji^{*}, Motofumi Usui^{**}, Daigoro Isobe^{***}

^{*}University of Tsukuba, Japan, ^{**}Japan Aerospace Exploration Agency, ^{***}University of Tsukuba, Japan

ABSTRACT

As the sizes of space antenna reflectors increase, the radio wave transmissions will become more susceptible to small structural deformations that occur in the reflectors. When the Engineering Test Satellite -VIII (ETS-VIII) communications satellite entered the Earth's shadow, radio wave transmissions from the large deployable reflector (LDR) to the Earth were observed to change [1]. Moreover, the temperature of the LDR was observed to decrease for about 200 °C. Therefore, it is conceivable that radio wave transmissions were significantly affected by temperature transition on the LDR. This phenomenon may become critical for the satellites because highly accurate beams are expected to be required for large space structures in the near future. Therefore, not only the means by using materials in which thermal deformation is hardly generated but also the means of active shape changing in orbit have been required to deal with various issues. In this study, the LDR model mounted on the ETS-VIII is constructed for investigation. As a result of numerical simulation of the deformation behavior under the actual thermal history detected on the ETS-VIII, the midpoint of the LDR was confirmed to deform by approximately 5 mm as the temperature decreased [2]. 5 mm deformation is equivalent to 65 km transition of the footprint of communication beam on the surface of the Earth, which explains the phenomena actually observed in the ETS-VIII. Based on these results, we developed an effective method for mechanically compensating the thermal deformation by adjusting the combined coefficient of thermal expansion of structural members which is calculated from the constituent ratio of CFRP and titanium alloy components, and by focusing on springs used to deploy a modular space structure. As a consequence, the thermal deformations at every apex that support the antenna reflector were all suppressed at a high correction rate. It is shown that the combination of these means is best for large space structure to actively suppress the thermal deformation in orbit. References [1] M. Usui, K. Wakita, L. T. T. Thanh, Y. Matsui, and D. Isobe: Suppression of thermal deformation of the large deployable reflector, Transactions of the Japan Society of Mechanical Engineers, Series C, Vol.77, No.777, 2011, pp.2107–2119 (in Japanese). [2] K. Shoji, D. Isobe and M. Usui: Numerical Investigations to Suppress Thermal Deformation of the Large Deployable Reflector during Earth Eclipse in Space, The Aeronautical Journal, Vol. 121, No. 1241, (2017), pp. 970-982, (<https://doi.org/10.1017/aer.2017.33>).

Unified Programming Framework for Parallel FEM Multi-physics Analysis

Tatsuhiro Shono^{*}, Gaku Hashimoto^{**}, Hiroshi Okuda^{***}

^{*}The University of Tokyo, ^{**}The University of Tokyo, ^{***}The University of Tokyo

ABSTRACT

For innovative manufacturing and design, multi-physics problem is important. Fluid-structure interaction analysis for blow molding and thermal fluid analysis for welding are good examples. Generally speaking, Multi-physics problems need longer computation time than mono-physics problems, and degrees of freedom becomes larger than conventional analysis when complex shape of products should be considered. Parallel computation is therefore effective in analysis of these problems. There are many programs for multi-physics analysis. On the other hand, there are more applicable programs to parallel computation, which is specialized in a particular analysis. FrontISTR[1], which is an open-source large-scale parallel FEM program for nonlinear structural analysis, is good example. It achieves high parallel efficiency based on overlapping domain decomposition, then has high applicability large-scale structural problems. Programming framework which extends parallel FEM program like FrontISTR for multi-physics problem is consequently beneficial for innovative manufacturing and design. In this presentation, we will show you a unified programming framework for parallel FEM multi-physics analysis. We will show you a unified programming framework for parallel FEM multi-physics analysis. In this presentation, we will deal with fluid-structure interaction problems and two-phase fluid flow problems. This framework is implemented on nonlinear structural analysis software without breaking a framework of original structural analysis. Additional loop is achieved two-way coupling scheme. Displacement of structures is replaced with flow velocity and pressure when element stiffness matrices at fluid element are calculated in the code. Elements in structures and elements in fluid share nodes at their interfaces, then boundary conditions for interaction between different physical fields are satisfied. This framework is implemented into FrontISTR to achieve high parallel efficiency. Some numerical results (flow over a thin elastic beam attached to a fixed square block[2], for example) solved by FrontISTR will also be shown as verification. [1] FrontISTR Forum, http://www.multi.k.u-tokyo.ac.jp/FrontISTR/index_en.php, 2018/01/10 accessed. [2] Wall, W. A., Fluid-Struktur-Interaktion mit stabilisierten Finiten Elementen, Ph. D. thesis, Institut für Baustatik, Universität Stuttgart.

Simulating the Tensile Response of a Composite Lap-Joint Using a Combined Discrete and Continuum Damage Modeling Approach

Ofir Shor*

*Rafael Advanced Defense Systems LTD

ABSTRACT

Designing structural components using composite materials often requires the use of connectors and joints, which are expected to withstand various structural loads. The talk will focus on the numerical simulation of a bi-material composite lap-joint under a tensile load, using a combination of discrete and continuum damage mechanics modeling approaches. An overall introduction of the modeling strategy will be given, followed by the description of the finite element model and the material models used in the analysis. The model was able to capture the ultimate tensile strength of the joint, as well as the joint's failure mode, which was initiated by delamination between the laminate plies, followed by the growth of intralaminar damage.

Calibration of a Conductive Thermal Model for SS 316L and 17-4 PH in Selective Laser Melting

Yi Shu^{*}, Adrian Lew^{**}, Daniel Galles^{***}

^{*}Stanford University, ^{**}Stanford University, ^{***}U.S. Army Research Laboratory

ABSTRACT

Precise thermal models for Additive Manufacturing are an important prerequisite for developing thermal control strategies as well as for predicting residual stresses for printed parts. We present a three dimensional finite element model for heat transfer in Selective Laser Melting (SLM) processes in which the laser beam parameters (power and its distribution) are calibrated by fitting the meltpool area section outlines in simulations with those in experiments. The experimental data are obtained by shining stainless steel 316L and 17-4 blocks with static and moving laser sources for different time periods, and samples are sectioned to extract the meltpool area profiles. The parametric spaces of possible meltpool profiles are constructed with various simulations with real, temperature-dependent material properties, in terms of appropriate non-dimensional parameters. We iterated the parameters and found those that produce least error between experimental meltpool outlines and simulated ones. With the optimal parameter values, we have achieved a good match of the meltpool outlines.

Trabecular-bone Adaptation to High-impact Exercise in Postmenopausal Women: A Combined Computational and Experimental Study

Vadim V Silberschmidt*, Juan Du**, Chris Hartley***, Katherine Brooke-Wavell****, Margaret A Paggiosi*****, Simin Li*****

*Loughborough University, UK, **Loughborough University, UK, ***Loughborough University, UK,
****Loughborough University, UK, *****University of Sheffield, UK, *****Loughborough University, UK

ABSTRACT

Osteoporosis is a common condition, with a bone loss and structural deterioration increasing risk of fracture [1]. Exercise can stimulate localised structural adaptation and increase bone density [2] that may reduce fracture risk. Different mathematical models were suggested to predict a bone-remodelling process improve understanding of this mechano-biological process, by which bone adapts to mechanical forces. To observe these changes, a few in-vivo mice models were develop; however, there is still no in-vivo assessment based on human models for investigation of the trabecular-bone adaptation in response to mechanical loading. In this study, a combined experimental and computational approach was used to predict this adaptation in postmenopausal women. caused by high-impact exercise A randomized controlled trial of a six-month unilateral exercise intervention was conducted with healthy postmenopausal women, with changes in an exercise leg compared to those in a control leg of the same participant. Microstructural changes in trabecular bone were assessed using high-resolution peripheral quantitative computed tomography (HR-pQCT; Scanco) at the distal tibia. 3D rigid registration was used to obtain resorption and formation areas between pre- and post-intervention scans. Finite-element (FE) models based on the obtained HR-pQCT data were used to determine a structural response of trabecular bone to loading – a high-impact hopping test; strain and strain gradients were used as two different mechanical stimuli. FE models were coupled with an algorithm for remodelling, a modification of a generic trilinear-curve relationship between the mechanical stimulus and adaptation for an equilibrium zone and two additional stages – over-loading and micro-damage. This is the first longitudinal study using HR-pQCT to investigate the effect of exercise on trabecular-bone adaptation across distal tibia. It demonstrated that this novel computational model is able to predict mechanoadaptation of trabecular bone to exercise of postmenopausal women. Such an approach could be used to design, investigate and optimise exercise strategies that target relevant physiological mechanisms. References 1. J. Kanis et al. (2002) Lancet 359(9321), 1929–1936. 2. S.J. Allison et al. (2015) J Bone Miner Res 30(9), 1709–16.

A Computational Investigation of Composites Augmented by Interfacially Bonded Mechanophores

Meredith Silberstein*, Meenakshi Manivannan**

*Cornell University, **Cornell University

ABSTRACT

Interfacial debonding is an important failure mode for polymer composites. A novel approach to manage this damage mechanism is to develop self-healing and self-reporting capabilities through the interfacial augmentation of chemicals termed mechanophores that have useful reactions in response to mechanical work (e.g. color change, chemiluminescence, small molecule release). We refer to such a composite system as an Interfacial Mechanophore Augmented Composite (IMAC). In this talk we will first present our study on activation of mechanophores at interfaces and then application of the key results to predict mechanophore activation in a particulate-filled composite. In the first study, we investigate the critical parameters for mechanophore-functionalized interfaces by building two computational models: a kinematic model with rigid non-interacting walls forming the interface and a molecular dynamics model with metallic substrates. In both the models the mechanophore is idealized as a coarse grained two-bead system governed by a double-well potential that emulates a force directed chemical reaction. Under substrate shear mechanophores progressively activate as interfacial displacement increases as long as detachment from the substrate requires more force than transitioning to the active mechanophore state. Further this activation progression is well approximated by a kinematic interpretation where change in the mechanophore attachment point separation is the dominant factor for determining mechanophore state. In the particulate composite analysis framework, this extensible link mechanophore concept is then used in conjunction with classical elasticity displacement field solutions for far field loading to determine the relative progression of damage and activation. Equibiaxial plain strain loading is used to explore the critical parameters governing mechanophore response within the composite. The results are summarized in terms of a design plot for selecting the appropriate critical mechanophore length change needed for a given composite. We will then also present results for uniaxial plain strain and full 3D uniaxial loading.

Peridynamic Models for Complex Materials

Stewart Silling*

*Sandia National Laboratories

ABSTRACT

Recent advances in the technology of metamaterials and nanoscale composites suggest the need to systematically derive a continuum mechanics material model from a given detailed small-scale description. Since long-range forces may be involved at the nanoscale, an appropriate continuum description would take these forces into account. Peridynamics may provide a suitable continuum mechanics theory for this purpose. In this talk, I will describe a new method for deriving a peridynamic micromodulus function, which is the fundamental peridynamic material property, from a small-scale model of a material. In this method, the material is discretized into cells that individually may contain many atoms or molecules. The mean displacement of the material within each cell is constrained to equal zero except for a single cell. Within this single cell, the mean displacement is a prescribed small nonzero vector. By solving the small-scale equilibrium equation subject to these constraints, we compute the position of every atom or molecule. The resulting net force between the perturbed cell and all of its neighboring cells provides the micromodulus function. This micromodulus function is suitable for peridynamic computations at the length scale of the cell spacing. The horizon emerges naturally from the method, since the micromodulus decays to nearly zero for cells separated by large distances. By constraining the time-averaged displacements of atoms and molecules, rather than their equilibrium displacements, a temperature-dependent micromodulus function can be derived similarly that allows for thermal oscillations.

Analysis of Extremely Flexible Structures Through a Geometrically Exact Bernoulli-Euler Rod Model

Cátia Silva^{*}, Sascha Maassen^{**}, Paulo Pimenta^{***}, Jörg Schröder^{****}

^{*}Polytechnic School at University of São Paulo, Brazil, ^{**}Universität Duisburg-Essen, Germany, ^{***}Polytechnic School at University of São Paulo, Brazil, ^{****}Universität Duisburg-Essen, Germany

ABSTRACT

This work presents a geometrically exact Bernoulli-Euler rod formulation that is an extension of [1,2] and based in [3]. Displacements and rotations can be unlimited large. Linear elastic constitutive equations for small strains are considered in the numerical examples. Energetically conjugated cross-sectional stresses and strains are defined. A straight reference configuration is assumed for the rod, but initially curved rods can be accomplished, if one regards the initial configuration as a stress-free deformed state from the plane position. The parameterization of the rotation field is done by the rotation tensor with the Rodrigues formula that makes the updating of the rotational variables very simple. A family of interpolation for the displacements for the torsion degree of freedom were applied in order to verify the most efficient combination. These were employed with the usual Finite Element Method, leading to adequate C1 continuity within the element. The connection between elements is enforced by Rodrigues parameter being equal on both connecting ends, this can be achieved by adding a penalty or Lagrangian term to the potential energy. The finite element method is used to discretize the potentials on a computational domain in terms of the nodal degrees of freedom. Bearing in mind that the potential is nonlinear a Newton-Raphson iteration scheme is chosen to solve this problem. A set of numerical benchmark examples illustrates the usefulness of the formulation and numerical implementation. These problems were performed, and presented satisfying results. Hence, it can be concluded that this formulation shows great promises to be extensively used for general 3D problems with flexible rods with a smooth connection scheme. 1. Pimenta P. M. and Yoho T., "Geometrically-exact analysis of spatial frames", Applied Mechanics Reviews, ASME, New York, v.46, 11, 118-128, 1993. 2. Viebahn, N., Pimenta, P.M. &&& Schroeder, J., "A simple triangular finite element for nonlinear thin shells - Statics, Dynamics and anisotropy", Computational Mechanics, online, 2016. 3. Silva, C.C., Maassen, S., Pimenta, P.M. &&& Schröder, J. "Geometrically exact analysis of Bernoulli-Euler rods" in preparation for Computer Methods In Applied Mechanics and Engineering, 2017.

Topology Optimization Applied to the Design of a Tesla Pump

Emílio Silva^{*}, Diego Alonso^{**}, Luís Sá^{***}, Juan Romero^{****}

^{*}Polytechnic School of the University of São Paulo, ^{**}Polytechnic School of the University of São Paulo,
^{***}Polytechnic School of the University of São Paulo, ^{****}Federal University of Espírito Santo

ABSTRACT

Tesla devices consist of rotating disks (without blades) and their operation principle is based on the boundary layer effect (i.e., viscous friction forces and Coandă effect). The Tesla pump may be used in various applications, however, its operation efficiency is quite low, which makes room for the optimization of its design. Therefore, in this work, a Topology Optimization formulation is proposed to optimize the Tesla pump rotor by using a 2D swirl flow model. The 2D swirl laminar fluid flow modelling is solved by using the finite element method. A traditional material model is adopted while considering nodal design variables, and is extended to take into account the optimization being performed in a rotating reference frame and the relative tangential velocity being smaller than the other velocity components. A multi-objective function is defined in order to minimize energy dissipation and vorticity. In order to reduce the generation of grayscale results, as it has been observed in previous works, an extra term is proposed in the vorticity function. An interior point optimization algorithm (IPOPT) is applied to solve the optimization problem. Numerical results taking into account some of the different aspects of the design of the rotor of a Tesla pump are presented.

Quasi-static and Dynamic FEM Simulation of Trabecular Bone with Bone Marrow Using a Constitutive Material Model Subject to Strain Rate and Anatomic Location

Juan Diego Silva Henao^{*}, Juan Pablo Casas Rodríguez^{**}, Alejandro Maraño Leon^{***}, Roberto Javier Rueda Esteban^{****}

^{*}Universidad de Los Andes, ^{**}Universidad de Los Andes, ^{***}Universidad de Los Andes, ^{****}Universidad de Los Andes

ABSTRACT

Previous studies have shown that mechanical properties of trabecular bone samples such as yield strength, modulus of elasticity and plateau stress are highly dependent on the anatomic location within the bone itself as well as strain rate. Several tests were conducted on specimens taken from different anatomical sites and orientations within the distal metaphysis of the femur in order to identify the dependency of mechanical properties with the anatomic location as well as their anisotropic behaviour. Samples were tested with and without bone marrow using three different tests devices: a conventional constant strain rate apparatus, a drop weight impact tests (DWIT) device and a split Hopkinson pressure bar system (SHPB) covering strain rates between 10^{-1} /s and 10^3 /s. A constitutive material model that predicts the behaviour of cancellous bone from several anatomic locations was derived from the experimental data gathered. FEM simulation were performed to validate the model estimation at several strain rates and its proximity to experimental data.

Optimized Phase Change Material Distribution for Adsorption Systems Using Topology Optimization Method in Axisymmetric Model

Diego Silva Prado*, Emílio Carlos Nelli Silva**

*Escola Politécnica da Universidade de São Paulo, **Escola Politécnica da Universidade de São Paulo

ABSTRACT

Gas transport and storage are two key factors to be considered when analysing potential solutions involving gas employment. The system efficiency and capacity often determine how attractive the gas solution is. One known solution for gas transport and storage is the adsorbed natural gas (ANG). It consists in the adhesion of gas in a porous matrix by the adsorption phenomena. Adsorption is an exothermic phenomenon, when gas is adsorbed, heat is liberated, heating up the system. One of the issues regarding ANG technology is the fact that increasing temperature causes adsorption capacity to decrease. To solve this problem, methods for controlling the temperature inside the vessel can be found in literature. One temperature control method consists in placing phase change material (PCM) bodies inside the vessel. In literature, it can be verified that placing PCM inside an adsorption tank can increase its adsorption and desorption capacity by reducing the system thermal amplitude. Results vary by changing the amount and position of PCM bodies at the tank interior. Employing a systematic tool for optimized material distribution, such as Topology Optimization Method (TOM) is an attractive solution for this material distribution problem. Several studies have been conducted regarding TOM capacities and implementations and it is considered a versatile tool for material distribution inside a domain. The study presented in this paper consists in the employment of a PCM model for porous media to create a topology optimization formulation capable of improving ANG tanks by optimizing PCM distribution at the vessel interior. The modelled tank consists in a cylindrical vessel with adsorbed material in its interior which is exposed to a pressure increase at the inlet. The FEniCS library is used to handle the differential equations problem and the routine is implemented in python. Sensitivities calculation are aided by dolfin-adjoint libraries. For TOM, the Project variable is set as the PCM distribution inside the vessel. For handling the non-linearity inherent of phase change problems, an analytical solution for phase change is linearized and applied in the numerical system. The portion of PCM at each phase is, then, determined by a variable presented in the mentioned model. This implementation benefits TOM once it avoids the necessity of adaptive mesh solutions, often needed when tackling phase change problems. Finally, PCM distribution inside a 2D axis symmetric ANG vessel is optimized by employing TOM. Optimization results are presented and the benefits the optimization brings are discussed.

AN ACCURATE APPROACH TO THE FINITE-ELEMENT SIMULATION OF FLUID-STRUCTURE INTERACTION WITH CURVILINEAR INTERFACES

VITORIANO RUAS* AND MARCO ANTONIO SILVA RAMOS[†]

* *∂*Alembert, Sorbonne Université - Campus de Jussieu
Couloir 55-65, 4^{ème} étage. 4 place Jussieu. 75005 Paris, France
and CNPq research grant holder, PUC-Rio, Brazil
ruas.vitoriano@gmail.com

[†] Department of Computer Science, Institute for Computing
Universidade Federal Fluminense, Niterói, Rio de Janeiro state, Brazil
marco@dcc.ic.uff.br

Key words: Curvilinear interface, Finite element, Hermite, High order, Simplex, Straight-edged.

Abstract. In many technical or scientific applications involving fluid-structure interaction, such as cardiovascular flow modeling, the solid walls are curved and therefore so is the flow domain. As long as velocity and displacement finite-element representations of order higher than one are employed, the interface degrees of freedom must be properly interpolated, otherwise method's theoretical accuracy will be eroded. We present a simple approach to avoid such a loss, based on a variational formulation that allows achieving this with straight-edged elements of the simplex type and polynomial algebra only. Examples with quadratic Lagrange and Hermite finite elements to represent displacements and classical mixed methods to approximate the primitive variables of viscous incompressible flow, illustrate the efficiency of the proposed approach.

1 WORK'S OVERVIEW

Among a few known techniques the isoparametric version of the finite element method (cf. [1]) for meshes consisting of curved triangles or tetrahedrons is the one most widely employed to solve partial differential equations with essential conditions prescribed on curved boundaries. It allows recovering optimal approximation properties that hold for elements of order greater than one in the energy norm for polytopic domains. However, besides a greater geometric complexity, this method requires the manipulation of rational functions and the use of numerical integration. We consider a simple alternative to deal with essential (i.e. Dirichlet) boundary conditions that bypasses these drawbacks, without eroding qualitative approximation properties.

Moreover, in contrast to other methods such as the isoparametric version of the finite element method, our technique is universal, for it applies to different types of degrees of freedom, such as normal components of vector or tensor fields. Actually the idea behind it was first disclosed during the talk given by the authors on a Hermite method with normal-derivative degrees of freedom, at ICNAAM - the International Conference of Numerical Analysis and Applied Mathematics -, which was held in Rhodes, Greece, in September 2016. Later on this work was published in the form of article [2]. In the present work we first recall the main principle the new technique is based upon, by taking as a model the solution of the Poisson equation with quadratic Lagrange finite elements. A detailed description thereof in both the two- and the three-dimensional case can be found in the open access article [3] and references therein. Then we show that the new method extends very naturally to both classical elasticity systems and viscous incompressible flow equations. This forms a basis for technique's application to fluid-structure finite-element modeling. In the particular case of the Stokes system, we show that the new method can be combined with any velocity-pressure pairing of global order greater than one. As an illustration we consider the classical Taylor-Hood (cf. [4]) and the Crouzeix-Raviart method, for which examples are given in two-dimension space. Some simulations of deformations of solid bodies of curved shape using our technique in connection with quadratic Lagrange finite elements are also supplied (see also [5]).

2 TECHNIQUE'S SHORT DESCRIPTION

First of all it is important to recall that the technique under consideration is aimed at interpolating Dirichlet conditions prescribed on curvilinear boundaries of bi- or tridimensional computational domains. It can provide a significant cost reduction of finite-element simulations in pure CFD or in fluid-structure modeling, as long as the method in use is of order greater than one. In this respect we can take as an example the popular Taylor-Hood method to solve the incompressible Navier-Stokes equations in a region delimited by two deformable excentric cylinders, both rotating with given angular velocities. The precision of this second order method to simulate the flow of an incompressible viscous fluid in such a domain will be considerably eroded, in case it is simply approximated by the polygon formed by the union of the straight-edged triangles, when a standard mesh is used. This effect will be amplified in case the deformation of the solid walls has to be taken into account, and a method of order greater than one is used to compute it, such as quadratic finite elements. A classical solution to overcome such an accuracy loss is to employ the isoparametric version of the finite element method to represent both the velocity of the fluid and the displacement of the solid walls, which requires the use of interface elements with parabolic edges. However, besides obvious geometric complications, this technique transforms the original local polynomial shape-functions into rational functions. Handling such functions can become a delicate issue. This is because the use of numerical integration is inevitable to compute the matrices inherent to the simulation, and the right choice of a quadrature rule is not always so clear. For those reasons our method provides an

efficient alternative, since it avoids the use of curved elements and handles only polynomial shape- and test-functions, thereby allowing for exact integration without any qualitative loss, as compared to the isoparametric technique.

Our method's guiding principle can be well understood in the framework of the finite-element solution of the following model-problem. Let us consider the Laplace equation $\Delta u = 0$ in a smooth curved plane domain Ω , with Dirichlet conditions $u=g$ on its boundary Γ , where g is assumed to be sufficiently smooth as well. Suppose that classical Lagrange finite elements are used to solve this problem, based on a straight-edged triangular mesh, in association with continuous functions which are a polynomial of degree less than or equal to k in each triangle.

Suppose again that Ω is approximated by the polygon Ω_h with boundary Γ_h , formed by the union of the triangles of a mesh with maximum edge-length equal to h . If the values of g at the nodes on Γ_h different from vertexes are taken from points on Γ close to them, it is well-known that, whatever $k > 1$, the error of the approximation of u in the energy norm will be an $O(h^{1.5})$ (see e.g. [6]), instead of the $O(h^k)$ one could hope for with this kind of interpolation. With the new technique it suffices to substitute the Lagrangian nodes in the interior of the edges contained in Γ_h , by nodes on Γ located nearby. The choice of the latter nodes is very wide, since anyway integration remains restricted to the triangles that form the polygon Ω_h . We further observe that the test-functions are not defined in this manner, but rather in the usual way for Lagrange finite elements. This is one of the main advantages of our method. In short this procedure allows generating approximations of optimal order k in the energy norm. A rigorous analysis of this property in both 2D and 3D can be found in two *arXiv* papers cited in [3].

A possible construction of the nodes located on Γ pertaining to the new method, generically denoted by P , is illustrated in Figure 1 for $k=3$.

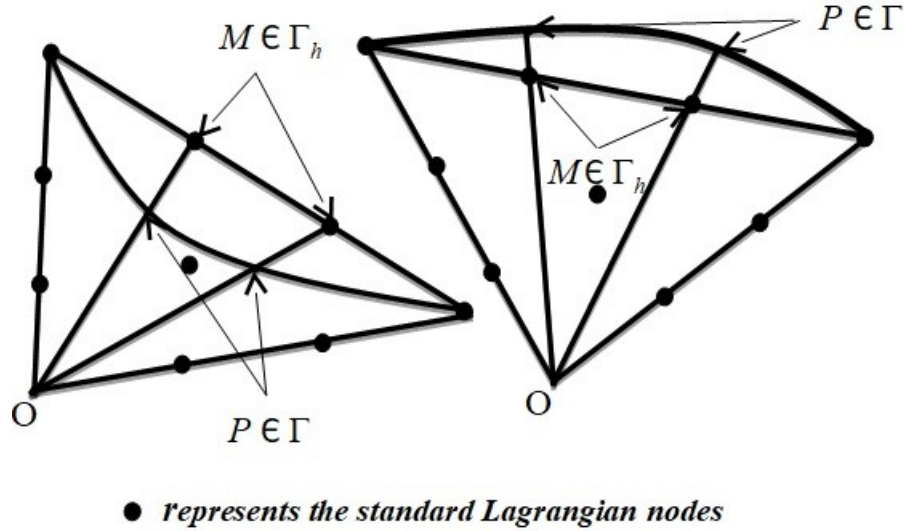


Figure 1- Lagrangian nodes $M \in \Gamma_h$ for $k=3$ and corresponding nodes $P \in \Gamma$ for typical boundary triangles

3 AN EXAMPLE WITH NORMAL-DERIVATIVE DEGREES OF FREEDOM

In this section we apply the principles described in Section 2 to a finite element method based on Hermite interpolation incorporating degrees of freedom of the normal-derivative type. The aim is to show that, in contrast to classical methods to handle Dirichlet conditions for second order boundary-value problems posed in curved domains, the technique studied in this work is as universal as can be. For this purpose we solve a model-problem using a variant of the classical Raviart-Thomas mixed finite element of the lowest order [7], commonly known as RT_0 . This variant studied in first author's work [8] among other papers of his, is to be employed in the framework of variational formulations mimicking corresponding mixed formulations. A Hermite interpolation with discontinuous piecewise quadratic functions allows for better accuracy of an approximate unknown field in the mean-square sense, as compared to the RT_0 finite element, though at equivalent cost. Solution's gradients in turn, are identically represented.

Suppose that we wish to determine the deflection u of an elastic membrane occupying a smooth plane domain Ω with edge Γ , under the action of a force density f perpendicular to its plane. It is well-known that this problem is governed by the Poisson equation $-c \Delta u = f$ in Ω , supplemented with appropriate boundary conditions, where c is a constant accounting for the mechanical properties of the material the membrane is made of. We consider that a portion Γ_0 of membrane's edge is kept fixed, that is, the essential boundary condition $u = 0$ holds on Γ_0 . On the other hand we assume zero traction on the complementary portion Γ_1 of Γ , which corresponds to the natural boundary condition $\partial u / \partial n = 0$ on Γ_1 , where $\partial u(\cdot) / \partial n$ denotes the outer normal derivative along Γ .

In order to solve this problem with our method, we first recast it in mixed form, by introducing the auxiliary field $\mathbf{p} = \text{grad } u$, which satisfies $\text{div } \mathbf{p} = -c^{-1}f$. The underlying mixed variational form writes: Find (\mathbf{p}, u) in $\mathbf{Q} \times W$ such that

$$\int_{\Omega} (v \text{div } \mathbf{p} + \mathbf{p} \cdot \mathbf{q} + u \text{div } \mathbf{q}) d\mathbf{x} = -c^{-1} \int_{\Omega} f v d\mathbf{x} \text{ for all } (\mathbf{q}, v) \text{ in } \mathbf{Q} \times W, \quad (1)$$

where W is the space of integrable functions in Ω (i.e. $W = L^2(\Omega)$), and \mathbf{Q} is a subspace of the space of vector fields which are square integrable in Ω , and whose divergence is also square-integrable in Ω , that is, the space $\mathbf{H}(\text{div}, \Omega)$ (cf. [7]). More precisely \mathbf{Q} is the subspace of $\mathbf{H}(\text{div}, \Omega)$ consisting of fields \mathbf{q} whose component $\mathbf{q} \cdot \mathbf{n}$ vanishes on Γ_1 , where \mathbf{n} is the outer normal vector to Γ .

It is important to recall that in the framework of formulation (1) the condition $\mathbf{p} \cdot \mathbf{n} = 0$ on Γ_1 is to be treated as an essential (Dirichlet) boundary condition, while the prescribed deflection $u = 0$ on Γ_0 is regarded as a natural (Neumann) boundary condition.

We actually solved a toy-problem with an empty Γ_0 . This requires taking an f satisfying the condition $\int_{\Omega} f d\mathbf{x} = 0$, and in this case u is defined up to an additive constant.

Now let \mathbf{T}_h be a mesh consisting of triangles with maximum edge length equal to h , satisfying the usual compatibility conditions (cf. [1]). Here again we denote by Ω_h the union of the triangles in \mathbf{T}_h and by Γ_h the boundary of this polygon. We define two subspaces \mathbf{Q}_h and W_h associated with \mathbf{T}_h , which are discrete counterparts of \mathbf{Q} and W . We recall that the Raviart-Thomas mixed method RT_0 consists of choosing W_h to be the space of functions which are constant in each triangle of the mesh. \mathbf{Q}_h in turn is the subspace of \mathbf{Q} consisting of fields of the form $a\mathbf{x} + \mathbf{b}$ in each triangle, where a is a real coefficient and \mathbf{b} is a vector of \mathbf{R}^2 , whose normal component is continuous on the edges of the elements in \mathbf{T}_h .

As for the Hermite variant of RT_0 , an approximation u_h of u is searched for in a space V_h defined as follows: In each triangle T of \mathbf{T}_h a function v in V_h is of the form $a\mathbf{x}^2/2 + \mathbf{b} \cdot \mathbf{x} + e$ where a and e are real coefficients and \mathbf{b} is a vector of \mathbf{R}^2 . Then, like the flux variable \mathbf{p} in the RT_0 method, the gradient of v is of the form $a\mathbf{x} + \mathbf{b}$ and its normal component along an edge is constant according to [7]. We require that this normal component of every v in V_h along a mesh edge be single valued if the edge is common to two triangles in the mesh, or to vanish if the edge is contained in Γ , in order to prescribe the zero traction condition on the edge of the membrane. Then following [8], we recast the finite-element counterpart of the mixed formulation (1) in the following variational form: Find u_h in V_h such that,

$$\sum_{T \in \mathbf{T}_h} \left[\int_T (v \Delta u_h + \text{grad } u_h \cdot \text{grad } v + u_h \Delta v) d\mathbf{x} \right] = -c^{-1} \int_{\Omega_h} f v d\mathbf{x} \quad \text{for all } v \text{ in } V_h. \quad (2)$$

Owing to these continuity requirements the local construction of functions in V_h must rely upon Hermite interpolation. Actually the degrees of freedom of V_h are precisely the (constant) normal derivatives along the edges, besides the function mean values in the elements of the mesh (cf. [8]). Since this method represents the gradient of the unknown field in the same way as the RT_0 mixed method, both methods differ only in the (discontinuous) representation of the deflection itself. Indeed in each triangle it is a linear function enriched with a quadratic term in the case of the Hermite method, whereas it is just constant for the mixed method. As long as Ω is a polygon, the Hermite variant of RT_0 described above is a second order method in the mean-square sense (cf. [8]), in contrast to the mixed method, which is just of the first order in the same sense.

Here we endeavor to show that, unless u_h is searched for in a suitable space U_h different from V_h such a property no longer holds, and moreover a substantial accuracy loss occurs in case Ω is a curved domain

Our choice of U_h is a space defined in the same way as V_h , except for elements in the subset of \mathbf{S}_h of \mathbf{T}_h consisting of triangles having an edge in Γ_h upon which a zero normal derivative condition must be enforced. However instead of enforcing this condition along such an edge, we require that the first order derivative of a function in U_h in the direction normal to it vanish along the tangent to the boundary at the intersection with it of the line joining the mid-point of this edge to the opposite vertex. This means that for each triangle in \mathbf{S}_h we pick up

the normal derivative where it is prescribed, that is, on the neighboring portion of the true boundary. This is precisely the counterpart of the Hermite finite element under study, for the technique designed to treat Dirichlet boundary conditions with Lagrange finite elements described in Section 2.

We next proceed to the numerical solution of our model-problem, taking $c = 1$ and Ω to be the ellipse with semi-axes equal to 0.5 and 1.0. We consider a manufactured exact solution given by $u(x,y) = (x^2/8 + y^2/32 - x^4/4 - y^4/64 - x^2y^2/8)$, f being defined accordingly. For symmetry reasons the computational domain is a quarter ellipse. We assess the convergence rates to the exact solution for three different approaches, namely, the classical RT_0 method, its Hermite variant taking $U_h = V_h$ and the latter combined with our method to approximate Dirichlet boundary conditions on curved boundaries. The meshes employed in these computations, indexed by an integer M with $h = 1/M$, are the transformation of a uniform mesh of the unit square into the mesh of the quarter ellipse, by letting polar coordinates play the role of cartesian coordinates.

From the error evolution measured in the mean-square norm, it turned out that the power of h in the corresponding **OACR** is roughly 1, 1.8 and 2, respectively, where the acronym **OACR** stands for observed asymptotic convergence rate. We refer to Table 1 for such data. Moreover we checked the evolution as the mesh is refined of numerical solution's maximum absolute value at the centroids of the elements in the mesh. The **OACR** in this sense is roughly an $O(h^2)$ for the three methods. Nevertheless it is noteworthy that the accuracy of the boundary-modified Hermite variant of RT_0 in this respect is considerably improved, even for the coarser meshes, taking into account that the maximum absolute value of the exact solution is 1.56250, up to the fifth decimal. This comparison is illustrated in Figure 2.

All these results indicate that the modification in order to enforce on the true boundary the normal derivative boundary condition, with the Hermite variant of RT_0 , is indeed necessary whenever Ω is a curved domain. Indeed in doing so one takes the same advantage thereof in terms of accuracy enhancement, as in the case of polygonal domains (cf. [8]).

$M \rightarrow$	8	16	32	64	128	OACR
$h \rightarrow$	0.01250000	0.00625000	0.00312500	0.00156250	0.00078125	\downarrow
Raviart-Thomas mixed method RT_0	0.53435×10^{-3}	0.20712×10^{-3}	0.90368×10^{-4}	0.42781×10^{-4}	0.21005×10^{-4}	$O(h^{-1.0})$
Hermite variant of RT_0 ($U_h = V_h$)	0.32559×10^{-3}	0.99666×10^{-4}	0.29191×10^{-4}	0.83411×10^{-5}	0.24152×10^{-5}	$O(h^{-1.8})$
Modified Hermite variant of RT_0	0.18500×10^{-3}	0.48191×10^{-4}	0.12493×10^{-4}	0.32565×10^{-5}	0.82059×10^{-6}	$O(h^{-2.0})$

Table 1 - Absolute errors of the solution to a toy-problem in an ellipse in the mean-square norm

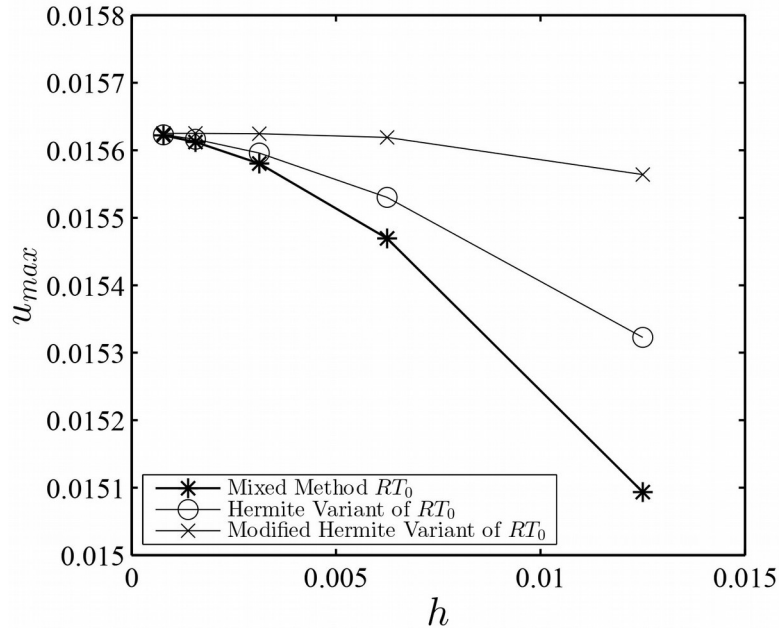


Figure 2 - Approximate solution's maximum absolute value u_{max} at the centroids of the elements

CONCLUSION

From the numerous experiments carried out so far with the new method to take into account Dirichlet boundary conditions prescribed on curved boundaries, it is possible to assert that it is a simple, reliable and accurate tool to handle interface conditions in fluid-structure or fluid-fluid higher order finite-element modeling. Moreover, as shown in this work, it is a universal technique, for it applies to different types of interpolations and degrees of freedom, and not only to those based only on function values, such as Lagrange finite elements.

ACKNOWLEDGEMENT

The first author gratefully acknowledges the financial support provided by CNPq through grant number 307996/2008-5.

REFERENCES

- [1] Zienkiewicz, O.C. and Taylor, R.L. The Finite Element Method. McGraw Hill, Vol. I., (1989), Vol. II., (1991).
- [2] Ruas, V. and Silva Ramos, M.A. A Hermite finite element method for Maxwell's equations. *Applied Mathematics and Information Sciences*, (2018) 12-2 : 271–283.
- [3] Ruas, V. Variational formulations yielding high-order finite-element solutions in smooth domains without curved elements. *Journal of Applied Mathematics and Physics*, (2017) 5-11: DOI:10.4236/jamp.2017.511174.
- [4] -, -. Accuracy enhancement for non-isoparametric finite-element simulations in curved domains; application to fluid flow. *Computer and Mathematics with Applications*, to appear.
- [5] -, -. Optimal Calculation of Solid-Body Deformations with Prescribed Degrees of Freedom over Smooth Boundaries. In: *Advanced Structured Materials*, H. Altenbach et al. Eds., Magdeburg, Springer International Publishing, Vol.1 (2018), 695–704.
- [6] Ciarlet, P.G., *The Finite Element Method for Elliptic Problems*, North-Holland, 1978.
- [7] Raviart, P.A. and Thomas, J.M. *Mixed Finite Element Methods for Second Order Elliptic Problems*, *Lecture Notes in Mathematics*, Springer Verlag, (1977) 292-315.
- [8] Ruas, V. Hermite finite elements for second order boundary value problems with sharp gradient discontinuities, *Journal of Computational and Applied Mathematics*, (2013) 246 : 234-242.

Numerical Evaluation of the Out-of-plane Response of Fiber Networks Using a Representative Volume Element

Jaan-Willem Simon*, Yujun Li**, Zengzhi Yu***

*Institute of Applied Mechanics, RWTH Aachen University, **Department of Advanced Manufacturing Engineering, Northwestern Polytechnical University, ***Institute of Applied Mechanics, RWTH Aachen University

ABSTRACT

Many natural and synthetic materials have fibrous microstructures, such as nonwoven fabrics, paper, and fiberboard. It is usually difficult to experimentally evaluate their out-of-plane mechanical behavior due to the small thickness compared to the in-plane dimension. Hence, to properly predict such properties, network-scale models are required to obtain homogenized material mechanics by considering fiber-scale mechanism. The current study demonstrates a three-dimensional representative volume element (RVE) for fiber networks using the finite element method. First the classical deposition procedure has been adopted to generate fiber networks with random or preferential fiber orientations. Thereafter, an artificial compression step has been performed to achieve the practical fiber volume fraction. The hollow fibers, described with elastic-plastic brick elements, have been joined by interface-based cohesive zone elements introduced in all fiber-fiber contact areas. Then, the fiber networks have been subjected to displacement boundary conditions, and their apparent mechanical responses have been evaluated by means of homogenization of resulting stresses. Further, an RVE size convergence study has been conducted in order to determine the appropriate RVE dimension. In particular, the out-of-plane responses in compression and in tension have been investigated by varying specimen length while keeping the specimen thickness constant. Finally, the apparent out-of-plane responses of the obtained RVE have been evaluated for several loading cases including out-of-plane compression, tension, simple shear, and pure shear. The results show a quite different mechanical behavior of fiber networks between all these out-of-plane loading cases, particularly between tension and compression. In addition, the study showed that the smallest RVE which represented a reasonable response has required at least 160 fibers. The framework established in this work can be used to model numerous kinds of fiber networks at the individual fiber level and pass the information up to the macro scale for further analysis. This model is suitable to analyze the out-of-plane deformation, where a model with beam elements shows difficulty.

Topological Optimization of Patient Specific Maxillofacial Implants

Janos Simonovics*, Peter Bujtar**

*Budapest University of Technology and Economics, Budapest, Hungary, **Monkland University Hospital,
Lanarkshire, Scotland

ABSTRACT

Head and neck tumors affecting the facial bones are a challenging area of reconstruction. Combined biological and mechanical understanding has already rewritten the scenario from scratch multiple occasions. Resection of the so called load-bearing buttress system alters the skeleto-musculo-neurological equilibrium. Segmental mandible defects, for this reason, benefit from engineering input to provide restitution of the original physiological estate. The current load-bearing workhorse, reconstruction plates or implants are manufactured in mass production. A mixture of locking and non-locking screws are used to anchor these into the residual skeleton. The implant currently in used were redesigned in the past on many occasion, still could not fulfill the multi-facetted demand requiring mechanical, aesthetical, radiological, restorative and functional aspects. Additive manufacturing offer the most recent option to rethink patient specific implants. In the current study, the data of a 57-year-old edentulous female, imaged with a Cone Beam Computer Tomography (CBCT - iCat), was selected to build a detailed Computer Aided Design (CAD) mandible model using reverse engineering techniques. The most frequently occurring segmental defects were modelled including some worst case defect scenarios. The cover surface was inserted as the design space for the reconstruction plate topology optimization. Topology, shape optimization and Finite Element Analysis (FEA) were used to reach desired development goals with literature based anatomical boundaries and loads during chewing. The stress values within the plate were recorded. We found the redesigned implants would provide more physiological load transfer, more likely to preserve and support the regeneration of bone. Eventually dental implant restoration would become more a viable option. The final implant weight was reduced with 60% compared to the original geometry while keeping the von Mises stress within the structural limits. It would be a unique novel feature of personalized implants to divert the micro strains ranges which would promote bone growing in resected areas. The availability of optimized implants can change the indication of resection. The current model can increase our understanding of the biomechanics and may help to translate additive manufacturing principles into the implant design practice.

A Micromorphic Approach Modelling the Anisotropic Material Behaviour of the Human Heart

Sebastian Skatulla^{*}, Markus von Hoegen^{**}, Joerg Schroeder^{***}, Ntobeko Ntusi^{****}

^{*}University of Cape Town, ^{**}Universität Duisburg-Essen, ^{***}Universität Duisburg-Essen, ^{****}University of Cape Town

ABSTRACT

Computational cardiac mechanics models need to take into account the complex underlying micro-structure of the cardiac tissue in a sufficiently accurate manner, address biological effects such as residual stresses, remodelling or rearrangement of micro-structural components and are numerically robust and efficient. It has been discovered that the initially crimped and coiled collagen fibres straighten during diastolic filling, the interconnected fibre sheets are able to slide over one another and fiber rearrangement and spatial reorientation is taking place. This work proposes a generalized continuum approach which features extra degrees of freedom and corresponding strain and stress measures. The approach can therefore account for the hierarchical fibrous characteristics of the myocardium which are associated with micro-structural deformation of muscle-fibre bundles as well as their motion relative to the bulk material representing the constraining cytoskeleton. The micromorphic generalised cardiac mechanics model is applied to finite element modelling of patient-specific hearts making use of cardiac magnetic resonance (CMR) scans provided for this investigation by the Cape Universities Body Imaging Centre (CUBIC). With the anatomical heart models calibrated, the fibre strain, fibre stress and active tension distributions are computed. The comparison with simulated results using a classical myocardial tissue model indicates clear differences due to elastic non-affine fibre reorientation which renders the tissue more compliant.

Numerical Investigations of the Out-of-plane Stiffness Behavior of Hybrid Core Sandwich Panels

Isabella C. Skrna-Jakl*, Dieter H. Pahr**

*TU Wien, Institute of Lightweight Design and Structural Biomechanics, **TU Wien, Institute of Lightweight Design and Structural Biomechanics; Karl Landsteiner Private University of Health and Science

ABSTRACT

Hybrid core sandwich structures, consisting of a foam core reinforced with thin composite beams, are among the most efficient lightweight design concepts. Besides aerospace applications, they are employed in industrial fields such as wind energy, transportation systems, ship building and roof constructions. The advantage of the hybrid core is that, due to the specific orientation of the anisotropic 1D reinforcements, a low weight sandwich design with an improved out-of-plane stiffness can be obtained. Aim of the present study is to numerically investigate the influence of specific core reinforcement design parameters on the out-of-plane stiffness behavior. Sandwich configurations with reinforcements oriented at $\pm 45^\circ$ are studied and Finite Element unit cell analyses are performed with boundary conditions corresponding to the standardized sandwich shear and compression tests. The effective out-of-plane engineering constants are computed, employing the homogenization software MEDTOOL [www.dr-pahr.at]. At first 3D-solid FE-models are analyzed and variations of the effective out-of-plane engineering constants due to • changes of the reinforcement material, • the presence of matrix joints in the crossing region of adjacent stiffeners, • stiffeners that penetrate each other at the crossing point, and • removal of the foam core are examined taking into account the weight of the investigated configurations. The results show that the specific values of the out-of-plane pressure and shear moduli can be increased up to 16-fold and 60-fold, respectively, in comparison to the data obtained from unit cell analyses of the unstiffened foam core sandwich. In a second step an FE-unit cell model was developed with the aim of reducing computational requirements for subsequent analyses. Therefore, the face sheets and the foam were modeled employing a coarse 3D-solid element mesh and beam elements were used for the reinforcements. The results show that particular modeling techniques are required to correctly model the transversally, isotropic material behavior of the beams as well as the connection of the beams to the face layers. Finally, FE-analyses of standardized sandwich shear and compression tests are performed. As the size of the standardized test samples and the size of the unit cell are of the same order of magnitude, „structural“ rather than periodicity boundary conditions must be used. The comparison of the effective out-of-plane engineering constants obtained by the numerical test and unit cell analyses, can be used to evaluate the experimental results.

Mesh Dependent Properties to Produce Mesh Independent Results in Fracture Mechanic Simulations

Damián Smilovich*, Raúl Radovitzky**, Eduardo Dvorkin***

*Sim&Tec, Buenos Aires, Argentina, **MIT, Cambridge, MA, USA, ***Sim&Tec, Buenos Aires, Argentina

ABSTRACT

The fundamental criteria that govern the fracture mechanics behavior of materials are (i) the fracture initiation criterion that controls the onset of fractures and (ii) the propagation criterion that controls the release of fracture energy when the already initiated fractures increment their opening. The Discontinuous Galerkin (DG) technique in conjunction with cohesive interface elements has been successfully used for many years in the modeling of fracture mechanic problems [1] [2] [3]. When simulating fracture propagation using the DG technique, a fracture opened at an interface element will propagate to a neighbor one when the initiation criterion is also fulfilled at it. The initiation criterion is usually stated as a function that combines the stress state at a point with the material ultimate stress; hence, it is a mesh independent criterion. However, it must be considered that the numerical model approximates the stress singularity at the crack tip using non-singular interpolation functions; therefore, the fulfillment of the initiation criterion depends on the mesh density at the crack tip; therefore, larger elements may numerically arrest the fracture propagation. To circumvent this problem and get results that are independent of the mesh it is possible to introduce in the initiation function a measure of the elements size. Numerical experiments are presented to back-up the proposed methodology illustrating that a mesh dependent initiation function decreases the dependence of the fracture mechanic results on the elements size. References [1] G. Camacho and M. Ortiz, "Computational modelling of impact damage in brittle materials," Int. J. of Solids and Structures, vol. 33, no. 20, pp. 2899-2938, 1996. [2] L. Noels and R. Radovitzky, "A general discontinuous Galerkin method for finite hyperelasticity. Formulation and numerical applications," Int. J. Numerical Methods Engrg., vol. 68, pp. 64-97, 2006. [3] R. Radovitzky, A. Seagraves, M. Tupek y L. Noels, "A scalable 3D fracture and fragmentation algorithm based on hybrid, discontinuous Galerkin, cohesive element method," Computer Methods Appl. Mech. and Engng., vol. 200, p. 326.344, 2011.

Topology Optimization of Primitives with Material Anisotropy

Hollis Smith^{*}, Julian Norato^{**}

^{*}University of Connecticut, ^{**}University of Connecticut

ABSTRACT

Anisotropic materials, such as fiber-reinforced bars or composite laminates, are widely used in industry to achieve lightweight structures with greater performance than is possible using homogeneous isotropic materials. In this presentation, we introduce a topology optimization method for the design of structures made of bars or plates that exhibit specified material anisotropy (e.g. fiber-reinforced bars or composite-laminate plates) within a 3-dimensional design region. The geometry and the elasticity tensor associated with each primitive are analytically and explicitly expressed in terms of their relevant geometric design parameters: position, orientation, and dimensions. In addition to these geometric variables, an auxiliary size variable is ascribed to each primitive and penalized in the spirit of solid isotropic material with penalization (SIMP) enabling the optimizer to entirely remove a primitive from the design if its size variable attains a near-zero value. To perform the primal and sensitivity analyses, we employ the geometry projection method to smoothly map the analytical geometry of the primitives onto a continuous density field defined over a fixed uniform finite element grid. Following the projection of the geometry, we use an ersatz material whereby the effective elasticity tensor at each finite element, and consequently its stiffness matrix, is modified by a suitable function of the projected density. The distinct advantage of this method is to enable topology optimization using readily-manufacturable anisotropic materials. Moreover, our method retains two significant advantages that existing free-form topology (i.e. density-based and level set-based) optimization techniques exhibit: 1) we circumvent re-meshing upon design changes because the projected ersatz material defined over the fixed finite element grid simplifies the primal and sensitivity analyses; and 2) the differentiability of the projection and the chain rule enable the implementation of efficient gradient-based optimization methods. We demonstrate the applicability of our proposed method by presenting several numerical examples.

Tendon Cell and Tissue Activation by Matrix Damage

Jess Snedeker^{*}, Fabian Passini^{**}, Stefania Wunderli^{***}

^{*}University and ETH Zurich, ^{**}University and ETH Zurich, ^{***}University and ETH Zurich

ABSTRACT

Introduction: Efforts to elucidate degenerative tendon disease mechanisms have been hindered by a lack of valid experimental models, a limitation that is at least partly attributable to large challenges in maintaining in vitro tissue homeostasis after explanting. Tendon tissue equilibrium very heavily depends on appropriate mechanical loading within a narrow, and still poorly defined, physiological range. We will present an overview of our recent work on the tendon cell-matrix interactions that drive tissue homeostasis, matrix remodeling and eventual tissue degeneration, and discuss a roadmap for unravelling these mechanically regulated signaling pathways for the development of effective treatment strategies. Results and Discussion: First results using a mouse tail tendon explant model to investigate the role of mechanical loads on tissue homeostasis and degeneration suggest that tissue damage accumulates in the tendon until “intrinsic repair mechanisms” are overwhelmed. At this point, the metabolic cost of extracellular matrix remodeling exceeds the locally available nutrient supply. We hypothesize that upon reaching this “Metabolic Tipping Point”, the vascular system is recruited along with accompanying nerve supply (and pain) and the tissue enters into a chronic disease state characterized by high matrix turnover and increasingly poor tissue quality. In this paradigm, a delicate mechanically regulated balance exists between recruitment and suppression of the extrinsic vascular system by the resident tendon core cells. Upon injury or damage, this regulation in turn steers the tissue towards either functional remodeling or chronic tendon disease. We believe that future research should focus on exploring the possibility of gaining control of the involvement of the intrinsic and extrinsic tendon compartment in the disease/repair process. Studying such synergetic involvement is experimentally challenging, but deserves our efforts when striving for resolving tendon disorders.

Integrated Computational Framework for Simulating the Failure Response of Materials with Complex Microstructures

Soheil Soghrati^{*}, Anand Nagarajan^{**}, Bowen Liang^{***}, Hossein Ahmadian^{****}, Ming Yang^{*****}

^{*}The Ohio State University, ^{**}The Ohio State University, ^{***}The Ohio State University, ^{****}The Ohio State University, ^{*****}The Ohio State University

ABSTRACT

We present an integrated computational framework relying on a new microstructure reconstruction algorithm and a non-iterative mesh generation technique, named Conforming to Interface Structured Adaptive Mesh Refinement (CISAMR), for creating high fidelity FE models of composite materials. A NURBS-based reconstruction algorithm is implemented to synthesize the material microstructure by packing arbitrary shaped particles, morphologies of which are extracted from digital data such as micro-computed tomography images. A genetic algorithm (GA) based optimization framework is also employed to simulate the target statistical microstructural descriptors such as the size distribution, volume fraction, and spatial arrangement of particles. CISAMR is then employed to create a FE model of the material by transforming a structured mesh into a high quality conforming mesh with low element aspect ratios and a negligible discretization error. This non-iterative transformation is carried out by combining customized versions of four algorithms: h-adaptivity, r-adaptivity, face-swap, and sub-tetrahedralization. Compared to enriched methods such as extended FEM, CISAMR obviates the additional computational burden associated with evaluating enrichment functions and provides a higher accuracy for recovering the gradient field. Further, unlike conventional mesh generation algorithms such as the Delaunay triangulation, CISAMR can easily handle problems with highly complex geometries without the use of iterative smoothing or relaxation algorithms to improve the elements quality. In this work, we show the application of this integrated reconstruction-meshing framework for simulating the failure response a variety of heterogeneous materials, including particulate and fiber-reinforced composites, as well as non-woven entangled materials such as fiberglass insulation packs. Multiple sources of material and geometrical nonlinearity, including the damage, contact, and cohesive debonding are considered in each simulation.

Numerical Experiments for Improvement of Material Deposition during OLED Manufacturing Process Using Direct Simulation Monte Carlo

Ilyoup Sohn^{*}, Insoo Seo^{**}, Sanghyun Lee^{***}, Sean Jeong^{****}

^{*}Korea Institute of Science and Technology Information, ^{**}Metariver Technology Co., Ltd., ^{***}Metariver Technology Co., Ltd., ^{****}Metariver Technology Co., Ltd.

ABSTRACT

OLED (Organic Light Emitting Diode) has a high degree of brightness, high speed response, low power and high resolution in the current display industry, increasing the scope of applications from computers and mobile devices. In 2012, a small size panel, such as smartphones, has been applied to tablet PCs and laptops, and has been applied to conventional TV screens with existing LCD screens to become an important part of the display panel. To obtain high demand and price competitiveness of the recent OLED panels, the effective mass production is required and the deposition process of a key material on a large panel with high degree of uniformity is required to produce a large amount of sub-panels. The most important technique in the face-qualification process is to increase the uniformity of the thin film thickness during the deposition process. However, it is a time-consuming process to predict and monitor the behavior of the evaporation, motion and deposition on panel of organic material under low pressure, rarefied condition experimentally. Also, since the organic materials are generally expensive, there is clearly a limit to perform experiments repeatedly. Therefore, a novel numerical analysis is essential so that it can effectively explain the behavior of deposition material under low pressure environment. Most studies of OLEDs have been conducted primarily about the studies of thermo-chemical behavior of materials, and the numerical analysis of the entire transport behavior of deposited materials within the low-pressure chamber was not actively studied. Therefore, Direct Simulation Monte Carlo (DSMC) method, which effectively simulates the behavior of the low pressure gas dynamics, is performed to simulate the actual model of the deposition of the evaporated organic material, and it is evaluated how the numerical solution obtained from DSMC calculations works for prediction of the actual OLED deposition process and improvement of uniformity of deposited materials on the display panel. This work primarily deals with two parts, one is a validation of a novel DSMC simulation operating on GPU architecture by comparing with measurements and another is an improvement of material uniformity with respect to the change of nozzle diameter where organic material is evaporated. REFERENCES 1. E. K. Lee, J. of the Semiconductor & Display Equipment Technology 8, 37-42 (2009). 2. M. S. Ivanov and S. F. Gimelshein, Annu. Rev. Fluid Mech 30, 469-505 (1998). 3. I. Sohn, J. Kim, J. Bae and J. Lee, IEEE Trans. Plasma Phys. 44 1823-1833 (2016).

Homogenization of Hyperelastic Composites with Stochastic Interface Defects

Damian Sokolowski*, Marcin Kamiński**

*Chair of Structural Reliability, Faculty of Civil Engineering, Architecture and Environmental Engineering, Lodz University of Technology, **Chair of Structural Reliability, Faculty of Civil Engineering, Architecture and Environmental Engineering, Lodz University of Technology

ABSTRACT

The main objective of this study is determination of degradation of the homogenized hyperelastic particulate composites stiffness resulting from the random interface defects between its components – the reinforcement and the matrix. These are introduced by means of an interphase coming from an artificial smearing of the stochastic defects of spherical shape, whose volume is the input Gaussian random variable. Both, the interphase and the matrix are hyper-elastic materials, while the reinforcement remains in the linear elastic regime. Homogenization is done with the use of unitary cubic Representative Volume Element (RVE) and the computations of probabilistic stiffness properties are performed within the framework of the Iterative Stochastic Finite Element Method (ISFEM). The ISFEM is implemented using the generalized stochastic perturbation method, whereas Monte-Carlo simulation as well as the semi-analytical approach serve as reference solutions. The non-linear Finite Element Method serves here as a basis for the ISFEM; the uniform uniaxial and biaxial deformations of this RVE are modeled in the system ABAQUS. Computational experiments include the deterministic results, basic probabilistic moments and coefficients (expectations, coefficients of variations, skewness and kurtosis) of the strain energy density potential. Principal novelty in this study is stochastic approach to probabilistic interface defects in composite made of hyperelastic and linear elastic constituents exhibiting a very high contrast of the stiffness. [1] A. Clément, C. Soize, J. Yvonnet, Computational nonlinear stochastic homogenization using a nonconcurrent multiscale approach for hyperelastic heterogeneous microstructures analysis. *Int. J. Numer. Meth. Eng.* 91: 799–824, 2012. [2] M. Kamiński, *The Stochastic Perturbation Technique for Computational Mechanics*, Wiley, Chichester, 2013. [3] D. Sokolowski, M. Kamiński, Computational homogenization of carbon/polymer composites with stochastic interface defects. *Compos. Struct.* 183: 434-449, 2018. Acknowledgements: The first Author would like to acknowledge financial support of the grant 2016/21/N/ST8/01224 from the National Science Center in Cracow, Poland.

Residual Limb Deformation and Mechanical Properties using Digital Image Correlation and Finite Element Analysis

Dana Solav^{*}, Hugh Herr^{**}, Kevin Moerman^{***}

^{*}Massachusetts Institute of Technology, ^{**}Massachusetts Institute of Technology, ^{***}Massachusetts Institute of Technology

ABSTRACT

Local changes in the volume, shape, and mechanical properties of the residual limb can be caused by adjacent joint motion, muscle activation, hydration, atrophy, and more. These changes affect socket fit quality and might cause inefficient load distribution, discomfort, and dermatological problems. Analyzing these effects is an important step in considering their influence on socket fit, and in accounting for their contribution within the socket design process. In this study, a 360° 3D digital image correlation (3D-DIC) system was developed for the full-field shape and deformation measurements of the residuum. A multi-camera rig was designed for capturing synchronized image sets as well as 6DOF force and torque measurements from a hand-held indentation device. Custom camera calibration and data-processing procedures were specifically designed to transform image data into 3D point clouds, and automatically merge data obtained from multiple views into continuous surfaces. Moreover, a specially developed data-analysis procedure was applied for correlating pairs of largely deformed images of speckled surfaces, from which displacements, deformation gradients, and strains were calculated. The entire procedure was validated by analyzing the strains of synthetically deformed 3D objects. First, a reference finite element (FE) model of a speckled cylinder was created. Then, different cases of prescribed deformation were simulated (e.g. homogeneous uniaxial tension, radial inflation, axial torsion). The simulated deformed objects contain the deformed state of reference speckle pattern. The reference and deformed models were then manufactured using a multi-color 3D printer, and were analyzed using the imaging system in order to evaluate its accuracy. Furthermore, the residuum skin of five transtibial amputees were speckled using a custom speckling stamp, and imaged in different configurations, e.g. in various knee angles and muscle contraction levels, different times after doffing of the prosthetic socket, and at different times of the day. The images were processed to obtain the associated full-field displacements and strains. Characterization of the full-field deformations provided essential insights into the patterns and sources of the phenomena. Furthermore, local and subject-specific soft tissue mechanical properties were obtained by analyzing simultaneous surface deformation and force measurements during indentation. The experiment were simulated using a Finite Element model, and the hyperelastic and viscoelastic material parameters were determined by minimizing the error between the experimental and FE data. These results can be used to accurately describe the residuum's biomechanical behavior and interaction with the prosthetic socket. Consequently, prosthetic socket designs which take into account these effects can be considered.

Partitioned Coupling for Simulations of Flow-Induced Vibration Using Quasi-Newton and Fictitious-Mass Approaches

Jerome Solberg*

*Lawrence Livermore National Laboratory

ABSTRACT

Flow-induced vibration is a significant engineering challenge, especially in the design of heat exchangers. The desire for increased efficiency and decreased plant footprint and cost necessitate thinner walled tubes, longer spans, greater packing density, and higher flow velocities. All these features lead to greater fluid-structure interaction, with the concomitant need for improved analytical tools. One approach common within the industry is one-way-coupled analysis, where the flow pressure loads, varying in time, are applied to the structure. The response of the fluid to structural motions is approximated via “added mass” and “added damping” terms included in the structural equations. These terms are generally a function of the fluid and the geometry, and can be difficult to calculate even for simple geometries [1]. Forward coupled analyses have great utility within the design cycle, but at high enough velocities a fully-coupled approach is necessary. A staggered approach is desirable because it allows disparate fluid and structural solvers to be coupled together whilst treating each solver as a “black box” in relation to the other. Such schemes can be slow to converge (or even not converge at all), because at low stiffness values of the structural components correct accounting for the “added mass” term is critical, as the well-known analysis of Causin and his coworkers has demonstrated. Recently, a related concept, that of “fictitious mass/damping” has been used in the context of a fully-coupled analysis where the fluid and structure solvers are solved in a staggered scheme incorporating relaxation [2]. In this work, we examine approaches based initially on [2] where the added mass/damping terms are monitored based on the progress of the solution. Solution strategies based on Quasi-Newton methods [3] are also explored, and the results from both approaches used to calibrate one-way-coupled analyses. The advantages of each of these methodologies is compared, with a special focus on their ability to inform one-way-coupled analyses. This presentation is a follow-on to work presented at the 2017 USNCCM conference. [1] Wambsganss, M. W., Chen, S.S., and Jendrzejczyk, J.A., 1974, "Added mass and damping of a vibrating rod in confined viscous fluid" ANL-CT-75-08, Report, Argonne National Laboratory, Argonne, Illinois. [2] Baek, H. and Karniadakis, G. E., "A convergence study of a new partitioned fluid-structure interaction algorithm based on fictitious mass and damping," *Journal of Computational Physics*, 231 (2012), 629-652. [3] Bogaers, A. E. J., Kok, S., Reddy, B. D. and Franz, T. "Quasi-Newton methods for implicit black-box FSI coupling" *Comp. Meth. in Appl. Mech. and Eng.*, 279 (2014), 113-132.

Simulation of Selective Beam Melting Processes Using Multi-Time-Stepping

Dominic Soldner^{*}, Julia Mergheim^{**}, Paul Steinmann^{***}

^{*}Institute of Applied Mechanics - Friedrich-Alexander-Universität Erlangen-Nürnberg, ^{**}Institute of Applied Mechanics - Friedrich-Alexander-Universität Erlangen-Nürnberg, ^{***}Institute of Applied Mechanics - Friedrich-Alexander-Universität Erlangen-Nürnberg

ABSTRACT

Additive manufacturing (AM) processes usually allow for more complex part geometries. In the context of powder bed based AM they are realised via the fusion of powdered material in locally defined regions by means of e.g. a laser or electron beam. Parts are then build in a layer-by-layer fashion. Simulating these manufacturing processes from a macroscopic point of view usually leads to computational demanding models, due to different scales in space and time, highly non-linear material behaviour, and the modelling of the layer-wise building process, i.e. dynamic growth of the computational domain. Therefore, multiple numerical methods are combined, aiming towards a reduction of the computational cost. Besides adaptive mesh refinement and coarsening, line heat input models, where the scan path is integrated in time, are often employed to reduce computational expenses. Yet the time step size of the model is constrained by the chosen resolution of the beam path, which clearly limits the size of the problem under investigation. Within the present contribution we decompose the computational domain and carry out the computations on the rendered sub-domains with distinct time step sizes in order to account for the different requirements of the temporal resolution of the model. This allows to employ smaller time step sizes in areas that are exposed to the beam, while other regions are discretised with a coarser temporal resolution.

Simulation of Red Blood Cells in Stenosed Vessels Using a Coupled Shell-fluid Analysis Purely Based on the Smoothed Particle Hydrodynamics (SPH) Method

Meisam Soleimani^{*}, Michele Marino^{**}, Peter Wriggers^{***}

^{*}Institute of Continuum Mechanics, Leibniz Universität Hannover, Germany, ^{**}Institute of Continuum Mechanics, Leibniz Universität Hannover, Germany, ^{***}Institute of Continuum Mechanics, Leibniz Universität Hannover, Germany

ABSTRACT

In this work, a novel 3D numerical method has been developed to simulate the mechanical response of Red Blood Cells (RBC) in the stenosed vessels. If the rheological behavior of the RBC changes, for example due to some infections, it is reflected in its deformability when it passes through the microvessels. It can severely affect its proper function which is providing the oxygen and nutrient to the living cells. By virtue of the numerical modeling, one can examine and predict the possibility of microvessel blockage due to less deformability of an infected RBC. If the RBC is healthy, it can easily squeeze while passing a capillary although the dimension of the capillaries is less than the RBC dimensions, see [1]. But in case of being infected by a disease such as Malaria, the RBC may stiffen as much as ten times and this can seriously hamper its passage through the microvessels. In extreme cases where vessel occlusion happens, it may result in death or coma. From the computational point of view, RBC is assumed to be a thin shell-like structure filled with an interior fluid (cytoplasm) and being submerged in an exterior fluid (plasma). The model is entirely based on the smoothed particle hydrodynamics (SPH) method for both fluid and the shell structure. Since the problem technically falls into the category of Fluid-Solid-Interaction (FSI), the presence of a moving interface (moving boundary condition) poses serious challenges in establishing coupling between the well-known fluid solvers (which are mainly Eulerian and grid-based) and solid solvers (which are generally Lagrangian and mesh-based). Utilizing the SPH method for both fluid and solid phases, one can significantly benefit from the Lagrangian and mesh-less features of this method. For example, no re-meshing is needed and the mesh movement is inherently and automatically handled. Adopting a Total Lagrangian (TL) formulation for the shell in the realm of finite deflection, the presented computational tool is capable of handling relatively large displacements and rotations appearing in RBC mechanical response. This work is actually a new application and extension to an in-house numerical code developed by the authors, see [2]. [1] Tenghu Wu, James J. Feng, Simulation of malaria-infected red blood cells in microfluidic channels: Passage and blockage, Biomicrofluidics (2013). [2] Meisam Soleimani, Peter Wriggers, Numerical simulation and experimental validation of biofilm in a multi-physics framework using an SPH based method, Computational Mechanics (2016).

Boundary Element Frame Fields for Hexahedral Meshing

Justin Solomon*, Amir Vaxman**

*MIT, **Utrecht University

ABSTRACT

A key geometric task in numerical partial differential equations (PDE) is hexahedral meshing, which involves dividing a volumetric domain into cube-shaped cells on which a physical quantity is approximated. Desiderata for the quality of a hexahedral mesh include uniformity of the shapes of the cubic cells as well as conformation to the geometry of the outer boundary; the latter constraint invalidates trivial grid-based techniques and implies complex topological structures for the set of elements. A promising approach for hexahedral meshing under exploration in the computer graphics community involves the design of frame fields. These fields assign six orthogonal directions to each point in a volumetric domain, used to guide the orientations of the cube elements; a subsequent discrete pass extracts individual elements aligned to the computed field. While the field-guided approach has many commonalities with popular two-dimensional quadrilateral meshing techniques, however, subtle challenges preclude direct extension of these algorithms to 3D, most prominently the non-commutative structure of rotations in 3D space. Instead, alternative structure emerges in the volumetric case. Whereas two-dimensional surfaces are curved, the volume bounded by the outer surface of the domain is homogeneous, inheriting the flat Euclidean metric from surrounding space. This allows the application of boundary element methods (BEM), which are effective for solving differential equations based on only boundary integrals. In this talk, we will discuss recent applications of boundary element techniques to frame-guided hexahedral meshing. This approach alleviates dependence of hexahedral meshing on an input tetrahedral mesh of the domain, suggesting the possibility of hexahedral meshing directly from a boundary representation and removing a key source of instability in existing techniques. Empirically, these algorithms also appear to generate smooth singular structures desirable for meshing in practice. In addition to describing details of two BEM-based hexahedral meshing pipelines, we will identify several open problems in this space in need of expertise in the BEM community.

Image Based Computational and Experimental Study on HIFU Ablation Close to Major Blood Vessels

Maxim Solovchuk*, Tony Sheu**

*National Health Research Institutes, **National Taiwan University

ABSTRACT

High intensity focused ultrasound is a rapidly developing technology for many therapeutic applications, including treatment of cancer. In comparison with the conventional treatment modalities, such as open surgery, radio- and chemotherapy, HIFU has the advantages of non-invasion, non-ionization and fewer complications after treatment. Despite the methods' clinical potential, it still remains challenging to treat several organs: including liver, breast, brain tumors. Accurate computer simulations are necessary in order to expand the application range of focused ultrasound and to predict and prevent unwanted secondary effects. It is still remain quite challenging to ablate the tumor close to blood vessel. The mathematical model has been developed to predict the treatment outcome which couples nonlinear acoustic equations with relaxation effects being taken into account, bioheat equations in tissue and blood domains, and hydrodynamic equations with acoustic streaming effect taken into account. In order to validate the model in vivo experiments have been performed in minipig. Temperature elevation during focused ultrasound therapy has been measured. The predicted results have been compared with experimental data and good agreement has been obtained. Numerical simulations have been performed in a patient specific geometry. Numerical modeling of thermal and acoustic fields plays a key role in the treatment planning of focused ultrasound ablation. It was shown that numerical simulations can help to reduce the treatment time.

Fracture Simulation Using a Damage Model Considering Contact and Frictional Sliding

Yuto Soma^{*}, Mao Kurumatani^{**}

^{*}Department of Urban and Civil Engineering, Ibaraki University, ^{**}Department of Urban and Civil Engineering, Ibaraki University

ABSTRACT

We present a method for simulating behavior of crack propagation including contact and frictional sliding of fracture surface. The crack propagation is analyzed using a damage model based on fracture mechanics for quasi-brittle material considering fracture energy as fracture property of material. The contact and the frictional sliding are modeled on the local coordinate system in which a first coordinate axis corresponds the contact direction. The contact is determined using the strain of the contact direction. The contact behavior is represented by maintaining the stiffness of damaged element of contact direction. The sliding is determined using the Coulomb friction and the shear strain on the local coordinate system. The frictional sliding is represented using the shear stress which consider the frictional force. First, we explain the modeling of crack propagation including contact and frictional sliding of fracture surface, and show the formulation of the damage model considering the contact and the frictional sliding. Next, several numerical examples are presented to demonstrate the performance of the proposed method. Finally, we compare the numerical results with the experimental results of direct shear tests to demonstrate the validity of the proposed method.

Computational Modeling of 3D Printed Parts for Analysis of Constitutive Behavior of Material

Madhukar Somireddy*, Aleksander Czekanski**

*York University, **York University

ABSTRACT

Abstract: Additive manufacturing techniques are gaining popularity in recent times and have been used for printing parts in industries such as aerospace, mechanical, electronics and biomedical [1]. These techniques fabricate a three-dimensional (3D) part by layer upon layer deposition of the material. In addition, fabrication of a complex geometry part is not a limitation unlike the subtractive machining methods. However, one of the main challenges with these latest fabrication methods is the anisotropy in the material properties of the printed parts [2]. Although isotropic material is used for printing the part, the final material properties are not same as initial. This change in the material properties is due to change in the mesostructure that is happening during the layer upon layer deposition of the material while printing the part. Printed parts from one of the AM techniques, fused deposition modeling, are considered here for the study. The present work addresses estimation of the final material properties of the printed parts using computational homogenization [3] and their constitutive material behavior. Then the failure analysis of printed parts based on fracture mechanics is studied. The investigation revealed that mechanical behavior of the printed parts is same as that of laminated composite structures and further, the behavior is influenced by their build orientation and thickness. Tensile and bending experimental investigation on printed parts revealed that the crack is initiated at interface of the fibers and then propagated across layer. The propagation of the crack occurs along the voids which exist at interface of the layers. The failure is then followed in the load carrying fibers of layers of the part. Potential damage modes such as debonding, fiber breaking in the 3D printed parts subject to tension and bending loads are identified for computational failure analysis. Then the procedure for computational modeling of printed parts for failure analysis using Abaqus is discussed. 1. Guo, N. and Leu, M.C., 2013. Additive manufacturing: technology, applications and research needs. *Frontiers of Mechanical Engineering*, 8(3), pp.215-243. 2. Parandoush, P. and Lin, D., 2017. A review on additive manufacturing of polymer-fiber composites. *Composite Structures*, 182, pp.36-53. 3. Hollister, S.J. and Kikuchi, N., 1992. A comparison of homogenization and standard mechanics analyses for periodic porous composites. *Computational Mechanics*, 10(2), pp.73-95.

Discrete Element Modeling and Simulation of Atomized and Spray Dried Granules of Metal Powder

Kwon Joong Son*

*Hongik University

ABSTRACT

This work presents the modeling and simulation of the dynamics of atomized and spray dried granules of metal powder using the discrete element method. The use of granules of metal powder in a powder metallurgy process improves the mechanical properties such as the density and tensile strength of sintered products compared to those from the conventional powder metallurgy or metal injection molding processes. Such an improvement can be achieved mainly due to the granule's better flowability during die filling and compactibility during die pressing than non-granulated fine powder. Despite many advantages from manufacturing aspects such as a high sintered density and a low sintering temperature, the granulated powders have not yet been widely used in powder metallurgy industries because of their relatively low material productivity and high cost. To increase the yield rate of the metal powder granules, further process optimizations are required in the rotary disc atomization and spray drying processes. The discrete element method (DEM) can be used as a computational tool to improve the granulation and drying of fine metal powders. DEM can compute particle-to-structure and particle-to-particle interactions with consideration of contact, impact, friction, bonding, and cohesion. Therefore, it can numerically investigate the effect of granule size, inter-particular cohesion and bonding, inter-granular adhesion, and spraying rate on the dynamics of granulated powders. This work particularly focuses on three types of discrete element simulations: (1) spraying of granules from the rotary disc atomizer (2) collision of a single granule with the drying chamber wall, and (3) discharging or clogging of granules at the spray dryer outlet. This computational work may contribute to the process optimizations in the metal powder granulation for powder metallurgy purposes.

DangShin: Intelligent Path Recommendation System for 3-Cusion Billiard Game

Kyuho Son^{*}, Dongsoo Han^{**}

^{*}Korea Advanced Institute of Science and Technology, ^{**}Korea Advanced Institute of Science and Technology

ABSTRACT

With the advances of computer vision techniques, many intelligent services continue to come out in various application domains utilizing the vision techniques. 3-Cusion billiard game is one of such applications. This paper proposes an intelligent path recommendation system for 3-cusion billiard game. The system is named DangShin. The system recommends successful play scenes in the real world billiard game for a given topology, which is the positions of three balls on a billiard table. To recommend the scenes, a topology is recognized with a picture of the table captured by a camera installed on the ceiling above the table. Then video scenes of successful hit with a similar topology are searched in a scene context database. Scene context is a bundle of scene data needed for the service. Initial topology and count of bounds to cushions are the examples. The system consists of a ball localizer, a position refiner, a context analyzer and a scene search engine. The ball localizer recognizes the positions of balls in each frame of a scene. The position refiner corrects time-series records of positions generated by the ball localizer based on background knowledge such as physics and billiard play rules. The context analyzer extracts scene contexts from the time-series ball positions refined by the position refiner. The scene search engine searches video scenes appropriate for recommendation in the scene context database. The system achieved an acceptable accuracy in the analysis of scene contexts for a practical service.

On the Equivalence between the S-method, XFEM and Ply-by-Ply Discretization for Delamination Analyses of Laminated Composites Using Shell Elements

Timothy Sonderman^{*}, Yang Jiao^{**}, Jacob Fish^{***}

^{*}Columbia University, ^{**}Columbia University, ^{***}Columbia University

ABSTRACT

Two hierarchical approaches, the s-method and the extended finite element method (XFEM), are compared to the classical ply-by-ply discretization approach in terms of their effectiveness in modeling delamination in laminated composites using shell elements. In the two hierarchical approaches, a smooth approximation field based on the mesh made of laminated shell elements is first introduced to resolve a delamination-free response of the composite structure. The initiation and propagation of delamination is modeled by either superposition of element patches (s-method) or by enrichment functions (XFEM). A cohesive zone model is employed to model decohesion at the inter-ply interfaces. In terms of representing strong discontinuities, the two hierarchical methods have been shown to represent an identical approximation space as the classical ply-by-ply discretization approach, even though the s-method gives rise to sparser matrix structure. In terms of representing weak discontinuities, the s-method has been shown to be equivalent to the ply-by-ply discretization approach and provides a seamless transition from weak to strong discontinuity.

Elastoplastic Analysis Using Scaled Boundary Finite Element Method

Chongmin Song*, Lei Liu**

*University of New South Wales, **University of New South Wales

ABSTRACT

The scaled boundary finite element method has been employed to formulate polygon and polyhedral elements (Ooi, et al. 2014; Talebi, et al. 2016). In complementary with this type of polygon and polyhedral elements, a quadtree/octree algorithm has been developed. Using these two developments, fully automatic stress analyses are performed on geometric models provided in CAD, digital image and STL formats (Talebi, et al. 2016; Saputra, et al. 2017; Liu et al. 2017). This study extends the technique for 2D elastoplastic analysis in Ooi, et al. (2014) to 3D. A novel, simple and efficient scaled boundary elastoplastic formulation with stabilisation is developed. In this formulation, the return-mapping calculation is only required to be performed at a single point in a polygon/polyhedral element, which improves the computational efficiency of the elastoplastic analysis and facilitates the implementation. Numerical examples are presented to validate the proposed technique and to demonstrate its applications. References Liu, Y., Saputra, A. and Song, Ch. (2017) "Automatic polyhedral mesh generation and scaled boundary finite element analysis of STL models", *Computer Methods in Applied Mechanics and Engineering*, Vol. 313, 106–132. Ooi, E. T., Song, Ch. and Tin-Loi, F. (2014) "A scaled boundary polygon formulation for elasto-plastic analyses", *Computer Methods in Applied Mechanics and Engineering*, Vol. 268, 905–937. Saputra, A., Talebi, H., Tran, D., Birk, C. and Song, Ch. (2017) "Automatic image-based stress analysis by the scaled boundary finite element method", *International Journal for Numerical Methods in Engineering*, Vol. 109, 697–738. Talebi, H., Saputra, A. and Song, Ch. (2016) "Stress analysis of 3D complex geometries using the scaled boundary polyhedral finite elements", *Computational Mechanics*, Vol. 58, 697–715.

Molecular Dynamics Study on Temperature-dependent Screw Dislocation Behavior in BCC Metal Nanopillars

Gyuho Song^{*}, Seok-Woo Lee^{**}

^{*}University of Connecticut, ^{**}University of Connecticut

ABSTRACT

Recent studies on body-centered-cubic (bcc) metal nanopillars revealed that dislocation are more easily multiplied in bcc structure than face-centered-cubic (fcc) structure. Computational studies in both bcc and fcc nanopillars suggested that cross-slip, which occurs at the free surface, plays an important role in dislocation multiplication at small length scales. Particularly for bcc structure, the relative difference in mobility between screw and edge dislocation is critical to induce the surface-controlled dislocation multiplication. The dislocation mobility of bcc metal is strongly dependent of intrinsic lattice resistance, which is a function of temperature, and the surface controlled multiplication behavior should also be dependent of temperature. In this study, therefore, we investigated how a single pure screw dislocation is multiplied through surface-controlled multiplication in a bcc nanopillars at a different stress, temperature (10~650 K), and nanopillars size by using constant stress molecular dynamics simulation. We chose [0 0 1]-oriented niobium and molybdenum nanopillars due to their different intrinsic lattice resistances. We created a single pure screw dislocation in a nanopillar, and applied the constant uni-axial compressive stress to drive the dislocation to move. We characterized the critical stress of dislocation multiplication as a function temperature and nanopillars size. Our results revealed the conservative decrease and increase in critical stress of multiplication with temperature, implying that surface-controlled multiplication is dependent of an absolute value of dislocation mobility as well as the relative difference in mobility between screw and edge dislocation. Also, we found that multiplication behavior has a distinct dependence on materials while being affected by the nanopillars size and the temperature. Our simulation results will be carefully analyzed to provide rationale for experimental results in literature. dislocation-free bcc nanopillars and dislocation-containing nanopillars at cryogenic temperatures. We will discuss how surface-controlled multiplication affects general dislocation multiplication behavior and strain burst size of bcc nanopillar. Our study will be able to bridge between experiment and computation on dislocation multiplication behavior in bcc structure at the nanometer scale.

Computational Design of Complex Ceramic Oxides from First-principles Calculations

Jun Song^{*}, Guoqiang Lan^{**}

^{*}McGill University, ^{**}McGill University

ABSTRACT

Complex ceramic oxides have found great use in aerospace applications, particularly on thermal insulation to enhance energy efficiency of turbine engines. However, the design and exploration of such materials is a daunting task given their complex structures and composition variation. In this talk, I will show that first-principles density functional theory (DFT) calculations, augmented by the Hubbard U correction, can serve as an effective computational route to accelerate the design and exploration of complex ceramic oxides. Focusing on rare-earth (RE) pyrochlores for thermal barrier coatings (TBCs), we performed a comprehensive set of DFT+U calculations, where the Hubbard U values were determined using the linear response approach. We show that the essential material properties, such as thermal conductivity and coefficient of thermal expansion, can be accurately predicted by first-principles calculations. With the first-principles based computational framework established, a design example of enhancing the performance of RE pyrochlores through alloying is then demonstrated.

The Shifted Boundary Method: A New Approach to Embedded Domain Computations of Waves and Shallow Water Flows

Ting Song^{*}, Alex Main^{**}, Guglielmo Scovazzi^{***}, Mario Ricchiuto^{****}

^{*}Duke University, ^{**}Duke University, ^{***}Duke University, ^{****}INRIA Bordeaux--Sud-Ouest

ABSTRACT

We present a new embedded boundary method for wave equation problems in time domain. Embedded boundary methods obviate the need for continual re-meshing in many applications involving rapid prototyping and design. Unfortunately, many finite element embedded boundary methods for incompressible flow are also difficult to implement due to the need to perform complex cell cutting operations at boundaries, and the consequences that these operations may have on the overall conditioning of the ensuing algebraic problems. We present a new, stable, and simple embedded boundary method, which we call “shifted boundary method” (SBM), that eliminates the need to perform cell cutting. Boundary conditions are imposed on a surrogate discrete boundary, lying on the interior of the true boundary interface. We then construct appropriate field extension operators, with the purpose of preserving accuracy when imposing the boundary conditions. We demonstrate the performance of the proposed method in simulations of problems in acoustics and shallow water flows.

A Material Point Method for Cavitating-fluid Flows

Yan Song^{*}, Xiong Zhang^{**}

^{*}School of Aerospace Engineering, Tsinghua University, ^{**}School of Aerospace Engineering, Tsinghua University

ABSTRACT

The material point method (MPM) is an effective way to simulate the fluid-structure coupling problem with large deformations, which combines the advantages of both Lagrangian method and Eulerian method. In the MPM, the history-dependent properties are carried by particles and the equations of motion are solved on background grid which is remeshed every time step. However, one of the major challenges of the MPM is the low rate of convergence and accuracy. A great improvement has been made by Sulsky and Gong in 2016, who improved the MPM (IMPM) based on the moving least squares (MLS) and Gaussian integration. This scheme eliminates the crossing errors and reaches second-order accuracy. The simulation of cavitating-fluid flows is an important aspect of marine-vehicle simulations. Because of the physical feature that the density changes severely across the fluid-vapor interfaces, the volume of a particle in the MPM may grow over than that of a grid cell, which causes the numerical fracture. On the other hand, the IMPM replaces material point integration in MPM by Gaussian integration, thus the particles only serve as the points where the physical properties such as the density, the pressure and the volume ratio of vapor in cavitating-fluid flows are indicated. In this paper, we propose a particle-reassignment algorithm which regenerates particles in a grid cell where the original particles are overcrowded or undercrowded based on the IMPM. This method can deal with the problem caused by the high density gradient in the cavitation region. Moreover, a simply and efficient method to impose the inflow and outflow boundary condition is proposed in the same way. We also formulate a MPM scheme to simulation cavitating-fluid flows. Numerical examples are also given to validate the proposed method.

A Localized Interface Scheme for Connecting Dissimilarly Partitioned Systems

Yeo-UI Song^{*}, K. C. Park^{**}, Sung-Kie Youn^{***}

^{*}Korea Hydro & Nuclear Power, ^{**}University of Colorado at Boulder, ^{***}KAIST

ABSTRACT

A new interface method for dissimilar interfaces is presented. Interface schemes in computational mechanics are widely used to handle large scaled systems effectively. Large scaled systems are partitioned into several subsystems which have independent meshes for individual target accuracy. When subsystems have flat interfaces, it is easy to control the interface constraint. However, the subsystems usually contain curved interfaces. These curved interfaces make gaps at the shared boundaries due to different mesh sizes. Various studies exist for the treatment of curved interfaces but they employ complicated projection procedures for the dissimilar meshes. Especially in arbitrary three-dimensional curved interfaces, complicated numerical integration is required. Present method introduces a gap element having zero strain condition. Localized Lagrange multiplier method is used to enforce the displacement compatibility. Several numerical examples are presented for the verification of the proposed method.

Modeling of Ice Fragmentations by Impact Based on Nonordinary State-Based Peridynamics

Ying Song^{*}, Shaofan Li^{**}, Zhuang Kang^{***}, Aman Zhang^{****}, Shaofei Ren^{*****}

^{*}College of Shipbuilding Engineering, Harbin Engineering University, Harbin 150001, China, ^{**}Department of Civil and Environmental Engineering, University of California, Berkeley, CA 94720, USA, ^{***}College of Shipbuilding Engineering, Harbin Engineering University, Harbin 150001, China, ^{****}College of Shipbuilding Engineering, Harbin Engineering University, Harbin 150001, China, ^{*****}College of Shipbuilding Engineering, Harbin Engineering University, Harbin 150001, China

ABSTRACT

Ice-structure interaction is currently one of the hot topic in engineering fields and has not yet been addressed. Traditional numerical methods derived from classical continuum mechanics have difficulties in resolving discontinuous problems of ice fragmentations. In the present paper, a non-ordinary state-based peridynamics formulation has been developed to simulate the behavior of the ice under impact loads applied by a rigid ball. Ice is assumed as an elastic-brittle materials and simulated by the modified Drucker-Prager plasticity model, the failure criterion of ice is defined based on fracture toughness. Furthermore, a continuous contact algorithm has been developed to detect the contact area between the rigid ball and ice particles. It is shown that numerical results are in good agreement with experimental data from open literatures, the behavior of ice under the impact loads can be assigned to four fragmentation classes, cratering, erosion, disruption, and total fragmentation, and the proposed peridynamics model can capture the detail fragmentation features of ice under low velocity impact loads.

MULTI-LINK VISCOELASTIC CONTACT MODEL FOR NUMERICAL SIMULATION OF SEISMIC POUNDING BETWEEN ADJACENT STRUCTURES

STEFANO SORACE^{*} and GLORIA TERENCE[†]

^{*} Polytechnic Department of Engineering and Architecture, University of Udine
Via delle Scienze 206, 33100
Udine, Italy
e-mail: stefano.sorace@uniud.it

[†] Department of Civil and Environmental Engineering, University of Florence
Via S. Marta 3, 50139
Florence, Italy
e-mail: gloria.terenzi@unifi.it

Key words: Seismic Pounding, Viscoelastic Analytical Model, Finite Element Contact Model.

Abstract. A special multi-link viscoelastic (MLV) finite element contact model is devised and calibrated in this study to reproduce Jankowski's non-linear viscoelastic analytical model in time-history analyses including the effects of seismic pounding. The MLV model is constituted by an in-series assemblage of n linear dampers and n associated in-parallel linear springs. Its response is based on the sequential activation and disconnection of the dampers, following the variation of the time-variable interpenetration depth $\delta(t)$ between the colliding structures. This way, the resulting equivalent damping coefficient $c(t)$ of the assemblage becomes a function of $\delta(t)$, and thus the relation between $c(t)$ and $\delta(t)$ can be easily reproduced in piece-wise linear form in the finite element computation. Detailed information on the practical implementation of the MLV model in time-history seismic analyses, as well as on the calibration of relevant geometrical and mechanical parameters, are offered in the paper, based on the results of a simple case study, represented by a couple of one-storey colliding reinforced concrete frames.

1 INTRODUCTION

Earthquake-induced pounding between closely spaced buildings is one of the highest sources of seismic vulnerability, as it can cause severe damage to non-structural and structural members, and even contribute to structural collapse. Pounding impacts derive from the out-of-phase vibrational response of the colliding structures induced by their different dynamic characteristics, when their separation joints at rest are not wide enough to accommodate the maximum relative displacements.

In order to assess the effects of pounding, a special multi-link viscoelastic (MLV) finite element contact model is devised and calibrated in this study to reproduce the classical Jankowski's non-linear viscoelastic analytical model [1]. Indeed, the damping coefficient of the latter is defined as a non-linear function of time, and thus it cannot be directly implemented in commercial structural calculus programs, because the damping coefficient of the damper elements included in their basic libraries is assumed to be a constant. A detailed description of the MLV model and information on its practical implementation in time-history seismic analyses, as well as on the calibration of relevant geometrical and mechanical parameters, are offered in the next Sections.

2 FINITE ELEMENT IMPACT MODEL FOR POUNDING ANALYSIS

Jankowski's model [1] (lower image in Figure 1) represents a substantial enhancement of the traditional Kelvin-Voigt rheological scheme[2] (upper image in Figure 1), given by in-parallel combination of an elastic spring with k_1 stiffness, which is capable of transmitting impact forces, and a linear viscous damper with damping coefficient c_1 , simulating the impact-related energy dissipation. The contact element becomes activated when the width of the separation gap at rest (gap_r in Figure 1) between the impacting structures—idealized as rigid masses, indicated with symbols m_1 and m_2 in Figure 1—shrinks. In Jankowski's model, a second gap element (gap_c in Figure 1) with initial width equal to zero is incorporated in series with the damper, so that the latter is activated at the approaching stage of the colliding structures only, rather than in the rebound phase too (i.e. when the relative velocity between m_1 and m_2 becomes negative). Moreover, an additional elastic spring with stiffness k_d is placed in parallel with the damper, so as to drive it to its pre-impact position before a new contact occurs.

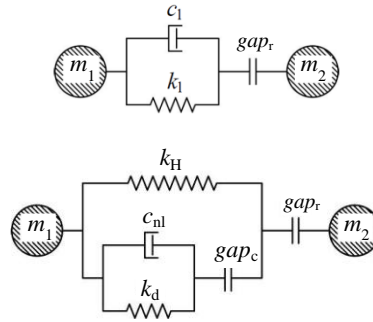


Figure 1. Rheological scheme of Kelvin-Voigt linear viscoelastic and Jankowski non-linear viscoelastic impact models

Further improvements of Jankowski's model as opposed to Kelvin-Voigt basic scheme consist in assuming non-linear behavioural characteristics both for the force-transmitting spring and the damper, consistently with the results of experimental studies carried out on

several different material and geometrical configurations of the impacting masses [3]. The response of the force-transmitting spring is governed by Hertz analytical law, which expresses the spring contact force, F_s , as a n -power law of the time-varying interpenetration depth $\delta(t)$ between the colliding members, with

$$\delta(t) = u_1(t) - u_2(t) - w_r \quad (1)$$

where $u_1(t)$, $u_2(t)$ are the displacements of the first and second mass, respectively, both functions of time, t , and w_r is the *gap_r* width. For pounding analyses, the n exponent in the Hertz-type expression of F_s is fixed at 3/2 [1,4], that is

$$F_s(t) = \beta \cdot \delta(t)^{3/2} \quad (2)$$

where β is the impact stiffness parameter of the spring, which has the dimensions of a force divided by a 3/2-power law of displacement. Based on this assumption, k_H stiffness of the force-transmitting spring is regarded as an “effective impact stiffness”, given by the following function of $\delta(t)$ [1]:

$$k_H(t) = \beta \cdot \sqrt{\delta(t)} \quad (3)$$

For impacting R/C frame structures β is normally set as equal to $2.75 \cdot 10^6 \text{ kN/m}^{3/2}$ [1]. The damping coefficient of the non-linear damper, c_{nl} , is defined as a non-linear function of $\delta(t)$ too, according to the following relation [1]:

$$c_{nl}(t) = 2\zeta \sqrt{\beta \sqrt{\delta(t)} \frac{m_1 m_2}{m_1 + m_2}} \quad (4)$$

where ζ is the impact damping ratio, expressed as [1]:

$$\zeta = \frac{9\sqrt{5}}{2} \frac{1 - e^2}{e[9\pi - 16] + 16} \quad (5)$$

In relation (5) e is the coefficient of restitution, which accounts for the energy dissipation related to the damage effects occurring during collision, defined as follows [3]:

$$e = \frac{v_1'(t) - v_2'(t)}{v_1(t) - v_2(t)} \quad (6)$$

being $v_1(t)$, $v_2(t)$ the approaching velocities of the two structures, and $v_1'(t)$, $v_2'(t)$ the post-impact (restitution) velocities. For concrete-to-concrete impact, a value of 0.65 is basically adopted for e [1,4]. Consequently, the impact ratio ζ given by (5) is equal to 0.373. Based on relations (1) through (5), the total viscoelastic non-linear contact force, F_t , results to be:

$$F_t = \beta \cdot \delta(t)^{\frac{3}{2}} + c_{nl}(t) \cdot \dot{\delta}(t) \quad (7a)$$

for $\delta(t) > 0$ and $\dot{\delta}(t) > 0$ (contact-approach phase)

$$F_t(t) = \beta \cdot \delta(t)^{3/2} \quad (7b)$$

for $\delta(t) > 0$ and $\dot{\delta}(t) \leq 0$ (contact-restitution phase)

$$F_t(t) = 0 \quad (7b)$$

for $\delta(t) \leq 0$ (no contact) with $\dot{\delta}(t)$ = interpenetration velocity.

As observed in the Introduction, the damper elements currently incorporated in the libraries of commercial finite element programs, like SAP2000NL software [6] used herein, are characterized by constant damping coefficients. Therefore, time-dependent expressions like (4) can only be reproduced by “equivalent” finite element modelling strategies, such as the above-mentioned MLV model, constituted by an in-series assemblage of m linear dampers and m associated in-parallel linear springs. The sequential activation (approaching stage) and disconnection (restitution stage) of dampers allows reproducing the time-history evolution of c_{nl} .

A numerical performance evaluation study of the MLV model carried out at previous stages of this research [7,8] highlighted that the 5-link version in Figure 2 offers the best balance between simulation capacities, very similar for m values greater than 5 (slightly poorer for $m=3$ and $m=4$), and computational effort, processing times being approximately an exponential function of the number of damper+gap+spring elements.

Dampers are denoted by relevant damping coefficients c_i (with $i=1,...,5$ in this case, and $i=1,...,m$ in general) in the model scheme drawn in Figure 2. The activation of each damper is governed by a gap (named gap_{ci} in Figure 2), to which a prefixed opening, w_i , is assigned. As the gap closes, the damper starts to react, adding its response to the already activated dampers. Similarly to the non-linear damper of the rheological scheme in Jankowski’s model in Figure 1, each element is combined in-parallel with a linear spring, with stiffness k_{di} , which drives it to its pre-impact position. The remaining components of the assembly (non-linear Hertzian spring, whose stiffness is denoted by symbol k_{HFE} in the finite element assembly, and the separation gap at rest gap_r in Figure 2) are the same as in Jankowski’s rheological scheme. For the practical implementation of the MLV model, the damping coefficients c_i of the dampers, the openings w_i of relevant gap elements gap_{ci} and the stiffness k_{di} of the linear springs must be specified. To this aim, the first step consists in tentatively predicting the maximum interpenetration depth, δ_{max} , expected from the time-history analysis. Then, the tentatively fixed value of δ_{max} , $\delta_{max,t}$, is discretized in m equal intervals with width $\Delta=\delta_{max,t}/m$, at the end of each one of which a new damper is activated. Therefore, the gap openings are obtained by the following rule: $w_i=(i-1) \cdot \Delta$. This holds $w_1=0$, consistently with the fact that the

first damper must be immediately activated when impact begins. Moreover, $w_m=(m-1) \cdot \Delta$, i.e. the m -th damper of the assembly is activated at the last step of the closing sequence of the gap elements.

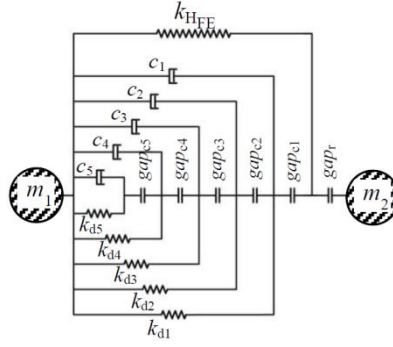


Figure 2. 5-link version of the MLV finite element model

Concerning the damping coefficients c_i , in the approaching phase the contribution of each damper is numerically added to the contribution of the already activated dampers, following the progressive increase in $\delta(t)$. As a result, each c_i value is assigned in such a way that the resulting “summed” damping coefficient of all the elements activated for a given interpenetration depth $\bar{\delta}$, $c_s(\bar{\delta})$, satisfactorily matches the corresponding analytical value $c_{nl}(\bar{\delta})$ calculated by (4). Then, the fitting process of c_s to c_{nl} is carried out by fixing the value of the “summed” damping coefficient reached at the activation of the i -th damper, c_{si} , as equal to the c_{nl} coefficient calculated by (4) for the δ value situated in the middle of the interval of activation of the same damper, δ_i , i.e. $c_{si} = c_{nl}(\delta_i)$, with $\delta_i = w_i + \frac{\Delta}{2}$. Finally, c_i is obtained as

follows: $c_i = c_{si} - \sum_{j=1}^{i-1} c_j$, i.e. by subtracting from c_{si} the sum of the damping coefficients of the

dampers activated before the i -th damper. This criterion for the selection of w_i and c_i parameters is iterative, as it starts from a reasonable $\delta_{max,t}$ estimate—as suggested in Section 3—and terminates when the δ_{max} value resulting from the time-history analysis converges to a constant.

The k_{di} stiffness values of the linear springs are calibrated, according to a trial-and-error process too, so as to help the springs disconnect the dampers completely (i.e. reopen the relevant gaps) in the restitution phase, before a new contact occurs. The analyses carried out on several R/C frames with different geometrical dimensions and number of stories suggest adopting for the k_{di} values the same mutual proportions as among the c_i coefficients calculated according to the criterion formulated above. This way, the tentative choice of the spring stiffness values is reduced only to k_{d1} . For several numerical test multi-storey R/C structures

examined in this study, k_{d1} resulted to vary from about 1000 kN/m to about 5000 kN/m. Thus, to properly start the iterative search of a set of k_{di} values, it is recommended to select k_{d1} within this range, and then to impose the relations: $k_{d2}=(c_2/c_1) \cdot k_{d1}$; $k_{d3}=(c_3/c_2) \cdot k_{d2}$; ...; $k_{dm}=(c_m/c_{m-1}) \cdot k_{dm-1}$, for k_{d2} through k_{dm} .

In addition to the mechanical parameters of the model discussed above, an internal elastic spring is assigned by default to the gaps and dampers constituting the MLV assembly, with the aim of preventing local unstable conditions in the solution of the equations governing the computational problem. Therefore, although such a spring has no direct physical meaning, the influence of relevant stiffness on the numerical performance of the model is evaluated in the next Section, along with the c_i , w_i and k_i parameters selected by the proposed criteria, for a simple numerical test pounding case study.

3 NUMERICAL TEST CASE STUDY FOR CALIBRATION OF MLV MODEL PARAMETERS

The two one-storey/one-span R/C frames sketched in Figure 3 are considered in this Section as pounding-prone numerical test structures. Both frames are square-shaped, with height and span of 5000 mm, and are situated at a 20 mm distance. Columns and beams were designed for gravitational loads only, so as to simulate a typical condition of most pre-normative pounding-prone R/C structures.

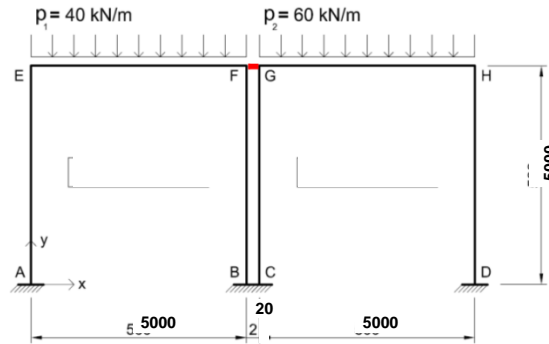


Figure 3. Geometrical (dimension in millimeters) and gravitational load scheme of the numerical test frames

The four columns and two beams have (350×350) mm×mm mutual cross sections, reinforced with 3 Φ 16 bars per side, and are made of concrete with cylindrical compressive strength equal to 25 MPa. The p_1 and p_2 uniformly distributed gravitational loads assigned to the beams, corresponding to the dead and live loads transferred by relevant floors (with greater tributary area for frame 2), are equal to 40 kN/m and 60 kN/m, respectively. The impacting masses, given by the contributions of p_1 and p_2 plus the weight of the beams, are: $m_1=21,9$ t and $m_2=32,1$ t. Time-history analyses were carried out by assuming a set of seven artificial ground motions as inputs, generated from the normative pseudo-acceleration elastic response

spectrum at 5% equivalent linear viscous damping ratio displayed in Figure 4, for two different earthquake levels (BDE and MCE, with peak ground accelerations of 0.234 g and 0.295 g, respectively, with g =acceleration of gravity). The response spectra of the two sets of ground motions are superimposed to relevant normative spectra in the two graphs of Figure 4.

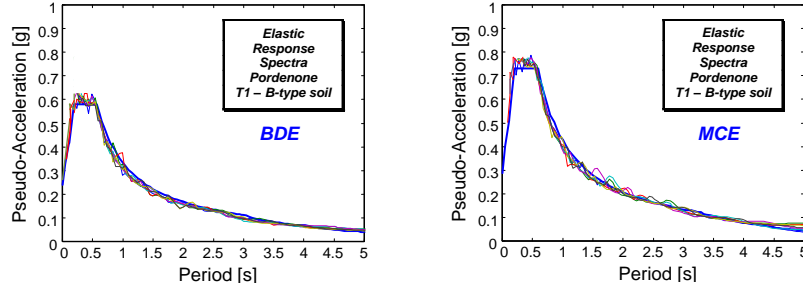


Figure 4. Reference normative pseudo-acceleration elastic response spectra, and superimposed spectra of the generated artificial ground motions

Beams and columns were modelled as elastic “frame”-type elements. The solution of the equations of motion was carried out with the Fast Non-linear Analysis method [9], implemented in SAP2000NL software for dynamic problems with a limited number of non-linear degrees-of-freedom.

The 5-link version of the MLV contact model was adopted, according with the observations in Section 2. The first step in the implementation of the model consists in fixing the gap openings w_i . These values are related to the tentatively predicted value of the maximum interpenetration depth δ_{\max} that will be achieved in the time-history analysis of the colliding structures. A numerical enquiry carried out on low-to-medium rise R/C frame structures with total heights up to 25 m showed δ_{\max} values always ranging between 2.5×10^{-4} and 5×10^{-4} times the height of the top contacting spots of the structures, h_{tcs} , for medium-to-severe input earthquake levels (i.e. for peak ground acceleration values of 0.2–0.3 g) [7,8]. Then, the tentative value of δ_{\max} , $\delta_{\max,t}$, can be selected within this range, e.g. as the mean value of it. For the considered numerical test case study, the peak ground acceleration for the BDE-scaled seismic action, equal to 0.234 g, is included in the reference PGA range above. Consistently, by considering that the height of the contact joints is equal to 5000 mm, $\delta_{\max,t}$ can be located in the range $[2.5 \times 10^{-4} \times 5000 = 1.25 \text{ mm} - 5 \times 10^{-4} \times 5000 = 2.5 \text{ mm}]$. The mean value is equal to 1.88 mm, which can be rounded to $\delta_{\max,t} = 2 \text{ mm}$ for this preliminary estimation. Therefore, for $m=5$, $\Delta = \delta_{\max,t}/m = 0.4 \text{ mm}$, which holds: $w_1=0$, $w_2=0.4 \text{ mm}$, $w_3=0.8 \text{ mm}$, $w_4=1.2 \text{ mm}$ and

$w_5=1.6 \text{ mm}$. Based on these w_i estimates, the following $\delta_i = w_i + \frac{\Delta}{2}$ mean interpenetration

depths are obtained for the five intervals: $\delta_1=0.2 \text{ mm}$; $\delta_2=0.6 \text{ mm}$; $\delta_3=1 \text{ mm}$; $\delta_4=1.4 \text{ mm}$; and $\delta_5=1.8 \text{ mm}$. The “summed” damping coefficients $c_{si} = c_{ni}(\delta_i)$ calculated by substituting in (4)

the standard ξ and β values discussed in Section 2 ($\xi=0.373$ and $\beta=2.75 \cdot 10^6 \text{ kN/m}^{3/2}$) and the m_1 , m_2 , and δ_1 through δ_5 values computed for this case study amount to: $c_{s1}=531 \text{ kN}\cdot\text{s/m}$; $c_{s2}=699 \text{ kN}\cdot\text{s/m}$; $c_{s3}=794 \text{ kN}\cdot\text{s/m}$; $c_{s4}=864 \text{ kN}\cdot\text{s/m}$; and $c_{s5}=920 \text{ kN}\cdot\text{s/m}$. Hence, the following

$c_i = c_{si} - \sum_{j=1}^{i-1} c_j$ damping coefficients of the five dampers are obtained: $c_1=c_{s1}=531 \text{ kN}\cdot\text{s/m}$;

$c_2=c_{s2}-c_1=168 \text{ kN}\cdot\text{s/m}$; $c_3=c_{s3}-c_1-c_2=95 \text{ kN}\cdot\text{s/m}$; $c_4=c_{s4}-c_1-c_2-c_3=70 \text{ kN}\cdot\text{s/m}$; and $c_5=c_{s5}-c_1-c_2-c_3-c_4=56 \text{ kN}\cdot\text{s/m}$.

The mean value of the [1000–5000] kN/m range indicated in Section 2 was adopted as tentative choice of the stiffness of the first damper-disconnecting spring, i.e. $k_{d1}=3000 \text{ kN/m}$.

By applying the relations reported in the same Section, the following tentative stiffness rounded values of the remaining springs are derived: $k_{d2}=(c_2/c_1) \cdot k_{d1}=950 \text{ kN/m}$;

$k_{d3}=(c_3/c_2) \cdot k_{d2}=540 \text{ kN/m}$; $k_{d4}=(c_4/c_3) \cdot k_{d3}=400 \text{ kN/m}$; $k_{d5}=(c_5/c_4) \cdot k_{d4}=320 \text{ kN/m}$.

Concerning the internal elastic spring of gaps and dampers of the MLV model, the users' manuals of several commercial structural analysis programs, including SAP2000NL, suggest to adopt stiffness values—named $k_{ies,gap}$ and $k_{ies,damp}$, respectively—significantly greater than the maximum axial stiffness of the elements connected to them (in this case represented by k_{HFE}), so as to avoid any spurious influence on the response of the latter. In particular, said α_{gap} and α_{damp} the multiplying coefficients to be applied to k_{HFE} to obtain $k_{ies,gap}$ and $k_{ies,damp}$, it is suggested to select α_{gap} and α_{damp} values no lower than 100. The maximum value of k_{HFE} , $k_{HFE,max}$, is computed by substituting $\delta_{max,t}=2 \text{ mm}$ in the corresponding k_H analytical expression (3). For $\beta=2.75 \cdot 10^6 \text{ kN/m}^{3/2}$, $k_{HFE,max}$ results to be equal to around 120,000 kN/m. Based on the users' manual indication above, both α_{gap} and α_{damp} were preliminarily fixed at 100. Therefore, the following initial values of $k_{ies,gap}$ and $k_{ies,damp}$ were assumed in the time-history analyses: $k_{ies,gap}=\alpha_{gap} \cdot k_{HFE,max}=12,000,000 \text{ kN/m}$, and $k_{ies,damp}=\alpha_{damp} \cdot k_{HFE,max}=12,000,000 \text{ kN/m}$. The F_t – δ response cycles of the MLV model obtained from the time-history analysis carried out with the most demanding of the seven input ground motions scaled at the BDE amplitude level are plotted in Figure 5, for the set of mechanical and numerical parameters assumed above.

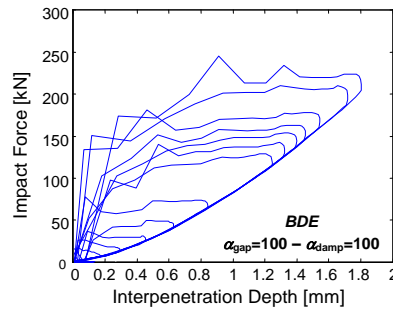


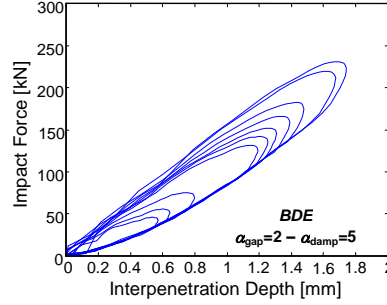
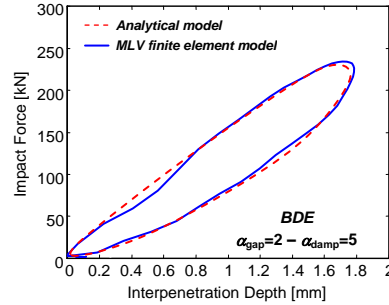
Figure 5. Response cycles of MLV model obtained for $\alpha_{gap}=100$ and $\alpha_{damp}=100$

Remarkable imperfections are noted in the approaching phase of all cycles, with saw-tooth shaped curves highlighting a too stiff response of gaps and dampers, due to the high $k_{ies,gap}$ and $k_{ies,damp}$ values initially adopted. As a consequence, the energy dissipated by the model, E_d , quantified by the area subtended by the cycles, is overestimated. On the other hand, the restitution branch of the cycles, ruled by the non-linear Hertzian spring, exactly follows equation (2). This demonstrates the effectiveness of the five damper-disconnecting springs, which allow the dampers disconnecting completely (i.e. reopening relevant gaps) in the restitution response phase. The δ_{max} value computed from the analysis is equal to 1.8 mm, close to the $\delta_{max,t}$ value of 1.88 mm, rounded to 2 mm, approximately estimated by the criterion presented above.

In order to improve the quality of MLV model response in the approaching pounding stage, the influence of $k_{ies,gap}$ and $k_{ies,damp}$ was analyzed by varying the α_{gap} and α_{damp} coefficients within the range [1–100]. The results of this analysis showed a negligible influence of α_{gap} and α_{damp} on δ_{max} , except for the case where they are both set as equal to 1. The number of contacts is rather insensitive too, since it is equal to 12 for α_{gap} and α_{damp} greater than 10, and 11 in the remaining cases. More appreciable differences come out for F_{max} , reaching around 15% between the highest and the smallest force values for α_{gap} and α_{damp} ranging from 100 and 2, and 25% for $\alpha_{gap}=\alpha_{damp}=1$. Differences are strong, instead, for E_d , which is a decreasing function of the internal stiffness of gaps and dampers, as a consequence of the progressive smoothing of the segmental saw-tooth shape of the approaching branch of response cycles. The processing time is a decreasing function of α_{gap} and α_{damp} too.

Based on the results of the numerical enquiry, the criterion followed to select the most appropriate α_{gap} and α_{damp} coefficient pair consisted in targeting the best correlation between the response cycles of the MLV numerical model and the corresponding cycles produced by Jankowski's analytical model. The latter were obtained by imposing the $\delta(t)$ time-history deduced from the response of the finite element model to the analytical model implemented via Excel software, and by computing relevant total contact force $F_t(t)$. The highest correlations were obtained for $\alpha_{gap}=2$ and α_{damp} ranging from 10 to 2, with the best superimposition reached for $\alpha_{damp}=5$. The cycles derived from the time-history analysis carried out with the same input accelerogram as in Figure 5, for the MLV model calibrated with $\alpha_{gap}=2$ and $\alpha_{damp}=5$, are displayed in Figure 6.

The maximum cycle extrapolated from the graph in Figure 6 is compared to the corresponding analytical cycle in Figure 7, highlighting a satisfactory superimposition, with nearly identical contained areas, and thus, coinciding amounts of dissipated energy. Therefore, it can be concluded that, whereas the basic users' manual suggestion concerning the adoption of α_{gap} and α_{damp} values no lower than 100 is well-suited for single non-linear link elements, it must be critically evaluated for assemblies of multiple elements, since it can negatively affect their hysteretic response, as ascertained for the MLV model examined here.

Figure 6. Response cycles of MLV model obtained for $\alpha_{\text{gap}}=2$ and $\alpha_{\text{damp}}=5$ Figure 7. Maximum response cycle of MLV model, for $\alpha_{\text{gap}}=2$ and $\alpha_{\text{damp}}=5$, and Jankowski's analytical model

Once the coefficient pair $\alpha_{\text{gap}}=2$, $\alpha_{\text{damp}}=5$ was fixed as the best performing choice for the calibration of the internal stiffness of gaps and dampers, the numerical enquiry was completed by evaluating the influence of the initial choices of the k_{di} stiffness values of the damper-disconnecting springs, and the openings w_i of the gaps. Concerning disconnecting springs, in addition to the basic value of 3000 kN/m, k_{d1} was varied over the entire [1000-5000] kN/m range suggested in Section 2, and k_{d2} through k_{d5} according to the mutual proportions expressed therein. The influence on the peak response quantities proved to be negligible, with F_{max} ranging from 236 kN ($k_{d1}=1000$ kN/m) to 230 kN ($k_{d1}=5000$ kN/m), and δ_{max} from 1.78 mm to 1.76 mm. The values of F_{max} and δ_{max} for $k_{d1}=3000$ kN/m coincide with the ones found for the upper limit of 5000 kN/m. More appreciable variations are found for E_d , as it ranges from 386 J ($k_{d1}=1000$ kN/m) to 491 J ($k_{d1}=5000$ kN/m), but with very small differences in the sub-range 3000–5000 kN/m, with E_d equal to 473 J for $k_{d1}=3000$ kN/m. Furthermore, for k_{d1} values below 3000 kN/m, a complete re-opening of the damper elements is not obtained, which causes small imperfections in the cycle contours at the restitution phase. These data show a stable response for the sub-range 3000–5000 kN/m, within which the basic choice of 3000 kN/m provides the most conservative results, as it determines the lowest E_d value (i.e. the lowest attenuation of pounding effects induced by the energy dissipation of contact elements).

The influence of the initial set of gap openings w_i was finally examined by varying their tentative choice based on the $\delta_{\max,t}=2$ mm value by which the calibration procedure was initialized. In particular, attention was focused on the consequences of $\delta_{\max,t}$ on the time-history analysis computation of the actual maximum interpenetration depth δ_{\max} . Relevant results show that, for $\delta_{\max,t}$ ranging from $\frac{1}{2}$ to 2 times the assumed basic value of 2 mm (i.e. ranging from 1 mm to 4 mm, with a step of 0.25 mm), δ_{\max} is nearly constant, as it varies from 1.79 mm to 1.77 mm, with a minimum of 1.76 mm for $\delta_{\max,t}$ equal to 1.25 mm through 2.5 mm. This underlines a substantial insensitivity of δ_{\max} with respect to $\delta_{\max,t}$, and thus the possibility of reaching a nearly “exact” calculation of δ_{\max} at the first round of the time-history analysis, for a reasonably wide range of $\delta_{\max,t}$ values around the basic choice suggested for the initial calibration of the MLV model. After the first round of the analysis, the w_i values are re-calculated for the computed δ_{\max} value, requiring a one step-only final calibration process of gap openings.

The parametric enquiry discussed here for the pair of one storey-one bay numerical R/C frames was carried out also for several other numerical test structures, by varying the number of storeys and bays from two to five, highlighting similar results. The choice ranges and criteria suggested above for the computational parameters involved in the analysis can thus be reasonably extended to the assessment of real case study pounding R/C structures.

6 CONCLUSIONS

The possibility of following the time-history evolution of impacts and related effects by non-linear force-transmitting springs and contact-energy dampers, offered by Jankowski’s analytical model for lumped colliding masses, can be duplicated in the computational analysis of complex structural systems by means of properly designed finite element assemblages, like the multi-link viscoelastic contact model devised and implemented in this research.

Specific remarks deriving from the results of the calibration analyses presented in this paper are summarized below.

- A remarkable influence of the stiffness of the internal elastic springs of gaps and dampers on the response cycles of the MLV model emerged from the analyses carried out on the two single-storey test frames. In particular, noticeable imperfections came out in the approaching phase, with saw-tooth shaped curves highlighting a too stiff response of both types of elements, when $k_{ies,gap}$ and $k_{ies,damp}$ were assumed—as basically suggested by SAP2000NL users’ manual—100 times greater than the axial stiffness of the connected element, represented in this case by the force-transmitting Hertzian spring.
- The parametric analysis developed on the stiffness multiplying coefficients α_{gap} and α_{damp} showed the highest correlation between the response cycles of MLV and Jankowski’s models for $\alpha_{gap}=2$ and α_{damp} ranging from 10 to 2, with the best superimposition reached for $\alpha_{damp}=5$. For these coefficient values, satisfactorily smooth curves were observed for the MLV model

cycles also in the approaching stage. Furthermore, nearly identical contained areas, and thus coinciding amounts of dissipated energy, were obtained, as compared to analytical cycles.

These results highlight that the users' manual suggestion of adopting α_{gap} and α_{damp} values no lower than 100, well-suited for single non-linear link elements, is not effective for the MLV model, and should always be critically evaluated when multi-link assembled models are implemented in time-history analyses.

– The influence of the mechanical parameters of the MLV model, i.e. the openings w_i of gap_{ci} elements, the c_i damping coefficients of dampers and the k_{di} stiffness values of damper-disconnecting springs, was relatively low on all response quantities, for parameter values selected within the tentative choice ranges determined according to the mathematical relations and empirical criteria presented in Section 2.

ACKNOWLEDGEMENTS

The study reported in this paper was sponsored by the Italian Department of Civil Protection within the ReLUIS-DPC Project 2016/2018, research Line 6: Isolation and Dissipation. The authors gratefully acknowledge this financial support.

REFERENCES

- [1] Jankowski, R. Non-linear viscoelastic modelling of earthquake-induced structural pounding. *Earthquake Engineering and Structural Dynamics* (2005) 34: 595–611.
- [2] Anagnostopoulos, S.A. Pounding of buildings in series during earthquakes. *Earthquake Engineering and Structural Dynamics* (1988) 16: 443–456.
- [3] Jankowski, R. Experimental study on earthquake-induced pounding between structural elements made of different building materials. *Earthquake Engineering and Structural Dynamics* (2010) 39: 343–354.
- [4] Davis, R. O. Pounding of buildings modelled by an impact oscillator. *Earthquake Engineering and Structural Dynamics* (1992) 21: 253–274.
- [5] Goldsmith, W. *Impact: the theory and physical behaviour of colliding solids*, Edward Arnold, London, UK (1960).
- [6] SAP2000NL. Theoretical and users' manual. Release 19.06. Berkeley (USA): Computers & Structures Inc. (2018).
- [7] Pratesi, F., Sorace, S. and Terenzi, G. Analysis and mitigation of seismic pounding of a slender R/C bell tower. *Engineering Structures* (2014) 71: 23–34.
- [8] Licari, M., Sorace, S. and Terenzi, G. Nonlinear modeling and mitigation of seismic pounding between R/C frame buildings. *Journal of Earthquake Engineering* (2015) 19: 431–460.
- [9] Wilson, E.L. *Three dimensional static and dynamic analysis of structures*, Computers and Structures Inc., Berkeley, California (2002).

Hydrodynamic Modeling by Macroscopic Balance Equations at Simultaneous Different Length Scales and for Different Time Durations

Shaul Sorek*

*Ben-Gurion University of the Negev

ABSTRACT

Averaging over a Representative Elementary Volume (REV), yield concurrent primary and secondary macroscopic balance equations that respectively consider the REV and a significantly smaller length scale (Sorek and Ohana, 2015). Two sets of assumptions address their corresponding primary and secondary macroscopic balance equations. One accounts for the advective flux of the extensive quantity as dominant over the dispersive flux; the other refers to the intensive quantity as dominant over the one deviating from it. At the REV scale, we obtain extended forms of the macroscopic Navier-Stokes (NS) equation. These can vary from inertia fluxes in the form of a nonlinear wave equation, Forchheimer's law expressing the microscopic fluid inertia transmitted to the solid matrix through their interface, or conform to Darcy's law when friction at that interface is dominant. The secondary balance equations are in the form of hyperbolic balance PDEs'. Field observations of colloidal motion at pores scale comply with these hyperbolic PDEs' being pure advection mass balance associated with the deviation from the average concentration and a wave driven migration propagating the deviation from the average intensive momentum quantity. Controlled experiments supplemented by numerical predication assessing the interaction between the primary and secondary macroscopic balance PDEs are needed to study the hydrodynamic interrelation between these two adjacent spatial scales. Further, we address the primary macroscopic balance PDE's concerning a fluid mass and momentum and a component mass, following an onset of pressure impulse. We obtain different forms of dominant PDE's at evolving temporal scales (Sorek, 1996). Numerical simulations were found to be consistent in excellent agreement with experimental observations. During the second time increment we address theoretically the efficiency of expansion wave for extracting solute from a saturated matrix. Simulations comparing between pumping using an approximate analytical form based on Darcy's equation and numerical prediction addressing the emitting of an expansion wave, suggest (Sorek and Ohana, 2015) that the latter extracts by far more solute mass for a spectrum of different porous media. References Sorek S. and Ohana Y., Macroscopic Balance Equations for Spatial or Temporal Scales of Porous Media Hydrodynamic Modeling, Austin J Hydrol., 2(1): 1-9, 2015. Sorek S. A model for solute transport following an abrupt pressure impact in saturated porous media, Transport in Porous Media. 22: 271-285, 1996.

Coupled CFD/CSD Simulations of Dust Production by Fragmenting Charges Using Stabilized Linear Tetrahedral Elements

Orlando Soto^{*}, Joseph Baum^{**}, Rainald Lohner^{***}, Robert Frank^{****}

^{*}Applied Simulations Inc., ^{**}Applied Simulations Inc., ^{***}George Mason University, ^{****}Applied Research Associates

ABSTRACT

This paper presents coupled Computational Fluid-Dynamics/Structural-Dynamics simulations of internal detonations of cased munitions against reinforced-concrete walls. These simulations are part of a test, analysis, and modeling effort studying air blast propagation through breached walls. The coupled simulations are providing additional insight and details not measured in the tests, as well as developing a synthetic database to supplement the test matrix. The simulations are performed to calibrate the CFD/CSD model and to determine the physics impacting the internal environments, wall breach, and blast propagation through the breach. Here we modeled the response of reinforced-concrete walls to loads from a cased charge, placed in close proximity to the center of wall-1. In the test, the detonation room (composed of two culverts) incurred a large amount of plastic damage due to the fragments and blast load, and both culverts failed. Test wall-1 initially breached over the middle third, with the wing walls removed by the later time blast loads. Debris from test wall 1 impacted test wall 2, which failed under the combined blast and debris. Initial coupled CFD/CSD simulations modeled the culverts as rigid, non-responding surfaces. These simulations reproduced the damage to the test walls, but the pressure histories matched the experimental data only out to 10 ms. Subsequent air blast reflections were significantly reduced, as if a large amount of energy has been evacuated from the facility. Post-test damage analysis showed significant fragment damage to the culverts, with the concrete stripped to the first layer of rebars. We estimate that the fragment impacts produced several hundred kilograms of dust that was ejected into the room. Repeat simulations, where the culvert response was modeled and the dust was allowed to absorb both kinetic and thermal energy, matched the experimental data significantly better. Furthermore, recent developments of stabilized linear-tetrahedral elements for non-linear CSD applications (see [1-2]) have shown a great improvement on capturing plastic localization zones and, therefore, fracture prediction in benchmark problems. Hence, this work addresses how the implementation of such techniques improves the accuracy and the computer time savings for real life applications. [1] Cervera, M., Chiumenti, M., Benedetti, L., Codina, R. "Mixed stabilized finite element methods in nonlinear solid mechanics. Part III: Compressible and incompressible plasticity". Computer Methods in Applied Mechanics and Engineering, 285, 752-775 (2015). [2] Soto, O.A., Baum, J.D., Löhner, R. "An efficient fluid-solid coupled finite element scheme for weapon fragmentation simulations". Eng. Fracture Mech., 77, 549-564 (2010).

A Higher Resolution MOOD Framework Using a Flow Oriented Gradient Reconstruction Applied to Water-Oil Displacements in Anisotropic and Heterogeneous Petroleum Reservoirs

Márcio Souza^{*}, Fernando Contreras^{**}, Paulo Lyra^{***}, Darlan Carvalho^{****}

^{*}Federal University of Paraíba, ^{**}Federal University of Pernambuco, ^{***}Federal University of Pernambuco,
^{****}Federal University of Pernambuco

ABSTRACT

First-order upwind method is routinely used to discretize the advective terms of general transport problems due to its robustness and reliability. Nevertheless, in the presence of steep gradients, its excessive numerical diffusion spuriously spreads out the shock representation. To remedy this, numerous higher-resolution strategies, based on the limited gradient reconstruction, have been proposed in literature [1]. In the finite volume approach, second-order of accuracy in space can be achieved by means of the suitable limited linear reconstruction with a MUSCL-type strategy [2]. This procedure, in general, captures discontinuities in the solution without producing spurious oscillations. However, due to its intrinsic 1-D nature, it is difficult to obtain monotone and accurate solutions for multidimensional flows. In this paper, a segregated mathematical model composed by a pressure equation and a saturation equation is approximated by a full finite volume formulation [1]. The saturation equation is explicitly approximated by a higher-resolution formulation using the Multidimensional Optimal Order Detection (MOOD) framework. This strategy, originally proposed in [2] and adapted to reservoir simulation in [1], produces monotone solutions by detecting, a-posteriori, the optimal order of each control volume (CV) in a multidimensional way. In our proposal, an alternative properly biased reconstruction strategy is adopted. In the gradient reconstruction step, we consider the local orientation of the flow to choose, only those neighbors CV classified as upwind regarding to the one evaluated. Thus, we achieve a flow oriented-based reconstruction instead of using that traditional non-biased used in [1] or even the conventional least-squares technique [2], which consider either full or face-based vicinity for building the reconstruction support. The pressure equation is implicitly solved by a robust Multi-Point Flux Approximation Method with a Diamond support (MPFA-D). This formulation used in [1] in reservoir simulation context is capable to produce convergent solutions, even for problems with non-diagonal permeability tensors and distorted meshes. The solution of some relevant benchmark problems with our formulation shows the enhancement of the accuracy and some reduction of grid orientation effects in the numerical solutions. References [1]. Contreras, F.; Souza, M.; Lyra, P.; Carvalho, D. K. A MPFA Method Using Harmonic Points Coupled to a Multidimensional Optimal Order Detection Method (MOOD) for the Simulation of Oil-Water Displacements in Petroleum Reservoirs. In XXXVII CILAMCE. 2016. Brasília. Brasil. [2]. Clain, S.; Diot, S.; Loubere, R. A. High-Order Finite Volume Method for Systems of Conservation Laws. Multi-Dimensional Optimal Order Detection (MOOD). Journal Comput. Physics. 2011; 230: 4028-4050.

3D Stochastic Bicontinuous Composites: Determination of Effective Elastic Properties through Computational Homogenization

Celal Soyarslan^{*}, Swantje Bargmann^{**}, Marc Pradas^{***}

^{*}Chair of Solid Mechanics, School of Mechanical Engineering and Safety Engineering, University of Wuppertal, Germany, ^{**}Chair of Solid Mechanics, School of Mechanical Engineering and Safety Engineering, University of Wuppertal, Germany, ^{***}School of Mathematics and Statistics, The Open University, Milton Keynes, United Kingdom

ABSTRACT

Considering linear and infinitesimal elasticity and using computational homogenization along with finite element method, we study effective elastic properties of 3D bicontinuous random composites. In generation of the microstructures, a leveled-wave model based on the work of J. W. Cahn [1] is used. The influence of box size, phase contrast, relative volume fraction of phases and applied boundary conditions on computed apparent elastic moduli is investigated. Only with periodic boundary conditions the effective properties can be determined at reasonable box sizes and up to a numerical error. For this minimum box size allowing the effective property determination, also referred to as the representative volume element (RVE) size, we scrutinize macroscopic response of gold-epoxy nanocomposites of various phase volume fractions. For all computations, kinematically uniform boundary conditions are found to be overestimating. This is especially the case for increasing phase contrast and volume fraction bias towards the weaker phase. Still, for the observed phase volume fraction interval, the apparent moduli computed using kinematically uniform boundary conditions fall much below the upper bounds of Hashin-Strihman, three-point Beran-Molyneux and Milton-Phan-Tien analytical bounds. Thus, computational homogenization devising periodic boundary conditions is justified to be the only tool in efficient and accurate determination of the effective properties of 3D bicontinuous random composites with high contrast and volume fraction bias towards the weaker phase. References 1. J.W. Cahn. Phase separation by spinodal decomposition in isotropic systems. The Journal of Chemical Physics, 42(1):93-99, 1965. 2. C. Soyarslan, S. Bargmann, M. Pradas, and J. Weissmüller. 3D stochastic bicontinuous microstructures: generation, topology and elasticity. Submitted, 2017. 3. C. Soyarslan, M. Pradas, and S. Bargmann. Determination of Effective Elastic Properties of 3-D Bicontinuous Random Composites through Computational Homogenization: Influence of Phase Contrast and Applied Boundary Conditions. Submitted, 2017.

Canonical Generalization of Lyapunov's Second Method and General Procedure of Utilization of Lyapunov Functions

Myroslav Sparavalo*

*NYC Transit Authority

ABSTRACT

The objective of the research is to develop a general method of constructing Lyapunov functions for non-linear non-autonomous differential inclusions described by ordinary differential equations with parameters. The goal has been attained through the following ideas and tools. First, three-point Poincaré strategy of the investigation of differential equations and manifolds has been used. Second, the geometric-topological structure of the non-linear non-autonomous parametric differential inclusions has been presented and analyzed in the framework of hierarchical fiber bundles. Third, a special canonizing transformation of the differential inclusions that allows to present them in special canonical form, for which certain standard forms of Lyapunov functions exist, has been found. The conditions establishing the relation between the local asymptotical stability of two corresponding particular integral curves of a given differential inclusion in its initial and canonical forms are ascertained. The global asymptotical stability of the entire free dynamical systems as some restrictions of a given parametric differential inclusion and the whole latter one per se has been investigated in terms of the classificational stability of the typical fiber of the meta-bundle. The general procedure of the utilization of Lyapunov functions is applied to the problem of the wide-sense robust control design for van der Pol nonlinear dynamics. References 1. Sparavalo, M. K. The Lyapunov Concept of Stability from the Standpoint of Poincaré Approach: General Procedure of Utilization of Lyapunov Functions for Nonlinear Non-Autonomous Parametric Differential Inclusions, 2014, arXiv:1403.5761, [cs.SY]. 2. Sparavalo, M. K. Lyapunov Functions in Nonlinear Unsteady Dynamics and Control: Poincaré's Approach from Metaphysical Theory to Down-to-Earth Practice, 1st Edition, NY, 2016, ISBN 9780692694244. 3. Sparavalo, M. K. Wide-Sense Robust and Stable in the Large Terminal Control for Van Der Pol Dynamics: Poincaré's-Approach-Based Backstepping Method, Procedia Engineering, Vol. 199, 2017, pp. 850-856.

A Comparison of NMAP and CTH for Modeling Projectile Impact on Steel Plates

Paul Sparks*, Jesse Sherburn**, William Heard***, David Roman-Castro****

*U.S. Army ERDC, **U.S. Army ERDC, ***U.S. Army ERDC, ****U.S. Army ERDC

ABSTRACT

Ballistic impact modeling of steel plates is of extreme importance to the military community. Research efforts have been devoted to developing analytical and numerical models to analyze and predict the outcome of ballistic impact problems [1, 2]. Dey et al. [1] carefully characterized the effect of different projectiles impacting steel targets and studying residual projectile velocity and the ballistic limit. The experimental test conducted in [1] provided the material constants necessary to model the failure criterion of Johnson and Cook [3]. The data from Dey can be used to calibrate and validate the numerical models. In this study, in-house experimental data produced from different projectiles impacting steel plates with velocities in the ordnance regime will be compared to two different numerical methods. Nonlinear Meshfree Analysis Program (NMAP) is a meshless based code which employs reproducing kernel particle methods (RKPM) in a semi-Lagrangian framework and CTH is an Eulerian shock physics based wave code. Both numerical codes are advantageous for modeling impact and penetration/perforation problems that predict deformation and material fragmentation. The effectiveness of each numerical codes is demonstrated by modeling and validating analogous impact experiments of steel plates to demonstrate the physical mechanisms in the perforation process. A discussion of the inherent strengths and weakness of each of the models will be discussed. [1] Dey, S., Børvik, T., Hopperstad, O., Leinum, J., Langseth, M. 2004. The effect of target strength on the perforation of steel plates using three different projectile nose shapes. *International Journal of Impact Engineering*. 30(8–9):1005–1038. Eighth International Symposium on Plasticity and Impact Mechanics (IMPLAST 2003). [2] Yreux, E., and Chen, J. S. 2016. A quasi-linear reproducing kernel particle method. *Int. J. Numer. Methods Eng.*, 109(7), 1045–1064. [3] Johnson, G. R., Cook, W.H. 1983. A constitutive model and data for metals subjected to large strains, high strain rates and high temperatures. *Proceedings of the Seventh International Symposium on Ballistics*, Hague. p. 541–7.

The Relaxation Properties of Poroelastic Scaffolds for Stem Cell Differentiation

Alexander Spector^{*}, Rahul Yerrabelli^{**}, Daniel Yuan^{***}

^{*}Johns Hopkins University, ^{**}Johns Hopkins University, ^{***}Johns Hopkins University

ABSTRACT

The mechanical properties of the extracellular matrix are significant to its interaction with the stem cells inside, affecting the processes of stem cell differentiation. Scaffolds mimic the structure and mechanical properties of the extracellular matrix and provide differentiation of the seeded stem cells similar to that in the native tissue. Stem cell differentiation is a dynamic process occurring on many time scales, a reflection of different biological events and signaling pathways involved. Thus, the time-dependent properties of the extracellular matrix (and scaffolds) must have a significant effect on stem cell differentiation, and it was recently confirmed by the experiments with stem cells in scaffolds with tunable stress relaxation [1] and strain creep parameters [2]. The question of the mechanism behind the relaxation/creep properties of the scaffolds and its relation to the scaffold structure is of key importance. Typically, the scaffolds are biphasic, including solid and fluid components. We consider porous-fibrous scaffolds and develop their poroelastic model that relates the relaxation properties to the diffusion of the fluid component through the scaffold. The problem reduces to the Bessel equation in terms of the Laplace transform of the displacement of the scaffold solid component. The model parameters are the Young's moduli in the fiber direction and perpendicular plane, corresponding Poisson's ratios, and the gel diffusion time that characterizes the scaffold fluid component. These parameters are estimated by fitting the theoretical time course of the applied force relaxing after the ramp loading to the experimental data on the relaxation of cylindrical specimens [3]. Using the estimated parameters, we compute the local mechanical factors sensed by the stem cell inside, including the stresses, pressure, and fluid velocity. The scaffold relaxation has a spectrum of times proportional to the gel diffusion time and satisfying a characteristic equation. The developed approach can be used for the effective design of scaffolds applied in stem cell therapies. [1] Chaudhuri et al. Hydrogels with tunable stress relaxation regulate stem cell fate and activity. *Nature Mats.*, 2015, 15, 326-334. [2] Cameron A.R. et al. The influence of substrate creep on mesenchymal stem cell behavior and phenotype. *Biomaterials*, 2011, 32, 5979-5993. [3] Cook, C. A. et al. Characterization of a novel bioreactor system for 3D cellular mechanobiology studies. *Botech&Bioeng.* 2016, 13, 1825–1837.

Isogeometric Analysis on Meshes with Polar Singularities: B-Spline Construction

Hendrik Speleers^{*}, Deepesh Toshniwal^{**}, Rene Hiemstra^{***}, Thomas Hughes^{****}

^{*}University of Rome "Tor Vergata", ^{**}University of Texas at Austin, ^{***}University of Texas at Austin, ^{****}University of Texas at Austin

ABSTRACT

One of the needs of CAD representations of arbitrary genus surfaces with finite number of polynomial patches is the introduction of holes surrounded by periodic configurations. Such holes can then be filled by means of polar spline surfaces, where the basic idea is to use periodic spline patches with one collapsed boundary invoking a polar singularity. Applications of this approach include subdivision surfaces, free-shape modeling, and, as we demonstrate here, isogeometric analysis. In order to obtain polar spline surfaces with specified continuity, the admissible set of control point configurations shrinks. In particular, imposition of C^k continuity constrains the inner k -rings of control points surrounding the singular point to a limited number of configurations. In hole-filling applications, the outer k -rings of control points are used to match the cross-derivative information at the hole boundary. In this talk, keeping in mind applications to design as well as analysis, we focus on C^k polar spline parametric patches with arbitrary degree and arbitrary number of elements at the hole boundary. We present a simple, geometric construction of B-spline basis functions over such polar parametric domains possessing interesting properties as non-negativity and partition of unity. In addition, the constructed spline spaces show optimal approximation behavior, even at the polar singular point [1]. [1] D. Toshniwal, H. Speleers, R.R. Hiemstra, and T.J.R. Hughes. "Multi-degree smooth polar splines: A framework for geometric modeling and isogeometric analysis", Comput. Methods Appl. Mech. Engrg. 316, 1005-1061, 2017.

Predicting Mechanical Properties of Epoxy from Molecular Models

Simcha Srebnik*, Irena Yungerman**

*Technion - Israel Institute of Technology, **Technion - Israel Institute of Technology

ABSTRACT

Epoxy resins are the most commonly used adhesives in industry due to their versatility, low cost, low toxicity, low shrinkage, high strength, resistance to moisture, and effective electrical resistance. Diverse mechanical properties can be obtained depending on the chemical structure of the curing agent and the conditions of the curing process. An outstanding goal is the ability to predict material properties and failure under stress based on the underlying chemistry of its constituents. In principle, all-atom simulations can be used to predict material properties without the need for empirical parameters. In practice, however, such simulations of epoxy resins that can be used to cheaply and systematically investigate chemistry-property relationship are only beginning to be realized due to the complexity of the system and the presence of unknown variables. Computational experiments are further complicated as the cross-linked system is nonergodic and sample dimensions are generally small, and therefore different realizations of the crosslinking reaction must be modeled to obtain sufficient statistical measurements. The small samples tend to show a wide scatter of properties, that also depend on the rate of deformation, whether thermal or mechanical. Moreover, the differences in spatial and temporal scales between mechanical experiments and molecular computations are vast and make it difficult to directly compare between the two. Coarse-grained simulations serve to bridge the gap between the length and temporal scales of the atomistic simulations with those of experiments, while retaining a non-constitutive model. Using bottom-up approach, we develop coarse-grained models parametrized against all-atom simulations for model epoxy and hardener, and analyze the behavior of the cross linked epoxy matrix under deformation. Failure at the interface of single walled carbon nanotube is examined for different nanotube diameters in an effort to understand the effect of curvature on adhesion at the interface.

VMS-based Error Estimation and Adaptivity in the Joint Physical and Stochastic Space

Vignesh Srinivasaragavan^{*}, Jason Li^{**}, Assad Oberai^{***}, Eric Phipps^{****}, Eric Cyr^{*****}, Onkar Sahni^{*****}

^{*}Rensselaer Polytechnic Institute, ^{**}Rensselaer Polytechnic Institute, ^{***}University of Southern California,
^{****}Sandia National Laboratories, ^{*****}Sandia National Laboratories, ^{*****}Rensselaer Polytechnic Institute

ABSTRACT

This presentation will focus on the formulation and application of an adaptive approach for stochastic PDEs with uncertain input data based on the variational multiscale (VMS) method. In this approach, we employ finite elements in the physical domain and spectral approximation (based on generalized polynomial chaos) in the stochastic domain. The VMS method allows in computing an accurate solution in a coarse space while accounting for the missing/fine scales through a model term. This model term is algebraically approximated within each element using the strong-form residual and a stochastic stabilization parameter, which is used in the variational statement for computing the numerical solution. Similarly, a model term is derived to estimate the error in the numerical solution in a local/element-wise fashion, where the model term for the local error is approximated using the same stabilization parameter used in computing the numerical solution, making error estimation computationally inexpensive. The procedure is designed to provide local and global error estimates and to drive adaptivity in the joint physical and stochastic space. By adaptivity in the joint space, we imply resolution control in the spatial approximation or the mesh (e.g., a graded or non-uniform unstructured mesh) together with the spectral approximation (e.g., a spatially varying spectral order over the mesh). We demonstrate the effectiveness of our approach on multiple example cases including transport problems spanning both advective and diffusive regimes in the stochastic domain as well as non-trivial geometries or physical domains.

Ductile Fracture of Multiphase Steel Sheets under Bending

Ankit Srivastava*, Yu Liu**

*Texas A & M University, College Station, TX 77843, **Texas A & M University, College Station, TX 77843

ABSTRACT

The fracture characteristics of steel sheets under bending mode are governed, at least in part, by the microstructural features such as the size, shape, distribution and properties of inclusions. Experiments suggest that the bend fracture of steel sheets of interest are determined by the size and location of large inclusions or clustered small inclusions (stringer of inclusions). The properties of inclusions have also been found to affect the damage nucleation process. Hence our aim is to analyze the collaborative effects of microstructural features on ductile fracture of steel sheets under bending. Here, finite element, finite deformation calculations are carried out using a constitutive framework for progressively cavitating ductile solids. In the finite element calculations, the individual phases of the multiphase steel together with the inclusions are discretely modeled. The extent to which the microstructural length scale originating from the multiphase microstructure and the length scale originating from the distribution of inclusions affect the ductile fracture of sheets under bending will be discussed.

An Implicit, Conservative, Hybrid Particle-kinetic-ion Fluid-electron Algorithm

Adam Stanier^{*}, Luis Chacon^{**}, Guangye Chen^{***}

^{*}Los Alamos National Laboratory, ^{**}Los Alamos National Laboratory, ^{***}Los Alamos National Laboratory

ABSTRACT

Bridging the inherent multi-scale nature of many important problems in plasma physics requires a combination of model reduction and algorithmic innovation. The hybrid model with full-orbit kinetic ions and fluid electrons is a promising approach to describe a wide range of space and laboratory plasmas. In particular, it has been recently demonstrated that the hybrid model is the minimum sufficient model to correctly capture the rate and global evolution of a reconnecting system for arbitrary guide magnetic field [1,2,3], with important consequences for space weather modeling. Here we focus on the quasi-neutral hybrid model using macro-particles to model the kinetic ion species, which avoids the need to solve for the distribution function in 6D (3D-3V) phase space, but is subject to discrete particle noise that scales as \sqrt{N} for the number of macro-particles N . The majority of existing algorithms employ explicit time-stepping, and much of the development has focused on the accuracy and stability of the time integration schemes. Key unresolved issues with these approaches involve the numerical instability of cold ion beams moving through the spatial grid due to aliasing errors [4], and the quadratic CFL condition ($dt \sim dx^2$) associated with fast dispersive Whistler waves. Recent work [5,6] has explored the use of fully implicit methods to step over such timescales in a stable manner, but have not addressed the topic of momentum or energy conservation. Here we present a novel fully implicit hybrid algorithm that features discrete mass, momentum and energy conservation, as well as discrete preservation of the solenoidal condition. The algorithm features sub-cycling and orbit averaging of the ions, with cell-centred finite differences and implicit midpoint time advance. To reduce numerical noise, the algorithm allows arbitrary-order shape functions and conservative smoothing on the gather and scatter operations. We discuss the implementation of the algorithm into a Jacobian-Free Newton Krylov solver framework, and then verify it for a number of test problems. These demonstrate the correctness of our implementation, the unique conservation properties, and its favorable stability properties. References: [1] A. Stanier et al., Phys. Plasmas 24, 022124 (2017). [2] J. Ng et al., Phys. Plasmas 22, 112104 (2015). [3] A. Stanier et al., Phys. Rev. Lett. 115, 175004 (2015). [4] P. W. Rambo, Journal of Computational Physics, 118, 152-158 (1995). [5] B. Sturdevant et al., Journal of Computational Physics, 316, 519 (2016). [6] J. Cheng et al., Journal of Computational Physics, 245, 364 (2013).

Parallel and Dirty CAD Tolerant Tetrahedral Mesh Generation with Feature Capture

Matt Staten^{*}, David Noble^{**}, Corey McBride^{***}, C. Riley Wilson^{****}, Manoj Bhardwaj^{*****}

^{*}Sandia National Laboratories, ^{**}Sandia National Laboratories, ^{***}ELEMENTAL TECHNOLOGIES INC, ^{****}Sandia National Laboratories, ^{*****}Sandia National Laboratories

ABSTRACT

With well documented and robust Delaunay and advancing-front algorithms, tetrahedral mesh generation is often considered a solved problem. However, automatic tetrahedral mesh generation on complex and dirty CAD assemblies on HPC systems remains an open problem due to the presence of small geometric features and imperfect geometry. We present the latest status on an effort to implement a massively parallel tet mesher for CAD assemblies using an overlay grid technique. Our approach extends to 3D CAD the 2D CISAMR [1] used successfully for material interface construction. We start by overlaying the CAD assembly with a cartesian hexahedral grid. Intersection points are computed where CAD vertices, curves, and surfaces intersect the overlay grid. Nodes in the overlay grid are snapped to closest intersection points, morphing the cartesian overlay. No cells are cut by geometry intersections. Finally, the hexahedral overlay grid cells are converted into tetrahedral elements following a Body Centered Cubic (BCC) structure [2]. By postponing the conversion of the overlay grid to tetrahedrons until after the grid is morphed, tetrahedral topology is chosen to maximize tetrahedral quality by considering the snapped node locations, eliminating need for post-processing smoothing and swapping. This approach to tetrahedral mesh generation implicitly captures CAD curves and vertices at the resolution of the overlay grid, while ignoring features smaller than the overlay grid resolution. The cell center node in the BCC pattern doubles the degrees of freedom for a given cell size. However, we choose the BCC pattern for the following reasons: First, it offers better quality tetrahedron than conversion of each cell into six tetrahedron; second, it allows for embarrassingly parallel conversion of the cells into tetrahedron; and third, it allows for better CAD approximation to non-planar CAD features by projecting the center node to the CAD. Future plans include replacing the hexahedral overlay grid with a balanced octree allowing for adaptive resolution of geometric features. [1] Soheil Soghrati, Anand Nagarajan, and Bowen Liang, Conforming to Interface Structured Adaptive Mesh Refinement: New Technique for the Automated Modeling of Materials With Complex Microstructures, Finite Elements in Analysis and Design, 125 (2017) 24-40. [2] Jun Wang, Zeyun Yu, Adaptive and Quality Tetrahedral Mesh Generation, Proceedings 19th International Meshing Roundtable, 2010. ^{*}Sandia National Laboratories is a multi-program laboratory managed and operated by Sandia Corporation, a wholly owned subsidiary of Lockheed Martin Corporation, for the U.S. Department of Energy's National Nuclear Security Administration under contract DE-AC04-94AL85000. SAND2018-0293 A

Computational Homogenization for Embossing of Thin Fibrous Structures based on FEM-FFT Coupling

Sarah Staub^{*}, Julia Orlik^{**}, Heiko Andrä^{***}

^{*}Fraunhofer Institute for Industrial Mathematics, ^{**}Fraunhofer Institute for Industrial Mathematics, ^{***}Fraunhofer Institute for Industrial Mathematics

ABSTRACT

Structured fiber networks play an important role in many different applications in the field of filter and hygiene media. Examples are different types of wipes as e.g. baby wipes or structured wipes for the trapping of dust. Another important class of embossed fiber networks are pleated filters. The current work focuses on the simulation of the structuring process of thin porous media. As the stamps applied for the embossing are large compared to the fibers of the network, a two-scale framework is elaborated. The structure mechanical equations on both scales are solved concurrently within a suitable homogenization framework similar to FE². The macroscopic scale is treated as heterogeneous thin plate, similar to [1], within a finite element method (FEM). In each integration point the membrane deformation and the deflection is computed and applied to formulate the microscopic boundary condition on a representative volume element (RVE). Within the nested solution scheme, the homogenized microscopic quantities yield the macroscopic effective properties and thus substitute the macroscopic constitutive behavior. At the microscale, the fibers and the bonds (melt points or resin) are captured in highly resolved voxelized RVEs, see [2] for examples. Due to the high porosity and the complexity of these structures a FEM formulation is not suitable at the microscale. Instead, a Fast-Fourier transform (FFT) based approach for the solution of the Lippmann-Schwinger (LS) integral equations in elasticity is applied. This approach allows the fast and effective solution of large and complex microstructures for an infinite material contrast. In contrast to LS-FFT methods in elasticity, which are based on second order elasticity operators with constant coefficients, here a fourth order bi-harmonic operator is considered instead. The novelty of the presented approach is the the scale coupling via the Green's function to this bi-harmonic operator. This allows the computation of the effective bending and torsion coefficients of the macroscopic plate, see [3]. References [1] E.W.C. Coenen, V.G. Kouznetsova and M.G.D. Geers "Computational homogenization for heterogeneous thin sheets", Int. J. Num. Meth. Eng. 83, 1180-1205, 2010. [2] S. Staub, H. Andrä and M. Kabel "Fast FFT based solver for rate-dependent deformations of composites and nonwovens", Int. J. Solids Struct., in press. [3] M. Hauck, A. Klar and J. Orlik "Design optimization in periodic structural plates under the constraint of anisotropy", Z. Angew. Math. Mech. 97, 1120-1235, 2017.

Bone Loss in Space Travellers: Systematic Review and Meta-analysis

Mariya Stavnichuk*, Corlett Tatsuya**, Svetlana Komarova***, Nicholas MikolajewiczShriners
Hospital for Children; Faculty of Dentistry, McGill University****, Martin Morris*****

*Shriners Hospital for Children, **Shriners Hospital for Children, ***Shriners Hospital for Children; Faculty of
Dentistry, McGill University, ****Shriners Hospital for Children; Faculty of Dentistry, McGill University, *****Schulich
Library of Science and Engineering, McGill University

ABSTRACT

Bone loss in astronauts is identified as a major challenge for long-duration space exploration. Understanding underlying mechanisms responsible for bone density changes observed in astronauts is imperative for a design of successful countermeasures. With the goal to examine the spatial and temporal aspects of microgravity-induced bone loss, the electronic databases were searched for studies presenting numerical values for measurements of bone health in astronauts. We identified 30 studies containing bone density estimates for 138 of 553 astronauts, obtained using X-ray radiography, single-energy photon and dual-energy X-ray absorptiometry or quantitative computed tomography before and immediately after the space flights that lasted from 4 to 252 days. Sample size-weighted changes in bone density compared to pre-flight in the region of head, shoulders and cervical vertebrae were +2.2% (95% confidence interval: 1.1, 3.3; n = 32 astronauts); in the region of forearms, thoracic vertebrae and ribs: -2.0% (-3.0, -0.9; n = 72); in the region of lumbar vertebrae and pelvic bones: -5.8% (-7.2, -4.5; n = 66); and in the region of lower extremities: -3.9% (-5.7, -2.2; n = 110). Bone density decreased with an increase in flight duration, at the rate of $-0.84 \pm 0.37\%$ per month. Changes in serum or urine biochemical markers of bone resorption and formation during space flight were available for 33 astronauts. Bone resorption markers consistently increased within the first 40 days and thereafter stabilized at 100-140% above baseline. Bone formation markers were more variable than bone resorption markers, however in general they remained unchanged or decreased during the first 30 days of the flight, and slowly increased thereafter. Comparison of the difference between bone formation and resorption markers to the changes in bone density demonstrated a notable disconnect in the time-dependent bone changes predicted by the markers, and the observed changes in bone density. This disconnect can be potentially explained by i) microgravity-specific effects uncoupling bone formation markers from bone gain; ii) temporal delay between bone formation markers and actual bone deposition, or iii) anatomical site differences in the effect of microgravity, with bone markers collecting information from the whole skeleton, while bone loss is observed only in lower half of the body.

SHAPE OPTIMIZATION OF UNIT CELLS FOR VIBRATION ISOLATION USING AUXETIC MATERIALS

Panagiotis I. Koutsianitis Georgios A. Drosopoulos Georgios K. Tairidis and
Georgios E. Stavroulakis

* Technical University of Crete
School of Production Engineering and Management
Institute of Computational Mechanics and Optimization
Chania, Crete, Greece
panoskout@gmail.com, Tairidis@gmail.com, gestavr@dpem.tuc.gr ;
<http://www.comeco.tuc.gr>

+ University of KwaZulu-Natal
Discipline of Civil Engineering
Structural Engineering & Computational Mechanics Group
Durban, South Africa
DrosopoulosG@ukzn.ac.za ; <http://secm.ukzn.ac.za>

Key words: Auxetic material, Band gaps, Vibration

Abstract. *In the present investigation, a band gap region, i.e. the isolation of certain frequencies, through the optimization of the shape of the unit cells of a lattice is considered. In general, a lattice is considered as an assembly of classical structural elements, such as beams, plates, etc. Each cell of the lattice is discretized using the finite element method, and more specifically with plane stress elements. The homogenized behavior of the system is extracted from the detailed investigation of the representative volume cell. In the present investigation, a lattice with a microstructure is considered. The shape of the unit cells can be triangular, quadratic, hexagonal, etc. The shape and the microstructure of the lattice can be optimized in order to achieve isolation of the desired frequencies. This can be done using either the trial and error method or global optimization methods, such as genetic algorithms. Auxetic materials can be useful in this direction.*

1 INTRODUCTION

Isolation of structures against vibrations which are caused by external loadings is a typical problem in engineering. There are a lot of techniques which are proposed in literature for this purpose. The design of a microstructure which consists of a lattice as an assembly of classical elements, such as beams and plates, is quite common. The overall mechanical behavior is determined from a representative unit cell and suitable loadings, using homogenization techniques. For dynamic loadings various directions of wave propagation and all frequencies of interest must be taken into account. The unit cells can be of several different shapes, e.g. square, triangular, hexagonal honeycomb etc. One can say that the mechanical behavior of a unit cell is determined by its shape, i.e. by its topology as described in [1]. In fact, the design parameters of the unit cell can

be tuned in order to find the band-gap regions, if any. As for the loading, a wave vector is applied at a particular cell, at the two directions x and y , thus it is a two-dimensional problem. This vector takes into account the periodic boundary conditions, which in turn are defined using the Floquet theorem [2].

The propagation of the waves can be considered according to the work of Brillouin and Kittel [3,4], where the motion can present pass and stop band gaps, that is specific frequencies where the wave is able or unable to propagate through the lattice. The wave propagation in two-dimensional periodic lattices is described in detail in [1,5]. More specifically, the Floquet-Bloch principles are considered in order to design lattices within a desired band. The objective is the study of wave propagation, i.e. bandgaps and wave directionality, in three regular honeycombs; hexagonal, square and triangular and in the semiregular Kagomé lattice. The results provide the dispersion curves for the different 2-D topologies of the studied unit cells.

Auxetics are mechanical metamaterials with negative Poisson ratio. Among their interesting properties is the enhanced vibration suppression [6]. An auxetic cell with star-shaped form is used here. A band gap analysis of star-shaped honeycombs with varied Poisson's ratio is studied in [7]. More specifically, star-shaped honeycombs with auxetic properties are analyzed in terms of their band gap properties, along with their equivalent mechanical behavior. The purpose of the selection of a material with auxetic behavior lies to its ability to provide enhanced Young's modulus of star-shaped structures. Moreover, it is known that band gap properties are observed not only in classical materials, but in ones with negative Poisson's ratio as well. In fact, negative values of this ratio can be an important factor in the design. Thus, the work presented in [7] can be used as a guide for the optimal design of such structures, with respect to band gap regions.

2 BLOCH THEOR

In general, the whole lattice can be obtained from the correlation of the unit cell with the basis vectors ε_i . However, the first step of the study should be the suitable definition of a unit cell. The lattice points r of a unit cell are in fact a small subset of the nodes of its finite element model. The displacement $q(r)$ of the lattice points of the unit cell for the case of plane waves is given as:

$$q(r_j) = q_j e^{(i\omega t - kr_j)} \quad (1)$$

where q_j is the amplitude, ω is frequency and k is the wave vector. The parameters n_1 and n_2 can identify any other cell which can be obtained by n translations across the e directions with respect to the unit cell of reference.

According to the Bloch's theorem, the displacement at the j^{th} point in any cell can be identified by a unique pair of integers n_1 and n_2 as:

$$q = q(r_j) e^{k(r - r_j)} = q(r_j) e^{(k_1 n_1 + k_2 n_2)} \quad (2)$$

where:

$$k_1 = k \cdot e_1 = \delta_1 + i\varepsilon_1 \quad (3)$$

$$k_2 = k e_2 = \delta_2 + i\varepsilon_2 \quad (4)$$

In the above equation, k_1 and k_2 denote the components of wave vector k which is propagated and at the same time dissipated along the vectors e_1 and e_2 . The real part δ denotes the attenuation constant, i.e. it is a measurement of the propagation of the wave among cells, while the imaginary part ε represents the change of the phase across the unit cell and it is called phase constant. Practically, this means that if a wave is propagating without any attenuation, then the real part δ is zero and thus, the wave vector can be given by:

$$k_1 = i\varepsilon_1 \quad (5)$$

$$k_2 = i\varepsilon_2 \quad (6)$$

The possible extraction of band gaps is based on the assumption of wave vectors which are following the Brillouin zone, i.e. vectors with edges restricted to the irreducible part of this zone^[2] as seen in Figure 1 below.

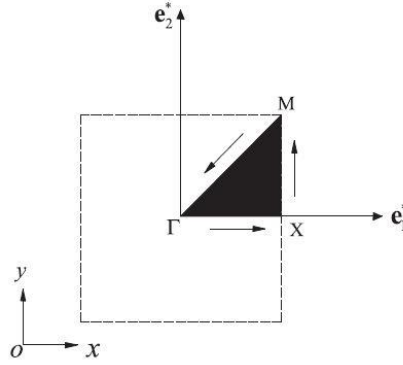


Figure 1: The first Brillouin zone and the irreducible Brillouin zone ($\Gamma - X - M$)

In general, periodic structures are systems with identical segments, coupled to their neighboring. More specifically, uniform 2-D structures can be considered as a special case of periodic structures which are homogeneous in x and y directions. These structures are, in fact, an assembly of rectangular segments with length to the x and y directions which equals to L_x and L_y respectively.

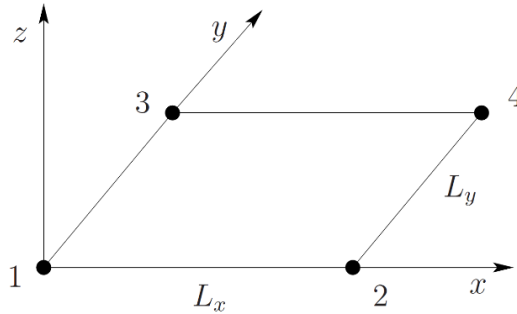


Figure 2: A rectangular segment with a 4-noded rectangular finite element

As seen in Figure 2, the degrees of freedom of the segment of reference can be considered with respect to the nodal degrees of freedom as:

$$q = [q_1^T \ q_2^T \ q_3^T \ q_4^T] \quad (7)$$

where q_j are the nodal degrees of freedom of the nodes of the j^{th} corner of the segment and T denotes the transpose.

The equation of motion of the element of reference is given as:

$$(-\omega^2 M + i\omega C + K)q = f \quad (8)$$

where M , C and K are the mass, damping and stiffness matrices respectively, ω is the natural frequency, f is the loading vector and i the imaginary number. Note that nodal forces dissipate the wave motion between the neighboring elements, thus the external loading vector is not zero, even though free wave motion is considered. The 2-D free wave propagates along the structure and thus it can be considered to be a Bloch wave [8]. Bloch's theorem is also called Floquet's theorem since it represents a generalisation of the Floquet's theorem for 1-D problems [9].

The propagation of the wave can then be obtained from the so-called propagation constants $\mu_x = \kappa_x L_x$ and $\mu_y = \kappa_y L_y$, which in turn, provide the relation among the periodic displacements q on the sides of the periodic element as:

$$q_2 = \lambda_x q_1, \quad q_3 = \lambda_y q_1, \quad q_4 = \lambda_x \lambda_y q_1 \quad (9)$$

where:

$$\lambda_x = e^{-i\mu_x}, \quad \lambda_y = e^{-i\mu_y} \quad (10)$$

As a result, the nodal degrees of freedom can be rewritten as:

$$q = \Lambda_R q_1 \quad (11)$$

where:

$$\Lambda_R = [I \ \lambda_x I \ \lambda_y I \ \lambda_x \lambda_y I] \quad (12)$$

In the free response case, i.e. when no external loading is considered, a possible equilibrium at node 1 leads to the restriction that the nodal forces of every element which is connected to node 1 is equal to zero. Thus, we have:

$$\Lambda_L f = 0 \quad (13)$$

where:

$$\Lambda_L = [I \ \lambda_x^{-1} I \ \lambda_y^{-1} I \ (\lambda_x \lambda_y)^{-1} I] \quad (14)$$

By substituting the equation (11) in the equation (8) and multiplying by Λ , the equation of the free wave motion takes the form:

$$(-\omega^2 \bar{M}(\mu_x, \mu_y) + i\omega \bar{C}(\mu_x, \mu_y) + \bar{K}(\mu_x, \mu_y)) q = f \quad (15)$$

where $\bar{M} = \Lambda_L M \Lambda_R$, $\bar{K} = \Lambda_L K \Lambda_R$ and $\bar{C} = \Lambda_L C \Lambda_R$ are the reduced mass, damping and stiffness matrices respectively.

The eigenvalue problem can be written as:

$$\bar{D}(\omega, \lambda_x, \lambda_y) = 0 \quad (16)$$

where \bar{D} is the reduced dynamic stiffness matrix.

3 AUXETIC MATERIALS

It is common for a structure that when a tensile external loading is applied on one dimension, the transverse cross-sectional length is reduced. On the other hand, when a compressive loading is applied, it is obvious that the opposite effect appears, i.e. there is an increase to the transverse cross-sectional length. This change of the length of elastic materials in the perpendicular direction is measured by Poisson's ratio, which usually takes positive values and more specifically values within the interval $0 < \nu < 0.5$.

However, there are materials which present a negative Poisson's ratio, which are called auxetic materials or simply auxetics. Auxetic materials are eventually microstructures that become thicker perpendicular to the direction of the applied load, under a tensile loading. This effect is caused by artificial hinges which appear inside the microstructure which in turn favor the occurrence of flexing. A typical star-shaped auxetic microstructure is shown in Figure 3 [10]. An important characteristic of structures with auxetic behavior is that they are composed of a repeated single pattern of identical microstructures, which in turn consist of a monolithic body with specific geometry. This geometry has a predefined deformation, i.e. it delivers the motion in a certain way under a certain loading, and thus, it can be considered as a compliant mechanism. More complicated auxetic microstructures can be designed using topology optimization techniques, see e.g. [11, 12]. It is worth noting that in the present investigation, the auxetic property of the microstructure is due to the shape of the element (star) and it is not related with a material with a negative Poisson's ratio.

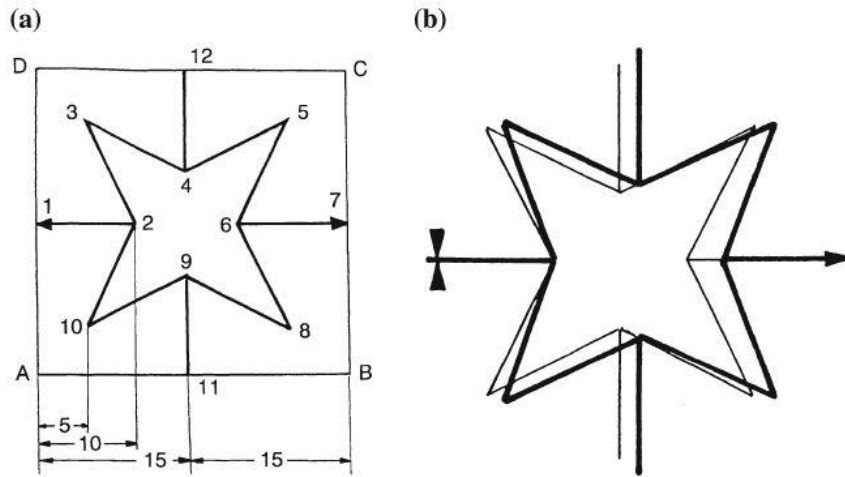


Figure 3: (a) Discretization of a star-shaped element and (b) its deformation

4 NUMERICAL RESULTS

In the present investigation, a square shaped unit cell was considered in order to study the possible appearance of band gaps. For this purpose, several cases were designed and studied. First, a simple unit cell without core was considered, corresponding to a simple homogeneous and isotropic material. A set of designs with an internal core, either with or without auxetic behavior, were studied in order to investigate whether the choice of the material influences the behavior of the unit cell in the dispersion curve, i.e. to detect possible appearance of band gaps. In the case of the auxetic material a further investigation was carried out, and more specifically, the thickness of the sides which connect the auxetic materials with their neighboring ones were changed, in order to test their behavior. The properties of the material which were considered are given in the following table:

	Material 1	Material 2
Young modulus (Pa)	$1 \cdot 10^9$	$100 \cdot 10^9$
Density (kg/m^3)	2000	7000
Poisson ratio	0.3	0.4

Table 1: Material properties

4.1 Study of unit cells with traditional materials

In the first investigation, a square lattice without core was considered. The dispersion curve for this case is shown in Figure 4 below. It is clearly observed that no band gap appears considering only a simple square-shaped unit cell.

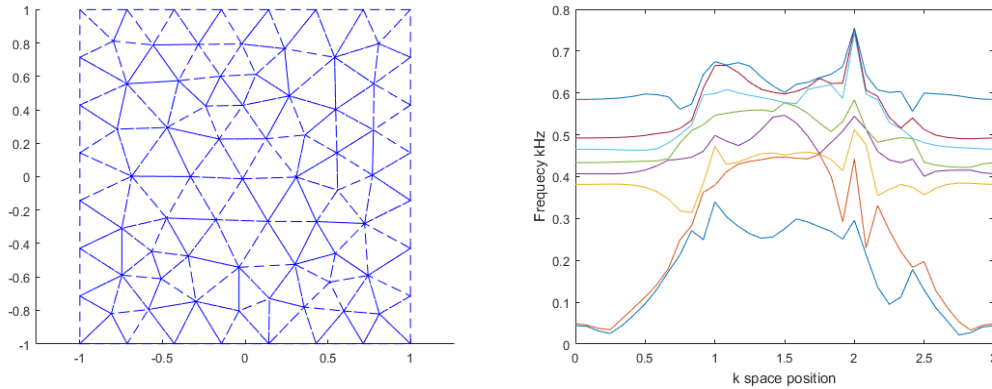


Figure 4: Square shape without core and its dispersion curve

Consequently, the case of a unit cell with an embedded stiff core was considered. This core is denoted with red color in Figure 5. In this case one can see that band gaps appear at some frequency areas, that is between the 2nd and the 3rd eigen frequencies.

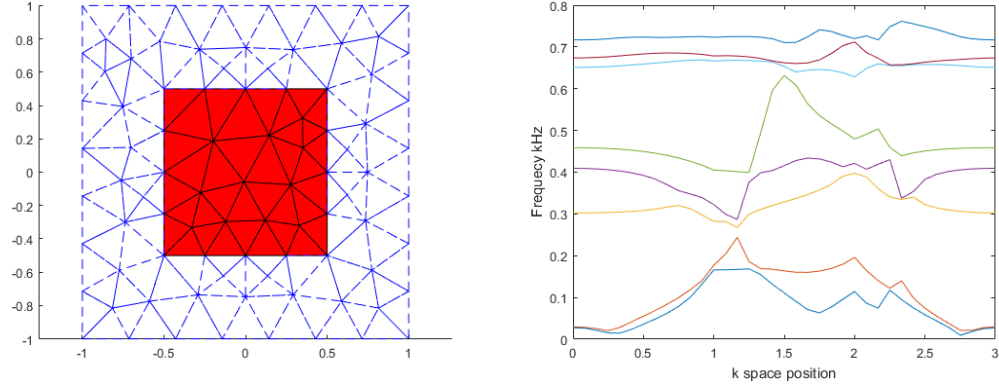


Figure 5: Square shape with core and its dispersion curve

4.2 Study of unit cells with auxetic materials

The following cases concern the design of an auxetic structure of a stiff material, with variable thickness as mentioned above. In this case we study not only the appearance of band gaps, but also the influence of the thickness of the auxetic material to the dispersion curve, as well as to the behavior of the band gap. In other words, we check if the change of the band gap is proportional to this thickness or not.

First, an auxetic star-shaped unit cell with thickness equals 0.1m is considered. In this case one can observe that some band gaps appear in a lot of regions, like between second and third eigenvalues, as seen in the following Figure 6.

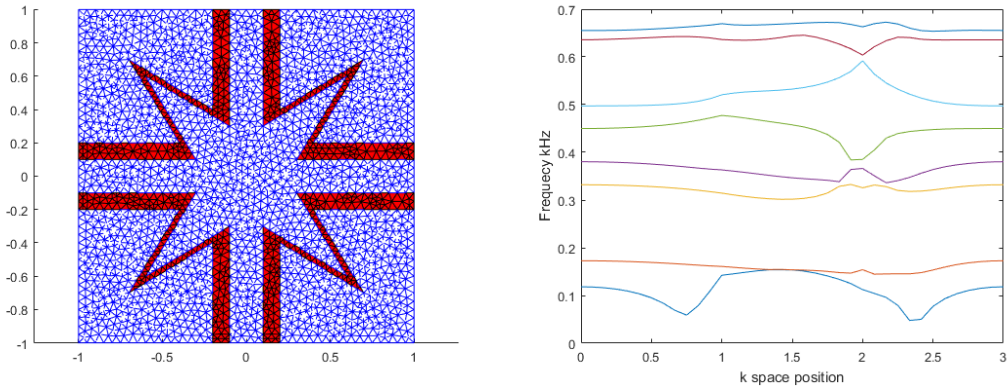


Figure 6: Square unit cell with auxetic core with thickness=0.1m and its dispersion curve

The second case is referred to an auxetic star unit cell with thickness of 0.2m. In this case we observe that no band gaps are created (see Figure 7).

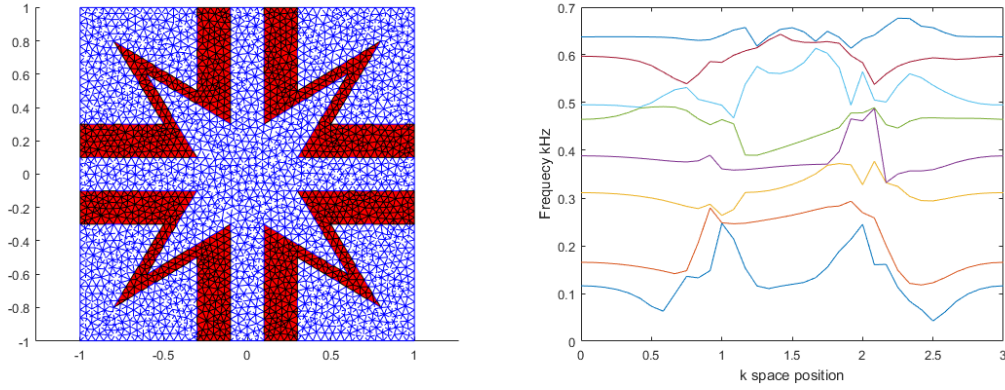


Figure 7: Square unit cell with auxetic core with thickness=0.2m and its dispersion curve

In the final case which is considered here, the auxetic star-shaped lattice has a thickness of 0.3m. It is clearly observed by Figure 8 that band gaps appear, however they are narrower compared to the case of thickness which equals to 0.1m.

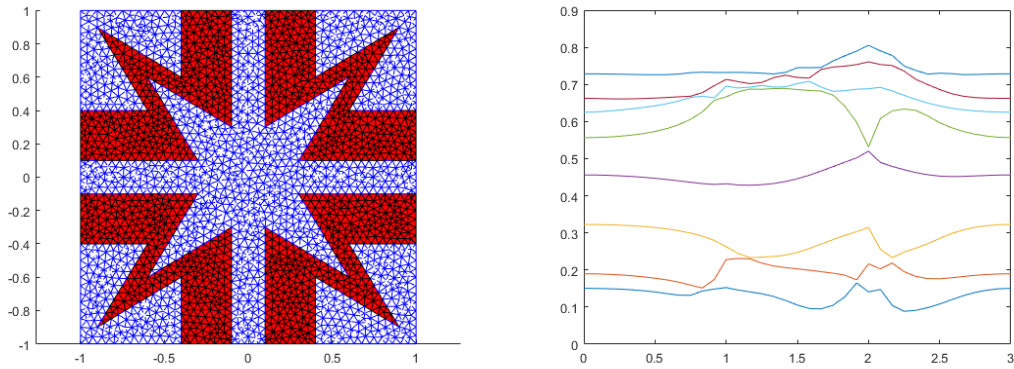


Figure 8: Square unit cell with auxetic core with thickness=0.3m and its dispersion curve

. CONCLUSIONS

The main goal of this investigation was the proper design and the analysis of a unit cell of a lattice in order to study wave propagation effects, the appearance of band gaps and eventually design with the purpose of blocking wave propagation through the structure. As a first step, several topologies of a square unit cell have been studied in order to understand the behavior of the dispersion curve, i.e. to investigate if a simple band gap was presented at the area of the first eight eigenvalues.

According to the present study, one can observe that with a simple square unit cell, no band gap occurs. Instead, with a core with enhanced mechanical properties, located in the middle of the square lattice, the first band gaps appeared. In addition, a star shape, part of the square cell, with auxetic behavior was selected in order to study the wave propagation through this hybrid unit cell. The star shape has the same mechanical properties with the previous core. Three cases with variable thickness of the star were considered. In two of the tree cases, a band gap area has achieved. However, the change

of the thickness does not affect proportionally the behavior of the dispersion curve and the band gaps.

In conclusion, the method proposed here is a systematic investigation for the dynamic behavior of the considered microstructure in the whole interval of frequencies. Based on this, optimization of band gaps is possible, according to the specific application. Extension to topology optimization in the future will allow the investigation of further, innovative auxetic microstructures.

ACKNOWLEDGEMENTS

The work of Panagiotis Koutsianitis has been supported by a doctoral grant of The Hellenic Foundation for Research and Innovation (H.F.R.I.) through the “First call for the financial support of doctoral candidates who already implement or wish to implement their doctoral theses in Greek Universities”.

REFERENCES

- [1] Spadoni, A., Ruzzene, M., Gonella, S. and Scarpa, F. Phononic properties of hexagonal chiral lattices. *Wave Motion* (2009) 46(7):435-450
- [2] Phani, A.S., Woodhouse, J. and Fleck, N.A. Wave propagation in two-dimensional periodic lattices. *J. Acoust. Soc. Am.* (2006) 119(4):1995-2005
- [3] Brillouin, L. *Wave Propagation in periodic structures*. 2nd ed. Dover, (1953)
- [4] Kittel, C. *Elementary solid state physics: A Short Course*. 1st ed. Wiley, New York, (1962)
- [5] Mace, B. R. and Manconi, E. Modelling wave propagation in two-dimensional structures using finite element analysis. *Journal of Sound and Vibration* (2008) 318:884–902
- [6] Ma, Y., Scarpa, F., Zhang, D., Zhu, B., Chen, L. and Hong, J. A nonlinear auxetic structural vibration damper with metal rubber particles. *Smart Materials and Structures*, (2013) 084012
- [7] Meng, J., Deng, Z., Zhang, K., Xu, X. and Wen, F. Band gap analysis of star-shaped honeycombs with varied Poisson’s ratio. *Smart Materials and Structures*. (2015) Vol. 24, No9
- [8] Bloch, F. *Über die quantenmechanik der elektronen in kristallgittern*. *Z. Physik*. (1928) 52:555–600
- [9] Floquet, G. *Sur les equations differentielles lineaires a coefficients periodiques*. *Annales scientifiques de l’Ecole Normale Superieure*. (1883) 12:47-88

- [10] Theocaris, P.S., Stavroulakis, G.E., Panagiotopoulos, P.D. Negative Poisson's ratios in composites with star-shaped inclusions: a numerical homogenization approach. *Arch. Appl. Mech.* (1997) 274–286
- [11] Kaminakis, N.T., Stavroulakis, G.E. Topology optimization for compliant mechanisms, using evolutionary-hybrid algorithms and application to the design of auxetic materials. *Composites Part B: Engineering* (2012) 43(6), 2655-2668
- [12] Kaminakis, N.T., Drosopoulos, G.A., Stavroulakis, G.E. Design and verification of auxetic microstructures using topology optimization and homogenization. *Arch. Appl. Mech.* (2015), 85(9-10), 1289-1306

An Efficient Computational Procedure for the Determination of the Stochastic Mechanical Properties of Defective Graphene Sheets

George Stefanou*, Dimitrios Savvas**

*Aristotle University of Thessaloniki, Greece, **National Technical University of Athens, Greece

ABSTRACT

In this paper, an efficient computational procedure is developed for the determination of the stochastic mechanical properties of graphene with different types and density of defects. The lattice of graphene is modeled using the molecular structural mechanics (MSM) approach, where the C-C covalent bonds are replaced by energetically equivalent beam elements [1]. Random fields describing the spatial variation of the anisotropic elasticity tensor of defective graphene sheets are determined using the moving window technique and Monte Carlo simulation [2, 3]. Three types of randomly dispersed defects are examined, namely Stone-Wales (SW), single vacancy (SV) and double vacancy (DV). The effect of window size, defect type and density on the random elastic properties of graphene sheets of area $100 \times 100 \text{ nm}^2$ is investigated. The results reveal that vacancy defects can reduce the axial stiffness of graphene up to 60% with respect to that of pristine graphene, whereas the effect of SW defects is less significant. Moreover, vacancy defects (especially DV defects) lead to substantial variability of the material properties. The computed random elasticity tensors can be used as input in the framework of stochastic finite element modeling of graphene structures. [1] C. Li, T.-W. Chou, A structural mechanics approach for the analysis of carbon nanotubes, *International Journal of Solids and Structures* 40 (10) (2003) 2487-2499. [2] S. Baxter, L. Graham, Characterization of random composites using moving-window technique, *Journal of Engineering Mechanics* 126 (4) (2000) 389-397. [3] D. Savvas, G. Stefanou, M. Papadrakakis, Determination of RVE size for random composites with local volume fraction variation, *Computer Methods in Applied Mechanics and Engineering* 305 (2016) 340-358.

Adaptive Systems in Lightweight Structures

Michael Stein*

*schlaich bergemann partner

ABSTRACT

The implementation of active control systems in the construction industry come with challenges due to safety requirements for any building in the public realm and the unpredictability of the performance of real world applications during a 50 or 100 year lifespan. Most of the times active systems are used to improve the performance of the structure or material, without being an essential part of the safety concept assuring the integrity of the structure. Two of these concepts, focused on applications in lightweight structures are shown in this presentation. The dynamic performance of pedestrian bridges is a great concern for owners and users with respect to safety and comfort. The most common solution to the problem is nowadays to install passive dampers at strategic locations and which are adjusted to basic dynamic performance parameters of the bridge. These parameters are strongly related to the active mass on the bridge itself. Light structures typically have low damping properties and experience high vibration sensitivity. The change in mass due to pedestrians on the bridge is relatively high and as passive dampers cannot react to this they loose their efficiency. For a stress ribbon bridge an active control system has been developed, which consists of sensor, controllers and actuators. The effectiveness of this measures in establishing a comfortable system for the pedestrian will be described in this presentation. The new BC Place Stadium Roof in Vancouver was designed to rest on an existing bowl structure, resulting in a lightweight cable fabric structure. However, large snow loads of 42psf plus snow drift had to be considered in the design. For the primary structure the prestress level in the cable system was chosen to avoid excessive deformations. The center part of the roof, which consists of deployable and inflatable fabric cushions was designed such, that only under these large snow loads the inside pressure of the cushions would have to be increased to keep their structural integrity. Thus, the detrimental growth of material creep under high long term stresses of the fabric cushions was reduced to acceptable levels. The technical challenge to implement this active control system will be described in this presentation.

Natural Boundary Conditions for Smoothing in Geometry Processing

Oded Stein^{*}, Eitan Grinspun^{**}, Max Wardetzky^{***}, Alec Jacobsen^{****}

^{*}Columbia University, ^{**}Columbia University, ^{***}Columbia University, ^{****}Columbia University

ABSTRACT

In geometry processing, smoothness energies are commonly used to model scattered data interpolation, dense data denoising, and regularization during shape optimization. The squared Laplacian energy is a popular choice of energy and has a corresponding standard implementation: squaring the discrete Laplacian matrix. For compact domains, when values along the boundary are not known in advance, this construction bakes in low-order boundary conditions. This causes the geometric shape of the boundary to strongly bias the solution. For many applications, this is undesirable. Instead, we propose using the squared Frobenius norm of the Hessian as a smoothness energy. Unlike the squared Laplacian energy, this energy's natural boundary conditions (those that best minimize the energy) correspond to meaningful high-order boundary conditions. These boundary conditions model free boundaries where the shape of the boundary should not bias the solution locally. Our analysis begins in the smooth setting and concludes with discretizations using finite-differences on 2D grids or mixed finite elements for triangle meshes. We demonstrate the core behavior of the squared Hessian as a smoothness energy for various tasks.

Grain Structures of Additive Manufactured Ni-base Superalloys Simulated by a Mesoscopic Phase-field Model

Ingo Steinbach^{*}, Mahesh Prasad^{**}, Oleg Shcayglo^{***}, Alexander Hartmaier^{****}

^{*}Ruhr-University Bochum, ICAMS, ^{**}Ruhr-University Bochum, ICAMS, ^{***}Ruhr-University Bochum, ICAMS,
^{****}Ruhr-University Bochum, ICAMS

ABSTRACT

Additive manufacturing is characterized by extreme thermal gradients which also change their orientation rapidly during the process depending on the track, speed and power of the incident beam. Correspondingly, the grain structure can vary from equiaxed to columnar with varying orientations. Also large single crystalline regions can be realized with epitaxial growth of successive layers. Numerical simulation of the competitive nucleation and growth in additive manufacturing of Ni-base superalloy samples using a mesoscopic phase field model are presented. The modelling approach takes orientation, speed and power of the incident beam as an input parameter and simulates the grain structure evolution in a mesoscopic region of the generated structure. Aspects of concurrent integration into a macroscopic simulation are discussed.

Experimental Observation of Three-Dimensional Hydraulic Fracture Dynamics in Heterogeneous Hydrogel

William Steinhardt*, Shmuel Rubinstein**

*Harvard University, **Harvard University

ABSTRACT

Hydraulic fractures occur miles underground, below complex, layered, heterogeneous rocks, making direct measurements of their dynamics or structure extremely challenging. As such, these fractures are typically studied in the lab within blocks of classically brittle materials like glass, PMMA, or rocks that are hydraulically broken with air or fluid (Bunger (2008), Alpern (2012)). Developments in polymer science have shown that heavily cross-linked hydrogels behave nearly identically both qualitatively and quantitatively to these same brittle materials and thus are another good material in which one can study hydraulic fractures (Livne et al (2004)). We have developed a system to study hydraulic fractures within these hydrogels, which have the benefits of highly tunable material properties, being optically clear, and fracture speeds and breakdown pressures 2-3 orders of magnitude lower than PMMA. Using a combination of fast camera photography and laser sheet microscopy, we can study the three dimensional morphology and dynamics of hydraulic fractures at extremely high spatiotemporal fidelity. While the fractures in the gels show excellent agreement with the tip asymptotics outlined in Rice (1968) and Spence and Sharp (1985). However, we also observe instabilities in the propagating fracture front that generate small steps, which leave behind “step lines” that segment an otherwise smooth fracture surface. We show that the density of these lines are the result of increasing mechanical heterogeneity, which we can control in our system, and that at high density, the lines interact resulting in a very rough and uneven fracture surface. This has important practical applications as roughness can be a dominant effect in hydraulic fracture propagation, as well as acting as a nucleation point for the clogging of proppants.

New Results for Stabilized Finite Element Methods for Reissner-Mindlin Plates

Rolf Stenberg*

*Department of Mathematics, Aalto University, Finland

ABSTRACT

We consider stabilized finite element methods for Reissner-Mindlin plates [1,2]. The advantages of these methods are: - They circumvent the “inf-sup” stability conditions needed for traditional mixed methods, i.e. the formulations are stable for all finite element spaces. - The conditioning of the stiffness matrix is optimal, which implies that iterative solution methods can be used [3]. A theoretical drawback of the method has been that the error analysis required the solution to be smooth, and due to this, the methods have often been questioned. We now present a new error analysis, which do not require additional smoothness. Numerical results supporting the analysis are presented. [1] T.J.R. Hughes, L.P. Franca. A mixed finite element formulation for Reissner-mindlin plate theory: Uniform convergence of all higher-order spaces. CMAME 67 (1988) 223--240 [2] R. Stenberg. A new finite element formulation for the plate bending problem. Asymptotic Methods for Elastic Structures. Proceedings of the International Conference, held in Lisbon, Portugal, October 4-8, 1993. P.G. Ciarlet, L. Trabucho and J.M. Viaño, Eds. Walter de Gruyter & Co. 1995, pp. 209–221 [3] J. Schöberl, R. Stenberg. Multigrid methods for a stabilized Reissner-Mindlin plate formulation. SIAM Journal of Numerical Analysis 47 (2009) 2735–2751

Process Modeling of LENS Manufacturing; Effects of Laser Scan Path on Residual Stress

Michael Stender^{*}, Lauren Beghini^{**}, Michael Veilleux^{***}, Joshua Sugar^{****}, Samuel Subia^{*****}

^{*}Sandia National Laboratories, Livermore, CA, USA, ^{**}Sandia National Laboratories, Livermore, CA, USA,

^{***}Sandia National Laboratories, Livermore, CA, USA, ^{****}Sandia National Laboratories, Livermore, CA, USA,

^{*****}Sandia National Laboratories, Albuquerque, NM, USA

ABSTRACT

This presentation will outline the application of a multi-physics process model of metal additive manufacturing (AM) to elucidate the effect of laser scan pattern on residual stress distribution following manufacturing. The AM process considered herein is referred to as Laser Engineered Net Shaping (LENS®); a subclass of directed energy deposition (DED) technologies. In the LENS process, a stream of metal powder is sprayed into the focal point of a laser heat source aimed at a moving stage. As the stage moves and the melt pool progressively cools, material is built up to create a final part geometry. In this work, a Lagrangian finite element analysis workflow is implemented to model the associated physical phenomena including: laser-induced heating; material deposition; heat transport through radiation, convection, and conduction; liquid-to-solid phase transition; re-melting; temperature and deformation-dependent evolution of material properties and, thermally driven deformation and residual stress accumulation. Through the application of this finite element process model, it is possible to simulate in situ LENS processing conditions as well as the resulting residual stresses, and distortions following manufacturing. A simple cylindrical part is considered and simulations are compared to experimental builds of similar laser scan patterns. Through modification of the simulated laser scan pattern, thermal conditions during manufacturing and the resulting residual stresses and distortions following manufacturing are shown to change. This work is useful in understanding the resulting properties and performance of LENS built parts and demonstrates the potential to engineer a desired residual stress state into a structure through control of LENS manufacturing strategy. *Sandia National Laboratories is a multimission laboratory managed and operated by National Technology and Engineering Solutions of Sandia, LLC., a wholly owned subsidiary of Honeywell International, Inc., for the U.S. Department of Energy's National Nuclear Security Administration under contract DE-NA0003525.

Structure-preserving Numerical Integrators for Relaxation Oscillators, with Application to Neuronal Dynamics

Ari Stern*

*Washington University in St. Louis

ABSTRACT

Relaxation oscillators pose a challenge for numerical integration, due to the presence of fast and slow time scales. Conventional exponential integrators (such as exponential Euler) allow for numerical stability at large time steps, but do a poor job at capturing the limit cycles governing oscillatory behavior unless the time step size is taken very small. In practice, this results in numerical solutions with the wrong amplitude and/or frequency of oscillation. We present a new family of methods that can maintain stability and preserve limit cycles for much larger time step sizes, with no increase in computational effort over exponential Euler. This is illustrated for the Van der Pol oscillator, as well as for the Hodgkin-Huxley model of neuronal dynamics (whose oscillations correspond to neuronal spiking). In particular, these methods allow for accurate simulation of neuronal dynamics at much lower computational cost than the methods currently used in computational neuroscience.

Ductile Fracture Representation Using the Phase-Field Model in SIERRA

Andrew Stershic^{*}, Brandon Talamini^{**}, Jakob Ostien^{***}, Michael Tupek^{****}

^{*}Sandia National Laboratories, California, ^{**}Sandia National Laboratories, California, ^{***}Sandia National Laboratories, California, ^{****}Sandia National Laboratories, New Mexico

ABSTRACT

The ability to computationally model the ductile fracture and failure of metals remains a compelling problem in the aerospace industry. This failure mechanism is preceded by significant plastic deformation and is characterized by a significant plastic zone at the blunted crack tip, rendering the typical brittle linear-elastic fracture models inadequate. In this work, we develop a phase-field model to represent the degradation of material condition in the vicinity of the strain localization. The introduction of a length-scale to limit the damage gradient acts to prevent spurious damage localization in the softening regime. This approach is implemented in SIERRA, a scalable multi-physics finite element code, and is applied to fundamental problems of interest to demonstrate its effectiveness. The specific choice of thermodynamic energy quantity used to drive the fracture process is discussed. Sandia National Laboratories is a multi-mission laboratory managed and operated by National Technology & Engineering Solutions of Sandia, LLC., a wholly owned subsidiary of Honeywell International, Inc., for the U.S. Department of Energy's National Nuclear Security Administration under contract DE-NA0003525.

The NRL Additive Manufacturing Multiphysics Discrete Element Method (NAMMDEM) Framework

John Steuben*, Athanasios Iliopoulos**, John Michopoulos***

*U.S. Naval Research Laboratory, **U.S. Naval Research Laboratory, ***U.S. Naval Research Laboratory

ABSTRACT

Additive Manufacturing (AM) has become a topic of great interest over a broad spectrum of research communities. These processes operate by successive depositions of mass and energy in a spatially resolved and highly non-uniform fashion. Feedstock materials are typically noncontinuum (i.e. large ensembles of powder particles), which are melted or sintered into a continuous object. Because of the irregular and highly localized time history of heat and mass deposition associated with these processes, a wide range of quality issues arise, including unusual microstructure morphologies, porosity, high residual stresses and strains, and generally reduced or indeterminate macro-scale mechanical properties. In powder-bed applications interaction of the recoater with both loose and sintered/melted particles, as well as atmospheric flow interaction with powder particles, have been observed to have major effects. This suggests that a simulation method that accounts for all these interactions must be implemented in order to enable the adoption of AM technologies for the production of performance-critical components. This work focuses on the development of a modeling and simulation framework for AM, based on the Discrete Element Method (DEM) [1]. Discussion of thermoplastic particle contact modeling and bond formation to capture the relevant multiphysics of the AM process will be presented. Other effects, such as gas pressure driven particle denudation are also included. Modeling of phase transformation using physics-informed level set methods will be introduced, as will appropriate boundary conditions to model relevant AM processes. This work also discusses the computational implementation of the NRL Additive Manufacturing Multiphysics Discrete Element Method (NAMMDEM) framework [2]. Particular focus will be paid to the necessity of high performance contact detection, which is required due to the highly polydisperse nature of AM feedstock powders. We will discuss improvements and optimizations to the contact detection algorithms of NAMMDEM, which have generated an order of magnitude performance improvement over its initial implementation. We will conclude with remarks regarding the integration of the NAMMDEM tool with continuum mechanics tools, such as point collocation or finite element methods. [1] Steuben, J. C., Iliopoulos, A. P., & Michopoulos, J. G. (2016). Discrete element modeling of particle-based additive manufacturing processes. *Computer Methods in Applied Mechanics and Engineering*, 305, 537-561. [2] Steuben, J. C., Iliopoulos, A. P., & Michopoulos, J. G. (2017, August). Recent Developments of the Multiphysics Discrete Element Method for Additive Manufacturing Modeling and Simulation. In *ASME 2017 IDETC/CIE* pp. V001T02A025-V001T02A025.

Computational Sciences and Math at Sandia – Algorithms, Software, and Applications

James Stewart*

*Sandia National Laboratories

ABSTRACT

The Computational Sciences and Math Group at Sandia National Laboratories fills a broad spectrum of R&D. Areas of focus include optimization, uncertainty quantification, multiphysics numerical methods, scalable numerical linear algebra, high-energy density physics, materials science spanning atomistic to continuum scales, and large-scale multiphysics application analysis. The group also develops widely-used, open-source software products including Dakota, many Trilinos packages, Albany, and LAMMPS. This talk will provide an overview of the group's research and present highlights of work across these areas of interest to the computational mechanics community.

Towards a Four-chamber Heart Model for Whole Heart Cardiac Motion Simulation

Marina Strocchi^{*}, Caroline Roney^{**}, Anton Prassl^{***}, Gernot Plank^{****}, Edward Vigmond^{*****},
Christopher Rinaldi^{*****}, Martin Bishop^{*****}, Justin Gould^{*****}, Steven Niederer^{*****}

^{*}King's College London, ^{**}King's College London, ^{***}Medical University of Graz, ^{****}Medical University of Graz,
^{*****}Fondation Bordeaux Université, ^{*****}King's College London - Guy's and St Thomas' NHS Foundation Trust,
^{*****}King's College London, ^{*****}King's College London - Guy's and St Thomas' NHS Foundation Trust,
^{*****}King's College London

ABSTRACT

Computational models of cardiac electromechanics are increasingly used for clinical applications simulating normal physiology, pathologies and treatments. Previous models have focused on the ventricles, which limit the capacity to simulate the effects of the atria, aorta and pulmonary artery on cardiac physiology. Developing models that explicitly present these surrounding structures will greatly improve simulations of changes in pre-load and afterload and move models closer to representing the clinical setting. In this work we present our four chamber cardiac modelling framework in a clinical case study. A four chamber heart model was generated from CT images with in and out-plane resolution of 0.36mm and 0.5mm, acquired from a 78-year-old female heart failure patient indicated for cardiac resynchronization therapy. Blood pools of the left ventricle, the right ventricle and the atria were automatically segmented and dilated of 6mm, 3.5mm and 2mm to obtain labels for the myocardium. The multi-label segmentation was then smoothed and upsampled to an isotropic resolution of 0.15mm, and finally meshed with an element target size of 0.8mm. The resulting tetrahedral mesh had 391551 nodes and 1875186 elements. Ventricular and atrial fibers were generated using two different rule-based mapping methods based on histological and DT-MRI measurements. Electrical excitation of the whole heart was simulated with a reaction-eikonal model. Atria and ventricles were stimulated at one right atrial and four ventricular endocardial sites. Cardiac tissue was modelled as a transversely isotropic conducting medium, with conduction velocities in the fiber and in the transverse direction tuned to achieve full atrial and ventricular activation within 90ms and 80ms, respectively. Mechanical deformations of the heart were modelled with the finite elasticity equations. Cardiac tissue was modelled as hyperelastic, incompressible, non-linear material. For the ventricles, we used a transversely isotropic constitutive law and a phenomenological active contraction model, while atria were modelled as isotropic and passive. Homogeneous Dirichlet boundary conditions were applied at the inflow tracts of the pulmonary veins, the left atrial appendage, the superior vena cava and the inferior vena cava. The model simulates the activation wave spreading across the heart. Apex-to-base shortening results in an ejection fraction of 27%. We have demonstrated in a single case the capacity to simulate both electrics and active mechanics in a four chamber heart and this provides the foundation framework for developing patient-specific four chamber heart models for studying the electrical and mechanical interaction between the atria and ventricles, in healthy and in diseased states.

Stochastic SFBEM Based on Erdogan's Solutions for Static Analysis of Crack Problems with Structural Uncertainties

Cheng Su^{*}, Zhi Xu^{**}, Zhongwei Guan^{***}, Xueming Fan^{****}

^{*}South China University of Technology, ^{**}South China University of Technology, ^{***}University of Liverpool,
^{****}South China University of Technology

ABSTRACT

Mathematical formulation and computational implementation of the stochastic spline fictitious boundary element method (SFBEM) are presented for static analysis of crack problems with structural parameters modeled as random fields. The stochastic governing differential equations of crack problems are decomposed into two sets of governing differential equations with respect to the means and the deviations of cracked plate responses by including the first order terms of deviations. These equations are in similar forms to those of deterministic crack problems, and they can be solved using deterministic fundamental solutions of cracked plates, namely the Erdogan's solutions, resulting in the means and covariances of the stress intensity factors and structural responses. The stress boundary conditions on the crack surface are automatically satisfied and the singular behaviour at the crack tip can be naturally reflected without setting boundary elements on the crack surfaces due to the use of the Erdogan's fundamental solutions. The proposed method is validated by comparing the solutions with those obtained by Monte Carlo simulation for a number of example problems.

A Phase-Field Study of the Grain-Size and Frequency Dependent Ferroelectric Characteristics of BaTiO₃ nanoceramics

Yu Su*

*Beijing Institute of Technology

ABSTRACT

In this work, we address a couple of fundamental issues in one of the most widely studied functional materials - ferroelectric ceramics, but with nano-sized grains. As the grain size decreases to the nanometer range, the characteristics of the ferroelectric nanoceramic can be ultimately determined by the competition between two effects: the intrinsic effect that is associated with the local properties of the grain boundary and the extrinsic effect that arises from the dynamics of domain structure which is highly influenced by the depolarization field caused by the grain boundary. In this work we investigate such a competition with a phase-field simulation based on the time-dependent Ginzburg-Landau (TDGL) kinetic equation. The study is performed on poled/unpoled nanoceramics under high- and low-amplitude bipolar alternating electric field with selected grain size and loading frequency. Our calculations for poled BaTiO₃ at 100 Hz show that, for the grain size from 170 to 50 nm, its properties are dominated by the extrinsic effect, and from 50 to 10 nm, they are dominated by the intrinsic one. As the grain size decreases, the dielectric and piezoelectric constants at the remnant state continuously rise in the extrinsic-dominated region and then drop sharply in the intrinsic-dominated region. Our frequency calculations from 10 to 2,500 Hz at the grain size of 100 nm indicate that the high-frequency behavior is very similar to that of the small grain-size, intrinsic-dominated one, whereas the low-frequency behavior is closely related to that of the large grain-size, extrinsic-dominated part, with the demarcation line occurring around 400 Hz. For the un-poled ceramics under small signal loading, the intrinsic effect is dominant over the entire range of grain size and frequency.

A Computational and Experimental Co-designed Framework for Confined Impact Test of Powder Materials

Waad Subber*, Sangmin Lee**, Karel Matous***

*University of Notre Dame, **University of Notre Dame, ***University of Notre Dame

ABSTRACT

The confined impact test is a common experiment to investigate the dynamical response of powder materials at high strain rates. The goal of the experiment is to generate the high internal pressure and temperature that can lead to synthesis of a new material, when reactive powder materials are used. The numerical simulations of such an experiment are challenging due to the high strain rates, large deformations, complex material behavior, and the high computational cost. To better understand the physical phenomena and to optimize the conditions under which a new material can be synthesized, a co-designed computational and experimental framework is investigated. The simulations of the experiment are performed using in-house massively parallel finite strain Lagrangian code PGFem3D equipped with a newly developed poro-viscoplastic constitutive model for powder material. Based on a sensitivity analysis we noticed that the dimensions governing the shape of the sample have equally important roles in achieving the maximum pressure inside the sample. To optimize the shape of the sample, we construct a probabilistic response surface based on Gaussian process (GP). A training dataset is used to build the response surface and an independent testing dataset is used to verify the prediction of the GP. The mean of the GP is exploited to obtain the optimal dimensions required to achieve the maximum pressure inside the sample. For validation under uncertainty, quantities of interest (QOIs) within subregions of the computational domain are introduced. The QOIs are the reaction force at the bottom face of the sample and the deformed shape represented by the displacement trajectory at the center point of the sample. To provide a confidence bound on the numerical predictions of the QOIs, the impact velocity is represented by a suitable stochastic expansion and propagated forward through the computational model. The numerical predictions of the QOIs with the associated confidence intervals are compared with the co-designed experimental results.

A Transformed Path Integral Approach for Linear-Quadratic Control

Gnana Subramaniam^{*}, Prakash Vedula^{**}

^{*}University of Oklahoma, ^{**}University of Oklahoma

ABSTRACT

We present an adaptive path integral based method for optimal, linear-quadratic (LQ) control of a nonlinear stochastic dynamical system. In our proposed approach, termed the transformed path integral control (TPIC), we utilize a short-time propagator formulation that allows the governing partial differential equation for LQ control to be solved in a transformed computational domain where the stochastic optimal controls are obtained, while preserving short-time properties of the underlying system dynamics. The formulation ensures non-negativity of the underlying probability density functions (PDFs) and realizability of the associated cost-functions, while better accommodating nonlinearities in drift and non-Gaussian behavior in PDFs. The choice of transformation considered, which maps a fixed grid in transformed space to a dynamically adaptive grid in the original state space, enables us to explore controls in desired domains of importance (or regions of high probability). The proposed method also allows for estimation of error bounds on the probability in the computational domain using Chebyshev's inequality. In addition, the method can accurately represent the underlying PDFs and better address challenges in processes with large diffusion, large drift and large concentration of the PDFs similar to the TPI method [1]. These features enable the TPIC approach to have better computational performance and efficiency, in comparison to conventional Monte Carlo and fixed grid based approaches. Additionally, we also present formulations to further enhance the computational efficiency of TPIC through application of Fast Gauss Transform techniques and bandlimiting approaches on the propagator matrices. We evaluate the performance of the TPIC method over conventional methods for LQ control of linear and nonlinear stochastic dynamical systems via consideration of canonical problems in one-dimensional and multi-dimensional state spaces. Generalization of the proposed framework to non-LQ context will also be discussed. [1] Gnana M Subramaniam and Prakash Vedula. "A transformed path integral approach for solution of the Fokker–Planck equation". In: Journal of Computational Physics 346 (2017), pp. 49– 70.

A Meshfree Generalized Finite Difference Method for Surface PDEs

Pratik Suchde^{*}, Joerg Kuhnert^{**}

^{*}Fraunhofer ITWM, Germany, ^{**}Fraunhofer ITWM, Germany

ABSTRACT

We propose a novel meshfree Generalized Finite Difference Method (GFDM) approach to discretize PDEs defined on manifolds. Derivative approximations for the same are done directly on the tangential plane at each point. As a result, the proposed method not only does not require a mesh, it also does not require an explicit reconstruction of the manifold. In contrast to existing methods for surface PDEs, it avoids the complexities of dealing with a manifold metric, while also avoiding the need to solve a PDE in the embedding space. As a result, a further advantage is that developments in usual (volume/bulk based) GFDM operators can be easily carried over, in this framework, to surface-based GFDM differential operators. We propose discretizations of the surface gradient operator, the surface Laplacian and surface Diffusion operators. Possibilities to deal with anisotropic and discontinuous surface properties (with large jumps in the diffusion coefficient, up to several orders of magnitude) are also introduced. The scope of using a moving Lagrangian framework for surface PDEs discretized using a meshfree GFDM will also be brought to light.

Computational Methods for Supporting Patient-Specific Treatment on Orthodontics

Kazuhiro Suga*

*Kogakuin University

ABSTRACT

It is an essential need for both patients and medical doctors to realize safe and effective treatments on orthodontics. Numerical prediction through computational mechanics has the potential to achieve it. However, a few trials have been carried out and there is no trial in clinical practice. We are developing a supporting system on orthodontics with the orthodontists in TMDU (Tokyo Medical and Dental University) in Japan. This report gives the goal of our support system and its current status in (1) a tooth-PDL modeling in order to predict the initial tooth movement for patient-specific clinical use, and (2) evaluation of orthodontic force and moment by a super elastic wire during tooth movement for designing treatment plan.

Ultimate State Simulations by Finite Cover Method with Damage Model

Hirofumi Sugiyama^{*}, Koji Saito^{**}, Kazumi Matsui^{***}, Shigenobu Okazawa^{****}

^{*}University of Yamanashi, ^{**}University of Yamanashi, ^{***}Yokohama National University, ^{****}University of Yamanashi

ABSTRACT

This paper examined the ultimate state of the metal, which called ductile fracture, by using finite cover method with damage model. Estimating the ultimate state is interests in many fields of engineering. In these days, high tensile strength steel and so on has used, finite element simulations play important roles to predict the complex material behavior. Especially, the ductile properties of metals are important to control the ultimate state of the metals. The continuum damage mechanics has been developed for that purpose, and relates the microscopic voids and the macroscopic damage parameters. The damage parameter is defined as between zero to one, which means the propagation of the ductile fracture. However, the propagation of the ductile fracture is described as the merely increase of the value. Therefore, this model is not able to represent the discontinuous deformation clearly. The conventional finite element simulation(FEM) is not good at handling the discontinuities, especially in crack propagation analysis because the FEM describes the discontinuities by elements boundaries. Some special techniques are necessary in order to describe the discontinuous deformation. Moreover, generalized finite element method have been developed mainly in fracture mechanics. extended finite element method(X-FEM) is well-known method. This method can easily simulate the nucleation and growth of discontinuities (cracks) by the character of enhanced approximation function. The X-FEM is mainly used for elastic body, thus the elasto-plastic analysis is less frequently. By contrast, finite cover method(FCM)is also proposed as one of the generalized finite element method. The FCM is able to describe the discontinuities obviously by multiple covers, which based on the basic concept of this method. In this paper, we examine the material behavior up to ultimate state by using FCM with damage model. Here firstly focuses on the force displacement curve at post peak and compare with some load condition by some shape of test pieces. Moreover, considering the crack initiation condition and some representative simulations are demonstrated. Consequently, we confirm proposed method using simple techniques is able to represent the ultimate state of material.

Spectral Finite Elements and Enriched Partition-of-unity Methods for Band Structure Calculations in Phononic Crystals

N. Sukumar^{*}, Ankit Srivastava^{**}

^{*}UC Davis, ^{**}IIT Chicago

ABSTRACT

Phononic crystals are periodic composites in 1-, 2- and 3-dimensions, which can be used to control vibration and waves (acoustic and/or elastodynamic) in these dimensions [1]. They differ from homogeneous materials most strikingly in the presence of the frequency bandgaps, which indicates regions of frequencies where such waves are prohibited from propagating in the crystal. Applications of phononic crystals range from noise and vibration control and collimation and refraction to determining their thermal properties (heat conductivity and heat capacity) and in topology design. The fundamental Bloch-periodic problem that is solved in the unit cell is: for a given wavevector (k -point) in the irreducible Brillouin zone, the solution of the elastodynamic eigenproblem provides the eigenpairs (eigenfrequencies and eigenmodes) that are used to construct the band structure. The most common approaches to solve the phononic eigenproblem are those based on planewaves (Fourier basis), variational methods such as the displacement-based finite element method, and multiple scattering, with recent advances including multiscale finite elements and Bloch-mode synthesis techniques. In this talk, we will first show the benefits of using spectral finite elements to compute the band structure of a two-phase 1-dimensional phononic crystal that has an exact solution. We will compare spectral finite elements to planewave expansion with displacement and mixed Rayleigh quotients [2], and show that spectral finite elements is particularly accurate and efficient when the two phases have sharp contrasts in material properties. For modeling a domain containing holes in two dimensions, we adopt a new numerical integration scheme [3] that permits use of a fixed Cartesian mesh with higher-order finite elements. Band structure calculations on perforated phononic materials will be presented to demonstrate the accuracy of the method. REFERENCES 1. M. I. Hussein, M. J. Leamy and M. Ruzzene, Dynamics of phononic materials and structures: Historical origins, recent progress and future outlook, *Applied Mechanics Reviews*, 66(4), 040802, 2014. 2. Y. Lu and A. Srivastava, Variational methods for phononic crystals, *Wave Motion*, 60, pp. 46-61, 2016. 3. E. B. Chin, J. B. Lasserre and N. Sukumar, Numerical integration of homogeneous functions on convex and nonconvex polygons and polyhedra, *Computational Mechanics*, 56(6), pp. 967-981, 2015.

THE STABILITY AND DYNAMIC BEHAVIOUR OF ELASTIC NON-LINEAR FLUID-LOADED STRUCTURES

R. SULIMAN^{*†}, O.F. OXTOPY[†], AND N. PEAKE^{*}

^{*}Department of Applied Mathematics and Theoretical Physics

University of Cambridge

Cambridge, Cambridgeshire, United Kingdom

R.Suliman@damtp.cam.ac.uk, N.Peake@damtp.cam.ac.uk

[†]Aeronautics System

Council for Scientific and Industrial Research

Pretoria, Gauteng, South Africa

ooxtoby@csir.co.za

Key words: Modal Analysis, Fluid-structure Interaction, Multiphysics Problems, Stability Analysis, Strong-coupling.

Abstract. The deformation of slender elastic structures due to the motion of fluid around it is a common multi-physics problem encountered in many applications. This work details the development and implementation of a numerical model capable of solving such strongly-coupled fluid-structure interaction problems.

In most fluid-structure interaction problems the deformation of the slender elastic bodies is significant and cannot be described by a purely linear analysis. We present a new formulation to model these larger displacements. By extending the standard modal analysis technique for linear structural analysis, the governing equations and boundary conditions are updated to account for the leading-order non-linear terms and a new modal formulation with quadratic modes is derived. The quadratic modal approach is tested on standard benchmark problems of increasing complexity and compared with analytical and full non-linear numerical solutions.

Two computational fluid-structure interaction approaches are then implemented in a partitioned manner: a finite volume method for discretisation of both the fluid and solid domains and the quadratic modal formulation for the structure coupled with a finite volume fluid solver. Strong-coupling is achieved by means of a fixed-point solver with dynamic relaxation. The fluid-structure interaction approaches are validated and compared on benchmark problems of increasing complexity and strength of coupling between the fluid and solid domains.

Fluid-structure interaction systems may become unstable due to the interaction between the fluid-induced pressure and structural rigidity. A thorough stability analysis of finite elastic plates in uniform flow is conducted by varying the structural length and flow velocity showing that these are critical parameters. Validation of the results with those from analytical methods is done. An analysis of the dynamic interactions between multiple finite plates in various configurations is also conducted.

1 INTRODUCTION

Computational mechanics is a growing discipline which uses computational methods to obtain approximate solutions to problems governed by the principles of mechanics. Fluid-structure interaction (FSI) constitutes a branch of computational mechanics in which there exists an intimate coupling between fluid and structural or solid domains; the behaviour of the system is influenced by the interaction of a moving fluid and a flexible solid structure. Examples of such FSI systems include wing flutter on aircraft, aeroelasticity of turbomachinery blades, flows in elastic pipes and blood vessels, heart valve dynamics, swimming of fish and in the processing of paper. In this work, we make use of a blend of mathematical and computational approaches to study strongly-coupled fluid-structure interaction problems involving long thin structures.

2 STRONGLY-COUPLED FLUID STRUCTURE INTERACTION APPROACHES

Two computational fluid structure interaction (FSI) approaches are implemented in a partitioned manner to model FSI problems. In the first approach a finite volume method is developed and implemented in *OpenFOAM* by coupling fluid and structural solvers. The finite element method has primarily been used for modelling the mechanics of solids¹. The finite volume method² has traditionally been more dominant in the field of fluid mechanics but has received increased attention for use in solid mechanics over the last two decades. Both schemes can be considered as methods of weighted residuals where they differ in the choice of weighting function³. In terms of computational FSI approaches, many recent studies have made use of a single discretisation scheme, either finite element^{4,5,6} or finite volume^{7,8,9}, to solve the entire domain. This simplifies the treatment at the interface of the fluid and solid domains. The fluid is assumed to be viscous, incompressible and isothermal with the governing equations given by the continuity and Navier-Stokes equations in an arbitrary-Lagrangian-Eulerian (ALE) reference frame. The solid is assumed to be a homogeneous isotropic elastic solid undergoing large, non-linear deformation with the motion governed by Cauchy's first equation of motion. We make use of the finite

volume method for discretisation of the entire domain. In the second approach a reduced-order modal approach for solving the structural equations is implemented and coupled with an incompressible finite volume fluid solver in *OpenFOAM*. Strong-coupling of the fluid and solid domains is achieved by means of a fixed-point solver using a dynamic relaxation parameter based on Aitken's method. It is a simple yet highly robust and efficient approach.

2.1 Governing Equations

The equations governing viscous incompressible isothermal fluid flow in an arbitrary-Lagrangian-Eulerian (ALE) reference frame¹⁰ are given by the continuity and Navier-Stokes equations. To close the governing equations, a constitutive relation for stress is required. We assume a Newtonian fluid to relate the stress to strain.

The partial differential equations that describe a homogeneous isotropic elastic solid undergoing large, non-linear deformation are given by Cauchy's first equation of motion¹¹. Assuming an isotropic hyperelastic St. Venant--Kirchhoff material model, the stress-strain relationship is given in terms of the second Piola--Kirchhoff stress. The first Piola--Kirchhoff stress is related to the second Piola--Kirchhoff stress by the deformation gradient, which relates quantities in the undeformed configuration to their counterparts in the deformed configuration. The constitutive stress-strain relationship is given in terms of the Green--Lagrange strain, which is related to the displacement field through the gradients of displacement.

The finite volume method of discretisation is used for the spatial discretisation of the equations above. This is done by placing them into weak form or integrating over an arbitrary control volume and applying the divergence theorem of Gauss.

2.2 Modal FSI Analysis

Tangential to the full finite volume FSI approach, a reduced-order modal approach to solving the structural equations has been used and coupled with an incompressible finite volume fluid solver in *OpenFOAM*.

For a modal structural analysis, Lagrange's equations of motion in the general case are used, which provides an expression for the eigenvalues or natural frequencies and eigenvectors or mode shapes.

2.3 Fluid-Solid Coupling

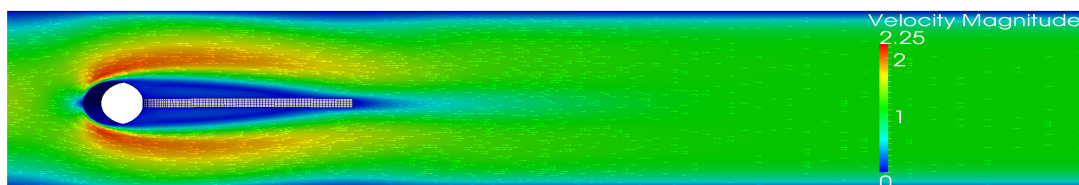
In this work we limit our analyses to incompressible flows and have made use of the incompressible *pimpleDyMFoam* flow solver. The coupling between the fluid and solid is done once at the beginning of every time-step when movement of the mesh occurs. The fluid flow provides a traction onto the structure. This results in a deformation of the structure which in turn affects the fluid flow. Coupling conditions for the traction, displacement and velocity are applied to ensure momentum conservation or force equilibrium at the interface, as well as to enforce the kinematic or geometric continuity and no-slip conditions respectively. The above conditions require an iterative procedure such that a strongly-coupled solution is obtained.

FSI systems can be solved using a single or monolithic solution method, which is inherently strongly-coupled, or a partitioned solution method, which can be strongly- or weakly-coupled. Monolithic methods ensure stability and convergence of the solution, since all equations are discretised and solved simultaneously. However, this approach may suffer from ill conditioning and convergence is generally slow. Conversely, partitioned approaches allow for the use of two independent solution techniques for solid and fluid equations in isolation. Weakly-coupled partitioned methods may diverge or result in inaccurate solutions when applied to problems where there are strong interactions between solid and fluid domains. The FSI implementation described above is a weakly-coupled one: the modal equations are solved as a boundary condition only once at the beginning of each time-step. If applied to strongly-coupled problems, the solver results in inaccurate solutions or diverges.

A separate coupling algorithm or additional outer iterations between the fluid and solid is therefore required to achieve strong-coupling. The most popular strongly-coupled FSI algorithms either use fixed point iteration or interface Newton--Krylov methods. Both approaches have their own shortcomings: fixed point methods are generally slow to converge as they make use of Gauss--Seidel iterations and methods to speed up convergence are needed, whilst Newton--Raphson methods require the computation of Jacobians that may be difficult to calculate exactly. A strongly-coupled fixed-point solver with dynamic relaxation, has been implemented in this work. It is the most basic of the above approaches yet is highly robust and efficient. The fixed point solver uses a relaxation parameter based on Aitken's method. The solver was modified to call the mesh movement algorithm after every iteration, thus allowing a re-calculation of interface forces, displacements and velocities with every iteration hence resulting in a fully-coupled scheme upon convergence.

2.4 Two-dimensional Flapping Beam

Both FSI approaches have been successfully validated and compared on benchmark cases and the results for a common FSI benchmark problem, proposed by Turek and Hron¹², of an elastic beam in the wake of a cylinder undergoing vortex-induced vibration are included here. The properties of the fluid and solid are as described in¹². A uniform constant fluid velocity, Reynolds number, $Re = 100$, was applied at the inlet while at the exit pressure was set to zero. Flow is assumed to be laminar. Snapshots of the beam deflection and velocity contours at various times are shown in Figure 1, showing large oscillations of the beam in its second mode of vibration as vortices are shed periodically from either side of it.



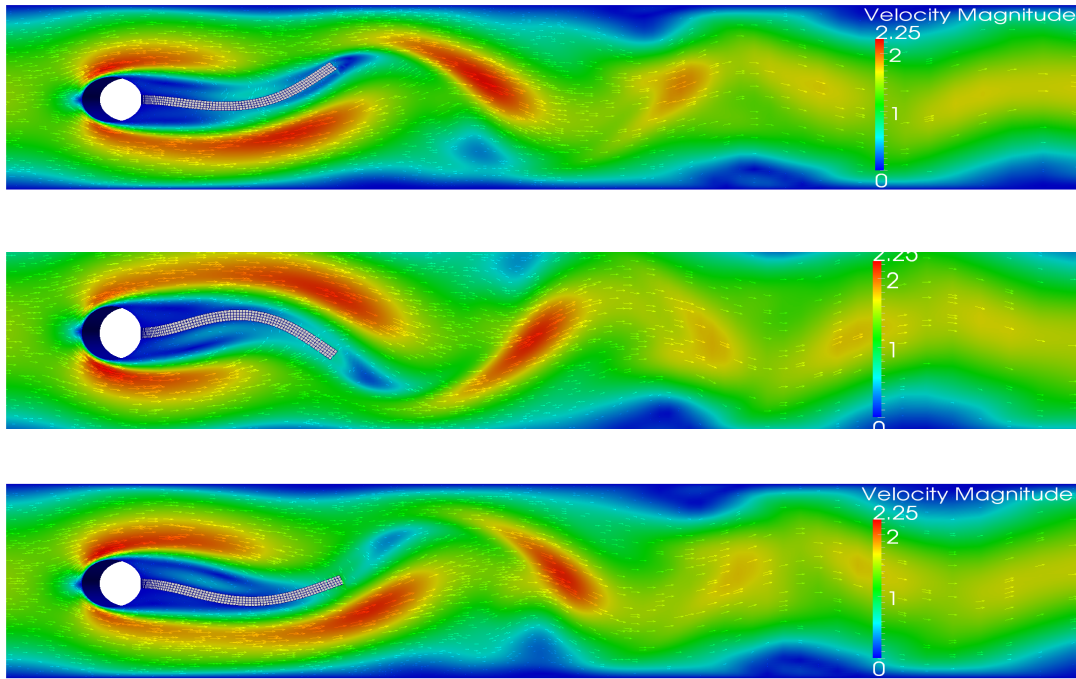


Figure 1: Velocity contours for a 2D beam oscillating in its second mode of vibration.

The vertical tip displacements of the beam using the modal FSI solver and the finite volume FSI method are compared with the results of Turek and Hron¹² in Figure 2. There is a good correlation between these results.

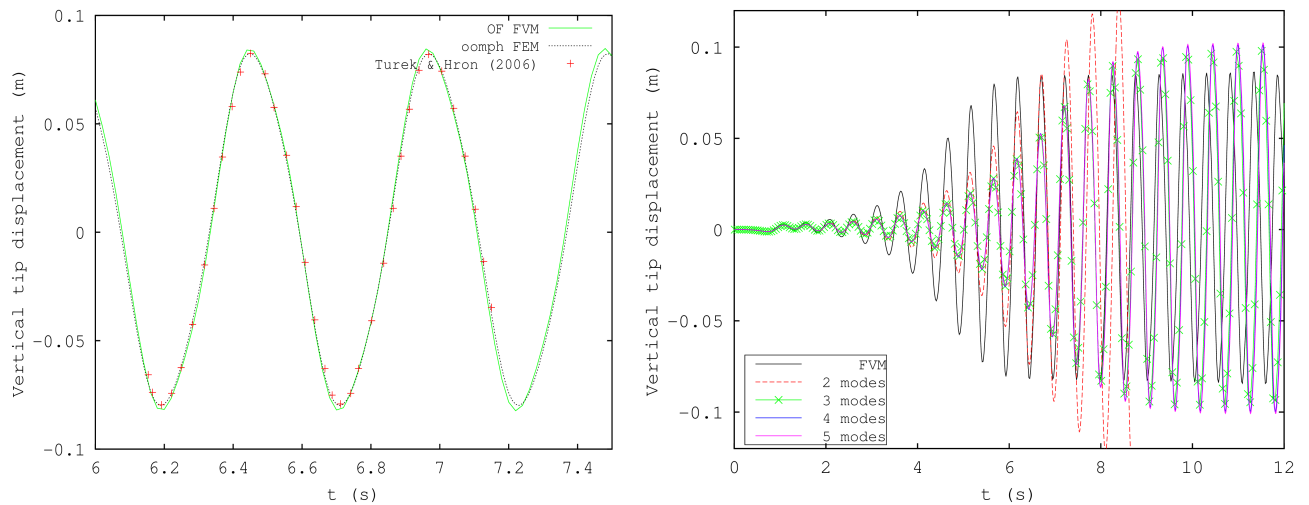


Figure 2: Vertical tip displacement for the Turek & Hron case using the finite volume method (left) and modal approach (right).

The finite volume FSI results, however, required a very fine mesh for the solid domain and consequently a long run-time. Upon further investigation of just a cantilever beam under a tip load it was found that the finite volume method for structural mechanics suffered from a phenomenon of shear locking. When the aspect ratio of the elements (ratio of element width to height) is large, a numerical shear strain component is produced in addition to a bending strain. This absorbs strain energy and results in a decrease in displacement or stiffening, as shown by the results in Figure 3 (left). In addition, an evaluation of the accuracy of the finite volume scheme shows that the scheme is only first-order accurate, see Figure 3 (right), which also explains the slow convergence in the result.

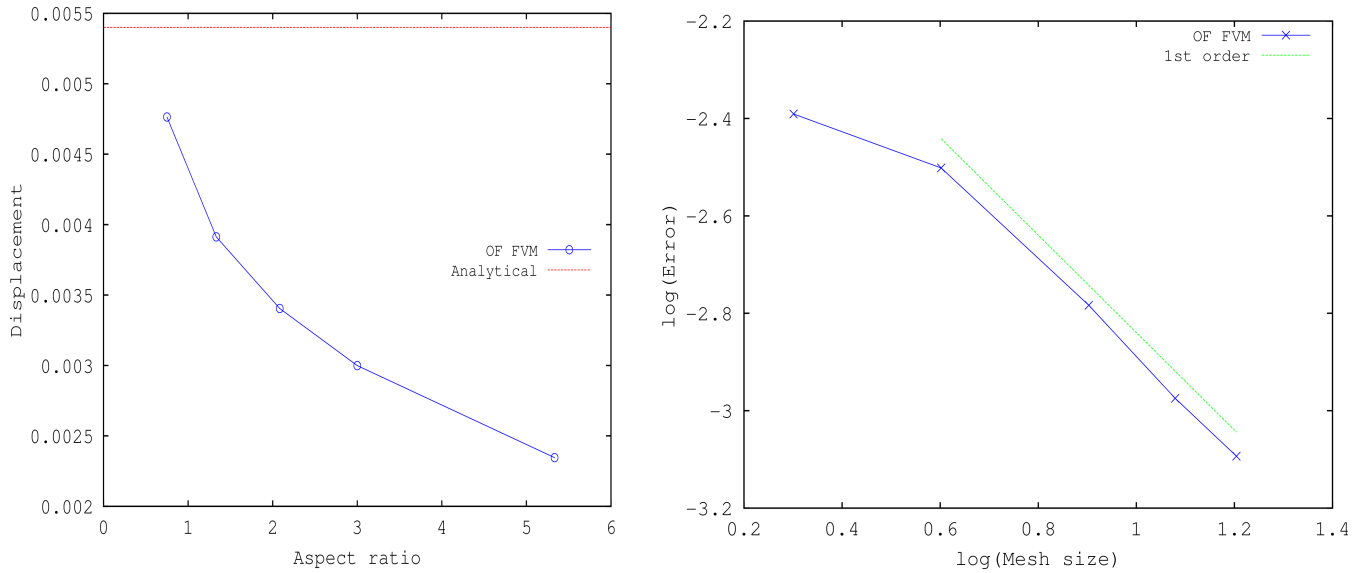


Figure 3: Analysis of a cantilever beam using the finite volume method: shear locking (left) and order of accuracy (right).

3 STABILITY ANALYSIS

The FSI system may become unstable due to the interaction between the fluid-induced pressure and structural rigidity, with flow velocity and structural length being critical parameters that influence the stability of the system. Three distinct theoretical approaches have traditionally been used to study the flapping stability of slender elastic structures immersed in axial flow. These include the traditional hydrodynamic stability theory, which can be viewed as a fluid-centric approach, the structural acoustic or wave-based approach and the aeroelastic theory or structure-centered approach. A number of detailed experimental studies have also been conducted including soap-film, water-tunnel and wind-tunnel experiments. If the flow velocity is below a certain critical value, the structure remains unmoved or in a so-called stretched-straight state. Above the critical flow velocity, the structure undergoes self-sustaining and regular flapping, while at a much greater velocity irregular and chaotic flapping results. In terms of structural length, it has been shown that below a critical length the structure always remains in the stretched-straight state. Most theoretical studies have been restricted to linear analyses and two

dimensions, whilst only a few studies have looked at the effect of multiple slender bodies. The use of computational methods may help to overcome these limitations.

The modal FSI approach was validated by application to a two-dimensional two degree-of-freedom airfoil. Theoretical methods predict a critical velocity of 51.5 m/s. The results from the transient analysis with an inlet velocity of 51.5m/s show constant amplitude flapping, Figure 4, which corresponds well with theoretical predictions.

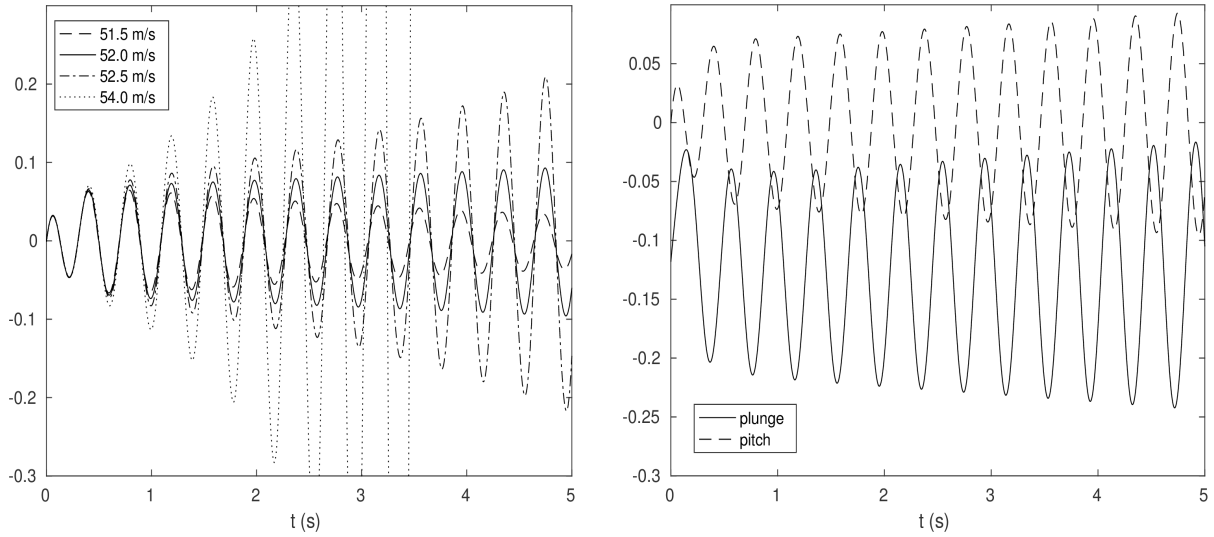


Figure 4: Flutter analysis of a two-degree-of-freedom airfoil.

A rigorous stability analysis of a two-dimensional finite plate under axial flow is conducted. The plate, which is initially at rest, is clamped at the leading edge and free at the trailing edge. A small initial perturbation is applied and the long-term transient behaviour of the plate is analysed. The bending rigidity of the structure stabilises the system, whilst an increase in aerodynamic pressure due to an increase in flow velocity destabilises the system and results in flutter. Following previous work^{13,14,15}, the critical stability curves can be defined in terms of the non-dimensional flag density and non-dimensional velocity. The critical stability curves are shown in Figure 5. Also shown on this figure are various points that were studied in this analysis. For comparison the flow is assumed to be inviscid in this case.

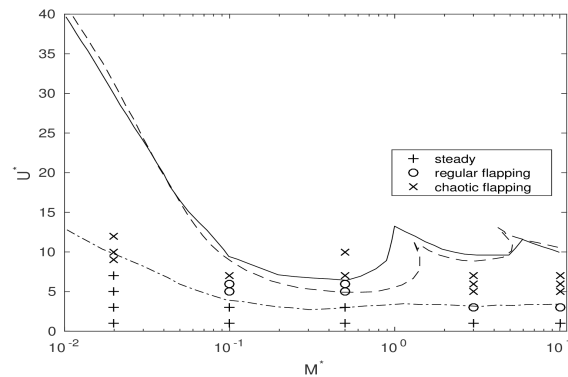


Figure 5: Critical stability curves for a finite flag under axial flow together with data points in this study.

The critical stability curves shown in Figure 5 contain branches that correspond to a different mode structure, as also observed experimentally by Eloy et al.¹⁴. The first branch for $M^* < 1$ corresponds with a flapping of the plate in its second mode of vibration, while the branch for $1 < M^* < 8$ corresponds with flapping in the third mode and $M^* > 8$ corresponds with the fourth mode. An analysis of the flapping behaviour shows good agreement with the results of Eloy et al.¹⁴ and Michelin et al.¹³. Snapshots of the flapping behaviour of the plate at $M^* = 0.002$ and $U^* = 9$ are shown in Figure 6. The second mode of vibration dominates this flapping behaviour and can be observed by the single node, or position of zero displacement, along the plate.

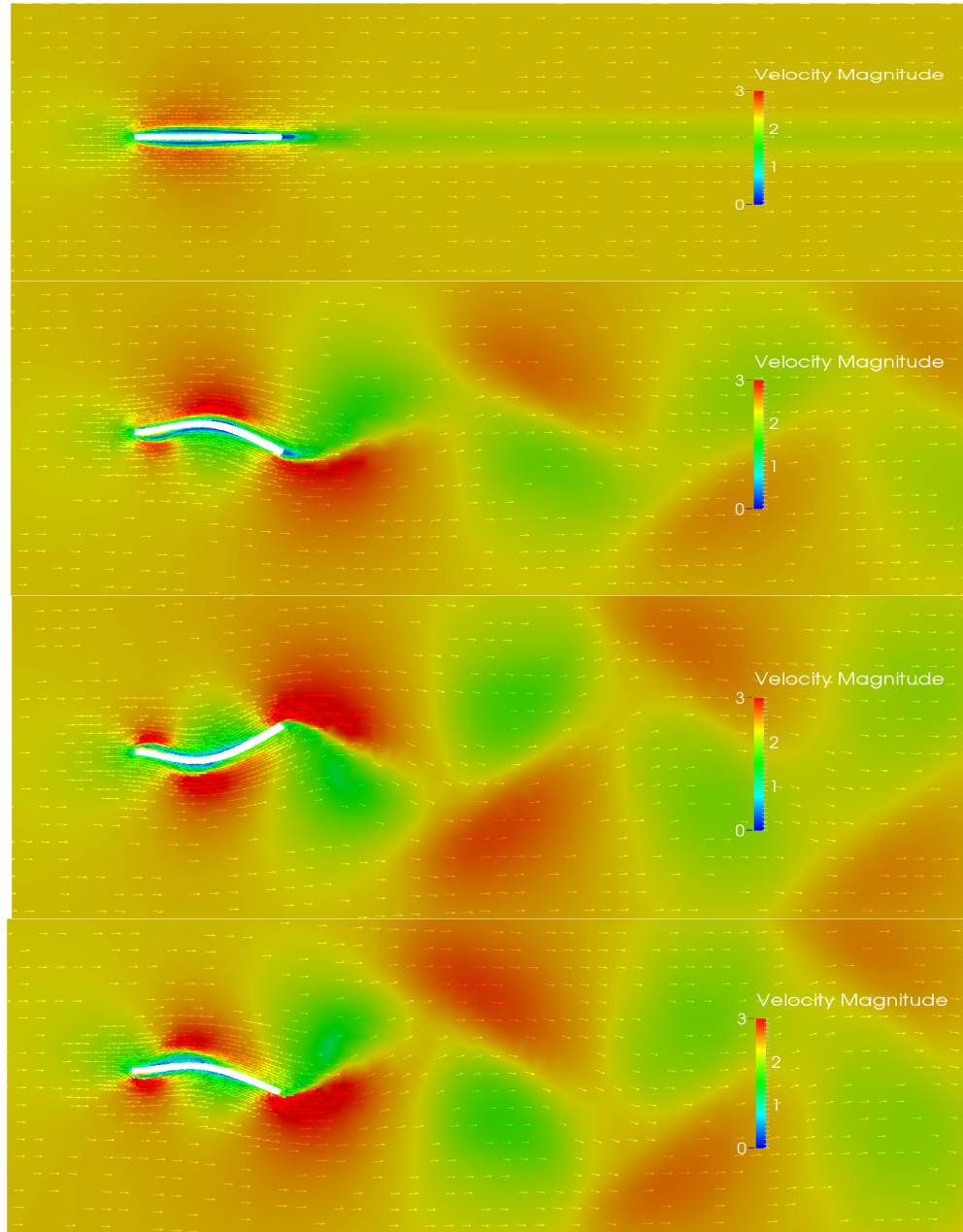


Figure 6: Snapshots of the flapping behaviour of the plate at $M^* = 0.002$ and $U^* = 9$.

12 REFERENCES

- [1] Zienkiewicz, O. C., and Taylor, R. L., 2000. *The Finite Element Method: Volume 2 - Solid Mechanics*, fifth ed. Butterworth-Heinemann, Oxford.
- [2] Patankar, S. V., 1980. *Numerical Heat Transfer and Fluid Flow*. McGraw-Hill, New York.
- [3] Suliman, R., Oxtoby, O., Malan, A., and Kok, S., 2014. "An enhanced finite volume method to model 2D linear elastic structures". *Applied Mathematical Modelling*, 38(7-8), pp. 2265–2279.
- [4] Hubner, B., Walhorn, E., and Dinkler, D., 2004. "A monolithic approach to fluid–structure interaction using spacetime finite elements". *Comput. Methods Appl. Mech. Engrg.*, 193, pp. 2087–2104.
- [5] Dettmer, W., and Peric, J., 2006. "A computational framework for fluid-structure interaction: Finite element formulation and application". *Computer Methods in Applied Mechanics and Engineering*, 195, pp. 5754–5779.
- [6] Teixeira, P., and Awruch, A., 2005. "Numerical simulation of fluid-structure interaction using the finite element method". *Computers and Fluids*, 34, pp. 249–273.
- [7] Slone, A., Pericleous, K., Bailey, C., and Cross, M., 2002. "Dynamic fluid-structure interaction using finite volume unstructured mesh procedures". *Computers and Structures*, 80, pp. 371–390.
- [8] Weller, C. G. H., 2005. "A unified formulation for continuum mechanics applied to fluid-structure interaction in flexible tubes". *International Journal for Numerical Methods in Engineering*, 64, pp. 1575–1593.
- [9] Suliman, R., Oxtoby, O., Malan, A., and Kok, S., 2015. "A matrix free, partitioned solution of fluid-structure interaction problems using finite volume and finite element methods". *European Journal of Mechanics - B/Fluids*, 49A, pp. 272–286.
- [10] Hirt, C., Amsden, A., and Cook, J., 1974. "An arbitrary Lagrangian-Eulerian computing method for all flow speeds". *Journal of Computational Physics*, 14, pp. 227–253.
- [11] Holzapfel, G., 2001. *Nonlinear Solid Mechanics: A continuum Approach for Engineering*. John Wiley & Sons Ltd., West Sussex, England.
- [12] Turek, S., and Hron, J., 2006. "Proposal for numerical benchmarking of fluid-structure interaction between an elastic object and laminar incompressible flow". *Lecture Notes in Computational Science and Engineering*, 53(371).
- [13] Michelin, S., Stefan, G., Smith, L., and Glover, B. J., 2008. "Vortex shedding model of a flapping flag". *Journal of Fluid Mechanics*, 617, Nov., p. 1.

- [14] Eloy, C., Lagrange, R., Souilliez, C., and Schouveiler, L., 2008. "Aeroelastic instability of cantilevered flexible plates in uniform flow". *Journal of Fluid Mechanics*, 611, Aug., pp. 97–106.
- [15] Alben, S., and Shelley, M. J., 2008 "Flapping States of a Flag in an Inviscid Fluid: Bistability and the Transition to Chaos". *Physical Review Letters*, 100(100), Jan., pp. 074301–1–074301–4.

Comparison between 1-D Versus 2-D Modelling Approach of Concrete Shell Design and Optimization

Concetta Sulpizio^{*}, Bruno Briseghella^{**}, Ivo Vanzì^{***}, Giuseppe Carlo Marano^{****}, Alessandra Fiore^{*****}

^{*}University of Chieti-Pescara "G. d'Annunzio", Pescara, Italy, ^{**}College of Civil Engineering, Fuzhou University, Fuzhou, Fujian, China, ^{***}University of Chieti-Pescara "G. d'Annunzio", Pescara, Italy, ^{****}Technical University of Bari, Bari, Italy, ^{*****}Technical University of Bari, Bari, Italy

ABSTRACT

During last years architecture is searching for new shapes inspired by natures. On the other hand, engineering is searching for lightweight structures and efficient application of materials. These are challenging goals for designers who want to combine these aspects. In this paper, different approach and related results have been compared. The first method is 1-D approach and it models the structure as a network of beams and nodes: this is the simplest one and it neglects some aspects. The second method is 2-D approach and it models the structure as a shell assembly: this is the finest one and can be useless for simplest cases. The aim of this work is to give to avantgarde designers an aid to optimal shape finding. He should use the right way in each case, avoiding serious mistakes choosing the simplest way when it is not applicable or the finest way when it is not necessary. The analyses involved two different types of surfaces: synclastic and anticlastic one. The optimization of shaping design could be conducted with different approaches. In this paper density methods has been used: Force Density Method FDM for 1-D and Surface Density Method SDM for 2-D. keywords: shell optimization, comparison approach, Force Density Method, Surface Density Method

Scaling laws in engineering science

Bohua Sun*

*Cape Peninsula University of Technology

ABSTRACT

The most powerful use of dimensional analysis (Bridgman [1]; Sedov [2]; Barenblatt [3]; Cantwell [4]; Sun [5, 6]) is to predict the outcome of an numerical experiment, depending on the variables, whilst providing theoretical insight [7]. Dimensional analysis may come across as simply trying to fit pieces of a puzzle together by trial and error. However, identifying the quantities that are relevant for a given problem is a demanding task, which requires deep physical insight [7]. The success or failure of using dimensional analysis depends on how to select the basic parameters of the problem. This may be done as follows: make a list of all quantities on which the answer must depend, then write down the dimensions of these quantities, and finally demand that these quantities should be combined into a functional form that provides the right dimension. This scheme was cast into a formal framework by Buckingham in 1921 and is often referred to as the Buckingham π -theorem [8]. Recently, the author has successfully applied the dimensional analysis to following complicated engineering problems [9–13]. In this paper, we will present our formulations for the problems of compressible turbulence, aquatic locomotion, capillary wrinkling of a thin film, as well as Kepler's third law of n-body periodic orbits in a Newtonian gravitation field. References [1] Bridgman, P.W. Dimensional Analysis. Yale University Press (1922) [2] Sedov, L.I. Similarity and Dimensional Analysis in Mechanics. Academic Press (1959) [3] Barenblatt, G.I. Similarity, Self-similarity and Intermediate Asymptotics. Cambridge University Press (1996) [4] Cantwell, B.J. Introduction to Symmetry Analysis. Cambridge University Press (2002) [5] Bohua Sun. Dimensional Analysis and Lie Group. China High Education Press (2016) [6] Bohua Sun. Dimensional analysis and applications. Phys. and Eng. (in Chinese) 26, 6(2016). [7] Hecksher, T. Insights through dimensions, Nature Physics, 13, 2017. [8] Buckingham, E. Phil. Mag. 42, 696–719 (1921). [9] Bohua Sun, The temporal scaling laws of compressible turbulence. Modern Physics Letters B, 30, 1650297 (2016) [10] Bohua Sun, Scaling laws of compressible turbulence, Applied Math Mech. 38(6):765–778 (2017) DOI 10.1007/s10483-017-2204-8 (the only Hot paper in the issue) [11] Bohua Sun, Scaling laws of aquatic locomotion, Sci. China-Phys. Mech. Astron. 60, 104711 (2017), doi: 10.1007/s11433-017-9073-1 [12] Bohua Sun, Capillary wrinkling scaling laws of floating elastic thin film with a liquid drop, Sci. China-Phys. Mech. Astron. 61, 024721 (2018), <https://doi.org/10.1007/s11433-017-9116-5>

Dynamic Free Surface of Thermocapillary-Buoyancy Convection in Liquid Column

Chengtong Sun*, Ruquan Liang**

*School of Mechanical and Vehicle Engineering, Linyi University, Shangdong, China, **School of Mechanical and Vehicle Engineering, Linyi University, Shangdong, China; Northeastern University, Shenyang, China

ABSTRACT

The coupling of buoyancy convection and thermocapillary convection can be observed in the residual gravity, and its corresponding phenomenon is universal and important for industrial processes, particularly the space technology (such as heat exchangers in space station, life support system, and growth of crystal. In this paper, we investigate numerically the thermocapillary-buoyancy convection for large Pr number fluid under the residual gravity based on the improved mass conserving level set approach and a new algorithm which is used to capture any micro-scale migrations of dynamic free surface. Against former studies, the coupling influence of thermocapillary-buoyancy convection on the change of flow pattern and the free surface movement has been investigated simultaneously for the first time. Present results show that the flow modes can be divided into four stages: the inchoate thermocapillary convection, the dominated buoyancy convection, the balanced thermocapillary-buoyancy convection ($Bod=1.005$), and the dominated thermocapillary convection. The free surface shape of liquid column changes from the “?”-shape to the twisted “M”-shape, the standard “M”-shape corresponding balanced stage of thermocapillary-buoyancy convection (at $t=975$, $Bod=1.005$), and finally becomes “S”-shape corresponding the fourth stage ($Bod=0.98$). Meanwhile, there is a weak response disturbance on the dynamic free surface during the transformation process of each stage. In this paper, some peculiar phenomena are found, which are not limited only to the research on thermocapillary convection but also can provide the necessary theoretical basis for the nonlinear dynamical system control and the study on complex behavior in chemical and biological systems. The present work is supported financially by the National Natural Science Foundation of China under the grants of 51676031 and 51376040. References [1] Liang R Q, Yang S, Li J Z. Thermocapillary convection in floating zone with axial magnetic fields. *Microgravity Sci. Technol.*, 25:285-293, (2014) [2] Kawaji M, Liang R Q, M. Nasr-Esfahany, Simic-Stefani S, Yoda S. The effect of small vibrations on Marangoni convection and the free surface of a liquid bridge. *Acta Astronautica*. 58 622-632, (2006)

Slope Stability Assessment by Mixed Cover Meshless Method

Pan Sun^{*}, Yudan Gou^{**}, Yongchang Cai^{***}, Hehua Zhu^{****}

^{*}Tongji Univeristy, ^{**}Tongji Univeristy, ^{***}Tongji Univeristy, ^{****}Tongji Univeristy

ABSTRACT

In slope stability analyses, the traditional finite element method (FEM) encounters the mesh alignment problem mainly due to the complex slope geometry, layered and staged excavation sequences, multiple material interfaces and joints/faults/bedding planes. In this work, a recently proposed meshless method, i.e., the mixed cover meshless method (MCMM), is utilized combined with the strength reduction method (SRM) to obtain the potential sliding surface and the safety factor in slope stability assessment. In MCMM, an arbitrary computational geometry is discretized using regular square cells and local h-refinement in key regions is readily implemented using the quadtree data structure. The MCMM alleviates the necessity of generating conforming meshes in FEM and has advantages of a simple formulation, convenient computer implementation and low computational cost compared to classic meshless methods such as the element-free Galerkin method (EFGM) and the meshless method based on Shepard function and partition of unity (MSPU). The developed technique was applied to some benchmark examples and the accuracy, efficiency and robustness were verified by the agreement between modelling results and reference solutions.

Deep-learning Enhanced Computational Failure Mechanics across Multiple Scales

WaiChing Sun*

*Columbia University

ABSTRACT

We introduce a new hybridized deep-learning/material modeling framework to capture localized failures, in particular, shear bands and fracture across multiple length scales. This modeling framework introduces deep learning as a mean to connect simulations and data across different scales through recursive homogenization. Directed graph, a concept to analyze the hierarchy of information will be used to generate optimal configurations of hybrid deep-learning/material models for a given set of data across length scale such that the effects of evolving microstructures due to micro-cracks, plastic slip and wear can be propagated to the macroscopic scales. To ensure efficiency, an ensemble of theoretical and deep-learning-based material models of different sophistication will be used to predict constitutive responses within a phase field framework. Each phase field represents the weights of a model of a particular scale in the ensembled constitutive predictions. By evolving the phase fields, the ensemble predictions will always capture the domain of interests, such as the moving crack tips during crack growth or shear bands forming in the softening regime, with the most sophisticated predictions, while the far field predictions will be adaptively simplified for efficiency. These evolutions of the phase fields in the space-time continuum is controlled by the driving force. This driving force is a scalar function that depends on the results of validations. Meanwhile, unconventional information from the microstructures, such as coordination number, fabric tensors, void size distribution, grain size distribution, will be analyzed and put into the directed graph that represents the hybridized constitutive laws without hand-crafting new phenomenological models as surrogates.

Adaptive Peridynamics-FEM Superposition

Wei Sun^{*}, Jacob Fish^{**}

^{*}State Key Laboratory of Hydrosience and Engineering, Tsinghua Univ., ^{**}Civil Engineering and Engineering Mechanics, Columbia Univ.

ABSTRACT

An Adaptive Peridynamics-FEM superposition scheme based on the enrichment theory is proposed. It features a superposition of a nonlocal peridynamics and the underlying FEM mesh, and the appropriate using of the principle of virtual work that enforce equilibrium. Furthermore, the adaptive scheme is also designed to take advantage of the superposition based method without any need of remeshing the underlying mesh. Numerical studies are conducted for one-, two- dimensional problems. It is shown that the proposed method is patch test consistency and no spurious force founded.

Nonlinear Dynamic Buckling of Viscoelastic Plate Considering Higher Order Modes

Yuanxiang Sun^{*}, Cheng Wang^{**}

^{*}Beijing Institute of Technology, ^{**}Beijing Institute of Technology

ABSTRACT

The nonlinear dynamic buckling of viscoelastic plates with large deflection is investigated in this paper by using chaotic and fractal theory. The problem of the simply-supported viscoelastic plate subjected to an in-plane periodic load is considered. The von Karman nonlinear geometry equations are introduced and standard linear solid model is employed. The nonlinear and dynamic governing equations of viscoelastic plates are the combination of the equilibrium equations and the deformation compatibility equation, which are nonlinear high-order integral partial differential dynamic equations. In order to obtain an accurate solution, the deflection function is expressed as a sinusoidal series with four terms rather than only one term in the computation (in the most of previous studies [1,2], the deflection function were expressed as a sinusoidal series with only one term). The Lyapunov exponent spectrum, the fractal dimension of strange attractors and the time evolution of deflection are obtained. The effect of high order modes on dynamic buckling of viscoelastic plate is obtained. References [1] Y.X. Sun, S.Y. Zhang. Chaotic dynamic analysis of viscoelastic plates. International Journal of Mechanical Sciences, 2001, 43: 1195-1208. [2] D. Touati, G. Cederbaum. Influence of large deflections on the dynamic stability of nonlinear viscoelastic plates. Acta Mechanica, 1995, 113, 215-231.

Effects of Geometric Parameters on the Fracture Mechanism of Bionic Suture Joint

Yupei Sun^{*}, Wenzhi Wang^{**}, Chao Zhang^{***}

^{*}Northwestern Polytechnical University, ^{**}Northwestern Polytechnical University, ^{***}Northwestern Polytechnical University

ABSTRACT

Fiber reinforced polymer composites have been widely used in the manufacture of high strength lightweight structures because of their superior mechanical properties. However, due to the brittle characteristic of the materials, the structure made of such materials has the defect of low fracture toughness. Moreover, this defect is magnified at the composite joint due to the stress concentration caused by the presence of drilling, adhesive and material stiffness mismatch, which eventually lead to structural premature failure. In the biological world, the long-term evolution process has created the rigid characteristics of bone structure. However, the connection between bone structures has taken a very special form - the suture joint. The suture joint can be described as a mixed connection composed of two rigid elements, which connected by a thin, relatively compliant interface layer. With the deepening of the research, the advantages of this kind of joint on the mechanical properties have been discovered: on the one hand, the suture joint ensures the connecting stiffness, mechanical strength and impact energy absorption characteristics of bone connection in the growing process; on the other hand, the change the suture joint makes the mechanical properties of the interface area change constantly, and keeps higher adaptability when the environment changes. Inspired by the above biological suture joint, the bionic composite suture joint was developed. In this study, we transform the typical triangular tooth connection interface into a parameterized model of the suture joint structure based on the fractal algorithm. According to the parameters of the baseline shape, tooth angle and arc baseline amplitude of the connection structure interface, the mechanical properties of this structure were studied by combining experimental and numerical simulation. In experimental, based on the parameterization construction method of the suture joint, these structure models with different parameters were made by 3D printing technology, and the structural bearing properties with different geometric parameters were obtained under tensile load. In numerical simulation, the parameterized numerical models of the suture joint were built and calculated based on the finite element method, and the correctness of the numerical model was validated by comparing with experimental. The experimental and numerical results displayed excellent performance of this kind of structure in controlling the fracture toughness, and the influences of geometric parameters on the fracture toughness were summarized.

The Mechanical Properties of the Boron Nitride Hexagonal Nanosheets

Yuzhou Sun*

*Zhongyuan University of Technology

ABSTRACT

This paper presents a multiscale method to study the mechanical properties of the hexagonal nanosheets of boron-nitride. A nanosheet is viewed as a higher-order gradient continuum planar sheet, in which the strain energy density depends not only on the first-order deformation gradient but also on the second-order deformation gradient. A representative cell is imaged on at a point where the constitutive response needs to be evaluated. The higher-order Cauchy-Born rule is used to approximate the bond vectors in the representative cell, and the minimizing of the strain energy density results with the constitutive relationships. The elastic constants, including Young's modulus, shear modulus, Poisson's ration and bending rigidity, are calculated by analyzing the physical meaning of the first- and second-order strain gradients. The developed model can also be used to study the nonlinear behavior of nanosheets under some simple loading situations, such as the uniform tension, torsion and bending. The stress-strain relationship of nanosheets is presented in the environment of uniform tension.

Optimization of Truss-Type Fiber Reinforced Plastic Composite Structures Based on Moving Morphable Components Method

Zhi Sun^{*}, Weisheng Zhang^{**}, Junfu Song^{***}, Xu Guo^{****}

^{*}Dalian University of Technology, ^{**}Dalian University of Technology, ^{***}Dalian University of Technology, ^{****}Dalian University of Technology

ABSTRACT

Fiber reinforced plastic (FRP) composite structures, which possess advanced specific stiffness and strength, have been widely used in various fields, for instance, transporting vehicles, wind turbine, and other light weight structures. For decades, extensive studies have been made, especially in the designing and analyzing of FRP composite structures, which further triggers the development of stacking sequence method and topology optimization method. However, typical FRP composite shell structures, including aircraft radar domes, composite overwrapped pressure vessel, and wind turbine blade, are designed into the geometry with changing curvature radius to meet aerodynamic or gas-tightness requirements. By using common plying or overwrapping process, the fiber angle and thickness of the aforementioned FRP composite structures would change along with the curvature radius of structure. However, the exist stacking sequence method and topology optimization method fail to consider the manufacture-driven change of fiber angle and thickness, and therefore left a gap to fill in. In this study, Moving Morphable Components (MMC) method, which is able to explicitly describe the geometry of structures, is used to perform topology optimization for FRP composite structures with beam-type or truss-type geometry. The FRP composite structures are considered to be manufactured based on geodesic winding, with fiber plying angle and thickness calculated according to the curvature radius of each beam. The stiffness and deformation of FRP composite structures are then analyzed by Finite Element Method. Composite frame of bicycle and vertical plate of aircraft wing are selected as numerical examples. The numerical results indicate the validity of the proposed optimization method.

Uncertainty in Cardiac Myofiber Orientation and Stiffnesses Dominate the Variability of Left Ventricle Deformation Response

Joakim Sundnes*, Rocio Rodriguez-Cantano**, Marie Rognes***

*Simula Research Laboratory, **Simula Research Laboratory, ***Simula Research Laboratory

ABSTRACT

Computational cardiac modelling is a mature area of biomedical computing, and is currently evolving from a pure research tool to aiding in clinical decision making. Assessing the reliability of computational model predictions is a key factor for clinical use, and uncertainty quantification (UQ) and sensitivity analysis are important parts of such an assessment. In this study, we apply new methods for UQ in computational heart mechanics to study uncertainty both in material parameters characterizing global myocardial stiffness and in the local muscle fiber orientation that governs tissue anisotropy. The uncertainty analysis is performed using the polynomial chaos expansion (PCE) method, which is a non-intrusive meta-modeling technique that surrogates the original computational model with a series of orthonormal polynomials over the random input parameter space. In addition, in order to study variability in the muscle fiber architecture, we model the uncertainty in orientation of the fiber field as an approximated random field using a truncated Karhunen-Loeve expansion. The former is used as a basis to build a reduced-dimensionality representation of the random field, essential to manage UQ analysis in extremely high-dimensional problems. Although the fiber arrangement exhibit a typical gross architecture, there are local and individual variations through the ventricular wall, as well as uncertainty derived from noisy measurements that may affect the global mechanical properties of the model. The results give insight into the applicability of the truncated KLE method for representing noisy fiber architecture fields, and demonstrate a substantial impact of fiber angle variations on the selected outputs, highlighting the need for accurate assignment of fiber orientation in computational heart mechanics models. Furthermore, the uncertainty and sensitivity analysis of global material parameters identify clear differences in their impact global output quantities. An interesting finding is that the impact of local uncertainty, or noise, in the fiber field appears to be significantly larger than the impact of uncertainty in the global parameters determining the fiber direction. This result indicates that as long as the organized, helical structure of fiber orientation is maintained, the actual helix angle has a moderate impact on the mechanical properties of the ventricle. However, as noise is introduced so that the helical structure is lost, the mechanical properties are severely affected.

Ductile Fracture Initiation Analyses with Consideration of Stress Triaxiality ahead of Axial Crack Fronts in Pressure Tubes of Hydrided Irradiated Zr-2.5Nb Materials without and with Split Circumferential Hydrides

Shin-Jang Sung*, Jwo Pan**, Poh-Sang Lam***, Douglas A. Scarth****

*University of Michigan, **University of Michigan, ***Savannah River National Laboratory, ****Kinectrics Inc.

ABSTRACT

Ductile fracture initiation with consideration of stress triaxiality ahead of the fronts of axial cracks in pressure tube (PT) specimens of hydrided irradiated Zr-2.5Nb materials without and with split circumferential hydrides at room temperature is examined by conducting three-dimensional finite element analyses with submodeling. First, a strain-based failure criterion with consideration of stress triaxiality is developed from the Gurson yield model with use of the experimental/computational results of transverse tensile tests and the effective plastic strain of the critical material element in CT specimens without hydride at fracture initiation. Next, three-dimensional finite element analyses of PT specimens of irradiated Zr-2.5Nb materials without and with three pairs of split circumferential hydrides are conducted with the similar mesh design, the same material definition, and the same applied stress intensity factor as those for CT specimens. The results of the three-dimensional finite element analysis of a PT specimen of irradiated Zr-2.5Nb materials without split circumferential hydrides suggest that circumferential hydrides ahead of the crack front in the middle of a PT specimen should fracture for the given internal pressure corresponding to the fracture toughness of the irradiated Zr-2.5Nb materials without circumferential hydrides. Based on the strain-based failure criterion with consideration of stress triaxiality, the applied stress intensity factor to reach the failure criterion at a critical distance ahead of the axial crack front in the middle of the thickness of an unhydrided irradiated PT specimen is 3% higher than that obtained from the computational results of unhydrided irradiated CT specimens. For a PT specimen with three pairs of split circumferential hydrides with various heights and ligament thicknesses along the crack front, three types of strain concentration are shown in the middle of the ligaments ahead of the crack front. The strain concentration is higher when the ratio of the ligament thickness to the hydride height is less than 3. The computational results suggest that with the strain-based failure criterion with consideration of stress triaxiality, only 60% to 70% of the internal pressure for fracture initiation of an unhydrided irradiated PT specimen is needed to fracture a hydrided irradiated PT specimen with many randomly distributed split circumferential hydrides along the crack front. The computational results can be used to explain the near 35% reduction of the fracture toughness at room temperature obtained from hydrided irradiated PT specimens when compared with that from unhydrided irradiated ones.

Non-Equilibrium Molecular Dynamics Simulations of Interfacial Wetting Behavior between Single Walled Carbon Nanotubes and Liquid Copper

Bryan Susi^{*}, Jay Tu^{**}

^{*}Applied Research Associates, Inc., ^{**}North Carolina State University

ABSTRACT

Multi-scale simulations with molecular resolution are more tractable now than ever and these simulations can have an overwhelmingly positive impact in many scientific disciplines if the practitioner fully understands the methods and models. These lessons are even more applicable for Non-Equilibrium Molecular Dynamics (NEMD) simulations. In this work, nano-scale NEMD simulations of a Single Walled carbon Nanotube (SWNT) intrusion into liquid copper in a Wilhelmy Balance configuration are performed to determine the propensity for incorporation of a SWNT in liquid copper. The objective of this research is ultimately to contribute to the understanding of how to fabricate Carbon Nanotube-Metal Matrix (CNT-MM) composites when the nanotubes are not wetted by the metal. This is a challenging problem with many underlying phenomena to investigate, but specific to this presentation will be results pertinent to selection of the appropriate MD pair-potential models, a new parameter set for the Morse potential model between carbon and copper which adequately describes their interfacial behavior, and an evaluation of the rate of carbon nanotube intrusion from the Wilhelmy-Balance simulations with emphasis on SWNT accommodation in the liquid medium. The primary contributions to the field are the new pair-potential coefficients to model the correct static contact angle between liquid copper and sp² hybridized carbon surfaces, a framework for accurate NEMD simulations of a nanoscale Wilhelmy-Balance experiment, and deviations between the molecular scale results and continuum fluid mechanics relationships as a function of nanotube intrusion rate.

Electrospinning Process Simulation for the Application in Predictive Cardiovascular Disease

Tijana Sustersic*, Liliana Liverani**, Aldo R. Boccaccini***, Nenad Filipovic****

*Faculty of Engineering, University of Kragujevac, 34000 Kragujevac, Serbia; Bioengineering Research and Development Center (BioIRC), 34000 Kragujevac, Serbia, **Institute of Biomaterials, University of Erlangen-Nuremberg, 91058 Erlangen, Germany, ***Institute of Biomaterials, University of Erlangen-Nuremberg, 91058 Erlangen, Germany, ****Faculty of Engineering, University of Kragujevac, 34000 Kragujevac, Serbia; Bioengineering Research and Development Center (BioIRC), 34000 Kragujevac, Serbia

ABSTRACT

The aim of this research was to simulate two-phase electrospinning jet from the syringe nozzle to the collector by using computational methods. Previous numerical studies have dealt only with one-phase flows or had too many simplifications when it comes to electrospinning process [1]. Since the application of electrospinning lies in manufacturing of cardiovascular implants (to allow and promote cell infiltration within the scaffolds), as well as in fiber modification methods for improving myocardial regeneration (various biodegradable polymers can be used for fiber fabrication) [2], these kind of simulations can offer a full insight into coupled physical laws that govern the process. This will be useful for optimization of the electrospinning parameters reducing the trial-and-error approach, decreasing the amount of chemicals, reducing waste management and equipment maintenance costs. Data obtained during experiments with 10wt% PVA solution were used as input for computational simulation. Three voltage pairs (15kV applied on the nozzle, 0kV on the collector; 13kV applied on the nozzle, -2kV on the collector; 20kV applied on the nozzle, 0kV on the collector) were investigated in order to examine their effect on jet shape and implicitly fiber structure. A two-phase flow model is simulated using turbulent k- ϵ model, volume of fluids (VOF) for the interphase region between the polymer and air and Magnetohydrodynamics(MHD) model for the behavior of the polymer in strong electric field. The simulation results show good agreement with experiments in terms of outcome - no fiber differences in experiments were present when proposed voltage pairs were used as boundary conditions, and similar jet shapes were obtained during simulations. These jet shapes for electrospinning are also visually very different from jet shapes when non-optimal parameters are used. This confirms the hypothesis that the jet shape during electrospinning can be a factor of indication whether the chosen electrospinning parameters would result in fibers with good quality. Differences that may occur between experiments and simulation can be a result of simplifications in simulations; influence of uniform and non-uniform electric field, as well as adopted parameters that were used based on literature values and could not be determined experimentally at this point. [1] Spivak, A. F., Dzenis, Y. A., & Reneker, D. H. (2000). A model of steady state jet in the electrospinning process. *Mechanics research communications*, 27(1), 37-42. [2] Kim, P. H., & Cho, J. Y. (2016). Myocardial tissue engineering using electrospun nanofiber composites. *BMB reports*, 49(1), 26.

Tunable Architected Metamaterials for Bone Implants

Alok Sutradhar*, Jaejong Park**

*The Ohio State University, **The Ohio State University

ABSTRACT

The design of medical bone implants involves multiscale consideration. The structure in macro level needs to satisfy the space, functional, aesthetic and load-transfer requirements. Additional considerations of stress-shielding and localized stress-concentrations to improve the effectiveness and functionality can be increased using architected metamaterials. For example, the mechanical properties of the bone implants and their adjacent bone need to be similar to reduce these effects. Topology optimization is a numerical tool that is suitable for obtaining optimized geometries under several constraints. Earlier efforts used inverse homogenization technique to attain the microstructures of scaffold geometries. These equivalent material model would be valid when there is a significant dimensional difference between the large and the small scales. With recent advances, 3D printing of multiscale multi-material structures is realizable. We present an approach to design tunable architected metamaterials for implants which may alleviate localized stress-concentration and stress-shielding. We develop a topology optimization framework to design the architecture materials in different scales which varies smoothly within the design domain. The preliminary study shows easy control in connectivity and provides more topological variability. The metamaterial implant models designed using the methodology in this work are 3D printed, and their performance is studied using mechanical testing.

Model Parameter Identification of Keloid-Skin Undergoing Large Deformations

Danas Sutula^{*}, Emmanuelle Jacquet^{**}, Jerome Chambert^{***}, Arnaud Lejeune^{****}, Franz Chouly^{*****}, Stéphane Bordas^{*****}

^{*}Université Bourgogne Franche-Comté, ^{**}Université Bourgogne Franche-Comté, ^{***}Université Bourgogne Franche-Comté, ^{****}Université Bourgogne Franche-Comté, ^{*****}Université Bourgogne Franche-Comté, ^{*****}Université du Luxembourg

ABSTRACT

The aim of this paper is to characterize the mechanical behavior of cutaneous tissues with the long-term goal to prevent keloid development in patients. Keloids are non cancerous tumors that grow continuously on the skin for several reasons. These specific tumors affect 11 million patients of all ages and are particularly common in Asian and African populations. The evolution of keloids is related to genetic, biological, biophysical, and biomechanical factors. Here we focus on the biomechanical influence, such as the state of stress inside a keloid and in the surrounding skin, which is known to play an important role. To predict the stresses in the keloid-skin, the patient-specific mechanical behavior of the keloid-skin needs to be determined. To this end, we present a patient-specific methodology for the identification of the hyper-elastic keloid-skin model parameters. In our approach, a keloid is observed on a patient using ultrasound and optical microscopy. The 3D image of the surface is used to develop the keloid-skin geometrical model. The hyper-elastic material model parameters for the healthy skin and the keloid are determined using an inverse analysis approach; essentially, the parameters are obtained by minimizing the mismatch between the numerical and the experimentally obtained displacements on the surface of the keloid-skin. The experimental measurements are obtained in-vivo using a custom-made extensometer and a digital image correlation technique. The inverse analysis is carried out incrementally over a series of loading steps. The motivation is to observe any variability in the model parameters during the different levels of loading. Significant variability in the model parameters would suggest a limitation of a particular hyper-elastic model to characterise the keloid-skin effectively due to the parameter dependence on the applied load. In the end, we are able to select a hyper-elastic model and determine the model parameters that adequately characterize the keloid-skin for the range of loading conditions of practical interest. We then investigate the nature of the stress field at the interface between the healthy skin and the keloid. The knowledge of the stress field has the potential to help design a specific device able to contain the growth of the keloid; this, however, is the topic of further investigation. Our next steps will focus on quantifying the sensitivity of the model parameters to the uncertainty in the experimental measurement data.

Generalized Fractional-Order Visco-Elasto-Plasticity with Damage for Anomalous Materials

Jorge Suzuki^{*}, Mohsen Zayernouri^{**}

^{*}Department of Computational Mathematics, Science, and Engineering (CMSE), Michigan State University,

^{**}Department of Computational Mathematics, Science and Engineering (CMSE); Department of Mechanical Engineering, Michigan State University

ABSTRACT

In this work we introduce an efficient framework that uses a generalized, fractional-order visco-elastic model, coupled to a fractional-visco-plastic component [1] and a modified Lemaitre damage model to introduce material degradation. The visco-plastic/damage coupling is thermodynamically consistent, with the constitutive laws derived using appropriate fractional-order Helmholtz free-energy potentials [2]. The dissipation potential for visco-plasticity is defined by the use of a time-fractional yield function. The damage potential has the same form as the classical Lemaitre approach, but the damage energy density release rate is described by a fractional-order potential. We perform a time-fractional integration of the resulting system of FODEs using a fractional return-mapping algorithm, with fast convolution scheme with computational complexity $O(n \log(n))$. The model is then implemented in a Finite Element framework for the analysis of geometrically nonlinear trusses. To the authors knowledge, this is the first contribution that couples a fractional visco-elasto-plastic model with damage in a thermodynamically consistent way. References: [1] J.L. Suzuki, M. Zayernouri, M.L. Bittencourt, and G.E. Karniadakis. Fractional-order uniaxial visco-elasto-plastic models for structural analysis. *Computer Methods and Applied Mechanics and Engineering*, 308:443 – 467, 2016. [2] A. Lion. On the thermodynamics of fractional damping elements. *Continuum Mech. Thermodyn.*, 9:83 – 96, 1997.

Three-stage Failure Simulation with Dynamic Frictional Contact Based on Co-rotational Technique

Shun Suzuki^{*}, Kenjiro Terada^{**}, Shuji Moriguchi^{***}, Norio Takeuchi^{****}

^{*}Tohoku University, ^{**}Tohoku University, ^{***}Tohoku University, ^{****}Hosei University

ABSTRACT

Based on the co-rotational formulation to deal with large displacements and rotations of a solid, we propose a method of three-stage failure simulation of brittle materials and structures involving dynamic contact behavior. On the premise of the standard three-dimensional finite element method with tetrahedral and hexahedral elements, a finite element model is composed of multiple blocks, each of which is constructed with several sets of elements. Here, the interface between adjacent blocks are assumed to be potential discontinuities equipped with the cohesive-zone model and the penalty method is employed to connect these sets of blocks, each of which is supposed to move and deform independently after complete separation without cohesive forces. Then, one of them possibly hits other blocks and divides some of them into several sub-blocks. The so-called node-to-segment approach is employed for non-matching meshes of blocks contacting with each other. In addition, the augmented Lagrangian method is applied to the constrained optimization problem associated with the bilateral contact with friction. In order to obtain stable solutions even after the complete failure, we adopt the energy-momentum conservation method for time-integration. To this end, the energy dissipation due to the stick/slip frictional behavior is also considered based on the Coulomb friction law. The three stages we are concerned with in our numerical simulations are the following: • At the first stage: a structure deforms in response to dynamic or static excitations and displays cracks along prescribed discontinuities so that it would be separated into several blocks. • At the second stage: several sets of blocks lose static equilibria and start to move dynamically. • At the third stage: moving blocks collide each other with friction and some of them further break up due to the shock generated by the collision. The proposed method has been designed to enable us to simulate all of these deformation and failure stages continuously. The implementation of the formulation is verified by conducting some numerical tests with a simple structure containing a potential discontinuity. Also, several numerical examples are presented to demonstrate the capability and performance of the proposed method to simulate three-stage failure processes involving large deformation and rotations with dynamic frictional-contact behavior.

Hysteretic Modeling Method by Recurrent Neural Network

Takuya Suzuki*, Yasutomo Matsuoka**

*Takenaka Corporation, **Takenaka Corporation

ABSTRACT

In nonlinear structural analyses, it is important to use an accurate hysteretic model. However, there are some materials and structural members that have too complex hysteresis to make hysteretic model for analysis for human. For such situations, we propose to use a recurrent neural network (RNN) system. A recurrent neural network is one of neural network. It can be changed by a system based on previous hysteresis inputs and outputs. The aim of this study was to confirm the applicability of RNN modeling method to the normal bilinear model of nonlinear hysteresis that is most popular model in structural analysis. First, we identified RNN model with long short-term memory (LSTM) using training data comprising bilinear historical displacement as input and force as output data. Then, it was confirmed that the identified RNN model could be applied to the system, and that it was equivalent to a theoretical bilinear model. As a result, following findings are obtained: (1) A RNN model with LSTM units is required for a bilinear system. This was determined using training data comprising theoretical bilinear input-output data. Comparison of the output of the identified RNN model with that of a theoretical model revealed good agreement. The changeability of an RNN by a system based on previous hysteresis inputs and outputs was confirmed in the case of basic hysteretic bilinear model, which is often used for structural seismic design. (2) The sparsity of the weight matrix of the identified RNN model was investigated. The weight matrix does not have sparsity when its layer contained "drop out". This indicated that the RNN model was very large and had many weight coefficients, which would make its analysis very difficult. The findings of this study show the applicability of RNN modeling to structural hysteresis. However, there is the need for further improvement of the procedure.

The Influence of Elastic Heterogeneity on the Strength of Dislocation-Obstacle Interactions

Benjamin Szajewski^{*}, Joshua Crone^{**}, Jarek Knap^{***}

^{*}Army Research Laboratory, ^{**}Army Research Laboratory, ^{***}Army Research Laboratory

ABSTRACT

The Influence of Elastic Heterogeneity on the Strength of Dislocation-Obstacle Interactions. B. A. Szajewski, 1, J. C. Crone, J. Knap Army Research Laboratory Abstract The interaction between glissile dislocations and spherical obstacles (e.g., voids and precipitates) within a continuum is responsible for marked increases in material strength. Due to their desirable engineering features, dislocation-obstacle interactions have been the subject of theoretical study for many decades [1,2]. Despite ongoing efforts, these studies have often been limited to crude approximations whose validity is difficult to assess. Towards enhancing our understanding of these complex interactions, we employ a three dimensional coupled dislocation dynamics and finite element method computational scheme [3] to directly compute the strength (i.e. Orowan stress) of a variety of dislocation-obstacle interactions. The coupled framework accounts for elastic mismatch between the host matrix and obstacles via the inclusion of elastic image stresses and stress concentrations computed through the finite elements. Our simulations span a range of elastic mismatch, linear obstacle densities, and sizes. Additionally, the influence of the surface formation energy on both the obstacle strength and critical dislocation nucleus size is explored via the introduction of a tunable parameter, γ_{surf} . Through our simulations, we demonstrate the influence of these four parameters on both the final stable configuration, and the dislocation-obstacle strength. We devise a simple mechanical model which yields insight into the results of both our numerical simulations as well as others found within the literature. 1. D. J. Bacon, U. F. Kocks and R. O. Scattergood, Philosophical Magazine 28:1241 (1973), DOI: 10.1080/14786437308227997 2. R. O. Scattergood and D. J. Bacon, Acta Metallurgica 30:1665 (1982), DOI: 10.1016/0001-6160(82)90188-2 3. J. C. Crone, P. W. Chung, K. W. Leiter, J. Knap, S. Aubry, G. Hommes, A. Arsenlis, Modelling and Simulation in Materials Science and Engineering 22:035014 (2014), DOI: 10.1088/0965-0393/22/3/035014

Altered Collagen Organization in Fatigue-Loaded Tendon Initiates Changes in Cell Mechanotransduction

Spencer Szczesny*, Tristan Driscoll**, Pen-Hsiu Chao***, Robert Mauck****

*Pennsylvania State University, **University of Pennsylvania, ***National Taiwan University, ****University of Pennsylvania

ABSTRACT

A primary cause of tendon degeneration is overuse (i.e., fatigue loading), which produces microscale damage of collagen fibrils and the accumulation of atypical tissue components (e.g., cartilaginous, fat, and calcium deposits) [1]. Why resident tenocytes produce these atypical matrix deposits rather than repair the native tissue structure is unknown. We hypothesized that fatigue damage induces changes in the tissue mechanical microenvironment (e.g., stiffness, topography), which alters the biophysical stimuli presented to tenocytes and leads to their adoption of abnormal (i.e., non-tenogenic) phenotypes. To test this hypothesis, we investigated the effects of fatigue loading on tendon microscale structure and mechanics using multiphoton microscopy and atomic force spectroscopy. Surprisingly, we found no change in the local tissue modulus after fatigue loading, despite widespread collagen fiber kinking and molecular denaturation. These data suggest that changes in tissue structure (i.e., altered collagen fiber crimping) may be responsible for early changes in tendon cell phenotype as a consequence of fatigue loading. To investigate this further, we used crimped electrospun nanofibrous scaffolds [2] to investigate the role of altered fiber crimping on cellular mechanobiology. Specifically, we used a fiber-reinforced structural constitutive model [2] to characterize the mechanics of these scaffolds as a function of fiber crimp and investigated the effect of crimping on mesenchymal stem cell (MSC) mechanotransduction. We found that MSCs seeded on crimped scaffolds (compared to straight fiber controls) had increased ERK activation in response to static stretch. Interestingly, nuclear aspect ratios were increased with stretch to similar amounts on both scaffold types, suggesting that the effect of the crimped scaffolds was not due to increased strain transmission from the scaffold to the cells. Instead, based on the results of our structural constitutive model, we found a significant stress response from fiber-fiber interactions/reorientations within the crimped scaffolds that are absent in the straight fiber controls. These results suggest that cell mechanotransduction is sensitive to the local fiber topography and that increased fiber reorientation associated with collagen disorganization in fatigue-loaded tendons may initiate the tissue remodeling responsible for tendon degeneration. Future work will investigate and model the effects of fatigue loading on the microscale mechanics and endogenous cellular mechanotransduction in live tendon explants. Such information will determine the role of mechanical loading in tendon degeneration and identify mechanotransduction signaling pathways as potential therapeutic targets. [1] Kannus &&& Jozsa 1991 JBJs 73:1507-25; [2] Szczesny et al. 2017 ACS Biomater Sci &&& Eng 3: 2869-2876.

Discrete Methods in Ice Accretion Modelling

Krzysztof Szilder*, Edward Lozowski**

*National Research Council Canada, **University of Alberta

ABSTRACT

Atmospheric icing due to freezing rain and freezing drizzle occurs when large, airborne supercooled water drops freeze on objects they encounter. The resulting ice can accumulate to a thickness of several centimetres during severe freezing rain events called ice storms. This ice can be hazardous for ground-based engineering structures such as overhead transmission lines, wind turbines, telecommunication masts and bridge cables. And it is especially hazardous to aircraft, where the build-up of ice due to impinging supercooled cloud droplets changes the stability and control characteristics of aerodynamic surfaces. Most current icing models are constrained in their verisimilitude by their reliance on solving continuous partial differential equations and their boundary conditions. By definition, continuous PDE's and their boundary conditions require that the simulated ice accretions have continuous properties, unless the discontinuities are known ahead of time. But typically they are not. We have circumvented these limitations by developing an original icing modelling capability, which we call "morphogenetic". It is based on a discrete formulation and simulation of ice formation physics. The original 2D development of this unique approach for the prediction of ice accretion shapes in the aerospace industry is given in [1]. Recent 3D modelling advances are described in [2-3]. The morphogenetic approach considers the behaviour of discrete ensembles of cloud drops, which impinge, move along the icing surface and freeze according to physically-based, stochastic rules. In essence, the method simulates ice accretion in the way it occurs naturally – drop by impinging drop. Because of this, it improves on existing ice accretion models. For example, it is capable of predicting complex ice accretions, such as simultaneous rime and glaze, ice accretions with variable density and discontinuous ice accretions such as rime feathers, lobster tails and icicles. It is also capable of predicting ice accretions on substrates with complex geometry, ranging from aircraft instrumentation and engines to power line insulators. [1] K. Szilder and E.P. Lozowski, "Novel Two-Dimensional Modeling Approach for Aircraft Icing", *Journal of Aircraft*, 41, 4, 854-861 (2004). [2] K. Szilder and E.P. Lozowski, "Three-Dimensional Numerical Simulation of Ice Accretion using a Discrete Morphogenetic Approach", *AIAA AVIATION Forum*, AIAA 2017-3418 (2017). [3] K. Szilder, "Theoretical and Experimental Study of Ice Accretion due to Freezing Rain on an Inclined Cylinder", *8th Int. Conference on Snow Engineering*, 183-192 (2016).

Fluid Structure Interaction Simulation for the Prediction of Car Water Crossing and Aquaplaning Using ESI Virtual Exterior Solution

Alain TRAMECON*, Matthias Schäfer**, Matia Oriani***

*ESI Group, **ESI Group, ***ESI Group

ABSTRACT

To develop cars and in particular electrical and autonomous cars, it is important to virtually test the car in real driving circumstances, including on wet road or under heavy rain conditions. ESI Group has introduced Virtual Exterior Solution which includes the Finite Point Method (FPM) technology as a CFD mesh free module to simulate the interaction of water with the car structure. It is used as a standard product in the industry for getting predictive airbag deployment simulation, tank sloshing and water drain applications and is now extended to other application fields like water crossing simulation and tire hydroplaning prediction. The objective is to enable a holistic prediction of the car behavior under realistic driving conditions, using a virtual car prototype. Detailed water behavior is accounted for, along with the deformation of structural part (tire, suspension, car body), in order to:

- Predict car drivability for water crossing for deep as well as shallow water crossing scenarios.
- Help tire design accounting for detailed thread geometry, tire pressure, and road conditions.
- Prevent accidental failures of structural parts due to water splash and brutal thermal effects by predicting the structural deformations in a fully coupled mode.

A technical introduction of the FPM mesh free technology, part of Virtual Exterior Solution will be shown. Validation cases vs. experimental results will be documented regarding fluid structure interaction. In a second part, current application examples will be presented covering deep car water crossing simulations and aquaplaning cases, focusing on fluid interaction with deformable structures.

A Fractional-order PID Controller Design Based on Fractional Calculus for Enhanced Performance of Dead-time Processes

LUAN VU TRUONG NGUYEN*, HOAI SON NGUYEN**, TAN HAI PHAN***, MAI VAN TRAN****

*FIRST AUTHOR AND CORRESPONDING AUTHOR, **CO-AUTHOR, ***CO-AUTHOR, ****CO-AUTHOR

ABSTRACT

A design method for the fractional-order proportional-integral-derivative controller based on fractional calculus is proposed in this paper. The analytical tuning rules are derived for achieving the performance improvement for both disturbance rejection and set-point tracking problems. Many illustrative examples are considered to confirm the effectiveness of the proposed algorithm for both integer and fractional order processes with time delays. In addition, the robust stability of fractional-order system is also carried out in order to demonstrate that the proposed fractional-order PID controller can hold well the robustness against perturbation uncertainty in the process models.

A Coupled Peridynamics/Finite Element Method for Modeling Dynamic Fracture

Alireza Tabarraei*, Shank Kulkarni**, Xiaonan Wang***

*University of North Carolina at Charlotte, **University of North Carolina at Charlotte, ***Ansys Software Company

ABSTRACT

Peridynamics is a nonlocal continuum model which, in contrast to other continuum models, uses integration instead of spatial derivations in its governing equations. Utilizing integration instead of derivatives is advantageous in modeling fracture since the governing equations remain valid even after the initiation or growth of discontinuities. Although peridynamics can model material behavior and fracture with a higher accuracy than classical continuum mechanics, however, nonlocal formulation makes peridynamics computationally expensive. To reduce the computational costs, we propose to couple peridynamics with local continuum domain (discretized by finite elements) using peridynamics only in small zones where higher accuracy is needed, e.g. vicinity of crack tips, and finite elements elsewhere where the solution is smooth. In the proposed multiscale model, peridynamics captures all the fine-scale behavior which finite element model is not able to capture. The main challenge in developing such a concurrent multiscale method is to eliminate the artifacts introduced by the interface of the two subdomains. One of the main issues that arises in dynamic coupling is spurious wave reflections; the high frequency (short wavelength) waves traveling from peridynamic cannot enter the finite element zone. The interface acts as a rigid boundary to the high-frequency waves, making them reflect back into the peridynamic zone. Hence, if the two subdomains are not appropriately linked to each other, the high-frequency waves get trapped in the peridynamic zone. This will lead to an increase in the energy of the peridynamic zone and will drastically reduce the computational accuracy. We propose a coupling technique which can effectively eliminate the spurious wave reflections at the interface of the two zones. The elimination of the spurious reflections is achieved by introducing an overlapping zone between the finite element and peridynamic zones. The consistency of the mechanical deformation in the overlapping zone is imposed using Lagrange multipliers while the high-frequency waves are damped by introducing a damping parameter in the equation of motion of the peridynamic nodes located in the overlapping zone. Using this approach we show that high-frequency waves are effectively damped before they reach the finite element zone.

A Study on Permeability Coefficient of Porous Media Using Immersed Boundary Method

Ikkoh Tachibana^{*}, Shuji Moriguchi^{**}, Kenjiro Terada^{***}, Takayuki Aoki^{****}

^{*}Tohoku University, ^{**}Tohoku University, ^{***}Tohoku University, ^{****}Tokyo Institute of Technology

ABSTRACT

This study aims to analyze the permeability behavior of porous media with the help of a numerical simulation which can represent microscopic flow behaviors. 3D Navier-Stokes equation is employed for the governing equation of fluid movement in the simulation, while the immersed boundary method [1] is utilized to embed spherical boundary on the grains' surface [2] in the finite difference formulation with the staggered grid system. In present study, a series of numerical permeability tests were carried out on the representing volume unit (RVE) of granular material, expressed as a cuboid region where solid spheres were randomly packed. Unidirectional flow was considered and static pressure gradient is applied as the boundary condition, while the other perpendicular directions were treated as periodic. The profile of each RVE as a granular material was controlled with its void ratio and distribution of inner particle diameter. Also, in order to compare results from different simulation conditions and inner structures, the Reynolds number for the porous media is taken into account. The results were compared to the former simulations with grid-wise uniformed inner structures conducted by the corresponding author [3] and several popular empirical formulae for an estimation of macroscopic permeability coefficient. The discussion is aimed at clarifying the relationship between present results and existing empirical formulae of permeability coefficient for soils within wide range of material profile index. References [1] C. Peskin, Flow patterns around heart valves: A numerical method, Journal of Computational Physics, 10-2, pp. 252-271, 1972 [2] M. Uhlmann, An immersed boundary method with direct forcing for the simulation of particulate flows, Journal of Computational Physics, 209-2, pp. 448-476, 2005 [3] I. Tachibana, S. Moriguchi, S. Takase, K. Terada, T. Aoki, K. Kamiya, and T. Kodaka, Characterization of transition from Darcy to non-Darcy flow with 3D pore-level simulations, Soils and Foundations, 57 pp. 707-719, 2017

Multiscale Modeling of 2D Heterostructures

Ellad Tadmor^{*}, Kuan Zhang^{**}, Mingjian Wen^{***}

^{*}University of Minnesota, ^{**}University of Minnesota, ^{***}University of Minnesota

ABSTRACT

The synthesis of graphene, a one-atom thick 2D graphitic sheet, was a revolution in materials physics. Since then a host of other 2D materials have been discovered that can be stacked to create layered heterostructures with remarkable properties. Due to the weak van der Waals interaction between layers, the resulting structures can be incommensurate and therefore challenging to model. We describe recent work on developing a hybrid continuum-atomistic computational method for simulating the mechanical response of 2D heterostructures. This multiscale framework includes a stack of finite element plate models interacting via a newly developed interlayer potential. In agreement with electron diffraction experiments, simulations of twisted bilayer graphene show a transformation from an initially incommensurate structure to commensurate structures separated by localized solitons [1]. This behavior is explained using a simple mechanics model. [1] “Structural and electron diffraction scaling of twisted graphene bilayers”, K. Zhang and E. B. Tadmor, Journal of the Mechanics and Physics of Solids, 112, 225–238 (2018).

NUMERICAL SIMULATION OF PROGRESSIVE COLLAPSE OF PERIMETER FRAME IN SUPER-HIGH-RISE FRAMED-TUBE STRUCTURE USING SIMPLE STRUCTURAL MODEL

Hiroyuki TAGAWA*, Misaki OKADA*, Noritoshi SUGIURA*

*Mukogawa Women's University
1-13 Tozaki-cho
Nishinomiya-shi, Hyogo, Japan
tagawa@mukogawa-u.ac.jp; <http://arch.mukogawa-u.ac.jp/>

Key words: Super-high-rise Framed-tube Structure, Progressive Collapse, Dynamic Stability, Perimeter Frame, Lateral-support, Minimum Eigenvalue.

Summary. Typical super-high-rise framed-tube structures have stiff beams and columns around the perimeter of the building and have no or few seismic beams inside the building. The rigid moment frames in the perimeters and floor system provide lateral-supports to prevent perimeter column buckling. However, when perimeter columns deform towards the outside of the structure simple connections between perimeter columns and floor system with small strength may break in tension. The lack of strong, stiff connections between perimeter frames and the floor system may result in minimum resistance to out-of-plane motion by the perimeter frames and may lead to unstable behavior when perimeter frames are separated from the floor systems as a result of accidental or earthquake loading. To investigate this behavior, simulations of the progressive collapse of these framed-tube systems were carried out using simple structural model, referred to as the coupled shear-flexural-beam model with links, consisting of lumped mass, spring and beam element. The hysteresis loop of link element connecting a shear-beam and a flexural-beam can simulate the behavior, including the tension break, of the frame-floor connections and tensile strength of link element is varied from 3% to 4% and 5% of the axial yield strength of the perimeter columns. Structural stability was evaluated by conducting eigenvalue analysis for mass and instantaneous stiffness matrices at each time-step of the nonlinear time-history analysis and a minimum eigenvalue was computed to assess the stability of the global structure. The results of this simulation shows that 1) when frame-floor connections do not break, continuous column effect resulting from elastic columns in perimeter frames is observed and drift concentration is mitigated, 2) when frame-floor connections have insufficient tensile strength and break in tension, progressive collapse of perimeter frames may occur due to out-of-plane motion of the frames, and 3) on-set of progressive collapse may be predicted by a negative instantaneous eigenvalue.

1 INTRODUCTION

Super-high-rise framed-tube structures such as the World Trade Center Building in New York typically have stiff beams and columns around the perimeter of the building and have no or few

seismic beams inside the building, as shown in Figure 1. This framing system is attractive to designers because they provide flexibility for floor layout. However, with this system, progressive collapse of the perimeter frames, due to instability resulting from failure of the floor-frame connections is a concern. The connections between the perimeter frame and floor system prevent buckling of the perimeter columns by limiting the column buckling length to the story height. If a perimeter column deforms towards the inside of the structure as shown in Figure 2(a), the floor system resists this motion and prevents buckling. However, if a perimeter column deforms towards the outside of the structure, as shown in Figure 2(b), large tensile forces may develop in the connection between the perimeter frame and floor-system. Since simple connections between the floor system and perimeter frame typically have relatively small strength, tensile failure may occur at these connections. Tensile failure of the frame-floor connection results in a longer column buckling length and, possibly, progressive collapse, as shown in Figure 3. Relatively low tensile capacity of the simple connections between the perimeter frames and floor-system is considered to be one of many factors that contributed to the progressive collapse of the World Trade Center Building in New York ^[1]. Previous study ^[2] investigated the progressive collapse of the high-rise U.S. type steel moment frame structure, which consists of the seismic frames located at the perimeters and the gravity frames inside the structure. In this study, the progressive collapse of perimeter frames in super-high-rise framed-tube structure is simulated numerically. Eigenvalue analysis is carried out at each time-step of the nonlinear time-history analysis to evaluate how the structure loses its stability and exhibits large deformations is evaluated as tensile failure of frame-floor connections progresses under earthquake loading.

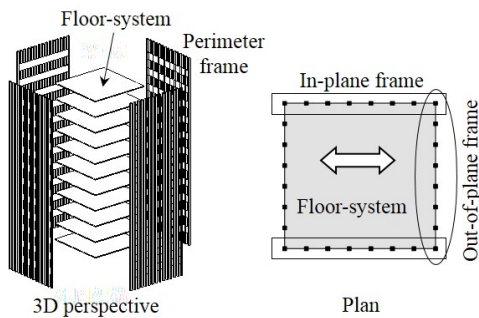
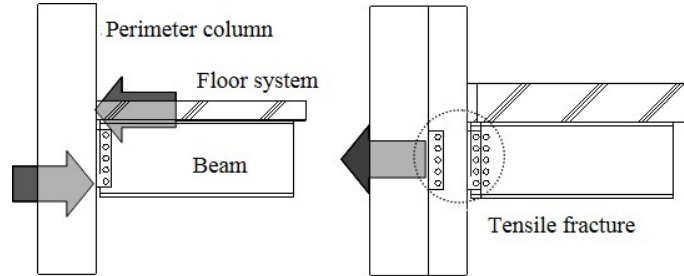
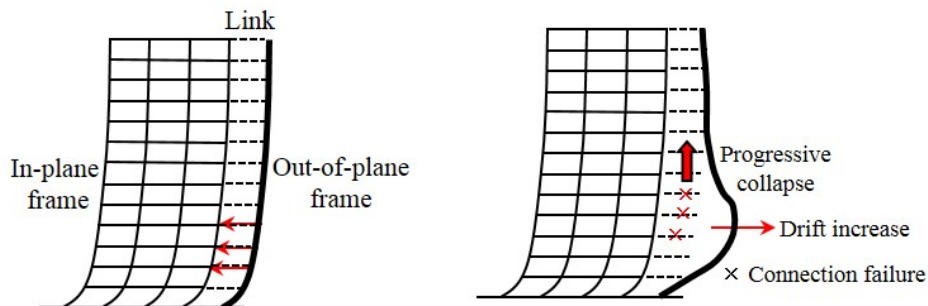


Figure 1. Framed-tube structure



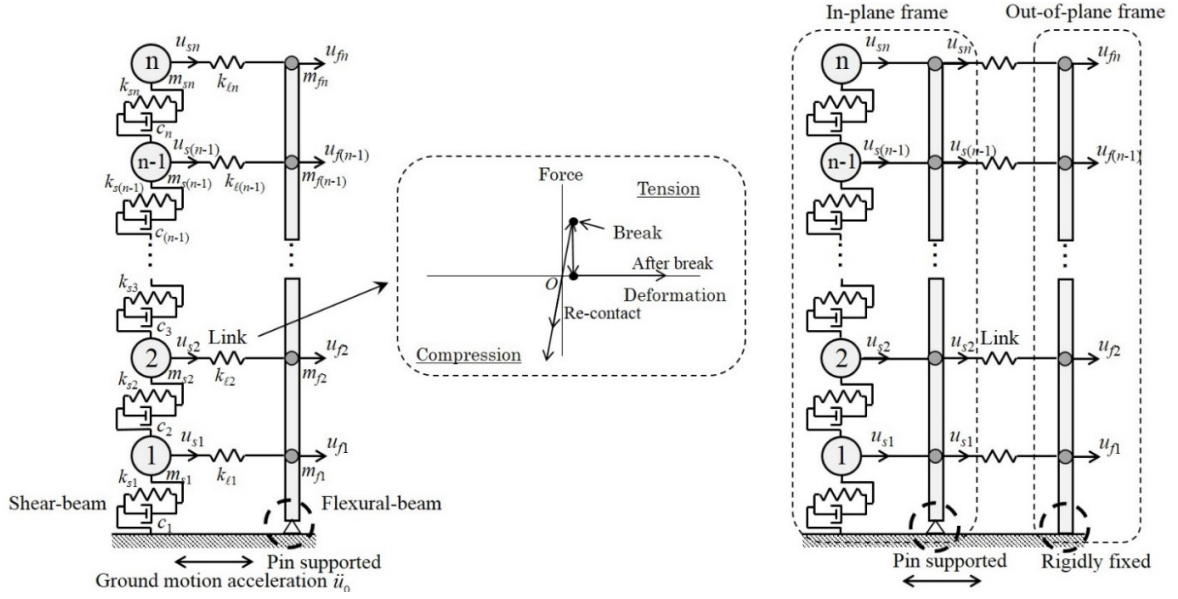
(a) Deform towards the inside (b) Deform towards the outside
Figure 2. Connection between perimeter column and floor system



(a) Before connection failure (b) After connection failure
Figure 3. Progressive collapse of perimeter frames due to connection failure in tensile direction

2 COUPLED SHEAR-FLEXURAL-BEAM MODEL WITH LINKS

The coupled shear-flexural-beam model with links is shown in Figure 4(a). This model consists of a shear-beam and a flexural-beam, which are connected with links. The model used in this study is shown in Figure 4(b), consisting of the shear-flexural-beam model representing the in-plane frame, the flexural-beam representing the out-of-plane frame, and connecting links.



(a) Coupled shear-flexural-beam model with links

(b) Model used for this study

Figure 4. Simple structural models

The formulation of the coupled shear-flexural-beam model with links is explained as bellow. The incremental form of equation of motion is given by Equation (1). Here, $[M]$ is mass matrix, $[C]$ is damping matrix, $[K(t)]$ is tangent stiffness matrix, $\{\Delta u_s\}$ and $\{\Delta u_f\}$ are the vectors of incremental displacements at each floor level for a shear-beam and flexural-beam, respectively, $\{\ell\}$ is a unit vector, and \ddot{u}_0 is the ground motion acceleration.

$$[M] \begin{Bmatrix} \{\Delta \ddot{u}_s\} \\ \{\Delta \ddot{u}_f\} \end{Bmatrix} + [C] \begin{Bmatrix} \{\Delta \dot{u}_s\} \\ \{\Delta \dot{u}_f\} \end{Bmatrix} + [K(t)] \begin{Bmatrix} \{\Delta u_s\} \\ \{\Delta u_f\} \end{Bmatrix} = -[M] \{\ell\} \Delta \ddot{u}_0 \quad (1)$$

Mass matrix is given by Equation (2). Here, $[M_s]$ and $[M_f]$ are the lumped mass matrices of the shear-beam and the flexural-beam, given by Equations (3) and (4), respectively.

$$[M] = \begin{bmatrix} [M_s] & [0] \\ [0] & [M_f] \end{bmatrix} \quad (2)$$

$$[M_s] = \begin{bmatrix} m_{s1} & 0 & 0 \\ 0 & \ddots & 0 \\ 0 & 0 & m_{sn} \end{bmatrix} \quad (3)$$

$$[M_f] = \begin{bmatrix} m_{f1} & 0 & 0 \\ 0 & \ddots & 0 \\ 0 & 0 & m_{fn} \end{bmatrix} \quad (4)$$

Tangent stiffness matrix is given by Equation (5).

$$[K(t)] = \begin{bmatrix} [K_s] + [K_l] & -[K_l] \\ -[K_l] & [K_F] + [K_l] \end{bmatrix} \quad (5)$$

Here, $[K_s]$ is the tangent stiffness matrix of the shear-beam given by Equation (6). Here, k_{si} is the tangent stiffness of the i^{th} -story spring in the shear-beam. If the geometrical nonlinearity, so called P - Δ effect in structural engineering, is considered, the tangent stiffness is reduced by $\theta_i^{P\Delta} = P_i/H_i$, where P_i is the weight of upper stories and H_i is the story height.

$$[K_s] = \begin{bmatrix} k_{s1} + k_{s2} & -k_{s2} & 0 & \cdots & 0 \\ -k_{s2} & k_{s2} + k_{s3} & \ddots & \ddots & \vdots \\ 0 & \ddots & \ddots & \ddots & 0 \\ \vdots & \ddots & \ddots & k_{s(n-1)} + k_{sn} & -k_{sn} \\ 0 & \cdots & 0 & -k_{sn} & k_{sn} \end{bmatrix} \quad (6)$$

$[K_f]$ is the stiffness matrix of the flexural-beam and the flexural-beam is assumed to be elastic in this study. The stiffness matrix of one beam element shown in Figure 5 is given by Equation (7). The stiffness matrix of the flexural-beam shown in Figure 6 is obtained by combining Equation (7) and rearranging the terms associated with displacement and rotation as given by Equation (8). By static condensation using the equilibrium condition, $\{M_i\} = \{0\}$, the stiffness matrix of the flexural-beam in terms of the force and the displacement is given by Equation (9). Finally, using the boundary condition, $u_0 = 0$, the stiffness matrix of the flexural-beam is given by Equation (10).

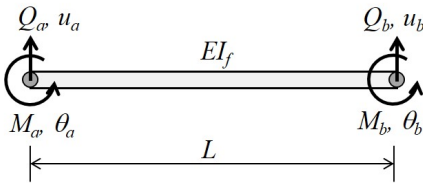


Figure 5. One beam element

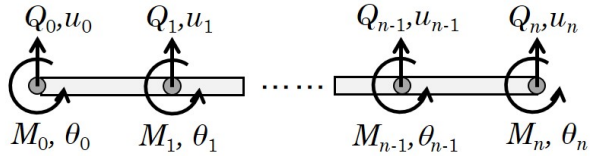


Figure 6. Flexural-beam

$$\begin{Bmatrix} Q_a \\ M_a \\ Q_b \\ M_b \end{Bmatrix} = \frac{EI_f}{L^3} \begin{bmatrix} 12 & 6L & -12 & 6L \\ & 4L^2 & -6L & 2L^2 \\ & & 12 & -6L \\ sym. & & & 4L^2 \end{bmatrix} \begin{Bmatrix} u_a \\ \theta_a \\ u_b \\ \theta_b \end{Bmatrix} \quad (7)$$

$$\begin{Bmatrix} \{Q_0, \dots, Q_n\}^T \\ \{M_0, \dots, M_n\}^T \end{Bmatrix} = \begin{bmatrix} [K_{11}]_{(n+1) \times (n+1)} & [K_{12}]_{(n+1) \times (n+1)} \\ [K_{21}]_{(n+1) \times (n+1)} & [K_{22}]_{(n+1) \times (n+1)} \end{bmatrix} \begin{Bmatrix} \{u_0, \dots, u_n\}^T \\ \{\theta_0, \dots, \theta_n\}^T \end{Bmatrix} \quad (8)$$

$$[\bar{K}_F]_{(n+1) \times (n+1)} = \frac{\{Q_0, \dots, Q_n\}^T}{\{u_0, \dots, u_n\}} = [K_{11}] - [K_{12}][K_{22}]^{-1}[K_{21}] \quad (9)$$

$$[K_F]_{n \times n} = [\overline{K_f}(2:n, 2:n)] \quad (10)$$

If geometrical nonlinearity is considered in beam element, the geometrical stiffness matrix given by Equation (11) is added to Equation (7), where P_i is the weight of upper stories and H_i is the story height. This geometrical stiffness matrix assumes small deformation.

$$[K_g] = \frac{-P_i}{H_i} \begin{bmatrix} \frac{6}{5} & \frac{H_i}{10} & -\frac{6}{5} & \frac{H_i}{10} \\ & \frac{2H_i^2}{15} & -\frac{H_i}{10} & -\frac{H_i^2}{30} \\ & & \frac{6}{5} & \frac{H_i}{10} \\ sym. & & & \frac{2H_i^2}{15} \end{bmatrix} \quad (11)$$

$[K_L]$ is the stiffness matrix of the link element and given by Equation (12).

$$[K_L] = \begin{bmatrix} [K_\ell] & -[K_\ell] \\ -[K_\ell] & [K_\ell] \end{bmatrix} \quad (12) \quad [K_\ell] = \begin{bmatrix} k_{\ell 1} & 0 & 0 & 0 & 0 \\ 0 & k_{\ell 2} & 0 & 0 & 0 \\ \vdots & 0 & \ddots & 0 & \vdots \\ 0 & 0 & 0 & k_{\ell(n-1)} & 0 \\ 0 & 0 & 0 & 0 & k_{\ell n} \end{bmatrix} \quad (13)$$

Rayleigh damping is used for $[C]$ as given by Equation (14). The values of a_0 and a_1 are determined so that the structure has 2% viscous damping ratio at the 1st natural period of the system and at $T=0.2$ [sec].

$$[C] = a_0 [M] + a_1 [K] \quad (14)$$

The Newmark- β method ($\alpha=1/2$, $\beta=1/4$) is used to solve the incremental equation of motion given by Equation (1). The modified Newton-Raphson iteration scheme is used to compute nonlinear incremental displacements corresponding to incremental external forces.

3 SIMULATION

3.1 Model parameters

Dynamic time-history analysis is carried out for the 15-story coupled shear-flexural-beam model with links shown in Figure 4(b) subjected to the NF 17 ground motions [3]. The 1st fundamental natural period of the entire structure is 1.81 [sec]. Every story has the same mass and the mass of the out-of-plane frame is assumed to be one fourth of the entire structure. The initial elastic stiffness of a horizontal spring in each story of the shear-beam is determined so that the shear-beam has the 1st fundamental natural of about 1.8 [sec] and the uniform story drift angle (SDA) under the horizontal design forces. This procedure is explained as follows. According to the UBC 1997 code [4], the 1st fundamental natural period of the structure can be estimated by Equation (15).

Here, f_i is the horizontal design force acting on the i^{th} story, δ_i is the elastic horizontal displacement on the i^{th} story for f_i , g is the gravitational acceleration and w_i is the weight of the i^{th} story.

$$T = 2\pi \sqrt{\frac{\sum_{i=1}^n w_i \delta_i^2}{g \sum_{i=1}^n f_i \delta_i}} \quad (15)$$

If the story drift angle of every story is uniform, which is defined as θ_{SDA} , and the height of the i^{th} story is h_i , δ_i is given by $h_i \cdot \theta_{SDA}$. Then, Equation (15) becomes Equation (16). Therefore, Equation (17) is obtained and the initial elastic stiffness of a horizontal spring in the i^{th} story, k_{si} , is given by Equation (18).

$$T = 2\pi \sqrt{\frac{\sum_{i=1}^n w_i (h_i \theta_{SDA})^2}{g \sum_{i=1}^n f_i (h_i \theta_{SDA})}} = 2\pi \sqrt{\frac{\sum_{i=1}^n m_{si} h_i^2}{\sum_{i=1}^n f_i h_i}} \theta_{SDA} \quad (16) \quad \therefore \theta_{SDA} = \frac{T^2}{4\pi^2} \frac{\sum_{i=1}^n f_i h_i}{\sum_{i=1}^n m_{si} h_i^2} \quad (17)$$

$$k_{si} = \frac{Q_i}{\theta_{SDA} (h_{i+1} - h_i)} = \frac{4\pi^2}{T^2} \frac{\sum_{i=1}^n m_{si} h_i^2}{\sum_{i=1}^n f_i h_i} \frac{\sum_{j=i}^n f_j}{(h_{i+1} - h_i)} \quad (18)$$

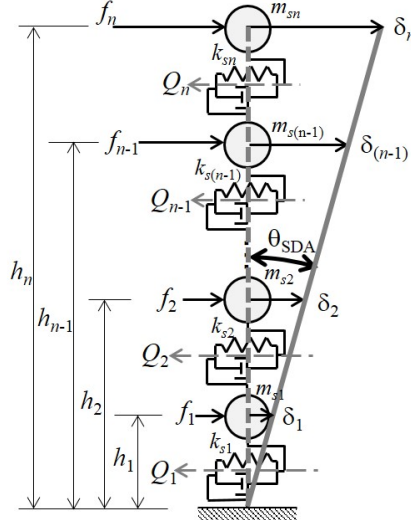


Figure 7. Uniform drift distribution of the shear-beam

Hysteresis loop of the horizontal spring of the shear-beam is set to be bilinear with kinematic hardening. The post-yield tangent stiffness ratio is set to be 3% and $P-\Delta$ effect is considered. The flexural-beam stiffness ratios, α_{cc} , of the in-plane frame and out-of-plane frame are 0.4 and 0.071, respectively. The axial force acting on the 1st-story perimeter column is assumed to be 30% of the axial yield strength of that column. The link element has the hysteresis loop shown in Figure 4(a) and the lateral-support strength is set to be from 3% to 4% and 5% of the axial yield strength of the 1st-story perimeter columns. The AIJ Recommendation for Limit State Design for Steel Structure [5] specifies lateral-support strength as 3% of the axial yield strength of columns.

3.2 Simulation results

Simulation results for the lateral-support strength ratio of 3%, 4% and 5% are presented below.

(a) 3% lateral-support strength ratio

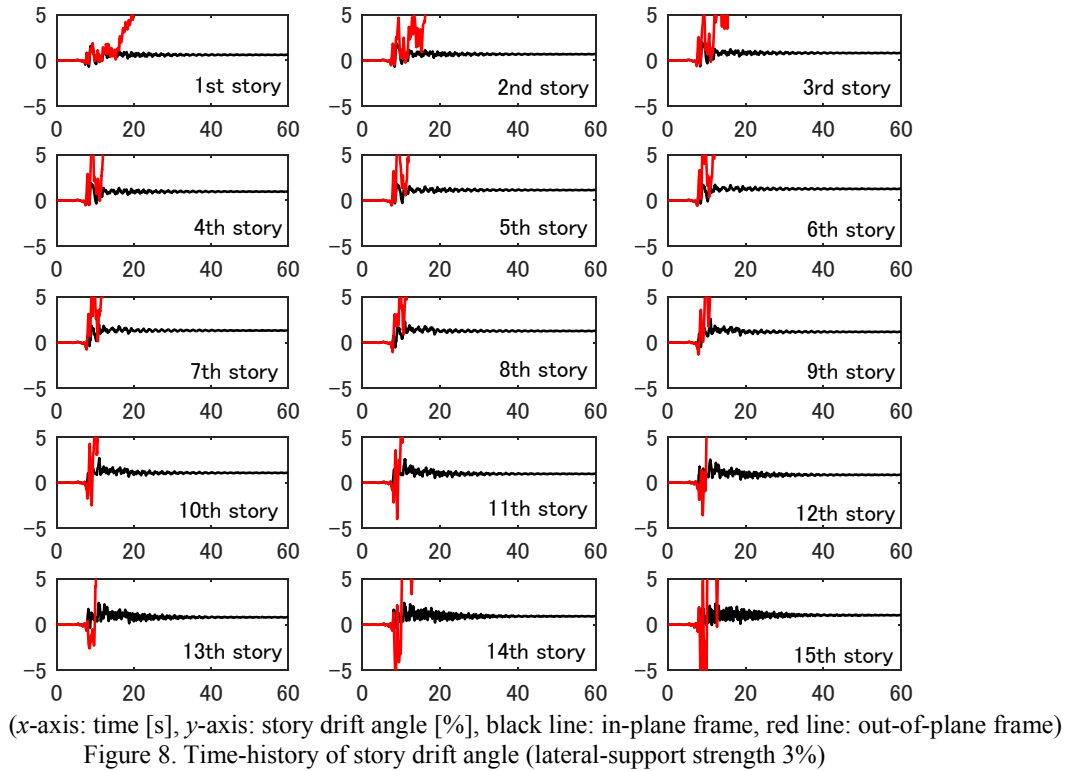
The time-history of the SDAs of the in-plane and out-of-plane frames for every story is shown in Figure 8. The in-plane and out-of-plane frames behave differently after about 10 [sec]. This is due to the tension breaks of the links. The relations of the axial force and axial deformation are shown in Figure 9. Distributions of the drifts of the in-plane and out-of-plane frames at connection failure are shown in Figure 10. The time-history of the minimum eigenvalue is shown in Figure 11. The minimum eigenvalue becomes negative after about 9 [sec], which results in unstable response and further, progressive collapse.

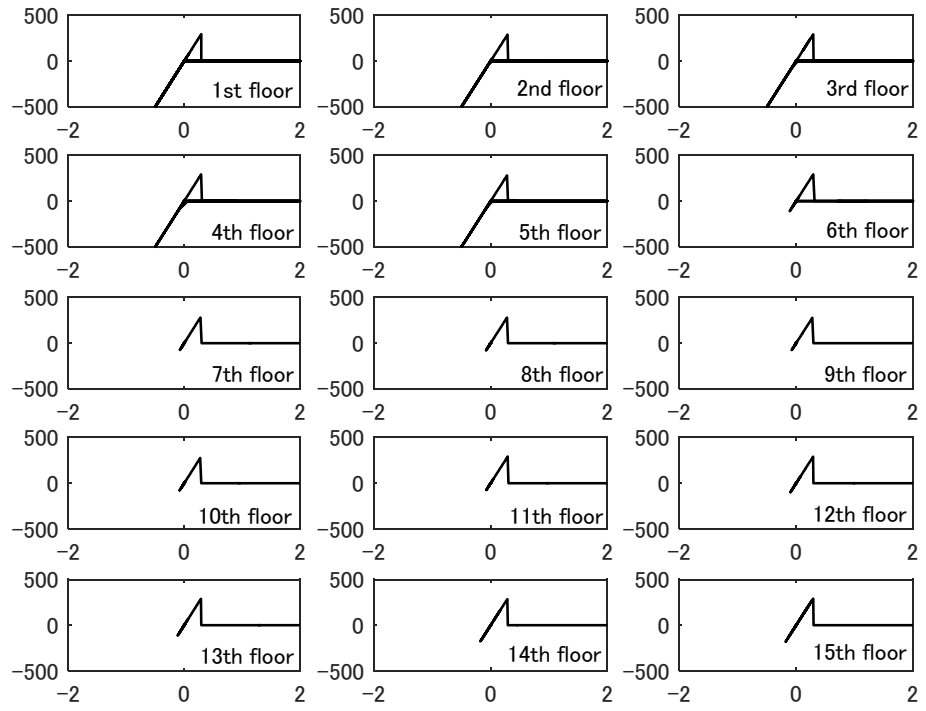
(b) 4% lateral-support strength ratio

The time-history of the SDAs is shown in Figure 12. Distributions of the drifts of the in-plane and out-of-plane frames at connection failure are shown in Figure 13. The minimum instantaneous eigenvalue continues to be negative as shown in Figure 14, which results in progressive collapse.

(c) 5% lateral-support strength ratio

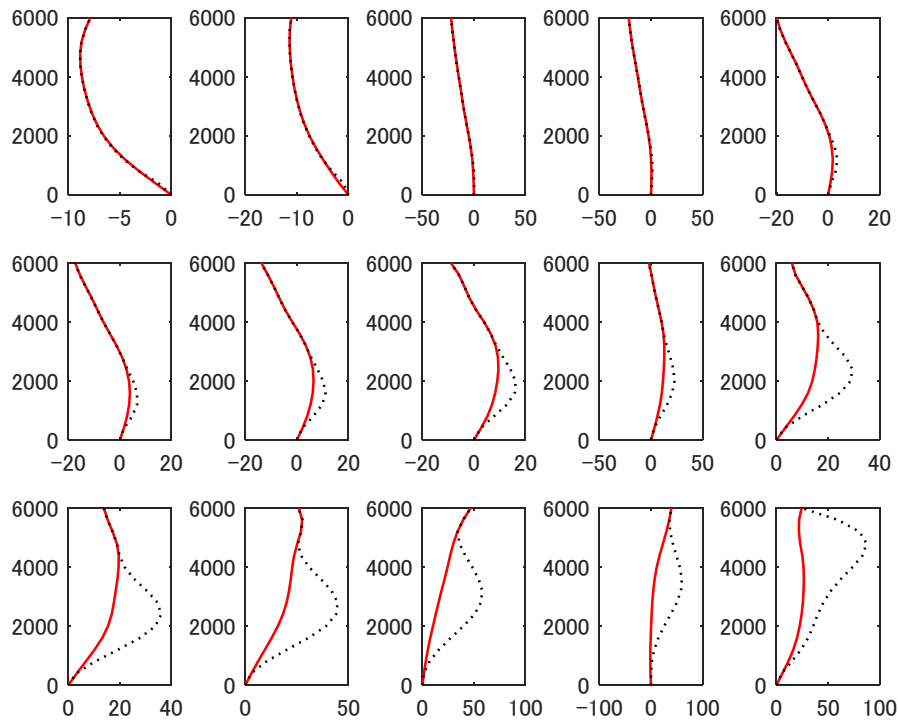
The time-history of the SDAs of the in-plane and out-of-plane frames is shown in Figure 15. The in-plane and out-of-plane frames behaves in slightly different manner since connection failure occurs at two links, at the 1st and 2nd floors, as shown in Figure 16. Distributions of the drifts of the in-plane and out-of-plane frames at connection failure are shown in Figure 17. The time-history of the minimum instantaneous eigenvalue is shown in Figure 18. The minimum eigenvalue is 0.437 and the instantaneous eigenvalue maintains positive value, which results in stable response.





(x-axis: axial deformation [cm], y-axis: axial force [kN])

Figure 9. Relation of axial force and deformation in link (lateral-support strength 3%)



(x-axis: Displacement [cm], y-axis: height [cm], solid line: in-plane frame, dotted line: out-of-plane frame)

Figure 10. Displacement distribution at breaks (lateral-support strength 3%)

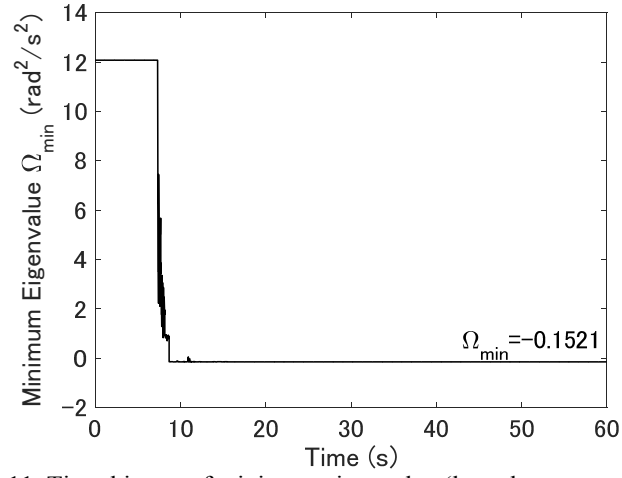


Figure 11. Time-history of minimum eigenvalue (lateral-support strength 3%)

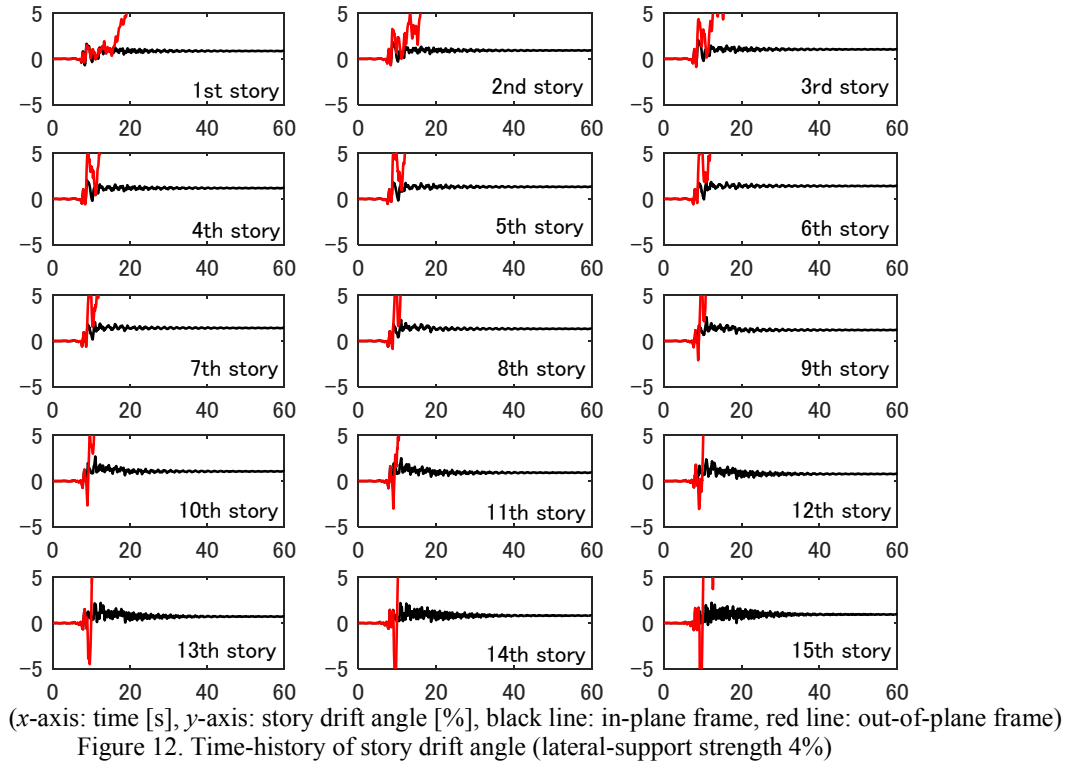
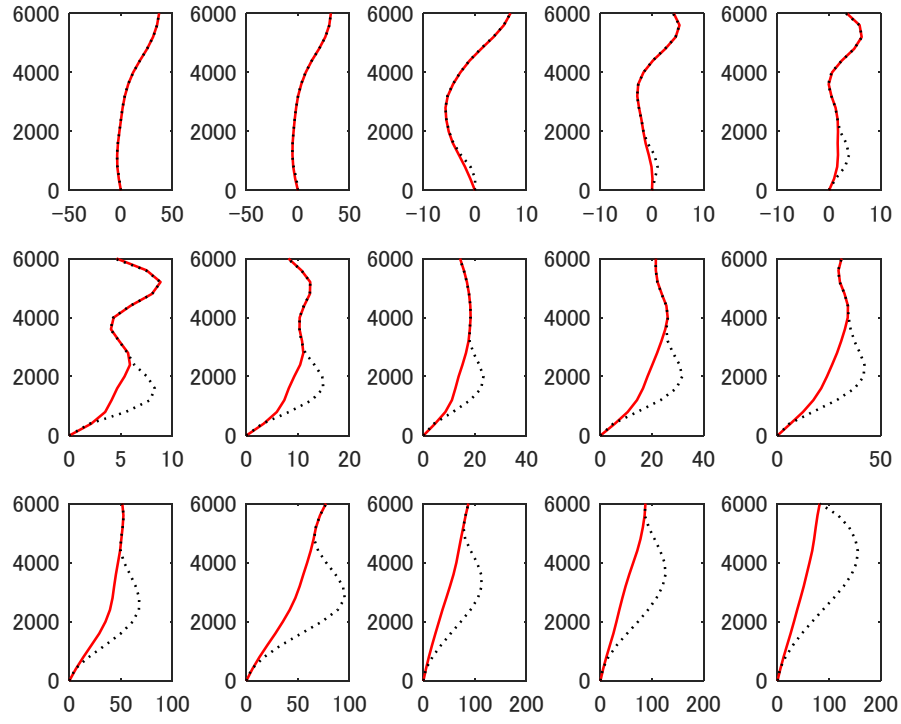


Figure 12. Time-history of story drift angle (lateral-support strength 4%)



(x-axis: Displacement [cm], y-axis: height [cm], solid line: in-plane frame, dotted line: out-of-plane frame)
Figure 13. Displacement distribution at breaks (lateral-support strength 4%)

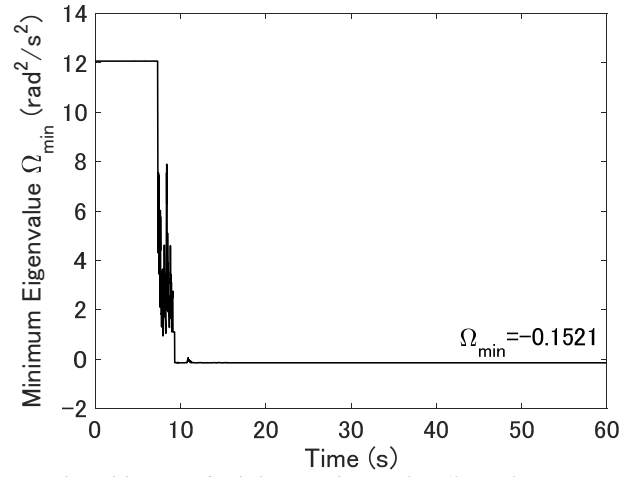
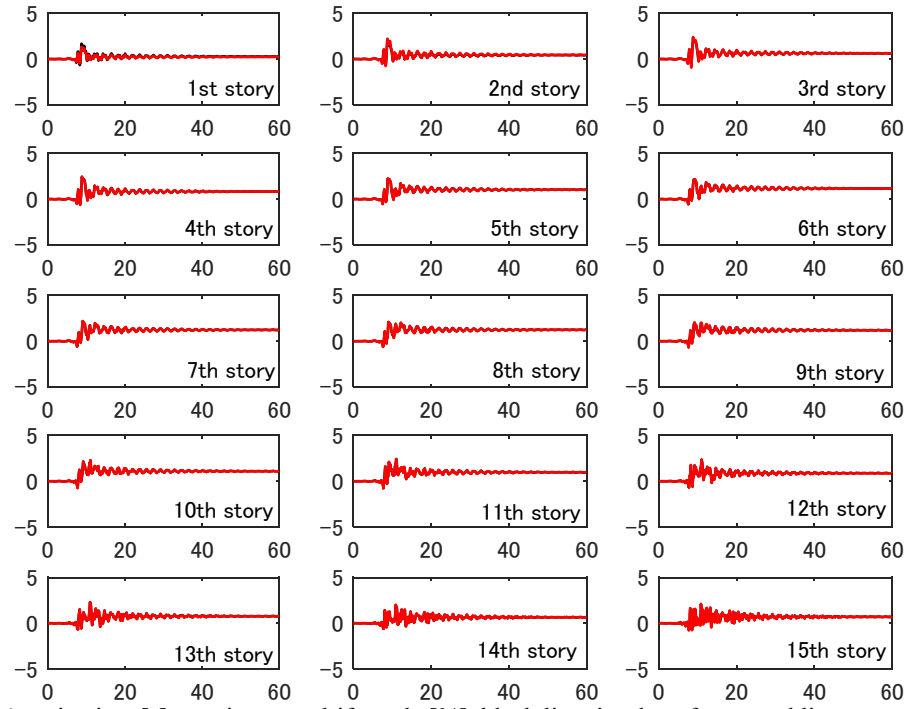
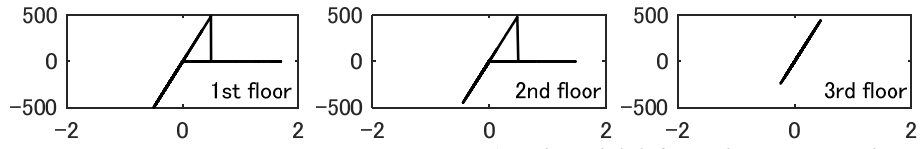


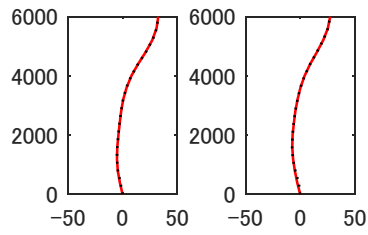
Figure 14. Time-history of minimum eigenvalue (lateral-support strength 4%)



(x-axis: time [s], y-axis: story drift angle [%], black line: in-plane frame, red line: out-of-plane frame)
Figure 15. Time-history of story drift angle (lateral-support strength 5%)



(x-axis: axial deformation [cm], y-axis: axial force [kN])
Figure 16. Relation of axial force and deformation in link (lateral-support strength 5%)



(x-axis: Displacement [cm], y-axis: height [cm], solid line: in-plane frame, dotted line: out-of-plane frame)
Figure 17. Displacement distribution at breaks (lateral-support strength 5%)

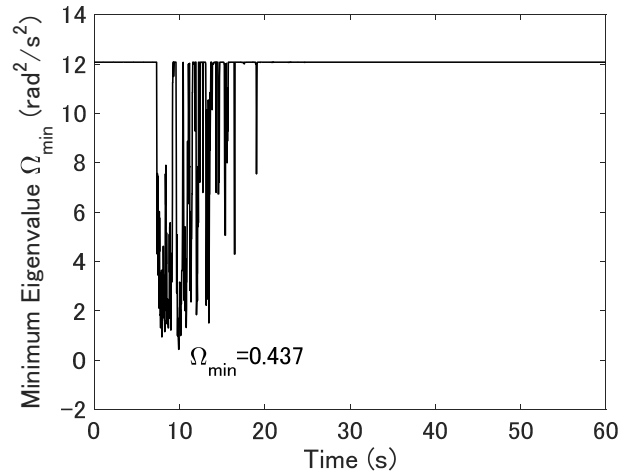


Figure 18. Time-history of minimum eigenvalue (lateral-support strength 5%)

4 CONCLUSIONS

In this study, the progressive collapse of super-high-rise framed-tube structure is simulated using simple shear-flexural-beam model with links. The link element simulates the restoring force of the simple connection between the perimeter, seismic frame and the floor-system. This link is modeled as possessing large stiffness and strength in compression and relatively small strength in tension. It was found that, when the tensile strength of the connection is 3% and 4%, the out-of-plane frame is separated from the in-plane frame and collapses as a result of severe earthquake loading. As the tensile strength of the links increases, the number of connection failures decreases and the in-plane and out-of-plane frames behaves as a single unit and in more stable manner.

REFERENCES

- [1] FEMA403, World Trade Center Building Performance Study, Data Collection, Preliminary Observations, and Recommendations, Appendix B, Structural Steel and Steel Connections, FEMA, Washington, DC. (2002).
- [2] Tagawa, H., MacRae, G., Lowes, L. and Wada, A. Analytical simulation of progressive collapse of perimeter frames due to out-of-plane behavior. The 14th World Conference on Earthquake Engineering, Beijing, China, October 12-17, (2008).
- [3] Somerville, P. et al. Development of Ground Motion Time Histories for Phase 2 of the FEMA/SAC Steel Project, Rep. No. SAC/BD97/04, SAC Joint Venture, Sacramento, California, (1997).
- [4] Uniform Building Code 1997 (UBC1997), International Conference of Building Officials, (1997)
- [5] Architectural Institute of Japan. Recommendations for Limit State Design of Steel Structures, (1998).

Coarse Graining DEM for a Non-spherical Particle System

Kazuya Takabatake*, Mikio Sakai**

*The University of Tokyo, **The University of Tokyo

ABSTRACT

Non-spherical particles are often encountered in chemical engineering. The behavior of non-spherical particles are too complicated to predict the translational and rotational motion. In designing a device for a powder process, introduction of numerical simulation technique is desired. The Discrete Element Method (DEM) is one of the most practical and efficient methods for the granular flow simulation. Although the adequacy and applicability of DEM have been proven in the numerous previous studies, there is a critical problem in the existing DEM regarding the calculation cost. In the DEM, the calculation cost depends on the number of calculation particles. In order to solve this problem, the coarse grain model was developed in our group, where the coarse particle whose diameter was larger than that of the original particle was used to simulate group of the original particles. Since the number of calculation particles can be drastically reduced by the coarse grain model, the large scale problem can be simulated by using a single computer in a reasonable time. When shape of the non-spherical particle is modeled, calculation costs would become expensive in the existing DEM. In order to solve this problem, the rolling friction model was proposed in the DEM. In the rolling friction model, the rolling resistance torque is calculated in order to reflect the non-spherical particle behavior. Since the rolling resistance torque works reversely against the angular velocity of the solid particle, the numerical oscillation occurs when the angular velocity is close to 0. In order to solve this issue, we develop a new rolling friction model in this study, which is more stable than the existing model. Besides, the rolling friction model is introduced into the coarse grain model for the first time to show the applicability to the large scale system. The adequacy of the model is proven through some verification tests. Consequently, the feasibility of a large-scale non-spherical particle system by using a single computer is shown in this study.

A Phase-field Lattice Boltzmann Method for Simulation of Microscopic Multiphase Flows

Naoki Takada*

*National Institute of Advanced Industrial Science and Technology (AIST)

ABSTRACT

Microscopic multiphase flows are widely encountered in various science and engineering fields. It is often difficult to experimentally observe the flows and measure the velocity, the pressure and the volume fraction simultaneously or to theoretically analyze them using the classical continuum dynamics approach based on a sharp-interface model. Computational fluid dynamics (CFD) simulations facilitate the understanding and prediction of the flows for flexible and accurate fluid-motion control, which result in the optimal design and efficient evaluation of micro-fluidic devices and processes. The phase-field model (PFM) has recently been attracting much attention from many researchers as one of the mesoscopic models that efficiently simulate the behavior of multi-phase systems based on the free-energy theory. The PFM describes an interface as a finite volumetric zone between different phases, across which physical properties vary steeply but continuously. Multiphase coexistence is allowed through minimizing a free-energy functional of the system without imposing topological constraints on the interface as phase boundary. The contact angle is set through a simple boundary condition on the solid surface with a wetting potential. As a result, PFM-CFD methods do not necessarily require conventional elaborate algorithms for the advection and reconstruction of interfaces. They therefore have an advantage over others, namely the efficient simulation of motions of multiple fluid-fluid interfaces attached to solid surfaces. This study aims to construct a PFM-CFD method for multiphase flow based on the previous two-phase and multiphase PFM-CFD methods [1,2]. For calculations of diffuse-interface advection and formation in the flow, the proposed method adopts the conservation-modified Allen-Cahn (AC) equation instead of the Cahn-Hilliard (CH) equation. The AC form is advantageous over the CH form in terms of volume conservation, interfacial tension effect, and computational efficiency, because the former is free from the interfacial-curvature effect on diffuse-interface dynamics and also has a second-order differential diffusion term instead of the fourth-order term in the latter. For solving the fluid-dynamics equations, the lattice-Boltzmann method (LBM) is employed in semi-Lagrangian form. The LBM is useful for high-performance computing because of the explicit and simple particle-kinematic operation with discrete conservation on an isotropic spatial grid. Through simple test simulations of three-phase rotational advection in two dimensions, it is confirmed that the PFM-CFD method has the potential to simulate multiphase flows accurately and efficiently. References: [1] N. Takada, et al., J. Comput. Sci. 17 (2016) 315-324. [2] H.G. Lee and J. Kim, Physica A 423 (2015) 33-50.

Dislocation Dynamics Simulation of Dislocation Shielding Effect at Crack Tip

Akiyuki Takahashi^{*}, Hayato Sugawara^{**}

^{*}Tokyo University of Science, ^{**}Tokyo University of Science

ABSTRACT

Ductile-brittle transition (DBT) in ferric steels is a critical issue to ensure the structural integrity of nuclear power plants. The main mechanism of the DBT is believed to be the shielding effect of dislocations at the crack tip. Therefore, in order to make a deep understanding of the DBT mechanisms, it is necessary to develop a computational method that can account for the dislocation nucleation, behavior and stress around the crack tip, and can derive the fracture toughness as a result of dislocation-crack interactions. This paper presents a dislocation dynamics (DD) simulation technique for the fracture toughness calculation with the consideration of dislocation shielding effect. In this study, the crack is represented with discrete dislocations, and the crack problem is solved using the DD method. The dislocation nucleation from the crack tip is simply modeled with a critical shear stress in the immediate vicinity of the crack tip. The nucleated dislocations move in the material, and produce the stress at the crack tip. The complex system of dislocation-crack interactions can be solved only with the DD method. In the DD method, the stress intensity factor at the crack tip can be easily computed by calculating the Peach-Koehler force, which is normally calculated in the DD simulations, acting at the crack tip dislocation. When the stress intensity factor reaches a critical value, the fracture toughness is determined using the analytical solution of stress intensity factor and the applied stress. To demonstrate the potential of the developed DD method, we performed a simulation of dislocation shielding effect with various dislocation mobility, which imitates the temperature dependence of dislocation behavior and fracture toughness. The numerical result clearly shows that the higher dislocation mobility gives higher fracture toughness, which is qualitatively in agreement with experimental results.

Tsunami Debris Simulation Considering Impact Loading Based on Finite Cover Method

Shinsuke Takase^{*}, Ryosuke Ogasawara^{**}, Kentaro Mori^{***}, Kenji Kaneko^{****}, Seizo Tanaka^{*****}, Kazuya Nojima^{*****}, Masaaki Sakuraba^{*****}

^{*}Hachinohe Institute of Technology, ^{**}Hachinohe Institute of Technology, ^{***}Hachinohe Institute of Technology, ^{****}Hachinohe Institute of Technology, ^{*****}University of Tsukuba, ^{*****}Nippon Koei Co., Ltd., ^{*****}Nippon Koei Co., Ltd.

ABSTRACT

We proposed a new fluid-structure interaction (FSI) analysis method, in which the finite cover method (FCM) is employed for interface capturing to properly evaluate the impact loading caused by tsunami debris. The stabilized finite element method is applied to solve the Navier-Stokes equations with a spatially fixed FE mesh, over which the Lagrangian meshes of structures are placed independently. In this study, the structures are assumed to be rigid bodies, and their motions and mutual contact are simulated with the discrete element method (DEM). Then, the key ingredient of the proposed method to accurately evaluate the impact loading caused by tsunami is the FCM, which enables us to realize appropriate discretization around the interfaces defined as intersections of the Eulerian mesh for fluids and the Lagrangian meshes for the rigid bodies. The continuity conditions of velocity and stress vectors at each interface are imposed with the penalty method. Also, we carry out the free surface flow simulations, for which the SUPG method is employed to discretize the Navier-Stokes equation. To capture the complex free surface motion such as breaking waves in case of tsunami impact, we apply the phase-field modeling with the conservation-modified Allen-Cahn equation. After verification analyses are carried out in comparison with experimental data, several representative numerical examples are presented to demonstrate the promise and performance of the proposed FSI analysis method. K.Terada, M. Asai, and Yamagishi : Finite Cover method for linear and nonlinear analyses of heterogeneous solids, Int. J. Numer. Meth. Engrg., 58, 1321-1346, 2003. N. Tanaka, J. Matsumoto and S. Matsumoto: Phase-field model-based simulation of motions of a two-phase fluid on solid surface, J. Comput. Sci. Technol, Vol.7 No.2, pp.322-337, 2013.

Multiscale Modeling of Piezoresistivity and Damage Induced Sensing Of Nanocomposite Bonded Explosive Materials Using Non-Local Damage Formulation

Krishna Talamadupula*, Gary Seidel**

*Virginia Tech, **Virginia Tech

ABSTRACT

Polymer bonded explosives (PBXs) are highly sensitive explosive composites that are susceptible to accidental detonation. They are composed of explosive grains at high volume fractions, for example RDX, HMX etc. surrounded by a polymer medium at low volume fractions such as epoxy, estane etc. The prognostication of life of PBX materials is of interest primarily due to its unstable nature. This work models the usage of CNT infused polymer binder in these explosive composites to give Nanocomposite Bonded Explosives (NCBXs). This leverages the ability of the CNTs to impart piezoresistive properties to the polymer and hence provide insitu sensing of strained and damaged states of NCBX materials. The effective piezoresistivity is derived from key multiscale aspects of the nanocomposite binder due to the presence of the CNTs such as electron hopping at the nanoscale, CNT bundle network formation and disruption at the microscale etc. The degree of piezoresistivity is informed in a hierarchical fashion from the lower scales to the microscale RVE being analyzed through a microscale gauge factor. Correlating the piezoresistive response of NCBXs to the model governing the mechanical behavior including damage will require a detailed understanding of the strain and damage sensing regimes. To this end, the use of local strain-softening damage laws has been found to lead to numerical instabilities and ill-posedness of boundary value problems or element size sensitivities. To move away from these limitations, this work adapts a non-local damage formulation in a continuum damage mechanics framework developed from previous research efforts and implements it in conjunction with a 2D finite element code with element deletion techniques. Interfacial damage between explosive grains and the surrounding nanocomposite binder is modeled with electromechanical cohesive zones. Quasi static tensile/compressive tests are conducted on selected RVEs of NCBXs. The non-local damage model and interfacial cohesive law should correctly reflect energy dissipation during the fracture process. Damage parameters are adjusted according to the material's fracture energy. Various damage modes within the RVE, final failure of the RVE and damage detection of individual damage modes through piezoresistive analysis are studied. The usage of the non-local damage formulations limits the spurious spreading of the damage band and leads to better crack convergence. The study of the damage mechanisms interlinked with the piezoresistive sensing response enhances the model's capabilities to track and describe various damage related phenomena. It is anticipated that this work will improve the prognosis of life of NCBX materials.

Advances in 10-node Composite Tetrahedral Elements for Solid Mechanics

Brandon Talamini^{*}, Jakob Ostien^{**}, Alejandro Mota^{***}, James Foulk^{****}, Kendall Pierson^{*****},
Nathan Crane^{*****}, Michael Veilleux^{*****}

^{*}Sandia National Laboratories, ^{**}Sandia National Laboratories, ^{***}Sandia National Laboratories, ^{****}Sandia National Laboratories, ^{*****}Sandia National Laboratories, ^{*****}Sandia National Laboratories, ^{*****}Sandia National Laboratories

ABSTRACT

In this work, we exhibit new developments to 10-node composite tetrahedral elements towards their use in demanding solid mechanics applications. First, we investigate the case of nearly incompressible material behavior, and find that use of the standard assumed gradient operator leads to volumetric locking. We reformulate the composite element through a generalized Hu-Washizu variational principle that allows independent approximations not just of the Piola stress and deformation gradient fields, but also the pressure and Jacobian. This allows the definition of lower order projections of the volumetric response in a variationally consistent way, thus preserving symmetry of the stiffness matrix. The element behavior is shown to be locking-free, without resorting to reduced integration, and without introducing spurious zero-energy modes. Second, we examine use of the composite tetrahedral elements in explicit dynamics analysis. We study the spectral properties of the time integration operator with various mass lumping schemes, and propose methods to estimate the largest stable time step size. Sandia National Laboratories is a multi-mission laboratory managed and operated by National Technology &&&&&&& Engineering Solutions of Sandia, LLC., a wholly owned subsidiary of Honeywell International, Inc., for the U.S. Department of Energy&&&&&&'s National Nuclear Security Administration under contract DE-NA0003525.

KEYNOTE: Multiscale Analysis of Progressive Damage in Composite Materials: Transverse Matrix Cracking as Example

Ramesh Talreja*

*Texas A&M; Univeristy

ABSTRACT

Damage in composite materials is necessarily progressive, i.e., it usually starts with a failure event that leads to a sequence of subsequent failure events, culminating in final failure. Depending on the fiber architecture and constituent material properties, and the imposed loading, the sequence of failure events occurs at multiple characteristic scales. The local stress fields change as the failure events rearrange the load sharing balance amongst the participating elements. The challenge of progressive damage analysis (PDA) is exacerbated by the multiple modes in which failure events collect themselves, e.g. as kink bands in axial compression versus random fiber breakage clusters in axial tension in unidirectional composites. In laminated configurations, the damage modes occur as multiple ply cracking and delamination, for example. While it is unrealistic to expect a single modeling approach to be able to address all damage modes, one can hope to find a strategy based on fundamental principles to lead to a common coherent approach. One such strategy will be put forth in this presentation. It will be guided by the laws of thermodynamics that govern all irreversible (energy dissipative) phenomena. The formation of a matrix crack in unidirectional polymer based composites under transverse tension will be taken as an example to illustrate the features of failure analysis at multiple scales, ranging from the molecular scale to the typical crack length of a few fiber diameters.

Second Gradient Poromechanics: Constitutive Modeling and Numerical Implementation in IGA-FEM

Claudio Tamagnini*, Carlos Plua**, Pierre Besuelle***

*University of Perugia, **Université Grenoble Alpes, ***CNRS

ABSTRACT

In this work, a fully coupled hydromechanical formulation for unsaturated 2nd gradient elastoplastic porous media is presented and applied to the numerical modeling of some geomechanics IBVP characterized by strain localization into shear bands. The introduction of internal length scales associated to the weakly non-local character of the constitutive equations effectively regularizes the numerical solutions. The 2nd gradient elastoplastic model adopted is based on two independent plastic mechanisms. The first one is provided by a three-invariant isotropic-hardening elastoplastic model similar to the one presented by Nova et al. (2003), extended to unsaturated soils. In lack of sufficient experimental evidence, the second-gradient mechanism is based on a simple elastic-perfectly plastic formulation. For the numerical solution of the governing system of non-linear PDEs, the Isogeometric (IGA) Finite Element Method (Hughes et al., 2005) has been adopted. When applied to constrained micromorphic media such as second-gradient materials, IGA offers the advantage of providing higher-order continuity of the approximating functions across element boundaries, which allows a more efficient and straightforward implementation of the discrete equilibrium problem, as compared to existing mixed FE formulations based on conventional polynomial shape functions, see Collin et al. (2006). This feature is also very important in coupled hydromechanical problems. In fact, the smoothness of the approximated displacements and pore pressure fields can mitigate significantly the requirements for minimum time steps. The simulation of some relevant consolidation problems demonstrates the good performance of the IGA implementation, and shows its effectiveness in regularizing the FE solutions when localization patterns occur in the strain field. References Collin, F., Chambon, R., & Charlier, R. (2006). A finite element method for poro mechanical modelling of geotechnical problems using local second gradient models. *International journal for numerical methods in engineering*, 65(11), 1749-1772. Hughes, T. J., Cottrell, J. A., & Bazilevs, Y. (2005). Isogeometric analysis: CAD, finite elements, NURBS, exact geometry and mesh refinement. *Computer methods in applied mechanics and engineering*, 194(39), 4135-4195. Nova, R., Castellanza, R., & Tamagnini, C. (2003). A constitutive model for bonded geomaterials subject to mechanical and/or chemical degradation. *International Journal for Numerical and Analytical Methods in Geomechanics*, 27(9), 705-732.

A Reformulation of Pressure Poisson Equation for the Least Squares Moving Particle Semi-implicit Methods

Tasuku Tamai*, Seiichi Koshizuka**

*Graduate School of Engineering, The University of Toyko, **Graduate School of Engineering, The University of Toyko

ABSTRACT

Least Squares Moving Particle Semi-implicit (LSMPS) method[1] is one of the particle methods for analyses of incompressible free-surface flow. In this study, in order to improve the satisfaction of incompressible constraint, a reformulation pressure Poisson equation for the LSMPS Method is presented. [1] T. Tamai and S. Koshizuka, Computational Particle Mechanics, Vol.1, 2014.

Space/Time Staggered Computational Framework and Reduced Order Modeling for Optimal Space-Time Discretizations

Kumar Tamma*, Rohit Deokar**

*University of Minnesota, **University of Minnesota

ABSTRACT

Novel developments in “Space/Time staggered computational framework and reduced order modeling for optimal Space-Time discretizations” in computational mechanics are presented and highlighted. The focus is on developments in the field of model order reduction framework in space and time for the Generalized single step single solve (GSSSS*) family of algorithms. It encompasses the following: a) The GSSSS framework has been developed in the past two decades as a unified theory encompassing all the computationally competitive time integration schemes for first and second order systems over the past 50 years or so. Using the underlying versatility of the GSSSS framework, a novel model order reduction procedure in space is proposed to eliminate spurious high frequency participation in dynamical systems. Numerically dissipative schemes which were originally proposed to deal with these high frequency participation lose energy over time and damp out the physics in the system. The proposed method for elimination of high frequency participation deals with this very problem by combining the advantages of the energy conserving and numerically dissipative algorithms through projection techniques. b) In addition, the so called “Finite element in time” framework for the GSSSS algorithms is developed using the weighted residual methodology. Based on the finite element in time methodology, a novel general purpose a posteriori error estimator for first and second order systems under the umbrella of GSSSS family of algorithms is proposed to foster adaptive time stepping. The applicability of the proposed estimator to several existing time integration algorithms including the well known schemes like the Newmark method, HHT-, Classical midpoint rule, Crank Nicolson and in addition, new algorithms and designs as well is demonstrated with single and multi-degree of freedom, linear and nonlinear dynamical problems. c) Lastly, model reduction in space and time through the so called staggered space-time MOR procedure is proposed which aims at refining the discretizations in space while employing a reduced dimension in time. Conversely, a reduced dimension in space is used to improve the discretization in time and the process is performed in an iterative fashion. Reference: * J. Har and K.K. Tamma, *Advances in Computational Dynamics of Particles, Materials and Structures*, John Wiley, 2012,

Numerical Framework for the Direct Micro-Macro Simulation of Micro-Heterogeneous Materials under Impact Loading

Erik Tamsen^{*}, Wolfgang Weber^{**}, Daniel Balzani^{***}

^{*}Technische Universität Dresden, ^{**}Helmut-Schmidt-Universität – Universität der Bundeswehr Hamburg,
^{***}Ruhr-Universität Bochum

ABSTRACT

Heterogeneities at the microscale give rise to sophisticated wave propagations and thus, a complex macroscopic material behavior under dynamic loading. For instance in strain-hardening cement-based composites, where the favorable energy absorbing behavior under impact loading results from breaking of the concrete matrix and fiber pullout, microscopic dynamic effects may be significant. To establish a valid model for the effective macroscopic material properties, the finite element method can be used. A suitable RVE can then be considered and based on its discretization a microscopic boundary value problem including dynamics can be solved to compute the homogenized mechanical fields at the macroscale. A direct micro-macro formulation based on kinematic admissibility and the principle of multiscale virtual power [1,2] is presented, which allows for an energetically consistent scale-bridging. The focus of the presentation lies on the derivation of consistent tangent moduli for large strains, which take into account effects resulting from inertia forces. These are required for a consistent direct micro-macro approach. Implementation aspects for the numerical simulation of reinforced concrete under impact loading will be discussed and selected numerical examples will be presented showing the resulting convergence behavior. [1] E.A. de Souza Neto, P.J. Blanco, P.J. Sánchez, R.A. Feijóo. An RVE-based multiscale theory of solids with micro-scale inertia and body force affects, *Mechanics of Materials*, 80:136-144, 2015. [2] C. Liu and C. Reina. Variational coars-graining procedure for dynamic homogenization. *Journal of the Mechanics and Physics of Solids*, 104:187-206, 2017

Neural Network Based Surrogate Models for Effective Mechanical Properties of Microstructures

RenKai Tan^{*}, Wenjing Ye^{**}

^{*}Hong Kong University of Science and Technology, ^{**}Hong Kong University of Science and Technology

ABSTRACT

Effective mechanical properties of microstructures are required in a number of applications. One example is in the design of metamaterials using topological optimization. A key step in the design procedure is the repetitive evaluation of effective properties of the microstructure, which evolves constantly during the process. For microstructures with complex shapes, this calculation using traditional numerical methods such as the FEM could be quite computational intensive and lead to a long design cycle. Recent advancement in the field of machine learning has attracted great attention of researchers in various fields to start utilizing the technology and integrating within their researches. The success of machine learning methods in taking up the role of a universal function approximator [1] could be very advantageous in replacing the computationally intensive finite element calculation. In this talk, we present neural network based surrogate models constructed to rapidly predict effective mechanical properties of a given microstructure. We utilize Convolutional Neural Network (CNN) to automatically extract features from microstructures which were represented as images [2] and use network to link the features with mechanical properties of microstructures. The network was trained using 20000 sets of data and tested with 2000 sets of data. The average accuracy of the CNN in the prediction of 9 dimensional material stiffness matrix from a 20 by 20 pixel topology image is around 0.5%, and the evaluation time for the property prediction is on the order of milliseconds. These preliminary results have demonstrated the potential of the developed approach, which is believed to be able to greatly reduce the total computational time for the topology optimization process. References: [1] Hornik, K., Stinchcombe, M., & White, H. Multilayer feedforward networks are universal approximators. *Neural networks*, 2(5), 359-366, 1989. [2] Russakovsky, O., Deng, J., Su, H. et al. ImageNet Large Scale Visual Recognition Challenge. *IJCV*, 2015.

3D Printing Employed for the Design and Manufacture of Metal Based Diamond Tools

Songcheng Tan^{*}, Zhan Yang^{**}, Longchen Duan^{***}, Xiaohong Fang^{****}

^{*}China University of Geosciences, Wuhan, ^{**}China University of Geosciences, Wuhan, ^{***}China University of Geosciences, Wuhan, ^{****}China University of Geosciences, Wuhan

ABSTRACT

Diamond tools are widely used in cutting, grinding and drilling areas. According to their raw materials and manufacture technology, diamond tools can be divided into metal based, ceramic based and resin based. Among them, the most common metal based diamond tools are all kinds of diamond bits and saws. However, the development of metal based diamond tools is restricted by the new manufacture technologies and material systems. Recently, 3D printing has been one of the hottest topics in manufacture area, and Selective Laser Melting (SLM) is rapidly developed at the same time. Thus, the SLM technology could provide a new opportunity to the metal based diamond tools manufacture industry. Nevertheless, when apply the SLM technology to the diamond composite material's manufacture, there are some special issues need to overcome, such as metal powder components and performance, diamond size and shape, etc. To verify the practicability of SLM employed for metal based diamond tools manufacture, some tests and analyses were conducted. In primary study, we manufactured 9 rectangular column composite samples by SLM, with dimensional of 8.5mm × 8.5mm × 15mm. The raw metal materials are FAM-201 pre-alloy powder and FJT-06 brazing pre-alloy powder. The sizes of the pre-alloy powder are 200 meshes, and their main components are copper, tin, iron, cobalt and nickel. Test results indicate that, it is feasible to produce a metal composite by the SLM, even though the raw metal powder are much coarser than the conventional size for the SLM. Based on the primary study, we manufactured 8 rectangular column diamond composite samples, with dimensional of 20mm × 20mm × 6mm. The raw metal powders are the same with the primary study. The volume ratio of diamond within composite is 5%, and the diamond size is 70 meshes to 80 meshes. The optimized SLM process parameters are: Laser power, 180W to 200W; Scanning speed, 700mm/s to 900mm/s; Scanning line interval, 0.07mm; Powder-bed depth, 0.15mm. Test results indicate that, strength of the diamond composite samples is stronger than the previous metal composite samples. Possible reasons may include the SLM process parameters are selected and optimized, and the diamond composite samples are much thinner than the previous. However, SEM tests indicate that, there are many pores and some cracks within the diamond composite matrix. Also, the SEM tests show that the SLM process would cause serious damage to the diamond grits.

Computational Modeling of Blast Wave Induced Traumatic Brain Injury and Model Validations

X. Gary Tan^{*}, Robert N. Saunders^{**}, Amit Bagchi^{***}

^{*}U.S. Naval Research Laboratory, Washington DC, USA, ^{**}U.S. Naval Research Laboratory, Washington DC, USA, ^{***}U.S. Naval Research Laboratory, Washington DC, USA

ABSTRACT

Modeling of human biomechanics and traumatic brain injury (TBI) resulting from blast exposure is very challenging because of the complex geometry and the substantial material heterogeneity in the human body. We developed a detailed finite element (FE) model of human body which represents both the geometry and the material realistically [1]. The high-fidelity computational models were developed based on high-resolution computed tomography (CT) and magnetic resonance imaging (MRI) scans. Hyper-viscoelastic models were used for soft tissues to capture the rate dependent behavior and large strain material nonlinearity. The shock wave interaction with the human due to a C4 explosion was simulated using the computational fluid dynamics (CFD) method, via an efficient combination of 1-D and 3-D numerical techniques. The shock wave loads were applied to the exterior of the FE models to simulate the pressure wave transmission through the body and capture the biomechanical response. The resulting large-scale CFD and FE problems were solved using the coupled Eulerian and Lagrangian solvers, respectively, in the highly scalable DoD Open Source code CoBi. The predicted brain tissue stress-strain fields were used to determine the areas susceptible to the injury by using published mechanical injury thresholds. The computational approaches were validated by comparing simulation results of head surrogate and full-scale animal models with recently collected data from shock/blast tube tests at specific instrumented locations [2]. The validated animal model and human model were also used to examine potential brain injury similarities and differences under identical loads. These results form the basis for correspondence rules that are able to relate insult-injury outcomes in an animal to those in the human. A key contribution of this work is to develop a multi-scale modeling approach to couple blast physics, whole body biodynamics and injury biomechanics for the blast event, as well as the multi-physics solver suitable for high-performance computing. The implications of these results suggest that computational models could be used to predict the biomechanical response in the blast TBI event, understand blast induced TBI mechanisms, develop animal-human injury correspondence rules, and help assess and improve the protection against the blast TBI. Reference: 1. Tan X.G., Przekwas A.J., & Gupta R.K., Computational Modeling of Blast Wave Interaction with a Human Body and Assessment of Traumatic Brain Injury, Shock Waves 2017. 2. Tan X.G., Saunders R.N., Bagchi A., Validation of a Full Porcine Finite Element Model for Blast Induced TBI using a Coupled Eulerian-Lagrangian Approach, ASME-IMECE 2017-70611.

MULTI-RESOLUTION TECHNIQUES FOR LEAST SQUARE MPS METHOD

MASAYUKI TANAKA*[†], RUI CARDOSO*, AND HAMID BAHAI*

*Brunel University London
Kingston Lane, Uxbridge
London, United Kingdom
masayuki.tanaka@brunel.ac.uk

[†]Toshiba Co., Ltd
33, Shinisogo-cho, Isogo-ku, Yokohama-shi
Kanagawa, Japan
masayuki11.tanaka@toshiba.co.jp

Key words: Least Square MPS Method, Multi-Resolution, Incompressible Fluid.

Abstract. The Moving Particle Semi-implicit (MPS) method is enhanced for multi-resolution simulations in this work. The spatial resolution is changed adaptively by the particle splitting and merging algorithms. The Least Square MPS (LSMPS) method is applied to obtain accurate results even if particles have different diameters. A new wall boundary scheme, which is represented by polygons, is also improved for a multi-resolution simulation. By conducting simulations for the Taylor Green vortex and for a dam break, the accuracy of the Multi-Resolution MPS method was verified. Also, it was shown that this method was able to reduce computational costs significantly.

1 INTRODUCTION

Full-Lagrangian particle methods have great advantages when compared with Eulerian methods due to the fact that the particle can move dynamically and there is no need to calculate the advection terms as in Eulerian methods. Originally, the Smoothed Particle Hydrodynamics (SPH) method, which is one of the most popular full-Lagrangian methods, was developed to simulate compressible fluid flows [10, 4]. On the other hand, the Moving Particle Semi-implicit (MPS) method was developed to simulate incompressible fluid flow strictly within a full-Lagrangian context [6].

However, the particle methods have some drawbacks such as longer computational time and inaccuracy. Generally, a particle method requires more computational resources when compared with an Eulerian method because of the extra computational effort required to handle particle interactions. Moreover, particle methods have been suffering from changing the resolution while Eulerian methods can easily change the sizes of meshes for different parts of the domain to reduce computational costs. In a Lagrangian description, however, the spatial resolution, i.e. diameters of

particles, is generally limited and non-uniform size diameters cannot be used. There have been several attempts to change the spatial resolution in the SPH methods: Kitsionas and Whitworth [5] proposed the particle splitting method to increase the spatial resolution locally. In this method a particle is split into thirteen particles to obtain a spherically symmetric kernel function; Lastiwka et al. [7] proposed changing resolution by adding or removing particles. They applied a first-order differentiation scheme and showed that it was accurate even if particles had non-uniform spacing; Liu et al. [9] proposed the Adaptive SPH method, in which a support domain was extended to non-spherical regions such as an ellipsoidal shape region for example; Adams et al. [1] proposed a method to change the spatial resolution adaptively. There have also been some noteworthy developments for multi-resolution techniques for the MPS method such as the works of Shibata et al. [12] on the overlapping technique and Tang et al. [17] for the extension of Shibata's work to three dimensions. Notwithstanding the great contributions of Shibata and Tang for multi-resolution methods for the MPS method, there is still a major drawback which is the inability of the technique to allow for two-way interactions between low-resolution and high-resolution domains. Tanaka et al. [15] developed further a multi-resolution technique for the MPS method in two dimensions, however, the formulation was derived for the classical MPS method and thus it suffers from inaccuracy and stability issues. Tang et al. [16] extended this method for three dimensions, however, no splitting or merging algorithms were adopted and therefore the spatial resolution cannot be changed dynamically.

In spite of a number of improvements, the particle methods have a key fundamental inaccuracy problem that can even lead to a total failure of simulations. The particle methods are usually formulated by assuming that particles are distributed uniformly. The source of inaccuracy starts to be more evident when consistency is lost due to the non-uniform arrangement of particles as the simulation goes on. The incompressible condition of the MPS method, which enforces the particle number density to be constant, is also one of the major sources for the loss of accuracy on the MPS method. Tamai and Koshizuka [13] have proposed the Least Square MPS (LSMPS) method to overcome the inaccuracies caused by the non-uniform particle distribution and other similar methods were proposed for the SPH method [2, 3].

In this work, the Multi-Resolution MPS method [14], which can change spatial resolution dynamically in incompressible fluid flow simulations is presented. A new boundary condition for a wall for multi-resolution simulations are also proposed.

2 MULTI-RESOLUTION MPS METHOD

2.1 Least Square Formulation

The LSMPS method [13], which recreates differential operators based on neighbouring particle positions for every time step, is applied in this work, because it can provide more accurate approximation even if diameters of particles differ. The formulation of the LSMPS for an arbitrary function f is shown next.

$$\mathbf{D}_x f(\mathbf{x}) = \mathbf{H}_i \mathbf{M}_i^{-1} \mathbf{b}_i \quad (1)$$

where \mathbf{x} is a coordinate, \mathbf{D}_x is a differential operator, \mathbf{H} is a matrix of coefficients, \mathbf{M} is a moment

matrix and \mathbf{b} is a moment vector. The second order formulation for two dimensions, for example, is represented as below:

$$\mathbf{D}_x = \left[\frac{\partial}{\partial x} \quad \frac{\partial}{\partial y} \quad \frac{\partial^2}{\partial x^2} \quad \frac{\partial^2}{\partial x \partial y} \quad \frac{\partial^2}{\partial y^2} \right]^T \quad (2)$$

$$\mathbf{H}_i = \text{diag}[L_i^{-1} \quad L_i^{-1} \quad 2L_i^{-1} \quad L_i^{-1} \quad 2L_i^{-1}] \quad (3)$$

$$\mathbf{M}_i = \sum_{j \neq i} w_{ij} \mathbf{p} \left(\frac{\mathbf{x}_j - \mathbf{x}_i}{L_i} \right) \otimes \mathbf{p} \left(\frac{\mathbf{x}_j - \mathbf{x}_i}{L_i} \right) \quad (4)$$

$$\mathbf{b}_i = \sum_{j \neq i} w_{ij} (f_j - f_i) \mathbf{p} \left(\frac{\mathbf{x}_j - \mathbf{x}_i}{L_i} \right) \quad (5)$$

$$\mathbf{p}(\mathbf{x}) = [x \quad y \quad x^2 \quad xy \quad y^2]^T \quad (6)$$

where L_i is a diameter of a particle and w is a weight function. By using this formulation, every derivative can then be calculated.

2.2 Incompressible Condition

In the Multi-Resolution MPS method [14], a higher order incompressible condition proposed by Nair and Tomar [11] is applied. The incompressible condition is given as:

$$\det \frac{\partial \mathbf{x}^{k+1}}{\partial \mathbf{x}^k} = 1 \quad (6)$$

If the time integration is calculated by using the Euler explicit scheme, the equation for pressure in 2D is denoted by

$$\mathbf{A}^k = \mathbf{I} + \Delta t \nabla^k \mathbf{u}^{k'} = \begin{pmatrix} a_{11} & a_{12} \\ a_{21} & a_{22} \end{pmatrix} \quad (8)$$

This incompressible condition is applied in the Multi-Resolution MPS method.

3 Multi-Resolution Techniques

In the Multi-Resolution MPS method, the size of the particles changes dynamically. A particle should be able to be split into smaller particles whenever a more refined resolution is required. Conversely, particles should be able to be merged into a larger particle whenever a coarser particle distribution is required. Splitting and merging are triggered by both the current diameter and a target diameter of each particle. The target diameter L^* can depend on many different parameters such as the position, the distance from a wall, the distance from a free surface, pressure, etc. The easiest way to define the target diameter is to make it to be a function of the coordinates, i.e., $L_i^* = L^*(\mathbf{x}_i)$. After evaluating the target diameter for each particle at every time step, then the particle can be judged to be split or merged according to the procedures described in the following sections.

2.3.1 Particle Splittin

A particle is split into two particles in this work. The particle volume, which is defined as $V = L^d$ by using the number of dimensions d , should be conserved during this particle splitting process, and then the diameter after splitting $L_{i'}$ is given as $L_{i'} = (1/2)^{1/d} L_i$. When the target diameter of a particle is much smaller than the current diameter, i.e. $L_i^* < \beta_s L_i$, the particle will be split. The threshold of the diameter to trigger the particle splitting should be in the middle of the current diameter L_i and the diameter after splitting $L_{i'}$, and then the splitting threshold β_s is defined as $\beta_s = 1/2\{(1/2)^{1/d} + 1\}$. The velocity for the new particles after splitting is obtained after the following interpolation:

$$\mathbf{u}_{i'} = \mathbf{u}_i + \langle \nabla \mathbf{u} \rangle_i (\mathbf{x}_{i'} - \mathbf{x}_i) \quad (10)$$

2.3.2 Particle Mer in

In this work, two particles are merged into a large particle. When the target diameter is much larger than the current diameter, i.e., $L_i^* > \beta_m L_i$, the particle i is merged with a neighbouring particle j . β_m is a merging threshold defined as $\beta_m = 2^{1/d}$. Particle j should be of the same kind of fluid as particle i and the distance between particles i and j should be smaller than a predefined threshold, i.e., $r_{ij} < \alpha \frac{L_i + L_j}{2}$. If there is no neighbouring particle which satisfies the above mentioned condition, then the merging process is terminated. Note that a particle which is going to be split should be ruled out from the merging judgement.

The position and velocity of the newly generated particles after merging are calculated so that the angular momentum and the linear momentum are conserved respectively:

$$\mathbf{x}_{i'} = \frac{V_i \mathbf{x}_i + V_j \mathbf{x}_j}{V_i + V_j} \quad (11)$$

$$\mathbf{u}_{i'} = \frac{V_i \mathbf{u}_i + V_j \mathbf{u}_j}{V_i + V_j} \quad (12)$$

The diameter of the new particle after merging is evaluated by considering volume conservation, i.e., $L_{i'} = (L_i^d + L_j^d)^{1/d}$.

2.4 Boundary Conditions for a Wall

In this work, wall geometries are represented by polygons and imaginary wall particles are generated on the boundaries at every time step, as shown in Figure 1. Note that the key difference from other conventional methods is that the imaginary wall particles are generated not beyond the boundary but right on the boundary. It would be much easier to impose boundary conditions for the viscosity and pressure terms if the imaginary particles were located right on the boundary because no interpolation technique would then be required for these particles. Note that this arrangement of the wall particles is only possible by the least square particle methods.

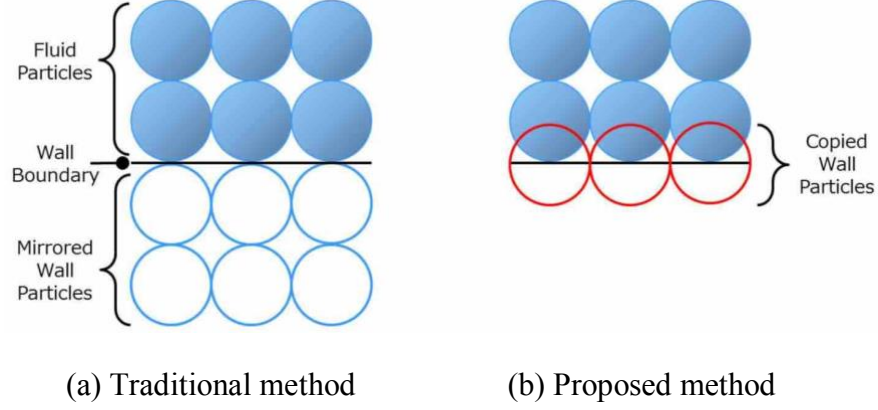


Figure 1: Imaginary wall particles

The boundary condition on the wall particles is defined as $\mathbf{u}^{k+1} \cdot \mathbf{n} = 0$. There are various ways to express the pressure boundary condition on wall particles. In this work, a semi-analytical wall boundary condition proposed Leroy et al. [8] is utilised:

$$\frac{1}{\rho} \nabla P \cdot \mathbf{n} = \frac{1}{\Delta t} \mathbf{u}^{k'} \cdot \mathbf{n} \quad (13)$$

The velocity of the wall is evaluated by using the velocities of the neighbouring particles.

3 RESULTS AND DISCUSSIONS

3.1 Taylor Green Vortex Simulation with Variable Resolution

The Taylor Green vortex example is simulated with the Multi-Resolution MPS method for the assessment of the conservation of energy and momentum. The Taylor Green vortex is a classical flow example with known analytical solution. The velocity $\mathbf{u}(x, y, t) = (u(x, y, t), v(x, y, t))$ and pressure $P(x, y, t)$ are expressed by using the coefficient $F(t) = U \exp(-2vt)$ as follows:

$$u(x, y, t) = F(t) \cos\left(2\pi \frac{x}{W}\right) \sin\left(2\pi \frac{y}{W}\right) \quad (14)$$

$$v(x, y, t) = -F(t) \sin\left(2\pi \frac{x}{W}\right) \cos\left(2\pi \frac{y}{W}\right) \quad (15)$$

$$P(x, y, t) = -\frac{\rho F(t)^2}{4} \left\{ \cos\left(4\pi \frac{x}{W}\right) + \cos\left(4\pi \frac{y}{W}\right) \right\} \quad (16)$$

where W is the size of the domain so that the coordinates are limited to $0 \leq x \leq W$ and $0 \leq y \leq W$, and U is the reference velocity.

The domain size used in the simulations was $W = 1$ m and the reference velocity was $U = 1$ m/s. The fluid density was 1000 kg/m^3 and the kinematic viscosity was $0 \text{ m}^2/\text{s}$. Because the viscosity term is neglected, the velocity and pressure distribution should remain still and the energy should be conserved. The particles whose diameters are 5 mm are located on the 200×200 grids in the

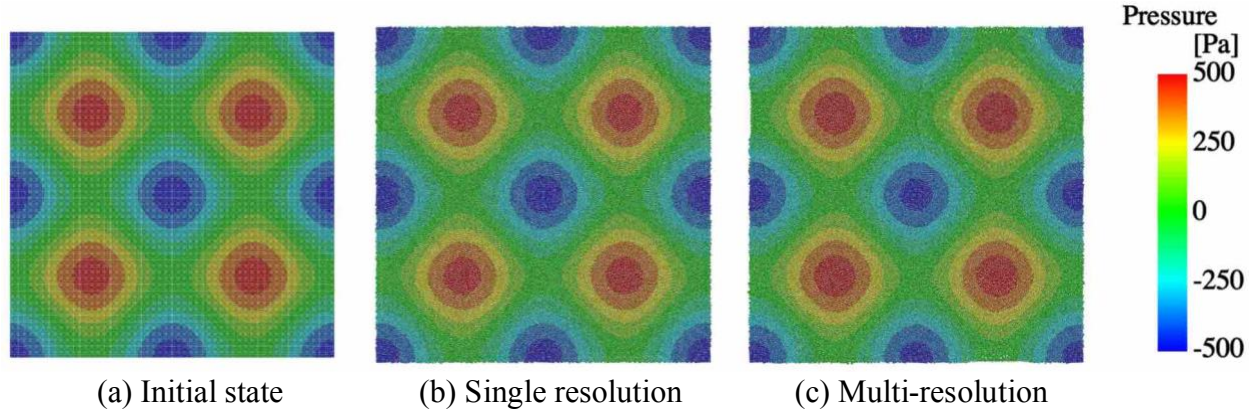


Figure 2: Pressure distribution of the Taylor Green vortex simulations

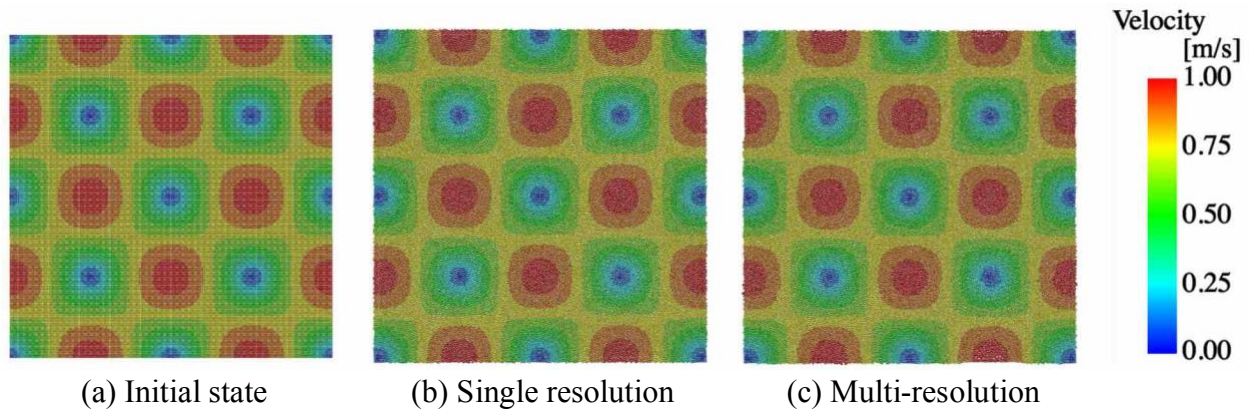


Figure 3: Velocity distribution of the Taylor Green vortex simulations

initial state for both single and multi-resolution simulations. In the multi-resolution simulation, the region within 0.25 m distance to the point (0.75 m, 0.75 m) is defined as the high resolution region, and the target diameter of the particles inside this region is 0.35 m. The simulations were conducted for a total time of 1.0 sec, which corresponds to one cycle for the vortex. The periodic boundary conditions are applied for X and Y directions by copying particles around edges of the simulation domain to the corresponding positions of the periodic boundary condition.

The pressure distribution and the velocity distribution before and after simulations are shown in Figure 2 and Figure 3 respectively. The distributions of the pressure and the velocity after both single and multi-resolution simulations are similar to the initial state although particles have moved for the time corresponding to one cycle of the vortex, and then it can be stated that the simulation was conducted accurately. The closeups of the regions where the resolution was changed are shown in Figure 4. In the left closeup, particles are moving from left to right direction and they are split when they enter the high resolution region. In the right closeup particles are moving from up to down direction and are merged whenever they get out of the high resolution region. In both the splitting and merging process, the velocity field was smooth and no strange particle arrangement was observed.

The pressure and velocity were measured on the evaluation points, shown in Figure 4, along the vertical line corresponding to $X = 0.75$ m and they were plotted together with the analytical

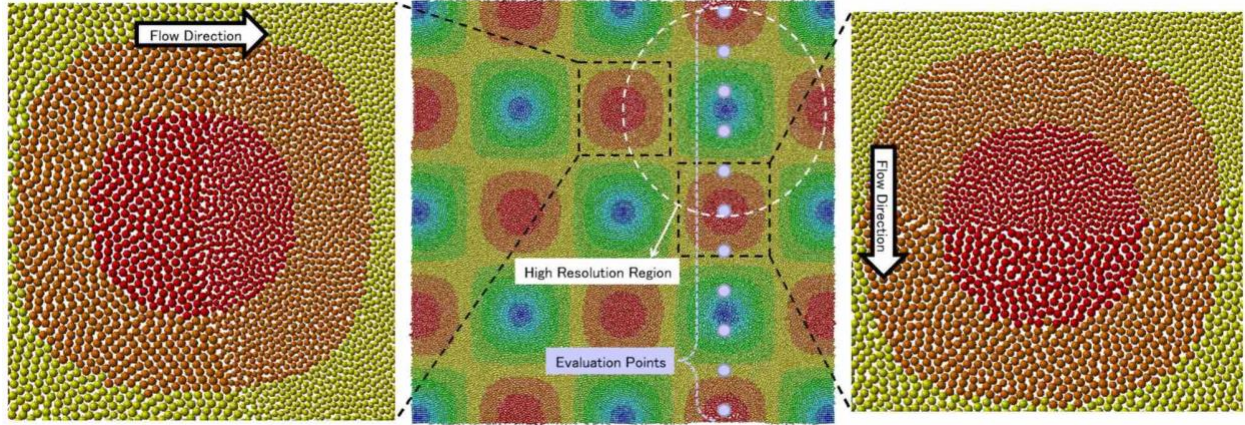


Figure 4: Closeups of resolution changing regions

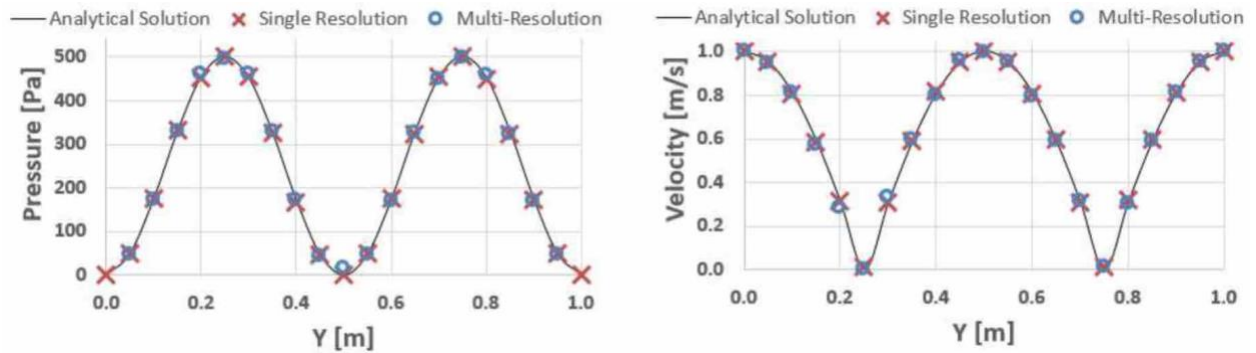


Figure 5: Comparison between the analytical solution and the simulation results

solutions in Figure 5. The results of both of the single and multi-resolution simulation were in good agreement with the analytical solutions although there was a slight difference for the pressure of the multi-resolution simulation around $Y = 0.5$ m. This point is near the interfacial region of the different size of particles and the error was supposed to be caused by changing the resolution. However the difference was small enough and did not affect the accuracy of the whole simulation. The linear and angular momentum and the total energy through the simulations were monitored in Figure 6. The errors for the momentum from the multi-resolution simulation was larger than those from the single resolution simulation although they are not significant. The error for the energy was as small as 0.1 % and thus it can be said that the accuracy of the Multi-Resolution MPS method is good enough so that the method can be successfully applied in the simulation of complex problems.

3.2 Multi-Resolution Dam Break Simulation with Free Surface

Dam break simulations are conducted by using the multi-resolution techniques. The initial size of the fluid is $100 \text{ mm} \times 250 \text{ mm}$. The vessel has the width of 400 mm with a small obstacle in the middle of the vessel, located at the bottom of the vessel. The obstacle is as small as $10 \text{ mm} \times 10 \text{ mm}$ and therefore particles as small as 1 mm for the diameter are required around the obstacle. The single resolution simulation with the diameter of 1 mm for the particles and the multi-resolution simulation with the diameter for the particles ranging from 1 mm to 5 mm are conducted. The

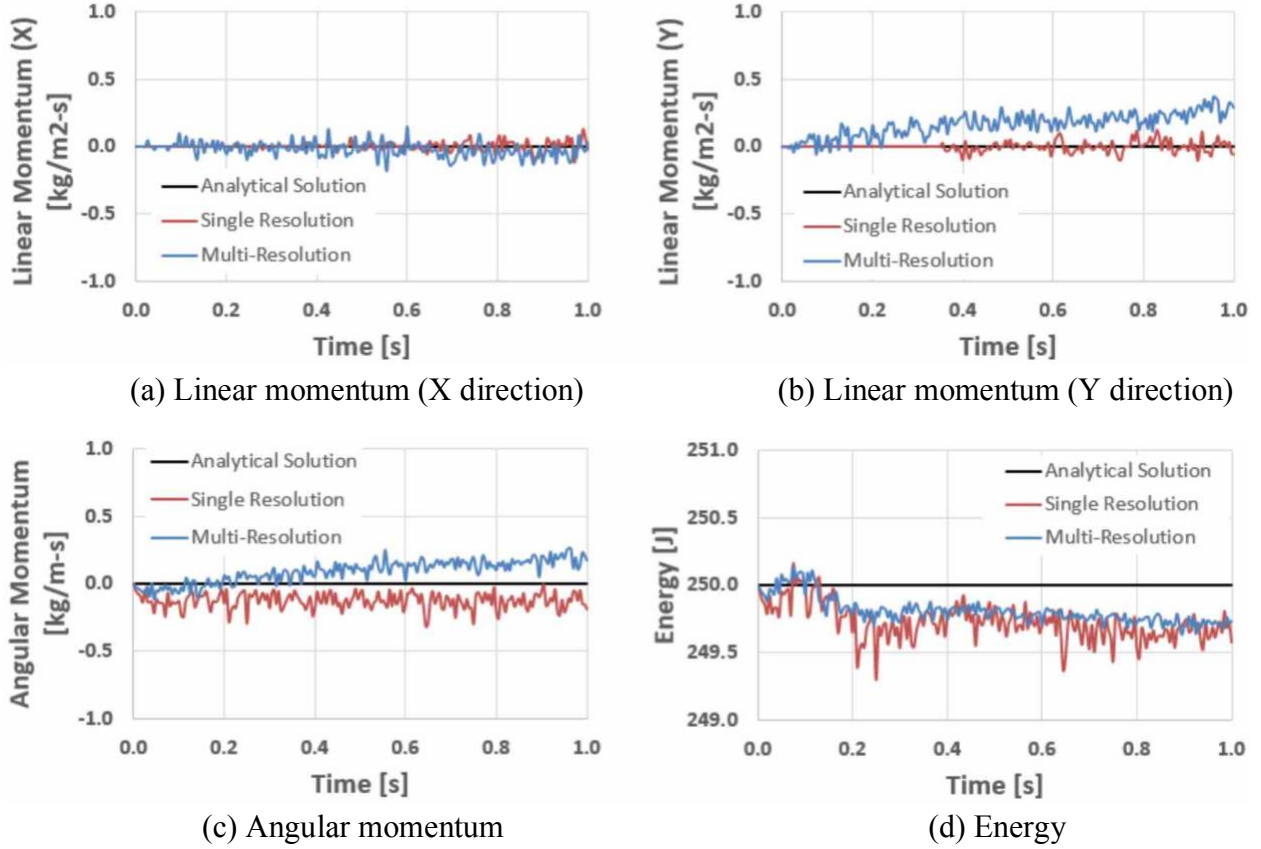


Figure 6: Profile of momentum and energy in the Taylor Green vortex simulation

target diameter in the multi-resolution simulation depends on the distance from the origin point, so that a finer resolution around the small obstacle can be obtained. The physical values and other simulation conditions are the same as for the first dam break example. The pressure and velocity values are monitored at the evaluation point which is 5 mm above the small obstacle.

Comparison of the pressure distribution between the single and multi-resolution simulations before colliding the small obstacle is shown in Figure 7. The fluid motion and the pressure distribution obtained by the multi-resolution simulation were similar in general to those by the single resolution simulation. Although some differences in the pressure distribution were observed around the small obstacle at 0.11 sec, this is due to the way the pressure value are computed as stated above. Such differences in pressure distribution did not influence the fluid motion crucially and then are considered to be acceptable.

The fluid motion and the velocity distribution after the collision with the small obstacle is illustrated in Figure 8. Both the fluid motion and the velocity field matched well up to 0.65 sec, however, the fluid shapes at 1.0 sec are different. This is because the characteristic part of the fluid is mainly in the region where the resolution is lower and so the simulation is not accurate anymore. Therefore the pre-selection for the configuration of the resolution should be done carefully.

The number of the fluid particles used in the multi-resolution simulation was 4,291 in average while it was 24,969 throughout the single resolution simulation. In other words, the number of

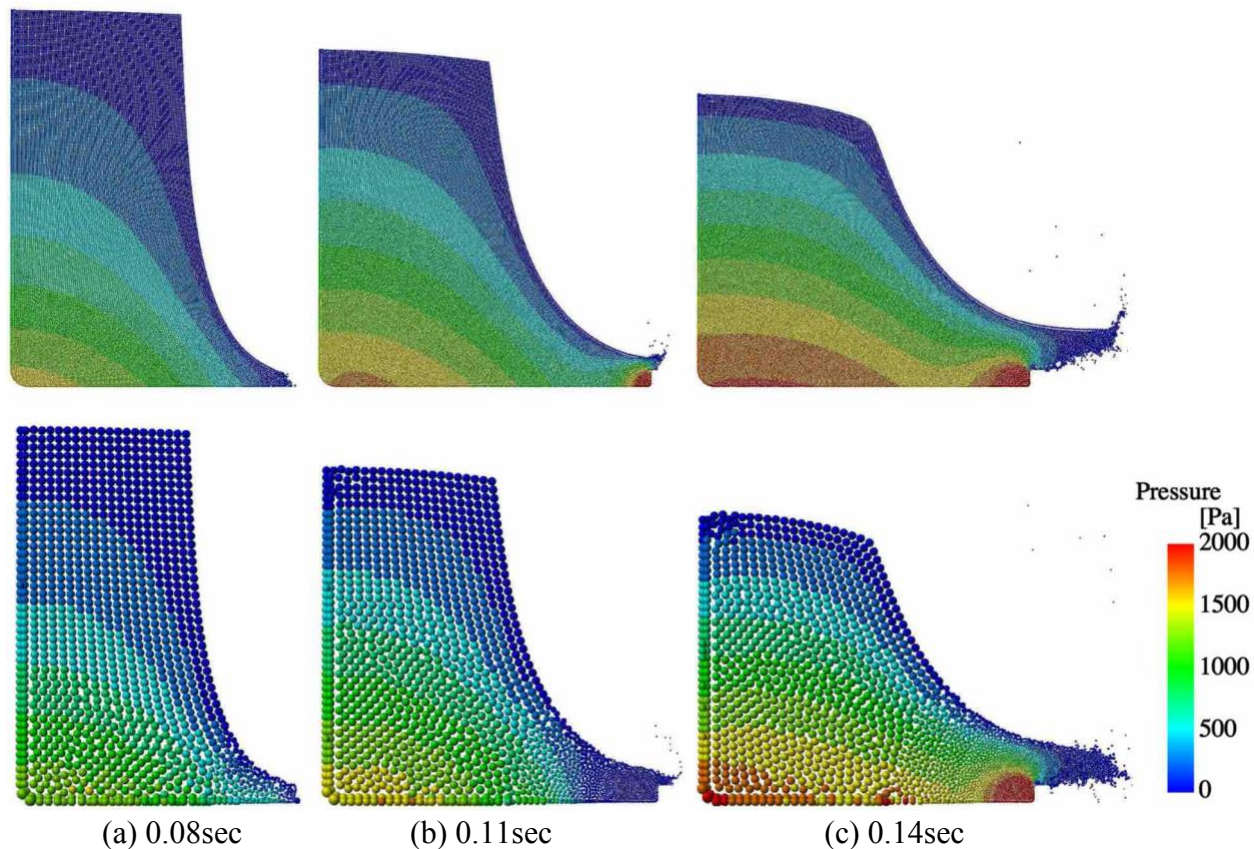


Figure 7: Comparison of the pressure distribution between the single and multi-resolution simulation (above: single resolution, bottom: multi-resolution)

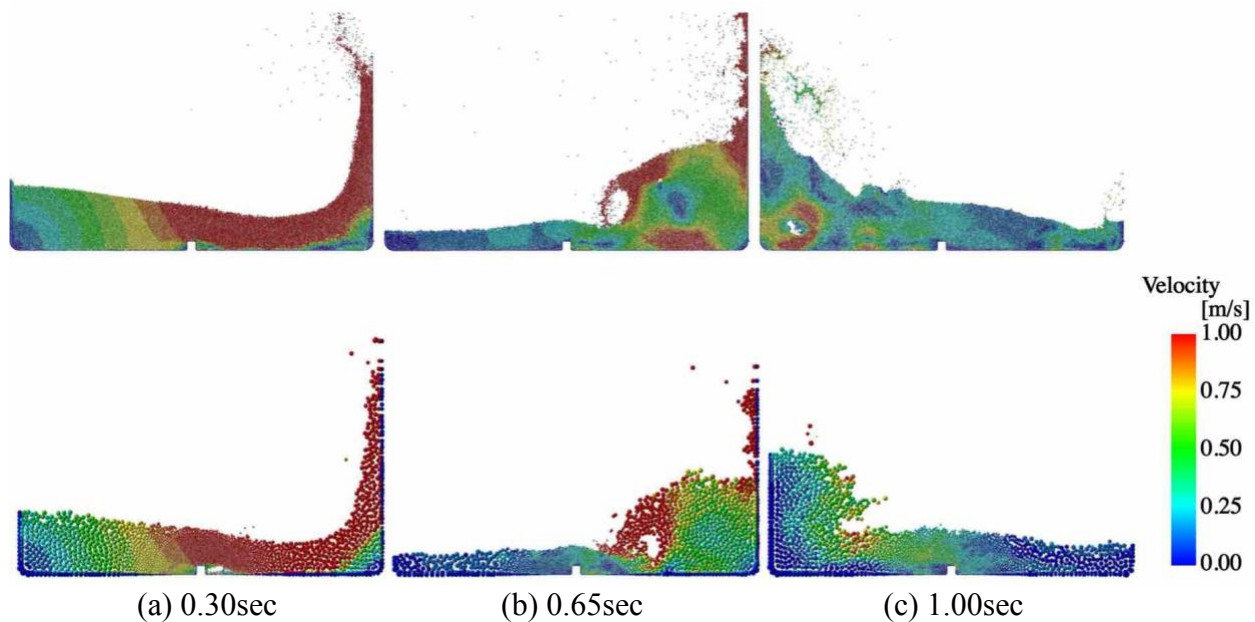


Figure 8: Velocity distribution of the dam break simulation with an obstacle (above: single resolution, bottom: multi-resolution)

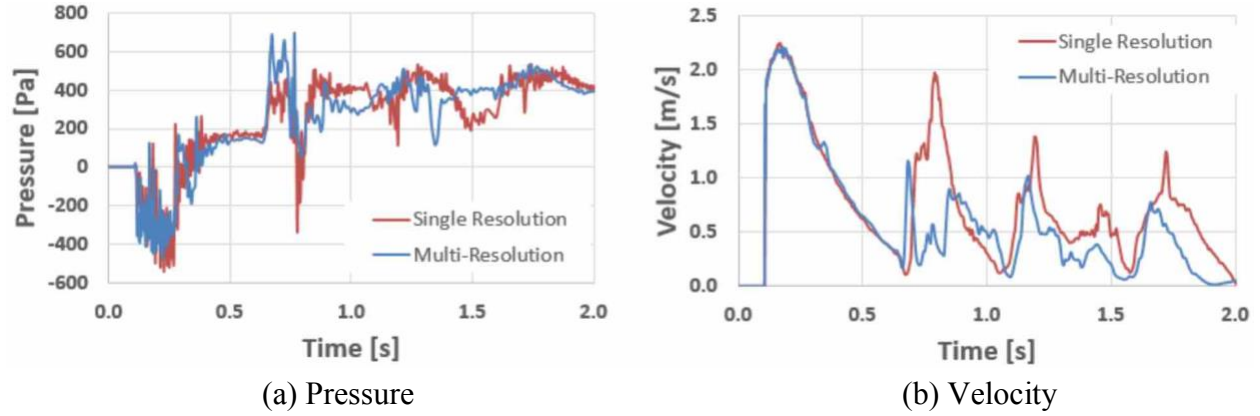


Figure 9: Pressure and velocity profile in the dam break simulation with an obstacle

fluid particles was reduced by 82.8 % by using the multi-resolution techniques, and as a result, the computational time was reduced by 93.4 %. In this case, the main reason why the reduction rate of the computational time is higher than that of the number of the fluid particles is because the size of the time step was able to be larger for the multi-resolution simulation. The particles which had the highest velocity were the splash particles after the fluid collided with the wall and the size of the splash particles in the multi-resolution simulation were larger than that in the single resolution simulation. Then, the time step could be larger in the multi-resolution simulation.

The pressure and velocity at the evaluation point located just above the obstacle were monitored for every 100 time steps as plotted in Figure 9. The results for the multi-resolution simulation provided similar pressure and velocity profiles with those of the single resolution simulation until 0.6 sec, but there were some differences observed as the simulation went on after that. This is mainly because a particle which had been in a lower resolution region came back to the higher resolution region carrying a bad level of accuracy with it as mentioned above. However, most importantly, the peak velocity at the first fluid impact around at 0.14 sec was almost the same. The multi-resolution technique is beneficial to reduce computational costs, but a proper resolution configuration for a proper problem to be simulated is required. This is a common issue not only for particle methods but also for many other numerical methods.

4 CONCLUSIONS

The Multi-Resolution MPS method is presented in this work. The spatial resolution is changed adaptively by the particle splitting and merging algorithms. The LSMPS method is applied to obtain accurate results even if particles have different diameters. A new wall boundary scheme, which is represented by polygons, is also improved for a multi-resolution simulation by copying fluid particles around walls and generating imaginary wall particles right on the boundaries. By conducting simulations for the Taylor Green vortex and for the dam break, the accuracy of the Multi-Resolution MPS method could be verified. Also, it was shown that this method was able to reduce computational costs significantly. Although only two dimensional simulations were conducted in this work, extension to three dimensions is straightforward.

REFERENCES

- [1] B. Adams, M. Pauly, R. Keiser, and L. J. Guibas. Adaptively sampled particle fluids. *ACM Transactions on Graphics - Proceedings of ACM SIGGRAPH 2007*, 26(3):Article No.48, 2007.
- [2] G. A. Dilts. Moving-least-squares-particle hydrodynamics-i. consistency and stability. *International Journal for Numerical Methods in Engineering*, 44(8):1115–1155, 1999.
- [3] G. A. Dilts. Moving least-squares particle hydrodynamics ii: conservation and boundaries. *International Journal for Numerical Methods in Engineering*, 48(10):1503–1524, 2000.
- [4] R. A. Gingold and J.J. Monaghan. Smoothed particle hydrodynamics - theory and application to non-spherical stars. *Monthly Notices of the Royal Astronomical Society*, 181:375–389, 1977.
- [5] S. Kitsionas and A. P. Whitworth. Smoothed particle hydrodynamics with particle splitting, applied to self-gravitating collapse. *Monthly Notices of the Royal Astronomical Society*, 330(1):129–136, 2002.
- [6] S. Koshizuka, H. Tamako, and Y. Oka. A particle method for incompressible viscous flow with fluid fragmentation. *Computational Fluid Dynamics Journal*, 4:29–46, 1995.
- [7] M. Lastiwka, N. Quinlan, and M. Basa. Adaptive particle distribution for smoothed particle hydrodynamics. *International Journal for Numerical Methods in Fluids*, 47(10-11):1403–1409, 2005.
- [8] A. Leroy, D. Violeau, M. Ferrand, and C. Kassiotis. Unified semi-analytical wall boundary conditions applied to 2-d incompressible sph. *Journal of Computational Physics*, 261:106–129, 2014.
- [9] M. B. Liu, G. R. Liu, and K. Y. Lam. Adaptive smoothed particle hydrodynamics for high strain hydrodynamics with material strength. *Shock Waves*, 15(1):21–29, 2006.
- [10] L. B. Lucy. A numerical approach to the testing of the fission hypothesis. *Astronomical Journal*, 82:1013–1024, 1977.
- [11] P. Nair and G. Tomar. Volume conservation issues in incompressible smoothed particle hydrodynamics. *Journal of Computational Physics*, 297(15):689–699, 2015.

- [12] K. Shibata, S. Koshizuka, and T. Tamai. Overlapping particle technique and application to green water on deck. International Conference on Violent Flows, Nantes, France, September, 2012. 106-111.
- [13] T. Tamai and S. Koshizuka. Least squares moving particle semi-implicit method. Computational Particle Mechanics, 1(2):277–305, 2014.
- [14] M. Tanaka, R. Cardoso, and H. Bahai. Multi-resolution mps method. Journal of Computational Physics, 359:106–136, 2018.
- [15] M. Tanaka, T. Masunaga, and Y. Nakagawa. Multi-resolution mps method. Transactions of Japan Society for Computational Engineering and Science, pages Paper No.20090001, in Japanese, 2009.
- [16] Z. Tang, D. Wan, G. Chen, and Q. Xiao. Numerical simulation of 3d violent free-surface flows by multi-resolution mps method. Journal of Ocean Engineering and Marine Energy, 2(3):355–364, 2016.
- [17] Z. Tang, Y. Zhang, and D. Wan. Numerical simulation of 3-d free surface flows by overlapping mps. Journal of Hydrodynamics, Ser. B, 28(2):306–312, 2016.

Discontinuous Galerkin Method for Advection Equation of Interface Capturing Method

Seizo Tanaka*

*University of Tsukuba

ABSTRACT

The protection system against water hazards, such as tsunami and flood have to have enough performance to save the residents. The design of protection system against the disaster should consider a dynamic impact force of water. Also the flood area should be estimated accurately. The numerical simulation is a useful tool estimate the forces and flood inundation area. In such a simulation, the high accurate solution requires not only stability and robustness but also mass conservation. We develop the free surface flow analysis method for tsunami wave propagation based on interface capturing approach. For treatment of free surface motion, interface capturing approach based on Volume of Fluid (VOF) method [1] is useful to apply dramatic free surface motion such as hydraulic jump, breaking waves. The accuracy of interface location expressed by interface function depends on the solution of advection equation in interface capturing method. The discontinuous Galerkin method [2] is applied to the advection equation as the governing equation of interface motion. And stabilized finite element method based on SUPG and PSPG method with continuous Galerkin method [3] is applied to the governing equation of incompressible viscous flow. As for the numerical example to verify the present method, broken-dam problem is carried out. [1] C. W. Hirt, B.D. Nicols: Volume of Fluid (VOF) method for dynamics of free boundaries, Journal of Computational Physics, Vol.39, pp.201-225, 1981. [2] B. Cockburn, G.E. Karniadakis, C.-W. Shu: Discontinuous Galerkin Methods, Theory, Computation and Applications, Springer, 2000. [3] S. Aliabadi, T.E. Tezduyar: Stabilized-finite element/Interface-capturing technique for parallel computing, Compute Methods Applied Mechanics and Engineering, Vol.190, pp.243-261, 2000.

Aero Acoustic Investigation of Backward-Facing Step Controlled by Suction and Blowing with Large Eddy Simulation

Kamil Furkan Taner*, Furkan Cosgun**, Baha zafer***

*Istanbul University, **Istanbul Technical University, ***Istanbul University

ABSTRACT

Kamil Furkan Taner*1 Furkan Cosgun2 Baha Zafer3 Istanbul University Istanbul Technical University Istanbul University *Corresponding Author Aero Acoustic investigation of Backward-Facing Step controlled by Suction and Blowing with Large Eddy Simulation Although Backward-Facing Step (BFS) studies have a simple geometry but exhibits a highly complex flow structure. Main problem retains their interests due to that this geometry is suitable to try new control methods such as active suction and blowing. Additionally, Backward-Facing Step geometry is frequently encountered in both military and industrial applications. In this study, Low Mach number transient incompressible flow field and aerodynamically generated noise of BFS flows will be investigated. BFS flow with steady Suction and Blowing control mechanisms will be numerically studied using Large Eddy Simulation (LES) and Subgrid-Scale Model of Kinetic-Energy Transport Equation. All unsteady flow field results are used to compute a BFS noise using Ffowcs William-Hawking (FW-H) Equation. Governing equations will be solved using segregated solver and non-iteratively which provides us to solve problem spending less time compared to iterative solvers using commercial FLUENT 16.0 with finite-volume method. All numerical solutions are compared with experimental data for unsteady flow field. References 1.C.-R. Zheng,Y.-C. Zhang and W.-Y. Zhang," Large eddy simulation of separation control over a backward-facing step flow by suction", International Journal of Computational Fluid Dynamics,25:2,59-74,2011. 2.B.Zafer,F. Cosgun,"Aeroacoustics investigation of unsteady incompressible cavity flow", Journal of the Faculty of Engineering and Architecture of Gazi University,31:3,665-675,2016. 3. Özsoy, E., Rambaud, R., Stitou, A. and Riethmuller, M.L., "Vortex characteristics in laminar cavity flow at very low Mach number", Experiments in Fluids, Tome 38, 133-145, 2005.

Mechanical Properties Regulate the Wrapping of Nanoparticles by the Cell Membrane

Huayuan Tang^{*}, Hongwu Zhang^{**}, Hongfei Ye^{***}, Yonggang Zheng^{****}

^{*}Dalian University of Technology, P. R. China, ^{**}Dalian University of Technology, P. R. China, ^{***}Dalian University of Technology, P. R. China, ^{****}Dalian University of Technology, P. R. China

ABSTRACT

Understanding how the cell membrane wraps nanoparticles (NPs), which are promising for many biomedical applications, is essential to improve the performance of the NP-based drug delivery carriers. Mechanical properties of the NP-membrane system, such as the shape and deformability of NPs, the flexibility and tension of the membrane, have complex influences on the wrapping behaviors of NPs by the cell membrane. Though extensive studies have been conducted in recent years, there is still a lack of a thorough understanding on these behaviors and the underlying mechanisms. In our recent work, we investigate how the shape and deformability of NPs regulate the cellular wrapping behaviors based on continuum models. The simulation results show that, accompanied with the rotation of the NP induced by the competition between the bending and membrane tension, the endocytosis of NP with irregular shape proceeds through the symmetric-asymmetric or asymmetric-symmetric-asymmetric wrapping pathway. For the wrapping of deformable NP, higher NP-membrane adhesion strength is required for the softer NP to be fully wrapped and the NP is easier to be fully wrapped but harder to be shallowly wrapped when the NP locates outside than inside the vesicle. For the wrapping of multiple NPs, the competition between the NP-NP adhesion and the membrane-mediated repulsion leads the NPs to be wrapped cooperatively or independently. For the system with elongated elliptic cross-sectional NPs, the NPs are more likely to be wrapped independently as the shapes become more anisotropic, while the soft NPs tend to be wrapped cooperatively compared with the stiff NPs. These results may provide guidelines to control the internalization pathway of NPs and for the design of NP-based drug delivery systems. References [1] Zheng, Y.; Tang, H.; Ye, H.; Zhang, H. Adhesion and Bending Rigidity-Mediated Wrapping of Carbon Nanotubes by a Substrate-Supported Cell Membrane. *RSC Adv.* 2015, 5, 43772. [2] Tang, H.; Ye, H.; Zhang, H.; Zheng, Y. Wrapping of Nanoparticles by the Cell Membrane: The Role of Interactions between the Nanoparticles. *Soft Matter* 2015, 11, 8674. [3] Tang, H.; Zhang, H.; Ye, H.; Zheng, Y. Wrapping of a Deformable Nanoparticle by the Cell Membrane: Insights into the Flexibility-Regulated Nanoparticle-Membrane Interaction. *J. Appl. Phys.* 2016, 120, 114701.

New Derivative-based Importance Criteria and Their Applications to a Plasma-Combustion Coupling Mechanism

Kunkun Tang^{*}, Jonathan Freund^{**}

^{*}University of Illinois at Urbana-Champaign, ^{**}University of Illinois at Urbana-Champaign

ABSTRACT

Sobol' and Kucherenko [1, 2] introduced two derivative-based sensitivity indices (DSI) and have shown a link between global sensitivity indices (GSI) and DSI. Even though GSI are considered superior to DSI as an importance ranking tool since they contain more model information, they can be impractical for many applications due to their high cost [2]. Monte Carlo algorithms for computing DSI and GSI have been developed and compared and the advantageous properties of the algorithm for DSI have been shown. DSI are particularly attractive since their computation can be much faster than GSI in applications with relatively low derivative variation. The approach proposed by Sudret and Mai [3] can compute the DSI [1] analytically from a polynomial chaos expansion. However, the extension of this for computing the improved DSI [2] seems difficult because of additional terms in the integrand. In the paper, we will introduce two new derivative-based measures that can be efficiently computed using an adaptive ANOVA approach, and use them to target multi-physics applications with hundreds of uncertain parameters. We will compare our variation of DSI to the standard approaches [1, 2], both theoretically and numerically. The cost advantage of our DSI will be shown. A simple extension of DSI for correlated inputs will also be presented. The overall methodology will be demonstrated for a plasma-combustion system in a dielectric-barrier discharge (DBD) actuated fuel jet. Experimental data of ignition burn boundary will be compared to predictions. We will consider challenging multi-physical uncertain parameters from submodels of chemical kinetics, laser ignition, and the DBD actuator. The total number of uncertain parameters in this application is 73. References [1] I.M. Sobol' and S. Kucherenko. Derivative based global sensitivity measures and their link with global sensitivity indices. *Mathematics and Computers in Simulation*, 79(10):3009–3017, 2009. [2] I.M. Sobol' and S. Kucherenko. A new derivative based importance criterion for groups of variables and its link with the global sensitivity indices. *Computer Physics Communications*, 181(7):1212–1217, 2010. [3] B. Sudret and C.V. Mai. Computing derivative-based global sensitivity measures using polynomial chaos expansions. *Reliability Engineering & System Safety*, 134:241–250, 2015.

Multiscale Molecular Simulation of Morphology Evolution of Active Layer of Small Molecule Organic Solar Cell during Vacuumed Deposition Process

Ping-Han Tang*, Chun-Wei Pao**

*Research Center for Applied Sciences, Academia Sinica, Taiwan, **Research Center for Applied Sciences, Academia Sinica, Taiwan

ABSTRACT

Recently, vacuum deposition of organic small molecule has been applied to the fabrication of many flexible optoelectronic device such as small molecule solar cells and organic light emitting diodes. In this study, we investigated the morphology evolution of DPDCPB:C70 small molecule solar cells during vacuum co-deposition processes by carrying out a series of GPU-accelerated, multiscale, coarse-grained molecular dynamics (CGMD) simulations. By coarsening DPDCPB and C70 molecules into ellipsoid beads, we were able to simulate morphology evolution of system with system length scale compatible with those with experiments (c.a. 50 nm). The Gay-Berne force field was parametrized using genetic algorithm to reproduce potential energy surfaces from respective all-atom molecular simulations. We systematically investigated morphology evolution of the active layer with different donor:acceptor ratio, as well as effects of substrate strains on resultant film morphologies. The present study demonstrates that, by using the ellipsoid-based coarse-grained model, it is possible to study morphology evolution of small molecule organic thin film during vacuum deposition processes with unprecedented details, which can provide valuable insights for experimental teams to further optimize device fabrication protocols for the next generation organic optoelectronic devices.

Fracture of Water-containing Soft Solids: Experiment and Phase Field Modeling

Shan Tang*

*Dalian University of Technology

ABSTRACT

A typical water-containing soft solid, hydrogel, is fabricated. Compression and three-point bending experiments on hydrogel blocks are carried out under plane strain conditions. To reveal the underlying physics behind the fracture behaviors at the large deformation regime observed in experiments, we reformulate a hyperelastic model for hydrogels with initial swelling that takes into account the initial volume fraction of water. In this model, the free energy is constructed based on decomposition of the deformation gradient into isochoric and volumetric parts. The model parameters are calibrated by curve fitting of the experimental results obtained under uniform compression. To simulate the fracture of hydrogels, a phase field modeling approach is adopted and incorporated into the hydrogel model. In the phase field formulation, the crack phase field only degrades the isochoric and positive volumetric parts of the deformation, which is a key for numerically stable fracture modeling. The present model is able to predict the crack initiation, fracture path and the force vs. displacement in good agreement with those in experiments. [1] Borden, M.J., Verhoosel, C.V., Scott, M.A., Hughes, T.J.R., Landis, C.M., 2012. A phase field description of dynamic brittle fracture. *Computer Methods in Applied Mechanics and Engineering* 217-220, 77-95. [2] Bourdin, B., Francfort, G.A., Marigo, J.J., 2000. Numerical experiments in revisited brittle fracture. *Journal of the Mechanics and Physics of Solids* 48, 797-826. [3] Tang, S., Kopacz, A.M., Chan, S., Olson, G.B., Liu, W.K., et al., 2013. Three dimensional ductile fracture analysis with a hybrid multiresolution approach and microtomography. *Journal of the Mechanics and Physics of Solids* 61, 2108-2124.

Multi-Level Hybridized Optimization Methods Coupling Local Search Deterministic and Global Search Evolutionary Algorithms

Zhili Tang^{*}, Lianhe Zhang^{**}, Jacques Periaux^{***}, Xiao Hu^{****}

^{*}NUAA, ^{**}ARI, ^{***}CIMNE, ^{****}NUAA

ABSTRACT

Efficient optimization methods coupling a stochastic evolutionary algorithm with a gradient based deterministic method are presented in this paper. Two kinds of hybridization are compared: one is a stochastic/deterministic alternate algorithm, the other is a stochastic/deterministic embedded algorithm. In the alternating hybridized algorithm, stochastic and deterministic optimizers are performed alternately, some individuals are selected from the previous population, and then to be sent to the deterministic algorithms for further optimization, the improved individuals were inserted into the above population to form a new population for stochastic algorithm. In the embedded hybridized algorithm, stochastic and deterministic optimization softwares run in parallel and independently, the connection between them is that deterministic optimizer works on an random selected individual (or the best individual) from the unevaluated population of stochastic algorithm, then its outcome (new individual) is re-injected into the evaluated population. Moreover, multi-level approximation (e.g. variable fidelity modeling and analysis, hierarchical approximate parameterization) is used in the algorithm, i.e. low fidelity modeling and rough parameterization are used to perform search on large population at lower level, and high fidelity modeling and detailed parameterization are used at higher level. After a validation of the methods on mathematical test cases, the methods are successfully applied to aerodynamic shape optimization of the fore-body of a hypersonic air breathing vehicle and provide significant acceleration in terms of CPU time.

Research on Thermo-hygro Coupling Problems of Early-age Concrete Based on Generalized Finite Difference Method

Zhuochao Tang^{*}, Zhuojia Fu^{**}, Rui Yang^{***}, Haitao Zhao^{****}

^{*}Center for Numerical Simulation Software in Engineering and Sciences, College of Mechanics and Materials, Hohai University, ^{**}Center for Numerical Simulation Software in Engineering and Sciences, College of Mechanics and Materials, Hohai University, ^{***}College of Civil and Transportation Engineering, Hohai University, ^{****}College of Civil and Transportation Engineering, Hohai University

ABSTRACT

Abstract: The microstructure of early-age concrete is constantly evolving due to hydration. Temperature and humidity of early-age concrete interact with each other and vary drastically, which has great influence on the formation and development of concrete. Thus, research on the quantitative relationship among temperature and humidity of early-age concrete has great significance to prevent deformation and cracking of concrete in early age. This paper applies a new-developed domain-type meshless method, the generalized finite difference method (GFDM), to solve thermo-hygro coupling problems of early-age concrete. The GFDM is free from mesh generation and numerical integration compared with the traditional finite difference method. And it is more flexible when the shape of the computational domain is irregular. Besides, the GFDM remains the merits of the simplicity and wide applicability in the classical finite difference method. For solving the coupling problems, the moving least squares theory and second-order Taylor series expansion have been used to construct the GFDM approximation formulation. And the second-order explicit Runge-Kutta method is used for time discretization. It is found that the generalized finite difference method combined with second-order explicit Runge-Kutta method provides the accurate numerical results in several numerical examples. Key words: early-age concrete; thermo-hygro coupling; the generalized finite difference method; second-order explicit Runge-Kutta method

Waves Scattering and Dissipation in Amorphous Materials

Anne Tanguy^{*}, Yaroslav Beltukov^{**}, Haoming Luo^{***}, Dmitry Parshin^{****}

^{*}INSA Lyon, France, ^{**}Ioffe Physical Technical Institute, St Petersburg, Russia, ^{***}INSA Lyon, France, ^{****}Saint Petersburg State Polytechnical University, Russia

ABSTRACT

In amorphous samples, acoustic waves scattering takes place at all scales. We show numerical results with evidence of simple scattering at long wave-lengths, multiple scattering at smaller wave-lengths, and mixed regimes in between. The transition from simple to multiple scattering, as well as possible localization regime, depends on the secificities of short range order.

Experimental and Modeling Strategies to Assess Micro and Nano-voids Growth and Coalescence in Irradiated Metallic Materials

Benoit Tanguy^{*}, J  r  my Hure^{**}, Pierre-Olivier Barrioz^{***}, Chao Ling^{****}, Jean-Michel Scherrer^{*****}, Jacques Besson^{*****}, Samuel Forest^{*****}

^{*}CEA Saclay , Universit   Paris–Saclay, ^{**}CEA Saclay, Universit   Paris–Saclay, ^{***}CEA Saclay, Universit   Paris–Saclay, ^{****}CEA Saclay, Universit   Paris–Saclay, ^{*****}CEA Saclay, Universit   Paris–Saclay, ^{*****}MINES ParisTech, PSL Research University, MAT – Centre des mat  riaux, ^{*****}MINES ParisTech, PSL Research University, MAT – Centre des mat  riaux

ABSTRACT

Microporous and nanoporous metallic materials are observed in many industrial applications such as structural alloys used in nuclear power plants under irradiation. These alloys show a marked decrease of fracture toughness with increasing level of fluence. Void growth to coalescence is the classical mechanism involved in ductile fracture of structural alloys, thus are the key features to better understand fracture toughness of these materials. Growth regime is characterized by a diffuse plastic flow around voids, while coalescence corresponds to localized plastic flow between adjacent voids. Analytical models, numerical simulations and experimental data have clearly shown that both regimes strongly depend on the mechanical behavior of the material around the voids, where yield stress, strain-hardening modulus and anisotropy are key parameters. Besides the growth and coalescence of micro-voids in an irradiated matrix, fracture toughness properties may be affected by the presence of nanovoids resulting of vacancies clustering under irradiation so that assessing the structural integrity of these components may require using homogenized models relevant for nanoporous materials. However, as voids size decreases to the nanoscale, size effects are expected in the fracture of ductile solids. The present paper details the strategies developed in order to assess the micro and nano-voids growth and coalescence in irradiated metallic materials. In the first part of the paper, few examples of experimental studies carried out on CFC materials will be given. These studies are based on the use of heavy ions irradiations to mimic both matrix hardening and softening resulting from irradiation and the creation of intragranular nanovoids population. In the second part of the paper, the modeling strategies will be detailed. Assessment of hardening, size and orientation effects is based on crystal plasticity framework. Finite element simulations of voided unit cells are performed with a single crystal plasticity model accounting for strain hardening and loss of strain hardening capability associated with irradiation induced defects. A first assessment of voids size effects is performed based on a single crystal strain gradient plasticity model derived at finite strains [1]. Finally, a recently implemented model taking into account the presence of an interface associated with an interfacial energy [2] and its comparison with finite element calculations on porous unit cells will be discussed. [1] C. Ling, S. Forest, J. Besson, B. Tanguy, F. Latourte, Int. Journal of Solids and Structures (2017) in-press [2] L. Dormieux, D. Kondo, Int. Journal of Eng. Science 48 (2010) 575–581

Matrix-free Isogeometric Analysis: The Computationally Efficient k -refinement

Mattia Tani^{*}, Giancarlo Sangalli^{**}

^{*}Università di Pavia, ^{**}Università di Pavia

ABSTRACT

One of the distinguishing features of Isogeometric Analysis (IGA) is the possibility of using high-degree high-regularity splines (the so-called k -refinement) as they deliver higher accuracy per degree-of-freedom in comparison to C^0 finite elements. Unfortunately, if the implementation is done following the approaches that are standard in the context of C^0 finite elements, the computational cost increases dramatically with the spline degree. This is true both for the formation of the linear system and for its numerical solution. As a consequence, the k -refinement is unfeasible for practical problems, where quadratic or cubic splines are typically preferred. Several improvements have been achieved recently. In [SIAM J. Sci. Comput., 38 (2016), pp. A3644--A3671], we discuss a preconditioner for scalar elliptic problems, based on an old idea, which is robust with respect to both the mesh size h and the spline degree p . Moreover, in [Comput. Methods Appl. Mech. Engrg., 316 (2017), pp. 606--622] a novel method is developed that allows the formation of the stiffness matrix with almost optimal complexity. In the work [arXiv:1712.08565, (2017), pp. 1--21], these two approaches are combined with a third ingredient: a matrix-free implementation. In this talk we discuss the overall strategy, which is very beneficial in terms of both memory and computational cost. In particular, we show that memory required is practically independent of p and that the cost depends on p only mildly. The numerical experiments show that, with the new implementation, the k -refinement becomes appealing from the computational point of view. Indeed, increasing the degree and continuity leads to orders of magnitude higher computational efficiency with respect to standard approaches.

Numerical Simulation of Liquid Drop Motions at the Edge

Hiroki Tanuma^{*}, Junya Onishi^{**}, Naoki Shikazono^{***}

^{*}The University of Tokyo, ^{**}The University of Tokyo, ^{***}The University of Tokyo

ABSTRACT

Contact line motion plays an important role in many industrial applications. For example, in the heat exchanger of an air conditioning system, the draining process of condensate water strongly influences the heat exchanger characteristics, such as pressure loss and heat transfer rate. Thus, accurate prediction of the contact line motion is highly demanded for designing optimal heat exchanger fins. It is well known that the contact line is pinned at the edge of a solid object. When the contact line is pinned at the edge with an edge angle ϕ an apparent contact angle increases from its equilibrium value θ_y (Young's angle) to a critical maximum value, θ_c , i.e., $\theta_c = \theta_y + (180 - \phi)$, which is also known as the Gibbs inequality condition (Gibbs, J. W. Scientific Papers 1906, 326.). Fang and Amirfazli (Fang, G.; Amirfazli, A. Langmuir 2012, 28, 9421–9430.) developed a free energy model of a droplet on a single pillar and illustrated four wetting cases at the edge. However, their model can only be applied to micro order droplets since they neglected the effect of gravity. Furthermore, when considering engineering application, an extension of their theory to more complex geometries is essential. To the best of our knowledge, there has been no attempts to study the edge effects of more complex objects. In this research, numerical simulations of the motion of a liquid drop at the right angle edge was conducted. In the present simulation, the continuity equation and the Navier-Stokes equation for incompressible viscous fluids are solved for both liquid and gas phases. To capture the motion of the interface between the liquid and gas phases, the level-set method is used. The boundary conditions at the liquid-gas interface are treated in a sharp manner with the use of the Ghost-fluid method. A numerical method based on the Cox theory is used for modeling the dynamics of the contact angle. Finally, the numerical results were validated with the experimental data.

Systematic Risk Analysis of Dam Groups Using Fussy Bayesian Network

Liang Tao^{*}, Yating Hu^{**}

^{*}Hohai University, ^{**}Hohai University

ABSTRACT

Nowadays, cascade development is the main trend in river development. The majority of risk analysis methods for dam groups are focused on the weighted superposition of risks of each dams in the river basin. However, the risk of individual dams in the whole river basin will be transmitted to each other. Once a certain dam is broken, it may lead to the collapse of downstream dams. Simply adding the risk of each dams in a basin does not objectively explain the systematic risk in the river basin. Here, based on the analysis of the mechanism of risk transmission in dam group, a fuzzy Bayesian network is used to establish the information fusion model for the risk of dam system in river basins. By example, we show the application of this model in the risk analysis of dam groups. The model has a good performance in the risk analysis of dam system in the basin, and can reasonably consider upstream and downstream risk transmission.

Computational-Experimental Approach to Evaluation of the Mechanical State of Laminate Composite Structures Using Embedded Fiber-Optic Strain Sensors

Mikhail Tashkinov^{*}, Valeriy Matveenkov^{**}, Igor Shardakov^{***}, Natalia Kosheleva^{****}, Grigoriy Serovae^{*****}

^{*}Perm National Research Polytechnic University, ^{**}Institute of Continuous Media Mechanics of RAS; Perm National Research Polytechnic University, ^{***}Institute of Continuous Media Mechanics of RAS; Perm National Research Polytechnic University, ^{****}Perm National Research Polytechnic University, ^{*****}Institute of Continuous Media Mechanics of RAS; Perm National Research Polytechnic University

ABSTRACT

In the recent years, research in smart materials and their fields of applications had been developing very actively. The idea of creating materials that along with prescribed basic functional tasks provide real-time information about their internal state is highly relevant for polymer composite materials and structures. The concept of smart composite materials with self-diagnostic functions had found its implementation with involvement of fiber-optic sensors, which, in particular, are able to measure various physical and mechanical quantities. Embedded into composites fiber-optic sensors have a wide range of advantages over other methods of strain measuring. They are able to withstand strains equal to strains of composite laminate, are affordable and easy to manufacture, are immune to electrical interference. Thus, under severe loading conditions fiber-optic sensors have advantages, including sensitivity, in comparison with other types of sensors. The proposed technique for predicting strength and mechanical behavior of composite structures is to compare the set of measurements from fiber-optic sensors with the results of numerical modelling with consideration of the features of the microstructure, including occurrence and development of defects. The computational component of the technique provides finite element simulations of mechanical behavior and failure of composite structure. The experimental part is based on strains measurements obtained by fiber-optical strain sensors on Bragg gratings embedded between the layers of composite. The mathematical models based on strains, measured by the optical fiber, are used for identifying stress concentration zones as well as for assessment of the possibility of application of fiber sensors to recording of internal defects appearance and propagation. The models were found to be applicable in case of introduction of the calibration coefficients for the sensors or when the strains along the fiber are much higher than the strains in the plane perpendicular to the fiber. The stress and strain fields were calculated taking into account microstructure in the vicinity of embedded fiber and the accompanying technological defect in the form of a resin pocket. The results of the approach illustrate a possibility of application of suggested non-destructive monitoring tools for correcting the parameters of the mechanical models. The latter allows to increase precision of numerical prediction of behavior and failure of composite materials and structures.

An Accurate, Fast, and Scalable Solver for High-frequency Wave Propagation

Matthias Taus^{*}, Leonardo Zepeda-Núñez^{**}, Russell Hewett^{***}, Laurent Demanet^{****}

^{*}MIT, ^{**}Lawrence Berkeley National Laboratory, ^{***}Total E&P, ^{****}MIT

ABSTRACT

In many science and engineering applications, solving time-harmonic high-frequency wave propagation problems quickly and accurately is of paramount importance. For example, in geophysics, particularly in oil exploration, such problems can be the forward problem in an iterative process for solving the inverse problem of subsurface inversion. It is important to solve these wave propagation problems accurately in order to efficiently obtain meaningful solutions of the inverse problems: low order forward modeling can hinder convergence. Additionally, due to the volume of data and the iterative nature of most optimization algorithms, the forward problem must be solved many times. Therefore, a fast solver is necessary to make solving the inverse problem feasible. For time-harmonic high-frequency wave propagation, obtaining both speed and accuracy is historically challenging. Recently, there have been many advances in the development of fast solvers for such problems, including methods which have linear complexity with respect to the number of degrees of freedom. While most methods scale optimally only in the context of low-order discretizations and smooth wave speed distributions, the method of polarized traces has been shown to retain optimal scaling for high-order discretizations, such as hybridizable discontinuous Galerkin methods and for highly heterogeneous (and even discontinuous) wave speeds. The resulting fast and accurate solver is consequently highly attractive for geophysical applications. To date, this method relies on a layered domain decomposition together with a preconditioner applied in a sweeping fashion, which has limited straight-forward parallelization. In this work, we introduce a new version of the method of polarized traces which reveals more parallel structure than previous versions while preserving all of its other advantages. We achieve this by further decomposing each layer and applying the preconditioner to these new components separately and in parallel. We demonstrate that this produces an even more effective and parallelizable preconditioner for a single right-hand side. As before, additional speed can be gained by pipelining several right-hand-sides.

Recent Advances in the Interventional Planning Stage of the Transseptal Puncture

Joao Tavares*, Pedro Morais**, Jan D'hooge***, João Vilaça****

*Instituto de Ciência e Inovação em Engenharia Mecânica e Engenharia Industrial, Faculdade de Engenharia, Universidade do Porto, Portugal, **Instituto de Ciência e Inovação em Engenharia Mecânica e Engenharia Industrial, Faculdade de Engenharia, Universidade do Porto, Portugal, ***Lab on Cardiovascular Imaging & Dynamics, Department of Cardiovascular Sciences, KULeuven - University of Leuven, Leuven, Belgium, ****DIGARC – Polytechnic Institute of Cávado and Ave, Barcelos, Portugal

ABSTRACT

Abstract Access to the left atrium (LA) is required for several minimally invasive cardiac interventions. Hereto, the atrial septum is punctured using a catheter inserted via the venous system using a technique termed transseptal puncture (TSP). Although the TSP has been commonly used, complications are still common. Besides, the exact puncture location is defined based on experience, being sub-optimal in specific situations. In this project, multiple contributions have been made to improve the state-of-the-art of the TSP. We initiated with a review [1] concerning the technique in terms of guidance technologies, pre-procedural planning and used surgical tools. Although multiple advances can be found regarding the medical tools and guidance technologies, few studies focused on the planning exist. Then, we proposed strategies to automate the planning of the TSP, namely: 1) an atrial region segmentation methodology [2]; 2) a strategy to identify the optimal puncture region, which is usually known as fossa ovalis (FO), and 3) a personalized atrial phantom model [3]. Both segmentation methods were validated on 41 computed tomographic images. The automated segmentations were compared against manual delineations, and an error lower than 1.7 mm was found as to the atrial region [1]. Regarding the identification of the FO, a performance comparable to the inter-observer variability was achieved. Moreover, both methods proved to be much faster than the traditional practice. Regarding the phantom model, it led to a highly accurate production and a highly realistic model in terms of intra-procedural imaging [3]. The developed strategies have shown high feasibility and accuracy, corroborating their potential for the automated planning of TSP. Acknowledgement: The authors acknowledge FCT, in Portugal, and the European Social Found, European Union, for funding support through the "Programa Operacional Capital Humano" in the scope of the PhD grant SFRH/BD/95438/2013, and also the funding of Projects NORTE-01-0145-FEDER-000013 and NORTE-01-0145-FEDER-000022, cofinanced by FEDER. References: [1] - P. Morais, J.L. Vilaça, J. Ector, J. D'hooge, and J.M.R.S. Tavares, "Novel solutions applied in transseptal puncture: a systematic review," *Journal of Medical Devices*, 2017. [2] - P. Morais, J.L. Vilaça, S. Queirós, F. Bourier, I. Deisenhofer, J.M.R.S. Tavares, and J. D'hooge, "A competitive strategy for atrial and aortic tract segmentation based on deformable models," *Medical Image Analysis*, 2017. [3] - P. Morais, J.M.R.S. Tavares, S. Queirós, F. Veloso, J. D'hooge, J.L. Vilaça, "Development of a patient-specific atrial phantom model for planning and training of inter-atrial interventions". *Medical Physics*, 2017.

Dynamic Spring Element Model for the Effective Simulation of the Longitudinal Tensile Failure of Polymer Composite

Rodrigo Tavares*, Fermin Otero**, Albert Turon***, Pedro Camanho****

*DEMec, Faculdade de Engenharia, Universidade do Porto; AMADE, Polytechnic School, University of Girona; INEGI, Porto, **INEGI, Porto, ***AMADE, Polytechnic School, University of Girona, ****DEMec, Faculdade de Engenharia, Universidade do Porto; INEGI, Porto

ABSTRACT

The need to understand the failure mechanisms in composite materials at the micro level has gained additional importance due to the pressing need to develop high performance materials for more demanding applications. This understanding makes it possible to develop a new generation of polymer composite materials in-silico. To understand fibre dominated failure it is necessary to have accurate models that are able to capture the main failure mechanisms in this type of failure. Although complex micromechanical models that capture these mechanisms exist, they are computationally expensive and can only be used for a limited representative volume element size. Simplified models are, therefore, necessary to allow faster predictions, although at the cost of some accuracy. The faster computation times of simplified models allow also the study of more material variations and can be used for optimization purposes. In this work, an extension of the Spring Element Model to a random fibre packing and hybrid composites is presented. Additionally, this model extends the Spring Element Model to consider the dynamic effects of fibre failure. The dynamic stress waves that propagates within the in the intact fibres increases that surround the broken one increase the stress concentrations and, therefore, increase the failure probability of these fibres. This dynamic effect will change the formation process of clusters of broken fibres, which will influence the predicted behaviour of the material. A study on the influence of the dynamic effects on the local stress fields surrounding a broken fibre and on the behaviour of the material is done for both non-hybrid and hybrid composites.

Novel NIST Databases to Aid Material Discovery

Francesca Tavazza^{*}, Kamal Choudhary^{**}, Gabriel Joshua^{***}, Richard Hennig^{****}

^{*}National Institute of Standard and Technology, ^{**}National Institute of Standard and Technology, ^{***}University of Florida, ^{****}University of Florida

ABSTRACT

Technological advances heavily rely on discovery and characterization of materials. Computational investigations, both at the classical and quantum level, have been proven to be extremely effective tools in characterizing material-properties starting from crystal structure information. As part of the Materials Genome Initiative, National Institute of Standards and Technology (NIST) has developed the Joint Automated Repository for Various Integrated Simulations (JARVIS) available at <https://jarvis.nist.gov/>. Jarvis contains repositories designed to automate materials discovery using classical force-field (JARVIS-FF)¹, density functional theory (JARVIS-DFT)², and machine learning (JARVIS-ML) calculations. The JARVIS-FF database currently consists of 20000 entries including energetics, elastic property, surface energy and vacancy formation energy calculations, and it is still increasing. It also includes computational tools for convex-hull plots and force-field comparisons. The data covers 1471 materials and 116 force-fields. Both the complete database and the software coding used in the process have been released for public use online. The JARVIS-DFT database consists of more than 25000 DFT calculations for three-dimensional (3D) bulk and single layer 2D materials of structural, electronic and elastic properties. A novel lattice-constant criterion is used to identify potentially new 2D, 1D, and 0D materials. We predicted at least 1485 2D materials based on such criterion. For bulk structures, the database also contains optoelectronic properties (bandgap and frequency dependent dielectric function) computed using two different exchange-correlation functionals, vdW-DF-optb88 and the Tran-Blaha modified Becke-Johnson functional. Lastly, while DFT presents an in-principle exact theory, various approximations are required to perform practical simulations. To this day, a systematic evaluation of the uncertainties related to such approximations is still lacking, and NIST is developing the DFT benchmarking database to estimate the uncertainty due to various choices of key controlled approximations. 1. Kamal Choudhary, Faical Yannick P. Congo, Tao Liang, Chandler Becker, Richard G. Hennig & Francesca Tavazza, "Evaluation and comparison of classical interatomic potentials through a user-friendly interactive web-interface", Scientific Data 4, Article number: 160125 (2017), doi:10.1038/sdata.2016.125 2. Kamal Choudhary, Irina Kalish, Ryan Beams & Francesca Tavazza, "High-throughput Identification and Characterization of Two-dimensional Materials using Density functional theory", Scientific Reports 7, Article number: 5179 (2017), doi:10.1038/s41598-017-05402-0

Patient-specific Modeling of Blood Flow

Charles Taylor*

*HeartFlow, Inc.

ABSTRACT

Patient-specific models of blood flow constructed from coronary CT angiography (cCTA) images and using computational fluid dynamics are transforming the diagnosis of heart disease by providing a safer, cheaper and more efficient procedure as compared to the standard of care that often involves nuclear imaging and invasive diagnostic cardiac catheterizations [1]. Such image-based computations require an accurate segmentation of the coronary artery lumen from cCTA images and leverage biologic principles relating form (anatomy) to function (physiology). Leveraging research originally performed at Stanford University, HeartFlow has developed a non-invasive test, FFRCT, based on computing flow and pressure in the coronary arteries [2]. FFRCT has been validated against invasive pressure measurements in more than 800 patients and demonstrated to improve care in numerous clinical studies to date [3]. At present, FFRCT has been used for more than 15,000 patients in routine practice for clinical decision making in the United States, Canada, Europe, and Japan. In the United States, the Centers for Medicare and Medicaid Services and the majority of private insurance companies reimburse physicians for using FFRCT. Patient data is uploaded to the HeartFlow application running on Amazon Web Services (AWS). Image analysis methods leveraging deep learning are used to create an initial patient-specific geometric model, and then a trained analyst inspects and corrects the model. Fully-automated mesh generation techniques are used to discretize the model and computational fluid dynamic analysis is performed on AWS to compute the blood flow solution. Results are returned to the physicians through a web interface or mobile application. New developments including treatment planning and evaluating rupture risk of coronary plaques will be discussed. The impact of computational methods developed by Professor Thomas J.R. Hughes on the field of patient-specific modeling of blood flow will be described. References [1] Taylor CA., Hughes TJR., Zarins CK, (1998) Finite Element Modeling of Blood Flow in Arteries. Computer Methods in Applied Mechanics and Engineering. Vol. 158, Nos. 1-2, pp. 155-196. [2] Taylor CA, Fonte TA, Min JK., Computational Fluid Dynamics Applied to Cardiac Computed Tomography for Noninvasive Quantification of Fractional Flow Reserve, J Am Coll Cardiol. 2013;61(22):2233-2241. [3] Douglas PS, De Bruyne B, Pontone G, Patel MR, Norgaard BL, Byrne RA, et al. 1-Year Outcomes of FFRCT-Guided Care in Patients With Suspected Coronary Disease: The PLATFORM Study. J Am Coll Cardiol 2016;68:435-445.

Physical Experimentation and Analytics of Near-Surface Cohesionless Soil Dynamics

Oliver-Denzil Taylor^{*}, Robert Walker^{**}, Amy Cunningham^{***}, Katheryn Martin^{****}, Mihan McKenna^{*****}

^{*}US Army Engineer Research & Development Center, ^{**}US Army Engineer Research & Development Center, ^{***}US Army Engineer Research & Development Center, ^{****}US Army Engineer Research & Development Center, ^{*****}US Army Engineer Research & Development Center

ABSTRACT

For analytical modeling of low-confinement soil models, the soil is considered both as an elastic media, and also as an inelastic media with a skeleton matrix of soil with pores filled with air and water. The inelastic model is implemented within a Terzaghi effective stress model, using the HONDO computational platform, in an attempt to replicate observed in situ wave propagation phenomenology and laboratory behavior. In this paper, we investigate the applicability of such models to describe the behavior of sand within the upper meter of the subsurface. Typically, the analytical model assumes that the input frequency is not an artifact of location on the wetting-drying time curve in order for the analytical outputs to be considered valid. However, as presented herein, experiments into tip-to-tip oriented bender elements indicate that this assumption is invalid. Furthermore, laboratory experiments on unconfined sand illustrates the significant shortcomings of trying to model cohesionless soil within the near surface, down to approximately 1 meter in depth with a free surface upper boundary.

Tom Hughes at 75: From FEA to IgA

Robert Taylor*

*University of California, Berkeley

ABSTRACT

This presentation honors Tom Hughes on the occasion of his 75th birthday and summarizes the influence he has had on my activities in computational mechanics during the last 45 years. Our early interactions in studies on plate bending, contact/impact problems, time integration methods and fluid dynamics took place while he was at Berkeley in the 1970's. Later we interacted on solution of viscoplastic problems, discontinuous Galerkin methods and Isogeometric analysis. Accordingly I summarize these and dedicate my presentation to Tom as he celebrates another important milestone in his life.

Analyses of Fatigue Crack Propagation with Smoothed Particle Hydrodynamics Method

Koki Tazoe^{*}, Hiroto Tanaka^{**}, Masanori Oka^{***}, Genki Yagawa^{****}

^{*}YANMAR CO., LTD., ^{**}YANMAR CO., LTD., ^{***}YANMAR CO., LTD., ^{****}The university of Tokyo and Toyo university

ABSTRACT

Fatigue fracture is one of the most serious problems in mechanical structures under cyclic loadings. Particularly, the fatigue crack propagation is one of the typical phenomena in fatigue damage. To assess the damage, accurate simulation of crack growth history is considered to be important [1]. Accordingly, some numerical analyses for the crack propagation problem with meshes, for example X-FEM, have been investigated [2]. Meshing analysis method, however, has problems when dealing with complex situations such as single crack separation, merging of multiple cracks, high kink angled initial crack and so on [2]. This means that, especially from the view point of engineering, it is not easy to handle such complex problems by using meshing analysis methods. On the other hand, particle methods, such as the SPH [3], are thought to be useful to solve above mentioned problems. However, as far as the present authors know, little studies have been published about fatigue crack propagation analyses by employing particle methods. In this study, the fatigue crack propagation is studied by using the SPH method. The developed computer program is based on linear fracture mechanics, where crack is assumed to propagate within particles located around crack front line, which is represented as a chain of particles including crack tips. We have solved planar fatigue crack propagation crossing a hole by this method, showing that a single initial crack is separated into two cracks at the edge of the hole and the two cracks merge at the other side in a smooth manner. After the merging, the kinked crack front shape [2] is disappeared automatically without any problems. It is concluded that the SPH method is a useful tool for simulation of the complex crack propagation history. References [1] Toyosada M, Gotoh K, Niwa T (2004) Fatigue life assessment for welded structures without initial defects: an algorithm for predicting fatigue crack growth from a sound site. *Int J Fatigue*. 26-9:993-1002 [2] Colombo D (2012) An implicit geometrical approach to level sets update for 3D non-planar X-FEM crack propagation. *Comp Meth Appl Mech Engng*. 237-240:39-50 [3] Lucy L B (1977) A numerical approach to the testing of the fission hypothesis. *Astronom. J* 8:1013-1024

Scale-resolving Simulations of Turbulent Boundary Layers: Effect of Inflow Unsteadiness

Pedram Tazraei*, Sharath Girimaji**

*Texas A&M; University, **Texas A&M; University

ABSTRACT

Scale-resolving simulations (SRS) offer a computationally viable alternative to direct numerical simulations (DNS) or large eddy simulations (LES) for many flows of engineering interest. In wall-bounded SRS simulations, it is desirable to perform RANS (Reynolds-averaged Navier-Stokes) in the close proximity of the wall and gradually introduce fluctuations through the log-layer and approach a reasonably resolved simulation as the free-stream is approached. Such a SRS computation can, in principle, be computationally reasonable and yet yield accurate results. In the current work, the near-wall modeling of SRS is addressed. The SRS approach considered in this study is the partially-averaged Navier-Stokes (PANS). The PANS provides a formal framework for adapting two-equation RANS models to model different degrees of scale resolution. The implicit filtering is carried out by imposing a cut-off in the energy spectrum, and the cut-off is specified by defining the ratios of the unresolved-to-total kinetic energy and unresolved-to-total dissipation rate. In this work, we will examine a key aspect of near-wall PANS modeling - the effect of inflow unsteadiness on the development of a SRS boundary layer. OpenFOAM software is used to perform the simulations. The multi-layered nature of the turbulent boundary layer (TBL) dictates clustering of grid points near the wall. For the boundary conditions, no-slip condition is prescribed at the wall. Zero pressure is defined at the upper boundary and outlet. And in the spanwise direction, cyclic condition is applied. In order to generate the turbulent inflow, the so-called "recycling/rescaling" method is invoked at the inlet. Implementation of the recycling/rescaling condition includes running two independent, precursor and main, simulations. The inflow data is recycled from a downstream enough perpendicular plane, and rescaled such that the momentum thickness of the precursor case matches the momentum thickness at the inlet of TBL. Several test cases are considered for discrete momentum thickness Reynolds number in the range of 830 to 2400. The accuracy of the simulations is examined by inspecting the first and second order turbulence statistics. Further, the organization of coherent structures in the near-wall region of a spatially developing boundary layer is examined. Multi-point physics based on the λ_2 criterion is examined by visualizing hairpin vortices and their organization in a packet form in a fully-developed turbulent boundary layer.

Asymmetric Capping of Biconvex Tablets: A FEM Study

Pierre Tchoreloff^{*}, Harona Diarra^{**}, Vincent Mazel^{***}

^{*}Université de Bordeaux, ^{**}Université de Bordeaux, ^{***}Université de Bordeaux

ABSTRACT

Capping is a classical problem during the manufacturing of pharmaceutical tablets. It corresponds to the separation of the top layer of the tablet and can be observed just at the ejection from the die or some days after. It is well known that biconvex tablets are more prone to capping than flat-faced ones. The reason is the mechanism that makes the tablet break [1]. During relaxation, the material in the cup can expand radially whereas the main body of the tablet cannot. This promotes the development of large shear stresses that can lead to capping. Considering this mechanism, if the compaction is applied symmetrically, capping should appear on both side of the tablet. Nevertheless it is well known that, sometimes, capping can be asymmetric, i.e. failure occurs only on one side of the tablet. When this phenomenon happens, capping always occurs on the side that is ejected first (i.e. the “upper side” on most of the machines). This dissymmetry is not explained by the mechanism proposed above. In this presentation we will study, using FEM modelling, how the ejection part of the compaction cycle could be responsible of this asymmetrical failure. Afterwards, influence of some process/product parameters on the capping tendency of biconvex tablet will be discussed, based on the phenomena found in the simulations. FEM simulations show that the ejection process can be separated into two phases. First, when the force applied by the lower punch is lower than the ejection force, the band of the tablet is fixed and the movement of the punch promotes a deformation of the tablet. At some point, the force needed to move the tablet is reached, and the tablet begins to move upward. During the first part of the unloading, the shear stress, that is responsible of the failure of the compact, increases on the upper side of the tablet and decreases on its lower side. The shear strength of the tablet may thus be reached because of the deformation of the tablet. This would promote capping only on the upper side of the tablet as sometimes observed during manufacturing. This mechanism makes it also possible to understand the influence of various process/product parameters on the capping tendency like lubrication or compaction speed.

1. Hiestand et al., J Pharm Sc., 1977, 66, 510-519.

Generating Statistically Equivalent Synthetic Microstructures of Additively Manufactured Stainless Steel

Kirubel Teferra^{*}, Lily Nguyen^{**}, David Rowenhorst^{***}

^{*}US Naval Research Laboratory, ^{**}US Naval Research Laboratory, ^{***}US Naval Research Laboratory

ABSTRACT

Additive manufacturing (AM) is a promising materials technology because of its ability to generate components according to prescribed CAD-based geometries with tight tolerances. The AM build process generates highly localized thermal cycles that induces rapid phase changes in the material. The frequency, localization, and speed of the thermally-driven phase changes is significantly different from the annealing processes associated with traditionally processed materials, often leading to different microstructural and constitutive properties. Since microstructure influences material properties, it is important to statistically characterize the features of these novel microstructures and develop models for their morphology. The three-dimensional microstructure of a material can be statistically characterized by reconstructing a specimen using electron backscatter diffraction (EBSD) coupled with mechanical serial sectioning. Since these datasets are extremely time consuming and costly to collect, synthetic microstructure models are trained to the data in order to generate statistically equivalent samples of the microstructure. Synthetic models for polycrystalline materials are usually variants of tessellation models. The microstructure of AM processed 316L is comprised of a highly chaotic morphology with very complex grain shapes that are not well characterized by only considering size and aspect ratio. This suggests that simple tessellation-based models are insufficient representations of the morphology, and novel models must be developed. This work studies the use of deep learning techniques to generate accurate representations of complex microstructures. Generative Adversarial Nets (GANs) is a methodology aimed at generating synthetic data that is indiscernible from real data. Two feed forward networks are simultaneously trained where one generates synthetic data, and the other builds a discriminator to distinguish the synthetic data from the real. The objective function is formulated to reach an equilibrium such that the discriminator returns an equal probability that the synthetic data is counterfeit or real. The efficacy of using GAN as a perturbation from an initial tessellation-based synthetic model in order to recover the error between the AM microstructure and the tessellation-based model will be studied. In addition, the Restricted Boltzman Machine, a generative model, will be employed to characterize the joint distribution of the model parameters such that statistically equivalent synthetic models can be simulated.

Machine Learning Materials Physics: Algorithms Predict Precipitate Morphology in an Alternative to Phase Field Dynamics

Gregory Teichert*, Emmanuelle Marquis**, Krishna Garikipati***

*University of Michigan, **University of Michigan, ***University of Michigan

ABSTRACT

Machine learning has been effective at detecting patterns and predicting the response of systems that behave free of natural laws. Examples include learning crowd dynamics, recommender systems and autonomous mobility. There also have been applications to the search for new materials that bear relations to big data classification problems. However, when it comes to physical systems governed by conservation laws, the role of machine learning has been more limited. Here, we present our recent work in exploring the role of machine learning methods in discovering or aiding the search for physics. Specifically, this talk will focus on using machine learning algorithms to represent high-dimensional free energy surfaces with the goal of identifying precipitate morphologies in alloy systems. Traditionally, this problem is approached by combining phase field models, which impose first-order dynamics, with elasticity, to traverse a free energy landscape in search of minima. Equilibrium precipitate morphologies occur at these minima. Here, we exploit the ability of machine learning methods to represent high-dimensional data, combined with surrogate optimization, reduced order modeling, and sensitivity analysis as an alternate approach to finding minimum energy states. This combination of data-driven methods offers an alternative to the imposition of first-order dynamics via phase field methods, and represents one approach to learning materials physics with machine learning.

DNS and LES of Scalar Transfer across a Wind-driven Air-water Interface Characterized by Gravity-capillary Waves

Andres Tejada-Martinez*, Amine Hafsi**, Fabrice Veron***

*aetejada@usf.edu, **University of South Florida, ***University of Delaware

ABSTRACT

Direct numerical simulation (DNS) of an initially quiescent coupled air-water interface driven by an air-flow with free stream speed of 5 m/s generates gravity-capillary waves on the interface and Langmuir turbulence characterized by small-scale (centimeter-scale) Langmuir circulation (LC) beneath the interface. LC consists of counter-rotating vortices in the direction of the wind and waves. In addition to LC, the water side turbulence consists of smaller turbulent eddies similar to the shear-driven eddies associated with the classical wall streaks in wall-bounded turbulent flow. Large-eddy simulation (LES) with momentum equation augmented with the well-known Craik-Leibovich (C-L) vortex force is used to understand the roles of the wave and shear-driven LC (i.e. the Langmuir turbulence) and the smaller shear-driven eddies (i.e. the shear turbulence) in determining molecular diffusive scalar flux from the air side to the water side and vertical scalar transport beneath. The C-L force consists of the cross product between the Stokes drift velocity (induced by the interfacial waves) and the flow vorticity. It is observed that Stokes drift shear intensifies the smaller eddies (with respect to purely wind-driven flow, i.e. without wave effects) leading to enhanced diffusive scalar flux at the air-water interface. These intensified smaller eddies are interpreted as part of the overall wave and shear-driven Langmuir turbulence. Furthermore, it is also observed that the larger scales (i.e. the LC) lead to increased vertical scalar transport at depths below the interface and thus greater scalar transfer efficiency. Both DNS and LES show that transition to Langmuir turbulence leads to a spike in scalar flux characterized by an order of magnitude increase. In the field, these episodic flux increases, if linked to gusts and overall unsteadiness in the wind, are expected to be an important contributor in determining the long-term average of air-sea gas fluxes.

Advanced Geometry-based Mesh Generation and Adaptation for Complex Flow Problems at Large Scale

Saurabh Tendulkar^{*}, Mark Beall^{**}, Rocco Nastasia^{***}

^{*}Simmetrix Inc., ^{**}Simmetrix Inc., ^{***}Simmetrix Inc.

ABSTRACT

This presentation will describe state of the art developments in unstructured and semistructured meshing technologies driven by the needs of flow problems involving complex geometries and physics. Applications of these technologies to active research areas in aircraft and ballistics systems design will be presented. For aircraft systems, the focus will be on generating and adapting large scale high quality meshes where high anisotropy and semistructured nature are desirable to model boundary layers in high speed flow. For ballistics the focus will be on evolving domains and adaptive meshing with support for discontinuous solution fields in projectile motion and propellant burn simulations. The ability to generate and adapt these meshes in parallel while maintaining fidelity to model geometry will be discussed.

Coupling of Particle Blast Method (PBM) with Discrete Element Method for Buried Mine Blast Simulation

Hailong Teng*

*Livermore Software Technology Corp.

ABSTRACT

This paper presents two meshless methods: particles blast method (PBM) and discrete element method (DEM). Particle blast method (PBM) is intend to model the gaseous behavior of high velocity, high temperature detonation products. PBM is developed based on corpuscular method (CPM), which has been successfully applied to airbag deployment simulation where the gas flow is slow. For blast simulation where gas flow is extremely high, the equilibrium assumption in CPM is no long valid. By reformulating the particle interaction algorithm, we proposed the PBM that is capable of modelling thermally non-equilibrium system and applied this method for the simulation of blast loading. DEM focus on the modeling of granular media, which might exhibit complex behavior under different condition. Finally, the paper present the coupling of PBM with DEM for buried mine blast simulation.

Optimization of Structural Stiffness under Dependent Load

Xiaoyan Teng*, Bingkun Mao*, Dongri Li*, Xudong Jiang†

*Harbin Engineering University, Harbin, Heilongjiang Province, China,
tengxiaoyan@hrbeu.edu.com

†Harbin University of Science and Technology, Harbin, Heilongjiang Province, China,
xudongjiang@sina.com

Key words: Topology Optimization, Dependent Load, Structural Stiffness, Multi-load Structures

Abstract.

Dependent load is a kind of load which fixed on the existence of structure, accompanied with the topological optimization of the whole structure. Gravitational load is the most typical one of dependent load. It is of great importance to take dead weight into consideration for topological optimization especially when it comes to large-scaled civil engineering structure design. Based on the calculation formula of sensitivity of the structural compliance, aiming at the design of structural topological optimization under the collaboration of gravitational load and independent load, evolutionary structural optimization under multiple load is proposed after analyzing the relevance of load to element stiffness. In the presence of dead weight, the optimization model has non-convexity. The sensitivity of gravity loading to structural flexibility is no longer constant to a negative value, that is compliance is no longer a monotonically decreasing function. Hence, in this case, if the treatment method of flexibility of the past is still followed, the optimal solution may not be obtained and the iteration may be terminated. In this paper, RAMP model is used to solve the problem of topological optimization under volume constraint and multi-load respectively by using Hard-kill and Soft-kill techniques based on bidirectional evolutionary structural optimization. The optimal results of approximation theory are obtained through a stable optimization iteration process. Numerical examples show that the sensitivities remain negative for the Hard-kill mode; the positive and negative results of the sensitivity sign change of the Soft-kill mode, and the results obtained after the absolute sensitivities are very close to the Hard-kill mode. The correctness of the two cell deletion methods is verified. Finally, taking bridge structure as an example, optimized analysis is carried out under concentrated load and uniform load respectively. The optimization results are close to the actual engineering structure, which verifies the validity of this method.

1 INTRODUCTION

Multi-load mentioned in this paper refers to the existence of the load attached to the unit, which is accompanied by the unit of additions and deletions. In the past, multi-load refers to a collection of concentrated loads or surface loads. The characteristics of these loads do not disappear, and the size and direction of the acting point and force are invariable and will not change with the unit. Therefore, there are essential differences between these two kinds of multi-loads[1]. The multi-load problem studied in this paper is to consider gravity as a dependent load. It is necessary and

necessary to consider gravity in practical topology optimization problems, especially for large-scale civil engineering structures. Bruyneel and Duysinx^[2] have studied and improved the discontinuous SIMP model and obtained the stable optimal structure under the assumption of self-gravity, which also proves that considering the self-gravity in the optimization process can affect the final topology. Some scholars, such as Yang^[3] and Ansola^[4], studied and improved ESO methods and studied continuum topology optimization considering their own gravity. Taking into account the shortcomings of the ESO method, BESO method in this area will be fully developed, this article will be discussed. Therefore, this paper will carry out the structural topology optimization design under the combined action of gravity load and non-dependent load. In the process of structural topology optimization, this paper introduces the dependent load (gravity load), the gravity is distributed on the node of each unit, vertically downward, and attached to the unit exists, in the iterative process, with the unit Additions and deletions are added and deleted, and the gravity of the structure is constantly changing.

2 MATHEMATICAL DESCRIPTION OF DEPENDENT LOAD OPTIMIZATION PROBLEMS

For structural stiffness optimization problems, no matter whether it is a single load or multiple loads, the deformation of any node is a linear change under the volume constraints. Therefore, the effect of multiple loads is the superposition of the effects of all independent loads, and ultimately the structural stiffness can also be maximized. The mathematical description of the optimization problem is the same under both load conditions. The description is as shown in equation (1).

$$\begin{aligned} \text{Find : } x &= (x_1, x_2, \dots, x_n)^T \\ \text{Min : } C(x) &= \frac{1}{2} \mathbf{f}^T \mathbf{u} \\ \text{Subject to : } &\begin{cases} V^* - \sum_{i=1}^n V_i x_i = 0 \\ x_i = \{x_{\min}, 1\} (i = 1, 2, \dots, n) \end{cases} \end{aligned} \quad (1)$$

In the formula, C is the average compliance of the structure, and \mathbf{f} and \mathbf{u} are the force vector and displacement vector of the dependent load and the external load, respectively. V_i is the volume of a single unit and V^* is the set total volume of the structure. This binary design variable x_i indicates the density of the i -th element. Normally, x_{\min} is given a relatively small value of 0.001. This value close to zero indicates that the corresponding element is an empty element.

3 DEPENDENT LOAD OPTIMIZATION THEORIES

3.1 Sensitivity analysis

The difference between the load and the fixed external load in the text is whether to consider the dependent gravity load. In the finite element analysis, the expression of this applied force vector is shown in equation (2).

$$\mathbf{f} = \sum_{i=1}^k \mathbf{f}_i + \mathbf{f}_0 = \mathbf{K} \mathbf{u} + \mathbf{f}_0 \quad (2)$$

In the formula, \mathbf{f}_i represents the self-weight load vector of the i -th unit, and \mathbf{f}_0 represents the additional fixed load. By introducing the Lagrangian multiplier λ , the sensitivity of the displacement and the force vector can be determined, so the expression of the objective function is

shown in equation (3).

$$C = \frac{1}{2} \mathbf{f}^T \mathbf{u} + \lambda^T (\mathbf{f} - \mathbf{K} \mathbf{u}) \quad (3)$$

In the formula, $\lambda^T (\mathbf{f} - \mathbf{K} \mathbf{u})$ is equal to 0, so the new objective function is equal to the old one. The sensitivity of the modified objective function is derived as shown in equation (4).

$$\frac{dC}{dx_i} = \frac{1}{2} \frac{\partial \mathbf{f}^T}{\partial x_i} (\mathbf{u} + 2\lambda) + \left(\frac{1}{2} \mathbf{f}^T - \lambda^T \mathbf{K} \right) \frac{\partial \mathbf{u}}{\partial x_i} - \lambda^T \frac{\partial \mathbf{K}}{\partial x_i} \mathbf{u} \quad (4)$$

Since it is a stiffness optimization, it is necessary to remove $\partial u / \partial x_i$ from the sensitivity expression, because λ can take any value, so that

$$\lambda = \frac{1}{2} \mathbf{u} \quad (5)$$

Then, substituting equation (5) into equation (4), the simplified form of the sensitivity expression is shown in equation (6).

$$\frac{dC}{dx_i} = \frac{\partial \mathbf{f}^T}{\partial x_i} \mathbf{u} - \frac{1}{2} \mathbf{u}^T \frac{\partial \mathbf{K}}{\partial x_i} \mathbf{u} \quad (6)$$

The sensitivity expression under the fixed external load (without considering the gravity load) is shown in formula (7).

$$\frac{\partial C}{\partial x_i} = -\frac{1}{2} \mathbf{u}_i^T \mathbf{K}_i^0 \mathbf{u}_i \quad (7)$$

According to equation (6), the sensitivity value of the compliance degree is determined by the algebraic sum of the two terms on the right side of the equation. However, according to the comparison formula (7), if the self-weight exists, the sensitivity symbol cannot be determined and can be positive or negative. In other words, as the design variables change, the sign of the sensitivity value also changes, which indicates the non-monotonic characteristics of the degree of compliance. Therefore, in this case, if the processing method of the compliance is still used in the past, it may result in that an optimal solution or even an iterative suspension may not be obtained. The following content will explain the sensitivity processing methods under these two loading conditions.

3.2 Material interpolation schemes and sensitivity values

The material interpolation scheme with penalty factor is widely used in the SIMP method, so a high-quality 0-1 design can be obtained. In order to achieve this goal with the BESO method, the Young modulus of the intermediate material will be used as an interpolation function of the cell density, as shown in equation (8).

$$\begin{cases} E(x_i) = E_0 x_i^p \\ \mathbf{K} = \sum_i^n x_i^p \mathbf{K}_i^0 \end{cases} \quad (8)$$

In the formula, E_0 represents the Young modulus of the real unit, and \mathbf{K}_i^0 represents the stiffness matrix of the real unit. It is assumed here that Poisson's ratio is independent of design variables.

If the above material interpolation model is applied, for the soft element, although the stiffness matrix becomes smaller due to the existence of the penalty factor, the material density of the

element is not weakened correspondingly. Therefore, the gravity received by the element does not follow the stiffness matrix, This is illogical. This results in the unit's displacement vector being an indeterminate quantity. Therefore, the value of $(\mathbf{f}_i \mathbf{u})$ cannot be determined. The algebraic sum of the two terms on the right side of equation (6) will lose control. On the other hand, considering the self-weight condition, the objective function becomes a non-convex function. Because of this factor, it is impossible to obtain a better 0-1 design.

Here, a new interpolation scheme (RAMP) will be considered, which was proposed by Stolpe and Svanberg [5]. This interpolation model overcomes the disadvantages of the power-exponent function interpolation scheme described above. The density model and the Young's modulus of the material model are expressed by Equation (9).

$$\begin{cases} \rho_i = x_i \rho_0 \\ E_i = \frac{x_i}{1 + p(1 - x_i)} E_0 \end{cases} \quad (9)$$

In the formula, ρ_0 and E_0 represent the density and Young modulus of a solid material, respectively, and p is a penalty factor greater than zero. For a three-dimensional model, when the structure is subjected to finite element meshing, for the 8-node cubic element, the load (self-weight) of the element is uniformly distributed on 8 nodes, assuming that the direction of gravity is Y direction, such as the formula (10) Shown.

$$\mathbf{f}_i = V_i \rho_i g \bar{\mathbf{f}} = V_i \rho_i g \left\{ 0, -\frac{1}{8}, 0, 0, -\frac{1}{8}, 0, 0, -\frac{1}{8}, 0, 0, -\frac{1}{8}, 0, 0, -\frac{1}{8}, 0, 0, -\frac{1}{8}, 0 \right\}^T \quad (10)$$

Assume that a unit change only affects the dependent load, and therefore, the relative change in the external load is shown in Equation (11).

$$\frac{\partial f}{\partial x_i} = V_i \rho^0 g \bar{\mathbf{f}}^T \mathbf{u}_i \quad (11)$$

The sensitivity of the average softness is shown in equation (12).

$$\frac{dC}{dx_i} = V_i \rho^0 g \bar{\mathbf{f}}^T \mathbf{u}_i - \frac{1 + p}{2[1 + p(1 - x_i)]^2} \mathbf{u}_i^T \mathbf{K}_i^0 \mathbf{u}_i \quad (12)$$

It can be seen that the element sensitivity depends on the value of the penalty factor. The formula (12) can directly determine the sensitivity of the empty and real elements, respectively, as shown in equation (13).

$$\alpha_i = -\frac{1}{p + 1} \frac{dC}{dx_i} = \begin{cases} -\frac{V_i \rho^0 g}{p + 1} \bar{\mathbf{f}}^T \mathbf{u}_i + \frac{1}{2} \mathbf{u}_i^T \mathbf{K}_i^0 \mathbf{u}_i & x_i = 1 \\ -\frac{V_i \rho^0 g}{p + 1} \bar{\mathbf{f}}^T \mathbf{u}_i + \frac{1}{2[1 + p(1 - x_{\min})]^2} \mathbf{u}_i^T \mathbf{K}_i^0 \mathbf{u}_i & x_i = x_{\min} \end{cases} \quad (13)$$

For the purpose of minimizing the compliance, the sensitivity value should be updated, the design variable x_i of the cell corresponding to the low sensitivity value is changed to x_{\min} , and the value of the design variable x_i of the cell having the high sensitivity value is changed to 1. Similar to the exponential function interpolated material scheme, this scheme also needs to select a larger penalty factor. With discrete design variables, the scheme can achieve convergence and a stable 0-1 design.

It should be noted that for the new interpolation scheme, when the penalty factor tends to be infinitely large, the sensitivity value of the soft cell tends to zero, and the expression of the

sensitivity value at this time is expressed by Equation (14).

$$\alpha_i = \begin{cases} \frac{1}{2} \mathbf{u}_i^T \mathbf{K}_i^0 \mathbf{u}_i & x_i = 1 \\ 0 & x_i = x_{\min} \end{cases} \quad (14)$$

In the formula, $x_i = 0$ replaces $x_i = x_{\min}$ because soft cells are equivalent to empty cells. Therefore, the above sensitivity value will be used for hard killed BESO method. For the hard kill method, it can be seen from equation (14) that the sensitivity expression of the structure subjected to self-weighted self-weight and fixed external load is the same.

Sensitivity analysis shows that the non-monotonicity of the objective function depends on the value of the penalty factor. The larger the value of the penalty factor, the less obvious is the non-monotonicity. For extreme cases where the penalty factor is infinitely large, the non-monotonic characteristic is completely disappeared. Unlike the topological optimization problem of fixed loads, the choice of penalty factors does affect the ordering of the sensitivity of the solid elements. Therefore, for Hard-kill, the first term on the right side of the sensitivity formula completely disappears, and the Soft-kill in contrast, there may be differences in the optimization results. However, the high computational efficiency of Hard-kill methods has prompted a large number of scholars to conduct continuous research [6].

4 NUMERICAL EXAMPLES

From the above, we can see that for the self-weight dependent load, if the soft killing method is used, the sensitivity expression shows that the objective function is non-monotonic, so it is not possible to perform the sensitivity update simply according to the magnitude of the strain energy, only according to the gradient and the energy method is optimized for calculation. Therefore, there are only Hard-kill and Soft-kill methods, but the Soft-kill method has too much calculation. Here is a simple example to compare the results of the two methods.

There are many types of dependent load optimization examples. The following examples are given by combining real objects: structures that are only subjected to gravity conditions, such as stone arch bridges; structures that are uniformly loaded, such as upper bearing arch bridges, middle bearing weights arch bridge and lower bearing arch bridge.

4.1 Stiffness optimization under concentrated loads

Example 1: The design domain size is 50mm x 20mm x 4mm. The four vertices of the bottom face are simply supported and restrained. The center of the top face is subjected to vertical downward force $F = 10\text{N}$, density $\rho = 1\text{g/mm}^3$, the elastic modulus of the material $E_1 = 1\text{GPa}$, and Poisson's ratio $\mu = 0.3$. The design domain is divided into $50 \times 20 \times 4$ mesh areas. The target volume is set to 50% of the total volume. The required parameter is: $ER = 0.02$, $r_{\min} = 3\text{mm}$.

Case1.1 Does not consider gravity ($G=0$, $F=10\text{N}$)

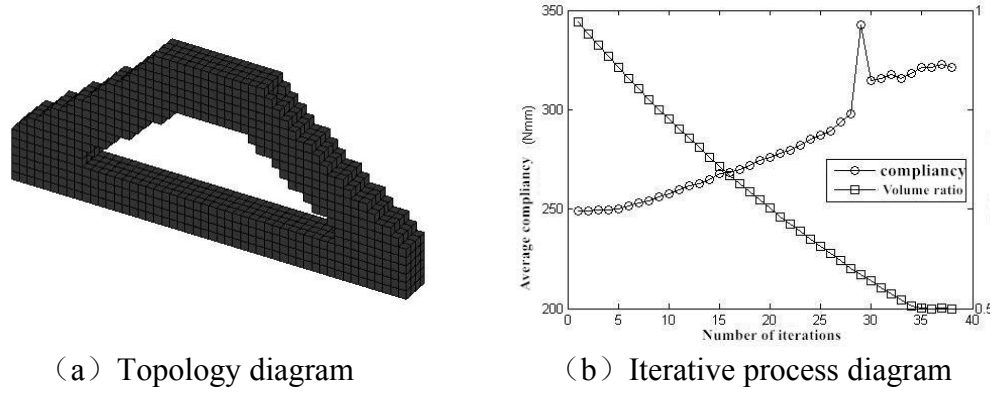


Fig. 1 Topological optimization results of simply supported beams under non-gravity

Case1.2 Under multiple loads ($G \neq 0$, $F=10N$)

For this example, Hard-kill and Soft-kill methods were used for comparison. The correctness of sensitivity treatment in Soft-kill was verified. The results are as follows:

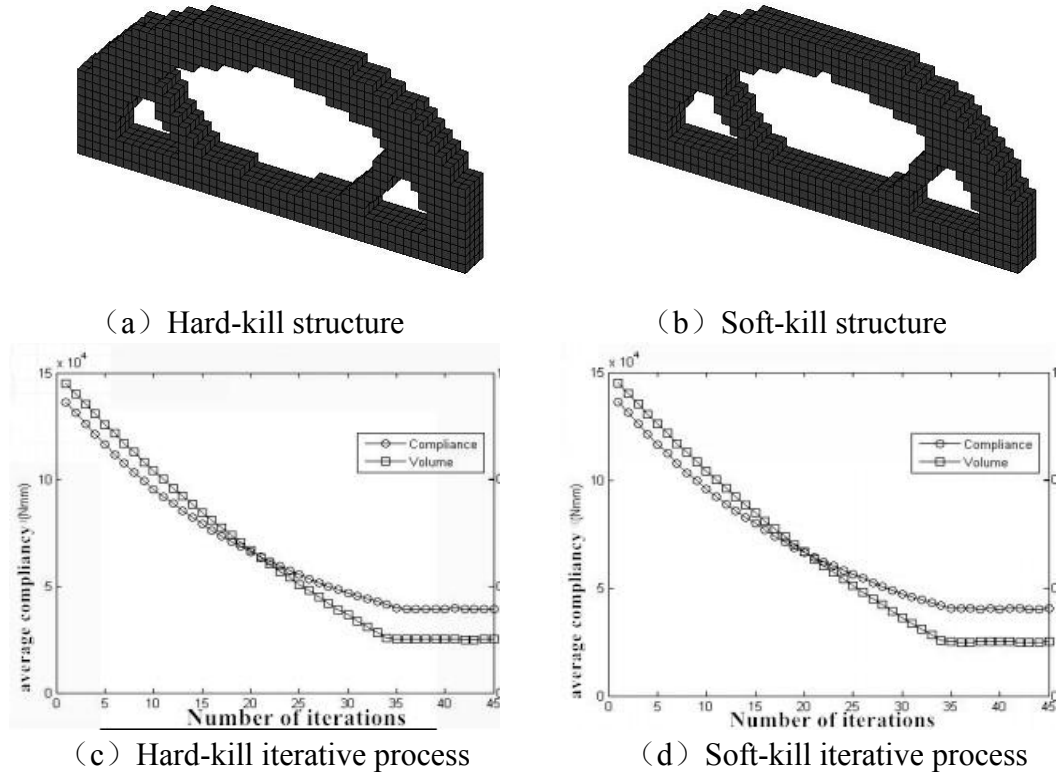


Fig. 2 Topological optimization results under gravity effect of simply supported beam (Hard-kill and Soft-kill)

Comparing Fig. 1(a) with Fig. 2(a)(b), it can be clearly seen that the structure undergoes a large change after the self-weight load is applied. The structure of Fig. 2 is more similar to the actual arch bridge structure. Comparing Fig. 2(a) with Fig. 2(b), the final structure of this method is very similar. Comparing Fig. 2(c) and Fig. 2(d), it can reach convergence smoothly, the convergence of the degree of flexibility makes the values: $C_1 = 39250 \text{ N} \cdot \text{mm}$ and $C_2 = 40390 \text{ N} \cdot \text{mm}$, respectively, and the difference is small. This verifies the correctness of the absolute value processing for Soft-

kill sensitivity values.

4.2 Stiffness optimization under uniform load

Through the example of the deck arch bridge, the half-through arch bridge and the through type arch bridge structure (as shown in Fig. 3), the initial design domain is established, and the structural topology optimization is performed under the joint action of the gravity load and the uniform load.

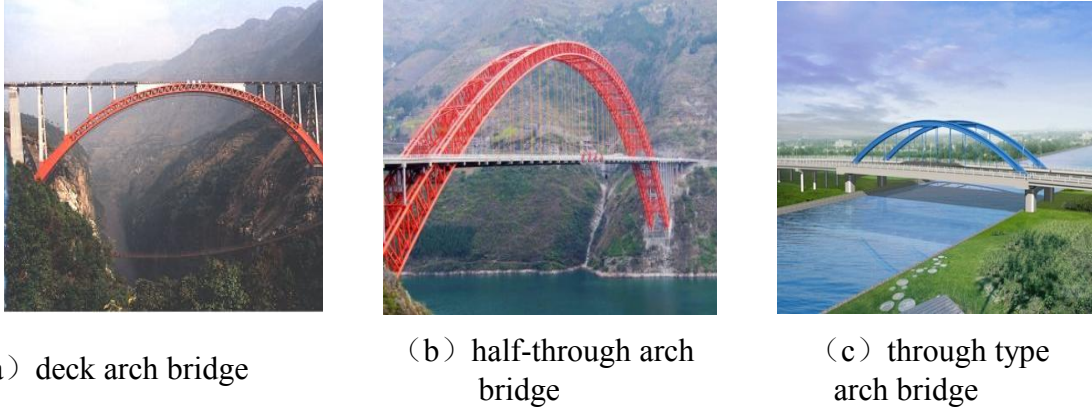


Fig. 3 Arch Bridge Engineering Structure

For the topology design of the bridge, the design domain will be divided into two categories: uniform load acting surfaces and non-active surfaces. In the iterative process, for the element corresponding to the action surface, not participating in the update of the variable, addition or deletion of the elements, is only used as a carrier of the external load, but the element corresponding to the Non-active surface is involved in updating the variable.

Example 2: Due to the different types of bridges, the design domain is also different: 1) Full design domain, the design domain size is $50\text{mm} \times 20\text{mm} \times 8\text{mm}$, the design domain is divided into $50 \times 20 \times 8$ mesh area; 2) The design domain is a U-shaped slot; 3) The design domain is an H-shaped slot. The four vertices of the bottom surface of the initial model corresponding to the three design domains are all clamped, and the top surface of the first design domain is uniformly distributed vertically downward; The inner surface of the bottom of the tank in the latter two design domains is subjected to vertical downward uniform load $F = 0.25\text{N/mm}^2$, density of material $\rho = 1\text{g/mm}^3$, elastic modulus $E_1 = 1\text{GPa}$, Poisson's ratio $\mu = 0.3$. The target volume is set to 40% of the total volume and the required parameter is: $ER=0.02$, $r_{\min} = 3\text{mm}$.

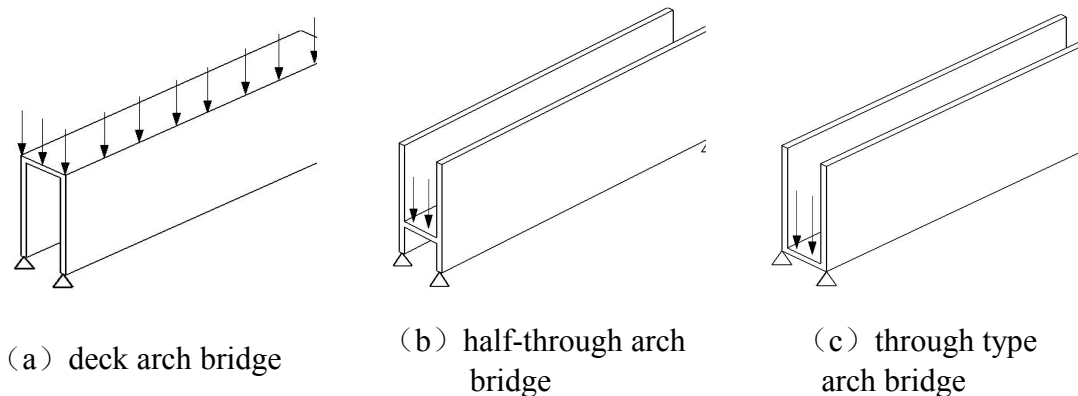
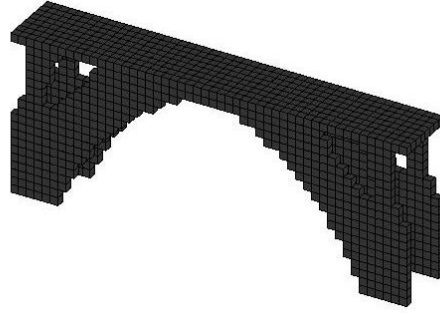
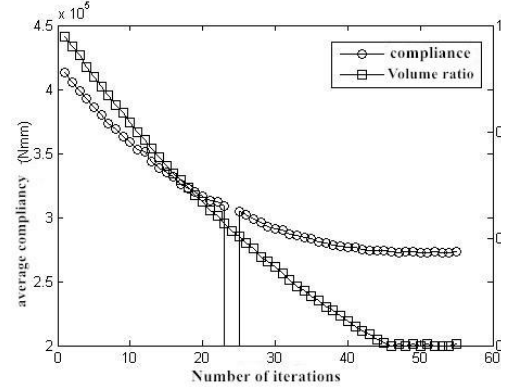


Fig. 4 Arch bridge design area

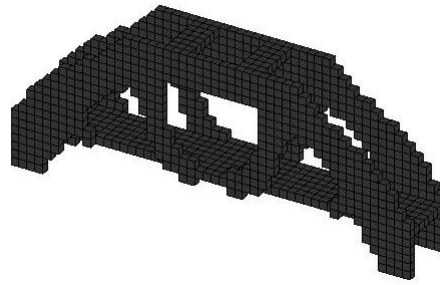
For the optimization of three arched bridges, the solution is as follows:



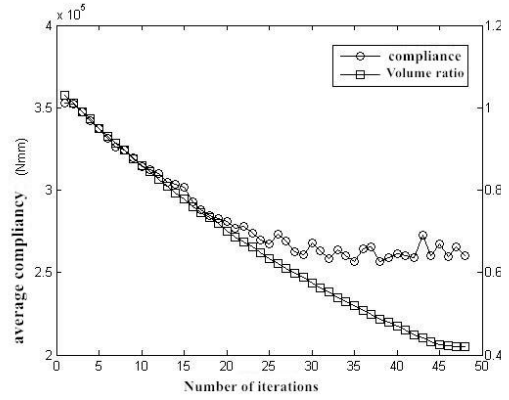
(a) Deck arch bridge topology



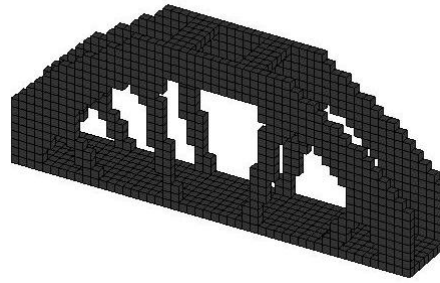
(b) Deck arch bridge iterative process chart



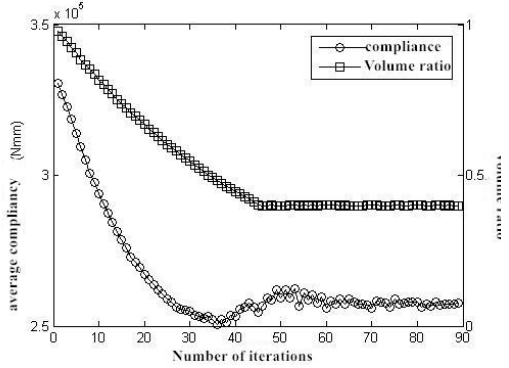
(c) half-through arch bridge topology



(d) half-through arch bridge iterative process chart



(e) through type arch bridge topology



(f) through type arch bridge iterative process chart

Fig. 5 Topology results of various bridges under uniform load conditions

For the above three results, it can be seen from the iterative process graph that the convergence value of flexibility are $2.734 \times 10^5 \text{ N}\cdot\text{mm}$, $2.601 \times 10^5 \text{ N}\cdot\text{mm}$ and $2.575 \times 10^5 \text{ N}\cdot\text{mm}$, respectively, and the overall stiffness of the three structures is from small to large.

From the above listed optimization results, it can be seen that although there are some differences in the structure of various bridges in reality, the main structures are similar, and the

results obtained are calculated by algorithms and are similar to those of bridges built through experience. This verifies that this method has important guiding significance in the design of actual buildings.

5 CONCLUSION

This paper mainly focuses on the structural topology optimization design under the joint action of gravity and non-dependent loads. The design correlation of load and element stiffness is analyzed, a progressive topology optimization method for multi-load structures is proposed.

The paper theoretically illustrates the difference from fixed external loads, which is mainly manifested in the difference in sensitivity, which is highlighted by the difference in the sensitivity expressions of hard killing and soft killing, mainly because the objective function becomes Non-convex function. The symbol of the Hard-kill sensitivity value is unchanged, the compliance is monotonous, the sensitivity of the Soft-kill is variable, the compliance is non-monotonic, which is the most significant difference between the two methods in this case. The numerical example shows that for hard killing, the result is independent of the type of load. For soft killing, the result obtained after absolute processing of the sensitivity value is very close to the result obtained by hard killing. This treatment method is reasonable. At the same time, the numerical examples also prove the correctness of the application of the dependent load in engineering and the necessity of considering the gravity load in the design of large-scale civil engineering structures.

ACKNOWLEDGEMENTS

This research is supported by the National Natural Science Foundation, of China (Grant No.51505096),and National Natural Science Foundation of Heilongjiang Province of China (Grant No.QC2016056,E2016024). The authors are thankful to Harbin Engineering University for English correction of the manuscript and subsidies.

REFERENCES

- [1] Hui Zhang, Shu-Tian Liu, Xiong Zhang. Topology optimization of 3D structures with design-dependent loads. *Acta. Mech. Sin.*, 2010, 26: 767-775P
- [2] M. Bruyneel, P. Duysinx. Note on topology optimization of continuum structures including self-weight. *Struct. Multidiscip. Optim.* 2005, 29: 245-256P
- [3] X.Y. Yang, Y.M. Xie, G.P. Steven. Evolutionary methods for topology optimization of continuous structures with design dependent loads. *Comput. Struct.*, 2005, 83: 956-963P
- [4] R. Ansola, J. Canales, J.A. Tarrago. An efficient sensitivity computation strategy for the evolutionary structural optimization (ESO) of continuum structures subjected to self-weight loads. *Finite Elem. Anal. Des.*, 2006, 42: 1220-1230P
- [5] Stolpe M, Svanbergn K. An alternative interpolation scheme for minimum compliance topology optimization. *Structural and Multidisciplinary Optimization*, 2001, 22(2): 116-124P
- [6] O.M. Querin, V. Young, G.P. Steven, Y.M. Xie. Computational efficiency and validation of bi-directional evolutionary structural optimization. *Comput. Methods Appl. Mech. Eng.*, 2000, 189: 559-573

Characterization of Macroscopic Mechanical Behavior of Dry Woven-fabrics in Consideration of Mesoscopic Frictional-contact between Fiber Bundles

Kenjiro Terada^{*}, Shinnosuke Nishi^{**}, ?lker Temizer^{***}

^{*}Tohoku University, ^{**}Tohoku University, ^{***}Bilkent University

ABSTRACT

With a view to application to two-scale decoupled draping simulations of dry woven fabrics, we characterize the macroscopic in-plane and out-of-plane mechanical behavior by considering the mesoscopic frictional-contact phenomena between fiber bundles. The method of isogeometric analysis (IGA) is applied to the numerical plate/shell testing (NPT) for their in-plane periodic unit structures [1] involving frictional contact at mesoscale. To accommodate large strains and rotations for both macro- and mesostructures, the NPT is also re-formulated within the framework of finite strain theory as an extension of the small strain counterparts [2]. The mesostructure having periodicity only in in-plane directions, which is referred to as an in-plane unit cell or a virtual specimen in this study, is identified with a representative volume element (RVE) to characterize the macroscopic plate/shell behavior that reflects the interfacial frictional-contact and locking phenomena between twisted fiber bundles. NURBS basis functions are utilized to accurately solve meso-scale frictional-contact problems, and either knot-to-surface (KTS) or mortar-based KTS algorithm is employed to evaluate the contact- and friction-related variables [3]. A weaving process is simulated as a preliminary analysis to obtain the initial state of an in-plane unit cell that is subjected to both bending of adjacent fiber bundles contacting each other and in-plane tensile loading. Several numerical examples are presented to validate the formulation and demonstrate the performance and capability of the proposed method of IGA-based NPT for characterizing the macroscopic in-plane and out-of-plane nonlinear structural behavior of dry woven-fabrics especially in response to macroscopic shear deformations. [1] Matsubara, S., Nishi, S., Terada, K. On the treatments of heterogeneities and periodic boundary conditions for isogeometric homogenization analysis, *Internat. J. Numer. Methods Engrg.*, Vol. 109 (2017) pp. 1523-1548. [2] K. Terada, N. Hirayama, K. Yamamoto, M. Muramatsu, S. Matsubara, S. Nishi, Numerical plate testing for linear two-scale analyses of composite plates with in-plane periodicity, *Internat. J. Numer. Methods Engrg.*, Vol. 105, pp. 111–137, 2016. [3] Temizer, ?., Wriggers, P., Hughes, T. J. R., Three-dimensional mortar-based frictional contact treatment in isogeometric analysis with NURBS, *Comput. Methods Appl. Mech. Engrg.*, Vol. 209-212, pp.115-128, 2012.

3-D FINITE ELEMENT IMPLEMENTATION OF HOUSNER FLUID-TANK DYNAMIC INTERACTION MODEL IN ELEVATED WATER TOWERS

GLORIA TERENCE^{*} and STEFANO SORACE[†]

^{*} Department of Civil and Environmental Engineering, University of Florence
Via S. Marta 3, 50139
Florence, Italy
e-mail: terenzi@dicea.unifi.it

[†] Polytechnic Department of Engineering and Architecture, University of Udine
Via delle Scienze 206, 33100
Udine, Italy
e-mail: stefano.sorace@uniud.it

Key words: Fluid-Tank Dynamic Interaction, Water Tanks, Housner model.

Abstract. A 3-D multi-mass finite element model simulating the dynamic fluid-structure interaction in water tanks is presented in this paper. The spatial scheme is derived from the classical Housner analytical model, consisting in a two-mass (impulsive plus convective) representation of the phenomenon, which is being commonly used in most international Seismic Standards and Design Guidelines, and is still a reference also for finite element computation. However, it provides an oversimplified idealization of the interaction effects in time-history seismic analyses, and requires proper adaptations when the tank vessel includes an internal manhole. The 3-D finite element generalization of Housner basic model proposed here allows spreading the hydrodynamic pressure in sloshing conditions on the entire surface of the vessel, as well as correctly transmitting them to the supporting structure, in the case of elevated tanks.

1 INTRODUCTION

Pre-normative elevated water storage tanks are among the most seismically vulnerable structures. This is a consequence of the tall and slender geometry of staging, of the little redundancy and low ductility of the constituting members, as well as of an unfavourable structural configuration with respect to seismic action, i.e. with the highest portion of masses (vessel plus contained liquid) concentrated on top. An effective study of this class of structures via numerical time-history analysis necessarily starts from an accurate simulation of fluid-tank dynamic interaction. The classical Housner analytical model [^{1,2}], consisting in a two-mass (impulsive plus convective) representation of the phenomenon, is being commonly used in most international Seismic Standards and Design Guidelines [³⁻⁵], and is still

suggested as a reference also for finite element computation. However, its basic 2-D formulation allows obtaining only a oversimplified schematization of the structural problem. In view of this, a three-dimensional generalization of the model is proposed in this study, so as to properly spread the hydrodynamic pressure effects on the entire surface of the vessel walls. This is obtained by subdividing the water volume in n equal fractions, and calibrating the n choice to meet a satisfactorily smoothed reproduction of the analytical hydrodynamic pressure distribution with reasonable computational effort.

Detailed information on the practical implementation of the 3-D generalized model in time-history seismic analyses is offered in the next Section. Then, the model is demonstratively applied to the analysis of a typical case study, represented by a Intze-type elevated water tower with reinforced concrete (R/C) structure situated in a medium seismicity area.

2 FLUID-STRUCTURE DYNAMIC INTERACTION MODEL

The two-mass equivalent model formulated by Housner in [1] and updated in [2] splits the total liquid mass m_L into an impulsive mass m_i , which oscillates synchronously with the tank wall, and a convective mass m_c , which is subject to sloshing motion. As shown in Figure 1, in the basic 2-D schematization of the model, m_i is rigidly connected to the tank wall, whereas m_c is linked by two elastic springs with identical stiffness $k_c/2$. Both masses are rigidly joined to the vessel wall in the vertical direction.

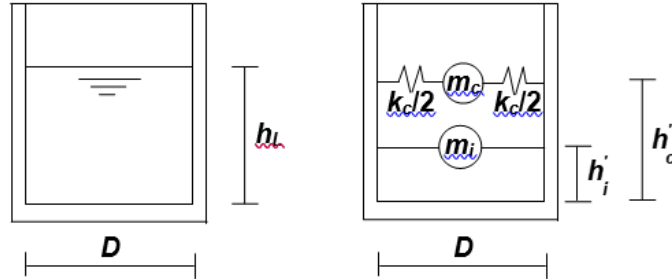


Figure 1. Two-mass model

Named h_i' , h_c' the heights of the two masses from the bottom of the tank wall, m_i , m_c , h_i' , h_c' and k_c are given by the following normative expressions for circular tanks with diameter D and maximum water free level h_L [3-5]:

$$\frac{m_i}{m_L} = \frac{\tanh\left(0.866 \frac{D}{h_L}\right)}{0.866 \frac{D}{h_L}} \quad (1)$$

$$\frac{m_c}{m_L} = 0.23 \frac{\tanh\left(3.68 \frac{h_L}{D}\right)}{\frac{h_L}{D}} \quad (2)$$

$$\frac{h_i'}{h_L} = 0.45 \quad \text{for} \quad \frac{D}{h_L} < 0.75 \quad (3a)$$

$$\frac{h_i'}{h_L} = \frac{0.866 \frac{D}{h_L}}{2 \tanh\left(0.866 \frac{D}{h_L}\right)} - 0.125 \quad \text{for} \quad \frac{D}{h_L} \geq 0.75 \quad (3b)$$

$$\frac{h_c'}{h_L} = 1 - \frac{\cosh\left(3.68 \frac{h_L}{D}\right) - 2.01}{3.68 \frac{h_L}{D} \cdot \sinh\left(3.68 \frac{h_L}{D}\right)} \quad (4)$$

$$k_c = 3.68 \frac{m_c \cdot g}{D} \tanh\left(3.68 \frac{h_L}{D}\right) \quad (5)$$

where g is the acceleration of gravity.

Expressions (1) through (5) are valid for tanks with rigid walls. This hypothesis is well suited for R/C containers, but is not always technically sound for steel ones. For cases where it cannot be accepted, in order to keep the hydrodynamic problem at a comparable level of simplification, a three-mass extension of Housner model including an additional mass linked to the tank wall by an elastic spring simulating wall flexibility can be adopted, as proposed in [2,6]. However, later studies [7] showed relatively little differences in m_i , m_c , h_i , h_c , h_i' , h_c' and k_c values obtained from rigid and flexible tank wall models; this motivates the assumption of the former as a reference for both R/C and steel tanks by the most important international Standards. Moreover, the two-mass model is identically adopted by all Standards for ground-supported and elevated tanks, where the latter additionally requires proper schematization of the supporting structure. As illustrated in Figure 2, this is basically idealized as a vertical cantilever with horizontal translation stiffness K_s and lumped structural mass m_s , including the mass of the container and a one-third portion of the mass of the staging [2,5], both in the normative seismic design of new tanks and the assessment of existing ones.

The vibration periods of the impulsive (i.e. m_i+m_s related) and convective modes of the resulting 2-degree-of-freedom (2-DOF) equivalent system, T_{i+s} and T_c , are

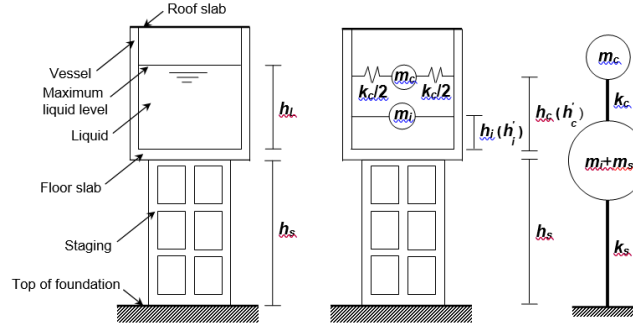


Figure 2. Two-mass idealization for elevated tanks

$$T_{i+s} = 2\pi \sqrt{\frac{m_i + m_s}{K_s}} \quad (6)$$

$$T_c = \frac{2\pi}{\sqrt{3.68 \tanh\left(3.68 \frac{h_L}{D}\right)}} \sqrt{\frac{D}{g}} \quad (7)$$

The 2-DOF model allows applying elementary dynamics relations to directly compute the maximum spectral response in terms of global parameters (base shear and moment, top drift, etc). These data are useful for a first-level quick evaluation of seismic performance of the structural system, as well as for checking the results of properly detailed finite element analyses, like the ones discussed in the next Sections. However, the 2-DOF model cannot be applied in its original schematization in the presence of an internal manhole.

In order to simulate the volumetric fluid-structure interaction, in the proposed model the water volume is subdivided in n equal fractions, each one being identified in plan with a circumferential angle Θ_n equal to $180^\circ/n$. Then, the alignments determined for half circumference are diametrically replicated for the other half, as shown in Figure 3, referred to tanks with a manhole.

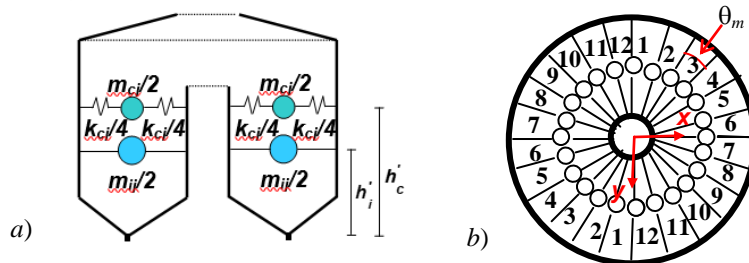


Figure 3. Reference parameters of the 3-D model for tanks with an internal manhole: section (a) and plan (b)

The influence of n on the finite element model response was evaluated by varying it from 6 (i.e. $\theta_n=30^\circ$) to 18 ($\theta_n=10^\circ$). The segmental reproduction of the analytical hydrodynamic pressure distribution on the vessel walls provided by the 3-D implementation of the two-mass model, progressively smoothing for increasing n values, was acceptable in all cases and totally satisfactory starting from $n=12$.

3 CASE STUDY WATER TOWER

The vertical cross section and the base plan of the water tower assumed as demonstrative case study for the application of the model are shown in the drawing on the left in Figure 4. The R/C vessel is Intze-type, constituted by two thin coaxial R/C cylindrical walls. The tank capacity and geometrical dimensions of the structure are as follows: maximum available water volume of 100 m^3 ; internal diameters of vessel and coaxial manhole equal to 6 m and 1 m, respectively; and external diameter of the staging base equal to 4.5 m.

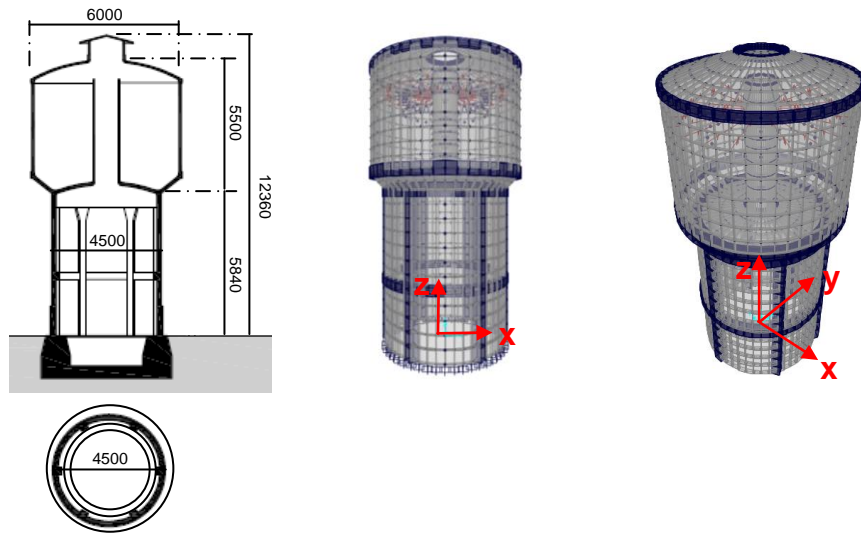


Figure 4. Cross section, base plan (dimensions in millimeters) and finite element model views of the water tower

The R/C shaft staging structure is constituted by a 150 mm-thick cylindrical wall ribbed by six columns with section of $(310 \times 310) \text{ mm} \times \text{mm}$, emerging on the internal side of the wall. The rib-columns are connected by a $(300 \times 300) \text{ mm} \times \text{mm}$ sized ring beam situated at their mid-height, and a $(150 \times 500) \text{ mm} \times \text{mm}$ sized top ring beam constituting the support of the vessel. The shaft wall has a 1200 mm-high thickening base of 50 mm, emerging on the external side. The external wall, manhole wall, bottom slab and floor slab of the vessel are 80, 80, 100 and 50 mm thick. The vessel is completed by an external inverted truncated cone

floor slabs and an internal cylindrical floor slab, bottom and top ring beams, a cylindrical roof slab, and a cylindrical lantern on top, with conical roof, for vessel aeration and natural illumination. The manhole is covered by a steel plug to prevent any fall of water in case of sloshing motion. The foundation consists of a 400 mm-thick base slab and a 1200 mm-high trapezoidal-shaped ring beam, with 1200 mm-wide lower base and 800 mm-wide upper base.

4 FINITE ELEMENT MODEL

The finite element model of the structure was generated by SAP2000NL calculus program [8]. Views of the model are displayed in Figure 4 too, along with the global reference coordinate systems, constituted by the Cartesian axes x , y and z . The mesh of the vessel and the shaft staging are made of shell-type elements. The upper small lantern was not expressly modelled, but its weight and the corresponding mass for the dynamic analyses were assigned to the underlying joints of the vessel.

The results of the modal and time-history analyses are presented in the following for $n=12$, to which $\theta_n=15^\circ$ corresponds. The horizontal and vertical cross sections of the finite element model, displayed in Figure 5, are referred to this choice.

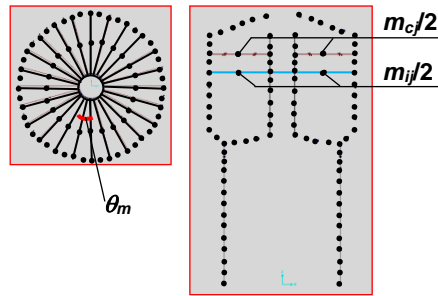


Figure 5. Horizontal and vertical sections of the finite element model of the tank

Concerning the 3-D implementation of the two-mass model, it should also be noted that, like in the 2-D scheme, the convective masses have only one relative DOF with respect to the tank walls to which they are connected, represented by the axial displacement of the associated springs (radial DOF in the 3-D layout). At the same time, the tangent and vertical relative displacements are null, since the convective masses are rigidly linked to the walls in these two directions. The former assumption corresponds to the fact that the horizontal hydrodynamic action of water is always exerted in radial direction. At the same time, the vertical rigid link compels the convective masses to respond jointly with the tank wall structure along this direction, similarly to the liquid impulsive masses, both in terms of modal analysis, for the “breathing” mode of the tank, and time-history analysis, for the response to the vertical ground motion component.

The m_i , m_c , h_i' , h_c' and k_c values calculated by means of Eqs. (1) through (5) are as follows: $m_i=71.800 \text{ kN}\cdot\text{s}^2/\text{m}$, $m_c=28.200 \text{ kN}\cdot\text{s}^2/\text{m}$, $h_i' = 2.41 \text{ m}$, $h_c' = 3.15 \text{ m}$ and $k_c=190 \text{ kN/m}$. For $n=12$, based on these values of the total water volume parameters, $m_{ij}=m_i/12=5.984 \text{ kN}\cdot\text{s}^2/\text{m}$, $m_{cj}=m_c/12=2.35 \text{ kN}\cdot\text{s}^2/\text{m}$, $k_{cj}=k_c/12=15.8 \text{ kN/m}$, for each water volume fraction, and $m_{ij}/2=2.992 \text{ kN}\cdot\text{s}^2/\text{m}$, $m_{cj}/2=1.175 \text{ kN}\cdot\text{s}^2/\text{m}$, $k_{cj}/4=3.95 \text{ kN/m}$, for the left and right portions of each volume fraction, are obtained. These data were introduced as input in the modal and time-history analyses of the structure.

A final observation about the 3-D finite element implementation of the two-mass model concerns the damping coefficients to be assigned to the two water masses for dynamic computations, which are fixed by all international Standards at 0.5% of the critical damping, for convective mass-governed modes, and at 5% for impulsive mass-governed modes. Consistently with these indications, a 0.5% value was associated in input to the translation DOF of each convective mass. At the same time, 5% was adopted for all the elements constituting the finite element meshes of the tank, impulsive water masses included, thus automatically involving all impulsive-related modal contributions.

Calculation of parameters m_c , m_i , k_c , as well as of h_i' and h_c' , was carried out by referring to an equivalent circular tank with a reduced diameter, D_r , instead of D , to obtain the same maximum water volume of 100 m^3 . As h_L is equal to 4 m , $D_r=5.62 \text{ m}$ results.

Figure 6 shows a graphical comparison of the maximum analytical (continuous line) and numerical (dotted line) hydrodynamic pressure distributions on the vessel wall, highlighting a satisfactory level of correlation for the $n=12$ value selected in this analysis. This confirms the results of previous numerical investigations [9] carried out with this n choice on water tanks with different structures.

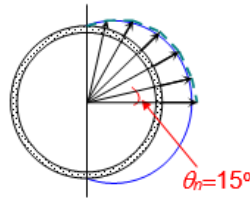


Figure 6. Maximum analytical (continuous line) and numerical (dotted line) hydrodynamic pressure distributions on the vessel wall

5 TIME-HISTORY PERFORMANCE ASSESSMENT ANALYSIS

The performance evaluation enquiry was carried out for the four reference seismic levels established by the Italian Standards [10], that is, Frequent Design Earthquake (FDE, with 81% probability of being exceeded over the reference time period V_R); Serviceability Design

Earthquake (SDE, with 50%/V_R probability); Basic Design Earthquake (BDE, with 10%/V_R probability); and Maximum Considered Earthquake (MCE, with 5%/V_R probability).

The V_R period is fixed at 75 years, which is obtained by multiplying the nominal structural life V_N of 50 years by a coefficient of use c_u equal to 1.5, imposed to structures whose seismic resistance is of importance in view of the consequences associated with their possible collapse. By referring to topographic category T1 (flat surface), and C-type soil (deep deposits of dense or medium-dense sand, gravel or stiff clay from several ten to several hundred meters thick), the resulting peak ground accelerations for the four seismic levels referred to the city of Florence, where the case study water tower is situated, are as follows: 0.082 g (FDE), 0.098 g (SDE), 0.223 g (BDE), and 0.27 g (MCE), for the horizontal motion components; and 0.017 g (FDE), 0.022 g (SDE), 0.079 g (BDE), and 0.111 g (MCE), for the vertical component.

The time-history analyses were developed by assuming artificial ground motions as inputs, generated by SIMQKE-II software [11] from the pseudo-acceleration elastic response spectra prescribed by the Italian Standards for Florence, graphed in Figure 7. The accelerograms were generated in families of seven both for the horizontal components (two families) and the vertical one (one family). As required by the Italian Standards, as well as by several other international seismic Codes and Regulations, in each time-history analysis the input motions were applied in groups of three simultaneous components, i.e. two horizontal components, with the first one selected from the first generated family of seven motions, and the second one selected from the second family, plus the vertical component.

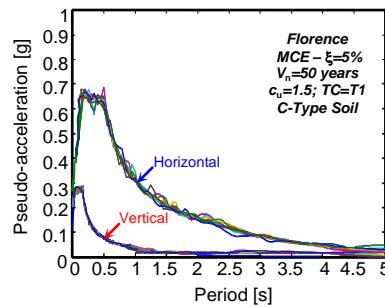


Figure 7. Normative pseudo-acceleration elastic response spectra for Florence — horizontal and vertical components

The results of the analyses carried out with the input motions scaled at the FDE and SDE levels show a completely elastic response, whereas the analyses at the BDE level highlight that an about 1.5 m-wide portion of the base section of the shaft staging is subjected to vertical tensile normal stresses greater than the strength of the vertical steel reinforcing bars situated in the same area (this portion is alternately generated on the opposite side, as a consequence of the alternate sign of seismic action). These data assess severely damaged

response conditions for the structure, but with residual margins towards structural collapse, which allows meeting the basic requirement of the Collapse Prevention (CP) performance level.

The analyses at the MCE level of seismic action represent the most significant step of the assessment study, owing to the importance class of the structure. Relevant results are synthesized in Figure 8, where the contour maps of the vertical normal stresses obtained from the most demanding among the seven groups of accelerograms are displayed on the finite element model of the structure.

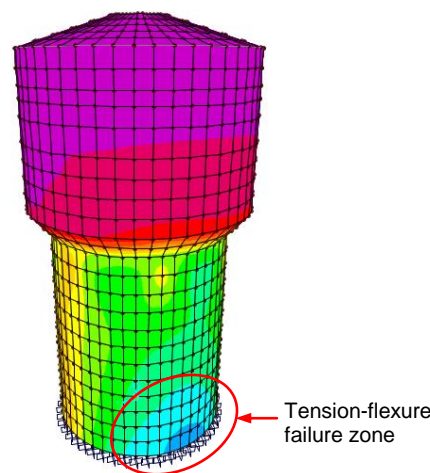


Figure 8. Contour maps of the vertical normal stresses obtained from the most demanding MCE-scaled group of input ground motions

This image shows that the portion of the base section subjected to vertical tensile normal stresses greater than the strength of the vertical reinforcing bars reaches about 4 meters. This wide tension-flexure failure zone is capable of causing overturning collapse mode of the shaft staging with respect to the foundation, similarly to the ones observed for the same type of elevated tanks in several earthquakes [^{12,13}].

The foundation is not involved in the overturning mechanism thanks to the massive dimensions of the constituting ring beam and base slab. Indeed, the stress states transferred to the substrate are always compressive, with maximum values equal to 0.3 MPa, which are absorbed by the substrate with wide safety margins. In addition, also the response of the R/C vessel structure is within its safe domain. By summing up, the results of the assessment analysis in current conditions highlight the need for a substantial retrofit intervention of the shaft staging structure.

6 CONCLUSIONS

The 3-D generalized finite element model proposed in this study for the computational simulation of fluid-tank dynamic interaction problems showed a satisfactory correlation with the hydrodynamic pressure distributions calculated via numerical analysis, starting from relatively low values of the n number of water volume fractions.

This enhanced implementation of Housner two mass plan model allows also easily taking into account the presence of manholes in the tank vessels, as well as correctly transmitting the hydrodynamic pressure-related stress states to the staging structure, for elevated tanks.

The water tower examined as demonstrative case study highlighted the feasibility of the 3-D model in practical applications, offering details for its use in elevated tanks with different geometrical characteristics.

ACKNOWLEDGEMENTS

The study reported in this paper was sponsored by the Italian Department of Civil Protection within the ReLUIS-DPC Project 2014/2016, research Line 6: Isolation and Dissipation. The authors gratefully acknowledge this financial support.

REFERENCES

- [1] Housner, G.W. Dynamic behavior of water tanks. *Bulletin of the Seismological Society of America* (1963) 53: 381–387.
- [2] Haroun, M.A. and Housner, G.W. Seismic design of liquid storage tanks. *ASCE Journal of Technical Councils*, (1981) 107: 191–207.
- [3] ACI 350.3-06. Seismic design of liquid-containing concrete structures. Farmington Hills, MI (USA), ACI, American Concrete Institute, (2006).
- [4] 371R-08. Guide for the analysis, design, and construction of elevated concrete and composite steel-concrete water storage tanks. Farmington Hills, MI (USA): ACI, American Concrete Institute (2008).
- [5] IITK-GSDMA. Guidelines for seismic design of liquid storage tanks. Kanpur, India: National Information Center of Earthquake Engineering (2007).
- [6] Veletsos, A.S. Seismic response and design of liquid storage tanks. In: *Guidelines for the seismic design of oil and gas pipeline systems*. New York, NY (USA): ASCE Technical Council on Lifeline Earthquake Engineering, (1984): 255–370 and 443–461.
- [7] Jaiswal, O.R., Rai, D.C. and Jain, S.K. Review of code provisions on seismic analysis of liquid storage tanks. Document IITK-GSDMA-EQ04-V1.0. IITK-GSDMA. Kanpur, India: Indian Institute of Technology Kanpur (2004).

- [8] SAP2000NL. Theoretical and users' manual. Release 16.05. Berkeley (USA): Computers & Structures Inc. (2014).
- [9] Sorace, S., Terenzi, G. and Mori, C. Passive energy dissipation-based retrofit strategies for R/C frame water storage tanks. *Engineering Structures* (2016) 106:385-398.
- [10] Technical Standards on Constructions. Rome, Italy: Italian Council of Public Works (2008) [in Italian].
- [11] Vanmarcke, E.H., Fenton, G.A. and Heredia-Zavoni, E. SIMQKE-II – Conditioned earthquake ground motion simulator: User's manual, version 2.1. Princeton University. Princeton (NJ) (1999).
- [12] Rai, D.C. Elevated tanks. In Jain, Lettis, Bardet and Murty (Eds.). 2001 Bhuj, India earthquake reconnaissance report. *Earthquake Spectra* (2002) Supplement A to 18: 279–295.
- [13] Moslemi, M., Kianoush, M.R. and Pogorzelski, W. Seismic response of liquid-filled elevated tanks. *Engineering Structures* (2011) 33: 2074–2084.

A Hybridizable Discontinuous Galerkin Method for Nonlinear Elastostatics and Elastodynamics

Sebastien Terrana^{*}, Ngoc-Cuong Nguyen^{**}, Jaime Peraire^{***}

^{*}Massachusetts Institute of Technology, ^{**}Massachusetts Institute of Technology, ^{***}Massachusetts Institute of Technology

ABSTRACT

We present a hybridizable discontinuous Galerkin (HDG) method for solving large deformations problems of elastic bodies. The HDG method is developed for three-field formulations of both static and dynamic nonlinear elasticity problems. Our approach is endowed with several attractive features that make it worthwhile for computational solid dynamics. First, with regards to robustness, the method is not prone to a variety of locking phenomena such as volumetric locking for nearly incompressible materials, or shear and membrane locking for thin structures. Second, with regards to accuracy, the method yields optimal convergence for the approximate strain and stress tensors, whereas other finite element methods often give only suboptimal convergence. And third, with regard to efficiency, the method reduces the globally coupled unknowns to the degrees of freedom of the numerical trace on the interior faces only, leading to substantial savings in computational time and memory storage. This feature is particularly beneficial for thin structures because the number of interior faces can be even less than the number of boundary faces. In addition, we discuss some details of the HDG implementation, particularly the choice of the stabilization parameter, the parallel iterative solver and the preconditioner. Numerical results are presented to verify the convergence of the HDG method through some simple analytical problems and some popular benchmark problems in the literature. Results for large realistic simulations will also be presented and discussed.

Toward Efficient Real-time Reconstruction of Elastic Deformations and Stresses in Plate and Shell Structures

Alexander Tessler*

*Distinguished Research Associate, Structural Mechanics and Concepts Branch, NASA Langley Research Center,
Hampton, VA 23681-2199

ABSTRACT

Since the inception of the inverse finite element method (iFEM) fifteen years ago [1], the field of structural health monitoring (SHM) has acquired a powerful computational tool for real-time reconstruction of full-field deformations and stress states in complex structures from in-situ strain measurements. The iFEM methodology is based on a weighted least-squares variational principle that provides the mathematical framework for formulating a wide range of finite elements similar to those used within the direct (forward) finite element method (FEM). The iFEM methodology can be readily implemented in any standard research or commercial finite element code. To date, iFEM-based models have been developed for shear-deformable beams, three-dimensional frames, flat plates and built-up shell structures. In recent years, iFEM has been explored further, validated experimentally, and applied to a variety of important industrial applications including aerospace, energy exploration, and marine applications. In this paper, theoretical fundamentals and new innovations in the iFEM technology will be discussed. The main focus will center around effective strategies that enhance iFEM from the standpoint of computational efficiency, accuracy, and robustness. To this end, several element-level regularization methods will be discussed that enable high-fidelity discretizations to be used in conjunction with relatively coarse distribution schemes of in-situ strain sensors, while ensuring the method's robustness and stability. Numerical examples will be presented that illustrate key features and advantages of this powerful enabling technology for structural health monitoring. [1] Tessler, A. and Spangler, J. L., A Variational Principle for Reconstruction of Elastic Deformations in Shear Deformable Plates and Shells. NASA/TM-2003-212445 (2003).

The Schwarz Alternating Method for Dynamic Multi-scale Coupling in Solid Mechanics

Irina Tezaur*, Alejandro Mota**

*Sandia National Laboratories, **Sandia National Laboratories

ABSTRACT

Concurrent multiscale methods for solid mechanics are essential for the understanding and prediction of behavior of engineering systems when a small-scale event will eventually determine the performance of the entire system. In [1], the domain-decomposition-based Schwarz alternating method was proposed as a means for concurrent multiscale coupling in finite deformation quasistatic solid mechanics. It was proven that the method converges to the single-domain solution provided each of the subdomain problems is well-posed, and that the convergence rate is geometric. The method was implemented in Sandia's Albany/LCM research code, and demonstrated to have a number of appealing features and advantages over completing multiscale coupling methods, most notably its concurrent nature (i.e., its ability to exchange information back and forth between small and large scales), its ability to couple non-conformal meshes with different element topologies, and its non-intrusive implementation into existing codes. Accuracy, convergence and scalability of the proposed method was demonstrated on several numerical examples. This talk will focus on some recent extensions of the Schwarz alternating formulation to dynamic solid mechanics problems. As with the quasi-static version of the method, the basic idea is to use the solution of a partial differential equation (PDE) on two or more regularly shaped domains comprising a more complex domain to iteratively build a solution for the more complex domain. Our dynamic Schwarz formulation is not based on a space-time discretization like other dynamic Schwarz-like methods; instead, it uses a governing time-stepping algorithm that controls time-integrators within each subdomain. As a result, the method is straight-forward to implement into existing codes (e.g, Albany/LCM), and allows the analyst to use different time-integrators with different time steps within each domain. We demonstrate on several test cases that coupling using the proposed method introduces no dynamic artifacts that are pervasive in other coupling methods (e.g., spurious wave reflections near domain boundaries), regardless of whether the coupling is done with different mesh resolutions, different element types like hexahedral or tetrahedral elements, or even different time integration schemes, like implicit and explicit. Furthermore, on dynamic problems where energy is conserved, we show that the method is able to preserve the property of energy conservation. REFERENCES [1] A. Mota, I. Tezaur, C. Alleman. "The alternating Schwarz method for concurrent multiscale coupling", Comput. Meth. Appl. Mech. Engng. 319 (2017) 19-51.

Stochastic Model Hyperreduction for Modeling and Quantifying Model-Form Uncertainties in Vibration Analysis

Radek Tezaur*, Charbel Farhat**, Todd Chapman***, Phil Avery****, Christian Soize*****

*Stanford University, **Stanford University, ***Stanford University, ****Stanford University, US Army Research Laboratory, *****Universite Paris-Est

ABSTRACT

A feasible, nonparametric, probabilistic approach for quantifying model-form uncertainties associated with a High-Dimensional computational Model (HDM) and/or a corresponding Hyperreduced Projection-based Reduced-Order Model (HPROM) [1,2] designed for the solution of generalized eigenvalue problems arising in vibration analysis, is presented. It is based on the construction of a Stochastic HPROM (SHPROM) associated with the HDM and its HPROM using three innovative ideas [3]: the substitution of the deterministic Reduced-Order Basis (ROB) with a Stochastic counterpart (SROB) that features a reduced number of hyperparameters; the construction of this SROB on a subset of a compact Stiefel manifold in order to guarantee the linear independence of its column vectors and the satisfaction of any applicable constraints; and the formulation and solution of a reduced-order inverse statistical problem to determine the hyperparameters so that the mean value and statistical fluctuations of the eigenvalues predicted in real time using the SHPROM match target values obtained from available data. If the data are experimental data, the proposed approach models and quantifies the model-form uncertainties associated with the HDM, while accounting for the modeling errors introduced by model reduction. If on the other hand the data are high-dimensional numerical data, the proposed approach models and quantifies the model-form uncertainties associated with the HPROM. Consequently, the proposed nonparametric, probabilistic approach for modeling and quantifying model-form uncertainties can also be interpreted as an effective means for extracting fundamental information or knowledge from data that is not captured by a deterministic computational model, and incorporating it in this model. Its potential for quantifying model-form uncertainties in eigenvalue computations is demonstrated for what-if? vibration analysis scenarios associated with shape changes for an engine nozzle. 1. C. Farhat, P. Avery, T. Chapman and J. Cortial, Dimensional Reduction of Nonlinear Finite Element Dynamic Models with Finite Rotations and Energy-Conserving Mesh Sampling and Weighting for Computational Efficiency, International Journal for Numerical Methods in Engineering, Vol. 98, pp. 625-662 (2014) 2. C. Farhat, T. Chapman and P. Avery, Structure-Preserving, Stability, and Accuracy Properties of the Energy-Conserving Sampling and Weighting (ECSW) Method for the Hyper Reduction of Nonlinear Finite Element Dynamic Models, International Journal for Numerical Methods in Engineering, Vol. 102, pp. 1077-1110 (2015) 3. C. Soize and C. Farhat, A Nonparametric Probabilistic Approach for Quantifying Uncertainties in Low- and High-Dimensional Nonlinear Models, International Journal for Numerical Methods in Engineering, Vol. 109, pp. 837-888 (2017)

A Novel Visco-hyper Elastic Constitutive Model for Elastomers to Capture Strain Rate Dependency

Rohan Thakkar*, Aleksander Czekanski**

*York University, **York University

ABSTRACT

Rubber-like materials undergo large deformations at relatively low stresses and recover their initial shape upon removal of the load. This exceptional ability makes them suitable and without doubt irreplaceable materials in vital engineering applications. This uncommon behavior of rubbers is caused by underlying coiled long chain polymer molecules. These chains straighten when the material is stretched and recoil upon removal of the load. As a result of molecular chains' rearrangement during loading process, they exhibit large strain elasticity and viscoelastic properties [1]. Generally, the framework of viscoelasticity can be classified into two distinct classes: a) Linear viscoelasticity & b) non-linear viscoelasticity. To summaries, linear viscoelasticity models are constituted by considering parallel and/or series arrangements of elastic springs and linear viscous dash-pots. These rheological analogies are superimposed by Boltzman's principle and the relaxation function is approximated with a prony series formulation. Whereas, non-linear viscoelastic constitutive relations are formulated by employing generalized integral based Kaye-BKZ theory. In this approach, numerous approximations of matrix stress functional defines the strain history on stresses. Rubber like materials involve highly non-linear deformation phenomena at finite strains and therefore, linear models are not adequate [2]. As a result, a quasi-linear viscoelastic frame work needs to be represented by 4-6 term prony series approximations. In contrast, the number of material constants can be reduced by articulating BKZ theory based nonlinear viscoelasticity [3]. Moreover, numerical implementation of such formulation is a straight forward and comparatively less time consuming process. For that reason, a novel power-exponential strain history functional has been proposed in nonlinear finite strain visco-hyperelastic framework to capture rate dependency in various types of elastomers. Derived constitutive relations are verified with respect to literature based high strain rate experimental data. Excellent agreement between numerical and experimental data have been achieved. The encouraging initial results leads to further expanding the scope of this work by implementing the newly developed model into commercial FE package.

Study of Turbulent Flows in an Air-filled Differentially-heated Cavity of Aspect Ratio 4: A Comparison between DNS, LES and Experimental Results

Nicolas Thiers^{*}, Olivier Skurtys^{**}, Romain Gers^{***}

^{*}Universidad Tecnica Federico Santa Maria, ^{**}Universidad Tecnica Federico Santa Maria, ^{***}Universidad Tecnica Federico Santa Maria

ABSTRACT

Natural convection in parallelepipedic enclosures of aspect ratio 4 (height / width) has been the subject of numerous studies over the past decades. Most of the numerical studies use simplified geometry considering a two dimensional case or an infinite depth assuming periodic conditions. In both cases, numerical results are significantly different of experimental data. In order to study the turbulent flows, three-dimensional Direct Numerical Simulation (DNS) and Large-Eddy Simulation (LES) were performed at $Ra_H = 10^{10}$, $Ra_H = 1.2 \times 10^{11}$ and $Ra_H = 10^{12}$. The aspect ratio width / depth was fixed to 1 and to be closer to experimental conditions, the non-slip boundary condition is imposed on the velocity at the six closing walls. To characterize the turbulent flows, stratification profile, the Nusselt number, Reynolds stress tensor, turbulent heat flux and PDF of the invariants for gradient velocity tensor were analyzed. Numerical results were compared with experimental data. The unsteady Boussinesq Navier-Stokes equations are solved using the high-order spectral element code Nek5000 for DNS and the Finite Volume Method (FVM) for LES where a OpenFoam solver was specially written. Simulations are performed at CCT-Val and NLHPC high performance clusters in Xeon X5675, 3.07GHz, 32GB RAM over 120 cores. The authors gratefully acknowledge financial support provided by Fondecyt research project n°1171281.

Revisiting Screw-propelled Vehicles Utilizing Experimental and Computational Methods

Andrew Thoesen^{*}, Sierra Ramirez^{**}, Hamidreza Marvi^{***}

^{*}Arizona State University, ^{**}Arizona State University, ^{***}Arizona State University

ABSTRACT

Screw-Propelled Vehicles (SPV's) have been widely used for terrestrial applications such as transportation over mud, snow, and amphibious environments. Similar vehicles have also been applied to industrial processes such as dewatering. Typical designs rely on a large pontoon shaft and relatively small blades to prevent unwanted sinkage or blade damage. Studies have looked at the mobility of SPV's on the surface of granular media but there are not any computational and experimental studies on characterizing propulsive buried screws. We will examine this problem using Discrete Element Method (DEM), Resistive Force Theory (RFT) and experimental approaches. First, we must evaluate performance of the propelling screws in a well characterized media. For this study, we've chosen Earth gravity and spherical glass beads of relative uniform size to minimize additional variables. In doing so we can begin to build a framework for more extensive design evaluation of screw propelled vehicles in more exotic materials and different gravities. Understanding the role of screw design and its angular velocity on thrust force is also key to the advancement and control of SPV's. In particular, our study examines a submerged, double-helix Archimedes screw generating propulsive force against a bed of soda-lime glass beads. Thus, this research forms the basis for design of a future miniaturized exploration vehicle for space applications. In our study, we used three different screw designs of 10 cm length and 5 cm diameter. They had pitches of 4, 6, and 8cm. They were submerged in 2mm glass beads of 90% roundness with 0.1mm standard deviation. These screws were run between 30 RPM and 120 RPM. We used EDEM, a DEM software for computational studies of the screw interactions with granular media. We also analyzed this problem using RFT. There is small discrepancy between our DEM, RFT, and experimental results and we will discuss possible sources of error and the potential for using DEM and RFT as a design tool for SPV's.

Modelling of Brine Conversion in Antarctic Sea Ice within the Theory of Porous Media (TPM)

Andrea Thom^{*}, Tim Ricken^{**}

^{*}Stuttgart University, Germany, ^{**}Stuttgart University, Germany

ABSTRACT

According to NASA, Antarctic sea ice has reached its lowest extent ever recorded by satellites at the end of summer 2017 in the southern hemisphere after decades of moderate sea ice expansion. Besides a strong influence on the global climate linking the exchange of energy and gases between the atmosphere and the ocean, changes in sea ice have also a biological respond concerning the ecosystem structure and function. These responds are strongly related to its physical and mechanical properties. Salt accumulations (brines) in growing sea ice are either rejected to the ocean, leading to a higher salinity of the upper ocean, or are trapped between ice crystals in pockets or channels, leading to a high salinity of the ice. Other inclusions like algae can serve as a food source for e.g. Antarctic krill in times of low resources in the water. A small-scale modelling of the porosity of the sea ice and its inclusions and the solid/brine multiphase microstructure, respectively, including thermodynamics of air-sea interactions as well as sea ice-biological linkages is a necessary tool to understand the heterogeneous sea ice nature better. Based on the Theory of Porous Media (TPM), cf. [1,2], the development of a thermodynamically consistent multiphase model which enables the continuum mechanical description of transport and phase transition phenomena in sea ice at a homogenized pore scale is presented. The model consists of a solid (ice), fluid and air phase including solvents and dissolved components in brine. The phase transition from water to ice is solved in each time step on the Gauss point scale as a coupled ODE system describing all dependencies of the thermodynamically un-equilibrium during phase transition. Its solution will be released to the upper scale via homogenization leading to an already established two-scale PDE-ODE approach for biomechanics applications [3]. [1] Ricken, Tim, and Joachim Bluhm. "Modeling of liquid and gas saturated porous solids under freezing and thawing cycles." *Aktuelle Forschung in der Bodenmechanik*, 2014. 23-42. [2] Ricken, Tim, et al. "Concentration driven phase transitions in multiphase porous media with application to methane oxidation in landfill cover layers." *ZAMM* 94.7?8 (2014): 609-622. [3] Ricken, Tim., et al. "Modeling function-perfusion behavior in liver lobules including tissue, blood, glucose, lactate and glycogen by use of a coupled two-scale PDE-ODE approach." *Biomechanics and modeling in mechanobiology* 14.3 (2015): 515-536.

Topological Optimization for Multi-Component Systems with Frequency and Stiffness Criteria

Simon Thomas^{*}, Qing Li^{**}, Grant Steven^{***}

^{*}University of Sydney, ^{**}University of Sydney, ^{***}University of Sydney

ABSTRACT

Numerous engineering structures consist of multiple components for manufacturing, transport and economic reasons, which are assembled by various connection elements. This study aimed to develop a computational design framework for seeking optimal topologies of the patterns/configurations of connection elements as well as the structural components based upon the frequency and stiffness criteria. Building upon our earlier work, multi-objective optimization is first developed to optimize the connection elements for stiffness and frequency criteria simultaneously. Then the proposed multi-objective design is extended to topology optimization by incorporating both connection elements and component configurations. In this study, an evolutionary structural optimization (ESO) procedure is adopted, where a finite element based discrete sensitivity is derived to numerically evaluate the effect of presence and absence of a connection element and/or component element on the design criteria. A series of illustrative examples are presented to demonstrate the effectiveness of the proposed method, allowing maximizing, minimizing or targeting the individual natural frequencies or separation between them. It is noted that the methodology can be conceptually extended to many other multi-component structural systems connected by screws, rivets, welds and the like. Finally, a real-world example is considered through design of an electricity transmission tower, where natural frequency is adjusted to help mitigate potential damage from aeolian vibration. The application of this method to other component bonding types, such as adhesive sprays or 3D printing, is also explored by achieving up to 36% improvement in its multi-criteria objective function when compared with its classically screw-bonded counterpart.

Modal Stochastic Models of an Industrial Stator Vane : Comparison with Experimental Datas

Fabrice Thouverez*, Jonathan Philippe**

*Ecole Centrale de Lyon, **SAFRAN

ABSTRACT

In the context of aeronautic engines, some components have a spatial periodicity almost perfect like bladed disks or stator vanes. This periodicity comes from the fact that one sector (including blade and a part of the disk) are perfectly repeated. This property leads to a specific strategy of modelling called “cyclic symmetry” allowing a quick and efficient computation of the dynamic of such components. In fact, we always have a small loss of cyclic properties which may lead to very large variation in the estimation of the response of the system. Indeed, the energy which, for a tuned case, periodically spread over the structure could become concentrated only on few blades in the mistuned case. This phenomenon is associated, in most cases, to a mistuning of the sectors between them. If we have to manage this mistuning, we will need to take into account the complete system which can lead to very large computation time for industrial applications. To avoid this, we propose to carry out two approximations the first one will be associated to the stochastic properties of the system and the second will be a sub-structuring technic to reduce the initial size of the system. We choose to develop a stochastic modal analysis allowing to express the stochastic flexibility in a very easy way. This expression will be used to calculate the dynamic response of the structure in terms of statistic momentum or maximum of amplitude. To estimate this stochastic modal basis, we will develop several kind of approximation of the stochastic solution. The first one will be based on a polynomial chaos expansion and the second will use a Multivariate Adaptive Regression Splines (MARS) method. A comparison between these two procedures is presented in terms of efficiency and precision. These calculations are possible because the proposed method includes a sub-structuring technic based on a double modal synthesis combining a Craig-Bampton approach and the estimation of a reduced based of the interface. This strategy has been validated in view of the necessary precisions of our computations. In order to validate the complete numerical strategy an industrial stator vane has been modeled and also experimentally tested. The experimental data collected will allow to situate the real structure in relation to the stochastic simulations.

Advanced Immersed Boundary Methods and Their Applications in Biological Flows

Fang-Bao Tian^{*}, Joseph Lai^{**}, Lincheng Xu^{***}, John Young^{****}, Li Wang^{*****}

^{*}School of Engineering and Information Technology University of New South Wales, Canberra, ACT 2600, Australian, ^{**}School of Engineering and Information Technology University of New South Wales, Canberra, ACT 2600, Australian, ^{***}School of Engineering and Information Technology University of New South Wales, Canberra, ACT 2600, Australian, ^{****}School of Engineering and Information Technology University of New South Wales, Canberra, ACT 2600, Australian, ^{*****}School of Engineering and Information Technology University of New South Wales, Canberra, ACT 2600, Australian

ABSTRACT

This talk first introduces our recent progresses on developing immersed boundary methods, including sharp-interface immersed boundary-finite difference method for fluid-structure interactions involving large deformations, adaptive immersed boundary-lattice Boltzmann method for fluid-structure interactions at moderate and high Reynolds numbers, and feedback immersed boundary method based on high-order finite difference method for fluid-structure interactions involving acoustics and shock waves. Several benchmark cases are then presented to validate the accurate and efficiency of these solvers. Finally, several applications of these methods in biological are briefly introduced to demonstrate their capabilities in complex flow computations.

Level-Set-Based Topology Optimization for Nonlinear Problems

Jiawei Tian^{*}, Shikui Chen^{**}

^{*}Department of Mechanical Engineering, State University of New York at Stony Brook, ^{**}Department of Mechanical Engineering, State University of New York at Stony Brook

ABSTRACT

Most structural topology optimization studies are limited to problems involving in linear elastic behaviors with small deformation. However, for some compliant mechanisms with soft rubber-like material undergoing large deformation, it is necessary to consider nonlinear elastic analysis into topology optimization, and hyperelastic model can accurately predict this mechanical behavior. In this paper, we model the mechanics of structures utilizing the compressible Neo-Hookean hyperelastic formulation and employ the level-set-based topology optimization method to get the optimized structure for nonlinear responses. In addition, the nonlinear global governing equation based on the residual form can be solved by using the Newton-Raphson algorithm. Shape sensitivity analysis is derived by using the adjoint variable method, and the design velocity field is calculated according to the gradient-based method. In order to verify the feasibility and the effectiveness of the above-presented method, several two-dimensional examples, including a cantilever beam, an MMB beam, and a stent are implemented and studied. The optimized result shows that the optimized structures can achieve the desired nonlinear large deformation.

Improved XFEM: Recent Advances

Rong Tian*

*Software center for high performance numerical simulation, Institute of Applied Physics and Computational Mathematics

ABSTRACT

The direct extension of singular tip enrichment of XFEM, the core of the method, to crack growth simulation has long been a difficulty due to: (a) elevated bad conditioning as crack propagating, (b) extra-dof dynamics and energy inconsistency, and (c) “null” critical time step size and mass lumping at crack tip. Based on an extra-dof-free partition of unity enrichment technique (Rong Tian. Comput. Methods Appl. Mech. Engrg. 266 (2013) 1–22), we have improved XFEM through a crack tip enrichment without extra dof (Rong Tian, Longfei Wen. Comput. Methods Appl. Mech. Engrg. 285 (2015) 639-658; Longfei Wen, Rong Tian. Comput. Methods Appl. Mech. Engrg. 308 (2015) 256-285). This paper will present a detailed introduction to the recent advances of the improved version of XFEM in both 2D and 3D as well as their parallel implementation. The improved XFEM's excellent stability, accuracy, and straightforwardness in implementation will be demonstrated.

Consistent Traction Boundary Conditions for Nonlocal Models

Xiaochuan Tian^{*}, Jianfeng Lu^{**}, Qiang Du^{***}, Xingjie Li^{****}

^{*}University of Texas at Austin, ^{**}Duke University, ^{***}Columbia University, ^{****}UNC Charlotte

ABSTRACT

It is a recurring problem in scientific computing to design efficient numerical algorithms for a problem imposed on unbounded domains. Such problem is multiscale in its nature since the fundamental difficulty usually roots in the existence of two widely separated spatial scales. The first is a large spatial scale representing the size of the space or the material body. The second is much smaller spatial scale of interest, for example, the part of the material body where crack or fracture actually happens or the the part of the body on which non-zero external forces exert. In this talk, we introduce a consistent nonlocal traction boundary condition for static nonlocal problems so that the computation limited to a finite domain still approximates the correct result for an unbounded domain. Such a traction boundary condition is also important in the engineering practice since it eliminates the surface effect of using nonlocal models on bounded domains. This is a joint work with Qiang Du, Xingjie Helen Li and Jianfeng Lu.

Bridging Between EMMS and Nonequilibrium Thermodynamics: Structure-Dependent Analysis of Energy Dissipation and CFD Validation

Yujie Tian*, Wei Wang**

*State Key Laboratory of Multiphase Complex Systems, Institute of Process Engineering, Chinese Academy of Sciences, **State Key Laboratory of Multiphase Complex Systems, Institute of Process Engineering, Chinese Academy of Sciences

ABSTRACT

Gas-solid fluidized bed is a typical nonlinear nonequilibrium dissipative system, featuring meso-scale structures with bimodal distribution of solid concentration and velocity. The energy-minimization multi-scale (EMMS) model focuses on such dissipative characteristics by decomposing the system into the dense-dilute two-phase structures which is inherently consistent with such bimodal distribution of parameters in gas-solid fluidized bed. However, the stability condition of EMMS model has not been fully understood, especially for its relationship with those extremum principles in nonequilibrium thermodynamic, for example, the Minimum Entropy Production Principle (Prigogine, 1967). In previous work, a structure-dependent multi-fluid model (SFM) (Hong et al., 2013) was proposed, the mass, momentum balance equations of which could be reduced to the hydrodynamic equations of two-fluid model (TFM) and those of the EMMS model under certain simplifications. In this work, SFM is further refined by applying the volume average method on a control volume considering the dense-dilute two-phase structures. Then, the structure-dependent energy dissipation rate is formulated, and extends to the extremum behavior of dissipation processes (Tian et al., 2017). It reveals that the results based on the minimum energy dissipation rate applies only to homogeneous, dilute flow states, but fails in the particle-fluid compromising fluidization regime, in particular, fails to predict choking transition. In contrast, the EMMS stability condition based on the principle of compromise in competition between dominant mechanisms well predicts the regime transition of fluidization. This work unfolds a fresh viewpoint to understand the relation between EMMS stability condition and nonequilibrium thermodynamics. Two-fluid model based CFD simulation is further performed, validating the advantage of EMMS approach for characterizing dissipative structure in fluidized beds. References: Prigogine, I., 1967. Introduction to Thermodynamics of irreversible processes, Interscience Publisher. New York. Hong, K., Shi, Z., Wang, W., Li, J., 2013. A structure-dependent multi-fluid model (SFM) for heterogeneous gas-solid flow. Chem. Eng. Sci. 99, 191–202. Tian, Y., Geng, J., Wang, W., 2017. Structure-dependent analysis of energy dissipation in gas-solid flows: Beyond nonequilibrium thermodynamics. Chem. Eng. Sci. 171, 271–281.

SPH ANALYSIS OF INKJET DROPLET IMPACT DYNAMICS

T. TILFORD*, J. BRAUN[†], J. C. JANHSEN[†], M. BURGARD[†], C. BAILEY*

*Computational Mechanics and Reliability Group, University of Greenwich, UK
Email T.Tilford@gre.ac.uk

[†] Fraunhofer-Institut für Produktionstechnik und Automatisierung, Germany

Key words: SPH, Additive Manufacturing, Microelectronics, Microfluidic Analysis

Abstract. This paper presents a novel Smoothed Particle Hydrodynamics (SPH) framework for analysis of droplet impact dynamics in a 3D inkjet printing process. Results obtained are validated against experimentally derived high-speed imaging data. The numerical framework is based on the Smoothed Particle Hydrodynamics approach of Monaghan et al [1] which has been proven to be efficient and effective for analysis of dynamic fluid flow problems involving free surface interfaces. The SPH approach has been augmented through addition of the kernel gradient correction scheme proposed by Belytschko et al [2] and stabilization terms of Marrone et al [3]. This correction provides a more accurate approximation of the boundary forces including surface tension which dominate at typical inkjet droplet lengthscales ($<100\ \mu\text{m}$). Analysis is expedited through adoption of the OpenACC programming paradigm to enable GPU based computation.

Numerical analyses have been validated against analytical solutions, reference macroscale problems and through comparison with experimental high speed imaging data of the inkjet printing process. The experimental setup consisted of a Fuji Dimatix SL-128 inkjet printhead jetting an acrylate based 3D printing build material onto a glass substrate. Images of a single inkjet droplet impacting onto the glass slide were captured at a rate of 100,000 frames per second, with droplet diameter assessed using a weight test approach.

Qualitative comparison of the numerical and experimental results showed a good agreement, indicating that the implemented framework is effective for analysis of the fluidic aspects of the printing process. The model is able to assist in tackling manufacturing issues that can detrimentally influence the quality of manufactured parts through provision of insight into the process.

1 INTRODUCTION

Additive manufacturing is becoming widely adopted across a range of industrial sectors and being applied to increasingly high value and high complexity products. Piezoelectric drop-on-demand inkjet printing systems can be used to form truly three dimensional, multi material objects with very high dimensional accuracy. The development of conductive pastes that can be dispensed using inkjet printers has enabled the approach to be utilised for development of microelectronics components.

The large number of academic research 3D printing systems targeting the electronics packaging sector [4-6] are now augmented by a number of commercially available systems intended for production of saleable products such as the Nano Dimension Dragonfly [7] and the Optomec [8] systems. The EU funded NextFactory [9-11] project has developed a 3D printing, micro-deposition, micro-assembly, and curing system, illustrated in Figure 1a, that can accurately deposit and cure both functional and structural materials and place/embed components in an integrated manner within a single platform. The system uses a hybrid approach in order to increase its flexibility, with an inkjet system augmented by microdeposition tools that enable conductive adhesive materials to be used alongside silver nano-inks for conductive features.

The system enables producers of micro-mechatronic systems to manufacture complete products on a single machine with the manufacturing process from CAD design to finished product taking a number of hours rather than more lengthy timescales typically associated with traditional manufacturing methods. The three-dimensional nature of the build process enables manufacture of complex 3D microsystems as readily as 2D and 2.5D devices.

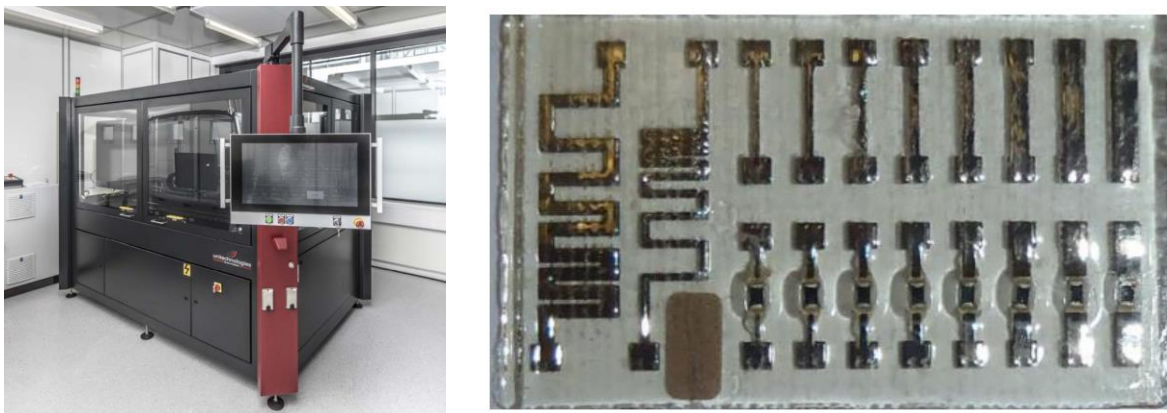


Figure 1(a): NextFactory 3-D additive manufacturing system and 1(b) 3-D printed microelectronics test structure

As is the norm for the electronics sector, new manufacturing approaches need to be considered in terms of the long term reliability of the final product. In addition to commonplace reliability qualification approaches such as JEDEC tests, there is an increasing drive to assess component quality during the manufacturing process. Condition based monitoring approaches measure key parameters associated with component quality during manufacture and continually optimise process parameters in real time to increase final quality and reliability of formed components [12, 13]. Such condition based monitoring systems need to be trained as to how variation of process parameters influences product quality. A numerical model, capable of detailed analysis of the process, can be used to underpin such an approach.

The primary requirement of the numerical model for inkjet deposition is to capture the complex physics involved when an inkjet droplet impacts a printed surface. There are a number of significant challenges in such an analysis. The primary challenge is that analysis of droplet impact upon an idealised flat surface is insufficient. Only the first layer of an inkjet printed structure will be deposited on the flat baseplate. The following layers will be deposited onto a layer of partially cured polymer droplets which form an uneven surface and will deform on impact. The material is not a simple Newtonian fluid such as water but a complex multi-component polymer which exhibits shear dependent viscous behaviour – a complex non-Newtonian material. Additionally, the impact is very severe with a droplet of diameter in the order of 40 microns impacting at approx. 5 metres per second.

Traditional computational fluid dynamics (CFD) approaches such as the Finite Volume Method [14] would be readily capable of modelling the impact dynamics of a small number of droplets. However, in order to consider prediction of the development of defects over a number of layers it is necessary to take advantage of a more efficient approach such as GPU enabled SPH. This approach has a number of advantages over traditional methods in that interfaces are explicitly captured rather than needing to be approximated but, more critically, incorporates a finite support distance enabling the problem domain to be subdivided into a large number of overlapping subdomains which can be assessed on a single core of a graphical processor unit.

2 Numerical Approach

The Smoothed Particle Hydrodynamics (SPH) approach was developed by Lucy [15] and by Gingold and Monaghan in 1977 [1]. It is a versatile discrete particle method for solution of a number of differing physical phenomena. It is a computationally highly effective method for solution of complex fluid flows, particularly in cases with interfaces and large deformations. The SPH approach considers the fluid as a collection of particles, each associated to a number of physical properties such as position, velocity, mass, density, etc. At the heart of the SPH approach is a means of evaluating spatial derivatives through integral interpolants which use kernels to approximate a delta function. The integral interpolant of any quantity function $A(r)$ is defined by:

$$A(r) = \int_{\Omega} A(r') W(r - r', h) dx \quad (1)$$

This relates the value of parameter A, a scalar variable such as pressure, at location r, through integration of the value of A over surrounding space Ω with a smoothing kernel W. This smoothing kernel essentially acts as a weighting factor which, critically, enables the variation of A at distances greater than a defined value to be ignored. This finite support radius enables the physical domain to be subdivided into a number of overlapping subdomains which greatly enhances the computational efficiency of the approach. In the standard SPH formulation, this can be written as:

$$A_i(r) = \sum_j A_j \frac{m}{\rho} W(ri - rj, h) \quad (2)$$

In which the value of A of particle i is evaluated by summing the values of A at all particles within the support radius as a function of their mass, m, density, ρ and kernel, W. This can be extended to spatial derivatives through the following functions:

$$\nabla A_i(r) = \sum_j A_j \frac{m}{\rho} \nabla W(ri - rj, h) \quad (3)$$

$$\nabla^2 A_i(r) = \sum_j A_j \frac{m}{\rho} \nabla^2 W(ri - rj, h) \quad (4)$$

A number of different kernels have been proposed in SPH literature, each with differing behaviour benefits and drawbacks. The cubic spline kernel has been adopted for this analysis as it is the most widely used and understood. The Cubic spline is given by the following function, with normalisation factors, σ , of $1/h$, $10/(7\pi h^2)$, and $1/(\pi h^3)$ in one, two and three dimensions respectively.

$$W(r, h) = \sigma \begin{cases} 1 - \frac{3}{2}q^2 + \frac{3}{4}q^3 & 0 \leq q \leq 1 \\ \frac{1}{2}(2 - q)^3 & 1 \leq q \leq 2 \\ 0 & q > 2 \end{cases} \quad (5)$$

This limited support radius enables the solution domain to be subdivided into cell each with dimension equal to the support radius. When each cell is linked with the 26 surrounding cells to form a sub-region, the domain is separated into a number of overlapping subdomains in that a particle inside the subregion will only have a valid interaction with particles in the same region as particles in other regions will be more than the support radius away. This is a key advantage of the SPH approach in that the computational cost of solving a number of small problems is significantly lower than solving one very large problem. Additionally, the numerical processing can be performed on a graphical processing unit (GPU) which comprises a relatively large number of relatively small cores which is ideally suited to such problems.

Within each subdomain it is necessary to determine the movement of each particle as a function of the acceleration due to interaction forces from surrounding particles. The fluid flow forces are governed by the Navier Stokes Equations, which can be written as:

$$\frac{\delta}{\delta t}(\rho u) + (\rho u \cdot \nabla) = -\nabla p + \mu \nabla^2 u + g \quad (6)$$

In the SPH approach these can be reformulated as a smoothed interaction force between each pair of particles. The acceleration of a particle can therefore be derived through summation of these forces over all particles within the support radius. The total acceleration force can be written as:

$$\frac{\delta \rho_i}{\delta t} = -\rho_i \sum_j (u_j - u_i) \cdot \nabla W(r_i - r_j, h) \frac{m_j}{\rho_j} \quad (7)$$

$$\begin{aligned} \frac{\delta}{\delta t}(\rho u_i) = & - \sum_j m_j \left[\left(\frac{p_i}{\rho_i^2} + \frac{p_j}{\rho_j^2} \right) \right. \\ & \left. - \frac{\varepsilon}{\rho_i \rho_j} \frac{4\mu_i \mu_j}{(\mu_i + \mu_j)} \frac{u_{ij} \cdot r_{ij}}{r_{ij}^2 + \eta^2} \right] \nabla W(r_i - r_j, h) \end{aligned} \quad (8)$$

In addition to the standard SPH formulation, a number of additional functions needed to be implemented in order to address specific challenges of the inkjet droplet impact problem. The first of these is to implement the dissipative SPH framework of Marrone et al [3] in order to better deal with the violent impact events. This framework involves modification of the interaction forces to incorporate additional stabilisation terms such that:

$$\begin{aligned} \frac{\delta \rho_i}{\delta t} = & -\rho_i \sum_j (u_j - u_i) \cdot \nabla W(r_i - r_j, h) \frac{m_j}{\rho_j} \\ & + \delta h c_0 \sum_j \psi_{ij} \cdot \nabla W(r_i - r_j, h) \frac{m_j}{\rho_j} \end{aligned} \quad (9)$$

where:

$$\psi_{ij} = 2(\rho_j - \rho_i) \frac{r_{ji}}{|r_{ij}|^2} - [(\nabla \rho_i) + (\nabla \rho_j)] \quad (10)$$

$$\pi_{ij} = \frac{(-u_i) \cdot r_{ji}}{|r_{ij}|^2} \quad (11)$$

The XSPH correction of Monaghan [16] has been implemented to stabilise the analysis, which modifies the particle velocity based on the velocity of the surrounding particles in a manner given by:

$$\frac{\delta r_i}{\delta t} = u_i + \varepsilon \sum_j \frac{m_{bj}}{\bar{\rho}_{ij}} u_{ji} W(r_i - r_j, h) \quad (12)$$

Furthermore, the kernel gradient correction approach of Belytschko [2] is implemented to correct the evaluation of the kernel and gradient values at interfaces. In these regions the support radius covers a region of liquid, represented by particles, and a region of air which, in this implementation, is represented by an absence of particles. The approach of Belytschko requires a 4x4 matrix to be inverted in order to determine the correction factors however this increases the accuracy of the analysis in the critical impact phase of the process. Time integration has been handled through use of a velocity Verlet scheme [17] while material cure behaviour has been handled through a viscosity modification term. A more detailed analysis of the cure kinetics and the non-Newtonian rheometry of the jetted fluids are required to improve the accuracy of the model.

$$\mathbf{A} = \sum_j W_i^s \begin{bmatrix} 1 & \delta x & \delta y & \delta z \\ \delta x & \delta x \delta x & \delta y \delta x & \delta z \delta x \\ \delta y & \delta x \delta y & \delta y \delta y & \delta z \delta y \\ \delta z & \delta x \delta z & \delta y \delta z & \delta z \delta z \end{bmatrix} \quad (13)$$

$$\mathbf{A} \alpha = \mathbf{I} \quad (14)$$

$$W_i^s = \frac{W_i}{\sum_j \left(\frac{m_j}{\rho_j} W_j \right)} \quad (15)$$

$$W = \alpha_{11} + \alpha_{12} \delta x + \alpha_{13} \delta y + \alpha_{14} \delta z \quad (16)$$

$$\nabla W_x = \alpha_{21} + \alpha_{22} \delta x + \alpha_{23} \delta y + \alpha_{24} \delta z \quad (17)$$

$$\nabla W_y = \alpha_{31} + \alpha_{32} \delta x + \alpha_{33} \delta y + \alpha_{34} \delta z \quad (18)$$

$$\nabla W_z = \alpha_{41} + \alpha_{42} \delta x + \alpha_{43} \delta y + \alpha_{44} \delta z \quad (19)$$

3 Droplet Impact Analysis

Analysis of a single droplet of uncured polymer has been performed using the model. The analysis has considered an initial state of a perfectly spherical droplet of diameter $23\mu\text{M}$ travelling toward a flat plane at 5 Ms^{-1} . The fluid is considered to have constant viscosity of $0.015\text{ Pa}\cdot\text{S}$ and density 1000.0 KgM^{-3} . Surface energy values for the fluid-air interface and fluid surface interface were taken as 72 mJM^{-2} . Polymer materials typically exhibit non-Newtonian behavior and the surface energy behavior is more complex than considered in the model and as such the accuracy of the analysis will be limited until the model is extended to capture these phenomena.

The development of the droplet shape during the impact, as predicted by the numerical model, is illustrated in Figure 2. The six images show the droplet at $1, 10, 20, 86, 200$ and $400\mu\text{s}$ after impact. The high impact speed causes relatively localized deformation in the immediate post impact phase before the kinetic energy is transferred into transverse momentum and significant viscous energy dissipation. The point at which the droplet has greatest transverse radius occurs at $86\mu\text{s}$, where momentum forces have been balanced by the surface tension forces resulting in zero velocity at the outermost extents of the droplet. Beyond this time, the surface tension forces draw the droplet back into a more spherical shape as shown in in the 200 and $400\mu\text{s}$ plots.

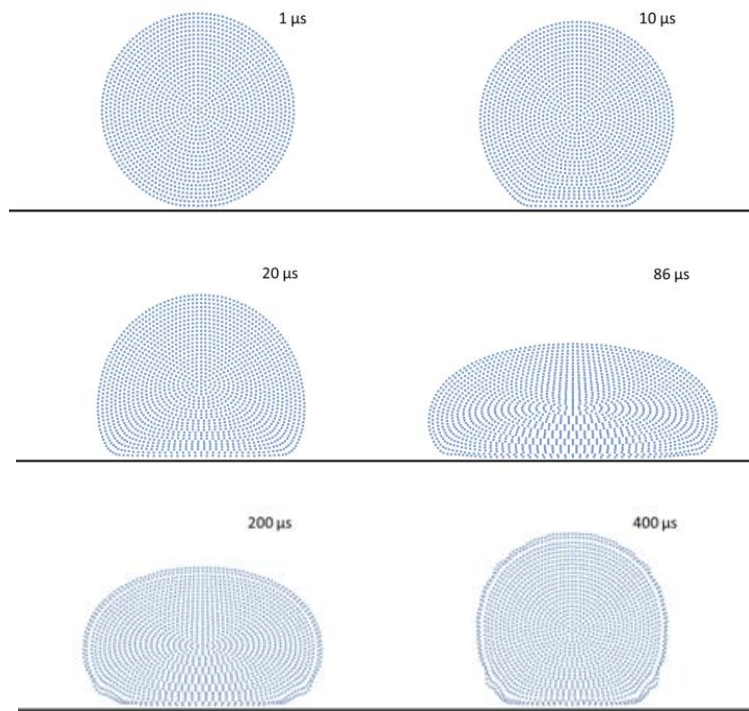


Figure 2: Single droplet impact sequence

These numerical results can be validated through qualitative comparison with high speed imaging data. The experimental setup consisted of a Fuji Dimatix SL-128 inkjet printhead jetting an acrylate based 3D printing build material onto a glass substrate. Images of a single inkjet droplet impacting onto the glass slide were captured at a rate of 100,000 frames per second, with droplet diameter being accurately assessed using a weight test approach. Figure 3 illustrates a droplet impact sequence showing on in every three images for conciseness. Comparison of these images with numerically derived results would suggest a discrepancy between the actual surface tension values and those considered in the model.

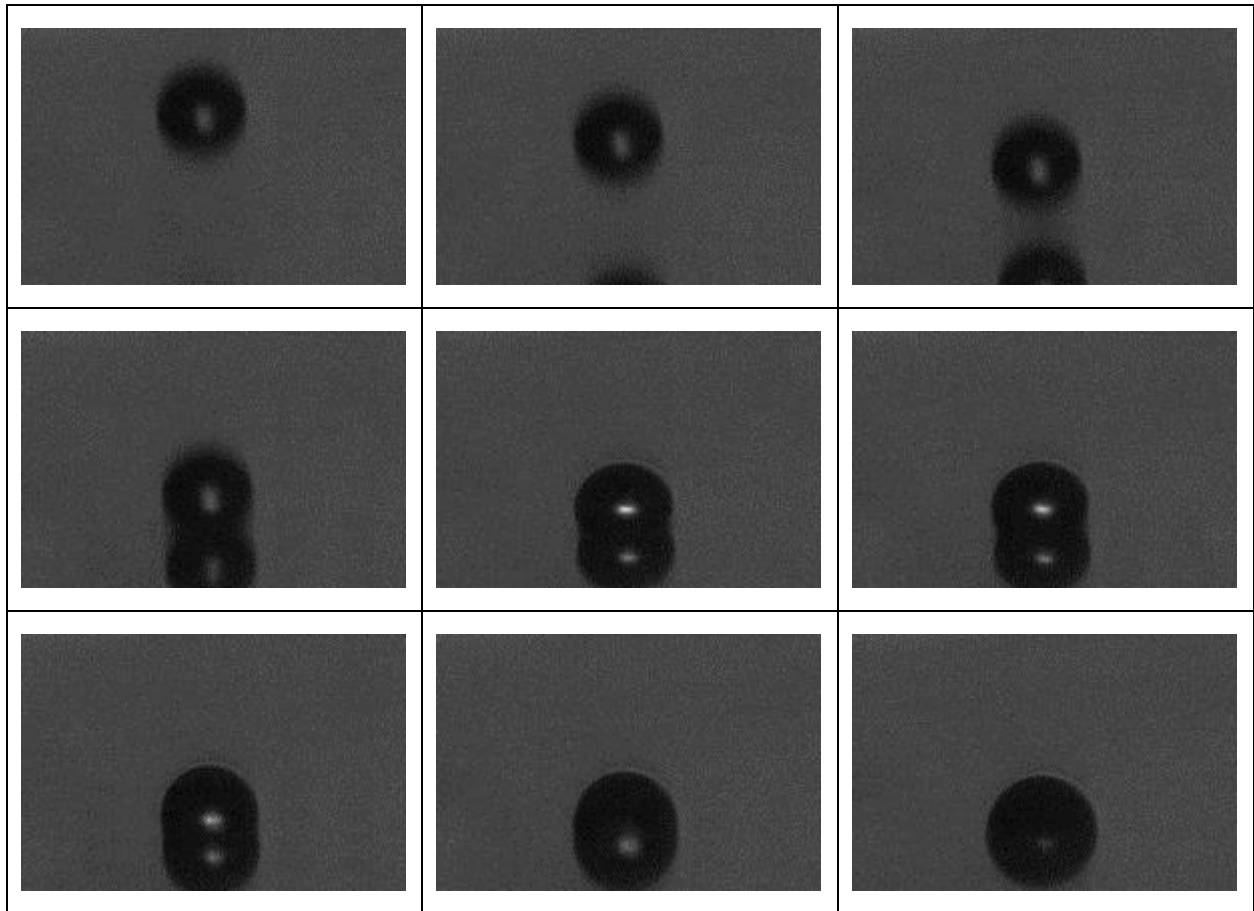


Figure 3: High-speed imaging droplet impact sequence

Conclusions

A new, effective approach for analysis of droplet impact dynamics associated with piezoelectric drop-on-demand inkjet printing systems was presented. The SPH formulation of Lucy and Gingold and Monaghan has been used as the basis for the model, with the δ -SPH terms of Marrone et al and gradient correction terms of Belytschko used to improve the accuracy and stability.

Qualitative comparison of results obtained from the numerical framework with experimentally derived high speed imaging data show the applicability of the approach. The approach could be further enhanced by implementation of an iterative incompressible approach such as that proposed by Ihmsen et al [18] and through integration of an appropriate cure kinetics model to capture post impact UV cure processes.

Acknowledgements

This paper is based on work supported by the NextFactory research project funded under the European Community's 7th Framework Programme (FP7/2007-2013) under grant agreement No. 608985 and through University of Greenwich REF/PP funding

REFERENCES

- [1] Monaghan, J. J., "On the Problem of Penetration in Particle Methods". Journal Computational Physics, Vol. 82, pp. 1-15, 1989
- [2] Belytschko, T., Krongauz, Y., Organ, D., Fleming, M., "Meshless methods: an overview and recent developments", Computer Methods in Applied Mechanics and Engineering, Vol. 139, Issues 1–4, pp. 3-47, 1996
- [3] Marrone, S., Antuono, M., Colagrossi, A., Le Touzé, D., Graziani, G., "δ-SPH Model for Simulating Violent Impact Flows", Computer Methods in Applied Mechanics and Engineering. Vol. 200, pp. 1526–1542, 2011
- [4] Kawahara, Y., Hodges, S., Cook, B. S., Zhang, C., Abowd, G. D., "Instant inkjet circuits: lab-based inkjet printing to support rapid prototyping of UbiComp devices", Proc UbiComp'13, September 8–12, 2013, Zurich, Switzerland, pp. 363-372
- [5] B. Khorramdel, J. Liljeholm, M. Laurila, T. Lammi, G. Mårtensson, T. Ebefors, F. Niklaus, M. Mäntysalo, Inkjet printing technology for increasing the I/O density of 3D TSV interposers, Microsystems and Nanoengineering, Vol. 3, 10.04.2017, p. 17002.
- [6] Integration of inkjet and RF SoC technologies to fabricate wireless physiological monitoring system, H. Sillanpää, A. Vehkaoja, D. Vorobiev, S. Nurmentaus, J. Lekkala, M. Mäntysalo, Proc. 5th Electronics System-integration Technology Conference (ESTC), Helsinki, 2014, doi:10.1109/ESTC.2014.6962739

- [7] <http://www.nano-di.com> [Accessed: 31 May 2018].
- [8] M O'Reilly and Jeff Leal, Jetting your way to fine pitch 3D interconnects, Chip Scale Review, Sept/Oct 2010
- [9] NextFactory, <http://www.nextfactory-project.eu> [Accessed: 31 May 2018].
- [10] Guentheil, J., Holzinger, D., Birch, R., Refle, O., "Process & Machine Development for the Integration of Conductive Paths Inside a 3D Printed Microsystem", Proc. Direct Digital Manufacturing Conference, Berlin, Germany, 2016
- [11] Tilford, Timothy, Stoyanov, Stoyan, Braun, Jessica, Janhsen, Jan Cristophe, Burgard, Matthias, Birch, Richard and Bailey, Christopher (2018) Design, manufacture and test for reliable 3D printed electronics packaging. Microelectronics Reliability, 85. pp. 109-117. ISSN 0026-2714 (doi:10.1016/j.microrel.2018.04.008)
- [12] Turloukis, G., Stoyanov, S., Tilford, T., Bailey, C., "Data driven approach to quality assessment of 3D printed electronic products", Proc. 38th International Spring Seminar on Electronics Technology, 2015, pp. 300 – 305
- [13] S. Stoyanov, C. Bailey, Machine learning for additive manufacturing of electronics, 40th International Spring Seminar on Electronics Technology (ISSE), 2017
- [14] Patankar, Suhas V., Numerical Heat Transfer and Fluid Flow, McGraw-Hill, 1980
- [15] Lucy, L., "A numerical approach to testing the fission hypothesis", Journal Astronomical., Vol. 82, pp. 1013-1924, 1977
- [16] Gingold, R. A., Monaghan, J. J., "Smoothed Particle Hydrodynamics: Theory and Application to non-Spherical Stars" Mon. Not. R. Astr. Soc., Vol. 181, pp. 375-389, 1977
- [17] L. Verlet, "Computer Experiments on Classical Fluids, I: Thermodynamical Properties of Lennard-Jones Molecules. Phys Rev, Vol. 159, pp. 98–103, 1967
- [18] M. Ihmsen, J. Cornelis, B. Solenthaler, C. Horvath, M. Teschner, Implicit Incompressible SPH, IEEE Transactions on Visualization and Computer Graphics, July 2013.

Multiscale Modelling of Transport Processes and ASR Induced Damage in Concrete

Jithender Jaswant Timothy*, Tagir Iskhakov**, Günther Meschke***

*Ruhr University Bochum, **Ruhr University Bochum, ***Ruhr University Bochum

ABSTRACT

Heterogeneous porous materials, such as concrete are often characterized by a pore-space spanning multiple length scales and a distributed network of microcracks, which either exists a priori, e.g. caused by the production process (shrinkage etc.), or which is later induced by the loading process. As a consequence, molecular transport, fluid flow and the load carrying capacity is strongly influenced specifically by the density and the topology (geometry, distribution, connectivity) of the pores and microcracks. In the first part of the presentation, using a combination of a recursive analytical micromechanics model [1] and direct numerical simulations, the effective transport properties for various isotropic and anisotropic damage configurations and pore-size distributions are computed. In the second part of the presentation, the effective transport properties are incorporated into a multiscale model for describing damage and deterioration in concrete due to Alkali-Silica Reaction (ASR) [2] while simultaneously being subject to combined mechanical, hygral and chemical loads. While microcrack propagation and evolution due to ASR gel pressure at the microscale is modelled within the framework of microporomechanics [3] and upscaled using mean-field homogenization, the kinetics of ASR is described at the aggregate scale using a finite element model. The overall capabilities of the model are shown using select examples and comparison with experimental data. References [1] Timothy, J. J. and Meschke, G. Cascade lattice micromechanics model for the effective permeability of materials with microcracks. *Journal of Nanomechanics and Micromechanics (ASCE)*, 6(4):04016009, 2016. [2] Bangert, F., Kuhl, D. and Meschke, G.,'Chemo-hygro-mechanical modelling and numerical simulation of concrete deterioration caused by alkali-silica reaction';, *International Journal for Numerical and Analytical Methods in Geomechanics* 28 (2004) 689-714. [3] Dormieux, L., Kondo, D. and Ulm, F.J. 'Microporomechanics';, (2006) Wiley & Sons.

Fast Simulation of Columnar Grain Growth During Laser Powder Bed Additive Manufacturing

Albert To^{*}, Jian Liu^{**}, Qian Chen^{***}, Yunhao Zhao^{****}, Wei Xiong^{*****}

^{*}University of Pittsburgh, ^{**}University of Pittsburgh, ^{***}University of Pittsburgh, ^{****}University of Pittsburgh,
^{*****}University of Pittsburgh

ABSTRACT

The goal of this work is to establish the link between process parameters and grain morphology and texture of laser power bed additive manufacturing (AM) processes. A quantitative method is proposed to predict the epitaxial growth of columnar grains within and across melt pools and texture formation during a metal AM process. Finite element simulation is used to predict the geometry and thermal profile of the melt pool. The thermal gradient distribution within the 3D melt pool determines the crystallography direction and growth direction of the columnar grains within each deposited single and multiple tracks. The multiple tracks with the predicted geometry are amalgamated together to represent the bulk part, and the epitaxial growth of grains across the boundary of neighboring tracks are quantitatively simulated. The proposed method will be validated by experimental studies of metal AM processed Inconel 718. The effects of process parameters and scan strategy on the grain texture will also be explored.

AFLOW: Integrated Infrastructure for Automated Computational Materials Design

Cormac Toher^{*}, Corey Oses^{**}, David Hicks^{***}, Frisco Rose^{****}, Eric Gossett^{*****}, Ohad Levy^{*****}, Marco Fornari^{*****}, Marco Buongiorno Nardelli^{*****}, Stefano Curtarolo^{*****}

^{*}Duke University, ^{**}Duke University, ^{***}Duke University, ^{****}Duke University, ^{*****}Duke University, ^{*****}Duke University, ^{*****}Central Michigan University, ^{*****}University of North Texas, ^{*****}Duke University

ABSTRACT

The AFLOW infrastructure for computational materials design [1] accelerates the development and the deployment of new technologies by automating high-throughput first principles calculations. AFLOW includes modules to analyze crystal symmetry, generate hypothetical materials structures by decorating crystallographic prototypes, model substitutional disorder, determine thermodynamic stability, as well as to calculate phonon dispersions, electronic structure and thermo-mechanical properties [2]. The results for more than 1.7 million materials entries are publicly accessible via the AFLOW data repository, which is available online at aflow.org. AFLOW data is being used to train machine-learning models, and to predict the synthesizability of disordered materials. Additional tools, such as the AFLUX Search-API [3] are available to programmatically search and process the data, and are integrated with the AFLOW framework. [1] C. Toher et al., The AFLOW Fleet for Materials Discovery, submitted arXiv:1712.00422 (2017). [2] C. Toher, C. Oses, J. J. Plata, D. Hicks, F. Rose, O. Levy, M. de Jong, M. D. Asta, M. Fornari, M. Buongiorno Nardelli, and S. Curtarolo, Combining the AFLOW GIBBS and Elastic Libraries to efficiently and robustly screen thermomechanical properties of solids, Phys. Rev. Materials 1, 015401 (2017). [3] F. Rose, C. Toher, E. Gossett, C. Oses, M. Buongiorno Nardelli, M. Fornari, and S. Curtarolo, AFLUX: The LUX materials search API for the AFLOW data repositories, Comput. Mater. Sci. 137, 362-370 (2017).

High-order Residual Distribution Scheme for the Euler Equations of Fluid Dynamics

Svetlana Tokareva^{*}, Remi Abgrall^{**}, Paola Bacigaluppi^{***}

^{*}University of Zurich, ^{**}University of Zurich, ^{***}University of Zurich

ABSTRACT

In the present work, a high order finite element type residual distribution scheme is designed in the framework of multidimensional compressible Euler equations of gas dynamics. The strengths of the proposed approximation rely on the generic spatial discretization of the model equations using a continuous finite element type approximation technique, while avoiding the solution of a large linear system with a sparse mass matrix which would come along with any standard ODE solver in a classical finite element approach to advance the solution in time. In this work, we propose a new Residual Distribution (RD) scheme, which provides an arbitrary explicit high order approximation of the smooth solutions of the Euler equations both in space and time. The design of the scheme allows for an efficient diagonalization of the mass matrix without any loss of accuracy. This is achieved by coupling the RD formulation [1] with a Deferred Correction (DeC) type method [2] for the discretization in time and choosing Bernstein polynomials as shape functions. This work is the extension of [3] to multidimensional systems. We have assessed our method on several challenging benchmark problems for one- and two-dimensional Euler equations and the scheme has proven to be robust and to achieve the theoretically predicted high order of accuracy on smooth solutions. As the second contribution, we show how to compute a relevant weak solution from a pressure-based formulation of the Euler equations of fluid mechanics using our high order RD approach. The pressure-based formulation is in particular useful when dealing with nonlinear equations of state since it is easier to compute the internal energy from the pressure than the opposite. This makes it possible to get oscillation-free solutions, contrarily to classical conservative methods. Finally, we present the extensions of the proposed RD scheme to some models of multiphase flow as well as Lagrangian hydrodynamics. [1] R. Abgrall, Residual distribution schemes: Current status and future trends, *Computers and Fluids* 35 (2006) 641--669. [2] Y. Liu, C.-W. Shu, M. Zhang, Strong stability preserving property of the deferred correction time discretisation, *Journal of Computational Mathematics* 26 (2008) 633-656. [3] R. Abgrall, High order schemes for hyperbolic problems using globally continuous approximation and avoiding mass matrices, *Journal of Scientific Computing* 73 (2017) 461-494

Exponential Integrators: Methods and Software

Mayya Tokman*

*University of California, Merced

ABSTRACT

Over the past decades, exponential integration emerged as a numerical technique that carries significant computational savings compared to current state-of-the-art approaches for certain classes of stiff problems. In this talk we will explain advantages exponential methods offer and discuss theoretical and practical aspects of designing and implementing different classes of efficient exponential integrators. We focus on Exponential Propagation Iterative Methods of Runge-Kutta type (EPIRK) that provide a general framework that can be adapted to construct exponential schemes based on the properties of the problem of interest. In particular, we will discuss the new class of implicit-exponential (IMEXP) methods. These time integrators provide an efficient alternative to implicit-explicit (IMEX) schemes for problems where both the linear and nonlinear forcing in the equations introduce stiffness. We will describe a software package EPIC that contains implementation of efficient exponential methods for serial and parallel computational platforms and illustrate performance gains these schemes provide using test problems and concrete applications.

Cerebrospinal Fluid-Brain Simulations Subject To Loading Conditions

Milan Toma^{*}, Paul Nguyen^{**}

^{*}New York Institute of Technology, ^{**}Emory University

ABSTRACT

A fluid-structure interaction (FSI) analysis is used to simulate the interaction between the brain and the cerebrospinal fluid in which the brain is submerged within the skull. Smoothed-particle hydrodynamics is used to represent the fluid flow within the head and its interaction with all the brain and skull structures. These simulations show the fluid particles moving and interacting with the brain gyri and sulci. Thus, the FSI model and its computational analysis have the capability to locate areas (down to the exact gyri and sulci) of the brain the most affected under given loading conditions and therefore assess the possible damage to the brain and consequently predict the symptoms. Closed brain injuries are a common danger in contact sports and motorized vehicular collisions. Mild closed brain injuries, such concussions, are not easily visualized by computed imaging or scans. Having a comprehensive head/brain model and using fluid-structure interaction simulations enable us to see the exact movement of the cerebrospinal fluid under such conditions and to identify the areas of brain most affected.

Meshless RBF-based Biomechanical Simulation of Human Respiratory Muscles

Igor Tominec^{*}, Nicola Cacciani^{**}, Pierre-Frédéric Villard^{***}, Elisabeth Larsson^{****}

^{*}Uppsala University, ^{**}Karolinska Institutet, ^{***}Université de Lorraine, ^{****}Uppsala University

ABSTRACT

The main objective of our research is to understand the functionality of a human diaphragm, the main muscle of the respiratory system. Its action affects the volume of the thorax cavity, such that the lungs can inflate and deflate, enabling a human to breathe. The aim is to enable medical researchers to perform studies on ventilator induced diaphragm dysfunction (VIDD). The diaphragm models in existing simulation tools are not advanced enough to capture the processes that lead to VIDD. Our approach is based on a continuum mechanics model that arises from nonlinear elasticity. The equations are solved on a 3D diaphragm geometry obtained from images of real patients. We aim to include the viscoelastic memory effect of the material, together with the anisotropic layout of the fibre bundles that form the muscle. The model is simulated using localized radial basis function methods in space and a quasistatic approach in time. Many numerical challenges are addressed, such as how to use anisotropic basis functions in order to treat the non-trivial high-aspect ratio geometry, convergence and computational speed of the nonlinear iterations, and the stability in time.

DNS of Plane Couette Flow with Roughness in the Transitional Region

Takeru Tomioka^{*}, Takahiro Tsukahara^{**}

^{*}Tokyo University of Science, ^{**}Tokyo University of Science

ABSTRACT

There are many investigations of wall-bounded turbulence, but few studies consider the influence of wall roughness on the transition process. From practical perspective, it is important to consider the roughness effect on the wall turbulence and its subcritical transition to turbulence. An earlier work by direct numerical simulation (DNS) of plane Couette flow (pCf) with roughened walls [1], reported a decrease in the lower critical Reynolds number (below which any disturbance decays) on roughened walls. It was also shown that turbulent intermittent structures arising in the transitional region were changed significantly due to the roughness given only on one wall. Details of such structure changes are still unknown. In this study, we focused on the intermittent structure observed in the transitional region of the roughened pCf. We analyzed the pCf driven by the top wall with adding the roughness to the bottom static wall. The roughness is mimicked by the body force rather than actually creating the roughness element [2]. This model term consists of roughness density, shape function, and average roughness height h . With fixing the former two parameters, we focused on the change of the intermittent structure through a parametric study with respect to h . In the absence of roughness, turbulent stripes (i.e., localized turbulence bands) form obliquely to the main stream direction, but non-oblique turbulence stripes (hereinafter called “vertical turbulent stripes”) were confirmed when h was high. We examined further how the structure would be changed by changing the Reynolds number and h in the parameter range where the vertical turbulence stripe was detected. The streamwise width of each band of the vertical turbulent stripes was found to decrease as the Reynolds number and/or h decrease, and when turbulent fraction falls below a certain value, the laminar flow occurs. Moreover, by expanding the calculation area in the streamwise direction, we observed a split of the vertical turbulence band into two bands. In the full paper, we will investigate the onset condition and mechanism of the vertical turbulent stripes. Reference [1] Ishida, T., Brethouwer, G., Duguet, Y., and Tsukahara, T., Laminar-turbulent patterns with rough walls. *Phys. Rev. Fluids*, 2, 073901 (2017) [2] Busse, A. and Sandham, N. D., Parametric forcing approach to rough-wall turbulent channel flow, *J. Fluid Mech.* 712, 169 (2012).

Structural Topology Optimization Considering Geometrical and Material Nonlinearities

Liyong Tong^{*}, Quantian Luo^{**}

^{*}The University of Sydney, ^{**}The University of Sydney

ABSTRACT

Multi-objective structural topology design optimization considering geometrical and material nonlinearities and multiple constraints is a challenging problem. Unlike linear structural topology optimization, it may involve repeated analyses of highly nonlinear structural systems and repetitive sensitivity analyses of topological designs if a gradient method is adopted. There exist several difficult issues in both nonlinear structural and sensitivity analyses. For example, how to represent an arbitrary topology of an element in nonlinear finite element formulations to ensure successful completion of each nonlinear analyses? How to use full nonlinear solutions, instead of approximate linear ones, in the updates of topological designs? In this study, the moving iso-surface threshold method is used to address this challenging optimization problem. A generalized mathematical formulation for nonlinear output displacement is derived. In this formulation, the displacement is expressed in terms of total mutual strain energy density calculated using virtual stresses and real strains of all incremental load steps in a nonlinear finite element analysis. This is different from the formulation where only the solution at the final load step is used in sensitivity analysis. This generalized formulation can easily fit in the formulation used in the moving iso-surface threshold method. Two optimization problems involving geometrical and material nonlinearities are considered. The first optimization problem is concerned with the topological design of nonlinear compliant mechanism with multi-objectives and multi-constraints. By using the problem formulation based on moving iso-surface threshold method, an effective algorithm is developed to maximize chosen displacements at multiple outputs for a compliant mechanism with displacement and volume constraints and nonlinear effects. Numerical results of the present algorithm for linear and nonlinear compliant mechanisms are obtained and compared with those linear ones available in the literature. The second optimization problem is about optimal topology design of pressurized cellular structures for potential application in morphing aircraft structures, in particular morphing aircraft wing camber variation using topology optimization to increase lift coefficient. First of all, optimal topology design of a pressurized unit cell is obtained. In the design iteration, super-elements are used to model pressure loading on structural boundaries with fluid-structure interaction and to obtain the optimal solution via a developed algorithm. Thereafter this pressurized unit cell is used as a building block to form integrated pressurized multi-cell wing rib structural component for wing camber morphing.

Comparison of Accuracy and Computational Cost of Different Numerical Boltzmann Solvers

Erik Torres^{*}, Jeff Haack^{**}, Irene Gamba^{***}, Thierry Magin^{****}

^{*}University of Minnesota, ^{**}Los Alamos National Laboratories, ^{***}University of Texas at Austin, ^{****}Von Karman Institute for Fluid Dynamics

ABSTRACT

In this work we compare two numerical methods for solving the Boltzmann Equation for neutral gas mixtures: a deterministic kinetic solver based on the Spectral-Lagrangian method [1] and the stochastic, particle-based Direct Simulation Monte Carlo (DSMC) method [2]. We measure the relative computational cost, both in terms of memory use and CPU run-times, to obtain a pre-set level of accuracy in the macroscopic moments. In order to perform a fair comparison, we will define clear metrics for assessing solution accuracy, given the differences inherent to the two numerical techniques (deterministic vs. stochastic). Three test cases are chosen to for this comparison, each one to stress-test a specific part of the two distinct methods. The first involves the time-unsteady, space-homogeneous relaxation of a mixture of mono-atomic gases, initially at different Maxwell-Boltzmann distributions. This allows us to directly compare the cost of solving the non-linear collision term for the two methods, without worrying about particle advection. The second test case is flow of a mono-atomic gas across a normal shock wave. We obtain the solution as a time-steady problem in the shock's frame of reference. The pre- and post-shock states, specified in terms of macroscopic moments are imposed as boundary conditions at the limits of a 1-D physical domain, whereas velocity space remains 3-D. The third test case involves heat transfer across a mono-atomic gas between two diffusely reflecting walls. Both the initial transient and final steady-state profiles of macroscopic moments are used for our comparison. For the Spectral-Lagrangian solver, the main factor in obtaining accurate solutions lies in sizing the velocity mesh to fully capture and resolve the velocity distribution function(s) of all components in the gas mixture. The computational cost increases with the 6th power of the number of velocity nodes used, and becomes the limiting factor for this method. In case of the DSMC method, statistical noise in the macroscopic moments is caused by the finite particle number used to approximate the velocity distributions in each physical location. This noise is of special concern at high gas temperatures and low stream velocities.

REFERENCES [1] I. M. Gamba and S. H. Tharkabhushanam, Spectral-Lagrangian methods for collisional models of non-equilibrium statistical states, J. Comp. Phys., 228(6), 2012-2036. [2] G.A. Bird, Molecular Gas Dynamics and the Direct Simulation of Gas Flows, Oxford Science Publications, 1994.

A Unified Framework for the Modeling and Simulation of Fluid Surfaces

Alejandro Torres-Sánchez*, Marino Arroyo**, Daniel Millán***

*Universitat Politècnica de Catalunya, **Universitat Politècnica de Catalunya, ***CONICET, Universidad Nacional de Cuyo

ABSTRACT

We develop a novel framework for the three-dimensional modeling and simulation of fluid surfaces from a continuum mechanics viewpoint. Fluid surfaces are ubiquitous in cell and tissue biology, with examples including lipid bilayers, the acto-myosin cortex, or epithelial monolayers. These surfaces usually involve a non-linear coupling between mechanical and chemical signals, which play a key role in important biophysical processes such as cell division, migration or morphogenesis. Thus, there is a growing interest in modeling and simulating these fluid interfaces. This, however, requires of a general framework that tackles the chemo-mechanical coupling transparently and deals with the geometric aspects of a time-evolving surface. To handle the multi-physics aspects of these surfaces, we base our approach on Onsager's variational principle, which provides a variational formulation for the dissipative dynamics of soft-matter systems. In addition to coupling different physical ingredients, modeling fluid surfaces inevitably requires the tools and language of differential geometry to describe a deforming surface evolving in Euclidean space. For instance, the classical rate-of-deformation tensor couples interfacial flows with shape changes in the presence of curvature. Furthermore, the fluid nature of these surfaces challenges classical Lagrangian or Eulerian descriptions of deforming bodies. Indeed, due to the fluid nature of the surface, Lagrangian parametrizations generate very large distortions that require a large amount of remeshing. On the other hand, since we need to track the position of the interface in Euclidean space, the meaning of an Eulerian description is unclear. Arbitrary Lagrangian-Eulerian formulations, well established for bulk media, appear as a natural choice but such a formulation for a deforming surface needs careful consideration. Finally, the three-dimensional simulation of lipid bilayers requires unconventional numerical methods since the resulting equations involve higher-order derivatives of the parametrization, lead to a mixed system of elliptic and hyperbolic partial differential equations and are stiff and difficult to integrate in time. Indeed, surface shape enters into the energy and dissipation expressions through curvature, which involves second-order derivatives of the parametrization. From a finite element method perspective, this implies that the basis functions used to represent the parametrization need to be smooth. Here, we propose a discretization based on subdivision surfaces. While the Galerkin FEM deals naturally with elliptic equations, hyperbolic systems such as the continuity equation modeling fluid transport require special treatment.

Hierarchical Boltzmann Simulations and M(odel)-refinement

Manuel Torrilhon*

*RWTH Aachen University

ABSTRACT

(to be announced)

Isogeometric Analysis on Meshes with Polar Singularities: Applications to High-order PDEs and Structure-preserving Discretizations

Deepesh Toshniwal^{*}, Hendrik Speleers^{**}, Thomas J R Hughes^{***}

^{*}University of Texas at Austin, ^{**}University of Rome Tor Vergata, ^{***}University of Texas at Austin

ABSTRACT

Representing arbitrary surfaces with a finite number of polynomial patches requires the introduction of polar points for high-valence neighborhoods in quadrilateral meshes. Such holes can be filled by means of polar spline surfaces, where the basic idea is to use periodic spline patches with one collapsed boundary. Building splines over such singularities requires special rules to ensure smoothness; ensuring suitability for design and analysis imposes further constraints. A general framework for building C^k polar spline parametric patches of arbitrary degree and with arbitrary number of elements at the hole boundary was presented in [1]. Apart from a simple, geometric construction of smooth basis functions, it was shown that it is possible to endow upon the spline basis interesting properties such as non-negativity and partition of unity. Numerical experiments indicating optimal approximation behavior, even at the singular point, were presented in [1]. In this talk, we will present applications of the technology developed in [1] to high-order PDEs, such as the Cahn-Hilliard equations, where the smoothness afforded by the spline basis allows straightforward numerical discretization and implementation. Moreover, using smooth polar splines as a basis for zero forms, we will construct basis functions for higher-order differential forms and present a pointwise divergence free discretization of the Stokes equation. [1] D. Toshniwal, H. Speleers, R.R. Hiemstra, and T.J.R. Hughes. "Multi-degree smooth polar splines: A framework for geometric modeling and isogeometric analysis", Comput. Methods Appl. Mech. Engrg. 316, 1005-1061, 2017.

Numerical Modeling of Nucleation Mechanisms for 3D Heterogeneous Microstructures

Thomas Toulorge^{*}, Marc Bernacki^{**}, Pierre-Olivier Bouchard^{***}, Modesa Shakoor^{****}, Victor Trejo Navas^{*****}

^{*}Mines ParisTech, ^{**}Mines Paris Tech, ^{***}Mines ParisTech, ^{****}Mines ParisTech, ^{*****}Mines ParisTech

ABSTRACT

Ductile fracture of metallic materials is known to be based on the mechanisms of voids nucleation, growth and coalescence. Voids nucleation is usually due either to failure of particles (fragmentation) or to failure at the interface between particles and the matrix (debonding). Coalescence is characterized by the initiation and propagation of micro-cracks between voids leading to final fracture. The most observed coalescence mode is due to internal necking between neighbouring voids with plastic localization in the intervvoid ligaments. For lower stress triaxiality ratios, a shear driven localization mode can also be observed. This mode, often called void-sheet coalescence, is not yet perfectly understood. This work focuses on the development of an efficient finite element approach for the modeling of failure mechanisms of complex 3D microstructures under large plastic strain and multi-axial loading conditions. Heterogeneous microstructures are represented by a matrix containing particles and voids defined by level-set functions and mesh adaption techniques [1]. A finite element analysis of 3D heterogeneous microstructures with randomly distributed particles is carried out so as to study the influence of particles debonding and fragmentation on void coalescence by internal necking [2]. Micromechanical simulations of a microstructure with 20% particle volume fraction show that voids nucleation leads to an early plastic strain localization mechanism that favors void coalescence and reduces ductility. This work was performed within the COMINSIDE project funded by the French Agence Nationale de la Recherche (ANR-14-CE07-0034-02 grant). REFERENCES [1] M. Shakoor, M. Bernacki and P.-O. Bouchard, A new body-fitted immersed volume method for the modeling of ductile fracture: analysis of void clusters and stress state effects on coalescence, *Engineering Fracture Mechanics*, 147, 398–417 (2015). [2] M. Shakoor, M. Bernacki and P.-O. Bouchard, Ductile fracture of a metal matrix composite studied using 3D numerical modeling of void nucleation and coalescence, *Engineering Fracture Mechanics*, in Press

Development of Augmented Reality Experience System of Indoor Damage due to Earthquake

Takuya Toyoshi^{*}, Daigoro Isobe^{**}, Takuzo Yamashita^{***}, Kazutoshi Matsuzaki^{****}, Hiromitsu Tomozawa^{*****}

^{*}National Research Institute for Earth Science and Disaster Resilience, ^{**}University of Tsukuba, ^{***}National Research Institute for Earth Science and Disaster Resilience, ^{****}Mizuho Information & Research Institute, Inc.,
^{*****}Mizuho Information & Research Institute, Inc.

ABSTRACT

Utilization of virtual reality (VR) and augmented reality (AR) technique is useful for education of disaster. The objective of this research is to develop a fusion technique to generate AR experience video for indoor damage using three-dimensional images with calculated results. National Research Institute for Earth Science and Disaster Resilience (NIED) is developing a virtual experience system of indoor disaster damage. This system consists of a data acquisition part and a data processing and playback part. The data acquisition part can measure and provide synchronized three-dimensional images, sound and acceleration. The system was applied to the E-Defense shake table test of the 10-story reinforced concrete (RC) building and a VR experience video of indoor damage was successfully generated. This video visualized on head mounted display (HMD) can provide a virtual experience of indoor disaster under seismic excitation [1]. A numerical analysis system called E-Simulator, which is under construction by NIED, can analyze motions and falls of indoor furniture and fixture under seismic excitation. A finite element method based on the adaptively shifted integration (ASI) – Gauss technique is used for this analysis. This method can simulate various indoor situations which are difficult to reproduce in actual experiments with high accuracy and low calculation cost using fewer elements [2]. To achieve the objective of this research, the data of indoor damages on the 10th floor of the 10-story RC building specimen excited on the shake-table test of the E-Defense was used. The acceleration data measured on the 10th floor was used for the motion analysis of furniture placed at various locations. A system to paste the texture from several furniture images was developed, and more realistic visualized data was produced. Furthermore, a fusion technique between numerical results and three-dimensional images was developed, in which the data are synchronized by linear interpolation. The generated images are to be shown in the presentation. References [1] Takuzo Yamashita, Mahendra Kumar Pal, Kazutoshi Matsuzaki and Hiromitsu Tomozawa, Development of Virtual Reality Experience System of Interior Damage due to Earthquake Utilizing E-Defense Shake Table Test, Journal of Disaster Research, pp. 882-890, 2017. [2] Daigoro Isobe, Takuzo Yamashita, Hiroyuki Tagawa, Mika Kaneko, Toru Takahashi and Shojiro Motoyui, Motion Analysis of Furniture under Seismic Excitation Using the Finite Element Method, Japan Architectural Review, doi: 10.1002/2475-8876.1015, 2017.

A Parametric Class of Composites with a Large Achievable Range of Effective Elastic Properties

Davi Colli Tozoni^{*}, Denis Zorin^{**}, Igor Ostanin^{***}, George Ovchinnikov^{****}

^{*}Courant Institute, New York University, ^{**}Courant Institute, New York University; Skolkovo Institute of Science and Technology, ^{***}Skolkovo Institute of Science and Technology, ^{****}Skolkovo Institute of Science and Technology

ABSTRACT

We investigate computationally an instance of the problem of G-closure for periodic metamaterials, i.e, the problem of determining what homogenized material properties can be achieved. We consider composites with isotropic homogenized elasticity tensor, obtained as a mixture of two isotropic materials, focusing on the case of a single material with voids. This problem is important, in particular, in the context of designing small-scale structures for metamaterials in the context of additive fabrication, making possible to obtain a range of material properties using a single base material. We demonstrate that two closely related simple parametric families based on the structure proposed by O. Sigmund attain good coverage of the space of isotropic properties satisfying Hashin-Shtrikman bounds. In particular, for positive Poisson ratio, we demonstrate that Hashin-Shtrikman bound can be approximated arbitrarily well, within limits imposed by numerical approximation: a strong evidence that these bounds are achievable in this case. For negative Poisson ratios, we numerically obtain a bound which we hypothesize to be close to optimal, at least for metamaterials with rotational symmetries of a regular triangle tiling.

A Comparison of Fluid-Structure-Interaction Approaches to Blood Flow Modeling with Vessel Prestress

Justin Tran^{*}, Vijay Vedula^{**}, Kathrin Baeumler^{***}, Alison Marsden^{****}

^{*}Stanford University, ^{**}Stanford University, ^{***}Stanford University, ^{****}Stanford University

ABSTRACT

Recent advances in computational modeling of blood flow include modeling the fluid-structure-interaction (FSI) effects between the vessel wall and the blood flow. These effects are crucial as the rigid wall assumption overestimates predictions of wall shear stress, disregards pressure wave propagation, and neglects the mechanical stresses experienced by the wall. Several methods were proposed to model vessel wall deformability. The Coupled Momentum Method (CMM) [1] approximates the vessel wall as a thin membrane where the interface traction is modeled as a body force in the linear elastodynamics equations. As the fluid mesh remains fixed, CMM incurs only a small increase in cost compared to rigid wall approximation, but is generally reliable for modest deformations of less than 10% of the vessel radius. The Arbitrary Lagrangian-Eulerian (ALE) [2] is a general framework for FSI that solves the fully coupled equations for fluid flow, nonlinear wall deformation, and time evolution of the computational mesh. A grid velocity is introduced into the convective term of the Navier-Stokes equations through a space-time Piola transform from an arbitrary mesh to a reference mesh, while satisfying the kinematic and dynamic constraints at the fluid-solid interface. ALE can accommodate large deformations on generic geometries, at a relatively higher cost. In this study, we compare the performance and computational results between using CMM and ALE for modeling blood flow in both idealized and patient-specific models. Additionally, we consider the effect of prestress in the vessel walls for both approaches [3]. Typically, when patient-specific models are constructed from image data, the walls are stressed and in equilibrium with the pressure and viscous forces from the fluid. This phenomenon is commonly neglected, but can lead to large differences when comparing simulation results to time-resolved clinical imaging data. This is especially true for CMM, where initialization requires inflation of the model so the displacements depart from a state of equilibrium with the fluid forces. This can lead to over-inflation which may not be correct. The main contributions of this work are a quantitative comparison of two common methods for FSI in cardiovascular applications both implemented in the same solver, and an analysis of including the effect of prestress for various idealized and patient-specific anatomic models. [1] Figueroa, C. Alberto, et al. Computer methods in applied mechanics and engineering. 2006. [2] Bazilevs, Yuri, et al. Computational Mechanics. 2006. [3] Hsu, Ming-Chen, and Yuri Bazilevs. Finite Elements in Analysis and Design. 2011.

ANALYTIC METHOD TO IDENTIFY TRAIN LOAD FROM INTEGRATED SLEEPER IN-SITU

L-H. TRAN^{*†}, T. HOANG^{*}, D. DUHAMEL^{*}, G. FORET^{*},
S. MESSAD[†] AND A. LOAËC[†]

^{*}Laboratoire Navier, UMR 8205, Ecole des Ponts ParisTech,
IFSTTAR, CNRS, UPE, Champs-sur-Marne, France
le-hung.tran@enpc.fr, tien.hoang@enpc.fr, denis.duhamel@enpc.fr, gilles.foret@enpc.fr

[†]SATEBA, 33 places des Corolles, 92400 Courbevoie, France
s.messad@sateba.com, a.loaec@sateba.com

Key words: Railway Dynamics, Instrumented Sleeper, Fiber Bragg gratings, Green’s function, Computation methods.

Abstract. The degradation of railway tracks can be observed through several measurement techniques. Recently, a method to diagnose the railway track using Fiber Bragg gratings (FBG) has been proposed. FBG are integrated inside the railway sleeper and is named a “Smart Sleeper”. To study the sleeper behavior, an analytical model for the dynamics of railway sleepers has been developed, which can calculate rapidly the sleeper responses. In this model, by using the relation between the rail forces and displacements of a periodically supported beam, the dynamic equation of the sleeper is written with the help of the Euler-Bernoulli beam equation and Dirac’s functions. Subsequently, thanks to the Green’s function of this system, the sleeper dynamic response is calculated analytically. A linear relation between the train loads and the sleeper strains is shown in the frequency domain. This article presents an application of this model to calculate the train loads from the strains measured by the FBG. Based on the analytical model, we obtain a matrix which presents the link between the loads and the sleeper responses. By integrating this matrix and the Fourier transform of the measurements recorded by the FBG at the middle and at the two rail-seats, the train loads can be quickly calculated by using the solver `mldivide` of MATLAB. The numerical application shows that the identified train loads are different for different wheels and different rails. This highlights the irregularity of the wheel-rail contact forces which can be used to detect the defaults in the rolling stock in future works.

1 INTRODUCTION

Generally, defective materials can be detected by several different methods. The easiest is the correlation by image analysis but it is slow and not exact. Measurement of elastic waves, electrical resistance or acoustic emission focus on a variation of the propagation time of waves and electrical resistance to detect the internal cracks of objects. The study of the dynamic properties of systems in the frequency domain (modal analysis) is then applied [1, 2, 3]. Material

damage would have abnormal resonant frequencies.

In recent years, a novel technology using the Fiber Bragg Grating (FBG) to diagnose the railway track has been developed. In 2010, Filograno et al. [12] posed the FBG sensors on the rail in different directions (vertical, horizontal and inclined at an angle 45°) for monitoring the high speed line from Madrid to Barcelona in real time. They could detect the train parameters: train speed and acceleration, the distance between the wheel and wheel number. Moreover, the dynamic charge can be calculated in a precise way. Wei et al. [13, 14] presented two methods: X-Crossing and D-Crossing to avoid the area where signals are noisy. Buggy et al. [15] has used the FBG to monitor the fishplate (junction of two rails). In the same year, Tam et al. [16] presented the system “Smart Railways” which has been developed by KCRS’s East Rail in Hong Kong. The FBG sensor has been demonstrated to be able to detect the rail imperfection [17, 18]. A railway sleeper “Smart Sleeper” [19] which has been developed by Sateba with 6 sensors allows us to measure the sleeper strain when the train is passing.

Substantial research using analytical and numerical methods for rail track has been carried out. Analytical models of the rail track have been developed by considering the model of an infinite beam placed on a continuous foundation [8, 9, 10] or a periodically supported beam [4, 5, 6, 7]. Some research focus on the pre-stressed concrete sleeper using FEM in 2D and in 3D [20, 21]. In 2017, Tran et al. [11] has developed an analytical model of the railway sleeper which allows us to rapidly calculate the sleeper response.

In this paper, based on the analytical model of the railway sleeper, an “inverse problem” has been developed to determine the train loads. By considering a beam resting on a Kelvin-Voigt foundation and by assuming a periodic charge, the sleeper strain and the train loads can be written as a linear relation in the frequency domain with the help of the Green’s function. The charges can be determined by using the MATLAB solver `mldivide`. We verified this problem to a good precision by back-calculating the train loads from a signal. That is a combination of imposed loads and random noise. Another application has been shown in this paper with the real measurements recorded by the “Smart Sleeper”. The results of this application shows the different charges applied on each rail which corresponds to different strain level recorded by the FGB of the sleeper.

2 GORVERNING EQUATIONS

2.1 Analytical model of the sleeper

A railway track can be modeled as shown in Fig. 1. In this track, the sleeper together with the ballast and foundation are modeled by an Euler-Bernoulli beam resting on a Kelvin-Voigt foundation. The sleeper length is $2L$ (from $-L$ to L) and the rail positions are at $x = \pm a$. The sleeper displacement $w_s(x, t)$ under a force $F(x, t)$ is driven by the dynamic equation of the Euler-Bernoulli pre-stressed beam as follows:

$$E_s I_s \frac{\partial^4 w_s(x, t)}{\partial x^4} + \rho_s S_s \frac{\partial^2 w_s(x, t)}{\partial t^2} - T \frac{\partial^2 w_s(x, t)}{\partial x^2} + k_f w_s(x, t) + \zeta_f \frac{\partial w_s(x, t)}{\partial t} = F(x, t) \quad (1)$$

where ρ_s , E_s , S_s and I_s are the density, the Young’s modulus, the section and the cross-sectional moment inertia of the sleeper respectively; k_f and ζ_f are the stiffness and damping coefficients

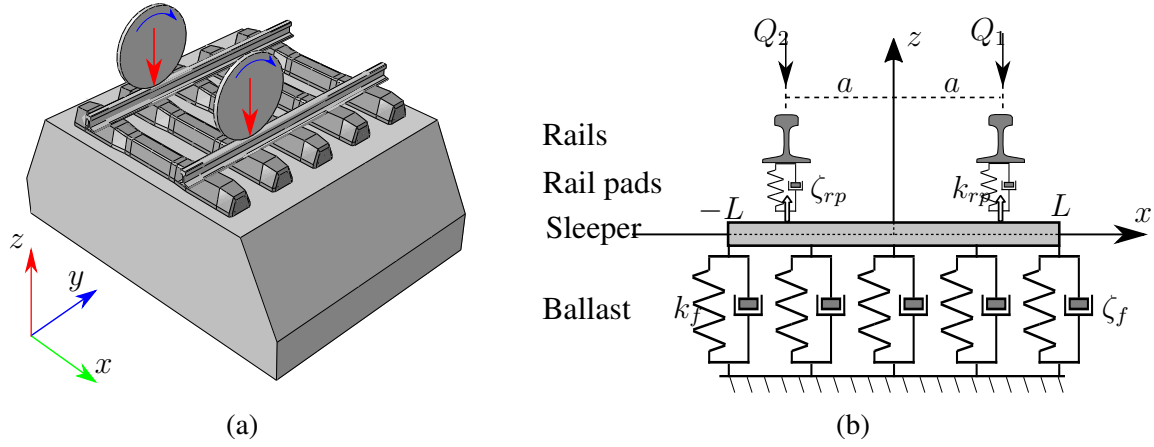


Figure 1: Railway track (a) and the analytical model representation (b)

of the foundation and T is the sleeper pre-stress. The force applied by the rails on the sleeper $F(x, t)$ can be written with the help of the Dirac's functions as follows :

$$F(x, t) = -R_1(t)\delta(x - a) - R_2\delta(x + a) \quad (2)$$

where R_1 and R_2 are the reaction forces applied on the rail positions ($x = \pm a$). For a free-free beam posed on the foundation, the moment (3a) and the shear force (3b) are vanishing at two extremities, thus these boundary conditions can be imposed by the 2nd and 3rd partial derivative with regard to x set to zero respectively:

$$\begin{cases} \frac{\partial^2 w_s}{\partial x^2}(-L, t) = \frac{\partial^2 w_s}{\partial x^2}(L, t) = 0 \\ \frac{\partial^3 w_s}{\partial x^3}(-L, t) = \frac{\partial^3 w_s}{\partial x^3}(L, t) = 0 \end{cases} \quad (3a)$$

$$\begin{cases} \frac{\partial^2 w_s}{\partial x^2}(-L, t) = \frac{\partial^2 w_s}{\partial x^2}(L, t) = 0 \\ \frac{\partial^3 w_s}{\partial x^3}(-L, t) = \frac{\partial^3 w_s}{\partial x^3}(L, t) = 0 \end{cases} \quad (3b)$$

Eq. (1) together with the boundary conditions (3) is a 4th order linear differential equation in the frequency domain which can be solved with help of the Green's function. (The calculation of the Green's function is shown in Appendix B). Hence, the sleeper response in the frequency domain $\hat{w}_s(x, \omega)$ can be written as follow:

$$\hat{w}_s(x, \omega) = \frac{-\hat{R}_1}{E_s I_s} G_a(x, \omega) + \frac{-\hat{R}_2}{E_s I_s} G_{-a}(x, \omega) \quad (4)$$

By substituting $x = a$ and $x = -a$ into the aforementioned equation, we obtain respectively the sleeper displacement at the rail positions:

$$\begin{aligned} \hat{w}_s(a, \omega) &= \frac{-\hat{R}_1}{E_s I_s} G_a(a, \omega) + \frac{-\hat{R}_2}{E_s I_s} G_{-a}(a, \omega) \\ \hat{w}_s(-a, \omega) &= \frac{-\hat{R}_1}{E_s I_s} G_a(-a, \omega) + \frac{-\hat{R}_2}{E_s I_s} G_{-a}(-a, \omega) \end{aligned} \quad (5)$$

The model of the periodically supported beam and together with the consecutive law of the rail pads shows the expression of the reaction force (see Appendix A). The combination at Eqs. (17) and (5) gives us the result of the reaction force of the sleeper on the two rails:

$$\begin{aligned}\hat{R}_1 &= \frac{E_s I_s}{\mathcal{K}} \frac{\mathcal{Q}_1 [G_{-a}(-a, \omega) + \chi] - \mathcal{Q}_2 G_{-a}(a, \omega)}{[\chi + G_a(a, \omega)] [\chi + G_{-a}(-a, \omega)] - G_a(-a, \omega) G_{-a}(a, \omega)} \\ \hat{R}_2 &= \frac{E_s I_s}{\mathcal{K}} \frac{\mathcal{Q}_2 [G_a(a, \omega) + \chi] - \mathcal{Q}_1 G_a(-a, \omega)}{[\chi + G_a(a, \omega)] [\chi + G_{-a}(-a, \omega)] - G_a(-a, \omega) G_{-a}(a, \omega)}\end{aligned}\quad (6)$$

where $\chi = E_s I_s \frac{k_p + \mathcal{K}}{k_p \mathcal{K}}$. Then, the sleeper displacement in the frequency domain can be obtained by replacing \hat{R}_1 and \hat{R}_2 in Eq. (4). The sleeper strain can be calculated using the beam theory and together with the equation of the sleeper response (4):

$$\hat{\varepsilon}_x(x, z, \omega) = z_s \left(\frac{\hat{R}_1}{E_s I_s} G_a''(x, \omega) + \frac{\hat{R}_2}{E_s I_s} G_{-a}''(x, \omega) \right) \quad (7)$$

where z_s is the distance to the beam's neutral axis. By using the inverse Fourier transform of Eqs. (4) and (7), we can get the sleeper response and the sleeper strain in the time domain.

2.2 Identification of the train load

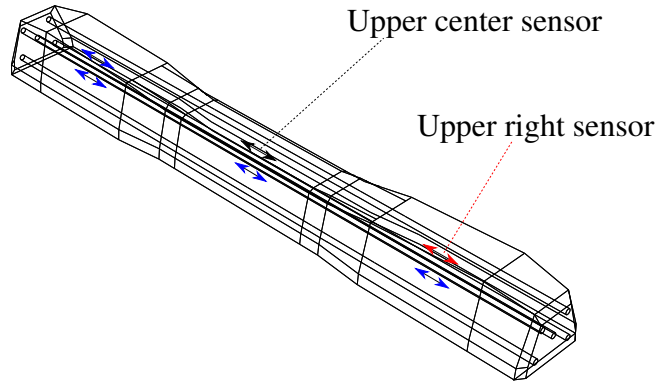


Figure 2: Instrumented sleeper: upper right sensor (red), and upper center sensor (black)

We will apply this analytical model to identify the train load from the sleeper strain. A “Smart Sleeper” which has been developed by Sateba with 6 Fibre Bragg Grating sensors (FBG) integrated in the longitudinal direction allow us to obtain the sleeper strain as the train passes. These sensors are situated at the two rail seats and at the middle of the sleeper. The signals are recorded by these sensors in the time domain and by using the Fourier transform, we can obtain these signals in the frequency domain. We can rewrite Eq. (7) as follows:

$$\hat{\varepsilon}_i(x_i, z_{s_i}, \omega) = \mathbf{A}_{i1}(x_i, z_{s_i}, \omega) \hat{R}_1(\omega) + \mathbf{A}_{i2}(x_i, z_{s_i}, \omega) \hat{R}_2(\omega) \quad (8)$$

where (x_i, z_{s_i}) are the positions of the sensors, $\mathbf{A}_{i1} = \left(\frac{z_{s_i}}{E_s I_s} G''_a(x_i, \omega) \right)$ and $\mathbf{A}_{i2} = \left(\frac{z_{s_i}}{E_s I_s} G''_{-a}(x_i, \omega) \right)$.

This equation can be also rewritten as:

$$[\hat{\varepsilon}(\omega)] = [\mathbf{A}_{i1}(\omega) \quad \mathbf{A}_{i2}(\omega)] \begin{bmatrix} \hat{R}_1(\omega) \\ \hat{R}_2(\omega) \end{bmatrix} \quad (9)$$

where $[\hat{\varepsilon}(\omega)]$ represents the vector signals in the frequency domain and has a dimension n_f that depends on the number of signals.

The reaction forces of the sleeper on the rail can be calculated by the equivalent charges \mathcal{Q}_k where $k = 1, 2$ which corresponds to right and left rails. From Eq. (6), we obtain:

$$\begin{bmatrix} \hat{R}_1(\omega) \\ \hat{R}_2(\omega) \end{bmatrix} = \begin{bmatrix} \mathbf{B}_{11}(\omega) & \mathbf{B}_{12}(\omega) \\ \mathbf{B}_{21}(\omega) & \mathbf{B}_{22}(\omega) \end{bmatrix} \begin{bmatrix} \mathcal{Q}_1(\omega) \\ \mathcal{Q}_2(\omega) \end{bmatrix} \quad (10)$$

where these 4 components \mathbf{B}_{ik} are 4 known constants. The equivalent charges \mathcal{Q}_k are calculated on each rail k (see Appendix A) as follows:

$$\mathcal{Q}_k(\omega) = \frac{\mathcal{K}(\omega)}{v E_r I_r \left[\left(\frac{\omega}{v} \right)^4 - \lambda_r^4 \right]} \sum_{j=1}^K Q_{kj} e^{-i\omega \frac{D_j}{v}} = [\mathbf{C}(\omega)] \mathbf{Q}_k \quad (11)$$

where $\mathbf{Q}_k = [Q_{kj}]_j$ is a column vector of all moving loads on the rail k . The matrix $[\mathbf{C}(\omega)]$ has dimensions $[n_f \times K]$ with n_f and K represent the length of the vector $[\hat{\varepsilon}(\omega)]$ and the wheel number respectively. Eq. (11) can be rewritten as follows:

$$\begin{bmatrix} \mathcal{Q}_1(\omega) \\ \mathcal{Q}_2(\omega) \end{bmatrix} = [\mathbf{C}(\omega)] \begin{bmatrix} \mathbf{Q}_1 \\ \mathbf{Q}_2 \end{bmatrix} \quad (12)$$

The combination of Eqs. (9), (10), and (12) allows us to deduce the relation between the sleeper strains and the train loads as follows:

$$[\hat{\varepsilon}(\omega)] = [\mathbf{A}_{i1}(\omega) \quad \mathbf{A}_{i2}(\omega)] \begin{bmatrix} \mathbf{B}_{11}(\omega) & \mathbf{B}_{12}(\omega) \\ \mathbf{B}_{21}(\omega) & \mathbf{B}_{22}(\omega) \end{bmatrix} [\mathbf{C}(\omega)] \begin{bmatrix} \mathbf{Q}_1 \\ \mathbf{Q}_2 \end{bmatrix} \quad (13)$$

And we can also rewritten the Eq. (13) as a linear equation:

$$[\hat{\varepsilon}(\omega)] = [\mathbf{F}_{i1}(\omega) \quad \mathbf{F}_{i2}(\omega)] \begin{bmatrix} \mathbf{Q}_1 \\ \mathbf{Q}_2 \end{bmatrix} = [\mathbf{F}(\omega)] [\mathbf{Q}] \quad (14)$$

Eq. (14) is a linear relation between the sleeper strains and train loads. Hence, we can use function `mldivide`¹ in MATLAB to solve this linear equation.

¹This solver has many methods of factorization to solve a system linear equation which depend on the dimension of the matrices (for example: Cholesky factorization for a matrix symmetric with real, positive diagonal element; Gaussian elimination to reduce the system to a triangular matrix if the matrix is upper Hessenberg etc.). In this case, the matrix $\mathbf{F}(\omega)$ is rectangular, thus method of QR factorization will be used in the `mldivide` solver

3 NUMERICAL APPLICATION

3.1 Verification

The objective of this section is to verify the precision of the inverse problem. By using the analytical signals generated by the analytical model, we apply it on the inverse problem to identify the train loads. The test will be done with the analytical signal and noise signal. The parameters of the railway track is shown in Table 1. These parameters allows us to generate the analytical signals for identifying the train loads.

Content	Unit	Notation	Value
Young's modulus of rail	GPa	E_r	210
Cross-sectional moment inertia of rail	m^4	I_r	3E-05
Rail density	kgm^{-3}	ρ_r	7850
Rail section area	m^2	S_r	7.69E-3
Young's modulus of sleeper	GPa	E_s	48
Cross-sectional moment inertia of sleeper	m^4	I_s	4.32E-4
Density of sleeper	kgm^{-3}	ρ_s	2475
Sleeper section area	m^2	S_s	54.9E-3
Length of sleeper	m	$2L$	2.41
Track gauge	m	$2a$	1.435
Stiffness of ballast	MNm^{-1}	k_f	240
Damping coefficient of ballast	$kNsm^{-1}$	ζ_f	58.8
Stiffness of rail pad	MNm^{-1}	k_{rp}	192
Damping coefficient of rail pad	$MNsm^{-1}$	ζ_{rp}	1.97
Train speed	ms^{-1}	v	50
Pre-stress of sleeper	kN	T	300
Sleeper spacing	m	l	0.6

Table 1: Parameters of the railway track

The charge per wheel on each rail has been generated randomly. Fig. 3 shows the superposition of the charges introduced and identified (blue line and red column respectively) on the left rail (a) and right rail(b). In the two figures, the blue line has the same value as the red columns in this figure because we found the same train loads. The relative error is about $3.7 \times 10^{-4} \%$. We can conclude that the inverse problem is verified with a good precision. The difference is due to small errors introduced during the numerical calculations.

Now, we add a random noise to the sleeper response to simulate the real measurments. Fig. 4 shows the sleeper strain as a red line and the noise signal as a blue line on the left rail (a) and right rail (b) in a time interval which corresponds to the time for the passing of a train. By using the inverse problem, the superposition of the train loads introduced and identified is shown in Fig. 5.

With the noise, the train loads have been found with a small difference. In this figure, the red column and blue line corresponding to trains loads introduced and identified don't have the same value. The table 2 shows the relative error with different levels of noise in the signal.

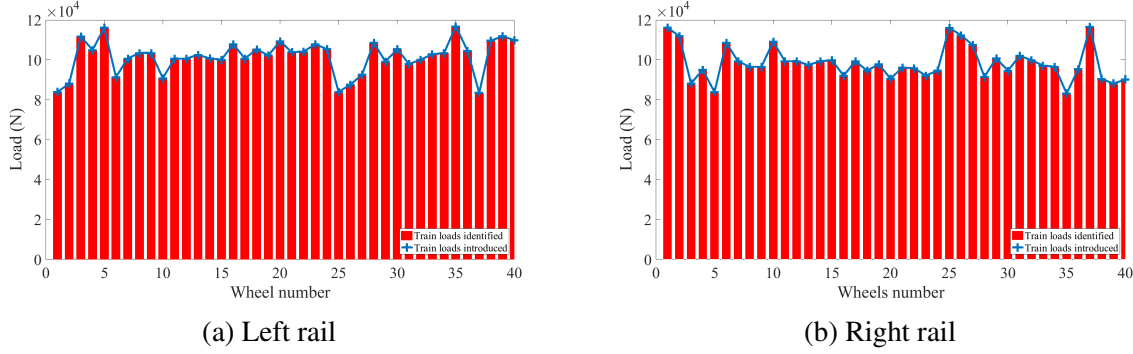


Figure 3: Superposition of the train loads introduced and identified on the left rail (a) and right rail (b)

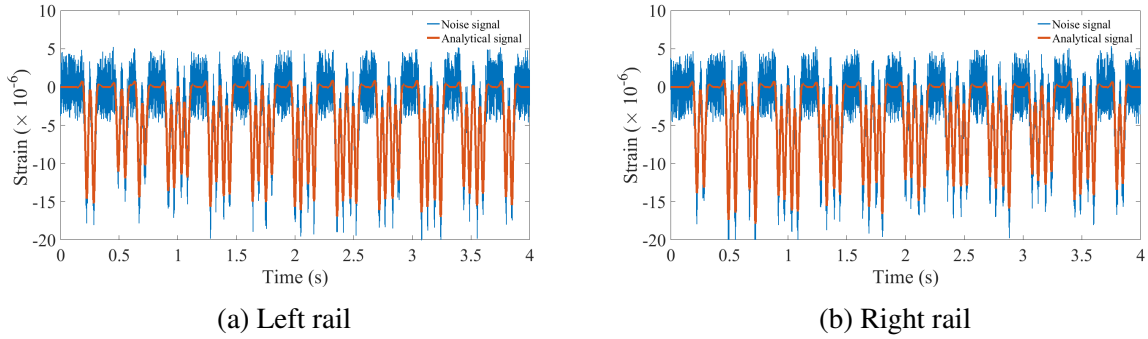


Figure 4: Analytical and noise signals on the left rail (a) and right rail (b)

Amplitude of noise	Left rail	Right rail	Average
Slightly noisy	0.281 %	0.285 %	0.283 %
Noisy	0.585 %	0.597 %	0.592 %
Very noisy	1.186 %	1.159 %	1.172 %
Strongly noisy	2.541 %	2.634 %	2.588 %

Table 2: Relative error between the train loads introduced and identified for different noise levels

Fig. 4 shows the case of large amount of introduced noise which the relative error is 1.17 %. With the strongly noisy signal, the relative error is about 2.6 %. Thus, we can conclude that the train loads identified have been found with a good precision.

3.2 Real signal

We will use the measurements recorded in-situ with the help of the “Smart Sleeper”. The measurement has been performed at Creil, France, on the 6th of May 2017. Fig. 7 shows the signal recorded by the “Smart Sleeper” during the passing of a train which contains 10 wagons

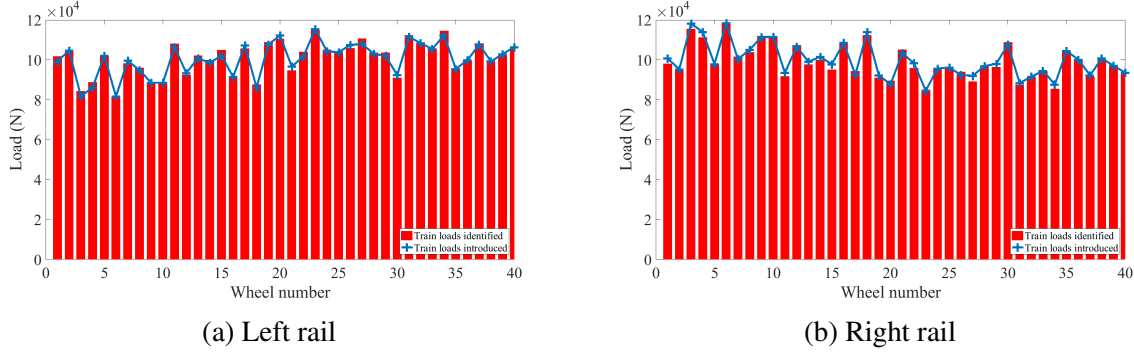


Figure 5: Superposition of the train loads introduced and identified on the left rail (a) and right rail (b)

including the locomotive. The green and red line represent the measurements on the left (a) and right (b) upper sensor respectively. The train loads on the two rails are shown in Fig. 6. The black in Fig. 7 represents the analytical sleeper response by using the identified train loads.

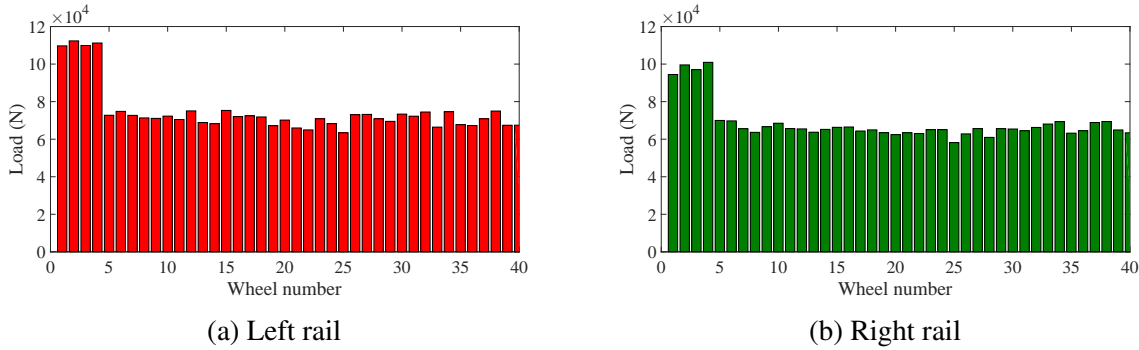


Figure 6: Train loads identified by using the measurements on the left rail (a) and right rail (b)

We note that the value of the first four loads on the two rails are bigger than the rest, corresponding to the locomotive of the train, which is normally heavier than the wagons. In the Fig. 7, the first four peaks are also superior to the rest.

Moreover, we note that the train loads on the two rails are not the same (in Fig 7, the sleeper strains on the left rail are superior to the right rail). By identifying the train loads, this phenomenon is demonstrated by the different charges on the two rails. The charges applied on the left rail are bigger than the right rail. This could be explained by the non-homogenous foundation or by the unbalanced of rolling stock.

4 CONCLUSION

Based on an analytical model of the railway sleeper the inverse problem has been developed to identify the train loads. In the frequency domain, the sleeper strain and the train loads can be linked by a linear relation. The train loads identified from the measurements in-situ demonstrate

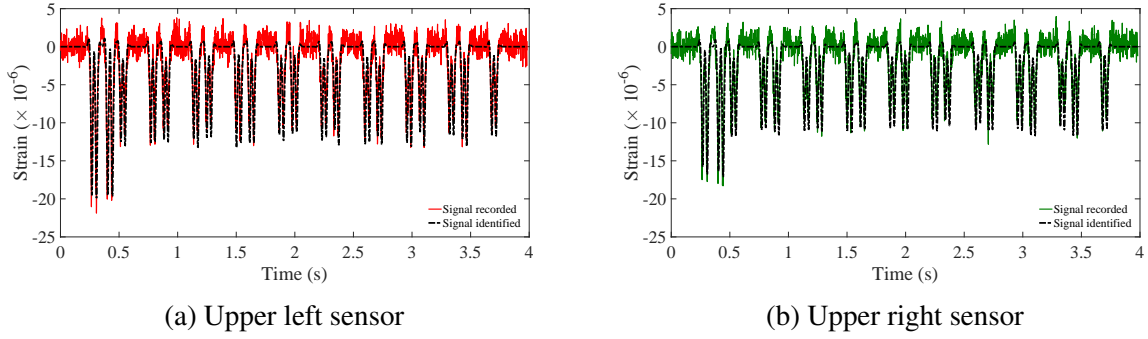


Figure 7: Sleeper response on the left rail (a) and right rail (b)

different values for each wheel of the train. Thus, this technique can detect the imperfection of the wheel-rail contact when the train load on one rail is much higher than the other. In future works, the model should be developed to identify other parameters of the railway track.

Acknowledgement

This work has been developed in the context of a partnership between Sateba (Consolis Group) and Ecole des Ponts ParisTech. The authors would like to thank the personnel of Sateba for their support.

A Periodically supported beam model

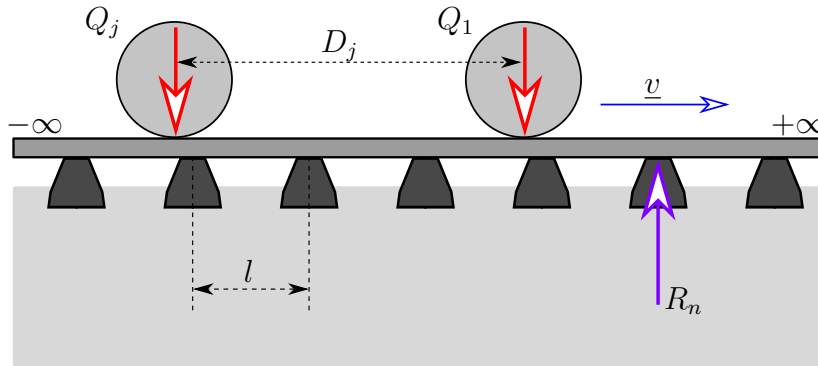


Figure 8

The periodically supported beam is shown in Fig. 8. When the rails are modeled by periodically supported beams [7], the forces R_k on each rail k in the frequency domain can be calculated as follows:

$$\hat{R}_k(\omega) = \mathcal{K} \hat{w}_r^{(k)}(\omega) + Q_k(\omega) \quad (15)$$

where \mathcal{K} is the equivalent stiffness, Q_k are the equivalent charges of the two rails which are determined. Let $w_r^{(k)}$ be the rail k displacements at the sleeper position respectively and $w_s(x, t)$

is the sleeper displacement where $x = \pm a$ corresponds to the positions of the rail seats. The forces \hat{R}_k can be expressed by the constitutive law of the rail pads in the frequency domain as follows:

$$\hat{R}_k(\omega) = -k_p (\hat{w}_r^{(k)}(\omega) - \hat{w}_s(a, \omega)) \quad (16)$$

where $k_p = k_{rp} + i\omega\zeta_{rp}$ is the dynamic stiffness of the rail pad and k_{rp} , ζ_{rp} are the stiffness and damping coefficients of the rail pads. By substituting Eq. (15) into Eq. (16), we obtain:

$$\hat{R}_k(\omega) = \frac{k_p \mathcal{K}}{k_p + \mathcal{K}} \hat{w}_s(a, \omega) + \frac{k_p}{k_p + \mathcal{K}} \mathcal{Q}_k(\omega) \quad (17)$$

B Green's function

By using the Fourier transform and combining equations (1), (2) and (3), this system dynamics equation can be rewritten in the frequency domain :

$$\begin{cases} \hat{w}_s''''(x, \omega) - \frac{T}{E_s I_s} \hat{w}_s''(x, \omega) - \frac{\rho_s S_s \omega^2 - k_b}{E_s I_s} \hat{w}_s(x, \omega) = -\frac{\hat{R}_1}{E_s I_s} \delta(x - a) - \frac{\hat{R}_2}{E_s I_s} \delta(x + a) \\ \hat{w}_s''(-L, \omega) = \hat{w}_s''(L, \omega) = 0 \\ \hat{w}_s'''(-L, \omega) = \hat{w}_s'''(L, \omega) = 0 \end{cases} \quad (18)$$

where (\square') stands for the partial derivative with regard to x and $k_b = k_f + i\omega\zeta_f$ is the foundation dynamic stiffness. The Green's function $G_a(x, \omega)$ of Eq. (18) is defined by :

$$\frac{\partial^4 G_a(x, \omega)}{\partial x^4} - \alpha_s^2 \frac{\partial^2 G_a(x, \omega)}{\partial x^2} - \lambda_s^4 G_a(x, \omega) = \delta(x - a) \quad (19)$$

where $\alpha_s = \sqrt{\frac{T}{E_s I_s}}$ and $\lambda_s = \sqrt[4]{\frac{\rho_s S_s \omega^2 - k_b}{E_s I_s}}$. This is a 4th order linear differential equation and its Green's function [22] can be written as follows:

$$G_a(x, \omega) = \begin{cases} A_1 e^{\lambda_1 x} + A_2 e^{\lambda_2 x} + A_3 e^{\lambda_3 x} + A_4 e^{\lambda_4 x} & \text{for } x \in [-L, a] \\ B_1 e^{\lambda_1 x} + B_2 e^{\lambda_2 x} + B_3 e^{\lambda_3 x} + B_4 e^{\lambda_4 x} & \text{for } x \in [a, L] \end{cases} \quad (20)$$

where A_i , B_i , and λ_i (with $1 \leq i \leq 4$) are parameters to be determined. λ_i is the 4 complex roots of the characteristic equation:

$$\mathcal{P}(\lambda) = \lambda^4 - \alpha_s^2 \lambda^2 - \lambda_s^4 \quad (21)$$

By using the boundary conditions of the free-free beam (continuity condition for displacement, slope and moments, discontinuity of magnitude one at the point force), we can obtain analytical expressions for A_i , B_i .

REFERENCES

- [1] H. F. Lam, Q. Hu and M. T. Wong, The Bayesian methodology for the detection of railway ballast damage under a concrete sleeper, *Engineering Structures* 81 (2005) 289–301.
- [2] A. Remennikov, S. Kaewunruen, Experimental Investigation on dynamic railway sleeper/ballast interaction, *Experimental Mechanics* 46 (1) (2006) 57–66.
- [3] M. Kodai, W. Tsutomu and S. Masamichi, Damage detection method for sleepers based on vibration properties, *EDP Sciences* 24 (2015).
- [4] D.J. Mead, Free wave propagation in periodically supported, infinite beams, *Journal of Sound and Vibration* 11 (2) (1970) 181–197.
- [5] D.J. Mead, Wave propagation in continuous periodic structures: research contributions from Southampton, *Journal of Sound and Vibration* 190 (3) (1996) 495–524.
- [6] X. Sheng, C. Jones and D. Thompson, Responses of infinite periodic structures to moving or stationary harmonic loads, *Journal of Sound and Vibration* 303 (3-5) (2007) 873–894.
- [7] T. Hoang, D. Duhamel, G. Foret, H. Yin, P. Joyez and R. Caby, Calculation of force distribution for a periodically supported beam subjected to moving loads, *Journal of Sound and Vibration* 388 (2017) 327–338.
- [8] H. Ding, L. Q. Chen, S. P. Yang, Convergence of Galerkin truncation for dynamic response of finite beams on nonlinear foundations under a moving load, *Journal of Sound and Vibration* 331 (10) (2012) 2426–2442.
- [9] V. H. Nguyen, D. Duhamel, Finite element procedures for nonlinear structures in moving coordinate. Part 1: Infinite bar under moving axial loads, *Computer & Structures* 84(21) (2006) 1368–1380.
- [10] V. H. Nguyen, D. Duhamel, Finite element procedures for nonlinear structures in moving coordinate. Part 2: Infinite beam under moving harmonic loads, *Computer & Structures* 86(21) 2056–2063.
- [11] L. H. Tran, T. Hoang, D. Duhamel, G. Foret, S. Messad, A. Loaïc, Analytical model of the dynamics of railway sleeper, 6th International Conference on Computational Methods in Structural Dynamics and Earthquake Engineering 2 (2017) 3937–3948.
- [12] M. L. Filograno et al., Real time monitoring of railway traffic using Fiber Bragg Grating sensors, *IEEE Sensors Journal* 12(1) (2012) 85–92.
- [13] C. Wei et al., A Fiber Bragg Grating sensor system for train axle counting, *IEEE Sensors Journal* 12(10) (2010) 1905–1912.
- [14] C. Wei et al., Real-Time train wheel condition monitoring by Fiber Bragg Grating sensors, *International Journal of Distributed Sensor Networks* 10 (2012).

- [15] S. J. Buggy et al., Railway track component condition monitoring using optical fibre Bragg Grating sensors, *Measurements Science and Technology* 27(5) (2016) 1–15.
- [16] H. Y. Tam et al., Utilization of fiber optic Bragg Grating sensing systems for health monitoring in railway applications, 6th International Workshop on Structural Health Monitoring, Stanford University, Stanford, CA, September 11-13, (2007) 1824.
- [17] R. Pimentel et al., Hybrid Fiber-Optic/Electrical measurement system for characterization of railway traffic and its effects on a short span bridge, *IEEE Sensors Journal* 8(7) (2008) 1243–1249.
- [18] S. L. Ho et al., Real time monitoring of railway traffic using Fiber Bragg Grating sensors, *IEEE Sensors Journal* (2006) 125–129.
- [19] L. Arnaud, P. Charles, Smart Sleeper : Measurement of bending moments in concrete sleepers laid on ballast tracks, *Transport Research Arena (TRA) 5th Conference: Transport Solutions from Research to Deployment*, (2014).
- [20] G. Kumaran, D. Menon and K. Krishnan Nair, Dynamic studies of railtrack sleepers in a track structure system, *Journal of Sound and Vibration*, 268(3) (2003) 485–501
- [21] A. A. Arab, S. S. Badie and M. T. Manzari, A methodological approach for finite element modeling of pretensioned concrete members at the release of pretensioning, *Engineering Structures*, 33(6) (2011) 1918–1929
- [22] E. Zauderer, *Partial differential equations of applied mathematics*, John Wiley Sons (1989).

An Engineering-oriented Simplified Methodology for Analysing Non-linear Behavior of Reinforced Concrete Structures

Nhu Cuong Tran*

*EDF R&D;

ABSTRACT

Modelling the non-linear behavior of damaged concrete structure is always a complex challenge for civil engineer. On one hand, application of non-linear damage models developed in the litterature for civil engineering structures is still difficult because of their complexity and their limited capacity. On the other hand, the elastic modelling approach used by many engineering services can overestimate stress inside structure especially in the case of displacement loading. In this work, we present a new structural modelling approach which is able to take into account the damage level of concrete without applying non-linear damage models. This approach is particularly suitable to the structures which mainly work in bending mode as beam or shell. The philosophy here is to do some iterative computations. The computation at current step uses a reduced Young modulu of damaged concrete which is determined as a function of strain computed in the previous step. The results obtained after three iterative computations using this approach are compared with the ones obtained in a real non-linear damage modelling. The difference between them which is lower than 10% is considered good for a civil engineering application. This simple, rapide and performant computation approach could be an alternative method to integrate into commercial software for engineering applications.

Simple Numerical Model for a Pipe-Lay on Uneven Seabed

Pavel Trapper*

*Ben-Gurion University of the Negev

ABSTRACT

Submarine pipeline installation process involves the pipe being laid from a barge into the water all the way to the bottom where it comes into contact with a seabed. The possible unevenness of the seabed, such as inclined plane, pits and hills may substantially affect pipeline configuration and lead to severe stress concentrations. In order to perform a proper design of the pipeline, one has to account for the pipe-seabed interaction. In the present study, a simple numerical model to analyze static pipeline configurations during the pipe-lay process on uneven seabed is presented. The technique also accounts for nonlinear stiffness of soil, and other environmental loading such as drag forces applied by the sea water. The solution technique is based on a finite difference discretization of nonlinear beam equation, which accounts for large deformations of the pipe. The whole pipeline is treated as single continuous segment. The solution is carried out in an incremental/iterative way, where the pipe is being gradually released from the barge into the water and laid on a seabed. During this process, pipe nodes are laid down and, one by one, come into a contact with the seabed. Active set of nodes beyond the touchdown point is updated iteratively, allowing for the separation due to irreversible plastic deformation of the seabed and emerging free spans. To demonstrate the method, several pipe-lay scenarios with different seabed topographies are presented. It is shown how on-bottom unevenness, including pits and hills, can affect pipeline configuration, formation of free spans, tension forces, shear forces, bending moments within the pipe, and its embedment into the seabed. The role of a top tension force applied by the laying barge is emphasized. The approach presents simple and computationally efficient way to analyze the pipe-lay on a seabed with complex geometry and nonlinear stiffness. The proposed model, contrary to time-consuming commercial packages, allows for performing the analysis in reasonable time on standard engineering computers.

A New Family of Hybrid Particle-mesh Methods for Conservation Laws

Nathaniel Trask^{*}, Pavel Bochev^{**}, Mauro Perego^{***}

^{*}Sandia National Laboratories, ^{**}Sandia National Laboratories, ^{***}Sandia National Laboratories

ABSTRACT

A key challenge in the practical application of traditional mesh-based methods is the dependence of the approximation upon the quality of an underlying mesh. This poses a bottleneck for engineering workflows, in which time to solution may be dominated by mesh-generation in preprocessing. Meshfree discretizations, on the other hand, possess a rich approximation theory that is by definition independent of any underlying mesh. Though accurate, pure meshfree schemes face their own challenges in developing notions of either discrete conservation or a stability theory; both properties taken for granted in mesh-based methods. In this talk, we present recent work using generalized moving least squares (GMLS) to address these issues and obtain the favorable properties of both worlds. By incorporating both meshfree approximation and an underlying mesh, we develop a family of hybrid particle/mesh schemes that may either be used in an Eulerian setting to enhance the accuracy and robustness of classical finite volume methods, or may be used in a Lagrangian setting to develop particle discretizations with notions of conservation and consistency.

Aeroelastic Analysis of an Inverted Wing Operating in Ground Effect Using Fluid-Structure Interaction

Ian Travell*, Rishi Abhyankar**

*Cranfield University / Multimatic Inc., **Cranfield University

ABSTRACT

A fluid-structure interaction model with strong coupling was developed for an inverted swept wing operating in ground effect. This model offered an improvement over traditional CFD models due to its ability to capture aeroelastic effects and provided the ability to investigate aeroelastic tailoring. A structural finite element model was used to determine a composite laminate structures for a simplified Formula 1 wing such that it would be sufficiently stiff to pass FIA rules mandated stiffness criteria. A 2D fluid model was used to validate the CFD solution using published experimental data for a Tyrrell 026 front wing aerofoil. The lift coefficient calculated in CFD correlated to experimental data to within 3 %. The fluid and structural models were then combined into a FSI model with strong two-way coupling. Causes of numerical instabilities from combining the two models were identified, discussed, addressed. Steady state solutions were attained for both a CFD model and a FSI model using the same 3D wing geometry, with the FSI model predicting an additional 2.19 % downforce over the CFD case. Aeroelastic tailoring was investigated by varying the laminate ply orientations and thicknesses and by changing the core material construction. A novel laminate structure was employed to couple the wing bending and torsion modes together. This resulted in the wing angle decreasing under fluid loading and provided a modest reduction in drag. A similar drag reduction effect was achieved by reducing the laminate thickness at the trailing edge to decrease the effective aerofoil camber when subjected to fluid loading. The laminate thickness at the leading edge was increased to maintain spanwise bending stiffness.

The Utility of Rapid Prototyping and 3D Virtual Modeling in Procedural Planning and Surgical Simulation for Congenital Heart Disease

Hannah Tredway*, Puneet Bhatla**, Michael Argilla***, Ralph Mosca****

*NYU School of Medicine, **Division of Pediatric Cardiology, Department of Radiology, NYU Langone Medical Center, ***Division of Pediatric Cardiology, NYU Langone Medical Center, ****Department of Cardiac Surgery, NYU Langone Medical Center

ABSTRACT

Background: Accurate characterization of cardiac anatomy is critical for the understanding and management of congenital heart disease (CHD). While traditional imaging methods allow for visualization of cardiac structures and depiction of morphologic defects, adequate understanding of the spatial relationships and complex cardiac connections remains a challenge. Rapid prototyping and three-dimensional (3D) models are gaining utility in the understanding and management of complex CHD as they allow for detailed portrayal of cardiac anatomy and visualization from multiple viewpoints. Here, we discuss our experience in creating patient-specific models and their utility in procedural simulation and planning. Methods: For each case, a virtual or physical 3D model was generated using computed tomography source data imported into an image post-processing workstation. Commercially available software was used to segment the blood pool and build a patient-specific heart replica. The models were cropped to highlight the anatomy of interest from various planes. When indicated, flexible models were printed using a polyjet printer. Cases: First, is an 11-month-old with numerous cardiac anomalies including multiple large muscular ventricular septal defects (VSD's). Following several failed attempts at closure with operative and interventional techniques, a virtual 3D model was requested to better characterize the complex interventricular communications. The model demonstrated a large residual VSD located adjacent to the initial closure device and another that was restricted by prominent muscular trabeculations. This depiction illuminated the potential challenge of traversing the in situ device with a catheter, allowing the interventionalist to elicit an optimal approach for device closure. The model also guided the echocardiographer in obtaining appropriate imaging angles to detect the success of the procedure. Next, is a 12-month-old with total anomalous pulmonary venous return that was surgically corrected via an anastomosis between the pulmonary veins and the right atrium. After one year, the patient presented in heart failure with significant left to right shunting across the residual interatrial communication. A model was requested to better elucidate the intracardiac anomalies. This physical model allowed the surgeon to manipulate the structures and elicit the feasibility of placing a baffle between the pulmonary veins and the left atrium, thereby redirecting blood flow and reducing intracardiac shunting. Conclusion: Virtual and printed 3D cardiac models can be invaluable in depicting the anatomy and complex spatial relationships of CHD. These models provide the means to visualize and manipulate the anatomy in any desired plane and thereby play a crucial role in guiding surgical and interventional strategies.

Flow Simulation in Heterogeneous Porous Media with the Moving Least-Squares Method

Dimitar Trenev^{*}, Laurent White^{**}, Rohan Panchadhara^{***}

^{*}ExxonMobil Research & Engineering, ^{**}ExxonMobil Research & Engineering, ^{***}ExxonMobil Research & Engineering

ABSTRACT

For historical reasons, as well as its speed of execution and simplicity, the two-point-flux finite-volume method is still the preferred technique for discretizing Darcy's law in most commercial reservoir simulators today. It is well known, however, that this method suffers from inaccuracies when applied to grids that are not K-orthogonal, which tends to occur more frequently as reservoir engineers rely on increasingly complex reservoir models. As reservoir simulations are used to guide the decisions during the development planning and production optimization of oil and gas fields, it is important to develop improved numerical methods for a more accurate and reliable prediction of the flow streams. In this talk, we present some novel enhancements of the moving least-squares method designed to specifically handle discontinuous and anisotropic permeability fields. This approach is an attractive alternative to the traditional discretization scheme based on the two-point-flux approximation for Darcy's law and a first-order finite-volume scheme for transport for two main reasons. First, the proposed cell-centered reconstruction scheme does not directly rely on mesh topology or whether the mesh is K-orthogonal. Second, increasing the number of neighboring points involved in the reconstruction results in a higher-order approximation of sharp flow fronts, offering an increased resolution when compared to the first-order approximation. We will present a set of numerical results – from solving Poisson's equation with discontinuous tensors on a non-K-orthogonal mesh, to a complete oil-water flow simulation in a complex, anisotropic reservoir – in support of these claims.

ON CONTROLLING, MONITORING AND HARVESTING ENERGY FROM STRUCTURAL VIBRATION USING NETWORKS OF DISTRIBUTED PIEZOELECTRIC PATCHES

M.A. TRINDADE, J.Q. VELÁSQUEZ, A.H. SHIGUEOKA,
H.J. CRUZ NETO, F.M. HORIY

Department of Mechanical Engineering,
São Carlos School of Engineering, University of São Paulo,
São Carlos, SP 13566-590, Brazil,
trindade@sc.usp.br, <http://www.eesc.usp.br/labdin>

Keywords: Vibration control, Piezoelectric materials, Sensors networks, Spatial modal filters.

Abstract. Piezoelectric materials are widely employed as thin layers or patches bonded on thin flexible structures forming multilayer composite structures, which may be used in automotive, aeronautical, aerospace, microelectronics and micromechanics applications, for sensing, vibration control, structural health monitoring, energy harvesting, among others. The search for performance improvement of these piezoelectric patches involves the optimization of the electromechanical coupling between piezoelectric patches and structural vibration modes. For that, there are several important aspects to account for, including the bonding effectiveness between patches and host structure, the location of each patch alone and the relative distribution of the patches. This work presents some recent advances on the optimization of networks of piezoelectric patches for applications in active structural vibration control and energy harvesting from structural vibrations.

1 INTRODUCTION

Piezoelectric materials are widely employed as thin layers or patches adhesively bonded on thin flexible structures forming multilayer composite structures, which may be used in automotive, aeronautical, aerospace or even microelectronics and micromechanics applications, for sensing, vibration control, structural health monitoring, energy harvesting, among others [1, 2, 3].

In vibration control applications, the piezoelectric patches may be used as sensors and/or actuators that enable the development of passive, active, semi-passive or active-passive vibration control solutions [1]. The performance and interest of active solutions are always limited by relatively weak actuation power of piezoelectric patches and cumbersome power electronics. One advantage of active-passive solutions is that they may combine the adaptivity of active control with the robustness of passive control. This could be achieved using an optimized combination of viscoelastic treatments for passive damping and piezoelectric actuators for active control [4, 5]. To

tackle the issue of required power for active control, some authors considered the use of resonant shunt circuits in series with the voltage source to improve the control authority [6, 7, 8, 9].

In this case, the advantage of a network of piezoelectric patches is that it allows targeting either a selected small number of vibration modes or even a specific single one. Thus, some authors proposed the use of adaptive/reconfigurable arrays or networks of sensors and actuators with the main objective of minimizing the power spilled to control non-interesting dynamics. Most methodologies proposed in these studies are based on the concept of modal, semi-modal or quasi-modal control using, for instance, spatial modal filters [10, 11, 12, 13, 14, 15]. These are particularly interesting for the attenuation of specific low-frequency vibration or sound radiation modes. In this case, the signals of the sensors in a network are combined to approximate the response of a selected mode-equivalent system, in which the contribution of undesired modes is excluded. By doing this, a feedback of such combined (or filtered) signal could lead to a focus of the control effort on the modes of interest and also would not affect the undesired modes.

Another way of profiting from a network of sensors for a focused active control is by considering a methodology so-called incomplete state feedback (ISF), also known as partial state feedback or optimal output feedback, as proposed by [16]. Its main advantage is to start from well-known LQR optimal control which provides good frequency properties, such as gain and phase margins. Instead of using a state observer, which increases system complexity, real-time computational effort and time delays, this technique considers only measured outputs for feedback. However, unlike LQR, the performance of ISF is dependent on system initial conditions. Therefore, some technique must be considered to guarantee robustness of the control performance for realistic unknown initial conditions [16, 17]. It is also important to consider the output matrix design, which includes the number, type and position of sensors. In analogy to the LQR control problem, a quadratic cost function may also be used to optimize ISF sensors locations [18, 17].

Presented results show that the active vibration control performance can be substantially increased with the use of such strategies. In addition, the adaptivity of solution is preserved in the sense that it can be modified in real time according to the operation and/or performance criteria.

In structural health monitoring (SHM) applications, networks of piezoelectric patches working as sensors may be used to detect damage by means of changes in the structural response signature [2]. This typically includes permanent mounted or embedded elements for sensing or data acquisition, signal processing and wireless communication [19]. Fortunately, piezoelectric materials high electromechanical coupling characteristic allows their use as sensor but also for micro power generation or energy harvesting [3]. In energy harvesting applications, networks of piezoelectric patches working in sensor mode connected to a harvester electric circuit are bonded onto flexible structures subjected to a vibration source, such that the vibration energy may be converted into usable electric energy. However, to improve the performance of piezoelectric energy harvesting of a sensors network, it is required to increase the electromechanical coupling between host structure and piezoelectric patches. For that, there are several important aspects to account for, including the bonding effectiveness between each patch and host structure, the location of each patch alone and the relative distribution of the patches. Besides, these important properties to be optimized may also be subjected to uncertainties [20, 21]. In this case, the advantage of a network of sensors is to facilitate localization of potential damages and also it may improve the amount of harvested energy with little added complexity. Therefore, once again, the use of a properly designed network of sensors may improve the overall multifunctional performance of system.

This work presents some recent results on the design of networks of sensors aiming at improving

active vibration control and energy harvesting performances based on a plate type host structure.

2 ACTIVE VIBRATION CONTROL USING PIEZOELECTRIC NETWORKS AND DISCRETE MODAL FILTERS

In this section, some results on the active vibration control of a plate type structure using a network of piezoelectric sensors and actuators are presented. The general design criteria is to allow using the very simple and practical direct output feedback control law. In the present study, for a given network of piezoelectric sensors and actuators bonded onto the host structure, three strategies to evaluate the optimal output feedback control gains are considered: i) using the network as a spatial modal filter to obtain an equivalent modal sensor which signal can be fed back as control voltage applied to piezoelectric actuators; ii) using a genetic algorithm optimization to evaluate control gains for each piezoelectric sensor output; and iii) using incomplete state feedback technique to evaluate control gains for each piezoelectric sensor output.

2.1 Problem description

An aluminum plate with dimensions $545 \times 400 \times 3$ mm, density of 2700 kg/m^3 , Young module of 69 GPa, Poisson's ratio 0.33, and clamped at all edges is considered as the host structure. 20 piezoelectric patches with dimensions $24 \times 25 \times 0.5$ mm and made of piezoceramic PZT5H are distributed over the host structure, such that a regular network of four by four sensors and another of two by two actuators are considered as shown in Figure 1. The finite element mesh together with the positions of sensors and actuators and input and output locations considered for the simulations are shown in Figure 2. The mobility of the first input/output (In1/Out1) will be considered for performance evaluation.

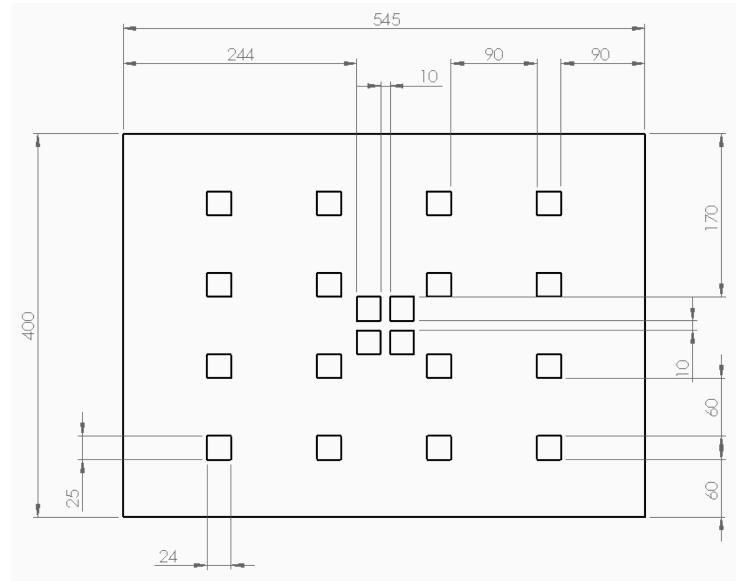


Figure 1: Regular network of piezoelectric patches, four by four sensors and four actuators in the center, 24×25 mm, bonded onto a clamped aluminum plate, $545 \times 400 \times 3$ mm.

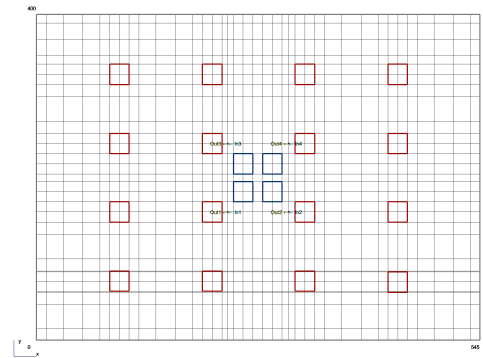


Figure 2: Finite element mesh, sensors/actuators positions and input/output locations.

Starting from a finite element model for the structure with piezoelectric patches with mechanical displacements and electric charges at patches as degrees of freedom, it is possible to write

electromechanical coupled equations of motion. A reduced-order model is then obtained, by projecting onto a reduced undamped modal basis, where the first m vibration modes are retained. This leads to the following equations of motion written in terms of modal coordinates, voltages induced in sensors and voltages applied to actuators,

$$\ddot{\boldsymbol{\eta}} + \Lambda \dot{\boldsymbol{\eta}} + \Omega^2 \boldsymbol{\eta} = \Phi^T \mathbf{f}(t) + \Phi^T \mathbf{K}_{uva} V_a \quad (1)$$

$$\mathbf{V}_s = -\mathbf{K}_{uqs}^T \Phi \boldsymbol{\eta}, \quad (2)$$

where Λ is a matrix of modal damping; Ω^2 is a diagonal matrix whose elements are the square of the natural frequencies; Φ is a matrix whose columns are the eigenvectors associated to the m first vibration modes normalized such that $\Phi^T \mathbf{M} \Phi = \mathbf{I}$, where \mathbf{I} is the identity matrix. The vector $\boldsymbol{\eta}$ is obtained from the transformation $\mathbf{u} = \Phi \boldsymbol{\eta}$. By defining the state vector as $\mathbf{z} = [\boldsymbol{\eta} \ \dot{\boldsymbol{\eta}}]^T$, it is possible to rewrite the system equations as

$$\dot{\mathbf{z}} = \mathbf{A} \mathbf{z} + \mathbf{B}_f \mathbf{f} + \mathbf{B}_a V_a, \quad (3)$$

$$y = \dot{u}_p = \mathbf{C}_y \mathbf{z}, \quad \mathbf{C}_y = [\mathbf{0} \quad \mathbf{C}_u \Phi], \quad (4)$$

$$\dot{\mathbf{V}}_s = \mathbf{C} \mathbf{z}, \quad \mathbf{C} = [\mathbf{0} \quad \mathbf{K}_{uqs}^T \Phi], \quad (5)$$

The output of the modal filter is, according to its definition,

$$V_f = \boldsymbol{\alpha}^T \mathbf{V}_s. \quad (6)$$

The control law of the form

$$V_a(t) = -K_f \dot{V}_f = -\mathbf{K} \dot{\mathbf{V}}_s = -\mathbf{K}_z \mathbf{z}, \quad \text{with } \mathbf{K} = K_f \boldsymbol{\alpha}^T, \quad \mathbf{K}_z = \mathbf{K} \mathbf{C}. \quad (7)$$

Thus, the control law can be either seen as the direct feedback of a single output \dot{V}_f with control gain K_f or as the direct feedback of multiple outputs $\dot{\mathbf{V}}_s$ with control gains \mathbf{K} . One way or another, given \mathbf{K} it is possible to factor out K_f to obtain a vector $\boldsymbol{\alpha}$ that establishes the relative gain distribution for each sensor.

By using Eqs. (3), (5), (6) and (7), it is possible to arrive at the state-space formulation of the closed-loop system. Then, by taking its Laplace Transform and isolating \mathbf{z} , the closed-loop displacement velocity measured at a given point and the control effort may then be calculated by combining to Eqs. (4), (5) and (7), resulting in

$$y(s) = \mathbf{C}_y (\mathbf{I}s - \mathbf{A} + K_f \mathbf{B}_a \boldsymbol{\alpha}^T \mathbf{C})^{-1} \mathbf{B}_f f(s) = H_{yf}(s) f(s) \quad (8)$$

$$V_a(s) = -K_f \boldsymbol{\alpha}^T \mathbf{C} (\mathbf{I}s - \mathbf{A} + K_f \mathbf{B}_a \boldsymbol{\alpha}^T \mathbf{C})^{-1} \mathbf{B}_f f(s) = H_{vaf}(s) f(s). \quad (9)$$

Thus the FRF with force input $f(\omega)$ and displacement velocity output $y(\omega)$, hereinafter denominated H_{yf} , may be found by evaluating Eq. (8) after applying the transformation $s = i\omega$ over the desired frequency range. Likewise, the FRF of the force input $f(s)$ and control effort output $V_a(s)$, henceforth denominated H_{vaf} , may be found after following the same procedure with Eq. (9).

2.2 Control design

2.2.1 Design of control gains based on spatial modal filters (LSQ)

The first method for designing the feedback control is based on the concept of spatial modal filters. It consists on first determining the optimal weighting coefficients $\boldsymbol{\alpha}$ based on the FRF of

each sensor in the network and the natural frequencies of the target vibration modes. Hence, the resulting filtered response (weighted sum of sensors outputs) can be designed to approximate a desired FRF. For instance, a desired FRF may be defined as the response of an equivalent system of one degree of freedom with natural frequency ω_j and damping factor ξ_j such that

$$g_j(\omega) = \frac{2\xi_j\omega_j^2}{\omega_j^2 - \omega^2 + 2i\xi_j\omega_j\omega} \quad (10)$$

Considering \mathbf{Y} as the discretized FRF matrix, with one column for each sensor in the network and one row for each frequency $\omega \in [\omega_1, \dots, \omega_m]$ and \mathbf{G}_j as the discretized target FRF, with one row for each frequency ω according to $g_j(\omega)$, one then searches for a vector of coefficients α_j such that

$$\mathbf{Y}\alpha_j = \mathbf{G}_j. \quad (11)$$

According to [14], the linear system defined by Eq. (11) in general admits only approximate solutions, which will be denoted α_j^* . The vector of weighting coefficients α_j^* represents the best solution, in the least-squares sense, for the design of a modal filter which isolates the j -th vibration mode response. The approximation of Eq. (11) can be obtained by traditional Moore-Penrose pseudo-inverse. Since \mathbf{Y} may be decomposed through QR decomposition, where \mathbf{Q}_Y is an orthonormal matrix and \mathbf{R}_Y is upper triangular, such that $\mathbf{Y} = \mathbf{Q}_Y\mathbf{R}_Y$, α_j^* can be written as

$$\alpha_j^* = \mathbf{R}_Y^{-1}\mathbf{Q}_Y^H\mathbf{G}_j \quad (12)$$

Alternatively, one may design a multi-modal target FRF by combining different mono-modal ones, such as $\mathbf{G}_c = \sum_j w_j \mathbf{G}_j$. w_j may be defined depending on the relative importance of each vibration mode to the feedback control performance criteria. The QR decomposition method was one of the methods employed in this work being convenient for the cases in which the FRF matrix has had full column rank. Besides, it can be shown that the pseudo-inverse method provides the least squares solution. Therefore, from now on, this method for evaluating the weighting coefficients will be denoted LSQ.

This technique may be effective for a given frequency range. However, [12] stated that the number of sensors required in the network should be at least the number of modes present in the frequency band of interest. Then, [14], have shown that is possible to decrease the number of required sensors by optimizing their locations. In any case, however, for practical applications in which the modal filter is not perfect, some further digital filtering could be required [15].

Then, with weighting coefficients α defined, the output feedback control gain K_f is evaluated using an dichotomy search algorithm so as to minimize the following cost function

$$J = \begin{cases} \sum_j W_j |H_{yf}(\omega_{r,j})|, & \text{if } \xi_j > 0.25\% \quad \text{and} \quad \max_{\omega_{r,j}} |H_{vaf}(\omega_{r,j})| \leq 200 \text{ V/N} \\ 10^6, & \text{otherwise} \end{cases} \quad (13)$$

where W_j are weighting coefficients and $\omega_{r,j}$ is the resonance frequency of the j -th vibration mode. Thus J is a weighted sum of all the peaks of the FRF H_{yf} provided all modal damping are above a given threshold (0.25%) and control voltage is below a stipulated limit (200 V/N). In practice, the control gain K_f is increased until either modal damping or control effort (or both) criteria is violated. If at least one is violated, a high value is set to the cost function to penalize the solution.

2.2.2 Design of control gains using Genetic Algorithm (GA)

Another strategy is to search for sensors signal weights that optimize the closed-loop response according to a given cost function [22]. Using this approach, the corresponding combined signal may not be related to that of a modal filter but its response is such that when fed back through the control actuators, the closed-loop response is improved. This is done through a direct search using genetic algorithm, which is an evolutive computation method based on a population that undergoes successive applications of mainly two operations, crossover and mutation, that will search the best individual. Each individual in a population is an instance of the design parameters. In the present case, one individual is a set of weighting coefficients α , whose probability of survival in the population depends on how well it scores with the objective function. For each individual, the control gain K_f is calculated according to the procedure described in the previous section. The fitness of each individual is then set to the performance index J used to find the optimal K_f .

2.2.3 Design of control gains using optimal output feedback (ISF)

The third method for evaluating the control gains is based on a technique put forward by Levine and Athans [16] that consists on solving an optimization problem considering a quadratic performance criterion, similar to LQR method, but for which the control input is proportional to a vector of outputs, unlike LQR for which the control input is proportional to the full state vector.

Considering the state space system defined in (3), (4) and (5), the control gain vector $\mathbf{K} = K_f \alpha^T$ is to be determined in order to minimize the following cost function

$$J = \int_0^\infty (\mathbf{z}^T \mathbf{Q} \mathbf{z} + R V_a^2) dt, \quad (14)$$

that represents a trade-off between control effort and performance. Considering that the system is stabilizable, it is possible to rewrite this function in the form

$$J = \text{tr} \{ \mathbf{P} \mathbf{Z} \} + \text{tr} \{ \mathbf{S} (\mathbf{A}_c^T \mathbf{P} + \mathbf{P} \mathbf{A}_c + \mathbf{Q} + \mathbf{K}^T \mathbf{R} \mathbf{K}) \} \quad (15)$$

in which \mathbf{Z} is a matrix given by the product $\mathbf{z}(0) \mathbf{z}^T(0)$, $\mathbf{S} \in \mathbb{R}^{2n \times 2n}$ is a symmetric matrix of Lagrange multipliers and \mathbf{A}_c is the closed loop matrix ($\mathbf{A}_c = \mathbf{A} - \mathbf{B}_a \mathbf{K} \mathbf{C}$). The first order necessary conditions for optimality are given by the partial derivatives of J with respect to the independent variables

$$\frac{\partial J}{\partial \mathbf{S}} = \mathbf{A}_c^T \mathbf{P} + \mathbf{P} \mathbf{A}_c + \mathbf{Q} + \mathbf{C}^T \mathbf{K}^T \mathbf{R} \mathbf{K} \mathbf{C} = 0, \quad (16)$$

$$\frac{\partial J}{\partial \mathbf{P}} = \mathbf{A}_c \mathbf{S} + \mathbf{S} \mathbf{A}_c^T + \mathbf{X} = 0, \quad (17)$$

$$\frac{1}{2} \frac{\partial J}{\partial \mathbf{K}} = \mathbf{R} \mathbf{K} \mathbf{C} \mathbf{S} \mathbf{C}^T - \mathbf{B}_a^T \mathbf{P} \mathbf{S} \mathbf{C}^T = 0. \quad (18)$$

Equations (16), (17) and (18) are the necessary conditions given by [16]. Differently from the case of full state feedback, it is not possible to manipulate these equations in order to obtain one equation in function of a single variable, which means that they must be solved simultaneously. With this purpose, two algorithms are proposed to obtain a solution. In the first one, it is used a least squares method with the Levenberg-Marquardt algorithm. Like the algorithms proposed for

the problem of optimal output feedback, only (18) is used in the least squares method, so that in the i -th iteration, given the value of K_i , (16) and (17) are solved for P_i and S_i using an algorithm to solve Sylvester equations.

The existence of an optimal output feedback control is related to the existence of a static output feedback that stabilizes the system. This investigation about stability can be done using control Lyapunov functions, which allows to determine not only which control law stabilizes flexible structures, but also an optimal control law. It can be shown [17] that, for a structure with low damping, a cost function given by the velocity squared of one of its points plus the control squared is minimized by the collocated control with negative velocity feedback of the same point. Another interesting aspect of this result is that it is a solution of the LQR problem with only one sensor.

One important issue of the methodology proposed is the dependence of the cost function and the optimal solution on system initial conditions. The method proposed here to overcome this difficulty is based on a robust formulation, which consists in optimizing the cost function for the worst case of the uncertainty. To present the methodology, the cost function is first rewritten using the fact that for every control gain \mathbf{K} that makes the closed loop system stable, the second term of the cost function vanishes, such that

$$J = \text{tr} \{ \mathbf{P} \mathbf{Z} \}, \quad (19)$$

then, it is possible to specify a set that may represent well the possible system initial conditions, in which \mathbf{z}_0 is a central value, such that the initial condition belongs to a box of dimension $2n$ centered at \mathbf{z}_0 with width Δ . Thus, the cost function for the worst case (\bar{J}) is

$$\bar{J} = \text{tr} \{ \mathbf{P} (\mathbf{z}_0 \mathbf{z}_0^T + \mathbf{z}_0 \Delta^T + \Delta \mathbf{z}_0^T + \Delta \Delta^T) \}. \quad (20)$$

2.3 Comparison between the optimum from LSQ, GA and ISF

First, a modal analysis of the plate was performed to determine the vibration modes that could contribute the most to acoustic radiation and evaluate their natural frequencies and electric potential induced in the patches. Based on this analysis, the first, fourth and eighth vibration modes were selected as target for the active vibration control. Then, an assessment of the closed-loop performance when considering the three control design strategies presented in the previous section (LSQ, GA and ISF) is performed.

For LSQ, a target FRF is defined as $\mathbf{G}_c = \sum_j w_j \mathbf{G}_j$, with $w_j = 1$ for $j = 1, 4, 8$ and $w_j = 0$ for all other modes. Then, the control gain K_f is evaluated according to the cost function J , with $W_j = 1$ for $j = 1, 4, 8$, $W_j = 0.1$ for $j = 2, 3, 5, 6, 7, 9, 10$ and $W_j = 0.01$ for $j > 10$. The same cost function is used for GA strategy, where both weighing coefficients and control gain are evaluated simultaneously. For ISF, matrix \mathbf{Q} is defined based on the total energy of the system, $\mathbf{Q} = \text{diag}(\omega_1^2, \dots, \omega_N^2, 1 \dots, 1)$, and effort weighting is defined by trial and error to guarantee a maximum of 200 V/N in the actuators, such that $R = 10^{-8}$. In all cases, the frequency range considered for control design is [0, 1500] Hz. These parameters lead to the control gains and weighing coefficients shown in Table 1.

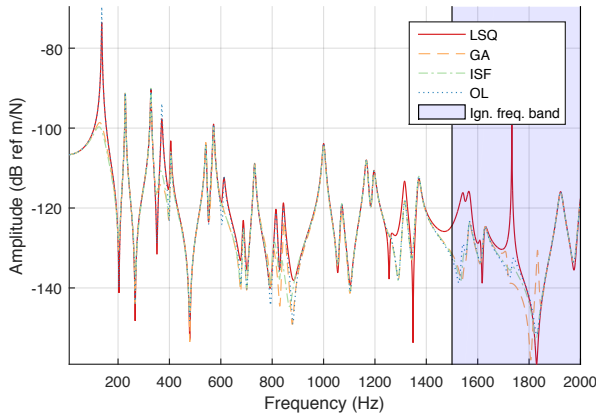
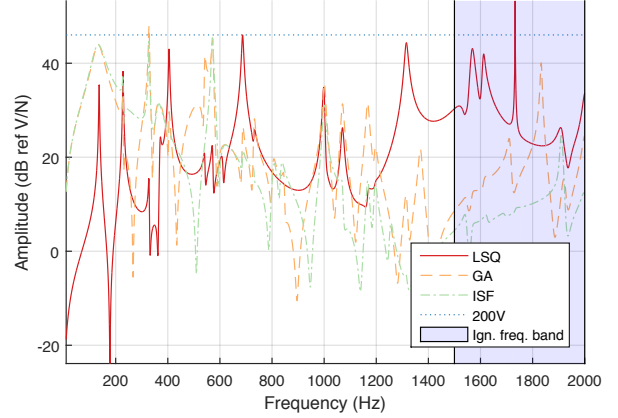
Figure 3 shows the closed-loop mobility using LSQ, GA and ISF strategies. Also, as reference, the open-loop mobility is also shown. It is noticeable that all strategies allow to reduce the peak amplitudes of the target modes (1, 4 and 8). However, LSQ performance is much smaller than GA and ISF ones. The amplitude reductions for the first, fourth and eighth modes are, respectively, 4, 4 and 0.5 dB for LSQ, 30, 23 and 8 dB for GA, and 31, 19 and 10 dB for ISF. The largest amplitude amplification is 3 dB for LSQ, 0.7 dB for GA, and 0.9 dB for ISF, within the design

Table 1: Control gains obtained with LSQ, GA and ISF strategies.

Sensor	K_f V/(V/s)	1	2	3	4	5	6	7	8
		9	10	11	12	13	14	15	16
LSQ	0.0064	-0.8631 0.5428	-0.5785 0.4526	0.6065 -0.2706	1.0000 -0.4946	0.1944 -0.4883	0.2146 -0.0748	0.1166 0.2504	-0.0271 0.5630
GA	0.0418	-0.1081 0.1163	-0.1127 0.8014	-0.0844 0.7584	0.1416 0.2967	0.2727 -0.1715	1.0000 -0.0756	0.7536 -0.1199	0.3876 -0.0104
ISF	0.0413	0.1184 0.3705	0.3269 1.0000	0.3559 0.9685	0.1584 0.4383	0.3414 0.1596	0.9492 0.3971	0.9274 0.4237	0.4286 0.1852

frequency range. The closed-loop modal damping factors for the first, fourth and eighth modes are, respectively, 0.8, 0.8 and 0.8% for LSQ, 15, 4 and 56% for GA, and 18, 5 and 8% for ISF.

Figure 4 shows the voltage control response for the LSQ, GA and ISF strategies in order to obtain the closed-loop performance shown in Figure 3. It is noticeable that the control effort frequency spectrum is quite different for the three strategies. Indeed, the resonance peak that limits the control effort and, thus, the closed-loop performance corresponds to the 9th, 3rd and 7th modes for LSQ, GA and ISF strategies, respectively.

**Figure 3:** Comparison between open-loop and closed-loop mobility using LSQ, GA and ISF strategies.**Figure 4:** Comparison between control effort using LSQ, GA and ISF strategies.

3 DISTRIBUTION OPTIMIZATION FOR ELECTROMECHANICAL COUPLING PERFORMANCE

In the literature, few works focused on the optimization of distributed networks of piezoelectric sensors to maximize their energy harvesting capabilities. Thus, some aspects affecting the electromechanical coupling of a piezoelectric sensors network, such as patches positioning, are studied here. This is done by, first, analyzing the effect on the electromechanical coupling of successive segmentation of piezoelectric material and the number of piezoelectric patches covering the host structure. Then, a genetic algorithm optimization is used to determine the optimal distribution of a fixed number of patches to maximize the electromechanical coupling. Results are obtained using a custom finite element model that accounts for adhesive layer properties.

3.1 Problem description

In the present work, it is considered that the potentially harvestable energy of a given piezoelectric element depends strongly on the effective electromechanical coupling coefficient (EMCCe) it provides to the structure. This represents the energy fraction that could be stored in the piezoelectric element when the structure vibrates in a given mode. The EMCCe of the structure depends on the electromechanical coupling coefficient (EMCC ou k_{ij}^2) of the material and on the mechanical coupling between the piezoelectric element and the host structure, consequently it can be expected that the EMCCe will be smaller than the material EMCC [23].

On the other hand, previous works indicate a potential reduction on the mechanical coupling between host structure and piezoelectric element due to the presence of an adhesive layer between them [20]. To evaluate the effect of the adhesive layer on the performance of surface-bonded piezoelectric patches working as energy harvesting devices, two analyses were proposed. In the first one, the effect of successive segmentation is investigated, once it is expected that segmentation could have a positive effect of mitigating electric charge cancellation but also a negative one due to an increase of border effects in the adhesive layer. In the second analysis, an optimization procedure is proposed to find a distribution of mechanically and electrically uncoupled piezoelectric patches that maximizes the EMCCe of the first five vibration modes.

3.2 Evaluation of effective electromechanical coupling (EMCCe)

For a generic flexible structure with a discrete distribution of piezoelectric patches, it is possible to evaluate the structure's EMCCe provided by each piezoelectric patch. A general procedure to calculate the EMCCe based on modeling has been proposed [23]. The i -th modal parameters, mode and natural frequency, of a structure with a discrete distribution of piezoelectric elements for SC and OC electric boundary conditions respectively can be found and, thus, the EMCCe of the structure, provided by a piezoelectric element, when it is vibrating in the i -th mode shape is defined as

$$k_i^2 = \frac{\omega_{OC}^i{}^2 - \omega_{SC}^i{}^2}{\omega_{OC}^i{}^2}. \quad (21)$$

3.3 Description of the proposed analyses

A network of piezoelectric patches is bonded onto a rectangular clamped plate aiming at harvesting energy from structural vibrations within a frequency-range that contains the first five resonant frequencies. The plate has dimensions $420 \times 320 \times 1 \text{ mm}^3$ and is made of aluminum with properties: Young modulus 70 GPa, Poisson's ratio 0.34 and mass density 2700 kg/m^3 . The piezoelectric patches have thickness 0.5 mm and are made of PZT-5H piezoceramic with properties taken from [20]. The patches are bonded to the structure using an adhesive layer with thickness 0.1 mm and properties: Young modulus 2.7 GPa, Poisson's ratio 0.4 and mass density 1140 kg/m^3 .

A uniform mesh of 42×32 elements was used to discretize aluminum plate, adhesive layer and piezoelectric patches. A modal analysis was performed and the first five mode shapes and natural frequencies of the clamped plate (without piezoelectric patches) are shown in Figure 5.

3.4 Analysis of a rectangular grid of piezoelectric patches

First, considering a patch size of $40 \times 40 \text{ mm}^2$, an analysis of the effective EMCC for varying number of patches in a rectangular grid is performed. In Table 2, the modal, average and specific

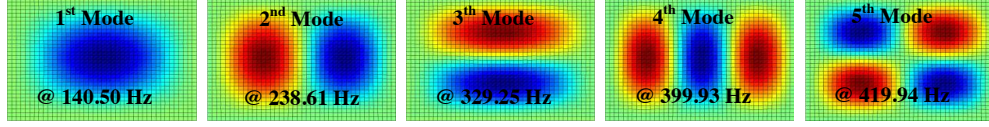


Figure 5: First five mode shapes of vibration and its natural frequencies for the clamped aluminum plate.

EMCCe by percentage of covered area are shown. Additionally, in the last one row, the ratio of average EMCCe per patch is also shown.

The biggest value of average EMCCe (9.2 %) found is for a configuration area with 48 patches (8x6). In terms of efficiency, 24 patches (6x4), 20 patches (5x4) and 16 patches (4x4) have similar values of specific EMCCe.

Table 2: Average and specific by percentage of covered area EMCCe values for all configurations of tested areas holding constant the patch size (40x40 mm²).

	Patches in x-direction									
	8		7		6		5		4	
Patches in y-direction	k_g^2	k_g^{2*}	k_g^2	k_g^{2*}	k_g^2	k_g^{2*}	k_g^2	k_g^{2*}	k_g^2	k_g^{2*}
7	8.8	13.2	8.3	14.2	7.3	14.6	6.1	14.6	4.9	14.6
6	9.2	16.2	8.7	17.4	7.7	17.9	6.4	17.9	5.1	17.8
5	9.0	18.8	8.5	20.3	7.4	20.8	6.2	20.8	4.9	20.7
4	7.7	20.3	7.3	21.8	6.4	22.4	5.3	22.3	4.2	22.1
3	5.8	20.4	5.5	21.9	4.8	22.3	3.9	22.0	3.1	21.9
2	3.8	19.7	3.5	21.1	3.0	21.2	2.5	20.8	2.0	20.7

3.5 Optimization of network distribution

Next, an optimization is performed to find the optimal distribution of a network of piezoelectric patches, which maximizes the average EMCCe for the first five modes of the structure. This is done using a genetic algorithm (GA) based optimization method. The objective is to find the vector x_{Np} , that represent the positions of N_p piezoelectric patches, which maximizes the cost function

$$J(x_{Np}) = \sum_{i=1}^{N_m=5} k_i (x_{Np})^2. \quad (25)$$

Results obtained in the previous parametric analyses were used as initial data to search for optimal distributions of a network of piezoelectric patches that maximize the average EMCCe of the structure and, consequently, its expected harvesting performance when working in a frequency-range that contains the first five natural frequencies. Thus, it has been chosen to find the optimal distribution of a network with 16, 20 and 24 piezoelectric patches of 40×40 mm². Network distributions found with GA are shown in Figure 6. Modal and average EMCCe values are presented in Table 3. They are also compared with values found from a rectangular centered network distribution with the same number of patches.

For 16 patches, a slight improve on the average EMCCe is obtained, compared to the corresponding rectangular grid, but it is also worthwhile to notice a reduction on the difference between maximum and minimum modal values which could be valuable to improve the global efficiency of a multimodal device. A similar conclusion could be drawn for the network with 20 patches. On

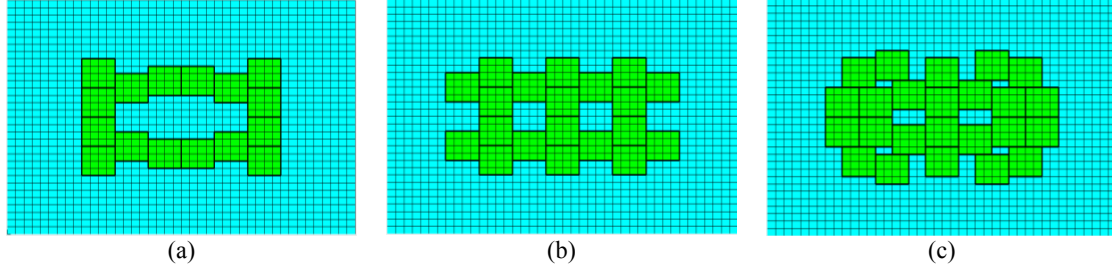


Figure 6: Optimized network configuration, with (a) sixteen, (b) twenty, and (c) twenty four patches.

the other hand, for the network with 24 patches, it was not possible to improve the global EMCCE, but the difference between maximum and minimum modal values are reduced.

Table 3: Comparison between modal and average EMCCE values obtained from optimized location of the piezoelectric patch network and from a rectangular distribution of the network.

	16 Patches		20 Patches		24 Patches	
	Optimized	Rectangular	Optimized	Rectangular	Optimized	Rectangular
Mode 1	4.2	7.1	6.4	8.1	7.3	8.6
Mode 2	5.7	3.3	6.5	5.4	7.9	7.4
Mode 3	3.9	4.7	4.6	5.2	5.2	5.5
Mode 4	4.0	3.7	5.3	4.1	6.1	5.4
Mode 5	4.4	2.3	4.6	3.7	5.2	5.0
EMCCeg	4.4	4.2	5.5	5.3	6.4	6.4
EMCCeg*	23.2	22.1	23.0	22.3	22.2	22.4
EMCCeg/P	0.28	0.26	0.27	0.26	0.26	0.27

4 CONCLUDING REMARKS

This work presented recent advances on the optimization of networks of piezoelectric patches for active structural vibration control and energy harvesting from structural vibrations. Results show that it is possible to profit from a network of sensors to improve and focus active vibration control strategies provided their gains is properly optimized. Three strategies to design the control gains are presented and analyzed. Aiming at energy harvesting from structural vibrations, another study was performed showing that by optimizing the distribution of sensors, it possible to improve the effective electromechanical coupling coefficient along a given frequency range.

ACKNOWLEDGEMENTS

Financial support of the National Council for Scientific and Technological Development (CNPq), through grants 574001/2008-5 and 309193/2014-1, is acknowledged.

REFERENCES

- [1] Ahmadian, M. and DeGuilio, A.P. Recent advances in the use of piezoceramics for vibration suppression. *Shock and Vibration Digest* (2001) **33**(1):15–22.
- [2] Gilbert, J.M., and Balouchi, F., Comparison of energy harvesting systems for wireless sensor networks, *International Journal of Automation and Computing* (2008) **5**(4):334–347.
- [3] Sodano, H.A., Inman, D.J., and Park, G., A review of power harvesting from vibration using piezoelectric materials, *Shock and Vibration Digest* (2004) **36**(3):197–206.

- [4] Trindade, M.A., Benjeddou, A. and Ohayon, R. Finite element modelling of hybrid active-passive vibration damping of multilayer piezoelectric sandwich beams – Part II: System analysis. *International Journal for Numerical Methods in Engineering* (2001) **51**(7):855–864.
- [5] Trindade, M.A. and Benjeddou, A. Hybrid active-passive damping treatments using viscoelastic and piezoelectric materials: review and assessment. *Journal of Vibration and Control* (2002) **8**:699–746.
- [6] Tang, J., Liu, Y. and Wang, K.-W. Semiactive and active-passive hybrid structural damping treatments via piezoelectric materials. *Shock and Vibration Digest* (2000) **32**(3):189–200.
- [7] Sirohi, J. and Chopra, I. Actuator power reduction using L-C oscillator circuits. *Journal of Intelligent Material Systems and Structures* (2001) **12**(12):867–877.
- [8] Godoy, T.C. and Trindade, M.A. Modeling and analysis of laminate composite plates with embedded active-passive piezoelectric networks. *Journal of Sound and Vibration* (2011) **330**:194–216.
- [9] Santos, H.F.L. and Trindade, M.A. Structural vibration control using extension and shear active-passive piezoelectric networks including sensitivity to electrical uncertainties. *Journal of the Brazilian Society of Mechanical Sciences and Engineering* (2011) **33**:287–301.
- [10] Meirovitch, L. and Baruh, H. Control of self-adjoint distributed-parameter systems. *Journal of Guidance, Control, and Dynamics* (1982) **5**(1):60–66.
- [11] Fripp, M.L. and Atalla, M.J. Review of modal sensing and actuation techniques. *Shock and Vibration Digest* (2001) **33**(1):3–14.
- [12] Preumont, A., François, A., De Man, P. and Piefort, V. Spatial filters in structural control. *Journal of Sound and Vibration* (2003) **265**(1):61–79.
- [13] Tanaka, N. and Sanada, T. Modal control of a rectangular plate using smart sensors and smart actuators. *Smart Materials and Structures* (2007) **16**(1):36–46.
- [14] Pagani Jr., C.C. and Trindade, M.A. Optimization of modal filters based on arrays of piezoelectric sensors. *Smart Materials and Structures* (2009) **18**(9):095046.
- [15] Trindade, M.A., Pagani Jr., C.C. and Oliveira, L.P.R., Semi-modal active vibration control of plates using discrete piezoelectric modal filters, *Journal of Sound and Vibration* (2015) **351**:17–28.
- [16] Levine, W. and Athans, M. On the determination of the optimal constant output feedback gains for linear multi-variable systems. *IEEE Transactions on Automatic Control* (1970) **15**(1):44–48.
- [17] Cruz Neto, H.J. and Trindade, M.A. Optimal placement of sensors for the output feedback control of structures using quadratic performance criterion. In *Proceedings of the 24th ABCM International Congress of Mechanical Engineering*, December 3-8, (2017), Curitiba, PR, Brazil.
- [18] Cai, G.P. and Lim, C. Continuous suboptimal control with partial state feedback. *Journal of Vibration and Control* (2005) **11**(4):561–578.
- [19] Le, M.Q., Capsal, J.F., Lallart, M., Hebrard, Y., Van Der Ham, A., Reffe, N., Geynet, L., and Cottinet, P.J. Review on energy harvesting for structural health monitoring in aeronautical applications. *Progress in Aerospace Sciences* (2015) **79**:147–157.
- [20] Trindade, M.A., Santos, H.F.L. and Godoy, T.C. Effect of bonding layer uncertainties on the performance of surface-mounted piezoelectric sensors and actuators. *XIV International Symposium on Dynamic Problems of Mechanics (DINAME)* (2013), Buzios, RJ, Brazil.
- [21] Velasquez, J.Q. and Trindade, M.A. Effect of adhesive layer properties on the performance of surface-mounted piezoelectric sensors and actuators. *Meeting on Aeronautical Composite Materials and Structures (MACMS)* (2015), São Carlos, SP, Brazil.
- [22] Horiy, F.M., Shigueoka, A.H., Trindade, M.A. Analysis of piezoelectric sensor networks for spatial modal filters and active vibration control. In *24th ABCM International Congress of Mechanical Engineering (COBEM)* (2017), Curitiba, PR, Brazil.
- [23] Trindade, M.A., and Benjeddou, A. Effective electromechanical coupling coefficients of piezoelectric adaptive structures: critical evaluation and optimization. *Mechanics of Advanced Materials and Structures* (2009) **16**(3):210–223.

Multi-fidelity Information Fusion Using Deep Neural Networks

Rohit Tripathy*, Ilias Bilionis**

*Purdue University, **Purdue University

ABSTRACT

A common scenario in computational science is the availability of a suite of simulators solving the same physical problem, such that the simulators are at varying levels of cost/fidelity. High fidelity simulators are more accurate but are computationally expensive, whereas low fidelity models can be evaluated cheaply while suffering from reduced accuracy. Additionally, many engineering applications are characterized by model parameters / boundary conditions / initial conditions etc. which are not known exactly. The surrogate-based approach to uncertainty quantification requires one to evaluate the forward model enough times such that one can construct a cheap (but accurate) approximation to the numerical solver. If the outputs from the simulators of varying fidelities are correlated, one can leverage information from low-fidelity simulators to augment information from a small number of evaluations of the high-fidelity simulator to construct an accurate surrogate model. In this work, we demonstrate a deep neural network (DNN) approach for constructing accurate surrogate models for uncertainty quantification by fusing information from multifidelity sources. DNNs are naturally suited for multi-fidelity information fusion because of the hierarchical representation of information. Our approach is validated on a synthetic example as well as an example from advanced manufacturing.

A Fast Statistical Homogenization Procedure (FSHP) for Random Composite

Patrizia Trovalusci*, Marco Pingaro**, Maria Laura De Bellis***, Emanuele Reccia****

*Sapienza University of Rome, **Sapienza University of Rome, ***University of Salento, ****Sapienza University of Rome

ABSTRACT

Composites materials are used in many engineering applications and typically exhibit a micro-structure made of randomly distributed inclusions (particles) embedded into a dissimilar matrix. A key aspect, recently investigated by many researchers, is the evaluation of appropriate mechanical properties to be adopted for the study of their behaviour. Homogenization procedures may be adopted for the definition of equivalent moduli able to take into account at the macroscale the material properties emerging from the internal micro-structure. In the case of materials with random micro-structure it is not possible to a priori define a Representative Volume Element (RVE), this being an unknown of the problem in contrast to the classical homogenization approach. A possible way to solve this problem is to approach the RVE using finite-size scaling of intermediate control volume elements, named Statistical Volume Elements (SVEs), and proceed to homogenization. Here a homogenization procedure, consistent with a generalized Hill-Mandel condition, is adopted in conjunction with a statistical procedure, by which scale-dependent bounds on classical moduli are obtained using Dirichlet and Neumann boundary conditions for solving Boundary Value Problems (BVPs) [1]. The outlined procedure has provided significant results, also extended to non-classical continuum formulations, but with high computational cost which prevents the possibility to perform series of parametric analyses. We here propose a so-called Fast Statistical Homogenization Procedure (FSHP) developed within an integrated framework that automates all the steps to perform: from the simulations of each random realization of the microstructure to the solutions of the boundary value problems for the SVEs, up to the evaluation of the final size of the RVE for the homogenization of the random medium. Within the FSHP the BVPs has been solved numerically adopting a mixed Virtual-Finite Element Method (VEM-FEM), with a single Virtual Element for the inclusions and triangular Finite Elements for the matrix, determined using random mesh generators. The computational strategies and the discretization adopted allow us to very efficiently solve the series (hundred) of BVPs and to rapidly converge to the RVE size detection. Several simulations are then performed by modifying the material contrast (ratio between the moduli of the materials components) deriving the size of the RVE for performing homogenization on various kinds of two-phases random composites. References Trovalusci, P., Ostoja-Starzewski, M., De Bellis, M.L., Murralli, A., "Scale-dependent homogenization of random composites as micropolar continua," Eur. J. Mech. A-Solid, 49, 396-407 (2015).

From Spinodal to Critical Fracture

Lev Truskinovsky*, Hudson Borja da Rocha**

*ESPCI, **ESPCI

ABSTRACT

Fracture in disordered solids is known to be intermittent across a vast range of scales from earthquakes to micro-peeling. The observed power law avalanche behavior has been previously linked to either spinodal or critical points. We use the simplest mean field model to show that both associations are relevant. The realization of a particular scenario in a quasi-statically driven system with over-damped athermal dynamics depends on the two parameters representing disorder and rigidity.

Creep Life Prediction of Ferritic-Martensitic Steels at High and Low Stresses Through Crystal Plasticity and Grain Boundary Modeling

Timothy Truster^{*}, Kristine Cochran^{**}, Mark Messner^{***}, Omar Nassif^{****}, David Parks^{*****}, Sam Sham^{*****}

^{*}University of Tennessee, ^{**}DR&C, Inc., ^{***}Argonne National Laboratory, ^{****}University of Tennessee, ^{*****}DR&C, Inc., ^{*****}Argonne National Laboratory

ABSTRACT

Advanced reactors designed to operate at higher temperatures than current light water reactors require structural materials with high creep strength and creep-fatigue resistance to achieve long design lives. Grade 91 is a ferritic/martensitic steel designed for long creep life at elevated temperatures. The time required to complete an experiment limits the availability of long-life creep data for Grade 91 and other structural materials. Design methods often extrapolate the available shorter-term experimental data to longer design lives. However, extrapolation methods tacitly assume the underlying material mechanisms causing creep for long-life/low-stress conditions are the same as the mechanisms controlling creep in the short-life/high-stress experiments. A change in mechanism for long-term creep could cause design methods based on extrapolation to be non-conservative. The goal for physically-based microstructural models is to accurately predict material response in experimentally-inaccessible regions of design space. Ideally, the individual mechanism models adhere to the material physics and not an empirical calibration to experimental data and so the model remains predictive for a wider range of loading conditions. This paper describes such a physically-based microstructural model for Grade 91 at 600° C. The model explicitly represents competing dislocation and diffusional mechanisms in both the grain bulk and grain boundaries using the crystal plasticity finite element method and cavity growth-based interface elements, respectively. The model accurately recovers the available experimental creep curves at higher stresses and the limited experimental data at lower stresses, predominately primary creep rates. The model predicts a mechanism shift for 600° C at approximately 100 MPa from a dislocation-dominated regime at higher stress to a diffusion-dominated regime at lower stress. This mechanism shift impacts the creep life, notch-sensitivity, and creep ductility of Grade 91. In particular, the model predicts existing extrapolation methods for creep life may be non-conservative when attempting to extrapolate data for higher stress creep tests to low stress, long-life conditions.

Modeling and Simulations of Fused Deposition Modeling

Gretar Tryggvason^{*}, Huanxiong Xia^{**}, Jiakai Lu^{***}

^{*}Johns Hopkins University, ^{**}Johns Hopkins University, ^{***}Johns Hopkins University

ABSTRACT

Additive manufacturing processes generally include complex multiphysics and multiscale processes, and an evaluation of suitable material/process models require accurate solutions of the governing equations, so that solutions can be compared with experimental results. Here, a fully resolved computational model is developed for the FDM (Fused Deposition Modeling) process, where objects are built by depositing filaments of hot polymers that fuse together when they solidify. The process is embedded in a hexahedral computational domain, where both the polymer and the ambient air are included. A finite volume/front tracking method and the one-fluid formulation are used to model the fluid flow, heat transfer, volume shrinkage, residual stress, as well as the moving immiscible interface. The extrusion of the polymer is modeled by using a volume source inside a rigid body with an open outlet, which is moving along a specific path. A temperature and shear-rate depend viscosity and a modified neo-Hooke stress model are used for the polymer to describe its viscoelastic behavior and find the solid stress. The model is solved by an implicit projection scheme with second-order accuracy both for time integration and space discretization. The accuracy and convergence properties are tested by grid refinement studies for a simple setup involving two short filaments, one on top of the other. The effect of the various injection parameters, such as nozzle speed, cooling condition, depositing and bridging space are briefly examined and the applicability of the approach to simulate the construction of simple multilayer objects is shown. In addition to helping evaluate the accuracy and fidelity of material models, fully resolved simulations also provide the “ground truth” for the simplified/reduced order model that are suitable for part-scale simulations.

Directly Aerodynamics Characteristics Simulation in Upper Airway by Medical Image

Tzu-I Tseng*, Fang-An Kuo**

*National Center for High-performance Computing, **National Center for High-performance Computing

ABSTRACT

The study predicts the flow characteristics in upper airway by using computational fluid dynamics (CFD) method to solve the flow governing Navier-Stokes equations. CFD simulations should be performed after image segmentation, geometry reconstruction and computing mesh generation. However, it requires a large amount of resources to reconstruct a suitable geometry for upper airway and generate the mesh. Because every medical image implied a two-dimensional mesh in Cartesian coordinate system, this study demonstrated a directly CFD technique based on the image-base grid calculates the flow characteristics in upper airway. The marked and cell (MAC) for structure mesh method is a popular and commonly used algorithm in computer graphics to discretize functions for fluid and other simulations. In addition, it is very simple to use and do the embarrassingly parallel computation by using the single instruction multiple data (SIMD) on the graphics processing unit (GPU) device. However, the MAC method was hard to trend the solid object with complex geometry especially applied in bio-mechanics simulation. The direct-forcing immersed boundary method (IBM) can correct the boundary effect from the interaction of the solid boundary and fluid flow and improve the accuracy the of flow simulation. In this study we employ the MAC method with direct-forcing IBM applied to solve the upper airway, by using massive floating-points-operation parallel computation on the GPU device. By using this technique compare to traditional procedure, the total processed time from an hour reduce to couple minutes.

Phase-field Simulation of the Effect of Temperature and Yield Stress Conditions on the Martensitic Transformation in Low-carbon Steel

Yuhki Tsukada^{*}, Emi Harata^{**}, Toshiyuki Koyama^{***}

^{*}Nagoya University, ^{**}Nagoya University, ^{***}Nagoya University

ABSTRACT

Microstructure evolution during the martensitic transformation (MT) in steels is strongly influenced by alloy composition and transformation temperature. The elastic strain energy derived from the MT influences the size and morphology of the martensite phase. A phase-field simulation study has shown that in low-carbon steels, the slip deformation during the MT plays an important role in the formation of habit plane between the parent and martensite phases [1]. Most recently, a phase-field model was developed which considered the elastic strain energy associated with the fcc-to-bct lattice deformation and slip deformation during the MT [2]. In the phase-field model, slip deformations of parent and martensite phases were calculated in the regions where the von Mises yield criterion was exceeded. In this study, the MTs in Fe-0.1mass%C were simulated at 600 K, 650 K and 700 K; at each temperature, the value of yield stress was varied for elucidating its effect on the martensite microstructure. Simulation results show that the MT progresses with forming the cluster composed of three tetragonal variants of the martensite phase. The equivalent plastic strain caused by the slip deformation is large in the interior of the martensite variant domains. However, the slip deformation of the parent phase is also confirmed to occur near the martensite phase. At 600 K and 650 K, the variant domain size decreases with increasing the value of yield stress. It is assumed that when the yield stress is high and the slip deformation is difficult to occur, the formation of minute multi-variant structure is effective for relaxing the elastic strain energy during the MT. On the other hand, at 700 K, the variant domain size is not influenced by the value of yield stress. It is presumed that at 700 K, the driving force for the MT is small and the transformation is slowed down; this leads to the increase in the slip deformation of the martensite phase and hence the formation of minute multi-variant structure is not an important factor for relaxing the elastic strain energy during the MT. References: [1] Y. Tsukada et al., ISIJ Int. 55 (2015) 2455-2462. [2] Y. Tsukada et al., Proc. of the 5th International Symposium on Steel Science (ISSS 2017), in press.

CFD Analysis in an Oil Hydraulic Vane Pump

Tetsuhiro Tsukiji^{*}, Shunsuke Akiyoshi^{**}, Yoshinari Nakamura^{***}, Kazunari Suzuki^{****}

^{*}Sophia University, ^{**}Sophia University, ^{***}KYB Corporation, ^{****}KYB Corporation

ABSTRACT

Abstract With the development of technology, hydraulic machinery, including hydraulic vane pumps, has recently become smaller, faster, and more durable against pressure. However, these trends make cavitation occur more easily, and cavitation causes problems with the performance of hydraulic machines because of the resulting vibration, noise, and erosion. Based on the experimental result of the outlet pressure measured using an actual vane pump, cavitation causes pressure fluctuation when the rotational speed exceeds a certain value. Pressure fluctuations make it difficult to control the pump and hydraulic system. Therefore, suppression of cavitation in the high-speed rotation region is important, and finally it is necessary to change the shape of the vane pump for operation at high speed. In this study, we aim to evaluate the accuracy of CFD analysis by conducting three-dimensional flow analysis of hydraulic vane pump and to improve pump performance by improving design of vane pump. We conducted a CFD analysis with consideration of internal leakage using the Zwart-Gerber-Belamri cavitation model[1]. Experimental values obtained by experiments were compared with CFD results to examine the accuracy of analysis. We also attempted to increase the volumetric flow rate and decrease the cavitation by changing the shape of the cam ring, using CFD analysis considering leakage. ANSYS Fluent 16.1 solver was used. The standard $k-\epsilon$ turbulent model was adopted to solve flow field. To solve Multi phase flow, the primary phase was set to "oil" and the secondary phase to "oil vapor". Main conclusions are as follows. 1. The CFD calculation of vane pump has sufficient accuracy to estimate the volumetric flow rate not only in the low speed rotation region but also in the high-speed rotation region where the cavitation is dominant by considering the internal leakage. 2. Changing the shape of the cam ring is effective for suppressing the cavitation phenomenon and the discharge flow rate also increased. Reference [1] P. J. Zwart, A. G. Gerber, T. Belamri, 2004, "A Two-Phase Flow Model for Predicting Cavitation Dynamics," ICMF International Conference on Multiphase Flow, Paper No. 152

Frictionless Contact Analysis in Finite Cover Method Using Nitsche's Method

Makoto Tsukino*, Takahiro Yamada**

*Quint Corporation, **Yokohama National University

ABSTRACT

The voxel-based analysis is used for not only structural analyses of mechanical parts but analyses in bioengineering or of microstructure of materials as an effective method for complex structure analyses because of its facility of mesh generation. In the voxel modeling, the surfaces of objects are represented as stepwise shape even if the original surfaces are smooth and hence it is difficult to analyze models that contain contact conditions. The finite cover method (FCM) [1], which is introduced the manifold method concept in which the mathematical cover and the physical domain are defined independently from each other, has capability to manage contact problems easier for its capability of geometry representation, although it holds an advantage in mesh generation. To apply the FCM to practical problems, a contact algorithm needs to be adopted. In general finite element analyses of contact problems, the penalty method is widely used thanks to its simple implementation. In the penalty method, a significant large penalty parameter needs to be employed to assure accuracy. However, such a penalty parameter may cause numerical instability since it makes the stiffness matrix ill-conditioned. Moreover, in the FCM formulation, the nodal points for displacements are located independently from the geometry representation and hence it is difficult to manage the positions of integration points for contact constraint, which may cause inaccurate distribution of the contact pressure due to the over-constraint with concentration of the integration points. To circumvent such difficulties, we apply the Nitsche's method for the contact algorithm in frictionless contact analyses formulated in [2] to FCM. In the Nitsche's approach, constraints for both the non-penetration condition and the equilibrium of stresses on the contacting surfaces are taken into account with a smaller penalty parameter for the stabilization term and that improve in problems associated with the penalty method. To show effectiveness of our approach, we calculate some 2D frictionless contact problems such as a Hertz contact problem. References [1] Jin C., Suzuki K., Ohtsubo H.: Linear Structural Analysis Using Cover Least Square Approximation, J. Appl. Mech., Vol.3, pp167-176, 2000. [2] Wriggers P., Zavarise G.: A formulation for frictionless contact problems using a weak form introduced by Nitsche, Comput. Mech., Vol.41, pp.407-420, 2008.

Modeling and Prediction of Particle Size Distribution in Milling Process using Discrete Element Method

Yuki Tsunazawa*, Chiharu Tokoro**

*National Institute of Advanced Industrial Science and Technology (AIST), Geological survey of Japan (GSJ),

**Waseda University

ABSTRACT

A milling process in mineral processing is the first and important process which determines the efficiency of the overall processes. To achieve the high efficiency of the later separation process, the particle size and its distribution should be appropriately controlled. The control of particle size distribution in the milling process is often difficult because the milling process is strongly affected by not only physical properties of raw ore but also operation conditions in the milling system. Numerical studies have been examined in order to investigate the optimal operation parameters and apparatus design of the milling system. Since these numerical studies were mostly concerned with the behavior of grinding media in the milling system, it has not been well-established that the prediction of particle size distribution during the milling process. The objective of this study was to develop a new method to predict particle size distribution during the milling process using the discrete element method (DEM). To develop the prediction method, we investigated a correlation between the experiments and the DEM simulations. In the experiments, copper ore, whose size was less than 2 mm, was grinded with a tumbling mill under various kinds of operation conditions. Based on the experimental results and the population balance model, we determined the grinding rate coefficient. In the DEM simulations, we only calculated grinding media in the tumbling mill and considered the effect of grinding samples. The DEM simulations were performed to calculate collision energy under the same operation conditions in the tumbling mill. As a result, we obtained a good correlation between collision energy obtained from the DEM simulations and the grinding rate coefficient obtained from the experiments. Therefore, this study proposed the prediction method of the particle size distribution in the milling systems using the DEM and the DEM simulations would contribute to determine milling conditions for appropriate control of particle size distribution during the milling process.

Accelerated Exploration and Learning of Complex Free Energy Landscapes

Mark Tuckerman*

*New York University

ABSTRACT

Theory, computation, machine-learning, and high-performance computers are playing an increasingly important role in helping us understand, design, and characterize a wide range of functional materials, chemical processes, biomolecular/biomimetic structure. The synergy of computation and experiment is fueling a powerful approach to address some of the most challenging scientific problems. In this talk, I will describe the efforts we are making in my group to develop new computational methodologies that address specific challenges in free energy exploration and generation. In particular, I will describe our recent development of enhanced free energy based methodologies for determining conformational preferences of bound and free oligopeptides, for predicting structure, polymorphism, and defects in molecular crystals, for studying crystal growth mechanisms, and for aiding in the understanding of first-order phase transitions. The strategies we are pursuing include large time-step molecular dynamics algorithms, heterogeneous multiscale modeling and learning techniques, which allow “landmark” locations (minima and saddles) on a high-dimensional free energy surface to be mapped out, and enhanced-sampling methods, which allow relative free energies of the landmarks to be generated efficiently and reliably. I will then discuss new schemes for using machine learning techniques to represent and perform computations using multidimensional free energy surfaces.

Monolithic Multigrid for Multiphysics Applications Arising from Resistive MHD

Raymond Tuminaro*, Eric Cyr**, Tobias Wiesner***, John Shadid****

*Sandia, **Sandia, ***Leica Geosystems AG, ****Sandia

ABSTRACT

We consider a resistive iso-thermal MHD formulation that includes dissipative terms for the momentum and magnetic induction equations. This model provides a base-level continuum description of charged fluids in the presence of electromagnetic fields (e.g. for understanding basic plasma physics mechanisms or for investigating magnetic confinement fusion systems). While multigrid methods are efficient for many single-field applications, the design of multigrid preconditioners for multiphysics systems is challenging when the coupling between different fields is strong. Multiphysics systems frequently give rise to matrices that are far from M-matrices, which are easily addressed by standard algebraic multigrid (AMG) methods. Often, standard relaxation algorithms do not smooth errors appropriately while AMG grid transfer procedures also have difficulties as these procedures often rely on positive-definite matrix properties. In this talk, we propose a multigrid strategy that takes advantage of the block structure associated with multiphysics systems. Here, blocks are defined by different physical quantities (or fields) and different equation types. Block diagonal prolongators are developed such that the Navier-Stokes and the Maxwell sub-pieces are interpolated separately. By using the same aggregates to build the prolongator blocks for the Navier-Stokes and Maxwell part, the co-location of unknowns at each mesh vertex is preserved throughout the multigrid hierarchy. Additionally, the proposed multigrid smoother is again based on a block idea (e.g., block Gauss-Seidel). While the talk focuses on a specific MHD context, we emphasize our more general purpose block framework. Specifically, the framework allows one to devise a wide variety of monolithic multigrid preconditioners. Different multigrid kernels (e.g., aggregation schemes, grid transfer strategies, smoothing algorithms) can be applied to different matrix sub-blocks and the results of these kernels can be combined in fairly flexible ways via an xml input deck. This flexible multigrid framework, provided by the MueLu package within Trilinos, drastically simplifies the implementation of block multigrid preconditioners for new types of applications. Additionally, the framework facilitates the definition of simple user interfaces to the resulting application-specific preconditioners. These simple interfaces reduce the number of exposed parameters for end users who want to apply the preconditioners in a production environment. We demonstrate the algorithms and framework for MHD multiphysics problems in the Drekar Finite Element MHD code and compare the performance of the resulting multigrid preconditioners with alternative preconditioning methods.

Variational Peridynamic Fracture: A Phase-field Inspired Framework for Peridynamic Damage Modeling

Michael Tupek*, David Littlewood**

*Sandia National Laboratories, **Sandia National Laboratories

ABSTRACT

A framework for deriving peridynamic bond-damage models which establishes a direct link to phase-field fracture methods [1] is proposed. In recent years, two approaches for modeling crack propagation in brittle materials have received significant attention: phase-field fracture and peridynamics. However, despite their obvious qualitative similarities, a direct relationship between them has yet to be established. By formulating peridynamics as an integral regularization of variational fracture, we introduce a unifying framework that: 1) can be used to derive both the well-known bond-breaking criterion [3] as well as newly proposed smoothly evolving bond-damage models, 2) provides a rigorous approach for extending brittle peridynamic damage models to non-bond-based peridynamic theories, and 3) enables the development of both Griffith and cohesive peridynamic damage models in the small peridynamic length scale limit. These improvements are both novel and important as they promise to address several outstanding issues in peridynamic failure modeling, including: 1) that the use of an instantaneous bond-breaking criteria can lead to abrupt energy releases leading to excessive numerical noise, poor accuracy, and lack of solver convergence, 2) computational convergence results for brittle state-based peridynamic damage models are relatively lacking, and 3) existing peridynamic fracture models are Griffith in the limit of the horizon going to zero, necessarily implying an unjustified and unnecessary relation between the peridynamic horizon and fracture process zone size. The proposed damage models are demonstrated using the open source peridynamics code Peridigm. REFERENCES [1] B. Bourdin, G.A. Francfort, and J.-J. Marigo. Numerical experiments in revisited brittle fracture. *J. Mech. Phys. Solids*, 48:797–826, 2000. [2] C. Miehe, F. Welschinger, and M. Hofacker. Thermodynamically consistent phase-field models of fracture: Variational principles and multi-field fe implementations. *International Journal for Numerical Methods in Engineering*, 83:1273–1311, 2010. [3] S.A. Silling, and E. Askari. A meshfree method based on the peridynamic model of solid mechanics. *Computers and Structures*, 83:1526–1535, 2005.

An Implicit Generalized Finite-Difference Method for Solving a Generalized Dual-Phase Lag Equation

Lukasz Turchan*

*Silesian University of Technology

ABSTRACT

Numerical solution of the bioheat transfer problem is discussed. The heat conduction in the domain considered is described by the generalized dual-phase lag model (GDPL) [1]. Such a model is created by a single partial differential equation and an additional formula concerning the dependence between blood and tissue temperatures. The model is supplemented by the appropriate boundary and initial conditions. At the stage of numerical computations an implicit scheme of generalized finite difference method (GFDM) is used [2]. In the first step of this method application, the time discretization is introduced using the differential quotients. In the next step, the cloud of nodes covering the interior and the boundary of domain considered is generated. Then the temperature function is expanded into the Taylor series. The approximation of the local values of the first and second spatial derivatives results from the least squares criterion. Introduction of this derivatives into differential equation produces a set of coupled linear equations which are valid for a given time step. In this way the nodal temperatures for the successive time steps are calculated [3]. The examples of computations, the comparison with the classical FDM solution and the conclusions will be presented in the final part of presentation. [1] Y. Zhang, Generalized dual-phase lag bioheat equations based on nonequilibrium heat transfer in living biological tissues, *International Journal of Heat and Mass Transfer*, 52 (21-22), 4829-4834, 2009. [2] B. Mochnicki, E. Majchrzak, Numerical modeling of casting solidification using generalized finite difference method, *THERMEC 2009, Materials Science Forum*, 638, 2676-2681, Trans. Tech. Publications, 2010. [3] L. Turchan, Solving the dual-phase lag bioheat transfer equation by the generalized finite difference method, *Archives of Mechanics*, 69 (4-5), 389-407, 2017.

Real-time High-Performance Robust Surgical Cutting Simulations

George Turkiyyah*, Julien Abinahed**, Ahmad Al-Ansari***, Nicolas Haddad****, Dinesh Manocha*****, Nikhil Navkar*****, Gorune Ohannessian*****, Zherong Pan*****, Georges Younes*****

*American University of Beirut, **Hamad Medical Corporation, ***Hamad Medical Corporation, ****American University of Beirut, *****University of North Carolina, *****Hamad Medical Corporation, *****American University of Beirut, *****University of North Carolina, *****Hamad Medical Corporation

ABSTRACT

Surgical simulation represents an extremely challenging class of computational science simulations where both high performance and absolute robustness are essential requisites for effectiveness. To be used as tools for planning personalized care or for rehearsing patient-specific procedures, surgical simulators must provide support for realistic and consistent geometric and mechanical behavior suitable for real-time interactions. Even a single contact that is not correctly detected and resolved, anywhere in space and at any time step, can result in completely erroneous and visually distracting simulation. The challenges of these simulations come from the need for: (1) interaction with non-linear deformable materials that undergo topological changes due to incisions and resections; (2) geometrically rich tool-tissue contact and interaction; and (3) dynamically changing tissue-tissue contact interactions. To ensure robustness in this environment, geometric computations and algorithms must interact at a fine-grained level with a finite element model of non-linear elastic deformations to resolve the dynamic contact conditions and update model deformations accordingly. Vertex-face and edge-edge contacts are identified and used to constrain the space of allowable deformations. These computations must be performed in real-time at several frames per second on models involving several tens of thousands of elements, pushing the limits of robust simulation in a high-performance computational simulation. In this work, we present incremental data structures and solution algorithms to support nonlinear elastic simulations in the dynamically changing environment of surgical cutting. Our geometric collision detection algorithms and finite element solution algorithms exploit hierarchical representations and incremental fast updates to the model, contact conditions, and solution. We perform continuous collision detection between discrete time steps so as not to miss any collision. This reduces to performing a high number of elementary tests corresponding to vertex-face and edge-edge combinations from triangle meshes, using efficient methods to accelerate the collision computation. The combination of these techniques result in simulation methods that exhibit only log-linear complexity allowing us to demonstrate robust real-time three-dimensional surgical cutting procedures at scale.

Leveraging Exascale Computational Resources to Accelerate Qualification of Additively Manufactured Parts

John Turner*, James Belak**

*Oak Ridge National Laboratory, **Lawrence Livermore National Laboratory

ABSTRACT

Additive manufacturing (AM), or 3D printing, of metals is transforming the fabrication of parts by reducing the weight of final parts, reducing waste (and hence energy) in the manufacturing process, and dramatically expanding the design space, allowing optimization of shape and topology. However, although the physical processes involved in AM are similar to those of welding, a field with a wealth of experimental, modeling, simulation, and characterization research over the past decades, qualification of AM parts remains a challenge. While modeling approaches and simulation tools for welding and similar processes are quite mature, they are proving inadequate for AM processes. We believe this is in part due to the fact that the process-structure-property-performance relationship is typically treated in an uncoupled manner, relying on tabular databases and hence unable to adequately capture the rapid dynamics and non-equilibrium nature of AM processes. The Exascale Additive Manufacturing Project (ExaAM) is a collaboration between U.S. Dept. of Energy laboratories as part of the Exascale Computing Project (ECP, <https://exascaleproject.org/>). ECP is a broad program including research efforts in hardware component and system design, system software, and science application development to deploy a computational ecosystem capable of delivering at least fifty times the performance of today's largest systems. ExaAM is one of the applications selected for the development and implementation of models that would not be possible on even the largest of today's computational systems. With the prospect of Exascale computing resources in mind, one of the goals of ExaAM is to remove some of the limitations noted above by coupling high-fidelity sub-grid simulations within continuum process simulations to determine microstructure, properties, and hence performance using local conditions. We briefly describe the approach being taken in ExaAM, which involves integrating and extending existing physics components for microstructure evolution, melt pool dynamics, polycrystalline properties, and part scale performance, most of which were not developed specifically for AM but which include the relevant high-fidelity physics capabilities. We also discuss plans for verification and validation of this new integrated simulation environment through collaboration with efforts such as AM-Bench (<https://www.nist.gov/ambench>), a set of benchmark test problems under development by a team led by NIST.

Influence of Sub-ply Voids in the Fracture Behavior of Fiber-reinforced Composites Using a Multiscale Analysis

Sergio Turteltaub*, Gijs de Jong**

*Delft University of Technology, **Delft University of Technology

ABSTRACT

The effective fracture behavior of a fiber-reinforced composite laminate depends on a series of design and manufacturing factors that include the material properties of the fiber and the matrix as well as the ply configuration (e.g., fiber volume fraction). An additional factor that influences the onset and propagation of micro-cracks at the sub-ply length scale are defects that appear during manufacturing. At that scale, defects may appear as micro-voids inside the matrix or as gaps between closely-spaced fibers that prevent filling. To study the influence of these micro-defects on the effective traction-separation response of a composite, a multiscale analysis is conducted where the defects are explicitly accounted for in finite element simulations. A recently-developed multiscale theory is expanded to account for voids in the computational domain. It is shown that the Hill-Mandel condition may be separated into two terms, one accounting for the actual crack and one for the voids that contribute to the crack process. The simulations are carried out using a separate traction-separation relation for each constituent (matrix, fiber and matrix-fiber interface) and for distinct mixed mode loading conditions until complete fracture is achieved. A convergence analysis is carried out to establish the existence of a representative volume element that includes voids of each type (matrix voids and fiber-gaps). Through a parametric analysis of configurations with a given void type and volume fraction, the influence of the void content on the effective fracture strength and the effective fracture energy of a composite can be quantified. Results show that for a mode II loading condition, both the effective fracture energy and strength decrease with increasing void content, while for mode I only the effective energy decreases. These effects only become significant when the void content exceeds a critical value, which depends on the type of voids evaluated.

Field Monte Carlo Potts-based Modeling of Discontinuous Dynamic Recrystallization under Finite Deformation

Abbas Tutcuoglu*, Dennis Kochmann**, Kaushik Bhattacharya***

*California Institute of Technology, **ETH Zurich, ***California Institute of Technology

ABSTRACT

Discontinuous dynamic recrystallization (DDRX) describes the process observed predominantly in low-to-medium stacking fault energy metals by which pristine grains with a new orientation nucleate at high energy sites and subsequently migrate to consume the surrounding plastically more severely distorted grains. In previous attempts to simulate DDRX, stochastic models such as the Monte Carlo Potts model (MCP) provided popular means by which the random nature of grain boundary migration and nucleation could be incorporated. Despite invaluable insights into the mathematical aspect of recrystallization, the underlying physical models were generally of simplified nature and thus failed to capture the full complexity inherent in the inelastic phenomena occurring on the microscale, including anisotropy, finite deformation or alternative strain accommodating processes such as twinning. A vertical homogenization approach is pursued to account for the multiscale nature of DDRX by introducing a representative volume element (RVE) on the mesoscale. The associated initial boundary value problem is solved using an improved spectral solver which allows for the presence of discontinuities inherent in high-angle grain boundaries without the occurrence of severe ringing artifacts. A crystal plasticity model is employed to capture the deformation state on the microscale based on a set of elastic and inelastic state variables, for the latter of which the temporal evolution is governed by the principle of minimum dissipation potential. Following the MCP ansatz, we formulate misorientation switches to model both grain boundary migration as well as nucleation, with the latter replacing ad-hoc nucleation models incorporating a hard threshold as employed in numerous previous attempts to simulate DDRX. An integral modification to classic MCP models consists in the amendment of the two aforementioned state switches by simultaneous changes of both elastic and inelastic states in the idea of a Field Monte Carlo Potts model (FMCP). The state changes, for which the respective definitions are motivated by experimental observations, are conducted in a novel time-continuous fashion. Using data on the microstructural evolution and the stress-strain response for copper during torsion experiments, we assess the performance of our FMCP model.

Relative Entropy and Applications to the Convergence of Thermomechanical Theories

Athanasios Tzavaras*

*King Abdullah University of Science and Technology

ABSTRACT

The relative entropy is a calculation originally developed for hyperbolic systems of conservation laws which exploits the entropy structure of hyperbolic systems in order to compare two appropriate solutions of the same or related thermomechanical systems. The method provides an appropriate metric in order to assess stability and convergence of numerical schemes. In this talk I will survey this method in two directions: (a) First, for general entropy dissipating hyperbolic-parabolic systems where the hyperbolic part is symmetrizable. This provides convergence for solutions from the system of thermoviscoelasticity to the system of adiabatic thermoelasticity in the limit as the viscosity and heat conduction tend to zero. (b) Second, for a class of dispersive systems that can be written as Euler flows generated by a variational structure induced by an energy functional. This class admits as examples the Euler-Korteweg system, the quantum hydrodynamics system, and various models of multi-component flows.

A Machine Learning Approach for Plastic Deformation History Using Spatial Strain Correlations

Michail Tzimas^{*}, Stefanos Papanikolaou^{**}, Stephen Langer^{***}, Andrew Reid^{****}, Hengxu Song^{*****}

^{*}West Virginia University, ^{**}West Virginia University, ^{***}National Institute of Standards and Technology,
^{****}National Institute of Standards and Technology, ^{*****}West Virginia University

ABSTRACT

We demonstrate a machine learning (ML) approach to quantify the deformation history of a specimen based on spatially resolved information that can be derived from a small-strain, non destructive mechanical test. The deformation history is encoded in the microstructure through the inhomogeneity of dislocation ensembles, and in the spatial correlations of dislocation patterns. Our playground consists of uni-axially compressed crystalline thin films of various widths generated by a discrete dislocation plasticity simulation. We explore the range of applicability of ML for typical protocols that are being used in mechanical testing, and as a function of possible size effects and stochasticity. While strain information is traditionally thought to not be a proper state variable for crystal plasticity, we find that spatially-resolved strain correlations contain much richer information that may be used to classify plastically predeformed samples in most cases. However, we also find that size effects and uncertainty may render unsupervised techniques unable to distinguish different plasticity regimes. Furthermore, we explore the applicability of this approach on quantifying source strength, recognizing statistical variations in source strength and recognizing the number of active slip systems in a sample.

Using Computational Modeling to Understand Radiation Damage Tolerance in Complex Oxides Both from the Bottom-up and the Top-down

Blas Pedro Uberuaga*

*Los Alamos National Laboratory

ABSTRACT

Meeting the ever-increasing demand for energy is a key challenge for the 21st century. Nuclear energy is a proven and green energy source that will be a key component of the world's energy profile. However, maximizing the efficiency of nuclear energy systems, both fission and fusion, requires materials that have significantly increased tolerance against radiation damage. Computational modeling has an important role in understanding and discovering new materials for next-generation nuclear energy systems. In this talk, we will describe research efforts that apply computational modeling to understand the response of materials to radiation damage. We will focus on a class of complex oxides, pyrochlores, that have been proposed for nuclear waste encapsulation. Pyrochlores, with the chemical formula $A_2B_2O_7$, are related to the simpler fluorite structure, with the added complication of having two cation species and oxygen structural vacancies. Past work by numerous groups has shown that the radiation tolerance of these materials is sensitive to the nature of the A and B cations and, in particular, their propensity to disorder. However, these observations are empirical at best and there is still a lack of understanding on the factors that govern the radiation response of these materials. We have tackled this problem from two different perspectives. First, using accelerated molecular dynamics, we have studied how cation disorder, often created during radiation damage, impacts defect kinetics and thus the transport mechanisms that dictate damage recovery. This bottom-up approach has revealed that a percolation transition occurs as disorder is introduced that leads to higher defect mobilities, which in turn promote self-healing of the damage. On the other hand, we have used materials informatics to analyze the role of pyrochlore chemistry on radiation tolerance. In this case, divorced from the complexities of making true predictions of performance, we instead use machine learning to take a top-down perspective and discover heuristic relationships between the material composition and the susceptibility of the material to amorphization. While neither study provides a complete understanding of radiation damage in these materials, together they provide a more complete picture of the factors that dictate their response to irradiation.

Coupled Simulation of Transportation and Electric Power Systems via EVs' Charging Behavior

Hideaki Uchida^{*}, Hideki Fujii^{**}, Shinobu Yoshimura^{***}

^{*}The University of Tokyo, ^{**}The University of Tokyo, ^{***}The University of Tokyo

ABSTRACT

Realization of a sustainable low-carbon society is required globally, and energy consumption reduction derived from fossil fuels has been emphasized. In the transportation sector, which accounts for a large percentage of energy consumption, EVs (Electric Vehicles) with high environmental performance has been popularized in recent years. To realize a low-carbon society, EVs are expected to play major roles, and it is important to use renewable energy for its charging effectively. Interactions between the road transport network in which gasoline-powered vehicles are used and the electric power system which is maintained by controllable energy systems have not been considered so far. However, the interactions are supposed to occur via EVs, which will popularize in the near future. Most of the previous studies about EVs' popularization focused on either the road transport network or the electric power system, and no sufficient simulation model has been studied for the interaction between both mechanisms. In this research, we proposed a coupled simulation model that can represent interactions between transport and electric power systems. We adopted MATES [1] (Multi-Agent Traffic and Environment Simulator) for simulating the transport mechanism, and implemented an EV agent and its charging behavior. Since the charging event is coupled to the electric power system mechanism, the spread of EVs will affect not only the road transport network but also the electric power system. For simulating the electric power system mechanism, we implemented the BFS (Backward Forward Sweep) method, which is one of the power flow calculation methods for low voltage distribution systems. Numerical experiments are executed in a certain area in the real world. Assuming high-output charging by quick charger at a charging station during long-distance trip and low-output charging by normal charger at home, we evaluated the time series change of the load flow in the urban power system by the EVs' charging events. As a result of the simulation, it was implied that the concentration of low-output charge after returning home might cause a voltage drop in the distribution system. This phenomenon became more prominent as the penetration rate of EV increased, and the possibility that it deviates from the legal range of the reference voltage is shown in some scenarios. [1] S.Yoshimura, "MATES : Multi-Agent based Traffic and Environmental Simulator – Theory, Implementation and Practical Application ", Computer Modeling in Engineering and Sciences, Vol.11, No.1, pp.17-25, (2006)

Development of a Three-dimensional Finite Element Model for a Unidirectional Carbon Fiber Reinforced Plastic Based on X-ray Computed Tomography Images and the Numerical Simulation on Kink Band Failure

Masahito Ueda^{*}, Iizuka Keisuke^{**}, Takuya Takahashi^{***}

^{*}Nihon University, ^{**}Nihon University, ^{***}Nihon University

ABSTRACT

A unidirectional carbon fiber reinforced plastic was scanned by an X-ray computed tomography system. Based on the X-ray computed tomography images, a three-dimensional model with random fiber waviness was developed. The constructed three-dimensional fiber model showed random waviness of each fiber in the unidirectional carbon fiber reinforced plastic. Finite element analysis was performed using the three-dimensional model. Simulation results showed bending and twisting deformations coupled with axial contractions during axial compression, which was developed due to fiber waviness. A reduction of the fiber directional Young's modulus due to fiber random waviness was quantitatively evaluated. Propagation of fiber kinking was also studied using the three-dimensional model. Initiation point of the kink-band failure was identified.

Multiscale Study on Origin of Magnetoelectric Effect in Multiferroic Composite Materials

Yasutomo Uetsuji*, Takeshi Wada**

*Osaka Institute of Technology, **Graduate School, Osaka Institute of Technology

ABSTRACT

A multiscale numerical investigation into the origin of the magnetoelectric effect in multiferroic composite materials was performed. Specifically, a well-known but unconfirmed mechanism for generating a macroscopic magnetoelectric effect through transmission of mechanical strain between the ferroelectric (FE) and ferromagnetic (FM) phases in an inhomogeneous microstructure was quantitatively established through multiscale finite element simulations. An asymptotic homogenization theory was employed for scale bridging between the macrostructure and the microstructure. Focusing first on a polycrystalline FE/FM composite, the relation between the physical properties and the FE phase content was investigated. Barium titanate was used for the FE phase and Terfenol-D is utilized for the FM phase. The orientation and allocation of FE and FM phases are set to be random. A uniform magnetic field was then applied to the macrostructure and the mechanical strain in the microstructure was investigated. The specific strain component exhibited an off-centered distribution when divided into FE and FM phases. The computation indicated that not only the shift in the mean strain in the microstructure, but also the homogenized piezoelectric stress constant must be increased to enhance the macro magnetoelectric effect. This conclusion is applicable to other inhomogeneous structures and it can explain the trend in the magnitude of the magnetoelectric effect for a random polycrystalline structure, a layered polycrystalline structure, and a layered single-crystal structure. The findings are helpful for the functional design of multiferroic composite materials. One of the authors (Y. Uetsuji) was financially supported by a Grant-in-Aid for Scientific Research (B) (Grant Number 17H03151) from the Ministry of Education, Culture, Sports, Science and Technology of Japan.

Continuum Model of Slow-fast Mode Transition of Crack Propagation in Viscoelastic Materials

Yoshitaka Umeno^{*}, Atsushi Kubo^{**}

^{*}The University of Tokyo, ^{**}The University of Tokyo

ABSTRACT

The slow-fast mode transition in crack propagation in viscoelastic materials is simulated within the framework of the finite element method (FEM). We successfully reproduced the phenomenon that a discontinuous jump of crack propagation velocity occurs as tensile strain energy increases in rubber and resin. A series of pure shear tests was carried out numerically with FEM simulations and crack velocities were measured under various values of tensile strain. By analyzing the principal stress in the vicinity of the crack tip, it was found that the mode transition is caused by a characteristic temporal change in stress on the crack tip; i.e., non-monotonic increase of stress.

A Molecular Modelling Approach for the Cross-Linking of Nanoparticle-Reinforced Epoxy Resins and Its Effect on Predicted Mechanical Properties

Robin Unger^{*}, Benedikt Daum^{**}, Johannes Fankhänel^{***}, Raimund Rolfes^{****}

^{*}Institute of Structural Analysis, Leibniz Universität Hannover, Germany, ^{**}Institute of Structural Analysis, Leibniz Universität Hannover, Germany, ^{***}Institute of Structural Analysis, Leibniz Universität Hannover, Germany, ^{****}Institute of Structural Analysis, Leibniz Universität Hannover, Germany

ABSTRACT

Nanoparticle-reinforced polymers are a novel class of materials and have gained large interest because of their outstanding material properties with respect to stiffness, strength and fracture toughness. Molecular dynamic simulations are an appropriate tool for computational material development and to study the underlying acting mechanisms, since they allow insights into particle-matrix interactions at the atomistic scale [1]. Recent research into the curing process of epoxy resins lead to a simulative cross-linking procedure [2], incorporated into the Molecular Dynamic Finite Element Method (MDFEM) [3] framework and calibrated by experimental in-situ near-infrared spectroscopy data. The calibrated procedure proved to generate simulation models with very good agreement in the curing kinetics and the final network structure. The present work extends the model generation to nanoparticle-reinforced epoxy resins, considering material combinations based on an epoxy system reinforced with boehmite nanoparticles with different partly reactive surface coatings. The present work focuses on two aspects. Firstly, the model generation is investigated, particularly the chemical linkage of the nanoparticle and the epoxy matrix with respect to the surface modifications, in view of the possible chemical reactions between particle and matrix. Since no reaction kinetic is predefined, steric effects and physical interactions, phenomena that are also dominant in reality, govern the bonding. An analysis of the cross-linking process is presented and the effect of the surface modifications on the resultant network structure is investigated. Secondly, material properties of the epoxy-boehmite composite with respect to the particle surface modifications and the particle-matrix interface are evaluated. Effective mechanical properties of the cross-linked nanocomposite are calculated and the correlation to the particle-matrix interaction is discussed. The objective of the contribution is to give an insight into the challenges and opportunities with respect to model generation for molecular dynamics simulations of nanocomposites with the purpose of virtual material development. References [1] Z. Wang et al., Effect of Interfacial Bonding on Interphase Properties in SiO₂/Epoxy Nanocomposite: A Molecular Dynamics Simulation Study, ACS Appl. Mater. Interfaces, 8(11), 2016 [2] R. Unger, B. Daum, U. Braun, R. Rolfes, Experimentally calibrated modelling technique for the cross linking mechanism of epoxy resin and its influence on mechanical properties, Proceedings ICCS20 - 20th International Conference on Composite Structures, 2017, ISBN 9788893850414 [3] L. Nasdala, A. Kempe, R. Rolfes, The molecular dynamic finite element method (MDFEM), CMC: Computers, Materials &&& Continua, 19(1), 2010

Creation of Analysis-Suitable Non-Uniform Rational B-Spline (NURBS) Volumes from Discrete Image-Based Models

Adam Updegrove^{*}, Jessica Zhang^{**}, Nathan Wilson^{***}, Shawn Shadden^{****}

^{*}University of California, Berkeley, ^{**}Carnegie Mellon University, ^{***}Open Source Medical Software Corporation,
^{****}University of California, Berkeley

ABSTRACT

In image-based biomedical research, a computer model is obtained by segmenting anatomical structures from medical image data. This typically results in a discrete boundary representation of an anatomy [1]. However, an analytic representation can significantly facilitate engineering design, analysis and computation. Moreover, if the parameterization is analysis suitable, it can enable direct simulation using isogeometric analysis (IGA). Robustly converting a discrete model into an analysis suitable representation is highly challenging and an active area of research [2]. We present a robust and automated method to convert discrete image-based models, particularly for cardiovascular applications, into analysis suitable CAD representations, and demonstrate resulting IGA analysis. Our framework to convert an image-based triangulated surface to a non-uniform rational b-spline (NURBS) volume can be summarized by the following steps: (1) Centerlines of the discrete input model are generated based on an automated cell thinning method creating a graph topology of the model (2) A polycube structure that mirrors this graph topology is generated, providing domains on which NURBS parameterizations will be formed. (3) The input model surfaces are partitioned into patches using the centerlines and centroidal voronoi clustering techniques. (4) Each model patch is mapped conformally to each polycube patch, while ensuring global consistency. (5) Structured parameterizations on the polycube are then mapped back to the original discrete model to provide a structured quadrilateral surface mesh. (6) Interpolation of this surface mesh is used to generate a structured hexahedral mesh volume, which acts as a scaffold onto which an analytic (volumetric NURBS) representation can be formed. The automatic conversion procedure has been tested on a variety of patient-specific vascular models from vascularmodel.org. Final volumetric conversions have been verified with quality metrics such as Hausdorff distance. With a volumetric analytic representation, IGA can be performed, and we will present examples of IGA simulation of blood flow and compare with finite-element modeling. Although these methods were developed primarily for vascular models, they can be utilized on non-vascular geometries that have an identifiable centerline structure as we will demonstrate. Future work includes extending these methods to even more complex anatomies (e.g. beyond genus 0 manifolds). References [1] Updegrove, Adam, et al. "Simvascular: An open source pipeline for cardiovascular simulation." *Annals of biomedical engineering* 45.3 (2017): 525-541. [2] Zhang, Yongjie Jessica. *Geometric modeling and mesh generation from scanned images*. Vol. 6. CRC Press, 2016.

Icing Simulation of NACA0012 Airfoil with Local Surface Heating

Sho Uranai^{*}, Hiroya Mamori^{**}, Naoya Fukushima^{***}, Katsuaki Morita^{****}, Makoto Yamamoto^{*****}

^{*}Tokyo University of Science, ^{**}Tokyo University of Science, ^{***}Tokai University, ^{****}Japan Aerospace Exploration Agency, ^{*****}Tokyo University of Science

ABSTRACT

Ice accretion is a phenomenon in which super-cooled water droplets impinge and accrete on solid surfaces. In airplanes, this phenomenon reduces the aerodynamics performance or can cause serious accidents. Therefore, de-/anti-icing systems for airfoils have been developed and used up to now, e.g., de-icer boots or bleed air system. An electro-thermal heater is also adopted as a de-/anti-icing device since this device is easy to be installed for airplanes. However, these devices require electric energy to melt the accreted ice on surfaces of airplanes. Therefore, the optimization for the heating device is necessary to be investigated. In this study, we preform icing simulations of NACA0012 airfoil with the surface heating to investigate effects of the heating area on the ice accretion. The numerical procedure consists of four steps: generation of the computational grids; computation of the flow field around an airfoil; computation of the droplet trajectories to obtain the distribution of the impinged droplets; computation of the thermodynamics to obtain ice shapes. The compressible turbulent flow was assumed. The governing equations are two-dimensional continuity, Navier-Stokes, and energy equations. The Kato-Launder $k-\epsilon$ model was used as a turbulence model. The droplet trajectories were tracked in the Lagrangian approach. We made two assumptions: the droplets follow the flow field, while they do not affect the flow field; the force acting on droplets is only aerodynamic drag. For the thermodynamic calculation, an "extended Messinger model" was used to calculate the amount of ice. Although the model imposes the adiabatic condition on the surface of the airfoil, in the present study we modified this model to satisfy the Dirichlet condition (i.e., constant surface temperature). In order to clarify the effect of heating area, we have conducted icing simulations for different heating areas. From the results of the velocity field around the airfoil without heating, the thickness of the velocity boundary layer after icing became thicker than that before icing. On the other hand, due to the surface heating, the amount of icing and its area became small as increasing the heating area. The drag coefficient of the airfoil after icing with the heating is smaller than that without heating. Moreover, the drag coefficient decreases as increasing the heating area.

Multiscale Modeling of Plastic Deformation in Amorphous Solids

Shingo Urata^{*}, Shaofan Li^{**}

^{*}Asahi Glass Co., Ltd. (AGC), ^{**}University of California, Berkeley

ABSTRACT

Structurally disordered amorphous materials are noncrystalline solids that include metallic glasses, glassy polymers, amorphous ceramics, oxide glasses and so forth. Some of these glassy materials may exhibit plastic deformation. However, the exact mechanism of ductility in amorphous materials is still not completely understood, thus it is very difficult to predict the inelastic mechanical behaviors of amorphous materials at macroscale by using numerical methods, which usually require empirical modeling to represent the inelastic nature. Although multiscale models, which couples atomistic to macroscale scale, are expected to give us reliable modeling without using any empirical and experimental information, only few methods are available to the glassy materials due to their disordered and random microstructure. In this work, we have developed a hierarchical multiscale method to model the inelastic deformation in amorphous materials at macroscale without using any empirical or phenomenological constitutive modeling. The novelties of the multiscale method are three-fold: (1) the multiscale method employs an atomistic-based representative sampling cell (r-cell) obtained through statistical inferences of molecular statics modeling and simulation to obtain macroscale constitutive relations at continuum level; (2) The evolution of the r-cell provides precisely quantification of defect rearrangement in atomistic-scale, and hence the ramification on flow stress, and (3) it uses a special type of Cauchy-Born rules based on the Parrinello-Rahman molecular dynamics to construct an atomistic-informed finite element method. We coined the multiscale method as the coarse-grained Parrinello-Rahman (CG-PR) method. By doing so, we have successfully simulate plastic deformation in the Lennard-Jones binary glass (LJBG) at macroscale without using any empirical continuum level inelastic constitutive relations. For example, strain rate dependence of stress-strain relation is considered by using CG-PR. In addition, even hysteresis of stress-strain curve of cyclic deformation is spontaneously estimated, because rearrangement of atoms in r-cell represents variation of the plasticity. Moreover, we have shown that the CG-PR method can accurately capture the shear band formations in amorphous materials by using macroscale a single-notched thin plate model. The CG-PR simulation results on the shear band formations are compared with large-scale molecular dynamics simulations.

MODELLING OF THE DYNAMICS OF GRAB CRANES WITH A COMPLEX KINEMATIC STRUCTURE, TAKING INTO ACCOUNT THE LINKS' FLEXIBILITY AND ADVANCED FRICTION MODELS

ANDRZEJ URBAŚ, KRZYSZTOF AUGUSTYNEK

University of Bielsko-Biala
43-309 Bielsko-Biala, Willowa 2, Poland
[aurbas,kaugustynek]@ath.bielsko.pl

Key words: Grab Crane, Dynamics, Rigid Finite Element Method, LuGre Friction Model

Abstract. A general mathematical model of a grab crane with a tree structure of a kinematic chain and the possibility of closed-loop subchains is presented in the paper. The formulated model takes into account the flexibility of the support system, links, drives and dry friction in joints. The joint coordinates and homogeneous transformation matrices, based on the Denavit-Hartenberg notation, are used to describe the motion of particular links. The equations of motion are derived using the Lagrange equations of the second kind. Flexible links are modelled using the rigid finite element method (RFEM). In this paper, the LuGre bristles' friction model is used. In numerical simulations, the grab crane consisting of a boom system forming an open-loop kinematic chain and two closed-loop subchains (formulated for hydraulic cylinders) is considered. The results of the calculations present an analysis of the influence of the friction and flexibility on the crane's dynamics.

NOMENCLATURE

$\alpha \in \{m_c, (s_c, 1), (s_c, 2)\}$ – indexes of main chain or subchains

g – acceleration of gravity

s – symbol of support

l – symbol of link

$rfe(\alpha, l, r)$ – symbol of r -th rigid finite element of link (α, l)

$sde(\alpha, l, s)$ – symbol of s -th spring-damping element of link (α, l)

$l^{(\alpha, l)}$ – length of link (α, l)

$m^{(\alpha, l)}$ – mass of link (α, l)

$\tilde{n}_{dof}^{(\alpha, l)}$ – number of generalised coordinates describing the motion of link (α, l)
with respect to the preceding link

$n_{dof}^{(\alpha, l)}$ – number of generalised coordinates describing the motion of link (α, l)
with respect to reference system $\{0\}$

- $n_{div}^{(\alpha,l)}$ – number of division of link (α,l)
 $n_{sde}^{(\alpha,l)}$ – number of sdes of link (α,l)
 $n_{rfe}^{(\alpha,l)}$ – number of rfes of link (α,l)
 $n_l^{(\alpha)}$ – number of links
 n_s – number of supports
 $s_\beta^{(sup,s)}, d_\beta^{(sup,s)} \Big|_{\beta \in \{x,y,z\}}$ – stiffness and damping coefficients of support s in β direction
 $s_\beta^{(\alpha,r)}, d_\beta^{(\alpha,r)} \Big|_{\beta \in \{\psi,\theta,\varphi\}}$ – stiffness and damping coefficients of rfe (α,l,r)
 $s_{dr}^{(\alpha,l)}, d_{dr}^{(\alpha,l)}$ – stiffness and damping coefficients of drive of link (α,l)
 $\sim^{(\alpha,l)}$ – vector of generalised coordinates describing the motion of link (α,l)
 with respect to the preceding link, $\sim^{(\alpha,l)} = \left(\begin{matrix} \sim^{(\alpha,l)} \\ i \end{matrix} \right)_{\substack{l=1,\dots,n_l^{(\alpha)} \\ i=1,\dots,\tilde{n}_{dof}^{(\alpha,l)}}}$
 $-(\alpha,l)$ – vector of generalised coordinates describing the motion of link (α,l)
 with respect to the base system
 (α,l) – vector of generalised coordinates describing the motion of link (α,l)
 with respect to reference system $\{0\}$, $(\alpha,l) = \left(\begin{matrix} (\alpha,l) \\ i \end{matrix} \right)_{\substack{l=1,\dots,n_l^{(\alpha)} \\ i=1,\dots,\tilde{n}_{dof}^{(\alpha,l)}}}$
 $\mathbf{r}^{(\alpha,l)}$ – vector of position of point defined in the local coordinate system of link (α,l)
 $\mathbf{t}_{dr}^{(\alpha,l)}, \mathbf{f}_{dr}^{(\alpha,l)}$ – driving torque or force of link (α,l)
 $\mathbf{t}_f^{(\alpha,l)}, \mathbf{f}_f^{(\alpha,l)}$ – friction torque or force
 $\mathbf{H}^{(\alpha,l)}$ – pseudo-inertia matrix of link (α,l)
 – reducing matrix, $\mathbf{H}^{(\alpha,l)} = \begin{bmatrix} 1 \\ 2 \\ 3 \end{bmatrix} = \begin{bmatrix} 1 & 0 & 0 & 0 \\ 0 & 1 & 0 & 0 \\ 0 & 0 & 1 & 0 \end{bmatrix}$
 $\tilde{\mathbf{T}}^{(\alpha,l)}$ – homogeneous transformation matrix from the local coordinate system of link (α,l) to the local reference system of the preceding link
 $\bar{\mathbf{T}}^{(\alpha,l)}$ – homogeneous transformation matrix from the local coordinate system of link (α,l) to the base system
 $\mathbf{T}^{(\alpha,l)}$ – homogeneous transformation matrix from the local coordinate system of link (α,l) to reference system $\{0\}$,
 $\mathbf{T}_i^{(\alpha,l)} = \frac{\partial \mathbf{T}^{(\alpha,l)}}{\partial \begin{matrix} (\alpha,l) \\ i \end{matrix}}, \quad \mathbf{T}_i^{(\alpha,l)} = \frac{\partial^2 \mathbf{T}^{(\alpha,l)}}{\partial \begin{matrix} (\alpha,l) \\ i \end{matrix} \partial \begin{matrix} (\alpha,l) \end{matrix}}$

Friction parameters

- $\sigma_0^{(m_c)}, \sigma_1^{(m_c)}, \sigma_2^{(m_c)}$ – vectors of stiffness, damping and viscous friction coefficients of bristles, respectively
- $\delta^{(m_c)}$ – vector of deflections of bristles
- $\mu^{(m_c)}$ – vector of friction coefficients
- $\mu_s^{(m_c)}, \mu_k^{(m_c)}$ – vectors of static and kinetic friction coefficients, respectively
- $v^{(m_c)}$ – vector of the Stribeck velocities

1 INTRODUCTION

For many years the control problems of handling equipment, including cranes, have been becoming more important. It is caused on the one hand by the desire to increase the efficiency of transshipment, on the other hand the care for the safety of service. The solution to these problems is to equip new constructions or to modify already existing ones by introducing measuring and executive systems. However, this approach can lead to significant increase in cost. Thanks to the use of computational methods in the area of simulation, the behavior of these devices in various operating conditions, it's possible to apply a strategy for the selection of appropriate control systems. For this purpose, dynamics models can be developed using commercial packages or using software dedicated to a specific construction. The developed mathematical models of grab cranes should take into account, e.g. the flexibility of the support system, links and drives. A significant influence on the dynamics response of the crane has also the friction phenomenon occurring in the joints.

The paper presents mathematical model of a grab crane¹⁻⁷ with a tree structure of a kinematic chain. This structure contains main chain (in the form of the open-loop kinematic chain) and two subchains (in the form closed-loop kinematic chains) which are models of hydraulic cylinders. The mathematical model takes into account the flexibility of the support system, links, drives and dry friction in joints^{6,7}. The clearance in joints is neglected. It is assumed, that the selected links of the crane are driven by torques or forces. These drives are modelled as flexible. The Denavit-Hartenberg notation based on the formalism of joint coordinates and homogeneous transformation matrices is used to describe kinematics of the grab crane⁸. The RFME is used to model the flexibility of links⁹. In this method, the rigid link is replaced by a system of rigid bodies interconnected by means of massless and dimensionless spring-damping elements. The main advantage of the RFEM is the ability to model flexible links using algorithms applied to the model of the rigid body systems with its small modification. Thanks to this, it is easy to use in computer implementation. The friction phenomenon is taken into account in all the joints of the main structure. The LuGre bristles' friction model is used to model this phenomenon¹⁰. This model allows to take into account the static and kinetic friction phases, and other effects like a preliminary displacement, the Stribeck effect and a frictional lag. The equations of motion are derived using the Lagrange equations of the second kind^{9,11}. These equations are supplemented by the Lagrange multipliers and constraint equations formulated for joints in which closed-loop kinematic chains are divided. The Baumgarte stabilization method is used for elimination of the constraint violation¹⁶.

The numerical calculations present the influence of the flexibility and friction in joints on the trajectory of the load and displacement of the crane's links.

2 MATHEMATICAL MODEL OF A GRAB CRANE WITH A FLEXIBLE LINK

The grab crane consists of the main structure (m_c) in the form of open-loop kinematic chain (number of links $n_l^{(m_c)} = 8$) and two subchains $((s_c, 1), (s_c, 2))$ in the form of closed-loop kinematic chains (number of links $\tilde{n}_l^{(\alpha)}|_{\alpha=\{(s_c, 1), (s_c, 2)\}} = 2$) (Fig. 1). The crane is connected to the ground by means of flexible supports ($n_s = 8$). The crane is driven by means of flexible drives in the form of torques ($\mathbf{t}_{dr}^{(m_c, 2)}, \mathbf{t}_{dr}^{(m_c, 8)}$) and forces ($\mathbf{f}_{dr}^{(m_c, 4)}, \mathbf{f}_{dr}^{(s_c, 1, 2)}, \mathbf{f}_{dr}^{(s_c, 2, 2)}$). It is assumed the friction phenomenon occurs only in the joints of the main structure.

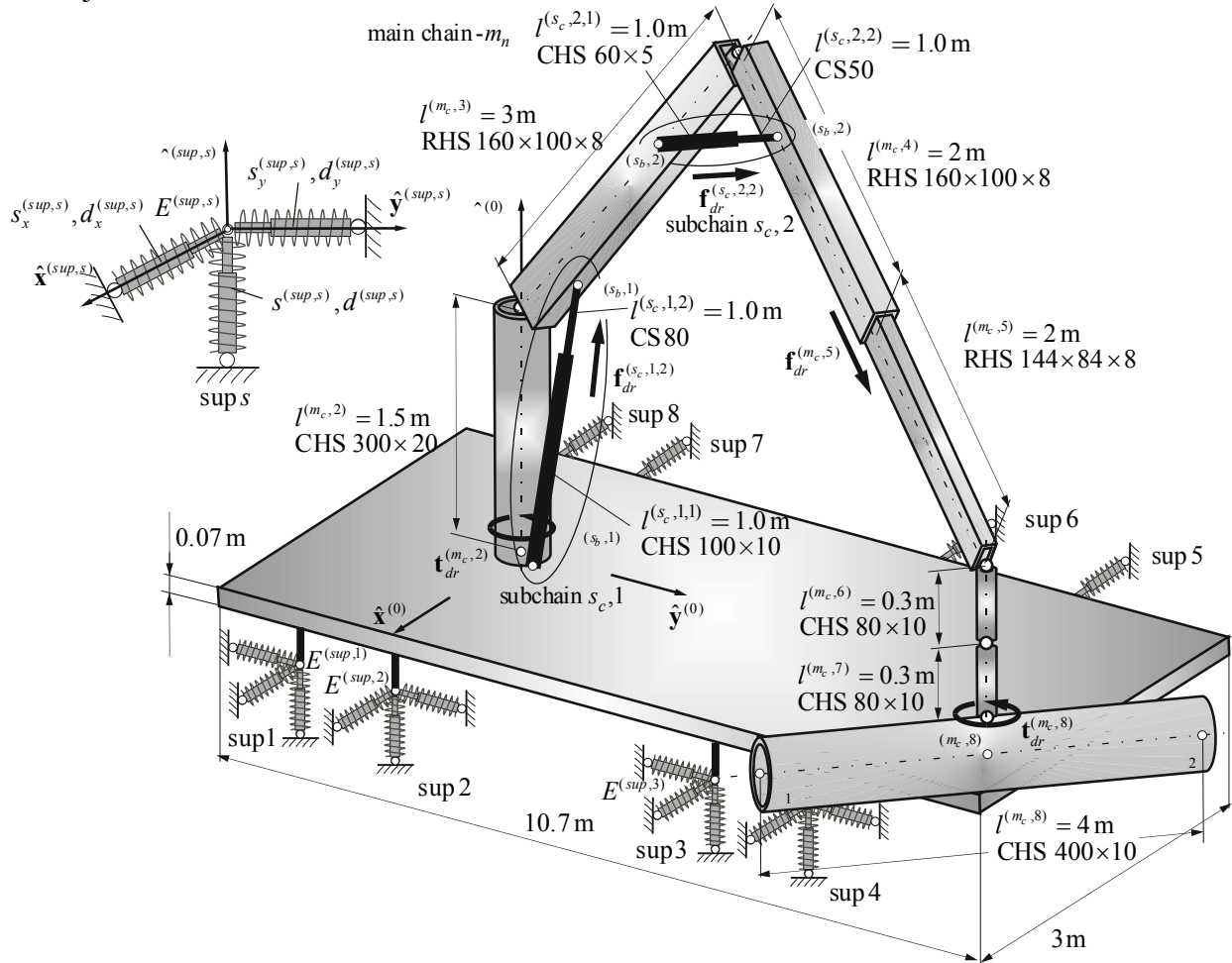


Fig. 1. Model of the grab crane

The joint coordinates together with the Denavit-Hartenberg notation, are used in order to describe the motion of particular links (Fig. 2). The RFEM is applied to discretise the flexible link. In this method, flexible link is replaced by the system of rigid elements (rfe) interconnected by means of spring-damping elements (sde).

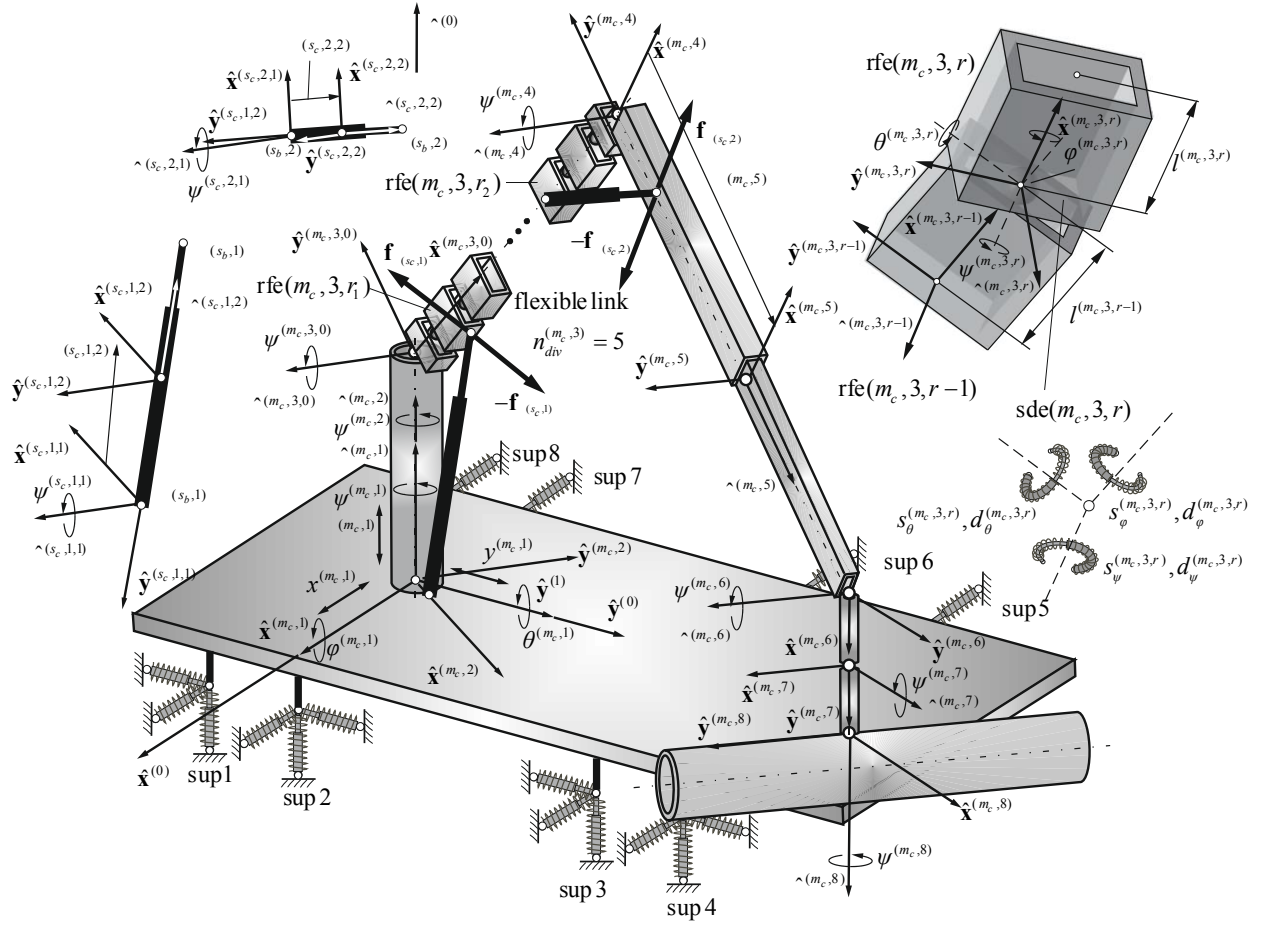


Fig.2. Denavit-Hartenberg notation

The motion of the grab crane is described by the vector of generalized coordinates:

$$= \left(i \right)_{i=1, \dots, n_{dof}} = \begin{bmatrix} (m_c) & -(s_c,1) & -(s_c,2) \end{bmatrix}, \quad (1)$$

where:

- for main chain m_c

$$(m_c) = \left(i \right)_{i=1, \dots, n_{dof}^{(m_c)}} = \begin{bmatrix} \sim(m_c,1) & \sim(m_c,2) & \sim(m_c,3) & \sim(m_c,4) & \sim(m_c,5) & \sim(m_c,6) & \sim(m_c,7) & \sim(m_c,8) \end{bmatrix},$$

$$\sim(m_c,1) = \begin{bmatrix} x^{(m_c,1)} & y^{(m_c,1)} & (m_c,1) & \psi^{(m_c,1)} & \theta^{(m_c,1)} & \phi^{(m_c,1)} \end{bmatrix},$$

$$\sim(m_c,2) = \begin{bmatrix} \psi^{(m_c,2)} \end{bmatrix}, \quad \sim(m_c,3) = \begin{bmatrix} \sim(m_c,3,0) & \dots & \sim(m_c,3,r) & \dots & \sim(m_c,3,n_{rfe}^{(m_c,3)}) \end{bmatrix},$$

$$\sim(m_c,3,0) = \begin{bmatrix} \psi^{(m_c,3,0)} \end{bmatrix}, \quad \sim(m_c,3,r) \Big|_{r=1, \dots, n_{rfe}^{(m_c,3)}} = \begin{bmatrix} \psi^{(m_c,3,r)} & \theta^{(m_c,3,r)} & \phi^{(m_c,3,r)} \end{bmatrix},$$

$$\sim(m_c,4) = \begin{bmatrix} \psi^{(m_c,4)} \end{bmatrix}, \quad \sim(m_c,5) = \begin{bmatrix} (m_c,5) \end{bmatrix}, \quad \sim(m_c,6) = \begin{bmatrix} \psi^{(m_c,6)} \end{bmatrix}, \quad \sim(m_c,7) = \begin{bmatrix} \psi^{(m_c,7)} \end{bmatrix}, \quad \sim(m_c,8) = \begin{bmatrix} \psi^{(m_c,8)} \end{bmatrix},$$

- for subchain $(s_c,1)$

$$\begin{aligned}
(s_c, 1) &= \begin{pmatrix} (s_c, 1) \\ i \end{pmatrix}_{i=1, \dots, n_{dof}^{(s_c, 1)}} = \begin{bmatrix} \sim(m_c, 1) & \sim(m_c, 2) & -(s_c, 1) \end{bmatrix}, \\
-(s_c, 1) &= \begin{pmatrix} -(s_c, 1) \\ i \end{pmatrix}_{i=1, \dots, n_{dof}^{(s_c, 1)}} = \begin{bmatrix} \sim(s_c, 1, 1) & \sim(s_c, 1, 2) \end{bmatrix}, \\
\sim(s_c, 1, 1) &= [\psi^{(s_c, 1, 1)}], \quad \sim(s_c, 1, 2) = [(s_c, 1, 2)],
\end{aligned}$$

- for subchain $(s_c, 2)$

$$\begin{aligned}
(s_c, 2) &= \begin{pmatrix} (s_c, 2) \\ i \end{pmatrix}_{i=1, \dots, n_{dof}^{(s_c, 2)}} = \begin{bmatrix} \sim(m_c, 1) & \sim(m_c, 2) & \sim(m_c, 3, 0) & \dots & \sim(m_c, 3, r_2) & -(s_c, 2) \end{bmatrix}, \\
-(s_c, 2) &= \begin{pmatrix} -(s_c, 2) \\ i \end{pmatrix}_{i=1, \dots, n_{dof}^{(s_c, 2)}} = \begin{bmatrix} \sim(s_c, 2, 1) & \sim(s_c, 2, 2) \end{bmatrix}, \\
\sim(s_c, 2, 1) &= [\psi^{(s_c, 2, 1)}], \quad \sim(s_c, 2, 2) = [(s_c, 2, 2)].
\end{aligned}$$

The local homogeneous transformation matrices have the following forms:

-for main chain m_c

$$\begin{aligned}
\tilde{\mathbf{T}}^{(b)} \Big|_{b=(m_c, 1)} &= \begin{bmatrix} c\psi^{(b)}c\theta^{(b)} & c\psi^{(b)}s\theta^{(b)}s\varphi^{(b)} - s\psi^{(b)}c\varphi^{(b)} & c\psi^{(b)}s\theta^{(b)}c\varphi^{(a)} + s\psi^{(b)}s\varphi^{(b)} & x^{(b)} \\ s\psi^{(b)}c\theta^{(b)} & s\psi^{(b)}s\theta^{(b)}s\varphi^{(b)} + c\psi^{(b)}c\varphi^{(b)} & s\psi^{(b)}s\theta^{(b)}c\varphi^{(b)} - c\psi^{(b)}s\varphi^{(b)} & y^{(b)} \\ -s\theta^{(b)} & c\theta^{(b)}s\varphi^{(b)} & c\theta^{(b)}c\varphi^{(b)} & z^{(b)} \\ 0 & 0 & 0 & 1 \end{bmatrix}, \\
\tilde{\mathbf{T}}^{(b)} \Big|_{b=(m_c, 2)} &= \begin{bmatrix} c\psi^{(b)} & -s\psi^{(b)} & 0 & 0 \\ s\psi^{(b)} & c\psi^{(b)} & 0 & 0 \\ 0 & 0 & 1 & 0 \\ 0 & 0 & 0 & 1 \end{bmatrix}, \quad \tilde{\mathbf{T}}^{(b)} \Big|_{b=(m_c, 3, 0)} = \begin{bmatrix} c\psi^{(b)} & -s\psi^{(b)} & 0 & 0 \\ 0 & 0 & -1 & 0 \\ s\psi^{(b)} & c\psi^{(b)} & 0 & l^{(m_c, 2)} \\ 0 & 0 & 0 & 1 \end{bmatrix}, \\
\tilde{\mathbf{T}}^{(b)} \Big|_{\substack{b=(m_c, 3, r) \\ r=1, \dots, n_{rfe}^{(m_c, 3)}}} &= \begin{bmatrix} c\psi^{(b)}c\theta^{(b)} & c\psi^{(b)}s\theta^{(b)}s\varphi^{(b)} - s\psi^{(b)}c\varphi^{(b)} & c\psi^{(b)}s\theta^{(b)}c\varphi^{(b)} + s\psi^{(b)}s\varphi^{(b)} & l^{(m_c, 3, r-1)} \\ s\psi^{(b)}c\theta^{(b)} & s\psi^{(b)}s\theta^{(b)}s\varphi^{(b)} + c\psi^{(b)}c\varphi^{(b)} & s\psi^{(b)}s\theta^{(b)}c\varphi^{(b)} - c\psi^{(b)}s\varphi^{(b)} & 0 \\ -s\theta^{(\alpha)} & c\theta^{(b)}s\varphi^{(b)} & c\theta^{(b)}c\varphi^{(b)} & 0 \\ 0 & 0 & 0 & 1 \end{bmatrix}, \\
\tilde{\mathbf{T}}^{(b)} \Big|_{b=(m_c, 4)} &= \begin{bmatrix} c\psi^{(b)} & -s\psi^{(b)} & 0 & l^{(m_c, 3, n_{rfe}^{(m_c, 3)})} \\ s\psi^{(b)} & c\psi^{(b)} & 0 & 0 \\ 0 & 0 & 1 & 0 \\ 0 & 0 & 0 & 1 \end{bmatrix}, \quad \tilde{\mathbf{T}}^{(b)} \Big|_{b=(m_c, 5)} = \begin{bmatrix} 1 & 0 & 0 & 0 \\ 0 & 0 & -1 & -^{(b)} \\ 0 & 1 & 0 & 0 \\ 0 & 0 & 0 & 1 \end{bmatrix}, \\
\tilde{\mathbf{T}}^{(b)} \Big|_{b=(m_c, 6)} &= \begin{bmatrix} c\psi^{(b)} & -s\psi^{(b)} & 0 & 0 \\ 0 & 0 & 1 & 0 \\ -s\psi^{(b)} & -c\psi^{(b)} & 0 & 0 \\ 0 & 0 & 0 & 1 \end{bmatrix}, \quad \tilde{\mathbf{T}}^{(b)} \Big|_{b=(m_c, 7)} = \begin{bmatrix} c\psi^{(b)} & -s\psi^{(b)} & 0 & l^{(m_c, 6)} \\ 0 & 0 & 1 & 0 \\ -s\psi^{(b)} & -c\psi^{(b)} & 0 & 0 \\ 0 & 0 & 0 & 1 \end{bmatrix},
\end{aligned}$$

$$\tilde{\mathbf{T}}^{(b)} \Big|_{b=(m_c,8)} = \begin{bmatrix} c\psi^{(b)} & -s\psi^{(b)} & 0 & 0 \\ 0 & 0 & 1 & l^{(m_c,7)} \\ -s\psi^{(b)} & -c\psi^{(b)} & 0 & 0 \\ 0 & 0 & 0 & 1 \end{bmatrix},$$

-for subchain $(s_c,1)$

$$\tilde{\mathbf{T}}^{(b)} \Big|_{b=(s_c,1,1)} = \begin{bmatrix} c\psi^{(b)} & -s\psi^{(b)} & 0 & x_{(s_c,1)}^{(m_c,2)} \\ 0 & 0 & -1 & y_{(s_c,1)}^{(m_c,2)} \\ s\psi^{(b)} & c\psi^{(b)} & 0 & (m_c,2)_{(s_c,1)} \\ 0 & 0 & 0 & 1 \end{bmatrix}, \quad \tilde{\mathbf{T}}^{(b)} \Big|_{b=(s_c,1,2)} = \begin{bmatrix} 1 & 0 & 0 & 0 \\ 0 & 0 & -1 & -^{(b)} \\ 0 & 1 & 0 & 0 \\ 0 & 0 & 0 & 1 \end{bmatrix},$$

-for subchain $(s_c,2)$

$$\tilde{\mathbf{T}}^{(b)} \Big|_{b=(s_c,2,1)} = \begin{bmatrix} c\psi^{(b)} & -s\psi^{(b)} & 0 & x_{(s_c,2)}^{(m_c,3,r)} \\ 0 & 0 & -1 & y_{(s_c,2)}^{(m_c,3,r)} \\ s\psi^{(b)} & c\psi^{(b)} & 0 & (m_c,3,r)_{(s_c,2)} \\ 0 & 0 & 0 & 1 \end{bmatrix}, \quad \tilde{\mathbf{T}}^{(b)} \Big|_{b=(s_c,2,2)} = \begin{bmatrix} 1 & 0 & 0 & 0 \\ 0 & 0 & -1 & -^{(b)} \\ 0 & 1 & 0 & 0 \\ 0 & 0 & 0 & 1 \end{bmatrix},$$

$$s\alpha^{(\beta)} = \sin\alpha^{(\beta)}, \quad c\alpha^{(\beta)} = \cos\alpha^{(\beta)}.$$

The transformation matrices to the global reference system are defined by following formulas:

$$\mathbf{T}^{(m_c,l)} \Big|_{l=1,\dots,n_l^{(m_c)}} = \mathbf{T}^{(m_c,l-1)} \tilde{\mathbf{T}}^{(m_c,l)}, \quad (2.1)$$

$$\mathbf{T}^{(s_c,1,l)} \Big|_{l=1,\dots,\tilde{n}_l^{(s_c,1)}} = \mathbf{T}^{(m_c,2)} \tilde{\mathbf{T}}^{(s_c,1,l)}, \quad (2.2)$$

$$\mathbf{T}^{(s_c,2,l)} \Big|_{l=1,\dots,\tilde{n}_l^{(s_c,2)}} = \mathbf{T}^{(m_c,3,r_2)} \tilde{\mathbf{T}}^{(s_c,1,l)}. \quad (2.3)$$

The equations of motion are derived using the Lagrange equations of the second kind. These equations are supplemented by constraint equations formulated for joints in which subchains are divided using the cut-joint technique.

The LuGre friction equations together with dynamics equations of motion can be written in following general form:

$$\dot{\cdot}^{(m_c)} = \mathbf{LuGre}(t, \cdot^{(m_c)}, {}^{(m_c)}), \quad (3.1)$$

$$\begin{bmatrix} \mathbf{M} & -\mathbf{C} \\ \mathbf{C} & \end{bmatrix} \begin{bmatrix} \ddot{\cdot} \\ \mathbf{f} \end{bmatrix} = \begin{bmatrix} \mathbf{e}(t, \cdot, \dot{\cdot}) - \mathbf{s}(\cdot, \dot{\cdot}) - \mathbf{d}(t, \cdot, \dot{\cdot}) - \mathbf{f}(t, {}^{(m_c)}, \dot{\cdot}^{(m_c)}) \\ \mathbf{c} \end{bmatrix}, \quad (3.2)$$

where:

$$(\mathbf{LuGre})_{i=1,\dots,7} = \frac{\cdot(m_c)}{n_l^{(1)}+i} \left(1 - \frac{\sigma_{0,i}^{(m_c)} z_i^{(m_c)} \operatorname{sgn}\left(\dot{q}_{n_l^{(1)}+i}^{(m_c)}\right)}{\mu_{,i}^{(m_c)} + \left(\mu_{s,i}^{(m_c)} - \mu_{,i}^{(m_c)}\right) \exp\left(-\left(\frac{\cdot(m_c)}{n_l^{(1)}+i}\right)^2\right)} \right),$$

$$\boldsymbol{\mu}^{(m_c)} = \boldsymbol{\sigma}_0^{(m_c)} \mathbf{z}^{(m_c)} + \boldsymbol{\sigma}_1^{(m_c)} \dot{\mathbf{z}}^{(m_c)} + \boldsymbol{\sigma}_2^{(m_c)} \dot{\mathbf{q}}^{(m_c)},$$

$$\mathbf{M} = \sum_{\alpha \in \{m_c, (s_c, 1), (s_c, 2)\}} \mathbf{M}^{(\alpha)}, \mathbf{f} = \begin{bmatrix} \mathbf{f}_{(s_c, 1)} \\ \mathbf{f}_{(s_c, 2)} \end{bmatrix},$$

$$\mathbf{M}^{(m_c)} = \begin{bmatrix} \mathbf{M}_{1,1}^{(m_c)} & \cdots & \mathbf{M}_{1,\cdot}^{(m_c)} & \cdots & \mathbf{M}_{1,n_l^{(m_c)}}^{(m_c)} \\ \vdots & \ddots & \vdots & \ddots & \vdots \\ \mathbf{M}_{i,1}^{(m_c)} & \cdots & \mathbf{M}_{i,\cdot}^{(m_c)} & \cdots & \mathbf{M}_{i,n_l^{(m_c)}}^{(m_c)} \\ \vdots & \ddots & \vdots & \ddots & \vdots \\ \mathbf{M}_{n_l^{(m_c)},1}^{(m_c)} & \cdots & \mathbf{M}_{n_l^{(m_c)},\cdot}^{(m_c)} & \cdots & \mathbf{M}_{n_l^{(m_c)},n_l^{(m_c)}}^{(m_c)} \end{bmatrix}, \mathbf{M}^{(s_c,1)} = \begin{bmatrix} \mathbf{M}_{1,1}^{(s_c,1)} & \cdots & \mathbf{M}_{1,n_l^{(s_c,1)}}^{(s_c,1)} \\ \vdots & \ddots & \vdots \\ \mathbf{M}_{n_l^{(s_c,1)},1}^{(s_c,1)} & \cdots & \mathbf{M}_{n_l^{(s_c,1)},n_l^{(s_c,1)}}^{(s_c,1)} \end{bmatrix},$$

$$\mathbf{M}^{(s_c,2)} = \begin{bmatrix} \mathbf{M}_{1,1}^{(s_c,2)} & \cdots & \mathbf{M}_{1,n_l^{(s_c,2)}}^{(s_c,2)} \\ \vdots & \ddots & \vdots \\ \mathbf{M}_{n_l^{(s_c,2)},1}^{(s_c,2)} & \cdots & \mathbf{M}_{n_l^{(s_c,2)},n_l^{(s_c,2)}}^{(s_c,2)} \end{bmatrix},$$

$$\mathbf{M}_{i,\cdot}^{(\alpha)} \Big|_{\alpha \in \{m_c, (s_c, 1), (s_c, 2)\}} = \sum_{l=\max\{i,\cdot\}}^{n_l^{(\alpha)}} \mathbf{M}_{i,\cdot}^{(\alpha,l)}, \mathbf{M}_{i,\cdot}^{(\alpha,l)} \Big|_{i,\cdot=1,\dots,l} = \left(m_{n_{dof}^{(\alpha,j-1)}+m,n_{dof}^{(\alpha,j-1)}+n}^{(\alpha,l)} \right)_{m=1,\dots,\tilde{n}_{dof}^{(\alpha,i)} \atop n=1,\dots,\tilde{n}_{dof}^{(\alpha,j)}},$$

$$m_{i,\cdot}^{(\alpha,l)} = \operatorname{tr} \left\{ \mathbf{T}_i^{(\alpha,l)} \mathbf{H}^{(\alpha,l)} \left(\mathbf{T}^{(\alpha,l)} \right) \right\},$$

$$\mathbf{C} = \begin{bmatrix} \mathbf{C}_{(s_c,1)} \\ \mathbf{C}_{(s_c,2)} \end{bmatrix},$$

$$\mathbf{C}_{(s_c,1)} = \begin{bmatrix} \mathbf{C}_{1\div \overline{n}_{dof}^{(m_c,3,r_1)}}^{(m_c,3,r_1)} & -\mathbf{C}_{1\div \overline{n}_{dof}^{(s_c,1,2)}}^{(s_c,1,2)} \end{bmatrix}, \mathbf{C}_{(s_c,2)} = \begin{bmatrix} \mathbf{C}_{1\div \overline{n}_{dof}^{(m_c,4)}}^{(m_c,4)} & -\mathbf{C}_{1\div \overline{n}_{dof}^{(s_c,2,2)}}^{(s_c,2,2)} \end{bmatrix},$$

$$\mathbf{C}^{(m_c,3,r_1)} = \begin{bmatrix} 1 \\ 3 \end{bmatrix} \begin{bmatrix} \overline{\mathbf{T}}_1^{(m_c,3,r_1)} \mathbf{r}_{(s_c,1)}^{(m_c,3,r_1)} & \cdots & \overline{\mathbf{T}}_{\overline{n}_{dof}^{(m_c,3,r_1)}}^{(m_c,3,r_1)} \mathbf{r}_{(s_c,1)}^{(m_c,3,r_1)} \end{bmatrix},$$

$$\mathbf{C}^{(s_c,1,2)} = \begin{bmatrix} 1 \\ 3 \end{bmatrix} \begin{bmatrix} \overline{\mathbf{T}}_1^{(s_c,1,2)} \mathbf{r}_{(s_c,1)}^{(s_c,1,2)} & \cdots & \overline{\mathbf{T}}_{\overline{n}_{dof}^{(s_c,1,2)}}^{(s_c,1,2)} \mathbf{r}_{(s_c,1)}^{(s_c,1,2)} \end{bmatrix},$$

$$\mathbf{C}^{(m_c,4)} = \begin{bmatrix} 1 \\ 2 \end{bmatrix} \begin{bmatrix} \overline{\mathbf{T}}_1^{(m_c,4)} \mathbf{r}_{(s_c,2)}^{(m_c,4)} & \cdots & \overline{\mathbf{T}}_{\overline{n}_{dof}^{(m_c,4)}}^{(m_c,4)} \mathbf{r}_{(s_c,2)}^{(m_c,4)} \end{bmatrix}, \mathbf{C}^{(s_c,2,2)} = \begin{bmatrix} 1 \\ 2 \end{bmatrix} \begin{bmatrix} \overline{\mathbf{T}}_1^{(s_c,2,2)} \mathbf{r}_{(s_c,2)}^{(s_c,2,2)} & \cdots & \overline{\mathbf{T}}_{\overline{n}_{dof}^{(s_c,2,2)}}^{(s_c,2,2)} \mathbf{r}_{(s_c,2)}^{(s_c,2,2)} \end{bmatrix},$$

$$\mathbf{e} = \sum_{\alpha \in \{m_c, (s_c, 1), (s_c, 2)\}} \mathbf{e}^{(\alpha)},$$

$$\mathbf{e}^{(m_c)} = \begin{bmatrix} \mathbf{e}_1^{(m_c)} \\ \vdots \\ \mathbf{e}_i^{(m_c)} \\ \vdots \\ \mathbf{e}_{n_l^{(m_c)}}^{(m_c)} \end{bmatrix}, \mathbf{e}^{(s_c,1)} = \begin{bmatrix} \mathbf{e}_1^{(s_c,1)} \\ \vdots \\ \mathbf{e}_i^{(s_c,1)} \\ \vdots \\ \mathbf{e}_{n_l^{(s_c,1)}}^{(s_c,1)} \end{bmatrix}, \mathbf{e}^{(s_c,2)} = \begin{bmatrix} \mathbf{e}_1^{(s_c,2)} \\ \vdots \\ \mathbf{e}_i^{(s_c,2)} \\ \vdots \\ \mathbf{e}_{n_l^{(s_c,2)}}^{(s_c,2)} \end{bmatrix}, \mathbf{e}_i^{(a)} \Big|_{a \in \{m_c, (s_c,1), (s_c,2)\}} = - \sum_{l=i}^{n_l^{(a)}} \left(\mathbf{h}_i^{(a,l)} + \mathbf{e}_i^{(a,l)} \right),$$

$$\mathbf{h}_i^{(a,l)} \Big|_{i=1,...,l} = \left(h_{n_{dof}^{(a,j-1)}+}^{(a,l)} \right)_{=1,...,\tilde{n}_{dof}^{(a,j)}}, h_i^{(a,l)} = \sum_{m=1}^{n_{dof}^{(a,l)}} \sum_{n=1}^{n_{dof}^{(a,l)}} \text{tr} \left\{ \mathbf{T}_i^{(a,l)} \mathbf{H}^{(a,l)} \left(\mathbf{T}_{m,n}^{(a,l)} \right) \right\} \cdot \left(\begin{matrix} a \\ m \end{matrix} \right) \cdot \left(\begin{matrix} a \\ n \end{matrix} \right),$$

$$\mathbf{g}_i^{(a,l)} \Big|_{i=1,...,l} = \left(g_{n_{dof}^{(a,j-1)}+}^{(a,l)} \right)_{=1,...,\tilde{n}_{dof}^{(a,j)}}, g_i^{(a,l)} = m^{(a,l)} g_3 \mathbf{T}_i^{(a,l)} \mathbf{r}_{(a,l)}^{(a,l)},$$

$$\mathbf{s} = \sum_{\beta \in \{sup,sde\}} \mathbf{s}^{(\beta)},$$

$$\mathbf{s}^{(sup)} = \left[\mathbf{f}^{(sup)} \right], \mathbf{f}^{(sup)} = \sum_{s=1}^{n_s} \left(\left(\frac{\partial \mathbf{e}^{(sup,s)}}{\partial \tilde{\mathbf{z}}^{(m_c,1)}} \right) \mathbf{S}^{(sup,s)} \mathbf{e}^{(sup,s)} + \left(\frac{\partial \dot{\mathbf{e}}^{(sup,s)}}{\partial \tilde{\mathbf{z}}^{(m_c,1)}} \right) \mathbf{D}^{(sup,s)} \dot{\mathbf{e}}^{(sup,s)} \right),$$

$$\mathbf{e}^{(sup,s)} = \mathbf{T}^{(m_c,1)} \mathbf{r}_{E^{(sup,s)}}^{(m_c,1)},$$

$$\mathbf{S}^{(sup,s)} = \text{diag} \left\{ s_x^{(sup,s)}, s_y^{(sup,s)}, s^{(sup,s)} \right\}, \mathbf{D}^{(sup,s)} = \text{diag} \left\{ d_x^{(sup,s)}, d_y^{(sup,s)}, d^{(sup,s)} \right\},$$

$$\mathbf{s}^{(sde)} = \left[\mathbf{f}^{(sde)} \right], \mathbf{f}^{(sde)} = \mathbf{S}^{(m_c,3)} \sim (m_c,3), \mathbf{S}^{(m_c,3)} = \text{diag} \left\{ 0, \mathbf{S}^{(m_c,3,1)}, ..., \mathbf{S}^{(m_c,3,r)}, ..., \mathbf{S}^{(m_c,3,n_{rfe}^{(m_c,3)})} \right\},$$

$$\mathbf{S}^{(m_c,3,r)} = \text{diag} \left\{ s_{\psi}^{(m_c,3,r)}, s_{\theta}^{(m_c,3,r)}, s_{\phi}^{(m_c,3,r)} \right\},$$

$$\mathbf{d} = \sum_{a \in \{m_c, (s_c,1), (s_c,2)\}} \mathbf{d}^{(a)}, \mathbf{d}^{(m_c)} = \begin{bmatrix} t_{dr}^{(m_c,2)} & f_{dr}^{(m_c,5)} & t_{dr}^{(m_c,8)} \end{bmatrix}, \mathbf{d}^{(s_c,1)} = \begin{bmatrix} f_{dr}^{(s_c,1,2)} \end{bmatrix},$$

$$\mathbf{d}^{(s_c,2)} = \begin{bmatrix} f_{dr}^{(s_c,2,2)} \end{bmatrix}, t_{dr}^{(m_c,i)} \Big|_{i \in \{2,8\}} = - \left[s_{dr}^{(m_c,i)} \left(\psi_{dr}^{(m_c,i)} - \psi^{(m_c,i)} \right) + d_{dr}^{(m_c,i)} \left(\dot{\psi}_{dr}^{(m_c,i)} - \dot{\psi}^{(m_c,i)} \right) \right],$$

$$f_{dr}^{(a)} \Big|_{a \in \{(m_c,5), (s_c,1,2), (s_c,2,2)\}} = \left[s_{dr}^{(a)} \left(\begin{matrix} a \\ dr \end{matrix} - \begin{matrix} a \end{matrix} \right) + d_{dr}^{(a)} \left(\begin{matrix} \cdot \\ dr \end{matrix} - \begin{matrix} \cdot \\ a \end{matrix} \right) \right],$$

$$\begin{matrix} (a) \\ dr \end{matrix} = \begin{cases} \begin{matrix} (a) \\ int \end{matrix} + 10 \frac{inc}{3} t^3 - 15 \frac{inc}{4} t^4 + 6 \frac{inc}{5} t^5 & \text{for } t < \\ \begin{matrix} (a) \\ fin \end{matrix} & \text{for } t \geq \end{cases}, \begin{matrix} (a) \\ inc \end{matrix} = \begin{matrix} (a) \\ fin \end{matrix} - \begin{matrix} (a) \\ int \end{matrix},$$

$$\mathbf{f} = \begin{bmatrix} t_f^{(m_c,2)} & t_f^{(m_c,3)} & t_f^{(m_c,4)} & f_f^{(m_c,5)} & t_f^{(m_c,6)} & t_f^{(m_c,7)} & t_f^{(m_c,8)} \end{bmatrix},$$

$$\mathbf{c} = \begin{bmatrix} \mathbf{c}_{(s_c,1)} \\ \mathbf{c}_{(s_c,2)} \end{bmatrix},$$

$$\mathbf{c}^{(s_c,1)} = \begin{bmatrix} 1 \\ 3 \end{bmatrix} \left[\left(\sum_{i,=1}^{\bar{n}_l^{(s_c,1,2)}} \bar{\mathbf{T}}_{i,}^{(s_c,1,2)} \cdot \begin{matrix} (s_c,1,2) \\ i \end{matrix} \cdot \begin{matrix} (s_c,1,2) \end{matrix} \right) \mathbf{r}_{(s_c,1)}^{(s_c,1,2)} - \left(\sum_{i,=1}^{\bar{n}_l^{(m_c,3,r_1)}} \bar{\mathbf{T}}_{i,}^{(m_c,3,r_1)} \cdot \begin{matrix} (m_c,3,r_1) \\ i \end{matrix} \cdot \begin{matrix} (m_c,3,r_1) \end{matrix} \right) \mathbf{r}_{(s_c,1)}^{(m_c,3,r_1)} \right],$$

$$\mathbf{c}^{(s_c,2)} = \begin{bmatrix} 1 \\ 2 \end{bmatrix} \left[\left(\sum_{i,=1}^{\bar{n}_l^{(s_c,2,2)}} \bar{\mathbf{T}}_{i,}^{(s_c,2,2)} \cdot \begin{matrix} (s_c,2,2) \\ i \end{matrix} \cdot \begin{matrix} (s_c,2,2) \end{matrix} \right) \mathbf{r}_{(s_c,2)}^{(s_c,2,2)} - \left(\sum_{i,=1}^{\bar{n}_l^{(m_c,4)}} \bar{\mathbf{T}}_{i,}^{(m_c,4)} \cdot \begin{matrix} (m_c,4) \\ i \end{matrix} \cdot \begin{matrix} (m_c,4) \end{matrix} \right) \mathbf{r}_{(s_c,2)}^{(m_c,4)} \right].$$

The dynamics of the grab crane forms the set of differential-algebraic equations with index 1. The constraint violations at the position and velocity level are eliminated by using the Baumgarte stabilization method.

3 SIMULATION RESULTS

For the assumed initial configuration of the crane the statics task is solved using the Newton-Raphson iterative method. Values of the joint coordinates obtained from this task take into account the influence of the deformation of flexible supports, links and drives due to the effects of gravity. The dynamics equations of motion and state equations, are integrated using the Runge-Kutta method of the fourth order with a constant step size. In each the integration step, the Newton-Euler recursive algorithm is applied to determine the joint forces and torques. These forces and torques are necessary to determine friction torques acting in rotational joints and friction forces acting in prismatic joints.

The parameters of the crane supports, drives and friction are presented in Tabs. 1-3, respectively.

Table 1: Parameters of the crane supports

sup s	1	2	3	4	5	6	7	8
$\mathbf{r}_{E^{(sup,s)}}^{(m_c,1)} [\text{m}]$	$\begin{bmatrix} 1.5 \\ 0 \\ -0.57 \\ 0 \end{bmatrix}$	$\begin{bmatrix} 1.5 \\ 1.0 \\ -0.57 \\ 0 \end{bmatrix}$	$\begin{bmatrix} 1.5 \\ 8.0 \\ -0.57 \\ 0 \end{bmatrix}$	$\begin{bmatrix} 1.5 \\ 9.0 \\ -0.57 \\ 0 \end{bmatrix}$	$\begin{bmatrix} -1.5 \\ 9.0 \\ -0.57 \\ 0 \end{bmatrix}$	$\begin{bmatrix} -1.5 \\ 8.0 \\ -0.57 \\ 0 \end{bmatrix}$	$\begin{bmatrix} 1.5 \\ 1.0 \\ -0.57 \\ 0 \end{bmatrix}$	$\begin{bmatrix} -1.5 \\ 0 \\ -0.57 \\ 0 \end{bmatrix}$
$\mathbf{S}^{(sup,s)} [\text{Nm}^{-1}]$	$\text{diag}\{3 \cdot 10^6, 3 \cdot 10^6, 1 \cdot 10^7\}$							
$\mathbf{D}^{(sup,s)} [\text{Ns m}^{-1}]$	$\text{diag}\{5 \cdot 10^4, 5 \cdot 10^4, 9 \cdot 10^4\}$							

Table 3: Drive parameters

drive	$(m_c, 2)$	$(s_c, 1, 2)$	$(s_c, 2, 2)$	$(m_c, 5)$	$(m_c, 8)$
$s_{int}^{(a)} [\text{deg}, \text{m}]$	0	1.9	0.55	1.0	270
$s_{fin}^{(a)} [\text{deg}, \text{m}]$	90	1.9	0.75	0.7	270
$s_{dr}^{(a)} [\text{Nradm}^{-1}, \text{Nm}^{-1}]$	10^7	10^8	10^8	10^8	10^7
$d_{dr}^{(a)} [\text{Nsradm}^{-1}, \text{Nsm}^{-1}]$	$7 \cdot 10^3$	$7 \cdot 10^3$	$7 \cdot 10^3$	$7 \cdot 10^3$	$7 \cdot 10^3$

Table 3: Friction parameters

joint	2	3	4	5	6	7	8
$\mu_s^{(m_c)}$	$[0.2 \ 0.2 \ 0.2 \ 0.2 \ 0.2 \ 0.2 \ 0.2]$						
$\mu^{(m_c)}$	$[0.1 \ 0.1 \ 0.1 \ 0.1 \ 0.1 \ 0.1 \ 0.1]$						
$\sigma_0^{(m_c)} [\text{rad}^{-1}, \text{m}^{-1}]$	$[10^2 \ 10^2 \ 10^2 \ 10^3 \ 10^2 \ 10^2 \ 10^2]$						
$\sigma_1^{(m_c)} [\text{srad}^{-1}, \text{s m}^{-1}]$	$[10 \ 10 \ 10 \ 10^{3/2} \ 10 \ 10 \ 10]$						
$\sigma_2^{(m_c)} [\text{srad}^{-1}, \text{s m}^{-1}]$							
$\cdot^{(m_c)} [\text{rads}^{-1}, \text{ms}^{-1}]$	$[1.75 \cdot 10^{-2} \ 1.75 \cdot 10^{-2} \ 1.75 \cdot 10^{-2} \ 0.001 \ 1.75 \cdot 10^{-2} \ 1.75 \cdot 10^{-2} \ 1.75 \cdot 10^{-2}]$						

The influence of the flexibility of link 3 and friction in the joints on the trajectories of selected points of load in $\hat{\mathbf{x}}^{(0)}\hat{\mathbf{y}}^{(0)}$ plane are presented in Fig. 3, whereas courses of $\alpha^{(0)}|_{\alpha=\{1, (8), 2\}}$ components are shown in Fig. 4. The courses of the driving forces in the actuators are presented in Fig. 5.

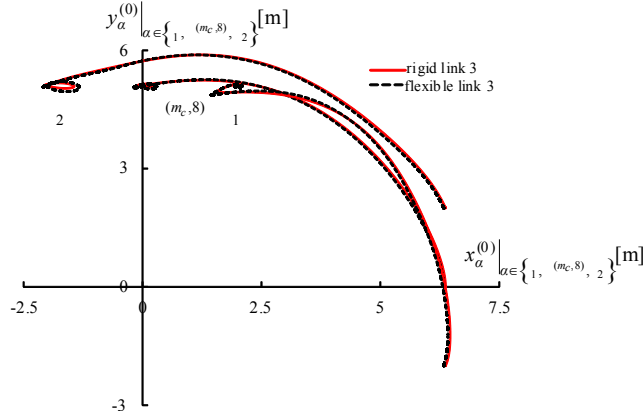


Fig. 3. Trajectories of selected points of the load

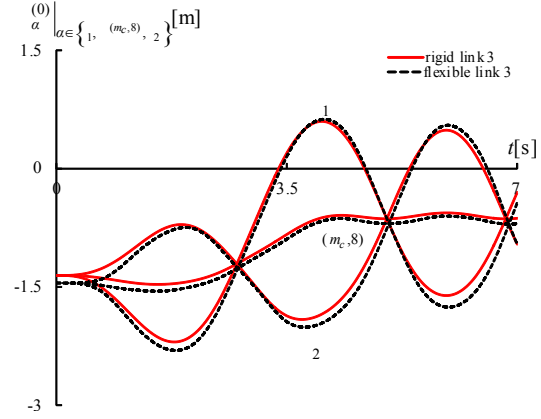


Fig. 4. Time courses of the α component

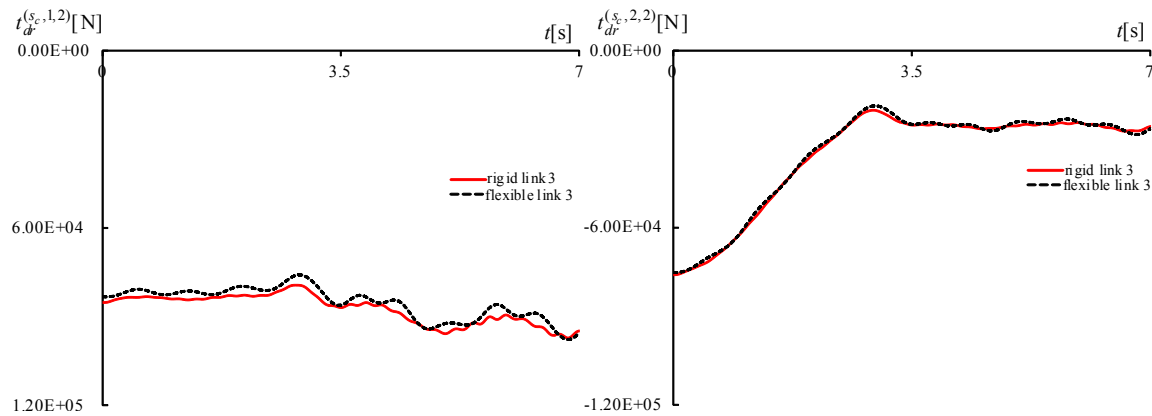


Fig. 5. Time courses of the driving forces

The performed calculations show that considered phenomena of the modeled crane have a influence on the crane dynamics. The flexibility introduce some oscillations in the time courses of the actuator driving function. These oscillations can arise when smaller actuators' stiffness values are taken in calculations.

4 CONCLUSIONS

The mathematical model of the grab crane presented in this paper has been used to analyse the influence of flexibility (supports, links and drives) and friction on crane's dynamics. The joint coordinates and homogeneous transformation matrices have been applied to describe the geometry of the grab crane. The dynamics equations of motion have been derived using the formalism of the Lagrange equations of the second kind. The RFEM has been used to discretize the flexible link. The LuGre bristles' friction model has been applied to model the friction in joints. The phenomena taken into account in the mathematical model of grab crane have the significant influence on

behavior of the handling load, and in the authors' opinion the presented results can be useful while a process of designing.

This paper is realized within the research project number 2017/01/X/ST8/01456 funded by the Polish National Science Centre.

REFERENCES

- [1] La Hera, P. X. and Morales, D. O. Non-linear dynamics modelling description for simulating the behavior of forestry cranes. *International Journal of Modelling Identification and Control*, 21, 2, 125-138, (2014).
- [2] La Hera, P. X. and Morales, D. O. Model-based development of control systems for forestry cranes. *Journal of Control and Science and Engineering*, vol., no. ID 256951, (2015). doi:10.1155/2015/256951
- [3] Posiadała, B. Modeling and analysis of the dynamics of load carrying system. in: *Proc. of World Congress on Engineering and Computer Science*, San Francisco, USA, (2012).
- [4] Papadopoulos, E. and Sarkar, S. On the dynamic modeling of an articulated electrohydraulic forestry machine. in: *Proc. of the 1996 AIAA Forum on Advanced Developments in Space Robotics*, WI, 1-2 August, (1996).
- [5] Papadopoulos, E., Frenette, R., Mu, B. and Gonthier, Y. On the modeling and control of an experimental harvester machine manipulator. in: *Proc. of IEEE/RSJ International Conference on Intelligent Robots and Systems*, Grenoble, France, 8-12 September, (1997).
- [6] Urbaś, A. Computational implementation of the rigid finite element method in the statics and dynamics analysis of forest cranes. *Applied Mathematical Modelling*, 46, June:750-762, (2017). doi: 10.1016/j.apm.2016.08.006
- [7] Urbaś, A. and Harlecki, A. Application of the rigid finite element method and the LuGre friction model in the dynamic analysis of the grab crane. in: *Proc. of 4th Joint International Conference on Multibody System Dynamics*, Montreal, Canada, May 29-June 2, (2016).
- [8] Craig, J. J. *Introduction to robotics. Mechanics and control*. Addison-Wesley Publishing Company, Inc., 1989.
- [9] Wittbrodt, E., Szczotka, M., Maczyński, A. and Wojciech, S. *Rigid Finite Element Method in Analysis of Dynamics of Offshore Structures*. Ocean Engineering & Oceanography, Springer, Berlin-Heidelberg, (2013).
- [10] Åström, K. J. and Canudas-de-Witt, C.. Revisiting the LuGre model. *IEEE Control Systems Magazine*, Institute of Electrical and Electronics Magazine, 28(6), (2008).
- [11] Jurevič, E. I. (ed.). *Dynamics of robot control*. Nauka, Moscow, (1984). (in Russian)

On the Implications of Hyperparameters Choices in Bayesian Inference of Random Fields

Felipe Uribe^{*}, Iason Papaioannou^{**}, Wolfgang Betz^{***}, Daniel Straub^{****}

^{*}Technische Universität München, ^{**}Technische Universität München, ^{***}Technische Universität München,
^{****}Technische Universität München

ABSTRACT

Inverse problems occur whenever one aims to infer information about a physical system based on observations. If the uncertain model parameters are expressed in terms of random fields, the complexity of the inverse problem is increased as uncertain parameters of random functions need to be identified, which generally renders the problem high-dimensional. We formulate the inference problem probabilistically using a Bayesian approach. A challenge in Bayesian inference with random fields is the definition of the prior distribution for the autocovariance kernel of the field. In practice, the prior knowledge is typically not sufficient to favor a particular kernel. One alternative is to define a hierarchical Bayesian model by decomposing the prior information about the autocovariance kernel into one or more conditional distributions of uncertain hyperparameters. In this paper, we employ the Karhunen-Loève expansion to represent the random field. The influence of different probabilistic modeling strategies for the hyperparameters, such as the truncation order of the expansion and the correlation length of the field, is investigated. We provide insight into the selection of prior probability distributions for the hyperparameters. We further analyze the computational implications of the adopted hierarchical Bayesian approach. The study is exemplarily performed on a structural beam with spatially variable flexibility.

Towards Support and Neutral Data Exchange for Isogeometric Analysis (IGA) in the ISO 10303 Standard

Benjamin Urick*, Allison Barnard Feeney**

*nVariate, Inc., **National Institute of Standards and Technology (NIST)

ABSTRACT

Isogeometric Analysis (IGA) is a computational analysis methodology that offers the possibility of integrating Finite Element Analysis (FEA) into conventional design tools, bridging the chasm between the current industrial verticals of Computer-Aided Design (CAD) and Computer-Aided Engineering (CAE). Although the benefits of IGA are vast and numerous as an engineering technology, one key problem is that conventional file formats limit the ability to share IGA modeling data between users. Currently users are forced to create their own file formats, rely on academic researchers' personal implementations, or use specific CAX application formats for the translation and storage of IGA data, often compromising the users' design intent. Support in current interchange formats, such as STEP, is limited as the standards were developed around conventional CAD and CAE, classically separated technologies prior to the invention of IGA. This has severely hindered both the potential for collaboration between users as well as the more critical objective: large-scale commercial adoption of IGA as an industrial technology. ISO 10303 plays an indispensable role as the de facto neutral file format in the world of CAD-CAE data exchange and has recently adopted critically important IGA features such as locally refined splines (e.g., T-splines, LR-splines, etc.), trivariate (volumetric) spline representations, etc. [1,2]. While these additions greatly increase the ability of IGA designers and analysts, it does not allow for the ability to exchange common unstructured mesh representations frequently encountered in industrial models, containing extraordinary points (E.P.s) of arbitrary valence. As part of its Digital Thread for Smart Manufacturing Project [3], The National Institute of Standards and Technology's (NIST) Engineering Laboratory (EL) has taken an active role in resolving the IGA data exchange problem. These activities have shed new insights on integrated CAX model representations in a IGA-centric view where CAD-CAE model definition is simultaneous. [1] T. Dokken, V. Skytt, J. Haenisch, K. Bengtsson, Isogeometric Representation and Analysis: Bridging the Gap Between CAD and Analysis, in: 47th AIAA Aerosp. Sci. Meet. New Horiz. Forum Aerosp. Expo., American Institute of Aeronautics and Astronautics, n.d. doi:10.2514/6.2009-1172. [2] V. Skytt, J. Haenisch, Extension of ISO 10303 with Isogeometric Model Capabilities, (2013). [3] Digital Thread for Smart Manufacturing, NIST. (2014). <https://www.nist.gov/programs-projects/digital-thread-smart-manufacturing>.

Experimental Verifications for Indirect Bridge Frequency Measurement

Shota Urushadze^{*}, Yeong-Bin Yang^{**}, Jong-Dar Yau^{***}

^{*}Institute of Theoretical and Applied Mechanics, ASCR, Prague, Czech Republic., ^{**}Chongqing University, China,
^{***}Tamkang University, Taiwan

ABSTRACT

According to the idea of indirect bridge frequency measurement proposed by Yang and co-workers [1-3], a moving test vehicle can be regarded as a message receiver to detect vibration data of the bridge that it passed. In the present study, an experimental setup will be carried out for indirect frequency measurement of a simply supported beam using a passing test vehicle with the feature of adjustable frequencies. The test vehicle is design as a single-degree-of-freedom unit in vertical vibration and guided by a set of tensile strings in self-equilibrium state so that it can drive the vehicle to move along the beam axis with full contact. To remain the test vehicle running over the beam at constant speed, this study proposed a set of cantilever spiral spring devices to adjust the frequency by regulating the arch length of the spiral springs. From the present experimental results, the indirect bridge inspection method is applicable to frequency monitoring of a bridge. Moreover, the harder stiffness adjusted by the spiral spring device can give a more accurate prediction for measuring bridge frequencies than the softer one. References [1] Yang, Y. B., Lin, C. W., and Yau, J. D., Extracting bridge frequencies from the dynamic response of a passing vehicle, J. Sound & Vibr., 272(3-5), 2004, 471-493. [2] Lin, C. W., and Yang, Y. B., Use of a passing vehicle to scan the bridge frequencies - an experimental verification, Eng. Struct., 27(13), 2005, 1865-1878. [3] Yang, Y. B., Li, Y.C., and Chang, K.C., Constructing the mode shapes of a bridge from a passing vehicle: a theoretical study, Smart Structures & Systems, An Int. J., 13(5), 2014, 797-819.

Numerical and Physical Modeling of Stringer Stiffened Silo Collapse Subject to Eccentric Discharge Flow

Gabriel Usera^{*}, Gonzalo Fernandez^{**}, Rocío Salles^{***}, Diego Olivert^{****}

^{*}UdelaR, Montevideo, Uruguay, ^{**}UdelaR, Montevideo, Uruguay, ^{***}UdelaR, Montevideo, Uruguay, ^{****}UdelaR, Montevideo, Uruguay

ABSTRACT

Stringer stiffened metal silos for grain and other bulk material storage are highly efficient structures designed to sustain axially symmetric loads. Accidental operation of eccentric outlets while the silo is loaded at full capacity might induce eccentric discharge flows under which severe non-symmetric loads develop onto the silo outer shell. These loads, being far from the structure design conditions, can cause localized buckling of the stringer stiffeners, loss of structural stability and, ultimately, its collapse. In this work both physical and numerical modeling of the interaction between granular flow and structural dynamic response are developed and compared for concentric and eccentric flow conditions. Small scale structured models of stringer stiffened silos, were assembled using aluminum foil for the outer shell and dried pasta straws for the vertical stringer stiffeners, while sand is used to model the granular flow. Thus, a complete structured small scale model with individual stringer stiffeners was developed with this approach. Experiments were performed varying the outlet positions, from concentric to mild (37%) and severe (74%) eccentric. Small to negligible deformations of the scale model were observed for concentric and mild eccentric flow conditions, while progressive individual stringer stiffeners buckling and full collapse of the structure was observed for severe eccentric flows. A numerical model of the structural dynamic response was implemented following Ivanov [1] proposal for a structural-DEM method. Shell elements were connected together with elongation, bending and torsional springs, modeling both the outer shell and the vertical stringer stiffeners. Full geometrical non-linearity and inertial behaviour is fully captured intrinsically by the DEM method. Load due to grain flow was modeled after Sadowski [2]. Numerical experiments again show small to negligible deformations for concentric flow conditions. Mildly eccentric flow produced limited localized deformations of the structure, with no buckling of the individual stringer stiffeners. Meanwhile, for severe eccentric flow, deep localized buckling, in the shape of 'smile' buckles, was observed followed by complete loss of structural stability and full collapse. Comprehensive physical and numerical modeling of structural behaviour of stringer stiffened silos was accomplished in this work, with novel approaches to the implementation of both physical models with individual stringer stiffeners and numerical modeling through a structural-DEM method.

Uncertainties in Geotechnical Laboratory Tests and Centrifuge Experiments

Ryosuke Uzuoka^{*}, Daiki Hizen^{**}, Katsutoshi Ueno^{***}

^{*}Kyoto University, ^{**}Tokushima University, ^{***}Tokushima University

ABSTRACT

Geomaterials are essentially inhomogeneous. Although a lot of their constitutive models have been proposed and some have been used in practice, numerical models considering inhomogeneity and uncertainties have not established. Centrifuge modelling is one of the most popular and reliable physical modelling for geomaterials; therefore the results of centrifuge experiments have been used for validation process of newly developed numerical method including constitutive models of soil. The material parameters of constitutive models have been calibrated with laboratory tests such as triaxial compression tests. However, uncertainties in the laboratory tests and the centrifuge experiments have not been considered in most validation cases of geotechnical problems although it was well known that geotechnical centrifuge modeling includes some uncertainties such as inhomogeneity of model ground and soil structures, unrepeatability of external loading. In this study many cases with the same target experimental conditions were performed through triaxial tests and centrifuge experiments for shear and consolidation behaviors of clay ground. The uncertainties in the deformation of clay ground were discussed.

Micromechanical Modeling and Simulation of Ductile Failure under Combined Tension and Shear

VISHAL VISHWAKARMA*, SHYAM KERALAVARMA**

*Department of Aerospace Engineering, Indian Institute of Technology Madras, Chennai 600036, India,

**Department of Aerospace Engineering, Indian Institute of Technology Madras, Chennai 600036, India

ABSTRACT

The Gurson (1977) model of ductile failure by void growth to coalescence is widely used in the structural integrity assessment of engineering components. Recent work has focused on addressing some well-known limitations of the Gurson model such as the inability to predict fracture at low stress triaxialities, incorporating the dependence of yield criterion on the Lode parameter, and the effect of “void coalescence” or plastic flow localization at the mesoscale of the voids. Recently, Keralavarma (2017) proposed a multi-surface plasticity model for a porous isotropic material by combining the Gurson void growth model with the void coalescence model of Keralavarma and Chockalingam (2016). Here, the theoretical framework of the multi-surface model is revisited and the model predictions are calibrated with micromechanical finite element simulations of void growth using the unit cell model. An initially cubic unit cell with a concentric spherical void is deformed to failure under a combination of triaxial tensile and shear loads. Periodic boundary conditions are used and the stresses are applied proportionally such that the macroscopic stress triaxiality, T , and lode parameter, L , remain constant throughout the loading history. The average stress-strain response, the evolution of porosity and the macroscopic strain at the onset of coalescence obtained from the simulations are compared with predictions from the multisurface model for a wide range values of T and L . It is shown that the effective response predicted by the multi-surface model is in good quantitative agreement with the cell model simulations for materials with low strain hardening capacity. The triaxiality and Lode parameter dependence of the strain to failure is correctly predicted by the model. For materials with high strain hardening capacity, the model is shown to significantly underestimate the ductility, especially under shear dominated loading conditions. A phenomenological extension of the model, motivated by the theory of strain localization in elasto-plastic materials, is shown to significantly improve the model predictions for hardening materials. References 1. Gurson, A.L. , 1977. Continuum theory of ductile rupture by void nucleation and growth: part i—yield criteria and flow rules for porous ductile media. *J. Eng. Mat. Tech.* 99, 2–15. 2. Keralavarma, S.M. , 2017. A multi-surface plasticity model for ductile fracture simulations. *J. Mech. Phys. Solids*, 103:100-120. 3. Keralavarma, S.M. , Chockalingam, S. , 2016. A criterion for void coalescence in anisotropic ductile materials. *Int. J. Plast.* 82, 159–176.

One-dimensional Fluid Model of In Vivo Pulmonary Arterial Hemodynamic Data

Daniela Valdez-Jasso*, Daniela Velez-Rendon**

*University of California at San Diego, **University of Illinois at Chicago

ABSTRACT

Pulmonary arterial hypertension (PAH) is a severe disease of the pulmonary vasculature that is characterized by high blood pressure in the lungs. During the development of PAH, the pulmonary vasculature undergoes structural remodeling that compromises its normal physiological function. Here, we investigate how the changes in wall mechanics contribute to the pulmonary vascular hemodynamics in PAH using a 1D fluid model. Using Euler equations and assuming an axisymmetric blood flow in the pulmonary arteries, the deformation of the arterial wall is prescribed using linear elasticity [1]. The initial-boundary value problem is initialized using in-vivo measurements of blood flow and pressure from the main pulmonary artery (MPA) at the inlet ((first node) to predict pressure and cross-sectional area propagation along the vessel length. Blood pressure, flow, outer diameter, wall thickness and in-situ length of the MPA are measurements from normo- and hypertensive male rats taken during open chest surgery. The pressure-area relation is a linearization of the thin shell model around the area value at no pressure [2]. The elastic modulus is the average of the right and left pulmonary artery elastic modulus measured under tubular biaxial tensile tests [3] immediately after hemodynamic measurements. In the current numerical scheme, no boundary conditions at the outlet are imposed. The system of equations was discretized in time and space, and was solved using Euler's method in MATLAB. Pressure and elastic modulus increased with the progression of PAH, but flow remained overall constant. By using these data, the model was able to predict pressure that closely resembles to that measured pressure at the inlet of the MPA. After three cardiac cycles, a slight decrease in the peak flow, pressure and cross-sectional area was observed. This could be interpreted as the attenuation of the waveform due to the buffering effect of the vessel. The computed dynamic cross-section area is about 26% higher than the measured value at zero stress during opening-angle experiments. When testing how the elastic modulus of one animal on another, we found the pressure and flow waveforms to remain unaffected. However, area predictions were amplified indicating the model being sensitive to wall stiffness. Boundary conditions will be investigated to determine how the changes in the wall mechanics influence the hemodynamics of the vasculature in PAH. [1] P Lee, et al. Biomech. Model. Mechanobiol., 2016. [2] MS Olufsen, Am. J. Physiol., 1999. [3] ER Pursell, et al. J. Biomech. Eng., 2016.

An Alternative Computational Approach to Evaluate the Directional Behavior of Periodic Media

Camilo Valencia^{*}, Pablo Zavattieri^{**}, Nicolas Guarin-Zapata^{***}, Juan Gomez^{****}, Juan Diego Jaramillo^{*****}

^{*}Universidad EAFIT, Medellin, Colombia., ^{**}Purdue University, U.S., ^{***}Universidad EAFIT, Medellin, Colombia.,
^{****}Universidad EAFIT, Medellin, Colombia., ^{*****}Universidad EAFIT, Medellin, Colombia.

ABSTRACT

One of the most relevant problems in the dynamic analysis of periodic media is the determination of the directional behavior of the material. As a result, the preferred propagation directions, which are a function of the material structure, are identified. In the typical analysis method one computes the material dispersion surfaces which result after solving a generalized eigenvalue problem corresponding to the imposition of the so-called Bloch periodic boundary conditions upon the unit cell. The preferred propagation directions are identified from the shapes appearing in the iso-frequency contour plots of the gradients over the first two modes of the dispersion surfaces. As a complement, it is also frequent to use a polar histogram of these gradients. This approach has a conceptual inconvenience. First, in the dispersion relations, the wave types and modes are usually mixed. For instance, it may be the case that information from several wave types originated at different Brillouin zones appear in the first mode. Similarly, since the approach is based on the first two modes the analysis might erroneously eliminate directional behavior associated to the high frequency regime. In this work we present an alternative approach to conduct directional analysis of periodic media where we consider the first N modes from the generalized eigenvalue problem. We compute the magnitude and directional distribution of a single vector field V computed after considering the N modes simultaneously. The results are then presented as a combination of phase velocity and a vector count held over V . Since we take information from several modes, as opposed to single mode biased methods, we obtain more representative descriptions of the directional response valid in the low and high frequency regime. Our presentation is organized as follows: - Description of the classical approach for directional analysis focusing on its two major drawbacks. - Detailed description of the proposed approach using N modes and a vector field. - Applications showing the validity and versatility of the proposed approach.

Direct Simulation of Granular Collapses Using $\mu(I)$ -like Rheology

Rudy Valette^{*}, Lucas Sardo^{**}, Elie Hachem^{***}

^{*}MINES-ParisTech, PSL Research University, ^{**}MINES-ParisTech, PSL Research University, ^{***}MINES-ParisTech, PSL Research University

ABSTRACT

We introduce an accurate numerical method for the computation of 2D and 3D granular collapse under gravity flows using different versions of the $\mu(I)$ rheology. We use a time-dependent regularization algorithm to solve the model using a finite element method, combined with anisotropic mesh adaptation to capture accurately the quasi-static vs. inertial flow zones, and using a variational multiscale method. A Level-Set method, based on self-reinitialization of the signed distance function, aims to capture and follow efficiently the interface between the fluid/air domains. We show that this rheology can capture the two experimentally observed types of spreading and the corresponding scaling laws, both in 2D and 3D collapses. Sensitivity analysis on rheological constants was performed for quasi-static and inertial parameters, in order to verify the universality (no dependency on grain type) of flow features such as relative spreading vs. aspect ratio, and normalized distance-time. We also demonstrate the effect of additional lengthscales on the dynamics of spreading, not discussed in previous literature.

A First Order System Discontinuous Petrov-Galerkin Method Using Continuous Trial Spaces

Eirik Valseth^{*}, Albert Romkes^{**}, Victor Calo^{***}

^{*}South Dakota School of Mines and Technology, ^{**}South Dakota School of Mines and Technology, ^{***}Curtin University

ABSTRACT

We present a new type discontinuous Petrov-Galerkin (DPG) method for finite element (FE) approximations of boundary value problems of second order linear partial differential equations (PDEs) in the spirit of the DPG method introduced by Demkowicz and Gopalakrishnan [1, 2]. The new DPG method uses a first order system weak representation of the governing PDEs, and distinguishes itself by using classical C_0 or continuous function spaces for the trial functions, in an effort to reduce computational cost. Discontinuous function spaces, however, are employed for the test functions and therefore the test functions can be solved locally at the element level by using the DPG philosophy in [1, 2]. Hence, they are optimal in the sense that they guarantee inherently stable FE approximations with best approximation properties in terms of the energy norm. The local contributions of test functions can be numerically solved on each element with high numerical accuracy and do not require the solution of global variational statements. 2D numerical verifications and convergence studies are to be presented for the solution of second order partial differential equations, including convection dominated convection-diffusion problems with highly oscillatory (diffusion) coefficients. [1] L. Demkowicz and J. Gopalakrishnan. Analysis of the DPG method for the Poisson equation. SIAM Journal on Numerical Analysis, 49(5):1788–1809, 2011. [2] L. Demkowicz and J. Gopalakrishnan. A class of discontinuous Petrov-Galerkin methods. II. Optimal test functions. Numerical Methods for Partial Differential Equations, 27(1):70–105, 2011.

Atomic-Microscale Modeling of Phonons in the Molecular Crystal RDX Using Accurate Phonon Lifetimes

Francis VanGessel^{*}, Daniel Elton^{**}, Gaurav Kumar^{***}, Peter Chung^{****}

^{*}University of Maryland, ^{**}University of Maryland, ^{***}University of Maryland, ^{****}University of Maryland

ABSTRACT

RDX is an energetic molecular crystal in which lattice vibrations are believed to play a large role in initiation mechanics. In addition to the short-ranged covalently-bonded interactions, which are found in the majority of solids in which phonons have been investigated in the literature, non-bonded long range forces play a significant role in the structural properties of RDX and other emerging materials such as so-called van der Waals solids. Here, we study of the microscale thermal transport properties of RDX via atomic and phonon Boltzmann transport equation modeling, using a recently developed anisotropic full Brillouin Zone model [1]. The full Brillouin zone model employs atomic models for its parameterization, allows for simulation of all lattice vibrational modes, and inherently captures anisotropy in thermal flow. Thus we will demonstrate how phonons are transported within the RDX crystal. Additionally, for the first time, we also calculate phonon lifetimes in RDX throughout the first Brillouin zone. This is accomplished by running lattice dynamics and molecular dynamics simulations and then fitting the mode projected spectral energy density. The use of mode specific lifetimes significantly increases the accuracy of the thermal conductivity values predicted with Boltzmann transport equation calculations, allowing for an additional source of anisotropy to appear in the thermal conductivity tensor. Our tabulation of mode specific lifetimes contains fine grained details about energy transport in RDX which may be of interest to those researching shock induced initiation and multiphonon up-pumping in RDX. In addition to addressing important questions regarding the behavior of phonons in RDX, this talk will further describe heat conduction mechanisms within anisotropic materials. Such mechanisms have become increasingly of interest due to the unique modalities of heat flow they enable, particularly flow-directional bias, and due to the promise of predictable and controllable thermoelectric behaviors at submicron scales. As such, new techniques have been developed to model these materials. However there still exist knowledge gaps regarding, for example, heat flow in non-covalently bonded crystals such as RDX where van der Waal's and Coulombic forces play a large role. Thus the aim of this talk is to both demonstrate anisotropic heat flow in RDX and by doing so improve model descriptions of phonon processes in non-covalently bonded crystals. [1] F. VanGessel and P. Chung, "An anisotropic full Brillouin zone model for the three dimensional phonon Boltzmann transport equation", Computer Methods in Applied Mechanics and Engineering, vol. 317, pp. 1012-1036, 2017.

DIMENSION ADAPTIVE PSEUDO-SPECTRAL PROJECTION FOR A PERMANENT SYNCHRONOUS MOTOR WITH UNCERTAIN PARAMETERS

CHRISTOPH KUBALA*, MICHAEL SCHICK*, AND ANTOINE VANDAMME*

*Robert Bosch GmbH

Stuttgart, Germany

{christoph.kubala; michael.schick3; antoine.vandamme}@de.bosch.com

Key words: Polynomial Chaos Expansion, Electrical Drives, Error Control, Uncertainty Quantification, Sparse Grids, Surrogate Modeling.

Summary. Many industrial problems are based on simulation models which require knowledge on parameter values. In practice, however, exact information is rarely available. For example, variations in component tolerances due to manufacturing processes may translate to parameter uncertainties influencing the outcome of simulation models. This makes uncertainty quantification crucial to establish the reliability of simulation results. Using the classical "Monte Carlo method" type design of experiment would randomly sample in parameter space, perform simulations for each sample and afterwards combine the results to estimate all statistical quantities of interest. The main drawback of this method is that usually many samples, i.e. many simulations, are required to reach a satisfactory error level in the statistical predictions (thousands to hundreds of thousands samples). In contrast, Polynomial Chaos Expansions (PCEs) are popular spectral surrogate models typically applied to solve uncertainty propagation problems. They quantify the effect of statistical fluctuations in simulation model outputs due to uncertainty in parameter space using orthogonal polynomials. Various techniques exist to compute the coefficients of PCEs. A canonical way is to approximate the coefficients by numerical quadrature, evaluate the simulation model at the quadrature nodes and post-process the results. However, this approach suffers from aliasing errors, which can be circumvented by tailoring the PCE to the numerical quadrature (in our case a "Smolyak sparse grid") in a special way. This gives rise to the so-called "Pseudo-Spectral Projection method" (PSP), which we consider in a dimension adaptive version (aPSP). The major advantage of aPSP is its automatic error control, which provides a robust error estimation on all adaptive iterations, and hence allows an estimation on the quality of each design of experiment. In this work, we investigate a PMSM (permanent magnet synchronous motor) with uncertain geometrical and physical parameters, for example the positioning of magnets. Our focus

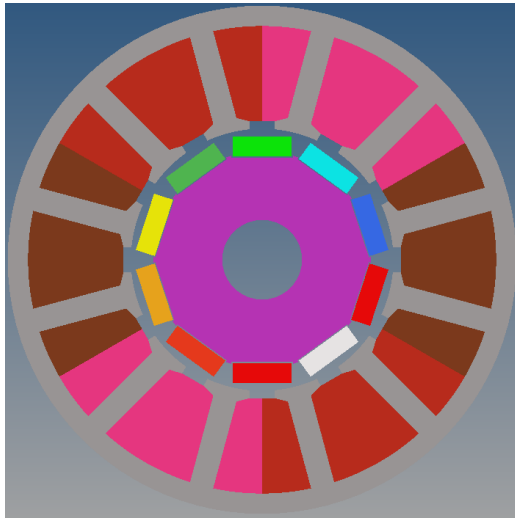
is on analyzing the convergence behavior of aPSP on different quantities of interest, such as the cogging torque, and their post-processing via Fast-Fourier-Transform. We measure convergence via the error estimation of aPSP and compare it to the convergence of root-mean-square errors, which is computed by point-wise squared differences of surrogate model evaluations and a test data set.

1 INTRODUCTION

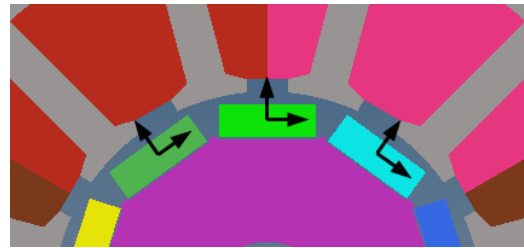
With regard to the development of the fuel prices and the world-wide CO_2 discussion the trend to electrification in motor vehicles is unbroken. More and more vehicles are equipped with e.g. electromotive supported steering systems, brake systems and the trend to electric mopeds (eScooter) and electromotive driven bicycles (eBikes) continues world-wide. The rising demand of electrical drives asks for designs with more power density, which are cheaper and more durable. Such solutions can be reached only with the most modern development methods. The main goal in the development of electric motors is to guarantee the demanded functions with minimal costs. The costs of an electrical machine consist not only of the material and the production costs, but also contain the costs by scrap during manufacturing. To minimize this scrap, it has to be guaranteed that the characteristics of the motor keep to the demanded limits under influence of manufacturing tolerances and noise factors. A motor design which fulfills this demand is called "robust". To evaluate the robustness of a motor design, classic approaches like Monte Carlo analysis or Latin Hypercube Sampling (LHS) could be used. Unfortunately these approaches suffer from a very high number of samples. If the computation time is high, e.g. due to the usage of finite element methods, the number of samples has to be reduced significantly. This need is even more important, when the robustness analysis has to be performed within a multi-objective optimization for each single design, see [7]. In this paper, the cogging torque of a permanent magnet synchronous surface-magnet motor is investigated, see Section 2. For this type of motor, the no-load torque is significantly disturbed by magnet tolerances, e.g. position and magnetic remanence and new orders appear in the spectrum of the torque signal. To assess how these tolerances affect the cogging torque, a dimension-adaptive pseudo spectral projection method (aPSP) is applied to a two-dimensional (spatial) magneto-static finite-element model to compute the stochastic cogging torque waveform along with the stochastic torque spectrum, see Section 3. In Section 4 the simulation results are compared with results achieved by a LHS method taken as reference to validate the aPSP method. The iteration dependent global error computed by the aPSP method is also documented to illustrate the method efficiency. Finally, a sensitivity analysis is performed on the stochastic cogging torque waveform obtained by the aPSP method to experience which parameters are dominating.

2 INVESTIGATED MOTOR

The presented methodology is used to analyze the cogging torque of a permanent magnet synchronous machine with 10 rotor poles and 12 stator teeth (see Fig. 1a). Here the cogging torque signal (no load torque), which is known to be sensitive to geometrical and material disturbances, is analyzed. We analyze the torque signal using a Fourier decomposition. In the nominal motor, without any disturbance, the cogging torque signal consists of only the order 60, the least common multiplier of the rotor poles and stator tooth, and multiples of it. Any disturbance in the rotor can affect these orders and, in case of asymmetrical disturbances, will also lead to the appearance of additional orders with the number of stator teeth and multiples (i.e. 12, 24, 36, ...), see [4]. Fig. 2a respectively 2b shows the cogging torque waveform respectively the related Fourier spectrum of a disturbed motor. In this paper, three magnets are chosen to be disturbed with 3 uncertain parameters each. The uncertain parameters of each magnet are: its position deviation in radial and tangential direction (see Fig. 1b) and its magnetic remanence. The parameters are assumed to be uniformly distributed within the interval $[-1;1]$.



(a) Sketch of a permanent magnet synchronous machine with 10 rotor poles and 12 stator teeth.



(b) Uncertain positioning of three magnets.

Figure 1: Sketch of motor magnet alignment. The positioning of three magnets is uncertain along the sketched directions. In addition, the value for the remanence of each of those magnets is also uncertain.

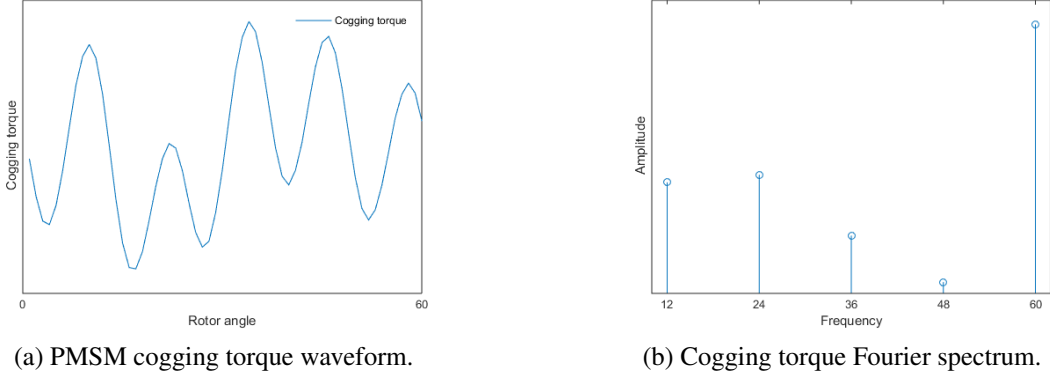


Figure 2: PMSM cogging torque waveform and related Fourier spectrum.

3 DIMENSION ADAPTIVE PSEUDO SPECTRAL PROJECTION

Mathematically speaking, the problem formulation as described in Section 2 is a forward uncertainty propagation task. The variation of the position of the three magnets and their corresponding remanence is modeled using 9 independent, uniformly distributed random variables denoted by $\xi = (\xi_1, \dots, \xi_9)$. We employ the generalized Polynomial Chaos expansion (PCE) [8, 3] to model the dependence of the cogging torque, denoted by Tq on the parameter vector ξ , i.e.,

$$Tq = Tq(\xi) = \sum_{i=0}^{\infty} Tq_i \psi_i(\xi). \quad (1)$$

Here, $\{\psi_i\}_{i=0}^{\infty}$ denote multivariate polynomials, which are orthogonal with respect to the Uniform probability density of the random vector ξ , i.e. each ψ_i is a multivariate Legendre polynomial. Two tasks remain: first, the infinite series in (1) must be truncated to become feasible for computation and second, the coefficients Tq_i must be computed numerically for all $i \in \mathbb{N}$ remaining in the truncated series. Afterwards, the PCE can be used in post-processing as a surrogate for the original simulation model to compute all relevant statistical information of Tq (mean, variance, probability density, sensitivity information, ...). Notably, there exist analytical expressions for the mean, the variance and the Sobol indices used in global sensitivity analysis, e.g. $\mathbb{E}(Tq) = Tq_0$ is the mean and $\sigma^2(Tq) = \sum_{i=1}^{\infty} Tq_i^2$ is the variance (if the polynomials are normalized with respect to the L^2 norm).

3.1 Truncation of the Polynomial Chaos expansion

In its standard formulation, the total polynomial degree of the PCE gets cut at some specified order $p \in \mathbb{N}$, which yields the approximated PCE:

$$Tq(\xi) \approx \sum_{i=0}^P Tq_i \psi_i(\xi). \quad (2)$$

The number of terms $P + 1$ is analytically determined via:

$$P + 1 = \frac{(p + M)!}{p!M!},$$

where $M \in \mathbb{N}$ denotes the number of uncertain parameters, i.e. in our case $M = 9$. After truncation, the coefficients Tq_i , $i = 0, \dots, P$ can be approximated by multivariate numerical quadrature - the so-called "non-intrusive spectral projection":

$$Tq_i(\xi) \approx \int Tq(\eta) \psi_i(\eta) w(\eta) d\eta = \sum_{j=1}^N w_j Tq(\xi^j) \psi_i(\xi^j), \quad i = 0, \dots, P, \quad (3)$$

where w denotes the joint probability density function of ξ , w_j and ξ^j denote the weights and nodes of the employed numerical quadrature rule of size N . However, when M increases the number of quadrature nodes required to keep a high accuracy grows exponentially. Often sparse grids [6] are employed to mitigate this so-called "curse of dimensionality". However, the approximation of the PCE coefficients by numerical quadrature suffers from aliasing errors due to a loss of discrete orthogonality if higher order polynomials are used in the truncated PCE [2, 1]. To overcome this drawback the PCE truncation can be tailored to the quadrature nodes of the sparse grid. It is based on applying the Smolyak algorithm used for construction of the sparse grid directly to the PCE system in (1). The method is then called "Pseudo-Spectral Projection" (see following section).

3.2 Pseudo-spectral projection

The PCE as defined in (1) uses a single enumeration index. It can be equivalently defined using a multi-index notation:

$$Tq(\xi) = \sum_{\alpha \in \mathbb{N}^M} Tq_\alpha \psi_\alpha(\xi), \quad (4)$$

where $\alpha = (\alpha_1, \dots, \alpha_M) \in \mathbb{N}^M$ is the multi-index, and $\psi_\alpha(\xi) := \prod_{i=1}^M \psi_{\alpha_i}^i(\xi_i)$. Here, $\psi_{\alpha_i}^i$ denote the univariate Legendre polynomial of degree α_i , which only depend on ξ_i ,

respectively. The multi-index notation has the advantage, that the truncation of the PCE can be defined in a more generic way:

$$Tq(\xi) \approx \sum_{\alpha \in \mathcal{I}} Tq_{\alpha} \psi_{\alpha}(\xi), \quad (5)$$

where $\mathcal{I} \subset \mathbb{N}^M$ denotes the index set used for truncation. There exists a one-to-one correspondence between the single and multi-index notation. For example, setting $\mathcal{I} = \{\alpha \in \mathbb{N}^M : \sum_{i=1}^M \alpha_i \leq p\}$ by enumeration one obtains the truncation specified in (2) for a given total order $p \in \mathbb{N}$.

The construction of sparse grids is based on Smolyak's algorithm. It can be applied directly to numerical quadrature rules and thereby it generates a set of sparse quadrature nodes and weights. In the Pseudo-Spectral Projection method, Smolyak's algorithm is applied to the polynomial basis of the PCE. The procedure is outlined in the following.

For each dimension $i = 1, \dots, M$ and polynomial degree $n \in \mathbb{N}$ we first define the projection operators \mathcal{P}_n^i by:

$$\mathcal{P}_n^i(Tq) := \sum_{j=0}^n Tq_j \psi_j^i, \quad (6)$$

with Tq_j , $j = 0, \dots, n$ defined as in (3). Then for each $i = 1, \dots, M$ define the one-dimensional hierarchical surplus operator by:

$$\begin{aligned} \Delta_{m(p)}^i &:= \mathcal{P}_{m(p)}^i - \mathcal{P}_{m(p-1)}^i, \quad p \geq 1, \\ \Delta_0^i &:= 0, \end{aligned}$$

where $m : \mathbb{N} \rightarrow \mathbb{N}$, $m(0) := 0$ is strictly increasing and called the "growth rule". Common choices for m are:

$$\begin{aligned} m(p) &:= p, \\ m(p) &:= 2p - 1, \quad m(0) := 0 \\ m(p) &:= 2^p - 1. \end{aligned}$$

For a given multi-index $k = (k_1, \dots, k_M)$ the multi-dimensional hierarchical surplus operator Δ_k is then defined by:

$$\Delta_k := \Delta_{m(k_1)}^1 \otimes \dots \otimes \Delta_{m(k_M)}^M. \quad (7)$$

Finally, Tq is approximated via:

$$Tq \approx \sum_{k \in \mathcal{I}} \Delta_k. \quad (8)$$

3.3 Error control and dimension adaptivity

The hierarchical surplus defined in (7) is used to define an error estimator ϵ_k^2 for each multi-index $k \in \mathcal{I}$:

$$\epsilon_k^2 := \|\Delta_k\|^2. \quad (9)$$

The norm $\|\cdot\|$ is typically chosen as the L^2 norm of the probability space of ξ . Having an error estimator, the remaining question is how to appropriately define the truncation index set \mathcal{I} . To this end, the dimension-adaptive sparse grid algorithm of Gerstner and Griebel [5, 1] can be easily adapted to the pseudo-spectral projection. It iteratively constructs the set \mathcal{I} based on the errors estimated by ϵ_k . Thereby, $\mathcal{I} := \mathcal{A} \cup \mathcal{O}$, with \mathcal{A} and \mathcal{O} denoting the so-called "active" (candidate set for further refinement) and "old" index sets, respectively. The overall error of the algorithm is measured using the global error

$$\epsilon := \sqrt{\sum_{k \in \mathcal{A}} \epsilon_k^2}. \quad (10)$$

It terminates when either the error falls below some threshold or some maximum number of iterations is achieved. The resulting method is then called "dimension adaptive Pseudo-Spectral Projection (aPSP)".

4 NUMERICAL RESULTS

In this section, the aPSP method is first applied to compute the stochastic cogging torque waveform. After computing the surrogate model with aPSP, the waveform is sampled using plain-vanilla Monte Carlo sampling to investigate the stochastic torque spectrum. All results are compared to reference results obtained by Latin Hypercube Sampling (LHS) of the original forward model. In addition, a global sensitivity analysis based on the "Analysis of Variance / Sobol indices" is performed on the waveform from the validated aPSP surrogate to identify dominant parameters.

4.1 Stochastic cogging torque waveform

The stochastic cogging torque waveforms computed by both LHS and aPSP methods (iteration 1 using 19 runs and iteration 7 using 103 runs) are shown in Fig. 3. The first aPSP iteration (only 19 runs required) is already capable to match the results computed with the LHS method very well. Increasing the iteration number, we observe a further convergence of the approximation error.

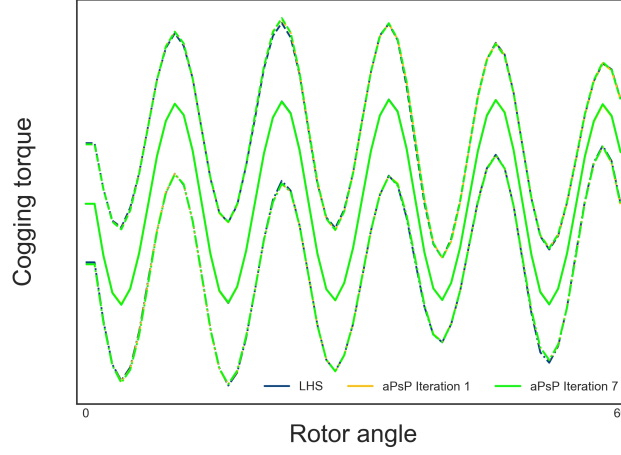


Figure 3: Stochastic cogging torque waveforms (average and 5% – 95% extrem quantiles).

4.2 Stochastic cogging torque spectrum

The stochastic cogging torque spectra computed by both LHS and aPSP methods are shown in Fig. 4.

The stochastic spectrum computed with the aPSP surrogate matches the one computed with the LHS method very well after a few iterations only (only 103 runs required).

4.3 Global error and sensitivity

The iteration dependent global error (see Section 3) during the stochastic cogging torque waveform computation is shown in Fig. 5a. The error decreases monotonically, yet in our belief its value overestimates the true error of the surrogate. We verified this statement by computing a root-mean square error (RMSE) relatively to the cogging torque waveform with respect to the LHS test data set, see Fig. 5b. The RMSE for the final iteration is of order 10^{-1} . The reason for the slow convergence of the global error is due to the strongly varying global sensitivity of the parameters as a function of the rotation angle, see Fig. 5c.

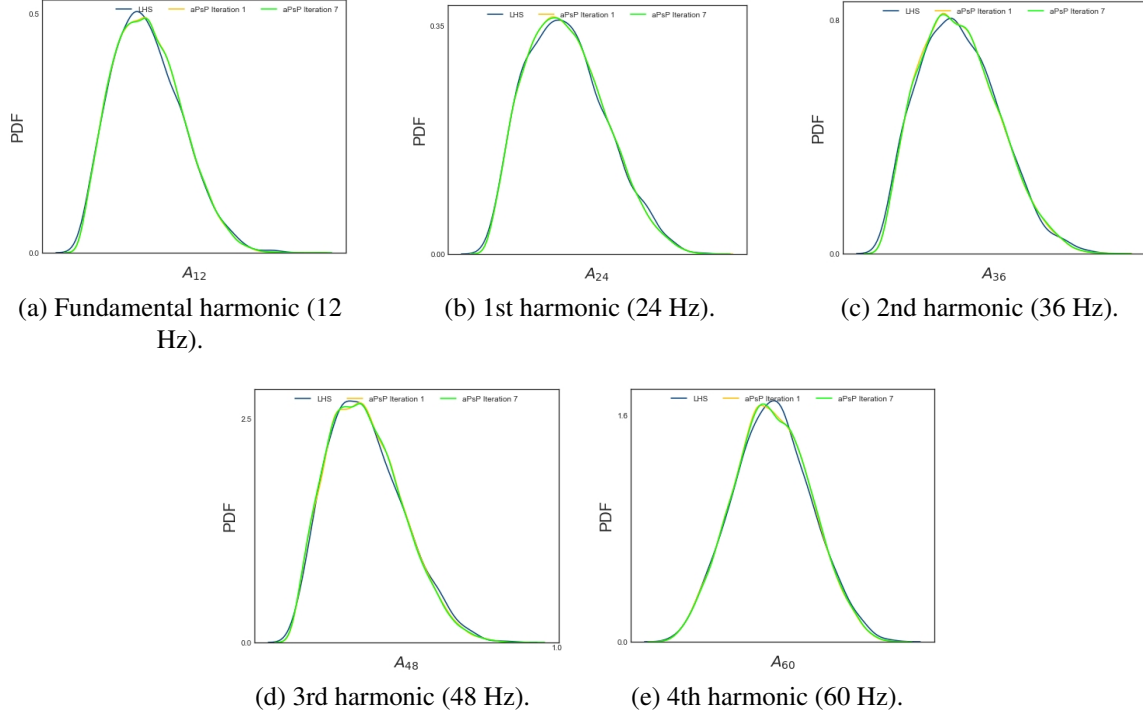
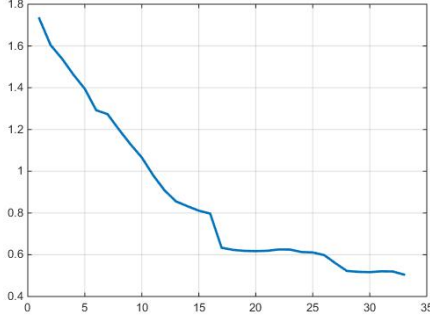


Figure 4: Cogging torque stochastic harmonic analysis.

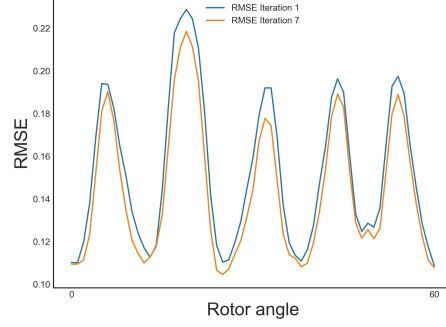
5 CONCLUSIONS

In this work we applied the dimension adaptive Pseudo-Spectral Projection method (aPSP) to a PSM with 9 uncertain parameters. The main difficulty is to obtain a forward uncertainty analysis of the PSM with high accuracy but using only a few model evaluations (due to the high computational cost associated with the solution of the forward model). The dimension adaptivity addresses this problem from two sides: the number of samples is kept low by only selecting "important" samples in the parameter space and a surrogate model (the Polynomial Chaos expansion) for which the aPSP provides an error estimator. To analyze the convergence behavior of the error estimator, we also compared the results to a reference obtained by Latin Hypercube Sampling applied to the original forward model.

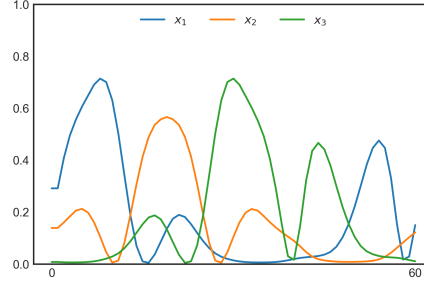
The numerical results demonstrate that the error estimation of the aPSP is slightly pessimistic but the reference data is matched very well using only few forward model evaluations. However, as the rotor's position is changed, the Sobol indices of the parameters also change in value making unimportant parameters more important and vice versa. This causes the error of the aPSP to decrease only slowly, since it is unclear how the rotor an-



(a) Global error vs. iteration number.



(b) RMSE vs. rotor position.



(c) Global sensitivity of parameters.

Figure 5: Convergence and sensitivity obtained by the aPSP method.

gle should be appropriately treated within the aPSP. We used averaging over the angle to obtain only scalar quantities, but in principle other choices may perform differently.

Our current research is on evaluating different strategies to deal with the angle dependency and in addition to apply the aPSP to a larger set of uncertain parameters in the PSM.

REFERENCES

- [1] Patrick R. Conrad and Youssef M. Marzouk. Adaptive smolyak pseudospectral approximations. *SIAM J. Sci. Comput.*, 35:2643–2670, 2013.
- [2] Paul G. Constantine, Michael S. Eldred, and Eric T. Phipps. Sparse pseudospectral approximation method. *Computer Methods in Applied Mechanics and Engineering*,

229-232:1 – 12, 2012.

- [3] Ernst, Oliver G., Mugler, Antje, Starkloff, Hans-Jörg, and Ullmann, Elisabeth. On the convergence of generalized polynomial chaos expansions. *ESAIM: M2AN*, 46(2):317–339, 2012.
- [4] L. Gasparin, A. Cernigoj, S. Markic, and R. Fiser. Additional cogging torque components in permanent-magnet motors due to manufacturing imperfections. *IEEE Transactions on Magnetics*, 45(3):1210–1213, March 2009.
- [5] T. Gerstner and M. Griebel. Dimension–adaptive tensor–product quadrature. *Computing*, 71(1):65–87, Aug 2003.
- [6] Thomas Gerstner and Michael Griebel. Numerical integration using sparse grids. *Numerical Algorithms*, 18(3):209, Jan 1998.
- [7] C. Kubala. Robust-design-optimierung von permanenterregten synchronmaschinen. *PhD thesis, TU Ilmenau*, 2015.
- [8] Dongbin Xiu and George Em Karniadakis. The wiener–askey polynomial chaos for stochastic differential equations. *SIAM J. Sci. Comput.*, 24:619–644, 2002.

The Origin of Tensile-compressive Asymmetry in Amorphous and Semicrystalline Polymers

Damien Vandembroucq*, Sara Jabbari-Farouji**

*ESPCI-PMMH, Paris, **Johannes Gutenberg University, Mainz

ABSTRACT

The mechanical properties of polymeric materials strongly depend on their morphology and spatial arrangements. Polymeric materials also exhibit asymmetric yield strength and strain hardening in tension and compression. We examine the microscopic origin of this asymmetry for amorphous and semicrystalline polymers by performing large-scale molecular dynamics simulations. We compute the tensile and compressive response of amorphous and semicrystalline polymers of a semiflexible bead-spring polymer model [1] for various chain lengths [1,2,3]. Investigating the microstructural evolution of polymers, we find that the asymmetry arises from a different arrangement of polymers during tensile and compressive deformation. In tension, the chains align themselves along the tensile axis that leads to a net global nematic ordering of the chains end-to-end vectors. During compression, the polymers arrange themselves in a plane perpendicular to the compressive axis and as a result a novel anti-nematic ordering of the chains end-to-end vectors emerges. Computing ratio of microscopic stretch of the polymers relative to the macroscopic stretch, we find that the semicrystalline polymers deform less affinely than their amorphous counterparts. Interestingly, the degree of non-affinity is smaller during compression. [1] H. Meyer and F. Muller-Plathe, J. Chem. Phys. 115, 7807 (2001). [2] S. Jabbari-Farouji, J. Rottler, M. Perez, O. Lame, A. Makke & J.-L. Barrat, Physical Review Letters 118 (21), 217802 (2017) [3] S. Jabbari-Farouji and D. Vandembroucq in preparation

Shear Banding and Finite Size Effects in a Mesoscopic Model of Amorphous Composites

Damien Vandembroucq^{*}, Botond Tyukodi^{**}, Claire Lemarchand^{***}, Jesper Hansen^{****}

^{*}ESPCI Paris, ^{**}Northeastern University, ^{***}CEA-DAM-DIF France, ^{****}Roskilde University

ABSTRACT

We study the plastic behavior of amorphous media reinforced by hard particles using a mesoscopic depinning-like lattice model. In this model, lattice sites represent coarse-grained shear transformations which interact via an Eshelby elastic interaction kernel. Hard inclusions are assigned larger yield thresholds than sites associated to the amorphous matrix. Results show a complex size dependence of the effective flow stress of the amorphous composite: one associated to the amorphous matrix and another one associated to the hard inclusions. While the former results in an $1/N$ dependence of the flow stress with the system size, the latter predicts a size dependent threshold concentration below which no reinforcement is observed. We show that the threshold concentrations correspond to the percolation of shear bands through the system in between the hard inclusions. Above the threshold concentration no shear bands can percolate without breaking through a hard site. In this regime we find that the distance of the flow stress to a linear mixing law scales as $(\log N/N)^{1/2}$ and the flow stress increases with the system size. The linear mixing law then gives an upper bound to the flow stress. We find that the increase in the flow stress is associated to the breakthrough of the weakest shear band over hard sites and the flow stress value is governed by the accumulation of plastic activity along the weakest band. We develop a simple model based on the weakest shear band hypothesis: although a simple linear mixing law is unable to predict the flow stress when applied to the bulk, we find that it works surprisingly well when applied to the weakest shear band. Our model turns out to predict well the flow stress value, its size dependence and even the flow stress fluctuations. [1] B. Tyukodi, C. Lemarchand, J. Hansen, D. Vandembroucq, "Finite size effects in a model for plasticity of amorphous composites", Physical Review E, 93, 023004 (2016) [2] B. Tyukodi, S. Patinet, D. Vandembroucq, S. Roux, "From depinning transition to plastic yielding of amorphous media: A soft-modes perspective", Physical Review E, 93, 063005 (2016)

Amorphous Plasticity from Atomic Scale to Mesoscopic Scale

Damien Vandembroucq^{*}, Armand Barbot^{**}, Matthias Lerbinger^{***}, Anier Hernandez Garcia^{****},
Reinaldo Garcia Garcia^{*****}, Botond Tyukodi^{*****}, Sylvain Patinet^{*****}

^{*}ESPCI Paris, ^{**}ESPCI Paris, ^{***}ESPCI Paris, ^{****}ESPCI Paris, ^{*****}ESPCI Paris, ^{*****}Northesater University
Boston, ^{*****}ESPCI Paris

ABSTRACT

In crystalline materials, plasticity results from the motion of defects of the crystalline lattice, dislocations. The absence of structural order in glasses requires to look for alternative microscopic mechanisms for the plastic deformation. A common hypothesis consists in considering series of localized rearrangements of the amorphous structure : Shear Transformations. In this talk we review recent results obtained for the characterization of such Shear Transformations at the atomic scale. We first present a recent numerical method allowing to characterize local yield thresholds in model 2D lennard-Jones glasses prepared by molecular dynamics. We discuss their connection to the plastic activity observed upon shearing and their dependence on the protocol of preparation of the glass. In particular we give quantitative evidence that the more relaxed the glass, the higher the local plastic thresholds. We also discuss the tensorial character of the Shear Transformations. We then present recent results obtained with lattice models of amorphous plasticity at a mesoscopic scale and discuss first attempts of coarse-graining the plastic behavior of glasses from atomic scale to mesoscopic scale. References : S. Patinet et al. Connecting Local Yield Stresses with Plastic Activity in Amorphous Solids, Phys. Rev. Lett. 117, 045501 (2016) A. Barbot et al. Local yield stress statistics in model amorphous solids, submitted to Phys. Rev. E B. Tyukodi et al. From depinning transition to plastic yielding of amorphous media: A soft-modes perspective, Phys Rev. E 93, 063005 (2016)

Numerical Treatment of Boundary Layers for High-Order DG Schemes by Using Basis Enrichment

Serena Vangelatos*, Claus-Dieter Munz**

*University of Stuttgart, **University of Stuttgart

ABSTRACT

Large Eddy Simulations (LES) of moderate and high Reynolds number flows becomes exceedingly expensive, if turbulent structures in the boundary layer have to be resolved. Several techniques for wall-modeled LES exist to model the near-wall turbulence and momentum transfer. The novel Extended Discontinuous Galerkin scheme (XDG) takes a priori properties of the expected form of the solution into account to resolve steep gradients. The underlying Discontinuous Galerkin (DG) scheme have gained a significant role in high-order spatial discretization techniques in computational sciences in the last decade. Some of the reasons for its steady growing popularity are the high order accuracy with geometrical flexibility, allowing adaptivity as well as easy parallelization based on the compact stencil. The main idea of the XDG approach is to extend the standard polynomial solution space of the Discontinuous Galerkin method by an appropriate enrichment function representing an approximate analytical solution of the flow, which cannot be resolved by the polynomials. In this way the solution is not prescribed, but the numerical method has the possibility to choose the appropriate solution out of the given function space via the Galerkin projection. In the application for turbulent boundary layer, we can make use of the universal properties of the mean velocity distribution in order to resolve the velocity gradients in the near-wall region with very coarse meshes. Several methods using an extended problem-tailored solution space such as the partition-of-unity method (PUM) or the extended finite element method (XFEM) have been developed. They are applied for approximation of solutions with jumps, singularities and other locally non-smooth features arising in cracks, solidification, shocks etc. Within the presentation, first the theoretical background of the XDG scheme is presented based on the discretization techniques of the DG method. With regard to turbulent boundary layers, the Singular Perturbation Problem for the linear scalar advection diffusion equation as well as for the non linear inviscid Burgers' equation in one dimension are considered in order to evaluate the ideas of basis enrichment numerically in the case of high gradients, which can not be represented by polynomials. In conclusion the application of XDG for the compressible Navier-Stokes equations to a turbulent channel flow in Implicit LES is shown with very coarse meshes.

Simulation of Blast Effects in Monumental Structures

Paolo Vannucci^{*}, Victor Maffi-Berthier^{**}, Filippo Masi^{***}, Ioannis Stefanou^{****}

^{*}University of Versailles and Saint Quentin, ^{**}INGEROP, France, ^{***}ENPC, ^{****}ENPC

ABSTRACT

Highly representative monuments are unfortunately too often the objective of destructions and the threats on them increase in the present situation. Research on the effects of an explosion inside monuments are hence interesting and topical. In the study of blast effects inside monumental structures, a particular attention must be paid to the procedure to be used for numerical simulations, that must account, on one hand, for the hypervelocity of the phenomenon and, on the other hand, for reflected shock waves. In fact, the internal geometry of a monument, often rather complex, can alter significantly the time history of the reflected blast pressure on the walls and some peculiar phenomena can happen, leading to an abnormal increase of the shock pressure and also to an unconventional time distribution of it. Another peculiarity of monumental structures is the type of the material. Normally composed of stones or masonry, the constitutive law of the material must be able to describe cracks produced by the blast and propagating into the body of the structure, which needs the use of a nonlinear model for the behavior of the material. In this communication, we propose first a comparative study on different methods for the evaluation of the blast pressure field inside a typical monumental structure: a vaulted hall. We compare empirical models (CONWEP and the recommendations TM5-1300 of USACE) with a completely numerical simulation, based upon the use of the JWL model. We give also new accurate analytical expressions for the Kingery and Bulmash experimental data, valid over the whole range of the scaled distance. The results of this study show that the shock waves reflected by the vault are focused leading to a large increase of the shock pressure. Such a result shows the importance of using numerical simulations for the calculation of blast pressure shock waves inside a monumental structure: recommendations using empirical formulations and relating to conventional geometries are inappropriate. We then apply this numerical approach to the study of a real structure: the Pantheon of Rome. A complete study, simulating the blast and the whole structure, is conducted and the consequences of the blast on the structure are completely simulated. Also in this case, we show that the focus of reflected waves is determinant in the structural collapse. The role played by the existing cracks in the Pantheon's dome is also analyzed.

Effect of Sclerostin Inhibition on Bone Mechanical Properties in a Murine Model of Osteogenesis Imperfecta as Revealed by Micro Finite Element Analysis

Peter Varga*

*AO Research Institute Davos

ABSTRACT

Osteogenesis imperfecta (OI) is a heritable bone fragility disorder caused in the majority of cases by mutations in type I collagen, leading to reduced bone mass, brittleness and deformities. Limitations in current treatment strategies may be overcome by anabolic sclerostin neutralizing antibody (Scl-Ab) therapy. The *Brl/+* mouse model of Type IV OI recapitulates the main features of the OI phenotype. The aim of this work is to determine the influence of Scl-Ab treatment on the mechanical behaviour of normal and *Brl/+* murine bone. In previous work, femora from two wildtype (WT) and two *Brl/+* male, 6 month old mice were treated with vehicle (saline) or Scl-Ab (BPS804, Mereo BioPharma) ($n=1/\text{genotype/treatment}$). Scl-Ab or vehicle was administered via intravenous injection for 5 weeks in a dose of 100 mg/kg/week. Each bone was scanned by lab micro computed tomography at 10 μm resolution and a mid-shaft region was imaged with phase-contrast synchrotron radiation-source CT (SR-CT, ESRF ID19, France) at 650 nm voxel size. In this study, micro finite element (microFE) models are developed to investigate the bone properties on two length scales. On the one hand, an organ-scale model of the entire femur is generated from the segmented microCT images. Material properties are assumed to be homogeneous and linear elastic, with Young's moduli of bone tissue in the WT and *Brl/+* femora determined from recent nanoindentation data [1]. The models are loaded in a four-point bending setup to evaluate stiffness and estimate strength. On the other hand, a meso-scale model is created from the segmented SR-CT images of the mid-shaft region and subjected to axial compression and bending. The role of tissue inhomogeneity is investigated by assigning individual elastic properties to the bone elements based on the local SR-CT density [2] and comparing the results to the homogeneous models. Further, the effect of cortical porosity is evaluated by turning lacunar porosity on/off in the models. The results of the WT and *Brl/+* mice are compared to evaluate the effect of the disease. The influence of the treatment is assessed by comparing the properties of the Scl-Ab-treated and the vehicle-treated animals. The findings will help to better understand the effect of Scl-Ab treatment on the mechanical properties of OI-bone and provide insight into the contributions of bone matrix heterogeneity and porosity. 1. Sinder et al. J Bone Miner Res. 2013, 28(1):73-80. 2. Razi et al. Acta Biomaterialia, 2015, 13:301-10.

Cross Migration of Surfactant-laden Viscous Droplets in a Transient Stokes Flow

Sharanya Varkala^{*}, Raja Sekhar G.P.^{**}, Christian Rohde^{***}

^{*}Department of Mathematics, Indian Institute of Technology, Kharagpur 721302, India, ^{**}Department of Mathematics, Indian Institute of Technology, Kharagpur 721302, India, ^{***}Institute of Applied Analysis and Numerical Simulation, University of Stuttgart, Pfaffenwaldring 57, 70569 Stuttgart, Germany

ABSTRACT

We consider the motion of a viscous drop in an arbitrary unsteady Stokes flow such that the surface of the drop is fully covered with a stagnant surfactant layer. In particular the regime of low surface Péclet number is analyzed and we account for the effect interfacial slip on the overall behavior of the flow field. The hydrodynamic problem is solved by the solenoidal decomposition method and the drag force is computed in terms of Faxén's laws, using a perturbation ansatz in powers of the surface Péclet number. The surface equation of the deformed sphere has been determined by an iterative method up to the first order approximation. Analytical expressions for the migration velocity of the drop are likewise given. Based on this analysis we can completely characterize various flow situations including a given ambient flow as uniform flow, Couette flow and Poiseuille flow. Moreover, we find out that a surfactant-induced cross-stream migration of the drop occurs towards the centre-line in both, Couette and Poiseuille flow cases. The variation of the drag force and the migration velocity is computed for different parameters such as the Péclet number and the Marangoni number. Finally, the theoretical findings are validated on with available experimental data.

Predictive Model for Porosity in Powder-bed Fusion Additive Manufacturing in the High Energy-density Regime

Guglielmo Vastola*, Pei Qing Xiang**, Yong-Wei Zhang***

*A*STAR Institute of High Performance Computing, **A*STAR Institute of High Performance Computing,

***A*STAR Institute of High Performance Computing

ABSTRACT

Process consistency and control are bottleneck issues to wider insertion of powder-bed fusion additive manufacturing in the industrial shopfloor. Of particular interest is the porosity of the components, which remains the limiting factor to high-cycle fatigue performance. Recent experiments have shown that, with increasing energy density, a surge in porosity is seen in selectively laser melted metals. In this high-energy density regime, porosity originates from mechanisms that have to be different from the well-known incomplete melting occurring in the low energy density regime. To shed light on this interesting phenomenon, we discuss the mechanism of bubble formation in the melt pool and possible trapping during the solidification, and then we formulate a predictive model for porosity in this regime. To compare with experimental results, we perform computer modelling and simulations (which have been validated by experiments) to determine the parameters of the model. We show that the model predictions are in reasonable qualitative and quantitative agreement with the experimental measurements. Hence, the proposed model can be used as a tool to predict porosity at increasing beam energy density, and further to control and possibly reduce it, paving the way for wider adoption of powder-bed fusion additive manufacturing in modern shopfloors.

Micro/meso-scale Modeling of 3D Woven Composites with Temperature Dependent Properties of Constituents

Kostiantyn Vasylevskyi*, Borys Drach**, Igor Tsukrov***

*University of New Hampshire, USA, **New Mexico State University, USA, ***University of New Hampshire, USA

ABSTRACT

In this research we investigate how the overall response and local stress concentrations in the 3D woven composites are influenced by the temperature dependence of constituents. We utilize our recently developed meso-scale finite element models of the material [1-2] and study responses of individual fiber tows and the entire composite unit cells. The considered loading cases include cooling of completely cured composite from curing to room temperature and thermo-mechanical loading in the range of service temperatures. Temperature dependent effective elastic properties and overall thermal expansion coefficients are obtained from the simulations. Studies of carbon reinforced epoxies show that the temperature dependent effects are well pronounced in the overall response and can lead to significant local stress concentrations. [1] A. Drach, B. Drach, I. Tsukrov. Processing of Fiber Architecture Data for Finite Element Modeling of 3D Woven Composites, *Advances in Engineering Software*, v 72, pp. 18–27, 2014. [2] I. Tsukrov, B. Drach, A. Drach, T. Gross. Utilizing Stress-based Failure Criteria for Prediction of Curing Induced Damage in 3d Woven Composites, *Proceedings of 21st International Conference on Composite Materials – ICCM21*, Xi'an, China, 2017.

Hierarchical Validation of the WIAMan LS-Dyna FEM for Application in Underbody Blast

Nicholas Vavalle^{*}, Christian Lomicka^{**}, Connor Pyles^{***}, Matthew Shanaman^{****}, Robert Armiger^{*****}, Mark Angelos^{*****}

^{*}Johns Hopkins Applied Physics Lab, ^{**}Johns Hopkins Applied Physics Lab, ^{***}Johns Hopkins Applied Physics Lab, ^{****}Johns Hopkins Applied Physics Lab, ^{*****}Johns Hopkins Applied Physics Lab, ^{*****}Johns Hopkins Applied Physics Lab

ABSTRACT

A finite element model (FEM) has been developed in conjunction with the development of the Warrior Injury Assessment Manikin (WIAMan) Anthropomorphic Test Device (ATD) and will serve as a state of the art Soldier surrogate for Underbody Blast (UBB) testing. The FEM will complement the physical ATD to predict injury response and assess operational risk of ATD failure. The objective of this work is to present the validation of the WIAMan FEM in sub-system and system-level simulations. The WIAMan FEM was developed and validated using a hierarchical approach. Component models were developed and validated individually and incorporated into the full system-level model. Validation of the component models occurred in two sets of experiments, non-injurious and injurious loading conditions. The test articles for these simulations were the lower leg, pelvis, and lumbar spine. The whole body model contains ~1.4 million nodes and was simulated in three loading conditions. Two whole body conditions were simulated from the Vertically Accelerated Load Transfer System (VALTS) test series, an upright posture and a reclined-seatback posture with the legs extended. The remaining simulation was of a test series run at the University of Michigan with the legs at an acute angle under the body. Model validation was quantified using correlation and analysis (CORA) which compares the model to experimental outputs with a rating from zero to one. The corridor portion of CORA was omitted because the variance in the physical ATD response was low. The typical simulation time for the whole body WIAMan FEM is approximately 13 hours for a 100 ms simulation on 100 processors. Preliminary results of the component simulations show good agreement with the experimental response. CORA scores for the components range from 0.62 to 0.83 across all input conditions. In whole body simulations, 33 signals were evaluated for each of the three whole body simulations including accelerations, rotations, forces, and moments. Preliminary results indicate a strong match to the experimental response with a CORA score of 0.76 in the nominal posture VALTS simulation. The validation results give confidence in the FEM's ability to predict the ATD response to a variety of loading conditions and encourage future use in designing safety measures for the warfighter in UBB. This study was part of the WIAMan Research sponsored by the U.S. Army Research Laboratory. The content included in this work does not necessarily reflect the position or policy of the U.S. government.

A Second-order Cone Interior-point Method for Initially Rigid Cohesive Fracture

Stephen Vavasis^{*}, Katerina Papoulia^{**}, Mohammadreza Hirmand^{***}

^{*}U. Waterloo, ^{**}U. Waterloo, ^{***}U. Waterloo

ABSTRACT

Initially rigid cohesive fracture is among the few techniques able to model complex and branching fracture with a sharp (nonsmeared) representation of the crack. Implicit time-stepping schemes are often favored in mechanics due to their ability to take larger time steps, but it is challenging to include an initially rigid cohesive model in an implicit scheme because the initiation of fracture corresponds to a nondifferentiability of the underlying potential. In this work, an interior-point method is proposed for implicit time stepping of initially rigid cohesive fracture. It uses techniques developed for convex second-order cone programming for the nonconvex problem at hand. The underlying cohesive model is taken from Papoulia (2017) and is based on a nondifferentiable energy function. That previous work proposed an algorithm based on successive smooth approximations to the nondifferential objective for solving the resulting optimization problem. It is argued herein that cone programming can capture the nondifferentiability without smoothing, and the resulting cone formulation is amenable to interior-point algorithms. A further benefit of the formulation is that other conic inequality constraints are straightforward to incorporate. A computational result is provided showing that certain contact constraints can be easily handled and that the method is practical.

Multiple Necking Pattern in Nonlinear Elastic Bars Subjected to Dynamic Stretching: The Role of Defects and Inertia

Alvaro Vaz-Romero^{*}, José Antonio Rodríguez-Martínez^{**}, Sébastien Mercier^{***}, Alain Molinari^{****}

^{*}University Carlos III of Madrid, ^{**}University Carlos III of Madrid, ^{***}Université de Lorraine, ^{****}Université de Lorraine

ABSTRACT

In this work we explore the inception and development of multiple necks in incompressible nonlinear elastic bars subjected to dynamic stretching. The goal is to elucidate the role played by a spatial-localized defect of the strain rate field in the necking pattern that emerges in the bars at large strains. For that task, we have used two different approaches: (1) finite element simulations and (2) linear stability analyses. The finite element simulations have revealed that, while the defect of the strain rate field speeds up the development of the necking pattern in the late stages of the localization process, the characteristic (average) neck spacing is largely independent of the defect within a wide range of defect amplitudes. The numerical results have been rationalized with the linear stability analyses, which enabled to explain the average spacing characterizing the necking pattern at high strain rates. Moreover, the numerical calculations have also shown that, due to inertia effects, the core of the localization process occurs during the post-uniform deformation regime of the bar, at strains larger than the one based on the Considère criterion. This phenomenon of neck retardation is shown to have a meaningful influence on the necking pattern.

Mechanical Instability of an Origami-Inspired Cellular Structure

Ashkan Vaziri^{*}, Soroush Kamrava^{**}

^{*}Northeastern University, ^{**}Northeastern University

ABSTRACT

In this project, we present a novel group of origami inspired cellular structures with reversible foldability and programmable instability. The mechanical instability of this structures relies on the properties of the material, hinge pattern, and hinge characteristics. The unit cell of the proposed cellular structure is a star-shaped sub-assembly with either one or two zero-energy states. Applying an external load on the unit cell, while it is initially in the first stable configuration and has zero energy, increases the level of energy up to a turning point and in some cases recovers the zero energy level corresponding to another stable configuration. Here, we investigate the instability of the structure experimentally and then explore the influence of geometrical parameters on the existence and quality of bi-stability through an analytical approach. The instability of the star-shaped unit cells can be further programmed by forming different styles of stars (three-pointed star, four-pointed star, and etc.) which alter the mechanical properties as well as the instability of the structure. The instability characteristics of the unit cells (mostly bi-stability) get transferred to a higher order structure which is made by tiling the star-shaped unit cells in three dimensions. Another fascinating feature of the star-shaped unit cell which gets extended to the cellular structure is auxeticity (i.e. negative Poisson's ratio). A careful observation indicates the reduction of the cross-sectional area of the unit cell under compressive load until it ends in a smaller cross-sectional area compared to the first zero-energy configuration.

Simulation of Flat Carbon Fibre Reinforced Laminated Composite Plates Subjected to Axial Crushing: Comparison of Two Intra-Laminar Damage Models in LS-DYNA and ABAQUS/Explicit

Reza Vaziri^{*}, Thomas Feser^{**}, Johannes Reiner^{***}, Navid Zobeiry^{****}, Matthias Waimer^{*****},
Dominik Schueler^{*****}, Nathalie Toso-Pentecôte^{*****}

^{*}Composites Research Network, The University of British Columbia, ^{**}Institute of Structures and Design, German Aerospace Center (DLR), ^{***}Composites Research Network, The University of British Columbia, ^{****}Composites Research Network, The University of British Columbia, ^{*****}Institute of Structures and Design, German Aerospace Center (DLR), ^{*****}Institute of Structures and Design, German Aerospace Center (DLR), ^{*****}Institute of Structures and Design, German Aerospace Center (DLR)

ABSTRACT

Carbon Fibre Reinforced Polymer (CFRP) systems are being widely used for crashworthy structural applications in the aerospace and automobile industry. The numerical prediction of the crushing response of CFRPs is challenging due to the complex nature of the various interacting failure modes that occur at different length scales. In this work, two intra-laminar damage models with different underlying assumptions are used to predict the mass-specific energy absorption (SEA) of flat coupon specimens made from IM7/8552 CFRP under dynamic axial crushing. The sub-laminate based continuum damage model, CODAM2 [1], implemented in LS-DYNA as the material model MAT_219 is compared to a ply-based damage model based on the Ladevèze theory [2] and implemented as a user subroutine (VUMAT) in ABAQUS/Explicit. The sensitivity of different CFRP layups on the SEA is numerically studied to investigate the capability of the two intra-laminar damage models to predict those layup variations. Results are compared with experimental data provided by the University of Utah [3]. This study demonstrates the capabilities, effects of various parameters and material model specific options and limitations of both damage models, thus contributing to further understanding and improvement of the structural analysis of composites under dynamic loading conditions such as crash or high velocity impact events. [1] A Forghani, N Zobeiry, A Poursartip and R Vaziri (2013). A structural modelling framework for prediction of damage development and failure of composite laminates, Journal of Composite Materials, 47(20-21), 2553–2573. [2] P Ladeveze, P and E LeDantec (1992). Damage modelling of the elementary ply for laminated composites. Composites science and technology, 43(3), 257-267. [3] M Perl, D Adams. Phase III Flat Coupon Crush Test Results, CMH-17 Crashworthiness WG Meeting, September 5, 2017.

A Multi-Physics Approach to Predicting Separation Forces in Constrained-Surface Stereolithography

Abhishek Venketeswaran*, Sonjoy Das**

*SUNY Buffalo, **SUNY Buffalo

ABSTRACT

Constrained-Surface Stereolithography (SL) is an additive manufacturing technology that prints three-dimensional objects by selectively exposing a liquid pool of photosensitive resin to UV radiation. A typical Constrained-surface SL apparatus consists of (a) Build platform (b) Resin vat and (c) Digital Imaging unit. The apparatus is used to print the object in a bottom-up approach, wherein the first layer is bonded onto the build platform and subsequently each new layer is printed in the gap between the bottom surface of the previously printed layer and the top surface of the resin vat. The build platform is maneuvered upwards upon the completion of each layer, to replenish the liquid volume in the gap. This separation is resisted by viscous adhesion due to the presence of the resin between the bottom surface of the part and the top surface of the vat. This adhesion poses a major hurdle to printing parts with a characteristic axial length of order of 10 mm. This adhesion can be attributed to a pressure gradient associated with the flow of the viscous resin into the gap. One of the most efficient strategies to reduce this adhesion is to coat the bottom surface of the vat with a thin film of an optically transparent and inert material (e.g. PDMS, Teflon, PTFE). The reduction in the adhesion is achieved via an elastohydrodynamics phenomenon involving a coupling of liquid flow and elastic deformations of the film in the gap. This work develops a theoretical framework to establish the dependence of the separation force on the mechanical properties of the liquid resin and the film coating. The flow of the resin into the thin gap between the part and the film is modeled using lubrication theory [2] while the elastic deformations of the thin film coating are modeled using perturbation theory [1]. A Finite Element (FE) model is developed on the basis of the resulting system of partial differential equations using a mixed Finite Element (FE) framework. Finally, the FE model is employed to predict the separation force on a printed part separating from a film for a constant build-platform speed. Bibliography [1] Argatov, Ivan and Gennady Mishuris. Contact Mechanics of Articular Cartilage Layers Asymptotic Model. Switzerland: Springer International Publishing, 2015. [2] Szeri, Andras Z. Fluid Film Lubrication: Theory and Design. Cambridge University Press, 2005.

Stabilization of XFEM Formulations by Tikhonov Regularization and Modified Barzilai-Borwein Iteration

Giulio Ventura*

*Department of Structural, Geotechnical and Building Engineering, Politecnico di Torino, Italy

ABSTRACT

In some cases the eXtended Finite Element Method may show ill-conditioning of the global system of equations at solution due to near linear dependency between element shape functions and enrichment functions. For example, this is easily observed when a discontinuity crosses nearby the element nodes and the Heaviside function enrichment is present. In [1] it has been shown that ill-conditioning has, as limiting case, the indeterminacy of the global system of equations. This originated the idea of improving system conditioning by biasing to zero a proper subset of the enrichment variables by a weak penalty term. This technique can be seen as a particular case of Tikhonov regularization [2], that is one of the most commonly used methods of regularization of ill-posed problems in statistics and analysis of inverse problems. The attractive properties of this stabilization technique is that it has no impact on the XFEM formulation, can be used for any set of enrichment functions and is of straightforward implementation. The introduction of the penalty term introduces a bias in the solution, whose entity can be considered acceptable in most applications. However, it is desirable that the solution is not affected by the stabilization procedure. To this end various alternatives has been explored: fixed point iteration with a correction term on the final solution system and several forms of the augmented lagrangian method. Nonetheless, all these alternatives were found not efficient from a computational point of view. Recently, an efficient way of eliminating the stabilization bias from the solution has been found by developing a new iteration formula that sets its roots on the method proposed by Barzilai and Borwein [3], who suggested formulas for the stepsize determination in steepest descent methods. The derived new iteration formula shows very good performance and leads to convergence in a few iterations. In the present contribution the derivation of the new iteration formula is shown and examples of its application to the stabilization of XFEM problems are given. [1] G. Ventura, C. Tesei. Stabilized X_FEM for Heaviside and nonlinear enrichments. In *Advances in Discretization Methods*, pages 209–228, Springer, 2016. [2] A.N. Tikhonov, A.V. Goncharsky, V.V. Stepanov, and A.G. Yagola. *Numerical methods for the solution of ill-posed problems*, volume 328. Springer Science & Business Media, 2013. [3] J. Barzilai, J.M. Borwein. Two-Point Step Size Gradient Methods, *IMA Journal of Numerical Analysis*, Volume 8, Issue 1, 1 January 1988, Pages 141–148.

Biomechanics of the Fetal Kicking Linked to Risk Factors for Developmental Dysplasia of the Hip

Stefaan W. Verbruggen^{*}, Bernhard Kainz^{**}, Susan C. Shelmerdine^{***}, Joseph V. Hajnal^{****},
Mary A. Rutherford^{*****}, Owen J. Arthurs^{*****}, Andrew T.M. Phillips^{*****}, Niamh C.
Nowlan^{*****}

^{*}Imperial College of London, ^{**}Imperial College of London, ^{***}Great Ormond Street Hospital, UK, ^{****}Kings College, London, ^{*****}Kings College, London, ^{*****}Great Ormond Street Hospital/University College, London, ^{*****}Imperial College, London, ^{*****}Imperial College, London

ABSTRACT

INTRODUCTION: Developmental dysplasia of the hip (DDH) is a common congenital joint shape malformation, associated with an increased risk of osteoarthritis in later life [1]. Risk factors for DDH are associated with restricted fetal movement, such as fetal breech position and low amniotic fluid volume (oligohydramnios) [2]. In addition, first-borns are significantly more likely than consecutive births to develop DDH [3]. However, counter-intuitively, DDH is not more common in twins despite significantly less space available for each fetus [4]. By quantifying the mechanical stimulation of the fetal skeleton for a range of uterine conditions which increase the risk of DDH, we test the hypothesis that a biomechanical link exists between fetal kicking and the occurrence of DDH. **METHODS:** Fetal biomechanics were modeled for cine-MRI scans of normal, cephalic fetuses, and fetuses in breech, oligohydramnios or twin pregnancies (n=3-7 per group) [5]. Muscle forces were applied to finite element models of two different geometries of fetal bones generated from post-mortem MRI. **RESULTS:** Maximum fetal kick force and resulting stress stimulation were significantly lower in breech and oligohydramnios scans, while there was no significant difference for twin kicks, compared to normal singletons (Figure 1B, C). The reaction force was significantly lower in firstborn fetal kicks, with downward trends in stress stimulation. **DISCUSSION:** This study reveals significant decreases in biomechanical stimulation of the hip joint in cases of breech and oligohydramnios, known risk factors for DDH. Furthermore, there were no significant differences between singleton and twin pregnancies, despite the more restrictive mechanical environment, possibly explaining the normal incidence of DDH in twins [4]. This work sheds new light on a potential biomechanical link between fetal movements and the development of DDH. **REFERENCES:** 1. Sandell, Nat Rev Rheumatol, 8:2, 2012 2. Hinderarker et al, Acta Orthopaedica, 65:3, 1994 3. de Hunt et al, Eur J Obst Gyn Reprod Biol, 165:1, 2012 4. De Pellegrin et al, J Pediat Ortho, 30:8, 2010 5. Verbruggen et al, Biomech Model Mechanobiol, 2016 **ACKNOWLEDGEMENTS:** Arthritis Research UK (20683) Wellcome Trust and EPSRC iFind project (102431), ERC dHCP project (FP2007-2013 319456), NIHR-CS-012-002, NIHR GOSH.

Skeleton-stabilized Immersed Isogeometric Analysis for Incompressible Flow Problems

Clemens Verhoosel*, Tuong Hoang**, Chao-Zhong Qin***, Ferdinando Auricchio****,
Alessandro Reali*****, Harald van Brummelen*****

*Eindhoven University of Technology, **Eindhoven University of Technology; University of Pavia, ***Eindhoven University of Technology, ****University of Pavia, *****University of Pavia, Technische Universität München, *****Eindhoven University of Technology

ABSTRACT

Isogeometric Analysis (IGA) of incompressible flow problems has been an active topic of research over the last decade. In particular, IGA of mixed formulations for incompressible flow problems based on inf-sup stable velocity-pressure pairs has been demonstrated to be very suitable, which has led to the development of a range of isogeometric element families. In recent years, it has been shown that direct application of these element families in an immersed (Isogeometric Finite Cell) setting leads to local oscillations in the pressure field near cut boundaries. In this contribution we present an alternative stabilization technique that avoids the stability problem observed for inf-sup stable velocity-pressure pairs in the Isogeometric Finite Cell method. The pivotal idea of the considered technique is to control the jump of high-order derivatives of the pressure field over the skeleton structure of the mesh. This skeleton-based stabilization technique allows utilizing identical discrete spaces for the velocity and pressure fields. To enable application of the skeleton-based stabilization technique in the Isogeometric Finite Cell setting, the system is complemented with a stabilization term for the velocity space similar to that of the pressure space. In contrast to the pressure stabilization, the velocity stabilization – which is referred to in the literature as Ghost-penalty stabilization – is only applied at the faces of the background mesh skeleton structure that are located near the cut boundaries. Since the proposed skeleton-based stabilization technique is applicable in the conforming setting, we have studied its performance for a range of Stokes flow and moderate Reynolds number Navier-Stokes flow benchmark problems on two and three-dimensional conforming meshes, including the case of a multi-patch NURBS-based Isogeometric Analysis. We have observed the skeleton-based stabilization method to yield solutions that are free of pressure oscillations and velocity locking effects, and to yield optimal rates of convergence under mesh refinement. The observations for the conforming isogeometric setting extend to the immersed setting, where we have considered a range of two and three-dimensional problems for incompressible flows. To demonstrate the versatility of the proposed simulation strategy we have considered the Isogeometric Finite Cell analysis of Stokes flow through a porous medium, where the geometry is extracted directly from three-dimensional scan data.

Theory and Simulation of Fast - Travelling Dislocations: An Atomistic Perspective

Jonas Verschueren^{*}, Beñat Gurrutxaga-Lerma^{**}, Daniele Dini^{***}, Daniel S. Balint^{****}, Adrian P. Sutton^{*****}

^{*}Imperial College London, Centre for Theory and Simulation of Materials and Department of Materials, ^{**}Trinity College Cambridge and Department of Engineering, University of Cambridge, ^{***}Imperial College London, Department of Mechanical Engineering, ^{****}Imperial College London, Department of Mechanical Engineering, ^{*****}Imperial College London, Department of Physics

ABSTRACT

Our understanding of dislocation mobility - quantifying the relationship between the force on a dislocation and its resulting velocity - is largely based on experiment. However, the validity of mobility laws extracted from this work breaks down for fast travelling dislocations moving with speeds comparable to the speed of sound in the medium. Debate on the topic of dislocation mobility in the pure glide regime has been ongoing for over half a century. At the heart of the discussion lies the problem that in this regime, the usual approximations by which elasticity theory is linearised are violated and the quasi-static approximation no longer holds. In the last 20 years, large-scale non-equilibrium molecular dynamics simulations have been used to produce qualitative mobility laws for fast travelling dislocations. Despite the breadth of physical phenomena that are captured in these simulations, they have failed to provide the community with a general understanding of dislocation mobility in this regime. We will show how lattice-dynamics models and simulations of uniformly moving dislocations may provide an accurate description of the dislocation - phonon interactions in metals. These interactions are widely believed to play a crucial part in physical descriptions of dislocation mobility. Quantitative comparisons between the lattice dynamics model and equivalent molecular dynamics simulations will be made. Furthermore, the effect of the dislocation core width on its mobility will be presented. Finally, the consequences of these results for a more general theory on dislocation mobility in the pure glide regime will be discussed. References W.G. Johnston, J.J. Gilman, J. Appl. Phys., 30 129 (1959) Z. Jin, H. Gao, P. Gumbsch, Phys. Rev. B, 77 094303 (2008) B. Gurrutxaga-Lerma, D.S. Balint, D. Dini, D.E. Eakins, A.P. Sutton, Proc. R. Soc. A, 469 2156 (2013)

Stabilised Finite Element Methods for Variational Inequalities

Juha Videman^{*}, Tom Gustafsson^{**}, Rolf Stenberg^{***}

^{*}Instituto Superior Técnico, University of Lisbon, Portugal, ^{**}Aalto University, Finland, ^{***}Aalto University, Finland

ABSTRACT

We survey our recent and ongoing work [1,2,3] on finite element methods for contact problems. In our approach, we first write the problem in mixed form where the contact pressure acts as a Lagrange multiplier. To avoid the problems related with a mixed finite element discretisation, we use a stabilised formulation, in which appropriately weighted residual terms are added to the discrete variational forms. We show that the discrete formulation is uniformly stable and that it leads to an optimal a priori error estimate. Using the stability of the continuous problem, we establish a posteriori estimates whose optimality is ensured by local lower bounds. In the implementation of the methods, the discrete Lagrange multiplier is locally eliminated, thus giving rise to a Nitsche-type method. We present a series of numerical results which support the optimality of our a posteriori estimates. [1] T. Gustafsson, R. Stenberg, J. Videman. Mixed and stabilized finite element methods for the obstacle problem. SIAM Journal of Numerical Analysis 55 (2017). 2718–2744 [2] T. Gustafsson, R. Stenberg, J. Videman. Stabilized methods for the plate obstacle problem. <https://arxiv.org/abs/1707.08396> [3] T. Gustafsson, R. Stenberg, J. Videman. Nitsche's method for boundary constraints (in preparation).

From Polymer Physics to Rubber Elasticity

Marina Vidrascu*

*INRIA and Sorbonne University

ABSTRACT

In this talk, I will present recent results on the ab-initio modelling of rubber-like materials. The starting point is a random network of interacting polymer chains, the free energies of which are explicit functions of the temperature, their numbers of monomers and their elongations. In a discrete-to-continuum homogenization regime, this model gives rise to continuum nonlinear elasticity. The associated energy density is characterized by an asymptotic (nonlinear) cell-problem on the discrete network. We shall describe the generation of the network, the numerical solution method, and present numerical results that compare favourably to both mechanical experiments (at the macroscopic level) and physical experiments (at the level of the network, recovering the so-called butterfly effect). This is based on joint works with L. Giovangigli and A. Gloria (Sorbonne Université), F. Lequeux (ESPCI), and P. Le Tallec (Ecole polytechnique)

On Hellinger-Reissner type Mixed Finite Elements for Hyperelasticity

Nils Viebahn*, Jörg Schröder**

*University Duisburg-Essen, **University Duisburg-Essen

ABSTRACT

The Mixed Finite Element Method is an excellent tool for the computation of boundary value problems that involve some kind of limiting behavior. In the framework of elasticity one of the most common applications is the case of incompressibility. It is well known, that classical displacement based finite element schemes suffer from so-called locking-phenomena in these situations, see [1], whereas mixed methods perform significantly better in many cases. In this framework the formulation proposed by Pian and Sumihara [2], which is based on the Hellinger-Reissner principle, is still one of most efficient formulations available. Unfortunately, due to the use of a complementary energy, the formulation is only available in the linear elastic case and very special and limited cases of nonlinear elasticity [3]. In this work we will propose some basic ideas on the extension of the Pian-Sumihara element into a general hyperelastic framework. It will be shown that, depending on the choice of your interpolating stress-quantity, hourglass modes may occur and a stabilization is necessary. [1] I. Babuska, M. Suri, Locking Effects in the Finite Element Approximation, Numer. Math., 62:439-463, 1992 [2] T.H.H. Pian, K. Sumihara. Rational Approach for assumed stress finite elements. International Journal for Numerical Methods in Engineering 20:1685-1695, 1984 [3] P. Wriggers. Mixed Finite-Element-Methods. In: Mixed Finite Element Technologies, CISM Courses and Lectures, vol 509. Edited by P. Wriggers and C. Carstensen, 2009

Multi-Scale Constitutive Modelling of Multiphase Alloys

Miguel Vieira de Carvalho*, Daniel de Bortoli**, Francisco Andrade Pires***

*Institute of Science and Innovation in Mechanical and Industrial Engineering, Portugal, **Institute of Science and Innovation in Mechanical and Industrial Engineering, Portugal, ***Faculty of Engineering of the University of Porto, Portugal

ABSTRACT

Multiphase alloys, such as TRIP (transformation induced plasticity) and dual-phase steels, enjoy considerable technological importance, due to their favourable mechanical properties such as a combination of high yield strength and elongation at failure. However, complex phenomena, such as plastic slip and martensitic phase transformations, pose a number of computational challenges. A variety of phenomenological and micromechanical constitutive models have been proposed in the literature, accounting for the major features of their macroscopic behaviour. However, a large number of material parameters is usually required, limiting their predictiveness and generalisability. In this context, multi-scale models are a natural fit due to their ability to both capture the fine-scale crystalline features and connect them to the macroscopic scale. The overall material behaviour can thus be directly obtained from modelling the multiple constituent phases – slip in FCC or BCC lattices, for the ferrite, martensite and stable austenite phases, and FCC-to-BCC phase transformations, for the meta-stable austenite crystallites. Here, a fully implicit rate-dependent formulation [1], using the volume-preserving exponential map [2] and strategies such as sub-stepping is employed. Thus, the issues of rate-independent formulations, such as non-smooth yield functions, active system set search and non-unique solutions are circumvented. Additionally, the effect of mechanically-induced martensitic transformations is introduced using a recently proposed generalisation of Patel and Cohen's [3] energy-based criterion. The resulting model also includes coupling effects with the evolution of austenite slip activity, bearing many similarities with the aforementioned crystal plasticity models. Thus, analogous computational difficulties arise and are tackled similarly. In order to study the macroscopic behaviour of multi-phase crystalline materials and its intrinsic connection to their complex microstructure, a large-strain fully implicit, RVE-based multi-scale finite element code is used. Both RVE homogenisation and fully coupled (FE2) analyses are performed to study the influence of microstructural parameters on the resulting behaviour for materials of interest, for which experimental data is available, such as metastable austenitic stainless steels and TRIP steels. References: [1] R. J. Asaro and A. Needleman. "Overview No. 42: Texture Development and Strain Hardening in Rate Dependent Polycrystals". In: *Acta Metallurgica* 33.6 (1985). [2] C. Miehe. "Exponential Map Algorithm for Stress Updates in Anisotropic Multiplicative Elastoplasticity for Single Crystals". In: *International Journal for Numerical Methods in Engineering* 39.19 (1996). [3] J. R. Patel and M. Cohen. "Criterion for the Action of Applied Stress in the Martensitic Transformation". In: *Acta Metallurgica* 1.5 (1953).

Solution for Strain Softening Problem in FEM and SPH

Rade Vignjevic*, Nenad Djordjevic**, Tom De Vuyat***, Simone Gemkov****

*Brunel University London, UK, **Brunel University London, UK, ***Brunel University London, UK, ****Cranfield University, UK

ABSTRACT

The main aim of this work was addressing localisation problem observed in the analysis of strain softening materials using finite element methods (FEM) and the smooth particle hydrodynamic (SPH) methods, combined with local continuum damage mechanics (CDM) approach. More specifically, the objective was to reduce and possibly remove mesh dependency of the numerical results and balance the effects of heterogeneous microstructure on local continua while keeping the boundary value problem of softening (damaged) continua well-posed. Strain softening is typically observed in damaged quasi brittle materials such as fibre reinforced composites and application of the CDM approach with the classic FEM features a number of anomalies, including mathematical (change of the type of partial differential equations leading to ill-posed boundary value problem), numerical (pronounced mesh dependency) and physical (infinitely small softening zone with the zero dissipated energy). Consequently, alternative definition of damage effects, called equivalent damage force (EDF) was proposed here, where the damage effects were solely contributing to the right-hand side of the momentum balance equations, whilst keeping the left hand side of the equation and also the type of partial differential equations unchanged, relative to the linear elastic response. The FEM and the SPH combined with a local continuum damage model (CDM) were used for analysis of a dynamic stress wave propagation problem, which was analytically solved in [1]. The analytical solution was compared to the numerical results, obtained by using a stable, Total-Lagrange form of SPH [2,3], and two material models implemented in the FEM based on: 1) classic CDM; and 2) equivalent damage force. The numerical results demonstrate that the size of the damaged zone is controlled by element size in classic FEM and the smoothing length in the SPH, which suggests that the SPH method is inherently non-local method and that the smoothing length should be linked to the material characteristic length scale in solid mechanics simulations.

1. Z.P. Bazant and T.B. Belytschko, Wave propagation in a Strain- Softening Bar: Exact Solution, Journal of Engineering Mechanics, 111, 381-389, 1985.
2. R. Vignjevic, N. Djordjevic, S. Gemkow, T. DeVuyt, J. Campbell, j., 2014. SPH as a nonlocal regularisation method: Solution for instabilities due to strain-softening. Computer Methods in Applied Mechanics and Engineering, 277, pp. 281-304.
3. R. Vignjevic, J. Campbell, J. Jaric, S. Powel, Derivation of SPH Equations in a moving referential coordinate system, Computer Methods in Applied Mechanics and Engineering, 198, 2403–2411, 2009.

A Three-dimensional, Mechanochemical Model of the Cellular Cortex

Guillermo Vilanova*, Alejandro Torres-Sánchez**, Daniel Santos-Oliván***, Marino Arroyo****

*Universitat Politecnica de Catalunya, **Universitat Politecnica de Catalunya, ***Universitat Politecnica de Catalunya, ****Universitat Politecnica de Catalunya

ABSTRACT

The cellular cortex is a thin layer underneath the plasma membrane of animal cells. It is composed by an intertwined network of actin fibers attached by crosslinkers and myosin motors that exert contractile forces among the fibers. The cortex plays a central role in global cellular mechanics, cell shape control, morphogenesis and cytokinesis. Its misregulation is involved in several diseases. However, the cortex mechanics remains not well understood. Here we developed a continuous mathematical model to study macromechanical responses of the cellular cortex under internal stimuli and external forces. In our framework, the cellular cortex is modeled as a viscoelastic fluid that generates active stresses. Furthermore, due to the small thickness of the actomyosin network compared to the dimensions of the cell we model the cortex as a surface. Using this approach, we investigate the behavior of cells subjected to forces at different time scales as the cellular cortex responds as an elastic network under short time-scale forces, while it behaves as a viscous fluid at longer time-scales. We also study the tightly coupled dynamics of the cortex layer and the cellular plasma and how they influence cell division and migration.

Numerical Simulation of Rivulets Formation Based on a Shallow Water Type Model

Philippe Villedieu*, Julien Lallement**, Pierre Trontin***, Claire Laurent****

*Institut de Mathématiques de Toulouse, INSA, France & ONERA The French Aerospace Lab, Toulouse, France,

ONERA The French Aerospace Lab, Toulouse, France, *ONERA The French Aerospace Lab, Toulouse, France, ****ONERA The French Aerospace Lab, Toulouse, France

ABSTRACT

This work deals with the numerical simulation of the motion of a thin partially wetting liquid film flowing on a solid substrate. One of our objectives is to be able to predict the formation of rivulets in the case of a water film sheared by an air flow. This type of situation is encountered, for example, in the case of thermal de-icing systems for aircraft wing. The liquid film which is formed in this case is generally unstable. Rivulets are formed which radically modify the exchange area between the film, the heated wing and the air flow, and therefore play a decisive role on the efficiency of the de-icing system. Classically, the dynamic of thin liquid film is modelled by the lubrication equation (see for example [1]). This equation involves fourth order derivatives to take into account the effects of capillary forces. This may lead to numerical issues, especially in our case where we want to use an unstructured mesh finite volume solver which is well suited for industrial applications. To avoid these difficulties, the lubrication equation has been replaced in the present work by a shallow water type model, written in conservative form and involving only second order derivatives thanks to the introduction of an additional transport equation for the gradient of the film thickness (as proposed in [2]). A non-singular disjoining pressure model has been used to account for the capillary forces in the vicinity of the film contact line [3]. In addition, an implicit cell-centred unstructured finite volume scheme has been developed and implemented for the discretization of the problem. Based on this approach, many 2D and 3D simulations have been performed to assess its capability to accurately reproduce both linear stability theoretical results and experimental results for partially wetting film configurations and rivulets formation. During the conference, the model, the numerical method and the simulation results will be presented and discussed. [1] JA Diez, L Kondic. On the breakup of fluid films of finite and infinite extent. *Physics of Fluids* 19 (7), 2007. [2] P. Noble, J.P. Vila, Stability Theory for Difference Approximations of Euler-Korteweg Equations and Application to Thin Film Flow, *SIAM J. Numer. Anal.* 52(6), 2014 [3] J. Lallement, Ph. Villedieu, P. Trontin and C. Laurent, A shallow water type model to describe the dynamic of thin partially wetting films, 23ème Congrès Français de Mécanique, Lille, 2017

Computational Design Optimisation for Local Control over Mechanical Properties in Heterogeneous Scaffolds

Claire Villette^{*}, Miguel Castilho^{**}, Jos Malda^{***}, Andrew Phillips^{****}

^{*}Imperial College London, Embody Orthopaedics Ltd, ^{**}Eindhoven University of Technology, University Medical Center Utrecht, ^{***}University Medical Center Utrecht, ^{****}Imperial College London

ABSTRACT

Introduction There is a compelling argument in favour of designing bone tissue engineering (BTE) scaffolds able to drive optimised bone formation by stimulating the mechanotransduction processes of the osteogenic cells in a controlled manner. However, in current BTE techniques, prediction, control and characterisation of the local mechanical environment created within the scaffold are insufficient. The importance of scaffold design parameters such as stiffness, pore size and pore shape for tissue growth has been established [1] but most scaffold designs still neglect the considerable heterogeneity observed in native bone architecture. The authors have implemented a digital tool for automated computer design of heterogeneous scaffolds with local mechanical properties and porosity optimized for user-specified objectives. The main goals of this study were to characterise the fidelity of the 3D printed constructs to the designs, validate the predictive computational scaffold models, and assess the performances of the optimisation procedures via in-silico and in-vitro testing. **Methods and results** The design tool was implemented in C# as a plugin to the 3D modelling software Rhinoceros 3D and its algorithmic modelling platform Grasshopper. This plugin supports automatic cellular topology generation and optimisation of thicknesses of the individual cell struts to meet both local strain and porosity targets under a specified load case, building on a heuristic strain-based optimisation algorithm derived by the authors [2]. The design framework was assessed in-silico and in-vitro for compression and three-point bending scenarios by comparing the resulting optimized designs with controls, defined as homogeneous scaffolds with same outer shape and same mass as the optimized designs. CAD models of all designs were manufactured in a photocurable acrylic resin using direct light processing and mechanically tested using the simulated scenarios. Manufacture artefacts such as left-in non-cured material were incorporated into the Finite Element (FE) models. A good fidelity of the prints to the designs was observed for scaffolds with resolution $\geq 0.1\text{mm}$. The computational models accurately predicted sample stiffness ($\pm 5\%$), material failure ($\pm 5\%$) and structural failure ($\pm 10\%$). The optimised samples showed up to 40% higher material failure load than the controls. Local mechanical characterisation will be conducted using microcomputed tomography. First public release of the design software is planned for June 2018 to support researchers and clinicians unfamiliar with programming and optimisation techniques in designing reliable BTE scaffolds. **References** [1] Hollister SJ, Nature Materials, 4, 2005. [2] Phillips ATM, et al., International Biomechanics, 2, 2015.

Adjoint Based Optimization of a Supersonic Separator

Ernani Vitillo Volpe^{*}, Jairo Paes Cavalcanti Filho^{**}, Ulisses Adonis Silva Costa^{***}, Marcelo Tanaka Hayashi^{****}

^{*}Univesity of São Paulo, ^{**}University of São Paulo, ^{***}University of São Paulo, ^{****}Federal University of ABC

ABSTRACT

An emerging technology for separating gaseous mixtures, these devices expand the fluid to supersonic speeds through a convergent-divergent nozzle, so as to condense components that have higher liquefaction temperatures. The introduction of swirl causes the heavier liquid phase to be centrifuged toward the wall, where it is collected. Widely recognized for their compactness and for the absence of moving parts, the supersonic separators are deemed an attractive alternative for removing contaminants from natural gas, wherever the available space is severely limited, such as in oil rigs. Yet they still pose some significant technical hurdles. Shock waves can seriously hamper the device efficiency, as a sudden rise in temperature may stop the liquefaction process or even cause the condensate to re-evaporate. Thermodynamics modeling of fluid behavior and state equations must account for the saturation region and phase change. In addition, the vanes that cause the flow to swirl must be carefully designed, so as not to interfere with the supersonic expansion, itself. In view of these challenges, we attempt an adjoint based computation of sensitivities and optimization of the device. To that end, we make use of the SU2, an open-source suite of tools for performing CFD simulations and optimization, which includes non-ideal gas models that are crucial for the problem. References: M. Pini, S. Vitale, P. Colonna, G. Gori, A. Guardone, T. Economon, J.J. Alonso and F. Palacios "SU2: the Open-Source Software for Non-ideal Compressible Flows"; 1st International Seminar on Non-Ideal Compressible-Fluid Dynamics for Propulsion & Power IOP Publishing IOP Conf. Series: Journal of Physics: Conf. Series 821 (2017) 012013 doi:10.1088/1742-6596/821/1/012013, 2017. S. Vitale, M. Pini, P. Colona, G. Gori, A. A. Guardone, T. D. Economon, F. Palcios and J.J. Alonso "Extension of the SU2 Open Source CFD code to the simulation of turbulent flows of fluids modelled with complex thermo-physical laws"; AIAA Paper, 2760, 2015.

Computational Unsaturated Poromechanics Enhanced by Deep Learning

Nikolaos Vlassis^{*}, Kun Wang^{**}, WaiChing Sun^{***}

^{*}Columbia University, ^{**}Columbia University, ^{***}Columbia University

ABSTRACT

Many engineering applications and geological processes involve unsaturated porous media across multiple length scales (e.g. rock joints, grain boundaries, deformation bands, and faults). Understanding the multiscale path-dependent hydro-mechanical responses of these interfaces across length scales is of ultimate importance for applications such as CO₂ sequestration and hydraulic fracture. Nevertheless, unlike the saturated counterpart, the path-dependent behaviors of the unsaturated porous media may originate from both the irreversible damage and plasticity of the solid skeleton, the hysteresis of the water retention behaviors and the resultant path-dependent hydraulic responses. For convenience, numerical models often neglect the hysteresis effect of the retention curves. This simplification often leads to unrealistic predictions. In this work, we introduce a hybrid hand-crafted/machine-learning model in which we combine a class of recurrent neural network model (based on long-short-term-memory neuron) that replicates the path-dependent water retention behaviors and classical constitutive critical state plasticity model to replicate the hydro-mechanical responses of unsaturated porous media. This approach allows one to bypass the need of deriving complex phenomenological law for the portion of the constitutive model that lacks clean physical underpinnings while retaining the part of the model that can be justified with sufficient physical arguments (e.g. critical state plasticity). A set of numerical experiments are used to demonstrate the robustness of the proposed model.

Designing Conforming Metamaterials in Irregular Domains Using Topology Optimization and Computational Conformal Geometry

Panagiotis Vogiatzis*, Ching Hung Chuang**, Hongyi Xu***, Shikui Chen****

*Department of Mechanical Engineering, State University of New York at Stony Brook, **Ford Research & Advanced Engineering, ***Ford Research & Advanced Engineering, ****Department of Mechanical Engineering, State University of New York at Stony Brook

ABSTRACT

Metamaterials are artificial materials which possess superior effective properties to conventional materials. The properties of these designs are based on the repetition in 2 or 3 dimensions of a unit cell, which acts as a building unit for a metamaterial structure. Over the last decades, topology optimization methods have joined traditional conceptual designing techniques, and have been widely employed in designing metamaterial unit cells. To use these materials in actual applications, it is common practice that the unit cell is placed in specific domains acting as an infill. Apart from special cases where the unit cell is used in a 2D or 3D rectangular domain, other applications may require multiple unit cell designs to be placed in an arbitrary external geometry. In these applications, the designer faces two challenges: connectivity problems between multiple metamaterial designs, and mapping a set of rectangular unit cells on an irregular domain. A simple approach for the former is adding a boundary box surrounding groups of metamaterials, or even every metamaterial design, which leads to limiting the designing freedom of potential designs by locking material at the boundaries during the optimization. For the latter, a current approach consists of a simple repetition of the unit cell to a perfect rectangular domain, placement of the resulted structure to the actual domain, and finally trimming the structure located outside the domain. However, this method has several drawbacks, including the potential existence of overhanging structures or abandoned material islands and the significant change of the effective properties of the partial unit cells near the boundaries of the domain. In this work, we employ the conformal mapping theory to map multiple metamaterial microstructures on irregular domains, considering geometric constraints during the optimization. Using conformal mapping leverages the problem currently faced. Conformal mapping, which is an angle-preserving Riemann mapping that preserves the local shape, can efficiently transform a rectangular unit cell to an irregular quadrilateral domain. Any arbitrary domain can be discretized into a quad domain, where the main part can consist of rectangular quads leaving irregular quads mainly near the boundaries. The proposed method successfully maps more than one different unit cell designs, conformed to the external boundaries. We investigate the preservation of the effective properties compared to the traditional trimming technique and the effective properties of the original unit cell.

Evaluation of Implicit-Explicit, Additive Runge-Kutta Method Efficiency in Simulating Global Non-Hydrostatic Atmospheric Dynamics for Earth System Modeling

Christopher Vogl^{*}, David Gardner^{**}, Daniel Reynolds^{***}, Paul Ullrich^{****}, Carol Woodward^{*****},
Andrew Steyer^{*****}

^{*}Lawrence Livermore National Laboratory, ^{**}Lawrence Livermore National Laboratory, ^{***}Southern Methodist University, ^{****}University of California Davis, ^{*****}Lawrence Livermore National Laboratory, ^{*****}Sandia National Laboratories

ABSTRACT

A standard global atmospheric model is comprised of the Euler equations coupled with an equation of state that is a modified ideal gas law. This system of equations includes acoustic waves that must be simulated in a stable manner despite that their effect on atmospheric dynamics is usually negligible. Furthermore, this system is solved on computational grids that are typically more refined in the vertical direction to account for the shorter vertical length scales present in atmospheric physics. Thus, the discretized system contains stiff elements both from the presence of acoustic waves in the model equations and from the domain discretization. For this discretized system, the use of explicit time integration methods imposes too strict of a timestep restriction for the timescales of earth system modeling. Fully implicit methods may circumvent this timestep restriction, but a global simulation results in a massive nonlinear system that is too computationally expensive to solve at every timestep. Thus, the class of Implicit-Explicit (IMEX), Additive Runge-Kutta (ARK) methods is investigated. In particular, the ability of these methods to accurately simulate atmospheric dynamics at large timesteps is evaluated. Various approaches to splitting the model equations into stiff components, which are treated implicitly, and non-stiff components, which are treated explicitly, are explored. The Suite of Nonlinear and Differential/Algebraic Equation Solvers (SUNDIALS) package is used to quickly incorporate IMEX, ARK methods into the High-Order Methods Modeling Environment (HOMME) dynamical core within the Energy Exascale Earth System Model (E3SM). Both existing methods, as well as ones that were recently developed for this specific discretized system, are considered. This work was performed under the auspices of the U.S. Department of Energy by Lawrence Livermore National Laboratory under contract DE-AC52-07NA27344. Lawrence Livermore National Security, LLC.

Computing Solution-compensation Spaces for Robust Non-linear Systems Design

Marc Eric Vogt^{*}, Helmut Harbrecht^{**}, Fabian Duddeck^{***}, Martin Wahle^{****}, Florian Stutz^{*****},
Markus Zimmermann^{*****}

^{*}Associate Professorship of Computational Mechanics, Technical University of Munich, ^{**}Research Group of Computational Mathematics, University of Basel, ^{***}Associate Professorship of Computational Mechanics, Technical University of Munich, ^{****}Department of Preliminary Design for Vehicle Dynamics, BMW, ^{*****}Research Group of Computational Mathematics, University of Basel, ^{*****}Institute of Product Development and Lightweight Design, Technical University of Munich

ABSTRACT

Tolerance to parameter variation due to lack-of-knowledge or epistemic uncertainty in mechanical non-linear systems design can be improved by computing so-called Solution Spaces. They are defined as sets of good designs reaching all design goals. Box-shaped Solution Spaces are subsets of the complete Solution Space. They can be expressed as the Cartesian product of permissible intervals for the design variables. These intervals are decoupled while also allowing for unintended variations of component properties. Since the size of the permissible intervals for crucial design variables is often not large enough to account for all uncertainties and to ensure feasibility, solution-compensation spaces where introduced. Solution-compensation spaces enable increased permissible intervals. In order to compute solution-compensation spaces the design variables are divided into two groups, early- and late-decision variables. Early-decision variables are associated with permissible intervals on which they may assume any value. Late-decision variables are associated with intervals where they can be adjusted to any specific value. Solution-compensation spaces are regions of early- and late-decision variables. For all values of early-decision variables values exist for late-decision variables such that all design requirements are satisfied. Existing algorithms optimize the size of box-shaped solution-compensation spaces for linear systems. A new approach to compute solution-compensation spaces for non-linear, high-dimensional design problems is introduced. It combines an existing heuristic with the solution-space algorithm introduced in [Zimmermann & Hoessle 2013]. Starting from a good design point, a candidate box is iteratively evaluated and modified. The evaluation is performed by Monte Carlo sampling for the early-decision variables in combination with heuristic optimization for the late-decision variables. This approach is applied to a non-linear design problem within the field of vehicle dynamics.

Sharp Algebraic and Total A Posteriori Error Bounds for h and p Finite Elements via a Multilevel Approach

Martin Vohralík^{*}, Jan Papež^{**}, Ulrich Rüde^{***}, Barbara Wohlmuth^{****}

^{*}Inria Paris and Ecole des Ponts ParisTech, ^{**}Inria Paris and Institute of Computer Sciences Prague,

^{***}Friedrich-Alexander-Universität Erlangen-Nürnberg, ^{****}Technische Universität München

ABSTRACT

We derive guaranteed, fully computable, constant-free, and sharp upper and lower a posteriori estimates on the algebraic, total, and discretization errors of finite element approximations of the Poisson equation obtained by an arbitrary iterative solver. The estimators are computed locally over patches of mesh elements around vertices and are based on suitable liftings of the total and algebraic residuals. The key ingredient is the decomposition of the algebraic error over a hierarchy of meshes, with a global solve on the coarsest mesh. Distinguishing the algebraic and discretization error components allows us to formulate safe stopping criteria ensuring that the algebraic error does not dominate the total error. We also prove equivalence of our total estimate with the total error, up to a generic polynomial-degree-independent constant. Numerical experiments illustrate sharp control of all error components and accurate prediction of their spatial distribution in several test problems. These include smooth and singular solutions, higher-order conforming finite elements, and different multigrid methods as well as the preconditioned conjugate gradient method as the iterative solver.

Modeling the Cellular Cortex as a Surface Active Gel

Axel Voigt*

*TU Dresden

ABSTRACT

We consider an active gel model for the cellular cortex, derive step by step the corresponding equations as a thin film limit, discuss numerical approaches for the proposed vector- and tensor-valued surface partial differential equations, show examples demonstrating the delicate interplay between topology, geometry and defect dynamics and relate the results to experiment for axis formation in *C. elegans* embryos.

Fracture as Material Sink

Konstantin Volokh*

*Technion

ABSTRACT

Cracks are created by massive breakage of molecular or atomic bonds. The latter, in its turn, leads to the highly localized loss of material, which is the reason why even closed cracks are visible by a naked eye. Thus, fracture can be interpreted as the local material sink. Mass conservation is violated locally in the area of material failure. We consider a theoretical formulation of the coupled mass and momenta balance equations for a description of fracture [1]. Our focus is on brittle fracture and we propose a finite strain hyperelastic thermodynamic framework for the coupled mass-flow-elastic boundary value problem. The attractiveness of the proposed framework as compared to the traditional continuum damage theories is that no internal parameters (like damage variables, phase fields etc.) are used while the regularization of the failure localization is provided by the physically sound law of mass balance. References [1] Volokh KY (2017) Fracture as a material sink. Materials Theory 1:3

Smarter Production Technology: an Example of a Smart Bending Machine

Vitalii Vorkov^{*}, Gonalo Costa Rodrigues^{**}, Joost R. Duflou^{***}

^{*}KU Leuven, ^{**}KU Leuven, ^{***}KU Leuven

ABSTRACT

The so-called third industrial revolution (or Industry 3.0) brought about computer-aided manufacturing and automation, which allowed achieving unprecedented precision and reliability of production processes. However, Industry 3.0 machines come as they are, and do not change throughout their lifetime. The current trend of automation and data exchange in manufacturing industry or Industry 4.0 strives to change this position towards cyber-physical machines that communicate within the production chain and learn from shared knowledge. In this work, we apply the methodology of Industry 4.0, namely Internet of things and machine learning, to the state-of-the-art sheet metal bending technology. Two typical problems of sheet metal forming are considered: an incorrect labeling of sheet metal plates or material identification, and an inaccurate prediction of the technological parameters or process characteristics prediction. These two problems are considered as building blocks of a smart bending machine and are solved for the test case of the air bending operation based on an available extensive experimental database. Material identification is implemented as a classification problem, where five classes of materials are considered (aluminum, structural steel, stainless steel and high-strength steel). A number of classification methods have been tested and the best of them allowed predicting the material class with 95% of accuracy based only on limited information (namely the springback value, and tooling and plate dimensions). Further, based on the identified material classes, a prediction model based on regression prediction has been trained. As for the material classification, a number of methods have been tested and compared as between different trained regression models, and also with the existing analytical model. The results revealed that even 200 tests are enough to train the regression model of the air bending process to achieve a springback prediction error below 5%, while the initial prediction error was above 12%. Given the communication between smart bending machines for the data acquisition, the material detection and bending parameters can be significantly improved very rapidly, since only a limited number of training data are necessary.

Multiscale Modeling of Ground Motions from Underground Explosions

Oleg Vorobiev*, Souheil Ezzedine**

*LLL, **LLNL

ABSTRACT

This work describes a methodology used for large scale modeling of wave generation and propagation from underground chemical explosions conducted at the Nevada National Security Site (NNSS) fractured granitic rock. We show that the discrete natures of rock masses as well as the spatial variability of the fabric of rock properties are very important to understand ground motions induced by underground explosions. Parallel codes are used to model physical processes at various scales. In the close vicinity of the source on the scale of 1-10 m, we apply a massively parallel Eulerian hydrocode, GEODYN with adaptive mesh refinement to model the shock wave generation around the source. This code supports large material deformations which may take place near the cavity created around the source. Eulerian solution is later remapped onto a Lagrangian parallel hydrocode, GEODYN-L, which explicitly accounts for discontinuities in the rock mass. The presence of joints and geologic layers may lead to elastic-plastic anisotropy of the rock mass. Explicit representation of these discontinuities is computationally expensive since it requires to use mesh resolution comparable to the joint density which is of the order of 1 m. We apply this method in the range where the rock mass response is not elastic (≤ 100 m). Beyond this range the rock mass can be considered elastic and can be represented by an anisotropic continuum model. Effective anisotropic stiffness for the rock mass is calculated by upscaling procedure where contribution of both the rock and the joints are used. This approach allows us to propagate seismic waves applying linear elastic anisotropic model to 1-10 km range. Thus, the ground motion generated in the near-field is propagated to the far field in a consistent way. We demonstrate the effectiveness of this method by modeling the ground motion observed during the Source Physics Experiment. This work performed under the auspices of the U.S. Department of Energy by Lawrence Livermore National Laboratory under Contract DE-AC52-07NA27344. LLNL-ABS-679820

A Theoretical and Computational Setting for a Gradient-enhanced Plasticity Theory : Small and Finite Deformations

George Voyiadjis*, Yooseob Song**

*Louisiana State University, **Louisiana State University

ABSTRACT

In this work, a coupled thermo-mechanical gradient-enhanced continuum plasticity formulation is developed within the thermodynamically consistent framework and corresponding two-dimensional finite element analysis is implemented to examine the micro-mechanical and thermal characteristics of the small-scale metallic volumes based on the small and large deformation theories. In the first part of the work, the theory based on the small deformation is proposed with the concept of thermal activation energy and the dislocations interaction mechanisms. The theory is also based on the decomposition of the thermodynamic microforces into energetic and dissipative counterparts, decomposition of free energy into the elastic, defect and thermal counterparts, and decomposition of dissipation potential into the mechanical and thermal counterparts. The temperature distribution in the system, due to the conversion of the plastic work into heat and the partial dissipation of the heat due to the fast transient time, is included into the model using a generalized heat equation. The derived constitutive model is validated through the comparison with the experimental observations conducted on micro-scale thin films. The proposed model is applied to the simple shear problem and the square plate problem respectively in order to investigate the thermo-mechanical behavior and the grain boundary effect of small-scale metallic materials. In the second part of the work, two-dimensional finite element simulation for the finite deformation incorporating the temperature effect is developed based on the implicit gradient-enhanced approach, F-bar method and radial return algorithm. The implicit gradient approach is well known for its computational strength, however, it is also commonly accepted that it cannot capture the size effect phenomenon observed in the small-scale experiments during the strain hardening regime. In order to resolve this issue, a modified implicit gradient approach which can capture the size effect under the finite deformation is constructed in this work. The simple shear problem is then solved to carry out the feasibility study of the proposed model on the size effect phenomenon. Lastly, the uniaxial plane strain tension problem is solved to perform the mesh sensitivity tests of the model during the strain softening regime.

Polygonal Analysis and Polytree-based Adaptive Topology Optimization of Fluid-submerged Breakwater Interaction

Truong Vu-Huu^{*}, Phuc Phung-Van^{**}, Hung Nguyen-Xuan^{***}, Magd Abdel-Wahab^{****}

^{*}Ghent University, ^{**}Ghent University, ^{***}HUTECH University, ^{****}Ghent University

ABSTRACT

This research presents the application, for the first time, of polygonal finite element method (PFEM) and polytree-based adaptive topology optimization technique to simulate and optimize fluid-submerged breakwater interaction problems. They are integrated to investigate fluid-structure interaction (FSI) problems between fluid and submerged breakwater (SBW). Then an optimal shape of SBW is main goal of this study. In addition, SBW is one of the most interesting protected solution in coastal structures because its distinguished features, particularly, protecting the landside from the erosion without any loss of beach amenity and negative aesthetic influents for the recent decade instead of seawall, groins, breakwater, etc. And It is always subjected the fluid interaction. In this study, some numerical examples are presented to demonstrate the effectiveness of the proposed method. A finite element commercial package, ABAQUS software, is used to produce reference solutions for the numerical examples written in MATLAB.

Plasma Actuators for Flow Control of Flapping Wing

CHINCHENG WANG*, Vedula Kumar**

*Yuan Ze University, **Yuan Ze University

ABSTRACT

The concept of fixed wing Micro Air Vehicle (MAV) has gained increasing interest over the past few decades, with the principal aim of carrying out surveillance missions. The design of flapping wing MAV is still in the infancy stage. On the other hand, researchers have been increasing interest in dielectric barrier discharge (DBD) plasma actuators for active flow control over ten years. The aim of this study is to investigate the performance of flapping wing MAV using active flow control (i.e. DBD plasma actuators). First, a study of a NACA 0012 airfoil will be performed for the aim of improving its aerodynamic performance with particular focus on the lift over drag coefficient. The fluid-structure interaction will be studied to show the versatility of DBD plasma actuators. The benchmark case will be validated with published literature. For the plasma-fluid interaction, we will use reduced-order model to solve plasma induced electric body force. The OpenFOAM CFD platform will be used to solve the problem. For the plasma induced turbulence in the flow regime, k- ϵ turbulence model will be adopted to address the interaction between plasma and fluid flows. In future, the combination of the flapping wing design with DBD plasma actuators would boast a maneuverability of MAV.

Cyclic Pseudoelasticity of Polycrystalline Shape Memory Alloys: Constitutive Modeling and Numerical Simulation

Jun WANG^{*}, Weihong ZHANG^{**}, Ziad MOUMNI^{***}

^{*}Institute of intelligence material and structure, Unmanned system technologies, Northwestern Polytechnical University, Xi'an, Shaanxi 710072, China, ^{**}State IJR Center of Aerospace Design and Additive Manufacturing, Northwestern Polytechnical University, Xi'an, Shaanxi 710072, China, ^{***}IMSIA, UMR 8193 CNRS-EDF-CEA-ENSTA, Universite Paris Saclay, 828 Boulevard des Marechaux, 91762 Palaiseau Cedex, France

ABSTRACT

This work presents a new 3D thermomechanical finite-strain constitutive model for cyclic pseudoelasticity of polycrystalline shape memory alloys (SMAs). The model considers four primary characteristics related to the cyclic behavior of SMA that have not been integrally addressed within the finite-strain framework: (i) large accumulated residual strain that results from the residual martensite and dislocations slipping during cycling; (ii) degeneration of pseudoelasticity and hysteresis loop due to the increase of dislocation density and internal stresses with the number of cycles; (iii) rate dependence that can be attributed to the thermomechanical coupling effect; (iv) evolution of the phase transformation from abrupt to smooth transition, as a consequence of the diversified crystallographic orientations of the grains, the heterogeneity of internal stresses, and the presence of non-transforming precipitates during cycling. Based on the decomposition of finite Hencky strain into elastic, transformation, residual and thermal components, the model is constructed within a thermodynamically consistent framework. Evolution equations associated with the internal variables are derived from the reduced form of energy balance, the Clausius-Duhem form of entropy inequality, and a Helmholtz free energy function that includes elastic, thermal, interaction and constraint energies. The model is used to simulate the cyclic tensile experiments on NiTi wire at different loading rates. The good agreement of the model predictions against the experimental data demonstrates the capabilities of the proposed model to well describe cyclic pseudoelasticity of polycrystalline SMAs, and to capture the aforementioned characteristics. Furthermore, in order to demonstrate the capability of the cyclic model to solve multi-axial problems, a finite elements simulation of a SMA torsion spring undergoing large strains and rotations resulting in local multi-axial non-proportional stress and strain evolution is performed.

Structural Optimization Design Method Considering SLM Manufacturing Constraints

YU WANG*

*South China Agricultural University

ABSTRACT

SLM (Selective Laser Melting) is one of the most widely used metal AM (additive manufacturing) technologies, which is able to manufacture metal components with complex geometries, and shorten the processing cycle. In the manufacturing process of SLM, the manufacturing abilities and parameters have a great effect on the mechanical properties of components. To design the structures meeting the manufacturing abilities, this paper presents a structural optimization design method with considering manufacturing constraints of SLM, to design components can be manufactured without the use of support material. The relationship between the limit height and angle of overhang when the component collapses is studied experimentally, the results of which are used to compose the corresponding self-supporting constraints embedded within the topology optimization framework. The optimized structures are manufactured via SLM technology to verify the effectiveness and correctness of the proposed method and manufacturing constraints.

Impact Characteristics Analysis and Fatigue Life Estimation of Recoil Spring

Zhifang WEI*, Yechang HU**

*North University of China, **North University of China

ABSTRACT

On automatic or semi-automatic guns, the recoil spring slows the rearward movement of the bolt moving components and pushes it back to the front, which is generally cylindrical helical compressing spring, with a single wire or three, four wire twisted cable. The recoil spring is mainly subjected to high speed impact load in the reciprocating movement. The spring deformation is very fast, and the deformation and stress distribution are very uneven. After long firing, the free length of spring can be shortened, the spring force is weakened and sometimes even fatigue crack or fracture can be produced. The failure of the spring will cause the action of automation to be fatigue and not in place, which will affect the firing accuracy. Therefore, the recoil spring impact characteristic analysis and fatigue life estimation is crucial. In this paper, the finite element simulation method was used to study the impact characteristics of the recoil spring and its fatigue life estimation method. Aimed at the 59 type 12.7 mm airborne machine gun, the dynamic response characteristics of the three-strand recoil spring under the impact of the bolt was analyzed with ABAQUS software, and the time history curve of the stress of the dangerous position was obtained. Then the curve was counted by the rain flow counting method to get the fatigue stress spectrum of recoil spring. According to the Miner damage theory, the fatigue life of the recoil spring was finally estimated based on the fatigue stress spectrum and the S-N curve of the spring material. The results show that the recoil spring has obvious transient in the impact process of the bolt, the impact velocity is far greater than the internal stress wave propagation speed of the spring, which is easy to make spring rings to merge together. And the stress wave is not reflected at the fixed end of the recoil spring during propagation, the maximum stress appears at the fixed end of the spring. Using the median fatigue curve (survival rate 50%), the estimated fatigue life of the recoil spring is about 6000 times, which is consistent with the overall life of the whole gun. The method presented in the paper can provide technical means for the fatigue life prediction and parameters design of multi-strand spring.

Barycentric Stencils

Eugene Wachspress*

*Columbia University

ABSTRACT

Dirichlet kernels provide a tool for analytic construction of harmonic barycentric coordinates (piecewise linear on the boundary) over any C^1 bounded region¹. These may be approximated well by more easily computed corresponding coordinates for inscribed polygons. A simple stencil is a ring with inner boundary the C^1 curve and outer boundary a similar curve or convex polygon. When the outer boundary is also a C^1 curve and a C^2 approximation is required within the ring, the Dirichlet barycentrics extrapolate into the ring while the polygon coordinates do not. Numerical studies with inner and outer ellipses are described. 1. Eugene Wachspress, Rational Bases and Generalized Barycentrics, Springer, 2016, pp 228-232

Phase-field Study of Dendritic Growth of Hexagonal Crystal in Thin Film

Koki Wada^{*}, Tomohiro Takaki^{**}

^{*}Kyoto Institute of Technology, ^{**}Kyoto Institute of Technology

ABSTRACT

Hot-dip galvanizing is a coating process to prevent steel from corrosion. In the process of hot-dip galvanizing, a steel material is immersed in a liquid bath of a molten zinc alloy, and the coating layer is formed through solidification. Then, very large grains with a (0001) orientation, termed spangles, are preferentially formed in the coating layer. Although it was reported that the (0001) texture of the coating layer was formed by a preferred (0001) nucleus orientation and preferential dendrite growth in a basal plane [A. Sémoroz et al., Metall. Mater. Trans. A, 33 (2002) 2695-2701], the detail morphological evolution and dendrite growth kinetics of the dendrite in such thin layer are not clear even now. In this study, we investigate the formation mechanism of the (0001) texture by performing dendrite growth simulations of a hexagonal crystal in thin film using a phase-field method, which is well accepted as the most accurate dendrite prediction model. Here, the phase-field simulations are systematically performed in the two- and three-dimensions by changing the crystal orientation and wetting angle between the dendrite and substrate surface. The dendrite growth velocity and morphology are investigated in detail.

Fundamental Study for Crack Propagation Forecast Using Machine Learning

Yoshitaka Wada^{*}, Makishi Takeyasu^{**}

^{*}Kindai University, ^{**}Kindai University

ABSTRACT

This paper presents the capability and applicability for fatigue crack propagation evaluation using a neural network system. Fatigue crack propagation includes several governing laws and computation methods which are elastic stress field, stress intensity factors, Paris's law, criterion of crack propagation direction. Crack propagation phenomenon simultaneously occurs with these laws and methods. In this paper, we compute crack propagation as training data in 2-dimension using s-version finite element method. Three training levels are defined. In 1st training level, crack position vector, propagation direction vector and stress intensity factors are learned. In 2nd training level, crack position vector, crack propagation direction vector, six stress components around crack tip are learned. In last training level, only crack position vector and crack propagation direction vector are trained. Last level requires only geometrical information to predict crack propagation phenomenon. In order to simplify the problem, all of parameters are completely determined as constant values. The simulation can represent curved crack path by incremental crack propagation computations. As a result of comparisons between the each level, the 1st level exhibits the highest reproducibility. If the same computation results as the 1st level, the last level requires 10 times training data and time to get convergence of the neural network system. We'd like to discuss the results of several learning examples and show the applicability of the neural network technology to the actual engineering problems.

Uncertainty Quantification of Data Collection and Data Processing in Materials Characterization

Noah Wade^{*}, Lori Grahman-Brady^{**}

^{*} Johns Hopkins University, ^{**} Johns Hopkins University

ABSTRACT

Serial sectioning techniques for the development of three dimensional microstructures are important to the advancement of material behavior modeling. Three dimensional microstructures provide valuable statistical information about the underlying structure and defects of a given material sample. However, due to the nature of serial sectioning techniques the material sample is destroyed in the process, and such methods often provide no quantitative measure of the accuracy to which they represent a physical sample as a digital microstructure. Furthermore, serial sectioning data sets are expensive in terms of time and resource allocation, meaning that error estimates based on analysis of multiple larger scale experiments is prohibitive. Without such measures of accuracy, error propagates unaccountably to material modeling and simulation experiments. To address the issues of error propagation, and experimental accuracy vs. experimental cost, a computational method was developed to simulate serial sectioning data collection. By simulating the data collection process for Electron Backscatter Diffraction (EBSD) and other serial sectioning techniques, the effect of many different experimental parameters can be study with respect to their impact on the total experimental error. User defined parameters such as resolution, slice thickness, dwell time, and polishing method all have a direct correlation to both the accuracy and experimental cost of a given serial sectioned data set. By varying each of these parameters the effects can be studied individually and provide bounds for both individual sources of error as well as the total error introduced through the experiment process. This is done by starting with a digital representation of a material, and simulating serial sectioning data collection on the digital material. The final results can be compared directly to their original source. Thus, providing a quantifiable comparisons of accuracy for different experimental parameters. Finally, this work seeks to demonstrate how each of these errors propagates from the experimental data collection stage through the modeling stage. Finite element simulations of virtually collected data illustrate changes in the final solution variables, and provides estimated bounds of the error introduced by changing different experimental parameters. Ultimately, this work this provides a method to account for inerrant errors of reconstructed microstructures and inform experimentalist on best methods for experimental uncertainty quantification.

Inverse Problems for Smart-City Applications

Julien Waeytens*

*Université Paris-Est, IFSTTAR

ABSTRACT

By 2050, about 75% of the world population would live in cities, despite the fact that most of the urbanites actually complain about their quality of life in cities, especially concerning the air pollution, the mobility/congestion and the thermal comfort in bad insulated buildings. Through the concept of Smart-City, by combining innovative sensors and new numerical technologies, new services can be proposed to the urbanites to facilitate their day-to-day living and new tools can be provided to the territorial collectivities to manage the cities. In addition, virtual testing and simulation can help selecting optimal urban plannings to move towards efficient, sustainable and green cities. In the presentation, we focus on the utility of inverse problems coupling sensor outputs and physical model for Smart-City applications. Firstly because of the costliness of some sensors, such as gaz sensor for air quality monitoring, their number and placement have to be optimized. In [1], we proposed an adjoint-based tool to evaluate the observability area associated to a given sensor position. Thus, air/water quality sensors can be optimally placed to localize indoor source emissions or to detect contaminants in drinking water networks. Then, the updating of model parameters by solving inverse problems can be of interest to reconstruct fields, like the flow in drinking water networks [2] for leak detection, and to monitor structures, like the localization and the quantification of damage in concrete structures [3] and in-situ evaluations of wall thermal resistance before and after rehabilitation works. Lastly, a new inverse problem formulation is presented to precisely predict quantities of interest and is applied to thermal building problems. Some of these experiments were conducted in the French equipment "Sense-City". [1] J. WAEYTENS, P. CHATELLIER, F. BOURQUIN, 2013, Sensitivity of inverse advection-diffusion-reaction to flow, sensor and control: a low computational cost tool, *Computers & Mathematics with Applications*, 66, 1082--1103. [2] J. WAEYTENS, P. CHATELLIER, F. BOURQUIN, 2015, Inverse Computational Fluid Dynamics: Influence of Discretization and Model Errors on Flows in Water Network Including Junctions, *Fluids Engineering*, 137 (9), 17p. [3] J. WAEYTENS, B. ROSIC, P-E. CHARBONNEL, E. MERLIOT, D. SIEGERT, X. CHAPELEAU, R. VIDAL, V. le CORVEC, L.-M. COTTINEAU, 2016, Model updating techniques for damage detection in concrete beam using optical fiber strain measurement device, *Engineering Structures*, 129, 2--10.

Multiscale Process-Structure Simulation for Additive Manufacturing in Metals Using a Cellular Automaton Model

Gregory Wagner^{*}, Yan Ping Lian^{**}, MJ Sarfi^{***}, Wing Kam Liu^{****}

^{*}Northwestern University, ^{**}Northwestern University, ^{***}Northwestern University, ^{****}Northwestern University

ABSTRACT

The material microstructure in parts produced through additive manufacturing is known to be very sensitive to the parameters governing the process. For example, in powder-bed or powder deposition processes, the porosity and the grain size and shape are affected by the laser power, path, and scan speed. Many of these effects can be traced to the complex thermal history at locations in the part as material is repeatedly melted, cooled, and reheated through multiple build layers and laser passes. In this work we model the development of metal microstructure during solidification by simulating the process at two different scales: the part scale, giving temperature fields throughout the part during the entire build, and the microscale, allowing microstructure development and growth to be simulated at select locations. At the part scale, we use an efficient finite element solution of the heat equations, including an effective heat capacity model informed by a database computed in ThermoCalc to capture the thermodynamics of solidification for a specific material. At the microscale, we use a cellular automata/finite element (CAFE) model to simulate the growth and interaction of individual grains. The two scales are coupled through the space- and time-varying temperature field. Through this approach we study the effects of various process parameters and toolpath designs on the resulting grain structures of the finished part.

Model-Based Control of Integrated Fluidic Actuators for Adaptive Structures

Julia Laura Wagner*, Michael Böhm**, Oliver Sawodny***

*Institute for System Dynamics, **Institute for System Dynamics, ***Institute for System Dynamics

ABSTRACT

Adaptive structures in structural engineering include sensors and actuators to influence the systems' response under stationary and dynamic loads. The induced structural stresses and displacements can be compensated by stationary adaption and dynamic control [1]. To provide a high integration level of the active elements, a new kind of fluidic actuator is developed. As proof of concept, a concrete beam is equipped with hydraulic pressure chambers which are arranged asymmetrical regarding the neutral axis. Thus the beam's deflection can be changed actively to reduce load induced displacements and achieve a more homogeneous stress distribution. In this work, a continuous model of the integrated fluidic actuator is formulated by means of a partial differential equation, based on the Euler-Bernoulli beam theory. The right hand side of the equation is realized using spatial characteristics in combination with time-dependent inputs. For this actuator, a control law is derived based on the equations of motion with the aim of controlling the deflection curve or the boundary forces and torques. We show that the derived model can also be used to find optimal actuator configurations in terms of geometry and position of the integrated pressure chambers [2]. Furthermore, both the controller design and actuator design problem can be combined in a holistic approach. The controller's effectiveness and the systems performance are shown by means of numerical results. [1] W. Sobek and P. Teuffel, "Adaptive systems in architecture and structural engineering," Proceedings of SPIE, vol. 4330, 2001, pp. 36–45. [2] M. Heidingsfeld, P. Rapp, M. Böhm, and O. Sawodny, "Gramian-based actuator placement with spillover reduction for active damping of adaptive structures," Proceedings of the 2017 IEEE/ASME International Conference on Advanced Intelligent Mechatronics (AIM 2017), 2017.

High Reynolds Aerothermal Simulations and Reduced Basis in Feel++

Jean-Baptiste Wahl^{*}, Romain Hild^{**}, Christophe Prud'homme^{***}, Vincent Chabannes^{****}

^{*}UNISTRA, ^{**}UNISTRA, ^{***}UNISTRA, ^{****}UNISTRA

ABSTRACT

We present in this talk our work on model order reduction for aero-thermal simulations. The model involves the resolution of coupled non-linear parametrized partial differential equations in which affine decomposition is not obtained. We consider the coupling between the incompressible Navier-Stokes equations and an advection diffusion equation for the temperature. Since the physical parameters induce high Reynolds and Peclet numbers, we have to introduce stabilisation operators in the discrete formulation in order to deal with the well known numerical stability issue. The chosen stabilization, applied to both fluid and heat equations, is the usual Streamline-Upwind/Petrov-Galerkin (SUPG). This method often produces non physical undershoots or overshoots in the edge of discontinuities, which can be critical. To tackle this discontinuity problem, we add in our model a new operator, known in the literature as shock capturing method. This new operator is non-linear and adds artificial diffusivity in the region of the discontinuities in order to treat under/overshoots. Although this method is particularly efficient, it induces a new difficulty, because the system becomes fully non-linear. We present in this talk our order reduction strategy for this model, based on Reduced Basis Method (RBM). In order to recover an affine decomposition for this complex model, we implemented a discrete variation of the Empirical Interpolation Method (EIM) which is a discrete version of the original EIM. This variant allows to build an approximated affine decomposition for complex operators such as in the case of SUPG. We also use this method for the non-linear operators induced by the shock capturing method. The construction of an EIM basis for non-linear operators, involves a potentially huge number of non-linear FEM resolutions - depending on the size of the sampling. Even if this basis is built during an offline phase, we usually cannot afford such expensive computational cost. We took advantage of the recent development of the Simultaneous EIM Reduced basis algorithm (SER) to tackle this issue. Enjoying the efficiency offered by reduced basis approximation, this method provides a huge computational gain and can require as little as $N+1$ finite element solves where N is the dimension of the RB approximation. As an illustration we present an application of a cooling system of a printed circuit board with different heat sources. The model is parametrized with different physical and geometrical parameters. This work has been funded by the ANR project CHORUS.

MATHEMATICAL AND COMPUTATIONAL MODELING FOR STUDYING THE VIBRATION OF A BEAM WITH MODIFIED STIFFNESS

ALEXANDRE DE M. WAHRHAFTIG*, AND THIAGO B. GROBA†

*Federal University of Bahia (UFBA), Polytechnic School, Department of Construction and Structures, Rua Aristides Novis, N° 02, 5° andar, Federação, Salvador – BA, Brazil, CEP: 40210-630.
e-mail: alixa@ufba.br

†Federal University of Bahia (UFBA), Polytechnic School, Department of Mechanical Engineering, Rua Aristides Novis, N° 02, 5° andar, Federação, Salvador – BA, Brazil, CEP: 40210-630.
e-mail: tbgroba@gmail.com

Key Words: Mathematical Analysis, Computational Modeling, Modified Stiffness, Vibration, Support of Machine.

Abstract: Vibration analysis is of extreme importance in industrial projects involving rotating machines and their supports. Vibration is an effect that reduces the accuracy of assembly systems, results in loss of production quality, increases the need for maintenance, generates excessive noise, as well as putting the health and safety of workers at risk. Almost all industrial divisions are subject to this problem. The dynamic characteristics of structures are known to depend on their stiffness and mass; these are key parameters in determining natural frequencies and modes of vibration. However, the initial stiffness of a structural system, calculated in its unloaded state, can be affected once loading forces are applied; this constitutes the so-called geometric stiffness. Mathematical analysis and computational modeling were performed to evaluate the influence of geometric stiffness on the fundamental frequency of a support system. The former provides a practical and efficient equation for calculating the altered system frequency. The latter allows the inclusion of elements that make it a sophisticated instrument in the search for solutions, thereby increasing the capacity of analysis. The mathematical analysis utilizes a model based on the Rayleigh method, which was developed to represent a beam with simple supports designed to function during periodic excitation. In this case, a compressive force reproduces the effects of a horizontal load, which alters the stiffness and consequently the natural vibrational frequency of the structure. Computational modeling, in turn, is constructed at different hierarchical levels using the finite element method. As the hierarchy of the models increases, more details can be incorporated, approaching the physical problem at ever higher levels of fidelity and with the possibility of incorporating structural components. This would not be possible in the most basic models. The results point to a close approximation between the mathematical solution and the various levels of computational modeling, with differences of less than 2%.

1. INTRODUCTION

Dynamic characteristics of a structure essentially depend on its stiffness and mass. Through these two elements, the natural frequencies and modes of vibration of the system are determined. However, the initial stiffness of a structure, as demonstrated in the unloaded state, is affected by the presence of loads, producing the so-called geometric stiffness (see ^{[1]-[6]}). This is the case for compressive loads. Brought to its limit, this decrease may lead to system instability.

Machine bases are an economically and strategically vital subset of national industry. They are subject to vibrations induced by the supported equipment. These vibrations can affect the safety of the structure and generate effects harmful to the equipment and detrimental to the quality of the product manufactured. They can also make the work environment unsafe. Moreover, the value of equipment commonly exceeds the value of support structures, both in terms of replacement costs, as well as due to incurred costs of downtime when operations must be suspended.

In particular, the model that was analyzed in this work represents a machine base composed of a steel pinned-roller beam simulating a rotary machine support. The presence of a normal compression force acting on the structural system decreases the stiffness of the beam and consequently its natural frequencies of vibration; this can lead to unexpected resonance regimes depending on the engine operating frequency. For this reason, the effects of loading on the stiffness of a beam as support were studied numerically by an exact mathematical solution and computational modeling.

2. MATHEMATICAL SOLUTION

From a dynamics point of view, a beam is a continuous system with infinite degrees of freedom. In many cases, a practical way of studying the beam motion is to associate it with a system possessing a single degree of freedom (SDOF). To do this, a certain function is assumed to ideally reproduce the desired form of vibration to study by applying it to the generalized coordinate, which is conveniently chosen to represent the oscillatory movement amplitude.

Thus, after deliberate study, the frequency can be found by equating the maximum strain energy developed during the motion with the maximum kinetic energy. The use of a function as previously mentioned was presented by Rayleigh^[7] in 1877 for studying vibration in mechanical systems. The concept behind this method is the conservation of energy principle, which can be applied not only to systems with a finite number of degrees of freedom but also to continuous systems for determining the fundamental period of vibration.

Consider a rotary machine mounted on a beam subjected to a compressive force. It is known that such forces affect the geometric stiffness and thus the values of the undamped free vibration frequencies. Designing the structure to possess frequencies that exceed the machine's service speed rotation may make it vulnerable to potentially dangerous resonance conditions due to geometric stiffness from frequency changes.

Assume Bernoulli-Euler beam theory for the following system (Figure 1). A support beam of length L and inertia I functions as the base to an engine E_g , which consists of linear elastic material that is represented by the modulus of elasticity E . A normal force of compression

reproduces the force that changes the stiffness and consequently the natural frequency of vibration of the structure f_n . The eccentricity between the engine axis and the part is initially ignored. The vertical displacement of the central joint is the generalized coordinate of the system. By using the Rayleigh method, the undamped vibration frequency in its first mode is obtained.

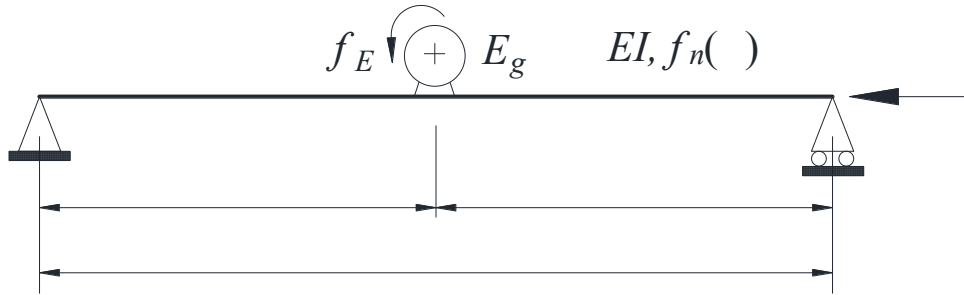


Figure 1. Beam as the base of an engine.

Consider also that the vertical displacement of a generic section of the beam in Figure 2 is given by

$$v(x, t) = \phi(x) (t), \quad (1)$$

in which $\phi(x)$ is a shape function that attempts to define the boundary conditions in the supports and value 1 in the central section of the beam, whose displacement with time is (t) .

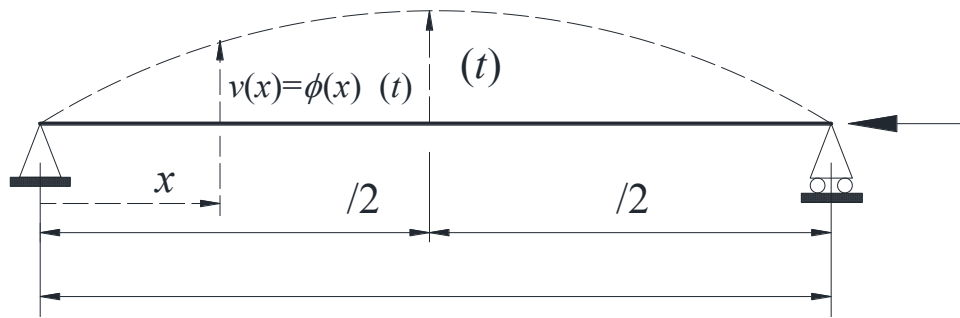


Figure 2. SDOF mathematical model of vibration.

In this case, one adopts the shape function given by Eq. (2):

$$\phi(x) = \sin\left(\frac{\pi x}{L}\right), \quad (2)$$

which is the exact solution of the problem without the load. A prime mark will denote a derivative of the function in relation to x .

Applying the Rayleigh method, one has the conventional bending stiffness, K_0 , as a function of the material elasticity and the geometry of the cross, which is equivalent to

$$K_0 = \int_0^L EI (\phi'')^2 dx, \quad (3)$$

where EI is the known flexural bending, which is represented by multiplication of the material modulus of elasticity with the inertia of the section in relation to the the vertical vibration mode. In turn, the geometric stiffness, K_g , as a function of the normal force of compression is equivalent to:

$$K_g = \int_0^L (\phi')^2 dx. \quad (4)$$

The total generalized mass of the system is found by calculating

$$M = M_c + M_v \quad (5)$$

where M_c is the concentrated mass at the middle span and M_v is the mass coming from the beam self-weight given by

$$M_v = \int_0^L m (\phi(x))^2 dx, \quad (6)$$

in which m represents the mass per length unit. Finally, the frequency of undamped free vibration (in rad/s) is found by way of Eq. (7):

$$\omega(\lambda) = \sqrt{\frac{K(\lambda)}{M}}. \quad (7)$$

Considering the total beam stiffness as a function of λ given by

$$K(\lambda) = K_0 - K_g(\lambda), \quad (8)$$

the free undamped frequency of vibration of the 1st mode is found, in Hertz, admitting the compressive force as positive, by:

$$f_n(\lambda) = \frac{\omega(\lambda)}{2\pi} = \frac{1}{2} \left[\frac{\pi^2 EI - \lambda^2}{3(m + 2Mc)} \right]^{\frac{1}{2}}. \quad (9)$$

The effects of geometric stiffness can be realized by considering a simple supported beam with theoretical length L equal to 2 m and cross-section as defined in Figure 3, where t is the thickness of the wall and h is the external side dimension of the square section adopted. The adopted dimensions of the beam are: $h = 50$ mm, $t = 1.5$ mm.

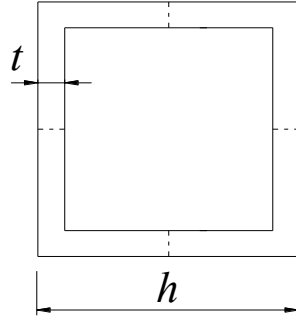


Figure 3. Adopted cross-section.

When considering Figure 4, it is observed that the presence of the compressive force truly reduces the beam stiffness and consequently its natural frequencies f_n (). If the engine operating frequency intercepts f_n (), it could lead to unexpected and potentially dangerous resonance regimes during operation.

The natural frequency of the beam has been calculated by using Eq. (9), taking a density of the material of 7850 kg/m^3 , a lumped mass at the central position of the span (engine mass) equal to 4.6 kg , and a modulus of elasticity of 205 GPa .

3. COMPUTATIONAL MODELING

Concerning the mathematical procedure, the formulation corresponding to the finite element method (FEM) is performed by finding the eigenvalues and eigenvectors by Eq.(10)

$$\{[K] - \omega^2 [M]\} \Phi = 0, \quad (10)$$

where $[M]$ is the mass matrix, and $[K]$ is the stiffness matrix, which for the geometric non-linear case includes the parcel of the geometric stiffness, configuring a similar formulation to that described in Eq.(8). The matrices in Eq.(10) for the different types of modeling can be found in Cook^[8].

The computational modeling as exemplified in Figure 4 was constructed in ANSYS Academic Version at different hierarchical levels of complexity with respect to the physics of the problem. Such modeling was based on the modified stiffness of the beam from a previous non-linear static analysis with the inclusion of the geometric stiffness parcel to obtain the total stiffness of the base, as described previously. This means that the stiffness matrix obtained at the end of the static processing was used to calculate the frequency of the first mode of vibration. A Poisson coefficient of 0.3 was added to the data described in the previous item.

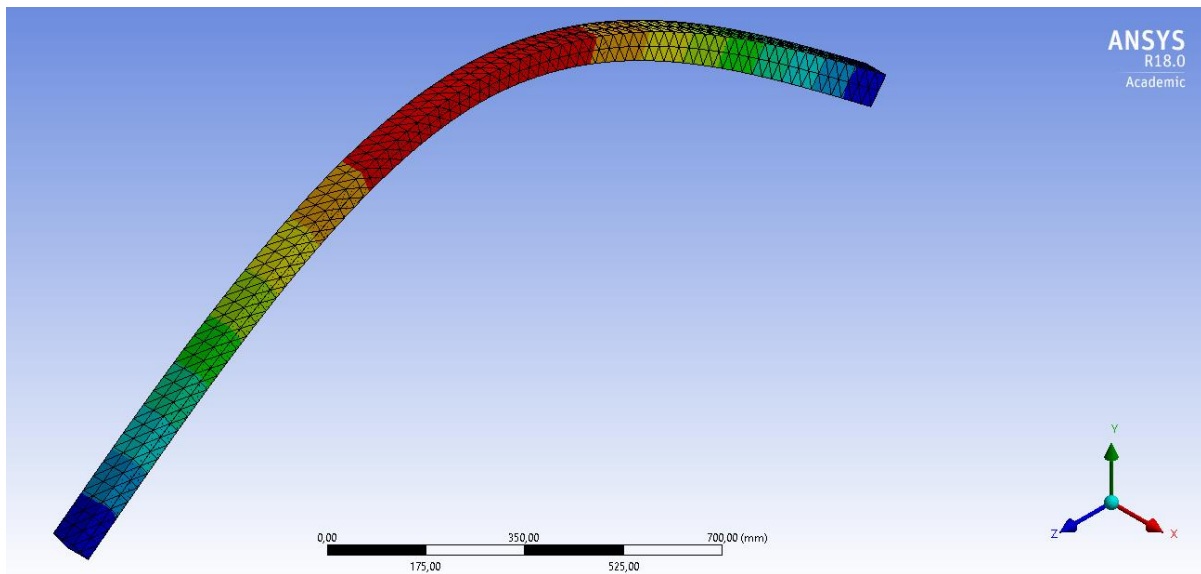


Figure 4. Computational model by FEM.

Three computational models were developed for studying the system at hierarchically increasing levels of complexity with respect to computational modeling: FEM 1D (unidimensional model with frame elements), FEM 2D (two-dimensional model with shell elements) and FEM 3D (tridimensional model with solid elements). The models are differentiated by the computational cost required for the finite element types used and by the possibility of generating more accurate results.

Moreover, as the hierarchy of models advances, more detail can be incorporated to approach the physical problem at ever higher fidelity levels and with the possibility of incorporating different structural components, which in the most basic models would not be possible. The models were elaborated according to the geometry defined for the mathematical simulation. The program was executed for the three hierarchical levels, thus making it possible to compare the results obtained with the analytical result as depicted in Figure 5.

As can be observed, the results generated in the computational modeling are adequate for the mathematical solution presented in Eq.(7), with an average difference of 1.5% between them. It should be noted that the FEM 3D model is the most complete and complex of all the models. For the 3D model, when the force reaches values close to 54 kN (near the collapse) a difference of 11.44% is found. This relates to the non-linear characteristic of the problem due to the internal stress level, which elevates the sensitivity of the model to the discretization used. It should be mentioned that this aspect was studied by Wahrhaftig^[9] who found in a similar context, a difference of up to 21% in the analyses performed (linear and non-linear).

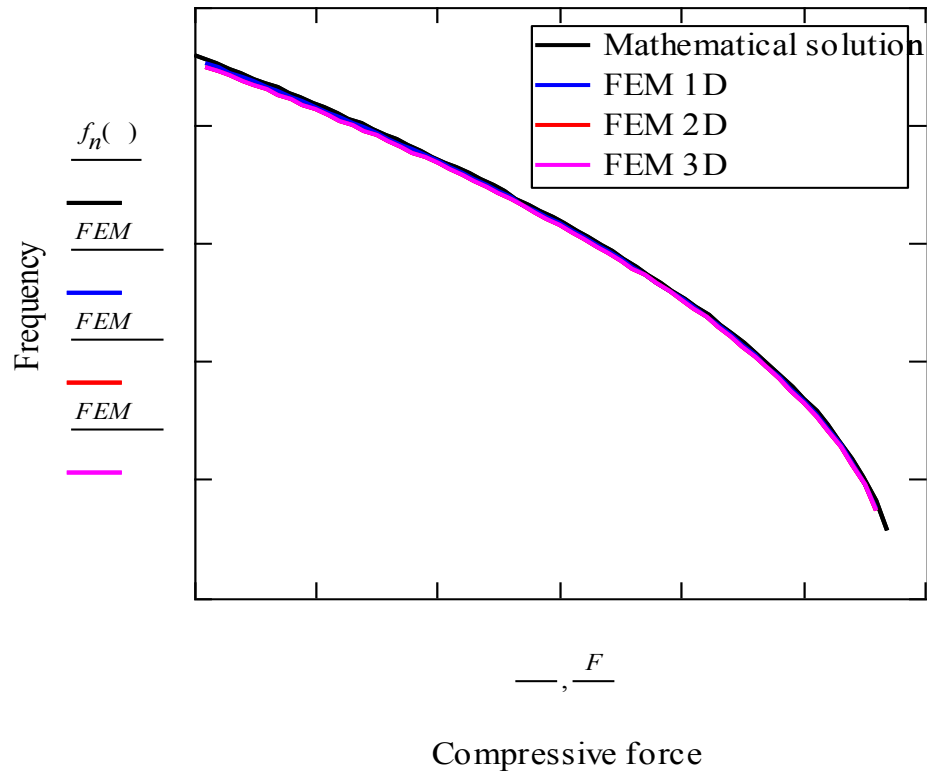


Figure 5. Comparison of results.

4. ACKNOWLEDGEMENT

This work was supported by the National Council of Scientific and Technological Development (CNPq) of Brazil through the Universal Call MCTI/CNPQ/14/2014, process 443044/2014-7.

5. CONCLUSION

- A vibration study of a beam with its stiffness geometrically altered was detailed by theoretical-analytical analysis and numerical-computational models.
- A model of a metallic pinned-roller beam operating under the effect of axial compression loads was elaborated upon to analyze the variation in its fundamental frequency while considering the applied forces.
- The effect on the geometric stiffness which is influenced by the horizontal loading and the corresponding possibility of introducing resonant regimes in the structural support system were demonstrated by calculating their frequencies.
- According to theory, increasing the axial compressive force can induce resonance conditions to manifest.
- In summary, it is possible to affirm that computational modeling yields a good approximation to the mathematical solution developed in this work.

REFERENCES

- [1] Wahrhaftig, A.M.; Brasil, R.M.L.R.F.; Balthazar, J.M. The first frequency of cantilevered bars with geometric effect: a mathematical and experimental evaluation. *J. Braz. Soc. Mech. Sci. & Eng.* (2013) 35:457–467.
- [2] Wahrhaftig, A.M.; Brasil, R.M.L.R.F. Vibration analysis of mobile phone mast system by Rayleigh method, *Appl. Math. Model.* (2016) 42:330–345.
- [3] Wahrhaftig, A.M.; Nascimento, L.S.M.S.C.; Brasil, R.M.L.R.F. Resonance evaluation with geometric stiffness and creep of slender beam of reinforced concrete. In *proceedings of the 11th European Conference on Computational Methods in Structural Dynamics and Earthquake Engineering (MCMSE)* (2017) 15–17 June, Rhodes Island, Greece.
- [4] Wahrhaftig, A.M.; Brasil, R.M.L.R.F. Initial undamped resonant frequency of slender structures considering nonlinear geometric effects: the case of a 60.8 m-high mobile phone mast. *J. Braz. Soc. Mech. Sci. & Eng.* (2017) 39:725–735.
- [5] Wahrhaftig, A.M. Analysis of the first modal shape using two case studies. *Int. J. Comput. Methods* (2017) 15:1840019–1840019-14.
- [6] Wahrhaftig, A.M.; Brasil, R.M.L.R.F.; César, S.F. Creep in the fundamental frequency and stability of a slender wooden column of composite section. *Rev. Árvore* (2016) 40:1119–1130.
- [7] Rayleigh, L. *Theory of sound* (two volumes), 2nd ed., Dover Publications, 1945 reissue, (1877).
- [8] Cook, R. D.; Malkus, D. S.; Plesha, M. E.; Witt, R. J. *Concepts and applications of finite element analysis*, 4th ed., Wiley, (2001).
- [9] Wahrhaftig, A.M. The technic of discretization in compressed bars, *Congress on Numerical Methods in Engineering* (2013) 25–28 June, Bilbao, Spain.

Free-form Optimization Method for Controlling Transient Response of a Linear Elastic Structure under Dynamic Loadings

Mamoru Wakasa*, Masatoshi Shimoda**

*Graduate School of Toyota Technological Institute, **Toyota Technological Institute Dept. of Advanced School
Science and Technology

ABSTRACT

Many natural vibration and frequency response problems were solved under the assumption of the harmonic vibration and the optimization methods for these two problems have been studied in many previous works because of the easy handling and conventionality. On the contrary, we propose a non-parametric shape optimization method to control the transient response of a linear elastic structure in this study. The estimation of the real response under the transient load is essential in the design of vehicles or structure under seismic loadings, where the loadings act dynamically, non-harmonically. We consider the viscous damping and the transient forced loads or the impulse loads are applied. In the development of the non-parametric shape optimization method, the free-form optimization method with H1 gradient method, is applied to the transient response problem. The design objective is to minimize the dynamic compliance, which is defined as the time integration of the each discretized time's compliance or to control the amplitude at arbitrary domains and times to the desired values. In these two optimization problems, the linear transient response is directly solved without converting the equivalent static loads method, which is often employed in the time-dependent non-linear optimization problems. The optimum design problems are formulated as a distributed-parameter optimization problem and the sensitivity functions for both optimization problems are theoretically derived using the material derivative and the adjoint methods. The derived sensitivity function is applied to the H1 gradient method to determine the optimal shape variation. With this method we can obtain the optimal free-form shape that reduces the objective functions while maintaining the surface smoothness. The some optimum design examples are demonstrated to show the effectiveness of the proposed method and the results are discussed.

Adjoint Based Data Assimilation for Quantification of Dynamic Mechanical Behavior of the Heart

Samuel Wall^{*}, Henrik Finsberg^{**}, Marie Rognes^{***}, Gabriel Balaban^{****}, Lik Chuan Lee^{*****}

^{*}Simula Research Laboratory, ^{**}Simula Research Laboratory, ^{***}Simula Research Laboratory, ^{****}Kings College, ^{*****}Michigan State University

ABSTRACT

Accurate biophysical models offer promise for improved understanding of cardiac functionality. However, the myocardium is a complex dynamic material, and while detailed models and constitutive laws describe its passive and active behaviour, fitting these models meaningfully to actual data is greatly complicated by the large number, and interaction of, required parameters. Although numerous techniques, from trial and error to advanced optimization, can be used to fit data, challenges still exist, often due to the computational requirements to search for optima. This is particularly challenging when considering real observations, where heterogeneous noisy data sets are the norm, and time constraints are present. Here we discuss the use of adjoint methods as an attractive, efficient means to rapidly assimilate large data sets into personalized models of cardiac mechanics. These optimization techniques allow us to fit models at a cost that does not significantly depend upon the numbers of parameters to be fit, and thereby provide an excellent means to assimilate high dimensional parameter spaces at a relatively low computational cost. These methods are enabled by the new generation of software tools that automatically create physical models and derive adjoint equations for problems of interest.[1,2] We describe the methodology, and show the utility of this method in a range of clinically driven applications.[2,3] In all these cases, we use an efficient pipeline to create cardiac models directly from medical imaging and applied adjoint based PDE constrained optimization to assimilate dynamic geometric information into fit models. These rapidly produced parameterized mechanical models demonstrate differences in active and passive properties of the myocardium in disease states, which may have diagnostic use as biomarkers. Reducing the computational cost of accurate models is a key step towards translating into greater utility, both for basic science and for eventual clinical adoption. We show that adjoint based PDE constrained optimization methods, and in particular their applicability for data assimilation, offer the means to accelerate the use of biophysical models. [1] Logg, A. et al. The FEniCS book (Vol. 84), 2012 [2] Farrell PE et al. Automated derivation of the adjoint of high-level transient finite element programs. SIAM Journal on Scientific Computing, 2013. [3] Balaban G et al. High resolution data assimilation of cardiac mechanics. International journal for numerical methods in biomedical engineering, 2017. [4] Finsberg et al. Estimating cardiac contraction through high resolution data assimilation of a personalized mechanical model. Journal of Computational Science, 2017.

An Improved Contact Method for Multi-material Eulerian Hydrocodes

Kenneth Walls*, David Littlefield**

*The University of Alabama at Birmingham, **The University of Alabama at Birmingham

ABSTRACT

Realistic and accurate modeling of contact for problems involving large deformations and severe distortions presents a host of computational challenges. Due to their natural description of surfaces, Lagrangian finite element methods are traditionally used for problems involving sliding contact. However, problems such as those involving ballistic penetrations, blast-structure interactions, and vehicular crash dynamics, can result in elements developing large aspect ratios, twisting, or even inverting. For this reason, Eulerian, and by extension Arbitrary Lagrangian-Eulerian (ALE), methods have become popular. However, additional complexities arise when these methods permit multiple materials to occupy a single finite element. Multi-material Eulerian formulations in computational structural mechanics are traditionally approached using mixed-element thermodynamic and constitutive models. These traditional approaches treat discontinuous pressure and stress fields that exist in elements with material interfaces by using a single approximated pressure and stress field. However, this approximation often has little basis in the physics taking place at the contact boundary and can easily lead to unphysical behavior. This work presents a significant departure from traditional Eulerian contact models by solving the conservation equations separately for each material and then imposing inequality constraints associated with contact to the solutions for each material with the appropriate tractions included. The advantages of this method have been demonstrated with several computational examples. This work concludes by drawing a comparison between the method put forth in this work and traditional treatment of multi-material contact in Eulerian methods.

Numerical Study of Effect of KC Number on the Vortex-Induced Vibration of a Flexible Riser in the Oscillatory Flow

Decheng Wan^{*}, Yuqi Zhang^{**}

^{*}Shanghai Jiao Tong University, ^{**}Shanghai Jiao Tong University

ABSTRACT

In offshore oil and gas drilling, relative oscillatory flow is generated between the platform and the riser by the effect of wind, waves and currents. The riser in the deep-water not only bears the weight and the top tension, but its amplitude increases obviously when the vortex shedding frequency is close to the natural frequency of the riser which does harm to the safety of the platform. So the study of Vortex-induced vibration (VIV) of an isolated riser in relative oscillatory flow is necessary to prevent the fatigue damage of the platform structure. In this paper, numerical simulations are carried out by our in-house CFD code viv-FOAM-SJTU, which is developed based on the open source code OpenFOAM. The strip theory and the Reynolds Averaged Navier-Stokes(RANS) equations are used to analyze the flow field. The Bernoulli-Euler beam theory with the FEM method is used to obtain the structural dynamics response. The oscillatory flow is simulated by forced excitation added at both ends. To achieve the fluid-structure interaction, interpolation module is developed to transmit data between the fluid and structure model. In this paper, numerical simulation of a flexible riser is carried out at first. Results are compared with the model test to verify the validity of the solver. Then, cases with different motion amplitudes and the same KC number are presented. Diameters of the cylinder change to assure the same KC number. Mechanism of the vibration are articulated through modal decomposition and wavelet transformation. Finally, cases with different KC number with the same motion amplitudes are simulated to explain the effect of KC number in the VIV of the riser in the oscillatory flow. Typical characteristics of the vibration are observed including the modal transition and the "build-up-lock-in-die-out" process.

A Matlab Tool for Scalable Uncertainty Evaluation and Its Use in Optimal Control

Yan Wan^{*}, Junfei Xie^{**}, Kevin Mills^{***}, James Filliben^{****}, Yu Lei^{*****}, Zongli Lin^{*****}, Frank Lewis^{*****}

^{*}University of Texas at Arlington, ^{**}Texas A&M; University - Corpus Christi, ^{***}National Institute of Standards and Technology, ^{****}National Institute of Standards and Technology, ^{*****}University of Texas at Arlington, ^{*****}University of Virginia, ^{*****}University of Texas at Arlington

ABSTRACT

Dynamical systems often operate in uncertain environments, which modulate the systems' dynamics and complicate the system analysis and control tasks. These uncertainties often possess the following features: 1) some of their statistical information can be obtained from environmental forecasting tools, 2) they are of high dimensionality, and 3) they cannot be represented by simple Gaussian noises, and 4) they modulate system dynamics in a nonlinear fashion. A critical step in the optimal control of these dynamical systems involves the evaluation of system output statistics under such uncertainties. Monte Carlo simulation and its variants have been used. However, they run into high computational load due to the nonlinear modulation of high dimensional uncertainties. We develop a Matlab tool for uncertainty evaluation, based on a method that we recently developed, called M-PCM-OFFD. As we have proven in [1,2], M-PCM-OFFD integrates the Multivariate Probabilistic Collocation Method (PCM) and Orthogonal Fractional Factorial Design (OFFD) procedures to achieve an accurate, robust, and scalable uncertainty evaluation performance. The Matlab tool takes the number of uncertain parameters, their statistical information, and the simulation model as inputs, and automatically generates a low-order approximated simulation model and estimated output statistics. In the presentation, we will illustrate the principles of the M-PCM-OFFD method, and then describe how the Matlab tool operates. We will also demonstrate how this tool can be used to solve practical optimal control and reinforcement-learning based control problems [3]. The tool and its supporting methodology contribute to the field by providing additional performance insights of OFFD and by, for the first time, bringing OFFD online to solve automatically uncertainty evaluation and optimal control problems. References: [1] J. Xie, Y. Wan, Y. Zhou, K. Mills, J. J. Filliben, Y. Lei, and Z. Lin, "Effective and Scalable Uncertainty Evaluation for Large-Scale Complex System Applications," in Proceedings of the 2014 Winter Simulation Conference, Savannah, GA, December 7-10, 2014. Journal version under review. [2] J. Xie, Y. Wan, Y. Zhou, K. Mills, J. J. Filliben, and Y. Lei, Effective Uncertainty Evaluation in Large-Scale Systems (book chapter), Principles of Cyber-Physical Systems, edited by S. Roy and S. Das, Cambridge University Press, in press, pp. 1-25, 2016. [3] J. Xie, K. Mills, J. J. Filliben, F. L. Lewis, "A Scalable Sampling Method to High-dimensional Uncertainties for Optimal and Reinforcement Learning-based Controls," IEEE Control Systems Letters, Vol. 1, No. 1, pp. 98-103, July 2017.

Mapped Finite Element Method for the Phase Field Approach to Fracture

Yang Wan^{*}, Yongxing Shen^{**}

^{*}University of Michigan-Shanghai Jiao Tong University Joint Institute, Shanghai Jiao Tong University, ^{**}University of Michigan-Shanghai Jiao Tong University Joint Institute, Shanghai Jiao Tong University

ABSTRACT

The phase field method to fracture has attracted widespread attention due to its ability to simulate crack initiation, propagation, merging and branching without extra criteria. However, the singularity around the crack tip deteriorates the convergence property of the method, just like the case of a discrete crack method. In this work, we apply the mapped finite element method proposed by Chiaramonte et al. [International Journal for Numerical Methods in Engineering, 111 (9) (2017) 864-900] to the phase field approach to fracture to attempt to recover the convergence property. The method is based on approximating a much smoother function in a parameterized domain by mapping the solution around the singularity. This reparameterized solution can be well approximated by the finite element method. With a parameter appropriately chosen, the finite element method can achieve an optimal convergence rate for any given order of interpolating polynomials. As the phase field evolves, our method is able to update the center of mapping, presumably the location of the singularity, allowing simulating crack propagation.

A Smoothed Implicit Material Point Method for Geotechnical Applications

Bin Wang^{*}, Quan Jiang^{**}, Xia-Ting Feng^{***}

^{*}Dr., ^{**}Dr., ^{***}Dr.

ABSTRACT

This paper presents a novel implicit material point method (MPM), where its formulations and numerical evaluations are detailed. On basis of the partition of unity (PU) concept, the shape functions from the classical finite element method (FEM) are used to construct the PU, while a radial polynomial basis function is employed to construct the nodal approximation. The new formulation synergizes the individual strengths of the traditional FEM and MPM. The inherent stress oscillations in MPM, which is caused by the discontinuities of the shape function gradients between the elements, is greatly improved. Several numerical examples are presented in the paper, including the 1-D bar vibration, 2-D cantilever beam, etc., with the results demonstrating that the proposed smoothed implicit material point method can achieve significantly better accuracy and higher convergence rate, as opposed to the traditional MPM.

A Multiscale Method for Analyzing Progressive Damage of 3D Braided Composite Structure by Using FFT

Bing Wang^{*}, Guodong Fang^{**}, Shuo Liu^{***}, Jun Liang^{****}

^{*}Harbin Institute of Technology, ^{**}Harbin Institute of Technology, ^{***}Harbin Institute of Technology, ^{****}Beijing Institute of Technology

ABSTRACT

Abstract: A more efficient multiscale coupling method is developed to study the progressive damage behavior of three dimensional (3D) braided composite structure. In the meso-scale, the fast Fourier transformation (FFT)-based method combining with variational principle is used to overcome the poor convergence for composites with large jumps of material properties. In the macro-scale, the mechanical response of the braided composites is analyzed by using finite element method, in which the stress and stiffness information of each material point can be transformed from the meso-scale results. It is verified that the predicted strength and dominated failure modes of the braided composites structure obtained by the proposed method combining with anisotropic stiffness degradation model are in good agreement with the experimental results. Meanwhile, the high computation efficiency is attractive for large complex structure taking into consideration the nonlinear mechanic behavior. Keywords: Multiscale analysis; Fast Fourier Transforms; Braided composites; Computation efficiency

Theory and Application of Assumed Stress Quasi-conforming Method

Changsheng Wang^{*}, Xiangkui Zhang^{**}, Ping Hu^{***}

^{*}Dalian University of Technology, ^{**}Dalian University of Technology, ^{***}Dalian University of Technology

ABSTRACT

Abstract: Quasi-conforming(QC) analysis is a flexible and characteristic finite element method, and the basic idea of the QC method is that the strain-displacement equations are weakened as well as the equilibrium equations. In the QC technique, the element strain fields are approximated using polynomials and integrated using interpolation functions. The assumed stress QC method starts from polynomials approximation of stress and the stress function matrix is chosen as weighted test function to weaken the strain-displacement equations. Unlike the hybrid Trefftz finite element method, the initial approximation of stress is flexible, which can be derived from analytical solutions of equilibrium equations or Taylor expansion. Appropriate approximation of initial stress will make the element formulation simple and concise, and no inner-field functions are needed for the strain integration. The assumed stress QC method has been used for plane stress analysis, couple stress analysis, static and free vibration of Reissner-Mindlin/laminated plates. The constructed elements exhibit advantages of QC technique, free from locking phenomenon and zero-energy modes and insensitive to mesh distortion. The characteristic of boundary integration makes the constructed quadrilateral QC elements can be used to mesh shape degenerates into triangle or concave quadrangle. The method can be generalized for the analysis of trimmed CAD surface in isogeometric analysis(IGA), which also provides an easy way to apply Dirichlet boundary conditions and incorporates IGA with existing finite element codes. Keywords: Quasi-conforming; assumed stress; boundary integration; mesh distortion; isogeometric analysis Reference [1]. Wang CS*, Zhang XK, Hu P. New formulation of quasi-conforming method: A simple membrane element for analysis of planar problems. *European Journal of Mechanics A/Solids*, 2016, 60:122-133. [2]. Wang CS*, Zhang XK, Hu P. A 4-node quasi-conforming quadrilateral element for couple stress theory immune to distorted mesh. *Computers & Structures*, 2016, 175: 52-64. [3]. Wang CS, Wang X, Zhang XK*, Hu P. Assumed stress quasi-conforming technique for static and free vibration analysis of Reissner-Mindlin plates. *International Journal for Numerical Methods in Engineering*, 112: 303-337, 2017.

Sizing and Shape Optimization for Peak Structural Responses under Long-term Processes of Stationary Stochastic Loads

Chien-Kai Wang*

*Tamkang University

ABSTRACT

Structural optimization has become a widely used tool to construct efficient structures for various applications due to its capability of providing design freedom and promise for saving material costs. Current optimization methods are usually utilized for optimal structural systems subjected to design constraints under certain definite loading distributions. However, engineering structures experience long-term processes of stationary stochastic loads, owing to various physical environments. In this paper, we develop a novel methodology of structural optimization for peak system responses during long-term processes of stationary stochastic loads. The proposed methodology provides an algorithm for generating structures with the optimal sizes and shapes for constraints on their extreme responses under environmental loads of various statistical features. The computational results confirm that material distribution of optimized structures for peak response constraints highly depends on correlated levels of stationary stochastic loads applied on different spots of the structures under long-term processes. Furthermore, conventional sizing and shape optimization of structures in statics for displacement constraints are also compared with the aforementioned optimized material distribution for peak response constraints under correlated environmental loads. Consequently, the developed methodology provides a powerful tool to investigate efficient structural designs under long-term load processes for fundamental engineering structures and related mechanics researches.

Heaviside Projection Based Aggregation in Stress-constrained Topology Optimization

Cunfu Wang^{*}, Xiaoping Qian^{**}

^{*}University of Wisconsin-Madison, ^{**}University of Wisconsin-Madison

ABSTRACT

The presentation introduces an approach to stress constrained topology optimization through Heaviside projection based constraint aggregation. The von Mises yield criterion is adopted to evaluate whether the material fails or not. Our main concern here is on developing a new way to enforce the element-wise local stress constraints. We apply the Heaviside function as an indicator to show the state of the material (safe or failed). If the stress exceeds the yield limit, the indicator function is marked as 1; otherwise 0. Then by integrating the indicator function over the whole design domain and normalizing over the total volume, we obtain the integral of Heaviside projection, which effectively means the volume fraction of the yielded material. As our objective is to make the stress constraint satisfied at every material point, all we need to do is to push the yielded material away, which can be implemented by constraining the Heaviside projection based integral (HPI) to be 0. Based on such Heaviside aggregation, a single global aggregated constraint is constructed. In practice, a smoothed Heaviside function is used as the stress state indicator for differentiability, and a small positive value epsilon rather than 0 is applied to bound the integral. The selection of epsilon is the key to successful enforcement of the stress constraint. If epsilon is too large, the global constraint would not be tight enough to remove the yielded material volume; if epsilon is too small, an over-conservative design would be obtained. In order to get an appropriate threshold epsilon, an adaptive scheme based on the gap between the maximum stress and the prescribed limit is also proposed. As the effectiveness of the global constraint is insensitive to the number of local constraints, this approach is applicable to large scale problems. Our 2D and 3D numerical experiments demonstrate that the single Heaviside aggregated stress constraint can efficiently control the local stress level. Compared to the traditional approaches based on the Kreisselmeier-Steihauser and p-norm aggregations, the Heaviside aggregation based single constraint can substantially reduce computational cost on sensitivity analysis. These advantages make the proposed approach to be applicable to large scale problems.

Topology Optimization of Continuum Structures with Load Position Uncertainty

Dong Wang*, Weifeng Gao**

*Northwestern Polytechnical University, 710072, P.R. China, **Northwestern Polytechnical University, 710072, P.R. China

ABSTRACT

In the structural design process, not only the structural parameters, such as, the geometry dimensions, material characteristics, boundary constraints, but also the external loads imposed on the structure often have some degrees of uncertainties due to the complicated loading environments. Therefore, in the optimal design of the structural configuration, these uncertainties should be involved properly so as to achieve the efficient load path for the external loads transferring toward the boundaries by allocating the given material more rationally, or for an improvement of the structural performance significantly. In this paper, the topology optimization of a continuum structure with the application position uncertainty of an external force is performed to gain the reliable load paths for transferring the load. Firstly, the position uncertainty of the external load is indicated with the interval variable in accordance with the non-probabilistic approach. Then on the basis of the design sensitivity analysis with respect to the load position movement [1], the structural compliance is expressed as the second-order Taylor series expansion with regard to the position disturbance of the external load. Furthermore, for the computational efficiency, the sensitivities of the structural compliance to the topology design variables are evaluated upon the compliance approximation. Finally, based on the SIMP model and the optimality criteria method [2], the compliance minimization problem is solved readily with consideration of the position uncertainty of the external load, and the numerical results are evaluated in detail against those obtained traditionally under the deterministic load position. Comparisons reveal that the topology optimal designs are obviously different with or without consideration of the load position uncertainty. It will be shown that the obtained topology optimization under consideration is of higher robustness to the disturbances of the load application points since new load paths are often created to accommodate the load position uncertainty. 1. Wang D. Sensitivity analysis of structural response to position of external applied load: in plane stress condition. *Structural Multidisciplinary Optimization*, 2014, 50: 605-622 2. Sigmund O. A 99 line topology optimization code written in Matlab. *Structural Multidisciplinary Optimization*, 2001, 21: 120-127.

Isogeometric Enriched Meshfree Analysis

Dongdong Wang^{*}, Hanjie Zhang^{**}, Junchao Wu^{***}

^{*}Department of Civil Engineering, Xiamen University, Xiamen, Fujian 361005, China, ^{**}Department of Civil Engineering, Xiamen University, Xiamen, Fujian 361005, China, ^{***}Department of Civil Engineering, Xiamen University, Xiamen, Fujian 361005, China

ABSTRACT

The B-spline and NURBS basis functions used in isogeometric analysis are naturally convex, which have a variation diminishing property and yield non-negative mass matrices for dynamic analysis. By contrast, the widely used moving least square or reproducing kernel meshfree approximants are non-convex. Thus the construction of convex meshfree approximations is an important recent topic for meshfree methods. The maximum entropy meshfree approximation is a typical convex meshfree approximation, but the extension of this approach to arbitrary order is still an open problem. In this work, the consistency conditions for isogeometric B-spline basis functions and meshfree shape functions are firstly presented in a unified manner. Thus, an isogeometric enriched quasi-convex meshfree method is proposed. The present quasi-convexity of the meshfree approximation is achieved by introducing the mixed reproducing points of isogeometric B-spline basis functions into the meshfree consistency conditions. The resulting meshfree shape functions have an identical form as the standard reproducing kernel meshfree shape functions, while the negative portions of the shape functions are significantly reduced. Consequently, generalization of the proposed formulation to arbitrary higher order basis functions is trivial. It is shown that this isogeometric enriched quasi-convex meshfree method yields better accuracy compared with the conventional meshfree method. The efficacy of the proposed method is demonstrated through several benchmark numerical examples. Key words: Isogeometric analysis; Meshfree method; Consistency condition; Quasi-convex approximation; Mixed reproducing points Acknowledgements: The support of this work by the National Natural Science Foundation of China (11772280, 11472233) and the Natural Science Foundation of Fujian Province of China (2014J06001) is gratefully acknowledged.

Electro-mechanical Characteristics Analysis of Influence Bone Remodeling

Fan Wang*

*Jinan University, Guangzhou, China

ABSTRACT

The Main factors affecting bone remodeling are bone stress, fluid pressure, fluid shear stress and the streaming potential. In this paper fluid pressure distribution in the bone, fluid shear stress and streaming potential in bone canalicules were studied when bone subjected to dynamic loads. The pore pressure and velocity solutions are obtained to examine the fluid transport behavior and pressure distribution in a loaded osteon on four different exterior surface cases.

The Atomistic Mechanism of Beta Relaxation Processes in Cu₅₀Zr₅₀ Metallic Glasses

Fei Wang^{*}, Shuo Li^{**}, Ping Huang^{***}

^{*}State Key Laboratory for Strength and Vibration of Mechanical Structures, School of Aerospace, Xi'an Jiaotong University, ^{**}State Key Laboratory for Strength and Vibration of Mechanical Structures, School of Aerospace, Xi'an Jiaotong University, ^{***}State Key Laboratory for Mechanical Behavior of Material, School of Materials Science and Engineering, Xi'an Jiaotong University

ABSTRACT

It has long been recognized that beta relaxation correlates with numerous mechanical properties of metallic glasses (MGs), while the underlying mechanisms and its structural origin are still under intense debate. In the present study, molecular dynamics simulations were used to examine the beta relaxation of three kinds of atomic structures of Cu₅₀Zr₅₀ MGs, i.e., the materials within and outside of shear band (SB) extracted from the plastically deformed MG, and the as-received MG. Despite their identical compositions, interestingly, the aforementioned MGs exhibit quite different beta relaxation behaviors. Compared to the un-deformed MG with no beta peak, the molecular dynamics simulations results indicated an independent beta peak appeared in the SB like structured specimen, while excess wing corresponding to beta relaxation was observed in the specimen with the deformed non-SB like structure. To the best of the author's knowledge, this is the first time to achieve such dramatic changes of beta relaxation in MGs with identical composition. In addition, the effects of free volume content, shear transformation zone (STZ) size on the quite different beta relaxation behaviors of the three kinds of specimens were characterized. By conducting tensile test via molecular dynamics simulations, the elastic and plastic deformation behaviors corresponding to the various beta relaxations were compared; and furthermore, detailed atomic structural evolution analysis based on the Voronoi polyhedral concept was conducted. The crucial parameters and atomic mechanisms that control the beta relaxation behaviors and mechanical properties of the Cu₅₀Zr₅₀ MGs were suggested and extended discussed. The simulation results presented here provide an in-depth understanding of the structural origin of beta relaxation in metallic glasses and may shed light on the way for synthesizing metallic glasses that could exhibit large tensile plasticity.

Molecular-mechanical Modeling of Fluid Structure at the Solid-fluid Interface and Transport under Nanoconfinement

Gerald Wang^{*}, Nicolas Hadjiconstantinou^{**}

^{*}MIT, ^{**}MIT

ABSTRACT

At the nanoscale, fluids in the vicinity of a solid boundary can arrange in layered structures that exhibit large density inhomogeneities as compared to the bulk fluid (far from the boundary). This effect, which is important for modeling fluid transport at the nanoscale, cannot be described via classical fluid mechanics. In this work, we present several results on mathematical and computational modeling of this layering phenomenon, and in particular the fluid layer directly adjacent to the solid, which we refer to as the first fluid layer. Using Nernst-Planck theory and molecular mechanics arguments we identify a dimensionless group – named the Wall number – that is closely connected with the magnitude of fluid layering at the interface. We also identify and model the relevant lengthscales and density magnitudes of the first fluid layer, such as its distance from the solid boundary, its characteristic width, and its total fluid particle content per unit area, referred to as the areal density. Our modeling results are validated using molecular dynamics simulations for a variety of fluid-solid systems. For the case of dense fluids, we find that the first layer density (defined as the layer areal density divided by its width) scales with the bulk fluid density with a proportionality constant that is only weakly dependent on temperature. Building on these models for interfacial fluid structure, we also present several results connecting fluid layering to anomalous transport under nanoconfinement. In particular, we study the anomalous diffusivity of a fluid confined within a nano-slit. We identify and discuss several key timescales for anomalous diffusive behavior, which are set by the Wall number and the confinement lengthscale. We show that anomalous diffusive behavior of fluid near the solid boundary is due to “dimensional restriction” of this fluid. We demonstrate that the relationship between nanoconfined fluid diffusivity and the confinement lengthscale can be accurately described by averaging the contributions of the bulk and interfacial regions. References: [1] Molecular mechanics and structure of the fluid-solid interface in simple fluids. G. J. Wang and N. G. Hadjiconstantinou. *Physical Review Fluids*, Vol. 2, No. 9, 094201 (2017). [2] Why are Fluid Densities So Low in Carbon Nanotubes? G. J. Wang and N. G. Hadjiconstantinou. *Physics of Fluids*, Vol. 27, No. 5, 052006 (2015).

Multiscale Poroelastic Modeling of Thermal Expansion of Concrete

Hui Wang*, Herbert Mang**, Yong Yuan***, Bernhard Pichler****

*Institute for Mechanics of Materials and Structures, Vienna University of Technology, **Institute for Mechanics of Materials and Structures, Vienna University of Technology, ***College of Civil Engineering, Tongji University, ****Institute for Mechanics of Materials and Structures, Vienna University of Technology

ABSTRACT

ABSTRACT The thermal expansion coefficient of concrete was reported to depend on the aggregate type, the volume fractions of the constituents, the age, and the internal relative humidity [1]. Concrete is a multiscale material consists of a cement paste matrix and aggregate inclusions. As for cement paste, the internal relative humidity increases with increasing temperature. This results in an unsymmetric bell-shaped dependence of the thermal expansion coefficient of cement paste on the internal relative humidity, varying between $8 \cdot 10^{-6} \text{ K}^{-1}$ to $22 \cdot 10^{-6} \text{ K}^{-1}$. The thermal expansion coefficient of the aggregate is typically smaller, ranging between $4 \cdot 10^{-6} \text{ K}^{-1}$ to $12 \cdot 10^{-6} \text{ K}^{-1}$, mainly depending on the mineral composition [1]. In this research, a multiscale poroelastic model for concrete is established, by resolving it down to nanoscopic hydration products. Measured changes of internal relative humidity serve as input, resulting in a variation of the effective pressure in both the gel and the capillary pores, as is the combined effect of the pore fluid pressure and the surface tension. The effective pore pressures are averaged as eigenstresses based on the proposed size distribution model of the pores [2,3]. Simultaneously, thermal eigenstresses are induced in the solid constituents, namely, solid hydrates, unhydrated clinkers, and aggregates, in case of a temperature change, linked to the macroscopic thermal expansion of the concrete with the multiscale model. The model is validated by comparing the predicted thermal expansion coefficients of cementitious materials with the experimental measurements. **ACKNOWLEDGEMENTS** Financial support by the Austrian Science Fund (FWF), provided within project P 281 31-N32 "Bridging the Gap by Means of Multiscale Structural Analyses", is gratefully acknowledged. The first author also gratefully acknowledges financial support by the China Scholarship Council. **REFERENCES** [1] J. H. Emanuel, J. L. Hulse, "Prediction of the thermal coefficient of expansion of concrete", *Journal of the American Concrete Institute*, 74(4), 149-155 (1997). [2] B. Pichler, C. Hellmich, "Estimation of influence tensors for eigenstressed multiphase elastic media with nonaligned inclusion phases of arbitrary ellipsoidal shape", *Journal of Engineering Mechanics*, 136(8), 1043-1053 (2010). [3] H. Wang, C. Hellmich, Y. Yuan, H. Mang, B. Pichler, "Does reversible water uptake/release by hydrates govern the thermal expansion of cement paste? – A scale transition analysis", *Cement and Concrete Research*, under revision.

A Simple Two-dimensional Mechanical Metamaterial with Negative Poisson's Ratio

Hui Wang^{*}, Yuxuan Zhang^{**}, Wanqing Lin^{***}

^{*}Henan University of Technology, ^{**}Henan University of Technology, ^{***}Henan University of Technology

ABSTRACT

Abstract Metamaterials with negative Poisson's ratio, also named as auxetics, have attracted much effort towards exploring their applications as foldable devices in multiple engineering fields such as the medical and the aerospace fields, due to their counter-intuitive mechanical properties. In this study, a simple two-dimensional structure exhibiting auxetic behavior in both compression and tension is designed, which is different to the popular re-entrant or chiral designs. This is achieved by introducing peanut-shaped holes with different locations and rotational angles in linear elastic medium. Several auxetic configurations are fabricated by 3D printing technique and then studied through the computational and experimental methods to reveal their deformation mechanisms and characterize their compressive and tensile mechanical properties. It is found that the present modeling yields explicit mechanical properties including Poisson's ratios, strength and stiffness under tension and compression. Therefore, the methodology used by this study could be effectively employed to design two-dimensional auxetic matamaterials for various applications. References [1] T. Frenzel, M. Kadic, M. Wegener. Three-dimensional mechanical metamaterials with a twist. *Science* (2017)358, 1072–1074 [2] L. Yang, O. Harrysson, H. West, D. Cormier. Modeling of uniaxial compression in a 3D periodic re-entrant lattice structure. *J Mater Sci* (2013)48: 1413–1422 [3] X. Ren, J. Shen, A. Ghaedizadeh, H. Tian, Y.M. Xie. A simple auxetic tubular structure with tuneable mechanical properties. *Smart Mater Struct* (2016)25: 065012

A Three-dimensional Explicit Constitutive Model for High-precision Simulation of Concrete Structures

Jiaji Wang^{*}, Muxuan Tao^{**}, Xin Nie^{***}

^{*}Tsinghua University, ^{**}Tsinghua University, ^{***}Tsinghua University

ABSTRACT

Recently, a three-dimensional (3D) explicit constitutive model has been developed for numerical simulation of reinforced concrete (RC) and steel concrete (SC) structures. The proposed model is based on smeared crack model and fixed angle crack assumption. The decoupling of normal and shear stress after cracking is assumed for the concrete material to simulate the spatial cracking phenomenon of RC and SC structures. The uniaxial constitutive law is adopted from many existing literatures and shows good agreement with existing test data in terms of the tension stiffening, shear softening and compression softening of concrete material. The material model is implemented in ABAQUS software for both the implicit solver and explicit solver. The proposed model is calibrated and validated by a large number of existing tests in the literatures, including the panel tests, the shear wall test and the beam tests. The modeling scheme, material constitutive law, and material parameters are illustrated in detail. The results of the proposed FE model agree fairly well with existing test results in terms of the overall load–displacement curve, ultimate capacity, and failure pattern.

Data-augmented Multi-scale Modeling of Intracranial Pressure Dynamics

Jian-Xun Wang^{*}, Xiao Hu^{**}, Shawn Shadden^{***}

^{*}University of California, Berkeley, ^{**}University of California, San Francisco, ^{***}University of California, Berkeley

ABSTRACT

Accurate intracranial pressure (ICP) monitoring is highly significant in a number of neurosurgical applications, and elevated ICP may lead to severe brain damage. The standard ways for clinical ICP monitoring are all invasive, which typically requires a hole drilled in the skull and transducer inserted into a ventricle [1]. This exposes the patient to infection and hemorrhage, and often requires a neurocritical care unit. Therefore, noninvasive estimation of ICP (nICP) is highly compelling for patient safety and broader access. Numerous past efforts on nICP attempt to identify ICP-related noninvasive signals or surrogates. These efforts while promising have not gained traction. To improve nICP prediction, we developed a data-augmented framework that combines a physical intracranial model and noninvasive signals using advanced data assimilation techniques. Conceptually, the proposed framework consists of three modules: (1) a forward model of the intracranial dynamics, (2) noninvasive measurement data, and (3) a data assimilation scheme. A multiscale cerebrovascular model [2] is used for simulating the forward intracranial dynamics. Noninvasive cerebral blood flow velocity (CBFV) measured by Transcranial Doppler Ultrasonography (TCD) is used for data assimilation. A regularizing iterative ensemble Kalman method is implemented to assimilate the TCD measured data into our physical model to improve predictive accuracy. For proof-of-concept, we first use synthetic TCD data to validate and examine the proposed framework. The synthetic observations are generated from the physical model with a set of specified model parameters as the “ground truth”. Only CBFV at the left and right middle cerebral arteries (MCA) are observed and 10% random noise is added. By assimilating these synthetic data, the unobserved intracranial states (e.g., ICP, CBFV at non-measurable arteries) can be significantly better estimated. Preliminary application of this framework to clinical data where invasive ICP has been measured concurrently with TCD also demonstrates significant improvement of mean ICP prediction. By using both synthetic and real TCD measurements, we demonstrated that estimation of intracranial dynamics can be significantly improved by combining an imprecise model with imprecise and indirect noninvasive measurements. Future work includes gearing the hemodynamics-based physical model more toward ICP dynamics and potentially assimilating measurements that are more directly related to ICP than MCA flow velocity. References [1] X. Zhang, et al., *Physiol Meas* 38, R143 (2017). [2] J. Ryu, X. Hu, S. C. Shadden, *J Biomech Eng* 137, 101009 (2015).

Development of Maneuvering Control Module in CFD Solver naoe-FOAM-SJTU

Jianhua Wang^{*}, Decheng Wan^{**}

^{*}Shanghai Jiao Tong University, ^{**}Shanghai Jiao Tong University

ABSTRACT

Maneuverability is one of the most concerned ship performance. So far, many studies have been done to predict maneuvering behavior using numerical methods, among which most are using the simplified model, either mathematical model or body force. Consequently, the detailed flow around ship hull, rotating propellers and moving rudders cannot be resolved during the maneuvering motion. In the present work, maneuvering control module is developed based on the CFD solver naoe-FOAM-SJTU, which has overset grid capability and a full 6 Degrees of Freedom (6DoF) motion module with a hierarchy of bodies. The implementation of the maneuvering control module is inherited from the motion module with a hierarchy of bodies, where moving components, such as propeller and rudder, are acted as the base of specific maneuvering controller. The control module adopts the feedback mechanism to deal with the motion of propellers and rudders. At present, three types of control module are achieved, i.e. heading controller, zigzag controller and turning circle controller. In addition, the open source toolbox waves2Foam is utilized to the present solver to simulate ship maneuver in waves. Based on the maneuvering control module, RANS computations are conducted to directly simulate free running ship maneuver with rotating propellers and moving rudders. The developed solver has been applied to various maneuvers, such as standard zigzag maneuver in both calm water and waves, turning circle maneuver in calm water and course keeping maneuver in various heading waves. During the simulation, the calculations start from the steady state of the self-propulsion calculation and the twin rudders are executed by a feedback control mechanism. The main parameters of ship maneuver, such as the overshoot angle, period, turning diameter and rudder deflection are obtained to compare with the available experiment data. Good agreement is achieved for both maneuvering parameters and ship motions. It shows that the present implementation of maneuvering control module is robust and reliable in simulating free running ship maneuver in both calm water and waves. Furthermore, the present approach can be easily extended to various control modules based on feedback control mechanism.

Phase Field Modeling of Ferroelectric Material with Isogeometric Analysis

Jie Wang^{*}, Chang Liu^{**}

^{*}School of Aeronautics and Astronautics, Zhejiang University., ^{**}School of Aeronautics and Astronautics, Zhejiang University.

ABSTRACT

Isogeometric analysis (IGA) is a recently developed technology in computational mechanics. Its main idea is to use the same smooth and higher-order basis functions, e.g. non-uniform rational B-splines (NURBS), for the representation of both the geometry in CAD and the approximation of solution fields in analysis. Thus, the complex geometry of materials can be modeled exactly. As a consequence, geometric errors are eliminated. In addition, the high order continuities of the basis functions are ideally suitable for solving high order partial differential equations, like the equation of flexoelectric problems and Cahn-Hilliard equation, which require at least C^1 continuous approximations. These attributes permitted us to derive accurate, efficient, and geometrically flexible methods for the problems with higher-order derivatives. In this paper, a NURBS-based variational formulation for the phase field equations of ferroelectric materials is established. Several numerical examples are provided in this paper to confirm the accuracy of this method. After that, the polarization distributions inside the PbTiO_3 material are simulated with the help of IGA. Moreover, the polarization distribution inside a three-dimensional ferroelectric material with the consideration of flexoelectricity is obtained in this paper.

Single and Multi-Objective Aerodynamic Shape Optimizations by Means of Stackelberg Game Coupled with Adjoint Method

Jing Wang*, Yao Zheng**, Jifa Zhang***, Fangfang Xie****, Jianjun Chen*****
Periaux*****, Zhili Tang*****

*Center for Engineering and Scientific Computation, and School of Aeronautics and Astronautics, Zhejiang University, Yuquan Campus, Hangzhou, Zhejiang, 310027, PR China, **Center for Engineering and Scientific Computation, and School of Aeronautics and Astronautics, Zhejiang University, Yuquan Campus, Hangzhou, Zhejiang, 310027, PR China, ***Center for Engineering and Scientific Computation, and School of Aeronautics and Astronautics, Zhejiang University, Yuquan Campus, Hangzhou, Zhejiang, 310027, PR China, ****Center for Engineering and Scientific Computation, and School of Aeronautics and Astronautics, Zhejiang University, Yuquan Campus, Hangzhou, Zhejiang, 310027, PR China, *****International Center for Numerical Methods in Engineering (CIMNE), Universidad Politecnica de Catalunya, Barcelona, Spain, *****College of Aerospace Engineering, Nanjing University of Aeronautics and Astronautics 29 Yudao Street?Nanjing, 210016, PR China

ABSTRACT

Aerodynamic shape optimization in aeronautical engineering, by its nature, is multi-objective. In general, two approaches are mainly used for solving multi-objective optimization problems: (1) The weighted average optimization method. It aggregates all the objective functions with different weights to form a single function for optimization. Consequently, the design results strongly depend on the choice of reasonable weights. (2) The non-dominated optimization method based on evolutionary algorithms. The evolutionary process is very time consuming due to a large number of function calls. Therefore, this method is limited to solve problems with simple configurations and a small number of design variables. In this study, the Stackelberg game strategy is coupled with the continuous adjoint method to solve multi-objective aerodynamic shape optimization problems. In the game, two types of players (leader and follower) are involved, and each pair of players is responsible for the optimization of one objective function. During the game, players perform optimizations alternately using the continuous adjoint method until the leader cannot improve its objective function further. When the leader and the follower optimize the same objective function, a “virtual” multi-objective problem is formulated, and this game can also be used to solve single-objective optimization problems. Note that the success of the proposed method highly depends on the choice of a few critical parameters, including the maximal number of iterations for each player, the splitting scheme of design variables, and the assignment of objective functions and design variables to different players. Therefore, impacts of these parameters are firstly assessed by a simple optimization case while some useful inferences are produced for the choice of these parameters. For the RAE2822 airfoil and the ONERA M6 wing, single-objective and multi-objective aerodynamic optimizations are conducted to verify the usefulness of these inferences, and to validate the efficiency and effectiveness of the proposed optimization method with a large number of design variables. Moreover, it is found that when solving single-objective problems, the proposed method can provide better optimization results with less computational cost than the original continuous adjoint method. Keywords: Stackelberg game, Continuous adjoint method, Single-objective optimization, Multi-objective optimization, Aerodynamic shape optimization

The Stability Problems in SPH Numerical Wave Tank

Jingyu Wang^{*}, Fei Xu^{**}, Yang Yang^{***}

^{*}School of Aeronautics, Northwestern Polytechnical University, 710072, Xi'an, P.R.China, ^{**}School of Aeronautics, Northwestern Polytechnical University, 710072, Xi'an, P.R.China, ^{***}School of Aeronautics, Northwestern Polytechnical University, 710072, Xi'an, P.R.China

ABSTRACT

The numerical wave tank is one of the effective tools to study the wave and its effect on the floating structure. Compared with the traditional methodology of CFD to construct the tank, the Smoothed Particle Hydrodynamics (SPH) method is superior in dealing with problems concerning complex boundary and extremely large deformation. When traditional SPH method is used to simulate wave propagation in a wave tank? it is usually observed that the wave height attenuates and the wave length elongates along the direction of wave propagation, owing to the stability problems in SPH. Although the instability cannot be removed under any circumstances in traditional SPH, it can be improved in several aspects. At first, the effect of boundary condition would be discussed. Repulsive boundary condition, dynamic boundary condition, as well as, mirror particle boundary condition has been used in this 2D numerical wave tank. Secondly, as we all know, the kernel function plays an important role in the stability of pressure, which may be the main reason of the problem. At the same time, the quality of wave varies with different smooth length in the kernel functions. Hence, the selection of kernel function and the smooth length would be talked in the paper. At last, some improvement of SPH methods, such as δ -SPH and GSPH, and other numerical processing techniques, would be taken into this wave tank to improve the stability of the numerical tank. Their adaptive in wave generation and propagation is shown in the simulations. By the research of these three aspects, a stable SPH numerical wave tank is established with little attenuation. Reference [1]Antuono M, Colagrossi A, Marrone S, et al. Propagation of gravity waves through an SPH scheme with numerical diffusive terms[J]. Computer Physics Communications, 2011, 182(4):866-877. [2]Kunal Puri, Prabhu Ramachandran. Approximate Riemann solvers for the Godunov SPH (GSPH)[J]. Journal of Computational Physics, 2014, 270(8):432-458. [3] Zhang J Z, Zheng J, Kai-Ping Y U, et al. A RESEARCH ON THE TENSILE INSTABILITY OF SPH IN FLUID DYNAMICS[J]. Engineering Mechanics, 2010, 27(2):65-72.

A Wavelet Method on the Solution of Nonlinear Problems in Computational Material Sciences

Jizeng Wang^{*}, Cong Xu^{**}, Youhe Zhou^{***}

^{*}College of Civil Engineering, Lanzhou University, ^{**}College of Civil Engineering, Lanzhou University, ^{***}College of Civil Engineering, Lanzhou University

ABSTRACT

A high-order wavelet method is developed for general nonlinear boundary value problems in mechanics. This method is established based on Coiflet approximation of multiple integrals of interval bounded functions combined with an accurate and adjustable boundary extension technique. The convergence order of this approximation has been proven to be N as long as the Coiflet with $N-1$ vanishing moment is adopted, which can be any positive even integers. Error analysis has proven that the proposed method is order N , and condition numbers of relevant matrices are almost independent of the number of collocation points. Examples of a wide range of strong nonlinear problems in engineering, especially in mechanics, including the extremely large deflection bending of plates and shells with complex shapes, demonstrate that accuracy of the proposed method is even greater than N , and most interestingly, such accuracy is independent of the order of the differential equation of the problem to be solved. Comparison to existing numerical methods further justifies the accuracy and efficiency of the proposed method.

Hybridizing Neural Network and Hand-crafted Critical State Plasticity Model for Forward Prediction of Geomaterials in a Directed Graph

Kun Wang^{*}, WaiChing Sun^{**}

^{*}Columbia University, ^{**}Columbia University

ABSTRACT

This work presents a novel component-based approach on the development of constitutive models for materials having complex path-dependent mechanical properties. Critical state plasticity models for capturing the complex cyclic response of sands have been proposed, yet lack the prediction accuracy against experiments. To extend the capability of the existing models, we propose the introduction of machine learning on experimental data into the conventional plasticity formulations. The directed graphs of the constitutive models are constructed, with the nodes representing the physical quantities (stress, strain, porosity, fabric tensor, etc.) and the edges representing the universal principles, definitions or constitutive equations relating these quantities. The discrepancy between the different constitutive models lies in the configuration of the directed graphs. The fully mathematical plasticity model involves yield surfaces, plasticity potentials, and evolution equation of internal variables. The fully data-driven constitutive model relates the stress to strain directly via the neurons in the artificial neural networks conserving material frame indifference. The development of hybrid data-driven plasticity model consists of selective replacement of mathematical formulation by machine learning. The choices of data-driven nodes and edges in the directed graph result in different configurations, hence lead to different hybrid models. We present a group of model designs with various degree of hybridization and compare them against experimental data on cyclic responses of sands. Their accuracy and computational efficiency are compared within our proposed model evaluation framework. This work offers the community a novel graph-based systematic approach on developing and assessment of hybrid data-driven constitutive models.

On the Use of Advanced Material Point Methods for Problems Involving Large Rotational Deformation

Lei Wang^{*}, Charles Augarde^{**}, William Coombs^{***}

^{*}University of Durham, ^{**}University of Durham, ^{***}University of Durham

ABSTRACT

The Material Point Method (MPM) is a quasi Eulerian-Lagrangian approach to solve solid mechanics problems involving large deformations. The standard MPM discretises the physical domain using material points which are advected through a standard finite element background mesh. The method of mapping state variables back and forth between the material points and background mesh nodes in the MPM significantly influences the results. In the standard MPM (sMPM), a material point only influences its parent element (i.e. the background element in which it is located), which can cause spurious stress oscillations when material points cross between elements. The instability is due to the sudden transfer of stiffness between elements. It can also result in some elements having very little stiffness or some internal elements losing all stiffness. Therefore, several extensions to the sMPM have been proposed, each of which replaces the material point with a deformable particle domain. The most notable of these extensions are the Generalised Interpolation Material Point (GIMP), the Convected Particle Domain Interpolation (CPDI1) and Second-order CPDI (CPDI2) methods. In this paper, the sMPM, CPDI1 and CPDI2 approaches are unified for geometrically non-linear elasto-plastic problems using an implicit solver and their performance investigated for large rotational problems. This type of deformation is common in applications in the area of soil mechanics, for example the vane shear test and, specifically of interest here, the installation of screw piles. Screw piles are currently used as an onshore foundation solution and research being undertaken at Durham, Dundee and Southampton universities is exploring their use in the area of offshore renewables. The numerical modelling using the MPM aims to predict the installation torque and vertical force as well as understanding the "state" of the soil around the screw pile which is critical in understanding the long term performance of the foundation. In the analysis, the pile is assumed to be a rigid body and no-slip boundary condition is used at the pile-soil interface. The boundary condition is imposed using the moving mesh concept within an unstructured mesh fixed to the pile. It will be shown that the CPDI2 approach produces erroneous torque due to particle domain distortion, while the CPDI1 approach and sMPM predict physically realistic mechanical responses.

Applications of Enhanced Sampling Methods in Protein-ligand Binding Free Energy Calculations

Lingle Wang*

*Schrodinger, Inc.

ABSTRACT

Accurate and reliable calculation of protein-ligand binding free energy is of central importance in computational biophysics and computer aided drug design. While alchemical free energy perturbation (FEP) methods provide an in-principle most rigorous approach for protein-ligand binding free energy calculations and are expected to yield the most accurate predictions, the accuracy of free energy calculations had been hindered by inadequate sampling of protein-ligand conformational space, blocking their applications in drug discovery projects. In this presentation, I am going to talk about the enhanced sampling method REST2 (Replica Exchange with Solute Tempering), designed to efficiently sample the complex potential energy surfaces of biological molecules. In particular, I am going to focus on the applications of REST2 on free energy calculations (through FEP/REST), and present the large-scale testing of FEP/REST on protein-ligand binding free energy calculations. We demonstrate that the combination of FEP/REST and the accurate force field OPLS3 achieves an unprecedented level of accuracy in protein-ligand binding free energy calculations across a broad range of target classes and ligands and a wide variety of chemical perturbations, and positions free energy calculations to play a guiding role in small molecule drug discovery.

Wave Propagations in Linear Elastic Peridynamic Media

Linjuan Wang^{*}, Jifeng Xu^{**}, Jianxiang Wang^{***}

^{*}Peking University, ^{**}Beijing Aeronautical Science and Technology Research Institute, ^{***}Peking University

ABSTRACT

The elastic waves in peridynamic media are different from those in the classical local media. The dispersive characteristics of waves in bond-based peridynamics have been studied in the literature, but the general properties of the waves in the state-based peridynamic media are less investigated. In particular, the integral forms raise great obstacles in mathematics to analytically investigating the properties of the state-based peridynamic theory. In this work, we focus on the dispersive characteristics of waves in state-based peridynamics. We examine in detail the dispersion relations, group velocity, phase velocity for different constitutive relations of the peridynamic media, and for different Poisson's ratios. We find that the wave velocity in peridynamic media with negative Poisson's ratios may be larger or less than that in the corresponding local media. These results have particular implications in analysing wave propagations in heterogeneous media.

VCUT Level Set: A Level Set Method with Variable Cutting Functions for Topology Optimization of Multiscale Structures

Michael Y Wang*

*Hong Kong University of Science and Technology

ABSTRACT

In this paper, we introduce a novel level set method with variable cutting, called VCUT Level Set, for designing topologically variable cellular structures through geometric modeling and structural optimization. In the conventional level set method for implicit representation of a structure as usually applied in structural topology optimization, the height level of the level set function is set at a constant value (i.e., zero). The basic idea of the VCUT level set approach is to replace the constant-valued cutting height (i.e., zero) with a variable-valued cutting function which is defined and characterized by a set of parameters, such as a piece-wise linear function or a parametric (nonlinear) function. These parameters of the variable cutting function are incorporated as variables as well in the numerical process of optimization. The VCUT level set method provides a greater capability and flexibility for optimizing not only solid macro-structures, but also cellular structures at micro- and meso- scales concurrently. In a demonstration of the VCUT level set method, we first define a global mesh over the design domain of the structure. The set of cutting heights are defined on the mesh nodes and they in turn interpolate a cutting function (linear or higher order) within each mesh element, to be applied locally to the level set function within the element. Since the cutting height is applied by the shared nodes and is interpolated within the mesh element, full geometric continuity in the level set representation is guaranteed at the face between two neighboring elements. In this paper, we apply the VCUT level set method for multiscale design of structures with spatially-varying mesoscale cells. The topology optimization seeks both the best cell geometry and the optimal distribution of graded cells. Numerical examples demonstrate the capabilities of the proposed VCUT level set method for optimizing multiscale structures with unprecedented macroscale topological features and mesoscale cellular distributions with smooth spatial gradient.

Strengthening Mechanisms in Surface Nano-crystallized Metals

Peng Wang^{*}, Shaoxing Qu^{**}, Zhanli Liu^{***}

^{*}Zhejiang University, ^{**}Zhejiang University, ^{***}Tsinghua University

ABSTRACT

Surface nano-crystallized (SNC) metals have great potential applications due to its good balance of strength and ductility. However, the strengthening and toughening mechanisms are still elusive because the grain size spans over four orders of magnitude in the gradient structure, suggesting that the corresponding constitutive behaviors vary obviously across several length scales. After analyzing the evolution of microstructure and mechanical characteristic of SNC copper at various scales, three different kinds of constitutive behaviors associated with the coarse grain (CG) layer, the transitional grain (TG) layer and the gradient nano-grain (GNG) layer are identified. Therefore, the evolution equations of dislocation density of these layers are needed to be established. Subsequently, we develop a general approach within the framework of dislocation mechanism based crystal plasticity to characterize the corresponding constitutive behaviors. Then, the strengthening mechanisms of SNC metals are analyzed within the framework. It is shown that the predictions based on the framework are in good agreement with the experimental results and the plastic strain gradient produce the non-local strengthening effect which is similar to the mechanism responsible for the strengthening of thin film passivated on one or both sides. The proposed general framework is capable of optimizing the mechanical properties and investigating the subsequent failure process in SNC materials. Keywords: Surface nano-crystallized metal, General constitutive model, Dislocation density evolution, Dislocation-based crystal plasticity, Non-local effect

Reliability Analysis of a MASH TL-3 Concrete Median Barrier Using Metamodels and FORM

Qian Wang^{*}, Hongbing Fang^{**}, Hanfeng Yin^{***}

^{*}Manhattan College, ^{**}The University of North Carolina at Charlotte, ^{***}Hunan University

ABSTRACT

Concrete median barriers are rigid barriers that are widely used on U.S. freeways. In this research work, reliability analyses of concrete median barriers under vehicle crashes were studied. The concrete barriers were under vehicular crashes according to the Manual for Assessing Safety Hardware (MASH) test level 3 (TL-3) requirements. In the proposed approach, a metamodeling method based on augmented radial basis function (RBF) was integrated with a First-Order Reliability Method (FORM). The random variables included impact parameters such as the vehicle weight and impact angle. Various crash responses were evaluated using computational methods and nonlinear transient finite element (FE) analyses. To reduce the computational effort due to the expensive numerical simulations, an approximation technique was applied and the augmented RBF metamodels were constructed to express the performance functions. One of the compactly supported RBFs augmented with linear polynomials was adopted, which was identified to be an accurate RBF from the authors' previous work. An alternate FORM was implemented once explicit expressions of the performance functions became available. This reliability analysis approach was tested for various mathematical and engineering examples. In the application to concrete barriers, different vehicular responses and occupant responses including those defined in the current crash standard were adopted and their limit values were selected. Reliability analyses were performed using the new approach and the failure probabilities and reliability indices were obtained. The reliability analysis results provided useful information for the assessment of concrete barriers. This proposed approach is useful for impact problems requiring expensive simulations and reliability analyses of these problems become more important for design optimization and decision making.

Contribution of Elastin and Collagen to Inter-Lamellar Bonding in the Arterial Wall

Ruizhi Wang*, Xunjie Yu**, Yunjie Wang***, Yanhang Zhang****

*Boston University, **Boston University, ***Boston University, ****Boston University

ABSTRACT

Arterial wall delamination begins with a tear cutting in the intima, which allows blood flow to enter the newly created lumen and split the media. To date, little is known about the distinct role of elastin and collagen plays in the initiation and propagation of aortic wall delamination. Elastin and collagen forms the primary load bearing extracellular matrix (ECM) components in the arterial wall. In fact, 27% of elastin was found to protrude obliquely from lamellar surfaces and terminate in inter-lamellar space, and 2% of elastin was found in the form of radial elastin struts that provides direct radial connection between adjacent lamellae [1]. This study aims to understand the contribution of elastin and collagen fibers to inter-lamellar bonding in the arterial wall. Peeling tests were performed on porcine thoracic aorta and purified elastin network. The peeling force/width in aortic media is about five times of that in elastin network, indicating the important role of inter-lamellar collagen in maintaining arterial wall integrity. In-situ multi-photon images revealed the presence of both inter-lamellar elastin and collagen fibers at the separation site between lamellar layers. A finite element model of peeling tests was created based on cohesive theories of fracture [2]. A hyperelastic and anisotropic constitutive law was used to model the tissue behavior [3]. Simulation results were fitted to experimental load-displacement curves to estimate the inter-lamellar bonding stiffness, stresses at damage initiation and fracture displacement in the cohesive zone for aortic media and elastin network. Resistance to inter-lamellar debonding was found to be the main contributor to the differences in peeling forces between aortic media and elastin. For cohesive interfaces following a bilinear traction-separation damage law, much higher bonding stiffness and damage initiation stresses were obtained in aortic media than in elastin network. Removal of collagen reduced inter-lamellar fiber density, which leads to the decreased bonding in elastin network. To consider the distinct role of elastin and collagen plays in the initiation and propagation of aortic wall delamination, a more realistic multiscale traction-separation relation for the cohesive zone was developed to include the structural and mechanical contributions of elastin and collagen fibers. [1] O'Connell M.K et al., *Matrix Biol*, 27:171–181, 2008. [2] Hillerborg A et al., *Cem Concr Res*, 6:773-782, 1976. [3] Holzapfel G.A et al., *J Elast*, 61:1-48, 2000.

Experimental Study on Mechanical Properties of Human Facial Skin in Vivo

Shibin Wang^{*}, Huixin Wei^{**}, Chuanwei Li^{***}, Linan Li^{****}, Anna Dai^{*****}, Lei Zhou^{*****}

^{*}Tianjin University, ^{**}Tianjin University, ^{***}Tianjin University, ^{****}Tianjin University, ^{*****}Tianjin University,
^{*****}Tianjin University

ABSTRACT

Characterising the mechanical behavior of human skin is of great importance for a number of applications including surgery, animation, dermatology and biomechanics. The human skin, which covers almost entirely the human body, is a complex multi-layer material, composed of epidermis, dermis and hypodermis. With nonlinear behavior, anisotropy, viscosity and preconditioning effects, it is a challenging endeavour to study mechanical properties of human skin. Furthermore, it depends on many factors, such as ageing, environment and in vivo or in vitro. In this study, the effect of different thickness of skin tissue and probe size have been investigated. To consider the bone, we propose a two-layer theoretical model. A novel loading device applied to the facial skin is developed. It can realize a precise three-dimensional (3D) translation, and the contact force can be measured with a loading cell. In order to ensure an indentation normal to the surface, we use a CCD camera combined with a transparent probe is employed to measure the contact area during loading and to analyze its contact state. The thickness of facial skin tissue are measured by the head CT photographs of subjects. We focus on the measurement of the mechanical behavior of facial skin tissue in vivo, combining the experimental test with the finite element method to study the mechanical constitutive mechanism of the facial soft tissue.

1?Cormac Flynn, Andrew Taberner, Poul Nielsen?Measurement of the force–displacement response of in vivo human skin under a rich set of deformations?Medical Engineering & Physics 33 (2011)?pages 610–619 2?Cormac Flynn, AndrewJ.Taberner, PoulM.F.Nielsen, SidneyFels?Simulating the three-dimensional deformation of in vivo facial skin? Journal of the Mechanical Behavior of Biomedical Materials, 28(2013)?pages 484-494.

Study on Formation Mechanism of Hydraulic Fracturing Network of Layered Shale

Tao Wang^{*}, Zhanli Liu^{**}, Yue Gao^{***}, Zhuo Zhuang^{****}

^{*}Tsinghua University, ^{**}Tsinghua University, ^{***}Tsinghua University, ^{****}Tsinghua University

ABSTRACT

Shale is a typical heterogeneous and anisotropic material whose properties are characterized primarily by locally oriented anisotropic clay minerals and naturally formed bedding planes. The nature of the bedding planes will greatly affect the hydraulic fracturing of the shale to form a large-scale stimulated reservoir volume (SRV). In this paper, the debonding behavior of bedding planes in the process of hydraulic fracture (HF) propagation is studied. Two dimensionless parameters are proposed to characterize the difficulties of tensile and shear debonding of the bedding planes. By analyzing the two dimensionless parameters, it can be found that the SRV is mainly caused by the shear failure of bedding planes in the actual hydraulic fracturing treatment. The larger the shear strength of the rock or the smaller the net fluid pressure, the smaller the SRV and the optimal perforation cluster spacing. Two dimensionless parameters (stimulating volume ratio and stimulating efficiency) are proposed to evaluate the stimulating effect. According to the theory of debonding in this paper, it is possible to guide the treatment of hydraulic fracturing, predict the SRV, optimize the spacing of perforation clusters, and improve the production of shale gas.

Meso-scale Nonequilibrium Features in a Gas-Fluidized Bed

Wei Wang^{*}, Haifeng Wang^{**}, Yanpei Chen^{***}

^{*}State Key Laboratory of Multiphase Complex Systems, Institute of Process Engineering, Chinese Academy of Sciences, Beijing 100190, P.R. China, ^{**}State Key Laboratory of Multiphase Complex Systems, Institute of Process Engineering, Chinese Academy of Sciences, Beijing 100190, P.R. China, ^{***}State Key Laboratory of Multiphase Complex Systems, Institute of Process Engineering, Chinese Academy of Sciences, Beijing 100190, P.R. China

ABSTRACT

To understand the meso-scale, far-from-equilibrium behavior in fluidization [1], we investigate, both numerically and experimentally, the nonequilibrium features in a pseudo 2D bubbling fluidized bed. In experiment, velocities of individual particles are measured by using a particle tracking velocimetry (PTV) method, and void fractions are obtained with Voronoi tessellation. A bimodal shape of probability density function (PDF) for particle vertical velocity is found in not only time-averaged but also time-varying statistics, which is caused by the transition between the dense and dilute phases and breaks the local-equilibrium assumption in continuum modeling of fluidized beds [1]. The results of time-varying radial distribution function and voidage distribution also confirm this finding. Moreover, analysis of voidage, velocity of particle, granular temperature and turbulent kinetic energy of particles shows that there is no scale-independent plateau over the interface, and it seems hard to find a scale-independent plateau to separate the micro- and meso-scales of fluidized beds, which require sub-grid meso-scale modeling for continuum or coarse-graining methods of gas-fluidized systems [2]. In numerical simulation, dense discrete particle method is used with the energy minimization multi-scale (EMMS) drag. Simulation results generally agree with the experiment. References [1] W. Wang, Y. Chen, Mesoscale modeling: Beyond local equilibrium assumption for multiphase flow, *Adv. Chem. Eng.* 47(2015) 193–277. [2] Y. Tian, J. Geng, W. Wang, Structure-dependent analysis of energy dissipation in gas-solid flows: Beyond nonequilibrium thermodynamics, *Chem. Eng. Sci.* 171 (2017) 271–281.

Probing the Mechanical Interactions of Cell Nuclear Pore Complex with Nanoparticles

Xiangqiao Wang^{*}, Liuyang Zhang^{**}

^{*}University of Georgia, ^{**}Xi'an Jiaotong University

ABSTRACT

Understanding and controlling the selective nanoparticle transport through the nuclear pore complex is critical to the development of nanomedicine applications. The transport happens about milliseconds and the length scale of hundreds of nanometers; however, the fundamental transport mechanism remains elusive due to lack of suitable experimental and/or computational tools. By taking into account the elastic structure of nucleus envelope, nucleus pore complex, and nanoparticle-FG protein hydrophobic affinity, we develop a coarse-grained model for the nucleus pore structure that can help us mimic and understand its process of nanoparticles' transport. We explore the roles played by nanoparticles' size, shape morphology, and surface coating in the transport process, and estimate the minimum force and energy required for a specific nanoparticle to pass through the nuclear pore complex. We believe that our findings can provide fundamental understanding in nuclear pore transport and some useful design principles for the nucleus-targeted drug delivery vectors.

Modeling the Crystal Growth of Semi-crystalline Polymers by a Phenomenological Phase-field Method

Xiaodong Wang^{*}, Jie Ouyang^{**}, Ying Liu^{***}

^{*}Northwestern Polytechnical University, ^{**}Northwestern Polytechnical University, ^{***}Shaanxi University of Science & Technology

ABSTRACT

Crystal growth of either polymers or metals commonly shows distinct anisotropic behaviors related to the anisotropy of interfacial free energy. Most of the phase-field models developed for solidification use a simple anisotropic function, which makes the interfacial free energy (the gradient term) depend on direction, to describe the anisotropic crystal growth [1]. The frequently used cubic anisotropic function in 3D [2], which has equal strength of anisotropy in the six main directions, only can be used to simulate the equiaxed dendritic growth pattern. For semi-crystalline polymers, because the alignment of molecular chains in some directions is often promoted or confined [3], the anisotropic crystal growth is seldom equiaxed. Therefore, it is necessary to derive new anisotropic functions special for semi-crystalline polymers. In this study, we have established a 3D phase-field model for investigating the crystal growth of semi-crystalline polymers. The model can be regarded as a generalization of the 2D phase-field model we ever presented. It couples a nonconserved crystal order parameter with a temperature field generated by latent heat of crystallization, and obtains its model parameters from the real material parameters. Unlike the models of metals and small molecular compounds, the current model considers the partially crystallization property of semi-crystalline polymers. Moreover, due to the long-chain molecular structure, polymer crystallizations usually exhibit complex anisotropy and have polymorphous nature. To account for the various anisotropy of interfacial energy in 3D, three anisotropic functions describing the anisotropic interfacial growth patterns are deduced phenomenologically based on a number of existing experimental facts. Simulation results have preliminarily demonstrated the good performance of our phase-field model in reproducing the complex and diverse morphology of semi-crystalline polymers in 3D. Several kinds of crystal patterns, which have been observed in experiments, can be reproduced. [1] Xu, H.J.; Matkar, R.; Kyu, T. Phase-field modeling on morphological landscape of isotactic polystyrene single crystals. *Phys. Rev. E* 2005, 72, 011804. [2] Karma, A.; Rappel, W.J. Quantitative phase-field modeling of dendritic growth in two and three dimensions. *Phys. Rev. E* 1998, 57, 4323–4349. [3] Wang, H.P.; Jong, K.K.; et al. Confined Crystallization of Polyethylene Oxide in Nanolayer Assemblies. *Science* 2009, 323, 757–760.

Explicit Multi-material Topology Optimization of Freely Vibrating Continuum Structures Using Moving Morphable Bars

Xuan Wang^{*}, Kai Long^{**}, Ping Hu^{***}

^{*}Dalian University of Technology, ^{**}North China Electric Power University, ^{***}Dalian University of Technology

ABSTRACT

It is accepted that the existing literature on dynamic optimization problem is all carried out in an implicit way, which involves a large number of design variables. More recently, a new class of optimization methods based on discrete geometric components has been proposed with the aim of doing topology optimization in an explicit and flexible way. In this paper, an explicit multi-material topology optimization method is developed for freely vibrating continuum structures, where the geometric parameters used to describe the size, shape and location of the moving bars are considered as design variables of the optimization problem. The moving bars corresponding to different material phases are mapped into two density fields on a fixed grid using a smoothed Heaviside function, which can not only avoid remeshing the grids but also enable us to use gradient-based algorithms to solve optimization problems. The explicit model of multi-material topology optimization using moving morphable bars and its sensitivity analysis is detailed for two different optimization problems, including maximization of the n -th eigenfrequency and Maximization of eigenfrequency gap. Numerical examples demonstrate the present formulation provides an effective means for multi-material topology optimization of freely vibrating continuum structures.

Adaptive Solution Transfer Between Non-matching Meshes for Coupling Climate Models

Xuebin Wang^{*}, Xiangmin Jiao^{**}, Qiao Chen^{***}, Yipeng Li^{****}

^{*}Stony Brook University, ^{**}Stony Brook University, ^{***}Stony Brook University, ^{****}Stony Brook University

ABSTRACT

Solution transfer is a critical component in global climate modeling, which requires coupling an atmospheric model with the ocean, land, sea-ice models, etc. These models may utilize different numerical discretization methods, and hence the interface meshes between them may be non-matching. Some of these models increasingly utilize high-order numerical methods and higher-resolutions meshes. It is necessary to develop more robust and efficient solution transfer methods, which must support high-order methods at various grid resolution. The commonly used solution-transfer methods are either pointwise-based (such as interpolation or moving least squares) or integral-based (such as the common-refinement or super-mesh based methods). The former is efficient but not conservative, while the latter is conservative but typically requires computing the intersections of the cells, which is geometrically complicated and computationally expensive. In this work, we propose an adaptive solution transfer method, which can achieve approximate local conservation in a weighted sense, without requiring the computation of intersections of the cells. To this end, our method uses the generalized Lagrange polynomial (GLP) basis functions in a Petrov-Galerkin formulation, in which the test functions are adapted to accommodate large gradients and potential discontinuities in the solution. Our method supports transferring node-based, cell-centered, or cell-averaged values in finite elements, finite volume, or spectral element methods. It can achieve high-order accuracy with excellent long-term stability. We demonstrate the approach using exchanges of heat and mass in a coupled atmosphere-ocean model.

Action Feedback Control of Elastic Wave Metamaterials

Yi-Ze Wang*, Yue-Sheng Wang**

*Institute of Engineering Mechanics, Beijing Jiaotong University, Beijing 100044, China, **Institute of Engineering Mechanics, Beijing Jiaotong University, Beijing 100044, China

ABSTRACT

There are a large number of investigations about elastic waves in periodic structures which are called as phononic crystals or elastic wave metamaterials. In this kind of systems, we can find the stop band in which acoustic and elastic waves cannot propagate. Based on this characteristic, these structures can be applied to noise and vibration isolation, elastic wave filters, etc. And a lot of investigations are reported on how to tuning methods of stop bands in elastic wave materials. Although there have been many methods applied to control the stop bands, they are mainly focused on the passive ones which are not easily changed according to the external situations. But we know that the automatic control system combines the merits of both electrical and mechanical devices. Then we can change our attention on the active control action with the automatic system. On the other hand, most of the previous investigations on elastic wave metamaterials are about the linear case, only a few studies have been reported on nonlinear elastic waves. But nonlinear elastic waves can show quite different characteristics from linear ones. In this work, the influence of active feedback control on nonlinear elastic wave metamaterials is discussed. From the results, we can conclude that the active control method can change both the location and width of stop bands, which are suitable to practical engineering. Acknowledgements: The presented work is supported by the National Natural Science Foundation of China under Grant Nos. 11772039 and 11532001.

A High-fidelity Computational Model for AM Models with Manufacturing Errors

Yingjun Wang*

*South China University of Technology

ABSTRACT

Additive manufacturing (AM), with material being added together layer by layer, can be used to produce objects of almost any shape or geometry. However, AM techniques cannot accurately build parts with large overhangs, especially for the large features close to horizontal, hanging over void. The overhangs will make the manufactured model deviate from the design model, which may cause the performance of the manufactured model cannot satisfy the design requirements. In this work, we will propose a new finite element (FE) model that includes the manufactured errors by mimicking the AM layer by layer construction process. In such FE model, an overhang coefficient is introduced to each FE, which is defined by the support elements in the lower layer. By mimicking the AM process from the bottom layer to the top layer, all the FE properties are updated based on their overhang coefficients, which makes the computational model is able to accurately predict the manufactured model with manufacturing errors. The proposed model can be used to predict the performance of the AM objects in the design stage, which will help the designers to improve their design by the simulation results.

Vortical Structure Development in a Riblet Controlled Boundary Layer Transition

Yiqian Wang^{*}, Song Fu^{**}, Chaoqun Liu^{***}

^{*}Tsinghua University, ^{**}Tsinghua University, ^{***}University of Texas at Arlington

ABSTRACT

The drag reduction mechanism of riblets with appropriate configuration is still unclear. In the present study, direct numerical simulations of flat plate and riblet controlled boundary layer transition are performed with Reynold number 1000 based on the inflow displacement thickness. It is found that the scalloped riblets investigated in this study induce streamwise vortices near the riblet tips which persist even after the flow become fully turbulence. In addition, a similar situation that the skin friction coefficient is highly correlated to the vortical structures in the log layer is found in both cases with and without riblet control, which justifies the need to study vortical structure development. The width and height of the scalloped riblet pose a great influence on the drag reduction performance. It is reported that riblets with width of wall unit 25-30 is optimised for drag reduction [1]. For the present study, the width of the scalloped riblet is 1.375 times inflow displacement thickness, which is in the range of 25-30 wall units. However, even though the averaged drag per unit area is substantially reduced around 20 percent, the total drag is not decreased at all because of the increase of we surface area. In this sense, a second case with same riblet shape, width and height, but with longer valley region is investigated. The results for this second case is still pending. The influence of riblets on the vortical structures will also be studied for the early transition stage. Klumpp et al. investigated how the same shape riblets advance or delay the boundary layer transition. In addition to their research, further detailed flow vortical structures will be given and their relationship to drag will also be investigated. [1] H. Choi, P. Moin and J. Kim, Direct numerical simulation of turbulent flow over riblets, Journal of Fluid Mechanisms, 1993, 255: 503-539. [2] S. Klumpp, M. Meinke, and W. Schroder, Numerical simulation of riblet controlled spatial transition in a zero-pressure-gradient boundary layer, Flow Turbulence & Combustion, 2010, 85, 57-71.

Steklov Geometry Processing: An Extrinsic Approach to Spectral Shape Analysis

Yu Wang^{*}, Mirela Ben-Chen^{**}, Iosif Polterovich^{***}, Justin Solomon^{****}

^{*}Massachusetts Institute of Technology (MIT), ^{**}Technion -- Israel Institute of Technology, ^{***}University of Montreal, ^{****}Massachusetts Institute of Technology (MIT)

ABSTRACT

We propose Steklov geometry processing, an extrinsic approach to spectral geometry processing and shape analysis. Intrinsic approaches, usually based on the Laplace--Beltrami operator, restrict consideration to quantities that can be measured without leaving the surface, and thus cannot distinguish shapes that deform isometrically. While extrinsic approaches hope to completely capture and characterize a shape including its spatial embedding, many previous extrinsic methods lack theoretical justification or require meshing of the volume enclosed by a surface. Instead, we propose a systematic surface-based approach to spectral analysis via Steklov eigenvalue problem, which involves computing the spectrum of the Dirichlet-to-Neumann operator of a surface bounding a volume. The Dirichlet-to-Neumann operator is the linear map from the boundary Dirichlet data of a Laplace equation to its corresponding Neumann data. A remarkable property of this operator is that it encodes the extrinsic and volumetric geometry up to rigid motion. For example, a recent result due to Polterovich and Sher [2015] shows the Steklov spectrum encodes extrinsic quantities including mean curvature. We use the boundary element method (BEM) to discretize the operator, accelerated by hierarchical numerical schemes and preconditioning; this pipeline allows us to solve eigenvalue and linear problems on large-scale meshes despite the density of the Dirichlet-to-Neumann matrix. Our experiments verify that the Steklov eigenfunctions are volumetric-shape-aware and that they encode the extrinsic features missed by intrinsic algorithms. We further demonstrate that our operators naturally fit into existing frameworks for geometry processing, making a shift from intrinsic to extrinsic geometry as simple as substituting the Laplace--Beltrami operator with the Dirichlet-to-Neumann operator. As a result, a large range of applications, including shape exploration, comparison, segmentation, correspondence, geometry descriptor computation, and spectral distance computation can benefit immediately from our operator, without the need of a volumetric discretization. Reference: [Polterovich and Sher 2015] Iosif Polterovich and David A Sher. Heat invariants of the Steklov problem. *The Journal of Geometric Analysis* 25, 2 (2015), 924–950. [Wang et al. 2017] Yu Wang, Mirela Ben-Chen, Iosif Polterovich, and Justin Solomon. Steklov Geometry Processing: An Extrinsic Approach to Spectral Shape Analysis. arXiv:1707.07070. Under review.

Experimental and Numerical Study of Surface Characteristics of Ti-6Al-4V Alloy in High Speed Cutting Based on SHPB System

Zengqiang Wang^{*}, Yuhang Cui^{**}, Hongliang Xue^{***}, Weiguo Guo^{****}, Zhanfei Zhang^{*****}

^{*}Key Laboratory of Ministry of Education for Contemporary Design and Integrated Manufacturing Technology, Northwestern Polytechnical University, Xi'an, China, ^{**}Xidian University, Xi'an, China, ^{***}Key Laboratory of Ministry of Education for Contemporary Design and Integrated Manufacturing Technology, Northwestern Polytechnical University, Xi'an, China, ^{****}School of Aeronautics, Northwestern Polytechnical University, Xi'an, China, ^{*****}Key Laboratory of Ministry of Education for Contemporary Design and Integrated Manufacturing Technology, Northwestern Polytechnical University, Xi'an, China

ABSTRACT

Abstract: This paper investigated the surface characteristics of Ti-6Al-4V in high speed cutting based on split Hopkinson pressure bar (SHPB) system with both experimental and numerical methods. The high-speed cutting of Ti-6Al-4V titanium alloy was simulated by three-dimensional finite element method to study the effects of cutting speed and cutting depth on cutting force and residual stress. Based on the simulation results, the high-speed cutting experiment based on SHPB was carried out. The cutting force was measured by strain gauge, the residual stress of the machined surface were measured by X-ray diffraction and the roughness of the machined surface were measured by needle scanning. The results show that with the experimental cutting speed (4.5-9.5m/s) and the cutting depth (0.1-0.6mm), the cutting forces, surface roughness and residual stress in the direction of the cutting speed decrease with the increasing cutting speed. As cutting depth increases, cutting forces and surface roughness increase. Therefore, better surface quality could be got by choosing a small cut depth and large cutting speed. By comparing the experimental results of cutting force and surface residual stress with numerical results, it is found that the two have good consistency. **Keywords:** High speed cutting; Finite element simulation; Surface characteristics; Hopkinson pressure bar; Ti-6Al-4V Alloys **References** [1] Gao C-Y, Zhang L-C, Liu P-H. The role of material model in the finite element simulation of high-speed machining of Ti6Al4V[J]. Proceedings of the Institution of Mechanical Engineers, Part C: Journal of Mechanical Engineering Science, 2016, 230(17): 2959-2967. [2] Larbi S, Djebali S, Bilek A. Study of High Speed Machining by Using Split Hopkinson Pressure Bar[J]. Procedia Engineering, 2015, 114: 314-321.

A Novel Reliability Analysis Technique Based on Adaptive Kriging and Error Estimation

Zeyu Wang^{*}, Abdollah Shafieezadeh^{**}

^{*}The Ohio State University, ^{**}The Ohio State University

ABSTRACT

As the complexity of numerical models, such as those based on FEM, increases and larger number of random variables are incorporated to enhance model completeness and predictability, the analysis of reliability of systems has become significantly more challenging. This is due to significant increase in the required number of calls to performance functions to achieve acceptable accuracy and increase in the computational time for each simulation. These challenges have motivated large efforts for development of reliability analysis algorithms that can substantially reduce the number of calls to performance functions, while maintaining high accuracy in reliability estimates. Surrogate model based approaches such as Support Vector Regression (SVR), Polynomial Chaos Expansion (PCE) and Kriging provide powerful tools for such reliability problems. Among these surrogate models, Kriging-based approaches can leverage statistical information via active learning to search for next best training points for model refinement. Well-known algorithms such as EGRA and AK-MCS leverage this property of Kriging to yield accurate estimates of failure probabilities. However, these algorithms lack the ability to determine error in their estimates of failure probability. Furthermore, the stopping criteria for the active learning process in these techniques are too strict, which can potentially lead to 'overfitting' phenomenon. To address the above limitations, the present paper introduces a new reliability analysis algorithm called Generalized Error Rate based Adaptive Kriging (GERAK). The structure of this algorithm is similar to AK-MCS. However, central limit theorem and its lemma De Moivre - Laplace theorem are employed to determine probabilistic properties of the number of realizations where the surrogate model yields wrong estimate for the sign of the limit state function. This feature is then used to reliably estimate an upper bound for error in failure probability estimates and subsequently as stopping criterion for refining the surrogate model. This along with the use of Maximum Uncertainty Function (MUF) as learning function that seeks for points with high uncertainty and probability density have led to very fast convergence of GERAK to true probability of failure. Several analytical examples are investigated in this study to showcase the significant advancements offered by GERAK compared to AK-MCS and other well-known methods.

Influence of Bubbles Growth and Detachment on a Catalytic Tubular Micromotor

Zhen Wang^{*}, Qingjia Chi^{**}, Lisheng Liu^{***}, Tao Bai^{****}, Qiang Wang^{*****}

^{*}Wuhan University of Technology, China, ^{**}Wuhan University of Technology, China, ^{***}Wuhan University of Technology, China, ^{****}Wuhan University of Technology, China, ^{*****}Wuhan University of Technology, China

ABSTRACT

Self-propelled micromotors that can convert environmental energy into mechanical movement are ubiquitous in our bodies. Particularly, the bubble-propelled tubular micromotors play an irreplaceable role in biomedicine and other fields. The performance of bubbles inside the catalytic micromotor should be clearly studied to meet the challenges in these widespread applications. Accumulated experiments have already revealed that the motion and lifetime of bubble-propelled tubular micromotors can be deeply influenced by bubble size and generation frequency. A mechanical model considering the bubble growth and detachment inside the tubular micromotor has been proposed. The effect of bubble size on locomotion of bubble-propelled tubular micromotors has been studied. Numerical investigations of the motility-related parameters, such as bubble size and generation frequency, the average velocity and track lines of the micromotor, are proved to be dependent of the geometry of the micromotor, roughness of the inner wall of the tubular micromotor and concentration of solution in the surrounding cues.

A Spectral-Element/Fourier Smoothed Profile Method for Large-Eddy Simulations of Industrial-Complexity Wake Flows

Zhicheng Wang^{*}, George Karniadakis^{**}, Michael Triantafyllou^{***}, Yiannis Constantinides^{****}

^{*}Massachusetts Institute of Technology, ^{**}Brown University, ^{***}Massachusetts Institute of Technology, ^{****}Chevron Energy Technology Company

ABSTRACT

An accurate, fast and robust spectral-element/Fourier smoothed profile method (SEFSPM) for turbulent flow past 3D complex-geometry moving bluff-bodies is developed and analyzed in this paper. Based on the concept of momentum thickness, a new formula for determining an interface thickness parameter is proposed. In order to overcome the numerical instability at high Reynolds number, the so-called Entropy Viscosity Method (EVM) is developed. To overcome resolution constraints pertaining to moving immersed bodies, the Coordinate Transformation Method (Mapping method) is incorporated in the current implementation. Moreover, a hybrid spectral element method using mixed triangular and quadrilateral elements is employed in conjunction with Fourier discretization along the third direction to efficiently represent body of revolution or long-aspect ratio bluff-body like risers and cables. The combination of the above coupling method are validated by prototype flows including flow past a stationary sphere at Reynolds number in the range [200,1,000], turbulent flow past a stationary and moving cylinder at Reynolds number in the range [80,10,000], as well as turbulent flow past a flexible dual-step cylinder at $Re_D=2000$. Finally, the application to predict the response of a self-excited flexible riser consisting of buoyancy-modules with aspect ratio over 50 at $Re_D=1000$ demonstrates that SEFSPM is a promising choice for industrial-complexity turbulent flows.

A Coupled Gradient-Based Shape and Topology Optimization Method

Zhijun Wang^{*}, Akke S.J. Suiker^{**}, Hèrm Hofmeyer^{***}, Twan van Hooff^{****}, Bert Blocken^{*****}

^{*}Eindhoven University of Technology, ^{**}Eindhoven University of Technology, ^{***}Eindhoven University of Technology, ^{****}Eindhoven University of Technology; KU Leuven, ^{*****}Eindhoven University of Technology; KU Leuven

ABSTRACT

Abstract: Topology optimization is a widely-used technique for finding the most favorable, internal structural lay-out with a minimal weight under the specific loading and boundary conditions applied[1,2]. Accordingly, within a finite element setting this technique searches for the optimal relative density of a fixed, discretized spatial domain representing the actual structure. To enable more diversity within the design domain and to enlarge the search space of optimal structural configurations, in the present work a coupled method for topology optimization and shape optimization is proposed. The method incorporates the shape design variables into a SIMP (Simplified Isotropic Material with Penalization) topology optimization formulation, whereby the shape and topology optimization steps are performed in a sequential manner. The computational efficiency of the method is warranted by using Non-Uniform Rational B-Splines (NURBS) for describing the outer shape of the design domain, and by combining gradient-based optimization solvers with analytically derived shape and topology sensitivities. The coupled method has been implemented in a finite element framework to analyze 2D, 2.5D, and 3D structural design problems. The results of representative case studies clearly show that the features of the design domain can have a large influence on the final topology calculated. Additionally, the optimization sequence in the coupled method may affect the path followed within the design space; however, this typically only has a minor effect on the final computational result. [1] Bendsøe, M.P., Sigmund, O. (2004). Topology optimization by distribution of isotropic Material. In Topology Optimization (pp. 1-69). Springer, Berlin, Heidelberg. [2] Sigmund, O., Maute, K. (2013). Topology optimization approaches. Structural and Multidisciplinary Optimization, 48(6), 1031-1055. Keywords: Structural design, Shape optimization, Topology optimization, Coupled model.

Numerical Modeling of Oligocrystalline Shape Memory Alloys

Zhiyi Wang^{*}, Raul Radovitzky^{**}, Bianca Giovanardi^{***}

^{*}MIT, ^{**}MIT, ^{***}MIT

ABSTRACT

Shape memory alloys (SMAs) are a class of metal alloys that can recover their original shapes when heated above a certain temperature. Unique features including the superelasticity and shape memory effect have made shape memory alloys attractive materials for a variety of fields ranging from bioengineering to aerospace engineering. In polycrystalline forms, the desirable properties of SMAs have been tremendously compromised by the brittleness problem due to severe premature intergranular fractures around grain boundaries and triple junctions. To overcome the problem of detrimental intergranular fracture, Chen et al. (2009) designed Cu-based SMAs in fine wire forms with bamboo-shaped oligocrystal microstructure. Experiments show that, by carefully designing the microstructure of oligocrystalline SMAs (oSMAs), mechanical properties approaching those of a single crystal can be achieved without being limited by various constraints involved in single crystal processing. It is, thus, of great importance to investigate how the microstructure and grain boundary characters affect the phase transformation and transformation-induced fracture of oSMAs. To study the impact of grain constraints on the ductility limits and investigate the mechanism of transformation-induced fracture in oSMAs from a numerical perspective, a three-dimensional anisotropic rate-dependent constitutive model is proposed. The model is based on the framework of the crystal-mechanics-based constitutive model by Thamburaja and Anand (2001) and features a robust explicit integration scheme to update the constitutive law. Finite element simulations are performed to model the mechanical response and martensite-austenite phase transformation of oSMA wires with triple junction structures. Quantitative analysis is conducted at the microstructural level to interpret the transformation-induced fracture. This model is able to predict the transformation-induced intergranular fracture in oSMA wires and provide insights on the mechanical response, energy absorption and microstructural design of oSMA wires.

Efficient Simulation of Tire Tread Block Dynamics

Matthias Wangenheim*

*Leibniz University of Hannover

ABSTRACT

All forces in vehicle-road contact are transmitted solely via the tire tread: Longitudinal forces - braking/acceleration maneuvers, lateral - cornering, vertical - vibration excitation). Tire tread blocks as the outermost layers of a tire are subject to highly dynamic load and load changes. To be able to simulate tread block dynamics under these transient conditions, efficient models are required. In this presentation I will derive an efficient 3D tread block model with rubber elastic and damping material properties. To optimize calculation time, model order reduction according to Craig & Bampton is applied. The local coefficient of friction between contact nodes and road surface is given in the form of friction characteristics in terms of temperature, sliding velocity and contact pressure; these characteristics originate from in house friction test results. The tread block is following a rolling trajectory, which is approximated to the one provided by the belt in real tires. As validation we vary the width of the tread blocks and compare the results with friction tests performed in our lab: The differences in traction potential between small blocks (winter tire) and wide blocks (summer tires) become obvious - the transmittable coefficient of friction of summer tires is significantly higher on dry road surfaces.

Investigating Dislocation Motion at Ordinary Timescales with Atomistic Simulations and Reaction Rate Theory

Derek Warner^{*}, Sepehr Saroukhani^{**}

^{*}Cornell University, ^{**}Cornell University

ABSTRACT

To fully utilize the potential of atomistic-to-continuum coupling techniques, their application to finite temperatures and long timescales must be developed. A key challenge in this task is that the success of long timescale atomistic simulations approaches is often specific to the process being examined. This talk will discuss our examination of thermally activated dislocation motion across a field of solutes. First, the accuracy of popular variants of the Harmonic Transition State Theory, as the most common approach, will be examined by comparing predictions to direct MD simulations. Next, the utility of the Transition Interface Sampling will be discussed, as the method was recently shown to be effective for predicting the rate of dislocation-precipitate interactions. For dislocation-solute interactions studied here, TIS was found to be accurate only when the dislocation overcomes multiple obstacles at a time, i.e. jerky motion, and it is inaccurate in the unpinning regime where the energy barrier is of diffusive nature. It will then be shown that the Partial Path TIS method - designed for diffusive barriers - provides accurate predictions in the unpinning regime. The use of the two methods to study the temperature and load dependence of the rate will be presented, where it was found that the Meyer-Neldel (MN) rule prediction of the entropy barrier is not as accurate as it is in the case of dislocation-precipitate interactions. In response, an alternative model will be proposed that provides an accurate prediction of the entropy barrier. This model can be combined with TST to offer an attractively simple rate prediction approach. Lastly, (PP)TIS predictions of the Strain Rate Sensitivity (SRS) factor at experimental strain rates and the predictions will be compared to experimental values.

Multi-Modal Sensor Fusion for State Estimation of an Adaptive Structures Test Bench

Alexander Warsewa^{*}, Oliver Sawodny^{**}, Cristina Tarín-Sauer^{***}, Flavio Guerra^{****}, Philipp Rapp^{*****}, Tobias Haist^{*****}, Wolfgang Osten^{*****}

^{*}Institute for System Dynamics, University of Stuttgart, Germany, ^{**}Institute for System Dynamics, University of Stuttgart, Germany, ^{***}Institute for System Dynamics, University of Stuttgart, Germany, ^{****}Institute of Applied Optics, University of Stuttgart, Germany, ^{*****}Institute for System Dynamics, University of Stuttgart, Germany, ^{*****}Institute of Applied Optics, University of Stuttgart, Germany, ^{*****}Institute of Applied Optics, University of Stuttgart, Germany

ABSTRACT

In this contribution, we consider the problem of state estimation for adaptive truss structures equipped with a multitude of sensors and actuators spanning different domains [1]. For reliable actuation of such a system, knowledge of the system state, consisting of the building deformation that can be quantified by the spatial deviation of certain building points, is required. However, in a general application, the state is not usually fully measurable, which is why state estimation techniques have to be employed [2]. A scale model of an adaptive truss structure with additional plates is available as an experimentation platform in our laboratory as a scaled version of an actual multi-story building. It is equipped with strain gauges, inertial measurement units and an optical measurement system. The optical measurement system consists of several light emitters, which are attached to the structure's outer faces and point to a remote camera. Using computer generated holograms and a multi-image technique, measurement of the emitter position is achieved with high precision. Sensor fusion is carried out and a complete state estimation is performed. Results obtained by an existing simulation model are experimentally validated on the test bench using actual measurement data. [1] W. Sobek and P. Teuffel, "Adaptive systems in architecture and structural engineering," Proceedings of SPIE, vol. 4330, 2001, pp. 36–45. [2] P. Rapp, M. Heidingsfeld, M. Böhm, O. Sawodny, and C. Tarín, "Multimodal Sensor Fusion of Inertial, Strain, and Distance Data for State Estimation of Adaptive Structures using Particle Filtering", Proceedings of the 2017 IEEE/ASME International Conference on Advanced Intelligent Mechatronics (AIM 2017), 2017.

Pelvic Response of a Total Human Body Finite Element (FE) Model During Simulated Under Body Blast (UBB) Impacts

Caitlin Weaver^{*}, Berkan Guleyupoglu^{**}, Joel Stitzel^{***}

^{*}U.S. Army Research Laboratory; Wake Forest University, School of Medicine, ^{**}Wake Forest University, School of Medicine, ^{***}Wake Forest University, School of Medicine

ABSTRACT

Under body blast (UBB) events in theater are the cause of many serious injuries sustained by the warfighter to the pelvis, spine, and lower extremities. Injury prediction for UBB events continues to be a challenge due to the limited availability of UBB-specific test studies. This study focuses on the pelvic injury response of the 50th percentile male Global Human Body Models Consortium (GHBMC) FE human body model. The input data used for this study was obtained from testing performed by the Warrior Injury Assessment Manikin (WIAMan) development effort. Evaluation of GHBMC model fidelity and injury response is based on biofidelity targets (corridors) created using pelvis accelerations obtained from experimental testing of UBB-type loading using post mortem human subjects (PMHS). In total, 10 simulations were performed at non-injurious velocities using experimentally recorded seat and floor pulses of 4 m/s. For these simulations, the GHBMC was positioned in a FE vehicle rig seat within the measured tolerances used to position the PMHS for experimental testing. Acceleration data from nodes in the S1 region of the pelvis of the GHBMC were extracted from the simulations. The extracted S1 acceleration data was compared to the biofidelity response corridors (BRCs) for the S1 region of the pelvis developed by the WIAMan program. Additionally, peak force data was extracted from FE cross-sections implemented in localized regions of the pelvis. An analysis was performed using an objective rating method (CORrelation and Analysis, CORA) using the BRC curves. The ± 0.5 and ± 1 SD curves were used for the inner and outer corridor limits, respectively. The average corridor curve was used as the cross-correlation reference. The CORA analysis showed good correlation (70% or higher) of the FE S1 acceleration for all 10 tests when compared to the BRCs. Additionally, the cross-sectional forces from these simulations were compared to pelvic fracture injury risk curves (IRCs) developed for the GHBMC. The peak force values from these simulations exhibited low risk of fracture (below 25%) in these cross-sectional regions. To date, the comparison of full body UBB experimental testing to drive and compare with full body FE simulation metrics for UBB is unique. This data was acquired with the explicit purpose of developing an enhanced capability to predict the risk of injury for mounted soldiers who are subjected to the effects of UBB loading with the goal of enhanced vehicle and soldier survivability.

Identifying and Applying State-Space Models Derived from High-Fidelity Physical Models of Li-ion Batteries

Peter Weddle^{*}, Tyrone Vincent^{**}, Huayang Zhu^{***}, Robert Kee^{****}

^{*}Colorado School of Mines, ^{**}Colorado School of Mines, ^{***}Colorado School of Mines, ^{****}Colorado School of Mines

ABSTRACT

- This paper develops and demonstrates a method to obtain and implement wide-bandwidth, linear, state-space models using binary perturbation. At specified operating conditions (e.g., temperature and state-of-charge), state-space models are identified from physically based battery models using pseudo-random binary sequences (PRBS). These state-space models predict the battery's current-voltage and current-temperature responses over specific frequency ranges. However, because the identified state-space models are accurate over limited frequency ranges, a "stitching" procedure is implemented to develop a single state-space model that is accurate over wide frequency ranges for particular operating conditions. The stitched state-space models, each accurate for particular operating conditions, are gain-scheduled to predict a battery's electrochemical and thermal responses over wide operating ranges. A validation study shows excellent agreement between the low-order gain-scheduled state-space models and the original large-scale physical model. Once validated, the state-space models may be incorporated into model-predictive-control (MPC) algorithms. In the present study, state-space models are identified from large-scale physical models. However, the computational approach is equally applicable to identifying and applying state-space models from experimental investigations.

Isogeometric Design Optimization of Nonlinear 3D Beam Structures for Multi-material 3D Printing and Soft Lattices

Oliver Weeger*, David W. Rosen**, Martin L. Dunn***, Sai-Kit Yeung****

*Singapore University of Technology and Design, **Singapore University of Technology and Design, ***University of Colorado Denver, ****Singapore University of Technology and Design

ABSTRACT

In recent years, many new possibilities for design and manufacturing of slender and light-weight structures have emerged through the advancement of advanced and additive manufacturing technologies. Existing and potential applications range from 3D printed micro-structures and meta-materials with slender members, to multi-functional, multi-material and composite structures with locally designed, spatially varying material properties, and to active, smart and self-assembling materials, structures and soft robots with compliant components and tailored large deformation behavior. These new perspectives call for novel design technologies that are capable of optimizing design, shape, and materials of structures subject to large deformations, material nonlinearities, graded and anisotropic materials, functional behavior, etc. In this work, we apply the concept of isogeometric design and analysis for combined shape, topology and design optimization of nonlinear, 3-dimensional beam structures. The mechanics of 3D beams are modelled by the geometrically exact, nonlinear Cosserat rod theory and discretized by an efficient and accurate, NURBS-based isogeometric collocation method [1]. By introducing spline parameterizations not only for the parameterization of geometry, here the centerline positions and cross-section orientations of the rods, but also for material and geometric cross-sections parameters of spatially-variable and functionally-graded rods, e.g. Young's moduli, radii, and layer-ratios of laminate cross-sections, as well as density, we can optimize shape, design and topology of rods and rod structures in a unified isogeometric framework. The resulting nonlinear optimization problem is implemented with analytical design sensitivities using the adjoint method and solved by standard gradient-based optimization methods. The approach is integrated into an isogeometric digital design and fabrication framework from CAD of rod structures, to analysis and optimization of their properties, and to additive manufacturing. We demonstrate our method in several additive manufacturing applications of functional rod structures, including multi-material 3D and 4D printed self-assembling structures [2] and soft, compliant lattice structures [3]. With our isogeometric design-to-manufacturing framework, we show the viability of using of isogeometric analysis and optimization for industrial-type applications. REFERENCES [1] O. Weeger, S.-K. Yeung, M. L. Dunn, "Isogeometric collocation methods for Cosserat rods and rod structures", *Comput. Methods Appl. Mech. Eng.*, Vol. 316, pp. 100–122, (2017). [2] O. Weeger, Y. S. B. Kang, S.-K. Yeung, M. L. Dunn, "Optimal Design and Manufacture of Active Rod Structures with Spatially Variable Materials", *3D Print. Addit. Manuf.*, Vol. 3(4), pp. 204–215, (2016). [3] O. Weeger, N. Boddeti, S.-K. Yeung, S. Kaijima, M. L. Dunn, "Digital Design and Manufacture of Soft Lattice Structures", *Addit. Manuf.*, under review, (2017).

Modeling and Design Optimization of Dynamic Structural Systems under Uncertainty: Application to Epicyclic Gearing

Erich Wehrle^{*}, Ilaria Palomba^{**}, Rafael Rojas^{***}, Renato Vidoni^{****}

^{*}Free University of Bozen-Bolzano, ^{**}Free University of Bozen-Bolzano, ^{***}Free University of Bozen-Bolzano,
^{****}Free University of Bozen-Bolzano

ABSTRACT

Modeling and design optimization of static mechanical systems has become routine in the development process, while for dynamic systems, challenges remain. Here, these challenges with dynamic structural and mechanical systems will be shown exemplary with epicyclic gearing. Epicyclic gearing has a wide range of applications and can be found in the drive trains of wind turbines, automotive automatic transmissions and automation systems. In this work, numerical optimization methods play a central role and are used to fit model parameters, for uncertainty analysis and to synthesize optimal designs. Parametric models of the dynamic and vibrational behavior are developed and applied to epicyclic gearing. Specifically, the resonance frequencies and frequency-response functions are calculated and used for design performance and limit measures. Results of experimental tests on a benchmark gear system validate these models and identify discrepancies. Numerical optimization is used to fit model parameters to tune values to meet experimental results. Intrinsic uncertainty is handled with interval methods, which bound the uncertain values instead of modeling them with probabilistic distributions. An efficient optimization-based minimization–maximization method is used to carry out uncertainty analyses. These give interval resonance frequencies and interval frequency-response functions, showing the upper- and lower-bound values, which in turn can be used in the design process to guarantee proper performance. Better performance is considered those designs that reduce the vibrational content for an operating case and, therefore, possible noise and fatigue problems. A general design optimization under uncertainty for dynamic systems is shown and used to find optimal designs and applied to a planetary gear system. Though, the same methodology can be used for other applications, such as the energy can also be maximized in cases of energy harvesting. Comparison of optimization methodologies is also shown: zeroth-order algorithms will be contrasted with first- and second-order algorithms as well as with approximation-based optimization in regards to computational effort, repeatability and performance of the optimal design found. Analytical sensitivity analysis allows for added numerical efficiency of the optimization methods. In addition, the sensitivities allow for postprocessing assessments of the optimal results, which assess the effect of the constraint limits (frequency ranges) and uncertainty levels (uncertain stiffnesses) on the objective function. Results are then summarized, providing insight on the design and analysis of dynamical systems and specifically planetary gear trains. This insight can be applied with and without the use of optimization methods, for the latter in the form of design rules.

Quasi-three-dimensional Phase Field Modeling of Martensitic Phase Transformation in Shape Memory Alloys

Cheng Wei^{*}, Changbo Ke^{**}, Shuibao Liang^{***}, Xinping Zhang^{****}

^{*}South China University of Technology, ^{**}South China University of Technology, ^{***}South China University of Technology, ^{****}South China University of Technology

ABSTRACT

ABSTRACT The physical and mechanical properties of materials with martensitic phase transformation are significantly influenced by the martensitic transformation process and so-obtained microstructures. In the past two decades, the phase field method has been developed to study the martensitic transformation (MT) behavior and evolution of martensitic microstructure [1-3]. Compared with two-dimensional (2D) simulation, the three-dimensional (3D) modeling of MT has all six components of the stress-free transformation strain. Therefore, all possible variants in MT can be characterized simultaneously by 3D phase field simulation. Further, the complex orientation relationship can be easily revealed in 3D space. However, much more computations are required in 3D phase field simulation. As a consequence, the 3D simulation system (or domain) is restricted to be very small, which is difficult to obtain useful information showing the whole scenario of martensitic transformation. In this study, a quasi-three-dimensional model based on phase field method is developed to reveal martensitic transformation characteristics in shape memory alloys. In the model, we introduce additional degrees of freedom to each node of the plane element in finite element method. So the all six components of the stress-free transformation strain could be expressed. Meanwhile, the order parameter gradient of the vertical direction is used as a new variable to show the angle between the interfacial plane and simulated plane in the microstructure. Thus, the model developed by the present study can well simulate martensitic transformation in arbitrary plane containing all possible variants. **Keywords:** Phase field; Quasi-three-dimensional modeling; Martensitic transformation; Finite element method **References** [1] Wang Y, Khachaturyan A G. Three-dimensional field model and computer modeling of martensitic transformations [J]. Acta Mater., 1997, 45: 759. [2] Ke C B, Ma X, Zhang X P. Phase field simulation of effects of pores on B2-R phase transformation in NiTi shape memory alloy [J]. Acta Metall. Sin., 2011, 47: 129 [3] Paranjape H M, Manjiraju S, Anderson P M. A phase field – Finite element approach to model the interaction between phase transformations and plasticity in shape memory alloys [J]. Int. J. Plasticity, 2016, 80: 1

A Mixed RKPM Formulation for Modeling Hydro-Mechanical Damage Processes in Multiphase Porous Media

Haoyan Wei^{*}, J. S. Chen^{**}

^{*}University of California, San Diego, ^{**}University of California, San Diego

ABSTRACT

In the first part of this work, a stabilized Reproducing Kernel Particle Method (RKPM) u-p formulation for hydro-mechanical modeling of multiphase porous media is developed [1]. In this approach, a stable equal-order u-p reproducing kernel approximation for the fluid-saturated porous media is developed by employing a fluid pressure projection method under a variationally consistent nodal integration framework [2] with a least-squares stabilization [3]. It has been shown that the fluid pressure projection method can be naturally integrated within the stabilized conforming nodal integration framework, and thus the non-physical fluid pressure oscillation due to a violation of the inf-sup condition as well as the spurious low-energy modes due to nodal integration can both be eliminated cost-effectively. Next, to capture the complex evolving crack patterns in porous geo-materials, the damage particle method [4] which approximates fractures by a set of damaged particles under the RKPM discretization is introduced. For each damaged particle, a regularized smeared description of the equivalent crack segment at the nodal position is adopted, which avoids spurious damage growth and ensures the objectivity of energy dissipation. The proposed methods are applied to the modeling of landslide and hydraulic fracturing processes. References [1] Wei, H., Chen, J. S., & Hillman, M. (2016). A stabilized nodally integrated meshfree formulation for fully coupled hydro-mechanical analysis of fluid-saturated porous media. *Computers & Fluids*, 141, 105-115. [2] Chen, J. S., Hillman, M., Rüter, M. (2013) An arbitrary order variationally consistent integration method for Galerkin meshfree methods. *International Journal for Numerical Methods in Engineering*, 95(5): 387-418. [3] Puso, M. A., Chen, J. S., Zywickz, E., & Elmer, W. (2008). Meshfree and finite element nodal integration methods. *International Journal for Numerical Methods in Engineering*, 74(3), 416-446. [4] Chen, J. S., Wei, H. (2018). A reproducing kernel damage particle method for multiscale modeling of fracture. *International Journal for Multiscale Computational Engineering* (to be submitted).

A Nonlocal Yield Criterion for Modeling Elastoplastic Deformation in Volume-Compensated Particle Model

Haoyang Wei^{*}, Hailong Chen^{**}, Yongming Liu^{***}

^{*}Arizona State University, ^{**}Idaho National laboratory, ^{***}Arizona State University

ABSTRACT

Abstract Volume-Compensated Particle Method (VCPM) [1] is a newly proposed nonlocal discontinuous formulation of classical continuum mechanics for mechanical problems with focus on spatial discontinuity. In VCPM, domain of interest is decomposed into discrete material points based on various lattice structures. Each material point interacts with neighboring material points up to certain distance. The interaction between a pair of material points depends on not only the deformations of the two material points themselves, but also the collectively deformation of all their neighbors. Model parameters for calculation of pairwise interactions are derived from material constants, such as Young's modulus and Poisson's Ratio, based on the strain energy equivalence between discontinuous formulation and its continuum counterpart. Since the equation of motion is governed by integro-differential equations, there are no singularity issues in VCPM for problems with spatial discontinuity, such as crack. Discontinuity initiation and propagation are the natural outcome of interaction removal. VCPM has been applied to study various behaviors of solid in the literature. For modeling ductile materials using VCPM, Chen et al. [2] proposed a one-dimensional bond-based critical stretch criterion to model elastoplastic deformation. This criterion only considers specific interaction between one neighboring particle and the particle of interest. The non-local multi-body effect is neglected in this criterion. In this work, a yield criterion for VCPM is proposed to account for the nonlocal effect from all neighbors. This proposed nonlocal yield criterion for each bond depends on not only the deformation of the two material points connected by this bond but also the deformation of all their neighbors. The Atomic Finite Element Method (AFEM) algorithm is implemented to determine the equilibrium state of solids under quasi-static loading. Because of the nonlinearity in an elastoplastic constitutive law, iteration method in combination with incremental loading method is used in the solution procedure. Numerical examples under various loading cases, i.e., uniaxial loading and multiaxial loading, are simulated using the proposed nonlocal yield criterion in VCPM. Good prediction accuracy is established by comparison between VCPM simulation results and ABAQUS simulation results. Reference [1] Chen, H., Jiao, Y., & Liu, Y. (2015). Investigating the microstructural effect on elastic and fracture behavior of polycrystals using a nonlocal lattice particle model. *Materials Science and Engineering: A*, 631, 173-180. [2] Chen, H., Lin, E., & Liu, Y. (2014). A novel Volume-Compensated Particle method for 2D elasticity and plasticity analysis. *International Journal of Solids and Structures*, 51(9), 1819-1833.

Blended B-Spline Construction on Unstructured Quadrilateral and Hexahedral Meshes with Optimal Convergence Rates in Isogeometric Analysis

Xiaodong Wei^{*}, Yongjie Zhang^{**}, Deepesh Toshniwal^{***}, Hendrik Speleers^{****}, Xin Li^{*****}, Carla Manni^{*****}, John Evans^{*****}, Thomas Hughes^{*****}

^{*}Carnegie Mellon University, ^{**}Carnegie Mellon University, ^{***}The University of Texas at Austin, ^{****}University of Rome, ^{*****}University of Science and Technology of China, ^{*****}University of Rome, ^{*****}University of Colorado Boulder, ^{*****}The University of Texas at Austin

ABSTRACT

We present a novel blended B-spline method to construct bicubic/tricubic splines over unstructured quadrilateral and hexahedral meshes for isogeometric analysis. C1 and (truncated) C2 B-spline functions are used in regular elements, whereas C0 and (truncated) C1 B-spline functions are adopted in boundary elements and interior irregular elements around extraordinary edges/vertices. The truncation mechanism is employed for a seamless transition from irregular to regular elements. The resulting regularity of the blended construction is C2-continuous everywhere except C0-continuous around extraordinary edges and C1-continuous across the interface between irregular and regular elements. The blended B-spline construction yields consistent parameterization during refinement and exhibits optimal convergence rates. Spline functions in the blended construction form a non-negative partition of unity, are linearly independent, and support Bézier extraction such that the construction can be used in existing finite element frameworks. Several examples provide numerical evidence of optimal convergence rates.

Graphene-substrate Interaction and Defects Guided Wrinkling in Graphene

Yujie Wei^{*}, Zhenqian Pang^{**}

^{*}LNM, Inst. of Mechanics, Chinese Academy of Sciences, ^{**}University of Chinese Academy of Sciences

ABSTRACT

The pattern of wrinkles is governed by the crystallographic planes of the substrates and the defects in the film. In this talk, we report how graphene-substrate interaction as well as commonly seen Stone-Wales defects and grain boundaries (GBs) influence the morphology of graphene on different planes of single crystalline copper substrate. Stone-Wales defects weaken the bending stiffness in graphene, and results in wrinkling along the defect direction. In the presence of GBs, primary wrinkles are always parallel to the GB direction, and there are also secondary wrinkles perpendicular to the GB. In combination with planes of the substrate and the orientation of defects, we demonstrate that we may manipulate wrinkling patterns for possible engineering applications.

A Biophysical Model for Neurodegeneration in the Aging Brain

Johannes Weickenmeier*

*Stevens Institute of Technology

ABSTRACT

Biochemical and morphological changes in the aging brain manifest in a progressive cognitive decline, loss of motor control and behavioral changes. We are slowly starting to understand some of the mechanisms of progressive neurodegenerative diseases, such as Alzheimer's disease, Parkinson's disease, and Lewy body dementia, which are generally associated with a propagation of toxic proteins through the brain which cause localized neuron cell death. While the involved misfolded proteins, or prions, such as amyloid-beta, tau, or Lewy bodies, differ for each disease, most neurodegenerative diseases show similar propagation patterns through the brain. Once an initial "toxic seed" appears, prions diffuse through the brain and aggregate in the cortical and subcortical layer. Local aggregation of mature senile plaques leads to the death of neurons and an accelerated spreading of the disease. This progressive neuron death manifests in gray and white matter loss with increasing age and the appearance of clinically known symptoms of neurodegenerative diseases. We present a finite element formulation that couples a reaction-diffusion equation for the prion propagation and classical growth mechanics for the gray and white matter loss in the aging brain. The spreading of prions is characterized by an isotropic propagation through the glial network and an anisotropic diffusion along white matter axons; volume loss due to neuron cell death is driven by the local prion concentration. Based on an anatomically accurate finite element model of the brain, we can reproduce characteristic propagation patterns [1] through the brain and the experimentally observed white and gray matter volume loss over time [2]. Our finite element framework serves as a model system to systematically test propagation mechanisms of individual toxic proteins and to provide new insight into the progression of neurodegenerative disease across temporal and spatial scales. References: [1] Jucker and Walker. Self-propagation of pathogenic protein aggregates in neurodegenerative diseases. Nature 2013. [2] Fjell et al. Critical ages in the life course of the adult brain: nonlinear subcortical aging. Neurobiology of Aging 2013

Generative Design of Lightweight Lattice Structures with Additive Manufacturing Constraints

David Weinberg*, Nam-Ho Kim**

*Autodesk, Inc., **University of Florida

ABSTRACT

For the past three decades, topology optimization has been remarkably popular in the engineering design community due to its capability on designing lightweight structures by optimally distributing materials to carry loads. Autodesk Nastran has implemented topology optimization since 2014 and rapidly enhancing its capabilities, including multidisciplinary optimization, hierarchical distributed computing, and various manufacturing method-oriented design. In particular, generating lightweight designs that can be producible by various manufacturing methods is critically important in industry. The topology optimization in Autodesk Nastran can include various manufacturing methods, such as minimum member size, multiple symmetry planes, extrusion, casting, milling, and 3D printing. In particular, 3D printing, or additive manufacturing, becomes an emerging technology as it allows manufacturing complex shapes that were not possible in conventional subtractive manufacturing technologies, such as milling. The current research trend in topology optimization for additive manufacturing focuses on how to design a structure so that the amount of supporting materials can be reduced or removed. However, the technology still remains in the regime of producing solid, isotropic materials. Due to remarkable advances in the additive manufacturing technology, it is now possible to build lattice structures, which involve repetitive patterns of a particular cell shape or type. In fact, lattice structures can be a unique feature for additive manufacturing. It has been demonstrated that lattice structures can reduce the structural weight with the same functionality as with homogeneous materials. This presentation discusses recent developments in topology optimization and lattice structures implemented in Autodesk Nastran. Autodesk Nastran supports lattice structures in topology optimization using Representative Volume Elements (RVEs) so that non-homogeneous tetra element meshes can be used to obtain optimized designs. Multiple design spaces are supported and each design space can have a different lattice material, cell size, member radius, and lattice type. Lattice and non-lattice design spaces can also be mixed. A standard topology optimization is run and the lattice material stiffness is updated every iteration and stresses and stability indexes are computed which reflect actual lattice beam member values. A smoothed STL and optional BREP geometry file are generated at the completion of each analysis which can be meshed using either RVEs (tet10 elements) or shell/beam elements (Autodesk Within) and analyzed for design verification. The presentation will cover the basic theory used in Autodesk Nastran topology optimization including stress and additive manufacturing constraints as well as several examples and classic benchmark problems.

Modelling Particle Segregation in Horizontal Rotating Drums

Thomas Weinhart^{*}, Deepak Tunuguntla^{**}, Anthony Thornton^{***}

^{*}University of Twente, ^{**}Dept. of Thermal and Fluid Engineering, University of Twente, ^{***}Dept. of Thermal and Fluid Engineering, University of Twente

ABSTRACT

In several industrial applications, granular materials are often vibrated (shaken) or rotated (sheared) while being processed and transported. As a result, particles or grains with similar characteristics such as the size, density, shape and et cetera typically end up together to find themselves arranged in a range of patterns. This is termed as particle segregation. For example, large particles in bidisperse-in-size mixtures rise towards the free surface when subjected to external vibrations (Brazil-nut effect [1]). On the other hand, small particles form a radial core surrounded by large particles in horizontal rotating drums [2]. Thereby, leading to particle segregation in the radial direction. This presentation focuses on the later scenario, which is particle segregation in horizontal rotated drums. In the past few decades, many experimental and simulational studies have observed and investigated particle segregation in horizontal rotating drums, e.g., [2,3]; however, only a handful of studies have focused on modelling particle segregation in these rotated systems, e.g., [4]. Thereby, as a stepping stone towards predicting particle segregation in mixtures comprising complex granular materials, this work focuses on modelling segregation in bidisperse mixtures comprising of spheres varying in, both, size and density. Similar to our previous modelling work regarding segregation in inclined channel flows [5,6], we will showcase recent advances in utilising the continuum theory for predicting particle segregation in horizontal rotating drums, which will be further validated by utilising experiments or particle simulations. References: [1] A. Rosato, K.J. Strandburg, F. Prinz and R. H. Swendsen, Phys. Rev. Lett. 58 (1987) [2] M. M. H. D. Arntz, H. H. Beertink, W. K. den Otter, W.J. Briels and R.M. Boom, AIChE J. 60 (2014) [3] C. R. K. Windows-Yule, B. J. Scheper, A. J. van der Horn, N. Hainsworth, J. Saunders, D. J. Parker and A. R. Thornton, New J. Phys. 18 (2016) [4] C. P. Schlick, Y. Fan, P. B. Umbanhowar, J. M. Ottino and R. M. Lueptow, J. Fluid Mech. 765 (2016) [5] D.R. Tunuguntla, O. Bokhove and A.R. Thornton, J. Fluid Mech. 749 (2014) [6] D.R. Tunuguntla, T. Weinhart and A.R. Thornton, Comp. Part. Mech. 4(4) (2017)

Contributions of the Osteocyte Canalicular Network to Mineral Homeostasis and Bone's Mechano-Sensitivity

Richard Weinkamer*, Alexander van Tol**, Andreas Roschger***, Junning Chen****, Felix Repp*****, Wolfgang Wagermaier*****, Philip Kollmannsberger*****, Paul Roschger Roschger*****, Peter Fratzl*****

*Max Planck Institute of Colloids and Interfaces, Department of Biomaterials, Potsdam, Germany, **Max Planck Institute of Colloids and Interfaces, Department of Biomaterials, Potsdam, Germany, ***Max Planck Institute of Colloids and Interfaces, Department of Biomaterials, Potsdam, Germany, ****Department of Engineering, University of Exeter, Exeter, United Kingdom, *****Max Planck Institute of Colloids and Interfaces, Department of Biomaterials, Potsdam, Germany, *****Max Planck Institute of Colloids and Interfaces, Department of Biomaterials, Potsdam, Germany, *****Center for Computational and Theoretical Biology, Universität Würzburg, Germany, *****Ludwig Boltzmann Institute of Osteology at the Hanusch Hospital of WGKK and AUVA Trauma Centre Meidling, Vienna, Austria, *****Max Planck Institute of Colloids and Interfaces, Department of Biomaterials, Potsdam, Germany

ABSTRACT

During bone formation, some of the bone-forming osteoblasts stay behind, are walled into the bone matrix and differentiate into osteocytes. These osteocytes use a network of cavities and sub-micrometer wide canals - lacunae and canaliculi - to house their cell bodies and processes, respectively, and to connect with other osteocytes. The importance of the osteocyte network and the corresponding porosity, the osteocyte lacuna-canalicular network (OLCN), has its reason in the ascribed multi-functionality of this structure [1]: (i) mechano-sensation via the detection of the fluid flow through canaliculi; (ii) contribution to mineral homeostasis by exploiting the large surface area provided by the network; (iii) transport of nutrients and signaling molecules. Using a combination of complementary experimental characterization methods, image analysis and computational modeling, we aimed, firstly, to detect spatial correlations between network density and mineral content of the bone to shed light on the network's role in mineral homeostasis, and, secondly, to assess the influence of the network topology [2] on fluid flow through the OLCN. The investigations were performed on human osteons in the femora of healthy middle-aged individuals. Samples were stained with rhodamine and the canalicular network was imaged using confocal laser scanning microscopy and quantified by the canalicular density [3], i.e. the total length of canaliculi per unit volume. The position-dependent mineral content of the same osteons was determined with quantitative backscattered electron imaging. To assess the fluid flow and pressure patterns induced by bone deformation under compression, a model analogous to electric circuits was implemented. A spatial correlation analysis between small regions of interest in the osteons showed that a locally dense canalicular network coincided with an increased mineral content. This accumulation of mineral hints at a mineral reservoir connected to the canalicular network. The fluid flow calculations demonstrated the importance of network density and connectivity for permeability. Particularly striking were the differences in the flow patterns between normal osteons and so-called osteons-in-osteons, where only a few canaliculi bridge the outer part to the inner part formed by remodeling. [1] Kerschnitzki, M., Kollmannsberger, P., Burghammer, M., Duda, G. N., Weinkamer, R., Wagermaier, W., Fratzl, P. (2013), JBMR 28, 1837. [2] Kollmannsberger, P., Kerschnitzki, M., Repp, F., Wagermaier, W., Weinkamer, R., Fratzl, P. (2017), New J.Phys. 19, 073019. [3] Repp, F., Kollmannsberger, P., Roschger, A., Kerschnitzki, M., Berzlanovich, A., Gruber, G. M., Roschger P., Wagermaier, W., Weinkamer, R. (2017), Bone Reports 6, 101.

Intravenous Drug Release from Different Peripheral Catheters

Dar Weiss*, Halit Yaakobovich**, Oren Rotman***, Shmuel Einav****

*Tel Aviv university, Tel Aviv, Israel, **Tel Aviv university, Tel Aviv, Israel, ***Stony Brook university, NY, USA,
****Tel Aviv university, Tel Aviv, Israel; Stony Brook university, NY, USA

ABSTRACT

Intravenous therapy is the most common method for administration of medicine or fluid directly into the blood stream using short peripheral catheters (SPCs). Common complication of SPCs' use is thrombophlebitis, a sterile inflammation of the vein wall. Previous studies have shown that up to 80% of patients receiving intravenous therapy develop thrombophlebitis. To date, the biomechanical interaction between the SPCs and the endothelial venous wall has been shown to irritate and activate the endothelial cells thus promote inflammation processes. Very short peripheral catheter (VSPC) is a novel catheter design aimed to reduce the contact between the catheter and the venous wall in order to minimize the biomechanical factor in thrombophlebitis development. The present study aims to explore and compare the dynamics of drug release through the existing SPC and our novel VSPC using experimental and numerical models. An open in-vitro flow loop was designed to simulate drug injection through each of the catheters. Soluble dye injections were recorded and analyzed by image processing methods. Two 3D computational models were created combining a vein section and each of the catheters. The following parameters were measured; (i) Drug washout time; (ii) Drug distribution within the vein; (iii) Drug velocity at the catheter outflow. The results have shown significant dynamic advantage of the VSPC over the SPC; both drug velocity and removal time were faster while injected through VSPC, as well as drug distribution that was located away from the vessel wall when compared to the current commercial SPC. For both of the catheters, increased vein flow rate and injection flow rate resulted in higher proximity of the drug to the vein opposite wall, faster washout time and faster drug velocity at the outflow of the catheter. The results indicate that beyond the bio-mechanical advantage, the VSPC also has a dynamic advantage on the SPC in terms of drug flush profile. Releasing the drug away from the vessel wall can minimize adverse drug effect reaction and potentially reduced the risk for thrombophlebitis.

Representative Models of Polycrystalline and Cellular Materials for Simulation of Properties and Processes at Various Length Scales

Tomasz Wejrzanowski*

*Faculty of Materials Science and Engineering, Warsaw University of Technology, Poland

ABSTRACT

The ability to model the structure and properties of a material in a natural way leads to an analysis of structure-property relationships. The mesoscopic models developed as part of these studies can be formed in such a way that geometrical features of the microstructural elements (grains, pores, particles) can be modified with respect to their size, shape, orientation, and spatial position. On the other hand, the properties of the microstructural elements are modeled at atomic scale by application of relevant simulation techniques. The methods developed or adopted here allow one to simulate specific properties and/or processes taking place in the material [1-4]. Three groups of materials are described in these studies: nanometals, particulate composites and open-cell foams. These groups, apparently different from each other when applications are considered, reveal very similar microstructures. Each of the microstructures contains a specific type of interfaces: phase boundary, grain boundary and free surface, respectively. Properties of interfaces and accompanying processes can be simulated at the atomic-scale and the results of such calculations may provide additional data for the design of novel materials. Examples of properties and processes related to the microstructure and structure of interfaces, for a selected group of materials, are presented and discussed here. 1. M. Lewandowska, T. Wejrzanowski, K.J. Kurzydowski, Grain growth in ultrafine grained aluminium processed by hydrostatic extrusion, *Journal of Materials Science*, 43, 2008, 7495–7500 2. J. Skibinski, K. Cwieka, T. Kowalkowski, B. Wysocki, T. Wejrzanowski, K.J. Kurzydowski, The influence of pore size variation on the pressure drop in open-cell foams, *Materials and Design*, Materials and Design 87 (2015) 650–655. 3. T. Wejrzanowski, M. Grybczuk, M. Chmielewski, K. Pietrzak, K.J. Kurzydowski, A. Strojny-Nedza, Thermal conductivity of metal-graphene composites, *Materials & Design* 99 (2016) 163-173 4. T. Wejrzanowski, S. Haj Ibrahim, K. Cwieka, M. Loeffler, J. Milewski, E. Zschech, C-G. Lee, Multi-modal porous microstructure for high temperature fuel cell application, *Journal of Power Sources* 373 (2018) 85–94

Performance Engineering – Welcome to the World of FLOPs, Bytes and Cycles!

Gerhard Wellein*, Jan Eitzinger**, Georg Hager***

*Friedrich-Alexander-University Erlangen-Nuremberg, **Erlangen Regional Computing Center, ***Erlangen Regional Computing Center

ABSTRACT

We consider Performance Engineering (PE) as a structured, iterative process for code optimization and parallelization. The key ingredient is a performance model which provides insights into the interaction between the code and the hardware. The model identifies the actual performance-limiting factors (“bottlenecks”), allowing for a selection of appropriate code changes. Once the impact of the code changes is validated the process restarts with a new bottleneck identified by the performance model. Since this model-based approach provides a thorough understanding of the impact of hardware features on code performance it is also useful in various other areas such as performance reproducibility, performance prediction for future architectures or education and training. We first introduce our PE concept and survey basic “white-box” performance models [1,2] appropriate for performance modelling at the core- and node-level. Choosing a widely used benchmark suite [3] we demonstrate, that automatic “black-box” performance modelling may lead to misleading results if not used with due care. Focusing on selected kernels from sparse and dense linear algebra as well as stencil computations [2] we show various aspects and application scenarios of our “white box” approach. These include data layout considerations for sparse matrix vector product, correct choice of optimization strategies and parameters for stencil computations or identification of performance bottlenecks of building block libraries which are widely considered to be optimal but still can be improved by up to 10x through simple measures. We conclude that code implementation and optimization efforts may greatly benefit in terms of hardware-efficiency, portability and sustainability from using PE in combination with basic white-box performance models. This work is supported by the German Research Foundation (DFG) through the Priority Programs 1648 “Software for Exascale Computing” under projects ESSEX-II (<https://blogs.fau.de/essex/>) and EXASTEEL-2 (<http://www.numerik.uni-koeln.de/14079.html>)

References [1] Williams, S., Waterman, A., and Patterson, D., Commun. ACM 52 (4), 65 (2009). [2] Stengel, H., Treibig, J., Hager, G., and Wellein, G., Proceedings of the 29th ACM on International Conference on Supercomputing (ICS 2015), 207 (2015). [3] McVoy, L. and Staelin, C., Proceedings of the 1996 annual conference on USENIX Annual Technical Conference (ATEC ’96). USENIX Association, Berkeley, CA, USA, 23-23.

Multilevel Monte Carlo Methods for Random Vibration Problems

Garth Wells^{*}, Unwin Helena^{**}, Nathan Sime^{***}

^{*}University of Cambridge, ^{**}University of Cambridge, ^{***}University of Cambridge

ABSTRACT

Uncertainty quantification is important for many vibration problems as small variations in model details can have profound effects on the response of a system. To analyse such systems, Monte Carlo methods are widely considered to be computationally too expensive for problems of practical interest, and this has led to the development of many modelling approaches to randomness for vibration problems. These modelling approaches typically lack the flexibility and generality of Monte Carlo methods. In this presentation, we consider the time cost complexity of Monte Carlo methods for eigenvalue problems to show that it is in fact much worse than is commonly thought, and show how the complexity can be conquered by multilevel methods. Multilevel Monte Carlo methods build on the control variate acceleration of Monte Carlo methods by sampling 'coarse' representations of a model, with a limited number of 'correction' samples using the full fidelity model. We present analysis and numerical examples showing that a multilevel approach can make Monte Carlo methods computationally tractable for a range of engineering random vibration problems.

Creep-fatigue-oxidation Crack Growth by Grain Boundary Cavitation

Jian-Feng Wen^{*}, Ankit Srivastava^{**}, Amine Benzerga^{***}, Shan-Tung Tu^{****}, Alan Needleman^{*****}

^{*}East China University of Science and Technology, ^{**}Texas A&M; University, ^{***}Texas A&M; University, ^{****}East China University of Science and Technology, ^{*****}Texas A&M; University

ABSTRACT

Intergranular cracking of polycrystalline metals in components at high temperatures, under both sustained and cyclic loads, is dominated by various time-dependent mechanisms at the crack tip. In the study, grain boundary cavitation, with cavity growth due to both creep and diffusion, is taken as the major failure mechanism contributing to crack growth. Plane strain finite deformation finite element calculations of mode I crack growth under small scale creep conditions are conducted. The crack growth calculations are based on a micromechanics constitutive relation that couples creep deformation and damage due to grain boundary cavitation. In some calculations, solute-induced grain boundary weakening is modelled by decreasing the critical spacing for grain boundary cavity coalescence. The influence on the crack growth rate of loading history parameters and solute diffusion are explored. Several features of the crack growth behavior observed in creep-fatigue tests naturally emerge; for example, a Paris law type relation is obtained for cyclic loading and the crack growth rate is accelerated by the solute induced grain boundary weakening.

A Combination Rule for Coplanar Cracks under Fatigue and Creep Conditions

Jian-Feng Wen^{*}, Yong Zhan^{**}, Fu-Zhen Xuan^{***}, Shan-Tung Tu^{****}

^{*}East China University of Science and Technology, ^{**}East China University of Science and Technology, ^{***}East China University of Science and Technology, ^{****}East China University of Science and Technology

ABSTRACT

It is not uncommon to detect multiple flaws in structures under cyclic loading or at high temperature. A proper prediction of the interaction effect of them is important to prevent a potentially catastrophic failure. In the study, fatigue/creep crack growth simulations, for a plate containing two coplanar surface flaws with both identical and dissimilar sizes, are undertaken in detail by a step-by-step finite element analysis. Combination rules for multiple coplanar flaws provided by fitness-for-service codes are critically assessed for the fatigue/creep failure mode. It is realized that the conservatism contained in existing criteria is highly dependent on the ratio of crack depth to the thickness. With the increase of crack size, as well as the similarity between two cracks, some criteria may lead to a higher risk of non-conservative estimation. Based on the fatigue/creep crack growth life, we suggest a new combination rule and conclude that it always yields a reasonable estimation with necessary conservatism, for various initial crack depths, material constants and relative sizes of two cracks. The difference of conservative degree of combination rules under fatigue and creep conditions is also demonstrated.

A Study on the Influence of Multiple Points Flexible Support Device on Arc-weld Additive Manufacture Process

Pin Wen^{*}, Hongling Ye^{**}, Qingsheng Yang^{***}

^{*}Department of Mechanical Engineering and Applied Electronic Technology, Beijing University of Technology,

^{**}Department of Mechanical Engineering and Applied Electronic Technology, Beijing University of Technology,

^{***}Department of Mechanical Engineering and Applied Electronic Technology, Beijing University of Technology

ABSTRACT

Layer additive manufacturing is a promising technique for the rapid manufacturing and repair of metallic components. In this field, weld-based rapid prototyping has drawn lots of attention due to the advantages including high productivity, cost saving, and high bonding strength of components. The thermal and residual stress distributions in the welding process have been widely investigated in this study. The thermal and residual stress were also studied by experiment, which are corresponded with the simulation result. Moreover, a multiple-point flexible support device has been novel designed to prevent the deformation of base panel with arc-welded stiffener. Then the validated model was utilized to study when and how big the applied force and release time by the device is proper. The results show that the release time after the end of weld reduce the final deformation, which are not considered in most researches. For instance, when the applied force is 20N and kept for 44s in the numerical example, the deformation in the vertical axis can be eliminated. The validated model was then extended to the case of multi-path multi-layer arc-weld additive manufacture. If the time dependent force transfer from triangular into rectangular, it will provide a more efficient energy consumption. This device will play an important role in the application of welding process of large plate.

Numerical Simulation of Bubble Rising by IMPS-based Multiphase Method

Xiao Wen^{*}, Decheng Wan^{**}

^{*}Shanghai Jiao Tong University, ^{**}Shanghai Jiao Tong University

ABSTRACT

The numerical simulation of bubble rising is challenging since the tracing of deformed multiphase interface. In this paper, a new mesh-less multiphase method is developed based on the IMPS (Improved Moving Particle Semi-implicit) method and applied to simulate the phenomena of bubble rising. In this method, the multiphase system is treated as the multi-density and multi-viscosity fluid. To consider the interaction between particles belonging to different phases, inter-particle viscosity defined by the harmonic mean viscosity is firstly adopted. Then the density smoothing technique is employed to reduce pressure discontinuity crossing the interface to obtain the continuous acceleration and velocity fields. Since the shape of bubble is dominated by the tension on the interface, a contoured continuum surface force (CCSF) model is utilized in the present method. The new multiphase MPS method is validated through comparisons with published numerical data. In particular, the multiphase MPS method is verified against Hysing et al.'s (2009) quantitative benchmark computations of two-dimensional bubble dynamics. Two benchmark cases have been studied by the present method and the evolution of a single bubble rising in a liquid column is concerned. In the first case which corresponds to a low Eötvös number, the present numerical result indicates that the bubble withstands a moderate deformation and ends up in the ellipsoidal regime, while in the second case with a high Eötvös number, the bubble undergoes significant topology change and breaks up eventually. For both cases, good agreements achieved for the benchmark quantities, including circularity, center of mass, and mean rise velocity, which demonstrate the accuracy and stability of the present multiphase MPS method.

Phase-field Approach to Modeling of High-temperature Oxidation of Metals and Alloys

Youhai Wen^{*}, Tianle Cheng^{**}, Jeffrey Hawk^{***}

^{*}U.S. Department of Energy - NETL, ^{**}U.S. Department of Energy - NETL, ^{***}U.S. Department of Energy - NETL

ABSTRACT

Structural alloys at high-temperatures invariably rely on formation of a slowly growing surface layer of oxide for the necessary oxidation resistance. The transition from internal to external oxidation is often a basis for design of the alloys. During internal oxidation, oxide dilatation is usually severe so that it leads to elastoplastic deformation of the alloy matrix and/or the oxide itself. In addition, the oxide-alloy interface may gradually lose coherency with the growth of oxide precipitation. Modeling of these issues are not trivial and it needs to be resolved prior to realistic simulation of morphological/microstructural evolution of oxide-alloy systems. First, a diffuse-interface electrochemical model is developed to study the fundamental processes during external oxidation in terms of ionic diffusion, diffusion-reaction and the electric field effects. Insights are gained in terms of the applicability of Wagner theory. Furthermore, we develop a thermodynamically consistent phase-field framework to incorporate plasticity and interfacial coherency loss, which paves the way for next-step development of a physics-based phase-field model to study internal oxidation and the transition to external oxidation.

Closure of Reduced Order Models Using Statistical Mechanics Approaches

Christopher Wentland^{*}, Eric Parish^{**}, Karthik Duraisamy^{***}

^{*}University of Michigan, Ann Arbor, ^{**}University of Michigan, Ann Arbor, ^{***}University of Michigan, Ann Arbor

ABSTRACT

Reduced order models of multi-scale problems require the modeling of the impact of the unresolved modes on the resolved modes. This is typically referred to as closure modeling. The first part of this talk will provide a brief overview of existing closure modeling approaches in the context of projection-based reduced order models. The second part of the talk will focus on the use of the Mori-Zwanzig formalism (MZ), an idea from non-equilibrium statistical mechanics, as a framework for closure. The MZ formalism offers a mathematically exact framework to derive coarse-grained representations and recasts unclosed terms in the form of a memory integral involving the time history of the resolved variables. As the memory integral is intractable for general problems, we develop a finite memory approximation of the MZ memory kernel and a scale-similarity hypothesis. The outcome of this modeling process is a parameter-free, mathematically-derived closure model. Results are presented for multi-scale problems of transport phenomena, with a focus on evaluating the predictive capability of the ROM.

Calculation Chain for the Sound Calculation of Gearboxes with Multibody Models

Denis Werner*, Bernd Graf**, Bernd Wender***, Stefan Falkenberger****, Jochen Neher*****

*University of Applied Sciences of Ulm, **University of Applied Sciences of Ulm, ***University of Applied Sciences of Ulm, ****Continental AG, *****MAN Diesel & Turbo SE

ABSTRACT

The goal of the laboratory of Structural Mechanics and Acoustics at the University of Applied Sciences of Ulm is the simulation of the sound radiation of gearboxes. The classical approach divides the gearbox into three systems: 1. The inner parts like shafts, gears and bearings as a multibody simulation model 2. The gearbox housing as a finite element model 3. The radiating housing surface and the surrounding fluid as an acoustic boundary or finite element model. With that concept, the exciting bearing forces are calculated with the first model. Those exciting forces (transferred into the frequency domain) are the input for a frequency response analysis of the gearbox housing. The results are the surface velocities as a boundary condition for the third acoustic model for the calculation of the radiated sound. The mayor difficulty here consists in the long computation time and the neglect of the interaction between the inner parts and the housing. One way to solve that problem is proposed in [1] by using a reduced order model of the housing in the multibody model. That means that the first two systems are connected in one multibody model so that the surface velocities of the radiating housing are calculated in the time domain. As the sound calculation is more efficient in the frequency domain, a FFT is applied to the velocities. Additionally this contribution includes further optimizations of the gearbox model needed for a higher calculation efficiency. Usually the gears are modelled with complex and time consuming 3D contacts. Various authors already presented suitable solutions for modelling gear pairs with generalized force elements that rely on pre-calculated stiffnesses [2]. The same concept is applied to the bearings where the manufacturer typically provides the stiffness maps. In order to validate this approach the interaction between the housing and the bearings is measured with a unique setup of newly developed sensors. This also allows determining the path contributions of each bearing to every radiating surface point via an Operational Transfer Path Analysis. To sum it up, a new approach for a time-efficient multibody gearbox model will be presented alongside with the according experimental validation techniques. [1]: Kirsch, Wegerhoff, Jacobs: Prognosemethodik für die Schallleistung von Getrieben während der Konstruktionsphase, FVA Nr. 587 II, Frankfurt, 2016 [2]: Palermo, Mundo, Hadjit, Desmet: Multibody element for spur and helical gear meshing based on detailed three-dimensional contact calculations, Mechanism and Machine Theory 62 (2013) 13-30

Multi-grain Phase-field Model for Ferroelectric Materials

Walter Werner^{*}, Manuel Hinterstein^{**}, Gunnar Picht^{***}, Britta Nestler^{****}, Daniel Schneider^{*****}

^{*}Institute of Materials and Processes (IMP), Karlsruhe University of Applied Sciences, ^{**}Institute of Applied Materials (IAM-KWT), Karlsruhe Institute of Technology (KIT), ^{***}Robert Bosch GmbH, Corporate Sector Research and Advance Engineering, Applied Research Materials, ^{****}Institute of Applied Materials (IAM-KWT), Karlsruhe Institute of Technology (KIT), ^{*****}Institute of Applied Materials (IAM-CMS), Karlsruhe Institute of Technology (KIT),

ABSTRACT

Ferroelectric materials with a perovskite crystal structure are widely used in applications like actuators, fuel injection systems, and sonar applications. The most widely spread commercial material is $\text{Pb}(\text{Zr}_{1-x}\text{Ti}_x)\text{O}_3$ due to its outstanding electromechanical properties and large temperature range for applications. Based on the Landau-Ginsburg-Devonshire (LGD) thermodynamic theory, Haun et al. was able to describe lead-based composition material. However, many effects do still not fit the prediction of LGD and need further investigation. One such phenomenon happens near the so-called morphotropic phase boundary (MPB). The MPB is hereby a compositional area in the phase diagram where the crystal structure changes from the tetragonal phase to the rhombohedral phase without changing the formulae type ABO_3 . In the vicinity of the MPB, the $\text{Pb}(\text{Zr}_{1-x}\text{Ti}_x)\text{O}_3$ -material passes through a minimum in the coercive field and a maximum in the obtainable strain. The experimentally determined strain is much larger than theoretically predicted. The reason for this discrepancy is the complex interplay of the different strain mechanisms and field induced phase transitions dependent on grain orientation [1]. For adjusting the theoretical prediction to the macroscopic observations, one possible approach [2] relies on measurements of the spontaneous strains for different phases using diffraction techniques. As a result, phase-dependent electrostrictive appliances QT and QR for tetragonal and rhombohedral phases are obtained. The aim of this work is to combine the LGD theory with a phase-field approach incorporating continuum mechanics of the elastic field [3] and to enable simulations of polarization domains inside the grain structures of different simultaneously present crystalline phases. In this presentation, the theory and fundamental model equations are explained and simulation results are shown in comparison with experimental data. [1] Hinterstein, M., Hoelzel, M., Rouquette, J., Haines, J., Glaum, J., Kungl, H. & Hoffman, M.: Interplay of strain mechanisms in morphotropic piezoceramics. *Acta Mater.* 94, 319 (2015). [2] Franzbach Daniel J, Seo Yo-Han, Studer Andrew J, Zhang Yichi, Glaum Julia, Daniels John E, Koruza Jurij, Benan Andreja, Mali Barbara, and Webber Kyle G. Electric-field-induced phase transitions in co-doped $\text{Pb}(\text{Zr}_{1-x}\text{Ti}_x)\text{O}_3$ at the morphotropic phase boundary. *Science and Technology of Advanced Materials*, 15, 02 2014. [3] Daniel Schneider, Felix Schwab, Ephraim Schoof, Andreas Reiter, Christoph Herrmann, Michael Selzer, Thomas Boehlke, and Britta Nestler. On the stress calculation within phase-field approaches: a model for finite deformations. *Computational Mechanics*, pages 1–15, 2017.

Improved Workflow for Unsupervised Multiphase Image Segmentation

Brendan West^{*}, Taylor Hodgdon^{**}, Matthew Parno^{***}, Arnold Song^{****}

^{*}ERDC-CRREL, ^{**}ERDC-CRREL, ^{***}ERDC-CRREL, ^{****}ERDC-CRREL

ABSTRACT

Quantitative image analysis often depends on accurate classification of pixels through a segmentation process. However, imaging artifacts such as the partial volume effect and sensor noise complicate the classification process. These effects increase the pixel intensity variance of each constituent class, causing intensity values of one class to overlap with another. This increased variance makes threshold based segmentation methods insufficient due to ambiguous overlap regions in the pixel intensity distributions. The class ambiguity becomes even more complex for systems with more than two constituent classes. We present an image processing workflow that improves segmentation accuracy for multiphase systems. First, the ambiguous transition regions between classes are identified and removed, which allows for global thresholding of single-class regions. Then the transition regions are classified using a distance function, and finally both segmentations are combined into one classified image. We present two methodologies for identifying transition pixels that use the results of a steerable filter and local deconvolution of the image pixels. We demonstrate on a variety of synthetic images that the misclassification errors and area differences calculated between each class of the synthetic images and the resultant segmented images range from 0.69-1.48% and 0.01-0.74%, respectively, showing the accuracy of this approach. We also present results demonstrating that this approach can accurately segment x-ray microtomography images of moist granular media using these computationally efficient methodologies.

Advances in Solution Schemes for Nonlinear Multiphase Flow and Transport in Porous Media

Mary Wheeler*, Gurpreet Singh**

*The University of Texas at Austin, **The University of Texas at Austin

ABSTRACT

This presentation consists of two developments. The first topic is on an approximate Jacobian nonlinear solver. This approach has been shown to outperform the two stage or CPR preconditioners conventionally designed for several multiphase flow problems. Here, we present an alternative to two-stage preconditioning (or CPR) for solving the aforementioned monolithic system after Newton linearization. This method relies upon an approximation in the nonlinear, fully discrete, variational formulation resulting in decoupling of the DOFs and consequent approximate Jacobian construction. The resulting linear system is easily reduced to one in pressure (reference phase) degrees of freedom (DOF) only circumventing the need for specialized preconditioners. Further, the linear system has fewer DOF owing to the elimination of saturations (or concentrations). The second topic is a space-time domain decomposition approach using the enhanced velocity mixed finite element method. This approach allows for non-matching subdomain discretizations both in space and time for non-linear flow and transport problems that are locally mass conservative. In order to accurately resolve these non-linearities, it is often necessary that a small time-step size be used during the numerical solve. Consequently, this approach is computationally prohibitive. We present a space-time domain decomposition approach that overcomes these difficulties.

Error Estimates of the Fixed Stress Iterative Scheme for Coupling Flow with Geomechanics

Mary Wheeler^{*}, Vivette Girault^{**}, Saumik Dana^{***}, Tameem Almani^{****}

^{*}University of Texas at Austin, ^{**}Pierre and Marie Curie University, ^{***}University of Texas at Austin, ^{****}Saudi Arabian Oil Company

ABSTRACT

Coupled poromechanical processes arise in various applications in the subsurface. Wellbore collapse, sand production, reservoir compaction and surface subsidence are examples of different classes of problems where fluid flow and geomechanics mutually affects the displacements and pressures in the ground. Thus, conducting a coupled porous and solid deformation analysis plays a critical role in simulating the field behavior. However, large scale modeling of coupled processes is a computational challenge that has been historically considered very complicated. Iterative methods for solving coupled flow and geomechanics have gained popularity in the last two decades for their simplicity and numerical efficiency. They are based on decoupling the equations using an intermediate sub-step; the flow, or the geomechanics, equations are solved first to obtain a solution for the other problem. This procedure is repeated at each time step until the solutions of the two problems converge to an acceptable tolerance. In this work, we consider a fixed- stress split algorithm to decouple the displacement equations from the flow equations for a large scale Biot system. The pressure flow equations are discretized by a mixed finite element method (MFEM) and the elastic displacement equations are discretized by a continuous Galerkin scheme (CG). A priori error estimates are derived with the expected order of accuracy provided the algorithm is sufficiently iterated at each time step. These error indicators are implemented in a large scale reservoir simulator (IPARS). A posteriori error estimators are also derived and implemented to help choose suitable mesh refinement. Numerical simulations are presented to confirm the theoretical results.

Gas Transport through the Pore Space of Seasonal Snow

Amber Whelsky^{*}, Mary Albert^{**}, Ed Waddington^{***}

^{*}Dartmouth College, ^{**}Dartmouth College, ^{***}University of Washington

ABSTRACT

Over half of the Earth's total land surface area in the northern hemisphere can be covered by snow in the winter. This large expanse of snow cover impacts many climate-sensitive phenomena including surface-atmosphere exchange processes, ground thermal regime, and water resources. Knowledge of the fundamental properties of seasonal snow is important for analysis in all of these areas. While transient models of gas diffusion through pore space of snow have been made, direct measurements of the gas diffusion through snow's complex pore space are lacking, despite a need for these measurements to ensure model accuracy. In this study we developed an advection-diffusion transport model of gas movement through seasonal snow and we present results from multiple experiments conducted on glass beads, used to verify correct interpretation of the transport physics. We further utilize the verified model, along with the first ever in-situ measurements of gas diffusion through snow, to describe the effective diffusivity of six different seasonal snow types, distinguished from one another by characteristic microstructure. Our transport model incorporates previous work on snow ventilation to account for subsurface air flow that is caused by wind flowing over features in the snow surface. Results suggest that steady winds blowing over surface roughness features can impact the transport of gas through the pore space of snow and therefore must be accounted for within transport models. After accounting for wind, our model and measurement results indicate a large discrepancy between our values and values from two common theoretical derivations of effective diffusivity in snow that are based mainly on measured density. Unlike derivations based on density, our results show that complex (non-spherical) crystal shape leads to interstitial gas diffusivity that is not captured by existing theoretical equations in part due to the original assumptions of isotropy and spherical ice grains. These results provide improved guidance for estimates of gas diffusivity in seasonal snow, to be used in surface-atmosphere gas-flux models. The transport model and experimental approach used in this work could be adjusted and incorporated into future studies of gas transport properties of other porous materials that are exposed to an advective flow.

Consistent Finite-Element Schemes for Subsurface Flow Simulation

Laurent White^{*}, Dimitar Trenev^{**}, Jeremy Brandman^{***}

^{*}ExxonMobil Research and Engineering, ^{**}ExxonMobil Research and Engineering, ^{***}ExxonMobil Research and Engineering

ABSTRACT

Computational simulation of coupled flow and transport in porous media plays an important role for reservoir development and management in the oil and gas industry, for predicting the fate of contaminants in groundwater formations as part of soil remediation efforts, and for studying the efficacy of geologic sequestration of carbon dioxide as a way of reducing emissions into the environment. Because these are important applications and can also incur significant capital expenses, the quest for accurate numerical prediction is ongoing. Computational models for these applications involve the coupling between a discrete approximation to the fluid velocity (or fluid velocities in case of multiphase-flow problems) and the discretized transport equation. In addition to carefully selecting computational approaches for each sub-problem – i.e., the appropriate schemes for velocity and transport discretizations – based on accuracy, speed and robustness, coupling these two computational approaches adds another layer of complexity and restrictions. In particular, the issue of mass conservation (both global and local) is often at the forefront, as spurious mass imbalances not only lead to inaccuracies but can also trigger numerical instabilities, especially for nonlinear multiphase-flow problems. Being heterogeneous and geometrically complex, geologic models and groundwater formations are best discretized by unstructured meshes. While the continuous finite-element method is a natural computational approach for handling such configurations, it has often been dismissed as a technique for simulating flow and transport because it lacks the proper mass-conservation properties. In particular, numerous statements have been made in the literature regarding the lack of conservation at the element level, i.e., mass imbalances that occur when summing up fluxes around element facets. While these statements are true, they fail to take a holistic approach and consider the coupled problem as a whole. We show that, as long as the flow equations and the transport equations are discretized consistently both in time and space, the continuous finite-element method can be a robust, accurate, and practical computational technique for solving these coupled flow and transport problems.

Topology Optimization with the Stress-based Finite Element Method of Solving the Equilibrium Problem

Zdzislaw Wieckowski*

*Lodz University of Technology

ABSTRACT

Abstract: The topology optimization problem for two-dimensional statically loaded structures has been considered. In contrast to commonly used approaches where the displacement field is applied as the main unknown variable in the solution of the equilibrium problem, the stress field has been utilized as the main unknown variable in the present paper. The optimization problem has been solved by the solid isotropic material with penalization (SIMP) approach. Several cases of structures optimized by applying both the displacement and stress-based finite element methods have been analyzed. The results obtained by the two methods have been compared. The optimization problem has been formulated so that the minimum of compliance is to be found provided that the material volume is constant and the stress field is the solution of the linear equilibrium problem [2,1]. The main differences in the present approach is that the compliance functional depends on the stress tensor directly and the equilibrium problem has been solved by minimization of complementary energy on the set of statically admissible stress fields. The equilibrium equations have been fulfilled inside the design domain by means of the Airy stress function which has been approximated using the rectangular element with 16 degrees of freedom which guarantees continuity of the approximated function and its first derivatives [3]. To satisfy the stress boundary conditions that have a form of linear constraints for degrees of freedom, the Lagrange multiplier technique has been applied [3]. A number of optimization tasks has been analyzed by the proposed technique and the well known approach presented in [1] where the rectangular element with 8 degrees of freedom has been applied. A significant smaller number of iterations needed to get the solution has been observed in the case of the present method. However, a single iteration takes more time in the case of stress-based approach where the calculations are more complicated. A sharper image of the optimized structure has been obtained by the stress-based method in the most of the considered cases. References [1] Andreassen E., Clausen A., Schevenels M., Lazarov B. S. and Sigmund O., Efficient topology optimization in MATLAB using 88 lines of code, Struct. Multidisc. Optim., 43 (1), 1-16 (2011). [2] Bendsoe M.P., Sigmund O., Topology Optimization, Springer Verlag, Berlin, 2003. [3] Wieckowski Z., Youn S.K., Moon B.S., Stress-based finite element analysis of plane plasticity problems, Int. J. Numer. Meth. Eng., 44, 1505-1525 (1999).

Hybrid Nonlinear Finite Elements and Peridynamics Using a Node-Based Force Scheme

Raymond Wildman*

*US Army Research Laboratory

ABSTRACT

A hybrid peridynamics/finite element method is discussed in which nonlinear finite elements (with a bi-linear stress-strain model) are used with a bond-based peridynamics method. In this approach, the peridynamics nodes are coincident with the finite element nodes and a force-blending scheme is used [1]. At each time step, both the peridynamic and finite element force is computed at each node, though peridynamics is only used at the onset of damage. The peridynamics constant is based on the tangent modulus of the surrounding finite elements, rather than the modulus in the linear region. A damage-adjusted bond breakage method [2] is used along with force-damping [3]. Damage-based blending is used at low-levels of damage, essentially before a full fracture surface separates a horizon. With this approach, a damage-dependent linear combination of the finite element force and peridynamic force is used at each node to smooth the transition from local to nonlocal model and to continue to capture the nonlinear effects. The main advantage of this approach is that using finite elements in the bulk is more accurate than peridynamics, while of course peridynamics is most useful for fracture modeling. Further, nonlinear finite element material models are more established than equivalent peridynamics models. Several numerical results demonstrate the efficacy of the method. [1] Wildman, Raymond A., James T. O'Grady, and George A. Gazonas. "A hybrid multiscale finite element/peridynamics method." *International Journal of Fracture* (2017): 1-13. [2] Ha, Youn Doh, and Florin Bobaru. "Characteristics of dynamic brittle fracture captured with peridynamics." *Engineering Fracture Mechanics* 78.6 (2011): 1156-1168. [3] Silling, Stewart. "Introduction to Peridynamics." *Handbook of Peridynamic Modeling*. Eds. Bobaru, Florin, et al.. CRC Press, 2016.

Scale Resolving Simulations of the Aerodynamic Flow around an Airfoil Using a Lattice Boltzmann Method

Sylvia Wilhelm^{*}, Jerome Jacob^{**}, Pierre Sagaut^{***}, Pierre Sagaut^{****}

^{*}Aix Marseille Univ, CNRS, Centrale Marseille, M2P2, Marseille, France, ^{**}Aix Marseille Univ, CNRS, Centrale Marseille, M2P2, Marseille, France, ^{***}Aix Marseille Univ, CNRS, Centrale Marseille, M2P2, Marseille, France, ^{****}Aix Marseille Univ, CNRS, Centrale Marseille, M2P2, Marseille, France

ABSTRACT

Scale resolving simulations based on the Lattice Boltzmann method are used to predict the flow around a NACA airfoil profile. The objective of this work is to predict the complex unsteady aerodynamic flow over clean and iced airfoils. The correct prediction of the maximum lift coefficient is important for safety reasons but is very challenging for iced airfoils since the flow is highly turbulent, three-dimensional and local separations may occur over the complex ice shapes. For this purpose, a hybrid RANS / LES model as well as wall-modeled LES are used with the Lattice Boltzmann Method (LBM). The LBM is an attractive alternative to the traditional Navier-Stokes approach due to its compact nature which makes it particularly suited for massively parallel simulations. It thus enables the study of geometrically and physically complex flows using scale resolving simulations at lower cost. The D3Q19 lattice model is used together with a regularized BGK collision model [1]. The LBM is applied on a multi-domain uniform mesh. An immersed solid boundary method is used to handle the connection between the volumetric mesh in the fluid and the surface mesh defining the solid domain. A reconstruction method of the distribution functions at the boundary nodes is used based on the evaluation of the macroscopic variables. Using a uniform grid, it would be too expensive to explicitly resolve the boundary layer. Therefore a wall model is implemented to evaluate the velocity at the boundary nodes. In this context, a Detached Eddy Simulation (DES) model is implemented based on the Spalart-Allmaras turbulence model. The behavior of this RANS turbulence model in the boundary layer is taken into account in the wall model. DES calculations of the flow around a clean NACA airfoil are conducted in order to validate the methodology. Wall-modeled LES of the clean airfoil are also performed. Several angles of attack are considered to reproduce the polar curve of the NACA profile. Light icing on the airfoil is taken into account by adding a roughness term in the wall model whereas horn type icing is explicitly resolved. Calculations are validated by comparison with experimental results and references of lift and drag coefficients as well as pressure coefficient distributions on the airfoil. [1] Latt, J., Chopard, B., Sep. 2006. Lattice Boltzmann method with regularized pre-collision distribution functions. *Mathematics and Computers in Simulation* 72 (2-6), 165–168.

Dislocation-based Crystal Plasticity Modeling of Dynamic Ductile Failure

Justin Wilkerson*, Thao Nguyen**, DJ Luscher***

*Texas A&M;, **Texas A&M;, ***LANL

ABSTRACT

A framework for dislocation-based viscoplasticity and dynamic ductile failure has been developed in (Nguyen et al., 2017) to model high strain rate deformation and damage in single crystals and polycrystals. The rate-dependence of the crystal plasticity formulation is based on the physics of relativistic dislocation kinetics suited for extremely high strain rates. The damage evolution is based on the dynamics of void growth, which are governed by both micro-inertia as well as dislocation kinetics and dislocation substructure evolution. An averaging scheme is proposed in order to approximate the evolution of the dislocation substructure in both the macroscale as well as its spatial distribution at the microscale. Additionally, a concept of a single equivalent dislocation density that effectively captures the collective influence of dislocation density on all active slip systems is proposed here. Together, these concepts and approximations enable the use of semi-analytic solutions for void growth dynamics developed in (Wilkerson and Ramesh, 2014), which greatly reduce the computational overhead that would otherwise be required. The resulting homogenized framework has been implemented into a commercially available finite element package, and a validation study against a suite of direct numerical simulations was carried out. Lastly, polycrystalline samples are studied at the mesoscale level through the explicit resolution of each grain, i.e. resolving each individual grain size, shape, and orientation, in a representative volume element. In these polycrystal simulations, failure naturally localizes along grain boundaries of particular misorientation in agreement with recent experimental observations, e.g. (Brown et al., 2015). Nguyen, T., Luscher, D.J., Wilkerson, J.W., "A dislocation-based crystal plasticity framework for dynamic ductile failure of single crystals," J. Mech. Phys. Solids, 108:1-29, 2017. Wilkerson, J.W., Ramesh, K.T., "A dynamic void growth model governed by dislocation kinetics," J. Mech. Phys. Solids, 70:262-280, 2014. Brown, A.D., Wayne, L., Pham, Q. et al., "Microstructural effects on damage nucleation in shock-loaded polycrystalline copper," Metall. and Mat. Trans. A, 46:4539, 2015.

Toward Validation of Meshfree Modeling of Underbody Blast Experiments

T. Neil Williams*, Stephen Akers**, Garrett Doles***, John Ehrgott, Jr.****

*U.S. Army Engineer Research and Development Center, **U.S. Army Engineer Research and Development Center, ***U.S. Army Engineer Research and Development Center, ****U.S. Army Engineer Research and Development Center

ABSTRACT

In the last twenty years, research has been conducted to determine the predominant factors affecting the impulse imparted by a buried charge to an overhead structure. It has been shown that the blast-loading environment is a function of many factors including the explosive type, configuration, mass, and depth of burial, the soil characteristics, and the distance between the ground surface and the target structure. As a part of this research, the U.S. Army Engineer Research and Development Center (ERDC) has focused considerable attention on understanding the relationship between a buried explosive charge and the surrounding geologic/soil materials and advancing our ability to predict these soil/explosive phenomena in high performance calculations. Through this research effort, it was found that there was a lack of consistent, repeatable, highly instrumented experiments to validate the computational simulations. This presentation discusses the meshfree modeling and results of recent underbody blast experiments with rigid and deformable targets that the ERDC conducted for software validation. The problem setup consists of a target at a given standoff from the ground surface with the explosive buried below the soil surface. The modeling involves significant mixing interactions of soils, explosive detonation products, air, and metal components. Comparisons of total impulse, deformation where applicable, and soil stress and velocity were made of the simulation and experimental results. The results obtained from this research provided detailed insight into the blast load environment created in a shallow-buried underbody blast event. This work also provided much needed critical validation experiment data that can be utilized to gain confidence in the models to predict the loading and deformation from a realistic underbody blast test event.

Reliable Thermophysical Property Data of Metal Systems for Integrated Computational Materials Design and the Next Generation Reporting Standard ThermoML 5.0

Boris Wilthan^{*}, Scott Townsend^{**}, Vladimir Diky^{***}, Andrei Kazakov^{****}, Kenneth Kroenlein^{*****}

^{*}National Institute of Standards and Technology (NIST), ^{**}National Institute of Standards and Technology (NIST),
^{***}National Institute of Standards and Technology (NIST), ^{****}National Institute of Standards and Technology
(NIST), ^{*****}National Institute of Standards and Technology (NIST)

ABSTRACT

The electronic availability of thermophysical property data in a well-structured machine-readable format is one of the cornerstones of a robust infrastructure for materials development. With Integrated Computational Materials Engineering (ICME) such a system promises substantially faster development and deployment of advanced materials at a fraction of the cost we face today. Equally important for a collection of well-characterized experimental thermophysical property data are their provenance and a clear statement regarding their quality quantified in statements of uncertainty. The Thermodynamics Research Center (TRC) within NIST has, for the last four years, actively engaged in addressing this challenges for the thermophysical property data for metals and alloys. This talk covers the progress in the continuous development of the free, publicly available NIST/TRC online resources (http://trc.nist.gov/metals_data) for metals and alloy data. It will include the progress made in capturing and structuring all relevant information from open literature into well-vetted datasets that can now be accessed and used via the Web through a human-oriented or computer-oriented (API) interface. Increased need for interoperability between data providers and data users also demands a data storage and exchange protocol for experimental and critically evaluated thermophysical and thermochemical property data. ThermoML is an XML-based IUPAC standard and the latest revision is a significant update to a more modern XML usage and adds the necessary elements for the representation of metal-based systems while maintaining compatibility to the traditional representation for organic-based systems. The latest efforts to expand the domain of applicability for this data communication standard, the active IUPAC project with the title "ThermoML-2017 REVISION OF AN XML BASED IUPAC STANDARD FOR THERMODYNAMIC PROPERTY DATA" will also be discussed.

Computational Fluid Mechanics without Equation Solver: A Meshless Point Collocation Method for Incompressible Navier-Stokes Equations

Adam Wittek*, Georgios Bourantas**, Grand Joldes***, Karol Miller****

*Intelligent Systems for Medicine Laboratory, Mechanical Engineering, The University of Western Australia, 35 Stirling Highway, Perth, WA 6009, Australia, **Intelligent Systems for Medicine Laboratory, Mechanical Engineering, The University of Western Australia, 35 Stirling Highway, Perth, WA 6009, Australia, ***Intelligent Systems for Medicine Laboratory, Mechanical Engineering, The University of Western Australia, 35 Stirling Highway, Perth, WA 6009, Australia, ****Intelligent Systems for Medicine Laboratory, Mechanical Engineering, The University of Western Australia, 35 Stirling Highway, Perth, WA 6009, Australia, School of Engineering, Cardiff University, The Parade, CF24 3AA Cardiff, United Kingdom

ABSTRACT

Abstract: We developed a very efficient numerical framework for non-stationary, incompressible Navier-Stokes (N-S) equations. The framework does not require an equation solver. We use strong form meshless collocation method to compute spatial derivatives on point cloud [1] and combine the flexibility of this method with the robustness of mesoscopic methods (we use Lattice-Boltzmann LB [3]) to numerically solve Poisson equations of mass conservation. We use explicit time integration schemes (Euler and 4th order Runge-Kutta RK4) with the critical time step determined using Gerschgorin circle theorem [2]. Application of this theorem facilitates rapid ("on-the-fly") time step computation. We implemented the proposed framework using MATLAB programming language and applied it to flow (incompressible N-S) equations in both their primitive variable (u-p) and velocity-vorticity (u- ω) formulations. The latter has been extended in 3D by using the vector potential method. We used lid-driven cavity problem in 2-D (rectangular domain) and 3-D (cubical domain) as benchmarks. The proposed framework can be easily parallelized, which makes it particularly attractive for GPU implementation. Furthermore, the Poisson type equation(s) can be solved through the traditional mesh-based methods, such as the Finite Element (FE) and the Finite Volume (FV), by using identical nodal distributions. The resulting linear systems are positive definite, diagonally dominant and symmetric and, therefore, robust iterative solvers (with appropriate preconditioners) have been developed over the past 30 years, ensuring a fast and accurate numerical solution. References [1] G. C. Bourantas, B. L. Cheesman, R. Ramaswamy, I. F. Sbalzarini. Using DC PSE operator discretization in Eulerian meshless collocation methods improves their robustness in complex geometries *Computers & Fluids* 136 285-300 (2016). [2] Isaacson, E. and Keller, H. B. 1966. *Analysis of Numerical Methods*, New York, Wiley, Library of Congress Catalog Card Number: 66-17630. [3] Chen S, Doolen GD. Lattice Boltzmann method for fluid flows *Annual Review of Fluid Mechanics* 30: 329-364 (1998).

Hierarchical Elastoplasticity of Bone: Theory, Algorithm, and Experimental Validation

Valentina Wittner*, Claire Morin**, Christian Hellmich***

*Institute for Mechanics of Materials and Structures, Vienna University of Technology, Vienna, Austria, **Ecole Nationale Supérieure des Mines, Saint-Étienne, France, ***Institute for Mechanics of Materials and Structures, Vienna University of Technology, Vienna, Austria

ABSTRACT

Introduction Bone is characterized by a hierarchically organized microstructure, exhibiting „universal” organizational patterns, whose „dosages”, however, vary between different species, organs, and anatomical locations - resulting in a great variety of mechanical properties. This complex internal structure leads to a necessity of taking into account all the different hierarchical components - some of which behave plastic - in order to explain the overall mechanical elastoplastic response of the bone. We here use a multiscale micromechanical model to predict the resistance to failure under mechanical load - the bone strength - based on the mechanical properties and volume fractions of its three elementary constituents: mineral, collagen and water. **Methods** Building on an earlier micromechanical explanation of bone strength (1) as well as on recent advances gained in the mechanics of crystalline structures (2) we developed an extended elastoplastic multiscale continuum micromechanics model for bone, based on the concept of concentration and influence tensors for eigenstressed microheterogeneous materials (3). The hierarchical organization of bone is considered in terms of six representative volume elements: cortical bone with cylindrical vascular pores, extravascular bone matrix with spherical lacunae pores and extracellular bone matrix consisting of cylindrical, mineralized collagen fibrils embedded into an extrafibrillar matrix, as well as wet mineral foam. The mineral is represented as an infinite number of cylindrical mineral phases oriented in all spatial directions interacting with spherical, water-filled pores within the extrafibrillar and the fibrillar space. The sole source of elastoplasticity lies in mutual sliding between those mineral phases, which are characterized by non-associated Mohr-Coulomb elastoplasticity; while the molecular collagen phase fails in a brittle manner, according to a Rankine criterion. Upscaling of these processes from the nano to the macroscale was made possible by a novel variant of the so-called return-map algorithm. **Results** The model is able to accurately predict the experimentally determined strength of bone tested in uniaxial tension and compression. While the strength is governed by the failure of the mineral during compression, the collagen failure defines the tensile strength. Furthermore, the sequence of plastic events and the stresses and strains can be determined across all hierarchical levels, illustrating the influence of the different components on the overall mechanical behavior of bone. **References** (1) Fritsch, Hellmich and Dormieux (2009), *Journal of Theoretical Biology* 260(2):230–252 (2) Morin, Vass and Hellmich (2017), *International Journal of Plasticity* 91:238–267 (3) Pichler and Hellmich (2010), *Journal of Engineering Mechanics* 136(8):1043–1053

A Generalized Algorithm for Finite Strain Plasticity

Gabriel Wittum^{*}, Alfio Grillo^{**}, Raphael Prohl^{***}

^{*}ECRC, KAUST, ^{**}Politecnico Torino, ^{***}G-CSC Frankfurt University

ABSTRACT

We introduce a generalized numerical algorithm for elasto-plastic problems at finite strains. Based on the Karush-Kuhn-Tucker system characterizing finite elastoplasticity, the presented algorithm solves linearized sub-problems iteratively. This linearization scheme may be extended to non-classical formulations of elastoplasticity, in which the plastic variables are not treated as internal variables. The generalized algorithm is compared to the classical Return Mapping Algorithm (RMA) with respect to the structural set-up and the computational effort. Especially some restrictions of the Return Mapping Algorithm in its classical form are pointed out. These can be overcome by means of the proposed method. Finally, the Generalized Plasticity Algorithm (GPA) and its convergence are tested by solving some benchmark problems.

Geometric Implications for Stress Concentration in Miura Origami

Zhongyuan Wo^{*}, Evgueni Filipov^{**}

^{*}University of Michigan, ^{**}University of Michigan

ABSTRACT

Origami principles have inspired foldable and reconfigurable thin-sheet structures for various engineering applications. At small length scales origami is well suited for creating metamaterials with adaptable and tunable properties. Analyzing stress distributions in the thin-sheet structures is important for improving robustness by predicting and potentially preventing failures. Additionally, origami systems which are intentionally designed to localize stresses can fail and collapse in predictive and preferred failure sequences [1]. In origami metamaterials, the controlled failure sequences could further expand the programmability and adaptability of the hierarchical systems. This work explores the Miura-ori pattern because it has attracted tremendous attention for its mechanical properties. The pattern is developable, rigid foldable and flat foldable, and can achieve negative Poisson's ratios, high stiffness-to-weight ratios, and tunable properties [2]. The Miura-ori typically fails at the origami vertices. These failures can be partly attributed to stress from folding a sheet with finite thickness, however, the restrictive geometry and sharp corners of the pattern also induce high stress concentrations at the vertices [3]. To realize the relationship between stress concentration and geometry of the Miura-ori, a finite element model where shells and rotational hinges are employed, simulates the stress distribution in the origami (idealized as zero-thickness). Three distinct loading cases are studied for the origami and the different geometric parameters of the Miura-ori are systematically varied. The panel side ratios (height/width), panel vertex angle of the Miura, as well as the fold angle all influence the load paths and stress distributions in the origami. [1] Ma J., and You Z. (2013). Energy absorption of thin-walled square tubes with a prefolded origami pattern-Part I: Geometry and numerical simulation. *Journal of Applied Mechanics*, 81: 011003. [2] Schenk, M., and Guest, S. D. (2013). Geometry of Miura-folded metamaterials. *Proceedings of the National Academy of Sciences*, 110(9), 3276–3281. <https://doi.org/10.1073/pnas.1217998110> [3] Witten, T. A. (2007). Stress focusing in elastic sheets. *Rev. Mod. Phys.*, 79(2), 643–675. <https://doi.org/10.1103/RevModPhys.79.643>

Using Graphs to Quantify Energetic and Structural (Dis)order in Organic Thin Films

Olga Wodo*

*University at Buffalo

ABSTRACT

The nanomorphology of polymer blend thin films critically affects performance especially in organic solar cells. However, many aspects of the underlying physics linking morphology to performance are still poorly understood. Furthermore, there is increasing evidence that atomic organization can hold the key to efficient charge transport within organic electronic devices. In order to fully capitalize on these recent evidence, there is a need to quantify the atomistic and energy features of morphologies with respect to basic steps of photovoltaic process. In this work, we take advantage of recent advances in molecular dynamic simulations and quantify atomic-scale morphological aspects of the thin films. Specifically, we present a graph-based technique that allows quantifying the point-cloud data (MD). In our approach, we first convert the point cloud data from atomistic simulation into a labelled, weighted, undirected graph and then use standard graph-based algorithms to calculate and quantify morphology features. The conversion of the CGMD-data into a graph preserves all the topological and geometric information about the internal structure, and local connectivity between individual atoms/beads (along and across the polymer chains). More importantly, the edges between individual beads on CGMD can be labelled by Euclidean distance, energy difference or hopping rate. Our method provides hierarchical information about the charge paths that a hole/electron needs to take to reach the electrode (path length, travel time, fraction of intra-molecular hops, path balance). We showcase capabilities of our approach by analyzing coarse grained molecular simulations of several oligothiophene blends. We present how graph-based method allows to provide quantitative insight into the origins of few orders of magnitude difference in mobility.

Computing Eddy-driven Effective Diffusivity Using Lagrangian Particles

Phillip Wolfram^{*}, Todd Ringler^{**}

^{*}Los Alamos National Laboratory, ^{**}Los Alamos National Laboratory

ABSTRACT

A novel method to derive effective diffusivity from Lagrangian particle trajectory data sets is developed and then analyzed relative to particle-derived meridional diffusivity for eddy-driven mixing in an idealized circumpolar current. Quantitative standard dispersion- and transport-based mixing diagnostics are defined, compared and contrasted to motivate the computation and use of effective diffusivity derived from Lagrangian particles. The effective diffusivity is computed by first performing scalar transport on Lagrangian control areas using stored trajectories computed from online Lagrangian In-situ Global High-performance particle Tracking (LIGHT) using the Model for Prediction Across Scales Ocean (MPAS-O). The Lagrangian scalar transport scheme is compared against an Eulerian scalar transport scheme. Spatially-variable effective diffusivities are computed from resulting time-varying cumulative concentrations that vary as a function of cumulative area. The transport-based Eulerian and Lagrangian effective diffusivity diagnostics are found to be qualitatively consistent with the dispersion-based diffusivity. All diffusivity estimates show a region of increased subsurface diffusivity within the core of an idealized circumpolar current and results are within a factor of two of each other. The Eulerian and Lagrangian effective diffusivities are most similar; smaller and more spatially diffused values are obtained with the dispersion-based diffusivity computed with particle clusters.

Validation of Multiscale Designer against AS4/8552, IM7/8552, and IM7/EP2202 NCAMP Data for Unidirectional Product Forms

Jeffrey Wollschlager^{*}, Zheng Yuan^{**}, Colin McAuliffe^{***}, Robert Crouch^{****}, Dimitrios Plakomytis^{*****}, Jacob Fish^{*****}

^{*}Altair Engineering, ^{**}Altair Engineering, ^{***}Altair Engineering, ^{****}Altair Engineering, ^{*****}Altair Engineering,
^{*****}Columbia University

ABSTRACT

Multiscale Designer is a stochastic multiscale material modelling framework that seeks to develop highly accurate and computationally efficient multiscale material models which rely on minimal testing. Multiscale Designer is a part of the Altair HyperWorks suite of tools. The presentation will first overview the methodology used to develop multiscale material models for unidirectional product forms from minimal testing; typically [0] tension/compression, [90] tension/compression, and [45/-45] tension. The second part of the presentation will present validation results for multiscale material models developed for AS4/8552, IM7/8552, and IM7/EP2202 NCAMP unidirectional materials against Unnotched Tension/Compression (UNT/C) and Open Hole Tension/Compression (OHT/C) data for the same material systems within the NCAMP database. The intention of the selected material systems is to show validation of the multiscale material models developed with the same methodology against material system combinations including different fiber / same matrix, and same fiber / different matrix.

STUDY ON THE IMPROVEMENT OF OXIDATIVE SCALE DUST COLLECTION ABILITY IN STEEL PROCESS

Sungyeun Won*, Soyeon Lee* and Changho Moon*

*Technical Research Laboratories, POSCO, Pohang, Korea
e-mail: sywon@posco.com, leesoyeon@posco.com, chmun@posco.com

Key words: Dust Collector, Oxidative Scale, Collecting Hood, Discrete Phase Model

Abstract. The purpose of this study is to remove the scales occurring in the steel sheet when manufacturing steel. The scale that occurs in all manufacturing processes will pollute the working environment and will have an absolute impact on the health of worker, thus requiring scale removal. Normally, removing the scale improves the performance of the dust collector, which is costly and not efficient. In order to analyze the behavior of the scale, Computational Fluid Dynamics was performed. Based on the CFD results, a dust hood was developed to capture the contaminants without improving the performance of the dust collector. Because the size of the scale is variable, ordinarily dust collector is not efficient, and a dust collecting hood with a different method of collecting dust according to the scale size was developed and the performance was doubled.

1 INTRODUCTION

Generation of fine dust is a big issue all over the world, and it is a serious problem especially in the East Asian region. Due to the generation of fine dusts, diseases such as respiratory diseases are caused, and inconvenience of living and social problems are caused. As a result, not only has public interest in environmental pollution increased, but also environmental pollution has been strengthened both domestically and internationally. [^{1, 2}] Thus, many devices and techniques for removing pollutants emitted to the atmosphere are being developed, and improvement of efficiency is a major concern as compared with the existing methods.

In the steel process, an oxide scale layer is formed on the surface of the strip by annealing. After the coils are wound up, the strips are loosened in the next process and the scales that fall off the surface of the steel sheet contaminate the equipment and the large scales are crushed to the size of the fine dust level. These oxide scales tend to contaminate the plant and escape to the factory door or window frame to increase the fine dust concentration in the atmosphere. There is a need to reduce the level of air pollution by eliminating the oxidation scale that occurs in industrial processes, improve the work environment in the plant and protect the health of workers.

The dust collecting method for removing air pollutants can be roughly divided into four types as filtration type, centrifugal type, washing type, and electric dust collecting type. In this study, we developed a hood that can improve the dust collecting efficiency of 10 μm or less by focusing on collecting contaminants instead of dust collecting methods. Because the fine dust - sized pollutants are light and are influenced by the flow of air, the Coanda effect is used to control the air flow. By controlling the flow of air, it is possible to control the behavior of the particles and to guide the scattered fine dust to the hood. [3]

The hood was designed using the Coanda effect [4] in order to accelerate the flow of air and the flow direction and the flow rate of air could be increased without any additional device. For this purpose, the hood design variables were determined and the optimal values were derived by determining the influence of each variable through the computational flow analysis. In order to simulate the actual flow of the scale particles, the behavior of the scales was investigated using the DPM(Discrete Phase Model) technique. [5]

2. PROBLEM DEFINITION

2.1 Analytical Model

The tension bridle roll which gives tension to the iron plate and the deflector roll which changes the direction use mainly similar size to maintain the equipment smoothly. The oxidized scale formed on the surface of the steel sheet after heat treatment is mainly in the hot-rolled steel sheet which is a hot-rolled steel sheet [6], and its thickness is more than about 2.0 mm.

Figure 1 shows the flow field for analyzing the behavior of micro-dust generation schematics and the behavior of oxidation scales. It is the most common type of line that can be seen in actual steel process. In this line, the oxidized scale layer formed on the surface of the steel plate is scattered while passing through the curved path of the steel plate, which adversely affects the surrounding environment pollution, equipment aging and health of workers. The red dotted line represents the behavior of fine dust scales detached from the steel sheet surface, and the blue box represents the area of the analytical flow field of interest in this study.

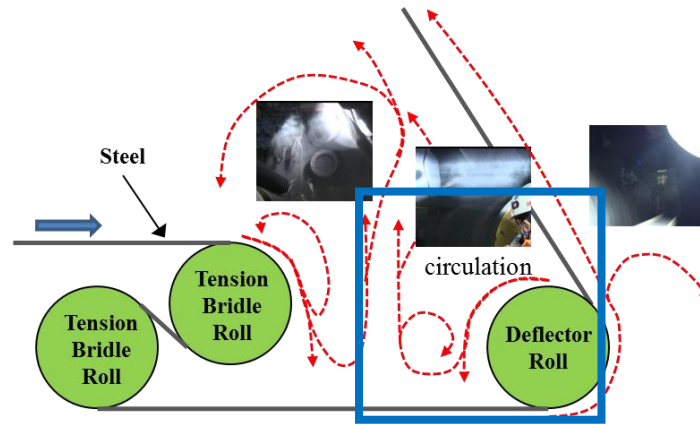


Figure 1 Process Schematic and Analytical Domain

The steel plate move in the direction from the lower part of the deflector roll to the upper left corner. The steel plate is bent in the tension bridle roll and the oxidized scales are dropped on the steel plate or floor. Due to this repeated situation, the scale is broken down and becomes smaller than the fine dust size, rising up to the upper part due to the flow of air due to the driving of the peripheral equipment.

For the analysis of the particle behavior on the flow field (blue line box) shown in Fig. 1, the lattice system is shown in Fig. 2 and nozzles with Coanda effect are installed on the upper and lower sides to remove fine dust scale. The air injected through the upper nozzle increase the air flow including the fine dust scale into the inside of the cover. The lower nozzle is also designed to capture the fine dust scale by increasing the air flow to the hood inlet while blocking the scale circulating on the roll.

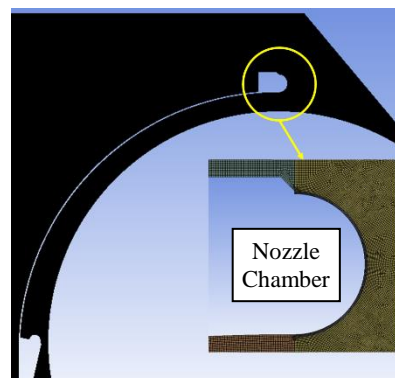


Figure 2 Mesh system

In order to understand the lattice dependence of the numerical solution, the number of

lattices was determined by comparing the numerical solutions according to the number of lattices and the number of lattices used in this numerical calculation was about 1.5millions. Especially, in order to verify the Coanda effect that can maximize the air flow around the nozzle, a large number of meshes are formed on the solid surface at the bottom of the nozzle.

2.2 Limitations of Floating Size

In the process, there is much unpredictable turbulence due to the operation of equipment, the closing of factory doors, and the difference in temperature in the plant. However, the size of the scale floating in a static state can be known based on the equation of motion.

The forces received by the particles in the atmosphere are gravity by mass, buoyancy by the fluid, and surface resistance against the flow direction of the fluid. The working force and the definition of each force are shown in Fig. 3.

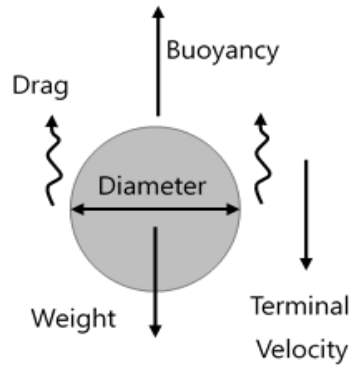


Figure 3 Forces acting on floating particle

The flow field in which the particles float can be assumed to be a creeping flow in which a very small flow is generated due to the driving of the plant. In the creeping flow field, the relation of all forces to the sphere is expressed as in Eq. (1), and the drag force in the flow field when Reynolds Number is less than 1 is expressed by Eq. (2) by the well-known Stoke's law.

$$F = m \frac{du}{dt} = F_w - F_b - F_d = mg - \frac{m\rho_a g}{\rho_s} - C_D A \frac{1}{2} \rho_a u_0^2$$

$$\text{here, } C_D = \frac{24}{\text{Re}} \quad (1)$$

$$F_d = 3\pi\mu u_0 D \quad (2)$$

Here, m is mass, g is gravitational acceleration, ρ_a is air density, ρ_s is density of scale, C_D is drag coefficient, μ is air viscosity, and Re is Reynolds number.

From these equations, drag force increases with increasing velocity of the particles falling in the fluid under gravity. Acceleration decreases with time, approaching zero and reaching a constant speed. This is called the terminal velocity. The terminal velocity of rounded particles is Eq. (3) with assuming that $du/dt = 0$ in Eq. (1).

$$u_t = \sqrt{\frac{4gD(\rho_s - \rho_a)}{3C_D\rho_a}} = \frac{gD^2(\rho_s - \rho_a)}{18\mu} \quad (3)$$

From this equation, the size of the particles reaching the termination speed can be expressed as Eq. (4).

$$D = \sqrt[3]{\frac{18Re\mu^2}{g\rho_a(\rho_s - \rho_a)}} = \frac{18\mu u_t}{g(\rho_s - \rho_a)} \quad (4)$$

From this, it can be seen that the size of the scale that floats without sinking in a static state is $0.23\mu m$ or less. However, in practice, the size of the scale that is floating due to the driving of the equipment and the surrounding of the door is larger than $0.23\mu m$. In this study, the behavior of particles with a fine particle size of $10\mu m$ is analyzed by controlling the air flow.

2. 3 Analysis of flow field

As shown in the analysis model in Section 2.1, numerical computation of fluid flow was performed assuming a 2 – dimensional since the roll is uniform in the longitudinal direction. The standard k- ϵ (SKE) turbulence model [7] was used to obtain numerical results of the flow field. The SKE model is known as the most used engineering turbulence model in the industry and has robust and reasonable accuracy. Compressibility, and buoyancy. The continuity equation, the momentum equation and the SKE transfer equation are shown in Eq. (5).

$$\begin{aligned} \frac{\partial \rho}{\partial t} + \frac{\partial}{\partial x_i}(\rho u_i) &= 0 \\ \frac{\partial}{\partial t}(\rho u_i) + \frac{\partial}{\partial x_j}(\rho u_i u_j) &= -\frac{\partial p}{\partial x_i} + \frac{\partial}{\partial x_j} \left[\mu \left(\frac{\partial u_i}{\partial x_j} + \frac{\partial u_j}{\partial x_i} - \frac{2}{3} \delta_{ij} \frac{\partial u_l}{\partial x_l} \right) \right] + \frac{\partial}{\partial x_j}(-\rho \overline{u'_i u'_j}) \end{aligned} \quad (5)$$

$$\begin{aligned}
 \frac{D(\rho k)}{Dt} &= \frac{\partial}{\partial x_j} \left[\left(\mu + \frac{\mu_t}{\sigma_k} \right) \frac{\partial k}{\partial x_j} \right] + G_k - \rho \varepsilon \\
 \frac{D(\rho \varepsilon)}{Dt} &= \frac{\partial}{\partial x_j} \left[\left(\mu + \frac{\mu_t}{\sigma_\varepsilon} \right) \frac{\partial \varepsilon}{\partial x_j} \right] + C_{\varepsilon 1} \frac{\varepsilon}{k} G_k - \rho C_{\varepsilon 2} \frac{\varepsilon^2}{k} \\
 C_\mu &= 0.09, \quad C_{\varepsilon 1} = 1.44, \quad C_{\varepsilon 2} = 1.92, \quad \sigma_k = 1.0, \quad \sigma_\varepsilon = 1.3
 \end{aligned} \tag{5}$$

Here, the ε - equation must use the wall function because it contains terms that are not computed from the wall. Generally, the effect is small for flows with large streamline curvature and large pressure gradient. In applying the general wall law, the momentum boundary condition is based on Launder-Spaulding law-of-the-wall and is shown in Eq. (6). A similar wall function was applied to energy.

$$U^* = \begin{cases} y^* & \text{for } y^* < y_v^* \\ \frac{1}{k} \ln(Ey^*) & \text{for } y^* > y_v^* \end{cases}, \quad U^* = \frac{U_p C_\mu^{1/4} k_p^{1/2}}{U_\tau^2}, \quad y^* = \frac{\rho C_\mu^{1/4} k_p^{1/2} y_p}{\mu} \tag{6}$$

2.4 Method of analyzing particle behavior

The DPM (Discrete Phase Model) technique was used to analyze the behavior of the fine dust scale in the flow field. The Lagrangian method was used to calculate the particle trajectory. The effect of the turbulence on the particles was the most common Stochastic tracking model. The above calculation was performed using FLUENT 17.2, the commercial CFD code. Additional minor features utilized default values given in commercial code.

2.5 Calculation Condition

The flow field is at atmospheric pressure and the rotation of the roll is 420 rpm in the counter clock wise direction and the linear velocity of the steel plate is 260 mpm. The scattered fine dust scale is composed of steel having a size of 0.1 ~ 10 μm and a rosin-rammler is applied to the diameter distribution. The flow rate was given as 10^{-20} kg / s. The specific gravity of the scale is 7.8 g / mm^3 , the density of air is 1.25 kg / m^3 , and the viscosity of air is 18×10^{-5} kg / m.s. The velocity at the top and bottom nozzles is given as 10.0 m / s.

2.6 Design parameters

In this study, the major parameters were set up for design to maximize collection efficiency. These design parameters are shown in Fig. 4. The parameters are the gap (S) of the nozzle tip injecting air, the nozzle bottom plate radius (R), the nozzle injection velocity (V) and the distance (H) from the roll.

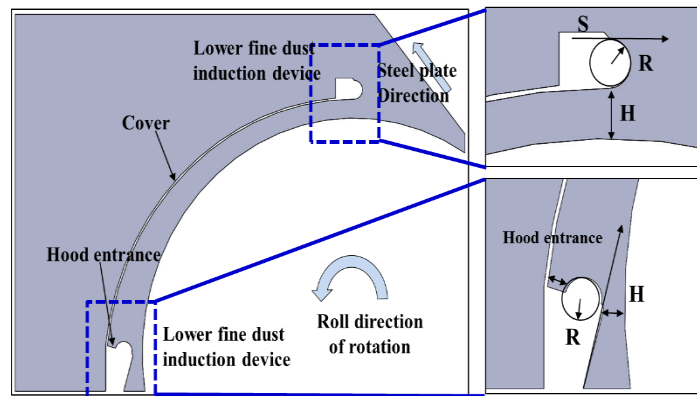


Figure 4 Design parameters

3. RESULTS AND DISCUSSION

3.1 Flow Characteristics

The flow characteristics of fine particle size scale particles in the flow field were investigated and the behavior and the collection efficiency of the particles when the particles were introduced into the calculated flow field were analyzed. The velocity and pressure distribution of the previous flow field is shown in Fig. 5.

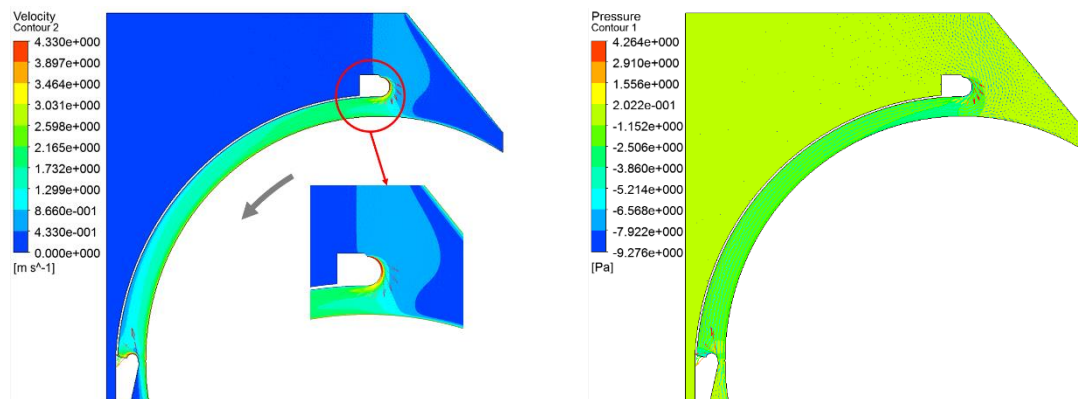


Figure 5 Contours of Velocity and Pressure

In this study, we focused on the nozzle which can induce the surrounding air and increase the flow rate, and it is confirmed that the flow field using this can realize the Coanda effect. By forming the curved surface of the lower part of the nozzle, the Coanda effect was obtained, and based on this, the design was established. The Coanda effect of air injected from the nozzle is shown in Fig. 6.

3.2 Effect of parameters

In this study, we analyzed the influence of major variables on design to maximize collection efficiency. It was found that there was no difference in the effect of the gap (S) of the nozzle tip injecting air and the nozzle bottom plate radius (R) was not significant. The faster the nozzle injection speed (V) was, the more favorable the effect was, but the effect was not clear. The Coanda effect, which changes the direction of flow along the lower curved surface, attracts more of the surrounding air, which means that it has a greater effect than the jet speed of the nozzle. However, the closer the flow plate height H is to the roll, the more effective it is to maximize the flow rate of the ambient air flow by the nozzle

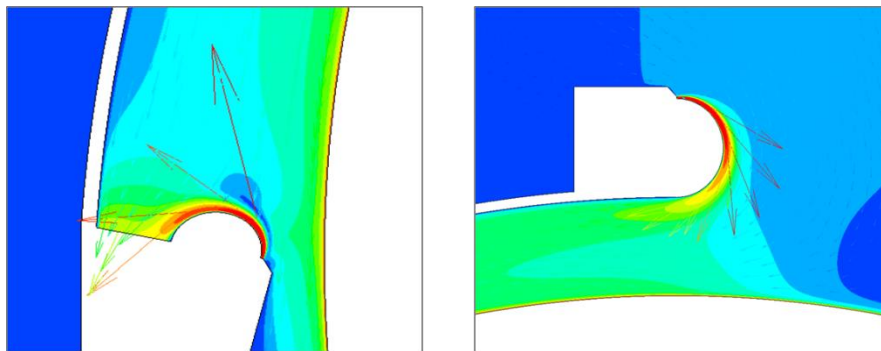


Figure 6 Coanda effect on the nozzle tip

4. CONCLUSION

Globally, especially in the East Asian region, the development of fine dust removal technology is ongoing to escape the threat of fine dust. In this study, we have developed a dust collecting system using numerical method in order to remove oxide scale of fine dust size floating off steel surface during steel manufacturing process. The principle of attracting the air flow and collecting the fine dust is applied to the fine dust scale of less than $10\mu\text{m}$ size which is influenced by the air flow. Nozzles were developed to utilize the Coanda effect to

induce airflow, thereby increasing ambient airflow. The influence of various design variables on the nozzle was analyzed and it was confirmed that the main factor, the nearby surface of the nozzle and the height of the flow plate in the roll.

In order to confirm the improvement of the dust collection efficiency, the dust concentration in the factory was measured and the standard of the Clean Air Conservation Act was achieved. The concentration of fine dust in the plant was 74%, lower than the legal standard, and the dust collection efficiency was doubled. This study will be helpful for the design of the dust collector in the future by designing the hood to capture the oxide scale of fine dust size.

REFERENCES

- [1] Environmental Performance Index-2016 Report, 2016
- [2] OECD, the Economic Consequences of Outdoor Air Pollution, 2016
- [3] Marin Rhodes, Introduction to Particle Technology, John Wiley & Sons, 2nd Ed., (2007)
- [4] S.Y. Jeong, J.S. Lee and J.H. Yoon, Optimal Nozzle Design of Bladeless Fan Using Design of Experiments, KSME, (2017), Vol.41, No. 8, 711-719
- [5] Z. Zhang, C. Yang, Y. Zhang and H. Zhu, Dynamic modeling method for infrared smoke based on enhanced discrete phase model, Infrared Physics & Technology, (2018), 89:315-324
- [6] H. Utsunomiya, K. Hara and R. Matsumoto, A. Azushima, Formation mechanism of surface defects in hot rolling process, CIRP Annals, (2014) Vol.63, Issue 1, 261-264
- [7] B.E. Launder and D.B. Spalding, The numerical computational of turbulent flow, Computer Methods in Applied Mechanics Engineering, (1974), 3:269-289

GPU Acceleration of Topology Optimization Methods

Jonathan Wong^{*}, Alexey Voronin^{**}, Dan White^{***}, Jun Kudo^{****}

^{*}Lawrence Livermore National Laboratory, ^{**}Lawrence Livermore National Laboratory, ^{***}Lawrence Livermore National Laboratory, ^{****}Lawrence Livermore National Laboratory

ABSTRACT

In topology optimization methods it is well known that the relatively straightforward finite element calculations for the cost and constraint function values and their sensitivities remain major high performance computing bottlenecks. Indeed, the iterative nature of topology optimization necessitates solving the finite element problem as quickly as possible since each iteration requires one or more finite element simulations. At the same time, we would like to obtain higher fidelity designs and therefore we need to work on highly refined meshes which further increases the computational burden. To mitigate computational cost, we investigate the use of Graphics Processing Units (GPUs). Several strategies are examined to reduce the finite element runtime over cube-like topology optimization design domains in excess of 10 million elements. We use matrix-free methods on the GPU to solve larger problems and increase the effective memory bandwidth for sparse matrix-vector (SpMV) operations. Microkernel optimizations are invoked to optimize GPU kernel performance at both small and large scales. Data movement and the use of GPU clusters are also examined. Lastly, we examine the effect of matrix-free Jacobi and geometric multigrid preconditioners. Topology optimization examples demonstrate the collective effectiveness of these different strategies on cube-like design domains that incorporate adaptive meshing.

Developments on Sub-Grid Scale Modeling of Failure Mechanisms for Flood Control Systems in a Hydrodynamic Storm Surge Model

Dylan Wood^{*}, Ethan Kubatko^{**}, Omar El-Khoury^{***}, Mehrzad Rahimi^{****}, Abdollah Shafieezadeh^{*****}

^{*}The Ohio State University, ^{**}The Ohio State University, ^{***}The Ohio State University, ^{****}The Ohio State University, ^{*****}The Ohio State University

ABSTRACT

Risk-informed decision making plays a critical role in mitigation of loss of life and assets during catastrophic events. This role is emphasized in coastal regions, which are susceptible to storm surge. Many factors, such as proximity to coastline and resilience of structures, directly influence the probable degree of risk posed to coastal regions by storm surge, though perhaps the most relevant and poorly understood factor is the ability of flood control systems to withstand forces attributed to storm surge and to protect coastal regions from inundation. Obtaining a proper understanding of this ability requires a multiphysics approach to modeling due to the intricate nature of the fluid-structure interactions involved during storm surge. Current available models are limited in their scope to provide information on this subject, e.g. current fragility based models frequently do not consider causal relationships and temporal correlations among multiple failure modes, and failure assessment often neglects the time evolution of processes leading to failure. We present on development of an adaptive-resolution storm surge model that responds to the changing state of flood control systems, designed to assist in overcoming of the aforementioned shortfalls. The storm surge model resolves failure mechanisms of flood control systems (e.g., wave run-up/overtopping, overflow, piping, sliding) as sub-grid scale processes. Results from the storm surge model are interfaced with geotechnical models in order to ensure the accuracy of the subgrid scale approaches. This presentation focuses on recent developments in resolving these failure mechanisms within a discontinuous Galerkin, shallow water equations based storm surge model (DG-SWEM [1]). Future goals include derivation of multi-dimensional time-dependent fragility models to be integrated with the storm surge model and ultimately lead to more informed decisions about catastrophic risk and infrastructure failure. [1] Dawson, C., Kubatko, E.J., Westerink, J.J., Trahana C., Mirabito, C., Michoskia C., Panda, N., Discontinuous Galerkin methods for modeling hurricane storm surge, *Advances in Water Resources*, 34, pp. 1165{1176, 2011.

A Symmetric Face-on-Face Contact Method for Implicit Nonlinear Solid Mechanics

Steven Wopschall*, Mark Rashid**

*Lawrence Livermore National Laboratory, **University of California, Davis

ABSTRACT

The implicit solution to contact problems in nonlinear solid mechanics poses many challenges. The discretization of the contact interface, form of the kinematic constraint, selection of a pressure basis, and the constraint enforcement method risk possible locking, contact force chatter in the presence of sliding, instability, non-physical or non-unique solutions, and equilibrium failure. This work seeks to address these issues whereby a symmetric face-on-face contact formulation is introduced for frictionless contact using three-dimensional, trilinear hexahedral finite elements. A set of opposing contact face-pairs is defined where a median plane methodology is used to construct local face-pair overlaps. These overlaps represent contact patches, the union of which constitutes the contact surface discretization. An up-to linear pressure basis is defined over each contact patch, whose active degrees of freedom are determined in a way that eliminates over-constraint. The resulting linear monomials are used as test functions for an integral form kinematic gap constraint. The gap constraints are enforced using a subcycle procedure that enforces both active and in-active constraints. This method is shown to handle complex contact interfaces in the presence of geometric and material nonlinearity resulting in physical and kinematically admissible solutions.

Treatment of Large Deformation Contact using VEM

Peter Wriggers*, Blaz Hudobivnik**

*Leibniz University Hannover, **Leibniz University Hannover

ABSTRACT

In most classical contact computations nodes are projected on parametrized surfaces where then contact constraints are enforced in tangential and normal direction to differentiate between stick and slip state. As an alternative, contact can be computed just by coupling of the nodes and assuming stick. The sliding case is then considered afterwards by letting the projected node follow a friction cone defined by normal and tangential tractions of Coulomb's law. This technique was applied to node-to-segment contact discretizations first in [1]. With the introduction of the Virtual Element Method [2] another possibility to formulate contact discretizations is offered by the flexibility of VEM to insert new nodes. Hence it will be possible to set up node-to-node formulations, even for sliding and for finite deformations. The approach is based on freely adding contact nodes to the original mesh [3] by this one easily overcomes differences in mesh size and surface interpolation. In combination with the moving cone description the VEM contact offers a simple formulation for surfaces in sliding contact. Contrary to classical node-to-node contact sliding movement is possible by adjusting the position of the contact nodes in the mesh according to the friction state. In the presentation a short introduction to the virtual element method for large deformations [4] is presented which will be the basis of the formulation. The projection algorithm for node-to-node contact is discussed next. Then the presentation will focus on the algorithmic scheme for the node adjustment due to the sliding motion. The resulting formulation will be compared to classical contact treatments with respect to performance and accuracy.

Pairwise Hydrodynamic Interactions of Vesicles in Applied Electric Fields

Bowei Wu^{*}, Shravan Veerapaneni^{**}

^{*}University of Michigan, ^{**}University of Michigan

ABSTRACT

The electrohydrodynamics (EHD) of vesicle suspensions is characterized by studying their pairwise interactions in applied DC electric fields in two dimensions. A boundary integral equation (BIE) based formulation for vesicle EHD is introduced, followed by a solution scheme based on Stokes and Laplace potential theory. In the dilute limit, the rheology of the suspension is shown to vary nonlinearly with the electric conductivity ratio of the interior and exterior fluids. We demonstrate our capability of simulating EHD phenomena including one vesicle deformation, pairwise interaction, and multiple vesicle interactions.

A Stable and Convergent Lagrangian Particle Method for Large Strain and Material Failure Analyses in Manufacturing Processes

CT Wu^{*}, Youcai Wu^{**}, Wei Hu^{***}

^{*}LSTC, ^{**}LSTC, ^{***}LSTC

ABSTRACT

In this paper, we present a new Lagrangian particle method for the simulation of manufacturing processes involving large strain and material failure. The starting point is to introduce some penalty terms as a means of circumventing the onerous zero-energy deformation in the Lagrangian particle method. The penalty terms are derived from the approximate strain vector by the combination of a constant and a strain derivative leading to a dual stress points algorithm for stabilization. The resultant stabilized Lagrangian particle formulation is a non-residual type which renders no artificial control parameters in stabilization procedure. Subsequently, the stabilized formulation is supplemented by an adaptive anisotropic Lagrangian kernel and a bond-based material failure criterion to sufficiently prevent the tension instability and excessive straining problems. Several numerical examples are utilized to examine the effectiveness and accuracy of present method for modeling large strain and material failure in manufacturing processes.

Several Key Concerns in the Development of Numerical Tank

Chengsheng Wu*, Feng Zhao**

*China Ship Scientific Research Center, **China Ship Scientific Research Center

ABSTRACT

CFD application is one of the most impressive progressions in the research on ship hydrodynamics. It is now becoming a powerful tool and involved intensively in the procedure of ship design. Numerical tank is a common vision for all the marine CFD man, which is presented to reinforce or even substitute model test in real tank. With the rapid development of CFD application and correlative technologies, "numerical tank" is now a hotspot in the research field of marine hydrodynamics. Nowadays, many attentions and efforts are paid on numerical tank. However, some key concerns about numerical tank are unclear. Such as, what is numerical tank? What are the technical contents and characters of numerical tank? How to ensure the accuracy of the result from numerical tank? These concerns are critical to the development of numerical tank. The research team of China Ship Scientific Research Center has made many efforts and is making continuing efforts now on the development of numerical tank. In this paper, the definition, technical contents and characters of numerical tank will be given out and discussed based on our research and practice. In our opinion, numerical tank is an application system based on reliable CFD technology which can provide service to the client as real tank does. The core value of numerical tank is practical application. The way of developing numerical tank can be knowledge packaged after attribute subdivision and can achieve the purpose of "developed by expert and used by common client". The differences between numerical tank and CFD in several aspects will also be analyzed, the two families of key technologies in the research of CFD and development of numerical tank will be presented and discussed. As an example, the key technology of confidence level assessment for the results of ship model resistance from numerical will be introduced in detail. The methodology of confidence level assessment is based on the procedure of "uncertainty analysis, validation of optimal solution, validation by big sample data". In which the uncertainty analysis is based on orthogonal design and variance analysis methods and statistic inference theory, the validation of optimal solution is based on effect analysis in orthogonal design and principle of minimum deviation; the virtual test method is validated by statistical analysis of comparison with a large numbers of model test data.

Properties and Functions of Soft Materials in a Honeybee Tongue

Jianing Wu*

*George W. Woodruff School of Mechanical Engineering, Georgia Tech

ABSTRACT

Many biological structures can perform highly-dexterous actions by using soft materials. To achieve high feeding efficiency but low energy expenditure during nectar feeding, the glossal surface of a honeybee undergoes shape changes, in which tongue hairs erect together with segment elongation in a drinking cycle. We discovered a transmission link embedded in the glossa from postmortem examination connected by intersegmental membranes which consists of chitin and protein. Compliance of soft materials provides more possibilities for its high deformation and kinematic synchronicity between tongue body and hairs. We measured the mechanical properties of this soft material and modeled the tongue structure as a compliant mechanism. It is validated that soft material contributes to not only a higher flexibility of the honeybee's tongue, but a higher capacity of elastic potential energy transfer rate. This work may arouse new prospects for conceptual design of micro-mechanical systems equipped with bio-inspired soft connections.

A Probabilistic Mean-Field-Homogenization Approach Applied to Study Unidirectional Composite Structures

Ling Wu^{*}, Laurent Adam^{**}, Ludovic Noels^{***}

^{*}University of Liege, ^{**}e-Xstream SA, ^{***}University of Liege

ABSTRACT

In order to account for micro-structural geometrical and material properties in an accurate way, homogenization-based multiscale approaches have been widely developed. However, most of the approaches assume the existence of a statistically Representative Volume Element (RVE), which does not always exist for composite materials due to the existing micro-structural uncertainties, in particular when studying the onset of failure. In this work we develop a stochastic multi-scale approach for unidirectional composite materials in order to predict scatter at the structural behavior. First Stochastic Volume Elements (SVE) [1] are built from experimental measurements. Toward this end, statistical functions of the fibers features are extracted from SEM images to generate statistical functions of the micro-structure. The dependent variables are then represented using the copula framework, allowing generating micro-structures, which respect the statistical information, using a fiber additive process [1]. Probabilistic meso-scale stochastic behaviors are then extracted from direct numerical simulations of the generated SVEs, defining random fields of homogenized properties [2]. Finally, in order to provide an efficient way of generating meso-scale random fields, while keeping information, such as stress/strain fields, at the micro-scale during the resolution of macro-scale stochastic finite element, a probabilistic Mean-Field-Homogenization (MFH) method is developed. To this end, the phase parameters of the MFH are seen as random fields defined by inverse stochastic identification of the stochastic homogenized properties obtained through the stochastic direct simulations of the SVEs. As a result, non-deterministic macro-scale behaviors can be studied while having access to the micro-scale different phases stress-strain evolution, allowing to predict composite failure in a probabilistic way. [1] M. Ostoja-Starzewski, X. Wang, Stochastic finite elements as a bridge between random material microstructure and global response, *Computer Methods in Applied Mechanics and Engineering* 168 (14) (1999) 35 - 49 [2] L. Wu, C.N. Chung, Z. Major, L. Adam, L. Noels. From SEM images to elastic responses: a stochastic multiscale analysis of UD fiber reinforced composites. Submitted to *Composite Structures* [3] V. Lucas, J.-C. Golinval, S. Paquay, V.-D. Nguyen, L. Noels, L. Wu, A stochastic computational multiscale approach; Application to MEMS resonators, *Computer Methods in Applied Mechanics and Engineering* 294 (2015) 141 - 167

Investigating Cross-Species Scaling for Traumatic Brain Injuries Using Finite Element Analysis

Taotao Wu^{*}, Jacobo Antona-Makoshi^{**}, Ahmed Alshareef^{***}, Matthew B. Panzer^{****}

^{*}University of Virginia, ^{**}Japan Automobile Research Institute, ^{***}University of Virginia, ^{****}University of Virginia

ABSTRACT

Animal injury models are widely used as surrogates for humans for the study of the mechanisms and the biomechanical thresholds of traumatic brain injury (TBI). However, one important question exists for translating animal responses to humans: how does the impact conditions and resulting biological response scale across species of various brain sizes and shapes. Simplified scaling methods based on structural similitude have guided the interpretation of animal data in the context of humans, but these methods are unvalidated and are criticized because they do not consider the differences in brain anatomy and shape of each species. Investigations using finite element (FE) models of brains from multiple species can address some of the limitations that exist with TBI scaling methods. Previously developed human (Mao et al. 2013) and non-human primate (Antona-Makoshi. 2016) FE brain models were modified to harmonize various modeling methods and anatomical features such as axonal tract information and brain tissue constitutive models. Where possible, the new brain models were validated against existing brain deformation test data and demonstrated good biofidelity. A parametric study was performed for each brain model simulated under a range of rotational head kinematics consistent with injury model data presented in the literature. Tissue-level injury metrics were recorded for each simulation, and model responses were compared across species under the assumption that comparable metrics result in comparable clinical outcome. Traditional scaling methods were evaluated against the predicted FE model data output. Relationships between tissue-level metrics, including maximum principal strain (MPS), the cumulative strain damage measure (CSDM) and maximum axonal strain (MAS), and applied head kinematics were formulated in angular acceleration-angular velocity space in a manner similar to Gabler et al. (2017). The metrics predicted by the FE models were different compared with those measured using traditional kinematic scaling methods. Compared with traditional scaling methods, using FE models to study cross-species TBI mechanics enabled the consideration for the differences between species in brain physical morphology, anatomy, tissue properties. Further efforts will focus on investigating the correlation between strain responses and pathology results. Overall, this study provided an improved method for scaling animal experiments and tissue injury metrics to humans. Reference Antona-Makoshi, J. (2016). PhD Thesis, Chalmers. Gabler, L. F. et al. (2017). J Biomech Eng. Mao H, et al. (2013). J Biomech Eng.135(11):111002.

Tightly Coupled, Partitioned Fluid-Structure Interaction Modeling Framework for Naval Applications: The Impact of Slamming Loads on High Speed Watercraft

Wensi Wu^{*}, Christopher Earls^{**}

^{*}Cornell University, ^{**}Cornell University

ABSTRACT

The current presentation reports on the effort to couple of our in-house computational structural dynamics software (CU-BEN) with a widely used computational fluid dynamics C++ API (OpenFOAM), in order to study the very challenging Fluid-Structure Interaction (FSI) problem known as “slamming.” Slamming occurs when shell surfaces, comprising the outer hull plating on high speed watercraft, impact the liquid phase in a way that has the shell normal nearly orthogonal to the free surface. Due to the relative densities between the liquid and solid phases, two-way coupling is required to handle the so-called “added mass effects.” Slamming loads cause very high strain rates and nonlinear responses within the solid domain; thus these aspects are considered in the CSD modeling. Additionally, the flat configuration of the structure, relative to the liquid free surface, presents significant opportunity for air to become trapped and compressed at the interface; thus a gas phase is admitted within our modeling. Given the tiny spatiotemporal scales in play within this particular phenomenology, experimental work has been limited; thus hampering the development of robust and accurate theoretical constructs. The present research aims at creating a kind of “FSI microscope”; to better investigate the context of slamming. Early applications of this simulation tool will inform experimental work of our collaborators; the results of which will subsequently be used as part of a formal model validation effort for the FSI simulation capability underdevelopment. The subsequently validated model will then be used, in conjunction with the experiments of our collaborators, to arrive at improved engineering theories describing slamming phenomena.

Turbulent-Turbulent Spot as the Inner-Layer Coherent Structure of Turbulent Boundary Layer

Xiaohua Wu*

*Royal Military College of Canada

ABSTRACT

There has been a general consensus that the dynamically important coherent structures inside the viscous sublayer and buffer layer of wall-bounded turbulent flows are low-momentum streaks and randomly distributed quasi-streamwise vortices. While this consensus is supported by direct numerical simulation (DNS) data for internal flows such as the fully-developed turbulent channel flow, there is actually very little supporting evidence coming from the external boundary layer flow. On the contrary, wind-tunnel experimental visualization in the 1970s by R.E. Falco on the viscous sublayer of the zero-pressure-gradient flat-plate boundary layer show that the viscous sublayer is dominated by pockets. Unfortunately, this important piece of evidence on viscous sublayer pockets has often been overlooked and ignored in the past because it contradicts with the mainstream idea of quasi-streamwise vortices and streaks. From our accurate, physically-realistic, spatially-developing DNS on the zero-pressure-gradient flat-plate boundary layer, we discovered that the inner layer of the turbulent boundary layer is dominated by turbulent-turbulent spots. These are defined as dense concentrations of small-scale vortices with high swirling strength originating from hairpin packets. Although structurally quite similar to the transitional-turbulent spots, these turbulent-turbulent spots are generated locally in the fully-turbulent environment, and they are persistent with a systematic variation of detection threshold level. The turbulent-turbulent spots exert indentation, segmentation and termination on the viscous sublayer streaks, thus creating pockets. The turbulent-turbulent spots coincide with local concentrations of high levels of Reynolds shear stress, enstrophy and temperature fluctuations, hence are dynamically important for turbulent transport processes. The sublayer streaks seem to be passive and are often simply the rims of the indentation pockets arising from the turbulent-turbulent spots. This work provides the first DNS confirmation on the existence of viscous sublayer pockets. Inside the viscous sublayer and the buffer layer, the dynamically important coherent structures of the boundary layer are turbulent-turbulent spots rather than quasi-streamwise vortices and streaks. The present boundary layer develops from a laminar Blasius solution at momentum-thickness Reynolds number 80 beneath a freestream decaying isotropic turbulence whose initial intensity is 3 percent. The boundary layer goes through a process of bypass transition in the narrow sense, reaching fully-turbulent state with an exit momentum-thickness Reynolds number of 3000. The accuracy of the DNS results is thoroughly validated against an array of existing experimental, numerical and theoretical data.

Wider Strain-rate Dependent Damage Constitutive Model and Application in Penetration Simulation for PBX explosives

Yanqing Wu^{*}, Xinyu Zhang^{**}, Fenglei Huang^{***}

^{*}Beijing Institute of Technology, ^{**}Beijing Institute of Technology, ^{***}Beijing Institute of Technology

ABSTRACT

Polymer-bonded explosives (PBXs) are a family of composite materials formulated with polymeric binder system and hard phase explosive crystals. Damage of PBXs caused by external stimulus influences not only the mechanical properties, but also the sensitivity, combustion and even detonation behavior of energetic materials because cracks, pores or debonding can act as fast reaction channels. The characteristic damage modes present in PBXs include intragranular voids, crystal fractures, and interfacial debonding. A three-dimensional viscoelastic model taking into account above three damage mechanisms has been developed to describe the mechanical response at wide strain rate range (10^{-3} ~ 10^4 s⁻¹). We can obtain the respective contributions of different damages to mechanical behavior, corresponding to different mechanical stimulus from quasi-static loading to high-strain-rate dynamic conditions. uniaxial compression tests were performed with the loading speed 5 mm/min and 1.0mm/min from 22°C to 75°C on some PBX. The Abaqus user subroutines UMAT and VUMAT were formulated based on the damage-coupled viscoelastic constitutive theory. Experimental quasi-static and dynamic compression data at some loading rates and different temperatures are used to validate the model and calibrate the constitutive parameters. The comparisons between simulated and experimental results under pure compressions loading show good agreements. When the projectile filled with explosive charge penetrates the target plate, the charge undergoes complex stress history, including the shock wave loading through the shell, and high inertial force, as well as loop loading and unloading due to shock wave reflection. The dynamic damage viscoelastic model is used to simulating the explosive charge filled in steel projectile in penetrating concrete target. Dissipation heat from plastic work, volume compression work and viscous flow work were included in the model. The penetration simulation showed that the compression stress wave is input into the explosive charge from the head and turn into tension reflected wave at the tail. By analyzing the damage distribution, the temperature distribution and the variations of plastic work and internal energy at different segment, the condition under which that explosive charge is prone to ignite can be predicted. Debonding damage tends to occur at the boundary elements near the shell inside surface. With the penetration proceeds, debonding damage diffuses from boarder area to the centerline area. The simulated results provide relevance between mechanical damage and ignition sensitivity of explosive charge, which are important for projectile structure design and safety evaluation.

Industrial Applications of the Smoothed Particle Galerkin (SPG) Method in Ductile Failure Analysis

Youcai Wu^{*}, C.T. Wu^{**}, Wei Hu^{***}

^{*}Livermore Software Technology Corporation (LSTC), ^{**}Livermore Software Technology Corporation (LSTC),

^{***}Livermore Software Technology Corporation (LSTC)

ABSTRACT

Abstract This work presents the industrial applications of the Smoothed Particle Galerkin (SPG) method [1, 2] in LS-DYNA® in ductile failure analysis. The SPG method is a new generation meshfree method developed for modeling semi-brittle and ductile material failure [3-5]. Different from the conventional finite element method (FEM) where the element erosion technique is utilized to mimic the material separation, the SPG method introduces a bond-based material failure mechanism to reproduce the strong discontinuity in displacement field without sacrificing the conservation properties of the system equations. The mathematical and numerical analyses have suggested that the SPG scheme is stable and convergent in modeling material failure processes. Currently, one of the major applications of the SPG method is the simulation of destructive manufacturing processes such as metal cutting, drilling, machining and shearing, and jointing processes such as riveting and screwing. The SPG method can also be applied to model the material failure in high velocity impact penetration problems. To show the effectiveness of the SPG method in analyzing ductile failure phenomena, industrial processes such as metal machining and high velocity impact penetration are modeled in this research. To further investigate the performance of the SPG method in those applications, parametric and convergence studies including the effects of bond failure criteria, nodal support size and domain discretization will be elaborated as well. Reference: [1] Wu CT, Koishi M, Hu W. A displacement smoothing induced strain gradient stabilization for the meshfree Galerkin nodal integration method. *Comput. Mech.* 56, 19-37, 2015. [2] Wu CT, Chi SW, Koishi M, Wu Y. Strain gradient stabilization with dual stress points for the meshfree nodal integration method in inelastic analysis. *Int. J. Numer. Methods Engrg.* 107, 3-30, 2016. [3] Wu CT, Bui TQ, Wu Y, Luo TL, Wang M, Liao CC, Chen PY, Lai YS. Numerical and experimental validation of a particle Galerkin method for metal grinding simulation. *Comput. Mech.* <https://doi.org/10.1007/s00466-017-1456-6>, 2017. [4] Wu CT, Wu Y, Crawford JE, Magallanes JM. Three-dimensional concrete impact and penetration simulations using the smoothed particle Galerkin method. *Int. J. Impact Engrg.* 106, 1-17, 2017. [5] Wu Y, Wu CT. Simulation of impact penetration and perforation of metal targets using the smoothed particle Galerkin method. In publication, *J. Engrg. Mech.* 2017.

Dynamic Buckling of Variable Angle Tow Composite Panels

Zhangming Wu*

*Cardiff University

ABSTRACT

Recently, variable angle tow (VAT) composites that offer an extended point wise stiffness tailoring capability for structural designers have attracted significant research interests. In this paper, the dynamic buckling behaviour of geometrically imperfect variable angle tow composite plates under longitudinal compressive pulse loading is studied. From the design point of view, even if a plate is capable of withstanding a particular amount of static in-plane compressive loading before buckling it may buckle earlier with a dynamic load of lower magnitude. The nature and duration of the dynamic load has a significant effect on the buckling behaviour. This work aims to explore the benign features offered by variable angle tow composites to enhance the dynamic buckling performance of rectangular plates. An efficient and robust semi-analytical modelling based on a mixed Hellinger-Reissner variational principle is developed to solve the dynamic buckling problem for VAT composite plates. Geometric imperfection, the nonlinearity induced by large deflections, and wave propagation effects given by in-plane inertia properties, are included in this newly developed dynamic buckling model. Both force and displacement controlled pulses loading are considered. Appropriate criteria are employed to assess the dynamic buckling behaviour under various loading types. Finite element model for the dynamic buckling analysis of VAT plates is also developed using the commercial package ABAQUS for the validation of numerical results given by the present model. The dynamic buckling behaviour characteristics of VAT plates subject to different in-plane boundary conditions are determined and analysed by studying their critical buckling loads and transverse deflection responses. Furthermore, a parametric study on the dynamic buckling response of VAT plates with linear variation of fibre angle is performed. The benefits of applying the VAT laminates to improve the dynamic buckling performance of rectangular plates are clearly demonstrated through comparing with the results of straight-fibre laminates. [1] Z. Gürdal, B.F. Tatting and C. K. Wu "Variable stiffness composite panels: Effects of stiffness variation on the in-plane and buckling response". Composites Part A: Applied Science and Manufacturing, Vol. 39, No. 5, pp 911-922, 2008. [2] Z. Wu, P.M. Weaver, G. Raju, and B. C. Kim "Buckling analysis and optimisation of variable angle tow composite plates". Thin-Walled Structures, Vol 60, pp163-172, 2012. [3] B. Budiansky, and John W. Hutchinson. "Dynamic buckling of imperfection-sensitive structures." Applied Mechanics. Springer Berlin Heidelberg, 1966. 636-651.

A File-Based Storage Approach to a Public Turbulence Database System and Applications to a Transitional Developing Boundary Layer Dataset

Zhao Wu^{*}, Rohit Ravoori^{**}, Tamer Zaki^{***}, Randal Burns^{****}, Charles Meneveau^{*****}

^{*}Department of Mechanical Engineering, Johns Hopkins University, 3400 North Charles Street, Baltimore, MD 21218, USA, ^{**}Department of Computer Science, Johns Hopkins University, 3400 North Charles Street, Baltimore, MD 21218, USA, ^{***}Department of Mechanical Engineering, Johns Hopkins University, 3400 North Charles Street, Baltimore, MD 21218, USA, ^{****}Department of Computer Science, Johns Hopkins University, 3400 North Charles Street, Baltimore, MD 21218, USA, ^{*****}Department of Mechanical Engineering, Johns Hopkins University, 3400 North Charles Street, Baltimore, MD 21218, USA

ABSTRACT

The Johns Hopkins Turbulence Databases (JHTDB, at <http://turbulence.pha.jhu.edu>) has been providing public access to several large DNS datasets through web services. In the previous version of JHTDB (Li et al., JoT, 2008; Kanov, thesis, 2015), the simulation data were converted and then ingested into SQL tables in SQL data servers. This ingestion process is complex and for 100 TB datasets may take months. This challenge has motivated the development of a new file-based data storage approach for JHTDB that enables easier and more streamlined setup of datasets. This approach is called FileDB; the databases are stored as files instead of SQL tables in the previous versions of JHTDB. As in the SQL-based system, in FileDB the simulation data are partitioned into data atoms of 8^3 . The atom is the fundamental unit of I/O operations. The size of the atom is chosen to balance the I/O time and disk seeking cost. The atom is indexed in z-order (also known as Morton order) for its good spatial locality. The converted data are then stored as binary files on data servers. For some datasets, the grid point number may not be a multiple of eight in one or more directions. In this case, the domain for which data are stored can be cut in that direction, or zero-padded. If the grid point numbers are not the same in all three directions, the atom z-indices can be discontinuous. In this case, a separate SQL table is created to store the atom z-indices that actually exist in the simulation domain. In this way, the JHTDB with FileDB can ingest more general simulation data, e.g. developing boundary layer (Lee and Zaki, APS/DFD, 2015). Three new datasets, a snapshot of isotropic turbulence on a 4096^3 grid, five snapshots of rotating stratified turbulence on a 4096^3 grid and a full time-history of a developing boundary layer flow over a smooth surface, are added to the JHTDB using fileDB. By avoiding the ingestion process, we have managed to achieve a massive speed up. For task parallelism when accessing these data on JHTDB, the data are distributed among nodes of the database cluster. The evaluation shows the performance of fileDB is as good as the previous SQL approach, with the added benefit of lower latency per request. Some sample results of analysis of geometric features of the turbulent/non-turbulent interface in the developing portion of the boundary layer will be presented.

An Application of State Space Method in Surface Instability Analysis for Graded Soft Materials

Zhigen Wu^{*}, Yihua Liu^{**}

^{*}Hefei University of Technology, ^{**}Hefei University of Technology

ABSTRACT

Surface instability of film-substrate system has been analyzed intensively for many years. For graded layers with depth-wise variation in material properties, the analytical solution for critical condition of surface instability cannot be obtained in general, thus the numerical method, such as the finite element method, was commonly employed for such cases. In the current presentation, we suggest a state space method for analyzing surface instability of graded layers with material properties varying in the thickness direction. Based on the governing equations for the surface instability of graded elastic layers and graded hydrogel layers, by discretizing the material properties into piecewise constant functions with homogeneous sub-layers, a state space method was developed to solve the eigenvalue problem and predict the critical condition for onset of surface instability. For the graded elastic system, results were presented for bilayers and continuously graded elastic layers. The state space solutions for elastic bilayers are in close agreement with the analytical solution for thin film wrinkling within the limit of linear elasticity. Numerical solutions for continuously graded elastic layers were compared to finite element results in a previous study (Lee et al., 2008, J. Mech. Phys. Solids 56, pp. 858–868). For the hydrogel system, the state space solutions for homogeneous hydrogel layers and hydrogel bilayers were compared to the finite difference results and analytical solutions. While the finite difference method often requires a large number of nodes to achieve convergence, the state space method requires relatively fewer sub-layers for continuously graded layers. The results for linearly and exponentially graded hydrogel layers show that the critical swelling ratio and corresponding critical wavelength both depend on the gradient profile of the crosslink density. In addition, the surface instability of graded elastic cylinders was also examined by the state space method. The state space solutions for three typical examples were acquired and show to be in good agreement with the numerical results by the finite element method, including the analytical solution for a thin cylindrical shell. In particular, a transition of the critical buckling mode for a soft cylinder covered by a bilayer was illustrated clearly by the present method. In contrast to the finite element method and finite difference method, the state space method is a semi-analytical approach with good convenience and higher computational efficiency for arbitrarily graded materials, including layered structures.

Multiscale Modeling for Instability Phenomena of Long Fiber Reinforced Composite with A Double Scale Microscopic Model

Rui XU*, Yanchuan HUI**, Qun HUANG***, Heng HU****, Hamid ZAHROUNI*****, Tarak BEN ZINEB*****, Shaobo ZHU*****

*1. Wuhan University 2. Laboratoire d'Etude des Microstructures et de Mécanique des Matériaux, Université de Lorraine, **1. Wuhan University, ***1. Wuhan University, ****1. Wuhan University, *****2. Laboratoire d'Etude des Microstructures et de Mécanique des Matériaux, Université de Lorraine, *****2. Laboratoire d'Etude des Microstructures et de Mécanique des Matériaux, Université de Lorraine, *****1. Wuhan University

ABSTRACT

The fiber microbuckling in long fiber composites may lead to the compressive failure of the macrostructure. To study such a multiscale problem, direct simulation is limited due to the expensive computation cost and difficulties in selecting non-linear calculation paths because there exists a lot of bifurcation points around the useful one. This work is to propose an efficient multiscale model for accurately simulating and analyzing the instability phenomena of long fiber reinforced materials. The multi-level finite element method [1] (FE^2) is adopted to realize the real-time interaction between macro- and microscopic levels: the macroscopic constitutive law is calculated on the Representative Volume Element (RVE), and the microscopic deformation gradient is transferred from the associated macroscopic Gauss point. However, the total computation cost may be still very high because the RVE on each Gauss point of macroscopic model needs a sufficient fine mesh to simulate the microbuckling of long fibers. Thus, a Fourier related double scale microscopic model [2] is developed to transform the fast varying microscopic unknowns into a series of slowly varying unknowns which only requires remarkably reduced meshes. In addition, the new RVE model allows one to control non-linear calculation paths easily by choosing the wavelength of the buckled fiber. The developed non-linear multiscale model is solved by the Asymptotic Numerical Method [3] (ANM), which is less time consuming and more stable than other classical iterative methods. The established multiscale model yields accurate results with a significantly improved computational efficiency. Keywords: Fourier series, Long fiber reinforced composites, RVE, FE^2 method, Instability. References [1] S. Nezamabadi, J. Yvonnet, H. Zahrouni, M. Potier-Ferry, A multilevel computational strategy for handling microscopic and macroscopic instabilities, *Computer Methods in Applied Mechanics and Engineering*, 198, 2099-2110, 2009. [2] Y. Liu, K. Yu, H. Hu, S. Belouettar, M. Potier-Ferry, N. Damil, A new Fourier-related double scale analysis for instability phenomena in sandwich structures, *International Journal of Solids and Structures*, 49, 3077-3088, 2012. [3] B. Cochelin, N. Damil, M. Potier-Ferry, Asymptotic-numerical methods and padé approximants for nonlinear elastic structures. *International Journal for Numerical Methods in Engineering*, 37, 1187-1213, 1994.

Negative Poisson's Ratio Design of the Cardiovascular Stent Using a Level Set-based Parameterization Method

HUIPENG XUE*, ZHEN LUO**

*University of Technology, Sydney, **University of Technology, Sydney

ABSTRACT

Abstract: Implanting stent is an important surgical way for treating a wide range of cardiovascular disease, but it will cause a physic injury for the vascular during the process, due to the variable shape of the vascular in the axial direction. So, the compliance of the stent is different in radial and axial directions. As for the former, the compliance should be minimized to support the vascular, while in another direction, the stent needs to comply the different shapes of the vascular as soon as possible. This paper presents a novel design work of the cardiovascular stent with a negative Poisson's ratio(NPR) to increase the compliance in the axial direction to reduce that damage. Moreover, the NPR stent is much shorter than the traditional one when ready for the implantation, no matter for self-expanding or balloon-expanding stent, which significantly increase the successful ratio of the operation. Although, there are many research studies on NPR design by using microstructure design method currently, this kind of metamaterials is hardly meeting the compliance requirements on the macro scale of the stent. So, this research proposes a new NPR design method. At first, the NPR structure will be obtained on the micro scale, and then it will transfer the microstructure to macrostructure by considering the working conditions in the vascular. During the microscale design, the macro compliance requirements will be considered in both directions to limit the structure of NPR, since the same NPR can have many different structures. In this paper, a level Set-based parameterization topology optimization method is used. It can obtain a structure with a clear boundary shape, which is an essential part of stent design because this research uses a micro scale design to get a macrostructure, and a small difference on the shape will lead to significant changes on the properties. Meanwhile, parameterization can control the boundary change very well. Finally, the new NPR stent structure will be tested by ANSYS. Keywords: Negative Poisson's ratio, stent, level set, parameterization, topology optimization

A Spectral Method to Study the Onset of Necking Instability for Dynamic Plane Strain

Mathieu Xavier^{*}, Dominique Jouve^{**}, Sébastien Mercier^{***}, Christophe Czarnota^{****}, Jean-Lin Dequiedt^{*****}, Alain Molinari^{*****}

^{*}CEA, ^{**}CEA, ^{***}Université de Lorraine, ^{****}Université de Lorraine, ^{*****}CEA, ^{*****}Université de Lorraine

ABSTRACT

During dynamic expansion of thin ductile metal cylinders, the deformation is first homogeneous. Then necking instabilities appear which generate local thinning, triggering plastic localization and finally the fragmentation of the structure. The present work aim is to provide new developments for the predictions of the fragment size and velocity. In order to study the onset of necking instability, linear stability analyses (LSA) are adopted to determine a critical wavelength which develops with the fastest growth rate. It has been shown that LSA can provide deep understandings of experimental results like the number of necks or their time of occurrence after some calibrations [1][2] However, the previous approaches suffer from some drawbacks. Indeed, based on a frozen coefficient theory, the model is salient when the time scale inherited from the development of the necking is smaller than the time scale of the background solution (homogeneous deformation without any imperfections). Such conditions are no more satisfied for stretching rate over 10000 per second. In the present talk, a new contribution is proposed. The time and space evolution of any perturbations is captured via a system of linearized equations. A Tau spectral method is adopted. Dynamic plane strain loading is investigated on a thin plate configuration, representative of a thin cylinder expansion. The material is incompressible. Its behavior is rigid viscoplastic, satisfying a J2 flow theory . As a result, different initial geometrical defects representative of material heterogeneities and forming defects have been considered. Their time and space evolution have been captured by the new method. It has been seen that while the perturbation evolution is highly depending on the shape of the defect in the early stage of the deformation process, their long term evolution is quite close to the one predicted by the classical LSA. We have checked that at least for strain rate lower than 1000 per second, the instantaneous growth rates predicted by the classical LSA and the new contribution are consistent. In a next step, larger strain rate loading will be investigated. In addition, to further validate the present approach, finite element simulations are planned. References: [1] Mercier and Molinari, Analysis of multiple necking in rings under rapid radial expansion, 2004, International Journal of Impact Engineering 30, 403-419 [2] Jouve, Étude analytique de l'instabilité plastique de striction pour une plaque sollicitée en traction biaxiale, 2010, École Polytechnique and Commissariat à l'Energie Atomique, France

Topology Optimization of Quasi-brittle Composites for Fracture Resistance with Phase Field Modeling of Crack Propagation

Liang Xia^{*}, Julien Yvonnet^{**}

^{*}Huazhong University of Science and Technology, ^{**}Université Paris-Est

ABSTRACT

In this work, we propose a numerical framework for optimizing the fracture resistance of quasi-brittle composites through a modification of the topology of the inclusion phase. The phase field method to fracturing is adopted within a regularized description of discontinuities, allowing to take into account cracking in regular meshes, which is highly advantageous for topology optimization purpose. Extended bi-directional evolutionary structural optimization (BESO) method is employed and formulated to find the optimal distribution of inclusion phase, given a target volume fraction of inclusion and seeking a maximal fracture resistance. A computationally efficient adjoint sensitivity formulation is derived to account for the whole fracturing process, involving crack initiation, propagation and complete failure of the specimen. The effectiveness of developed framework is illustrated through a series of 2D and 3D benchmark tests. It has been shown that significant improvement of the fracture resistance of composites has been achieved for designs accounting for full failure when compared to conventional linear designs. Compared to previous studies in the literature on the subject, this work provides a much more efficient alternative for the design of high fracture resistant composites. There exist twofold merits of the developed design framework: on the one hand, the adoption of topology optimization provides uttermost design freedom, yielding higher fracture resistant designs; on the other hand, limited number of iterations is required for the design for the sake of using gradient information, which is of essential importance dealing with computationally demanding fracturing simulation.

Achieving Temperature Transferable Coarse-Graining of Polymers and Glass-Forming Materials via Energy Renormalization

Wenjie Xia*

*National Institute of Standards and Technology

ABSTRACT

The bottom-up prediction of the properties of polymeric and glass-forming materials based on molecular dynamics simulation is a grand challenge in soft matter physics. Coarse-grained (CG) modeling is often employed to access greater spatiotemporal scales required for many applications. However, there is currently no temperature transferable and chemically specific coarse-graining method that allows for modeling of polymer dynamics over a wide temperature range. Here, we pragmatically address this issue by “correcting” for deviations in activation free energies that occur upon coarse-graining. In particular, we propose an energy-renormalization (ER) strategy to coarse-graining polymers based on relationships drawn from the Adam-Gibbs theory of glass formation, in conjunction with the localization model of relaxation. By testing different glass-forming materials ranging from fragile polymers to small molecules, we show that our ER approach can faithfully estimate the diffusive, segmental and glassy dynamics of the AA model over a large temperature range spanning from the Arrhenius melt to the non-equilibrium glassy states. Our proposed CG approach offers a promising strategy for developing thermodynamically consistent CG models with temperature transferability.

Exact Geometry Based Quasi-Conforming Analysis: Isogeometric Analysis Method with Quasi-Conforming Techniques

Yang Xia^{*}, Ping Hu^{**}

^{*}Dalian University of Technology, ^{**}Dalian University of Technology

ABSTRACT

Isogeometric analysis (IGA) is proposed by Prof. T.J.R. Hughes et al. as an alternative solution for computer aided engineering. In the past decade it has been developed into a powerful numerical method which has solid mathematical theory, excellent numerical efficiency, precision and versatile ability for engineering applications. The innovative idea to use splines as approximate functions for both geometry and unknown physical fields in isogeometric analysis provides solution for the integration of computer aided design and engineering, and also promotes the development of approximation theory with splines. Quasi-conforming (QC) technique is initially developed within traditional finite element framework by Prof. L.M. Tang. The major advantage of QC technique in the formulation is that the approximate space for displacements and strains are separately defined and the displacement-strain equation is transformed from partial differential form into weakened integration form. Inspired by isogeometric method, the quasi-conforming techniques are developed into exact geometry based quasi-conforming analysis method (EGQC) which uses NURBS based geometry as input model rather than traditional mesh. The contributions of the proposed EGQC method are listed as below. First, the displacements and strains are separately approximated according to the property of solved problem to achieve better performance. Second, the basis functions to describe the unknown physical fields are chosen according to the solved problems which are not limited to splines. Applications with the EGQC method on structural analysis have been developed. First the algorithms for analysis of beam structure with Euler and Timoshenko beam theories are proposed. The polynomial basis is used in simulation of Euler beam to improve the computational efficiency [1]. An order-reduction method with Timoshenko beam theory is proposed to cure the locking problem [2]. The method behaves great in simulation of beam structure and is expanded to the simulation of Reissner-Mindlin shell problems. In future works the EGQC method will be expanded to problems with extra constraints for the solution space, such as the simulation for incompressible material. References [1]Ping Hu Yang Xia Changsheng Wang, Exact geometry based quasi-conforming analysis for Euler-Bernoulli beam. Theoretical & Applied Mechanics Letters, 2012, 2(5), 6-9. [2]Ping Hu, Qingyuan Hu, Yang Xia, Order reduction method for locking free isogeometric analysis of Timoshenko beams, Computer Methods in Applied Mechanics and Engineering, Volume 308, 2016, Pages 1-22.

Numerical Simulations of the Ignition Dynamics in an Annular Combustor

Yifan Xia^{*}, Yao Zheng^{**}, Dongmei Zhao^{***}, Haiwen Ge^{****}, Gaofeng Wang^{*****}

^{*}Zhejiang University, ^{**}Zhejiang University, ^{***}University of Science and Technology of China, ^{****}Texas Tech University, ^{*****}Zhejiang University

ABSTRACT

An annular combustor which comprises multiple swirling injectors is an universal and crucial configuration for modern aero-engines. In present work, the transient flame front propagation during ignition process in a laboratory-scale annular combustor is numerically investigated in Large-eddy simulation (LES) and RANS to understand the ignition dynamics. The annular combustor comprises sixteen swirling injectors injecting lean premixed propane/air mixtures and two transparent quartz concentric cylindrical walls of the combustion chamber, which provides optical access to high-speed imaging to diagnosis the chemiluminescence of flame front. Various experiments have been conducted on the annular combustor which provide the database to validate the numerical results. Three stages of ignition process are distinctly exposed towards understanding of gas turbine ignition. The ignition process is numerically investigated by LES and RANS with detailed chemistry in this paper. The factors, such as fuel to air ratio and flow characteristics, influencing light-round ignition process are extensively explored. The numerical results of LES and RANS are well consistent to each other. Meanwhile, the ignition sequences of light-round process are compared with experimental data, which show an overall good agreement. The non-symmetric circumferential flame propagation is observed in simulations and experiments, which is induced by circumferential flow characteristics due to the arrangement of multiple swirling injectors. The circumferential flow characteristics and flame/flow interactions are analyzed in the numerical simulations. The simulations reveal that the turbulent wrinkling and thermal expansion are the main effects to the flame front propagation. The wrinkling factor of the flame front is calculated to qualify the influence of flame/turbulence interaction in the flame front propagation, which is hardly obtained by experiments. The thermal expansion rate across the flame front is studied by the temperature distribution. The simulations enable detailed data analysis compared to experimental measurements. The light-around time and circumferential flame propagation speed are quantitatively calculated to characterize the ignition dynamics during the light-around ignition.

2D Analysis of Cracked Viscoelastic Media Using Singular Element

Li Xiang^{*}, Hu Xiaofei^{**}, Yao Weian^{***}

^{*}Dalian University of Technology, ^{**}Dalian University of Technology, ^{***}Dalian University of Technology

ABSTRACT

In this paper, crack problem in linear viscoelastic material is studied numerically by using a singular element which was derived based on the Symplectic Eigen Solution (SES) for crack. Firstly, the fundamental equations of 2D viscoelastic problem are transformed into a series of elastic crack problems by using the method of precise time-domain expanding algorithm. These time independent elastic crack problems are connected through the time-domain expanding coefficients of displacement and stress in a recursive manner. Secondly, the elastic crack problems are solved by using finite element method and the singular element is applied to solve the stress singularity problem. The circle singular element occupies the area around the crack tip and is connected to the conventional elements meshed in the other area through export nodes. Mesh refinement near the crack tip is unnecessary and hence the computational costs are significantly reduced. Taking advantages of the proposed method, the viscoelastic fracture parameters such as stress intensity factor, crack opening and sliding displacement and strain energy release rate are all related to the symplectic eigen expanding coefficients and can be solved directly without any post-processing. Finally, numerical examples are provided to demonstrate the proposed method. Numerical predictions are also compared with those obtained by other numerical methods, such as, extended finite element method, enriched finite element method, boundary element method and numerical manifold method. The comparisons show that the present method is convenient, accurate and efficient.

A Stress State Dependent Constitutive Model for Finite Deformation of Soft Elastomers

Yuhai Xiang^{*}, Peng Wang^{**}, Danming Zhong^{***}, Shaoxing Qu^{****}

^{*}Zhejiang University, ^{**}Zhejiang University, ^{***}Zhejiang University, ^{****}Zhejiang University

ABSTRACT

Predicting the constitutive behavior of finite deformation of soft elastomers under complex stress state is a long-standing challenge because a large number of constitutive models calibrated from uniaxial stress state cannot accurately characterize the responses under complex stress state. Therefore, we developed a stress state dependent constitutive model based on a new microscopic picture, in which the stress is decomposed into two parts: one comes from cross-linked network and another comes from entangled network. Then the experimental results of vulcanized rubber, natural rubber, Entec Enflex S4035A thermoplastic elastomer (TPE), silicone rubber and Tera-PEG gel under the uniaxial, biaxial and pure shear loading conditions are used to calibrate and verify the proposed constitutive model. Meanwhile, a comparison is made with other similar constitutive models (extended tube model and nonaffine network model). It is shown that the proposed model can not only capture softening with a stress plateau, hardening with a sharp rise in stress, but also can accurately characterize the constitutive behaviors of soft rubberlike material under complex stress state with only three material parameters. Furthermore, the stress state dependent constitutive model can accurately simulate the deformation process of the complex structure, thus proving that the proposed model have great potential applications in the area of soft robots, soft electronics and polymer manufacture.

Geometrically Nonlinear Finite Element Method Based on the Willis-Form Equations

Zhihai Xiang*, Yixiao Sun**

*Tsinghua University, **Tsinghua University

ABSTRACT

It has been proved that linear elastic equations for inhomogeneous media are in Willis-forms with a displacement coupling term related with the gradient of pre-stresses [1]. This has also been verified by an experiment on rotational springs [2]. Since the pre-stress is crucial to finite deformation analysis, we propose a new geometrically nonlinear finite element method in updated Lagrangian formulation based on the Willis-form equations. This method is featured with an additional stiffness matrix, which contains the gradient of pre-stress of previous load step. In this way, efficient Newton-Raphson iteration is conducted by using a secant stiffness matrix. Acknowledgement This work is supported by National Science Foundation of China with grant number 11672144. References [1] ZH Xiang and RW Yao. Realizing the Willis equations with pre-stresses. *Journal of the Mechanics and Physics of Solids*, 87, 2016: 1-6. [2] RW Yao, HX Gao, YX Sun, XD Yuan, ZH Xiang. An experimental verification of the one-dimensional static Willis-form equations. *International Journal of Solids and Structures*, 2017, doi.org/10.1016/j.ijsolstr.2017.06.005.

A 3D Mesoscopic Model for the Dynamic Behavior of an Al/PTFE Composite

Yang Xiang Li^{*}, He Yong^{**}, Wang Chuang Ting^{***}, He Yuan^{****}

^{*}Xing Li Yang, ^{**}Yong He, ^{***}Chuang Ting Wang, ^{****}Yuan He

ABSTRACT

Abstract: reactive materials or impact-initiated materials are known to be reactive under dynamic impacting and released large quantity of energy. As a typical impact-initiated composite, Al/PTFE composite has been investigated extensively those years. The mechanical behavior of an Al/PTFE composite under dynamic loading with numerical simulation and experiments. The composite was produced with powder mixed, suppression and sintering. The microstructure of the composite was obtained with micro CT facility, a 3D mesoscopic model was established by following a series of image processing procedures. Gas gun launched impact experiments were conducted to investigate the mechanical behavior of composite under dynamic loading. The results of simulations agreed well with the experiment results. It is indicated that the 3D mesoscopic model procedure used in this paper is an efficient method to predict the dynamic behavior of composites under impact loading.

Large-Eddy Simulation of a Screeching Axisymmetric Jet in the Helical Mode

Li Xiangru*, He Feng**

*School of Aerospace, Tsinghua University, **School of Aerospace, Tsinghua University

ABSTRACT

Large eddy simulation is performed for investigating the screech noise generation and shock-vortex interactions of a screeching axisymmetric jet in the helical C mode issuing from a convergent nozzle at a nozzle pressure ratio of 3.4. The nozzle pressure ratio, exit diameter and lip thickness of nozzle are the same as the experiment condition in [1]. The Favre filtered compressible Navier–Stokes equations in cylindrical coordinates have been solved by using a finite difference method. The large eddy simulation code employs a seven-order weighted essentially non-oscillatory scheme [2] for the convective fluxes, a sixth-order centered difference approach for the viscous fluxes, and a four-stage third-order strong-stability-preserving Runge–Kutta technique in time. The simulated mean velocity field, shock cell structures and screeching frequency are all in good agreement with the experimental measurements. The large helical vortex structures appear in the jet shear layer which coincide with the helical screeching mode. It is also found in numerical results that shock structures oscillate periodically with the screeching frequency. The helical shock motions of the forth shock structure is complicated. In our research, the organized vortices in the jet shear layer change shock formations by modifying the sonic line. The fluctuating velocities of numerical data have been analysed by proper orthogonal decomposition(POD). The first two modes of POD containing more energy than other modes. The mode 1 and mode 2 would look visually the same but a spatial phase shift ensures orthogonality between mode 1 and 2. The POD results in several different planes indicate that the helical vortices in jet shear layer are the dominant dynamic flow structures and they are related with screeching sound waves strongly. [1] Edgington-Mitchell, D., et al. (2014). “Coherent structure and sound production in the helical mode of a screeching axisymmetric jet.” *Journal of Fluid Mechanics* 748: 822-847. [2] Balsara, D. S. and C.-W. Shu (2000). “Monotonicity Preserving Weighted Essentially Non-oscillatory Schemes with Increasingly High Order of Accuracy.” *Journal of Computational Physics* 160(2): 405-452.

Development of a Transferable Reactive Force Field of P/H Systems: Application to the Chemical and Mechanical Properties of Phosphorene

Hang Xiao^{*}, Xiaoyang Shi^{**}, Feng Hao^{***}, Xiangbiao Liao^{****}, Yayun Zhang^{*****}, Xi Chen^{*****}

^{*}Columbia University, ^{**}Columbia University, ^{***}Columbia University, ^{****}Columbia University, ^{*****}Columbia University, ^{*****}Columbia University

ABSTRACT

We developed ReaxFF parameters for phosphorus and hydrogen to give a good description of the chemical and mechanical properties of pristine and defected black phosphorene. ReaxFF for P/H is transferable to a wide range of phosphorus and hydrogen containing systems including bulk black phosphorus, blue phosphorene, edge-hydrogenated phosphorene, phosphorus clusters and phosphorus hydride molecules. The potential parameters were obtained by conducting global optimization with respect to a set of reference data generated by extensive ab initio calculations. We extended ReaxFF by adding a 60° correction term which significantly improved the description of phosphorus clusters. Emphasis was placed on the mechanical response of black phosphorene with different types of defects. Compared to the nonreactive SW potential,¹ ReaxFF for P/H systems provides a significant improvement in describing the mechanical properties of the pristine and defected black phosphorene, as well as the thermal stability of phosphorene nanotubes. A counterintuitive phenomenon is observed that single vacancies weaken the black phosphorene more than double vacancies with higher formation energy. Our results also showed that the mechanical response of black phosphorene is more sensitive to defects in the zigzag direction than that in the armchair direction. In addition, we developed a preliminary set of ReaxFF parameters for P/H/O/C to demonstrate that the ReaxFF parameters developed in this work could be generalized to oxidized phosphorene and P-containing 2D van der Waals heterostructures. That is, the proposed ReaxFF parameters for P/H systems establish a solid foundation for modelling of a wide range of P-containing materials.

A 2D Local Discontinuous Galerkin Finite Element Method Solution of the Richards's Equation

Yilong Xiao^{*}, Ethan Kubatko^{**}

^{*}The Ohio State University, ^{**}The Ohio State University

ABSTRACT

Unsaturated flows in porous media influenced by hydraulic conductivity and capillary pressure are governed by the Richards's equation. Many available numerical Richards's equation solvers are based on conforming finite element methods, which could experience numerical difficulties when soil water content undergoes abrupt changes and/or in the presence of natural heterogeneities in porous media. In light of such challenges, a two-dimensional numerical solver is formulated based on the local discontinuous Galerkin finite element method (LDG-FEM) --- a class of finite element method that employs piecewise continuous trial spaces and allows solution discontinuity across element boundaries. Soil water content measurement will be acquired from the National Oceanic and Atmospheric Administration (NOAA) for model validation. Extension of this LDG solver as a general framework in solving other convection-diffusion problems is expected in future.

Electromechanical Response and Effective Properties of Piezoelectric Fiber Composite with Arbitrary Shape Inclusion

Cihang Xie^{*}, Ying Wu^{**}

^{*}Xi'an Jiaotong University, ^{**}Xi'an Jiaotong University

ABSTRACT

The piezoelectric fiber composite has achieved great application in vibration control of aeronautic and aerospace structures, which contains an active layer constructed by piezoceramic fibers embedded in polymer matrix. In this paper, an analytical framework based on the complex potential theory and the generalized self-consistent method has been developed to predict the electromechanical fields and the effective properties of piezoelectric fiber composite. A three-phase model is presented, which assumes a representative cell containing an arbitrary shape piezoelectric fiber and non- piezoelectric matrix is embedded in infinite equivalent piezoelectric composite. Both of in-plane strain with transverse electric fields and anti-plane shear with in-plane electric fields are considered. Firstly, a new conformal mapping method is proposed to translate arbitrary two connected domain into annular domain, and arbitrary simply connected domain into circle domain. Then, the general solutions of the complex potential for each component can be expressed in series form with unknown coefficients. The continuity conditions of the interfaces and the homogeneous conditions are used to build up a set of equations to determine the unknown coefficients. After the complex potentials are solved, the exact electromechanical response and effective properties of piezoelectric fiber composite with arbitrary shape inclusion are obtained. It is shown that the inclusion shape has a significant influence on the stress and electric field distribution at the interface between the matrix and piezoelectric fibers. Furthermore, the proposed analytical framework provides a powerful instrument for solving the related problems about fibrous composites with imperfect interfaces or with coated phase.

Interfacial Stress Evolution during the Isothermal Growth of Mixed Oxide Layer in Thermal Barrier Coating System

Feng Xie^{*}, Weixu Zhang^{**}

^{*}State Key Laboratory for Strength and Vibration of Mechanical Structures, Xi'an Jiaotong University, ^{**}State Key Laboratory for Strength and Vibration of Mechanical Structures, Xi'an Jiaotong University

ABSTRACT

Abstract: Thermal barrier coating system (TBCs) is widely used in hot-section component parts of gas turbine. A prepared TBCs typically consists of a bond coat (BC) and a ceramic top coat (TC). An additional thermal growth oxidation (TGO) layer will form in pre-treatment or in service. During TGO growth, a layer of α -Al₂O₃ appears first, which provides oxidation protection. Then with time evolution, mixed oxide (MO) forms. MO grows much faster than α -Al₂O₃. It expands significantly and is one of main causes for the failure of TBCs. During the isothermal growth of MO in TBCs, severe stresses are generated and may induce micro-cracks and delamination. This work analyzes the local stress evolution around the convex morphology of MO by establishing the evolution equations on stress. A modified finite difference method is implemented to solve the problem. The effects of growth rate and volume expansion ratio of MO on the local stresses are considered. Through numerical analysis, we found that the stress induced by the growth of MO is much larger than that of α -Al₂O₃. The radial stress of α -Al₂O₃/MO interface gradually changes from compression to tension with the growth of MO. The radial tensile stress results in the initiation of the delamination. The growth of MO also induces the hoop tensile stress near the TC/MO interface and leads to the occurrence of the micro-cracks, which is in accordance with the experimental observation. Key words: local stress evolution, thermal barrier coating system, mixed oxide, oxidation growth, sphere model

In Situ Observation and Numerical Simulation of the Thermal Distortion during Direct Energy Deposition Process

Ruishan Xie^{*}, Gaoqiang Chen^{**}, Yue Zhao^{***}, Wentao Yan^{****}, Qingyu Shi^{*****}, Xin Lin^{*****}

^{*}Tsinghua University, ^{**}Tsinghua University, ^{***}Tsinghua University, ^{****}Northwestern University, ^{*****}Tsinghua University, ^{*****}Northwestern Polytechnical University

ABSTRACT

Part distortion is a technical bottleneck in the field of metal additive manufacturing, which depends on the thermo-mechanical behavior the material experienced during deposition process. This study successfully obtained the continuous full-field strain of a Ti-6Al-4V thin-wall during the direct energy deposition additive manufacturing process using digital image correlation (DIC) method. The finite element method was established based on the same deposition process with the experiments. The numerical simulation results agree well with experiments. The longitudinal strain increased rapidly to tensile strain as the laser beam approached, whereas the vertical strain decreased rapidly to a compressive strain and gradually transformed to tensile strain. The strains accumulated and rose periodically for the first several layers, which then decreased periodically during the following deposition. The strain accumulation behavior varied with the location of the deposited part, which caused the uneven distortion both in longitudinal and vertical directions. Increasing interlayer cooling time could significantly reduce the transient distortion of the deposited part during deposition, while it was not good for the final distortion. The in-situ strain field of additive manufactured part obtained in this study can be an effective validation for theoretic and computation studies, which also provides valuable guidance for real-time monitoring and controlling of stress and distortion for industry production.

Topology Optimization Analysis of Tensegrity Torus Based on Niche Genetic Algorithm

Shengda Xie^{*}, Xingfei Yuan^{**}, Shuo Ma^{***}

^{*}Zhejiang University, ^{**}Zhejiang University, ^{***}Zhejiang University

ABSTRACT

An absolute self-balancing cable dome can be created by adopting tensegrity torus as ring girders. A topology optimization method based on improved genetic algorithm with the sharing function niche mechanism, pre-selection niche mechanism and adaptive technique is proposed by considering the flexibility and mechanical properties of tensegrity torus. The minimum structural weight is taken as the optimal objective of the method. The four constraint conditions of the method are feasible integral structural pre-stressing, none cross collision of bars, constraint of members stress and limitation of structure displacements. In order to obtain the static analysis results of tensegrity torus of different topological conditions efficiently, a self-compiled program of vector form intrinsic finite element is applied in the algorithm. Finally, the analysis results of several examples of different spans and topological conditions solved by ANSYS prove the effectiveness of the proposed computing method. The improved niche genetic algorithm provides a new computing method for the topology optimization of tensegrity torus?

A New MMC-based Isogeometric Topology Optimization Using R-functions and Collocation Schemes

Xianda Xie^{*}, Shuting Wang^{**}, Manman Xu^{***}, Yingjun Wang^{****}

^{*}Huazhong University of Science and Technology, ^{**}Huazhong University of Science and Technology,
^{***}Huazhong University of Science and Technology, ^{****}South China University of Technology

ABSTRACT

A new isogeometric topology optimization (TO) method based on moving morphable components (MMC) is presented, where R-functions are used to represent the topology description functions (TDF) to overcome the C1 discontinuity problem of the overlapping regions of components. Three new ersatz material models based on uniform, Gauss and Greville abscissae collocation schemes are used to represent both the Young's modulus of material and the density field based on the Heaviside values of collocation points. Three benchmark examples are tested to evaluate the proposed method, where the collocation schemes are compared as well as the difference between isogeometric analysis (IGA) and finite element method (FEM). The results show that the convergence rate using R-functions have been improved in a range of 17%-40% for different cases in both FEM and IGA frameworks, and the Greville collocation scheme outperforms the other two schemes in the MMC-based TO.

COMPUTATIONAL HOMOGENIZATION SIMULATION ON STEEL REINFORCED RESIN USED IN THE INJECTED BOLTED CONNECTIONS

Haohui Xin, Martin P. Nijgh, Milan Veljkovic

Faculty of Civil Engineering and Geosciences, Delft University of Technology
Stevinweg 1, room 2.60 (Stevin II)

Delft University of Technology, Delft, The Netherlands

H.Xin@tudelft.nl; M.P.Nijgh@tudelft.nl; M.Veljkovic@tudelft.nl

Key words: Steel reinforced resin, linear Drucker-Prager plastic model , Finite element simulation, Computational homogenization.

Abstract: Injected bolts are regarded as a suitable alternative for a renovation of riveted connections of large span structures. Recently, the injected material, epoxy resin is modified at TU Delft by adding the steel shots to improve injected bolts performance suitable for reusable composite (steel-concrete) structures. The shots serves as reinforcement into epoxy resin serving as matrix. Increase of compressive strength and stiffness, and improvement of creep characteristics of the reinforced injected materials are expected. In a bolt hole the reinforce resin appears in confinement environment and will improve performance of connections exposed to monotonic and cyclic loading. In this paper, numerical homogenization, where combined non-linear isotropic/kinematic cyclic hardening model is employed to define the steel plasticity, linear Drucker-Prager plastic criterion was used to simulate resin damage, and the cohesive surfaces reflecting the relationship between traction and displacement at the interface were employed to simulate the steel-resin interface, is conducted to predict the tensile and shear behaviour of steel reinforced resin after validated by compressive material test results. The friction angle β , the ratio of the yield stress in triaxial tension to the yield stress in triaxial compression K , and the dilation angle ψ of linear Drucker-Prager plastic model are obtained based on experiments and numerical homogenization simulation. The confinement effects on steel reinforced resin could be effectively simulated. Finite element simulations on unconfined/confined steel reinforced resin material tests were conducted to validate the material parameters proposed in this paper. A good agreement is observed, indicating the model and parameters proposed in this paper could be effectively used in the finite element simulation of injected bolts.

1 INTRODUCTION

Injected bolts are regarded as a suitable alternative for a renovation of fitted bolts, riveted or preloaded connections of large span structures [1–3]. A hole is included in the head of the bolt in order to inject the bolt-hole clearance with a resin. After injection and curing of the resin, the connection is slip resistant. Recently, the injected material, epoxy resin is modified at TU Delft by adding the steel shots (reused after abrasive blast cleaning of steel surface) to increase initial stiffness of the connection for reusable composite (steel-concrete) structures[4]. The shots serves as reinforcement of an epoxy resin serving as matrix. Additional increase of compressive strength and expected improvement of creep characteristics of the reinforced injected material, especially in an oversized bolt clearance connection, will improve performance of connections exposed to monotonic and cyclic loading.

Besides the experimental research, numerical simulations may play an important role in the qualification and certification of short- and long- term behaviour of injection bolts. The material models of resin/steel reinforced resin are investigated before conducting finite element simulation on structural elements containing connection with injection bolts. However, the material behaviour of reinforced resin depends on the type of resin, type of the reinforcing material, the volume fraction of resin and steel shots and the size of the hole clearance. It is appropriate to adopt a multi-scale analysis to determine the mechanical properties of the steel-reinforced resin. Numerical homogenization method [5], which could accurately consider the geometry and spatial distribution of the phases, and also could precisely estimate the propagation of damage in order to accurately predict the failure strength, is considered to be an effective modelling tool for analysis of steel reinforced resin performance. Fish et al. [6–9] successfully use the statistically computational homogenization methods to predict the macroscopic behaviour of concrete, FRP material and even femur fracture. Xin et al. [10–12] adopted a multi-scale analysis in determining mechanical properties of pultruded GFRP laminates and successfully predict the mechanical behaviour of a pultruded GFRP bridge deck. Gonzalez and LLorca [13] analysed the mechanical response of a unidirectional FRP subjected to transverse compression. Vaughan and McCarthy [14] investigate the effect of fiber–matrix debonding and thermal residual stress on the transverse damage behavior of unidirectional FRP.

Computational homogenization methods of fine scale models provide a pathway to use high fidelity models to predict macroscopic mechanical responses of steel reinforced resin. However, the high fidelity numerical homogenization methods are reported computationally expensive [15–18]. The hierarchical strategy, where experimental results and high fidelity model (HFM) are employed to train a low fidelity model (LFM) and to supplement experimental database is adopted to model the material behaviour of steel reinforced resin [18]. The performance of the steel reinforced resin is effectively predicted by an elaborate but computationally inexpensive low fidelity model identified by a more fundamental but computationally taxing high fidelity model, which has been calibrated to the experimental results.

In this paper, first-order numerical homogenization is employed as high fidelity model, where combined non-linear isotropic/kinematic cyclic hardening model is employed to define the steel plasticity, linear Drucker-Prager plastic criterion was used to simulate resin damage, and the cohesive surfaces reflecting the relationship between traction and displacement at the interface. The linear Drucker-Prager plastic model is used as low fidelity model. The friction angle β , the ratio of the yield stress in triaxial tension to the yield stress in triaxial compression K , and the dilation angle ψ of linear Drucker-Prager plastic model are obtained based on experiments and

numerical homogenization simulation. Finite element simulations on unconfined/confined steel reinforced resin material tests were conducted to validate the proposed material parameters. This research may contribute to numerical simulation and practical design of injection bolts.

2 COMPUTATIONAL HOMOGENIZATION

2.1 Computational Homogenization and Periodic Boundary Condition

The link between micro-scale and macro-scale behaviour could be established based on Hill-Mandel computational homogenization method. The macro-scale Cauchy stress is obtained by averaging the micro scale Cauchy stress, in the unit cell domain, expressed as below [5]:

$$\sigma_{ij} = \frac{1}{|\Theta|} \int_{\Theta} \tilde{\sigma}_{ij} d\Theta \quad (1)$$

where: σ_{ij} is the macro-scale Cauchy stress, $\tilde{\sigma}_{ij}$ is the micro-scale Cauchy stress, Θ is the domain of the unit cell.

The boundary was implemented by so called “mixed boundary conditions” via constraint equations, is expressed by the following equations [5,19]:

$$\int_{\partial\Theta_Y} (u_i^f(x, y) - \varepsilon_{ik}^c y_k) N_j^\Theta d\gamma_Y = 0 \quad (2)$$

$$|u_i^f(x, y) - \varepsilon_{ik}^c y_k| N_j^\Theta \leq Tol \quad (3)$$

where: N_j^Θ is the unit normal to the unit cell boundary $\partial\Theta_y$.

2.2 Material Constitutive law

(1) Steel

The combined non-linear isotropic/kinematic cyclic hardening model is employed to define the steel plasticity [20]. The yield surface generally consists of two components, (i) a nonlinear kinematic hardening component, which describe the translation of the yield surface in stress space through the back-stress; and (ii) an isotropic hardening component, which describe the change of the equivalent stress defining the size of the yield surface as a function of plastic deformation. The pressure-independent yield surface is defined as below:

$$F_1 = f(\sigma - \alpha) - \sigma^0 = 0 \quad (4)$$

where σ^0 is the yield stress and $f(\sigma - \alpha)$ is the equivalent Mises stress with respect to the back-stress α . The non-linear kinematic/isotropic hardening is employed to describe the translation of the yield surface in stress space. The kinematic hardening is specified by half-cycle input material data. For each input material data point $(\sigma_i, \varepsilon_i^{pl})$, a value of back-stress α_i is obtained from the input data as:

$$\alpha_i = \sigma_i - \sigma_i^0 \quad (5)$$

where σ_i^0 is the user-defined size of the yield surface at the corresponding plastic strain for the isotropic hardening component. Integration of the backstress evolution laws over a half cycle yields the expression:

$$\alpha = \sum_{k=1}^N \left[\frac{C_k}{\gamma_k} \left(1 - e^{-\gamma_k \varepsilon_k^{pl}} \right) \right] \quad (6)$$

where N is number of back-stress, C_k and γ_k are material parameters and calibrated through material data.

(2) Resin

The plastic behaviour of resin was assumed to be governed by the linear Drucker-Prager model. The yield surface of the linear Drucker-Prager model [20] is given below.

$$F_2 = t - p \tan \beta - d = 0 \quad (7)$$

$$t = \frac{1}{2} q \left[1 + \frac{1}{K} - \left(1 - \frac{1}{K} \right) \left(\frac{r}{q} \right)^3 \right] \quad (8)$$

where β is the slope of the linear yield surface and is commonly referred as the friction angle of the material, d is the cohesion of the material, K is the ratio of the yield stress in triaxial tension to the yield stress in triaxial compression, and controls the dependence of the yield surface on the value of the intermediate principal stress. The flow potential of linear Drucker-Prager model is chosen as below equations:

$$G = t - p \tan \psi \quad (9)$$

where ψ is the dilation angle.

(3) Steel-Resin Interface

The cohesive surfaces reflecting the relationship between traction and displacement at the interface were used to simulate the steel-resin interface. The cohesive element is always subjected to complicated loading condition; the quadratic stress failure criterion [20] is used to evaluate the initial damage.

$$\left\{ \frac{\langle t_n \rangle}{t_n^0} \right\}^2 + \left\{ \frac{t_s}{t_s^0} \right\}^2 + \left\{ \frac{t_t}{t_t^0} \right\}^2 = 1 \quad (10)$$

where: t_n , t_s and t_t are traction components related to pure modes *I*, *II* and *III*, t_n^0 , t_s^0 and t_t^0 are interfacial strength of pure modes *I*, *II* and *III*. In the damage evolution period, the interfacial stiffness degraded from initial K_0 to $(1-d) K_0$, where d is a damaged variable. The Benzeggagh-Kenane fracture criterion (BK Law) [20,21] is particularly used to predict damage propagation of mixed-mode loadings in terms of the critical fracture energies during deformation purely along the first and the second shear directions are the same.

$$G^C = G_n^C + \left(G_s^C - G_n^C \right) \left\{ \frac{G_s + G_t}{G_n + G_s + G_t} \right\}^\eta \quad (11)$$

where: G_n , G_s , and G_t are the corresponding energy release rates under pure modes *I*, *II*, and *III*, the additional subscript “*C*” denotes critical case, which can be determined based on a standard fracture toughness test and η is a material parameter.

3. STRESS-STRAIN RELATIONSHIP OF RESIN

The uniaxial compressive behaviour of resin is described by combining the damage mechanics and Ramberg-Osgood relationship [22], as below:

$$\sigma = (1 - D) \sigma^{R-O}(\varepsilon) \quad (12)$$

$$\varepsilon = \frac{\sigma^{R-O}}{E} + K \left(\frac{\sigma^{R-O}}{E} \right)^n \quad (13)$$

where: D is damage variable. The damage variable is defined as below:

$$D = \begin{cases} 0 & \varepsilon < \varepsilon_0^f \\ \frac{\varepsilon - \varepsilon_0^f}{\varepsilon_u^f - \varepsilon_0^f} & \varepsilon \geq \varepsilon_0^f \end{cases} \quad (14)$$

where: ε_0^f is plastic strain at fracture initiation, ε_u^f is the plastic strain at the failure. The fracture initiation strain ε_0^f is assumed to be the corresponding strain at the peak load while the failure strain is obtained by extended the softening stage. The parameters relationship is fitted based on the experimental results before damage occurred. The fitted material parameters are listed in Tables 1.

Table 1 Ramberg-Osgood Relationship Parameters of Resin and Steel-reinforced Resin

Item		K	n	R ²	ε_0^f (%)	ε_u^f (%)
Resin	Nominal Stress	6.07×10^{11}	8.27	0.98	1.01	4.07
	True Stress	1.62×10^{16}	10.62	0.95	1.03	1.03

The friction angle β , the ratio of the yield stress in triaxial tension to the yield stress in triaxial compression K, and the dilation angle ψ is calculated based on experiments and listed in Table 2.

Table 2 Material Parameters of linear Drucker-Prager model

Material	Associated flow			Non-dilatant flow		
	β	K	ψ	β	K	ψ
Resin	12.16^0	0.92	12.16^0	12.18^0	1.00	0^0
Steel reinforced resin	49.80^0	0.78	49.80^0	52.04^0	1.00	0^0

4. COMPUTATIONAL HOMOGENIZATION

It is very difficult to make a dog-bone shape tensile specimens in order to experimentally obtain tensile behaviour. The computational homogenization method provide an alternative way to obtain the tensile and shear behaviour numerically after validating the multiscale model with compressive test results. The unit cell is shown in Fig. 1. Material model and parameter used in Section 3 is employed to simulate the resin behaviour in the computational homogenization modelling. S235 grade steel is employed to describe the behaviour of steel shot based on Eurocode EN 1993-1-1 nominal data, [23]. The “mixed periodic boundary conditions” are applied to the unit cell via constraint equations. Surface cohesive model is used to describe the interface behaviour between steel and resin. The interface parameters are calibrated based on compressive test results. The normal interface stiffness is calibrated as 5.53×10^5 N/mm³, and the

shear interface stiffness is calibrated as $2.01 \times 10^5 \text{ N/mm}^3$. The normal interface strength obtained after the calibration is 40.8 MPa. The shear interface strength is calibrated to 41.5 MPa. The normal critical fracture energies G_n^c is determined as 0.04 kJ.mm^{-1} , and the shear critical fracture energies G_s^c and G_t^c is determined as 0.45 kJ.mm^{-1} . The material parameter is assumed to be 1.8 based on references [11,12]. The viscosity coefficient for the cohesive surface is assumed to be 0.001 s.

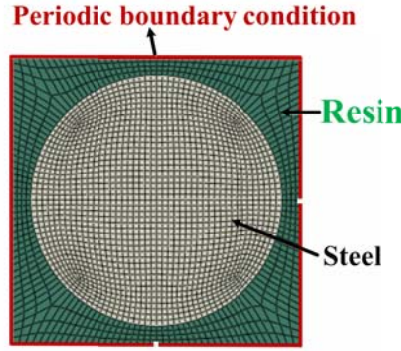


Figure (1): Unit cell of steel reinforced resin

Compressive stress-strain relationship comparisons between numerical homogenization and experiments of unconfined steel reinforced resin is shown in Fig.2. The macro scale stress is obtained based on Eq.(1), so the homogenization results is compared with true stress and strain relationship. A good agreement is observed, indicating it is reliable to use computational homogenization method to predict the tensile and shear behaviour of steel reinforced resin.

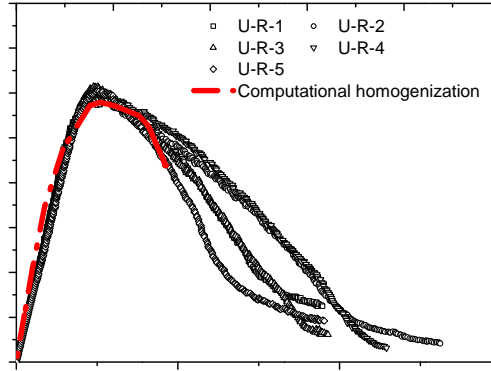
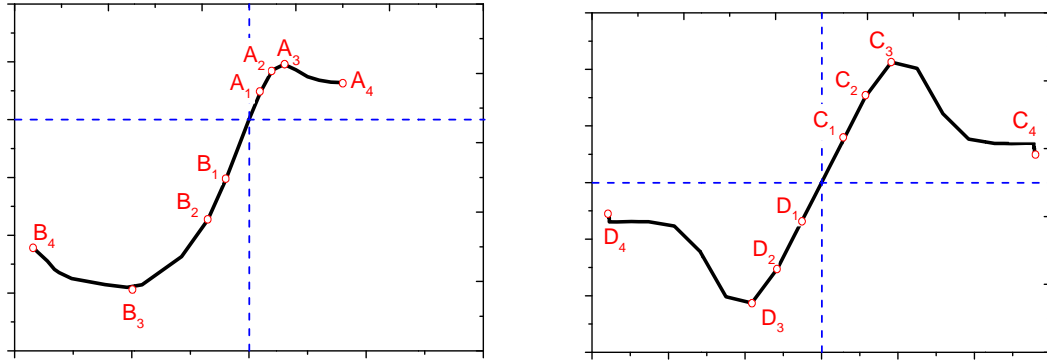


Figure (2): Stress-strain relationship comparisons between numerical homogenization and experiments of unconfined steel reinforced resin

The uniaxial stress and strain relationship, shear stress and strain relationship based on numerical homogenization method is shown in Fig. 3. The ultimate tensile strength of steel reinforced resin is 39.8Mpa. The Mises stress distribution and deformation of unit cell is shown in Fig. 4 and Fig .5 at different stages in Fig. 3. The principal plastic strain at the failure of the unit cell is shown in Fig. 6. The numerical multiscale simulation indicated that the damage and failure of steel reinforced resin is governed by the resin and interface while the steel is in the elastic stage during uniaxial and shear loading. The friction angle β , the ratio of the yield stress in triaxial

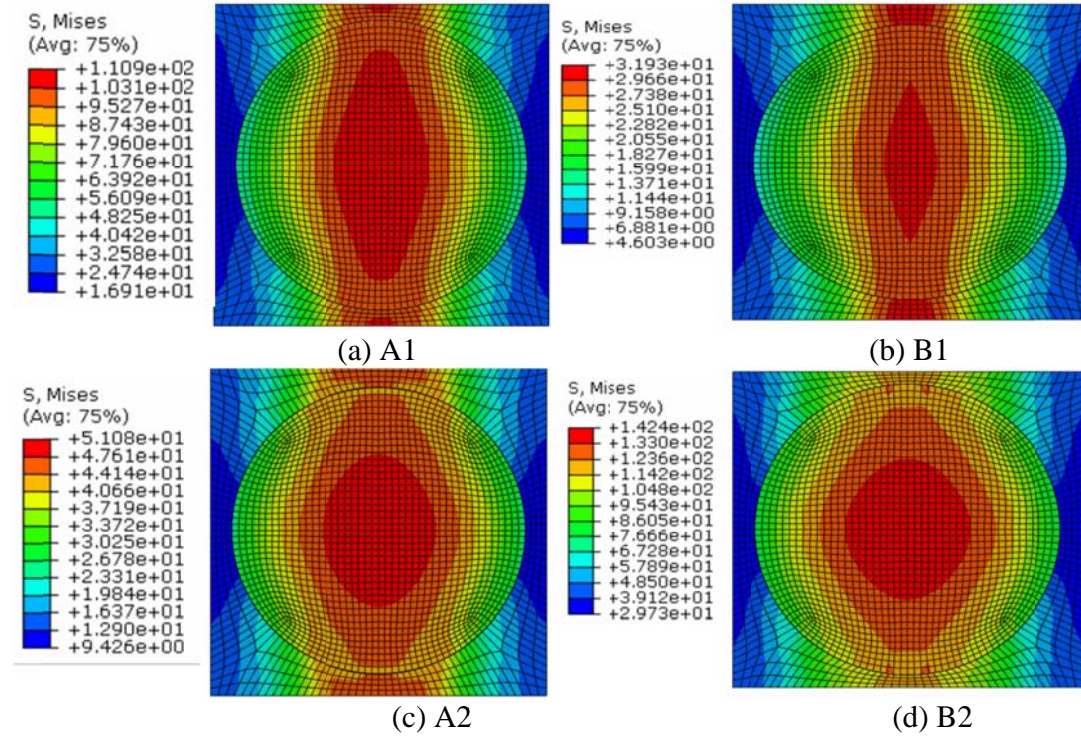
tension to the yield stress in triaxial compression K , and the dilation angle ψ is calculated based on multiscale simulation results. The steel reinforced resin material parameters of the linear Drucker-Prager model is summarized in Table 2.



(a)

(b)

Figure (3): Stress-strain relationship of steel reinforced resin calibrated by the numerical homogenization



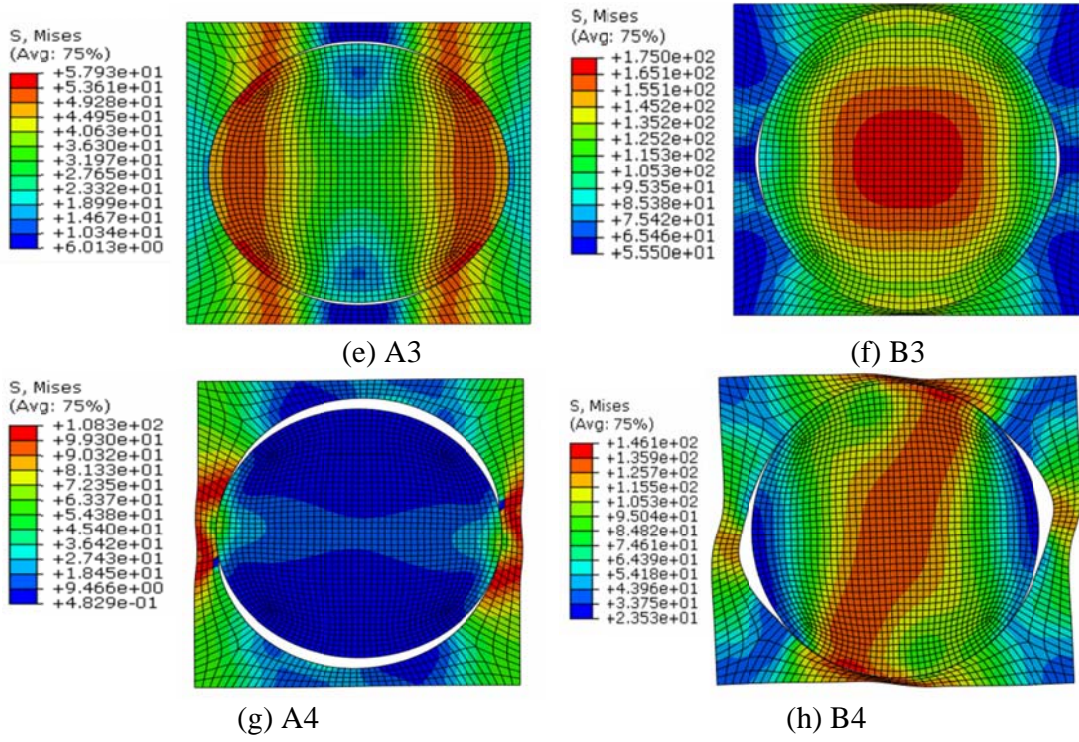
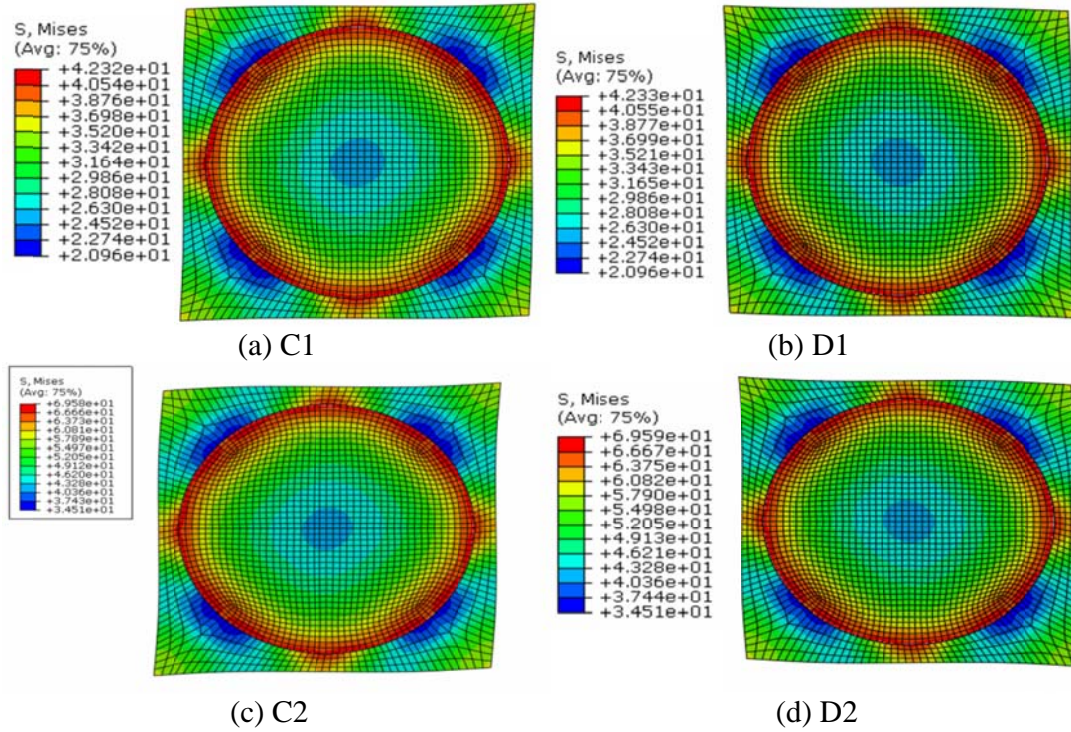


Figure (4): Mises stress distribution of unit cell under uniaxial loading in compression A1 to A4 and in tension B1 to B4 (in Fig.2)



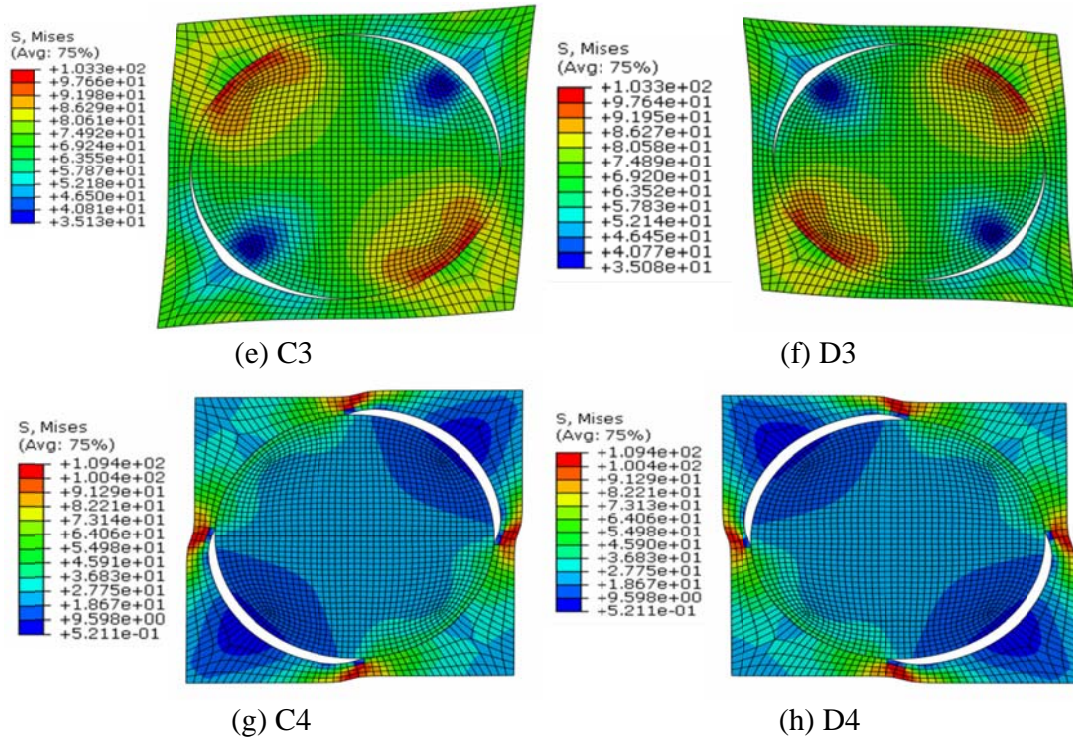


Figure (5): Mises stress distribution of unit cell under shear loading under shear loading C1 to C4 and D1 to D4 (in Fig.2)

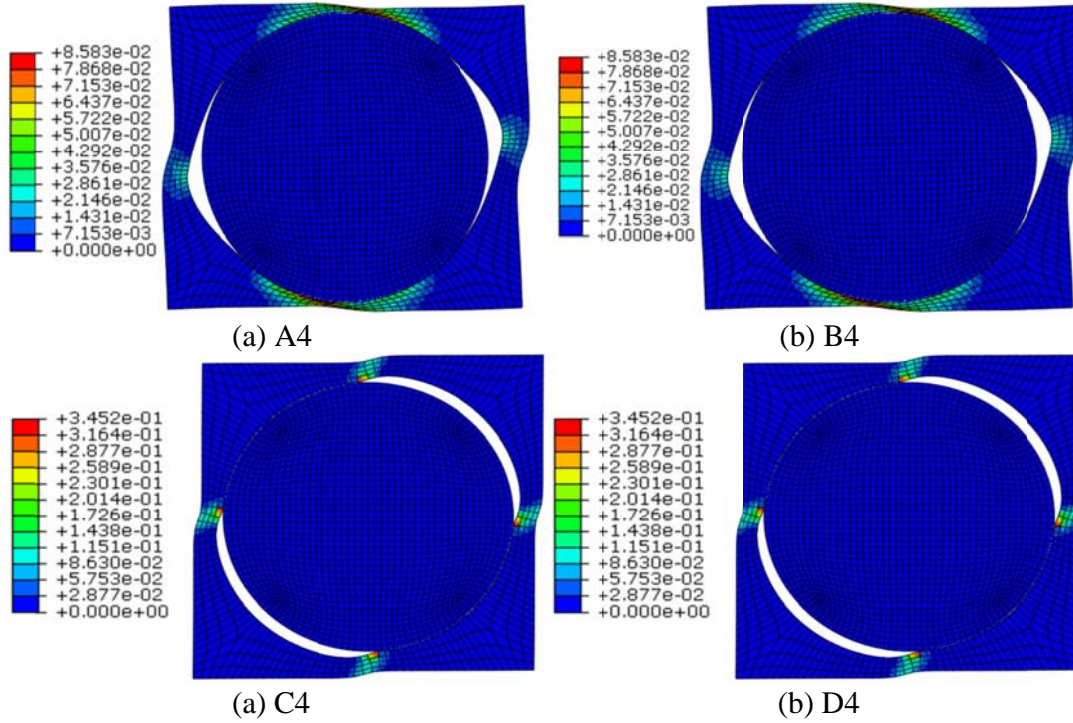


Figure (6): Principal plastic strain of unit cell at failure

5. VALIDATIONS

The unconfined steel reinforced resin compressive tests were simulated numerically using solid element C3D8R[20] see Fig.7. The uniaxial true stress and strain relationship and material parameters of the linear Drucker-Prager model are based on the multiscale simulation. The nominal stress-strain relationship of unconfined steel reinforced resin comparisons between finite element simulation and experimental results is shown in Fig. 8. A good agreement is observed. Finite element model of the confined resin experiments was built to validate the efficiency of the linear Drucker-Prager model when predicting resin behaviour with confinement. The nominal stress-strain of confined resin comparisons between finite element simulation and experimental results is shown in Fig. 8. A good agreement is observed, indicating the Drucker-Prager model could effectively model the confined condition of the resin. The fracture initiation strain at the peak load from “nondilatant flow” model is a little larger than if the “associated flow” model is used.

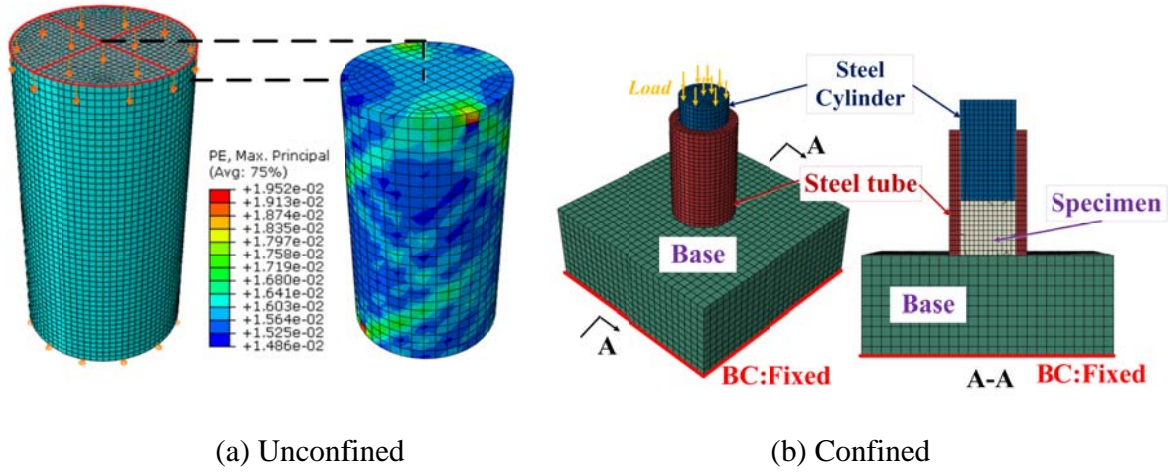


Figure (7): Finite element model of steel reinforced resin tests

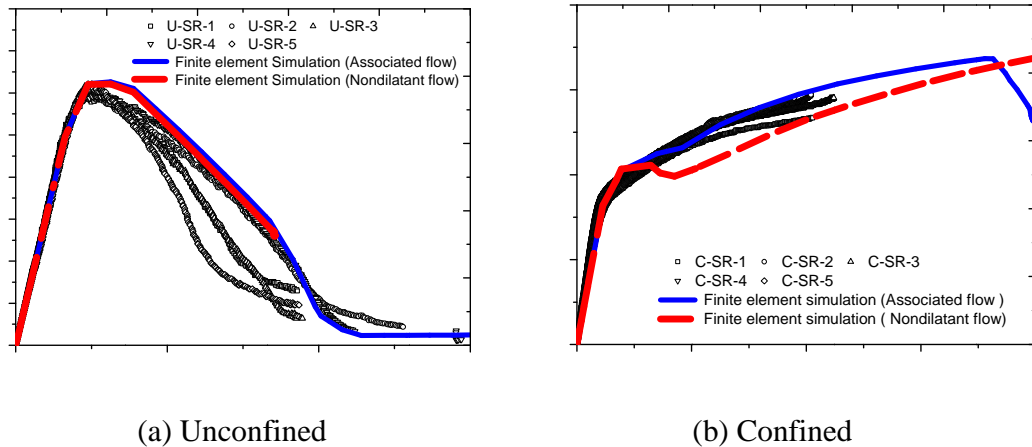


Figure (8): Predicted stress-strain relationship and experimental results of steel reinforced resin specimens

6 CONCLUSION

- The friction angle β , the ratio of the yield stress in triaxial tension to the yield stress in triaxial compression K, and the dilation angle ψ of the linear Drucker-Prager plastic model is obtained based on numerical homogenization to efficiently consider the confinement effects on steel reinforced resin. For associated flow hardening, the friction angle is 12.16° and 49.80° , the ratio K is 0.92 and 0.78, and the dilation angle ψ is 12.16° and 49.80° respectively for resin and steel reinforced resin. For non-dilatant flow, the friction angle is 49.80° and 52.04° , the ratio K is 1.00 and 1.00, and the dilation angle ψ is 0.0° and 0.0° respectively for resin and steel reinforced resin.

REFERENCES

- [1] Correia J, De Jesus AMP, Pinto JCM, Calçada RAB, Pedrosa B, Rebelo C, et al. Fatigue behaviour of single and double shear connections with resin-injected preloaded bolts. 19th Congr. IABSE Stock., 2016.
- [2] de Oliveira Correia JAF, Pedrosa BAS, Raposo PC, De Jesus AMP, dos Santos Gervásio HM, Lesiuk GS, et al. Fatigue Strength Evaluation of Resin-Injected Bolted Connections Using Statistical Analysis. Engineering 2017.
- [3] Kolstein H, Li J, Koper A, Gard W, Nijgh M, Veljkovic M. Behaviour of double shear connections with injection bolts. Steel Constr 2017;10:287–94.
- [4] Nijgh MP. New Materials for Injected Bolted Connections-A feasibility study for demountable connections. Delft University of Technology, 2017.
- [5] Fish J. Practical Multiscale John Wiley & Sons, 2013
- [6] Tal D, Fish J. Stochastic multiscale modeling and simulation framework for concrete. Cem Concr Compos 2018;90:61–81.
- [7] Fish J, Hu N. Multiscale modeling of femur fracture. Int J Numer Methods Eng 2017;111:3–25.
- [8] Hu N, Fish J, McAuliffe C. An adaptive stochastic inverse solver for multiscale characterization of composite materials. Int J Numer Methods Eng 2017;109:1679–700.
- [9] Tal D, Fish J. Generating a statistically equivalent representative volume element with discrete defects. Compos Struct 2016;153:791–803.
- [10] Xin H, Liu Y, Mosallam AS, He J, Du A. Evaluation on material behaviors of pultruded glass fiber reinforced polymer (GFRP) laminates. Compos Struct 2017;182:283–300.
- [11] Xin H, Mosallam A, Liu Y, Xiao Y, He J, Wang C, et al. Experimental and numerical investigation on in-plane compression and shear performance of a pultruded GFRP composite bridge deck. Compos Struct 2017;180:914–32.
- [12] Xin H, Mosallam A, Liu Y, Wang C, Zhang Y. Analytical and experimental evaluation of flexural behavior of FRP pultruded composite profiles for bridge deck structural design. Constr Build Mater 2017;150:123–49.

- [13] Romanowicz M. A numerical approach for predicting the failure locus of fiber reinforced composites under combined transverse compression and axial tension. *Comput Mater Sci* 2012;51:7–12. doi:10.1016/j.commatsci.2011.07.039.
- [14] Vaughan TJ, McCarthy CT. Micromechanical modelling of the transverse damage behaviour in fibre reinforced composites. *Compos Sci Technol* 2011;71:388–96. doi:10.1016/j.compscitech.2010.12.006.
- [15] Xin H, Sun S, Fish J. A surrogate modeling approach for additive-manufactured materials. *Int J Multiscale Comput Eng* 2017.
- [16] Liu Y, Sun W, Fish J. Determining material parameters for critical state plasticity models based on multilevel extended digital database. *J Appl Mech* 2016;83:11003.
- [17] Xin H, Sun W, Fish J. Discrete element simulations of powder-bed sintering-based additive manufacturing. *Int J Mech Sci* 2017.
- [18] Fish J, Yuan Z, Kumar R. Computational certification under limited experiments. *Int J Numer Methods Eng* 2018;114:172–95.
- [19] Fish J, Fan R. Mathematical homogenization of nonperiodic heterogeneous media subjected to large deformation transient loading 2008:1044–64. doi:10.1002/nme.
- [20] Abaqus V. 6.14 Documentation. Dassault Syst Simulia Corp 2014.
- [21] Benzeggagh ML, Kenane M. Measurement of mixed-mode delamination fracture toughness of unidirectional glass/epoxy composites with mixed-mode bending apparatus. *Compos Sci Technol* 1996;56:439–49.
- [22] Ramberg W, Osgood WR. Description of stress-strain curves by three parameters 1943.
- [23] EN1993-1-1. Eurocode 3: Design of steel structures – Part 1.1: General rules – General rules and rules for buildings. Brussels CEN 2005.

Evaluation of Stress Intensity Factors in Cracked Plates and Shells Using Irwin's Integral and High-order XFEM

Chen Xing^{*}, Yongxiang Wang^{**}, Haim Waisman^{***}

^{*}1 State Key Laboratory of Mechanics and Control of Mechanical Structures, Nanjing University of Aeronautics and Astronautics, Nanjing, Jiangsu 210016, China 2 Department of Civil Engineering and Engineering Mechanics, Columbia University, New York, 10027, NY, USA, ^{**}Department of Civil Engineering and Engineering Mechanics, Columbia University, New York, 10027, NY, USA, ^{***}Department of Civil Engineering and Engineering Mechanics, Columbia University, New York, 10027, NY, USA

ABSTRACT

This paper presents a novel framework based on Irwin's integral for evaluation of stress intensity factors (SIFs) in cracked plates and shells, using the extended finite element method (XFEM) with high order enrichment terms. The mixed interpolation of tensorial components (MITC) plate element based on the Mindlin-Reissner theory is used and enriched with discontinuous and high-order near tip functions. Irwin's integral is first reformulated for plates and shells and then evaluated using enriched degrees of freedom in XFEM. In this way, SIFs can be obtained in a closed-form and thus no special post-processing is needed. The accuracy of the formulation is studied on several benchmark examples of cracked plates. We consider an inclined crack problem with structured and unstructured quadrilateral meshes, and two cracks approaching each other. In both cases the method shows good accuracy and in particular the latter case shows the advantage of this method over the classical J-integral method. Finally, we demonstrate excellent performance on a shell problem of a cylinder with a circumferential crack subject to tension or torsion.

An Adaptive Galerkin Finite Element Method for Forced Vibration of Skeletal Structures in Structural Engineering

Qinyan Xing^{*}, Qinghao Yang^{**}, Chenyu Lu^{***}, Yiyi Dong^{****}, Si Yuan^{*****}

^{*}Tsinghua University, ^{**}Tsinghua University, ^{***}Tsinghua University, ^{****}Tsinghua University, ^{*****}Tsinghua University

ABSTRACT

As an advanced means of finite element method (FEM), the adaptive finite element method (AFEM) has been deeply studied and widely used in mechanics and engineering ever since it was proposed in 1980s. The basic idea of adaptivity is that, the user pre-specifies an error tolerance instead of a well-designed mesh in conventional FEM, the algorithm itself adjusts and generates an adaptive mesh, and finally a solution satisfying the error tolerance in certain norm is obtained. Actually the present research originates from the adaptive solution of one-dimensional steady convection-diffusion problem, for which the conventional Bubnov-Galerkin FEM may produce a bad result because of numerical oscillation, as we all known. Based on the Energy Element Projection (EEP) method for super-convergence computation of both the function and its derivatives in the post-processing stage of FEM, an efficient adaptive Galerkin FEM was established for boundary-value problems (BVPs) of ordinary differential equations (ODEs). And then it was extended to the adaptive solution of initial-value problems (IVPs) of ODEs, which in structural engineering are usually resulted from the finite element discretization of dynamic problems. The Galerkin weak form for IVPs and the adaptive strategy using EEP super-convergent solutions to estimate errors and guide the mesh refinement will be presented firstly. The forced vibration of skeletal structures, which is fundamental in structural dynamics, is a time- and space-dependent problem of partial differential equations (PDEs) in mathematics. Discretizing the structure along the axial direction of members with the conventional FEM, a system of IVPs is obtained and then solved with the adaptive strategy mentioned above, i.e. the adaptive analysis of time domain is realized. After that, the similar strategy is implemented to the axial coordinate of the members, i.e. the adaptive analysis of space domain is realized as well. As a result, an optimal time-space mesh and the corresponding dynamic solution with satisfying accuracy are obtained. The basic idea and the implementation algorithm of this adaptive Galerkin FEM for time- and space-dependent problems will be elaborated secondly. Several representative examples including Euler or Timoshenko beams and the plane frame under harmonic loads or seismic loads will be given to demonstrate the efficiency of the method finally. This work is part of the project supported by the National Natural Science Foundation of China (No. 51508305).

A Scaled Boundary Finite Element Based Node-to-Node Scheme for Three Dimensional Frictional Contact Problems

Weiwei Xing^{*}, Junqi Zhang^{**}, Chongmin Song^{***}, Francis Tin-Loi^{****}

^{*}University of New South Wales, ^{**}University of New South Wales, ^{***}University of New South Wales, ^{****}University of New South Wales

ABSTRACT

A new node-to-node scheme is proposed for three dimensional frictional contact analysis involving large sliding, with the aid of the scaled boundary finite element method. Treatment of non-matching contact interface which may result from different meshes of contact bodies or large tangential slippage remains to be one of the key obstacles in contact mechanics. Methods based on the finite element method often fail the patch test and/or require a complicated implementation, especially in three dimensional problems [1]. Moreover, initial penetrations and gaps introduced by non-matching meshes in curved contact interface may cause difficulty in contact pair identification and hence affect solution convergence. In the proposed method, non-matching meshes are treated using polyhedral elements constructed in the scaled boundary finite element method. The polyhedral elements may have an arbitrary number of faces. Only the boundary of a polyhedral element is discretised thereby providing highly flexibility in mesh transition [2]. Non-matching meshes can be easily converted to matching ones with a surface remeshing procedure which inserts nodes along the contact interface. The method allows the use of the simple and robust node-to-node contact analysis algorithm. The initial penetrations and gaps can also be eliminated. The surface remeshing procedure is limited to the contact interface only and no volume remeshing is required in the scaled boundary finite element method. The contact constraint is formulated and solved directly as a mathematical programming problem known as a mixed complementarity problem. Contact constraints of non-penetration and stick slide condition are described directly in a complementarity format. The constraints are strictly satisfied without having to resort to user-specified control parameters. The irreversibility of friction is accommodated in a rate formulation that is solved in a sufficiently accurate stepwise fashion. Through numerical examples, it is demonstrated that the proposed method not only can pass the patch test but also is stable and accurate, especially in conjunction with higher order elements. References: [1] V. A. Yastrebov, Numerical Methods in Contact Mechanics, John Wiley & Sons, 2013. [2] E. T. Ooi, C. Song, F. Tin-Loi, A scaled boundary polygon formulation for elasto-plastic analyses, Computer Methods in Applied Mechanics and Engineering 268 (2014) 905-937.

Numerical Simulation of Damage Effects of a Carbon Fiber Composite Cylinder Subjected to Laser Irradiation and Axial Compression

Xiaodong Xing^{*}, Weilong Guo^{**}, Te Ma^{***}, Hongwei Song^{****}

^{*}Harbin Engineering University, ^{**}Harbin Engineering University, ^{***}Harbin Engineering University, ^{****}Chinese Academy of Sciences

ABSTRACT

The specific aim of this study is to investigate damage effects of the carbon fiber composite subjected to compression load and laser irradiation simultaneously. The intense laser irradiation can lead to ablation and damage of materials. Because the damage effects of composites irradiated by laser are very complex, only the thermal decomposition and oxidation reaction are taken into account in our study. The ALE adaptive grid method and a UMESHMOTION subroutine in ABAQUS are applied to simulate the ablation progress. The three-dimensional ablation evolution of a carbon fiber composite cylindrical shell is obtained and the influence of the related parameters on the critical buckling load is discussed as well.

Predicting Dislocation-Interface Reactions from the Atomistic to the Microscale

Liming Xiong*, Valery Levitas**

*Assistant Professor, **Professor

ABSTRACT

The dislocation-interface reaction in materials is inherently multiscale since both the atomic structure of the interfaces and the long-range fields of the dislocation pile-up at the interface come into play. In this work, we present a concurrent atomistic-continuum (CAC) method for multiscale modeling and simulations of dislocation-interfaces interactions. The interfaces to be investigated include twin boundaries in bi-crystalline metallic materials, phase boundaries in amorphous/crystalline and crystalline/crystalline multilayered metallic composites. The CAC method is based on a finite element implementation of a multiscale formulation in which the reconfiguration of crystal structures and slip systems in crystalline solids are embedded. CAC models of typical material systems, such as bi-crystalline Cu and Al with twin boundaries, multilayered $\text{Cu}_x\text{Zr}_{1-x}/\text{Cu}$, and fcc/bcc/fcc composites, are constructed. With a fully atomistic resolution at the interface and coarse-grained atomistic resolution in the regions away from interfaces, CAC models require significantly less computational cost than that by fully atomistic simulation. Most importantly, the atomistic natures of dislocation nucleation, migration, and interactions are preserved in the coarse region away from the atomic-scale interfaces. CAC simulations reveal main mechanisms underlying dislocation-interface interactions from the atomic to the microscale. In bi-crystalline Cu and Al specimens, the dislocation-twin boundary reaction is found to always follow the recombination-redissociation process, without forming any twin boundary dislocations in process of recombination. In $\text{Cu}_x\text{Zr}_{1-x}/\text{Cu}$, with the dislocations being "piled-up" at the amorphous/crystalline interfaces, strong local stress concentrations near the amorphous-crystalline interface lead to the devitrifications in amorphous layers. In contrast, in fcc/bcc/fcc nanolaminates, dislocation pile-ups at the fcc/bcc interface is found to assist phase transformation from bcc to fcc. Our results elucidate the discrepancies between atomistic simulations and experimental observations of dislocation-interface reactions and highlight the importance of directly modeling dislocation-interfaces interactions using concurrent multiscale models.

Modeling and Simulation of Nonequilibrium Complex Flows

Aiguo Xu*, Guangcai Zhang**

*Institute of Applied Physics and Computational Mathematics, P. R. China and Peking University, P. R. China,

**Institute of Applied Physics and Computational Mathematics, P. R. China

ABSTRACT

Nonequilibrium complex flows are ubiquitous in nature and play an important role in both the engineering fields and our daily lives. The existing various interfaces, complex forcing and relaxation processes results in very complicated hydrodynamic and thermodynamic responses. It is known that a Navier-Stokes(NS) model is not sufficient to capture the complicated non-equilibrium behaviors, and the spatial and temporal scales which the microscopic molecular dynamics simulation can access are too small to be comparable with experiments. The Monte Carlo simulation has a similar constraint on the system size and evolution time. Under such cases, a kinetic model based on the Boltzmann equation is more preferable. In this talk, we will briefly review the progress of discrete Boltzmann modeling, simulation and analysis of nonequilibrium complex flows in our group in recent years. The topics are relevant to multiphase flows, shock waves, combustions and hydrodynamic instabilities. Mathematically, the only difference of discrete Boltzmann from the traditional hydrodynamic modeling is that the NS equations are replaced by a discrete Boltzmann equation. But physically, besides the macroscopic behaviors described by the NS model, the discrete Boltzmann model(DBM) presents more kinetic information on the Thermodynamic Non-Equilibrium (TNE). Via the DBM, it is convenient to perform simulations on systems with flexible Knudsen number. The observations on TNE have been used to estimate the deviation amplitude from thermal equilibrium state, to recover the main feature of real distribution function, to distinguish different stages of phase transition, to discriminate and capture various interfaces, etc. References [1] A. Xu, C. Lin, G. Zhang, Y. Li, Multiple-relaxation-time lattice Boltzmann kinetic model for combustion, *Physical Review E* 91, 043306 (2015). [2] Y. Gan, A. Xu*, G. Zhang, S. Succi, Discrete boltzmann modeling of multiphase flows: hydrodynamic and thermodynamic non-equilibrium effects, *Soft Matter* 11, 5336 (2015). [3] H. Lai, A. Xu*, G. Zhang, Y. Gan, Y. Ying, S. Succi, Nonequilibrium thermohydrodynamic effects on the Rayleigh-Taylor instability in compressible flows, *Physical Review E* 94, 023106 (2016).

Atomistic Modeling and Simulations on Mechanics and Thermal Transport of Heterostructures.

Baoxing Xu*

*University of Virginia Charlottesville

ABSTRACT

Heterostructures that are assembled by interfacing two-dimensional (2D) materials in an either lateral or vertical manner offer a unique platform for future energy efficient and multifunctional nanoelectronics. Unfortunately, the inherent difference of material lattice structures between layer components or external loading conditions will render mechanical deformation in heterostructures. The mechanical deformation could easily alter phonon activities by coupling with atom vibration, and thus changes thermal properties of heterostructures. Given the feature thickness (one to several atomic) of heterostructures, the thermal properties, which play an important role in thermal management of various electronic and thermal devices, are critical for maintaining optimal functionality of these devices, and yet is far less investigated due to their couplings with mechanical deformation. Understanding the fundamental thermal transport of heterostructures under mechanical deformation will be crucial for designing emerging heterostructures of relevance to applications in stretchable electronic and thermal devices with controllable heat-power dissipation and thermal management. In the present study, we develop atomistic modeling and simulation techniques to probe the effect of mechanical deformation on thermal transports in both vertical and lateral heterostructures, and to design heterostructures with mechanically controllable thermal properties. The fundamental thermal transport mechanism of both vertical and lateral heterostructures under various mechanical deformation are elucidated with the help of atomistic simulations. Further, guided by atomistic simulations, we present several proof-of-concept designs of heterostructures and demonstrate their mechanically tunable performance.

Resonant Attenuation of Stress Wave in a Particulate Composite

Dandan Xu*

*College of Mechanical Engineering, Zhejiang University of Technology, Hangzhou, China

ABSTRACT

Efficient wave attenuation is crucial for the protection of strong shock wave. In this presentation, a numerical study of resonant attenuation of stress wave in a particulate composite is performed using Finite Element Method (FEM). Coated particles, which are embedded in an elastic matrix, play roles of resonance units. Each unit consists of a core of high density and a soft interface, and it works like a mass-spring oscillator. Local resonance occurs when the natural frequency of the particle matches the frequency of incident wave. For a given incident wave, by designing the corresponding natural frequency of the coated particles, the local resonance is stimulated. Thus, a maximum amount of the incident energy transforms to the kinetic energy of the particles, leading to significant wave attenuation during the propagation in the composite. In this study, the effects of particle size and material properties on the natural frequency are also investigated.

SPH Simulation of Water Spray Generated by Aircraft Chine-Tire on the Contaminated Runway

Fei Xu^{*}, Xuanqi Ren^{**}, Xianpeng Zhang^{***}, Xiangyang Gao^{****}

^{*}Institute for Computational Mechanics and Its Applications? Northwestern Polytechnical University, ^{**}Institute for Computational Mechanics and Its Applications? Northwest Polytechnical University, ^{***}Institute for Computational Mechanics and Its Applications? Northwest Polytechnical University, ^{****}Institute for Computational Mechanics and Its Applications? Northwest Polytechnical University

ABSTRACT

The spray produced by aircraft tire running on contaminated runway may enter the inlet of engines, and lead to the compressor stall, surge, or even combustor flameout. Scholars used to study this problem by full-scale aircraft spray test, which may cost a lot, and get only a little valid data. According to the analysis of the interaction between tire and water, the numerical models of an elastic chined tire rolling in the water are established by coupled smoothed particle hydrodynamics (SPH) and finite element method (FEM). Then, the mechanism of the chine effect on the water spray is studied and the shape of chine is analyzed to avoid the potential danger. However, from the full-scale tests, we found that the chine tires could effectively suppress the spray at lower taxiing speed of aircraft, while it would suddenly lose effectiveness at higher speed. In order to discover the problem, we tried several steps. (1) A falling test of aircraft tire is constructed to investigate the suppression effect of the chine. The influence of the chine height is discussed in detail. (2) To reveal the reduction of suppression effect at high taxiing speed, several factors of the chine geometry, the water depth and the taxiing speed are considered. A quantitatively study is performed to analyze the inhibitory effect with respect to the hydroplaning speed of an aircraft tire and the height of chine. The results shows that when the height of chine exceeds a certain value, very small increment may cause significant ineffectiveness to suppress the water spray. (3) Based on the above understandings, a new configuration of aircraft chine-tire is proposed, which would be effective at a wide range of taxiing speed.

Strongly-coupled Direct Numerical Simulation of Thermal Turbulence in Channel with Rib-tabulator and Surface-roughness

Hongyi Xu*, Duo Wang**

*Fudan University, **Fudan University

ABSTRACT

Abstract - The paper applied the state-of-the-art flow numerical simulation method, i.e. Direct Numerical Simulation (DNS), and strongly coupled the DNS with the heat-transfer governing equation to solve the thermal-turbulence phenomena in a cooling channel with rib-tabulator of turbine-blade, see Ref [1]. In order to capture the turbulent thermal-fluid phenomena in reality and subsequently to build more accurate flow and heat-transfer models, three innovative approaches were applied to the studies. On the computational side, the current research developed a highly efficient and reliable parallel solution technology based on the Flexible-cycle Additive-correction Multi-grid method (Ref [2]). The surface roughness of the cooling vane was considered by including the roughness geometry in the DNS and an innovative Immersed-Boundary (IB) method, see Ref [3], was applied to handle the geometry complexities due to the existence of surface-roughness. On the flow physics side, the time-sequencing fully-developed turbulent inflow conditions were generated through a temporal DNS of turbulence in a channel, which permitted to accurately resolve the fully-developed thermal turbulence problem in the cooling vane with rib and surface roughness structures in the modern aero-engine. The computational results were expected to provide a variety of advantages over the conventional Reynolds-averaged Navier-Stokes (RANS) approach, including the more accurate mean flow field and the heat-transfer performance predictions. The results presented the typical wall-turbulence characteristics, such as the near-wall coherent structures for a regular smoothed wall and more interesting flow structures caused by a wall roughness as well as their effects on the heat transfer properties. The strongly-coupled flow and heat-transfer simulation captured the temperature and its derivative fields, exhibiting the attractive coherent streaky patterns associated with the turbulence. These research will advance the current knowledge of the surface-roughness on the flow field and heat transfer. References [1] J.C. Han, Recent Studies in Turbine Blade Cooling, International Journal of Rotating Machinery, 10(6): 443–457, 2004. [2] H. Xu, W. Yuan, M. Khalid, Design of a high-performance unsteady Navier-Stokes solver using flexible-cycle additive-correction multi-grid technique. Journal of Computational Physics, 209: 504–540, 2005. [3] H. Xu, Developing LES/DNS Simulation Capability based on Immersed Boundary Method coupled with FCAC Multigrid and AMR Techniques, The 18th International Conference on Finite Elements in Flow Problem, Taipei, 2015.

Mechanical Integrity and Electrical Behaviors of Lithium-ion Pouch Cells under Dynamic Mechanical Loadings

Jun Xu^{*}, Yikai Jia^{**}

^{*}Beihang University, ^{**}Beihang University

ABSTRACT

Dynamic mechanical loading is one of the major catastrophic factors that trigger short-circuit, thermal runaway, or even fire/explosion consequences of lithium-ion batteries (LIBs). In this study, the mechanical integrity and electrical coupling behaviors of lithium-ion pouch cells under dynamical loading were investigated. Two types of experiments, namely compression and drop weight tests, were designed. The state-of-charge (SOC) and strain rate (or impact energy in drop weight tests) dependencies of batteries, as well as their coupling effect, were examined. Furthermore, the electrical performance of battery was investigated through real-time monitoring of voltage change during loading. Experiments on LiCoO₂ lithium-ion pouch cells show that the increase in SOC or strain rates may increase battery structure stiffness. In addition, strain rate may intensify battery structure stiffening with the SOC effect. Experiments show that open-circuit voltage of battery has a relationship with compression deformation. The gradient of voltage drop increases with strain rates, thereby leading to changes in failure mode and rapid deterioration of batteries. Results may provide useful insights into the fundamental understanding of electrical and mechanical coupled integrity of LIBs and lay a solid basis for their crash safety design.

A Novel High-order Time Integration Method for Structural Dynamics

Junjie Xu^{*}, Duozi Wang^{**}, Zhe Qu^{***}

^{*}Key Laboratory of Earthquake Engineering and Engineering Vibration, Institute of Engineering Mechanics, China Earthquake Administration, ^{**}Key Laboratory of Earthquake Engineering and Engineering Vibration, Institute of Engineering Mechanics, China Earthquake Administration, ^{***}Key Laboratory of Earthquake Engineering and Engineering Vibration, Institute of Engineering Mechanics, China Earthquake Administration

ABSTRACT

A novel high-order time integration method for structural dynamic analysis is proposed. The main idea of the proposed method is to implement an error estimation and recovery based on the weak form Galerkin method. By implementing the recovery scheme, displacement, velocity and acceleration with fourth order accuracy can be calculated, which is more accurate than the common algorithms with second order accuracy such as the Newmark method. Examples of a SDOF, a Multi-DOF system and a frame structure are given to verify the accuracy of the proposed method. Simple numerical tests show a significant reduction in the computation time for the proposed method in comparison to that for the Newmark method.

Mesh Refinement Strategies Based Multiscale Isogeometric Optimization of Lattice Material

Manman Xu^{*}, Shuting Wang^{**}, Xianda Xie^{***}

^{*}Huazhong University of Science and Technology, ^{**}Huazhong University of Science and Technology,

^{***}Huazhong University of Science and Technology

ABSTRACT

This paper presents a new approach to design the structures made of heterogeneous lattice structured material. The optimization problem is formulated as minimizing the macroscopic structural compliance under a prescribed material volume constraint while accounting for microstructures of the lattice material. This approach is based on isogeometric analysis(IGA) method and bidirectional evolutionary structural optimization(BESO) technique. IGA is adopted for computing stiffness matrix and nodal displacements of elements on macro-scale. The elements on micro-scale is obtained by mesh refinement strategies of IGA and the effective mechanical properties of microscopic elements is calculated by IGA and asymptotic homogenization(AH). To concurrently optimize the topology of structure and topology of elements on micro-scale, BESO is used as the optimization algorithm. Solutions of numerical tests show that the mesh refinement strategy based isogeometric optimization scheme can address the nonlinearity two-scales problem.

Effect of Twin Boundary on the Deformation Behaviors of Magnesium Nanopillars: A Molecular Dynamics Study

Shuang Xu^{*}, Lisheng Liu^{**}, Hai Mei^{***}

^{*}Wuhan University of Technology, ^{**}Wuhan University of Technology, ^{***}Wuhan University of Technology

ABSTRACT

The plasticity of magnesium and its alloys, which causes the limited formability and restricts the wide application, is currently an active field of research. Deformation twinning plays a crucial role in hexagonal close-packed metals, because it can change the crystal orientation and accommodate the plastic deformation. In this work, deformation behaviors of magnesium nanopillar with two different modes of twin boundaries (TBs) during uniaxial tension and compression were investigated using molecular dynamics simulations. The effect of TB density on the mechanical behaviors and related mechanisms were considered. Simulation results showed strong asymmetry mechanical properties between tension and compression for both TB modes. Furthermore, it found that enough number of {10-11} TBs has the potential to make the flow stress increases with strain in a rather smooth manner. References [1] H. Somekawa, A. Singh, C. A. Schuh, Effect of twin boundaries on indentation behavior of magnesium alloys, *Journal of Alloys and Compounds* 685 (2016) 1016–1023. [2] Q. Yu, L. Qi, K. Chen, R. K. Mishra, J. Li, A. M. Minor, The nanostructured origin of deformation twinning, *Nano Letters* 12 (2012) 887–892. [3] M. Pozuelo, S. Mathaudhu, S. Kim, B. Li, W. Kao, J.-M. Yang, Nanotwins in nanocrystalline MgAl alloys: an insight from high-resolution TEM and molecular dynamics simulation, *Philosophical Magazine Letters* 93 (2013) 640–647.

Mesoscale Modeling of Dislocations in Face-Centered Cubic Metals

Shuozhi Xu^{*}, Jaber Mianroodi^{**}, Abigail Hunter^{***}, Irene Beyerlein^{****}, Bob Svendsen^{*****}

^{*}University of California, Santa Barbara, ^{**}RWTH Aachen and Max-Planck-Institut für Eisenforschung GmbH,
^{***}Los Alamos National Laboratory, ^{****}University of California, Santa Barbara, ^{*****}RWTH Aachen and
Max-Planck-Institut für Eisenforschung GmbH

ABSTRACT

The motions of dislocations, linear crystalline defects with cores that are nanometers wide, control the plastic deformation of metallic crystals. While atomistic simulations are desirable in studying dislocations, they are limited to nano/submicron length scale even with dedicated high-performance computing resources. On the other hand, classical continuum models do not naturally incorporate the discrete atomic-scale degrees of freedom and other evolving internal state variables needed to define the dislocation core structure. Since their inception in the early 1990s, atomistic/continuum coupling approaches have been developed to combine the atomistic domain (for short-range dislocation core) with the continuum domain (for addressing long-range dislocation elastic fields). By employing coarse-grained or reduced order models in regions away from those requiring short-range accuracy, these methods can simulate problems at the micron-scale that is not accessible to typical fully-resolved atomistics. In this work, we explore the core structure/energy/stress of dislocations in face-centered cubic metals using the concurrent atomistic-continuum (CAC) method [1]. Employing the underlying interatomic potential as the only constitutive relation, CAC admits a two-way exchange of displacement discontinuities through a lattice between atomistic and coarse-grained domains. As a result, it is more accurate than one-way linking multiscale strategies. In this talk, results of CAC simulations are compared against fully resolved atomistics, as well as two other meso-scale dislocation models, i.e., phase-field dislocation dynamics [2] and atomistic phase-field microelasticity [3]. The generalized stacking fault energy surface is calculated using density functional theory and employed within the phase field model. Possible sources of differences among these mesoscale calculations are discussed. The issues of core energy double counting in phase field methods and grid/mesh sensitivity are explored. Two atomic-level stress formulations are employed and compared. A dislocation loop is then modelled using all three mesoscale approaches to shed light on their abilities to describe more realistic mixed-type configurations, potentially assisting in designing stronger metallic materials. References: [1] Shuozhi Xu, Rui Che, Liming Xiong, Youping Chen, David L. McDowell, A quasistatic implementation of the concurrent atomistic-continuum method for FCC crystals, *Int. J. Plast.* 72 (2015) 91-126 [2] Irene J. Beyerlein, Abigail Hunter, Understanding dislocation mechanics at the mesoscale using phase field dislocation dynamics, *Phil. Trans. R. Soc. A* 374 (2016) 20150166 [3] Jaber R. Mianroodi, Bob Svendsen, Atomistically determined phase-field modeling of dislocation dissociation, stacking fault formation, dislocation slip, and reactions in fcc systems, *J. Mech. Phys. Solids* 77 (2015) 109-122

Investigation of High-pressure Induced Densification of Silicate-based Glasses Using Atomistically-informed Peridynamic Model

Wentao Xu^{*}, Jacob Fish^{**}, Yang Jiao^{***}

^{*}Columbia University, ^{**}Columbia University, ^{***}Columbia University

ABSTRACT

An atomistically-informed peridynamic model is proposed for the study of high-pressure induced densification of silica glass. Start by employing a molecular dynamic(MD) model of amorphous silica($a\text{-SiO}_2$), which is described by enforcing Tersoff potential on the continuous random network of SiO_2 . Constitutive relations, as well as densification mechanism are thoroughly investigated within the MD framework. It's shown that the results obtained from MD simulation are in good agreement with available experimental data. Based on the results from MD simulation, a constitutive model that accounts for the anomalous densification behavior is proposed and next reformulated to a state-based peridynamic model. We argue that the peridynamic model is capable of reproducing coarse-scale quantities of interest from MD simulation and yet being able to simulate at component level. Numerical simulations of the atomistically-informed peridynamic model are carried out and validated against the results from MD simulation.

Multimaterial Topology Optimization of Thermoelectric Devices

Xiaoqiang Xu^{*}, Yongjia Wu^{**}, Lei Zuo^{***}, Shikui Chen^{****}

^{*}Department of Mechanical Engineering, State University of New York at Stony Brook, ^{**}Department of Mechanical Engineering, Virginia Tech., ^{***}Department of Mechanical Engineering, Virginia Tech., ^{****}Department of Mechanical Engineering, State University of New York at Stony Brook

ABSTRACT

Since it is not feasible to achieve high efficiency of the thermoelectric generator (TEG) consisting of only one single thermoelectric material in a wide temperature range, this paper proposes a novel methodology based on topology optimization for finding the optimal geometry of a TEG made of multiple materials. The conversion efficiency of the TEG is formulated as the objective to be optimized. The proposed method is implemented using the Solid Isotropic Material with Penalization (SIMP) method. Simple relationships are established between the density function of SIMP and the corresponding physical properties of thermoelectric materials within each temperature sub-interval. This method can maximize the potential of different thermoelectric materials by distributing each material into its optimal working temperature range. Several numerical examples are provided to demonstrate the validity of the proposed method and some comparisons between the single-material TEG are given as well.

Research on Curing Deformation of Thermosetting Resin Matrix Composites During Autoclave Forming

Yingjie Xu^{*}, Tenglong Gao^{**}, Weihong Zhang^{***}, Jianbo Xi^{****}, Enwei Yan^{*****}

^{*}State IJR Center of Aerospace Design and Additive Manufacturing, Northwestern Polytechnical University, Xi'an, Shaanxi 710072, China; Shaanxi Engineering Laboratory of Aerospace Structure Design and Application, Northwestern Polytechnical University, Xi'an, Shaanxi 710072, China, ^{**}State IJR Center of Aerospace Design and Additive Manufacturing, Northwestern Polytechnical University, Xi'an, Shaanxi 710072, China, ^{***}State IJR Center of Aerospace Design and Additive Manufacturing, Northwestern Polytechnical University, Xi'an, Shaanxi 710072, China, ^{****}AVIC Xi'an Aircraft Industry (Group) Company LTD., Xi'an, Shaanxi 710089, China, ^{*****}AVIC Xi'an Aircraft Industry (Group) Company LTD., Xi'an, Shaanxi 710089, China

ABSTRACT

During autoclave processing, the thermal expansion of composites, chemical shrinkage of resin as well as the interaction with the mold can result into shape distortion in composites structures, which has a very negative factor on the performance of composite products. In this paper, the cure kinetics reaction of prepreg system was firstly investigated, then the temperature and degree of cure during curing process were predicted by means of ABAQUS. Moreover, a thermodynamics and mesomechanics constitutive model was developed to study the curing deformation with numerical simulation method, in which the properties of density, special heat capacity, thermal expansion and thermal conductivity coefficients varies with the temperature and curing degree. The time varying characteristic of these parameters were measured with the instruments of differential scanning calorimetry (DSC), dilatometry (DIL) and laser flash apparatus (LFA), respectively. Further, the influence of layup and processing parameters on curing deformation was studied by finite element analysis. Acknowledgements This work is supported by National Key Research and Development Program of China (2017YFB1102800), Shaanxi international science and technology cooperation and exchange program (2016KW-057) and Seed Foundation of Innovation and Creation for Graduate Students in Northwestern Polytechnical University.

On the Gradient of Lode's Angle

Yuanjie Xu^{*}, Minglong Zhang^{**}, Zuoguang Fu^{***}

^{*}Wuhan University, ^{**}Wuhan University, ^{***}Wuhan University

ABSTRACT

One of most important ways to model the complex behaviors of loading-path dependent geomaterials within the framework of plasticity theory is construct the yield criterion and/or the plastic potential as functions of stress invariants, including Lode's angle. Consequently, the gradient of Lode's angle with respect to stress tensor plays an essential role both in elasto-plastic constitutive equations and in the finite element analysis. From the theoretic and computation perspectives, the first-order gradient of the plastic potential with respect to stress tensor is indispensable in the orthogonal flow rule, while that of the yield criterion is used to impose the consistency condition, and the second-order gradient of plastic potential is required in computing local Jacobi matrix to guarantee the second-order convergence rate in Newton-Raphson iteration. The formulas of the gradient of Lode's angle in literatures were highly nonlinear and cumbersome. Moreover, they became singular when the stress state happened to be an axisymmetric one. The objective of this study is to derive the simple and concise formulas for the first- and second-order gradient of Lode's angle with respect to the stress tensor in principal stress space, respectively. The formulas have completeness and can be expressed explicitly. Numerical examples show that the resulted formulas simplify the calculation of plastic flow direction, plastic strain tensor, and local Jacobi matrix. They render the return-mapping algorithm more efficient for FE analysis with complex elasto-plastic constitutive relations. Furthermore, we proposed a new perturbation scheme that enables the perturbation error of the first-order gradient tensor of Lode's angle to be evaluated when a stress state is axisymmetric. Finally, some important properties of our findings are also provided.

Orthotropic A-FEM for Static Strength Prediction in Composite Laminates

Yunwei Xu^{*}, Qingda Yang^{**}

^{*}University of Miami, ^{**}University of Miami

ABSTRACT

Typical composites exhibit complex, multiple fatigue damage events that are strongly coupled and developed in a stochastic microstructure. The gradual progression of such damages is of primary concern for safety and tolerance design of composite structures. Those traditional methods based on linear elastic fracture mechanics are not effective and efficient for such complex damage processes. In order to accurately assess/predict the composite fatigue life, it is necessary to explicitly account for the progressive evolution of all major types of discrete damage events with high fidelity. In this paper, we extended a recently developed augmented finite element method (AFEM) that can accurately and efficiently account arbitrary cracking in isotropic materials to deal with the much more complicated multiple fracture problems in composites. A composite laminate may develop multiple types of cracks (matrix cracking, fiber rupture in tension/kinking in compression, and delamination) at different locations depending on the in-situ stress environments. Moreover, these modes of damages are not isolated in most of the practical application, i.e. intra-ply transverse cracking will lead to inter-ply delamination and delamination propagation may lead effect fiber damage. Also, typical composite exhibits complex asymmetric mechanical behaviors between tension- and compression-dominant stress state. Strong nonlinearity in shear stress-strain is also critically important for delamination crack growth. Therefore in our A-FEM formulation, we adopt the mechanism-based Sun's criteria for crack initiation under general in-situ stress states. Upon satisfaction of a certain criteria, i.e., matrix tension/compression/shear crack, fiber tension rupture crack, fiber-compression kink band formation, a cohesive crack will be initiated within an element. The element will be augmented into two subdomains connected by a specified mixed-mode cohesive law of the initiated crack type. The elemental equilibrium of this augmented problem will be solved using a newly developed consistency-check based algorithm, which has been proven to have mathematical exactness for piece-wise linear cohesive laws. A rigorous verification and validation process will be presented to demonstrate that the developed orthotropic A-FE can initiate and propagate various types of cracks under different stress environments, and can predict the entire (linear or nonlinear) stress-strain curves all the way to two-part failure for any quasi-static laminates tension tests. Further, we shall demonstrate that, this element can be used together with any cohesive interface elements to account for the important damage coupling between ply cracking and interlaminar delamination.

An Active Compliant Micro-assembly Control Method Based on Micro-force Sensing

Zhenyuan Xu^{*}, Wenrong Wu^{**}, Juan Zhang^{***}, Hong Yang^{****}, Lie Bi^{*****}, Xi Dai^{*****}

^{*}Laser Fusion Research Center, China Academy of Engineering Physics, Mianyang, China, ^{**}Laser Fusion Research Center, China Academy of Engineering Physics, Mianyang, China, ^{***}Laser Fusion Research Center, China Academy of Engineering Physics, Mianyang, China, ^{****}Laser Fusion Research Center, China Academy of Engineering Physics, Mianyang, China, ^{*****}Laser Fusion Research Center, China Academy of Engineering Physics, Mianyang, China, ^{*****}Laser Fusion Research Center, China Academy of Engineering Physics, Mianyang, China

ABSTRACT

This paper studies the spatial nondestructive assembly problem of vulnerable micro-parts, and presents an active compliant assembly control method based on micro-force. By analyzing the various contact states of vulnerable micro-parts, the relationship model between the output of six-dimensional micro-force sensor and position-pose error of peg-in-hole micro-assembly is established. Specifically, a method to solve the uncertainty of contact state based on active constraint state is presented. This method makes the relationship between the position-pose error of peg-in-hole and the force condition of micro-parts corresponded to each other, therefore, the position-pose error of peg-in-hole can be estimated by micro-force and micro torque. Furthermore, an automatic control method based on two dimensional micro-forces and two dimensional micro torques is proposed to solve the coupling problem between multi-dimensional forces and position, multi-dimensional torques and pose angle. Especially for the peg-in-hole micro-assembly task with initial position-pose deviation, the experimental results verify the effectiveness of the proposed method. Finally, the interference fit of peg-in-hole micro-assembly is also analyzed, and the experimental results verify the active compliant micro-assembly control method can be applied as well. The solution of these problems will avoid the micro-assembly jammed, which is beneficial to the nondestructive assembly of the vulnerable micro-parts and has important application significance. Keywords: micro-assembly, micro force, position-pose control, interference fit, compliant control

Dynamic Analysis of Crack Problems by SFBEM Based on Erdogan's Solutions

Zhi Xu^{*}, Miao Chen^{**}, Cheng Su^{***}, Xueming Fan^{****}

^{*}South China University of Technology, ^{**}South China University of Technology, ^{***}South China University of Technology, ^{****}South China University of Technology

ABSTRACT

The appearance of cracks on engineering structures has large influence on the structural dynamic characteristics. The Erdogan's solutions for static analysis of an infinite cracked plate are introduced in this paper. Based on the above fundamental solutions, mathematical formulation and computational implementation of the spline fictitious boundary element method (SFBEM) are presented for dynamic analysis of linear-elastic cracked plates, in which the stress boundary conditions on the crack surface are automatically satisfied and the singular behaviour at the crack tip can be naturally captured. The eigenvalues and mode shapes of cracked plates can be obtained using the proposed method. The dynamic stress intensity factors and structural responses of cracked plates can also be achieved with the present approach. Numerical examples are given to demonstrate that the proposed method is superior to the traditional finite element method (FEM) in terms of accuracy and efficiency.

THE OPTIMIZATION ANALYSIS OF THE VIBRATION CHARACTERISTICS OF A BUS FRAME

Xue AN^{*}; Hae Chang Gea[†]; Dongyan SHI[†]

^{*} College of Mechanical and Electrical Engineering, Harbin Engineering University

Harbin, China;

Email: sara@hrbeu.edu.cn;

[†]College of Mechanical and Aerospace Engineering, Rutgers, The State University of New Jersey, USA

Email: gea@soe.rutgers.edu;

[†]College of Mechanical and Electrical Engineering, Harbin Engineering University

Harbin, China;

Email: shidongyan@hrbeu.edu.cn;

Keywords: Adams, Workbench, deceleration zone, simulation analysis

Summary: *In this paper, Adams and Workbench simulation software are used to explore the vibration characteristics of a passenger car when driving through the deceleration belt with different loads. The vibration frequency of the bus-body is taken as an evaluation index, when the passenger car passes through the deceleration belt. By comparing the excitation frequency and the natural frequency of the body frame in the suspension system, When the frequency values are close, the resonance phenomenon is easy to occur, and the dangerous position of the body frame is determined. Finally, by improving the structure of the dangerous parts, the vibration characteristics of the body are optimized and the resonance phenomenon is avoided.*

1 INTRUDUCTION

With the improvement of people's living standard, private cars are also gradually increasing, However, people's demand for the comfort of the car is getting higher and higher, and the comfort of the car is mainly related to the vibration of the body and the noise environment in the car. At the same time, the rapid development of automobile manufacturing industry is devoted to the development of high performance, economic and comfortable products. Abnormal vibration can affect the life, safety and reliability of the vehicle when the car passes some special road surface.

In this paper, the passenger car driving simulation analysis is carried out under the special traffic speed, vehicle vibration characteristics, in order to further study the road condition to provide theoretical basis for the influence of body structure, and for better optimization of body structure provides the certain reference value.

The author has published two papers on this subject, and on this basis^[1,2], further research has been done.

2 THE ESTABLISHMENT AND ANAL SIS OF THE SIMULATION MODEL OF DECELERATION BELT

2.1 The simulation model of deceleration belt is established

In this paper, the wheel diameter of the simulation model is 0.64 m, and according to the relevant provisions of JT/T713-2008 rubber speed belt standard^[3].The simulation model of deceleration belt is selected, whose width is $a=0.32$ m, and the height is $h=0.05$ m.

Then run the road file in Adams/View software to see the speed bump model, as shown in figure 2-1^[4].

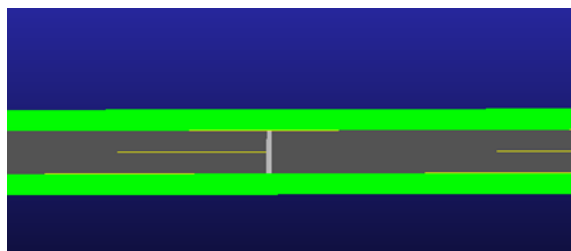


Fig. 2-1 The model of road deceleration

2.2 The simulation experiment of speed reduction belt pavement is carried out

The final simulation model of vehicle model and road surface model is determined in Adams/View analysis module^[5-7], as shown in fig.2-2. When the passenger trains at different speed and different loads to drive through the deceleration belt, the simulation test of the ride

smoothness is carried out, and the vibration frequency of the body in the vertical direction acceleration is output.

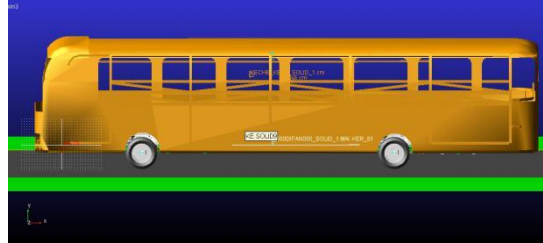
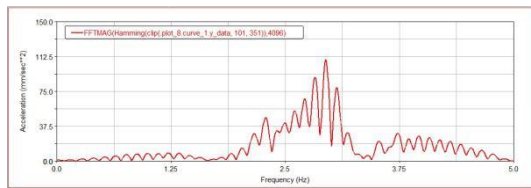


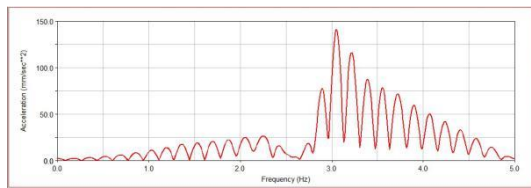
Fig. 2-2 the simulation model of the bus passing the speed bump

The speed of the bus is set at 15km/h, 20km/h, 25km/h, 30km/h. When the passenger car is in no-load, medium and full load, it outputs the vibration of the body in the vertical direction. The simulation results are as follows, See figure 2.3-2.4:

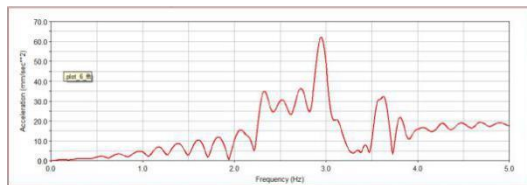
(1) When the bus was empty, driving at different speeds, the simulation results are shown in figure 2.3 :



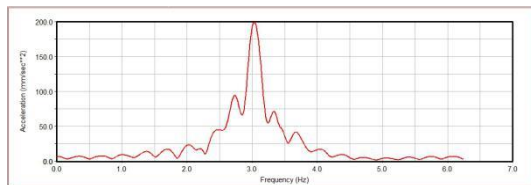
(a) The driving speed is 15km/h



(b) The driving speed is 20km/h



(c) The driving speed is 25km/h



(d) The driving speed is 30km/h

Fig. 2-4 The simulation results under different speeds at no-load

(2) When the bus is with medium load, driving at different speeds, the simulation results are shown in figure 2.4:

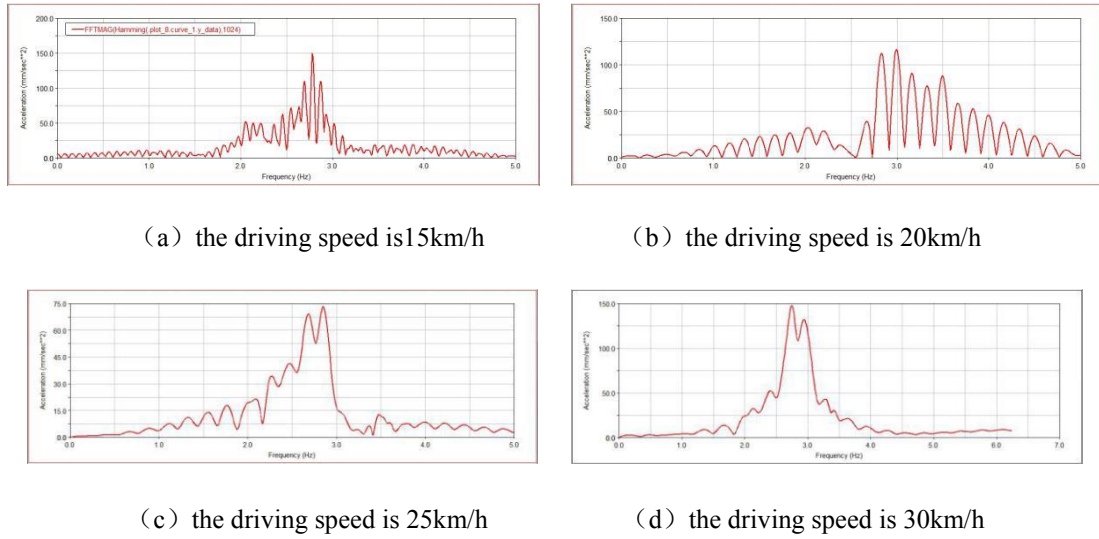


Fig. 2-4 The simulation results under different speeds at half-load

(3) When the bus is with full load, driving at different speeds, the simulation results are shown in figure 2.5:

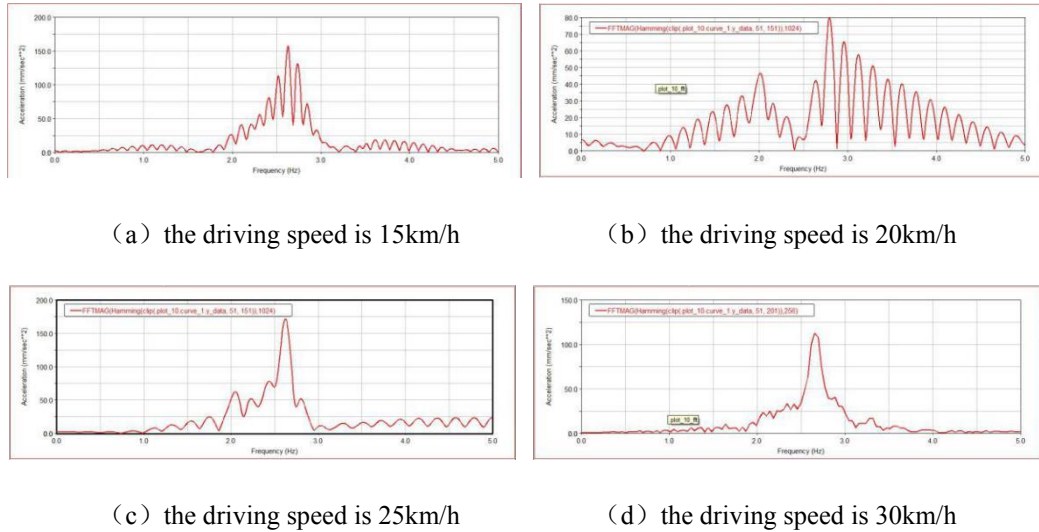


Fig. 2-5 The simulation results under different speeds at full load

The above simulation results are calculated, as shown in table 2-1:

Tab 2-1 The results of simulation

Speed Load	15km/h	20km/h	25km/h	30km/h
Full load	2.6 (Hz)	2.8 (Hz)	2.7 (Hz)	2.6 (Hz)
Middle load	2.8 (Hz)	3.0 (Hz)	2.9 (Hz)	2.8 (Hz)
No load	2.9 (Hz)	3.1 (Hz)	2.9 (Hz)	3.0 (Hz)

The experimental results show that the vibration frequency of the maximum acceleration of the body in the vertical direction is the evaluation index, and the acceleration of the vertical direction is significantly increased when the bus passes the speed bump. When the vibration acceleration of the body is the maximum, the corresponding vibration frequency of the vehicle is the vibration frequency of the passenger car.

When the bus is traveling at a speed of 15km/h- 30km/h, the frequency range of the body is 2.6-3.1Hz.

3 MODAL ANALYSIS OF BODY SKELETON

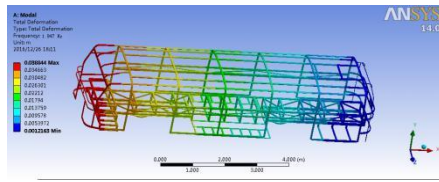
Using PRO/E software to build body frame model, import the finite element analysis software Workbench to conduct modal analysis. Main parameters are defined: the elastic modulus is 2.1×10^{11} , poisson ratio is 0.3, and the density is 7800 kg/m^3 [8,9]. A finite element model is obtained for the mesh partition of the body frame model, as shown in fig.3-1^[10].



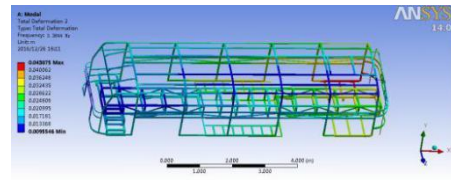
Fig. 3-1 Finite element model of bus body

3.1 Analysis of the results

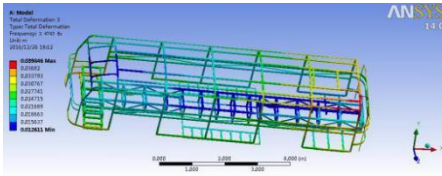
This paper mainly studies the low-frequency characteristics of the body frame, so in the simulation test, only the first six order natural frequencies and corresponding modes of vibration are recorded. Before the optimization of the body structure, finite element analysis of the body skeleton was carried out, and the vibration patterns were obtained, as shown in fig.3-2



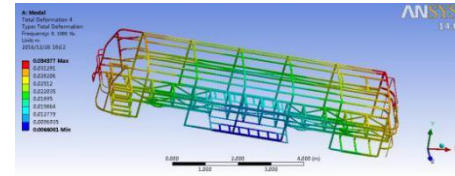
The first order vibration graph



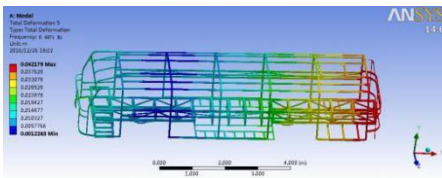
The second order vibration graph



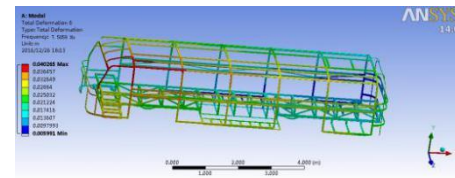
The third order vibration graph



The forth order vibration graph



The fifth order vibration graph



The sixth order vibration graph

Fig. 3-2 The front of the body is a six-order modal mode

The intrinsic frequency of the vehicle body skeleton modal analysis is shown in table 3-1.

Tab 3-1 Natural frequency of body frame

Order	Frequency (Hz)	The main characteristics
1	2.868	The front part of the car bends longitudinally
2	3.384	Local deformation at the end of the car
3	3.474	Local deformation of front and rear
4	6.109	Heavy deformation of the front and rear
5	6.497	The small deformation of the locomotive and the large deformation of the car
6	7.506	Integral mode and local mode mixing

Comparing the natural frequency with the excitation frequency, the comparison curves are drawn, as shown in figure 3-3

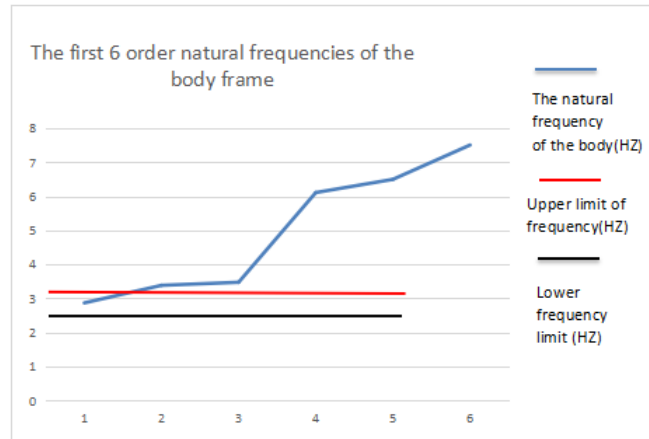


Fig. 3-3 Analysis of simulation results

The vibration frequency range of the body in vibration system is 2.6-3.1 Hz by Adams software. Comparison of modal analysis results can be obtained: The first order natural frequency of the body frame is 2.868 Hz, The first order natural frequency of the body frame is 2.868 Hz, In the range of vibration frequency of the vehicle during the deceleration zone ,By analyzing the mode of vibration, it can be concluded that the head position is easy to be resonant.

3.2 Local improvement of bus body structure

By comparing the results of two simulations, the resonant frequency was obtained, and the resonant position of the body was determined by the corresponding mode of vibration, then The improved position of body frame structure is determined. In order to not affect the life and performance of the body structure during the design process and meet the structural strength and stiffness requirements of the body,Therefore, local improvement of body frame structure is carried out.

3.2.1 Structural improvement method

In the case of not making too much change in the structure of the body frame, the area of resonance in the frame structure is optimized. Thus, the final structure improvement method is determined. Main content is: Based on the mode diagram, the resonance location is determined, then change the regional body frame structure geometry size in China, or to increase or decrease of beam, and then analyzed many experiments on the points adjustment, which change the inherent characteristics of body structure, and finally determine the improvement plan. Then, change the geometrical dimensions of the body skeleton structure in the region, or increase or decrease the number of beams. The optimal improvement scheme is finally obtained through several test and analysis.

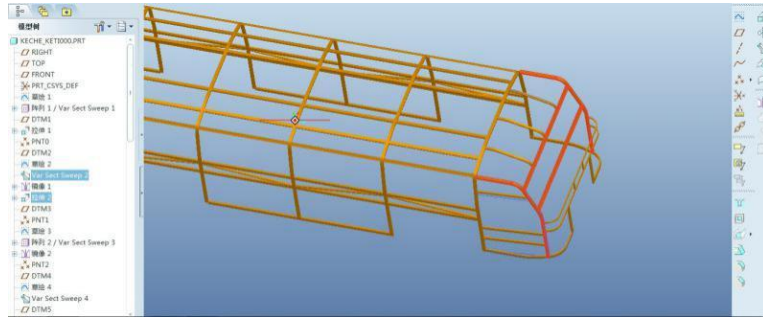


Fig. 3-4 The position of structure improved

The specific improvement parameters are: four square steel pipes of the front position, and the thickness of steel tube δ is changed from 1mm to 2mm. See figure 3-5.

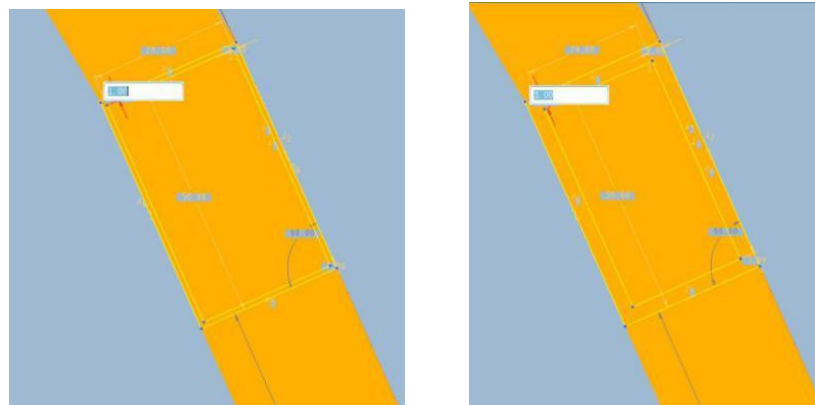
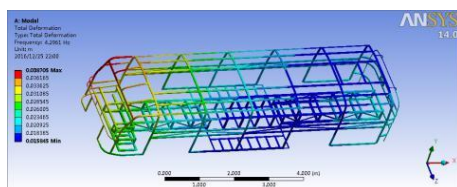


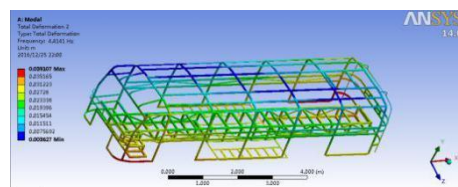
Fig. 3-5 The measurement of structure improved

3.2.2 Finite element analysis after modification

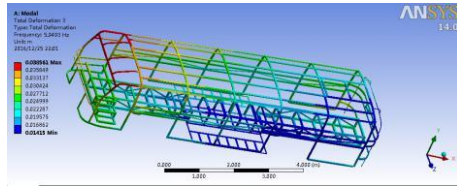
The modal analysis of the locally modified body skeleton model is carried out again. The grid is divided according to the size of the cell, and the modal analysis is performed after the grid division. The modal diagram is shown in Fig. 3-6.



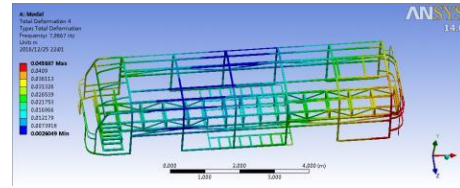
The first order vibration graph



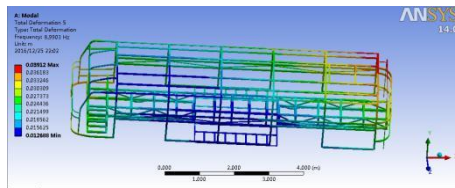
The second order vibration graph



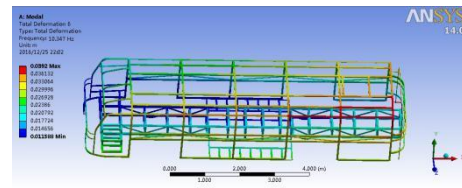
The third order vibration graph



The forth order vibration graph



The fifth order vibration graph



The sixth order vibration graph

Fig. 3-6 The first six order modal shapes of the body after structural improvement

After the structural improvement, the natural frequency of the bus body skeleton modal analysis is shown in table 3-2

Tab 3-2 Natural frequency of structure improvement

Order	frequency (Hz)	The main characteristics
1	4.296	Front position X-axis distortion
2	4.414	Integral mode and local mode mixing
3	5.9493	Local deformation of the front part
4	7.9867	Local deformation of front and rear
5	8.9903	Local deformation of locomotive
6	10.347	Integral mode and local mode mixing

4 MPARING OF RESULTS BEFORE AND AFTER OPTIMI ATION

The natural frequency comparison chart of each order before and after the improvement of the frame structure of the body is drawn, as shown in fig.4-1.

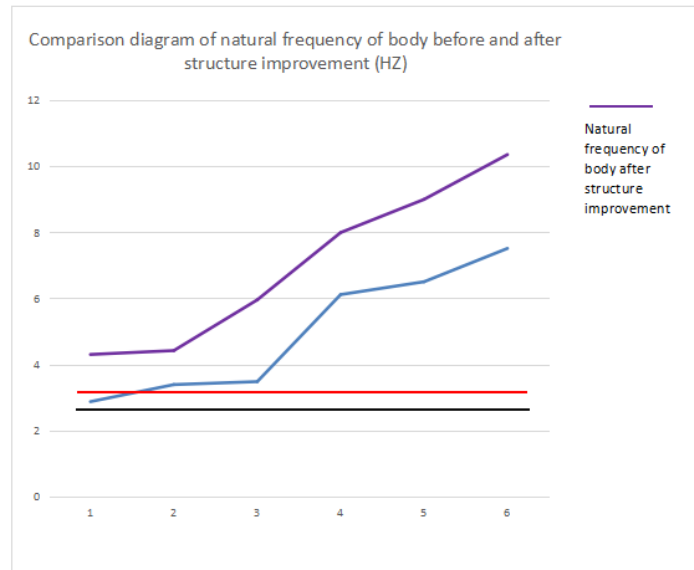


Fig. 4-1 Analysis of simulation results

After structure optimization, body frame of each order natural frequency significantly deviate from the body in the process of driving vibration frequency range, especially prone to the first order natural frequency of resonance, effectively avoid the possibility of resonance body and suspension system.

CONCLUSION

- (1) The vertical vibration frequency range of the passenger car is 2.6-3.1Hz with the speed of 15km/h-30km/h and different loads.
- (2) When the coach is driving through the deceleration zone, there will be a resonant phenomenon in the position of the bus head
- (3) The inherent frequency of the body is obviously deviated from the resonant frequency range, so the resonance phenomenon can be avoided effectively.

ACKNOWLEDGEMENTS

This paper is funded by the International Exchange Program of Harbin Engineering University for Innovation-oriented Talents Cultivation. The works also supported by the National Natural Science Foundation of China (No. 51679056), and Natural Science Foundation of Heilongjiang Province of China (E2016024).

REFERENCE

- [1] AN Xue,WEN Xuezhu Analysis on the Vibration by Bus crossing the Speed Bumps Based On MATLAB[J],Mechanical Engineer, 2016(3):34-36.
- [2] AN Xue,WEN Xuezhu Modal Analysis of bus suspension and bus body framework,The technology and research of passenger cars, 2016, 38(5):13-15.
- [3] MA Jun,DU Lingling Study and Establishment of Trade Standard of "Pavement Rubber Bump"COMMUNICATIONS STANDARDIZATION,2008:27-29.
- [4] Zheng Qiu-feng Vibration analysis of speed bump[J],ChengShi Jianshe LiLun Yan Jiu,2013(35)
- [5] Fang Hong-bin The Modeling of Electric Vehicle based on ADAMS and Performance Analysis and Configuration Improvement,Jilin University,2009.
- [6] Liu Gaojun,Yin Huaixian,Zhang Tiezhu,Simulation of ride comfort of hybrid bus based on ADAMS / Car
- [7] Zhang Xiuqin,Yang Bo,Simulation analysis of ride comfort of random pavement based on ADAMS[J],Shanghai Auto, 2011(8):18-23
- [8] Zhang Gongxue,TianYang,Finite element analysis of a bus body frame based on ANSYS[J],Journal of Shan Xi University of Science &Technology, 2008, 26(6):150-153.
- [9] WeiNingbo.TheFiniteElementofAnalysisofIntegratedCoachBodyBasedonANSYS[D],Chang'an University,2011.
- [10]Hu Shuqing,LiuChengwu,ZhangQingyiong,Finite element analysis of a bus body frame based on ANSYS[J],Mechanical & Electrical Technology,2013(1):9-13.

Flux Flow along a Grain Boundary within a High Temperature Superconductor: A Molecular Dynamics Simulation

Feng Xue^{*}, Yu Liu^{**}, Xiaofang Gou^{***}

^{*}College of Mechanics and Materials, Hohai University, ^{**}College of Mechanics and Materials, Hohai University,

^{***}College of Mechanics and Materials, Hohai University

ABSTRACT

Abstract: With the rapid development of high-temperature superconductors, it is of great importance to understand the precise current density and flux distribution around grain boundaries (GBs) of superconducting materials. In this paper, we simulate the flux dynamics by the molecular dynamics method. All the flux lines and pin centers are regarded as point particles, whereas those along the GB are different with the ones in grains. An extra force is added on the flux lines within the width of a GB to reflect the anisotropy of the potential function between flux lines and pin centers around the GB. Details of flux flow along the GB are displayed in this work, and the critical forces and the I-V curve are obtained. The simulated results, as well as a theoretical model [1] we proposed, are discussed in this paper which can be helpful for understanding the underlying mechanism of critical current density of polycrystalline superconductors. Key words: superconducting film, molecular dynamics method, grain boundary. REFERENCE [1] F. Xue, Y. Gu, and X. Gou, J. Supercond. Nov. Magn. 29, 2711 (2016).

A Fully Eulerian Finite Element Approach to Predicting Largely Deforming and Phase Changing Solids

Tianju Xue^{*}, Maurizio Chiaramonte^{**}

^{*}Princeton University, ^{**}Princeton University

ABSTRACT

Problems with severe solid deformations or even phase-changes are ubiquitous in many applications in engineering and sciences alike. Typical ones might be liquefaction and re-consolidation of granular continua as observed in earthquakes and landslides. Traditionally, the continuum mechanics perspective of solids has followed the Lagrangian paradigm, where the governing equations are posed for a fixed material point. Contrastingly, for fluids the governing equations are posed for a fixed spatial point, which is also referred to as the Eulerian reference frame. The contrast between Lagrangian vs Eulerian formulation of solids and fluids stems from the nature of different constitutive relations. The approaches to solve for solids and fluids problems are hence dichotomous. This brings trouble when solids and fluids coexist and need to be simulated simultaneously with good efficiency. The proposed approach is to formulate the problem, regardless of the state of the material being fluid or solid, using an Eulerian frame of reference. The primary variable is taken as the inverse of the deformation mapping to a reference configuration similarly to [1]. By noting that the material derivative of the reference coordinates along a fixed particle is actually zero, one may recover the inverse mapping by solving an additional advection equation. With the inverse mapping at hand, both the total deformation for solid constituents as well as rates of deformation for fluid constituents may be obtained. Some recent efforts have been invested in this area and some of the relevant work can be found in [1, 2]. To handle the evolving free surface, we propose to introduce an order parameter advected along the deformation of the solid. Additional fields, such as the phase field of fracture mechanics, as well as internal state variables for inelastic materials are also advected along the flow. We will develop higher order Discontinuous Galerkin methods in order to solve the resulting system of governing equations. Sample problems will showcase the capabilities of the proposed method in relation to state-of-the-practice tools. References: [1] K. Kamrin, C. H. Rycroft, and J.-C. Nave. "Reference map technique for finite-strain elasticity and fluid solid interaction". In: *Journal of the Mechanics and Physics of Solids* 60.11 (2012), pp. 1952-1969. [2] D. I. W. Levin, J. Litven, G. L. Jones, S. Sueda, and D. K. Pai. "Eulerian solid simulation with contact". In: *ACM Transactions on Graphics* 30.4 (2011), p. 1.

A 3D h-Adaptive Methodology for Simulating Metal Forming Processes with Crack Initiation and Propagation Using a Hexa-tetra Based Multi Level Remeshing Technique

Fangtao YANG*, Alain RASSINEUX**, Carl LABERGERE***, Khemais Saanouni****

*Université de Technologie de Compiègne, France, **Université de Technologie de Compiègne, France,

Université de Technologie de Troyes, France, *Université de Technologie de Troyes, France

ABSTRACT

We propose an h-adaptive 3D FE methodology in an explicit solver to represent the initiation and propagation of cracks in ductile materials in which cracks are represented as locations of all the fully damaged elements [1]. The size of the loading sequence is adapted to control both the size and the number of the damaged elements to be deleted. An elasto-plastic model fully coupled with damage is used [2]. Size indicators based on plasticity, damage and their dissipation are proposed. The goal is to refine the mesh in active areas as well as coarsen the mesh in inactive areas. An original multi deformable octree technique is proposed in order to adapt (refine and coarsen) the tetrahedron mesh with robustness and efficiency, at a reduce computational cost. No unstructured mesh generator is used nor local remeshing technique. A first coarse hexahedral mesh is created and each element is thereafter considered as an octree which can be deformed throughout the simulation. The remeshing process is purely analytical based on octree refinement or coarsening. Once all octrees have been created, a tetrahedron mesh is created in each octant with conforming meshes at the interface between octrees. After a loading step, the mesh is deformed and the newly created octrees are reconstructed while taking into account the structure deformation. Issues to reduce numerical diffusion and to preserve peak value which may occur during the transfer of variables are discussed and a hybrid transfer operator based on enhanced diffuse approximation is presented [3]. Solutions based on surface subdivision are proposed to smooth the crack along inactive areas and enable contact. [1] Yang, F.T., Rassineux, A., Labergere, C., Saanouni, K., A 3D h-adaptive local remeshing technique for simulating the initiation and propagation of cracks in ductile materials (2018) Computer Methods in Applied Mechanics and Engineering, 330, pp. 102-122. [2] Saanouni, K., 2013. Damage mechanics in metal forming: Advanced modeling and numerical simulation. John Wiley & Sons. [3] Yang, F.T., Rassineux, A., Labergere, C., A hybrid Meshless-FEM field transfer technique minimizing numerical diffusion and preserving extreme values: Application to ductile crack simulation, Finite Elements in Analysis & Design, in press, 2018.

A New Model for Fiber Bridging in Cementitious Composites Based on Large Deflection Beam Theory

Jie YAO*, Christopher K Y LEUNG**

*The Hong Kong University of Science and Technology, **The Hong Kong University of Science and Technology

ABSTRACT

The behavior of Engineered Cementitious Composites (ECC) is strongly affected by the relationship between total fiber bridging stress and crack opening width. In order to extract this relationship, the single fiber pull-out behavior is usually studied first. From experimental data, when a fiber inclined to the crack surface is pulled along the direction perpendicular to the crack, the peak pull-out load is commonly observed to increase with the inclination angle. This is often explained in terms of the snubbing effect for flexible strings passing over a frictional pulley, but such an explanation is not satisfactory because the bending stiffness of the fiber used in ECC is not negligible. In this study, a new model for fiber bridging is proposed. The fiber on each side of the crack is treated as a continuously supported beam lying on the elastic foundation (which represents the matrix) plus a free length protruded into the crack. The protruded part is treated as a cantilever supported at its end by an equivalent spring group representing the part of fiber inside the matrix. The relationship between bridging stress and crack opening width is then calculated by the combination of pulling, bending as well as shearing. Since the protruded part is very likely to undergo large deflection, large deflection theory of bending is applied. From the simulation results on PVA fibers, although fiber's slip-hardening effect and the frictional pulley at the fiber exiting matrix point are not taken into account, bridging stress can still exhibit the increasing trend with the inclination angle. The shear deflection can also be proven to be unimportant compared to fiber's bending, thus this model gives a new physical explanation to the empirical snubbing effect as the consequence of increasing bending forces. In addition, other two models based on small deflection are also developed. Through the comparison with large deflection model, it turns out consideration of both bending stiffness provided by axial force and large deflection is necessary. The effects of different parameters such as embedded length and fiber/matrix stiffness ratio are then studied, and it is found that the ratio of inclined fiber's maximum pullout force to the corresponding aligned fiber's maximum pullout force increases with the fiber/matrix stiffness ratio and decreases with increasing embedded length.

Deterioration of Atomistic Mechanisms That Bind Mutated Type IV Collagens with Integrin

JINGJIE YEO*, YIMIN QIU**, GANGSEOB JUNG***, YONG-WEI ZHANG****, DAVID L. KAPLAN*****, MARKUS J. BUEHLER*****

*High Performance Computing, A*STARMassachusetts Institute of Technology; Institute of, **Tufts University, ***Massachusetts Institute of Technology, ****Institute of High Performance Computing, A*STAR, *****Tufts University, *****Massachusetts Institute of Technology

ABSTRACT

Human type IV collagen constitutes a major component of extracellular scaffolds for the assembly and mechanical stability of certain types of tissues, especially that of glomerular basement membranes. Type IV collagen is also a vital component for interacting with cells, which is crucial for cell adhesion and differentiation. Approximately 80% of Alport Syndrome cases are caused by mutations in the COL4A5 gene encoding the $\alpha 5$ chain of type IV collagen. The effect of Gly missense mutation within and adjacent to the predicted integrin binding sequence on collagen-integrin binding was investigated by combining atomistic molecular simulations and recombinant collagen experiments. The introduction of any reported Gly substitution in Alport syndrome (Gly - Glu, Gly - Val and Gly - Asp) in the recombinant collagen abolished its integrin binding affinity, even if the mutation site was not located within the essential integrin binding site. To probe this phenomenon in detail on a molecular level, the atomistic mechanisms of the binding process were analyzed with atomistic molecular dynamics simulations. The integrin-binding domain of each wild-type and mutant model collagen-like peptide were constructed and structurally aligned to the experimentally determined crystal structure of type I collagen bound to integrin&amp;amp;apos;s $\alpha 2$ inserted (I)-domain (PDB: 1DZI). These bound structures were then refined through replica exchange simulations with solute tempering in explicit solvent. Similarly, the integrin $\alpha 1$ I-domain (PDB: 1PT6) was modelled and refined through structural alignment with the integrin $\alpha 2$ I-domain to create a second set of collagen-integrin complexes. Through this approach, we will be able to determine the hydrogen-bonding topology, structural and conformational changes in the collagens and integrins, as well as quantitatively measure the binding free energy through enhanced sampling with methods such as adaptive biasing force.

Topology Optimization of Particle-matrix Composites for Optimal Fracture Resistance

Julien YVONNET^{*}, Daicong DA^{**}, Liang XIA^{***}, Guangyao LI^{****}

^{*}Université Paris-Est, ^{**}Université Paris-Est, ^{***}Huazhong University of Science and Technology, Wuhan,
^{****}Hunan University, Changsha, China

ABSTRACT

We propose a topology optimization framework for optimizing the fracture resistance of two-phase composites through a redistribution of the inclusion phases [1,2]. A phase field method [3] for fracture capable initiation, propagation and interactions of complex microcracks networks is adopted. This formulation avoids the burden of remeshing problems during crack propagation and is well adapted to topology optimization purpose. An efficient design sensitivity analysis is performed by using the adjoint method, and the optimization problem is solved by an extended bi-directional evolutionary structural optimization (BESO) method. The sensitivity formulation accounts for the whole fracturing process involving cracks nucleation, propagation and interaction, either from the interfaces and then through the solid phases, or the opposite. The spatial distribution of material phases are optimally designed using the extended BESO method to improve the fractural resistance. We demonstrate through several examples that the fracture resistance of the composite can be significantly increased at constant volume fraction of inclusions by the topology optimization process. References [1] L. Xia, D. Da, J. Yvonnet, Topology optimization for maximizing the fracture resistance of quasi-brittle composites, *Computer Methods in Applied Mechanics and Engineering*, 2018, in press. [2] D. Da, J. Yvonnet, L. Xia, G. Li, Topology optimization of particle-matrix composites for optimal fracture resistance taking into account interfacial damage, submitted. [3] B. Bourdin, G. A. Francfort, J. J. Marigo, The variational approach to fracture, *Journal of elasticity* 91 (1-3) (2008) 5–148.

Multi-Time Scale Simulations of Coupled Transient Electro-Mechanical Fields for Modeling Finite Strain Piezoelectricity

Reza Yaghmaie*, Somnath Ghosh**

*Johns Hopkins University, **Johns Hopkins University

ABSTRACT

Abstract: This paper presents the wavelet transformation based multi-time scaling algorithm for finite element simulations of piezoelectric materials in finite strain theory. The free energy for piezoelectric materials in finite deformation is derived through a consistent thermodynamic framework, from which the constitutive equations for the mechanical stress, Maxwell stress and electrical displacement are formulated in terms of strain and electric fields. A fully coupled total Lagrangian finite element formulation is devised for rigorously modeling piezoelectric materials with highly nonlinear constitutive laws and time dependent material effects. One major challenge in computational modeling of many piezoelectric devices including actuator and sensor structures is the large discrepancies in the frequencies of electrical signal and mechanical vibrations and this requires simulating a large number of cycles with electric excitation time period for reaching to a state of mechanical deformation in the time domain. The conventional single time-scale integration schemes are constrained by the stability and convergence requirements of the highest frequency response and therefore are insufficient to advance with the changes in the low frequency field. The present work addresses these issues by developing the wavelet transformation based multi-time scaling (WATMUS) algorithm for dynamic piezoelectric simulations in the finite element framework [1,2,3]. The wavelet transformation projects the high frequency (fine time scale) electric potential and its first time derivative, displacement and velocity fields through translation and dilation of an appropriate set of scaling functions on the low frequency (coarse time scale) response with monotonic evolution. The method significantly enhances the computational efficiency in comparison with conventional single time scale integration methods. The performance of the WATMUS method is demonstrated by several examples proving its accuracy and efficiency for solving nonlinear coupled systems. References: [1] Yaghmaie, R. and Guo, S. and Ghosh, S. (2016). "Wavelet transformation induced multi-time scaling (WATMUS) model for coupled transient electro-magnetic and structural dynamics finite element analysis." Comput. Methods Appl. Mech. Eng. 303, 341–373, <https://doi.org/10.1016/j.cma.2016.01.016>. [2] Yaghmaie, R. and Ghosh, S. (2017). "Multi-time scaling based modeling of transient electro-magnetic fields in vibrating media with antenna applications." Comput. Mech. 60 (1), 117–141, <https://doi.org/10.1007/s00466-017-1396-1>. [3] Yaghmaie, R. and Ghosh, S. (Submitted). "A computational model coupling transient electro-mechanical fields for analyzing finite deformation piezoelectric material behavior"

Development of Multi-Stage Failure Simulation Using the Principle of Hybrid-type Virtual Work

Tadao Yagi^{*}, Norio Takeuchi^{**}, Kiyomichi Yamaguchi^{***}, Kazuto Yamamura^{****}, Kenjiro Terada^{*****}

^{*}Ishimoto Architectural & Engineering Firm, Inc., ^{**}Hosei University, ^{***}Hosei University, ^{****}Nippon Steel & Sumitomo Metal Corporation, ^{*****}Tohoku University

ABSTRACT

ABSTRACT Multi Stage Failure Simulation (MSFS) is a simulation that seamlessly analyzes various destruction states of structures. We propose an explicit dynamic model to solve sequentially large deformation behavior as MFSF. In order to realize MSFS, we focus on the following two points. (1) Determine of mechanism, (2) Analysis on the rigid body motion after the collapse. In this proposal, we use the Hybrid-type Penalty Method (HPM) [1] suitable for MSFS. In this method for calculating the displacement field, it is assumed that an independent linear displacement field for the axial direction and an independent displacement field for the bending of each element are combined. The continuity conditions of displacement are incorporated by using a penalty function. The elastic solution obtained with this method is consistent with the exact solution. Moreover, the approach of the dynamic model after collapse is similar to the Distinct Element Method (DEM), it is possible to explain the behavior of the failure mechanism after the formation [2] [3]. In this paper, we include the similar mechanism judgment method of structural stability in this algorithm. Possibility of applying MSFS in various collapse patterns is proposed by this. The effectiveness of the proposed method is demonstrated by the simple numerical examples. REFERENCES [1] K. Yamaguchi and N. Takeuchi, Discrete Limit Analysis for Framed Structures by using Hybrid-type Penalty Method, Bulletin of Research Center for Computing and Multimedia Studies, Hosei University, 30, 2016. [2] T. Yagi, N. Takeuchi, K. Yamamura, and M. Kusabuka, An explicit dynamic method for a discrete element model using the principle of hybrid-type virtual work, Proceedings of the 11th World Congress on Computational Mechanics, Barcelona, Spain, 2014. [3] T. Yagi and N. Takeuchi, An explicit dynamic method of Rigid Bodies-Spring Model, International Journal of Computational Method, 12, 1540014, 2015.

Application of Hamiltonian Flows to Exploring Parameters of Mathematical Models in Situations with Insufficient Data

Takaharu Yaguchi*, Mizuka Komatsu**

*Kobe University / JST PRESTO, **Kobe University

ABSTRACT

Although parameter estimation is essential in mathematical modeling of phenomena in the real world, enough number of data is not necessarily available because experiments are often labor intensive or require expensive equipment. In these cases, the problem of parameter estimation often yields an underdetermined least squares problem, and optimal parameters in the models are not determined uniquely. To choose an appropriate set of parameters, it is necessary to enumerate qualitatively different sets of parameters. To facilitate this problem, we propose an application of Hamiltonian flows to explore the set of optimal solutions. In our algorithm, a set of optimal parameters is first assumed to be obtained by, e.g., a quasi-Newton method. Then a set of optimal parameters are explored by following the Hamiltonian flows of which the energy function is defined by using the objective function. Because the Hamilton equation preserves the energy, all points on the orbits are optimal solutions if the initial conditions are imposed by using an optimal solution.

Comparison between numerical approaches to simulate a supersonic nozzle

Paulo V. M. Yamabe*, Bruno C. Souza**, Emilio C. N. Silva***, Jairo P. Cavalcante Filho****,
Breno A. Avancini*****, Ernani V. Volpe*****, Marcelo T. Hayashi*****, Ulisses A. S.
Costa*****, Douglas Serson*****, José R. S. Moreira*****, Julio R.
Meneghini*****, Reinaldo M. Orselli*****, Julián Restrepo*****

*Polytechnic School of University of Sao Paulo, **Polytechnic School of University of Sao Paulo, ***Polytechnic School of University of Sao Paulo, ****Polytechnic School of University of Sao Paulo, *****Polytechnic School of University of Sao Paulo, *****Federal University of ABC, *****Polytechnic School of University of Sao Paulo, *****Polytechnic School of University of Sao Paulo, *****Polytechnic School of University of Sao Paulo, *****Polytechnic School of University of Sao Paulo, *****Polytechnic School of University of Sao Paulo, *****Polytechnic School of University of Sao Paulo, *****Polytechnic School of University of Sao Paulo

ABSTRACT

The supersonic separator is a new compact and efficient technology for CO₂ separation from Natural Gas with high CO₂ fraction. It consists of a supersonic nozzle with a swirling flow. The cooling caused by the expansion of the flow leads to condensation of the CO₂, which then moves to the outer portions of the nozzle due to centrifugal effects, where it can be collected. As a preliminary step on a comprehensive study of this complex device, we compare the use of different computational fluid dynamics (CFD) packages for the simplified problem of a supersonic divergent-convergent nozzle, both in terms of accuracy and of computational cost for the same number of degrees of freedom. The codes we consider are: Ansys Fluent, a widely-used commercial software based on finite volume methods; SU2, an open-source suite of tools for performing CFD simulations and optimization, also based on finite volume methods; Nektar++, an open-source high-order spectral/hp element framework, which includes a compressible flow solver using the Discontinuous Galerkin method; and a least square solver implemented using the FEniCS project, which is an open-source finite element computing platform. The simulations results of a planar nozzle with the same area distribution and pressure ratio as Arina (2004) are presented and compared with experimental data. References: Renzo Arina 2004, Numerical simulation of near-critical fluids. Applied Numerical Mathematics, 51 (4), 409-426.

Method of Manufactured Solutions in Large Deformation Problems of Hyperelasticity

Takahiro Yamada*

*Yokohama National University

ABSTRACT

In recent years, numerical simulations have been contributed to crucial decision making in the various fields such as medical engineering. Then we need to give the information on the credibility of modeling and numerical simulations to the public. Verification and validation are attracting great attention as a framework to provide such information on modeling and simulations. In this work, we apply the method of manufactured solution (MMS), which is a technique of verification proposed by Roache[1] for fluid dynamics, to nonlinear problems of solid mechanics. In the conventional method of manufactured solution, spatial derivatives of stresses derived from given solutions are required to calculate body forces. Such derivatives can hardly be evaluated in problems of nonlinear materials and hence it has not been popular in solid mechanics. The author developed an alternative technique to calculate equivalent nodal vectors associated with body forces in the method of nearby problems[2] for finite element method. In this approach, calculation of the second order derivative of solutions can be avoided by utilizing the weak formulation and finite element discretization. The actual procedure to calculate equivalent nodal force vectors is similar to the evaluation of internal force in the standard nonlinear finite element procedures, in which the work product of the stress and virtual strain is integrated over the domain. We have applied our procedure to the problems of elasto-plasticity, which is a typical model of nonlinear materials. In this paper, we apply this approach to the method of manufactured solution for large deformation problems of hyperelasticity, which is often used to describe rubber-like materials. In the method of manufactured solutions, an arbitrary displacement field can be prescribed formally. However incompressible or nearly incompressible properties need to be considered in the large deformation problems of hyperelasticity and manufactured solutions that ignore such properties may lead to physically unreasonable external loads or numerical instabilities. Thus we developed a procedure to construct displacement fields in which volumetric changes are controlled in the large deformation state. [1] P. J. Roache and S. Steinberg: Symbolic manipulation and computational fluid dynamics," AIAA Journal, Vol. 22, No. 10, pp. 1390-1394, 1998. [2] T. Yamada: Verification Procedure Based on Method of Nearby Problems for Finite Element Analysis of Solid, ASME 2015 Verification and Validation Symposium, 2015.

Optimum Design of Microstructures Considering Wave Dispersion Using the High Order Homogenization Method

Takayuki Yamada^{*}, Grégoire Allaire^{**}

^{*}Kyoto University, ^{**}Ecole Polytechnique

ABSTRACT

The wave dispersion is a phenomenon appearing in heterogeneous media, by which waves with different wavelengths propagate with different velocities [1]. These effects are modeled by an additional fourth-order term (namely Burnett coefficient) in the homogenized wave equation. Considering the dispersion phenomenon is important in industrial applications, since the periodic size of the microstructures is finite. To begin with, this presentation shows optimum design of microstructures considering wave dispersion [2]. Additionally, the high order homogenized wave equation with an obtained optimal solution is computed using the first Fourier transform Method. References [1] F. Santosa, W. W. Symes, A Dispersive Effective Medium for Wave Propagation in Periodic Composites, SIAM Journal on Applied Mathematics, 1991, Vol.51, pp.984–1005. [2] G. Allaire, T. Yamada, Optimization of dispersive coefficients in the homogenization of the wave equation in periodic structures, HAL Id: hal-01341082.

Interfacial Fracture of Surface Coating under Impact Loading Produced by Pulsed Laser Irradiation

Takeshi Yamada^{*}, Hiroki Watanabe^{**}, Yusaku Saito^{***}, Akio Yonezu^{****}

^{*}Chuo University, ^{**}Chuo University, ^{***}Chuo University, ^{****}Chuo University

ABSTRACT

This study aims to evaluate coating adhesion, i.e. the interfacial strength of coatings and thin films by using pulsed-laser irradiation technique. This method uses strong ultrasonic wave induced by pulsed laser irradiation, such that interfacial fracture of coating occurs due to strong wave. For this irradiation, grease layer is applied to the back of the substrate and a pulsed laser is irradiated, so that ablation occurs in grease layer, inducing strong elastic wave. The elastic wave propagates from the back surface of substrate to the coating surface, and tensile stress acts on the coating/substrate interface. Since such pulsed laser irradiations cause the coating delamination and spallation, this technique is also called laser spallation method. In parallel, the out of plane displacement is measured by using a laser ultrasonic interferometer (continuous wave CW laser). First, to determine critical laser energy of interfacial fracture, pulsed laser irradiation is conducted with various levels of irradiation laser energy. The delamination can be detected from the observation of coating surface morphology and out-of-plane displacement waveform. This study evaluates adhesion of various coating, such as the oxide film on carbon steel substrate and electroplated coatings etc. Furthermore, computation of elastic wave propagation using FDTD (Finite difference time domain) and FEM (Finite Element Method) are carried out to estimate tensile stress developed at the coating film/substrate interface. Based on the above results, the interfacial strength is estimated quantitatively. In addition, the durability of interfacial adhesion is investigated by repeated laser irradiation with similar manner of the above (laser spallation method). In other words, we try to investigate cyclic fatigue of interfacial fracture. In this test, repetitive lower stress loading is applied to the interface using repeated laser irradiations. It is found that repetitive loading encourages interfacial fracture, whose stress level is lower than that of single (monotonic) laser irradiation (of above laser spallation method). Upon various levels of irradiation laser energy, interfacial adhesion durability is investigated. In parallel, numerical simulation (FDTD and FEM) is conducted to estimate interfacial stress for delamination. This result may be useful for adhesion durability, when a coating/film is used under cyclic loading in long time period. Reference: Quantitative evaluation of adhesion quality of surface coating by using pulse laser-induced ultrasonic waves, Surface and Coatings Technology, Vol.286(2016) pp.231-238 Measurement of interfacial fracture toughness of surface coatings using pulsed-laser-induced ultrasonic waves, Journal of Nondestructive Evaluation, Vol.37,2 (2018) pp.1-11]

Development of Hyperelastic Analysis Using Meshfree Particle Method

Nobuki Yamagata^{*}, Masakazu Ichimiya^{**}, Noritaka Matsuoka^{***}, Pedro Marcal^{****}

^{*}Advanced Creative Technology Co., Ltd., ^{**}Advanced Creative Technology Co., Ltd., ^{***}Sumitomo Riko Company Limited, ^{****}MPACT Corp.

ABSTRACT

Development of Hyperelastic Analysis using Meshfree Particle Method Nobuki Yamagata¹, Masakazu Ichimiya¹, Noritaka Matsuoka² and Pedro V. Marcal³ 1 Advanced Creative Technology Co., Ltd., 2 Sumitomo Riko Company Limited, 3 MPACT Corp. Key Words: MeshFree Particle Method, SSPH, Hyperelastic Material, Large Deformation. The large deformation analysis approaches using finite element method (FEM) to simulate the incompressible and the nearly incompressible behavior of hyperelastic materials such as rubber have been carried out to handle the mesh distortions and the volumetric locking resulting from the incompressibility constraint. And on the other hand, in order to solve large deformation problem of solid materials, the SPH method is used which is a kind of particle method based on the meshfree Lagrangian scheme. This method can handle the governing equations and existing constitutive models for structural analysis problems and can solve large deformation problems without mesh distortion. However, this conventional SPH method has disadvantages of impossibility to apply to static and thermal stress analyses in the solid mechanics. To remove these disadvantages, other meshfree methods have been proposed such as Corrected Smoothed Particle Method (CSPM), Reproducing Kernel Particle Method (RKPM), Symmetric Smoothed Particle Hydrodynamics Method (SSPH) and so on. The SSPH method has an advantage over any other meshfree methods because the basic functions have continuous capabilities of derivatives up to the expected order. In this study, using the Improved SPH method (SSPH) the nonlinear formulation for the large deformation analysis of rubber materials, which are considered to be hyperelastic and nearly incompressible, is presented. In a same manner as FEM, the behaviour of rubber is classified as hyperelastic in which the strain energy density function can be defined in this study. The choice of reference configuration influences the kinematics, constitutive law, and SSPH formulation. The original configuration is selected as the reference configuration in the SSPH calculation. The second Piola-Kirchhoff stress and Green-Lagrangian strain are used as the stress and strain measures, respectively. Several numerical examples are presented to study the characteristics of SSPH and to demonstrate the effectiveness of this method in large deformation analyses of hyperelastic materials. And it is also demonstrated that this method has a superior performance to the conventional finite element methods in dealing with large material distortions.

Solid-liquid Coupled Material Point Method for 3-D Simulations of Soil Deformation and Flow

Yuya Yamaguchi^{*}, Shinsuke Takase^{**}, Kenjiro Terada^{***}, Shuji Moriguchi^{****}

^{*}Department of Civil and Environmental Engineering, Tohoku University, ^{**}Department of Civil Engineering and Architecture, Hachinohe Institute of Technology, ^{***}International Research Institute of Disaster Science, Tohoku University, ^{****}International Research Institute of Disaster Science, Tohoku University

ABSTRACT

A new solid-liquid coupled material point method is developed to accurately predict a collapse process of ground structures such as slopes and embankments subjected to excess pore pressure during a heavy rainfall, which involves a transition process from a soil structure to flowing mixture. The governing equations are formulated based on Biot's two-phase mixture theory and separate sets of Lagrangian material points are used to discretize unknown variables of solid and liquid phases in reference to the literature [1][2]. The material behavior of solid phase is represented by the Drucker-Prager's type plastic flow model combined with Hencky's hyperelasticity, whereas the liquid is assumed to be a Newtonian fluid. To improve the accuracy, robustness and efficiency in comparison with the previous studies, the incompressibility is assumed for not only solid grains, but also pore liquids, which necessitates the continuity equation of the liquid phase. By applying the Chorin's projection method to the momentum equation of the liquid phase, pore water pressure can be obtained as a solution of Poisson equation. For the discretization in space, we employ B-spline basis functions [3], which suppress numerical oscillations when a material point crosses the mesh boundary. Since MPM does not require us to search for adjacent particles, the computing costs are significantly small, the proposed method is also suitable for parallel computing with an appropriate domain decomposition so that large-scale 3-D simulations would be possible. Several numerical examples are presented to demonstrate the capability of the proposed method that inherits the beneficial features of MPM. A collapse analysis of an embankment with water inflow boundary conditions is a typical example problem to incorporate the performance, by which the superiority in computational efficiency over existing approaches can be confirmed. References [1] Bandara, S., Soga, K., Coupling of soil deformation and pore fluid flow using material point method. *Computers and Geotechnics*, 63, 2015, pp. 199–214. [2] Bui, H. H., Nguyen, G. D., A coupled fluid-solid SPH approach to modelling flow through deformable porous media. *Internat. J. Solids Struct.*, 125, 2017, pp. 244–264. [3] Steffen, M., Kirby, R. M., Berzins, M., Analysis and reduction of quadrature errors in the material point method (MPM). *Internat. J. Numer. Method Engrg.*, 76(6), 2008, pp. 922–948.

Advanced Multi-Physics CFD Simulations for Engineering Problems

Makoto Yamamoto*

*Tokyo University of Science

ABSTRACT

Computational Fluid Dynamics (CFD) has been completely matured in the engineering sense. Nowadays, we can use CFD for research and development of various machines. However, most targets of current CFD are limited to single-phase flows. Thus, in near future, we have to focus on multi-phase flows which are typically of multi-scale and multi-physics. Based on this consideration, I have been tackling the modeling and simulations of multi-physics engineering problems such as ice accretion, particle deposition and sand erosion in a jet engine. In these problems, the flow fields strongly depend on surface deformation. For example, ice layer whose thickness is few mm is formed on fan blades of a jet engine in icing environments. Such a thin ice layer can lead to 10% performance degradation. Therefore, exact reproduction of surface deformation is critical in the simulations. At first, I adopted a finite difference method (i.e. grid-based method) because of my long experience. Using a finite difference method, I and my students succeeded in simulating the temporal changes of flow field, wall surface and machine performance due to icing, deposition and erosion. However, in the simulations, we had to smooth the wall surface so that we could re-generate the grid along the deformed or rough surface. This might reduce or destroy the accuracy of simulations. (It is too difficult to verify and validate this point.) So, I decided to change the strategy, and introduced a particle-based method, since it does not need any grid system. It should be noted that a particle-based method has one big disadvantage, that is, it is too time-consuming. Therefore, a hybrid grid and particle-based method is recently developed. The macroscopic field is computed by a grid-based method, while microscopic or mesoscopic phenomenon on and over a wall surface is computed by a particle-based method. Doing so, I expect that this hybrid method can improve the accuracy of multi-physics simulations in both quality and quantity. In the final paper and my presentation, the numerical procedures of the hybrid grid and particle-based method is introduced, with showing the numerical results on ice accretion and particle deposition phenomena in a jet engine.

Large Deformation Analysis with Connecting Shell and Solid Elements by Using Nitsche's Method

Takeki Yamamoto^{*}, Isao Saiki^{**}, Takahiro Yamada^{***}, Kazumi Matsui^{****}

^{*}Tohoku University, ^{**}Tohoku University, ^{***}Yokohama National University, ^{****}Yokohama National University

ABSTRACT

Structures can be constructed with various shape of components which can be modeled as solids, plates, and beams. In the finite element analysis, the whole domain of such structures is often discretized with one type of element only. This approach does not seem to be appropriate in general cases, and it may indicate difficulty in some cases. For example, in the structure composed with an assemblage of solids and plates, if the whole domain is discretized with continuum elements, the local behavior can be evaluated effectively, but huge computational cost may be required. On the other hand, if the entire region is discretized with structural elements, simple bending behavior of thin-walled structures can be predicted efficiently, but they are not sufficient to evaluate local behaviors. Thus, the more effective procedure of discretizing the whole domain of the problem of interest can be constructed by selecting different types of elements according to the shape. This paper presents a numerical procedure to connect shell and solid elements by using the Nitsche's method[1]. The continuity of displacements can be satisfied approximately with the penalty method[2], which is effective for setting the penalty parameter to a sufficiently large value. When the continuity of only displacements on the interface is applied between shell and solid elements, an unreasonable deformation may be observed near the interface. In this work, the continuity of stress vectors on the interface is considered by employing the Nitsche's method, and hence a deformation on the interface can be improved. Several numerical examples of large deformation analysis are presented to examine the fundamental performance of the proposed procedure. The behavior of the proposed simulation model is compared with that of the whole domain discretized with solid elements only. [1] J. Nitsche: Über ein variationsprinzip zur Lösung von Dirichlet-Problemen bei verwendung von teilräumen, die keinen randbedingungen unterworfen sind, Abhandlungen aus dem Mathematischen Seminar der Universität Hamburg, 36, 9–15, 1971. [2] G. R. Liu, S. S. Quek: The Finite Element Method: A Practical Course, 2nd eds., Butterworth-Heinemann, 2013.

Analysis of Brick Masonry Structures for Coke Oven Using the Hybrid-type Penalty Method

Kazuto Yamamura^{*}, Yasuyuki Tajiri^{**}, Norio Takeuchi^{***}

^{*}Nippon Steel and Sumitomo Metal Corporation, ^{**}Nippon Steel & Sumikin Technology Co.,Ltd., ^{***}Hosei University

ABSTRACT

The coke oven which produce coke by carbonization of coal is one of high temperature furnaces in the iron and steel industry and cokes are used to improve efficiency of operation for blast furnace. The walls of coking chamber are brick masonry structures using over 20000 shaped bricks(per chamber) and are subject to repeated thermal and mechanical stresses during operations of the coal charging , carbonization and coke discharging in daily. As the results, chamber walls will be damaged associated with their characteristics in multi-body contact structures and showed complex behavior such as deformation with joint opening, wall thinning, crack initiation and its growth(through crack), corner defect of brick , collapse of wall etc. A numerical predictions of these phenomena are effective not only stable operation and prolonging life of structures but also optimal design of brick structures for damage prevention. To meet above needs, analysis tool of brick masonry structures using the Hybrid-type Penalty Method(HPM)[1] has been developed. In the HPM, analysis field is divided subdomain and the compatibility of the displacement on the element boundary edge is approximately introduced using the penalty as a spring constant of Lagrangian multiplier in the formulation of the hybrid-type virtual work. And surface tractions on boundary of elements are calculated and it is made possible to analyze slip and opening between elements. In this report, outline of development of analysis tool for brick masonry structures using HPM and practical predictions of wall behavior and strength of coking chamber with cracks are introduced. [1] Takeuchi,N. et al.; Development of modified RBSM for rock mechanics using principle of hybrid-type virtual work, pp.395-403 Research Publishing Service, Singapore, 2009

Generation of Three-Dimensional Video Image of Indoor Damage Due to an Earthquake Using Point Cloud

Takuzo Yamashita^{*}, Kazutoshi Matsuzaki^{**}, Mahendra Kumar Pal^{***}, Hiromitsu Tomozawa^{****},
Toru Hagiwara^{*****}, Yuji Mori^{*****}

^{*}National Research Institute for Earth Science and Disaster Resilience, ^{**}Mizuho Information and Research Institute, Inc., ^{***}National Research Institute for Earth Science and Disaster Resilience, ^{****}Mizuho Information and Research Institute, Inc., ^{*****}Mizuho Information and Research Institute, Inc., ^{*****}Mizuho Information and Research Institute, Inc.

ABSTRACT

Virtual reality (VR) experience of indoor damage due to earthquake has a great potential for promotion of earthquake-resistant countermeasures and earthquake disaster drill. E-Defense of the National Research Institute for Earth Science and Disaster Resilience, or NIED, possesses the world's largest shaking table by which real scale buildings can be shaken against large earthquake such as the 1995 Kobe earthquake. We aim to develop a VR experience system using data of indoor damage reproduced by E-Defense shake table tests. As data for VR experience system, synchronized video image, sound and floor acceleration were obtained for shake table tests of a 10-story reinforced concrete (RC) structure. Then, VR visualization system was developed in which 360-degree video image which was generated by mapping multiple video images into sphere surface is displayed in a head mount display (HMD) [1]. However, such a 360-degree video image cannot consider the position movement of the user. In this research, we aim to generate three-dimensional video image which can consider the position movement by using point cloud. Shooting target is the same room mentioned above. Firstly, we develop shooting system of point cloud. Kinect v2 is employed to obtain RGB image and depth data. To capture the entire area of the room, eight Kinect v2 devices are installed in this system and network system is constructed to operate synchronized data measurement from outside the shake table. Secondly, to merge data measured at all devices, program that coordinate data of coordinate system of each devices is transformed into those in the unified coordinate system is developed. Finally, to display in a HMD, the amount of data size is eliminated by using voxel grid filter and two different visualization methods are developed; one by using polygon generated by point cloud and another by adjusting the size of the point cloud in accordance with the distance from the view point. In the former case, visualization quality is not satisfactory because data includes negligible noise which leads to zigzag-type elements. In the latter case, VR visualization image to grasp the indoor damage from arbitrary position can be displayed in the HMD. Reference [1] T. Yamashita, M. K. Pal, K. Matsuzaki and H. Tomozawa: Development of a Virtual Reality Experience System for Interior Damage due to an Earthquake -Utilizing E-Defense Shake Table Test-, Journal of Disaster Research, Vol.12, No.5, pp.882-890, 2017.10

A Fully Coupled Finite Element Formulation for Liquid-solid-gas Thermo-fluid Flow with Melting and Solidification and Its Application to Additive Manufacturing

Jinhui Yan^{*}, Wentao Yan^{**}, Stephen Lin^{***}, Greg Wagner^{****}

^{*}Northwestern University, ^{**}Northwestern University, ^{***}Northwestern University, ^{****}Northwestern University

ABSTRACT

Many important industrial processes, such as additive manufacturing, involve rapid mass, flow and heat transport between gas, liquid and solid phases. Various associated challenges, such as the large density ratio between gas and condensed phases, make accurate, robust thermal multi-phase flow simulations of these processes very difficult. In order to address some of the associated challenges, a computational framework for thermal multi-phase flows is developed based on the finite element method (FEM). A unified model for thermal multi-phase flows similar to the models widely used in the manufacturing community is adopted. The combination of the level-set method and residual-based variational multi-scale formulation (RBVMS) is used to solve the governing equations of thermal multi-phase flows. Phase transitions between solid and liquid phases, i.e., melting and solidification, are considered. Interfacial forces, including surface tension and Marangoni stress, are taken into account and handled by a density-scaled continuum surface force model. A robust fully coupled solution strategy is adopted to handle various numerical difficulties associated with thermal multi-phase flow simulations, and implemented by means of a matrix-free technique using Flexible GMRES. The mathematical formulation and its algorithmic implementation are described in detail. Several numerical examples and the applications to additive manufacturing will be shown. The computational results are compared with analytical, experimental and simulation data from other researchers, with good agreement in cases where such data is available.

Quantifying the Uncertainty of AM Models: from High-fidelity to Low-fidelity

Wentao Yan^{*}, Paul Witherell^{**}, Wing Liu^{***}

^{*}Northwestern University & NIST, ^{**}NIST, ^{***}Northwestern University

ABSTRACT

Computational modeling for additive manufacturing has proven to be a powerful tool to understand the physical mechanisms, predict fabrication quality, and guide design and optimization. However, various models have been developed with different assumptions and purposes, and these models are sometimes difficult to choose, especially for end-users, due to the lack of quantitative comparison and standardization. Thus, this study is focused on quantifying the uncertainty due to the modeling assumptions, and evaluating the difference due to whether or not some physical factors are incorporated. Multiple models with different assumptions, from high-fidelity to low-fidelity, are run with a variety of manufacturing process parameters, while experiments are performed to validate the models. The models include: a thermal-fluid flow model resolving individual powder particles, a heat transfer model simplifying powder bed as continuum material and an analytical thermal model. This study will provide guidance on how to select models and how much accuracy to be expected, based on the specific purpose. Moreover, the quantification of each physical factor will also contribute to further developing simplified models, i.e. which factors can be reasonably simplified or ignored. [1] Wentao Yan, Wenjun Ge, Jacob Smith, Stephen Lin, Orion Kafka, Feng Lin, Wing Kam Liu, Multiscale modeling of electron beam melting of functionally graded materials, *Acta Materialia*, 2016. 115: 403-412 [2] Wentao Yan, Wenjun Ge, Ya Qian, Stephen Lin, Gregory Wagner, Feng Lin, Wing Kam Liu, Multi-physics modeling of single/multiple-track defect mechanisms in Electron Beam Selective Melting. *Acta Materialia*, 2017. 134:324-333 [3] Wentao Yan, Ya Qian, Wenjun Ge, Stephen Lin, Gregory Wagner, Feng Lin, Wing Kam Liu, Meso-scale modeling of multiple-layer fabrication process in Selective Electron Beam Melting. *Materials & Design*

Numerical Study on Clad-substrate Interfacial Quality of Laser Cladding for Additive Restoration of Mold Steels Using Crucible Steel

Wenyi Yan^{*}, Chaitanya Vundru^{**}, Santanu Paul^{***}, Ramesh Singh^{****}

^{*}Monash University, ^{**}Indian Institute of Technology Bombay, ^{***}Indian Institute of Technology Bombay, ^{****}Indian Institute of Technology Bombay

ABSTRACT

Laser cladding is increasingly used for the repair/restoration of critical structural components in aerospace and automobile industries. To enhance the integrity and functional life of the restored components, improving the clad quality and maintaining the integrity of clad-substrate interface is of primary importance. The quality and life of the restored components will depend on the residual stresses, which are induced due to the temperature gradients, the dissimilarity of the coefficients of thermal expansion and the elastoplastic behavior of the clad and the substrate materials. Further, due to high cooling rates, additional strains are developed due to metallurgical transformation induced plasticity and volumetric dilation. And this temperature gradient and the change in the coefficient of thermal expansion is steep at the interface. Thus the interface can sometimes become the probable cause of weakness of the cladding. In addition, a significant clad diffusion would have occurred across the clad-substrate interface, which affects the microstructure of bonding interface. Complete metallurgical bond between the clad and the substrate is also governed by the melting at the interface. In this study, a coupled metallo-thermomechanical finite element model for laser cladding of CPM9V powder on H13 tool steel is developed to predict the evolution of residual stress due to thermomechanical interactions and metallurgical transformations. This model is employed to predict the transient temperatures, both longitudinal and traverse (to the scanning direction) residual stresses at the clad-substrate interface. To attain minimal dilution, the melt line should lie as close as possible to the clad-substrate interface. This effort of minimize dilution appears to increase the possibility of tensile transverse and longitudinal residual stresses in the clad-substrate interface. Occurrence of a tensile residual stress at the clad-substrate interface could result in the premature failure of the cladding. On the other hand, compressive residual stress at the clad-substrate interface could improve its service life. So the state of the residual stress of the clad-substrate interface is explored. The pre-scanning of the substrate has been noted to improve clad-substrate quality. Micro-hardness is estimated both numerically and experimentally at the clad-substrate interface.

Influence of Various Parameters on the Cutting and Failure Mechanism of Unidirectional CFRP Composites Based on Finite Element Analysis

Xiaoye Yan^{*}, Jianguo Guo^{**}, Xingtao Dong^{***}

^{*}Northwestern Polytechnical University, ^{**}Northwestern Polytechnical University, ^{***}Shandong institute of space electronic technology

ABSTRACT

A three-dimensional micro-scale finite element (FE) model of cutting unidirectional carbon fiber reinforced polymer (UD-CFRP) materials is developed in this paper. Fiber, matrix and the fiber-matrix interface are modeled separately to predict fiber breakage, matrix cracking and fiber-matrix debonding. The fibers are assumed to be linearly elastic up to sudden failure defined by the maximum stress criterion. Matrix material is modeled as elastoplastic in combination with a damage evolution behavior. The debonding at the interface is assumed to occur when the displacements of the cohesive elements exceed their displacement limits. Experiments on orthogonal cutting of UD-CFRP workpiece with various fiber orientations have been conducted and compared to the micro-scale FE predictions. The good correlation between experimental data and numerical results allows for an in-depth FE analysis to explain the cutting mechanism beneath the experimental observations such as cutting forces and surface morphology. The dissipative energies associated with damage in fiber, matrix and the interface, friction in the rake face-composite chip contact zone, friction along the fiber and matrix interface, and plastic deformation of matrix have been evaluated and correlated to the dominating failure mechanisms. The chip formation mechanisms and the surface quality are analyzed and it is found that the former is mainly associated with fiber damage modes, while the latter is related to fiber damage modes and the direction of propagation of fiber-matrix debonding.

Meshless RBF Galerkin Method for Band Structure Calculation of Phononic Crystals

Zhizhong Yan^{*}, Chuanzeng Zhang^{**}

^{*}Beijing Institute of Technology, ^{**}University of Siegen

ABSTRACT

Meshless RBF Galerkin Method for Band Structure Calculation of Phononic Crystals Zhizhong Yan¹, Chuanzeng Zhang² ¹Beijing Institute of Technology zzyan@bit.edu.cn ²University of Siegen In recent years, phononic crystals which are periodically-structured media and possess acoustic/elastic wave band gaps have attracted great attentions due to a variety of important applications. Up to now, some methods have been developed for the calculation of acoustic/elastic wave band gaps, including the plane wave expansion (PWE) method, the wavelet method, the finite element method (FEM) and so on. These methods have their own advantages and disadvantages. Therefore, it has been one of the main contents of phononic crystals research to find the accurate and efficient numerical methods. Recently, meshless methods based on radial basis functions (RBFs) have become attractive for solving partial differential equations (PDEs) using a set of nodes within the domain of interest. In this paper, a new meshless RBF Galerkin (weak form) method is proposed for modeling phononic crystals. When modeling the phononic crystals an eigenvalue problem with periodic boundary conditions is formed. The wave equation is transferred into an integral form by the variational principle, the unknown functions are approximated by a set of RBFs, then the eigenvalue problem of a general matrix is obtained. The Gauss integral method is used to improve the accuracy and solve the discontinuity of the material parameters of phononic crystals. The results obtained from the meshless RBF weak form method are found to be in good agreement with the wavelet method. Meshless RBF local weak form method has obvious advantages compared with the traditional numerical methods. It does not require a grid or mesh, and the RBF is defined as the distance function, which is not sensitive to the dimension. Meanwhile, the use of RBFs for the problems with a discontinuity of material parameters is found to reduce the Gibbs phenomenon. In addition, the Gauss integral method is used to calculate the numerical integral, and the calculation speed is improved as compared to the traditional method. The proposed meshless method are proved to be a promising scheme for calculating the band gaps. References [1] Sigalas M M, Soukoulis C M. Elastic-wave propagation through disordered and/or absorptive layered systems. *Phys Rev B*, 1995, 51: 2780—2789 [2] G.R. Liu, Y.T. Gu, A meshfree method: meshfree weak-strong (mws) from methods, for 2-d solids, *Journal of Computational Mechanics* 33 (1) (2002) 2–14

A MICROMECHANICS-BASED HIERARCHICAL COMPUTATIONAL MODEL TO PREDICT FUNCTIONAL BEHAVIORS OF ELECTRIFIED CEMENTITIOUS COMPOSITES

B. J. Yang[†], Haemin Jeon[‡], and Bong-Rae Kim^{*}

[†]Institute of Advanced Composite Materials, Korea Institute of Science and Technology
92 Chudong-ro, Bongdong-eup, Wanju-gun, Jeollabuk-do 55324, Republic of Korea
Email address; bj.yang@kist.re.kr

[‡]Department of Civil and Environmental Engineering, Hanbat National University
125 Dongseodae-ro, Yuseong-gu, Daejeon 34014, Republic of Korea
Email address; hjeon@hanbat.ac.kr

^{*}Civil and Architectural Engineering Dept., KEPCO E&C
269 Hyeoksin-ro, Gimcheon-si, Gyeongsangbuk-do 39660, Republic of Korea
Email address; bongraekim@kepc-enc.com

Key words: Micromechanics, Hierarchical approach, Cementitious composites, Functional Filler, Genetic algorithm

Abstract. The cementitious composite with functional fillers has attracted with considerable attention in the major scientific and engineering field due to its excellent mechanical and functional characteristics such as high load-carrying capacity and self-detecting of damage. With increasing interest in this multi-functional material, the need for advanced computational modelling such as multiscale modelling has also grown significantly. In this study, a hierarchical computational model based on micromechanics and genetic algorithm is proposed to predict functional behaviors of electrified cementitious composites. In order to consider the tunnelling effect and interface characteristics of conductive fillers in the electrified cementitious composite, the Cauchy's probabilistic model is applied to the concept of an effective medium theory. The model parameters regarding conductive network are estimated by genetic algorithm, and the determined parameters are applied to the micromechanical model. Based on the proposed hierarchical approach, a series of numerical simulations including the experimental comparisons of the electrified cementitious composites with functional fillers are carried out to elucidate the potential of the proposed model.

1 INTRODUCTION

Cementitious material is one of the widely used traditional materials in the civil infrastructure applications owing to its stable mechanical and chemical properties [1]. Recently, the request for multifunctional characteristics is being imposed upon the cementitious material as well as its original functionality such as high load-carrying capacity. As a result, the cementitious material with functional fillers has attracted with considerable attention due to their excellent mechanical and functional characteristics. Among a variety of functional characteristics, the most studied area is conductive cementitious material that can be utilized for electromagnetic shielding [2], self-monitoring [3], deicing pavement [4], etc.

With increasing interest in these multi-functional materials, the need for advanced computational modelling such as multiscale modelling has also grown significantly. In this study, a computational method that quantitatively predicts the functional characteristics of electrified cementitious composite is proposed. A hierarchical computational model based on micromechanics and genetic algorithm is developed, and the electrified cementitious composite corresponding to the mixing ratio of multi-walled carbon nanotube (MWCNT) and carbon fiber (CF), and the water-cement ratio (w/c) is experimentally tested. The experimentally measured data are utilized to estimate the model constants of the proposed method. Figure 1 shows a schematic illustration of MWCNT and CF-embedded cementitious composite considered in this study.

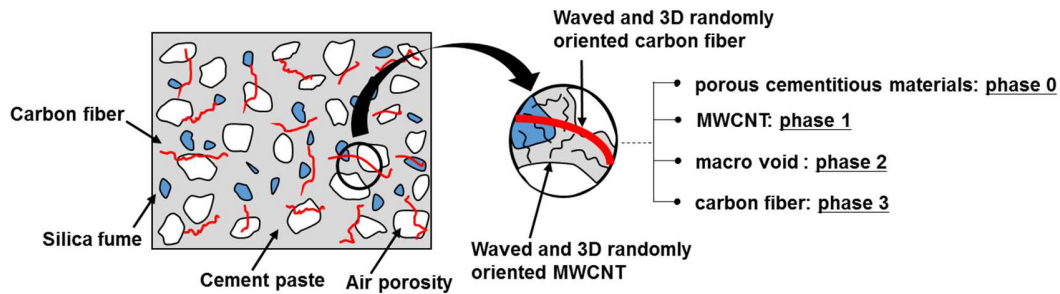


Figure 1. Schematic illustration of MWCNT and CF-embedded cementitious composite

In order to consider the tunneling effect and interface characteristics of conductive fillers in the electrified cementitious composite, the Cauchy's probabilistic model is applied to the concept of an effective medium theory [5]. The model parameters regarding conductive network are estimated by genetic algorithm, and the determined parameters are applied to the micromechanical model [6]. Based on the proposed hierarchical approach, a series of numerical simulations including the experimental comparisons of the electrified cementitious composites with functional fillers are carried out to elucidate the potential of the proposed model.

2 MICROMECHANICS-BASED HIERARCHICAL COMPUTATIONAL MODEL

As shown in Figure 1, this study deals with the electrified cementitious composite having the cementitious material, MWCNT, CF, and porosity. Let us consider the multi-phase material which consists of cementitious material (phase 0), MWCNT (phase 1), porosity (phase 2), and CF (phase 3). It is assumed that the MWCNT, porosity, and CF are randomly and uniformly dispersed in the cementitious material as shown in Figure 1. To simulate the functional behavior of the electrified cementitious composite theoretically, we carried out a micromechanics-based homogenization process consisting of three steps as shown in Figure 2.

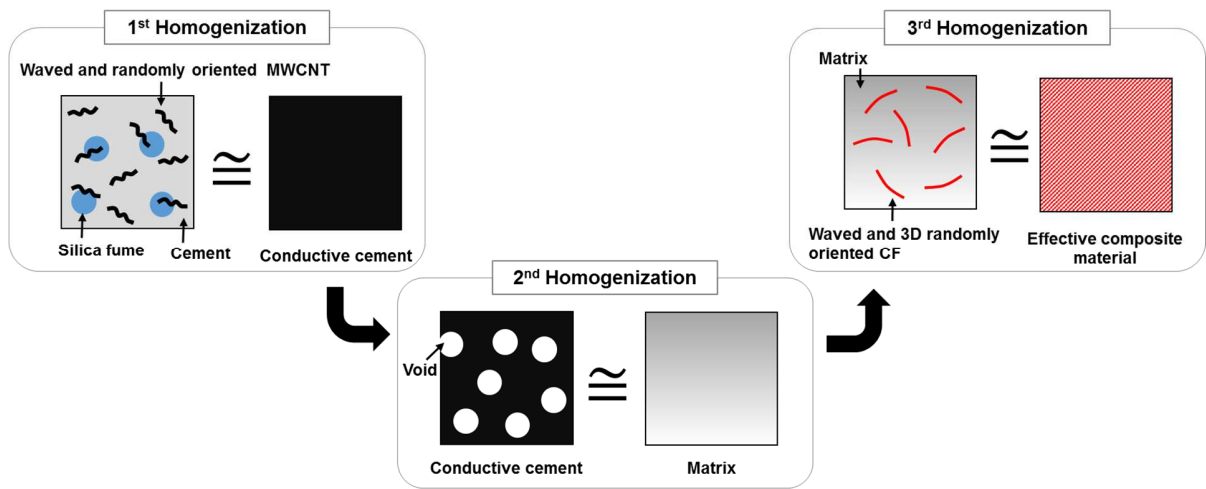


Figure 2. Schematic of micromechanics-based homogenization process consisting of three steps

For homogenization, the effective medium theory (EMT) [5] and the modified Mori-Tanaka (MT) [7] models are considered herein. The EMT and MT models have proven to be suitable theory for predicting the electrical conductivity of composite through many literatures. The effective conductivity of electrified cementitious composites can be expressed as follows using EMT and MT model:

$$(1 - \phi_1) \left[(\mathbf{L}_0 - \mathbf{L}_{cc})^{-1} + \mathbf{L}_0^{-1} / 3 \right]^{-1} + \phi_1 \left[\left\{ (\mathbf{L}_1)^t - \mathbf{L}_{cc} \right\}^{-1} + \mathbf{S}_1 \mathbf{L}_{cc}^{-1} \right]^{-1} = 0 \quad (1)$$

$$\mathbf{L}_m = \mathbf{L}_{cc} + \phi_2 \left[\mathbf{I} - \phi_2 \mathbf{T} : \mathbf{L}_{cc}^{-1} / 3 \right]^{-1} : \mathbf{T} \quad (2)$$

$$\mathbf{T} = \left\{ (\mathbf{L}_2 - \mathbf{L}_{cc})^{-1} + \mathbf{L}_{cc}^{-1} / 3 \right\}^{-1} \quad (3)$$

$$(1 - \phi_3) \left[(\mathbf{L}_m - \mathbf{L}_e)^{-1} + \mathbf{L}_m^{-1} / 3 \right]^{-1} + \phi_3 \left[\left\{ (\mathbf{L}_3)^t - \mathbf{L}_m \right\}^{-1} + \mathbf{S}_3 \mathbf{L}_e^{-1} \right]^{-1} = 0 \quad (4)$$

where \mathbf{L}_r denotes the electrical conductivity of r -phase, and the subscripts cc , m , and e mean the conductive cement, matrix, and effective composite material at each homogenization stage, respectively. The superscript i denotes the interface between the inclusion and matrix. In addition, \mathbf{S}_r and ϕ_r are the aspect ratio-dependent depolarization tensor [7] which can be estimated by genetic algorithm and volume fraction of inclusions, respectively.

3 CHARACTERISTICS OF ELECTRIFIED CEMENTITIOUS COMPOSITE

The electrical resistivity corresponding to the mixing ratio of MWCNT and CF, and the w/c ratios is measured to investigate the electrical characteristics of multifunctional cementitious composite. Figure 3 shows the electrical resistivity of the specimens with respect to weight fraction of MWCNT and CF, and w/c ratios. Here, F0, F1, and F5 mean that CF is contained in the cement matrix for 0, 1, and 5% by weight ratio, respectively.

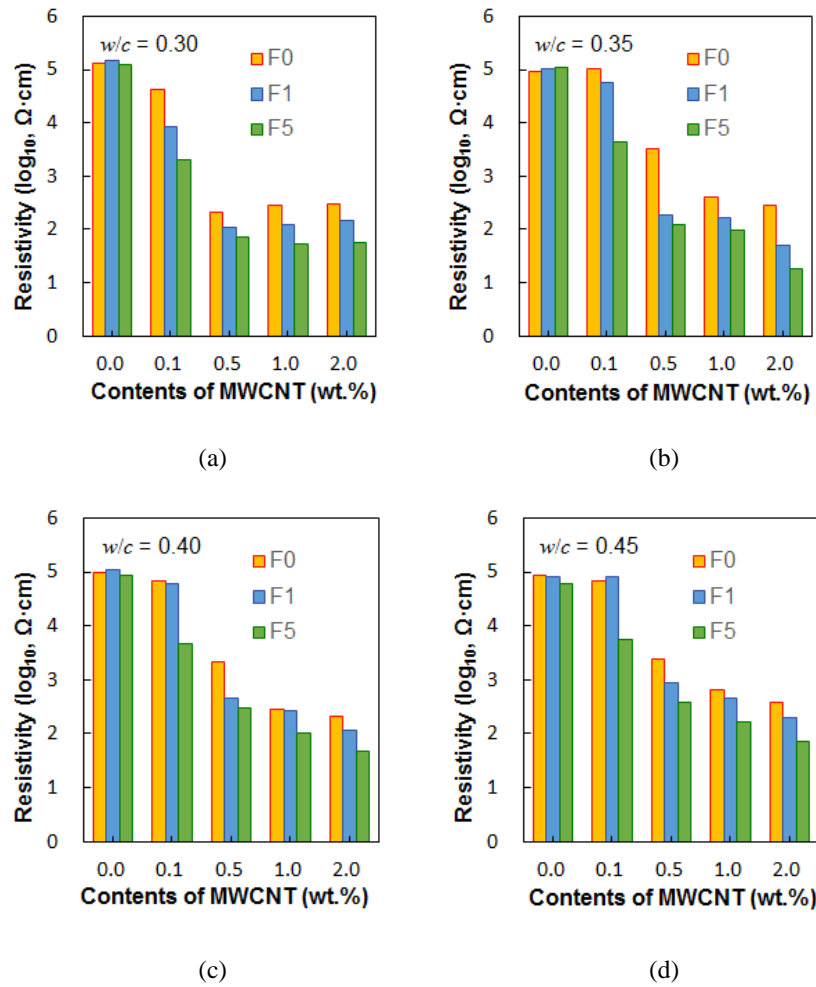


Figure 3. Electrical resistivity of the specimens corresponding to weight fraction of MWCNT, CF, and w/c ratio

Experimental results show that the electrical resistivity of specimens decreases as the amount of MWCNT incorporated into the cement increases, and as the w/c ratio decreases. However, the difference rate of resistivity with the w/c ratio is smaller than that of the reported results from the existing literatures, which is caused by the hierarchical conductive pathway, bridging CF and MWCNT. A related scanning electron microscope (SEM) image that can explain this mechanism (tunneling effect) is shown in Figure 4.

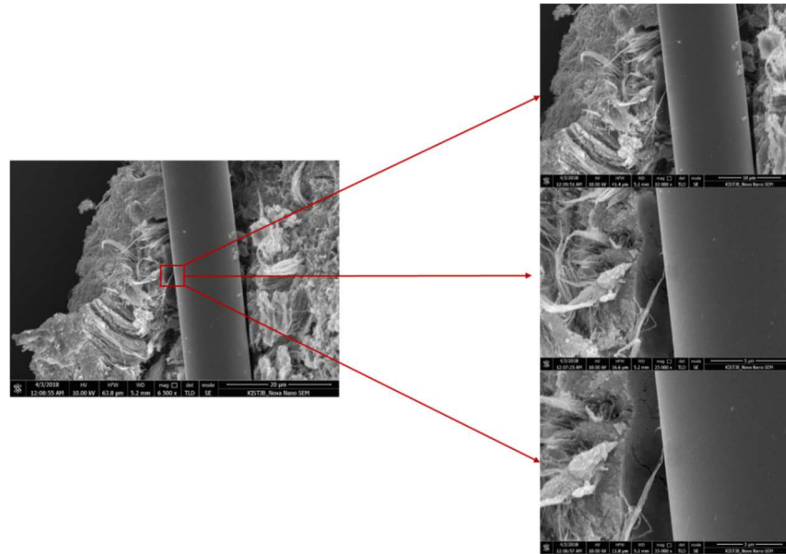


Figure 4. SEM image illustrating hierarchical conductive pathway, bridging CF and MWCNT

4 CONCLUSIONS

This study presents the micromechanics-based hierarchical computational model for electrified cementitious composites. In particular, the proposed computational approach, in which the computational method (micromechanics and generic algorithm) and a series of experiments are properly associated, enables accurate prediction of functional behavior of electrified cementitious composites, not only with respect to electrical properties but also internal conductivity network mechanism. Figure 5 shows the representative comparison of electrical resistivity between predictions and experimental results of electrified cementitious composites, in which the predictions are in good agreement with the experimental results. Although this study is focused on the electrified cementitious composite having MWCNT and CF, the proposed computational approach could be utilized to predict the functional characteristics of the cementitious composites with different functional fillers.

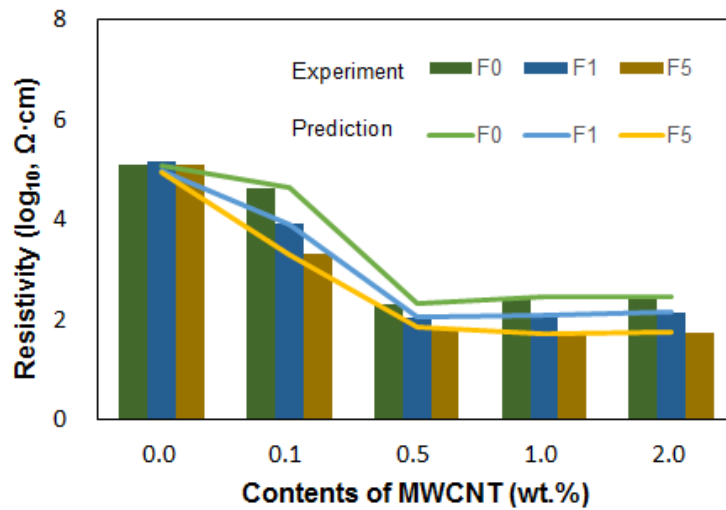


Figure 5. Representative comparison of electrical resistivity between predictions and experimental results of the cementitious composite

REFERENCES

- [1] Hewlett P. Lea's chemistry of cement and concrete. Elsevier (2003).
- [2] Guan H., Liu S., Duan Y., Cheng J. Cement based electromagnetic shielding and absorbing building materials. *Cement Conc. Compos.* (2006) 28:468-474.
- [3] Sun M.Q., Liew R.J., Zhang M.H., Li W. Development of cement-based strain sensor for health monitoring of ultra high strength concrete. *Const. Build. Mater.* (2014) 29:630-637.
- [4] Yehia S., Tuan C.Y., Ferdon D., Chen B. Conductive concrete overlay for bridge deck deicing: mixture proportioning, optimization, and properties. *ACI Mater. J.* (2000) 97:172-181.
- [5] Hashemi R. and Weng G.J. A theoretical treatment of graphene nanocomposites with percolation threshold, tunneling-assisted conductivity and microcapacitor effect in AC and DC electrical settings. *Carbon* (2016) 96: 474-490.
- [6] Yang B.J., Jang J.U., Eem S.H., Kim S.Y. A probabilistic micromechanical modeling for electrical properties of nanocomposites with multi-walled carbon nanotube morphology. *Compos. Part A. Appl. Sci. Manuf.* (2017) 92: 108-117.
- [7] Wang Y., Weng G.J., Meguid S.A., Hamouda A.M. A continuum model with a percolation threshold and tunneling-assisted interfacial conductivity for carbon nanotube-based nanocomposites. *J. Appl. Phys.* (2014) 21: 193706.

Nonlinear Finite Element Methods and Applications in Automobile Industry

Bin Yang^{*}, Xiaonong Meng^{**}, Arthur Schubert^{***}

^{*}Altair Engineering, Inc, ^{**}Altair Engineering, Inc, ^{***}Altair Engineering (Germany), GmbH

ABSTRACT

With the rapidly developing computing power, nonlinear finite element methods (FEM) have been widely applied to solve challenging engineering problems. Great research efforts have been devoted to improve the accuracy of the solution and the stability and robustness of the solution process. Some cutting edge research work has been done and become available in commercial finite element software. This paper presents some recent developments in the application of nonlinear FEM, particularly in automobile industry. A few practical industrial cases are presented to show the performance of these developments.

Symplectic Semi-analytical Method for the Multilayered Two-dimensional Decagonal Quasicrystal Plates with Heat Effect

Changyu Yang^{*}, Qingpeng Tan^{**}, Xueqian Fang^{***}, Mingqian Xu^{****}

^{*}Shijiazhuang Tiedao University, ^{**}Shijiazhuang Tiedao University, ^{***}Shijiazhuang Tiedao University,
^{****}Shijiazhuang Tiedao University

ABSTRACT

The mixed finite element--symplectic semi-analytical approach is proposed in this article to analyze the multilayered two-dimensional decagonal quasicrystal plates under simply supported displacement boundary conditions with the heat effect. The basic equations of the Hamiltonian formalism is derived by introducing the total free energy functions composed by the phonon field and the phason field. The problem is solved in an in-plane finite element discretization in a single layer and then in the multilayer solution with the symplectic state space method. The correctness of the proposed semi-analytical method is verified with open literature. Numerical results show that stacking sequences, coupling constants and thermal fields take a great role in the stress fields of the multilayered quasicrystal plates. The numerical results can also be used as analyzing laminated composites made of two-dimensional quasicrystals.

NONLINEAR ANALYSIS OF UNDERWATER MARINE RISER RECOIL USING HIGHLY EFFICIENT MULTIBODY DYNAMICS METHOD

CHENG YANG*, JIANBIN DU*, ZAIBIN CHENG[†], CHAOWEI LI[†], AND YI WU[†]

* Tsinghua University, School of Aerospace Engineering
Room N-1008, MengMinWei Science and Technology Building
Beijing, China
cyang15@mails.tsinghua.edu.cn; dujb@mail.tsinghua.edu.cn

[†]CNOOC Research Institute
ROOM A-710, CNOOC Plaza, NO.6, Taiyanggong South Street
Beijing, China
chengzb@cnooc.com.cn; lichw6@cnooc.com.cn; wuyi11@cnooc.com.cn

Key words: Marine Riser; Flexible Multibody Dynamics; Recoil; Auxiliary Pipelines; Nonlinear Analysis.

Abstract. A flexible multibody methodology for full-scale marine riser system considering static, modal and recoil case is presented in this paper. Lagrangian equations together with numerical methods for static, modal and emergency disconnect recoil cases are developed in detail. Finite element method has been widely used in the recoil research of marine riser in the recent decades, but the corresponding applications of multibody dynamics still consider the riser with finite segment method or directly simplify it as a mass-spring system to make the number of degrees of freedom of system small. In this paper, a full-scale flexible multibody dynamics model of marine riser is built with geometrically exact beam that is modified for ocean environment in 1547-meter water depth and mud discharging. A numerical example is built and calculated for static, modal and recoil cases to compared with the commercial finite element software DEEPRISER, 93% agreement is gained for all cases and the presented flexible multibody method is 3 time faster in the recoil case. The auxiliary pipelines on the riser are always simplified by an equivalent mass which is added to that of marine riser in the finite element method. To verify this, a more detailed example is built with the auxiliary pipelines modeled by respective beam lines and connected to riser by hundreds of constraint joints. The associate mass model of auxiliary pipelines is only suitable for static and modal calculation, but not for the recoil dynamic calculation, where the dangerous case of riser may be mistakenly seen as safe case. But the simplified model considering both associate mass and associate stiffness is suitable for recoil dynamic calculation which is almost the same as the detailed auxiliary model.

1. INTRODUCTION

The methods of studying marine riser system can be mainly divided into three categories: analytical method ^[1-6], finite element method ^[7-19] and multibody dynamic method ^[20-21], along with real tests on drillships ^[12,29-31] and increasing interests in nonlinearity of riser recoil ^[11-19,29-31] and drillstring/riser involved contacts ^[22-24,27-28].

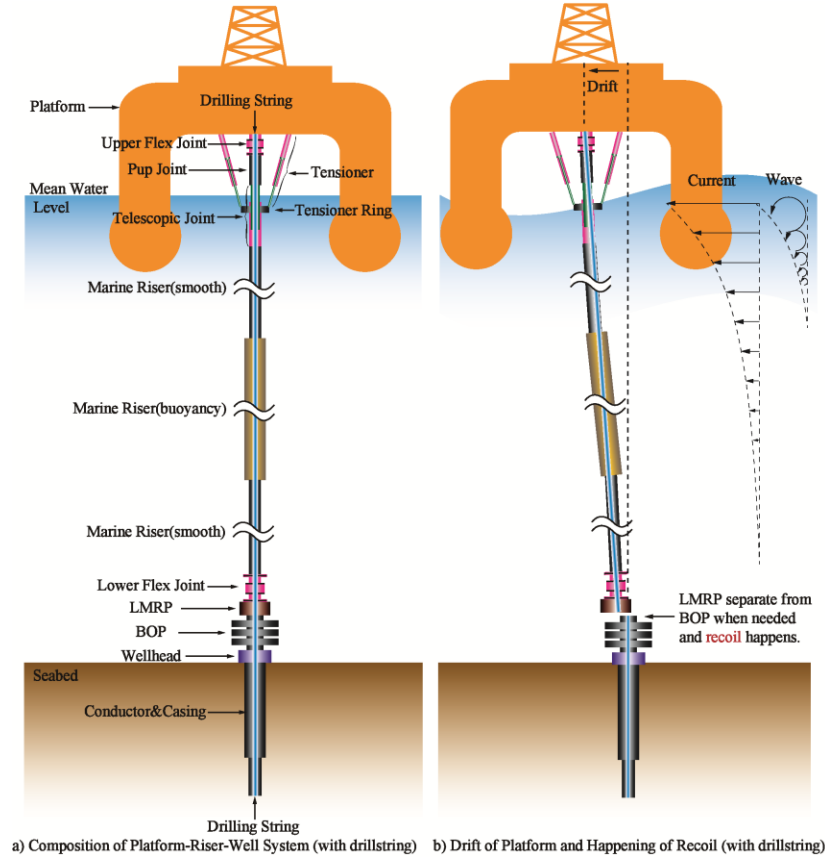


Fig. 1 Plateform-Riser-Well System

Analytical equations of marine riser mechanics are built in differential equation form and intuitive conclusion can be derived with some basic simplification. Then either with series solution method ^[1] employed by Fischer and Ludwig, or with finite difference methods used by Tidwell, Ilfrey ^[2] and Sexton ^[3], or with Runge Kutta integration method applied by Burke ^[4], these equations are solved. Systematic analysis methodology for various issues of marine riser has been summarized in specific books ^[5-6], where ^[5] uses excel files to verify the findings by comparing with the results of different calculation methods and ^[6] focuses on closed form solutions of static and dynamic stable solution mainly by series solution method.

Finite element method has been the major tool for marine riser analysis in the recent decades. In 1973, Gardner and Kitch ^[7] took the small angle, large deflection theory in the finite formulation of riser, then Gnone ^[8] considered the three-dimensional case in 1975, followed by Kirk ^[9] who employed normal mode solution for dynamic response in 1979, and Bernitsas ^[10] presented a large deformation within small strain theory and coupled the torsion and bending in

1985. With the development of nonlinear theory, a number of specific commercial software based on finite element method have developed their methodology respectively on simulating the disconnect and recoil of marine riser. Yong and Hock^[11-13] compared the 3700-ft-water-depth emergency disconnect analysis results of a modified RISTEN program with that of a full-scale test on drillship Discover 534 in 1992; Lang and Real^[14] employed iterative procedures to solve differential equations for tensioner and finite volume equations for mud column respectively in the recoil analysis with software DEEPRISER, and several static and dynamic stages were proposed to get the initial status of the detailed tensioner; Grytøyr and Sharma^[15-16] proposed a disconnection analysis methodology for simulating the CWO riser and drilling riser in software RIFLEX, and more detailed description can be found in the theses of Brynstad^[17] and Grønevik^[18]. Pestana^[19] also introduced a method of recoil simulation in software ORCAFLEX. The marine riser system researches based on finite element software take the advantages of built-in ocean environment loads and riser flexibility, but suffer from simulating moving joints and numerical stiffness caused by realistic tensioner spring coefficients and recoil impulse.

There are only a few applications of multibody dynamics in the marine riser system. In 2003, Raman^[20] used the Kane's formalism to build the marine riser with lumped masses which were connected by extensional and rotational springs, and Runge-Kutta method is chosen to integrate in MATLAB, 3.86 hours were spent for a 500s simulation with 10 lumped masses on a Pentium III PC. In 2015, Lee^[21] employed the discrete Euler-Lagrange equation of rigid multibody dynamics for wireline tensioner simulation with realistic tension spring coefficient, where the tensioner was modeled with 6 rigid bodies and the riser simplified as a mass-spring-damping system. Full-scale model with flexible riser and corresponding efficient numerical scheme for large degrees of freedom haven't been developed for the steady/recoil research of marine riser system.

A methodology for full-scale flexible riser system based on multibody dynamics is presented in this paper, Lagrangian equations together with numerical methods for static, modal and emergency disconnect recoil cases are developed in detail, in which a highly efficient algorithm for drillstring-riser contact is proposed. In the first section, the modeling of marine riser system in flexible multibody dynamics is presented. In the second section, example based on realistic drillship is performed and the numerical results of static, modal and recoil cases are compared with those of finite element commercial software DEEPRISER to verify the correctness and efficiency of the proposed method. In the third section, a detailed auxiliary pipelines model is analyzed and corresponding simplification rule for FEM method is suggested.

2. MODELING OF MARINE RISER SYSTEM IN FLEXIBLE MULTIBODY DYNAMICS

In the flexible multibody model, the pup joints, telescopic joint, marine riser, drillstring and conductor in the soil are discretized with beam elements; other parts are simplified as rigid bodies. The marine beam element for marine riser and drillstring is based on the ordinary beam element, with considering hydrostatic, hydrodynamic and friction loads on the inner and outer surfaces of the riser.

The upper flex joint (UFJ) is simulated by a ball hinge together with a group of torsion springs, and it is the same to the lower flex joint (LFJ). Two cylindrical pairs are set respectively at the upper end of the telescopic cylinder and the lower end of the telescopic rod. A ball hinge connects the tensioner rod and the tensioner ring at an offset from the center line of the

telescopic joint. The lower end of the conductor is constrained to the seabed with a ball hinge. The drillstring is connected to platform with a ball hinge + torsion springs, although there is another tensioner subsystem for drillstring, a simplicity of ball hinge connection is enough for the simulation of contact between drillstring and riser.

The marine riser disconnect is simulated by releasing the time-dependent fixed hinge between LMRP and BOP at a given time, to make the recoil analysis. This model is also applicable for a system with wire line tensioner, with a slight adjustment by removing the tensioner rod and replacing direct-acting tensioner force with wire line tensioner force.

2.1 Lagrange governing equation

Lagrange equations of the first kind is adopted to state the flexible multibody system [29] in this paper, it costs additional number of degrees of freedom for constraint multipliers to avoid degrees merging of linked bodies introduced by the second kind, but it is fortunate that the additional degrees of freedom of constraint multipliers is quiet small compared to those of flexible parts with finite element discrete format (not simplified flexible body with modal method). The system governing equations are

$$\begin{cases} \underbrace{\frac{d}{dt} \left(\frac{\partial L(\mathbf{q}, \dot{\mathbf{q}})}{\partial \dot{\mathbf{q}}} \right) - \frac{\partial L(\mathbf{q}, \dot{\mathbf{q}})}{\partial \mathbf{q}}}_{\mathbf{F}_L} + \mathbf{F}_{ex} + \left(\frac{\partial \Phi}{\partial \mathbf{q}} \right)^T \boldsymbol{\lambda} = \mathbf{0} \\ \Phi(\mathbf{q}) = \mathbf{0} \end{cases} \quad (1)$$

wherein t is the time variable, $\mathbf{q} \in \mathbb{R}^{n_q}$ is the general coordinate of rigid and flexible bodies, $\boldsymbol{\lambda} \in \mathbb{R}^{n_\lambda}$ is the Lagrange multiplier of constraints, $L(\mathbf{q}, \dot{\mathbf{q}}) = T - V$ is the Lagrange function with kinematic energy T and potential energy V , $\Phi(\mathbf{q})$ is the equations for complete constraints of number of degrees n_λ . The potential general force gained from Lagrange function is also noted as \mathbf{F}_L , together with general force of non-potential force $\mathbf{F}_{ex}(\mathbf{q}, \dot{\mathbf{q}}, t)$ and constraint force $\left(\frac{\partial \Phi}{\partial \mathbf{q}} \right)^T \boldsymbol{\lambda}$ to get a zero vector.

The following work to assemble the governing equations of the platform-riser-well system is to give out the detailed expression of \mathbf{F}_L and \mathbf{F}_{ex} for rigid body and marine riser, and constraints Φ between them. Ocean environment loads such as sea current, sea wave, internal load i.e. mud discharge friction force are considered.

2.2 Geometrically exact beam

Geometrically exact beam^[30-31] with rotation vector as attitude parameter is adopted to present the quality and elasticity of marine riser. A total Lagrangian framework is chosen for beam as the marine riser for drilling is normally stiff enough to stay in the linear elastic constitutive model.

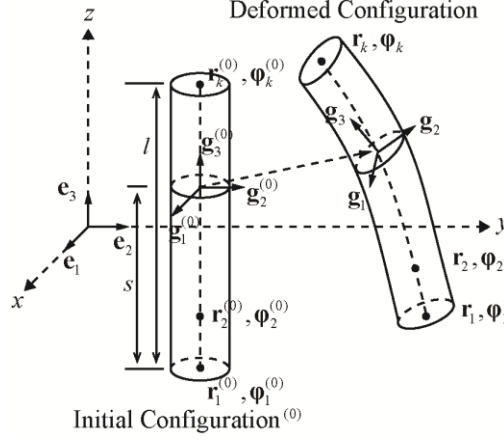


Fig. 2 Initial and Deformed Configuration of Beam

As shown in Fig. 2, if there is k ($2 \sim 5$) nodes in an element, each node takes 6 coordinate $(\mathbf{r}_i, \varphi_i)$ as general coordinate just as that of a rigid body. The shape functions note as $N_i(\xi)$, where $\xi = s/l$ is the normalized length along the beam axis, s is the arc length, l is the element length. Then the position and attitude at ξ is interpolated with

$$\begin{aligned} \mathbf{r}(\xi) &= \sum_{i=1}^k N_i(\xi) \mathbf{r}_i \\ \varphi(\xi) &= \sum_{i=1}^k N_i(\xi) \varphi_i \end{aligned} \quad (2)$$

2.3 Current & wave & mud discharging

Morison empirical formula is adopted to simulate the force of wave and current ^[15-16]

$$F_{morison} = \rho \pi \frac{D^2}{4} C_m a + \frac{\rho}{2} C_d D |u| u \quad (3)$$

Wherein u is the quantity of relative velocity \mathbf{u} , ρ is the density of sea water, D is the outer diameter of riser, C_m is the coefficient of added mass, C_d is the coefficient of drag, u is the transverse component of relative speed of the sea water to marine riser. The speed vector of sea wave can be calculated with stokes formula or any other wave model.

One-dimensional fluid Euler equation [17] and finite volume method is adopted to form the friction force of discharging mud [18]. After the linear density of friction F_{fric} is calculated, the general force of mud friction is

$$\mathbf{F}_{in}^{fric} = \int_0^l F_{fric} [(\dot{\mathbf{x}} \cdot \mathbf{G}_3) \mathbf{G}_3]^T \frac{\partial \mathbf{x}}{\partial \mathbf{q}} dl \quad (4)$$

In addition, hydrostatic pressure should be applied at the section where the interfaces of riser joints have different inside or outside diameter; hydrostatic pressure should be applied to the bottom of LMRP when the rise is cut off under the LMRP to disconnected from the wellhead and the pressured area should the sum of last riser joint's section and those of auxiliary pipelines.

3. NUMERICAL RESULTS

A platform-riser-well model base on a real system is built in both DEEPRISER (a specialized commercial software for marine riser related problems) and homemade codes with the same physical parameters which are shown in Tab. 1 .

Tab. 1 Parameters of Platform-Riser-Well System

<p>Platform</p> <p>1565.2m</p> <p>1564.67m</p> <p>1543.78m</p> <p>1519.4m</p> <p>1463.01m</p> <p>908.27m</p> <p>16.73m</p> <p>16.13m</p> <p>10.79m</p> <p>1m</p> <p>seabed 0m</p> <p>-70m</p> <p>UFJ</p> <p>Pup joints</p> <p>Telescopic joint</p> <p>Riser 1 (smooth)</p> <p>Riser 2 (buoyance)</p> <p>Riser 3 (smooth)</p> <p>LFJ</p> <p>LMRP</p> <p>BOP</p> <p>wellhead</p> <p>conductor</p>	Name		Value						
	Riser/Conductor material		steel						
	Riser element length		3m						
	Riser 1	Outside diameter	533.4mm						
		Inside diameter	508.0mm						
		Length of a joint	22.86m						
		Weight in air (a joint)	15331kg						
		Weight in water(a joint)	13335kg						
	Riser 2	Outside diameter of buoyance	1371.6mm						
		Outside diameter	533.4mm						
		Inside diameter	511.2mm						
		Length of a joint	22.86m						
		Weight in air(a joint)	14605kg						
		Weight in water(a joint)	12700kg						
		Buoyance weight in air(a joint)	9661 kg						
Buoyance Weight in water(a joint)	-11022 kg								
Riser 3	Outside diameter	533.4mm							
	Inside diameter	514.4mm							
	Length of a joint	22.86m							
	Weight in air (a joint)	13698kg							
	Weight in water(a joint)	11929kg							
LMRP	Weight in air	148846kg							
	Weight in water	129496kg							
Auxiliary pipeline	<i>Serial number</i>	<i>1</i>	<i>2</i>	<i>3</i>	<i>4</i>	<i>5</i>	<i>6</i>		
	OD(mm)	152.4	152.4	127	63.5	63.5	66.7		
	ID(mm)	101.6	101.6	101.6	50.8	50.8	50.8		

3.1 Equilibrium, Vibration and Recoil Results

The comparison of equilibrium configuration results is shown in Fig. 3, horizontal displacement of riser under different drift off values of platform are compared.

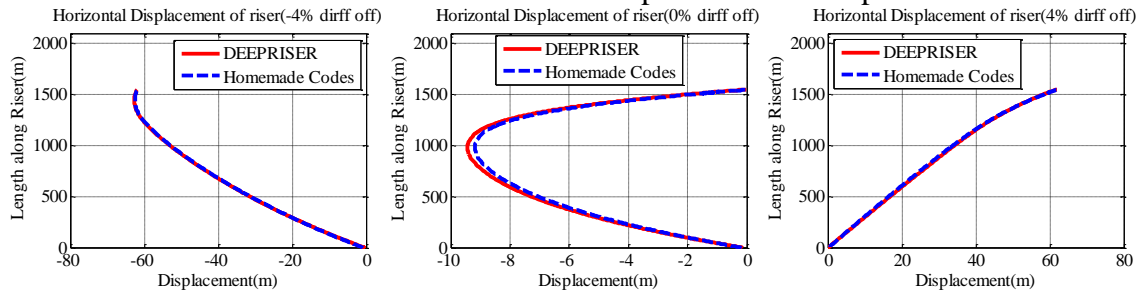


Fig. 3 Equilibrium Results of -4%,0%,4% Drift Off (current, top tension 5800kN)

The comparison of vibration results around equilibrium configuration is shown in Fig. 4, the vibration is calculated under 0% drift off of platform with once a year current. Natural frequency and vibration mode near the equilibrium configuration are compared. The top tension is set as 5800kN.

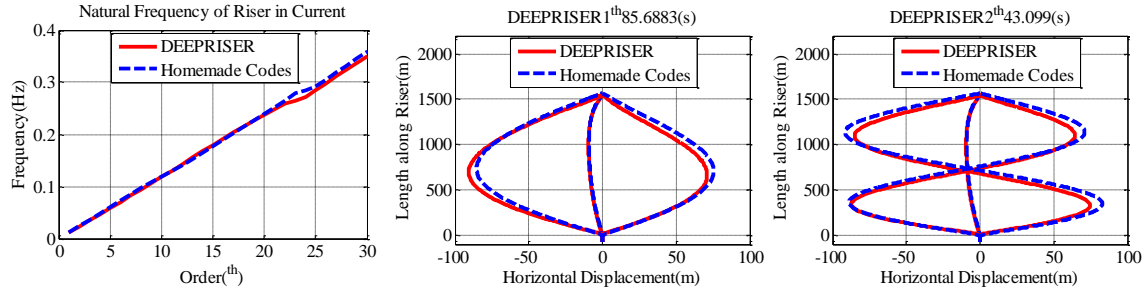


Fig. 4 Vibration Results Under 0% Drift Off (current, top tension 5800kN)

The comparison of recoil results is shown in Fig. 5, the LMRP is cut off at 46th second, numerical results of 4 mainly engineering criteria are compared, including telescopic joint stroke, tensioner ring tension, elevation of LMRP, and envelope of effective tension of riser.

As shown in Tab. 2, a minimum coincidence degree of 93.4% is gained between DEEPRISER and the homemade codes with presented flexible multibody dynamic method. The results of DEEPRISER are set as reference values for the calculation of coincidence degrees, and the coincidence of recoil is the minimum of coincidence degrees of the four criteria.

Consider the method difference between DEEPRISER and homemade codes, the results of homemade codes are verified to be correct for equilibrium configuration calculation, vibration calculation and dynamic response of recoil calculation.

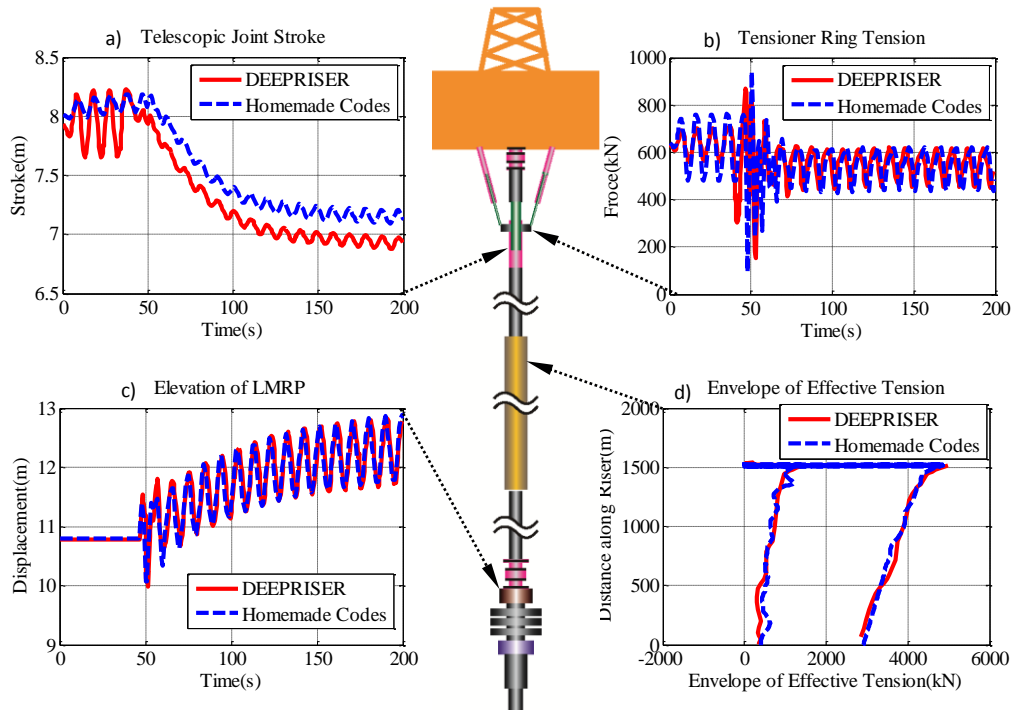


Fig. 5 Recoil results of dynamic response (wave, current, 0% drift off, top tension 3500kN)

Tab. 2 Coincidence between DEEPRISER and The Homemade Codes

<i>Case</i>	<i>Equilibrium</i>			<i>Vibration</i>	<i>Recoil</i>
Items	-4% drift off	4% drift off	0% drift off	frequency	
Coincidence	98.2%	95.8%	93.4%	95.1%	93.5%

3.2 Efficiency of flexible multibody method

The recoil model is calculated by DEEPRISER and the homemade codes on the same computer with configuration, although parallel computing is available for the homemade codes, single core mode is set for the homemade codes to keep the same with DEEPRISER in the efficiency comparison of recoil simulation. As shown in Tab. 3, the homemade codes gained a X3.2 speed up compared to DEEPRISER, mainly because the step sizes in multibody dynamics are much bigger than those of DEEPRISER as shown in Fig. 6. The multibody dynamics adopts smart variable step-size implicit integration algorithm of BDF, however DEEPRISER uses constant-step-size explicit algorithm in recoil simulation so far.

Tab. 3 CPU Time for Recoil Calculation (single core)

<i>Software</i>	<i>CPU time</i>
DEEPRISER	12min
Homemade Codes	3.7 min
Speed up	3.2

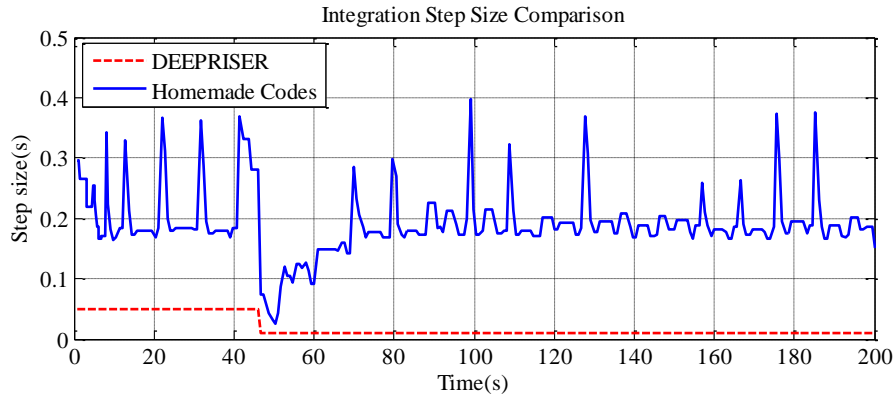


Fig. 6 Integration Step Size Comparison

4. Detailed auxiliary pipeline model

In the modeling of the marine riser in many FEM commercial software simulating marine riser system, including DEEPRISER, the auxiliary pipelines are considered by added mass which is uniformly applied to the riser and the stiffness of auxiliary pipelines is ignored. As shown in Fig. 7 a), only the mass contribution of auxiliary pipelines is considered. However, in flexible multibody dynamics, it is very easy to connect flexible parts, rigid parts with constraints and the method can allow many constraints in the system and encounter no problem in numerical

calculation. So as shown in Fig. 7 b), a detailed auxiliary pipeline model is considered and calculated with flexible multibody dynamics. Each pipeline is simulated with a beam and they are connected to the riser at every joint end by fixed constraints. For 6 auxiliary pipelines in the model, there are more than 300 fixed constraints in the detailed auxiliary model and the number of degrees of freedom is multiplied by more than 7 times. To make a complete comparison, a model considering both added mass and added stiffness of auxiliary pipelines is also built and calculated.

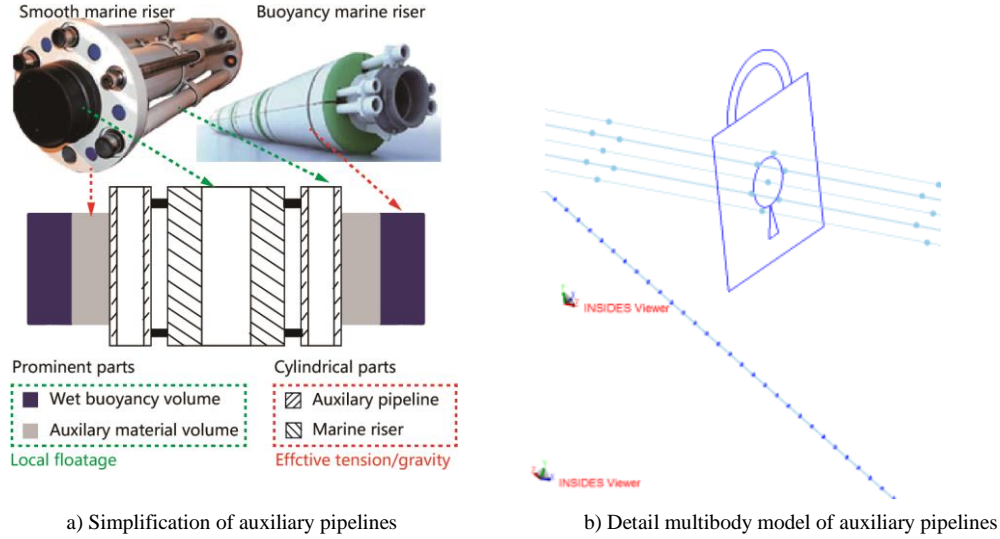


Fig. 7 Detailed Flexible Multibody Model

The calculated results are shown in Fig. 8~Fig. 9 for static equilibrium, vibration modes and recoil dynamics. The results are summarized in Tab. 4, it shows for static calculation, the added mass model of auxiliary pipelines is only suitable for static and modal calculation, but not for the recoil dynamic calculation, where the dangerous case of riser may be mistakenly seen as safe case. But the simplified model considering both added mass and added stiffness is suitable for recoil dynamic calculation which is almost the same as the detailed auxiliary model.

Tab. 4 Results Summary of Detailed Auxiliary Model

<i>Analysis Type</i>	<i>Detailed Model</i>	<i>Multibody</i>	<i>Single Beam (Associate Mass)</i>	<i>Single Beam (Associate Mass & Stiffness)</i>
Static	Ref.	✓	✓	✓
Modal	Ref.	✓	✗	✗
Recoil	Ref.	✗	✗	✓

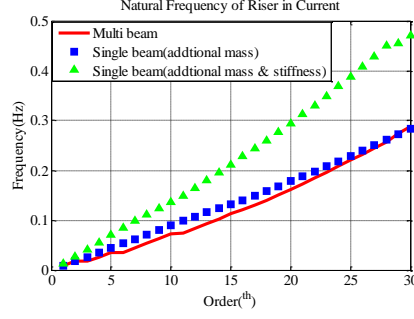


Fig. 8 Vibration Results Under 0% Drift Off (current, top tension 5800kN)

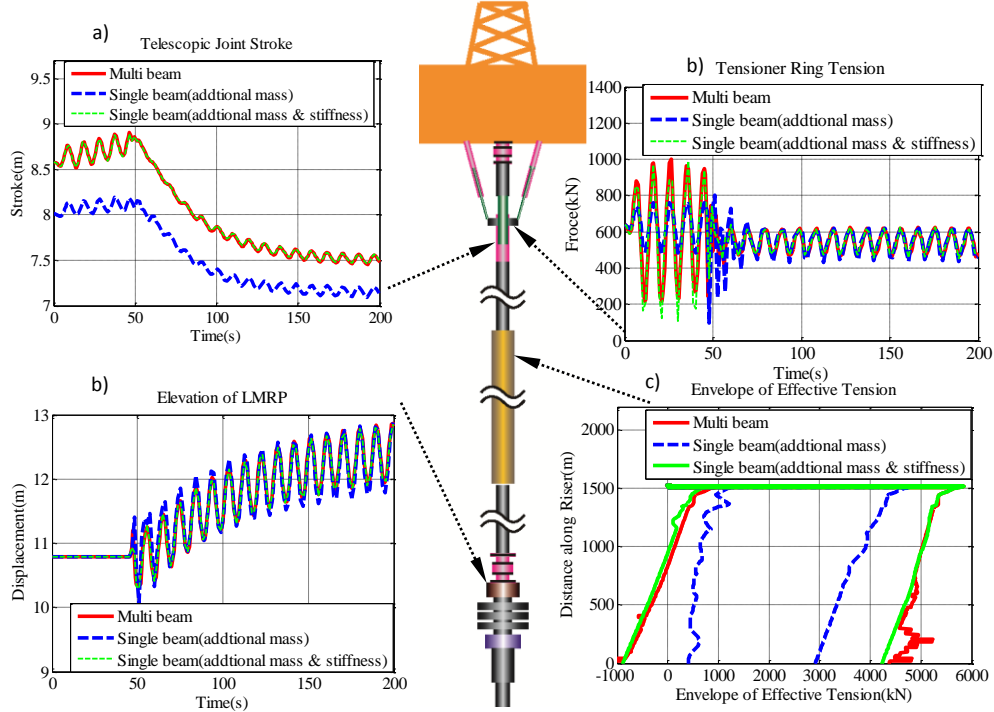


Fig. 9 Recoil Results of Dynamic Response (wave, current, 0% drift off, top tension 3500kN)

5. CONCLUSIONS

This article models the marine riser system in flexible multibody dynamics considering static, modal and recoil cases in full-scale. Lagrangian equations of first class and geometrically exact beam are adopted to present the riser system. Buoyance, wave, current and mud discharge are included in the numerical calculations. Basic examples coincide with DEEPRISER, a commercial marine riser software with FEM method, and gains 3 times speedup. Detailed auxiliary pipelines model is built in flexible multibody dynamics and the results show that the simplified model considering auxiliary pipelines as associate mass may lead to wrong estimation of safety in the recoil simulation. It suggests the associated stiffness should also be included if simplify the auxiliary pipeline in recoil case, but the static and modal cases could ignored it.

ACKNOWLEDGEMENT

The research is supported by NSFC (11772170, 11372154) and National Basic Research Program of China (2015CB251203) which is gratefully acknowledged by the authors.

REFERENCES

- [1] Fischer W, Ludwig M. Design of Floating Vessel Drilling Riser[J]. Journal of Petroleum Technology, 1966, 18(3):272-280.
- [2] Tidwell D R, Ilfrey W T. Developments in marine drilling riser technology[C]//MECHANICAL ENGINEERING. 345 E 47TH ST, NEW YORK, NY 10017: ASME-AMER SOC MECHANICAL ENG, 1969, 91(11): 62.
- [3] Sexton R M, Agbezuge L K. Random wave and vessel motion effects on drilling riser dynamics[C]//Offshore technology conference. Offshore Technology Conference, 1976.
- [4] Burke B G. An analysis of marine risers for deep water[J]. Journal of petroleum technology, 1974, 26(04): 455-465.
- [5] Sparks C P. Fundamentals of marine riser mechanics: basic principles and simplified analyses[M]. PennWell Books, 2007.
- [6] Dareing D W. Mechanics of Drillstrings and Marine Risers [M]. ASME Press, 2012.
- [7] Gardner T N, Kotch M A. Dynamic analysis of risers and caissons by the element method[C]//Offshore Technology Conference. Offshore Technology Conference, 1976.
- [8] Gnone E, Signorelli P, Giuliano V. Three-dimensional static and dynamic analysis of deep-water sealines and risers[C]//Offshore Technology Conference. Offshore Technology Conference, 1975.
- [9] Kirk C L, Etok E U, Cooper M T. Dynamic and static analysis of a marine riser[J]. Applied Ocean Research, 1979, 1(3): 125-135.
- [10] [Bernitsas M M, Kokarakis J E, Imron A. Large deformation three-dimensional static analysis of deep water marine risers[J]. Applied ocean research, 1985, 7(4): 178-187.
- [11] Young R D, Hock C J, Karlsen G, et al. Analysis and design of anti-recoil system for emergency disconnect of a deepwater riser: case study[C]//Offshore Technology Conference. Offshore Technology Conference, 1992.
- [12] Young R D, Hock C J, Karlsen G, et al. Comparison of analysis and full-scale testing of anti-recoil system for emergency disconnect of deepwater riser[C]//Offshore Technology Conference. Offshore Technology Conference, 1992.
- [13] [Hock C J, Young R D. A deepwater riser emergency disconnect antirecoil system[J]. Journal of Petroleum Technology, 1993, 45(08): 744-751.
- [14] Lang D W, Real J, Lane M. Recent developments in drilling riser disconnect and recoil analysis for deepwater applications[C]//Proceedings of the ASME 2009 28th International Conference on Ocean, Offshore and Arctic Engineering, Honolulu, HI, June, OMAE2009-79427. 2009.
- [15] Grytøyr G. Improving operating window for disconnect operations of CWO risers[J]. OMAE2010-20976, 2010.
- [16] Grytøyr G, Sharma P, Vishnubotla S. Marine drilling riser disconnect and recoil analysis[C]//Proceedings of the AADE National Technical Conference and Exhibition. 2011.
- [17] Brynstad B I. DISCONNECTION OF WORKOVER RISERS ON VERY DEEP WATER[D]. Norwegian University of Science and Technology, 2012.

- [18] Grønevik A. Simulation of drilling riser disconnection-Recoil analysis[D]. Norwegian University of Science and Technology, 2013.
- [19] Pestana R G, Roveri F E, Franciss R, et al. Marine riser emergency disconnection analysis using scalar elements for tensioner modelling[J]. *Applied Ocean Research*, 2016, 59: 83-92.
- [20] Raman-Nair W, Baddour R E. Three-dimensional dynamics of a flexible marine riser undergoing large elastic deformations[J]. *Multibody System Dynamics*, 2003, 10(4): 393-423.
- [21] Lee H, Roh M I, Ham S H, et al. Dynamic simulation of the wireline riser tensioner system for a mobile offshore drilling unit based on multibody system dynamics[J]. *Ocean Engineering*, 2015, 106: 485-495.
- [22] Bueno R C S, Morooka C K. Analysis method for contact forces between drillstring-well-riser[C]//International Petroleum Conference and Exhibition of Mexico. Society of Petroleum Engineers, 1994.
- [23] Han C, Yan T, Tong Y. The analysis on coupling vibration of drill string and marine riser in deep-water drilling[J]. *The International Journal of Multiphysics*, 2016, 7(1).
- [24] Hao L P, Dung T Q. Applying the contact element for simulation of interaction between drillstring and holewall [J]. *Vietnam Journal of Mechanics*, 2003, 25(2): 97-112.
- [25] Pogorelov D, Mikheev G, Lysikov N, et al. A multibody system approach to drill string dynamics modeling[C]//2012 Proceedings of the ASME 11th Biennial Conference on Engineering Systems Design and Analysis (ESDA2012). 2012, 4: 53-62.
- [26] Cheng Z B, Jiang W, Ren G X, et al. A multibody dynamical model for full hole drillstring dynamics[C]//Applied Mechanics and Materials. Trans Tech Publications, 2013, 378: 91-96.
- [27] Wang N, Cheng Z, Lu Y, et al. A multibody dynamics model of contact between the drillstring and the wellbore and the rock penetration process[J]. *Advances in Mechanical Engineering*, 2015, 7(5): 1687814015582117.
- [28] Arbatani S, Callejo A, Kövecses J, et al. An approach to directional drilling simulation: finite element and finite segment methods with contact[J]. *Computational Mechanics*, 2016, 57(6): 1001-1015.
- [29] Shabana A A. Dynamics of multibody systems[M]. Cambridge university press, 2013.
- [30] Simo J C, Vu-Quoc L. A three-dimensional finite-strain rod model. Part II: Computational aspects[J]. *Computer methods in applied mechanics and engineering*, 1986, 58(1): 79-116.
- [31] Simo J C, Vu-Quoc L. On the dynamics in space of rods undergoing large motions—a geometrically exact approach[J]. *Computer methods in applied mechanics and engineering*, 1988, 66(2): 125-161.

The Multi-scale Modeling for Progressive Failure Analysis of Woven Composite Using Domain Superposition Technique

Guangmeng Yang*, Meiying Zhao**

*Northwestern Polytechnical University, Xi'an, PR of China, **Northwestern Polytechnical University, Xi'an, PR of China

ABSTRACT

A robust multi-scale computational strategy allowing reliable prediction of the progressive failure behaviors is developed for woven composite, which can deal with the mesh generation for arbitrary architecture. In micro-scale modeling, the statistical representative volume element (SRVE) under periodic boundary condition (PBC) is setup to approximate the microstructure of the composite using initially periodic shaking method. For the matrix, the elastic-plastic model taking into account hydrostatic stresses is introduced, as well as ductile damage criteria. Cohesive zone model based on the power law is used to simulate the fiber/matrix debonding whose parameters are explored in details. In the meso-scale approach, the Hashin criteria is formed for yarn to predict the damage initiation in progressive damage model, with Von Mises criteria being considered for matrix since the main failure mechanism is dominated by the fracture in yarns [1]. In order to overcome the difficulty in mesh partition due to the complex internal architecture and geometric degeneracies, the domain superposition technique (DST) is proposed to realize fast modeling in FEA. The model adopts the global domain geometry superimposed with the reinforcement phase material domain geometries, therefore, facilitating the generation of hexahedral elements, which is also easy to apply PBC. Using the DST model, the reinforcement FE meshes are couple into global mesh by nodal degree of freedom coupling technique. Accordingly, the material models of reinforcement phase are adjusted to ensure the accurate representation of the actual composites system. The above multi-scale progressive damage model is incorporated into a finite element code ABAQUS, via a user-defined material subroutine. The comparison between the numerical results and experimental data taken from Naik [2] are carried out in terms of stress-strain curves and failure strength. The predictions are in good agreement with the experimental results. The damage process indicates that the warp longitudinal failure occurs first, followed by the fill transverse failure. All these failure modes are accompanied by the failure of matrix until the final fracture caused by the longitudinal failure. The multi-scale modeling approach opens a path to provide accurate prediction in fast parametric modeling. [1] Yuan Zhou et al, Progressive damage analysis and strength prediction of 2D plain weave composites, 47(2013) 220-229 [2] N. K. Naik, V. K. Ganesh. Failure behavior of plain weave fabric laminates under on-axis uniaxial tensile loading:II—analytical predictions, 30 (1992) 1779-1822

Nolinear Simulation of Capsule Tent on Material Properties and Structural Features to Guide Membrane Design

Hong Yang^{*}, Zhibing He^{**}, Baibin Jiang^{***}, Zhenyuan Xu^{****}, Shasha Gao^{*****}, Guanghui Yuan^{*****}, Jun Xie^{*****}, Sheng Wei^{*****}, Wei Ren^{*****}, Juxi Liang^{*****}, Qiang Yin^{*****}

^{*}Research Center of Laser Fusion, China Academy of Engineering Physics, ^{**}Research Center of Laser Fusion, China Academy of Engineering Physics, ^{***}Research Center of Laser Fusion, China Academy of Engineering Physics, ^{****}Research Center of Laser Fusion, China Academy of Engineering Physics, ^{*****}Research Center of Laser Fusion, China Academy of Engineering Physics, ^{*****}Research Center of Laser Fusion, China Academy of Engineering Physics, ^{*****}Research Center of Laser Fusion, China Academy of Engineering Physics, ^{*****}Research Center of Laser Fusion, China Academy of Engineering Physics, ^{*****}Research Center of Laser Fusion, China Academy of Engineering Physics, ^{*****}Research Center of Laser Fusion, China Academy of Engineering Physics, ^{*****}Research Center of Laser Fusion, China Academy of Engineering Physics, ^{*****}Research Center of Laser Fusion, China Academy of Engineering Physics, ^{*****}Research Center of Laser Fusion, China Academy of Engineering Physics, ^{*****}Research Center of Laser Fusion, China Academy of Engineering Physics

ABSTRACT

Retaining a sphere with two closed membranes like a tent is a classical and reliable method of holding a capsule in the hohlraum center, which is widely researched as a concept of inertial confinement fusion (ICF). The capsule and hohlraum are only several millimeters in diameter. Physical experiments have demonstrated adverse influence on capsule implosion stability by applying retaining membranes with 100 nanometers in thickness. Much thinner retaining membrane is imperative in future ICF targets. However, a free-standing membrane with dozens of nanometers in thickness is suspect on target fabrication feasibility. The primary issue focuses on material failure of the upper and lower membranes when they close capsule during an assembling procedure. Since the hollow capsule and its retaining membranes are always made from polymer, gravity influence can be neglected. The main causes on material failure due to large deformation when membranes are adapted to capsule profile. After assembling, an ICF target containing capsule tent will be transported and loaded into laser drive. Uncertain impacts may cause capsule misregistration and even membrane rupture before target shot. Physical experiments and capsule fuel characterization have rigorous requirements on the misalignment between capsule and hohlraum center. To guide the ultrathin capsule tent design in ICF target engineering, a bilinear isotropic hardening model is introduced to calculate static and dynamic mechanical responses of membranes in specified geometry parameters. Mechanical properties including elastic modulus, yield strength and tangential modulus are researched in a wide range and concluded regularity on the capsule tent performance. Besides, membrane structural features such as equilibrium holes and defects are modeled and analyzed based on several design types and material conditions.

Strain Analysis Damage Identification Method for Crane Girder Based on Peridynamics

Huichao Yang^{*}, Feiyun Xu^{**}, Bowei Li^{***}

^{*}School of Mechanical Engineering, Southeast University, ^{**}School of Mechanical Engineering, Southeast University, ^{***}School of Mechanical Engineering, Southeast University

ABSTRACT

Peridynamics is a new numerical calculation theory of mechanics, and is widely used in studies of discontinuous mechanical problems, damage simulation and identification and other complex mechanical behaviors. Because of working impact loads, the crane girder is often damaged in the forms of crack initiation and growth. Considering of the advantages of peridynamics, a numerical calculation of strain signals based on peridynamics of the crane girder being subject to working impact loads was studied. In this study, the mathematical model of the crane girder was established, and the strain signals of checkpoints were simulated. By analysis these strain signals, the characteristics of the strain signals was got, the damage mechanism of the crane girder was researched. Firstly, the mathematical model of the crane girder was established based on peridynamics and the working impact load was simulated as weigh emergency braking. Secondly, some checkpoints were arranged in different locations on the crane girder according to sensor optimization theory, and the strain signals of these checkpoints were acquired. Then, the characteristics of the strain signals were obtained through time-frequency analysis, and the relationship of between strain signal and damage degree was interpreted, then the damage mechanism of the crane girder was got. Finally, the application of this method was implemented by some experiments, and the results demonstrated that this method can effectively identify the damage of the crane girder.

A Taylor-based Meshless Method for Non-linear PDEs

Jie Yang^{*}, Michel Potier-Ferry^{**}, Heng Hu^{***}, Yao Koutsawa^{****}, Qian Shao^{*****}

^{*}Université de Lorraine, ^{**}Université de Lorraine, ^{***}Wuhan University, ^{****}Luxembourg Institute of Sciences and Technology, ^{*****}Wuhan University

ABSTRACT

In this talk, Taylor series are applied to the spatial discretization of partial differential equations, a topic on which there are very few papers in the literature. As in Trefftz methods, one uses a complete family of quasi-exact solutions of the PDE in each subdomain, which permits to discretize only the boundary and the interfaces. Here the most original point is the algorithm to build these quasi-exact polynomial solutions, by vanishing the Taylor series of the residual. The latter procedure can be applied to generic partial differential systems, possibly by means of algorithmic differentiation, which has been achieved for non-linear Poisson equations (Yang et al, J. Comp. Physics 2017), hyperelasticity or Navier-Stokes equation, including when fluid flows are coupled with double diffusion or heat propagation. Within Trefftz methods, various techniques are available to connect several analytical solutions in various subdomains. Here a meshless integrationless procedure based on least-square collocation is used. This full procedure, called Taylor meshless method (TMM), proves to be robust and efficient. It converges with the degree of the polynomials (p-convergence) and/or with the number of subdomains (h-convergence). As often with Trefftz methods, the main difficulty is the loss of accuracy due to matrix ill-conditioning, but according to a number of numerical tests, the method was able to provide highly accurate solutions (up to 10^{-10}), with a rather large degree (up to $p=15-20$), with a strong reduction of the number of unknowns as compared with classical methods (typically a ratio of 20-50 with respect to FEM) and for large scale problems (the equivalent FEM mesh involving millions of unknowns), see Yang et al, Int. J. Num. Eng. 2017. This talk will focus on applications in fluid mechanics.

Two-Mass Vehicle Model for Extracting Bridge Frequencies

Judy Yang^{*}, Bo-How Chen^{**}

^{*}National Chiao Tung University, ^{**}National Chiao Tung University

ABSTRACT

In the past decade, the dynamic response of a passing vehicle has been utilized to extract the frequencies of the supporting bridge. Particularly, the test vehicle was modeled as a single-degree-of-freedom sprung mass moving over a simple beam in most previous studies, which suffers from the drawback that the sprung mass may be affected by the vehicle motion. As such, the present work presents a two-mass vehicle model for extracting the bridge frequencies, which contains a sprung mass (vehicle body) and an unsprung mass (axle mass). By using the response of the unsprung mass, the bridge response can be extracted more realistically. The main results of the present work are listed as follows: (1) with the aid of unsprung mass in the vehicle model, the dynamic responses of both the vehicle and bridge can be faithfully revealed, (2) increasing the unsprung mass can effectively help the extraction of bridge frequencies, including the second frequency, (3) the proposed model can identify the bridge frequencies even under high levels of road roughness, while the traditional single-mass model cannot, and (4) the proposed model can identify the bridge frequencies under high levels of road roughness without additional techniques of processing in the presence of vehicle damping.

Edge Orientations of Mechanically Exfoliated Anisotropic Two-dimensional Materials

Juntan Yang^{*}, Haimin Yao^{**}

^{*}The Hong Kong Polytechnic University, ^{**}The Hong Kong Polytechnic University

ABSTRACT

Mechanical exfoliation is an approach widely applied to prepare high-quality two-dimensional (2D) materials for investigating their intrinsic physical properties. During mechanical exfoliation, in-plane cleavage results in new edges whose orientations play an important role in determining the properties of the as-exfoliated 2D materials especially those with high anisotropy. Here, we systematically investigate the factors affecting the edge orientation of 2D materials obtained by mechanical exfoliation. Our theoretical study manifests that the fractured direction during mechanical exfoliation is determined synergistically by the tearing direction and material anisotropy of fracture energy. For a specific 2D material, our theory enables us to predict the possible edge orientations of the exfoliated flakes as well as their occurring probabilities. The theoretical prediction is experimentally verified by examining the inter-edge angles of the exfoliated flakes of four typical 2D materials including graphene, MoS₂, PtS₂, and black phosphorus. This work not only sheds light on the mechanics of exfoliation of the 2D materials but also provides a new approach to deriving information of edge orientations of mechanically exfoliated 2D materials by data mining of their macroscopic geometric features.

A Novel Self-locked Tube System for Energy Absorption

Kuijian Yang^{*}, Chuan Qiao^{**}, Yuli Chen^{***}

^{*}Institute of Solid Mechanics, Beihang University, ^{**}Department of Mechanical Engineering, McGill University,
^{***}Institute of Solid Mechanics, Beihang University

ABSTRACT

Thin-walled round tubes are widely used in impact protection due to its low cost and high energy absorption. However, round tube system requires internal connections and boundary constraints to suppress the lateral splashing of tubes. Complicated constraints can increase installation time and thus make round tube system unsuitable for emergent protection. To break this limitation, a novel self-locked tube system is proposed [1]. The proposed system is composed of dumbbell-shaped self-locked tubes. When subjected to lateral impact, the dumbbell-shaped tubes can mesh with each other and thus provide lateral constraints to prevent lateral splashing. Therefore, the self-locked system can work immediately after the tubes are put together, with no need of any internal connections or boundary constraints. The self-locking effect of the proposed system is validated by impact experiments and finite element method (FEM) simulations. A plastic hinge model is developed to estimate the energy absorbing properties of the single self-lock tube [2], which is validated by both FEM simulation and experiments. Based on the theoretical analysis, the effects of geometry of the tube on energy absorption are studied and the optimal geometry design of the tube is discussed. Besides, the stacking arrangement of the multiple-tube system is investigated by FEM simulations, and a general guideline on the structural design of proposed multiple-tube system is provided. Furthermore, an internally nested self-locked tube system is proposed to improve the energy absorption capacity [3]. The basic unit is a dumbbell-shaped tube nested by round tubes inside, and is investigated by plastic hinge model, experiment and FEM simulation. The geometric parameters of inner tubes are investigated, and suggestions on designing an internally nested self-locked tube system are provided. References: [1] Chen Y., Qiao C., Qiu X., Zhao S., Zhen C., Liu B., A novel self-locked energy absorbing system, *Journal of the Mechanics & Physics of Solids*, 87 (2016) 130-149. [2] Qiao C., Chen Y., Wang S., Yang K., Qiu X., Theoretical analysis on the collapse of dumbbell-shaped tubes, *International Journal of Mechanical Sciences*, 123 (2017) 20-33. [3] Yang K., Chen Y., Liu S., Qiao C., Yang J., Internally nested self-locked tube system for energy absorption, *Thin-Walled Structures*, 119 (2017).

Finite Element Simulation of Metallic Sandwich Plates with Graded Lattice Cores Subjected to Blast Loading

Lihong Yang^{*}, Guocai Yu^{**}, Jia Qu^{***}, Linzhi Wu^{****}, Xiao Han^{*****}

^{*}Key Laboratory of Advanced Ship Materials and Mechanics, College of Aerospace and Civil Engineering, Harbin Engineering University, 150001, Harbin, China, ^{**}Key Laboratory of Advanced Ship Materials and Mechanics, College of Aerospace and Civil Engineering, Harbin Engineering University, 150001, Harbin, China, ^{***}Key Laboratory of Advanced Ship Materials and Mechanics, College of Aerospace and Civil Engineering, Harbin Engineering University, 150001, Harbin, China, ^{****}Key Laboratory of Advanced Ship Materials and Mechanics, College of Aerospace and Civil Engineering, Harbin Engineering University, 150001, Harbin, China, ^{*****}Key Laboratory of Advanced Ship Materials and Mechanics, College of Aerospace and Civil Engineering, Harbin Engineering University, 150001, Harbin, China

ABSTRACT

Sandwich plates with cellular cores have been increasingly exploited as explosion protection structures [1]. Among a number of cellular cores, lattice truss core structure has been identified as one of the most promising candidates for ultra-lightweight core constructions due to its open topological configuration and more controllable optimization design process [2]. To further enhance the blast resistance of sandwich structures, graded lattice truss cores, where the relative density of cores itself vary layer-by-layer, can be utilized in sandwich structures. Due to the superior core compression and the wave dissipation characteristics of the graded core layers, the energy absorption capability of core layers and the blast resistance of the sandwich structure can be improved. In this research, 3D finite element simulations of metallic sandwich plates with graded lattice truss cores under blast loading have been carried out using the ABAQUS/Explicit software. The applied impulsive pressure distribution on the surface of the plates was calculated using the CONWEP code. The relative density of core layer was regulated to vary with sectional dimension of core truss members. The panels were made of stainless steel AL6XN which was assumed to follow bilinear strain hardening and strain rate-dependence. It is observed that the blast resistance capability of sandwich plates was sensitive to graded arrangement of the core relative density. The graded sandwich plates would exhibit a better blast resistance than the ungraded ones. Keywords: graded lattice cores; sandwich plates; finite element simulation; blast resistance

Investigation on Mechanical Properties and Memory Shape Effect of CNT-Reinforced SMP by Using MD Simulation

Qing-Sheng Yang*, Xue-Jiao Zhang**, Xia Liu***

*Beijing University of Technology, **Beijing University of Technology, ***Beijing University of Technology

ABSTRACT

Shape memory polymers (SMPs) are promising smart materials that can recover their original shape upon exposure to external stimuli from temporary shape. It offers wide potential applications due to unique shape-changing functionality. However, SMPs with high mechanical strength are increasingly needed. The reinforcement mechanism of nano inclusions on the mechanical properties of nanocomposites is still a controversial issue. In this work, physical and mechanical properties of polyethylene (PE) polymer nanocomposites infusing different content of single-walled-carbon-nanotube (SWNT) were investigated by molecular dynamics (MD) simulations. The effect of nano inclusions on primitive chain network of PE matrices was also considered. It is found that mean squared displacement of the PE matrix infused with SWNT junction is smaller than that of pure PE. However, these nano inclusions did not significantly alter the underlying mesh of primitive chain network of PE matrices. The change of mechanical properties associated with these nano inclusions should be directly attributed to the interaction between polymer matrices and nano inclusions. For this purpose, we carried out the analysis on the thermodynamic cycle of the shape memory polymer at different tensile strain, and obtained the effect of the various content of SWNT on the mechanical properties of the SCNT/PE composites. The effect of nanofiller dispersion on the glass transition temperature of the nanocomposites was studied. The stress-strain relationship under uniaxial tension at different temperatures were obtained, which demonstrates the mechanical properties at different phases. These results illustrate the mechanism of shape memory effect and recovery in amorphous polymers.

Structural Analyses with Explicit Considerations of Microscopic Damage Evolution for Virtual Testing of Composites

Qingda Yang*

*The University of Miami

ABSTRACT

The rapid advances in novel computational mechanics theories, computing power, coupled with ultra-high resolution experimental characterization for interior progressive damage processes in structural materials, are enabling a new paradigm for rapid invention of new structural materials with novel microstructures for multifunctional applications. This method advocates a comprehensive multi-scale approach that utilizes a system of hierarchical models, engineering tests, and specialized laboratory experiments. To achieve practical applications of such methods in routine engineering design processes, these methods have to demonstrate that they can faithfully assess the safety and durability of a structure that is subjected to the intended loading environment during its entire lifespan. However, it is inevitable that the majority of engineering materials exhibit progressive damage evolution during their lifetime. In a typical composite structure, the progressive damage evolution process involves the initiation of numerous discrete, small cracks at locations that cannot be predetermined, their coupled evolution with local delamination to form one or several major cracks of structural criticality, which lead to the catastrophic structural failure. It is thus critical to be able to explicitly account for the progressive evolution of all major types of discrete damage events with high fidelity in a structural model. In this paper, we extend a recently developed method named augmented finite element method (A-FEM), which can account for arbitrary multiple cracking events in composites with orders of magnitude improve in numerical efficiency and accuracy, to explicitly include damage accumulation descriptions of various damage modes in composites (i.e., matrix cracking, fiber rupture in tension/kinking in compression, and delamination) under general thermal-mechanical loading. It will be demonstrated with ample validated examples that the A-FEM based simulation platform is able to predict key structural performance characteristics for structural design engineers, including the static strength, strength degradation under thermal-mechanical cyclic loading, the influence of temperature history to the static and fatigue strength, and more importantly, the probability of structural failure at any loading history. A rigorous multiscale validation procedure involving standard engineering tests for macroscopic quantification and in-situ micro-CT for tracing internal damage accumulation in real materials will also be included to promote further discussions on how to assess the credibility of simulated results.

A Reproducing Kernel Finite Volume Method

Saili Yang^{*}, Michael Hillman^{**}

^{*}The Pennsylvania State University, ^{**}The Pennsylvania State University

ABSTRACT

Meshfree methods have evolved into a powerful technique for solving challenging scientific and engineering problems where traditional methods fall short. However, several treatments are required to obtain an efficient, stable, and convergent Galerkin implementation [1], and enforcement of essential boundary conditions is non-trivial [2]. On the other hand, strong-form collocation meshfree methods do not suffer from these issues, yet require expensive higher order derivatives, and in order to converge many collocation points must be employed [3]. This work introduces a reproducing kernel finite volume method. A particular weight function is selected which leads to a set of collocation equations, and offers ease of implementation, and an efficient nodal collocation-type method which does not require higher order derivatives. The formulation automatically satisfies the Variational Consistency conditions, and gives optimal convergence without special treatment. No unstable modes are observed, and thus apparently the method also offers stability without additional techniques. Finally, the essential boundary conditions are directly enforced, which leads to additional ease of implementation. The method is developed for elastostatics and elastodynamics, and several benchmark problems are solved to show its effectiveness in terms of stability, accuracy, and efficiency. References: [1] M. Hillman, J.-S. Chen, "An accelerated, convergent, and stable nodal integration in Galerkin meshfree methods for linear and nonlinear mechanics," Int. J. Numer. Methods Eng. (107) 603–630, 2016. [2] S. Fernández-Méndez, A. Huerta, "Imposing essential boundary conditions in mesh-free methods," Comput. Methods Appl. Mech. Eng. (193) 12, 1257–1275, 2004. [3] H.-Y. Hu, C.-K. Lai, J.-S. Chen, "A study on convergence and complexity of reproducing kernel collocation method," Interact. Multiscale Mech. (2) 3, 295–319, 2009.

Thermomechanical Multiscale Modeling of Boron Nitride Reinforced Nanocomposites

Seunghwa Yang^{*}, Seoyeon Choi^{**}, Kyeongmin Lee^{***}, Yelim Ki^{****}, Man Young Lee^{*****},
Maenghyo Cho^{*****}

^{*}Chung-Ang University, ^{**}Chung-Ang University, ^{***}Chung-Ang University, ^{****}Chung-Ang University, ^{*****}Agency
for Defense Development, ^{*****}Seoul National University

ABSTRACT

Boron nitride (BN) has promising mechanical, dielectric and thermal transport properties comparable to graphene and carbon nanotube (CNT) with greater thermal stability than the two nanocarbon structure. Moreover, BN has excellent radiation shielding characteristics which makes it a good reinforcement for deep space polymer nanocomposites. The BN has two representative forms of BN nanosheet and BN nanotube (BNNT) each of which has exactly same configuration to the graphene and CNT respectively. Therefore, BN reinforced nanocomposites can be modeled as infinite cylinder type or penny shaped inclusion type inclusion problem in micromechanics model. Since characteristics length scale of BN nanosheet and BNNT are in nanometer scale, molecular modeling and simulation of BNT reinforced nanocomposites representative volume element (RVE) can also be addressed in analysis and design of nanocomposites. In this presentation, the thermomechanical properties of BN reinforced nanocomposites are determined from classical molecular dynamics (MD) simulations. In MD simulations, nanocomposites RVEs consisting of single BN and amorphous polymer matrix are constructed and elastic and thermal properties are determined according to the volume fraction of BN. Once thermomechanical properties of BN, polymer, and BN nanocomposites are determined, interface condition between BN and polymer matrix are characterized by means of inverse multiscale modeling approach or BN/polymer laminated interface molecular structures. Since interfacial sliding or phonon scattering are of primary importance for the effective load transport or thermal energy transport, a micromechanics model which can describe these interfacial properties are developed from conventional micromechanics models. Once the thermomechanical multiscale modeling framework is completed, some validation studies are performed to evaluate the accuracy and efficiency of the proposed model by comparing with experimental results or MD simulation results.

Influence of Delay and Noise on the Stability of Periodic Attractor in Nonlinear Vibration Isolator

Tao Yang^{*}, Qingjie Cao^{**}

^{*}Harbin Institute of Technology, ^{**}Harbin Institute of Technology

ABSTRACT

In this paper, we present a detailed study of time-delayed feedback control of the quasi-zero-stiffness SD (smooth and discontinuous) oscillator driven by stochastic environmental fluctuations. This oscillator is composed of a lumped mass connected with a vertical spring and a pair of horizontally springs, which can achieve the quasi-zero-stiffness widely used in vibration isolation. We investigate the effects of time-delayed control force and nonlinear damping on the mean first passage time from the periodic attractors to reveal the complicated nonlinear stochastic dynamics of this system. Varying the intensities of noise sources, it is possible to analyze the behavior of the switching time from the unstable periodic attractor to the stable one in different delay regimes. Moreover, the optimum time delay is obtained based on the consideration for the phenomena of noise- and delay-enhanced stability. Finally, a quantitative measure for amplitude response has been carried out to evaluate the isolation performance of the controlled system. This paper established the relationship between the parameters and vibration properties of the damping and stiffness nonlinearities SD oscillator which provides the guidance for optimizing time-delayed control for vibration isolation of the nonlinear systems.

Optimizing Battery Design Using Multifidelity Model

Xiu Yang^{*}, Wenxiao Pan^{**}, Jie Bao^{***}, Michelle Wang^{****}

^{*}Pacific Northwest National Laboratory, ^{**}University of Wisconsin at Madison, ^{***}Pacific Northwest National Laboratory, ^{****}Harvard University

ABSTRACT

We develop a mathematical framework to study the optimal design of air electrode microstructures for lithium-oxygen (Li-O₂) batteries. The design parameters to characterize an air-electrode microstructure include the porosity, surface-to-volume ratio, and parameters associated with the pore-size distribution. A surrogate model for discharge capacity is first constructed as a function of these design parameters. In particular, a Gaussian process regression method, co-kriging, is employed due to its accuracy and efficiency in predicting high-dimensional responses from a combination of multifidelity data. Specifically, a small sample of data from high-fidelity simulations are combined with a large sample of data obtained from computationally efficient low-fidelity simulations. The high-fidelity simulation is based on a multiscale modeling approach that couples the microscale while the low-fidelity simulation is based on an empirical macroscale model. The constructed response surface provides quantitative understanding and prediction about how air electrode microstructures affect the discharge capacity of Li-O₂ batteries. The succeeding sensitivity analysis via Sobol indexes and optimization via genetic algorithm offer reliable guidance on the optimal design of air electrode microstructures.

An Enhanced Generalized Algorithm for Finite Particle Method

Yang Yang^{*}, Fei Xu^{**}, Lu Wang^{***}, Jingyu Wang^{****}

^{*}Northwestern Polytechnical University, ^{**}Northwestern Polytechnical University, ^{***}Northwestern Polytechnical University, ^{****}Northwestern Polytechnical University

ABSTRACT

Finite Particle Method (FPM) is a significant improvement to the traditional SPH method, which can greatly improve the computational accuracy for the whole computational domain, including both interior area and boundary area. However, long computational time is always a big obstacle to the development of FPM, which is caused by the large amount of calculation on solving the linear equations for each particle in the computational domain. Therefore, how to obtain a higher computational accuracy in the limited computational expense is becoming more and more attentive. Based on our previous Specified FPM (SFPM) algorithm, a developed generalized FPM method (GFPM) is derived, which introduces the additional information of the Taylor remainder into the calculation of traditional FPM. Then by combining the FPM and GFPM, an enhanced generalized Finite Particle Method (EGFPM) is proposed. Numerical results show that, (1) the function and the derivative values calculated by EGFPM obtain an improvement of about three-order of magnitude and one-order of magnitude over FPM respectively. (2) For a given computational accuracy, EGFPM needs fewer particles distributed in the computational domain than FPM. (3) The computational time by EGFPM show just slight longer than FPM, and the time difference is just average 4‰ of traditional FPM.

The Molecular Dynamics Simulation on Mechanical Properties of Y2O3/Ni Composites

Yanjie Yang^{*}, Mabao Liu^{**}, Shuan Ma^{***}, Shiqi Zhou^{****}, Ang Li^{*****}

^{*}Xi'an Jiaotong University, ^{**}Xi'an Jiaotong University, ^{***}Xi'an Jiaotong University, ^{****}Xi'an Jiaotong University, ^{*****}Xi'an Jiaotong University

ABSTRACT

Molecular dynamics (MD) simulations were carried out to investigate the influence of Y2O3 contents and dispersity on the mechanical properties of Y2O3/Ni composites. The well-dispersed addition of 1.0wt%, 2.0wt%, 3.0wt%, 4.0wt%, 5.0wt%, 6.0wt% Y2O3 to Ni matrix are studied, whose results show the 2.0wt% Y2O3/Ni composite provides the best Young's modulus and bulk modulus when Y2O3 disperses uniformly in the Ni matrix. Shear modulus of the composites reaches the highest at the content of Y2O3 being 3.0wt% while 2.0wt%Y2O3/Ni composite has the nearly same value of shear modulus with 3.0wt%Y2O3/Ni (78.2672GPa and 78.3469GPa respectively). The influence of dispersity on Y2O3/Ni composites was also studied by MD simulation, which indicates the aggregation of Y2O3 causes a sharp decline on both Young's modulus and shear modulus. A series of experiments were also carried out to test the MD simulations. Mechanical alloying (MA) and Spark Plasma Sintering (SPS) were adopted to produce the Y2O3/Ni composites with the content of Y2O3 being 1.0wt%, 2.0wt%, 3.0wt%, 5.0wt%. XRD, SEM and compressive tests were taken to analyze the properties of the developed composites. SEM results indicate the appearance of aggregation occurs in the composites with the addition of Y2O3 above 2.0wt%, which leads to a sharp decrease in mechanical properties, as the same as the MD simulation results. Compared with previous researches done by W Chen et al[2] whose results show the most appropriate Y2O3 content is 1.5wt% due to the poor dispersion of Y2O3, the present experimental study shows a larger proper Y2O3 content (2.0wt%) which is consistent with the MD simulations. References: [1] J.D. Giallonardo, U. Erb, K.T. Aust, et al. The Influence of Grain Size and Texture on the Young's Modulus of Nanocrystalline Nickel and Nickel-iron Alloys[J]. Philosophical Magazine, 2011, 91(36):4594-4605. [2] Chen W, Xiong W, Zhang X. Effect of Y2O3 Content and Sintering Temperature on Mechanical Properties of ODS Nickel-Based Superalloy[J]. Rare Metal Materials & Engineering, 2010, 39(1):112-116.

Identification of Bridge Modal Properties from the Contact-point Response of a Moving Test Vehicle

Yeong-bin Yang^{*}, Bin Zhang^{**}, Yao Qian^{***}, Yuntian Wu^{****}

^{*}Chongqing University, ^{**}Chongqing University, ^{***}Chongqing University, ^{****}Chongqing University

ABSTRACT

The response of the contact point of the vehicle with the bridge, rather than the vehicle itself, is firstly proposed for modal identification of bridges by a moving test vehicle. To begin, approximate closed-form solutions were derived for the vehicle and contact-point responses, and verified by finite element solutions. The contact-point acceleration is born to be free of the vehicle frequency, an annoying effect that may overshadow the bridge frequencies in case of rough surface. From the frequency response function (FRF) of the vehicle with respect to the contact point, it was shown that the contact-point response generally outperforms the vehicle response in extracting the bridge frequencies in that more frequencies can be identified. In the numerical simulations, the contact-point response was compared with the vehicle response for various scenarios. It is concluded that in each case, say, for varying vehicle speeds or frequencies, for smooth or rough road surfaces, with or without existing traffic, the contact-point response outperforms the vehicle response in extracting either the frequencies or mode shapes of the bridge.

A Triple-scale Asymptotic Homogenization for Coupled Conduction-radiation Problems in Porous Materials with Multi-level Configurations

Zhiqiang Yang^{*}, Zihao Yang^{**}

^{*}Harbin Institute of Technology, China, ^{**}Northwestern Polytechnical University, China

ABSTRACT

The novelty of the newly method developed is by implementation on heat conduction-radiation problems in porous materials with multiple heterogeneities. The heterogeneities of porous structures are considered by periodic layouts of unit cells on the microscale and mesoscale. A new micro-meso-macro formula based on reiterated homogenization methods and multiscale asymptotic expansions is established. The equivalent coefficients are obtained by up-scaling procedure and homogenized problem are derived. In this method, both the mesoscopic and microscopic information is combined with homogenization solution to catch local oscillation inside the material. The numerical results show that the three-scale asymptotic expansion proposed in this manuscript can be useful for determination of the heat transfer properties of porous materials and demonstrate its potential applications in engineering and technology.

Model Reduction of Parametrized Aerodynamic Flows: Adaptive Discontinuous-Galerkin Reduced-basis Empirical Quadrature Procedure

Masayuki Yano*

*University of Toronto

ABSTRACT

We present a model reduction formulation for parametrized nonlinear partial differential equations (PDEs) with emphasis on steady aerodynamic flows modeled by the compressible Reynolds-averaged Navier-Stokes (RANS) equations. The approach builds on four key ingredients: the discontinuous Galerkin (DG) method which provides high-order accuracy and stability for convection-dominated flows; an anisotropic adaptive mesh refinement strategy which quantifies and efficiently controls the spatial finite-element discretization error; reduced basis (RB) spaces which provide rapidly convergent approximations to the parametric manifold; sparse empirical quadrature rules which provide "hyperreduction" to enable rapid evaluation of the nonlinear DG residual and output forms associated with the RB spaces. The quadrature rules are identified by a DG extension of a linear program (LP) empirical quadrature procedure (EQP) [1] which (i) admits efficient solution by a simplex method, (ii) guarantees energy stability, and (iii) directly controls the solution error induced by the approximate quadrature. The errors associated with the spatial discretization, reduced basis approximation, and hyperreduction are simultaneously controlled in a systematic and automated manner by a greedy algorithm in the offline stage. We demonstrate the approach for parametrized steady aerodynamic flows with variations in physical flow conditions or mathematical model parameters. The former enables rapid exploration of the design space. The latter enables combined model and discretization uncertainty quantification (UQ) of the RANS equations with the Spalart-Allmaras (SA) turbulence model, where the model error arises from the uncertainty in SA model parameters. In both scenarios, the DG-RB-EQP method achieves significant computational savings while tightly controlling the discretization error associated with the spatial, reduced basis, and quadrature approximations. The rapid predictions provided by the DG-RB-EQP method also enables control of the Monte Carlo (MC) sampling error in the context of UQ. [1] AT Patera and M Yano, An LP empirical quadrature procedure for parametrized functions, *Comptes Rendus Mathematique*, accepted.

Computational Studies on the Failure Problems in Lithium-ion Batteries

Haimin Yao*

*The Hong Kong Polytechnic University

ABSTRACT

Developing batteries with high capacity and long cycle life would not only be of significant value to industries but help alleviate pressure from energy shortage. High-capacity batteries require electrode materials with high capacity which, however, tend to be accompanied with large volume change during lithiation and delithiation process. For example, Silicon (Si), an anode material with the highest capacity, experiences 300-400% volume change during the charge/discharge processes. Such large volume change is the Achilles' heel of Si because it would cause a series of failure problems such as fracture of the electrode materials and delamination from current collector, resulting in loss of electric conductivity and capacity fading. In the past a few years, we have been studying, by using computational mechanics approaches, the lithiation-induced failure problems in a variety of anode materials including SnO₂ nanowires [1], carbon-coated silicon core-shell nanoparticles [2] and yolk-shell carbon-coated silicon nanoparticle [3]. Our results not only shed light on the mechanisms of these failure phenomena, but also provide guidance for alleviating or even solving the associated problems. References: 1. Q. Li, W. Li, Q. Feng, P. Wang, M. Mao, J. Liu, L.M. Zhou, H. Wang, H. Yao*, 2014. Thickness-dependent fracture of amorphous carbon coating on SnO₂ nanowire electrodes, Carbon 80, 793-798. 2. W. Li, K. Cao, H. Wang, J. Liu, L.M. Zhou, H. Yao*, 2016. Carbon coating may expedite the fracture of carbon-coated silicon core-shell nanoparticles during lithiation, Nanoscale 8, 5254-5259. 3. W. Li, Q. Wang, K. Cao, J. Tang, H. Wang, L.M. Zhou*, H. Yao*, 2016. Mechanics-based optimization of yolk-shell carbon-coated silicon nanoparticle as electrode materials for high-capacity lithium ion battery, Composites Communications 1, 1-5.

Stochastic Reconstruction of Complex Heavy Oil Molecules Using an Artificial Neural Network

Muzaffer Yasar*, Celal Utku Deniz**, Hande Sebnem Ozoren Yasar***, Michael T. Klein****

*Chemical Engineering Department, Istanbul University Avcilar, Istanbul 34820, **Hitit University, Corum, Turkey,

Istanbul University Avcilar, Istanbul 34820, *Chemical and Biomolecular Engineering Department, University of Delaware Newark, Delaware 19716

ABSTRACT

An approach for the stochastic reconstruction of petroleum fractions based on the joint use of artificial neural networks and genetic algorithms was developed. This hybrid approach reduced the time required for optimization of the composition of the petroleum fraction without sacrificing accuracy. A reasonable initial structural parameter set in the optimization space was determined using an artificial neural network. Then, the initial parameter set was optimized using a genetic algorithm. The simulations show that the time savings were between 62 and 74 percent for the samples used. This development is critical, considering that the characteristic time required for the optimization procedure is hours or even days for stochastic reconstruction. In addition, the stand-alone use of the artificial neural network step that produces instantaneous results may help where it is necessary to make quick decisions.

Effect of Boiling Point and Density Prediction Methods on Stochastic Reconstruction

Sebnem Hande Ozoren Yasar*, Celal Utku Deniz**, Muzaffer Yasar***, Michael T. Klein****

*Vocational School of Technical Science, Istanbul University Avcilar, Istanbul 34820, **Hitit University, Corum, Turkey, ***Chemical Engineering Department Istanbul University Avcilar, Istanbul 34820, ****Chemical and Biomolecular Engineering Department, University of Delaware Newark, Delaware 19716

ABSTRACT

Stochastic Reconstruction (SR) methods are used to generate a series of molecules that mimic the properties of complex mixtures using partial analytical data. Determining a quantitative composition using these methods is limited by the property prediction methods used. This paper addresses the use of two key measurements in the characterization of petroleum fractions, namely, density and boiling point distributions. It is known that the different methods used in estimating these two basic properties have different error rates. Boiling point prediction performances of the various group contribution methods were tested by means of the molecular library established for the molecules that can be present in the petroleum fractions. It has been observed that the combined use of these methods causes about 50% smaller sum of squared errors than any method alone. The predictive performances of the density calculation methods were similarly tested. The best-calculated density results were found by the combination of the linear mixing rule based on molar fractions and the Yen - Woods method.

Contact along Virtual Interfaces for Wear Simulation: Coupling the X-FEM with the Mortar Discretization

Vladislav A. Yastrebov^{*}, Basava Raju Akula^{**}, Julien Vignollet^{***}

^{*}MINES ParisTech, PSL Research University, Centre des Matériaux, CNRS UMR 7633, ^{**}MINES ParisTech, PSL Research University, Centre des Matériaux, CNRS UMR 7633, ^{***}Safran Tech, Safran Group

ABSTRACT

Interaction between solids involving contact, friction, adhesion and wear are complex both with regard to their mathematical description and numerical treatment. The interfacial nature of these phenomena lays a strong emphasis on the interface discretization scheme. Stability and appropriate patch-test performance of these schemes are necessary ingredients to ensure the overall accuracy and robustness of the contact treatment. A relative motion between contacting bodies can lead to material removal (wear) of rubbing solids. The change of geometry change the contact pressures, and thus leads to alteration of the system's global response and affects the further evolution of wear. Numerical simulation of wear usually involve (1) constitutive local wear laws determining the wear depth evolution at every effective cycle, (2) remeshing procedures to capture the shape changes at the interface, and (3) field remapping in case of material behavior involving internal variables. In this presentation we will suggest a novel method enabling to simplify the treatment of wear problems and ensuring optimal convergence as well as accurate representation of surface tractions, which is essential for wear simulation. Face-to-face discretization techniques combined with penalty-based or Lagrange-multiplier based treatment of contact/friction constraints form the state of the art methods enabling to handle contact interaction along non-conformal interfaces in a robust way and ensure the accuracy of surface tractions [1]. The extended finite element method (X-FEM) presents a different technique to handle intra-mesh discontinuities: shock waves, oxidation fronts, composite materials, voids and cracks [2]. Combining the face-to-face contact formulation with the X-FEM method presents an attractive option to treat contact problems along virtual surfaces/interfaces with incompatible meshes: the face-to-face discretization ensures an accurate treatment of contact and the X-FEM ensures independence of interfaces of the finite element mesh. The virtual contact surface embedded in the volumetric mesh can incorporate geometrical aspects, such as roughness, and can evolve in time due to wear and/or third body accumulation. The main aspects of such a coupling between the mortar and the X-FEM methods will be presented as well as a few examples. [1] M. Gitterle, A. Popp, M. W. Gee, and W. A. Wall (2010). Finite deformation frictional mortar contact using a semi-smooth newton method with consistent linearization. *Int J Num Methods Eng*, 84(5):543-571. [2] N. Sukumar, D.L. Chopp, N. Moës, and T. Belytschko (2001). Modeling holes and inclusions by level sets in the extended finite-element method. *Comp Methods Appl Mech Eng*, 190(46):6183-6200.

Trend of Patents about Utilization of AI Technology in Extended Computer Aided Engineering Region ~ The Field of Application and the Proposal of Development Policy of AI Technology in Manufacturing Industry ~

Kenji Yasutake*

*Asteroid Research Inc.

ABSTRACT

These days, the third generation AI technology characterized by deep machine learning is developing rapidly and it is widely utilized in various industrial fields, for example image recognition and automatic driving etc. CAE (Computer Aided Engineering) technology has been quite important for the design and development of new products and ecosystems in the enterprises. However the AI technology is not yet widely available for the Working-Level design process in the manufacturing industry. In this paper, the patent trends of AI technology about "Extended CAE" are described. First, a concept of "Extended CAE" in the industrial manufacturing process is defined. Next, the patent trends of AI technology about the Extended CAE for manufacturing industry about (1) an automated production in a factory, (2) high efficiency operation in a construction site and (3) semi-automated patent search and application are mentioned. Finally, the future development plans of AI technology about industrial manufacturing process in the enterprises are proposed.

Finite Strain Meshfree Co-rotational Formulation for Hyperelastic Solids

Louie Yaw*

*Walla Walla University

ABSTRACT

Prior research in finite element analysis with incompressible materials has established improved performance when the analysis is placed within a co-rotational formulation. The present work aims to show that these benefits also transfer to the meshfree setting. In this work a finite strain meshfree formulation is included within a co-rotational framework, which to our knowledge has not been done heretofore. Advantage is taken of the close relation between local engineering strains and Biot strains (advocated by Crisfield [1], Moita [2]) in the refined nodal discretization limit. Under such conditions individual nodal stresses approach a state of homogeneous local stress. Biot stresses and strains allow the incorporation of finite strains and hyperelastic material models. For the meshfree formulation, any set of meshfree basis functions is suitable; herein, we adopt maximum-entropy basis functions (Yaw et al [3]). Nodal integration over a Voronoi cell background with stabilization is employed. The formulation passes the large strain patch test for the case of pure shear. Results for plane stress stretched membrane, plane strain axial extrusion, and Cook's membrane are among the benchmark problems presented. We will conclude with the promise and outlook of finite strain meshfree-based co-rotational formulations. [1] M. A., Crisfield. Non-linear Finite Element Analysis of Solids and Structures – Vol 2 Advanced Topics. John Wiley & Sons Ltd., Chichester, England, 1997. [2] G. F., Moita. "Non-linear finite element analysis of continua with emphasis on hyperelasticity", Ph.D. Thesis, Imperial College, London, 1994. [3] L. L. Yaw, N. Sukumar, and S. K. Kunnath. Meshfree co-rotational formulation for two-dimensional continua. International Journal for Numerical Methods in Engineering, 79(8):979–1003, 2009.

Electric Field-Induced Adjustable Mechanical Property and Deformation Behavior of Fluid-Filled Carbon Nanotubes

Hongfei Ye^{*}, Zhen Chen^{**}, Hongwu Zhang^{***}, Xiaolong Gao^{****}, Yonggang Zheng^{*****}

^{*}Dalian University of Technology, ^{**}Dalian University of Technology & University of Missouri, ^{***}Dalian University of Technology, ^{****}Dalian University of Technology, ^{*****}Dalian University of Technology

ABSTRACT

Water-filled carbon nanotubes (CNTs) have been successfully fabricated and separated in laboratory. It has also been demonstrated that the ions could enter the CNTs spontaneously. Hence, it is possible to further fabricate the salt water-filled CNTs based on the present experimental technology. As an ideal candidates for structural elements or functional components in nanoscale systems, the CNTs are expected to be accurately and conveniently controlled, including their mechanical property, deformation and so on, which has great potential applications in micro-electro-mechanical systems, microfluidic chips, etc. Due to the sensitivity of polar water molecules and ions to electric field, the controllable performance may be feasible for fluid-filled CNTs. In this report, the systematic study on the mechanical property and deformation response of pure water and salt water-filled CNTs under the electric field are presented, including the compression test, torsion deformation, size dependence, pre-strained effect, controllable tension and bending, etc. For the water-filled CNTs, the results based on the molecular dynamics (MD) simulations indicate that the mechanical properties (the elastic modulus, Poisson's ratio, critical buckling stress) would vary with the electric field intensity, which exhibit a nonlinear dependence on the diameter of CNTs. As for the salt water-filled CNTs, the electric field could result in the tension and bending deformations. Some theoretical models are also constructed to verify the deformation behavior of the fluid-filled CNTs. Furthermore, the mentioned controllable performances are also utilized to design molecular sieving and nanoscale trigger. The present research reveals the adjustable performance of fluid-filled CNTs and provides theoretical guidance and reference for the experimental works. By means of the controllable deformation of fluid-filled CNTs, the present investigation also opens up a new avenue in the design and fabrication of nanoscale controlling units, high-sensitive sensors, etc. The supports from the National Natural Science Foundation of China (Nos. 11672063, 11672062, 11772082, 11472117 and 11232003), the 111 Project (No. B08014), Young Science and Technology Star Program of Dalian (2016RQ018) and Fundamental Research Funds for the Central Universities are gratefully acknowledged.

Extended Level Set Methods (X-LSM) for Shape and Topology Optimization on Manifolds

Qian Ye^{*}, Yang Guo^{**}, Shikui Chen^{***}, Xianfeng Gu^{****}

^{*}Department of Mechanical Engineering, State University of New York at Stony Brook, ^{**}Department of Computer Science, State University of New York at Stony Brook, ^{***}Department of Mechanical Engineering, State University of New York at Stony Brook, ^{****}Department of Computer Science and Applied Mathematics, State University of New York at Stony Brook

ABSTRACT

The level-set-based topology optimization (TO) approach has been considered as a powerful tool in generating innovative designs. However, the conventional level set functions are defined in the Euclidean space (R^2 and R^3), which cannot satisfy the demand of TO on general freeform surfaces. In this paper, we propose a new method to address the problem of structural shape and topology optimization on free-form surfaces which is mathematically defined as manifolds. By using conformal parameterization, we extend the level set based topology optimization framework from the Euclidean space (R^2 and R^3) to surfaces with arbitrary topologies. In our method, a manifold is conformally mapped onto a 2D rectangular domain, where the level set functions are defined afterward. We prove that by using this conformal mapping, the corresponding covariant derivatives on a manifold can be represented by the Euclidean differential operators after a scalar multiplication. Therefore, the topology optimization problem on free-form surfaces can be formulated as a 2D problem in the Euclidean space. To update the level set function, we can define and solve a new set of partial differential equations (PDEs), including the modified Hamilton-Jacobi Equation in 2D instead of on the free-form surface. Compared with other established approaches which need to project the Euclidean differential operators to the surface, the computational difficulty of the X-Level Set method is highly reduced. In addition, the conformal mapping between the free-form surfaces and the 2D domain is an explicit approach. Moreover, it is intuitive to observe the design revolution on the manifold. Two benchmark examples of the mean compliance topology optimization problems on free-form shell structures are studied, and the optimized solutions are presented to demonstrate the validity and effectiveness of the proposed method.

Coupled Physics Simulation of Fracture in Nuclear Fuel Pellets Induced by Resistive Heating

Ju-Yuan Yeh^{*}, Benjamin Spencer^{**}, Mary Lou Dunzik-Gougar^{***}

^{*}Idaho State University, ^{**}Idaho National Laboratory, ^{***}Idaho State University

ABSTRACT

Nuclear light water reactors (LWRs), which make up the majority of the commercial power reactors currently in use worldwide, use ceramic uranium oxide fuel pellets stacked within long cylindrical metallic fuel rods. During normal operation, these fuel pellets experience significant gradients in temperature, and as a result, corresponding high stresses induced by nonuniform thermal expansion. This causes the fuel pellets to fracture very early in their service life. While this fracturing is not a direct safety concern, it does significantly affect a number of aspects of the performance of the nuclear fuel system. There are ongoing efforts to base the material behavior models used for LWR fuel performance on physical behavior rather than on empirical models that represent those effects indirectly. To that end, capabilities have been added to the BISON nuclear fuel performance code developed at Idaho National Laboratory to use several techniques for modeling fracture within multiphysics fuel performance models. These techniques include the extended finite element method (XFEM), smeared cracking, and peridynamics. As these fracture models have matured, the need for validation data has become clear. Because it is extremely difficult to monitor the processes of fracture propagation within a nuclear reactor, separate-effects validation experiments of fracturing fuel outside the reactor, but under thermal conditions comparable to those seen in the reactor are being planned. One of these experiments employs the use of resistive heating by applying a current through a fuel pellet to obtain volumetric heating similar to that provided by fission processes in the nuclear reactor. This is expected to produce temperatures that are much higher on the inside of the pellet than on the outside, and which will result in thermally-induced cracking similar to that observed under normal LWR operation conditions. The BISON code is an inherently multiphysics simulation environment, and has been extended to model electrical fields coupled with the thermal and mechanical fields typically simulated in that tool. With this added capability, it is being used to simulate fracture induced by an electric current applied to a pellet. This is being used to guide the development of these validation experiments, and the outcomes of those tests will be used to improve the accuracy of the models for fracture in BISON. This talk will describe the coupled physics models, the solution methods used, and show the results of their application to this problem.

Modelling of landslides with the Material Point Method

Alba Yerro Colom*, Jonathan Bray**, Kenichi Soga***

*Virginia Tech, **Virginia Tech, ***University of California, Berkeley

ABSTRACT

Landslides and slope instabilities represent one of the most important problems in geotechnics and cause significant damage to properties as well as human life around the world. Understanding the mechanics of the slope deformation process is of particular importance for risk assessment. Traditionally, most geotechnical analyses focus on failure prediction (i.e. onset of failure); however, despite the probability of failure at the initiation stage of a landslide is often small, it is essential to understand the post-failure behavior in order to minimize the risk of catastrophic damages. Hence, there is an urgent need to develop numerical schemes capable of simulating failure initiation and post-failure dynamics of landslides in a unique framework. In this work, the Material Point Method (MPM) is presented as a numerical technique capable of modelling large deformation problems and interaction between different materials. MPM discretizes the continuum into a set of material points that represent and move attached to the material, while main governing equations are solved at the nodes of a background computational mesh. With this dual description of the media, MPM can deal with large deformations of history-dependent materials without limitations of mesh tangling, and contact between different bodies is automatically solved. During the last decade, MPM has been applied to different engineering fields such as ice dynamics and fracture of wood, and recently it has received increasing attention in the geotechnical field, in particular in the analysis of landslides. In this work, different theoretical and real cases will be discussed in order to present the capabilities of MPM to analyze complex landsliding problems. Special emphasis will be dedicated to examine the Oso Landslide, which occurred in the State of Washington, USA on 22 March 2014. The Oso Landslide is one of the worst landslide disasters in the US history with 43 fatalities. It took place in multiple failure stages, travelled nearly 1 km over the floodplain involving several failure surfaces and significant soil softening.

The Elastic-Plastic Decomposition of Crystal Deformation at the Micro-nano Scale

Yu Yifan^{*}, Cui Junzhi^{**}

^{*}Academy of Mathematics and Systems Science, Chinese Academy of Sciences, ^{**}Academy of Mathematics and Systems Science, Chinese Academy of Sciences

ABSTRACT

With the development of computer performance, it has become very popular to make use of molecular dynamics simulation to study mechanical properties of materials at micro-nano scales. From the instantaneous positions of atoms, some macroscopic mechanical properties of materials, such as the elastic constants, can be calculated. The usual procedure is as follows: firstly, taking the snapshots of an atomistic system at two different instants, the total deformation gradient can be evaluated by piecewise polynomial interpolation. However, the elastic and plastic deformation gradients can't directly obtained from the total deformation gradient. Thus, some predecessors extended the multiplicative decomposition of the total deformation gradients to the micro-nano scale, and developed some decomposition methods, which make success in some extent. But there are still some flaws in dealing with the atomic locations after unloading. Therefore it is necessary to develop a new decomposition algorithm on the elastic and plastic deformation gradients from total deformation gradient. In this paper, we develop a new algorithm to calculate the post-unloading configurations based on the fact that unloaded materials should be on a stable state, that is, the internal atomic arrangement of materials correspond with atomic locations of minimum total potential energy. Our algorithm is to decompose the total deformation gradient field into the elastic deformation gradient field and the plastic deformation gradient field, where the elastic deformation gradient comes from the microscopic lattice structure of unloading configurations retaining defects. Our algorithm successfully solves the flaws of the previous methods. And it is the basis for further studying the elastic-plastic properties based on MD simulation. The framework of this paper is as follows: first part is to point out the necessary of developing a new decomposition algorithm, and introduce the high order deformation elements based on the BCC/FCC lattice to calculate the total deformation gradient field. The second is to devote to the algorithm of obtaining post-unloading configurations, and the new decomposition algorithm. Final part is an example on tensed nanowire to verify the correctness of our algorithm.

N-S Equations and Relativistic Structures and Engineering Applications

Wang Yiping*

*Qianjiang Mathematics and Power Engineering Institute

ABSTRACT

In this talk, we propose a novel fluid mechanics calculation method and the universality of asymmetric energy, and manufacture an asymmetric energy engine. Mechanics calculation: It is proposed that eddy currents and turbulent flows are infinite multi-scale vortex flow states defined as a point state, the logarithm-based logarithm of the non-dimensional quantities and the three logarithmically invariant circular log-dynamic equations are established, , For a variety of high-power polynomials formed by the state of flow, for concise, self-consistent, accurate solution. Engineering Application: Propose the principle and mechanism of asymmetric super-energy engine to solve the design and manufacture of long vortex vane and super-symmetric heat engine controlled by six programs. Manufacture of asymmetric super-engine, won the Chinese national invention patents: (1), Macro-type: positive and reverse flow can produce asymmetric transformers. That is, a fuel-free engine that is used to generate electricity. Project: "eccentric rotation engine", a small batch production. If the meeting allows, can bring to the show. (2), The concept of medium-sized: high and low heat can transform asymmetric super energy, resulting in 10 to 20 times more than traditional internal combustion engine, for transportation, power generation. Project: "a two-way vortex air-cooled negative pressure aerodynamic hydrogen engine" (ZL201410052227.0); "double-scroll negative pressure internal combustion engine" (ZL201510187088.7). (3) , Micro-type: The asymmetric super-energy is generated by the positive and negative nuclear energy conversion controlled by six programs. The project is "Small Safety and Environmental Protection Nuclear Power Engine".

Anisotropy of Microstructure in Compacted Granular Solids

Bereket Yohannes^{*}, Xue Liu^{**}, Alberto Cuitino^{***}

^{*}Rutgers University, ^{**}BASF, ^{***}Rutgers University

ABSTRACT

Compaction is one of the most common industrial processes used to achieve densification of powders and to develop tensile strength or resistance to crushing. Several factors, including powder properties, applied compaction pressure, and the shape of tooling affect the compaction process itself and the final microstructure. Even though several prior studies have addressed this topic in detail, the compaction process is still not well understood, particularly in terms of developing a mechanistic relationship between particle scale properties and the powder compact properties such as relative density and tensile strength. In order to understand the effect of particle properties, such as particle size, plasticity, elasticity, and surface bonding energy, on the powder compact, we ran several experiments and discrete particle simulations. We studied commonly used excipients for pharmaceutical products and metallic powders. The exact particle size distributions of the powders are represented in the simulations, and the mechanical properties of the particles are calibrated using the powder compaction experiment results. Then, we validated our simulation results based on experimental indirect tensile strength test. We found that the simulation results are quantitatively similar to experimental results. Once the simulations are validated, we used the simulations to investigate the microstructure evolution during the compaction process and the effect of particle properties, particularly that of the size and the mechanical properties of the particles. In this presentation, we will discuss the experimental and simulation methods and results in detail.

Evaluation of Dynamic Impact Analysis on Curved Surface Structure Using Isogeometric Elements

Yuta Yokoyama^{*}, Hirofumi Sugiyama^{**}, Shigenobu Okazawa^{***}

^{*}University of Yamanashi, ^{**}University of Yamanashi, ^{***}University of Yamanashi

ABSTRACT

In recent years, the model that can be handled by CAE (Computer Aided Engineering) is also complicated due to rapid improvement in computer performance, and the number of divisions of elements is also enormous, so the problem increasing the time required for the whole analysis due to the complication of the target in performing the analysis, the time taken to mesh the CAD (Computer Aided Design) model occupies most of the time of the whole analysis. Isogeometric analysis method was proposed to solve this problem. Isogeometric analysis is different from conventional FEM (Finite Element Method) analysis and it can be applied to CAD by using B-spline / NURBS (Non Uniform Rational B-Spline) basis function as shape function it is possible to use the created model directly for analysis, it is possible to shorten the time and improve the calculation accuracy. In this study, focusing on the high model reproducibility of the Isogeometric element, dynamic impact analysis of a structure having a curved surface was carried out and the performance of the Isogeometric element was evaluated. Impact analysis was performed dynamically using bonnet, door panel, etc. as a structure having a curved surface. In order to evaluate the performance of isotropic element, it was compared with the analysis result of a model made by ordinary finite element method. This study concludes, in order to verify the accuracy verification of the Isogeometric element and the FEM, we analyzed using a model with curved surface and comparative verification. Then we investigated the influence and analysis accuracy in dynamic collision analysis using Isogeometric element, and showed future prospects.

An Improved Extended Material Point Method for Crack Problems

Liang Yong*, Zhang Xiong**

*Tsinghua University, China, **Tsinghua University, China

ABSTRACT

The extended material point method (XMPM)[1] has demonstrated its capabilities in the simulation of crack growth problems. Because of the use of the jump function as the enrichment function around the crack, the XMPM can describe the discontinuous displacement and velocities by only one set of background grid mesh. However, the jump enrichment function is unable to describe the crack tip direction and the crack length in the cell where the crack tip is located in. In this work, the asymptotic crack tip functions are used to enrich the nodes around the crack tip to make the XMPM able to simulate the crack direction and length in one cell. Naturally, the result around the crack tip and the prediction of the crack growth is more accurate. In addition, the original XMPM is based on the conventional MPM[2] framework. It also suffers the cell crossing noise. To deal with the above issue, we use one-point quadrature with the quadrature point located at the center of the element and the nodal velocity is obtained by the moving least squares method (MLS). This improved XMPM scheme needs additional handling at the boundary and the generalized interpolation material point (GIMP)[3] shape function is also used. Numerical examples show that the asymptotic crack tip enrichment function can make the XMPM give more accurate result around the crack tip than before. For a manufactured solution with large deformation, the use of one-point quadrature, MLS for the nodal velocity and the GIMP shape function show that the cell crossing noise is eliminated and the accuracy is much better. REFERENCES [1] Liang Y, Benedek T, Zhang X, et al. "Material point method with enriched shape function for crack problems[J]"; Computer Methods in Applied Mechanics and Engineering, 2017, 322: 541-562. [2] Sulsky, Deborah, Zhen Chen, and Howard L. Schreyer. "A particle method for history-dependent materials." Computer methods in applied mechanics and engineering 118.1 (1994): 179-196. [3] S.G. Bardenhagen, E.M. Kober. "The generalized interpolation material point method." Computer Modeling in Engineering and Sciences 5 (6) (2004) 477-495.

Iron Ore Particle Production through Liquid CO₂ Penetration and High Pressure Gas Propulsion by CDEM (Continuous-Discontinuous Element Method)

Fan Yongbo^{*}, Li Shihai^{**}, Qiao Jiyan^{***}, Feng Chun^{****}, Cheng Pengda^{*****}

^{*}Institute of Mechanics, Chinese Academy of Sciences, ^{**}Institute of Mechanics, Chinese Academy of Sciences,
^{***}Institute of Mechanics, Chinese Academy of Sciences, ^{****}Institute of Mechanics, Chinese Academy of
Sciences, ^{*****}Institute of Mechanics, Chinese Academy of Sciences

ABSTRACT

An average iron content of iron ore is less than 30%, rough crushing, fine crushing, milling and other processing must be executed before they can be smelted. Currently iron ore broken by mechanical grinding demands higher cost. We describe a novel methodology named CDEM (Continuous-Discontinuous element method), coupling finite element method and discrete element method, can accurately realize crack initiation, crack propagation based on porosity seepage model and block rupture model, which facilitate micron-sized iron ore particle production through liquid CO₂ penetration and high pressure gas propulsion. On the conditions of iron ore permeability coefficient, porosity and tensile strength test, a series of numerical experiments of iron ore powdering have been carried out under different initial pressure of the liquid CO₂ and different initial pressure of gas. The higher the initial pressure of gas, the higher the number of fine particles obtained. Together with the powdering experiments conclusion, we can provide theoretical guidance for industrialization of iron ore powdering. The liquid CO₂ penetration and high pressure gas propulsion method is much more environmentally friendly, efficient, energy saving, and effective.

Newly Optimized Silicene Interatomic Potential Model for Elastic Constants

SangHyuk Yoo^{*}, Keonwook Kang^{**}, Byeongchan Lee^{***}

^{*}Yonsei University, ^{**}Yonsei University, ^{***}Kyong Hee University

ABSTRACT

Silicene is the 2D structured silicon, which can be used as opto-electric devices such as FET due to the promising electrical properties [1]. However, silicene can be deformed by mechanical stress during fabrication or operation, and electric properties transition will be occurred. For this reason, research of correlation between stress and deformations would support to control the manufacture process or operation environments. Previous results of mechanical tests by molecular statics simulations in the elastic regime are not accorded with the results of DFT calculation. The reason of this outcome is induced by that most of interatomic potential models were developed to predict elastic behaviors of 3D structures. In this study, authors conducted parameter optimizations of Tersoff potential model in order to predict elastic constants consistent with DFT values, including Young's modulus, Poisson's ratio and Bending modulus [2]. REFERENCES [1] L. Tao et al.: Silicene field-effect transistors operating at room temperature, Nat. Nano., Vol.10, pp.227—231, 2015. [2] J. Tersoff, Phys. Rev. B, 37, 12, (1988) 6991–6999

Topology Optimization with Finite Element Based k-e Turbulent Model

Gil Ho Yoon*

*hanyang university

ABSTRACT

In this research, a new finite element (FE) based topology optimization (TO) for turbulent flow was developed using the k-e model, which is one of the Reynolds-Averaged Navier-Stokes (RANS) equations. Despite many innovative works on the subject of fluidic TO, it is still difficult to consider the impact of turbulent flow in TO. To consider the effect of complex turbulent fluid motion, this research considered the k-e finite element model. To conduct a successful TO, one issue is modification of the k-e turbulent model to account for topological evolution during the optimization process. To address this issue, we proposed the addition of penalization terms to the original governing equations. To show the validity of the present approach and the effect of turbulent flow on optimal layouts, some two dimensional benchmark designs studied for laminar flow were reconsidered. By considering the effect of turbulent flow, the eddy viscosity values were increased at some local regions due to the Boussinesq hypothesis, and naturally optimal layouts affected by the spatially varying viscosity were obtained in turbulent flow.

Molecular Dynamic study of Immobilization of the Laccase on Graphene Sheet

Tae Young Yoon*, Sungsoo Na**

*Korea University, **Korea University

ABSTRACT

Biofuel cells are the most anticipated future energy material. These biofuel cells get energy from the bio-material for variety of kinds. Many researchers have developed wearable biofuel cells that consumes the energy from the tears and blood [1]. These materials from our human body, contains enzymes that produce and accept electrons. Electron producing enzyme, especially the Glucose Oxidases are inserted in the anode of the fuel cell and Laccase that accepts electron are placed in cathode. Therefore, by the mechanism of the enzyme, biofuel cells are able to storage the electron then produce electricity as a battery. The most limitation of the biofuel cell is the power level. The power level of the fuel cells, have been progressed by enzyme immobilization methods. The most immobilization methods are the electrode modification of the biofuel cells. Carbon materials like graphene sheet or CNT are used because of good electric conductivity. These methods have been made remarkable progress to power level, but still, biofuel cells are not practical as other kind of ordinary batteries. In this paper, we conducted conformation and interaction studies of the Laccase in nano-scale with molecular dynamic simulation. As mentioned above, Laccase are the most well-used enzyme for the cathode that accepts the electron. Therefore, we have simulated molecular dynamics simulation with Laccase immobilized on graphene sheet. We then, analyzed conformation change of the laccase, graphene binding site, and the interaction energy between laccase and graphene sheet.

Multiscale and Multiphysics Integrated Simulations for Offshore Wind Farm Using K-Computer : An Overview

Shinobu Yoshimura^{*}, Tomonori Yamada^{**}, Takanori Uchida^{***}, Hiroshi Imamura^{****}, Yoshinobu Yamade^{*****}, Chisachi Kato^{*****}, Akiyoshi Iida^{*****}, Yasunori Yusa^{*****}, Naoto Mitsume^{*****}, Yuko Ueda^{*****}

^{*}The University of Tokyo, ^{**}The University of Tokyo, ^{***}Kyushu University, ^{****}Wind Energy Institute of Tokyo, Inc., ^{*****}Mizuho Information & Research Institute, Inc., ^{*****}The University of Tokyo, ^{*****}Toyohashi University of Technology, ^{*****}Tokyo University of Science, ^{*****}The University of Tokyo, ^{*****}Wind Energy Institute of Tokyo, Inc.

ABSTRACT

An offshore wind farm for power generation consists of tens to hundred of large scale wind turbines. To promote the use of natural energy in Japan, the Japanese government has planned to develop wind farms generating totally 4 million kw of power by 2030. To do so, we need to take care of heavier weather conditions and narrower offshore sites in Japan, compared with European and US environments. To improve the performance of power generation of wind farms and the reliability of individual wind turbine, it is necessary not only to concentrate on the improvement of the individual wind turbine, but also to improve the accuracy of evaluating the degradation of power generation of wind turbine affected by wake interaction. Moreover, it is necessary to improve the reliability evaluation of individual wind turbine exposed to the wake. As a part of the post K-computer project (Flagship 2020 project), we have been developing multiscale and multiphysics integrated simulations for an entire offshore wind farm. The simulations consist of the following components, (a) Large-scale flow simulation of a wind farm taking into weather and terrain, (b) Large-scale LES simulation of two tandem wind turbines to evaluate an effect of wake into power generation taking into account multiscale phenomena in time and space domains such as atmospheric flow, wind turbine wake, turbine blade boundary layer, and (c) Flow induced vibration of wind turbine based on FSI simulation. In this presentation, we describe an overview of the simulation system.

Application of the Variational Phase Field Method to Hydraulic Fracturing: A Comparative Study

Keita Yoshioka^{*}, Thomas Nagel^{**}

^{*}Helmholtz Centre for Environmental Research - UFZ, ^{**}Helmholtz Centre for Environmental Research - UFZ

ABSTRACT

The ability to predict complex hydraulic fracturing behaviour beyond conventional planar assumption in sub-surface e.g. in unconventional resources has been crucially important in order to understand and control the hydraulic fracturing process in the energy resource industry. Due to the complex boundary conditions and its multi-physical nature in sub-surface environments, modelling of hydraulic fracturing at a laboratory scale is difficult to extrapolate to a field scale. Among the many numerical techniques studied such as discrete element or extended finite element methods, an approach termed variational phase field model, which was originally proposed by Bourdin, Francfort and Marigo in 2000, has become increasingly popular within the hydraulic fracturing modelling community in the recent years. One of its strengths, the ability to handle complex un-prescribed crack paths, is a fundamental for the numerical simulation of hydraulic fracturing, and its unified formulation of fracture nucleation and propagation in any propagation mode with an arbitrary number of fractures is a very attractive feature of such a numerical implementation. From the original implementation of Bourdin et al., however, several adaptations are required for hydraulic fracturing applications, which are: 1) extension to porous media, 2) computation of fracture width, 3) coupling with fluid flow, and 4) compressive-tensile split of the strain energy for geo-materials. Thus, in this study, we focus our development on these points and compare how different phase-field formulations address these issues in somewhat different manners. Finally, we discuss our endeavour to improve the numerical efficiency in coupling of the multi-physical processes.

Personalized FEA of Femurs - A Leap to Clinical Practice

Zohar Yosibash*, Nir Trabelsi**, Amir Sternheim***

*School of Mechanical Engineering, Tel Aviv University, Ramat Aviv, Israel, **Mechanical Engineering, Shamoon College of Engineering, Beer Sheva, Israel, ***National Unit of Orthopaedic Oncology, Tel-Aviv Medical Center, Tel-Aviv, Israel

ABSTRACT

Patient-specific CT-based high-order finite element models (p-FEMs) accurately predict ex-vivo experimental observations on human femurs, including risk of fracture [1,2]. They account for the exact geometry and inhomogeneous material properties, are created in a semi-automated manner from CT scans and validated on a large cohort of fresh frozen femurs. CT-based p-FEMs were applied to predict bone strength in patients with bone tumors to their femur [3], demonstrating excellent prediction capabilities. The first part of the talk addresses the methodology to semi-automatically generate the femurs' FEM from CT scans, assign material properties, apply the stance position load and interpret the FE results according to surgeon's need. Application of FE methodology in clinical practice is subject to obstacles and surprises, however, at the same time is accompanied by tremendous satisfaction when it helps patients and saves pain and agony. The second part of the talk will address the steps undertaken to bring the methodology into clinical practice. We shall present two clinical studies for using our CT-based p-FEA: one related to the need of a prophylactic surgery of femurs with metastatic tumors and the other related to the risk of a contralateral fracture of the femur proximal part following fractures in the elderly population. Several cases analyzed during the clinical trials and the potential use of p-FEA in clinical practice will be presented. References: [1] N. Trabelsi et al. Patient-specific finite element analysis of the human femur - a double-blinded biomechanical validation. J. Biomech., 44:1666-1672, 2011. [2] Z. Yosibash, et al. Predicting the yield of the proximal femur using high order finite element analysis with inhomogeneous orthotropic material properties. Phil. Tran. of the Roy Soc.: A, 368:2707-2723, 2010. [3] Z. Yosibash, et al. Predicting the stiffness and strength of human femurs with realistic metastatic tumors. Bone, 69:180-190, 2014.

A Meshfree Quadrature Rule for Non-local Mechanics

Huaigian You^{*}, Nathaniel Trask^{**}, Michael Parks^{***}, Yue Yu^{****}

^{*}Lehigh University, ^{**}Sandia National Lab, ^{***}Sandia National Lab, ^{****}Lehigh University

ABSTRACT

We present a meshfree quadrature rule for compactly supported non-local integro-differential equations (IDEs) with radial kernels. We apply this rule to develop a meshfree discretization of a peridynamic solid mechanics model that requires no background mesh. Existing discretizations of peridynamic models have been shown to exhibit a lack of asymptotic compatibility to the corresponding linearly elastic local solution. By posing the quadrature rule as an equality constrained least squares problem, we obtain asymptotic convergence by introducing polynomial reproduction constraints. Our approach naturally handles traction-free conditions, surface effects, and damage modelling for both static and dynamic problems. We demonstrate high-order convergence to the local theory by comparing to manufactured solutions and to cases with crack singularities for which an analytic solution is available. Finally, we verify the applicability of the approach to realistic problems by reproducing high-velocity impact results from the Kalthoff-Winkler experiments.

Mechanotransduction of a Vesicle Membrane and Its Implication in Cellular Mechanotransduction

Yuan-Nan Young*, Onshun Pak**, Zhangli Peng***

*New Jersey Institute of Technology, **Santa Clara University, ***University of Notre Dame

ABSTRACT

Mechanosensation is an important process in biological fluid–structure interaction. To understand the biophysics underlying mechanosensation, it is essential to quantify the correlation between membrane deformation, membrane tension, external fluid shear stress, and conformation of mechanosensitive (MS) channels. A multiscale continuum model is constructed for a MS channel gated by tension in a lipid bilayer membrane under stresses due to fluid flows. We illustrate that for typical physiological conditions vesicle hydrodynamics driven by a fluid flow may render the membrane tension sufficiently large to gate a MS channel open. In particular, we focus on the dynamic opening/closing of a MS channel in a vesicle membrane under a planar shear flow and a pressure-driven flow across a constriction channel. Our modeling and numerical simulation results quantify the critical flow strength or flow channel geometry for intracellular transport through a MS channel. The modeling and simulation (both boundary integral and dissipative particle dynamics simulations) results imply that for fluid flows that are physiologically relevant and realizable in microfluidic configurations stress-induced intra-cellular transport across the lipid membrane can be achieved by the gating of reconstituted MS channels, which can be useful for designing drug delivery in medical therapy and understanding complicated mechanotransduction. We then use this model to investigate the cellular mechanotransduction by primary cilia in the force-by-lipid paradigm.

A Simple A Posteriori Estimate on General Polytopal Meshes with Applications to Complex Porous Media Flows

Soleiman Yousef*, Martin Vohralik**

*IFP Energies nouvelles, France, **Inria Paris, & Université Paris-Est, CERMICS (ENPC), France

ABSTRACT

In this work we develop an a posteriori error estimate for lowest-order locally conservative methods on meshes consisting of general polytopal elements. We focus on the ease of implementation of the methodology based on H^1 -conforming potential reconstructions and $H(\text{div}, \Omega)$ -conforming flux reconstructions. In particular, the evaluation of our estimates for steady linear diffusion equations merely consists in some local matrix-vector multiplications, where, on each mesh element, the matrices are either directly inherited from the given numerical method, or easily constructed from the element geometry, while the vectors are the flux and potential values on the given element. We next extend our approach to steady nonlinear problems. We obtain a guaranteed upper bound on the total error in the fluxes that is still obtained by local matrix-vector multiplications, with the same element matrices as above. Moreover, the estimate holds true on any linearization and algebraic solver step and allows to distinguish the different error components. Finally, we apply this methodology to unsteady nonlinear coupled degenerate problems describing complex multiphase flows in porous media. Also here, on each step of the time-marching scheme, linearization procedure, and linear algebraic solver, the estimate takes the simple matrix-vector multiplication form and distinguishes the different error components. It leads to an easy-to-implement and fast-to-run adaptive algorithm with guaranteed overall precision, adaptive stopping criteria, and adaptive space and time mesh refinements. Numerous numerical experiments on practical problems in two and three space dimensions illustrate the performance of our methodology.

Inverse Transient Heat Flux Boundary Condition and Computation of Thermal Stress

Bo Yu^{*}, Chuanbao Nie^{**}, Huanlin Zhou^{***}, Chuang Xu^{****}

^{*}Hefei University of Technology, ^{**}Hefei University of Technology, ^{***}Hefei University of Technology, ^{****}Hefei University of Technology

ABSTRACT

The structure can be sometimes affected by the high heat flux in real engineering, such as the high heat flux of spacecraft surface when it returns the atmosphere, but the high heat flux usually cannot be measured directly. A novel non-iterative inverse method based on the precise integration finite element method (PIFEM) is established for estimating the transient boundary conditions in this paper. First of all, we obtain the temperature of measured points by solving the direct problem based on PIFEM. After that, the matrices formed by the PIFEM need to be reassembled, and then the unknown transient heat flux of boundary can be obtained by the least-square method. Finally, we can use the inversed heat flux boundary condition to compute the temperature and thermal stress distributions of the structure by PIFEM. Numerical results show that the present method can obtain the great performance on the inversing accuracy, the computing efficiency is better than intelligent evolutionary algorithm, and the measured errors and the number of measured points have little effect on the inverse results.

Data-driven Reduced-order Modeling of Microvoid Evolution for Ductile Fracture

Cheng Yu^{*}, Modesar Shakoor^{**}, Orion Kafka^{***}, Wing Kam Liu^{****}

^{*}Northwestern University, ^{**}Northwestern University, ^{***}Northwestern University, ^{****}Northwestern University

ABSTRACT

Microvoid evolution plays an important role in the ductile fracture process. Although various Gurson-type models have been developed to account for microvoid morphology and distribution, as well as matrix hardening and plasticity anisotropy with considerable fitting parameters, it is difficult to derive a unified constitutive model that considers all of these parameters. This presentation introduces a data-driven reduced order computational homogenization method by explicitly modeling microvoid evolution for ductile fracture analysis. Instead of using a phenomenological constitutive law, the material behavior of each integration point in a macroscopic part is computed on-the-fly using a statistical volume element (SVE) with embedded microvoids and periodic boundary conditions. The matrix of the SVE is modeled with a single/poly crystal plasticity law which accounts for plastic flow anisotropy and creep. Microvoids are reconstructed to reflect the real material microstructure morphology and distribution. To simulate the fracture process within a reasonable computational time, we adopt a recently developed data-driven order reduction technique, called self-consistent clustering analysis (Liu, Z., Bessa, M.A. & Liu, W.K., 2016. Computer Methods in Applied Mechanics and Engineering, 306, pp.319–341.), for the SVE problem. The predicted void evolution in a SVE under uniaxial tension is validated by comparing with in-situ X-ray tomography observation of void-driven fracturing in an additively manufactured Nickel-based superalloy. Fracture toughness tests of a high strength steel using compact tension specimens are also simulated with the primary particles modeled using finite elements at the macroscale and secondary particles modeled in the microscale SVEs. The fracture toughness measurements and crack path are compared to experiments. The proposed method might be used for ultimate strength and fracture toughness optimization by controlling the microstructure.

High Performance Fully-Coupled Fluid-Solid-Acoustic Solver

Feimi Yu*, Lucy Zhang**

*Rensselaer Polytechnic Institute, **Rensselaer Polytechnic Institute

ABSTRACT

The evaluation of the acoustic perturbation with low Mach number in fluid-structure interactions is challenging. Due to the large discrepancy in time scale between the fluid and the acoustic behavior, the computational time is significantly increased if directly numerical simulation is to be used. In this talk, we will introduce an aeroacoustic model for nearly incompressible isentropic flows used in Navier-Stokes equations, which is then incorporated into a fluid-structure interaction framework to evaluate the impact of pressure fluctuation on a deformable solid. A finite element library, deal.II, is utilized to modularize the finite element program to solve the modified Navier-Stokes equations for the ease of modification of the parameters and increasing the overall performance of the computation. The fully-coupled fluid-solid-acoustic solver requires the linearization and optimization of an effective preconditioner. Test cases are performed to validate the computation performance and the accuracy of the presented model. As an application, we will present a vocal fold vibration simulation where fluid-solid-acoustic fields are coupled to simulate the acoustic fields produced by slightly compressible flow that interacts with the vocal fold tissues.

The Nacelle's Position Effect on Aerodynamics of Blended-Wing-Body Airplane

Gang Yu^{*}, Yue Shu^{**}, Dong Li^{***}, Zeyu Zhang^{****}

^{*}PhD Student, Northwestern Polytechnical University, Xi'an, P.R. China, ^{**}Master Student, Northwestern Polytechnical University, Xi'an, P.R. China, ^{***}Professor, Northwestern Polytechnical University, Xi'an, P.R. China, ^{****}PhD Student, Northwestern Polytechnical University, Xi'an, P.R. China

ABSTRACT

The Blended-Wing-Body (BWB) airplane concept represents a potential revolution in subsonic transport efficiency for large airplanes[1]. Except the Wing-Body blended way, the propulsion airframe integration of BWB airplane also takes a very important role for its good aerodynamic performances. The wing engine mounting distorts lift distribution may creating poor cruise aerodynamics. Therefore, its need to be minimized through careful propulsion airframe integration design[2]. The nacelle's position effect on aerodynamics of Blended-Wing-Body airplane is analyzed in this paper. First, the aerodynamics of clean BWB configuration (wing-body without nacelle) and with nacelle's initial configuration are compared to get an idea of nacelle's effect on the wing-body's aerodynamics. Then, the nacelle at different positions effect on aerodynamics of wing-body are analyzed to see the nacelle's position effect on the wing-body's aerodynamics. And moreover, the wing-body's effect to nacelle's aerodynamics is also compared. The initial model of 300 seating civil BWB airplane is shown as Fig.1. It is designed by the Aerodynamic Concept Design Institute of Northwestern Polytechnical University (NWPU) located in Xi'an, China. The pylon is deleted from the model to make clear the problem is only the Nacelle's position effect. The N-S equations[3] are used as the governing equations to solve the BWB's flow field. The Finite Volume method is used to discrete the equations, and the spatial discretization using the Roe's scheme. The turbulence flow model is Menter's k- ω sst model. The mesh is an O-H multi-block structure mesh as shown in Fig.2. And the calculate condition is Mach=0.8, Re=145 \times 10⁶, AOA=2°. The nacelle's position changed way is shown in Table. 1. Table. 1

Direction	Lower Bound(mm)	Upper Bound(mm)	Interval(mm)
X	-600	600	100
Y	-500	500	100
Z	-300	300	100

Some results are shown in Figures below. It could be seen from the results that there are three main effects of nacelle's position on aerodynamics of BWB: 1. The high pressure area caused by nacelle's leading edge stagnation point; 2. The shockwave interface between nacelle and wing-body; 3. The flow separation induced by the shock between nacelle and wing-body; Reference [1] R. Liebeck, M. Page, B. Rawdon. Blended-Wing-Body subsonic commercial transport[R]. AIAA 98-0438, 1998. [2] G. Hill, R. Thomas, Challenges and opportunities for noise reduction through advanced aircraft propulsion airframe integration and configurations, in: 8th CEAS Workshop: Aeroacoustics of New Aircraft and Engine Configurations, Budapest, Hungary, 2004, pp.1–13. [3] John D. Anderson, Computational Fluid Dynamics, Tsinghua University Press.

An I-integral Method for Crack Analysis in Ferroelectrics under Large-scale Switching

Hongjun Yu^{*}, Meinhard Kuna^{**}, Licheng Guo^{***}

^{*}Harbin Institute of Technology, China, ^{**}Technische Universität Bergakademie Freiberg, Germany, ^{***}Harbin Institute of Technology, China

ABSTRACT

It is a great challenge to extract the crack-tip fracture parameters of ferroelectrics under large-scale domain switching. A successful attempt is the establishment of the interaction integral (I-integral), whereas hereby the integration region must exclude grain boundaries. This paper breaks this limitation and develops an enhanced I-integral. The enhanced I-integral exhibits several merits over previous switching-toughening models in determining the crack-tip intensity factors. First, restriction to small-scale switching is overcome. Second, the intensity factors of different modes are decoupled. Third, it is independent of integration area size, regardless of the presence of grain boundaries and domain walls. These advantages ensure the successful utility of the area-independent I-integral in ferroelectric polycrystals under large-scale domain switching. The phase field model is combined with the I-integral method to form an effective approach to predict the polarization distributions and to evaluate the crack-tip intensity factor. Using this approach, a tensile test of PbTiO₃ ferroelectric polycrystals with an impermeable crack is simulated. The crack-tip mechanical and electrical field intensity factors obtained by the I-integral agree well with those by the extrapolation technique, and the I-integral shows good area-independence even when grain boundaries and domain walls exist in the integration area. For polycrystals, domain switching initiates not only from the crack tip but also from the grain boundaries due to high polarization gradient and stress concentration. Domain switching is triggered by a critical load, which greatly reduces the mode-I stress intensity factors. The critical load is much lower for polycrystals than for single crystals and sometimes vanishes due to grain orientations.

Direct Numerical Simulation of Thermal Turbulence and Conjugated Heat Transfer in Film-cooling Structures

Ting Yu^{*}, Hongyi Xu^{**}, Duo Wang^{***}

^{*}Fudan University, ^{**}Fudan University, ^{***}Fudan University

ABSTRACT

Direct Numerical Simulation of Thermal Turbulence and Conjugated Heat Transfer in Film-cooling Structures
Abstract - Nowadays, the film-cooling technology was widely applied in the design of the heated components in aero-engines, including the combustor and the turbine blades. The early researches within the field included both experimental and numerical simulation works, such as Pedersen et al[1] and Walters et al[2]. The current paper focused on the film-cooling flows in a typical simplify cylindrical-hole structure. The state-of-the-art direct numerical simulation (DNS) was used to capture the turbulent flow and the heat-transfer phenomena in the structures. In order to accurately simulate the heat-transfer in the thermal flows on both heating and cooling sides, and to strongly couple the heat-conduction calculation in the metal in between the flows, the interfacial thermal boundary conditions between the fluid and solid were implemented by the continuous conditions of both temperature and heat conduction on the heating and cooling surfaces. This simulation strategy permitted an accurate capture of the conjugated heat-transfer process in both thermal fluids and solid metal. The accurate DNS-solution techniques were achieved by the reliable and robust Flexible-cycle Additive-correction Multi-grid (FC-AC MG) method first introduced in Xu[3]. The computation provided the detailed mechanisms of the cooling-film flow formation and the closely-related thermal effects on the cooling surfaces. These results permitted an in-depth investigations of the cooling structure performance, such as the distributions of the cooling effectiveness, the flow and temperature details inside the cooling hole as well as the transient heat-conduction process inside the metal, which will eventually lead to significant improvements for the design of the current film-cooling structures. References [1]Pedersen D R, Eckertl E R G, Filming cooling with large density differences between the main stream and secondary fluid measured by heat-mass transfer analogy [J], ASME Journal of Heat Transfer, 1997, 119(1), 59-98. [2]Walters D K, Leylek J H, A detailed analysis of film cooling physics, part1-streamwise injection with cylindrical holes [J], ASME Journal of Turbo Machinery, 1996, 31(3), 195-216. [3]Lakehal D, Theodoridis G, Rodi W, Three dimensional flow and heat transfer calculations of film cooling at the leading edge of a symmetrical turbine blade model [J], Int. Journal of Heat & Fluid Flow, 2001, 22(2), 156-160

Numerical Study on Longitudinal Vibration of Roller Chain Drive

Wenguang Yu^{*}, Binglei Zhang^{**}

^{*}Shanghai Electric Group Co., Ltd., Central Academe, ^{**}Shanghai Electric Group Co., Ltd., Central Academe

ABSTRACT

A refined dynamic model of a roller chain drive is developed and applied to the analysis of dynamic behavior of roller chain drive in Escalator. The roller chain drive model is composed of the two sprockets, the chain made of rollers and links, which are represented by elastic boundary constraint, lumped mass and springs–damper assemblies respectively. The chain elasticity, the mass of slack spans, torsional stiffness and inertia of sprockets are taken into account in the dynamic model. The boundary condition of the chain model are discussed in detail. The dynamic model is implemented in a computational code based on APDL to study the dynamics of the chain drive, including the frequency of longitudinal vibration and the transient vibration response of the engaging rollers under the polygonal effect. The numerical model is updated according to comparison with experiment results. Finally the updated numerical model is used to predict dynamic performance of similar roller chain drives and investigate the impacts of different factors, like length of span and mass of chain, on the dynamic behavior.

A Discrete Fiber Network Model of Arterial Elastin

Xunjie Yu^{*}, Katherine Yanhang Zhang^{**}

^{*}Boston University, ^{**}Boston University

ABSTRACT

Abstract Discrete fiber network (DFN) model has been used to study biological fibrous materials with fiber-level geometric realism. DFN model is able to capture the microstructural kinematics of fibrous tissue at large strains. In most DFN models, the crosslinks were usually modeled as pin joints [1]. In this study, a DFN model of elastin network in the arterial wall was developed based on measured geometric features to study the nature of crosslinks in contributing to extracellular matrix (ECM) mechanics and fiber kinematics. Multiphoton microscopy was performed on purified elastin network from porcine thoracic aorta to characterize fiber orientation distribution, areal fraction, and fiber diameter. A DFN model was generated by randomly placing line segments into the given domain following the obtained orientation distribution until the desired fiber areal fraction was reached. The intersections of two segments were treated as crosslinks. Periodic boundary conditions were prescribed, and the DFN network is continuous when tiled up in both horizontal and vertical directions. Dangling ends, which are the free ends of line segments projecting beyond the crosslinks, were removed since they do not contribute to the rigidity of the network. Finite element simulations of DFN under equi- and nonequi- biaxial stretch were performed in Abaqus. Timoshenko beam element B21H was selected to represent a single fiber. The elastin fiber is modeled using an entropy-based freely-jointed chain with material parameters determined based on tissue-level stress vs. stretch relationship obtained from biaxial tensile tests [2]. The inter-fiber crosslinks were modeled with rotational stiffness that varies systematically from 0 (pin-joined) to infinity (rigid). The reorientation of the fibers in the DFN model was studied and compared with MPM images of elastin network. The DFN model showed excellent fitting and predicting capabilities of elastin network under equi- and nonequi-biaxial loading conditions. In previous structural based constitutive models of arteries, interactions among ECM fibers are often ignored [3]. The rotational stiffness of the crosslinks was found to play an important role in fiber realignment when elastin network is subjected to mechanical loading. References 1. Mauri, A., et al., (2016). J Mech Behav of Biomed Mater, 58, 45–56. 2. Wang, Y., et al., (2016). J Biomech, 49(12), 2358-2365.. 3. Chow, M. J., et al., (2014). Biophys. J, 106(12), 2684–2692.

Error Estimates for Dynamic Augmented Lagrangian Boundary Condition Enforcement, with Application to Immersogeometric Fluid--Structure Interaction

Yue Yu^{*}, Xin Yang Lu^{**}, David Kamensky^{***}, Ming-Chen Hsu^{****}, Thomas Hughes^{*****}, Yuri Bazilevs^{*****}

^{*}Lehigh University, ^{**}McGill University, ^{***}University of California, San Diego, ^{****}Iowa State University, ^{*****}The University of Texas at Austin, ^{*****}University of California, San Diego

ABSTRACT

In this work, we analyze the convergence of the recent numerical method for enforcing fluid--structure interaction (FSI) kinematic constraints in the immersogeometric framework for cardiovascular fluid--structure interaction. In the immersogeometric framework, the structure is modeled as a thin shell, and its influence on the fluid subproblem is imposed as a forcing term. This force has the interpretation of a Lagrange multiplier field supplemented by penalty forces, in an augmented Lagrangian formulation of the FSI kinematic constraints. Because of the non-matching fluid and structure discretizations used, no discrete inf-sup condition can be assumed. To avoid solving (potentially unstable) discrete saddle point problems, the penalty forces are treated implicitly and the multiplier field is updated explicitly. In the present contribution, we introduce the term dynamic augmented Lagrangian (DAL) to describe this time integration scheme. We formulate the DAL algorithm for a linearized parabolic model problem, analyze the regularity of solutions to this problem, and provide error estimates for the DAL method in both the $L^\infty(H^1)$ and $L^\infty(L^2)$ norms. We also prove error estimates for a recently-proposed extension of the DAL method, with improved conservation properties. Numerical experiments indicate that the derived estimates are sharp and that the results of the model problem analysis can be extrapolated to the setting of nonlinear FSI, for which the numerical method was originally proposed.

Interfacial Behavior of Adhesively Bonded Pipe Joints Subjected to Combined Thermal and Mechanical Loadings

Hong Yuan*, Jun Han**

*Jinan University, **Jinan University

ABSTRACT

Pipe structures are a very important structural form for energy, aerospace and construction industries. In consideration of whole weight, strength and maintenance workload, it is commonly accepted that there should be less joints in a piping system at first design. Due to the limitation of transportation, installation and rehabilitation, a joint seems essential for a large structure system containing different components. The limitations of the overall system performance usually come from the capacity of pipe joints. For most piping system, the joints can be divided into three types: flange coupling, welding and adhesive bonding. The first two traditional connections have the same shortage, such as high stress concentration. However, the adhesively bonded pipe joint can effectively lower the stress concentration. Among all the possible loading configurations, tensional loading is one of the fundamental loading types. Because of the difficulties in the analysis of interfacial behavior, there are just a few theoretical studies available in the previous references. All the existing analytical studies were focused on the elastic region of interfacial behavior. However, the interfacial failure always experiences much more complicated processes. So the softening and debonding of the adhesively bonded interface should be taken into consideration. To understand the interfacial behavior of plane joints exposed to different temperature variations, the pull test can be used. The results can reflect the combined effects of a number of factors, including temperature-induced interfacial shear stresses change in the bondline as well as the adherends if the temperature becomes sufficiently high. The whole joints should be subjected to normal work high temperature because a large temperature variation will induce complicity of the interface bond property. Interfacial behavior is the key factor that affects the total performance of bonded joints. This paper presents an analytical solution for the full-range behavior of an adhesively bonded pipe joint under combined thermal and mechanical loadings in which interfacial softening and debonding have been taken into consideration. The expressions for the interface slip and shear stress are derived for the different failure stages. The present research improves and clarifies the understanding of the interfacial debonding of bonded pipe joints under combined thermal and mechanical loadings. The predictions of the closed-form solutions agree with the ABAQUS finite element results very well. By modifying different material parameters, the present results may be further extended to composite pipe joints, composite-metal pipe joints or metallic pipe joints.

Computational Mechanics Modeling of a Continuum Soft Robot

Hongyan Yuan^{*}, Bahador Marzban^{**}, Richard Sperling^{***}

^{*}University of Rhode Island, ^{**}University of Rhode Island, ^{***}University of Rhode Island

ABSTRACT

Compliant and low-weight soft robots have many advantages, compared to traditional rigid robots, including safe operation in constrained environments, dexterity and adaptivity in unstructured environments, relative simplicity in fabrication, low-energy consumption, and low-cost. One of many challenges in developing soft robots is the mechanics modeling and control of soft robots due to continuum elastic deformation of the soft materials. In this work, we develop a computational mechanics program for simulation and control of a novel cable-driven continuum soft robot. A 3D finite-element rod model is adopted to convert the continuum robot arm into discrete rigid bodies in the computational program. Computational multibody dynamics algorithms are adopted to carry out dynamic simulations of the robot arm driven by the motor-cable forces. The friction and contact of robot arm with the environment are simulated. The computational mechanics program is used to guide and optimize the design of the continuum soft robots for specific tasks such as locomotion. Simulations from the computational program are also used in a machine-learning algorithm to develop an adaptive control method for the soft robots.

A Modified Zerilli–Armstrong Model Incorporating the Anisotropy and Anomalous Stress Peak : Application to the Laser Additive Manufactured Inconel 718

Kangbo Yuan^{*}, Weiguo Guo^{**}, Penghui Li^{***}, Jianjun Wang^{****}, Longyang Chen^{*****}

^{*}School of Aeronautics, Northwestern Polytechnical University, Xi'an, China, ^{**}School of Aeronautics, Northwestern Polytechnical University, Xi'an, China, ^{***}School of Aeronautics, Northwestern Polytechnical University, Xi'an, China, ^{****}School of Aeronautics, Northwestern Polytechnical University, Xi'an, China, ^{*****}School of Astronautics, Northwestern Polytechnical University, Xi'an, China

ABSTRACT

Abstract: The lack of accurate description of dynamic thermomechanical behaviors in extreme high-strain-rate and high-temperature loading environment could be a major obstacle to extending the laser additive manufactured (LAMED) Inconel 718 to engineering applications. In this study, to obtain further understandings of plastic flow behaviour of the LAMED Inconel 718, uniaxial compression experiments were conducted over a wide range of temperatures (298–1193 K) and strain rates (0.001–5300/s). Not only the anisotropy of compressive strength, but the influences of temperature and strain rate on plastic flow stress were analyzed. The flow stress of the as-deposited alloy in laser scanning direction is higher than that in deposition direction, which is attributed to the columnar crystal epitaxially growing along the build direction. A anomalous stress peak in flow stress vs. temperature relation was found and proved to be the third-type of strain aging effect. The flow stress of the alloy exhibits inconspicuous strain-rate sensitivity over the range of strain rate below 1000 /s, while increases sharply with the strain rate once it exceeds 1000 /s. Taking into account the anisotropy, as well as the anomalous temperature and strain rate dependencies of the flow stress, a modified Zerilli–Armstrong constitutive model for the LAMED In718 was developed. A directional factor was introduced to indicate the equivalent size of columnar crystals, the strain rate hardening has been enhanced once the strain rate exceeds a certain level, and a normal distribution with temperature was used to describe the 3rd SA effect. The model was shown to be able to accurately predict the plastic flow behaviour of the LAMED Inconel 718 over a wide range of temperatures and strain rates.

Keywords: Laser additive manufactured Inconel 718, anisotropy, temperature, strain rate, constitutive model

References [1] Zerilli, F. J., Armstrong, R. W. (1987). Dislocation – mechanics - based constitutive relations for material dynamics calculations. *Journal of Applied Physics*, 61(5), 1816-1825. [2] Wang, J., Guo, W. G., et. al (2015). The third-type of strain aging and the constitutive modeling of a Q235B steel over a wide range of temperatures and strain rates. *International Journal of Plasticity*, 65, 85-107.

A Parallel Adaptive Mesh Flow Solver Based on PHG Toolbox

Li Yuan*

*ICMSEC, Academy of Mathematics and Systems Science, Chinese Academy of Sciences

ABSTRACT

Nowadays unstructured tetrahedral grids are widely used in scientific and engineering computing. Adaptive mesh strategies can improve accuracy for a given number of grid scales, or reduce grid scales for a given accuracy. In the past two decades a lot of parallel unstructured flow solvers have been developed. However, development of parallel adaptive mesh codes needs a series of efforts ranging from domain repartition to keep load balance to data transfer among processors, which are barriers for many people only caring numerical schemes or engineering applications. The emergence of a PHG (Parallel Hierarchical Grid) platform provides interface functions for carrying out common and difficult tasks in parallel adaptive finite element programs, such as parallel adaptive mesh refinement, dynamic load balancing, and linear solvers. PHG is an open source toolbox for writing scalable parallel adaptive finite element programs. In this work, we have developed a C++ h-adaptive code – Libfvphg for numerical solution of hyperbolic conservation laws / Euler equations on three-dimensional tetrahedral grids based on the PHG platform. Libfvphg uses finite volume method with linear reconstructions but it is easily extendable to discontinuous Galerkin methods directly. This is because PHG supports DG finite element as well as other types of element. The finite volume method uses only the piecewise constant element. Libfvphg not only encompasses a variant of partial differential equations (conservation laws, Euler), reconstruction strategies (Green Gauss, least squares) and numerical flux functions (LF, HLLC, Roe), but also supports various posteriori error estimates for adaptive mesh. We show that the development of Libfvphg using PHG is like writing a serial code, where the DOF of PHG is used as the flow variables. The needed neighboring cell information in other process and parallel adaptive mesh management are automatically done in PHG. We describe the C++ object hierarchy, the sets of equations used in the current version, and the available choices for numerical discretization, particularly, the second-order high resolution multidimensional limiting process (MLP). Finally, we give a set of relevant validation and verification test cases. These include spherical explosion, transonic flow past a wing-body combination. Numerical effects of using different reconstructions and posteriori error estimates are examined. The parallel efficiency is shown to be 80-40% from 32 up to 1024 processes for 20 million tetrahedrons. We intend to illustrate that parallel unstructured grid flow solver can be built relatively easy if using the PHG platform.

N-Scale Eigenstrain-Based Reduced Order Homogenization

Zheng Yuan*

*Altair Engineering

ABSTRACT

A hierarchical model reduction approach aimed at systematically reducing computational complexity of multiple scale homogenization for nonlinear history-dependent problems is developed. The method consists of the following salient features: (1) formulation of non-linear unit cell problems at multiple scales in terms of eigenstrain modes that a priori satisfy equilibrium equations at multiple scales and thus eliminating the need for costly solution of discretized non-linear equilibrium, (2) hierarchical solution strategy that requires sequential solution of single-scale problems, and (3) recursive formulation of N-scale stress updates that essentially simplifies the implementation to a regular two-scale case.

A Generalized Dual-Purposed Reduced-Order-Homogenization Model for Multiscale Fatigue Damage

Zifeng Yuan^{*}, Jacob Fish^{**}

^{*}Columbia University, in the City of New York, ^{**}Columbia University, in the City of New York

ABSTRACT

Composite material is widely used as a thin-wall structure, where the characteristic length in thickness direction (out-of-plane direction) is much smaller than the rest two directions (in-plane direction). In addition, the composite structure is made of a number of layups with different orientations. Accordingly, delamination may take place between layups where the mismatch stress reaches the corresponding strength. In the presentation, we describe a Generalized Dual-Purpose Model (GDPM). The GDPM is able to predict interlayer delamination under mode I, II, III, or generalized mixed-mode, where the intralayer can be arbitrary plane-stress model. Specifically, the intralayer adopts a plane stress multiscale reduced-order-homogenization model to simulate fatigue damage accumulation of a Polymer Matrix Composite (PMC) material. An isotropic fatigue damage model and hybrid fatigue damage and plasticity model are introduced to simulate the fiber and matrix phase, respectively. Comparison of the numerical results with experimental measurement is given as well.

Experimental and Numerical Investigations of 6082-T6 Aluminum Alloy Beams with Hollow Sections

ZHAO Yuanzheng*, ZHAI Ximei**

*School of Civil Engineering, Harbin Institute of Technology, **School of Civil Engineering, Harbin Institute of Technology

ABSTRACT

This paper presents experimental and numerical studies of aluminum alloy beams with square (SHS), rectangular (RHS) and circular (CHS) hollow sections. Three-point bending and four-point bending tests were performed to the hinged-ended beams made of cold-extruded 6082-T6 aluminum alloy and measurement of the initial geometric imperfection and material strength for the members was conducted before the tests. A finite element (FE) model was proposed using non-linear FE analysis software ABAQUS and the model was verified against the experimental results. Considering the distinct nonlinear property of aluminum alloy, material and geometric nonlinearities were incorporated into the FE model. The simulation results showed that the FE model was accurate enough to predict the failure modes, buckling resistance and deformability of the experimental beams. A parametric study was conducted to access the effect of the key parameters such as sectional dimension, radius-thickness ratio and slenderness ratio on the deformation capacity and strength of the hinged-ended aluminum alloy beams by the FE model. Based on the comparison of the beam strengths obtained from the parametric study and the design strength predicted by several current design specifications, the verification of the Chinese code (GB 50429-2007), the American code (ADM-2005) and the European code (Eurocode 9) were performed and the revised suggestions for GB 50429-2007 were presented. The reliability analysis for the design rules were performed to investigate whether the reliability levels can reach the goals.

CFD Based Multidisciplinary Design Optimization for Offshore Aquaculture Platform

FENG Yukun^{*}, DAI Yi^{**}, CHEN Zuogang^{***}, CAI Jiqiang^{****}, WANG Fei^{*****}, CHEN Zhixin^{*****}

^{*}State Key Laboratory of Ocean Engineering, Shanghai Jiao Tong University, ^{**}State Key Laboratory of Ocean Engineering, Shanghai Jiao Tong University; Collaborative Innovation Center for Advanced Ship and Deep-Sea Exploration, Shanghai Jiao Tong University., ^{***}State Key Laboratory of Ocean Engineering, Shanghai Jiao Tong University; Collaborative Innovation Center for Advanced Ship and Deep-Sea Exploration, Shanghai Jiao Tong University., ^{****}Fishery Machinery and Instrument Research Institute, Chinese Academy of Fishery Sciences., ^{*****}State Key Laboratory of Ocean Engineering, Shanghai Jiao Tong University; Collaborative Innovation Center for Advanced Ship and Deep-Sea Exploration, Shanghai Jiao Tong University., ^{*****}Fishery Machinery and Instrument Research Institute, Chinese Academy of Fishery Sciences.

ABSTRACT

The shape of the hull has a significant impact on the resistance and propulsive performance of the ship, especially for the fat ship. In this research, the experimental and numerical analysis of an offshore aquaculture platform are carried out, while the multidisciplinary design optimization of the platform shape is also conducted. RANS solver is applied for the numerical analysis. Validity of the numerical method is proved by comparing numerical results of the original shape with experimental results. An optimization framework using Latin hypercube design, free-form deformation (FFD) method, Kriging surrogate model and Genetic algorithm (GA) are developed. Nine design variables have been employed to modify the shape of the platform. Because of a tradeoff between the minimum resistance and the minimum nonuniformity of wake flow, the optimum solution of the hull shape is selected from the Pareto front to balance the two objectives. Model tests for the optimized shape are then performed to validate the design results. The results show that the resistance and the nonuniformity of the wake flow of the optimized shape are reduced by 1.59% and 17.80% respectively in comparison with the results of the original shape.

A Probabilistic Progressive Damage Simulation Model for Braided Composites

Gunjin Yun^{*}, Sungwoo Jeong^{**}, Chao Zhang^{***}

^{*}Seoul National University, ^{**}Seoul National University, ^{***}Northwestern Polytechnical University

ABSTRACT

A Probabilistic Progressive Damage Simulation Model for Braided Composites Sungwoo Jeong Department of Mechanical & Aerospace Engineering, Seoul National University, South Korea Chao Zhang School of Aeronautics, Northwestern Polytechnical University, China Gunjin Yun Department of Mechanical & Aerospace Engineering, Seoul National University, South Korea Abstract This paper presents a probabilistic progressive damage simulation model for braided composites. Damage mechanisms considered in this paper are fiber tow damage and tow-to-tow interface delamination. Deterministic predictions by the existing damage progressive analysis model of braided composites could be very different from the experimental global strength and failure modes due to effects of material uncertainties. Therefore, uncertainties of constituents' physical properties were taken into account in this study. An anisotropic damage model was used for damage initiation and evolution of fiber tows. A cohesive-zone model under mixed-modes was also adopted for delamination between fiber bundles. Strength and critical fracture energies of fiber tows were simulated as spatially varying random fields through the Karhunen-Loeve expansion method. For demonstrations of the proposed probabilistic damage analysis, a three-dimensional meso-scale finite element model of a single-layered unit cell was developed. Sensitivity of statistical parameters of the random material properties to sequential local and global damage behavior was evaluated. Both statistical local damage and global response of the braided composite were simulated and compared with experimental observations and we identified the most sensitive statistical model parameters. Keywords: spatial variability, probabilistic damage progression, braided composites, random fields, stochastic analysis, Karhunen-Loeve expansion

Large-scale Thermal Elastic-Plastic Welding Analysis Using Domain Decomposition Method

Yasunori Yusa^{*}, Yuma Murakami^{**}, Shota Miyauchi^{***}, Hiroshi Okada^{****}

^{*}Tokyo University of Science, ^{**}Tokyo University of Science, ^{***}Tokyo University of Science, ^{****}Tokyo University of Science

ABSTRACT

To estimate mechanical behaviors of a welding problem, such as residual stress and residual deformation, thermal elastic-plastic analysis is helpful. Also, when the problem is a real structure, large-scale parallel computation technique is necessary. Thus, we are developing a system that can analyze a large-scale welding problem by thermal elastic-plastic modeling. This system is based on domain decomposition method, which is frequently used in parallel finite element analysis. In domain decomposition method, the analysis domain is decomposed into multiple subdomains. Then, a linear system of equations, which is linearized by Newton-Raphson method, is statically condensed into subdomain interface degrees of freedom. The condensed linear system of equations is solved by conjugate gradient method with a preconditioner such as balancing domain decomposition. In the presentation, we will show the methodology that is specially required in the large-scale welding analysis. For example, the consideration of a moving heat source needs MPI (message passing interface) communications at every time step. Moreover, the convergence properties of Newton-Raphson method as well as conjugate gradient method are carefully investigated. This is because the thermal elastic-plastic problem with temperature-dependent material parameters is known to be a strongly nonlinear problem especially in the vicinity of the heat source. A part of the present work has been supported by JSPS KAKENHI Grant Number JP16K05988.

Sharp Volumetric Billboard Based Multilevel Modeling and Multigrid Method

Dewen Yushu^{*}, Karel Matouš^{**}

^{*}University of Notre Dame, ^{**}University of Notre Dame

ABSTRACT

Numerical modeling of heterogeneous materials is challenging due to the extremely high computational cost required to resolve all of the geometrical complexities. Despite the recent development of high performance computational frameworks and homogenization techniques, accurately predicting highly nonlinear material response with prominent localized behavior remains elusive. In this talk, we will introduce a novel sharp volumetric billboard (SVB) based multilevel modeling and multigrid computational technique, which enables accurate predictions of mechanical behavior of high energy ball milled (HEBM) Ni/Al composites. This SVB based modeling is an image based modeling technique, which stems from the volumetric billboard (VB) method, a Google Earth like multi-resolution modeling strategy in computer graphics. By creating VB series of an object, the data amount is greatly decreased while object shape is visually retained. In our work, we analyze the statistical and physical implications of the VB technique, and enhance it through the SVB scheme. A sharpening filter is created to reconstruct the original material contrast on coarser microstructures. We propose a contrast-based minimization problem and a corresponding numerical algorithm that approximates the minima through a fast sweeping strategy with local volume preservation. In our work, we focus on the Ni/Al reactive composites produced by HEBM. We utilize a fine scale microstructure from microtomography, and create levels of detail (LODs) from the SVB scheme. The first and second order probability functions are computed, and both exhibit consistency after large data reduction. Then, we use a parallel generalized finite element code, PGFem3D, to compute the mechanical behavior under a tension-relaxation loading profile using crystal plasticity constitutive equations. We adopt both identical and random texture. The macro- and micro-mechanical robustness of data compression is demonstrated through corresponding error analysis. The close properties of SVB LODs and their data structures naturally lend themselves in the development of multigrid methods. Our recent study shows that the SVB LODs contains reliable coarse microstructures, which can instruct the formulation of the key component – the intergrid operators -- in a multigrid method. Moreover, the coarse SVB LODs can also act as reliable preliminary to large computations. This is because the coarse SVB LODs generate coarse problems that can be used to approximate finer solution using significantly lower computational resources with acceptable numerical error.

Investigating the Influence of Buccal Bone Thickness on Bone Remodeling around Maxillary Anterior Implantation

KEKE ZHENG^{*}, Nobuhiro Yoda^{**}, Junning Chen^{***}, Zhipeng Liao^{****}, Keiichi Sasaki^{*****},
Michael Swain^{*****}, Qing Li^{*****}

^{*}School of Aerospace, Mechanical and Mechatronic Engineering, The University of Sydney, ^{**}School of Dentistry, Tohoku University, ^{***}College of Engineering Mathematics and Physical Sciences, University of Exeter, ^{****}School of Aerospace, Mechanical and Mechatronic Engineering, The University of Sydney, ^{*****}School of Dentistry, Tohoku University, ^{*****}School of Aerospace, Mechanical and Mechatronic Engineering, The University of Sydney, ^{*****}School of Aerospace, Mechanical and Mechatronic Engineering, The University of Sydney

ABSTRACT

Due to the anatomical registration in the maxillary anterior region during implantation, such as insufficient bone volume, part of the buccal bone will be lost after bone remodeling, with the consequence of a high risk of soft tissue recession [1]. Therefore, the critical buccal bone morphology around implants is widely considered as a primary factor to deaccelerate bone resorption around implants [2], as increasing the buccal bone thickness (BBT) above the implant [3]. This study established a framework that combined the in-vivo clinical quantification with in-silico computational modeling to investigate the effects of BBT on the bone remodeling outcome. One specific patient who had undergone an implant treatment in the anterior maxilla and experienced the buccal bone resorption on the implant was studied. A three-dimensional heterogeneous nonlinear FE model was constructed based on the CT images of this patient, and a validated bone remodeling algorithm was employed to simulate up to 48-month bone remodeling behavior in the bone region around the implant. The anterior incisory bone region of this model was then varied systematically to simulate five different BBTs (0.5, 1.0, 1.5, 2.0, and 2.5 mm), and the optimal BBT was inversely determined to minimize the risk of resorption. Our findings indicated that the initial BBT appeared to play a critical role in distributing mechanobiological stimuli, thereby determining subsequent variation in BBT. For this particular patient, the simulated results revealed that the increased BBT decreases the bone resorption rate in the peri-implant region. However, a 1.5 mm of BBT is recommended in this case as the extra bone volume does not indicate improving the remodeling outcome. This study revealed that the initial BBT significantly affected mechanobiological responses, which consequentially determines the bone remodeling process. An optimal initial BBT is considered essential to assure a long-term stability of implant treatment. Reference 1. Grunder U, et al. 2005. Influence of the 3-d bone-to-implant relationship on esthetics. *Int J Periodontics Restorative Dent*. 2. Merheb J, et al. 2014. Critical buccal bone dimensions along implants. *Periodontology* 3. Veltri M, et al. 2015. Three-dimensional buccal bone anatomy and aesthetic outcome of single dental implants replacing maxillary incisors. *Clinical oral implants research*.

Bayesian Deep Convolutional Encoder-Decoder Networks for Surrogate Modeling and Uncertainty Quantification

Nicholas Zabaras*, Yin hao Zhu**

*Center for Informatics and Computational Science, University of Notre Dame, **Center for Informatics and Computational Science, University of Notre Dame

ABSTRACT

We are interested in the development of surrogate models for uncertainty quantification and propagation in problems governed by stochastic PDEs using a deep convolutional encoder-decoder network in a similar fashion to approaches used in deep learning for image to image regression tasks. To evaluate the performance of this approach, we consider standard uncertainty quantification benchmark problems including flow in heterogeneous media defined in terms of limited data-driven permeability realizations. The performance of the surrogate model developed is surprisingly good even though there is no underlying structure shared between the input (permeability) and output (flow/pressure) fields as is often the case in the image-to-image regression models used in computer vision problems. Since normal neural networks are data intensive and cannot provide predictive uncertainty, we propose a Bayesian approach to convolutional neural nets. A recently introduced variational gradient descent algorithm based on Stein's method is scaled to deep convolutional networks to perform approximate Bayesian inference on millions of uncertain network parameters. This approach achieves state of the art performance in terms of predictive accuracy and uncertainty quantification in comparison to other approaches in Bayesian neural networks as well as techniques such as Gaussian processes and ensemble methods even when the training data size is relatively small. Uncertainty propagation tasks are considered and the predictive output Bayesian statistics are compared to those obtained with Monte Carlo estimates.

Computational Homogenization of MREs: Effect of Boundary Conditions, RVE Size and Microstructure Composition

Reza Zabihyan^{*}, Julia Mergheim^{**}, Jean-Paul Pelteret^{***}, Benjamin Brands^{****}, Paul Steinmann^{*****}

^{*}Chair of Applied Mechanics, Friedrich-Alexander-Universität Erlangen-Nürnberg, Germany, ^{**}Chair of Applied Mechanics, Friedrich-Alexander-Universität Erlangen-Nürnberg, Germany, ^{***}Chair of Applied Mechanics, Friedrich-Alexander-Universität Erlangen-Nürnberg, Germany, ^{****}Chair of Applied Mechanics, Friedrich-Alexander-Universität Erlangen-Nürnberg, Germany, ^{*****}Chair of Applied Mechanics, Friedrich-Alexander-Universität Erlangen-Nürnberg, Germany

ABSTRACT

Magnetorheological elastomers (MREs) are composites whose mechanical behaviour highly depends on the applied magnetic field. Since explicit constitutive laws for such heterogeneous materials are not specified, their effective macroscopic properties can be estimated from the response of the underlying micro-structures using homogenization procedure. In the present work, the behaviour of heterogeneous magnetorheological composites subjected to large deformations and external magnetic fields is studied. A fully-coupled FE² computational homogenization framework is used to derive the macroscopic material response from the averaged responses of the underlying periodic and random microstructures. The microstructures consist of two materials and are far smaller than the characteristic length of the macroscopic problem. Different types of boundary conditions based on the primary variables of the magneto-elastic enthalpy and energy functionals are applied to solve the problem at the micro-scale. The results indicate that the application of each set of boundary conditions presents a different macroscopic responses. However, increasing the size of the RVE, solutions from different boundary conditions and microstructures converge to the response obtained from periodic boundary conditions.

Why Aortic Valve Functions The Way It Does

Rana Zakerzadeh*, Ming-Chen Hsu**, Michael Sacks***

*Institute for Computational Engineering and Science, Department of Biomedical Engineering, University of Texas at Austin, **Department of Mechanical Engineering, Iowa State University, ***Institute for Computational Engineering and Science, Department of Biomedical Engineering, University of Texas at Austin

ABSTRACT

Understanding the mechanics of the aortic valve (AV) has been a research focus for many years, with the aim of improving our understanding of its function in health and disease, as well as guiding the design of prosthetic replacements. Yet, we still do not fully understand how the AV is “designed,” including what features are most critical to ensure its efficient operation during the cardiac cycle. In the present study, we utilized a computational framework to determine how key characteristics of the AV interact and vary, while still maintaining proper valve function. Major AV features simulated included leaflet geometry and anatomical asymmetry, heterogeneity, prestrain, anisotropy, and layer contributions, as well as the shape and mechanical behaviors of the aortic sinus and aortic walls. AV dynamics and performance were assessed by a number of metrics, including effective orifice area, wall shear stresses, and leaflet coaptation, stress and strain fields within the leaflets and aortic root. To achieve this computationally, we simulated the coupling of the deforming aortic root, heart valves, and the surrounding blood flow under physiological conditions through several cardiac cycles using our immersogeometric fluid-structure interaction (FSI) methodology. Leaflets were modeled as a thin shell structures using various material behaviors and structural features. In particular, effects of leaflet shape, heterogenous structure, and interactions with the aortic root and sinus were studied in detail. We observed a noticeable influence of the surface curvature on the effective orifice area of the valve and the overall leaflet deformation. Sensitivity results also demonstrated that incorporating an anisotropic material model for leaflets had a significant influence on the valve deformation during diastolic closure. The basis for this was noted in part that in dynamic simulation of the AV during the opening phase the leaflet was in the small strain regime, when the majority of the collagen fibers were not recruited, so that the isotropic like tissue matrix dominated the valve deformation. Geometric studies clearly delineated the range of leaflet shapes acceptable for physiological function, and in particular what characteristics might be allowable in prosthetic valve devices. The results of this study demonstrate the effectiveness of the proposed platform for analyzing the heart valve function with greater levels of physical realism, and can provide guidelines for detecting anomalies in the natural valve or improving leaflet tissue's design in the artificial valves to enhance valve durability.

Numerical Simulation of Free Fall Penetrometer Deployment Using MPM

Luis Zambrano-Cruzatty*, Alba Yerro Colom**, Nina Stark***

*Virginia Polytechnic Institute and State University, **Virginia Polytechnic Institute and State University, ***Virginia Polytechnic Institute and State University

ABSTRACT

The number of engineering activities in offshore and nearshore environments is increasing because of the growing population in coastal areas, the necessity to obtain energy and minerals from the seafloor, and the current advances in ocean and offshore energy harvesting. In-situ characterization of seabed sediments is essential to most of such projects. However, current standard methods such as Cone Penetration Testing is expensive, time-consuming, and challenged by environmental conditions. Free fall penetrometers (FFP) promise the characterization of surficial seabed sediments efficiently and can be adapted to different environmental conditions. FFPs can be described as torpedo-like bodies equipped with various sensors. Recently, focus was given to devices that only measure accelerations and pore pressure in the interest to design more robust devices. The penetrometer free falls through the water column and impacts the surface at 3-6 m/s. The reaction force on the tip is computed using acceleration recordings, and sediment strength properties are deduced. However, soil behavior during high and transient velocities impacts is not fully understood, yet. Hence, there is a need to perform numerical simulations to investigate the problem. Modelling of a FFP deployment is complex because represents a soil-structure interaction problem involving high-velocity motions, large deformations, and hydro-mechanical coupling between soil particles and porous water. Several numerical technics have been previously used, including Finite Element Method (FEM), Arbitrary Lagrangian-Eulerian Method (ALE), and Coupled Eulerian-Lagrangian method (CEL). However, FEM is limited to small deformations, while ALE and CEL require remeshing techniques to deal with large strains. In this study, the Material Point Method (MPM) is proposed to analyze the FFP performance. MPM can accommodate large deformations without mesh tangling limitations, contact between soil and structure can be easily simulated, and coupled hydro-mechanical formulations can be considered. A set of numerical analysis will be performed to determine the capabilities of MPM to model FFP deployments. A moving mesh technique will be considered together with a mesh convergence analyses to optimize the computational resources and to maximize the results accuracy. The interaction between penetrometer and soil will be simulated considering different contact properties using a contact algorithm. A hydro-mechanical formulation will be considered to simulate the behavior of saturated soil. The numerical results will be compared and benchmarked with experimental data. Finally, a parametric study will be conducted to investigate the relationships between dynamic bearing capacity, FFP velocity, and soil strength properties.

Mean Field Theory of Plasticity and Yielding of Glasses

Francesco Zamponi*

*CNRS and Ecole Normale Supérieure, Paris

ABSTRACT

I will discuss a microscopic mean field theory of glasses. The theory is based on an exact solution of interacting particle systems in the abstract limit of infinite dimensions. Within the theory, one can follow the response of a glass state to several perturbations, including compression and shear. I will focus in particular on the response to shear, and discuss how the theory can reproduce some known features of glasses, such as plasticity and yielding. I will also discuss the limitations of the theory, and how to go beyond mean field. The talk is based on [1] Shear yielding and shear jamming of dense hard sphere glasses - P.Urbani, F.Zamponi - Phys.Rev.Lett. 118, 038001 (2017) [2] Following the Evolution of Hard Sphere Glasses in Infinite Dimensions under External Perturbations: Compression and Shear Strain - C.Rainone, P.Urbani, H.Yoshino, F.Zamponi - Phys.Rev.Lett. 114, 015701 (2015)

A COMPUTATIONAL APPROACH FOR INVESTIGATION OF THE EFFECT OF ELECTROMAGNETIC PHENOMENA IN MAGNETORHEOLOGICAL SQUEEZE FILM DAMPERS ON THE VIBRATION ATTENUATION OF RIGID ROTORS

JAROSLAV ZAPOMĚL¹, PETR FERFECKI², ANILRAJ SUDHAKAR³, AND JAN KOZÁNEK⁴

^{1,4}Institute of Thermomechanics ASCR
Department of Dynamics and Vibration
Dolejšková 5, Prague 8, 182 00 Czech Republic
¹zapomel@it.cas.cz, ⁴kozanek@it.cas.cz

^{1,2,3}VŠB - Technical University of Ostrava
Department of Applied Mechanics
17. listopadu 15, Ostrava - Poruba, 70833 Czech Republic
¹jaroslav.zapomel@vsb.cz, ²petr.ferfecki@vsb.cz, ³anilraj.sudhakar@vsb.cz

²VŠB - Technical University of Ostrava
IT4Innovations
17. listopadu 15, Ostrava - Poruba, 70833 Czech Republic
²petr.ferfecki@vsb.cz

Key words: magnetorheological squeeze film dampers, variable magnetic reluctance, transient electromagnetic phenomena, current and voltage control, rotor vibration attenuation

Abstract. The optimum performance of damping devices placed between the rotor and its stationary part is achieved by adapting their damping effect to the current running conditions. This is enabled by application of magnetorheological squeeze film dampers, the damping force magnitude of which is controlled by changing magnetic flux passing through a thin layer of lubricating film. The magnetic flux is generated in electric coils embedded in the damper body. The change of the thickness of the oil film around the damper circumference due to the rotor vibration changes reluctance of the magnetic circuit. It induces the electromotoric voltage that reduces the applied current and thus leads to decreasing of amount of the damping effect. In the developed mathematical model of the damper the magnetorheological oil was represented by a bilinear material. The dependence of the yielding shear stress on magnetic induction was described by a power function, the pressure distribution in the oil film by the modified Reynolds equation, and the electromagnetic phenomena by the equation of the voltage equilibrium and the Hopkins law. The developed mathematical model was used to compare the influence of two strategies for controlling the damping effect, the current and voltage control, on vibration suppression of rotor systems. The development of the enhanced mathematical model of the magnetorheological squeeze

film damper and learning more on the influence of the control regimes on behaviour of rigid rotors are the main contributions of this paper.

1 INTRODUCTION

The lateral vibration of rotating machines is attenuated by damping devices inserted in the rotor supports. As discussed in [1] to achieve their optimum performance their damping effect must be adaptable to the current operating speed.

The work of controllable damping devices is based on utilization of various physical principles, like hydraulic [2], mechanical-hydraulic [3] or electromagnetic [4].

A new approach to controlling the damping forces is utilized in the magnetorheological dampers, which are lubricated by liquids sensitive to a magnetic field. The damping force is controlled by a magnetic flux passing through the lubrication layer. The design, function, experimental investigations and application of magnetorheological dampers for the vibration attenuation of rotating machines are discussed in a number of journal articles and conference papers, e.g. in [5,6]. Zapoměl et al. [7] developed the mathematical model of a short squeeze film magnetorheological damper, in which bilinear material was employed to represent the magnetorheological oil. This arrived at stable computational procedures, in which this damper model was implemented. The study reported in [8] deals with the distribution of the magnetic flux in the damper body and of the magnetic induction in the lubricating film.

This article extends the mathematical model of a magnetorheological squeeze film damper by taking into account variable reluctance of the magnetic circuit and deals with the influence of the induced electromagnetic phenomena during the damper operation on the time delay of the damping effect and consequently, on vibration attenuation of rigid rotors. The developed mathematical model was used to compare the influence of two strategies for controlling the damping force, the current and voltage control, focusing on the vibration suppression of rotor systems.

2 MECHANICAL AND HYDRAULIC MODEL OF THE DAMPER

The principle of work of magnetorheological squeeze film dampers (Fig. 1) is described in detail in [7,9]. The damping effect is produced by squeezing a thin layer of a magnetorheological oil between two concentric rings. The inner ring is connected with the shaft journal by a rolling element bearing and with the damper housing by a flexible cage spring. The magnetic flux generated in electric coils embedded in the damper passes through the lubricant. As resistance against the flow of magnetorheological oils depends on magnetic induction, the change of the coil feeding voltage can control the amount of the damping force.

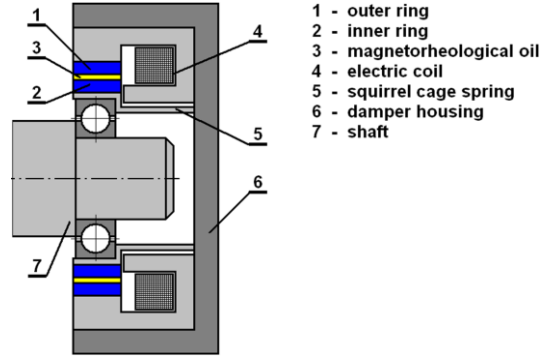


Fig. 1. Scheme of the magnetorheological squeeze film damper.

The pressure distribution in the oil film is described by the Reynolds equation adapted to bilinear material. The derivation and details on solution of the governing equations can be found in [7].

$$\frac{\partial}{\partial Z} \left(\frac{1}{\eta_c} h^3 p' \right) = 12\dot{h} \quad \text{for} \quad 0 \leq Z \leq Z_c, \quad (1)$$

$$\frac{\partial}{\partial Z} \left[\frac{1}{\eta} \left(h^3 p' + 3h^2 \tau_y + 8 \frac{\tau_c^3}{p'^2} - 12 \frac{\tau_y \tau_c^2}{p'^2} \right) - \frac{8}{\eta_c} \frac{\tau_c^3}{p'^2} \right] = 12\dot{h} \quad \text{for} \quad \dot{h} < 0 \quad \text{and} \quad Z > Z_c, \quad (2)$$

$$Z_c = -\frac{\tau_c h^2}{6\eta_c \dot{h}}, \quad (3)$$

$$p'_c = -\frac{2\tau_c}{h}. \quad (4)$$

Here, p is the pressure, p' stands for the pressure gradient in the axial direction, Z is the axial coordinate perpendicular to axes X and Y (Fig. 2), h is the oil film thickness, τ_y is the yielding shear stress, τ_c is the shear stress at the core border (the core is the region in the oil layer where the velocity rate is low and the oil behaves almost as a solid matter [10]), η_c , η are the dynamic viscosities of the oil inside and outside the core area, respectively, Z_c defines the axial coordinate of the location where the core touches the rings surfaces, p'_c denotes the pressure gradient in the axial direction at location Z_c , and $(\dot{})$ denotes the first derivative with respect to time.

At locations where the thickness of the oil layer rises with time ($\dot{h} > 0$), a cavitation is assumed. It is supposed that the pressure remains constant in cavitated areas and is equal to the pressure in the ambient space [11].

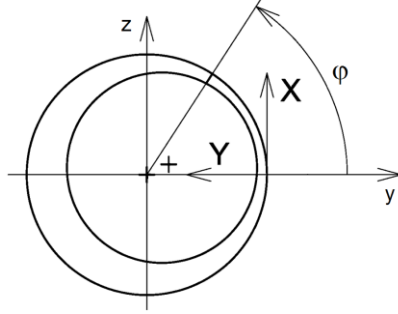


Fig. 2. The coordinate system of the damper.

The components of the hydraulic force acting on the rotor journal in the y and z directions (F_{mry} , F_{mrz}) are given by the integration of the pressure distribution p_d in the damper gap

$$F_{mry} = -2R_D \int_0^{\frac{L_D}{2}} \int_0^{2\pi} p_d \cos \varphi \, d\varphi \, dZ, \quad (5)$$

$$F_{mrz} = -2R_D \int_0^{\frac{L_D}{2}} \int_0^{2\pi} p_d \sin \varphi \, d\varphi \, dZ \quad (6)$$

taking into account different pressure profiles in noncavitated and cavitated regions. R_D is the mean gap radius, L_D is the damper length, and φ is the circumferential coordinate (Fig. 2).

3 ELECTROMAGNETIC MODEL OF THE DAMPER

The damper body is considered to be consisted of a set of meridian segments and each segment as a divided core of an electromagnet. This enables to express magnetic induction B and consequently, the yielding shear stress at any location in the oil film [7,9]

$$B = k_B \mu_0 \mu_{MR} \frac{I}{h} \quad (7)$$

$$\tau_y = k_y B^{n_y} \quad (8)$$

Here, μ_0 is the vacuum permeability, μ_{MR} is the magnetorheological oil relative permeability, I is the applied current, k_B is the design parameter, and k_y and n_y are the proportional and exponential material constants of the magnetorheological oil. More details on determination of the design parametre k_B can be found in [8].

Lateral vibration of the inner damper ring changes the width of the damper gap and thus the magnetic flux passing through the oil layer. The relation between the applied voltage, applied current and the magnetic flux is governed by the equation of the voltage equilibrium

$$\frac{d\Phi}{dt} + RI = U, \quad (9)$$

Φ is the magnetic flux generated in the coil, R is the ohmic resistivity of the electric circuit, U is the applied voltage, and t is the time.

The Hopkins law and the assumption that relative permeability of the damper steel part is much larger than that of the magnetorheological oil gives the relation for the amount of the magnetic flux passing through each meridian segment

$$N_C I = \Phi_i \frac{h_i}{\mu_{MR} R_D L_D \Delta\varphi}, \quad (10)$$

$\Delta\varphi$ is the increment of the circumferential coordinate, N_C reads for the number of the coil turns.

The total magnetic flux is equal to the sum of magnetic fluxes passing through all meridian segments

$$\Phi = \sum_{i=1}^{N_s} \Phi_i, \quad (11)$$

where N_s is the number of the meridian segments.

Next it is assumed that the segments are of an infinitesimal thickness. Then introducing

$$A = \int_0^{2\pi} \frac{d\varphi}{h(\varphi)}, \quad (12)$$

expressing Φ_i from (10) and utilization of (11) and (12) give the relation for the total magnetic flux

$$\Phi = \mu_{MR} N_C I R_D L_D A(t). \quad (13)$$

The differentiation of (13) with respect to time and its substitution into (9) yields the governing equation for the time history of the current in dependence of the applied voltage

$$\dot{I} + \left(\frac{\dot{A}}{A} + \frac{R}{\mu_{MR} N_C R_D L_D A} \right) I = \frac{U}{\mu_{MR} N_C R_D L_D A}. \quad (14)$$

4 THE INVESTIGATED ROTOR

The rotor of the analysed rotating machine consists of a shaft and of one disc (Fig. 3). The rotor is connected with the stationary part by two magnetorheological dampers at both its ends. It turns at constant angular speed, is loaded by its weight, and is excited by the disc unbalance. The cage springs of both dampers are prestressed to eliminate their deflection caused by the rotor weight. The rotor and the stationary part can be considered as absolutely rigid and the whole system as symmetric with respect to the disc middle plane.

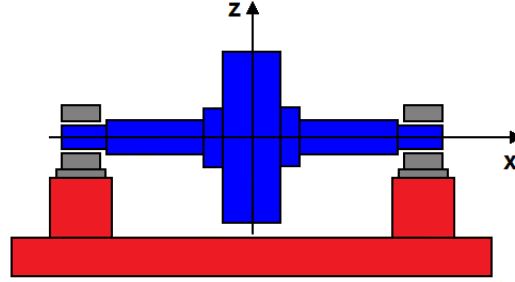


Fig. 3. The investigated rotating machine.

The task was to compare two approaches to controlling the damping force produced by the magnetorheological dampers, the current and voltage control, by analysing the rotor response on the change of the damping effect.

In the computational model the rotor is considered as absolutely rigid body and the magnetorheological dampers are represented by springs and force couplings.

The vibration of the system, taking into account its symmetry, is governed by a set of two nonlinear motion equations

$$m_R \ddot{y} + b_P \dot{y} + 2k_D y = 2F_{mry} + m_R e_T \omega^2 \cos \omega t + F_{psy}. \quad (15)$$

$$m_R \ddot{z} + b_P \dot{z} + 2k_D z = 2F_{mrz} + m_R e_T \omega^2 \sin \omega t + F_{psz} - m_R g. \quad (16)$$

m_R is the rotor mass, b_P is the coefficient of external damping, k_D is the stiffness of the cage spring, ω is the angular speed of the rotor rotation, e_T is the eccentricity of the rotor unbalance, y, z are the displacements of the rotor centre, F_{psy}, F_{psz} are the y and z components of the prestress force, g is the gravity acceleration, and $(\ddot{})$ denotes the second derivative with respect to time.

To perform the solution the equations of motion were transformed to the state space. In the case of the voltage control the equation governing the dependence of the current on the applied voltage feeding the magnetorheological dampers was added. The Adams-Moulton method was applied to solve the resulting equations.

5 THE SIMULATION RESULTS

The parameters of the studied rotor are: the rotor mass 430 kg, the coefficient of linear damping of the rotor caused by the environment 200 Ns/m, the stiffness of one cage spring 3.0 MN/m, the eccentricity of the rotor unbalance 60 μm , the magnetorheological squeeze film damper length/diameter 50/150 mm, the width of the damper gap 1.0 mm, the oil dynamic viscosity outside the core 0.3 Pas, the oil dynamic viscosity in the core 300 Pas, the magnetorheological oil proportional and exponential constants 2000, 1.1, respectively, the oil relative permeability 5, the damper design parameter 120, the resistivity of the electric circuit 10 Ω , and the number of the coil turns 240.

A simple dynamical analysis shows that the critical speed of the undamped rotating system is about 118 rad/s.

The goal of the investigation was to analyse the rotor response on increase of the damping effect for several angular velocities of the rotor rotation (100, 120, 250, 500 rad/s). They correspond to the speeds below, close to, and above the critical one. The rise of damping in the magnetorheological dampers was controlled by the uniform increase of the current (current control) or voltage (voltage control) during the time period of 10 ms. The increase was 0.5A/5V, 0.5A/5V, 2A/20V, 3A/30V for speeds of 100, 120, 250, 500 rad/s, respectively.

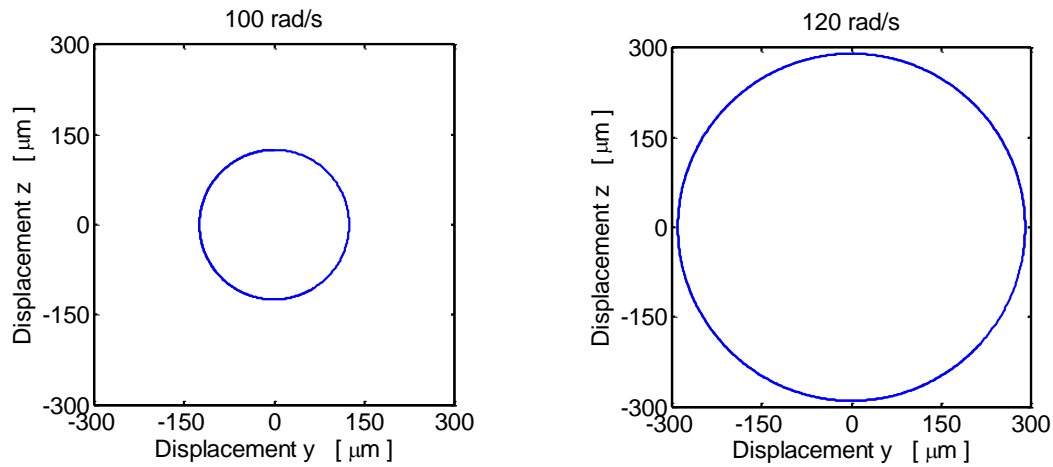


Fig. 4. The steady state orbits of the rotor centre for two running speeds (100, 120 rad/s) and no applied current.

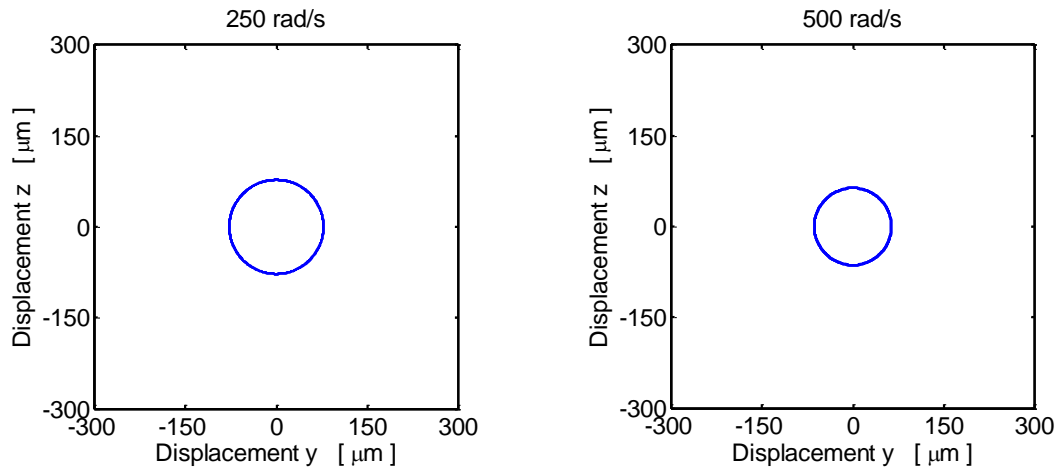


Fig. 5. The steady state orbits of the rotor centre for two running speeds (250, 500 rad/s) and no applied current.

The steady state orbits of the rotor centre for the case of zero applied current are drawn in Figs. 4 and 5. It is evident that the orbit reaches its maximum size for the speed of the rotor rotation close to the critical one and that the vibration amplitude of the rotor turning at speed

sufficiently higher than the critical one is close to the eccentricity of the rotor unbalance ($60\text{ }\mu\text{m}$).

The increase of the current feeding the coils of magnetorheological dampers for different speeds of the rotor rotation is drawn in Figs. 6 - 9. The results are related to the current (CC) and voltage (VC) control regimes. The show the time delay of the current history if the voltage control is applied.

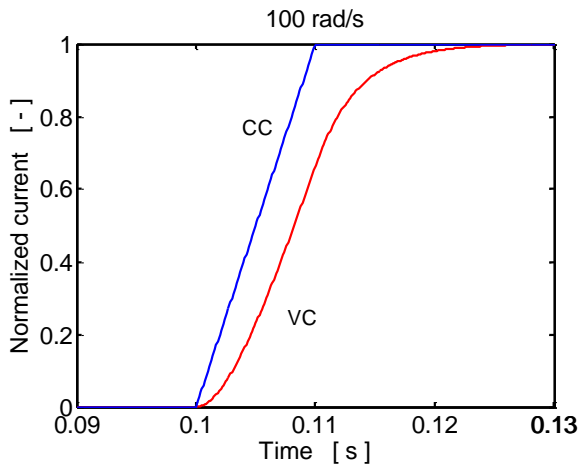


Fig. 6. Normalized current (100 rad/s).

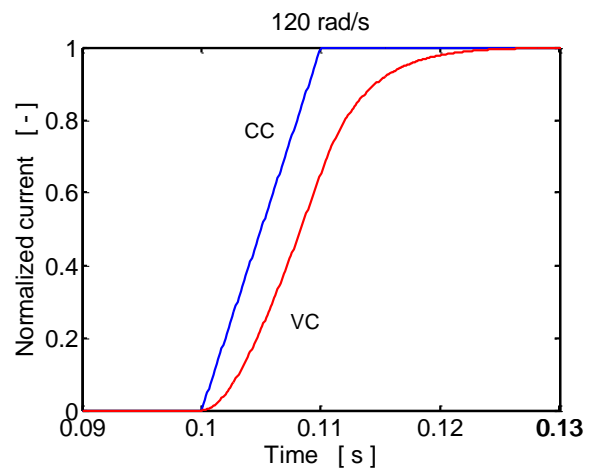


Fig. 7. Normalized current (120 rad/s).

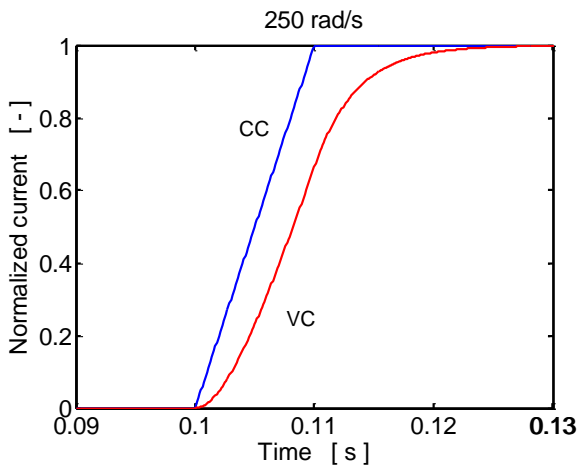


Fig. 8. Normalized current (250 rad/s).

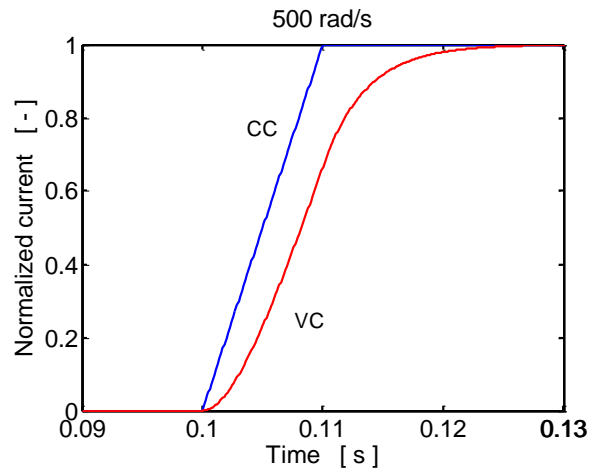


Fig. 9. Normalized current (500 rad/s).

Figs. 10 - 13 show the time history of the rotor centre eccentricity (the total rotor vibration amplitude) after increasing the damping effect in the rotor supports. The eccentricity goes down approximately in a monotonic way for the rotational speeds lower than the critical one while for higher angular speeds the time history of the eccentricity has an oscillatory

character. The delay of the rotor response is evident in all investigated cases if the damping is controlled by the change of voltage.

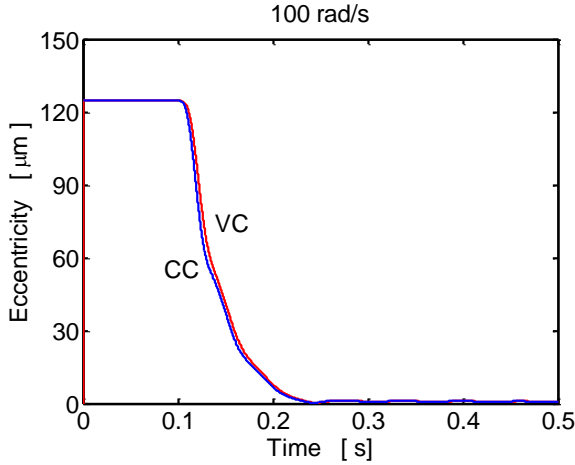


Fig. 10. The rotor centre eccentricity (100 rad/s).

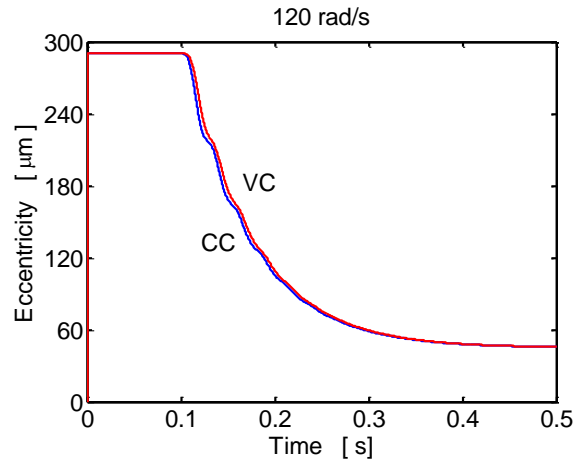


Fig. 11. The rotor centre eccentricity (120 rad/s).

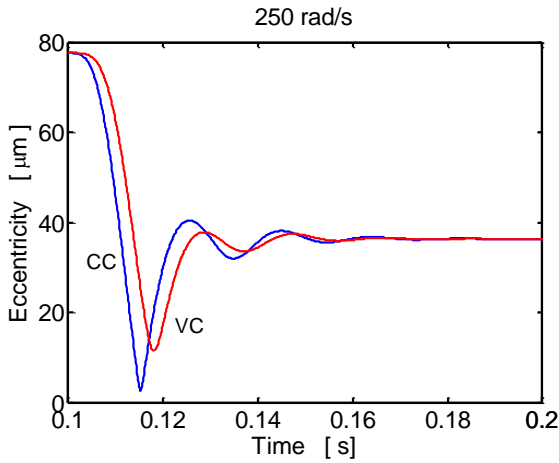


Fig. 12. The rotor centre eccentricity (250 rad/s).

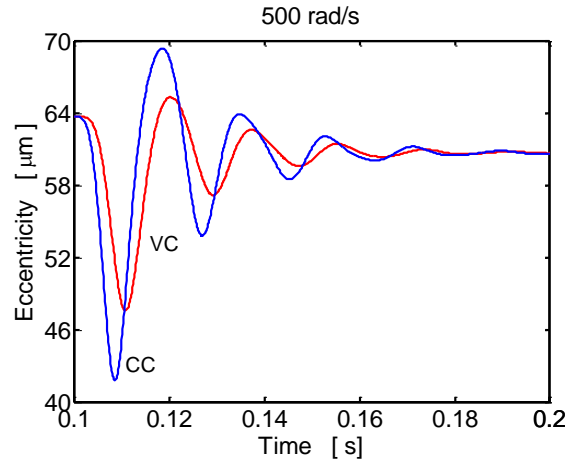


Fig. 13. The rotor centre eccentricity (500 rad/s).

The time histories of the normalized current (ratio of the instantaneous to desired current value) for the cases of the current and voltage control regimes and shorter time of rising the damping effect (1 ms) for two rotor rotational speeds are drawn in Figs. 14 and 15.

Figs. 16 - 17 show the corresponding rotor responses. The disturbance of the vibration (comparing with Figs. 12 and 13) is higher. The time delay of the rotor response if the damping effect is controlled by the voltage is evident. Maximum magnitude of the rotor centre eccentricity is higher if the current control strategy is used.

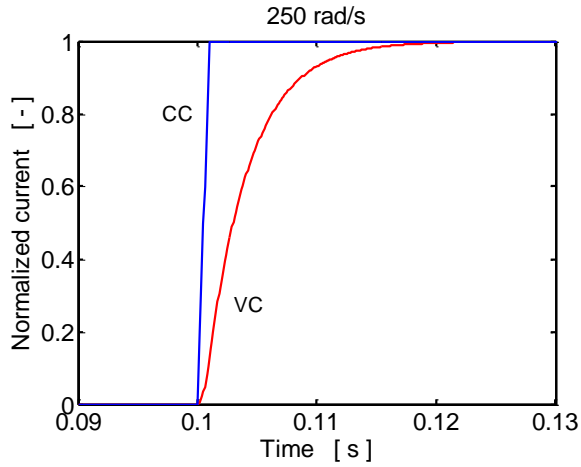


Fig. 14. Normalized current (250 rad/s, 1 ms action).

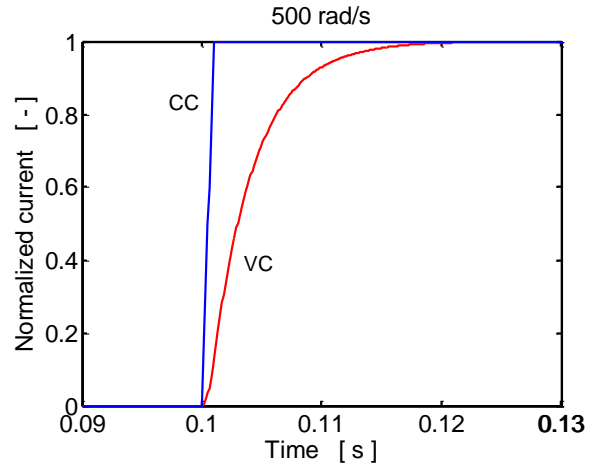


Fig. 15. Normalized current (500 rad/s, 1 ms action).

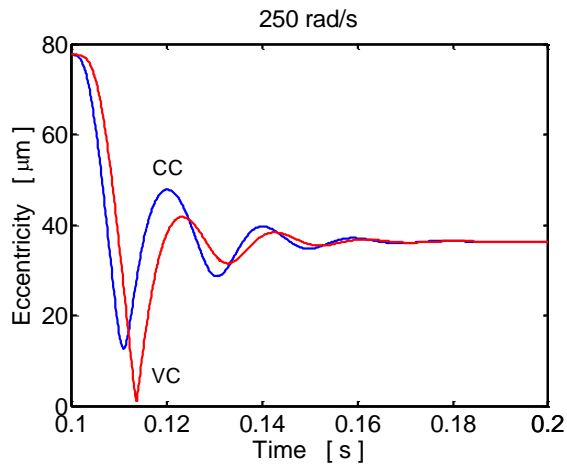


Fig. 16. The rotor eccentricity (250 rad/s, 1 ms action).

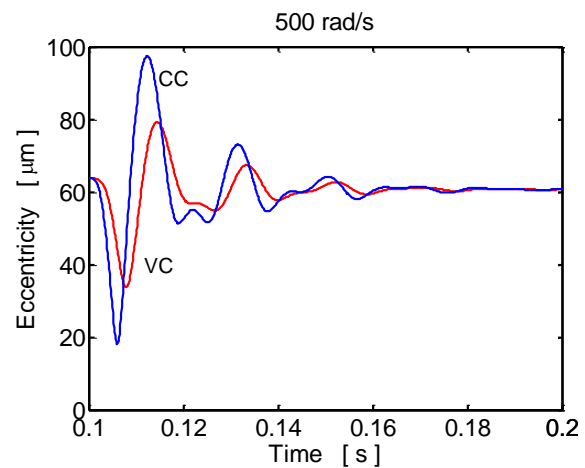


Fig. 17. The rotor eccentricity (500 rad/s, 1 ms action).

6 CONCLUSIONS

This paper presents an enhanced mathematical model of a short magnetorheological squeeze film damper and its utilization for comparing two strategies to control of the damping effect.

The new mathematical model is multiphysical. It takes into account the mutual interaction between the hydraulic forces, transient electromagnetic phenomena, and the mechanical vibration. Its development is based on assumptions of the classical theory of lubrication. The oil is represented by bilinear material. The pressure distribution in the full oil film in the damper gap is governed by the adapted Reynolds equation.

The damping force can be regulated either by means of the current or voltage control. The former controls the voltage with the aim to achieve the required time history of the current while the latter controls the voltage with the goal to achieve its required time course. It implies the voltage control strategy is technologically less complicated and thus more reliable than controlling the current. The efficiency of both strategies from the point of view of suppressing the rotor vibration was compared by means of computer simulations, during which the response of a rigid rotor excited by the unbalance was investigated. The results show that (i) the response of the rotor is faster if the current control is applied, if the voltage control is used, the response is delayed, (ii) in all investigated cases when the damping effect was controlled by the voltage the eccentricity of the rotor centre (the total amplitude of the rotor vibration) never exceeded the magnitude of the vibration when the current control was applied, and (iii) the disturbance of the vibration of the rotor running at angular velocity higher than the critical one was greater in the cases when the period of the manipulation action (the change of the voltage or current) was shorter and the disturbance did not depend on the damping control regime.

The development of the enhanced mathematical model of the magnetorheological squeeze film damper contributed to learning more on properties of magnetorheological damping devices and on their influence on vibration attenuation of rigid rotors.

Acknowledgements. The research work reported in this article was made possible by the National Programme of Sustainability (project LQ1602 - IT4Innovations excellence in science) and by the research project of the Institute of Thermomechanics AS CR (RVO: 61388998). The support is highly acknowledged.

REFERENCES

- [1] Zapoměl, J., Ferfecki, P. and Kozánek, J. Determination of the transient vibrations of a rigid rotor attenuated by a semiactive magnetorheological damping device by means of computational modelling. *Appl. Comput. Mech.* (2013) 7: 223-234
- [2] Mu, C., Darling, J. and Burrows, C.R. An appraisal of a proposed active squeeze film damper. *ASME J. Tribol.* (1991) 113: 750-754
- [3] El-Shafei, A. and El-Hakim, M. Experimental investigation of adaptive control applied to HSFD supported rotors. *ASME J. Eng. Gas Turbine Power* (2000) 122: 685-692
- [4] Tonoli, A., Silvagni, M., Amati, N., Staples, B. and Karpenko, E. Design of electromagnetic damper for aero-engine applications. *Proceedings of the International Conference on Vibration in Rotating Machinery*, Exeter, England. (2008) 761-774.
- [5] Forte, P., Paterno, M., and Rustighi, E. A magnetorheological fluid damper for rotor applications. *Int. J. Rotating Mach.* (2004) 10: 175-182.
- [6] Aravindhan, T.S. and Gupta, K. Application of magnetorheological fluid dampers to rotor vibration control. *Adv. Mech. Eng.* (2006) 5: 369-380

- [7] Zapoměl, J., Ferfecki, P. and Forte P. A new mathematical model of a short magnetorheological squeeze film damper for rotordynamic applications based on a bilinear oil representation - derivation of the governing equations. *Appl. Math. Model.* (2017) 52: 558-575
- [8] Ferfecki, P., Zapoměl, J. and Kozánek, J. Analysis of the vibration attenuation of rotors supported by magnetorheological squeeze film dampers as a multiphysical finite element problem. *Adv. in Eng. Soft.* (2017) 104: 1-11
- [9] Zapoměl, J., Ferfecki, P. and Forte, P. A computational investigation of the transient response of an unbalanced rigid rotor flexibly supported and damped by short magnetorheological squeeze film dampers. *Smart Mater. Struct.* (2012) 21: 105011
- [10] Çeşmeci, Ş. and Engin, T.: Modeling and testing of a field-controllable magnetorheological fluid damper. *Int. J. Mech. Sci.* (2010) 52: 1036-1046
- [11] Zeidan, F.Y. and Vance, J.M. Cavitation leading to a two phase fluid in a squeeze film damper. *Tribol. Trans.* (1989) 32: 100-104

A Load Balance Strategy for Partitioned Multi-physics Applications

J. Miguel Zavala-Aké*, Daniel Mira**, Mariano Vázquez***, Guillaume Houzeaux****

*BSC, **BSC, ***BSC, ****BSC

ABSTRACT

One of the main challenges of multi-physics problems is the development of approaches and algorithms with the capability of solving efficiently large-scale problems on extreme scale architectures. An approach widely used to solve multi-physics applications is based on the partition of the computational domain into regions. Each of these partitions is governed by a particular physical field principle. In this approach, the solution of the whole domain can be reconstructed from each partition through an iterative coupling algorithm. The main drawback of this approach is related to the unbalance introduced when an inappropriate selection in the allocation of the available resources is done. The aim of this paper is to introduce and validate a load balance strategy for partitioned multi-physics applications which enables reaching an optimal parallel performance. As a result, it is possible to estimate the behaviour of the parallel performance metrics of any partitioned multi-physics application composed of two parallel partitions. Finally, the proposed strategy is applied to a conjugate heat transfer problem with up to 2048 CPU-cores where it is shown the validity of the approach.

Clever Mechanisms and Strategies Found in the Architecture of Some Naturally Occurring Materials

Pablo Zavattieri^{*}, Nobphadon Suksangpanya^{**}, David Restrepo^{***}, Adwait Trikanad^{****}, Di Wang^{*****}, Alireza Zaheri^{*****}, Nick Yaraghi^{*****}, Horacio Espinosa^{*****}, David Kisailus^{*****}

^{*}Purdue University, ^{**}Purdue University, ^{***}Purdue University, ^{****}Purdue University, ^{*****}Purdue University, ^{*****}Northwestern University, ^{*****}University of California Riverside, ^{*****}Northwestern University, ^{*****}University of California Riverside

ABSTRACT

There is a strong demand for new paradigms of design and development of advanced high-performance structural materials with high specific strength, stiffness and toughness for new technological needs. Yet, most engineering materials have an inverse relation between these desired properties. By natural selection, Nature has evolved efficient strategies to synthesize materials that often exhibit exceptional mechanical properties that significantly break the trade-offs often achieved by man-made materials. In fact, most biological composite materials achieve higher toughness without sacrificing stiffness and strength in comparison with typical engineering material. Interrogating how Nature employs these strategies and decoding the structure-function relationship of these materials is a challenging task that requires (i) knowledge about the actual loading and environmental conditions of the material in their natural habitat, (ii) a complete characterization of their constituents and hierarchical architecture through the use of modern tools such as in-situ electron microscopy, small-scale mechanical testing capabilities, and (iii) solving some interesting solid mechanics problems that involve analytical and numerical models, as well as additive manufacturing. This talk will be focused on the convergent evolution of impact resistant naturally occurring materials and how we can use computational tools and mechanics to evaluate some important hypotheses about the key morphological features of the microstructure and toughening mechanisms that are unique in these hierarchical materials.

SHAKING-TABLE TEST WITH HEAD-MOUNTED DISPLAY AND VIRTUAL REALITY TO QUANTIFY ANXIETY DURING STRONG MOTION

FENG ZENG*, MASAKI WADA*, MASAYA ISHIDA*, SATOSHI ISHIKAWA*, AND
TORU TAKAHASHI*

*Chiba University
1-33, Yayoicho, Inage-ku,
Chiba, 263-8522, Japan

takahashi.toru@faculty.chiba-u.jp; <http://www.chiba-u.ac.jp/>

Key words: Quantifying anxiety, Head mount display (HMD), Virtual reality (VR), Shaking table test, Questionnaire.

Abstract. In present-day Japan, not only structural reliability, but human safety and comfort during strong motion are important issues for structural engineering. Quantifying the level of anxiety that occurs during strong motion is valuable for clarifying the structural performance needed for human comfort and will facilitate the communication between structural designers and clients about risk. In this study, a shaking-table test for humans who are wearing a head-mounted display (HMD) was performed to quantify the levels of anxiety during strong motion. To determine the influence of falling furniture during strong motion, a scenario consisting of a living room with several pieces of furniture was also simulated using virtual reality (VR). The vibration period, speed, and shape of the input motion were varied for each VR-based situation. The results of the test show that a longer shaking period produced lower levels of anxiety. View direction, which changed the direction in which the television and bookshelf fell relative to the participant, was observed to affect levels of anxiety, but these results are limited. The results of this study will further advance our understanding about how vibration in a building affects the anxiety of its occupants during earthquake events.

1. INTRODUCTION

In present-day Japan, not only structural reliability, but human safety and comfort during strong motion are important issues for structural engineering. When earthquakes occur, evaluating the ability to evacuate according to factors such as human psychology and falling furniture is very important for ensuring indoor safety. In past studies that looked at the injuries that occurred during a magnitude 7 earthquake, the proportion of injuries due to falling furniture was higher than those caused by the collapse of the building [1,2]. Moreover, human behavior is related to the movement of furniture in such situations [3]. Therefore, quantifying anxiety during strong motion is valuable for clarifying the structural performance needed for human comfort and facilitates the communication between structural designers and clients about risk. In this study, a shaking-table test for humans using a head-mounted display (HMD) was performed to quantify anxiety during strong motion. To evaluate the influence of falling furniture during strong motion, virtual reality (VR) was used to simulate a living room with a table, sofa, chairs, television, bookshelf, and sideboard during strong motion. The aim

was to assess the difference in the level of anxiety experienced by subjects using a shaking table and an HMD that displayed two different views of a virtual scene in which the furniture either fell to the side or forward with respect to the observer under the same vibration [^{4,5,6}].

2. SHAKING-TABLE TEST

The shaking-table tests were performed from Nov 8th to Dec 15th, 2017. We conducted experiments on 15 subjects (all males), using a simple vibration table installed in the Building Engineering Laboratory at Chiba University, Japan. We asked subjects to answer a questionnaire after experiencing multiple excitations that were presented with two different views of a virtual scene of falling furniture, displayed under the same vibration conditions. In each experiment, the subject's bioinformatics were measured and the acceleration was measured by accelerometers attached to the shaking table and one subject's head.

2.1 HMD

While they experienced the vibration of the shaking table, the subjects wore an HMD (Fig. 1) that displayed a virtual scene synchronized with the vibration to simulate an actual earthquake situation. Each virtual scene shows the two directions in which furniture tends to fall: along the x-direction, i.e., side to side (room x; Fig. 2) and along the y-direction, i.e., forwards and backwards (room y; Fig. 3).



Fig. 1 HMD and experimental setup



Fig. 2 Virtual scene in which furniture collapses in the x direction (room x): (left) before and (right) after vibration.

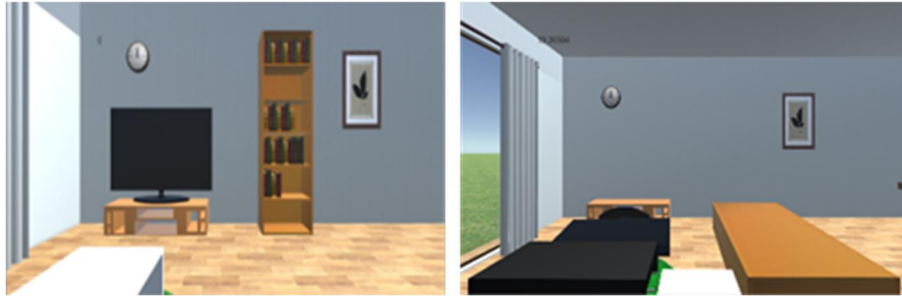


Fig. 3 Virtual scene in which furniture collapses in the y direction (room y): (left) before and (right) after vibration.

2.2 Vibration Waves and Inputs

In the tests, six vibration periods (0.4, 0.6, 1.0, 2.0, 3.0, and 4.0 s), four levels of input motion (0.1, 0.15, 0.3, and 0.6 m/s), and five input directions (x-direction, y-direction, O-shape, 8-shape, and ∞ -shape) were performed for each viewpoint of the virtual scene. However, some of these inputs were abandoned because of the limitations of the stroke and maximum acceleration of the vibration table. Therefore, each participant was subjected to a total of 142 inputs in this experiment. Vibration was continued for a duration of 12 to 32 s, and the excitation sequence was random to take into account the psychological impact on the subject. The magnitude of the internal change has a significant impact on three indoor conditions: whether the bookshelf falls, the television falls, or the table falls.

2.3 Questionnaire

The subjects were asked to answer a questionnaire after each shaking-table vibration was completed. The questionnaire evaluated three main aspects: the degree of anxiety (on a scale from 0 to 4), ability to take action (on a scale from 0 to 2), and sense of shaking (“forward and backward,” “side to side,” or “not sure”). The questions are shown in Table 1.

Table 1. Questionnaire

(A) How did you feel in the shaking table experiments? (Degree of anxiety)	
0. I had no anxiety.	1. I felt a little anxiety.
2. I felt anxiety.	3. I felt some anxiety.
4. I felt a lot of anxiety.	
(B) Do you think you could take action if it were the real earthquake? (Ability to take action)	
0. I can take action.	1. I am not sure whether I can take action or not.
2. I do not think I can take action.	
(C) Which shaky feeling is stronger, when the furniture falls side to side or forward and backward under the same vibration?	
0. I felt more strongly forward and backward.	1. I am not sure.
2. I felt more strongly side to side.	

3. TEST RESULTS

3.1 Questionnaire analysis method

The results of the questionnaire after each input motion are presented in this paper. In the bubble charts in Fig. 4, the horizontal axis is the maximum input speed of and the vertical axis indicates the score of the questionnaire item. The size of the bubble is related to the number of subjects who gave that answer. Finally, a straight line was fitted to the data using the weighted least squares method. In this study, we focus on the degree of anxiety in the questionnaire results.

3.2 Comparison of Room x and y

In general, the results for the four periods (0.4, 0.6, 1.0, and 2.0 s), fluctuate substantially, while the effects of environmental changes are small and the virtual scene is not much different at 3.0 s and 4.0 s (Fig. 4).

First, we compare the x-direction with the 8-shaped vibration patterns in room x, which creates large changes in the room. At 15 cm/s speed, which has no effect on the indoor environment, more people in room x have a high degree of anxiety during short-period vibrations and more participants have a high level of anxiety in room y during long-period vibrations, depending on the video. It is hard to determine how anxiety is influenced by the video. However, in the case of large indoor changes at 60 cm/s, there are many participants with a high level of anxiety in all rooms except during the x-direction vibration with a period of 0.4 s. In particular, there is an especially big difference between the 1.0 and 2.0 s of the 8-shaped vibration cycle. All other results differ by about one or two people.

Next, we compared the effects of y-direction and vibration patterns in room y with large variations. At the 15 cm/s rate, there was no effect on the indoor environment for the y-direction periods of 0.4, 0.6, 1.0, and 2.0 s and the ∞ -shape periods of 0.4 and 1.0 s. Room x generated a high degree of anxiety for ∞ -shape motion with a period of 2.0 s. The number of people with high anxiety in room y was high, and this number did not change according to the

video. It is also difficult to determine the influence on these results. However, when indoor changes are affected by speeds as high as 60 cm/s, except for the ∞ -shape period of 0.6 and 2.0 s, all other conditions in room y lead to high levels of anxiety. Here, there is also a difference in answers of about 1 or 2 people.

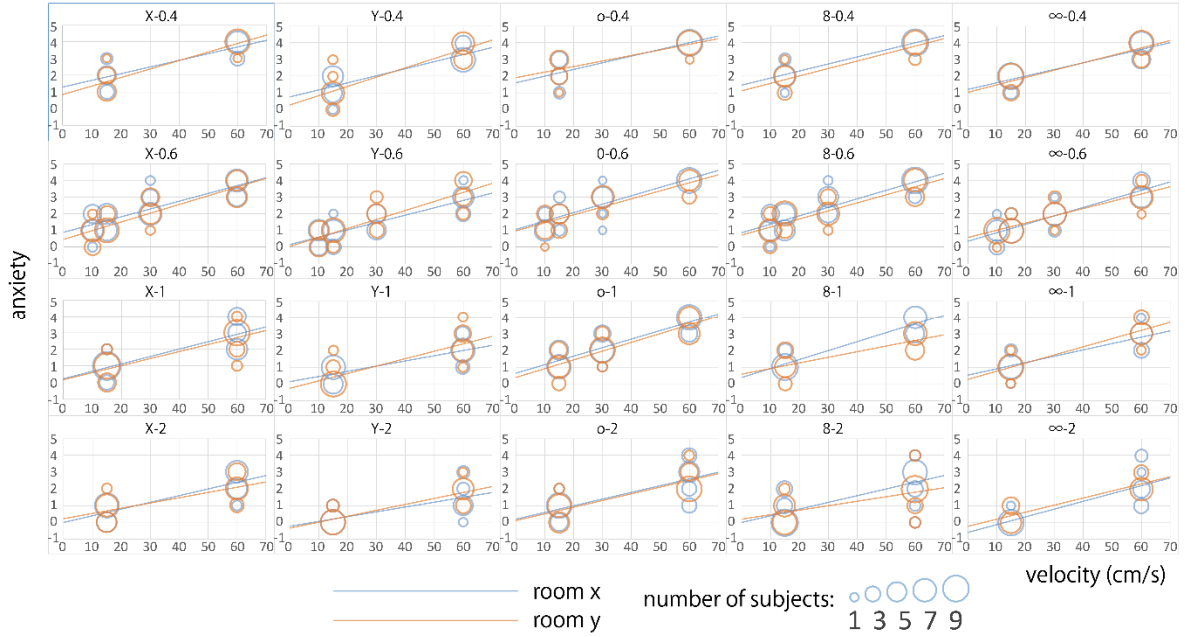


Fig. 4 Degree of anxiety for each virtual scene

Finally, for the o-shaped vibration pattern of the same degree in rooms x and y, the number of participants with high anxiety in room x are high at 0.4 s and 15 cm/s. Moreover, many participants had high anxiety in room x.

To summarize these results, it is very difficult to determine the change in discomfort based on a comparison of the virtual scene only because of the small number of test subjects. However, an individual's anxiety level has a large impact on the changes in the chart. Regardless, there are some effects at a speed of about 60 cm/s or more; the results show that there is some influence on the degree of anxiety.

3.3 Performance evaluation curve

From the questionnaire results, we determined an approximate curve corresponding to the anxiety evaluation values and speeds depending on the different types of vibrations and periods. Considering the full cycle, we plotted the period using the horizontal and vertical axes for each evaluation. By performing this operation for each vibration shape, a performance evaluation curve is obtained (Fig. 5).

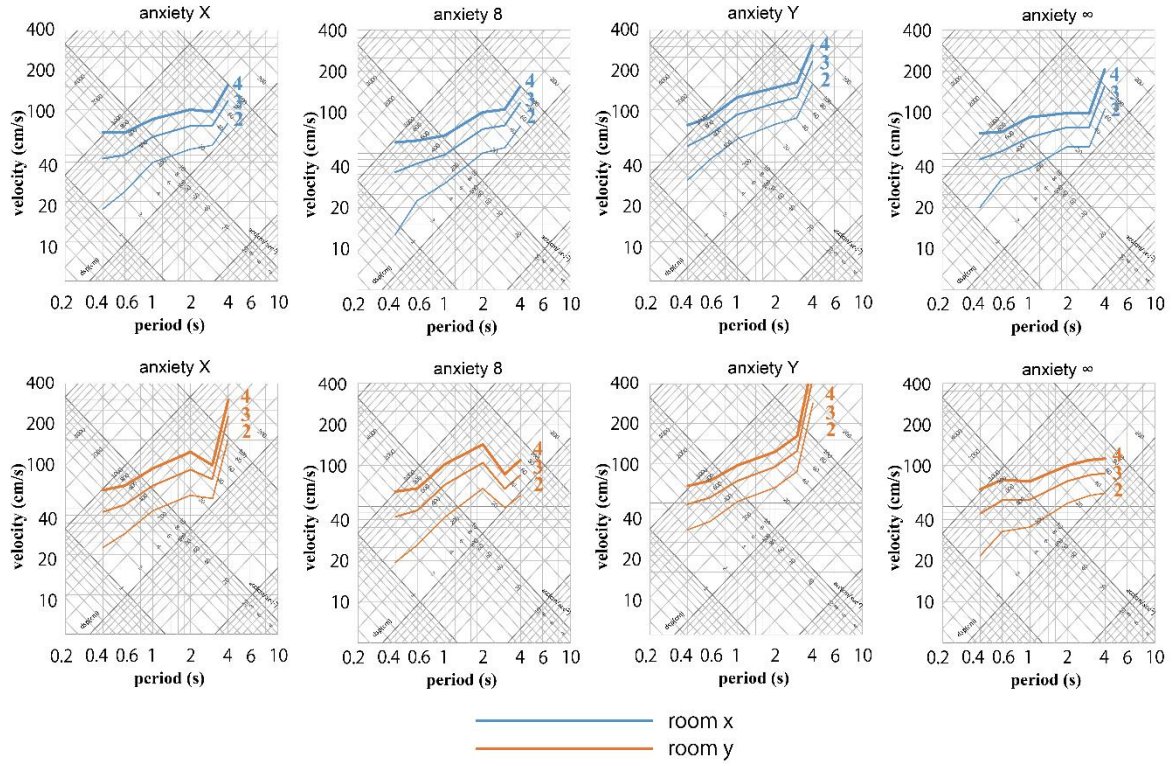


Fig. 5 Comparison of performance evaluation curves

First, room x has a lower curve than room y when comparing the x-direction and 8-shape graphs. In other words, room x is more likely to make people feel anxious. Second, comparing the y-direction with ∞ -shape graphs, the room y has a lower curve than room x. In other words, room y is more likely to make people feel uneasy.

Thus, based on a comparison of the performance evaluation curves, we believe that the virtual scenes have an effect on the degree of anxiety. However, compared with the results in Fig. 4, because the influence of each anxiety level is large and the difference in the performance evaluation curve is small, it is difficult to precisely describe the effect of the virtual scene.

3.4 Comparison of the conclusions of the previous result

Using fitted lines, we compare the results for room x and y in 2017 with the results obtained in Oct 13th to Nov 15th, 2015 and Feb 15th to Mar 14th, 2017 [7]. We used the same oscillation conditions, vibrations at speeds of 10, 15, 30 and 60 cm/s, and 0.6 s (Fig. 6).

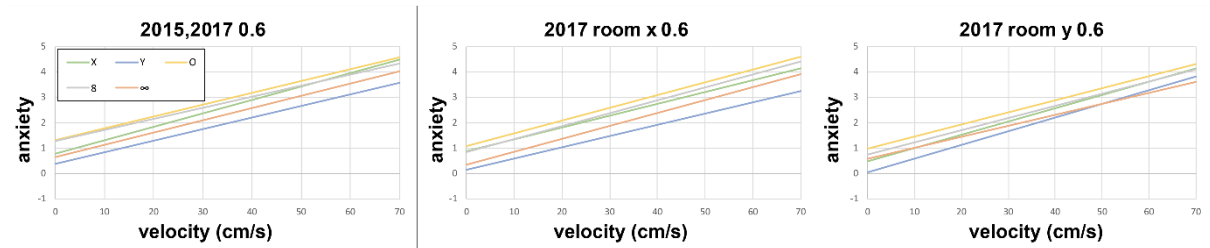


Fig. 6 Comparison of the results from 2015 to 2017.

In all charts, the O-shape vibration generates the highest degree of anxiety. This is thought to be due to the centrifugal sensation that the O-shape vibration produces, which is like a smooth circle. The O-shape vibration does not create a very different variation in the condition of each virtual scene, and the virtual scene appears to have no special influence on the results. Therefore, regardless of which room is used in 2017, any virtual scene will cause participants to feel very uncomfortable. Moreover, the x-direction vibration excitation generates a greater degree of anxiety than the y-direction vibration excitation. This is because the experiment is performed on a chair with a leg structure that can alleviate the impact of the subject's shaking. In contrast, there is no support in the left and right directions. Alternatively, it may be that when people first sit in a chair and receive vibrations, the side-to-side shakes are more likely to cause anxiety than forward-and-backward shaking. In room y, the x-direction vibration with less indoor variation generates more anxiety than the y-direction vibration with greater indoor environment variation and is not affected by the virtual scene. Alternatively, it could be that despite the influence of the virtual scene, the influence of the direction of vibration is greater.

4. CONCLUSIONS

The results of this experiment show that indoor changes may have an impact on people's anxiety. In addition, it is necessary to note the difference in the degree of anxiety between the x-direction vibration and the y-direction vibration. However, because the total number of experimental data is still very small, these results may not be very accurate. In future, the number of experiments and the total number of data should be increased.

In addition, it is necessary to verify the reliability of this conclusion from various viewpoints of these data, such as the ability to take action, the strong sense of shaking direction, biological information, and acceleration.

REFERENCES

- [1] T. Takahashi, T. Suzuki, T. Saito, T. Azuhata, and K. Morita: Shaking Table Test for Indoor Human Response and Evacuation Limit, Joint Proc. 7CUEE & 5ICEE, Tokyo Institute of Technology, Paper No. 17, pp. 187-193, 2010.
- [2] T. Takahashi, M. Sadahiro, T. Saito, T. Azuhata, K. Morita, K. Noguchi, and C. Minowa: Shaking Table Test on Indoor Seismic Safety of High-rise Buildings, Part I. Performance Test on BRI Large Stroke Shaking Table. Part II. Movement of Furniture Under Long

- Period Earthquake Ground Motion, Proc. 14WCEE, Paper IDs: S10-024 and S10-014, 2008.
- [3] T. Takahashi, M. Sadahiro, T. Suzuki, T. Saito, T. Azuhata, K. Noguchi, and C. Minowa: Shaking Table Test on Indoor Human Performance Limit in Strong Motion for High-Rise Buildings, Proc. 8th Pacific Conference on Earthquake Engineering, Paper No.131, 2007.
 - [4] T. Takahashi, A. Mazaki, T. Saito, T. Azuhata, and K. Noguchi: Shaking Table Test on Indoor Human Performance Limit in Strong Motion, Proc. 12JEES, Paper No. 0322, 2006.
 - [5] T. Takahashi, T. Azuhata, T. Saito, and K. Ohtomo: Structural Performance Considering Human Response Limit During Strong Earthquake, Proc. JCROSSAR2003, JSME, Vol. 5, pp. 825-828, 2003.
 - [6] T. Takahashi, T. Azuhata, K. Noguchi, D. Kounsana, and Y. Watanabe: Shaking table test on indoor human response and its feeling in strong ground motion, Summaries of Technical Papers of Annual Meeting of the AIJ, B2 pp. 861–864, 2001.
 - [7] M. Wada, A. Masuzawa, T. Yamashita and T. Takahashi: Experimental Study on Quantification of Anxiety under Strong Motion using Two Dimensional Small Shaking Table, Architectural Institute of Japan, Journal of Structural Engineering, Vol. 64B, pp. 345-350, March 2018.

Analysis of Nonequilibrium Scale Effects in the Shock Wave-Boundary Layer Interactions

Ming Zeng^{*}, Hao Zhang^{**}, Dongfang Wang^{***}, Zhenxia Chai^{****}, Wei Liu^{*****}

^{*}National University of Defense Technology, ^{**}National University of Defense Technology, ^{***}National University of Defense Technology, ^{****}National University of Defense Technology, ^{*****}National University of Defense Technology

ABSTRACT

Abstract? Reduced scale models are generally used in the laboratory simulation of flow with shock wave-boundary layer interactions. If chemical reactions take place in the flow, it is important to take into account of the nonequilibrium scale effects which result from the finite rate of the chemical kinetics. The simulated parameter of scale effects is the product of free stream density ρ_0 and the characteristic length L ($\rho_0 L$, binary scaling parameter) for dissociation nonequilibrium flow and $\rho_0^* \rho_0 L$ for recombination nonequilibrium flow, while for equilibrium or frozen flow, there are not scale effects except for those result from viscosity. For hypersonic flow over blunt body where the binary dissociations are dominant behind the detached bow shock, the binary scaling parameter $\rho_0 L$ can simulate the nonequilibrium scale effects, and at the same time the Reynolds number which embodies the viscous effects can also be sufficed. However, for the flow with shock wave-boundary layer interactions, the three-body recombination reactions can not be neglected in the boundary layer near the cold wall. Moreover, if the flow separation occurs, the recombination reactions may be comparable with dissociation reactions in the separation zone. Therefore, the nonequilibrium scale effects are somewhat complex for the shock wave-boundary layer interaction flow, and the simulation parameter for nonequilibrium scale effects for the flow should be investigated further. Taking the shock tunnel test model, a two dimensional compression corner (with total length of 0.6096m and the front plate length of 0.3048m) as the base one, the flow over models with 2 and 5 times scales are all simulated numerically for the analysis of the nonequilibrium scale effects. Twelve free stream conditions are selected with speed range from 3000 to 6000m/s and the values of $\rho_0 L$ range from 0.003 to 0.03 kg/m². The hypersonic nonequilibrium compression corner flow for three corner angles (15, 18 and 24 degrees) and three different model scales are numerically simulated. The behaviour of nonequilibrium scale effects on the flow structure and separation properties are analyzed for the various free stream conditions which corresponding to various flow thermochemical states. Through combining the numerical analysis and Triple Deck theory in the analytical treatment of shock wave boundary layer interactions, the similarity law for nonequilibrium flow is studied, the determination of nonequilibrium scale effects simulation parameter as well as its validity range is investigated. key words? nonequilibrium flow, nonequilibrium scale effects, compression corner flow, flow separation, numerical simulation

The Evaluation of Reverse Shoulder Lateralization on Scapular Fracture Risk: a Computational Study based on Different Failure Criteria

Wei Zeng^{*}, Kathleen Lewicki^{**}, Douglas Citters^{***}, Zi Chen^{****}

^{*}University of Virginia; Dartmouth College, ^{**}Dartmouth College, ^{***}Dartmouth College, ^{****}Dartmouth College

ABSTRACT

As an effective solution for patients with glenohumeral joint disease, reverse shoulder arthroplasty (RSA) can treat severe rotator cuff deficiency, but its medialization design of the shoulder's center of rotation (CoR) has been associated with scapular notching caused by impingement. Recent studies have shown that lateralization has beneficial effects on decreasing of notching and improving rotational capability in RSA. However, few studies have quantified the relationship between fracture failure risk of scapular and the specific design variations, especially lateralization. In this work, we estimated the impact of glenosphere lateralization to scapular strain/stress state by computational modeling, which can identify potential risk of scapular fracture. The comparison study showed larger lateralization produced higher strain/stress concentrations in scapular spine (Levy Region Type II), with approximately 10% increase for 12 mm lateralized loading scenario. The FE results were analyzed using three most representative failure measures. The occurrence of fracture risk predicted by maximum principal strain behaved similarly as the maximum principal stress measure since the bone was assumed to be isotropic. However, the largest area of high fracture risk predicted using von Mises stress measure identified a different risk pattern. Studying the effects of RSA lateralization on scapular fracture risk can help guide continued optimization of RSA performance and surgical techniques. The findings on the connections between loading style and bone failure measures can provide valuable insight into future research on the assessment and improvement of the generality of bone failure criteria.

Embedded Boundaries in ALE Flow Computations for Shock Hydrodynamics and Multi-Fluid Simulations

Xianyi Zeng^{*}, Guglielmo Scovazzi^{**}, Kangan Li^{***}

^{*}University of Texas at El Paso, ^{**}Duke University, ^{***}Duke University

ABSTRACT

We present a computational framework that combines an embedded boundary method and an arbitrary Lagrangian-Eulerian (ALE) method for multiphase flow computations of compressible fluids. This methodology is capable of handling geometrically complex material interfaces on moving grids and is suitable for multi-material flow computations in the context of ALE shock hydrodynamics. Specifically, we use a variational multiscale stabilized finite element method to update the fluid state of each material, and define ghost values to enforce the transmission condition at the embedded material interface, which is captured using a level-set approach. Two different strategies to populate ghost values are considered and compared, namely the constant extrapolation and a multi-material Riemann solver. The accuracy and conservation properties of both ghost value population strategies are assessed using benchmark shock tube problems and blast/bubble interaction problems. The method is then extended to solve multi-fluid problems with more than two fluids such as the triple-point problem, where multiple material interfaces are captured by the projected level set method; and it is also extended for numerical simulation of a liquid-gas-solid interaction problem, where body-fitted grids are used to track the multi-fluid/solid interface and an embedded boundary separates the liquid from the gas.

Numerical Investigation of the Role of Cell-Cell Interactions on Cell Locomotion in a Tightly Packed Epithelial Monolayer Sheet

Xiaowei Zeng^{*}, Liqiang Lin^{**}, Jie Bai^{***}

^{*}University of Texas at San Antonio, ^{**}University of Texas at San Antonio, ^{***}University of Texas at San Antonio

ABSTRACT

In epithelium, cells are tightly anchored and attached to each other through cell-cell adhesions. Forces exerted between cells determine tissue homeostasis as well as reorganization during embryonic development, wound healing and disease development. To understand how cell-cell interaction forces will influence the tissue state, we develop a novel vertex based simulation model for adhesive cell clusters and monolayers. In this presentation, we shall present our latest results on cell locomotion in a tightly packed epithelial monolayer sheet based on cell growth, division, remodeling and migration. In the simulation, a 2D epithelial monolayer sheet was generated. The macroscale cell is modeled as soft materials, and cell-cell/substrate interactions are governed by a recently developed interfacial zone model. The polygonal shape of epithelial cells is generated using Voronoi tessellation techniques. We have developed and implemented the related computational algorithms into simulation code for the described cell growth, division, remodeling and migration model. The simulation shows that the cell locomotion depends on cell-cell interaction, and the stronger cell-cell adhesion may play a role on “jammed” state in an epithelial cell cluster.

Derivation of Conical Indentation Model for Hyperelastic Materials Assisted by Dimensional Analysis and Finite Element Analysis

Yuxing Zhan^{*}, Xinrui Niu^{**}

^{*}Shenzhen Research Institute of City University of Hong Kong, ^{**}Shenzhen Research Institute of City University of Hong Kong

ABSTRACT

Classical conical indentation model, which is based on linear elastic assumption, is not suitable to extract mechanical parameters of hyperelastic materials for the following two reasons. Firstly, the parameter obtained from classical model is not accurate when dealing with single-parameter hyperelastic materials, because hyperelasticity is not considered in the model. The error will be larger if the half angle of the conical indenter is small, because hyperelasticity will significantly violate the linear elastic assumption under sharp indenters. Secondly, because classical model can provide only one material parameter, it's not capable to deal with double-parameter hyperelastic materials. Moreover, it is mathematically impossible to extract the parameters of double-parameter hyperelastic materials through single indentation experiment, no matter what model is used, because the uniqueness of the parameters can't be guaranteed. To solve the above two problems, dimensional analysis and finite element analysis are applied in this work. Dimensional analysis is to construct the mathematical form of conical indentation model. To solve the non-unique problem, dual-indenter method is adopted and the mathematical form of the corresponding indentation model is also constructed by dimensional analysis. Finite element analysis is to determine the model parameters in the constructed models. Because severe element distortion will be induced by conical indenter during finite element analysis, re-meshing processes are inserted in simulation to obtain accurate results. After constructing the indentation models, the stability of the models are analyzed. Conical indentation models for single- and double-parameter hyperelastic materials were constructed in this work. By adopting the models, conical indentation experiment, which is simple to conduct and can obtain local property of material, can be applied to capture mechanical properties of hyperelastic materials.

Numerical Simulation of Underwater Contact Explosion Based on the Coupled SPH-FEM Method

Aman Zhang^{*}, Pingping Wang^{**}, Furen Ming^{***}, Zifei Meng^{****}

^{*}Harbin Engineering University, ^{**}Harbin Engineering University, ^{***}Harbin Engineering University, ^{****}Harbin Engineering University

ABSTRACT

It often brings deadly threat to the warship subjected to underwater contact explosion. Therefore, studies on the load characteristics and damage mechanism are of great significant. The loads of contact explosion consist of shock waves, high-velocity fragments, water-gas jet induced by detonation, bubble jet, etc., which are characterized by high temperature, high pressure and high speed shocks, and accompanied by large deformation, tearing, attacking, and splashing and so on, which makes it hard to solve with traditional mesh-based method. As a meshless particle method, the smooth particle hydrodynamics (SPH) can easily track the moving interface and well deal with the large deformation problems. Thus, the coupled SPH-FEM method is employed to simulate this phenomenon in this paper. In the present work, a novel nonreflecting boundary condition is proposed to economize calculating time, and the Riemann-solver is adopted to reduce the pressure oscillation at the interface of water and detonation products. The numerical results are compared with experimental or theoretical results to validate the applicability of the current procedure. Furthermore, the load characteristics of contact underwater explosion and the damage mechanism of the nearby ship structures are studied, which provides some references for the structural design of naval architecture of underwater explosion. Key words: SPH-FEM; Underwater contact explosion; Nonreflecting boundary; Riemann-solver Reference: Zhang A, Wen-shan Y, Xiong-liang Y. Numerical simulation of underwater contact explosion[J]. Applied Ocean Research, 2012, 34: 10-20. Liu M B, Liu G R, Lam K Y, et al. Smoothed particle hydrodynamics for numerical simulation of underwater explosion[J]. Computational Mechanics, 2003, 30(2): 106-118.

Numerical Simulation of Mechanical-electrical-thermal Failure for Lithium-ion Batteries under Impact Loads

Chao Zhang^{*}, Shriram Santhanagopalan^{**}, Honggang Li^{***}

^{*}Northwestern Polytechnical University, ^{**}National Renewable Energy Laboratory, ^{***}Northwestern Polytechnical University

ABSTRACT

Crashworthiness and mechanical crash induced internal short circuit are critical concerns for the deployment of lithium-ion batteries on electrical-driven vehicles. In this work, we intend to investigate mechanical failure, the initiation of short circuit and the propagation of thermal events for lithium-ion battery cells under impact loads. The lithium-ion cell can be considered as a multi-layer stacked structure made of anodes, cathodes and separators. To model it, we introduce a multi-scale approach to solve the stress status of each component while treating each battery cell as a homogenized layer in macro scale. Extensive tensile and compressive tests are conducted to characterize the basic mechanical properties of each cell component, which are implemented into the multi-scale model through a user-defined material model. Also, experimental results of single battery cell are used to validate the material model. We build the model using the mechanical solver and Multiphysics solver of finite element software LS_DYNA. The stress history is utilized to predict the mechanical failure for each representative element of the battery cell and to calculate electrical contact resistance based on the failure status of cell components. The coupled mechanical-electrical-thermal failure (including force response, voltage response and temperature history profiles) of a pouch lithium-ion battery cell under impact is then studied numerically and compared with experimental results. Through numerical parameter study, we elaborate the effect of impact conditions on the consequential failure behavior of battery cells, and highlight important physical properties that impacts the coupled responses. The results and modeling approach presented in this study form the basis for safety studies of lithium-ion batteries, and are especially useful for the design and optimization of battery structures for electrical-driven vehicle applications.

Bi-directional Coupling between a PDE-domain and an Adjacent Data-domain Equipped with Multi-fidelity Sensors

Dongkun Zhang^{*}, Liu Yang^{**}, George Karniadakis^{***}

^{*}Brown University, ^{**}Brown University, ^{***}Brown University

ABSTRACT

We consider a new prototype problem in domain decomposition with the solution in one domain governed by a known partial differential equation (PDE) whereas in an adjacent domain the solution is reconstructed by information gathered via distributed sensors (data) of variable fidelity. The PDE-domain and the Data-domain are tightly coupled, as the PDE solution is driven by the collected data, while the information gathered from its associated network sensors is influenced by the PDE solution. Our overall methodology is based on the Schwarz alternating method and on recent advances in Gaussian process regression (GPR) using multi-fidelity data. The effectiveness of the proposed domain decomposition algorithm is demonstrated using examples of Helmholtz equations in both 1D and 2D domains.

Multifield Formulation for Fluid-structure Interactions

Duan Zhang*

*Los Alamos National Laboratory

ABSTRACT

Interface tracking and reconstruction methods are used often for fluid-structure interaction problems. Most of these methods start with some initial interfaces. However, there are cases where material interfaces are not known a priori. The examples range from crack or spall surface formation under impact loading to flaking of mud in a slowly drying puddle. This presentation introduces a fully coupled numerical scheme for material interactions, in which the material locations and the interfaces are described by the volume fraction fields of the materials. The numerical scheme is based on the ensemble phase averaging method. Interactions among the materials are considered through the closure relations of the averaged equations. This treatment of the material interactions has an additional advantage that the equations are applicable to material interactions occurring inside body of the materials, such as fluid-solid interactions in a porous material. Interactions on the material interfaces are treated in the same manner as the body interactions. No special treatment for interfaces is necessary. Numerically, the equations for the solid material are solved using the dual domain material point method, which uses Lagrangian points to track history dependent state variables, such as damage, failure, and plastic strain of the solid. The distribution of the material points provides natural description of the material locations and interfaces. The material point method also uses Eulerian description for the material. In the numerical scheme described here, the Eulerian description is used to couple with the calculation of fluids. To ensure consistence of the Lagrangian and Eulerian descriptions, a weak solution method is introduced to enforce the continuity condition. The numerical method is shown to be quite versatile. Many advanced material models can be implemented to study complex fluid-structure problems with large deformations of the solids. After reviewing basic concepts of the material point method and its recent advances, I will present examples of crack formation in a ductile material subjected to blast loading using a rate-dependent tensile plasticity model [1,2]. This work was performed under the auspices of the United States Department of Energy. [1] J. Johnson, F. Addessio, Tensile plasticity and ductile fracture, J. Appl. Phys. 64 (12) (1988) 6699–6712. [2]. F. L. Addessio, J. N. Johnson, Rate-dependent ductile failure model, Journal of Applied Physics 74 (1993) 1640–1648.

3D Tensor Field Design

Eugene Zhang*

*Oregon State University

ABSTRACT

Hexahedral mesh generation is a delicate process. Recent advances in the area make use of a 3D frame field to guide the orientation of the mesh elements. In this talk, we will explore the design of 3D tensor fields, which can be used as a frame field. We will discuss how to control the smoothness of the tensor field as well as its topological structures, which have implications in controlling the irregular vertices in the resulting mesh.

A Multi-material Topology Optimization Method for Energy Absorbing Designs with Viscoelastic and Hyperelastic Materials

Guodong Zhang^{*}, Kapil Khandelwal^{**}

^{*}University of Notre Dame, ^{**}University of Notre Dame

ABSTRACT

Energy absorbing designs are of great importance in many engineering applications. Traditional experimental/experience based design methods for such applications are time consuming, however. As an alternative, topology optimization (TO) can be used as a conceptual design method. As desired in practical applications, energy absorbing designs should have optimal energy absorbing capacity together with necessary stiffness. To achieve this objective, a multi-material TO considering finite deformation is presented in which a viscoelastic material – that provides dissipation – is combined with a hyperelastic material – that provides stiffness. Several issues pertaining to the multi-material design framework are discussed and addressed. In particular, for the developed multi-material density-based TO, a material interpolation scheme is proposed for mixing viscoelastic and hyperelastic phases. Besides, due to the use of incompressible viscoelastic material, F-bar formulation is adopted to handle the volumetric locking. Moreover, a constitutive model interpolation approach is proposed to address the mesh distortion issue induced by the use of fictitious domain in TO. Finally, an analytic path-dependent adjoint sensitivity analysis is given that is necessary for gradient-based optimizers. The proposed framework is demonstrated to be effective through several numerical examples.

Uncertainty Quantification and Propagation of Imprecise Probabilities with Copula Dependence Modeling for Composite Material Properties

Jiaxin Zhang^{*}, Michael Shields^{**}

^{*} Johns Hopkins University, ^{**} Johns Hopkins University

ABSTRACT

Abstract Imprecise probability, as a generalized probability theory, allows for partial probability specifications and is applicable when data is so scarce that a unique probability distribution cannot be identified. The primary research challenges in imprecise probabilities relate to quantification of epistemic uncertainty and improving the efficiency of uncertainty propagation with imprecise probabilities – particularly for complex systems in high dimensions, at the same time considering dependence among random variables. The conventional method to address variable dependence from limited information is to assume that the random variables are coupled by a Gaussian dependence structure and rely on a transformation into independent variables. This assumption is often inaccurate, subjective, and not justified by the data. A novel UQ methodology has been recently developed by the authors [1, 2] for quantifying and efficiently propagating imprecise probabilities with independent uncertainties created by the scarcity of data. In this study, we generalize this novel UQ methodology to overcome the limitations of the independence assumption by modeling the dependence structure using imprecise vine copulas theory [3]. A data-driven Bayesian approach is investigated to quantify the uncertainties of copula dependence modeling for two composite material models with different dependent structures, including E-Glass fiber/LY556 Polyester Resin model and AS4 Carbon fiber/3501-6 Epoxy Resin model. The generalized approach achieves particularly precise estimates for uncertainty quantification and efficient uncertainty propagation of imprecise probabilities in copula dependence modeling for composite material properties. References [1] Jiaxin Zhang and Michael D. Shields. On the quantification and efficient propagation of imprecise probabilities resulting from small datasets. *Mechanical Systems and Signal Processing* 98 (2018): 465-483. [2] Jiaxin Zhang and Michael D. Shields. The effect of prior probabilities on quantification and propagation of imprecise probabilities resulting from small datasets. *Computer Methods in Applied Mechanics and Engineering*, 2017. (In Review) [3] Harry Joe. *Dependence modeling with copulas*. CRC Press, 2014.

3D Microstructure-based Finite Element Modeling of Deformation and Fracture of SiCp/Al Composites

Jie Zhang*

*State Key Laboratory of Metal Matrix Composites, Shanghai Jiao Tong University

ABSTRACT

The mechanical behavior, with particular emphasis on the damage mechanisms, of SiCp/Al composites was studied by both experiments and finite element analysis in this paper. A 3D microstructure-based finite element model was developed to predict the elasto-plastic response and fracture behavior of a 7vol.% SiCp/Al composite. The 3D microstructure of SiCp/Al composite was reconstructed by implementing a Camisizer XT particle size analysis device and a random sequential adsorption algorithm. The constitutive behavior of the elastoplastic-damage in the metal matrix, the elastic-brittle failure for the particle reinforcement, and the traction-separation for interfaces, were independently simulated in this model. The validity of the modeling results were validated by the agreement of the experimental stress-strain curve and the morphology of fracture section with those predicted by the simulation. The visual elasto-plastic deformation process, along with crack generation and propagation was well simulated in this model. The numerical results were used to provide insight into the damage mechanisms of SiCp/Al composites, and the effects of interfacial strength and particle strength on material properties were also discussed in detail.

Accuracy Analysis of a Composite Implicit Time Integration Scheme and Application to Linear and Nonlinear Structural Dynamics

Jie Zhang*

*Sun Yat-sen University, Zhuhai, 519082, China

ABSTRACT

The concept of two sub-steps composite implicit time integration scheme is extended in a generalized manner. A rigorous accuracy analysis in acceleration, velocity and displacement is performed, and the presented and proved accuracy condition enables the displacement, velocity, and acceleration achieving second-order accuracy simultaneously. The numerical dissipation and dispersion and the initial magnitude errors from the algorithmic amplification matrix's eigenvalues and eigenvectors are investigated physically. An optimal algorithm-Bathe composite method is revealed with unconditional stability, no overshooting in displacement, velocity, and acceleration and excellent performance compared with many other algorithms. The composite time integration scheme applying to linear and nonlinear structural dynamics cases is also performed, especially to solving the nonlinear dynamics problem of shell structures by combining the degenerated shell finite element method. References [1] Jie Zhang, Yinghua Liu, Donghuan Liu. Accuracy of a composite implicit time integration scheme for structural dynamics. *International Journal for Numerical Methods in Engineering*, 109(3): 368-406, 2017. [2] Jie Zhang, Donghuan Liu, Yinghua Liu. Degenerated shell element with composite implicit time integration scheme for geometric nonlinear analysis. *International Journal for Numerical Methods in Engineering*, 105(7): 483-513, 2016. [3] Klaus-Jürgen Bathe, Mirza M. Irfan Baig. On a composite implicit time integration procedure for nonlinear dynamics. *Computers & Structures*, 83(31-32): 2513-2524, 2005.

Automatic Polyhedral Mesh Generation for Scaled Boundary Finite Element Analysis

Junqi Zhang^{*}, Chongmin Song^{**}

^{*}University of New South Wales, ^{**}University of New South Wales

ABSTRACT

Mesh generation of geometric models is an imperative task in the finite element analysis. Presently, the mesh generation process requires frequent human interventions, which are time consuming and error prone. Possible flaws and defects in the geometric models further increase the difficulty in mesh generation. It is recently shown that the polyhedral element formulated in the scaled boundary finite element method provides a higher degree of flexibility in mesh generation than standard finite elements [1]. This type of polyhedral elements may have arbitrary number of nodes, edges and faces. Only boundary discretization is required. What's more, a polyhedron doesn't need to be closed, leading to a convenient and accurate way to model concave shapes. In this paper, an automatic polyhedral mesh generation method is developed based on a modified octree scheme and Laplacian smoothing. A special technique is proposed to handle concave corners in the model. The steps of the proposed method are illustrated as follows. A uniform background grid is generated to cover the 3D model. The grid is refined on the surface of the model until a specified resolution is reached. The octree grid is trimmed by the surface so that a conforming mesh of arbitrary polyhedral elements can be generated. The mesh near the surface is optimized using Laplacian smoothing. The nodes on corners of the geometric model will not be moved during smoothing while the nodes on edges can be moved on the same edges only. The mesh quality can be significantly improved and sharp features are preserved. When a polyhedron containing concave corner is detected, a so-called scaling center is defined at the concave corner. This type of concave polyhedral elements can be analyzed directly by the scaled boundary finite element method. It improves the stability in mesh generation as well as the accuracy in stress analysis. Volume discretization is not required in the scaled boundary finite element method. Several numerical results are presented to verify the proposed method. [1] Liu, Y., Saputra, A. A., Wang, J., Tin-Loi, F., & Song, C. (2017). Automatic polyhedral mesh generation and scaled boundary finite element analysis of STL models. *Computer Methods in Applied Mechanics and Engineering*, 313, 106-132.

Reconstruction of Microstructure and Mechanical Properties of Short Fiber-reinforced Thermoplastic Considering Fiber Orientation and Length Distribution

Ke Zhang^{*}, Bo Wang^{**}, Peng Hao^{***}, Xiangfei Yang^{****}

^{*}State Key Laboratory of Structural Analysis for Industrial Equipment, Department of Engineering Mechanics, Dalian University of Technology, ^{**}State Key Laboratory of Structural Analysis for Industrial Equipment, Department of Engineering Mechanics, Dalian University of Technology, ^{***}State Key Laboratory of Structural Analysis for Industrial Equipment, Department of Engineering Mechanics, Dalian University of Technology, ^{****}State Key Laboratory of Structural Analysis for Industrial Equipment, Department of Engineering Mechanics, Dalian University of Technology

ABSTRACT

Accurate predictions of mechanical properties are of primary importance for the application of short fiber reinforced thermoplastic composites. Microstructure features are neglected for traditional methods when calculating effective elastic properties. In this study, we employed a random sequential adsorption algorithm to generate a representative volume element (RVE) based on fiber orientation distribution function (ODF) reconstructed by second-order fiber orientation tensor, which simulated the material microstructure of short fiber reinforced thermoplastic composites. Meanwhile, we performed finite element analysis on RVE samples with a homogenization procedure in parallel to evaluate the effective elastic properties of the whole composite. The illustrative example demonstrated that reconstructing ODF can predict precisely elastic properties compared to traditional methods. Furthermore, a modified random sequential adsorption algorithm was proposed to generate a RVE based on ODF and length distribution function (LDF), and the prediction accuracy can be further improved. Finally, the effects of the number-average fiber length and the weight-average fiber length on the mechanical properties were investigated.

An Energy-Based DG Method for Second Order Wave Equations

Lu Zhang^{*}, Daniel Appelo^{**}, Thomas Hagstrom^{***}

^{*}Southern Methodist University, ^{**}University of Colorado, Boulder, ^{***}Southern Methodist University

ABSTRACT

We present a new method for constructing discontinuous Galerkin methods for wave equations in second order form. The weak form works directly with the Lagrangian of the system. By Noether's Theorem, given any symmetry of the Lagrangian, one can derive a conservation law on a given element. Our method is built on such conservation laws, with the weak form chosen so that the rate of change of the conserved quantity is determined by the flux through the element boundaries. These can be chosen either to exactly preserve a discretization of the conserved quantity or to dissipate it in proportion to jumps across the inter-element boundaries. If the conserved quantity is positive definite, as in the energy for typical physical systems, we can conclude that the method is stable and convergent. We have applied our construction to a variety of problems ranging from the simple scalar wave equation (Appelo and Hagstrom, SINUM, 53, 2015) to linear elasticity (Appelo and Hagstrom, CMAME, in revision). In this talk we focus on its application to the convective wave equation. Here some new features arise. First, the energy is not associated purely with time symmetry, but rather with a specific combination of space and time symmetry. Second, depending on whether the background flow projected in the direction normal to the element boundary is subsonic or supersonic, upwind fluxes must be defined in different ways. We will outline the convergence analysis of the method in this case and demonstrate optimal high-order convergence for some simple examples.

A Micromorphic Model for Strength Analysis on Carbon Nanotube Reinforced Concrete: Modeling and Experiments

Lu-Wen Zhang*

*Shanghai Jiao Tong University

ABSTRACT

Concrete exhibits a large number of microcracks during the application of any external loads, which have a significant effect on the mechanical behavior of concrete and contribute to nonlinear behavior at low stress levels. CNTs can act as crack bridges inside concrete, making it less porous and improving its flexural strength and toughness significantly. In order to dig deeper into the mechanical properties of CNT-reinforced concrete composite, a multiscale micromorphic framework is established to simulate the phases and interface in different constitutive models, for the purpose of linking continuum behavior of CNT reinforced concrete and its microstructure. In this investigation, the geometry of RVE is considered in which the CNT and matrix are taken as elastic continua. A morphological kinematic descriptor is used to characterize the fiber-matrix bond-slip mechanism). The equilibrium equations of conventional Cauchy stress at the macroscale, as well as generalized microstress at the mesoscale, are established. A staggered algorithm is implemented to solve the coupled problem, including the additional DOFs associated with the micromorphic fields. The mixture theory is used as the methodological approach to model reinforced composites. The iterative solution procedure using the Newton–Raphson method with displacement control is employed to solve the system of equations for each incremental step. Several numerical examples are carried out to demonstrate the proposed model's capability of representing adequately the effects of microscopic bond sliding on the overall macroscopic deformation of CNT-reinforced cement composite structures.

Adaptive Interface for the Immersed Finite Element Method

Lucy Zhang^{*}, Jie Cheng^{**}

^{*}Rensselaer Polytechnic Institute, ^{**}Rensselaer Polytechnic Institute

ABSTRACT

Despite the great advantage of not having to constantly re-meshing the computational domain, one of the major challenges in the immersed methods is the resolution or the sharpness at the fluid-structure interface. When dealing with non-conformed meshes, the interaction is handled by the interpolation between meshes. As a result of the interpolation, the interface is often not sharp enough to reflect accurately the physical quantity changes or jumps such as the intrinsic material properties and resolved physical quantities between the phases such as stress and pressure. In this talk, we utilize the quad-tree mesh structure of an open-source finite element library deal.II, where the cells in the grid can be conveniently split or merged based on a locally defined criterion. We choose to use the second order derivative of the “fluid-structure interaction force” as an indicator of mesh adaption in the neighborhood of the fluid-structure interface in the background fluid grid. Upon the adaptive refinement, the interface is precisely tracked and represented during the dynamic fluid-structure interactions, yet the total number of degrees of freedom is controlled in a reasonable range without knowing the general solid location a prior. This adaptive interface is conveniently implemented in our refactored immersed finite element method (IFEM) code. Our newly developed open source, high performance IFEM code, open-IFEM, utilizes a series of open source libraries, and is published on Github. We welcome potential users to use and contribute to this open-source project.

Calibrated Growth Model for In-stent Restenosis Using Patient Data

Lucy Zhang*, Jie Cheng**

*Rensselaer Polytechnic Institute, **Rensselaer Polytechnic Institute

ABSTRACT

The in-stent restenosis is a common adverse event of vascular procedures. It pertains to stenting treatment for arteries or blood vessels that have become narrowed, and subsequently become re-narrowed as a result of the stent placement. In this talk, we use a growth model to simulate tissue growth and remodeling based on mechanical stimulants such as stent deployment. The growth model is calibrated based on patient data to produce binary in-stent restenosis prediction. The tissue wall shear stress is considered as the major mechanical stimulant. The multi-time scale coupling between short-term fluid-induced shear stress during the blood pulsatile flow within a cardiac cycle and long-term tissue growth is performed using the concept of small-on-large. This study provides a useful simulation approach to predict the risks of in-stent restenosis, which ultimately provides better patient care and planning.

A Rheology Model Incorporating Scale Effect for Rockfills

Minglong Zhang^{*}, Zuoguang Fu^{**}, Yuanjie Xu^{***}

^{*}Wuhan University, ^{**}Wuhan University, ^{***}Wuhan University

ABSTRACT

Scale effect of rockfills can hardly be captured by classical constitutive models because those models are independent of scale. Based on Cosserat continuum theory, this study extended the Perzyna's viscoplastic model for describing the scale effect in the rheological behavior of rockfills. We derived the constitutive integration algorithm and the closed form of the consistent tangent modulus for this model. This model was implemented in ABAQUS by means of User Element Interface (UEL). the results of numerical simulations were compared to those typical experiments as tri-axial creep tests of soft rock, stress relaxation tests of black slate rockfill and creep tests of granite rockfill. The numerical results were in a good agreement with the experimental data so that the validity of this model was proved. We introduced parameters, such as the sphericity index, roundness index, and mean diameter of the particle, into our model, by relating the internal length with those parameters via the equation suggested by Voyiadjis. Then, we investigated the influence of particle size and shape on axial strain, deviator strain and deviator stress using this viscoplastic model. Time-dependent deformation of a typical Concrete-Faced Rockfill Dam was analyzed using FEM with this viscoplastic model as the constitutive equation of rockfills. The settlement of the dam predicted by the simulation agrees well with the result from site observation.

Effect of Phase Transition on Mechanical Properties of NIPA Hydrogel by Tensile Test

Ni Zhang^{*}, Shoujing Zheng^{**}, Zishun Liu^{***}

^{*}Xi'an Jiaotong University, ^{**}Xi'an Jiaotong University, ^{***}Xi'an Jiaotong University

ABSTRACT

Poly(N-isopropylacrylamide) (NIPA) hydrogel is one of the most extensively studied temperature-sensitive hydrogel, displaying a lower critical solution temperature (LCST) in aqueous solution and undergoing an abrupt thermo-reversible change in volume as the external temperature cycles around LCST (type α phase transition). Due to the lower temperature of phase transition (30°C - 35°C), the NIPA hydrogels have attracted great interest for a wide variety of applications, such as artificial organs, actuators, drug delivery, on-off switches, etc. Moreover, phase transition can also be induced by tensile force (type β phase transition) in some experimental phenomenon. However, the mechanical behaviors of NIPA hydrogel induced by two types phase transitions are still not well understood. Therefore, in this study, two types phase transitions as well as their coupling effect on mechanical properties of NIPA hydrogel are quantitatively studied from simulation and experiment. The mechanical properties of self-prepared NIPA hydrogel with LCST around 35°C under monotonic load and cyclic load using tensile test are studied with different temperatures. It is found that type β phase transition greatly influenced the mechanical properties of NIPA hydrogel during the tensile process. The maximum nominal stress and maximum stretch above the LCST are larger than those of below the LCST. We also find that the samples around LCST are easy to rupture, because of phase coexistent. The gels under type β phase transition, to some extent, behave some toughening characteristics, in particular, under cyclic load. Furthermore, the phase transition induced by tensile force is irreversible. In addition, adopting the existing theory of temperature-sensitive hydrogel, numerical simulations are carried out using parameters' value that determined by experiments. It can be found that the simulation results agreed well with the experimental results.

Simulation of Seismic Energy Dissipation in Concrete Gravity Dams Using a Smeared Crack Approach

Pei Zhang^{*}, Qingwen Ren^{**}

^{*}Hohai University, ^{**}Hohai University

ABSTRACT

Abstract: Seismic energy dissipation analysis of concrete gravity dams is presented based on an improved smeared crack model. The hysteretic behavior for concrete under tension-compression reversals due to the crack closing and reopening mechanism is simulated by the proposed model. Cracked shear modulus is suggested as a function of the normal strain in the directions perpendicular to the crack plane. The conservation of fracture energy and strain-rate effect are considered at the same time. Two-dimensional seismic response analyses of Koyna dam are performed to demonstrate the application of the proposed model. The influence of hysteretic behavior under tension-compression reversals on the seismic cracking and dissipation energy accumulation of concrete dams are discussed. The main novelty of the present paper is the proposed model considering the hysteretic behavior for concrete under tension-compression reversals. The effect of earthquake duration on the seismic energy dissipation of concrete dams can be taken into account by means of the proposed model, which is significant for the seismic damage assessment of concrete dams.

An Improved Staggered Iteration Scheme for the Modelling of Cohesive Zone Based Fracture by Phase Field Method

Peng Zhang^{*}, Weian Yao^{**}, Xiaofei Hu^{***}

^{*}Dalian University of Technology, ^{**}Dalian University of Technology, ^{***}Dalian University of Technology

ABSTRACT

Recently phase field model has gained popularity because of its convenience of analyzing crack initiation and propagation. In the present study a cohesive law based phase field model is implemented in the commercial finite software Abaqus with the user subroutine UEL (user defined element). The traction-separation relationship involved in the cohesive model has increased the solving difficulty of modeling significantly. Especially for the convergence issue which could result in the abortion of simulation without proper iteration algorithm. In order to improve the robustness and efficiency of the model, existing iteration algorithms are discussed in detail by using an analogical method. Based on the obtained results, a new improved iteration algorithm based on the staggered iteration scheme is proposed for the modelling of cohesive fracture. Numerical results show that both the crack path and load versus displacement curve predicted by the proposed method are in good agreement with the experimental observation and other numerical results. Furthermore, through the comparison of the iteration numbers of each incremental load between the present improved algorithm and the staggered iteration algorithm, it is proven that the proposed method is more effective for phase field modeling of cohesive fracture.

Tunable Metamaterials for Manipulating Elastic Wave through Transformation Method

Quan Zhang^{*}, Yiwen Li^{**}, Kai Zhang^{***}, Gengkai Hu^{****}

^{*}School of Aerospace Engineering, Beijing Institute of Technology, Beijing, 100081, China, ^{**}School of Aerospace Engineering, Beijing Institute of Technology, Beijing, 100081, China, ^{***}School of Aerospace Engineering, Beijing Institute of Technology, Beijing, 100081, China, ^{****}School of Aerospace Engineering, Beijing Institute of Technology, Beijing, 100081, China

ABSTRACT

Elastic metamaterials have attracted significant interest in recent years because of their broad range of applications, including vibration isolation, wave guiding, cloaking, and focusing [1]. Practically, traditional elastic metamaterials only operate at fixed frequency ranges due to the fixed microstructure, limiting additional potential applications. To address this issue, electromagnets, shape memory effect, structural deformation, fluid-structure interaction, and piezo-shunting have been employed to achieve elastic metamaterials with tunable band gaps [2,3]. These current strategies for designing tunable locally resonant metamaterials are all based on tuning the stiffness of the resonator. The most notable shortcoming of this approach is that the high frequency effective mass density is a constant, contrary to the request of transformation method based on density regulation. The high frequency effective mass density of locally resonant metamaterials is simply determined by the mass of substrate, which can be easily tuned if the mass distribution between resonator and substrate is changeable. Here, this paper reports a type of tunable locally elastic metamaterial, which consists of several liquid or gas inclusions in a solid matrix, controlled through a pair of embedded pumps. Both band gaps and effective mass density at high frequency can be tuned by controlling the liquid distribution in the unit cell, as demonstrated through a combination of theoretical analysis, numerical simulation, and experimental testing. Finally, we point out that our method can be utilized in steering wave propagation through transformation method based on density regulation. Our study offers a new perspective to design tunable metamaterials through controlling mass distribution, providing new avenues for vibration isolation and wave guiding. Reference: [1] O.R. Bilal, A. Foehr, C. Daraio, Adv. Mater. 2017, 29, 1700628. [2] Z. Wang, Q. Zhang, K. Zhang, G. Hu, Adv. Mater. 2016, 28, 9857. [3] P. Wang, F. Casadei, S. Shan, J.C. Weaver, K. Bertoldi, Phys. Rev. Lett. 2014, 113, 014301.

A Multiscale Space-time Computational Framework for Fracture and Fatigue Failure Simulation

Rui Zhang^{*}, Shogo Wada^{**}, Clint Nicely^{***}, Dong Qian^{****}

^{*}The University of Texas at Dallas, ^{**}The University of Texas at Dallas, ^{***}The University of Texas at Dallas,
^{****}The University of Texas at Dallas

ABSTRACT

We present a multiscale computational framework based on the coupling of time-discontinuous Galerkin (TDG) based space-time finite element method with either a two-scale damage model or Peridynamics (PD) for the purpose of fracture and fatigue failure simulation. This approach takes full advantage of the space-time FEM and its extended version (XTFEM) [1-3] in capturing multiple temporal scales, sharp gradients and discontinuities that are frequently encountered in these applications. An accelerated implementation of space-time FEM is developed to further improve its numerical efficiency. After outlining the basic framework, we first describe the integration with a two-scale models based on continuum damage mechanics. Sets of parameters for these damage models are calibrated by fatigue experiments of materials such as steel and synthetic rubber. We then present the work on the coupling of XTFEM simulation with PD simulation to capture crack initiation and propagation. To accommodate the evolving nature of the dynamic fracture, an adaptive scheme is developed so that the PD simulation is prescribed dynamically at the region near crack tip. Finally, a physics-based projection approach is introduced to realize seamless coupling between the two methods. Direct numerical simulations of high cycle fatigue over one million cycles are successfully performed with the presented framework. The results are validated through comparison with experiments and comparisons with full PD simulation of brittle fracture propagation. References: [1] S. Bhamare, T. Eason, S. Spottswood, S. R. Mannava, V. K. Vasudevan, and D. Qian, "A multi-temporal scale approach to high cycle fatigue simulation," Computational Mechanics, vol. 53, pp. 387-400, 2014. [2] R. Zhang, L. Wen, S. Naboulsi, T. Eason, V. K. Vasudevan, and D. Qian, "Accelerated multiscale space-time finite element simulation and application to high cycle fatigue life prediction," Computational Mechanics, vol. 58, pp. 329-349, 2016. [3] S. Wada, R. Zhang, S. R. Mannava, V. K. Vasudevan, and D. Qian, "Simulation-based prediction of cyclic failure in rubbery materials using nonlinear space-time finite element method coupled with continuum damage mechanics," Finite Elements in Analysis and Design, vol. 138, pp. 21-30, 2018.

A Phase Field Model for Simulation of Crack Propagation in Anisotropic Materials and Its Application to Predict Fracture Behavior in Silicon Carbide

Shuaifang Zhang^{*}, Cheng Liu^{**}, Izabela Szlufarska^{***}, Michael Tonks^{****}

^{*}University of Florida, ^{**}University of Wisconsin-Madison, ^{***}University of Wisconsin-Madison, ^{****}University of Florida

ABSTRACT

Crack initiation and fracture is of utmost concern in all engineering applications. Understanding fracture is complicated by its high sensitivity to the material microstructure, with defects typically serving as locations for crack initiation. Phase field modeling has been proved to an efficient tool for simulating crack initiation and propagation in materials, and several successful fracture models have been developed for isotropic materials in the recent past. However, the anisotropic nature of most crystal lattices necessitates a model that account for anisotropic material behavior. In this presentation, we present an anisotropic phase field model that can account for the impact of material microstructure on crack initiation and propagation. First, numerical examples are shown for verification of this phase field fracture model. Then, results from molecular dynamics simulations are used to parameterize the model for SiC. Finally, the model is used to predict fracture in polycrystalline SiC.

Understanding Wrinkles and Folds in Elastic Thin Sheets via a Lattice Model

Teng Zhang*

*Syracuse University

ABSTRACT

Thin elastic sheets can undergo complicated instabilities even under simple loads, examples including wrinkles and folds of a floating thin sheets due to liquid surface tension. A very rich instability phase diagram can emerge in thin sheets with simple geometries, such as annular and rectangular strip, which is determined by the nonlinear interplay of bending energy, gravity potential, surface energy and external work. In this talk, I will show from two examples, annular wrinkles and folds in a strip, that a triangle lattice model can efficiently and robustly capture these nonlinear instability modes. For the annular wrinkling problem, we will compare numerical predictions from the lattice model with experiments, perturbation theory at the near-threshold instability, and energy methods at the far-from threshold instability. It will be shown that the lattice model are all in very good agreements with the existing experiments and theories. For the folds in a strip under compression, we will explicitly account for the geometry nonlinearity of the gravity potential and self-contact of the solid film to avoid penetration. We will validate the lattice model by comparing it with an exact solution from full nonlinear analysis before self-contact and a reduced one-dimensional rod model.

A Moving Morphable Void (MMV)-based Explicit Approach for Topology Optimization Considering Stress Constraints

Weisheng Zhang^{*}, Xu Guo^{**}

^{*}Dalian University of Technology, ^{**}Dalian University of Technology

ABSTRACT

Topology optimization considering stress constraints has received ever-increasing attention in recent years for both of its academic challenges and great potential in real-world engineering applications. Traditionally, stress-constrained topology optimization problems are solved with approaches where structural geometry/topology is represented in an implicit way. This treatment, however, would lead to problems such as the existence of singular optima, the risk of low accuracy of calculated stress magnitude, and the lack of direct link between optimized results and computer-aided design/engineering (CAD/CAE) systems. With the aim of resolving the aforementioned issues in a systematic and straightforward way, a Moving Morphable Void (MMV)-based approach is proposed in the present study. Compared with existing approaches, the distinctive advantage of the proposed approach is that the structural geometry/topology is described in a completely explicit way. This feature provides the possibility of obtaining optimized designs with crisp and explicitly parameterized boundaries using much fewer numbers of degrees of freedom for finite element analysis and design variables for optimization, respectively. Several numerical examples provided demonstrate the effectiveness and advantages of the proposed approach.

Infrared Grating Thermal Wave Imaging for Detection of Damage in Thin Film System

Weixu Zhang*

*State Key Laboratory for Strength and Vibration of Mechanical Structures, Xi'an Jiaotong University

ABSTRACT

Interfacial damage significantly influences the reliability of thin film. For a very thin multi-layer film, how to accurately locate the damage is a big challenge. We introduced a new infrared grating thermal wave imaging to detect the damage in the thin film. The fundamental theoretical analysis of this approach will be presented. The effectiveness of this approach is validated by numerical simulation and experiment. The new approach is of high accuracy to locate the position of damage in principle.

A Contact Analysis Study for Rough Surfaces Considering Sliding-impact Behavior

Wenbo Zhang^{*}, Yunxia Chen^{**}, Jingjing He^{***}

^{*}Beihang University, ^{**}Beihang University, ^{***}Beihang University

ABSTRACT

Most of the typical coupling sliding-impact behavior are caused by thermal-solid-liquid complex operational environment. It may result in contact interface damage and even catastrophic consequences. The key point to solve this problem is to reveal the contact damage mechanism of sliding-impact behavior which happens on the typical contact interface. The actual damage can be caused by permanent deformation of two rough surfaces. This paper presents a theoretical study on the contact deformation process based on the elastoplastic deformation theory and the fractal theory. It can reveal the micro elastic-plastic contact mechanism and the statistical characteristics of macro contact with in consideration of the coupling sliding/impact behavior. Firstly, a revised W-M fractal contact model under the fixed load has been established. Then, the influence of impact on the contact variables of the revised W-M fractal contact model, such as the mean contact pressure, the contact area and the contact load are further analyzed by changing the magnitude of the impact energy and fixed contact loads. In addition, the equivalent contact load of uncertain time-varying impact under different contact mechanisms is also included.

Initial Solution Estimation for One-step Inverse Isogeometric Analysis in Sheet Metal Stamping

Xiangkui Zhang^{*}, Xuefeng Zhu^{**}, Changsheng Wang^{***}

^{*}School of Automotive Engineering, State Key Laboratory of Structural Analysis for Industrial Equipment, Dalian University of Technology, Dalian 116024, China, ^{**}School of Automotive Engineering, State Key Laboratory of Structural Analysis for Industrial Equipment, Dalian University of Technology, Dalian 116024, China, ^{***}School of Automotive Engineering, State Key Laboratory of Structural Analysis for Industrial Equipment, Dalian University of Technology, Dalian 116024, China

ABSTRACT

Recently, Isogeometric Analysis (IGA) based on incremental methods for simulating the stamping process has been researched. To the best of our knowledge, however, few studies have combined IGA and One-step inverse approach which is based on total deformation theory of plasticity. A key step for One-step inverse IGA is to estimate a good initial solution. Traditional mesh-based initial solution algorithms for One-step inverse approach are not suitable for One-step inverse NURBS-based IGA. In this paper, we presented a method which can rapidly unfold the undevelopable NURBS surface onto a planar domain and obtain a good initial solution estimation for One-step inverse IGA. The key idea of the presented method is unfolding the control net of a NURBS surface for isogeometric analysis by energy-based initial solution estimation algorithm. In addition, we developed a “cutting-stitching” algorithm which can separate a complex control net into several parts with simple shapes. Numerical examples illustrate the initial solutions using the presented method are approaching the final results by One-step inverse finite element method. This implies that the iterative steps and computational time of One-step inverse IGA will be reduced significantly compared with that of One-step inverse finite element method.

CFD Simulation of Piston-cylinder Jet Flows in Marine Propulsion

Xiaosong Zhang^{*}, Decheng Wan^{**}, James Huan^{***}

^{*}Shanghai Jiao Tong University, ^{**}Shanghai Jiao Tong University, ^{***}Optimax Dynamic

ABSTRACT

As a result of natural selection, fast moving marine animals choose impulsive modes to swim. Examples are: a squid generates an impulsive jet for thrust through its body muscle contraction, and a fish, through a control of the flapping of its caudal fin, is able to create an impulsive jet with a feature of thrust vectoring. A great amount of experimental work has been carried out to study impulsive jets and the associated vortex rings through the starting flows generated from a piston-cylinder apparatus. The research showed the efficiency advantage of an impulsive jet for propulsion lies in the utilization of the largest possible isolated vortex ring an impulsive jet can generate before its pinch-off from the trailing jet. With growing interests for a practical use of impulsive jet in marine propulsion, numerical simulation capabilities for impulsive jet flows become of obvious importance. Numerical simulation capabilities are challenged by the highly transient and vortical nature in the impulsive jet flows. Most of studies in the numerical simulations for the impulsive jet flows, especially the starting flows from a piston-cylinder apparatus, were for low Reynolds numbers in the scale of marine animals. Few numerical simulations were found for impulsive jetting into a background flow. CFD solver based on OpenFOAM was applied to simulate the starting flows by a piston-cylinder apparatus at Reynolds numbers from low to high covering marine animals and practical marine propulsors, and with various background flows. Numerical aspects such as numerical schemes, grid sensitivity and convergence quality in terms of the accuracy in capturing the flow vortical structures in the transient flow fields were studied. The numerical simulations were first validated and verified against those from the experimental and numerical studies found in the literature in the low Reynolds number range with and without background flows. The simulation tool was then applied to the predictions of the impulsive jet flows in the high Reynolds number range in practical marine propulsion with background flows.

Winkle Patterns on Torus

Xiaoxiao Zhang^{*}, Teng Zhang^{**}

^{*}Syracuse University, ^{**}Syracuse University

ABSTRACT

We investigate wrinkle patterns in a torus tripe-layer, where a thin outer layer is under expansion to drive the formation and evolution of wrinkles and an inner core has a tunable modulus to adjust the confinement of global expansion of the torus. We show from large-scale finite element simulations that hexagonal patterns will form at strong confinements (i.e. a stiff core) and strip wrinkles will develop at weak confinements (i.e. a soft core). Hexagons and strips can co-exist to form hybrid patterns at an intermediate confinement. As the outer layer further expands, strip and hexagon patterns will evolve into Zigzag and segment labyrinth, respectively. In addition, we observe strip wrinkles tend to initiate from the inner surface of the torus while hexagon wrinkles start from the outer surface. We further quantitatively analyze the topological defect distribution for a representative hexagonal pattern.

Numerical Modeling and Experimental Validation of Hyper Velocity Impact of a Multi-Layer Fabric Coated Aluminum Plate

Xiong Zhang^{*}, Zhiping Ye^{**}

^{*}Tsinghua University, ^{**}Tsinghua University

ABSTRACT

Due to their excellent impact-resistance, anti-fatigue and energy absorption capacity, fabrics and flexible composites are frequently used in protective structures to enhance their protective capacity. For example, a multi-layer fabric coated aluminum plate is usually used in the hard-upper torso of a space suit to protect astronauts from getting hurt by space dust, where the multi-layer fabric consists of an outer-layer fabric, a multi-layer insulation (MLI) layer and a liner layer. In this work, the protective performance of the multi-layer fabric coated aluminum plate is investigated both experimentally and numerically. To provide benchmarks for validating our numerical method, thirteen hyper velocity impact tests with different impact velocities (maximum velocity is 6.19km/s) and projectile diameters have been conducted. Due to the limitations of test equipment capacity, the hypervelocity impact tests with impact velocity higher than 6.2km/s are hard to be conducted. Therefore, a material point method (MPM) model is established for the multi-layer fabric coated aluminum plate and validated/corrected using our test results for impact velocity less than 6.2km/s. An equivalent laminated plate model of the MLI layer, which is composed of aluminized films separated by gauzes, is established to avoid discretizing its each single-layer which is too thin. A ballistic limit equation is established for the multi-layer fabric coated aluminum plate for space suit design by using the hyper velocity test results for impact velocity less than 6.2km/s and the MPM simulation results for impact velocity greater than 6.2 km/s. It shows that the critical diameter obtained by the validated MPM model for impact velocity less than 6.2km/s agrees well to the established ballistic limit equation, although which is established based on the test results for these velocity range. The corrected MPM model and the ballistic limit equation developed for the multi-layer fabric coated aluminum plate provide an effective tool for the space suit design.

The Nonlinear Controlling Effectiveness and Failure Mechanism of the MSCS

Xun'an Zhang^{*}, Zheng Wei^{**}, Ping Jiao^{***}

^{*}Professor, Department of Civil Engineering, Northwestern Polytechnical University, Postal Code: 710072, Xi'an, PRC., ^{**}PhD Student, Department of Civil Engineering, Northwestern Polytechnical University, Postal Code: 710072, Xi'an, PRC., ^{***}Vice Profession, Department of Civil Engineering, Northwestern Polytechnical University, Postal Code: 710072, Xi'an, PRC.

ABSTRACT

Mega-sub controlled structure (MSCS) is a new form of super tall buildings which is installed dissipation dampers to consume dynamic energy associated with excellent earthquake-resistant capability, and is stronger nonlinearity. However, as the nonlinear controlling effectiveness and failure mechanism of a practical MSCSS is different from the traditional mega sub structure (MSS), it is necessary to further investigate its nonlinear controlling effectiveness and failure mechanism. This paper focuses on the Mega-Sub Controlled Structure Systems (MSCSS) performances and characteristics regarding the new control principle contained in MSCSS subjected to strong earthquake excitations. The adopted control scheme consists of modulated sub-structures where the control action is achieved by viscous dampers and sub-structure own configuration. The elastic-plastic time history analysis under severe earthquake excitation is analyzed base on the Finite Element Analysis Method (FEAM), and some comparison results are also given in this paper. The result shows that the MSCSS systems can remarkably reduce vibrations effects more than the mega-sub structure (MSS). The study illustrates that the improved MSCSS presents good seismic resistance ability even at 1.2g and can absorb seismic energy in the structure, thus imply that structural members cross section can be reduce and achieve to good economic characteristics. Furthermore, the elasto-plastic analysis demonstrates that the MSCSS is accurate enough regarding international building evaluation and design codes. This paper also shows that the elasto-plastic dynamic analysis method is a reasonable and reliable analysis method for structures subjected to strong earthquake excitations and that the computed results are more precise. Keywords: controlling effectiveness, Elasto-plastic dynamic analysis, Mega-Sub Controlled Structure, Plastic hinge pattern.

Multi-scale Concurrent Topology Optimization for Macrostructures with Multi-patch Microstructures

Yan Zhang^{*}, Mi Xiao^{**}, Hao Li^{***}, Liang Gao^{****}

^{*}State Key Laboratory of Digital Manufacturing Equipment and Technology, Huazhong University of Science and Technology, ^{**}State Key Laboratory of Digital Manufacturing Equipment and Technology, Huazhong University of Science and Technology, ^{***}State Key Laboratory of Digital Manufacturing Equipment and Technology, Huazhong University of Science and Technology, ^{****}State Key Laboratory of Digital Manufacturing Equipment and Technology, Huazhong University of Science and Technology

ABSTRACT

Due to the capability of the fully exploring materials distribution at the macroscopic and materials configuration at the microscopic, the multi-scale concurrent topology optimization can obtain more excellent structural performance than the monoscale design by either sole macrostructures optimization or materials design. The intensive computational cost on material microstructures varying from point to point at the macroscopic scale is the main restriction on applications of the multi-scale concurrent topology optimization. This work develops a novel multi-scale concurrent design framework for topology optimization of material and structure to obtain the most excellent structural performance with a given material usage and an affordable computation cost. In this framework, the macrostructure consists of multiple kinds of material microstructures. Firstly, an ordered SIMP interpolation method, which is efficient to solve multi-material topology optimization problems without introducing any new variables, is presented to generate an optimized structure layout with the predetermined element density at macro scale. Then, all macro elements with the same density are considered to have the same microstructural configuration at micro scale. A parametric level set method is applied to the evolution of the shape and topology of the microstructures, whose effective properties are evaluated by the numerical homogenization approach. The kinematical connective constraint approach is employed to guarantee the connectivity of neighboring microstructures. In this way, the proposed method can simultaneously generate optimized macro material distribution patterns as well as optimized material microstructural configurations. Finally, some reasonable design solutions of the macrostructure and several material microstructures are obtained under the significantly reduced computation cost.

A New Design of Joint-bonded Triangular Cell Lattice Metamaterial with High Stiffness and Unbounded Thermal Expansion

Yongcun Zhang*, Yujing Liang**, Shutian Liu***

*State Key Laboratory of Structural Analysis for Industrial Equipment, Dalian University of Technology, Dalian, 116024, China, **State Key Laboratory of Structural Analysis for Industrial Equipment, Dalian University of Technology, Dalian, 116024, China, ***State Key Laboratory of Structural Analysis for Industrial Equipment, Dalian University of Technology, Dalian, 116024, China

ABSTRACT

Triangular cell lattice metamaterials composed of bi-layer curved rib elements (called the Lehman-Lakes lattice) possess unbounded thermal expansion, high stiffness and sheer impossibility of thermal buckling, which are highly desirable in many engineering structural application subjected to large fluctuations in temperature. However, the requirement of such lattice metamaterial must be pin-connected joints. The fabrication complexity makes them less than ideal for consideration especially on microstructural scales. In this study, a newly designed bi-layer curved rib element that the layer one is partially covered with layer two is proposed, which can assemble the joint-bonded lattice metamaterials with any cell topologies. As an example, the joint-bonded triangular cell lattice metamaterial (JTCLM) that is presented, which can achieve high stiffness and the desired CETs from infinite small (negative) to infinite great (positive) by intentionally adjusting the used materials and geometric parameters of rib elements. The thermomechanical properties of JTCLM are given by the closed-form analytical solution. The validity of the analytical models is illustrated and proved by the numerical simulations. Furthermore, the used materials are considered to be invar and steel, two design targets of JTCLM are obtained by optimizing the geometric parameters of rib element. One target is the stiffest JTCLM with the highest tunability for realizing large positive or negative CTEs, and the other is the stiffest JTCLM with zero CTE. Compared with the Lehman-Lakes lattice, the JTCLM with the same large positive or negative CTEs can achieve more than four times stiffness improvement; the JTCLM with zero CTE has more than 56% improvement in stiffness and simultaneously have a 34% reduction in weight. The better manufacturability and multifunctional properties of the new proposed JTCLM display a great potential for a wide range of applications.

Study on a Delamination Control Method for Composite Materials Based on Shape Memory Alloy

Yu Zhang^{*}, Meiying Zhao^{**}, Chao Zhang^{***}

^{*}Northwestern Polytechnical University, ^{**}Northwestern Polytechnical University, ^{***}Northwestern Polytechnical University

ABSTRACT

Carbon fiber reinforced composite laminates have been widely used in the field of aerospace for the high specific strength and specific stiffness. However, the laminated characteristics of resin-based composites cause relatively low interlaminar mechanical properties, and the large area delamination caused by low-velocity impact would further lead to the deterioration of structural buckling characteristics. In order to reduce the damage under low-velocity impact and control the delamination area of resin-based composites, a new damage control method of embedding shape memory alloy (SMA) into composite material was proposed in this study. And based on the pseudo-elastic property of SMA, the impact damage characterization method of SMA reinforced resin-based composites laminates were explored. The numerical model of SMA reinforced resin-composites include three different parts, SMA wire, laminates layer and interface between layers. In this paper, a macroscopic thermodynamic constitutive model of SMA was studied based on previous research on phenomenological constitutive model, and this material model was used to describe the deformation process of SMA wire which combined into classical laminates numerical model. Here, to describe characteristics of interface damage between layers, the cohesive method was applied. In order to preliminarily calibrate the material parameters, the tensile test of SMA reinforced resin-based composites laminates was carried out, some parameters of material are determined by comparing the numerical model with the experimental results. After that, a numerical model of SMA reinforced resin-based composite laminates under low-velocity impact loading was established based on above method. According to the numerical results, the phenomena of delamination control for composite materials by SMA was analysed. Furthermore, the damage mechanism of SMA reinforced resin-based composites laminates was summarized.

Sensitivity of Topology Features in Stress Tensor Fields over Mesh Refinement

Yue Zhang*

*Oregon State University

ABSTRACT

Hexahedral meshes are important in tensor field visualization, such as the stress and strain tensors obtained from finite element modeling of solid mechanics. In this talk, we discuss features in 3D tensor fields that are sensitive to mesh refinement and how to classify features that are topology artifacts that are due to improper meshes.

Stress- and Temperature-Induced Phase Transformation in Architecture Materials

Yunlan Zhang^{*}, David Restrepo^{**}, Miriam Velay^{***}, Nilesh Mankame^{****}, Pablo Zavattieri^{*****}

^{*}Purdue University, ^{**}Purdue University, ^{***}Purdue University, ^{****}General Motors, ^{*****}Purdue University

ABSTRACT

Phase transforming cellular materials are architected materials whose unit cells have multiple stable configurations. If designed correctly, these materials can absorb energy by allowing controlled snap-through mechanisms as the cells transform between different stable configurations. Most previous works on architecture materials with snap-through mechanisms focused on material behavior when the material is loaded in one direction. Mostly because, most of the designs were limited to 1D behavior. In this work, we propose a new family of 2D structures defined by the number of axis of symmetry through a combined analytical, computational and experimental approach. This includes a new family of cellular architectures that employ cylindrical shell elements dissipate energy by triggering local snap-through instabilities. Physical samples were manufactured and tested in loading and unloading cycles. Ancillary analytical and computational analysis guided the design and help understand the different mechanisms acting in the system for energy dissipation. Our mechanical tests have shown key similarities in deformation modes with the simulations, and verified that there is significant energy dissipation due to snapping instabilities as expected. We also look at the application of these mechanisms to the design of temperature-induced phase transformation taking into advantage design and combination of materials to produce shape memory and actuation capabilities.

Numerical and Experimental Studies on Microstructures and Mechanical Properties in Friction Stir Additive Manufacturing

Zhao Zhang^{*}, Zhijun Tan^{**}, Jianyu Li^{***}, Zhenyu Wan^{****}, Xinxin Yao^{*****}, Honglei Yuan^{*****}

^{*}Department of Engineering Mechanics, Dalian University of Technology, Dalian 116024, China, ^{**}Department of Engineering Mechanics, Dalian University of Technology, Dalian 116024, China, ^{***}Department of Engineering Mechanics, Dalian University of Technology, Dalian 116024, China, ^{****}Department of Engineering Mechanics, Dalian University of Technology, Dalian 116024, China, ^{*****}Department of Engineering Mechanics, Dalian University of Technology, Dalian 116024, China, ^{*****}Department of Engineering Mechanics, Dalian University of Technology, Dalian 116024, China

ABSTRACT

Friction Stir Additive Manufacturing (FSAM) is a new developed technology based on friction stir welding. The plates can be joined together in a solid state by the friction from the rotating tool. In FSAM, recrystallization occurs and then the grains can be coarsened by the following temperature variations. The recrystallization and grain coarsening can be simulated by Monte Carlo method. The precipitate evolution can be also investigated. The pinning effect of precipitates is studied. The mechanical property can be divided into different components including the contributions from dislocation density, from the crystal plasticity for pure aluminum, from solid solutions, and from the precipitates. Each component is calculated and results show that the contribution from the precipitates is the main factor for the determination of the final mechanical property of aluminum in FSAM. Experiments are performed to validate the final predicted mechanical property. Acknowledgements: This study is funded by the National Natural Science Foundation of China (No. 11572074) and the Fundamental Research Funds for the Central Universities.

Optimized Design of 3D Printed Trachea for Cancer Patients

Zhi Zhang^{*}, Jaejong Park^{**}, Shaheen Islam^{***}, Alok Sutradhar^{****}

^{*}The Ohio State University, ^{**}The Ohio State University, ^{***}The Ohio State University, ^{****}The Ohio State University

ABSTRACT

The tracheal stent is widely used in the treatment of airway malformation may be caused by stenosis, malacia, traumatic injury, and external compression from cancer. However, these stents present some critical problems which include the growth of obstructed granulation tissue inside of trachea, and frequent migration of the stent. Improvements of tracheal stent design have been primarily focused on using new stent materials (e.g., metal, silicone, carbon nano-composite, shape memory materials). Customized patient-specific designs to ease obstructions or alleviate compressions and/or closing of trachea openings have not been explored in a systematic way. In this research, we take a systematic approach to study the airflow behavior in trachea airway due to obstruction focused for cancer patients. Using patient-specific computed tomography (CT) images, we propose an approach to solve the post-stent implantation problem and find the optimized design. Parametric studies on the length of branches and the angle between branches in the silicone stent, the flow rate, pressure drop were carried out. Computational fluid dynamics (CFD) approach was used to evaluate the performance of design with these variable parameters. Different obstructions pattern in the stent were also analyzed using CFD to imitate the shape change caused by the external compression from cancer around the trachea. Additionally, the geometry of trachea from CT images was modified with obstructions to simulate how external compression from cancer can disturb airflow behavior.

3D Crystal-Plastic Particle-in-Cell Simulation of Open-Cell Metal Foam

Dongfang Zhao^{*}, Jayden Plumb^{**}, James Guilkey^{***}, Ashley Spear^{****}

^{*}University of Utah, ^{**}University of Utah, ^{***}University of Utah, ^{****}University of Utah

ABSTRACT

Open-cell metallic foams are hierarchical structural-material systems that have applications as light-weight impact absorbers, noise insulators, and heat sinks, to name a few. Their hierarchical structure includes the grain scale, the scale of individual ligaments, and the topological scale of the foam. Many researchers have related the bulk mechanical properties of these cellular solids to the nominal density and to other metrics at the topological scale. Far fewer studies have investigated the dependence of bulk and local mechanical response on grain-scale structure of the foam. This talk will describe a high-fidelity numerical framework that captures the deformation mechanisms across multiple length scales in open-cell aluminum foam. Due to large deformations at the ligament scale in the foam during compressive loading, the finite element method tends to produce divergent results as Lagrangian meshes become extremely distorted and entangled. Utilizing the material point method (MPM), the framework presented here accommodates large deformations in the foam, since the background grid is incrementally reset during the simulation while state variables are stored at the MPM particles. Convected-particle tetrahedral domain integration (CPTI) is used, which enables a conformal representation of the ligament morphologies and grain boundaries within each ligament. To accurately predict the local, micromechanical deformations at the grain scale, a crystal-plasticity constitutive model has been incorporated into the MPM driver. The crystal-plastic material point-based (CPMPM) framework is demonstrated to simulate the deformation of foam at a mesoscale and enables simulation of the compressive behavior all the way to the foam-densification regimes. A parallel effort involves multi-scale experiments to map 3D grain structure in a real sample of open-cell aluminum foam using far-field high-energy X-ray diffraction microscopy (HEDM). The measured grain-scale data is used in the subsequent virtual reconstruction of foam geometry and generation of CPMPM models. Four cases with different grain instantiations (one measured and three synthetic) are investigated to quantitatively analyze the size effects of ligaments on the mechanical behaviors of open-cell metallic foam using the CPMPM framework. The simulation results provide insight into the correlation of local and global mechanical properties with foam microstructural features. With this new insight, well-established microstructure-based design criteria will facilitate performance-based optimization of open-cell metallic foams.

Experimental Study and State-based Peridynamic Simulation of Crack/Crack System Propagation and Coalescence in Pre-cracked Sandstone Disks under Compressive Loading

Shijun Zhao^{*}, Qing Zhang^{**}

^{*}Hohai University, ^{**}Hohai University

ABSTRACT

Abstract The rock is a natural formation of mineral aggregates, generally contains different scale voids, cracks, damage and other defects. In this work, crack/crack system propagation and coalescence in pre-cracked Brazilian disks are studied by experiment and numerical simulation. Firstly, in the experiment, sandstone disks with different single pre-cracked angles and pre-cracked crack system are under compressive line loading. Secondly, most of the current numerical analysis methods must satisfy the continuity conditions in order to solve the space differential equation, the traditional numerical methods of continuum mechanics cannot accurately describe the progressive failure process of rock complex damage accumulation, macro crack initiation and crack propagation. State-based Peridynamic model is employed to simulate crack/crack system propagation and coalescence in pre-cracked sandstone disks. The state-based Peridynamic model describes a material point in a continuum interacts directly with other neighborhood material points across a finite distance. Furthermore, compared the experimental results with numerical simulation results, it is found that the numerical results by state-based Peridynamic theory are in good agreement with the experimental results. The state-based Peridynamic model has natural advantages in analyzing crack propagation and coalescence problems. Keywords Rock mechanics; Experimental study; Numerical simulation; Peridynamic; Crack propagation

A Coupled Peridynamics-Immersed Boundary-Lattice Boltzmann Scheme for Fluid-Structure Interaction Problems

Teng Zhao^{*}, Yongxing Shen^{**}

^{*}University of Michigan-Shanghai Jiao Tong University Joint Institute, Shanghai Jiao Tong University, ^{**}University of Michigan-Shanghai Jiao Tong University Joint Institute, Shanghai Jiao Tong University

ABSTRACT

Fluid-structure interaction is a long-standing challenging problem in engineering due to complex behaviors of solids and fluids. Thus a widely extensible computational method is emerging. In this study, we provide a general computational framework aiming at solving fluid-structure interaction problems in complex media. This scheme utilizes a nonordinary state-based peridynamics model for solid deformation and the lattice Boltzmann method for fluid flow. To avoid tracking the fraction of different phases in large deformation and fracture process of the solid, we employ a modified immersed boundary method. The numerical method is compared with analytical solutions to demonstrate convergence. It is worth noting that the peridynamics model is solved by meshless method and the lattice Boltzmann method is based on a structured mesh. So, the influence of different discretization parameters is studied in the numerical examples. This scheme is applicable to a wide range of materials and fluids, including dynamic fracture in hydraulic fracturing process. Numerical results of hydraulic fracturing simulation is shown, which is in general agreement with literature and experiments.

Bubble Assemblies in Ternary Systems with Long Range Interaction

Yanxiang Zhao*

*George Washington University

ABSTRACT

A nonlocal diffuse interface model, based on the Nakazawa-Ohta density functional theory for triblock copolymers, is used to study bubble assemblies in ternary systems. The model has three parameters weighing three types of long range interaction and two parameters that fix the total area of each constituent. As the parameters vary, a large number of morphological phases appear as stable stationary states. One open question related to the polarity direction of double bubble assemblies is answered numerically. Moreover, it is shown that the average size of bubbles in a single bubble assembly depends on the sum of the minority constituent areas and the long range interaction coefficients. One further identifies the ranges for area fractions and the long range interaction coefficients for double bubble assemblies.

The Application of Hybrid Stress-function Method in Piezoelectric Materials

Yingtao Zhao^{*}, Tianbing Zhao^{**}, Yunhui Sun^{***}

^{*}Key Laboratory of Dynamics and Control of Flight Vehicle, Ministry of Education, School of Aerospace Engineering, Beijing Institute of Technology, Beijing 100081, People's Republic of China, ^{**}Key Laboratory of Dynamics and Control of Flight Vehicle, Ministry of Education, School of Aerospace Engineering, Beijing Institute of Technology, Beijing 100081, People's Republic of China, ^{***}Key Laboratory of Dynamics and Control of Flight Vehicle, Ministry of Education, School of Aerospace Engineering, Beijing Institute of Technology, Beijing 100081, People's Republic of China

ABSTRACT

The finite element method (FEM) has been widely used as one of the most important tools to engineering and scientific analysis. However, FEM has been suffered from mesh distortion. Recently, a novel finite element method is developed named as hybrid stress-function (HS-F) method. The resulting plane element is immune to mesh distortion and possesses excellent performance even when the quadrilateral element is degenerated into a triangular or concave one. By applying the fundamental analytical solutions of stress field to FEM, the HS-F opens a new way to develop shape-free finite element models. In this paper, we generalize the high-performance HS-F method to piezoelectric materials. Firstly, a systematic approach to determine the polynomial stress function for piezoelectric plane problems is presented based on Lekhnitskii's anisotropic elastic theory and Sosa's analytical method. Secondly, by introducing the first 23 generalized stress functions, a new HGSF-23 element is constructed based on the principle of minimum mechanical enthalpy. Finally, several numerical examples of classic problems are given to test the new element. The results show that the element inherits the advantages of HS-F method. It is a new mesh-free method for analysis of piezoelectric materials and also has very high accuracy. Moreover, the procedure may provide a guidance to develop other high-performance elements for coupling fields based on HS-F method.

Investigation of Solidification Conditions in Electron Beam Melting Using Computational thermal-Fluid Dynamics Simulation

Yufan Zhao^{*}, Yuichiro Koizumi^{**}, Kenta Aoyagi^{***}, Kenta Yamanaka^{****}, Akihiko Chiba^{*****}

^{*}Grad. School of Eng., Tohoku Univ., ^{**}Institute for Materials Research, Tohoku Univ. (Current: Grad. School of Eng., Osaka Univ.), ^{***}Institute for Materials Research, Tohoku Univ., ^{****}Institute for Materials Research, Tohoku Univ., ^{*****}Institute for Materials Research, Tohoku Univ.

ABSTRACT

Electron beam melting (EBM), an additive manufacturing (AM) technology, is capable of fabricating dense metallic components using a high-intensity electron beam to melt powder layer by layer. Compared with laser powder-bed fusion process, EBM has high power density, fast melting rate and low residual stresses [1, 2]. For wide applications of EBM-built alloys, flexible control of not only the geometry but also the microstructures are highly demanded. The grains grow epitaxially from the base-metal in nature, easily producing columnar grains. For grain structure control, solidification conditions ((i) constitutional undercooling, (ii) convective fluid flow and (iii) molten pool geometry) are worthy of attention. The interaction between high-energy beam and material causes strong fluid flow in the molten pool and affect final grain morphology. In this study, the computational thermal-fluid dynamics (CtFD) simulation was applied to analyze the heat transfer, fluid flow and resultant solidification conditions, and then to inspect the effects of solidification conditions on grain morphology. CtFD simulation, which is based on a finite-difference methods (FDM), can track the front of the molten metal by the volume-of-fluid (VOF) method and predict temperature field and fluid flow. The proof-of-concept experiments were carried out in EBM apparatus using biomedical Co-Cr-Mo (CCM) alloy by way of example. The local solidification conditions, including temperature gradient (G), solidification rate (R) and fluid velocity (U) at the solidification front, were extracted from simulation results. Through the analysis of the simulated data and the experimental result, the solidification behavior within dynamic molten pool was studied. The study revealed the profound influence of fluid flow rather than G and R on grain morphology. Higher fluid velocity (U) at solidification front was found to be a quite important factor to promote CET in EBM process of CCM alloy. In addition, greatly variable normal direction of solidification front also contributes to the formation of equiaxed grains. This study also showed great prospect of controlling grain structure with the aid of quantitatively numerical simulation, which will contribute to the development of EBM-built alloys with desired property. References [1] SS Gajapathi, SK Mitra, PF Mendez. Int. J. Heat Mass Transfer, 54.25 (2011): 5545-5553. [2] Sochalski-Kolbus, L. M., et al. Metall. Mater. Trans. A, 46.3 (2015): 1419-1432.

Application of Surface Nanocrystallization in the Energy Absorption Devices

Zhen Zhao^{*}, Jufang Jia^{**}, Wei Wang^{***}, C W Lim^{****}, Xinsheng Xu^{*****}

^{*}Dalian University of Technology; City University of Hong Kong; City University of Hong Kong Shenzhen Research Institute., ^{**}Dalian University of Technology, ^{***}Dalian University of Technology, ^{****}City University of Hong Kong; City University of Hong Kong Shenzhen Research Institute., ^{*****}Dalian University of Technology; City University of Hong Kong Shenzhen Research Institute.

ABSTRACT

The increasing of motor vehicles leads to frequent occurrence of traffic accidents. To improve the safety performance of automobiles, enhancing the buffering effect of the energy absorption devices during the collision accidents has become a key issue in the automobile manufacturing industry. The thin-walled structure is the most extensively used fundamental component in the energy absorption devices, which buckles easily under axial impact and absorbs a large amount of energy. Experimental results show that the geometric parameters and material properties have significant influence on the energy absorption capacity. In other words, the high-order buckling modes of the thin-walled structure can be induced by optimized parameters, which could directly improve the energy absorption effect. At present, classical design of energy absorption devices, e.g., changing external configuration of the overall structure, adding adjunctive structures to the main body, usually increases the processing difficulty and manufacturing costs. Therefore, there is a great demand for developing a high energy absorption device without any modification of the configuration of the fundamental component. A novel surface nanocrystallization technology is an emerging technology to enhance the mechanical properties of metal material. By using the nanocrystallization technology, the local material properties of thin-walled structures are strengthened and the nanocrystallization layouts are designed easily. Thus, it provides a simple way to induce the high-order buckling modes of the thin-walled structures under impact loads. In the present study, an accurate simulation method is proposed to analyze and optimize the local nanocrystallization energy absorption devices. Firstly, on this basis of the theoretical equations, the dynamic analysis algorithm for the local nanocrystallization energy absorption devices is developed under the framework of ANSYS LS-DANA. The produce of the energy absorption is accurately predicted by the proposed algorithm. Secondly, the local nanocrystallization layouts and geometric parameters are optimized by using a structural optimization theory. The relation between the buckling mode and the key influencing factors are obtained. Compared with the thin-walled structures without nanocrystallization, the treated ones show higher energy absorption capacity and stability. It provides a new technique of designing and manufacturing such energy absorption devices for the automobiles during the collision accidents. The present study not only promotes the development in energy absorption design but also provides guidance to the practical engineering manufacturing in various industries.

Multi-scale Finite Element Modeling on the Impact Behavior of Triaxially Braided Composites

Zhenqiang Zhao^{*}, Chao Zhang^{**}, Yulong Li^{***}, Gunjin Yun^{****}

^{*}Northwestern Polytechnical University, ^{**}Northwestern Polytechnical University, ^{***}Northwestern Polytechnical University, ^{****}Seoul National University

ABSTRACT

Carbon fiber reinforced textile/braided composite now has gradually been used in aerospace and automotive structures to defend the external impact load due to its outstanding impact resistance. For instance, the two-dimensional tri-axially braided composite (2DTBC) is introduced to fabricate engine fan case structure, which exhibits excellent damage tolerance and reduces significantly the weight of the aero-engine. Design and optimization of large-scale structures, such as the fan blade and containment casing of aero engine, is a formidable and costly task. Fortunately, finite element simulation approach has been validated for its capability in predicting the failure behavior and mechanical performance of braided composite. In addition, previous studies suggest that accurate determination of basic mechanical properties are very essential for the proper implementation of material models in impact simulations. Thus, in this work, a multi-scale method is proposed to investigate the impact response of 2DTBC. Firstly, a micromechanical model is used to obtain the properties of fiber tows which are intertwined to form the layer of 2DTBC, based on the properties of fiber and matrix extracted from literatures. Then, a validated meso-scale finite element (FE) model is adopted to simulate the failure behavior of the braided composites under different load conditions, taking into consideration the realistic test boundary conditions. Finally, an enhanced macro-scale subcell model for a six-layer braided composite plate is developed to study the impact behavior of the 2DTBC. The homogenized material properties of the subcell model is acquired by using the volume averaging method from the effective stress-strain responses of the subcell elements for the representative unit cell. The presented modeling framework presents a new tool for impact simulation of textile composites and shows advantages in capturing the failure initiation and progression during an impact load. The impact simulation results compare well with the experimental results and provide insights on the impact failure characters of this material.

Generalized Variational Principles for Fully Coupled Thermo-Chemo-Mechanical System Based on Continuum Thermodynamics

JIAHONG ZHENG*, CONGYING JIANG*, ZHENG ZHONG*[†],
AND XIAOLONG ZHANG*

*Tongji University
No.1239, Siping Road, Yangpu District,
Shanghai, China
Email: 1510038jhz@tongji.edu.cn

[†]Harbin Institute of Technology, Shenzhen
No.6, First Pingshan Road, Nanshan District,
Shenzhen, Guangdong, China
Email: zhongk@tongji.edu.cn; <http://www.hitsz.edu.cn/teacher/view/id-1287.html#>

Key words: Generalized Variational Principle, Functional, Multi-Field Coupling,
Chemical Reaction, Continuum Thermodynamics

Abstract: Multi-scale and multi-physics coupling governs many complex engineering problems. Such issues with chemical or electrochemical reactions are essential for many industrial applications, such as energy storage and conversion technologies. Discussions regarding thermo-chemo-mechanical coupled problems have drawn great attention in recent years. Our previous research substantiates that the reaction extent can be treated as an internal variable for modeling multi-physics problems by means of continuum mechanics. However, few efforts have been devoted to develop variational principles and associated numerical modeling technologies of this kind of problems. Herein, two complementary generalized variational principles for fully coupled thermo-chemo-mechanical problems are established. The equivalence between the proposed generalized variational principles and the partial differential equations governing the fully coupled thermo-chemo-mechanical problems is then demonstrated. The analogy of different physical essences are discussed, which reveals the intrinsic relationship between different fields. Introducing proper preconditions simplifies corresponding variational principles to be valid for single field problems, two-field coupled or half coupled problems. Some remarkable simplifications of present theory are obtained. These simplifications corroborate former studies, indicating that all existed theories share the same theoretical basis. This work may provide a way for numerical simulating multi-physics problems, for which some numerical validations are given.

*Corresponding author. ZHENG Jiahong. Email: 1510038jhz@tongji.edu.cn; Tel: 86-18301958023.

Nomenclature

U	=Internal energy(= $E + \Phi$) / (J)	Φ	=Dissipative potential energy / (J)
E	=Free internal energy / (J)	Ψ	=Dissipative potential density / (J/m ³)
e^r	=Free internal energy density / (J/m ³)	ϕ	=Dissipative power density / (W/m ³)
\mathbf{u}	=Displacement / (m)	$\boldsymbol{\varepsilon}$	=Total strain / (-)
$\boldsymbol{\varepsilon}^r$	=Thermodynamic reversible strain / (-)	$\boldsymbol{\sigma}$	=Stress / (Pa)
$\boldsymbol{\varepsilon}^i$	=Irreversible strain / (-)	\mathbf{f}	=Body force / (N)
η^r	=Reversible entropy per unit volume / (J/K/m ³)		=Temperature / (K)
	=Heat flux density / (J/m ² /s)		=Thermal dissipative intensity / (K/m)
c_α	=Number of moleculars of α influx per unit volume / (mol/m ³)	μ_α	=Chemical potential of α / (J/mol)
m_α	=Mass flux of α / (mol/m ² /s)	μ_α	=Diffusion dissipative intensity of α / (J/mol/m)
$\ell^{(\gamma)}$	=Extent of reaction γ / (mol/m ³)	γ	=Chemical affinity / (J/mol)
r_α	=Source density of α / (mol/m ³)	$\nu_\alpha^{(\gamma)}$	=Stoichiometric coefficient of α in reaction γ / (-)
	=Work done by external forces / (J)	\mathbf{n}	=Unit vector normal to boundary
$\bar{\mathbf{u}}$	=Prescribed boundary displacement / (m)	$\bar{\mathbf{T}}$	=Prescribed boundary force / (N/m ³)
\bar{m}_α	=Prescribed boundary mass flux of α / (mol/m ² /s)	$\bar{\mu}_\alpha$	=Prescribed boundary chemical potential of α / (J/mol)
$\bar{}$	=Prescribed boundary modified heat flux / (J/K/m ² /s)	$\bar{}$	=Prescribed boundary temperature / (K)
<i>ubscripts uperscripts</i>			
*	=Complementary part		=Related to heat conduction
r	=Thermodynamic reversible	i	=Irreversible (dissipative)
α	=Chemical species α	γ	= γ th reaction
	= th internal variable	m	=Related to mass diffusion

For convenience, we assume Einstein's summation convention for subscribe/superscript α and γ herein.

1 INTRODUCTION

The strong coupling of various physical quantities can be found in advanced functional materials^[1, 2], energy storage and conversion devices^[3, 4], natural porous media^[5-7], natural fiber reinforced composites^[8-10] and biological tissues^[11]. For example, gels or polyelectrolytes have typical coupling performances such that ion transportation and electrochemical reaction take place simultaneously with hyperelastic responses^[12].

Great efforts have been devoted to theoretical studies on such multi-field coupling problems in the past decades. Based on thermodynamics for mechano-chemistry^[13] and poroelasticity^[14], Rice

and Cleary^[15] solved some basic stress-diffusion problems. With more physical phenomena involved, such as temperature effect, chemical reaction and electrical response, some phenomenological models have been developed^[16-19]. In order to develop an efficient numerical method for multidisciplinary simulation, variational principles for multi-field problems attracted great research interests. Luo^[20, 21] derived generalized variational principles for thermo-mechanical and electro-mechanical coupling problems. Yang and Qin^[22] proposed a variational principle and corresponding finite element formulation of coupled thermo-electro- chemo-mechanical problems. Hu and Shen^[23] obtained a series of quasi variational principles for thermal-mechanical- chemical coupling problems by using different forms of free energy and constitutive equations. Recently, Zhang and Zhong^[24] developed a fully coupled theoretical framework for chemically active and deformable solids with mass diffusion and heat conduction, treating reaction extent as an independent variable so that the contributions of chemical reaction can be distinguished from those of species diffusion.

Generalized variational principles of Hu-Washizu type and Hellinger-Reissner type are direct theoretical basis of constructing mixed finite element method which can avoid some numerically ill-posed issues in conventional finite element method. For multi-field problems, such generalized variational principle has never been reported yet. Therefore, the main purpose of this work is to construct a suitable generalized variational principle for fully coupled thermo-chemo-mechanical problems based on the theoretical framework of Zhang and Zhong^[24], and to show the capability of the framework through examples numerically implemented.

The present work is organized as follows. First, basic equations for fully coupled multi-field problems are discussed in Section 2. Then the generalized variational principles of potential energy type and complementary energy type are established and demonstrated respectively. Section 3 is devoted to clarify the consistency with those in literature through a simplified version of proposed generalized variational principle. In Section 4, a numerical example of a reaction-diffusion process reveals the progress in present approach. Results are shown in Section 4 as well.

2 THEORETICAL MODEL

On the basis of previous studies, a thermodynamic framework considering chemical extent as an independent internal state variable was established in Ref.[24-26]. This framework governs typical thermo-chemo-mechanical coupling problems. Consider a macroscopically homogeneous body B made of a chemically active medium (a host solid with absorbed chemical species) and bounded by surface S. With deformation, mass diffusion, heat conduction and chemical reaction considered, after slight adjustment governing equations can be expressed as follows:

First constitutive equations (state equations)

$$\boldsymbol{\sigma} = \frac{\partial e^r}{\partial \boldsymbol{\varepsilon}^r} = \frac{\partial e^r}{\partial \boldsymbol{\eta}^r} \quad \mu_\alpha = \frac{\partial e^r}{\partial c_\alpha} \quad (\gamma) = -\frac{\partial e^r}{\partial \ell^{(\gamma)}} \quad (1)$$

Second constitutive equations (evolving equations)

$$\dot{\boldsymbol{\varepsilon}}^i = \frac{\partial \phi^*}{\partial \boldsymbol{\sigma}} = \frac{\partial \phi^*}{\partial} \quad \dot{m}_\alpha = \frac{\partial \phi^*}{\partial c_\alpha} \quad \dot{\ell}^{(\gamma)} = \frac{\partial \phi^*}{\partial \ell^{(\gamma)}} \quad (2)$$

Gradient equations

$$\frac{1}{2}(\nabla \mathbf{u} + \mathbf{u} \nabla) = \boldsymbol{\varepsilon}^r + \boldsymbol{\varepsilon}^i \quad + \nabla \cdot = 0 \quad \mu_\alpha + \nabla \mu_\alpha = 0 \quad (3)$$

Balance equations

$$\nabla \cdot \boldsymbol{\sigma} + \mathbf{f} = 0 \quad \dot{\eta}^r + \nabla \cdot = 0 \quad \dot{c}_\alpha + \nabla \cdot \mu_\alpha = 0 \quad (4)$$

while boundary conditions are listed as follows:

Dirichlet type boundary conditions

$$\mathbf{u} = \bar{\mathbf{u}} \text{ (on } \partial\Omega_u) \quad =^- \text{ (on } \partial\Omega_T) \quad \mu_\alpha = \bar{\mu}_\alpha \text{ (on } \partial\Omega_{\mu_\alpha}) \quad (5)$$

Neumann type boundary conditions

$$\boldsymbol{\sigma} \cdot \mathbf{n} = \bar{\mathbf{T}} \text{ (on } \partial\Omega_\sigma) \quad \cdot \mathbf{n} =^- \text{ (on } \partial\Omega_J) \quad \mu_\alpha \cdot \mathbf{n} = \bar{\mu}_\alpha^m \text{ (on } \partial\Omega_{\mu_\alpha}^m) \quad (6)$$

where Ω is the control volume of body B with the outward unit vector \mathbf{n} normal to its boundary $\partial\Omega$, $\partial\Omega = \partial\Omega_u \cup \partial\Omega_\sigma = \partial\Omega \cup \partial\Omega_T = \partial\Omega_\mu \cup \partial\Omega_{\mu_\alpha}$, $\partial\Omega_u \cap \partial\Omega_\sigma = \partial\Omega \cap \partial\Omega_T = \partial\Omega_\mu \cap \partial\Omega_{\mu_\alpha} = \emptyset$, and a bar over a quantity denotes its prescribed boundary value.

Then complementary generalized variational principles can be established. A potential energy type functional is constructed as:

$$\begin{aligned} \Pi(\mathbf{u}, \boldsymbol{\varepsilon}^r, \boldsymbol{\varepsilon}^i, \boldsymbol{\sigma}, \eta^r, c_\alpha, \mu_\alpha, \mu_\alpha^m, \ell^{(\gamma)}, \ell^{(\gamma)}) \\ = E + \Phi - \int_1 + \int_2 + \int_3 + \int_4 + \int_5 + \int_6 \end{aligned} \quad (7)$$

where

$$\begin{aligned} E &= E(\boldsymbol{\varepsilon}^r, \eta^r, c_\alpha, \ell^{(\gamma)}) = \int_\Omega e^r(\boldsymbol{\varepsilon}^r, \eta^r, c_\alpha, \ell^{(\gamma)}) d \\ \Phi &= \int_t \int_\Omega \left[\boldsymbol{\sigma} : \dot{\boldsymbol{\varepsilon}}^i + \dot{\eta}^r + \mu_\alpha \cdot \dot{c}_\alpha + \ell^{(\gamma)} \dot{\ell}^{(\gamma)} - \phi^*(\boldsymbol{\sigma}, \eta^r, \mu_\alpha, \ell^{(\gamma)}) \right] d \, dt \\ &= \int_\Omega \mathbf{f} \cdot \mathbf{u} d + \int_{\partial\Omega_\sigma} \bar{\mathbf{T}} \cdot \mathbf{u} d - \int_t \int_{\partial\Omega_T} \cdot \mathbf{n} d \, dt - \int_t \int_{\partial\Omega_{\mu_\alpha}} \bar{\mu}_\alpha^m \cdot \mathbf{n} d \, dt \\ \int_1 &= \int_\Omega \left[\frac{1}{2}(\nabla \mathbf{u} + \mathbf{u} \nabla) - (\boldsymbol{\varepsilon}^r + \boldsymbol{\varepsilon}^i) \right] : \boldsymbol{\sigma} d \quad \int_2 = - \int_t \int_\Omega (\dot{\eta}^r + \nabla \cdot) d \, dt \quad \int_3 = - \int_t \int_\Omega (\dot{c}_\alpha + \nabla \cdot \mu_\alpha^m) \mu_\alpha d \, dt \\ \int_4 &= \int_{\partial\Omega_u} (\bar{\mathbf{u}} - \mathbf{u}) \cdot \boldsymbol{\sigma} \cdot \mathbf{n} d \quad \int_5 = \int_t \int_{\partial\Omega_J} (\cdot \mathbf{n} - \cdot^-) d \, dt \quad \int_6 = \int_t \int_{\partial\Omega_{\mu_\alpha}^m} \mu_\alpha (\mu_\alpha^m \cdot \mathbf{n} - \mu_\alpha^m) d \, dt \end{aligned}$$

Correspondingly, a complementary energy type functional is constructed as:

$$\begin{aligned} \Pi^*(\mathbf{u}, \boldsymbol{\varepsilon}^r, \boldsymbol{\varepsilon}^i, \boldsymbol{\sigma}, \eta^r, c_\alpha, \mu_\alpha, \mu_\alpha^m, \ell^{(\gamma)}, \ell^{(\gamma)}) \\ = E^* + \Phi^* - \int_1^* + \int_2^* + \int_3^* + \int_4^* + \int_5^* + \int_6^* \end{aligned} \quad (8)$$

where

$$E^* = E^*(\boldsymbol{\sigma}, \mu_\alpha, \ell^{(\gamma)}) = \int_\Omega \left[\boldsymbol{\sigma} : \boldsymbol{\varepsilon}^r + \eta^r + \mu_\alpha c_\alpha - \ell^{(\gamma)} \ell^{(\gamma)} - e^r(\boldsymbol{\varepsilon}^r, \eta^r, c_\alpha, \ell^{(\gamma)}) \right] d$$

Theorem: the first variation of Π or Π^* vanishes, if and only if $\mathbf{u}, \boldsymbol{\varepsilon}^r, \boldsymbol{\varepsilon}^i, \boldsymbol{\sigma}, \boldsymbol{\eta}^r, , c_\alpha, \mu_\alpha, , ,$
 $\ell^{(\gamma)}, \quad (\gamma)$ are the exact solution of above mentioned boundary value problem (1)~(6).

For one example, let first constitutive relations, second constitutive relations, gradient relations and Dirichlet boundary conditions be prescribed, that is taking (1)~(3) and (5) as preconditions. Thus, the thermo-chemo Gibbs type functional should be:

$$\Pi_g(\mathbf{\epsilon}^r, \mathbf{\epsilon}^i, \mu_\alpha, {}^{(\gamma)}) = \mathbf{\epsilon}^r + \Phi_g - \mathbf{\epsilon}^i_g \quad (9)$$

$$\mathbf{r} = \mathbf{r}(\boldsymbol{\varepsilon}^{\mathbf{r}}, \boldsymbol{\mu}_\alpha, \ell^{(\gamma)}) = \int_{\Omega} g^{\mathbf{r}}(\boldsymbol{\varepsilon}^{\mathbf{r}}, \boldsymbol{\mu}_\alpha, \ell^{(\gamma)}) d = \int_{\Omega} \left[e^{\mathbf{r}}(\boldsymbol{\varepsilon}^{\mathbf{r}}, \boldsymbol{\eta}^{\mathbf{r}}, \mathbf{c}_\alpha, \ell^{(\gamma)}) - \boldsymbol{\eta}^{\mathbf{r}} - \boldsymbol{\mu}_\alpha \mathbf{c}_\alpha + \ell^{(\gamma)} \right] d$$

$$\Phi_g = \Phi_g(\dot{\mathbf{x}}^i, \quad , \quad ^\mu_{\alpha}, \quad ^{(\gamma)}, t) = \int_t \int_\Omega [\boldsymbol{\sigma} : \dot{\mathbf{x}}^i - \phi^*(\boldsymbol{\sigma}, \quad , \quad ^\mu_{\alpha}, \quad ^{(\gamma)})] d \quad dt$$

$$g = f - q - c = \int_{\Omega} \mathbf{f} \cdot \mathbf{u} d\mathbf{x} + \int_{\partial\Omega_{\sigma}} \bar{\mathbf{T}} \cdot \mathbf{u} d\mathbf{x} + \int_t \int_{\partial\Omega_j} -d \, dt + \int_t \int_{\partial\Omega_m} \mu_{\alpha}^{-m} d \, dt$$

Then

$$\begin{aligned} \delta \Pi_g = & \int_{\partial \Omega_\sigma} (\boldsymbol{\sigma} \cdot \mathbf{n} - \bar{\mathbf{T}}) \cdot \delta \mathbf{u} d\mathbf{x} - \int_{\Omega} (\nabla \cdot \boldsymbol{\sigma} + \mathbf{f}) \cdot \delta \mathbf{u} d\mathbf{x} + \int_t \int_{\partial \Omega_j} (\mathbf{u} \cdot \mathbf{n} - \bar{u}) \delta \mathbf{u} d\mathbf{x} dt \\ & + \int_t \int_{\partial \Omega_m} (\mathbf{u} \cdot \mathbf{n} - \bar{u}) \delta \mu_\alpha d\mathbf{x} dt - \int_t \int_{\Omega} (\dot{c}_\alpha + \nabla \cdot \mathbf{m}_\alpha) \delta \mu_\alpha d\mathbf{x} dt - \int_t \int_{\Omega} (\dot{\eta}^r + \nabla \cdot \mathbf{h}) \delta \eta^r d\mathbf{x} dt \end{aligned} \quad (10)$$

Considering thermodynamic reversible strain $\boldsymbol{\varepsilon}^r = \boldsymbol{\varepsilon} - \boldsymbol{\varepsilon}^i$, current concentration $\tilde{c}_\alpha = c_\alpha + r_\alpha = c_\alpha + v_\alpha^{(\gamma)} \ell^{(\gamma)}$, chemical affinity $\eta^{(\gamma)} = -\mu_\alpha v_\alpha^{(\gamma)}$ and dissipative power $\dot{\psi}(\eta^i) = \dot{\eta}^i$ with $\dot{\eta} = \dot{\eta}^r + \dot{\eta}^i$, one has

$$\begin{aligned} g^r(\boldsymbol{\varepsilon}^r, \mu_\alpha, \eta^{(\gamma)}) &= e^r(\boldsymbol{\varepsilon}^r, \eta^r, c_\alpha, \ell^{(\gamma)}) + \psi - \eta^r - \mu_\alpha c_\alpha + \eta^{(\gamma)} \ell^{(\gamma)} - \eta^i + \hat{\eta}^i \\ &= e(\boldsymbol{\varepsilon}^r, \eta, \tilde{c}_\alpha) - \eta - \mu_\alpha \tilde{c}_\alpha + \hat{\eta}^i = g_c(\boldsymbol{\varepsilon}^r, \mu_\alpha) + \hat{\eta}^i \\ \psi_g &= \int_t \left[\boldsymbol{\sigma} : \dot{\boldsymbol{\varepsilon}}^i - \phi^*(\boldsymbol{\sigma}, \mu_\alpha, \eta^{(\gamma)}) \right] dt = \int_t \dot{d}_{gc} dt = d_{gc} \end{aligned} \quad (11)$$

in which a superposed hat (^) denotes a variable to be held fixed during variation, $g_c(\boldsymbol{\varepsilon}^r, \mu_\alpha)$ and d_{gc} are respectively the Gibbs free energy density and corresponding dissipative energy density that Kuang^[27-29] and Shen et. al^[23, 30-31] adopted. The reduced form deduced here equals to the Gibbs type quasi variational principle for multi-field problem that Kuang and Shen proposed.

It's important to emphasize that, Yu and Shen^[30] introducing quasi variational term $\delta \hat{\eta}^i = -\int_\Omega \hat{\eta}^i \delta d$ of (11) into the heat source term δB_Q^* , by the interpretation of “the irreversible part of the complement of heat corresponding to the inner complement dissipative energy”^[23]. That term ingeniously avoid energy imbalance during deducing principles from free energy density g_c and dissipative energy density d_{gc} separately. However, derivation in this section shows that the division of total internal energy simplifies the formulas and derivation of variational principles significantly. And a variational principle with an explicit functional has great advantage than those quasi variational principles in future application.

4 NUMERICAL EXAMPLE

To illustrate the main progress in present approach, we consider a chemical active thin plate bonded to a rigid substrate, immersed in a liquid as Fig.1. This plate deforms gradually due to chemical reaction and mass diffusion on isothermal assumption. Assuming we have linear constitutive laws, such a chemo-mechanical coupling problems can be described in a weak-form of equivalent integral equation based on the theoretical model mentioned above. Solved by PDE toolbox of COMSOL Multi-physics[®], the displacement distributions in the normal direction during different reaction-diffusion process are shown in Fig.2.

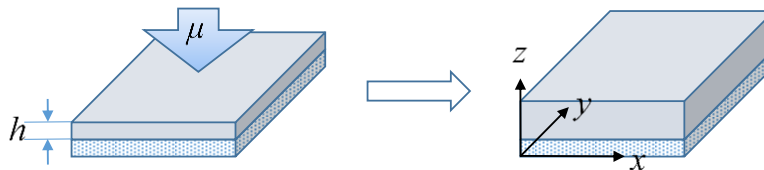
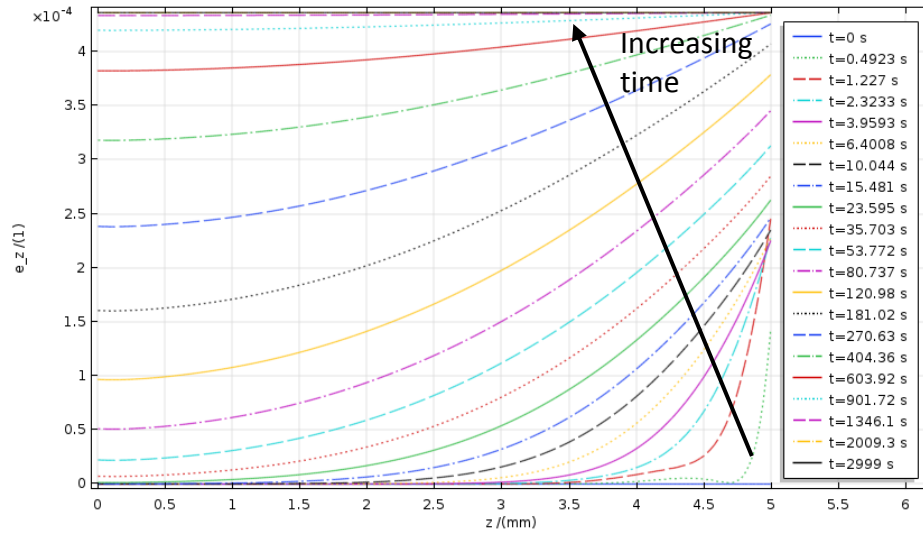
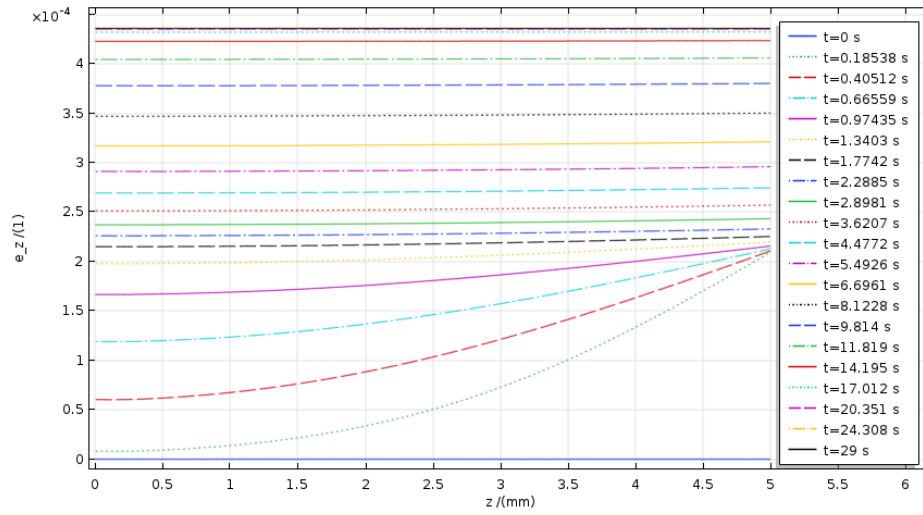


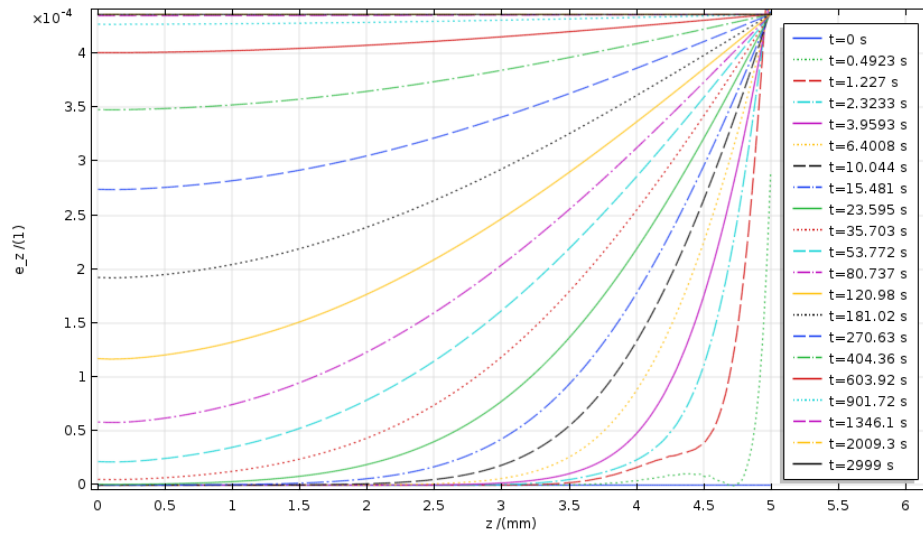
Fig.1 Schematic diagram



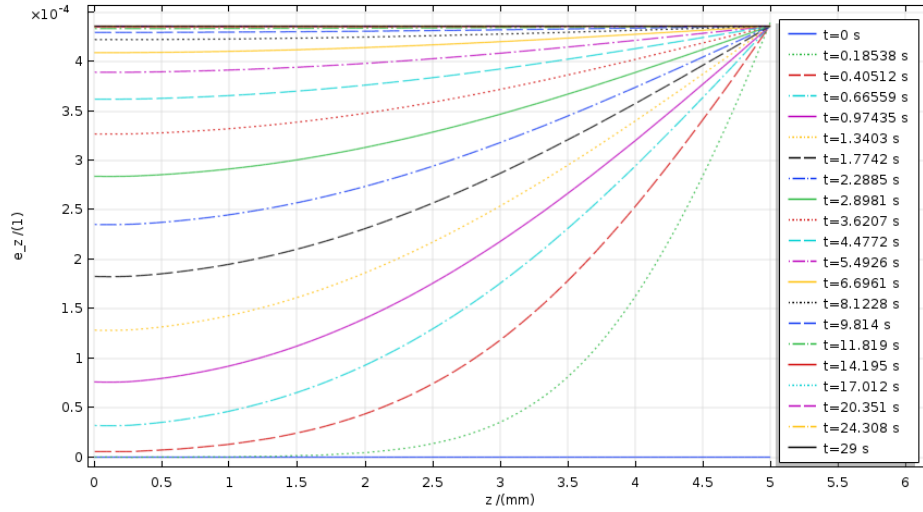
(a) $=4e-7[\text{mol}^2/(\text{m}^*\text{J}^*\text{s})]$, $nct=2e-3[1/\text{s}]$



(b) $=4e-5[\text{mol}^2/(\text{m}^*\text{J}^*\text{s})]$, $nct=2e-3[1/\text{s}]$



(c) $=4e-7[\text{mol}^2/(\text{m}^*\text{J}^*\text{s})]$, $nct=2e1[1/\text{s}]$



$$(d) = 4e-5[\text{mol}^2/(\text{m}^3\text{J}\cdot\text{s})], \quad nct=2e1[1/\text{s}]$$

Fig.2 Displacement u distribution in z direction for different reaction-diffusion process

Results in Fig.2 indicate the different evolving process under different diffusion rate (measured by diffusion coefficient D) and different reaction rate (measured by reaction rate constant nct). Fig.2(b) reveals a typical reaction control process while Fig.2(c) a diffusion control process. Fig.2(a) and Fig.2(d) present the competition of contributions from diffusion and chemical reaction in different time scale. Such results agree well with those analytical conclusions of Zhang and Zhong^[24].

CONCLUSIONS

- Two complementary generalized variational principles for fully coupled thermo-chemo-mechanical problems are established. Discussion on simplification to theories in literature indicates the conciseness of proposed theory.
- Simulations show that weak-form integral equations based on the theoretical model mentioned above is suitable for simulating such multi-physics problems. This approach reveals the difference under different process.

REFERENCES

- [1] Bekas, D.G., Tsirka, K., Baltzis, D. and Paipetis, A. S. Self-healing materials: a review of advances in materials, evaluation, characterization and monitoring techniques. *Compos. Part B*. (2016) 87:92-119.
- [2] Chester, S. A., and Anand, L. A coupled theory of fluid permeation and large deformations for elastomeric materials. *J. Mech. Phys. Solids*. (2010) 58:1879-1906.
- [3] Swaminathan, N. and Qu, J. M. Interactions between non-stoichiometric stresses and defect transport in a tubular electrolyte. *Fuel Cells*. (2007) 7:453-462.
- [4] Brassart, L. and Suo, Z. Reactive flow in large-deformation electrodes of lithium-ion batteries. *Int. J. Appl. Mec.* (2012) 4:1250023.

- [5] Huyghe, J. and Janssen, J. D. Thermo-chemo-electro-mechanical formulation of saturated charged porous solids. *Transp. Porous. Med.* (1999) 34:129-141.
- [6] Coussy, O. *Poromechanics*. Poromechanics. John Wiley & Sons, Ltd, West Sussex, (2004).
- [7] Coussy, O. *Mechanics and Physics of Porous Solids*. Wiley, West Sussex, (2010).
- [8] Pan, Y. and Zhong, Z. Compos. Modeling of the mechanical degradation induced by moisture absorption in short natural fiber reinforced composites. *Sci. Technol.* (2014) 103:22-27.
- [9] Pan, Y. and Zhong, Z. A nonlinear constitutive model of unidirectional natural fiber reinforced composites considering moisture absorption. *J. Mech. Phys. Solids.* (2014) 69:132-142.
- [10] Pan, Y. and Zhong, Z. The effect of hybridization on moisture absorption and mechanical degradation of natural fiber composites: An analytical approach. *Compos. Sci. Technol.* (2015) 110:132-137.
- [11] Peradzynski, Z. Diffusion of calcium in biological tissues and accompanying mechano-chemical effects *Arch. Mech.* (2010) 62:423-440.
- [12] Yang, C. H., Zhou, S., Shian, S., Clarke, D. R. and Suo, Z. Organic liquid-crystal devices based on ionic conductors. *Mater. Horiz.* (2017) 4:1102-1109.
- [13] Gibbs, J. W. *The Scientific Papers of J. Willard Gibbs*. (1878) 184, 201, 215.
- [14] Biot, M. A. General Theory of Three-Dimensional Consolidation. *J. Appl. Phys.* (1941) 12:155.
- [15] Rice, J. R. and Cleary, M. P. Some basic stress diffusion solutions for fluid - saturated elastic porous media with compressible constituents. *Rev. Geophys.* (2010) 14:227-241.
- [16] Rambert, G., Jugla, G., Grandidier, J. C. and Cangemi, L. A modelling of the direct couplings between heat transfer, mass transport, chemical reactions and mechanical behaviour. Numerical implementation to explosive decompression. *Compos. Part A.* (2006) 37:571-584.
- [17] Rambert, G., Grandidier, J. C. and Aifantis, E. C. On the direct interactions between heat transfer, mass transport and chemical processes within gradient elasticity. *Eur. J. Mech. A* (2007) 26:68-87.
- [18] Loeffel, K. and Anand, L. A chemo-thermo-mechanically coupled theory for elastic-viscoplastic deformation, diffusion, and volumetric swelling due to a chemical reaction. *Int. J. Plast.* (2011) 27:1409-1431.
- [19] Loeffel, K., Anand, L. and Gasem, Z. M. On modeling the oxidation of high-temperature alloys. *Acta Mater.* (2013) 61:399-424.
- [20] Luo, E., Kuang, J., Huang, W. and Luo, Z. Unconventional Hamilton-type variational principles for nonlinear coupled thermoelastodynamics. *Sci. China Math.* (2002) 45:783-794.

-
- [21] Huang, W. J., Luo, E., She, H.L. Unconventional Hamilton-type variational principles for dynamics of Reissner sandwich plate. *Appl. Math. Mech.* (2006) 27:75-82.
- [22] Yang, Q., Qin, Q., Ma, L., Lu, X. Z. and Cui, C. A theoretical model and finite element formulation for coupled thermo-electro-chemo-mechanical media. *Mech. Mater.* (2010) 42:148-156.
- [23] Hu, S. and Shen, S. Non-equilibrium thermodynamics and variational principles for fully coupled thermal-mechanical-chemical processes. *Acta Mech.* (2013) 224:2895-2910.
- [24] Zhang, X. and Zhong, Z. A coupled theory for chemically active and deformable solids with mass diffusion and heat conduction. *J. Mech. Phys. Solids.* (2017) 107:49-75.
- [25] Zhong, Z. and Zhang, X. L. Research advances and perspectives of thermo-chemo-mechanically coupling continuum theories for solids. *Chin. Quart Mech.* (2017) 38:593-618.
- [26] Zhang, X. L. and Zhong, Z. A thermodynamic framework for thermo-chemo-elastic interactions in chemically active materials. *Sci. China Phys. Mech. Astron.* (2017) 60:084611.
- [27] Kuang, Z. B. Variational principles for generalized dynamical theory of thermopiezoelectricity. *Acta Mech.* (2009) 203:1.
- [28] Kuang, Z. B. Variational principles for generalized thermodiffusion theory in pyroelectricity. *Acta Mech.* (2010) 214:275-298.
- [29] Kuang, Z. B. Energy and entropy equations in coupled nonequilibrium thermal mechanical diffusive chemical heterogeneous system. *Sci. Bull.* (2015) 60:952-957.
- [30] Yu, P. and Shen, S. A fully coupled theory and variational principle for thermal–electrical–chemical–mechanical processes. *J. Appl. Mech. T. ASME*, (2014) 81:111005.
- [31] Chen, J., Wang, H., Yu, P. and Shen, S. A Finite element implementation of a fully coupled mechanical-chemical theory. *Int. J. Appl. Mech.* (2017) 9:1750040.
- [32] Demirel, Y. Modeling of thermodynamically coupled reaction-transport systems. *Chem. Eng. J.* (2008) 139:106-117.
- [33] Hu, H. C. On some variational principles in the theory of elasticity and the theory of plasticity. *Acta Phys. Sin.* (1954) 10:259.
- [34] Hu, H. C. Variational principles of elasticity and its application. Science Press, Beijing, (1981).
- [35] Yang, Q. S., Qin, Q. H., Ma L. H., Lu, X. Z. and C. Q. Cui, *Mech. Mater.* 42, 148 (2010).

Large-scale and Parallel Pre-processing Researches and SuperMesh Development

Peng Zheng*, Quan Xu**, Juelling Leng***, Yang Yang****, Jianjun Chen*****, Zeyao Mo*****

*Institute Of Computer Application/High Performance Numerical Simulation Software Center, China Academy Of Physics, **High Performance Numerical Simulation Software Center, China Academy Of Physics, ***High Performance Numerical Simulation Software Center, China Academy Of Physics, ****High Performance Numerical Simulation Software Center, China Academy Of Physics, *****aCenter for Engineering and Scientific Computation, Zhejiang University, *****High Performance Numerical Simulation Software Center, China Academy Of Physics

ABSTRACT

One of the key technologies to improving the availability of high performance numerical simulation is the large-scale and parallel pre-process technology, which serves to generate large-scale, high precision and high resolution grids quickly and with high quality. Facing the challenge of whole system and three-dimensional simulation running on peta-flop supercomputer, and in order to meet the needs of 'cloak meshing', the pre-processing engine SuperMesh is developed. We presents an accurate and highly automatic geometry processing and mesh generation pipeline of SuperMesh and its flexible extensible architecture here, which could generates large-scale structured and unstructured mesh for complicated CAD Model, and could be butted seamlessly with the parallel programming framework JASMIN, JAUMIN and JCOGIN. Since 2013, SuperMesh has been used in customizing specific packages for several high performance numerical simulation software based on those programming framework. Currently, in order to face the challenge of 100 peta-flop computing, researches have been carried out in automatic model cleaning based on mixed representation and multilevel parallel mesh generation. Firstly, mixed representation of Brep model and discrete model is used to change Brep model synchronously when processing discrete model for coordinated mesh generation. Then, Brep model partition and mesh size prediction method are applied in first level parallel mesh generation. Finally, a background mesh partition method is used and the subsequent steps of surface meshing, volume meshing and mesh improvement in sub-region are executed in a complete parallel manner, all these related novel algorithms are going to be incorporated in SuperMesh. References [1] Jianjun Chen, Zhiwei Liu, Yao Zheng, Peng Zheng, Jianjing Zheng, Zhoufang Xiao, Chuang Yu. Automatic sizing ?functions for 3D unstructured mesh generation. Procedia Engineering, (In: Proc. of the 26th International Meshing Roundtable, Barcelona, Spain, Sep 18-21 2017) 2017; 203: 245-257. [2] Zeyao Mo, Aiqing Zhang, Xiaolin Cao, Qingkai Liu, Xiaowen Xu, Hengbin An, Wenbing Pei, Shaoping Zhu. JASMIN: a parallel software infrastructure for scientific computing[J], Front. Comput. Sci. China, 4(4): 480-488, 2010. [3] Peng Zheng, Wei Fang, Quan Xu, Juelling Leng, Min Xiong, Changhua Yu. Parallel AFT Tetrahedral Mesh Generation for JAUMIN[J/OL]. Journal of Frontiers of Computer Science and Technolgy, [2017-12-21].<http://kns.cnki.net/kcms/detail/11.5602.TP.20170103.1036.006.html>.

The Numerical Study of Phase Transition of Temperature Sensitive Hydrogel under Mechanical Constraint

Shoujing Zheng*, Zishun Liu**

*International Center for Applied Mechanics, State Key Laboratory for Strength and Vibration of Mechanical Structures, Xi'an Jiaotong University, Xi'an, 710049, People's Republic of China, **International Center for Applied Mechanics, State Key Laboratory for Strength and Vibration of Mechanical Structures, Xi'an Jiaotong University, Xi'an, 710049, People's Republic of China

ABSTRACT

The numerical study of phase transition of temperature sensitive hydrogel under mechanical constraint Shoujing Zheng, Zishun Liu* International Center for Applied Mechanics, State Key Laboratory for Strength and Vibration of Mechanical Structures, Xi'an Jiaotong University, Xi'an, 710049, People's Republic of China *Corresponding Author: zishunliu@mail.xjtu.edu.cn Abstract Temperature sensitive hydrogel is blessed with outstanding properties which may be utilized for innovative appliance. However, this is not achievable if the phase transition property of it is not well understood. Under certain mechanical constraint or temperature stimuli, the hydrogel shows the phase transition, a very special phenomenon that shows huge volume change. Based on the theory that can predict this volumetric deformation, we developed a numerical method to study the phase transition under mechanical constraints. In the simulation, the subroutine of ABAQUS is used to calculate the stress of the hydrogel under the uniaxial load. The subroutine is in the UHYPER form, which is developed by our group previously (Ding et al., 2013). Using the code, we found that the mechanical behavior is intrinsically different before and after the phase transition. We also found that near the phase transition, multiple curves can be obtained in the stress-stretch figure. In other words, near the phase transition region, one stress can correspond to at least two stretches, one representing the swollen state, one representing the shrunk state. The calculation above can prove the existence of phase transition numerically. Furthermore, using Dynamic Mechanical Analysis, we have conducted experiments to quantitatively investigate this peculiar behavior. Based on the experimental data, a new decision rule is formulated to determine the critical stress. Finally, with a proper fitting parameter and a transformation from referential state to free swelling state, we can compare the numerical prediction of the stress-stretch curve with results from experiments (Zheng and Liu, 2017). References Ding, Z., Liu, Z., Hu, J., Swaddiwudhipong, S., Yang, Z., 2013. Inhomogeneous large deformation study of temperature-sensitive hydrogel. International Journal of Solids and Structures 50, 2610-2619. Zheng, S., Liu, Z., 2017. Phase transition of temperature sensitive hydrogel under mechanical constraint. Journal of Applied Mechanics.

Extended Multiscale Finite Element Methods for the Localization and Crack Propagation Analyses of Heterogeneous Materials

Yonggang Zheng^{*}, Mengkai Lu^{**}, Hongwu Zhang^{***}

^{*}Dalian University of Technology, P. R. China, ^{**}Dalian University of Technology, P. R. China, ^{***}Dalian University of Technology, P. R. China

ABSTRACT

Based on the embedded strong discontinuity model, we have developed recently the extended multiscale finite element methods for the strain localization and crack propagation analyses of homogeneous and heterogeneous materials. In these methods, the kinematic descriptions of the localization and crack are considered based on a set of fine-scale meshes with the strong discontinuity model. Then an enhanced coarse element strategy, in which additional coarse nodes can be adaptively added according to the propagation of shear band or discontinuity line, is used to construct the multiscale numerical base functions that can well capture the localization or discontinuous characteristics and transform the information between the fine scale and coarse scale. The mechanical problems are then solved in a coarse-scale mesh by upscaling from the fine-scale meshes based on the developed enhanced coarse element strategy. The displacement decomposition technique is adopted to modify the downscale computations by adding the perturbation solutions and thus the microscopic displacement can also be accurately obtained. Various representative numerical examples were carried out to demonstrate the effectiveness and high efficiency of the proposed methods. References [1] Lu, M.K.; Zhang, H.W.; Zheng, Y.G.*; Zhang, L. A Multiscale Finite Element Method for the Localization Analysis of Homogeneous and Heterogeneous Saturated Porous Media with Embedded Strong Discontinuity Model. *Int. J. Numer. Methods Eng.*, 2017, 112, 1439. [2] Lu, M.K.; Zhang, H.W.; Zheng, Y.G.*; Zhang, L. A Multiscale Finite Element Method with Embedded Strong Discontinuity Model for the Simulation of Cohesive Cracks in Solids. *Comput. Methods Appl. Mech. Eng.*, 2016, 311, 576. [3] Zhang, H.W.*; Lu, M.K.; Zheng, Y.G.; Zhang, S. General Coupling Extended Multiscale FEM for Elasto-Plastic Consolidation Analysis of Heterogeneous Saturated Porous Media. *Int. J. Numer. Anal. Methods Geomech.*, 2015, 39, 63.

Investigation of Thermal Alleviation on Cold Dwell Fatigue

Zebang Zheng*, Fionn Dunne**

*Imperial College London, **Imperial College London

ABSTRACT

Dwell sensitivity is well known in titanium alloys, and is found to cause high peak stresses that can lead to failure. The mechanism of dwell debit is thought to be related to very particular crystallographic orientation combinations. A polycrystalline aggregate containing a combination of a primary hard grain with c-axis nearly parallel to the loading direction and adjacent soft grains with c-axis nearly normal to the loading direction, commonly known as a rogue grain combination, was studied under a dwell fatigue condition using crystal plasticity model with dual phase morphology explicitly represented. Load shedding was found to occur within the rogue grain combination, in which stress is redistributed from the soft grain to the hard grain during a hold at peak applied stress. Load shedding was also found to be strongly affected by temperature: the amount of stress redistribution is significantly reduced when temperature increased from 20°C to 300°C. The temperature sensitivity of load shedding is a result of the diminishment in strain rate sensitivity at high temperatures. Engine rig spin tests under isothermal conditions and realistic in-service engine loading histories (non-isothermal) was modelled and compared using dual phase polycrystal model. The evolution of effective plastic strain and dislocation density around the hard-soft grain boundary was captured and quantified. The peak stress developed during the loading under in-service conditions was found to be lower than the critical value to initiate facet crack due to the inhibition of load shedding at high temperature.

Study on Sharp V-notch Problem Using Symplectic Analytical Singular Element

Cai Zhiyu^{*}, Hu Xiaofei^{**}, Yao Weian^{***}

^{*}Dalian University of technology, ^{**}Dalian University of technology, ^{***}Dalian University of technology

ABSTRACT

V-notch problem with dynamic loading condition is considered in this paper. In the time domain, the precise time domain expanding algorithm is employed, in which a self-adaptive technique is carried out to improve computing accuracy. By expanding variables in each time interval, the recursive finite element formulas is derived. In the space domain, a Symplectic Analytical Singular Element (SASE) is constructed within the framework of finite element method (FEM). The vicinity of the crack tip is represented by using the SASE, and the other area is meshed by using conventional elements. Due to the advantage of the SASE, the dynamic stress intensity factors (DSIFs) can be obtained directly via the relationship between the the eigen expanding coefficients and the DSIFs, without any post-processing. Numerical examples are conducted to investigate the accuracy and the stability. Results show that the proposed SASE for dynamic V-notch problem is effective and efficient.

In-vivo Effects of Different Orthodontic Loading on Root Resorption and Correlation to Mechanobiological Stimulus in Periodontal Ligament

Jingxiao Zhong^{*}, Junning Chen^{**}, Richard Weinkamer^{***}, M. Ali Darendeliler^{****}, Michael V. Swain^{*****}, Andrian Sue^{*****}, Keke Zheng^{*****}, Qing Li^{*****}

^{*}University of Sydney, ^{**}University of Exeter, ^{***}Max Planck Institute of Colloids and Interfaces, ^{****}University of Sydney, ^{*****}University of Sydney, ^{*****}University of Sydney, ^{*****}University of Sydney, ^{*****}University of Sydney

ABSTRACT

Orthodontic root resorption (ORR) is a common side effect of orthodontic therapy. In orthodontic practice, the treatment-related risk factors are of particular interest to clinicians, and orthodontic load magnitude is believed to be one of the primary controlling factors. High pressure in the periodontal ligament (PDL) generated by orthodontic forces will trigger recruitment of odontoclasts, leaving resorption craters on root surfaces. However, due to intricate anatomical and physiological environment for ORR, odontoclast's in-vivo responses to mechanobiological loading have yet to be studied. The patterns of resorption craters are the traces of odontoclast activity. Therefore, this study aimed to investigate the mechanobiological relationship influencing the extent and distribution of orthodontic root resorption, considering the resorptive patterns as evidences of in-vivo cellular responses to two different levels of orthodontic loadings. First, the resorption craters were quantitatively assessed in a 3D manner using microCT. The spatial information and individual crater characteristics were analysed to provide insights into in-vivo odontoclast activities and their patterns, with reference to known regulations of osteoclast behaviour. Furthermore, 3D subject-specific nonlinear finite element (FE) models were created based on the microCT images to evaluate the corresponding mechanobiological stimuli induced by different orthodontic loadings. With combination of experimental and numerical characterisation, the correlation between ORR and orthodontic loading can be analysed. Results indicated that the heavy force (225 g) led to a larger total resorption volume than the light force (25 g), mainly by presenting larger individual crater volumes ($p < 0.001$) than increasing crater numbers, suggesting that increased mechano-stimulus predominantly boosted cellular resorption activity rather than recruiting more odontoclasts. Furthermore, buccal-cervical and lingual-apical regions in both loading groups were found to have significantly larger resorption volumes than other regions ($p < 0.005$). These clinical observations are complimented by the finite element analysis (FEA) results, which indicated that when the volume average compressive hydrostatic pressure exceeded the capillary blood pressure (4.7kPa), root resorption was more likely to be induced. This work provides new insights into the odontoclastic activities in-vivo and helps in predicting therapeutical outcomes, for potential improvement in the generally sophisticated surgical procedure.

Dual-basis Dimensional Reduction for Non-dissipative Explicit Dynamic Discrete Element Simulations with High-frequency Noises

Xinran Zhong^{*}, Kun Wang^{**}, WaiChing Sun^{***}

^{*}Columbia University, ^{**}Columbia University, ^{***}Columbia University

ABSTRACT

We present, for the first time, a dimensional reduction model based on proper orthogonal decomposition (POD) for non-dissipative explicit dynamic discrete element method (DEM) simulations. Two individual POD bases are obtained by the method of snapshots for the displacement and rotation degrees of freedom of the discrete element particles, respectively. The POD basis for rotation is extracted from the vector space of angular velocity. Since the rotation vectors are pseudovectors which adopt a different algebra, explicit Lie-group time integrator is introduced for the integration of particle rotations, while the time integrator for the displacement field is in the Euclidean space. As such, the two set of snapshots are taken from the simulations with numerically dissipative schemes. Then the derived reduced dimension bases are employed in energy-momentum conserving DEM simulations. This approach brings four important benefits. First, one may filter out the high-frequency noises and obtain accurate results without introducing artificial damping that sometimes leads to inconsistent results and reduced wave propagation speed. Second, the number of snapshots used for displacement and rotation can be different, depending on the nature of the problems. Third, since this method requires no injection of artificial or numerical damping, there is no need to tune damping parameters. Finally, the suppression of high-frequency responses allows larger time step for faster explicit integration. The proposed POD-DEM scheme is important for analyzing wave propagation, mixing, rate-dependent simulations for particular materials in which how the external work applied on the system converts into internal energy and dissipation are critical to the outcomes.

Simulation of Crack Growth by Method of Updating Sub-partition and Substructure

Chuwei Zhou^{*}, Chen Xing^{**}

^{*}Nanjing University of Aeronautics and Astronautics, ^{**}Nanjing University of Aeronautics and Astronautics

ABSTRACT

A method of updating sub-partition and substructure in finite element frame is proposed to simulate the crack propagation in planar and plate structures. Using this method crack configuration is modeled independently to global element mesh. The element cut apart by crack is sub-partitioned into ordinary sub-elements while an element cut into by crack tip is sub-partitioned into several singular sub-elements. Whole sub-partitioned elements which overlap a crack constitute a substructure. The sub-partition and substructure is updated (or to be generated) corresponding to the propagation of existing crack grows (or nucleation of a new crack). In this way global re-meshing is avoided for FE simulating crack extension along arbitrary path or crack initiating anywhere. The additional nodal freedom degrees introduced by element sub-partition in the substructure are condensed to boundary nodes of the substructure which are just the original mesh nodes. Thus, freedom degrees of global structure analysis are invariable. The proposed method is within ordinary FEM frame, so all the existing constitutions of material and models of element can be employed directly. It avoids the difficulty of formulating asymptotic function at crack tip for non-linear problems which conventional XFEM faces with. 5-node singular planar and shell elements are constructed to represent the singularities at crack tips for planar and plate bending problems, respectively. These elements connect with the ordinary four-node linear planar or plate elements directly. The proposed method and singular elements are used in fracture analysis for both planar and plate bending structures. Good accuracy of the crack tip fields prediction and good adaptability of moving crack simulation are demonstrated through examples.

Progressive Failure Modelling for Heterogeneous Media with Strain Strength Distribution and Microplane Model

Dong Zhou*

*Institute of Mechanics, Chinese Academy of Sciences

ABSTRACT

A progressive damage model based on strain strength distribution criterion and microplane model is proposed. In the strain strength distribution criterion (Li & Zhou, 2013), the strain strength of the heterogeneous material is assumed to be distributive in space in mesoscopic view. Thus in the failure process, fracture plane in any direction of the representative volume element (RVE) for the material is considered to be composed of elastic area and fracture area. The interactions on the elastic area remains elasticity, while on the fracture plane it turns into contact and complies with the Coulomb's friction law. The ratio of the fracture area to the total area of the fracture plane is defined as the fracture degree, which can be explicitly and quantitatively expressed with a certain distribution function. In the 3D microplane model (Brocca, Brinson & Bažant, 2002), the stress-strain relations are defined independently on planes of all possible orientations in the microstructure. Different constitutive laws for the microplane are defined and proposed. However, the reasonable model with specific physical meaning and being capable of describing the heterogeneous properties are still need to be developed. The progressive damage model proposed in this paper combines the advantages of the above two models. The framework of the model is established with the principle of virtual work that is similar to the microplane model. A spherical RVE is defined and the stress-strain relationship in any direction of the spherical surface is given by the strain strength distribution model. There are no artificial parameters introduced in this model except the distribution function of the strength within the material. Theoretical and numerical results show that, if the material is not damaged, the model will degenerate into the 3D generalized Hooke's law, while in the failure process, the nonlinear and strain softening can be naturally obtained. Li S, Dong Z. Progressive failure constitutive model of fracture plane in geomaterial based on strain strength distribution[J]. International Journal of Solids & Structures, 2013, 50(3-4):570-577. Brocca M, Brinson L C, Bažant Z P. Three-dimensional constitutive model for shape memory alloys based on microplane model[J]. Journal of the Mechanics & Physics of Solids, 2002, 50(5):1051-1077.

A Non-ordinary State-based Godunov-Peridynamics Formulation for Shocks in Solids

Guohua Zhou*, Michael Hillman**

*The Pennsylvania State University, **The Pennsylvania State University

ABSTRACT

The theory and meshfree implementation of Peridynamics has been proposed to model problems involving strong transient discontinuities such as impact-induced fragmentation. For effective application of numerical methods to these events, essential shock physics and Gibbs instability should also be addressed. So far, the artificial viscosity technique has been employed [1-3] in Peridynamics to treat shocks. This technique is simple to implement, but involves tunable parameters which is undesirable, and can lead to results which are not objective. On the other hand, the Godunov scheme has been shown to be an effective approach for shock modeling which does not involve any tunable parameters and directly embeds shock physics into the formulation with the Gibbs instability addressed in an effective way. However, this scheme was originally developed based on mesh-based frameworks, and to incorporate it into meshfree methods such as Peridynamics is not straightforward. This work introduces a physics-based shock modeling formulation for non-ordinary state-based Peridynamics, in which Godunov scheme is introduced by embedding Riemann solution into the force state. Several benchmark problems are solved with high accuracy to demonstrate the effectiveness of the proposed formulation. [1] Ren, B., Fan, H., Bergel, G.L., Regueiro, R.A., Lai, X. and Li, S., 2015. A peridynamics–SPH coupling approach to simulate soil fragmentation induced by shock waves. *Computational Mechanics*, 55(2), pp.287-302. [2] Lai, X., Liu, L., Li, S., Zeleke, M., Liu, Q. and Wang, Z., 2018. A non-ordinary state-based peridynamics modeling of fractures in quasi-brittle materials. *International Journal of Impact Engineering*, 111, pp.130-146. [3] Silling, S.A., Parks, M.L., Kamm, J.R., Weckner, O. and Rassaian, M., 2017. Modeling shockwaves and impact phenomena with Eulerian peridynamics. *International Journal of Impact Engineering*, 107, pp.47-57.

Shape Identification for Inverse Geometry Heat Conduction Problems by FEM without Iteration

Huanlin Zhou*

*School of Civil Engineering, Hefei University of Technology, Hefei, P.R.China

ABSTRACT

The boundary geometry shape is identified by the finite element method (FEM) without iteration and mesh reconstruction for two-dimensional (2-D) and three-dimensional (3-D) inverse heat conduction problems. Firstly, the direct heat conduction problem with the exact domain is solved by the FEM and the temperatures of measurement points are obtained. Then, by introducing a virtual boundary, a virtual domain is formed. By minimizing the difference between the temperatures of measurement points in the exact domain and those in the virtual domain, the temperatures of the points on the virtual boundary are calculated based on the least square error method and the Tikhonov regularization. Finally, the objective geometry shape can be estimated by the method of searching the isothermal curve or isothermal surface for 2-D or 3-D problems, respectively. In the process, no iterative calculation is needed. The proposed method has a tremendous advantage in reducing the computational time for the inverse geometry problems. Numerical examples are presented to test the validity of the proposed approach. Meanwhile, the influences of measurement noise, virtual boundary, measurement point number and measurement point position on the boundary geometry prediction are also investigated in the examples. The solutions show that the method is accurate and efficient to identify the unknown boundary geometry configurations for 2-D and 3-D heat conduction problems.

Design for Additive Manufacturing

Ming Zhou^{*}, Fabian Fuerle^{**}, Raphael Fleury^{***}

^{*}Altair Engineering, ^{**}Altair Engineering, ^{***}Altair Engineering

ABSTRACT

In recent years additive manufacturing, in popular term 3D-Printing, has become a broad technology movement. By large its fame is driven by rapidly growing consumer adoption. However, rapid growth has been seen in biomedical applications, and initial successes have also been showcased for aerospace and other fields. 3D-Printing brings almost unlimited freedom for design shape and form, hence offers the perfect combination with topology optimization for creation of most efficient structures. Many successful designs created with topology optimization have been presented in real product environment by leading global companies. In recent years the authors have developed several advanced features in OptiStruct to address unique needs from additive manufacturing. These include: (1) design of blended solid/lattice structures; (2) topology optimization considering support elimination or penalization. This paper offers a general treatment around design for additive manufacturing, including software tools for final geometry creation and printing processing. We will also discuss further development of optimization capabilities including dual utilization of lattice serving both structural and printing support purposes.

Topology Optimization of Coupled Thermofluidic-mechanical Problems for Channel-cooling Structures

Mingdong Zhou^{*}, Xi Zhao^{**}

^{*}Shanghai Jiao Tong University, ^{**}Dalian University of Technology

ABSTRACT

This work introduces an efficient topology optimization approach for coupled thermofluidic-mechanical problems to design structures containing straight cooling channels. Instead of using a full-blown but computationally expensive thermofluidic solver, a simplified thermofluidic model together with a multiphase parameterization based on the Solid Isotropic Material with Penalization (SIMP) model are developed to design the cross section of the device that consists of solid, fluid and void. A design dependent convection boundary scheme is proposed to allow continuous interpolation of heat sinks among multi-phases for topological design as well as a pertinent thermofluidic simulation. Numerical examples which take engineering requirements on lightweight, uniform structural deformation and temperature distribution into account are given to demonstrate the applicability of the approach. Verifications of the optimized 3D structures by a full-blown thermofluidic simulation show that the proposed approach can yield lightweight channel-cooling structures with desirable heat-transfer and load-carrying performances subject to external heat flux and static load.

Damage Resistance Properties of Hybrid Fiber Reinforced Magnesium Alloy Laminates Subjected to Low Velocity Impact

Xia Zhou^{*}, Mengjiao Du^{**}, Guohui Qu^{***}, Xingchi Chen^{****}

^{*}Dalian University of Technology, Dalian, 116024, P. R. China, ^{**}Dalian University of Technology, Dalian, 116024, P. R. China, ^{***}Dalian Xinzhong Group Company LTD., Dalian 116113, China, ^{****}Dalian University of Technology, Dalian, 116024, P. R. China

ABSTRACT

In order to investigate the low-velocity impact response of novel fiber reinforced magnesium alloy laminates, the numerical simulations of low velocity drop weight impact tests on AZ31B magnesium alloy laminates reinforced with glass fiber, carbon fiber and their hybrids under different impact energies were conducted. The simulation predictions are also compared with the existing experimental results [1]. The magnesium alloy, the interfacial delamination between two neighboring layers and the fiber/epoxy composites in the fiber/AZ31B Mg laminates were modeled through an anisotropic plastic constitutive model, an exponential cohesive zone model, and 3D Hashin failure criteria incorporated with the stiffness reduction of failed elements respectively. In addition, the numerical analyses of low-velocity impact for different fiber/Mg alloy laminates were carried out by using ABAQUS/Explicit with a user-defined subroutine (VUMAT) to predict the dynamic impact response and delamination as well as damage evolution rules under conditions of different impact energies. Meantime, the variations of impact force, deformation and energy absorption with time were also analyzed. The results show that the matrix cracking for different fiber/Mg alloy laminates firstly occurred in the backside at the lower impact energy (20J), while the matrix cracking and fiber breakage could also appear in the impact side as the impact energy increases from 20 J to 50 J. Compared with the single carbon fiber/Mg alloy laminate, the single glass fiber/Mg alloy laminate can absorb more energy under an impact load. Hybrid carbon fiber and glass fiber reinforced Mg alloy laminates can improve the impact-resistant properties when the glass-fibers plies are set at the appropriate layers. When the impact energy is in the range of 20-50 J and the glass-fibers plies are located on the second layer of 3/2 hybrid fiber/Mg alloy laminates, the hybrid carbon fiber and glass fiber reinforced Mg alloy based laminates have the best impact toughness and good impact damage resistance properties. The simulation and experimental results are in good agreement in terms of the damage morphology, the curves of force-time and force-deflection. The mechanical response and the damage trends of the fiber magnesium laminates under low velocity impact can be well predicted using the VUMAT subroutine. [1] T. Pärnänen, R. Alderliesten, C. Rans, T. Brander, O. Saarela. Applicability of AZ31B-H24 magnesium in Fibre Metal Laminates – An experimental impact research [J]. Composites Part A Applied Science & Manufacturing, 2012, 43(9):1578-1586.

Ultralight and Super-elastic Honeycomb Plate of Graphene Aerogel

Xiao-Huan Zhou*, Xia Liu**

*Beijing University of Technology, **Beijing University of Technology

ABSTRACT

Graphene is a one-atom-thick layer of carbon atoms arranged in a hexagonal pattern, which makes it the strongest material in the world. Controlled preparation of graphene aerogel from graphene can be achieved by freeze-drying, self-assembly, template growth and 3D printing. In this paper, a continuous honeycomb plate out of graphene aerogel was presented and analyzed. In the honeycomb plate, the framework of the plate is used as the template for unidirectional growth of the graphene aerogel. Then, multiscale simulations were performed on the honeycomb plate by combining finite element method and coarse-grained molecular dynamics method. Firstly, a coarse-grained molecular dynamics model of the honeycomb plate of graphene aerogel was built. The cyclic compressive and bending tests of a unit cell of the honeycomb plate were simulated to study its mechanical properties and microstructural evolution. Then, the deformation response of plate was simulated using ABAQUS. The results showed that the plate is able to recover its initial shape even after large deformation. It is attributed to the three-dimensional honeycomb structure and the graphene aerogel microstructure.

Dual-anisotropic Solid Metamaterials for Elastic Wave Manipulation

Xiaoming Zhou^{*}, Yong Cheng^{**}

^{*}Key Laboratory of Dynamics and Control of Flight Vehicle, Ministry of Education and School of Aerospace Engineering, Beijing Institute of Technology, Beijing 100081, China, ^{**}Key Laboratory of Dynamics and Control of Flight Vehicle, Ministry of Education and School of Aerospace Engineering, Beijing Institute of Technology, Beijing 100081, China

ABSTRACT

Dual-anisotropic solid materials refer to those with anisotropic stiffness and anisotropic inertial density simultaneously. They are found to be vital to the realization of elastic wave control according to the transformation elasticity theory. In this study, we propose a new type of structured metamaterials with the dual-anisotropic property. The proposed metamaterial is a periodic composite material, with the unit cell consisting of the stiff hexagonal lattice serving as the host, in which the soft two-bar inclusions are embedded. The anisotropic stiffness can be acquired by tailoring the geometry of the hexagonal lattice. The sharpened bar inclusion is designed by mimicking the slipping-boundary effect in fluid-solid interfaces in order to pursue the broadband anisotropic inertial density. We have developed an effective-medium model to retrieve the effective stiffness and density from the band-structure results. Effective-medium results verify the almost constant dual-anisotropic properties achieved in the broad frequency range. The cloaking structure is a device that can prevent elastic wave penetration into its interior. Based on the linear-transformation mapping, we construct a carpet cloaking device and derive the dual-anisotropic material parameters from the transformation method. Based on the proposed model, we design the metamaterial elements that fulfill the parameter requirement and assemble them into the cloaking structure. Numerical simulations show that the interior strain field amplitude can be greatly lowered in the broad frequency range due to the protection of the metamaterial cover. Our studies are expected to open a new route to the broadband elastic wave mitigation using dual-anisotropic solid metamaterials. Reference: Yong Cheng, Xiaoming Zhou, and Gengkai Hu, Broadband dual-anisotropic solid metamaterials, Scientific Reports, 7, 13197, 2017.

Examples of Uncertainties of Molecular Dynamics Simulations

Xiaowang Zhou^{*}, Ryan B. Sills^{**}, Richard A. Karnesky^{***}, Reese E. Jones^{****}

^{*}Sandia National Laboratories, Livermore, CA 94550, ^{**}Sandia National Laboratories, Livermore, CA 94550,
^{***}Sandia National Laboratories, Livermore, CA 94550, ^{****}Sandia National Laboratories, Livermore, CA 94550

ABSTRACT

Properties of materials always exhibit variabilities due to the statistical nature of microstructural details. Understanding such variabilities is critical for engineering design. Unfortunately, material models usually create additional variabilities due to the statistical nature of numerical procedures. It is therefore challenging to model the microstructure-induced variabilities without first reducing the model-induced variabilities. Here we discuss the variabilities commonly created by molecular dynamics models using three examples: dislocation energy calculations, diffusion studies, and vapor deposition simulations. Counter-intuitively, we found that molecular statics simulations can create much larger variabilities than molecular dynamics simulations especially for large systems containing many metastable states. In some cases, the variabilities of time-averaged molecular dynamics simulations can be reduced to almost zero. In other cases where the variabilities are not zero, molecular dynamics simulations can still provide convincing insights that help improve materials in experiments. Acknowledgement: Sandia National Laboratories is a multi-mission laboratory managed and operated by National Technology and Engineering Solutions of Sandia, LLC., a wholly owned subsidiary of Honeywell International, Inc., for the U.S. Department of Energy's National Nuclear Security Administration under contract DE-NA-0003525.

Kinetic Analysis of Multi-DOF Motion Simulator

Yuefa Zhou^{*}, Liang Xu^{**}, Wenbo Zhou^{***}, Zhiyong Zhang^{****}

^{*}College of Aerospace Engineering and Civil Engineering, Harbin Engineering University, Room 3055, Building 11, No.145, Nantong Street, Nan gang District, 150001 Harbin, Heilongjiang Province, P.R. China, ^{**}College of Aerospace Science and Engineering, National University of Defense Technology, 410073, Changsha, Hunan Province, P.R. China, ^{***}College of Science and Engineering, the University of Edinburgh, Edinburgh, EH9 3JG, UK, ^{****}College of Aerospace Engineering and Civil Engineering, Harbin Engineering University, Room 3055, Building 11, No.145, Nantong Street, Nan gang District, 150001 Harbin, Heilongjiang Province, P.R. China

ABSTRACT

This thesis studies on the multi-degree of freedom electro-hydraulic hybrid turntable, which composed by the six-DOF parallel turntable (Stewart turntable) and three-axis turntable. The upper body in the Stewart platform can realize six-DOF movement in the space through six hydraulic drive lever; outer ring, central ring and inner ring(working space) of three-axle table can infinitely rotate in any orientation space. The establishment of Hybrid Turntable, comprehensive two kinds of platforms, realizes the control in any positions and any directions, which not only compensates range limits of Stewart platform rotation, but also to make up the bound that three-axis turntable cannot move randomly, making the study more theoretical significance and the actual value. This paper analyzes the multi-degree of freedom electro-hydraulic hybrid turntable from kinematics and dynamics aspects, the kinematics and dynamics equations are obtained; using the software program of MATLAB to the motion model for motion simulation and dynamic simulation and draw simulation graphs, And then through analyzing and summarizing, draw conclusions. The simulation results coincide with the actual motion of simulator. The results obtained would be useful for the design and analysis of practical manufacture.

A Study of Stress Singularities Arising at the Interface in One-Dimensional Hexagonal Piezoelectric Quasicrystals

Zhenhuan Zhou^{*}, Zhenting Yang^{**}, Wang Xu^{***}, Xiong Yu^{****}, Xinsheng Xu^{*****}

^{*}Dalian University of Technology; City University of Hong Kong Shenzhen Research Institute, ^{**}Dalian University of Technology, ^{***}Dalian University of Technology, ^{****}Dalian University of Technology, ^{*****}Dalian University of Technology; City University of Hong Kong Shenzhen Research Institute

ABSTRACT

Quasicrystals (QCs) are a special class of quasi-periodic alloys which possess a series of ideal properties such as high hardness, low adhesion, low coefficient of friction, low porosity, low electrical and thermal conductivity. Due to their piezoelectric effects, QCs can be used in manufacturing the sensor and actuator in the smart systems. The present study proposed a simple method for the determination of fracture parameters of the one-dimensional hexagonal piezoelectric QC with an interface V-notch. The present method is carried out in two steps. In the first step, the physical domain is meshed by the conventional element for QCs and is divided into a finite size singular region near the notch tip and a regular region far away from the notch tip. In the second step, exact solution of V-notched QCs which can be represents by a series of analytical symplectic eigenfuntions is derived by establishing a Hamiltonian system. By using the obtained solutions, the large number of nodal unknowns in the singular region are transformed into a small set of undetermined coefficients of a symplectic series. The nodal unknowns in the regular region remain as usual. Consequently, high-accuracy generalized intensity factors are obtained by the first several coefficients of the series. Explicit expressions in the singular fields are obtained simultaneously. Numerical results are compared with the existing solutions and found to be in good agreement. Some new results are given also. Compared with other numerical methods, the present has three advantages. First, based on the symplectic eigenfunction expansion of the near region, the number of unknown variables is reduced to a very low level. This results in reducing the computational time and the memory requirement for fracture analysis of cracked structures. Second, no special finite elements and post-processing are needed to determine the generalized intensity factors and the exact solutions in the near fields are obtained simultaneously. Third, as the analytical solution is embodied in the transformation, the accuracy of the predicted generalized intensity factors and their derivatives is high.

Control Acoustic Wave at the Deep Sub Wavelength Scale with Anisotropic Metasurface

Jie Zhu*

*Hong Kong Polytechnic University

ABSTRACT

Manipulating acoustic wave at the deep sub wavelength scale is of great interests. In this talk we introduce the design of gradient-index metasurface that can manipulate airborne acoustic wave at subwavelength scale. From the dispersion relation of surface mode, an explicit expression can be obtained to map the effective refractive index into the hole depth of the unit cell. Arbitrary GRIN profile with effective refractive index higher than that of air can thus be straightforwardly implemented by simply adjusting the spatial distribution of the hole depth. Our work provides a feasible pathway to the subwavelength manipulation of airborne sound as well as an ideal experimental platform to directly observe the wave propagation and energy flow inside GRIN media.

Uncertainty Propagation in Thermo-mechanical Behaviors of Functionally Graded Plates Existing Unknown-but-Bounded Parameters

Jingjing Zhu^{*}, Zhiping Qiu^{**}, Zheng Lv^{***}

^{*}Beihang University, ^{**}Beihang University, ^{***}Beihang University

ABSTRACT

Functionally graded (FG) materials, which are composed of two or more phases with different material properties, offer excellent performance in high-temperature environment. However, due to the limitations of technology and operation condition, the errors of manufacturing and processing lead to the uncertainty in material properties. The deterministic analyses are insufficient to provide a complete prediction of the structural response. Therefore, it is indispensable to develop uncertainty propagation model to reflect the effects of uncertain material properties on the mechanical behaviors of functionally graded structures. This presentation focuses on the effects of the uncertainty in material properties on the free vibration characteristics of rectangular FG plates in thermal environment. The deterministic model for thermo-mechanical behavior is presented in the framework of classic thin plate theory. Then a non-deterministic model for the free vibration of rectangular FG plates, in which temperature effect and uncertain material properties are considered, is developed. For probabilistic methods, sufficient information about the uncertainty is often impossible or very expensive to obtain to define the precise probability distributions. Meanwhile, even small variations from real values may result in large errors in probability distributions of the design space. In order to overcome the demerits of probabilistic approach in the case of inadequate data, the material uncertainties are quantified as interval variables. Based on the set theory, an interval iterative method (IIM) for solving this model is proposed to seek the bounds of uncertain natural frequencies. Meanwhile, the Monte Carlo simulation (MCS) is employed as the referenced result to validate the accuracy and efficiency of the IIM. Subsequently, extensive investigations are performed to reveal the combined effects of the material uncertainties and power law index, aspect ratio, thickness to length ratio as well as temperature change on the natural frequencies. Finally, some conclusions are summarized, which are meaningful in practical engineering applications to realize a safe and reliable design.

A Background Mesh Approach to Fluid-Structure Interaction Using PFEM

Minjie Zhu^{*}, Michael Scott^{**}

^{*}Oregon State University, ^{**}Oregon State University

ABSTRACT

Both fixed and moving finite element (FE) mesh can be used with Lagrangian based fluid analysis (Idelsohn et al 2013). Although the fixed mesh is always of good computational quality, it is difficult to be extended to fluid-structure interaction (FSI). As in Becker et al (2015), the structural domain with the hypoelastic model is simulated with a fluid-like formulation in order to use the fixed mesh for the structures. However, arbitrary structural types, such as beams and columns, cannot always be modeled with a fixed mesh. On the other hand, the moving mesh is flexible for any structural type and simulating the complex interaction between fluid and structure, but the quality and size of elements are difficult to control due to the random locations of fluid particles. The background mesh approach combines the advantages of both methods, using a fixed mesh for the fluid only domain and a moving mesh for the FSI domain. Massless fluid particles transport fluid properties over the fixed mesh as in Becker et al (2015). The problem with the fixed mesh for FSI is the arbitrary locations of structural nodes which can be very close to the fixed nodes of the fixed mesh when the structure undergoes large displacements. To resolve this problem, when fluid particles enter the FSI domain, the fixed nodes that are close to structural nodes are removed and the Delaunay Triangulation is used to generate a moving mesh between the remaining fixed nodes and structural nodes. As a result, the majority of the fluid domain uses the good quality fixed mesh and the moving FSI mesh is flexible for different structural types. The current fully Lagrangian FSI solvers (Zhu and Scott 2014) for the particle finite element method (PFEM) can be used without modification and its efficiency is increased with the partial fixed mesh. Becker, P., Idelsohn, S., and Oñate, E. (2015). "A unified monolithic approach for multi-fluid flows and fluid-structure interaction using the particle finite element method with fixed mesh." *Computational Mechanics*, 55(6), 1091–1104. Idelsohn, S. R., Nigro, N. M., Gimenez, J. M., Rossi, R., and Marti, J. M. (2013). "A fast and accurate method to solve the incompressible Navier-Stokes equations." *Engineering Computations*, 30(2), 197–222. Zhu, M. and Scott, M. H. (2014). "Improved fractional step method for simulating fluid-structure interaction using the PFEM." *International Journal for Numerical Methods in Engineering*, 99(12), 925–944.

Integrating Computational Modeling with in situ TEM for Understanding the Degradation in Lithium-ion Battery Electrodes

Ting Zhu*

*Georgia Institute of Technology

ABSTRACT

Lithium-ion batteries play a pivotal role in the emerging renewable energy landscape. However, they suffer from the electrochemically-induced mechanical degradation in high-capacity electrodes, resulting in fast capacity fade and short cycle life. We have developed a unique nanoscale battery cell inside transmission electron microscope (TEM), which enables the real-time observations of reaction, deformation and degradation in individual nanowire and nanoparticle electrodes. In this talk, I will present our recent studies that integrate computational modeling with in situ TEM for understanding the degradation in Lithium-ion battery electrodes. Examples include the lithiation of Si nanowires with different types of coatings, delithiation of Ge nanoparticles, and lithiation of composite Si/Ge nanowire electrodes. Our results provide new insights into the microstructural evolution and mechanical degradation in battery electrodes, and have broad implications for designing the durable electrodes in high-performance rechargeable batteries.

B++ Splines with Applications in XIGA, Topology Optimization and Sheet Metal Forming

Xuefeng Zhu^{*}, Ping Hu^{**}, Zheng-Dong Ma^{***}

^{*}Dalian University of Technology, ^{**}Dalian University of Technology, ^{***}The University of Michigan

ABSTRACT

In the fields of XIGA, topology optimization and IGA-based sheet metal forming for trimmed CAD geometries, imposing strong Dirichlet boundary conditions on the complex geometric boundaries is still a challenge. In this paper, we will introduce recent researches in the fields of XIGA, topology optimization and sheet metal forming using B++ splines. B++ splines mean “Boundary Plus Plus Splines”. B++ Splines can integrate the boundary description and background meshes into a unity representation which allows imposing strong Dirichlet boundary conditions. We have developed bivariate B++ splines for trimmed NURBS surfaces [1] and trivariate B++ splines for B-rep models respectively. Recently, we applied B++ Splines to the fields of XIGA, topology optimization and sheet metal forming. First, we proposed XIGA based on B++ splines. Compared with traditional XIGA, the presented method allows imposing strong Dirichlet boundary conditions in the weak or strong discontinuous interfaces. Second, we developed a topology optimization method using B++ splines. Compared with traditional topology optimization methods using Heaviside functions, our method does not rely on Heaviside functions and simplifies the analysis procedure significantly. Third, inspired by the pioneering work by Benson et al. [2] in sheet metal forming, we developed an initial solution estimation algorithm [3] for One-step inverse IGA and B++ spline-based isogeometric shell analysis of trimmed CAD surfaces, which are expected to be applied into the simulations of sheet metal forming. The aforementioned researches imply that B++ splines have a wide range of applications in the field of isogeometric analysis, especially for the simulation of the engineering problems with complex geometric boundaries. [1] Zhu, X., Hu, P., & Ma, Z. D. (2016). B++ splines with applications to isogeometric analysis. *Computer Methods in Applied Mechanics and Engineering*, 311, 503-536. [2] Benson, D. J., Bazilevs, Y., Hsu, M. C., & Hughes, T. J. R. (2011). A large deformation, rotation-free, isogeometric shell. *Computer Methods in Applied Mechanics and Engineering*, 200(13), 1367-1378. [3] Zhang, X., Zhu, X.*, Wang, C., Liu, H., Zhou, Y., Gai, Y., ... & Ma, Z. D. (2018). Initial solution estimation for one-step inverse isogeometric analysis in sheet metal stamping. *Computer Methods in Applied Mechanics and Engineering*, 330, 629-645.

A Multi-Fidelity Stochastic Collocation Method for Time-Dependent Problems

Xueyu Zhu^{*}, Dongbin Xiu^{**}

^{*}University of Iowa, ^{**}Ohio State University

ABSTRACT

In this talk, we shall discuss a collocation method with multi-fidelity simulation models to efficiently reconstruct the time trajectory of time-dependent parameterized problems. By utilizing the time trajectories of low/high-fidelity solutions to construct the approximation space, this method is demonstrated to offer two substantial advantages: (1) it is able to produce more accurate results with a limited number of high-fidelity simulations; (2) it avoids instability issues of time-dependent problems due to the nonintrusive nature. We also provide several numerical examples to illustrate the effectiveness and applicability of the method.

Study of Fish Self-adapting Behaviour in Karman Vortex Street Using Reinforcement Learning

Yi Zhu^{*}, Daoyi Dong^{**}, Fang-Bao Tian^{***}, John Young^{****}, Joseph Lai^{*****}

^{*}School of Engineering and Information Technology, UNSW Canberra, ^{**}School of Engineering and Information Technology, UNSW Canberra, ^{***}School of Engineering and Information Technology, UNSW Canberra, ^{****}School of Engineering and Information Technology, UNSW Canberra, ^{*****}School of Engineering and Information Technology, UNSW Canberra

ABSTRACT

Rocks and other objects in the flow can generate a repeating pattern of swirling vortices, known as the Karman vortex street. Fish (like rainbow trout) in these vortices show a large-amplitude lateral motion of the body occurring at a low frequency, to achieve high efficient swimming (Stewart et al., 2016). This behaviour involves two essential processes: sensing the ambient flow using the lateral line (Liao, 2006) and dynamically adjusting swimming pattern to maximize the performance in respond to the flow. However, it is still unclear how fish achieve these complex processes. What flow information is really useful in this process? How the fish respond to the information? What is the basic flow mechanism behind it? In this work, we intend to gain a deeper understanding of these questions by building a numerical model of a fish to optimize its performance in a Karman vortex street. This is achieved by combining an immersed boundary--lattice-Boltzmann method (IB-LBM) and the reinforcement learning algorithm. The IB-LBM is employed to calculate the flow dynamics caused by a fish-like foil movement due to its simplicity and high efficiency. The foil is put in a vortex street generated by a cylinder in a uniform stream. The foil employs a reinforcement learning algorithm to alter its swimming kinematics. The algorithm tries different swimming amplitudes and frequencies (states, actions) and observes the change in flow velocity and pressure in the ambient flow (rewards). By analysing these states, actions and rewards, the fish automatically finds a way to achieve optimal performance with a sequence of actions in different states. To the best of our knowledge, this work is the first attempt to simulate the fish self-adapting behaviour in a Karman vortex street including both the flow sensing and feedback control processes. It will provide deeper understanding of this behaviour and benefit the design of maneuverable autonomous underwater vehicles. Liao, J. C. (2006). The role of the lateral line and vision on body kinematics and hydrodynamic preference of rainbow trout in turbulent flow. *Journal of Experimental Biology*, 209(20), 4077-4090. Stewart, W. J., Tian, F. B., Akanyeti, O., Walker, C. J., & Liao, J. C. (2016). Refuging rainbow trout selectively exploit flows behind tandem cylinders. *Journal of Experimental Biology*, 219(14), 2182-2191.

Homogenisation of Dislocation System and Dislocation Pattern Formation

Yichao Zhu*

*Dalian University of Technology

ABSTRACT

Proper formulation of multiple-scale dislocation interactions is crucial for continuum model of dislocation to capture the various types of dislocation patterns formed in crystalline materials. In this talk, starting with discussion on homogenising the behaviour of a row of dislocation dipoles, we will show by matched asymptotic expansion that discrete dislocation dynamics (DDD) can be effectively upscaled by a set of evolution equations for dislocation densities along with a set of equilibrium equations for variables characterising the self-locked dislocation structures (SLDSs) which can be treated quasi-steadily on the continuum scale. The stress to unlock the SLDSs, i.e. the flow stress, can be determined by checking the solvability conditions of the local equations that govern the steady state of SLDSs. Based on these findings, a general strategy of summarising the collective behaviour of many dislocations will be presented. Under this guideline, a (continuum) flow stress formula for multi-slip systems, which resolves more details from the underlying dynamics than the ubiquitously adopted Taylor-type formulae, is derived. Moreover, the continuum dynamics of the formation, migration and dissociation of SLDSs on parallel slip planes can be successfully formulated in good accordance with the underlying DDD.

Numerical Simulation of PMMA Foaming Process Assisted by Supercritical Carbon Dioxide: Bubble Growth Dynamics

Yuxuan Zhu^{*}, Guoqiang Luo^{**}, Qiwen Liu^{***}, Ruizhi Zhang^{****}, Jian Zhang^{*****}, Qiang Shen^{*****}, Lianmeng Zhang^{*****}

^{*}State Key Lab of Advanced Technology for Materials Synthesis and Processing, Wuhan University of Technology,

^{**}State Key Lab of Advanced Technology for Materials Synthesis and Processing, Wuhan University of Technology, ^{***}Department of Mechanics and Engineering Structure, Wuhan University of Technology, ^{****}State Key Lab of Advanced Technology for Materials Synthesis and Processing, Wuhan University of Technology,

^{*****}State Key Lab of Advanced Technology for Materials Synthesis and Processing, Wuhan University of Technology, ^{*****}State Key Lab of Advanced Technology for Materials Synthesis and Processing, Wuhan University of Technology, ^{*****}State Key Lab of Advanced Technology for Materials Synthesis and Processing, Wuhan University of Technology

ABSTRACT

In this paper, the bubble growth process of PMMA/supercritical carbon dioxide system in an isothermal condition was simulated. Based on the cell model, a mathematical model for bubble growth was established by solving the continuity equation, momentum equation, mass equation, diffusion equation and constitutive equation. Through the numerical simulation of MATLAB, the effects of process parameters on bubble growth were investigated. The results show that the foaming temperature and the saturation pressure significantly affect the cell growth process, in which the foaming temperature significantly affects the viscosity of the matrix, the nucleation rate of the cell, the amount of carbon dioxide adsorbed and the diffusion rate to the cell. The saturation pressure significantly affects the nucleation rate and the amount of carbon dioxide absorption. The simulation results prove that with the foaming temperature increasing, the size of bubble increases exponentially and the bubble size decreases linearly with the increasing of saturation pressure. The numerical simulation results in this paper have significant guidance on the foaming process.

Theoretical and Numerical Models to Predict and Optimize Fracking in Shale

Zhuo Zhuang^{*}, Zhanli Liu^{**}, Tao Wang^{***}

^{*}School of Aerospace Engineering, Tsinghua University, Beijing 100084, China, ^{**}School of Aerospace Engineering, Tsinghua University, Beijing 100084, China, ^{***}School of Aerospace Engineering, Tsinghua University, Beijing 100084, China

ABSTRACT

Hydraulic fracture (fracking) technology in gas or oil shale field engineering is highly developed last decades in North America and also recent years in China, but the knowledge of actual fracturing process is mostly empirical and makes a mechanician wonder: Why the fracking works? In this work, the theoretical and numerical models to predict and optimize fracking are proposed for fracking simulation in shale rock. The first work is fracking prediction. The self-consistent fracture condition based on extended finite element method (XFEM) is resulting in fluid flux, perforation entry loss and energy release rate to drive multi-scale fracture growth or arrest. However, there are million smeared fractures in the horizontal perforation wellbore, which is beyond computation capacity. XFEM is only suitable for major fractures, so the multi-scale self-consistent model of damage volume ratio is developed to predict pressured fluid flow in wellbore and global production in field engineering from the stimulated reservoir volume (SRV) based on the required fracture spacing order, reservoir pressure and propand size, as well as the other given conditions. Some examples are provided to test and verify the models. The second work is fracking optimization. Shale is a typical layered and anisotropic material whose properties are characterized primarily by locally oriented anisotropic clay minerals and naturally formed bedding planes. The debonding of bedding planes will greatly influence the shale fracking to form a large-scale highly permeable fracture network, named SRV. Both theoretical and numerical models are developed to quantitatively predict the growth of debonding zone in layered shale under fracking, and the good agreement is obtained between the theoretical and numerical prediction results. Some parameters are proposed to characterize the corresponding conditions of tensile and shear debonding of bedding planes. It is found that debonding is mainly caused by the shear failure of bedding planes in the actual reservoir. Then the theoretical model is applied to design the perforation cluster spacing to optimize SRV, which is a critical issue in fracking. If the spacing is too small, there are overlapping areas of SRV and the fracking efficiency is much lower. If the spacing is too large, some stratum can't be stimulated. Simultaneously, the parameters of SRV and efficiency are proposed. Through maximizing the values of these parameters, the SRV and optimal perforation cluster spacing range can be quantitatively calculated to guide the fracking treatment design. These results are comparable with the data from field engineering. Keywords: Hydraulic fracture, Stimulate reservoir volume, Theoretical and numerical models, Fracking prediction and optimization, Shale rock

References 1. Bažant, Z.P., Salviato, M., Chau, V.T., Visnawathan, H., and Zubelewicz, A. 2014, "Why Fracking Works." J. Applied Mech. ASME 81 (10), 101010-1-10. 2. Brice Lecampion, Jean Desroches, Simultaneous initiation and growth of multiple radial hydraulic fractures from a horizontal wellbore, J. Mech. Phys. Solids, 2015, (82): 235-258 3. QL Zeng ZL Liu, DD Xu, H Wang, Z Zhuang, Modeling arbitrary crack propagation in coupled shell/solid structures with X-FEM, Int. J. Numer. Meth. Engng 2016; 106:1018–1040 4. Qinglei Zeng, Tao Wang, Zhanli Liu, Zhuo Zhuang, Simulation based unitary fracking condition and multi-scale self-consistent fracture network formation in shale, J. Applied Mechanics, 2017.05, 84: 051004-1 5. Tao Wang, Zhanli Liu, Qinglie Zeng, Yue Gao, Zhuo Zhuang, XFEM modeling of hydraulic fracture in porous rocks with natural fractures, Science China Physics, Mechanics & Astronomy, 2017, 60(8):084612 6. Zhuo Zhuang, Zhanli Liu, etc., Extended finite element method, Elsevier/Tsinghua University Press, 2014

The Strategy for Modeling and Solving Uncertainly Defined Boundary Value Problems

Eugeniusz Zieniuk*, Marta Kapturczak**, Agnieszka Boltuc***

*University of Bialystok, **University of Bialystok, ***University of Bialystok

ABSTRACT

Solving different types of problems most often leads to solving different types of partial differential equations. As it is known from the literature, they can be elliptic, parabolic or hyperbolic type. The great variety of these equations gives many possibilities for modeling and solving various practical problems. To solve them, numerical methods are used, among which the finite and boundary element methods or meshless methods should be mentioned. A common feature of all mentioned differential equations and the methods of solving them is that their physical definition requires input data determined in a precise manner, i.e. the shape of the boundary, boundary conditions and other parameters are given in the form of exact numerical values. This is some idealization of reality, because these data are measured, and hence contains errors related to the inaccuracy of a measuring device. To take into account all these inaccuracies, an effective strategy for comprehensive modeling of uncertainty of the boundary problem should be developed. In the literature some preliminary papers are presented allowing for a consideration of the uncertainty of the system's parameters or boundary conditions. However, there are no papers about the uncertainly defined shapes or papers comprehensively considering all the above-mentioned uncertainties. The main aim of the research is to develop a comprehensive modeling strategy for these uncertainties, as well as a method for solving such defined problems. For this purpose, the parametric integral equation system (PIES) previously developed by one of the co-authors and successfully used to solve various precisely defined problems should be generalized [1]. It consists in the assumption that the input data are defined using interval arithmetic. Therefore, it must be included everywhere in the PIES mathematical apparatus by appropriate modifications. However, after many tests, it was decided to use the directed interval arithmetic, not classical one. Nevertheless, even this arithmetic has to be modified in order to properly model uncertainty. Such modified arithmetic was also applied for numerical solution of interval PIES. The paper presents examples of modeling and solving uncertainly defined potential boundary value problems using the proposed strategy. References: [1] Zieniuk E., Sawicki D., Boltuc A.: Parametric integral equations systems in 2D transient heat conduction analysis, Int. J. Heat Mass Transf., 78 (2014), s. 571 – 587.

The Effect of Cavitation on the Temperature Elevation during Focused Ultrasound Therapy

Ekaterina Zilonova^{*}, Maxim Solovchuk^{**}, Tony Sheu^{***}

^{*}National Taiwan University, ^{**}National Health Research Institutes, ^{***}National Taiwan University

ABSTRACT

The present study investigates the cavitation presence impact on the HIFU thermal therapy process in soft tissue. The key aspects have been covered: dependency of the bubble dynamics on soft tissue viscoelastic properties, temperature elevation inside and outside the bubble, bubble-bubble interaction and corresponding to it translational motion of the bubbles, the comparison with real experiments. For the mentioned purposes, new coupled models have been proposed, describing bubble dynamics with Gilmore-Akulichev model, soft tissue with Zener viscoelastic model, temperature elevation with interrelated heat equations for bubble's interior and exterior. Bubble-bubble interaction was modeled using Doinikov's model. The comparison with experiments has been performed on the basis of the predicted temperature elevation in a soft tissue with cavitations effect taken into account.

A Finite Element Algorithm for Large Deformation Frictional Contact of Multiphasic Materials with Multiple Neutral and Charged Solutes

Brandon Zimmerman^{*}, Krista Durney^{**}, Gerard Ateshian^{***}

^{*}Columbia University, ^{**}Columbia University, ^{***}Columbia University

ABSTRACT

Contact of multiphasic soft tissues is an important topic in biomechanics, particularly in understanding damage and failure mechanisms in diarthrodial joints, where opposing cartilage surfaces undergo reciprocal contact loading for thousands of cycles per day. Previous work [1] on injurious frictional loading of juvenile bovine cartilage has shown damage to collagen fibrils and the concomitant formation of a swollen blister, which forms due to mechanoelectrochemical interactions between ionic species in the interstitial fluid and charged molecules bound to the solid matrix. Capturing the salient characteristics of this damage cascade in a computational framework necessitates multiphysics modeling of these solutes, and their interactions with the charged solid matrix, under frictional contact conditions. To date, however, finite element algorithms for multiphasic contact are restricted to frictionless conditions, precluding the simulation of friction-mediated processes. FEBio is a free finite element software package designed to meet the computational needs of the biomechanics and biophysics community (febio.org) [2]. This study describes the formulation of a novel finite element algorithm for frictional contact of multiphasic materials and its implementation and verification in FEBio. Previously [3] we developed a finite element algorithm for frictional contact of biphasic materials that coupled interstitial fluid pressurization to the frictional response. The extension to multiphasic contact is more challenging, as it requires coupling of chemical and osmotic interactions with the mechanical and fluid pressurization response, and has yet to be achieved. We propose to overcome these challenges by implementing our model of multiphasic friction in a large deformation finite element algorithm that relates the frictional traction to the effective fluid pressure inside the tissue. In a multiphasic analysis, it is well known that fluid pressures are not continuous and thus cannot be used as nodal variables. However, the effective fluid pressure, which is inclusive of osmotic effects, is continuous and thus may be used as a nodal variable. In this framework, the frictional traction in a multiphasic material is proportional only to the fraction of normal traction transmitted via solid-solid interactions across the contact interface. Consequently, an elevated effective fluid pressure, whether due to osmotic or mechanical effects, will reduce the friction coefficient, achieving the desired mechanoelectrochemical coupling. The model is validated against our experimental investigations of osmotic pressure-driven frictional behavior, successfully demonstrating unique behaviors previously unobtainable by finite element methods. References [1] Durney, KM+, SB3C 1071, 2016 [2] Maas, S+, J Biomech Eng, 2012 [3] Zimmerman, BK+, SB3C 179, 2017

Assessing the Fracture Strength of Geological and Related Materials in Fluid Environments via an Atomistically Based J-integral

Jonathan Zimmerman^{*}, Reese Jones^{**}, Louise Criscenti^{***}, Jessica Rimsza^{****}

^{*}Sandia, ^{**}Sandia, ^{***}Sandia, ^{****}Sandia

ABSTRACT

Predicting fracture initiation and propagation in low-permeability geomaterials is a critical yet unsolved problem crucial to assessing shale caprocks at carbon dioxide sequestration sites, and controlling fracturing for gas and oil extraction. Experiments indicate that chemical reactions at fluid-geomaterial interfaces play a major role in subcritical crack growth by weakening the material and altering crack nucleation and growth rates. Engineering the subsurface fracture environment, however, has been hindered by a lack of understanding of the mechanisms relating chemical environment to mechanical outcome, and a lack of capability directly linking atomistic insight to macroscale observables. We have developed a fundamental atomic-level understanding of the chemical-mechanical mechanisms that control subcritical cracks through coarse-graining data from reactive molecular simulations. Previous studies of fracture at the atomic level have typically been limited to producing stress-strain curves, quantifying either the system-level stress or energy at which fracture propagation occurs. As such, these curves are neither characteristic of nor insightful regarding fracture features local to the crack tip. In contrast, configurational forces, such as the J-integral, are specific to the crack in that they measure the energy available to move the crack and truly quantify fracture resistance. By development and use of field estimators consistent with the continuum conservation properties we are able to connect the data produced by atomistic simulation to the continuum-level theory of fracture mechanics and thus inform engineering decisions. In order to trust this connection we have performed theoretical consistency tests and validation with experimental data. Although we have targeted geomaterials, this capability can have direct impact on other unsolved technological problems such as predicting the corrosion and embrittlement of metals and ceramics. Sandia National Laboratories is a multimission laboratory managed and operated by National Technology and Engineering Solutions of Sandia, LLC., a wholly owned subsidiary of Honeywell International, Inc., for the U.S. Department of Energy's National Nuclear Security Administration under contract DE-NA-0003525

Role of Bone's Multi-scale Structure in Resisting Deformation and Fracture

Elizabeth A. Zimmermann*, Björn Busse**, Robert O. Ritchie***

*Shriners Hospital for Children-Canada, **University Medical Center-Hamburg Eppendorf, ***University of California Berkeley

ABSTRACT

Bone is an extremely tough and yet lightweight material that provides structural support to organisms. In this context, bone provides mechanical resistance to physiological forces with the additional capacity for self-repair and adaptation to changing loading environments. Bone's mechanical resistance derives from its complex hierarchical structure, which spans from macroscopic length-scales including bone's macro-architecture to the nanometer scale, consisting of collagen molecules and mineral platelets. Specifically, bone's strength and ductility originate primarily at the nano to submicrometer structure through deformation of its mineralized collagen fibrils. Bone toughness (i.e., resistance to crack initiation and growth) is generated at much larger, micro- to near-millimeter, scales from crack-tip shielding associated with interactions between the crack path and the microstructure. Here, we discuss how these multi-scale deformation and toughening mechanisms resist fracture in more complex physiological loading conditions. For instance, in high strain rate conditions, time-dependent, viscous mechanical component is suppressed, which affects the tissue's capacity for fibrillar sliding and crack deflection mechanisms that generate toughness at lower strain rates. Furthermore, we discuss how fracture resistance becomes degraded in biological aging and disease conditions, leading to increased risk of fracture. The aging- and disease-related change in mechanical properties stems from alterations to the structural features at multiple length-scales, including the collagen cross-linking environment, the homogeneity of mineralization, and the density of the osteonal structures. Studying the origins of bone's fracture resistance in physiological and disease conditions aids further progress in the diagnosis, prevention, and treatment of diseases that increase the fracture risk or affect the mechanical integrity of human cortical bone.

Bridging the Gap between Domain Experts and Computer Scientists with Tiger Teams in the bwHPC-C5 Project

Thorsten Zirwes^{*}, Jordan A. Denev^{**}, Robert Barthel^{***}, Olaf Schneider^{****}

^{*}Steinbuch Centre for Computing, Karlsruhe Institute of Technology, Hermann-von-Helmholtz-Platz 1, 76344 Eggenstein-Leopoldshafen, Germany, ^{**}Steinbuch Centre for Computing, Karlsruhe Institute of Technology, Hermann-von-Helmholtz-Platz 1, 76344 Eggenstein-Leopoldshafen, Germany, ^{***}Steinbuch Centre for Computing, Karlsruhe Institute of Technology, Hermann-von-Helmholtz-Platz 1, 76344 Eggenstein-Leopoldshafen, Germany, ^{****}Steinbuch Centre for Computing, Karlsruhe Institute of Technology, Hermann-von-Helmholtz-Platz 1, 76344 Eggenstein-Leopoldshafen, Germany

ABSTRACT

The Coordinated Compute Cluster Competence Centers ("bwHPC-C5") are a state-funded project with the participation of eleven universities, which offers federated support for users of six High Performance Computing (HPC) clusters in the state of Baden-Württemberg, Germany. Users of these HPC systems can request "Tiger Teams", which are formed by the users (domain experts) as well as members of the computing centers (computer scientists). The work performed in the Tiger Teams includes advising users for optimal usage of HPC systems, porting code to other clusters, parallelization of sequential parts of code and optimization of data management as well as performance of user applications. One example of a Tiger Team from the "Competence Center Engineering" is given by a user, whose application requires a lot of memory per process due to a complex particle tracking code that is coupled to the open-source CFD code OpenFOAM. In a Tiger Team, the user's application was ported to the "JUSTUS" cluster, which has been specifically designed for quantum chemistry codes and thus has more memory per node. Besides the work of the Tiger Teams, we also present an example for performance optimization of a CFD code for combustion processes. The code is a coupling between OpenFOAM and the open-source chemistry library Cantera. A large part of total simulation time was spent on computing chemical reaction rates. The user provides a text file which contains the set of chemical reactions. This text file is read at the start of the simulation and used to compute the chemical reaction rates during simulation. In order to speed this up, a converter tool was developed which automatically converts the text file into C++ source code. The code contains all routines needed for computing the chemical reaction rates and is generated in a way that makes it easy for the compiler to perform optimizations. For example, the data is laid out in a way that loops can easily be auto-vectorized, which will become more important on future architectures. Due to OpenFOAM's runtime selection mechanism, the user can quickly modify the simulation setup to incorporate the new routines. By using the optimized routines, total simulation time could be reduced by 40%. In addition to these serial optimizations, parallel performance analysis tools like ScoreP/Vampir and Extrae/Paraver have been applied in order to improve load balancing. The optimized application shows nearly ideal speedup and has been run on up to 28,800 CPU cores.

An XFEM/DG Method for the Simulation of Valve Dynamics through a Fluid-Structure Interaction Problem

Stefano Zonca*, Christian Vergara**, Luca Formaggia***

*MOX, Dipartimento di Matematica, Politecnico di Milano, **MOX, Dipartimento di Matematica, Politecnico di Milano, ***MOX, Dipartimento di Matematica, Politecnico di Milano

ABSTRACT

We present an unfitted numerical method for the simulation of fluid-structure interaction (FSI) problems in the case of an incompressible fluid that interacts with an immersed elastic structure. In particular, we consider a full three-dimensional model for the structure, though its thickness is smaller than its characteristic size. We apply this strategy to the simulation of heart valves dynamics. The proposed method is based on the eXtended Finite Element Method (XFEM) which relies on unfitted and overlapping meshes, in particular the structure mesh overlaps the fluid one. The advantage of this approach is that the structure mesh is allowed to move independently of the fluid (background) one, which is fixed. As result, the fluid-structure interface intersects the background elements in an arbitrary configuration. This generates cut-elements of generic (polyhedral) shape that require a special treatment for integration and accuracy purposes. The coupling between the fluid and structure problems is taken into account by means of a Discontinuous Galerkin (DG) mortaring applied to the fluid-structure interface. We present several 3D numerical results featuring realistic Reynolds numbers that highlight the suitability of the proposed method.

Field-aligned Parametrization and Quad Layout Construction

Denis Zorin^{*}, Marcel Campen^{**}

^{*}Courant Institute, New York University, ^{**}Osnabrück University

ABSTRACT

A variety of techniques were proposed to model smooth surfaces of arbitrary topology based on tensor product splines (e.g. subdivision surfaces, free-form splines, T-splines). Conversion of an input surface into such a representation is commonly achieved by constructing a global seamless parametrization, possibly aligned to a guiding cross-field and using this parametrization as a domain to construct the spline-based surface. (Informally, seamless parametrizations can be thought of as parametrizations of surfaces cut to disks, with isoparametric line directions and spacing on the surface matching perfectly across the cuts). A quad layout can be constructed from such parametrizations. One major fundamental difficulty in designing robust algorithms for this task is the fact that for common types, e.g. that spline surfaces or subdivision surfaces, reliably obtaining a suitable parametrization that has the same topological structure as the guiding field, in particular, having exactly the same singularities, poses a major challenge. Even worse, not all fields admit compatible parametrizations: in some cases, singularities need to be added, or the field modified in other ways. In other words, it is not known for what singularity choices defined by the user or automatically, there is a matching spline layout. I will discuss our recent work that addresses the problem. In particular, I will present a complete solution based on the new concept of seamless similarity maps (a relaxation of the seamless parametrization definition, allowing scale jumps across cuts) and a matching spline construction. It turns out, that for any given guiding field structure, a compatible parametrization of this kind exists and can be computed by a relatively simple algorithm; at the same time, for any such parametrization, a smooth piecewise rational surface with exactly the same structure as the input field can be constructed from it. Further I will discuss a solution that imposes more restrictive requirements (but still allows essentially arbitrary singularity configurations) but does not require using similarity maps. Both of these approaches lead to fully automatic construction of high-order approximations of arbitrary surfaces, even with highly complex topology, potentially enabling, e.g., robust automatic conversion of surfaces to isogeometric form.

Experiments, Continuous and Discrete Simulations of the Role of an Inclined Bottom on the Lateral Discharge Flow of Granular Media from Silos

Zhenhai Zou^{*}, Pascale Aussillous^{**}, Pierre Ruyer^{***}, Pierre-Yves Lagrée^{****}

^{*}Institut de Radioprotection et de Sûreté Nucléaire (IRSN), ^{**}Aix-Marseille Univ, CNRS, IUSTI, ^{***}Institut de Radioprotection et de Sûreté Nucléaire (IRSN), ^{****}Sorbonne Universités, UPMC Université Paris 06, CNRS UMR 7190

ABSTRACT

In the context of safety studies of nuclear power plants, we consider an hypothetical scenario of a control rod ejection leading to a reactivity insertion. During such an accident, the cladding of the fuel rods is severely stressed and standard safety studies ensure its integrity. In this study, we go beyond this statement and assume the failure of the cladding of some fuel rods. Fuel fragments and fission gas at high temperature could then be ejected toward the surrounding coolant and exchange rapidly a large amount of heat. The violence of this interaction depends particularly on the discharge flow rate of fragments toward the fluid. In the present work, we represent the fuel fragments as a dry granular media and the clad as a vertical reservoir, a silo. The ejection of fuel fragment is simulated by the discharge of the granular media through an orifice on one lateral side of the silo. We focus especially on the influence of the internal geometry of the reservoir on the discharge flow thanks to experiments, continuous and discrete numerical simulations. Continuous simulations are done thanks to an implementation of frictional rheology in a volume of fluid incompressible free code (Basilisk) which solves Navier-Stokes equations. Discrete simulations use the free solver LMGC90 implementation of the contact dynamic method. More precisely, the reservoir has an inclined bottom which ends up at the lateral orifice. The controlled parameters are the height of the orifice D , the thickness of the silo W , the bottom inclination angle and the particles size. The measured parameters are the mass flow rate and the velocity field near the orifice, obtained thanks to Particle Image Velocimetry. We have compared laboratory experiments, continuous and discrete numerical simulations and observed an excellent agreement between experimental and simulation results. We found that the grains velocity at the center of the orifice only depends on its size. Two granular flow regimes have been identified. The first regime is observed for small inclination of the bottom : the granular flow orientation is controlled by the aspect ratio D/W , the higher D/W , the more the flow is aligned with gravity. The second regime is observed for large inclination of the bottom : the flow orientation is strongly correlated with the angle. Finally, we present a model that predicts the discharge flow rate of particles from a rectangular silo with an inclined bottom according to its aspect ratio.

Applying Isogeometric Shells to Unstructured U-spline Surfaces

Zhihui Zou^{*}, Michael Scott^{**}, Derek Thomas^{***}, Bastian Oesterle^{****}, Manfred Bischoff^{*****},
Wolfgang Dornisch^{*****}, Tom Hughes^{*****}

^{*}Brigham Young University, ^{**}Brigham Young University, ^{***}Coreform LLC, ^{****}University of Stuttgart,
^{*****}University of Stuttgart, ^{*****}Technische Universität Kaiserslautern, ^{*****}The University of Texas at Austin

ABSTRACT

In this talk we will describe our efforts to extend the isogeometric Kirchhoff-Love and geometrically exact Reissner-Mindlin shells to a newly developed spline representation called U-splines. A U-spline surface allows unstructured meshes and overcomes the analysis-suitability restrictions of a T-spline while preserving the mathematical properties required by analysis. This enables us to apply isogeometric shell formulations to complex engineering structures. We also explore the imposition of C1 continuity constraints around the extraordinary points in U-spline, which makes the higher order isogeometric shells applicable to complex meshes with extraordinary points. We demonstrate the effectiveness of the approach on several carefully selected numerical benchmarks.

On a New Mixed Formulation of Kirchhoff and Reissner-Mindlin Plates

Walter Zulehner*, Katharina Rafetseder**

*Johannes Kepler University Linz, **Johannes Kepler University Linz

ABSTRACT

In 3D linear elasticity it is well-known that stress tensor fields satisfying the homogeneous equilibrium equation can be expressed in terms of the Beltrami stress functions provided the domain is topologically simple. There is a similar result for the tensor field of bending and twisting moments in plate models, if the mid-surface of the plate is simply connected. While the stress tensor field in 3D linear elasticity can be written as a second-order differential operator applied to the Beltrami stress functions, the tensor field of bending and twisting moments in plate models is only a first-order differential operator applied to some 2D vector field. We will show how this result can be used to reformulate the Kirchhoff and the Reissner-Mindlin plate models as well-posed second-order systems. The incorporation of mixed boundary conditions describing clamped, simply supported, and free parts of the plate's boundary as well as corner conditions are discussed. For the Kirchhoff model the second-order system consists of three (consecutively to solve) standard second-order elliptic problems, see [1,2]. For the Reissner-Mindlin model the ideas from [1,2] are combined with the formulation in [3] (presented there, more generally, for shells) and result in two second-order elliptic problems and one saddle point problem. The reformulation of the plate models as second-order systems allows for discretization methods in approximation spaces with continuous functions. This includes standard continuous Lagrangian finite element methods and spline spaces from isogeometric analysis on multi-patch domains with continuous patching only. [1] W. Krendl, K. Rafetseder, and W. Zulehner. A decomposition result for biharmonic problems and the Hellan-Herrmann-Johnson method, ETNA, Electron. Trans. Numer. Anal., 45, pp. 257–282, 2016. [2] K. Rafetseder and W. Zulehner. A decomposition result for Kirchhoff plate bending problems and a new discretization approach. ArXiv e-prints, arXiv:1703.07962, pp. 1-27, March 2017. [3] R. Echter, B. Oesterle and M. Bischoff. A hierarchic family of isogeometric shell finite elements, Comput. Methods Appl. Mech. Engrg., 254, pp. 170–180, 2013.

A Fictitious Domain Method for Fluid-Structure Interaction

Patrick Zulian^{*}, Maria Nestola^{**}, Rolf Krause^{***}

^{*}Institute of Computational Science, Università della Svizzera italiana, ^{**}Institute of Computational Science, Università della Svizzera italiana, ^{***}Institute of Computational Science, Università della Svizzera italiana

ABSTRACT

We present a new and completely parallel approach for fluid-structure interaction with contact between the elastic structures. Our approach is inspired by the fictitious domain method [1] and exploits variational transfer techniques for coupling the solid and the fluid and on the possibly contacting surfaces between solids [2]. The main idea of the fictitious domain method is modeling the solid phase as immersed in a background fluid phase. The fluid is described in an Eulerian fashion (fixed mesh), while we use Lagrangian meshes for the solid structure. The coupling between the two phases is achieved with overlapping domain decomposition. Specifically, our coupling is constructed by means of L2-projections where a Lagrange multiplier is used to weakly enforce the velocity vector constraint along the interface-boundary between the solid and the fluid. For solving the arising nonlinear-system of discrete equations we adopt a staggered approach within a fixed-point iteration, hence the fluid and the solid problems are solved separately with the following four steps: First, we transfer velocities from the solid mesh to the fluid mesh. Second, we solve the fluid dynamics problem by imposing the velocity constraint in the overlapping region. Third, we compute and transfer the reaction force from the fluid mesh to the boundary of the solid mesh. At last, we solve the solid mechanics problem by imposing the reaction force on the solid (Neumann) boundary. We present the discretization, the setup of the parallel variational transfer [3], methods for the solution of the arising non-linear problems, and the related software libraries we developed. We present 2D and 3D benchmarks, and a tricuspid heart valve. [1] F. P. Baaijens. A fictitious domain/mortar element method for fluid-structure interaction. *International Journal for Numerical Methods in Fluids*, 35(7):743–761, 2001. [2] T. Dickopf and R. Krause. Efficient simulation of multi-body contact problems on complex geometries: A flexible decomposition approach using constrained minimization. *International journal for numerical methods in engineering*, 77(13):1834–1862, 2009. [3] R. Krause and P. Zulian. A parallel approach to the variational transfer of discrete fields between arbitrarily distributed unstructured finite element meshes. *SIAM Journal on Scientific Computing*, 38(3):C307–C333, 2016.

ADVANTAGES OF AUTOMATIC-DIFFERENTIATION-BASED FORMULATION AND SENSITIVITY ANALYSIS BASED IMPLEMENTATION OF MULTISCALE METHODS

NINA ZUPAN*, JOŽE KORELC†

* University of Ljubljana
Faculty of Civil and Geodetic Engineering
Jamova cesta 2
Ljubljana, Slovenia
e-mail: nina.zupan@fgg.uni-lj.si, <http://www3.fgg.uni-lj.si>

† University of Ljubljana
Faculty of Civil and Geodetic Engineering
Jamova cesta 2
Ljubljana, Slovenia
e-mail: joze.korelc@fgg.uni-lj.si, <http://www3.fgg.uni-lj.si>

Key words: Multiscale methods, MIEL, FE^2 , sensitivity analysis, path dependent problems, convergence

Summary. Multiscale methods became a strong field in computational mechanics, partly because of a need for detailed analysis of response with respect to material and geometric nonlinearities and thanks to growing computer capabilities. In this paper, focus is on advantages of Automatic-Differentiation-Based formulation and sensitivity analysis based implementation, especially convergence rate of two frequently used multiscale methods, MIEL and FE^2 . Their implementation is carried out with AceGen and AceFEM based on analytical sensitivity analysis and is compared to Schur complement based one. Sensitivity analysis based implementation assures efficient and consistent multiscale modeling. It is shown that quadratic convergence is achieved also for path dependent problems with two interacting continuation methods.

1 INTRODUCTION

Multiscale methods are growing trend in computational mechanics, especially with increasing capabilities of computers. Many of the multiscale methods originate from the demand to model heterogeneous materials [1]. Roughly, multiscale methods can be divided into two groups: methods that are based on homogenization techniques and domain decomposition methods. For purpose of convergence comparison, one method from each group was implemented, FE^2 and MIEL. Numerical schemes for implementation

of MIEL and FE² multiscale methods, based on sensitivity analysis and with use of Schur complement, are presented. Implementation is done with the Mathematica packages AceGen and AceFEM [2]. These programs enable analytical sensitivity analysis of first and second order, which can be used for efficient implementation of multiscale finite element methods. Computational environment was created, where the multiscale program code is automatically derived and various types of multiscale and single scale approaches can be freely mixed, while retaining quadratic convergence of the two-level Newton-Raphson procedure.

2 AUTOMATION OF PRIMAL AND SENSITIVITY ANALYSIS

The AceGen is an advanced automatic code generator, where automatic differentiation technique, automatic code optimization and generation are combined with computer algebra system Mathematica [3]. The AceFEM package is a general finite element environment designed to solve multi-physics and multi-field problems. Automation of primal and sensitivity analysis is done with AceGen. The automatic differentiation technique (AD) can be used for the evaluation of the exact derivatives of any arbitrary complex function via chain rule and represents an alternative solution to the numerical differentiation and symbolic differentiation. The result of AD procedure is called "computational derivative" [4].

For automation of multiscale analysis the automation of primal analysis as well as first and second order sensitivity analysis are needed. In primal analysis the response of the system is evaluated, whereas in sensitivity analysis the derivatives of the response, e.g. displacements, strains, stresses or work, with respect to arbitrary design parameter ϕ_i are sought. The primal problem is solved by the standard Newton-Raphson iterative procedure (see e.g. [5]). For the automation of the multiscale methods the sensitivity analysis with respect to prescribed essential boundary conditions is needed.

For the path independent problems, the primal problem is defined with the residual equation $\mathbf{R}(\mathbf{p}) = \mathbf{0}$, where \mathbf{p} represents a set of nodal unknowns of the problem. For the boundary condition sensitivity analysis we define the residuals and the vectors of unknown as a function of a vector of design parameters $\boldsymbol{\phi}$ by

$$\mathbf{R}(\mathbf{p}(\boldsymbol{\phi}), \bar{\mathbf{p}}(\boldsymbol{\phi})) = \mathbf{0} \quad (1)$$

where $\bar{\mathbf{p}}$ represents a set of nodal unknowns with prescribed essential boundary conditions.

The sensitivity problem can be obtained from the primal problem by differentiating (1) with respect to design parameters (2). Equation (2) represents a system of linear equations (4) for the unknown sensitivities of the primal unknowns of the problem $\frac{D\mathbf{p}}{D\phi_i}$. The right hand side is called "first order sensitivity pseudo load vector". The vector $\frac{D\bar{\mathbf{p}}}{D\phi_i}$ represents the rate of the change of the prescribed essential boundary conditions, with respect to the change of design parameter and is called "prescribed boundary condition velocity field".

The sensitivity problem is solved after the convergence of the primal problem has been reached. For the automation we need only the ADB form (see [5]) of pseudo load vector ${}^I\tilde{\mathbf{R}}$ evaluated at the integration point of the individual finite element ${}^I\tilde{\mathbf{R}}_g$. The global pseudo load vector is then obtained by the standard integration over the element domain and the standard finite element assembly procedure of element contributions to global vector ${}^I\tilde{\mathbf{R}}_g$.

$$\frac{\partial \mathbf{R}}{\partial \mathbf{p}} \frac{D\mathbf{p}}{D\phi_i} + \frac{\partial \mathbf{R}}{\partial \bar{\mathbf{p}}} \frac{D\bar{\mathbf{p}}}{D\phi_i} = \mathbf{0} \quad (2)$$

$${}^I\tilde{\mathbf{R}} = -\frac{\partial \mathbf{R}}{\partial \bar{\mathbf{p}}} \frac{D\bar{\mathbf{p}}}{D\phi_i} \quad (3)$$

$$\mathbf{K} \frac{D\mathbf{p}}{D\phi_i} = -{}^I\tilde{\mathbf{R}} \quad (4)$$

The second order sensitivity problem is obtained from the first order problem, by differentiating (2) with respect to design parameter ϕ_i . It results in

$$\begin{aligned} & \frac{\partial^2 \mathbf{R}}{\partial \mathbf{p}^2} \frac{D\mathbf{p}}{D\phi_i} \frac{D\mathbf{p}}{D\phi_j} + \frac{\partial^2 \mathbf{R}}{\partial \mathbf{p} \partial \bar{\mathbf{p}}} \frac{D\bar{\mathbf{p}}}{D\phi_j} \frac{D\mathbf{p}}{D\phi_i} + \frac{\partial \mathbf{R}}{\partial \mathbf{p}} \frac{D^2 \mathbf{p}}{D\phi_i D\phi_j} + \frac{\partial^2 \mathbf{R}}{\partial \bar{\mathbf{p}} \partial \mathbf{p}} \frac{D\mathbf{p}}{D\phi_j} \frac{D\bar{\mathbf{p}}}{D\phi_i} + \\ & + \frac{\partial^2 \mathbf{R}}{\partial \bar{\mathbf{p}}^2} \frac{D\bar{\mathbf{p}}}{D\phi_i} \frac{D\bar{\mathbf{p}}}{D\phi_j} + \frac{D\mathbf{R}}{D\bar{\mathbf{p}}} \frac{\partial^2 \bar{\mathbf{p}}}{\partial \phi_i \partial \phi_j} = \mathbf{0} \end{aligned} \quad (5)$$

$$\mathbf{K} \frac{D^2 \mathbf{p}}{D\phi_i D\phi_j} = -{}^{II}\tilde{\mathbf{R}} \quad (6)$$

where ${}^{II}\tilde{\mathbf{R}}$ represents the second order sensitivity pseudo load vector.

All first order sensitivities have to be calculated in order to be able to calculate the second order sensitivities. Equation (5) represents a system of linear equations (6) for the unknown sensitivities of the primal unknowns of the problem $\frac{D^2 \mathbf{p}}{D\phi_i D\phi_j}$. For ADB formulation (see [6]).

3 MULTISCALE METHODS

For overview of multiscale methods reader is referred to [7,8]. FE^2 is a standard two-level finite element homogenization approach [9], that is appropriate for the problems where scales are separated far enough and are only weakly coupled. In some cases, for example when difference between two scales is finite, or when in the region of high gradients, the FE^2 multi-scale approach fails, thus we need to use some sort of domain decomposition method. One possibility is the mesh-in-element or MIEL scheme described in [10].

3.1 FE^2 method

The FE^2 method is a two-level scheme, where we have one FE model for the macro scale (problem to be solved) and the second one at each material integration point (micro problem), as shown in Fig. 1. All information about micro-structure is obtained from

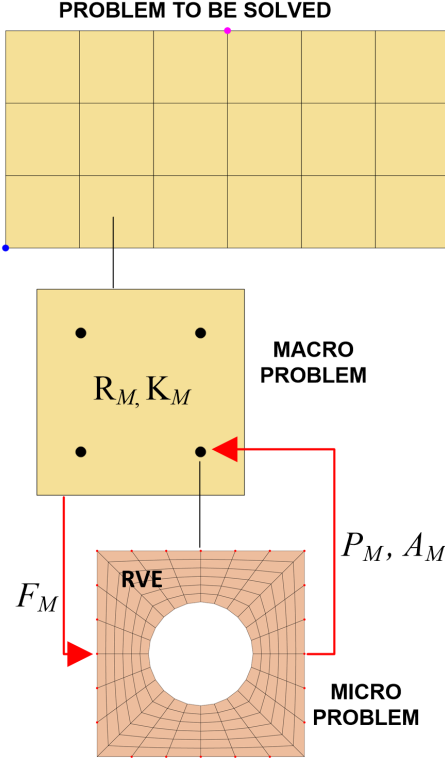


Figure 1: FE² procedure

computations on RVE-level by averaging the material response characterized by an appropriate stress measure and constitutive tangent matrix over RVE. RVE is attached to each integration point of the macroscopic FE problem. For a typical finite strain problem that leads to $\mathbf{P}_M = \{\mathbf{P}_m\}$ and $\mathbf{A}_M = \{\frac{\partial \mathbf{P}_m}{\partial \mathbf{F}_M}\}$, where \mathbf{P}_M and \mathbf{P}_m are the first Piola-Kirchhoff stress tensors at macro and micro level, \mathbf{F}_M is the macroscopic deformation gradient and \mathbf{A}_M a macroscopic constitutive matrix. This information is then used at the macro level for the evaluation of integration point contribution to element residual \mathbf{R}_{Mg} and tangent matrix \mathbf{K}_{Mg} at the macro level, as follows

$$\mathbf{R}_{Mg} = \mathbf{P}_M : \frac{\partial \mathbf{F}_M}{\partial \mathbf{p}_{Me}} \quad (7)$$

$$\mathbf{K}_{Mg} = \frac{\partial \mathbf{R}_M}{\partial \mathbf{p}_{Me}} + \frac{\partial \mathbf{R}_M}{\partial \mathbf{P}_M} \mathbf{A}_M \frac{\partial \mathbf{F}_M}{\partial \mathbf{p}_{Me}} \quad (8)$$

where \mathbf{p}_{Me} represents a set of nodal unknowns of macro element. The FE² method can be implemented in different ways (see e.g. [9,11]). For efficiency of the method efficient calculation of the macroscopic constitutive matrix \mathbf{A}_M is important. In a conventional way of computing macroscopic constitutive tangent, computation of a Schur complement of RVEs tangent matrix is needed [9]. An alternative is calculation of consistent

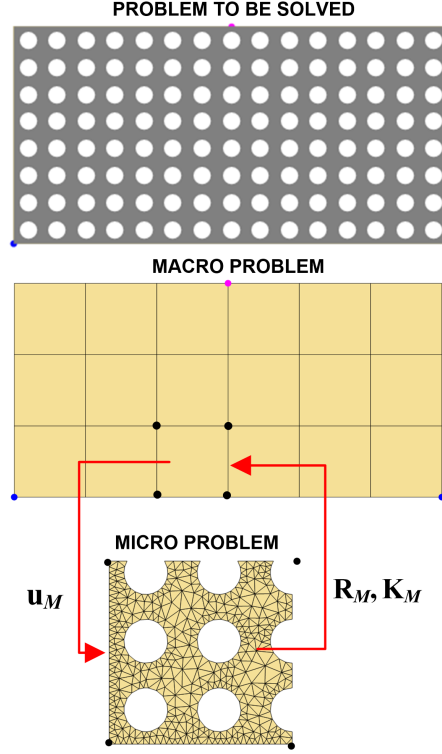


Figure 2: MIEL procedure

macroscopic stiffness matrix by sensitivity analysis of the micro-structure, with respect to macro strain measure used to impose boundary conditions on RVE. Sensitivity parameters of the problem are components of the macro deformation gradient \mathbf{F}_M , thus $\boldsymbol{\Phi} = \{F_{M,11}, F_{M,12}, F_{M,13}, F_{M,21}, \dots\}$. For the complete formulation of the prescribed boundary condition sensitivity problem, prescribed boundary condition velocity field $\frac{D\bar{\mathbf{p}}}{D\boldsymbol{\Phi}}$ is needed.

3.2 MIEL method

In case of MIEL the finite element models at different scales communicate between each other through degrees of freedom of the finite element at the macro scale. The residual and tangent matrix are for each macro element obtained directly from the micro scale problem. Each macro element thus represents one micro problem. MIEL procedure is presented in Fig. 2.

Macro tangent matrix is typically evaluated with the Schur complement of the global micro tangent matrix, thus elimination of inner DOFs. Here alternative implementation in AceFEM is presented, where macro tangent matrix is calculated through second order sensitivity analysis, with respect to prescribed essential boundary conditions. In that way, we get values of implicit dependencies of micro displacements on macro displacements.

Let \mathbf{p}_{Me} be a vector of unknowns in the nodes of the macro element, \mathbf{p}_{me} a vector of unknowns in the nodes of the characteristic micro problem element and W strain energy function. The outer shape of the micro problem is the same as the shape of the corresponding macro element. The prescribed essential boundary conditions (displacements) are identical to the displacements at the boundary of the corresponding macro element. The integration point contribution (g -th integration point in the e -th element of the micro mesh) to the macro residual and macro tangent matrix is then

$$\mathbf{R}_{Mg} = \frac{\partial W(\mathbf{p}_{me}(\mathbf{p}_{Me}))}{\partial \mathbf{p}_{Me}} = \frac{\partial W}{\partial \mathbf{p}_{me}} \frac{D\mathbf{p}_{me}}{D\mathbf{p}_{Me}} \quad (9)$$

$$\mathbf{K}_{Mg} = \frac{\partial \mathbf{R}_{Mg}}{\partial \mathbf{p}_{Me}} = \frac{\partial^2 W}{\partial \mathbf{p}_{me}^2} \frac{D\mathbf{p}_{me}}{D\mathbf{p}_{Me}} + \frac{\partial W}{\partial \mathbf{p}_{me}} \frac{D^2 \mathbf{p}_{me}}{D\mathbf{p}_{Me}^2}. \quad (10)$$

The implicit dependencies $\frac{D\mathbf{p}_{me}}{D\mathbf{p}_{Me}}$ and $\frac{D^2 \mathbf{p}_{me}}{D\mathbf{p}_{Me}^2}$ are obtained by the first and second order sensitivity analysis. Thus, the sensitivity analysis based automation of the MIEL scheme requires the second order sensitivity analysis for a set of sensitivity parameters \mathbf{p}_{Me} .

For the complete formulation of the prescribed boundary condition sensitivity problem, the first and the second order prescribed boundary condition velocity fields are needed, for details see e.g. [5] where the concept is extended to path dependent problems.

4 ADVANTAGES OF PROPOSED IMPLEMENTATION

In this section among other advantages improvement of convergence rate of implicit multiscale methods is presented, due to the automatic-differentiation-based formulation and sensitivity analysis based implementation, in comparison with Schur complement based implementation.

Solving of nonlinear problems is done implicitly with a two-level Newton-Raphson type iterative solution procedure. Here the macro path is parametrized by macro load level (λ_M). For every load step at macro level ($\Delta\lambda_M$), several substeps can be done at micro level ($\Delta\lambda_m$) where (λ_m) represents additional parameter at micro level used to parametrize micro problem within one macro load step. Since we have two scales, we have in general a path following procedure at both levels, resulting in two-level path following procedure presented in Fig. 3. Traditionally, each step at macro level is followed by only one step at micro level. Sensitivity analysis based multiscale analysis allows extension to more general case, where each macro step can be followed by an arbitrary number of micro substeps. For every substep at micro level, sensitivity has to be updated, otherwise for path dependent problems the quadratic convergence is lost.

As a numerical example, bending of a three-dimensional simply supported beam with enforced vertical displacement $w = 0.1$ cm was investigated, see Fig. 4. Supports of the beam were modeled in a way of preventing displacements in all three directions on one side and released displacement in x direction on the other side. The dimensions of a beam were $10 \times 2.5 \times 2.5$ cm with macro mesh division $16 \times 4 \times 4$. At macro level finite elements

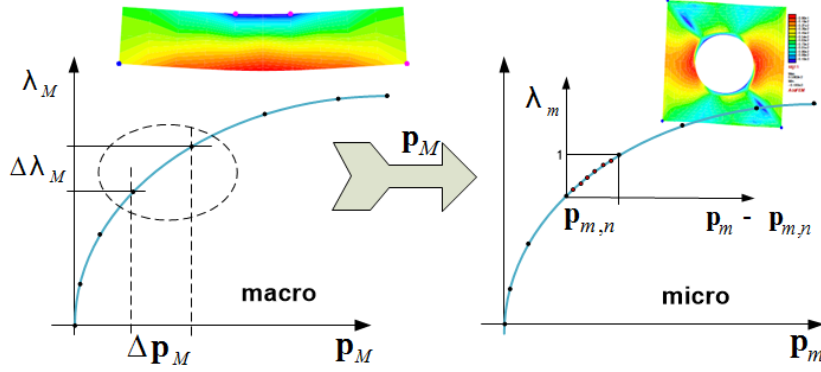


Figure 3: Two-level path following procedure.

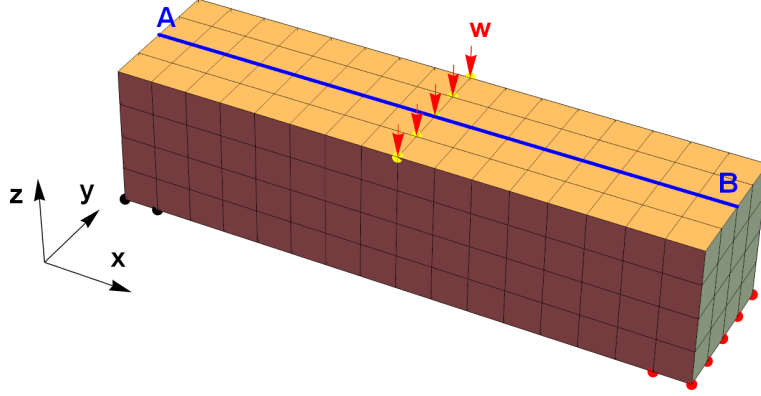


Figure 4: Numerical example: simply supported beam

were hexahedron (H1) and for micro mesh tetrahedron elements (O1) were used. The complete response was evaluated using adaptive path following procedure. The material properties were: Youngs modulus $E = 210$ GPa, Poissons ratio $\nu = 0.3$ and yield stress $\sigma_y = 0.024$ GPa.

Numerical example was evaluated with FE^2 procedure. Results of convergence rate of the Newton-Raphson method for one macro load step in nonlinear region are shown in Table 1, for small strain plasticity (PL). With meaning of labels in Table 1 as follows: PL 1/1 Schur - elasto-plastic material, each macro load step is followed by one micro load step, Schur complement based implementation; PL 1/1 Sens. - elasto-plastic material, each macro load step is followed by one micro load step, sensitivity analysis based implementation; PL 1/5 Schur - elasto-plastic material, each micro increment is divided into 5 substeps, Schur complement based implementation; PL 1/5 Sens. - elasto-plastic material, each micro increment is divided into 5 substeps, sensitivity analysis based implementation, sensitivity is updated; PL 1/5 Sens. uncon. - elasto-plastic material, each micro increment is divided into 5 substeps, sensitivity analysis based implementation, sensitivity is not updated.

In case of sensitivity analysis based implementation of FE^2 convergence is quadratic, while for Schur complement implementation that is not true. Additionally 5 substeps for each macro load step were enforced. In the last column results are shown for case where sensitivity was not updated after every substep, leading to disappearance of quadratic convergence. For MIEL we arrived to similar conclusions as for FE^2 .

Table 1: Comparison of convergence rate for FE^2 scheme

it.	PL 1/1 Schur	PL 1/1 Sens.	PL 1/5 Schur	PL 1/5 Sens.	PL 1/5 Sens. uncons.
1	6.995×10^{-3}	5.004×10^{-3}	5.906×10^{-3}	4.967×10^{-3}	4.974×10^{-3}
2	1.740×10^{-3}	1.186×10^{-4}	9.571×10^{-4}	1.019×10^{-4}	9.569×10^{-5}
3	9.599×10^{-4}	2.888×10^{-6}	7.029×10^{-4}	3.343×10^{-6}	2.566×10^{-5}
4	1.342×10^{-4}	5.568×10^{-9}	4.463×10^{-4}	4.518×10^{-9}	1.846×10^{-5}
5	2.816×10^{-4}		1.404×10^{-4}		1.065×10^{-6}
-	-		-		-
17	1.614×10^{-7}		7.292×10^{-8}		5.825×10^{-9}
-	-		-		
20	1.155×10^{-8}		9.050×10^{-9}		
-	-				
22	5.249×10^{-9}				

Additionally, proposed approach enables unification and automation of various multi-scale approaches for an arbitrary nonlinear, time dependent coupled problem (e.g. general finite strain plasticity). Different multiscale methods FE^2 , MIEL and also single-scale schemes can be used together in one model. With that optimal domain discretization is possible. Implementation of the presented multiscale computational approach in Ace-FEM is fully parallelized for multi-core processors. The setup is also appropriate for the implementation on clusters.

5 CONCLUSIONS

Essential boundary condition sensitivity analysis based implementation of multiscale FE^2 and MIEL was proposed, as an alternative to more traditional implementation based on Schur complement, which is numerically demanding mathematical operation that additionally requires a lot of disc space. The differences between the sensitivity analysis based implementation of FE^2 and MIEL method are in essential boundary condition of micro problem and in essential boundary condition velocity fields needed for the sensitivity

analysis. For FE^2 first order sensitivity is enough, whereas for MIEL second order sensitivity is needed. Ergo, beforehand implementing multiscale methods, efficient analytical sensitivity analysis for first and second order was needed.

Investigation of convergence rate was done on numerical examples for FE^2 and MIEL method, with both ways of implementing them. As a fact, for hyperelastic material, convergence rate is quadratic also for inconsistent sensitivity analysis, regardless of the number of micro substeps, because the problem is not path dependent. The most important asset of automatic-differentiation-based (ADB) formulation and sensitivity based implementation is that quadratic convergence is retained also for nonlinear path dependent problems with substepping at micro level. For path dependent problems only correctly done sensitivity analysis at micro level leads to algorithmically consistent macro tangent matrix and to quadratic convergence. For every substep at micro level, sensitivity has to be updated, otherwise for path dependent problems the quadratic convergence is lost.

Acknowledgement The financial support for this work was obtained from the Slovenian Research Agency within the PhD Grant Agreement (annex No: 630-34/2015-7).

REFERENCES

- [1] Lamut, M., Korelc, J., Rodič, T. Multiscale modelling of heterogeneous materials. *Materials and technology*. (2011) 45: 421-426.
- [2] Korelc, J., Wriggers, P. *Automation of finite element methods*. Springer, Switzerland (2016).
- [3] Mathematica 11.2, Wolfram Research Inc., <http://www.wolfram.com> (2017).
- [4] Korelc, J. Automatic generation of finite-element code by simultaneous optimization of expressions. *Theoretical computer science*. (1997) 187: 231-248.
- [5] Korelc, J. Automation of primal and sensitivity analysis of transient coupled problems. *Computational Mechanics*. (2009) 44: 631-649.
- [6] Sorić, J., Wriggers, P., Allix, O. (Eds.) *Multiscale Modeling of Heterogeneous Structures*. Springer International Publishing, (2018).
- [7] Geers, M.G.D., Kouznetsova, V.G., Brekelmans, W.A.M. Multi-scale computational homogenization: Trends and challenges. *Journal of Computational and Applied Mathematics*. (2010) 234: 2175-2182.
- [8] Efendiev, Y., Hou, T. Y. *Multiscale Finite Element Methods: Theory and Applications*. Springer, Dordrecht, (2008).
- [9] Kouznetsova, V., Brekelmans, W.A.M., Baaijens F.P.T. An approach to micro-macro modelling of heterogeneous materials. *Computational Mechanics*. (2001) 27: 37-48.

- [10] Markovič, D., Ibrahimbegović, A. On micro-macro interface conditions for micro scale based FEM for inelastic behaviour of heterogeneous materials. Computer methods in applied mechanics and engineering. (2004) 193: 5503-5523.
- [11] Šolinc, U., Korelc, J. A simple way to improved formulation of FE^2 analysis. Computational Mechanics. (2015) 56: 905-915.

Analysis of a Railway Wheel-rail Connection during Intensive Braking Using Coupled Thermal and Stress FE Simulations

Péter T. Zwierczyk*, Károly Váradi**

*Assistant Professor, Ph.D.; Budapest University of Technology and Economics, **Professor; Budapest University of Technology and Economics

ABSTRACT

In a railway wheel-rail connection, we can define several tread surface failures of the wheels. This research is focusing on the so-called micro-thermal and sub-surface fatigue cracks. These are two of the most frequent failure types both of the wheel and the rail. The aim of our investigation was to map the appearance and the generation background of these failures using a multistage FE modelling procedure which consisted of coupled transient thermal and elastic-plastic contact FE simulations [1]. During intensive wheel-braking of the railway vehicles, equipped with disk brake only, it appears that the wheel slides on the rail. While the macroscopic sliding speed is restricted it is not eliminated by the WSP (Wheel Slide Protection System). Through the sliding process considerable heat is generated between the connecting parts. This heat may cause micro-cracks on and under the wheel tread. Previously, as it was presented in [2], [3], a modelling method was developed in ANSYS Workbench V14.5 software which could help understand the generation procedure of these micro-cracks caused by the heat generation. In the current state of the research, using an extended FE model, the effect of the different operation conditions (movement speed, different coefficient of friction, etc.) and the coupled effect of the micro-cracks and the subsurface fatigue cracks can be observed. The results showed that which are the sliding speed limits of the WSP systems (beside different braking conditions), where it may not cause micro-cracks on the surface of the wheel tread. Using the results of the elaborated calculations the setup of the WSP systems can be modified under different braking conditions which helps minimize the failures of the wheels and the rail. The recent study and publication was realized within the Knorr-Bremse Scholarship Program supported by the Knorr-Bremse Rail Systems Budapest. [1] P. T. Zwierczyk, "Thermal and stress analysis of a railway wheel rail rolling sliding contact," in PhD. thesis, Budapest University of Technology and Economics, 2015. [2] P. T. Zwierczyk and K. Váradi, "Thermal and stress analyses of a railway wheel-rail connection during intensive sliding-rolling braking," presented at the 12th World Congress on Computational Mechanics (WCCM XII), Seoul, South Korea, 2016, p. 1. [3] P. T. Zwierczyk and K. Váradi, "Thermal Stress Analysis of a Railway Wheel in Sliding-Rolling Motion," J. Tribol., vol. 136, no. 3, pp. 031401–1 – 031401–8, May 2014.

TYPICAL AEROSPACE MOUNT DESIGN BY TOPOLOGY OPTIMIZATION AND MANUFACTURED BY ADDITIVE MANUFACTURING

Guanghai SHI^{*†}, Dongliang QUAN^{*}, Chengqi GUAN^{*}, Feng SONG^{*}, Dongtao^{*} WU

^{*}Beijing Aerospace Technology Institute
No.40, Yungangbeili, Fengtai District, Beijing , China

[†]Shgh5@126.com

Key words: Topology optimization; Thermo-elastic; additive manufacturing; SLM; Aerospace bracket

Abstract. Combination of optimization and additive manufacture could make structure optimization, especially for topology optimization, more effectively in improving structure performance and mass reduction. A large load bearing aerospace bracket structure had been design under the guidance of thermo-elastic topology optimization theory and manufactured with additive manufacture method. And on the basic of topology optimization, taking the lightweight structure and optimal performance as ultimate target, taking the necessary installation space requirement into account, the parameterized bracket model had been reconstructed for size optimization. Further, the optimized bracket lightweight structure design had finished. Then, the formability improvement had been done, additional test bars are added in the manufacturing process for performance testing, and process support is added inside the specimen to meet the requirements of the hanging angle process. Finally the bracket was printed with the selective laser melting (SLM) equipment from Bright Laser Technology Company. The mechanical properties test of the test rod shows that the mechanical properties of the specimen meet the requirements. The main contributions are focused on the following points. In order to meet the requirement of thermal load optimization for the aerospace bracket, a new thermo-elastic topology optimization and sensitive analysis formulation had been adopted. The additive manufacture method had been considered in the same processing with topology initial structure reconstruct after topology optimization, which could improve the lightweight level of optimized structure, without the constrain of traditional manufacture requirement, such as openness requirement. In order to cooperate with the SLM equipment, elaborately designed structure rotation and process support had been done, which guaranteed the final structural quality by additive manufacture.

1 INTRODUCTION

Additive manufacturing, which is a technique of layer-by-layer build-up of a product from a computer aided design model^[1], has seen unprecedented growth as a manufacturing tool in some

corporations for reducing mass and shortening reaction cycle^[2]. Additive manufacturing has been adopted in engineering applications^[3-6].

Topology optimization, which is a technique to seek the best structural configuration, has been widely accepted and adopted as an innovative design method in both academic research^[7] and applications in aircraft, aerospace and mechanical engineering^[8].

Combination of topology optimization and additive manufacturing technologies provides an effective approach for the development of high performance structures. For example, EADS Innovation Works obtained the innovative design of the hinge bracket of Airbus A320 using topology optimization and additive manufacturing technologies. Compared to the original design, a significant mass reduction of 64% is obtained.

Thermo-elastic topology optimization is also extended to the design of compliant mechanism^[9], simultaneous optimization of the microstructure of homogeneous porous material and macrostructure topology^[10] and dynamic compliance minimization in a temperature field^[11]. Besides, multiple materials were taken into account by introducing the concept of thermal stress coefficient (TSC)^[12].

This work focuses on the application of the thermo-elastic topology optimization. An aerospace bracket is designed by thermo-elastic topology optimization and manufactured by additive manufacturing technology. The rest of this paper is organized as follows. In Section 2, the topology optimization method of thermo-elastic structures is introduced. In Section 3, the considered aerospace bracket is presented. In the last section, the conclusions are presented.

2 THERMO-ELASTIC TOPOLOGY OPTIMIZATION

For a typical structural domain Ω , the equation that is solved for the thermo-elastic static linear analysis can be stated as:

$$\mathbf{K}\mathbf{u} = \mathbf{F}^a + \mathbf{F}^{th} \quad (1)$$

Herein, \mathbf{K} is the global stiffness matrix and \mathbf{u} is the nodal displacement vector. \mathbf{F}^a and \mathbf{F}^{th} are the nodal vector of the applied force and of the thermal stress load, respectively. At the finite element level, the element stiffness matrix and the nodal vector of thermal stress load of element e can be expressed as:

$$\begin{aligned} \mathbf{K}_e &= \int_{V_e} \mathbf{B}_e^T \mathbf{D}_e \mathbf{B}_e dV \\ \mathbf{F}_e^{th} &= \beta_e \bar{\mathbf{F}}_e^{th} \quad \bar{\mathbf{F}}_e^{th} = \int_{\Omega_e} \mathbf{B}_e^T \boldsymbol{\phi} \Delta t_e d\Omega \end{aligned} \quad (2)$$

Here, the element strain-displacement matrix \mathbf{B}_e consists of derivatives of element shape functions Δt_e denotes the temperature rise of element e and $\boldsymbol{\phi}=[1 \ 1 \ 0 \ 0 \ 0]$ for 3D problems. \mathbf{D} is the elasticity matrix depending on Young's modulus and Poisson's ratio. The thermal stress coefficient β , which can be treated as a material property, is defined as a function of the Young's modulus (E), thermal expansion coefficient (α) and Poisson's ratio (μ)^[12].

$$\beta_e = \frac{E_e \alpha_e}{1 - 2\mu_e} \quad (3)$$

In this work, a minimization of the global compliance subjected to the volume constraint is implemented to obtain the optimal configuration. The formulation of this optimization problem is expressed as:

$$\begin{aligned}
&\text{find:} && \mathbf{x} = \{x_i\} \quad (i = 1, \dots, n) \\
&\text{minimize:} && C = \mathbf{u}^T \mathbf{K}(\mathbf{x}) \mathbf{u} \\
&\text{subject to:} && \mathbf{K}(\mathbf{x}) \mathbf{u} = \mathbf{F}^a + \mathbf{F}^{th}(\mathbf{x}) \\
&&& \mathbf{H}(\mathbf{x}) \mathbf{t} = \mathbf{P} \\
&&& V \leq \overline{vf} \cdot V^{(0)} \\
&&& 0 < x_{\min} \leq x_i \leq 1
\end{aligned} \tag{4}$$

\mathbf{P} , \mathbf{t} and \mathbf{H} are the global thermal load vector, nodal temperature vector and heat conductivity matrix. Herein, the thermal stress load vector \mathbf{F}^{th} distinctly depends on the design variables while the applied mechanical force \mathbf{F}^a and thermal load \mathbf{P} are assumed to be design-independent.

n is the number of the designable finite elements and subscripts i indicates the i th designable element. \mathbf{x} denotes the set of design variables and a lower bound of the design variables, e.g., $x_{\min}=10^{-9}$ is introduced to avoid the singularity of the structural stiffness matrix and heat conductivity matrix in finite element analysis.

3 TOPOLOGY OPTIMIZATION OF THE BRACKET

3.1 Design processing

In this section, bracket optimization numerical example is tested to illustrate the proposed method. A sensitivity filtering technique is adopted to yield checkerboard-free topology configuration.

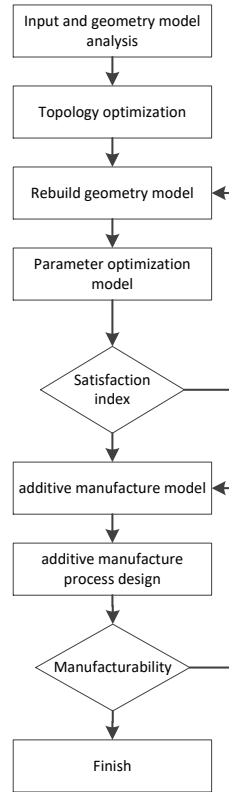


Figure 1 Optimization and additive manufacturing process

The optimization and additive manufacturing flow of the bracket is illustrated in Figure 1, which contains the following steps. First, input and geometry models are analyzed. Based on the initial design structure, the topology optimization space is magnified reasonably, design domain and non-design domain are determined; load and boundary conditions are simplified in this step. Secondly, the topology optimization numerical simulations are carried out to obtain the optimized structure. Thirdly, reconstruct lightweight bracket for additive manufacture based on topology optimization, taking the assemble space, operating space into consideration, the openness requirement of traditional machining is not considered. Fourth, based on the reconstructed geometric model, the parameters optimizations are carried out to complete detail design. Fifth, based on the detailed design model, carry out the process design of additive manufacturing, which including the manufacturing position, auxiliary supporting, et al. Last, finish manufacture of optimized bracket.

3.2 Bracket introduction

A single spacecraft consists of a symmetrical pair of bracket. In theory, the pair of symmetric brackets bear the same load. For assembly process, the asymmetry caused by engine deformation is guaranteed by considering certain safety factor in the bracket design. In this paper, the topology optimization of bracket along the course on the right side is analyzed, and the other side is considered to be completely symmetrical structure. As a centrally loaded component and subjected to certain thermal loads, it is necessary to have good thermal strength and elastic plastic properties, and TC4 titanium alloy material is considered comprehensively.

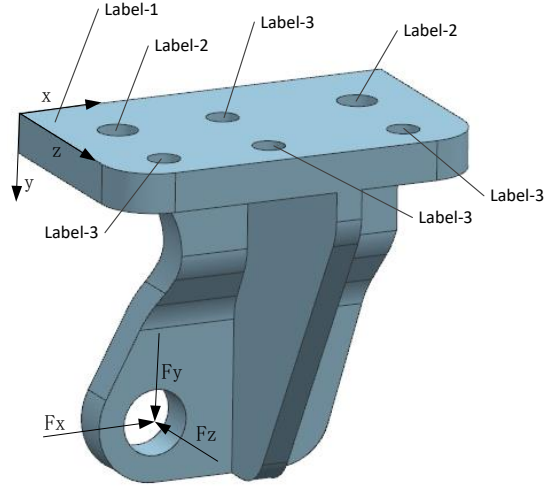


Figure 2 Initial bracket structure and corresponding loads and boundaries

Table 1 Bracket Work Load

Load Direction	X direction	Y direction	Z direction
Load N	-50000	-15000	-7500

Figure 2 display the initial bracket structure, which could meet the functional requirements, but still have potential for mass reduction and stiffness enhancement. The load in bracket includes the following three aspects. Firstly, thrust load of the course direction produced by the engine; Secondly, transverse and vertical mass force load caused by engine self over load; Thirdly, longitudinal frictional force produced by thermal deformation of engine. Consider a certain safety factor, the load in bracket are listed in Table 1.

Table 2 Boundary condition for bracket optimization

Label	Boundary condition	Description
Lable-1	$U_y=0$ $\theta_x = 0; \theta_z = 0$	Bottom face of bracket
Lable-2	$U_x=0, U_y=0, U_z=0$ $\theta_x = 0; \theta_z = 0$	Locating hole
Lable-3	$U_y=0$ $\theta_x = 0; \theta_z = 0$	Bolt hole

The Lable-1 in Figure 2 is the bottom face of bracket. The Lable-2s in Figure 2 are double locating holes. The Label-3s in Figure 2 are four bolt holes. The load and boundary conditions are reasonably simplified, acting on the bottom of the bracket and the connection holes, as shown in Table 2.

The topology optimization was carried out on the basis of re-matching the occupied space of the bracket. Before the topology optimization, the design domain was enlarged so that there would be enough design space in the topology optimization process, the enlarged design space are shown in Figure 3. In addition, according to the previous optimization example, given the necessary non-design domain of the load and constraint boundary, the main transmission line of

the structure can be clearer in topology optimization result. According to the loading and fixing requirements from experiences , give the top margin hole 10mm, bottom hole margin 5mm as the non-design domain, as shown in Figure 3.

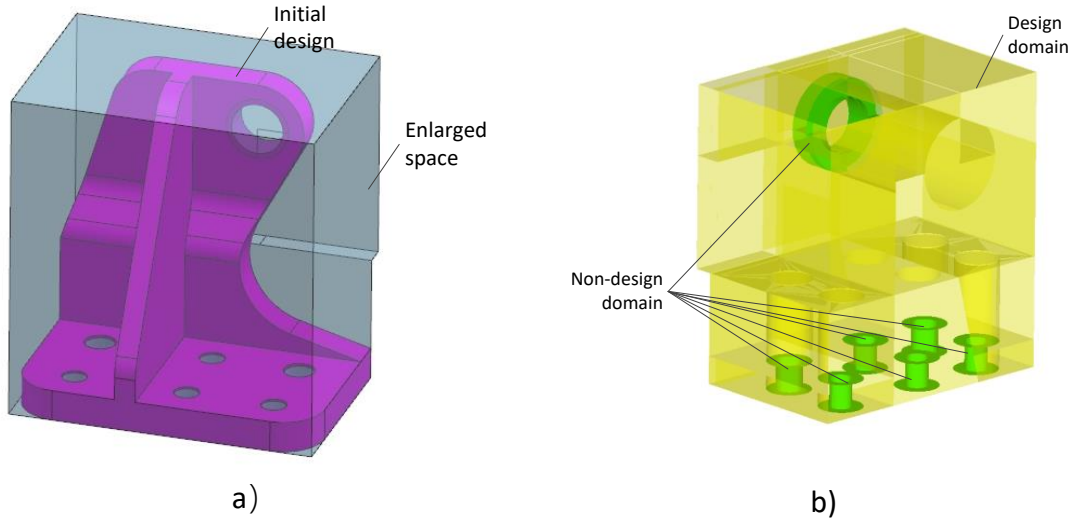


Figure 3 Enlarged space for topology optimization

a) Enlarged design zone; b) Design domain and non-design domain in optimization model

Based on the load, boundary condition and topology model, the optimization formulation is as follows.

$$\begin{aligned}
 & \text{Min : Compliance} \\
 & s.t \quad volfrac \leq a \\
 & \quad \quad Dis \leq b
 \end{aligned} \tag{5}$$

Among them, Compliance is the optimized model strain energy, which is the objective function in the optimization process; the optimization constraint contains three kinds of constraints, volfrac is volume fraction constraint, and its upper bound are a, which contains three numbers, corresponding to three optimization examples, the values are as follows: 0.15、 0.2、 0.25. For example, number 0.15 means that the optimized volume does not exceed 15% of the model volume before optimization. Dis is the displacement constrain in load center, and its upper bound is b=0.5mm, which is determined by analyzing the initial bracket structure.

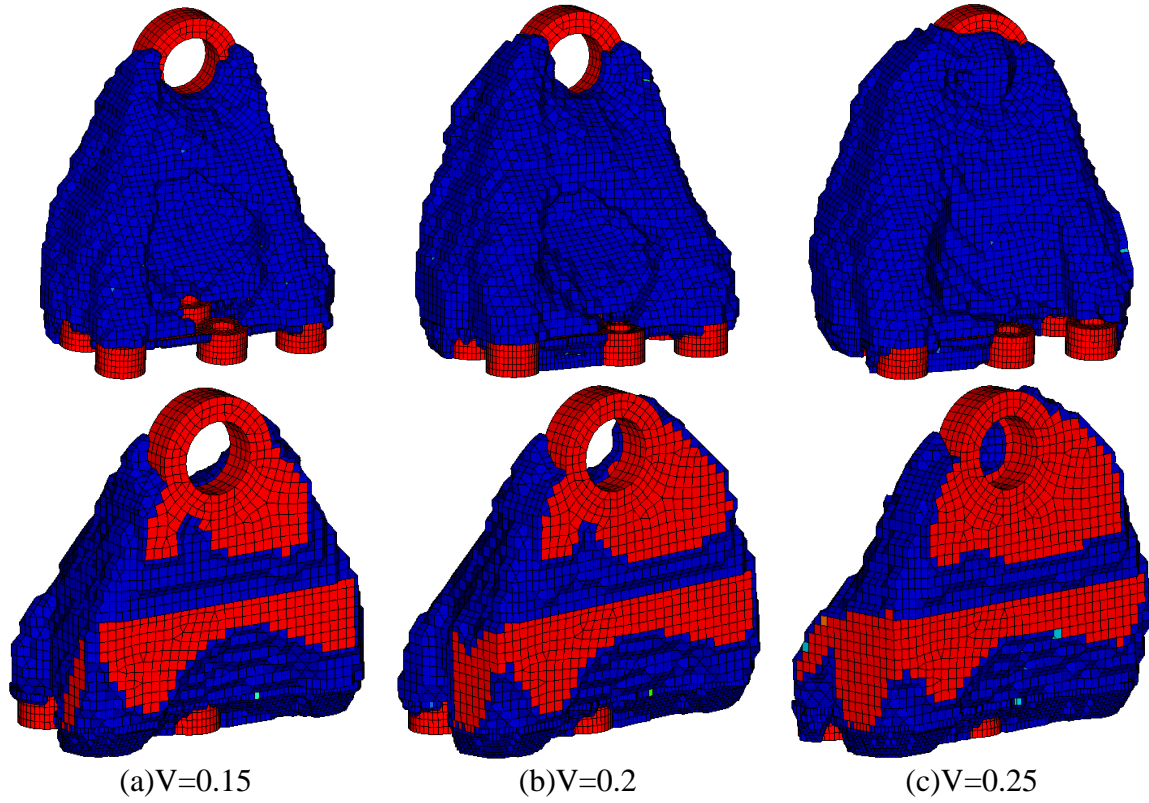


Figure 4 Structure after topology optimization (Element density >0.5)

As shown in Figure 4, the optimization results are given under the given volume constraints of 15%, 20% and 25% respectively. The figure gives the optimized material density distribution, which is the density greater than 0.5, the red area is density closed to 1, the density in the optimization result means the corresponding carrying capacity. The numerical examples shows that the volfrac constrain with upper bound 0.15 and 0.2 have better density distribution. The optimized result shown that the material density, distributed between load area and fixed boundary, is closed to 1. The rest of the area forms an approximately boxed structure, which connected the fixed plate and loading hole area at one end.

The model geometry model is reconstructed based on topology optimization results. The following principles are followed in the process of model reconstruction. Firstly, take the function requirement constrain, for example, the bolt installation and operation space. Secondly, refer to topology optimization results as far as possible. Thirdly, in addition to the location of the installation hole, it is not necessary to consider the openness requirements of machining manufacturing, and the manufacturing process limit is considered based on the additive manufacturing method. Fourth, reduce the structural mass as much as possible. Fifth, The stiffness index is not lower than the initial design model.

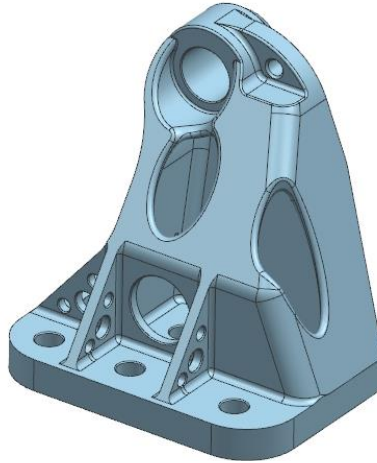


Figure 5 Reconstructed aerospace bracket

Table 3 Comparison of the original and optimized designs

	Mass (kg)	Displacement of KP (mm)	Max von-Mises stress (MPa)	Buckling factor
Existing design	3.48	0.39	400.0	46.7
Reconstructed design	2.85	0.36	635.8	62.0

Comparisons of the original and reconstructed designs are illustrated in Table 2. Benefiting from topology and size optimization, the mass of the aerospace bracket is reduced by 18.1%.

4 Conclusions

A heavy-loaded aerospace bracket is optimized using topology optimization for mass reduction. To meet the requirement of the aerospace bracket design, a formulation of thermo-elastic topology optimization is proposed and the sensitivity analysis is detailed. By means of the adoption of the structural optimization method, more than 18% of the structural mass of the aerospace bracket is reduced and all mechanical performances are satisfied. Following, size optimization based on reconstructed design and additive manufacture by SLM technique will be done.

This work indicates that the combination of topology optimization and additive manufacturing technology provides a powerful tool kit to the engineering designers and they are an amazingly good fit.

Acknowledgements

This work is supported by the National Key Research and Development Program of China (2016YFB0201605, 2016YFB0201600, 2017YFB1102805, 2017YFB1102800).

REFERENCES

- [1] Gu DD, Meiners W, Wissenbach K and Poprawe R (2012) Laser additive manufacturing of metallic components: materials, processes and mechanisms. *Int Mater Rev* 57: 133-164
- [2] Ford SLN (2014) Additive Manufacturing Technology: Potential Implications for U.S. Manufacturing Competitiveness. *Journal of International Commerce and Economics*
- [3] Schiller GJ (2015) Additive Manufacturing for Aerospace. 2015 Ieee Aerospace Conference
- [4] Shapiro AA, Borgonia JP, Chen QN, Dillon RP, McEnerney B, Polit-Casillas R and Soloway L (2016) Additive Manufacturing for Aerospace Flight Applications. *J Spacecraft Rockets* 53: 952-959
- [5] Froes FH, Boyer R and Dutta B (2017) Additive Manufacturing for Aerospace Applications-Part I. *Adv Mater Process* 175: 36-40
- [6] Zhu WJ, Zhao XL, Zhang W, Ren K, Zhang ZY and Li DC (2014) Design and Evaluation of Fully Configured Models Built by Additive Manufacturing. *AIAA J* 52: 1441-1451
- [7] Sigmund O and Maute K (2013) Topology optimization approaches: A comparative review. *Struct Multidisc Optim* 48: 1031-1055 DOI 10.1007/s00158-013-0978-6
- [8] Zhu J, Zhang W and Xia L (2015) Topology Optimization in Aircraft and Aerospace Structures Design. *Arch Comput Method Eng*: 1-28 DOI 10.1007/s11831-015-9151-2
- [9] Ansola R, Vegueria E and Canales J (2010) An element addition strategy for thermally actuated compliant mechanism topology optimization. *Engineering Computations* 27: 694-711 DOI 10.1108/02644401011062090
- [10] Deng J, Yan J and Cheng G (2013) Multi-objective concurrent topology optimization of thermoelastic structures composed of homogeneous porous material. *Struct Multidisc Optim* 47: 583-597 DOI 10.1007/s00158-012-0849-6
- [11] Yang X and Li Y (2014) Structural topology optimization on dynamic compliance at resonance frequency in thermal environments. *Struct Multidisc Optim* 49: 81-91 DOI 10.1007/s00158-013-0961-2
- [12] Gao T and Zhang WH (2010) Topology optimization involving thermo-elastic stress loads. *Struct Multidisc Optim* 42: 725-738 DOI 10.1007/s00158-010-0527-5

Correct Energy Behavior of Stabilized Formulations

Marco ten Eikelder*, Ido Akkerman**

*Delft University of Technology, **Delft University of Technology

ABSTRACT

Energy errors in the numerical formulation of PDEs can lead to inaccurate results. This occurs in the context of two-fluid flow problems, where many numerical methods create artificial energy at the interface. Even a small energy error can cause highly unstable behavior [1]. This talk concerns the construction of stabilized finite element methods with correct energy behavior. The streamline upwind Petrov-Galerkin method (SUPG), the Galerkin/least-squares method (GLS), and the variational multiscale method (VMS) are very popular stabilized methods of the last decades. These methods are well-established but do not show correct energy behavior. Taking a multiscale point of view, we rectify this discrepancy with dynamic and orthogonal small-scales. The newly constructed methodology is presented for the convection-diffusion equations [2] and the incompressible Navier-Stokes equations [3]. The convection-diffusion case demands the large- and small-scales to be H_0^1 -orthogonal to arrive at a method with desired energy behavior. Its counterpart in case of the incompressible Navier-Stokes equations is to apply an orthogonality induced by the Stokes equations. This needs to be augmented with divergence-free H_0^1 -small-scales to ensure correct energy evolution. The resulting formulation is of GLS-type and enjoys several favorable properties. These include (i) divergence-free solutions, (ii) the conservation of linear and angular momentum and (iii) divergence-free small-scales. A key observation is that the demand for correct energy behavior creates a link between the VMS, SUPG and GLS methodologies. Numerical results show that the dissipation due to the small-scales can be negative in standard stabilized methods. Computations of a turbulent flow show improved energy behavior of the constructed method compared to the standard VMS method. The implementations use the IGA concept (i) to ensure pointwise divergence-free solutions and (ii) to deal with smooth basis functions convenient for the computation of second derivatives. [1] I. Akkerman, Y. Bazilevs, D.J. Benson, C.E. Kees, M.W. Farthing, Free-surface flow and fluid-object interaction modeling with emphasis on ship hydrodynamics, J. Appl. Mech. 79: 010905, 2012. [2] M.F.P. ten Eikelder, I. Akkerman, Correct energy evolution of stabilized formulations: The relation between the variational multiscale approach and the Galerkin/least-squares method via dynamic orthogonal small-scales and isogeometric analysis. I: The convective-diffusive context, Comput. Methods Appl. Mech. Engrg. 331: 259-280, 2018. [3] M.F.P. ten Eikelder, I. Akkerman, Correct energy evolution of stabilized formulations: The relation between the variational multiscale approach and the Galerkin/least-squares method via dynamic orthogonal small-scales and isogeometric analysis. II: The incompressible Navier-Stokes equations, under review.

The Computational Analysis of Resonances of Bubble Clouds and Fish Schools with the Boundary Element Method

Elwin van 't Wout^{*}, Christopher Feuillade^{**}, Carlos Jerez-Hanckes^{***}

^{*}Pontificia Universidad Católica de Chile, ^{**}Pontificia Universidad Católica de Chile, ^{***}Pontificia Universidad Católica de Chile

ABSTRACT

At specific frequencies, schools of fish can exhibit a high reflectivity of acoustic signals from sonar systems, resulting in a strong impact on the quality of the sonar signal used for underwater surveillance. This phenomenon happens for fish that have swim bladders filled with air. Because of the high contrast in density between air and water, a clear low-frequency resonance is present. These resonances, also known as Minnaert resonances, have been observed in practice and can be explained theoretically. Although the resonance frequency of a single air bubble in water can be determined analytically with Mie series, numerical methods need to be used to investigate the impact of the shape as well as the number of bubbles in the system. Specifically, the resonance frequency of a cloud of bubbles depends on the configuration and distances between them. When bubbles are close to each other, high-accuracy numerical methods need to be used to compute the resonance frequency of the coupled system. The boundary element method (BEM) for the multiple traces formulation (MTF) of the Helmholtz transmission problem will be used to analyse the low-frequency resonances accurately. The numerical results are compared with a method based on transmission matrices, demonstrating that the BEM effectively predicts the pronounced frequency shifts in the resonances of the clouds of bubbles. [1] R. Hiptmair and C. Jerez-Hanckes, "Multiple traces boundary integral formulation for Helmholtz transmission problems." *Adv. Comput. Math.*, vol. 37 (2012), pp. 39-91. [2] M. Raveau and C. Feuillade, "Resonance scattering by fish schools: A comparison of two models." *J. Acoust. Soc. Am.*, vol. 139 (2016), pp. 163-175. [3] W. Smigaj, T. Betcke, S. Arridge, J. Phillips, and M. Schweiger, "Solving Boundary Integral Problems with BEM++." *ACM Trans. Math. Softw.*, vol. 41 (2016), pp. 6:1-6:40.

An Adaptive IGA Method for Elasto-capillary FSI

Harald van Brummelen*, Mahnaz Shokrpour-Roudbari**, Jacco Snoeijer***, Gertjan van Zwieten****

*Eindhoven University of Technology, **Eindhoven University of Technology, ***Twente University, ****Evalf computing

ABSTRACT

Binary fluids are fluids that comprise two constituents, viz. two phases of the same fluid (gas or liquid) or two distinct species (e.g. water and air). A distinctive feature of binary-fluids is the presence of a fluid–fluid interface that separates the two components. This interface generally carries surface energy and accordingly it introduces capillary forces. The interaction of a binary-fluid with a deformable solid engenders a variety of intricate physical phenomena, collectively referred to as elasto-capillarity. The solid–fluid interface also carries surface energy and, generally, this surface energy is distinct for the two components of the binary fluid. Consequently, the binary-fluid–solid problem will exhibit wetting behavior. Elasto-capillarity underlies miscellaneous complex physical phenomena such as durotaxis, i.e. seemingly spontaneous migration of liquid droplets on solid substrates with an elasticity gradient; capillary origami, i.e. large-scale solid deformations by capillary forces. Binary-fluid–solid interaction is moreover of fundamental technological relevance in a wide variety of high-tech industrial applications, such as inkjet printing and additive manufacturing. In this presentation, we consider a computational model for elasto-capillary fluid-solid interaction based on a diffuse-interface model for the binary fluid and a hyperelastic-material model for the solid. The diffuse-interface binary-fluid model is furnished by quasi incompressible Navier–Stokes–Cahn–Hilliard equations with a preferential-wetting boundary conditions at the fluid-solid interface. To resolve the scale difference between the characteristic length scale of the problem (e.g. droplet radius) and the width of the diffuse fluid-fluid interface we apply an adaptive hierarchical B-spline approximation. we consider a monolithic approach to ensure robustness of the solution procedure for the coupled FSI problem. We consider several aspects of the model, of the formulation and of the considered numerical techniques.

Demonstration of a Computationally Efficient Method for Stacking Sequence Blending of Composite Laminates

Julien van Campen*, Ellen van den Oord**

*TU Delft, **TU Delft

ABSTRACT

Stacking sequence optimisation can be used to increase the strength or stiffness of a composite laminate, or to reduce its weight subject to a strength or stiffness constraint. Optimisation of larger composite structures consisting of multiple panels may result in stacking sequences of adjacent panels that are incompatible with one another. The act of enforcing stacking sequence continuity to ensure structural integrity and manufacturability of a laminated composite laminate is known as blending. This term was first introduced by Zabinsky (1994). In literature, many methods can be found to implement structural continuity by means of stacking sequence blending in one way or another. The complexity of the problem makes the blending of a structure with a large number of adjacent design regions, and thus stacking sequences, prohibitive. This work introduces a computationally efficient method for stacking sequence blending of composite laminates. The presented method is inspired by cellular automata (CA) and relies on the application of a set of simple rules to solve the blending problem. The presented method is demonstrated using the benchmark 18-panel horseshoe blending problem, Soremekun et al. (2002). Each panel is initialized using a genetic algorithm (GA). The result is fed into the CA-scheme. The obtained results are equal to or better than those reported in the literature and were obtained requiring very little operations. This can be attributed to the increased design space of the presented method compared to literature. The computational efficiency makes the presented method especially interesting for composite structures with a large number of design regions. An outlook on the scalability of the presented method and its limits will be given. Soremekun, G. A., Gürdal, Z., Kassapoglou, C. and Toni, D. (2002), 'Stacking sequence blending of multiple composite laminates using genetic algorithm', *Composite Structures* 56(1), 53–62. Zabinsky, Z. B. (1994), 'Global optimization for composite structural design', Monthly technical progress report, under contracts NAS1-18889 (report No. 58) and NAS1-20013, task 2 (report 4).

Interaction Between a Moving Oscillator and an Infinite Beam on Elastic Foundation with Transition Zone in Stiffness – Green's Function Approach

Karel N. van Dalen^{*}, Traian Mazilu^{**}, Andrei B. Fîrîgău^{***}, Tao Lu^{****}

^{*}Delft University of Technology, ^{**}University Politehnica of Bucharest, ^{***}Delft University of Technology, ^{****}Delft University of Technology

ABSTRACT

Transition zones in railway lines are areas between different track structures such as the transition from conventional track (ballasted track) to slab track, to a tunnel or a viaduct. The main feature of a transition zone is that it exhibits a dramatic change in structural behaviour to bridge the difference in the adjacent track parts. This change causes high dynamic loads which contribute to quality deterioration of the track. Two main factors influence the magnitude of the interaction forces between trains and track in transition zones. Firstly, the abrupt change in track stiffness. This stiffness is determined by the mechanical features of the entire track structure; the conventional track is a compliant structure, while slab track, tunnels and viaducts are relatively stiff. A train passing a stiffness change induces a variation of track deflection under the moving dead loads and, consequently, also a variation in the wheelset's vertical momentum leading to higher (dynamic) loads. Secondly, settlements of the backfill and its foundation are typically larger than those of stiff structures, leading to unevenness of the track. This abstract deals with the issue of the dynamic analysis of an infinite Euler-Bernoulli beam on elastic foundation with transition in foundation stiffness, subjected to a moving oscillator. This model is one of the simplest ones for a vehicle passing a transition zone. The equations of motion are solved by means of the time-domain Green's function method using convolution integrals in terms of the unknown contact force. Considering the track as an aperiodic structure, the Green's functions (receptances) are calculated in a stationary reference frame (i.e., non-moving sources). Two methods of solution are investigated. The first one is based on the Laplace Transform, where the response consists of a contribution from the initial conditions and one from the moving contact force. By choosing the initial conditions in accordance with the response of a beam with homogenous foundation subjected to a moving load, the free vibrations and waves due to oscillator entrance are suppressed and steady-state behaviour is achieved before the oscillator reaches the transition zone. The second method is based on the Fourier Transform, which automatically ensures this steady-state behaviour. Both methods are exemplified in the paper. The influence of the length of the transition zone and the speed of the moving oscillator on the contact force are analysed; both sub-critical and super-critical speeds are considered.

Reduced-order Modelling and Design Sensitivity Analysis in Topology Optimization of Geometrically Nonlinear Shell Structures

Fred van Keulen*, Yi Zhang**, Dirk Munro***, Xiaoqian Chen****

*Department of Precision and Microsystems Engineering (Mechanical, Maritime and Materials Engineering Faculty), Delft University of Technology, Delft, The Netherlands, **College of Aeronautics and Astronautics, National University of Defense Technology, Changsha, Hunan, China, ***Department of Precision and Microsystems Engineering (Mechanical, Maritime and Materials Engineering Faculty), Delft University of Technology, Delft, The Netherlands, ****National Innovation Institute of Defense Technology, Chinese Academy of Military Science, Beijing, China

ABSTRACT

In structural topology optimization a computational bottleneck occurs in the finite element analysis (FEA) of the physics of the problem [1]. If geometric nonlinearity is taken into account in the analysis of the structural behaviour, then the FEA is an expensive incremental solution procedure (Newton-Raphson) [2]. Reduced-order modelling (ROM) concepts have been employed in the analysis of nonlinear structural behaviour to alleviate the computational burden [3]. ROM techniques are computationally efficient because the bottleneck referred to above is proportional to the number of degrees of freedom in the discretized analysis domain. In this work we study ROM concepts in topology optimization of shell structures subjected to out of plane loading. The aforementioned configuration mitigates numerical issues related to the distortion of low-density elements, which permits, in turn, a focussed study on the computational properties of the ROM in the optimization loop. We present, compare and evaluate sensitivity calculation with four different formulations. In all the formulations the ROM is utilised to speed-up the Newton-Raphson procedure in the analysis phase. The ROM basis vectors are made-up of the orthonormalised solution vectors of a set number of load increments. The first formulation entails correction of the equilibrium solution obtained with the ROM, with the FOM, and a standard full-order adjoint sensitivity calculation. The second formulation is a consistent ROM adjoint sensitivity formulation without full-order correction. The third formulation provides approximate sensitivity information by neglecting the terms associated to the basis vectors in the consistent adjoint formulation. The fourth and final formulation entails projection of the reduced-order solution to the full-order solution space (without correction), and the approximate equilibrium solution is used directly in the standard full-order adjoint formulation. The four options are compared with the standard FOM formulation, which serves as benchmark. The numerical experiments confirm the expected efficiency of the ROM, but the results also indicate that both approximate formulations provide a good balance between accuracy and efficiency. [1] N. Aage, E. Andreassen, B.S. Lazarov, and O. Sigmund. Giga-voxel computational morphogenesis for structural design. *Nature*, 550(7674):84-86, 2017 [2] T.E. Bruns and D.A. Tortorelli. Topology optimization of non-linear elastic structures and compliant mechanism. *Computer Methods in Applied Mechanics and Engineering*, 190(26):3443-3459, 2001. [3] A.K. Noor and J.M. Peters. Reduced basis technique for nonlinear analysis of structures. *AIAA Journals*, 18(4):455-456, 1980

Multiscale Conditional Sampling of PDEs with Random Field Inputs

Hans-Werner van Wyk*

*Auburn University

ABSTRACT

The statistical prediction and design of physical systems described by partial differential equations with uncertain, complex material properties often carries a prohibitive computational cost. This is attributable to a combination of two bottlenecks: i) the steep cost of evaluating sample paths and ii) the complexity of the underlying parameter space. In order to stay within a given computational budget, some form of adaptivity must be employed. In this talk we adaptively vary parametric complexity, by using Gaussian Markov random fields to model the spatially varying input parameters for our PDE. This allows us to exploit readily available local dependency information of the parameter field in conjunction with standard finite element error estimates and local sensitivities to identify spatial regions that contribute statistically to the error in the computed quantity of interest. We illustrate our approach by means of numerical examples.

Efficient Multiscale/Multiphysics Modeling of Hygrothermal Fatigue in Laminated Composites

Frans van der Meer*, Bert Sluys**, Iuri Rocha***

*Delft University of Technology, **Delft University of Technology, ***Knowledge Centre WMC / Delft University of Technology

ABSTRACT

Accurate lifetime prediction in composite laminates subjected to a combination of fatigue loads and exposure to extreme environmental conditions is a challenging task. Although of crucial importance in design, a comprehensive knowledge of material behavior under these circumstances is still lacking, leading to inefficient designs with wide safety margins. In order to fill this knowledge gap, it is necessary to move away from traditional characterization techniques based on coupon testing and macroscale modeling and focus on the microscopic mechanisms that drive failure and aging. By explicitly modeling fibers, resin and interfaces, phenomena such as plasticization, hydrolysis, oxidation, molecular relaxation, differential swelling and debonding can be accurately captured. In order to obtain macroscopic information relevant for design, concurrent multiscale techniques providing a continuous two-way coupling between scales can be used. A major obstacle in using such multiscale techniques is the high computational effort involved. Concurrent scale coupling implies that for each macroscopic analysis step multiple micromodels are executed, each of which features dense finite element meshes and high-fidelity constitutive models with expensive stress update procedures. Furthermore, fatigue loads and aging mechanisms usually act in two distinct time scales, leading to analyses with a very large number of time steps. It is therefore important to employ techniques to decrease the effort associated to solving the microscopic equilibrium problem while minimizing any resultant loss of accuracy. In this work, a number of reduced-order modeling techniques is used to allow for fast and accurate multiscale/multiphysics analysis of laminated composites. At the macroscale, the stress equilibrium problem is combined with a Fickian diffusion analysis in order to solve for the water concentration field that drives aging. The micromodels consist of linear-elastic fibers, viscoelastic/viscoplastic/damage resin and cohesive interfaces. The resultant two-scale model is used to predict material degradation after a number of immersion/drying cycles combined with cyclic mechanical loads. In order to accelerate micromodel computation, a combination of the Proper Orthogonal Decomposition (POD) and Empirical Cubature Method (ECM) techniques is employed. In order to efficiently recover stresses and material history at all integration points, Gappy Data least-squares reconstruction is used in combination with a k-means clustering algorithm. The gains in execution time brought by the acceleration techniques are assessed and the resultant lifetime predictions are compared with experimental results.

Experimental and Numerical Multi-scale Mechanics of High Toughness Fibrillating Interfaces with Large Elastic Mismatch

Olaf van der Sluis*, Tijmen Vermeij**, Jan Neggers***, Bart Vossen****, Marc van Maris*****,
Marc Geers*****, Johan Hoefnagels*****

*Eindhoven University of Technology & Philips Research Laboratories, **Eindhoven University of Technology,
Eindhoven University of Technology, *Eindhoven University of Technology, *****Eindhoven University of
Technology, *****Eindhoven University of Technology, *****Eindhoven University of Technology

ABSTRACT

A multi-scale experimental and numerical analysis, encompassing a range of analysis techniques, has been employed to unravel the physical origin behind the remarkably high macroscopic work-of-separation of large elastic mismatch fibrillating interfaces, particularly the copper/PDMS system which is often encountered in stretchable electronics, as function of the interface roughness. The experimental investigation, including 0°, 90°, and 180° peel tests, conclusively revealed that the delamination process is a multi-scale problem spanning all length scales. The progressing peel front was imaged in-situ in an Environmental Scanning Electron Microscope (ESEM). Front-view visualization at high magnification revealed that, at the peel front, a fibrillation process occurs, while high-magnification side-view visualization clearly showed that the fibrils initiate at the peaks of the copper roughness profiles. The fibril shape, distribution and location were found to be governed by the copper topography, which was explained by a mechanism of fibril nucleation resulting from a combination of mechanical interlocking at roughness valleys and cavitation at the roughness peaks. Quantification of the PDMS residue on the delaminated copper surface revealed that the delamination propagates primarily by fibril rupture instead of interface decohesion, while quantitative matching of the two crack surface topologies showed that the PDMS material deforms in a fully hyper-elastic manner. With these microscopic observations at hand, a single fibril model was developed, which was calibrated to dedicated PDMS single fibril experiments. The single fibril simulations showed that, contrary to the frequently used exponentially decaying Traction-Separation Law, the fibril exhibits a nonlinear increase in traction with increasing opening displacement up to the point of a sudden loss of traction due to fibril fracture. A discrete multiple fibril model that incorporates this abrupt fibril rupture was employed to analyze the mutual interaction between the fibrils as well as the local transfer of loads to the adjacent bulk rubber. The high work-of-separation values were explained by the unstable dynamic release of stored elastic energy in the PDMS bulk, the spatial discreteness of the fibrils, including the interaction of the fibrils with the adjacent deforming bulk materials, and the highly nonlinear behavior of the PDMS at large strains. The results established an experimentally validated quantitative relation between the peel front height and the macroscopic interface toughness, which was confirmed by independent results from the 180° peel test.

Redundancy Distribution and Adaptive Structures

Malte von Scheven*, Ekkehard Ramm**, Manfred Bischoff***

*Institute for Structural Mechanics, University of Stuttgart, **Institute for Structural Mechanics, University of Stuttgart, ***Institute for Structural Mechanics, University of Stuttgart

ABSTRACT

Already for the design of a passive load bearing system redundancy and thus the degree of static indeterminacy plays an important role. According to Ströbel [1] the distribution of the static indeterminacy in the system (Figure 1) can be described by the redundancy contribution of each element of a truss. The sum of the redundancy contributions of all elements is equal to the degree of indeterminacy of the entire structure. The extension of this notion presented for truss systems by Ströbel to frames and continua or thin-walled structures yields valuable insight into the load bearing of a structure but at the same time it poses some scientific challenges. Also for the integrative design of efficient adaptive structures in civil engineering the redundancy distribution can be applied. The redundancy matrix, containing the redundancy contributions of all elements, is directly related to the space of adaptability. During the design process the eigen vectors of this space can be used to evaluate how good the stress distribution of a system can be adapted without specifying the number or positions of the actuators. The space of adaptability can also be used to find favourable positions for the actuators taking into account the controllability without application of complex and time consuming optimization algorithms. The aim of this work is to get a better insight into the load bearing behaviour of adaptive systems and characterize them. Thereby an integrative design of optimal adaptive structures based on insights to the load bearing behaviour and not on complex optimization algorithms should be enabled. [1] D. Ströbel. Die Anwendung der Ausgleichsrechnung auf elastomechanische Systeme. Doktorarbeit. Institut für Anwendungen der Geodäsie im Bauwesen, Universität Stuttgart. 1995.

Machine Learning Materials Physics: Hierarchical Multiscale Modeling of Porous Battery Materials by Deep Neural Networks

zhenlin wang^{*}, Krishna Garikipati^{**}

^{*}University of Michigan, ^{**}University of Michigan

ABSTRACT

In this work, we study deep neural networks as a paradigm for abstracting the complexity of porous microstructures of battery electrodes. This investigation is part of a larger exploration of the roles of machine learning in materials physics. The porous electrodes are obtained as arbitrarily chosen configurations of spherical active particles in a fluid electrolyte. Porous separators are similar realizations of cylindrical polymer particles surrounded by the electrolyte. Direct numerical simulations (DNS) are performed for the coupled electro-chemo-thermo-mechanics of the charging-discharging cycle of the cell. Our goal is to incorporate this particle scale physics in homogenized models of the electrode and separator. We have previously used simplified response functions that vary with the evolving porosity in these homogenized models (Wang et al. J. Electrochem. Soc. 164, 2017). Our DNS of the particle scale physics generate training data for deep neural network (DNN) representations of the swelling functions, diffusivity and reaction kinetics. For lithium batteries, the concentrations of Li atoms, Li^+ ions, and porous microstructure variables are the input features to the DNNs. This study offers the opportunity to contrast the DNN representations with previous experimental fits of the response functions that were parameterized by the average porosity.

Constitutive Modelling for Fiber Reinforced Thermoplastic Composites

shenghua wu^{*}, F. M. Andrade Pires^{**}, Lallit Anand^{***}

^{*}MIT & FEUP, ^{**}FEUP, ^{***}MIT

ABSTRACT

Fiber-reinforced composite materials offer considerable performance advantages over conventional materials and play a crucial role in light-weight applications, especially for current developments in the field of electro mobility, aeronautical industry, automotive industry etc. However, thermoplastic composites exhibit a highly complex deformation behavior. The understanding of their mechanical behavior, particularly the plastic deformation mechanisms presented by the thermoplastic matrix, is of critical importance to the design and the improvement of their mechanical properties. In this contribution, a microstructural representative volume element (RVE), composed by a thermoplastic polyamide matrix and reinforcement fibers, is initially considered to study the deformation response of these materials. The RVE is subjected to a comprehensive set of stress states and the observed deformation mechanisms together with the nonlinear homogenized response of the composite are analyzed in detail. Based on these micromechanical results, a constitutive model is proposed based on crystal plastic approach and numerically implemented into an implicit integration scheme. The material parameters in the proposed constitutive model are calibrated with micromechanical tests. The proposed model then is used to predict the mechanical behavior of structural composites.

Progressive Damage and Rupture in Soft Viscoelastic Media

shenghua wu*, yunwei mao**

*MIT & FEUP, **MIT

ABSTRACT

Soft viscoelastic media has wide applications, such as tissue engineering and drug delivery. To fully exploit the potential of these materials, the understanding on progressive degradation, damage and rupture in such materials is critical. However, the intrinsic viscoelasticity of these materials hinges the understanding. Here we present an idea which can capture the progressive damage and rupture in soft viscoelastic media, by embedding two essential ideas: a). The free energy of elastomers is not entirely entropic in nature—there is also an energetic contribution from the deformation of the bonds in the chains. This energetic part in the free energy is the driving force for progressive damage and fracture. b). In contrast to the instantaneous nature of the energetically controlled elasticity, the conformational or entropic changes in polymeric materials are processes whose rates are sensitive to the local molecular mobility. The viscous-elastic effects in soft viscoelastic media are considered as effective entropy controlled process in soft media. Using this model, we can estimate the rupture stretch of viscoelastic materials from fundamental quantities describing the polymer network and viscosity of the media. We also demonstrate that in linear viscoelastic region, de Gennes's scaling law is recovered from our model.

Theoretical Views on the Yielding Transition in Amorphous Solids

matthieu wyart*

*EPFL

ABSTRACT

Glassy systems with long-range interactions often present avalanche type-response under slow driving, whose statistics is similar to that of earthquakes. They also present a vanishing density of excitation at low energy or “pseudo gap”. I will explain why these facts must come together, and discuss in particular the plasticity of amorphous solids (for example, how does a mayonnaise flow when one slowly pushes it with a spoon). I will argue that the mean-field description of plasticity maps into the problem of Levy Flights near an absorbing boundary, and draw consequences of this analogy.

Study of Coherent Structures of Turbulent Boundary Layer by DNS and Experiment

panpan yan^{*}, Chaoqun liu^{**}, yanang guo^{***}, xiaoshu cai^{****}

^{*}Beijing Jiaotong University, Beijing, 100044, China, ^{**}University of Texas at Arlington, Arlington, Texas 76019, USA, ^{***}University of Shanghai for Science and Technology, Shanghai, 200093, China, ^{****}University of Shanghai for Science and Technology, Shanghai, 200093, China

ABSTRACT

To study the characteristics of coherent structures of the turbulent boundary layer, the motion single frame and long exposure imaging (MSFLE) method is proposed and an elaborate direct numerical simulation experiment was also conducted. MSFLE method is a Lagrangian measurement method, the speed of the camera is kept the same as the speed of the coherent structure, and the particle trajectory was captured by long exposure. By calculating the trace of the points on a chosen plane of the DNS result, we can obtain the particle trajectory like MSFLE method. Multilayer of vortex structures was observed and the evolution of the vortex packets with time was recorded. The result of the DNS simulation agrees well with the experiment. The size of the vortex of the different layer is almost the same, and no vortex breakdown was observed. The formation of the small-scale vortex is caused by sweeps and ejections of the larger coherent structures rather than the breakdown process.

Numerical Investigation on Dynamic Mechanical Property of Polyurea by Coarse-Grained Molecular-Dynamics Model

kaili yao^{*}, zhuo zhuang^{**}, zhanli liu^{***}

^{*}Tsinghua University, ^{**}Tsinghua University, ^{***}Tsinghua University

ABSTRACT

The main goal of this work is to establish relationship between the chain structure and dynamic mechanical properties of polyurea. Molecular-level simulations of polyurea are realized by molecular dynamics (MD). The coarse graining (CG) model is developed to bridge the size disparity from nano to meso scales to reduce the computational cost and make the problem realistic to investigate. The dynamic mechanical properties of polyurea are then calculated from the results obtained by MD simulation using the Green-Kubo method, including the storage modulus, loss modulus and loss factor. They are functions related to frequency, which can characterize the abilities of the material to store and dissipate energy under periodic loading with certain frequencies. The CG procedure mainly includes two parts, static structure mapping and dynamic behavior mapping, respectively. In case of static structure mapping, the all-atoms geometric model of polyurea is divided into the appropriate CG geometric model and use IBI method to obtain the potential energy parameters of the model. Because the dynamics of CG-MD simulations are speed up, it is necessary to revise the dynamic behavior by correcting the time scale and modulus of CG-MD simulation results. MD simulation process is realized by LAMMPS software. The CG method speeds up MD simulation at least four orders of magnitude and makes it possible to study the macromolecule relaxation problems under current computational tool. In order to obtain the macroscopic mechanical properties of the material from the meso scale model, the shear relaxation function is calculated by the Green-Kubo method and then the storage modulus, loss modulus and loss factor are obtained. After confirming reliability of the model described above, the structure of molecular chain is changed, that is the length of chain and ratio of soft and hard segments. Then, the analysis is made for their effect on the dynamic mechanical properties of polyurea. The computational solutions display that if the molecular chain is longer, there is the longer shear modulus, the longer relaxation time, the higher storage modulus and loss modulus. Comparing homopolymer with the same chain length, the copolymer has the higher modulus and longer relaxation time. By reducing the ratio of soft and hard segments, it increases the shear modulus, lengthens the relaxation time and greatly increases the storage modulus and loss modulus. Finally, the CG-MD simulation results are compared with the data from DMA experiments and ultrasonic experiments to verify and calibrate the CG-MD model.

Dynamic Load Identification of Three Dimensional Structures Based on LMS Adaptive Delay Inverse System

yuanxi yin^{*}, xunxuan gong^{**}

^{*}Harbin Engineering University, ^{**}Harbin Engineering University

ABSTRACT

The problem of load identification has been a popular research topic in the field of ship and aerospace. Unknown loads usually exist in the dynamic system of the ship or the aircraft which may destroy the structure. For the sake of structural safety and structural optimization, the unknown load needs to be accurately identified. The load identification is composed to the frequency domain method and the time domain method. The time domain method has advantages in the nonlinear problem, which is more suitable for practical complex engineering applications. Based on the LMS Adaptive Inverse Delay System Identification Excitation Method, a three-dimensional acceleration response data identification is proposed to identify the periodic load, impact load and random load time history acting on the three-dimensional structure. The dynamic load can cause multi-directional coupling vibration on the three-dimensional elastic body. The three-dimensional elastic structure is established by Virtual.Lab simulation to obtain the time history data of dynamic load and acceleration responses in different directions. In MATLAB, the LMS adaptive algorithm is used to calculate the load Identify and the recognition effect in different directions are ideal. In a complex structure which is closer to the real engineering structure (double floating valve structure with vibration isolator), the recognition effect of multi-directional coupling vibration response of three-dimensional structure caused by dynamic load is verified by experiment, which proves the feasibility of this method.

Response Analysis of Moving Load on Stepped Cantilever Beam

bo zhang^{*}, Hongliang Li^{**}

^{*}Harbin Engineering University, ^{**}Harbin Engineering University

ABSTRACT

With the development of modern industry, more and more variable cross-section structure are used in machinery manufacturing, military industry, bridge construction and civil engineering. Beams with variable cross-section show excellent mechanical properties, it will get benefit from studies on variable cross-section structure. In previous research, when concerning about the dynamic response of the variable cross-section structure under moving load, the structures are usually simplified to equal section beam structure. However, the accuracy of the simplified cross-section beam will be reduced, which may not meet the production requirements. In this paper, in order to reduce the deviation, the variable section beams are simplified as ladder beams. This paper will take the stepped cantilever beam as an example, based on the vibration theory and the numerical calculation method, the free vibration characteristics and the forced vibration characteristics of the cantilever ladder beam are analyzed. According to the ladder beam vibration equation and boundary conditions, the natural frequency and mode function of each section of the ladder beam are deduced by using the transfer matrix method. In order to simplify the calculation process, on the premise of guaranteeing accuracy, use the modal truncation method to intercepted the first four natural frequencies for analysis, the first four natural frequencies and the corresponding mode functions are obtained. By using the resulting natural frequencies and mode functions ,under the action of the moving load ,each part of the forced vibration response can be solved by using Newmark algorithm and connect each beam by continuity conditions. The numerical calculation process is done in matlab, the time-response curve of the cantilevered ladder beam under moving loads can be obtained. The research method in this paper can be used to calculate the stepped beam with arbitrary segments and arbitrary boundaries. This research has a good engineering application. Using this method can reduce the calculation deviation and provide data support for designing and manufacturing. This abstract is funded by the International Exchange Program of Harbin Engineering University for Innovation-oriented Talents Cultivation

Visualization Research of Key Blocks of Tunnel in Multi Parallel Fracture Cutting

Yin Zhao^{*}, Shen Huang^{**}, Xuan Wu^{***}

^{*}Hohai University, ^{**}Hohai University, ^{***}Hohai University

ABSTRACT

In order to research key blocks in whole block rock cutted by multiple fractures, take a hydraulic tunnel as an example, based on the analysis of geological datas, achieved the statistics of fractures, average spacing, cohesion, according to block theory, found rock structural plane in three-dimensional network simulation, displayed the movable block of the tunnel, and the display of the most critical block in rocks cutting buy multi groups of fractures, reveal the sliding mode and analyzed the safety factor, satisfied the requirement of the three-dimensional display in the engineering.